A publication of the
American Pharmaceutical Association—
the National Professional Society
of Pharmacists

JOURNAL OF PHARMACEUTICAL SCIENCES

INDEX TO AUTHORS
INDEX TO SUBJECTS

VOLUME 68
JANUARY TO DECEMBER, 1979

Published monthly under the supervision of the Board of Trustees

MARY H. FERGUSON
Editor

SHELLY ELLIOTT
Production Editor

MARCIA GARTRELL
Copy Editor

NICOLETTE TRIANTAFELLU
Copy Editor

EDWARD G. FELDMANN
Contributing Editor

SAMUEL W. GOLDSTEIN
Contributing Editor

BELLE R. BECK
Editorial Secretary

DAVID BOHARDT
Director of Publications

L. LUAN CORRIGAN
Assistant Director of Publications

EDITORIAL ADVISORY BOARD

John Autian
Norman R. Farnsworth
William O. Foye
William J. Jusko
Herbert A. Lieberman
David E. Mann, Jr.
Gerald J. Papariello
Edward G. Rippie

JANUARY 1979
VOLUME 68 NUMBER 1

JOURNAL OF PHARMACEUTICAL SCIENCES

MARY H. FERGUSON
Editor

SHELLY ELLIOTT
Production Editor

JANIS KELLY
Copy Editor

EDWARD G. FELDMANN
Contributing Editor

SAMUEL W. GOLDSTEIN
Contributing Editor

BELLE R. BECK
Editorial Secretary

DAVID BOHARDT
Director of Publications

L. LUAN CORRIGAN
Assistant Director of Publications

EDITORIAL ADVISORY BOARD

JOHN AUTIAN
NORMAN R. FARNSWORTH
WILLIAM O. FOYE
WILLIAM J. JUSKO
HERBERT A. LIEBERMAN
DAVID E. MANN, JR.
GERALD J. PAPARIELLO
EDWARD G. RIPPIE

The *Journal of Pharmaceutical Sciences* is published monthly by the American Pharmaceutical Association (APhA) at 2215 Constitution Ave., N.W., Washington, DC 20037. Second-class postage paid at Washington, D.C., and at additional mailing office.

All expressions of opinion and statements of supposed fact appearing in articles or editorials carried in this journal are published on the authority of the writer over whose name they appear and are not to be regarded as necessarily expressing the policies or views of APhA.

Offices—Editorial, Advertising, and Subscription: 2215 Constitution Ave., N.W., Washington, DC 20037. Printing: 20th & Northampton Streets, Easton, PA 18042.

Annual Subscriptions—United States and foreign, industrial and government institutions $50, educational institutions $50, individuals *for personal use only* $30; single copies $5. All foreign subscriptions add $5 for postage. Subscription rates are subject to change without notice. Members of APhA may elect to receive the *Journal of Pharmaceutical Sciences* as a part of their annual $70 (foreign $75) APhA membership dues.

Claims—Missing numbers will not be supplied if dues or subscriptions are in arrears for more than 60 days or if claims are received more than 60 days after the date of the issue, or if loss was due to failure to give notice of change of address. APhA cannot accept responsibility for foreign delivery when its records indicate shipment has been made.

Change of Address—Members and subscribers should notify at once both the Post Office and APhA of any change of address.

Photocopying—The code at the foot of the first page of an article indicates that APhA has granted permission for copying of the article beyond the limits permitted by Sections 107 and 108 of the U.S. Copyright Law provided that the copier sends the per copy fee stated in the code to the Copyright Clearance Center, Inc., P. O. Box 765, Schenectady, NY 12301. Copies may be made for personal or internal use only and not for general distribution.

Microfilm—Available from University Microfilms International, 300 N. Zeeb Road, Ann Arbor, MI 48106.

© Copyright 1979, American Pharmaceutical Association, 2215 Constitution Ave., N.W., Washington, DC 20037; all rights reserved.

CONSISTENCY IN STABILITY TESTING

For various reasons, we don't watch much in the way of television programs at our house, but the other evening we took in a football game. During this battle of the gridiron, one of the commercials was an advertising spot for a long-life automobile battery. The emphasis of this advertising pitch was the confidence the motorist could place in the reliability of the product to start his or her automobile "month after month after month."

To a significant extent, pharmacists, physicians, and patients expect—and even assume—that this kind of long-term potency will be found to at least a comparable degree in the drug products that they dispense, prescribe, or consume. Unfortunately, however, such faith is sometimes misplaced. Drug products generally deteriorate with time; some do so faster than others, to the point that a significant possibility may exist that the product—just as the rundown auto battery on the coldest day of winter—won't work, or do the job expected of it, when it is really needed.

Solution of this problem is complex and involves at least three broad elements: (*a*) stability testing to determine if the product deteriorates, how it does so, and at what rate; (*b*) packaging and storage conditions that can be employed to minimize instability and enhance effective shelflife; and (*c*) expiration dating to inform users how long the product can be relied upon to perform satisfactorily given the proper conditions of packaging and storage.

Over the past decade, industry, regulatory agencies, the official compendia, and the pharmacy profession have all been deeply involved in the subjects of packaging, storage, and expiration dating of drugs. Specifications have been developed and implemented for "tight" and "well-closed" containers; sharper standards have been developed for light protection; numerical definitions have been established for storage temperatures, such as "cold," "cool," "room temperature," "warm," and "excessive heat"; guidelines for expiration date timetables, and requirements as to the drugs to be covered, have been established; and so on.

However, less apparent progress has been made in reaching agreement on criteria in the first and most fundamental area; namely, how stability testing is to be conducted. Specifically, agreement is needed on uniformity of approach with regard to systematic, consistent, and standardized testing and test procedures.

But it now appears that this gap is about to be filled. At several conferences for drug industry technical and scientific personnel this past October, Food and Drug Administration spokesmen devoted their presentations to the subject of stability testing. In one instance, the FDA official predicted that FDA would be issuing stability "guidelines" within a month or two. If his prediction is accurate as to timing, the promised guidelines may have appeared before this column is published.

At another conference, a second FDA speaker focused on some specifics in describing "what FDA expects from stability testing." He stated, for example, that accelerated study data to establish a tentative two-year expiration date on a drug product should contain at least three months of storage at 37 to 40° Celsius and 75% or higher relative humidity. He also touched on the test intervals to be employed in conducting stability tests; specifically, he recommended *"at the initial date of manufacture, three, six, nine, 12, 18, and 24 months, and each year thereafter. The tentative expiry date may in this manner be extended to whatever shelflife may be justified by data from these studies."*

Enough in the way of details was provided to suggest that what FDA has on the drawing board will offer clear and understandable directions, whether or not there is agreement outside the agency as to their scientific validity in fulfilling the intended purpose.

Hence, without in any way prejudging the anticipated guidelines in this latter regard, it is welcome news that some definitive proposals are well along in the regulatory pipeline. The existence of guidelines alone should go far in resolving the present hodge-podge approach to stability testing of drug products.

Open Letter to Phytochemists

Inspired by papers delivered at the recent conference at Kew on the systematics and biology of Leguminosae, I reiterate a plea issued previously[1]. Those of us attempting to understand the effects of herbivores on plants and the responses of plants to herbivory are dependent on the work of chemists, natural products chemists, phytochemists, and pharmacologists for the identification of the secondary compounds in plants. However, secondary compounds do not occur in Latin binomials, and herbivores do not eat Latin binomials.

Secondary compounds occur in plant parts. A report of a new alkaloid in *Xus albus*, even assuming the plant to be correctly identified, is absolutely useless to the animal–plant biologist (except perhaps in giving some later phytochemist a clue as to what to look for in diagnosing a toxic diet). There is no excuse for the numerous papers that do not clearly identify the plant part from which the chemical was obtained. It takes one sentence to report it and only a few seconds to determine it. Secondary compounds are not evenly distributed in kind or quantity throughout the plant (in space and often in time as well). Animals respond accordingly.

It is easier to understand why the phytochemist is reluctant to determine content per unit of tissue, but let me simply beg for such information. Most secondary compound effects on animals are dosage dependent[2]. Without statements of concentration, we are powerless to interpret refusals of foods containing these chemicals. Furthermore, artificial diets testing the compounds cannot be realistic unless the concentrations are known from real dietary items. Even statements of the approximate concentration enormously increase the value of a chemical identification.

Seeds and their contained chemicals are of particular interest to me, and seed chemistry data are gross offenders. Seedcoats are from 1 to 70% of the dry weight of a seed[3] and are usually made of largely inert cellulose–lignin–tannin complexes; at the least, secondary compounds found in the seedcoat are not repeated in the seed contents and vice versa. When a bag of seeds is ground up and analyzed, concentrations of secondary compounds as then measured are extremely misleading. The animals that eat seeds almost invariably discard, avoid, or defecate the seedcoat undigested. The kind and concentration of secondary compounds in the seed contents normally matter to the animal, and this information is almost never recorded. Please do it.

The time is ripe for a person with a strong flair for organization to initiate and develop an international museum of secondary compounds. Such a "museum" would perform all those analogous functions provided by more conventional museums of organisms. The burgeoning population of workers on the interface between animals and plants are desperate for a technology or a system that will cut through the contemporary block to the identification, characterization, and provision of secondary compounds for experimental and feeding studies. Secondary compounds are, after all, practically the entire basis for the enormous and complex structure of the interaction between herbivores and plants, which makes them largely responsible for the diversity of plant and animal life on this planet.

Daniel H. Janzen
Department of Biology
University of Pennsylvania
Philadelphia, PA 19104

Received November 13, 1978.

[1] D. H. Janzen, *Ann. Missouri Bot. Gard.*, **64**, 706 (1978).
[2] D. H. Janzen, *Phytochemistry*, **16**, 223 (1977).
[3] D. H. Janzen, *Ecology*, **58**, 921 (1977).

Propoxyphene Bioavailability

A recent letter[1] by Mr. Chmielewski on "Propoxyphene Bioavailability" in the Open Forum indicated that no technical information was forthcoming from the authors after written requests. As we certainly have no reason for not responding to any inquiry, we checked our files and discovered that Mr. Chmielewski's request, along with six other requests, had been filed as sent. However, there were no copies of correspondence indicating that these requests were answered. We have recently sent the requested information to the requestors with our regrets for the delay. We thank Mr. Chmielewski for bringing this matter to our attention.

In regard to some conclusions drawn from the aforementioned Open Forum letter, we would like to make the following comments:

1. The research lots reported[2] in our bioavailability article were 100,000 capsule lots (one-tenth full size manufactured lots), which were manufactured on the exact equipment to be used for the full-sized marketed lots.
2. The research lots in question met all current existing FDA requirements and could have been submitted as part of an abbreviated NDA and been marketed.
3. The research lot that was bioinequivalent was not marketed for that very reason. We firmly believe that it is better to test for the bioequivalence of products before they are put on the market rather than after marketing.
4. The research lot that passed bioavailability testing was not marketed. The tablet dosage form was marketed instead.

Our original article was not published with political motivation. The data were sent to the FDA well before publication. The intent of the article was to point out that existing FDA requirements for approval of propoxyphene capsules were, in our opinion, inadequate. Furthermore, Mr. Chmielewski's request that only marketed generic formulations be tested for bioinequivalence would indicate that he is in favor of marketing products without any bioavailability testing. We do not believe that the blind approach of testing for bioequivalence only after the products have been marketed will improve the quality of the products on the market. It is quite possible that there are existing marketed generic formulations of propoxyphene capsules that are bioinequivalent. However, since there is little, if any, testing of this product for bioinequivalence, we sincerely doubt that any publications will be forthcoming.

K. A. DeSante
D. G. Kaiser
A. R. DiSanto,
The Upjohn Co.
Kalamazoo, MI 49001

R. G. Stoll
Arnar-Stone Laboratories
North Chicago, Ill.

Received November 2, 1978.

[1] D. H. Chmielewski, *J. Pharm. Sci.*, **67**(9), IV (1978).
[2] K. A. DeSante, R. G. Stoll, D. G. Kaiser, and A. R. DiSanto, *ibid.*, **66**, 1713 (1977).

Open Letter to Phytochemists

Inspired by papers delivered at the recent conference at Kew on the systematics and biology of Leguminosae, I reiterate a plea issued previously[1]. Those of us attempting to understand the effects of herbivores on plants and the responses of plants to herbivory are dependent on the work of chemists, natural products chemists, phytochemists, and pharmacologists for the identification of the secondary compounds in plants. However, secondary compounds do not occur in Latin binomials, and herbivores do not eat Latin binomials.

Secondary compounds occur in plant parts. A report of a new alkaloid in *Xus albus*, even assuming the plant to be correctly identified, is absolutely useless to the animal–plant biologist (except perhaps in giving some later phytochemist a clue as to what to look for in diagnosing a toxic diet). There is no excuse for the numerous papers that do not clearly identify the plant part from which the chemical was obtained. It takes one sentence to report it and only a few seconds to determine it. Secondary compounds are not evenly distributed in kind or quantity throughout the plant (in space and often in time as well). Animals respond accordingly.

It is easier to understand why the phytochemist is reluctant to determine content per unit of tissue, but let me simply beg for such information. Most secondary compound effects on animals are dosage dependent[2]. Without statements of concentration, we are powerless to interpret refusals of foods containing these chemicals. Furthermore, artificial diets testing the compounds cannot be realistic unless the concentrations are known from real dietary items. Even statements of the approximate concentration enormously increase the value of a chemical identification.

Seeds and their contained chemicals are of particular interest to me, and seed chemistry data are gross offenders. Seedcoats are from 1 to 70% of the dry weight of a seed[3] and are usually made of largely inert cellulose–lignin–tannin complexes; at the least, secondary compounds found in the seedcoat are not repeated in the seed contents and vice versa. When a bag of seeds is ground up and analyzed, concentrations of secondary compounds as then measured are extremely misleading. The animals that eat seeds almost invariably discard, avoid, or defecate the seedcoat undigested. The kind and concentration of secondary compounds in the seed contents normally matter to the animal, and this information is almost never recorded. Please do it.

The time is ripe for a person with a strong flair for organization to initiate and develop an international museum of secondary compounds. Such a "museum" would perform all those analogous functions provided by more conventional museums of organisms. The burgeoning population of workers on the interface between animals and plants are desperate for a technology or a system that will cut through the contemporary block to the identification, characterization, and provision of secondary compounds for experimental and feeding studies. Secondary compounds are, after all, practically the entire basis for the enormous and complex structure of the interaction between herbivores and plants, which makes them largely responsible for the diversity of plant and animal life on this planet.

Daniel H. Janzen
Department of Biology
University of Pennsylvania
Philadelphia, PA 19104

Received November 13, 1978.

[1] D. H. Janzen, *Ann. Missouri Bot. Gard.*, **64**, 706 (1978).
[2] D. H. Janzen, *Phytochemistry*, **16**, 223 (1977).
[3] D. H. Janzen, *Ecology*, **58**, 921 (1977).

Propoxyphene Bioavailability

A recent letter[1] by Mr. Chmielewski on "Propoxyphene Bioavailability" in the Open Forum indicated that no technical information was forthcoming from the authors after written requests. As we certainly have no reason for not responding to any inquiry, we checked our files and discovered that Mr. Chmielewski's request, along with six other requests, had been filed as sent. However, there were no copies of correspondence indicating that these requests were answered. We have recently sent the requested information to the requestors with our regrets for the delay. We thank Mr. Chmielewski for bringing this matter to our attention.

In regard to some conclusions drawn from the aforementioned Open Forum letter, we would like to make the following comments:

1. The research lots reported[2] in our bioavailability article were 100,000 capsule lots (one-tenth full size manufactured lots), which were manufactured on the exact equipment to be used for the full-sized marketed lots.
2. The research lots in question met all current existing FDA requirements and could have been submitted as part of an abbreviated NDA and been marketed.
3. The research lot that was bioinequivalent was not marketed for that very reason. We firmly believe that it is better to test for the bioequivalence of products before they are put on the market rather than after marketing.
4. The research lot that passed bioavailability testing was not marketed. The tablet dosage form was marketed instead.

Our original article was not published with political motivation. The data were sent to the FDA well before publication. The intent of the article was to point out that existing FDA requirements for approval of propoxyphene capsules were, in our opinion, inadequate. Furthermore, Mr. Chmielewski's request that only marketed generic formulations be tested for bioinequivalence would indicate that he is in favor of marketing products without any bioavailability testing. We do not believe that the blind approach of testing for bioequivalence only after the products have been marketed will improve the quality of the products on the market. It is quite possible that there are existing marketed generic formulations of propoxyphene capsules that are bioinequivalent. However, since there is little, if any, testing of this product for bioinequivalence, we sincerely doubt that any publications will be forthcoming.

K. A. DeSante
D. G. Kaiser
A. R. DiSanto,
The Upjohn Co.
Kalamazoo, MI 49001

R. G. Stoll
Arnar-Stone Laboratories
North Chicago, Ill.

Received November 2, 1978.

[1] D. H. Chmielewski, *J. Pharm. Sci.*, **67**(9), IV (1978).
[2] K. A. DeSante, R. G. Stoll, D. G. Kaiser, and A. R. DiSanto, *ibid.*, **66**, 1713 (1977).

JOURNAL OF PHARMACEUTICAL SCIENCES

JANUARY 1979
VOLUME 68 NUMBER 1

RESEARCH ARTICLES

Effect of Salicylic Acid on Pharmacokinetics of Free and Plasma Protein-Bound Bilirubin in Experimental Unconjugated Hyperbilirubinemia

SVEIN ØIE and GERHARD LEVY ˣ

Received March 31, 1978, from the *Department of Pharmaceutics, School of Pharmacy, State University of New York at Buffalo, Amherst, NY 14260.* Accepted for publication May 19, 1978.

Abstract □ The effect of salicylic acid injection and infusion on the concentrations of free and total (sum of free and bound) unconjugated bilirubin in plasma was studied in hyperbilirubinemic rats. *In vitro* addition of salicylic acid, 5–30 mg/100 ml, to rat plasma containing bilirubin, 12.7 mg/100 ml, caused a pronounced, salicylate concentration-dependent increase in the free bilirubin concentration. Normal rats were made hyperbilirubinemic by continuous intravenous infusion of bilirubin; the concentrations of free and total unconjugated bilirubin in plasma, and of total unconjugated bilirubin in whole blood, were determined as a function of time. Rapid intravenous injection of salicylate caused a rapid and pronounced decrease of total bilirubin concentrations in plasma and whole blood but had no apparent effect on the concentration of free bilirubin in plasma. Similar effects were obtained with slow infusions of salicylate, except that total bilirubin concentrations decreased gradually. These observations are consistent with the theory that the clearance rate of bilirubin by the body is proportional to the concentration of free bilirubin in plasma and that the steady-state concentration of free bilirubin depends only on the formation rate and intrinsic clearance of the pigment and is not affected by displacement of bilirubin from plasma protein binding sites. Occasional cases of acute apparent bilirubin intoxication were associated with unusually elevated concentrations of free bilirubin, reflecting a decreased intrinsic metabolic clearance of the pigment.

Keyphrases □ Salicylic acid—effect on pharmacokinetics of free and total bilirubin in hyperbilirubinemic rats □ Bilirubin, free and total—pharmacokinetics, effect of salicylic acid in hyperbilirubinemic rats □ Pharmacokinetics—free and total bilirubin, effect of salicylic acid in hyperbilirubinemic rats

The increased incidence of kernicterus and fatalities in premature infants treated with sulfisoxazole (1, 2) demonstrated the hazards of administering to hyperbilirubinemic neonates drugs that can displace the potentially neurotoxic heme pigment bilirubin from plasma protein binding sites. Studies in humans and animals (3–8) showed that drugs such as sulfisoxazole and salicylate, which displace bilirubin from plasma albumin, cause a redistribution of the pigment from plasma to extravascular tissues, including the brain. The concentration of free, diffusible (rather than total) bilirubin in plasma is, therefore, considered to be a key determinant of kernicterus in hyperbilirubinemic neonates (9). Many drugs displace bilirubin from binding sites on plasma albumin.

The displacement of bilirubin from albumin by a drug results in a permanent (disregarding stability considerations) increase in the concentration of free bilirubin in a closed *in vitro* system and may be thought to have a similar effect *in vivo*. However, according to recently developed pharmacokinetic theory (10, 11) and preliminary experimental data (12), such an increase should not occur. There is increasing evidence that the metabolic clearance rate of partly plasma protein-bound substances is proportional to their free (rather than total) concentration in plasma[1]. Under these conditions:

$$\text{total clearance} = \text{intrinsic clearance} \times \text{free fraction} \quad \text{(Eq. 1)}$$

where the intrinsic clearance is a measure of the activity of the enzyme system(s) responsible for the rate-determining step in the biotransformation process(es) and the free fraction is the ratio of free to total concentration of the substance in plasma.

According to Eq. 1, a plot of total clearance *versus* free fraction should be linear and go through the origin. This result has, in fact, been demonstrated in animals and humans for several extensively plasma protein-bound drugs (11, 14). This relationship also applies to bilirubin (12), indicating that the metabolic clearance rate of bilirubin is proportional to the concentration of free bilirubin in plasma.

The steady-state (plateau) concentration of total bilirubin in plasma, C_∞, is determined by the formation rate, R, and the total clearance of the pigment:

$$C_\infty = R/\text{total clearance} \quad \text{(Eq. 2)}$$

[1] Exceptions are those few (but clinically important) drugs and endogenous compounds whose elimination rate is limited by blood flow rate (13) or metabolic capacity.

0022-3549/79/0100-0001$01.00/0
© 1979, American Pharmaceutical Association

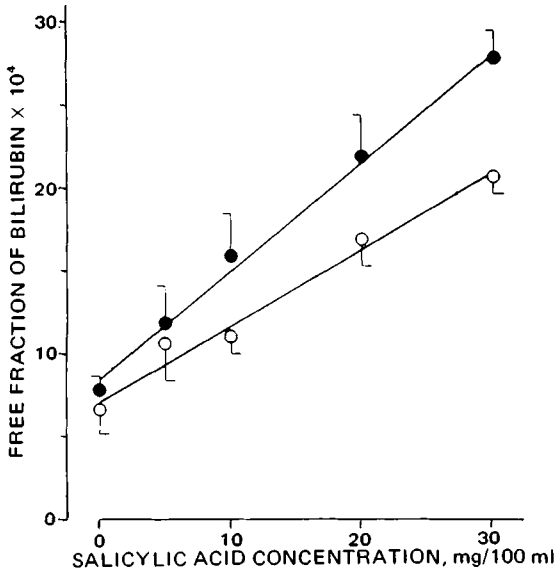

Figure 1—*Effect of various concentrations of salicylic acid on the protein binding of bilirubin at 37° in pooled plasma from four rats. Key: ●, 12.7 mg of total bilirubin/100 ml; and ○, 6.4 mg of total bilirubin/100 ml. Data are averages of five determinations with 1 SD shown in one direction only for clarity of presentation.*

The steady-state concentration of *free* bilirubin in plasma, $C_{\infty f}$, is determined by the formation rate and the *intrinsic* clearance of the pigment:

$$C_{\infty f} = R/\text{intrinsic clearance} \qquad \text{(Eq. 3)}$$

Equation 3 is obtained by substituting Eq. 1 into Eq. 2. Since total clearance is affected by changes in protein binding while intrinsic clearance is not so affected, a decrease in the plasma protein binding of bilirubin should decrease the steady-state concentration of total bilirubin but should have no effect on the steady-state concentration of free bilirubin in plasma. Administration of a drug that displaces bilirubin from plasma albumin should result in only a temporary perturbation of the steady-state situation until the "excess" bilirubin has been cleared by the body, unless that drug also modifies the intrinsic clearance (for example, by enzyme induction or inhibition) or the formation rate of bilirubin.

In the present study, this hypothesis was tested by determining the effects of a rapid injection and a slow infusion of salicylate on the concentrations of free and total bilirubin in the plasma and total bilirubin in whole blood of rats made hyperbilirubinemic by a continuous intravenous infusion of bilirubin. Contrary to common practice, the plasma concentrations of drug and bilirubin were maintained in a clinically realistic range (drug to albumin and bilirubin to albumin molar concentration ratios less than unity), and the concentration of free bilirubin was determined in undiluted plasma.

EXPERIMENTAL

Male Sprague–Dawley rats[2], 310–450 g, were maintained on a standard diet[3]. Two days before an experiment, a silicone rubber–polyethylene cannula was placed permanently in the right jugular vein to facilitate intravenous infusion, injection, and frequent withdrawal of blood samples (15, 16).

On the day of an experiment, a solution of bilirubin and sodium taurocholate (1:1.1 weight ratio in 0.7% sodium chloride adjusted to pH 7.4) was infused at a rate equivalent to 0.8 mg of bilirubin/kg/min (3.2 ml/hr/rat) for 15 min and then at 0.32 mg of bilirubin/kg/min for 105 min. Three rats then received an intravenous injection of salicylic acid, 67 mg/kg, as sodium salicylate in 0.5 ml of water, and the infusion was continued for 120 min with bilirubin, 0.32 mg/kg/min, and salicylic acid, 0.148 mg/kg/min. Three other rats received the same bilirubin infusion regimen for the first 2 hr, followed by an infusion of salicylic acid, 0.6 mg/kg/min, and bilirubin, 0.32 mg/kg/min, for the next 2 hr. Another four rats received both injection and infusion of salicylate in separate crossover experiments, about 2 weeks apart.

Additional rats served as controls and received bilirubin infusion but no salicylic acid. Some of the control rats received an intravenous injection of 0.5 ml of 1.8% sodium chloride (approximately the same tonicity as the sodium salicylate injection solution) at 2 hr. All infusion equipment, including syringes and cannulas, was covered with aluminum foil to protect bilirubin from light.

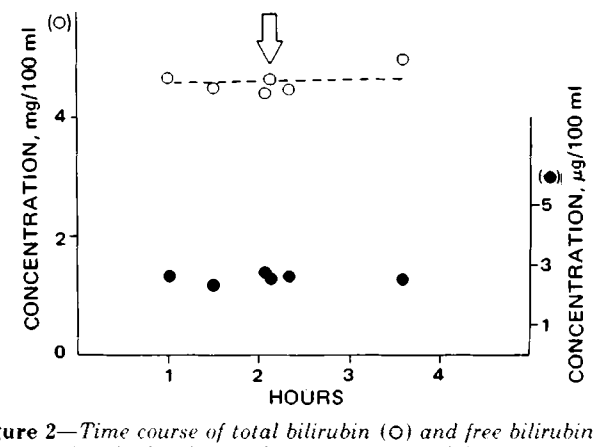

Figure 2—*Time course of total bilirubin (○) and free bilirubin (●) concentrations in the plasma of a rat infused with bilirubin at a rate of 0.80 mg/kg/min for 15 min and then at a rate of 0.32 mg/kg/min. The arrow indicates the time of injection of 0.5 ml of 1.8% NaCl. (Note the use of more than one scale in this and some of the following figures.)*

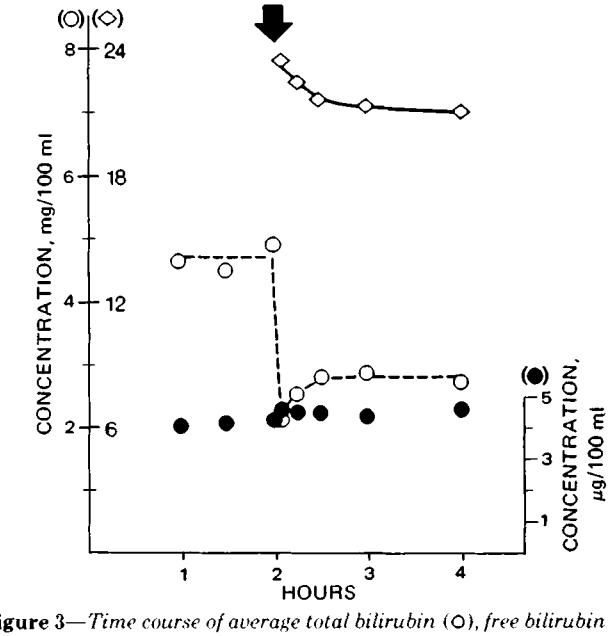

Figure 3—*Time course of average total bilirubin (○), free bilirubin (●), and salicylic acid (◇) concentrations in plasma of four rats infused with bilirubin, 0.8 mg/kg/min, for 15 min and then at a rate of 0.32 mg/kg/min until the end of the experiment. The arrow indicates the time of injection of salicylic acid, 67 mg/kg, which was followed by an infusion of 0.148 mg/kg/min.*

[2] Blue Spruce Farms, Altamount, N.Y.
[3] Charles River Formula 4RF.

Table I—Effect of Salicylic Acid Injection or Infusion on Total and Free Unconjugated Bilirubin and Salicylic Acid Concentrations in Plasma of Rats with Experimental Unconjugated Hyperbilirubinemia

	Salicylic Acid Injection			Salicylic Acid Infusion		
Hours	Total Bilirubin Concentration, mg/100 ml	Free Bilirubin Concentration, μg/100 ml	Salicylic Acid Concentration, mg/100 ml	Total Bilirubin Concentration, mg/100 ml	Free Bilirubin Concentration, μg/100 ml	Salicylic Acid Concentration, mg/100 ml
1.0	4.88 ± 0.48[a]	3.96 ± 0.99	0	5.07 ± 0.90	3.78 ± 0.96	0
1.5	4.93 ± 0.77	4.12 ± 1.33	0	5.22 ± 0.94	3.70 ± 1.16	0
2.0[b]	5.30 ± 0.66	4.13 ± 1.27	0	5.19 ± 0.90	3.82 ± 0.95	0
2.08	1.87 ± 0.69	4.44 ± 1.05	24.8 ± 2.2	—[c]	—[c]	—[c]
2.25	2.37 ± 0.70	4.21 ± 1.38	22.2 ± 1.8	4.41 ± 0.89	4.17 ± 1.28	6.46 ± 1.51
2.5	2.86 ± 0.77	4.45 ± 1.64	21.1 ± 1.55	3.65 ± 0.83	3.91 ± 1.20	10.1 ■ 1.1
3.0	2.89 ± 0.39	4.26 ± 1.52	21.0 ± 1.2	3.15 ± 0.71	4.31 ± 1.37	14.3 ± 1.0
4.0	2.87 ± 0.57	4.24 ± 1.33	20.8 ± 0.8	2.47 ± 0.78	4.08 ± 1.63	20.6 ± 1.5

[a] All data are means ± *SD*, $n = 7$. Four of the seven rats in each group were used in crossover experiments. [b] Time of salicylate injection. [c] Blood sample was not obtained at this time.

Heparinized blood samples (0.6 ml) were collected at 1, 1.5, and 2 hr and then again 15, 30, 60, and 120 min after the salicylate injection or the start of the salicylate infusion. An additional blood sample was obtained 5 min after the salicylate injection. Plasma was separated by centrifugation and analyzed for free (17) and total unconjugated bilirubin (18) and for salicylic acid (19). In some cases, the erythrocytes were lysed by freezing, thawing, and addition of 1 ml of 6% ascorbic acid in 0.2 *M* phosphate buffer, pH 8.2, to 0.1 ml of erythrocytes. This solution was analyzed for total unconjugated bilirubin (18).

Considerable care was taken to obtain "mainstream" blood samples uncontaminated by the bilirubin infusion solution. The infusion pump was disconnected from the indwelling intravenous cannula, and the cannula was flushed with 0.1–0.2 ml of normal saline solution containing heparin, 20 units/ml (volume sufficient to fill the cannula without entering the bloodstream), using a syringe attached to the cannula with a three-way stopcock. The saline solution was then drawn back into the syringe, thereby filling the catheter with blood. About 0.5 ml of blood was then drawn into a second syringe, the blood sample of 0.6 ml was drawn into a third syringe, and the 0.5 ml of blood from the second syringe was reinjected and followed by about 0.1–0.2 ml of heparinized normal saline solution to empty the cannula of blood. The bilirubin infusion was then resumed. The entire procedure required about 1 min.

The concentration of free bilirubin was determined in undiluted plasma by measuring the rate of the peroxidase-catalyzed degradation of bilirubin by peroxide. A 0.1-ml aliquot of 0.1 *M* phosphate buffer, pH 7.4, containing 0.01 *M* edetate disodium was evaporated to dryness in a 10-ml centrifuge tube. Plasma, 0.1 ml, was added, and the dried buffer was dissolved in it by vortexing. Then 10 μl of peroxidase solution (8 purpurogallin units of horseradish peroxidase[4]/ml of 0.1 *M* phosphate buffer, pH 7.4) was added. The reaction was started by adding 5 μl of peroxide solution (0.2% ethyl hydrogen peroxide in 0.1 *M* phosphate buffer, pH 7.4) and stopped after 1–2 min by addition of 1 ml of 6% ascorbic acid in 0.2 *M* phosphate buffer, pH 8.2. The entire reaction was carried out in a water bath at 37°.

The concentration of total unconjugated bilirubin before and after the reaction was determined spectrophotometrically after chloroform extraction (18), using a bilirubin control[5] as the standard. *In vitro* studies of bilirubin binding in plasma were carried out in the same manner, except that about 25 μl of bilirubin solution (crystalline bilirubin[6] dissolved in water with the aid of a few drops of 2 *M* NaOH) was added to 1 ml of pooled plasma from several rats to obtain the desired bilirubin concentration, and salicylate was added as 5 μl of an aqueous solution/100 μl of plasma.

RESULTS

Bilirubin added *in vitro* to pooled rat plasma in concentrations of 6.4 and 12.7 mg/100 ml was 99.935 and 99.925% bound, respectively, to plasma proteins. Salicylic acid decreased the protein binding of bilirubin in a concentration-dependent manner (Fig. 1). At a concentration of 30 mg/100 ml, salicylic acid decreased bilirubin binding to 99.794 and 99.721%, respectively. These changes are equal to 3.2- and 3.7-fold increases in the free fraction of bilirubin in plasma containing 6.4 and 12.7 mg of bilirubin/100 ml, respectively.

The bilirubin infusion schedule resulted in an average plasma concentration of total bilirubin of about 5 mg/100 ml, which, with three exceptions that are not included in the tabulation for reasons explained subsequently, remained constant in any one animal for the duration of the experiment (Fig. 2) or until salicylate was administered (Table I). The total bilirubin concentration in plasma decreased rapidly and substantially with salicylate injection and then increased slightly to a new plateau (lower than preinjection) as salicylate concentrations declined to a steady state (Fig. 3 and Table I). Salicylate concentrations were at a maximum immediately after injection, with a subsequent distribution phase, and then approached a plateau due to continuing infusion of the drug. Despite the significant changes in the concentrations of salicylate and total bilirubin, the free bilirubin concentration remained essentially constant throughout the experiment.

Slow infusion of salicylate over 2 hr resulted in a gradual decrease in the total bilirubin concentration, but the concentration of free bilirubin again remained essentially constant at all times (Fig. 4 and Table I). Both methods of salicylate administration were designed to, and did, produce about the same drug concentration in plasma at 4 hr, but the injection lowered the total bilirubin concentration by a maximum of 65% while the infusion caused a maximum decrease of 52% on the average (Table I). This difference was due to the higher salicylate concentration immediately after drug injection (*i.e.*, the predistributive concentration maximum) since the relationship between salicylate and total bilirubin concentrations in plasma was the same with both modes of salicylate administration (Fig. 5).

The rapid decrease of total bilirubin concentrations in plasma following injection of salicylate was accompanied by a significant increase in the concentration of bilirubin in erythrocytes (Table II). However, the bilirubin concentration in whole blood decreased (Fig. 6), indicating that some bilirubin was redistributed from blood to extravascular tissues. The elevated bilirubin concentration in the erythrocytes persisted for the duration of the experiment, suggesting that diffusion of the pigment out of the erythrocytes is very slow, perhaps due to precipitation of bilirubin in these cells.

Three rats (one injection control, one receiving salicylate injection, and one receiving salicylate infusion) developed signs of bilirubin intoxication and were excluded from the results summarized in Table I. At about the 3rd hr of bilirubin infusion, the skin of these animals became noticeably yellow, their breathing slowed, and they became prostrate. The time course of bilirubin concentrations in the plasma of one of these animals is shown in Fig. 7. Total and free plasma bilirubin concentrations increased substantially and continuously after the sodium chloride (control)

Table II—Effect of Salicylic Acid Injection on Total Unconjugated Bilirubin Concentration in Erythrocytes of Rats with Experimental Unconjugated Hyperbilirubinemia

Hours	Bilirubin Concentration[a], mg/100 ml
1.0	0.57 ± 0.24
1.5	0.58 ± 0.21
2.0[b]	0.61 ± 0.18
2.08	1.55 ± 0.83[c]
2.25	1.84 ± 0.65[c]
2.5	1.90 ± 0.60[c]
3.0	2.08 ± 0.63[c]
4.0	1.87 ± 0.55[c]

[a] Mean ± *SD*. $n = 4$. [b] Time of salicylate injection. [c] Significantly different from control period ($p < 0.02$).

[4] Sigma type I.
[5] Dade Division, American Hospital Supply Corp., Miami, Fla.
[6] Sigma.

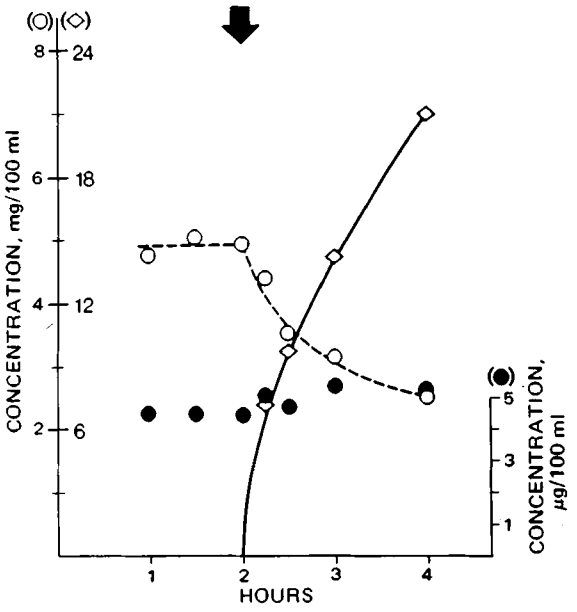

Figure 4—*Effect of salicylic acid infusion (0.6 mg/kg/min, starting at the time shown by the arrow) on average free and total bilirubin concentrations in plasma of four rats. Bilirubin infusion rate and symbols are as in Fig. 3. Note the similarity of presalicylic acid bilirubin concentrations in the salicylic acid infusion (this figure) and injection experiments (Fig. 3), which were carried out on the same animals in a crossover study.*

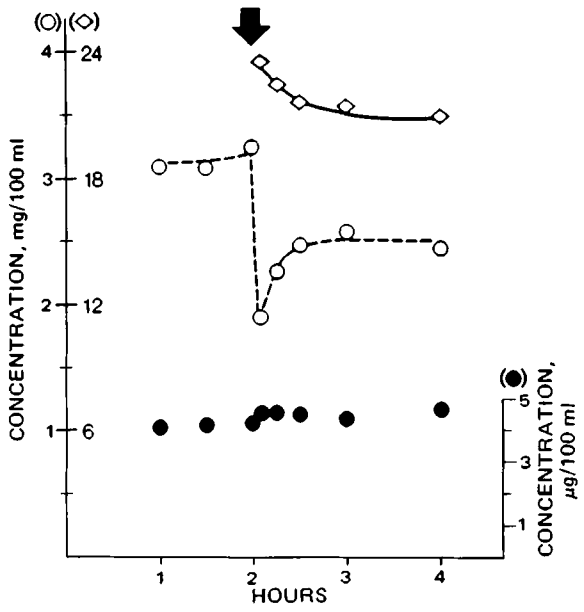

Figure 6—*The same experiment as in Fig. 3, except that open circles represent average total bilirubin concentrations in whole blood rather than in plasma. A similar but more gradual decrease of total bilirubin concentrations in whole blood was observed when salicylate was administered by slow infusion without initial rapid injection.*

injection. The concentration of free bilirubin increased relatively more than the concentration of total pigment, indicating a decrease in the protein binding of bilirubin.

This decrease is more readily apparent in Fig. 8, which shows the free fraction values as a function of total bilirubin concentration in pooled plasma from four normal rats and in plasma of the sick rat. The free fraction values of bilirubin in the intoxicated rat were normal for the first 150 min of the experiment (during which the animal appeared healthy) but then rose substantially above normal as the animal began to show signs of intoxication.

A different picture was apparent in another rat with signs of bilirubin intoxication. The free and total bilirubin concentrations in the plasma of that animal, which received a sodium salicylate injection at 2 hr, remained relatively constant over 3 hr while the skin of the animal became increasingly yellow. However, the concentration of free bilirubin and the free fraction value of bilirubin were about five times higher than in the normal animals. The albumin and total protein concentrations in the plasma of this intoxicated animal were only 2.24 and 6.75 g/100 ml, respectively, compared to an average of 3.75 and 7.96 g/100 ml, respectively, in 42 normal animals from the same source (20).

DISCUSSION

Salicylate, in therapeutically realistic concentrations, had a pronounced displacing effect on protein-bound bilirubin in undiluted rat plasma. The bilirubin concentrations were in the range encountered in jaundiced neonates and did not exceed the capacity of the strong binding sites of albumin in plasma.

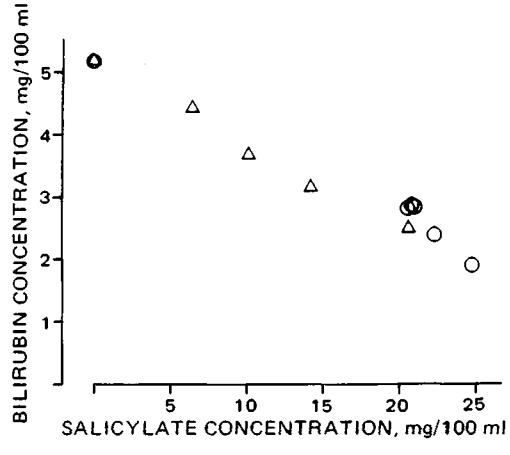

Figure 5—*Relationship between plasma concentrations of total bilirubin and salicylic acid in rats infused (△) or injected (○) with salicylic acid and infused with bilirubin. Each data point represents the mean of seven animals.*

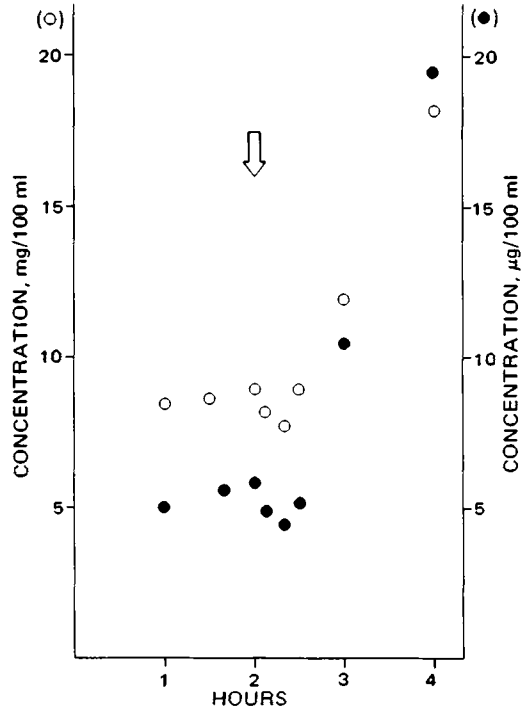

Figure 7—*Time course of total (○) and free (●) bilirubin concentrations in plasma of a rat infused with bilirubin and showing toxic symptoms. The arrow indicates the time of injection of 0.5 ml of 1.8% NaCl.*

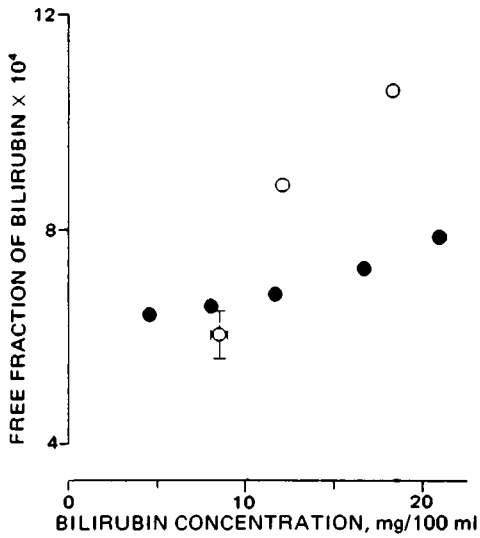

Figure 8—*Free fraction of bilirubin as a function of total bilirubin concentration in pooled plasma from four rats (●) and in plasma of the sick rat described in Fig. 7 (○). The open circle with bars represents the mean value ± 1 SD of the first six pairs of data points in Fig. 7.*

Rapid intravenous injection of salicylate to rats made hyperbilirubinemic by a constant infusion of bilirubin caused a rapid and pronounced decrease of plasma total bilirubin concentrations and a concomitant increase of bilirubin in the erythrocytes. This redistribution of bilirubin was not limited to the blood since the total bilirubin concentration in blood decreased. Thus, salicylate caused a transfer of bilirubin to extravascular sites as observed previously (6).

Administration of salicylate by slow infusion caused a much more gradual decrease of total bilirubin concentrations in plasma. More important, the maximum average decrease of the total bilirubin concentration in plasma (52%) was somewhat less pronounced than that after salicylate injection and occurred at the end of the experiment when the salicylate concentration had increased to about 20 mg/100 ml. When the same salicylate concentration was approached from "above," *i.e.*, by rapid injection followed by a maintenance infusion, the total bilirubin concentration in plasma was temporarily decreased by a maximum of 65% on the average. This difference should be even more pronounced with bilirubin-displacing drugs that have a larger distribution phase (as reflected by the difference between the concentration of drug in plasma immediately after rapid injection and the intercept on the concentration axis at zero time obtained by back-extrapolation of the terminal semilogarithmic concentration decay curve).

Administration of salicylate to neonatal guinea pigs while they were infused with bilirubin at a constant rate decreased total bilirubin concentrations in serum and increased bilirubin in the brain (6). In view of this reciprocal relationship, it is possible (but has not yet been demonstrated experimentally) that the magnitude of redistribution of bilirubin from plasma to the brain caused by displacement of bilirubin from plasma protein binding sites by a drug can be reduced by administering that drug slowly so as to prevent the predistributive drug concentration peaks associated with rapid intravenous injection. As stated previously (21) in a different context: "Since the equilibrium of bilirubin between tissue and albumin occurs very rapidly, kernicterus may develop from bilirubin displaced during transient high serum concentrations of a competing drug attained by rapid infusion. As the drug is cleared, binding will revert to normal (the perfect crime)."

The results of this investigation are in agreement with the predictions based on the theoretical pharmacokinetic considerations presented in the introductory paragraphs. A decrease in plasma protein binding of bilirubin caused by administration of a displacing agent decreased the plasma concentration of total bilirubin but had no effect on the steady-state concentration of free bilirubin. The redistribution of the pigment following salicylate injection was so rapid that no increase in the concentration of free bilirubin in plasma was apparent 5 min after injection. However, such temporary elevations of free bilirubin concentrations in plasma were observed shortly after rapid injection of another displacing agent, sulfisoxazole (22).

Since the concentration of bilirubin in extravascular tissues, including the brain, is apparently a function of the free concentration in plasma, a decrease in plasma protein binding *per se* (*i.e.*, without concomitant change in tissue binding) should have no effect on the *steady-state* concentration of total bilirubin in the tissues. However, the return to tissue steady-state conditions may be quite slow. This investigation showed that elevated bilirubin concentrations in erythrocytes persisted for at least 2 hr (Table II). Bilirubin concentrations in the brain of Gunn rats were elevated 2 hr after sulfadimethoxine administration (23). This persistence of bilirubin in tissues may be due, at least in part, to precipitation of the pigment and slow dissolution of the crystalline precipitate. Crystals of bilirubin were observed in the brain, kidneys, bone marrow, cerebrospinal fluid, and blood cells of hyperbilirubinemic infants (24, 25).

While the steady-state concentration of free bilirubin in plasma is not affected by protein binding, it should be increased if the rate of formation of bilirubin increases and/or if the intrinsic metabolic clearance of bilirubin decreases (Eq. 3). Such an increase in the plasma concentration of free bilirubin was observed in three animals during this investigation and was associated with typical signs and symptoms of acute bilirubin intoxication. Thus, in one rat that received bilirubin infusion but no salicylate, the concentration of free bilirubin rose after 3 hr from about 5 to about 19 μg/100 ml (Fig. 7). In addition, the protein binding of bilirubin decreased significantly (Fig. 8) relative to that in plasma of healthy animals. Both of these perturbations are consistent with impairment of hepatic function. The rise in the free bilirubin concentration could have been the result of decreased intrinsic metabolic clearance of the pigment while the diminished protein binding may have been due to an increase in the concentration of endogenous substances in plasma that are capable of displacing bilirubin from protein binding sites and are rapidly cleared by the normal liver.

Another case of acute bilirubin intoxication was observed in a rat subsequently found to be hypoalbuminemic. Had the intrinsic bilirubin clearance by the liver been normal, then the steady-state plasma concentration of total bilirubin in this animal would have been below normal but the concentration of free bilirubin in plasma should have been in the normal range. In fact, the total plasma bilirubin concentration was not decreased and the free bilirubin concentration in plasma was substantially above normal throughout the experiment, suggesting that this animal had impaired liver function from the beginning of the experiment. The hypoalbuminemia is consistent with this conclusion.

Diamond and Schmid (6), in their classic paper on experimental bilirubin encephalopathy, stated that the most significant limitation of the study was their inability to estimate directly the unbound plasma bilirubin fraction available for transfer into the brain. With the use of recently developed experimental methodology for determining free bilirubin concentrations in undiluted plasma (17), this limitation was overcome. The results emphasize the need for monitoring free rather than total unconjugated bilirubin concentrations in the plasma of newborn infants since the total bilirubin concentration may be decreased by endogenous or exogenous (drug or drug metabolite) displacing agents or by hypoalbuminemia.

A potentially serious problem may be the "hit-and-run" nature of bilirubin-displacing agents. For example, administration of a single dose of a bilirubin-displacing drug to a jaundiced patient may cause a pronounced shift of the heme pigment from plasma to extravascular sites, including the brain. If such a drug has a very short half-life or if it is injected intravenously and has a pronounced distribution phase, blood samples obtained even a relatively short time after drug administration may show normal rather than elevated bilirubin free fraction values in plasma. However, this "perfect crime" does leave a clue, namely, the more persistent elevation of bilirubin concentrations in erythrocytes. It will be important to determine how long these elevations persist, if they occur following administration of drugs other than salicylate, and if monitoring of bilirubin concentrations not only in plasma but also in erythrocytes can be of clinical diagnostic value.

REFERENCES

(1) W. A. Silverman, D. H. Anderson, W. A. Blanc, and D. N. Crozier, *Pediatrics*, **18**, 614 (1956).

(2) R. C. Harris, J. F. Lucey, and J. R. MacLean, *ibid.*, **20**, 875 (1958).

(3) L. Johnson, M. L. Garcia, E. Figueroa, and F. Sarmiento, *Am. J. Dis. Child.*, **101**, 322 (1961).

(4) D. Watson, *Clin. Sci.*, **22**, 435 (1962).

(5) R. Schmid, I. Diamond, L. Hammaker, and C. B. Gundersen, *Nature*, **206**, 1041 (1965).

(6) I. Diamond and R. Schmid, *J. Clin. Invest.*, **45**, 678 (1966).
(7) J. C. Topham and R. D. Board, *Biochem. Pharmacol.*, **20**, 718 (1971).
(8) R. A. Yeary and D. R. Davis, *Toxicol. Appl. Pharmacol.*, **28**, 269 (1974).
(9) M. J. Maisels, *Pediatr. Clin. North Am.*, **19**, 447 (1972).
(10) G. Levy and A. Yacobi, *J. Pharm. Sci.*, **63**, 805 (1974).
(11) G. Levy, in "The Effect of Disease States on Drug Pharmacokinetics," L. Z. Benet, Ed., American Pharmaceutical Association, Washington, D.C., 1976, chap. 9.
(12) S. Øie and G. Levy, *J. Pharm. Sci.*, **64**, 1433 (1975).
(13) G. R. Wilkinson and D. G. Shand, *Clin. Pharmacol. Ther.*, **18**, 377 (1975).
(14) C.-M. Lai and G. Levy, *J. Pharm. Sci.*, **66**, 1739 (1977).
(15) J. R. Weeks and J. D. Davis, *J. Appl. Physiol.*, **19**, 540 (1964).
(16) J. J. Ashley and G. Levy, *Res. Commun. Chem. Pathol. Pharmacol.*, **4**, 297 (1972).
(17) J. Jacobsen and O. Fedders, *Scand. J. Clin. Lab. Invest.*, **26**, 237 (1970).
(18) R. Brodersen and I. Vind, *ibid.*, **15**, 107 (1963).
(19) B. B. Brodie, S. Udenfriend, and A. F. Coburn, *J. Pharmacol. Exp. Ther.*, **80**, 114 (1944).
(20) A. Yacobi and G. Levy, *J. Pharm. Sci.*, **64**, 1660 (1975).
(21) R. P. Wennberg and L. F. Rasmussen, *J. Pediatr.*, **87**, 1007 (i975).
(22) S. Øie and G. Levy, *J. Pharm. Sci.*, **68**, 6 (1979).
(23) D. R. Davis and R. A. Yeary, *Pediatr. Res.*, **9**, 846 (1975).
(24) T. J. Vietti, in "Kernicterus," A. Sass-Kortsák, Ed., University of Toronto Press, Toronto, Canada, 1960, p. 153.
(25) L. M. Gartner, R. N. Snyder, R. S. Chabon, and J. Bernstein, *Pediatrics*, **45**, 906 (1970).

ACKNOWLEDGMENTS

Supported in part by Grant GM 19568 from the National Institute of General Medical Sciences, National Institutes of Health, and by an unrestricted grant from an anonymous donor.

Effect of Sulfisoxazole on Pharmacokinetics of Free and Plasma Protein-Bound Bilirubin in Experimental Unconjugated Hyperbilirubinemia

SVEIN ØIE and GERHARD LEVY ˣ

Received April 7, 1978, from the *Department of Pharmaceutics, School of Pharmacy, State University of New York at Buffalo, Amherst, NY 14260.* Accepted for publication May 26, 1978.

Abstract □ The effect of sulfisoxazole on the time course of free (unbound) bilirubin concentrations in plasma was studied. Normal adult rats were made hyperbilirubinemic by continuous intravenous infusion of bilirubin. Sulfisoxazole was administered by either rapid intravenous injection or slow intravenous infusion, and the plasma concentrations of free and total (free plus bound) unconjugated bilirubin were determined as a function of time. Rapid injection of sulfisoxazole caused a rapid and pronounced decrease of total bilirubin concentrations in plasma but had only a transient effect on the concentration of free bilirubin. Slow infusion of sulfisoxazole caused a gradual and eventually pronounced decrease of total bilirubin concentrations in plasma but had no apparent effect on the concentration of free bilirubin at any time. These results are consistent with recently developed pharmacokinetic theory according to which the plasma clearance of total bilirubin should increase upon administration of a displacing agent while the plasma clearance of free bilirubin should remain unchanged. Bilirubin-induced encephalopathy caused by sulfisoxazole or other displacing agents may be due to very transient elevations of free bilirubin concentrations in plasma of infants with elevated plasma concentrations of total bilirubin and the consequent redistribution of the pigment to extravascular sites, including the brain.

Keyphrases □ Sulfisoxazole—effect on pharmacokinetics of bilirubin in hyperbilirubinemic rats □ Pharmacokinetics—bilirubin in hyperbilirubinemic rats, effect of sulfisoxazole □ Bilirubin—pharmacokinetics in hyperbilirubinemic rats, effect of sulfisoxazole □ Antibacterials—sulfisoxazole, effect on pharmacokinetics of bilirubin in hyperbilirubinemic rats

Administration of sulfisoxazole to premature infants with neonatal jaundice has caused kernicterus (brain damage), often with fatal outcome (1, 2). Typically, this effect has been associated with a decrease of bilirubin concentrations in plasma. The same phenomenon was observed in rats with unconjugated hyperbilirubinemia (3). Sulfisoxazole is a potent displacer of plasma protein-bound bilirubin (4), and some of this displaced bilirubin is redistributed to extravascular sites, including the brain where it exerts its toxic effect (5).

Previous *in vivo* studies of the interaction between sulfisoxazole and bilirubin were limited by the lack of suitable methodology for the determination of free (unbound) unconjugated bilirubin in plasma. The more recently developed reaction rate method (6) permits determination of free bilirubin in undiluted plasma under clinically realistic conditions, *i.e.*, at bilirubin to albumin molar ratios of less than unity (6, 7). Therefore, an investigation was initiated to explore the kinetics of the interaction between sulfisoxazole and bilirubin in rats with experimental unconjugated hyperbilirubinemia, with emphasis on the temporal pattern of free and total (sum of free and protein-bound) unconjugated bilirubin concentrations in plasma and total unconjugated bilirubin concentrations in erythrocytes before and after intravenous injection or infusion of sulfisoxazole.

BACKGROUND

Bilirubin is eliminated almost entirely by conjugation in the liver and subsequent excretion of the conjugates in the bile and urine (8). The total plasma clearance of bilirubin is about 10% of the plasma perfusion rate of the liver (9), and the concentration of total bilirubin in erythrocytes is about 10% of the concentration in plasma of rats with experimental hyperbilirubinemia under otherwise normal physiological conditions (Ref. 10 and results of this study). Therefore, the following pharmacokinetic relationships may be expected to apply (11):

$$TC = f_p k'' \quad \text{(Eq. 1)}$$

$$C_\infty = R^0/TC \quad \text{(Eq. 2)}$$

$$f_p C_\infty = R^0/k'' \quad \text{(Eq. 3)}$$

0022-3549/79/0100-0006$01.00/0
© 1979, American Pharmaceutical Association

(6) I. Diamond and R. Schmid, *J. Clin. Invest.*, **45**, 678 (1966).
(7) J. C. Topham and R. D. Board, *Biochem. Pharmacol.*, **20**, 718 (1971).
(8) R. A. Yeary and D. R. Davis, *Toxicol. Appl. Pharmacol.*, **28**, 269 (1974).
(9) M. J. Maisels, *Pediatr. Clin. North Am.*, **19**, 447 (1972).
(10) G. Levy and A. Yacobi, *J. Pharm. Sci.*, **63**, 805 (1974).
(11) G. Levy, in "The Effect of Disease States on Drug Pharmacokinetics," L. Z. Benet, Ed., American Pharmaceutical Association, Washington, D.C., 1976, chap. 9.
(12) S. Øie and G. Levy, *J. Pharm. Sci.*, **64**, 1433 (1975).
(13) G. R. Wilkinson and D. G. Shand, *Clin. Pharmacol. Ther.*, **18**, 377 (1975).
(14) C.-M. Lai and G. Levy, *J. Pharm. Sci.*, **66**, 1739 (1977).
(15) J. R. Weeks and J. D. Davis, *J. Appl. Physiol.*, **19**, 540 (1964).
(16) J. J. Ashley and G. Levy, *Res. Commun. Chem. Pathol. Pharmacol.*, **4**, 297 (1972).
(17) J. Jacobsen and O. Fedders, *Scand. J. Clin. Lab. Invest.*, **26**, 237 (1970).
(18) R. Brodersen and I. Vind, *ibid.*, **15**, 107 (1963).
(19) B. B. Brodie, S. Udenfriend, and A. F. Coburn, *J. Pharmacol. Exp. Ther.*, **80**, 114 (1944).
(20) A. Yacobi and G. Levy, *J. Pharm. Sci.*, **64**, 1660 (1975).
(21) R. P. Wennberg and L. F. Rasmussen, *J. Pediatr.*, **87**, 1007 (i975).
(22) S. Øie and G. Levy, *J. Pharm. Sci.*, **68**, 6 (1979).
(23) D. R. Davis and R. A. Yeary, *Pediatr. Res.*, **9**, 846 (1975).
(24) T. J. Vietti, in "Kernicterus," A. Sass-Kortsák, Ed., University of Toronto Press, Toronto, Canada, 1960, p. 153.
(25) L. M. Gartner, R. N. Snyder, R. S. Chabon, and J. Bernstein, *Pediatrics*, **45**, 906 (1970).

ACKNOWLEDGMENTS

Supported in part by Grant GM 19568 from the National Institute of General Medical Sciences, National Institutes of Health, and by an unrestricted grant from an anonymous donor.

Effect of Sulfisoxazole on Pharmacokinetics of Free and Plasma Protein-Bound Bilirubin in Experimental Unconjugated Hyperbilirubinemia

SVEIN ØIE and GERHARD LEVY ˣ

Received April 7, 1978, from the *Department of Pharmaceutics, School of Pharmacy, State University of New York at Buffalo, Amherst, NY 14260.* Accepted for publication May 26, 1978.

Abstract □ The effect of sulfisoxazole on the time course of free (unbound) bilirubin concentrations in plasma was studied. Normal adult rats were made hyperbilirubinemic by continuous intravenous infusion of bilirubin. Sulfisoxazole was administered by either rapid intravenous injection or slow intravenous infusion, and the plasma concentrations of free and total (free plus bound) unconjugated bilirubin were determined as a function of time. Rapid injection of sulfisoxazole caused a rapid and pronounced decrease of total bilirubin concentrations in plasma but had only a transient effect on the concentration of free bilirubin. Slow infusion of sulfisoxazole caused a gradual and eventually pronounced decrease of total bilirubin concentrations in plasma but had no apparent effect on the concentration of free bilirubin at any time. These results are consistent with recently developed pharmacokinetic theory according to which the plasma clearance of total bilirubin should increase upon administration of a displacing agent while the plasma clearance of free bilirubin should remain unchanged. Bilirubin-induced encephalopathy caused by sulfisoxazole or other displacing agents may be due to very transient elevations of free bilirubin concentrations in plasma of infants with elevated plasma concentrations of total bilirubin and the consequent redistribution of the pigment to extravascular sites, including the brain.

Keyphrases □ Sulfisoxazole—effect on pharmacokinetics of bilirubin in hyperbilirubinemic rats □ Pharmacokinetics—bilirubin in hyperbilirubinemic rats, effect of sulfisoxazole □ Bilirubin—pharmacokinetics in hyperbilirubinemic rats, effect of sulfisoxazole □ Antibacterials—sulfisoxazole, effect on pharmacokinetics of bilirubin in hyperbilirubinemic rats

Administration of sulfisoxazole to premature infants with neonatal jaundice has caused kernicterus (brain damage), often with fatal outcome (1, 2). Typically, this effect has been associated with a decrease of bilirubin concentrations in plasma. The same phenomenon was observed in rats with unconjugated hyperbilirubinemia (3). Sulfisoxazole is a potent displacer of plasma protein-bound bilirubin (4), and some of this displaced bilirubin is redistributed to extravascular sites, including the brain where it exerts its toxic effect (5).

Previous *in vivo* studies of the interaction between sulfisoxazole and bilirubin were limited by the lack of suitable methodology for the determination of free (unbound) unconjugated bilirubin in plasma. The more recently developed reaction rate method (6) permits determination of free bilirubin in undiluted plasma under clinically realistic conditions, *i.e.*, at bilirubin to albumin molar ratios of less than unity (6, 7). Therefore, an investigation was initiated to explore the kinetics of the interaction between sulfisoxazole and bilirubin in rats with experimental unconjugated hyperbilirubinemia, with emphasis on the temporal pattern of free and total (sum of free and protein-bound) unconjugated bilirubin concentrations in plasma and total unconjugated bilirubin concentrations in erythrocytes before and after intravenous injection or infusion of sulfisoxazole.

BACKGROUND

Bilirubin is eliminated almost entirely by conjugation in the liver and subsequent excretion of the conjugates in the bile and urine (8). The total plasma clearance of bilirubin is about 10% of the plasma perfusion rate of the liver (9), and the concentration of total bilirubin in erythrocytes is about 10% of the concentration in plasma of rats with experimental hyperbilirubinemia under otherwise normal physiological conditions (Ref. 10 and results of this study). Therefore, the following pharmacokinetic relationships may be expected to apply (11):

$$TC = f_p k'' \quad \text{(Eq. 1)}$$

$$C_\infty = R^0/TC \quad \text{(Eq. 2)}$$

$$f_p C_\infty = R^0/k'' \quad \text{(Eq. 3)}$$

0022-3549/79/0100-0006$01.00/0
© 1979, American Pharmaceutical Association

where TC is the total plasma clearance, k'' is the intrinsic clearance (reflecting the activity of the enzyme systems involved in the rate-determining steps of bilirubin conjugation), f_p is the free fraction of bilirubin in plasma (*i.e.*, the ratio of free to total bilirubin concentrations), C_∞ is the steady-state plasma concentration of total bilirubin, f_pC_∞ is the steady-state plasma concentration of free bilirubin, and R^0 is the sum of the production and infusion rates of bilirubin. When the infusion rate is sufficient to produce marked hyperbilirubinemia in normal animals (as in this study), $R^0 \simeq$ infusion rate.

Equation 1 was confirmed experimentally in rats (12). Accordingly, administration of a displacing agent, resulting in an increased f_p, should cause a decrease of C_∞ (Eqs. 1 and 2) but should have no effect on the *steady-state* plasma concentration of free bilirubin as long as the displacing agent has no effect on k'' (*i.e.*, on the activity of the enzyme systems responsible for the biotransformation of bilirubin). This prediction was confirmed with respect to salicylic acid (10). From a toxicologic point of view, pharmacokinetic studies of interactions between bilirubin and displacing agents should focus particularly on the temporary perturbations of bilirubin kinetics and not solely on the steady state before and after (or during continued) administration of the displacing agent. The investigation of the interaction between bilirubin and sulfisoxazole described here was designed on the basis of these considerations.

EXPERIMENTAL

Male Sprague–Dawley rats[1], 360–460 g, were maintained on a standard diet[2]. Two days before an experiment, a silicone rubber–polyethylene cannula was placed permanently in the right jugular vein to facilitate intravenous infusion, injection, and frequent withdrawal of blood samples (13, 14). On the day of an experiment, a solution of bilirubin and sodium taurocholate (1:1.1 weight ratio, in 0.7% sodium chloride adjusted to pH 7.4) was infused at a rate of 0.8 mg of bilirubin/kg/min for 15 min and then at 0.32 mg of bilirubin/kg/min for 105 min.

Half of the rats then received an intravenous injection of sulfisoxazole, 40 mg/kg, in 0.5 ml of pH 7.4 phosphate buffer, and the infusion was continued for an additional 120 min with bilirubin, 0.32 mg/kg/min, and sulfisoxazole, 0.20 mg/kg/min. The other rats received the same bilirubin infusion regimen for the first 2 hr, followed by an infusion of sulfisoxazole, 0.44 mg/kg/min, and bilirubin, 0.32 mg/kg/min, for the next 2 hr. About 1 week later, crossover experiments were performed. All infusion equipment, including syringes and cannulas, was covered with aluminum foil to protect bilirubin from light.

Heparinized blood samples (0.6 ml) were collected at 1, 1.5, and 2 hr and then again at 15, 30, 60, and 120 min after the sulfisoxazole injection or the start of the sulfisoxazole infusion. An additional blood sample was obtained 5 min after the sulfisoxazole injection. Considerable care was taken to obtain "mainstream" blood samples uncontaminated by the bilirubin infusion solution (14). Plasma and erythrocytes were separated by centrifugation and analyzed for free (4, 6) and total unconjugated bilirubin (15) and for sulfisoxazole (16). Whole blood concentrations of unconjugated bilirubin were calculated from the concentrations in plasma and erythrocytes and the fractional volumes of these phases in whole blood.

RESULTS

The bilirubin infusion schedule resulted in steady-state plasma concentrations of total bilirubin between 5.7 and 10.3 mg/100 ml until sulfisoxazole was administered. The total bilirubin concentration in plasma decreased rapidly and substantially from 7.43 ± 1.91 mg/100 ml (mean ± *SD*) immediately before sulfisoxazole injection to 4.10 ± 1.24 mg/100 ml 5 min after injection ($p < 0.02$) and then increased slightly as sulfisoxazole concentrations in plasma declined with time (Fig. 1). The concentration of free bilirubin increased about threefold immediately after sulfisoxazole injection but returned to the presulfisoxazole level soon thereafter. This temporary increase occurred in all four rats but differed significantly in magnitude among animals. Therefore, four additional animals were studied.

The average (± *SD*) concentration of free bilirubin in the plasma of all eight rats immediately before sulfisoxazole injection was 3.4 ± 0.8 μg/100 ml; it increased to 12.6 ± 10.2 μg/100 ml 5 min after sulfisoxazole injection ($p < 0.05$ by paired t-test; $p < 0.004$ by sign test). The concentration of total unconjugated bilirubin in whole blood decreased from

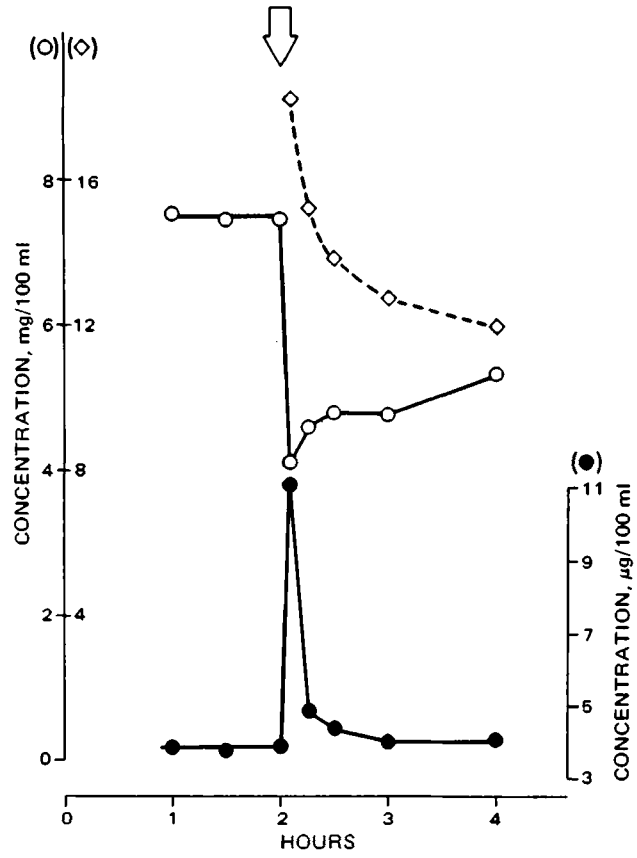

Figure 1—*Time course of free bilirubin (●), total bilirubin (○), and sulfisoxazole (◇) concentrations in plasma of four rats with experimental unconjugated hyperbilirubinemia. The arrow indicates the time of injection of sulfisoxazole, 40 mg/kg. Following the injection, sulfisoxazole was infused at a rate of 0.20 mg/kg/min.*

4.54 ± 1.06 immediately before to 3.12 ± 1.02 mg/100 ml 5 min after sulfisoxazole injection ($p < 0.05$).

Slow infusion of sulfisoxazole over 2 hr resulted in a gradual decrease in the total bilirubin concentration while the concentration of free bilirubin remained essentially constant at all times (Fig. 2), but blood was not sampled 5 min after the start of the sulfisoxazole infusion. The total bilirubin concentration in plasma at the end of the 2-hr sulfisoxazole infusion was significantly lower than immediately before the start of the infusion ($p < 0.005$). An examination of the data shows that a given sulfisoxazole concentration produces the same quantitative decrease in the concentration of total bilirubin in plasma whether sulfisoxazole concentrations were decreasing (after injection) or increasing (during infusion) with time (Fig. 3).

The total bilirubin concentrations in the erythrocytes during the sulfisoxazole injection and infusion experiments are listed in Table I. These concentrations increased upon administration of sulfisoxazole, indicating a shift of bilirubin from plasma to erythrocytes. Notably, the elevation of erythrocyte bilirubin concentrations persisted for the duration of the experiments.

DISCUSSION

The results of this investigation are consistent with and confirm the applicability to bilirubin of the pharmacokinetic relationships represented by Eqs. 1–3. The plasma concentration of total bilirubin decreased upon administration of sulfisoxazole. The magnitude of this effect increased with increasing concentrations of sulfisoxazole, consistent with the concentration-dependent displacing effect of this drug on plasma protein-bound bilirubin (4). On the other hand, the concentration of unbound bilirubin remained constant, except for a temporary increase immediately after injection pending reestablishment of the steady state. This finding indicates that sulfisoxazole had no effect on the intrinsic clearance, k'', of bilirubin under the conditions of this investigation.

Direct and indirect evidence indicates that the concentration of free rather than total bilirubin in plasma determines, among other factors,

[1] Blue Spruce Farms, Altamont, N.Y.
[2] Charles River Formula 4RF.

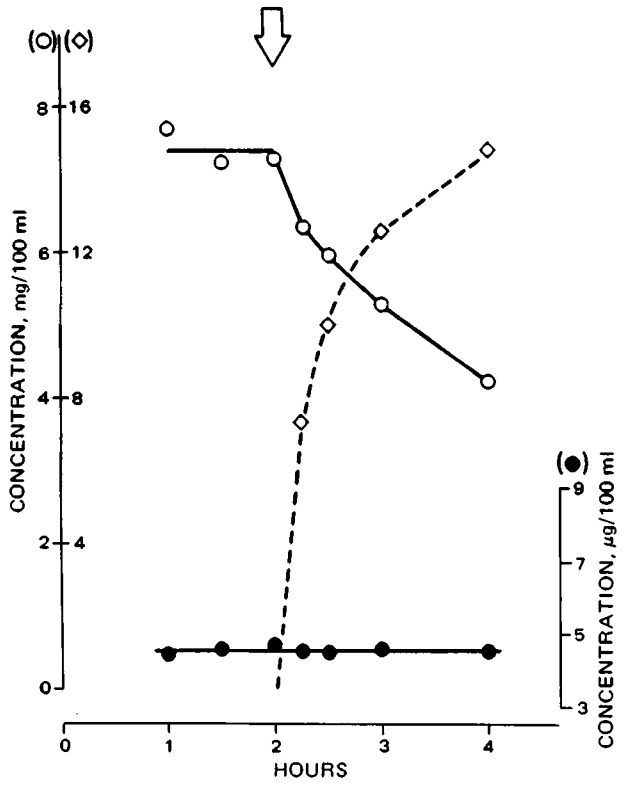

Figure 2—*Time course of free bilirubin (●), total bilirubin (○), and sulfisoxazole (◇) concentrations in plasma of four rats with experimental unconjugated hyperbilirubinemia. The arrow indicates the beginning of an infusion of sulfisoxazole at a rate of 0.44 mg/kg/min.*

the risk of brain damage in hyperbilirubinemic infants (17). Based on the results of this investigation, the bilirubin-induced encephalopathy caused by sulfisoxazole or other drugs capable of displacing bilirubin from plasma albumin is probably due to transient elevations of free bilirubin concentrations in plasma of jaundiced infants associated with perturbation of steady-state conditions and the consequent redistribution of bilirubin from plasma to other sites. These other sites include the brain (5) and erythrocytes.

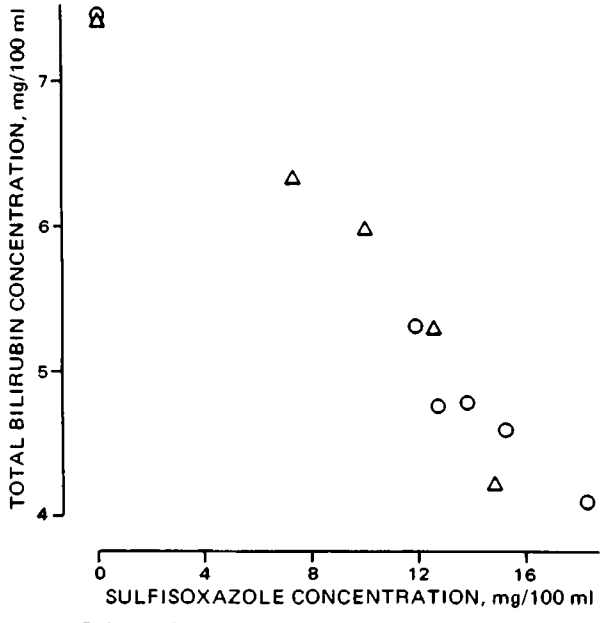

Figure 3—*Relationship between the plasma concentrations of total bilirubin and sulfisoxazole after rapid injection (○) and during infusion (△) of sulfisoxazole. Each data point represents the mean of four animals.*

Table I—Effect of Sulfisoxazole Injection or Infusion on Total Bilirubin Concentration in Erythrocytes of Rats with Experimental Unconjugated Hyperbilirubinemia

Hours	Concentration, mg/100 ml (mean ± *SD*, *n* = 4) Injection	Infusion
1.0	0.84 ± 0.13	0.80 ± 0.13
1.5	0.76 ± 0.07	0.74 ± 0.03
2.0	0.77 ± 0.08	0.82 ± 0.16
2.08	1.77 ± 0.70[a]	—[b]
2.25	1.58 ± 0.39[a]	1.31 ± 0.26[a]
2.5	1.57 ± 0.44[a]	1.62 ± 0.38[a]
3.0	1.48 ± 0.38[a]	1.42 ± 0.21[a]
4.0	1.47 ± 0.48[a]	1.41 ± 0.28[a]

[a] Statistically significantly different from control (1.0–2.0 hr) period, $p < 0.005$. [b] No blood sample was taken at this time.

As in a previous study with salicylate (10), the elevated concentrations of bilirubin in the erythrocytes persisted throughout the experiment (*i.e.*, for at least 2 hr), unlike the total bilirubin concentrations in plasma which reversed readily as drug concentrations declined (Figs. 1 and 3). Studies in hyperbilirubinemic rats and in human infants have shown persistence of bilirubin in the brain (18). Precipitation of the very poorly water-soluble pigment in the brain and erythrocytes may be responsible for this persistence; crystals of bilirubin have been found in both tissues (19, 20).

The results of this investigation suggest that clinical assessment of jaundiced infants may be facilitated by the determination of bilirubin concentrations in erythrocytes in addition to the determination of the free bilirubin concentration in plasma, particularly if the patients have been treated with drugs that can displace bilirubin from binding sites on plasma proteins. The potential usefulness of this procedure will have to be assessed in a prospective clinical trial.

The effects of salicylic acid (10) and sulfisoxazole on the plasma protein binding and pharmacokinetics of bilirubin are similar in most respects but strikingly different in one: rapid intravenous injection of salicylate was not associated with an elevation of free bilirubin concentrations in plasma 5 min later (10) while sulfisoxazole injection caused a pronounced, though temporary, rise in these concentrations under the same conditions (Fig. 1). The diffusion of free bilirubin from plasma to extravascular sites (but apparently not from plasma to erythrocytes) appears to be slower after injection of sulfisoxazole than after injection of salicylate. The relevance of this observation to the induction of encephalopathy by bilirubin and the mechanism of the apparent difference in the distribution kinetics of bilirubin in the presence of salicylate or sulfisoxazole remain to be determined.

REFERENCES

(1) W. A. Silverman, D. H. Anderson, W. A. Blanc, and D. N. Crozier, *Pediatrics*, **18**, 614 (1956).

(2) R. C. Harris, J. F. Lucey, and J. R. MacLean, *ibid.*, **20**, 875 (1958).

(3) L. Johnson, M. L. Garcia, E. Figueroa, and F. Sarmiento, *Am. J. Dis. Child.*, **101**, 322 (1961).

(4) S. Øie and G. Levy, *Clin. Pharmacol. Ther.*, **21**, 627 (1977).

(5) I. Diamond and R. Schmid, *J. Clin. Invest.*, **45**, 678 (1966).

(6) J. Jacobsen and O. Fedders, *Scand. J. Clin. Lab. Invest.*, **26**, 237 (1970).

(7) S. Øie, Ph.D. thesis, State University of New York at Buffalo, Amherst, N.Y., 1975.

(8) R. Schmid, *N. Engl. J. Med.*, **287**, 703 (1972).

(9) S. Øie and G. Levy, *J. Pharm. Sci.*, **67**, 45 (1978).

(10) *Ibid.*, **68**, 1 (1979).

(11) G. Levy, in "The Effect of Disease States on Drug Pharmacokinetics," L. Z. Benet, Ed., American Pharmaceutical Association, Washington, D.C., 1976, chap. 9.

(12) S. Øie and G. Levy, *J. Pharm. Sci.*, **64**, 1433 (1975).

(13) J. R. Weeks and J. D. Davis, *J. Appl. Physiol.*, **19**, 540 (1964).

(14) J. J. Ashley and G. Levy, *Res. Commun. Chem. Pathol. Pharmacol.*, **4**, 297 (1972).

(15) R. Brodersen and I. Vind, *Scand. J. Clin. Lab. Invest.*, **15**, 107 (1963).

(16) A. C. Bratton and E. K. Marshall, Jr., *J. Biol. Chem.*, **128**, 537 (1939).

(17) P. Zamet, H. Nakamura, S. Perez-Robles, J. C. Larroche, and N. Minkowski, *Biol. Neonat.*, **26**, 274 (1975).

(18) D. R. Davis and R. A. Yeary, *Pediatr. Res.*, **9**, 846 (1975).
(19) T. J. Vietti, in "Kernicterus," A. Sass-Kortsák, Ed., University of Toronto Press, Toronto, Canada, 1960, p. 153.
(20) L. M. Gartner, R. N. Snyder, R. S. Chabon, and J. Bernstein, *Pediatrics*, **45**, 906 (1970).

ACKNOWLEDGMENTS

Supported in part by Grant GM 19568 from the National Institute of General Medical Sciences, National Institutes of Health, and by an unrestricted grant from an anonymous donor.

Spectrophotometric Determination of Theophylline Formulations

M. ABDEL-HADY ELSAYED *x, H. ABDINE, and YOUSRY M. ELSAYED

Received May 23, 1977, from the *Faculty of Pharmacy, University of Alexandria, Alexandria, Egypt.* Accepted for publication February 8, 1978. *Present address: Department of Pharmacy, Faculty of Biological and Pharmaceutical Sciences, University of Nigeria, Nsukka, Nigeria.

Abstract □ Minophylline (theophylline ethanoate of piperazine) and aminophylline (theophylline ethylenediamine) were determined spectrophotometrically in dosage forms without interference from excipients and/or preservatives. A mixture of minophylline, in about 30-fold concentration, with phenobarbital was assayed for both components with good accuracy and high reproducibility.

Keyphrases □ Minophylline—spectrophotometric analysis in pharmaceutical formulations □ Aminophylline—spectrophotometric analysis in pharmaceutical formulations □ Spectrophotometry—analyses, minophylline and aminophylline in pharmaceutical formulations □ Diuretic-vasodilators—minophylline, spectrophotometric analysis in pharmaceutical formulations □ Relaxants, smooth muscle—aminophylline, spectrophotometric analysis in pharmaceutical formulations

The assay of binary mixtures in pharmaceutical formulations is challenging. One example is minophylline[1] and phenobarbital mixtures, especially when the latter component is present in small amounts. The interference of excipients and/or preservatives increases the severity of the problem.

BACKGROUND

The various methods dealing with the correction of interfering absorbances were reviewed (1, 2). The correction of linear interferance can be carried out graphically (3) or algebraically (4–7). By applying the algebraic version to the correction of linear impurity absorption, the concentration, C, can be determined from:

$$C = \frac{A_1(\lambda_2 - \lambda_3) - A_2(\lambda_1 - \lambda_3) + A_3(\lambda_1 - \lambda_2)}{E_1(\lambda_2 - \lambda_3) - E_2(\lambda_1 - \lambda_3) + E_3(\lambda_1 - \lambda_2)} \quad \text{(Eq. 1)}$$

in which A_1, A_2, and A_3 are the absorbances at λ_1, λ_2, and λ_3, respectively; E_1, E_2, and E_3 are the corresponding 1-cm path length absorbances of a 1% solution. Dividing both numerator and denominator by $(\lambda_1 - \lambda_3)$ and substituting h for $(\lambda_2 - \lambda_3)/(\lambda_1 - \lambda_3)$ give the following equation after simple rearrangement:

$$A_2 - hA_1 - (1 - h)A_3 = C[E_2 - hE_1 - (1 - h)E_3] \quad \text{(Eq. 2)}$$

Substitution of the left-hand term by corrected A (A_c) and the second term in the right-hand side by K yields:

$$A_c = CK \quad \text{(Eq. 3)}$$

A linear relationship is obtained by plotting A_c *versus* C.

Another method for the correction of interfering absorbances is Glenn's method of orthogonal function (8), in which absorbance A is replaced by the coefficient of the orthogonal function, p_j. This coefficient is proportional to concentration. To extract the coefficient of a given polynomial from an absorption curve, it is necessary to obtain absorbances at a number of equally spaced wavelengths. Thus, to extract the coefficient of the quadratic polynomial p_2, for example, six absorbance measurements at six equally spaced wavelengths are needed. By plotting the p_2 at different intervals *versus* λ_m (the mean set of wavelengths), a convoluted absorption curve is obtained (9).

The present paper reports the determination of minophylline in the presence of the tablet base, sweetening agent, coloring agent, and preservatives usually existing in pharmaceutical preparations; the determination of aminophylline in ampuls containing benzyl alcohol as a preservative; and an assay for a minophylline–phenobarbital mixture in syrup. Determination of phenobarbital in this mixture is difficult since it is present in a small amount.

EXPERIMENTAL

Materials—Minophylline[2] and aminophylline[3] standard solutions were at a concentration of 1 mg/ml in 0.1 *N* H_2SO_4. Phenobarbital sodium[4] standard solution was 1 mg/ml in water. Minophylline tablets[2], Batch 7, contained 250 mg/tablet; minophylline ampuls[2], Batch 29, contained 200 mg/2 ml.

Minophylline–phenobarbital[2], Batch 101,004, contained 2.0 g of minophylline and 0.06 g of phenobarbital/100 ml. Aminophylline ampuls[5], Batch S/52D, contained 500 mg of aminophylline/2 ml and 0.04 ml of benzyl alcohol as the preservative.

Reagents—Analytical grade 0.1 *N* H_2SO_4, 0.5 *N* NaOH, 0.25 *M* Na_2CO_3 (anhydrous), 0.25 *M* $NaHCO_3$, and alcohol were used.

Instruments—A photoelectric spectrophotometer[6] with 1-cm silica cells was used.

Procedures—*Standard Curves for Minophylline and Aminophylline Using* A_c *Method*—Different solutions containing 0.3, 0.6, 0.9, 1.2, 1.5, and 1.8 mg % minophylline were prepared by dilution with 0.1 *N* H_2SO_4. The absorbance of each solution was measured at λ_1 246 nm, λ_2 274 nm, and λ_3 295 nm.

For aminophylline, the concentrations prepared were 0.3, 0.6, 0.9, 1.2, 1.5, 1.8, and 2.1 mg %; λ_1, λ_2, and λ_3 were 242, 270, and 287 nm, respectively. The A_c for each concentration of minophylline or aminophylline was calculated.

Standard Curve for Minophylline Using p_2 *Method*—The absorbances of the same solutions were measured at 266, 270, 274, 278, 282, and 286 nm. The coefficient p_2 for each concentration was calculated.

Standard Curve for Phenobarbital Applying ΔA *Method*—Two sets of solutions were prepared so that each contained 0.5, 1, 1.5, 2, 2.5, 3, 3.5, 4, 4.5, and 5 mg % phenobarbital. One set was prepared in 0.1 *N* NaOH (Solution A), and the other was prepared in a mixture of 0.025 *M* Na_2CO_3 (anhydrous) and 0.025 *M* $NaHCO_3$ (Solution B). The absorbance of Solution B was measured at 238 nm using Solution A as a blank. Then Solution A was measured at 260 nm using Solution B as a blank. The $\Sigma \Delta A_{238}$ and ΔA_{260} for each concentration were calculated.

Assay for Pharmaceutical Preparations—*Minophylline Tablets*—From powdered tablets (10 tablets were powdered and mixed), an

[1] The theophylline ethanoate of piperazine. The International Nonproprietary Name is acefylline piperazine.

[2] Alexandria Company for Pharmaceutical and Chemical Industries.
[3] Boehringer Ingelheim, Germany.
[4] VEB Chemische Werk, Germany.
[5] Burroughs Wellcome and Co.
[6] Prolabo, Paris, France.

0022-3549/79/0100-0009$01.00/0
© 1979, American Pharmaceutical Association

(18) D. R. Davis and R. A. Yeary, *Pediatr. Res.*, **9**, 846 (1975).
(19) T. J. Vietti, in "Kernicterus," A. Sass-Kortsák, Ed., University of Toronto Press, Toronto, Canada, 1960, p. 153.
(20) L. M. Gartner, R. N. Snyder, R. S. Chabon, and J. Bernstein, *Pediatrics*, **45**, 906 (1970).

ACKNOWLEDGMENTS

Supported in part by Grant GM 19568 from the National Institute of General Medical Sciences, National Institutes of Health, and by an unrestricted grant from an anonymous donor.

Spectrophotometric Determination of Theophylline Formulations

M. ABDEL-HADY ELSAYED *x, H. ABDINE, and YOUSRY M. ELSAYED

Received May 23, 1977, from the *Faculty of Pharmacy, University of Alexandria, Alexandria, Egypt.* Accepted for publication February 8, 1978. *Present address: Department of Pharmacy, Faculty of Biological and Pharmaceutical Sciences, University of Nigeria, Nsukka, Nigeria.

Abstract □ Minophylline (theophylline ethanoate of piperazine) and aminophylline (theophylline ethylenediamine) were determined spectrophotometrically in dosage forms without interference from excipients and/or preservatives. A mixture of minophylline, in about 30-fold concentration, with phenobarbital was assayed for both components with good accuracy and high reproducibility.

Keyphrases □ Minophylline—spectrophotometric analysis in pharmaceutical formulations □ Aminophylline—spectrophotometric analysis in pharmaceutical formulations □ Spectrophotometry—analyses, minophylline and aminophylline in pharmaceutical formulations □ Diuretic-vasodilators—minophylline, spectrophotometric analysis in pharmaceutical formulations □ Relaxants, smooth muscle—aminophylline, spectrophotometric analysis in pharmaceutical formulations

The assay of binary mixtures in pharmaceutical formulations is challenging. One example is minophylline[1] and phenobarbital mixtures, especially when the latter component is present in small amounts. The interference of excipients and/or preservatives increases the severity of the problem.

BACKGROUND

The various methods dealing with the correction of interfering absorbances were reviewed (1, 2). The correction of linear interferance can be carried out graphically (3) or algebraically (4–7). By applying the algebraic version to the correction of linear impurity absorption, the concentration, C, can be determined from:

$$C = \frac{A_1(\lambda_2 - \lambda_3) - A_2(\lambda_1 - \lambda_3) + A_3(\lambda_1 - \lambda_2)}{E_1(\lambda_2 - \lambda_3) - E_2(\lambda_1 - \lambda_3) + E_3(\lambda_1 - \lambda_2)} \quad \text{(Eq. 1)}$$

in which A_1, A_2, and A_3 are the absorbances at λ_1, λ_2, and λ_3, respectively; E_1, E_2, and E_3 are the corresponding 1-cm path length absorbances of a 1% solution. Dividing both numerator and denominator by $(\lambda_1 - \lambda_3)$ and substituting h for $(\lambda_2 - \lambda_3)/(\lambda_1 - \lambda_3)$ give the following equation after simple rearrangement:

$$A_2 - hA_1 - (1 - h)A_3 = C[E_2 - hE_1 - (1 - h)E_3] \quad \text{(Eq. 2)}$$

Substitution of the left-hand term by corrected A (A_c) and the second term in the right-hand side by K yields:

$$A_c = CK \quad \text{(Eq. 3)}$$

A linear relationship is obtained by plotting A_c *versus* C.

Another method for the correction of interfering absorbances is Glenn's method of orthogonal function (8), in which absorbance A is replaced by the coefficient of the orthogonal function, p_j. This coefficient is proportional to concentration. To extract the coefficient of a given polynomial from an absorption curve, it is necessary to obtain absorbances at a number of equally spaced wavelengths. Thus, to extract the coefficient of the quadratic polynomial p_2, for example, six absorbance measurements at six equally spaced wavelengths are needed. By plotting the p_2 at different intervals *versus* λ_m (the mean set of wavelengths), a convoluted absorption curve is obtained (9).

The present paper reports the determination of minophylline in the presence of the tablet base, sweetening agent, coloring agent, and preservatives usually existing in pharmaceutical preparations; the determination of aminophylline in ampuls containing benzyl alcohol as a preservative; and an assay for a minophylline–phenobarbital mixture in syrup. Determination of phenobarbital in this mixture is difficult since it is present in a small amount.

EXPERIMENTAL

Materials—Minophylline[2] and aminophylline[3] standard solutions were at a concentration of 1 mg/ml in 0.1 *N* H_2SO_4. Phenobarbital sodium[4] standard solution was 1 mg/ml in water. Minophylline tablets[2], Batch 7, contained 250 mg/tablet; minophylline ampuls[2], Batch 29, contained 200 mg/2 ml.

Minophylline–phenobarbital[2], Batch 101,004, contained 2.0 g of minophylline and 0.06 g of phenobarbital/100 ml. Aminophylline ampuls[5], Batch S/52D, contained 500 mg of aminophylline/2 ml and 0.04 ml of benzyl alcohol as the preservative.

Reagents—Analytical grade 0.1 *N* H_2SO_4, 0.5 *N* NaOH, 0.25 *M* Na_2CO_3 (anhydrous), 0.25 *M* $NaHCO_3$, and alcohol were used.

Instruments—A photoelectric spectrophotometer[6] with 1-cm silica cells was used.

Procedures—*Standard Curves for Minophylline and Aminophylline Using* A_c *Method*—Different solutions containing 0.3, 0.6, 0.9, 1.2, 1.5, and 1.8 mg % minophylline were prepared by dilution with 0.1 *N* H_2SO_4. The absorbance of each solution was measured at λ_1 246 nm, λ_2 274 nm, and λ_3 295 nm.

For aminophylline, the concentrations prepared were 0.3, 0.6, 0.9, 1.2, 1.5, 1.8, and 2.1 mg %; λ_1, λ_2, and λ_3 were 242, 270, and 287 nm, respectively. The A_c for each concentration of minophylline or aminophylline was calculated.

Standard Curve for Minophylline Using p_2 *Method*—The absorbances of the same solutions were measured at 266, 270, 274, 278, 282, and 286 nm. The coefficient p_2 for each concentration was calculated.

Standard Curve for Phenobarbital Applying ΔA *Method*—Two sets of solutions were prepared so that each contained 0.5, 1, 1.5, 2, 2.5, 3, 3.5, 4, 4.5, and 5 mg % phenobarbital. One set was prepared in 0.1 *N* NaOH (Solution A), and the other was prepared in a mixture of 0.025 *M* Na_2CO_3 (anhydrous) and 0.025 *M* $NaHCO_3$ (Solution B). The absorbance of Solution B was measured at 238 nm using Solution A as a blank. Then Solution A was measured at 260 nm using Solution B as a blank. The $\Sigma \Delta A_{238}$ and ΔA_{260} for each concentration were calculated.

Assay for Pharmaceutical Preparations—*Minophylline Tablets*—From powdered tablets (10 tablets were powdered and mixed), an

[1] The theophylline ethanoate of piperazine. The International Nonproprietary Name is acefylline piperazine.

[2] Alexandria Company for Pharmaceutical and Chemical Industries.
[3] Boehringer Ingelheim, Germany.
[4] VEB Chemische Werk, Germany.
[5] Burroughs Wellcome and Co.
[6] Prolabo, Paris, France.

0022-3549/79/0100-0009$01.00/0
© 1979, American Pharmaceutical Association

Table I—Assay Results for Theophylline Formulations

Preparation	n	Mean Percentage ± CV, %		
		A_c Method	A Method	p_2 Method
		Minophylline Tablets and Ampuls		
Tablets[a]	12	99.65 ± 0.78 (2.27)[b]	100.47 ± 0.98	99.64 ± 1.49 (3.07)
Commercial tablets	12	101.77 ± 0.82 (2.66)	102.66 ± 0.79	101.17 ± 1.70 (2.71)
Ampuls	8	93.56 ± 0.61 (7.94)	96.79 ± 1.03	93.00 ± 1.55 (6.12)
		Aminophylline Ampuls		
Solution[c]	5	99.94 ± 0.79 (9.41)	104.73 ± 0.78	—
Ampuls	5	100.31 ± 0.34 (13.25)	105.57 ± 0.78	—
		Minophylline–Phenobarbital Mixture		
Minophylline	11	101.15 ± 0.71 (17.85)	107.49 ± 0.87	99.30 ± 1.16 (18.29)
		ΔA_{238} Method	ΔA_{260} Method	ΔA_T Method
Phenobarbital	8	92.75 ± 2.91	103.90 ± 3.00	98.36 ± 1.21

[a] The tablet powder was prepared in the laboratory by weighing 250 mg of minophylline and adding 0.5 g of commercial lactose. [b] The figures in parentheses are the calculated t values with reference to the A method; theoretical t (α = 0.05) = 2.306 (for df 8), 2.145 (for df 14), 2.086 (for df 20), and 2.074 (for df 22). [c] A volume of 10 ml of aminophylline solution (250 mg/ml) to which 0.2 ml of benzyl alcohol was added.

accurately weighed quantity equal to about 0.7 g was extracted with three 30-ml portions of 0.1 N H_2SO_4 and suitably diluted for spectrophotometric measurement.

Minophylline Ampuls—The contents of five ampuls were mixed together in a dry conical flask. A measured volume was suitably diluted with 0.1 N H_2SO_4 for spectrophotometric measurement.

Aminophylline Ampuls—This assay was as described for minophylline ampuls.

Minophylline–Phenobarbital Syrup—Minophylline was determined as described for minophylline ampuls by suitably diluting a measured volume with 0.1 N H_2SO_4. Phenobarbital was assayed by transferring a measured volume to a separator. The solution was acidified with dilute sulfuric acid and extracted with four 25-ml portions of chloroform. The extract was evaporated on a water bath, and the residue was dissolved in ethanol and quantitatively transferred to a volumetric flask (50 ml).

Two similar volumes were transferred into 50-ml measuring flasks, one containing 5 ml of 1 N NaOH (Solution C) and the other containing a mixture of 5 ml of 0.25 M Na_2CO_3 and 5 ml of 0.25 M $NaHCO_3$ (Solution D). The contents were diluted to volume. The absorbance (ΔA_{238}) of Solution D was measured at 238 nm using Solution C as a blank, followed by measurement of Solution C against Solution D at 260 nm.

RESULTS AND DISCUSSION

With the conventional spectrophotometric method, the absorbances of the prepared solutions in 0.1 N H_2SO_4 were measured at λ_{max} 274 nm for minophylline and at 270 nm for aminophylline. Beer's law was valid within concentration range of 0.3–1.8 mg % for minophylline and of 0.3–2.1 mg % for aminophylline. The calibration curves can be described by the following regression equations:

$$A_{274} = -0.0002 + 0.0290C \text{ (for minophylline)} \quad \text{(Eq. 4)}$$

$$A_{270} = -0.002 + 0.4251C \text{ (for aminophylline)} \quad \text{(Eq. 5)}$$

On application of the A method, a high mean percent recovery (Table I) was obtained. The contribution of irrelevant absorbance led to high results.

The absorbances of interfering substances, *e.g.*, sweetening agents, binders, diluents, and fillers, varied linearly with wavelength (10). To correct the linear impurity absorbance, the absorbances of the minophylline solution were measured at λ_1 246 nm, λ_2 274 nm, and λ_3 295 nm (Fig. 1). For the aminophylline solution, λ_1, λ_2, and λ_3 were 242, 270, and 287 nm, respectively.

The A_c can be calculated from the following formulas:

$$A_c = A_{274} - (21/49)A_{246} - (28/49)A_{295} \text{ (for minophylline)} \quad \text{(Eq. 6)}$$

and:

$$A_c = A_{270} - (17/45)A_{242} - (28/45)A_{287} \text{ (for aminophylline)} \quad \text{(Eq. 7)}$$

Within a concentration range of 0.3–1.8 mg % for minophylline and of 0.3–2.1 mg % for aminophylline, A_c *versus* C showed a linear relationship. The corresponding calibration curves can be described from the following regression equations:

$$A_c = 0.0010 + 0.1697C \text{ (for minophylline)} \quad \text{(Eq. 8)}$$

$$A_c = 0.0040 + 0.3030C \text{ (for aminophylline)} \quad \text{(Eq. 9)}$$

With the orthogonal function method, the absorbances of minophylline solution were measured over the 266–286-nm wavelength range at 4-nm intervals. The quadratic coefficient was calculated by:

$$p_2 = [(+5)A_{266} + (-1)A_{270} + (-4)A_{274} + (-4)A_{278} + (-1)A_{282} + (+5)A_{286}]/84 \quad \text{(Eq. 10)}$$

The numbers between brackets are given in standard texts (11, 12), and the divisor 84 is the normalizing factor. Within a concentration range of 0.3–1.8 mg %, p_2 *versus* C showed a linear relationship. The calibration curve can be described by:

$$p_2 \times 10^3 = -0.1410 - 8.1465C \quad \text{(Eq. 11)}$$

The wavelength range (Fig. 1) of 266–286 nm (λ_m 276) at 4-nm intervals was chosen as the analytical set, because the p_2 value is maximum and q_2 (where $q_2 = p_2\sqrt{N}$ and N is the normalizing factor 84) for a solution of 1.9 mg % (w/v) minophylline in 0.1 N H_2SO_4 was found to exceed 0.140[10].

The results of the assay for different pharmaceutical preparations are presented in Table I. The following conclusions were made.

The mean percentage from results of the A method is either slightly or distinctly higher than that of the A_c and p_2 methods. These data were

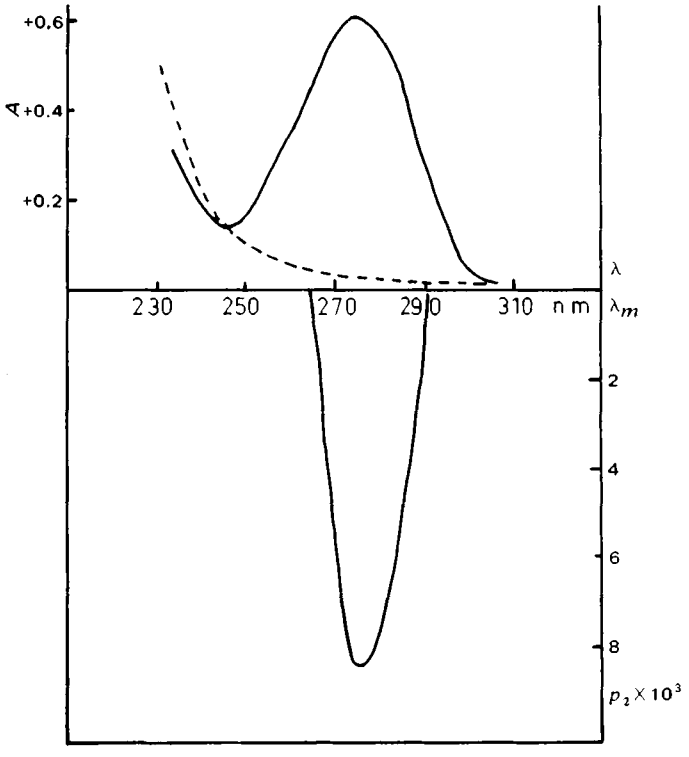

Figure 1—*Spectra of minophylline (—) (1 mg %) and convoluted curve therefrom and phenobarbital (- - -) (2 mg %). (The solvent was 0.1 N H_2SO_4.)*

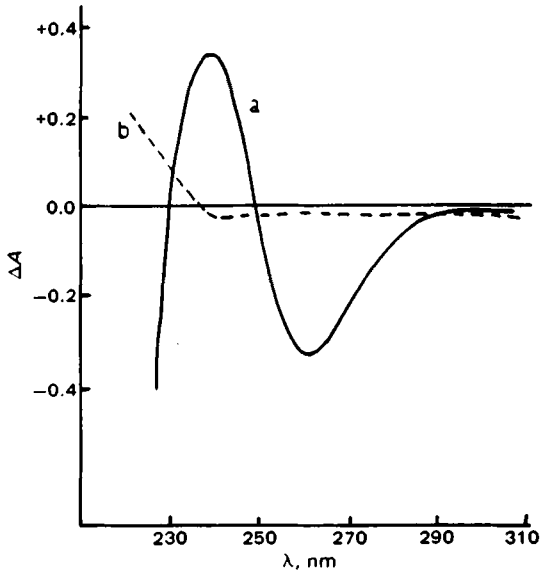

Figure 2—*Curve of phenobarbital (a) (2 mg %) and minophylline (b) (0.5 mg %).*

subjected to statistical analysis. Since the calculated t value ($\alpha = 0.05$) is higher than the theoretical value (Table I), the null hypothesis is rejected (13) and the results of the A_c and p_2 methods are considered more accurate. Therefore, the irrelevant absorbance due to excipients in pharmaceutical formulations can be corrected by using the A_c and p_2 methods.

The irrelevant absorbance due to benzyl alcohol is corrected by applying the A_c method, although the spectrum of benzyl alcohol exhibits typical benzenoid structure. It exhibits maxima at 254 ($A^{1\%}_{1cm} \simeq 40$) and 260 ($A^{1\%}_{1cm} \simeq 34$) nm. Because of the low absorptivity and relatively small concentration (*i.e.*, in a ratio of ~1:12.5 to aminophylline) of benzyl alcohol, canceling of its irrelevant absorbance by application of the A_c method is possible.

The coefficient of variation from the results of the p_2 method is always high compared with the A and A_c methods. Such error in the p_2 method can be attributed to wavelength-setting errors since extinction measurements are usually made on the slopes of the absorption curves (14). Therefore, for its simplicity and high reproducibility, the A_c method is preferable to the p_2 method.

The presence of minophylline and phenobarbital in a ratio of about 30:1 in syrup necessitates the separation of phenobarbital prior to its estimation. In the assay of minophylline in the presence of phenobarbital, there is no problem since the latter absorbs minimally. Furthermore, the absorbance of phenobarbital in an acid medium is small and varies linearly with wavelength (Fig. 1). Such absorbance was treated as irrelevant absorbance, *i.e.*, corrected by the A_c and p_2 methods (Table I).

Phenobarbital was determined by the application of the ΔA method (15) at λ_{238} (ΔA_{238}) and λ_{260} (ΔA_{260}) nm. The contribution of the differential absorbance of minophylline (that could be extracted with phenobarbital) is negligible (Fig. 2). For both ΔA_{238} and ΔA_{260} methods, Beer's law is valid within a 0.5–5-mg % concentration range. The regression equations are:

$$\Delta A_{238} = 0.0119 + 0.1605C \quad \text{(Eq. 12)}$$

$$\Delta A_{260} = 0.0243 + 0.1530C \quad \text{(Eq. 13)}$$

$$\Delta A_T = 0.0363 + 0.3135C \quad \text{(Eq. 14)}$$

where ΔA_T is ($\Delta A_{238} + \Delta A_{260}$).

The results obtained from ΔA_{238}, ΔA_{260}, and ΔA_T are presented in Table I.

The ΔA_{238} method gave lower results than the ΔA_{260} method while ΔA_T gave a mean value for both. The low results of ΔA_{238} are attributed to the differential absorbance of minophylline (Fig. 2), *i.e.*, negative error is obtained. Such error becomes positive on reversing the cells in the ΔA_{260} method. On summing ΔA_{238} and ΔA_{260}, these errors cancel each other. Therefore, it is not surprising that ΔA_T results are more accurate and give lower coefficients of variation. Moreover, on summing ΔA_{238} and ΔA_{260}, a higher slope value is obtained, which renders ΔA_T more sensitive.

REFERENCES

(1) E. J. Mulder, F. J. Sprint, and K. J. Kenning, *Pharm. Weekbl.*, **98**, 745 (1963).

(2) R. G. White, *Prog. Infrared Spectrosc.*, **2**, 275 (1964); through "Absorption Spectrophotometry," 3rd ed., G. E. Lothian, Ed., Adam Hilger Ltd., London, England, 1969, p. 94.

(3) N. Wright, *Ind. Eng. Chem. Anal. Ed.*, **13**, 1 (1941).

(4) R. A. Morton and A. L. Stubbs, *Analyst*, **71**, 348 (1946).

(5) H. C. Shaw and J. P. Jefferies, *ibid.*, **78**, 519 (1953).

(6) S. H. Ynen, J. E. Bogness, and D. Myles, *ibid.*, **92**, 375 (1967).

(7) A. M. Wahbi and S. Ebel, *Anal. Chim. Acta*, **70**, 57 (1974).

(8) A. L. Glenn, *J. Pharm. Pharmacol.*, **15**, 123T (1963).

(9) I. U. Agwu and A. L. Glenn, *ibid., Suppl.*, **19**, 763 (1967).

(10) H. Abdine, A. M. Wahbi, and M. A. Korany, *ibid.*, **23**, 444 (1971).

(11) W. E. Milne, "Numerical Calculus," 1st ed., Princeton University Press, Princeton, N.J., 1949, pp. 265, 375.

(12) R. A. Fisher and F. Yates, "Statistical Tables for Biological, Agricultural and Medical Research," 4th ed., Oliver and Boyd, Edinburgh, Scotland, 1953, p. 80.

(13) "Statistical Manual for Chemistry," L. Bauer, Ed., Academic, London, England, 1971.

(14) M. Ismail and A. L. Glenn, *J. Pharm. Pharmacol.*, **10**, 150T (1964).

(15) H. Goodman, A. LaMonde, G. S. Banker, and A. M. Knevel, *Can. J. Pharm. Sci.*, **6**, 70 (1971).

ACKNOWLEDGMENTS

The authors thank the director and staff members of the Alexandria Company for Pharmaceutical and Chemical Industries, Alexandria, Egypt, for providing the analyzed samples.

Effect of Nonsteroidal Anti-Inflammatory and Other Pharmacological Agents on Tuberculin Reaction

R. J. WOJNAR ˣ, R. J. BRITTAIN, and E. DZELZKALNS

Received March 30, 1978, from the *Department of Experimental Pathology, Squibb Institute for Medical Research, Princeton, NJ 08540.* Accepted for publication May 19, 1978.

Abstract □ Nonsteroidal anti-inflammatory and other pharmacological agents were tested in the efferent arc of the tuberculin skin reaction in the guinea pig. A low but significant inhibition was produced by the acidic anti-inflammatory agents, including the arylalkanoic acids, the anthranilic acids, indomethacin, and phenylbutazone. Some nonacidic anti-inflammatory agents also were inhibitory; benzydamine caused a high inhibition. Except for methotrexate, the antineoplastic–antimetabolite agents were not potent inhibitors. Inhibition without toxicity was produced by the coumarin anticoagulants, the diuretics, chloroquine, tilorone, and the following immunoregulators: antithymocyte γ-globulin, cyclophosphamide, and penicillamine. Levamisole, colchicine, heparin, and niridazole were inhibitory but produced lethality either at or above the effective dose.

Keyphrases □ Tuberculin reaction—effect of nonsteroidal anti-inflammatory and various other pharmacological agents in guinea pigs □ Anti-inflammatory agents, nonsteroidal—effect on tuberculin reaction in guinea pigs □ Immune systems, cell mediated—tuberculin reaction, effect of nonsteroidal anti-inflammatory and various other pharmacological agents in guinea pigs

The pathogenesis of rheumatoid arthritis involves various immunological aspects. The participation of cellular immunity is suggested by studies of rheumatoid joints (1–5), synovitis (6), and the response of circulating lymphocytes to products of rheumatoid joint tissues and fluids (7–10).

Many nonsteroidal anti-inflammatory agents now in use for rheumatoid arthritis were identified principally with a model of acute inflammation, carrageenan-induced edema (11), and a model with both immunological and inflammatory components, adjuvant-induced arthritis (12).

In view of the suggested role of cellular immunity in rheumatoid arthritis, it was of interest to determine if nonsteroidal anti-inflammatory agents could affect a cell-mediated immune system, particularly at a stage apart from sensitization. These agents were tested in the efferent arc (13) of the tuberculin reaction in the guinea pig. This immunologically specific system has been characterized by its infiltration of mononuclear cells and its presumptive mediation by lymphokines (14, 15).

This study was extended to other pharmacologically active agents, some previously tested and others not tested in the tuberculin reaction. These data could identify new agents that might affect cell-mediated immune reactions and thus form the basis for a new chemical design of therapeutic agents for rheumatoid arthritis.

EXPERIMENTAL

Tuberculin System—The tuberculin reaction in the guinea pig was produced essentially as described previously (16). Briefly, male albino guinea pigs were sensitized to *Mycobacterium tuberculosis*[1] in Freund's incomplete adjuvant[1] as described or by injection intradermally into the right hind footpad and subcutaneously into two sites in the nape of the neck. Three to four weeks later, the animals were challenged with 0.6 μg of tuberculin[2], and the diameters and thicknesses of the lesions were measured after 24 hr.

Table I—Effect of Anti-Inflammatory-Antirheumatic Agents on the Tuberculin Reaction

Agent	Percent Inhibition, D/T[a] 50-mg/kg Dose[b]	100-mg/kg Dose[b]
Arylalkanoic acids		
Alclofenac	7 ± 2/32 ± 5 (13)	10 ± 3/30 ± 6 (12)
Aspirin	7 ± 3/19 ± 7 (11)	7 ± 1/25 ± 4 (18)
Cicloprofen	7 ± 2/28 ± 4 (14)	
Ibufenac	9 ± 2/29 ± 4 (35)	
Ibuprofen	17 ± 1/43 ± 4 (29)	
Naproxen	8 ± 2/27 ± 9 (15)	
Sodium salicylate		[c] −2 ± 2/4 ± 7 (12)
Tolmetin sodium	6 ± 1/17 ± 6 (11)	10 ± 2/22 ± 4 (18)
Anthranilic acids		
Diclofenac sodium	5 ± 2/14 ± 8[c] (18)	10 ± 4/41 ± 15 (7)[d]
Flufenamic acid	10 ± 2/30 ± 4 (28)	
Meclofenamic acid	6 ± 3/31 ± 8 (11)	
Mefenamic acid	7 ± 4/18 ± 9 (15)	
Niflumic acid	[c] 3 ± 2/8 ± 6[c] (27)	[c] −2 ± 7/28 ± 9 (9)
Other agents		
Aurothioglucose	18 ± 2/36 ± 6 (17)	13 ± 3/24 ± 8 (6)
Benzydamine hydrochloride	13 ± 3/60 ± 5 (18)	
Flazalone hydrochloride	19 ± 3/41 ± 6 (8)	12 ± 5/39 ± 10 (7)
Indomethacin	[c] 4 ± 4/10 ± 7[c] (17)	12 ± 2/19 ± 6 (14)
Phenylbutazone	[c] 1 ± 3/−3 ± 7[c] (22)	[c] 2 ± 2/−2 ± 7[c] (11)

[a] In this and subsequent tables, percent inhibition diameter/thickness ± *SE* (number of animals). [b] In this and subsequent tables, compounds were administered each time at the listed dose. Unless otherwise indicated, the compounds were administered twice, subcutaneously, as in *Experimental*. [c] Not significant. All other values in this and subsequent tables were significant at $p < 0.05$, unless indicated as not significant. [d] Delayed death of three out of seven animals.

Tuberculin, Turpentine, and Histamine System—The reactions for all three agents were produced on the same animal. Animals were sensitized and challenged with tuberculin, as described. Reactions to turpentine[3] were produced as described previously (16) or, as in later experiments, by intradermal injection of 0.05 ml of turpentine–buffer[4] (1:9 v/v) emulsified by repeated passage through a syringe needle. Turpentine was administered 5 hr after challenge with tuberculin, just after the second administration of the test compound. Evaluation was performed in a manner similar to, and at the same time as, the tuberculin reaction. After evaluation of the reactions to tuberculin and turpentine, reactions to histamine were produced and measured as described previously (16).

Administration of Test Compounds—The test compounds in sesame oil were administered twice, at 30 min before and again at 5 hr after tuberculin, either subcutaneously at ventral sites or orally by gavage, unless otherwise stated. Compounds were tested in groups of four to seven animals. The average inhibition ± *SE* was calculated for the test compound-treated groups in comparison to the control sesame oil-treated groups. Variability within and among the groups of animals was taken into account.

For the control animals, the average diameter, D, and thickness, T, ± *SD* of the lesions from tuberculin were 18.3 ± 1.3 and 0.79 ± 0.13 mm (75 groups), respectively. From turpentine, these values were 18.5 ± 1.7 and 0.87 ± 0.12 mm (six groups), respectively. From histamine, the av-

[1] *M. tuberculosis* H37 RA and adjuvant, Difco Laboratories, Detroit, Mich.

[2] Tuberculin purified protein derivative (I) as lyophilized material, lot 974562C, Parke, Davis and Co., Detroit, Mich. Each milligram of I was equivalent in potency to 50,000 tuberculin units.

[3] Rectified turpentine, Winsor and Newton, Secaucus, N.J.

[4] Hemagglutination buffer, Difco Laboratories, Detroit, Mich.

0022-3549/79/0100-0012$01.00/0
© 1979, American Pharmaceutical Association

Table II—Effect of Anti-Inflammatory-Antirheumatic Agents on the Tuberculin Reaction

Agent	Dose, mg/kg	Percent Inhibition, D/T
Benzydamine	25	7 ± 3/30 ± 8 (16)
	150[a,b]	18 ± 5/55 ± 9 (5)
Indomethacin	100[c]	12 ± 2/36 ± 10 (14)
	150[a]	19 ± 4/50 ± 6 (11)[d]
Niflumic acid	100[c]	10 ± 2/32 ± 9 (14)
	150[a]	14 ± 6/57 ± 14 (8)[d]
Phenylbutazone	100[c]	19 ± 3/59 ± 7 (13)[d]
	150[a]	7 ± 2/28 ± 6 (11)

[a] Oral administration. [b] In saline. [c] Administered once daily at 2 and 1 days before challenge and twice on the day of challenge. [d] Death of animals: with indomethacin, 1/11; with niflumic acid, 2/10; and with phenylbutazone, 2/14.

erage diameter and intensity, I, were 13.6 ± 1.0 mm and 2.9 ± 0.7 (six groups), respectively.

The compounds tested are grouped in Tables I–V according to their listed therapeutic use (17).

RESULTS AND DISCUSSION

The temporal difference between the afferent and efferent arcs in the tuberculin reaction (13) allows for evaluation of compounds in the separate stages. Compounds were tested on the events following the interaction of sensitized cells and antigen, the efferent arc, thereby focusing on their potential therapeutic activity.

Anti-Inflammatory-Antirheumatic Agents (Tables I and II)—Statistically significant, but low, inhibitions of the tuberculin reaction were produced by the acidic anti-inflammatory agents, including the arylalkanoic acids, the anthranilic acids, indomethacin, and phenylbutazone, except sodium salicylate. For the arylalkanoic acids, the extent of inhibition appeared to plateau generally at 10% for diameter and 30% for thickness. These values were attained by the other active acidic agents even after administration for multiple days. In instances where this level of inhibition was exceeded, lethality was noted, as shown with indomethacin, niflumic acid, and phenylbutazone (Table II). This greater inhibition might have been due to this lethality.

The similar inhibition shared by these acidic anti-inflammatory agents suggests that they inhibit a common path in the tuberculin reaction. The inhibition of prostaglandin synthesis by these agents (18–21) and the correlation of anti-inflammatory effects and this mechanism (19) suggest that their inhibition of the tuberculin reaction could have occurred through inhibition of prostaglandin synthesis.

Some support for this view comes from the proposal that prostaglandins serve as potentiators of inflammation in the guinea pig, as shown with the tuberculin reaction (22). Furthermore, prostaglandins have been associated with cutaneous inflammation (23), including allergic contact dermatitis, a delayed hypersensitivity reaction. The prostaglandin pathway also has been altered in skin, including that of the guinea pig (24), by indomethacin and aspirin (23).

Phenylbutazone, the least potent acidic anti-inflammatory agent, previously had a slight (25) or no (26) effect in the tuberculin reaction. Sodium salicylate in this and previous (25) studies was inactive. In an assessment of delayed hypersensitivity in the human, aspirin at therapeutic doses had no effect (27). The low activity of aspirin in the present studies may not be demonstrable in humans.

Among the effective nonacidic anti-inflammatory agents, benzydamine inhibited the tuberculin reaction greater than the plateau level achieved by the acidic agents. This result suggests that benzydamine was active by a mechanism separate from or in addition to that for the acidic agents. Benzydamine, as well as flazalone, modulate the prostaglandin pathway (20) but at a site different from that of some acidic agents (28).

In nonimmunologically induced reactions, benzydamine moderately inhibited the turpentine-induced reaction and only slightly inhibited the histamine-induced reaction (Table VI). Some similarity could be noted

Table III—Effect of Antineoplastic-Antimetabolite Agents on the Tuberculin Reaction

Agent	Dose, mg/kg	Percent Inhibition, D/T
Azathioprine	100	[a]10 ± 5/12 ± 12[a] (5)
	150	[a]4 ± 5/6 ± 12[a] (6)
	200[b]	[a]5 ± 4/11 ± 8[a] (5)
	300[b]	13 ± 2/50 ± 4 (10)
Hydroxyurea	50	13 ± 4/13 ± 14[a] (9)
	100	15 ± 5/12 ± 12[a] (11)
Mercaptopurine	100	[a]10 ± 5/25 ± 10[a] (6)
	150	[a]7 ± 5/14 ± 13[a] (6)
	200[b]	20 ± 3/31 ± 8 (5)
	300[b]	13 ± 2/24 ± 4 (10)
Methotrexate	25	[a]12 ± 6/28 ± 20[a] (4)
	50	15 ± 5/37 ± 11 (8)
Oxisuran	50	[a]1 ± 4/11 ± 7[a] (10)
	100	[a]7 ± 4/14 ± 9[a] (5)
	150[c]	[a]3 ± 5/17 ± 10[a] (6)

[a] Not significant. [b] Oral administration. [c] Intraperitoneal administration in saline once daily for 3 days with challenge on the 3rd day.

Table IV—Effect of Anticoagulants on the Tuberculin Reaction

Agent	Dose, mg/kg	Percent Inhibition, D/T
Acenocoumarol	50	[a]−2 ± 5/18 ± 10[a] (4)
Anisindione	50	[a]1 ± 2/16 ± 8[a] (4)
Dicumarol	50	[a]3 ± 2/15 ± 7[a] (6)
	10[b]	15 ± 2/61 ± 5 (7)
	50[b]	28 ± 2/77 ± 4 (7)
Heparin sodium	10[c]	18 ± 4/27 ± 8 (11)[d]
	50	34 ± 2/44 ± 3 (10)[d]
	10[b]	18 ± 2/35 ± 4 (5)[d]
Warfarin	10[b]	19 ± 2/59 ± 5 (7)
	50[b]	22 ± 2/50 ± 6 (7)

[a] Not significant. [b] Administered once daily at 2 and 1 days before challenge and twice on the day of challenge. [c] Heparin, 10 mg = 1600 units. [d] Deaths of animals at 10 and 50 mg/kg, given for 1 day, were 1/12 and 9/16, respectively; at 10 mg/kg, given for multiple days, death of animals was 2/7.

Table V—Effect of Various Pharmacological Agents on the Tuberculin Reaction

Agent	Dose, mg/kg	Percent Inhibition, D/T
Antigout		
Colchicine	0.1	10 ± 3/24 ± 8 (11)
	0.2	20 ± 2/65 ± 4 (12)
	0.4	26 ± 2/59 ± 8 (5)[a]
	0.8	—[a]
Antihistamine		
Chlorpheniramine maleate	50	15 ± 1/38 ± 7 (13)
	100	29 ± 6/93 ± 1 (2)[a]
Pyribenzamine hydrochloride	25	20 ± 2/61 ± 6 (10)
	50	36 ± 14/76 ± 24 (2)[a]
Antiparasitic		
Chloroquine phosphate	50	15 ± 3/52 ± 8 (12)
	100	21 ± 3/70 ± 7 (6)
Levamisole hydrochloride	50	7 ± 2/17 ± 9[b] (20)
	100	19 ± 1/57 ± 4 (19)[a]
	150	—[a]
Niridazole	50	10 ± 3/16 ± 9[b] (20)
	100	23 ± 2/64 ± 4 (6)
	100[c,d]	13 ± 2/46 ± 5 (5)
	100[c]	—[a]
Antiviral		
Tilorone hydrochloride	50	12 ± 3/29 ± 8 (11)
	100	24 ± 1/63 ± 5 (17)
	100[c]	18 ± 3/51 ± 6 (6)
Chelating agent		
Penicillamine	100	6 ± 3/22 ± 11[b] (13)
	150	[b]0 ± 4/13 ± 15[b] (6)
	50[c,e]	[b]7 ± 3/39 ± 5 (7)
Diuretic		
Chlorothiazide	50	11 ± 1/41 ± 6 (12)
	100	12 ± 2/56 ± 6 (6)
Furosemide	50	29 ± 2/75 ± 6 (8)
Immunoregulator		
Cyclophosphamide	50	[b]3 ± 5/18 ± 8[b] (4)
	100	15 ± 2/32 ± 7 (12)
	150	19 ± 2/53 ± 7 (12)

[a] Death of animals; with colchicine, 7/12 at 0.4 and 6/6 at 0.8 mg/kg; with chlorpheniramine maleate, 4/6; with pyribenzamine hydrochloride, 2/4; with levamisole hydrochloride, 13/32 at 100 and 6/6 at 150 mg/kg; and with niridazole, 6/6. [b] Not significant. [c] Oral administration. [d] Administered only 30 min before challenge. [e] Administered once daily at 2 and 1 days before challenge and twice on the day of challenge.

Table VI—Effect of Agents on Immunological *versus* Nonimmunological Reactions

Agent	Dose and Route, mg/kg	Percent Inhibition		
		Tuberculin *D/T*	Turpentine *D/T*	Histamine *D/I*
Benzydamine hydrochloride	50 sc	15 ± 2/60 ± 6 (9)	16 ± 3/49 ± 7	[a]6 ± 4/18 ± 9
Chlorpheniramine maleate	25 po	[a]1 ± 4/−4 ± 12[a] (7)	[a]5 ± 2/−2 ± 7[a]	26 ± 2/47 ± 7
	50 po	7 ± 3/45 ± 7 (7)	16 ± 2/26 ± 6	61 ± 10/88 ± 3
	100 po	9 ± 3/77 ± 3 (7)	18 ± 2/61 ± 7	100 ± 0/100 ± 0
Antithymocyte γ-globulin	50 ip[b]	36 ± 3/94 ± 3 (5)	16 ± 4/10 ± 13[a]	[a]−8 ± 6/3 ± 13[a]

[a] Not significant. [b] Intraperitoneal administration in 0.3 *M* glycine buffer, pH 7.4, at 50 mg of IgG/kg twice daily on the day before and on the day of challenge.

between benzydamine and the 9-benzyladenines (16) in their inhibitory activities against immunological and nonimmunological reactions and in their spatial atomic arrangements as constructed with Corey–Pauling–Koltun models.

Antineoplastic–Antimetabolite Agents (Table III)—Except for methotrexate, these agents generally were not effective or potent inhibitors of the efferent arc of the tuberculin reaction, at least after acute administration. Significant inhibition did occur with mercaptopurine or its analog, azathioprine, but only after oral administration of large doses. In other studies, inhibition of expression was observed with mercaptopurine[5] (29) and azathioprine (30) after administration for multiple but not single (25) days; however, multiple administration of mercaptopurine was near the time of sensitization (29) or was associated with lethality[5]. Methotrexate, inhibitory in the present studies, had variable effects (25, 31). Oxisuran did not inhibit the tuberculin reaction, unlike its inhibitory activity in ovalbumin-induced hypersensitivity in the guinea pig (32).

Anticoagulants (Table IV)—The anticoagulants were effective inhibitors of the tuberculin reaction, confirming previous reports (33, 34). The coumarin derivatives were effective only after administration for days before challenge, consistent with their proposed mode of action (35). Heparin sodium was inhibitory whether administered before or only at the time of challenge; lethality accompanied all levels of inhibition. The relationship of the clotting process and direct evidence of its activation in the course of the delayed hypersensitivity reaction were described (34, 36, 37). The induration of the tuberculin reaction may be due to the retention of extravascular fluid by the fibrin meshwork (36, 38). Consistent with this hypothesis was the marked inhibition of this reaction by the tested diuretic agents (Table V).

Various Pharmacological Agents (Table V)—Colchicine, an antigout agent, significantly inhibited the tuberculin reaction, as shown in this study and a previous report (39). Its dose–response range was very narrow, with noted lethality at about four times its minimally effective dose. Its mechanism of action in the tuberculin reaction is suggested by the indication that microtubular disruptive agents promote macrophage migration and counteract the influence of the macrophage migration inhibitory factor (39) without influencing the production of this factor (40, 41). Nonetheless, colchicine, although effective in gout (42), is not clinically effective in rheumatoid arthritis. Its narrow therapeutic index, as shown with the tuberculin reaction, may preclude its activity against cell-mediated immune aspects in rheumatoid arthritis.

Both antihistamines greatly inhibited the tuberculin reaction; lethality was noted at the larger dose. In a comparison to nonimmunologically induced reactions, chlorpheniramine maleate at two 25-mg/kg po doses markedly inhibited the histamine-induced reaction without significantly inhibiting the tuberculin and turpentine-induced reactions (Table VI). These two latter reactions were inhibited as the dose was increased to levels that abolished the histamine-induced reaction. Exclusion of a role for histamine in the tuberculin reaction cannot be made from these data, even though half of the reactivity to histamine can be abolished without significantly affecting the tuberculin reaction. An increase of histamine (43–45) as well as the histamine-forming capacity (46) has been found at the site of delayed hypersensitivity reactions; however, its significance in guinea pigs is currently unknown (47, 48).

The antiparasitic agents effectively inhibited the tuberculin reaction. Chloroquine phosphate was inhibitory without any noted toxicity, as in a previous study (25). Its biological effects are numerous (49), and clinically it is of value in rheumatoid arthritis (50–52). Niridazole, orally administered, suppressed delayed hypersensitivity in guinea pigs (53), mice (54), and humans (55). Data in the present study extend this activity of niridazole after both oral and parenteral administrations to the tuberculin reaction in the guinea pig. Activity occurred without overt toxicity, but lethality was noted at larger oral doses. Studies suggest that administration of niridazole prevented production of the macrophage migration inhibitory factor (53).

Another antiparasitic agent, levamisole, enhanced the cell-mediated immune response (56) and was effective in rheumatoid arthritis (57). Penicillamine, a chelating agent, is similar to levamisole in its immunostimulatory properties (58) and its effectiveness in rheumatoid arthritis (59–61). In the present studies, at identical parenteral doses, levamisole suppressed the tuberculin reaction only in association with lethality and penicillamine was inactive. Inhibition by penicillamine was observed after oral administration for multiple days, a regimen similar to that resulting in enhancement of pertussis vaccine pleurisy in the rat (58). Failure to enhance the tuberculin reaction could have resulted because the stimulatory effects were most marked in compromised animals (56) while the animals in the present study were optimally sensitized.

A cell-specific immunoregulator, anti-guinea pig thymocyte γ-globulin[6], essentially abolished the thickness and markedly inhibited the diameter of the tuberculin reaction. Associated with this inhibition was a 50% reduction in the peripheral lymphocytes. Turpentine- and histamine-induced reactions were not inhibited significantly (Table VI). Previously, contact dermatitis was inhibited by antithymocyte serum (62), and the tuberculin reaction was inhibited by antilymphocyte serum (63, 64). Another immunoregulator, cyclophosphamide, administered acutely, did not cause significant inhibition at small test doses in this and a previous (25) study but was active at the larger doses. Inhibition of the tuberculin reaction also occurred after administration of multiple doses after sensitization (30, 65). Thus, apart from its immunosuppressive effect, cyclophosphamide can inhibit the efferent arc of the tuberculin reaction.

Tilorone, an antiviral agent, suppressed tuberculin skin reactivity (66) and adjuvant arthritis (66, 67) in the rat and tuberculin footpad reactivity in the mouse (68). In adjuvant disease, the inhibitory effect occurred when the compound was administered during sensitization (66, 67) but not after sensitization (67). In the present study, tilorone significantly inhibited tuberculin reactivity at the efferent arc without overt toxicity.

Overall, expression of a cell-mediated immune reaction has been inhibited to various extents by different pharmacological agents. In view of the proposed involvement of this type of immunity in rheumatoid arthritis, as well as other disease states, and the possible therapeutic value from inhibition of this immunity, those agents that displayed significant activity apart from lethality warrant continued studies on their mode of action. The low inhibition of the acidic anti-inflammatory agents suggests limitation in this regard, although they may be active on other aspects of the disease state. Significant activity is suggested by such agents as the coumarin anticoagulants, antithymocyte (lymphocyte) γ-globulin, benzydamine, chloroquine, niridazole, and tilorone.

REFERENCES

(1) D. T. Y. Yu and J. B. Peter, *Semin. Arthritis Rheum.*, **4**, 25 (1974).

(2) P. Stastny, M. Rosenthal, M. Andreis, and M. Ziff, *Arthritis Rheum.*, **18**, 237 (1975).

(3) H. Ishikawa and M. Ziff, *ibid.*, **19**, 1 (1976).

(4) A. D. Bankhurst, G. Husby, and R. C. Williams, Jr., *ibid.*, **19**, 555 (1976).

(5) J. A. Van Boxel and S. A. Paget, *N. Engl. J. Med.*, **293**, 517 (1975).

(6) V. M. Goldberg, E. M. Lance, and P. Davis, *Arthritis Rheum.*, **17**, 993 (1974).

[5] Unpublished data.

[6] Horse anti-guinea pig thymocyte γ-globulin, lot 51, courtesy of Dr. G. Gray, The Upjohn Co., Kalamazoo, Mich.

(7) P. A. Bacon, R. Bluestone, A. Cracchiolo, and L. S. Goldberg, *Lancet*, **2,** 699 (1973).
(8) E. J.-M. A. Thonar and M. B. E. Sweet, *Arthritis Rheum.*, **19,** 539 (1976).
(9) J. E. Crout, F. C. McDuffie, and R. E. Ritts, Jr., *ibid.*, **19,** 523 (1976).
(10) T. D. Kinsella, *Ann. Rheum. Dis.*, **35,** 8 (1976).
(11) C. A. Winter, E. A. Risley, and G. W. Nuss, *Proc. Soc. Exp. Biol. Med.*, **111,** 544 (1962).
(12) M. E. Rosenthal and C. L. Nagra, *ibid.*, **125,** 149 (1967).
(13) J. L. Turk and D. A. Willoughby, *Antibiot. Chemother.*, **15,** 267 (1969).
(14) B. Benacerraf and I. Green, *Annu. Rev. Med.*, **20,** 141 (1969).
(15) J. R. David and R. R. David, *Progr. Allergy*, **16,** 300 (1972).
(16) R. J. Wojnar and R. J. Brittain, *Agents Actions*, **5,** 152 (1975).
(17) "USAN and the USP Dictionary of Drug Names," M. C. Griffiths, M. J. Dickerman, and L. C. Miller, Eds., U.S. Pharmacopeial Convention, Rockville, Md., 1976.
(18) J. R. Vane, *Nature New Biol.*, **231,** 232 (1971).
(19) R. Flower, R. Gryglewski, K. Herbaczyńska-Cedro, and J. R. Vane, *ibid.*, **238,** 104 (1972).
(20) D. W. Cushman and H. S. Cheung, *Biochim. Biophys. Acta*, **424,** 449 (1976).
(21) R. J. Taylor, Jr., and J. J. Salata, *Biochem. Pharmacol.*, **25,** 2479 (1976).
(22) T. J. Williams and J. Morley, *Nature (London)*, **246,** 215 (1973).
(23) M. E. Goldyne, *J. Invest. Dermatol.*, **64,** 377 (1975).
(24) D. S. Snyder, *Prostaglandins*, **11,** 631 (1976).
(25) G. L. Floersheim, *Helv. Physiol. Acta*, **22,** 92 (1964).
(26) J. F. Borel, C. Feurer, C. Magnée, and H. Stähelin, *Immunology*, **32,** 1017 (1977).
(27) M. W. Duncan, D. A. Person, R. R. Rich, and J. T. Sharp, *Arthritis Rheum.*, **20,** 1174 (1977).
(28) S. Moncada, P. Needleman, S. Bunting, and J. R. Vane, *ibid.*, **12,** 323 (1976).
(29) S. M. Phillips and B. Zweiman, *J. Exp. Med.*, **137,** 1494 (1973).
(30) R. Arinoviche and G. Loewi, *Ann. Rheum. Dis.*, **29,** 32 (1970).
(31) R. M. Friedman, *Proc. Soc. Exp. Biol. Med.*, **116,** 471 (1964).
(32) A. E. Fox, J. L. Gingold, and H. H. Freedman, *Infect. Immun.*, **8,** 549 (1973).
(33) D. S. Nelson, *Immunology*, **9,** 219 (1965).
(34) S. Cohn, B. Benacerraf, R. T. McCluskey, and Z. Ovary, *J. Immunol.*, **98,** 351 (1967).
(35) "The Pharmacological Basis of Therapeutics," L. S. Goodman and A. Gilman, Eds., Macmillan, New York, N.Y., 1975, p. 1350.
(36) R. B. Colvin, R. A. Johnson, M. C. Mihm, Jr., and H. F. Dvorak, *J. Exp. Med.*, **138,** 686 (1973).
(37) R. B. Colvin and H. F. Dvorak, *J. Immunol.*, **114,** 377 (1975).
(38) R. B. Colvin, M. C. Mihm, Jr., and H. F. Dvorak, *N. Engl. J. Med.*, **295,** 734 (1976).
(39) E. Pick and H. Abrahamer, *Int. Arch. Allergy Appl. Immunol.*, **44,** 215 (1973).
(40) E. Pick, *Immunology*, **26,** 649 (1974).
(41) B. R. Bloom, J. Gaffney, and L. Jimenez, *J. Immunol.*, **109,** 1395 (1972).
(42) S. L. Wallace, D. Bernstein, and H. Diamond, *J. Am. Med. Assoc.*, **199,** 93 (1967).
(43) T. Inderbitzen, *Int. Arch. Allergy Appl. Immunol.*, **7,** 140 (1955).
(44) J. Prochazka Fisher and R. A. Cooke, *J. Allergy*, **29,** 396 (1958).
(45) M. A. Goldman, B. A. Simpson, and H. F. Dvorak, *J. Immunol.*, **110,** 1511 (1973).
(46) R. W. Schayer and O. H. Ganley, *Am. J. Physiol.*, **197,** 721 (1959).
(47) H. O. Schild and D. A. Willoughby, *Br. Med. Bull.*, **23,** 46 (1967).
(48) J. P. Phair, A. J. Eisenfeld, R. J. Levine, and F. S. Kantor, *Immunology*, **18,** 611 (1970).
(49) W. M. Sams, Jr., *Mayo. Clin. Proc.*, **42,** 300 (1967).
(50) A. W. Bagnall, *Can. Med. Assoc. J.*, **77,** 182 (1957).
(51) A. Freedman and V. L. Steinberg, *Ann. Rheum. Dis.*, **19,** 243 (1960).
(52) A. J. Popert, K. A. E. Meijers, J. Sharp, and F. Bier, *ibid.*, **20,** 18 (1961).
(53) J. C. Daniels, K. S. Warren, and J. R. David, *J. Immunol.*, **115,** 1414 (1975).
(54) A. A. F. Mahmoud, M. A. Mandel, K. S. Warren, and L. T. Webster, Jr., *ibid.*, **114,** 279 (1975).
(55) L. T. Webster, Jr., A. E. Butterworth, A. A. F. Mahmoud, E. N. Mngola, and K. S. Warren, *N. Engl. J. Med.*, **292,** 1144 (1975).
(56) J. Symoens and M. Rosenthal, *J. Reticuloendothel. Soc.*, **21,** 175 (1977).
(57) U. Trabert, M. Rosenthal, and W. Müller, *Schweiz. Med. Wochenschr.*, **106,** 1293 (1976).
(58) P. A. Dieppe, D. A. Willoughby, E. C. Huskisson, and E. Arrigoni-Martelli, *Agents Actions*, **6,** 618 (1976).
(59) I. A. Jaffe, *Arthritis Rheum.*, **13,** 436 (1970).
(60) Multicentre Trial Group, *Lancet*, **1,** 275 (1973).
(61) M. H. Gordon and G. E. Ehrlich, *J. Am. Med. Assoc.*, **229,** 1342 (1974).
(62) J. L. Turk, D. A. Willoughby, and J. E. Stevens, *Immunology*, **14,** 683 (1968).
(63) B. H. Waksman, S. Arbouys, and B. G. Arnason, *J. Exp. Med.*, **114,** 997 (1961).
(64) H. B. Richerson, H. F. Dvorak, and S. Leskowtiz, *ibid.*, **132,** 546 (1970).
(65) J. M. Gumpel, P. M. Ford, and F. W. S. Webb, *Ann. Rheum. Dis.*, **30,** 78 (1971).
(66) H. Megel, A. Raychaudhuri, S. Goldstein, C. R. Kinsolving, I. Shemano, and J. G. Michael, *Proc. Soc. Exp. Biol. Med.*, **145,** 513 (1974).
(67) Y.-H. Chang, *J. Pharmacol. Exp. Ther.*, **203,** 156 (1977).
(68) F. M. Collins, *Antimicrob. Agents Chemother.*, **7,** 447 (1975).

ACKNOWLEDGMENTS

The authors are grateful to the various pharmaceutical companies for providing samples of compounds. They also thank M. Miraglia for assistance.

Fluorescence Assay of Hydroxynaphthoquinones

JOHAN G. VAN DAMME * and ROELAND E. DE NÈVE ˣ

Received November 17, 1977, from the *Laboratorium voor Galenische en Magistrale Farmacie, Farmaceutisch Insituut, Vrije Universiteit Brussel, Paardenstraat, 67, B-Sint-Genesius-Rode, Brussels, Belgium.* Accepted for publication April 5, 1978. *Present address: S. A. Unda-Harzé, B 4071 Aywaille, Belgium.

Abstract □ Three procedures for fluorescence assay of hydroxynaphthoquinones are reported. The first procedure, based on prior sodium dithionite reduction and determination of the fluorophore in butyl acetate, is applicable to all of the hydroxynaphthoquinones investigated (detection limit: ± 0.020 μg of quinone/g of butyl acetate). The second method, specific for 5-hydroxy-1,4-naphthoquinones (juglone series), involves warm reduction with stannous chloride in an acid medium and determination of the fluorophore in chloroform (detection limit: ±0.020 μg of quinone/g of chloroform). The third method, based on the reaction of Guilbault and Kramer, is applicable to 5-hydroxy- and 5,8-dihydroxy-1,4-naphthoquinones having both free quinonoid positions (detection limit: ±0.020 μg of juglone/g of dimethyl sulfoxide and 0.070 μg of *p*-naphthazarin/g of dimethyl sulfoxide). The nature of the fluorophores also was investigated.

Keyphrases □ Hydroxynaphthoquinones, various—fluorometric analyses, three different procedures □ Fluorometry—analyses, various hydroxynaphthoquinones, three different procedures

Hydroxynaphthoquinones of considerable interest (1) include the perihydroxy-1,4-naphthoquinones, juglone [occurring in the green parts of *Juglans regia* L. (Juglandaceae)], and plumbagin [in the roots and leaves of Plumbaginaceae and in *Drosera rotundifolia* L. (Droseraceae)], as well as lawsone [in *Lawsonia inermis* L. (Lythracaea)], lapachol (in the heartwood of several genera of the Bignoniaceae, especially the tribe Tecomeae), and phthiocol (isolated from *Mycobacterium tuberculosis*).

Dried plants, crude extracts, tinctures, or the pure quinones are still in use. In Belgium and France, tincture of Drosera is reputed to be of value in chronic bronchitis; but, since the drug deteriorates even when carefully stored, it is often inert (2). Henna (powder of dried leaves of *Lawsonia*) has been used in intestinal amoebiasis (3) and is perhaps one of the oldest cosmetics still in use. The fungicidal and bactericidal properties of pure plumbagin and juglone also have found medicinal use (4), and the antitumor properties of lapachol are presently of interest (5).

The chemistry of the hydroxynaphthoquinones has been studied extensively, especially lapachol (6) and juglone (1). However, the usual colorimetric and spectrophotometric methods for quantitative analysis of these compounds suffer from a lack of sensitivity and specificity. Fluorometric methods have not been reported until now and have to be based on chemical conversion because hydroxynaphthoquinones are nonfluorescent.

This paper describes simple fluorometric procedures for the pure compounds, permitting determinations at the submicrogram level. The most general method involves biphasic reduction with sodium dithionite solutions and determination of the fluorophore in butyl acetate. Since the procedure is also applicable to naphthoquinones with alkyl or prenyl (3-methyl-2-butenyl) groups (7), the method is not specific but is highly sensitive. Another procedure is based on warm reduction with stannous chloride followed by determination of the fluorophore formed in chloroform. The method is specific for 5-hydroxy-1,4-naphthoquinones (juglone and plumbagin) and is sensitive. A third procedure uses the reaction of Guilbault and Kramer (8) (nucleophilic addition of potassium cyanide) and appears to be specific for 5-hydroxy- and 5,8-dihydroxy-1,4-naphthoquinones with both quinonoid positions free.

EXPERIMENTAL

Instrumentation—The fluorescence spectrometer, equipped with a xenon arc[1] fed by a dc current supply[2], had a magnetic stabilizer[3], two quartz prism monochromators[4] with continuously adjustable slit widths, fluorescence attachment[5], a potted photomultiplier[6], and a microammeter[7] coupled to a transmission concentration converter[8] with four-digit display. The coarse gain of the instrument was variable in steps up to 15,000×, and the instrumental sensitivity in terms of quinine sulfate units is 1 μg/ml of 0.1 *N* H_2SO_4, obtaining full-scale deviation (100 in arbitrary units) by a gain of 3000×, an excitation maximum of 355 nm (slit width 10 nm), and an emission maximum of 460 nm (slit width 10 nm). The blank under these circumstances was 0.1 in arbitrary units.

For recording (uncorrected) spectra, the monochromators were equipped with wavelength drives and the transmission concentration converter was coupled to a one-axis recorder[9] with a wavelength marker.

Absorption spectra were obtained on a recording spectrophotometer[10].

Materials—Lawsone[11], lapachol[12], and juglone[12] were used without further purification, and *p*-naphthazarin[13] was purified by recrystallization in benzene. Plumbagin was prepared and purified by the method of de Buruaga (9) (mp[14] 75°). Phthiocol also was prepared (10) and purified by preparative TLC[15] (mp 172°).

All reagents were analytical or reagent grade purity. The assay solutions, prepared in double-distilled water, were 15% sodium dithionite, 1% potassium cyanide in phosphate buffer (pH 7.5), and 5% stannous chloride in 4 *M* HCl.

Chloroform[16] and dimethyl sulfoxide[16] were fluorescent grade, and butyl acetate[16] was analytical grade.

All glassware was treated with chromic acid (24 hr) and, after rinsing with distilled water, oven dried. To avoid adsorption losses, the inner surfaces were deactivated by soaking for 10 min in a 1% solution of a siliconizing agent[17]. The glassware was then rinsed thoroughly and oven dried (105°, 30 min).

Quartz cells were treated with fuming nitric acid (11).

Procedure A—The appropriate quantity of quinone was dissolved in 5 ml of butyl acetate in a screw-capped tube. Then 5 ml of sodium dithionite reagent was added, and the mixture was shaken for 15 min at 200

[1] Type Osram X B O 450 W mounted in a housing LX 501, C. Zeiss.
[2] Type V X 501 r, C. Zeiss.
[3] Type B V X 200 K, C. Zeiss.
[4] Type M 4 Q III, C. Zeiss.
[5] Type Z F M 4 C, C. Zeiss.
[6] RCA 1 P 28.
[7] P M Q II, C. Zeiss.
[8] TKR, C. Zeiss.
[9] Servogor S Type RE 541, Goerz-Austria.
[10] Perkin-Elmer model 124.
[11] Fluka AG, Switzerland.
[12] Aldrich Chemical Co.
[13] Bayer A. G., West Germany.
[14] Uncorrected on a Tottoli apparatus, Buchi.
[15] On 20 × 20-cm precoated silica gel plates with 2-mm layers (E. Merck, Darmstadt, West Germany . The eluent was heptane–butyl acetate (1:9); the R_f of phthiocol was 0.55.
[16] E. Merck, Darmstadt, West Germany.
[17] Siliclad, Clay-Adams, New York, N.Y.

0022-3549/79/0100-0016$01.00/0
© 1979, American Pharmaceutical Association

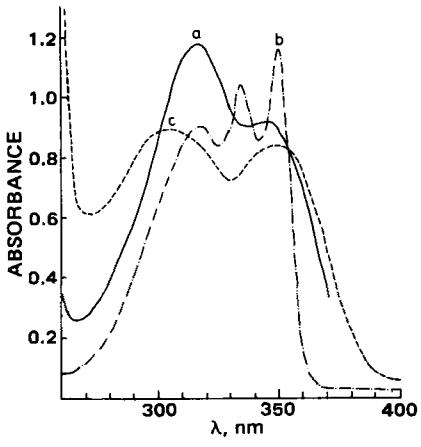

Figure 1—*UV spectra in butyl acetate. Key: a, reduced lawsone, 7.0 × 10^{-5} M; b, reduced juglone, 6.5 × 10^{-5} M; and c, reduced* p*-naphthazarin, 6.0 × 10^{-5} M.*

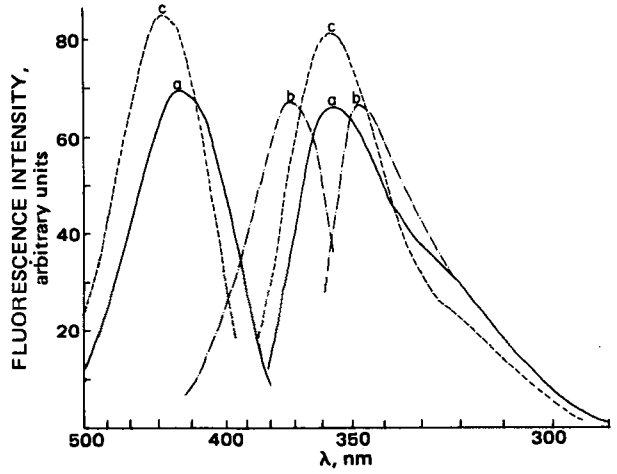

Figure 2—*Uncorrected excitation and emission spectra in butyl acetate. Key: a, reduced lawsone, 1.4 × 10^{-4} M; b, reduced juglone, 1.3 × 10^{-4} M; and c, reduced* p*-naphthazarin, 1.2 × 10^{-4} M.*

movements/min on a horizontal shaker. In a nitrogen atmosphere, about 3 ml of the butyl acetate phase was transferred to a 1-cm path quartz cell.

Procedure B—The appropriate quantity of quinone was dissolved in 1 ml of ethanol in a screw-capped tube. Then 5 ml of stannous chloride reagent was added; the mixture was covered with a small funnel and left for 1 hr over a boiling water bath (evaporation of the ethanol). After cooling, 5 ml of chloroform was added, and the mixture was shaken for 5 min at 200 movements/min. Following a brief centrifugation (5 min at 3000×*g*), about 3 ml of the organic phase was transferred to a 1-cm path quartz cell.

Procedure C—The appropriate quantity of quinone was dissolved in 5 ml of dimethyl sulfoxide, 0.5 ml of the potassium cyanide reagent was added, and the mixture was left to stand for 10 min. About 3 ml was transferred to a 1-cm path quartz cell prior to measurement.

Assay—For the determination of linearity, two concentration regions were chosen. In each region, seven samples and one reagent blank were tested. The samples were: Procedure A, 0.5–2 and 1–10 μg of quinone/g of butyl acetate; Procedure B, 1–10 and 5–25 μg of quinone; and Procedure C, 0.4–4 and 2–10 μg of quinone/g of dimethyl sulfoxide.

To determine the precision of the method, 12 blanks and 12 1-μg quinone standards were analyzed, starting with the weight operation, and the standard deviation was calculated.

The detection and determination limits as defined by Currie (12) were determined for each procedure.

RESULTS AND DISCUSSION

Nature of the Fluorophores—*Procedure A*—By applying the biphasic dithionite procedure to alkyl- and phenylnaphthoquinones, it was shown that the fluorophores formed were the corresponding hydroquinones; furthermore, the conversion of the quinone into the hydroquinone was nearly complete (7).

Although formation of hydroquinones should logically be involved for hydroxynaphthoquinones, the problem is more complex because of interferences due to phenol–keto tautomerism. Indeed, in contrast to the alkylnaphthohydroquinones where the phenolic form predominates in solution and only one form exists in the solid state (13), different tautomeric forms with perihydroxynaphthohydroquinones have been obtained in the solid state. In this case, the term "isomerism" instead of tautomerism must be used (14).

According to Fieser and Gates (10), dithionite reduction of phthiocol yields 3-methyl-1,2,4-trihydroxynaphthalene, and the phenolic tautomer predominates in solution.

Absorptiometric analysis, showing the similarity of the spectra of reduced lawsone and phthiocol, indicates that lawsone also yielded 1,2,4-trihydroxynaphthalene upon dithionite reduction (Fig. 1).

The reaction product with juglone was isolated by performing the procedure with ethyl acetate instead of butyl acetate and evaporating the solvent at room temperature in a nitrogen atmosphere. The melting point (170°) and chemical properties (15) of the compound indicate the presence of an α-hydrojuglone (1,4,5-trihydroxynaphthalene). The absorption spectrum (Fig. 1) of α-hydrojuglone in butyl acetate is very characteristic with three maxima: 317, 334, and 349 nm. Dithionite-reduced plumbagin yielded a similar spectrum, showing the formation of α-hydroplumbagin.

The reaction product of *p*-naphthazarin was obtained in a similar manner; physical and chemical properties (16) (*e.g.*, violet fluorescence in ethanol, mp 140°) suggest the presence of 1,4,5,8-tetrahydroxynaphthalene. As shown by the absorption spectrum (Fig. 1), the phenolic tautomer must also predominate in solution.

In contrast to the biphasic dithionite reduction, other reduction procedures (stannous and titanous chloride and zinc powder plus hydrochloric acid) did not always give the phenolic tautomers. With *p*-naphthazarin, cold stannous chloride reduction did not yield a fluorophore upon extraction in butyl acetate; on the other hand, addition of alcoholic hydrochloric acid to α-hydronaphthazarin solution in butyl acetate yielded fluorescence quenching. The formation of β-hydronaphthazarin (see Procedure B) is also unlikely, so another tautomer is probably involved.

From fluorescence analysis, it appears that one can distinguish between 2-hydroxynaphthoquinones (lawsone, lapachol, and phthiocol) and 5-hydroxynaphthoquinones (juglone and plumbagin), the spectra being identical within the same group (Fig. 2).

Procedure B—According to Thomson (17), warm stannous chloride reduction of juglone gives a mixture of α- and β-hydrojuglone in a 35:65 ratio, the latter being extractable with chloroform. Zahn and Ochwat (18) showed that the probable structure of β-hydrojuglone is 5-hydroxy-1,4-dioxo-1,2,3,4-tetrahydronaphthalene.

The fluorescent species obtained with juglone by application of Procedure B is thus probably β-hydrojuglone and is, as shown by its excitation and emission spectra, completely different from α-hydrojuglone (Fig. 3). With plumbagin, a fluorophore also was obtained, which is different from α-hydroplumbagin. Since the absorption spectrum of the compound in chloroform is similar to the spectrum of β-hydrojuglone (with respect to a bathochromic shift of approximately 40 nm), the fluorescent species is presumably a 1,4-dioxo-1,2,3,4-tetrahydronaphthalene compound (β-hydroplumbagin).

In contrast, warm stannous chloride reduction of *p*-naphthazarin did not yield fluorophores upon extraction either in chloroform or in butyl acetate, which illustrates that the formation of either α- or β-hydronaphthazarin is not probable.

Procedure C—Thiele and Meisenheimer (19) observed that hydrogen cyanide yields a diaddition product with 1,4-benzoquinone: 2,3-dicyano-1,4-dihydroxybenzene. The fluorescent properties of this compound were reported by Guilbault and Kramer (8), who demonstrated that the same compound is obtained upon reaction with potassium cyanide in dimethyl sulfoxide and that the green fluorescence must be assigned to a tautomeric ionic form.

Reynolds and Van Allen (20) showed that 2,3-dicyano-1,4-naphthalenediol is obtained with 2,3-dichloro-1,4-naphthoquinone and sodium cyanide. 1,4-Naphthoquinone should react much more slowly and presumably yield the same compound.

Performance of the Guilbault–Kramer procedure on 2,3-dichloro-1,4-naphthoquinone yielded a yellow fluorescent solution, and no ap-

Table I—Quantitative Determinations (Procedure A)

Parameter	2-Hydroxy-1,4-naphthoquinones			5-Hydroxy-1,4-naphthoquinones		
	Lawsone	Phthiocol	Lapachol	Juglone	Plumbagin	Naphthazarin
Excitation (slit width[a])	355 (3.6)	343 (3.6)	345 (6)	350 (9)	350 (6)	360 (6)
Emission (slit width[a])	429 (22)	432 (23)	430 (24)	370 (14)	375 (14)	440 (24)
Gain	9500×	12,000×	12,000×	12,000×	15,000×	12,000×
Blank[b]	0.5 ± 0.1[c]	1.5 ± 0.2[c]	2.5 ± 0.2[c]	0.5 ± 0.2[c]	0.2 ± 0.2[c]	2.2 ± 0.2[c]
1-μg standard[b]	49.0 ± 0.2[c]	62.5 ± 0.3[c]	57.0 ± 0.3[c]	52.0 ± 0.3[c]	53.5 ± 0.3[c]	61.6 ± 0.3[c]
Detection limit[d]	0.015	0.020	0.022	0.023	0.022	0.020
Lower determination limit[d]	0.045	0.060	0.066	0.071	0.066	0.061

[a] In nanometers. [b] In arbitrary units. [c] Standard deviation. [d] In micrograms of quinone per gram of solvent (butyl acetate).

preciable fluorescence was noted with 1,4-naphthoquinone after a reaction time of 10 min. Application of the same procedure on perihydroxynaphthoquinones with both quinonoid positions free (juglone and naphthazarin) yielded highly fluorescent species, and no fluorescence upon reaction with plumbagin was detectable. From fluorescence spectra, it appears that only one fluorophore (Fig. 4) was involved with juglone and that several fluorophores were formed with *p*-naphthazarin (Fig. 5). In the last case, the presence of more than one fluorescent component was suspected because the shape of the emission spectrum changed when the wavelength of the exciting light was varied (21).

Since no monoaddition product could be isolated (8, 19, 20) with juglone upon reaction with *p*-benzoquinone, *p*-naphthoquinone, and 2,3-dichloro-1,4-naphthoquinone, formation of a diaddition compound again was presumed.

Choice of Solvent—*Procedure A*—Biphasic reduction with butyl acetate is preferred, although the procedure yields similar results with amyl alcohol and ether. The use of an ester such as butyl acetate is indicated, because the solubility of this solvent for the dithionite reagent is extremely low. On standing, dithionite solutions become turbid through sulfur precipitation.

The aprotic character of the solvent is of interest since interferences due to electrolytic excited-state dissociation, as found with naphthols (22) and naphthalenediols (23), are avoided. Furthermore, absorption, excitation, and emission spectra in butyl acetate are bathochromically shifted compared to the spectra in cyclohexane (24), illustrating hydrogen bonding. Bathochromic shifts may be important, because the energy output of the light source is higher in the near UV region of the spectrum, resulting in a higher instrumental sensitivity.

Procedure B—Although β-hydroquinones are fluorescent in solvents such as ether, butyl acetate, and amyl alcohol, they are also fluorescent in chloroform, in contrast to the α-hydroquinones which produce nonfluorescent chloroform solutions because of an external heavy atom effect (25). Interferences of other quinones due to simultaneous reduction to hydroquinones are avoided, and the selectivity of the method is greatly enhanced. The absence of an external heavy atom effect (spin orbit coupling) in β-hydroquinones can be explained by intramolecular hydrogen bonding.

Procedure C—Guilbault and Kramer (8) observed that the maximum rates of reaction and fluorescence were obtained with benzoquinone in a solvent with a high dielectric constant such as dimethyl sulfoxide. This finding illustrates that the fluorescent species in an ionic molecule and solvents favoring the ionic form should be best. The effect of water and pH of the added reagent also was reported (8). With benzoquinone, the total water content should not exceed 9% (v/v) to avoid a deleterious effect on the reaction rate, and the pH should be held at 6.5–7.5 for the reaction to proceed smoothly.

With juglone, similar results were obtained. The maximum fluorescence intensity and reaction rate were obtained in dimethyl sulfoxide with a total water content not exceeding 2% (v/v). The potassium cyanide reagent should also be made up in a pH 7.5 phosphate buffer.

Quantitative Results—*Procedure A*—As indicated in Table I, the precision of the method is high, mainly due to the high photochemical stability of the fluorophores formed and the stoichiometric progress of the reduction. Moreover, working in a nitrogen atmosphere is not required for reliable results.

The luminescence blank is low, and the main factors contributing to the blank are the luminescence of the cell, the surroundings, and scattered light. Insertion of properly chosen stray light filters at the exits of excitation and emission monochromators is recommended. The dithionite reagent itself does not contribute to the blank.

From excitation and emission maxima or spectra, it appears that 2-hydroxy- and 5-hydroxy-1,4-naphthoquinones can be determined separately in mixtures. Separate determinations of 5-hydroxy- and 5,8-dihydroxy-1,4-naphthoquinones seem rather difficult to perform. The (lower) determination limit, defined as the concentration for which the relative standard deviation is 10%, is calculated as indicated by Currie (12). The obtained values (±0.020 μg/g of solvent) show the high sensitivity of the method.

To determine the linearity, the upper determination limit was defined as the concentration for which a 10% deviation of the regression line is obtained, calculated from the first seven points. A value of 4 μg/g of solvent was obtained, showing the deviation from linearity due to concentration quenching.

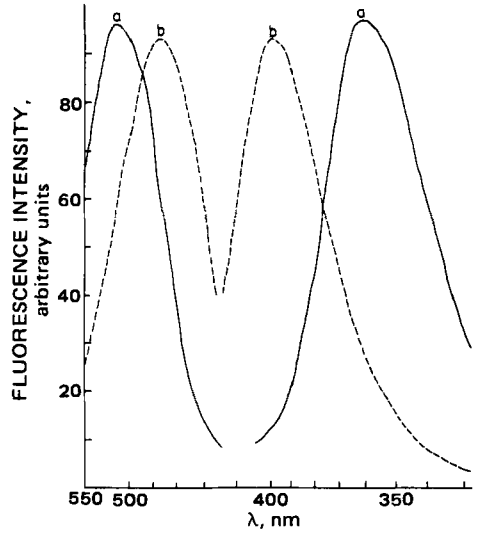

Figure 3—*Uncorrected excitation and emission spectra in chloroform. Key: a, β-hydrojuglone, 3.3 × 10⁻⁵ M; and b, β-hydroplumbagin, 3.7 × 10⁻⁵ M.*

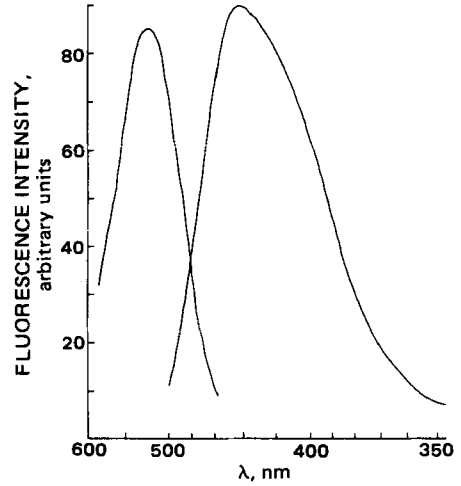

Figure 4—*Uncorrected excitation and emission spectra of the fluorophores of 1.2 × 10⁻⁴ M juglone (Procedure C).*

Table II—Quantitative Determinations (Procedure B)

Parameter	Juglone	Plumbagin
Excitation (slit width[a])	363 (13)	397 (18)
Emission (slit width[a])	510 (38)	474 (30)
Gain	1500×	750×
Blank[b]	2.9 ± 0.1[c]	2.0 ± 0.1[c]
1-μg standard[b]	31.3 ± 0.1[c]	27.5 ± 0.1[c]
Detection limit[d]	0.016	0.018
Lower determination limit[d]	0.050	0.054

[a] In nanometers. [b] In arbitrary units. [c] Standard deviation. [d] In micrograms of quinone per gram of solvent (chloroform).

Correlation coefficients were calculated from the first seven points (the first concentration region) and were not less than 0.998.

Procedure B—Quantitative results are summarized in Table II. The fluorophores formed do not suffer from either photodecomposition or reoxidation by air. Furthermore, as indicated by the precision of the method, the isomerization ratio of α- to β-hydrojuglones is independent of the concentration involved.

The luminescence blank is sufficiently low. In contrast to Procedure A, the reagents contribute to the blank, as shown by insertion of a spectrograde labeled chloroform blank.

From excitation and emission maxima, it appears that juglone and plumbagin can be determined separately in mixtures. The lower and upper determination limits in both cases were 0.020 and 4 μg/g of chloroform, respectively, which indicates a sufficiently large linearity.

Correlation coefficients calculated for the first seven points (first concentration region) were not less than 0.999.

The method is highly specific for 5-hydroxy-1,4-naphthoquinones; other quinones do not interfere when chloroform is the solvent.

Procedure C—Although more fluorophores are involved with *p*-naphthazarin, reliable quantitative results were obtained of a sufficiently high precision at a 375-nm emission maximum (Table III). The detection and lower determination limits of *p*-naphthazarin were three times higher than the juglone limits, and the upper determination limits were 5 and 7 μg/g of dimethyl sulfoxide with juglone and naphthazarin, respectively.

Fluorescent grade labeled dimethyl sulfoxide is recommended as the solvent since analytical grade solvents yield high blanks, probably due to impurities.

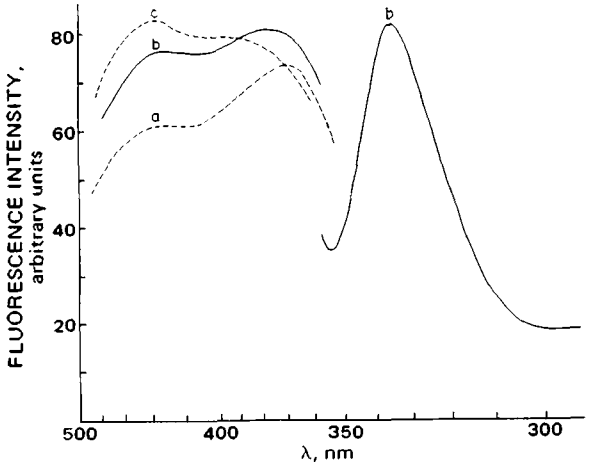

Figure 5—*Uncorrected excitation and emission spectra of the fluorophores of 1.2 × 10⁻⁴ M p-naphthazarin. Key: a, emission spectrum (excitation = 330 nm); b, emission spectrum (excitation = 335 nm); and c, emission spectrum (excitation = 340 nm).*

Table III—Quantitative Determinations (Procedure C)

Parameter	Juglone	Naphthazarin
Excitation (slit width[a])	444 (24)	337 (12)
Emission (slit width[a])	525 (45)	375 (14)
Gain	1500×	9000×
Blank[b]	0.5 ± 0.1[c]	1.4 ± 0.1[c]
1-μg standard[b]	21.0 ± 0.1[c]	12 ± 0.2[c]
Detection limit[d]	0.023	0.070
Lower determination limit[d]	0.070	0.210

[a] In nanometers. [b] In arbitrary units. [c] Standard deviation. [d] In micrograms of quinone per gram of solvent (dimethyl sulfoxide).

p-Benzoquinone and 2,3-dichloro-1,4-naphthoquinone also yield a positive reaction.

REFERENCES

(1) R. H. Thomson, "Naturally Occurring Quinones," 2nd ed., Academic, New York, N.Y., 1971.

(2) R. Paris and H. Moyse, "Matière Médicale," vol. 2, Masson, Paris, France, 1967, pp. 225–229.

(3) M. E. Hanke and S. M. Talaat, *Trans. R. Soc. Trop. Med. Hyg.*, **55**, 56 (1961).

(4) P. Lebeau and M. Janot, "Traité de Pharmacie Chimique," vol. 2, Masson, Paris, France, 1955, pp. 1160–1164.

(5) K. V. Rao, T. C. McBride, and J. J. Oleson, *Cancer Res.*, **28**, 1952 (1968).

(6) "The Constitution and Properties of Lapachol, Lomatiol and Other Hydroxynaphthoquinone Derivatives," L. F. Fieser, Ed., 1937.

(7) J. G. Van Damme, Ph.D. thesis, Vrije Universiteit Brussel, Brussels, Belgium, 1977.

(8) G. G. Guilbault and D. N. Kramer, *Anal. Chem.*, **37**, 1395 (1965).

(9) S. de Buruaga, *An. Soc. Fis. Quin.*, **31**, 134 (1933).

(10) L. F. Fieser and J. W. Gates, *J. Am. Chem. Soc.*, **63**, 2948 (1941).

(11) J. R. Edisbury, "Practical Hints on Absorption Spectrometry," Hilger and Watts, London, England, 1966, pp. 127–132.

(12) L. A. Currie, *Anal. Chem.*, **40**, 586 (1968).

(13) G. W. Wheland, "Resonance in Organic Chemistry," Wiley, New York, N.Y., 1955, pp. 401–405.

(14) B. Pullmann and A. Pullmann, "Les Théories Électroniques de la Chimie Organique," Masson, Paris, France, 1952, pp. 247, 248.

(15) "Elsevier's Encyclopaedia of Organic Chemistry," Carboisocyclic Condensed Compounds, No. 3, vol. 12B, F. Radt, Ed., Elsevier, New York, N.Y., 1950, p. 2155.

(16) *Ibid.*, pp. 2179–2181.

(17) R. H. Thomson, *J. Chem. Soc.*, **1950**, 1737.

(18) K. Zahn and P. Ochwat, *Ann. Chem.*, **462**, 72 (1928).

(19) J. Thiele and L. Meisenheimer, *Chem. Ber.*, **33**, 675 (1900).

(20) G. Reynolds and J. Van Allen, *J. Org. Chem.*, **29**, 3591 (1964).

(21) C. A. Parker, "Photoluminescence of Solutions," Elsevier, New York, N.Y., 1968, p. 19.

(22) A. Weller, *Z. Phys. Chem.*, **17**, 224 (1958).

(23) L. D. Derkacheva, *Opt. Spektrosk.*, **9**, 110 (1958) (English).

(24) I. Berlman, "Handbook of Fluorescence Spectra of Aromatic Molecules," Academic, New York, N.Y., 1965, pp. 112–115.

(25) C. A. Parker, "Photoluminescence of Solutions," Elsevier, New York, N.Y., 1968, pp. 373–386.

ACKNOWLEDGMENTS

Abstracted from a thesis submitted by J. G. Van Damme to the Vrije Universiteit Brussel in partial fulfillment of the Doctor of Philosophy degree requirements.

Supported in part by the Nationaal Fonds voor Geneeskundig Onderzoek.

Development of an Estriol-Releasing Intrauterine Device

R. W. BAKER *x, **M. E. TUTTLE** *, **H. K. LONSDALE** *, and **J. W. AYRES** ‡

Received December 27, 1977, from *Bend Research, Inc., Bend, OR 97701, and the ‡School of Pharmacy, Oregon State University, Corvallis, OR 97331. Accepted for publication May 19, 1978.

Abstract □ Estriol-releasing intrauterine devices were developed for experimental use in animals and humans. The devices consist of a reservoir containing the steroid surrounded by a rate-limiting polyurethane membrane. After an initial transient, the drug is released from the device at a constant rate for 1 year or more; devices with a much longer release period can be fabricated readily. A constant release rate is achieved by maintaining solid drug in the reservoir and good physical contact between the drug and the inside wall of the device. The methods used to fabricate the devices are described along with release rate and stability data.

Keyphrases □ Intrauterine devices—estriol releasing, prepared, release rate and stability evaluated □ Estriol—delivered by intrauterine devices, release rate and stability evaluated □ Dosage forms—intrauterine devices, estriol releasing, prepared, release rate and stability evaluated □ Estrogens—estriol, delivered by intrauterine devices, release rate and stability evaluated

Scommegna *et al.* (1) first described the preparation and use of a drug-releasing intrauterine device (IUD) for fertility control. A low dose of a steroid, applied locally to the entrometrial tissue of the uterus, provided a contraceptive effect by a mechanism other than simple irritation with its concomitant side effects. The delivery of the naturally occurring steroid progesterone at a constant dosage rate of 70 μg/day (or 26 mg/year) from such an IUD can maintain contraception (2–7). This dosage rate is well below that required to maintain contraception when the same drug is given systemically.

This paper describes the development and *in vitro* behavior of two similar estriol-releasing IUD's. One device is intended for use in experimental studies in animals; the other is intended for use in humans, following approval by the Food and Drug Administration. Prior animal studies (8) suggested that estriol is effective at concentrations lower than those required with progesterone, suggesting that such a device could be effective *in vivo* for several years.

The design of the human device closely follows that developed earlier (5), which, in turn, was based on the "T" shape first proposed by Tatum (9). The design of the device and its approximate dimensions are presented in Fig. 1. The devices for use in animals consisted essentially of only the stem of the T shown in Fig. 1. That is, they were rod-shaped devices, with a nominal outside diameter of 2–3 mm and lengths of 1–2 cm.

Devices with a range of release rates from 0.5 to 12.5 μg/day were required for use in animals to study the effect of release rate on contraceptive efficacy, tissue development, and other physiological parameters. Furthermore, the release rates had to be essentially invariant over the intended period of use, *i.e.*, from several months to 1 year or more.

THEORETICAL

Constant or zero-order release of a drug from a device can be achieved by maintaining a constant thermodynamic driving force across a fixed, rate-limiting membrane. This concept follows from Fick's first or steady-state law. Thus, the flux, J, across a membrane in one dimension is given by:

$$J = D\,\Delta C_m/l \qquad \text{(Eq. 1)}$$

where ΔC_m is the difference in drug concentration within the membrane of thickness l, and D is the diffusion coefficient of the drug in the membrane. The drug concentration within the membrane is simply related to that in the external phases in contact with the membrane through a partition coefficient, K. Thus, Eq. 1 can be restated in more useful terms as:

$$J = DK\,\Delta C/l \qquad \text{(Eq. 2)}$$

where ΔC is the concentration difference in the two solutions external to the membrane. Therefore, the flux will be constant as long as ΔC is maintained constant.

The developed devices were conceptually of this type. Solid drug was contained within the reservoir created by the tube-shaped stem of the T shown in Fig. 1. The steady-state release rate from such a cylindrical reservoir device is given by (10):

$$Q = \frac{2\pi hDK\,\Delta C}{\ln(r_o/r_i)} \qquad \text{(Eq. 3)}$$

where Q is expressed in mass per unit time (*e.g.*, micrograms per day), h is the filled length of the cylinder, and r_o and r_i are the outer and inner radii, respectively, of the cylinder. With solid drug present in the reservoir, the internal concentration is fixed; when the IUD is in use *in vivo*, the external concentration also is fixed at essentially zero. Thus, the release rate remains constant and is determined only by device dimensions and the permeability of the rate-limiting membrane.

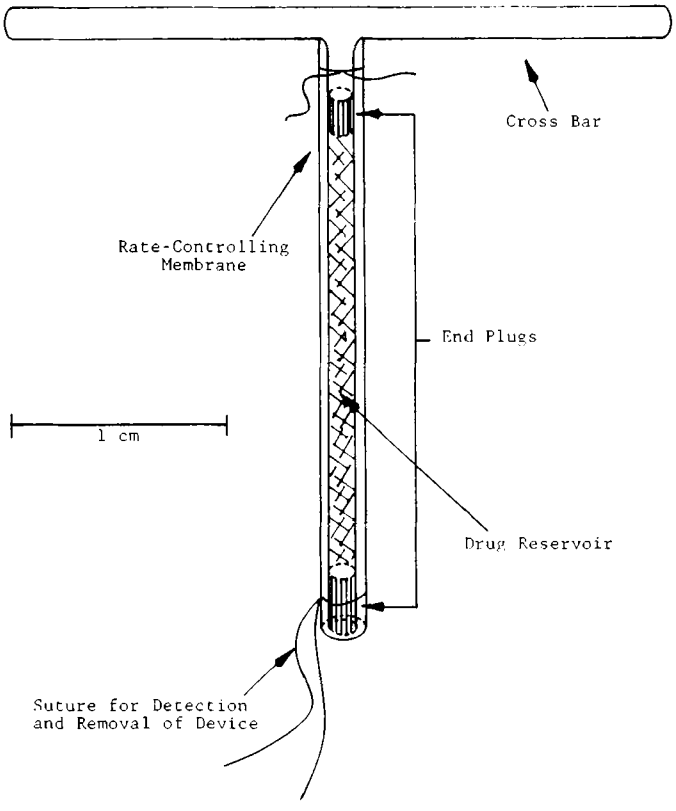

Figure 1—*Schematic of the drug-delivering IUD.*

0022-3549/79/0100-0020$01.00/0
© 1979, American Pharmaceutical Association

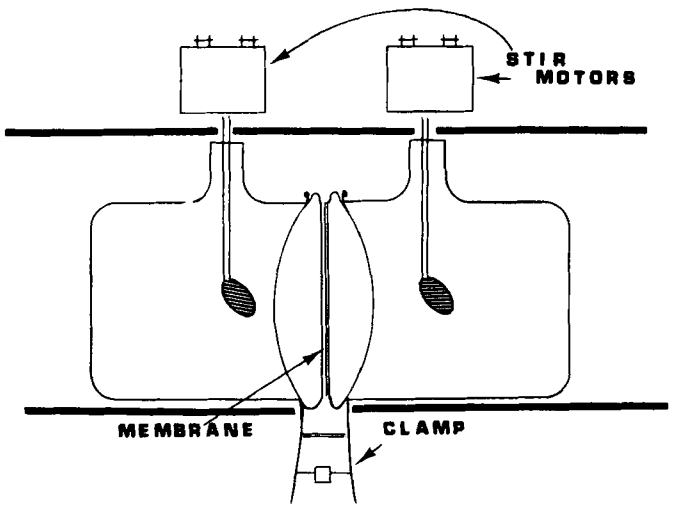

Figure 2—*Permeability cell.*

EXPERIMENTAL

Constraints—Several constraints on the device affected material selection and the final design:

1. The reservoir must hold sufficient drug to achieve constant release for the intended period of use. For devices releasing 12.5 μg of estriol/day for more than 1 year, the reservoir must be sufficiently large to hold at least 5 mg of estriol; *i.e.*, the reservoir volume must be at least 5×10^{-3} cm^3. Because of the necessity to include excipients, the minimum acceptable reservoir volume is about 10×10^{-3} cm^3.
2. The device must be flexible, so as to be nonirritating, but sufficiently strong to withstand uterine contractions without expulsion or failure of the device walls. Furthermore, the walls must be sufficiently thick that they can be fabricated to a reproducible thickness. In practice, these constraints limited the usable range of wall thicknesses to 0.15–0.50 mm.
3. The portion of the reservoir to be filled with drug must be less than the total length of the device, to allow for plugging the ends, but sufficient to allow the reservoir to be filled reproducibly. The desired range of filled reservoir lengths is 5–15 mm.

With reference now to Eq. 3, these constraints and the required range of drug release rates define the quantities Q, h, r_o, and r_i. This equation then defines the requisite permeability of the membrane to the drug. In the present work, a "normalized flux" is used to express this permeability. The normalized flux is the flux, expressed in micrograms per square centimeter per day, through a flat sheet membrane 1 mm thick when one side of the membrane is exposed to a saturated solution of the permeant and the other side is maintained free of permeant. The normalized flux is thus $DK\ \Delta C$ (or Jl in Eq. 2), and it has dimensions micrograms-millimeters per square centimeter-day. The permissible range of normalized fluxes that will satisfy all device constraints is 1–6 μg-mm/cm^2-day, and the desired value is approximately 4 μg-mm/cm^2-day. With a single rate-limiting membrane material, all the required release rates can be achieved, by appropriate changes in reservoir length and wall thickness, if the permeability of the membrane to the drug is of this magnitude.

Permeabilities—Membrane permeability measurements were carried out in conventional, two-compartment, stirred glass cells at 37° (Fig. 2).

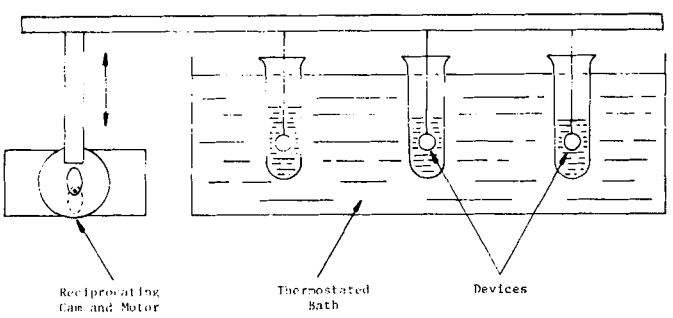

Figure 3—*Apparatus used to measure release rates from devices.*

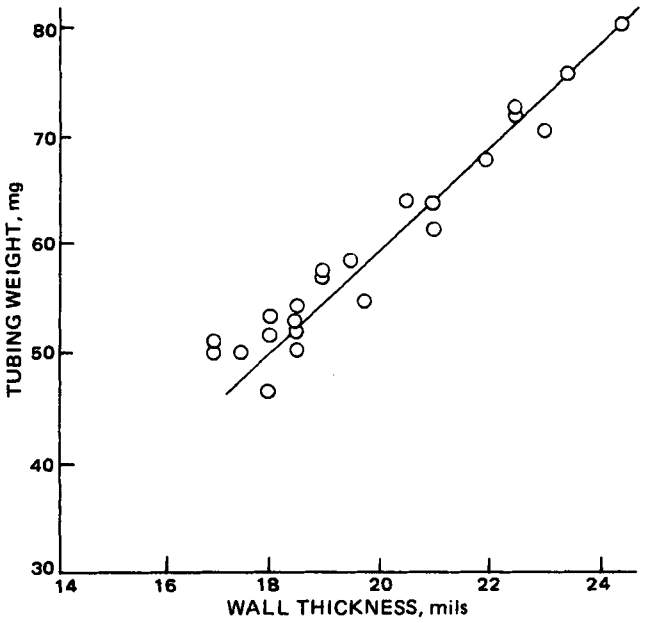

Figure 4—*Weight* versus *wall thickness for 20-mm long 45-mil bore Polymer 12 tubing.*

One compartment was filled with a saturated solution of estriol while the other compartment was maintained at a concentration (<1 ppm) well below saturation (~15 ppm for estriol). Stirring sufficient to minimize boundary layer effects was maintained in both cell compartments. The low concentration compartment was sampled periodically by pipetting a small, known aliquot and replacing it with fresh solution.

Test films for permeability measurements were prepared by conventional methods, *i.e.*, melt pressing or solution casting. Some films were used as supplied by the manufacturer. Others were annealed in air to alter their permeability. Silicone rubber films were prepared by melt pressing the unvulcanized polymer in the presence of a peroxide catalyst at 100° to effect cross-linking.

Release rate measurements on assembled devices were made by periodically suspending the devices from a reciprocating arm in 25-ml vials of distilled water at 37° for about 1 day (Fig. 3). This elution solution then was analyzed. Between release rate measurements, the devices were stored in a flowing water bath at 37°.

The permeability and release rate data were obtained using radiolabeled estriol and standard scintillation counting techniques.

A number of rubbery polymers were initially screened for their permeability to estriol, including three grades of silicone rubber, chlorinated polyethylene, three grades of ethylene–vinyl acetate copolymers of varying vinyl acetate content, and several ester-based and ether-based polyurethanes.

Device Fabrication—Two types of devices were prepared: animal devices, which were simple tubes containing the drug and plugged at both ends, and human devices, which were similar filled tubes sutured to an inert cross bar (Fig. 1).

The tubing was made by dip coating stainless steel rods with a 10% (w/v) solution of polyurethane Polymer 12[1] in tetrahydrofuran. Typically, a rod was immersed in the viscous polymer solution and then slowly and smoothly withdrawn vertically from the solution with a motor drive. The tetrahydrofuran was allowed to evaporate, and the dipping was repeated a sufficient number of times to build up a wall of sufficient thickness. Once completed, the tubing was removed from the rod by swelling it by brief immersion in ethanol or methanol. About 30 cm of the rod was coated with polymer, and there was a slight variation in thickness along the length of the tubing caused by gravity flow of the polymer solution during the removal and drying steps. Therefore, the tubing was cut into short lengths, somewhat longer than required for the devices. Thickness variation along these segments was not significant.

All the required devices could be fabricated from tubing made with stainless steel rods of three different diameters: 29, 45, and 63 mils (0.73, 1.13, and 1.58 mm, respectively); compensation for wall thickness variations could be made through variations in the filled length. Initially, the

[1] Estane 5714.

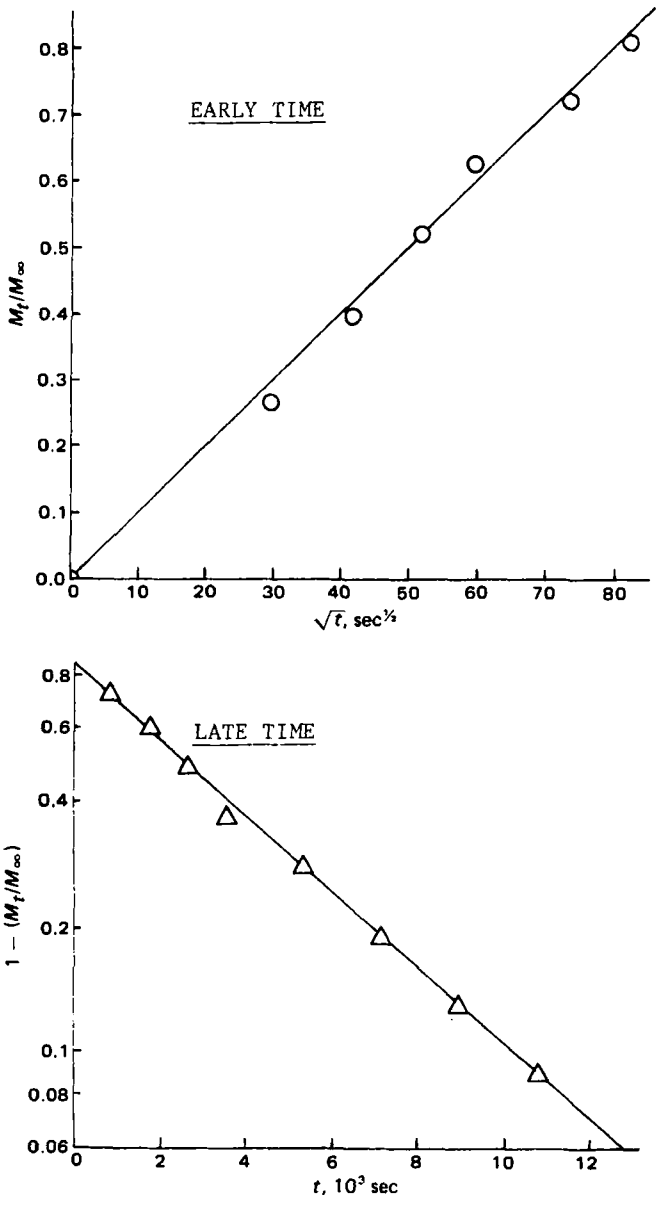

Figure 5—*Estriol desorption from Polymer 12 membranes.*

wall thickness was determined by measuring the outside diameters individually with a microscope. Later, however, a simpler and more reliable method was developed in which tubing of 20 mm length was weighed and a correlation between weight and wall thickness was established (Fig. 4). Tubing of a given inside diameter was then simply weighed, and its wall thickness was read off the curve. The release rate was then fixed by appropriate adjustment in the length of the tubing to be filled.

Devices were prepared by: (*a*) taking a piece of tubing of the correct length and selected wall thickness, (*b*) creating a plug of nominally 2-mm length in one end with a room temperature-curing silicone resin[2], (*c*) filling the tubing with powdered estriol or a suspension of estriol in a suitable drug carrier, including 6–10% (w/w) of barium sulfate added to render the devices radioopaque, and (*d*) sealing the other end with another 2-mm plug of the silicone resin. A short length of 4–0 nylon monofilament, to be used to remove the devices from the animals, was then sutured through one plugged end.

Several liquid carriers for the estriol in the reservoir of the device were evaluated, including water, cocoa butter, and a triglyceride[3]. The evaluation was based on release rate measurements made with devices containing a fixed amount of carrier but decreasing amounts of drug to duplicate the depletion that would occur in use.

All devices were sterilized with pure ethylene oxide for 15 hr by standard procedures.

Clinical devices and the individual components were subjected to a series of stability tests. The purity and stability of the estriol prior to and during these tests were determined by standard GLC and TLC methods. The tests were run for 6 months at storage temperatures of 0, 25, 37, and 50°. The stability of the components was checked individually, in combination with one another, and in the presence of water.

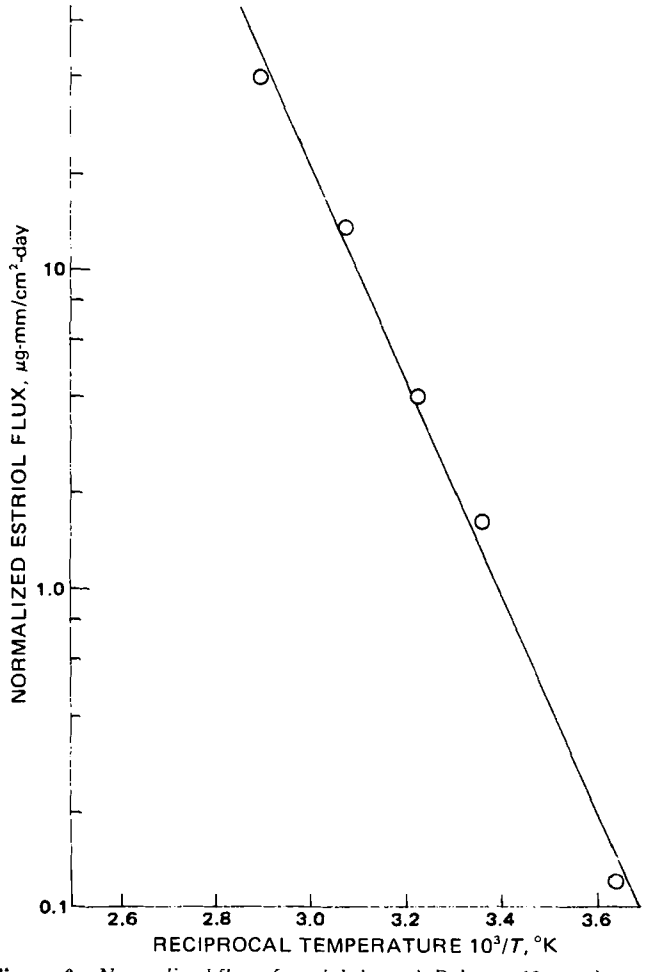

Figure 6—*Normalized flux of estriol through Polymer 12 membranes* versus *reciprocal temperature.*

RESULTS AND DISCUSSION

Permeabilities—Membrane permeabilities, expressed in terms of the normalized flux, are presented in Table I. The tabulated results are generally averages of two runs on separate films; reproducibility was generally quite good. Of the membranes tested, only the polyurethanes had the requisite permeability (Table I). The ester-based polyurethanes were discounted because of their instability to hydrolysis during use *in*

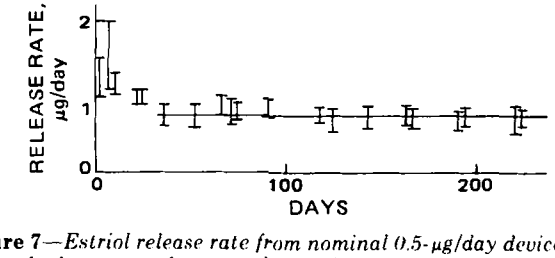

Figure 7—*Estriol release rate from nominal 0.5-μg/day devices. The range of release rates from two devices is shown.*

[2] Dow Corning Silastic A.
[3] Dynamit Nobel Witespol H-5.

Table I—Permeability of Polymers to Estriol

Polymer Generic Name	Normalized Flux, μg-mm/cm²-day
Silicone rubber[a]	<0.1
Silicone rubber[b]	<0.1
Silicone rubber[c]	<0.1
Chlorinated polyethylene[d]	<0.1
Chlorinated polyethylene[e]	<0.1
Ethylene vinyl acetate[f] (9% vinyl acetate)	<0.1
Ethylene vinyl acetate[g] (18% vinyl acetate)	~0.1
Ethylene vinyl acetate[h] (40% vinyl acetate)	0.8
Polyurethane (ester)[i]	<0.1
Polyurethane (ester)[j]	0.4
Polyurethane (ester)[k]	2.7
Polyurethane (ester)[l]	0.3
Polyurethane (ether)[m]	1.9
Polyurethane (ether)[n]	0.3
Polyurethane (ether)[o]	3.3

[a] Dow Corning, 46514. [b] Dow Corning, 46515. [c] Dow Corning, 46516. [d] Dow Chemical, 3623. [e] Dow Chemical, 4213. [f] USI, UE638. [g] USI, UE630. [h] DuPont, Elvax 40. [i] Goodrich, Tuftane 800. [j] Uniroyal, Roylar E9. [k] Goodrich, Estane 5702. [l] Goodrich, Estane 5710. [m] Uniroyal, Roylar 84N. [n] Upjohn, Pellethane 80A. [o] Goodrich, Estane 5714.

vivo (11). Therefore, a more detailed study of the permeability of ether-based polyurethanes was carried out (Table II).

Several materials exhibited the required permeability. However, the permeability of Polymer 10 and 11 films was history dependent. When the manufacturer-supplied film was heated in air for several hours at 120°, the permeability to estriol increased severalfold. Polymer 12 appeared to offer the best combination of properties, and all the devices were prepared from this material.

To characterize further the Polymer 12 membranes, the solubility and diffusivity of estriol were measured by the sorption–desorption method (12). A film of the polymer was immersed in a saturated aqueous solution of estriol until equilibrium was obtained and the film was saturated with drug. The film was removed from the solution, rapidly rinsed to remove any solution adhering to the surface, and placed in a large volume of pure water. The rate of desorption of drug from the film was measured by periodically removing and analyzing samples of the water.

The diffusion coefficient was calculated by applying Fick's second law. There are two approximate solutions to this law for the present boundary conditions, an early time solution given by:

$$\frac{M_t}{M_\infty} = 4(Dt/\pi l^2)^{1/2} \qquad \text{for } 0 \le M_t/M_\infty \le 0.6 \qquad \text{(Eq. 4)}$$

and a late-time solution given by:

$$\frac{M_t}{M_\infty} = 1 - \frac{8}{\pi^2}\exp(-\pi^2 Dt/l^2) \qquad \text{for } 0.4 \le M_t/M_\infty \le 1.0 \quad \text{(Eq. 5)}$$

where M_t is the amount of drug desorbed after time t, M_∞ is the total amount desorbed, and l is the thickness of the film.

Typical plots of experimental data, presented in the manner suggested by Eqs. 4 and 5, are shown in Fig. 5. From such plots, the diffusion coefficient of estriol in Polymer 12 was calculated to be 2×10^{-9} cm²/sec at 30°. The solubility of the drug in the polymer, obtained from the same data, is 0.2% (w/w).

An Arrhenius plot of the normalized flux *versus* temperature is presented in Fig. 6. The slope of the line yields an activation energy of 7 kcal/mole. This value is relatively low, reflecting the rubbery nature of the polymer. Thus, a 1° change in body temperature at 37° would produce a 6% change in release rate, an amount too small to be of concern.

Table II—Estriol Permeability of Several Ether-Based Polyurethanes

Polymer[a]	Method of Preparation	Normalized Flux, μg-mm/cm²-day
1	Melt pressed	16
2	Melt pressed	5.8
3	Solution cast[b]	5.4
4	Solution cast	3.7
5	Solution cast	7.7
6	Solution cast	2.9
7	Melt pressed	6.3
8	Melt pressed	5.5
9	Melt pressed	1.3
10	Supplied as film	0.3–0.6
10	Film heat treated at 120° for 12 hr	2.4
10	Solution cast	2.2
11	Melt pressed	1.4
12	Melt pressed	3.3
12	Solution cast	3.9

[a] Suppliers and trade names are: Polymer 1, K. J. Quinn, PE-49; Polymer 2, K. J. Quinn, PE-55; Polymer 3, K. J. Quinn, PE-55; Polymer 4, K. J. Quinn, PE-18; Polymer 5, K. J. Quinn, PE-19; Polymer 6, Hooker Chemical, Rucothane P-602-3; Polymer 7, Uniroyal, Roylar A-895; Polymer 8, Goodrich, Tuftane TF-410; Polymer 9, American Cyanamid, Cyanaprene 9341; Polymer 10, Upjohn, Pellethane 80A; Polymer 11, Upjohn, Pellethane 55D; and Polymer 12, Goodrich, Estane 5714. [b] All solution-cast films in this table were cast from tetrahydrofuran solutions.

Release Rates—*Animal Devices*—Release rates from animal devices filled with dry estriol are presented in Figs. 7–9. The various release rates were achieved by varying the wall thickness of the device as well as the length of the reservoir. Long-term constant release rates were obtained with all of the devices, usually in reasonable agreement with the target release rates.

Not readily apparent in the figures is the fact that there was generally a complex "burst effect." This effect is more clearly evident in the early portion of the release curves; one is shown in more detail in Fig. 10. There was an obvious peak in the release rate at about 3 days. After approximately 10 days, the rate reached a steady-state value.

For devices freshly prepared, one would expect a "time lag" effect where the release rate is initially less than the steady-state value. For devices stored under conditions where the estriol is not eluted (*e.g.*, stored in air), one would expect a burst effect where the release rate is initially higher than the steady-state rate (10). Because of the way the devices were stored, the observed release rates did not follow either simple pattern.

The device depicted in Fig. 10 had been stored in air at room temperature for 2–4 weeks before the release rate measurements were begun. During this time, the polyurethane walls became saturated with drug at room temperature. When the device was then taken to 37° for release rate measurements, a new equilibrium was approached. It was this discontinuity in estriol concentration in the wall of the device that resulted in the peaked release rate curve shown in Fig. 10. This behavior is typical of that obtained throughout this study, although the magnitude and duration of the burst effect depended on the device geometry. A similar effect was observed in *in vitro* measurements of release rates of testosterone from silicone rubber implant devices (13).

The burst effect was examined in some detail, because of its effect on the early release rate profiles from devices. The time for the flux through a cylinder to reach its steady-state value is equal to about four "time lags"

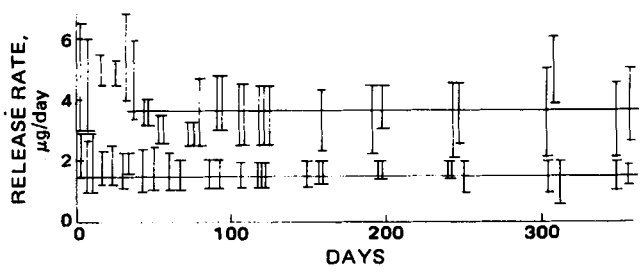

Figure 8—*Estriol release rate from nominal 1.25- and 3.75-μg/day devices. The range of release rates from two devices is shown.*

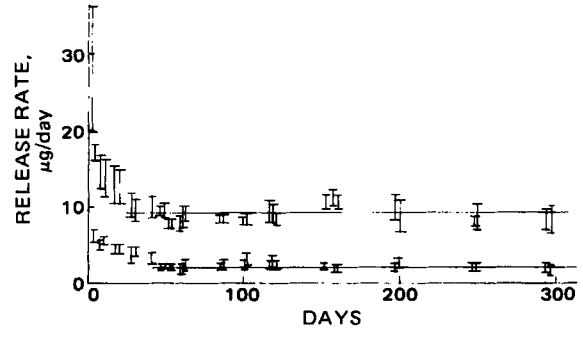

Figure 9—*Estriol release rate from nominal 3- and 9-μg/day devices. The range of release rates from three devices is shown.*

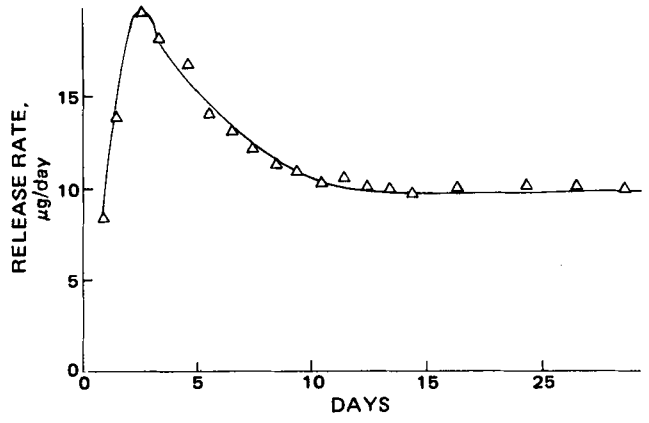

Figure 10—*Early time estriol release rate from a nominal 12.5-μg/day device.*

(14), *i.e.*:

$$\text{time to steady state} = \frac{r_i^2 - r_o^2 + (r_i^2 + r_o^2)\ln(r_o/r_i)}{D \ln(r_o/r_i)} \quad \text{(Eq. 6)}$$

where r_i and r_o are the inner and outer radii of the cylinder, respectively, and D is the diffusion coefficient. With this expression, the time to reach the steady-state release rate from the devices can be computed.

The results are shown in Fig. 11 as a plot of time to steady state *versus* r_o/r_i. Three plots are presented, one for each of the radii used. The time to steady state also is denoted on the figure. There was some variation in these times because of the range of wall thicknesses used to prepare each set of devices. The small-bore, thick-walled devices (*i.e.*, those with large r_o/r_i) with low steady-state release rates required a long time to reach steady state; *i.e.*, they exhibited a prolonged burst effect. The thin-walled devices with higher release rates had a shorter burst effect. Release rates measured after the burst effect agreed reasonably well with values predicted on the basis of permeability measurements.

Release rate data for the 12.5-μg/day animal devices are not presented here. The devices prepared for animal studies were, in fact, replicates of

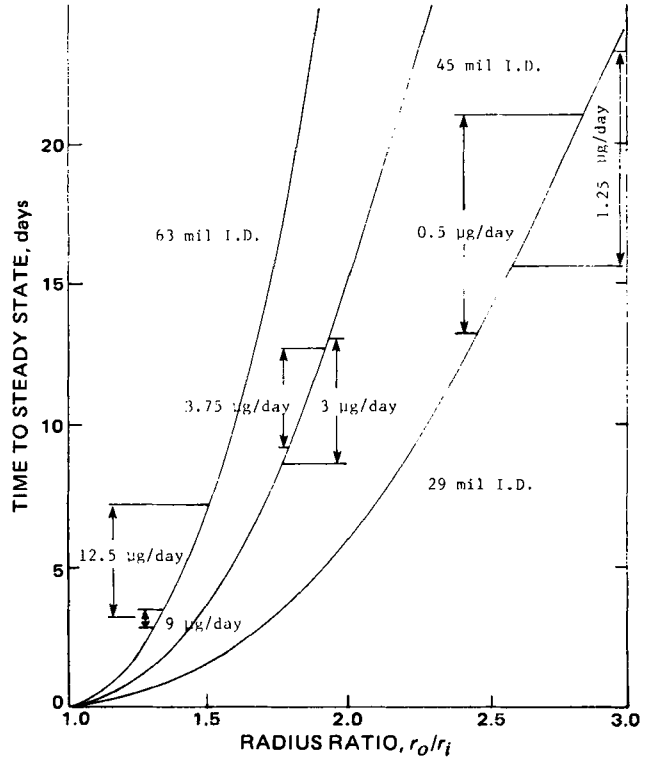

Figure 11—*Time to steady state for a cylinder* versus r_o/r_i. *The three curves refer to the three inner radii. The times to steady state for all of the actual devices are shown.*

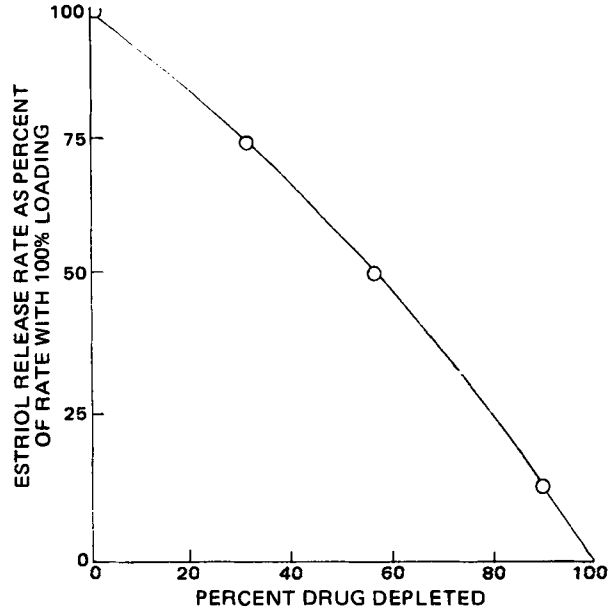

Figure 12—*Estriol release rate as a percentage of the release rate of a fully loaded device* versus *percent of drug depleted.*

the clinical devices. The release characteristics of these devices are discussed under *Clinical Devices.*

One can predict that the release rate from devices filled with only powdered drug will fall with time, because the contact between the drug and the inner wall of the device decreases as the device becomes depleted. This effect was simulated by preparing devices incompletely filled with drug. The measured steady-state release rates, expressed as a percentage of the release rate from a completely filled device, are plotted against the simulated fractional depletion of drug in Fig. 12. This phenomenon did not significantly affect the animal devices, because they contained a several years' supply of drug while the *in vivo* experiments were designed for a duration of only a few months. As discussed in more detail later, drug depletion and the resultant reduction in release rate would be important in devices intended for long-term use in humans.

Clinical Devices—The problem of drug depletion would become acute for devices in use *in vivo* for many months. It can be solved, however, by incorporating a suitable liquid carrier within the reservoir. The carrier is maintained saturated with drug as long as any solid drug is present in

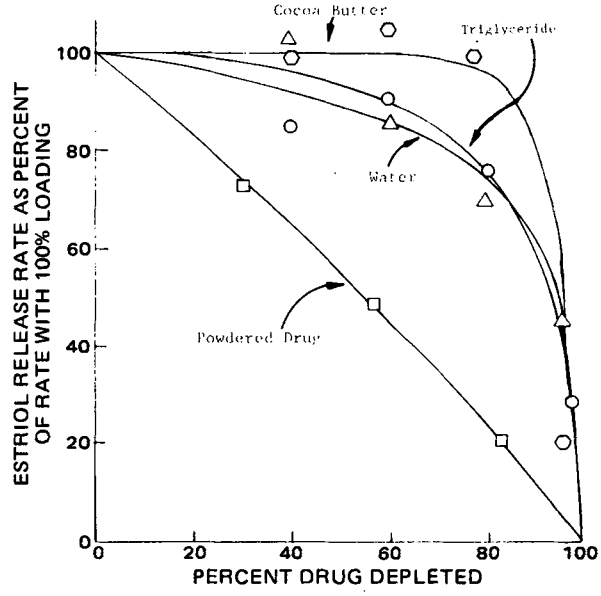

Figure 13—*Estriol release rate as a percentage of the rate of a fully loaded device* versus *drug depletion for devices incorporating different carrier agents.*

Table III—Summary of Device Release Rates

Type	Target Release Rate, μg/day	Actual Steady-State Release Rate, μg/day
Animal	0.5	0.7
	1.25	1.5
	3.0	3
	3.75	3.7
	9	9
	12.5	11
Human	12.5	11

the reservoir. The carrier thus provides intimate contact between the inside wall of the device and the reservoir. The concept of using a saturated solution to achieve a constant driving force within a reservoir dates back to Fick's original 1855 paper. The first application of this phenomenon to achieve controlled release, however, was in 1967 (15). It was further described in a U.S. patent in 1969 (16).

Figure 13 presents the results of carrier tests. Estriol release rate as a percentage of the rate of a fully loaded device is plotted *versus* the drug loading expressed as the percentage of drug depletion. All of the carriers provided a more nearly constant release over the device lifetime than did the dry-filled device. The best results were obtained with cocoa butter, which has a solubility for estriol of 70 μg/ml. Therefore, all of the clinical devices were prepared with cocoa butter in the reservoir.

Release rate data from cocoa butter-filled clinical devices are presented in Fig. 14. There was again a burst effect, following which zero-order release was observed for as long as the test was run. In these experimental human devices, sufficient drug was incorporated to sustain a constant release rate for more than 1 year. By simply incorporating more drug, a device lifetime of at least 5 years could be readily achieved.

Stability of Clinical Devices—GLC and TLC analyses of the estriol and cocoa butter present in the clinical devices showed that both agents were unaffected by the sterilization procedure. No degradation of the components was observed in the stability tests. The release rates of devices stored for 3 and 6 months are compared with the release rates obtained with devices placed on test within 2 weeks of preparation in Fig. 15. As can be seen by comparing these plots, there was no significant change in release rate on storage.

SUMMARY AND CONCLUSIONS

Estriol-releasing IUD's for use in animal studies and T-shaped devices that could be used in clinical trials were developed and subjected to stability tests. The release rates from these devices are summarized in Table III. The devices appear to be stable on long-term storage with respect to both release rate and the chemical nature of the drug and other components.

These devices consist of a simple reservoir containing the drug, surrounded by a rate-limiting polyurethane membrane. For long-term use, it is necessary to include a liquid carrier agent in the reservoir to assure intimate contact with the interior device walls. Devices containing sufficient estriol to provide a constant release rate of 12 μg/day for several years could be made by simple alterations in the geometry of the device.

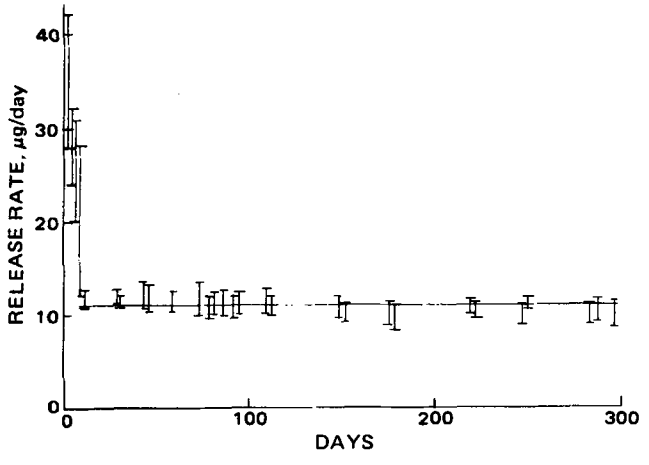

Figure 14—*Estriol release rate from clinical devices* versus *time. The range of release rates from four devices is shown.*

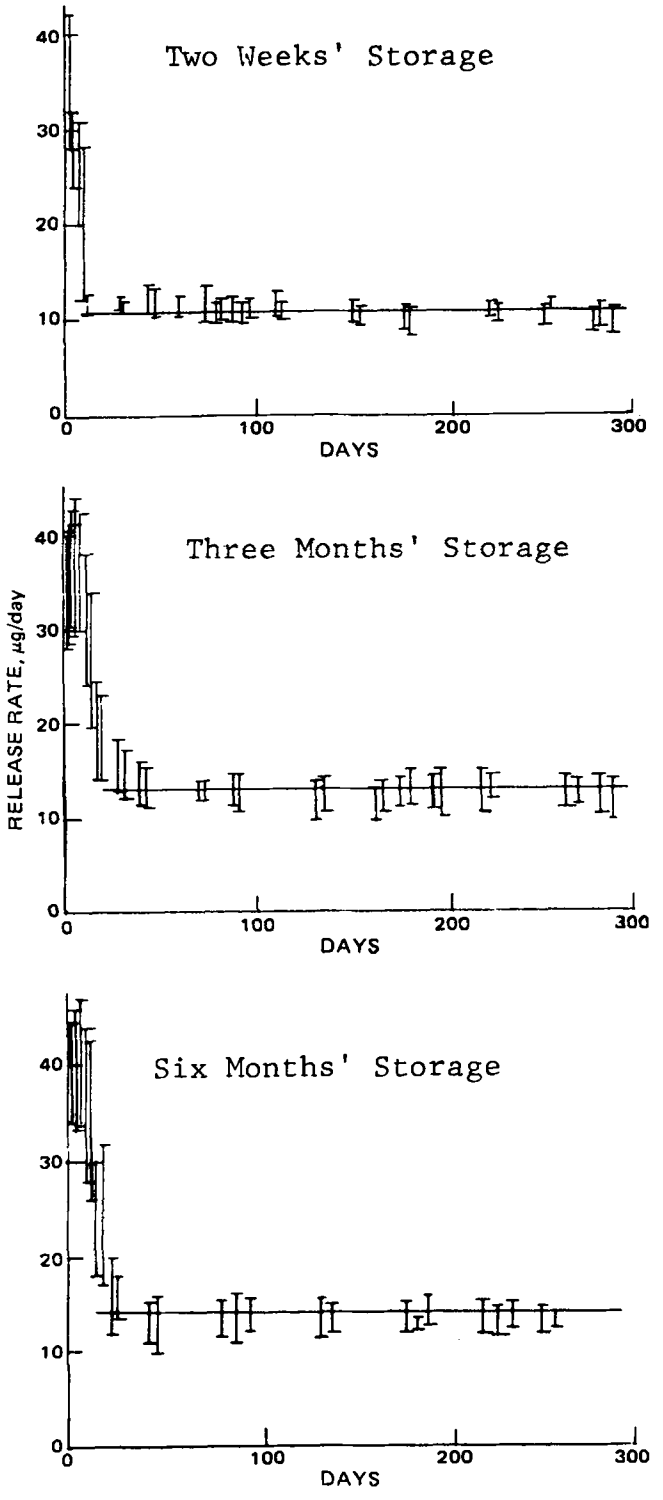

Figure 15—*Estriol release rate from clinical devices stored for 2 weeks, 3 months, and 6 months. The range of release rates from four, eight, and eight devices, respectively, is shown.*

REFERENCES

(1) A. Scommegna, G. N. Pandya, M. Christ, A. W. Lee, and M. R. Cohen, paper presented at the 25th Meeting of the American Fertility Society, Miami, Fla., Apr. 1969. *Fertil. Steril.*, **21**, 201 (1970).

(2) A. Lifchez and A. Scommegna, *ibid.*, **21**, 426 (1970).

(3) Y. Gibor, S. Bhuvarasarma, and A. Scommegna, *ibid.*, **22**, 671 (1971).
(4) B. D. Kulkani, T. D. Avila, B. B. Pharriss, and A. Scommegna, *Contraception*, **8**, 299 (1973).
(5) A. Scommegna, T. Avila, M. Luna, R. Rao, and W. P. Dmowski, *Obstet. Gynecol.*, **43**, 769 (1974).
(6) S. A. Tillson, M. Marion, R. Hudson, P. Wong, B. B. Pharriss, R. Aznar, and J. Martinez-Manautou, *Contraception*, **11**, 179 (1975).
(7) B. B. Pharriss, R. Erickson, J. Bashaw, S. Hoff, V. A. Place, and A. Zaffaroni, *Fertil. Steril.*, **25**, 915 (1974).
(8) W. P. Dmowski, A. Shih, J. Wilhelm, F. Auletta, and A. Scommegna, *ibid.*, **28**, 262 (1977).
(9) H. J. Tatum, *Am. J. Gynecol.*, **112**, 1000 (1972).
(10) R. W. Baker and H. K. Lonsdale, in "Controlled Release of Biologically Active Agents," A. C. Tanquary and R. E. Lacey, Eds., Plenum, New York, N.Y., 1974.
(11) J. W. Boretos, D. E. Detmer, and J. H. Donachy, *J. Biomed. Mater. Res.*, **5**, 373 (1971).
(12) H. K. Lonsdale, U. Merten, and R. L. Riley, *J. Appl. Polym. Sci.*, **9**, 1341 (1965).
(13) R. L. Shippy, S. T. Hwang, and R. G. Bunge, *J. Biomed. Mater. Res.*, **7**, 115 (1973).
(14) J. Crank, "The Mathematics of Diffusion," Oxford University Press, Oxford, England, 1967.
(15) K. Lehmann, *Drugs Made Ger.*, **10**, 115 (1967).
(16) C. A. Noll and L. J. LaSalvia, U.S. pat. 3,468,796 (Sept. 23, 1969).

ACKNOWLEDGMENTS

This work was carried out under subcontract to the Michael Reese Hospital and Medical Center of Chicago under their prime Contract 1-HD-3-2739 with the National Institute of Child Health and Human Development, National Institutes of Health.

The authors are indebted to both the technical director of the project at Michael Reese Hospital, Dr. W. Paul Dmowski, and to the contract administrator for NIH, Dr. Henry Gabelnick. Technical discussions with them and with Dr. Antonio Scommegna of Michael Reese Hospital were invaluable. They also thank their coworkers at Bend Research, D. B. Davis, J. C. Kleiber, and R. J. Ray, and well as Dr. J. H. Block of the School of Pharmacy, Oregon State University, for technical assistance.

Pharmacokinetics of Morphine and Its Surrogates II: Methods of Separation of Stabilized Heroin and Its Metabolites from Hydrolyzing Biological Fluids and Applications to Protein Binding and Red Blood Cell Partition Studies

EDWARD R. GARRETT ˣ **and TÜRKAN GÜRKAN** *

Received January 27, 1978, from *The Beehive, College of Pharmacy, J. Hillis Miller Health Center, University of Florida, Gainesville, FL 32610.* Accepted for publication May 26, 1978. *Present address: Department of Analytical Chemistry, Faculty of Pharmacy, University of Istanbul, Istanbul, Turkey.

Abstract □ The inhibition of the spontaneous hydrolysis of heroin in fresh dog plasma and blood ($t_{1/2}$ = 8 min) is effected by 10 mg of sodium fluoride/ml ($t_{1/2}$ = 40 min) and 35 μg of tetraethyl pyrophosphate/ml ($t_{1/2}$ = 415 min). Tetraethyl pyrophosphate is the inhibitor of choice and gives the same stability for heroin as in phosphate buffer. Aged plasma loses its enzymatic efficiency. Heroin in cerebrospinal fluid hydrolyzes at rates similar to those in buffer. Modified extraction procedures developed for enzyme-inhibited plasma at pH 4.5 have high extraction efficiencies (86–100%) and permit isolation of undegraded heroin from its metabolites. Separations of heroin and metabolites from enzyme-inhibited plasma were effected by described high-pressure liquid chromatographic systems and from TLC with elution of pertinent developed spots. Efficiencies of these TLC recoveries were 81 ± 1% for heroin and 82 ± 1% for morphine. Contrary to the literature, heroin has significant protein binding where 40% of that not bound to an ultrafiltration membrane is bound to dog plasma proteins. The apparent partition coefficient is 1.4 ± 0.2 between red blood cells and plasma water, and it is 0.8 ± 0.1 between red blood cells and dog plasma.

Keyphrases □ Heroin—hydrolysis in dog plasma and blood, effect of sodium fluoride and tetraethyl pyrophosphate, protein binding and partition coefficient evaluated □ Hydrolysis—heroin in dog plasma and blood, effect of sodium fluoride and tetraethyl pyrophosphate □ Enzyme inhibition—by sodium fluoride and tetraethyl pyrophosphate, dog plasma and blood, effect on heroin hydrolysis □ Protein binding—heroin in enzyme-inhibited dog plasma □ Partition coefficient—heroin between red blood cells and enzyme-inhibited dog plasma □ Narcotics—heroin, hydrolysis in dog plasma and blood, effect of enzyme inhibitors, protein binding and partition coefficient evaluated

3,6-Diacetylmorphine (heroin) is rapidly hydrolyzed in the body to 6-monoacetylmorphine and then to morphine (1–3). These latter compounds, along with morphine 3-glucuronide, are the major metabolites of heroin excreted in urine (4–8), although minor or negligible amounts of normorphine and its glucuronide as well as morphine 6-glucuronide and 6-acetylmorphine were reported in human urine after heroin administration (9–11).

BACKGROUND

Other than the heroin assay of Way *et al.* (2, 3) on homogenized mice after intravenous administration of heroin ($t_{1/2}$ for heroin = ~2.5 min), the inability to monitor heroin levels in plasma or biological fluid due to its fast hydrolysis and/or metabolism has prevented the study of heroin pharmacokinetics *per se*. Pharmacokinetic studies on heroin administration were thus limited to the estimation of half-lives of urinary excretions of the major heroin metabolites with apparent $t_{1/2}$ values of 1–3 hr (8, 10).

0022-3549/79/0100-0026$01.00/0
© 1979, American Pharmaceutical Association

(3) Y. Gibor, S. Bhuvarasarma, and A. Scommegna, *ibid.*, **22**, 671 (1971).
(4) B. D. Kulkani, T. D. Avila, B. B. Pharriss, and A. Scommegna, *Contraception*, **8**, 299 (1973).
(5) A. Scommegna, T. Avila, M. Luna, R. Rao, and W. P. Dmowski, *Obstet. Gynecol.*, **43**, 769 (1974).
(6) S. A. Tillson, M. Marion, R. Hudson, P. Wong, B. B. Pharriss, R. Aznar, and J. Martinez-Manautou, *Contraception*, **11**, 179 (1975).
(7) B. B. Pharriss, R. Erickson, J. Bashaw, S. Hoff, V. A. Place, and A. Zaffaroni, *Fertil. Steril.*, **25**, 915 (1974).
(8) W. P. Dmowski, A. Shih, J. Wilhelm, F. Auletta, and A. Scommegna, *ibid.*, **28**, 262 (1977).
(9) H. J. Tatum, *Am. J. Gynecol.*, **112**, 1000 (1972).
(10) R. W. Baker and H. K. Lonsdale, in "Controlled Release of Biologically Active Agents," A. C. Tanquary and R. E. Lacey, Eds., Plenum, New York, N.Y., 1974.
(11) J. W. Boretos, D. E. Detmer, and J. H. Donachy, *J. Biomed. Mater. Res.*, **5**, 373 (1971).
(12) H. K. Lonsdale, U. Merten, and R. L. Riley, *J. Appl. Polym. Sci.*, **9**, 1341 (1965).
(13) R. L. Shippy, S. T. Hwang, and R. G. Bunge, *J. Biomed. Mater. Res.*, **7**, 115 (1973).
(14) J. Crank, "The Mathematics of Diffusion," Oxford University Press, Oxford, England, 1967.
(15) K. Lehmann, *Drugs Made Ger.*, **10**, 115 (1967).
(16) C. A. Noll and L. J. LaSalvia, U.S. pat. 3,468,796 (Sept. 23, 1969).

ACKNOWLEDGMENTS

This work was carried out under subcontract to the Michael Reese Hospital and Medical Center of Chicago under their prime Contract 1-HD-3-2739 with the National Institute of Child Health and Human Development, National Institutes of Health.

The authors are indebted to both the technical director of the project at Michael Reese Hospital, Dr. W. Paul Dmowski, and to the contract administrator for NIH, Dr. Henry Gabelnick. Technical discussions with them and with Dr. Antonio Scommegna of Michael Reese Hospital were invaluable. They also thank their coworkers at Bend Research, D. B. Davis, J. C. Kleiber, and R. J. Ray, and well as Dr. J. H. Block of the School of Pharmacy, Oregon State University, for technical assistance.

Pharmacokinetics of Morphine and Its Surrogates II: Methods of Separation of Stabilized Heroin and Its Metabolites from Hydrolyzing Biological Fluids and Applications to Protein Binding and Red Blood Cell Partition Studies

EDWARD R. GARRETT ˣ **and TÜRKAN GÜRKAN** *

Received January 27, 1978, from *The Beehive, College of Pharmacy, J. Hillis Miller Health Center, University of Florida, Gainesville, FL 32610.* Accepted for publication May 26, 1978. *Present address: Department of Analytical Chemistry, Faculty of Pharmacy, University of Istanbul, Istanbul, Turkey.

Abstract □ The inhibition of the spontaneous hydrolysis of heroin in fresh dog plasma and blood ($t_{1/2}$ = 8 min) is effected by 10 mg of sodium fluoride/ml ($t_{1/2}$ = 40 min) and 35 μg of tetraethyl pyrophosphate/ml ($t_{1/2}$ = 415 min). Tetraethyl pyrophosphate is the inhibitor of choice and gives the same stability for heroin as in phosphate buffer. Aged plasma loses its enzymatic efficiency. Heroin in cerebrospinal fluid hydrolyzes at rates similar to those in buffer. Modified extraction procedures developed for enzyme-inhibited plasma at pH 4.5 have high extraction efficiencies (86–100%) and permit isolation of undegraded heroin from its metabolites. Separations of heroin and metabolites from enzyme-inhibited plasma were effected by described high-pressure liquid chromatographic systems and from TLC with elution of pertinent developed spots. Efficiencies of these TLC recoveries were 81 ± 1% for heroin and 82 ± 1% for morphine. Contrary to the literature, heroin has significant protein binding where 40% of that not bound to an ultrafiltration membrane is bound to dog plasma proteins. The apparent partition coefficient is 1.4 ± 0.2 between red blood cells and plasma water, and it is 0.8 ± 0.1 between red blood cells and dog plasma.

Keyphrases □ Heroin—hydrolysis in dog plasma and blood, effect of sodium fluoride and tetraethyl pyrophosphate, protein binding and partition coefficient evaluated □ Hydrolysis—heroin in dog plasma and blood, effect of sodium fluoride and tetraethyl pyrophosphate □ Enzyme inhibition—by sodium fluoride and tetraethyl pyrophosphate, dog plasma and blood, effect on heroin hydrolysis □ Protein binding—heroin in enzyme-inhibited dog plasma □ Partition coefficient—heroin between red blood cells and enzyme-inhibited dog plasma □ Narcotics—heroin, hydrolysis in dog plasma and blood, effect of enzyme inhibitors, protein binding and partition coefficient evaluated

3,6-Diacetylmorphine (heroin) is rapidly hydrolyzed in the body to 6-monoacetylmorphine and then to morphine (1–3). These latter compounds, along with morphine 3-glucuronide, are the major metabolites of heroin excreted in urine (4–8), although minor or negligible amounts of normorphine and its glucuronide as well as morphine 6-glucuronide and 6-acetylmorphine were reported in human urine after heroin administration (9–11).

BACKGROUND

Other than the heroin assay of Way *et al.* (2, 3) on homogenized mice after intravenous administration of heroin ($t_{1/2}$ for heroin = ~2.5 min), the inability to monitor heroin levels in plasma or biological fluid due to its fast hydrolysis and/or metabolism has prevented the study of heroin pharmacokinetics *per se*. Pharmacokinetic studies on heroin administration were thus limited to the estimation of half-lives of urinary excretions of the major heroin metabolites with apparent $t_{1/2}$ values of 1–3 hr (8, 10).

0022-3549/79/0100-0026$01.00/0
© 1979, American Pharmaceutical Association

The apparent fast metabolism of heroin *in vivo* is confounded further by its rapid *in vitro* hydrolysis in aqueous solutions and biological fluids (12). The limited studies available showed that heroin hydrolyzes to 6-*O*-acetylmorphine in 0.5 *M* sodium carbonate with a half-life of 4.2 min whereas the subsequent hydrolysis to morphine has a half-life of 55.5 min (12). Human blood was reported to be devoid of 6-monoacetylmorphine esterase, although the rate of morphine liberation was slightly faster than in nontreated serum (13). Heroin was stable at pH 7.3 in phosphate buffer at 37.5° (12) but not in enzyme-deactivated human serum (13).

Hydrolysis in whole human blood ($t_{1/2}$ = 12.6 min) was faster than the hydrolysis in serum ($t_{1/2}$ = 19.8 min). Nakamura *et al.* (12) also implied that 1% sodium fluoride might inhibit *post-mortem* hydrolysis of, or bacterial action on, heroin in plasma.

These heroin instabilities in aqueous solutions and biological fluids cast suspicion on the validity of stated heroin quantifications in such fluids when they are not qualified for stability or when biological tissue treatment has used pH adjustment to 8 or 9 prior to the presumed extraction of heroin. Thus, the one available study of the heroin time course by analysis of homogenized organs and mouse tissue is also suspect (3). Furthermore, the inability to assay heroin after adjustment of blood and urine to pH 8.5–8.7 with saturated sodium bicarbonate prior to the presumed extraction (8) may be due to heroin degradation during the analytical processes as well as to its fast transformation *in vivo*. Tissue treatment with 10% trichloroacetic acid, with homogenization prior to subsequent extraction of the neutralized suspension (14), should give invalid estimates of easily hydrolyzable heroin and its products of acid solvolysis.

This paper presents methods of extraction and separation, such as high-pressure liquid chromatography (HPLC) and TLC, of heroin and its metabolites from biological fluids that minimize their spontaneous hydrolysis and permit quantitative assays. The efficiencies of various processes are given.

Sodium fluoride (12) and tetraethyl pyrophosphate (13) might inhibit the enzymic hydrolysis of heroin in plasma. The latter may be a preferred inhibitor since it was effective against a wide spectrum of esterases. The studies described here were designed to determine which inhibitor was the best to add to plasma prior to extraction under conditions where spontaneous hydrolysis would be minimized.

The only previous studies (15) to determine the protein and red blood cell binding of heroin were conducted by equilibrium dialyses over 18 hr with human serum. No consideration apparently was given to the possible hydrolysis of heroin in such systems, and the protein binding analysis was based on the assumption that the measured radioactivity in the compartments after equilibration would serve as a basis for calculation. But the results were contradictory and confusing. ^{14}C-Heroin showed no significant binding, but significant binding (20–39%) was observed when cold heroin was added to human serum. Similar results were obtained with washed human erythrocytes and red cell ghosts. It was concluded that "free heroin and morphine probably float unbound in the blood before . . . metabolism."

The probable instability of heroin under the experimental conditions of equilibrium dialysis of serum (15) demands a faster method to study protein binding, with an enzymic inhibitor to prevent heroin solvolysis. This paper considers the protein binding and red blood cell partition of heroin when these factors have been taken into account.

EXPERIMENTAL

Materials—*N-Methyl*-^{14}C-morphine[1], morphine sulfate crystalline USP[2], 6-*O*-acetylmorphine[3], and tetraethyl pyrophosphate[4] were used. All solvents were analytical grade[5]. Precoated silica gel plates[6], preparative and analytical, were used for TLC separation. The pH of the isotonic phosphate buffer was 7.45 (5.15 g of sodium chloride[5], 132 ml of 0.067 *M* KH_2PO_4[5], and *q.s.* to 1000 ml with 0.067 *M* $Na_2HPO_4 \cdot 7H_2O$[5]).

Freshly prepared 1 *M* $NaHCO_3$[5] was adjusted to pH 8.9 with 1 *M* NaOH[5]. Sodium acetate[5], 1 *M*, was adjusted to pH 4.8 with 1 *M* acetic acid[5]. Sodium carbonate[5], sodium fluoride[5], acetic anhydride[5], and pyridine[5] also were used.

Special high quality methanol[7] was used for HPLC separation. Ultrafiltration cones[8], cone supports[8], and tubes[8] were used for protein binding studies. Iodoplatinate spray was prepared from platinum chloride[5], according to the procedure of Stahl (16).

A toluene base scintillation fluid[9] was used for radioactive counting with a liquid scintillation counter[10]. All samples were counted for 5 min, with a blank inserted at the start. The degree of quench of each sample was estimated by the channel ratio method and based on an established quench curve. All samples were allowed to adapt to the dark for at least 6 hr. The systems and procedures used gave counting efficiencies of 95% when plasma was assayed and 92% when urine was assayed.

The chromatograph[11] was equipped with a 421.8-kg/cm^2 (6000-psi) constant flow pump and a 254-nm UV detector. A low polarity reversed-phase column[12] was used.

All glassware was silylated[13].

Preparation of ^{14}C-Heroin—The ^{14}C-heroin was synthesized by acetylation of ^{14}C-morphine (59 mCi/mmole). ^{14}C-Morphine was mixed with unlabeled crystalline morphine sulfate to obtain a theoretical 10–15 mCi/mmole specific activity. The mixture (10–15 mg as morphine base) was acetylated with acetic anhydride (0.5 ml) in the presence of pyridine (5–10 μl) for 3 hr in a tightly capped 15-ml test tube submerged in a 70° water bath[14] and was maintained at room temperature for 2 days. Excess acetic anhydride was evaporated under a nitrogen stream at 50°, and 2 ml of 5% sodium carbonate solution was added to the brown–pinkish residue.

The heroin was extracted from the aqueous solution five or six times with 5 ml of chloroform or until a small amount of chloroform solution spotted on a TLC plate did not give a positive reaction with iodoplatinate spray. The combined chloroform phases were evaporated to 1 ml under a nitrogen stream at 50° in a water bath. This solution was applied to a preparative TLC (silica gel) plate, and the plate was developed with chloroform–methanol (80:20). The heroin band (R_f 0.77) was scraped from the plate and extracted several times with 20 ml of acetone until the TLC spotted extracts showed no positive reaction with iodoplatinate spray.

The combined acetone phases were evaporated under a nitrogen stream on a heating block[15] at 55°. The obtained heroin was of high purity (97.5%); only small amounts of radioactivity were obtained on the 6-*O*-acetylmorphine (2.24%, R_f 0.50) and morphine (0.12%, R_f 0.22) spots.

Nonlabeled heroin was prepared according to the procedure of Hays *et al.* (17).

Analysis of ^{14}C-Radiolabeled Heroin, 6-*O*-Acetylmorphine, and Morphine in Plasma—The procedure was used to determine the products of plasma solvolysis of ^{14}C-heroin. Tetraethyl pyrophosphate (10 μl) in an acetone solution of 17.3 mg/ml was added to a vial, and the acetone was evaporated. Plasma containing heroin (1.0 ml) was added to the vial, and the pH was adjusted to 4.8 with 1 ml of 1 *M* acetate buffer of the same pH. It was extracted immediately with 22 ml of benzene–butanol (85:15).

The organic phase (20 ml) was transferred to a scintillation vial and evaporated under a nitrogen stream in a water bath at 60°. The dry residue was dissolved in 0.5 ml of methanol, and 10 ml of scintillation fluid was added. The capped vials were dark adapted for at least 6 hr before counting. This procedure extracts heroin into the organic phase, and the remaining aqueous solution contains 6-*O*-acetylmorphine and morphine.

Carbonate buffer (2 ml) adjusted to pH 8.9 was added to the aqueous solution (pH 8.9), and 6-*O*-acetylmorphine and morphine were extracted with 2 × 5 ml of ethyl acetate–isopropyl alcohol (85:15). The combined organic phases in a 15-ml centrifuge tube were evaporated under a nitrogen stream in a water bath at 60°. The walls were rinsed with 0.5 ml of the same solvent. The solution was again evaporated to dryness. The dry residue was then dissolved in 25 μl of the same solvent with a vortex mixer, 15 μl was spotted on a silica gel TLC plate, and the plate was developed with chloroform–methanol (80:20).

6-*O*-Acetylmorphine and morphine standards were spotted on the same plate to determine their positions. The standards were visualized

[1] Amersham/Searle Co., Arlington Heights, Ill.
[2] Merck and Co., Rahway, N.J.
[3] Batch 1934-886-50, Department of Health, Education, and Welfare, Public Health Service, National Institute of Mental Education.
[4] Chemical Procurement Laboratories, College Point, N.Y.
[5] Mallinckrodt Chemical Works, St. Louis, Mo.
[6] Silica gel 60, E. Merck Laboratories, Elmsford, N.Y.
[7] Burdick and Jackson Laboratories, Muskegon, Mich.
[8] Type 2100 CF-50, Amicon Corp., Lexington, Mass.
[9] Scinti Verse, Fisher Scientific Co., Fair Lawn, N.J.
[10] Model LS 330, Beckman Instruments, Fullerton, Calif.
[11] Model ALC 202, Waters Associates, Milford, Mass.
[12] μBondapak C_{18} Porasil, Waters Associates, Milford, Mass.
[13] Silyl-8, Pierce Chemical Co., Rockford, Ill.
[14] Meyer N-Evap, Organomation Associates, Shrewsbury, Mass.
[15] Reacti-Therm heating module, Pierce Chemical Co., Rockford, Ill.

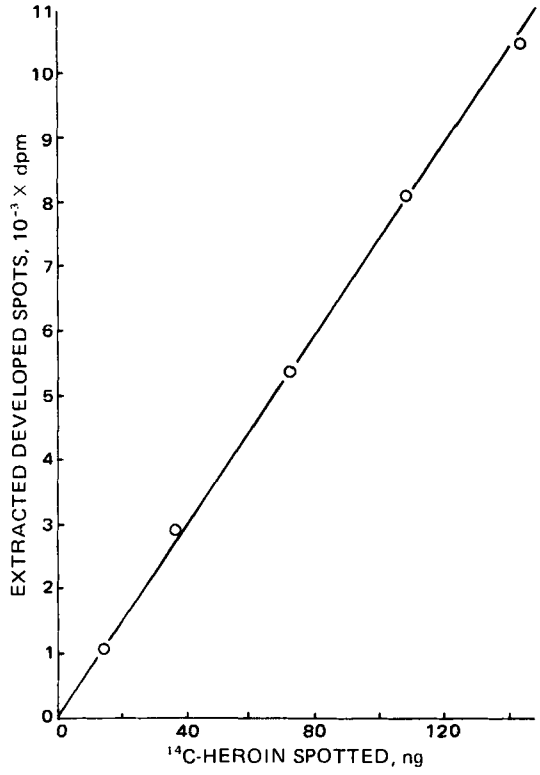

Figure 1—*Plot of disintegrations per minute of heroin extracted with 0.5 ml of methanol from spots at appropriate* R_f *values (0.77) on a TLC silica gel plate developed with chloroform–methanol (80:20) against the nanograms of* ^{14}*C-heroin spotted in 10 μl of acetone at the origin.*

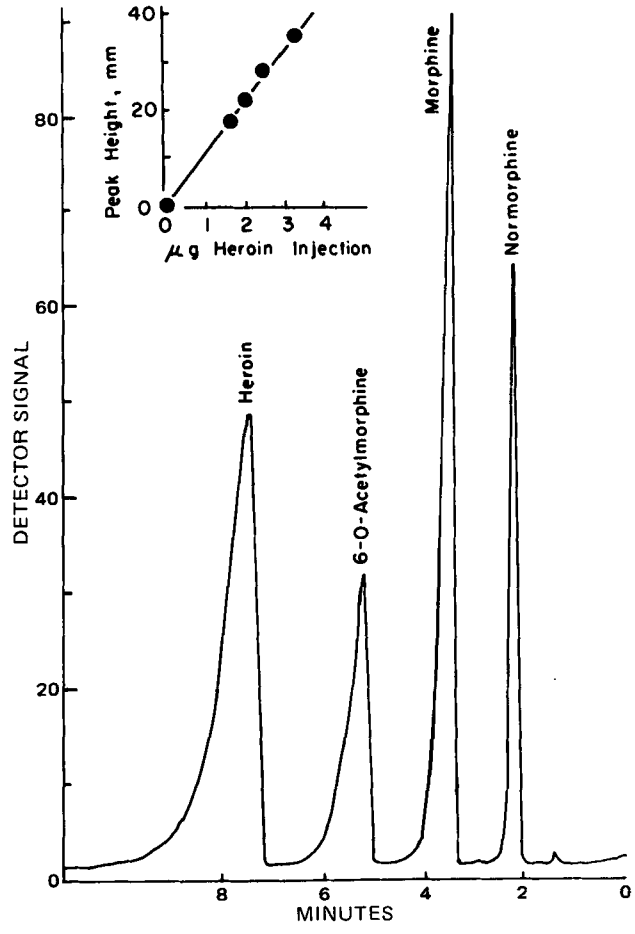

Figure 2—*HPLC reversed-phase chromatogram of a 10-μl aqueous solution of a mixture of heroin, 6-O-acetylmorphine, morphine, and normorphine developed by 55:45 methanol–buffer (2 ml/min) where the buffer contained 0.1% $(NH_4)_2CO_3$ and 0.01 M $(NH_4)_2HPO_4$. The inset is a typical calibration curve in millimeters of height of the heroin peak against the nanograms of heroin injected.*

with iodoplatinate spray. The marked spots were scraped from the plate, and the powdered silica was transferred to a vial and agitated with 0.5 ml of methanol for 5 min. Scintillation liquid (10 ml) was added, and the capped vials were counted after 6 hr of dark adaptation.

Hydrolysis Kinetics of Heroin in Body Fluids—The hydrolysis kinetics of heroin were studied in buffer, plasma, whole blood, and cerebrospinal fluid. The kinetics of heroin hydrolysis in dog plasma were studied with and without the enzyme inhibitors sodium fluoride and tetraethyl pyrophosphate. An aliquot (25 ml) of dog plasma was spiked with varying amounts of ^{14}C-labeled heroin in the normal range expected on heroin administration, and 0.5 or 1 ml of this mixture was assayed by liquid scintillation counting for the heroin extracted at pH 4.7 at various times up to 1–2 hr.

The study was repeated with sodium fluoride (20 mg/ml of plasma) and tetraethyl pyrophosphate (34.7 μg/ml of plasma). Similar studies were repeated in 10 ml of fresh (3 hr) dog blood with and without an enzyme inhibitor. Four milliliters of chloroform completely extracted added radiolabeled ^{14}C-heroin from 1.0 ml of plasma. The hydrolysis kinetics of heroin were studied in fresh dog cerebrospinal fluid (6.5 ml) and isotonic phosphate buffer (10 ml) without an enzyme inhibitor.

The stock solutions of heroin and tetraethyl pyrophosphate were prepared in acetone. Appropriate volumes were then transferred to a centrifuge tube, and the solvent was evaporated under a nitrogen stream at room temperature. The dry residue was dissolved in 20 μl of ethanol, and the biological fluids were added.

The hydrolysis kinetics of 6-*O*-acetylmorphine in dog plasma were studied by spiking 10 ml of fresh dog plasma with unlabeled 6-*O*-acetylmorphine (80 μg). Aliquots (1 ml) were taken at 0, 5, 10, 15, 20, and 40 min. The samples were extracted and analyzed by TLC as described previously. Only the 6-*O*-acetylmorphine spot was seen; no spot attributable to morphine was observed.

Plasma Protein Binding of Heroin—The binding of heroin in heparinized dog plasma was determined by ultrafiltration (18). Standard radiolabeled heroin solutions (9–5500 ng/ml) were prepared in enzyme-inhibited (tetraethyl pyrophosphate, 100 or 115 μg/ml) plasma and plasma water. An aliquot (0.5 ml) was taken prior to centrifugation to determine the total radioactivity. The plasma (3 ml) was put in ultrafiltration cones and centrifuged at 3000 rpm for about 10 min until half of the plasma was filtered. The radioactivity of 0.5 ml of the ultrafiltrate was determined. The membrane binding of heroin was calculated similarly by the ultrafiltration of spiked samples of plasma water prepared from the ultrafiltration of plasma.

Red Blood Cell–Plasma Partitions of Heroin—Pseudoplasma was prepared by ultrafiltration of dog plasma through the membrane cones. Aliquots of a previously analyzed ^{14}C-heroin solution were added to pseudoblood, prepared by adding packed red blood cells (1.00 ml) to this pseudoplasma (1.00 ml) containing the tetraethyl pyrophosphate inhibitor. The red blood cells, obtained from the centrifugation of heparinized dog blood, were washed twice with isotonic saline and recentrifuged. No significant hemolysis was observed.

The mixture was then mixed gently in a centrifuge tube and allowed to equilibrate, usually for 20 min. A hematocrit was taken, and the tube was usually centrifuged for 10 min at 1500 rpm. An aliquot (0.2 ml) of the separated plasma was transferred into a vial for radioactivity determination by liquid scintillation counting. The partition coefficients between plasma water and red blood cells were determined also as functions of drug concentration and time.

The study was repeated with a given concentration of ^{14}C-heroin in a synthetic blood prepared from dog plasma and packed washed blood cells.

HPLC Separation of Heroin, 6-*O*-Acetylmorphine, and Morphine—Reversed-phase HPLC was used to separate heroin, 6-*O*-acetylmorphine, morphine, and normorphine by injection of an aliquot of a mixture of the three alkaloids at a flow rate of 2 ml/min. The compounds were monitored by UV detection, with a bonded phase column[12] used for separation. Solvent systems were 60:40 or 55:45 methanol–buffer where the buffer contained 0.1% $(NH_4)_2CO_3$ and 0.01 *M* $(NH_4)_2HPO_4$.

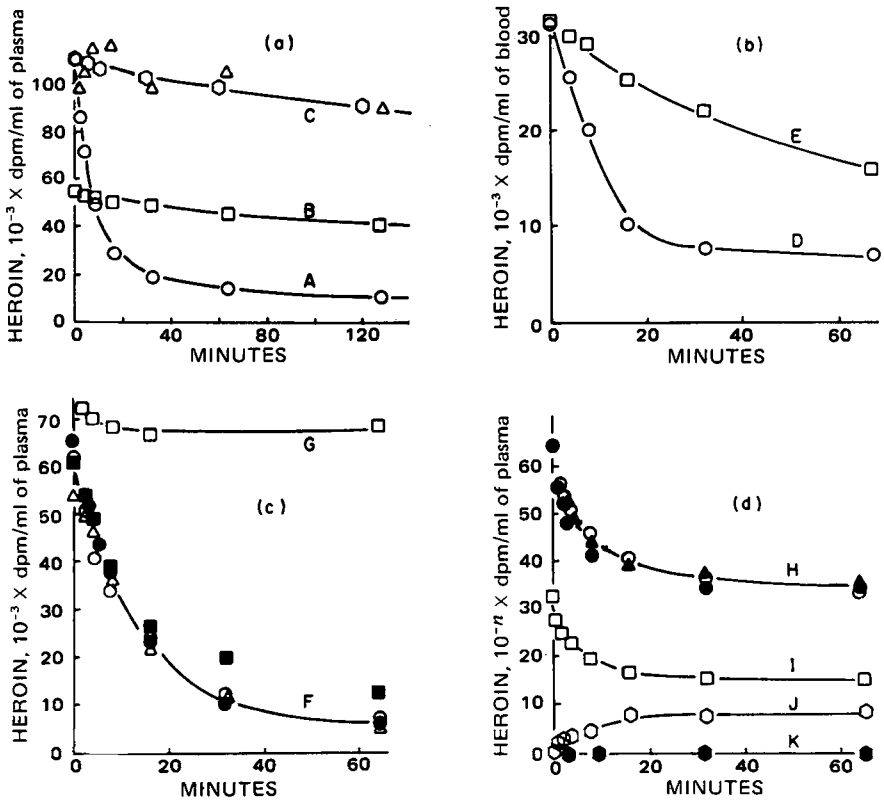

Figure 3—*Instability of heroin in various fluids at room temperature under various conditions. (a) ^{14}C-Heroin (1.2 μg/ml at a specific activity of 91.06 dpm/ng) was completely extracted with chloroform at pH 4.7, and the radiolabeled heroin was assayed by liquid scintillation counting. Key: A (○), fresh dog plasma, no inhibitor; B (□), fresh dog plasma containing 20 mg of sodium fluoride/ml and diluted 1:1 with 0.004 M phosphate buffer (pH 7.4) to give disintegrations per minute per 0.5 ml of plasma; and C, fresh dog plasma (○) containing 34.7 μg of tetraethyl pyrophosphate/ml or 0.004 M phosphate buffer (pH 7.4) containing no inhibitor (△). (b) ^{14}C-Heroin (1.36 μg/ml of blood at a specific activity of 26.9 dpm/ng) was extracted from fresh dog blood with chloroform at pH 4.7, and the radiolabeled heroin was assayed by liquid scintillation counting. Key: D (○), fresh dog blood containing no inhibitor; and E (□), fresh dog blood containing 10 mg of sodium fluoride/ml of blood. (c) Curve F is for ^{14}C-heroin (72 × 10^3 dpm/ml of fresh dog plasma without inhibitors with time as determined by liquid scintillation counting assay of chloroform extraction at pH 4.7). Key: ○, 0.79 μg/ml of plasma; ■, 3.11 μg/ml of plasma; △, 5.43 μg/ml of plasma; and ●, 7.71 μg/ml of plasma. Curve G is for ^{14}C-heroin [82 × 10^3 dpm/ml of fresh dog cerebrospinal fluid without inhibition as determined by liquid scintillation counting assay of benzene–butanol (8.5:1.5) extract]. (d) Curve H, n = 2, is for ^{14}C-heroin (0.216 μg/ml of plasma at a specific activity of 29.9 dpm/ng) extracted from dog plasma of pH 4.7 with 20 ml of benzene–butanol (8.5:1.5)/ml of fresh dog plasma without inhibition. The extract was assayed by liquid scintillation counting. Key: ●, heroin alone; ○, heroin plus 1.6 μg of cold 6-O-acetylmorphine/ml of plasma; and ▲, heroin plus 1.6 μg of cold morphine/ml of plasma. Ethanol (10 μl) had been added to reconstitute evaporated organic solutions of drugs before addition of 25 ml of plasma. ^{14}C-Heroin (1.08 μg/ml of fresh dog plasma at a specific activity of 29.9 dpm/ng) was assayed (n = 3) as for curve H with time (curve I, □). 6-O-Acetylmorphine (curve J, ○) and morphine (curve K, ●) were assayed (n = 3) by liquid scintillation counting of the second extraction after pH adjustment of the heroin-extracted plasma to pH 8.9.*

RESULTS AND DISCUSSION

Separation and Analysis of Heroin and Metabolites—Cold methods for the analyses of morphine after efficient extraction from biological fluids by GLC with electron-capture detection of pentafluoropropionyl derivatives were reported recently (19). The morphine glucuronide metabolite, readily separated from the extracted morphine, was completely hydrolyzed to, and assayed as, morphine.

Heroin and its metabolites (6-*O*-acetylmorphine, morphine, and morphine glucuronide) in biological fluids such as plasma can be analyzed in the same way as morphine after: (*a*) selective sequential extraction procedures as given under *Experimental*, (*b*) TLC separation with subsequent elution of spots at referenced R_f values, and (*c*) separation with HPLC systems. In the HPLC case, UV monitoring can give direct assay of the separated peaks at higher concentrations. Alternatively, the appropriate retention volumes can be collected, acid hydrolyzed to morphine, and assayed by the more sensitive morphine assay methods reported previously (19).

Extraction Efficiencies—Radiolabeled heroin (97% pure by HPLC) was added to plasma where the heroin was inhibited from plasmolysis by added tetraethyl pyrophosphate. Chloroform (4 ml) completely extracted the radioactivity from plasma (1 ml) at an adjusted plasma pH of 4.7.

Benzene–butanol (8.5:1.5), 20 ml, was used to extract ^{14}C-heroin in tetraethyl pyrophosphate-inhibited (173 μg/ml) plasma (1 ml + 1 ml of pH 4.7 buffer), and the organic phase was assayed for radioactivity by liquid scintillation counting. The extraction efficiency was 86.3 ± 1.1% (*SD*) and was independent of the concentration of heroin in the plasma in the range of 285–2280 ng/ml. The specific values were (nanograms of heroin per milliliter of plasma and extraction efficiency): 285, 86.0%; 570, 86.1%; 1140, 84.8%; 1710, 87.6%; and 2280, 87.04%. When the same procedures were conducted with ^{14}C-morphine in plasma, 7 and 9% of the total radioactivity were extracted at pH 4.8.

^{14}C-Morphine was extracted twice from 1 ml of plasma (0.66 μg/ml), mixed with 1 ml of pH 4.8 acetate buffer and 2 ml of pH 8.89 carbonate buffer, by 5 ml of ethyl acetate–isopropyl alcohol (8.5:1.5). The organic phase was then assayed for radioactivity by liquid scintillation counting. The extraction efficiency was 97.53 ± 0.23% (*SD*). In a second study, replicated four times, 0.5 ml of plasma, mixed with 1.5 ml of carbonate buffer (pH 8.9), was extracted with 5 ml of the same organic solvent. The extraction efficiency was 97.31 ± 0.91% (*SE*).

The extraction efficiency of morphine under the conditions for hydrolysis of the morphine glucuronide to morphine was studied also. ^{14}C-Morphine (0.66 μg) was added to 1 ml of plasma, which was mixed with 1 ml of pH 4.7 acetate buffer, 2 ml of pH 8.9 carbonate buffer, and 4 ml of 6 *N* HCl to which 1.15 mg of solid sodium carbonate was added, with the pH adjusted to 8.9. This mixture was extracted with 30 ml of benzene–butanol (8.5:1.5), the organic solution was evaporated, the

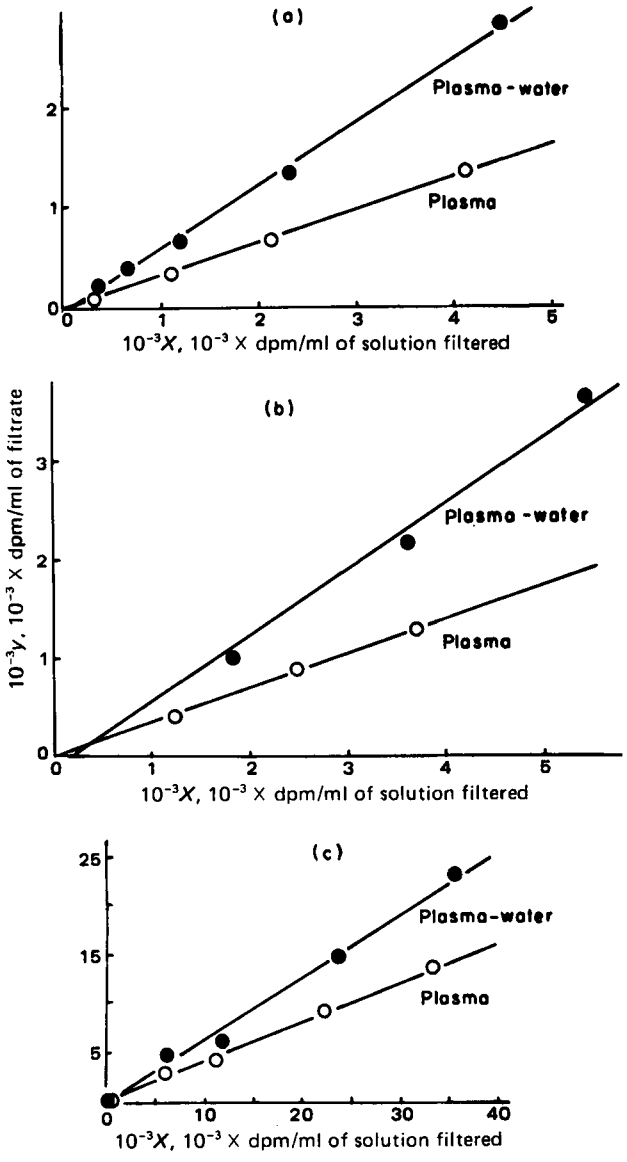

Figure 4—*Plots of disintegrations per minute per milliliter in ultrafiltrate (y) against disintegrations per minute per milliliter of filtered plasma and plasma water solution (x) of ^{14}C-heroin whose hydrolysis was inhibited with tetraethyl pyrophosphate (108 or 115 μg/ml). The drawn lines are those fitted by linear regression in accordance with* $y(\pm SE_y) = m(\pm SE_m)x + b(\pm SE_b)$, *where the* SE_i*'s are the standard errors of estimate. The coefficient of determination is* r^2. *(a) 9–144 ng of ^{14}C-heroin/ml; specific activity = 29.9 dpm/ng. Plasma water:* $y(\pm 60.3) = 0.640(\pm 0.018)x - 57(\pm 42)$; $r^2 = 0.9976$. *Plasma:* $y(\pm 26) = 0.338(\pm 0.009)x - 32(\pm 21)$; $r^2 = 0.9986$. *(b) 180–550 ng of ^{14}C-heroin/ml; specific activity = 6.11 dpm/ng. Plasma water:* $y(\pm 165) = 0.664(\pm 0.041)x - 103(\pm 139)$; $r^2 = 0.9925$. *Plasma:* $y(\pm 10) = 0.345(\pm 0.004) - 0.04(\pm 9)$; $r^2 = 0.9998$. *(c) 920–5500 ng of ^{14}C-heroin/ml; specific activity = 6.11 dpm/ng. Plasma water:* $y(\pm 1056) = 0.633(\pm 0.037)x - 100(\pm 740)$; $r^2 = 0.9900$. *Plasma:* $y(\pm 214) = 0.402(\pm 0.008)x + 42(\pm 150)$; $r^2 = 0.9988$.

residue was reconstituted in 0.5 ml of methanol, and the radioactivity was assayed by liquid scintillation counting. The recoveries of radioactivity were 91.1 and 93.1%.

TLC Separation and Extraction Efficiencies of Developed TLC Spots—Development of mixtures and separate solutions on a TLC silica gel plate with chloroform–methanol (80:20) widely separated morphine (R_f 0.22) from 6-*O*-acetylmorphine (R_f 0.50) and heroin (R_f 0.77). The morphine glucuronide stayed at the origin. ^{14}C-Heroin, 14.5, 36.2, 72.4, 108.6, and 144.7 ng, was spotted and developed on TLC plates. The developed spots were scraped, the scrapings were extracted with 0.5 ml of methanol, and the radioactivity was assayed by liquid scintillation counting. The extraction efficiency from the scrapings was 80.9 ± 1.2% (*SD*) and was independent of the amount spotted (Fig. 1).

Similar studies with spotted ^{14}C-morphine gave an extraction efficiency of 82.3 ± 1.1% (*SD*).

HPLC Separations—Several HPLC systems were developed for separation and analyses of morphine and its metabolites. A typical separation for normorphine, morphine, 6-*O*-acetylmorphine, and heroin by 55:45 methanol–buffer, with the pH 6.98 buffer containing 0.1% $(NH_4)_2CO_3$ and 0.01 *M* $(NH_4)_2HPO_4$, is given in Fig. 2. When the purified synthesized ^{14}C-heroin was analyzed by HPLC in such a system, 96.5% of the administered radioactivity was collected at the retention volume of heroin (9.5–13 min), 2.49% at that of morphine (2.5–4 min), and 0.83% at that of 6-*O*-acetylmorphine (4.5–6.5 min).

Organic solvent extracts of inhibited plasma (1 ml), obtained with 20 ml of ethyl acetate–isopropyl alcohol or benzene–butanol (8.5:1.5) from the plasma mixed with 1 ml of pH 8.9 carbonate buffer, contained heroin, 6-*O*-acetylmorphine, and morphine. The extracts were reconstituted in 50 μl of acetone, of which 10 μl was injected in the liquid chromatograph and developed by the previously stated procedures. The fractions were monitored directly by UV, using the peak heights, peak areas, or their ratios to the respective values of an internal standard such as normorphine.

In the apparatus used, the sensitivity of the direct UV assay was 0.1 μg/injection (inset, Fig. 2) and thus equivalent to 0.5 μg/ml of plasma. Greater sensitivity could be obtained by acid hydrolysis of the collected pertinent fractions with assay as morphine by the previously described (19) GLC method for the derivatized compound or liquid scintillation counting of the radiolabeled dansyl derivatization product. Direct liquid scintillation counting could assay the fraction if ^{14}C-heroin were administered to the animal.

Instability of Heroin and Its Inhibition in Plasma—Heroin underwent some spontaneous hydrolysis in pH 7.4 phosphate buffer (curve C, Fig. 3*a*) with an estimated apparent half-life of 415 min. The hydrolysis accelerated in fresh dog plasma with an apparent half-life of 8 min (curve A, Fig. 3*a*). The presence of 20 mg of sodium fluoride/ml of plasma (curve B, Fig. 3*a*) and 34.7 μg of tetraethyl pyrophosphate/ml of plasma (curve C, Fig. 3*a*) reduced the hydrolysis rate to that of buffer. The instability of heroin in fresh cerebrospinal fluid (curve G, Fig. 3*c*) was close to that in buffer alone (curve C, Fig. 3*a*).

The addition of 10 mg of sodium fluoride/ml to dog blood significantly increased the estimated half-life of heroin instability from 8 min (curve D, Fig. 3*b*) to 40 min (curve E, Fig. 3*b*). Unfortunately, sodium fluoride ruptured red blood cells and denatured plasma protein. Thus, tetraethyl pyrophosphate was the inhibitor of choice.

Additional studies of heroin instability in other dog plasma (curve F, Fig. 3*c*) also showed apparent half-lives of 8 min and were independent of heroin concentrations in the studied range of 0.79–7.7 μg/ml of plasma.

When these plasmas (curve F, Fig. 3*c*) were kept at room temperature for 24 hr and respiked with heroin, no significant loss of the added heroin was observed. The 24-hr sample that originally had 0.79 μg of heroin/ml of plasma was adjusted to 416,700 dpm/ml assayed as heroin and, 10 min later, the assayed heroin was still 478,500. Similarly, the original 7.71 μg/ml of plasma was adjusted to 478,500 dpm/ml with ^{14}C-heroin, and the count of assayed extract after 10 min was 481,000 dpm/ml. Also, negligible hydrolysis of ^{14}C-heroin was observed in stored plasma in several instances. These studies imply that the catalysts or enzymes in plasma that promote heroin hydrolysis are inactivated on storage.

When similar studies were conducted with fresh dog plasma that was not stored for such a long interval, the catalytic activity was maintained. A plasma containing 1037 ng/ml assayed 83,760 dpm/ml as heroin at zero time and 8112 at 63 min. When additional ^{14}C-heroin, 1570 μg/ml, was added to the plasma, the assays were 128,500 dpm/ml at 65 min and 23,216 dpm/ml at 125 min.

For several plasmas stored for varying times, incompletely catalyzed hydrolysis was observed (curve H, Fig. 3*c*). The possiblity of product-inhibited hydrolysis was denied by the demonstration that heroin alone, heroin plus 6-*O*-acetylmorphine, and heroin plus morphine demonstrated the same kinetics of heroin hydrolysis in plasma (curve H, Fig. 3*c*).

The major observed product of plasma-catalyzed heroin hydrolysis was 6-*O*-acetylmorphine; negligible radioactivity assignable to morphine was observed (curves I–K, Fig. 3*d*). A specific study was made of the attempted hydrolysis of 6-*O*-acetylmorphine (8 μg/ml) in fresh plasma and plasma inhibited with tetraethyl pyrophosphate. Extraction with 5 ml of ethyl acetate–isopropyl alcohol (8.5:1.5) of 1.00-ml plasma samples adjusted to pH 8.9 with 2 ml of carbonate buffer with subsequent solvent evaporation, reconstitution in 25 μl of ethyl acetate–isopropyl alcohol,

Table I—Summary of Membrane and Plasma Protein Binding Studies of ^{14}C-Heroin by Ultrafiltration

Heroin Concentration, ng/ml	Tetraethyl Pyrophosphate Concentration, μg/ml	Assay Levels	Assay Level Replicates	Specific Activity, dpm/ng	Fraction in Plasma Water Not Bound to Membrane ±*SD*[a] (a)	Fraction in Plasma: Not Bound to Membrane and Plasma Protein[b] ±*SD* (b)	Fraction in Plasma: Not Bound to Plasma Protein[c] (c)	Fraction of Free Heroin Bound to Plasma Protein[d]
9–144	108	5	3	29.9	0.596 ± 0.032	0.313 ± 0.016	0.283	0.475
21–127	108	3	1	39.0	0.690 ± 0.008	0.470 ± 0.018	0.220	0.319
293	115	1	4	6.81	0.655	0.372	0.283	0.432
183–550	115	3	3	6.11	0.609 ± 0.054	0.344 ± 0.05	0.265	0.435
920–5500	115	4	3	6.10	0.64* ± 0.12	0.411 ± 0.029	0.231	0.360
Average ± *SD*					0.64 ± 0.04	0.38 ± 0.06	0.26 ± 0.03	0.40 ± 0.06

[a] Disintegrations per minute per milliliter of plasma water filtrate ÷ disintegrations per minute per milliliter of plasma water before filtration. Assayed values in plasma water before and after filtration were used in all cases. [b] Disintegrations per minute per milliliter of plasma filtrate ÷ disintegrations per minute per milliliter of plasma before filtration. Assayed values in plasma were used in all cases except for the 920–5500-ng/ml plasma studies where the disintegrations per minute per milliliter of plasma before filtration were calculated from the known specific activity and the amount of ^{14}C-heroin added to the plasma. [c] Calculated from a − b. [d] Calculated from (a − b)/a = (c/a).

and TLC development of 15 μl showed only the presence of 6-*O*-acetylmorphine and no morphine after 0, 5, 10, 15, 20, and 40 min of reaction in the plasma. This result strongly indicates that only heroin hydrolysis is catalyzed by fresh plasma.

Plasma Protein Binding of ^{14}C-Heroin by Ultrafiltration—The ultrafiltration of ^{14}C-heroin from tetraethyl pyrophosphate-inhibited plasma water and plasma demonstrated linear relations between the concentrations of radiolabeled material in the filtrate and the solutions filtered (Fig. 4), with intercepts not significantly different from zero. The respective slopes were estimates of the fraction unbound to membrane, S_{PW}, and unbound to plasma proteins plus membrane, S_P, for the filtration of plasma water and plasma, respectively. These plots showed that the fractions membrane bound, $1 - S_{PW}$, were 0.360 ± 0.018 (*SE*) for 9–144 ng of heroin/ml, 0.336 ± 0.041 for 180–550 ng of heroin/ml, and 0.367 ± 0.037 for 920–5500 ng of heroin/ml. The fractions, both membrane and plasma protein bound, $1 - S_P$, were 0.662 ± 0.009, 0.655 ± 0.004, and 0.598 ± 0.037, respectively. Thus, it can be concluded that the fractions bound of heroin were concentration independent in the 9–550-ng/ml range. The fractions of heroin not bound to the membrane but bound to plasma protein, $(S_{PW} - S_P)/S_{PW}$, were 0.472, 0.480, and 0.365, respectively.

A summary of membrane and plasma protein binding for all studies conducted, calculated from the averages of the data, is given in Table I. The values were calculated differently from the methods given in Fig. 4. The overall average of the fraction of free heroin, *i.e.*, unbound to membrane, that was bound to plasma protein was 0.40 ± 0.06 *SD*.

Additional studies were conducted at 1467 ng of ^{14}C-heroin/ml of plasma; aliquots of the plasma were filtered at 0, 4, 8, 16, and 32 min. There were no significant differences among the assays of the filtrates obtained at different times. In two studies, the fractions bound to membrane plus plasma proteins were 0.624 ± 0.049 *SD* and 0.647 ± 0.017 *SD*, $n = 5$. It must be concluded that equilibration between plasma protein and heroin was established well within the time necessary for processing the plasma.

Table II—Summary of Red Blood Cell–Plasma Water Partition Studies[a]

Partition System	*H*, hematocrit/100	ng of ^{14}C-Heroin / ml of System	A_B, dpm of ^{14}C-Heroin / ml of System	A_P, dpm of ^{14}C-Heroin / ml of Plasma or Plasma Water	*D*[b] (Partition Coefficient), RBC/plasma water	Equilibration Time, min	Centrifugation Time, min
A Plasma water–red blood cells	0.345	38.0	1532	1320	1.47	20	10
	0.356	59.6	2298	2010	1.41	20	10
	0.350	75.4	3064	2560	1.56	20	10
	0.350	94.9	3830	3155	1.61	20	10
	0.352	94.9	3830	3210	1.55	20	10
	0.350	94.9	3830	3140	1.63	20	10
	0.345	190	7660	6755	1.39	20	10
Average ± *SD*					1.52 ± 0.10		
B Plasma water–red blood cells	0.345	94.9	3830	3320	1.45	2	10
	0.345	94.9	3830	3390	1.38	0	10
Average					1.41		
C Plasma water–red blood cells	0.301	94.9	3830	3130	1.74	0	3
	0.295	94.9	3830	3510	1.31	4	3
	0.296	94.9	3830	3465	1.36	8	3
	0.298	94.9	3830	3425	1.40	16	3
	0.295	94.9	3830	3837	0.99	32	3
Average ± *SD*					1.36 ± 0.27		
D Plasma water–red blood cells	0.300	39.3	1523	1381	1.34	20	10
	0.300	39.3	1523	1499	1.05	20	10
	0.300	39.3	1523	1480	1.10	20	10
	0.305	39.3	1523	1503	1.04	20	10
Average ± *SD*					1.13 ± 0.14		
E Plasma water–red blood cells	0.232	16.8	689	568	1.92	20	10
	0.228	16.8	648	598	1.37	20	10
	0.233	16.8	655	599	1.40	20	10
	0.235	16.8	647	568	1.59	20	10
Average ± *SD*					1.57 ± 0.25		
F Plasma–red blood cells	0.253	104.5	1892	1947	1.48	20	10
	0.285	104.5	1892	2030	1.27	20	10
	0.268	104.5	1892	1963	1.44	20	10
	0.274	104.5	1892	2037	1.23	20	10
Average ± *SD*					1.36 ± 0.12[c]		

[a] Plasma water–red blood cell systems were inhibited with 86.5 μg of tetraethyl pyrophosphate/ml. The plasma–red blood cell system was inhibited with 104.5 μg of tetraethyl pyrophosphate/ml. The fraction bound, *f*, was taken as zero for the plasma water–red blood cells systems and as 0.4 for the plasma–red blood cells system. [b] Average of averages was 1.39 ± 0.15 *SD*. [c] If $f = 0$ were taken rather than $f = 0.4$, the calculated *D* would be 0.814 ± 0.074 *SD*.

Partitioning of ^{14}C-Heroin between Plasma Water and Red Blood Cells—The results of the several studies conducted on the partitioning of ^{14}C-heroin between plasma water and red blood cells (RBC) are summarized in Table II. The heroin in the systems was inhibited from plasmolysis with 86.5 or 104.5 μg of tetraethyl pyrophosphate/ml. The partition coefficient, D, was calculated from (20):

$$D = \frac{[A_{RBC}]}{[A_p^u]} = \left\{ \frac{[A_B]}{[A_p](1-H)(1-f)} - \frac{f}{1-f} - 1 \right\} \frac{1-H}{H} \quad \text{(Eq. 1)}$$

where $[A_{RBC}]$, $[A_B]$, and $[A_p]$ are the ^{14}C-heroin concentrations in the red blood cells, blood, and plasma, respectively, and $[A_p^u]$ is the drug concentration in the plasma that is unbound to plasma proteins. The hematocrit ÷ 100 is H, and f is the fraction of drug in plasma bound to plasma proteins. The value of f was taken as zero in the plasma water systems and as 0.4 in the plasma–red blood cell mixture.

The results of Study A (Table II) showed no significant differences among the partition coefficients, D, within the range of 38–190 ng of ^{14}C-heroin/ml of pseudoblood. Any time of equilibration greater than zero for ^{14}C-heroin in the pseudoblood did not affect significantly the determined partition coefficients (compare Studies A–C in Table II). Also, times of centrifugation, 3 and 10 min, of the plasma water–red blood cell mixtures to separate the plasma water to be assayed did not significantly affect the results. Only Study D appeared to differ slightly from the total results where the average of the averages given in Table II was 1.39 ± 0.15 *SD*.

Study E was performed after separation of the plasma water from Study D, where the red blood cells containing the equilibrated ^{14}C-heroin were reequilibrated with fresh plasma water and subsequently centrifuged to determine the new partition coefficient. Study E was on a synthetic blood, prepared from plasma and red blood cells, and the partition coefficient determined from Eq. 1 for a protein-bound fraction of $f = 0.4$ was the same as that from the plasma water–red blood cell systems. If the fraction bound had been ignored, *i.e.*, $f = 0$, the calculated apparent D would have been 0.814 ± 0.074 *SD*, which differs widely from the plasma water systems since the protein binding makes a fraction of the heroin unavailable for partition into the red blood cells.

REFERENCES

(1) C. I. Wright, *J. Pharmacol. Exp. Ther.*, **71**, 164 (1947).

(2) E. L. Way, J. W. Kemp, J. M. Young, and D. R. Grassetti, *ibid.*, **129**, 144 (1960).

(3) E. L. Way, J. M. Young, and J. W. Kemp, *Bull. Narc.*, **17** (1), 15 (1965).

(4) T. M. Shen, *J. Clin. Pharm. Assoc.*, **1**, 124 (1936); through *Chem. Abstr.*, **31**, 730 (1937).

(5) F. W. Oberst, *J. Pharmacol. Exp. Ther.*, **73**, 401 (1941).

(6) F. W. Oberst, *ibid.*, **79**, 266 (1943).

(7) P. N. Mo and E. L. Way, *ibid.*, **154**, 142 (1966).

(8) H. W. Elliott, K. D. Parker, J. A. Wright, and N. Nomoff, *Clin. Pharmacol. Ther.*, **12**, 806 (1971).

(9) S. Y. Yeh and R. L. McQuinn, *J. Pharm. Sci.*, **64**, 1237 (1975).

(10) S. Y. Yeh, C. W. Gorodetzky, and R. L. McQuinn, *J. Pharmacol. Exp. Ther.*, **196**, 249 (1976).

(11) S. Y. Yeh, R. L. McQuinn, and C. W. Gorodetzky, *J. Pharm. Sci.*, **66**, 201 (1977).

(12) G. R. Nakamura, J. I. Thornton, and T. T. Noguchi, *J. Chromatogr.*, **110**, 81 (1975).

(13) S. Ellis, *J. Pharmacol. Exp. Ther.*, **94**, 130 (1948).

(14) G. L. Cohn, J. A. Cramer, and H. D. Kleber, *Proc. Soc. Exp. Biol. Med.*, **144**, 351 (1973).

(15) G. L. Cohn, J. A. Cramer, W. McBride, R. C. Brown, and H. D. Kleber, *ibid.*, **147**, 664 (1974).

(16) E. Stahl, "Thin Layer Chromatography," Springer-Verlag, New York, N.Y., 1965, p. 493.

(17) S. E. Hays, L. T. Grady, and A. V. Kruegel, *J. Pharm. Sci.*, **62**, 1509 (1973).

(18) P. H. Hinderling, J. Brès, and E. R. Garrett, *ibid.*, **63**, 1684 (1974).

(19) E. R. Garrett and T. Gürkan, *ibid.*, **67**, 1512 (1978).

(20) E. R. Garrett and H. J. Lambert, *ibid.*, **62**, 550 (1973).

ACKNOWLEDGMENTS

Supported in part by Grant 2-R01-DA-00743-04 from the National Institute on Drug Abuse, Rockville, MD 20852. A portion of T. Gürkan's stay was supported by a grant from the government of Turkey.

The technical assistance of Kathleen L. Eberst and George L. Perry is gratefully acknowledged.

Liquid Chromatography in Pharmaceutical Analysis XI: Determination of Muscle Relaxant–Analgesic Mixtures Using Reversed-Phase and Ion-Pair Techniques

J. T. STEWART, I. L. HONIGBERG ˣ, and J. W. COLDREN

Received February 7, 1978, from the *Department of Medicinal Chemistry, School of Pharmacy, University of Georgia, Athens, GA 30602.* Accepted for publication May 19, 1978.

Abstract □ High-pressure liquid chromatography using reversed-phase and/or ion-pair techniques was used to optimize resolution of aspirin-containing muscle relaxant mixtures as well as other therapeutic agents commonly found in muscle relaxant–analgesic mixtures. The compounds were chromatographed on an octadecylsilane column using methanol–water solvent systems, some of which contained tetrabutylammonium cation as counterion. Mixtures of methocarbamol–aspirin and chlorzoxazone–acetaminophen were selected to demonstrate separation and quantification. The methocarbamol–aspirin mixture was chromatographed with methanol–water (40:60, pH 6.8) containing 0.01 *M* tetrabutylammonium cation at a flow rate of 2.0 ml/min. The chlorzoxazone–acetaminophen mixture was chromatographed with methanol–water (50:50) at a 2.0-ml/min flow rate. The separation and quantitation of each mixture were achieved in approximately 8 min with accuracy in the 2–3% range.

Keyphrases □ Muscle relaxant–analgesic mixtures, various—high-pressure liquid chromatographic analyses of components □ Analgesic–muscle relaxant mixtures, various—high-pressure liquid chromatographic analyses of components □ High-pressure liquid chromatography—analyses, components of various muscle relaxant–analgesic mixtures

Previous high-pressure liquid chromatographic (HPLC) investigations with muscle relaxant–analgesic agents such as meprobamate, methocarbamol, carisoprodol, chlorzoxazone, acetaminophen, aspirin, caffeine, and phenacetin (1) indicated that the aspirin-containing combinations were difficult to chromatograph using nonpolar solvents

0022-3549/79/0100-0032$01.00/0

© 1979, American Pharmaceutical Association

Partitioning of ^{14}C-Heroin between Plasma Water and Red Blood Cells—The results of the several studies conducted on the partitioning of ^{14}C-heroin between plasma water and red blood cells (RBC) are summarized in Table II. The heroin in the systems was inhibited from plasmolysis with 86.5 or 104.5 μg of tetraethyl pyrophosphate/ml. The partition coefficient, D, was calculated from (20):

$$D = \frac{[A_{RBC}]}{[A_p^u]} = \left\{ \frac{[A_B]}{[A_p](1-H)(1-f)} - \frac{f}{1-f} - 1 \right\} \frac{1-H}{H} \quad \text{(Eq. 1)}$$

where $[A_{RBC}]$, $[A_B]$, and $[A_p]$ are the ^{14}C-heroin concentrations in the red blood cells, blood, and plasma, respectively, and $[A_p^u]$ is the drug concentration in the plasma that is unbound to plasma proteins. The hematocrit ÷ 100 is H, and f is the fraction of drug in plasma bound to plasma proteins. The value of f was taken as zero in the plasma water systems and as 0.4 in the plasma–red blood cell mixture.

The results of Study A (Table II) showed no significant differences among the partition coefficients, D, within the range of 38–190 ng of ^{14}C-heroin/ml of pseudoblood. Any time of equilibration greater than zero for ^{14}C-heroin in the pseudoblood did not affect significantly the determined partition coefficients (compare Studies A–C in Table II). Also, times of centrifugation, 3 and 10 min, of the plasma water–red blood cell mixtures to separate the plasma water to be assayed did not significantly affect the results. Only Study D appeared to differ slightly from the total results where the average of the averages given in Table II was 1.39 ± 0.15 *SD*.

Study E was performed after separation of the plasma water from Study D, where the red blood cells containing the equilibrated ^{14}C-heroin were reequilibrated with fresh plasma water and subsequently centrifuged to determine the new partition coefficient. Study E was on a synthetic blood, prepared from plasma and red blood cells, and the partition coefficient determined from Eq. 1 for a protein-bound fraction of $f = 0.4$ was the same as that from the plasma water–red blood cell systems. If the fraction bound had been ignored, *i.e.*, $f = 0$, the calculated apparent D would have been 0.814 ± 0.074 *SD*, which differs widely from the plasma water systems since the protein binding makes a fraction of the heroin unavailable for partition into the red blood cells.

REFERENCES

(1) C. I. Wright, *J. Pharmacol. Exp. Ther.*, **71**, 164 (1947).

(2) E. L. Way, J. W. Kemp, J. M. Young, and D. R. Grassetti, *ibid.*, **129**, 144 (1960).

(3) E. L. Way, J. M. Young, and J. W. Kemp, *Bull. Narc.*, **17** (1), 15 (1965).

(4) T. M. Shen, *J. Clin. Pharm. Assoc.*, **1**, 124 (1936); through *Chem. Abstr.*, **31**, 730 (1937).

(5) F. W. Oberst, *J. Pharmacol. Exp. Ther.*, **73**, 401 (1941).

(6) F. W. Oberst, *ibid.*, **79**, 266 (1943).

(7) P. N. Mo and E. L. Way, *ibid.*, **154**, 142 (1966).

(8) H. W. Elliott, K. D. Parker, J. A. Wright, and N. Nomoff, *Clin. Pharmacol. Ther.*, **12**, 806 (1971).

(9) S. Y. Yeh and R. L. McQuinn, *J. Pharm. Sci.*, **64**, 1237 (1975).

(10) S. Y. Yeh, C. W. Gorodetzky, and R. L. McQuinn, *J. Pharmacol. Exp. Ther.*, **196**, 249 (1976).

(11) S. Y. Yeh, R. L. McQuinn, and C. W. Gorodetzky, *J. Pharm. Sci.*, **66**, 201 (1977).

(12) G. R. Nakamura, J. I. Thornton, and T. T. Noguchi, *J. Chromatogr.*, **110**, 81 (1975).

(13) S. Ellis, *J. Pharmacol. Exp. Ther.*, **94**, 130 (1948).

(14) G. L. Cohn, J. A. Cramer, and H. D. Kleber, *Proc. Soc. Exp. Biol. Med.*, **144**, 351 (1973).

(15) G. L. Cohn, J. A. Cramer, W. McBride, R. C. Brown, and H. D. Kleber, *ibid.*, **147**, 664 (1974).

(16) E. Stahl, "Thin Layer Chromatography," Springer-Verlag, New York, N.Y., 1965, p. 493.

(17) S. E. Hays, L. T. Grady, and A. V. Kruegel, *J. Pharm. Sci.*, **62**, 1509 (1973).

(18) P. H. Hinderling, J. Brès, and E. R. Garrett, *ibid.*, **63**, 1684 (1974).

(19) E. R. Garrett and T. Gürkan, *ibid.*, **67**, 1512 (1978).

(20) E. R. Garrett and H. J. Lambert, *ibid.*, **62**, 550 (1973).

ACKNOWLEDGMENTS

Supported in part by Grant 2-R01-DA-00743-04 from the National Institute on Drug Abuse, Rockville, MD 20852. A portion of T. Gürkan's stay was supported by a grant from the government of Turkey.

The technical assistance of Kathleen L. Eberst and George L. Perry is gratefully acknowledged.

Liquid Chromatography in Pharmaceutical Analysis XI: Determination of Muscle Relaxant–Analgesic Mixtures Using Reversed-Phase and Ion-Pair Techniques

J. T. STEWART, I. L. HONIGBERG ˣ, and J. W. COLDREN

Received February 7, 1978, from the *Department of Medicinal Chemistry, School of Pharmacy, University of Georgia, Athens, GA 30602.* Accepted for publication May 19, 1978.

Abstract □ High-pressure liquid chromatography using reversed-phase and/or ion-pair techniques was used to optimize resolution of aspirin-containing muscle relaxant mixtures as well as other therapeutic agents commonly found in muscle relaxant–analgesic mixtures. The compounds were chromatographed on an octadecylsilane column using methanol–water solvent systems, some of which contained tetrabutylammonium cation as counterion. Mixtures of methocarbamol–aspirin and chlorzoxazone–acetaminophen were selected to demonstrate separation and quantification. The methocarbamol–aspirin mixture was chromatographed with methanol–water (40:60, pH 6.8) containing 0.01 *M* tetrabutylammonium cation at a flow rate of 2.0 ml/min. The chlorzoxazone–acetaminophen mixture was chromatographed with methanol–water (50:50) at a 2.0-ml/min flow rate. The separation and quantitation of each mixture were achieved in approximately 8 min with accuracy in the 2–3% range.

Keyphrases □ Muscle relaxant–analgesic mixtures, various—high-pressure liquid chromatographic analyses of components □ Analgesic–muscle relaxant mixtures, various—high-pressure liquid chromatographic analyses of components □ High-pressure liquid chromatography—analyses, components of various muscle relaxant–analgesic mixtures

Previous high-pressure liquid chromatographic (HPLC) investigations with muscle relaxant–analgesic agents such as meprobamate, methocarbamol, carisoprodol, chlorzoxazone, acetaminophen, aspirin, caffeine, and phenacetin (1) indicated that the aspirin-containing combinations were difficult to chromatograph using nonpolar solvents

0022-3549/79/0100-0032$01.00/0

© 1979, American Pharmaceutical Association

Table I—Effect of the Mobile Phase on Retention Time [a]

Mobile Phase [b]	Meprobamate	Methocarbamol	Carisoprodol	Chlorzoxazone	Acetaminophen	Aspirin	Caffeine	Phenacetin
A	120	110	232	160	88	80	104	130
	(14)[c]	(16)	(20)	(16)	(14)	(16)	(14)	(16)
B	192	152	532	300	100	84	120	220
	(20)	(26)	(52)	(36)	(12)	(26)	(14)	(24)
C	392	245	1580	580	116	88	168	392
	(36)	(31)	(520)	(60)	(14)	(16)	(20)	(32)
D	124	108	212	172	72	101	104	136
	(12)	(20)	(20)	(20)	(14)	(12)	(12)	(20)
E	177	144	464	312	96	125	116	200
	(20)	(16)	(28)	(28)	(14)	(20)	(16)	(24)
F	324	217	1206	660	116	151	148	352
	(34)	(20)	(111)	(52)	(16)	(20)	(20)	(28)
G	116	120	224	188	88	105	104	144
	(12)	(10)	(24)	(20)	(10)	(16)	(14)	(16)
H	164	148	448	292	96	126	112	216
	(16)	(20)	(42)	(24)	(10)	(16)	(12)	(20)
I	296	226	1080	532	104	184	134	355
	(24)	(28)	(88)	(28)	(10)	(24)	(16)	(48)

[a] Retention time expressed as seconds measured as elapsed time between injection and the chromatographic peak maximum. The eluted peaks were monitored using refractive index detection. [b] A, B, and C are 60:40, 50:50, and 40:60 mixes of methanol and water, respectively. D, E and F are 60:40, 50:50, and 40:60 mixes of methanol and water, respectively, containing 0.01 *M* tetrabutylammonium cation and 0.01 *M* dibasic sodium phosphate and buffered to pH 8 with phosphoric acid. G, H, and I are 60:40, 50:50, and 40:60 mixes of methanol and water, respectively, containing 0.01 *M* tetrabutylammonium cation and 0.01 *M* dibasic sodium phosphate and buffered to pH 6.8 with phosphoric acid. [c] Base peak width expressed as seconds.

and normal phase chromatography. Generally, aspirin eluted close to the solvent front in approximately 50% of the solvents tested or had extremely long retention times in about 25% of the solvents.

Earlier experience with ion-pair chromatography (2, 3) suggested that resolution of acidic components from nonpolar constituents of these muscle relaxant–analgesic mixtures by this technique would be a more successful approach. Therefore, ion-pair formation with tetrabutylammonium cation was investigated, especially with mixtures containing aspirin. The use of tetrabutylammonium cation as a suitable counterion in HPLC was investigated previously (4–6). Ion-pair formation also was utilized (7–9) as a tool for effecting chromatographic analysis of selected organic ions. Included in the present study were investigations of HPLC separations of nonaspirin muscle relaxant–analgesic mixtures using reversed-phase chromatography without ion-pair formation.

The chromatographic data can be applied readily to the separation of selected multidrug dosage forms. This paper reports the separation and quantitation at unit-dose levels of methocarbamol–aspirin using ion-pair and reversed-phase chromatography and of chlorzoxazone–acetaminophen using reversed-phase chromatography.

EXPERIMENTAL[1]

Reagents and Chemicals—Powdered samples of meprobamate[2], methocarbamol[3], carisoprodol[2], chlorzoxazone[4], acetaminophen[5], aspirin[6], caffeine[5], and phenacetin[5] were used. All other chemicals and solvents were the highest purity of the commercially available materials.

Mobile Phases—The mobile phases, consisting of varying proportions of absolute methanol–distilled water, were prepared fresh daily. Certain mobile phases (D–I in Table I) were made 0.01 *M* with respect to the tetrabutylammonium cation in the following manner. An appropriate quantity of tetrabutylammonium iodide[6], calculated to give the desired molar concentration of tetrabutylammonium cation in the final solvent mix, was dissolved in absolute methanol and stirred at room temperature for 1 hr with an equivalent quantity of finely divided silver oxide. The silver oxide was removed by filtration, and a quantity of the methanolic solution was mixed with distilled water to give the desired solvent ratio.

Dibasic sodium phosphate also was added to the distilled water prior to mixing such that its concentration in the final solvent mix was 0.01 *M*. Then the pH of Solvents D–F and G–I was adjusted to 8 and 6.8, respectively, with concentrated phosphoric acid.

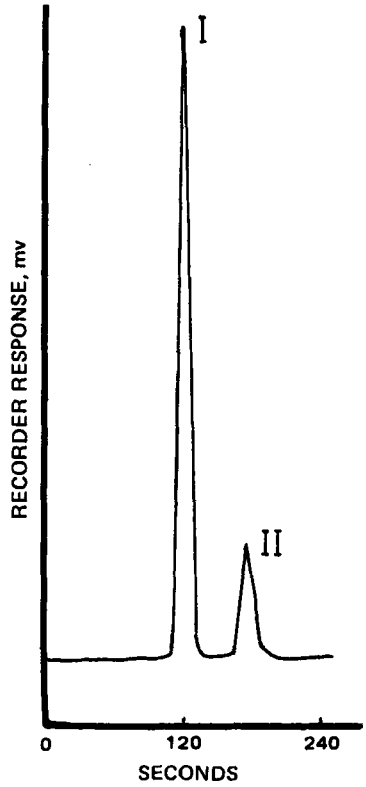

Figure 1—*Liquid chromatogram of simulated meprobamate–aspirin dosage form using refractive index detection on an octadecyl column with absolute methanol–water (50:50, pH 8.0) containing 0.01* M *tetrabutylammonium cation. Concentrations of meprobamate and aspirin were 15 and 25 mg, respectively, dissolved in 25 ml of the mobile phase. A 50-μl injection was made. Key: I, aspirin; and II, meprobamate.*

[1] A Waters Associates liquid chromatograph (model ALC 202), equipped with an M-6000 pump, a U6K injector, UV (254 nm) and differential RI detectors, a Spectra-Physics autolab minigrator with digital printout, and a Waters packed column, 4 mm i.d. × 30 cm, was used.

[2] Wallace Laboratories, Cranbury, N.J.

[3] A. H. Robins, Richmond, Va.

[4] McNeil Laboratories, Fort Washington, Pa.

[5] Eastman Chemicals, Rochester, N.Y.

[6] Aldrich Chemicals, Milwaukee, Wis.

Table II—Typical Calibration Data for Standard Drug Solutions

Compound	Final Concentration, mg[a]	*D/IS* Ratio[b]	Slope	Intercept	$r \pm s_{y \cdot x}$[c]
Methocarbamol	4.0	0.1157 ± 0.0006[d]	0.0303	−0.0041	0.9999 ± 0.0026
	8.0	0.2405 ± 0.0076			
	16.0	0.4802 ± 0.0056			
Aspirin	3.25	0.1816 ± 0.0034	0.0560	0.0011	0.9999 ± 0.0026
	6.50	0.3670 ± 0.0052			
	13.00	0.7281 ± 0.0006			

[a] Total mg/25 ml of solution. [b] Data represent three replicate injections of standard solutions; *D/IS* is the ratio of the integrated area of the drug at some concentration divided by the integrated area of phenacetin at a concentration of 1 mg/25 ml. [c] Standard error of the estimate of *y (D/IS)* on *x* (concentration). [d] Confidence limits at $p = 0.05$.

Drug Solutions—Solutions of each drug (5–10 mg/ml) were prepared by dissolving each powder in the appropriate mobile phase.

Internal Standard Solutions—For methocarbamol–aspirin, 100 mg of phenacetin was dissolved in 100 ml of absolute methanol. For chlorzoxazone–acetaminophen, 49 mg of phenacetin was dissolved in 25 ml of absolute methanol–distilled water (50:50).

Stock Solutions for Calibration Curves—*For Methocarbamol–Aspirin*—Separate stock solutions of methocarbamol (200 mg/100 ml) and aspirin (162.5 mg/100 ml) were prepared in absolute methanol. Accurately pipetted volumes of 2.0, 4.0, and 8.0 ml of each stock solution were placed in 25-ml volumetric flasks. The internal standard stock solution, 1 ml, was added to each flask, followed by the addition of absolute methanol to volume. The three concentrations of each drug were subjected to regression analysis, and the slope and intercept were calculated (Table II).

For Chlorzoxazone–Acetaminophen—Separate stock solutions of chlorzoxazone (62.8 mg/25 ml) and acetaminophen (75.0 mg/25 ml) were prepared in absolute methanol–distilled water (50:50). Accurately pipetted volumes of 0.5, 1.0, and 2.0 ml of each stock solution were placed in 5-ml volumetric flasks. The internal standard stock solution, 1 ml, was added to each flask, followed by the addition of absolute methanol–distilled water (50:50) to volume. The three concentrations of each drug were subjected to regression analysis and the slope and intercept were calculated (Table III).

Chromatographic Separation and Quantification—The degassed mobile phase was pumped through an octadecylsilane[7] column at a flow rate of 2.0 ml/min (2000 psig) at room temperature until a stable baseline was obtained. Replicate 20- and 40-μl injections of sample and standard solutions for the methocarbamol–aspirin and chlorzoxazone–acetaminophen studies, respectively, were made using a 100-μl syringe[8]. The chart recorder provided a record of drug elution from the column as peaks on a chromatogram. In all cases, the solute was measured by electronic integration of the peak area[1].

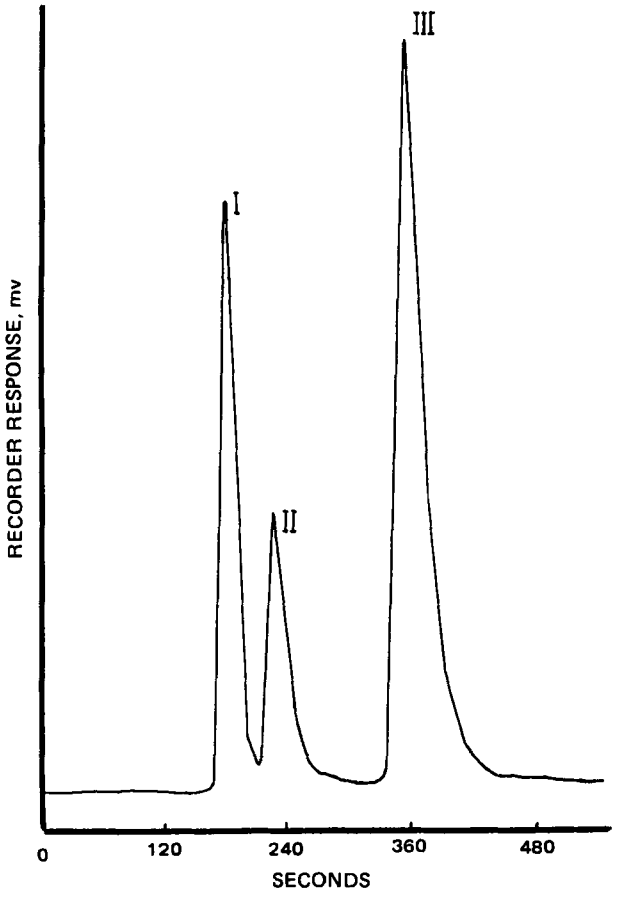

Figure 2—*Liquid chromatogram of simulated methocarbamol–aspirin dosage form at 254 nm on an octadecyl column with absolute methanol–water (40:60, pH 6.8) containing 0.01 M tetrabutylammonium cation. Concentrations of methocarbamol and aspirin were 8 and 6.5 mg, respectively, dissolved in 25 ml of the mobile phase. A 20-μl injection was made. The phenacetin concentration was 1 mg/25 ml. Key: I, aspirin; II, methocarbamol; and III, phenacetin (internal standard).*

RESULTS AND DISCUSSION

Optimization of resolution of the therapeutic agents most commonly found in muscle relaxant–analgesic mixtures necessitated: (*a*) examination of variation in solvent composition combining absolute methanol with changing concentrations of distilled water, and (*b*) addition of tet-

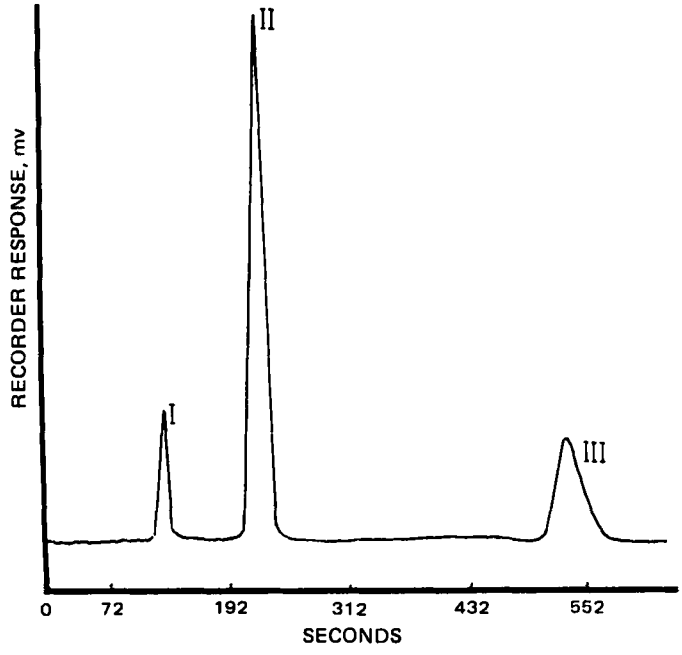

Figure 3—*Liquid chromatogram of simulated carisoprodol–phenacetin–caffeine dosage form using refractive index detection on an octadecyl column with absolute methanol–water (50:50). Concentrations of carisoprodol, phenacetin, and caffeine were 20, 16, and 3.2 mg, respectively, dissolved in 5 ml of the mobile phase. A 10-μl injection was made. Key: I, caffeine; II, phenacetin; and III, carisoprodol.*

[7] μBondapak C_{18}, <10 μm, Waters Associates, Milford, Mass.
[8] Model B-110, Precision Sampling Corp., Baton Rouge, La.

Table III—Typical Calibration Data for Standard Drug Solutions

Compound	Final Concentration, mg[a]	*D/IS* Ratio[b]	Slope	Intercept	$r \pm s_{y,x}$[c]
Chlorzoxazone	1.26	0.5534 ± 0.0430[d]	0.4295	0.0136	0.9999 ± 0.0027
	2.51	1.0939 ± 0.0146			
	5.02	2.1692 ± 0.0547			
Acetaminophen	1.5	0.6402 ± 0.0360	0.4086	0.0322	0.9999 ± 0.0093
	3.0	1.2656 ± 0.0136			
	6.0	2.4816 ± 0.0304			

[a] Total mg/5 ml of solution. [b] Data represent three replicate injections of standard solutions; *D/IS* is the ratio of the integrated area of the drug at some concentration divided by the integrated area of phenacetin at a concentration of 1.96 mg/5 ml. [c] Standard error of the estimate of *y (D/IS)* on *x* (concentration). [d] Confidence limits at $p = 0.05$.

rabutylammonium cation to the mobile phase to effect ion-pair formation, especially in mixtures containing aspirin. The stationary phase was limited to octadecylsilane chemically bonded to a porous silica support.

The effects of these parameters on retention times and base peak widths of the drugs are shown in Table I. The eluted peaks were monitored using refractive index detection since many of the muscle relaxants were aliphatic compounds and did not possess satisfactory UV absorption. For pH stabilization, dibasic sodium phosphate was added to mobile phases containing tetrabutylammonium cation.

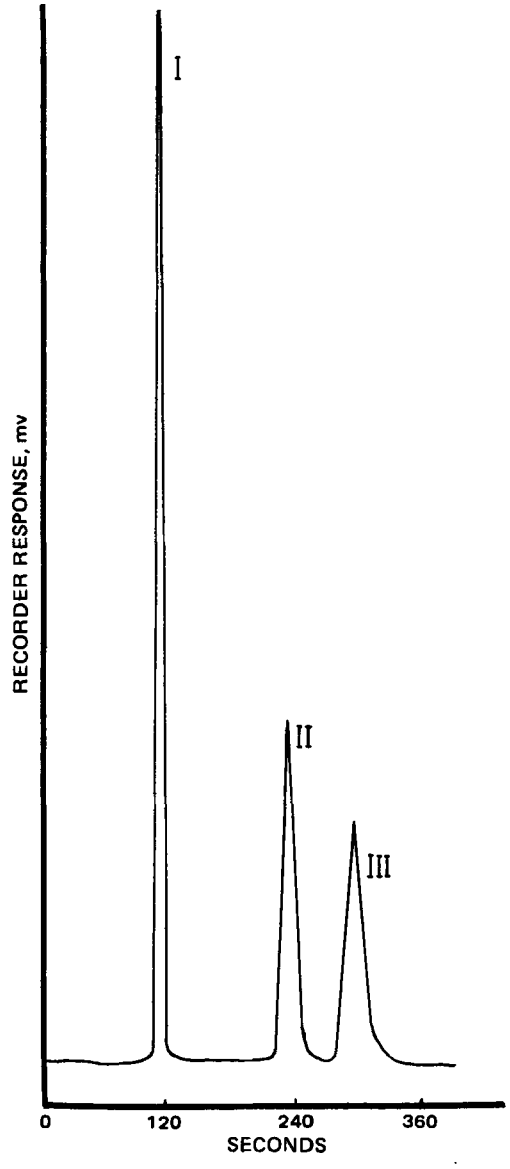

Figure 4—*Liquid chromatogram of simulated chlorzoxazone–acetaminophen dosage form using refractive index detection on an octadecyl column with absolute methanol–water (50:50). Concentrations of chlorzoxazone and acetaminophen were 2.51 and 3.0 mg, respectively, dissolved in 5 ml of mobile phase. A 40-μl injection was made. The phenacetin concentration was 1.96 mg/5 ml. Key: I, acetaminophen; II, phenacetin (internal standard); and III, chlorzoxazone.*

Reasonably high concentrations of methanol were used instead of the pentanol-saturated mobile phase recommended previously (5, 6). This substitution, especially in studies involving tetrabutylammonium cation, desensitizes the mobile and stationary phases to fluctuations in ambient temperature, which could have a large effect on pentanol saturation levels (5, 6). In addition, routine column cleanup procedures can be performed without a prolonged reequilibration step. The stripping of pentanol from a reversed-phase stationary support was documented (6).

The following generalizations can be inferred from the data in Table I. Retention times for all drugs increased as the mobile phase polarity increased. The noncharged solutes such as meprobamate, carisoprodol, and methocarbamol had a wide range of retention times in methanol–water systems ($k' = 0.2$–18). Increasing the polarity of the mobile phase (Solvents A → C) predictably increased the k' value for any selected neutral solute. The addition of tetrabutylammonium counterion to the mobile phase (*e.g.*, Solvent C *versus* Solvent F or I) should have further increased the mobile phase polarity, leading to an additional increase in retention time. This increase was not observed. The retention times for the neutral solutes in tetrabutylammonium-containing solvents were the same as or, in many cases, shorter than those observed with methanol–water. This anomaly in the observed retention time can be cited as evidence for the association of tetrabutylammonium counterion with the hydrophobic stationary phase, which renders this phase more polar than when the solvent contains only methanol–water. As a result, the neutral solutes have a lower affinity for the stationary phase and elute in shorter retention times.

Meprobamate was eluted using all solvents employed. A meprobamate–aspirin mixture was separated with any solvent system except G. However, in Solvents A–C, aspirin traveled close to the solvent front and was difficult to distinguish from other components present at the front. Figure 1 illustrates a separation of meprobamate–aspirin using Solvent E, which contained the tetrabutylammonium cation.

All solvent systems were also satisfactory for the elution of methocarbamol. A typical mixture of methocarbamol and aspirin was separated with Solvents A–C, F, and I (Fig. 2).

All solvents were useful for the elution of carisoprodol on the octadecylsilane column. The mixture carisoprodol, phenacetin, and caffeine was separated by any of the mobile phases listed in Table I (Fig. 3).

Chlorzoxazone was satisfactorily eluted on the octadecylsilane column using Solvents A–I. A chlorzoxazone–acetaminophen mixture was separated using any of the solvent systems (Fig. 4).

The elution of acetaminophen was best accomplished with Solvents B, C, F, and I. The retention time for the drug in the remaining solvents was at or near the solvent front, thus rendering it difficult to distinguish clearly between acetaminophen and other components present at the front.

Aspirin traveled at or near the solvent front in the methanol–water systems containing no tetrabutylammonium ion. Addition of tetrabutylammonium ion to the mobile phase caused retention of aspirin on the column, with the retention time increasing as the polarity of the mobile phase increased. There were slight differences in retention time for aspirin in the pH 8 *versus* 6.8 mobile phases.

Caffeine and phenacetin were eluted successfully with all solvent systems. A typical aspirin, phenacetin, and caffeine mixture was satisfactorily separated by Solvents A–C and I.

Satisfactory quantitation of a multicomponent dosage form depends on adequate component resolution. The theoretical parameter, R_s (10), is a reasonable measure of the separation of two species on a column. It can be approximated for any two drugs included in this study from the

Table IV—Analysis of Methocarbamol–Aspirin and Chlorzoxazone–Acetaminophen in Known Mixtures

Mixture	Components	Amount Added, mg	Amount Found[a], mg	Accuracy, %
A	Methocarbamol	8.00[b]	8.19 ± 0.12[c]	2.38
	Aspirin	6.50	6.67 ± 0.13	2.62
B	Acetaminophen	3.00[d]	3.08 ± 0.08[c]	2.67
	Chlorzoxazone	2.51	2.59 ± 0.05	3.19

[a] Based on four replicate determinations of the known mixture. [b] Total mg/25 ml of solution. [c] Confidence limits at $p = 0.05$. [d] Total mg/5 ml of solution.

data contained in Table I[9]. Simulated dosage form mixtures containing methocarbamol–aspirin[10] and chlorzoxazone–acetaminophen[11] were selected for quantitation to exemplify this situation with Solvents I and B, respectively. Both solvent systems allowed good overall resolution with reasonable retention times.

Typical chromatograms of the drug mixtures are shown in Figs. 2 and 4. Various concentrations of stock solutions of each drug dissolved in the appropriate mobile phase (see *Experimental*) were chromatographed using the octadecylsilane column. Phenacetin was added to each solution as the internal standard. The area under the curve for each peak on the chromatograms was determined with an electronic integrator. The ratio of each drug peak area to the area of the internal standard was calculated for each chromatogram. Regression analysis of these data at the various concentrations of each drug gave the slope, intercept, and correlation coefficient for each calibration curve (Tables II and III).

Solutions containing known quantities of methocarbamol–aspirin and/or chlorzoxazone–acetaminophen in ratios equivalent to those found in the commercial dosage forms were chromatographed, and the ratios of drug peak areas to internal standard peak areas (*D/IS*) were calculated for each drug. The slope and intercept data from the regression analysis for each drug (Tables II and III) were used to solve for drug concentration [*D/IS* = (slope × concentration) + intercept][12] in these simulated dosage form mixtures.

The data in Table IV demonstrate the quantitative results obtained for the mixtures. The utility of HPLC in the analysis of methocarbamol–aspirin and chlorzoxazone–acetaminophen mixtures is clearly demonstrated with accuracy in the 2–3% range.

[9] It is possible to calculate the approximate resolution, R_s, of two components by the equation $R_s = 2(t_2 - t_1)/(w_1 + w_2)$, where t_1 and t_2 are retention times and w_1 and w_2 are base peak widths of Compounds 1 and 2, respectively. In past experience, two components with an R_s value >1.50 showed satisfactory resolution for quantification by this analytical technique if the peak areas were approximately equal. A significant difference in peak areas for two components may require an R_s value of 2 or greater.

[10] Robaxisal, A. H. Robins, Richmond, Va.

[11] Parafon-Forte, McNeil Laboratories, Fort Washington, Pa.

[12] Olivetti-Underwood programma 101.

REFERENCES

(1) I. L. Honigberg, J. T. Stewart, and M. Smith, *J. Pharm. Sci.*, **67**, 675 (1978).

(2) J. T. Stewart, I. L. Honigberg, J. P. Brant, W. A. Murray, J. L. Webb, and J. B. Smith, *ibid.*, **65**, 1536 (1976).

(3) S. J. Saxena, J. T. Stewart, I. L. Honigberg, J. G. Washington, and G. R. Keene, *ibid.*, **66**, 813 (1977).

(4) G. Schill, K. O. Borg, R. Modin, and B. A. Persson, in "Handbook of Derivatives for Chromatography," K. Blau and G. S. King, Eds., Heyden and Sons, London, England, 1977, pp. 500–529.

(5) K. G. Wahlund, *J. Chromatogr.*, **115**, 411 (1975).

(6) K. G. Wahlund and U. Lund, *ibid.*, **122**, 269 (1976).

(7) B. L. Karger and B. A. Persson, *J. Chromatogr. Sci.*, **12**, 521 (1974).

(8) B. L. Karger, S. C. Su, S. Marchese, and B. A. Persson, *ibid.*, **12**, 678 (1974).

(9) D. P. Wittmer, N. O. Nuessle, and W. G. Haney, *Anal. Chem.*, **47**, 1422 (1975).

(10) B. L. Karger, L. R. Snyder, and C. Horvath, "An Introduction to Separation Science," Wiley, New York, N.Y., 1973, pp. 146–150.

ACKNOWLEDGMENTS

Presented in part at the Pharmaceutical Analysis and Control Section, APhA Academy of Pharmaceutical Sciences, New York meeting, May 1977.

The authors acknowledge the technical assistance of M. Smith.

Formation of a Thio Analog of Noracronine

J. R. DIMMOCK *x, A. J. REPTA ‡, and JAMES J. KAMINSKI ‡§

Received March 13, 1978, from the **College of Pharmacy, University of Saskatchewan, Saskatoon, Saskatchewan, Canada*, and the ‡*Department of Pharmaceutical Chemistry, University of Kansas, Lawrence, KS 66044.* Accepted for publication May 29, 1978. §Present address: Interx Research Corp., Lawrence, KS 66044.

Abstract □ Acronine was heated with tetraphosphorus decasulfide in benzene to give a mixture of products, the major component (A) being identified tentatively as an unstable product derived from four molecules of noracronine with one molecule of tetraphosphorus decasulfide. Treatment of Compound A with various solvents and heat converted it into a maroon solid (B), which was shown to be 7-thionoracronine.

Keyphrases □ 7-Thionoracronine—synthesized from acronine and tetraphosphorus decasulfide □ Noracronine thio analog—7-thionoracronine synthesized from acronine and tetraphosphorus decasulfide □ Prodrugs, potential—7-thionoracronine synthesized from acronine and tetraphosphorus decasulfide

The alkaloid acronine[1] (I) has a wide spectrum of anticancer activity (1) but the disadvantage of low aqueous solubility. Various attempts have been made (2) to improve the formulation of I, including the preparation of molecular complexes of the alkaloid with povidone and gentisic acid. A prodrug (II) that regenerates acronine quantitatively and shows improved water solubility was prepared but suffers from the disadvantage of being hydrolyzed too rapidly under physiological conditions (3). Reaction of II with aniline gave a rapid quantitative yield of anil[2], and the hydrolysis rates were similar for a series of analogs of II in which the acetyl group was replaced by other acyl functions (2).

Recent studies revealed that hydrolysis in water of II

[1] Previously referred to as acronycine (NSC 403169).

[2] B. Kreilgard, Royal Danish School of Pharmacy, Copenhagen, Denmark, unpublished data.

0022-3549/79/0100-0036$01.00/0

© 1979, American Pharmaceutical Association

Table IV—Analysis of Methocarbamol–Aspirin and Chlorzoxazone–Acetaminophen in Known Mixtures

Mixture	Components	Amount Added, mg	Amount Found[a], mg	Accuracy, %
A	Methocarbamol	8.00[b]	8.19 ± 0.12[c]	2.38
	Aspirin	6.50	6.67 ± 0.13	2.62
B	Acetaminophen	3.00[d]	3.08 ± 0.08[c]	2.67
	Chlorzoxazone	2.51	2.59 ± 0.05	3.19

[a] Based on four replicate determinations of the known mixture. [b] Total mg/25 ml of solution. [c] Confidence limits at $p = 0.05$. [d] Total mg/5 ml of solution.

data contained in Table I[9]. Simulated dosage form mixtures containing methocarbamol–aspirin[10] and chlorzoxazone–acetaminophen[11] were selected for quantitation to exemplify this situation with Solvents I and B, respectively. Both solvent systems allowed good overall resolution with reasonable retention times.

Typical chromatograms of the drug mixtures are shown in Figs. 2 and 4. Various concentrations of stock solutions of each drug dissolved in the appropriate mobile phase (see *Experimental*) were chromatographed using the octadecylsilane column. Phenacetin was added to each solution as the internal standard. The area under the curve for each peak on the chromatograms was determined with an electronic integrator. The ratio of each drug peak area to the area of the internal standard was calculated for each chromatogram. Regression analysis of these data at the various concentrations of each drug gave the slope, intercept, and correlation coefficient for each calibration curve (Tables II and III).

Solutions containing known quantities of methocarbamol–aspirin and/or chlorzoxazone–acetaminophen in ratios equivalent to those found in the commercial dosage forms were chromatographed, and the ratios of drug peak areas to internal standard peak areas (*D/IS*) were calculated for each drug. The slope and intercept data from the regression analysis for each drug (Tables II and III) were used to solve for drug concentration [*D/IS* = (slope × concentration) + intercept][12] in these simulated dosage form mixtures.

The data in Table IV demonstrate the quantitative results obtained for the mixtures. The utility of HPLC in the analysis of methocarbamol–aspirin and chlorzoxazone–acetaminophen mixtures is clearly demonstrated with accuracy in the 2–3% range.

[9] It is possible to calculate the approximate resolution, R_s, of two components by the equation $R_s = 2(t_2 - t_1)/(w_1 + w_2)$, where t_1 and t_2 are retention times and w_1 and w_2 are base peak widths of Compounds 1 and 2, respectively. In past experience, two components with an R_s value >1.50 showed satisfactory resolution for quantification by this analytical technique if the peak areas were approximately equal. A significant difference in peak areas for two components may require an R_s value of 2 or greater.

[10] Robaxisal, A. H. Robins, Richmond, Va.

[11] Parafon-Forte, McNeil Laboratories, Fort Washington, Pa.

[12] Olivetti-Underwood programma 101.

REFERENCES

(1) I. L. Honigberg, J. T. Stewart, and M. Smith, *J. Pharm. Sci.*, **67**, 675 (1978).

(2) J. T. Stewart, I. L. Honigberg, J. P. Brant, W. A. Murray, J. L. Webb, and J. B. Smith, *ibid.*, **65**, 1536 (1976).

(3) S. J. Saxena, J. T. Stewart, I. L. Honigberg, J. G. Washington, and G. R. Keene, *ibid.*, **66**, 813 (1977).

(4) G. Schill, K. O. Borg, R. Modin, and B. A. Persson, in "Handbook of Derivatives for Chromatography," K. Blau and G. S. King, Eds., Heyden and Sons, London, England, 1977, pp. 500–529.

(5) K. G. Wahlund, *J. Chromatogr.*, **115**, 411 (1975).

(6) K. G. Wahlund and U. Lund, *ibid.*, **122**, 269 (1976).

(7) B. L. Karger and B. A. Persson, *J. Chromatogr. Sci.*, **12**, 521 (1974).

(8) B. L. Karger, S. C. Su, S. Marchese, and B. A. Persson, *ibid.*, **12**, 678 (1974).

(9) D. P. Wittmer, N. O. Nuessle, and W. G. Haney, *Anal. Chem.*, **47**, 1422 (1975).

(10) B. L. Karger, L. R. Snyder, and C. Horvath, "An Introduction to Separation Science," Wiley, New York, N.Y., 1973, pp. 146–150.

ACKNOWLEDGMENTS

Presented in part at the Pharmaceutical Analysis and Control Section, APhA Academy of Pharmaceutical Sciences, New York meeting, May 1977.

The authors acknowledge the technical assistance of M. Smith.

Formation of a Thio Analog of Noracronine

J. R. DIMMOCK *x, A. J. REPTA ‡, and JAMES J. KAMINSKI ‡§

Received March 13, 1978, from the **College of Pharmacy, University of Saskatchewan, Saskatoon, Saskatchewan, Canada*, and the ‡*Department of Pharmaceutical Chemistry, University of Kansas, Lawrence, KS 66044.* Accepted for publication May 29, 1978. §Present address: Interx Research Corp., Lawrence, KS 66044.

Abstract □ Acronine was heated with tetraphosphorus decasulfide in benzene to give a mixture of products, the major component (A) being identified tentatively as an unstable product derived from four molecules of noracronine with one molecule of tetraphosphorus decasulfide. Treatment of Compound A with various solvents and heat converted it into a maroon solid (B), which was shown to be 7-thionoracronine.

Keyphrases □ 7-Thionoracronine—synthesized from acronine and tetraphosphorus decasulfide □ Noracronine thio analog—7-thionoracronine synthesized from acronine and tetraphosphorus decasulfide □ Prodrugs, potential—7-thionoracronine synthesized from acronine and tetraphosphorus decasulfide

The alkaloid acronine[1] (I) has a wide spectrum of anticancer activity (1) but the disadvantage of low aqueous solubility. Various attempts have been made (2) to improve the formulation of I, including the preparation of molecular complexes of the alkaloid with povidone and gentisic acid. A prodrug (II) that regenerates acronine quantitatively and shows improved water solubility was prepared but suffers from the disadvantage of being hydrolyzed too rapidly under physiological conditions (3). Reaction of II with aniline gave a rapid quantitative yield of anil[2], and the hydrolysis rates were similar for a series of analogs of II in which the acetyl group was replaced by other acyl functions (2).

Recent studies revealed that hydrolysis in water of II

[1] Previously referred to as acronycine (NSC 403169).

[2] B. Kreilgard, Royal Danish School of Pharmacy, Copenhagen, Denmark, unpublished data.

0022-3549/79/0100-0036$01.00/0

© 1979, American Pharmaceutical Association

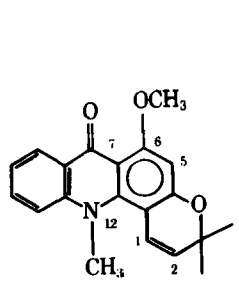

I

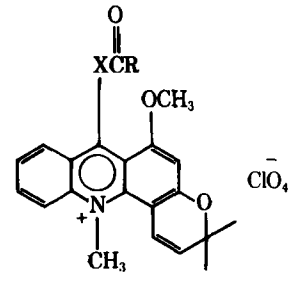

II: X = O
III: X = S

proceeded by aryl–oxygen cleavage to the extent of about 30% (4). It was considered that molecular modification of II to give the thioesters (III) would enhance the propensity for acyl–sulfur fission since the carbon–sulfur bond would be less susceptible to rupture than the carbon–oxygen bond of II. If this theory is validated in practice, variation in the nature of the thioester function would permit controlled alteration in the hydrolysis rate of III to thioacronine, which could undergo biotransformation to acronine. Such replacement of sulfur by oxygen in drug molecules is well established (5, 6).

DISCUSSION

A synthetic route to produce III (R = CH_3) involved the conversion of acronine to 7-thioacronine (IV), followed by treatment with perchloric acid and acylation with acetic anhydride. Various synthetic procedures are available for converting oxo derivatives to the corresponding thio analogs, including the use of tetraphosphorus decasulfide (P_4S_{10}) in several organic solvents (7, 8). Reaction of acronine with tetraphosphorus decasulfide gave a maroon solid; TLC showed that the principal component (A) was present to an extent of 64%. Preparative TLC led to the isolation of small quantities of Compound A, which was unstable to both heat and solvents, invariably breaking down to Compound B, which appeared to be stable. Mass spectrometry of both A and B showed molecular ions at 323 mass units.

The structure of the stable compound (B), which was formed by heating the crude reaction product between acronine and tetraphosphorus decasulfide in methanol, was investigated since knowledge of its structure might elucidate the nature of Compound A. Elemental analysis of B revealed the presence of carbon, hydrogen, nitrogen, oxygen, and sulfur. Since the molecular weight of 323 was found by mass spectrometry, an elemental formula for B of $C_{19}H_{17}NO_2S$ was suggested; *i.e.*, in comparison to acronine ($C_{20}H_{19}NO_3$), a methylene group appears to have been lost and one of the oxygen atoms replaced by sulfur.

Two possibilities for the structure of B would be replacement of the 6-methoxy group by sulfur to give V and, alternatively, replacement of the 7-oxo function by sulfur during or subsequent to *O*-demethylation to give VI. It is well established that acronine undergoes *O*-demethylation in the presence of heat and acid (9, 10), and Compound B gave a black color with alcoholic ferric chloride solution.

Electronic absorption spectroscopy was considered a useful tool to differentiate between V and VI since thioketones absorb at much longer wavelengths than the analogous ketones (11) and, with thiophenols and phenols, the long wavelength absorptions differ by less than 15 nm (12). The model Compounds VII and VIII were prepared, and the long wavelength absorptions of the thio VIII were greater than VII by 91 nm (Table I). Thus, if Compound B had Structure V, it would be expected to absorb

Table I—Long Wavelength Electronic Absorptions of VII, VIII, I, IX, and B

Compound	λ_{max}, nm (ϵ)
VII	400 (8555)
VIII	491 (32,750)
I	390 (6820)
IX	410 (5030)
B	490 (5610)

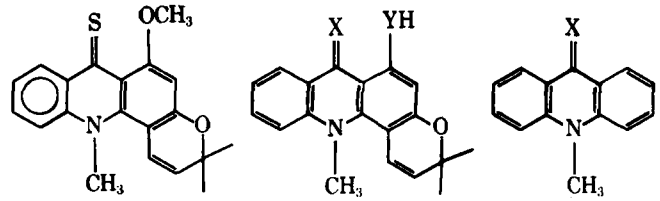

IV

V: X = O, Y = S
VI: X = S, Y = O

VII: X = O
VIII: X = S

at similar wavelengths to 6-noracronine (IX), whose preparation was described previously (9, 10); VI would be predicted to exhibit an absorption maximum at approximately 90 nm greater than that of noracronine.

The visible spectrum of B showed a long wavelength absorption at 80 nm higher than noracronine and at virtually the same wavelength as 10-methyl-9-thioacridone (VIII). The virtual insolubility of B in organic solvents and water prevented its examination by both PMR spectroscopy and pKa determinations and, although positions for IR C=S absorptions were quoted (13, 14), it also was concluded (15) that meaningful assignments cannot be made. Thus, on the basis of elemental analysis, electronic absorption spectroscopy, and mass spectrometry, it appears that B may be best represented as the thioketone VI.

The question arises as to the nature of the unstable purple component (A) isolated in the initial reaction between acronine and tetraphosphorus decasulfide. Elemental analysis revealed the presence of carbon, hydrogen, oxygen, nitrogen, sulfur, and phosphorus. While the instability of the molecule precludes a dogmatic assertion of its identity, a molecular formula of $C_{76}H_{68}N_4O_{12}P_4S_{10}$, corresponding to an organophosphorus complex of four molecules of noracronine with one molecule of tetraphosphorus decasulfide, appears feasible. Such a complex could be formed after initial *O*-demethylation of the 6-methoxy group of acronine to produce noracronine (IX), which could react with each sulfur atom of the P=S linkage of tetraphosphorus decasulfide, whose molecular architecture is clearly documented (16) (Scheme I)[3].

Although such organophosphorus intermediates are unstable and rarely isolated, hydrogen bonding between the 6-hydroxy group of noracronine and the nearby sulfur atoms may stabilize the intermediate. Such a structure as A resembles trithianes, which are decomposed by heat to yield the monomeric thiones (17); hence, A could break down to B in the presence of heat or solvent. Finally, reaction of noracronine with tetraphosphorus decasulfide yielded the purple Compound A, which strengthens further the hypothesis that a 6-hydroxy group is present in A.

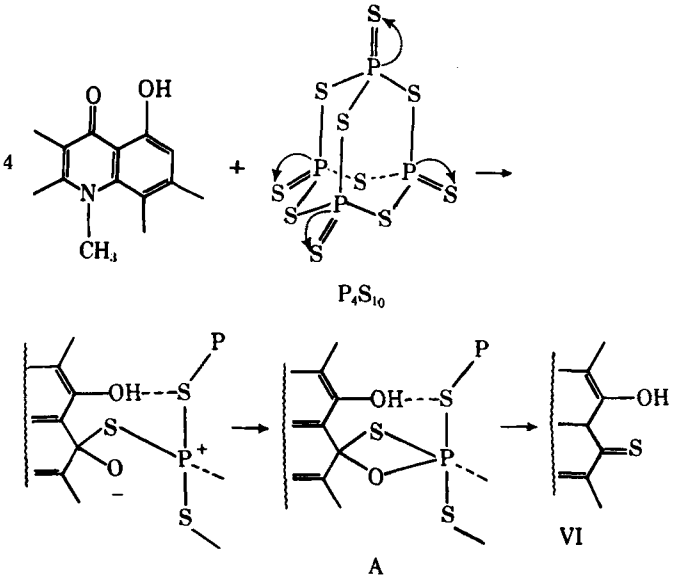

Scheme I

[3] Reaction of only one molecule of noracronine with tetraphosphorus decasulfide is shown. It is postulated that one molecule of IX reacts with each of the four P=S bonds of tetraphosphorus decasulfide.

Other attempts were made to produce 7-thioacronine (IV) through reaction of 7-acetylacroninium perchlorate with sodium hydrogen sulfide and the thioacetate ion in aqueous solution. In these cases, it was anticipated that the sulfur nucleophile would displace the acetate group (4) of II. Only B was obtained from these reactions, indicating the lability of the 6-methoxy group of the precursor ester.

Alternative synthetic pathways to the desired thio analog of acronine apparently are required to avoid the demethylation of the 6-methoxy group of acronine and/or the acroninium esters.

EXPERIMENTAL[4]

Melting points are uncorrected. Solvents were dried initially over anhydrous magnesium sulfate and then stored over drying granules[5]. IR spectra[6] were determined as potassium bromide disks, the instrument being previously calibrated with polystyrene. NMR spectra[7] were run in deuterochloroform or trifluoroacetic acid, and tetramethylsilane was used as the internal and external standard. Electronic absorption spectra[8] were determined by dissolving the compound in dimethylacetamide (1 ml) and diluting the solution to 100 ml with methylene chloride; further dilutions with methylene chloride were undertaken when required.

TLC was conducted on silica gel plastic sheets[9], 0.25 mm thick; where appropriate, quantitative estimations[10] of the chromatograms were made. Preparative TLC employed 2-mm silica gel plates[11]. Acronine[12] had λ_{max} 390 nm (ϵ 6820) and R_f 0.28 on silica gel with benzene–acetone (2:1) as the developing solvent.

Reaction of Acronine with Tetraphosphorus Decasulfide—A mixture of acronine (0.5975 g, 0.001861 mole) and tetraphosphorus decasulfide (0.6 g, 0.002703 mole) in dry benzene (18 ml) was heated under reflux with stirring for 2 hr. The mixture was decanted while hot, leaving a maroon solid. This material was removed from the reaction vessel, dried in a vacuum desiccator, and weighed (0.9363 g). TLC on silica gel plastic sheets using benzene–acetone (2:1) revealed the presence of compounds at R_f 0, 0.026, 0.073, 0.28, and 0.59. When viewed under long wavelength UV light, an additional spot, R_f 0.36, became apparent.

Under these conditions, acronine has an R_f value of 0.31 and fluoresces under long wavelength UV light; no acronine was detected in this experiment. Quantitation of the chromatogram indicated that the purple component (A), R_f 0.28, was present to the extent of 64%. When the reaction was carried out in the presence of carbon dioxide, A represented 44% of the mixture.

A small quantity of the crude reaction mixture (0.15 g) was triturated rapidly with chloroform–methanol (9:1), placed on two preparative silica gel plates, and chromatographed with benzene–acetone (2:1). The purple layer was removed and extracted several times with methylene chloride, and the organic extract was dried (anhydrous sodium sulfate). Removal of the solvent *in vacuo* at room temperature yielded A as purple crystals (0.010 g), and TLC showed one component; mass spectrum: parent ion *m/e*: 323.09658 (calc. for $C_{19}H_{17}NO_2S$: 323.09790).

Anal.—Calc. for $C_{76}H_{68}N_4O_{12}P_4S_{10}$: C, 54.23; H, 4.10; N, 3.35; P, 7.40; S, 19.16. Found: C, 57.73; H, 6.39; N, 2.46; P, 6.64; S, 17.72.

The stability of Compound A was investigated. A small quantity of the crude reaction product was chromatographed on silica gel, and the purple layer containing A was removed. Approximately equal quantities of silica gel containing A were placed in stoppered containers and triturated with the following solvents: benzene, acetone, chloroform, methylene chloride, chloroform–methanol (9:1 v/v), pyridine, and methanol. After 20 min, a small quantity of the slurry was placed on a silica gel plastic sheet and chromatographed with benzene–acetone (2:1). An orange spot, R_f 0.54, was found in the pyridine solution while the methanol extract showed the presence of the major component at the point of application. The remaining solutions showed the presence of only Compound A.

After 3 days, chromatograms of each solution showed the presence of an orange spot, R_f 0.59; in solutions of benzene and pyridine, no other compounds were seen. In another experiment, small quantities of A were placed in each of six stoppered containers. Three vials were stored at room temperature, 4°, and −17°; one was stored at room temperature under nitrogen; and another vial was stored at room temperature protected from light. In each case, TLC on the following day showed only A; a sixth sample, heated to 70° overnight, gave an orange spot, R_f 0.57, as the major component.

Preparation of 7-Thionoracronine (VI)—The crude mixture (4.9946 g) obtained by reacting acronine with tetraphosphorus decasulfide was heated under reflux with methanol (50 ml) for 37 min, and the hot mixture was filtered. The maroon residue obtained (0.7948 g), mp 193°, was recrystallized repeatedly from ethyl acetate to give VI (0.4046 g), mp 223° dec., as maroon prisms. An alcoholic solution of the compound gave a black color with alcoholic ferric chloride solution. High-resolution mass spectrometry indicated a molecular ion of 323.09572 (calc. for $C_{19}H_{17}NO_2S$: 323.09790); IR: 2270 w, 1630 s, and 1595 s cm^{-1}; UV (λ_{max}): 490 (ϵ 5610) and 410 (18,100) nm.

Anal.—Calc. for $C_{19}H_{17}NO_2S$: C, 70.57; H, 5.29; N, 4.33; O, 9.90; S, 9.90. Found: C, 70.24; H, 5.32; N, 4.03; O, 10.10; S, 9.81.

Preparation of Noracronine—Acronine hydrochloride, prepared from 5.0 g of acronine, was heated at 145–174° for 94 min (9, 10) to give a gold-yellow mass, mp 118.5–194° (4.23 g), shown by quantitative TLC to consist of noracronine (79%) and acronine (21%). Four recrystallizations from ethanol gave pure noracronine (1.42 g, 30%), mp 200° [lit. (10) mp 198–200°], as pale-orange crystals; NMR (deuterochloroform): δ 1.54 [s, 6H, 3-$(CH_3)_2$], 3.89 [s, 3H, $N(CH_3)_2$], 5.51 (d, J = 5 Hz, 1H, 2-H), 6.28 (s, 1H, 5-H), 6.57 (d, J = 5 Hz, 1H, 1-H), 7.12–8.50 (m, 4H, H at C-8, C-9, C-10, and C-11), and 14.78 (s, 1H, 6-OH, exchanged with D_2O) ppm; UV (λ_{max}): 410 (ϵ 5030) nm.

Noracronine (0.15 g, 0.00049 mole) and tetraphosphorus decasulfide (0.15 g, 0.00068 mole) were heated together in dry benzene (55 ml) for 2 hr, and the hot mother liquid was decanted. The residue (0.2110 g) was dried in a desiccator. TLC showed a purple spot, R_f 0.44, as the major component and minor products at R_f 0.65 and 0.097, as well as some material at the point of application. Compounds VI and VIII, when chromatographed simultaneously, had R_f values of 0.61 and 0.59, respectively.

Preparation of 10-Methyl-9(10*H*)-acridone (VII)—Acridine (1.4677 g, 0.00820 mole) and dimethyl sulfate (4.00 g, 0.0317 mole) were heated together in dry benzene (15 ml) for 70 min, and the deposited yellow crystals were removed by filtration to give 10-methylacridinium methylsulfate (2.1 g), mp 214–215° dec. The methylsulfate was oxidized with potassium ferricyanide in potassium hydroxide solution, using the reported method for the preparation of 1,3-dimethoxy-10-methylacridone from the corresponding methylsulfate (18), to give a light-brown crystalline mass, which was shaken with chloroform and water. The chloroform extract was separated, washed with water, and dried (anhydrous magnesium sulfate). Evaporation of the solvent gave yellow crystals, which were recrystallized from methanol to yield VII (50%), mp 202–202.5° [lit. (19) mp 202°]; UV (λ_{max}): 400 (ϵ 11,750) and 380 (8555) nm.

Preparation of 10-Methyl-9(10*H*)-thioacridone (VIII)—10-Methyl-9-chloroacridinium dichlorophosphate, prepared from VII (11.00 g) by a reported method (20), was added to a stirred solution of sodium hydrogen sulfide dihydrate (4.27 g) in ethanol (119 ml). After stirring at room temperature for 1 hr, the precipitate was collected by filtration, washed repeatedly with water to remove unreacted sodium hydrogen sulfide dihydrate, and dried to give deep-red needles (11.64 g). Eight recrystallizations from dry xylene gave VIII (2.68 g, 23%), mp 265.5–267° [lit. (21) mp 263°]; UV (λ_{max}): 491 (ϵ 32,750) and 461 (17,960) nm.

Reaction of Acetylacroninium Perchlorate with Sodium Hydrogen Sulfide and Thioacetic Acid—A solution of sodium hydrogen sulfide dihydrate (0.04 g, 0.00043 mole) in water (10 ml) was added to a stirring solution of acetylacroninium perchlorate (0.0261 g, 0.000056 mole) in water (100 ml). After the mixture had stirred at room temperature for 1 hr, the precipitate was collected and dried at room temperature in a desiccator. TLC indicated the presence of four compounds with R_f values of 0.014, 0.070, and 0.34 and an orange spot with a value of 0.65. Another spot, R_f 0.52, was visible under short wavelength UV light. TLC of the acetylacroninium perchlorate sample indicated components with similar R_f values and color corresponding to the spots with the three lowest R_f values of the compound isolated in the reaction.

Increasing the molar ratio of sodium hydrogen sulfide dihydrate and acetylacroninium perchlorate to 111:1 gave a product with similar TLC

---

[4] Elemental analyses were carried out by Mr. T. N. Nguyen, Department of Medicinal Chemistry, College of Pharmacy, University of Kansas, Lawrence, KS 66044, Schwarzkopf Microanalytical Laboratories, Woodside, NY 11377, and Mr. R. G. Teed, Department of Chemistry and Chemical Engineering, University of Saskatchewan, Saskatoon, Saskatchewan, Canada. Mass spectra were determined by Mr. R. Drake, Department of Chemistry, University of Kansas, Lawrence, KS 66044, on a CH-5 instrument (Varian Associates, Chicago, IL 60670).

[5] Linde molecular sieve, type 4A, Union Carbide Corp., Chicago, IL 60638.

[6] Beckman AccuLab 4, Irvine, CA 92664.

[7] T-60 spectrometer, Varian Associates, Chicago, IL 60670.

[8] Cary 15 spectrophotometer, Varian Associates, Chicago, IL 60670.

[9] Polygram, Brinkmann Instruments, Westbury, NY 11590.

[10] TLC densitometer (Kontes, Vineland, NJ 08360) attached to a potentiometric amplifier, dc offset module, and strip-chart recorder (Heath Co., Benton Harbor, MI 49022).

[11] Silica gel 60, F-254 TLC plates, Brinkmann Instruments, Des Plaines, IL 60016.

[12] Obtained from the National Cancer Institute, Bethesda, MD 20014.

characteristics as in the previous experiment, although the intensity of the orange compound was increased.

A solution of sodium hydrogen sulfide dihydrate (0.3146 g, 0.0034 mole) in propylene glycol (3.7 ml) and a solution of acetylacroninium perchlorate (0.0110 g, 0.000034 mole) in propylene glycol (4.7 ml) were stirred at room temperature for 1 hr. The resultant viscous, orange solution was poured into water (20 ml), and the yellow precipitate was collected and dried. TLC showed a yellow component (with similar R_f value and fluorescence properties as acronine) and an orange component, R_f 0.70, as the major product.

In a further experiment, acetylacroninium perchlorate (0.0245 g, 0.0000528 mole) was added to a stirred solution of thioacetic acid (0.4296 g, 0.00565 mole) and sodium hydroxide (0.20 g, 0.005 mole) in water (100 ml). After stirring at room temperature for 1 hr, the precipitate was collected and dried. TLC showed a yellow spot, R_f 0.39, fluorescing under UV light and an orange component, R_f 0.68, in major amount.

REFERENCES

(1) G. H. Svoboda, G. A. Poore, P. J. Simpson, and G. B. Bodor, *J. Pharm. Sci.*, **55**, 758 (1966).

(2) A. J. Repta, in "Prodrugs as Novel Drug Delivery Systems," T. Higuchi and V. Stella, Eds., American Chemical Society, Washington, D.C., 1975, p. 196.

(3) D. W. A. Bourne, T. Higuchi, and A. J. Repta, *J. Pharm. Sci.*, **66**, 628 (1977).

(4) A. J. Repta, J. R. Dimmock, B. Kreilgard, and J. J. Kaminski, *ibid.*, **66**, 1501 (1977).

(5) "The Pharmacological Basis of Therapeutics," 3rd ed., L. S. Goodman and A. Gilman, Eds., Macmillan, New York, N.Y., 1965, p. 120.

(6) A. Albert, "Selective Toxicity," 3rd ed., Wiley, New York, N.Y., 1965, p. 281.

(7) H. de Diesbach and H. Kramer, *Helv. Chim. Acta*, **28**, 1399 (1945).

(8) W. Baker, J. B. Harborne, and W. D. Ollis, *J. Chem. Soc.*, **1952**, 1303.

(9) R. D. Brown, L. J. Drummond, F. N. Lahey, and W. C. Thomas, *Aust. J. Sci. Res.*, **A2**, 622 (1949).

(10) T. R. Govindachari, B. R. Pai, and P. S. Subramanian, *Tetrahedron*, **22**, 3245 (1966).

(11) H. H. Jaffe and M. Orchin, "Theory and Applications of Ultraviolet Spectroscopy," Wiley, New York, N.Y., 1962, p. 182.

(12) *Ibid.*, p. 477.

(13) K. Nakaniski, "Infrared Absorption Spectroscopy–Practical," Holden-Day, San Francisco, Calif., 1962, p. 54.

(14) R. M. Silverstein and G. C. Bassler, "Spectrometric Identification of Organic Compounds," 2nd ed., Wiley, New York, N.Y., 1967, p. 76.

(15) L. J. Bellamy, "The Infra-Red Spectra of Complex Molecules," Wiley, New York, N.Y., 1954, p. 293, and references cited therein.

(16) R. B. Heslop and K. Jones, "Inorganic Chemistry and a Guide to Advanced Study," Elsevier, Amsterdam, The Netherlands, 1976, p. 444.

(17) E. Campaigne, in "The Chemistry of Carbonyl Compounds," S. Patai, Ed., Interscience, London, England, 1966, p. 931, and references cited therein.

(18) G. K. Hughes and E. Ritchie, *Aust. J. Sci. Res.*, **A2**, 423 (1949).

(19) K. D. Legg and D. M. Hercules, *J. Am. Chem. Soc.*, **91**, 1902 (1969).

(20) A. Albert, "The Acridines," Edward Arnold, London, England, 1951, p. 228.

(21) K. Gleu and S. Nitzsche, *J. Prakt. Chem.*, **153**, 225 (1939).

ACKNOWLEDGMENTS

Supported in part by Contract N01 CM 23217 from the Drug Development Branch, Division of Cancer Treatment, National Cancer Institute, National Institutes of Health, Bethesda, Md.

The authors acknowledge the assistance of Wanda Waugh, Stan Rippel, and D. L. Kirkpatrick. Dr. J. R. Dimmock acknowledges that much of the work was made possible by the sabbatical leave provided him by the College of Pharmacy, University of Saskatchewan.

Molecular Connectivity Study of Halocarbon Anesthetics

THÉRÈSE DI PAOLO *¶×, LEMONT B. KIER ‡, and LOWELL H. HALL §

Received February 3, 1978, from the **Massachusetts College of Pharmacy, Boston, MA 02115*, the ‡*Department of Pharmaceutical Chemistry, Medical College of Virginia, Richmond, VA 23298*, and the §*Department of Chemistry, Eastern Nazarene College, Quincy, MA 02169.* Accepted for publication May 19, 1978. ¶Present address: Medical Research Council Group in Molecular Endocrinology, Centre Hospitalier de l'Université Laval, Quebec G1V 4G2, Canada.

Abstract □ The structure–activity relationships of 45 halogenated hydrocarbons using molecular connectivity were studied. A very good correlation was obtained between the anesthetic activity and the molecular connectivity term ${}^0\chi^v$ in addition to the polar hydrogen factor, Q_H. The equation reported accounts for and quantifies the known structure–activity observations on general anesthetics. The results are discussed briefly with reference to the mechanisms of action of general anesthetics.

Keyphrases □ Molecular connectivity indexes—related to anesthetic activity of various halogenated hydrocarbons □ Halogenated hydrocarbons, various—molecular connectivity indexes related to anesthetic activity □ Anesthetic activity—various halogenated hydrocarbons, related to molecular connectivity indexes □ Structure–activity relationships—molecular connectivity indexes related to anesthetic activity of various halogenated hydrocarbons □ Topological indexes—molecular connectivity, related to anesthetic activity of various halogenated hydrocarbons

To derive information about the mechanism of action of anesthetic gases, some investigators attempted to relate potency to physicochemical properties, including boiling points, solubilities, partition coefficients, molar volumes, molar refractions, and van der Waals equation constants. The finding of a significant correlation indicated that mechanisms of action parallel the physicochemical property.

These property studies (1) did not give any direct insight into the structural features influencing potency. The first real effort to gain such insight used a calculation of molecular structure known as molecular connectivity (2). That study, on a diverse group of anesthetic gases, resulted in a good correlation between potency and a combination of a molecular connectivity index and an electronic charge description. The correlation (r = 0.982) was good enough

0022-3549/79/0100-0039$01.00/0

© 1979, American Pharmaceutical Association

characteristics as in the previous experiment, although the intensity of the orange compound was increased.

A solution of sodium hydrogen sulfide dihydrate (0.3146 g, 0.0034 mole) in propylene glycol (3.7 ml) and a solution of acetylacroninium perchlorate (0.0110 g, 0.000034 mole) in propylene glycol (4.7 ml) were stirred at room temperature for 1 hr. The resultant viscous, orange solution was poured into water (20 ml), and the yellow precipitate was collected and dried. TLC showed a yellow component (with similar R_f value and fluorescence properties as acronine) and an orange component, R_f 0.70, as the major product.

In a further experiment, acetylacroninium perchlorate (0.0245 g, 0.0000528 mole) was added to a stirred solution of thioacetic acid (0.4296 g, 0.00565 mole) and sodium hydroxide (0.20 g, 0.005 mole) in water (100 ml). After stirring at room temperature for 1 hr, the precipitate was collected and dried. TLC showed a yellow spot, R_f 0.39, fluorescing under UV light and an orange component, R_f 0.68, in major amount.

REFERENCES

(1) G. H. Svoboda, G. A. Poore, P. J. Simpson, and G. B. Bodor, *J. Pharm. Sci.*, **55**, 758 (1966).

(2) A. J. Repta, in "Prodrugs as Novel Drug Delivery Systems," T. Higuchi and V. Stella, Eds., American Chemical Society, Washington, D.C., 1975, p. 196.

(3) D. W. A. Bourne, T. Higuchi, and A. J. Repta, *J. Pharm. Sci.*, **66**, 628 (1977).

(4) A. J. Repta, J. R. Dimmock, B. Kreilgard, and J. J. Kaminski, *ibid.*, **66**, 1501 (1977).

(5) "The Pharmacological Basis of Therapeutics," 3rd ed., L. S. Goodman and A. Gilman, Eds., Macmillan, New York, N.Y., 1965, p. 120.

(6) A. Albert, "Selective Toxicity," 3rd ed., Wiley, New York, N.Y., 1965, p. 281.

(7) H. de Diesbach and H. Kramer, *Helv. Chim. Acta*, **28**, 1399 (1945).

(8) W. Baker, J. B. Harborne, and W. D. Ollis, *J. Chem. Soc.*, **1952**, 1303.

(9) R. D. Brown, L. J. Drummond, F. N. Lahey, and W. C. Thomas, *Aust. J. Sci. Res.*, **A2**, 622 (1949).

(10) T. R. Govindachari, B. R. Pai, and P. S. Subramanian, *Tetrahedron*, **22**, 3245 (1966).

(11) H. H. Jaffe and M. Orchin, "Theory and Applications of Ultraviolet Spectroscopy," Wiley, New York, N.Y., 1962, p. 182.

(12) *Ibid.*, p. 477.

(13) K. Nakaniski, "Infrared Absorption Spectroscopy–Practical," Holden-Day, San Francisco, Calif., 1962, p. 54.

(14) R. M. Silverstein and G. C. Bassler, "Spectrometric Identification of Organic Compounds," 2nd ed., Wiley, New York, N.Y., 1967, p. 76.

(15) L. J. Bellamy, "The Infra-Red Spectra of Complex Molecules," Wiley, New York, N.Y., 1954, p. 293, and references cited therein.

(16) R. B. Heslop and K. Jones, "Inorganic Chemistry and a Guide to Advanced Study," Elsevier, Amsterdam, The Netherlands, 1976, p. 444.

(17) E. Campaigne, in "The Chemistry of Carbonyl Compounds," S. Patai, Ed., Interscience, London, England, 1966, p. 931, and references cited therein.

(18) G. K. Hughes and E. Ritchie, *Aust. J. Sci. Res.*, **A2**, 423 (1949).

(19) K. D. Legg and D. M. Hercules, *J. Am. Chem. Soc.*, **91**, 1902 (1969).

(20) A. Albert, "The Acridines," Edward Arnold, London, England, 1951, p. 228.

(21) K. Gleu and S. Nitzsche, *J. Prakt. Chem.*, **153**, 225 (1939).

ACKNOWLEDGMENTS

Supported in part by Contract N01 CM 23217 from the Drug Development Branch, Division of Cancer Treatment, National Cancer Institute, National Institutes of Health, Bethesda, Md.

The authors acknowledge the assistance of Wanda Waugh, Stan Rippel, and D. L. Kirkpatrick. Dr. J. R. Dimmock acknowledges that much of the work was made possible by the sabbatical leave provided him by the College of Pharmacy, University of Saskatchewan.

Molecular Connectivity Study of Halocarbon Anesthetics

THÉRÈSE DI PAOLO *¶×, LEMONT B. KIER ‡, and LOWELL H. HALL §

Received February 3, 1978, from the **Massachusetts College of Pharmacy, Boston, MA 02115*, the ‡*Department of Pharmaceutical Chemistry, Medical College of Virginia, Richmond, VA 23298*, and the §*Department of Chemistry, Eastern Nazarene College, Quincy, MA 02169.* Accepted for publication May 19, 1978. ¶Present address: Medical Research Council Group in Molecular Endocrinology, Centre Hospitalier de l'Université Laval, Quebec G1V 4G2, Canada.

Abstract □ The structure–activity relationships of 45 halogenated hydrocarbons using molecular connectivity were studied. A very good correlation was obtained between the anesthetic activity and the molecular connectivity term ${}^0\chi^v$ in addition to the polar hydrogen factor, Q_H. The equation reported accounts for and quantifies the known structure–activity observations on general anesthetics. The results are discussed briefly with reference to the mechanisms of action of general anesthetics.

Keyphrases □ Molecular connectivity indexes—related to anesthetic activity of various halogenated hydrocarbons □ Halogenated hydrocarbons, various—molecular connectivity indexes related to anesthetic activity □ Anesthetic activity—various halogenated hydrocarbons, related to molecular connectivity indexes □ Structure–activity relationships—molecular connectivity indexes related to anesthetic activity of various halogenated hydrocarbons □ Topological indexes—molecular connectivity, related to anesthetic activity of various halogenated hydrocarbons

To derive information about the mechanism of action of anesthetic gases, some investigators attempted to relate potency to physicochemical properties, including boiling points, solubilities, partition coefficients, molar volumes, molar refractions, and van der Waals equation constants. The finding of a significant correlation indicated that mechanisms of action parallel the physicochemical property.

These property studies (1) did not give any direct insight into the structural features influencing potency. The first real effort to gain such insight used a calculation of molecular structure known as molecular connectivity (2). That study, on a diverse group of anesthetic gases, resulted in a good correlation between potency and a combination of a molecular connectivity index and an electronic charge description. The correlation (r = 0.982) was good enough

0022-3549/79/0100-0039$01.00/0

© 1979, American Pharmaceutical Association

Table I—CH Bond Polarity Indexes

Halogen	Q_H Contribution
F	0.43
Cl	0.41
Br	0.44
I	0.40
α-F	0.13
α-Cl	0.10
α-Br	0.09
β-F	0.05
β-Cl	0.05
β-Br	0.05

to permit the prediction of the potency trend in eight other anesthetic gases. Of equal importance was the utility of the relating equation for describing some important structural features influencing the anesthetic potency.

Structure–activity relationship studies of anesthetic activity were pursued on other groups of molecules to study and isolate the factors affecting activity. A structure–activity study on a group of anesthetic ethers where the polarity of the hydrogens is fairly constant gave very high correlations with a molecular connectivity term (3). A nonlinear structure–activity study of a group of hydrocarbon, ether, and ketone anesthetics also gave very good correlations with two molecular connectivity terms (4).

Another group of molecules with general anesthetic potency is the halocarbons. The potency of 45 halocarbons was reported (5) and served as a basis for the present study of the structure–activity relationship. This study extends the opportunity to probe the important structural features influencing anesthetic potency and, more specifically, the effect of polar hydrogens.

EXPERIMENTAL

The method of structural description, molecular connectivity, describes numerically the branching, unsaturation, cyclization, and heteroatom presence and position in a molecule (2, 6–9).

The polar nature of hydrogen atoms previously was found to be an important structural characteristic (2). Similarly, in this study, the polar hydrogen was found to influence potency. The quantification of this polarity was undertaken at a subquantum mechanical level, because the general utility of a possible structure–activity correlation lies in the general ease with which such an index may be calculated.

Accordingly, a polar hydrogen index was computed as a derivative of the Swain and Lupton F values (10, 11). The F value is the relative field effect (as opposed to the resonance effect) on an atom or group influencing the Hammet σ constant.

The F values are used directly as an index of the polarity of CH bonds. The F value (Table I) of chlorine is 0.41. This index is used to describe the polarity of the CH bond in the fragment ClCH. The total polarity index of the CH bond is a sum of the effects arising from all halogens; therefore, the CH bond polarity index in chloroform is 3 (0.41) = 1.23. In dichloromethane, the two equivalent CH bonds must be reckoned as $2 \times 0.41 = 0.82$ each.

For the influence of halogen atoms on carbon atoms attached to the primary CH fragment, a diminished influence is used in the Swain and Lupton system. From the F values for the fragment ClCCH, the influence of an α-chlorine atom on the CH bond polarity value is 0.10. Halogens on β-carbons were approximated as only contributing 0.05 each to the CH bond polarity total.

Summation of all polarity influencing values, Q_{Hi}, gives a total CH bond polarity, Q_H, which might also be used as a structural descriptor coupled with connectivity indexes in an analysis of halocarbon structure–activity relationships.

In cases where no halogen is attached to a CH fragment, the Q_H is taken as zero, as in V, VII, IX, X, XIX, XXVIII, XXX, XXXV, and XLIII–XLV. Two exceptions to this rule are XXIX and XXXIV, in which a methylene group is flanked by two halogen-substituted methyl groups. Here, the computed total Q_H value was obtained as a sum of both CH fragments.

RESULTS AND DISCUSSION

For the analysis of the data set, the molecular connectivity indexes ${}^m\chi_t$ were calculated through the third order ($m = 3$) for the path indexes ($t = P$) and for the ${}^3\chi_c$ index. Also, the corresponding valence indexes ${}^m\chi_t{}^v$ were calculated and entered into the data file. For each observation, then, there are 10 indexes as variables. Multiple linear correlations were run between the variables and the anesthetic potency, considering all possible single variables as well as all pairs and triplets.

The single χ index giving the best correlation against log AD_{50} was ${}^0\chi^v$. No other variable gave a correlation significantly close to that for ${}^0\chi^v$, $r = 0.70$. This result is consistent with that found for two other sets of general anesthetics (2, 3).

To obtain an equation that accurately represents the data, the questions to be resolved center on the characterization of the polar hydrogen atoms. Should the effects of all such hydrogens be summed? Do all polar hydrogens affect the anesthetic potency equivalently?

A plot of log AD_{50} *versus* ${}^0\chi^v$ gives some helpful indications. Compounds with nonpolar or only very slightly polar hydrogens fall along the same line as compounds with no hydrogen atoms. The compounds with polar hydrogens fall below that line; the more polar the hydrogen, or the greater the number of polar hydrogens, the further below the line they fall. This general observation suggests that there is a minimum value for polarity to activate the hydrogen atom in the physiological process.

Following this line of thought, polarity variables were calculated for each hydrogen, Q_{Hi}, in a molecule as already described and regressions were run along with the variable ${}^0\chi^v$. The following equations were obtained:

$$\log_e AD_{50} = 5.14 - 0.959{}^0\chi^v - 1.53Q_{H1} \quad \text{(Eq. 1)}$$

$$r = 0.86 \quad s = 0.63 \quad F = 59 \quad n = 45$$

$$\log_e AD_{50} = 6.04 - 1.05{}^0\chi^v - 1.68Q_{H1} - 1.49Q_{H2} \quad \text{(Eq. 2)}$$

$$r = 0.96 \quad s = 0.34 \quad F = 177 \quad n = 45$$

$$\log_e AD_{50} = 6.15 - 1.06{}^0\chi^v - 1.71Q_{H1} - 1.34Q_{H2} - 0.549Q_{H3} \quad \text{(Eq. 3)}$$

$$r = 0.97 \quad s = 0.32 \quad F = 151 \quad n = 45$$

where Q_{H1} represents the most polar CH bond, Q_{H2} represents the second most polar, and so on. Examination of residuals clearly indicates that compounds with slightly polar hydrogens (V, IX, XXVIII, XXX, XXXV, and XLIII–XLV) are predicted too small, indicating that Q_{Hi} should be set to zero up to a threshold value. The Q_H values for these hydrogens range up to about 0.36. There is a significant break in the Q_H values up to about 0.67. Thus, a useful threshold value of about 0.50 can be tested. The statistical results are as follows:

$$\log_e AD_{50} = 4.78 - 0.94{}^0\chi^v - 1.30Q_{H1} \quad \text{(Eq. 4)}$$

$$r = 0.87 \quad s = 0.60 \quad F = 67 \quad n = 45$$

$$\log_e AD_{50} = 5.17 - 1.00{}^0\chi^v - 1.12Q_{H1} - 1.32Q_{H2} \quad \text{(Eq. 5)}$$

$$r = 0.97 \quad s = 0.32 \quad F = 194 \quad n = 45$$

$$\log_e AD_{50} = 5.19 - 0.993{}^0\chi^v - 1.13Q_{H1} - 1.12Q_{H2} - 0.800Q_{H3} \quad \text{(Eq. 6)}$$

$$r = 0.976 \quad s = 0.27 \quad F = 204 \quad n = 45$$

There is some improvement in the correlation statistics and achievement of a better distribution of residuals.

From Eqs. 4–6, it appears that the influence of each polar hydrogen is not greatly different. Hence, it is of interest to investigate a Q_H variable that is a summation of all the polar hydrogen terms (above the threshold).

The equation based upon ${}^0\chi^v$ and $Q_H = \Sigma Q_{Hi}$ gives the best statistical results:

$$\log_e AD_{50} = 5.229\ (\pm 0.171) - 1.026\ (\pm 0.044){}^0\chi^v - 1.054\ (\pm 0.053)Q_H \quad \text{(Eq. 7)}$$

$$r = 0.975 \quad s = 0.27 \quad F = 411 \quad n = 45\ (p < 0.001)$$

The quantities in parenthesis for each regression parameter in Eq. 7 are the standard deviations calculated in the regression routine for each parameter. The calculated values shown in Table II are based on Eq. 7.

Equation 7 accounts for 95% (R^2) of the variance in $\log_e AD_{50}$. These results are in line with previous results for a mixed group of anesthetics

Table II—Correlation of Anesthetic Activity of Halogenated Hydrocarbons

Compound	$^0\chi^v$	Q_H	$\log_e AD_{50}$ Obs.	$\log_e AD_{50}$ Calc.[a]	$\lvert\Delta\log_e AD_{50}\rvert$
		Methane Derivatives			
I CHF_2Cl	1.334	1.27	3.02	2.52	0.50
II $CHFCl_2$	2.761	1.25	1.12	1.08	0.04
III CH_2Cl_2	3.115	1.64	0.49	0.30	0.19
IV $CHFClBr$	3.542	1.28	0.18	0.25	0.07
		Ethane Derivatives			
V CF_2ClCH_3	2.257	0.00	3.14	2.91	0.23
VI CF_3CHFCl	1.387	1.22	2.74	2.52	0.22
VII $CF_3CFClBr$	3.294	0.00	2.28	1.85	0.43
VIII CF_2BrCHF_2	2.167	1.21	1.94	1.73	0.21
IX $CFCl_2CH_3$	3.684	0.00	1.85	1.45	0.40
X $CF_2ClCFCl_2$	3.941	0.00	1.70	1.19	0.51
XI $CF_2ClCHFCl$	2.814	1.19	1.11	1.09	0.02
XII CF_3CHCl_2	2.814	1.20	0.87	1.08	0.21
XIII CHF_2CH_2Cl	2.041	2.30	0.77	0.71	0.06
XIV CHF_2CH_2Br	2.821	2.35	0.26	−0.14	0.40
XV CF_2ClCH_2Cl	3.168	1.54	0.25	0.36	0.11
XVI $CF_2ClCHFBr$	3.595	1.23	0.18	0.24	0.06
XVII $CF_2BrCHFCl$	3.595	1.19	0.11	0.29	0.18
XVIII $CF_3CHClBr$	3.595	1.23	−0.16	0.24	0.40
XIX $CFCl_2CFCl_2$	5.368	0.00	−0.22	−0.28	0.06
XX CF_2ClCH_2Br	3.948	1.60	−0.22	−0.51	0.29
XXI CF_2BrCH_2Cl	3.948	1.52	−0.29	−0.42	0.13
XXII $CF_2ClCHCl_2$	4.242	1.18	−0.22	−0.37	0.15
XXIII $CFCl_2CHFCl$	4.242	1.17	−0.54	−0.36	0.18
XXIV $CF_2BrCHFBr$	4.375	1.22	−0.43	−0.55	0.12
XXV CF_3CHBr_2	4.375	1.26	−0.63	−0.59	0.04
XXVI $CHFClCHFCl$	3.115	2.14	−0.60	−0.22	0.38
XXVII $CF_2ClCHClBr$	5.022	1.21	−0.78	−1.20	0.42
		Propane Derivatives			
XXVIII $CF_2ClCH_2CH_3$	2.964	0.00	2.08	2.19	0.11
XXIX $CF_3CH_2CF_2Cl$	1.793	1.48	1.66	1.83	0.17
XXX $CF_3CCl_2CH_3$	3.737	0.00	1.39	1.39	0.00
XXXI $CF_3CHBrCH_3$	3.391	0.82	0.78	0.89	0.11
XXXII $CH_2ClCF_2CH_3$	2.964	1.34	0.77	0.78	0.01
XXXIII CF_2ClCF_2CHFCl	2.867	1.25	0.69	0.97	0.28
XXXIV $CF_3CH_2CF_2Br$	2.573	1.46	0.64	1.05	0.41
XXXV $CFCl_2CH_2CH_3$	4.391	0.00	0.40	0.72	0.32
XXXVI $CH_2BrCF_2CH_3$	3.744	1.40	0.22	−0.09	0.31
XXXVII $CHF_2CF_2CH_2Cl$	2.094	2.69	0.18	0.24	0.06
XXXVIII $CF_2ClCHClCH_3$	4.038	0.77	−0.04	0.27	0.31
XXXIX $CF_2ClCHBrCH_3$	4.818	0.80	−0.58	−0.56	0.02
XL $CHF_2CF_2CH_2Br$	2.874	2.77	−0.63	−0.64	0.01
XLI $CHF_2CF_2CHClBr$	3.948	2.43	−1.66	−1.38	0.28
XLII $CF_3CHBrCH_2Br$	5.082	2.27	−2.30	−2.38	0.08
		Butane Derivatives			
XLIII $CH_3CF_2CF_2CH_3$	2.106	0.00	2.99	3.07	0.08
XLIV $CH_3CF_2CH_2CH_3$	2.760	0.00	1.79	2.40	0.61
XLV $CH_3CF_2CFClCH_3$	3.533	0.00	1.22	1.60	0.38

[a] Using Eq. 7.

(5) where $^0\chi^v$ was also the best connectivity term to correlate with activity. This correlation also accounts well for the qualitative structure–activity relationships of the general anesthetics (12, 13):

1. Halogenation of hydrocarbons increases potency in the following order: F < Cl < Br (Table III). Compare also XII and XXII, XVI and XXIV, XVIII and XXVII, XV and XX, XV and XXI, V and IX, XIII and XIV, XXXIV and XXIX, XXXVII and XL, XXXI and XXXIX, XXXVIII and XXXIX, XXXII and XXXVI, and XLIII and XLV. In all of these cases, this structure–activity observation is quantitatively accounted for by Eq. 7.

2. Fluorination usually decreases potency, as can be seen in the examples in Table III for halogen substitution.

3. Compounds substituted as dibromides and dichlorides tend to be more potent than their monosubstituted analogs. The dibromo compounds are more potent than the dichloro derivatives. Compare, for example, XII and XV.

4. Increased potency in a homologous series is observed. This result is quantified in the homologous pairs V and XXVIII and IX and XXXV.

5. The polar hydrogen factor Q_H accounts well for the structure–activity observations that compounds containing CHFCl, CHFBr, and CHClBr produce good anesthesia and that one or more hydrogen atoms in the molecule are necessary for effective central nervous system depression. Equation 7 shows that a fully activated acidic hydrogen increases anesthetic activity by 1.4 $\log_e$ units and that the influence of more than one acid hydrogen can be well approximated by a simple additive relation.

The predictive value of the structure–activity equation is demonstrated by its ability to predict activities not in the original data (Table IV). One iodo compound is included and well predicted. With Eq. 7, the predicted anesthetic activity for the convulsant $CF_3CH_2OCH_2CF_3$ (indoklon) (14) is 4.66; for its anesthetic isomer $(CF_3)_2CHOCH_3$ (14), it is 3.67. Equation 7 predicts an extremely low anesthetic activity for indoklon and a value and order of magnitude higher for its anesthetic isomer.

The equation obtained in this study is analogous to equations obtained previously with a mixed group of anesthetics (5), and it can be interpreted similarly in the light of theories of anesthesia. In this study, polar hydrogens were evaluated with a term derived from the Swain and Lupton (10) field-based F. Experimentally, these polar hydrogens were better donors in a hydrogen bond than aliphatic CH (14, 15). Halogenated hydrocarbon anesthetics also break hydrogen bonds of the NH···N, OH···O, and NH···O=C types in solution (16–21). Thus, the polar hydrogens can contribute to anesthetic activity because of their hydrogen bonding ability and their ability to perturb existing hydrogen bonds. These results are consistent with the observed disordering effect of anesthetics on membranes and protein structure (1) and the concepts of the critical volume hypothesis.

Only one other structure–activity study on this data set was reported (5). A nonpolar term, P_0, was appropriately related to van der Waals interaction terms by an approximate additivity scheme (5). In addition,

Table III—Anesthetic Potency as a Function of Halogen

Compound	$\log_e$ AD_{50} Obs.	Calc.[a]
VI CF_3CHFCl	2.74	2.52
XII CF_3CHCl_2	0.87	1.08
XVIII $CF_3CHClBr$	−0.16	0.24
XXV CF_3CHBr_2	−0.63	−0.59
VIII CF_2BrCHF_2	1.94	1.73
XVII $CF_2BrCHFCl$	0.11	0.29
XXIV $CF_2BrCHFBr$	−0.43	−0.55
XI $CF_2ClCHFCl$	1.11	1.09
XVI $CF_2ClCHFBr$	0.18	0.24
XXII $CF_2ClCHCl_2$	−0.22	−0.37
XXVII $CF_2ClCHClBr$	−0.78	−1.20
VI $CHFClCF_3$	2.74	2.52
XI $CHFClCF_2Cl$	1.11	1.09
XVII $CHFClCF_2Br$	0.11	0.29
XXIII $CHFClCFCl_2$	−0.54	−0.36
I CHF_2Cl	3.02	2.52
II $CHFCl_2$	1.12	1.08
III CH_2Cl_2	0.49	0.30
IV $CHFClBr$	0.18	0.25

[a] Using Eq. 7.

an additivity scheme was employed for estimating the acidity of hydrogen atoms by taking the contribution to the electron demand by each halogen as a constant. The total electron demand on the ith hydrogen is called H_{ai}. The developed relation (5) was a six-parameter equation with an unusual form for multiple regression:

$$\log_e AD_{50} = a_1 + a_2P_0 + a_3\delta_1H_{a1} + a_4\delta_1 + a_5\delta_2H_{a2} + a_6\delta_2 \quad \text{(Eq. 8)}$$

Table IV—Predicted Anesthetic Activity

Compound	$^0\chi^v$	Q_H	$\log_e$ AD_{50} Obs.[a]	Calc.[b]
CF_3CH_3	0.829	0.00	3.91	4.38
CF_3CH_2Cl	1.740	1.60	2.08	1.76
CF_3CH_2Br	2.520	1.66	1.03	0.89
CF_3CH_2I	3.101	1.58	0.22	0.38
$CF_3CH{=}CH_2$	1.114	0.00	4.09	4.09
$CF_3CH_2CH_3$	1.536	0.00	3.91	3.65
$CF_3CH_2CH_2Cl$	2.247	1.12	1.10	1.54
$CF_3CH_2CH_2Br$	3.227	1.18	0.41	0.67
$CF_3CHClCH_2Cl$	3.521	2.22	−0.92, −0.69	−0.72
$CF_3CH_2CF_3$	0.365	1.56	2.40	3.21
$CHF_2CHClCH_3$	2.911	1.63	0.53	0.52
$CF_3CH_2CHCl_2$	3.521	0.97	−0.58	0.59
$CF_2ClCH_2CH_2Cl$	3.875	1.12	−0.11	0.07
$CF_2ClCHClCFCl_2$	5.722	1.10	−0.51	−1.80
$CH_3CF_2CH{=}CH_2$	2.337	0.00	2.12	2.83
$CF_3CH_2CF_2CH_3$	1.589	1.30	1.61	2.23
$CH_3CFClCH_2CH_3$	4.187	0.00	0.59	0.93
$CH_3CF_2CH_2CHCl_2$	4.745	0.92	−1.05	−0.61
$CH_3CF_2CHClCH_2Cl$	4.745	1.99	−1.61	−1.74

[a] From Ref. 22. [b] Calculated using Eq. 7.

where the terms a_1–a_6 are the regression parameters and the δ_i's are Kronecker deltas used to introduce the threshold idea. However, the threshold variable δ_i is also entered separately in two places in the equation, affecting two pairs of regression parameters: a_3 and a_4 and a_5 and a_6.

The correlation of P_0 with log AD_{50} yields $r = 0.69$. Equation 8 leads to $r = 0.988$ and $s = 0.20$, the only statistics reported for Eq. 8. Therefore, it is rather difficult to compare Eqs. 7 and 8 because of the differing number of regression parameters, 3 compared to 6, and the rather peculiar manner in which the threshold variable influences the regression. Equation 7 is a more readily applied form of analysis and was used in two other anesthetic structure–activity studies.

In addition to statistical analysis, Eq. 7 is capable of structural interpretation and prediction as already discussed.

REFERENCES

(1) J. C. Miller and K. W. Miller, in "MTP International Review of Science—Biochemistry Series," vol. 12, H. K. F. Blaschoko, Ed., Butterworths, London, England, 1975.

(2) T. Di Paolo, L. Kier, and L. Hall, *Mol. Pharmacol.*, **13,** 31 (1977).

(3) T. Di Paolo, *J. Pharm. Sci.*, **67,** 564 (1978).

(4) *Ibid.*, **67,** 566 (1978).

(5) R. H. Davies, R. D. Bagnall, and W. G. M. Jones, *Int. J. Quantum Chem.*, **1,** 201 (1974).

(6) L. B. Kier, L. H. Hall, W. J. Murray, and M. Randic, *J. Pharm. Sci.*, **64,** 1971 (1975).

(7) L. B. Kier, W. J. Murray, and L. H. Hall, *J. Med. Chem.*, **18,** 1272 (1975).

(8) L. H. Hall and L. B. Kier, *J. Pharm. Sci.*, **66,** 642 (1977).

(9) L. B. Kier and L. H. Hall, "Molecular Connectivity Theory in Chemistry and Drug Research," Academic, New York, N.Y., 1976.

(10) C. G. Swain and E. C. Lupton, Jr., *J. Am. Chem. Soc.*, **90,** 4328 (1968).

(11) C. Hansch, A. Leo, S. H. Unger, K. H. Kim, D. Nikaitani, and E. J. Lien, *J. Med. Chem.*, **16,** 1207 (1973).

(12) J. C. Krantz, Jr., and F. G. Rudo, "Handbook of Experimental Pharmacology," vol. XX/I, Springer, Berlin, Germany, 1966, p. 501.

(13) E. R. Larsen, *Fluorine Chem. Rev.*, **3,** 1 (1969).

(14) S. Cohen, A. Goldschmidt, G. Shtacher, S. Srebrenik, and S. Gitter, *Mol. Pharmacol.*, **11,** 379 (1975).

(15) L. J. Bellamy, "Advances in Infrared Group Frequencies," vol. II, Chapman and Hall, London, England, 1975.

(16) R. B. Green, "Hydrogen Bonding by C-H Groups," Wiley, New York, N.Y., 1974.

(17) T. Di Paolo and C. Sandorfy, *J. Med. Chem.*, **17,** 809 (1974).

(18) T. Di Paolo and C. Sandorfy, *Nature*, **252,** 471 (1974).

(19) A. Nagyrevi and C. Sandorfy, *Can. J. Chem.*, **55,** 1593 (1977).

(20) R. Massuda and C. Sandorfy, *ibid.*, **55,** 3211 (1977).

(21) J. M. Brown and P. A. Chalone, *ibid.*, **55,** 3380 (1977).

(22) B. H. Robbins, *J. Pharmacol. Exp. Ther.*, **86,** 197 (1946).

ACKNOWLEDGMENTS

The authors appreciate the use of the facilities in the Computer Centers at Eastern Nazarene College and Massachusetts College of Pharmacy.

Quantitative GLC Determination of Oxycodone in Human Plasma

NED L. RENZI, Jr. [x], **and JOSIAH N. TAM**

Received February 24, 1978, from *Biochemical Research, McNeil Laboratories, Fort Washington, PA 19034.* Accepted for publication May 26, 1978.

Abstract □ A GLC assay was developed for the determination of oxycodone levels in human plasma using a nitrogen-specific detector. The assay was developed for use in bioavailability studies of therapeutic doses of oxycodone. After ingestion of a commercial tablet containing 4.5 mg of oxycodone hydrochloride and 0.38 mg of oxycodone terephthalate by six volunteers, the mean peak oxycodone concentration in plasma was 18.4 ng/ml at 1 hr.

Keyphrases □ Oxycodone—GLC analysis in plasma □ GLC—analysis, oxycodone in plasma □ Narcotic analgesics—oxycodone, GLC analysis in plasma

Oxycodone (14-hydroxydihydrocodeinone) (I) is a narcotic analgesic (1) and antitussive agent (2). For many years, the detection and determination of oxycodone were based largely on TLC and UV spectrophotometry (3–5). Recently, a GLC procedure for the quantitation of oxycodone hydrochloride in pharmaceutical preparations was reported (6).

However, methods of determining oxycodone levels in human plasma have not been available. This problem is inevitably coupled with the fact that the circulating oxycodone in blood from normal subjects after a single therapeutic dose is extremely low. The existing spectrophotometric and GLC methods are not suitable since the lower limit of detection is approximately 1 μg.

This report describes a GLC assay for oxycodone [with corydine hydrochloride (II) as the internal standard] in plasma using a nitrogen-specific detector. The assay requires 5 ml of plasma and is capable of determining 2 ng of oxycodone/ml.

EXPERIMENTAL

Materials—Nanograde quality methanol and chloroform[1] were used without further purification. Thirty-milliliter glass bottles[2] with polyethylene screw caps[3] were used for the plasma extraction, and 12-ml glass-stoppered centrifuge tubes[4] were used for the final solvent evaporation. Volumetric glass pipets were utilized for all solvent transfers. All glassware was soaked in chromic acid for at least 1 hr, rinsed thoroughly with distilled water, and heat treated for 3 hr at 270°. Polyethylene screw caps were soaked in *n*-heptane for at least 1 hr and dried at 60° prior to use.

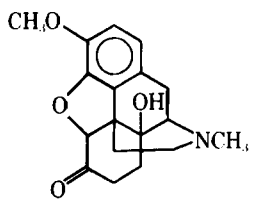

I

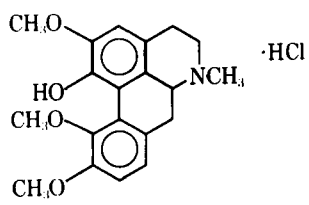

II

Stock solutions of oxycodone and corydine (1-hydroxy-2,10,11-trimethoxyaporphine), an internal standard, were prepared in chloroform using oxycodone hydrochloride[1] and corydine hydrochloride[5] with all concentrations expressed in terms of the free base. Both compounds showed satisfactory UV, IR, NMR, and TLC properties. Clinical control plasma[6] was used in the preparation of the oxycodone plasma standards.

Apparatus—A gas chromatograph[7] equipped with a nitrogen–phosphorus-specific detector was used. The GLC column was a 0.91-m × 2-mm i.d. silanized glass column packed with 2% OV-101 on 100–120-mesh Chromosorb WHP[8]. The column was conditioned at 270° overnight with a helium flow of 30 ml/min.

Chromatographic temperatures were: column oven, 240°; injection port, 260°; and detector, 300°. The helium carrier gas flow rate was 30 ml/min, the hydrogen flow rate was 3 ml/min, and the air flow rate was 100 ml/min.

For the positive identification of oxycodone in human plasma, a quadrupole mass spectrometer[9] and a data system[10] were used in conjunction with the gas chromatograph[11]. A 1.51-m × 2-mm i.d. silanized glass column packed with 3% OV-1 on 60–80-mesh Gas Chrom Q[12] was conditioned at 270° overnight with a helium carrier gas flow rate of 20 ml/min. During analysis, the interface oven and the transfer line in the GLC–mass spectrometry system were at 250°. The column temperature was 235°, and the injection port temperature was 280°.

The methane[13] pressure was adjusted to provide an ion source pressure

Figure 1—*Typical gas chromatogram of a plasma sample seeded with 10 ng of oxycodone/ml of plasma.*

[1] Mallinckrodt Chemicals.
[2] Wheaton Co.
[3] Standard Cap Corp.
[4] Arthur H. Thomas Co.
[5] Eastman Organic Chemicals.
[6] Interstate Blood Bank, Philadelphia, Pa.
[7] Hewlett-Packard model 5710A.
[8] Hewlett-Packard.
[9] Finnigan model 3300.
[10] Finnigan model 6110.
[11] Finnigan model 9500.
[12] Applied Science Laboratories.
[13] Instrument purity, Matheson.

0022-3549/79/0100-0043$01.00/0
© 1979, American Pharmaceutical Association

Table I—Means, Standard Deviations, and Coefficients of Variation of Area Ratios at Various Oxycodone Concentrations

Oxycodone Concentration, ng/ml	Number of Determinations	Area Ratios		
		Mean	*SD*	*CV*
2	5	0.163	0.49	0.30
5	10	0.257	0.061	0.23
10	9	0.517	0.111	0.21
20	9	1.084	0.171	0.16
30	9	1.608	0.277	0.17
50	5	2.802	0.224	0.08

of 1 torr. The ion source settings were: ion energy, 2 v; ion repeller, 0 v (chemical ionization), 35 v (electron impact); ion lens, 40 v; and filament, 70 v (electron impact), 150 v (chemical ionization). The electron beam total emission was regulated at 0.55 mamp, while the source was operated without external heating.

Assay Procedure—Five milliliters of plasma, 10.0 ml of internal standard in chloroform solution (20 ng of corydine/ml), and 1.0 ml of 1 *N* NaOH were added to a 30-ml bottle, and the mixture was shaken on a tabletop shaker[14] at 120 oscillations/min for 15 min. After centrifugation[15] at 2000 rpm, the aqueous phase was removed and discarded. To the organic phase was added 5.5 ml of 0.05 *N* HCl. The mixture was then shaken for 15 min and centrifuged for 10 min.

Five milliliters of the aqueous layer was transferred to a 30-ml bottle containing 10.0 ml of chloroform and 1.0 ml of 1 *N* NaOH. The mixture was shaken for 15 min and centrifuged for 10 min, and the aqueous phase was removed and discarded. Then 8 ml of the organic phase was pipetted into a 12-ml centrifuge tube, and the solvent was evaporated under a nitrogen stream at 40°. The residue was reconstituted in 20 μl of methanol, and 10 μl was injected into the gas chromatograph.

Oxycodone Single-Dose Human Plasma Samples—Six healthy adult male volunteers were fasted for at least 12 hr prior to dosing and 1 hr postdosing. Each subject was dosed with a single tablet[16] and 200 ml of distilled water. Blood samples of 20 ml were collected in heparinized vacuum tubes by venipuncture at 0 (predose), 10, 20, 40, 60, and 90 min and 2, 3, 4, 5, 6, and 8 hr after dosing. The plasma was separated by centrifugation immediately after collection, and the clear plasma was stored frozen at −10° in polypropylene snap-cap tubes until assayed (within several weeks).

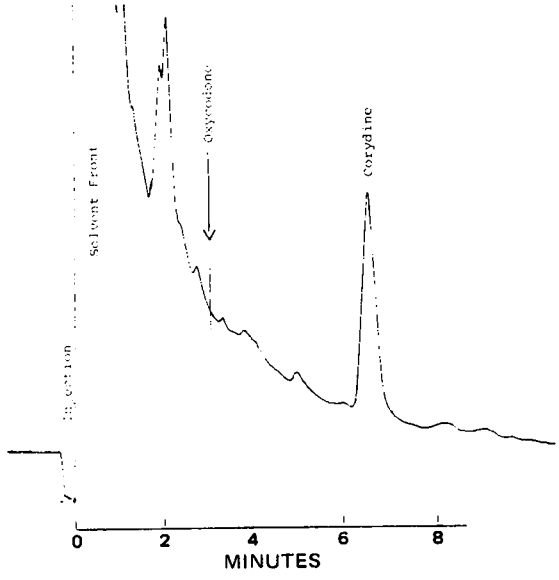

Figure 2—*Typical gas chromatogram of a blank plasma sample containing corydine as an internal standard.*

[14] Eberbach Corp.
[15] International Centrifuge.
[16] Percodan, Endo Laboratories, Inc. Each tablet contained 4.5 mg of oxycodone hydrochloride, 0.38 mg of oxycodone terephthalate, 224 mg of aspirin, 160 mg of phenacetin, and 32 mg of caffeine.

Table II—Plasma Oxycodone Levels (Nanograms per Milliliter) in Six Subjects after Oral Administration of 4.5 mg of Oxycodone Hydrochloride and 0.38 mg of Oxycodone Terephthalate

Time after Administration	Subject						
	1	2	3	4	5	6	Mean
0	0	—	0	0	0	0	0
10 min	0	0.8	0	0	0	0	0.1
20 min	6.3	2.0	0	5.5	1.8	0	2.6
40 min	13.0	19.8	6.3	21.0	13.0	5.7	13.1
60 min	36.5	12.9	16.5	20.0	16.0	8.5	18.4
90 min	12.5	22.8	19.5	15.3	25.0	8.7	17.3
2 hr	10.7	18.9	17.0	12.3	18.3	17.0	15.7
3 hr	10.0	11.5	12.3	7.0	13.8	6.0	10.1
4 hr	8.0	8.8	10.7	9.6	11.9	7.3	9.4
5 hr	6.0	7.0	9.9	9.0	11.3	4.3	7.9
6 hr	3.7	6.3	5.5	5.0	10.0	1.7	5.4
8 hr	3.0	4.0	2.3	3.5	14.3	1.0	4.7

RESULTS AND DISCUSSION

The plasma level profiles of oxycodone in humans have not been reported, undoubtedly because of the difficulties in measuring low levels of oxycodone after a single oral therapeutic dose. The TLC and UV spectrophotometric assays (3–5) as well as the GLC method, using flame-ionization detection (6), do not offer enough sensitivity for determining oxycodone levels in human plasma samples.

Due to the lack of an electron-capturing moiety in the oxycodone molecule, the electron-capture detector has no better sensitivity than the flame-ionization detector toward oxycodone. Derivatization of oxycodone with acetic anhydride and propionic anhydride was unsuccessful (5). Other available derivatization reagents for electron-capture detection appeared not to react with oxycodone. The nitrogen-phosphorus-specific detector used in the nitrogen mode, however, shows good sensitivity in detecting oxycodone. The lower limit of detection is 2 ng or better, and the detector response is linear between 2 and 50 ng.

Oxycodone is a weak base with a pKa of 8.53 (7); the compound can be extracted from plasma into an organic solvent, such as chloroform, in the presence of a strong base. Oxycodone forms salts with strong acids such as hydrochloric, and these salts are readily soluble in water. With the present extraction procedure, the mean extraction efficiencies ± *SD* for 10 determinations were 72.8 ± 10.8% for oxycodone at concentrations of 10 ng/ml and 71.6 ± 15.3% at 20 ng/ml. Corydine had a mean extraction efficiency of 54.1 ± 6.3% (n = 6) at 20 ng/ml (concentration used in the assay).

Figure 1, a typical oxycodone chromatogram tracing, shows the separation of oxycodone and corydine peaks. The retention times under the experimental conditions were 3.3 and 6.9 min for oxycodone and corydine, respectively. Shown in Fig. 2 is the chromatogram tracing of a blank plasma extract. No plasma peaks interfered with the assay.

The peak area ratios of replicate samples (expressed as oxycodone to corydine), obtained from the addition of known amounts of oxycodone to control blank plasma followed by processing according to the described procedure, are summarized in Table I. A least-squares analysis gave a straight-line standard curve with a correlation coefficient of 0.9992, a slope of 0.056 ± 0.01, and an intercept of −0.010 ± 0.029, which, within experimental error, showed that the line passed through the origin. The assay is reproducible, as shown by coefficients of variation in Table I.

In the assay development, the hydrochloride salt of oxycodone was used to prepare oxycodone standards. However, the hydrochloride salt is hygroscopic, and the terephthalate salt is a better compound for this purpose[17].

The identity of the GLC peak was confirmed by GLC–mass spectrometry using both electron-impact and chemical-ionization modes of analysis. The electron-impact spectrum exhibited a molecular ion at m/e 316 for the component in the GLC peak, which is identical to the spectrum of authentic oxycodone obtained by the direct inlet technique. The chemical-ionization spectrum showed mass peaks at m/e 316 (M + 1), 344 (M + 29), and 356 (M + 41), which are characteristic peaks in the chemical-ionization spectrum of oxycodone with methane as a reagent gas. Furthermore, the chemical-ionization spectrum of the component in the GLC peak was also identical to that of authentic oxycodone by the direct inlet method.

[17] Pharmacy Research Department, McNeil Laboratories, unpublished results.

Since the metabolism of oxycodone has not been fully established, the GLC characteristics of the metabolite(s) are yet unknown. However, from the expected metabolic pathways of iminoethanophenanthrofurans (8), it may be speculated that the metabolites have different retention in the GLC column than oxycodone under the same chromatographic conditions. Drugs usually coadministered with oxycodone such as acetaminophen, aspirin, caffeine, and phenacetin do not interfere in the assay. Without derivatization, acetaminophen and aspirin do not pass through the GLC column while phenacetin and caffeine appear to be eluted with the solvent.

The results of single-dose administrations of 4.5 mg of oxycodone hydrochloride and 0.38 mg of oxycodone terephthalate to human subjects are listed in Table II. The maximum plasma oxycodone levels ranged from 17.0 to 36.5 ng/ml in the six subjects. After 8 hr, the oxycodone levels ranged from 1.0 to 14.3 ng/ml.

REFERENCES

(1) C. G. Moertel, D. L. Ahmann, W. F. Taylor, and N. Schwartan, *J. Am. Med. Assoc.*, **229**, 55 (1974).

(2) L. O. Boreus, *Eur. J. Pharmacol.*, **15**, 127 (1971).

(3) K. Teichert, E. Mutschler, and H. Rochelmeyer, *Dsch. Apoth-Ztg.*, **100**, 477 (1960).

(4) J. Zarnack and S. Pfeifer, *Pharmazie*, **19**, 216 (1964).

(5) S. J. Mulé, *Anal. Chem.*, **36**, 1907 (1964).

(6) M. Ono, M. Shimamini, K. Takahashi, and E. S. Hokoku, **93**, 92(1975); through *Chem. Abstr.*, **84**, 184984n.

(7) G. O. Jolliffe and M. M. Attmad, *Bull. Narcotics*, **23**(4), 37 (1971).

(8) T. K. Adler, J. M. Fujimoto, E. L. Way, and E. M. Baker, *J. Pharmacol. Exp. Ther.*, **114**, 251 (1955).

Interaction of the Antimalarial α-Dibutylaminomethyl-2,6-bis(trifluoromethylphenyl)-4-pyridinemethanol with Human Serum Albumin

O. J. BOUWSMA *, J. T. STEWART ˣ, and J. J. VALLNER

Received February 22, 1978, from the *Departments of Pharmacy and Medicinal Chemistry, School of Pharmacy, University of Georgia, Athens, GA 30602.* Accepted for publication June 2, 1978. *Present address: Institute for Lipid Research, Baylor College of Medicine, Houston, Tex.

Abstract □ Binding of the antimalarial α-dibutylaminomethyl-2,6-bis(trifluoromethylphenyl)-4-pyridinemethanol with human serum albumin was studied using difference spectroscopy, fluorescence quenching, and equilibrium dialysis. Results indicated that the number of high affinity binding sites of the drug on protein is 0.45, with the total number of binding sites being 3.3–4.0. The binding constants were in the range of 0.57–4.00 × 10^6 M^{-1}. The drug was bound more strongly to a nonionic detergent than to either a cationic or anionic detergent. Interpretation of these data and fluorescence quenching results indicated that the drug is possibly bound to a hydrophobic site on human serum albumin.

Keyphrases □ Pyridinemethanol, substituted—binding to human serum albumin □ Binding, protein—substituted pyridinemethanol to human serum albumin □ Antimalarials—α-dibutylaminomethyl-2,6-bis(trifluoromethylphenyl)-4-pyridinemethanol, binding to human serum albumin □ α-Dibutylaminomethyl-2,6-bis(trifluoromethylphenyl)-4-pyridinemethanol—binding to human serum albumin

Interest in protein binding of drugs led to an investigation of the antimalarial α-dibutylaminomethyl-2,6-bis(trifluoromethylphenyl)-4-pyridinemethanol[1] (I). The drug is 22 times more effective than quinine and is active against highly chloroquine-resistant *Plasmodium berghei* in mice[2]. There is a lack of information about binding of such pyridinemethanols to serum proteins. Such data are important to an understanding of the distribution, metabolism, and excretion of these antimalarials since only the fraction of drug unbound exerts chemotherapeutic activity (1, 2).

The hydrophobic alkyl side chains, the aromatic π-electrons, the hydrogen-bonding site (OH group), and the possible electrostatic interactions suggest that the drug

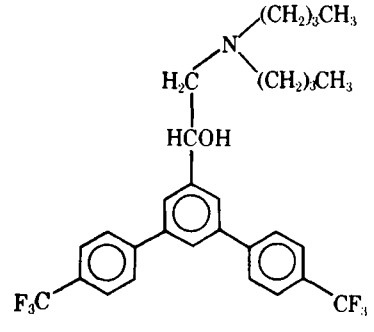

I

may have a high affinity for serum albumin (3). The limited water solubility of the drug, even as the hydrochloride salt, makes the examination of binding affinity difficult. In this paper, the interaction of I with human serum albumin is examined by difference spectrophotometry, fluorescence quenching, and equilibrium dialysis.

EXPERIMENTAL

Apparatus and Chemicals—Compound I was supplied as the hydrochloride salt[3]. Its purity was verified by TLC in three different solvent systems (4) and by mass spectral analysis. Human serum albumin[4] was investigated for purity (5). The $E^{1\%}_{1cm}$ values for the albumin were 6.36 at 279 nm and 190 at 210 nm. Sorensen phosphate buffer, adjusted to pH 7.4, was used.

The dialysis membrane was prepared according to literature methods (6–8). Rigid, clear acrylic plastic dialysis cells (10 ml) were washed repeatedly with distilled water and sonicated overnight in distilled water. Electronic absorption spectra[5] were taken in 1-cm silica cells. Fluores-

[1] WR 148,946.

[2] P. S. Loizeaux, Walter Reed Army Institute for Research, personal communication, 1976.

[3] Walter Reed Army Institute of Research, Washington, D.C.

[4] Armour and Co.

[5] Cary spectrophotometer, model 118, Varian Instrument, Palo Alto, Calif.

0022-3549/79/0100-0045$01.00/0

© 1979, American Pharmaceutical Association

Since the metabolism of oxycodone has not been fully established, the GLC characteristics of the metabolite(s) are yet unknown. However, from the expected metabolic pathways of iminoethanophenanthrofurans (8), it may be speculated that the metabolites have different retention in the GLC column than oxycodone under the same chromatographic conditions. Drugs usually coadministered with oxycodone such as acetaminophen, aspirin, caffeine, and phenacetin do not interfere in the assay. Without derivatization, acetaminophen and aspirin do not pass through the GLC column while phenacetin and caffeine appear to be eluted with the solvent.

The results of single-dose administrations of 4.5 mg of oxycodone hydrochloride and 0.38 mg of oxycodone terephthalate to human subjects are listed in Table II. The maximum plasma oxycodone levels ranged from 17.0 to 36.5 ng/ml in the six subjects. After 8 hr, the oxycodone levels ranged from 1.0 to 14.3 ng/ml.

REFERENCES

(1) C. G. Moertel, D. L. Ahmann, W. F. Taylor, and N. Schwartan, *J. Am. Med. Assoc.*, **229**, 55 (1974).

(2) L. O. Boreus, *Eur. J. Pharmacol.*, **15**, 127 (1971).

(3) K. Teichert, E. Mutschler, and H. Rochelmeyer, *Dsch. Apoth-Ztg.*, **100**, 477 (1960).

(4) J. Zarnack and S. Pfeifer, *Pharmazie*, **19**, 216 (1964).

(5) S. J. Mulé, *Anal. Chem.*, **36**, 1907 (1964).

(6) M. Ono, M. Shimamini, K. Takahashi, and E. S. Hokoku, **93**, 92(1975); through *Chem. Abstr.*, **84**, 184984n.

(7) G. O. Jolliffe and M. M. Attmad, *Bull. Narcotics*, **23**(4), 37 (1971).

(8) T. K. Adler, J. M. Fujimoto, E. L. Way, and E. M. Baker, *J. Pharmacol. Exp. Ther.*, **114**, 251 (1955).

Interaction of the Antimalarial α-Dibutylaminomethyl-2,6-bis(trifluoromethylphenyl)-4-pyridinemethanol with Human Serum Albumin

O. J. BOUWSMA *, J. T. STEWART ˣ, and J. J. VALLNER

Received February 22, 1978, from the *Departments of Pharmacy and Medicinal Chemistry, School of Pharmacy, University of Georgia, Athens, GA 30602.* Accepted for publication June 2, 1978. *Present address: Institute for Lipid Research, Baylor College of Medicine, Houston, Tex.

Abstract □ Binding of the antimalarial α-dibutylaminomethyl-2,6-bis(trifluoromethylphenyl)-4-pyridinemethanol with human serum albumin was studied using difference spectroscopy, fluorescence quenching, and equilibrium dialysis. Results indicated that the number of high affinity binding sites of the drug on protein is 0.45, with the total number of binding sites being 3.3–4.0. The binding constants were in the range of 0.57–4.00 × 10^6 M^{-1}. The drug was bound more strongly to a nonionic detergent than to either a cationic or anionic detergent. Interpretation of these data and fluorescence quenching results indicated that the drug is possibly bound to a hydrophobic site on human serum albumin.

Keyphrases □ Pyridinemethanol, substituted—binding to human serum albumin □ Binding, protein—substituted pyridinemethanol to human serum albumin □ Antimalarials—α-dibutylaminomethyl-2,6-bis(trifluoromethylphenyl)-4-pyridinemethanol, binding to human serum albumin □ α-Dibutylaminomethyl-2,6-bis(trifluoromethylphenyl)-4-pyridinemethanol—binding to human serum albumin

Interest in protein binding of drugs led to an investigation of the antimalarial α-dibutylaminomethyl-2,6-bis(trifluoromethylphenyl)-4-pyridinemethanol[1] (I). The drug is 22 times more effective than quinine and is active against highly chloroquine-resistant *Plasmodium berghei* in mice[2]. There is a lack of information about binding of such pyridinemethanols to serum proteins. Such data are important to an understanding of the distribution, metabolism, and excretion of these antimalarials since only the fraction of drug unbound exerts chemotherapeutic activity (1, 2).

The hydrophobic alkyl side chains, the aromatic π-electrons, the hydrogen-bonding site (OH group), and the possible electrostatic interactions suggest that the drug

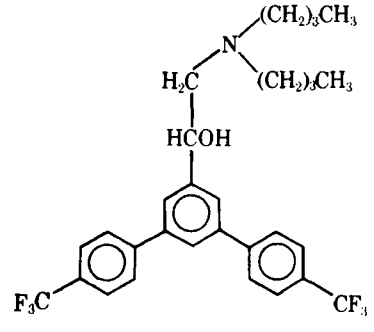

I

may have a high affinity for serum albumin (3). The limited water solubility of the drug, even as the hydrochloride salt, makes the examination of binding affinity difficult. In this paper, the interaction of I with human serum albumin is examined by difference spectrophotometry, fluorescence quenching, and equilibrium dialysis.

EXPERIMENTAL

Apparatus and Chemicals—Compound I was supplied as the hydrochloride salt[3]. Its purity was verified by TLC in three different solvent systems (4) and by mass spectral analysis. Human serum albumin[4] was investigated for purity (5). The $E^{1\%}_{1cm}$ values for the albumin were 6.36 at 279 nm and 190 at 210 nm. Sorensen phosphate buffer, adjusted to pH 7.4, was used.

The dialysis membrane was prepared according to literature methods (6–8). Rigid, clear acrylic plastic dialysis cells (10 ml) were washed repeatedly with distilled water and sonicated overnight in distilled water. Electronic absorption spectra[5] were taken in 1-cm silica cells. Fluores-

[1] WR 148,946.

[2] P. S. Loizeaux, Walter Reed Army Institute for Research, personal communication, 1976.

[3] Walter Reed Army Institute of Research, Washington, D.C.

[4] Armour and Co.

[5] Cary spectrophotometer, model 118, Varian Instrument, Palo Alto, Calif.

0022-3549/79/0100-0045$01.00/0

© 1979, American Pharmaceutical Association

cence spectra were recorded on a spectrophotofluorometer[6] equipped with a corrected spectra attachment. Microliter syringes[7] were used to deliver quantities of solutions accurately. All other chemicals were the highest grade of commercially available materials.

Difference Spectrophotometry—The tandom technique (9) was used to study interactions between I (5×10^{-4} *M*) and albumin ($0.362–7.25 \times 10^{-5}$ *M*). Identical 50-μl increments of drug were added to the buffer cell in the reference beam and to the protein cell in the sample beam. To maintain a constant protein concentration in each beam after drug addition, a volume of protein equal to that of drug added but double the concentration of the protein already in the cell was added to the protein cell. Drug concentration was equalized by the addition of an identical volume of buffer to the buffer cell in the reference compartment. The resulting difference spectrum was then recorded for each added increment of drug over the albumin concentration range studied.

Drug–Surfactant Interactions—Difference spectroscopy studies were repeated in an identical manner to that already described except that a 0.025% cetrimonium bromide (cetrimide), 0.025% sodium lauryl sulfate, or 0.1% octoxynol[8] solution was used in place of the protein. These solutions represent cationic, anionic, or nonionic surfactants, respectively, at concentrations above the critical micelle concentration.

Fluorescence Quenching—Solutions of albumin were prepared over the concentration range of $1.45–14.5 \times 10^{-6}$ *M*. The fluorescence intensity of the native protein was recorded at excitation and emission wavelengths of 284 and 334 nm, respectively. The effects of 50-μl additions of drug (5×10^{-4} *M*) on the fluorescence of albumin were recorded.

The fluorometric titrations were performed as follows: 2.0 or 3.0 ml of a protein solution of an appropriate concentration, contained within a 1-cm quartz cell, was titrated by successive additions of drug solution. A concurrent titration of albumin and buffer was performed so that dilution effects could be considered and the magnitude of the fluorescence quenching could be adjusted appropriately. All fluorescence titrations were performed at an ambient temperature of 22 ± 1°.

Equilibrium Dialysis—Accurately pipetted samples (5–7.5 ml) of an albumin solution ($1.45–14.5 \times 10^{-6}$ *M*) were added to one-half of a dialysis cell, and an identical volume of I ($0.1–20 \times 10^{-6}$ *M*) in phosphate buffer was added to the other half. Equilibrium was obtained in 24 hr as determined by preliminary experiments. After dialysis was complete, an aliquot was removed from the drug side and concentrated sulfuric acid was added so that the final acid normality was 9.

The solution was then assayed fluorometrically using excitation and emission wavelengths of 322 and 381 nm, respectively (4). A blank buffer solution was concurrently assayed and subtracted from the sample reading. The total concentration of free drug was calculated from the resulting fluorescence intensity, taking into account drug bound to the dialysis membrane and cells.

RESULTS AND DISCUSSION

Compound I was shown to bind to human serum albumin by the techniques of difference spectroscopy, fluorescence quenching, and equilibrium dialysis. An example of difference absorption spectra obtained for the association of drug with protein is shown in Fig. 1. The spectra were characterized by positive peaks at 212, 243 ± 3, and 294 nm and negative peaks at 225 ± 4 and 324 ± 4 nm. The UV absorption spectrum of I at pH 7.4 was characterized by absorption bands at 296 (max) and 286 nm (10). Families of curves were generated by incremental additions of I to albumin solutions of fixed concentrations (0.025, 0.05, 0.1, 0.2, and 0.5%).

Absorbance titration curves (Fig. 2) were generated by plotting the change in absorbance (measured as the difference in intensity of the peak at 243 nm and the trough at 225 nm) *versus* concentrations of I added. Increasing concentrations of drug produced increasing absorbance changes that did not deviate from linearity until the drug to protein concentration was greater than 20. Limited drug solubility ($<10^{-4}$ *M*) prohibited a more accurate approximation of the saturation of protein binding sites. Thus, amounts of bound and free drug could not be determined since a complete saturation of protein is necessary for the calculations.

An example of data derived in the fluorescence quenching experiments is shown in Fig. 3. Linear portions of the titration curve extrapolated from the *x* and *y* axes gave the stoichiometric point from which the mole ratio of I bound to albumin was obtained. The association constants for the interaction of drug with protein were calculated from the curve using the methods of Attallah and Lata (11) (Table I).

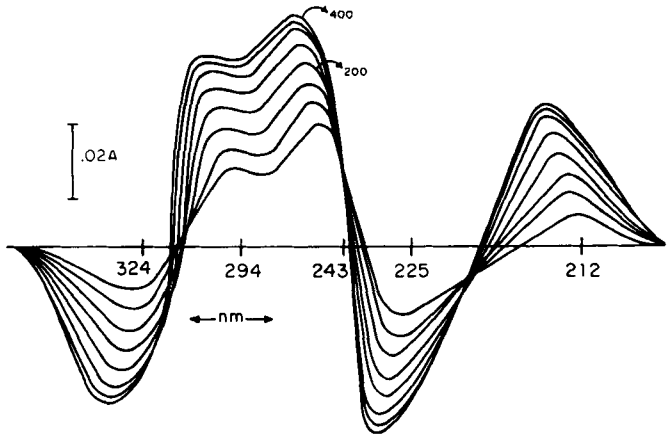

Figure 1—*Difference spectrophotometric titration curves of 3.62×10^{-6} M human serum albumin with I (5×10^{-4} M). The numbers 200 and 400 denote microliters of drug added.*

Data obtained from the equilibrium dialysis studies were graphed (Fig. 4) according to Scatchard (12).

Table II shows a comparison of binding sites and binding constants for the I–protein interaction obtained by the three experimental techniques. The data from the equilibrium dialysis experiments indicate that the number of high affinity binding sites was 0.45[9]. A number closer to 1.0, indicating a one-to-one interaction of drug to protein, would be more easily understood. One possible explanation for the low number is the dimerization of human serum albumin followed by its interaction with one drug molecule. However, this behavior is not likely at the low levels of protein utilized. Another explanation, the association of one drug molecule with two molecules of protein, is plausible because the drug has a high molecular weight and is relatively planar in conformation. Thus, it could conceivably bind between two protein molecules.

Data from the equilibrium dialysis experiments further indicate that the number of secondary binding sites was 2.85, yielding a total number of sites of 3.30. These values compare favorably with primary and sec-

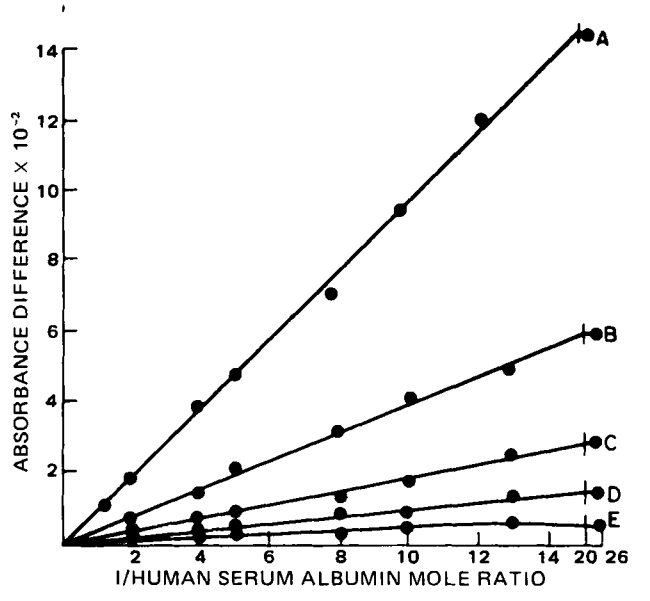

Figure 2—*Plots of absorbance difference [243 (peak)–225 (trough) nm] versus the mole ratio of I to human serum albumin. Slopes A–E represent the addition of increasing increments of I (5×10^{-4} M) to 3.62×10^{-6}, 7.25×10^{-6}, 1.45×10^{-5}, 2.90×10^{-5}, and 7.25×10^{-5} M human serum albumin, respectively.*

[6] Model MPF-4, Perkin-Elmer Corp., Norwalk, Conn.
[7] Hamilton Co., Reno, Nev.
[8] Triton X-100, Rohm and Haas, Philadelphia, Pa.

[9] Scatchard plots typically do not contain adequate numbers of *r* values less than 1.0, usually due to the method of analysis chosen for the investigation of the albumin–drug complex or the resultant free drug concentration. The fluorescence assay used in this study enabled the determination of many points below $r = 1.0$.

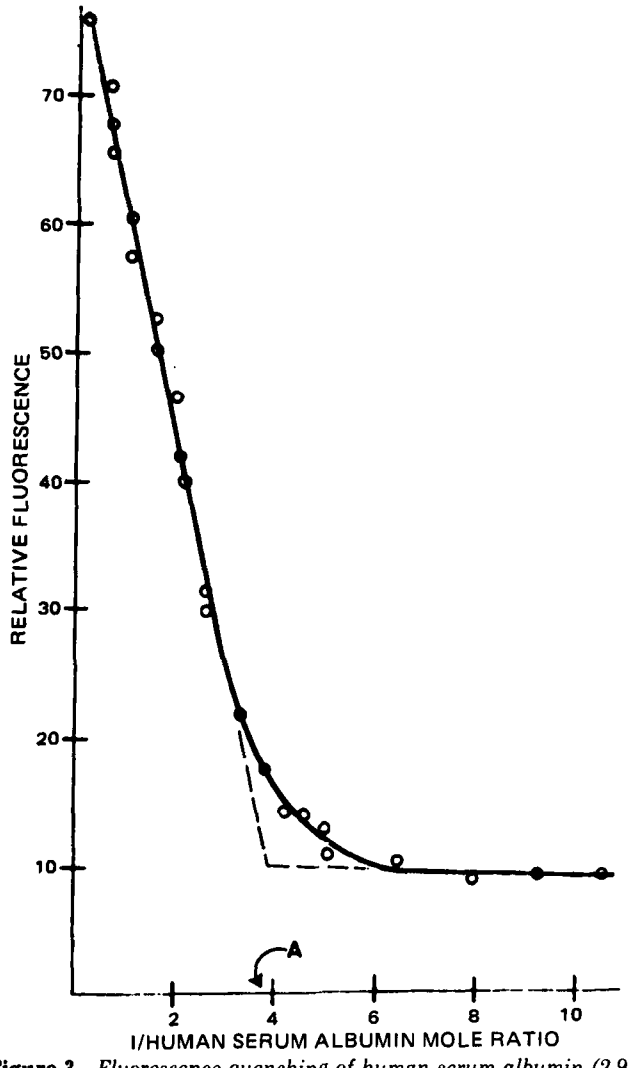

Figure 3—*Fluorescence quenching of human serum albumin (2.9 × 10^{-6} M) with increasing additions of I (5 × 10^{-4} M). Fluorescence intensity was monitored using excitation and emission wavelengths of 284 and 334 nm, respectively. The point at A represents 3.75 binding sites.*

ondary binding sites of 0.39 and 3.15, respectively, determined by Mais *et al.* (13) for quinidine, a drug conformationally similar to I. An earlier study (14) reported that quinidine binds to a single class of sites with $n = 1$ and $k = 7700$.

Fluorescence quenching experiments did not differentiate between primary and secondary binding sites but yielded an average total number of binding sites that compared favorably with the 3.30 from equilibrium dialysis experiments.

In contrast to equilibrium dialysis and fluorescence quenching, difference spectroscopy did not yield specific information concerning the total number of binding sites. At the lowest level of protein (0.025%) and the highest level of drug, a graph of spectral differences from 243 to 225 nm *versus* drug concentration revealed that the protein was becoming

Table I—Quenching of Native Human Serum Albumin Fluorescence by I [a]

Albumin Concentration, $M \times 10^{-6}$	Mole Ratio, n	Association Constant, $\times 10^{-6}\ M^{-1}$
1.45	3.50	1.64
2.90	3.75	1.22
7.30	4.00	1.58
10.2	3.60	1.35
14.5	4.00	0.57

[a] Excitation and emission wavelengths were 284 and 334 nm, respectively, in 1-cm quartz cells at 22 ± 1°.

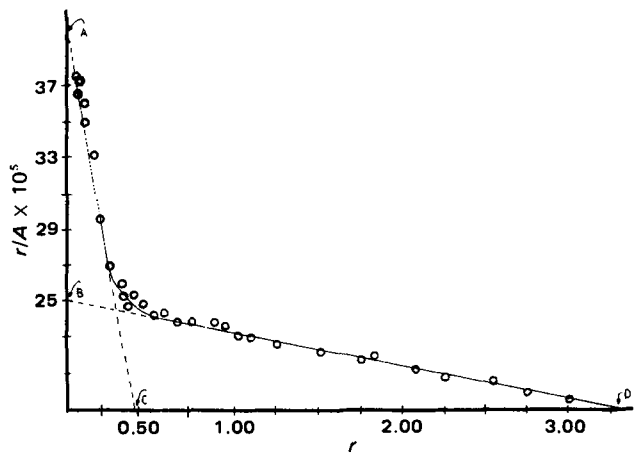

Figure 4—*Scatchard plot of* r/A versus r *for the human serum albumin–I titration for an albumin concentration of 1.45 × 10^{-6} M. A and B represent the binding constants for primary and secondary binding sites, respectively; C and D represent the number of primary and secondary binding sites, respectively.*

saturated with drug at a 20:1 drug to protein ratio. Binding constants for I calculated from both equilibrium dialysis and fluorescence quenching experiments were comparable and were in the range of 0.57–4.00 × 10^6 M^{-1}.

To elucidate the types of binding sites of I on albumin, the characteristics of curves generated by adding I to solutions of surface-active agents were studied. Difference spectra were generated as described previously, except that surface-active agents were substituted for protein. Addition of drug to an anionic surfactant produced negligible changes in absorbance. Addition of drug to a cationic surfactant produced small absorbance changes at 267 (peak) and 258 (trough) nm. Difference spectra with a nonionic surfactant (Fig. 5) produced a bathochromic shift similar to that observed between drug and albumin, indicating that binding was possibly occurring at a nonionic or hydrophobic site on the protein. Troughs appeared at 320 and 275 nm, and a peak appeared at 248 nm. The intensity of the peak was proportional to the quantity of drug added.

The hydrophobic or hydrophilic nature of binding sites on human serum albumin also was studied by other investigators (15, 16). Sudlow *et al.* (15) used dansyl sulfonamide and dansyl sarcosine as specific fluorescence markers to study two distinct binding sites on the albumin for anionic drugs such as warfarin, iophenoxic acid, and flufenamic acid. Gabay and Huang (16) used difference spectroscopy and fluorescence quenching experiments to demonstrate binding of phenothiazines to hydrophobic sites on human serum albumin. Sjoholm and Ljungstedt (17) found that the portion of albumin containing tryptophan is hydrophobic in nature.

The observed fluorescence quenching of albumin by I in the present studies could indicate that the drug is being bound near tryptophan at a hydrophobic site. Since the fluorescence of albumin arises mainly (>90%) from the aromatic tryptophan residue (one tryptophan per albumin molecule) and since that region of the albumin is hydrophobic (16, 17), a decreased fluorescence on titration of the albumin with I indicates that the tryptophan region is involved. Also binding studies of several tranquilizers and depressants with pKa values similar to I (pKa 8.3) revealed that those drugs with high binding constants ($\geq 10^5\ M^{-1}$) are bound hydrophobically (18).

It is not clear which portions of the structure of I are involved in hydrophobic binding to the albumin. Previous data obtained at pH 7.4

Table II—Binding Sites and Binding Constants for the Interaction of I and Human Serum Albumin

Method	Binding Site, n	Binding Constant, $\times 10^{-6}\ M^{-1}$
Equilibrium dialysis	Primary (0.45)	4.00
	Secondary (2.85)	0.76
Fluorescence quenching	Total (3.5–4.0)	0.57–1.64
Difference spectroscopy	>20[a]	—[b]

[a] Does not represent n but represents total sites occupied before the protein is saturated with drug. [b] Preliminary estimates of k, using methodology similar to that in enzyme kinetics yielding K_m, suggest a value of $7 \times 10^5\ M^{-1}$.

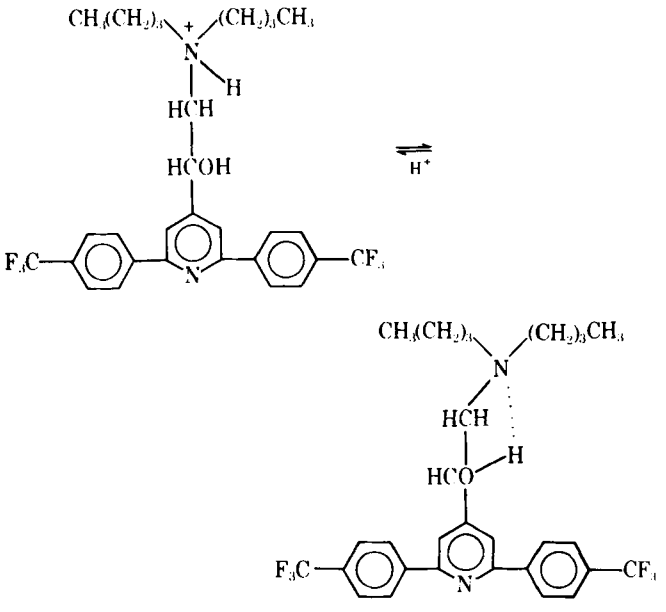

Scheme I

showed that the monocation is the predominant species (10) and that the neutral form of the drug (occurring to the extent of 10–12%) exists as an intramolecular-bonded species (Scheme I). Additional studies also demonstrated that the pyridinic nitrogen is not protonated at pH 7.4 (10). Further investigation indicated that the pKa of the pyridinic nitrogen is 0.0, a low pKa for such a nitrogen (the pKa of pyridine is 5.2). The low value was attributed to both steric and inductive effects of the two trifluoromethylphenyl substituents. These effects should diminish possible binding of albumin at the pyridinic nitrogen of I and further support the possibility for hydrophobic forces being responsible for the drug–albumin interaction.

There is possibly additional attachment of I to human serum albumin at pH 7.4 *via* the quaternary nitrogen functionality. Most antimalarials exist as mono- or dications at physiological pH (19) and can potentially

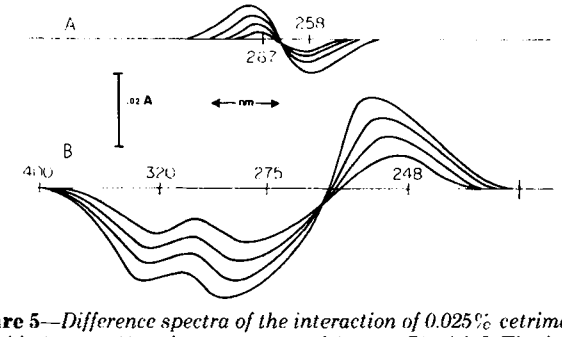

Figure 5—*Difference spectra of the interaction of 0.025% cetrimonium bromide (curves A) and 0.1% octoxynol (curves B) with I. The families of curves were generated by titrating each substance with 50-μl increments of I (5 × 10⁻⁴ M).*

interact with protein *via* the charged site. In the case of chloroquine (pKa 7.78), both species are available at pH 7.4; however, Parker and Irvin (20) showed that only the monocation interacts reversibly with bovine serum albumin. Evidence in this study for the possible attachment of I to albumin *via* the quaternary nitrogen functionality is the occurrence of red shifts of up to 10 nm obtained from difference spectroscopy experiments on addition of drug to albumin (or of albumin to drug). These shifts may represent a small change in the tertiary or quaternary structure of the protein. These types of shifts were also reported in the difference spectral study of chloroquine (19).

In summary, binding sites and binding constant data for I by equilibrium dialysis and fluorescence quenching methods are comparable. The data indicate that human serum albumin has between three and four binding sites per molecule for I, with a binding constant of approximately $1 \times 10^6\ M^{-1}$. Fluorescence quenching experiments and drug–surfactant interaction studies revealed that binding of the drug is possibly occurring at a hydrophobic site on the albumin. Difference spectroscopy data provided some evidence for additional attachment of drug to albumin *via* the charged exocyclic nitrogen.

REFERENCES

(1) W. J. Jusko and M. Gretch, *Drug Metab. Rev.*, **5**, 43 (1976).

(2) J. J. Vallner, *J. Pharm. Sci.*, **66**, 447 (1977).

(3) J. W. Bridges and A. G. E. Wilson, "Progress in Drug Metabolism," vol. 1, Wiley, New York, N.Y., 1976, pp. 193–245.

(4) O. J. Bouwsma and J. T. Stewart, *Anal. Lett.*, **9**, 1003 (1976).

(5) J. H. Perrin and J. J. Vallner, *J. Pharm. Sci.*, **64**, 1508 (1975).

(6) L. G. Craig, in "Methods in Enzymology," vol. 11, C. H. W. Hirs, Ed., Academic, New York, N.Y., 1967, p. 877.

(7) M. V. Simpson, in "Methods in Enzymology," vol. 30, K. Moldave and L. Grossman, Eds., Academic, New York, N.Y., 1974, p. 403.

(8) U. Z. Littauer, in "Methods in Enzymology," vol. 20, K. Moldave and L. Grossman, Eds., Academic, New York, N.Y., 1971, p. 72.

(9) A. S. Brill and H. E. Sandberg, *Biophys. J.*, **8**, 669 (1969).

(10) O. J. Bouwsma, J. T. Stewart, and A. C. Capomacchia, *J. Pharm. Sci.*, **67**, 1224 (1978).

(11) N. A. Attallah and G. F. Lata, *Biochim. Biophys. Acta*, **168**, 321 (1968).

(12) G. Scatchard, *Ann. N.Y. Acad. Sci.*, **51**, 660 (1949).

(13) R. F. Mais, S. Keresztes-Nagy, J. F. Zaroslinski, and Y. T. Oester, *J. Pharm. Sci.*, **63**, 1423 (1974).

(14) H. L. Conn and R. J. Luchi, *J. Clin. Invest.*, **40**, 509 (1961).

(15) G. Sudlow, D. J. Birkett, and D. N. Wade, *Mol. Pharmacol.*, **12**, 1052 (1976).

(16) S. Gabay and P. C. Huang, "The Phenothiazines and Structurally Related Drugs," I. S. Forrest, C. J. Carr, and E. Usdin, Eds., Raven, New York, N.Y., 1974, pp. 175–189.

(17) I. Sjoholm and I. Ljungstedt, *J. Biol. Chem.*, **248**, 8434 (1973).

(18) P. C. Huang and S. Gabay, *Biochem. Pharmacol.*, **23**, 957 (1974).

(19) A. Korolkovas and J. H. Burckhalter, "Essentials of Medicinal Chemistry," Wiley, New York, N.Y., 1976, pp. 403–422.

(20) I. S. Parker and J. L. Irvin, *J. Biol. Chem.*, **199**, 889 (1952).

ACKNOWLEDGMENTS

Abstracted in part from a dissertation submitted by O. J. Bouwsma to the Graduate Faculty, University of Georgia, in partial fulfillment of the Doctor of Philosophy degree requirements.

Reliability of Arrhenius Equation in Predicting Vitamin A Stability in Multivitamin Tablets

J. G. SLATER ˣ, H. A. STONE, B. T. PALERMO, and R. N. DUVALL

Received August 8, 1977, from the *Pharmacy Research Department, Consumer Products Division, Miles Laboratories, Inc., Elkhart, IN 46515.* Accepted for publication June 1, 1978.

Abstract □ Shelflife predictions of vitamin A stability in multivitamin tablets were calculated based on data obtained from the analyses of six multivitamin tablet preparations by the classical Arrhenius treatment. This approach gave excessive variation in the predictions. The same data were treated by a modified Arrhenius method, which reduced the variation. Long-term room temperature data show that incorrect slopes were predicted in three of the six sets of data with the modified approach. The data indicate that erroneous predictions can result when applying the Arrhenius treatment to accelerated data and that this approach should be used with extreme caution in establishing the expiration date of a multivitamin tablet product, especially where the limiting ingredient for expiration dating is a preprocessed raw material and not a single-entity chemical.

Keyphrases □ Vitamin A—stability in multivitamin tablets, predicted using Arrhenius equation □ Stability—vitamin A in multivitamin tablets, predicted using Arrhenius equation □ Arrhenius equation—use in predicting stability of vitamin A in multivitamin tablets

The prediction of chemical stability of pharmaceutical dosage forms is important to the pharmaceutical industry in view of impending governmental proposals on expiration dating. The technique usually used to predict shelflife has been application of the Arrhenius equation. This technique was applied first (1) to the color stability of a liquid multisulfa preparation and later to the stability of certain vitamins in liquid multivitamin preparations (2, 3).

The Arrhenius technique was used to predict expiration dates of liquid multiple-vitamin preparations (4) and vitamin A, thiamine, and ascorbic acid stability in sugar-coated multiple-vitamin tablets (5). The latter study validated the room temperature-predicted degradation rates by assaying, at various intervals, tablets that were stored at room temperature for 3 years. All of these studies were conducted under very tight controls. They all used constant-temperature baths containing oil or water to maintain their accelerated temperature-controlled conditions.

This paper presents the results of the classical and of a modified application of the Arrhenius equation in predicting vitamin A stability in several multivitamin tablet products. Since vitamin A stability in multiple-vitamin tablets is important to the total product stability (5), it is desirable to have a reliable method for its prediction. The purpose of this study was to determine the accuracy of the Arrhenius predictions for vitamin A stability in multivitamin products.

Commercially available dry vitamin A in itself is a formulated product. Its stability in bulk form and when included in a multicomponent system is largely dependent on the purity and integrity of the crystalline vitamin A, the components of the "beading" formula, and the method of achieving the final product. Thus, it is not a single, pure chemical entity to begin with, and it will vary from supplier to supplier.

EXPERIMENTAL

The two sugar-coated tablet formulations, Products A and B, had the following active ingredient composition per tablet: vitamin A, 6850 IU; vitamin D, 875 IU; ascorbic acid, 55.0 mg; thiamine, 2.5 mg; riboflavin, 2.575 mg; niacinamide, 20.4 mg; pyridoxine, 1.05 mg; cyanocobalamin, 1.35 μg; and pantothenic acid, 1.77 mg.

Four chewable tablet formulations, Products C–F, were used. Product C had the following active ingredient composition per tablet: vitamin A, 5720 IU; vitamin D, 500 IU; ascorbic acid, 57.5 mg; thiamine, 2.06 mg; riboflavin, 2.5 mg; niacinamide, 20.0 mg; pyridoxine, 1.05 mg; and cyanocobalamin, 1.15 μg. Products D–F had the same active ingredient composition as Product C but contained 6250 IU of vitamin A/tablet.

All of these compositions are theoretical levels based on bulk label and do not include supplier overages.

The official USP UV absorption method (6) was used to assay for vitamin A content in these tablets. Random samples were taken from the population of each of the six products. One sample was set aside for initial testing of vitamin A content while the other samples were packaged in screw-capped glass containers and placed in temperature-controlled conditions at 50[1], 40[1], 25[1], 55[2], or 45[2] ± 1°.

Products A–D were placed at 50, 45, 40, and 25°. For Products A and B, samples at 50° were withdrawn and assayed every 2nd week for 8 weeks; those at 45° were withdrawn every 3rd week for 12 weeks; those at 40° were withdrawn every 4th week for 16 weeks; and those at 25° were assayed at 26, 52, 95, and 156 weeks. For Products C and D, samples at 50, 45, and 40° were withdrawn and assayed every 4th week for 16 weeks; those at 25° were assayed at 26, 52, 78, 104, and 156 weeks.

Products E and F were placed at 55, 50, 45, 40, and 25°. Samples at 55° were assayed every week for 6 weeks; those at 50° were assayed every 2nd week for 10 weeks; those at 45 and 40° were assayed every 4th week for 16 weeks; and those at 25° were assayed at 13, 26, 35, 52, and 104 weeks (Product E) and at 13, 26, 52, 104, and 156 weeks (Product F).

RESULTS

Figure 1 shows a typical plot of the thermodegradation of vitamin A in these products. The open circle (at time zero) is the average of six assays of five tablets each run by two individuals in triplicate. The other points on the graph are averages of four assays of five tablets each run by two individuals in duplicate. This general format was followed for the six products.

Table I contains the thermodegradation data for the six products. Standard statistical techniques (7–10) were used to calculate the table

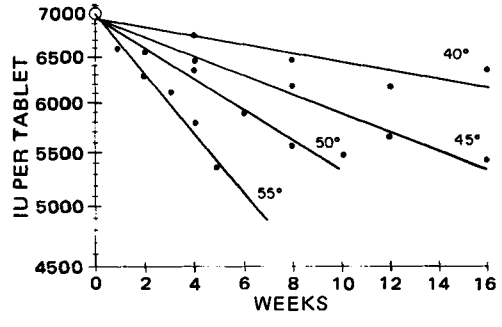

Figure 1—*Typical pseudo-first-order plots of the thermodegradation of vitamin A.*

[1] Walk-in storage areas, Tyler Refrigeration Corp.
[2] Thelco model 4 bench top unit, Precision Scientific Co.

0022-3549/79/0100-0049$01.00/0
© 1979, American Pharmaceutical Association

Table I—Initial Vitamin A and Values of Calculated Rate Constants and Intercepts with 95% Confidence Limits for Each Thermodegradation Curve

Product	ln (Average Initial Potency)	40°		45°		50°		55°	
		k, weeks^{-1}	b, ln potency	k, weeks^{-1}	b, ln potency	k, weeks^{-1}	b, ln potency	k, weeks^{-1}	b, ln potency
A	8.83	0.0353 ± 0.00415	8.82 ± 0.0371	0.0723 ± 0.00495	8.84 ± 0.0332	0.132 ± 0.00924	8.81 ± 0.0413	—	—
B	8.93	0.0570 ± 0.00418	8.95 ± 0.0374	0.132 ± 0.00608	8.96 ± 0.0408	0.247 ± 0.0218	8.85 ± 0.0976	—	—
C	8.70	0.0136 ± 0.00227	8.70 ± 0.0212	0.0188 ± 0.00246	8.70 ± 0.0230	0.0282 ± 0.00399	8.69 ± 0.0373	—	—
D	8.82	0.00680 ± 0.00134	8.82 ± 0.0125	0.0112 ± 0.00207	8.82 ± 0.0191	0.0194 ± 0.00210	8.81 ± 0.0196	—	—
E	8.83	0.00597 ± 0.00119	8.82 ± 0.0111	0.0141 ± 0.00180	8.83 ± 0.0168	0.0259 ± 0.00306	8.83 ± 0.0178	0.0459 ± 0.00708	8.81 ± 0.0237
F	8.85	0.00729 ± 0.00232	8.84 ± 0.0217	0.0164 ± 0.00196	8.85 ± 0.0183	0.0268 ± 0.00285	8.85 ± 0.0152	0.0520 ± 0.00493	8.85 ± 0.0172

Table II—Range of Room Temperature k Values from Confidence Limits of Arrhenius Plot, Predicted Range of Vitamin A Potency from k Values and Room Temperature Intercept at t = 156, k Values and Intercepts with Confidence Limits from Room Temperature Data, 95% Confidence Limits, Range of Vitamin A Potency at t = 156 Weeks, and Overlap Data

Product	Arrhenius Plot Data: Range of Predicted k Values, weeks^{-1}	Arrhenius Plot Data: Range of Predicted Vitamin A Potency, IU/tablet	25° Data: k, weeks^{-1}	25° Data: b, ln Intercept ±95% Confidence Limits	25° Data: 95% Confidence Limits, IU/tablet	Overlap
A	0.000844-0.0208	273-6100	0.00129	8.85 ± 0.0346	5410-5990	Over entire range
B	0.000221-0.134	0-7390	0.00153	8.94 ± 0.0298	5770-6290	Over entire range
C	0.000943-0.0177	380-5130	0.00164	8.69 ± 0.0385	4380-4840	Over entire range
D	0.000494-0.00304	4200-6240	0.000560	8.82 ± 0.0171	6050-6300	Over entire range
E	0.000282-0.00169	5280-6580	0.00214	8.84 ± 0.0283	4600-5270	0-45.8 weeks and after 162.6 weeks
F	0.000402-0.00214	5020-6590	0.00150	8.86 ± 0.0120	5460-5640	Over entire range

values. The intercepts and the average of the initial assay values agreed well; in fact, the initial values are in the range of the limits of the intercept, which indicates that the pseudo-first-order degradation model is correct.

The Arrhenius equation data were plotted by Arrhenius plotting techniques and are typically represented by Product E in Fig. 2. This figure was generated using the least-squares fitting technique (7–10). After the Arrhenius equations were determined, a range of predicted room temperature rate constants were determined from the confidence limit curves. This range is shown by broken lines in Fig. 3 for Product E when inserted into the room temperature degradation equation (11). The statistically treated room temperature data for Product E are represented by the solid line and curves in Fig. 3.

To determine accurately the overlap between y values found from predicted k values and the values found from the 95% confidence limits about the room temperature data, the point or points of intersection must be determined. Algebraic manipulation of the equations gives rise to a quadratic equation to solve for x (12). The range of k values obtained from the confidence limits about the Arrhenius plot regression line, the predicted range of vitamin A potency at t = 156 weeks, the 25° data equations as determined by least-squares fitting, the range of vitamin A potency from the 95% confidence limits about the room temperature regression line at t = 156 weeks, and the overlap values for the six products are listed in Table II.

The potency of the vitamin A remaining was obtained by substituting the predicted k values into the room temperature degradation equation, setting t = 156 weeks, setting ln C_0 equal to the 25° data equation intercept, and taking the antilogarithm. Inspection of Table II reveals that the predicted k values and 95% confidence limits overlapped over the entire 156 weeks for all products except E. It also can be concluded that the classical application of the Arrhenius techniques gives such a wide range of k values and subsequent potency at 3 years as to be of little value. For instance, the prediction for Product B is from 0 to 7390 IU/tablet, which is meaningless.

It was, therefore, decided to use a modified application of the Arrhenius technique[3].

The degradation rate constants, k, were calculated by the formula (13):

$$m = \frac{y_1 - y_2}{x_1 - x_2} \qquad \text{(Eq. 1)}$$

where y_1 = ln [Σ initial vitamin A potency/n], y_2 = ln [Σ vitamin A potency at time x_2/n], $x_1 = 0$, and x_2 = time in weeks at y_2. For comparison to the classical method, an average k at each temperature and the 95% confidence limits on k were calculated (14, 15). These values for all six products at each temperature are given in Table III. A comparison of Tables I and III reveals that the range of k values overlapped in all cases,

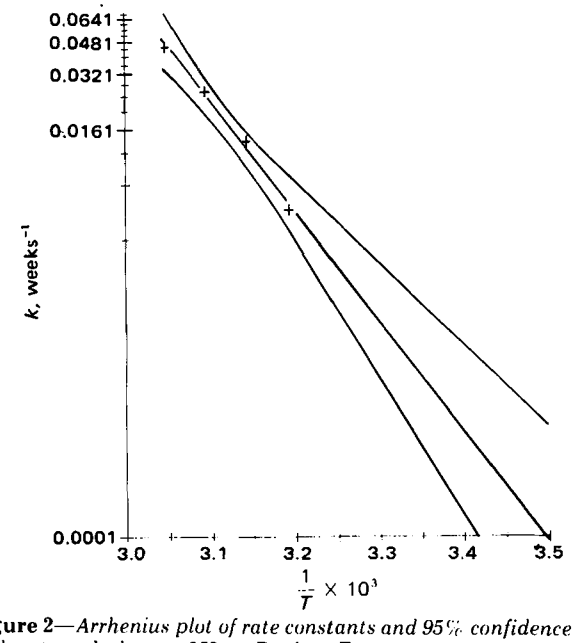

Figure 2—*Arrhenius plot of rate constants and 95% confidence limits with extrapolations to 25° on Product E.*

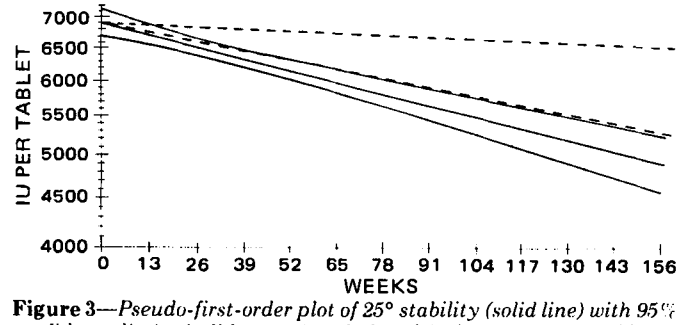

Figure 3—*Pseudo-first-order plot of 25° stability (solid line) with 95% confidence limits (solid curves) and plot of Arrhenius upper and lower predicted* k *values (broken lines) on Product E.*

[3] Suggested by J. T. Carstensen to B. T. Palermo, June 16, 1976.

Table III—Average k Values and 95% Confidence Limits for Each Thermodegradation Curve

Product	40°	45°	50°	55°
A	0.0370 ± 0.00455	0.0746 ± 0.0120	0.145 ± 0.0205	—
B	0.0521 ± 0.00790	0.123 ± 0.0151	0.285 ± 0.0626	—
C	0.0138 ± 0.00341	0.0197 ± 0.00652	0.0315 ± 0.00932	—
D	0.00703 ± 0.00305	0.0117 ± 0.00229	0.0214 ± 0.00330	—
E	0.00722 ± 0.00199	0.0128 ± 0.00306	0.0275 ± 0.00333	0.0560 ± 0.0177
F	0.00965 ± 0.00416	0.0180 ± 0.00424	0.0280 ± 0.00354	0.0527 ± 0.00506

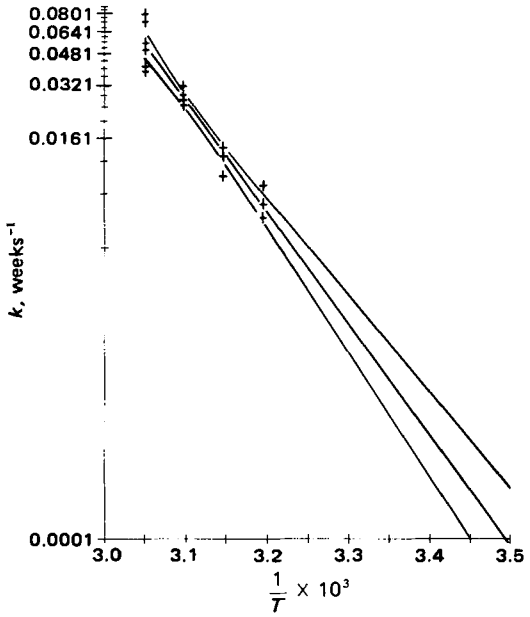

Figure 4—*Arrhenius plot of rate constants derived from modified application and 95% confidence limits with extrapolations to 25° on Product E.*

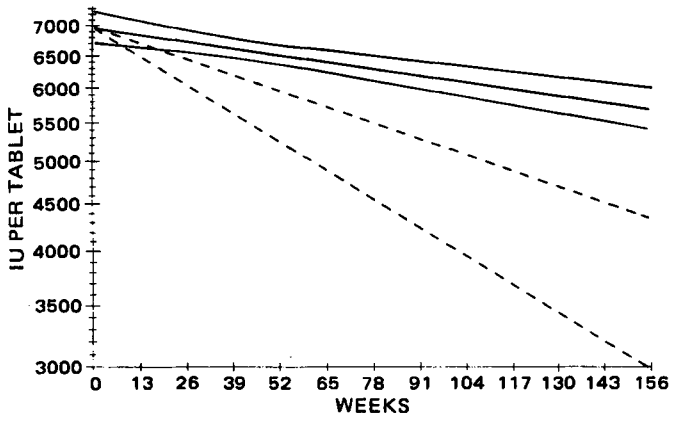

Figure 5—*Pseudo-first-order plot of 25° stability (solid line) with 95% confidence limits (solid curves) and plot of Arrhenius upper and lower predicted* k *values (broken lines) from modified application on Product A.*

indicating that the k values were not altered significantly from the classical approach.

The modified Arrhenius equation plot is typically represented by Product E in Fig. 4. These data were treated as were the previous Arrhenius plot data to give a range of k values and are shown by broken lines in Fig. 5 for Product A when inserted into the room temperature degradation equation. The actual room temperature data found for Product A also are represented in Fig. 5 by the solid line and curves. The range of k values, predicted vitamin A potency at t = 156 weeks, and overlap data are given in Table IV for all six products.

Comparison of the lower and upper k values in Tables II and IV reveals that this procedure predicts k values within the range predicted by the classical procedure, which indicates that the Arrhenius equation plot was not changed significantly. This comparison also reveals that the modified procedure results in a much smaller range of k values and, consequently, a tighter limit of vitamin A potency at 3 years. This result is due to the difference in the degrees of freedom (two for the classical application and 17 for the modified application for Product E), with a resulting smaller t value for the modified application of the Arrhenius plot. Table IV also shows that the Arrhenius plot did not accurately predict the room temperature degradation pattern in three of the six products.

Table IV—Range of k Values Obtained from Modified Application of the Arrhenius Technique, Predicted Range of Vitamin A Potency from k Values and Room Temperature Intercept at t = 156, and Overlap Data

Product	Range of Predicted k Values, weeks^{-1}	Range of Predicted Vitamin A Potency, IU/tablet	Overlap
A	0.00302–0.00539	3010–4350	0–17.0 weeks
B	0.00233–0.00469	3670–5310	0–28.7 weeks
C	0.00193–0.00639	2190–4400	Over entire range
D	0.000571–0.00195	4990–6190	Over entire range
E	0.000451–0.00109	5830–6440	0–20.7 weeks
F	0.00102–0.00211	5070–6010	Over entire range

DISCUSSION

The shelflife of a product is determined by the stability of its most unstable ingredient. In the multiple-vitamin products, vitamin A is the limiting ingredient. The problem is to find a method that will establish accurately the stability pattern of vitamin A in these products at room temperature. When vitamin A data generated at elevated temperatures are treated by the classical application of the Arrhenius plot, the resulting predicted range of room temperature k values is very wide. The modified application simply increases the degrees of freedom by determining a greater number of rate constants from the available data, which decreases the range of predicted k values without altering the Arrhenius equation.

The predicted room temperature degradation lines as determined by the k values should be inside the actual room temperature confidence limits or encompass those limits. Since three of the six products tested did not meet these criteria, it was concluded that the Arrhenius equation did not give the same room temperature k value as was calculated from the room temperature data. Therefore, 25° stability data must be generated to determine the shelflife accurately.

This study did not corroborate Tardif's (5) findings that the room temperature stability data validate the predicted degradation rates of vitamin A. Tardif used constant-temperature oil baths and different temperatures than were used in this study. Both studies indicated that the pseudo-first-order reaction rate is the correct model; however, this study generated an incorrect predicted k in three out of six cases.

REFERENCES

(1) E. R. Garrett and R. F. Carper, *J. Am. Pharm. Assoc., Sci. Ed.*, **44**, 515 (1955).

(2) E. R. Garrett, *ibid.*, **45**, 171 (1956).

(3) E. R. Garrett, *ibid.*, **45**, 470 (1956).

(4) N. A. McLeod, O. Pelletier, and J. A. Campbell, *Can. Pharm. J.*, **3**, 948 (1964).

(5) R. Tardif, *J. Pharm. Sci.*, **54**, 281 (1965).

(6) "The United States Pharmacopeia," 17th rev., Mack Publishing Co., Easton, Pa., 1965, p. 890.

(7) W. J. Dixon and F. J. Massey, Jr., "Introduction to Statistical Analysis," 2nd ed., McGraw-Hill, New York, N.Y., 1957, p. 191.

(8) J. T. Carstensen, "Theory of Pharmaceutical Systems," vol. 1, Academic, New York, N.Y., 1972, p. 179.
(9) D. V. Huntsberger, "Elements of Statistical Inference," Allyn and Bacon, Boston, Mass., 1961, p. 198.
(10) W. J. Dixon and F. J. Massey, Jr., "Introduction to Statistical Analysis," 2nd ed., McGraw-Hill, New York, N.Y., 1957, p. 195.
(11) J. T. Carstensen, "Theory of Pharmaceutical Systems," vol. 1, Academic, New York, N.Y., 1972, p. 171.
(12) G. E. Moore, "Algebra, College Outline Series," 1st ed. rev., Barnes and Noble, New York, N.Y., 1951, p. 73.
(13) W. A. Wilson and J. I. Tracy, "Analytic Geometry," 3rd ed., D. C. Heath, Boston, Mass., 1949, p. 52.
(14) W. J. Dixon and F. J. Massey, Jr., "Introduction to Statistical Analysis," 2nd ed., McGraw-Hill, New York, N.Y., 1957, p. 16.
(15) W. J. Dixon and F. J. Massey, Jr., *ibid.*, p. 128.

ACKNOWLEDGMENTS

The authors are grateful to Dr. J. T. Carstensen, University of Wisconsin, Madison, Wis., for suggestions and review of the manuscript.

Formulation and Evaluation of Ethiodized Oil Emulsion for Intravenous Hepatography

GEORGE GRIMES *, MICHAEL VERMESS ‡, JOSEPH F. GALLELLI *, MARY GIRTON ‡, and DULAL C. CHATTERJI *x

Received April 28, 1978, from the **Pharmacy Department and the* ‡*Diagnostic Radiology Department, The Clinical Center, National Institutes of Health, Bethesda, MD 20014.* Accepted for publication June 12, 1978.

Abstract □ A study was conducted to prepare and evaluate an ethiodized oil emulsion for intravenous administration that would selectively opacify the liver. Several formulations with differing globule size were prepared and compared for their *in vivo* activity (degree of liver opacification obtained) and stability. Results of studies conducted in rabbits and monkeys revealed that the oil globules that concentrate most in liver were 2.0–3.0 μm in diameter. The formulation of choice was stable for 6 months at refrigeration temperature (2–6°). In monkeys, this formulation produced an improved diagnostic image of the liver using computerized tomography at a dose of 0.2 ml/kg. The potential use of such emulsions in diagnostic radiology is briefly discussed.

Keyphrases □ Ethiodized oil—various emulsions for intravenous administration prepared, effect of oil globule size on liver opacification in rabbits and monkeys □ Radiopaque media—ethiodized oil, various emulsions for intravenous administration prepared, effect of oil globule size on liver opacification in rabbits and monkeys □ Hepatography, intravenous—various emulsions of ethiodized oil prepared, effect of oil globule size on liver opacification in rabbits and monkeys

There have been numerous previous attempts to opacify the liver and spleen by intravenously administered contrast material. As early as 1930, Keith and Briggs (1) used intravenously injected emulsified oil to opacify the liver and spleen in rats. Degkwitz (2) produced an iodine-containing oily contrast material[1] (I), which was used in clinical studies (3) following experiments in animals.

Experimental work (4) with I in mice, rabbits, and guinea pigs indicated that intravenous injection did opacify the spleen, liver, and placenta. This same contrast material was used in nine patients but was too toxic for routine clinical examinations (5). Emulsified ethyl diiodostearate was injected in 10 patients, most of whom had severe toxic reactions (6). Experimental work (7) in dogs used an emulsified oily contrast medium of ethiodized oil[2]. The average globule size of the emulsion (7) was 0.3 μm, and it opacified the liver and spleen.

Recently, two experimental emulsified forms of iodized oil[3], II*a* and II*b*, were produced. Their basic difference was the average globule size of the emulsion, II*a* (emulsion grossiere) having the larger globule size and II*b* (emulsion fine) the smaller. Emulsion II*b*, mode diameter of 1.3 μm (range 0.16–7 μm), was used intravenously in two clinical studies (8, 9), but up to 75% of the patients had disturbing reactions such as fever, chill, anorexia, nausea, vomiting, and a 10–20% drop in platelet counts. These reactions appeared to be dose related and almost constant above the 1.2-ml/kg dose level. In another study (10) with 32 rhesus monkeys, a 2.0-ml/kg iv dose of the same emulsion produced an opacified diagnostic image of the liver and spleen on X-ray examination.

A recent revolutionary discovery in diagnostic roentgenology, computerized tomography (CT), with its improved contrast resolution, raised hopes that a fraction of the previously utilized dose would opacify the liver sufficiently for diagnostic evaluation without undesirable side effects. With this new equipment, Vermess *et al.* (11) opacified the liver and demonstrated carcinogen-induced hepatic tumor in the rhesus monkey with an intravenous dose as low as 0.1–0.2 ml of II*b*/kg.

The possible use of such small doses in human subjects renewed interest in the ethiodized oil emulsion for clinical hepatography. Unfortunately, II*b* was no longer available. Therefore, a study was initiated to prepare an ethiodized oil emulsion for intravenous hepatography. In addition, since none of the mentioned reports attempted to correlate the size of the oil globules with the opacifying ability and since no quantitative data related the dose to the density of the liver scans, a more systematic study of the subject appeared to be warranted.

The size of the oil globules is of primary importance in the opacification of the various tissues, in accordance with Degkwitz's theory that different tissues absorb oil globules of different sizes (2). This fact compounded the problem

[1] Jodsol.
[2] Ethiodol, iodinated ester of poppyseed oil, iodine content 37% (w/v), is routinely used for lymphography; Savage Laboratories, Houston, TX 77036.
[3] II*a* is AG-52-315 and II*b* is AG 60-99; Lipidol UF, Laboratoires Andre Guerbet, Aulnay sur Bois, France.

0022-3549/79/0100-0052$01.00/0
© 1979, American Pharmaceutical Association

(8) J. T. Carstensen, "Theory of Pharmaceutical Systems," vol. 1, Academic, New York, N.Y., 1972, p. 179.
(9) D. V. Huntsberger, "Elements of Statistical Inference," Allyn and Bacon, Boston, Mass., 1961, p. 198.
(10) W. J. Dixon and F. J. Massey, Jr., "Introduction to Statistical Analysis," 2nd ed., McGraw-Hill, New York, N.Y., 1957, p. 195.
(11) J. T. Carstensen, "Theory of Pharmaceutical Systems," vol. 1, Academic, New York, N.Y., 1972, p. 171.
(12) G. E. Moore, "Algebra, College Outline Series," 1st ed. rev., Barnes and Noble, New York, N.Y., 1951, p. 73.
(13) W. A. Wilson and J. I. Tracy, "Analytic Geometry," 3rd ed., D. C. Heath, Boston, Mass., 1949, p. 52.
(14) W. J. Dixon and F. J. Massey, Jr., "Introduction to Statistical Analysis," 2nd ed., McGraw-Hill, New York, N.Y., 1957, p. 16.
(15) W. J. Dixon and F. J. Massey, Jr., *ibid.*, p. 128.

ACKNOWLEDGMENTS

The authors are grateful to Dr. J. T. Carstensen, University of Wisconsin, Madison, Wis., for suggestions and review of the manuscript.

Formulation and Evaluation of Ethiodized Oil Emulsion for Intravenous Hepatography

GEORGE GRIMES *, MICHAEL VERMESS ‡, JOSEPH F. GALLELLI *, MARY GIRTON ‡, and DULAL C. CHATTERJI *x

Received April 28, 1978, from the **Pharmacy Department and the* ‡*Diagnostic Radiology Department, The Clinical Center, National Institutes of Health, Bethesda, MD 20014.* Accepted for publication June 12, 1978.

Abstract □ A study was conducted to prepare and evaluate an ethiodized oil emulsion for intravenous administration that would selectively opacify the liver. Several formulations with differing globule size were prepared and compared for their *in vivo* activity (degree of liver opacification obtained) and stability. Results of studies conducted in rabbits and monkeys revealed that the oil globules that concentrate most in liver were 2.0–3.0 μm in diameter. The formulation of choice was stable for 6 months at refrigeration temperature (2–6°). In monkeys, this formulation produced an improved diagnostic image of the liver using computerized tomography at a dose of 0.2 ml/kg. The potential use of such emulsions in diagnostic radiology is briefly discussed.

Keyphrases □ Ethiodized oil—various emulsions for intravenous administration prepared, effect of oil globule size on liver opacification in rabbits and monkeys □ Radiopaque media—ethiodized oil, various emulsions for intravenous administration prepared, effect of oil globule size on liver opacification in rabbits and monkeys □ Hepatography, intravenous—various emulsions of ethiodized oil prepared, effect of oil globule size on liver opacification in rabbits and monkeys

There have been numerous previous attempts to opacify the liver and spleen by intravenously administered contrast material. As early as 1930, Keith and Briggs (1) used intravenously injected emulsified oil to opacify the liver and spleen in rats. Degkwitz (2) produced an iodine-containing oily contrast material[1] (I), which was used in clinical studies (3) following experiments in animals.

Experimental work (4) with I in mice, rabbits, and guinea pigs indicated that intravenous injection did opacify the spleen, liver, and placenta. This same contrast material was used in nine patients but was too toxic for routine clinical examinations (5). Emulsified ethyl diiodostearate was injected in 10 patients, most of whom had severe toxic reactions (6). Experimental work (7) in dogs used an emulsified oily contrast medium of ethiodized oil[2]. The average globule size of the emulsion (7) was 0.3 μm, and it opacified the liver and spleen.

Recently, two experimental emulsified forms of iodized oil[3], II*a* and II*b*, were produced. Their basic difference was the average globule size of the emulsion, II*a* (emulsion grossiere) having the larger globule size and II*b* (emulsion fine) the smaller. Emulsion II*b*, mode diameter of 1.3 μm (range 0.16–7 μm), was used intravenously in two clinical studies (8, 9), but up to 75% of the patients had disturbing reactions such as fever, chill, anorexia, nausea, vomiting, and a 10–20% drop in platelet counts. These reactions appeared to be dose related and almost constant above the 1.2-ml/kg dose level. In another study (10) with 32 rhesus monkeys, a 2.0-ml/kg iv dose of the same emulsion produced an opacified diagnostic image of the liver and spleen on X-ray examination.

A recent revolutionary discovery in diagnostic roentgenology, computerized tomography (CT), with its improved contrast resolution, raised hopes that a fraction of the previously utilized dose would opacify the liver sufficiently for diagnostic evaluation without undesirable side effects. With this new equipment, Vermess *et al.* (11) opacified the liver and demonstrated carcinogen-induced hepatic tumor in the rhesus monkey with an intravenous dose as low as 0.1–0.2 ml of II*b*/kg.

The possible use of such small doses in human subjects renewed interest in the ethiodized oil emulsion for clinical hepatography. Unfortunately, II*b* was no longer available. Therefore, a study was initiated to prepare an ethiodized oil emulsion for intravenous hepatography. In addition, since none of the mentioned reports attempted to correlate the size of the oil globules with the opacifying ability and since no quantitative data related the dose to the density of the liver scans, a more systematic study of the subject appeared to be warranted.

The size of the oil globules is of primary importance in the opacification of the various tissues, in accordance with Degkwitz's theory that different tissues absorb oil globules of different sizes (2). This fact compounded the problem

[1] Jodsol.
[2] Ethiodol, iodinated ester of poppyseed oil, iodine content 37% (w/v), is routinely used for lymphography; Savage Laboratories, Houston, TX 77036.
[3] II*a* is AG-52-315 and II*b* is AG 60-99; Lipidol UF, Laboratoires Andre Guerbet, Aulnay sur Bois, France.

0022-3549/79/0100-0052$01.00/0
© 1979, American Pharmaceutical Association

of making the emulsion; aside from the usual safety problems associated with intravenous emulsions (12, 13), the globule size needed to be within a narrow range so that maximum selective opacification of the liver could be obtained.

Various intravenous emulsions of different globule sizes were prepared and tested in rabbits and monkeys. Since such emulsions lose their effectiveness with age (10, 14), probably due to the instability of the emulsion, studies also were conducted to determine the stability and the reproducibility of various emulsion formulations with respect to globule size, distribution, and retention of *in vivo* activity. The feasibility of preparing a sterile emulsion also was investigated.

EXPERIMENTAL

Materials and Equipment—Water for injection[4], ethiodized oil[2], polysorbate 80[5], sorbitan monooleate[5], phosphatidyl choline[6], and particle-free electrolyte solution[7] were used as received. All other chemicals were reagent grade.

An alcoholic extract of lecithin was prepared as follows. About 200 ml of absolute ethanol was added to 50 g of soy lecithin-refined[8], and the mixture was stirred for 20 min and filtered through a fine muslin and then through a filter paper[9]. The remaining slurry and filters were rinsed with enough alcohol to give a final volume of 200 ml of filtrate. When analyzed for solid content (by drying in a steam bath to constant weight), each milliliter of the extract was found to contain 45 mg of solids.

Emulsions were prepared using a homogenizer[10], and their globule size was evaluated using an electronic counter[11]. Computerized tomographic scans for liver were performed with a computerized body scanner[12].

Preparation of Emulsions—In each emulsion, the contents of four 10-ml ampuls of ethiodized oil (total volume of 40 ml, 53 g) were emulsified and brought to a total volume of 100 ml. Thus, the emulsions contained 53% (w/v) of ethiodized oil, equivalent to approximately 0.2 g of iodine/ml of emulsion. Emulsions were prepared by dissolving water-soluble ingredients and emulsifiers in water and oil-soluble emulsifiers in oil. The alcoholic extract of lecithin, when required in the formulation, was also added to the oil phase.

Each phase was heated separately, with mechanical stirring, to 60°. The oil phase was then poured slowly into the stirring aqueous phase. Stirring was continued for 3 min to form the primary oil-in-water emulsion. The volume of the mixture was adjusted to 100 ml with water, and the mixture was then poured into a 500-ml homogenizer flask and milled at specific speed settings (medium, medium high, or high) for a specified time. The rotor shaft of the homogenizer contained two sharp propeller blades, each 3 cm long and 1.5 cm apart at an angle of 30° to each other. The lower blade was fixed at the extreme end of the shaft and adjusted to 6 mm above the bottom surface of the homogenizing flask.

Sterile emulsions were prepared by passing each phase through sterile 0.22-μm filters[13] into sterile flasks and carrying out the remaining procedures (as already described) using the aseptic technique and sterile equipment and supplies where needed. The emulsions were then aseptically transferred to sterile 50-ml multiple-dose vials, which were stoppered with sterile rubber closures and crimped with aluminum caps. The vials were stored at room and refrigeration (2–6°) temperatures.

Experimental Evaluation *In Vitro*—*Gross Observation*—Each emulsion was periodically checked visually for sedimentation, viscosity changes, and redispersibility of layers.

Microscopic Observation—Approximately 0.5 ml of a well-shaken emulsion was diluted with 20 ml of distilled water and again mixed well. One drop of this dilution was placed on a microscope slide and observed at ×1125 magnification. A grid attachment (1.8 μm/grid square) in the ocular lens was used to measure globule size.

In general, a good emulsification resulted in a maximum number of globules in the 1–3-μm size range. Particular attention was given to the number of globules above 5 μm (diameter) or to any unusual or undissolved particles.

Electronic Counter Analysis—The electronic counter was used for quantitating the globule size of the emulsions. To prepare samples for analysis, the emulsions were diluted to a 1:40,000 concentration by first taking 50 μl of an emulsion and then diluting it with 2 ml of electrolyte solution[7]. A 20-μl aliquot of this dilution was further diluted to 20 ml with electrolyte solution[7] in a disposable, particle-free, plastic beaker[14]. Counts were then performed using a 30-μm apperture tube and a 50-μl sampling volume, which generally contained from 80,000 to 100,000 globules above 0.75 μm in diameter.

The counter was calibrated with 2.02-μm monosized, polystyrene beads[15]. Counts representing the number of globules above a specified diameter were obtained[16]. The count between any size range was calculated by the difference between the cumulative counts above the extremes. The average volume of the globules in a given size range was calculated by the geometric mean of the extremes of the range. Globules below 0.75 μm in diameter were not considered in calculations or evaluation because they were thought to be unimportant in opacifying the liver and because the total volume of this range would not significantly contribute to error in the volume calculations of the larger globules (the contribution of d^3 factor decreases rapidly as diameter, d, decreases). Both the number and volume distribution of the oil globules in the emulsions were calculated.

A potential source of error with this counting procedure should be discussed. During the counting, it appeared that counts for globules larger than 2.0 μm decreased with time (in the diluted emulsion) whereas counts for particles around 1.0 and 1.5 μm remained relatively constant. This result is contrary to the general behavior of emulsions, which, after dilution with saline solutions, usually give higher counts of larger globules, apparently due to coalescence of smaller globules (15, 16). No explanation is apparent for the unusual behavior of ethiodized oil emulsion diluted in electrolyte solution. To minimize this error, the counts were taken as quickly as possible after mixing, starting from the largest size (7 μm) and working down to the 1-μm level. All data presented are the average of at least three runs.

Experimental Evaluation *In Vivo*—The *in vivo* evaluation of the emulsions was performed in three stages. Not all emulsions were examined at all three stages; many were eliminated at the first- or second-stage level.

First-Stage Experiments—First-stage experiments were done with groups of four New Zealand White rabbits, 1.0–3.3 kg. Following the cannulation of an ear vein, the animals were lightly anesthetized with a 2% solution of thiamylal sodium. The initial dose was 1 ml/kg; additional small doses were administered as required to keep the animal under light anesthesia. A 2-ml/kg dose of the experimental emulsion was then injected through the same venipuncture, with the injection rate approximately 1 ml/min.

Prior to the intravenous injection of the emulsion, a preliminary abdominal radiograph was obtained on each animal. Following the completion of the injection, additional X-rays were obtained at 0.5, 1, 1.5, 2, and 3 hr. The increase of the opacity of the livers and spleens was then visually compared, and the effectiveness of the emulsion was evaluated on the basis of the comparison.

Second-Stage Experiments—New Zealand White rabbits were again utilized in groups of four. The preliminary anesthesia was performed as in Stage I. Three of the four rabbits received 0.5 ml/kg of the test emulsions *via* the intravenous cannula, with the injection rate the same as in Stage I. One rabbit in the group was used as a control and injected with 0.5 ml of normal saline/kg. Following the injection, the animals were kept under light anesthesia for 1 hr and then sacrificed by rapid intravenous injection of thiamylal sodium until the cessation of respiration and heartbeat.

The dead animals were refrigerated for 2 hr, after which computerized tomographic scans of the livers and, occasionally, the spleens were obtained. The computerized tomographic scans were performed with a computerized body scanner[12] utilizing the 25.4-cm scanning circle and

[4] Abbott Laboratories, North Chicago, Ill.
[5] Atlas Chemical Industries, Wilmington, Del.
[6] Phospholipon-80, containing 80% phosphatidyl choline, American Lecithin Co., Atlanta, Ga.
[7] Isoton II, conducting fluid for Coulter Counter measurements, Coulter Diagnostics, Hialeah, Fla.
[8] ICN Pharmaceuticals, Cleveland, Ohio.
[9] No. 2, Whatman, Clifton, N.J.
[10] Homogenizer 45, Virtis Research Equipment, Gardiner, N.Y.
[11] Model B, Coulter Electronics, Hialeah, Fla.
[12] Model EMI 5005, Electric and Musical Industries, Northbrook, Ill.
[13] Millipore Corp., Bedford, Mass.
[14] Accuvette II, Coulter Diagnostics, Hialeah, Fla.
[15] Coulter Electronics, Hialeah, Fla.
[16] Corrected for coincidence as directed in the instrument manual.

Table I—Formulation of Emulsions

Emulsion	Emulsifier/100 ml	Mix Speed[a]	Comments
III	Polysorbate 80, 4.5 g, and sorbitan monooleate, 1.5 g	Medium	Opacified spleen but did not significantly opacify liver; average globule size smallest of all emulsions and least effective
IV	Polysorbate 80, 2.25 g, and sorbitan monooleate, 0.75 g	Medium high	Opacified liver well but not as well as V and VI
V	Alcoholic extract of lecithin[b], 10 ml	Medium high	Most effective of all emulsions in liver opacification, reproducibility, and clarity
VI	Lecithin in ethanol, 3.0 g/10 ml	Medium high	Opacified as well as V but not as reproducible
II*b*	Lecithin, 3 g, and polyoxyl 40 stearate, 1.2 g		Unavailable commercial product, used for comparison purposes

[a] The mix time was 3 min for Emulsions III–VI. [b] Extract from 2.5 g of lecithin; representing 0.45 g of extracted solids.

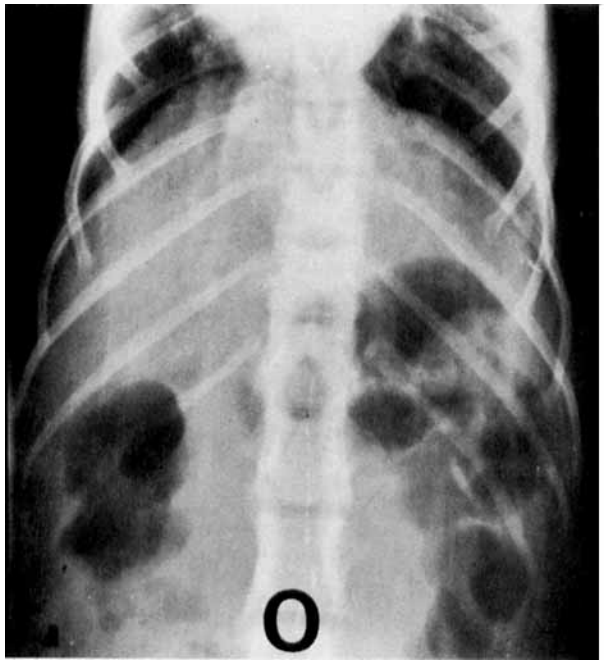

a

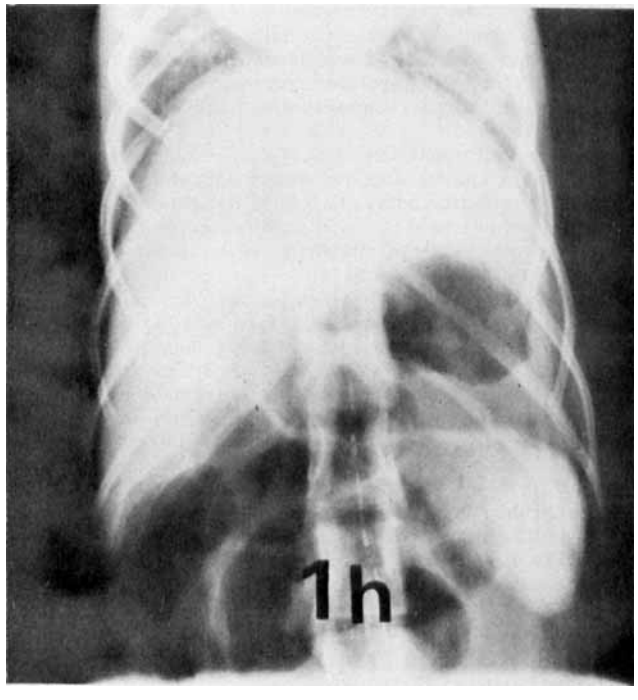

b

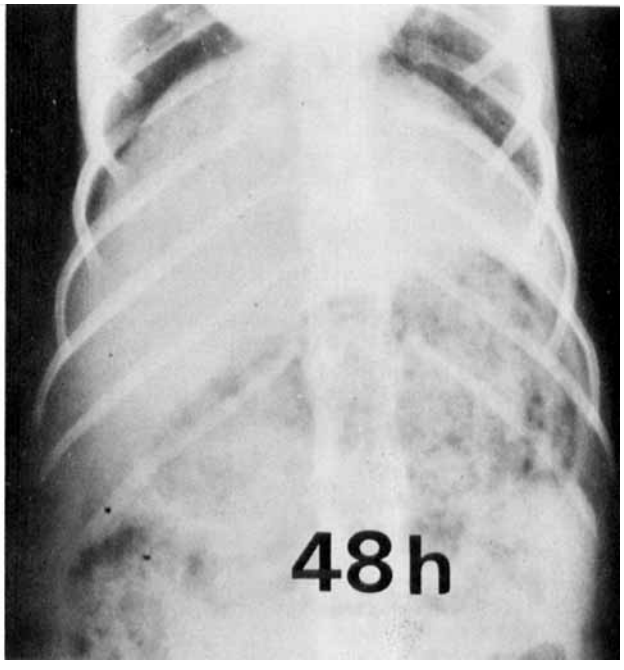

c

Figure 1—*Radiographs of rhesus monkey livers before* (a), *1 hr* (b), *and 48 hr* (c) *after the intravenous injection of 2 ml of Emulsion V/kg. Note marked increase in the density of liver and spleen after 1 hr and almost complete clearance of the contrast material 48 hr after the injection.*

80-sec scanning time. The slice thickness of the scans was 13 mm, and the scans were performed at 1-cm distances. The number of slices necessary to obtain proper visualization of the liver parenchyma varied according to the size of the livers. The densities of the livers and, occasionally, the spleens were measured both visually on the measure mode and by the computer-generated mean attenuation value of a selected homogeneous area of the liver on the independent viewing console.

Third-Stage Experiments—These experiments were conducted on three female and two male normal rhesus monkeys, 3–6 kg. The animals were sedated and anesthetized as described previously (11). To prevent respiratory motion during the 80-sec exposure of the computerized tomographic scanning, the animals were intubated and connected to a respirator. Spontaneous respiration was eliminated by intravenous administration of 3 mg of tubocurarine chloride. Preliminary scans of the liver and, occasionally, the spleen were obtained utilizing the equipment and technique described in Stage II.

Following the preliminary scans, 0.2 ml of the experimental emulsion/kg was slowly injected (over approximately 1 min) into a peripheral vein. Thirty minutes after completion of the injection, the scans of the liver were repeated. In most experiments, the animals were also rescanned 60 min after the injection.

The density of the livers was measured on preliminary, 30-, and 60-min scans, as described in the Stage II experiments, both visually and by the computer-generated mean attenuation expressed in EMI Units (EU) on the 500 scale. The increases in the density of the livers after 30 and 60 min were compared to the preliminary scan and evaluated.

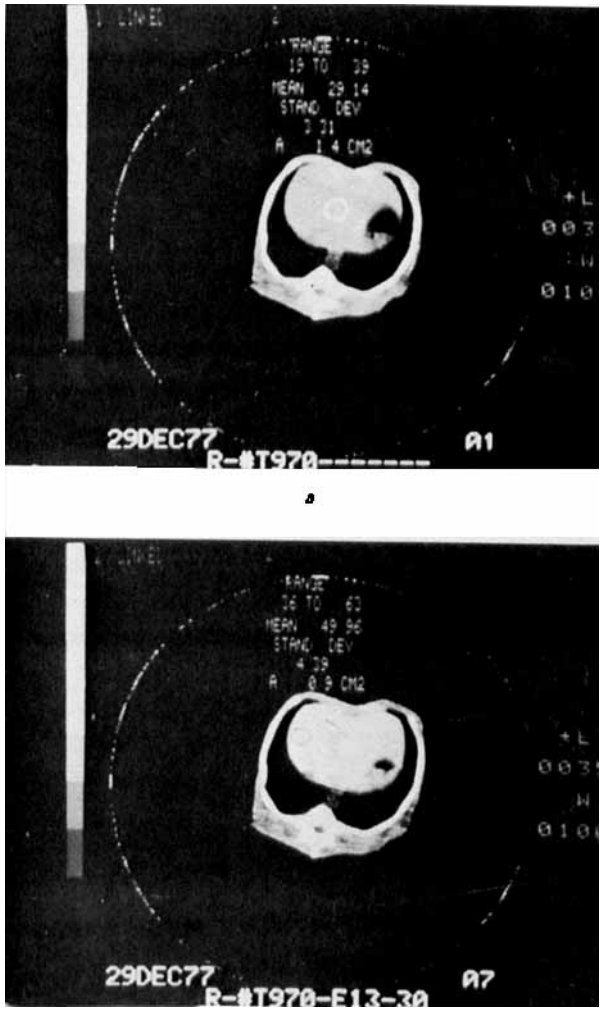

a b

Figure 2—*Computerized tomographic images of rhesus monkey livers before* (a) *and 1 hr after* (b) *the intravenous injection of 0.2 ml of Emulsion V/kg. Computer-generated density measurements indicated an increase in liver attenuation by 21 EMI Units.*

RESULTS AND DISCUSSION

The success of Emulsion II*b* in opacifying the liver (10) prompted efforts to formulate a similar emulsion. With the same formulation (3% purified soy lecithin and 1.2% polyoxyl 40 stearate as emulsifier), initial attempts were made to prepare an emulsion with a maximum number of globules around 1.3 μm in diameter. However, considerable difficulty was encountered during preparation of the emulsion. The lecithin was not completely soluble, even in hot (60°) ethiodized oil, and, more important, the resulting emulsion contained large spongy masses (8–10 μm) that could not be filtered through a 5-μm stainless steel filter. Therefore, several different procedures were attempted.

Table I lists the formulations and procedures used in preparation of five emulsions along with their relative *in vivo* results. The data on Emulsion II*b* are included for comparison. However, at the time of *in vivo* testing, II*b* was at least 1 year old and was not representative of the true potency of a freshly prepared compound.

Emulsion III (Table I) was prepared using the formulation of Hom *et al.* (17). This emulsion, when examined under a microscope, revealed that most of the globules were around 1 μm in diameter; a few were between 1.5–2.0 μm, and very few were above 2 μm. Emulsion III, at a dose of 2.0 ml/kg, was tested in rabbits by the conventional radiographic technique and showed only minimal opacification of the liver. An emulsion with a globule size smaller than that of Emulsion III also opacified the liver poorly. Therefore, an emulsion with a larger globule size was investigated.

Emulsion IV was made with the same polysorbate 80–sorbitan monooleate emulsifier combination as Emulsion III, but a smaller amount of emulsifier was used (Table I). On microscopic observation, Emulsion IV showed a good number of globules in the 1.5–2.0-μm range and very few above the 3–5-μm range. Although Emulsion IV opacified the liver in rabbits, it was somewhat less effective than II*b*. Thus, this emulsion showed promise and probably could have been improved further by changing the emulsifier concentration to increase the globule size. However, work on these emulsifier combinations was discontinued because of the lack of toxicity data on their intravenous use in humans.

The use of lecithin was investigated once again. To eliminate the major problem of spongy masses observed with refined soy lecithin, the lecithin was purified further by extraction in ethanol. When the alcoholic extract was used along with the addition of enough alcohol to make the final alcohol concentration 10% (v/v) in the emulsion, it no longer contained spongy masses and appeared clean under the microscope. Therefore, variations of the formulation were examined by changing the emulsifier concentration or stirring speed, which resulted in the preparation of Emulsion V (Table I).

Emulsion V, at doses of 2.0 ml/kg for conventional X-ray and 0.2 ml/kg for computerized tomography, produced denser liver scans than Emulsions III and IV. Microscopic observation of Emulsion V revealed that the globule sizes were generally larger than those in Emulsions III and IV, and a large number of globules were in the 2-μm range. A further increase in the size of the globules in Emulsion V (obtained by changing the stirring speed or homogenizing time) resulted in an emulsion that gave unsatisfactory liver scans.

Since Emulsion V was made using an alcoholic extract of soy lecithin, it was thought that a purer commercial extract of lecithin, used without further processing, would give a more reproducible emulsion. Therefore, various alcohol-soluble lecithins containing various amounts of phosphatidyl choline were evaluated. Phosphatidyl choline 80%[6] was studied most because of its high alcohol solubility. Emulsion VI (Table I), prepared with 3% (w/v) phosphatidyl choline, resulted in globule sizes that were larger than those of Emulsion V, but a good number of globules were in the 2–2.5-μm range. However, relatively fewer globules were below 1.5 μm and more globules were larger than 3 μm compared to Emulsions III–V.

The potency of Emulsion VI in opacifying the liver was comparable to that of Emulsion V. However, during the preparation of Emulsion VI, the temperature of the oil and water phases had to be very strictly adhered to (otherwise the primary emulsion gelled), and the procedure did not prove to be reproducible. Furthermore, the concentration of the emulsifier in Emulsion VI was much higher than that in Emulsion V (3% compared to 0.45% in Emulsion V), and attempts to reduce it resulted in an even poorer emulsion. Therefore, Emulsion V was chosen for toxicity and clinical studies.

Animal Studies—Figure 1 shows the successive stages of opacification of liver using Emulsion V in conventional X-ray radiography. Maximum opacification was reached in about 1 hr. Other emulsions (Emulsions IV–VI and II*b*) behaved qualitatively the same way, although their scan density was different. The ability of Emulsion V to opacify the liver at a dose of 0.2 ml/kg in monkeys when analyzed by computerized tomography is shown in Fig. 2 and concurs with previous reports (11). This dose is only one-tenth of the previously used doses (2.0 ml/kg) and should reduce the potential toxicity problems associated with ethiodized oil emulsion. Detailed toxicological studies of Emulsion V are being conducted on rats and primates[17].

Stability of Emulsions—Emulsions IV–VI after storage at 4–8° for 6 months showed slight flocculent sedimentation, which rapidly redispersed on mild shaking. The emulsions did not show any significant changes in globule size distribution or hepatographic potency when tested in animals during this storage period. The stability of these emulsions at room temperature also appeared to be similar; but based on experiences with storage of other intravenous lipid emulsions, storage at refrigeration temperatures is recommended. Freezing broke the emulsion and should be avoided.

Sterilization of Emulsions V and VI by autoclaving in the final container was attempted. Autoclaving for 15 min at 121° or for 3.5 min at 132° was tried. In both cases, emulsions were completely broken. Emulsion VI could not be redispersed on shaking. Emulsion V was redispersed on shaking, but redispersed Emulsion V showed large globules (up to 30 μm in diameter) along with smaller globules (1–4 μm). Therefore, sterilization by autoclaving was judged to be unsuccessful.

[17] Toxicity studies at Hazelton Laboratories, Vienna, VA 22180, carried out on rats showed the LD_{50} at 15.6 ml/kg.

Table II—Globule Size Distribution of Emulsions

Size Range, μm	Emulsion III Number, %	Emulsion III Volume, %	Emulsion IV Number, %	Emulsion IV Volume, %	Emulsion V Number, %	Emulsion V Volume, %	Emulsion VI Number, %	Emulsion VI Volume, %	Emulsion IIb Number, %	Emulsion IIb Volume, %
0.75–1.0	59.77	28.1	41.67	10.73	46.94	6.03	31.09	2.62	31.43	2.31
1.0–1.5	33.92	45.1	34.61	25.21	24.9	9.05	28.75	6.86	26.96	5.61
1.5–2.0	5.69	21.4	18.08	37.24	11.91	12.24	17.2	11.6	15.6	9.2
2.0–2.5	0.5	3.8	2.2	9.6	7.0	15.5	9.8	14.3	10.8	13.7
2.5–3.0	0.1	1.6	1.4	11.2	4.5	18.2	6.3	16.7	6.2	14.5
3.0–4.0	—	—	0.3	5.1	3.4	28.4	5.4	29.3	6.9	32.3
4.0–5.0	—	—	0.03	1.1	0.5	9.0	1.4	16.2	1.9	19.6
5.0–7.0	—	—	—	—	0.03	1.6	0.08	2.4	0.12	2.7
Relative density of liver scans[a]	<40		47		57		56		50	

[a] In rabbits at a dose of 0.5 ml/kg using computerized tomography; density of control animal was 32. Numbers expressed in EMI Units (EU) on the 500 scale.

All batches were made using aseptic techniques and were found to be sterile and pyrogen free.

Correlation of Globule Size and Density of Liver Scans—Table II shows the globule size distribution, both by number and volume (mass), of various emulsions along with the results of their *in vivo* testing. Since only the volume of the oil absorbed in the liver affects the degree of opacification, the density of liver scans was correlated with the volume distribution and not the number distribution of the globules. The size range of less than 1.5 μm was ruled out completely because Emulsion III, which contained the highest amount of oil in this range, was relatively inactive. Likewise, the size range of 1.5–2.0 μm was ruled out because, although Emulsion IV contained 37.2% oil of this size, it opacified the liver poorly as compared to Emulsions V, VI, and II*b*, which all contained far less oil in this range. Size above 3.0 μm was also ruled out because II*b*, which contained the highest amount of oil in this range, opacified the liver less than Emulsions V and VI.

It appeared, therefore, that opacification of the liver was related to the amount of the oil in the 2.0–3.0-μm range. Also, there was a direct rank-order correlation between the volume of the oil in the 2.0–3.0-μm size range and the density of the liver scans (Table II). Another indication of the importance of the 2–3-μm size range was observed when Emulsion IV, after being stored at room temperature for several months, opacified the liver better than when freshly prepared and had a potency comparable to Emulsions V and VI. A globule size analysis of the aged Emulsion IV showed that globules had generally increased in size and that 32% (v/v) of the oil was now in the 2.0–3.0-μm range (compared to 20.7% in fresh Emulsion IV, Table II). Therefore, it can be assumed that the increased potency of the aged Emulsion IV was due to an increase in the volume of the oil in the 2.0–3.0-μm range.

A correlation of the density of the liver scans with the volume fraction of the oil in a particular size range has been shown to be very important. Therefore, to prepare the best emulsion, the formulator should attempt to prepare emulsions such that most of the oil globules are in the specific size range needed, rather than homogenizing the emulsion to a globule size less the 1 μm as has often been done (7, 17, 18). As seen from Table II, only about a third of the oil in Emulsion V was in the 2.0–3.0-μm range. Since the liver appears to take up oil globules preferentially between 2.0 and 3.0 μm, if an emulsion could be prepared in which all the oil was in this range, it might be possible to reduce the emulsion dose to perhaps one-third and still deposit the same amount of iodinated oil in the liver. Such a preparation would have an added advantage of sparing other tissues from unnecessary exposure to iodinated oil.

The results of the present investigation indicate that at least one organ, the liver, has preference regarding the size of the oil globules it absorbs. If similar specificity exists for other tissues and organs, it would be possible to prepare emulsions of different globule size that preferentially opacify a particular organ or tissue. Work is in progress to prepare emulsions with a more uniform globule size and to test this hypothesis.

REFERENCES

(1) W. S. Keith and D. R. Briggs, *Proc. Soc. Exp. Biol.*, **27**, 538 (1930).

(2) R. Degkwitz, *Fortschr. Geb. Roentgenstr. Nuklearmed.*, **58**, 472 (1938).

(3) F. Beckermann and C. Popken, *ibid.*, **58**, 519 (1938).

(4) M. E. Grossmann and G. H. Cooray, *J. Fac. Radiol.*, **1**, 112 (1949).

(5) O. Olsson, *Acta Radiol.*, **22**, 749 (1941).

(6) S. M. Berger, *Am. J. Roentgenol.*, **76**, 39 (1956).

(7) J. G. Teplick, M. E. Haskin, and J. Skelley, *Radiology*, **82**, 478 (1964).

(8) M. Laval-Jeantet, J. L. Lamarque, P. Dreux, A. M. Laval-Jeantet, and J. Launay, *Acta Radiol. Diagn.*, **17**, 49 (1976).

(9) A. Pinet, V. T. Minh, M. Boucherat, A. Dubrenil, and J. P. Magis, *ibid.*, **17**, 41 (1976).

(10) M. Vermess, R. H. Adamson, J. L. Doppman, A. S. Rabson, and J. R. Herdt, *Radiology*, **119**, 31 (1976).

(11) M. Vermess, R. H. Adamson, J. L. Doppman, and M. Girton, *ibid.*, **125**, 711 (1977).

(12) T. J. Macek, *J. Pharm. Sci.*, **52**, 694 (1963).

(13) M. J. Groves, *ibid.*, **57**, 1273 (1968).

(14) S. F. Thomas, *Radiology*, **78**, 435 (1962).

(15) W. S. Singleton and M. L. Brown, *J. Am. Oil Chem. Soc.*, **42**, 312 (1965).

(16) E. Shotton and S. S. Davis, *J. Pharm. Pharmacol.*, **20**, 825 (1968).

(17) F. S. Hom, J. Autian, A. N. Martin, J. E. Berk, and J. G. Teplick, *J. Am. Pharm. Assoc., Sci. Ed.*, **46**, 254 (1957).

(18) H. A. Baltaxe, B. Katzen, D. R. Alonzo, and D. Wixson, *Radiology*, **119**, 27 (1976).

Pharmacokinetics and Bioavailability of Intravenous, Intramuscular, and Oral Lorazepam in Humans

DAVID J. GREENBLATT *x, RICHARD I. SHADER ‡, KATE FRANKE *, DEAN S. MacLAUGHLIN *, JEROLD S. HARMATZ ‡, MARCIA DIVOLL ALLEN *, ANN WERNER *, and ELAINE WOO *

Received February 21, 1978, from the *Clinical Pharmacology Unit, Massachusetts General Hospital, Boston, MA 02114, and the ‡Psychopharmacology Research Laboratory, Massachusetts Mental Health Center, Boston, MA 02115. Accepted for publication June 8, 1978.

Abstract □ Six healthy volunteers received single 2- and 4-mg doses of lorazepam by 5-min intravenous infusion, in tablet form by mouth in the fasting state, and by deltoid intramuscular injection in a six-way crossover study. A seventh subject received the 4-mg iv, po, and im doses. Concentrations of lorazepam and its glucuronide metabolite in multiple plasma samples and in all urine collected during 72 hr after each dose were determined by electron-capture GLC. Mean kinetic variables for intravenous lorazepam after 2- and 4-mg doses, respectively, were: volume of distribution (V_d), 1.14 and 1.30 liters/kg; elimination half-life ($t_{1/2\beta}$), 14.3 and 14.6 hr; total clearance, 1.05 and 1.10 ml/min/kg; and cumulative urinary excretion of lorazepam glucuronide, 81.1 and 82.3% of the dose. With the possible exception of V_d, all kinetic variables were dose independent. Following a lag time averaging 15–17 min, absorption of oral lorazepam was first order, with apparent absorption half-life ($t_{1/2a}$) values averaging 40 (2-mg dose) and 22 (4-mg dose) min. Absorption was 91–95% complete. No lag times were observed after intramuscular injection of lorazepam; absorption was first order, with $t_{1/2a}$ values averaging 12 (2-mg dose) and 19 (4-mg dose) min. The completeness of absorption was 83–100%. Absorption kinetics for both oral and intramuscular lorazepam were dose independent. Plasma $t_{1/2\beta}$ for intact lorazepam was independent of dose and administration route.

Keyphrases □ Lorazepam—pharmacokinetics and bioavailability in humans, various administration routes compared □ Pharmacokinetics—lorazepam in humans, various administration routes compared □ Bioavailability—lorazepam in humans, various administration routes compared □ Benzodiazepines—lorazepam, pharmacokinetics and bioavailability in humans, various administration routes compared

Lorazepam (I, Scheme I), a 3-hydroxy-1,4-benzodiazepine derivative, is extensively used as a sedative and antianxiety agent (1, 2). Previous studies (3–8) investigated the disposition of lorazepam in humans following intravenous, intramuscular, and oral administration to different groups of subjects. However, the effect of dose on lorazepam pharmacokinetics and the absolute bioavailability of extravascular modes of administration are not established.

The present study assessed the pharmacokinetics of intravenous lorazepam at two doses within the usual therapeutic range. Also assessed were the rate and completeness of absorption of oral and intramuscular lorazepam in the same subjects at two different dosage levels.

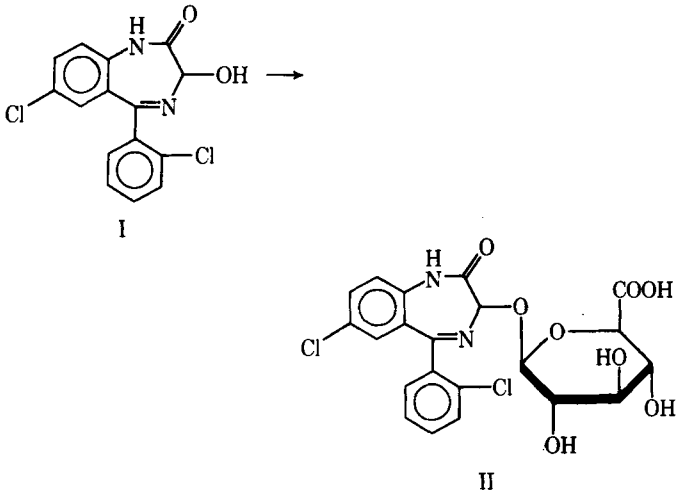

Scheme I

EXPERIMENTAL

Subjects—The seven healthy male and female volunteers[1] (Table I) ranged in age from 23 to 31 years and were within 10% of ideal body weight. All subjects had normal hematologic profiles and laboratory screening tests[2] and had no identifiable medical disease. They had no history of current or chronic psychotropic drug use.

Procedure—The first six subjects received single doses (2 or 4 mg iv, po, or im) of lorazepam on six occasions separated by at least 1 week. The seventh subject (EM) terminated participation after four trials; only data from the three 4-mg trials are included in the analysis. Table I shows the sequence of drug administration for each subject.

For intravenous administration, 1 ml of injectable lorazepam solution, containing 2 or 4 mg dissolved in its customary solvent[3], was diluted to 50 ml with 5% dextrose in water. The dose was infused into an antecubital vein over 5 min using a constant-rate infusion pump. For intramuscular administration, 1 ml of injectable lorazepam, containing 2 or 4 mg, was administered as a single deltoid injection. Oral lorazepam was administered as one or two 2-mg tablets together with 100 ml of water following an overnight fast.

Venous blood samples were drawn from an indwelling scalp vein cannula or by separate venipuncture at the following times after the termination of the intravenous infusion or the oral and intramuscular doses: 0.25, 0.5, 0.75, 1.0, 1.5, 2.0, 2.5, 3, 4, 6, 8, 12, 18, 24, 30, 36, and 48 hr. Following intravenous administration, additional samples were drawn just at the termination of the infusion and at 2 and 5 min postinfusion. All blood specimens were collected in heparinized vacuum tubes.

All urine was collected for 72 hr after each dose in intervals divided as follows: 0–4, 4–8, 8–24, 24–48, and 48–72 hr.

Plasma samples and aliquots of all urine collections were stored at −20° until assayed.

Analysis of Plasma and Urine—Concentrations of intact lorazepam in 1-ml samples of plasma and urine were determined by electron-capture GLC as described elsewhere (9). Urinary concentrations of lorazepam glucuronide (II, Scheme I), the major human metabolite of lorazepam, were likewise determined after enzymatic deconjugation with β-glucuronidase. Oxazepam served as the internal standard for all analyses, and the two compounds were chromatographed without prior derivatization. The sensitivity of the method was 1–3 ng of lorazepam/ml of original sample. The variation of identical samples did not exceed 5%.

Data Analysis—Postinfusion plasma lorazepam concentrations were analyzed by weighted iterative nonlinear least-squares regression analysis (10, 11). The iterative process was allowed to proceed until the convergence criteria were met or a total of 50 iterative steps was completed. Since concentration values generally spanned two log scales, each residual error, prior to squaring, was weighted by a factor equal to the reciprocal

[1] Written informed consent was obtained.
[2] SMA-20.
[3] Containing 0.02 ml of benzyl alcohol and 0.18 ml of polyethylene glycol; volume adjusted to 1.0 ml with propylene glycol.

0022-3549/79/0100-0057$01.00/0
© 1979, American Pharmaceutical Association

Table I—Characteristics of Subjects and Sequence of Lorazepam Administrations

Subject	Age, years	Sex	Weight, kg	Sequence of Trials (Dose and Route)					
				1[a]	2	3	4	5	6
JH	30	F	53.6	2 im	4 po	2 iv	4 im	2 po	4 iv
JK	26	M	76.4	2 im	4 iv	2 po	4 im	2 iv	4 po
HJP	25	M	79.5	2 po	4 iv	2 im	4 im	4 po	2 iv
DJG	31	M	69.5	2 im	4 iv	2 po	4 im	2 iv	4 po
EO	29	F	65.9	2 po	4 iv	2 im	4 po	4 im	2 iv
LW	27	F	53.6	2 po	4 im	2 im	4 po	4 iv	2 iv
EM[b]	23	F	56.8	2 iv	4 po	4 im	4 iv		

[a] Trial number. [b] This subject withdrew from the study after four trials; findings from the 2-mg iv trial were not included in the analysis.

Table II—Pharmacokinetics of Intravenous Lorazepam[a]

Subject	V_1, liters/kg	V_d, liters/kg	$t_{1/2\alpha}$, min	$t_{1/2\beta}$, hr	Clearance, ml/min/kg	$AUC_{0\rightarrow\infty}$, ng/ml × hr	72-hr Excretion of Lorazepam as Glucuronide, % of dose	Half-Life Determined from Lorazepam Glucuronide Excretion Rate *versus* Time, hr	Projected Cumulative Excretion of Lorazepam as Glucuronide, % of dose
					Dose = 2 mg				
JH[b]	0.30	1.30	1.4	12.4	1.22	511.7	64.9	14.1	66.9
JK	0.12	1.13	1.9	8.4	1.56	279.7	82.1	11.0	83.3
HJP	0.48	1.05	10.4	9.9	1.23	341.1	87.7	16.6	93.1
DJG	0.28	1.11	1.1	24.9	0.52	924.4	63.2	23.4	72.9
EO	—[c]	1.16	0.0	12.8	1.04	485.6	91.0	16.8	96.1
LW	0.36	1.14	1.3	17.6	0.74	836.0	67.5	19.5	74.2
Mean	0.30	1.14	2.7	14.3	1.05	563.1	76.1	16.9	81.1
±*SE*	±0.05	±0.03	±1.6	±2.5	±0.15	±107.0	±5.0	±1.7	±4.8
					Dose = 4 mg				
JH	0.94	1.43	18.9	14.0	1.18	1053.8	81.5	14.8	85.0
JK[d]	0.51	1.25	2.0	12.6	1.15	760.4	78.7	12.2	80.2
HJP	0.40	1.10	0.9	12.6	1.01	828.4	88.2	14.6	91.8
DJG	1.15	1.24	12.0	22.0	0.65	1468.4	49.4	24.6	58.1
EO	0.32	1.30	2.1	12.3	1.22	830.5	92.0	14.2	95.2
LW	0.66	1.21	27.9	18.0	0.78	1600.2	66.0	14.5	70.0
EM	1.10	1.62	5.1	10.6	1.77	664.3	94.6	10.4	95.7
Mean	0.72	1.30	9.8	14.6	1.10	1029.4	78.6	15.1	82.3
±*SE*	±0.12	±0.06	±3.9	±1.5	±0.13	±138.4	±6.1	±1.7	±5.3

[a] See text for explanation of abbreviations. [b] Intermediate pi half-life of 0.49 hr following 2-mg dose. [c] Indeterminant V_1 due to large value of alpha. [d] Intermediate pi half-life of 0.37 hr following 4-mg dose.

Table III—Pharmacokinetics of Oral Lorazepam[a]

Subject	Lag Time, min	Peak Concentration, ng/ml	Time of Peak Concentration, hr after dose	$t_{1/2a}$, min	$t_{1/2\beta}$, hr	Half-Life Determined from Lorazepam Glucuronide Excretion Rate *versus* Time, hr
			Dose = 2 mg			
JH	0	36.2	1.0	56.9	15.2	13.4
JK	5.9	21.5	2.5	50.2	9.3	13.6
HJP	16.2	23.3	2.0	26.0	9.0	13.4
DJG	—[b]	26.0	6.0	—[b]	25.9	38.3
EO	12.5	27.3	2.0	60.2	18.6	12.8
LW	41.5	31.5	1.5	8.5	19.3	16.2
Mean	15.2	27.6	2.50	40.4	16.2	18.0
±*SE*	±7.1	±2.2	±0.73	±10.0	±2.6	±4.1
			Dose = 4 mg			
JH	14.4	45.1	1.0	1.0	16.7	15.2
JK	0	47.5	1.5	44.1	14.0	12.8
HJP	24.5	47.8	2.5	17.3	11.1	14.8
DJG	26.5	38.8	1.5	17.3	25.0	31.4
EO	42.8	44.2	1.5	30.3	15.5	12.6
LW	0	68.1	2.0	30.8	15.9	14.9
EM	11.3	44.4	1.0	14.3	10.8	12.3
Mean	17.1	48.0	1.57	22.1	15.6	16.3
±*SE*	±5.8	±3.5	±0.20	±5.3	±1.8	±2.6

[a] See text for explanation of abbreviations. [b] Absorption pattern not consistent with a first-order process.

of that plasma concentration. Data points were fitted to the following function:

$$C = Ae^{-\alpha t} + Be^{-\beta t} \quad \text{(Eq. 1)}$$

where C is the plasma lorazepam concentration at time t after the end of the infusion; A and B are hybrid intercept terms that were subsequently corrected for the infusion period (12); and α and β are hybrid exponents, representing apparent phases of drug distribution and elimination, respectively (6–8, 13–16). For two of the 13 subject trials, Eq. 1 did not explain the data adequately. Accordingly, the points were fitted to an equation of the following form:

$$C = Ae^{-\alpha t} + Pe^{-\pi t} + Be^{-\beta t} \quad \text{(Eq. 2)}$$

Use of this equation in these two cases considerably improved the quality of the fit and substantially reduced the residual error.

Coefficients and exponents from the fitted function were used to calculate the following pharmacokinetic variables: volume of the central compartment (V_1), total apparent volume of distribution using the "area"

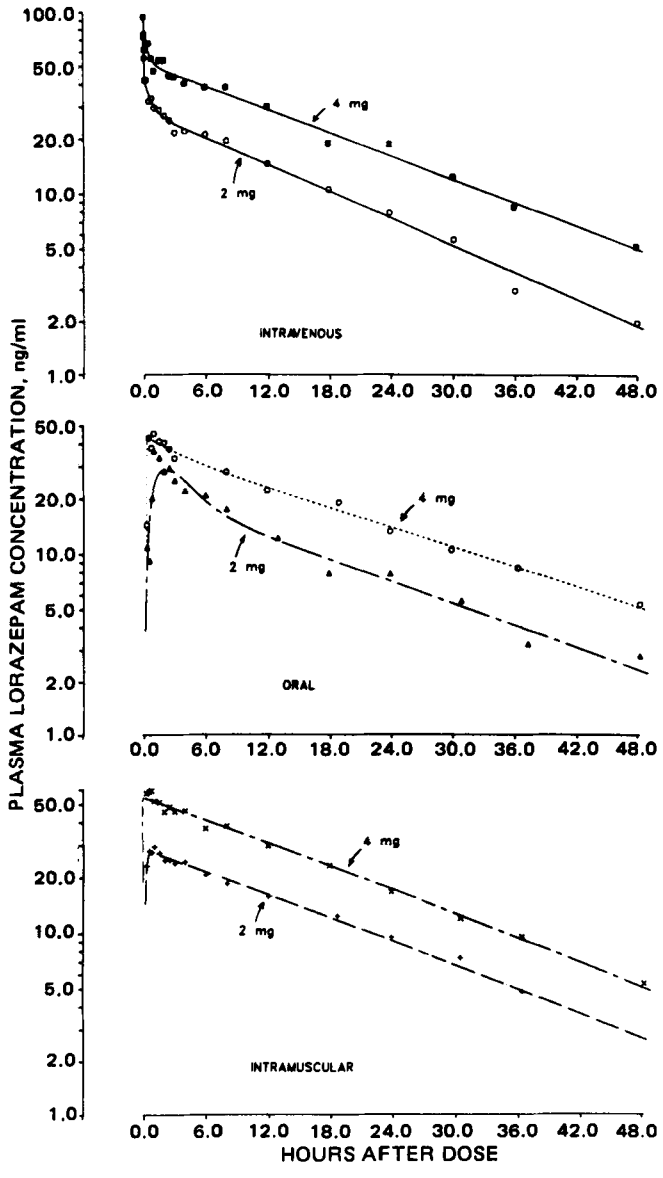

Figure 1—*Plasma lorazepam concentrations and pharmacokinetic functions for Subject JH.*

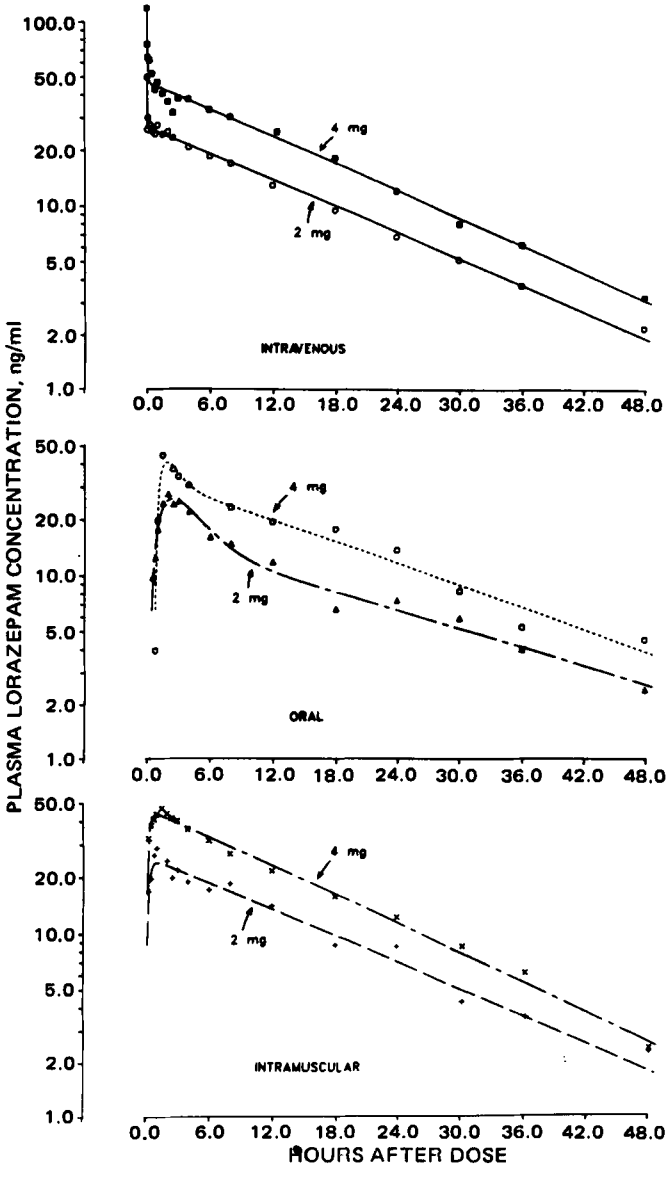

Figure 2—*Plasma lorazepam concentrations and pharmacokinetic functions for Subject EO.*

method (V_d), apparent distribution half-life ($t_{1/2\alpha}$), apparent elimination half-life ($t_{1/2\beta}$), and total clearance (6–8, 13–16). When appropriate, an intermediate "pi" half-life ($t_{1/2\pi}$) also was calculated. Individual "micro" transfer and elimination rate constants corresponding to the two- or three-compartment open pharmacokinetic models were not determined since these constants are dependent on the ambiguous configuration of compartments within the model (17, 18). The micro rate constants can be calculated using the data presented under *Results*.

The half-life also was determined from the slope of the terminal log-linear portion of a plot of the average urinary excretion rate (interval excretion divided by interval length) *versus* the midpoint of the collection interval. The amount of lorazepam glucuronide remaining to be excreted between 72 hr and "infinity" was determined as the quotient of the projected excretion rate at 72 hr and the apparent urinary excretion rate constant. This quantity was added to the 72-hr cumulative excretion to give the cumulative excretion of lorazepam glucuronide from time zero to infinity.

Plasma lorazepam concentrations following extravascular modes of administration were analyzed by similar methods. Since concentration values generally spanned one log scale, the weighting factor for each residual error prior to squaring was the reciprocal of the square root of the plasma concentration. Data points were fitted to each of the following two functions:

$$C = A(e^{-\beta t} - e^{-k_a t}) \qquad \text{(Eq. 3)}$$

$$C = -(A + B)e^{-k_a t} + Ae^{-\alpha t} + Be^{-\beta t} \qquad \text{(Eq. 4)}$$

As in Eqs. 1 and 2, C is the plasma lorazepam concentration at time t after the dosage; A and B are hybrid intercept terms; α and β are hybrid exponents; and k_a is the apparent first-order absorption rate constant, which was used to calculate the apparent first-order absorption half-life ($t_{1/2a}$). The constant k_a serves as only an apparent rate constant and does not necessarily correspond to a microconstant associated with any particular pharmacokinetic model (15–18).

In all subject trials, the choice between Eqs. 3 and 4 as function of best fit was determined by assessment of the randomness of scatter of actual data points about the fitted function and by comparison of the sum of squares of weighted residual errors (19). In most subject trials following oral lorazepam administration, Eqs. 3 and 4 required further modification by introduction of a lag time (t_0), which elapsed prior to the start of absorption.

The apparent systemic availability of oral and intramuscular lorazepam was determined using the following three variables: (*a*) the total area under the plasma lorazepam concentration–time curve from time zero to infinity ($AUC_{0\to\infty}$), calculated using the appropriate pharmacokinetic

Table IV—Pharmacokinetics of Intramuscular Lorazepam [a]

Subject	Peak Concentration, ng/ml	Time of Peak Concentration, hr after dose	$t_{1/2\alpha}$, min	$t_{1/2\beta}$, hr	Half-Life Determined from Lorazepam Glucuronide Excretion Rate *versus* Time, hr
			Dose = 2 mg		
JH	29.0	1.0	5.4	14.3	13.0
JK	26.7	2.0	11.4	15.8	11.3
HJP	23.3	1.0	15.0	11.6	14.5
DJG	24.3	1.5	18.6	23.3	31.7
EO	28.2	1.0	9.6	12.6	15.7
LW	29.4	0.75	12.6	16.8	16.0
Mean	26.8	1.20	12.1	15.7	17.0
±*SE*	±1.0	±0.18	±1.8	±1.7	±3.0
			Dose = 4 mg		
JH	58.6	0.75	~0	14.1	13.7
JK	62.9	1.0	28.2	12.4	13.5
HJP	34.3	0.75	10.8	10.5	14.6
DJG	42.0	0.75	17.4	25.6	26.5
EO	46.3	1.5	9.0	11.5	13.5
LW	51.9	1.0	16.8	24.7	18.9
EM	36.2	2.5	50.6	13.9	12.3
Mean	47.5	1.17	19.0	16.1	16.1
±*SE*	±4.1	±0.24	±6.2	±2.4	±1.9

[a] See text for explanation of abbreviations.

Table V—Bioavailability of Oral Lorazepam

Subject	$AUC_{0\to\infty}$ ng/ml × hr	$AUC_{0\to\infty}$ % of iv value	72-hr Excretion of Lorazepam as Glucuronide % of dose	72-hr Excretion of Lorazepam as Glucuronide % of iv value	Projected Cumulative Excretion of Lorazepam as Glucuronide % of dose	Projected Cumulative Excretion of Lorazepam as Glucuronide % of iv value
			Dose = 2 mg			
JH	491.6	96.1	86.2	132.8	88.2	131.8
JK	307.4	109.9	50.9	62.0	52.5	63.0
HJP	317.9	93.2	62.1	70.8	64.1	68.9
DJG	905.7	98.0	59.2	93.7	82.4	113.0
EO	467.1	96.2	82.4	90.5	84.5	87.9
LW	537.7	64.3	56.6	83.9	59.9	80.6
Mean	504.6	92.9	66.2	88.9	71.9	90.9
±*SE*	±88.9	±6.2	±5.9	±10.1	±6.1	±10.9
			Dose = 4 mg			
JH	898.3	85.2	76.4	93.7	80.5	94.7
JK	664.4	87.4	101.2	128.6	104.1	129.8
HJP	782.2	94.4	62.1	70.4	65.9	71.8
DJG	1405.3	95.7	44.3	89.7	57.2	98.4
EO	737.2	88.8	83.7	91.0	85.7	90.0
LW	1496.4	93.5	60.6	91.8	63.4	90.5
EM	691.7	104.1	82.4	87.1	84.1	87.9
Mean	953.6	92.7	73.0	93.2	77.3	94.7
±*SE*	±131.8	±2.4	±7.1	±6.6	±6.1	±6.6

function; (*b*) the 72-hr urinary excretion of lorazepam glucuronide; and (*c*) the projected cumulative excretion of lorazepam glucuronide (13–16, 20). Each variable was compared to the corresponding value following intravenous administration of the same dose to the same subject.

Statistical methods included analysis of variance and the Student *t* test (21).

RESULTS

Intravenous Lorazepam—*Subjective Effects*—Subjective central nervous system (CNS) effects appeared rapidly after the intravenous infusion and included drowsiness, ataxia, dysarthria, and loss of recall. These effects abated gradually between 2 and 12 hr after dosage and had essentially disappeared 24 hr after dosage. No serious untoward consequences were encountered. The effects of the 2-mg dose were qualitatively similar but less intense and of shorter duration than those of the 4-mg dose.

Pharmacokinetics—Disappearance of lorazepam from plasma was consistent with Eq. 1 in 11 subject trials and with Eq. 2 in the other two (Table II). The initial distribution phase proceeded rapidly, with distribution half-life values of less than 20 min in all but one subject trial. The apparent elimination half-life averaged 14–15 hr, and the total clearance averaged about 1.1 ml/min/kg. Mean total apparent volumes of distribution were slightly larger than body weight.

The 72-hr urinary excretion of intact lorazepam did not exceed 0.5% of the dose in any subject. In contrast, a mean of 76–79% of the dose was excreted as lorazepam glucuronide in 72 hr; the projected cumulative excretion of lorazepam glucuronide averaged more than 80% of the dose. The half-life determined from the lorazepam glucuronide excretion rate *versus* time data averaged 15–17 hr and was highly correlated with the apparent plasma elimination half-life of intact lorazepam for both the 4- ($r = 0.89$) and 2- ($r = 0.91$) mg doses.

Based on the six subjects who received both doses of intravenous lorazepam, there was no significant difference between the two dosage levels in V_1 (paired $t = 0.97$), $t_{1/2_\alpha}$ ($t = 1.49$), $t_{1/2\beta}$ ($t = 0.89$), clearance ($t = 0.58$), 72-hr and projected cumulative excretion of lorazepam glucuronide ($t = 0.02$ and 0.23), and apparent excretion half-life of lorazepam glucuronide ($t = 1.04$). The apparent volume of distribution (V_d) after the 4-mg dose was significantly larger ($t = 7.01$) than after the 2-mg dose, but the actual difference between the two mean values was small. Figures 1 and 2 illustrate representative plasma lorazepam concentration–time curves.

Oral Lorazepam—*Subjective Effects*—Subjective CNS effects appeared within 2 hr of dosage and generally were maximal between 1 and 4 hr after dosage, after which they gradually abated. Again, the intensity and duration of clinical manifestations were greater with the 4- than with the 2-mg dose.

Pharmacokinetics—In 10 of the 13 subject trials, a lag time of 6–43

Table VI—Bioavailability of Intramuscular Lorazepam

Subject	$AUC_{0\to\infty}$ ng/ml × hr	$AUC_{0\to\infty}$ % of iv value	72-hr Excretion of Lorazepam as Glucuronide % of dose	72-hr Excretion of Lorazepam as Glucuronide % of iv value	Projected Cumulative Excretion of Lorazepam as Glucuronide % of dose	Projected Cumulative Excretion of Lorazepam as Glucuronide % of iv value
			Dose = 2 mg			
JH	573.3	112.0	70.1	108.0	72.0	107.5
JK	404.0	144.4	56.3	68.6	57.1	68.6
HJP	410.0	120.2	82.2	93.7	85.7	92.0
DJG	840.5	90.9	63.6	100.1	82.7	113.5
EO	454.4	93.6	77.4	85.1	81.3	84.6
LW	717.3	85.8	56.8	84.1	61.6	83.0
Mean	556.5	107.8	67.7	90.0	73.4	91.5
±*SE*	±73.3	±9.1	±4.4	±5.7	±4.9	±6.8
			Dose = 4 mg			
JH	1096.1	104.0	79.0	96.9	83.2	97.9
JK	756.9	99.5	52.4	66.6	53.7	66.9
HJP	547.1	66.0	73.1	82.9	76.1	82.9
DJG	1476.9	100.6	46.5	93.9	56.2	96.7
EO	757.1	91.2	77.4	83.9	79.9	83.9
LW	1413.2	88.3	54.8	83.0	59.7	85.3
EM	620.6	93.4	72.2	76.3	73.8	77.1
Mean	952.6	91.9	65.1	83.4	68.9	84.4
±*SE*	±143.0	±4.8	±5.1	±3.9	±4.6	±4.1

min elapsed prior to the start of absorption (Table III). With the exception of Subject DJG following the 2-mg dose, absorption proceeded as an apparent first-order process, with absorption half-life values ranging from 8 to 60 min. In all but one case, peak lorazepam concentrations were reached within 2.5 hr after the dosage.

There was a trend toward less rapid absorption of the 2- than of the 4-mg dose. However, based on the six subjects who received both doses, differences between doses in time of peak concentration (t = 1.08) and in apparent absorption half-life (t = 0.66) did not reach significance. The apparent plasma elimination half-life of lorazepam and the half-life determined from lorazepam glucuronide rate *versus* time data were nearly identical between the two doses (t = 0.11 and 0.78, respectively). Representative plasma concentration curves are shown in Figs. 1 and 2.

Intramuscular Lorazepam—*Subjective Effects*—Mild to moderate local discomfort associated with both intramuscular injections was reported by three of the seven subjects. The discomfort spontaneously resolved after the injection. In no case was severe pain described, nor were there any residual local complications. The onset of subjective effects was rapid, generally within 1 hr of the injection.

Pharmacokinetics—Absorption of intramuscular lorazepam proceeded as a first-order process, with no apparent lag time, in all subjects (Table IV). The mean apparent absorption half-life averaged less than 20 min after both doses, and the peak concentration was reached an average of 1.2 hr after injection (Figs. 1 and 2). There was no significant difference between the two dose levels either in the apparent absorption half-life (t = 0.48) or in the time of peak concentration (t = 1.07).

The apparent plasma elimination half-life of lorazepam and the half-life determined from the lorazepam glucoronide excretion rate *versus* time data were similar to those observed following intravenous and oral dosage. Again, there was no significant difference between the two dose levels (t = 0.45 and 0.20, respectively).

Bioavailability—Tables V and VI show the apparent systemic availability of oral and intramuscular lorazepam at both dose levels using all three measures of bioavailability. Systemic availability of the 2-mg oral dose by all three measures averaged 89–93% of the intravenous value. The availability of the 4-mg oral dose averaged 93–95%. The bioavailability of the 2-mg im dose of lorazepam averaged 90–100%, while that of the 4-mg im dose averaged 84–92% (Fig. 3).

A two-way analysis of variance was used to assess differences among the three routes of administration in the three measures of systemic availability (Table VII). For the 2-mg dose, none of the differences approached significance. Differences were of borderline significance for the 4-mg dose.

Effect of Route on Lorazepam Elimination—The effect of route of administration on the apparent elimination half-life of intact lorazepam from plasma and on the half-life determined from lorazepam glucuronide excretion rate was assessed at both dose levels using a two-way analysis of variance (Table VIII). The route of administration had no significant influence on either of these variables at either dose level (see also Fig. 4).

DISCUSSION

Distribution of lorazepam following intravenous infusion proceeded rapidly, with mean distribution half-life values of less than 10 min. This result is consistent with the prompt onset of clinical sedative effects following intravenous infusion observed in this and other studies (22–26). However, the present study was not designed to provide precise quantitation of the time course and intensity of CNS effects nor of the relation between subjective manifestations and pharmacokinetic variables.

The apparent volume of distribution of lorazepam on the average was slightly larger than body weight, indicating moderately extensive tissue uptake. The apparent elimination half-life averaged 14–15 hr, similar to values reported previously (4–9). Consistent with earlier studies (5–9, 27, 28), conjugation to glucuronic acid appeared to be the major route of lorazepam clearance. A mean of 76–79% of the dose was recovered in the urine as lorazepam glucuronide during the 72 hr after drug administration. The projected cumulative excretion of lorazepam glucuronide exceeded 80% of the dose. In contrast, excretion of intact lorazepam did not exceed 0.5% of the dose in any subject. The parallel pattern of elimination

Table VII—Bioavailability of Lorazepam: Two-Way Analysis of Variance among Three Routes of Administration

Bioavailability Measure	Dose = 2 mg F	Dose = 2 mg $d.f.$	Dose = 2 mg p	Dose = 4 mg F	Dose = 4 mg $d.f.$	Dose = 4 mg p
$AUC_{0\to\infty}$	1.42	2, 10	0.29	2.20	2, 12	0.15
72-hr excretion of lorazepam glucuronide	1.66	2, 10	0.24	2.92	2, 12	0.09
Projected cumulative excretion of lorazepam glucuronide	1.14	2, 10	0.36	2.72	2, 12	0.11

Table VIII—Effect of Route of Administration on Lorazepam Elimination

Variable	Dose = 2 mg F	Dose = 2 mg $d.f.$	Dose = 2 mg p	Dose = 4 mg F	Dose = 4 mg $d.f.$	Dose = 4 mg p
Plasma elimination half-life of intact lorazepam ($t_{1/2\beta}$)	0.98	2, 10	0.41	0.75	2, 12	0.49
Half-life determined from lorazepam glucuronide excretion rate *versus* time	0.15	2, 10	0.87	1.09	2, 12	0.37

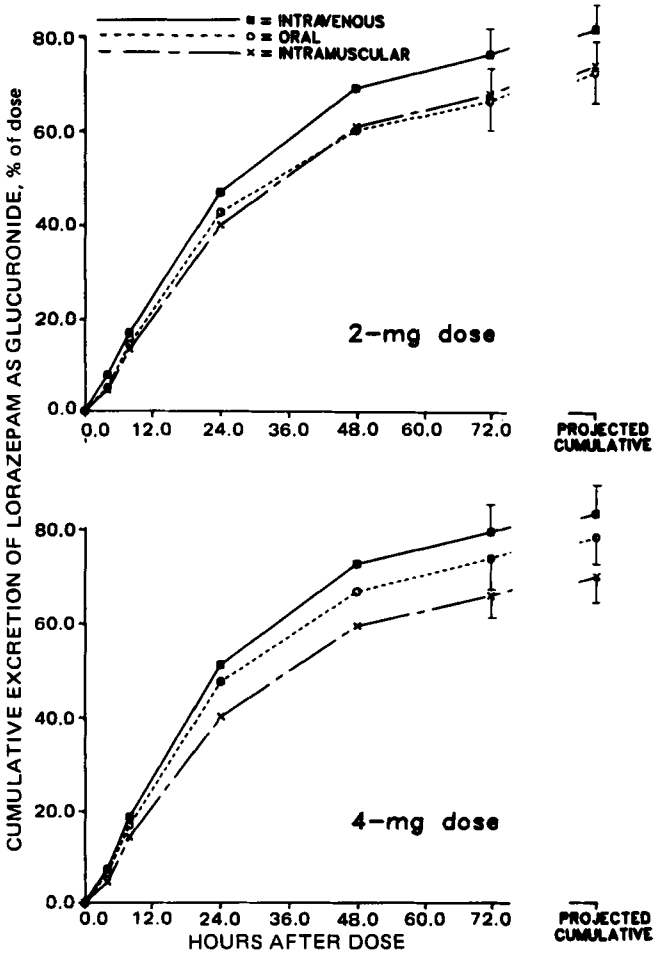

Figure 3—*Urinary excretion of lorazepam glucuronide following 2- (top) and 4- (bottom) mg doses administered by three routes. Each point is the mean (±SE when indicated) for all subjects at that point in time.*

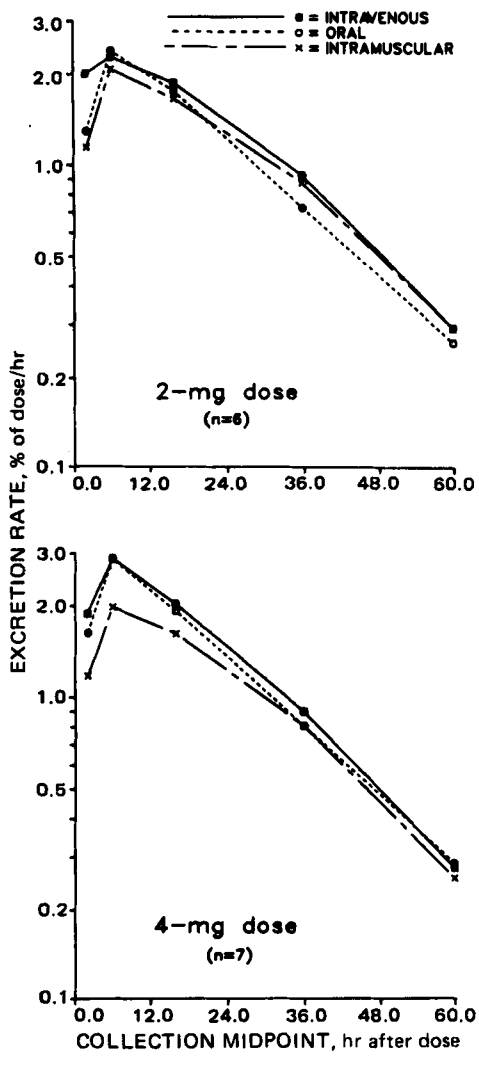

Figure 4—*Urinary excretion rate of lorazepam glucuronide following 2- (top) and 4- (bottom) mg doses administered by three routes. Each point is the mean for all subjects at that point in time. (Standard errors, omitted for clarity, are available from the authors upon request.)*

of the parent compound from plasma and of its endogenously formed metabolite in urine strongly suggests that the elimination rate of lorazepam glucuronide is determined by its formation rate rather than by its intrinsic clearance (16, 29, 30). Pharmacokinetic studies of lorazepam glucuronide administered as such would be required to determine the characteristics of clearance of this metabolic product.

With the assumptions that hepatic biotransformation accounts for essentially all of the total clearance of lorazepam and that hepatic blood flow is approximately 21 ml/kg/min in a healthy individual, the low hepatic extraction ratio of lorazepam indicates that only a fraction of an orally administered dose would fail to reach the systemic circulation due to first-pass metabolism (16, 31). Finally, none of the pharmacokinetic variables for lorazepam differed significantly between the two dose levels.

A lag time averaging 15–17 min elapsed prior to the start of absorption of oral lorazepam. Lag times were observed in previous pharmacokinetic studies of lorazepam (6) and of other benzodiazepines (32–34) and probably are attributable to the time necessary for dissolution of the oral dosage form and/or gastric emptying time. Thereafter, absorption proceeded as an apparent first-order process in all but one subject trial. There was variability between subjects and within subjects at the two dosage levels in values of apparent absorption half-life. However, there was no evidence of any systematic dose-dependent variation in absorption. In all but one subject trial, peak lorazepam levels were attained within 2.5 hr after dosage. Furthermore, the peak level attained was approximately proportional to the dose. Following attainment of peak concentrations, lorazepam elimination from plasma and apparent excretion of lorazepam glucuronide in urine proceeded at rates similar to those observed following intravenous injection of lorazepam. As reported previously with chlordiazepoxide (34, 35) and diazepam (36), the absorption of oral lorazepam appeared to be more than 90% complete.

Intramuscular injection of lorazepam did not produce excessive local discomfort. Injection site pain was described previously (23, 37, 38) but in most studies was not a clinically important problem (7, 39–47). Absorption of intramuscular lorazepam was consistently rapid, and in no case did a lag time elapse prior to the start of absorption. Peak concentrations were reached within 2.5 hr of the dosage in all subjects, and values of the apparent first-order absorption half-life averaged less than 20 min at both dosage levels. As with oral lorazepam, the peak concentration was approximately proportional to the dose. The pattern of elimination of lorazepam and the excretion of lorazepam glucuronide were very similar to those observed following intravenous and oral dosage. On the average, absorption of intramuscular lorazepam was 83–100% complete. The pharmacokinetics of intramuscular lorazepam contrast sharply with findings with intramuscular chlordiazepoxide (34, 35, 48) and diazepam (49–53). Absorption of the latter two benzodiazepine derivatives is slow and erratic and can produce unreliable clinical effects (49, 51–55). Furthermore, injection of chlordiazepoxide and diazepam is associated with considerable pain (56). The absorption profile of intramuscular lorazepam suggests that this compound may have benefits over existing benzodiazepine derivatives in some clinical situations.

REFERENCES

(1) D. J. Greenblatt and R. I. Shader, "Benzodiazepines in Clinical Practice," Raven, New York, N.Y., 1974.

(2) D. J. Greenblatt, in "Psychopharmacology: A Generation of

Progress," M. A. Lipton, A. DiMascio, and K. F. Killam, Eds., Raven, New York, N.Y., 1978, p. 1381.

(3) H. W. Elliott, *Br. J. Anaesth.*, **48**, 1017 (1976).

(4) R. Verbeeck, T. B. Tjandramaga, R. Verberckmoes, and P. J. DeSchepper, *Br. J. Clin. Pharmacol.*, **3**, 1033 (1976).

(5) A. A. Kyriakopoulos, in "Pharmacokinetics of Psychoactive Drugs: Blood Levels and Clinical Response," L. A. Gottschalk and S. Merlis, Eds., Spectrum Publications, Flushing, N.Y., 1976, p. 45.

(6) D. J. Greenblatt, R. T. Schillings, A. A. Kyriakopoulos, R. I. Shader, S. F. Sisenwine, J. A. Knowles, and H. W. Ruelius, *Clin. Pharmacol. Ther.*, **20**, 329 (1976).

(7) D. J. Greenblatt, T. H. Joyce, W. H. Comer, J. A. Knowles, R. I. Shader, A. A. Kyriakopoulos, D. S. MacLaughlin, and H. W. Ruelius, *ibid.*, **21**, 222 (1977).

(8) D. J. Greenblatt, W. H. Comer, H. W. Elliott, R. I. Shader, J. A. Knowles, and H. W. Ruelius, *J. Clin. Pharmacol.*, **17**, 495 (1977).

(9) D. J. Greenblatt, K. Franke, and R. I. Shader, *J. Chromatogr.*, **146**, 311 (1978).

(10) D. W. Marquardt, *J. Soc. Ind. Appl. Math.*, **11**, 431 (1963).

(11) R. A. Usanis, "NLIN–Nonlinear Least Squares Estimation of Parameters (Library Services Series Document No. LSR-089-1)," Triangle Universities Computation Center, Research Triangle Park, N.C., 1972.

(12) J. C. K. Loo and S. Riegelman, *J. Pharm. Sci.*, **59**, 53 (1970).

(13) D. J. Greenblatt and J. Koch-Weser, *N. Engl. J. Med.*, **293**, 702, 964 (1975).

(14) D. J. Greenblatt, H. J. Pfeifer, H. R. Ochs, K. Franke, D. S. MacLaughlin, T. W. Smith, and J. Koch-Weser, *J. Pharmacol. Exp. Ther.*, **202**, 365 (1977).

(15) J. G. Wagner, "Fundamentals of Clinical Pharmacokinetics," Drug Intelligence Publications, Hamilton, Ill., 1975.

(16) M. Gibaldi and D. Perrier, "Pharmacokinetics," Dekker, New York, N.Y., 1975.

(17) J. G. Wagner, *J. Pharmacokinet. Biopharm.*, **4**, 443 (1976).

(18) *Ibid.*, **4**, 395 (1976).

(19) H. G. Boxenbaum, S. Riegelman, and R. M. Elashoff, *J. Pharmacokinet. Biopharm.*, **2**, 123 (1974).

(20) D. J. Greenblatt, T. W. Smith, and J. Koch-Weser, *Clin. Pharmacokinet.*, **1**, 36 (1976).

(21) G. W. Snedecor and W. G. Cochran, "Statistical Methods," University of Iowa Press, Ames, Iowa, 1967.

(22) W. H. Comer, H. W. Elliott, N. Nomof, G. Navarro, N. Kokka, H. W. Ruelius, and J. A. Knowles, *J. Int. Med. Res.*, **1**, 216 (1973).

(23) C. D. Blitt, W. C. Petty, W. A. Wright, and B. Wright, *Anesth. Analg. (Cleveland)*, **55**, 522 (1976).

(24) K. A. George and J. W. Dundee, *Br. J. Clin. Pharmacol.*, **4**, 45 (1977).

(25) P. Gomez-Lozano, *Curr. Ther. Res. Clin. Exp.*, **19**, 469 (1976).

(26) S. K. Pandit, D. V. Heisterkamp, and P. J. Cohen, *Anesthesiology*, **45**, 495 (1976).

(27) R. T. Schillings, S. R. Shrader, and H. W. Ruelius, *Arzneim.-Forsch.*, **21**, 1059 (1971).

(28) J. A. Knowles, W. H. Comer, and H. W. Ruelius, *ibid.*, **21**, 1055 (1971).

(29) J. W. Dundee and K. A. George, *Acta Anaesthesiol. Belg.*, **27** (Suppl.), 3 (1976).

(30) P. R. Byron and R. E. Notari, *J. Pharm. Sci.*, **65**, 1140 (1976).

(31) G. R. Wilkinson and D. G. Shand, *Clin. Pharmacol. Ther.*, **18**, 377 (1975).

(32) S. M. MacLeod, H. G. Giles, G. Patzalek, J. J. Thiessen, and E. M. Sellers, *Eur. J. Clin. Pharmacol.*, **11**, 345 (1977).

(33) D. J. Greenblatt, R. I. Shader, D. R. Weinberger, M. D. Allen, and D. S. MacLaughlin, *Psychopharmacology*, **57**, 199 (1978).

(34) H. G. Boxenbaum, K. A. Geitner, M. L. Jack, W. R. Dixon, H. E. Spiegel, J. Symington, R. Christian, J. D. Moore, L. Weissman, and S. A. Kaplan, *J. Pharmacokinet. Biopharm.*, **5**, 3 (1977).

(35) D. J. Greenblatt, R. I. Shader, S. M. MacLeod, E. M. Sellers, K. Franke, and H. G. Giles, *Eur. J. Clin. Pharmacol.*, **13**, 267 (1978).

(36) S. A. Kaplan, M. L. Jack, K. Alexander, and R. E. Weinfeld, *J. Pharm. Sci.*, **62**, 1789 (1973).

(37) J. W. Dundee, J. K. Lilburn, S. G. Nair, and K. A. George, *Br. J. Anaesth.*, **49**, 1047 (1977).

(38) G. Gale and S. Galloon, *Can. Anaesth. Soc. J.*, **23**, 22 (1976).

(39) M. I. Aleniewski, B. J. Bulas, L. Maderazo, and C. Mendoza, *Anesth. Analg. (Cleveland)*, **56**, 489 (1977).

(40) P. Mundeleer, *Acta Anaesthesiol. Belg.*, **27** (Suppl.), 12 (1976).

(41) R. J. Fragen and N. Caldwell, *Anesth. Analg. (Cleveland)*, **55**, 795 (1976).

(42) R. S. Cormack, J. S. Milledge, and C. D. Hanning, *Br. J. Anaesth.*, **49**, 351 (1977).

(43) N. J. Paymaster, *Curr. Med. Res. Opin.*, **4**, 388 (1976).

(44) R. Verschraegen and G. Rolly, *Acta Anaesthesiol. Belg.*, **25**, 68 (1974).

(45) J. Bobon, S. Bourdouxhe, M. Breulet, M. Parent, and D. P. Bobon, *Psychopharmacologia*, **33**, 377 (1973).

(46) J. C. Gasser, R. D. Kaufman, and J. W. Bellville, *Clin. Pharmacol. Ther.*, **18**, 170 (1975).

(47) R. B. Knapp and L. Fierro, *Anesth. Analg. (Cleveland)*, **53**, 122 (1974).

(48) D. J. Greenblatt, R. I. Shader, J. Koch-Weser, and K. Franke, *N. Engl. J. Med.*, **291**, 1116 (1974).

(49) L. Hillestad, T. Hansen, H. Melsom, and A. Drivenes, *Clin. Pharmacol. Ther.*, **16**, 479 (1974).

(50) J. A. S. Gamble, J. W. Dundee, and R. A. E. Assaf, *Anaesthesia*, **30**, 164 (1975).

(51) K. Korttila and M. Linnoila, *Br. J. Anaesth.*, **47**, 857 (1975).

(52) R. A. E. Assaf, J. W. Dundee, and J. A. S. Gamble, *Anaesthesia*, **30**, 152 (1975).

(53) J. Kanto, *Int. J. Clin. Pharmacol.*, **12**, 427 (1975).

(54) W. H. Forrest, C. R. Brown, and B. W. Brown, *Anesthesiology*, **47**, 241 (1977).

(55) M. L. Palestine and E. Alatorre, *Curr. Ther. Res. Clin. Exp.*, **20**, 289 (1976).

(56) D. J. Greenblatt, R. I. Shader, and J. Koch-Weser, *J. Clin. Pharmacol.*, **16**, 118 (1976).

ACKNOWLEDGMENTS

Supported in part by Grant MH-12279 from the U.S. Public Health Service, by Grant 77-611 from the Foundations' Fund for Research in Psychiatry, and by a grant-in-aid from Wyeth Laboratories, Radnor, Pa. D. S. MacLaughlin was supported by U.S. Public Health Service Grant GM-23430 to the Boston Collaborative Drug Surveillance Program.

Carbon-13 Magnetic Resonance Spectroscopy of Drugs III: Penicillins

CHING-JER CHANG *x **and STANLEY L. HEM** ‡

Received April 3, 1978, from the *Department of Medicinal Chemistry and Pharmacognosy and the ‡Department of Industrial and Physical Pharmacy, School of Pharmacy and Pharmacal Sciences, Purdue University, West Lafayette, IN 47907. Accepted for publication June 14, 1978.

Abstract □ The natural abundance ^{13}C-NMR spectra of a series of penicillins (penicillin V methyl ester, penicillin V, penicillin G, methicillin, oxacillin, cloxacillin, and dicloxacillin) were studied. The chemical shifts were assigned using the pulse Fourier transform technique with the aid of long-range carbon-13 hydrogen coupling. The previous assignments of penicillin V methyl ester were revised.

Keyphrases □ Penicillins, various—^{13}C-NMR spectra, chemical shifts assigned □ ^{13}C-NMR spectroscopy—various penicillins, chemical shifts assigned □ Antibacterials—various penicillins, ^{13}C-NMR spectra, chemical shifts assigned

β-Lactam antibiotics are some of the most widely used drugs (1–3). Current research is focused in chemical manipulation (1–6) to produce antibiotics effective against resistant organisms. This advance depends heavily on the use of modern analytical techniques (1, 2, 7, 8).

Proton NMR spectroscopy (^{1}H-NMR) has been useful in determining configuration and conformation of β-lactam compounds (1–3, 8–14). Carbon-13 NMR (^{13}C-NMR) spectroscopy is becoming increasingly important in the study of drugs (15–20). The carbon-13 chemical shift analysis of simple compounds can be accomplished by the traditional approach based on the structural dissimilarity and the additivity principle of chemical shift (15–17, 21, 22). However, this approach often leaves some uncertainty in the assignments of all close signals because subtle steric and electronic effects cannot be precisely assessed. The differentiation of these carbon signals, however, is critical in biosynthetic studies and in elucidating the interactions of β-lactam drugs with biological molecules (23–27).

In this study, the nuclear spin–spin coupling patterns were applied to the ^{13}C-NMR analysis of penicillins.

EXPERIMENTAL

The NMR spectra[1] of about 1 *M* solutions in dimethyl sulfoxide-d_6 and 2 *M* in all other deuterated solvents were obtained in 10-mm (^{13}C-NMR) and 5-mm (^{1}H-NMR) spinning tubes. The carbon-13 resonances of the deuterated solvents and methanol (in deuterium oxide) served as the internal reference, and chemical shift values were converted to the tetramethylsilane (VIII) scale using the following equations:

$$\delta(\text{VIII}) = \delta(\text{dimethyl sulfoxide-}d_6) + 39.6 \text{ ppm} \quad \text{(Eq. 1)}$$

$$\delta(\text{VIII}) = \delta(\text{chloroform-}d_3) + 76.9 \text{ ppm} \quad \text{(Eq. 2)}$$

$$\delta(\text{VIII}) = \delta(\text{methanol-}d) + 49.0 \text{ ppm} \quad \text{(Eq. 3)}$$

$$\delta(\text{VIII}) = \delta(\text{methanol}) + 49.3 \text{ ppm} \quad \text{(Eq. 4)}$$

The carbon-13 spectra were recorded at ambient temperature and 50°. All proton lines were decoupled by a broad band (2.5 kHz) irradiation from an incoherent 99.99-MHz source. The chemical shifts were measured for a 5000-Hz sweepwidth. The carbon-13–hydrogen coupling constants or splittings were measured from proton-coupled spectra. The typical pulse width was 23.5 μsec, and the repetition time between pulses was 4 sec.

All penicillins were USP grade. Penicillin V methyl ester was prepared by treating penicillin V free acid with diazomethane in ether solution for 1 hr. Its ^{1}H- and ^{13}C-NMR and mass spectra confirm the structure. The partially deuterated methyl ether was made from the deuterated penicillin V, which was obtained by exchanging the labile protons with monodeuterated methanol. The mass spectrum of the product indicates that it contains monodeutero-, dideutero-, and trideuteromethyl groups.

RESULTS AND DISCUSSION

Single-frequency proton decoupling was used for the assignments of the methine carbon resonances of methyl and benzyl esters of penicillin derivatives (9, 28) and phenethicillin potassium (29). A complete interpretation of the ^{1}H-NMR spectrum is absolutely necessary for this approach. It is difficult to determine the methine proton resonances (H_5 and H_6) of penicillins, especially in solutions above the critical micelle concentration (30).

A more convenient method for distinguishing these peaks is the direct measurement of ^{13}C–^{1}H one-bond coupling constants ($^1J_{CH}$), as shown in the proton-coupled spectrum of penicillin V methyl ester (I) (Fig. 1). Based on the electronegativity of the adjacent groups (18, 21, 22, 31), it is reasonable to predict the relative coupling constant magnitude in the following order: $^1J(C_5\text{–}H_5) > {}^1J(C_6\text{–}H_6) > {}^1J(C_3\text{–}H_3)$. The values obtained for I confirm this prediction [$^1J(C_5\text{–}H_5)$ = 178.5, $^1J(C_6\text{–}H_6)$ = 153.2, and $^1J(C_3\text{–}H_3)$ = 145.3 Hz]. This method provides the unambiguous assignments of C_3, C_5, and C_6 resonances of all other penicillins in different solvents (Tables I and II).

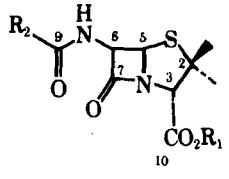

10

I: $R_1 = CH_3$, R_2 =

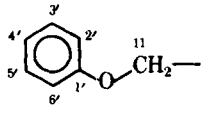

I-*d*: $R_1 = CH_2D + CHD_2 + CD_3$, R_2 =

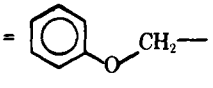

II: R_1 = K, R_2 =

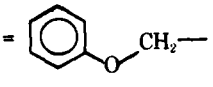

III: R_1 = K, R_2 =

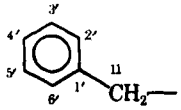

IV: R_1 = Na, R_2 =

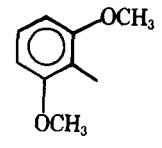

[1] Jeol PFT-100 spectrometer, operating at 23.5 kg and interfaced with a Jeol EC-100 20K computer, and a Varian EM-360 60-MHz spectrometer.

0022-3549/79/0100-0064$01.00/0
© 1979, American Pharmaceutical Association

Table I—^{13}C-NMR Data of Penicillins in Deuterium Oxide Solution [a]

Carbon	I	II	III	IV	V	VI	VII
2	65.4 m[b]	64.8 m	64.6 m	64.8 m	64.9 m	64.9 m	65.1 m
3	71.7 dm 145.3 (H_3)	73.4 bd 147.1 (H_3)	73.5 bd 146.7 (H_3)	73.7 bd 145.2 (H_3)	73.5 bd 145.3 (H_3)	73.4 bd 143.4 (H_3)	73.5 bd 144.7 (H_3)
5	68.6 ddd 178.5 (H_5) 5.7 } H_3 4.1 } H_6	66.8 bd 180.0 (H_5)	66.9 bd 178.2 (H_5)	66.9 bd 180.1 (H_5)	66.4 bd 178.2 (H_5)	66.2 bd 177.6 (H_6)	66.3 bd 180.0 (H_6)
6	59.4 dd 153.2 (H_6) 2.5 (H_5)	57.5 bd 155.0 (H_6)	58.1 bd 153.8 (H_6)	57.9 bd 153.8 (H_6)	58.0 bd 154.4 (H_6)	57.7 bd 154.4 (H_6)	57.8 bd 155.0 (H_6)
7	173.5 ddd 10.8 } H_3 7.2 } H_5 3.7 } H_6	174.0 m	174.7 ddd 9.2 } H_3 7.0 } H_5 5.1 } H_6	175.0 dt 9.0 } H_3 4.9 } H_5 } H_6	174.9 m	174.7 m	174.5 dt 8.6 } H_3 4.6 } H_5 } H_6
9	169.8 td 4.5 (H_{11}) 2.6 (H_6)	169.6 bt 4.3 (H_{11})	173.1 bt 6.7 (H_{11})	167.1 bs	162.6 d 2.5 (H_6)	161.9 d 3.0 (H_6)	161.5 bs
10	169.1 qui 4.3 (H_3, OCH_3)	173.8 d 4.3 (H_3)	174.1 d 4.3 (H_3)	174.2 d 4.3 (H_3)	174.9 m	174.2 d 4.3 (H_3)	174.0 d 3.7 (H_3)
11	67.7 t 147.4 (H_{11})	66.8 t 148.3 (H_{11})	42.3 t 129.7 (H_{11})				
2α-CH_3	27.0 qm 128.2 (2α-CH_3)	26.8 qm 127.0 (2α-CH_3)	26.9 bq 127.8 (2α-CH_3)	27.0 bq 128.2 (2α-CH_3)	27.0 bq 129.4 (2α-CH_3)	27.0 bq 129.4 (2α-CH_3)	26.9 bq 125.7 (2α-CH_3)
2β-CH_3	32.2 qm 128.2 (2β-CH_3)	31.6 qm 127.0 (2β-CH_3)	31.1 bq 128.0 (2β-CH_3)	30.0 bq 128.8 (2β-CH_3)	31.0 bq 129.4 (2β-CH_3)	31.3 bq 129.4 (2β-CH_3)	31.8 bq 124.5 (2β-CH_3)
1′	158.3 bt 9.1 (H'_3, H'_5)	156.9 bt 9.5 (H'_3, H'_5)	134.7 bs 4.9 (H'_3, H'_5)	113.2 t 4.9 (H'_3, H'_5)	110.5 q 2.4 (2′-CH_3)	111.3 q 2.4 (2′-CH_3)	111.0 q 2.4 (2′-CH_3)
2′	115.6 ddd 159.5 (H'_2)	114.9 ddd 160.4 (H'_2)	129.5 bd 158.1 (H'_2)	157.5 m 6.7 (2′-CH_3)	174.3 q 6.7 (2′-CH_3)	174.7 q 6.7 (2′-CH_3)	175.8 q 6.9 (2′-CH_3)
3′	130.5 dd 160.8 (H'_3) 8.3 (H'_5)	130.1 dd 161.1 (H'_3) 8.5 (H'_5)	128.9 dd 160.2 (H'_3) 6.6 (H'_5)	104.7 dd 164.8 (H'_3) 6.7 (H'_5)			
4′	122.7 dt 162.1 (H'_4) 7.2 (H'_2, H'_6)	122.2 dt 161.8 (H'_4) 7.0 (H'_2, H'_6)	127.3 bd 161.1 (H'_4)	132.3 d 163.0 (H'_4)			
5′	130.5 dd 160.8 (H'_5) 8.3 (H'_3)	130.1 dd 161.1 (H'_3) 8.5 (H'_5)	128.9 dd 160.2 (H'_5) 6.6 (H'_3)	104.7 dd 164.8 (H'_5) 6.7 (H'_3)	160.7 bs	158.8 bs	156.5 s
6′	115.6 ddd 159.5 (H'_6) 7.8 (H'_4) 4.8 (H'_2)	114.9 ddd 160.4 (H'_6) 7.2 (H'_4) 4.4 (H'_2)	129.5 bs 158.1 (H'_6)	157.5 m	127.2 m	126.6 bt 4.9 (H'_8, H'_{10})	126.0 m
7′					128.8 bd 129.5 dd 163.0 (H'_8) 6.3 (H'_{10})	133.5 m 132.7[d] bd 165.4 (H'_8)	135.7 (135.5) m 129.4 (129.3) bd 170.6 (H'_8)
8′							
9′					131.0 bd 159.9 (H'_9)	131.9[b] bd 163.6 (H'_9)	133.4 bd 168.9 (H'_9)
10′					129.5 dd 163.0 (H_{10}) 6.3 (H'_8)	128.2 bd 164.8 (H'_{10})	129.3 (129.4) 170.6 (H'_{10})
11′					128.8 bd 162.4 (H'_{11})	130.9[b] bd 166.6 (H'_{11})	133.5 (133.7) m
2′-CH_3				56.2 q 145.9 (2′-OCH_3)	12.7 q 131.8 (2′-CH_3)	13.0 q 131.8 (2′-CH_3)	13.1 q (131.8) (2′-CH_3)

[a] The data of each carbon resonance are shown in the following order: chemical shift in deuterium oxide, multiplicity, and spin–spin splittings (coupled protons). All spectra were measured in deuterium oxide at about 25°, except the spectrum of I, which was measured in methanol-*d*, and the spectrum of VII, which was measured at 50°; b = broad, qui = quintet, and m = unresolved multiplet. [b] Signals in any vertical column may be reversed.

Table II—^{13}C-NMR Data of Penicillins in Dimethyl Sulfoxide-d_6 Solution [a]

Carbon	II	III	IV	V	VI	VII
2	64.9 m	64.4 m	64.5 m	64.8 m	64.7 m	64.8 m
3	74.0 dm 142.8 (H_3)	74.0 dm 140.4 (H_3)	74.3 dm 141.6 (H_3)	73.9 bd 141.6 (H_3)	73.9 dm 142.2 (H_3)	73.8 dm 144.0 (H_3)
5	67.1 ddd 176.1 (H_5) 5.2 H_3 3.1 H_6	66.9 dt 175.4 (H_5) 3.8 (H_3, H_6)	67.4 dt 173.3 (H_5) 3.6 (H_3, H_6)	67.2 dt 178.2 (H_5) 3.6 (H_3, H_6)	66.9 dt 178.2 (H_5) 4.2 (H_3, H_6)	67.1 ddd 180.7 5.4 H_3 3.7 H_6
6	57.5 dd 152.0 (H_6) 2.5 (H_5)	57.9 dd 151.0 (H_6) 1.5 (H_5)	58.0 bd 150.8 (H_6)	58.9 bd 152.6 (H_6)	58.3 bd 152.6 (H_6)	58.4 dd 153.2 (H_6) 2.7 (H_5)
7	172.6 ddd 8.6, 6.4, 4.3 (H_3, H_5, H_6)	172.7 ddd 9.8, 7.0, 4.9 (H_3, H_5, H_6)	174.3 dt 9.8, 5.1 (H_3, H_5, H_6)	172.5 ddd 9.8, 7.0, 4.9 (H_3, H_5, H_6)	173.1 m	172.8 m
9	167.9 q 4.9 (H_6, H_{11})	170.4 td 6.4 (H_{11})	165.1 d 3.4 (H_6)	161.7 bs	160.7 d 2.5 (H_6)	159.8 d 4.3 (H_6)
10	169.7 d 3.7 (H_3)	169.8 d 4.2 (H_3)	171.8 d 4.3 (H_3)	171.3 d 4.3 (H_3)	171.6 d 4.3 (H_3)	171.5 d 4.3 (H_3)
11	66.4 t 147.1 (H_{11})	41.6 bt 129.4 (H_{11})				
2α-CH_3	27.6 qm 127.6 (2α-CH_3)	27.5 qm 127.6 (2α-CH_3)	27.9 qm 127.6 (2α-CH_3)	27.6 qm 127.6 (2α-CH_3)	27.6 qm 125.9 (2α-CH_3)	27.5 qm 128.8 (2α-CH_3)
2β-CH_3	32.5 qm 127.6 (2β-CH_3)	31.8 qm 127.6 (2β-CH_3)	31.3 qm 127.6 (2β-CH_3)	32.1 bq 129.4 (2β-CH_3)	32.2 qm 128.1 (2β-CH_3)	32.5 qm 129.4 (2β-CH_3)
1′	157.7 m	135.8 m	115.8 t 5.8 (H'_3, H'_5)	112.0 q 2.4 (2′-CH_3)	112.8 q 2.4 (2′-CH_3)	112.3 d 3.0 (2′-CH_3)
2′	114.8 ddd 160.2 (H'_2) 7.9 (H'_4) 4.6 (H_6)	129.8 dm 157.3 (H'_2)	157.2 dq 10.7 (H'_4) 4.9 (OCH_3)	170.8 q 7.0 (2′-CH_3)	171.9 q 6.7 (2′-CH_3)	172.8 q 7.1 (2′-CH_3)
3′	129.8 dd 160.8 (H'_3) 8.1 (H'_5)	129.0 dd 159.9 (H'_3) 4.9 (H'_5)	104.6 dd 163.3 (H'_3) 7.7 (H'_5)			
4′	121.6 dt 162.3 (H'_4) 7.2 (H_2, H'_6)	126.4 dm 163.0 (H'_4)	130.9 d 160.5 (H'_4)			
5′	129.8 dd 160.8 (H'_3) 8.1 (H'_5)	129.0 dd 159.9 (H'_5) 4.9 (H'_3)	104.6 dd 163.3 (H'_5) 7.7 (H'_3)	160.3 t 3.7 (H'_7, H'_{11})	159.5 bs	157.4 s
6′	114.8 ddd 160.2 (H'_6) 7.9 (H'_4) 4.6 (H_2)	129.8 dm 157.3 (H'_6)	130.9 d 160.5 (H'_6)	128.3 t 6.7 (H'_6)	127.5 m	126.9 m
7′				128.1 dd 161.8 (H'_7) 6.1 (H_9, H'_{11})	133.0[b] m	135.1[b] m
8′				129.0 ddd 162.6 (H'_8) 5.7 (H'_{10}) 2.6 (H_7, or H'_9)	132.0[b] bm 165.4 (H'_8)	129.0 dm 169.7 (H'_8)
9′				130.3 dt 161.8 (H'_9) 7.2 (H'_7, H'_{11})	132.0[b] bm 165.4 (H'_9)	133.0 d 167.8 (H'_9)
10′				129.0 ddd 162.6 (H'_{10}) 5.7 (H'_8) 2.6 (H_9 or H'_{11})	127.8 dm 165.4 (H'_{10})	129.0 dm 169.7 (H'_{10})
11′				128.1 dt 161.8 (H'_{11}) 6.1 (H_9, H'_7)	130.2[b] dm 168.5 (H'_{11})	134.9[b] m

[a] The data of each carbon resonance are shown in the following order: chemical shift, multiplicity, and coupling constants (coupled protons). The chemical shift and multiplicity were measured at about 25 and 50°, respectively; b = broad, and m = unresolved multiplet. [b] Signals in any vertical column may be reversed.

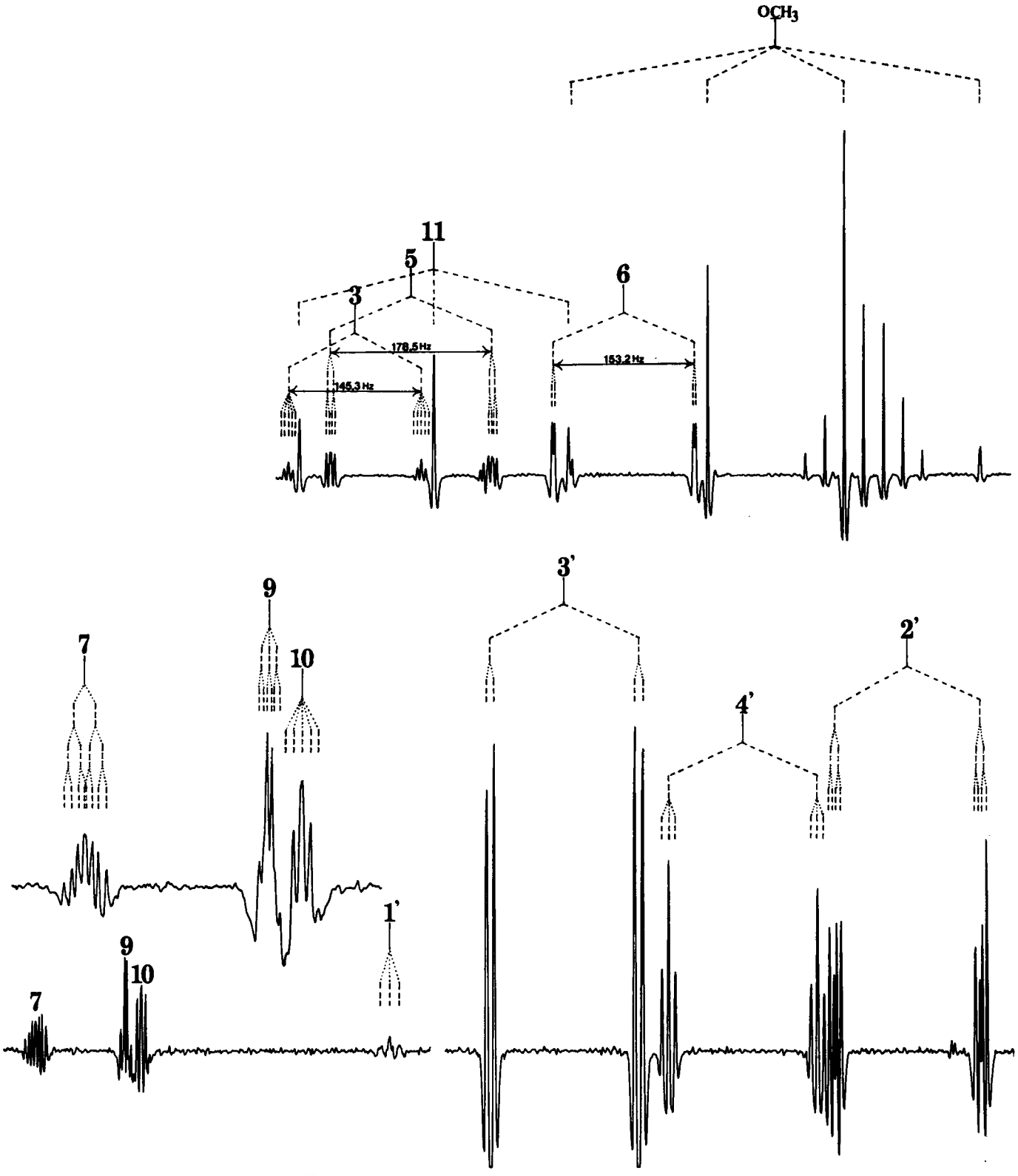

Figure 1—*High-resolution proton-coupled ^{13}C-NMR spectrum of penicillin V methyl ester (I) in methanol-d. A narrow (100–500 Hz) exponential (−3) window is used to measure small splittings.*

The application of ^{13}C–^{1}H one-bond coupling information in the ^{13}C-spectral analysis is limited to the protonated carbons. Coupling information also can be applied to the nonprotonated carbons (18, 19, 31–35). This application can be demonstrated fully in the chemical shift analysis of C_7, C_9, and C_{10} of penicillins.

In a previous report (28) on the ^{13}C-NMR assignments of I, the most downfield peak (172.6 ppm) was assigned to C_{10} and the 167.6-ppm peak was assigned to both C_7 and C_9. The proton-coupled spectrum of I was studied in methanol-*d*, chloroform-d_3, and dimethyl sulfoxide-d_6 solutions. The most downfield signal at about 173 ppm can be recognized as a doublet of double doublet (ddd) or a double quartet (dq) (Fig. 1). It thus can be designated to either C_7 (ddd) or C_{10} (dq).

To clarify this uncertainty, a deuteromethyl ester of penicillin V (I-*d*) was prepared. The proton-coupled spectrum of I-*d* shows that the most

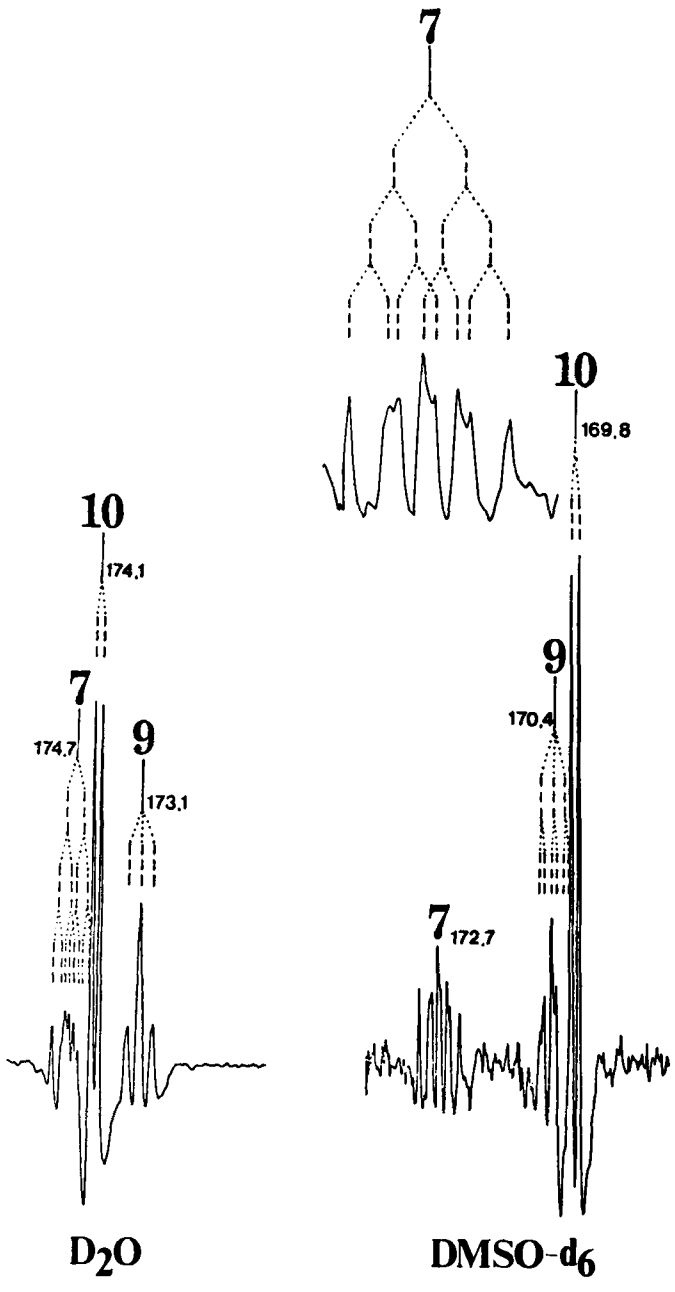

Figure 2—*High-resolution proton-coupled ^{13}C-NMR spectra of penicillin G potassium salt (III) in deuterium oxide and dimethyl sulfoxide-d_6 solutions. Only the carbonyl carbon signals are shown. A narrow (100–500 Hz) exponential (−3) window is used to measure small splittings.*

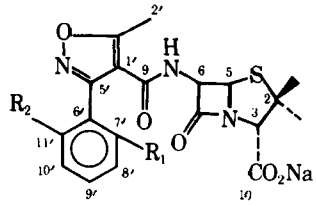

V: $R_1 = R_2 = H$
VI: $R_1 = Cl$, $R_2 = H$
VII: $R_1 = R_2 = Cl$

downfield peak at 173.5 ppm remains intact while the 169.1-ppm peak becomes an unresolved multiplet, arising from the ^{13}C–deuterium coupling. Therefore, the 169.1-ppm peak (quintet) must be assigned to C_{10} [$^2J(C_{10}\text{–}H_3) \approx {}^3J(C_{10}\text{–}CH_3) = 4.3$ Hz] in contradiction to the previous assignment (28). The C_9 signal appears as a triple doublet due to its coupling with H_{11} and H_6. This finding clearly demonstrates the invalidity of simple chemical shift theory or the additivity principle in the differentiation of the close resonance signals.

The ^{13}C–hydrogen coupling patterns of the phenoxy portion of I (Fig. 1 and Table I) can be analyzed by analogy to the coupling of phenols (33). The typical three-bond couplings of aromatic systems are seen. The magnitude of $^3J(C'_2\text{–}H'_6)$ is smaller than the usual three-bond coupling constants due to coupling through an oxygen-substituted carbon (32–34). Thus, C'_2 appears as a doublet of double doublet [$^1J(C'_2\text{–}H'_2 = 159.5$, $^3J(C'_2\text{–}H'_4) = 7.8$, and $^3J(C'_2\text{–}H'_6) = 4.8$ Hz]. Most aromatic carbon resonances of other penicillins can be determined similarly.

The proton-coupled spectra of penicillin in deuterium oxide solution display some useful features of ^{13}C–hydrogen long-range splitting patterns. The C_{10} signal always appears as a doublet because of the two-bond couplings with H_3. The C_7 resonance peak is shown as a doublet of double doublet or a double triplet due to the couplings with H_3, H_5, and H_6, revealing characteristics reminiscent of the spectrum of I.

The splitting patterns of C_9 vary according to the structure of the side chain (R_2). The broad linewidth often prohibits the measurement of the small coupling between C_9 and H_6. The coupling is apparent in the spectra of sodium salts of oxacillin (V) and cloxacillin (VI).

The chemical shift analysis of the isoxazole moiety is straightforward. The C'_1 resonance signal occurs at the highest field among all sp^2 carbon peaks and is the only carbon without a two- or three-bond proton in V and VI. The C'_2 signal can be differentiated from C_7 and C_{10} simply because of its unique two-bond coupling with C'_2–CH_3.

The C'_6, C'_7, and C'_{10} signals of VI can be determined from chemical shift calculations (15, 16, 21, 22). However, C'_8, C'_9, and C'_{10} cannot be firmly assigned since the calculated values are close and the rotation around the C'_5–C'_6 bond is probably partially restricted. This restricted rotation is indicated by the splitting of C'_7 (C'_{11}) and C'_8 (C'_{10}) of dicloxacillin (VII) into doublets in deuterium oxide.

Direct measurements from the proton-coupled spectra may sometimes provide line splittings instead of precise coupling constants due to the virtual couplings of the proton nuclei. However, the directly observed line splittings (coupling patterns) may be more useful.

Concentrated aqueous solutions of penicillins are too viscous to give fine spectra with good resolution, partially because of the formation of micellar solutions (30). The instability of penicillin in water prevents spectral determination at elevated temperatures. To confirm the coupling patterns, the ^{13}C-NMR spectra of penicillins were taken in dimethyl sulfoxide-d_6 at 50°. The linewidth was considerably reduced, allowing the measurement of the fine splittings of most carbon signals.

Comparative studies of the chemical shift in deuterium oxide and dimethyl sulfoxide-d_6 (Fig. 2) indicate that the solvent affects the relative chemical shift (Tables I and II) (15, 16, 21, 22). This effect prevents the use of simple chemical shift calculations to deduce the chemical shift directly from one solvent to the other solvent. However, the coupling patterns are not perturbed by the solvent effect (Fig. 2) unless a slowly exchangeable proton is involved.

REFERENCES

(1) E. H. Flynn, "Cephalosporins and Penicillins: Chemistry and Biology," Academic, New York, N.Y., 1972.

(2) M. S. Manhas and A. K. Bose, "β-Lactams: Natural and Synthetic," Wiley-Interscience, New York, N.Y., 1971.

(3) M. S. Manhas and A. K. Bose, "Synthesis of Penicillin and Cephalosporin C and Analogs," Dekker, New York, N.Y., 1969.

(4) P. G. Sammes, *Chem. Rev.*, **76**, 113 (1976).

(5) C. H. Nightingale, D. S. Greene, and R. Quintiliani, *J. Pharm. Sci.*, **64**, 1899 (1975).

(6) W. J. Wheeler, *Lloydia*, **40**, 519 (1977).

(7) L. A. Mitscher, H. D. H. Showalter, K. Shirahata, and R. L. Foltz, *J. Antibiotics*, **28**, 668 (1975).

(8) A. F. Casy, "PMR Spectroscopy in Medicinal and Biological Chemistry," Academic, New York, N.Y., 1971.

(9) S. Kukolja, N. D. Jones, M. O. Chaney, T. K. Elzey, M. R. Gleissner, J. W. Paschal, and D. E. Dorman, *J. Org. Chem.*, **16**, 2388 (1975).

(10) G. V. Fazakerley and G. E. Jackson, *J. Chem. Soc. Perkin Trans. II*, **1975**, 567.

(11) C. M. Dobson, L. O. Ford, S. E. Summers, and R. J. P. Williams, *J. Chem. Soc. Farady Trans. II*, **1975**, 1145.
(12) W. L. Wilson, H. W. Avdovich, and D. W. Hughes, *J. Assoc. Off. Anal. Chem.*, **57**, 1300 (1974).
(13) L. S. Kan, F. K. Schweighardt, S. Kao, and N. C. Li, *Biochem. Biophys. Res. Commun.*, **46**, 22 (1972).
(14) J. B. Lowry and N. V. Riggs, *Tetrahedron Lett.*, **1964**, 2911.
(15) E. W. Wehrli and T. Wirthlin, "Interpretation of Carbon-13 NMR Spectra," Heyden, London, England, 1976.
(16) E. Breitmaier and W. Voelter, "^{13}C NMR Spectroscopy," Verlag Chemie, Weinheim, West Germany, 1974.
(17) G. C. Levy, "Topics in Carbon-13 NMR Spectroscopy," vol. 2, Wiley-Interscience, New York, N.Y., 1976.
(18) C.-j. Chang and G. E. Peck, *J. Pharm. Sci.*, **65**, 1019 (1976).
(19) C.-j. Chang, H. G. Floss, and G. E. Peck, *J. Med. Chem.*, **18**, 505 (1975).
(20) N. J. Bach, H. E. Boaz, E. C. Kornfeld, C.-j. Chang, H. G. Floss, E. W. Hagaman, and E. Wenkert, *J. Org. Chem.*, **39**, 1274 (1974).
(21) G. C. Levy and G. L. Nelson, "Carbon-13 Nuclear Magnetic Resonance for Organic Chemists," Wiley-Interscience, New York, N.Y., 1972.
(22) J. B. Stothers, "Carbon-13 NMR Spectroscopy," Academic, New York, N.Y., 1972.
(23) D. J. Aberhart, *Tetrahedron*, **33**, 1545 (1977).
(24) S. Hem, E. J. Russo, S. M. Bahal, and R. S. Levi, *J. Pharm. Sci.*, **62**, 267 (1973).
(25) D. E. Tutt and M. A. Schwartz, *J. Am. Chem. Soc.*, **93**, 767 (1971).
(26) K. Izaki, M. Matsukashi, and J. L. Strominger, *J. Biol. Chem.*, **243**, 3180 (1968).
(27) J. J. Fischer and O. Jardetzky, *J. Am. Chem. Soc.*, **87**, 3237 (1965).
(28) R. A. Archer, R. D. G. Cooper, and P. V. Demarco, *J. Chem. Soc. Chem. Commun.*, **1970**, 129.
(29) W. L. Wilson, H. W. Avdovich, D. W. Hughes, and G. W. Buchanan, *J. Pharm. Sci.*, **66**, 1079 (1977).
(30) J. T. H. Ong and H. B. Kostenbauder, *ibid.*, **64**, 1378 (1975).
(31) L. H. Hurley, M. Zmijewski, and C.-j. Chang, *J. Am. Chem. Soc.*, **97**, 4372 (1975).
(32) C.-j. Chang, T.-L. Shieh, and H. G. Floss, *J. Med. Chem.* **20**, 176 (1977).
(33) C.-j. Chang, *J. Org. Chem.*, **41**, 1881 (1976).
(34) C.-j. Chang, H. G. Floss, and W. Steck, *ibid.*, **42**, 1337 (1977).
(35) C.-j. Chang, H. G. Floss, L. H. Hurley, and M. Zmijewski, *ibid.*, **41**, 2932 (1976).

ACKNOWLEDGMENTS

The authors are grateful to Mrs. T.-L. Shieh for technical assistance.

First-Pass Effect after Rectal Administration of Thiazinamium Methylsulfate

J. H. G. JONKMAN *x, L. E. van BORK ‡, J. WIJSBEEK *, A. S. BOLHUIS-de VRIES *, R. A. de ZEEUW *, N. G. M. ORIE ‡, and H. L. M. COX §

Received March 24, 1978, from the **Department of Pharmaceutical and Analytical Chemistry and the* ‡*Pulmonary Division of the Department of Internal Medicine, State University of Groningen, Antonius Deusinglaan 2, Groningen, The Netherlands,* and the §*Laboratory of the Dutch Pharmacists, The Hague, The Netherlands.* Accepted for publication June 5, 1978.

Abstract □ The absorption and metabolism of the quaternary ammonium compound thiazinamium methylsulfate were studied in humans using plasma concentration data and urinary excretion measurements. After giving a dose of 150 mg in suppositories, the relative bioavailability was 5.8 ± 3.2 (*SD*) % of the dose, comparable to the values obtained following oral administration. The degree of first-pass effect observed after rectal administration was comparable with that after oral administration.

Keyphrases □ Thiazinamium methylsulfate—rectal absorption and metabolism in humans □ Absorption, rectal—thiazinamium methylsulfate in humans □ Metabolism—thiazinamium methylsulfate in humans □ Phenothiazine derivatives—thiazinamium methylsulfate, rectal absorption and metabolism in humans □ Antihistaminics—thiazinamium methylsulfate, rectal absorption and metabolism in humans

It has been widely assumed that, after rectal administration, drugs mainly enter the general circulation without an initial passage through the liver, provided that the suppository does not reach the higher parts of the rectum (1, 2). The drug supposedly enters the inferior or middle rectal veins, which drain into the vena cava inferior. The blood in the superior rectal vein flows to the portal vein and subsequently enters the liver.

After oral administration, most drugs enter the portal vein, so a 100% passage through the liver is involved. Once a drug enters the general circulation, approximately 20% of the total blood flow passes through the liver during each circulation, whatever the route of administration. However, when drugs are administered parenterally, the total first passage through the liver does not occur. It has been assumed that the same condition would apply for the rectal route. For this reason, rectal administration has been recommended as a noninvasive alternative for drugs largely metabolized by the liver or excreted in the bile and for drugs subject to degradation in the GI tract.

Thiazinamium methylsulfate[1] (I) is a phenothiazine derivative with a quaternary ammonium group in the molecule. The drug is used for the treatment of some generalized obstructive lung diseases because it causes bronchodilatation (especially after intramuscular injection) as a result of substantial anticholinergic and antihistaminic properties (3–9).

[1] Multergan, Specia, Rhône Poulenc, Paris, France.

0022-3549/79/0100-0069$01.00/0
© 1979, American Pharmaceutical Association

(11) C. M. Dobson, L. O. Ford, S. E. Summers, and R. J. P. Williams, *J. Chem. Soc. Farady Trans. II*, **1975**, 1145.
(12) W. L. Wilson, H. W. Avdovich, and D. W. Hughes, *J. Assoc. Off. Anal. Chem.*, **57**, 1300 (1974).
(13) L. S. Kan, F. K. Schweighardt, S. Kao, and N. C. Li, *Biochem. Biophys. Res. Commun.*, **46**, 22 (1972).
(14) J. B. Lowry and N. V. Riggs, *Tetrahedron Lett.*, **1964**, 2911.
(15) E. W. Wehrli and T. Wirthlin, "Interpretation of Carbon-13 NMR Spectra," Heyden, London, England, 1976.
(16) E. Breitmaier and W. Voelter, "^{13}C NMR Spectroscopy," Verlag Chemie, Weinheim, West Germany, 1974.
(17) G. C. Levy, "Topics in Carbon-13 NMR Spectroscopy," vol. 2, Wiley-Interscience, New York, N.Y., 1976.
(18) C.-j. Chang and G. E. Peck, *J. Pharm. Sci.*, **65**, 1019 (1976).
(19) C.-j. Chang, H. G. Floss, and G. E. Peck, *J. Med. Chem.*, **18**, 505 (1975).
(20) N. J. Bach, H. E. Boaz, E. C. Kornfeld, C.-j. Chang, H. G. Floss, E. W. Hagaman, and E. Wenkert, *J. Org. Chem.*, **39**, 1274 (1974).
(21) G. C. Levy and G. L. Nelson, "Carbon-13 Nuclear Magnetic Resonance for Organic Chemists," Wiley-Interscience, New York, N.Y., 1972.
(22) J. B. Stothers, "Carbon-13 NMR Spectroscopy," Academic, New York, N.Y., 1972.
(23) D. J. Aberhart, *Tetrahedron*, **33**, 1545 (1977).
(24) S. Hem, E. J. Russo, S. M. Bahal, and R. S. Levi, *J. Pharm. Sci.*, **62**, 267 (1973).
(25) D. E. Tutt and M. A. Schwartz, *J. Am. Chem. Soc.*, **93**, 767 (1971).
(26) K. Izaki, M. Matsukashi, and J. L. Strominger, *J. Biol. Chem.*, **243**, 3180 (1968).
(27) J. J. Fischer and O. Jardetzky, *J. Am. Chem. Soc.*, **87**, 3237 (1965).
(28) R. A. Archer, R. D. G. Cooper, and P. V. Demarco, *J. Chem. Soc. Chem. Commun.*, **1970**, 129.
(29) W. L. Wilson, H. W. Avdovich, D. W. Hughes, and G. W. Buchanan, *J. Pharm. Sci.*, **66**, 1079 (1977).
(30) J. T. H. Ong and H. B. Kostenbauder, *ibid.*, **64**, 1378 (1975).
(31) L. H. Hurley, M. Zmijewski, and C.-j. Chang, *J. Am. Chem. Soc.*, **97**, 4372 (1975).
(32) C.-j. Chang, T.-L. Shieh, and H. G. Floss, *J. Med. Chem.* **20**, 176 (1977).
(33) C.-j. Chang, *J. Org. Chem.*, **41**, 1881 (1976).
(34) C.-j. Chang, H. G. Floss, and W. Steck, *ibid.*, **42**, 1337 (1977).
(35) C.-j. Chang, H. G. Floss, L. H. Hurley, and M. Zmijewski, *ibid.*, **41**, 2932 (1976).

ACKNOWLEDGMENTS

The authors are grateful to Mrs. T.-L. Shieh for technical assistance.

First-Pass Effect after Rectal Administration of Thiazinamium Methylsulfate

J. H. G. JONKMAN *x, L. E. van BORK ‡, J. WIJSBEEK *, A. S. BOLHUIS-de VRIES *, R. A. de ZEEUW *, N. G. M. ORIE ‡, and H. L. M. COX §

Received March 24, 1978, from the **Department of Pharmaceutical and Analytical Chemistry and the* ‡*Pulmonary Division of the Department of Internal Medicine, State University of Groningen, Antonius Deusinglaan 2, Groningen, The Netherlands,* and the §*Laboratory of the Dutch Pharmacists, The Hague, The Netherlands.* Accepted for publication June 5, 1978.

Abstract □ The absorption and metabolism of the quaternary ammonium compound thiazinamium methylsulfate were studied in humans using plasma concentration data and urinary excretion measurements. After giving a dose of 150 mg in suppositories, the relative bioavailability was 5.8 ± 3.2 (*SD*) % of the dose, comparable to the values obtained following oral administration. The degree of first-pass effect observed after rectal administration was comparable with that after oral administration.

Keyphrases □ Thiazinamium methylsulfate—rectal absorption and metabolism in humans □ Absorption, rectal—thiazinamium methylsulfate in humans □ Metabolism—thiazinamium methylsulfate in humans □ Phenothiazine derivatives—thiazinamium methylsulfate, rectal absorption and metabolism in humans □ Antihistaminics—thiazinamium methylsulfate, rectal absorption and metabolism in humans

It has been widely assumed that, after rectal administration, drugs mainly enter the general circulation without an initial passage through the liver, provided that the suppository does not reach the higher parts of the rectum (1, 2). The drug supposedly enters the inferior or middle rectal veins, which drain into the vena cava inferior. The blood in the superior rectal vein flows to the portal vein and subsequently enters the liver.

After oral administration, most drugs enter the portal vein, so a 100% passage through the liver is involved. Once a drug enters the general circulation, approximately 20% of the total blood flow passes through the liver during each circulation, whatever the route of administration. However, when drugs are administered parenterally, the total first passage through the liver does not occur. It has been assumed that the same condition would apply for the rectal route. For this reason, rectal administration has been recommended as a noninvasive alternative for drugs largely metabolized by the liver or excreted in the bile and for drugs subject to degradation in the GI tract.

Thiazinamium methylsulfate[1] (I) is a phenothiazine derivative with a quaternary ammonium group in the molecule. The drug is used for the treatment of some generalized obstructive lung diseases because it causes bronchodilatation (especially after intramuscular injection) as a result of substantial anticholinergic and antihistaminic properties (3–9).

[1] Multergan, Specia, Rhône Poulenc, Paris, France.

0022-3549/79/0100-0069$01.00/0
© 1979, American Pharmaceutical Association

Table I—Absorption Characteristics of Thiazinamium Methylsulfate after Rectal Administration of a 150-mg Dose

Parameter	Patient GL	Patient PH	Patient WM	Patient HH	Patient WB	Patient MF	Patient TJ	Mean ± *SD*
Age, years	57	62	52	63	26	71	68	57 ± 15
Body weight, kg	74	86	79	67	70	72	75	75 ± 6
Height, m	1.78	1.74	1.81	1.76	1.74	1.76	1.77	1.77 ± 0.02
Dose, mg/kg	2.63	2.26	2.46	2.90	2.78	2.70	2.59	2.62 ± 0.21
c_{max}[a], ng/ml	72	54	142	63	45	290	53	103 ± 89
t_{max}[b], min	45	90	45	120	105	15	20	63 ± 42
F_{rel}[c], % of dose	6.3	6.6	11.0	6.9	0.7	5.8	3.4	5.8 ± 3.2
$(F_{rel})_{tot}$[d], % of dose	6.6	6.8	11.6	8.1	0.7	5.8	3.7	6.2 ± 3.4

[a] Maximum plasma concentration. [b] Time at which c_{max} was reached. [c] Relative bioavailability (compared to intramuscular injection). [d] Estimated values obtained after extrapolation except for Patients WB and MF (measured values).

In excretion and metabolism studies (10, 11), an extensive first-pass effect apparently occurred when thiazinamium cations were administered orally. Moreover, a high proportion of both the unchanged drug and the metabolite was found in bile (12).

The purpose of this study was to investigate whether rectal administration of I would offer better systemic bioavailability.

EXPERIMENTAL

Dosage Form—The lipophilic (fatty) base was a mixture[2] of some mono-, di-, and triglycerides of naturally occurring saturated fatty acids (C_{12}–C_{18}), with a melting range of 33.5–35.5° and a congealing range of 32.5–34.5°. The specific gravity of the base at 20° is 0.950–0.980; it has an iodine number less than three, a saponification value of 230–240, and a hydroxyl value of less than 15 (13).

Its melting behavior both *in vitro* and *in vivo* was described by Ritschel (14), who showed that a suppository of the lipophilic base without additional drug substances melted almost completely in the human rectum within 10 min.

For all experiments involving rectal administration, a dose of 0.4747 m*M* (150 mg) of thiazinamium base (calculated as the hydroxide), equal to 194.6 mg of the methylsulfate, was selected. The drug was passed through a sieve to obtain particles <150 μm in size. The suppositories were prepared by the fusion method, *i.e.*, a suspension of the powder was mixed with 2 mg of colloidal silica[3] in the molten base (about 50°). The liquid then was poured into 2-ml molds at 34–35°.

The drug content in the suppositories was determined by an amphimetric titration to be 100.3% (n = 3) of the stated amount (10). The dissolution rate of the suppositories was determined as described previously (15, 16). The dissolution half-life was 6 min.

Analytical Methods—The amount of thiazinamium cations in plasma and urine was determined as described previously (17). The procedure is based on ion-pair extraction of the compound with iodide as a counterion, followed by GLC with an alkali flame-ionization detector.

Thiazinamium sulfoxide cations were isolated from the urine by means of column chromatography using an ion-exchange resin[4], followed by two-dimensional TLC (18). The sensitivity of the latter method was not sufficient to allow the measurement of metabolite concentrations in plasma.

Protocol—Seven male patients with generalized obstructive lung disease (Table I) had no abnormalities in their blood composition, kidney function, liver function, and digestive tract. None of the patients used other drugs during the investigation or the preceding week. Patients fasted overnight. After drug administration at 9.00 am, the patients stayed in bed for 1 hr.

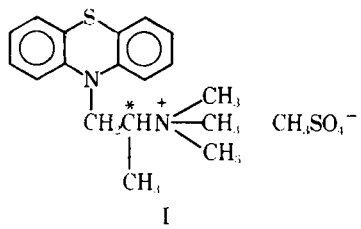

I

Blood sampling took place at 0, 3, 6, 10, 15, 20, 30, 45, 60, 75, 90, 105, 120, 150, 180, 210, 330, and 420 min following drug administration. The samples (~10 ml) were drawn from a permanent cannula[5] with a three-way stopcock[6] placed in the right cubital vein. The blood was collected in 15-ml glass tubes with screw caps[7]; each contained 1 drop of heparin solution (5 mg = 500 U of heparin sodium/ml of distilled water). The samples were immediately stored in a refrigerator at 4°.

Within 2 hr of collection, the samples were centrifuged for 20 min at 6000×*g*. Next, 4.0 ml of the plasma layer was transferred to a 50-ml centrifuge tube[8] and stored at −20°. It was analyzed within 2 months. Within this period, no significant decrease in the concentrations could be detected (10).

Immediately after drug administration, each patient was allowed to drink 200 ml of water. After 90 and 210 min, the patients were given a light meal (rusks with sugar and a glass of orange lemonade). During the experiment, the patients were allowed to drink water upon request.

Urine was collected every hour, if possible, during the first 7 hr of the investigation and up to 24 hr afterwards.

Determination of Relative Bioavailability—The areas under the plasma concentration–time curves were determined by cutting and weighing a standard high-quality paper. The relative bioavailability *versus* an intramuscular injection of 12.5 mg (which was found to have an absolute bioavailability of 100% during the time of the experiment) in the same patients was calculated by comparing the areas under the curves after correction for the dose. This comparison was allowed because the pharmacokinetics of this drug are not dose dependent (10).

RESULTS AND DISCUSSION

Bioavailability—Typical plasma concentration–time curves are given in Fig. 1. Plasma concentrations were generally low. In most patients, absorption started rather quickly. The t_{max} values varied from 15 to 120 min with a mean value of 63 ± 42 (*SD*) min, suggesting that thiazinamium cations are rapidly liberated from the base in the rectum. This finding is in agreement with the *in vitro* experiment.

The values for c_{max} varied from 54 to 290 ng/ml, with a mean value of 103 ± 89 (*SD*) ng/ml. In most patients, a more or less pronounced plateau

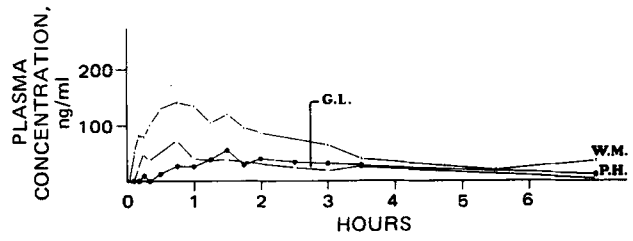

Figure 1—*Typical examples of individual plasma concentration–time curves obtained after rectal administration of a suppository containing 150 mg of thiazinamium.*

[2] Witepsol H-15, Dynamit Nobel A.G., Chemische Werke Witten, Witten, German Federal Republic.
[3] Aerosil.
[4] Amberlite XAD-2.
[5] Indwelling catheter, Braunule T with LOK, B. Braun, Melsungen, German Federal Republic.
[6] K-75a, Pharmseal, Herstal, Belgium.
[7] Sovirel, Levallois-Perret, France.
[8] Quickfit.

Table II—Cumulative Urinary Excretion of Thiazinamium Cations (I) and Thiazinamium Sulfoxide Cations (II) after Rectal Administration of a 150-mg Dose[a]

Parameter	Patient GL	Patient PH	Patient WM	Patient WB	Patient MF	Patient TJ[b]	Mean ± *SD*[c]
I, % of dose	2.2	1.9	5.3	0.6	2.5	1.4	2.5 ± 1.7
I, % of F_{rel}	35.1	28.7	47.9	96.9	43.4	33.3	55.9 ± 16.5
II, % of dose	2.0	1.8	4.6	1.0	1.2	1.6	2.1 ± 1.5
II, % of F_{rel}	32.1	26.7	42.2	161.5	20.4	38.0	56.6 ± 59.2
I + II, % of dose	4.2	3.7	9.9	1.6	3.7	3.0	4.0 ± 3.1
I + II, % of F_{rel}	67.2	55.4	90.1	258.4	63.8	71.3	106.9 ± 85.6
I to II ratio	1:0.92	1:0.93	1:0.88	1:1.67	1:0.47	1:1.14	1:1.01
Intramuscular I to II ratio[d]	1:0.16	1:0.25	1:0.29	1:0.17[e]	1:0.26	1:0.34	1:0.25

[a] No urinary excretion data are available for Patient HH. [b] Until 390 min after administration. [c] Mean of data of five patients (TJ omitted). [d] For comparison, the ratio between unchanged drug and metabolite in urine as observed after intramuscular injection of a 12.5-mg dose is also given. [e] Until 420 min after injection.

level was found where the plasma concentration remained relatively constant. This finding may indicate that the absorption of the drug continues for an extended period.

From the plasma concentration–time curves during the experiments, a mean relative bioavailability, F_{rel}, of 11.5 ± 6.0 (*SD*) mg of thiazinamium methylsulfate was calculated, which equals 5.8 ± 3.2 (*SD*) % of the dose. In two patients, the curve had already declined to zero at 7 hr after administration; in five patients, extrapolation to zero was possible, which led to an estimated total relative bioavailability, $(F_{rel})_{tot}$, of 6.2 ± 3.4 (*SD*) % of the dose. These data are of the same order of magnitude as those following oral administration (11).

Biotransformation and Urinary Excretion—Earlier investigations (10) showed that only one metabolite, thiazinamium sulfoxide, was formed in humans. Figure 2 represents the cumulative renal excretion of thiazinamium cations and thiazinamium sulfoxide cations in Patient GL. Table II lists the quantities of these compounds excreted during the experiment.

The excretion of thiazinamium cations appeared to be rapid. In general, the patients had already excreted in 7 hr ~90% of the total amount excreted in 24 hr. The amount of unchanged drug excreted over 24 hr varied from 28.7 to 96.9% of the calculated value of the bioavailability.

However, the 96.9% value (Patient WB) was much higher than the values obtained from the other patients, so WB may represent a special case. Without this value, the excretion varied between 28.7 and 47.9% of the calculated bioavailability [mean value of 38.8 ± 8.6 (*SD*) %].

Figure 2 shows that the renal excretion rate of thiazinamium sulfoxide cations was almost identical to that of the unchanged drug. The mean value of the amount of thiazinamium sulfoxide cations found in the urine of Patients GL, PH, WM, WB, and MF accounted for 30.4 ± 9.2 (*SD*) % of the bioavailability.

The mean ratio between the unchanged drug and metabolite (Table II) was 1:1.01. Without the value for Patient WB, a mean ratio of 1:0.78 was found. After an intramuscular injection of a dose of 12.5 mg in the same patients, the mean value for the ratio between the unchanged drug and metabolite was much lower, namely 1:0.25.

The difference between these ratios strongly suggests that a substantial first-pass effect occurs after rectal administration. Comparison with data obtained after oral and intramuscular administrations in another group of patients (10, 19) indicates that the first-pass effect following rectal administration is of the same degree as that after oral administration (ratio 1:0.94).

This finding implies that thiazinamium cations only partially bypass the first liver passage when administered rectally. This conclusion is rather surprising because, although there is no concrete evidence, it is currently accepted (1, 2) that rectally administered drugs enter the systemic circulation largely without initial passage through the liver (provided that the suppository does not reach the higher parts of the rectum).

To explain a first-pass effect after rectal administration of thiazinamium cations, it must be assumed that this drug enters the systemic circulation almost exclusively by way of the smaller rectal vessels, which drain into the portal vein and subsequently the liver, just as in the case of oral administration. As pointed out previously, only the veins of the higher part of the rectum drain directly into the portal veins. Therefore, the drug must have been transported largely by way of the superior rectal veins.

If part of the drug is absorbed in the inferior or middle rectal veins, it probably then reaches the superior rectal veins by way of the numerous connections (anastomoses) between them. Another possibility is that the molten suppository quickly reaches the higher parts of the rectum and that the drug is directly absorbed into the superior rectal veins.

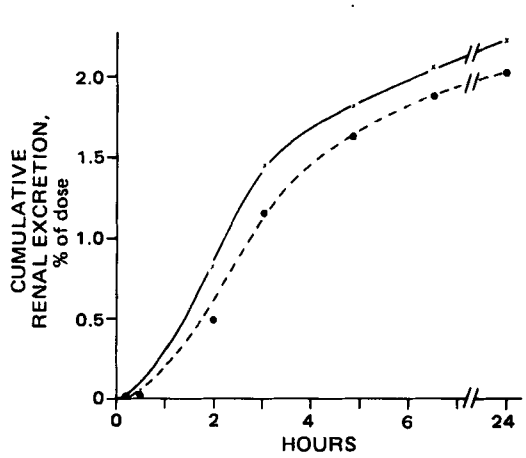

Figure 2—*Typical example of cumulative renal excretion curves of thiazinamium cations* (×) *and thiazinamium sulfoxide cations* (●) *after rectal administration of 150 mg to Patient GL.*

REFERENCES

(1) "The Pharmacological Basis of Therapeutics," L. S. Goodman and A. Gilman, Eds., Macmillan, New York, N.Y., 1975, p. 7.

(2) C. Jacquot, J. Cariou, J. R. Rapin, and Y. Cohen, in "Formulation and Preparation of Dosage Forms," J. Polderman, Ed., Elsevier, Amsterdam, The Netherlands, 1977, p. 153.

(3) H. Booy-Noord, N. G. M. Orie, W. C. Berg, and K. de Vries, *J. Allergy*, **46**, 1 (1970).

(4) H. Booy-Noord, N. G. M. Orie, H. J. Ten Cate, S. Ten Sloots, and D. Bolt, *Int. Arch. Allergy*, **10**, 321 (1957).

(5) L. E. van Bork, J. H. G. Jonkman, R. A. de Zeeuw, N. G. M. Orie, R. Peset, and K. de Vries, *Ned. T. Geneesk.*, **121**, 1196 (1977).

(6) R. Ducrot and P. Decourt, *CR Soc. Biol.*, **144**, 908 (1950).

(7) *Ibid.*, **144**, 911 (1950).

(8) H. J. Sluiter and K. de Vries, *Ned. T. Geneesk.*, **117**, 1084 (1974).

(9) A. Bouhuys and J. Ortega, *Pneumonologie*, **153**, 135 (1976).

(10) J. H. G. Jonkman, Ph.D. thesis, State University of Groningen, The Netherlands, 1977.

(11) J. H. G. Jonkman, L. E. van Bork, J. Wijsbeek, R. A. de Zeeuw, and N. G. M. Orie, *Clin. Pharmacol. Ther.*, **21**, 457 (1977).

(12) K. Neef, J. H. G. Jonkman, and D. K. F. Meijer, *J. Pharm. Sci.*, **67**, 1147 (1978).

(13) "Witepsol® für Suppositorien," Dynamit Nobel A. G., Chemische Werke Witten, Witten, German Federal Republic, 1967.

(14) W. A. Ritschel, "Angewandte Biopharmazie," Wissenschaftliche Verlagsgesellschaft, Stuttgart, German Federal Republic, 1973.

(15) H. L. M. Cox and D. D. Breimer, "Abstracts of the 33th International Congress of Pharmaceutical Sciences," Stockholm, Sweden, 1973.

(16) C. J. de Blaey and J. J. Rutten-Kingma, *Pharm. Acta Helv.*, **52**, 11 (1977).

(17) J. H. G. Jonkman, J. Wijsbeek, S. Hollenbeek Brouwer-de Boer, R. A. de Zeeuw, L. E. van Bork, and N. G. M. Orie, *J. Pharm. Pharmacol.*, 27, 849 (1975).

(18) J. H. G. Jonkman, J. Wijsbeek, J. E. Greving, R. E. M. van Gorp, and R. A. de Zeeuw, *J. Chromatogr.*, 128, 208 (1976).

(19) J. H. G. Jonkman, L. E. van Bork, J. Wijsbeek, R. A. de Zeeuw, and N. G. M. Orie, *Pharm. Weekbl.*, 111, 1209 (1976).

ACKNOWLEDGMENTS

Supported in part by Grant G.O. 741-62 of the Gezondheidsorganisatie T.N.O., The Hague, The Netherlands.

The authors thank Prof. Dr. J. S. Faber for stimulating discussions, Mrs. Ria Hemmer-Kuiper for preparing the manuscript, and Mrs. Grietje Hayer-Herder for the illustrations.

Determination of Submicrogram Quantities of Clonidine in Biological Fluids

L.-C. CHU ˣ, W. F. BAYNE, F. T. TAO, L. G. SCHMITT, and J. E. SHAW

Received January 12, 1978, from the *Alza Corporation, Palo Alto, CA 94304.* Accepted for publication June 15, 1978.

Abstract □ A sensitive and specific GLC method using electron-capture detection was developed for clonidine in plasma and urine. Di-perfluoroacyl derivatives of both clonidine and the 4-methyl analog of clonidine (used as an internal standard) were formed, and an extraction process was developed for the removal of excess derivatization reagent and endogenous biological compounds; the assay permitted quantification of 25 pg of clonidine/ml in a 4-ml plasma sample. The assay was used to elucidate the time course of plasma concentrations in a normotensive subject following oral administration of 50, 100, and 200 μg of clonidine hydrochloride and also to determine unchanged drug excreted in the urine.

Keyphrases □ Clonidine—GLC analysis in plasma and urine □ GLC—analysis, clonidine in plasma and urine □ Antihypertensives—clonidine, GLC analysis in plasma and urine

Clonidine, 2-[(2,6-dichlorophenyl)imino]imidazolidine, is a potent drug used in the treatment of arterial hypertension. The sympatico-inhibitory activity of clonidine is predominantly due to its influence on α-adrenergic receptors in the brain stem (1). The hypotensive effect of clonidine is absent in tetraplegic subjects with transection of the cervical spinal cord above the sympathetic outflow (2). The absence of the hypotensive effect in these subjects indicates that the action of the drug is centrally mediated in humans.

The therapeutic dose of clonidine is a few tenths of a milligram per day. Clonidine is lipophilic in nature with a large volume of distribution (3). Thus, the resulting plasma concentrations following oral administration of therapeutic doses are in the submicrogram range.

BACKGROUND

The metabolism and disposition of clonidine in various animal species were studied (4) using ^{14}C-labeled clonidine. The time course of total radioactivity in the plasma following oral administration of either 390 or 1440 μg of clonidine was determined. The plasma concentrations of unchanged drug were not ascertained, although approximately 45% of the orally administered dose was excreted in the urine as unchanged drug.

The plasma levels, renal excretion, and urinary metabolic pattern were determined (5) in normotensive subjects. Three hours following oral administration of 300 μg of ^{14}C-labeled clonidine, clonidine contributed less than 50% of the total ^{14}C-radioactivity in the plasma.

A recently developed GLC–mass spectrometric method permits the measurement of clonidine in plasma and urine following administration of unlabeled therapeutic doses to humans (6). The method is based on the selective monitoring of mass fragments produced from clonidine and from a deuterated internal standard under electron-impact ionization. The sensitivity of the method and the chromatographic properties of clonidine and the internal standard were improved by formation of their dimethyl derivative through on-column methylation with trimethylanilinium hydroxide (7). The precision of the method at 0.25 ng/ml was ±11% *SD* with 4 ml of plasma. Davies *et al.* (8) used the improved GLC–mass spectral method to study the pharmacokinetics and pharmacodynamics of clonidine following oral and intravenous administration of 300 μg of clonidine hydrochloride[1].

Cho and Curry (9) developed a GLC method using a ^{90}Sr-ionization detector to determine clonidine levels in the blood and tissues of rats administered 500 μg of drug/kg iv. The minimum detectable quantity of clonidine was 2–3 ng. The drug, which was not derivatized, tended to adsorb onto the chromatographic support, especially with the longer columns, thus decreasing the sensitivity of the assay.

A GLC method with electron-capture detection of the pentafluorobenzyl derivative of clonidine was reported (10). This method was used to determine the temporal pattern of plasma concentrations in rats following administration of 500 μg of clonidine hydrochloride/kg, about 100 times the dose received by humans.

This paper reports an electron-capture GLC method for the determination of clonidine in plasma and urine using a di-heptafluorobutyryl derivative of clonidine and an internal standard. The electron-capture-sensitive background is reduced through the use of silica gel columns. This method was used to elucidate the time course of plasma concentrations in a normotensive subject following oral administration of 50, 100, and 200 μg of clonidine hydrochloride.

EXPERIMENTAL

Materials—Methylene chloride, benzene, and hexane, employed in the extraction procedures, were used as obtained[2]. Ethyl acetate[3], purchased in quart bottles and sealed under nitrogen, was used as the solvent for the derivatization of clonidine and the internal standard.

The carbonate buffers, 1 *M* (pH 9.75) and 0.1 *M* (pH 9.2), were made from potassium bicarbonate and adjusted to the appropriate pH with freshly prepared potassium hydroxide solution. Sulfuric acid (0.1 *N*) was diluted from the concentrated acid.

Heptafluorobutyric anhydride[4] was obtained in 1-ml glass ampuls. After the ampul was opened, the contents were stored in a 3-ml minivial for protection from moisture. A new ampul was used daily.

The internal standard, 2-[(2,6-dichloro-4-methylphenyl)imino]imidazolidine, was used as received[5].

Dimethyldichlorosilane, 5% in toluene, was used to silanize all glassware for at least 2 hr; the glassware was then rinsed with toluene, methanol,

[1] Catapres, Boehringer Ingelheim.
[2] Nanograde solvents, Mallinckrodt, St. Louis, Mo.
[3] Burdick & Jackson Laboratories, Muskegon, Mich.
[4] Pierce Chemical Co., Rockford, Ill.
[5] C. H. Boehringer Sohn, Ingelheim, Germany.

0022-3549/79/0100-0072$01.00/0
© 1979, American Pharmaceutical Association

(17) J. H. G. Jonkman, J. Wijsbeek, S. Hollenbeek Brouwer-de Boer, R. A. de Zeeuw, L. E. van Bork, and N. G. M. Orie, *J. Pharm. Pharmacol.*, 27, 849 (1975).

(18) J. H. G. Jonkman, J. Wijsbeek, J. E. Greving, R. E. M. van Gorp, and R. A. de Zeeuw, *J. Chromatogr.*, 128, 208 (1976).

(19) J. H. G. Jonkman, L. E. van Bork, J. Wijsbeek, R. A. de Zeeuw, and N. G. M. Orie, *Pharm. Weekbl.*, 111, 1209 (1976).

ACKNOWLEDGMENTS

Supported in part by Grant G.O. 741-62 of the Gezondheidsorganisatie T.N.O., The Hague, The Netherlands.

The authors thank Prof. Dr. J. S. Faber for stimulating discussions, Mrs. Ria Hemmer-Kuiper for preparing the manuscript, and Mrs. Grietje Hayer-Herder for the illustrations.

Determination of Submicrogram Quantities of Clonidine in Biological Fluids

L.-C. CHU ˣ, W. F. BAYNE, F. T. TAO, L. G. SCHMITT, and J. E. SHAW

Received January 12, 1978, from the *Alza Corporation, Palo Alto, CA 94304.* Accepted for publication June 15, 1978.

Abstract □ A sensitive and specific GLC method using electron-capture detection was developed for clonidine in plasma and urine. Di-perfluoroacyl derivatives of both clonidine and the 4-methyl analog of clonidine (used as an internal standard) were formed, and an extraction process was developed for the removal of excess derivatization reagent and endogenous biological compounds; the assay permitted quantification of 25 pg of clonidine/ml in a 4-ml plasma sample. The assay was used to elucidate the time course of plasma concentrations in a normotensive subject following oral administration of 50, 100, and 200 μg of clonidine hydrochloride and also to determine unchanged drug excreted in the urine.

Keyphrases □ Clonidine—GLC analysis in plasma and urine □ GLC—analysis, clonidine in plasma and urine □ Antihypertensives—clonidine, GLC analysis in plasma and urine

Clonidine, 2-[(2,6-dichlorophenyl)imino]imidazolidine, is a potent drug used in the treatment of arterial hypertension. The sympatico-inhibitory activity of clonidine is predominantly due to its influence on α-adrenergic receptors in the brain stem (1). The hypotensive effect of clonidine is absent in tetraplegic subjects with transection of the cervical spinal cord above the sympathetic outflow (2). The absence of the hypotensive effect in these subjects indicates that the action of the drug is centrally mediated in humans.

The therapeutic dose of clonidine is a few tenths of a milligram per day. Clonidine is lipophilic in nature with a large volume of distribution (3). Thus, the resulting plasma concentrations following oral administration of therapeutic doses are in the submicrogram range.

BACKGROUND

The metabolism and disposition of clonidine in various animal species were studied (4) using ^{14}C-labeled clonidine. The time course of total radioactivity in the plasma following oral administration of either 390 or 1440 μg of clonidine was determined. The plasma concentrations of unchanged drug were not ascertained, although approximately 45% of the orally administered dose was excreted in the urine as unchanged drug.

The plasma levels, renal excretion, and urinary metabolic pattern were determined (5) in normotensive subjects. Three hours following oral administration of 300 μg of ^{14}C-labeled clonidine, clonidine contributed less than 50% of the total ^{14}C-radioactivity in the plasma.

A recently developed GLC–mass spectrometric method permits the measurement of clonidine in plasma and urine following administration of unlabeled therapeutic doses to humans (6). The method is based on the selective monitoring of mass fragments produced from clonidine and from a deuterated internal standard under electron-impact ionization. The sensitivity of the method and the chromatographic properties of clonidine and the internal standard were improved by formation of their dimethyl derivative through on-column methylation with trimethylanilinium hydroxide (7). The precision of the method at 0.25 ng/ml was ±11% *SD* with 4 ml of plasma. Davies *et al.* (8) used the improved GLC–mass spectral method to study the pharmacokinetics and pharmacodynamics of clonidine following oral and intravenous administration of 300 μg of clonidine hydrochloride[1].

Cho and Curry (9) developed a GLC method using a ^{90}Sr-ionization detector to determine clonidine levels in the blood and tissues of rats administered 500 μg of drug/kg iv. The minimum detectable quantity of clonidine was 2–3 ng. The drug, which was not derivatized, tended to adsorb onto the chromatographic support, especially with the longer columns, thus decreasing the sensitivity of the assay.

A GLC method with electron-capture detection of the pentafluorobenzyl derivative of clonidine was reported (10). This method was used to determine the temporal pattern of plasma concentrations in rats following administration of 500 μg of clonidine hydrochloride/kg, about 100 times the dose received by humans.

This paper reports an electron-capture GLC method for the determination of clonidine in plasma and urine using a di-heptafluorobutyryl derivative of clonidine and an internal standard. The electron-capture-sensitive background is reduced through the use of silica gel columns. This method was used to elucidate the time course of plasma concentrations in a normotensive subject following oral administration of 50, 100, and 200 μg of clonidine hydrochloride.

EXPERIMENTAL

Materials—Methylene chloride, benzene, and hexane, employed in the extraction procedures, were used as obtained[2]. Ethyl acetate[3], purchased in quart bottles and sealed under nitrogen, was used as the solvent for the derivatization of clonidine and the internal standard.

The carbonate buffers, 1 *M* (pH 9.75) and 0.1 *M* (pH 9.2), were made from potassium bicarbonate and adjusted to the appropriate pH with freshly prepared potassium hydroxide solution. Sulfuric acid (0.1 *N*) was diluted from the concentrated acid.

Heptafluorobutyric anhydride[4] was obtained in 1-ml glass ampuls. After the ampul was opened, the contents were stored in a 3-ml minivial for protection from moisture. A new ampul was used daily.

The internal standard, 2-[(2,6-dichloro-4-methylphenyl)imino]imidazolidine, was used as received[5].

Dimethyldichlorosilane, 5% in toluene, was used to silanize all glassware for at least 2 hr; the glassware was then rinsed with toluene, methanol,

[1] Catapres, Boehringer Ingelheim.
[2] Nanograde solvents, Mallinckrodt, St. Louis, Mo.
[3] Burdick & Jackson Laboratories, Muskegon, Mich.
[4] Pierce Chemical Co., Rockford, Ill.
[5] C. H. Boehringer Sohn, Ingelheim, Germany.

0022-3549/79/0100-0072$01.00/0
© 1979, American Pharmaceutical Association

and methylene chloride. Microcolumns were used to reduce chromatographic interferences. Each short silanized Pasteur pipet was packed with a plug of silanized glass wool and 0.5 cm of silica gel adsorbent[6].

Apparatus—The derivatives of clonidine and the internal standard were chromatographed on a gas chromatograph[7] equipped with a scandium tritide detector. A 2-mm i.d. × 1.8-m silanized glass column packed with 3% OV-17 on 100–120-mesh Chromosorb W, AW, DMCS[8], was used. The support was inactivated and coated with the liquid phase according to a method described previously (11). Nitrogen was used as the carrier gas.

The retention times for the derivatives of clonidine and the internal standard were 5 and 6.5 min, respectively, at a column temperature of 175° and a gas flow of 25 ml/min. The injector temperature was 220°, and the detector temperature was 250°.

A quadrupole mass spectrometer[9], interfaced with a gas chromatograph[10], was used to establish the structure of the derivatives. The electron energy of the ionization source was 70 ev. A GLC column similar to that already described was employed.

Derivatization of Microgram Quantities of Clonidine—Clonidine base (9.85 mg) was dissolved in 10 ml of ethyl acetate and stored at 0°. A 30-μl aliquot of this solution was placed in a 12-ml conical centrifuge tube with a polytef stopper and taken to dryness with a nitrogen stream. The dried clonidine base was reconstituted in 100 μl of dry ethyl acetate (water content of 50 ppm), followed by the addition of 4 μl of heptafluorobutyric anhydride.

After vortexing, the centrifuge tube was immersed in a water bath at 45° for 15 min. The contents were then taken to dryness under a nitrogen stream. Hexane (400 μl) was added to the dried residue, followed by 1 ml of 0.1 *M* potassium carbonate buffer (pH 9.2). The contents were then vortexed and centrifuged.

The organic layer was transferred to another 12-ml conical centrifuge tube and taken to dryness with a nitrogen stream. The residue was dissolved in 50 μl of methylene chloride, and a flame-ionization detector was employed to check the completeness of derivatization.

Derivatization of Submicrogram Quantities of Clonidine—The working standard of clonidine in ethyl acetate (described in the previous section) was diluted to contain 50–1000 pg/μl, depending on the quantity of clonidine to be derivatized. Aliquots of the diluted solutions were added to 12-ml centrifuge tubes, and the ethyl acetate was removed with a nitrogen stream. Derivatization was conducted as already described; however, the hexane phase following the carbonate wash was not evaporated to dryness.

Reduction of Electron-Capture-Sensitive Background—Microcolumns, prepared as already described and washed with two column heights of benzene followed by two column heights of hexane, were used to reduce the electron-capture-sensitive background. The hexane phase, obtained in the previous procedure, was loaded on a microcolumn. An additional 400 μl of hexane was used to wash the aqueous carbonate phase and also was added to the microcolumn. The microcolumn was then washed with 1.2 ml of hexane.

Elution of the clonidine derivative was effected by washing the microcolumns with 2 ml of 25% (v/v) benzene in hexane. The eluate was taken to dryness with nitrogen at 40°, and the residue was dissolved in 25–50 μl of 20% ethyl acetate in hexane. Aliquots ranging from 2 to 5 μl were injected into the gas chromatograph, and the derivative was detected with the electron-capture detector. The microcolumns could be reused on the same day by washing with two column heights of benzene followed by two column heights of hexane.

Extraction of Clonidine and Internal Standard from Plasma—Extractions of 4-ml plasma samples containing clonidine and the internal standard were performed in 30-ml silanized, separatory centrifuge funnels[11]. A 2-ml aliquot of 1 *M* carbonate buffer (pH 9.75) was added to the plasma. The buffered plasma sample was extracted with 12 ml of 10% ethyl acetate in methylene chloride. The contents were shaken horizontally in a modified shaker[12] for 10 min and centrifuged at 1200 rpm.

The organic layer was then removed through the polytef valve in the bottom of the separator into a second separator. The organic extract was back-extracted with 3 ml of 0.1 *N* H_2SO_4, and the organic phase was discarded. The retained aqueous phase was adjusted to pH 10 with a saturated aqueous solution of sodium carbonate (approximately 5 drops required) and extracted with 3 ml of benzene. The benzene extract was transferred to a 12-ml conical centrifuge tube and taken to dryness at 40° with a nitrogen stream.

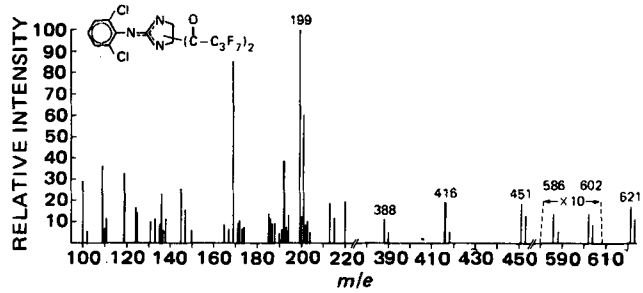

Figure 1—*Mass spectrum of di-heptafluorobutyryl derivative of clonidine obtained with an electron energy of 70 ev and an emission current of 1 mamp.*

Standard Curve for Clonidine in Plasma—Aliquots of human plasma (4 ml) were spiked with varying amounts of clonidine (100 pg–5 ng) and a constant amount of the internal standard (4 ng). A blank plasma sample, containing no clonidine or internal standard, also was carried through the assay. The plasma samples were extracted, derivatized, and chromatographed on the microcolumns as described.

The samples were then injected into the gas chromatograph, and the responses of the derivatives of clonidine and the internal standard were recorded. The areas of the chromatographic peaks were approximated by the product of the height and width at half-height. The standard curve was generated using a linear least-squares analysis of the ratio of the peak areas for the derivatives (clonidine to the internal standard) *versus* the amount of clonidine (slope of 0.392 and correlation coefficient of 0.997).

Assay in Urine—The assay of urine samples was the same as that described for plasma samples, except that 1-ml aliquots of urine and 24 ng of the internal standard were used.

***In Vivo* Studies**—One normotensive subject received 50, 100, and 200 μg of clonidine hydrochloride. Following each dose, 10-ml blood samples were withdrawn into heparin-containing evacuated glass tubes at predetermined times. The blood was centrifuged, and the plasma was separated and frozen until analyzed. Urine was collected over 12-hr intervals for 48 hr.

RESULTS AND DISCUSSION

Ethyl acetate was the solvent of choice for the derivatization of clonidine and the internal standard with heptafluorobutyric anhydride. Complete conversion to a single derivative was achieved with microgram quantities of clonidine, as indicated by the presence of a single peak in the chromatogram obtained with a flame-ionization detector. When acetonitrile was used as a solvent for the derivatization, three peaks were

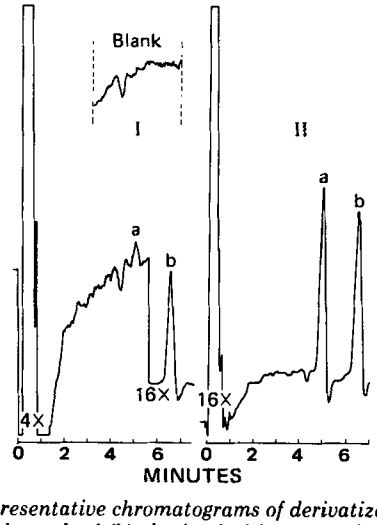

Figure 2—*Representative chromatograms of derivatized clonidine (a) and the internal standard (b) obtained with 100 pg of clonidine (I) and 2.5 ng of clonidine added to 4 ml plasma (II).*

[6] Separations Group, Hesperia, Calif.
[7] Model 2100, Varian, Walnut Creek, Calif.
[8] Johns-Manville, Denver, Colo.
[9] Model 1015 SL, Finnigan, Sunnyvale, Calif.
[10] Model 1700, Varian, Palo Alto, Calif.
[11] Labcrest, Warminster, Pa.
[12] Model 6000, Eberbach, Ann Arbor, Mich.

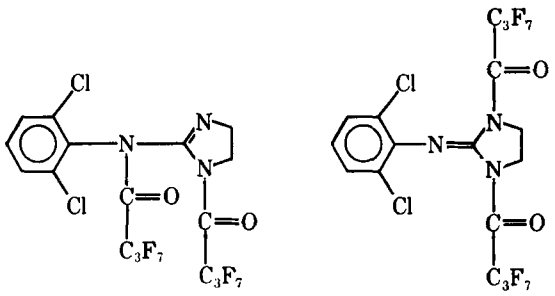

Ia

Ib

present in the chromatogram obtained with the flame-ionization detector. The major peak corresponded to that obtained with ethyl acetate as the solvent, and none of the chromatographic peaks had a retention time corresponding to that of underivatized clonidine. With GLC–mass spectrometry, the two other peaks present in the chromatogram subsequently were identified as mono-heptafluorobutyryl derivatives of clonidine.

The mass spectrum of the compound that gave the single chromatographic peak, obtained with ethyl acetate as the solvent for derivatization, is shown in Fig. 1. The spectrum exhibited a molecular ion at *m/e* 621, consistent with the incorporation of two heptafluorobutyryl groups into the clonidine molecule. The loss of one fluorine atom and the loss of one chlorine atom from the molecular ion produced the *m/e* 602 and 586 fragments, respectively. The ion at *m/e* 451 was due to the loss of the C_3F_7 group and a hydrogen atom, and this ion decomposed with expulsion of a chlorine atom to give the *m/e* 416 ion. This ion further fragmented with the loss of carbon monoxide to give *m/e* 388. The base peak for the di-heptafluorobutyryl derivative was observed at *m/e* 199 and can be formulated as arising from the loss of the two acyl groups plus the two methylene groups from the imidazole ring.

There were no prominent ions in the mass spectrum of the di-heptafluorobutyryl derivative to establish unequivocably the exact position of the acyl incorporation. Two possible structural isomers (I*a* and I*b*) can result from the incorporation of two acyl groups into the clonidine molecule.

To establish the structure of the diacyl derivative, macroquantities of the derivative could be made and analyzed using either ^1H- or ^{13}C-NMR spectroscopy. Since one isomer possesses a C_2 symmetry element lacking in the other, the proton pattern resulting from the hyperfine interaction of the methylene protons or the ^{13}C-resonances of the methylene carbons would be expected to differ in the two isomers.

The precision of the assay at 60 pg of clonidine/ml in 4 ml of plasma was ±8% *SD*. The recovery of clonidine carried through the entire procedure was 60% relative to an external standard, which was prepared by diluting microgram quantities of derivatized clonidine.

Chromatograms from spiked plasma samples are shown in Fig. 2. The blank plasma sample indicated the absence of interferences. The small positive response in the chromatogram for the 4-ml plasma sample with a clonidine concentration of 25 pg/ml represents approximately 5–6 pg of the clonidine derivative.

To achieve the levels of detection obtained with the method, it was necessary to inactivate the support material in the GLC column. Otherwise, loss in sensitivity resulted due to adsorption of the derivatives on the support. Sufficient inactivation was achieved with the vapor phase silanization technique (11). Furthermore, it was necessary to remove the electron-capture-sensitive background with the microcolumns, following derivatization, to achieve the desired sensitivity. The microcolumns probably removed endogenous biological interferences.

In the electron-capture GLC method developed by Edlund and Paalzow (10), the minimum detectable quantity of the derivative was 3.3 pg. The precision of this method at 0.2 ng in plasma (volume presumably 500 μl) was less than ±20% *SD*. The dose per unit body weight administered to the rats was greater than 100 times that administered to humans for therapeutic benefit, and the volume of the rat plasma sample assayed was generally one-tenth to one-twentieth the volume of the human plasma samples used in this newly developed method. Both factors tend to minimize interference of the chromatographic peaks of interest by endogenous biological materials.

The major known metabolite of clonidine, the *p*-hydroxy analog, was

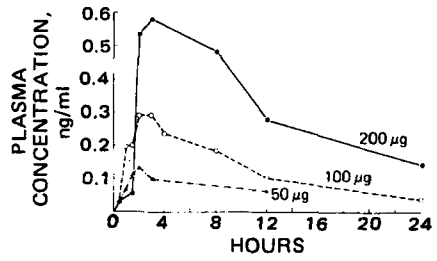

Figure 3—*Plasma concentration–time curves of subject administered three oral doses of clonidine hydrochloride.*

neither extracted nor derivatized under the assay conditions. Chloroform extracts of urine from subjects given ^{14}C-labeled clonidine were shown by TLC to contain only clonidine (5). Metabolites, including the *p*-hydroxy analog, that were more polar than clonidine were extracted with butanol. Chromatograms of patients receiving clonidine therapy and diuretics (either chlorthalidone or hydrochlorothiazide) exhibited no interfering peaks. The peak shapes, in particular peak width, were the same in these chromatograms as those obtained from samples prepared by spiking plasma with clonidine. Moreover, endogenous compounds, at least from individuals not receiving clonidine, did not interfere with the clonidine peaks (insert in Fig. 2). Therefore, except for the remote possibility that a diuretic or one of its metabolites is carried through the assay and has the same chromatographic characteristics as the clonidine derivative, the assay is specific.

The temporal patterns of plasma concentration in the normotensive subject administered 50, 100, and 200 μg po of clonidine hydrochloride are shown in Fig. 3. The maximum plasma concentrations and the times at which they occurred were 133 (2 hr), 292 (3 hr), and 582 (3 hr) pg/ml, respectively. The peak plasma concentrations were in the ratio 1:2.2:4.4 while the corresponding doses were in the ratio 1:2:4. Since an apparent proportionality existed between peak plasma concentration and dose, the subject apparently behaved as a linear system over the dosing range.

The analysis of unchanged drug excreted in the urine presented no problems since the urinary concentrations were generally two orders of magnitude larger than those in the plasma. Interferences by endogenous compounds were absent. The urinary recoveries were in the range of previously reported values (4, 7, 8).

REFERENCES

(1) P. A. Van Zwieten, "Progress in Pharmacology," vol. 1, no. 1, Gustav Fischer Verlag, Stuttgart, West Germany, 1975.

(2) J. L. Reid, L. M. H. Wing, C. J. Mathias, H. L. Frankel, and E. Neill, *Clin. Pharmacol. Ther.*, **21**, 375 (1977).

(3) C. T. Dollery, D. S. Davies, G. H. Draffan, H. J. Dargie, C. R. Dean, J. L. Reid, R. A. Clare, and S. Murray, *ibid.*, **19**, 11 (1976).

(4) D. Rehbinder, in "Modern Aspects in the Treatment of Arterial Hypertension," A. Zanchetti and M. Enrico, Eds., Boehringer Ingelheim, Florence, Italy, 1974, p. 3.

(5) S. Darda, in "Recent Advances in Hypertension," vol. 2, P. Milliez and M. Safar, Eds., International Symposium on Hypertension, Monaco, 1975, p. 375.

(6) G. H. Draffan, R. A. Clare, S. Murray, G. D. Bellward, D. S. Davies, and C. T. Dollery, "Proceedings of the Third International Symposium on Mass Spectrometry in Biochemistry and Medicine," Sardinia, Italy, June 1975.

(7) G. H. Draffan, G. D. Bellward, R. A. Clare, H. J. Dargie, C. T. Dollery, S. Murray, J. L. Reid, L. Wing, and D. S. Davies, "Proceedings of the Second International Conference on Stable Isotopes," Oak Brook, Ill., Oct. 1975, p. 149.

(8) D. S. Davies, L. M. H. Wing, J. L. Reid, E. Neill, P. Tippett, and C. T. Dollery, *Clin. Pharmacol. Ther.*, **21**, 593 (1977).

(9) A. K. Cho and S. H. Curry, *Biochem. Pharmacol.*, **18**, 511 (1969).

(10) P. O. Edlund and L. K. Paalzow, *Acta Pharmacol. Toxicol.*, **40**, 145 (1977).

(11) R. J. Leibrand and L. L. Dunham, *Res. Dev.*, **Sept. 1973**, 32.

Metabolism and Measurement of Chloroprocaine, an Ester-Type Local Anesthetic

JAMES E. O'BRIEN *x, VICKI ABBEY *, ORVILLE HINSVARK *, JAMES PEREL ‡, and MIECZYSLAW FINSTER ‡

Received March 6, 1978, from the **Analytical Chemistry Department, Pharmaceutical Division, Pennwalt Corporation, Rochester, NY 14623,* and the ‡*Departments of Pharmacology and Anesthesiology, College of Physicians and Surgeons, Columbia University, New York, NY 10032.* Accepted for publication June 5, 1978.

Abstract □ Blood levels of intact chloroprocaine were determined using a GLC procedure capable of detecting as little as 10 ng of chloroprocaine/ml of blood. It was necessary to deactivate plasma cholinesterases in collected samples by adding echothiophate iodide to blood sampling tubes. An extraction procedure, followed by a TLC separation and spectrodensitometric assay, was developed for measurement of the metabolite 2-chloro-4-aminobenzoic acid in plasma and urine. With these procedures, data were obtained showing that chloroprocaine is hydrolyzed rapidly by plasma cholinesterases. No unchanged drug could be detected in any blood samples obtained from volunteers who received chloroprocaine by intravenous infusion or from obstetric patients who had epidural anesthesia during labor and delivery. Blood levels of 2-chloro-4-aminobenzoic acid rose promptly with the administration of chloroprocaine and declined rapidly after drug administration. Most of the metabolite was recovered in urine.

Keyphrases □ Chloroprocaine—GLC analysis in plasma and urine, metabolism and elimination in humans □ GLC—analysis, chloroprocaine in plasma and urine □ Metabolism—chloroprocaine in humans □ Elimination—chloroprocaine in humans □ Anesthetics, local—chloroprocaine, GLC analysis in plasma and urine, metabolism and elimination in humans

Structurally, the local anesthetics commonly used to relieve pain during surgical and obstetrical procedures are of two main types: amides and esters. The amide-type agents tend to be longer acting, because they are more stable toward hydrolysis and are not rapidly metabolized. As a consequence, when administered repeatedly to obstetric patients during labor, these agents may accumulate in high or even toxic concentrations in the maternal and fetal blood. Neonatal depression, fetal bradycardia, methemoglobinemia, and even fetal deaths have been attributed to the toxicity of these drugs (1–4). In contrast, chloroprocaine[1] (I), an ester-type local anesthetic, is hydrolyzed rapidly by the maternal and fetal plasma pseudocholinesterase into two relatively nontoxic metabolites, 2-chloro-4-aminobenzoic acid (II) and 2-diethylaminoethanol[2] (III) (Scheme I) (6, 7).

The objective of this study was to ascertain whether the apparent low toxicity (8) of I can be attributed to its rapid metabolism resulting in low levels of intact drug in the maternal and/or fetal blood. Therefore, it was necessary to develop sensitive and selective procedures capable of measuring the intact agent and a metabolite, II, in biological fluids. The approach described involves: (*a*) collection of blood samples over echothiophate, which completely inhibits plasma cholinesterase activity; (*b*) separation of the plasma fraction to facilitate handling and shipping of the samples; (*c*) extraction of either I or II into an organic solvent; and (*d*) measurement of the drug or metabolite by GLC or by the emitted fluorescence of a treated TLC plate.

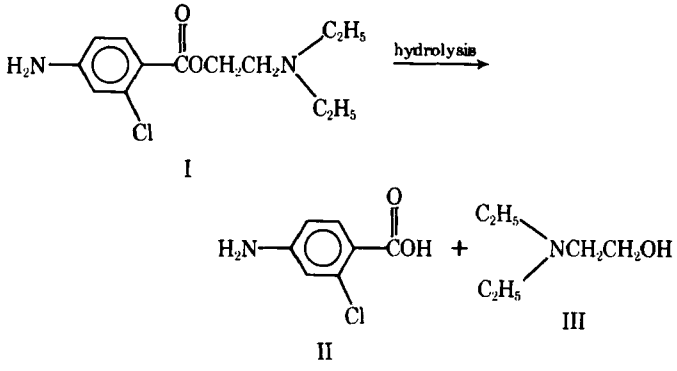

Scheme I

EXPERIMENTAL

GLC Determination of Chloroprocaine (I)—The following modified procedure of Somogyi (9) was employed to precipitate protein. A 5-ml aliquot of 1.8% (w/v) $Ba(OH)_2 \cdot 8H_2O$ was added to 2 ml of plasma in a 50-ml centrifuge tube, and the mixture was shaken for 45 sec. This time was long enough to ensure good contact and complete protein precipitation, yet short enough to minimize losses due to alkaline hydrolysis[3]. A 5-ml aliquot of 2% (w/v) $ZnSO_4 \cdot 7H_2O$ was added to the sample. Compound I dissolved in this neutral solution was stable throughout the remainder of the procedure.

The precipitated protein was separated from the liquid by centrifugation, and the supernate was decanted into a 50-ml graduated tube. The precipitate was washed twice, by repeating the above procedure, using 2 ml of 1.8% $Ba(OH)_2$ and 2 ml of 2% $ZnSO_4$. These washes were added to the initial liquor, the combined volume was read, and the entire sample was transferred to a 30-ml separator. The pH was adjusted to 8.5 with 2% (w/v) sodium bicarbonate.

The aqueous phase then was extracted with methylene chloride[4] three times; 5 ml was used for the initial two extracts, and 2 ml was used for the final one. The extracts were placed into a 15-ml centrifuge tube, and the combined volume was recorded. At this time, the internal standard [100 μl of 0.001% (w/v) procaine in methylene chloride] was added to the extract. To act as a scavenger and to minimize drug losses that may occur by adsorption on glass surfaces, 1 ml of 0.02% (w/v) triethanolamine in methylene chloride was then added.

The methylene chloride was removed under a gentle stream of nitrogen at 50°. The walls of the tube were washed down with 2 ml of methylene chloride, and again the solvent was removed. The residue was reconstituted with 100 μl of methylene chloride, and a 5-μl sample was injected into a biomedical gas chromatograph[5]. The instrument, operated isothermally at 220°, was equipped with a flame-ionization detector and a 1.2-m long × 3-mm i.d. glass column packed with 10% SE-30 on 80–100-mesh Chromosorb W. The injection port temperature was 230°, and the detector temperature was 270°. The flow rates were 40 ml/min at 40

[1] Nesacaine, Pennwalt Corp., Rochester, N.Y.

[2] A recently published paper by Raj *et al.* (5) described a spectrophotometric approach to measuring I levels directly in plasma. Efforts to duplicate the procedure were not successful, primarily because of sample opacity and/or component interference.

[3] The ester linkage of I is susceptible to hydrolysis, either through base catalysis or by plasma cholinesterases. For that reason, the contact time at the elevated pH must be minimized and the enzymic hydrolysis must be inhibited completely to obtain reliable data.

[4] Pesticide grade, Fisher Scientific.

[5] Hewlett-Packard model 7610 A.

0022-3549/79/0100-0075$01.00/0
© 1979, American Pharmaceutical Association

Table I—Recovery of Chloroprocaine Added to Whole Blood

I Added, ng/ml of blood	Amount Recovered, ng/ml	Percent Recovery
100	97	97
100	100	100
250	252	101
250	234	94
625	628	100
625	656	105
1250	1242	99
1250	1311	105
2500	2524	101
2500	2483	99
Mean		100
SD		3

psig for the carrier gas (helium), 35 ml/min for hydrogen, and 300 ml/min for air.

A typical chromatogram is shown in Fig. 1. Under these conditions, the practical lower limit of detection for I was ≃ 10 ng/ml of plasma.

Quantitative TLC Estimation of 2-Chloro-4-aminobenzoic Acid (II)—A volume of fluid (for samples taken during anesthetic procedures, usually 5 ml of plasma or 2 ml of urine) containing a minimum of 50 ng of II was made acidic (pH 1–3) by addition of 1 ml of a saturated ammonium chloride solution and a few drops of concentrated hydrochloric acid. The metabolite was extracted into an equivalent volume of ethyl acetate as the mixture was agitated on a rotary mixer[6] for 10 min.

The two phases were separated by centrifugation and spotted on a F-254 silica gel (0.25 mm thickness) TLC plate[7]. The individual components were separated by acetic acid–methanol–chloroform (2:18:80 v/v). A pilot run may be required so that the volume spotted and/or the concentration of the ethyl acetate solution can be adjusted to obtain a spot containing 50–200 ng of II, the linear range of response by the spectrodensitometer[8].

The plate was developed to within 2 cm of the top and dried. It was then exposed to acetic acid vapors and sprayed with 0.01% fluorescamine[9]. The amount of fluorescence developed at the incident wavelength of 370 nm was quantitated with the spectrodensitometer. The intensity of the emitted green fluorescence (wavelength around 450 nm) approximated a linear relationship with concentration over a range of 50–200 ng/spot.

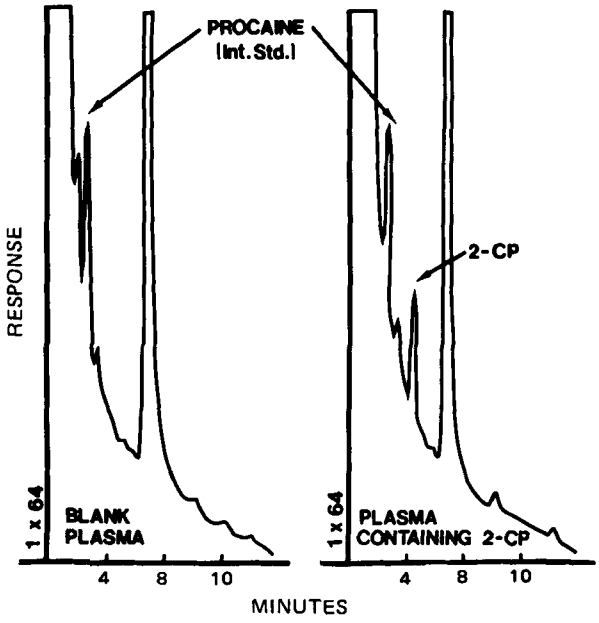

Figure 1—*Typical chromatograms of extracts of human plasma (2-CP = chloroprocaine).*

[6] Lab Quake, Labindustries, Berkeley, Calif.
[7] E. Merck, Brinkmann Instruments, Westbury, N.Y.
[8] Model SC3000, Schoeffel Instruments, Westwood, N.J.
[9] Fluram, Roche Diagnostics, Nutley, N.J.

Table II—Recovery of 2-Chloro-4-aminobenzoic Acid Added to Plasma or Urine

Plasma		Urine	
Added, μg/ml	Percent Recovery	Added, μg/ml	Percent Recovery
5.0	112	100.4	94
5.0	102	100.4	95
5.0	106	100.4	94
10.1	97	100.4	90
10.1	97	376.4	88
10.1	98	376.4	91
		376.4	91
		376.4	92
Mean	102		92
SD	6		2

Most of II is excreted in the urine as conjugates, which were hydrolyzed by treating with an equivalent volume of 1 *N* NaOH at 100° for 20 hr. If acid hydrolysis is employed in lieu of the base treatment, decarboxylation, resulting in the formation of 2-chloroaniline, will occur.

***In Vitro* Estimation of Hydrolysis Rate**—Protein precipitation was initially used to diminish the background interference caused by substances endogenous to plasma; subsequently, it was employed to terminate enzymatic hydrolysis in preparation for the acquisition of kinetic data.

Blood samples from obstetrical patients and cord blood from their newborns, as well as blood from healthy volunteers, were collected in heparinized blood sampling tubes[10].

While the sample was agitated on a vortex mixer, a known amount of I was added rapidly as an aqueous solution (20 μl of approximately 250 ng of I/μl of water) to 2 ml of blood or plasma at 23°. At a preselected time, the enzymatic hydrolysis was terminated by protein precipitation and the residual II was extracted and determined as described. Since the reaction is very rapid, it was necessary for the analyst to act expeditiously. Pilot measurements indicated that a half-life of 10–30 sec can be expected for the intact drug in normal plasma. With this criterion, sampling times of 2, 10, 20, and 60 sec were adequate.

***In Vivo* Studies**—*Sampling Procedures*—It would not have been practical to terminate enzymatic action *via* protein precipitation while blood was being drawn from patients or volunteers. Therefore, a program was initiated to investigate cholinesterase inhibitors. Echothiophate iodide rapidly and completely inhibited the cholinesterase activity of blood, and it was used to modify sample tubes according to the following procedure.

Commercially available, heparinized, 10-ml blood sampling tubes[10] were modified by the addition of 50 mg of echothiophate iodide[11] (aqueous solution, 100 μl of 0.5 g/ml) to each tube. The tubes were then stoppered, and a vacuum of 200 torr was reestablished. To preserve the integrity of the inhibitor, the tubes were refrigerated until used.

Intravenous Infusion Studies—Seven healthy volunteers, four males and three nonpregnant females, each received 250 mg of I (2% concentration) by constant rate intravenous infusion. These seven volunteers were divided into two groups. The first group of three received the infusion over 60 min. Since no side effects were observed, the infusion rate was then increased to 250 mg/30 min for the second group of four.

A total of 12 blood samples per individual was drawn into the modified tubes from the antecubital vein in the contralateral arm at preselected times during the infusion and up to 30 min after it was terminated. Urine samples were collected 60 and 90 min after the beginning of infusion, and their volumes were measured and recorded. Plasma fractions were separated promptly by centrifugation and frozen along with the urine samples until analyzed. Attempts to measure I were made on all samples. Determination of II levels were made only in the second group of four volunteers.

Obstetric Epidural Anesthesia—One patient in labor received continuous epidural anesthesia over 3 hr preceding delivery. Anesthesia was induced and maintained with 2% I, for a total dose of 740 mg. Maternal venous blood samples were drawn into echothiophate-containing tubes at 10, 20, 30, and 60 min after the induction of anesthesia. Another maternal sample was obtained at delivery, along with fetal samples from the umbilical artery and vein. These samples were analyzed for I only.

Two other patients receiving continuous epidural anesthesia during labor were studied. At birth, maternal venous, umbilical venous, and umbilical arterial samples were collected for determination of I and II.

[10] Vacutainer, Becton-Dickinson, Rutherford, N.J.
[11] Ayerst Laboratories, New York, N.Y.

Table III—Half-Life (Seconds) of Chloroprocaine in Maternal and Umbilical Cord Blood

Subject	Maternal	Umbilical Cord
1	13	23
2	15	38
3	19	37
4	21	45
5	22	58
6	27	47
7	29	50
Mean	21[a]	43[a]

[a] Paired t test; $p < 0.001$.

Table IV—Half-Life (Seconds) of Chloroprocaine in Samples of Whole Blood Obtained from Male and Female Controls

	Males	Females
	14	24
	22	27
	25	31
	22	21
	20	22
		26
Mean	21[a]	25[a]
SD	4	4

[a] Pooled t test; $0.10 < p < 0.20$.

RESULTS AND DISCUSSION

GLC Determination of I—The feasibility of using GLC techniques was demonstrated for the determination of I in biological fluids. An initial protein precipitation was required to reduce background interference from endogenous plasma constituents. While Table I provides data showing recovery of a known addition of I (100–2500 ng/ml) from fresh prepoisoned human blood, a practical detection limit of 10 ng/ml could be attained[12].

Quantitative TLC Estimation of II—In all of the subjects studied, I was hydrolyzed so rapidly that the intact drug could not be detected. Therefore, the drug disposition was followed indirectly by determining levels of one of its primary metabolites, II, by the previously described extraction and quantitative TLC procedure.

To evaluate the method, known amounts of II were added to blood and urine samples. According to the described procedures, these samples were acidified and extracted with ethyl acetate and then the metabolite content of the extract was determined by the quantitative TLC procedure. The data in Table II show good agreement between the amounts added and those recovered. The practical detectable limit was about 50 ng of II/spot.

While the procedure is applicable to whole blood measurement, it is more convenient to use the plasma fraction. Therefore, the possibility of preferential distribution between the erythrocyte fraction and plasma must be considered. A known amount of II was added to each of four whole blood samples, which were then incubated at 37° for 1 hr. The plasma from two of the samples was then separated. The II content of these fractions was compared to that in the remaining two whole blood samples, and no significant differences in concentration could be observed. Because of the relative ease of handling, plasma samples were used for subsequent measurements.

***In Vitro* Estimation of Hydrolysis Rate**—To gain insight into the detoxification mechanisms of I, its hydrolysis rates were determined in maternal and fetal plasma samples (Table III), as well as in samples obtained from healthy male and nonpregnant female volunteers (Table IV). These determinations were performed at room temperature (23°). The rates of *in vivo* metabolism at 37° should be faster.

Since the cholinesterase activity of the neonate's plasma appears to be related to that of the mother, and since the sampling of the male and female population was independent, the statistical comparison of maternal and cord plasma was made by a paired t test while the comparison between male and female plasma was made according to a pooled t test. The observed mean plasma half-life of I was shorter in males than in females; however, this difference was not significant. In contrast, the hydrolysis of I was much faster in maternal than in fetal plasma; the differences of observed mean values of approximately 21 and 43 sec, respectively, were highly significant.

[12] Unpublished data.

Table V—Plasma Cholinesterase Inhibition by Various Substances

Inhibitor	Concentration of Inhibitor in Blood, mg/ml	Percent Recovery of Drug after 30 min
Protein precipitation	—	100
Sodium arsenite	5–50	10–50
Sodium fluoride	5–15	50
Dimethylcarbamate of (2-hydroxy-5-phenylbenzyl)trimethylammonium bromide[a]	0.5–5	50
Sodium fluoride plus dimethylcarbamate	0.5–15	50
Echothiophate iodide[b]	0.5	80
	1.0	90
	2.0	100

[a] Hoffmann-La Roche Inc. [b] Ayerst Laboratories.

Table VI—Recovery of Chloroprocaine Showing the Effectiveness of Echothiophate-Modified Tubes

Subject	n[a]	Percent Recovery	
		Mean	*SD*
1	6	74	4
2	5	79	6
3	6	73	3
4	6	74	3

[a] Three samples per subject in duplicate (one tube for Subject 2 was lost).

***In Vivo* Studies**—*Sampling Procedures*—To prevent artifactual drug hydrolysis in the collected samples, it was necessary to develop an effective and convenient technique of completely inhibiting cholinesterase in the sampling tube. Several potential inhibitors were compared relative to protein precipitation (Table V). To be acceptable, the material had to meet the following requirements: (*a*) complete and rapid inhibition of cholinesterase activity, (*b*) lack of interference in the final GLC measurements, and (c) convenience in clinical usage. Only echothiophate at the 2-mg/ml level possessed the required characteristics.

To confirm further the general acceptability of echothiophate as an inhibitor, a known quantity of I (3.8 μg/tube) was added to heparinized blood sampling tubes, previously modified with echothiophate. These tubes were used for blood collection from four healthy volunteers. The samples were then analyzed for residual I content (Table VI). From the 23 measurements, a mean recovery of 75% (SD = 4) was obtained, indicating that approximately 25% of the drug was hydrolyzed prior to complete enzyme deactivation. Obviously, a finite time lapse is unavoidable before the required contact between blood cholinesterases and echothiophate can be established. This interval is apparently sufficient to allow hydrolysis of 25% of the added drug. Despite this problem, the data demonstrate that echothiophate is an excellent agent for terminating enzymatic hydrolysis of I and that its use provides reliable blood samples for subsequent assay.

Table VII—2-Chloro-4-aminobenzoic Acid Content (Micrograms per Milliliter) of Plasma in Subjects Receiving 250 mg of Chloroprocaine/30 min by Intravenous Infusion

Minutes	Subject 1	Subject 2	Subject 3	Subject 4
2	Trace	Trace	0.2	0.71
5	0.2	0.9	1.2	2.7
10	2.2	2.2	2.6	2.4
15	3.0	2.6	3.9	2.9
30	—[a]	3.5	4.3	3.6
Infusion terminated				
35	2.6	—[a]	2.2	1.5
40	2.6	0.7	2.0	1.0
45	2.2	0.6	1.8	0.7
60	0.8	Nil	0.6	0.6

[a] Lost sample.

Table VIII—Recovery of 2-Chloro-4-aminobenzoic Acid and Its Conjugates Emitted in the Urine 60 and 90 min after the Beginning of an Intravenous Infusion of 250 mg of Chloroprocaine/30 min

	60 min				90 min				Total			
	Free		Conjugate		Free		Conjugate		Free		Conjugate	
Subject	mg	% dose	mg	% dose	mg	% dose	mg	% dose	mg	% dose	mg	% dose
1	10.3	6.6	13.9	8.9	0.5	0.3	20.2	13.0	10.8	6.8	34.1	21.9
2	2.0	1.3	14.5	9.3	8.3	5.3	74.8	47.9	10.3	6.6	89.3	57.1
3	3.9	2.5	43.1	25.1	Trace	—	17.6	11.3	3.9	2.5	60.7	38.8
4	13.0	8.3	50.9	32.6	0.4	0.4	36.6	23.3	13.4	8.6	87.5	56.0

Intravenous Infusion Studies—Compound I could not be detected in any sample from volunteers receiving an intravenous infusion. These results suggest either that essentially all of the drug disappeared from the circulation at a rate equal to or greater than the rate at which it was being infused or that plasma cholinesterases had not been deactivated completely by the inhibitor during sample collection. If the latter were the case, hydrolysis would continue until the protein precipitation procedure was carried out.

The extremely rapid hydrolysis rate shown by *in vitro* experiments suggested that the first alternative was more likely. Nonetheless, to test the second alternative, known quantities of I were added to aliquots of blood samples obtained in the abovementioned protocol. After the samples stood for several minutes, they were assayed for residual compound. No loss of drug occurred, indicating that echothiophate had, indeed, deactivated the plasma cholinesterases.

Initial measurements for I were negative. No intact drug could be observed in any of the seven subjects. The distribution and excretion of I were then determined indirectly by measuring II concentrations in blood and urine of the group of four who received the drug over 30 min (Table VII). The acid metabolic fragment, II, was present. Its concentrations increased with time, rapidly at first, and then tended to plateau. After the infusion was terminated, the blood levels of II declined at rapid rates, either because of further metabolism or through an excretory process.

As shown in Table VIII, urinary elimination was the primary means of removing this metabolite. The listed results were derived from urine samples collected from the same four volunteers at 60 and 90 min from the beginning of infusion. As much as 65% of the administered dose was found in the urine after 90 min. Most of the II was excreted as a conjugate of which no definite identification has been made, although β-glucuronidase and sulfatase had no effect upon the release of II. In analogy to unsubstituted benzoic acid and salicylic acid, the glycine conjugate could be among the more likely products (10). Regardless of its composition, the proportion of the conjugate to the free metabolite increased with time.

Table IX—Levels (Micrograms per Milliliter of Plasma) of Anesthetic and Its Metabolite in Maternal and Umbilical Cord Plasma of Two Patients Who Received Approximately 800 mg of Chloroprocaine for Obstetric Epidural Anesthesia

	I		II	
Sample	Patient 1	Patient 2	Patient 1	Patient 2
Umbilical artery	Nil	Nil	0.03	0.09
Umbilical vein	Nil	Nil	0.07	0.45
Maternal vein	Nil	Nil	1.97	2.78

Obstetric Epidural Anesthesia—No intact I could be found in the maternal or umbilical cord blood samples following obstetric epidural anesthesia. Rapid metabolism within the maternal circulation probably prevented the drug from reaching the fetus. Measurable quantities of II were found in all samples (Table IX). They were higher in the umbilical venous than umbilical arterial blood, suggesting the transfer of the metabolite into the fetus. However, the low ratios of fetal to maternal levels of II indicate that the placental transfer of this compound was very limited.

REFERENCES

(1) H. O. Morishima, S. S. Daniels, M. Finster, P. J. Poppers, and L. S. James, *Anesthesiology*, **27**, 147 (1966).

(2) K. Teramo and Q. Widholm, *Acta Obstet. Gynaecol. Scand., Suppl.*, **46**, 1 (1967).

(3) P. J. Poppers and M. Finster, *Anesthesiology*, **29**, 1124 (1968).

(4) K. Teramo, "Fetal Pharmacology," L. Boreus, Ed., Raven, New York, N.Y., 1973, p. 281.

(5) P. P. Raj, R. Rosenblatt, J. Miller, R. Katz, and E. Carden, *Anesth. Analg. (Cleveland)*, **56**, 110 (1977).

(6) F. F. Foldes, D. L. Davis, and O. J. Plekss, *Anesthesiology*, **17**, 187 (1956).

(7) F. F. Foldes and M. H. Aven, *Science*, **114**, 206 (1951).

(8) C. W. Nellermore, D. C. Moore, L. D. Bridenbaugh, G. N. Casady, and B. Braly, *Anesthesiology*, **21**, 269 (1960).

(9) M. Somogyi, *J. Biol. Chem.*, **160**, (1945).

(10) C. Bedford, A. J. Cummings, and B. K. Martin, *Br. J. Pharmacol.*, **24**, 418 (1965).

ACKNOWLEDGMENTS

Supported in part by NIGMS Grant GM-09069.

The authors thank Dr. Kare Gundersen and Dr. John Giering of the Medical Department, Pharmaceutical Division, Pennwalt Corp., for their advice and assistance and Dr. Robert Lehman of Ayerst Laboratories for supplying the echothiophate iodide.

Magnetic Microspheres: Synthesis of a Novel Parenteral Drug Carrier

KENNETH WIDDER *x, GEORGE FLOURET ‡, and ANDREW SENYEI *

Received February 2, 1978, from the *Department of Pathology and The Cancer Center and the ‡Department of Physiology, Northwestern University Medical School, Chicago, IL 60611. Accepted for publication June 16, 1978.

Abstract □ The synthesis and characterization of a novel parenteral drug carrier capable of area specific localization by magnetic means are described. The carrier consists of human serum albumin microspheres, average of 1 μm in diameter, in which a magnetizable material (magnetite) and a prototype drug (doxorubicin) are entrapped. Stabilization of the microsphere matrix by formaldehyde, 2,3-butanedione, and heat conferred equal stability to the matrix but differentially affected the *in vitro* drug release rate. Released doxorubicin was chemically identical to the starting material.

Keyphrases □ Microspheres, magnetic—synthesized as drug carriers, effect of stabilization and heat on drug release *in vitro* □ Carriers, drug—magnetic microspheres synthesized, effect of stabilization and heat on drug release *in vitro* □ Delivery, drug—magnetic microspheres synthesized as drug carriers, effect of stabilization and heat on drug release *in vitro*

Several types of carriers intended to modify the systemic distribution of soluble chemotherapeutic agents recently were proposed as possible drug vehicles. Kramer (1) entrapped daunorubicin hydrochloride and mercaptopurine in human serum albumin microspheres and suggested their use *in vivo*. The *in vivo* distribution of dactinomycin and a variety of other agents was modified by entrapping them into liposomes (2, 3).

The *in vivo* distribution of a carrier may be influenced mechanically by varying its size, as with albumin microspheres (4, 5), or chemically by altering its surface charge, as with liposomes (6, 7). In addition, the attachment of antibodies to the carrier surface was suggested as a mechanism for targeting to specific cell surface antigens (8, 9). However, intravascular administration of any such carriers, modified or not, results in their undesired accumulation by the reticuloendothelial system (10, 11). A mechanism for selectively restricting the carrier and, hence, the drug to a desired body site with minimal interference of the reticuloendothelial system is highly desirable.

This report describes the preparation and characterization of a novel delivery system for water-soluble drugs. It consists of albumin microspheres (average of 1 μm in diameter) containing ultrafine magnetic particles, magnetite (ferrosoferric oxide), and a prototype drug, doxorubicin hydrochloride. Magnetic microspheres injected intravascularly can be localized to a desired target site *in vivo* by an externally applied magnetic field of appropriate strength (12). Moreover, the intra-arterial injection of carrier-delivered doxorubicin resulted in the same target site concentrations as a 100-fold higher dose of free doxorubicin administered intravenously.

This site-specific delivery of chemotherapeutic agents allows for maximum concentration of an agent at a desired body site, thus permitting the use of much smaller doses than are normally required with generalized systemic administration. Such smaller doses would also result in decreased toxicity of the administered agent.

EXPERIMENTAL

Preparation of Microspheres—A modified emulsion polymerization method, similar to that developed by Scheffel *et al.* (13), was used to prepare the microspheres. Stabilization of the albumin matrix of the microspheres was accomplished by either heat denaturation at various temperatures or cross linking with carbonyl compounds in an ether phase reaction.

Heat-Stabilized Microspheres—An aqueous solution was prepared containing, per milliliter, 250 mg of human serum albumin[1] (I), 0.02 ml of ^{125}I-bovine serum albumin[2] (II), 32 mg of bulk purified doxorubicin hydrochloride[3] (III), and 72 mg of magnetite[4] (IV) particles 10–20 nm in diameter. A 0.5-ml aliquot of this suspension was added to 30 ml of cottonseed oil[5] and the resultant emulsion was homogenized by sonication[6] (100 w) for 1 min at 4°. The homogenate was then added dropwise into 100 ml of stirred (1600 rpm) cottonseed oil preheated to a desired temperature (110–165°).

The duration of heating (10 min) was held constant regardless of the temperature selected. After 10 min, the oil was allowed to cool to 25° with constant stirring. The microspheres were washed free of oil by adding 60 ml of anhydrous ether[7], centrifuging[8] for 15 min at 2000×*g*, and decanting the supernate. After the fourth wash, the pellet of microspheres was allowed to air dry in the dark for 24 hr at 4°. The resultant microspheres were lyophilized[9] to remove any remaining water and stored at 4° until they were used.

Carbonyl-Stabilized Microspheres—An oil homogenate of I–IV was prepared as described. The homogenate was added dropwise into 100 ml of constantly stirred (1600 rpm) cottonseed oil at 25°. After 10 min of stirring, the microspheres were washed free of oil with ether. The microspheres were then resuspended in ether (40 mg of microspheres/100 ml of ether) containing either 0.2 *M* 2,3-butanedione[10] or 0.1 *M* formaldehyde[11] as the cross-linking agent.

The suspension was stirred rapidly for either 15 or 60 min. Excess carbonyl reagent was removed by immediately adding 100 ml of ether, pelleting the microspheres by centrifuging at 2000×*g* for 10 min, and decanting the supernate. The microspheres were washed four times in this manner and subsequently lyophilized and stored at 4°.

Analysis of Microspheres—Aliquots of the lyophilized microspheres suspended in ether were taken, and the size of the microspheres in each aliquot was determined by scanning electron microscopy.

The stability of III released from an aqueous suspension of both types of microspheres (1 mg/ml) was determined by TLC on 5 × 20-cm precoated silica gel 60[12] plates, using chloroform–methanol–acetic acid–water (60:20:14:6). The R_f values of III and its aglycone breakdown products were obtained by visualizing the native fluorescence of the drugs with a shortwave UV lamp[13]. The experimental R_f value was then compared to a reference R_f value of stock III.

The percent starting parent compound remaining intact after release from the microspheres was determined quantitatively by scraping the appropriate areas of the chromatographic plates and eluting the compounds from the silica with 5% HCl in ethanol for 12 hr at 4°. The con-

[1] Sigma Chemical.
[2] Specific activity of 1.51 mCi/mg, 1.42 mCi/ml, New England Nuclear.
[3] Adriamycin, Adria Laboratories.
[4] Ferrosoferric oxide (Fe_3O_4) in aqueous suspension, Ferrofluidics Corp.
[5] Sargent-Welch.
[6] Branson sonifier model 185.
[7] Mallinckrodt Chemicals.
[8] Sorval model RC2-B.
[9] Model 10-010, Virtis Co.
[10] Aldrich Chemical Co.
[11] Scientific Products. The 2,3-butanedione is soluble in ether; however, formaldehyde must be extracted into the ether phase. This extraction was accomplished by the vigorous shaking for 10 min of a 1:5 solution of 37% aqueous formaldehyde–ether with the addition of a saturating amount of ammonium sulfate.
[12] EM Laboratories.
[13] Model UVS-12, Ultraviolet Products.

0022-3549/79/0100-0079$01.00/0
© 1979, American Pharmaceutical Association

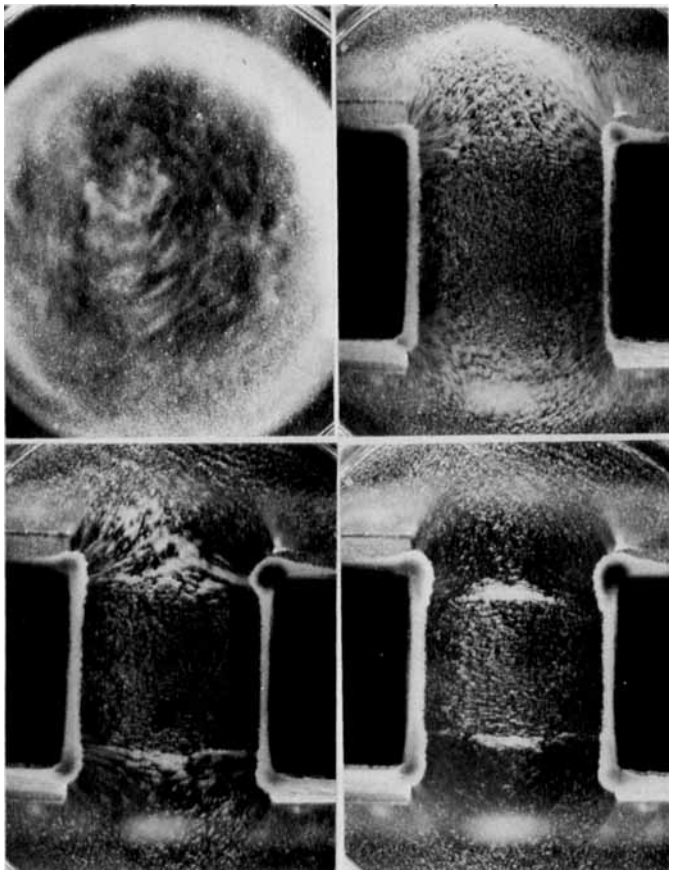

Figure 1—*Sequential time sequence photographs of magnetically responsive drug-bearing microspheres in aqueous suspension after horseshoe magnet is applied. Progressive alignment of microspheres (negative contrast) along magnetic field lines is evident. Elapsed time between photographs 1 and 4 is approximately 2 sec.*

centration of III and the pooled group of aglycone breakdown products was determined by spectrophotofluorometry[14].

The magnetite contained within the microspheres was determined quantitatively by hydrolyzing an aliquot of the microspheres in concentrated nitric acid and assaying the resultant hydrolysate for iron by atomic absorption spectroscopy[15]. Transmission electron microscopy of the microspheres was utilized to assess incorporation of magnetite into the albumin matrix and was described in detail elsewhere (14).

The efficiency of III incorporation was checked by extraction of the drug as follows. A 1-mg portion of the drug-containing carrier was incubated in 5 ml of 5% HCl in ethanol for 24 hr at 4°. The suspension of microspheres was then centrifuged for 10 min at 2000×*g*, and the III content was determined by spectrophotofluorometric analysis of the supernate as described. Extraction of the drug from the microspheres by this method was essentially complete since subsequent incubation of the microspheres for 24 hr at 25° in both saline and acid alcohol failed to show detectable III in the supernates.

The structural integrity of the albumin matrix of the microspheres before and after cross linking or heat denaturation was determined by the following procedure. The microspheres were suspended (0.5 mg/ml) in 0.154 *N* NaCl with 0.1% polysorbate 80[16] (V) and sonicated for 5 min in an ultrasonic water bath[17]. The sonicated suspensions were allowed to incubate at 37° for either 24 or 48 hr. After incubation, an aliquot of the suspension was centrifuged for 10 min at 2000×*g* to remove microspheres not totally disrupted. The resulting supernate was removed and treated with 24% aqueous trichloroacetic acid for 2 hr to precipitate free albumin and then centrifuged at 2000×*g* for 10 min.

The trichloroacetic acid-soluble supernate represents iodine-125 not

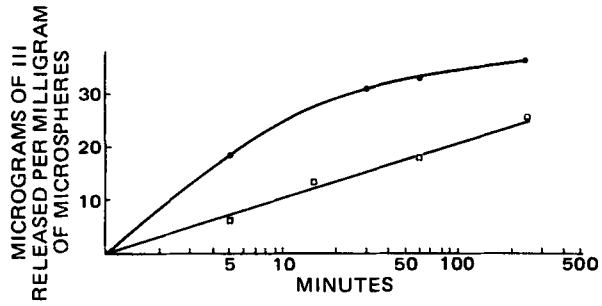

Figure 2—*Release of III from 0.1* M *formaldehyde-stabilized microspheres in saline-polysorbate 80 at 37°. Key: ●, cross linked 15 min; and □, cross linked 60 min.*

associated with albumin, whereas the trichloroacetic acid-precipitable pellet represents ^{125}I-albumin released from the albumin matrix. The deterioration of the microsphere matrix was then determined from the trichloroacetic acid-precipitable ^{125}I-albumin counts[18] and expressed as a percentage of the initial counts of ^{125}I-albumin associated with the microspheres prior to suspension and sonication.

Drug Release—The drug release rate from the microspheres *in vitro* was determined as follows. An 8-mg portion of microspheres (1 mg/ml) suspended in V was sonicated for 2 min in the ultrasonic water bath to produce a homogeneous suspension of microspheres. The magnetically responsive microspheres were pulled to one side of the vessel using a horseshoe magnet[19]. The supernate, containing drug released from the microspheres during sonication, was removed. Microspheres were then rapidly resuspended in 8 ml of V and gently hand agitated for 10 sec.

The reaction vessels were then placed in a water bath at 37° and covered to protect III from light. At appropriate time intervals, microsphere-free supernate samples were obtained by magnetically drawing the microspheres to the side of the vessel and removing a 1-ml aliquot of the supernate. The amount of drug released over time was determined spectrophotofluorometrically as described.

RESULTS AND DISCUSSION

A relatively homogeneous population of microspheres is produced by the methods described with microspheres ranging from 0.2 to 1.5 μm and having an average diameter of 1 μm. The magnetic responsiveness of the drug carrier is shown in Fig. 1 where the sequential alignment of the microspheres along magnetic field lines and also around the poles of the magnet is evident. Details of their magnetic responsiveness under flow conditions corresponding to the human circulation were reported elsewhere (14, 15).

Doxorubicin was relatively stable to temperatures used in the preparation of heat-stabilized microspheres as determined by TLC, with only a moderate increase in aglycone breakdown products. Control starting III (nonheated) consisted of 97% pharmacologically active drug and 3% aglycones. The aglycones are pharmacologically inactive (16). Compounds released from microspheres prepared at 135–145° for 10 min consisted of 74% pharmacologically active III (identical R_f as starting III) with the remaining 26% consisting of aglycones.

Carbonyl-stabilized microspheres showed no increase in aglycone formation when compared to control III. Under the conditions employed, the carbonyl agents did not appear to react with the free amine of the released III as evidenced by TLC. The *in vitro* biological activity of III released from heat-stabilized microspheres will be described in detail elsewhere[20]; both starting and released III can identically and stoichiometrically inhibit ^{3}H-uridine uptake by rat fibrosarcoma cells.

Despite the fact that microspheres prepared at 25° retain their morphology in ether, they require some form of stabilization if they are to be transferred to an aqueous solvent. In fact, structural integrity of the microspheres as judged by sonication was directly related to stabilizing treatment. When microspheres were prepared at 25° with no stabilizing treatment, there was 16% deterioration after 24 hr of incubation at 37° and 37% deterioration after 48 hr as determined by ^{125}I-albumin disassociated from the microspheres. In contrast, ≤3% deterioration of the microspheres was detected after 24 and 48 hr when microspheres were

[14] American Instrument Co. model SPF-1255 (excitation = 470 nm, and emission = 585 nm); level of detectability was 1×10^{-6} *M* III.
[15] Iron analysis performed by Scientific Control Labs, Chicago, Ill.
[16] Tween 80 (Sigma Chemical Co.) in 0.154 *N* NaCl.
[17] Model M.E. 2.1, Mettler Electronics Corp.

[18] ^{125}I-Activity was determined in a Packard model 578 well-type γ-counter.
[19] Edmund Scientific No. 70,572.
[20] Paper in preparation.

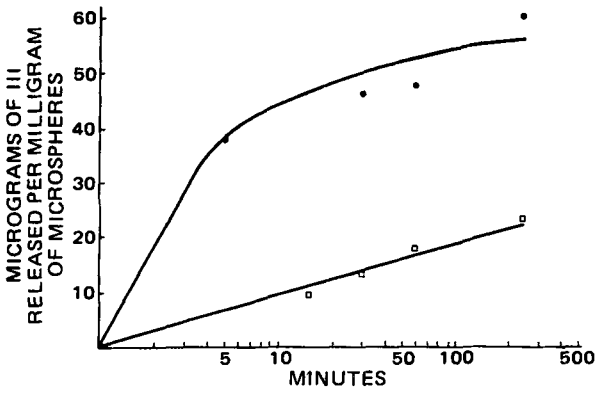

Figure 3—*Release of III from 0.2 M 2,3-butanedione-stabilized microspheres in saline–polysorbate 80 at 37°. Key: ●, cross linked 15 min; and □, cross linked 60 min.*

cross linked for 15 min or longer with either 2,3-butanedione or formaldehyde. Heat treatment above 100° had a similar effect.

By varying the amount of magnetite added to the starting solution, the percent magnetite dry weight composition of the microspheres could readily be controlled. The magnetite content has important implications with respect to the magnetic responsiveness of the carrier. Though increasing the magnetite content would confer greater magnetic responsiveness to the microsphere and thus permit the use of smaller extracorporeal fields, it would decrease the available drug space in the microsphere, thus requiring larger dosages of carrier to deliver equivalent drug concentrations. Depending on the type of drug and the desired target site, the optimum magnetite content would range between 20 and 50% magnetite by dry weight of the drug–carrier complex (14, 15).

After preparation of the carrier, essentially all of the starting III was associated with the resultant microspheres as judged by extraction with acid alcohol. Regardless of the method of preparation, of the 90 μg of III associated with 1 mg of carrier, approximately 40% (36 μg) was liberated rapidly on sonication in an aqueous solvent. The rate of III release from heat-stabilized and carbonyl-stabilized microspheres is shown in Figs. 2–5. As expected, increased stabilization of the microspheres, either by longer cross-linking treatment or by increased temperature, decreased the release rate of III. The generated release curves are comparable to those presented by Scheu *et al.* (17) for coacervate-produced microspheres.

Detailed kinetic studies were not warranted in this study since a significant amount of drug was still associated with the carrier at $t = 5$ min in both heat- and carbonyl-stabilized preparations. This time period represents a realistic interval for carrier injection and *in vivo* transit time to the desired target site. Furthermore, *in vivo* extrapolation from *in vitro* data is not readily feasible because of a number of complex blood flow variables. However, data from Fig. 5, where microspheres were incubated in human serum, reveal an inhibited release of III compared to Fig. 4, in which the release medium was V. This result suggests that *in vivo* release times would correspond more closely to Fig. 5 than Fig. 4. Experimental work is in progress to evaluate the biological fate of the magnetite *in vivo* after carrier administration. Preliminary acute (7 days) and chronic (90

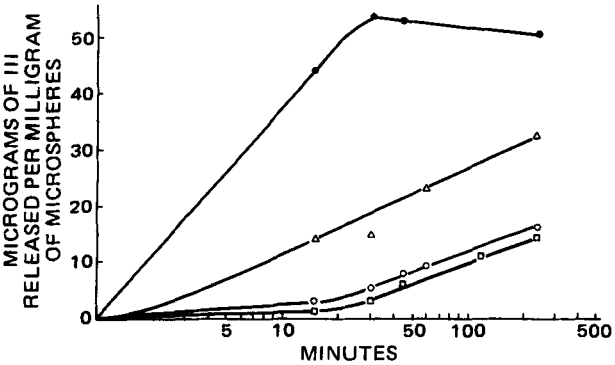

Figure 4—*Release of III in saline–polysorbate 80 at 37° from heat-stabilized (10 min) microspheres prepared at various temperatures. Key: ●, 25°; △, 115–127°; ○, 125–135°; and □, 135–145°.*

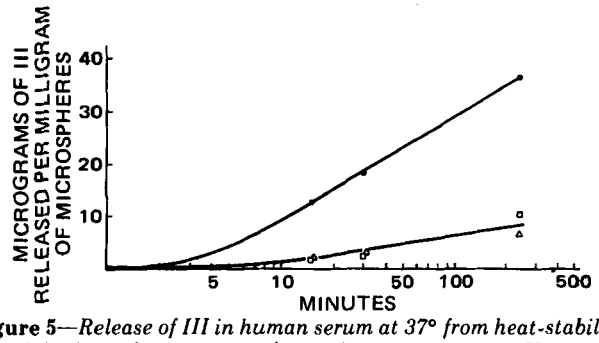

Figure 5—*Release of III in human serum at 37° from heat-stabilized (10 min) microspheres prepared at various temperatures. Key: ●, 25°; △, 115–127°; and □, 135–145°.*

days) toxicity studies in BDF_1 mice showed minimal adverse effects (12).

The described low temperature conditions employing either carbonyl reagents or no deliberate denaturing step at all should permit encapsulation of many temperature-sensitive drugs that formerly could not be incorporated into solid albumin microspheres. Several theoretical explanations may be offered for the formation of stable microspheres without "overt" denaturation of the albumin. One that seems likely is that albumin molecules, aligning on the oil–water interface, undergo a change in conformation such that hydrophobic regions of the molecules are preferentially exposed externally to the oil. Thus, a hydrophobic "crust" or mantle is formed that is not reversible for a period of time, which permits microspheres to maintain their morphology for a limited time when transferred to an aqueous environment.

Using model phospholipid interfaces, Kimelberg (18) described conformational changes of proteins aligning at such interfaces. What has not been reported to date is that nonstabilized microspheres are durable enough to maintain morphologic integrity in aqueous suspension for a sufficient time to permit their use as either therapeutic vehicles or substrates for subsequent denaturation by low temperature methods. The nonaqueous carbonyl reagent method of stabilizing the albumin matrix, in addition to maintaining the spherical morphology of the carrier generated in the oil emulsion, appears to slow the diffusion of III from the carrier.

The use of microspheres or any drug–macromolecular complex as vehicles for targeting chemotherapeutic agents rests solely on the ability of the carrier to achieve either cell or area specificity. Efforts at cell-specific targeting of cancer chemotherapeutic agents are mainly focused on exploitation of biochemical differences between cells (19, 20). Unfortunately, target cell specificity has not been achieved in most cases, as evidenced by the numerous side effects apparent with generalized systemic drug administration.

Area-specific drug delivery using a carrier may be of value not only in greatly decreasing unwanted systemic distribution of drugs but also in eradicating localized disease states. Magnetic microspheres offer a new modality for drug delivery. The narrow and relatively uniform size range of these microspheres makes them ideal for small vessel passage, thus permitting uniform saturation of target capillary beds. With the ability to control the rate of drug release from the carrier and the ability to localize both carrier and drug *in vivo* to a desired site, a different modality of drug delivery may be readily explored.

REFERENCES

(1) P. A. Kramer, *J. Pharm. Sci.*, **63**, 1646 (1974).

(2) D. E. Neerunjun and G. Gregoriadis, *Biochem. Soc. Trans.*, **2**, 868 (1974).

(3) Y. Rahman, E. A. Cerny, S. L. Tallaksen, B. J. Wright, S. O. Nance, and J. F. Thompson, *Proc. Soc. Exp. Biol. Med.*, **146**, 1173 (1974).

(4) H. N. Wagner, B. A. Rhodes, Y. Sasaki, and J. P. Ryan, *Invest. Radiol.*, **4**, 374 (1969).

(5) I. Zolle, B. A. Rhodes, and H. N. Wagner, *Int. J. Appl. Radiat.*, **21**, 155 (1970).

(6) G. Gregoriadis and E. D. Neerunjun, *Eur. J. Biochem.*, **47**, 179 (1974).

(7) R. L. Juliano and D. Stamp, *Biochem. Biophys. Res. Commun.*, **63**, 651 (1975).

(8) G. Gregoriadis and E. D. Neerunjun, *ibid.*, **65**, 537 (1975).

(9) G. Weissmann, *Hosp. Pract.*, **11**, 49 (1976).
(10) G. Gregoriadis and B. E. Ryman, *Eur. J. Biochem.*, **24**, 485 (1972).
(11) I. Zolle, F. Hosain, and B. A. Rhodes, *J. Nucl. Med.*, **11**, 379 (1970).
(12) K. J. Widder, A. E. Senyei, and D. G. Scarpelli, *Proc. Soc. Exp. Biol. Med.*, **158**, 141 (1978).
(13) U. Scheffel, B. A. Rhodes, T. K. Natarajan, and H. N. Wagner, *J. Nucl. Med.*, **13**, 498 (1972).
(14) A. Senyei, K. Widder, and G. Czerlinski, *J. Appl. Phys.*, **49**, 3578 (1978).
(15) K. J. Widder and A. E. Senyei, U.S. pat. pending Serial No. 820,812 (1977).
(16) A. DiMarco, *Cancer Chemother. Rep. Part 3*, **6**, 91 (1975).
(17) J. D. Scheu, G. J. Sperandio, S. M. Shaw, R. R. Landolt, and G. E. Peck, *J. Pharm. Sci.*, **66**, 172 (1977).
(18) H. K. Kimelberg, *Mol. Cell. Biochem.*, **10**, 171 (1976).
(19) E. Hurwitz, R. Levy, R. Maron, M. Wilchek, R. Aron, and M. Sela, *Cancer Res.*, **35**, 1175 (1975).
(20) G. F. Rowland, G. J. O'Neill, and D. A. L. Davies, *Nature*, **255**, 487 (1975).

ACKNOWLEDGMENTS

The authors thank Dr. Steven D. Reich for advice and Ms. Paula Giroux for help.

Antifungal Properties of *n*-Alkoxyacetic Acids and Their Methyl Esters

HERMAN GERSHON ˣ, LARRY SHANKS, and ALAN DeANGELIS

Received February 17, 1978, from *Boyce Thompson Institute for Plant Research at Cornell University, Ithaca, NY 14853.* Accepted for publication June 27, 1978.

Abstract □ Eleven *n*-alkoxyacetic acids and their methyl esters, in which the alkyl group was C_1–C_9, C_{11}, or C_{13}, were tested against *Aspergillus niger*, *Trichoderma viride*, and *Myrothecium verrucaria* in Sabouraud dextrose agar at pH 4.0 and 5.6. Toxicity to *Candida albicans*, *Trichophyton mentagrophytes*, and *Mucor mucedo* was determined in the same medium at pH 5.6 and 7.0 in the absence and presence of 10% beef serum. The fungitoxicity of the acids was influenced by chain length, pH of the medium, and absence or presence of adsorbents. The toxicity of the esters was influenced primarily by chain length and to a lesser extent by the medium pH and the presence of beef serum. The order of activity of the *n*-alkoxyacetic acids was according to the number of linear atoms in the chain: 11 > 12 > 10 > 9 > 8 > 7 > 6 > 14 > 16. *T. mentagrophytes* was the organism most strongly affected by these compounds, with the esters being slightly more active than the acids. Compared to other fatty acid analogs, the order of fungitoxicity, on a weight basis, was 2-alkynoic acids > 2-alkenoic acids > alkanoic acids > 2-bromoalkanoic acids > 2-fluoroalkanoic acids > *n*-alkoxyacetic acids.

Keyphrases □ *n*-Alkoxyacetic acids and methyl esters—antifungal activity evaluated *in vitro*, effect of chain length, pH, and adsorbents □ Antifungal activity—*n*-alkoxyacetic acids and methyl esters evaluated *in vitro*, effect of chain length, pH, and adsorbents □ Structure–activity relationships—*n*-alkoxyacetic acids and methyl esters, antifungal activity evaluated *in vitro*

As part of a search for fungitoxic agents, the structure–activity relationships of fatty acids were studied (1–6). In addition, compounds were evaluated for potential use against opportunistic fungi, which are frequent invaders of immunosuppressed and debilitated patients (4–10). Such fungi include species of *Candida*, *Aspergillus*, *Mucor*, and *Cryptococcus* (11).

BACKGROUND

Fatty acids possess significant antifungal activity. For systemic use, in spite of their low toxicities, they have been ineffective, possibly because they are metabolized readily by the host through the usual fatty acid pathways. The fungitoxicity of 2-fluoro fatty acids paralleled that of the nonfluorinated fatty acids (1). Since it is believed that 2-fluoro fatty acids do not undergo β-oxidation (12), they possess at least one potential advantage over the nonfluorinated fatty acids for systemic antifungal activity.

Another approach for preparing fatty acids that do not undergo β-oxidation is to replace the β-methylene group with an oxygen (13). In the structure $ROCH_2COOH$, the C–O–C angle is 111° and the corresponding C–C–C angle is 112°. The C–O bond length is 1.43 Å, and the length of the C–C bond is 1.54 Å. Replacement of the CH_2 group by O would not greatly alter the steric configuration of the analog, and it would not be β-oxidizable because of the lack of β-hydrogens.

The major factors influencing the fungitoxicity of fatty acids and derivatives are the partition coefficient and the absence or presence of adsorbents such as albumin in the growth medium. Chain length, pKa of the acid, and pH of the medium are among the factors determining the partition coefficient of the test compound (6). The deactivating effect of the adsorbent can be explained as being due to hydrogen bonding (5).

No systematic antimicrobial studies with 3-oxa acids or esters have been reported. 11-Fluoroundecyloxyacetic acid and several other 3-oxa acids inhibited *Mycobacterium tuberculosis in vitro* at 50 μg/ml (14).

The present study was concerned with the preparation of the straight-chain 3-alkoxyacetic acids and their methyl esters in which the alkyl groups included 1–9, 11, or 13 carbon atoms. Methoxy- and ethoxyacetic acids were purchased[1]. The following acids were prepared by published methods: *n*-propyloxyacetic acid, *n*-butyloxyacetic acid, *n*-pentyloxyacetic acid, *n*-hexyloxyacetic acid, *n*-heptyloxyacetic acid, *n*-octyloxyacetic acid (15), *n*-undecyloxyacetic acid, and *n*-tridecyloxyacetic acid (13).

The following methyl esters were also previously reported: methyl methoxyacetate, methyl ethoxyacetate, methyl *n*-propyloxyacetate (16), methyl *n*-butyloxyacetate (17), and methyl *n*-octyloxyacetate (18). *n*-Nonyloxyacetic acid was prepared by condensing *n*-nonyl alcohol with chloroacetic acid by means of sodium in toluene, and the previously unknown methyl esters were obtained from the acids by heating with methyl alcohol in the presence of a catalytic quantity of thionyl chloride.

The data characterizing the new compounds are in Table I. The purity of all compounds was verified by GLC.

The fungi used were *Aspergillus niger* (ATCC 1004), *Trichoderma viride* (ATCC 8678), *Myrothecium verrucaria* (ATCC 9095C), *Candida albicans* (ATCC 10231), *Trichophyton mentagrophytes* (ATCC 9129), and *Mucor mucedo* (ATCC 7941).

The compounds were screened against *A. niger*, *T. viride*, and *M. verrucaria* in Sabouraud dextrose agar[2] at pH 4.0 and 5.6 according to published methods (1). Graded levels of test compound dissolved in dimethyl sulfoxide were incorporated into the growth medium, which was then inoculated with the respective fungus. The inoculum consisted of

[1] Eastman Kodak Co., Rochester, N.Y.
[2] Difco, Detroit, Mich.

0022-3549/79/0100-0082$01.00/0
© 1979, American Pharmaceutical Association

(9) G. Weissmann, *Hosp. Pract.*, **11**, 49 (1976).
(10) G. Gregoriadis and B. E. Ryman, *Eur. J. Biochem.*, **24**, 485 (1972).
(11) I. Zolle, F. Hosain, and B. A. Rhodes, *J. Nucl. Med.*, **11**, 379 (1970).
(12) K. J. Widder, A. E. Senyei, and D. G. Scarpelli, *Proc. Soc. Exp. Biol. Med.*, **158**, 141 (1978).
(13) U. Scheffel, B. A. Rhodes, T. K. Natarajan, and H. N. Wagner, *J. Nucl. Med.*, **13**, 498 (1972).
(14) A. Senyei, K. Widder, and G. Czerlinski, *J. Appl. Phys.*, **49**, 3578 (1978).
(15) K. J. Widder and A. E. Senyei, U.S. pat. pending Serial No. 820,812 (1977).
(16) A. DiMarco, *Cancer Chemother. Rep. Part 3*, **6**, 91 (1975).
(17) J. D. Scheu, G. J. Sperandio, S. M. Shaw, R. R. Landolt, and G. E. Peck, *J. Pharm. Sci.*, **66**, 172 (1977).
(18) H. K. Kimelberg, *Mol. Cell. Biochem.*, **10**, 171 (1976).
(19) E. Hurwitz, R. Levy, R. Maron, M. Wilchek, R. Aron, and M. Sela, *Cancer Res.*, **35**, 1175 (1975).
(20) G. F. Rowland, G. J. O'Neill, and D. A. L. Davies, *Nature*, **255**, 487 (1975).

ACKNOWLEDGMENTS

The authors thank Dr. Steven D. Reich for advice and Ms. Paula Giroux for help.

Antifungal Properties of *n*-Alkoxyacetic Acids and Their Methyl Esters

HERMAN GERSHON ˣ, LARRY SHANKS, and ALAN DeANGELIS

Received February 17, 1978, from *Boyce Thompson Institute for Plant Research at Cornell University, Ithaca, NY 14853.* Accepted for publication June 27, 1978.

Abstract □ Eleven *n*-alkoxyacetic acids and their methyl esters, in which the alkyl group was C_1–C_9, C_{11}, or C_{13}, were tested against *Aspergillus niger*, *Trichoderma viride*, and *Myrothecium verrucaria* in Sabouraud dextrose agar at pH 4.0 and 5.6. Toxicity to *Candida albicans*, *Trichophyton mentagrophytes*, and *Mucor mucedo* was determined in the same medium at pH 5.6 and 7.0 in the absence and presence of 10% beef serum. The fungitoxicity of the acids was influenced by chain length, pH of the medium, and absence or presence of adsorbents. The toxicity of the esters was influenced primarily by chain length and to a lesser extent by the medium pH and the presence of beef serum. The order of activity of the *n*-alkoxyacetic acids was according to the number of linear atoms in the chain: 11 > 12 > 10 > 9 > 8 > 7 > 6 > 14 > 16. *T. mentagrophytes* was the organism most strongly affected by these compounds, with the esters being slightly more active than the acids. Compared to other fatty acid analogs, the order of fungitoxicity, on a weight basis, was 2-alkynoic acids > 2-alkenoic acids > alkanoic acids > 2-bromoalkanoic acids > 2-fluoroalkanoic acids > *n*-alkoxyacetic acids.

Keyphrases □ *n*-Alkoxyacetic acids and methyl esters—antifungal activity evaluated *in vitro*, effect of chain length, pH, and adsorbents □ Antifungal activity—*n*-alkoxyacetic acids and methyl esters evaluated *in vitro*, effect of chain length, pH, and adsorbents □ Structure–activity relationships—*n*-alkoxyacetic acids and methyl esters, antifungal activity evaluated *in vitro*

As part of a search for fungitoxic agents, the structure–activity relationships of fatty acids were studied (1–6). In addition, compounds were evaluated for potential use against opportunistic fungi, which are frequent invaders of immunosuppressed and debilitated patients (4–10). Such fungi include species of *Candida*, *Aspergillus*, *Mucor*, and *Cryptococcus* (11).

BACKGROUND

Fatty acids possess significant antifungal activity. For systemic use, in spite of their low toxicities, they have been ineffective, possibly because they are metabolized readily by the host through the usual fatty acid pathways. The fungitoxicity of 2-fluoro fatty acids paralleled that of the nonfluorinated fatty acids (1). Since it is believed that 2-fluoro fatty acids do not undergo β-oxidation (12), they possess at least one potential advantage over the nonfluorinated fatty acids for systemic antifungal activity.

Another approach for preparing fatty acids that do not undergo β-oxidation is to replace the β-methylene group with an oxygen (13). In the structure $ROCH_2COOH$, the C–O–C angle is 111° and the corresponding C–C–C angle is 112°. The C–O bond length is 1.43 Å, and the length of the C–C bond is 1.54 Å. Replacement of the CH_2 group by O would not greatly alter the steric configuration of the analog, and it would not be β-oxidizable because of the lack of β-hydrogens.

The major factors influencing the fungitoxicity of fatty acids and derivatives are the partition coefficient and the absence or presence of adsorbents such as albumin in the growth medium. Chain length, pKa of the acid, and pH of the medium are among the factors determining the partition coefficient of the test compound (6). The deactivating effect of the adsorbent can be explained as being due to hydrogen bonding (5).

No systematic antimicrobial studies with 3-oxa acids or esters have been reported. 11-Fluoroundecyloxyacetic acid and several other 3-oxa acids inhibited *Mycobacterium tuberculosis in vitro* at 50 μg/ml (14).

The present study was concerned with the preparation of the straight-chain 3-alkoxyacetic acids and their methyl esters in which the alkyl groups included 1–9, 11, or 13 carbon atoms. Methoxy- and ethoxyacetic acids were purchased[1]. The following acids were prepared by published methods: *n*-propyloxyacetic acid, *n*-butyloxyacetic acid, *n*-pentyloxyacetic acid, *n*-hexyloxyacetic acid, *n*-heptyloxyacetic acid, *n*-octyloxyacetic acid (15), *n*-undecyloxyacetic acid, and *n*-tridecyloxyacetic acid (13).

The following methyl esters were also previously reported: methyl methoxyacetate, methyl ethoxyacetate, methyl *n*-propyloxyacetate (16), methyl *n*-butyloxyacetate (17), and methyl *n*-octyloxyacetate (18). *n*-Nonyloxyacetic acid was prepared by condensing *n*-nonyl alcohol with chloroacetic acid by means of sodium in toluene, and the previously unknown methyl esters were obtained from the acids by heating with methyl alcohol in the presence of a catalytic quantity of thionyl chloride.

The data characterizing the new compounds are in Table I. The purity of all compounds was verified by GLC.

The fungi used were *Aspergillus niger* (ATCC 1004), *Trichoderma viride* (ATCC 8678), *Myrothecium verrucaria* (ATCC 9095C), *Candida albicans* (ATCC 10231), *Trichophyton mentagrophytes* (ATCC 9129), and *Mucor mucedo* (ATCC 7941).

The compounds were screened against *A. niger*, *T. viride*, and *M. verrucaria* in Sabouraud dextrose agar[2] at pH 4.0 and 5.6 according to published methods (1). Graded levels of test compound dissolved in dimethyl sulfoxide were incorporated into the growth medium, which was then inoculated with the respective fungus. The inoculum consisted of

[1] Eastman Kodak Co., Rochester, N.Y.
[2] Difco, Detroit, Mich.

0022-3549/79/0100-0082$01.00/0
© 1979, American Pharmaceutical Association

Table I—*n*-Alkoxyacetic Acids and Methyl Esters (n-$R_1OCH_2COOR_2$)

R_1	R_2	Yield, %	Boiling Point (mm)[a]	$n_D^{25°}$	ν neat, cm^{-1} C=O	ν neat, cm^{-1} -O-	Formula		Analysis, % Calc.	Analysis, % Found
n-C_9H_{19}	H	47	123° (0.3)[b]	—	1725	1142	$C_{11}H_{22}O_3$	C	65.31	65.20
								H	10.96	11.05
n-C_5H_{11}	CH_3	77	42° (0.4)	1.4230	1770	1142	$C_8H_{16}O_3$	C	59.97	60.11
								H	10.07	9.96
n-C_6H_{13}	CH_3	77	52° (0.3)	1.4184	1780	1148	$C_9H_{17}O_3$	C	62.04	62.00
								H	10.41	10.27
n-C_7H_{15}	CH_3	82	62° (0.3)	1.4235	1780	1146	$C_{10}H_{20}O_3$	C	63.79	63.79
								H	10.71	10.86
n-C_9H_{19}	CH_3	82	64° (0.25)	1.4284	1771	1145	$C_{12}H_{24}O_3$	C	66.63	66.65
								H	11.18	11.11
n-$C_{11}H_{23}$	CH_3	80	108° (0.25)	1.4343	1772	1145	$C_{14}H_{28}O_3$	C	68.85	68.55
								H	11.52	11.37
n-$C_{13}H_{27}$	CH_3	57	127° (0.25)	1.4385	1776	1147	$C_{16}H_{32}O_3$	C	70.54	70.35
								H	11.84	11.70

[a] Analytical sample. [b] Mp 32.5–33.5° (hexane).

Table II—Antifungal Activity of *n*-Alkoxyacetic Acids and Their Methyl Esters at pH 4.0 and 5.6 in Sabouraud Dextrose Agar after 5 Days at 28° against *A. niger*, *T. viride*, and *M. verrucaria*

R	Levels of Inhibition at pH 4.0[a] *A. niger*	*T. viride*	*M. verrucaria*	Antifungal Spectrum Index[b]	Levels of Inhibition at pH 5.6 *A. niger*	*T. viride*	*M. verrucaria*	Antifungal Spectrum Index[b]
				$ROCH_2COOH$				
CH_3	0	1	1	4	0	0	0	0
C_2H_5	0	1	1	4	0	0	0	0
n-C_3H_7	0	1	1	4	0	1	1	4
n-C_4H_9	1	1	1	9	0	1	1	4
n-C_5H_{11}	1	1	2	12	1	1	1	9
n-C_6H_{13}	1	2	2	15	1	2	2	15
n-C_7H_{15}	2	3	2	21	1	2	2	15
n-C_8H_{17}	2	3	3	24	2	3	3	24
n-C_9H_{19}	2	3	3	24	2	3	3	24
n-$C_{11}H_{23}$	0	3	3	12	0	3	3	12
n-$C_{13}H_{27}$	0	1	1	4	0	1	1	4
				$ROCH_2COOCH_3$				
CH_3	1	0	1	4	1	0	1	4
C_2H_5	0	0	0	0	0	0	0	0
n-C_3H_7	0	1	1	4	0	1	1	4
n-C_4H_9	0	1	1	4	0	1	1	4
n-C_5H_{11}	11	1	1	9	1	1	1	9
n-C_6H_{13}	1	1	1	9	1	1	1	9
n-C_7H_{15}	1	1	2	12	1	1	2	12
n-C_8H_{17}	1	2	2	15	1	2	2	15
n-C_9H_{19}	1	2	3	18	1	2	3	18
n-$C_{11}H_{23}$	0	0	0	0	0	0	0	0
n-$C_{13}H_{27}$	0	0	0	0	0	0	0	0

[a] Compounds were incorporated in test medium at 10^4, 10^3, and 10^2 μg/ml; 3 = inhibition at all levels of compound, 2 = inhibition at the two highest levels, 1 = inhibition at the highest level only, and 0 = compound inactive at highest level tested. [b] Antifungal spectrum index = the total number of levels of inhibition multiplied by the number of organisms inhibited.

1 drop of spore suspension containing 6×10^6 spores/ml in 0.85% NaCl solution. Incubation took place at 28° for 5 days.

For *T. mentagrophytes*, *C. albicans*, and *M. mucedo*, the methods described previously were used (7). To the Sabouraud dextrose agar at pH 5.6 and 7.0, both with and without 10% beef serum[3], were added graded levels of test compound dissolved in dimethyl sulfoxide. The inocula of *T. mentagrophytes* and *M. mucedo* consisted of 1 drop of spore suspension containing 6×10^6 spores/ml in 0.85% NaCl solution; the inoculum of *C. albicans* was 1 drop of a suspension obtained from a 20-hr culture in Sabouraud dextrose broth[2] incubated at 37°.

The results reported are numbers of levels of compound causing 100% inhibition of the test organisms. The compounds were tested at 10^4, 10^3, and 10^2 μg/ml. All tests were carried out in duplicate in "I" plate petri dishes[4]. The results were weighted by calculating the antifungal spectrum index, which is defined as the sum of the number of levels of complete inhibition multiplied by the number of organisms inhibited within the defined system (19, 20).

The test results against *A. niger*, *T. viride*, and *M. verrucaria* are presented in Table II; those against *C. albicans*, *T. mentagrophytes*, and *M. mucedo* are in Table III.

[3] Miles Laboratories, Kankakee, Ill.
[4] Falcon.

EXPERIMENTAL[5]

***n*-Nonyloxyacetic Acid**—Sodium metal (30.6 g, 1.33 g-atom) was added to 2000 ml of dry toluene and heated to boiling with vigorous stirring. *n*-Nonyl alcohol (95.9 g, 0.66 mole) dissolved in 300 ml of toluene was added dropwise with continued heating and stirring. When all of the alcohol was converted to the alkoxide, as evidenced by cessation of hydrogen evolution, chloroacetic acid (62.6 g, 0.66 mole) dissolved in 500 ml of toluene was added, and the mixture was stirred and heated overnight.

The toluene suspension was extracted several times with water to dissolve the salts, and the combined aqueous extracts were extracted several times with ether to remove occluded toluene and unreacted octanol. The water solution was acidified with 6 *N* HCl and extracted with ether to remove the oxa acid. The ether extract was dried (sodium sul-

[5] Melting points were taken in a Thomas-Hoover apparatus and are uncorrected. GLC was performed on a Varian Aerograph model 1200 gas chromatograph with a flame-ionization detector to which was attached a Varian Aerograph model 20 recorder. The purity of the acids was established by analyzing the silyl esters on a column containing 3% Dexsil 400 on 90–100-mesh Anachrom A (Analabs, New Haven, Conn.). All samples tested microbiologically were at least 95% pure. IR spectra were obtained with a Perkin-Elmer model 221 spectrophotometer, and refractive indexes were taken with an Abbe-3L B & L refractometer.

Table III—Antifungal Activity of *n*-Alkoxyacetic Acids and Their Methyl Esters at pH 5.6 and 7.0 in Sabouraud Dextrose Agar in the Absence and Presence of Beef Serum against *C. albicans*, *T. mentagrophytes*, and *M. mucedo* [a]

R	Levels of Inhibition [b]												Antifungal [c] Spectrum Index
	C. albicans				*T. mentagrophytes*				*M. mucedo*				
	pH 5.6		pH 7.0		pH 5.6		pH 7.0		pH 5.6		pH 7.0		
	Without Serum	With Serum	Without Serum	With Serum	Without Serum	With Serum	Without Serum	With Serum	Without Serum	With Serum	Without Serum	With Serum	
						$ROCH_2COOH$							
CH_3	0	0	0	0	1	0	0	0	0	0	0	0	1
C_2H_5	0	0	0	0	1	0	0	0	0	0	0	0	1
n-C_3H_7	0	0	0	0	1	1	0	0	1	1	1	1	12
n-C_4H_9	0	0	0	0	2	1	0	0	1	1	1	1	14
n-C_5H_{11}	1	1	0	0	2	2	1	1	2	1	1	1	39
n-C_6H_{13}	1	1	1	1	2	2	1	1	2	2	1	1	48
n-C_7H_{15}	1	1	1	1	3	2	2	1	2	2	2	2	60
n-C_8H_{17}	2	2	1	1	3	3	2	2	2	2	2	2	72
n-C_9H_{19}	2	2	1	1	3	3	2	2	2	2	1	1	66
n-$C_{11}H_{23}$	0	0	0	0	3	3	3	2	0	0	0	0	11
n-$C_{13}H_{27}$	0	0	0	0	3	2	3	2	0	0	0	0	10
						$ROCH_2COOCH_3$							
CH_3	1	1	1	1	1	1	1	1	1	1	1	1	36
C_2H_5	0	0	0	0	1	0	0	0	1	1	1	1	10
n-C_3H_7	0	0	0	0	1	1	1	1	1	1	1	1	16
n-C_4H_9	1	1	1	1	1	1	1	1	1	1	1	1	36
n-C_5H_{11}	1	1	1	1	1	1	1	1	1	1	1	1	36
n-C_6H_{13}	1	1	1	1	1	1	1	1	2	1	1	1	39
n-C_7H_{15}	1	1	1	1	3	2	2	1	1	1	1	1	48
n-C_8H_{17}	1	1	1	1	3	3	3	3	1	1	1	1	60
n-C_9H_{19}	0	0	0	0	3	3	3	2	0	0	0	0	11
n-$C_{11}H_{23}$	0	0	0	0	3	3	3	2	0	0	0	0	11
n-$C_{13}H_{27}$	0	0	0	0	3	3	3	2	0	0	0	0	11

[a] *C. albicans* and *M. mucedo* were incubated at 37° for 20 hr, and *T. mentagrophytes* was incubated at 28° for 5 days. [b] Same as footnote *a* in Table I. [c] Same as footnote *b* in Table II.

fate), and the solvent was removed in a rotary still. The residue then was fractionated under reduced pressure.

Methyl *n*-Nonyloxyacetate—To 20 g (0.099 mole) of *n*-nonyloxyacetic acid dissolved in 200 ml of methyl alcohol was added 2 ml of thionyl chloride. The mixture was heated under reflux overnight. The solvent was removed in a rotary evaporator, and the residue was distilled fractionally under reduced pressure.

RESULTS AND DISCUSSION

The fungitoxicity of compounds can be compared by using the combined antifungal spectrum indexes at pH 4.0 and 5.6. The 2-alkoxyacetic acids (Table II) were most toxic to *A. niger*, *T. viride*, and *M. verrucaria* at chain lengths of seven to 14 atoms. The methyl esters showed their greatest activity at chain lengths of six to 12 atoms. The order of fungitoxicity of the acids was at chain lengths of 12 = 11 > 10 > 9 > 14 > 8 > 7 > 6 = 16 atoms; for the esters, the order was 12 > 11 > 10 > 9 = 8 > 7 = 6. The antifungal activity of the acids was greater in many cases at pH 4.0 than at pH 5.6, and the activity of the esters was unaffected by the medium pH. The fungitoxicity of the acids was considerably greater than that of the esters.

With respect to *C. albicans*, *T. mentagrophytes*, and *M. mucedo*, the most fungitoxic acids were at chain lengths of six to 16 atoms and the most fungitoxic esters were at chain lengths of three to 16 atoms (Table III). When the pH of the medium was raised and beef serum was added, antifungal activity decreased. The same was true for the esters but to a lesser extent. The organism most affected was *T. mentagrophytes*, with the esters being slightly more active than the acids. The order of toxicity of the alkoxyacetic acids to these fungi according to chain length was 11 > 12 > 10 > 9 > 8 > 7 > 6 > 14 > 16 atoms; for the esters, the order was 11 > 10 > 9 > 8 = 7 = 4 > 6 > 12 = 14 = 16 > 5.

Totaling of the antifungal spectrum indexes of the seven most active acids at pH 4.0 and 5.6 for *A. niger*, *T. viride*, and *M. verrucaria* showed that, on a weight basis, the order of fungitoxicity of five types of fatty acids was: 2-alkynoic acids > 2-alkenoic acids > alkanoic acids > 2-bromoalkanoic acids > 2-fluoroalkanoic acids (6). The present results place the alkoxyacetic acids slightly below the activity of the 2-fluoroalkanoic acids. However, as for the 2-fluoroalkanoic acids, the alkoxyacetic acids should possess a longer life within the host and, consequently, reach the parasite in greater concentration than acids susceptible to β-oxidation.

The relative contributions of α-, β-, and ω-oxidative pathways to fatty acid oxidation in rat liver were studied (21). It was reported that α-oxidation was negligible and that β-oxidation of stearic acid was 25 times as rapid as ω-oxidation. For palmitic acid, β-oxidation was even more rapid than for stearic acid.

REFERENCES

(1) H. Gershon and R. Parmegiani, *J. Med. Chem.*, **10**, 186 (1967).

(2) H. Gershon, R. L. Rodin, R. Parmegiani, and P. K. Godfrey, *ibid.*, **13**, 1237 (1970).

(3) H. Gershon, R. L. Rodin, R. Parmegiani, and P. K. Godfrey, *Contrib. Boyce Thompson Inst.*, **24**, 245 (1970).

(4) H. Gershon, M. W. McNeil, R. Parmegiani, P. K. Godfrey, and J. M. Baricko, *Antimicrob. Agents Chemother.*, **4**, 435 (1973).

(5) H. Gershon and L. Shanks, *Can. J. Microbiol.*, **22**, 1198 (1976).

(6) *Ibid.*, **24**, 593 (1978).

(7) *Ibid.*, **21**, 1317 (1975).

(8) H. Gershon, L. Shanks, and D. E. Gawiak, *J. Med. Chem.*, **19**, 1069 (1976).

(9) H. Gershon and L. Shanks, *ibid.*, **20**, 606 (1977).

(10) H. Gershon and L. Shanks, *J. Pharm. Sci.*, **67**, 578 (1978).

(11) A. S. Levine, R. G. Graw, Jr., and R. C. Young, *Semin. Hematol.*, **9**, 141 (1972).

(12) F. L. M. Pattison, R. L. Buchanan, and F. H. Dean, *Can. J. Chem.*, **43**, 1700 (1965).

(13) B. Mayer and J. Asselineau, *C. R. Hébd. Scéances Acad. Sci., Ser. C*, **262**, 668 (1966).

(14) B. Mayer and J. Asselineau, *Chim. Ther.*, **3**, 325 (1968).

(15) H. G. Rule, W. Hay, and J. Paul, *J. Chem. Soc.*, **1928**, 1317.

(16) L. Schreiner, *Justus Liebigs Ann. Chem.*, **197**, 1 (1879).

(17) H. M. Palomaa, *Ann. Acad. Sci. Fenn. Ser. A4*, 1 (1913); through *Chem. Abstr.*, **8**, 1772 (1914).

(18) E. A. Falco, P. B. Russell, and G. H. Hitchings, *J. Am. Chem. Soc.*, **73**, 3753 (1951).

(19) H. Gershon and R. Parmegiani, *Appl. Microbiol.*, **10**, 348 (1962).

(20) H. Gershon, R. Parmegiani, and W. J. Nickerson, *ibid.*, **10**, 556 (1962).

(21) G. J. Antony and B. R. Landau, *J. Lipid Res.*, **9**, 267 (1968).

ACKNOWLEDGMENTS

The authors thank Robin S. Gershon for technical assistance.

Macromerine and Normacromerine Biosynthesis in *Coryphantha macromeris* var. *runyonii*

WILLIAM J. KELLER

Received April 17, 1978, from the *School of Pharmacy, Northeast Louisiana University, Monroe, LA 71209.* Accepted for publication June 22, 1978.

Abstract □ The biosynthetic conversion of epinephrine to normacromerine in *Coryphantha macromeris* (Engelm.) Br. and R. var. *runyonii* (Br. and R.) L. Benson (Cactaceae) has been studied. Metanephrine, which has been isolated from this cactus and is a normal metabolite of epinephrine in mammalian systems, appeared to be the likely intermediate between epinephrine and normacromerine. Normacromerine turnover studies suggested a 16-day interval between metanephrine administration and harvest of the cacti. During this incubation period, the cacti specifically converted 4.77% of the administered DL-7-^{3}H-metanephrine to normacromerine. Based on biochemical precedents, the postulated metabolic fate of normacromerine in the cactus was an enzymatic *N*-methylation to give macromerine. However, radiolabeled normacromerine was a very inefficient precursor to macromerine.

Keyphrases □ Epinephrine—biosynthetic conversion to normacromerine in *Coryphantha macromeris* cactus □ Normacromerine—biosynthetic conversion from epinephrine in *Coryphantha macromeris* cactus □ Macromerine—biosynthetic conversion from epinephrine in *Coryphantha macromeris* cactus □ *Coryphantha macromeris* cactus—biosynthetic conversion of epinephrine to normacromerine

The peyote cactus, *Lophophora williamsii* (Lem.) Coult., is a well-known hallucinogen because of its mescaline (3,4,5-trimethoxyphenethylamine) content (1, 2). The Dona Ana cactus, *Coryphantha macromeris* (Engelm.) Br. and R., is currently being promoted as a legal psychedelic agent and has about one-fifth the potency of peyote (3–7). By far the most abundant alkaloid in *C. macromeris* and its *runyonii* variety is the epinephrine analog normacromerine (*N*-methyl-3,4-dimethoxy-β-hydroxyphenethylamine) (8, 9). A recent study (10), using a battery of tests to evaluate the behavioral effects of various mind-altering substances in laboratory animals, showed normacromerine to be psychoactive. The behavioral effects produced by normacromerine correlated most closely with those associated with mescaline administration.

Keller *et al.* (9) initiated a preliminary study of the biosynthetic pathway leading to the formation of the psychoactive normacromerine in *C. macromeris* var. *runyonii*. A C_6–C_2 pathway, where tyrosine was decarboxylated and the resulting tyramine was converted stepwise to normacromerine, was established (9). Dopa and dopamine were not precursors of normacromerine. The natural occurrence of both epinephrine and norepinephrine in *C. macromeris* var. *runyonii* and the specific conversion of these catecholamines to normacromerine were demonstrated (11). The fact that norepinephrine was metabolized to normacromerine less efficiently than either tyramine or epinephrine indicated a branched biosynthetic pathway.

Metanephrine, a metabolite of epinephrine in mammals (12), was isolated from *C. macromeris* var. *runyonii* (8). Thus, metanephrine appears to be the logical intermediate during the biosynthetic conversion of epinephrine to normacromerine. Once formed in the cactus, normacromerine could undergo *N*-methylation to give macromerine. The present study used radiolabeled metanephrine and normacromerine to investigate this possible biochemical sequence in the cactus.

EXPERIMENTAL[1]

Plant Material—Living specimens of *C. macromeris* var. *runyonii* were obtained commercially[2]. Reference photos of the plants are on file, and live plants are being maintained in a controlled environment chamber[3]. The cacti were watered bimonthly and were maintained on a diurnal cycle of 14 hr of light and 10 hr of dark. The temperature was maintained at 32° during the light period and at 18° during the dark period.

Radioactivity Measurements—Organic samples were solubilized in 2 ml of 95% ethanol before the addition of 10 ml of the scintillation solvent. The solvent consisted of 0.5% 2,5-diphenyloxazole and 0.05% 1,4-bis[2-(4-methyl-5-phenyloxazolyl)]benzene in a toluene–*p*-dioxane (1:1) mixture. Silica gel scrapings were extracted with 2 ml of 95% ethanol before addition of 10 ml of the scintillation solvent. Glass screw-capped liquid scintillation vials were used for all samples.

All radioactive samples were analyzed using a scintillation counter. Three samples were counted routinely, and the reported activities represent an average of these three values. Samples were counted to an error of less than ±1%. The counter efficiency was determined for each sample by the internal standard method using ^{14}C-toluene. A blank value was obtained routinely to determine the magnitude of background radiation.

Chromatography—Analytical silica gel GF-254 TLC plates were prepared in the usual manner, developed with benzene–chloroform–methanol–28% ammonium hydroxide (8:6:5:1), and visualized under shortwave UV light.

Preparative TLC was conducted as previously described (8, 9). Resolution of the nonphenolic alkaloid mixture was accomplished on 1-mm layers of silica gel PF-254 with the previously mentioned solvent system. From 12 to 16 plates were necessary for each isolation of normacromerine and macromerine. After the alkaloids were eluted from the silica gel with methanol, the eluates were filtered, combined, and concentrated under reduced pressure.

Labeled Compounds—DL-7-^{3}H-Metanephrine (label in the β-position) was assayed for chromatographic homogeneity as suggested by the supplier[4], and its radioactivity was determined immediately prior to administration to the cacti.

Generous quantities of (−)-7-^{14}C-normacromerine (label in the β-position) were available from a previous study (11). Chromatographic homogeneity and exact radioactivity were determined immediately before use.

Administration of Precursors—Administration of the precursors was accomplished by injecting aqueous solutions into selected specimens at several aboveground sites. Groups of five plants were used for the normacromerine and macromerine turnover studies while groups of four plants were employed to obtain percent incorporation data. After the precursor solutions were slowly injected, the needle was left in place for a few seconds to allow dispersion. The plants were watered and returned to the growth chamber for incubation immediately after administration of the radioactive compounds.

[1] Melting points were determined using a Fisher model 355 digital melting-point analyzer and are uncorrected. Scintillation counting was conducted using a Beckman model LS-230.

[2] Abbey Garden, Carpenteria, Calif.

[3] Scientific Systems, Baton Rouge, La.

[4] New England Nuclear Corp., Boston, Mass.

0022-3549/79/0100-0085$01.00/0
© 1979, American Pharmaceutical Association

Table I—Specific Activity of Labeled Normacromerine Hydrochloride, Formaldemethone, and Veratraldehyde Semicarbazone from Plants Injected with DL-7-^{3}H-Metanephrine (9.276 mCi/mmole; 540 μCi Administered)

Compound	Crystallization	Yield, mg	Melting Point	Literature Melting Point	Specific Activity, dpm/mmole
Normacromerine	1	460	130–131°	132–133° (14)	3.07×10^7
	2	405	131–132°	—	3.05×10^7
	3	351	131–132°	—	3.04×10^7
Veratraldehyde semicarbazone	1	56	175–176°	177° (15)	2.92×10^7
	2	29	175–176°	—	2.91×10^7
Formaldemethone	1	46	192–193°	193–194° (16)	1.72×10^3

Extraction of Alkaloids—Following the incubation period, the plants were freed from adhering soil, weighed, and processed as previously described (8).

Determination of Optimum Harvesttime—To determine an ideal incubation period, normacromerine turnover was studied after the administration of DL-7-^{3}H-metanephrine. Macromerine turnover also was examined after 7-^{14}C-normacromerine administration.

In each case, identical volumes of an aqueous solution of precursors were injected into each specimen of *C. macromeris* var. *runyonii*. The plants were watered and returned to the controlled environment chamber for incubation. A harvest interval of 4 days was maintained for the metanephrine-treated cacti, with the sacrifice of one plant constituting a harvest. Individual normacromerine-injected plants were harvested after 9, 18, 36, 54, and 72 days. The harvested plant was extracted to yield its nonphenolic alkaloids. A modification of the procedure suggested by Fleming and Clark (13) was used to quantitate the radioactivity associated with the macromerine and/or normacromerine after analytical TLC. Details of this method were described previously (9).

Isolation and Identification of Macromerine and Normacromerine—In all cases where macromerine and normacromerine were isolated from the nonphenolic fraction, preparative TLC was used. The identity of the isolated alkaloid was established by cochromatography and melting-point determinations on the hydrochloride derivative. The normacromerine hydrochloride was crystallized three times to establish radiochemical purity; the radioactivity of 5-mg portions was determined in triplicate after each crystallization. Macromerine hydrochloride was crystallized one time, and its radioactivity was determined in triplicate following this single crystallization.

Periodate Degradation of Normacromerine—The isolated normacromerine from the DL-7-^{3}H-metanephrine-treated cacti was degraded with sodium periodate to locate the position of the tritium label in the molecule to determine the degree of label randomization and/or the presence of radioactive contaminants. A portion of the isolated normacromerine hydrochloride (200 mg) was dissolved in 10 ml of 0.1 *M* phosphate buffer (pH 6.2), and 220 mg of sodium periodate was added to this solution. After stirring at room temperature for 15 min, the pH of the reaction mixture was adjusted to 4.0 (pH paper) with 10% acetic acid, followed by the immediate addition of 40 ml of 0.5% dimedone (5,5-dimethyl-1,3-cyclohexanedione). After 3 hr of refrigeration, the dimedone derivative of the liberated formaldehyde (formaldemethone) was filtered and recrystallized from ethanol–water.

The filtrate was extracted with two 50-ml volumes of ether, and the ether extract was evaporated *in vacuo*. After the residue was dissolved in 10 ml of an ethanol–water mixture, 100 mg of semicarbazide hydrochloride and 150 mg of sodium acetate were added, followed by 1 min of boiling. Overnight refrigeration induced the crystallization of veratraldehyde semicarbazone. This derivative was filtered and recrystallized from an ethanol–water mixture. The radioactivity associated with each degradation product was measured as previously described.

RESULTS AND DISCUSSION

Keller (11) observed that the radioactivity associated with normacromerine reached a maximum between 20 and 24 days after administration of DL-7-^{14}C-epinephrine. When considering that metanephrine is only one biosynthetic step from normacromerine, an incubation period of 20–24 days may not be ideal for the suspected precursor. To investigate this possibility, normacromerine turnover was examined in the living cacti after the administration of DL-7-^{3}H-metanephrine. Maximum incorporation of radioactivity into normacromerine occurred within 16 days after precursor administration. Consequently, in the subsequent experiment, the plants were harvested and processed 16 days after administration of labeled metanephrine.

Table II—Percent Distribution of Activity per Millimole after Administration of (−)-7-^{14}C-Normacromerine

Harvest Day	Normacromerine	Macromerine
9	99	1
18	97	3
36	96	4
54	98	2
72	100	0

To evaluate the significance of metanephrine in normacromerine biosynthesis, four cacti were injected with aqueous DL-7-^{3}H-metanephrine. These plants yielded 460 mg of normacromerine hydrochloride after the first crystallization. After the hydrochloride was recrystallized twice from absolute ethanol–ether, the specific activity remained relatively constant. Based on the total activity of DL-7-^{3}H-metanephrine administered to the cacti, 4.77% was recovered as crystalline normacromerine hydrochloride. The periodate degradation revealed that 96% of the activity in the labeled normacromerine hydrochloride was associated with the β-position (Table I).

Once formed in the cactus, the most logical metabolic fate of normacromerine appears to be *N*-methylation to give macromerine. To examine this possibility, four plants were injected with an aqueous solution of (−)-7-^{14}C-normacromerine hydrochloride (2.82 μCi/mmole; 0.57 μCi administered). After an 18-day incubation, these plants were harvested and extracted as usual. The nonphenolic fraction yielded 75 mg of macromerine hydrochloride. The radioactivity associated with this material was barely above background values. Based on the total activity of (−)-7-^{14}C-normacromerine hydrochloride administered to the cacti, only 0.0005% was recovered as crystalline macromerine hydrochloride. Because of this very low activity, the isolated macromerine hydrochloride was not chemically degraded.

One possible explanation for the poor incorporation of normacromerine into macromerine might be that the *N*-methylation of normacromerine is a very slow process in the cactus. This possibility was explored by measuring macromerine turnover after administration of (−)-7-^{14}C-normacromerine. The cacti were harvested at selected intervals over 72 days. The radioactivity associated with normacromerine also was determined for each harvest. Table II presents the percent of the total macromerine–normacromerine activity associated with the individual compounds from each harvest.

The results of this investigation indicate metanephrine to be the immediate precursor to normacromerine in *C. macromeris* var. *runyonii*. Since very little normacromerine was converted to macromerine over 72 days, *N*-methylation of normacromerine appears not to be a major biosynthetic route. Macromerine may be biosynthetically derived from *N*-methylmetanephrine, a compound known to occur in the cactus (8). Alternatively, macromerine may be demethylated to form normacromerine. Experiments designed to answer these questions are in progress.

REFERENCES

(1) G. J. Kapadia and M. B. E. Fayez, *Lloydia*, **36**, 9 (1973).

(2) P. Brawley and J. C. Duffield, *Pharmacol. Rev.*, **24**, 31 (1972).

(3) H. Grubber, "Growing the Hallucinogens," Level Press, San Francisco, Calif., 1973, p. 13.

(4) A. Gottlieb, "Peyote and Other Psychoactive Cacti," Kistone Press, San Francisco, Calif., 1977, p. 6.

(5) J. Mann, "The First Book of Sacraments of the Tree of Life," Tree of Life Press, San Francisco, Calif., 1972, p. 15.

(6) M. J. Superweed, "Home Grown Highs," Stone Kingdom Syndicate, San Francisco, Calif., 1972, p. 6.

(7) M. J. Superweed, "Herbal Highs," Stone Kingdom Syndicate, San Francisco, Calif., 1970, p. 5.

(8) W. J. Keller, J. L. McLaughlin, and L. R. Brady, *J. Pharm. Sci.*, **62**, 408 (1973).

(9) W. J. Keller, L. A. Spitznagle, L. R. Brady, and J. L. McLaughlin, *Lloydia*, **36**, 397 (1973).

(10) W. M. Bourn, W. J. Keller, and J. F. Bonfiglio, *Life Sci.*, **23**, 1175 (1978).

(11) W. J. Keller, *Lloydia*, **41**, 37 (1978).
(12) P. B. Molinoff and J. Axelrod, *Annu. Rev. Biochem.*, **40**, 465 (1971).
(13) R. M. Fleming and W. G. Clark, *J. Chromatogr.*, **52**, 305 (1970).
(14) W. J. Keller and J. L. McLaughlin, *J. Pharm. Sci.*, **61**, 147 (1972).
(15) R. L. Shriner, R. C. Fuson, and D. Y. Curtin, "The Systematic Identification of Organic Compounds," Wiley, New York, N.Y., 1965, p. 321.
(16) D. G. O'Donovan and H. Horan, *J. Chem. Soc. C*, **1968**, 2791.

ACKNOWLEDGMENTS

Supported by grants from the Cactus and Succulent Society of America and the Northeast Louisiana University Research Council.

Papaver bracteatum Lindl.: Quantitative Extraction and Determination of Thebaine

P. G. VINCENT *x, W. A. GENTNER *, F. J. E. M. KÜPPERS ‡, and C. A. SALEMINK ‡

Received April 24, 1978, from the **Science and Education Administration, Federal Research, Beltsville Agricultural Research Center, U.S. Department of Agriculture, Beltsville, MD 20705*, and the ‡*Department of Organic Chemistry of Natural Products, State University of Utrecht, Utrecht, The Netherlands.* Accepted for publication June 22, 1978.

Abstract □ An interlaboratory procedure for the quantitative extraction and analysis of thebaine from different tissues of *Papaver bracteatum* Lindl. is presented. Each step was evaluated for the yield of thebaine by use of 1-^{3}H-thebaine and GLC. The method of drying and milling of tissue and the size of resultant particles were important factors in the quantitative recovery of thebaine.

Keyphrases □ *Papaver bracteatum*—various plant tissues, extraction and analysis of thebaine □ Thebaine—extraction and analysis from various plant tissues of *Papaver bracteatum* □ Alkaloids—thebaine, extraction and analysis from various plant tissues of *Papaver bracteatum* □ Narcotics—thebaine, extraction and analysis from various plant tissues of *Papaver bracteatum*

Papaver bracteatum Lindl. is being evaluated as a source of the alkaloid thebaine from which codeine may be derived (1, 2). Methods for the analysis of thebaine include quantitative TLC followed by spectrophotometry (3), colorimetry (4), GLC (5, 6), and high-speed liquid chromatography (7, 8).

A United Nations Working Group on *P. bracteatum* (9) recommended a general method for thebaine analysis. In this study, each step of the method is presented for the analysis of thebaine in roots, leaves, and capsules of *P. bracteatum*. The purposes of this investigation were to maximize the yield of thebaine and to provide a basis for comparison of interlaboratory results of analysis of thebaine in such tissues.

EXPERIMENTAL

Plant Culture—The seed source and plant culture were previously described[1] (6).

Preparation of Tritiated Thebaine—1-^{3}H-Thebaine was prepared by the acid-catalyzed tritiation of salutaridine, followed by borohydride reduction to the epimeric salutaridinols and subsequent conversion to thebaine. The entire sequence was first performed on the deuterated analogs, which permitted unambiguous assignment of the label to the 1-position by NMR and mass spectrometry. The specific activity was 6.17 μCi/mg.

Sample Preparation—The effects on thebaine yield of oven drying (60°) *versus* freeze drying of plant tissue were compared. The effect of ball[2] or blade[3] milling was evaluated, as was the influence of particle size on thebaine recovery. The residual water content of samples before analyses was determined. Thebaine extractions with 5% aqueous acid and methanol–ammonium hydroxide (98:2) were compared. The efficiencies of other extracting solvents (5) are also discussed.

Assay—Thebaine was determined as previously described (6).

RESULTS AND DISCUSSION

(−)-Thebaine (I) (except for the position of the double bonds), (−)-codeine (II), and (−)-morphine (III) have the same skeletal structure and absolute configuration.

Apparently, thebaine was not stable at 60°. Thebaine, present at time of harvest, may have been transformed during heat drying into other compounds, as evidenced by the appearance of unidentified "alkaloidal" substances on thin-layer chromatograms following drying and by the appearance of several radioactive substances following addition of 1-^{3}H-thebaine to plant tissues before drying. The mechanism and nature of the additional substances derived from thebaine during oven drying have not been studied adequately; however, enzymatic and/or physical factors undoubtedly are involved in the transformation processes. No additional products from thebaine were observed when tissues were freeze dried, as measured by TLC of tissue extracts to which 1-^{3}H-thebaine had been added.

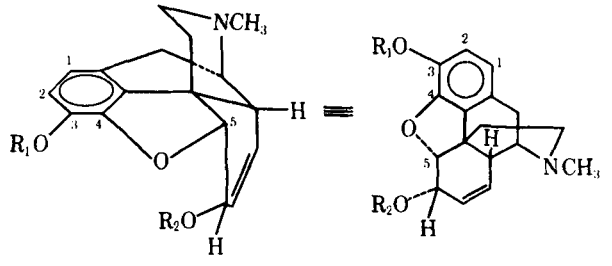

I: $R_1 = R_2 = CH_3$ (double bonds between C6—7 and C8—14)
II: $R_1 = CH_3$, $R_2 = H$
III: $R_1 = R_2 = H$

[1] The plant material was identified as *Papaver bracteatum* Lindl. by Dr. P. G. Vincent and M. L. Stiff, U.S. Department of Agriculture, Beltsville, Md. A voucher (preserved and living) specimen (see Ref. 6 for numbers) representing material collected for this investigation is available for inspection at the U.S. Department of Agriculture, Beltsville, Md.

[2] Dangoumau quantitative microgrinder; Prolabo, Microbroyeur Quantitatif Dangoumau, Appareil No. 07-449.02, France.

[3] Wiley.

0022-3549/79/0100-0087$01.00/0
© 1979, American Pharmaceutical Association

(11) W. J. Keller, *Lloydia*, **41**, 37 (1978).
(12) P. B. Molinoff and J. Axelrod, *Annu. Rev. Biochem.*, **40**, 465 (1971).
(13) R. M. Fleming and W. G. Clark, *J. Chromatogr.*, **52**, 305 (1970).
(14) W. J. Keller and J. L. McLaughlin, *J. Pharm. Sci.*, **61**, 147 (1972).
(15) R. L. Shriner, R. C. Fuson, and D. Y. Curtin, "The Systematic Identification of Organic Compounds," Wiley, New York, N.Y., 1965, p. 321.
(16) D. G. O'Donovan and H. Horan, *J. Chem. Soc. C*, **1968**, 2791.

ACKNOWLEDGMENTS

Supported by grants from the Cactus and Succulent Society of America and the Northeast Louisiana University Research Council.

Papaver bracteatum Lindl.: Quantitative Extraction and Determination of Thebaine

P. G. VINCENT *x, W. A. GENTNER *, F. J. E. M. KÜPPERS ‡, and C. A. SALEMINK ‡

Received April 24, 1978, from the **Science and Education Administration, Federal Research, Beltsville Agricultural Research Center, U.S. Department of Agriculture, Beltsville, MD 20705*, and the ‡*Department of Organic Chemistry of Natural Products, State University of Utrecht, Utrecht, The Netherlands.* Accepted for publication June 22, 1978.

Abstract □ An interlaboratory procedure for the quantitative extraction and analysis of thebaine from different tissues of *Papaver bracteatum* Lindl. is presented. Each step was evaluated for the yield of thebaine by use of 1-^{3}H-thebaine and GLC. The method of drying and milling of tissue and the size of resultant particles were important factors in the quantitative recovery of thebaine.

Keyphrases □ *Papaver bracteatum*—various plant tissues, extraction and analysis of thebaine □ Thebaine—extraction and analysis from various plant tissues of *Papaver bracteatum* □ Alkaloids—thebaine, extraction and analysis from various plant tissues of *Papaver bracteatum* □ Narcotics—thebaine, extraction and analysis from various plant tissues of *Papaver bracteatum*

Papaver bracteatum Lindl. is being evaluated as a source of the alkaloid thebaine from which codeine may be derived (1, 2). Methods for the analysis of thebaine include quantitative TLC followed by spectrophotometry (3), colorimetry (4), GLC (5, 6), and high-speed liquid chromatography (7, 8).

A United Nations Working Group on *P. bracteatum* (9) recommended a general method for thebaine analysis. In this study, each step of the method is presented for the analysis of thebaine in roots, leaves, and capsules of *P. bracteatum*. The purposes of this investigation were to maximize the yield of thebaine and to provide a basis for comparison of interlaboratory results of analysis of thebaine in such tissues.

EXPERIMENTAL

Plant Culture—The seed source and plant culture were previously described[1] (6).

Preparation of Tritiated Thebaine—1-^{3}H-Thebaine was prepared by the acid-catalyzed tritiation of salutaridine, followed by borohydride reduction to the epimeric salutaridinols and subsequent conversion to thebaine. The entire sequence was first performed on the deuterated analogs, which permitted unambiguous assignment of the label to the 1-position by NMR and mass spectrometry. The specific activity was 6.17 μCi/mg.

Sample Preparation—The effects on thebaine yield of oven drying (60°) *versus* freeze drying of plant tissue were compared. The effect of ball[2] or blade[3] milling was evaluated, as was the influence of particle size on thebaine recovery. The residual water content of samples before analyses was determined. Thebaine extractions with 5% aqueous acid and methanol–ammonium hydroxide (98:2) were compared. The efficiencies of other extracting solvents (5) are also discussed.

Assay—Thebaine was determined as previously described (6).

RESULTS AND DISCUSSION

(−)-Thebaine (I) (except for the position of the double bonds), (−)-codeine (II), and (−)-morphine (III) have the same skeletal structure and absolute configuration.

Apparently, thebaine was not stable at 60°. Thebaine, present at time of harvest, may have been transformed during heat drying into other compounds, as evidenced by the appearance of unidentified "alkaloidal" substances on thin-layer chromatograms following drying and by the appearance of several radioactive substances following addition of 1-^{3}H-thebaine to plant tissues before drying. The mechanism and nature of the additional substances derived from thebaine during oven drying have not been studied adequately; however, enzymatic and/or physical factors undoubtedly are involved in the transformation processes. No additional products from thebaine were observed when tissues were freeze dried, as measured by TLC of tissue extracts to which 1-^{3}H-thebaine had been added.

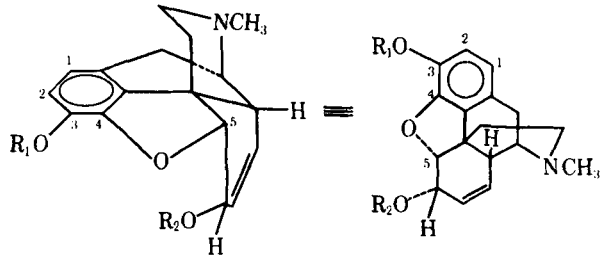

I: $R_1 = R_2 = CH_3$ (double bonds between C6—7 and C8—14)
II: $R_1 = CH_3$, $R_2 = H$
III: $R_1 = R_2 = H$

[1] The plant material was identified as *Papaver bracteatum* Lindl. by Dr. P. G. Vincent and M. L. Stiff, U.S. Department of Agriculture, Beltsville, Md. A voucher (preserved and living) specimen (see Ref. 6 for numbers) representing material collected for this investigation is available for inspection at the U.S. Department of Agriculture, Beltsville, Md.

[2] Dangoumau quantitative microgrinder; Prolabo, Microbroyeur Quantitatif Dangoumau, Appareil No. 07-449.02, France.

[3] Wiley.

0022-3549/79/0100-0087$01.00/0
© 1979, American Pharmaceutical Association

Table I—Distribution of Particle Sizes from Root Tissues of *P. bracteatum* Prepared by Ball Milling or by Blade Milling

Particle Size[a]	Ball Mill		Blade Mill	
	g	%	g	%
>40 (420 μm)	0.333	2.6	0.137	0.8
40–70 (420–210 μm)	0.533	4.2	2.647	16.1
70–140 (210–105 μm)	6.503	51.2	10.162	61.9
140–260 (105–56 μm)	2.713	21.4	1.772	10.8
<260 (56 μm)	2.618	20.6	1.707	10.4

[a] Particle size was determined by sieving after 2 min of ball milling and after passing 40- and 60-mesh sieves of blade milling.

Table II—Effect of Type of Milling on Recovery of Thebaine from Root and Capsule Tissues from *P. bracteatum*

Mill Type	Mean Thebaine[a], μg		
	Capsule	Root	Capsule[b]
Blade	2927	843	—
Ball	2730	1266	—
Total elution[c]	3497	1579	3385

[a] Triplicate GLC analyses from three replicate 250-mg samples of milled tissue. Samples were adjusted for residual water content. [b] Capsule tissue spiked with 1-^{3}H-thebaine. [c] Total elution refers to 250-mg tissue samples placed on a glass chromatographic column with glass wool at the bottom and 1 liter of 5% aqueous acetic acid eluted over the sample during 12 hr. Tissue was ball milled.

Drying of Plant Tissue—Oven drying of plant tissue at 60° and freeze drying at −55° were compared. In all tissue types extracted (*i.e.*, root, aboveground parts, stem, and capsule), 13–17% less thebaine was extracted from the oven-dried tissues than from freeze-dried tissues. Root tissue from identical sources prepared in a manner differing only in the method of drying gave thebaine values of 5.91 μg/mg of tissue *versus* 7.14 μg/mg of tissue for oven-dried and freeze-dried tissue, respectively. Fairbairn and Helliwell (10) reported that drying at 105° rather than 60° led to no loss of thebaine, but they did not evaluate freeze drying.

Extraction Solvent—The efficacy of acetic acid (5% aqueous) and methanol–ammonium hydroxide (98:2) as extraction solvents was evaluated since these two systems are widely used. Other solvent systems and various extraction conditions were studied previously (5). Numerous analyses of all types of plant tissues consistently showed that the aqueous acetic acid (5%) extraction was 22–25% more efficient in extracting thebaine than methanol–ammonium hydroxide (98:2). The acetic acid extraction may have been more efficient because thebaine probably exists as a quaternary salt in the plant and protonation of the molecule under dilute acid conditions in an aqueous system favors "release" of the alkaloid.

One problem that may exist with tissue extraction under mild acid conditions is that acid-catalyzed reactions may result from protonation of the nitrogen atom and produce reactive salts. Acid-catalyzed reaction products were detected and will be the subject of a future study.

Purification Protocol—The procedure for extraction and purification of plant tissues is as follows.

Harvest the plant, freeze dry the plant parts (24-hr minimum), and grind the material (2 min by ball milling). Weigh a 100–500-mg sample and place it in a flask with 30 ml of extraction solvent [5% aqueous acetic acid (v/v)]. Weigh a sample for dry weight determination and determine the dry weight after 12 hr at 100°.

Agitate the sample in the extraction solvent for 1 hr. With a Büchner funnel, filter[4] the sample. Wash the flask three times with 10-ml portions of extracting solvent and also wash the sides of the funnel. Rinse out a 500-ml evaporating flask and a funnel with 10 ml of extracting solvent. Pour the filtered sample through the funnel into the evaporating flask and wash the flask with 10 ml of extracting solvent.

Combine the extracts. Wash the extracts three times with 25 ml of ether when pigments, *i.e.*, from stems and leaf tissue, are to be removed. Adjust the aqueous phase to pH 9.5 with concentrated ammonium hydroxide and add it to a separator. Wash the beaker with 10 ml of chloroform. Then add 20 ml of redistilled chloroform, shake, and release gas three times.

Tap off the chloroform phase containing the alkaloids (bottom phase) and keep it. Add 30 ml of chloroform to the water phase (top phase) and shake. Repeat the procedure two more times. Backwash the chloroform phase with 30 ml of 0.1 *N* NH_4OH and discard the water phase (top phase).

Collect the chloroform phase in an evaporating flask and evaporate it to dryness *in vacuo* (50°) under nitrogen. (Residual water, if present, may be removed under a stream of dry nitrogen gas.) Add 1 ml of ethanol containing an internal standard[5]. Then inject a 1–2-μl aliquot into the chromatograph and compare the peaks to the standards.

The GLC columns were glass, packed with 2% OV-17 on 100–120-mesh Gas Chrom Q.

Sample Preparation—Particle size and weight correction were important in the determination of thebaine from tissues of *P. bracteatum* prepared by ball milling or blade milling (Table I). Data showed a greater percentage of fines; *i.e.*, more 105–56-μm particles were produced by ball milling than by blade milling. A finer particle size offered a greater surface area for solvent extraction. A similar percent distribution of particle sizes was found when leaf, stem, or capsule tissues were ball or blade milled. Blade milling of capsule tissue was difficult because tissues gummed behind the blades; gumming resulted from the high lipid content even though seeds were removed before processing.

Table II shows the effect of milling type on the recovery of thebaine from root and capsule tissue of *P. bracteatum*. The thebaine content of capsule tissue did not differ between the two milling types, but large differences were evident for root tissue, *i.e.*, 33% less in blade-milled than in ball-milled tissue. To determine the maximum thebaine recoverable, 1 g of capsule tissue was placed in a 5-cm diameter glass column and eluted with 5% aqueous acetic acid. One liter of the acid was allowed to pass over the tissue for 12 hr, and the eluant was collected in a flask containing ammonium hydroxide. In some experiments, 1-^{3}H-thebaine was added to the capsule tissue before elution.

For total elution of unspiked and spiked thebaine tissue, an average of 3442 ± 80 μg of thebaine was recovered. Total elution (Table II) with 5% aqueous acetic acid of capsule tissue yielded ~18% more thebaine than tissue incubated in the same solvent 1 hr before shake extraction, regardless of the type of milling. When 1-^{3}H-thebaine was added to any of the particle classes of tissues and extracted with aqueous acid for 1 hr, about 99% of the radioactivity was in the extract and supernate. About 0.06% of the radioactivity remained in the marc. For root tissue, 17 and 45% less thebaine were recovered after ball and blade milling, respectively, than after total elution. In root and capsule tissue, 1% of the isotope was recovered from the marc. No isotope exchange or degradation of the 1-^{3}H-thebaine was observed.

Particle size and, hence, effective surface area affected thebaine yield. On a total dry weight basis, the fines yielded the greatest quantity of thebaine, although there were few differences between the particle-size classes on a concentration basis. In the formation of particle classes, some cell-type segregation may occur; *i.e.*, lacticifers are much finer cell types than sclerenchyma. Physical processes are probably also involved such as surface area phenomena, speed of diffusion from the particle, irreversible absorption or adsorption to the particle, "bound" thebaine (10), and other complex interactions.

These data suggested that there were inherent difficulties in comparison of thebaine content in tissues milled by different techniques. Thus, milling devices should be standardized for interlaboratory comparisons. Thebaine yield apparently was higher and more consistent when ball milling was used. Therefore, the effect of time of ball milling of *P. bracteatum* capsule tissue on the distribution of particle size and thebaine content was studied (Table III).

In each of the four time periods, thebaine yields were consistently the highest in the >260-mesh fraction and lowest in the <40-mesh fraction. A milling time of 2 min gave the highest average yield of thebaine. Thebaine yields decreased as milling time was increased beyond 2 min. This decrease may have resulted, in part, from heat generated from friction by the high velocity movement of the balls. The heat produced may have acted as a catalyst in the presence of natural plant acids for the decomposition of thebaine.

Sample Size—A wide weight range (5 mg–1 g) of sample sizes of the plant tissues was analyzed for thebaine. Reproducibility was greatest in samples with weights of 250 mg because of tissue availability (<2% deviation between replicates), although 100-mg samples were adequate providing they were taken from a homogeneous source. Particle segregation during storage gave samples for extraction and GLC analysis that were highly variable. Therefore, stored milled tissues were mixed thoroughly before subsampling for thebaine analysis.

GLC Determination of Thebaine—Thebaine was determined quantitatively by GLC, and the results were corroborated by TLC and spectrophotometry at 285 nm (6). Working limits for linear detector re-

[4] Whatman No. 3 paper.

[5] Internal standards were cholesterol acetate and tetrahydrothebaine (1 mg/ml).

Table III—Effect of Time of Ball Milling of *P. bracteatum* Capsule Tissues on Distribution of Particle Size and Thebaine Content [a]

Milling Time, min	Mesh Size	Sieve Weight g	Sieve Weight %	Thebaine Weight, %	$\bar{x}$	Δ%[b]
1.0	>40	4.77	27	1.12		
	40–70	4.62	26	1.20		
	70–140	6.41	36	1.31	1.264	−1.7
	140–260	1.19	6	1.60		
	<260	0.95	5	1.64		
2.0	>40	0.92	4	0.99		
	40–70	4.14	17	1.06		
	70–140	11.63	47	1.21	1.286	—
	140–260	4.59	19	1.51		
	<260	3.26	13	1.62		
3.0	>40	0.22	2	0.95		
	40–70	1.18	8	0.96		
	70–140	7.30	48	1.07	1.229	−4.4
	140–260	1.90	13	1.35		
	<260	4.30	29	1.53		
4.5	>40	0.09	1	0.83		
	40–70	0.33	2	0.89		
	70–140	7.12	47	1.06	1.227	−4.6
	140–260	3.10	20	1.31		
	<260	4.57	30	1.47		

[a] Capsules were deseeded, crushed, freeze dried for 24 hr, and ball milled. [b] Percent difference from 2 min of milling time thebaine yields.

sponse were 0.1–1.0 μg of thebaine/sample. Detector and/or integrator saturation occurred when the thebaine concentration per GLC injection exceeded ~2 μg. Reproducibility between triplicate analyses at each concentration of alkaloid was ±1%. Integrator responses to samples yielding $<10^5$ μv/sec were reanalyzed to give counts $>10^5$ either by adjustment of the injection volume or by increased electrometer sensitivity.

Linear detector responses for isothebaine, papaverine, alpinigenine, laudanosine, salutaridine, reticuline, and several additional alkaloids from *Papaver* except morphine were similar. The detector response was not linear with morphine because it severely tailed under GLC conditions, possibly because of adsorption onto the column. Morphine was calibrated as its *N,O*-bis(trimethylsilyl)acetamide derivative for samples suspected of containing this alkaloid but was not usually included in standard calibration mixtures.

GLC flame-ionization responses to varying concentrations of thebaine *versus* a constant level of cholesterol acetate were linear throughout the range analyzed. Linear ratio detector responses also were obtained when tetrahydrothebaine was used as an internal standard. The disadvantage of tetrahydrothebaine in routine analyses, alone or in combination with cholesterol acetate, was its relatively short retention time, especially at high column temperatures. Tetrahydrothebaine usually eluted from the GLC column as a rider to the solvent peak, which may have complicated manual peak area determinations. Laudanosine, antipyrine, and tetrahydropalmatine were not suitable for use as internal standards in GLC analyses, although they were recommended by the Third Working Group on *P. bracteatum* (9).

A small quantity of thebaine (<1%) always adsorbed to new OV-17–Gas Chrom Q columns. Saturating the columns with an alkaloid standard containing thebaine (~0.2–0.4 μg) by injection of standard mixtures obviated this problem. Calibration solutions consisted of 1 μg of cholesterol acetate plus 0.2–1 μg each of thebaine, isothebaine, and codeine in 1 ml of absolute ethanol.

By carefully standardizing and checking each step of the procedure for loss of thebaine, it was determined that this procedure can be used for comparison of intra- and interlaboratory analyses.

REFERENCES

(1) United Nations Division of Narcotic Drugs, Scientific Research on *P. bracteatum*, ST/SOA/SER.J/1, Geneva, Switzerland, 1973.

(2) United Nations Division of Narcotic Drugs, Scientific Research on *P. bracteatum*, ST/SOA/SER.J/2, Geneva, Switzerland, 1973.

(3) J. W. Fairbairn and F. Hakim, *J. Pharm. Pharmacol.*, **25**, 353 (1973).

(4) H. Sakuri, *J. Pharm. Soc. Jpn.*, **30**, 909 (1960).

(5) P. G. Vincent and W. A. Gentner, United Nations Secretariat, Division of Narcotic Drugs, Scientific Research on *P. Bracteatum*, ST/SOA/SER.J/9, Geneva, Switzerland, 1974.

(6) P. G. Vincent, C. E. Bare, and W. A. Gentner, *J. Pharm. Sci.*, **66**, 1716 (1977).

(7) R. Verpoorte and A. B. Svendsen, *J. Chromatogr.*, **100**, 227 (1974).

(8) D. W. Smith, T. H. Beasley, Jr., R. L. Charles, and H. W. Zieler, *J. Pharm. Sci.*, **62**, 1961 (1973).

(9) United Nations Division of Narcotic Drugs, Scientific Research on *P. bracteatum*, Document ST/SOA/SER.J/15, Geneva, Switzerland, 1974.

(10) J. W. Fairbairn and K. Helliwell, *J. Pharm. Pharmacol.*, **27**, 217 (1975).

ACKNOWLEDGMENTS

The authors thank Merck Sharp and Dohme for providing 1-^{3}H-thebaine.

^{13}C-NMR Spectra of Strychnos Alkaloids: Brucine and Strychnine

SHIVA P. SINGH *, VIRGIL I. STENBERG ‡, SURENDRA S. PARMAR *ˣ, and SYLVIA A. FARNUM ‡

Received October 14, 1977, from the **Department of Physiology, School of Medicine, and the* ‡*Department of Chemistry, University of North Dakota, Grand Forks, ND 58202.* Accepted for publication June 27, 1978.

Abstract □ The natural abundance ^{13}C-NMR spectra of brucine and strychnine were obtained using the pulse Fourier transform technique. The chemical shifts of various carbon resonances were assigned on the basis of substituent effects on benzene shifts, intensities of signals, multiplicities generated in single-frequency off-resonance-decoupled spectra, and comparisons with the chemical shifts of structurally related compounds.

Keyphrases □ Brucine—^{13}C-NMR spectrometry, chemical shifts assigned □ Strychnine—^{13}C-NMR spectrometry, chemical shifts assigned □ ^{13}C-NMR spectrometry—brucine and strychnine, chemical shifts assigned

Several literature reports show the correlation of the structure of the various classes of alkaloids with their ^{13}C-NMR spectra (1–6). The structure and stereochemistry of strychnos alkaloids, brucine (I) and strychnine (II), were characterized (7, 8), but no reports are available concerning the assignments of their carbon resonances.

© 1979, American Pharmaceutical Association

Table III—Effect of Time of Ball Milling of *P. bracteatum* Capsule Tissues on Distribution of Particle Size and Thebaine Content [a]

Milling Time, min	Mesh Size	Sieve Weight g	Sieve Weight %	Thebaine Weight, %	$\bar{x}$	Δ%[b]
1.0	>40	4.77	27	1.12		
	40–70	4.62	26	1.20		
	70–140	6.41	36	1.31	1.264	−1.7
	140–260	1.19	6	1.60		
	<260	0.95	5	1.64		
2.0	>40	0.92	4	0.99		
	40–70	4.14	17	1.06		
	70–140	11.63	47	1.21	1.286	—
	140–260	4.59	19	1.51		
	<260	3.26	13	1.62		
3.0	>40	0.22	2	0.95		
	40–70	1.18	8	0.96		
	70–140	7.30	48	1.07	1.229	−4.4
	140–260	1.90	13	1.35		
	<260	4.30	29	1.53		
4.5	>40	0.09	1	0.83		
	40–70	0.33	2	0.89		
	70–140	7.12	47	1.06	1.227	−4.6
	140–260	3.10	20	1.31		
	<260	4.57	30	1.47		

[a] Capsules were deseeded, crushed, freeze dried for 24 hr, and ball milled. [b] Percent difference from 2 min of milling time thebaine yields.

sponse were 0.1–1.0 μg of thebaine/sample. Detector and/or integrator saturation occurred when the thebaine concentration per GLC injection exceeded ~2 μg. Reproducibility between triplicate analyses at each concentration of alkaloid was ±1%. Integrator responses to samples yielding $<10^5$ μv/sec were reanalyzed to give counts $>10^5$ either by adjustment of the injection volume or by increased electrometer sensitivity.

Linear detector responses for isothebaine, papaverine, alpinigenine, laudanosine, salutaridine, reticuline, and several additional alkaloids from *Papaver* except morphine were similar. The detector response was not linear with morphine because it severely tailed under GLC conditions, possibly because of adsorption onto the column. Morphine was calibrated as its *N,O*-bis(trimethylsilyl)acetamide derivative for samples suspected of containing this alkaloid but was not usually included in standard calibration mixtures.

GLC flame-ionization responses to varying concentrations of thebaine *versus* a constant level of cholesterol acetate were linear throughout the range analyzed. Linear ratio detector responses also were obtained when tetrahydrothebaine was used as an internal standard. The disadvantage of tetrahydrothebaine in routine analyses, alone or in combination with cholesterol acetate, was its relatively short retention time, especially at high column temperatures. Tetrahydrothebaine usually eluted from the GLC column as a rider to the solvent peak, which may have complicated manual peak area determinations. Laudanosine, antipyrine, and tetrahydropalmatine were not suitable for use as internal standards in GLC analyses, although they were recommended by the Third Working Group on *P. bracteatum* (9).

A small quantity of thebaine (<1%) always adsorbed to new OV-17–Gas Chrom Q columns. Saturating the columns with an alkaloid standard containing thebaine (~0.2–0.4 μg) by injection of standard mixtures obviated this problem. Calibration solutions consisted of 1 μg of cholesterol acetate plus 0.2–1 μg each of thebaine, isothebaine, and codeine in 1 ml of absolute ethanol.

By carefully standardizing and checking each step of the procedure for loss of thebaine, it was determined that this procedure can be used for comparison of intra- and interlaboratory analyses.

REFERENCES

(1) United Nations Division of Narcotic Drugs, Scientific Research on *P. bracteatum*, ST/SOA/SER.J/1, Geneva, Switzerland, 1973.

(2) United Nations Division of Narcotic Drugs, Scientific Research on *P. bracteatum*, ST/SOA/SER.J/2, Geneva, Switzerland, 1973.

(3) J. W. Fairbairn and F. Hakim, *J. Pharm. Pharmacol.*, **25**, 353 (1973).

(4) H. Sakuri, *J. Pharm. Soc. Jpn.*, **30**, 909 (1960).

(5) P. G. Vincent and W. A. Gentner, United Nations Secretariat, Division of Narcotic Drugs, Scientific Research on *P. Bracteatum*, ST/SOA/SER.J/9, Geneva, Switzerland, 1974.

(6) P. G. Vincent, C. E. Bare, and W. A. Gentner, *J. Pharm. Sci.*, **66**, 1716 (1977).

(7) R. Verpoorte and A. B. Svendsen, *J. Chromatogr.*, **100**, 227 (1974).

(8) D. W. Smith, T. H. Beasley, Jr., R. L. Charles, and H. W. Zieler, *J. Pharm. Sci.*, **62**, 1961 (1973).

(9) United Nations Division of Narcotic Drugs, Scientific Research on *P. bracteatum*, Document ST/SOA/SER.J/15, Geneva, Switzerland, 1974.

(10) J. W. Fairbairn and K. Helliwell, *J. Pharm. Pharmacol.*, **27**, 217 (1975).

ACKNOWLEDGMENTS

The authors thank Merck Sharp and Dohme for providing 1-^{3}H-thebaine.

^{13}C-NMR Spectra of Strychnos Alkaloids: Brucine and Strychnine

SHIVA P. SINGH *, VIRGIL I. STENBERG ‡, SURENDRA S. PARMAR *ˣ, and SYLVIA A. FARNUM ‡

Received October 14, 1977, from the **Department of Physiology, School of Medicine, and the* ‡*Department of Chemistry, University of North Dakota, Grand Forks, ND 58202.* Accepted for publication June 27, 1978.

Abstract □ The natural abundance ^{13}C-NMR spectra of brucine and strychnine were obtained using the pulse Fourier transform technique. The chemical shifts of various carbon resonances were assigned on the basis of substituent effects on benzene shifts, intensities of signals, multiplicities generated in single-frequency off-resonance-decoupled spectra, and comparisons with the chemical shifts of structurally related compounds.

Keyphrases □ Brucine—^{13}C-NMR spectrometry, chemical shifts assigned □ Strychnine—^{13}C-NMR spectrometry, chemical shifts assigned □ ^{13}C-NMR spectrometry—brucine and strychnine, chemical shifts assigned

Several literature reports show the correlation of the structure of the various classes of alkaloids with their ^{13}C-NMR spectra (1–6). The structure and stereochemistry of strychnos alkaloids, brucine (I) and strychnine (II), were characterized (7, 8), but no reports are available concerning the assignments of their carbon resonances.

© 1979, American Pharmaceutical Association

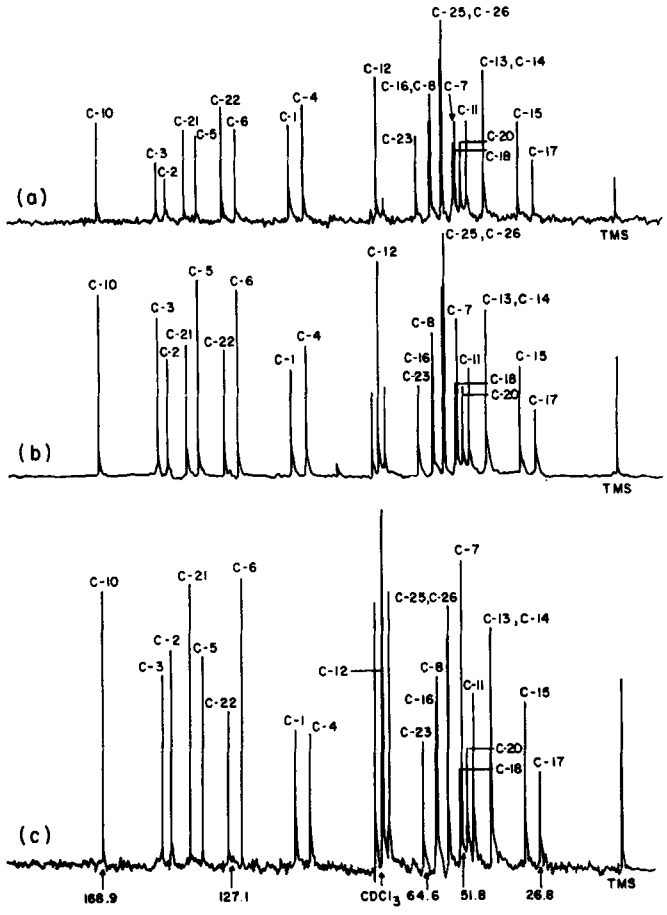

Figure 1—*Proton noise-decoupled ^{13}C-NMR spectrum of brucine. Key: (a), pulse repetition of 2.5 sec; (b), pulse repetition of 7 sec; and (c), pulse repetition of 25 sec.*

Previous efforts in assigning the ^{13}C-NMR chemical shifts of synthetic and natural therapeutic agents (9–12) initiated the ^{13}C-NMR analysis of brucine and strychnine. Strychnine is a powerful convulsant and is not used therapeutically because of its high toxicity.

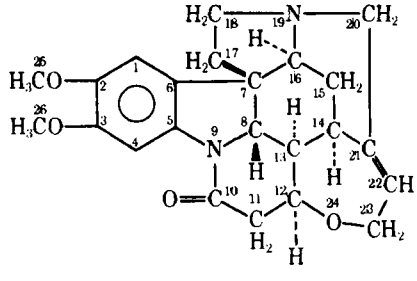

I

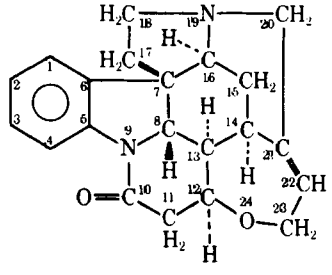

II

Table I—^{13}C-Chemical Shifts of Brucine

Assignment	Multiplicity	Chemical Shift
C-10	s	168.9
C-3	s	149.2
C-2	s	146.2
C-21	s	140.6
C-5	s	136.0
C-22	d	127.1
C-6	s	123.6
C-1	d	105.6
C-4	d	101.1
C-12	d	77.3
C-23	t	64.6
C-16[a]	d	60.3
C-8[a]	d	59.9
C-26[b]	q	56.4
C-25[b]	q	56.1
C-18	—[c]	52.6
C-7	—[c]	51.8
C-20	—[c]	50.2
C-11	—[c]	48.2
C-13	d	42.4
C-14	d	42.4
C-15	t	31.6
C-17	t	26.8

[a] These values may be interchanged. [b] These values may be interchanged. [c] The signal multiplicities are not clear.

The natural abundance ^{13}C-NMR spectra of brucine and strychnine were recorded in 30% (w/v) deuterochloroform as an internal lock and solvent with tetramethylsilane as a reference. In each case, a proton noise-decoupled and single-frequency off-resonance-decoupled (SFORD) spectra were run. The SFORD spectra differentiated the various types of carbons. The assignments of the carbon resonances were made on the basis of chemical shift theory, multiplicities generated in SFORD spectra, signal intensities, and comparisons with other structurally related compounds.

EXPERIMENTAL

The ^{13}C-NMR spectra[1] of brucine[2] and strychnine[3] (recrystallized from chloroform) were run in 10-mm tubes with spectrometer settings as follows: spectra width, 4 kHz; pulse width, 12 μsec (90°); repetition rate, 2.5, 7, 25, and 35 sec; and data points, 4 K.

RESULTS AND DISCUSSION

Brucine—The ^{13}C-NMR chemical shifts of brucine are recorded in Table I. The various carbon resonances are illustrated in Fig. 1. Twenty-two separate signals account for all 23 carbon resonances of I. The nine signals in the lower field region of the 102–169-ppm chemical shift are due to aromatic carbons, amidic carbon, and ethylenic carbons. The 13 signals in the higher field region of the 26–78-ppm chemical shift are due to the remaining 14 carbons.

The six singlets in the lower field region represent the carbon resonances of C-2, C-3, C-5, C-6, C-10, and C-21. The singlet at the farthest downfield region (168.9 ppm) is assigned to C-10 on the basis of the chemical shift theory of the carbonyl carbons of amides (13). Earlier studies indicated that a directly bonded methoxy group to the benzene nucleus produces a 31.4-ppm downfield shift at the same carbon and a 14.4-ppm upfield shift at the *ortho*-carbon (13). Since C-2 and C-3 in I are attached to a methoxy group and are *ortho* to the methoxy group, the singlets observed at 149.2 and 146.2 ppm are thus assigned to C-3 and C-2, respectively. The resonance of C-3 observed at the lower field in comparison to C-2 is due to the *meta* and *para* effect of nitrogen (13) on C-3 and C-2, respectively.

The assignments of various carbon resonances of I compare well with the chemical shifts of carbons in III and IV (1), with the exception of the

[1] Jeol FX60 spectrometer operating at 15.00 kHz.
[2] Fisher Scientific Co., New York, N.Y.
[3] J. T. Baker Chemical Co., Phillipsburg, N.J.

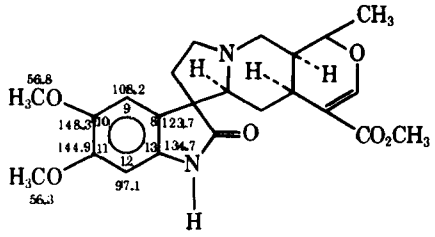

III

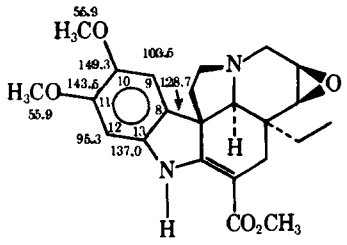

IV

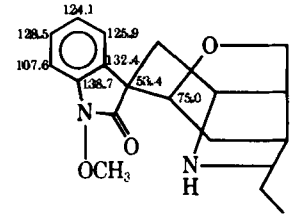

VII

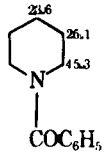

VIII

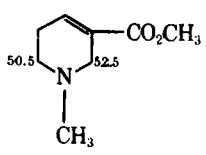

IX

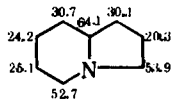

X

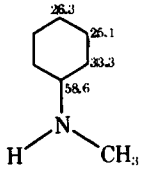

XI

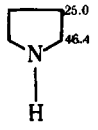

XII

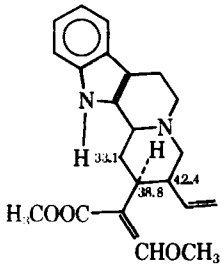

XIII

chemical shifts of C-10 and C-11. Contrary to the earlier studies (1), the assignments of C-10 (148.3 ppm) and C-11 (144.9 ppm) in III and C-10 (149.3 ppm) and C-11 (143.5 ppm) in IV should be reversed since in both cases C-11 is *meta* and C-10 is *para* to the nitrogen atom (13) and the chemical shifts assigned for C-3 (128.7 ppm) and C-4 (124.1 ppm) of acetanilide (V) (14). The carbon resonances of C-5 and C-6 are represented by chemical shifts at 136.0 and 123.6 ppm, respectively, by comparison with the chemical shift of the corresponding carbons of the analogous compounds, III and IV (1).

The C-22 has one α-carbon while C-21 has two α-carbons and two β-carbons, and these carbons account for the downfield chemical shift (13). Since oxygen produces an upfield chemical shift to its β-carbon and nitrogen exhibits a downfield chemical shift to its β-carbon, the remaining singlet at 140.6 ppm and a doublet centered at 127.0 ppm are thus attributed to C-21 and C-22 resonances, respectively. The assignments of these signals are in agreement with the chemical shifts reported for pimaradiene (VI) (15). Similar signals are also present in the ^{13}C-NMR spectra of II where the electronic environment of all aromatic carbons is completely different than that of I.

By comparing the assignment of chemical shift of III and IV, it can be assumed that the two doublets centered at 105.1 and 101.1 ppm are best assigned to C-1 and C-4, respectively.

The assignment of the chemical shift of carbon resonances in the lower field region is somewhat difficult. The C-12 and C-23 are directly attached to an oxygen atom, which produces more downfield shift at the same carbon than the nitrogen (13). Since the C-12 has the greater number of α- and β-carbons as compared to C-23, the chemical shift observed at the lower field is due to C-12. These observations provide support for the assignments of the doublet centered at 77.3-ppm and the triplet centered at 64.6-ppm chemical shifts to C-12 and C-23, respectively. The assignment of the chemical shifts of the analogous compound, gelsedine (VII) (16), provides further support for the assignments in I.

The quartets centered at 56.4 and 56.1 ppm are attributed to C-25 and C-26, respectively, as in III and VI (1), which, however, changed. This assignment is also supported by the absence of these signals in II. The C-8, C-16, C-18, and C-20 are directly bonded to nitrogen atoms, and thus the resonances due to these carbons are observed at a lower field in comparison to the remaining carbons (13). By comparison with the assignments of the chemical shift in VIII, IX, X (3), and XI (13), the doublets centered at 60.3 and 59.9 ppm and the signals at 52.6 and 50.2 ppm are assigned to C-16, C-8, C-18, and C-20, respectively, and the resonances for C-8 and C-16 are interchangeable. The methylene carbon C-11 is represented by the signal at 48.2 ppm.

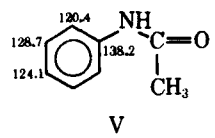

V

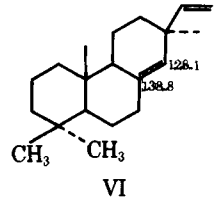

VI

The farthest upfield triplet at 26.5 ppm is assigned to C-17 due to the splitting pattern and comparison of the assignments of X and XII (3). This assignment is at a lower field in comparison to the corresponding carbon resonance of X, because it possesses a greater number of β-carbons. The chemical shift of C-15 is observed at 31.6 ppm while the carbon resonances of both C-13 and C-14 are represented at 42.4 ppm by comparing the assignment of chemical shifts of XIII (3) and XI (13).

In the present study, the proton noise-decoupled spectrum of I was also recorded at three different pulsing sequences of 2.5, 7.0, and 25.0 sec. These results, exhibiting the relaxing time (T_1) of different carbon atoms, are represented in Fig. 1. The presence of a longer T_1 for quaternary carbons as compared to other carbons indicated that the increase in time between pulsing sequences provides these carbons more time to relax, which consequently results in their larger peaks with respect to the peaks observed with carbons with a shorter T_1.

These results provide a clear distinction between quaternary carbons and other carbon atoms. The heights of the signal due to the carbon resonances of C-3, C-2, C-21, C-5, C-6, and C-7 are longer with an increase in the pulse time as compared to other carbons. The signal at 51.8 ppm is thus assigned to the quaternary carbon C-7, which is also supported by the chemical shifts of VII and XIV (1). The chemical shifts observed with II exhibited a similar signal at 52.0 ppm for C-7 in the proton noise-decoupled spectra of II (Fig. 2).

Strychnine—The ^{13}C-NMR chemical shifts of strychnine relative to tetramethylsilane are recorded in Table II. The various carbon resonances of II are shown in Fig. 2. The nine separate signals downfield in the 116–170-ppm region are assigned to aromatic carbons, amidic carbon, and ethylenic carbons. The 11 separate signals upfield in the 26–77-ppm

Table II—^{13}C-Chemical Shifts of Strychnine

Assignment	Multiplicity	Chemical Shift
C-10	s	169.3
C-5	s	142.3
C-21	s	140.5
C-6	s	132.7
C-3	d	128.6
C-22	d	127.5
C-1	d	124.2
C-2	d	122.3
C-4	d	116.3
C-12	d	77.2
C-23	t	64.6
C-8 and C-16	d	60.2
C-18	—[a]	52.8
C-7	—[a]	52.0
C-20	—[a]	50.4
C-11	—[a]	48.2
C-13[b]	d	42.9
C-14[b]	d	42.5
C-15	t	31.7
C-17	t	26.9

[a] The signal multiplicities are not clear. [b] These values may be interchanged.

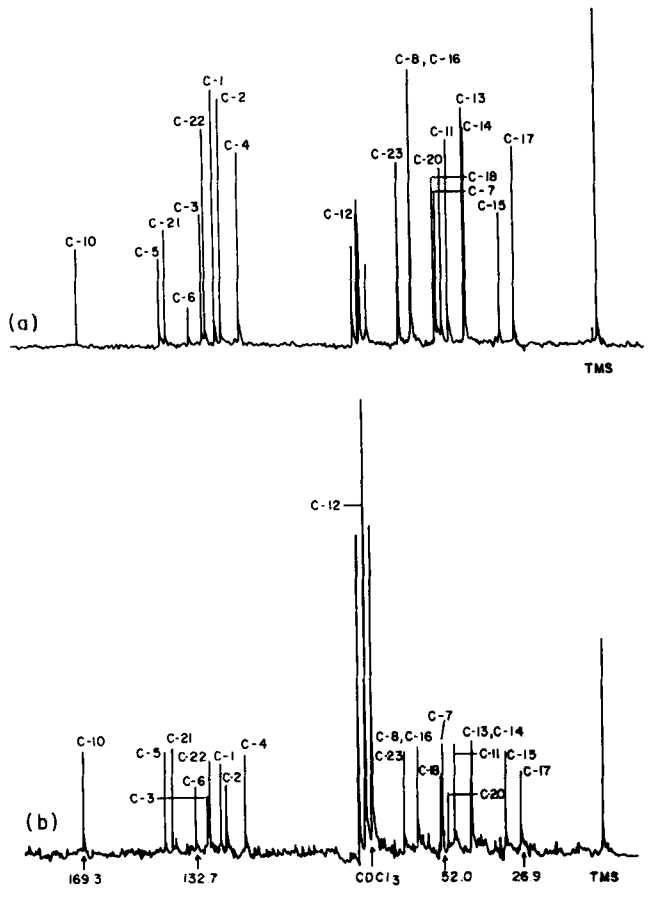

Figure 2 *--Proton noise-decoupled ^{13}C-NMR spectrum of strychnine. Key: (a), pulse repetition of 3 sec; and (b), pulse repetition of 35 sec.*

chemical shift region represent the carbon resonances of the remaining 12 carbons of II.

The farthest downfield singlet in the ^{13}C-NMR spectrum of II is attributed to C-10 on the basis of chemical shift theory of the carbonyl carbons of amides (13). By comparison with the chemical shifts of I, the singlet at 140.4 ppm and the doublet centered at 127.4 ppm are assigned to C-21 and C-22, respectively. The remaining two singlets at 142.3 and 132.6 ppm are due to the carbon resonances of C-5 and C-6, respectively. These assignments are comparable with the chemical shifts of VII (16) and XV (3). On the basis of the chemical shift theory for aromatic substitution and comparison with the chemical shifts of VII and XV, the four doublets centered at 124.2, 122.2, 128.6, and 116.3 ppm are represented by the carbon resonances of C-1, C-2, C-3, and C-4, respectively.

The remaining carbons, which exhibit their resonances in the upfield region, are in the same electronic environment as the corresponding carbons of I. Hence, the chemical shifts of these carbons observed in the ^{13}C-NMR spectrum of II are assigned by comparing the chemical shift observed due to the corresponding carbons of I (Table II).

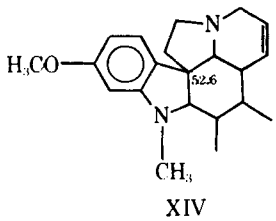

XIV

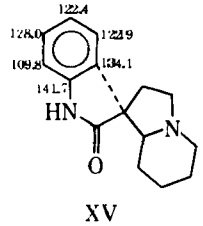

XV

REFERENCES

(1) E. Wenkert, D. W. Cochran, E. W. Hagaman, F. M. Schell, N. Neuss, A. S. Katner, P. Potier, C. Kan, M. Plat, M. Koch, H. Mehri, J. Poisson, N. Kunesch, and Y. Rolland, *J. Am. Chem. Soc.*, **95,** 4990 (1973).

(2) N. Neuss, H. E. Boaz, J. L. Occolowitz, E. Wenkert, F. M. Schell, P. Potier, C. Kan, M. M. Plat, and M. Plat, *Helv. Chim. Acta*, **56,** 2660 (1973).

(3) E. Wenkert, J. S. Bindra, C. J. Chang, D. W. Cochran, and F. M. Schell, *Acc. Chem. Res.*, **7,** 46 (1974).

(4) A. Rabaron, M. Koch, M. Plat, J. Peyroux, E. Wenkert, and D. W. Cochran, *J. Am. Chem. Soc.*, **93,** 6270 (1971).

(5) C. G. Moreland, A. Philip, and F. I. Carroll, *J. Org. Chem.*, **39,** 2413 (1974).

(6) F. I. Carroll, C. G. Moreland, G. A. Brine, and J. A. Kepler, *ibid.*, **41,** 996 (1976).

(7) H. L. Holmes, in "The Alkaloids," vol. I, R. H. Manske, Ed., Academic, New York, N.Y., 1950, chap. 7.

(8) J. B. Hendrickson, in "The Alkaloids," vol. VI, R. H. Manske, Ed., Academic, New York, N.Y., 1960, chap. 6.

(9) V. I. Stenberg, N. K. Narain, and S. P. Singh, *J. Heterocycl. Chem.*, **14,** 225 (1977).

(10) V. I. Stenberg, N. K. Narain, S. P. Singh, R. H. Obenauf, and M. J. Albright, *ibid.*, **14,** 407 (1977).

(11) S. P. Singh, S. S. Parmar, and V. I. Stenberg, *ibid.*, **15,** 9 (1978).

(12) S. P. Singh, S. S. Parmar, V. I. Stenberg, and S. A. Farnum, *ibid.*, **15,** 13 (1978).

(13) G. C. Levy and G. L. Nelson, "Carbon-13 Nuclear Magnetic Resonance for Organic Chemists," Wiley-Interscience, New York, N.Y., 1972, pp. 38, 47, 53, 80, 120.

(14) L. F. Johnson and W. C. Jankowski, "Carbon-13 NMR Spectra," Wiley-Interscience, New York, N.Y., 1972, p. 295.

(15) E. Wenkert and B. L. Buckwalter, *J. Am. Chem. Soc.*, **94,** 4367 (1972).

(16) E. Wenkert, C. J. Chang, D. W. Cochran, and R. Pellicciari, *Experientia*, **28,** 377 (1972).

ACKNOWLEDGMENTS

Supported in part by National Institute on Drug Abuse Grant 7-R01-DA01893-01, Eagles' Max Baer Heart Fund, and Contract N00014-76-C-0219 between the Office of Naval Research, Department of the Navy, and the University of North Dakota.

The authors thank Dr. S. J. Brumleve and Dr. T. K. Akers for their advice and encouragement. Grateful acknowledgment is made to the North West Area Foundation, St. Paul, Minn., for providing a Hill Professorship to S. S. Parmar.

Loss of a Hydrophobic Amine from Solution by Adsorption onto Container Surfaces

KAILAS D. THAKKER, TAKERU HIGUCHI, and LARRY A. STERNSON ×

Received April 18, 1978, from the *Department of Pharmaceutical Chemistry, University of Kansas, Lawrence, KS 66045.* Accepted for publication June 22, 1978.

Abstract □ The apparent loss of the hydrophobic amine drug α-[(dibutylamino)methyl]-6,8-dichloro-2-(3′,4′-dichlorophenyl)-4-quinolinemethanol monohydrochloride from solution due to its adsorption onto the surface of its storage container was studied. The drug appeared to be adsorbed only as the free base. Therefore, any perturbations to the solution phase that will help solubilize the drug and thus lower its chemical potential will minimize adsorption. Multilayer drug adsorption to the container surfaces appeared to take place, with some evidence of a highly organized system in the adsorbed phase. Adsorption was minimized when the heterogeneous polar functionalities on glass surfaces were covered by a layer of silicone or methacrylate polymer, which yielded less reactive, more hydrophobic surfaces. Loss was also minimized when the environment was kept acidic (pH ≤ 4.8), the drug was dissolved in a proton-donating solvent (*e.g.*, chloroform), and an ion-pairing agent (*e.g.*, trichloroacetate) was present to solubilize further the monocationic form of the drug in organic media.

Keyphrases □ α-[(Dibutylamino)methyl]-6,8-dichloro-2-(3′,4′-dichlorophenyl)-4-quinolinemethanol—adsorption onto container surfaces □ Adsorption—α-[(dibutylamino)methyl]-6,8-dichloro-2-(3′,4′-dichlorophenyl)-4-quinolinemethanol onto container surfaces

Quantitative analysis at the submicrogram level poses challenges not encountered in the determination of analytes at higher levels. One problem often encountered, particularly with analysis of hydrophobic drugs, is the apparent loss of compound from solution by adsorption onto container surfaces (1, 2). The experimental antimalarial α-[(dibutylamino)methyl]-6,8-dichloro-2-(3′,4′-dichlorophenyl)-4-quinolinemethanol monohydrochloride (I) and its free base (II) adsorb to container surfaces to a significant and readily measurable extent. The loss of I from solution in hydroxylic solvents by adsorption was studied, and methods to minimize this source of error were investigated.

EXPERIMENTAL

Materials—Compounds I and II were used as received[1]. Glass containers (10-ml volumetric flasks) were siliconized by immersion in a 1% silicone[2] solution for 5 min. The silicone solution was then discarded, and the glassware was rinsed with double-distilled water and dried in an oven at 100° for ~24 hr.

The inner surfaces of volumetric flasks were coated with methacrylate polymer[3] by filling the container with a 10% solution of polymer for ~10 min. The solution was then evaporated, the inner surfaces were rinsed with methanol, and the flasks were dried at 100° for 48 hr in an oven.

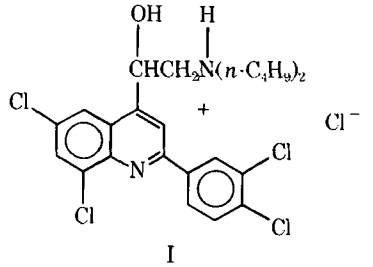

I

Adsorption Experiments—Solutions were prepared containing 5 ml of 0.02 *M* H_2SO_4 [or 0.02 *M* phosphate buffer (pH 5.8)], an appropriate volume of stock solution of I (10–40 μg/ml in methanol), and sufficient methanol to bring the total volume to 10 ml. The solution was stirred at a constant rate and monitored fluorometrically (λ_{ex} 272 nm and λ_{em} 370 nm) as a function of time. The solutions then were discarded, and the inner surface of the vessel was rinsed with 2-ml portions of a wash solvent for prescribed periods with shaking. Each rinse was assayed fluorometrically for desorbed I.

Equilibrium Desorption of Adsorbed Phase—Methanolic solutions of I were allowed to stir for about 20 days at 25°. The I concentration remaining in solution was determined fluorometrically; intensities were compared with standard curves made at the time of analysis. Drug adsorption to surfaces of the flasks was assumed to be complete when four consecutive concentration measurements were constant. The solutions were stirred for 3 weeks after adsorption was assumed complete.

The total amount of the drug adsorbed was calculated by difference (the total amount added and the amount remaining in solution). The solution was then discarded. Solvent (2 ml) was added to the flasks, and the flasks were shaken in a vertical position for 0.5 hr. The amount of the drug desorbed in 0.5 hr was determined fluorometrically. The solution was discarded, and 2 ml of fresh solvent was added. A number of successive washes was made, until no drug could be detected in the wash solution. The volume of the solvent (2 ml) and the time of shaking the solution (0.5 hr) were kept constant for all washes.

In all cases, volumes were kept constant. When a plastic container or a glass container coated with silicone or methacrylate polymer solutions was used, a Pyrex glass container of the same dimensions was used as a standard for comparison.

RESULTS AND DISCUSSION

Loss of I from Solution—In early investigations with aqueous solutions of I and II, the drug concentration in solution appeared to decrease rapidly when monitored spectrophotometrically.

When solutions of I [0.08 μg/ml in water–methanol (50:50 v/v), buffered at pH 5.8] were stirred at 430 rpm, 50% of the compound was lost to the surface of each container within 28 min. The stirring rate had a considerable effect on the depletion of the drug from solution. A reduction in the stirring rate from 430 to 315 rpm increased the I half-life in solution from 28 to 168 min. Although these data are insufficient to draw definitive conclusions, the results are consistent with the assumption that mass transfer *via* drug diffusion to the container surface is rate determining in adsorption.

The extent of drug adsorption was dependent on the amount of drug already adsorbed on the container surface. When 0.78 μg of drug was adsorbed to the surface of a 20-ml beaker, 0.03 μg of drug/ml remained in solution; when 2.25 μg of drug was adsorbed to an identical container, the I concentration in solution was 0.05 μg/ml. The I concentration remaining in solution in equilibrium with its adsorbed phase was also dependent on the total amount of the drug adsorbed. These results may be explained by assuming that the chemical potential of the drug in the adsorbed phase may be different when different amounts of the drug are totally adsorbed, as would be the case if the drug were adsorbed in layers on the container surface.

Influence of pH on Adsorption—The pH of the solvent system in which I was dissolved had a pronounced effect on adsorption. Whereas the half-life of I in methanol–water (50:50) buffered at pH 5.8 was approximately 28 min (Fig. 1), adsorption occurred more slowly ($t_{1/2}$ = ~15 hr) in the presence of pH 4.2 buffer (Fig. 2) and was eliminated substantially in the presence of 0.01 *M* H_2SO_4 at the same stirring rate (430 rpm) and at the same initial drug concentration (0.08 μg/ml).

[1] Walter Reed Army Research Institute.
[2] Siliclad, Becton-Dickinson.
[3] Plexiglas.

0022-3549/79/0100-0093$01.00/0
© 1979, American Pharmaceutical Association

Table I—Adsorption of I [a] from Solution [b] to Surface of Various Containers

Time	Percent of Drug Remaining in Solution after Agitation in: Glass Beaker[c]	Polypropylene Beaker[c]	Polyfluoroethylene Beakers A[c]	Polyfluoroethylene Beakers B[d]
5 min	94	96	88	84
15 min	89	95	88	65
30 min	90	94	87	55
45 min	—	—	84	53
60 min	87	94	82	46
3 hr	78	85	81	36
5.5 hr	71	74	—	—
6 hr	65	—	—	—
9 hr	—	59	80	27
10 hr	36	—	—	—

[a] 0.11 μg/ml in water–methanol (1:1). [b] Analyzed fluorometrically at 370 nm (excitation wavelength 272 nm). [c] In the presence of 1×10^{-2} *M* H_2SO_4. [d] In the presence of pH 5.8 phosphate buffer.

At or below pH 4.2, the predominant species in solution is the monocationic form of the drug [$pKa_1^* = 0.5$ and $pKa_2^* = 6.3$ determined in water–methanol (75:25) in this laboratory]. The decreased drug adsorption in relatively acidic solutions may well be due to the predominance of the more polar monocationic form of the drug, which is better solubilized in hydroalcoholic solution than is the free base. The reduced adsorption at lower pH suggests that only the free base, II, adsorbs to container surfaces; *i.e.*, the thermodynamic activity of the free base in hydroalcoholic solution is greater than the activity of the monocation in the same solvent. It is presumed that the acidic environment does not significantly affect the container surface, which would modify adsorption characteristics.

Equilibrium Desorption of Free Base (II)—After a solution containing I or II was equilibrated with its adsorbed phase, addition of a fresh volume of solvent resulted in desorption of the drug until equilibrium was reestablished.

Equilibrium desorption of II, when a range of 10–60 μg was initially adsorbed on glass containers, is shown in Fig. 3. Each point represents a single desorption step with 2 ml of wash solution [methanol–water (1:1)].

The apparent constancy in the amount of drug desorbed as a function of the amount remaining adsorbed suggests multilayer drug adsorption on the surface as opposed to precipitation of the slightly soluble drug onto the surface. It was not possible to desorb the drug with the methanol–water (1:1) solution when less than 5 μg was adsorbed, suggesting that this amount may represent monolayer formation on the specific containers used. Simple calculations, with the assumption that 5 μg of the drug formed a monolayer on the beakers used, indicated the surface area per molecule of I to be about 18–19 $Å^2$. This value is comparable with the reported surface area per molecule for stearic acid in monolayers (about 22 $Å^2$) (3), lending support to the assumption that 5 μg of II adsorbed to the surfaces of these containers may represent a monolayer.

When 10–60 μg is adsorbed to the same container, several layers of the drug may be expected to form on the container surface and these layers

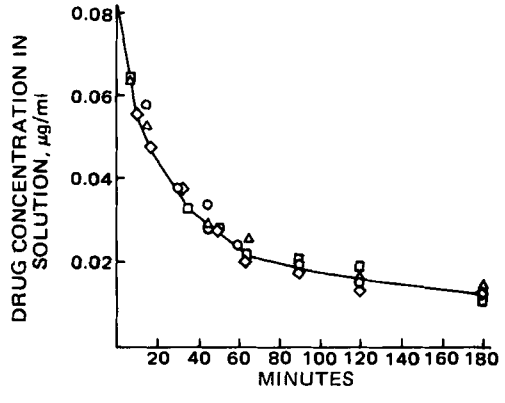

Figure 1—*Adsorption of the drug from solutions (0.08 μg/ml) in water–methanol (1:1) in the presence of pH 5.8 phosphate buffer to surfaces of four identical containers (△, ○, □, and ◇).*

Table II—Adsorption of I from Solution [a] to the Surfaces of 10-ml Volumetric Flasks

Time	Percent of Drug Remaining in Solution[b] in: Uncoated Flasks	Flasks Coated with Methacrylate Solution	Flasks Coated with Silicone Solution
5 min	92	100	99
15 min	—	100	96
35 min	83	100	95
60 min	78	99	94
4 hr	76	97	91
8 hr	—	98	85

[a] 0.098 μg/ml in water–methanol (1:1) in the presence of 1×10^{-2} *M* H_2SO_4. [b] Analyzed fluorometrically at 370 nm (excitation wavelength 272 nm).

may possess a definite order, *i.e.*, layers of decreasing chemical potential in proceeding from the outerlayer to the monolayer. The desorption of such an ordered phase may occur in several steps, with one or more layers desorbing at the same time. The general pattern for desorption in Fig. 3 conforms with the hypothesized ordered layering of II in the adsorptive phase if it is assumed that 5 μg of the drug represents a monolayer and that approximately two layers of drug desorb simultaneously.

The scatter in the data in Fig. 3 may result from the long periods required to reach equilibrium, making the analytical technique rather inaccurate, and the nonhomogeneity of container surfaces, offering sites of different energy to the drug being adsorbed. This situation may result in exposure of different layers to the solvent at the same time during desorption.

Reduction or Prevention of Drug Adsorption to Surfaces of Containers—Drug adsorption to surfaces of different types of containers was studied to see if any reduction or prevention of adsorption to surfaces other than glass occurred. The adsorption of II from solutions [in water–methanol (1:1)] to surfaces of different containers is presented in Tables I and II. Except when otherwise indicated, solutions were made 0.01 *M* in sulfuric acid since an acid environment minimized adsorption.

Vessel composition did not appear to affect adsorption since losses of drug from solution to the surface of polyfluoroethylene beakers (20% loss) and polypropylene beakers (25% loss) were similar to each other and similar to glass beakers (29% loss) of identical surface area when adsorption was studied over 5 hr (Table I). However, the coating of glass vessels with materials that increase surface hydrophobicity did affect the propensity for adsorption. When II was dissolved in methanol–water solution (containing 0.01 *M* H_2SO_4) in 10-ml volumetric flasks coated with a silicone solution (Table II), only 9% of the drug was lost from solution in 4 hr and 15% in 8 hr. Alternatively, when the flasks were coated with a methacrylate polymer solution, less than 2% of drug was adsorbed over 8 hr.

Container surfaces were not examined in microscopic detail, so no attempts were made to explain the effect of the surface on drug adsorption. The effect of environmental pH on adsorption was demonstrated further by the observations that only 20% of drug was lost to the surface of polyfluoroethylene beakers in 10 hr in the presence of 0.01 *M* H_2SO_4 but that 70% was lost when pH 5.8 phosphate buffer was used in place of the acid (Table I). Adsorption of II occurred to all surfaces investigated; however, adsorption occurred to a much lesser extent with methacrylate- and silicone-coated containers.

The desorption of II from glass surfaces into the solution phase was

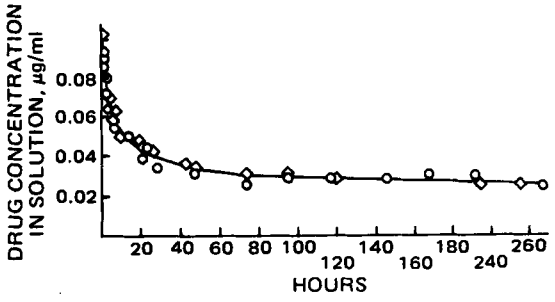

Figure 2—*Adsorption of the drug from solutions (0.105 μg/ml) in water–methanol (1:1) in the presence of pH 4.2 succinate buffer to surfaces of two identical containers (○ and ◇).*

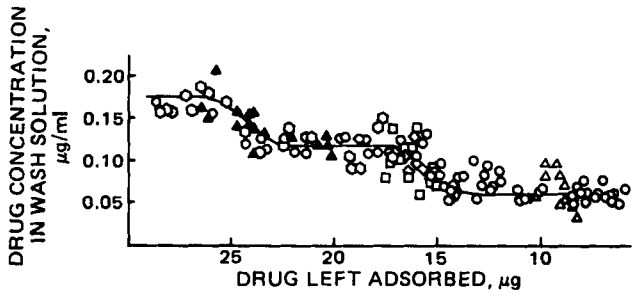

Figure 3—*Equilibrium desorption [into 2 ml of water–methanol (1:1)] of the drug when 60 (○), 40.7 (▲), 30 (○), 17.6 (□), 17.3 (◇), or 10.6 (△) μg was adsorbed initially.*

studied with several organic solvents (Table III). Methanol and ether failed to desorb any detectable quantity of the drug in 30 min. The presence of 20% (v/v) chloroform in methanol facilitated the transfer into the solution phase, resulting in the desorption of 42% of the free base. A relatively efficient transfer (92%) was obtained when chloroform alone was the transfer reagent. Chloroform, a proton-donating solvent, is capable of solubilizing II more efficiently through hydrogen bonding with electron-rich sites (nitrogen and chlorine) on II.

In all cases, the transfer efficiency was increased by the addition of acid to the solvents (Table III). In the presence of 0.01 *M* H_2SO_4 in methanol, a fairly high transfer occurred over the range studied (the 0.2 and 2.0 μg adsorbed initially could be desorbed to an extent of 56 and 88%, respectively). Addition of 33% (v/v) chloroform to that solvent favored the solution phase, making transfer to the solution even more efficient (97%). Acids capable of forming ion-pairs with I, *e.g.*, trichloroacetate, resulted in a 100% transfer of the drug to the solution phase (dichloromethane or chloroform).

General trends observed during the transfer of the adsorbed phase (Table III) suggest that transfer into the solution phase was more favored as the total amount of the free base adsorbed increased. With smaller amounts of adsorbed drug, the adsorbed phase was preferred over the solution phase, except in chloroform solutions. Furthermore, drug transfer from the adsorbed phase into solution (for any solvent system tried) was more efficient when silicone-coated (or methacrylate-coated) containers were used as compared to Pyrex glassware. The Pyrex glass surface is more heterogeneous than the surface of a silicone-coated container. Therefore, adsorption of hydrophobic drug molecules may be stronger onto a glass surface.

In conclusion, the drug appears to adsorb onto container surface in layers possessing a definite energetic order. Minimum adsorption occurred to glassware made hydrophobic by coating with silicone or methacrylate. Desorption was achieved most efficiently with solvent systems that most effectively solvate the drug. The presence of an acid environment converted II to a more polar monocationic species, which was efficiently solvated as an ion-pair in proton-donating solvents (chloroform and dichloromethane), thus eliminating the adsorption of I to container surfaces.

Table III—Transfer of the Drug from the Adsorbed Phase [a] to the Solution Phase

Solvent Used for Transfer	Drug Adsorbed, μg	Drug Transferred, μg	Drug Transferred, %
2 ml of methanol	0.21	0.0	0
	0.21[b]	0.0	0
	2.06	0.0	0
	2.06[b]	0.12	6.0
2 ml of ether	1.92	0.0	0
	1.92[b]	0.0	0
1.6 ml of chloroform and 0.4 ml of methanol	1.09	0.52	48
	1.11[b]	0.47	42
	0.43	0.0	0
	0.43[b]	0.26	61
1.6 ml of chloroform and 0.4 ml of hexane	1.93	1.0	52
	1.93[b]	1.7	88
	0.19	0.0	0
	0.19[b]	0.1	52
2 ml of chloroform	1.28	0.59	45
	1.28[b]	1.18	92
2.0 ml of methanol and 0.03 ml of 3 *M* H_2SO_4	0.24	0.0	0
	0.21[b]	0.18	88
	2.06	0.70	34
	2.06[b]	1.14	55
2.0 ml of methanol, 0.1 ml of 1 *M* H_2SO_4, and 1.0 ml of chloroform	2.38	1.15	48
	0.24	0.13	56
	2.06[b]	2.01	97
	0.21[b]	0.15	75
2.0 ml of chloroform containing 4% CCl_3COOH	0.22[b]	0.22	100
	1.66	1.41	85
	0.22	0.18	82
2.0 ml of dichloromethane containing 4% CCl_3COOH	0.22[b]	0.22	100

[a] The drug was allowed to adsorb onto surfaces of 10-ml volumetric flasks from water–methanol (1:1) solutions. [b] Ten-milliliter volumetric flasks coated with a silicone solution were used.

REFERENCES

(1) L. H. Bird, *N.Z. Sci. Technol.*, **30**, 344 (1949).

(2) K. T. H. Farrer and W. C. J. Hollenberg, *Analyst*, **78**, 730 (1953).

(3) I. Langmuir, *J. Am. Chem. Soc.*, **39**, 1865 (1917).

Trace Determination of Acetaminophen in Serum

DAVID J. MINER and PETER T. KISSINGER ˣ

Received October 31, 1977, from the *Department of Chemistry, Purdue University, West Lafayette, IN 47907.* Accepted for publication May 5, 1978.

Abstract □ A simple and accurate method for measuring acetaminophen in serum was developed using liquid chromatography with electrochemical detection. Acetaminophen can be quantitated in 100 μl of serum over the range of 20 ng/ml–20 μg/ml. The method is linear (r = 0.9997) and reproducible (RSD = 3.0% at 2 μg/ml, RSD = 5.1% at 200 ng/ml, n = 6). An internal standard (N-propionyl-p-aminophenol) is used, and a single extraction is performed.

Keyphrases □ Acetaminophen—liquid chromatographic analysis in serum □ Liquid chromatography—analysis, acetaminophen in serum □ Analgesics—acetaminophen, liquid chromatographic analysis in serum

The determination of free acetaminophen and its metabolites in biological fluids is a subject of continuing interest. Therapeutic and overdose levels are easily measured by several techniques including spectrophotometry, GLC, TLC, and liquid chromatography. Current methods are often inadequate, however, for microliter samples from newborns and experimental animals. Subtherapeutic levels, which are of interest in drug metabolism (pharmacokinetic) studies, also push most methods to their detection limits where data are subject to poor precision and specificity. The most sensitive methods are based on liquid chromatography with electrochemical detection (1), liquid chromatography with UV detection (2–5), or GLC (6, 7). The detection limit of these methods is roughly 100 ng/ml with 1 ml of serum.

Liquid chromatography with electrochemical detection has steadily gained acceptance for clinical determinations (8). This paper reports improvements in an earlier procedure (1) that allow accurate quantitation at levels lower than those previously reported (20 ng/ml) while requiring 10-fold less serum and little sample preparation.

EXPERIMENTAL

Reagents—Acetaminophen[1] was obtained commercially. Standard solutions were prepared in 1 M phosphate buffer (pH 7). The internal standard, N-propionyl-p-aminophenol, was synthesized by a standard method (9). Methanol[2] was distilled once prior to use. Tap water was deionized and distilled prior to use.

Instrumentation—A stainless steel liquid chromatograph[3] was equipped with a 20-μl injection loop and a carbon paste electrochemical detector. The working electrode potential was +0.65 v *versus* a silver-silver chloride reference electrode. The column (15 cm × 4.6 mm) was slurry packed with microparticulate reversed-phase packing material[4].

The mobile phase was prepared by mixing 390 ml of water, 34 ml of 1 M ammonium acetate, 70 ml of methanol, and 9 ml of 1 M acetic acid. A flow rate of 1.17 ml/min was used. All data were manually recorded from peak height measurements. Culture tubes were silanized with trimethylchlorosilane by a gas phase technique analogous to that described by Fenimore *et al.* (10).

Analysis—Solid sodium chloride (~0.07 g), 100 μl of serum, and 100 μl of 1.0 M phosphate buffer (pH 7) (saturated with sodium chloride and containing 2 mg of N-propionyl-p-aminophenol/liter) were added to a silanized 3-ml culture tube. Two milliliters of dichloromethane–2-propanol–ether (5:1:2) was added, and the tubes were capped and shaken for 10 min on a reciprocal shaker. Then the tubes were centrifuged briefly, and the organic layer was removed and evaporated at 40° under dry nitrogen. The residue was reconstituted in 500 μl of mobile phase. Standards for calibrating instrumental response were prepared by spiking drug-free serum and processing it with each set of samples.

RESULTS AND DISCUSSION

A typical chromatogram is shown in Fig. 1C for serum containing 200 ng of acetaminophen/ml. The detection limits of previously published methods were roughly at this level. Since one complete chromatogram requires 12 min, five samples can be processed per hour. The time required per sample can be significantly reduced when only therapeutic levels are measured and/or if the internal standard is not used (with some sacrifice in precision).

With the electrochemical detector operating at high sensitivity, a chromatogram for drug-free serum could be obtained as illustrated in Fig. 1A. The chromatographic conditions were chosen to minimize interferences so that low levels of acetaminophen could be measured (Fig. 1B). With the specified chromatographic conditions, no significant endogenous interferences were found in nine drug-free serum samples tested. Ultimately, however, the method became blank limited. The minimum detectable concentration of acetaminophen was 3 ng/ml of serum. In the absence of the serum matrix, a minimum of 2 pg injected in the 20-μl loop could be detected (S/N = ~2). Since the method is not detector limited, further sample cleanup procedures or more efficient chromatography would undoubtedly improve the detection limits.

Other drugs were tested as possible interferences, but none interfered. Barbiturates, theophylline, theobromine, salicylamide, caffeine, and aspirin were not electrochemically active at the electrode potential employed. Salicylic acid was poorly extracted and detectable with much less sensitivity than acetaminophen at the potential employed. Phenacetin was more strongly retained than N-propionyl-p-aminophenol and could be quantitated by increasing the working electrode potential.

The organic extractant used (dichloromethane–2-propanol–ether) gave slightly cleaner extracts than did ethyl acetate. Ether was also tried, but,

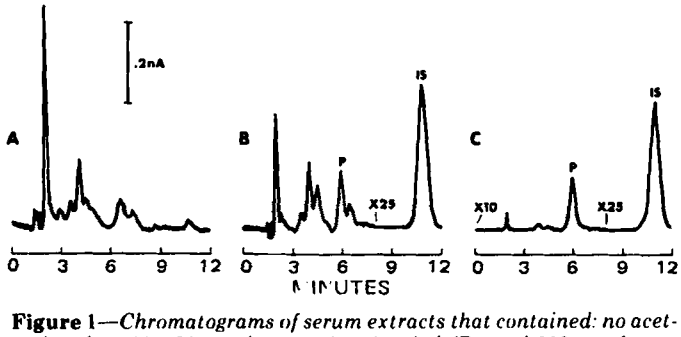

Figure 1—*Chromatograms of serum extracts that contained: no acetaminophen (A), 20 ng of acetaminophen/ml (B), and 200 ng of acetaminophen/ml (C). Key: P, acetaminophen; and IS, internal standard.*

[1] Sigma Chemical Co., St. Louis, Mo.
[2] Technical grade.
[3] LC-50, Bioanalytical Systems, Lafayette, Ind.
[4] μBondapak, Waters Associates, Milford, Mass.

0022-3549/79/0100-0096$01.00/0
© 1979, American Pharmaceutical Association

while it gave cleaner extracts, the efficiency of extraction for acetaminophen was significantly lower. Acetaminophen and the internal standard partitioned nearly identically to one another. Absolute recovery of acetaminophen was 80–90%, and recovery relative to a matrix-free standard was 109%.

Linearity was evaluated by spiking drug-free serum with 10 standard solutions over the range of 20 ng/ml–20 μg/ml. The correlation coefficient obtained was 0.9997. Reproducibility was determined by spiking six different drug-free serum samples. The relative standard deviation at 2 μg/ml was 3.0%; at 200 ng/ml, it was 5.1%.

Reversed-phase chromatography with electrochemical detection is a useful means of quantitating acetaminophen metabolites in blood, urine, and liver homogenates. Since all major metabolites are more polar than the free drug or oxidize at significantly more positive potentials, they do not interfere in the present method.

REFERENCES

(1) R. M. Riggin, A. L. Schmidt, and P. T. Kissinger, *J. Pharm. Sci.*, **64**, 680 (1975).

(2) G. R. Gotelli, P. M. Kabra, and L. J. Marton, *Clin. Chem.*, **23**, 957 (1977).

(3) L. T. Wong, G. Solomonrai, and B. H. Thomas, *J. Pharm. Sci.*, **65**, 1064 (1976).

(4) R. A. Horvitz and P. I. Jatlow, *Clin. Chem.*, **23**, 1596 (1977).

(5) D. Howie, P. I. Adriaenssens, and L. F. Prescott, *J. Pharm. Pharmacol.*, **29**, 235 (1977).

(6) W. A. Garland, K. C. Ksiao, E. J. Pantuck, and A. H. Conney, *J. Pharm. Sci.*, **66**, 340 (1977).

(7) M. A. Evans and R. D. Harbison, *ibid.*, **66**, 1628 (1977).

(8) P. T. Kissinger, *Anal. Chem.*, **49**, 447A (1977).

(9) L. R. Fieser and M. Fieser, "Advanced Organic Chemistry," Reinhold, New York, N.Y., 1961, p. 758.

(10) D. C. Fenimore, C. M. Davis, J. H. Whitford, and C. A. Harrington, *Anal. Chem.*, **48**, 2289 (1976).

ACKNOWLEDGMENTS

Supported by grants from the National Science Foundation and the National Institute of General Medical Sciences.

Extraction and TLC Separation of Food, Drug, and Cosmetic Dyes from Tablet-Coating Formulations

FRANK A. FADIL ˣ and WILLIAM O. McSHARRY

Received February 22, 1978, from the *Quality Control Department, Hoffmann-La Roche, Inc., Nutley, NJ 07110.* Accepted for publication May 19, 1978.

Abstract □ A rapid method for extraction of dyes from tablet-coating formulations is described. The dyes were released from their lakes by treatment with concentrated phosphoric acid and dissolved in methanol. After being made alkaline with ammonium hydroxide, the mixture was centrifuged to obtain a clear supernate for application to the TLC plate. With ethyl acetate–methanol–water–concentrated ammonium hydroxide (150:40:35:5) on silica gel, 20 dyes were separated sufficiently to confirm their presence in the coating formulation.

Keyphrases □ Dyes, various—TLC determination in tablet-coating formulations □ TLC—determination, various dyes in tablet-coating formulations □ Tablet-coating formulations—TLC determination of various dyes

The widespread use of coloring agents in pharmaceutical preparations, combined with stringent and changing regulations on their use, makes a simple and rapid method for identifying the components of a colorant mixture highly desirable. TLC has been used extensively for this purpose, and several systems for the separation of dyes were published (1–4). If the dyes are components of a formulation, a suitable preparative scheme must be employed before the sample is applied to the thin-layer plate. Since tablet-coating formulations are relatively simple[1], published systems for extracting dyes from foods and drugs (5–7) are unnecessarily complex.

The aim of this work was to develop a combination of preparative scheme and TLC system that could be applied uniformly to various formulations.

[1] Formulations contained one or more lakes, titanium dioxide, and one or more of the following: sucrose, povidone, hydroxypropylcellulose, sodium benzoate, alcohol, and water.

Table I—Summary of R_f Values

Dye	R_f
FD&C Yellow No. 5	0.06
FD&C Green No. 3	0.07
FD&C Red No. 2[a] (amaranth)	0.07
FD&C Blue No. 1	0.16
D&C Blue No. 4	0.17
FD&C Yellow No. 6	0.22
FD&C Red No. 40	0.22
FD&C Red No. 33	0.23
FD&C Red No. 4	0.24
FD&C Violet No. 1[a]	0.26
FD&C Red No. 7	0.27
D&C Green No. 5	0.31
FD&C Red No. 3 (erythrosine sodium)	0.31
FD&C Red No. 28	0.33
FD&C Orange No. 4	0.36
D&C Red No. 19	0.36
D&C Yellow No. 10	0.37
D&C Yellow No. 11	0.77
D&C Red No. 36	0.81
D&C Green No. 6	0.85

[a] Use no longer permitted in the United States.

EXPERIMENTAL

Extraction of Dyes—Ten drops (~0.4 ml) of phosphoric acid (85%) were placed in a 50-ml centrifuge tube, and an appropriate amount of tablet-coating liquid (up to 1 ml), pure dye or lake, was added. The contents of the tube were mixed by swirling intermittently for 5 min. Methanol, 10 ml, was added, and the tube was shaken for 1 min. Then 1 ml of concentrated ammonium hydroxide (29%) was added, and the tube again was shaken for 1 min. Solids were removed by centrifuging, and 10 μl of the supernate was applied to the thin-layer plate.

TLC Plates—Silica gel G[2] plates, 20 × 20 cm, 0.25 mm thick, were

[2] E. M. Reagents, E. Merck, Darmstadt, West Germany.

0022-3549/79/0100-0097$01.00/0

© 1979, American Pharmaceutical Association

while it gave cleaner extracts, the efficiency of extraction for acetaminophen was significantly lower. Acetaminophen and the internal standard partitioned nearly identically to one another. Absolute recovery of acetaminophen was 80–90%, and recovery relative to a matrix-free standard was 109%.

Linearity was evaluated by spiking drug-free serum with 10 standard solutions over the range of 20 ng/ml–20 μg/ml. The correlation coefficient obtained was 0.9997. Reproducibility was determined by spiking six different drug-free serum samples. The relative standard deviation at 2 μg/ml was 3.0%; at 200 ng/ml, it was 5.1%.

Reversed-phase chromatography with electrochemical detection is a useful means of quantitating acetaminophen metabolites in blood, urine, and liver homogenates. Since all major metabolites are more polar than the free drug or oxidize at significantly more positive potentials, they do not interfere in the present method.

REFERENCES

(1) R. M. Riggin, A. L. Schmidt, and P. T. Kissinger, *J. Pharm. Sci.*, **64**, 680 (1975).

(2) G. R. Gotelli, P. M. Kabra, and L. J. Marton, *Clin. Chem.*, **23**, 957 (1977).

(3) L. T. Wong, G. Solomonrai, and B. H. Thomas, *J. Pharm. Sci.*, **65**, 1064 (1976).

(4) R. A. Horvitz and P. I. Jatlow, *Clin. Chem.*, **23**, 1596 (1977).

(5) D. Howie, P. I. Adriaenssens, and L. F. Prescott, *J. Pharm. Pharmacol.*, **29**, 235 (1977).

(6) W. A. Garland, K. C. Ksiao, E. J. Pantuck, and A. H. Conney, *J. Pharm. Sci.*, **66**, 340 (1977).

(7) M. A. Evans and R. D. Harbison, *ibid.*, **66**, 1628 (1977).

(8) P. T. Kissinger, *Anal. Chem.*, **49**, 447A (1977).

(9) L. R. Fieser and M. Fieser, "Advanced Organic Chemistry," Reinhold, New York, N.Y., 1961, p. 758.

(10) D. C. Fenimore, C. M. Davis, J. H. Whitford, and C. A. Harrington, *Anal. Chem.*, **48**, 2289 (1976).

ACKNOWLEDGMENTS

Supported by grants from the National Science Foundation and the National Institute of General Medical Sciences.

Extraction and TLC Separation of Food, Drug, and Cosmetic Dyes from Tablet-Coating Formulations

FRANK A. FADIL ˣ and WILLIAM O. McSHARRY

Received February 22, 1978, from the *Quality Control Department, Hoffmann-La Roche, Inc., Nutley, NJ 07110.* Accepted for publication May 19, 1978.

Abstract □ A rapid method for extraction of dyes from tablet-coating formulations is described. The dyes were released from their lakes by treatment with concentrated phosphoric acid and dissolved in methanol. After being made alkaline with ammonium hydroxide, the mixture was centrifuged to obtain a clear supernate for application to the TLC plate. With ethyl acetate–methanol–water–concentrated ammonium hydroxide (150:40:35:5) on silica gel, 20 dyes were separated sufficiently to confirm their presence in the coating formulation.

Keyphrases □ Dyes, various—TLC determination in tablet-coating formulations □ TLC—determination, various dyes in tablet-coating formulations □ Tablet-coating formulations—TLC determination of various dyes

The widespread use of coloring agents in pharmaceutical preparations, combined with stringent and changing regulations on their use, makes a simple and rapid method for identifying the components of a colorant mixture highly desirable. TLC has been used extensively for this purpose, and several systems for the separation of dyes were published (1–4). If the dyes are components of a formulation, a suitable preparative scheme must be employed before the sample is applied to the thin-layer plate. Since tablet-coating formulations are relatively simple[1], published systems for extracting dyes from foods and drugs (5–7) are unnecessarily complex.

The aim of this work was to develop a combination of preparative scheme and TLC system that could be applied uniformly to various formulations.

[1] Formulations contained one or more lakes, titanium dioxide, and one or more of the following: sucrose, povidone, hydroxypropylcellulose, sodium benzoate, alcohol, and water.

Table I—Summary of R_f Values

Dye	R_f
FD&C Yellow No. 5	0.06
FD&C Green No. 3	0.07
FD&C Red No. 2[a] (amaranth)	0.07
FD&C Blue No. 1	0.16
D&C Blue No. 4	0.17
FD&C Yellow No. 6	0.22
FD&C Red No. 40	0.22
FD&C Red No. 33	0.23
FD&C Red No. 4	0.24
FD&C Violet No. 1[a]	0.26
FD&C Red No. 7	0.27
D&C Green No. 5	0.31
FD&C Red No. 3 (erythrosine sodium)	0.31
FD&C Red No. 28	0.33
FD&C Orange No. 4	0.36
D&C Red No. 19	0.36
D&C Yellow No. 10	0.37
D&C Yellow No. 11	0.77
D&C Red No. 36	0.81
D&C Green No. 6	0.85

[a] Use no longer permitted in the United States.

EXPERIMENTAL

Extraction of Dyes—Ten drops (~0.4 ml) of phosphoric acid (85%) were placed in a 50-ml centrifuge tube, and an appropriate amount of tablet-coating liquid (up to 1 ml), pure dye or lake, was added. The contents of the tube were mixed by swirling intermittently for 5 min. Methanol, 10 ml, was added, and the tube was shaken for 1 min. Then 1 ml of concentrated ammonium hydroxide (29%) was added, and the tube again was shaken for 1 min. Solids were removed by centrifuging, and 10 μl of the supernate was applied to the thin-layer plate.

TLC Plates—Silica gel G[2] plates, 20 × 20 cm, 0.25 mm thick, were

[2] E. M. Reagents, E. Merck, Darmstadt, West Germany.

0022-3549/79/0100-0097$01.00/0

© 1979, American Pharmaceutical Association

prepared using an automatic TLC plate coater[3]. Plates were dried at 40° and activated by heating at 105° for 15 min just prior to use.

Solvent—Ethyl acetate–methanol–water–concentrated ammonium hydroxide (150:40:35:5) was mixed and transferred to the chromatographic chamber just prior to use.

Chamber—A paper-lined glass tank, ~30 × 9 × 27 cm, was saturated with solvent just prior to use.

RESULTS AND DISCUSSION

Essentially complete extraction of dyes from the tablet-coating formulation was indicated by the lack of color in the centrifuged solid residue. Development of the thin-layer chromatogram required about 50–60 min.

The R_f values were not affected by applying all dyes in combination or by varying quantities applied from 0.1 to 10 μg. Other components of the tablet-coating formulations had no effect.

Average R_f values for the 20 dyes are shown in Table I. The spots were generally compact horizontal bands that were visually distinct even when the R_f values were very close. Distinction was aided by hue differences even among dyes of the same color group. The possibility of discriminating among all dyes of a given color group was confirmed by applying mixtures. Any of several similar published systems (2, 3) probably could be used to resolve any possible confusion.

The method has been applied successfully to more than a dozen different color-coating formulations to date.

[3] Camag model 21 602, Muttenz, Switzerland.

REFERENCES

(1) F. Bandelin and J. Tuschhoff, *J. Am. Pharm. Assoc., Sci. Ed.*, **49**, 302 (1960).

(2) M. Penner, *J. Pharm. Sci.*, **57**, 2132 (1968).

(3) R. Hoodless, K. Pitman, T. Stewart, J. Thomson, and J. Arnold, *J. Chromatogr.*, **54**, 393 (1971).

(4) H. De Clercq and D. Massart, *ibid.*, **93**, 243 (1974).

(5) C. Graichen and J. Molitor, *J. Assoc. Off. Anal. Chem.*, **46**, 1022 (1963).

(6) G. Lehmann, P. Collet, H. G. Hahn, and M. Ashworth, *ibid.*, **53**, 1182 (1970).

(7) C. Graichen, *ibid.*, **58**, 278 (1975).

Collaborative Study of a GLC Method for Vitamin E

ALAN J. SHEPPARD ˣ and WILLARD D. HUBBARD

Received March 9, 1978, from the *Division of Nutrition, Food and Drug Administration, Washington, DC 20204.* Accepted for publication May 4, 1978.

Abstract □ The official GLC method of the Association of Official Analytical Chemists (AOAC) for determining vitamin E was modified and collaboratively studied for the National Formulary (NF). The internal standard hexadecyl hexadecanoate (cetyl palmitate) was substituted for the dotriacontane used in the AOAC method, and some other minor changes were made. Eleven samples, representing all types of NF formulations and NF bulk materials, were analyzed by 11 laboratories. The coefficients of variation of the reproducibility and repeatability were 4.5 and 2.4%, respectively, for all laboratories and samples. The values were 3.4 and 1.6%, respectively, when the one laboratory statistically determined to be an outlier was excluded. The coefficients of variation of reproducibility and repeatability for α-tocopheryl acid succinate were 2.1 and 1.5%, respectively. All of these values lie within the 5% limit required by the NF.

Keyphrases □ Vitamin E—GLC analysis, collaborative study of 11 samples by 11 laboratories □ GLC—analysis, vitamin E, collaborative study of 11 samples by 11 laboratories

Interest in GLC as compendial or official methodology for the quantitative measurement of α-tocopherol, α-tocopheryl acetate, and α-tocopheryl acid succinate has developed during the past 10 years. Sheppard *et al.* (1) conducted a collaborative study of a GLC method for determining vitamin E and demonstrated the superiority of GLC over the colorimetric method (2, 3). An external calibration procedure was used for calculating the quantity of specific vitamin E isomers in pharmaceutical preparations. The Association of Official Analytical Chemists (AOAC) adopted the GLC method (4, 5).

BACKGROUND

An extensive collaborative study of the GLC method for determining vitamin E was initiated in April 1970 by the Pharmaceutical Manufacturers Association Quality Control Section (PMAQCS) at the request of the National Formulary (NF) for a better, more specific compendial assay for vitamin E and vitamin E decavitamin preparations (6). A preliminary intralaboratory GLC study comparing the dotriacontane internal standard method with the AOAC external standard method showed no significant difference in the results. Since the two calibration methods were apparently equally valid, the less complicated internal standard method was chosen for the PMAQCS study.

The GLC method was again demonstrated to be more specific and rapid than the compendial colorimetric methods (2, 3). The internal standard calibration method used in the PMAQCS study gave improved precision over that of the AOAC method (1), which used an external calibration technique. On the basis of the PMAQCS study, the AOAC adopted the GLC method with the dotriacontane internal standard as a primary calibration method; the external standard method became an alternative calibration method (7).

Concurrently, the NF staff was studying the PMAQCS collaborative study results and planned to include a GLC method based on that study in NF XIV (8). However, this GLC method was the subject of much discussion and debate. Therefore, the NF decided to adopt the AOAC method as an interim method until a generally agreed-upon GLC method could be studied collaboratively. The NF incorporated the AOAC method, without the external calibration alternative, into NF XIV (8).

A meeting of persons from domestic and foreign industry, the AOAC, and the Food and Drug Administration was held in 1974 to resolve various issues and to agree upon methodology. Hexadecyl hexadecanoate (cetyl palmitate) was chosen to replace dotriacontane as the internal standard. Electronic integration was considered mandatory. Other minor modifications were made in the AOAC method, and the revised method was then converted to NF monograph form and circulated to the attendees for approval. The method was then collaboratively studied in 1975. The results of that study are presented here.

EXPERIMENTAL

Method—The collaborators were instructed to follow the official AOAC method (7) with the following changes: column temperature, 245–265°; and inert carrier gas flow, adjusted so that the α-tocopheryl acetate peak appears about 20 min after sample injection.

The internal standard solution is prepared by dissolving 500 mg of

0022-3549/79/0100-0098$01.00/0

© 1979, American Pharmaceutical Association

prepared using an automatic TLC plate coater[3]. Plates were dried at 40° and activated by heating at 105° for 15 min just prior to use.

Solvent—Ethyl acetate–methanol–water–concentrated ammonium hydroxide (150:40:35:5) was mixed and transferred to the chromatographic chamber just prior to use.

Chamber—A paper-lined glass tank, ~30 × 9 × 27 cm, was saturated with solvent just prior to use.

RESULTS AND DISCUSSION

Essentially complete extraction of dyes from the tablet-coating formulation was indicated by the lack of color in the centrifuged solid residue. Development of the thin-layer chromatogram required about 50–60 min.

The R_f values were not affected by applying all dyes in combination or by varying quantities applied from 0.1 to 10 μg. Other components of the tablet-coating formulations had no effect.

Average R_f values for the 20 dyes are shown in Table I. The spots were generally compact horizontal bands that were visually distinct even when the R_f values were very close. Distinction was aided by hue differences even among dyes of the same color group. The possibility of discriminating among all dyes of a given color group was confirmed by applying mixtures. Any of several similar published systems (2, 3) probably could be used to resolve any possible confusion.

The method has been applied successfully to more than a dozen different color-coating formulations to date.

[3] Camag model 21 602, Muttenz, Switzerland.

REFERENCES

(1) F. Bandelin and J. Tuschhoff, *J. Am. Pharm. Assoc., Sci. Ed.*, **49**, 302 (1960).

(2) M. Penner, *J. Pharm. Sci.*, **57**, 2132 (1968).

(3) R. Hoodless, K. Pitman, T. Stewart, J. Thomson, and J. Arnold, *J. Chromatogr.*, **54**, 393 (1971).

(4) H. De Clercq and D. Massart, *ibid.*, **93**, 243 (1974).

(5) C. Graichen and J. Molitor, *J. Assoc. Off. Anal. Chem.*, **46**, 1022 (1963).

(6) G. Lehmann, P. Collet, H. G. Hahn, and M. Ashworth, *ibid.*, **53**, 1182 (1970).

(7) C. Graichen, *ibid.*, **58**, 278 (1975).

Collaborative Study of a GLC Method for Vitamin E

ALAN J. SHEPPARD ˣ and WILLARD D. HUBBARD

Received March 9, 1978, from the *Division of Nutrition, Food and Drug Administration, Washington, DC 20204.* Accepted for publication May 4, 1978.

Abstract □ The official GLC method of the Association of Official Analytical Chemists (AOAC) for determining vitamin E was modified and collaboratively studied for the National Formulary (NF). The internal standard hexadecyl hexadecanoate (cetyl palmitate) was substituted for the dotriacontane used in the AOAC method, and some other minor changes were made. Eleven samples, representing all types of NF formulations and NF bulk materials, were analyzed by 11 laboratories. The coefficients of variation of the reproducibility and repeatability were 4.5 and 2.4%, respectively, for all laboratories and samples. The values were 3.4 and 1.6%, respectively, when the one laboratory statistically determined to be an outlier was excluded. The coefficients of variation of reproducibility and repeatability for α-tocopheryl acid succinate were 2.1 and 1.5%, respectively. All of these values lie within the 5% limit required by the NF.

Keyphrases □ Vitamin E—GLC analysis, collaborative study of 11 samples by 11 laboratories □ GLC—analysis, vitamin E, collaborative study of 11 samples by 11 laboratories

Interest in GLC as compendial or official methodology for the quantitative measurement of α-tocopherol, α-tocopheryl acetate, and α-tocopheryl acid succinate has developed during the past 10 years. Sheppard *et al.* (1) conducted a collaborative study of a GLC method for determining vitamin E and demonstrated the superiority of GLC over the colorimetric method (2, 3). An external calibration procedure was used for calculating the quantity of specific vitamin E isomers in pharmaceutical preparations. The Association of Official Analytical Chemists (AOAC) adopted the GLC method (4, 5).

BACKGROUND

An extensive collaborative study of the GLC method for determining vitamin E was initiated in April 1970 by the Pharmaceutical Manufacturers Association Quality Control Section (PMAQCS) at the request of the National Formulary (NF) for a better, more specific compendial assay for vitamin E and vitamin E decavitamin preparations (6). A preliminary intralaboratory GLC study comparing the dotriacontane internal standard method with the AOAC external standard method showed no significant difference in the results. Since the two calibration methods were apparently equally valid, the less complicated internal standard method was chosen for the PMAQCS study.

The GLC method was again demonstrated to be more specific and rapid than the compendial colorimetric methods (2, 3). The internal standard calibration method used in the PMAQCS study gave improved precision over that of the AOAC method (1), which used an external calibration technique. On the basis of the PMAQCS study, the AOAC adopted the GLC method with the dotriacontane internal standard as a primary calibration method; the external standard method became an alternative calibration method (7).

Concurrently, the NF staff was studying the PMAQCS collaborative study results and planned to include a GLC method based on that study in NF XIV (8). However, this GLC method was the subject of much discussion and debate. Therefore, the NF decided to adopt the AOAC method as an interim method until a generally agreed-upon GLC method could be studied collaboratively. The NF incorporated the AOAC method, without the external calibration alternative, into NF XIV (8).

A meeting of persons from domestic and foreign industry, the AOAC, and the Food and Drug Administration was held in 1974 to resolve various issues and to agree upon methodology. Hexadecyl hexadecanoate (cetyl palmitate) was chosen to replace dotriacontane as the internal standard. Electronic integration was considered mandatory. Other minor modifications were made in the AOAC method, and the revised method was then converted to NF monograph form and circulated to the attendees for approval. The method was then collaboratively studied in 1975. The results of that study are presented here.

EXPERIMENTAL

Method—The collaborators were instructed to follow the official AOAC method (7) with the following changes: column temperature, 245–265°; and inert carrier gas flow, adjusted so that the α-tocopheryl acetate peak appears about 20 min after sample injection.

The internal standard solution is prepared by dissolving 500 mg of

0022-3549/79/0100-0098$01.00/0

© 1979, American Pharmaceutical Association

hexadecyl hexadecanoate in n-hexane in a 500-ml volumetric flask and diluting to volume with n-hexane.

The column is conditioned for 1 hr at 300° with no carrier gas flow. The column is then cooled, and the carrier gas flow is begun and maintained for 4 hr.

Tablets and capsules are prepared according to Ref. 7. Bulk materials are treated the same as the standards. Other preparations are diluted with internal standard solution so that the final concentration is 1 mg of vitamin E/ml.

The instrument is calibrated by injecting 2 μl of standard solution(s).

Retention times, relative to the internal standard, are: α-tocopherol, 0.53; α-tocopheryl acid succinate, 0.54; and α-tocopheryl acetate, 0.62.

Collaborative Study—Eleven samples and instructions were sent to 11 laboratories in the United States and the Federal Republic of Germany. All collaborators were experienced in GLC analysis of vitamin E and were familiar with the official AOAC method. Nine industrial laboratories plus this laboratory and the USP Drug Research and Testing Laboratory participated. The collaborators were instructed to analyze the samples in duplicate, using a single injection. "Duplicate," as used in the study, is a second subsample carried through the entire method, terminating with a single GLC analysis.

The samples[1] were NF formulations and bulk materials especially selected and prepared for the study to be representative of the many situations that confront the quality control, formulary, or regulatory chemist performing a routine analysis. The samples were coded in this laboratory and were packed and shipped by the NF. The shipment also included the reference and internal standards furnished by the NF.

Sample 1 was a practice sample, *dl*-α-tocopheryl acetate, 400 IU of vitamin E/capsule. Sample 2 was a vitamin E capsule, *dl*-acetate, 200 IU. Sample 3 was a vitamin E capsule, *d*-acetate, 400 IU. Sample 4 was a vitamin E capsule, *d*-alcohol, 400 IU. Sample 5 was *dl*-α-tocopheryl acetate, pharmaceutical grade, 500-mg ampuls.

Sample 6 was *dl*-α-tocopherol, pharmaceutical grade, 600-mg ampuls. Sample 7 was *d*-α-tocopheryl acetate, 94.0 g of vitamin E/100 g. Sample 8 was *d*-α-tocopheryl acid succinate, minimum assay 97%. Sample 9 was *d*-α-tocopherol, mixed tocopherols, minimum assay 671 mg/g. Sample 10 was an unknown, and Sample 11 was an unknown, 489 mg of α-tocopheryl acetate.

Samples 1–9 were labeled as to content claim; Samples 10 and 11 bore only sample numbers. Sample 10 was a blind duplicate of Sample 4. For Sample 10, the analyst was required to identify the tocopheryl isomer or isomers present and to determine quantitatively the amount of the specific isomer present.

The GLC method, instructions to collaborators, and sample number label information were sent under separate cover to each collaborator.

RESULTS AND DISCUSSION

The analytical results are summarized in Table I. The statistical summary is presented in Table II. Repeatability as used here relates to within-laboratory measurements, and reproducibility refers to between-laboratory measurements.

A two-way analysis of variance for the data from all laboratories and all samples was performed. A significant difference ($p < 0.01$) was found among laboratories. A significant ($p < 0.01$) laboratory × sample interaction also was found, because the majority of the laboratories did not obtain consistent results for all samples. For some samples, a laboratory obtained higher results in comparison to other laboratories; for other samples, the same laboratory obtained lower results in comparison to other laboratories.

A one-way analysis of variance was performed for each sample, both with and without Laboratory 5 (statistically determined to be an outlier). When this laboratory was excluded, a significant difference (at least $p < 0.05$) was found among laboratories for each sample. When Laboratory 5 was included, there were no significant ($p > 0.05$) differences among laboratories for Samples 2, 3, 5, and 10. In every instance, the coefficients of variation for repeatability and reproducibility were either equal or smaller when Laboratory 5 was excluded from the analysis.

A two-way analysis of variance was performed to compare the duplicate samples, 4 and 10, and a significant difference ($p < 0.05$) was found among laboratories. When Laboratory 5 was excluded, there was a significant

Table I—Collaborative Results (International Units) of the GLC Determination of Vitamin E[a]

Sample	Laboratory										
	1	2	3	4	5	6	7	8	9	10	11
1	385, 382	360, 364	385, 390	404, 402	400, 401	377, 393	394, 393	382, 384	409, 400	357, 363	387, 391
2	221, 207	188, 187	202, 203	202, 203	177, 244	196, 193	212, 201	204, 206	213, 209	202, 194	201, 204
3	294, 326	299, 299	309, 305	290, 303	329, 266	297, 296	324, 324	307, 309	334, 318	289, 288	309, 316
4	271, 262	289, 282	302, 302	327, 322	263, 286	274, 272	275, 265	292, 295	297, 310	284, 277	304, 315
5	1000, 982	910, 910	952, 970	970, 969	990, 910	935, 949	955, 939	960, 1000	929, 932	942, 937	958, 968
6	1021, 1069	1004, 1004	1004, 997	1048, 1045	890, 902	1000, 986	999, 988	1017, 1016	1000, 975	1011, 1031	990, 1014
7	983, 949	897, 871	970, 961	952, 958	950, 880	945, 947	901, 959	950, 953	940, 929	959, 959	958, 969
8	1030, 1039	985, 1003	1000, 1039	1047, 1038	970, 939	972, 993	1004, 1005	989, 1008	995, 1002	1003, 998	984, 1023
9	687, 707	708, 726	764, 787	810, 799	659, 600	731, 739	757, 766	748, 763	761, 759	729, 744	758, 757
10	275, 274	300, 310	298, 262	329, 328	332, 269	277, 274	306, 306	293, 294	308, 307	286, 292	305, 315
11	491, 486	486, 490	515, 510	494, 487	457, 431	489, 479	512, 516	487, 489	500, 524	507, 494	494, 497

[a] Duplicate analyses.

[1] Sample 1 was purchased on the open market. Samples 2–4 and 10 were provided by R. P. Scherer, Detroit, Mich. Samples 5 and 6 were obtained from Hoffmann-La Roche, Nutley, N.J. Sample 7 was given by General Mills Chemicals, Minneapolis, Minn. Samples 8, 9, and 11 were provided by Distillation Products Industries, Rochester, N.Y.

Table II—Statistical Summary of Collaborative Results of GLC Analysis of Vitamin E

Statistic	Sample[a] 1	2	3	4	5	6	7	8	9	10	11
All laboratories											
Mean	385.9	203.0	306.0	289.4	953.1	1000.5	945.5	1003.0	738.9	297.3	492.5
Reproducibility	15.1	16.0	16.3	19.4	27.2	41.2	28.5	26.4	47.6	20.0	20.4
CV, %	3.9	7.9	5.3	6.7	2.9	4.1	3.0	2.6	6.4	6.7	4.2
Repeatability	3.0	16.0	15.8	7.2	20.5	14.2	18.0	15.6	15.8	15.8	8.7
CV, %	0.8	7.9	5.2	2.5	2.2	1.4	1.9	1.6	2.1	5.3	1.8
Without Laboratory 5											
Mean	384.4	202.5	306.8	290.8	953.4	1011.0	948.5	1007.8	749.8	297.0	497.4
Reproducibility	15.1	8.4	13.6	19.4	25.7	23.4	25.8	21.4	31.0	18.6	12.6
CV, %	3.9	4.1	4.4	6.7	2.7	2.3	2.7	2.1	4.1	6.2	2.5
Repeatability	3.2	4.6	8.7	5.5	11.9	14.6	10.5	14.8	10.0	8.8	7.0
CV, %	0.8	2.3	2.8	2.6	1.3	1.4	1.1	1.5	1.3	3.0	1.4

[a] For all laboratories and samples, the mean was 601.4, the reproducibility was 27.1 with a coefficient of variation of 4.5%, and the repeatability was 14.5 with a coefficient of variation of 2.4%. When Laboratory 5 was eliminated, the mean was 604.5, the reproducibility was 20.6 with a coefficient of variation of 3.4%, and the repeatability was 9.8 with a coefficient of variation of 1.6%.

($p < 0.01$) laboratory × sample interaction. Six of the laboratories obtained consistent results for both samples. Four of the five remaining laboratories obtained results that were considerably higher for Sample 10, while one laboratory reported considerably higher results for Sample 4. Because of the significant laboratory × sample interaction, no significant difference ($p < 0.05$) was found between Samples 4 and 10.

One laboratory failed to identify properly the isomer present in Sample 10. It was learned that the procedure had not been followed correctly. Therefore, in this instance, the procedure was not at fault. All other laboratories identified the isomer present in Sample 10. The required isomer identification was properly carried out for all other samples by all laboratories.

CONCLUSION

Even with the data of the poorest performing laboratory included, coefficients of variation of 4.5% for reproducibility and 2.4% for repeatability are within the 5% required by NF. The laboratory exhibiting the poorest performance can be eliminated statistically, and the resulting coefficients of variation are 3.4 and 1.6% for reproducibility and repeatability, respectively. The reproducibility of 2.1% and the repeatability of 1.5% for the α-tocopheryl acid succinate are exceptionally gratifying since this compound is suspected of breaking down during GLC analysis and would be expected to exhibit larger coefficients of variation. The method, as collaboratively studied, appears to meet the requirements for an NF compendial method.

REFERENCES

(1) A. J. Sheppard, W. D. Hubbard, and A. R. Prosser, *J. Assoc. Offic. Anal. Chem.*, **52**, 442 (1969).

(2) "The National Formulary," 13th ed., Mack Publishing Co., Easton, Pa., 1970, p. 758.

(3) "The United States Pharmacopeia," 18th rev., Mack Publishing Co., Easton, Pa., 1970, p. 913.

(4) *J. Assoc. Offic. Anal. Chem.*, **52**, 335 (1969).

(5) "Official Methods of Analysis," 11th ed., Association of Official Analytical Chemists, Washington, D.C., 1970, secs. 39.063–39.070.

(6) B. C. Rudy, F. P. Mahn, B. Z. Senkowski, A. J. Sheppard, and W. D. Hubbard, *J. Assoc. Offic. Anal. Chem.*, **55**, 1211 (1972).

(7) "Official Methods of Analysis," 12th ed., Association of Official Analytical Chemists, Washington, D.C., 1975, secs. 43.078–43.085.

(8) "The National Formulary," 14th ed., Mack Publishing Co., Easton, Pa., 1975, p. 758.

ACKNOWLEDGMENTS

Presented at the 91st annual meeting of the Association of Official Analytical Chemists, Washington, D.C., October 1977.

The authors acknowledge A. P. Besancon, Distillation Products Industries; B. Stuckey, Eastman Chemical Products; P. R. Heinze, BASF Wyandotte Corp.; G. G. Wilson, General Mills Chemicals; B. C. Rudy, Hoffmann-La Roche; and C. H. Barnstein, National Formulary, for their many contributions during the early stages of this study. The authors also thank the following collaborators who participated in this study: F. J. Cioffi, E. R. Squibb and Sons, New Brunswick, N.J.; H. D. Fisher, General Mills Chemicals, Minneapolis, Minn.; S. A. Fusari, Parke-Davis and Co., Detroit, Mich.; D. K. Wyatt, USP Drug Research and Testing Laboratory, Rockville, Md.; M. Jacobs, Distillation Products Industries, Rochester, N.Y.; G. W. Kurtz, R. P. Scherer Corp., Detroit, Mich.; F. P. Mahan, Hoffmann-La Roche, Nutley, N.J.; P. Morrison, Eastman Chemical Products, Kingsport, Tenn.; P. D. Rysenga, The Upjohn Co., Kalamazoo, Mich.; and U. Thiele, BASF Aktungesellschaft, Ludwigshafen, Federal Republic of Germany.

Absence of Povidone-Iodine-Induced Mutagenicity in Mice and Hamsters

JUTTA MERKLE ˣ and HEINRICH ZELLER

Received November 3, 1977, from the *Department of Industrial Hygiene and Toxicology, BASF Aktiengesellschaft, D-6700 Ludwigshafen/Rh., Federal Republic of Germany.* Accepted for publication May 19, 1978.

Abstract □ Povidone-iodine USP was tested for mutagenicity in mice by the dominant lethal assay or micronucleus test and in Chinese hamsters by the bone marrow test. None of the three tests revealed any evidence of mutagenic effect.

Keyphrases □ Povidone-iodine—evaluated for mutagenicity in mice and hamsters □ Mutagenicity—povidone-iodine evaluated in mice and hamsters □ Anti-infectives, topical—povidone-iodine, evaluated for mutagenicity in mice and hamsters

According to Wlodkowski *et al.* (1), povidone-iodine blocked growth of the DNA polymerase-deficient *Escherichia coli* strain whereas no mutagenic effects were found with *Salmonella typhimurium* in the same (Ames) test. In the fluctuation test, povidone-iodine was mutagenic only for *S. typhimurium* T 1530 and not for *S. typhimu-*

0022-3549/79/0100-0100$01.00/0

© 1979, American Pharmaceutical Association

Table II—Statistical Summary of Collaborative Results of GLC Analysis of Vitamin E

Statistic	Sample[a] 1	2	3	4	5	6	7	8	9	10	11
All laboratories											
Mean	385.9	203.0	306.0	289.4	953.1	1000.5	945.5	1003.0	738.9	297.3	492.5
Reproducibility	15.1	16.0	16.3	19.4	27.2	41.2	28.5	26.4	47.6	20.0	20.4
CV, %	3.9	7.9	5.3	6.7	2.9	4.1	3.0	2.6	6.4	6.7	4.2
Repeatability	3.0	16.0	15.8	7.2	20.5	14.2	18.0	15.6	15.8	15.8	8.7
CV, %	0.8	7.9	5.2	2.5	2.2	1.4	1.9	1.6	2.1	5.3	1.8
Without Laboratory 5											
Mean	384.4	202.5	306.8	290.8	953.4	1011.0	948.5	1007.8	749.8	297.0	497.4
Reproducibility	15.1	8.4	13.6	19.4	25.7	23.4	25.8	21.4	31.0	18.6	12.6
CV, %	3.9	4.1	4.4	6.7	2.7	2.3	2.7	2.1	4.1	6.2	2.5
Repeatability	3.2	4.6	8.7	5.5	11.9	14.6	10.5	14.8	10.0	8.8	7.0
CV, %	0.8	2.3	2.8	2.6	1.3	1.4	1.1	1.5	1.3	3.0	1.4

[a] For all laboratories and samples, the mean was 601.4, the reproducibility was 27.1 with a coefficient of variation of 4.5%, and the repeatability was 14.5 with a coefficient of variation of 2.4%. When Laboratory 5 was eliminated, the mean was 604.5, the reproducibility was 20.6 with a coefficient of variation of 3.4%, and the repeatability was 9.8 with a coefficient of variation of 1.6%.

($p < 0.01$) laboratory × sample interaction. Six of the laboratories obtained consistent results for both samples. Four of the five remaining laboratories obtained results that were considerably higher for Sample 10, while one laboratory reported considerably higher results for Sample 4. Because of the significant laboratory × sample interaction, no significant difference ($p < 0.05$) was found between Samples 4 and 10.

One laboratory failed to identify properly the isomer present in Sample 10. It was learned that the procedure had not been followed correctly. Therefore, in this instance, the procedure was not at fault. All other laboratories identified the isomer present in Sample 10. The required isomer identification was properly carried out for all other samples by all laboratories.

CONCLUSION

Even with the data of the poorest performing laboratory included, coefficients of variation of 4.5% for reproducibility and 2.4% for repeatability are within the 5% required by NF. The laboratory exhibiting the poorest performance can be eliminated statistically, and the resulting coefficients of variation are 3.4 and 1.6% for reproducibility and repeatability, respectively. The reproducibility of 2.1% and the repeatability of 1.5% for the α-tocopheryl acid succinate are exceptionally gratifying since this compound is suspected of breaking down during GLC analysis and would be expected to exhibit larger coefficients of variation. The method, as collaboratively studied, appears to meet the requirements for an NF compendial method.

REFERENCES

(1) A. J. Sheppard, W. D. Hubbard, and A. R. Prosser, *J. Assoc. Offic. Anal. Chem.*, **52**, 442 (1969).

(2) "The National Formulary," 13th ed., Mack Publishing Co., Easton, Pa., 1970, p. 758.

(3) "The United States Pharmacopeia," 18th rev., Mack Publishing Co., Easton, Pa., 1970, p. 913.

(4) *J. Assoc. Offic. Anal. Chem.*, **52**, 335 (1969).

(5) "Official Methods of Analysis," 11th ed., Association of Official Analytical Chemists, Washington, D.C., 1970, secs. 39.063–39.070.

(6) B. C. Rudy, F. P. Mahn, B. Z. Senkowski, A. J. Sheppard, and W. D. Hubbard, *J. Assoc. Offic. Anal. Chem.*, **55**, 1211 (1972).

(7) "Official Methods of Analysis," 12th ed., Association of Official Analytical Chemists, Washington, D.C., 1975, secs. 43.078–43.085.

(8) "The National Formulary," 14th ed., Mack Publishing Co., Easton, Pa., 1975, p. 758.

ACKNOWLEDGMENTS

Presented at the 91st annual meeting of the Association of Official Analytical Chemists, Washington, D.C., October 1977.

The authors acknowledge A. P. Besancon, Distillation Products Industries; B. Stuckey, Eastman Chemical Products; P. R. Heinze, BASF Wyandotte Corp.; G. G. Wilson, General Mills Chemicals; B. C. Rudy, Hoffmann-La Roche; and C. H. Barnstein, National Formulary, for their many contributions during the early stages of this study. The authors also thank the following collaborators who participated in this study: F. J. Cioffi, E. R. Squibb and Sons, New Brunswick, N.J.; H. D. Fisher, General Mills Chemicals, Minneapolis, Minn.; S. A. Fusari, Parke-Davis and Co., Detroit, Mich.; D. K. Wyatt, USP Drug Research and Testing Laboratory, Rockville, Md.; M. Jacobs, Distillation Products Industries, Rochester, N.Y.; G. W. Kurtz, R. P. Scherer Corp., Detroit, Mich.; F. P. Mahan, Hoffmann-La Roche, Nutley, N.J.; P. Morrison, Eastman Chemical Products, Kingsport, Tenn.; P. D. Rysenga, The Upjohn Co., Kalamazoo, Mich.; and U. Thiele, BASF Aktungesellschaft, Ludwigshafen, Federal Republic of Germany.

Absence of Povidone-Iodine-Induced Mutagenicity in Mice and Hamsters

JUTTA MERKLE ˣ and HEINRICH ZELLER

Received November 3, 1977, from the *Department of Industrial Hygiene and Toxicology, BASF Aktiengesellschaft, D-6700 Ludwigshafen/Rh., Federal Republic of Germany.* Accepted for publication May 19, 1978.

Abstract □ Povidone-iodine USP was tested for mutagenicity in mice by the dominant lethal assay or micronucleus test and in Chinese hamsters by the bone marrow test. None of the three tests revealed any evidence of mutagenic effect.

Keyphrases □ Povidone-iodine—evaluated for mutagenicity in mice and hamsters □ Mutagenicity—povidone-iodine evaluated in mice and hamsters □ Anti-infectives, topical—povidone-iodine, evaluated for mutagenicity in mice and hamsters

According to Wlodkowski *et al.* (1), povidone-iodine blocked growth of the DNA polymerase-deficient *Escherichia coli* strain whereas no mutagenic effects were found with *Salmonella typhimurium* in the same (Ames) test. In the fluctuation test, povidone-iodine was mutagenic only for *S. typhimurium* T 1530 and not for *S. typhimu-*

0022-3549/79/0100-0100$01.00/0

© 1979, American Pharmaceutical Association

Table I—Testing of Povidone-Iodine in the Dominant Lethal Test on Male NMRI Mice when Applied in a Single Intraperitoneal Dose[a]

Dose	Mating Week	Females with Implantations		Total Implantations		Live Embryos		Dead Implantations		Mutagenicity Index
		Number	%	Number	Per Female	Number	Per Female	Number	Per Female	
0	1	48	80.0	548	11.4	491	10.2	57	1.2	10.4
	2	58	96.7	771	13.3	705	12.2	66	1.1	8.6
	3	58	96.7	750	12.9	690	11.9	60	1.0	8.0
	4	56	93.3	734	13.1	671	12.0	63	1.1	8.6
	5	57	95.0	737	12.9	666	11.7	71	1.2	9.6
	6	58	96.7	736	12.7	655	11.3	81	1.4	11.0
	7	58	96.7	761	13.1	705	12.2	56	1.0	7.4
	8	54	90.0	731	13.5	652	12.1	79	1.5	10.8
Control: 10 ml of distilled water/kg	1	43	71.7	516	12.0	473	11.0	43	1.0	8.3
	2	54	90.0	721	13.4	652	12.1	69	1.3	9.6
	3	57	95.0	717	12.6	646	11.3	71	1.2	9.9
	4	56	93.3	761	13.6	671	12.0	90	1.6	11.8[b]
	5	59	98.3	776	13.2	699	11.8	77	1.3	9.9
	6	58	96.7	802	13.8	716	12.3	86	1.5	10.7
	7	60	100.0	772	12.9	716	11.9	56	0.9	7.3
	8	56	93.3	779	13.9	712	12.7	67	1.2	8.6
72 mg/kg	1	33	55.0[c]	345	10.5	296	9.0	49	1.5	14.2
	2	58	96.8	772	13.3	695	12.0	77	1.3	10.0
	3	59	98.3	735	12.5	653	11.1	82	1.4	11.2
	4	58	96.7	772	13.3	716	12.3	56	1.0	7.3
	5	59	98.3	784	13.3	719	12.2	65	1.1	8.3
	6	58	96.7	811	14.0	744	12.8	67	1.2	8.3
	7	56	93.3	679	12.1	607	10.8	72	1.3	10.6[b]
	8	57	95.0	749	13.1	674	11.8	75	1.3	10.0

[a] Mating was one male to three females. [b] $p < 0.05$. [c] $p < 0.01$.

rium T 1538.

The fluctuation test showed an increase in the mutant frequency of a Valin-sensitive *E. coli* K 12 strain under the influence of povidone-iodine at an incubation temperature of 4° only and not at 37°[1].

According to investigations carried out by Speck *et al.* (2), povidone-iodine is capable of selectively altering the DNA of human diploid cells growing in culture. These investigations, and the importance of povidone-iodine as a local antiseptic, prompted the testing of povidone-iodine for mutagenicity in various animal test systems.

EXPERIMENTAL

Male and female NMRI mice[2] and male and female Chinese hamsters[3] (*Gricetulus griseus*) received standardized feed[4], and drinking water was available *ad libitum*. The animals were housed in plastic (polycarbonate) cages in air-conditioned rooms at 20 ± 2° and 55 ± 5% humidity. The day/night rhythm was 12 hr.

Povidone-iodine USP (iodine as I_3^-[1] ion complex bonded to povidone; available iodine 11.2%) dissolved in distilled water was administered intraperitoneally. The results were checked for significant differences using the χ^2 test or U test.

Dominant Lethal Assay—This assay is an indirect method of detecting induced mutations in the germ cells of male animals, because the results are found in female animals mated with (treated) males. An increase in the number of dead implantations is the main evidence of induced dominant lethal mutation. The conception rate and the average number of implantations also are used for evaluation purposes.

The test procedure used was that of Röhrborn and Vogel (3). One group of 20 male mice received 72 mg of povidone-iodine/kg (one-fifth LD_{50}).

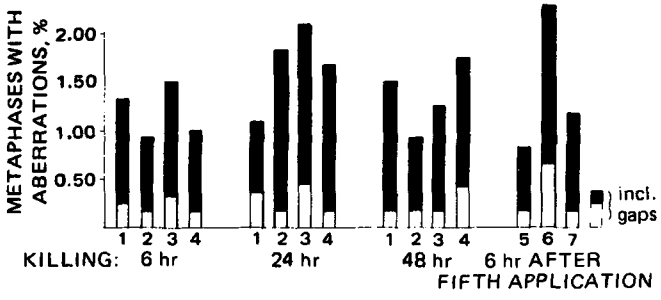

Figure 1—*Bone marrow test results in hamsters after intraperitoneal application of povidone-iodine. Key: Group 1, control; Group 2, control (sodium chloride); Group 3, 1 × 38.3 mg/kg; Group 4, 1 × 82.5 mg/kg; Group 5, control; Group 6, control (sodium chloride); and Group 7, 5 × 38.3 mg/kg.*

Table II—Testing of Povidone-Iodine in the Micronucleus Test on NMRI Mice with Double Intraperitoneal Application

Dose	0	2 × 10 ml of Distilled Water/kg	2 × 36 mg/kg
Number of animals	10	10	10
Analyzed normochromatic erythrocytes	40,000	40,000	40,000
With micronuclei, ‰	2.15	3.17	2.52
Minimum, ‰	0.12	0.12	0.15
Maximum, ‰	0.35	0.45	0.35
1 micronucleus, ‰	1.90	2.82	2.35
2 micronuclei, ‰	0.22	0.30	0.15
3 micronuclei, ‰	0.00	0.05	0.00
More than 3 micronuclei, ‰	0.02	0.00	0.02
Analyzed polychromatic erythrocytes	20,000	20,000	20,000
With micronuclei, ‰	3.70	2.95	4.30[a]
Minimum, ‰	0.20	0.20	0.20
Maximum, ‰	0.50	0.50	0.65
1 micronucleus, ‰	3.60	2.75	4.20
2 micronuclei, ‰	0.10	0.20	0.05
3 micronuclei, ‰	0.00	0.00	0.05
More than 3 micronuclei, ‰	0.00	0.00	0.00

[a] $p < 0.05$.

[1] F. Lingens, Universität Hohenheim, Institut für Mikrobiologie, Garbenstrasse 30, D-7000 Stuttgart 70, Federal Republic of Germany, personal communication.

[2] Supplied by Wiga Co., Sulzfeld, Federal Republic of Germany.

[3] Supplied by Thomae Co., Biberach, Federal Republic of Germany.

[4] Altromin R, supplied by Altromin Co., Lage/Lippe, Federal Republic of Germany; or Ssniff H, supplied by Intermast GmbH, Boeckum-Hoevel, Federal Republic of Germany.

Table III—Testing of Povidone-Iodine in the Bone Marrow Test on Chinese Hamsters with Single Intraperitoneal Application

Dose	Untreated			10 ml of Saline/kg			38.3 mg/kg			82.5 mg/kg		
Put to death after, hr	6	24	48	6	24	48	6	24	48	6	24	48
Number of animals	12	11	12	12	12	12	12	11	12	12	12	12
Analyzed metaphases	1200	1100	1200	1200	1200	1200	1200	1100	1200	1200	1200	1200
Animals with aberrant metaphases	8	8	9	7	9	6	9	8	8	6	9	9
Metaphases with aberrations												
Including gaps	16	12	18	11	22	11	18	23	15	12	20	21
Excluding gaps	3	4	2	2	2	2	4	5	2	2	2	5
Gaps (chromatide)	9	8	14	7	15	9	10	15	10	7	12	16
Gaps (isochromatide)	4	0	2	2	5	0	4	3	3	3	6	0
Breaks (chromatide)	0	2	1	1	0	2	2	2	2	1	0	2
Breaks (isochromatide)	0	0	0	0	1	0	0	0	0	0	0	0
Acentric fragments	3	1	1	0	1	0	2	3	0	1	1	3
Multiple aberrations	0	1	0	1	0	0	0	0	0	0	1	0

A second group of 20 male mice received 10 ml of distilled water/kg in a single application. The third group of 20 male mice remained untreated. One male was mated to three females.

Micronucleus Test—This test is a conventional screening method of indirectly discovering induced structural and numeric chromosome aberrations in somatic cells. Increased appearance of micronuclei in erythrocytes can be an indication of indirect mutations and also of spindle poisons.

The test procedure used was that of Boller and Schmid (4) or Schmid (5). The three groups were each comprised of five male and five female mice. One group received 36 mg of povidone-iodine/kg (one-tenth LD_{50}), and another group received 10 ml of distilled water/kg twice at an interval of 24 hr. The third group of animals remained untreated. Six hours after the final dose, the animals were sacrificed, the femurs were removed, and bone marrow smears were prepared; 4000 normochromatic and 2000 polychromatic erythrocytes were examined per animal.

Bone Marrow Test—This test was carried out in accordance with published recommendations (6) and involved 15 groups of six male and six female Chinese hamsters each. This test is used for direct analysis of induced structural and numerical chromosome aberrations in somatic cells.

Three groups of animals received a single 38.3-mg/kg (one-quarter LD_{50}) or 82.5-mg/kg (one-half LD_{50}) dose of povidone-iodine or 10 ml of saline solution/kg. Three groups remained untreated. Two other groups received five applications of 38.3 mg of povidone-iodine/kg or five 10-ml/kg applications of saline solution on 5 successive days. Another group of animals remained untreated. The animals were sacrificed 6, 24, or 48 hr after the single application or 6 hr after the fifth application; 100 metaphases were evaluated per animal.

Table IV—Testing of Povidone-Iodine in the Bone Marrow Test on Chinese Hamsters with Five Intraperitoneal Injections [a]

Dose	Untreated	5 × 10 ml of Saline/kg	5 × 38.3 mg/kg
Number of animals	12	11	11
Analyzed metaphases	1200	1100	1100
Animals with aberrant metaphases	7	8	7
Metaphases with aberrations			
Including gaps	10	25	13
Excluding gaps	2	7	2
Gaps (chromatide)	8	17	8
Gaps (isochromatide)	0	1	3
Breaks (chromatide)	1	6	2
Breaks (isochromatide)	0	0	0
Acentric fragments	0	1	0
Multiple aberrations	1	0	0

[a] Animals put to death 6 hr after the fifth application.

RESULTS

Dominant Lethal Assay (Table I)—The animals tolerated a single application of povidone-iodine without symptoms. The conception rate decreased significantly during the 1st week, but the average number of implantations and the mutagenicity index were not affected. During the other mating periods, all parameters varied in a similar manner as in the control animals.

Micronucleus Test (Table II)—The animals tolerated administration of povidone-iodine without symptoms. There was merely a slight increase in polychromatic erythrocytes containing micronuclei, but even this increase was within the normal range.

Bone Marrow Test (Tables III and IV and Fig. 1)—The animals tolerated povidone-iodine with no symptoms when administered in a single dose, but repeated application caused the animals to show signs of pain lasting for ~1 min. There was no increase in the percentage of aberrant metaphases when the substance was administered singly or repeatedly. The type of aberration was the same with treated and untreated animals.

DISCUSSION

Contrary to previous results (1, 2), povidone-iodine did not have any mutagenic effect in the dominant lethal assay, the micronucleus test, or the bone marrow test.

Because of its available iodine content, povidone-iodine has an antibacterial effect. The mutagenic effect with an *E. coli* or *S. typhimurium* strain could be due to lower sensitivity, which can result from a mutation. However, this hypothesis is unlikely since resistance does not develop following the use of povidone-iodine. Possibly, povidone-iodine also is inactivated so quickly in mammalian metabolism that genetic damage cannot result. Some genetic experts think that mutagenicity testing of microorganisms does not in any way represent ultimate testing for obtaining information, mutagenic or otherwise, and that positive *in vitro* tests cannot be used as an argument in favor of mutagenic hazard in humans when tests on mammals turn out negative.

The findings of the present animal experiments suggest that povidone-iodine has no mutagenic effects since no mutagenic effect was detected even when extremely high doses were administered.

REFERENCES

(1) T. J. Wlodkowski, W. T. Speck, and H. S. Rosenkranz, *J. Pharm. Sci.*, **64**, 1235 (1975).

(2) W. T. Speck, H. S. Carr, and H. S. Rosenkranz, *J. Toxicol. Environ. Health*, **1**, 977 (1976).

(3) G. Röhrborn and F. Vogel, *Dtsch. Med. Wochenschr.*, **92**, 2315 (1967).

(4) K. Boller and W. Schmid, *Humangenetik*, **11**, 35 (1970).

(5) W. Schmid, *Mutat. Res.*, **31**, 9 (1975).

(6) *Toxicol. Appl. Pharmacol.*, **22**, 269 (1972).

GLC Determination of Butylated Hydroxyanisole in Human Plasma and Urine

R. EL-RASHIDY and SARFARAZ NIAZI ˣ

Received December 30, 1977, from the *Department of Pharmacy, College of Pharmacy, University of Illinois at the Medical Center, Chicago, IL 60612.* Accepted for publication May 26, 1978.

Abstract □ A highly sensitive and specific GLC method was developed for the analysis of butylated hydroxyanisole, a commonly used antioxidant. Concentrations below 100 ng/ml could be detected in human plasma and urine. Preliminary pharmacokinetic studies demonstrated that, upon administration of 100 mg po, butylated hydroxyanisole was quickly absorbed and removed from the plasma with a high degree of intersubject variability.

Keyphrases □ Butylated hydroxyanisole—GLC analysis in plasma and urine □ GLC—analysis, butylated hydroxyanisole in plasma and urine □ Antioxidants—butylated hydroxyanisole, GLC analysis in plasma and urine

Butylated hydroxyanisole (I) is a commonly used food antioxidant (1) in this country (average intake: 35–140 mg/day). Although generally regarded as safe (GRAS list), several studies reported various pharmacological and toxicological properties (2–4). No study, however, has addressed its disposition characteristics in humans. Previously (5), concentration-dependent binding of I to human serum albumin was reported.

The purpose of this investigation was to develop a specific and sensitive technique for the analysis of I in plasma and urine that can be used to study the kinetics of the absorption and disposition of I.

EXPERIMENTAL

Apparatus—A gas chromatograph[1] was equipped with a flame-ionization detector. A 1.8-m long, 3.13-mm o.d., and 2.13-mm i.d. stainless steel column[2] was packed with 5% QF-1 as the stationary phase coated on 80–100-mesh Gas Chrom WAW as the supporting phase[2]. The column, detector, and injection port temperatures were 165, 225, and 215°, respectively. The carrier gas (nitrogen), hydrogen, and air flow rates were 30, 40, and 300 ml/min, respectively. Injections of 2–3 μl were made with a 10-μl syringe[3].

Reagents and Chemicals—Pure samples of I and butylated hydroxytoluene (II), the internal standard, were obtained commercially[4]. All other reagents were reagent grade[5].

Analysis of I in Plasma and Urine—To 1 ml of plasma or 5 ml of urine in a 15-ml centrifuge tube, a 0.2-ml solution of II (10 μg/ml) was added. A 4-ml portion of petroleum ether[5] also was added to the tube, which was then stoppered with an aluminum foil-lined closure and shaken[6] for 10 min. The organic layer was transferred to another centrifuge tube containing 3 ml of 5% sodium bicarbonate, and this tube was stoppered and shaken for another 10 min. A 3-ml aliquot of the organic layer was transferred to another tube and evaporated to dryness under a gentle stream of nitrogen in a beaker water bath held at 30°. The residue was dissolved in 50 μl of carbon disulfide, and aliquots of 2–3 μl were injected onto the column for quantification.

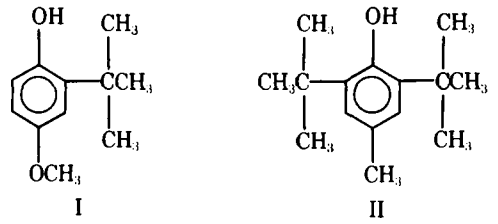

I II

The calibration curves were constructed by adding 0.25, 0.50, 0.75, 1.0, and 2.0 μg of I to 1 ml of human plasma or 5 ml of human urine. The peak height ratios of I and II plotted against spiked concentrations of I gave good linear correlations.

Human Experiments—Two healthy adult male volunteers, 55 and 60 kg, who had not ingested any products containing I or II for 2 weeks were each given 100 mg of I in a gelatin capsule with 200 ml of water after overnight fasting. Blood samples were withdrawn at 0.5, 1, 2, 4, 6, and 8 hr following administration; pooled urine samples were collected for 0–8-, 8–16-, 16–24-, and 24–36-hr intervals. All samples were kept frozen and protected from light until analyzed.

RESULTS AND DISCUSSION

Several analytical methods for the detection of I in food products (6–11) require large samples, are not very sensitive, and are not applicable to the analysis of biological samples.

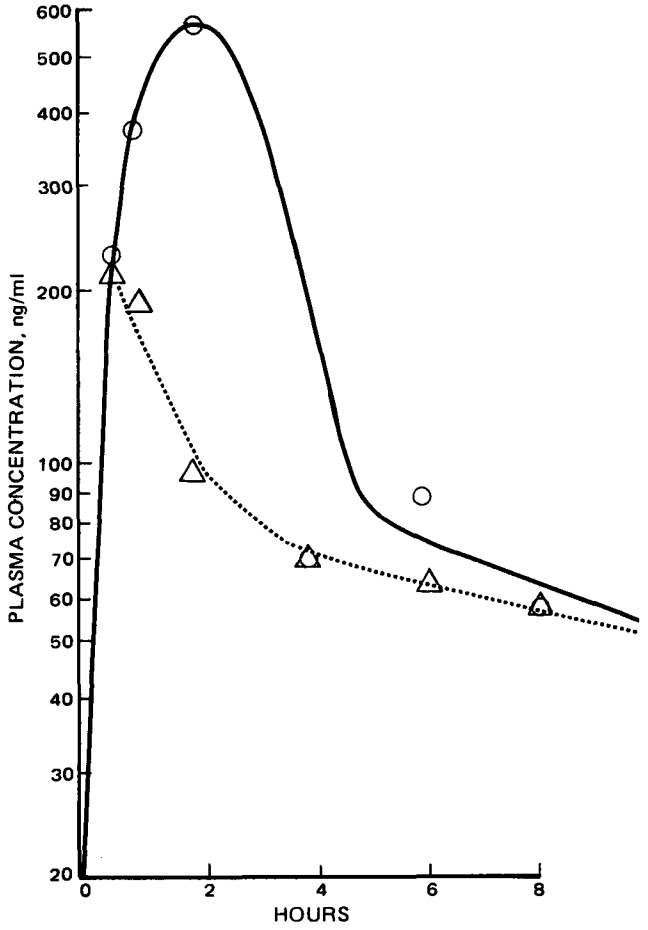

Figure 1—*Plasma concentration profiles of free butylated hydroxyanisole following oral administration of 100 mg in two subjects.*

[1] Varian Aerograph model 1400, Varian, Park Ridge, Ill.
[2] Alltech Associates, Arlington Heights, Ill.
[3] Hamilton Co., Reno, Nev.
[4] Nutritional Biochemicals Corp., Cleveland, Ohio.
[5] Fisher Scientific Co., Fair Lawn, N.J.
[6] Precision Scientific Corp., Chicago, Ill.

0022-3549/79/0100-0103$01.00/0
© 1979, American Pharmaceutical Association

Table I—Precision and Accuracy of the Assay Applied to Spiked Human Plasma Samples

Spiked Concentration, ng/ml	Determined Concentration, ng/ml ± *SEM*[a]	Range
200	200 ± 1.0	194–205
500	500 ± 0.8	488–512
1000	998 ± 1.0	970–1026
3000	3087 ± 2.5	2870–3303

[a] $n = 6$.

The extraction procedure suggested here results in a noise-free blank for the plasma and urine. The spiked samples (prepared from a stock solution of 1 mg/ml in ethanol) showed excellent resolution. The retention time for I was 4 min, whereas the internal standard (II) appeared at 3.0 min. These short retention times are highly desirable, allowing large numbers of samples to be analyzed in a short time. The extraction efficiency was calculated to range from 75 to 80% when compared with the standard solutions prepared in carbon disulfide.

The sensitivity of the column under these conditions allowed detection of quantities as low as 10 ng injected onto the column; however, the concentration of I that could easily be detected in plasma and urine was below 100 ng/ml. The precision and accuracy of the analytical method were discerned by spiking the plasma samples with concentrations ranging from 200 to 3000 ng/ml. Table I reports the determined concentrations of the spiked samples.

The plasma I levels following administration of a 100-mg oral dose are shown in Fig. 1. Each data point represents the average of six determinations. A large degree of intersubject variation was noted in terms of the time and magnitude of the peak concentration. After a rapid rise in the plasma concentration, a sharp decline resulted in the lowering of the concentration to below 100 ng/ml within 2 hr for Subject 1 and 6 hr for Subject 2. Therefore, the bioavailability of I and its rate of absorption may differ greatly between subjects.

Less than 1% of the administered dose of I was eliminated in the urine as intact drug (Table II), which is in concurrence with a previous study (1).

Table II—Recovery of Free Butylated Hydroxyanisole in Urine[a]

Hours	Subject 1	Subject 2
0–8	0.080 ± 0.012	0.050 ± 0.011
8–16	0.570 ± 0.009	0.431 ± 0.009
16–24	0.033 ± 0.0017	0.027 ± 0.025
24–36	0.00	0.00

[a] Percent of administered dose ± *SEM*.

Detailed pharmacokinetic studies are in progress.

REFERENCES

(1) B. D. Astill, J. Mills, D. W. Fassett, R. L. Roudabush, and C. J. Terhaar, *Am. J. Agric. Food Chem.*, **10**, 315 (1962).

(2) Technical Report Series No. 228, World Health Organization, 1962.

(3) A. Takanaka, R. Kato, and Y. Omori, *Shokuhim Eiseigaku Zasshi*, **10**, 260 (1969).

(4) D. M. Conning and T. McElligott, *Proc. Eur. Soc. Study Drug Toxic.*, **11**, 203 (1970).

(5) R. El-Rashidy and S. Niazi, *J. Pharm. Sci.*, **67**, 967 (1978).

(6) W. A. B. Thompson, *J. Chromatogr.*, **19**, 599 (1965).

(7) T. K. Choy, J. J. Quattrone, Jr., and N. J. Alicino, *ibid.*, **12**, 171 (1963).

(8) D. Takahashi, *J. Assoc. Off. Anal. Chem.*, **51**, 943 (1968).

(9) *Ibid.*, **50**, 880 (1967).

(10) S. Dilli and K. Robards, *Analyst*, **102**, 201 (1977).

(11) B. D. Page and B. P. C. Kennedy, *J. Assoc. Off. Anal. Chem.*, **59**, 1208 (1976).

ACKNOWLEDGMENTS

Supported in part by a grant from the Graduate College Campus Research Board, University of Illinois at the Medical Center.

Bioavailability and Related Heart Function Index of Digoxin Capsules and Tablets in Cardiac Patients

E. ASTORRI *x, G. BIANCHI *, G. LA CANNA *, D. ASSANELLI *, O. VISIOLI *, and A. MARZO ‡

Received August 9, 1977, from the **Istituto di Clinica Medica Ia, Cattedra di Malattie Cardiovascolari, University of Parma, Via Gramsci, 14-I-43100 Parma, Italy*, and the ‡*Istituto Simes di Cardiologia Sperimentale, Via C. Colombi, 18-I-20161 Milan, Italy.* Accepted for publication May 23, 1978.

Abstract □ A loading dose of digoxin (750 μg) in two commercial formulations was administered to 14 patients with heart disease according to a crossover design. One formulation consisted of soft gelatin capsules containing a solution of digoxin; the other formulation was compressed tablets. All parameters investigated, *i.e.*, serum peak height, time of the peak, area under the serum level–time curve (*AUC*), and area above the Q–S_2I (electromechanical systole) decrease (obtained from polycardiographic evaluation), showed better bioavailability of digoxin capsules than tablets, averaging 36.3%. The better bioavailability of digoxin capsules than tablets seems to be more evident in heart disease patients than that encountered previously in healthy subjects. The *AUC* and the area above the Q–S_2I decrease were linearly correlated only with digoxin capsules.

Keyphrases □ Bioavailability—digoxin capsules and tablets compared in cardiac patients □ Heart function index—digoxin capsules and tablets compared in cardiac patients □ Digoxin—bioavailability and heart function index, capsules and tablets compared in cardiac patients □ Cardiotonic agents—digoxin, bioavailability and heart function index, capsules and tablets compared in cardiac patients

A marked lack of uniformity in content and bioavailability of digoxin tablets was reported (1–5) for different formulations as well as for different batches of the same marketed product. In the last few years, a fairly satisfactory bioavailability level has been achieved in most commercial preparations of digoxin tablets that meet the Food and Drug Administration's recent specific requirements (6). The most important development in this field is the

0022-3549/79/0100-0104$01.00/0

© 1979, American Pharmaceutical Association

Table I—Precision and Accuracy of the Assay Applied to Spiked Human Plasma Samples

Spiked Concentration, ng/ml	Determined Concentration, ng/ml ± *SEM*[a]	Range
200	200 ± 1.0	194–205
500	500 ± 0.8	488–512
1000	998 ± 1.0	970–1026
3000	3087 ± 2.5	2870–3303

[a] $n = 6$.

The extraction procedure suggested here results in a noise-free blank for the plasma and urine. The spiked samples (prepared from a stock solution of 1 mg/ml in ethanol) showed excellent resolution. The retention time for I was 4 min, whereas the internal standard (II) appeared at 3.0 min. These short retention times are highly desirable, allowing large numbers of samples to be analyzed in a short time. The extraction efficiency was calculated to range from 75 to 80% when compared with the standard solutions prepared in carbon disulfide.

The sensitivity of the column under these conditions allowed detection of quantities as low as 10 ng injected onto the column; however, the concentration of I that could easily be detected in plasma and urine was below 100 ng/ml. The precision and accuracy of the analytical method were discerned by spiking the plasma samples with concentrations ranging from 200 to 3000 ng/ml. Table I reports the determined concentrations of the spiked samples.

The plasma I levels following administration of a 100-mg oral dose are shown in Fig. 1. Each data point represents the average of six determinations. A large degree of intersubject variation was noted in terms of the time and magnitude of the peak concentration. After a rapid rise in the plasma concentration, a sharp decline resulted in the lowering of the concentration to below 100 ng/ml within 2 hr for Subject 1 and 6 hr for Subject 2. Therefore, the bioavailability of I and its rate of absorption may differ greatly between subjects.

Less than 1% of the administered dose of I was eliminated in the urine as intact drug (Table II), which is in concurrence with a previous study (1).

Table II—Recovery of Free Butylated Hydroxyanisole in Urine[a]

Hours	Subject 1	Subject 2
0–8	0.080 ± 0.012	0.050 ± 0.011
8–16	0.570 ± 0.009	0.431 ± 0.009
16–24	0.033 ± 0.0017	0.027 ± 0.025
24–36	0.00	0.00

[a] Percent of administered dose ± *SEM*.

Detailed pharmacokinetic studies are in progress.

REFERENCES

(1) B. D. Astill, J. Mills, D. W. Fassett, R. L. Roudabush, and C. J. Terhaar, *Am. J. Agric. Food Chem.*, **10**, 315 (1962).

(2) Technical Report Series No. 228, World Health Organization, 1962.

(3) A. Takanaka, R. Kato, and Y. Omori, *Shokuhim Eiseigaku Zasshi*, **10**, 260 (1969).

(4) D. M. Conning and T. McElligott, *Proc. Eur. Soc. Study Drug Toxic.*, **11**, 203 (1970).

(5) R. El-Rashidy and S. Niazi, *J. Pharm. Sci.*, **67**, 967 (1978).

(6) W. A. B. Thompson, *J. Chromatogr.*, **19**, 599 (1965).

(7) T. K. Choy, J. J. Quattrone, Jr., and N. J. Alicino, *ibid.*, **12**, 171 (1963).

(8) D. Takahashi, *J. Assoc. Off. Anal. Chem.*, **51**, 943 (1968).

(9) *Ibid.*, **50**, 880 (1967).

(10) S. Dilli and K. Robards, *Analyst*, **102**, 201 (1977).

(11) B. D. Page and B. P. C. Kennedy, *J. Assoc. Off. Anal. Chem.*, **59**, 1208 (1976).

ACKNOWLEDGMENTS

Supported in part by a grant from the Graduate College Campus Research Board, University of Illinois at the Medical Center.

Bioavailability and Related Heart Function Index of Digoxin Capsules and Tablets in Cardiac Patients

E. ASTORRI *x, G. BIANCHI *, G. LA CANNA *, D. ASSANELLI *, O. VISIOLI *, and A. MARZO ‡

Received August 9, 1977, from the **Istituto di Clinica Medica Ia, Cattedra di Malattie Cardiovascolari, University of Parma, Via Gramsci, 14-I-43100 Parma, Italy*, and the ‡*Istituto Simes di Cardiologia Sperimentale, Via C. Colombi, 18-I-20161 Milan, Italy.* Accepted for publication May 23, 1978.

Abstract □ A loading dose of digoxin (750 μg) in two commercial formulations was administered to 14 patients with heart disease according to a crossover design. One formulation consisted of soft gelatin capsules containing a solution of digoxin; the other formulation was compressed tablets. All parameters investigated, *i.e.*, serum peak height, time of the peak, area under the serum level–time curve (*AUC*), and area above the Q–S_2I (electromechanical systole) decrease (obtained from polycardiographic evaluation), showed better bioavailability of digoxin capsules than tablets, averaging 36.3%. The better bioavailability of digoxin capsules than tablets seems to be more evident in heart disease patients than that encountered previously in healthy subjects. The *AUC* and the area above the Q–S_2I decrease were linearly correlated only with digoxin capsules.

Keyphrases □ Bioavailability—digoxin capsules and tablets compared in cardiac patients □ Heart function index—digoxin capsules and tablets compared in cardiac patients □ Digoxin—bioavailability and heart function index, capsules and tablets compared in cardiac patients □ Cardiotonic agents—digoxin, bioavailability and heart function index, capsules and tablets compared in cardiac patients

A marked lack of uniformity in content and bioavailability of digoxin tablets was reported (1–5) for different formulations as well as for different batches of the same marketed product. In the last few years, a fairly satisfactory bioavailability level has been achieved in most commercial preparations of digoxin tablets that meet the Food and Drug Administration's recent specific requirements (6). The most important development in this field is the

0022-3549/79/0100-0104$01.00/0

© 1979, American Pharmaceutical Association

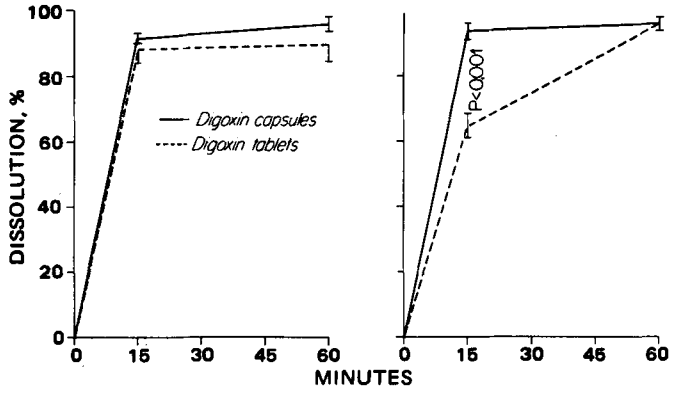

Figure 1—*Dissolution of digoxin capsules and tablets using both the paddle-water (left) and paddle-acid (right) methods (mean values of six experiments ± SE). Values of* p *were computed using the Student* t *test for independent samples.*

soft gelatin liquid-filled capsule, a new pharmaceutical formulation, which contains the glycoside in a dissolved form and allows a more satisfactory bioavailability range than tablets.

This paper reports a comparative study of the bioavailability of digoxin in capsules and tablets in volunteer patients who suffered from heart disease and used digoxin. A polycardiographic investigation enabled a useful statistical comparison between bioavailability and the related index of heart function for both formulations.

EXPERIMENTAL

Drug—The digoxin capsules[1] contained 0.25 mg of digoxin dissolved in 1.5 mg of *N,N*-dimethylacetamide and 139 mg of polyethylene glycol 400. The digoxin tablets[2] also contained 0.25 mg of the cardiac glycoside. The dissolution rate of both formulations was evaluated according to the *Federal Register* (6), using both the paddle-acid and paddle-water methods.

Treatment—The 14 patients were of both sexes and were 40–64 years old; they had an average body weight of 75 kg. They were in normal sinusal rhythm and were affected by atherosclerotic and/or hypertensive heart disease. A series of laboratory tests and clinical observations showed that the patients had no other serious diseases and that inorganic ions, serum proteins, creatinine clearance, and thyroid, GI, and renal functions were normal.

All subjects received three digoxin capsules and three digoxin tablets (750 μg of digoxin) in a crossover design at an interval of 10 days. A blood sample (5 ml) was taken from each subject before treatment and at 15, 30, and 45 min and 1, 2, 3, and 4 hr after treatment. Serum digoxin concentrations were measured with the radioimmunoassay[3] method of Smith *et al.* (7). At the same times, polycardiographic measurements were recorded[4].

Variations in systolic intervals were measured and adjusted for heart rate and sex according to Weissler *et al.* (8). Of the parameters evaluated, electromechanical systole ($Q–S_2I$) was selected as the most representative of the action of digitalis on the heart. In effect, $Q–S_2I$ is a useful index in terms of the decrease in both the preejective period and the left ventricular ejection time (9).

RESULTS

Dissolution with the paddle-acid method was complete in 15 min with capsules but was markedly slower with tablets ($p < 0.001$). Both formulations were completely dissolved in 60 min. With the paddle-water method, digoxin tablets gave a dissolution rate slightly lower than capsules, but this difference was not statistically significant (Fig. 1).

[1] Eudigox, lot A9-74, Simes.
[2] Lanoxin, lot 4 B16, Wellcome.
[3] Kits were supplied by Sorin Biomedica, Saluggia (Vercelli) Italy.
[4] Elema Schonander Mongograf 61.

Table I—Peak Height, Peak Time, Area under the Serum Level–Time Curve (*AUC*), and Area above the $Q–S_2I$ Decreases in 14 Heart Patients after Administration of a Loading Dose of Digoxin (750 μg) in Capsules and Tablets[a]

Parameter	Digoxin Capsules	Digoxin Tablets	Δ%[b]	t[c]	p[c]
Peak height, ng/ml	5.3 ± 0.5	3.6 ± 0.4	32	3.7	<0.01
Peak time, min	107 ± 19	153 ± 19	−43	−3.3	<0.01
AUC, ng/ml × hr	12.3 ± 1.6	7.6 ± 0.6	38	3.4	<0.01
Area above $Q–S_2I$ decrease, msec hr	7.0 ± 1.0	4.7 ± 0.6	32	3.0	<0.02

[a] Mean values ± *SE*. [b] Δ% = [(capsules − tablets)/capsules] × 100. [c] Evaluated with the Student *t* test for paired samples.

The peak height was significantly higher and was attained earlier with the capsules than with the tablets. The areas under the serum level–time curve (*AUC*) and above the decrement of electromechanical systole were significantly higher with the capsules than with the tablets (Table I). When a regression straight-line relationship between the *AUC* and the area above the $Q–S_2I$ decrease was calculated, a linear regression coefficient of 0.49 ($p < 0.05$) was obtained with the capsules, in contrast to 0.15 (p without any statistical significance) with the tablets.

DISCUSSION

The better bioavailability of digoxin capsules than tablets was previously encountered in dogs (10) and in healthy subjects after a single dose (11–15) and in a steady-state condition (16). The originality of this investigation lies in the experimental design, which consists of administration of a loading dose of digoxin (750 μg) in capsules and tablets to heart patients in a crossover pattern and the evaluation of bioavailability and related heart function index. The need to measure evident variations in cardiomechanical parameters indicated a loading dose of 750 μg of digoxin. The bioavailability of digoxin capsules was 36% higher than that of tablets (mean of the four Δ% in Table I) in heart patients. This difference in healthy human subjects was around 20 (12) and 27% (13) after a single dose and 26% (16) in a steady-state condition. The difference in bioavailability between digoxin capsules and tablets thus seems to be more evident in heart patients than in healthy subjects. In addition, the *AUC* and the area above the $Q–S_2I$ decrease were linearly correlated with capsules ($p < 0.05$) but not with tablets. In no case was there any evidence of GI or cardiac toxicity.

Considerable individual variability in plasma digoxin levels was observed in healthy subjects using tablets with a high dissolution rate, capsules, and, in particular, an oral solution of digoxin (12, 13, 15–17). Data from the cardiac patients in this investigation were similar to the previous healthy subject data regarding individual variability. In addition, the objective situation of the cardiopathic patients involves a specific lack of individual variability due to inadequate circulation, the liver status, and, in many cases, confinement to bed. The variability of response in digoxin absorption seems to be related mainly to the daily situation of each patient, whereas the entity of enteral absorption is closely related to the pharmaceutical formulation used.

REFERENCES

(1) J. Lindenbaum, M. H. Mellow, M. O. Blackstone, and V. P. Butler, *N. Engl. J. Med.*, **285**, 1344 (1971).

(2) J. G. Wagner, M. Christensen, E. Sakmar, D. Blair, J. D. Yates, P. W. Willis, A. J. Sedman, and R. G. Stoll, *J. Am. Med. Assoc.*, **224**, 199 (1973).

(3) M. C. B. Van Oudtshoorn, *Lancet*, **2**, 1153 (1972).

(4) D. H. Huffman, C. V. Manion, and D. L. Azarnoff, *Clin. Pharmacol. Ther.*, **16**, 310 (1974).

(5) G. Levy and M. Gibaldi, *Circulation*, **49**, 391 (1974).

(6) *Fed. Regist.*, **39** (15), 2471 (1974).

(7) T. W. Smith, V. P. Butler, and E. Haber, *N. Engl. J. Med.*, **281**, 1212 (1969).

(8) A. M. Weissler, W. S. Harris, and C. D. Schoenfield, *Circulation*, **37**, 149 (1968).

(9) W. Forester, R. P. Lewis, M. A. Weissler, and T. A. Wilke, *ibid.*, **49**, 517 (1974).

(10) A. Marzo, P. Ghirardi, G. C. Merotti, and C. Gandolfi, *Boll. Soc. Ital. Cardiol.*, **21**, 1781 (1976).

(11) P. Ghirardi, G. Catenazzo, O. Mantero, G. C. Merotti, and A.

Marzo, *J. Pharm. Sci.*, **66**, 267 (1977).
(12) I. G. Mallis, D. H. Schmidt, and J. Lindenbaum, *Clin. Pharmacol. Ther.*, **18**, 761 (1975).
(13) J. Lindenbaum, *ibid.*, **21**, 278 (1977).
(14) B. F. Johnson, C. Bye, G. Jones, and G. A. Sabey, *ibid.*, **19**, 746 (1976).
(15) P. F. Binnion, *J. Clin. Pharmacol.*, **16**, 461 (1976).
(16) C. Longhini, V. Alvisi, B. Bagni, F. Portaluppi, and C. Fersini, *Curr. Ther. Res.*, **21**, 909 (1977).
(17) D. J. Greenblatt, D. W. Duhme, J. Koch-Weser, and T. W. Smith, *Clin. Pharmacol. Ther.*, **16**, 444 (1974).

ACKNOWLEDGMENTS

The authors thank Dr. Cesare Gandolfi of Sorin Biomedica, Saluggia (Vercelli) Italy, for providing the radioimmunoassay kits.

Quantitative Determination of Chlorthalidone in Pharmaceutical Dosage Forms by High-Pressure Liquid Chromatography

MICHAEL J. O'HARE ˣ, EULALIA TAN, and JOSEPH E. MOODY

Received October 25, 1977, from the *Department of Analytical Research and Development, USV Pharmaceutical Corporation, Tuckahoe, NY 10707.* Accepted for publication May 29, 1978.

Abstract □ A reliable and selective high-pressure liquid chromatographic procedure for the quantitative determination of chlorthalidone in pharmaceutical dosage forms is described. A comparison of this stability-indicating procedure with the USP spectrophotometric assay is presented for chlorthalidone tablets and chlorthalidone tablets containing reserpine.

Keyphrases □ Chlorthalidone—high-pressure liquid chromatographic analysis in pharmaceutical dosage forms □ High-pressure liquid chromatography—analysis, chlorthalidone in pharmaceutical dosage forms □ Diuretics—chlorthalidone, high-pressure liquid chromatographic analysis in pharmaceutical dosage forms

Chlorthalidone (I), 2-chloro-5-(1-hydroxy-3-oxo-1-isoindolinyl)benzenesulfonamide, is an oral antihypertensive–diuretic administered alone and in combination with reserpine in tablets[1]. Several methods have been reported for the determination of chlorthalidone in biological media (1–4) and for its chromatographic separation and detection in the presence of other substances (5, 6). At present, there is no simple direct method for the quantitative and stability determinations of chlorthalidone in pharmaceutical dosage forms.

The USP method (7) consists of solvent extraction of the powdered tablet material and subsequent quantitative comparison of the UV absorption of a solution of the extracted chlorthalidone with the absorption of a solution of USP reference standard chlorthalidone run concomitantly. The compendial method lacks analytical specificity and selectivity for the active drug substance and is, therefore, not a reliable stability-indicating assay.

This report describes a high-pressure liquid chromatographic (HPLC) procedure that is simple, direct, and specific for chlorthalidone in tablets as the single active drug substance and in combination with reserpine.

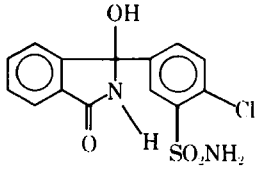

I

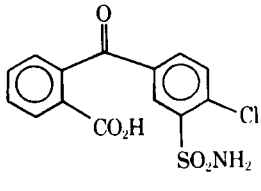

II

[1] Marketed by the USV Pharmaceutical Corp. under the trade name of Hygroton and in combination with reserpine under the trade name of Regroton.

EXPERIMENTAL

Reagents—Commercial distilled-in-glass solvents[2] and analytical reagent grade acetic acid[3] were used without additional purification.

Apparatus—A high-pressure liquid chromatograph[4], interfaced to an electronic integrator[5], was equipped with a fixed wavelength (254 nm) UV absorption detector and a constant volume injection valve[6].

Column—The column consisted of a stainless steel tube (1m × 2.2 mm i.d.) prepacked with a polyamide-coated stationary phase[7].

External Standard Solution—The external standard solution was prepared by accurately weighing approximately 50 mg of chlorthalidone reference standard[8], transferring the sample to a 25.0-ml volumetric flask, and dissolving and diluting it to volume with acetonitrile–water (9:1 v/v).

Sample Preparation—Twenty tablets were weighed and ground to a fine powder. An accurately weighed sample of the ground powder, equivalent to approximately 50 mg of chlorthalidone, was extracted with 25.0 ml of acetonitrile–water (9:1 v/v) in a 50-ml screw-capped centrifuge tube by vigorous agitation on a mixer[9] for 15 min. Then the sample was centrifuged, and the supernate was saved for chromatographic analysis.

Assay—The mobile phase, 2-propanol–acetic acid–water–*n*-hexane (30:1.5:0.5:68 v/v) was pumped through the column at a flow rate of 2 ml/min with a column head pressure of approximately 35 kg/cm². The fixed wavelength detector was operated at an attenuation of 0.32 aufs, and the column oven was maintained at 35° throughout the analysis.

Aliquots (10 μl) of the standard and sample solutions were injected in

[2] Burdick and Jackson Laboratories, Muskegon, Mich.
[3] Mallinckrodt, St. Louis, Mo.
[4] Model 830, E. I. DuPont de Nemours, Wilmington, Del.
[5] Autolab, System IV B, Spectra-Physics, Santa Clara, Calif.
[6] Six port equipped with 10-μl loop, Valco Instruments Co., Houston, Tex.
[7] Pellamidon, Whatman, Clifton, N.J.
[8] USP reference standard.
[9] Vortex Genie, Scientific Industries, Bohemia, N.Y.

0022-3549/79/0100-0106$01.00/0
© 1979, American Pharmaceutical Association

Marzo, *J. Pharm. Sci.*, **66**, 267 (1977).
(12) I. G. Mallis, D. H. Schmidt, and J. Lindenbaum, *Clin. Pharmacol. Ther.*, **18**, 761 (1975).
(13) J. Lindenbaum, *ibid.*, **21**, 278 (1977).
(14) B. F. Johnson, C. Bye, G. Jones, and G. A. Sabey, *ibid.*, **19**, 746 (1976).
(15) P. F. Binnion, *J. Clin. Pharmacol.*, **16**, 461 (1976).
(16) C. Longhini, V. Alvisi, B. Bagni, F. Portaluppi, and C. Fersini, *Curr. Ther. Res.*, **21**, 909 (1977).
(17) D. J. Greenblatt, D. W. Duhme, J. Koch-Weser, and T. W. Smith, *Clin. Pharmacol. Ther.*, **16**, 444 (1974).

ACKNOWLEDGMENTS

The authors thank Dr. Cesare Gandolfi of Sorin Biomedica, Saluggia (Vercelli) Italy, for providing the radioimmunoassay kits.

Quantitative Determination of Chlorthalidone in Pharmaceutical Dosage Forms by High-Pressure Liquid Chromatography

MICHAEL J. O'HARE ˣ, EULALIA TAN, and JOSEPH E. MOODY

Received October 25, 1977, from the *Department of Analytical Research and Development, USV Pharmaceutical Corporation, Tuckahoe, NY 10707.* Accepted for publication May 29, 1978.

Abstract □ A reliable and selective high-pressure liquid chromatographic procedure for the quantitative determination of chlorthalidone in pharmaceutical dosage forms is described. A comparison of this stability-indicating procedure with the USP spectrophotometric assay is presented for chlorthalidone tablets and chlorthalidone tablets containing reserpine.

Keyphrases □ Chlorthalidone—high-pressure liquid chromatographic analysis in pharmaceutical dosage forms □ High-pressure liquid chromatography—analysis, chlorthalidone in pharmaceutical dosage forms □ Diuretics—chlorthalidone, high-pressure liquid chromatographic analysis in pharmaceutical dosage forms

Chlorthalidone (I), 2-chloro-5-(1-hydroxy-3-oxo-1-isoindolinyl)benzenesulfonamide, is an oral antihypertensive–diuretic administered alone and in combination with reserpine in tablets[1]. Several methods have been reported for the determination of chlorthalidone in biological media (1–4) and for its chromatographic separation and detection in the presence of other substances (5, 6). At present, there is no simple direct method for the quantitative and stability determinations of chlorthalidone in pharmaceutical dosage forms.

The USP method (7) consists of solvent extraction of the powdered tablet material and subsequent quantitative comparison of the UV absorption of a solution of the extracted chlorthalidone with the absorption of a solution of USP reference standard chlorthalidone run concomitantly. The compendial method lacks analytical specificity and selectivity for the active drug substance and is, therefore, not a reliable stability-indicating assay.

This report describes a high-pressure liquid chromatographic (HPLC) procedure that is simple, direct, and specific for chlorthalidone in tablets as the single active drug substance and in combination with reserpine.

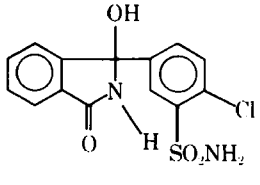

I

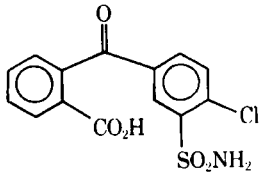

II

[1] Marketed by the USV Pharmaceutical Corp. under the trade name of Hygroton and in combination with reserpine under the trade name of Regroton.

EXPERIMENTAL

Reagents—Commercial distilled-in-glass solvents[2] and analytical reagent grade acetic acid[3] were used without additional purification.

Apparatus—A high-pressure liquid chromatograph[4], interfaced to an electronic integrator[5], was equipped with a fixed wavelength (254 nm) UV absorption detector and a constant volume injection valve[6].

Column—The column consisted of a stainless steel tube (1m × 2.2 mm i.d.) prepacked with a polyamide-coated stationary phase[7].

External Standard Solution—The external standard solution was prepared by accurately weighing approximately 50 mg of chlorthalidone reference standard[8], transferring the sample to a 25.0-ml volumetric flask, and dissolving and diluting it to volume with acetonitrile–water (9:1 v/v).

Sample Preparation—Twenty tablets were weighed and ground to a fine powder. An accurately weighed sample of the ground powder, equivalent to approximately 50 mg of chlorthalidone, was extracted with 25.0 ml of acetonitrile–water (9:1 v/v) in a 50-ml screw-capped centrifuge tube by vigorous agitation on a mixer[9] for 15 min. Then the sample was centrifuged, and the supernate was saved for chromatographic analysis.

Assay—The mobile phase, 2-propanol–acetic acid–water–*n*-hexane (30:1.5:0.5:68 v/v) was pumped through the column at a flow rate of 2 ml/min with a column head pressure of approximately 35 kg/cm². The fixed wavelength detector was operated at an attenuation of 0.32 aufs, and the column oven was maintained at 35° throughout the analysis.

Aliquots (10 μl) of the standard and sample solutions were injected in

[2] Burdick and Jackson Laboratories, Muskegon, Mich.
[3] Mallinckrodt, St. Louis, Mo.
[4] Model 830, E. I. DuPont de Nemours, Wilmington, Del.
[5] Autolab, System IV B, Spectra-Physics, Santa Clara, Calif.
[6] Six port equipped with 10-μl loop, Valco Instruments Co., Houston, Tex.
[7] Pellamidon, Whatman, Clifton, N.J.
[8] USP reference standard.
[9] Vortex Genie, Scientific Industries, Bohemia, N.Y.

0022-3549/79/0100-0106$01.00/0
© 1979, American Pharmaceutical Association

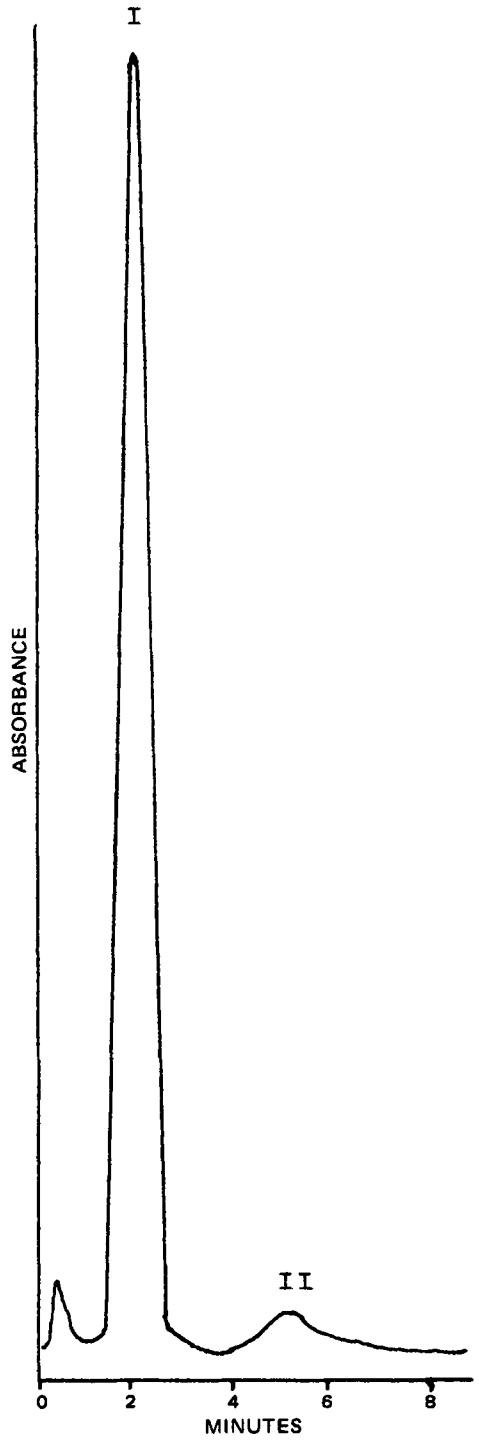

Figure 1—*Representative high-pressure liquid chromatogram.*

duplicate through the constant volume injection valve. Peak heights, determined manually, were used to calculate the average tablet content of chlorthalidone with the following equation:

$$\text{mg of chlorthalidone/tablet} = F \times H \times \frac{\text{average tablet weight (mg)}}{\text{weight of sample (mg)}} \quad \text{(Eq. 1)}$$

where H is the peak height of chlorthalidone in the sample solution and F is the ratio of the standard weight (milligrams) to the peak height of chlorthalidone in the standard solution.

Alternatively, satisfactory results were obtained on an electronic integrator programmed to measure peak area and to calculate the dosage of chlorthalidone per tablet.

Table I—Accuracy, Precision, and Percent Recovery of Chlorthalidone from Spiked Tablet Placebo by HPLC

Standard Mixture	Placebo, mg	Chlorthalidone, mg Added	Chlorthalidone, mg Found	Recovery, %
1	140	50.47	49.6	98.3
2	140	50.23	49.6	99.3
3	140	50.86	51.4	101.1
4	140	50.92	50.4	99.0
5	280	50.16	50.2	100.1
6	280	50.72	50.8	100.2
7	280	50.47	50.5	100.1
8	280	50.60	50.1	99.0
9	560	50.62	50.0	98.8
10	560	50.57	50.8	100.5
11	560	50.69	52.0	102.6
12	560	50.17	50.4	100.5
Average				100.0
Average deviation				0.89
SD				1.18

RESULTS AND DISCUSSION

The quantitative determination of chlorthalidone in experimental tablets with and without reserpine was accomplished by HPLC using a stainless steel column packed with a polyamide stationary phase. The polyamide column separates organic substances according to subtle differences in polarity and degree of hydrogen bonding (8).

The separation of chlorthalidone from its hydrolysis product (3), 4′-chloro-3′-sulfamoyl-2-benzophenone carboxylic acid (II), by the proposed method is shown in Fig. 1. The chromatogram was obtained by the analysis of a solution spiked with I and II. A trace amount of water was added to the described mobile phase to prevent unwanted effects caused by column dehydration. Acetic acid was necessary to control the extent of hydrogen bonding to the stationary phase, thereby providing a comparatively sharp symmetrical peak. Thus, by maintaining the recommended composition of the mobile phase, a reliable and quantitative separation of chlorthalidone was achieved. Since reserpine and normal tablet excipients have shorter retention times, they do not interfere with the analysis.

A statistical evaluation of this method is presented in Table I. The results on 12 consecutive analyses of standard mixtures, consisting of the addition of chlorthalidone to the tablet placebo, demonstrate its accuracy and precision. A linear relationship of sample size *versus* peak height was obtained over the concentration range of interest by varying the addition of chlorthalidone from 40 to 60 mg. Since no internal standard could be found, the concentrations of chlorthalidone in unknown samples were determined by comparison of peak heights of the drug in unknown samples with those in standard mixtures. Excellent results were obtained when the chromatographic injections were performed with a constant volume injection valve. The relative standard deviation for this procedure was 1.2%, and the repetitive analysis of a single solution of chlorthalidone gave a relative standard deviation of 0.89%.

Table II—Comparison between the HPLC and USP Methods on Chlorthalidone in Experimental Tablets

Sample[a]	Dosage Claimed, mg/tablet	Chlorthalidone Found, mg/tablet HPLC	Chlorthalidone Found, mg/tablet USP
1	12.5	12.8	12.4
2	25.0	25.2	24.2
3	50.0	50.3	50.8
4	100.0	99.1	100.0
5	75.0	74.6	74.8
6	100.0	98.8	100.0
7	100.0	101.4	100.0
8	100.0	101.2	100.7
9	100.0	99.0	100.6
10	50.0	50.3	50.8
11	50.0	49.1	51.8
12	50.0	50.5	51.0
13	50.0	50.3	50.6
14	50.0	49.2	50.8
15	50.0	50.0	50.9
16	50.0	50.2	51.3

[a] Experimental tablets without reserpine are Samples 1–12; experimental tablets with reserpine are Samples 13–16.

The experimental data in Table II were obtained on randomly selected samples of experimental tablets containing chlorthalidone with and without reserpine. The samples were analyzed in duplicate for chlorthalidone by the HPLC method and the conventional USP procedure. The results from both methods are comparable. However, since the HPLC method is stability indicating with respect to the hydrolysis product, II, this procedure is more reliable than the USP method and more accurately reflects the actual concentration of chlorthalidone per tablet dose.

REFERENCES

(1) M. Ervik and K. Gustavii, *Anal. Chem.*, **46**, 39 (1974).

(2) M. G. Tweeddale and R. I. Ogilvie, *J. Pharm. Sci.*, **63**, 1065 (1974).

(3) R. Pulver, H. Wirz, and E. G. Stenger, *Schweiz. Med. Wochenschr.*, **89**, 1130 (1959).

(4) P. H. Degen and A. Schweizer, *J. Chromatogr.*, **142**, 549 (1977).

(5) L. R. A. Bradshaw, *ibid.*, **44**, 422 (1969).

(6) R. Maes, M. Gijbels, and L. Laruelle, *ibid.*, **53**, 408 (1970).

(7) "The United States Pharmacopeia," 19th rev., Mack Publishing Co., Easton, Pa., 1975, pp. 90, 91.

(8) F. M. Rabel, *Anal. Chem.*, **45**, 957 (1973).

ACKNOWLEDGMENTS

The authors thank Dr. J. C. Barclay for advice and Dr. J. Sapio and Ms. C. Paveenbampen for assistance.

Anticonvulsant Activity of Alkyl-Substituted *N*-Benzylcyanoacetamides

CHARLES M. DARLING ˣ **and PAMELA PRYOR**

Received February 6, 1978, from the *School of Pharmacy, Auburn University, Auburn, AL 36830.* Accepted for publication June 1, 1978.

Abstract □ Thirteen new derivatives of 2-alkyl- and 2,2-dialkyl-*N*-benzylcyanoacetamide, a cyano analog of beclamide, were synthesized and tested for anticonvulsant activity. The unsubstituted compound was more active and more toxic than the derivatives. No activity was observed when the alkyl substituents in the symmetrically disubstituted derivatives contained a total of six or more carbon atoms or when benzyl was a substituent. The monosubstituted compounds were more toxic than the disubstituted compounds.

Keyphrases □ *N*-Benzylcyanoacetamides, alkyl substituted—synthesized, evaluated for anticonvulsant activity in mice □ Anticonvulsant activity—alkyl-substituted *N*-benzylcyanoacetamides evaluated in mice □ Structure-activity relationships—*N*-benzylcyanoacetamides evaluated for anticonvulsant activity in mice

Although early reports (1–3) of the use of beclamide (I) in the treatment of grand mal and psychomotor seizures were promising, the usefulness of the agent has proved to be disappointing. Beclamide has the characteristic structural arrangement of the common antiepileptics (1), as shown in II. The fact that the α-carbon atom only bears a single substitution has been suggested as the reason for the variable results obtained clinically.

Schwartz *et al.* (4, 5) reported the anticonvulsant activity of a number of substituted cyanoacetamides. Although several C-monoalkyl cyanoacetamides were prepared as intermediates, only the C-dialkylated products were tested for anticonvulsant activity. Activity against electroshock, sedative activity, and toxicity increased with increasing hydrocarbon substitution on the α-carbon atom up to dipropyl, which was the most highly substituted compound tested (4). Also, *N*-methylation and *N*-dimethylation caused a significant decrease in potency, while

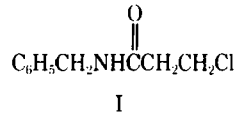

I

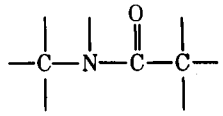

II

N-propylation and *N*-cyclization (pyrrolidine, piperidine, and morpholine) led to inactive compounds (4).

This report describes the preparation and activity of several substituted *N*-benzylcyanoacetamides as cyano analogs of beclamide. The substituents were chosen to study the effectiveness of substituting a nitrile group for a chloromethyl group in beclamide and the degree of hydrocarbon substitution that would retain activity in this series of cyanoacetamides.

EXPERIMENTAL[1]

2-Substituted *N*-Benzylcyanoacetamides (IV–XI and XVI)—These compounds were synthesized by a modification of the reported method (5). Compound III (6) (17.4 g, 0.10 mole) was added to a solution of potassium hydroxide (5.6 g, 0.10 mole, or 11.2 g, 0.20 mole) in formamide (50–75 ml). The mixture was stirred at ambient temperature for 1 hr, and the appropriate alkyl bromide (0.10 or 0.20 mole) was added.

For the preparation of the monosubstituted compounds, the mixture was stirred at ambient temperature for 3 hr; for the disubstituted derivatives, the mixture was refluxed for 1–3 hr. Then the reaction mixture was poured into ice water with stirring and filtered. The residue was recrystallized from the appropriate solvent (Table I) and activated charcoal.

The NMR spectra were consistent with the proposed structures. The NMR spectra of IV–XI showed the following common absorption peaks ($CDCl_3$): δ 7.15–7.25 (s, 5H or 10H, ArH) and 4.30–4.40 (d, 2H, NCH_2Ar) ppm. Additional absorption peaks were noted for: IV, 1.60 (s, 6H, CH_3) ppm; and V, VII, IX, and XI, 3.30–3.35 (m, 1H, CH) ppm. Depending on the alkyl substituent (V–X), the absorption in the hydrocarbon region ranged from δ 0.70 to 2.50 ppm with a multiplet splitting pattern. Each spectrum integrated for the correct number of protons. For XVI, the NMR spectrum showed the following absorption peaks ($CDCl_3$): δ 7.20 (s, 15H, ArH), 4.20 (d, 2H, NCH_2Ar), and 3.20 (q, 4H, CCH_2Ar) ppm.

***N*-Benzyl-2-benzyl-2-methylcyanoacetamide (XII)**—To a solution of potassium hydroxide (2.80 g, 0.05 mole) and formamide (10 ml) in dimethyl sulfoxide (30 ml) was added XI (13.2 g, 0.05 mole), and the mixture was stirred for 30 min. Potassium iodide (0.1 g) and methyl iodide

[1] Melting points were determined in open capillary tubes and are uncorrected. Elemental analyses were performed by Atlantic Microlab, Atlanta, Ga. NMR data were recorded on a Varian Associates T-60A spectrophotometer.

0022-3549/79/0100-0108$01.00/0

© 1979, American Pharmaceutical Association

The experimental data in Table II were obtained on randomly selected samples of experimental tablets containing chlorthalidone with and without reserpine. The samples were analyzed in duplicate for chlorthalidone by the HPLC method and the conventional USP procedure. The results from both methods are comparable. However, since the HPLC method is stability indicating with respect to the hydrolysis product, II, this procedure is more reliable than the USP method and more accurately reflects the actual concentration of chlorthalidone per tablet dose.

REFERENCES

(1) M. Ervik and K. Gustavii, *Anal. Chem.*, **46**, 39 (1974).

(2) M. G. Tweeddale and R. I. Ogilvie, *J. Pharm. Sci.*, **63**, 1065 (1974).

(3) R. Pulver, H. Wirz, and E. G. Stenger, *Schweiz. Med. Wochenschr.*, **89**, 1130 (1959).

(4) P. H. Degen and A. Schweizer, *J. Chromatogr.*, **142**, 549 (1977).

(5) L. R. A. Bradshaw, *ibid.*, **44**, 422 (1969).

(6) R. Maes, M. Gijbels, and L. Laruelle, *ibid.*, **53**, 408 (1970).

(7) "The United States Pharmacopeia," 19th rev., Mack Publishing Co., Easton, Pa., 1975, pp. 90, 91.

(8) F. M. Rabel, *Anal. Chem.*, **45**, 957 (1973).

ACKNOWLEDGMENTS

The authors thank Dr. J. C. Barclay for advice and Dr. J. Sapio and Ms. C. Paveenbampen for assistance.

Anticonvulsant Activity of Alkyl-Substituted *N*-Benzylcyanoacetamides

CHARLES M. DARLING ˣ **and PAMELA PRYOR**

Received February 6, 1978, from the *School of Pharmacy, Auburn University, Auburn, AL 36830.* Accepted for publication June 1, 1978.

Abstract □ Thirteen new derivatives of 2-alkyl- and 2,2-dialkyl-*N*-benzylcyanoacetamide, a cyano analog of beclamide, were synthesized and tested for anticonvulsant activity. The unsubstituted compound was more active and more toxic than the derivatives. No activity was observed when the alkyl substituents in the symmetrically disubstituted derivatives contained a total of six or more carbon atoms or when benzyl was a substituent. The monosubstituted compounds were more toxic than the disubstituted compounds.

Keyphrases □ *N*-Benzylcyanoacetamides, alkyl substituted—synthesized, evaluated for anticonvulsant activity in mice □ Anticonvulsant activity—alkyl-substituted *N*-benzylcyanoacetamides evaluated in mice □ Structure-activity relationships—*N*-benzylcyanoacetamides evaluated for anticonvulsant activity in mice

Although early reports (1–3) of the use of beclamide (I) in the treatment of grand mal and psychomotor seizures were promising, the usefulness of the agent has proved to be disappointing. Beclamide has the characteristic structural arrangement of the common antiepileptics (1), as shown in II. The fact that the α-carbon atom only bears a single substitution has been suggested as the reason for the variable results obtained clinically.

Schwartz *et al.* (4, 5) reported the anticonvulsant activity of a number of substituted cyanoacetamides. Although several C-monoalkyl cyanoacetamides were prepared as intermediates, only the C-dialkylated products were tested for anticonvulsant activity. Activity against electroshock, sedative activity, and toxicity increased with increasing hydrocarbon substitution on the α-carbon atom up to dipropyl, which was the most highly substituted compound tested (4). Also, *N*-methylation and *N*-dimethylation caused a significant decrease in potency, while

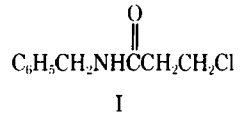

I

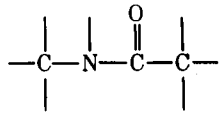

II

N-propylation and *N*-cyclization (pyrrolidine, piperidine, and morpholine) led to inactive compounds (4).

This report describes the preparation and activity of several substituted *N*-benzylcyanoacetamides as cyano analogs of beclamide. The substituents were chosen to study the effectiveness of substituting a nitrile group for a chloromethyl group in beclamide and the degree of hydrocarbon substitution that would retain activity in this series of cyanoacetamides.

EXPERIMENTAL[1]

2-Substituted *N*-Benzylcyanoacetamides (IV–XI and XVI)—These compounds were synthesized by a modification of the reported method (5). Compound III (6) (17.4 g, 0.10 mole) was added to a solution of potassium hydroxide (5.6 g, 0.10 mole, or 11.2 g, 0.20 mole) in formamide (50–75 ml). The mixture was stirred at ambient temperature for 1 hr, and the appropriate alkyl bromide (0.10 or 0.20 mole) was added.

For the preparation of the monosubstituted compounds, the mixture was stirred at ambient temperature for 3 hr; for the disubstituted derivatives, the mixture was refluxed for 1–3 hr. Then the reaction mixture was poured into ice water with stirring and filtered. The residue was recrystallized from the appropriate solvent (Table I) and activated charcoal.

The NMR spectra were consistent with the proposed structures. The NMR spectra of IV–XI showed the following common absorption peaks ($CDCl_3$): δ 7.15–7.25 (s, 5H or 10H, ArH) and 4.30–4.40 (d, 2H, NCH_2Ar) ppm. Additional absorption peaks were noted for: IV, 1.60 (s, 6H, CH_3) ppm; and V, VII, IX, and XI, 3.30–3.35 (m, 1H, CH) ppm. Depending on the alkyl substituent (V–X), the absorption in the hydrocarbon region ranged from δ 0.70 to 2.50 ppm with a multiplet splitting pattern. Each spectrum integrated for the correct number of protons. For XVI, the NMR spectrum showed the following absorption peaks ($CDCl_3$): δ 7.20 (s, 15H, ArH), 4.20 (d, 2H, NCH_2Ar), and 3.20 (q, 4H, CCH_2Ar) ppm.

***N*-Benzyl-2-benzyl-2-methylcyanoacetamide (XII)**—To a solution of potassium hydroxide (2.80 g, 0.05 mole) and formamide (10 ml) in dimethyl sulfoxide (30 ml) was added XI (13.2 g, 0.05 mole), and the mixture was stirred for 30 min. Potassium iodide (0.1 g) and methyl iodide

[1] Melting points were determined in open capillary tubes and are uncorrected. Elemental analyses were performed by Atlantic Microlab, Atlanta, Ga. NMR data were recorded on a Varian Associates T-60A spectrophotometer.

0022-3549/79/0100-0108$01.00/0

© 1979, American Pharmaceutical Association

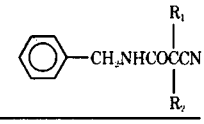

Table I—*N*-Benzylcyanoacetamides

Compound	R_1	R_2	Recrystallization Solvent[a]	Yield, %	Melting Point	Formula	Analysis, %	Calc.	Found
III	H	H	A	—	121–124°[b]			—	—
IV	CH_3	CH_3	B	39.1	64–66°	$C_{12}H_{14}N_2O$	C	71.26	71.28
							H	6.98	6.98
							N	13.85	13.78
V	CH_2CH_3	H	A	20.0	87–89°	$C_{12}H_{14}N_2O$	C	71.26	71.35
							H	6.98	7.01
							N	13.85	13.84
VI	CH_2CH_3	CH_2CH_3	A	32.1	97–99°	$C_{14}H_{18}N_2O$	C	73.01	73.06
							H	7.88	7.92
							N	12.16	12.15
VII	$CH_2CH_2CH_3$	H	A	30.5	83–86°	$C_{13}H_{16}N_2O$	C	72.19	72.20
							H	7.46	7.51
							N	12.95	12.82
VIII	$CH_2CH_2CH_3$	$CH_2CH_2CH_3$	A	7.6	77–79°	$C_{16}H_{22}N_2O$	C	74.38	74.44
							H	8.58	8.56
							N	10.84	10.90
IX	$CH_2CH_2CH_2CH_3$	H	B	15.5	70–72°	$C_{14}H_{18}N_2O$	C	73.01	73.05
							H	7.88	7.90
							N	12.16	12.16
X	$CH_2CH_2CH_2CH_3$	$CH_2CH_2CH_2CH_3$	A	60.8	76–79°	$C_{18}H_{26}N_2O$	C	75.48	75.61
							H	9.15	9.21
							N	9.78	9.73
XI	H	$CH_2C_6H_5$	C	12.7	123–125°	$C_{17}H_{16}N_2O$	C	77.25	77.30
							H	6.10	6.14
							N	10.60	10.57
XII	CH_3	$CH_2C_6H_5$	B	29.4	80–83°	$C_{18}H_{18}N_2O$	C	77.67	77.66
							H	6.52	6.55
							N	10.06	9.99
XIII	CH_2CH_3	$CH_2C_6H_5$	A	25.5	99–101°	$C_{19}H_{20}N_2O$	C	78.05	78.02
							H	6.90	6.92
							N	9.58	9.52
XIV	$CH_2CH_2CH_3$	$CH_2C_6H_5$	A	75.6	144–145°	$C_{20}H_{22}N_2O$	C	78.40	78.41
							H	7.24	7.25
							N	9.14	9.17
XV	$CH_2CH_2CH_2CH_3$	$CH_2C_6H_5$	A	49.8	128–130°	$C_{21}H_{24}N_2O$	C	78.71	78.67
							H	7.55	7.66
							N	8.74	8.68
XVI	$CH_2C_6H_5$	$CH_2C_6H_5$	A	76.2	141–143°	$C_{24}H_{22}N_2O$	C	81.33	81.27
							H	6.26	6.28
							N	7.90	7.92

[a] A = 95% ethanol, B = isopropyl ether, and C = toluene. [b] Lit. (5) mp 123–124.5°.

(7.10 g, 0.05 mole) were added, and the mixture was stirred at ambient temperature for 22 hr. The mixture was poured into ice water, and the water layer was decanted. The semisolid residue was washed with water, air dried, and recrystallized from isopropyl ether (Table I).

The NMR spectrum was consistent with the proposed structure; NMR ($CDCl_3$): δ 7.20 (s, 10H, ArH), 4.30 (d, 2H, NCH_2Ar), 3.05 (q, 2H, CCH_2Ar), and 1.60 (s, 3H, CH_3) ppm.

***N*-Benzyl-2-alkyl-2-benzylcyanoacetamides (XIII–XV)**—To a solution of sodium metal (0.89 g, 0.0387 mole) in absolute ethanol (50 ml) was added the appropriate monosubstituted *N*-benzylcyanoacetamide (V, VII, or IX) (0.035 mole). After heating at reflux for 30 min, benzyl chloride (4.90 g, 0.0387 mole) was added dropwise, and the mixture was heated at reflux for 2 hr. After cooling, water (50 ml) was added, and the solution was extracted with chloroform (3 × 60 ml). The combined chloroform extracts were dried (anhydrous magnesium sulfate) and concentrated *in vacuo*. The residue was recrystallized from 95% ethanol and activated charcoal (Table I).

Table II—Anticonvulsant and Toxic Effects

Compound	MES Activity[a] 0.5 hr	MES Activity[a] 4 hr	scMet Activity[a] 0.5 hr	scMet Activity[a] 4 hr	Toxicity[a] 0.5 hr	Toxicity[a] 4 hr
I[b]	+	—	+	—	—	—
III	+	+	++	—	++	+
IV	+	—	—	—	—	—
V	+	—	+	—	++	—
VI	—	—	+	—	—	—
VII	+	—	+	+	+	—
IX	+	—	+	—	+	—

[a] Activity and toxicity at 30, 100, or 300 mg/kg are represented by +++, ++, or +, respectively; — denotes no activity or toxicity observed at 300 mg/kg. Compounds VIII and X–XVI demonstrated no activity or toxicity at 300 mg/kg. [b] The reported (6) values for MES ED_{50}, scMet ED_{50}, and median toxic dose in the rotorod test are 183 (161–208) mg/kg, 175 (132–233) mg/kg, and 273 (246–303) mg/kg, respectively.

The NMR data agreed with the proposed structures. The NMR spectra exhibited the following common absorption peaks ($CDCl_3$): δ 7.20–7.25 (s, 10H, ArH), 4.30 (d, 2H, NCH_2Ar), and 3.05–3.10 (q, 2H, CCH_2Ar) ppm. Absorption in the hydrocarbon region (δ 0.70–2.20 ppm) exhibited a multiplet splitting pattern and integrated for the correct number of protons assigned to each structure.

Anticonvulsant Testing—All compounds were tested for anticonvulsant activity[2] using the Anticonvulsant Screening Project test systems (7). Three tests were performed in male Carworth Farms No. 1 mice: the maximal electroshock seizure test (MES), the subcutaneous pentylenetetrazol seizure threshold test (scMet), and the rotorod test to evaluate neurotoxicity.

All compounds were tested at three dose levels (30, 100, and 300 mg/kg) at 30 min and 4 hr after their intraperitoneal administration. Typically, four animals were injected with each dose, solubilized or suspended in 30% polyethylene glycol 400, and examined 30 min later for toxicity in the rotorod test. Anticonvulsant activity was evaluated immediately thereafter by subjecting one mouse to the maximal electroshock seizure test and another to the subcutaneous pentylenetetrazol seizure threshold test. The same tests were repeated after 4 hr on the two remaining mice.

Anticonvulsant activity in the maximal electroshock seizure test is defined as abolition of the limb tonic extensor component of the maximal

[2] Antiepileptic Drug Development Program, Epilepsy Branch, National Institute of Neurological and Communicative Disorders and Stroke, National Institutes of Health, Bethesda, MD 20014.

electroshock seizure elicited in mice with a 60-Hz alternating current of 50 mamp delivered for 0.2 sec *via* corneal electrodes. Activity in the subcutaneous pentylenetetrazol seizure threshold test is defined as failure to observe even a threshold seizure (a single episode of clonic spasms of at least 5 sec in duration) at a dose of 85 mg/kg.

RESULTS AND DISCUSSION

The results of the anticonvulsant activity tests (Table II) suggest that the substitution of a nitrile group for a chloromethyl group in beclamide leads to an increase in toxicity with a retention in activity against maximal electroshock and pentylenetetrazol-induced seizures. Compound III, having no carbon substitution, showed activity at a comparable or lower dose than beclamide (I). However, additional testing is required to determine whether the differences in potencies and toxicity are significant.

Of the four monosubstituted compounds tested, V, VII, and IX exhibited weak activity against maximal electroshock and pentylenetetrazol-induced seizures and neurotoxicity as evaluated by the rotorod test. Compound V appeared to be more toxic than VII or IX. Whether higher monosubstituted homologs would be active and/or toxic was not determined. No activity or toxicity was observed for the benzyl-substituted derivative (XI).

No activity was observed when the alkyl substituents in the symmetrically disubstituted derivatives contained six or more carbon atoms. Unlike the monosubstituted compounds, the active disubstituted derivatives (IV and VI) exhibited no toxicity at the dose levels tested.

REFERENCES

(1) J. Mercier, in "International Encyclopedia of Pharmacology and Therapeutics," sect. 19, vol. 1, J. Mercier, Ed., Pergamon, New York, N.Y., 1973, p. 226.

(2) B. B. Gallagher, in "Anticonvulsants," vol. 15, J. A. Vida, Ed., Academic, New York, N.Y., 1977, p. 43.

(3) W. J. Murray and L. B. Kier, *ibid.*, p. 594.

(4) H. F. Schwartz, R. G. Brown, E. I. Isaacson, and J. N. Delgado, *J. Pharm. Sci.*, **57**, 1530 (1968).

(5) H. F. Schwartz, L. F. Worrell, and J. N. Delgado, *ibid.*, **56**, 80 (1967).

(6) O. C. Dermer and J. King, *J. Org. Chem.*, **8**, 168 (1943).

(7) Anticonvulsant Screening Project, Antiepileptic Drug Development Program, National Institutes of Health, DHEW Publication No. (NIH) 76-1093, Bethesda, MD 20014.

Direct Spectrophotometric Assay of Quaternary Ammonium Compounds Using Bromthymol Blue

J. B. LOWRY

Received August 9, 1976, from *Flow Pharmaceuticals, Inc., Palo Alto, CA 94303.* Accepted for publication May 29, 1978. Present address: Cooper Laboratories, Inc., Moutain View, CA 94043.

Abstract □ Benzalkonium chloride, benzethonium chloride, and chlorhexidine gluconate were assayed quantitatively by a direct spectrophotometric method with bromthymol blue buffered at pH 7.5. The method shows good results at concentrations of 0–300 μg/ml and in the presence of epinephrine bitartrate, phenylephrine hydrochloride, pilocarpine hydrochloride, and polyvinyl alcohol.

Keyphrases □ Quaternary ammonium compounds, various—spectrophotometric analyses in prepared and commercial solutions □ Spectrophotometry—analyses, various quaternary ammonium compounds in prepared and commercial solutions □ Bromthymol blue—used in spectrophotometric analyses of various quaternary ammonium compounds in prepared and commercial solutions □ Preservatives—various quaternary ammonium compounds, spectrophotometric analyses in prepared and commercial solutions

Low concentrations of quaternary ammonium compounds such as benzalkonium chloride, benzethonium chloride, and chlorhexidine gluconate, which are used in clear ophthalmic solutions, are difficult to determine quantitatively and reproducibly. Most methods rely on complexing the quaternary ammonium compound with an acid dye such as methyl orange or bromphenol blue and extracting the complex with a chlorinated hydrocarbon solvent (1, 2). These methods have difficulties and inaccuracies arising from incomplete extraction or the emulsions formed with the hydrocarbon solvent and the quaternary ammonium compound-containing solution.

In response to the problems resulting from extraction of the dye complex, a direct method was developed using bromthymol blue buffered at pH 7.5; the reduction in absorbance was measured at 610 nm. The method was tested with benzalkonium chloride, benzethonium chloride, and chlorhexidine gluconate.

Table I—Standard Curves for Benzalkonium Chloride, Benzethonium Chloride, and Chlorhexidine Gluconate

Concentration, μg/ml	Absorbance		
	Benzalkonium Chloride	Benzethonium Chloride	Chlorhexidine Gluconate
0	0.804	0.804	0.804
100	0.593	0.659	0.667
200	0.370	0.471	0.538
300	0.225	0.325	0.438

EXPERIMENTAL

Apparatus—A pH meter and a spectrophotometer with 1-cm cells were used[1].

Reagents—Benzalkonium chloride USP, benzethonium chloride USP, epinephrine hydrochloride USP, polyvinyl alcohol, pilocarpine hydrochloride USP, phenylephrine hydrochloride USP, chlorhexidine gluconate BP, and hydroxyethylcellulose[2] were used as received. All other chemicals were reagent grade.

Buffer Solutions—Stock solutions of 0.05 and 0.25 *M* dibasic potassium phosphate and monobasic potassium phosphate were used in buffer preparation. A buffer of pH 7.5 was prepared by mixing either the 0.05 *M* solutions together or the 0.25 *M* solutions together until a pH of 7.5 was obtained.

[1] Beckman DU spectrophotometer.

[2] The 250 MR grade, Hercules Inc., Wilmington, Del.

0022-3549/79/0100-0110$01.00/0

© 1979, American Pharmaceutical Association

electroshock seizure elicited in mice with a 60-Hz alternating current of 50 mamp delivered for 0.2 sec *via* corneal electrodes. Activity in the subcutaneous pentylenetetrazol seizure threshold test is defined as failure to observe even a threshold seizure (a single episode of clonic spasms of at least 5 sec in duration) at a dose of 85 mg/kg.

RESULTS AND DISCUSSION

The results of the anticonvulsant activity tests (Table II) suggest that the substitution of a nitrile group for a chloromethyl group in beclamide leads to an increase in toxicity with a retention in activity against maximal electroshock and pentylenetetrazol-induced seizures. Compound III, having no carbon substitution, showed activity at a comparable or lower dose than beclamide (I). However, additional testing is required to determine whether the differences in potencies and toxicity are significant.

Of the four monosubstituted compounds tested, V, VII, and IX exhibited weak activity against maximal electroshock and pentylenetetrazol-induced seizures and neurotoxicity as evaluated by the rotorod test. Compound V appeared to be more toxic than VII or IX. Whether higher monosubstituted homologs would be active and/or toxic was not determined. No activity or toxicity was observed for the benzyl-substituted derivative (XI).

No activity was observed when the alkyl substituents in the symmetrically disubstituted derivatives contained six or more carbon atoms. Unlike the monosubstituted compounds, the active disubstituted derivatives (IV and VI) exhibited no toxicity at the dose levels tested.

REFERENCES

(1) J. Mercier, in "International Encyclopedia of Pharmacology and Therapeutics," sect. 19, vol. 1, J. Mercier, Ed., Pergamon, New York, N.Y., 1973, p. 226.

(2) B. B. Gallagher, in "Anticonvulsants," vol. 15, J. A. Vida, Ed., Academic, New York, N.Y., 1977, p. 43.

(3) W. J. Murray and L. B. Kier, *ibid.*, p. 594.

(4) H. F. Schwartz, R. G. Brown, E. I. Isaacson, and J. N. Delgado, *J. Pharm. Sci.*, **57**, 1530 (1968).

(5) H. F. Schwartz, L. F. Worrell, and J. N. Delgado, *ibid.*, **56**, 80 (1967).

(6) O. C. Dermer and J. King, *J. Org. Chem.*, **8**, 168 (1943).

(7) Anticonvulsant Screening Project, Antiepileptic Drug Development Program, National Institutes of Health, DHEW Publication No. (NIH) 76-1093, Bethesda, MD 20014.

Direct Spectrophotometric Assay of Quaternary Ammonium Compounds Using Bromthymol Blue

J. B. LOWRY

Received August 9, 1976, from *Flow Pharmaceuticals, Inc., Palo Alto, CA 94303.* Accepted for publication May 29, 1978. Present address: Cooper Laboratories, Inc., Moutain View, CA 94043.

Abstract □ Benzalkonium chloride, benzethonium chloride, and chlorhexidine gluconate were assayed quantitatively by a direct spectrophotometric method with bromthymol blue buffered at pH 7.5. The method shows good results at concentrations of 0–300 μg/ml and in the presence of epinephrine bitartrate, phenylephrine hydrochloride, pilocarpine hydrochloride, and polyvinyl alcohol.

Keyphrases □ Quaternary ammonium compounds, various—spectrophotometric analyses in prepared and commercial solutions □ Spectrophotometry—analyses, various quaternary ammonium compounds in prepared and commercial solutions □ Bromthymol blue—used in spectrophotometric analyses of various quaternary ammonium compounds in prepared and commercial solutions □ Preservatives—various quaternary ammonium compounds, spectrophotometric analyses in prepared and commercial solutions

Low concentrations of quaternary ammonium compounds such as benzalkonium chloride, benzethonium chloride, and chlorhexidine gluconate, which are used in clear ophthalmic solutions, are difficult to determine quantitatively and reproducibly. Most methods rely on complexing the quaternary ammonium compound with an acid dye such as methyl orange or bromphenol blue and extracting the complex with a chlorinated hydrocarbon solvent (1, 2). These methods have difficulties and inaccuracies arising from incomplete extraction or the emulsions formed with the hydrocarbon solvent and the quaternary ammonium compound-containing solution.

In response to the problems resulting from extraction of the dye complex, a direct method was developed using bromthymol blue buffered at pH 7.5; the reduction in absorbance was measured at 610 nm. The method was tested with benzalkonium chloride, benzethonium chloride, and chlorhexidine gluconate.

Table I—Standard Curves for Benzalkonium Chloride, Benzethonium Chloride, and Chlorhexidine Gluconate

Concentration, μg/ml	Absorbance		
	Benzalkonium Chloride	Benzethonium Chloride	Chlorhexidine Gluconate
0	0.804	0.804	0.804
100	0.593	0.659	0.667
200	0.370	0.471	0.538
300	0.225	0.325	0.438

EXPERIMENTAL

Apparatus—A pH meter and a spectrophotometer with 1-cm cells were used[1].

Reagents—Benzalkonium chloride USP, benzethonium chloride USP, epinephrine hydrochloride USP, polyvinyl alcohol, pilocarpine hydrochloride USP, phenylephrine hydrochloride USP, chlorhexidine gluconate BP, and hydroxyethylcellulose[2] were used as received. All other chemicals were reagent grade.

Buffer Solutions—Stock solutions of 0.05 and 0.25 *M* dibasic potassium phosphate and monobasic potassium phosphate were used in buffer preparation. A buffer of pH 7.5 was prepared by mixing either the 0.05 *M* solutions together or the 0.25 *M* solutions together until a pH of 7.5 was obtained.

[1] Beckman DU spectrophotometer.

[2] The 250 MR grade, Hercules Inc., Wilmington, Del.

0022-3549/79/0100-0110$01.00/0

© 1979, American Pharmaceutical Association

Table II—Assay of Benzalkonium Chloride with Various Compounds

Compound Present	Benzalkonium Chloride Found, μg/ml
Control	100
Epinephrine bitartrate, 10 mg/ml	104
Phenylephrine hydrochloride, 100 mg/ml	105
Pilocarpine hydrochloride, 40 mg/ml	102
Polyvinyl alcohol, 100 mg/ml	102

Dye Solutions—Bromthymol blue, 60 mg, was dissolved in 100 ml of ethanol.

Hydroxyethylcellulose Solution—Hydroxyethylcellulose, 500 mg, was dissolved in 100 ml of water.

Stock and Working Solutions—Stock benzalkonium chloride, benzethonium chloride, and chlorhexidine gluconate were prepared by dissolving accurately weighed amounts of the compounds in water. Working solutions were prepared by diluting aliquots of the stock solutions.

Test Solutions—A test solution was made by adding 1 g of epinephrine bitartrate and diluting it to 100 ml with the 100-μg/ml benzalkonium chloride working solution. This step was repeated using 10 g of phenylephrine hydrochloride and 4 g of pilocarpine hydrochloride and diluting to 100 ml with 100-μg/ml benzalkonium chloride working solution. For a contact lens wetting solution, a commercial product containing 10 mg of polyvinyl alcohol/ml was used.

Assay—In a 25-ml volumetric flask, 2.0 ml of hydroxyethylcellulose solution and 250 mg of sodium chloride were mixed with 5–10 ml of 0.05 *M* buffer solution. Then 50–300 μg/ml of a working quaternary ammonium solution and sufficient buffer to bring the volume to 25 ml were added. After mixing, the absorbance was measured at 610 nm on a spectrophotometer. A blank was prepared in the same manner but without the quaternary ammonium compound, and its absorbance was measured.

For the test solution, 2.0 ml of each was used. A 0.25 *M* buffer was substituted for the 0.05 *M* buffer when pilocarpine hydrochloride or epinephrine bitartrate was present since these compounds are acidic and a stronger buffer is needed to hold the pH at 7.5.

RESULTS AND DISCUSSION

Absorbances were measured between 400 and 700 nm using a blank solution and a 300-μg/ml working solution of each quaternary ammonium compound. The maximum reductions in absorbance occurred at 610 nm (Fig. 1). A standard linear curve was determined between 0 and 300 μg/ml at 610 nm (Table I).

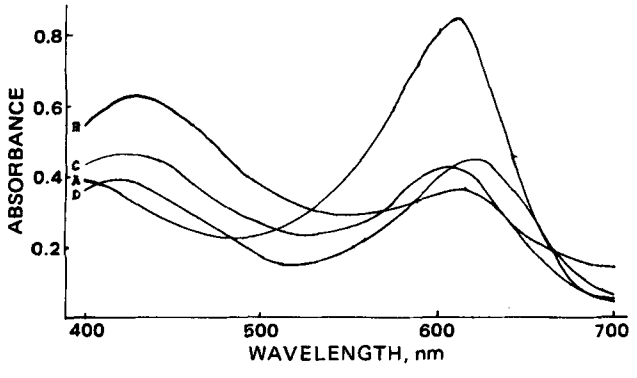

Figure 1—*Spectra of bromthymol blue (A), bromthymol blue and benzalkonium chloride (B), bromthymol blue and benzethonium chloride (C), and bromthymol blue and chlorhexidine gluconate (D).*

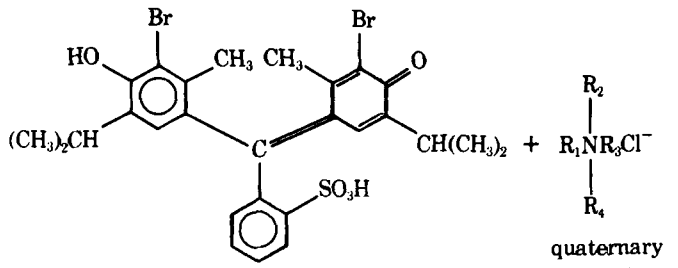

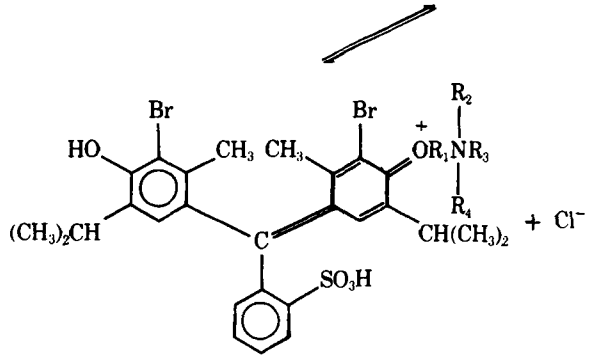

Scheme I

The method was then tested with some solutions that commonly contain benzalkonium chloride as a preservative. A sample of contact lens wetting solution containing 10 mg of polyvinyl alcohol/ml and 100 μg of benzalkonium chloride/ml was assayed. A value of 102 μg of benzalkonium chloride/ml was obtained by this method *versus* a value of 104 μg of benzalkonium chloride/ml obtained by a method using a methyl orange–benzalkonium chloride dye complex extracted with 1,2-dichloroethane (2).

The method was tried with a 10-mg/ml epinephrine bitartrate solution, a 100-mg/ml phenylephrine hydrochloride solution, and a 40-mg/ml pilocarpine hydrochloride solution, each containing 100 μg of benzalkonium chloride/ml. The results were compared to a 100-μg/ml benzalkonium chloride working solution. The results (Table II) showed little change from the working solution.

The mechanism of action is probably similar to the color change of bromthymol blue (I) in the presence of an acid or base (Scheme I).

This method offers advantages in determining quaternary ammonium compounds when extraction difficulties arise with other spectrophotometric methods.

REFERENCES

(1) L. C. Chatten and K. O. Okamura, *J. Pharm. Sci.*, **62**, 1328 (1973).

(2) R. S. Santoro, *J. Am. Pharm. Assoc., Sci. Ed.*, **49**, 666 (1960).

ACKNOWLEDGMENTS

The author thanks Dr. Joseph Z. Krezanoski for his help.

Enantiomeric Purity of Naproxen by Liquid Chromatographic Analysis of Its Diastereomeric Octyl Esters

DAVID M. JOHNSON ˣ, ANNA REUTER, JUDITH M. COLLINS, and GEOFFREY F. THOMPSON

Received May 18, 1978, from the *Pharmaceutical Analysis Department, Syntex Research, Palo Alto, CA 94304.* Accepted for publication June 14, 1978.

Abstract □ A sensitive and specific analytical method was developed to determine the enantiomeric purity of naproxen. A simple derivatization of naproxen with (*S*)-(+)-2-octanol proceeded quantitatively and gave a mixture of diastereomeric esters displaying baseline separation on liquid chromatography. The ratio of these esters was the same as the ratio of enantiomers present in naproxen samples assayed. Reproducibility of the method was excellent.

Keyphrases □ Naproxen—liquid chromatographic analysis of enantiomers □ Liquid chromatography—analysis, enantiomers of naproxen □ Enantiomers—of naproxen, liquid chromatographic analysis □ Anti-inflammatory agents—naproxen, liquid chromatographic analysis of enantiomers

The anti-inflammatory drug naproxen is the (*S*)-(+)-enantiomer of 2-(6′-methoxy-2′-naphthyl)propionic acid (I) (1, 2). During naproxen development, it became necessary to develop a simple, yet sensitive, analytical method for the determination of the enantiomeric purity of this drug.

A chromatographic method was chosen over an NMR or direct rotation measurement because of the small sample size required and to gain the specificity necessary to separate I from any of a variety of potentially optically active compounds (*i.e.*, degradation products, impurities, and metabolites). To provide chromatographic separation of the enantiomers of I, another chiral species must be introduced and a diastereomeric relationship established. The most commonly used technique involves reaction of the enantiomeric mixture with an optically active reagent to form a pair of diastereomers that can be separated using ordinary chromatographic materials[1,2]. For this method to be rigorous (*i.e.*, for the ratio of diastereomers produced to mirror exactly the ratio of enantiomers present in the original sample), the reagent used must be enantiomerically pure and there must be no kinetic resolution or racemization in the reaction that transforms the enantiomer mixture into a diastereomer mixture (6).

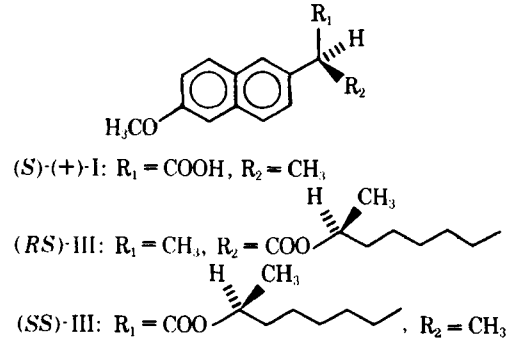

This paper describes a simple method for the quantitative reaction of I with (*S*)-(+)-2-octanol [(*S*)-(+)-II] to give the diastereomeric esters (*SS*)-III and (*RS*)-III. The liquid chromatographic separation and quantitation of these esters are also discussed.

EXPERIMENTAL

Materials—The syntheses of naproxen[3] and 2-(6′-hydroxy-2′-naphthyl)propionic acid[3] were reported previously (1, 2). (*S*)-(+)-2-Octanol (>99% optically pure) was obtained commercially[4]. The reagent grade toluene was purified by washing with concentrated sulfuric acid until the acid remained colorless. The toluene was then washed with water until neutral and then with saturated sodium bicarbonate solution. A final wash with water until neutral and drying over anhydrous sodium sulfate afforded toluene of sufficient purity for use as the esterification reaction solvent.

Glass-distilled hexane and ethyl acetate were obtained commercially[5] and were dried prior to use by percolation through neutral aluminum oxide[6] (activity grade I). All other solvents were reagent grade.

Liquid Chromatography Equipment and Operating Conditions—A liquid chromatograph[7] equipped with a variable wavelength UV detector[8] and a 100-μl fixed loop injector[9] were used. The wavelength chosen for detection was 332 nm (0.04 aufs); at lower wavelengths, an impurity found in all batches of octanol gave a detectable peak coincident with that for (*SS*)-III. Integration of peak areas was obtained through the use of a programmed digital integration system[10] interfaced to the detector. A 25-cm × 3-mm (i.d.) commercially available microparticle silica[11] column was operated at ambient temperature. With 0.5% (v/v) ethyl acetate in hexane as the mobile phase and a flow rate of 1.2 ml/min, the column developed a pressure of approximately 49.21 atmospheres.

Esterification Procedure—Approximately 1 mg of I was weighed into a test tube fitted with a polytef-faced screw cap. To this solid was added 100 μl of (*S*)-(+)-II and, on dissolution, 900 μl of purified toluene and 5 μl of concentrated sulfuric acid were also added. The capped tubes were placed in an oil bath for 2 hr at 100°[12]. After cooling to room temperature, 1 ml of 0.02 *M* sodium bicarbonate was added and the mixture was agitated vigorously.

The toluene layer was transferred to a new tube and dried over sodium sulfate. A 100-μl aliquot of this solution was then brought to 10 ml with the mobile phase, and the resulting solution (~10 μg/ml) was analyzed by injecting 100 μl (1 μg) into the chromatograph. The percent (*SS*)-III is then calculated from:

$$\text{percent (SS)-III} = \frac{\text{area peak 1}}{\text{area peak 1} + \text{area peak 2}} \times 100 \quad \text{(Eq. 1)}$$

[1] For an excellent review of the separation of diastereomers by GLC, see Ref. 3.

[2] Direct chromatographic separation of enantiomers by GLC (4) and liquid chromatographic (5) methods, utilizing optically active stationary or mobile phases, has been reported.

[3] Institute of Organic Chemistry, Syntex Corp., Palo Alto, Calif.

[4] Norse Laboratories.

[5] Burdick and Jackson Laboratories.

[6] Woelm, ICN Pharmaceuticals.

[7] Spectra-Physics model 3500B.

[8] Schoeffel model 770.

[9] Valco universal inlet.

[10] Spectra-Physics Systems I.

[11] Spectra-Physics prepacked with 5-μm Spherisorb silica.

[12] The progress of the reaction was followed by TLC. The reaction mixture (50 μl) was spotted directly onto silica gel GF plates and developed with hexane–tetrahydrofuran–acetic acid (50:50:1). In this solvent system, I (R_f 0.71) and III (R_f 0.86) are well separated.

0022-3549/79/0100-0112$01.00/0
© 1979, American Pharmaceutical Association

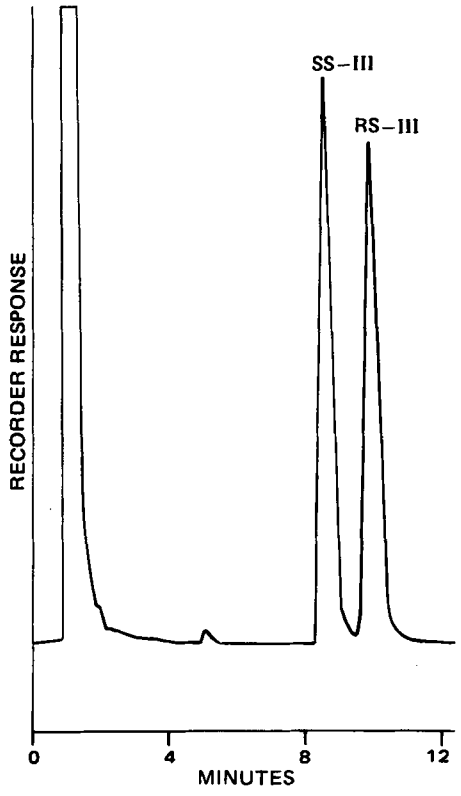

Figure 1—*Chromatogram of the mixture of diastereomeric octyl esters (III) prepared from racemic I and* (S)-(+)-*II.*

where peak 1 is the first eluting peak and corresponds to the (*SS*)-ester and the second peak corresponds to the (*RS*)-ester[13].

Scale-up of this reaction gave a crystalline product (mp 53°) upon workup whose spectral properties were consistent with those of the expected ester III.

Calibration Curve—Approximately 10 mg of (*S*)-(+)-I of high optical purity[14], $[\alpha]_D^{25}$ +67.4° (c 1.0, $CHCl_3$), was accurately weighed into a 10-ml volumetric flask. The solid was dissolved by addition of 1 ml of (*S*)-(+)-II, and the resulting solution was brought to 10 ml with purified toluene. This procedure was repeated using racemic I. Into six culture tubes were added aliquots of the solutions as shown below to give a final volume of 1 ml in each tube:

volume of (*S*)-(+)-I, ml	volume of (±)-I, ml	approximate enantiomeric purity, %
1.0	0	100
0.8	0.2	80
0.6	0.4	60
0.4	0.6	40
0.2	0.8	20
0	1.0	0

To each sample was added 5 μl of concentrated sulfuric acid, and the resulting reaction mixtures were treated as described and analyzed by liquid chromatography. The enantiomeric purity of (*S*)-(+)-I in each calibration sample can be calculated from the following equation[15]:

$$\text{percent enantiomeric purity} = 200\left[\frac{V_+W_+F + \frac{1}{2}V_\pm W_\pm}{V_+W_+ + V_\pm W_\pm}\right] - 100 \quad \text{(Eq. 2)}$$

[13] Actually each peak represents an enantiomeric pair. Peak 1 represents both (*SS*)-III and (*RR*)-III while peak 2 represents both (*RS*)-III and (*SR*)-III. Due to the high degree of optical purity of (*S*)-(+)-II, contributions that (*RR*)-III and (*SR*)-III may make to each peak were ignored.

[14] Optical rotations were measured on a Perkin-Elmer model 141 polarimeter.

[15] If $W_+ = W_\pm$, *i.e.*, if the weights used to prepare the two standard solutions are the same, then Eq. 2 simplifies to:

$$\text{percent enantiomeric purity} = 200\,[V_+F + \tfrac{1}{2}V_\pm/V_+ + V_\pm] - 100$$

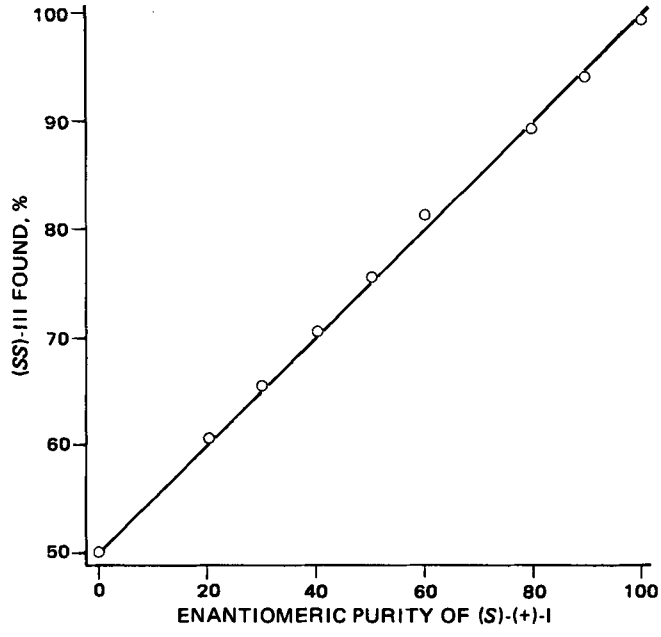

Figure 2—*Calibration plot showing the relationship between the known enantiomeric purity (by weight) of prepared samples of I and the diastereomeric composition of III found after esterification.*

where:

V_+ = volume of (*S*)-(+)-I standard solution in milliliters
$V_\pm$ = volume of racemic I standard solution in milliliters
W_+ = weight of (*S*)-(+)-I used to prepare the standard solution
$W_\pm$ = weight of racemic I used to prepare the standard solution
F = mole fraction of the (*S*)-(+) enantiomer known to be in the batch of I used to prepare the (*S*)-(+)-I standard solution

RESULTS AND DISCUSSION

The esterification reaction rate was followed by TLC. The reaction was complete in approximately 1.5 hr at 100° under the conditions specified. Complete loss of I was observed, and no side products were apparent by TLC. When (*S*)-(+)-I and (*S*)-(+)-II were allowed to react for 23 hr under these same conditions, no evidence of degradation of the ester [(*SS*)-III] was observed by TLC and liquid chromatography. Racemization of I or epimerization of (*SS*)-III under these severe conditions was also ruled out since the percent (*SS*)-diastereomer found (98%) compares well with that found after only 2 hr of reaction (99%). These results indicate that the reaction of I with (*S*)-(+)-II gives only III with no competing reactions and that this ester is completely stable, both chemically and stereochemically, under the reaction conditions.

The liquid chromatographic method used to analyze the reaction mixtures displayed baseline separation of the (*SS*)- and (*RS*)-diastereomers of III (Fig. 1). The specificity of the method for I in the presence of 2-(6′-hydroxy-2′-naphthyl)propionic acid (IV), a major metabolite in humans (7, 8), was also demonstrated by the large separation found between the octyl esters of I and IV on liquid chromatography.

A plot of the percent (*SS*)-III found experimentally *versus* the known enantiomeric purity of (*S*)-(+)-I in each sample is shown in Fig. 2. The excellent fit of the points in this calibration curve to a line of slope 0.5

Table I—Enantiomeric Purity of Several Samples of I [a] by Esterification followed by Liquid Chromatography

Sample	Enantiomeric Purity of (*S*)-(+)-I, %
1	79.2
2	79.9
3	79.8
4	79.2
5	79.9
Mean ± *SD*	79.6 ± 0.4

[a] Samples are 80.0% enantiomerically pure.

clearly demonstrates that for each sample the ratio of the diastereomeric esters produced is identical to the ratio of enantiomers present in the original sample. If, however, enantiomerically impure (*S*)-(+)-II were used, the slope of the line in Fig. 2 would be less than 0.5 and could be calculated from:

$$\text{slope} = \frac{\text{enantiomeric purity of (S)-(+)-II}}{200} \qquad \text{(Eq. 3)}$$

Table I shows the results of the liquid chromatographic analysis of five samples of (*S*)-(+)-I (80% enantiomerically pure). The data clearly demonstrate the excellent reproducibility of the method. This result is expected since the measurement is not dependent on quantitative recovery of III but rather involves comparison of relative peak areas of two closely eluting diastereomers. The applicability of this method to other

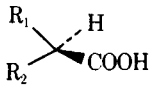

A

carboxylic acids of this type (Structure A) can only be speculative but is perhaps not unlikely if R_1 and R_2 are sufficiently dissimilar.

REFERENCES

(1) I. T. Harrison, B. Lewis, P. Nelson, W. Rooks, A. Roszkowski, A. Tomolonis, and J. H. Fried, *J. Med. Chem.*, **13**, 203 (1970).

(2) J. Riegl, M. L. Maddox, and I. T. Harrison, *ibid.*, **17**, 377 (1974).

(3) E. Gil-Av and D. Nurok, *Adv. Chromatogr.*, **10**, 99 (1974), and references cited therein.

(4) C. H. Lochmuller and R. W. Souter, *J. Chromatogr. Chromatogr. Rev.*, **113**, 283 (1975), and references cited therein.

(5) W. H. Pirkle and D. L. Sikkenga, *J. Chromatogr.*, **123**, 400 (1976), and references cited therein.

(6) M. Raban and K. Mislow, in "Topics in Stereochemistry," vol. II, N. L. Allinger and E. L. Eliel, Eds., Wiley-Interscience, New York, N.Y., 1967, p. 211.

(7) R. Runkel, M. Chaplin, G. Boost, E. Segre, and E. Forchielli, *J. Pharm. Sci.*, **61**, 703 (1972).

(8) G. F. Thompson and J. M. Collins, *ibid.*, **62**, 937 (1973).

Stability of E-Type Prostaglandins in Triacetin

S. H. YALKOWSKY ˣ **and T. J. ROSEMAN**

Received January 11, 1978, from *The Upjohn Company, Kalamazoo, MI 49001.* Accepted for publication June 1, 1978.

Abstract □ A drug delivery system for E-type prostaglandins is described. In this system, consisting of drug dissolved in triacetin and filled into soft gelatin capsules, normally unstable prostaglandins show excellent stability at room temperature.

Keyphrases □ Prostaglandins, E type—stability in triacetin drug delivery system □ Stability—E-type prostaglandins in triacetin drug delivery system □ Delivery, drug—E-type prostaglandins in triacetin system, stability

Prostaglandins are a class of biologically active compounds with a wide spectrum of pharmacological responses. Their application in human reproduction (1) and antiulcer therapy (2) demonstrates their clinical usefulness. The general instability of prostaglandins has resulted in the arduous task of developing stable formulations for biological, toxicological, and clinical testing.

The number of asymmetric carbon centers in the molecule can result in the formation of stereoisomers through various degradative pathways. For example, in the F series, dinoprost (prostaglandin $F_{2\alpha}$) undergoes acid-catalyzed epimerization to form the 15-epi derivative (3). Prostaglandins of the E series [*e.g.*, prostaglandin E_1 and prostaglandin E_2 (dinoprostone)] are more labile due to the facile dehydration of the 11-β hydroxyl group in the cyclopentanone ring, forming prostaglandins of the A series; in some cases, subsequent isomerization to B series prostaglandins occurs (4). Recently (5), a more detailed kinetic scheme was elucidated for the decomposition of prostaglandins E_1 and E_2 to include other degradative steps leading to the formation of 8-iso, 15-epi, and 13,15-rearrangement products of the respective prostaglandins.

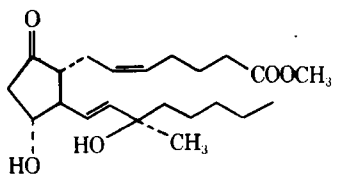

I

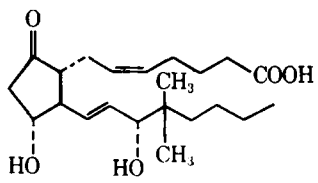

II

Table I—Stability of II in Triacetin

Time	Temperature	Triacetin Solution, % label[a]	Soft Elastic Capsule[b], % label
Initial	4°	102	100
1 month	4°	102	108
3 months	4°	103	98.8
6 months	4°	105	91.1
9 months	4°	108	105
12 months	4°	98.7	106[c]
Initial	25°	102	100
1 month	25°	98.8	95.3
3 months	25°	103	93.5
6 months	25°	102	87.9
9 months	25°	103	100
12 months	25°	94.7	94.5
Initial	40°	102[d]	100
1 month	40°	99.1[d]	101
3 months	40°	87.7[d]	91.5
6 months	40°	87.3[d]	70.3

[a] Average values from theoretical concentrations of 0.5 and 2.2 mg/ml unless otherwise indicated. [b] Theoretical concentration was 0.85 mg/ml. [c] Value was for 11 months. [d] Value from a theoretical concentration of 2.2 mg/ml.

This paper reports the use of triacetin for stabilizing stock solutions of (15*R*)-15-methyl prostaglandin E_2 methyl ester (I) and 16,16-dimethyl prostaglandin E_2 (II) for experimental studies and in dosage form design. Nonaqueous solvents usually are employed for solubilizing water-insoluble drugs (6, 7). With prostaglandins, a variety of solvent vehicles also was employed to enhance stability (8) and to provide a milieu for rapid drug dissolution.

0022-3549/79/0100-0114$01.00/0

© 1979, American Pharmaceutical Association

clearly demonstrates that for each sample the ratio of the diastereomeric esters produced is identical to the ratio of enantiomers present in the original sample. If, however, enantiomerically impure (*S*)-(+)-II were used, the slope of the line in Fig. 2 would be less than 0.5 and could be calculated from:

$$\text{slope} = \frac{\text{enantiomeric purity of (S)-(+)-II}}{200} \qquad \text{(Eq. 3)}$$

Table I shows the results of the liquid chromatographic analysis of five samples of (*S*)-(+)-I (80% enantiomerically pure). The data clearly demonstrate the excellent reproducibility of the method. This result is expected since the measurement is not dependent on quantitative recovery of III but rather involves comparison of relative peak areas of two closely eluting diastereomers. The applicability of this method to other

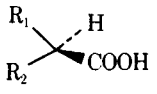

A

carboxylic acids of this type (Structure A) can only be speculative but is perhaps not unlikely if R_1 and R_2 are sufficiently dissimilar.

REFERENCES

(1) I. T. Harrison, B. Lewis, P. Nelson, W. Rooks, A. Roszkowski, A. Tomolonis, and J. H. Fried, *J. Med. Chem.*, **13**, 203 (1970).

(2) J. Riegl, M. L. Maddox, and I. T. Harrison, *ibid.*, **17**, 377 (1974).

(3) E. Gil-Av and D. Nurok, *Adv. Chromatogr.*, **10**, 99 (1974), and references cited therein.

(4) C. H. Lochmuller and R. W. Souter, *J. Chromatogr. Chromatogr. Rev.*, **113**, 283 (1975), and references cited therein.

(5) W. H. Pirkle and D. L. Sikkenga, *J. Chromatogr.*, **123**, 400 (1976), and references cited therein.

(6) M. Raban and K. Mislow, in "Topics in Stereochemistry," vol. II, N. L. Allinger and E. L. Eliel, Eds., Wiley-Interscience, New York, N.Y., 1967, p. 211.

(7) R. Runkel, M. Chaplin, G. Boost, E. Segre, and E. Forchielli, *J. Pharm. Sci.*, **61**, 703 (1972).

(8) G. F. Thompson and J. M. Collins, *ibid.*, **62**, 937 (1973).

Stability of E-Type Prostaglandins in Triacetin

S. H. YALKOWSKY ˣ **and T. J. ROSEMAN**

Received January 11, 1978, from *The Upjohn Company, Kalamazoo, MI 49001.* Accepted for publication June 1, 1978.

Abstract □ A drug delivery system for E-type prostaglandins is described. In this system, consisting of drug dissolved in triacetin and filled into soft gelatin capsules, normally unstable prostaglandins show excellent stability at room temperature.

Keyphrases □ Prostaglandins, E type—stability in triacetin drug delivery system □ Stability—E-type prostaglandins in triacetin drug delivery system □ Delivery, drug—E-type prostaglandins in triacetin system, stability

Prostaglandins are a class of biologically active compounds with a wide spectrum of pharmacological responses. Their application in human reproduction (1) and antiulcer therapy (2) demonstrates their clinical usefulness. The general instability of prostaglandins has resulted in the arduous task of developing stable formulations for biological, toxicological, and clinical testing.

The number of asymmetric carbon centers in the molecule can result in the formation of stereoisomers through various degradative pathways. For example, in the F series, dinoprost (prostaglandin $F_{2\alpha}$) undergoes acid-catalyzed epimerization to form the 15-epi derivative (3). Prostaglandins of the E series [*e.g.*, prostaglandin E_1 and prostaglandin E_2 (dinoprostone)] are more labile due to the facile dehydration of the 11-β hydroxyl group in the cyclopentanone ring, forming prostaglandins of the A series; in some cases, subsequent isomerization to B series prostaglandins occurs (4). Recently (5), a more detailed kinetic scheme was elucidated for the decomposition of prostaglandins E_1 and E_2 to include other degradative steps leading to the formation of 8-iso, 15-epi, and 13,15-rearrangement products of the respective prostaglandins.

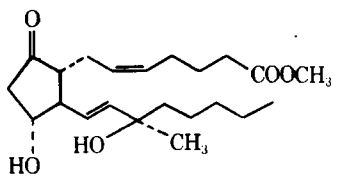

I

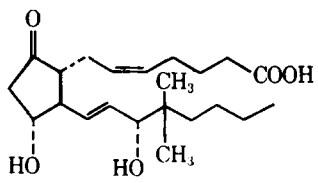

II

Table I—Stability of II in Triacetin

Time	Temperature	Triacetin Solution, % label[a]	Soft Elastic Capsule[b], % label
Initial	4°	102	100
1 month	4°	102	108
3 months	4°	103	98.8
6 months	4°	105	91.1
9 months	4°	108	105
12 months	4°	98.7	106[c]
Initial	25°	102	100
1 month	25°	98.8	95.3
3 months	25°	103	93.5
6 months	25°	102	87.9
9 months	25°	103	100
12 months	25°	94.7	94.5
Initial	40°	102[d]	100
1 month	40°	99.1[d]	101
3 months	40°	87.7[d]	91.5
6 months	40°	87.3[d]	70.3

[a] Average values from theoretical concentrations of 0.5 and 2.2 mg/ml unless otherwise indicated. [b] Theoretical concentration was 0.85 mg/ml. [c] Value was for 11 months. [d] Value from a theoretical concentration of 2.2 mg/ml.

This paper reports the use of triacetin for stabilizing stock solutions of (15*R*)-15-methyl prostaglandin E_2 methyl ester (I) and 16,16-dimethyl prostaglandin E_2 (II) for experimental studies and in dosage form design. Nonaqueous solvents usually are employed for solubilizing water-insoluble drugs (6, 7). With prostaglandins, a variety of solvent vehicles also was employed to enhance stability (8) and to provide a milieu for rapid drug dissolution.

0022-3549/79/0100-0114$01.00/0

© 1979, American Pharmaceutical Association

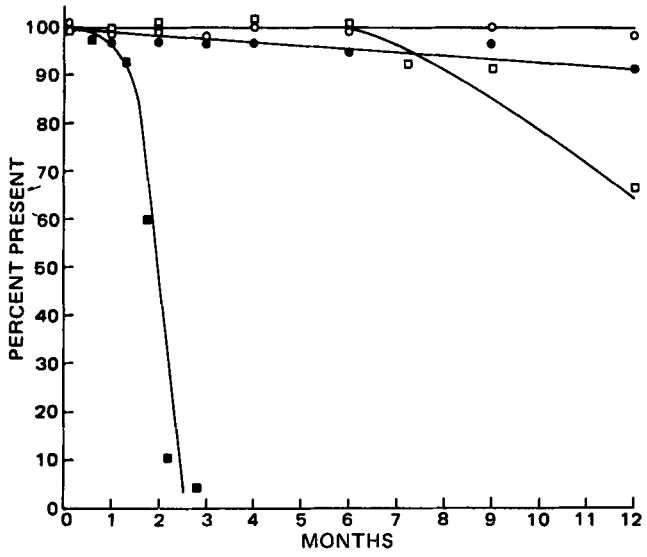

Figure 1—*Stability of I in the solid state and triacetin solutions. Data for solutions are average values for theoretical concentrations from 0.10 to 12 mg/ml. Key: □, 25° bulk drug; ■, 47° bulk drug; ○, 25° triacetin solution; and ●, 47° triacetin solution.*

EXPERIMENTAL

Materials—Compounds I (9) and II (10) were synthesized[1] as described previously. Triacetin[2] was purchased.

Stability Studies—Both I and II were tested for stability as bulk drug and in triacetin solution. Stability[3] was monitored at 4, 25, and 47° for up to 12 months (Table I and Fig. 1).

[1] At The Upjohn Co.
[2] Aldrich Chemical Co. or Union Carbide Chemicals Co., New York, N.Y.
[3] Analyses were performed by the Control Division, The Upjohn Co., using high-pressure liquid chromatography.

RESULTS AND DISCUSSION

The solid-state stability of I is shown in Fig. 1. Degradation occurred at 47 and 25°. At these temperatures, the drug was stable at early times and then rapidly decomposed. As the prostaglandin degraded, a physical transformation of the solid resulted, producing an oil phase. The marked change in the slopes at 25 and 47° may have been due to subsequent catalysis by the decomposed liquid phase. In sharp contrast to the stability of bulk drug, I was quite stable in triacetin solutions at 25°, and there was a marked improvement of stability at the elevated temperature of 47° (Fig. 1).

Table I shows the stability of another E series prostaglandin drug in triacetin. Analysis of these data further substantiates the stability-enhancing property of this solvent. Triacetin dosage forms prepared with II were clinically effective as inhibitors of simulated gastric secretion in humans, indicating that the drug is bioavailable from these dosage forms (11).

REFERENCES

(1) "Prostaglandins and Reproduction," S. M. M. Karim, Ed., MTP Press, St. Leonard's House, Great Britain, 1975.

(2) A. Robert, in "Advances in Prostaglandin and Thromboxane Research," vol. 2, B. Samuelsson and R. Paoletti, Eds., Raven, New York, N.Y., 1976, p. 507.

(3) T. J. Roseman, S. S. Butler, and S. L. Douglas, *J. Pharm. Sci.*, **65**, 673 (1976).

(4) D. C. Monkhouse, L. Van Campen, and A. J. Aguiar, *ibid.*, **62**, 576 (1973).

(5) R. G. Stehle and T. O. Oesterling, *ibid.*, **66**, 1590 (1977).

(6) A. J. Spiegel and M. M. Noseworthy, *ibid.*, **52**, 917 (1963).

(7) S. H. Yalkowsky and S. C. Valvani, *Drug Intel. Clin. Pharm.*, **11**, 417 (1977).

(8) The Upjohn Co., U.S. pat. 3,749,800 (1973). The Upjohn Co., U.S. pat. 3,829,579 (1974). Syntex Corp., U.S. pat. 3,833,725 (1974). The Upjohn Co., U.S. pat. 3,966,962 (1976).

(9) E. W. Yankee, U.F. Axen, and G. L. Bundy, *J. Am. Chem. Soc.*, **96**, 5865 (1974).

(10) B. J. Magerlein, D. W. DuCharme, W. E. Magee, W. L. Miller, A. Robert, and J. R. Weeks, *Prostaglandins*, **4**, 143 (1973).

(11) D. E. Wilson, J. Quertermus, M. Raiser, J. Curran, and A. Robert, *Ann. Intern. Med.*, **84**, 688 (1976).

Fluorinated Phenytoin Anticonvulsant Analogs

WENDEL L. NELSON ˣ, YOUNG G. KWON, GARY L. MARSHALL, JAMES L. HOOVER, and GARY T. PFEFFER

Received March 20, 1978, from the *Department of Pharmaceutical Sciences, School of Pharmacy, University of Washington, Seattle, WA 98195.* Accepted for publication June 8, 1978.

Abstract □ Six ring-fluorinated phenytoin analogs were synthesized, and their anticonvulsant activity in the maximal electroshock seizure and subcutaneous pentylenetetrazol assays was determined. 5-(4-Fluorophenyl)-5-phenylhydantoin, 5-(3-fluorophenyl)-5-phenylhydantoin, and 5,5-bis(4-fluorophenyl)hydantoin were active in the maximal electroshock seizure assay. The compounds were much less potent than phenytoin but showed an extremely long duration of action.

Keyphrases □ Phenytoin analogs, fluorinated—synthesized, evaluated for anticonvulsant activity in mice □ Anticonvulsant activity—fluorinated phenytoin analogs evaluated in mice □ Fluorinated phenytoin analogs—synthesized, evaluated for anticonvulsant activity in mice □ Structure-activity relationships—fluorinated phenytoin analogs evaluated for anticonvulsant activity in mice

Phenytoin (5,5-diphenylhydantoin) has been used as an effective agent for the treatment of many different seizure disorders for about 40 years. The principal route of metabolism in humans and dogs is *para*-hydroxylation, affording optically active 5-(4-hydroxyphenyl)-5-phenylhydantoin (1, 2). This compound is eliminated as a urinary conjugate, making up 60–70% of the daily dose (2). Other metabolites of aromatic hydroxylation also have been reported, including 5-(3-hydroxyphenyl)-5-phenylhydantoin (3), 5-(3-dihydroxyphenyl)-5-phenylhydantoin (4, 5), 5,5-bis(4-hydroxyphenyl)hydantoin (6), 5-(3-methoxyphenyl)-5-phenylhydantoin (4, 5), and the dihydrodiol 5-(3,4-dihydroxy-1,5-cyclohexadienyl)-5-phenylhydantoin (7). Further oxidized phenytoin conjugates, a trihydroxyphenytoin glucuronide and a dihydroxymethoxyphenytoin glucuronide, were identified as metabolites of 5,5-bis(4-hydroxyphenyl)hydantoin (6).

Since the primary route of metabolism, aromatic hydroxylation in the *para*-position, provides inactive me-

0022-3549/79/0100-0115$01.00/0
© 1979, American Pharmaceutical Association

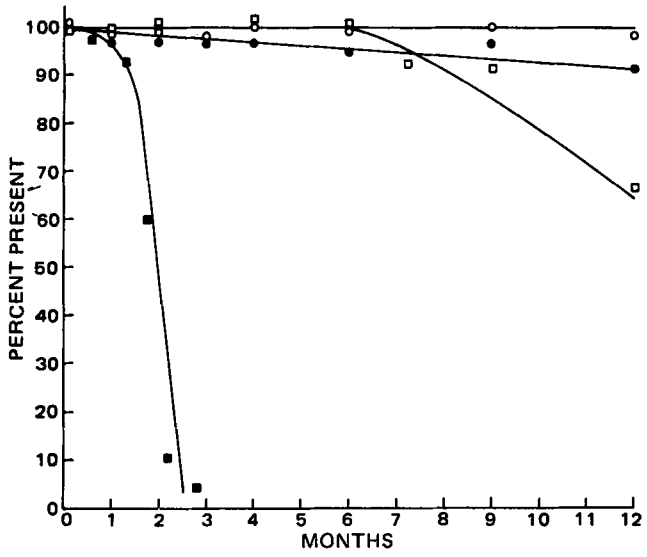

Figure 1—*Stability of I in the solid state and triacetin solutions. Data for solutions are average values for theoretical concentrations from 0.10 to 12 mg/ml. Key: □, 25° bulk drug; ■, 47° bulk drug; ○, 25° triacetin solution; and ●, 47° triacetin solution.*

EXPERIMENTAL

Materials—Compounds I (9) and II (10) were synthesized[1] as described previously. Triacetin[2] was purchased.

Stability Studies—Both I and II were tested for stability as bulk drug and in triacetin solution. Stability[3] was monitored at 4, 25, and 47° for up to 12 months (Table I and Fig. 1).

[1] At The Upjohn Co.
[2] Aldrich Chemical Co. or Union Carbide Chemicals Co., New York, N.Y.
[3] Analyses were performed by the Control Division, The Upjohn Co., using high-pressure liquid chromatography.

RESULTS AND DISCUSSION

The solid-state stability of I is shown in Fig. 1. Degradation occurred at 47 and 25°. At these temperatures, the drug was stable at early times and then rapidly decomposed. As the prostaglandin degraded, a physical transformation of the solid resulted, producing an oil phase. The marked change in the slopes at 25 and 47° may have been due to subsequent catalysis by the decomposed liquid phase. In sharp contrast to the stability of bulk drug, I was quite stable in triacetin solutions at 25°, and there was a marked improvement of stability at the elevated temperature of 47° (Fig. 1).

Table I shows the stability of another E series prostaglandin drug in triacetin. Analysis of these data further substantiates the stability-enhancing property of this solvent. Triacetin dosage forms prepared with II were clinically effective as inhibitors of simulated gastric secretion in humans, indicating that the drug is bioavailable from these dosage forms (11).

REFERENCES

(1) "Prostaglandins and Reproduction," S. M. M. Karim, Ed., MTP Press, St. Leonard's House, Great Britain, 1975.

(2) A. Robert, in "Advances in Prostaglandin and Thromboxane Research," vol. 2, B. Samuelsson and R. Paoletti, Eds., Raven, New York, N.Y., 1976, p. 507.

(3) T. J. Roseman, S. S. Butler, and S. L. Douglas, *J. Pharm. Sci.*, **65**, 673 (1976).

(4) D. C. Monkhouse, L. Van Campen, and A. J. Aguiar, *ibid.*, **62**, 576 (1973).

(5) R. G. Stehle and T. O. Oesterling, *ibid.*, **66**, 1590 (1977).

(6) A. J. Spiegel and M. M. Noseworthy, *ibid.*, **52**, 917 (1963).

(7) S. H. Yalkowsky and S. C. Valvani, *Drug Intel. Clin. Pharm.*, **11**, 417 (1977).

(8) The Upjohn Co., U.S. pat. 3,749,800 (1973). The Upjohn Co., U.S. pat. 3,829,579 (1974). Syntex Corp., U.S. pat. 3,833,725 (1974). The Upjohn Co., U.S. pat. 3,966,962 (1976).

(9) E. W. Yankee, U.F. Axen, and G. L. Bundy, *J. Am. Chem. Soc.*, **96**, 5865 (1974).

(10) B. J. Magerlein, D. W. DuCharme, W. E. Magee, W. L. Miller, A. Robert, and J. R. Weeks, *Prostaglandins*, **4**, 143 (1973).

(11) D. E. Wilson, J. Quertermus, M. Raiser, J. Curran, and A. Robert, *Ann. Intern. Med.*, **84**, 688 (1976).

Fluorinated Phenytoin Anticonvulsant Analogs

WENDEL L. NELSON ˣ, YOUNG G. KWON, GARY L. MARSHALL, JAMES L. HOOVER, and GARY T. PFEFFER

Received March 20, 1978, from the *Department of Pharmaceutical Sciences, School of Pharmacy, University of Washington, Seattle, WA 98195.* Accepted for publication June 8, 1978.

Abstract □ Six ring-fluorinated phenytoin analogs were synthesized, and their anticonvulsant activity in the maximal electroshock seizure and subcutaneous pentylenetetrazol assays was determined. 5-(4-Fluorophenyl)-5-phenylhydantoin, 5-(3-fluorophenyl)-5-phenylhydantoin, and 5,5-bis(4-fluorophenyl)hydantoin were active in the maximal electroshock seizure assay. The compounds were much less potent than phenytoin but showed an extremely long duration of action.

Keyphrases □ Phenytoin analogs, fluorinated—synthesized, evaluated for anticonvulsant activity in mice □ Anticonvulsant activity—fluorinated phenytoin analogs evaluated in mice □ Fluorinated phenytoin analogs—synthesized, evaluated for anticonvulsant activity in mice □ Structure-activity relationships—fluorinated phenytoin analogs evaluated for anticonvulsant activity in mice

Phenytoin (5,5-diphenylhydantoin) has been used as an effective agent for the treatment of many different seizure disorders for about 40 years. The principal route of metabolism in humans and dogs is *para*-hydroxylation, affording optically active 5-(4-hydroxyphenyl)-5-phenylhydantoin (1, 2). This compound is eliminated as a urinary conjugate, making up 60–70% of the daily dose (2). Other metabolites of aromatic hydroxylation also have been reported, including 5-(3-hydroxyphenyl)-5-phenylhydantoin (3), 5-(3-dihydroxyphenyl)-5-phenylhydantoin (4, 5), 5,5-bis(4-hydroxyphenyl)hydantoin (6), 5-(3-methoxyphenyl)-5-phenylhydantoin (4, 5), and the dihydrodiol 5-(3,4-dihydroxy-1,5-cyclohexadienyl)-5-phenylhydantoin (7). Further oxidized phenytoin conjugates, a trihydroxyphenytoin glucuronide and a dihydroxymethoxyphenytoin glucuronide, were identified as metabolites of 5,5-bis(4-hydroxyphenyl)hydantoin (6).

Since the primary route of metabolism, aromatic hydroxylation in the *para*-position, provides inactive me-

0022-3549/79/0100-0115$01.00/0
© 1979, American Pharmaceutical Association

Table I—Anticonvulsant Activity and Neurotoxicity

Compound	MES 0.5 hr	MES 4 hr	ED_{50}	Toxicity[a]	Additional Notes
I	–	+[b]	61 (44–71)[c] at 6 hr	1190 (982–1712) at 24 hr	Onset of MES activity was 2–4 hr. Doses of 133 mg/kg showed protection at 24 hr. Doses of 1000–1500 mg/kg showed a slow onset of neurotoxicity (8–20 hr), lasting more than 48 hr.
II	–	–	nd[d]	nd	—
III	+++	+++	23 (20–26) at 4 hr	158 (117–183) at 6 hr	—
IV	–	–	See note	Nontoxic at 2000 mg/kg	At 2000 mg/kg, 4/8 animals were protected at 192 hr. At 1000 mg/kg, maximum protection was at 24 hr, and 4/8 remained protected at 48 hr.
V	–	–	nd	nd	—
VI	–	–	270 (227–321) at 8 hr	Nontoxic at 2000 mg/kg	—

[a] A description of the assay methods appears in the *Experimental* section. [b] The +++, ++, and + signify activity at 30, 100, and 300 mg/kg, respectively; – indicates no activity was observed. [c] The 95% confidence limits. [d] Not done.

tabolites, it has a significant influence on blood levels and the duration of action of phenytoin. It was reasoned that by addition of fluorine atoms to the aromatic ring, it might be possible to slow or block this metabolic pathway and thus provide compounds of a longer duration of action than phenytoin. This change also offered the potential of providing compounds with a different spectrum of anticonvulsant activity.

The addition of fluorine atoms offered the advantage of being the smallest possible change to the phenytoin molecule next to isotopic substitution. Also, it was thought that these compounds could serve as standards for work related to ^{18}F-phenytoin derivatives as potential organ-scanning agents (8, 9). The synthesis of six different fluorinated phenytoin analogs is reported here, with results of initial screening in anticonvulsant assays.

RESULTS AND DISCUSSION

Fluorinated phenytoin analogs I–IV and VI were prepared by a Bucherer synthesis, modified by the method of Henze and Isbell (10), from the corresponding benzophenone, potassium cyanide, and ammonium carbonate with acetamide as solvent. Compound V was prepared from urea and 3,3-difluorobenzil, available through the benzoin condensation of 3-fluorobenzaldehyde.

The results of maximum electroshock seizure (MES) assays of I–VI appear in Table I. The compounds were not active in subcutaneous pentylenetetrazol (sc-Met) assays. The observed restriction of activity to the maximum electroshock seizure assay was similar to that of phenytoin. Activity was noted in I, IV, and VI, which contain a fluorine atom in at least one 4-position, and in 5-(2-fluorophenyl)-5-phenylhydantoin (III). The compounds were considerably less active than phenytoin [ED_{50} = 9.5 mg/kg for phenytoin (11)]. Although not potent, I, IV, and VI were of an extremely long duration of action: up to more than 7 days duration for IV and 8–48 hr for the doses of I and VI tested. Additionally, the compounds were very slow in onset of activity, requiring several hours to reach peak activity.

If the substitution of a fluorine atom at the *para*-position in phenytoin yielded a compound protected from metabolic conversion to an inactive metabolite, I and IV would be less readily hydroxylated and would be more potent than phenytoin, but this behavior was not observed. Additionally, since IV has fluorines at both *para*-positions, it should be more active than I since I retains one possible site for metabolic inactivation. This hypothesis is also contrary to the results observed.

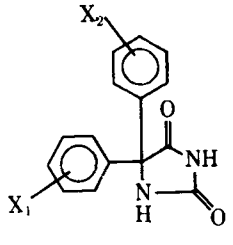

I: X_1 = 4-F, X_2 = H
II: X_1 = 3-F, X_2 = H
III: X_1 = 2-F, X_2 = H
IV: X_1 = 4-F, X_2 = 4-F
V: X_1 = 3-F, X_2 = 3-F
VI: X_1 = 4-F, X_2 = 3-F

Since the addition of fluorines in the *para*-position results in compounds with reduced activity compared to phenytoin, factors other than metabolic deactivation (*e.g.*, steric, electronic, and partitioning) must contribute to the observed low activity. The reported absence of activity of other *para*-substituted phenytoin analogs, especially halogenated or methyl-substituted analogs (12, 13), is similar to that observed with these fluorinated analogs.

The slow onset of action is difficult to explain satisfactorily. A latent period before onset of pharmacological activity is usually interpreted to indicate that activity may be mediated by formation of an active metabolite or alteration of enzyme levels by alteration of the rate of synthesis or degradation, which requires some time for these changes to occur. These interpretations assume that drug absorption is not rate limiting, which seems to be valid in these cases since the compounds are very similar to phenytoin. Although these possibilities potentially exist for the fluorinated phenytoin derivatives, no evidence in this work supports such an explanation.

The presence of activity in *para*-substituted compounds and not in *meta*-substituted compounds (II and V) is also puzzling. However, in view of the low potency of the *p*-fluoro-substituted compounds, this difference is not worthy of protracted speculation. Too few *meta*-substituted systems have been studied to allow valid comparison of II and V with other related compounds.

Only III, 5-(2-fluorophenyl)-5-phenylhydantoin, showed reasonable activity, being slightly less than half as potent as phenytoin on a molar basis and less than half as neurotoxic (TD_{50} = 158 *versus* 65 mg/kg).

In conclusion, the long duration of activity of I, IV, and VI is notable. However, the low potency of these compounds suggests that preparation of other compounds is probably of higher priority than intensive investigation of the behavior of these phenytoin analogs. The significant decrease in activity of the analogs suggests that there may be only a very limited number of successful modifications of the aromatic ring possible, at least at the *meta*- and *para*-positions.

EXPERIMENTAL

5-(4-Fluorophenyl)-5-phenylhydantoin (I)—A mixture of 2.00 g (0.010 mole) of 4-fluorobenzophenone, 0.75 g (0.011 mole) of potassium cyanide, 1.0 ml of water, and 3.00 g (0.032 mole) of powdered ammonium carbonate in 20.0 g of acetamide was heated in a Parr bomb at 125–130° for 24 hr. After cooling, the bomb was opened and 300 ml of water was added. The resulting mixture was acidified (hood, hydrogen cyanide evolved), and the precipitate removed by filtration. Recrystallization from ethanol–water afforded I as off-white crystals, 2.70 g (52% yield), mp 274–276°.

Anal.—Calc. for $C_{15}H_{11}FN_2O_2$: C, 66.67; H, 4.07; N, 10.35. Found: C, 66.42; H, 4.01; N, 10.29.

5-(3-Fluorophenyl)-5-phenylhydantoin (II)—3-Fluorobenzophenone was prepared from 3-fluorobenzoyl chloride, which was prepared by refluxing 3-fluorobenzoic acid with 50% molar excess of thionyl chloride for 1 hr followed by distillation, and benzene in the presence of anhydrous aluminum chloride. 3-Fluorobenzophenone was obtained in a 50% yield, bp 112–114°/0.9 mm, mp 52–54° [lit. (14) mp 53°]. 3-Fluorobenzophenone was converted to II by the procedure described for the preparation of I. Compound II was obtained in a 48% yield, mp 246–251° (ethanol–water).

Anal.—Calc. for $C_{15}H_{11}FN_2O_2$: C, 66.67; H, 4.07; F, 7.04; N, 10.35. Found: C, 66.39; H, 3.98; F, 7.31; N, 10.41.

5-(2-Fluorophenyl)-5-phenylhydantoin (III)—By a procedure analogous to that for the preparation of I, the title compound was prepared from 2-fluorobenzophenone in a 27% yield, mp 264–266°.

Anal.—Calc. for $C_{15}H_{11}FN_2O_2$: C, 66.67; H, 4.07; N, 10.35. Found: C, 66.15; H, 3.99; N, 10.51.

5,5-Bis(4-fluorophenyl)hydantoin (IV)—By a procedure analogous to that for the preparation of I, the title compound was prepared from 4,4′-difluorobenzophenone in a 50% yield, mp 310–312°.

Anal.—Calc. for $C_{15}H_{10}F_2N_2O_2$: C, 62.50; H, 3.47; F, 13.16; N, 9.72. Found: C, 62.03; H, 3.46; F, 13.37; N, 9.59.

5,5-Bis(3-fluorophenyl)hydantoin (V)—This compound was prepared from 3,3′-difluorobenzil and urea by the general hydantoin synthesis described by Adams *et al.* (15). A mixture of 1.95 g (0.03 mole) of potassium cyanide, 15 ml of water, 30 ml of ethanol, and 18.60 g (0.15 mole) of 3-fluorobenzaldehyde was refluxed for 30 min and cooled in an ice bath to effect crystallization. The crude product was collected, washed with cold 50% aqueous alcohol and water, and dried, affording 11.40 g (66% of theory) of the benzoin, mp 77–79°.

A mixture of 9.93 g (0.04 mole) of the crude benzoin, 40 ml of acetic acid, and 2.80 g (0.34 mole) of concentrated nitric acid was heated on a steam bath for 3 hr. Then water, 150 ml, was added. On cooling, the crude benzil was deposited, 9.20 g (93% yield).

A mixture of 1.80 g (4.06 mmoles) of the benzil, 0.50 g (8.33 mmoles) of urea, 15 ml of ethanol, and 13 ml of 30% aqueous potassium hydroxide was refluxed for 2 hr. Then 25 ml of water was added, and the solution was filtered. Acidification afforded the desired hydantoin, 325 mg (28% yield), mp 238–240°.

Anal.—Calc. for $C_{15}H_{10}F_2N_2O_2$: C, 62.50; H, 3.47; F, 13.16; N, 9.72. Found: C, 62.04; H, 3.41; F, 12.89; N, 9.85.

5-(3-Fluorophenyl)-5-(4-phenyl)hydantoin (VI)—This compound was prepared from 3,4′-difluorobenzophenone by a procedure similar to that for the preparation of I. The product was obtained in 58% yield, mp 279–280° (dioxane–water).

Anal.—Calc. for $C_{15}H_{10}F_2N_2O_2$: C, 62.50; H, 3.47; F, 13.16; N, 9.72. Found: C, 62.21; H, 3.59; F, 13.08; N, 9.48.

Pharmacological Testing[1]—All tests were performed on male Carworth Farms No. 1 mice. All compounds were tested initially at three dosage levels (30, 100, and 300 mg/kg) at 30 min and 4 hr after their intraperitoneal administration. Four animals were injected with each dose. Thirty minutes later, each animal was examined for toxicity in the rotorod test. Immediately thereafter, anticonvulsant activity was evaluated by subjecting one mouse to the protection against the maximal electroshock seizure test and another to the subcutaneous pentylenetetrazol (sc-Met) test.

The same tests were repeated 4 hr later on the two remaining mice. All compounds were solubilized in 30% polyethylene glycol 400 and administered intraperitoneally in a volume of 0.01 ml/g. The ED_{50} and TD_{50} values and their confidence limits were determined by probit analysis and/or by the method of Litchfield and Wilcoxon (16).

Maximum electroshock seizure activity is defined as abolition of the hindlimb tonic extensor component of the maximal electroshock seizure elicited in mice with a 60-Hz alternating current of 50 mamp delivered for 0.2 sec *via* corneal electrodes. Subcutaneous pentylenetetrazol activity is defined as failure to observe even a threshold seizure (a single episode of clonic spasms of at least 5 sec). Neurologic toxicity is defined as failure of an animal to remain for 1 min on a 2.54-cm diameter knurled plastic rod rotating at 6 rpm.

[1] Compounds were tested for anticonvulsant activity by the Anticonvulsant Screening Project, Antiepileptic Drug Development Program, Epilepsy Branch, National Institute of Neurological and Communicative Disorders and Stroke, National Institutes of Health, Bethesda, MD 20014.

REFERENCES

(1) J. H. Poupaert, R. Cavalier, M. H. Claesen, and P. A. Dunvort, *J. Med. Chem.*, **18**, 1268 (1975).

(2) T. C. Butler, *J. Pharmacol. Exp. Ther.*, **119**, 1 (1957).

(3) A. J. Atkinson, J. MacGee, J. Strong, D. Garteiz, and T. E. Gaffney, *Biochem. Pharmacol.*, **19**, 2483 (1970).

(4) T. Chang, R. A. Okerholm, and A. J. Glazko, *Anal. Lett.*, **5**, 195 (1972).

(5) T. Chang, R. A. Okerholm, and A. J. Glazko, *Res. Commun. Chem. Pathol. Pharmacol.*, **4**, 13 (1972).

(6) R. M. Thompson, J. Beghin, W. F. Fife, and N. Gerber, *Drug Metab. Dispos.*, **4**, 349 (1976).

(7) T. Chang, A. Savoy, and A. J. Glazko, *Biochem. Biophys. Res. Commun.*, **34**, 444 (1970).

(8) K. Nakamura, Y. Masudo, and K. Nakatsuji, *Arch. Int. Pharmacodyn. Ther.*, **165**, 103 (1967).

(9) R. E. Counsell, V. V. Ranade, W. Kline, B. H. Hong, and A. A. Buswink, *J. Pharm. Sci.*, **65**, 285 (1976).

(10) H. R. Henze and A. F. Isbell, *J. Am. Chem. Soc.*, **76**, 4152 (1952).

(11) Anticonvulsant Screening Project, Antiepileptic Drug Development Program, NINCDS, NIH, DHEW Publication (NIH) 76-1093, 1976. E. A. Swinyard, W. C. Brown, and L. S. Goodman, *J. Pharmacol. Exp. Ther.*, **106**, 319 (1952).

(12) H. H. Merritt and T. J. Putnam, *Epilepsia*, **3**, 51 (1945).

(13) W. J. Close and M. A. Spielman, in "Medicinal Chemistry," vol. V, W. H. Hartung, Ed., Wiley, New York, N.Y., 1961, pp. 1–350.

(14) E. J. Moriconi, W. F. O'Connor, and W. F. Forbes, *J. Am. Chem. Soc.*, **84**, 3928 (1962).

(15) R. Adams, J. R. Johnson, and C. F. Wilcox, "Laboratory Experiments in Organic Chemistry," 6th ed., Collier–Macmillan, London, England, 1970.

(16) J. T. Litchfield and F. Wilcoxon, *J. Pharmacol. Exp. Ther.*, **96**, 99 (1949).

Applications of Paired Ion High-Pressure Liquid Chromatography: Quantitative Determination of Potassium Guaiacolsulfonate and Other Ingredients in Cough Syrups

V. DAS GUPTA

Received March 21, 1978, from the *College of Pharmacy, University of Houston, Houston, TX 77004.* Accepted for publication June 9, 1978.

Abstract □ A method for the quantitative determination of potassium guaiacolsulfonate and phenylephrine hydrochloride in commercial dosage forms was developed. The method is based on paired ion high-pressure liquid chromatography with tetrabutylammonium as the counterion. The method not only separates potassium guaiacolsulfonate from phenylephrine hydrochloride but also from some other ingredients: chlorpheniramine maleate, sodium benzoate, colors, and flavors. Furthermore, two isomers of potassium guaiacolsulfonate, potassium salts of 4- and 5-guaiacolsulfonic acid, also separate from each other. The method was tried on five different commercial dosage forms (all with different colors) with excellent results on three. In the other two samples, which also contained codeine, there may have been a stability problem.

Keyphrases □ Potassium guaiacolsulfonate—high-pressure liquid chromatographic analysis in pharmaceutical preparations □ Phenylephrine hydrochloride—high-pressure liquid chromatographic analysis in pharmaceutical preparations □ High-pressure liquid chromatography—analyses, potassium guaiacolsulfonate and phenylephrine hydrochloride in pharmaceutical preparations □ Adrenergics—phenylephrine hydrochloride, high-pressure liquid chromatographic analysis in pharmaceutical preparations □ Expectorants—potassium guaiacolsulfonate, high-pressure liquid chromatographic analysis in pharmaceutical preparations

Many cough syrups contain potassium guaiacolsulfonate (I), which is an expectorant, and other active and inactive ingredients. The literature for the quantitative determination of I was reviewed previously (1). A new colorimetric procedure for its quantitative determination, based on the oxidation of I in an alkaline borate buffer solution and subsequent coupling with 4-aminoantipyrine, was developed (1). Since phenylephrine hydrochloride (II) also undergoes this coupling, it interferes with the quantitative determination of I.

BACKGROUND

Potassium guaiacolsulfonate is a mixture of two isomers (2), potassium salts of 4- and 5-guaiacolsulfonic acid, but the presently available methods (1, 3–5) for the quantitative determination of I do not distinguish between them.

Recently, paired ion high-pressure liquid chromatography (HPLC) has become popular for increasing the retention times of weak acids and bases by the addition of a counterion in the mobile phase (6). Alkyl sulfonates are used for basic compounds, and quaternary ammonium compounds are used for acidic compounds (6).

Paired ion chromatography is an effective means of separating ionic compounds (6). It was used for the separation of thyroid hormones and sulfa drugs (7); and the analysis of FD&C dyes, such as tartrazine, was reported with tertiary or quaternary amines as the counterion in the mobile phase (8). Reversed-phase paired ion HPLC was used for the separation of hydrocortisone from hydrocortisone phosphate (9). This approach also was applied to the simultaneous determination of niacin and niacinamide in multivitamin preparations with dioctyl sulfonate as the counterion (10).

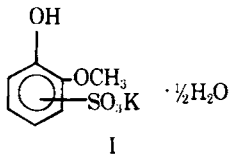

I

The purpose of this report is to present a method for: (*a*) the quantitative determination of I in the presence of II, (*b*) the separation of the two isomers of I, and (*c*) the quantitative determination of I in the presence of some other active and inactive ingredients present in commercial dosage forms used to relieve the symptoms of coughs and colds. The developed method is based on paired ion HPLC with tetrabutylammonium (III) as the counterion. An identical method in which the ammonium ion was substituted for III also was tried without success.

EXPERIMENTAL

Reagents and Chemicals—All reagents and chemicals were ACS, USP, or NF quality and were used without further purification. Brompheniramine hydrochloride[1] (IV), chlorpheniramine maleate[2] (V), codeine phosphate[3] (VI), dextromethorphan hydrobromide[4] (VII), diphenhydramine hydrochloride[1] (VIII), potassium guaiacolsulfonate[3], phenylephrine hydrochloride[5], promethazine hydrochloride[6] (IX), and sodium benzoate[3] (X) were used as received.

Apparatus—The high-pressure liquid chromatograph[7] was connected to a multiple wavelength detector[8], a recorder[9], and an integrator[10].

Column—The column[11] (30 cm × 4 mm i.d.) was of a very nonpolar material, consisting of a monomolecular layer of octadecyltrichlorosilane permanently bonded by silicone–carbon bonds.

Chromatographic Conditions—Solvent A consisted of 0.005 *M* dibasic ammonium phosphate in water containing 8.5% (v/v) methanol. The pH was adjusted to 7.75[12] (±0.05) with dilute phosphoric acid (1:100 in water). Solvent B was the same as A except that tetrabutylammonium hydroxide (from a 40% aqueous solution) was substituted for dibasic ammonium phosphate.

The temperature was ambient. The flow rate was 4.0 ml/min except for the first 2 min with Solvent A when it was 2.0 ml/min. The detector was set at a sensitivity of 0.1 (254 nm) for Solvent A and at 0.04 for Solvent B. The chart speed was 30.5 cm/hr.

Preparation of Solutions—The stock solutions of all drugs, I, II, and IV–X, were prepared by dissolving 0.250 g of the drug in enough water to make 100.0 ml. The standard solutions were prepared by diluting the stock solution with the appropriate chromatographic solvent as needed. A standard mixture of six ingredients, I, II, V, VI, IX, and X, was prepared by mixing 10.0 ml of each stock solution and then bringing to volume (100.0 ml) with the appropriate chromatographic solvent. This mixture was diluted further with the chromatographic solvent as needed.

Dilutions of Commercial Dosage Forms for Analysis—A 10.0-ml aliquot of the dosage form was diluted to 100.0 ml with water. An appropriate quantity of this solution was diluted further with an appropriate chromatographic solvent to obtain a concentration of 250.0 μg of I/ml. For the analysis of II, which was present in only one dosage form, the first dilution in water, *i.e.*, 10.0–100 ml, was used. This dilution contained 100 μg of II/ml.

Assay—A 20.0-μl aliquot of the assay solution was injected into the chromatograph using the described conditions (chromatographic Solvent B). For comparison, an identical volume of the appropriate standard

[1] Parke-Davis & Co., Detroit, Mich.
[2] Schering Corp., Bloomfield, N.J.
[3] Merck & Co., Rahway, N.J.
[4] Hoffmann-La Roche, Nutley, N.J.
[5] Winthrop Laboratories, New York, N.Y.
[6] Wyeth Laboratories, Philadelphia, Pa.
[7] Waters ALC 202 equipped with a U6K universal injector, Waters Associates, Milford, Mass.
[8] Spectroflow monitor SF770, Schoeffel Instrument Corp., Westwood, N.J.
[9] Omniscribe 5213-12, Houston Instruments, Austin, Tex.
[10] Autolab minigrator, Spectra-Physics, Santa Clara, Calif.
[11] Waters μBondapak C_{18}, Catalog No. 27324.
[12] Model 4500 digital pH meter, Beckman Instruments, Irvine, Calif.

0022-3549/79/0100-0118$01.00/0
© 1979, American Pharmaceutical Association

Table I—Results on Potassium Guaiacolsulfonate and Phenylephrine Hydrochloride in Various Commercial Dosage Forms

Dosage Form (Expectorant)	Color	pH[a]	Concentration of I, mg/ml	Percent[b] of Label Claim Found On I Using Developed Method	On I Using Literature Method	On II Using Developed Method
1[c]	Green	5.2	8.8	99.5	100.0	—[d]
2[e]	Yellowish brown	5.2	8.8	99.4	124.4[f]	97.0
3[g]	Yellow	5.2	8.8	99.9	100.5	—[d]
4[h]	Dark red	5.2	8.8	88.7	100.5	—[d]
5[i]	Red	5.7	16	90.9	95.3	—[d]
RSD, %[j]				1.14	1.29	

[a] After diluting 10 ml to 100 ml with water. [b] Average of two. [c] Other listed ingredients per 5 ml of the dosage form were: IX, 5 mg; ipecac fluid extract, 0.01 ml; chloroform, 0.015 ml; citric acid anhydrous, 60 mg; and sodium citrate, 197 mg. [d] Did not contain phenylephrine hydrochloride. [e] Also contained all ingredients listed under footnote c plus 1 mg of II/ml. [f] Results are high due to interference from II (see Ref. 1). [g] Also contained all ingredients listed under footnote c plus 1.5 mg of dextromethorphan hydrobromide/ml. [h] Also contained all ingredients listed under footnote c plus 2 mg of VI/ml. [i] Other listed ingredients per 5 ml of the dosage were: IV, 3.75 mg; VIII, 8.75 mg; ammonium chloride, 80 mg; methanol, 0.5 mg; and codeine sulfate, 10 mg. [j] Based on five injections of the standard mixture. Similar deviations were recorded on different days of the experiment.

solution (containing 250 μg of I/ml or 100 μg of II/ml) or mixture was injected after the assay solution eluted.

Calculations—Since preliminary investigations indicated that the peak areas (peaks heights also) were related directly to the concentrations (range of 1.25–5.0 μg) of each ingredient, the results were calculated using:

$$\frac{A_a}{A_s} \times 100 = \text{percent of label claim} \qquad \text{(Eq. 1)}$$

where A_a is the peak area of the assay solution and A_s is the peak area of the standard solution.

With I, the area of the larger peak (first peak from one of the two isomers) was used. The second peak was too small for accurate results. The results are presented in Table I, and the sample chromatograms are presented in Figs. 1A–1C and 2. A chromatogram that was developed using Solvent A is presented in Fig. 1D. Potassium guaiacolsulfonate also was assayed using the colorimetric method (1). The results are presented in Table I.

RESULTS AND DISCUSSION

The results clearly indicate that paired ion HPLC is useful for the separation of a number of active ingredients (Fig. 1C): chlorpheniramine maleate, potassium guaiacolsulfonate, phenylephrine hydrochloride, and sodium benzoate. Under identical conditions without the addition of the counterion tetrabutylammonium, this separation was not possible (Fig. 1D). The addition of the counterion not only separated these ingredients but also the two isomers of potassium guaiacolsulfonate from each other. A number of other ingredients, bromdiphenhydramine hydrochloride, codeine phosphate, diphenhydramine hydrochloride, dextromethorphan hydrobromide, methylparaben, propylparaben, promethazine hydrochloride, colorants, and flavors, did not interfere with analysis. The concentrations tested were much higher (5 mg/ml, based on the original dosage form) than are usually found in commercial dosage forms.

The addition of a counterion such as III increases the retention times of weak acids (8, 9). However, it appears that it considerably decreased the retention time of phenylephrine hydrochloride, a zwitterion (Figs. 1C and 1D).

The developed method can be used for the quantitative determination of I in pharmaceutical dosage forms (Table I). The relative percent standard deviation based on five injections of the standard mixture was 1.29. Phenylephrine hydrochloride in combination with I also may be determined (Table I). The separation of I and II from each other appears to be excellent (Figs. 1C and 2A). It was not possible to determine the concentration of I and II separately using the method reported earlier (1).

Furthermore, it was estimated that the first four expectorants (Table I) contained ~0.02% sodium benzoate as the preservative while the fifth expectorant did not contain sodium benzoate. It was possible to determine the concentration of sodium benzoate without a separate analysis or additional injections into the chromatograph. With HPLC, additional ingredients can be determined without additional labor or cost.

The results on potassium guaiacolsulfonate in Expectorants 4 and 5 (Table I) were lower with the developed method than with the literature method (1) because the developed method separated the two isomers of I. Neither the literature method (1) nor the NF method (3) distinguishes between the two isomers. In the developed method, the larger peak (first peak from I) was used to determine the concentrations of I because the second peak was too small for accurate determinations. The ratio of peak heights of the two isomers was about 7:1 in the standard mixture (Fig. 1C, peaks 3 and 4) and in other expectorants (Figs. 2A and 2B, peaks 2 and 3) except 4 and 5 (Table I), both of which contained codeine.

In Expectorants 4 and 5, the ratios were significantly different, 5:1 (Fig. 2C, peaks 2 and 3) and 6.3:1, respectively. Therefore, there may be a stability problem in the presence of codeine. The difference in the ratios of the two isomers in the presence of codeine in the two samples may have been due to: (*a*) pH differences (Table I); (*b*) the difference in codeine

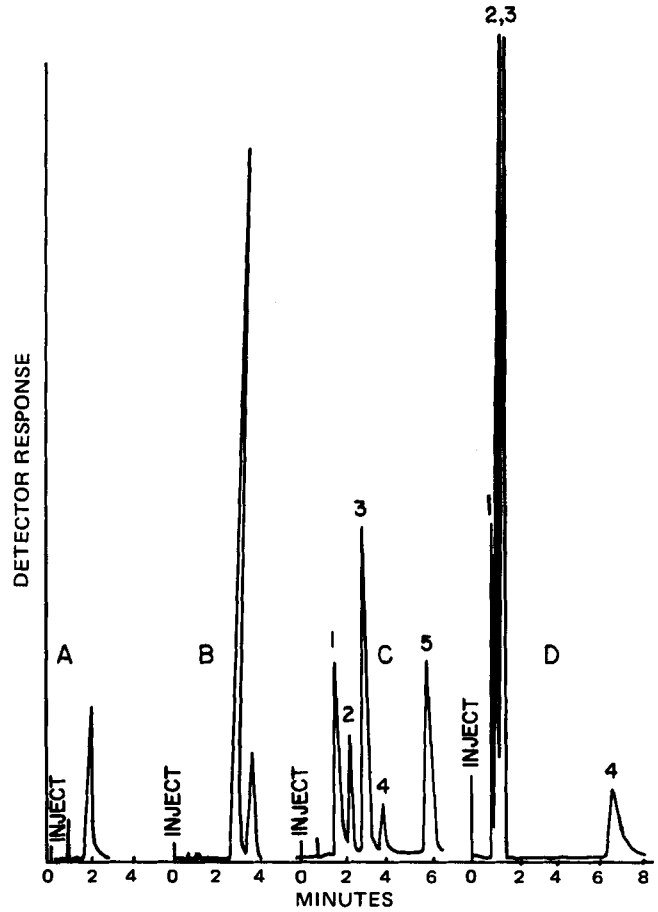

Figure 1—*Sample chromatograms. Solvent B was used for A–C, and Solvent A was used for D. Chromatogram A is from a standard solution of II in water (100 μg/ml). Chromatogram B is from a standard solution of I (250 μg/ml). Both peaks are from I. Chromatogram C is from a mixture containing 125 μg/ml each of I, II, V, VI, IX, and X. Peak 1 is from V, 2 is from II, 3 and 4 are from I, and 5 is from X. No peaks were recorded from the other two ingredients. Chromatogram D is the same as C, except that the solvent was A and the concentration of each ingredient was 250 μg/ml. Peak 1 is from V, 2 is from I, 3 is from X, and 4 is from II.*

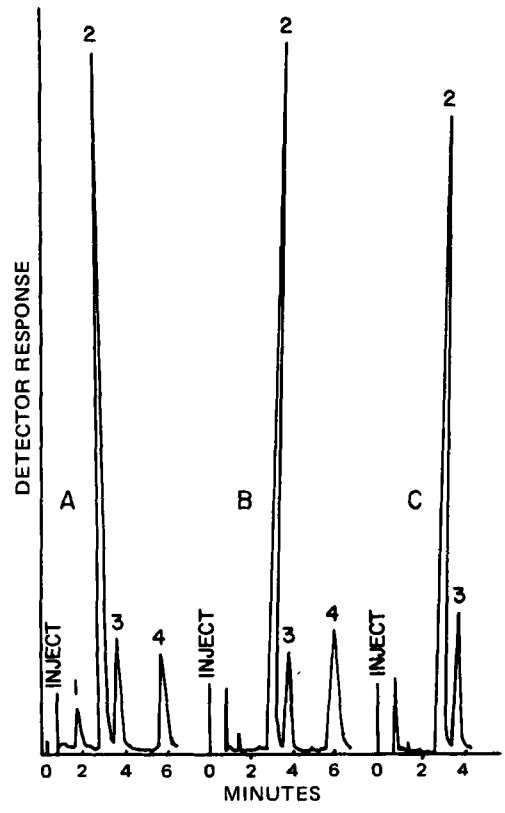

Figure 2—*Sample chromatograms developed using Solvent B. Chromatogram A is from a commercial expectorant (2 in Table I). Peak 1 is from II, 2 and 3 are from I, and 4 is from X. Chromatogram B is from Expectorant 1 in Table I. Peaks are the same as in A except that it did not contain II. Chromatogram C is from Expectorant 4 in Table I. Peaks are the same.*

salts: codeine phosphate in Expectorant 4 *versus* codeine sulfate in Expectorant 5; (*c*) a higher concentration of codeine in Expectorant 4 relative to the concentration of potassium guaiacolsulfonate, *i.e.*, codeine was 2 mg/ml in each sample *versus* only 8.8 mg of I/ml in Expectorant 4 and 16 mg of I/ml in Expectorant 5; (*d*) different buffering systems: citrates in Expectorant 4 *versus* ammonium chloride in 5; and (*e*) the ages of the samples, which were not determined. The standard mixture did contain codeine, and the ratio (about 7:1) of the peak heights of the two isomers had not changed even after standing for about 7 days. Without further intensive investigations, it is not possible to determine whether this change in ratio affects the therapeutic value.

Expectorants 1–4 (Table I) gave an additional unidentified peak after about 13.5 min. Expectorant 5 gave at least two unidentified peaks after about 7 and 13.3 min. These peaks, which were recorded using Solvent B, could be from the colorants, flavors, or preservative. This matter was not pursued further because detailed formulas of the dosage forms were not available.

REFERENCES

(1) V. D. Gupta and A. J. L. de Lara, *J. Pharm. Sci.*, **64**, 2001 (1975).

(2) "The Merck Index," 9th ed., Merck & Co., Rahway, N.J., no. 7415.

(3) "The National Formulary," 13th ed., Mack Publishing Co., Easton, Pa., p. 574.

(4) A. S. D'Souza and K. G. Shenoy, *Indian J. Pharm.*, **29**, 327 (1967).

(5) S. B. Gandhi, P. R. Patel, and K. H. Misarwala, *ibid.*, **30**, 45 (1968).

(6) "Paired Ion Chromatography," Bulletin D61, Waters Associates, Milford, Mass., Dec. 1975.

(7) B. L. Karger, S. C. Su, S. Marchese, and B. Persson, *J. Chromatogr. Sci.*, **12**, 678 (1974).

(8) D. P. Wittmer, N. O. Nuessle, and W. G. Haney, Jr., *Anal. Chem.*, **47**, 1422 (1975).

(9) J. Kopri, D. P. Wittmer, B. J. Sandmann, and W. G. Haney, Jr., *J. Pharm. Sci.*, **65**, 1087 (1976).

(10) S. P. Sood, D. P. Wittmer, S. A. Ismaiel, and W. G. Haney, Jr., *ibid.*, **66**, 40 (1977).

Molecular Connectivity Analyses of Structure Influencing Chromatographic Retention Indexes

LEMONT B. KIER *x **and LOWELL H. HALL** ‡

Received March 6, 1978, from the **Department of Pharmaceutical Chemistry, Medical College of Virginia, Richmond, VA 23298,* and the *‡Department of Chemistry, Eastern Nazarene College, Quincy, MA 02170.* Accepted for publication June 15, 1978.

Abstract □ The molecular connectivity indexes of various aliphatic alcohols, ketones, ethers, and esters were used to describe structural features influencing chromatographic retention indexes. Good correlations were obtained within chemical classes for a particular stationary phase.

Keyphrases □ Molecular connectivity indexes—correlated with structural features influencing chromatographic retention indexes, various organic compounds □ Chromatographic retention indexes—correlated with molecular connectivity indexes, various organic compounds □ Topological indexes—molecular connectivity indexes correlated with structural features influencing chromatographic retention indexes

The chromatographic retention index is a quantification of a dynamic physicochemical process involving the equilibration of a solute between two liquids passing each other at an interface (liquid–liquid chromatography) or the interchange state between gas and solution phases (gas–liquid chromatography). The retention index for a particular molecule in a particular system depends on the structure of that molecule and the nature of that system. A rigorous definition of the structure of a molecule should make it possible to arrive at an accurate value for a retention index for a given system.

BACKGROUND

Previously (1), it was shown that definition of molecular structure at the level of topology could provide sufficient information for close correlations with numerous physicochemical properties. This definition of molecular structure is called molecular connectivity (2). To the extent that chromatographic retention indexes are influenced by topological

0022-3549/79/0100-0120$01.00/0
© 1979, American Pharmaceutical Association

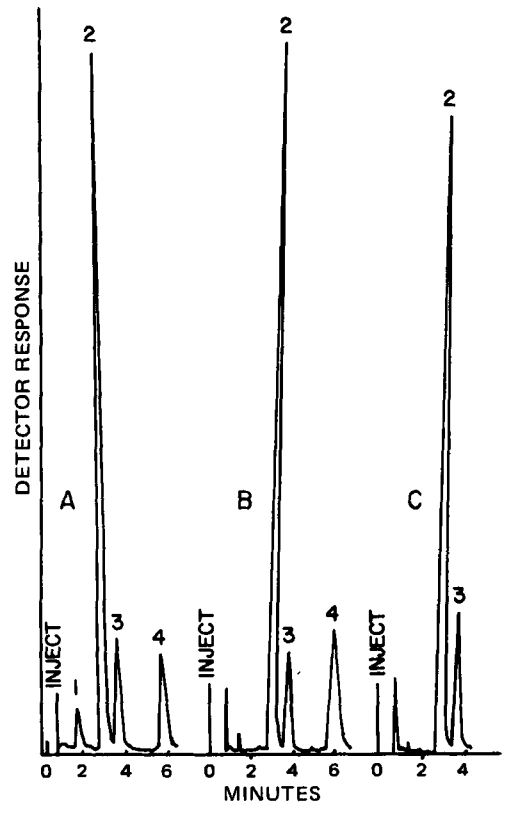

Figure 2—*Sample chromatograms developed using Solvent B. Chromatogram A is from a commercial expectorant (2 in Table I). Peak 1 is from II, 2 and 3 are from I, and 4 is from X. Chromatogram B is from Expectorant 1 in Table I. Peaks are the same as in A except that it did not contain II. Chromatogram C is from Expectorant 4 in Table I. Peaks are the same.*

salts: codeine phosphate in Expectorant 4 *versus* codeine sulfate in Expectorant 5; (*c*) a higher concentration of codeine in Expectorant 4 relative to the concentration of potassium guaiacolsulfonate, *i.e.*, codeine was 2 mg/ml in each sample *versus* only 8.8 mg of I/ml in Expectorant 4 and 16 mg of I/ml in Expectorant 5; (*d*) different buffering systems: citrates in Expectorant 4 *versus* ammonium chloride in 5; and (*e*) the ages of the samples, which were not determined. The standard mixture did contain codeine, and the ratio (about 7:1) of the peak heights of the two isomers had not changed even after standing for about 7 days. Without further intensive investigations, it is not possible to determine whether this change in ratio affects the therapeutic value.

Expectorants 1–4 (Table I) gave an additional unidentified peak after about 13.5 min. Expectorant 5 gave at least two unidentified peaks after about 7 and 13.3 min. These peaks, which were recorded using Solvent B, could be from the colorants, flavors, or preservative. This matter was not pursued further because detailed formulas of the dosage forms were not available.

REFERENCES

(1) V. D. Gupta and A. J. L. de Lara, *J. Pharm. Sci.*, **64**, 2001 (1975).

(2) "The Merck Index," 9th ed., Merck & Co., Rahway, N.J., no. 7415.

(3) "The National Formulary," 13th ed., Mack Publishing Co., Easton, Pa., p. 574.

(4) A. S. D'Souza and K. G. Shenoy, *Indian J. Pharm.*, **29**, 327 (1967).

(5) S. B. Gandhi, P. R. Patel, and K. H. Misarwala, *ibid.*, **30**, 45 (1968).

(6) "Paired Ion Chromatography," Bulletin D61, Waters Associates, Milford, Mass., Dec. 1975.

(7) B. L. Karger, S. C. Su, S. Marchese, and B. Persson, *J. Chromatogr. Sci.*, **12**, 678 (1974).

(8) D. P. Wittmer, N. O. Nuessle, and W. G. Haney, Jr., *Anal. Chem.*, **47**, 1422 (1975).

(9) J. Kopri, D. P. Wittmer, B. J. Sandmann, and W. G. Haney, Jr., *J. Pharm. Sci.*, **65**, 1087 (1976).

(10) S. P. Sood, D. P. Wittmer, S. A. Ismaiel, and W. G. Haney, Jr., *ibid.*, **66**, 40 (1977).

Molecular Connectivity Analyses of Structure Influencing Chromatographic Retention Indexes

LEMONT B. KIER *x **and LOWELL H. HALL** ‡

Received March 6, 1978, from the **Department of Pharmaceutical Chemistry, Medical College of Virginia, Richmond, VA 23298,* and the *‡Department of Chemistry, Eastern Nazarene College, Quincy, MA 02170.* Accepted for publication June 15, 1978.

Abstract □ The molecular connectivity indexes of various aliphatic alcohols, ketones, ethers, and esters were used to describe structural features influencing chromatographic retention indexes. Good correlations were obtained within chemical classes for a particular stationary phase.

Keyphrases □ Molecular connectivity indexes—correlated with structural features influencing chromatographic retention indexes, various organic compounds □ Chromatographic retention indexes—correlated with molecular connectivity indexes, various organic compounds □ Topological indexes—molecular connectivity indexes correlated with structural features influencing chromatographic retention indexes

The chromatographic retention index is a quantification of a dynamic physicochemical process involving the equilibration of a solute between two liquids passing each other at an interface (liquid–liquid chromatography) or the interchange state between gas and solution phases (gas–liquid chromatography). The retention index for a particular molecule in a particular system depends on the structure of that molecule and the nature of that system. A rigorous definition of the structure of a molecule should make it possible to arrive at an accurate value for a retention index for a given system.

BACKGROUND

Previously (1), it was shown that definition of molecular structure at the level of topology could provide sufficient information for close correlations with numerous physicochemical properties. This definition of molecular structure is called molecular connectivity (2). To the extent that chromatographic retention indexes are influenced by topological

0022-3549/79/0100-0120$01.00/0
© 1979, American Pharmaceutical Association

Table I—GLC Retention Indexes

Compound	Stationary Phase[a] I	II	III	IV
Methanol	1027	1156	311	652
Ethanol	1062	1159	395	730
Propanol	1163	1257	511	828
Butanol	1274	1366	621	941
Pentanol	1384	1467	731	1053
3-Pentanol	1221	1318	673	954
Hexanol	1479	1565	830	1160
2-Hexanol	1345	1571	771	1080
3-Hexanol	1312	1401	771	1058
Heptanol	1575	1665	935	1268
Octanol	1674	1742	1028	1367
2-Methyl-2-butanol	1128	1229	—	920
3-Methyl-2-butanol	—	1296	652	949
2,2-Dimethyl-1-propanol	1214	1298	637	935
2-Methyl-2-pentanol	1215	1308	714	1002
3-Methyl-2-pentanol	1307	1396	772	1055
4-Methyl-2-pentanol	1286	1369	732	1035
2-Methyl-3-pentanol	1263	1357	752	1021
3-Methyl-3-pentanol	1229	1336	738	1023
2,4-Dimethyl-3-pentanol	1280	1390	818	1083
3-Ethyl-3-pentanol	1315	1436	—	1135
Cyclohexanol	1538	1679	858	1215
Acetone	915	1141	438	895
2-Butanone	995	1162	551	980
2-Pentanone	1072	1276	639	1070
3-Pentanone	1068	1286	651	1056
3-Methyl-2-butanone	1026	1227	—	1042
2-Hexanone	1173	1373	742	1182
3-Hexanone	1141	1332	741	1141
3-Methyl-2-pentanone	1114	1311	711	1140
4-Methyl-2-pentanone	1099	1293	—	1125
2-Heptanone	1276	1471	845	1286
3-Heptanone	1239	1393	842	1250
2,4-Dimethyl-3-pentanone	1083	1264	763	1132
2-Nonanone	1483	1676	—	1501
5-Nonanone	1425	1604	—	1443
Ether	668	793	486	647
Methyl butyl ether	795	914	610	785
Methyl propyl ether	692	819	506	676
Isobutyl methyl ether	726	820	569	722
tert-Butyl methyl ether	746	868	555	758
Dipropyl ether	811	922	673	792
Isopropyl propyl ether	756	857	631	751
Ethyl formate	885	1092	466	842
Propyl formate	982	1196	569	947
Methyl acetate	896	1100	474	877
Ethyl acetate	951	1157	560	949
Propyl acetate	1043	1242	654	1043
Isopropyl acetate	958	1137	601	981
Butyl acetate	1141	1335	769	1153
sec-Butyl acetate	1054	1223	712	1080
Methyl propionate	971	1179	575	951
Ethyl propionate	1022	1212	657	1014
Methyl butyrate	1052	1252	679	1035
Ethyl butyrate	1100	1284	751	1106
Pentyl acetate	1242	—	856	1262

[a] I = Carbowax 300, 100°; II = diethylene glycol succinate, 120°; III = squalane, 100°; and IV = Zonyl E7, 120°.

structural characteristics, it is reasonable to suppose that molecular connectivity may permit a close correlation between structure and this physicochemical property.

Two studies (3, 4) related molecular connectivity indexes with chromatographic retention indexes. With a series of pyrazine derivatives, good correlation was obtained between $^1\chi$ and the R_m value by TLC (3). Michotte and Massart (4) attempted to relate a single molecular connectivity index to gas–liquid retention indexes in four different stationary phases.

Since both studies were performed before the complete development of molecular connectivity had been published, the full power of the method was not brought to bear on these problems. The present study demonstrates that molecular connectivity can successfully describe structural features influencing chromatographic indexes.

EXPERIMENTAL

Molecular connectivity calculations were described previously (1, 2, 5–8). This study reexamined GLC retention data previously studied by Michotte and Massart (4) and originally derived by McReynolds (9). The Michotte and Massart study considered 22 aliphatic alcohols, 14 aliphatic ketones, seven aliphatic ethers, and 13 aliphatic esters; their retention indexes are listed in Table I. GLC systems included stationary phases composed of squalene, diethylene glycol succinate, polyethylene glycol 300, and a fluoroalkyl ester surfactant[1].

Simple connectivity and valence connectivity indexes were computed for each molecule through the fourth order. The best pair of indexes was searched for in a multiple linear regression analysis for all molecular classes but the ethers, where the limited sample size permitted only one molecular connectivity index. The results are shown in Table II as indexes and the correlation coefficients.

Table II—Best Correlation Coefficients between Retention Indexes and χ Indexes[a]

Class	Squalene	Diethylene Glycol Succinate	Polyethylene Glycol 300	Fluoroalkyl Ester Surfactant
Alcohols	0.994 ($^1\chi$)	0.967 ($^1\chi$, $^0\chi^v$)	0.977 ($^1\chi$, $^0\chi^v$)	0.992 ($^1\chi$, $^0\chi^v$)
Esters	0.991 ($^1\chi$)	0.982 ($^2\chi$, $^3\chi^v_C$)	0.990 ($^1\chi$, $^4\chi_P$)	0.991 ($^2\chi$, $^3\chi^v_C$)
Ketones	0.996 ($^1\chi$)	0.988 ($^2\chi$, $^3\chi^v_C$)	0.995 ($^2\chi$, $^3\chi^v_C$)	0.997 ($^1\chi$, $^1\chi^v$)
Ethers	0.968 ($^1\chi$)	0.930 ($^3\chi^v_P$)	0.958 ($^3\chi^v_P$)	0.966 ($^3\chi^v_P$)

[a] Terms in parentheses are best one or two χ indexes giving the *r* value.

DISCUSSION

Molecular connectivity indexes can provide a description of structure within a chemical class that is very adequate in the correlation with chromatographic behavior (Table II). Chromatographic behavior across chemical classes, *e.g.*, alcohols and ketones, depends on what may be regarded as nontopological structural characteristics in addition to features described by χ indexes. Thus, the intermolecular and hydrogen bonding exhibited by alcohols and ketones would obviously be different in these two classes, leading to different but parallel chromatographic behavior.

Michotte and Massart (4) discovered this fact but failed to note its significance. Their lack of success in collecting all of the molecules in Table II into a single molecular connectivity correlation with retention was taken as a failure of the method. Different molecular classes will behave differently in GLC systems because of both topological and electronic structural differences.

Michotte and Massart (4) presumed that GLC retention behavior mirrored biological phenomena. Clearly, this property is not a general model for any biological event except perhaps the absorption of a gaseous general anesthetic. Even with general anesthetics, it is necessary to include an electronic term to merge different chemical classes in a successful structure–activity relationship (6, 10, 11).

It can be concluded that selected molecular connectivity indexes give good correlations with GLC retention indexes within chemical classes for a particular stationary phase. The GLC phenomenon is not a property relating to general biological phenomena; it must not be confused with the more biologically related property of liquid–liquid chromatography. The study further illustrates the utility of molecular connectivity to describe structure in structure–activity relationship studies.

REFERENCES

(1) L. B. Kier and L. H. Hall, "Molecular Connectivity in Chemistry and Drug Research," Academic, New York, N.Y., 1976.

(2) L. B. Kier, L. H. Hall, J. W. Murray, and M. Randic, *J. Pharm. Sci.*, **64**, 1971 (1975).

(3) R. Kaliszan and H. Folks, *Chromatographia*, **10**, 346 (1977).

(4) Y. Michotte and D. L. Massart, *J. Pharm. Sci.*, **66**, 1630 (1977).

(5) L. B. Kier and L. H. Hall, *J. Med. Chem.*, **20**, 1631 (1977).

(6) T. DiPaolo, L. B. Kier, and L. H. Hall, *Mol. Pharmacol.*, **13**, 31 (1977).

(7) L. B. Kier and L. H. Hall, *Eur. J. Med. Chem.*, **12**, 307 (1977).

[1] Zonyl E7.

(8) L. B. Kier, T. DiPaolo, and L. H. Hall, *J. Theoret. Biol.*, **67**, 585 (1977).
(9) W. O. M. McReynolds, "Gas Chromatographic Retention Indices," Preston Technical Abstracts, Evanston, Ill., 1964.
(10) R. H. Davies, R. D. Bagnall, and W. G. M. Jones, *Int. J. Quantum Chem.*, **1**, 201 (1974).
(11) C. Hansch, A. Vittoria, C. Silipo, and P. Y. Jow, *J. Med. Chem.*, **18**, 546 (1975).

Determination of Water in Aluminum Chlorohydrate and Effervescent Tablets by Karl Fischer Analysis

HARVEY D. SPITZ

Received September 29, 1976, from *Health Care Division Research, Johnson & Johnson, New Brunswick, NJ 08903.* Accepted for publication June 21, 1978.

Abstract □ A procedure was developed for the quantitative determination of loosely bound water in aluminum chlorohydrate and the water content in denture cleanser effervescent tablets. The basic method involves extracting the water from the sample into dioxane followed by titration of the dioxane in methanol with Karl Fischer reagent. Matrix ingredients did not interfere.

Keyphrases □ Aluminum chlorohydrate—water content analyzed by Karl Fischer titration □ Water content—aluminum chlorohydrate, Karl Fischer titration □ Karl Fischer titration—water content of aluminum chlorohydrate analyzed □ Astringents—aluminum chlorohydrate, water content analyzed by Karl Fischer titration

Aluminum chlorohydrate adsorbs free water depending on the surrounding humidity. In dry powder aerosol formulations containing aluminum chlorohydrate, free water can affect product performance. Similarly, in effervescent tablets in sealed packages, water may cause unwanted reactions that can alter the seal integrity or the product itself.

Thermogravimetric analysis and differential scanning calorimetry were used to show the presence of loosely bound water and hydrated water in aluminum chlorohydrate (1). Although free water can be determined by an electrometric approach (1), the method requires a conductivity apparatus, highly purified water, and a standard curve. Moisture in effervescent tablets may be determined by drying over a desiccant, but this procedure is time consuming and the potential for error is increased due to volatile components.

This paper reports the use of the Karl Fischer technique to determine loosely bound water (free water) in aluminum chlorohydrate and water in denture cleanser effervescent tablets without interference from the matrix ingredients.

EXPERIMENTAL

Analysis of Water in Effervescent Tablets—*Reagents*—Karl Fischer reagent[1], the diluent for Karl Fischer reagent[2], and *p*-dioxane[3] were used as received. Diluted Karl Fischer reagent was prepared by diluting 50 ml of Karl Fischer reagent[1] to 250 ml with the diluent for Karl Fischer reagent[2]. A water standard was prepared by weighing 0.06 g of purified water into a preweighed 50-ml volumetric flask. The flask was diluted to the mark with dioxane[3], which usually contains less than 0.005% water.

Apparatus—Karl Fischer titrations were performed with an automatic titrator[4]. A wrist-action shaker[5] was used at its maximum setting. Commercially available 50-ml glass-stoppered centrifuge tubes were dried in an oven at 105°.

Standardization Procedure—Add 100 ml of methanol to a dry titration vessel and titrate with Karl Fischer reagent to the electrometric end-point. Accurately measure the volume of Karl Fischer reagent required to titrate 100 ml of methanol, remove the reagent from the buret, and substitute with diluted Karl Fischer reagent. Discard the titrated methanol and replace it with a fresh 100 ml of methanol. To the fresh methanol, add from a Mohr pipet approximately 0.5 ml less Karl Fischer reagent than the amount required to reach the end-point. Complete the titration using the diluted reagent to the electrometric end-point.

Pipet 10.0 ml of dioxane into the methanolic solution just titrated. Titrate with the diluted Karl Fischer reagent to the electrometric end-point. Record the volume of diluted Karl Fischer reagent used to titrate this system. This sample represents the dioxane reagent blank.

Pipet accurately 10.0 ml of water standard directly into the same titration vessel and titrate with diluted Karl Fischer reagent to the electrometric end-point. Record the volume of diluted Karl Fischer reagent used.

Sample Preparation—Weigh together, to the nearest 10 mg, five tablets that have been crushed within their individual sealed packets (to avoid moisture adsorption from the environment[6]) and empty them into a dry 50-ml centrifuge tube. Reweigh the empty packets and calculate the sample weight by difference.

Pipet accurately 25.0 ml of dioxane into the centrifuge tube and shake on a wrist-action shaker for 15 min. Centrifuge the tube for 5 min.

Procedure—Pipet carefully (without disturbing the insoluble material) 10.0 ml of the dioxane solution into the Karl Fischer titration vessel containing 100 ml of methanol titrated with diluted Karl Fischer reagent to the electrometric end-point. Titrate this sample solution to the electrometric end-point. Record the volume of titrant used. Additional samples can be analyzed by pipetting 10.0 ml of the dioxane solution from another sample into the sample solution just titrated and titrating with the diluted Karl Fischer reagent to the electrometric end-point. Record the volume of titrant used.

Four samples can be analyzed concurrently in the same titrated system. If there is a few minutes of delay between sample analysis, one should titrate the methanolic solution before the next sample is added because of the possibility of moisture entering the titrated system (this titration value need not be recorded).

Calculations—The following equations were used:

$$T = \frac{W}{(V - D)} \qquad \text{(Eq. 1)}$$

[1] Catalog No. SO-K-3, Fisher Scientific Co., Fair Lawn, N.J.
[2] Catalog No. SO-K-5, Fisher Scientific Co., Fair Lawn, N.J.
[3] J. T. Baker Chemical Co., Phillipsburg, N.J.
[4] Precision Auto-Aquatrator, Precision Scientific Co., Chicago, Ill.
[5] Burrell Corp., Pittsburgh, Pa.
[6] Crushing tablets exposed to the atmosphere produces erroneously high results because of water adsorption from the environment.

0022-3549/79/0100-0122$01.00/0
© 1979, American Pharmaceutical Association

(8) L. B. Kier, T. DiPaolo, and L. H. Hall, *J. Theoret. Biol.*, **67**, 585 (1977).
(9) W. O. M. McReynolds, "Gas Chromatographic Retention Indices," Preston Technical Abstracts, Evanston, Ill., 1964.
(10) R. H. Davies, R. D. Bagnall, and W. G. M. Jones, *Int. J. Quantum Chem.*, **1**, 201 (1974).
(11) C. Hansch, A. Vittoria, C. Silipo, and P. Y. Jow, *J. Med. Chem.*, **18**, 546 (1975).

Determination of Water in Aluminum Chlorohydrate and Effervescent Tablets by Karl Fischer Analysis

HARVEY D. SPITZ

Received September 29, 1976, from *Health Care Division Research, Johnson & Johnson, New Brunswick, NJ 08903.* Accepted for publication June 21, 1978.

Abstract □ A procedure was developed for the quantitative determination of loosely bound water in aluminum chlorohydrate and the water content in denture cleanser effervescent tablets. The basic method involves extracting the water from the sample into dioxane followed by titration of the dioxane in methanol with Karl Fischer reagent. Matrix ingredients did not interfere.

Keyphrases □ Aluminum chlorohydrate—water content analyzed by Karl Fischer titration □ Water content—aluminum chlorohydrate, Karl Fischer titration □ Karl Fischer titration—water content of aluminum chlorohydrate analyzed □ Astringents—aluminum chlorohydrate, water content analyzed by Karl Fischer titration

Aluminum chlorohydrate adsorbs free water depending on the surrounding humidity. In dry powder aerosol formulations containing aluminum chlorohydrate, free water can affect product performance. Similarly, in effervescent tablets in sealed packages, water may cause unwanted reactions that can alter the seal integrity or the product itself.

Thermogravimetric analysis and differential scanning calorimetry were used to show the presence of loosely bound water and hydrated water in aluminum chlorohydrate (1). Although free water can be determined by an electrometric approach (1), the method requires a conductivity apparatus, highly purified water, and a standard curve. Moisture in effervescent tablets may be determined by drying over a desiccant, but this procedure is time consuming and the potential for error is increased due to volatile components.

This paper reports the use of the Karl Fischer technique to determine loosely bound water (free water) in aluminum chlorohydrate and water in denture cleanser effervescent tablets without interference from the matrix ingredients.

EXPERIMENTAL

Analysis of Water in Effervescent Tablets—*Reagents*—Karl Fischer reagent[1], the diluent for Karl Fischer reagent[2], and *p*-dioxane[3] were used as received. Diluted Karl Fischer reagent was prepared by diluting 50 ml of Karl Fischer reagent[1] to 250 ml with the diluent for Karl Fischer reagent[2]. A water standard was prepared by weighing 0.06 g of purified water into a preweighed 50-ml volumetric flask. The flask was diluted to the mark with dioxane[3], which usually contains less than 0.005% water.

Apparatus—Karl Fischer titrations were performed with an automatic titrator[4]. A wrist-action shaker[5] was used at its maximum setting. Commercially available 50-ml glass-stoppered centrifuge tubes were dried in an oven at 105°.

Standardization Procedure—Add 100 ml of methanol to a dry titration vessel and titrate with Karl Fischer reagent to the electrometric end-point. Accurately measure the volume of Karl Fischer reagent required to titrate 100 ml of methanol, remove the reagent from the buret, and substitute with diluted Karl Fischer reagent. Discard the titrated methanol and replace it with a fresh 100 ml of methanol. To the fresh methanol, add from a Mohr pipet approximately 0.5 ml less Karl Fischer reagent than the amount required to reach the end-point. Complete the titration using the diluted reagent to the electrometric end-point.

Pipet 10.0 ml of dioxane into the methanolic solution just titrated. Titrate with the diluted Karl Fischer reagent to the electrometric end-point. Record the volume of diluted Karl Fischer reagent used to titrate this system. This sample represents the dioxane reagent blank.

Pipet accurately 10.0 ml of water standard directly into the same titration vessel and titrate with diluted Karl Fischer reagent to the electrometric end-point. Record the volume of diluted Karl Fischer reagent used.

Sample Preparation—Weigh together, to the nearest 10 mg, five tablets that have been crushed within their individual sealed packets (to avoid moisture adsorption from the environment[6]) and empty them into a dry 50-ml centrifuge tube. Reweigh the empty packets and calculate the sample weight by difference.

Pipet accurately 25.0 ml of dioxane into the centrifuge tube and shake on a wrist-action shaker for 15 min. Centrifuge the tube for 5 min.

Procedure—Pipet carefully (without disturbing the insoluble material) 10.0 ml of the dioxane solution into the Karl Fischer titration vessel containing 100 ml of methanol titrated with diluted Karl Fischer reagent to the electrometric end-point. Titrate this sample solution to the electrometric end-point. Record the volume of titrant used. Additional samples can be analyzed by pipetting 10.0 ml of the dioxane solution from another sample into the sample solution just titrated and titrating with the diluted Karl Fischer reagent to the electrometric end-point. Record the volume of titrant used.

Four samples can be analyzed concurrently in the same titrated system. If there is a few minutes of delay between sample analysis, one should titrate the methanolic solution before the next sample is added because of the possibility of moisture entering the titrated system (this titration value need not be recorded).

Calculations—The following equations were used:

$$T = \frac{W}{(V - D)} \qquad \text{(Eq. 1)}$$

[1] Catalog No. SO-K-3, Fisher Scientific Co., Fair Lawn, N.J.
[2] Catalog No. SO-K-5, Fisher Scientific Co., Fair Lawn, N.J.
[3] J. T. Baker Chemical Co., Phillipsburg, N.J.
[4] Precision Auto-Aquatrator, Precision Scientific Co., Chicago, Ill.
[5] Burrell Corp., Pittsburgh, Pa.
[6] Crushing tablets exposed to the atmosphere produces erroneously high results because of water adsorption from the environment.

0022-3549/79/0100-0122$01.00/0
© 1979, American Pharmaceutical Association

Table I—Recovery of Water from Effervescent Tablets

Sample	A[a]	B	C	D	E	Water Recovered, %
1	9.45	5.67	11.48	17.15	17.62	102.7
2	7.93	4.76	11.48	16.24	16.91	104.1
3	12.30	7.40	11.48	18.88	19.17	101.5

[a] A = milligrams of water left in the original tablets before spiking (determined from a 10-ml aliquot for analysis from a total of 25 ml of dioxane). B = milligrams of water left in the remaining 15 ml of dioxane after a 10-ml aliquot was taken for analysis. C = milligrams of water spiked into B. D = total milligrams of water from B + C. E = milligrams of water found in spiked Sample D.

where T is the titer of diluted Karl Fischer reagent (milligrams of water per milliliter of diluted Karl Fischer reagent), W is the milligrams of water in the 10-ml aliquot used for standardization, V is the milliliters of diluted Karl Fischer reagent used to titrate the standard water, and D is the volume of diluted Karl Fischer reagent used to titrate the dioxane (blank).

The percent water found in the sample (P) was calculated using:

$$P = \frac{(K - D) \times T \times 2.5}{S} \times 100 \qquad \text{(Eq. 2)}$$

where K is the milliliters of diluted Karl Fischer reagent used to titrate the sample, D is the volume of diluted Karl Fischer reagent used to titrate the dioxane blank, T is the titer of diluted Karl Fischer reagent, S is the sample weight (milligrams), and 2.5 is the aliquot factor.

Analysis of Loosely Bound Water in Aluminum Chlorohydrate—*Reagents and Apparatus*—The reagents and apparatus required are the same as those described for the analysis of effervescent tablets except that the Karl Fischer reagent is not diluted and the standardization is simplified.

Standardization Procedure—To 100 ml of methanol titrated with Karl Fischer reagent, add 10.0 ml of dioxane and titrate to the electrometric end-point. Record this volume (blank). Accurately weigh, to the nearest 0.1 mg, about 120 mg of purified water directly into the titration vessel and titrate with Karl Fischer reagent to the electrometric end-point. Record the volume.

Sample Preparation—Weigh accurately and quickly, to the nearest milligram, about 10.0 g of aluminum chlorohydrate into a dry 50-ml centrifuge tube. Pipet accurately 25.0 ml of dioxane into the centrifuge tube; shake on a wrist-action shaker for 0.5 hr. Centrifuge the tube for 5 min.

Procedure—Pipet carefully (without disturbing the aluminum chlorohydrate) 10.0 ml of the dioxane solution into the Karl Fischer titration vessel containing 100 ml of methanol titrated with Karl Fischer reagent to the electrometric end-point. Titrate the resulting sample solution to the electrometric end-point. Record the volume of titrant used for the titration.

Several sample solutions can be titrated concurrently in the same titrated solution.

Calculations—Water content can be calculated using the same basic format employed for the effervescent tablet calculations.

Recovery Study—A recovery study was performed on denture cleanser effervescent tablets to determine if water could be recovered at the desired level (less than 0.1%) and if any ingredient in the matrix interfered in the analysis. Tablets first were analyzed for their water content according to the procedure previously described. To the remaining extracted tablets and 15 ml of dioxane (still in the centrifuge tube), a known amount of water (in dioxane) was added. The tablets were extracted once again, and the water content was determined as before.

Recovery data were calculated after determining the amount of water in the original tablets before spiking, the amount of water left in the remaining dioxane after an aliquot was taken for analysis, and the amount of water added to the sample.

RESULTS AND DISCUSSION

Since only the free water content in aluminum chlorohydrate was of interest, and not its water of hydration, the method had to differentiate between the different types of water. Likewise, the procedure had to determine the water in effervescent denture cleanser tablets without interference from other ingredients in the formulation. Analytical techniques involving GLC, distillation, spectroscopy, oven drying, and other methods were also considered for the analysis of water, but the speed, specificity, simplicity, and adaptability of the Karl Fischer technique to the variety of samples tested made it the first choice.

Dioxane was selected (1–5) as the extractant because aluminum chlorohydrate is insoluble in dioxane and it extracts only the loosely bound water from the insoluble aluminum chlorohydrate and not the water of hydration. Likewise, dioxane extracts only the free water in denture cleanser effervescent tablets, leaving behind the interfering insoluble sodium bicarbonate and other potential interfering ingredients. Under ordinary circumstances, Karl Fischer reagent reacts with sodium bicarbonate (5) and also appears to titrate all of the water in aluminum chlorohydrate, which can amount to 25%. Sodium bicarbonate does not interfere since it is rendered insoluble in dioxane and is removed before titrating the dioxane solution.

Although it was reported that the Karl Fischer method was not successful (1) because of the reactivity of aluminum chlorohydrate to Karl Fischer reagent, the dioxane extraction technique eliminates this problem. However, alcohol is necessary in the titration vessel, because titrating dioxane alone gives a premature end-point.

The recovery data of water in effervescent tablets are shown in Table I. At least 500 analyses were performed on denture cleanser effervescent tablets using this modified Karl Fischer procedure.

Experimental tablets as well as commercially available denture cleanser tablets were found to contain between 0.02 and 0.1% water. Samples of aluminum chlorohydrate also were analyzed for loosely bound water. The results obtained agreed well with samples supplied (1) with known levels of loosely bound water at the 0.5 and 2.0% level.

The foregoing methods, although somewhat different, both contain the same basic dioxane extraction technique followed by the Karl Fischer titration. The concept and simplicity of this approach can be adapted to other similar matrixes. This procedure, with some modification, was applied successfully to aerosol formulations containing sodium bicarbonate or aluminum chlorohydrate. The basic technique is to expel a known amount of sample through a plastic tube leading from the actuator directly into dioxane. The propellant is evaporated above room temperature, and the water analysis is conducted as previously described. This technique determines the total available free water within the aerosol product.

This dioxane extraction–titration technique is simple and rapid and should be applicable to a wide variety of products that formerly could not be analyzed by the basic Karl Fischer titration procedure.

REFERENCES

(1) R. Somkaite, R. G. Dell, and R. D. Desai, *Drug Cosmet. Ind.*, **113**, 52 (Dec. 1973).

(2) N. A. Armstrong and R. V. Griffiths, *Powder Technol.*, **1**, 374 (1967–68).

(3) T. G. Banner, *Analyst*, **71**, 483 (1946).

(4) E. Bonauguri and G. Seniga, *Ann. Chim.*, **45**, 805 (1955b).

(5) J. Mitchell, D. M. Smith, E. C. Ashby, and W. M. D. Bryant, *J. Am. Chem. Soc.*, **63**, 2927 (1941).

ACKNOWLEDGMENTS

The author is indebted to Dr. Rozalija Somkaite of Reheis Chemical Co. for providing samples of aluminum chlorohydrate and for her interest and helpful suggestions in the developmental stages of this work. He also thanks Mr. Carl Graham for technical assistance.

South American Plants II: Taspine Isolation and Anti-Inflammatory Activity

GEORGIA PERSINOS PERDUE [x], RALPH N. BLOMSTER [*], DAVID A. BLAKE [‡], and NORMAN R. FARNSWORTH [§]

Received January 30, 1978, from *Natural Products Advocates, Rockville, MD 20852.* Accepted for publication June 21, 1978. *Present address: School of Pharmacy, University of Maryland, Baltimore, MD 21201. ‡Present address: School of Medicine, Johns Hopkins University, Baltimore, MD 21205. §Present address: College of Pharmacy, University of Illinois, Chicago, IL 60612.

Abstract □ *Croton lechleri* L. (Euphorbiaceae), a plant from the Upper Amazon Valley of Peru, yielded the alkaloid taspine. The anti-inflammatory activity of taspine hydrochloride was studied using the carrageenan-induced pedal edema method, the cotton pellet-induced granuloma method, and the adjuvant polyarthritis model.

Keyphrases □ Taspine—isolated from *Croton lechleri* bark, evaluated for anti-inflammatory activity in rats □ *Croton lechleri* bark—taspine isolated, evaluated for anti-inflammatory activity in rats □ Anti-inflammatory activity—taspine isolated from *Croton lechleri* bark, evaluated in rats

Croton lechleri L. (Euphorbiaceae)[1], commonly called Sangre de grado, is a tree of the upper Amazon Valley of Peru. The bark, when slashed, produces a red viscous sap. Sangre de grado sap is used by the Peruvian Indians for several medicinal purposes, including rheumatism. Taspine (I) was isolated from the sap, and its hydrochloride salt was shown to elicit anti-inflammatory activity[2] in three different standard pharmacological models. Taspine previously was isolated from *Leontice eversmanii* Bge. (Berberidaceae) of Central Asia, Iran, and Afghanistan (1).

EXPERIMENTAL[3]

Isolation of Taspine—A sample (250 ml) of red viscous exudate (sap), obtained by slashing the bark of mature trees of *C. lechleri*, was diluted with distilled water and made alkaline with 28% NH_4OH. This sample was extracted with chloroform (4 × 1 liter). The chloroform layers were combined, reduced *in vacuo* to ~1000 ml, filtered, and refrigerated. An amorphous yellow compound formed, which was removed by filtration and dried.

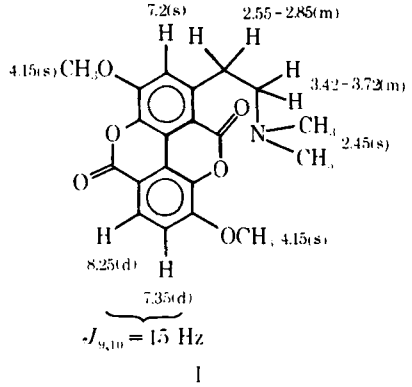

I

Following TLC of this material on plates of aluminum oxide G[4], eluted with 1-butanol–acetic acid–water (4:1:1), and spraying of the dried chromatograms with Dragendorff's reagent, a single spot at R_f 0.77 was observed. This material was crystallized from hot methanol to yield taspine on chilling. This crystalline compound also showed a single Dragendorff-positive spot on TLC at R_f 0.77.

Identification of Taspine—Recrystallization from methanol afforded an analytical sample of taspine base, mp 370° dec. and $[\alpha]_D^{24}$ +7.6° (c 0.64, pyridine), in agreement with those constants reported (2) for taspine.

Anal.—Calc. for $C_{20}H_{19}NO_6$: C, 65.03; H, 5.18; N, 3.79; O, 25.99; OCH_3, 16.80. Found: C, 65.16; H, 5.29; N, 3.77; O, 25.72; OCH_3, 17.18.

The elemental analysis was consistent for taspine and was supported by mass spectral data, which showed a molecular weight of 369. The compound exhibited a UV spectrum with absorption maxima at $\lambda_{max}^{methanol}$ 348 (ε 3800), 333 (3100), 285 (4200), and 245 (25,800) nm, which is typical for a substituted ellagic acid and consistent with that reported previously (3).

An NMR spectrum of the alkaloid base was also consistent with taspine and that reported previously (3). It revealed the presence of two methoxy groups, as evidenced by a singlet at δ 4.15 ppm (six protons), two *N*-methyl groups occurring as a singlet at δ 2.46 ppm (six protons), and four bridged methylene protons present as complex multiplets at δ 2.55–2.85 ppm (two protons) and δ 3.42–3.72 ppm (two protons). The three aromatic protons were shown as a singlet for the lone aromatic proton at δ 7.2 ppm, and the signals for the two adjacent aromatic protons appeared as doublets at δ 7.35 (J = 15 Hz) and 8.25 (J = 15 Hz) ppm.

Preparation of Taspine Hydrochloride—Hydrogen chloride gas was passed through a chloroform solution of alkaloid base until maximal precipitation occurred. The crude alkaloid hydrochloride was refrigerated for 24 hr and then removed by filtration, washed with chloroform, resuspended in chloroform, and filtered. The solid product was dried *in vacuo* at 100° for 24 hr. The procedure was repeated until the filtrate was colorless.

Carrageenan-Induced Pedal Edema Method—A modification of the procedure of Winter *et al.* (4) was used to evaluate the acute anti-inflammatory potency of taspine hydrochloride. Male Wistar rats (150–200 g) in groups of eight were treated by stomach tube with taspine hydrochloride or phenylbutazone as a suspension in 0.25% agar at the doses shown in Table I. One hour later, 0.1 ml of a 1% suspension of carrageenan[5] in 0.9% sodium chloride was injected into the plantar aponeurosis of the right hindpaw. The volume of the injected paw was recorded immediately (zero-time value) by immersion in mercury to a premarked ankle level, and pressure changes were recorded by means of a modified plethysmograph connected to a two-channel polygraph[6]. This system was precalibrated to record milliliters of volume displacement.

Paw volume measurements were repeated at 3 hr. Significant differences ($p < 0.05$) between control and drug treatments were determined by a one-way analysis of variance for equal replication. The ED_{50} and confidence limits were determined on the combined data from four experiments by the method of Litchfield and Wilcoxon (5).

Cotton Pellet-Induced Granuloma Method—The method of Winter *et al.* (6) was used to test for granuloma inhibition. Male Wistar rats (150–200 g) were used in groups of eight animals per dose. Cotton pellets were made by cutting cotton dental rolls[7] into 5-mm sections and adding an aqueous solution of ampicillin (to prevent bacterial abscess). The pellets were dried in a desiccator and weighed individually. Two pellets

[1] Voucher specimens were identified by Dr. John Wurdack, Smithsonian Institution, and are deposited in the Smithsonian Institution, Washington, D.C.

[2] U.S. pat. 3,694,557, granted to Amazon Natural Drug Co.

[3] Elemental analysis was performed by Geller Laboratories, Saddle River, N.J. Melting points were taken on a Mel-Temp apparatus and are uncorrected. UV spectra were recorded on a Beckman model DK2 spectrophotometer. Mass spectra were recorded with an LKB-9000 spectrophotometer. NMR spectra were recorded on a Varian model T-60 instrument.

[4] Woelm, Alupharm Chemicals, New Orleans, La.

[5] Algin Corporation of America.

[6] Hewlett-Packard.

[7] Johnson & Johnson No. 1.

0022-3549/79/0100-0124$01.00/0
© 1979, American Pharmaceutical Association

Table I—Antiedema Activity of Taspine Hydrochloride

Assay[a]	Compound	Dose, mg/kg	Mean Increase in Paw Volume, ml ± *SE*[b]	Percent of Control
A	Agar		1.40 ± 0.12	100
	Phenylbutazone	250	0.71 ± 0.05	51
	Taspine hydrochloride	50	0.58 ± 0.06	41
	Taspine hydrochloride	125	0.78 ± 0.08	56
	Taspine hydrochloride	250	0.67 ± 0.09	48
B	Agar		1.16 ± 0.12	100
	Phenylbutazone	200	0.50 ± 0.07	43
	Taspine hydrochloride	50	0.71 ± 0.11	61
	Taspine hydrochloride	125	0.53 ± 0.06	45
	Taspine hydrochloride	250	0.39 ± 0.07	34
C	Agar		1.08 ± 0.12	100
	Phenylbutazone	200	0.43 ± 0.08	40
	Taspine hydrochloride	10	0.45 ± 0.08	42
	Taspine hydrochloride	50	0.43 ± 0.04	40
	Taspine hydrochloride	50	0.43 ± 0.04	40
	Taspine hydrochloride	125	0.33 ± 0.06	31
	Taspine hydrochloride	250	0.22 ± 0.05	20
D	Agar		1.18 ± 0.06	100
	Phenylbutazone	200	0.55 ± 0.07	47
	Taspine hydrochloride	50	0.70 ± 0.04	59
	Taspine hydrochloride	125	0.50 ± 0.06	42
	Taspine hydrochloride	250	0.40 ± 0.05	34

[a] Assay procedures are as indicated in the text. [b] All treated groups were significantly different from agar controls (< 0.05) in all four assays.

were implanted subcutaneously, under ether anesthesia, one on each side of the animal. After the wounds were autoclipped, the animals were allowed to recover from anesthesia and were dosed with agar suspension, taspine hydrochloride (20 mg/kg), or indomethacin (0.5 or 1.0 mg/kg).

Daily dosing was continued for 6 days. The animals were sacrificed 1 day later; the pellets, together with the adherent granuloma, were carefully dissected from surrounding tissue, and the dry weight was obtained. An increased weight of pellet served as a measure of granulomatous inflammatory response. Tests for significant differences between treatment groups were calculated according to the Student t and F tests (7).

Adjuvant Polyarthritis—The anti-inflammatory activity of taspine hydrochloride was compared with that of indomethacin in the adjuvant-induced arthritic rat model by a procedure similar to that of Ward and Cloud (8). Male Fischer rats (150–200 g), in treatment groups of eight animals, were dosed daily for 20 days with an agar suspension of taspine hydrochloride (20 mg/kg/day), indomethacin (1 mg/kg/day), or agar vehicle. On the 3rd day of dosing, 0.1 ml of *Mycobacterium butyricum* (adjuvant) suspension (5 mg/ml of light petrolatum) was injected into the plantar aponeurosis of the right hindpaw.

Paw volume measurements were performed immediately after adjuvant injection (Day 0) and at 3, 6, 9, 12, 15, and 18 days by the procedure described for carrageenan pedal edema. The t and F tests for significant differences ($p < 0.05$) between agar and drug treatment groups were performed on the data obtained on Day 18.

Lethal Potency—The LD_{50} of taspine hydrochloride was determined in male Wistar rats for both a single oral dose and seven daily doses. In the single-dose study, taspine hydrochloride was dissolved in saline and

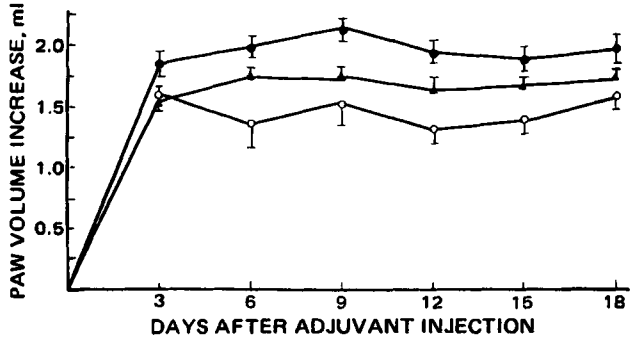

Figure 1—*Adjuvant-induced polyarthritic assay. Treatments were administered from Day −2 to 18. Values are means ± SE for groups of eight rats. Key: ●, agar; ▲, indomethacin (1 mg/ml); and ○, taspine hydrochloride (20 mg/kg).*

Table II—Antigranulation Effect of Taspine Hydrochloride

Assay[a]	Compound	Dose, mg/kg	Average Weight of Granulation Tissue, mg ± *SE*[b]	Inhibition, %
A	Agar	0.25%	144 ± 14	15
	Indomethacin	0.5	122 ± 7	34
	Taspine hydrochloride	20	95 ± 11[c]	
B	Agar	0.25%	160 ± 4	
	Indomethacin	1	132 ± 5[c]	17
	Taspine hydrochloride	20	136 ± 8[c]	15

[a] Assay procedures are as indicated in text. [b] The weight of two dried granulomatous pellets per animal removed 1 day after last treatment minus the weight of the original dried pellets. [c] Significantly different from vehicle control ($p < 0.05$).

administered by gavage tube to groups of 10 rats at doses of 0, 450, 500, and 600 mg/kg. In the seven-dose study, groups of six rats were dosed at 0, 50, 100, 200, and 300 mg/kg. Animals were weighed daily for 7 days after the last dose, and their appearance was noted. Dead animals were autopsied, and the presence of gross lesions was noted. The LD_{50} values and their 95% confidence limits were calculated by the method of Litchfield and Wilcoxon (5).

RESULTS AND DISCUSSION

Taspine was isolated from the red viscous exudate of *C. lechleri*. Its structure was determined by UV, NMR, and mass spectrometry, elemental analysis, and melting-point determinations. The hydrochloride salt of taspine possessed anti-inflammatory activity.

When administered orally, 1 hr prior to the injection of carrageenan, taspine hydrochloride induced a dose-related inhibition of paw swelling measured at 3 hr (Table I). A dose–response relationship was evident in three of four assays (B–D). The oral ED_{50} value calculated for taspine hydrochloride with the combined data of the four assays was 58 mg/kg, although the dose–response curve was relatively shallow. For comparison, phenylbutazone at 200–250 mg/kg inhibited the edematous response by approximately 50%. Thus, in the carrageenan-induced pedal edema method, taspine hydrochloride appeared to be three to four times more potent than phenylbutazone.

In two duplicate assays, taspine hydrochloride (20 mg/kg) inhibited granuloma formation significantly over 1 week (Table II). Indomethacin (1 mg/kg) caused a similar degree of granuloma response inhibition (Assay B).

Figure 1 shows the effects of oral taspine hydrochloride (20 mg/kg/day) and indomethacin (1 mg/kg/day) on the increased paw volume response to a single injection of adjuvant. Both the immediate (Day 3) and sustained (Days 3–18) increases in paw volume were reduced significantly from those of agar controls by both indomethacin and taspine hydrochloride. There was no significant difference in the body weight gain between treatment groups throughout the dosing period.

The oral lethal potencies (LD_{50}) of taspine hydrochloride in male Wistar rats were 518 mg/kg (434–537, 95% confidence limits) for a single dose and 100 mg/kg (55–145) for seven daily doses. In the multiple-dose study, diarrhea and weight loss were observed for 2–3 days prior to death. Death occurred on the 7th day in the 100-mg/kg group and on the 5th–7th days in the 200–300-mg/kg groups. A crusted blood-tinged nasal discharge was often noted on the day preceding death, and autopsied animals had marked congestion of the lungs.

These results demonstrate that taspine hydrochloride has significant anti-inflammatory activity in three standard pharmacological assays at dosage levels considerably below those producing lethal effects in rats.

REFERENCES

(1) A. P. Oryekov and R. A. Konovalvov, *Acad. Pharm.*, **270**, 329 (1932).

(2) T. F. Plantanova, A. D. Kuzavkov, and Y. N. Sheinker, *J. Gen. Chem. USSR*, **26**, 2957 (1956).

(3) M. Shamma and J. L. Moniot, *Chem. Commun.*, **1971**, 1065.

(4) C. A. Winter, E. A. Risley, and G. W. Nuss, *Proc. Soc. Exp. Biol. Med.*, **111**, 544 (1962).

(5) J. T. Litchfield, Jr., and F. Wilcoxon, *J. Pharmacol. Exp. Ther.*, **96**, 99 (1949).

(6) C. A. Winter, E. A. Risley, C. C. Porter, and G. W. Nuss, *J. Am. Pharm. Assoc., Sci. Ed.*, **46**, 515 (1957).

(7) C. I. Bliss, "Outline of Biometry," Yale Co-op, New Haven, Conn., 1954, p. 86.
(8) J. N. Ward and R. S. Cloud, *J. Pharmacol. Exp. Ther.*, **152**, 116 (1966).

ACKNOWLEDGMENTS

Presented at the Pharmacognosy and Natural Products Section, APhA Academy of Pharmaceutical Sciences, Chicago meeting, August 1974.

COMMUNICATIONS

Errors in Chlorothiazide Bioavailability Estimates Based on a Bratton–Marshall Colorimetric Method for Chlorothiazide in Urine

Keyphrases □ Chlorothiazide—bioavailability in dogs, colorimetric and high-pressure liquid chromatographic analyses compared □ Bioavailability—chlorothiazide in dogs, colorimetric and high-pressure liquid chromatographic analyses compared □ Colorimetry—analysis, chlorothiazide in urine, bioavailability estimates compared to high-pressure liquid chromatographic analysis in dogs □ High-pressure liquid chromatography—analysis, chlorothiazide in urine, bioavailability estimates compared to colorimetric analysis in dogs □ Diuretics—chlorothiazide, bioavailability in dogs, colorimetric and high-pressure liquid chromatographic analyses compared

To the Editor:

Chlorothiazide (6-chloro-2*H*-1,2,4-benzothiadiazine-7-sulfonamide 1,1-dioxide) is a weakly acidic (pKa_1 = 6.7 and pKa_2 = 9.5) and poorly absorbed (1, 2) diuretic used in the treatment of hypertension, congestive heart failure, and other edematous conditions in humans and dogs. The pharmacokinetics of chlorothiazide in both species are not well characterized, and the potential use of the dog as an animal model in comparative bioavailability studies on various commercial chlorothiazide tablet and aqueous suspension products remains unexplored.

Based on comparisons of urinary excretion data obtained with a high-pressure liquid chromatographic (HPLC) method (3, 4) and several Bratton–Marshall-based colorimetric methods (2, 5, 6) for chlorothiazide in urine, the Food and Drug Administration tentatively concluded that the appreciable intersubject variation in chlorothiazide tablet bioavailability observed in human studies employing a colorimetric method of analysis was due, in part, to variable assay interference by urine constituents (3, 4). During oral and intravenous studies on the effect of dose on the pharmacokinetics of chlorothiazide absorption and disposition[1], we assessed whether chlorothiazide bioavailability estimates in male mongrel dogs were also a function of the assay used to determine unchanged chlorothiazide in urine. This communication reports the results of these determinations.

In two complete crossover studies, four fasting male mongrel dogs received 125–750 mg po[2] and 250 mg iv[3] of chlorothiazide. Urine samples were collected at predetermined intervals for 48–72 hr and assayed by both a slight modification[1,4] of a specific HPLC method (7) and a modified Bratton–Marshall method purported to reduce assay interference by urine constituents (2).

The original colorimetric method (2) was slightly modified to allow for quantitative recovery and to eliminate turbidity in samples subjected to the Bratton–Marshall reaction for color development. Chlorothiazide was hydrolyzed quantitatively to 6-amino-4-chlorobenzene-1,3-disulfonamide by heating a mixture of 1.0 ml of 3.75 *N* NaOH and 5.0 ml of diluted urine (1:25 or 1:50), containing 6.25–37.5 μg of chlorothiazide, at 100° for 1 hr. The solution was cooled to room temperature and extracted three times with 4.0 ml of ethyl acetate.

The combined ethyl acetate extracts were evaporated to dryness at 60–70° under a gentle stream of nitrogen, and the residue was reconstituted with 0.5 ml of 0.5 *N* NaOH and 5.5 ml of distilled water. Then the solution was filtered[5], and a 5.0-ml aliquot of the filtrate was acidified with 1.0 ml of 6 *N* HCl and mixed with 0.5 ml of 0.1% sodium nitrite. After 3 min, 0.5 ml of 0.5% ammonium sulfamate was added, and the mixture was vortexed[6]. Five minutes later, 0.5 ml of 0.1% *N*-(1-naphthyl)ethylenediamine dihydrochloride was added, and the reaction mixture was stored in the dark for 10 min to allow for maximum color development.

The absorbance of the colored solution was measured[7] (within 2 hr of color development) at 518 nm. The coefficient of variation of the modified method, based on 10 replicate determinations of a standard urine sample containing 60 μg of chlorothiazide/ml, was 7.6%. Twenty-four hour blank urine specimens subjected to this procedure yielded a mean "apparent chlorothiazide" excretion value (n = 4, $\pm SD$) of 0.63 ± 0.2 mg or 0.037 ± 0.01 mg/kg.

Although there was an apparent linear relationship (Fig. 1) between the cumulative urinary excretion values based on the HPLC and Bratton–Marshall assay results, only eight of 24 urinary excretion values determined by the colorimetric method were within ±10% of the values determined by the specific HPLC method. The interanimal variability in chlorothiazide excretion was greater after oral

[1] To be published.
[2] One-half, one, two, or three 250-mg Diuril tablets (lot V4092, Merck Sharp and Dohme), purchased on the open market.
[3] Aqueous solution of the sodium salt.
[4] The original HPLC method (7) was modified to include an ethyl acetate extraction step and sulfadiazine as the internal standard. An HPLC unit (model 204) was equipped with a μBondapak C_{18} reversed-phase column and a UV monitor (model 440) operated at 280 nm (Waters Associates, Milford, MA 01757). The mobile phase was 10% acetonitrile in 0.01 *M* phosphoric acid at a constant flow of 2.0 ml/min. The retention times for sulfadiazine and chlorothiazide were 5.61 and 6.97 min, respectively. No interference by urine constituents was observed. The coefficient of variation of the modified method, based on 10 replicate determinations of a standard urine sample containing 60 μg of chlorothiazide/ml, was 1.2%.
[5] Swinnex-13 filter unit with 0.45-μm pore size filters (type HA), Millipore Corp., Bedford, MA 01730.
[6] Vortex-Genie, Fisher Scientific Co., Rochester, NY 14624.
[7] Beckman DB-G spectrophotometer, Beckman Instruments, Mountainside, NJ 07091.

0022-3549/79/0100-0126$01.00/0
© 1979, American Pharmaceutical Association

(7) C. I. Bliss, "Outline of Biometry," Yale Co-op, New Haven, Conn., 1954, p. 86.
(8) J. N. Ward and R. S. Cloud, *J. Pharmacol. Exp. Ther.*, **152**, 116 (1966).

ACKNOWLEDGMENTS

Presented at the Pharmacognosy and Natural Products Section, APhA Academy of Pharmaceutical Sciences, Chicago meeting, August 1974.

COMMUNICATIONS

Errors in Chlorothiazide Bioavailability Estimates Based on a Bratton–Marshall Colorimetric Method for Chlorothiazide in Urine

Keyphrases □ Chlorothiazide—bioavailability in dogs, colorimetric and high-pressure liquid chromatographic analyses compared □ Bioavailability—chlorothiazide in dogs, colorimetric and high-pressure liquid chromatographic analyses compared □ Colorimetry—analysis, chlorothiazide in urine, bioavailability estimates compared to high-pressure liquid chromatographic analysis in dogs □ High-pressure liquid chromatography—analysis, chlorothiazide in urine, bioavailability estimates compared to colorimetric analysis in dogs □ Diuretics—chlorothiazide, bioavailability in dogs, colorimetric and high-pressure liquid chromatographic analyses compared

To the Editor:

Chlorothiazide (6-chloro-2*H*-1,2,4-benzothiadiazine-7-sulfonamide 1,1-dioxide) is a weakly acidic (pKa_1 = 6.7 and pKa_2 = 9.5) and poorly absorbed (1, 2) diuretic used in the treatment of hypertension, congestive heart failure, and other edematous conditions in humans and dogs. The pharmacokinetics of chlorothiazide in both species are not well characterized, and the potential use of the dog as an animal model in comparative bioavailability studies on various commercial chlorothiazide tablet and aqueous suspension products remains unexplored.

Based on comparisons of urinary excretion data obtained with a high-pressure liquid chromatographic (HPLC) method (3, 4) and several Bratton–Marshall-based colorimetric methods (2, 5, 6) for chlorothiazide in urine, the Food and Drug Administration tentatively concluded that the appreciable intersubject variation in chlorothiazide tablet bioavailability observed in human studies employing a colorimetric method of analysis was due, in part, to variable assay interference by urine constituents (3, 4). During oral and intravenous studies on the effect of dose on the pharmacokinetics of chlorothiazide absorption and disposition[1], we assessed whether chlorothiazide bioavailability estimates in male mongrel dogs were also a function of the assay used to determine unchanged chlorothiazide in urine. This communication reports the results of these determinations.

In two complete crossover studies, four fasting male mongrel dogs received 125–750 mg po[2] and 250 mg iv[3] of chlorothiazide. Urine samples were collected at predetermined intervals for 48–72 hr and assayed by both a slight modification[1,4] of a specific HPLC method (7) and a modified Bratton–Marshall method purported to reduce assay interference by urine constituents (2).

The original colorimetric method (2) was slightly modified to allow for quantitative recovery and to eliminate turbidity in samples subjected to the Bratton–Marshall reaction for color development. Chlorothiazide was hydrolyzed quantitatively to 6-amino-4-chlorobenzene-1,3-disulfonamide by heating a mixture of 1.0 ml of 3.75 *N* NaOH and 5.0 ml of diluted urine (1:25 or 1:50), containing 6.25–37.5 μg of chlorothiazide, at 100° for 1 hr. The solution was cooled to room temperature and extracted three times with 4.0 ml of ethyl acetate.

The combined ethyl acetate extracts were evaporated to dryness at 60–70° under a gentle stream of nitrogen, and the residue was reconstituted with 0.5 ml of 0.5 *N* NaOH and 5.5 ml of distilled water. Then the solution was filtered[5], and a 5.0-ml aliquot of the filtrate was acidified with 1.0 ml of 6 *N* HCl and mixed with 0.5 ml of 0.1% sodium nitrite. After 3 min, 0.5 ml of 0.5% ammonium sulfamate was added, and the mixture was vortexed[6]. Five minutes later, 0.5 ml of 0.1% *N*-(1-naphthyl)ethylenediamine dihydrochloride was added, and the reaction mixture was stored in the dark for 10 min to allow for maximum color development.

The absorbance of the colored solution was measured[7] (within 2 hr of color development) at 518 nm. The coefficient of variation of the modified method, based on 10 replicate determinations of a standard urine sample containing 60 μg of chlorothiazide/ml, was 7.6%. Twenty-four hour blank urine specimens subjected to this procedure yielded a mean "apparent chlorothiazide" excretion value (n = 4, $\pm SD$) of 0.63 ± 0.2 mg or 0.037 ± 0.01 mg/kg.

Although there was an apparent linear relationship (Fig. 1) between the cumulative urinary excretion values based on the HPLC and Bratton–Marshall assay results, only eight of 24 urinary excretion values determined by the colorimetric method were within ±10% of the values determined by the specific HPLC method. The interanimal variability in chlorothiazide excretion was greater after oral

[1] To be published.
[2] One-half, one, two, or three 250-mg Diuril tablets (lot V4092, Merck Sharp and Dohme), purchased on the open market.
[3] Aqueous solution of the sodium salt.
[4] The original HPLC method (7) was modified to include an ethyl acetate extraction step and sulfadiazine as the internal standard. An HPLC unit (model 204) was equipped with a μBondapak C_{18} reversed-phase column and a UV monitor (model 440) operated at 280 nm (Waters Associates, Milford, MA 01757). The mobile phase was 10% acetonitrile in 0.01 *M* phosphoric acid at a constant flow of 2.0 ml/min. The retention times for sulfadiazine and chlorothiazide were 5.61 and 6.97 min, respectively. No interference by urine constituents was observed. The coefficient of variation of the modified method, based on 10 replicate determinations of a standard urine sample containing 60 μg of chlorothiazide/ml, was 1.2%.
[5] Swinnex-13 filter unit with 0.45-μm pore size filters (type HA), Millipore Corp., Bedford, MA 01730.
[6] Vortex-Genie, Fisher Scientific Co., Rochester, NY 14624.
[7] Beckman DB-G spectrophotometer, Beckman Instruments, Mountainside, NJ 07091.

0022-3549/79/0100-0126$01.00/0
© 1979, American Pharmaceutical Association

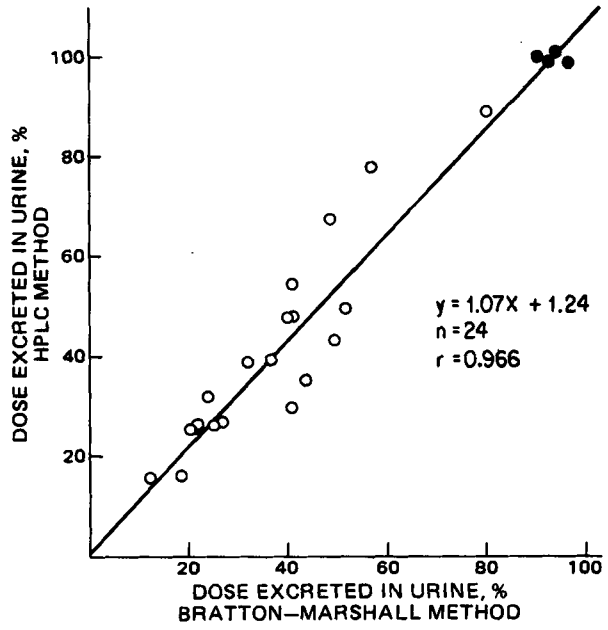

Figure 1—*Relationship between the percent of chlorothiazide dose excreted in the urine of four dogs as determined by HPLC and Bratton–Marshall methods. Key:* ○, *125–750 mg po; and* ●, *250 mg iv.*

administration of chlorothiazide (coefficient of variation of 26–50% for the various doses irrespective of analytical method) than after intravenous administration (coefficient of variation was 1.0% by the HPLC method and 2.5% by the Bratton–Marshall method).

These results clearly indicate that interferences by urinary constituents, which vary during the experimental period and with the extent of dilution of the urine specimen (3, 4, 8), can cause appreciable errors in chlorothiazide bioavailability estimates based on the colorimetric procedure and that HPLC should be the analytical method of choice in all future urinary excretion-based bioavailability studies on chlorothiazide and, perhaps, other thiazide diuretics.

(1) R. E. Kauffman and D. L. Azarnoff, *Clin. Pharmacol. Ther.*, **14**, 886 (1973).

(2) M. C. Meyer and A. B. Straughn, *Curr. Ther. Res.*, **22**, 573 (1977).

(3) V. P. Shah, V. K. Prasad, B. E. Cabana, and P. Sojka, *ibid.*, **24**, 366 (1978).

(4) J. P. Hunt, V. P. Shah, V. K. Prasad, and B. E. Cabana, *APhA Acad. Pharm. Sci. Abstr.*, 8 (1), 195 (1978).

(5) J. E. Baer, H. L. Leedy, A. V. Brooks, and K. H. Beyer, *J. Pharmacol. Exp. Ther.*, **125**, 295 (1959).

(6) H. Sheppard, T. F. Mowles, and A. J. Plummer, *J. Am. Pharm. Assoc., Sci. Ed.*, **49**, 722 (1960).

(7) E. T. Lin and L. Z. Benet, *APhA Acad. Pharm. Sci. Abstr.*, 8 (1), 194 (1978).

(8) J. H. Gustafson, *ibid.*, 5 (2), 162 (1975).

Dennis E. Resetarits
Theodore R. Bates ˣ

Department of Pharmaceutics
School of Pharmacy
State University of New York at Buffalo
Amherst, NY 14260

Received July 20, 1978.

Accepted for publication October 17, 1978.

Presented in part at the Basic Pharmaceutics Section, APhA Academy of Pharmaceutical Sciences, Hollywood, Fla., meeting, November 1978.

Supported in part by Grants GM-20852 and GRS-RR0545415 from the National Institutes of Health.

Localization of Isoproterenol-Induced Contractions of Canine Small Intestine

Keyphrases □ Isoproterenol—*in vivo* effects on small intestinal motor activities, dogs □ Motor activities *in vitro*—effect of isoproterenol on muscularis mucosa and muscularis externa motility

To the Editor:

The proposition is generally accepted that the catecholamines produce relaxation of the small intestinal musculature of a number of species *via* α- and β-receptor mechanisms. This acceptance was gained because exceptions to this rule were rarely noted and were usually inconsistent or segment related. These scattered observations have not been systematically analyzed to determine what possible common threads connected them.

For all practical purposes, most experimental evidence for the small intestinal relaxatory activities of the catecholamines has derived from *in vitro* and *in situ* studies involving dogs, cats, rats, rabbits, mice, and guinea pigs. The only serious disagreement arises with the canine ileum. Some years ago, it was reported (1, 2) that occasionally high dosages of isoproterenol produced marked stimulation of the ileum of the anesthetized dog *in situ*, but no explanation for this phenomenon was advanced. Since that time, we have observed similar anomalous effects of isoproterenol stimulation on the canine small intestine. Thus, the purpose of this communication is to propose a unifying theory with respect to the excitatory activities of catecholamines on the mammalian GI tract.

Kokas and Gordon (3) reported that the villi of the canine small intestine were specifically stimulated by β-adrenergic agents and that this effect was enhanced by α-adrenolytics. Later, we also observed that stimulatory effects of β-adrenergic agents on canine ileal segmenting activities in the chloralose–urethan anesthetized animal became predictably reproducible following pretreatment by α-adrenolytics. Intravenous doses of isoproterenol usually produced marked jejunal and ileal segmenting activity. Both bilateral vagotomy and atropine were ineffective in blocking this small intestinal response. Prior administration of the α-adrenolytic phenoxybenzamine potentiated the response (Fig. 1), which was blocked by dichloroisoproterenol (not depicted).

We subsequently decoupled the canine ileal tunica muscularis from the muscularis mucosa (4) and demonstrated that the β-excitatory effect upon the latter occurs *pari passu* with the inhibitory effect on the former. Again, the excitatory effects of the β-agonists are enhanced by pretreatment with α-adrenolytics. In experiments using the classical tissue bath technique, contractions of the circular and longitudinal components of the muscularis were recorded (Fig. 2). Isoproterenol had opposite effects in different parts of the ileum of the same animal. The tunica muscularis portion of the ileum exhibited a relaxation response to a fixed dose of isoproterenol, whereas the muscularis mucosa portion exhibited only a tonic contractile response to the same dose of the β-agonist. These observations using mechanically decoupled effector systems are identical to the results obtained by Kokas and Gordon (3) without decoupling but by specific observations of the motility of the villi.

0022-3549/79/0100-0127$01.00/0
© 1979, American Pharmaceutical Association

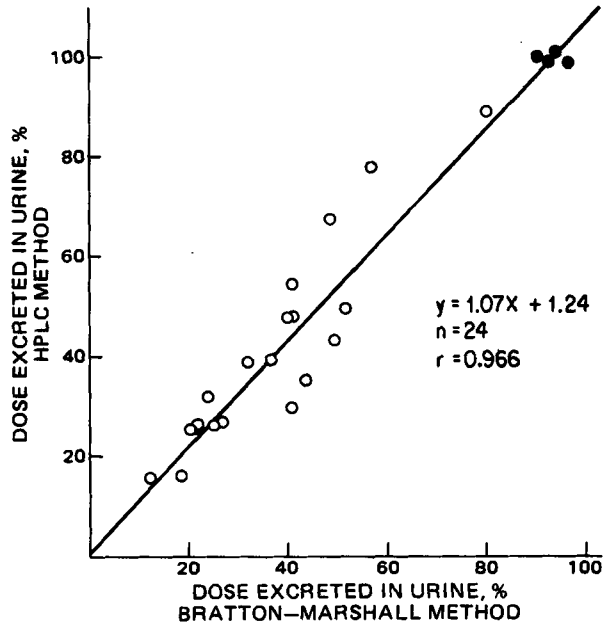

Figure 1—*Relationship between the percent of chlorothiazide dose excreted in the urine of four dogs as determined by HPLC and Bratton–Marshall methods. Key:* ○, *125–750 mg po; and* ●, *250 mg iv.*

administration of chlorothiazide (coefficient of variation of 26–50% for the various doses irrespective of analytical method) than after intravenous administration (coefficient of variation was 1.0% by the HPLC method and 2.5% by the Bratton–Marshall method).

These results clearly indicate that interferences by urinary constituents, which vary during the experimental period and with the extent of dilution of the urine specimen (3, 4, 8), can cause appreciable errors in chlorothiazide bioavailability estimates based on the colorimetric procedure and that HPLC should be the analytical method of choice in all future urinary excretion-based bioavailability studies on chlorothiazide and, perhaps, other thiazide diuretics.

(1) R. E. Kauffman and D. L. Azarnoff, *Clin. Pharmacol. Ther.*, **14**, 886 (1973).

(2) M. C. Meyer and A. B. Straughn, *Curr. Ther. Res.*, **22**, 573 (1977).

(3) V. P. Shah, V. K. Prasad, B. E. Cabana, and P. Sojka, *ibid.*, **24**, 366 (1978).

(4) J. P. Hunt, V. P. Shah, V. K. Prasad, and B. E. Cabana, *APhA Acad. Pharm. Sci. Abstr.*, 8 (1), 195 (1978).

(5) J. E. Baer, H. L. Leedy, A. V. Brooks, and K. H. Beyer, *J. Pharmacol. Exp. Ther.*, **125**, 295 (1959).

(6) H. Sheppard, T. F. Mowles, and A. J. Plummer, *J. Am. Pharm. Assoc., Sci. Ed.*, **49**, 722 (1960).

(7) E. T. Lin and L. Z. Benet, *APhA Acad. Pharm. Sci. Abstr.*, 8 (1), 194 (1978).

(8) J. H. Gustafson, *ibid.*, 5 (2), 162 (1975).

Dennis E. Resetarits
Theodore R. Bates ˣ

Department of Pharmaceutics
School of Pharmacy
State University of New York at Buffalo
Amherst, NY 14260

Received July 20, 1978.

Accepted for publication October 17, 1978.

Presented in part at the Basic Pharmaceutics Section, APhA Academy of Pharmaceutical Sciences, Hollywood, Fla., meeting, November 1978.

Supported in part by Grants GM-20852 and GRS-RR0545415 from the National Institutes of Health.

Localization of Isoproterenol-Induced Contractions of Canine Small Intestine

Keyphrases □ Isoproterenol—*in vivo* effects on small intestinal motor activities, dogs □ Motor activities *in vitro*—effect of isoproterenol on muscularis mucosa and muscularis externa motility

To the Editor:

The proposition is generally accepted that the catecholamines produce relaxation of the small intestinal musculature of a number of species *via* α- and β-receptor mechanisms. This acceptance was gained because exceptions to this rule were rarely noted and were usually inconsistent or segment related. These scattered observations have not been systematically analyzed to determine what possible common threads connected them.

For all practical purposes, most experimental evidence for the small intestinal relaxatory activities of the catecholamines has derived from *in vitro* and *in situ* studies involving dogs, cats, rats, rabbits, mice, and guinea pigs. The only serious disagreement arises with the canine ileum. Some years ago, it was reported (1, 2) that occasionally high dosages of isoproterenol produced marked stimulation of the ileum of the anesthetized dog *in situ*, but no explanation for this phenomenon was advanced. Since that time, we have observed similar anomalous effects of isoproterenol stimulation on the canine small intestine. Thus, the purpose of this communication is to propose a unifying theory with respect to the excitatory activities of catecholamines on the mammalian GI tract.

Kokas and Gordon (3) reported that the villi of the canine small intestine were specifically stimulated by β-adrenergic agents and that this effect was enhanced by α-adrenolytics. Later, we also observed that stimulatory effects of β-adrenergic agents on canine ileal segmenting activities in the chloralose–urethan anesthetized animal became predictably reproducible following pretreatment by α-adrenolytics. Intravenous doses of isoproterenol usually produced marked jejunal and ileal segmenting activity. Both bilateral vagotomy and atropine were ineffective in blocking this small intestinal response. Prior administration of the α-adrenolytic phenoxybenzamine potentiated the response (Fig. 1), which was blocked by dichloroisoproterenol (not depicted).

We subsequently decoupled the canine ileal tunica muscularis from the muscularis mucosa (4) and demonstrated that the β-excitatory effect upon the latter occurs *pari passu* with the inhibitory effect on the former. Again, the excitatory effects of the β-agonists are enhanced by pretreatment with α-adrenolytics. In experiments using the classical tissue bath technique, contractions of the circular and longitudinal components of the muscularis were recorded (Fig. 2). Isoproterenol had opposite effects in different parts of the ileum of the same animal. The tunica muscularis portion of the ileum exhibited a relaxation response to a fixed dose of isoproterenol, whereas the muscularis mucosa portion exhibited only a tonic contractile response to the same dose of the β-agonist. These observations using mechanically decoupled effector systems are identical to the results obtained by Kokas and Gordon (3) without decoupling but by specific observations of the motility of the villi.

0022-3549/79/0100-0127$01.00/0
© 1979, American Pharmaceutical Association

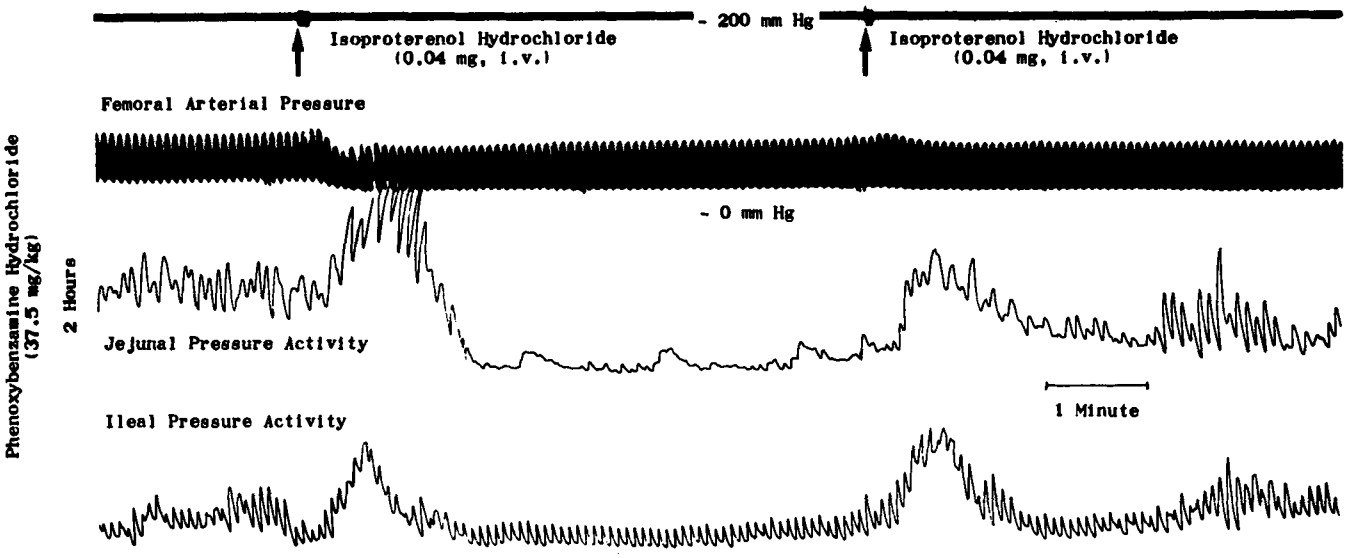

Figure 1—*Polygram showing the effect of intravenous isoproterenol, repeated once, on a phenoxybenzamine background on femoral arterial blood pressure and jejunal and ileal intraluminal pressure activities.*

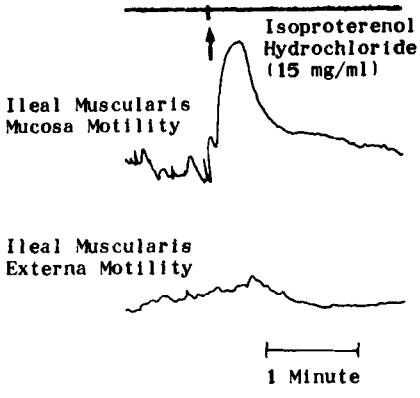

Figure 2—*Polygram showing* in vitro *effects of isoproterenol on the muscular components of the canine ileum.*

A systematic review of the literature indicates that, insofar as gross organ motility is concerned, the canine ileum is the one system observed *in vitro* or *in situ* in which the adrenergic effect is not always inhibitory. Basic histology also tells us that this is the only system that exists in the aforementioned species, from the cardia to the rectum, in which the muscularis mucosa forms a physically significant effector layer (similar to humans) in terms of the ratio of layer thickness to inner layer radius.

Therefore, we advance the general proposition that β-adrenergic agents in high doses are usually stimulatory to the muscularis mucosa and that they are potentiated by α-adrenolytics. We also support the proposition that the β-agents are inhibitory of the motility of the tunica muscularis. In terms of gross organ motility, we believe that the net effect of any agent will be primarily determined by its effect on the more physically significant of the coupled effector systems.

(1) R. P. Ahlquist, *Am. J. Physiol.*, **153**, 586 (1948).
(2) R. P. Ahlquist and B. Levy, *J. Pharmacol. Exp. Ther.*, **127**, 146 (1959).
(3) E. Kokas and H. A. Gordon, *ibid.*, **180**, 56 (1972).
(4) M. F. Tansy, J. S. Martin, W. E. Landin, and F. M. Kendall, *Fed. Proc.*, **37**, 373 (1978).

Martin F. Tansy ˣ
John S. Martin
Wendell E. Landin
Frank M. Kendall
Department of Physiology and Biophysics
Health Sciences Center
Temple University
Philadelphia, PA 19140

Received August 4, 1978.
Accepted for publication October 20, 1978.

Bioavailability under Variable Renal Clearance Conditions

Keyphrases □ Bioavailability—method for assessment under variable renal clearance conditions □ Renal clearance conditions, variable—effect on bioavailability □ Pharmacokinetics—bioavailability under variable renal clearance conditions

To the Editor:

Several methods are used to calculate the bioavailability of a drug, *i.e.*, the fraction of the administered dose that reaches the general circulation. Bioavailability can be determined from single (1–4) or multiple (5) doses, as well as at steady state (6).

The most popular methods for assessing bioavailability involve single test and reference doses. A comparison determination of the total area under the plasma concentration *versus* time curve, AUC_0^∞, or the total amount excreted unchanged in urine from time = 0 to time = ∞, A_R^∞, between the test dose and a reference dose is made. The assumptions in these methods are:

1. Total plasma clearance is the same in the test dose and reference studies when the areas are used for bioavailability assessment.
2. The fraction excreted unchanged in the urine, f_e, is

0022-3549/79/0100-0128$01.00/0
© 1979, American Pharmaceutical Association

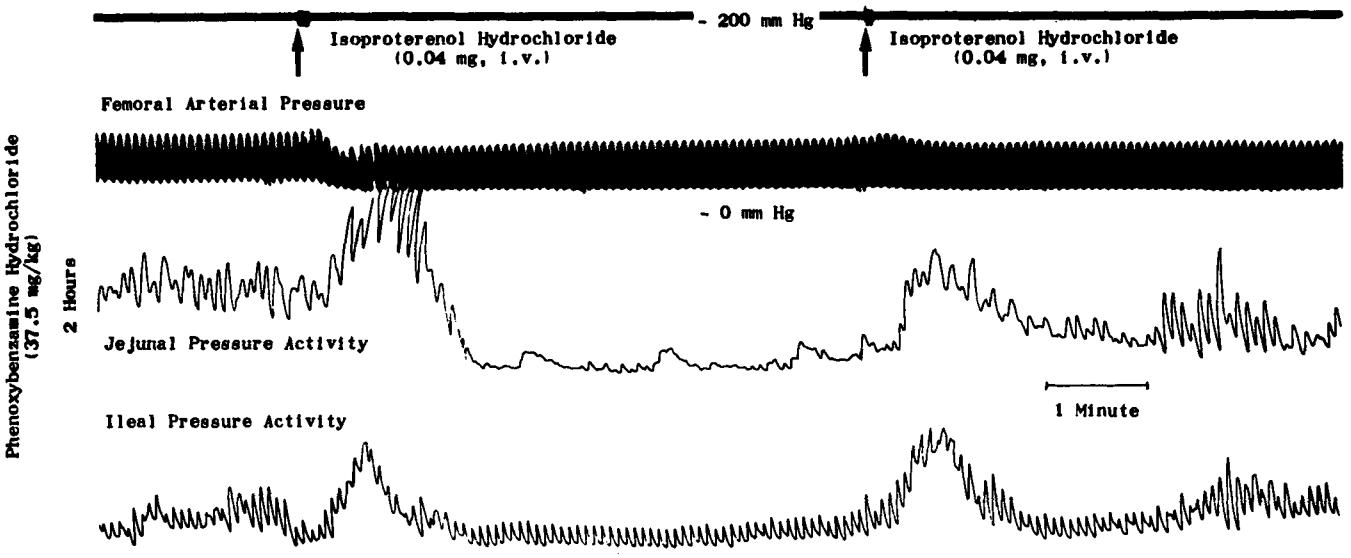

Figure 1—*Polygram showing the effect of intravenous isoproterenol, repeated once, on a phenoxybenzamine background on femoral arterial blood pressure and jejunal and ileal intraluminal pressure activities.*

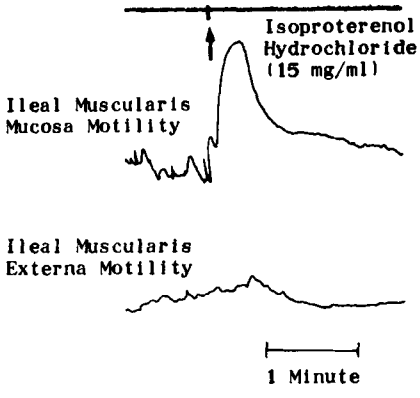

Figure 2—*Polygram showing* in vitro *effects of isoproterenol on the muscular components of the canine ileum.*

A systematic review of the literature indicates that, insofar as gross organ motility is concerned, the canine ileum is the one system observed *in vitro* or *in situ* in which the adrenergic effect is not always inhibitory. Basic histology also tells us that this is the only system that exists in the aforementioned species, from the cardia to the rectum, in which the muscularis mucosa forms a physically significant effector layer (similar to humans) in terms of the ratio of layer thickness to inner layer radius.

Therefore, we advance the general proposition that β-adrenergic agents in high doses are usually stimulatory to the muscularis mucosa and that they are potentiated by α-adrenolytics. We also support the proposition that the β-agents are inhibitory of the motility of the tunica muscularis. In terms of gross organ motility, we believe that the net effect of any agent will be primarily determined by its effect on the more physically significant of the coupled effector systems.

(1) R. P. Ahlquist, *Am. J. Physiol.*, **153**, 586 (1948).
(2) R. P. Ahlquist and B. Levy, *J. Pharmacol. Exp. Ther.*, **127**, 146 (1959).
(3) E. Kokas and H. A. Gordon, *ibid.*, **180**, 56 (1972).
(4) M. F. Tansy, J. S. Martin, W. E. Landin, and F. M. Kendall, *Fed. Proc.*, **37**, 373 (1978).

Martin F. Tansy ˣ
John S. Martin
Wendell E. Landin
Frank M. Kendall
Department of Physiology and Biophysics
Health Sciences Center
Temple University
Philadelphia, PA 19140

Received August 4, 1978.
Accepted for publication October 20, 1978.

Bioavailability under Variable Renal Clearance Conditions

Keyphrases □ Bioavailability—method for assessment under variable renal clearance conditions □ Renal clearance conditions, variable—effect on bioavailability □ Pharmacokinetics—bioavailability under variable renal clearance conditions

To the Editor:

Several methods are used to calculate the bioavailability of a drug, *i.e.*, the fraction of the administered dose that reaches the general circulation. Bioavailability can be determined from single (1–4) or multiple (5) doses, as well as at steady state (6).

The most popular methods for assessing bioavailability involve single test and reference doses. A comparison determination of the total area under the plasma concentration *versus* time curve, AUC_0^∞, or the total amount excreted unchanged in urine from time = 0 to time = ∞, A_R^∞, between the test dose and a reference dose is made. The assumptions in these methods are:

1. Total plasma clearance is the same in the test dose and reference studies when the areas are used for bioavailability assessment.
2. The fraction excreted unchanged in the urine, f_e, is

0022-3549/79/0100-0128$01.00/0
© 1979, American Pharmaceutical Association

the same in the reference and test studies when the total amount excreted unchanged in the urine is used for determination of bioavailability.

A number of drugs, however, demonstrate urine pH and urine flow dependent renal clearance; unless the experimental conditions are rigidly controlled by acidifying or alkalinizing the urine pH with ammonium chloride or sodium bicarbonate while maintaining constant fluid intake, renal plasma clearance, Cl_R, is likely to vary between and within test and reference studies.

Kwan and Till (7) suggested a method to circumvent this situation. When renal plasma clearance differs between studies, the renal plasma clearance can be determined from the renal excretion rates and the plasma concentrations of the unchanged drug between the experiments. The assumptions in this method are that renal clearance is constant within an experiment (but, of course, can vary between studies) and that the extrarenal plasma clearance is the same between studies.

The assumption of constant renal plasma clearance throughout the individual studies is, at best, an approximation. When studies have to be carried out over longer periods, the renal clearance may vary due to fluctuations in urine flow and urine pH throughout the day, providing the renal clearance is urine pH and urine flow dependent.

We propose a method for the determination of bioavailability that does not require constant renal clearance, neither between experiments nor within an experiment. This method allows for the determination of the bioavailability of a drug without rigid control of urine pH or urine flow, provided the extrarenal plasma clearance is unaltered.

The elimination rate, dA_e/dt, can be described by:

$$\frac{dA_e}{dt} = \frac{dA_{xr}}{dt} + \frac{dA_r}{dt} \qquad \text{(Eq. 1)}$$

where dA_{xr}/dt is the rate of extrarenal elimination and dA_r/dt is the rate of renal excretion.

The extrarenal elimination can be expressed by:

$$\frac{dA_{xr}}{dt} = (Cl_{xr})(C_p) \qquad \text{(Eq. 2)}$$

where Cl_{xr} is the extrarenal clearance and C_p is the plasma concentration.

Substitution of Eq. 2 in Eq. 1 and rearrangement give:

$$dA_e = (Cl_{xr})(C_p)(dt) + dA_r \qquad \text{(Eq. 3)}$$

The total amount eliminated from the body from time = 0 to time = ∞ must be equal to the total amount entering the general circulation, *FD, and* the total amount excreted in the urine from time = 0 to time = ∞ must be equal to the total amount recovered in the urine, A_R^∞.

Therefore, integrating Eq. 3 from time = 0 to time = ∞ gives:

$$FD = \int_0^\infty (Cl_{xr})(C_p)(dt) + A_R^\infty \qquad \text{(Eq. 4)}$$

where F is the bioavailability of the dosage form and D is the amount of drug administered.

Since $\int_0^\infty (C_p)(dt) = AUC_0^\infty$ and Cl_{xr} is assumed to be a constant, the following relationship is obtained:

$$FD = (Cl_{xr})(AUC_0^\infty) + A_R^\infty \qquad \text{(Eq. 5)}$$

When the bioavailability of the reference dose is F^s and the bioavailability of the test dosage form is F^T, F^T can simply be determined by:

$$F^T = \frac{(F^sD^s - A_R^{\infty s})\dfrac{AUC_0^{\infty T}}{AUC_0^{\infty s}} + A_R^{\infty T}}{D^T} \qquad \text{(Eq. 6)}$$

When the reference dose is an intravenous bolus dose where the bioavailability is equal to 1, Eq. 6 can be expressed by:

$$F^T = \frac{(D^s - A_R^{\infty s})\dfrac{AUC_0^{\infty T}}{AUC_0^{\infty s}} + A_R^{\infty T}}{D^T} \qquad \text{(Eq. 7)}$$

To use this method, the total area under the plasma concentration *versus* time curve and the amount excreted unchanged in the urine from time = 0 to time = ∞ for both the test drug and the standard are needed. Except for the assumption of extrarenal plasma clearance constancy, this method does not require a constant renal clearance and fraction excreted unchanged nor an assessment of the pharmacokinetic model. From Eq. 6, it can be seen that this method cannot be used to assess the relative bioavailability of a drug, F^T/F^s, and is only useful when the reference dosage form is an intravenous bolus or if the bioavailability of the reference dose is known.

(1) M. Gibaldi and D. Perrier, "Pharmacokinetics," Dekker, New York, N.Y., 1975.

(2) J. G. Wagner and J. W. Ayres, *J. Pharmacokinet. Biopharm.*, **5**, 533 (1977).

(3) J. G. Wagner, *Arzneim.-Forsch.*, **26**, 105 (1976).

(4) P. J. Niebergall, E. T. Sugita, and R. L. Schnaare, *J. Pharm. Sci.*, **64**, 1721 (1975).

(5) K. C. Kwan, J. V. Bondi, and K. C. Yeh, *ibid.*, **64**, 1639 (1975).

(6) T. N. Tozer, in "Principles and Perspectives in Drug Availability," J. Blanchard, R. J. Sawchuck, and B. B. Brodie, Eds., S. Karger, Basel, Switzerland, 1978, chap. 5.

(7) K. C. Kwan and A. Till, *J. Pharm. Sci.*, **62**, 1494 (1973).

Svein Øie ˣ
Donald Jung
Department of Pharmacy
School of Pharmacy
University of California
San Francisco, CA 94143

Received August 28, 1978.
Accepted for publication October 20, 1978.

Novel Method for Determining Protein Binding of Theophylline

Keyphrases □ Theophylline—protein binding determined by ultrafiltration method □ Protein binding—theophylline, determined by ultrafiltration method □ Binding, protein—theophylline, determined by ultrafiltration method □ Ultrafiltration method—determination of theophylline protein binding □ Relaxants, smooth muscle—theophylline, protein binding determined by ultrafiltration method

To the Editor:

The kinetics of drug elimination and the apparent biological half-life of a drug may be influenced by drug–protein interactions (1). Although interpatient and intrapatient variations in theophylline clearance rates are gen-

0022-3549/79/0100-0129$01.00/0

© 1979, American Pharmaceutical Association

the same in the reference and test studies when the total amount excreted unchanged in the urine is used for determination of bioavailability.

A number of drugs, however, demonstrate urine pH and urine flow dependent renal clearance; unless the experimental conditions are rigidly controlled by acidifying or alkalinizing the urine pH with ammonium chloride or sodium bicarbonate while maintaining constant fluid intake, renal plasma clearance, Cl_R, is likely to vary between and within test and reference studies.

Kwan and Till (7) suggested a method to circumvent this situation. When renal plasma clearance differs between studies, the renal plasma clearance can be determined from the renal excretion rates and the plasma concentrations of the unchanged drug between the experiments. The assumptions in this method are that renal clearance is constant within an experiment (but, of course, can vary between studies) and that the extrarenal plasma clearance is the same between studies.

The assumption of constant renal plasma clearance throughout the individual studies is, at best, an approximation. When studies have to be carried out over longer periods, the renal clearance may vary due to fluctuations in urine flow and urine pH throughout the day, providing the renal clearance is urine pH and urine flow dependent.

We propose a method for the determination of bioavailability that does not require constant renal clearance, neither between experiments nor within an experiment. This method allows for the determination of the bioavailability of a drug without rigid control of urine pH or urine flow, provided the extrarenal plasma clearance is unaltered.

The elimination rate, dA_e/dt, can be described by:

$$\frac{dA_e}{dt} = \frac{dA_{xr}}{dt} + \frac{dA_r}{dt} \qquad \text{(Eq. 1)}$$

where dA_{xr}/dt is the rate of extrarenal elimination and dA_r/dt is the rate of renal excretion.

The extrarenal elimination can be expressed by:

$$\frac{dA_{xr}}{dt} = (Cl_{xr})(C_p) \qquad \text{(Eq. 2)}$$

where Cl_{xr} is the extrarenal clearance and C_p is the plasma concentration.

Substitution of Eq. 2 in Eq. 1 and rearrangement give:

$$dA_e = (Cl_{xr})(C_p)(dt) + dA_r \qquad \text{(Eq. 3)}$$

The total amount eliminated from the body from time = 0 to time = ∞ must be equal to the total amount entering the general circulation, *FD, and* the total amount excreted in the urine from time = 0 to time = ∞ must be equal to the total amount recovered in the urine, A_R^∞.

Therefore, integrating Eq. 3 from time = 0 to time = ∞ gives:

$$FD = \int_0^\infty (Cl_{xr})(C_p)(dt) + A_R^\infty \qquad \text{(Eq. 4)}$$

where F is the bioavailability of the dosage form and D is the amount of drug administered.

Since $\int_0^\infty (C_p)(dt) = AUC_0^\infty$ and Cl_{xr} is assumed to be a constant, the following relationship is obtained:

$$FD = (Cl_{xr})(AUC_0^\infty) + A_R^\infty \qquad \text{(Eq. 5)}$$

When the bioavailability of the reference dose is F^s and the bioavailability of the test dosage form is F^T, F^T can simply be determined by:

$$F^T = \frac{(F^sD^s - A_R^{\infty s})\dfrac{AUC_0^{\infty T}}{AUC_0^{\infty s}} + A_R^{\infty T}}{D^T} \qquad \text{(Eq. 6)}$$

When the reference dose is an intravenous bolus dose where the bioavailability is equal to 1, Eq. 6 can be expressed by:

$$F^T = \frac{(D^s - A_R^{\infty s})\dfrac{AUC_0^{\infty T}}{AUC_0^{\infty s}} + A_R^{\infty T}}{D^T} \qquad \text{(Eq. 7)}$$

To use this method, the total area under the plasma concentration *versus* time curve and the amount excreted unchanged in the urine from time = 0 to time = ∞ for both the test drug and the standard are needed. Except for the assumption of extrarenal plasma clearance constancy, this method does not require a constant renal clearance and fraction excreted unchanged nor an assessment of the pharmacokinetic model. From Eq. 6, it can be seen that this method cannot be used to assess the relative bioavailability of a drug, F^T/F^s, and is only useful when the reference dosage form is an intravenous bolus or if the bioavailability of the reference dose is known.

(1) M. Gibaldi and D. Perrier, "Pharmacokinetics," Dekker, New York, N.Y., 1975.

(2) J. G. Wagner and J. W. Ayres, *J. Pharmacokinet. Biopharm.*, **5**, 533 (1977).

(3) J. G. Wagner, *Arzneim.-Forsch.*, **26**, 105 (1976).

(4) P. J. Niebergall, E. T. Sugita, and R. L. Schnaare, *J. Pharm. Sci.*, **64**, 1721 (1975).

(5) K. C. Kwan, J. V. Bondi, and K. C. Yeh, *ibid.*, **64**, 1639 (1975).

(6) T. N. Tozer, in "Principles and Perspectives in Drug Availability," J. Blanchard, R. J. Sawchuck, and B. B. Brodie, Eds., S. Karger, Basel, Switzerland, 1978, chap. 5.

(7) K. C. Kwan and A. Till, *J. Pharm. Sci.*, **62**, 1494 (1973).

Svein Øie ˣ
Donald Jung
Department of Pharmacy
School of Pharmacy
University of California
San Francisco, CA 94143

Received August 28, 1978.
Accepted for publication October 20, 1978.

Novel Method for Determining Protein Binding of Theophylline

Keyphrases □ Theophylline—protein binding determined by ultrafiltration method □ Protein binding—theophylline, determined by ultrafiltration method □ Binding, protein—theophylline, determined by ultrafiltration method □ Ultrafiltration method—determination of theophylline protein binding □ Relaxants, smooth muscle—theophylline, protein binding determined by ultrafiltration method

To the Editor:

The kinetics of drug elimination and the apparent biological half-life of a drug may be influenced by drug–protein interactions (1). Although interpatient and intrapatient variations in theophylline clearance rates are gen-

0022-3549/79/0100-0129$01.00/0

© 1979, American Pharmaceutical Association

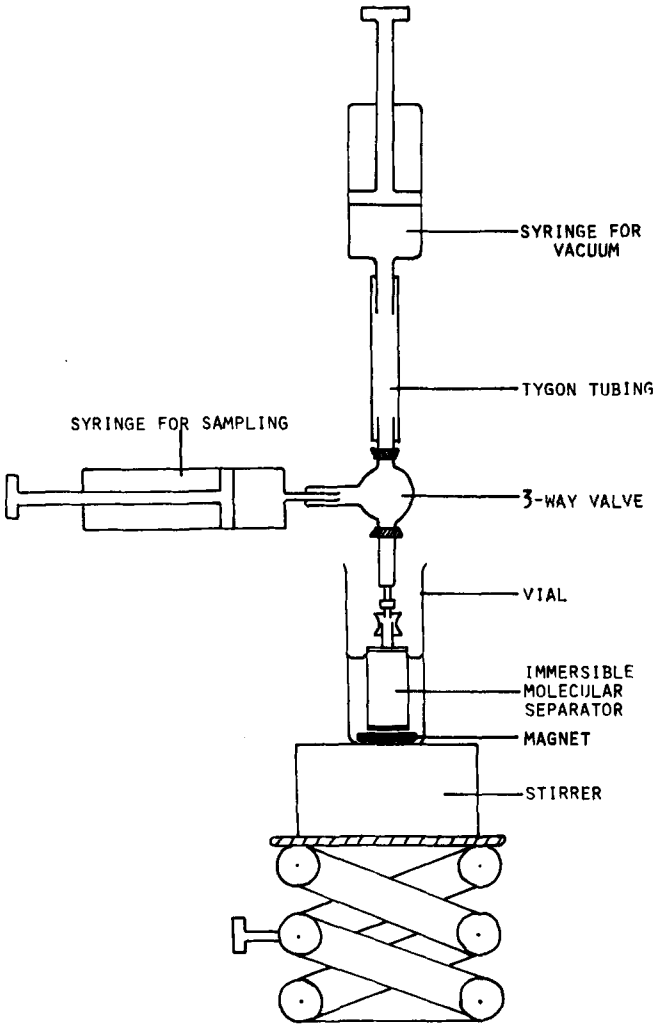

Figure 1—*Ultrafiltration apparatus using the immersible membrane cartridge.*

erally attributed to factors such as age, smoking, ingestion of other drugs, and hepatic dysfunction (2), protein binding of theophylline also could influence clearance.

Theophylline binding to bovine serum albumin (fraction V) (3) and human plasma (4) has been determined by equilibrium dialysis, but this technique is slow and unsuitable for routine clinical use. Conventional ultrafiltration is more rapid and has been used to study the binding of theophylline to serum and human milk (5). Ultrafiltration cones have been employed to measure protein binding of theophylline in small (2 ml) plasma samples (6). A controlled-temperature centrifuge is required for reproducible results with these ultrafiltration techniques.

The extent of theophylline binding to human serum and bovine serum albumin (fraction V) was determined using an ultrafiltration method that eliminates centrifugation. An immersible cartridge[1] was used, consisting of a noncellulosic ultrafiltration membrane sealed to a plastic core. Each cartridge was connected to a 3-ml disposable syringe *via* a three-way valve (Fig. 1). The syringe provided a sufficient vacuum to effect ultrafiltration when the cartridge was immersed in the test material. The ultrafiltrate was sampled using the second syringe.

The human serum and bovine serum albumin solution (4%) in phosphate buffer, pH 7.4, contained 15 μg of theophylline/ml. The immersible cartridge unit was flushed with pH 7.4 buffer prior to use, and excess buffer was removed by suction. The cartridge was immersed in 2–4 ml of the theophylline–protein specimen to be analyzed, and the sample was agitated gently with a magnetic stirring bar while avoiding physical damage to the separator membrane. A vacuum was applied to the core until sufficient protein-free filtrate was obtained. The aliquot collected in protein-binding studies by ultrafiltration did not exceed 10% of the initial volume. Samples of the filtrate and retentate were removed and assayed for theophylline using high-performance liquid chromatography (7). The extent of binding was calculated using:

$$\text{fraction bound} = \frac{D_b}{D_t} = \frac{D_t - D_f}{D_t} \qquad \text{(Eq. 1)}$$

where D_b is the amount of drug bound, D_t is the total amount of drug present, and D_f is the amount of free drug. Each immersible cartridge unit was reused several times after careful washing according to the procedure recommended by the manufacturer.

The immersible cartridge and ultrafiltration cone[2] methods were compared at room temperature. The cones were soaked in pH 7.4 phosphate buffer, removed, and wiped dry. Protein solution or serum containing theophylline, 2–4 ml, was placed in the cone and centrifuged at 800×*g*. The samples were spun three times (2–6 min each) to provide three 100-μl aliquots. The second and third aliquots were assayed for theophylline to give the concentration of free drug in the original sample. The solution in the cone was analyzed for total concentration of theophylline.

Both ultrafiltration cones and immersible cartridge units permitted protein leakage into the filtrate if the membrane was not functioning correctly or was damaged. Such leakage would invalidate results since the protein transports bound theophylline. A sensitive colorimetric semiquantitative estimate for protein[3] was used to test all filtrates.

The percentage binding of theophylline at concentrations of 15 μg/ml to serum or bovine serum albumin (fraction V) was similar when determined by the immersible cartridge and ultrafiltration cone methods. With the 4% bovine serum albumin, theophylline protein binding was 56.3 ± 7.4% using the immersible cartridge and 51.7 ± 11.4% using the ultrafiltration cones. In pooled human serums, theophylline protein binding was 67.8 ± 5.5% using the immersible cartridge and 66.3 ± 4.6% using the ultrafiltration cones. The results obtained from the immersible cartridge and cones were not significantly different ($p < 0.05$).

Determination of theophylline protein binding using immersible cartridges is convenient and rapid. The ultrafiltration membrane has a nominal molecular weight cutoff of 10,000, which provides effective separation of

[1] Immersible molecular separator, Millipore Ltd., Mississauga, Ontario, L4V 1L2, Canada.

[2] Centriflo CF 50-A cones, Amicon Corp., Lexington, MA 02173.

[3] Albustix, Ames Co. Division, Miles Laboratories, Ltd., Rexdale, Ontario, Canada.

theophylline from serum or plasma proteins. The apparatus is portable and does not require a refrigerated centrifuge for ultrafiltration. The procedure is ideal for clinical investigations because of the small volume of sample required. It has potential application to the study of protein binding of a wide range of xenobiotic compounds.

(1) J. J. Vallner, *J. Pharm. Sci.*, **66**, 447 (1977).
(2) R. Wyatt, M. Weinberger, and L. Hendeles, *J. Pediatr.*, **92**, 125 (1978).
(3) M. L. Eichman, D. E. Guttman, Q. van Winkle, and E. P. Guth, *J. Pharm. Sci.*, **51**, 66 (1962).
(4) R. Koysooko, E. F. Ellis, and G. Levy, *Clin. Pharmacol. Ther.*, **15**, 454 (1974).
(5) A. M. Yurchak and W. J. Jusko, *Pediatrics*, **53**, 518 (1976).
(6) J. V. Aranda, D. S. Sitar, W. D. Parsons, P. M. Loughnan, and A. H. Niems, *N. Engl. J. Med.*, **295**, 413 (1976).
(7) D. S. Sitar, K. M. Piafsky, R. E. Rango, and R. I. Ogilvie, *Clin. Chem.*, **21**, 1774 (1975).

Colin J. Briggs [x]

D. W. Mulhall
Keith J. Simons
Faculty of Pharmacy
University of Manitoba
Winnipeg, Manitoba
Canada R3T 2N2

F. Estelle R. Simons
Section of Allergy and Clinical Immunology
Department of Pediatrics
Faculty of Medicine
University of Manitoba
Winnipeg, Manitoba
Canada R3E 0W1

Received June 19, 1978.
Accepted for publication September 28, 1978.
Supported by the Children's Hospital of Winnipeg Research Foundation.
D. W. Mulhall was the recipient of a Summer Studentship from the Medical Research Council of Canada. F. E. R. Simons is the recipient of a Queen Elizabeth II Scientist Award.

BOOKS

REVIEWS

Formulation and Preparation of Dosage Forms. Edited by J. POLDERMAN. Elsevier/North-Holland, 52 Vanderbilt Ave., New York, NY 10017. 1977. 307 pp. 16 × 24 cm. Price $37.95.

This volume presents the proceedings of the 37th International Congress of Pharmaceutical Sciences (F.I.P.) held in The Hague, The Netherlands, September 5–9, 1977. The editor states that the book takes its title from the main theme of the Congress.

The first of five sections is Formulation and Preparation of Dosage Forms. Three reviews are given on formulation factors affecting drugs given by oral route, surface applied drugs, and drugs given parenterally. These reviews are preceded by a General Introduction and followed by Conclusions and Perspectives. The introduction was more informative and better documented than the presentations on the oral route and the parenteral route.

The second section is Drug Substance-Pro-Drugs. The presentation, Drug Substances in Particular Pro-Drugs: Problems and Methods of Approach, was excellent and provided a wealth of references. The report, Analytical Aspects on Pro-Drugs, was informative and well documented. Pro-Drugs: Structure Activity Relationships suffers by comparison with the other presentations.

The third section, First Pass Effects, is composed of three lectures covering the influence of the route of administration of a substance on its bioavailability, drug metabolism associated with the routes of administration, and first pass effects and consequences for the routes of administration and dosage form design. The section describes the first pass effects and cites examples; however, some statements are redundant. Perhaps this repetition is unavoidable with the multiauthor presentations of a symposium.

The fourth section, Mechanism of Drug Release, consists of three presentations. Physico-chemical Aspects of Drug Release discusses theories of dissolution and dissolution of particles and binary mixtures. Solid Dosage Forms: Mechanism of Drug Release gives a simple view of the effect of formulation on release. Liberation of Medicaments from Semi-solid Bodies Applied to the Skin considers penetration conditions of chemical substances through the skin and the role of carrier materials in the rate of release of medicaments applied to the skin.

The final section, Physico-chemical and Technological Aspects, was also composed of three presentations. Powder technology was discussed superficially. A description of physicochemical and technological aspects of granulation techniques was elemental. A review of the process involved in tablet formulation provided some interesting scanning electron micrographs of compressed tablets; however, it did not explain or document what might be occurring in the compaction process. The final section was the least informative of the five sections.

As expected in a symposium presented by 17 authors in three languages, even after translation into English, the style is not uniform and repetition does occur; however, the volume is easily read and provides facts and references of interest to anyone concerned with dosage forms.

Reviewed by Eugene L. Parrott
College of Pharmacy
University of Iowa
Iowa City, IA 52242

Cardiovascular Drugs. Vol. 1: Antiarrhythmic, Antihypertensive and Lipid Lowering Drugs. Vol. 2: β-Adrenoceptor Blocking Drugs. Edited by GRAEME S. AVERY. University Park Press, 233 East Redwood St., Baltimore, MD 21202. 1978. 16 × 24 cm. Vol. 1: 176 pp. Vol. 2: 230 pp.

These two volumes comprise two parts of a three-part series entitled "Cardiovascular Drugs." The chapters have been revised from popular review articles previously published in the Australasian Drug Information Services press journal, *Drugs*. Written by internationally recognized authorities in their respective fields, this collected series provides a concise and convenient review of the current state of the art in cardiovascular drug therapy.

Volume 1 contains four chapters that review lipid lowering drugs and hyperlipidemia, antihypertensive drug therapy, antiarrhythmic agents, and clinical pharmacology and therapeutic uses of digitalis glycosides. With 51 figures, 19 tables, over 500 references, and an extensive subject index, this volume provides valuable and practical information concerning the appropriate therapeutic use of antiarrhythmic, hypotensive, and hypolipidemic drugs. Also included are discussions concerning the pharmacological actions, adverse reactions, and combination drug interactions of these cardiovascular agents.

Volume 2 contains nine chapters covering the pharmacodynamics and pharmacokinetics of β-adrenoreceptor blocking drugs; β-adrenoceptor blocking agents in the treatment of hypertension, angina pectoris, cardiac arrhythmias, and hyperthyroidism; clinical toxicology of propranolol and practolol; adverse effects of β-adrenoceptor blocking agents on respiration; and autoimmune and autoallergy phenomena in patients treated with β-blockers. With 20 figures, 27 tables, over 1000 references, and a subject index, this book provides a comprehensive review of β-adrenergic blocking drugs.

These well-written and comprehensive volumes are excellent reference sources and clinical guides to scientists working in cardiovascular re-

theophylline from serum or plasma proteins. The apparatus is portable and does not require a refrigerated centrifuge for ultrafiltration. The procedure is ideal for clinical investigations because of the small volume of sample required. It has potential application to the study of protein binding of a wide range of xenobiotic compounds.

(1) J. J. Vallner, *J. Pharm. Sci.*, **66**, 447 (1977).
(2) R. Wyatt, M. Weinberger, and L. Hendeles, *J. Pediatr.*, **92**, 125 (1978).
(3) M. L. Eichman, D. E. Guttman, Q. van Winkle, and E. P. Guth, *J. Pharm. Sci.*, **51**, 66 (1962).
(4) R. Koysooko, E. F. Ellis, and G. Levy, *Clin. Pharmacol. Ther.*, **15**, 454 (1974).
(5) A. M. Yurchak and W. J. Jusko, *Pediatrics*, **53**, 518 (1976).
(6) J. V. Aranda, D. S. Sitar, W. D. Parsons, P. M. Loughnan, and A. H. Niems, *N. Engl. J. Med.*, **295**, 413 (1976).
(7) D. S. Sitar, K. M. Piafsky, R. E. Rango, and R. I. Ogilvie, *Clin. Chem.*, **21**, 1774 (1975).

Colin J. Briggs [x]

D. W. Mulhall
Keith J. Simons
Faculty of Pharmacy
University of Manitoba
Winnipeg, Manitoba
Canada R3T 2N2

F. Estelle R. Simons
Section of Allergy and Clinical Immunology
Department of Pediatrics
Faculty of Medicine
University of Manitoba
Winnipeg, Manitoba
Canada R3E 0W1

Received June 19, 1978.
Accepted for publication September 28, 1978.
Supported by the Children's Hospital of Winnipeg Research Foundation.
D. W. Mulhall was the recipient of a Summer Studentship from the Medical Research Council of Canada. F. E. R. Simons is the recipient of a Queen Elizabeth II Scientist Award.

BOOKS

REVIEWS

Formulation and Preparation of Dosage Forms. Edited by J. POLDERMAN. Elsevier/North-Holland, 52 Vanderbilt Ave., New York, NY 10017. 1977. 307 pp. 16 × 24 cm. Price $37.95.

This volume presents the proceedings of the 37th International Congress of Pharmaceutical Sciences (F.I.P.) held in The Hague, The Netherlands, September 5–9, 1977. The editor states that the book takes its title from the main theme of the Congress.

The first of five sections is Formulation and Preparation of Dosage Forms. Three reviews are given on formulation factors affecting drugs given by oral route, surface applied drugs, and drugs given parenterally. These reviews are preceded by a General Introduction and followed by Conclusions and Perspectives. The introduction was more informative and better documented than the presentations on the oral route and the parenteral route.

The second section is Drug Substance-Pro-Drugs. The presentation, Drug Substances in Particular Pro-Drugs: Problems and Methods of Approach, was excellent and provided a wealth of references. The report, Analytical Aspects on Pro-Drugs, was informative and well documented. Pro-Drugs: Structure Activity Relationships suffers by comparison with the other presentations.

The third section, First Pass Effects, is composed of three lectures covering the influence of the route of administration of a substance on its bioavailability, drug metabolism associated with the routes of administration, and first pass effects and consequences for the routes of administration and dosage form design. The section describes the first pass effects and cites examples; however, some statements are redundant. Perhaps this repetition is unavoidable with the multiauthor presentations of a symposium.

The fourth section, Mechanism of Drug Release, consists of three presentations. Physico-chemical Aspects of Drug Release discusses theories of dissolution and dissolution of particles and binary mixtures. Solid Dosage Forms: Mechanism of Drug Release gives a simple view of the effect of formulation on release. Liberation of Medicaments from Semi-solid Bodies Applied to the Skin considers penetration conditions of chemical substances through the skin and the role of carrier materials in the rate of release of medicaments applied to the skin.

The final section, Physico-chemical and Technological Aspects, was also composed of three presentations. Powder technology was discussed superficially. A description of physicochemical and technological aspects of granulation techniques was elemental. A review of the process involved in tablet formulation provided some interesting scanning electron micrographs of compressed tablets; however, it did not explain or document what might be occurring in the compaction process. The final section was the least informative of the five sections.

As expected in a symposium presented by 17 authors in three languages, even after translation into English, the style is not uniform and repetition does occur; however, the volume is easily read and provides facts and references of interest to anyone concerned with dosage forms.

Reviewed by Eugene L. Parrott
College of Pharmacy
University of Iowa
Iowa City, IA 52242

Cardiovascular Drugs. Vol. 1: Antiarrhythmic, Antihypertensive and Lipid Lowering Drugs. Vol. 2: β-Adrenoceptor Blocking Drugs. Edited by GRAEME S. AVERY. University Park Press, 233 East Redwood St., Baltimore, MD 21202. 1978. 16 × 24 cm. Vol. 1: 176 pp. Vol. 2: 230 pp.

These two volumes comprise two parts of a three-part series entitled "Cardiovascular Drugs." The chapters have been revised from popular review articles previously published in the Australasian Drug Information Services press journal, *Drugs*. Written by internationally recognized authorities in their respective fields, this collected series provides a concise and convenient review of the current state of the art in cardiovascular drug therapy.

Volume 1 contains four chapters that review lipid lowering drugs and hyperlipidemia, antihypertensive drug therapy, antiarrhythmic agents, and clinical pharmacology and therapeutic uses of digitalis glycosides. With 51 figures, 19 tables, over 500 references, and an extensive subject index, this volume provides valuable and practical information concerning the appropriate therapeutic use of antiarrhythmic, hypotensive, and hypolipidemic drugs. Also included are discussions concerning the pharmacological actions, adverse reactions, and combination drug interactions of these cardiovascular agents.

Volume 2 contains nine chapters covering the pharmacodynamics and pharmacokinetics of β-adrenoreceptor blocking drugs; β-adrenoceptor blocking agents in the treatment of hypertension, angina pectoris, cardiac arrhythmias, and hyperthyroidism; clinical toxicology of propranolol and practolol; adverse effects of β-adrenoceptor blocking agents on respiration; and autoimmune and autoallergy phenomena in patients treated with β-blockers. With 20 figures, 27 tables, over 1000 references, and a subject index, this book provides a comprehensive review of β-adrenergic blocking drugs.

These well-written and comprehensive volumes are excellent reference sources and clinical guides to scientists working in cardiovascular re-

theophylline from serum or plasma proteins. The apparatus is portable and does not require a refrigerated centrifuge for ultrafiltration. The procedure is ideal for clinical investigations because of the small volume of sample required. It has potential application to the study of protein binding of a wide range of xenobiotic compounds.

(1) J. J. Vallner, *J. Pharm. Sci.*, **66**, 447 (1977).
(2) R. Wyatt, M. Weinberger, and L. Hendeles, *J. Pediatr.*, **92**, 125 (1978).
(3) M. L. Eichman, D. E. Guttman, Q. van Winkle, and E. P. Guth, *J. Pharm. Sci.*, **51**, 66 (1962).
(4) R. Koysooko, E. F. Ellis, and G. Levy, *Clin. Pharmacol. Ther.*, **15**, 454 (1974).
(5) A. M. Yurchak and W. J. Jusko, *Pediatrics*, **53**, 518 (1976).
(6) J. V. Aranda, D. S. Sitar, W. D. Parsons, P. M. Loughnan, and A. H. Niems, *N. Engl. J. Med.*, **295**, 413 (1976).
(7) D. S. Sitar, K. M. Piafsky, R. E. Rango, and R. I. Ogilvie, *Clin. Chem.*, **21**, 1774 (1975).

Colin J. Briggs [x]

D. W. Mulhall
Keith J. Simons
Faculty of Pharmacy
University of Manitoba
Winnipeg, Manitoba
Canada R3T 2N2

F. Estelle R. Simons
Section of Allergy and Clinical Immunology
Department of Pediatrics
Faculty of Medicine
University of Manitoba
Winnipeg, Manitoba
Canada R3E 0W1

Received June 19, 1978.
Accepted for publication September 28, 1978.
Supported by the Children's Hospital of Winnipeg Research Foundation.
D. W. Mulhall was the recipient of a Summer Studentship from the Medical Research Council of Canada. F. E. R. Simons is the recipient of a Queen Elizabeth II Scientist Award.

BOOKS

REVIEWS

Formulation and Preparation of Dosage Forms. Edited by J. POLDERMAN. Elsevier/North-Holland, 52 Vanderbilt Ave., New York, NY 10017. 1977. 307 pp. 16 × 24 cm. Price $37.95.

This volume presents the proceedings of the 37th International Congress of Pharmaceutical Sciences (F.I.P.) held in The Hague, The Netherlands, September 5–9, 1977. The editor states that the book takes its title from the main theme of the Congress.

The first of five sections is Formulation and Preparation of Dosage Forms. Three reviews are given on formulation factors affecting drugs given by oral route, surface applied drugs, and drugs given parenterally. These reviews are preceded by a General Introduction and followed by Conclusions and Perspectives. The introduction was more informative and better documented than the presentations on the oral route and the parenteral route.

The second section is Drug Substance-Pro-Drugs. The presentation, Drug Substances in Particular Pro-Drugs: Problems and Methods of Approach, was excellent and provided a wealth of references. The report, Analytical Aspects on Pro-Drugs, was informative and well documented. Pro-Drugs: Structure Activity Relationships suffers by comparison with the other presentations.

The third section, First Pass Effects, is composed of three lectures covering the influence of the route of administration of a substance on its bioavailability, drug metabolism associated with the routes of administration, and first pass effects and consequences for the routes of administration and dosage form design. The section describes the first pass effects and cites examples; however, some statements are redundant. Perhaps this repetition is unavoidable with the multiauthor presentations of a symposium.

The fourth section, Mechanism of Drug Release, consists of three presentations. Physico-chemical Aspects of Drug Release discusses theories of dissolution and dissolution of particles and binary mixtures. Solid Dosage Forms: Mechanism of Drug Release gives a simple view of the effect of formulation on release. Liberation of Medicaments from Semi-solid Bodies Applied to the Skin considers penetration conditions of chemical substances through the skin and the role of carrier materials in the rate of release of medicaments applied to the skin.

The final section, Physico-chemical and Technological Aspects, was also composed of three presentations. Powder technology was discussed superficially. A description of physicochemical and technological aspects of granulation techniques was elemental. A review of the process involved in tablet formulation provided some interesting scanning electron micrographs of compressed tablets; however, it did not explain or document what might be occurring in the compaction process. The final section was the least informative of the five sections.

As expected in a symposium presented by 17 authors in three languages, even after translation into English, the style is not uniform and repetition does occur; however, the volume is easily read and provides facts and references of interest to anyone concerned with dosage forms.

Reviewed by Eugene L. Parrott
College of Pharmacy
University of Iowa
Iowa City, IA 52242

Cardiovascular Drugs. Vol. 1: Antiarrhythmic, Antihypertensive and Lipid Lowering Drugs. Vol. 2: β-Adrenoceptor Blocking Drugs. Edited by GRAEME S. AVERY. University Park Press, 233 East Redwood St., Baltimore, MD 21202. 1978. 16 × 24 cm. Vol. 1: 176 pp. Vol. 2: 230 pp.

These two volumes comprise two parts of a three-part series entitled "Cardiovascular Drugs." The chapters have been revised from popular review articles previously published in the Australasian Drug Information Services press journal, *Drugs*. Written by internationally recognized authorities in their respective fields, this collected series provides a concise and convenient review of the current state of the art in cardiovascular drug therapy.

Volume 1 contains four chapters that review lipid lowering drugs and hyperlipidemia, antihypertensive drug therapy, antiarrhythmic agents, and clinical pharmacology and therapeutic uses of digitalis glycosides. With 51 figures, 19 tables, over 500 references, and an extensive subject index, this volume provides valuable and practical information concerning the appropriate therapeutic use of antiarrhythmic, hypotensive, and hypolipidemic drugs. Also included are discussions concerning the pharmacological actions, adverse reactions, and combination drug interactions of these cardiovascular agents.

Volume 2 contains nine chapters covering the pharmacodynamics and pharmacokinetics of β-adrenoreceptor blocking drugs; β-adrenoceptor blocking agents in the treatment of hypertension, angina pectoris, cardiac arrhythmias, and hyperthyroidism; clinical toxicology of propranolol and practolol; adverse effects of β-adrenoceptor blocking agents on respiration; and autoimmune and autoallergy phenomena in patients treated with β-blockers. With 20 figures, 27 tables, over 1000 references, and a subject index, this book provides a comprehensive review of β-adrenergic blocking drugs.

These well-written and comprehensive volumes are excellent reference sources and clinical guides to scientists working in cardiovascular re-

search. They are of particular interest to physicians, pharmacologists, and toxicologists involved in clinical pharmacology and toxicology. Volume 3, "Platelets, Thrombosis and Drugs," will conclude the "Cardiovascular Drugs" series.

Reviewed by William P. Heilman
Life Science Division
T. R. Evans Research Center
Diamond Shamrock Corporation
Painesville, OH 44077

Quantitative Drug Design: A Critical Introduction. Medicinal Research Series Vol. 8. By YVONNE CONNOLLY MARTIN. Dekker, 270 Madison Ave., New York, NY 10016. 1978. 425 pp. 15 × 23 cm. Price $38.50.

This "how to do it" text is a must for anyone interested in the application of quantitative structure–activity relationship methods to molecular design. It will introduce the concepts to the beginner, guide the efforts of the intermediate, and provide convenient reference material for the professional.

The introduction gives the topics covered and emphasizes the steps in drug design: (*a*) find a lead, (*b*) synthesize and test an exploratory series, (*c*) develop quantitative structure–activity relationship models, and (*d*) optimize the lead with quantitative structure–activity relationships. The author then plunges into the "guts and workings" of quantitative structure–activity relationships. Some topics covered are: extrathermodynamic and *de novo* approaches, noncovalent interactions, physical properties, biological data, equations relating potency and physical properties, regression analysis, statistical evaluation, and a detailed example of extrathermodynamic calculations.

The text is well written, clear, easy to follow, current, well illustrated, and well referenced. Of particular importance are the treatment of statistics, the detailed examples, the discussion of biological data, and the very practical discussion in Chapter 11, Synthesis to Follow up a Lead: How to Start and When to Stop. The Appendixes, which are very useful, contain equations and definitions, substituent constants, Wiswesser line notation, and sources of computer programs and data bases.

This book was much needed and has come at a time when the field is exploding. It is highly recommended for those interested in quantitative structure–activity relationships who want to find out what can and cannot be done with the methods and for those working every day with quantitative structure–activity relationships who want most of the information in one handy place.

Reviewed by William P. Purcell
Drug Design Laboratory
University of Tennessee Center for the Health Sciences
Memphis, TN 38103

Marihuana Research Findings: 1976. NIDA Research Monograph 14. Edited by ROBERT C. PETERSEN. National Institute on Drug Abuse, 11400 Rockville Pike, Rockville, MD 20852. 1977. 251 pp. 15 × 23 cm.

The National Institute on Drug Abuse (NIDA) regularly publishes research monographs on various aspects of abused drugs. This book, like many of its predecessors, is useful to workers in the area or those contemplating future endeavors in that area. The book contains nine chapters, each representing an area of research interest that in general reflects NIDA grant activity in marihuana research. Most chapters have been written by experts in the field. A preliminary summary of marihuana findings by the editor is quite readable and was the text for the sixth edition of the *Marihuana and Health Report*.

Chapter 1, written by William McGlothlin, gives an excellent overview on the epidemiological research findings with marihuana usage during the past 10 years, with emphasis on recent findings. Chapters 2 and 3, by Ralph Karler, cover the chemistry, metabolism, toxicology, and pharmacology of marihuana. These chapters appear to be the weakest in the book. The reader has considerable difficulty following the text without benefit of chemical structures. Particularly was this problem true with the synthetic analogs of marihuana. Surprisingly, there was no mention in Chapter 2 of the NIDA-sponsored symposium on marihuana assays in humans detailed in Monograph 7. (In the summary by the editor, *cf.*, p 12, this symposium was referenced.)

Chapters 4–6, by Douglas Peter Ferraro, cover the research on behavioral effects, most of which comes from animal studies. Chapter 7, by Reese Jones, is the best organized and perhaps the most useful to researchers starting in this area. This chapter covers the myriad of human effects known to occur from marihuana smoking or administration of individual cannabinoids. Chapter 8, by Steven Matsuyama and Lissy Javrick, details the rather limited knowledge available on genetic and immune responses in animals and humans. The final chapter, by Sidney Cohen, takes a sort of anecdotal approach to therapeutic aspects of marihuana use. Sections on intraocular pressure reduction, bronchodilation, and anticonvulsant work certainly emphasized some positive effects found for various cannabinoids which are not necessarily found in marihuana.

The book is an excellent source for recent references in the marihuana area and is recommended mainly for that reason. Yet the newcomer in marihuana research should be forewarned that this short thesis cannot completely cover the vast literature of this field.

Reviewed by Jimmie L. Valentine
BioAnalytic Laboratory
School of Pharmacy
University of Missouri–Kansas City
Kansas City, MO 64108

Aliphatic Chemistry, Vol. 5, A Specialist Periodical Report. Edited by A. McKILLOP *et al.* The Chemical Society, Burlington House, London WIV OBN, England. 1977. xii + 337 pp. 14.5 × 22 cm. Price $47.00. Available from Special Issues Sales, American Chemical Society, 1155 Sixteenth St., N.W., Washington, DC 20036.

In the fifth volume of the Specialist Periodical Reports on aliphatic chemistry, the authors and editor maintain the excellent quality and the well-organized format of the previous volumes. This volume is composed of four chapters that survey the literature published during 1975 and one chapter (Chapter 5) that summarizes the literature for the 2-year period of 1974–1975.

The literature dealing with alkanes, acetylenes, allenes, and olefins was contributed by J. C. Saunders and B. P. Swann, who were also coauthors of the corresponding chapter in Volume 4. The task of compiling Chapter 2—by far the longest in this volume—on compounds with other functional groups (carboxylic acids and their derivatives, nitriles and isocyanides, aldehydes and ketones, alcohols, amines, alkyl halides, ethers, and other types of aliphatic compounds) was performed by E. F. V. Scriven. Dr. Scriven maintains the high standards set by E. W. Colvin, who so ably contributed the analogous chapters in all of the preceding volumes.

Progress in the areas of naturally occurring polyolefinic and polyacetylenic compounds (Chapter 3) is reviewed for the fourth consecutive year by G. Pattenden. This chapter summarizes reports dealing with detection and isolation, structure elucidation, and syntheses of these unsaturated natural products. Included are not only open-chain, alicyclic, and simple heterocyclic natural products containing polyolefinic and polyacetylenic moieties but also more complex compounds, such as the macrolide and ansamycin antibiotics. The view, formerly held, that halogen-containing compounds are rare in nature is refuted by this chapter and its predecessors in earlier volumes, particularly by the sections that treat compounds from marine sources.

Chapter 4 on prostaglandins by K. W. Mallion reflects a resurgence of interest in syntheses of prostaglandins and their analogs. Synthesis routes are amply illustrated with structures and schemes. In Chapter 5, F. D. Gunstone surveys the literature of 1974 and 1975 on the biology, chemistry, and biochemistry of fatty acids and related compounds.

It is becoming difficult to review the volumes of this series without becoming repetitiously laudatory. The fact remains that this volume and its predecessors provide admirable surveys of the annual literature in the specified areas; collectively, they constitute valuable reviews of the recent literature (1970–1975) of these areas. It is still a marvel that such comprehensive coverage of specific (Chapters 3–5) and general (Chapters 1–2) topics is presented in a concise, informative, and well-organized style.

Reviewed by Y. F. Shealy
Southern Research Institute
Birmingham, AL 35205

search. They are of particular interest to physicians, pharmacologists, and toxicologists involved in clinical pharmacology and toxicology. Volume 3, "Platelets, Thrombosis and Drugs," will conclude the "Cardiovascular Drugs" series.

Reviewed by William P. Heilman
Life Science Division
T. R. Evans Research Center
Diamond Shamrock Corporation
Painesville, OH 44077

Quantitative Drug Design: A Critical Introduction. Medicinal Research Series Vol. 8. By YVONNE CONNOLLY MARTIN. Dekker, 270 Madison Ave., New York, NY 10016. 1978. 425 pp. 15 × 23 cm. Price $38.50.

This "how to do it" text is a must for anyone interested in the application of quantitative structure–activity relationship methods to molecular design. It will introduce the concepts to the beginner, guide the efforts of the intermediate, and provide convenient reference material for the professional.

The introduction gives the topics covered and emphasizes the steps in drug design: (*a*) find a lead, (*b*) synthesize and test an exploratory series, (*c*) develop quantitative structure–activity relationship models, and (*d*) optimize the lead with quantitative structure–activity relationships. The author then plunges into the "guts and workings" of quantitative structure–activity relationships. Some topics covered are: extrathermodynamic and *de novo* approaches, noncovalent interactions, physical properties, biological data, equations relating potency and physical properties, regression analysis, statistical evaluation, and a detailed example of extrathermodynamic calculations.

The text is well written, clear, easy to follow, current, well illustrated, and well referenced. Of particular importance are the treatment of statistics, the detailed examples, the discussion of biological data, and the very practical discussion in Chapter 11, Synthesis to Follow up a Lead: How to Start and When to Stop. The Appendixes, which are very useful, contain equations and definitions, substituent constants, Wiswesser line notation, and sources of computer programs and data bases.

This book was much needed and has come at a time when the field is exploding. It is highly recommended for those interested in quantitative structure–activity relationships who want to find out what can and cannot be done with the methods and for those working every day with quantitative structure–activity relationships who want most of the information in one handy place.

Reviewed by William P. Purcell
Drug Design Laboratory
University of Tennessee Center for the Health Sciences
Memphis, TN 38103

Marihuana Research Findings: 1976. NIDA Research Monograph 14. Edited by ROBERT C. PETERSEN. National Institute on Drug Abuse, 11400 Rockville Pike, Rockville, MD 20852. 1977. 251 pp. 15 × 23 cm.

The National Institute on Drug Abuse (NIDA) regularly publishes research monographs on various aspects of abused drugs. This book, like many of its predecessors, is useful to workers in the area or those contemplating future endeavors in that area. The book contains nine chapters, each representing an area of research interest that in general reflects NIDA grant activity in marihuana research. Most chapters have been written by experts in the field. A preliminary summary of marihuana findings by the editor is quite readable and was the text for the sixth edition of the *Marihuana and Health Report*.

Chapter 1, written by William McGlothlin, gives an excellent overview on the epidemiological research findings with marihuana usage during the past 10 years, with emphasis on recent findings. Chapters 2 and 3, by Ralph Karler, cover the chemistry, metabolism, toxicology, and pharmacology of marihuana. These chapters appear to be the weakest in the book. The reader has considerable difficulty following the text without benefit of chemical structures. Particularly was this problem true with the synthetic analogs of marihuana. Surprisingly, there was no mention in Chapter 2 of the NIDA-sponsored symposium on marihuana assays in humans detailed in Monograph 7. (In the summary by the editor, *cf.*, p 12, this symposium was referenced.)

Chapters 4–6, by Douglas Peter Ferraro, cover the research on behavioral effects, most of which comes from animal studies. Chapter 7, by Reese Jones, is the best organized and perhaps the most useful to researchers starting in this area. This chapter covers the myriad of human effects known to occur from marihuana smoking or administration of individual cannabinoids. Chapter 8, by Steven Matsuyama and Lissy Javrick, details the rather limited knowledge available on genetic and immune responses in animals and humans. The final chapter, by Sidney Cohen, takes a sort of anecdotal approach to therapeutic aspects of marihuana use. Sections on intraocular pressure reduction, bronchodilation, and anticonvulsant work certainly emphasized some positive effects found for various cannabinoids which are not necessarily found in marihuana.

The book is an excellent source for recent references in the marihuana area and is recommended mainly for that reason. Yet the newcomer in marihuana research should be forewarned that this short thesis cannot completely cover the vast literature of this field.

Reviewed by Jimmie L. Valentine
BioAnalytic Laboratory
School of Pharmacy
University of Missouri–Kansas City
Kansas City, MO 64108

Aliphatic Chemistry, Vol. 5, A Specialist Periodical Report. Edited by A. McKILLOP *et al.* The Chemical Society, Burlington House, London WIV OBN, England. 1977. xii + 337 pp. 14.5 × 22 cm. Price $47.00. Available from Special Issues Sales, American Chemical Society, 1155 Sixteenth St., N.W., Washington, DC 20036.

In the fifth volume of the Specialist Periodical Reports on aliphatic chemistry, the authors and editor maintain the excellent quality and the well-organized format of the previous volumes. This volume is composed of four chapters that survey the literature published during 1975 and one chapter (Chapter 5) that summarizes the literature for the 2-year period of 1974–1975.

The literature dealing with alkanes, acetylenes, allenes, and olefins was contributed by J. C. Saunders and B. P. Swann, who were also coauthors of the corresponding chapter in Volume 4. The task of compiling Chapter 2—by far the longest in this volume—on compounds with other functional groups (carboxylic acids and their derivatives, nitriles and isocyanides, aldehydes and ketones, alcohols, amines, alkyl halides, ethers, and other types of aliphatic compounds) was performed by E. F. V. Scriven. Dr. Scriven maintains the high standards set by E. W. Colvin, who so ably contributed the analogous chapters in all of the preceding volumes.

Progress in the areas of naturally occurring polyolefinic and polyacetylenic compounds (Chapter 3) is reviewed for the fourth consecutive year by G. Pattenden. This chapter summarizes reports dealing with detection and isolation, structure elucidation, and syntheses of these unsaturated natural products. Included are not only open-chain, alicyclic, and simple heterocyclic natural products containing polyolefinic and polyacetylenic moieties but also more complex compounds, such as the macrolide and ansamycin antibiotics. The view, formerly held, that halogen-containing compounds are rare in nature is refuted by this chapter and its predecessors in earlier volumes, particularly by the sections that treat compounds from marine sources.

Chapter 4 on prostaglandins by K. W. Mallion reflects a resurgence of interest in syntheses of prostaglandins and their analogs. Synthesis routes are amply illustrated with structures and schemes. In Chapter 5, F. D. Gunstone surveys the literature of 1974 and 1975 on the biology, chemistry, and biochemistry of fatty acids and related compounds.

It is becoming difficult to review the volumes of this series without becoming repetitiously laudatory. The fact remains that this volume and its predecessors provide admirable surveys of the annual literature in the specified areas; collectively, they constitute valuable reviews of the recent literature (1970–1975) of these areas. It is still a marvel that such comprehensive coverage of specific (Chapters 3–5) and general (Chapters 1–2) topics is presented in a concise, informative, and well-organized style.

Reviewed by Y. F. Shealy
Southern Research Institute
Birmingham, AL 35205

search. They are of particular interest to physicians, pharmacologists, and toxicologists involved in clinical pharmacology and toxicology. Volume 3, "Platelets, Thrombosis and Drugs," will conclude the "Cardiovascular Drugs" series.

Reviewed by William P. Heilman
Life Science Division
T. R. Evans Research Center
Diamond Shamrock Corporation
Painesville, OH 44077

Quantitative Drug Design: A Critical Introduction. Medicinal Research Series Vol. 8. By YVONNE CONNOLLY MARTIN. Dekker, 270 Madison Ave., New York, NY 10016. 1978. 425 pp. 15 × 23 cm. Price $38.50.

This "how to do it" text is a must for anyone interested in the application of quantitative structure–activity relationship methods to molecular design. It will introduce the concepts to the beginner, guide the efforts of the intermediate, and provide convenient reference material for the professional.

The introduction gives the topics covered and emphasizes the steps in drug design: (*a*) find a lead, (*b*) synthesize and test an exploratory series, (*c*) develop quantitative structure–activity relationship models, and (*d*) optimize the lead with quantitative structure–activity relationships. The author then plunges into the "guts and workings" of quantitative structure–activity relationships. Some topics covered are: extrathermodynamic and *de novo* approaches, noncovalent interactions, physical properties, biological data, equations relating potency and physical properties, regression analysis, statistical evaluation, and a detailed example of extrathermodynamic calculations.

The text is well written, clear, easy to follow, current, well illustrated, and well referenced. Of particular importance are the treatment of statistics, the detailed examples, the discussion of biological data, and the very practical discussion in Chapter 11, Synthesis to Follow up a Lead: How to Start and When to Stop. The Appendixes, which are very useful, contain equations and definitions, substituent constants, Wiswesser line notation, and sources of computer programs and data bases.

This book was much needed and has come at a time when the field is exploding. It is highly recommended for those interested in quantitative structure–activity relationships who want to find out what can and cannot be done with the methods and for those working every day with quantitative structure–activity relationships who want most of the information in one handy place.

Reviewed by William P. Purcell
Drug Design Laboratory
University of Tennessee Center for the Health Sciences
Memphis, TN 38103

Marihuana Research Findings: 1976. NIDA Research Monograph 14. Edited by ROBERT C. PETERSEN. National Institute on Drug Abuse, 11400 Rockville Pike, Rockville, MD 20852. 1977. 251 pp. 15 × 23 cm.

The National Institute on Drug Abuse (NIDA) regularly publishes research monographs on various aspects of abused drugs. This book, like many of its predecessors, is useful to workers in the area or those contemplating future endeavors in that area. The book contains nine chapters, each representing an area of research interest that in general reflects NIDA grant activity in marihuana research. Most chapters have been written by experts in the field. A preliminary summary of marihuana findings by the editor is quite readable and was the text for the sixth edition of the *Marihuana and Health Report*.

Chapter 1, written by William McGlothlin, gives an excellent overview on the epidemiological research findings with marihuana usage during the past 10 years, with emphasis on recent findings. Chapters 2 and 3, by Ralph Karler, cover the chemistry, metabolism, toxicology, and pharmacology of marihuana. These chapters appear to be the weakest in the book. The reader has considerable difficulty following the text without benefit of chemical structures. Particularly was this problem true with the synthetic analogs of marihuana. Surprisingly, there was no mention in Chapter 2 of the NIDA-sponsored symposium on marihuana assays in humans detailed in Monograph 7. (In the summary by the editor, *cf.*, p 12, this symposium was referenced.)

Chapters 4–6, by Douglas Peter Ferraro, cover the research on behavioral effects, most of which comes from animal studies. Chapter 7, by Reese Jones, is the best organized and perhaps the most useful to researchers starting in this area. This chapter covers the myriad of human effects known to occur from marihuana smoking or administration of individual cannabinoids. Chapter 8, by Steven Matsuyama and Lissy Javrick, details the rather limited knowledge available on genetic and immune responses in animals and humans. The final chapter, by Sidney Cohen, takes a sort of anecdotal approach to therapeutic aspects of marihuana use. Sections on intraocular pressure reduction, bronchodilation, and anticonvulsant work certainly emphasized some positive effects found for various cannabinoids which are not necessarily found in marihuana.

The book is an excellent source for recent references in the marihuana area and is recommended mainly for that reason. Yet the newcomer in marihuana research should be forewarned that this short thesis cannot completely cover the vast literature of this field.

Reviewed by Jimmie L. Valentine
BioAnalytic Laboratory
School of Pharmacy
University of Missouri–Kansas City
Kansas City, MO 64108

Aliphatic Chemistry, Vol. 5, A Specialist Periodical Report. Edited by A. McKILLOP *et al.* The Chemical Society, Burlington House, London WIV OBN, England. 1977. xii + 337 pp. 14.5 × 22 cm. Price $47.00. Available from Special Issues Sales, American Chemical Society, 1155 Sixteenth St., N.W., Washington, DC 20036.

In the fifth volume of the Specialist Periodical Reports on aliphatic chemistry, the authors and editor maintain the excellent quality and the well-organized format of the previous volumes. This volume is composed of four chapters that survey the literature published during 1975 and one chapter (Chapter 5) that summarizes the literature for the 2-year period of 1974–1975.

The literature dealing with alkanes, acetylenes, allenes, and olefins was contributed by J. C. Saunders and B. P. Swann, who were also coauthors of the corresponding chapter in Volume 4. The task of compiling Chapter 2—by far the longest in this volume—on compounds with other functional groups (carboxylic acids and their derivatives, nitriles and isocyanides, aldehydes and ketones, alcohols, amines, alkyl halides, ethers, and other types of aliphatic compounds) was performed by E. F. V. Scriven. Dr. Scriven maintains the high standards set by E. W. Colvin, who so ably contributed the analogous chapters in all of the preceding volumes.

Progress in the areas of naturally occurring polyolefinic and polyacetylenic compounds (Chapter 3) is reviewed for the fourth consecutive year by G. Pattenden. This chapter summarizes reports dealing with detection and isolation, structure elucidation, and syntheses of these unsaturated natural products. Included are not only open-chain, alicyclic, and simple heterocyclic natural products containing polyolefinic and polyacetylenic moieties but also more complex compounds, such as the macrolide and ansamycin antibiotics. The view, formerly held, that halogen-containing compounds are rare in nature is refuted by this chapter and its predecessors in earlier volumes, particularly by the sections that treat compounds from marine sources.

Chapter 4 on prostaglandins by K. W. Mallion reflects a resurgence of interest in syntheses of prostaglandins and their analogs. Synthesis routes are amply illustrated with structures and schemes. In Chapter 5, F. D. Gunstone surveys the literature of 1974 and 1975 on the biology, chemistry, and biochemistry of fatty acids and related compounds.

It is becoming difficult to review the volumes of this series without becoming repetitiously laudatory. The fact remains that this volume and its predecessors provide admirable surveys of the annual literature in the specified areas; collectively, they constitute valuable reviews of the recent literature (1970–1975) of these areas. It is still a marvel that such comprehensive coverage of specific (Chapters 3–5) and general (Chapters 1–2) topics is presented in a concise, informative, and well-organized style.

Reviewed by Y. F. Shealy
Southern Research Institute
Birmingham, AL 35205

search. They are of particular interest to physicians, pharmacologists, and toxicologists involved in clinical pharmacology and toxicology. Volume 3, "Platelets, Thrombosis and Drugs," will conclude the "Cardiovascular Drugs" series.

Reviewed by William P. Heilman
Life Science Division
T. R. Evans Research Center
Diamond Shamrock Corporation
Painesville, OH 44077

Quantitative Drug Design: A Critical Introduction. Medicinal Research Series Vol. 8. By YVONNE CONNOLLY MARTIN. Dekker, 270 Madison Ave., New York, NY 10016. 1978. 425 pp. 15 × 23 cm. Price $38.50.

This "how to do it" text is a must for anyone interested in the application of quantitative structure–activity relationship methods to molecular design. It will introduce the concepts to the beginner, guide the efforts of the intermediate, and provide convenient reference material for the professional.

The introduction gives the topics covered and emphasizes the steps in drug design: (*a*) find a lead, (*b*) synthesize and test an exploratory series, (*c*) develop quantitative structure–activity relationship models, and (*d*) optimize the lead with quantitative structure–activity relationships. The author then plunges into the "guts and workings" of quantitative structure–activity relationships. Some topics covered are: extrathermodynamic and *de novo* approaches, noncovalent interactions, physical properties, biological data, equations relating potency and physical properties, regression analysis, statistical evaluation, and a detailed example of extrathermodynamic calculations.

The text is well written, clear, easy to follow, current, well illustrated, and well referenced. Of particular importance are the treatment of statistics, the detailed examples, the discussion of biological data, and the very practical discussion in Chapter 11, Synthesis to Follow up a Lead: How to Start and When to Stop. The Appendixes, which are very useful, contain equations and definitions, substituent constants, Wiswesser line notation, and sources of computer programs and data bases.

This book was much needed and has come at a time when the field is exploding. It is highly recommended for those interested in quantitative structure–activity relationships who want to find out what can and cannot be done with the methods and for those working every day with quantitative structure–activity relationships who want most of the information in one handy place.

Reviewed by William P. Purcell
Drug Design Laboratory
University of Tennessee Center for the Health Sciences
Memphis, TN 38103

Marihuana Research Findings: 1976. NIDA Research Monograph 14. Edited by ROBERT C. PETERSEN. National Institute on Drug Abuse, 11400 Rockville Pike, Rockville, MD 20852. 1977. 251 pp. 15 × 23 cm.

The National Institute on Drug Abuse (NIDA) regularly publishes research monographs on various aspects of abused drugs. This book, like many of its predecessors, is useful to workers in the area or those contemplating future endeavors in that area. The book contains nine chapters, each representing an area of research interest that in general reflects NIDA grant activity in marihuana research. Most chapters have been written by experts in the field. A preliminary summary of marihuana findings by the editor is quite readable and was the text for the sixth edition of the *Marihuana and Health Report*.

Chapter 1, written by William McGlothlin, gives an excellent overview on the epidemiological research findings with marihuana usage during the past 10 years, with emphasis on recent findings. Chapters 2 and 3, by Ralph Karler, cover the chemistry, metabolism, toxicology, and pharmacology of marihuana. These chapters appear to be the weakest in the book. The reader has considerable difficulty following the text without benefit of chemical structures. Particularly was this problem true with the synthetic analogs of marihuana. Surprisingly, there was no mention in Chapter 2 of the NIDA-sponsored symposium on marihuana assays in humans detailed in Monograph 7. (In the summary by the editor, *cf.*, p 12, this symposium was referenced.)

Chapters 4–6, by Douglas Peter Ferraro, cover the research on behavioral effects, most of which comes from animal studies. Chapter 7, by Reese Jones, is the best organized and perhaps the most useful to researchers starting in this area. This chapter covers the myriad of human effects known to occur from marihuana smoking or administration of individual cannabinoids. Chapter 8, by Steven Matsuyama and Lissy Javrick, details the rather limited knowledge available on genetic and immune responses in animals and humans. The final chapter, by Sidney Cohen, takes a sort of anecdotal approach to therapeutic aspects of marihuana use. Sections on intraocular pressure reduction, bronchodilation, and anticonvulsant work certainly emphasized some positive effects found for various cannabinoids which are not necessarily found in marihuana.

The book is an excellent source for recent references in the marihuana area and is recommended mainly for that reason. Yet the newcomer in marihuana research should be forewarned that this short thesis cannot completely cover the vast literature of this field.

Reviewed by Jimmie L. Valentine
BioAnalytic Laboratory
School of Pharmacy
University of Missouri–Kansas City
Kansas City, MO 64108

Aliphatic Chemistry, Vol. 5, A Specialist Periodical Report. Edited by A. McKILLOP *et al.* The Chemical Society, Burlington House, London WIV OBN, England. 1977. xii + 337 pp. 14.5 × 22 cm. Price $47.00. Available from Special Issues Sales, American Chemical Society, 1155 Sixteenth St., N.W., Washington, DC 20036.

In the fifth volume of the Specialist Periodical Reports on aliphatic chemistry, the authors and editor maintain the excellent quality and the well-organized format of the previous volumes. This volume is composed of four chapters that survey the literature published during 1975 and one chapter (Chapter 5) that summarizes the literature for the 2-year period of 1974–1975.

The literature dealing with alkanes, acetylenes, allenes, and olefins was contributed by J. C. Saunders and B. P. Swann, who were also coauthors of the corresponding chapter in Volume 4. The task of compiling Chapter 2—by far the longest in this volume—on compounds with other functional groups (carboxylic acids and their derivatives, nitriles and isocyanides, aldehydes and ketones, alcohols, amines, alkyl halides, ethers, and other types of aliphatic compounds) was performed by E. F. V. Scriven. Dr. Scriven maintains the high standards set by E. W. Colvin, who so ably contributed the analogous chapters in all of the preceding volumes.

Progress in the areas of naturally occurring polyolefinic and polyacetylenic compounds (Chapter 3) is reviewed for the fourth consecutive year by G. Pattenden. This chapter summarizes reports dealing with detection and isolation, structure elucidation, and syntheses of these unsaturated natural products. Included are not only open-chain, alicyclic, and simple heterocyclic natural products containing polyolefinic and polyacetylenic moieties but also more complex compounds, such as the macrolide and ansamycin antibiotics. The view, formerly held, that halogen-containing compounds are rare in nature is refuted by this chapter and its predecessors in earlier volumes, particularly by the sections that treat compounds from marine sources.

Chapter 4 on prostaglandins by K. W. Mallion reflects a resurgence of interest in syntheses of prostaglandins and their analogs. Synthesis routes are amply illustrated with structures and schemes. In Chapter 5, F. D. Gunstone surveys the literature of 1974 and 1975 on the biology, chemistry, and biochemistry of fatty acids and related compounds.

It is becoming difficult to review the volumes of this series without becoming repetitiously laudatory. The fact remains that this volume and its predecessors provide admirable surveys of the annual literature in the specified areas; collectively, they constitute valuable reviews of the recent literature (1970–1975) of these areas. It is still a marvel that such comprehensive coverage of specific (Chapters 3–5) and general (Chapters 1–2) topics is presented in a concise, informative, and well-organized style.

Reviewed by Y. F. Shealy
Southern Research Institute
Birmingham, AL 35205

A publication of the
American Pharmaceutical Association—
the National Professional Society
of Pharmacists

JOURNAL OF PHARMACEUTICAL SCIENCES

INDEX TO AUTHORS
INDEX TO SUBJECTS

VOLUME 68
JANUARY TO DECEMBER, 1979

Published monthly under the supervision of the Board of Trustees

MARY H. FERGUSON
Editor

SHELLY ELLIOTT
Production Editor

MARCIA GARTRELL
Copy Editor

NICOLETTE TRIANTAFELLU
Copy Editor

EDWARD G. FELDMANN
Contributing Editor

SAMUEL W. GOLDSTEIN
Contributing Editor

BELLE R. BECK
Editorial Secretary

DAVID BOHARDT
Director of Publications

L. LUAN CORRIGAN
Assistant Director of Publications

EDITORIAL ADVISORY BOARD

John Autian
Norman R. Farnsworth
William O. Foye
William J. Jusko
Herbert A. Lieberman
David E. Mann, Jr.
Gerald J. Papariello
Edward G. Rippie

FEBRUARY 1979
VOLUME 68 NUMBER 2

JOURNAL OF PHARMACEUTICAL SCIENCES

MARY H. FERGUSON
Editor

SHELLY ELLIOTT
Production Editor

JANIS KELLY
Copy Editor

EDWARD G. FELDMANN
Contributing Editor

SAMUEL W. GOLDSTEIN
Contributing Editor

BELLE R. BECK
Editorial Secretary

DAVID BOHARDT
Director of Publications

L. LUAN CORRIGAN
Assistant Director of Publications

EDITORIAL ADVISORY BOARD

JOHN AUTIAN	HERBERT A. LIEBERMAN
NORMAN R. FARNSWORTH	DAVID E. MANN, JR.
WILLIAM O. FOYE	GERALD J. PAPARIELLO
WILLIAM J. JUSKO	EDWARD G. RIPPIE

The *Journal of Pharmaceutical Sciences* is published monthly by the American Pharmaceutical Association (APhA) at 2215 Constitution Ave., N.W., Washington, DC 20037. Second-class postage paid at Washington, D.C., and at additional mailing office.

All expressions of opinion and statements of supposed fact appearing in articles or editorials carried in this journal are published on the authority of the writer over whose name they appear and are not to be regarded as necessarily expressing the policies or views of APhA.

Offices—Editorial, Advertising, and Subscription: 2215 Constitution Ave., N.W., Washington, DC 20037. Printing: 20th & Northampton Streets, Easton, PA 18042.

Annual Subscriptions—United States and foreign, industrial and government institutions $50, educational institutions $50, individuals *for personal use only* $30; single copies $5. All foreign subscriptions add $5 for postage. Subscription rates are subject to change without notice. Members of APhA may elect to receive the *Journal of Pharmaceutical Sciences* as a part of their annual $70 (foreign $75) APhA membership dues.

Claims—Missing numbers will not be supplied if dues or subscriptions are in arrears for more than 60 days or if claims are received more than 60 days after the date of the issue, or if loss was due to failure to give notice of change of address. APhA cannot accept responsibility for foreign delivery when its records indicate shipment has been made.

Change of Address—Members and subscribers should notify at once both the Post Office and APhA of any change of address.

Photocopying—The code at the foot of the first page of an article indicates that APhA has granted permission for copying of the article beyond the limits permitted by Sections 107 and 108 of the U.S. Copyright Law provided that the copier sends the per copy fee stated in the code to the Copyright Clearance Center, Inc., P. O. Box 765, Schenectady, NY 12301. Copies may be made for personal or internal use only and not for general distribution.

Microfilm—Available from University Microfilms International, 300 N. Zeeb Road, Ann Arbor, MI 48106.

© Copyright 1979, American Pharmaceutical Association, 2215 Constitution Ave., N.W., Washington, DC 20037; all rights reserved.

ANTIBIOTIC CERTIFICATION—OBSOLETE AND ARCHAIC

All too often laws and regulations, once enacted or finalized, go on *ad infinitum*. Various observers have commented that they become "chiseled in stone" or "fixed in concrete." However they are described, the point is that such rules or legislation may have been appropriate and valid at one time but now have outlived their usefulness. As such, they ought to be reexamined and the continued need for them should be reassessed in the context of the contemporary situation.

Although many examples might be mentioned, building codes are frequently cited as illustrations of this phenomenon. A local community may have adopted standards and specifications for plumbing installations fifty years ago when cast-iron, threaded pipe was the only reliable system. Subsequently, copper tubing with soldered joints for water service and polyethylene or polypropylene plastic pipe for waste drains were developed and now offer more reliability as well as greater simplicity in installation. But the building code calling for cast-iron pipe remains virtually frozen, and only through lengthy and laborious processes is it modified and changed to take into account the advances in plumbing technology.

So it is in other regulatory areas, including drug quality monitoring and surveillance.

In particular, we were reminded of this situation when APhA Academy of Pharmaceutical Sciences former president George Schneller, speaking at the November meeting of the subdivision, addressed the subject of Food and Drug Administration routine batch certification of antibiotics.

Dr. Schneller labeled this federal requirement as *"obsolete and archaic, and increases the cost of these medicines to the public while contributing nothing to public safety or health."*

He further charged that it is an example of *"oppressive regulation which is a substantive cause of inflation."* To correct the matter, he recommended that the rule be deleted, and in its place "*. . . a much more rational and economical alternative would be to control the quality of antibiotic products by the same machinery as other drugs—namely, through the publication of appropriate tests and standards in the USP and through the FDA's regular enforcement activities directed to assuring compliance with those standards.*"

For our part, we completely agree with Dr. Schneller's views. In fact, we commented along this line [see *J. Am. Pharm. Assoc.*, NS2, p. 640 (Nov. 1962)] in the final days of enactment of the Kefauver–Harris Drug Amendments. That article argued the very same scientific points that Dr. Schneller just recently reiterated and reemphasized; namely, that when the initial antibiotic agents were first marketed in the 1940s, *"they were extremely crude concentrates of extractives from microbial culture media. Conventional methods of drug analysis were not applicable to them and would not assure a true measure of their potency.* [But subsequent] *rapid advances in the manufacturing processes of production, synthesis, and purification soon made it possible to produce these antibiotics as essentially pure, crystalline substances with a degree of purity comparable to other fine chemicals."*

The article went on to state that these advances in technology eliminated the original justification for batch certification of antibiotics; and, furthermore, the result made it illogical to treat antibiotics any differently than all other potent medicinal agents on the market.

However, as in the case of the long outdated local plumbing code which refuses to recognize or accept comparable improvements in the plumbing field, current federal drug regulation continues to prescribe testing requirements for antibiotics which Dr. Schneller has properly labeled as "obsolete and archaic."

The limited resources available to FDA in terms of both scientific personnel and test facilities could be put to much better use in many other areas of drug monitoring and surveillance.

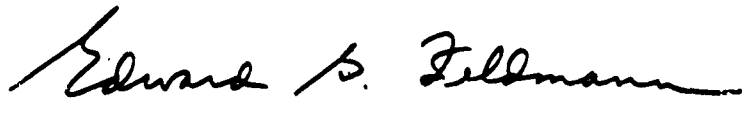

Call for Papers

In response to the suggestion of some of Professor T. O. Soine's former students and friends, as well as on the advice of the Editor of *J. Pharm. Sci.* concerning the publication of a group of papers in one issue in memory of Dr. Soine of Minnesota, we would like to set up the following guidelines:

1. All manuscripts submitted for this purpose should be addressed to:

Dr. Mary H. Ferguson, Editor
Journal of Pharmaceutical Sciences
2215 Constitution Avenue, N.W.
Washington, DC 20037

2. All papers should be indicated as "Dedicated to the memory of the late Professor Soine." This dedication should appear in the first footnote of the paper and be attached to the paper on a separate sheet.

3. The deadline for receipt of these papers is May 1, 1979.

Kuo-Hsiung Lee
Department of Medicinal Chemistry
School of Pharmacy
University of North Carolina
Chapel Hill, NC 27514

Received January 10, 1979.

Nondisintegration of a Capsule's Contents

A recent article in this Journal[1] forceably called my attention, again, to the fact that our pharmaceutical industry scientists have not yet developed a good capsule disintegrant. Or, if they have, it is a well-guarded secret, known only to a select few. In view of the public posture espoused by Eli Lilly and Co. in regard to the innate quality of all products from the top manufacturers, it is difficult for this writer to conceive that they would produce a capsule product (in this case, aspirin) that was an intentionally "slowed" or "timed" release product without claiming that they did so deliberately.

The reader is referred to Figs. 2–5 in the above-cited article. By four different methods, aspirin dissolved more slowly at a stirring rate of 75 rpm from the capsule formulation than from two readily available tablet formulations. It is clear that the authors were studying dissolution rate methodologies and not dosage forms *per se*. Their results, however, agree quite well in magnitude and direction with much earlier work[2] whose intention was to compare dissolution rate availability of tablets and capsules as dosage forms. Apparently, no one has paid much attention to Paikoff and Drumm[3] either since they reported that the contents of a capsule remained in a holder like a "sausage" after the gelatin shell was gone.

Once again, the challenge is expressed: capsule formulators need a good disintegrant, one as good as compressed starch in a tablet. The experimentor who develops one good enough (and cheap enough) will have created a "new" dosage form from a very old dosage form and should probably make a bundle.

Willis E. Moore
College of Pharmacy and Allied Health Professions
Wayne State University
Detroit, MI 48202

Received November 20, 1978.

[1] T. E. Needham, K. Shah, J. Kotzan, and H. Zia, *J. Pharm. Sci.*, **67**, 1070 (1978).
[2] P. T. Shah and W. E. Moore, *ibid.*, **59**, 1034 (1970).
[3] M. Paikoff and G. Drumm, *ibid.*, **54**, 1693 (1965).

FACULTY POSITION

Assistant Professor of Pharmacology. Ph.D. preferred but not essential. Undergraduate degree in pharmacy desirable. Primarily undergraduate teaching of pharmacology and biochemistry. University town of 14,000 on eastern edge of South Dakota.

Send resume to

Dean Raymond E. Hopponen
College of Pharmacy
South Dakota State University
Brookings, SD 57007

Affirmative Action/Equal Opportunity Employer

Development Pharmacist

The Upjohn Company's Veterinary Pharmacy area has an opening for a pharmacist to carry out research and development of various dosage forms intended for use in animal health. This job encompasses development of sterile parenterals, oral liquids and various solid dosage forms. Candidates should have a BS or MS in pharmacy.

Kalamazoo is a medium sized midwestern community offering an excellent mix of cultural/recreational pursuits. Comprehensive benefits and relocation programs. Submit resume in confidence to:

Upjohn

Myra W. Johnson
The Upjohn Company
7171 Portage Road
Kalamazoo, MI 49001

An Equal Opportunity Employer M/F

University of Georgia School of Pharmacy

Faculty Position in Pharmaceutics/Biopharmaceutics

Applicants are invited to apply for a full-time (12 months) faculty position at the Assistant Professor or Associate Professor level in the Department of Pharmacy of the University of Georgia School of Pharmacy. The starting date is flexible. Applicants should possess a B.S. degree in Pharmacy and a Ph.D. degree in Pharmaceutics and must be qualified to teach undergraduate and graduate courses in dosage form technology, biopharmaceutics and physical pharmacy. A strong background in analytical chemistry is desirable. The successful applicant is expected to participate in the graduate program and develop independent research programs. The salary is competitive and will be commensurate with qualifications and experience. The closing date for application is March 1, 1979, or until a suitable candidate is selected.

Interested candidates should send a letter of application accompanied by a curriculum vita and the names of three references to: **D. E. Cadwallader, Ph.D., Head, Department of Pharmacy, School of Pharmacy, University of Georgia, Athens, Georgia 30602.**

The University of Georgia is an equal opportunity affirmative action employer.

FACULTY POSITION IN PHARMACEUTICS/INDUSTRIAL PHARMACY

Due to retirement, a faculty vacancy on a tenure track will exist in September, 1979. In addition to participation in teaching the course sequence in pharmaceutics, the successful applicant will develop and teach elective courses in industrial pharmacy.

Located in a modern, air conditioned building constructed in 1972, the well equipped manufacturing laboratories, adjacent to the nuclear pharmacy and a sterile products laboratory, offer excellent potential for research activity.

The 1978 Fall enrollment in the School of Pharmacy is about 450 students in the last three years of a 2-3 program.

Ferris State College, with an enrollment of over 10,000 students, is situated on a relatively new campus, 55 miles north of Grand Rapids (Michigan's second largest city) and 40 miles south of Michigan's winter and summer resort and lake areas.

The candidate must have a Ph.D. with a major in pharmaceutics or related area and preferably be a registered pharmacist. Rank and salary are open and will be determined by educational background and experience.

Applicants should submit a letter of application and resume to: **Dean Ian W. Mathison, Ph.D., School of Pharmacy, Ferris State College, Big Rapids, Michigan 49307 (616) 796-2641, Ext. 3300.**

Equal Opportunity/Affirmative Action Employer

Call for Papers

In response to the suggestion of some of Professor T. O. Soine's former students and friends, as well as on the advice of the Editor of *J. Pharm. Sci.* concerning the publication of a group of papers in one issue in memory of Dr. Soine of Minnesota, we would like to set up the following guidelines:

1. All manuscripts submitted for this purpose should be addressed to:

Dr. Mary H. Ferguson, Editor
Journal of Pharmaceutical Sciences
2215 Constitution Avenue, N.W.
Washington, DC 20037

2. All papers should be indicated as "Dedicated to the memory of the late Professor Soine." This dedication should appear in the first footnote of the paper and be attached to the paper on a separate sheet.

3. The deadline for receipt of these papers is May 1, 1979.

Kuo-Hsiung Lee
Department of Medicinal Chemistry
School of Pharmacy
University of North Carolina
Chapel Hill, NC 27514

Received January 10, 1979.

Nondisintegration of a Capsule's Contents

A recent article in this Journal[1] forceably called my attention, again, to the fact that our pharmaceutical industry scientists have not yet developed a good capsule disintegrant. Or, if they have, it is a well-guarded secret, known only to a select few. In view of the public posture espoused by Eli Lilly and Co. in regard to the innate quality of all products from the top manufacturers, it is difficult for this writer to conceive that they would produce a capsule product (in this case, aspirin) that was an intentionally "slowed" or "timed" release product without claiming that they did so deliberately.

The reader is referred to Figs. 2–5 in the above-cited article. By four different methods, aspirin dissolved more slowly at a stirring rate of 75 rpm from the capsule formulation than from two readily available tablet formulations. It is clear that the authors were studying dissolution rate methodologies and not dosage forms *per se*. Their results, however, agree quite well in magnitude and direction with much earlier work[2] whose intention was to compare dissolution rate availability of tablets and capsules as dosage forms. Apparently, no one has paid much attention to Paikoff and Drumm[3] either since they reported that the contents of a capsule remained in a holder like a "sausage" after the gelatin shell was gone.

Once again, the challenge is expressed: capsule formulators need a good disintegrant, one as good as compressed starch in a tablet. The experimentor who develops one good enough (and cheap enough) will have created a "new" dosage form from a very old dosage form and should probably make a bundle.

Willis E. Moore
College of Pharmacy and Allied Health Professions
Wayne State University
Detroit, MI 48202

Received November 20, 1978.

[1] T. E. Needham, K. Shah, J. Kotzan, and H. Zia, *J. Pharm. Sci.*, **67**, 1070 (1978).
[2] P. T. Shah and W. E. Moore, *ibid.*, **59**, 1034 (1970).
[3] M. Paikoff and G. Drumm, *ibid.*, **54**, 1693 (1965).

FACULTY POSITION

Assistant Professor of Pharmacology. Ph.D. preferred but not essential. Undergraduate degree in pharmacy desirable. Primarily undergraduate teaching of pharmacology and biochemistry. University town of 14,000 on eastern edge of South Dakota.

Send resume to

Dean Raymond E. Hopponen
College of Pharmacy
South Dakota State University
Brookings, SD 57007

Affirmative Action/Equal Opportunity Employer

Development Pharmacist

The Upjohn Company's Veterinary Pharmacy area has an opening for a pharmacist to carry out research and development of various dosage forms intended for use in animal health. This job encompasses development of sterile parenterals, oral liquids and various solid dosage forms. Candidates should have a BS or MS in pharmacy.

Kalamazoo is a medium sized midwestern community offering an excellent mix of cultural/recreational pursuits. Comprehensive benefits and relocation programs. Submit resume in confidence to:

Upjohn

Myra W. Johnson
The Upjohn Company
7171 Portage Road
Kalamazoo, MI 49001

An Equal Opportunity Employer M/F

University of Georgia School of Pharmacy

Faculty Position in Pharmaceutics/Biopharmaceutics

Applicants are invited to apply for a full-time (12 months) faculty position at the Assistant Professor or Associate Professor level in the Department of Pharmacy of the University of Georgia School of Pharmacy. The starting date is flexible. Applicants should possess a B.S. degree in Pharmacy and a Ph.D. degree in Pharmaceutics and must be qualified to teach undergraduate and graduate courses in dosage form technology, biopharmaceutics and physical pharmacy. A strong background in analytical chemistry is desirable. The successful applicant is expected to participate in the graduate program and develop independent research programs. The salary is competitive and will be commensurate with qualifications and experience. The closing date for application is March 1, 1979, or until a suitable candidate is selected.

Interested candidates should send a letter of application accompanied by a curriculum vita and the names of three references to: **D. E. Cadwallader, Ph.D., Head, Department of Pharmacy, School of Pharmacy, University of Georgia, Athens, Georgia 30602.**

The University of Georgia is an equal opportunity affirmative action employer.

FACULTY POSITION IN PHARMACEUTICS/INDUSTRIAL PHARMACY

Due to retirement, a faculty vacancy on a tenure track will exist in September, 1979. In addition to participation in teaching the course sequence in pharmaceutics, the successful applicant will develop and teach elective courses in industrial pharmacy.

Located in a modern, air conditioned building constructed in 1972, the well equipped manufacturing laboratories, adjacent to the nuclear pharmacy and a sterile products laboratory, offer excellent potential for research activity.

The 1978 Fall enrollment in the School of Pharmacy is about 450 students in the last three years of a 2-3 program.

Ferris State College, with an enrollment of over 10,000 students, is situated on a relatively new campus, 55 miles north of Grand Rapids (Michigan's second largest city) and 40 miles south of Michigan's winter and summer resort and lake areas.

The candidate must have a Ph.D. with a major in pharmaceutics or related area and preferably be a registered pharmacist. Rank and salary are open and will be determined by educational background and experience.

Applicants should submit a letter of application and resume to: **Dean Ian W. Mathison, Ph.D., School of Pharmacy, Ferris State College, Big Rapids, Michigan 49307 (616) 796-2641, Ext. 3300.**

Equal Opportunity/Affirmative Action Employer

JOURNAL OF PHARMACEUTICAL SCIENCES

FEBRUARY 1979
VOLUME 68 NUMBER 2

RESEARCH ARTICLES

Isolation and Identification of Morphine N-Oxide α- and β-Dihydromorphines, β- or γ-Isomorphine, and Hydroxylated Morphine as Morphine Metabolites in Several Mammalian Species

S. Y. YEH ˣ, H. A. KREBS, and C. W. GORODETZKY

Received April 17, 1978, from the *National Institute on Drug Abuse, Division of Research, Addiction Research Center, Lexington, KY 40583.* Accepted for publication July 10, 1978.

Abstract □ New morphine metabolites in the urine of guinea pigs, rats, rabbits, cats, monkeys, and humans were isolated with column chromatography, solvent extraction, and TLC and identified with TLC, GLC, and GLC–mass spectrometry. In addition to the known morphine metabolites, morphine N-oxide was isolated from the urine of guinea pigs, and α- and β-dihydromorphines were isolated or detected in the urine of guinea pigs, rats, and rabbits. Monohydroxymorphine was identified tentatively in the urine of guinea pigs, rats, rabbits, and cats. Dihydroxymorphine was identified tentatively in the urine of guinea pigs, rats, and, possibly, rabbits. Finally, β- or γ-isomorphine was identified tentatively in the urine of guinea pigs. The newly described morphine metabolites may be involved in some long lasting pharmacological effects of morphine.

Keyphrases □ Morphine—metabolites isolated and identified in various mammalian species □ Metabolites—of morphine, isolated and identified in various mammalian species □ Narcotic analgesics—morphine, metabolites isolated and identified in various mammalian species

Studies in various laboratory animals and in humans have shown that morphine is metabolized by the following pathways: (*a*) conjugation to give morphine 3-glucuronide, morphine 6-glucuronide, morphine 3,6-diglucuronide, and morphine 3-ethereal sulfate (1–9); (*b*) N-demethylation to yield normorphine, which is conjugated to yield normorphine 3-glucuronide and normorphine 6-glucuronide (6, 10–18); and (*c*) oxidation to form dihydromorphinone (6, 19).

Recently, a minor metabolite, tentatively identified as morphine-2,3-quinone, was reported in the urine of rats administered morphine and after incubation of morphine with rat brain homogenates (20). Also, 2-methoxymorphine was observed in rabbit liver homogenate incubated with morphine and [^{14}C-*methyl*]-S-adenosylmethionine (21). The formation of 2-methoxymorphine may have occurred through hydroxylation of morphine to form a catechol-like compound, which was further methylated. Although O-methylation of morphine to codeine was reported (22, 23), this metabolic pathway was not confirmed (24, 25).

The present paper reports the isolation and identification of free and conjugated morphine N-oxide, free and conjugated α- and β-dihydromorphines[1], and, tentatively, β/γ-isomorphine[1], monohydroxymorphine, and dihydroxymorphine.

EXPERIMENTAL

Drugs—Morphine sulfate, dihydromorphinone hydrochloride, and normorphine hydrochloride were obtained commercially. α-Isomorphine, α-dihydromorphine, and β-dihydromorphine were synthesized as described previously (26). Morphine N-oxide was synthesized according to the procedure of Freund and Speyer (27). [^{14}C-*N-Methyl*]morphine, synthesized according to the procedure of Anderson and Woods (28), had a specific activity of 4 μCi/mg. The purity of the labeled drug was determined with instant TLC impregnated with silica gel[2].

Morphine 3-glucuronide, morphine 6-glucuronide, morphine 3-ethereal sulfate, and normorphine 6-glucuronide were isolated from the urine of humans, dogs, and cats administered morphine (3, 6, 9). Normorphine 3-glucuronide was isolated from the urine of dogs administered normorphine (18). Dihydromorphinone 3-glucuronide and dihydromorphine 3-glucuronide were isolated from the urine of animals administered dihydromorphinone and dihydromorphine, respectively[3]. The characteristics of dihydromorphinone 3-glucuronide and dihydromorphine 3-glucuronide were identical with those reported previously (29).

Animal Experiments—*Short-Term Morphine Administration*—

[1] The alcoholic hydroxyl groups of α- and β-dihydromorphines are at the C-6 position but with different configurations. The hydroxyl groups of morphine and α-isomorphine are at the C-6 position with different configurations, and the double bond is at the C-7–8 position; the hydroxyl groups of β- and γ-isomorphines are at the C-8 position with different configurations, and the double bond is at the C-6–7 position.

[2] Gelman Instrument Co., Ann Arbor, Mich.

[3] Unpublished data.

0022-3549/79/0200-0133$01.00/0
© 1979, American Pharmaceutical Association

Morphine sulfate solution was administered as follows: (*a*) 20 mg/kg sc to two male and two female dogs (8–15 kg), (*b*) 10 mg/kg ip to two male and two female cats (2–4 kg) daily for 3 days, (*c*) 25 mg/kg ip to two New Zealand female and two male rabbits (1.2–3.6 kg) daily for 3 days, (*d*) doses increasing from 12.5 to 50 mg/kg ip to four albino Wistar male rats (300–400 g) twice a day for 4 days, and (*e*) 25 mg/kg ip to five male guinea pigs (0.7–1.0 kg) daily for 28 days. On Days 0, 7, 14, 21, and 28, the same dose of [^{14}C-*N-methyl*]morphine (1 μCi/kg) was substituted for the regular dose of morphine and administered to the guinea pigs by the same route.

After drug administration, animals were individually housed in stainless steel metabolic cages. Urine was collected daily during the entire drug administration period and for 24 hr following the last dose and frozen until drug analysis. Food and water were given *ad libitum*.

Long-Term Morphine Administration—Urine samples were collected from animals and humans chronically administered morphine as follows: (*a*) three male and three female rhesus monkeys[4] (*Macaca mulata*) administered morphine sulfate, 4 mg/kg sc three times a day for at least 1 month; (*b*) two male and two female beagle dogs chronically infused with morphine sulfate for several months in doses up to 500–1000 mg iv/day; and (*c*) four healthy, male, former narcotic addict volunteers stabilized on morphine sulfate, 60 mg sc four times a day for 4 weeks (16).

After drug administration, animals were individually housed in stainless steel metabolic cages. Urine was collected for 24-hr periods and frozen until drug analysis. Food and water were given *ad libitum*. Urine from the human subjects was collected for 24-hr periods by the volunteers and refrigerated until analysis.

Extraction of Morphine and Its Metabolites—Samples with and without hydrolysis were adjusted to pH ~10, buffered with 2 ml of 40% K_2HPO_4, salted, and extracted with 15 ml of 1,2-dichloroethane (glass distilled) containing 30% 2-propanol according to the procedure described by Yeh (16). For determination of morphine *N*-oxide, samples were extracted twice with 10 ml of 1,2-dichloroethane containing 50% 2-propanol (30). After evaporation of the extracts to dryness, the residues were used for TLC, GLC, and GLC–mass spectral identification. The extracts were derivatized with *N*-trimethylsilylimidazole in pyridine[5] in a sealed tube at 90° for 1 hr (16) for GLC and GLC–mass spectral identification.

Hydrolysis of Conjugated Metabolites—Acid hydrolysis and enzymatic hydrolysis of the urine and the isolated metabolites were performed as described previously (16).

Glucuronide and Free Phenol Tests—The glucuronide test was performed according to the procedure of Dische (31). Free phenol was determined by a modified procedure of Volterra (32) with the reagents of Folin and Ciocalteu. (One-tenth of the stated volume of samples and reagents was used.)

TLC—TLC fiber sheets impregnated with silica gel or glass plates precoated with silica gel and an absorbent area[6] were used. The chromatograms were developed either with 1-butanol–acetic acid–water (35:3:10) (Solvent A) or ethyl acetate–methanol–ammonium hydroxide (17:2:1) (Solvent B) and visualized after spraying with iodoplatinate.

In experiments with radioisotopes, TLC sheets were scanned for radioactive spots by cutting the chromatogram into 1-cm strips. These strips were then placed in counting vials, moistened with 0.5 ml of methanol–water (1:1), and evaluated in a liquid scintillation spectrometer[7] after addition of 10 ml of Bray's solution[8].

GLC—A gas chromatograph[9] was equipped with a 0.9-m × 2-mm glass column packed with 3% OV-17 coated on 60–80-mesh Gas Chrom Q. The temperatures of the injector, column, and detector were 255, 220, and 295°, respectively; gas flow rates were 30 ml/min for nitrogen and hydrogen and 300–400 ml/min for dried compressed air.

GLC–Mass Spectrometry—Chemical-ionization mass spectral data were obtained on a gas chromatograph–mass spectrometer[10] equipped with an interactive data system[11] and a 0.9-m × 2-mm glass column packed with 3% OV-17 coated on 60–80-mesh Gas Chrom Q. The temperatures of the injector, column, and ion source were 230, 210, and 100°, respectively. The gas chromatograph was coupled to the mass spectrometer by a 0.31-cm glass-lined stainless steel tube and venting valve.

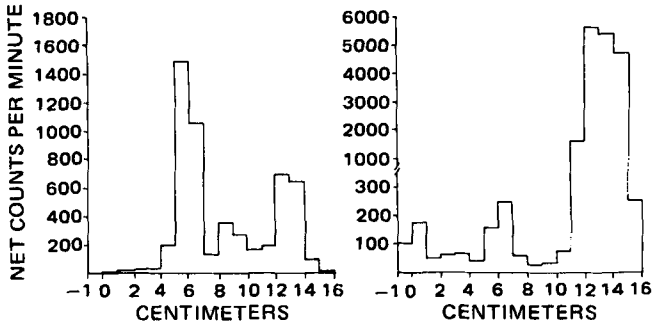

Figure 1—*Radiochromatograms of the organic phase (right panel) showing three spots with* R_f *0.1, 0.4 (as Fraction A), and 0.85 and of the aqueous phase (left panel) showing three spots with* R_f *0.35 (as Fraction M), 0.6 (as Fraction N), and 0.85 (as Fraction O).*

Methane, with a flow rate giving an ion chamber pressure of about 1000 μm, was used as the carrier gas as well as the chemical-ionization reagent gas in the ion source. The electron energy was 80 ev, and the ion repeller voltage was 3 v. Aliquots of 3–5 μl of the silylated sample were injected. After injection, the venting valve was opened for the first 30 sec, allowing excess derivatizing reagent and solvent to escape without entering the ionization chamber.

The obvious GLC peaks were analyzed by examining the mass fragment pattern. In addition, the whole chromatogram was scanned for predicted possible morphine metabolite ions (as silyl derivatives) such as normorphine (*m/e* 416), dihydromorphine (*m/e* 432), monohydroxymorphine (*m/e* 518), dihydroxymorphine (*m/e* 606 and 534) (if one of the four hydroxyl groups was not silanized), codeine (*m/e* 372), norcodeine (*m/e* 358), morphine-2,3-quinone (*m/e* 372), 2-methoxymorphine, and hydroxycodeine (*m/e* 460).

Isolation of Morphine Metabolites in Urine—The 24-hr urine was pooled for animals of the same species receiving the same drug dose. Each 100 ml of the pooled urine was centrifuged to remove the insoluble substances and passed with a flow rate of 2–4 ml/min through a resin[12] column (2.1 × 40 cm) previously washed with methanol and water. The column was washed with 150 ml of distilled water and eluted with 300 ml of methanol containing 2.5% NH_4OH. The effluent was collected in 20-ml tubes.

In experiments with labeled morphine, radioactivity in the urine and the effluent was monitored by counting a 0.5-ml aliquot of each tube with 10 ml of scintillation solution in a liquid scintillation spectrometer. In experiments with nonlabeled drug, morphine and its metabolites in the effluent were monitored with TLC. The methanol eluate, which contained radioactivity or iodoplatinate positive spots, was recombined and evaporated to a syrupy residue with a rotary evaporator under reduced pressure in a water bath at ~50°. (All evaporations were done in this way.) The residue was suspended in 5 ml of 5% NH_4OH solution and extracted three times with 1,2-dichloroethane containing 30% 2-propanol to yield organic and aqueous phases. Several batches of urine were thus processed, and the organic and aqueous phases were pooled for subsequent purification.

The organic phase was evaporated to dryness, and the residue was dissolved in methanol. An aliquot of the methanol solution was chromatographed on instant TLC sheets impregnated with silica gel. The chromatogram was developed with Solvent B and showed three iodoplatinate positive and radioactive spots, R_f 0.0, 0.4, and 0.9 (Fig. 1). A large volume of the methanol solution was chromatographed on large instant TLC sheets impregnated with silica gel (20 × 20 cm). The whole chromatogram was horizontally cut into three sections according to the zones corresponding to R_f 0.0–0.3, 0.3–0.6, and 0.6–1.0.

The substances located in the zone corresponding to 0.0–0.3 were eluted with water; in the zones of 0.3–0.6 and 0.6–1.0, the substances were eluted with methanol. The eluate obtained from the R_f 0.3–0.6 region was marked as Fraction A. The eluate obtained from the R_f 0.0–0.3 region was rechromatographed on instant TLC sheets impregnated with silica gel and developed with Solvent A. The chromatogram showed two spots, R_f 0.35 and 0.85, which were eluted with aqueous methanol and methanol,

[4] Courtesy of Dr. L. S. Harris, Department of Pharmacology, Medical College of Virginia, Richmond, Va.

[5] Tri-Sil-Z, Pierce Chemical Co., Rockford, Ill.

[6] Quantum Industries, Fairfield, N.J.

[7] Mark III, model 6880, Searle Analytic Inc., Des Plaines, Ill.

[8] Composed of naphthalene, 60 g; 2,5-diphenyloxazole, 4 g; 1,4-bis[2-(5-phenyloxazolyl)]benzene, 200 mg; methanol, 100 ml; ethylene glycol, 20 ml; and *p*-dioxane, *q.s.* to 1 liter.

[9] Model 2700, Varian Aerograph, Walnut Creek, Calif.

[10] Model 3300, Finnigan, Sunnyvale, Calif.

[11] Model 6000, Finnigan, Sunnyvale, Calif.

[12] Amberlite, XAD-2 resin, a styrene–divinylbenzene copolymer, Rohm & Haas Chemical Co., Philadelphia, Pa.

Table I—TLC, GLC, and Chemical-Ionization GLC–Mass Spectral Characteristics of Authentic Standards of Potential Morphine Metabolites

Authentic Standard	Instant TLC R_f, Solvent A	Instant TLC R_f, Solvent B	TLC R_f, Solvent B	Phenol Test	Glucuronide Test	As Trimethylsilyl Derivative: GLC R_T, min	GLC–Mass Spectrometry, m/e: $(M-15)^+$	$(M+1)^+$	$(M+29)^+$
Morphine	0.85	0.9	0.4	+	−	5.6	414	430	458
α-Isomorphine	0.85	0.9	0.4	+	−	4.1	414	430	458
Morphine *N*-oxide	0.8	0.4	0	+	−	5.6	414	430	458
Normorphine	0.7	0.8	0.2	+	−	6.8	400	416	444
Dihydromorphinone	0.9	0.9	0.4	+	−	5.6	414	430	458
α-Dihydromorphine	0.8	0.9	0.3	+	−	3.4	416	432	460
β-Dihydromorphine	0.8	0.9	0.3	+	−	3.9	416	432	460
Morphine 3-glucuronide	0.35	0	0	−	+				
Morphine 6-glucuronide	0.5	0	0	+	+				
Morphine 3,6-diglucuronide	0	0	0	−	+				
Morphine 3-ethereal sulfate	0.6	0.4	0	−	−	5.6	414	430	458
Dihydromorphinone 3-glucuronide	0.4	0	0	−	+				
Dihydromorphine 3-glucuronide	0.3	0	0	−	+				
Normorphine 3-glucuronide	0.3	0	0	−	+				
Normorphine 6-glucuronide	0.6	0	0	+	+				
β- and/or γ-Isomorphine[a]				+	−		414	430	458
Monohydroxymorphine[a]				+	−		502	518	546
Dihydroxymorphine[a]							590	606	634

[a] The chemistry and mass spectral data for these compounds are proposed in the absence of authentic standards.

respectively, to yield Fractions B and C. The eluate obtained from the R_f 0.6–1.0 region was rechromatographed on TLC plates, and the chromatogram was developed with Solvent B. The regions corresponding to R_f 0.1–0.3, 0.3–0.5, and 0.5–1.0 were eluted separately with methanol to yield Fractions D, E, and F, respectively.

An aliquot of the aqueous phase was chromatographed on an instant TLC plate impregnated with silica gel. The chromatogram was developed with Solvent A and showed three spots, R_f 0.35, 0.6, and 0.85, corresponding to morphine 3-glucuronide, morphine 6-glucuronide, and free base drugs (morphine, dihydromorphine, and β/γ-isomorphine), respectively (Fig. 1). The aqueous phase, after solvent extraction, was evaporated to a syrupy residue. The residue was triturated with methanol to yield methanol-soluble and methanol-insoluble fractions. The methanol-insoluble fraction was marked as Fraction G. This process was repeated several times to obtain the maximum yield of methanol-insoluble metabolites.

The methanol-soluble fraction was purified by adsorption on 10 g of neutral alumina and added onto a 50-g neutral alumina column (2.5 × 15 cm). The column was eluted with 100 ml of methanol and then with 100 ml each of methanol–water in ratios of 75:25, 50:50, and 25:75. Finally, it was eluted with 500 ml of water, and the effluent was collected in 20-ml tubes. Each tube was monitored for radioactivity in radioisotope experiments (by liquid scintillation spectrometry) or by iodoplatinate positive spots in nonradioactive experiments (shown by TLC). Iodoplatinate positive substances or radioactivity appeared in tubes 8–11 and 24–44. The eluates in these tubes were pooled separately and concentrated. The eluates from tubes 8–11 were purified further on TLC plates developed with Solvent B, as already described, to yield Fractions H–K.

The eluates from tubes 24–44 were evaporated to dryness, and the residue was triturated with methanol to yield methanol-soluble and methanol-insoluble metabolites. The methanol-insoluble metabolites were combined with Fraction G for identification. The methanol-soluble fraction was streaked on large instant TLC sheets, impregnated with silica gel, and developed with Solvent A. The chromatogram showed four spots. The regions corresponded to R_f 0.0–0.1, 0.2–0.5, 0.5–0.7, and 0.7–1.0 and were eluted with water–methanol to yield Fractions L, M, N, and O, respectively.

RESULTS

Identification of Morphine Metabolites in Urine of Guinea Pigs—Approximately 60–70% of the radioactivity present in the urine was recovered in the methanol eluate; 6–10% was recovered in the effluent, including the water washing. The results of glucuronide and free phenol tests and TLC, GLC, and GLC–mass spectral characteristics of authentic standards and of each fraction are presented in Tables I and II.

Identification of Morphine N-*Oxide*—The metabolite isolated in Fraction A was positive in the free phenol test and negative in the glucuronide test and showed the same TLC (Fig. 1), GLC, and GLC–mass spectral characteristics as authentic morphine *N*-oxide. The UV spectrum of this metabolite in alkaline solution showed a bathochromic shift. Furthermore, the metabolite was reduced with sodium bisulfite or titanous chloride to yield morphine (identified by TLC). Based on this evidence, the metabolite was identified as morphine *N*-oxide.

For quantitative estimation of morphine *N*-oxide, the chromatogram was cut into 1-cm strips, and the radioactivity of each strip was measured with liquid scintillation spectrometry after addition of 10 ml of scintillation solution. The amount of morphine *N*-oxide was 2% of the amount of free morphine.

Identification of Free α- and β-Dihydromorphines and β- or γ-Isomorphine—The metabolite isolated in Fraction D was positive in the phenol test. The gas chromatogram showed four peaks (Fig. 2), three of which (peaks 2–4) corresponded in retention times to α- and β-dihydromorphines and morphine, respectively. The mass spectra of peaks 2 (spectrum No. 58) and 3 (No. 65) showed mass ions of 342, 416, 432, and 460, characteristic of dihydromorphine (Fig. 3); peak 4 (No. 96) showed mass ions 340, 414, 430, and 458, characteristic of morphine.

The mass ion of 518, corresponding to the m + 1 ion of monohydroxymorphine, was also seen in the spectrum of peak 4. This compound would be expected to yield a fragment ion of 428 after elimination of one molecule of $(CH_3)_3SiOH$. A small 428 fragment ion was seen in the spectrum of peak 4; however, it could be an isotope mass of the 430 fragment. This peak may be a mixture of morphine and monohydroxymorphine. It is also possible that the morphine may have been a decomposition product of monohydroxymorphine.

The spectrum of peak 1 (No. 48) showed mass ions of 340, 414, 430, and

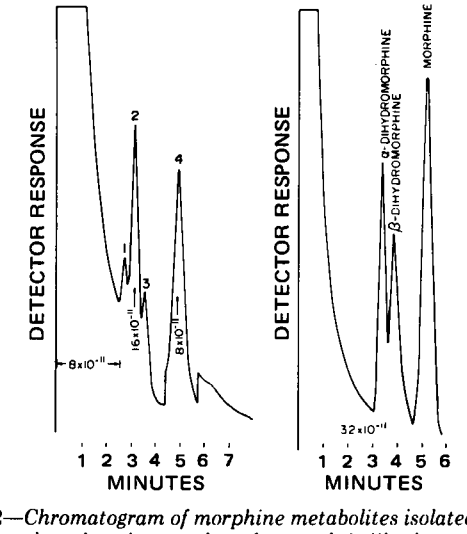

Figure 2—*Chromatogram of morphine metabolites isolated in Fraction D (left) and authentic samples of α- and β-dihydromorphines and morphine (right).*

Table II—TLC, GLC, and Chemical-Ionization GLC–Mass Spectral Characteristics of Morphine Metabolites Isolated from the Urine of Guinea Pig

Isolated Sample	Instant TLC R_f Solvent A	Instant TLC R_f Solvent B	TLC R_f, Solvent B	Phenol Test	Glucuronide Test	As Trimethylsilyl Derivative: GLC R_T, min	GLC–Mass Spectrometry, m/e $(M-15)^+$	$(M+1)^+$	$(M+29)^+$	Identified as
Fraction A	0.85	0.4	0.03	+	−	5.6	414	430	458	Morphine *N*-oxide
Fraction B	0.35	0	0	−	+					Morphine 3-glucuronide
Hydrolyzed B	0.85	0.9	0.4	+	−	5.6	414	430	458	
Fraction C	0.85	0.9	0.4	+	−	5.6	414	430	458	Morphine
Fraction D	0.8	0.8	0.2	+	−	3.0	414	430	458	β-/γ-Isomorphine
						3.4	416	432	460	α-Dihydromorphine
						3.9	416	432	460	β-Dihydromorphine
						5.6	414	430	458	Morphine
								518		Monohydroxymorphine
Fraction E	0.85	0.9	0.4	+	−	5.6	414	432	458	Morphine
Fraction F		0.6–1		+	−	7.1				
Fraction G	0.35	0	0	−	+					3-Glucuronides of:
Hydrolyzed G	0.85	0.9	0.4	+	−	3.0	414	430	458	β-/γ-Isomorphine
						3.4	416	432	460	α-Dihydromorphine
						3.9	416	432	460	β-Dihydromorphine
		0.4				5.6	414	430	458	Morphine, morphine *N*-oxide
		0.7				6.8	400	416	444	Normorphine
Fraction H	0.85	0.4		+	−	4.5				
Fraction I	0.85	0.6–1	0.2	+	−	3.4	416	432		α-Dihydromorphine
						5.6	414	430		Morphine
								518		Monohydroxymorphine
Fraction J	0.85	0.5–1	0.4	+	−	5.6	414	430		Morphine
Fraction K	0.85	0.6–1		+	−	7.1				
Fraction L	0	0	0	−	+					Morphine 3,6-diglucuronide
Hydrolyzed L	0.85	0.9	0.4	+	−	5.6	414	430	458	
Fraction M	0.35	0	0	−	+					3-Glucuronides of:
Hydrolyzed M	0.85	0.9	0.4	+	−	3.0	414	430	458	β-/γ-Isomorphine
		0.7				3.4	416	432	460	α-Dihydromorphine
		0.4				3.9	416	432	460	β-Dihydromorphine
		0.7				5.6	414	430	458	Morphine, morphine *N*-oxide
						6.8	400	416	444	Normorphine
Fraction N	0.6	0	0	+	+					6-Glucuronides of:
Hydrolyzed N	0.85	0.9	0.4	+	−	3.0	414	430		β-/γ-Isomorphine
		0.7				3.4	416	432	460	α-Dihydromorphine
						3.9	416	432		β-Dihydromorphine
						5.6	414	430	458	Morphine
Fraction O	0.85	0.9	0.4	+	−	5.6	414	430	458	Morphine

458, characteristic of morphine. Since the retention time of peak 1 (No. 48) differed from that of morphine and α-isomorphine, it was tentatively identified as β- or γ-isomorphine. Authentic standards of monohydroxymorphine, β-isomorphine, and γ-isomorphine were not available for comparison.

Identification of C-3 Glucuronides of Morphine N-Oxide, Morphine, α- and β-Dihydromorphines, β- or γ-Isomorphine, and Normorphine—The metabolites isolated in Fractions G and M appeared identical and were positive in the glucuronide test and negative in the phenol test. After acid or enzymatic hydrolysis with β-glucuronidase, they were positive in the phenol test. After acid hydrolysis, solvent extraction, and chromatography of Fraction M, the chromatogram on instant TLC sheets, impregnated with silica gel and developed with Solvent B, showed three spots, corresponding to morphine *N*-oxide (0.4); normorphine (0.8); and morphine, β/γ-isomorphine, and dihydromorphine (0.9). The gas chromatogram showed peaks with retention times and mass spectra consistent with α- and β-dihydromorphines, morphine, normorphine, and β- or γ-isomorphine. These results indicate that morphine was biotransformed to morphine *N*-oxide, α- and β-dihydromorphines, normorphine, and, possibly, β- or γ-isomorphine, which were conjugated as glucuronides at the C-3 position.

Identification of C-6 Glucuronides of Morphine and α-Dihydromorphine—The metabolite isolated in Fraction N was positive in the phenol and glucuronide tests, and its R_f value corresponded to morphine 6-glucuronide. After acid hydrolysis or enzymatic hydrolysis with β-glucuronidase, solvent extraction, and chromatography, the chromatogram on instant TLC sheets, impregnated with silica gel and developed with Solvent B, showed one spot, R_f 0.9 (morphine and dihydromorphine). The gas chromatogram showed two peaks with retention times and mass spectra corresponding to α-dihydromorphine and morphine. These results indicate that morphine was biotransformed to α-dihydromorphine 6-glucuronide and morphine 6-glucuronide.

Identification of Morphine 3,6-Diglucuronide—The metabolites isolated in Fraction L were positive in the glucuronide test and negative in the phenol test, and the R_f value was the same as morphine 3,6-diglucuronide previously isolated from human urine (6). The fraction was rechromatographed on instant TLC sheets impregnated with silica gel and developed with Solvent A; the chromatogram showed spots corresponding to morphine 3-glucuronide and morphine. This result may have been due to the instability of morphine 3,6-diglucuronide. A GLC peak was not observed in the fraction prior to hydrolysis. After hydrolysis, a GLC peak with retention time and mass spectra corresponding to morphine was observed.

Tentative Identification of Monohydroxy- and Dihydroxymorphines—A mass ion, *m/e* 518, consistent with the m + 1 ion of monohydroxymorphine was observed in the mass spectrum of the metabolite isolated in Fractions D (Fig. 3) and I (not shown) and the extract of acid-hydrolyzed urine. In addition to this ion, an ion consistent with the mass m + 1 ion of dihydroxymorphine, *m/e* 606, was observed in the extract of acid-hydrolyzed urine (Fig. 4). Masses of 518 and 606 appeared in the spectrum of the same peak. Monohydroxymorphine may be a decomposition product of dihydroxymorphine.

Identification of Morphine Metabolites in Urine of Rabbits—Morphine 3-glucuronide, morphine 6-glucuronide, free and conjugated normorphines, conjugated α- and β-dihydromorphines, dihydromorphinone, and morphine 3,6-diglucuronide were isolated and identified as morphine metabolites in the urine of rabbits administered morphine. Monohydroxymorphine was tentatively identified (Fig. 5).

Identification of Morphine Metabolites in Urine of Rats—Morphine 3-glucuronide, morphine 6-glucuronide, normorphine, dihydromorphinone, and α-dihydromorphine were identified as morphine metabolites in rats (Fig. 6). In addition to the ion of monohydroxymorphine, *m/e* 518, an ion consistent with the m + 1 ion of dihydroxymorphine, *m/e* 606, was observed. A mass of *m/e* 534 also was observed, which could have been due to silanization of only three of the four hydroxyl groups of dihydroxymorphine.

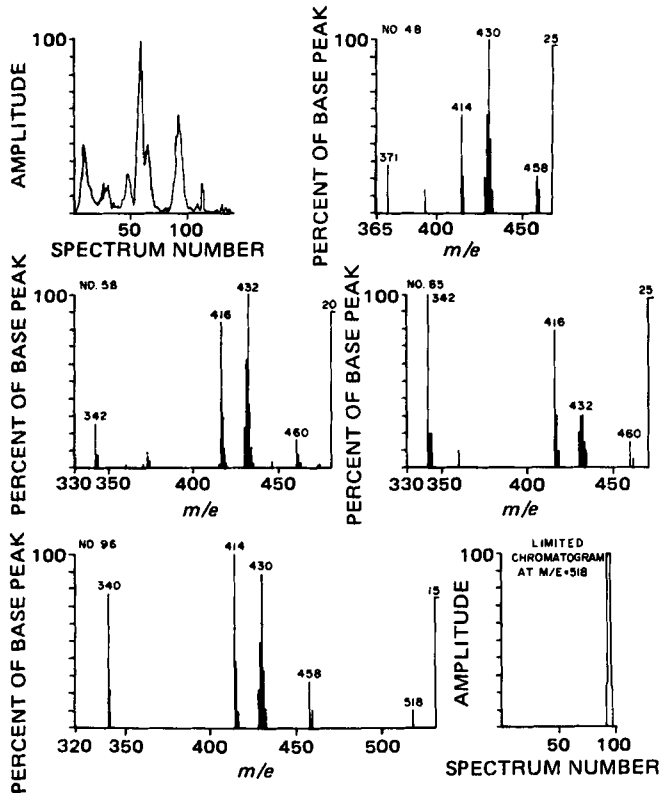

Figure 3—*Integrated total ion current and mass spectra of morphine metabolites isolated in Fraction D. Key: No. 48, β- or γ-isomorphine (tentative); No. 58, α-dihydromorphine; No. 65, β-dihydromorphine; and No. 96, monohydroxymorphine (tentative).*

Identification of Morphine Metabolites in Urine of Monkeys—Morphine 3-glucuronide, morphine 6-glucuronide, normorphine, and dihydromorphinone were identified as morphine metabolites in the urine of morphine-dependent monkeys.

Identification of Morphine Metabolites in Urine of Cats—Morphine 3-ethereal sulfate (a major metabolite), morphine 3-glucuronide, and normorphine were identified as morphine metabolites in the urine of cats (9). Monohydroxymorphine was tentatively identified (Fig. 7).

Identification of Morphine Metabolites in Urine of Dogs—The isolation and identification of morphine metabolites in the urine of dogs

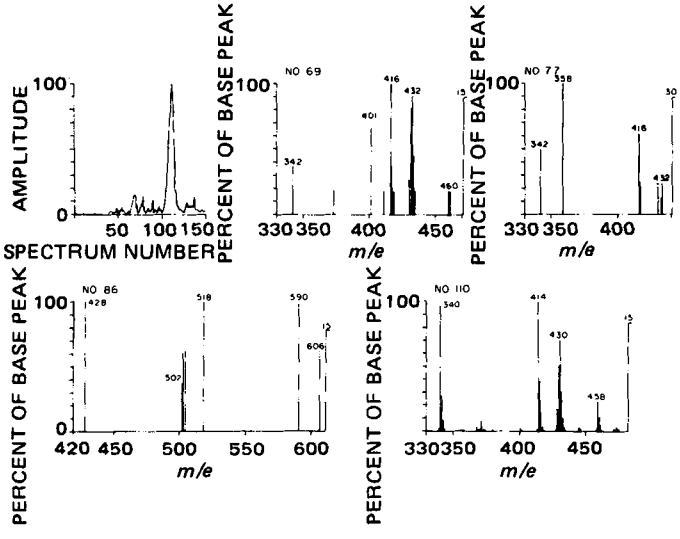

Figure 4—*Integrated total ion current chromatogram and mass spectra of acid-hydrolyzed urine of guinea pigs. Key: No. 69, α-dihydromorphine; No. 77, β-dihydromorphine; No. 86, dihydroxymorphine (tentative); and No. 110, morphine.*

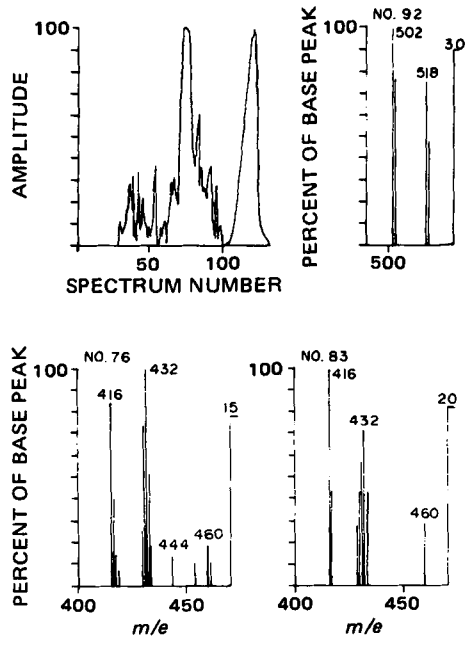

Figure 5—*Integrated total ion current chromatogram and mass spectra of the extract of acid-hydrolyzed urine of rabbits. Key: No. 76, α-dihydromorphine; No. 83, β-dihydromorphine; No. 92, monohydroxymorphine (tentative); and No. 120, morphine (not shown).*

were reported previously (4). In the present study, the extract of acid-hydrolyzed urine was derivatized and screened with GLC and GLC–mass spectrometry for the possible metabolites dihydromorphinone, dihydromorphine, monohydroxymorphine, and dihydroxymorphine. No evidence of these compounds was found.

Identification of Morphine Metabolites in Urine of Morphine-Dependent Humans—The details of a systematic isolation and identification of morphine metabolites in the urine of morphine-dependent subjects were reported previously (6). In the present study, the extract of acid-hydrolyzed urine was derivatized and screened for other possible metabolites. No evidence indicated the presence of dihydromorphine, monohydroxymorphine, dihydroxymorphine, and β- or γ-isomorphine. However, the urine was refrigerated for 3–4 years prior to analysis.

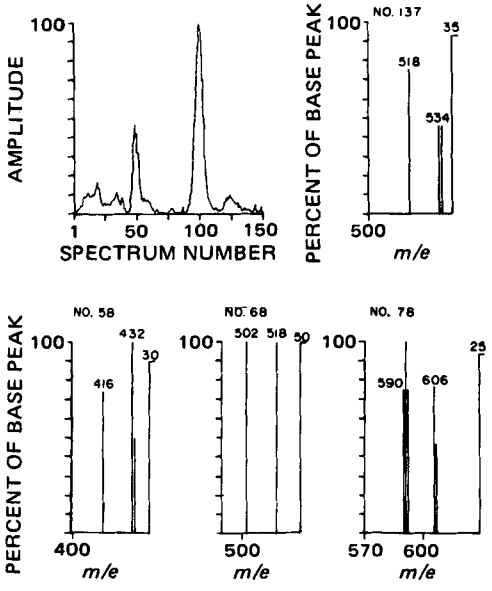

Figure 6—*Integrated total ion current chromatogram and mass spectra of the extract of acid-hydrolyzed urine of rats. Key: No. 58, α-dihydromorphine; No. 68, monohydroxymorphine (tentative); No. 78, dihydroxymorphine (tentative); No. 100, morphine (not shown); No. 125, normorphine (not shown); and No. 137, dihydroxymorphine (assuming only three hydroxyl groups were silanized) (tentative).*

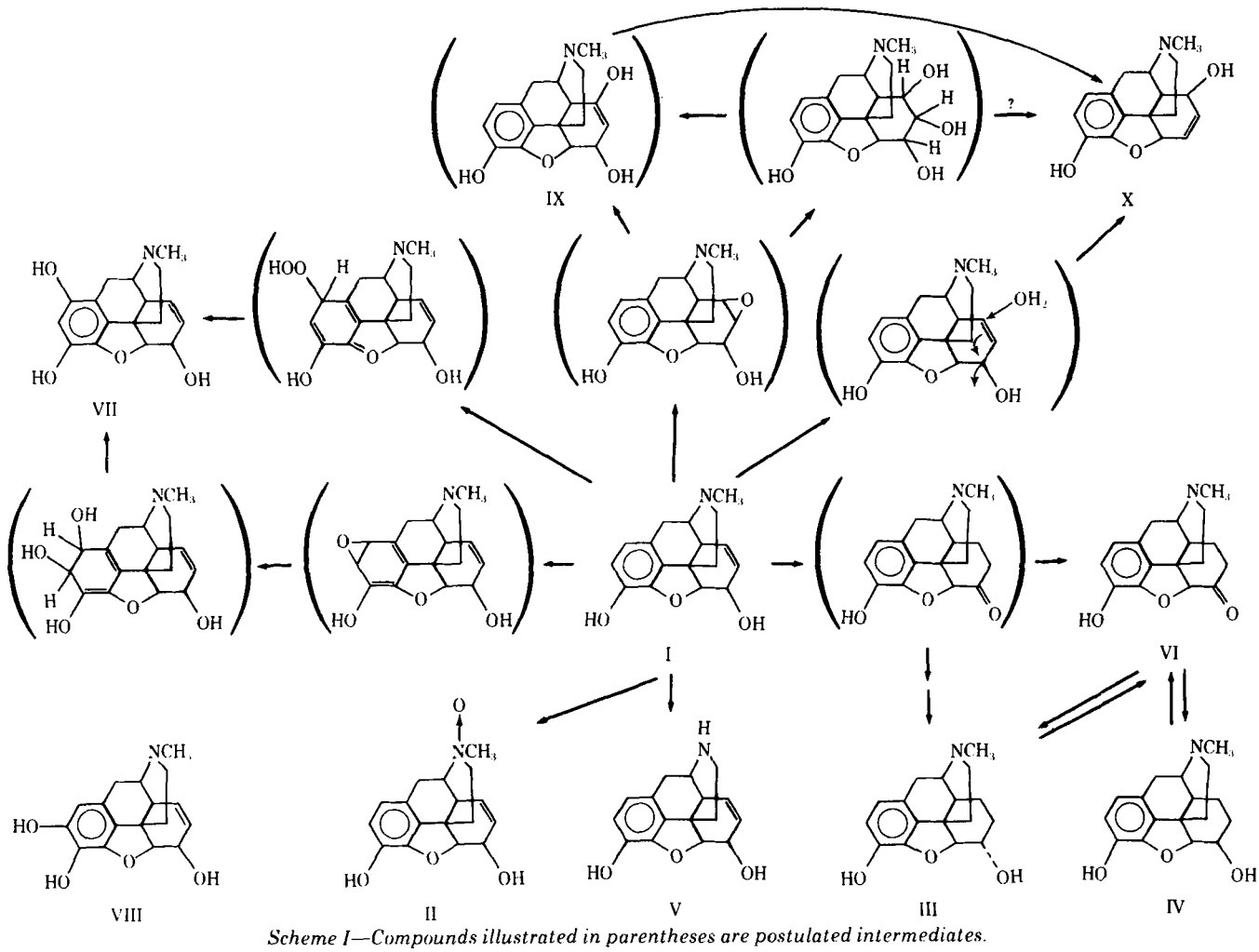

Scheme I—Compounds illustrated in parentheses are postulated intermediates.

DISCUSSION

Although direct evidence is lacking for some steps, it seems reasonable to suggest, based on the metabolism of other compounds, the pathway for the metabolism of morphine (I) shown in Scheme I. Morphine *N*-oxide (II), α-dihydromorphine (III), and β-dihydromorphine (IV), in addition to normorphine (V) and dihydromorphinone (VI), were isolated or detected in the urine. In addition, 1-hydroxymorphine (VII), 2-hydroxymorphine (VIII), 8-hydroxymorphine (IX), dihydroxymorphines, and β- or γ-isomorphine (X) were identified tentatively.

Biotransformation of Morphine to Morphine *N*-Oxide and Normorphine—*N*-Oxide formation, a product of oxidation of a tertiary amine catalyzed by amine oxidase, appears to be a minor metabolic pathway of narcotics. *N*-Oxides of narcotics have been isolated *in vitro* (33–41). The isolation and identification of morphine *N*-oxide in the urine of guinea pigs, therefore, was no surprise. However, it was not isolated and identified in the urine of the other species. Morphine *N*-oxide also might have formed in the body of other species but been reduced in the body or in the urine. Indeed, reduction of morphine *N*-oxide to morphine in rats (30) and of propoxyphene *N*-oxide to propoxyphene in dogs (42) was reported. Furthermore, morphine *N*-oxide may have been present in the urine of the other species at concentrations below the detectable limits of the methods used.

The amine oxidase is present in the liver of pigs, rats, and humans (33–35) and differs from *N*-demethylase. It has a pH optimum at 8.4 and catalyzes oxidation of tertiary amines to their *N*-oxides and secondary amines to hydroxyamines. The *N*-demethylase has a pH optimum at 7.4 and catalyzes oxidation of the *N*-methyl group to form an alcohol and then an aldehyde. The end-product of *N*-demethylation of morphine is normorphine. The factors affecting *N*-demethylase of morphine were discussed previously (16).

Biotransformation of Morphine to Dihydromorphinone and Dihydromorphine—The reduction of the 7,8-double bond of morphine appears similar to reactions occurring in steroid metabolism in the formation of 5α- and 5β-hydroxy metabolites of testosterone, progesterone, and corticoids (43–45). These enzymes do not appear to be substrate specific. Δ′-3-Keto steroids are readily reduced both *in vivo* (43) and *in vitro* (44, 45). Morphine would likely undergo a similar reaction.

Oxidoreductases (dehydrogenases) that reversibly oxidize secondary alcohols to ketones have been evaluated in the study of steroid hormone metabolism. These enzymes can utilize both di- and tripyridine nucleotides as cofactors and do not appear to be substrate specific. Biotransformation of morphine to dihydromorphinone was reported in several species (17, 19). Biotransformation of dihydromorphinone to dihydromorphine was observed in rabbits (29). The reduction of naloxone and naltrexone *in vitro* and *in vivo* to α- and β-naloxols and α- and β-naltrexols, respectively, also was reported (46–53).

Biotransformation of Morphine to Monohydroxy- and Dihydroxymorphines—Ions with a mass *m/e* 518 and 606 equal to the mass of monohydroxymorphine and dihydroxymorphine (as silyl derivatives)

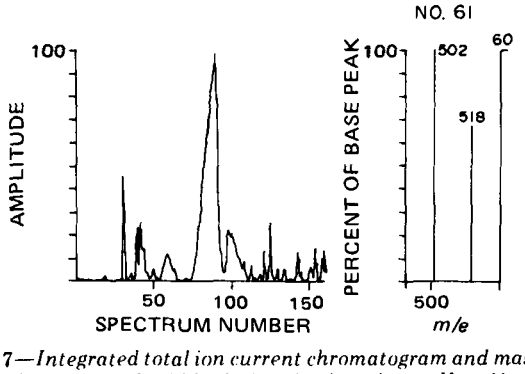

Figure 7—*Integrated total ion current chromatogram and mass spectrum of the extract of acid hydrolyzed urine of cats. Key: No. 61, monohydroxymorphine (tentative); No. 88, morphine (not shown); and No. 100, normorphine (not shown).*

Table III—Morphine Metabolites Identified in the Urine of Several Mammalian Species

Species	Morphine Metabolites[a]											
	XII	V	XIII	XIV	XV	VI[b]	III/IV	X[c]	II	VII/VIII/IX	*m/e* 534[c]	*m/e* 506[c]
Human[d]	+	+	+	+	+	−	−	−	−	−	−	
Guinea pig	+	+	+	−	+	+	+	+	+	+	−	−
Rat	+	+	+	−	±	+	+	−	−	+	+	+
Rabbit	+	+	+	−	±	+	+	−	−	+	+	−
Monkey	+	+	+	−	±	+	−	−	−	−	−	−
Cat	+	+	−	+	−	−	−	−	−	+	−	−
	Minor			Major								
Dog[e]	+	+	+	+		−	−	−	−	−		

[a] XII, morphine 3-glucuronide; V, normorphine; XIII, morphine 6-glucuronide; XIV, morphine 3-ethereal sulfate; XV, morphine 3,6-diglucuronide; VI, dihydromorphinone; III, α-dihydromorphine; IV, β-dihydromorphine; X, β- or γ-isomorphine; II, morphine *N*-oxide; and VII, VIII, and IX, 1-, 2-, and 8-hydroxymorphines, respectively. [b] From Ref. 17. [c] Identifications are tentative. [d] From Ref. 6. [e] From Ref. 4.

were not detected in the hydrolyzed control urine but were seen in the urine extract of some animals administered morphine. It is usual for the chemical-ionization (methane) spectrum of a substance, particularly drugs, to consist only of the m + 1 ion. These compounds were identified tentatively as metabolites of morphine. A paucity of these metabolites and a lack of authentic standards of monohydroxymorphine and dihydroxymorphine for comparison precluded further verification of their identity.

Studies of the metabolism of naloxone and naltrexone, morphine antagonists with structures similar to morphine, in humans and monkeys revealed compounds in the extract of hydrolyzed urine tentatively identified as methoxynaloxone and methoxynaltrexone (as silyl derivatives)[13,14]. In a later study[14], the structures were conclusively shown to be 2-methoxynaloxone and 2-methoxynaltrexone as compared with authentic samples. The formation of 2-methoxy derivatives of morphine, nalorphine, levorphanol, and phenazocine was observed in rabbit liver microsomes (21). The formation rate of the catechol-like compound appears to be correlated with the lipid solubility of the substrate. A similar biotransformation of morphine (*i.e.*, hydroxylation) might have occurred and resulted in the mass spectra detected in the extract of urine of some animals, as already noted.

Hydroxylation of morphine could be taking place in the aromatic as well as in the aliphatic ring. 2-Hydroxy-, 10-hydroxy-, and 14-hydroxymorphines, 14-hydroxydihydromorphine, 14-hydroxycodeine, and 14-hydroxycodeinone have been synthesized (55–59). The hydroxylation of the aromatic ring at position 1 could proceed either by the well-known epoxide pathway or by the hydroperoxide pathway, as in butylated hydroxytoluene metabolism (60). Since morphinedihydrodiol was not detected, the second pathway appears to be more attractive, although the epoxide pathway cannot be ignored. One hydroxyl group of dihydroxymorphine might be in the aromatic ring while the other one is in the aliphatic ring.

The tentatively identified monohydroxy- and dihydroxymorphines might be the end-products of morphine metabolism *via* an epoxide pathway. The epoxide can bind covalently to macromolecules, *e.g.*, receptor sites, protein, or other molecules and might be released slowly from the body. The possible metabolic intermediates or the reaction product between intermediates and a macromolecule or a degradation product of that adduct might be responsible for some long-term effects of morphine. Protracted abstinence observed in humans and animals (61–63), prolonged tolerance (64), and a decrease in growth rate of offspring of morphine-treated rats and mice (65–67) might be due to the intermediate metabolite(s) of morphine bound to the macromolecule.

Biotransformation of Morphine to β- or γ-Isomorphine—Two possible pathways could lead to the conversion of morphine to isomorphine: hydroxide-ion direct attack at the C-8 position or formation of morphine 7,8-epoxide. Attempts to synthesize morphine 7,8-epoxide by modifying the procedure of Craig and Purushothaman (68) and Kishi *et al.* (69) failed. TLC of the reaction product showed two spots. The R_f of the major spot corresponded to that of morphine *N*-oxide. A small peak with mass consistent with monohydroxymorphine, in addition to morphine, was observed in the reaction product. Possibly, the 7,8-epoxide is a transient intermediate and is converted to isomorphine spontaneously. Further *in vitro* studies are needed to verify these suggestions.

Glucuronides of Morphine, Morphine *N*-Oxide, Dihydromorphinone, and Dihydromorphine—Glucuronidation is a universal metabolic pathway for biotransformation of foreign compounds having a phenolic or alcoholic hydroxyl group. Conjugation of morphine, dihydromorphine, normorphine, and dihydromorphinone with glucuronic acid at the 3- and/or 6-positions has been reported. The finding of glucuronides of morphine *N*-oxide and α- and β-dihydromorphines in the present studies was expected. Chromatograms of the methanol effluent or the aqueous phase after solvent extraction of the methanol effluent (obtained from the urine of rats, rabbits, and monkeys) on instant TLC sheets, impregnated with silica gel and developed with Solvent A, showed a spot with R_f 0.0–0.1, corresponding to that of morphine 3,6-diglucuronide. No attempt was made to establish the identity of this fraction.

Ethereal Sulfate Conjugation of Morphine—The major metabolite of morphine in cats was morphine ethereal sulfate; morphine glucuronide was a minor metabolite. There is a deficiency of glucuronyl transferase in the cat, but this enzyme is present in major quantities in the other species.

SUMMARY

Morphine metabolites isolated or detected in the species studied are summarized in Table III. Normorphine, morphine 3-glucuronide, and morphine 6-glucuronide were found in humans, guinea pigs, rats, rabbits, monkeys, dogs, and cats. In cats, morphine 3-glucuronide was a minor metabolite and morphine 6-glucuronide was not observed. Morphine ethereal sulfate was observed in humans and cats. Dihydromorphinone was observed in guinea pigs, rats, rabbits, and monkeys. Both α- and β-dihydromorphines were observed in guinea pigs, rats, and rabbits.

Morphine *N*-oxide and β- or γ-isomorphine were observed in guinea pigs. Hydroxylated morphine was observed in guinea pigs, rats, rabbits, and cats. In these studies, the metabolism of morphine in guinea pigs was investigated more thoroughly than in the other species using radioactively labeled drug. The minor metabolites found in guinea pigs but not in other species might also be present in the urine of other species but not in a sufficient concentration to be detected by the methods used.

Codeine, norcodeine, methoxyhydroxymorphine (2-hydroxycodeine), and morphine-2,3-quinone were not detected.

REFERENCES

(1) L. A. Woods, *J. Pharmacol. Exp. Ther.*, **112**, 158 (1954).

(2) J. M. Fujimoto and E. L. Way, *ibid.*, **121**, 340 (1957).

(3) S. Y. Yeh and L. A. Woods, *ibid.*, **175**, 69 (1970).

(4) A. L. Misra, S. Y. Yeh, and L. A. Woods, *Biochem. Pharmacol.*, **19**, 1536 (1970).

(5) K. Oguir, S. Ida, and H. Yochimura, *Chem. Pharm. Bull.*, **18**, 2414 (1970).

(6) S. Y. Yeh, C. W. Gorodetzky, and H. A. Krebs, *J. Pharm. Sci.*, **66**, 1288 (1977).

(7) L. A. Woods and H. I. Chernov, *Pharmacologist*, **8**, 206 (1966).

(8) J. M. Fujimoto and V. B. Haarstad, *J. Pharmacol. Exp. Ther.*, **165**, 45 (1969).

(9) S. Y. Yeh, H. I. Chernov, and L. A. Woods, *J. Pharm. Sci.*, **60**, 469 (1971).

(10) H. W. Elliott, B. M. Tolbert, T. K. Alder, and H. H. Anderson, *Proc. Soc. Exp. Biol. Med.*, **85**, 77 (1954).

(11) J. Axelrod, *J. Pharmacol. Exp. Ther.*, **117**, 322 (1956).

(12) A. L. Misra, S. J. Mulé, and L. A. Woods, *ibid.*, **132**, 317 (1961).

(13) K. Milther, *Acta Pharmacol. Toxicol.*, **18**, 199 (1961).

(14) L. Tampier and A. Penna-Herreros, *Arch. Biol. Med. Exp.*, **3**, 146 (1966).

[13] Data reported in the report of Committee on Problems of Drug Dependence, 1975.

[14] E. J. Cone and C. W. Gorodetzky, personal communication.

(15) S. F. Brunk and M. Delle, *Clin. Pharmacol. Ther.*, **16**, 51 (1974).
(16) S. Y. Yeh, *J. Pharmacol. Exp. Ther.*, **192**, 201 (1975).
(17) S. Y. Yeh, R. L. McQuinn, and C. W. Gorodetzky, *Drug Metab. Dispos.*, **5**, 335 (1977).
(18) S. Y. Yeh, R. L. McQuinn, H. A. Krebs, and C. W. Gorodetzky, *J. Pharm. Sci.*, **67**, 878 (1978).
(19) A. Klutch, *Drug Metab. Dispos.*, **2**, 23 (1974).
(20) A. L. Misra, N. L. Vadlamani, R. B. Pontani, and S. J. Mulé, *Biochem. Pharmacol.*, **22**, 2129 (1973).
(21) J. Daly, J. K. Inscoe, and J. Axelrod, *J. Med. Chem.*, **8**, 1953 (1965).
(22) C. Elison and H. W. Elliott, *J. Pharmacol. Exp. Ther.*, **144**, 265 (1964).
(23) U. Börner and S. Abbott, *Experientia*, **29**, 180 (1973).
(24) S. Y. Yeh, *ibid.*, **30**, 264 (1974).
(25) L. S. Abrams and H. W. Elliott, *J. Pharmacol. Exp. Ther.*, **189**, 285 (1974).
(26) L. F. Small, N. B. Eddy, and E. Mosettig, in "Studies on Drug Addiction with Special Reference to Chemical Structure of Opium Derivatives and Allied Synthetic Substances and Their Physiological Action," Supplement No. 138 to Public Health Reports, U.S. Government Printing Office, Washington, D.C., 1938.
(27) M. Freund and E. Speyer, *Chem. Abstr.*, **5**, 702 (1911).
(28) K. S. Anderson and L. A. Woods, *J. Org. Chem.*, **24**, 274 (1959).
(29) S. Roerig, J. M. Fujimoto, and R. I. H. Wang, *Proc. Soc. Exp. Biol. Med.*, **143**, 230 (1973).
(30) A. L. Misra and C. L. Mitchell, *Biochem. Med.*, **5**, 379 (1971).
(31) Z. Dische, *J. Biol. Chem.*, **167**, 189 (1947).
(32) M. Volterra, *Am. J. Clin. Pathol.*, **12**, 525 (1942).
(33) D. M. Ziegler, C. H. Mitchell, and D. Jollow, in "Microsomes and Drug Oxidations," J. R. Gillette, A. H. Conney, G. J. Cosmides, R. W. Estabrook, J. R. Fouts, and G. J. Mannering, Eds., Academic, New York, N.Y., 1969, p. 173.
(34) M. L. Das and D. M. Ziegler, *Arch. Biochem. Biophys.*, **140**, 300 (1970).
(35) M. S. Gold and D. M. Ziegler, *Xenobiotica*, **3**, 179 (1973).
(36) J. T. C. Woo, G. A. Gaff, and M. R. Fennessy, *J. Pharm. Pharmacol.*, **20**, 763 (1968).
(37) A. H. Beckett, M. Mitchard, and A. A. Shihab, *ibid.*, **23**, 347 (1971).
(38) A. H. Beckett, D. P. Vaughan, and E. E. Essien, *ibid.*, **24**, 244 (1972).
(39) M. Mitchard, M. J. Kendall, and K. Chan, *ibid.*, **24**, 913 (1972).
(40) W. G. Stillwell, C. S. Myran, and J. T. Stewart, *Res. Commun. Chem. Pathol. Pharmacol.*, **14**, 603 (1976).
(41) J. D. Phillipson, S. S. Handa, and S. W. El-Dabbas, *Phytochemistry*, **15**, 1297 (1976).
(42) R. E. McMahon and H. R. Sullivan, *Xenobiotica*, **7**, 377 (1977).
(43) F. Unger and R. I. Dorfman, *Science*, **115**, 115 (1952).
(44) G. M. Tomkins, *J. Biol. Chem.*, **218**, 437 (1956).
(45) A. Vermeulen and E. Caspi, *ibid.*, **233**, 54 (1958).
(46) E. J. Cone, *Tetrahedron Lett.*, **28**, 2607 (1973).
(47) E. J. Cone, C. W. Gorodetzky, and S. Y. Yeh, *Drug Metab. Dispos.*, **2**, 506 (1974).
(48) E. J. Cone, C. W. Gorodetzky, and S. Y. Yeh, *J. Pharm. Sci.*, **64**, 618 (1975).
(49) N. Chatterjie, J. M. Fujimoto, C. E. Inturrisi, S. Roerig, R. I. H. Wang, D. V. Bowen, F. H. Field, and D. D. Clarke, *Drug Metab. Dispos.*, **2**, 401 (1974).
(50) L. Malspeis, M. S. Bathala, T. M. Ludden, H. B. Bhat, S. G. Frank, T. D. Sokoloski, B. E. Morrison, and R. H. Reuning, *Res. Commun. Chem. Pathol. Pharmacol.*, **12**, 43 (1975).
(51) L. Malspeis, T. M. Ludden, M. S. Bathala, B. E. Morrison, D. R. Feller, and R. H. Reuning, *ibid.*, **14**, 393 (1976).
(52) S. Roerig, J. M. Fujimoto, R. I. H. Wang, S. H. Pollock, and D. Lange, *Drug Metab. Dispos.*, **4**, 53 (1976).
(53) H. E. Dayton and C. E. Inturris, *ibid.*, **4**, 474 (1976).
(54) K. Verebey, M. A. Chedekel, S. J. Mulé, and D. Rosenthal, *Res. Commun. Chem. Pathol. Pharmacol.*, **12**, 67 (1975).
(55) H. Wieland and P. Kappemeier, *Ann.*, **382**, 306 (1911).
(56) H. Rapoport and S. Masamune, *J. Am. Chem. Soc.*, **77**, 6359 (1956).
(57) U. Weiss, *Chem. Abstr.*, **56**, 4810b (1962).
(58) U. Weiss and S. Daum, *J. Med. Chem.*, **8**, 123 (1965).
(59) I. Seki, *Takamine Kenkyusho Nempo*, **12**, 52 (1960); through *Chem. Abstr.*, **55**, 7458f (1961).
(60) C. Chen and Y. S. Shaw, *Biochem. J.*, **144**, 497 (1974).
(61) W. R. Martin, A. Wikler, C. G. Eades, and F. T. Pescor, *Psychopharmacologia*, **4**, 247 (1963).
(62) W. R. Martin and D. R. Jasinski, *J. Psychiatr. Res.*, **1**, 9 (1969).
(63) W. R. Martin, C. G. Eades, W. O. Thompson, J. A. Thompson, and H. G. Flanary, *J. Pharmacol. Exp. Ther.*, **189**, 759 (1974).
(64) J. Cochin and C. Kornetsky, *ibid.*, **145**, 1 (1964).
(65) G. Friedler and J. Cochin, *Pharmacologist*, **9**, 230 (1967).
(66) G. Friedler and J. Cochin, *Fed. Proc.*, **27**, 754 (1968).
(67) G. Friedler, *Pharmacologist*, **13**, 262 (1971).
(68) J. C. Craig and K. K. Purushothaman, *J. Org. Chem.*, **35**, 1721 (1970).
(69) Y. Kishi, M. Aratani, H. Tanino, T. Fukuyama, and T. Goto, *Chem. Commun. (J. Chem. Soc. D)*, **1972**, 64.

ACKNOWLEDGMENTS

The authors thank Dr. E. J. Cone of the National Institute on Drug Abuse and Professor Chiadao Chen of the Department of Biochemistry, Medical School, Northwestern University, Chicago, Ill., for helpful discussions.

A preliminary report of part of this work appeared in *Pharmacologist*, **18**, 178 (1976).

Kinetics of Absorption and Elimination of Pralidoxime Chloride in Dogs

EDWARD F. LEMANOWICZ *x, EDWIN T. SUGITA, PAUL J. NIEBERGALL ‡, and ROGER L. SCHNAARE

Received December 8, 1977, from the *Department of Pharmacy, Philadelphia College of Pharmacy and Science, Philadelphia, PA 19104.* Accepted for publication June 21, 1978. *Present address: McNeil Laboratories, Fort Washington, PA 19034. ‡Present address: Marion Laboratories, Kansas City, MO 64137.

Abstract □ The kinetics of the absorption and elimination of pralidoxime chloride were investigated in the dog. Similar apparent elimination rate constants were obtained after intravenous, intramuscular, and oral administration. Although oral absorption occurred slowly, intramuscular absorption proceeded rapidly. With *in situ* techniques, it was found that no absorption occurred from the isolated stomach and duodenum but that absorption did take place from the jejunum and ileum.

Keyphrases □ Pralidoxime chloride—absorption and elimination kinetics in dogs □ Absorption, GI—pralidoxime chloride, kinetics in dogs □ Elimination—pralidoxime chloride, kinetics in dogs □ Kinetics—absorption and elimination of pralidoxime chloride in dogs □ Cholinesterase reactivators—pralidoxime chloride, absorption and elimination kinetics in dogs

Most charged drugs are poorly absorbed after oral administration. However, quaternary ammonium compounds that are charged and have low lipid solubility undergo varied absorption. About 10% of a dose of tetraethylammonium chloride was absorbed at the end of 3 hr, using *in vivo* intestinal loops in dogs (1). The disappearance of 10–30% of a dose of a number of quaternary ammonium anticholinergics was found in the rat using isolated intestinal loops (2, 3). *N,N*-Bis(phenylcarbamoylmethyl)-dimethylammonium chloride, an antiarrhythmic agent, was poorly and erratically absorbed in rats (4) and humans (5). The bioavailability of thiazinamium methylsulfate after oral administration in humans is approximately 10% (6).

Levine and Steinberg (7) reported almost complete absorption of the methanesulfonate, phosphate, methochloride, and methiodide salts of pralidoxime in the rat. However, other investigators indicated that large doses of this drug were required to obtain significant plasma levels in humans (8–10).

To understand more fully the erratic absorption behavior of quaternary ammonium compounds, the complete absorption and elimination profile of pralidoxime chloride (2-[(hydroxyimino)methyl]-1-methylpyridinium chloride) was investigated in the dog. This drug is used clinically to reactivate cholinesterase in the therapy of organophosphate poisoning.

EXPERIMENTAL

Test Animals—Thirty-one male mongrel dogs, 8.6–11.4 kg, were permitted to adjust to the environment for at least 48 hr. Water was permitted *ad libitum*, and food was withheld for 24 hr prior to use.

Chemicals—Pralidoxime chloride[1] was used as received. All other chemicals were reagent grade.

Anesthesia—Pentobarbital sodium, given intravenously at a dosage of 30 mg/kg, was used as the anesthetic.

Blood Sampling—Venous blood sampling in anesthetized animals was accomplished with inside needle catheters[2].

The catheter was inserted in the femoral vein after anesthesia, and heparin sodium was then administered at a dosage of 1000 units/kg as an anticoagulant. Venous blood samples were collected in heparinized tubes[3]. In unanesthetized animals, samples were obtained by venipuncture.

Pralidoxime Assay—A previously described analytical technique, (11) was utilized to determine the pralidoxime content in biological fluids. Standard aqueous solutions containing 0.750–9.00 mg of pralidoxime/ml were prepared; to each 10.0-ml sample, 0.40 ml of 20% NaOH was added. The standard curve obeyed the Beer–Lambert law.

Intravenous Administration—The drug was dissolved in 10 ml of sterile water for injection and administered intravenously *via* the cephalic vein over 3 sec. Three dogs received a 150-mg dose, and three other dogs received a 300-mg dose. Blood samples, 3 ml, were taken from each dog at 0, 1, 2, 3, 4, 6, 8, 10, 15, 20, 25, 30, 40, 60, 75, 90, 105, 120, and 150 min.

Drug Disappearance from GI Tract—*Stomach*—A midline abdominal incision was made 8 cm in length and equidistant from the base of the sternum. The stomach was exposed and kept moist by bathing in physiological saline at 37°. The stomach was tied off just below the entry of the esophagus and just above the pyloric sphincter. A small slit was made in the cardiac portion and in the pyloric region of the stomach approximately 2 cm from each tie. Foley catheters[4] were inserted into each slit, inflated, and fixed in position using a purse string suture.

The stomach was returned to the abdominal cavity and rinsed with 100 ml of physiological saline at 37° by way of a syringe attached to the catheter at the cardiac portion. After rinsing, air was forced through the syringe to expel any remaining wash. A 50-ml vented calibrated syringe was attached to each catheter; 15 min after washing, 1 g of drug dissolved in 50 ml of water at 37° was administered through the catheter at the cardiac portion. A positive backward pressure was exerted on each catheter to prevent inward movement.

At 0, 15, 30, 45, 60, 75, 90, 105, and 120 min after drug administration, the total volume of the stomach contents was measured by withdrawing the fluid into the syringe at the pyloric portion. A 0.20-ml sample was removed and analyzed.

Duodenum, Jejunum, and Ileum—The procedure used was similar to that described for the stomach. The entire duodenum, with blood, nerve, and lymph supplies intact, was isolated and tied at the pylorus and the duodenal–jejunal flexure and catheterized as described previously. The bile duct and pancreatic duct were ligated. Washing, drug administration, and sampling procedures were identical to those used with the stomach.

A 1-g dose of pralidoxime chloride in 50 ml of water at 37° was administered to four dogs. Duodenal contents were removed by way of the distal syringe, the volume was determined, and a 0.20-ml sample was removed for assay at 0, 15, 30, 45, 60, 75, 90, 105, and 120 min after drug administration. During each experiment, 3-ml blood samples also were taken at 15-min intervals up to 2 hr.

Jejunal and ileal washing, drug administration, and sampling techniques were as described for the stomach and duodenum. The midsection of the jejunum was isolated; a segment drained by three branches of the common mesenteric vein was tied off with its blood, nerve, and lymph supplies intact. A slit was made central to each ligation, and a catheter was inserted. The loop was then returned to the abdominal cavity.

For ileal disappearance, the ileum was isolated. A section drained by three branches of the common mesenteric vein (starting at the second

[1] Aldrich Chemical Co., Milwaukee, Wis.

[2] Bardic, C. R. Bard.

[3] Vacutainer, Becton-Dickinson.

[4] Bardex, C. R. Bard.

0022-3549/79/0200-0141$01.00/0
© 1979, American Pharmaceutical Association

Table I—Pharmacokinetic Parameters after Rapid Intravenous Injection of Pralidoxime Chloride

Dose, mg	Dog	A, μg/ml	α, min^{-1}	C, μg/ml	γ, min^{-1}	B, μg/ml	β, min^{-1}
150	1	190	2.06	68	0.201	12	0.0179
	5	680	1.69	82	0.110	14	0.0131
	16	220	1.51	88	0.173	14	0.0124
							0.0145 ± 0.006[a]
300	1	450	1.40	150	0.120	27	0.0171
	17	290	0.82	94	0.116	34	0.0180
	18	420	1.58	78	0.140	19	0.0167
							0.0173 ± 0.0013[a]

[a] Mean ± 95% confidence limits.

branch after the ileocecal juncture) was ligated. The segment was catheterized and returned to the abdominal cavity. Jejunal and ileal contents were removed by the distal syringe, the volume was determined, and a 0.20-ml sample was removed for assay. Blood samples, 3 ml, also were taken at 15-min intervals up to 4 hr.

Back-diffusion of drug from the plasma into each GI area was determined by isolating the area as described previously and injecting a 300-mg iv dose at 0 and 60 min. Samples, 0.2 ml, were taken from the isolated areas at 0, 15, 30, 45, 60, and 120 min and assayed.

Oral Administration—Pralidoxime chloride, 1 g, was administered *via* stomach tube to unanesthetized dogs as solutions (50 ml) and as tablets[5]. Three dogs were used for each dosage form. Immediately after administration of the tablets, 50 ml of water was given by way of a stomach tube. Blood samples were taken at 1, 3, 5, and 7 hr after administration and analyzed for drug. Three days later, the animals were dosed again and blood samples were taken at 2, 4, 6, and 8 hr.

The same procedure was followed for oral administration in anesthetized dogs. Tablets were administered just prior to anesthesia. Blood samples, 3 ml, were taken at 30-min intervals up to 11 hr.

Intramuscular Administration—Drug, 150 mg in 3 ml of sterile water for injection, was administered into the triceps muscle. Blood samples were taken for assay at 5, 10, 15, 20, 25, 30, 45, 60, 75, 90, 105, 120, and 135 min.

Statistical Comparison—Statistical comparisons were made using analysis of variance. Significance was tested at the $p \leq 0.05$ level.

RESULTS

Intravenous Administration—The plasma concentration–time profiles after rapid intravenous injection of pralidoxime chloride at both 150 and 300 mg were characterized by a triexponential equation:

$$C_p = Ae^{-\alpha t} + Be^{-\beta t} + Ce^{-\gamma t} \qquad \text{(Eq. 1)}$$

This equation can be represented as a three-compartment open model for drug disposition. Table I lists the values for the various parameters for each dog. There was no significant difference between elimination rate constants (β) obtained with the 150- and 300-mg doses. Also, there was no difference within each dose. In a single experiment where ether was used as the anesthetic instead of pentobarbital, an elimination rate constant of 1.77×10^{-2} min^{-1} was obtained after a 150-mg dose.

Drug Disappearance from Different Segments of GI Tract—No measurable disappearance of plasma pralidoxime levels was observed at any time in experiments utilizing isolated stomach or duodenum.

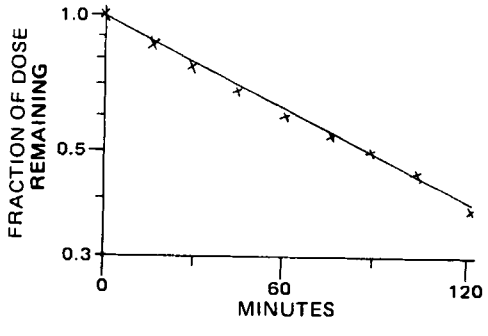

Figure 1—*Fraction of dose remaining in jejunal loop (Dog 25).*

[5] Protopam tablets, 0.5 g, Ayerst.

Drug disappearance from the isolated jejunum followed first-order kinetics, where the observed rate constant was defined as k_a (Fig. 1).

Similar results were observed for drug disappearance from the ileum, except that first-order loss was not observed until approximately 60 min. The pattern for the initial period in all dogs was similar; the data illustrated erratic behavior and nonlinearity when plotted for first-order kinetics. The best estimates of k_a, the disappearance rate constants, were obtained from the terminal linear segment using regression analysis. As can be seen in Table II, the rate constants and percent losses observed after 2 hr from the ileum were significantly greater than those obtained from the jejunum. No differences were observed within each set of animals at each intestinal area.

Plasma levels after intestinal drug administration indicate higher levels from the ileum than from the jejunum (Fig. 2). Although the results shown are for Dogs 9 and 17, similar results were obtained for the other two dogs in each set. Longer blood sampling in the jejunum experiments may have shown a slow, continual rise in plasma levels since this trend was observed in all three animals. However, since blood levels beyond the 2-hr experiment were difficult to obtain, this hypothesis could not be verified. Since samples also were not collected at every interval or with every dog within the 2-hr interval, average results have not been given.

No detectable amounts of drug could be found in the stomach, the duodenum, the jejunum, or the ileum at 0, 15, 30, 45, 60, and 120 min following the intravenous administration of a 300-mg dose at 0 and 60 min, indicating no back-transfer of drug into these areas. Two dogs were observed at each level.

Oral Administration—No plasma levels were observed in anesthetized dogs following oral administration of 1 g of pralidoxime chloride as a solution and as tablets. Tablets passed compendial standards for disintegration, weight variation, and potency and contained an average of 511 mg of drug. Mean plasma levels after oral administration of a 1-g dose in solution and as tablets to three unanesthetized dogs are presented in Figs. 3 and 4.

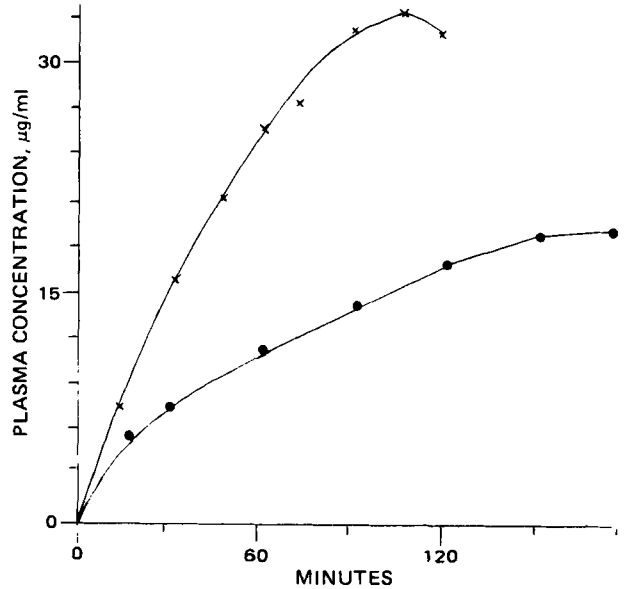

Figure 2—*Plasma concentration after jejunal and ileal administration of 1 g of pralidoxime chloride. Key: ●, jejunal, Dog 9; and ×, ileal, Dog 17.*

Table II—Disappearance Rate Constant, k_a, and Percent Loss of Pralidoxime Chloride from the *In Situ* Isolated Stomach, Duodenum, Jejunum, and Ileum

GI Area	Dog	$k_a \times 10^3$, min^{-1}	Loss after 2 hr, %
Stomach	36, 43	—	—[a]
Duodenum	19, 20, 22, 24	—	—[a]
Jejunum	9	6.87	56.8
	12	7.79	58.4
	15	8.81	63.7
	25	8.12	64.3
		7.89 ± 1.09[b]	60.8 ± 5.18[b]
Ileum	17	18.8	83.7
	21	17.7	84.2
	23	17.0	80.8
	26	16.3	80.5
		17.5 ± 1.46[b]	82.3 ± 2.65[b]

[a] No measurable loss. [b] Mean ± 95% confidence limits.

The individual and average data were fitted adequately to a one-compartment open model with first-order absorption. The following equation describes the plasma level after administration with both dosage forms:

$$C_p = P_1'(e^{-k_a't} - e^{-\beta t}) \qquad \text{(Eq. 2)}$$

where P_1' is a constant, k_a' is the apparent absorption rate constant, β is the elimination rate constant, and C_p is the plasma level at time t.

A tetraexponential equation would be expected since a three-compartment model was observed after intravenous administration. However, this model is difficult to observe after oral administration since it is not feasible to obtain the large number of blood samples required to describe absorption and disposition adequately. For this reason, a less complicated model is often used to delineate blood level curves after oral drug administration (12).

The parameters of Eq. 2 were obtained using the method of residuals and nonlinear least-squares regression analysis to obtain the best estimates of the constants (13). Individual apparent absorption rate constants, elimination rate constants, areas under the plasma level–time curve from zero to infinity, and bioavailabilities, F, are presented in Table III.

There was no significant difference in the absorption rate constants and elimination rate constants obtained with either the solution or tablet. No difference was observed for values obtained within each dosage form. However, the area under the curve from zero to infinity for the solution

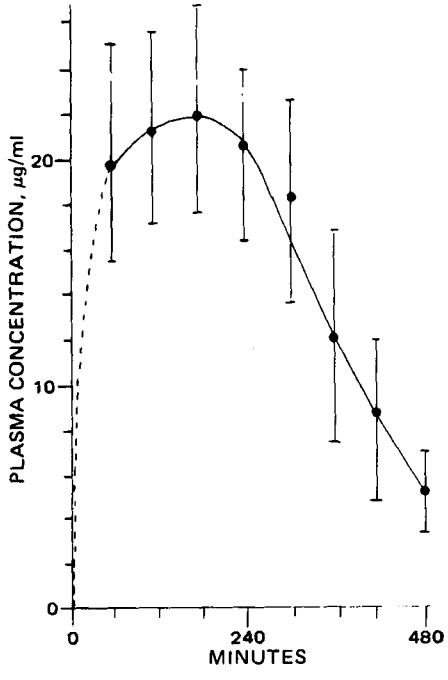

Figure 3—*Mean plasma concentration ± 95% confidence limits after oral administration of 1 g of pralidoxime chloride in solution.*

Table III—Absorption Rate Constants, Elimination Rate Constants, Area under the Plasma Level–Time Curve from Zero to Infinity, and Bioavailability Obtained after Oral Administration of 1 g of Pralidoxime Chloride

Dosage Form	Dog	$k_a' \times 10^3$, min^{-1}	$\beta \times 10^2$, min^{-1}	Area under Curve, μg-hr/ml	Bioavailability, F[a]
Solution	40	8.13	1.24	118	0.61
	41	6.21	1.15	145	0.75
	42	7.46	1.21	153	0.79
		7.26 ± 1.96[b]	1.20 ± 0.092[b]	139 ± 20.7[b]	0.72[c]
Tablet	43	7.08	1.72	76.6	0.40
	44	7.10	1.23	80.1	0.41
	45	7.78	1.09	89.2	0.46
		7.32 ± 0.74[b]	1.35 ± 0.67[b]	82.0 ± 7.36[b]	0.42[c]

[a] Calculated using the average of the individual areas under the curve for the 150-mg iv dose. [b] Mean ± 95% confidence limits. [c] Mean value.

was 70% larger than for the tablet, and these values were statistically different. Using the average of the individual areas under the curve for the 150-mg iv dose, the approximate bioavailabilities for the solution and tablet were 0.72 and 0.42, respectively.

Intramuscular Administration—Mean plasma levels after administration of 150 mg of pralidoxime chloride to three dogs are shown in Fig. 5. The following equation describes the plasma levels after intramuscular administration:

$$C_p = P_1''(e^{-\beta t} - e^{k_a''t}) \qquad \text{(Eq. 3)}$$

where P_1'' is a constant, β is the elimination rate constant, k_a'' is the apparent absorption rate constant, and C_p is the plasma level at time t.

Although a tetraexponential equation would be expected since a three-compartment model was observed after intravenous injection, as discussed under *Oral Administration*, less complicated models are often observed with other routes of administration.

The parameters of Eq. 3 were obtained using the method of residuals and nonlinear regression analysis to obtain the best estimates of the constants. Individual absorption rate constants and elimination rate constants are given in Table IV.

No significant difference was observed among the elimination rate constants obtained after intravenous, oral, or intramuscular administration. Values obtained within each route of administration were similar. The absorption rate constant after intramuscular administration was approximately eight times larger than after oral administration. Table V summarizes the results for each route.

DISCUSSION

After intravenous drug administration, the elimination kinetics are readily analyzed because no simultaneous absorption processes are oc-

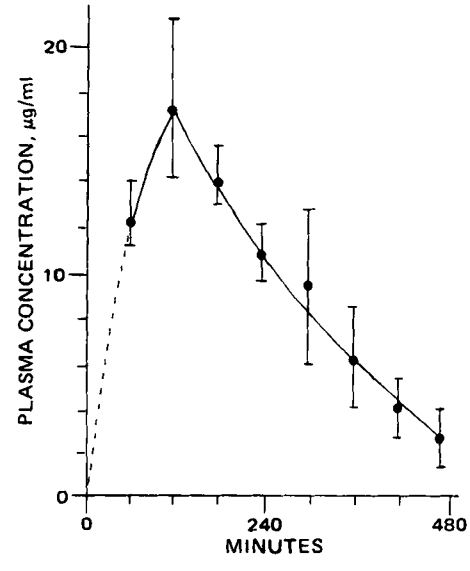

Figure 4—*Mean plasma concentration ± 95% confidence limits after oral administration of two 0.5-g pralidoxime chloride tablets.*

Table IV—Apparent Absorption Rate Constants and Elimination Rate Constants Obtained after Administration of 150 mg im of Pralidoxime Chloride

Dog	$k_a'' \times 10^2$, min^{-1}	$\beta \times 10^2$, min^{-1}
43	7.16	1.18
44	5.20	1.69
45	5.11	1.50
	5.82 ± 2.35[a]	1.46 ± 0.52[a]

[a] Mean ± 95% confidence limits.

curring. The intravenous study of pralidoxime was undertaken to determine the elimination rate constant. Plasma levels after intravascular drug administration in dogs at doses of 150 and 300 mg were described by a triexponential equation.

A three-compartment open model after rapid intravenous injection also was described for 5-(dimethyltriazeno)imidazole-4-carboxamide in the dog (14). A two-compartment open model was used to describe the pharmacokinetics for pralidoxime given intravenously to humans (15). In this latter study, blood sampling was not initiated until 5 min after injection, and only four samples were obtained between 5 and 30 min. Had samples been obtained at earlier times, perhaps a more complex model would have been observed, as was found in the dog where blood sampling began at zero time. Delayed sampling and a lack of frequent sampling at very early times may place the starting point of the plasma curve at a point in time beyond which the value of the first exponential is significant.

In addition to obtaining a plasma level profile of pralidoxime, the objective of the intravenous study was to determine the elimination rate constant, β. After intravenous injection of 150- and 300-mg doses, mean β values of 1.45×10^{-2} and 1.73×10^{-2} min^{-1} were found, respectively. No significant difference existed between these values, indicating that changing the dose within the range utilized had no effect on the drug elimination pattern in dogs. Elimination rate constants of 0.0128 min^{-1} (16) for pralidoxime iodide, 0.0084 min^{-1} (17) for pralidoxime methanesulfonate, and 0.010 min^{-1} (15), 0.0089 min^{-1} (17), and 0.00973 min^{-1} (18) for pralidoxime chloride were reported after intravenous administration to humans.

The rapid drug disappearance from the plasma in both dogs and humans probably is due to the fact that pralidoxime is eliminated from the kidneys by both glomerular filtration and tubular secretion (19). The excreted substances are the unchanged drug and an altered derivative, possibly an aldehyde (19).

When ether was used in place of pentobarbital as the anesthetic, a β of 1.77×10^{-2} min^{-1} was obtained. This value, which is of the same magnitude as those obtained with pentobarbital anesthesia, indicates that the latter probably has no effect on plasma pralidoxime disappearance after a single dose.

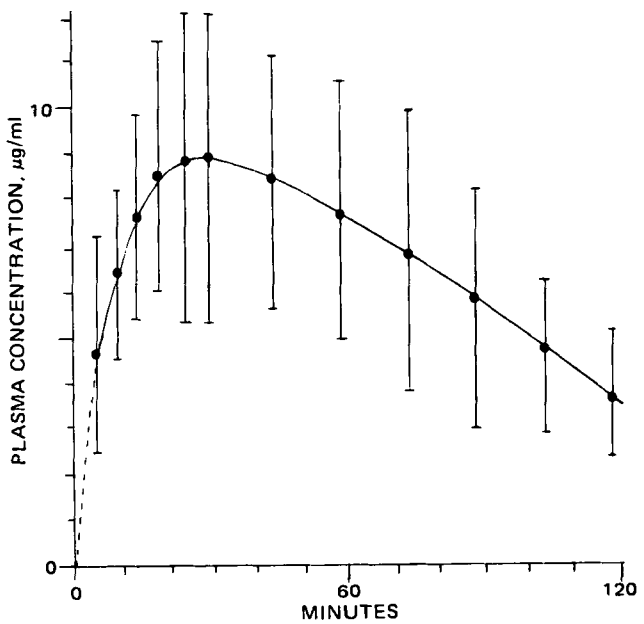

Figure 5—*Mean plasma concentration ± 95% confidence limits after intramuscular administration of 150 mg of pralidoxime chloride.*

Table V—Results for Each Route of Administration

Route of Administration	Dose	β ± 95% Confidence Limits, min^{-1}	k_a ± 95% Confidence Limits, min^{-1}
Intravenous	150 mg	0.0145 ± 0.006	—
	300 mg	0.0173 ± 0.0013	—
Oral solution	1 g	0.0120 ± 0.00092	0.00726 ± 0.00196
Oral tablets	1 g	0.0135 ± 0.0067	0.00732 ± 0.00074
Intramuscular	150 mg	0.0146 ± 0.0052	0.0582 ± 0.0235
Jejunum	1 g	—	0.00789 ± 0.00109
Ileum	1 g	—	0.0175 ± 0.00146
Stomach	1 g	—	0.00
Duodenum	1 g	—	0.00

Once a profile of elimination from the plasma after intravenous administration was obtained, the absorption pattern and absorption rates from the various areas of the GI tract were examined in an *in situ* preparation. The method involved the use of isolated areas of the GI tract, which permitted serial sampling from the area and also blood sampling. No detectable loss of drug was observed from the isolated stomach or duodenum after administration of a 50-ml solution containing 1 g of drug. Plasma levels were also not detectable after drug instillation into each area. Based on these results, it appears that absorption of the compound from the isolated stomach and duodenum of anesthetized dogs is negligible. Kakemi *et al.* (20), using the isolated stomach of the rat, also reported no absorption of pralidoxime methiodide.

The lack of absorption is predictable based on the physicochemical properties of quaternary ammonium compounds. Since the drug is a charged compound and not lipid soluble, passage through a lipid barrier would be expected to be low. The lack of absorption probably cannot be attributed to inadequate blood flow since blood flow in the stomach and duodenum is sufficient in the pentobarbital-anesthetized dog (21).

However, drug disappearance from the isolated jejunum and ileum was observed. The loss of pralidoxime from the jejunum exhibited first-order kinetics. In the ileum, the drug disappeared rapidly, although erratically, during the initial 60 min, followed by a slower, first-order disappearance. This behavior may be the result of some interaction of pralidoxime with the ileal mucosa, resulting in the establishment of a pseudoequilibrium condition or the secretion of fluid in the ileum, which could possibly slow drug absorption. A rapid initial absorption rate with a subsequent decline in the rate for pralidoxime chloride and other monoaldoximes in rats was observed previously (7).

In the jejunum and ileum, the mean absorption rate constants were 7.89×10^{-3} and 1.75×10^{-2} min^{-1} and the percent loss after 2 hr was 61 and 82%, respectively. These results illustrate that drug absorption from the jejunum proceeded at a slower rate than from the ileum in isolated segments of the dog. The differences are probably not the result of a change in pH since the pH of the intestinal contents during the experiment was 7.3 in both segments. Also, blood flow in the jejunum and ileum was reported as identical in the pentobarbital-anesthetized dog (21).

The differences observed in absorption from the jejunum and ileum were possibly the result of differences in some membrane characteristic or constituent. Ion-pair formation may play a role in the absorption of quaternary ammonium compounds (4, 22); adjunctive substances present in the membrane may combine with the drug and facilitate its absorption (23). The absorption rate of the methiodide salt of 2-pyridine aldoxime in the rat reached a maximum with an increasing concentration of drug (20), which is consistent with ion-pair formation or may suggest the possible existence of another transport system.

If such substances or transport systems do, in fact, exist, variability in the nature and distribution in different areas of the GI tract could possibly cause differences in the absorption rate. Pralidoxime may possibly be absorbed *via* the pore route since the pores are not static structures. The ability of the pores to change dimensions may differ at the various levels of the GI tract. Based on elasticity theory, a small change in the linear dimension of a membrane will cause a much greater change in the dimensions of the pores (24).

Plasma levels after drug administration in the isolated jejunum and ileum indicate a more rapid rise from the ileum than from the jejunum. This result is consistent with more rapid absorption from the ileum than from the jejunum. Plasma levels beyond the 2-hr experiment were difficult to obtain since clotting occurred and excessive bleeding was en-

countered when surgically prepared animals were heparinized. Therefore, it is not known whether plasma levels would have continued to increase slowly had sampling been successful beyond approximately 2 hr.

No back-transfer of drug was observed from the plasma into the isolated stomach, duodenum, jejunum, or ileum after intravenous administration at 0 and 60 min. This finding indicates that the disappearance results of pralidoxime from the various areas of the GI tract of the dog were measures of absorption. The *in situ* preparation used in studying absorption from the various areas of the GI tract of the dog appears to be a good technique and provides a means of kinetically following drug disappearance from the isolated area.

After absorption in certain isolated areas of the GI tract was observed, studies were conducted to investigate absorption of drug in the intact animal following oral administration. No absorption occurred in pentobarbital-anesthetized dogs; this result may possibly be explained in terms of the lack of absorption from the stomach. In the anesthetized dog, stomach emptying may be delayed or eliminated, preventing drug absorption from the intestinal tract. In the unanesthetized dog, stomach emptying is not affected and, therefore, absorption occurs.

Plasma levels after oral administration of both dosage forms to unanesthetized dogs were described by Eq. 2. Evaluation of the data showed that the terminal phase of the plasma level–time profile represented the apparent absorption rate constant rather than the elimination rate constant. This effect can occur if absorption is slower than elimination (25). The rate constants were assignable since the elimination rate constant was known from the prior intravenous study.

Byron and Notari (26) clearly demonstrated the problems associated with assignment of rate constants when absorption is assumed to be rate limiting. In recognition of these problems, the use of apparent absorption rate constants was adopted.

The mean apparent absorption rate constants after oral administration of drug in solution and as tablets were 7.26×10^{-3} and 7.32×10^{-3} min^{-1}, respectively. These values are of the same magnitude as the apparent absorption rate constant obtained from the jejunum, 7.89×10^{-3} min^{-1}. This result suggests that absorption may occur principally from the jejunum, as would be predicted since the jejunum constitutes the major portion of the small intestine. However, the isolated ileal experiments showed a faster absorption rate constant. Therefore, if drug is still available during intestinal transit, it could also be absorbed in this region.

This discussion may provide an explanation for the discrepancy between the reported constants after intravenous and oral administration of pralidoxime salts in humans. Elimination rate constants of 0.010 (15), 0.00973 (18), and 0.0089 (17) min^{-1} were reported after intravenous administration while values of 0.0047 (10), 0.0068 (9), and 0.0068 (27) min^{-1} were found after oral administration. Sidell *et al.* (27) utilized the usual one-compartment open model with a first-order absorption equation to obtain values for the various constants. However, the assignments were in error since the elimination rate constant was larger than the absorption rate constant. Reevaluation of the data in the oral studies indicated that the elimination rate constants were 0.0122 (10), 0.0133 (9), and 0.0112 (27) min^{-1}, respectively. These values are of the same magnitude as those obtained following intravenous administration, suggesting that the reported constants are apparent absorption rate constants.

No statistically significant difference was observed in rate constants obtained after oral administration of drug in solution and as tablets to dogs. A difference between the area under the curve obtained with the solution and with tablets was observed. This result indicated that, although the absorption rate was not affected, the drug was less available from the tablet dosage form.

Since the same dogs were not used in the oral and intravenous studies, only an approximate measure of the bioavailability of drug from the solution and tablet dosage forms could be obtained.

The results indicate that although pralidoxime is a charged molecule, considerable intestinal absorption occurs, supporting similar evidence reported by Levine and Steinberg (7).

After intramuscular administration, however, the opposite is observed. Reasonable plasma levels are obtained with a dose of 150 mg, and the descending portion of the plasma level–time curve corresponds to apparent elimination since absorption is rapid. Generally after intramuscular administration of drugs in aqueous solution, absorption is rapid and complete. An elimination rate constant of 0.0093 min^{-1} was reported in humans (15) as compared to a mean of 0.0146 min^{-1} obtained in this investigation.

Elimination with intravenous, intramuscular, and oral administration was rapid. Comparison of apparent elimination rate constants for different routes of administration indicates no significant difference in these values.

In the dog, large oral doses of drug apparently are necessary to achieve measurable plasma levels since elimination occurs at a faster rate than absorption. This conclusion can be reached only after comparison of intravenous and oral administration. Low plasma pralidoxime levels may, therefore, result from slow absorption coupled with rapid elimination rather than negligible or poor absorption. In contrast, after intramuscular administration, absorption is more rapid than elimination and low doses produce measurable plasma levels.

CONCLUSIONS

The results suggest that, in dogs, pralidoxime is absorbed best in the jejunal and ileal areas of the small intestine. Absorption from the isolated stomach and duodenum is negligible. Based on the results of intravenous and oral administration, it was concluded that although there is reasonable bioavailability of drug from oral dosage forms, low plasma levels are observed due to more rapid elimination than absorption. The reverse was observed with intramuscular administration.

REFERENCES

(1) B. R. Rennick, G. K. Moe, R. H. Lyons, S. W. Hoobler, and R. Neligh, *J. Pharmacol. Exp. Ther.*, **91**, 210 (1947).

(2) R. R. Levine and E. W. Pelikan, *ibid.*, **131**, 319 (1961).

(3) R. R. Levine, *ibid.*, **131**, 328 (1961).

(4) M. Gibaldi and B. Grundhofer, *J. Pharm. Sci.*, **62**, 343 (1973).

(5) L. Ryden, A. Berlin, and L. R. Treiber, *Eur. J. Clin. Pharmacol.*, **8**, 277 (1975).

(6) J. H. G. Jonkman, L. E. Van Bork, J. Wijsbeek, R. A. De Zeeuw, and N. G. M. Orie, *Clin. Pharmacol. Ther.*, **21**, 457 (1977).

(7) R. R. Levine and G. M. Steinberg, *Nature*, **209**, 269 (1966).

(8) A. Sundwall, *Biochem. Pharmacol.*, **5**, 225 (1960).

(9) A. A. Kondritzer, P. Zvirblis, A. Goodman, and S. H. Paplanus, *J. Pharm. Sci.*, **57**, 1142 (1968).

(10) F. R. Sidell, W. A. Groff, and R. I. Ellin, *ibid.*, **58**, 1093 (1969).

(11) J. R. May, P. Zvirblis, and A. A. Kondritzer, *ibid.*, **54**, 1508 (1965).

(12) J. G. Wagner, *ibid.*, **59**, 1049 (1970).

(13) P. J. Niebergall, R. L. Schnaare, and E. T. Sugita, *ibid.*, **60**, 1393 (1971).

(14) T. L. Loo, B. B. Tanner, G. E. Housholder, and B. J. Shepard, *ibid.*, **57**, 2126 (1968).

(15) F. R. Sidell and W. A. Groff, *ibid.*, **60**, 1224 (1971).

(16) B. V. Jager, G. N. Stagg, N. Green, and L. Jager, *Bull. Johns Hopkins Hosp.*, **102**, 225 (1958).

(17) F. R. Sidell, W. A. Groff, and A. Kaminskis, *J. Pharm. Sci.*, **61**, 1765 (1972).

(18) R. D. Swartz and F. R. Sidell, *Clin. Pharmacol. Ther.*, **14**, 83 (1973).

(19) F. Berglund, C. E. Elwin, and A. Sundwall, *Biochem. Pharmacol.*, **11**, 383 (1962).

(20) K. Kakemi, H. Sezaki, and T. Kondo, *Chem. Pharm. Bull.*, **17**, 1864 (1969).

(21) B. Goodhead, *Can. J. Physiol. Pharmacol.*, **47**, 787 (1969).

(22) G. Fiese and J. H. Perrin, *J. Pharm. Sci.*, **58**, 599 (1969).

(23) G. M. Irwin, H. B. Kostenbauder, L. W. Dittert, R. Staples, A. Misher, and J. V. Swintosky, *ibid.*, **58**, 313 (1969).

(24) A. C. Burton, in "Permeability and Function of Biological Membranes," L. Bolis, A. Katchalsky, R. D. Keynes, W. R. Loewenstein, and B. A. Pethica, Eds., North Holland Publishing, Amsterdam, The Netherlands, 1970, pp. 1–29.

(25) J. T. Doluisio, J. C. LaPiana, and L. W. Dittert, *J. Pharm. Sci.*, **60**, 715 (1971).

(26) P. R. Byron and R. E. Notari, *ibid.*, **65**, 1140 (1976).

(27) F. R. Sidell, W. A. Groff, and A. Kaminskis, *ibid.*, **61**, 1136 (1972).

ACKNOWLEDGMENTS

Abstracted in part from a dissertation submitted by E. F. Lemanowicz to the Graduate School, Philadelphia College of Pharmacy and Science, in partial fulfillment of the Doctor of Philosophy degree requirements.

Supported in part by Research Fellowship Award GM36443 to E. F. Lemanowicz from the U.S. Public Health Service.

Sensitivity of *Pseudomonas aeruginosa* Envelope Mutants to Alkylbenzyldimethylammonium Chlorides

M. R. W. BROWN [x] **and E. TOMLINSON** *

Received January 16, 1978, from the *Microbiology Laboratory, Department of Pharmacy, University of Aston in Birmingham, Gosta Green, Birmingham, B4 7ET, England.* Accepted for publication June 23, 1978. *Present address: School of Pharmacy, University of Bath, Bath, Avon, BA2 7AY, England.

Abstract □ A series of stepwise polymyxin-resistant envelope mutants of *Pseudomonas aeruginosa* was used to test the activity of a homologous series (C_{10}–C_{18}) of alkylbenzyldimethylammonium chlorides. A sterilization kinetics procedure in deionized water was devised to avoid amounts of quaternary compound above the critical micelle concentration. In all cases, there was a linear relationship between the logarithm of the rate of change of the colony count with time and the logarithm of the homolog concentration. For all strains, there was a linear relationship between alkyl chain length and the concentration required to reduce the colony count to 10% in 2 hr. The stepwise series of polymyxin-resistant strains increased in resistance to polymyxin about threefold for each step. In general, this increase resulted in a similar increase in resistance to the quaternary compound. It is proposed that death in this system may primarily be a consequence of damage to the outer membrane rather than to the cytoplasmic membrane.

Keyphrases □ Alkylbenzyldimethylammonium chlorides, various—antibacterial activity evaluated in series of *Pseudomonas aeruginosa* envelope mutants □ Antibacterial activity—various quaternary ammonium chlorides evaluated in series of *Pseudomonas aeruginosa* envelope mutants □ Quaternary ammonium chlorides, various—antibacterial activity evaluated in series of *Pseudomonas aeruginosa* envelope mutants □ Structure–activity relationships—various alkylbenzyldimethylammonium chlorides, antibacterial activity evaluated in series of *Pseudomonas aeruginosa* envelope mutants

The envelope of *Pseudomonas aeruginosa* and other Gram-negative bacteria is profoundly implicated in drug resistance (1–3). A series of stepwise polymyxin-resistant envelope mutants of *P. aeruginosa* became resistant to several other chemical agents including benzalkonium chloride (4). In the present study, this model series was used to evaluate the effectiveness of a homologous series of alkylbenzyldimethylammonium chlorides (I). A minimum inhibitory concentration (MIC) test procedure gave rise to artifacts due to colloidal association of I (5). Consequently, a test sensitive enough to avoid amounts of I above the critical micelle concentration (CMC) was developed.

In the absence of colloidal association, linear relationships were found between antipseudomonal activity and lipophilicity of the homologs of I. Thus, the universal validity of the parabolic relationship reported to exist between antibacterial activity and lipophilicity of many quaternary ammonium salts is questionable. These results are discussed in terms of the two membranes present in the envelope of the Gram-negative *P. aeruginosa*. Death in this test system may follow as a consequence of damage to the outer membrane rather than primarily being due to a disorganized cytoplasmic membrane.

Since Domagk (6) observed that alkylbenzyldimethylammonium chlorides were antibacterial, they have become accepted as effective agents in aqueous pharmaceutical formulations. The mode of action of these membrane-active agents was reviewed (7, 8); resistance to them is associated with their exclusion from the target cytoplasmic membrane (1, 9, 10). A literature review (5) suggested that many studies of benzalkonium chloride activity were carried out in a concentration range above the CMC. Consequently, some reported parabolic lipophilicity–activity relationships may be artifacts.

Table I—Results and Storage Procedure for the Selective Training of *P. aeruginosa* to Polymyxin Resistance

Culture[a]	Polymyxin, units/ml	Store
A(W)	last + ve = 7.2	A1
A1	last + ve = 18	A2
A2	last + ve = 48	A3
A3	last + ve = 180	A4
A4	last + ve = 560	A5
A5	last + ve = 2160	A6
A6	last + ve = 6300	A7

[a] Each inoculum was 10^7 cells. A(W) refers to the wild-type *P. aeruginosa* (ATCC 9027). Stores were designated as cultures twice washed by centrifugation in the simple salts medium free of polymyxin, subcultured in this medium, and kept at 20°.

EXPERIMENTAL

To measure the antimicrobial activities of a series of alkylbenzyldimethylammonium chlorides (I) against polymyxin-resistant *P. aeruginosa*, an initial study was performed using an MIC test procedure. Although reproducible end-points could be determined for the wild-type organism and also for organisms having low resistance to polymyxin, it was not possible to obtain end-points for the higher order polymyxin-resistant strains even when extremely high concentrations of the quaternary compound were used. In part, this result was attributed to micelle formation of these surface-active molecules interfering with the system (5), the effect being compounded by the presence of high concentrations of nutrient salts in the test environment. Therefore, a sterilization kinetics procedure was developed in which a salt-free environment existed; it was intrinsically more sensitive to the action of the compounds. Under these circumstances, artifacts in activity of I due to micelle formation were avoided.

Polymyxin B Sulfates—Freeze-dried powder[1] was reconstituted by dissolution in sterile deionized distilled water, stored at 10°, and used within 2 weeks of reconstitution.

Chemically Defined Media—Simple salts (as previously defined) giving oxygen-depleted liquid cultures (5) were used unless otherwise stated.

Organism—*P. aeruginosa* (ATCC 9027), originally obtained as a freeze-dried culture, was resuspended in nutrient broth, subcultured into the chemically defined medium, and stored at 10° on this medium solidified with agar.

Alkylbenzyldimethylammonium Chlorides[2] (I)—Four homologs having alkyl chain lengths of 10, 12, 14, and 18, with their purity as previously described (5), were studied in detail.

Selection of Resistant Variants—To produce a series of strains with a regularly changing and reproducible resistance to polymyxin, a training procedure in the chemically defined medium was used. The method involved a fixed inoculum of 10^7 cells and fixed volumes of medium containing a range of concentrations of polymyxin differing in amount by an arbitrary 20%. The inoculum consisted of an oxygen-depleted culture

[1] Donated by Dr. J. D. Gurney, Wellcome Research Laboratories, Beckenham, Kent, England.

[2] Donated by Dr. R. A. Cutler, Sterling-Winthrop Research Institute, Rensselaer, N.Y.

0022-3549/79/0200-0146$01.00/0
© 1979, American Pharmaceutical Association

Table II—Regression and Correlation Coefficients for Eq. 2[a]

	Level of Resistance to Polymyxin B Sulfate															
	Wild-Type Organism				130 units/ml				500 units/ml				1750 units/ml			
n	*a*	*b*	*N*	*r*	*a*	*b*	*N*	*r*	*a*	*b*	*N*	*r*	*a*	*b*	*N*	*r*
10	2.479	8.785	5	0.992	2.542	9.462	5	0.990	2.170	6.206	4	0.980	2.020	−4.680	5	0.985
12	2.411	9.704	6	0.987	1.665	6.408	4	0.992	1.625	5.092	5	0.973	2.521	7.415	4	0.928
14	2.449	11.244	5	0.989	2.262	10.621	5	0.995	2.295	8.912	5	0.991	1.585	4.927	5	0.984
18	0.786	2.964	6	0.933	0.990	4.335	4	0.948	1.433	6.315	5	0.992	1.734	7.149	5	0.992

[a] The *n* is the carbon number of the alkyl chain of the quaternary ammonium salt, *a* and *b* are the regression coefficients for the expression, and *N* and *r* are the number of data points used and the correlation coefficient, respectively.

of *P. aeruginosa* adjusted to 10^8 cells/ml from optical density measurements with a spectrophotometer[3]. The end-point was selected by incubating the test tubes at 37° for 7 days.

Cells from the tubes containing the highest concentration of polymyxin permitting growth were used as the inocula for the subsequent production of the next resistant step. A sample of such cells was washed twice in the growth medium after centrifugation, grown overnight, and designated as stores; such stores were kept at 20°. Stores were subcultured weekly into fresh medium, and the MIC of polymyxin against the subculture was checked monthly. If cells were needed from a store for subsequent experimentation, they were first incubated by shaking at 37° for 18 hr in the medium containing the maximum concentration of polymyxin in which the stored cells were known to show growth. For some tests, the polymyxin-resistant cells were not stored but utilized immediately subsequent to emergence.

Sterilization Kinetics Procedure—A sterilization kinetics test system in which there can be no significant alteration of the thermodynamic activity of the quaternary ammonium compounds by the growth nutrient salts was developed. Bacteria were harvested from an agar slope, added to 25 ml of a liquid medium, and shaken overnight at 37°. A 0.5-ml aliquot of this stock culture then was added to a further 25 ml of the medium, which was shaken for 18 hr at 37°. A portion of this final culture was allowed to cool to room temperature and spun at 3000 rpm for 5 min. The cells were washed sequentially in media of strengths 100, 80, 50, and 20% and then washed twice in deionized water. This procedure avoided damage by osmotic shock (11).

The optical density of this aqueous suspension was measured, and the cell concentration was adjusted to 1.5×10^5 cells/ml with deionized water. This final suspension was slowly warmed to 37°, and 0.5 ml was added to 24.5-ml sterile aqueous concentrations of I under test such that an initial nominal cell count of 3×10^3/ml was achieved. Studies were carried out with stirred suspensions at 37°. After various times of contact of bacteria with the quaternary ammonium salt, a 0.5-ml aliquot was removed from the test system and added to 2.0 ml of polysorbate 80–lecithin broth to inactivate I (12). After a further 5 min, 0.5-ml aliquots were spread on the surface of three overdried nutrient agar plates. The plates were then incubated at 37° for approximately 16 hr, and the number of colonies was counted.

Additional experimentation was carried out to determine whether the initial transfer of the overnight culture into an eventual deionized water environment (11) and the transfer into the inactivation media significantly affected subsequent viable counts. In both cases, no effect could be observed. The initial incubation procedure ensured that cell clumping did not occur, as shown by microscopic examination. During the test procedure, cells were added to a system free of I; if the viable count of this suspension altered significantly during the time of the test, the experiment on that cell culture was discontinued.

To test that *P. aeruginosa* (ATCC 9027) remained constant in its sensitivity to the quaternary ammonium salts, an MIC procedure with dodecylbenzyldimethylammonium chloride was performed periodically. The sensitivity of the test organism remained constant. Of the series of stepwise resistant pseudomonads produced, three strains were able to grow in the medium with added polymyxin at levels of 130, 500, and 1750 units/ml. The four alkylbenzyldimethylammonium chlorides were examined at different concentration levels against the wild type and polymyxin-resistant organisms.

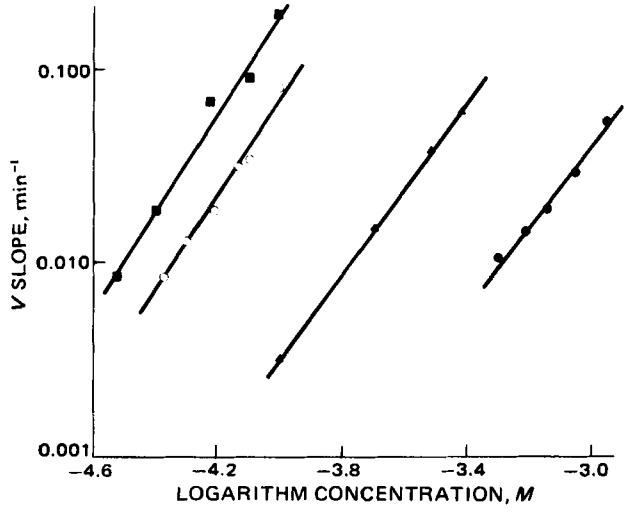

Figure 1—*Effectiveness of various concentrations of decylbenzyldimethylammonium chloride against polymyxin-resistant* P. aeruginosa. *The* V *slope refers to the rate of decrease in the viable count with time. Key:* ■, *wild-type organism;* ○, *organism resistant to 130 units of polymyxin/ml;* ▲, *organism resistant to 500 units of polymyxin/ml; and* ●, *organism resistant to 1750 units of polymyxin/ml.*

[3] Pye Unicam SP 600, Cambridge, England.

RESULTS AND DISCUSSION

By selective training of *P. aeruginosa* using aqueous solutions of polymyxin B sulfate in simple salts medium, several series of stepwise resistant pseudomonads were produced. Table I shows the results obtained for a typical series. There was an approximately threefold increase in the resistance to polymyxin with each step.

With the sterilization kinetics procedure, death-time curves were obtained for all homologs. The relationship between viable count and time was exponential (5) and given by:

$$V_t/V_0 = e^{-kt} \qquad \text{(Eq. 1)}$$

where V_0 and V_t refer to the number of viable bacteria in the reaction vessel at time zero and time t, respectively, and k is a constant for the

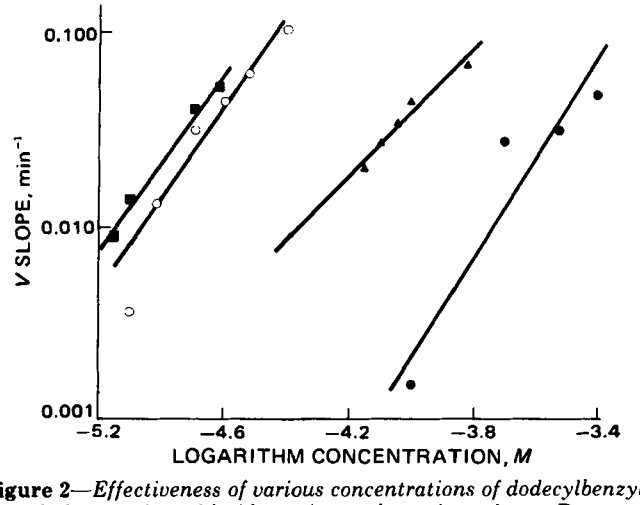

Figure 2—*Effectiveness of various concentrations of dodecylbenzyldimethylammonium chloride against polymyxin-resistant* P. aeruginosa. *Key: same as Fig. 1.*

Table III—Computed Molarity of Quaternary Homologs Required to Reduce the Viable Count to 10% of the Original in 2 hr [a]

	Level of Resistance to Polymyxin B Sulfate			
n	Wild Type	130 units/ml	500 units/ml	1750 units/ml
10	4.139×10^{-5}	2.884×10^{-5}	1.523×10^{-4}	4.506×10^{-4}
12	1.298×10^{-5}	7.998×10^{-6}	3.871×10^{-5}	1.713×10^{-4}
14	3.625×10^{-6}	2.429×10^{-6}	1.625×10^{-5}	3.804×10^{-5}
18	3.861×10^{-7}	3.337×10^{-7}	1.382×10^{-6}	4.772×10^{-7}

[a] See footnote to Table II.

system depending on the sensitivity of the organism and the concentration of quaternary salt used.

The log of the rates of change of log viable count with time, log (d log V/dt) for each quaternary at each concentration level, and against all organisms was derived using least-squares regression according to the expression:

$$\log (d \log V/dt) = a \log (\text{quaternary concentration}) + b \quad \text{(Eq. 2)}$$

The end-point of activity for I in the sterilization kinetics test was that concentration of quaternary producing a reduction in viable count to 10% of the original in 2 hr. All derived regression and correlation coefficients are given in Table II. All correlations obtained were significant at the $\alpha = 0.001$ level.

Figures 1–4 show those relationships existing between antimicrobial effectiveness of the four homologs against each organism studied and at each concentration of quaternary. In all cases, there was a linear relationship between the logarithm of the concentration and the logarithm of the rates of change of colony count with time. Table III gives the computed 2-hr end-point for all compounds against all organisms. The dose–response curves (Figs. 1–4) were generally parallel for each quaternary compound, suggesting a similar mode of action against each resistant strain (5).

Figure 5 demonstrates the relationship between the chain length of the I homologs and the concentrations calculated to produce the required end-point. There was a straight-line relationship between alkyl chain length and activity.

Relationships between the levels of resistance to polymyxin and the levels of resistance to the quaternaries were presented graphically. Figure 6 shows the results for tetradecylbenzyldimethylammonium chloride, using a linear–linear scale. Figure 7 shows the comparative resistance levels of all homologs toward all organisms studied, using the 2-hr end-point and analysis on a log–log basis. In all cases, the strain trained to be resistant to a maximum of 130 units of polymyxin/ml was the most sensitive to the quaternary compounds. An increase in polymyxin resistance above this value, however, increased resistance to quaternary action. The increase in sensitivity of the 130-units/ml strain over the wild type is shown more markedly on the log–log plot due to scaling factors. The pattern of sensitivity of this series to both drugs is a consequence of changes in envelope structure (3, 4, 13).

Portions of the plots (Fig. 7) having positive slopes show that approximately four times the amount of each quaternary was necessary for each step in resistance to each strain of *P. aeruginosa*, although this value varied both between chain lengths and between polymyxin resistance levels. The value of this increase in quaternary concentration necessary to be effective against higher order polymyxin-resistant strains is useful in comparing pseudomonal resistance to both chemical types. The three resistant organisms were between 3.5 and 3.8 times more resistant to polymyxin than their next step variant, which is similar in magnitude to the value obtained when considering the alkylbenzyldimethylammonium chlorides.

The rate at which low molecular weight organic nonelectrolytes diffuse across biological membranes correlates with their lipid–water partition coefficient within limits. Lien *et al.* (14) studied a large range of mainly membrane-active antibacterial agents for activity against Gram-positive and Gram-negative bacteria. The ideal lipophilic character (log P_0) for a set of congeneric drugs was much higher for Gram-positive bacteria (about 6) than for Gram-negative bacteria (about 4) (14). This difference was attributed to the relatively lipid-rich wall of Gram-negative bacteria that retained lipophilic drugs and hindered penetration. However, colloidal association may have contributed to the interpretation of these

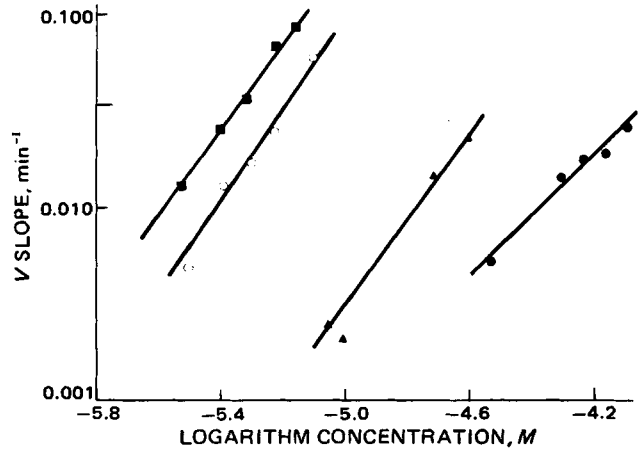

Figure 3—*Effectiveness of various concentrations of tetradecylbenzyldimethylammonium chloride against polymyxin-resistant* P. aeruginosa. *Key: same as Fig. 1.*

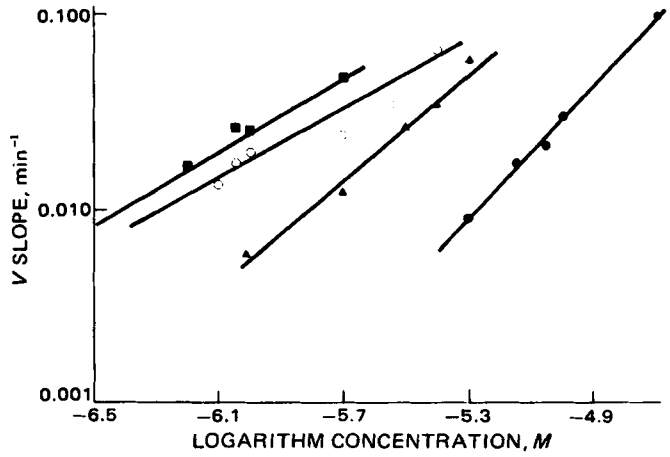

Figure 4—*Effectiveness of various concentrations of octadecylbenzyldimethylammonium chloride against polymyxin-resistant* P. aeruginosa. *Key: same as Fig. 1.*

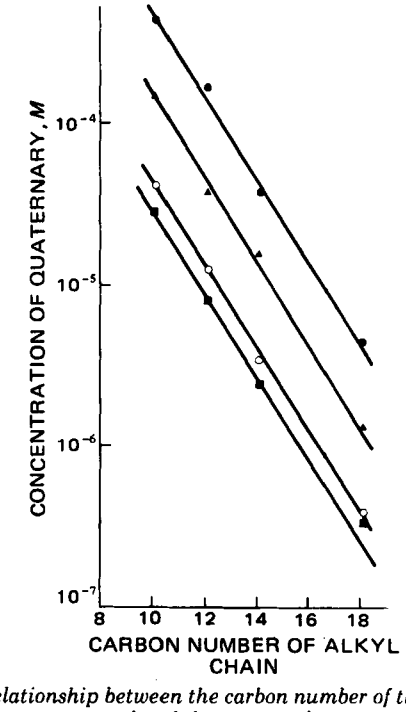

Figure 5—*Relationship between the carbon number of the alkyl chain of the quaternary compound and the computed concentrations required to reduce the viable count of different polymyxin-resistant strains to 10% of the original in 2 hr. Key: same as Fig. 1.*

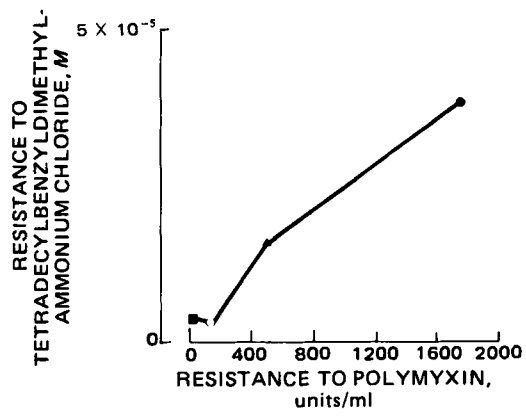

Figure 6—*Relationship between levels of resistance to polymyxin and levels of resistance to tetradecylbenzyldimethylammonium chloride for the various pseudomonads studied. Key: same as Fig. 1.*

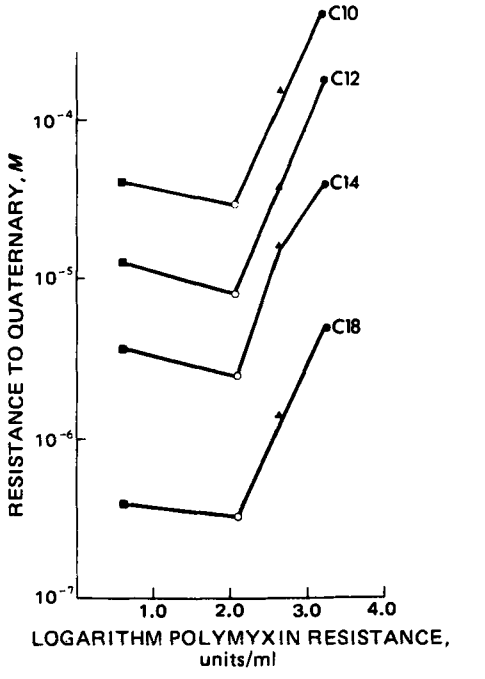

Figure 7—*Composite diagram showing relationships between levels of resistance to polymyxin and to all homologs studied. Key: same as Fig. 1.*

data (5). Furthermore, the outer membrane of Gram-negative bacteria is not a simple lipid barrier (1, 2) and may possibly have water-filled pores lined with protein as an aid to penetration by hydrophilic molecules (3, 15).

The linear relationship between carbon number and antibacterial activity (Fig. 5) is interesting. Probably the differential possibilities of uptake by hydrophobic outer membrane sites, diffusion through outer membrane pores (I, mol. wt. 276–388), and micelle formation in the periplasmic space result in a nonlinear carbon number–activity relationship for a primary effect on the cytoplasmic membrane. The results are consistent with the hypothesis that bacterial death was a consequence of quaternary action primarily at the outer membrane. Under these circumstances, increasing lipophilicity would be associated with increased outer membrane disruption without the drawback of retention by a prior lipid site. These effects tend to be enhanced by this hypotonic test system. A similar lethal outer membrane effect was proposed for polymyxin action (16).

REFERENCES

(1) M. R. W. Brown, in "Resistance of *Pseudomonas aeruginosa*," M. R. W. Brown, Ed., Wiley, London, England, 1975, p. 71.

(2) J. W. Costerton and K.-J. Cheng, *J. Antimicrob. Chemother.*, **1**, 363 (1975).

(3) H. Nikaido, *Biochim. Biophys. Acta*, **433**, 118 (1976).

(4) M. R. W. Brown and W. M. Watkins, *Nature*, **227**, 1360 (1970).

(5) E. Tomlinson, M. R. W. Brown, and S. S. Davis, *J. Med. Chem.*, **20**, 1277 (1977).

(6) G. Domagk, *Dtsch. Med. Wochenschr.*, **61**, 829 (1935); through *Chem. Abstr.*, **29**, 7018 (1935).

(7) E. F. Gale, E. Cundliffe, P. E. Reynolds, M. H. Richmond, and M. J. Waring, in "The Molecular Basis of Antibiotic Action," Wiley, London, England, 1972.

(8) D. W. Blois and J. Swarbrick, *J. Pharm. Sci.*, **61**, 390 (1972).

(9) T. J. Franklin, *Crit. Rev. Microbiol.*, **2**, 253 (1973).

(10) W. A. Hamilton, *Membr: Struct. Funct., Fed. Eur. Biochem. Soc., Meet., 6th, 1969*, **20**, 71 (1970).

(11) M. R. W. Brown and B. A. Winsley, *J. Gen. Microbiol.*, **56**, 99 (1969).

(12) S. R. Kohn, L. Gershenfeld, and M. Barr, *J. Pharm. Sci.*, **52**, 967 (1963).

(13) J. B. Dame and B. Shapiro, *J. Bacteriol.*, **127**, 961 (1976).

(14) E. J. Lien, C. Hansch, and S. M. Anderson, *J. Med. Chem.*, **11**, 430 (1968).

(15) Y. Kamio and H. Nikaido, *Biochim. Biophys. Acta*, **464**, 589 (1977).

(16) D. C. LaPorte, K. S. Rosenthal, and D. R. Storm, *Biochemistry*, **16**, 1642 (1977).

ACKNOWLEDGMENTS

The authors are grateful to Fisons Ltd. for a grant that supported this work, including a Fellowship for E. Tomlinson.

Plasma Levels following Single and Repeated Doses of Erythromycin Estolate and Erythromycin Stearate

P. G. WELLING *x, R. L. ELLIOTT, M. E. PITTERLE, H. P. CORRICK-WEST, and L. L. LYONS

Received February 6, 1978, from the *Center for Health Sciences, School of Pharmacy, University of Wisconsin, Madison, WI 53706.* Accepted for publication June 21, 1978. *Present address: Department of Clinical Pharmacology and Therapeutics, School of Medicine, University of Birmingham, Birmingham, B15 2TJ, England.

Abstract □ The pharmacokinetics of erythromycin and erythromycin 2′-propanoate were studied in healthy male volunteers following single and repeated doses of erythromycin stearate tablets, erythromycin estolate capsules, and a suspension. Estolate dosages gave rise to higher plasma levels of total drug than the stearate. However, the stearate yielded higher plasma levels of erythromycin base. Absorption of all dosage forms, except the suspension, was delayed, and pharmacokinetic interpretation of both single- and multiple-dose data required incorporation of an absorption lag time. The absorption of erythromycin stearate was inhibited by food and also by low fluid volumes in fasted subjects. Absorption of erythromycin estolate was increased in the presence of food and was not greatly affected by fluid volume. Although single-dose data poorly predicted circulating levels of erythromycin following repeated doses, trends observed after single doses were maintained during chronic treatment.

Keyphrases □ Erythromycin base and 2′-propanoate—bioavailability in humans, effect of food and fluid volume □ Bioavailability—erythromycin base and 2′-propanoate in humans, effect of food and fluid volumes □ Antibacterials—erythromycin base and 2′-propanoate, bioavailability in humans, effect of food and fluid volume

Despite the widespread use of erythromycin, there is still uncertainty regarding its optimum oral dosage form. Erythromycin absorption from formulations containing erythromycin base and from different esters and salts varied (1–6).

Factors influencing erythromycin absorption recently were reviewed (7). Most studies reported delayed or reduced absorption of erythromycin base or stearate in the presence of food (8–11). Absorption of erythromycin estolate appeared not to be influenced markedly while that of erythromycin ethylsuccinate increased in nonfasted individuals (10–14). Suspension formulations apparently were not influenced by the absence or presence of food (12, 15). However, results vary greatly.

The subject of erythromycin absorption has been confused by observations that the bioavailability of erythromycin stearate is inhibited by reduced fluid volumes (16) and that absorption characteristics from a single dose may have no relation to those following repeated doses (17). The notion that absorption of erythromycin estolate is superior to most other erythromycin dosage forms was challenged by Wiegand and Chun (18).

In the present study, circulating drug levels were compared following single and repeated doses of erythromycin stearate and erythromycin estolate. Plasma levels of erythromycin base and the propanoate ester were measured separately after dosing erythromycin estolate by a modification of the method of Tserng and Wagner (19).

EXPERIMENTAL

Ten healthy male volunteers, 21–42 years old (mean 29) and between 61 and 89 kg (mean 73), were in good physical condition with normal blood and urine laboratory values. There were no histories of drug allergy. Informed consent was obtained from each subject.

Table I—Summary of Treatments

Number[a]	Description
1	2 × 250-mg erythromycin estolate capsules with 250 ml of water after breakfast
2	2 × 250-mg erythromycin estolate capsules with 250 ml of water after overnight fast
3	2 × 250-mg erythromycin estolate capsules with 25 ml of water after overnight fast
4	Erythromycin estolate suspension, 5 mg/kg, with 250 ml of water after overnight fast
5	2 × 250-mg erythromycin stearate tablets with 250 ml of water after breakfast
6	2 × 250-mg erythromycin stearate tablets with 250 ml of water after overnight fast
7	2 × 250-mg erythromycin stearate tablets with 25 ml of water after overnight fast

[a] Each treatment was administered as a single dose and again following repeated doses.

Protocols—Subjects[1] were requested to take no drugs for 1 week before a study and no drugs other than required erythromycin doses during a study. Subjects conducted their normal daily tasks during the entire experiment.

Each subject received seven different treatments (Table I) randomized using one 7 × 7 Latin square and three rows of another. At least 2 weeks were allowed between treatments. Each treatment was administered as a single and repeated dosage regimen.

Dosing and Sampling Schedules—Subjects fasted overnight before a treatment and ate no food except test meals until 4 hr postdosing. On the morning of a treatment, subjects drank 250 ml of water at least 1 hr before dosing. Drugs were administered at 8 am. Blood samples (~6 ml) were taken from a forearm vein into vacuum tubes[2] containing heparin as an anticoagulant at 0, 0.5, 1, 2, 4, 6, 8, and 12 hr. Five additional and identical doses were given at 6-hr intervals starting 24 hr after the initial dose, the final dose being given at 8 am on the 3rd day. Further blood samples were then taken as after the initial dose.

In Treatments 1 and 5, the first and last doses of erythromycin estolate or erythromycin stearate were given immediately following a standard breakfast of corn flakes with milk, two slices of buttered toast, coffee with cream, and 2 teaspoonfuls of sugar. Intermediate doses were taken immediately following normal meals, the 2-am dose being taken following a light snack. In all other treatments, the first and last doses were given in the fasting state while intermediate doses were taken at least 2 hr before or after meals. With all single and repeated doses, the volume of water ingested with the drug dose was as indicated in Table I.

The dose of the suspension in Treatment 4 was selected on the basis of a recent recommendation that erythromycin suspension should be dosed at a level of 20 mg/ml/day for the treatment of streptococcal pharyngitis in children (20). Although this dosage is somewhat lower than that of the tablets and capsules, the dosage range was similar for a given individual. Therefore, the suspension data were considered together with those from other treatments, with adjustments where appropriate, while providing information on plasma drug levels obtained with this particular regimen.

Erythromycin estolate capsules[3] and suspension[4] and erythromycin stearate tablets[5] were commercial products.

[1] Faculty, technical staff, or graduate students.
[2] Vacutainers.
[3] Ilosone capsules, 250 mg, Eli Lilly and Co., Indianapolis, Ind.
[4] Ilosone liquid suspension, Eli Lilly and Co., Indianapolis, Ind.
[5] Filmtabs, Abbott Laboratories, Chicago, Ill.; purchased from University Hospitals, Madison, Wis.

0022-3549/79/0200-0150$01.00/0
© 1979, American Pharmaceutical Association

Table II—Results of Statistical Comparison of Drug Levels in Plasma following Single-Dose Treatments [a]

Drug Level Compared	0.5 hr	1 hr	2 hr	4 hr	6 hr	8 hr	12 hr
Ester[b]	4 > 1,3	2-4 > 1 4 > 3	NSD[c]	1 > 2-4	1 > 2-4	1 > 2-4	1 > 2-4
Base[d]	2,4 > 1,5 4 > 3	1 > 2-7 5-7 > 2-4	6,7 > 1-5	1 > 2,4 5-7 > 2-4	1 > 2,4 5-7 > 2-4	1 > 2-4,5,7 6 > 2,5,7 5-7 > 4	1 > 2,4,6,7 5-7 > 2
Total[e]	4 > 1-3,5-7	2-4,6 > 1 2,3 > 5,7 4 > 3,5-7	4,6 > 5	1 > 2-7	1 > 2-7 2-4 > 7	1 > 2-7 2,3,6 > 5,7	1 > 2-7 2-4 > 5-7

[a] All data were analyzed by an analysis of variance while individual treatments were compared by a paired t test. Differences were considered significant when $p < 0.05$. [b] Plasma levels compared among Treatments 1–4. [c] No significant differences. [d] Plasma levels compared among Treatments 1–7. [e] Comparison included total levels from all treatments, plasma levels of erythromycin base from Treatments 5–7 being considered as total levels.

Assay—Plasma samples from subjects receiving erythromycin stearate were promptly frozen (−20°) until assayed. These samples were assayed for antibiotic activity with a microbiological cup–plate diffusion method. Samples were diluted when necessary with 0.05 *M* phosphate buffer, pH 7.9. The test organism was *Sarcina lutea* (ATCC 9341) growing on neomycin assay agar[6].

All assays were done in triplicate. The relationship between the inhibition zone of bacterial growth and the logarithm of erythromycin concentration was linear over plasma erythromycin concentrations of 0.1–20.0 μg/ml. Assay reproducibility was ±8% at the lower concentration range and ±3% at the higher.

Plasmas from subjects receiving erythromycin estolate were assayed for both erythromycin 2′-propanoate and erythromycin base by a method adapted from one described previously (19). The major modification consisted of substituting the microbiological end-point for the fluorometric method used originally (19). The microbiological method was adopted because of its relative simplicity compared to the fluorometric procedure and also to avoid any interference by microbiologically inactive but fluorescing metabolites.

Further small modifications were incorporated, and the method finally used was as follows. Immediately following separation from whole blood, plasma was divided to obtain two 1-ml portions. One portion was acidified with 2 ml of 0.1 *M* phosphate buffer, pH 5.7, and extracted twice with 2 ml of ether. The ether extracts were combined. The other plasma portion was made basic with 2 ml of 0.1 *M* phosphate buffer, pH 8.5, and similarly extracted twice with 2 ml of ether. The ether extract of the acidified sample contained erythromycin 2′-propanoate while that of the basified sample contained both erythromycin 2′-propanoate and erythromycin base (19). Ether extracts were dried under nitrogen, and the residues were frozen until assayed.

On the day of the assay, 2 ml of 0.05 *M* phosphate buffer, pH 7.9, was added to each tube. Tubes then were incubated with occasional shaking at 37° for 5 hr to ensure complete ester hydrolysis. Final dilutions, when required, were done with 0.05 *M* phosphate buffer, pH 7.9, and the hydrolyzed samples were analyzed by the microbiological method described for erythromycin stearate.

This procedure yielded plasma levels of both combined ester and free base and also of erythromycin 2′-propanoate only. Levels of free base were obtained by subtraction. Repeated experiments with high purity drug standards showed that the assay achieved quantitative separation of erythromycin ester and free base. Equivalent amounts of erythromycin 2′-propanoate and free base gave identical assay readings in repeated trials following the 5-hr hydrolysis at 37° and pH 7.9, indicating complete conversion of the bacterially inactive ester to the base during the hydrolysis or during both the hydrolysis and incubation steps.

Analysis—Circulating levels of erythromycin following intravenous doses were described in terms of a two-compartment model (21); levels following oral doses were described in terms of a one-compartment model with either first-order (16, 22) or zero-order (17) absorption.

To differentiate the two oral dosing models, individual data sets for erythromycin following Treatments 5–7 and for both the propanoate ester and total erythromycin activity following Treatments 1–4 were analyzed using the one-compartment model with first- and zero-order absorption. Circulating levels of erythromycin base from Treatments 1–4 were not sufficiently defined for pharmacokinetic analysis.

In the first-order analysis, individual data sets were fitted to Eq. 1 following single doses and appropriate expansions of this equation following repeated doses:

$$C = \frac{FD}{V}\left(\frac{k_a}{k_a - k_{el}}\right)\left[e^{-k_{el}(t-t_{lag})} - e^{-k_a(t-t_{lag})}\right] \qquad \text{(Eq. 1)}$$

where C is the drug concentration in plasma; F is the fraction of the dose D absorbed; V is the apparent drug distribution volume; k_a and k_{el} are first-order rate constants for drug absorption and elimination, respectively; t is the time since dosing; and t_{lag} is the time elapsed between dosing and the time of appearance of measurable drug in plasma.

In the zero-order analysis, individual data sets from single doses were fitted simultaneously to Eqs. 2 and 3 for times less than and greater than the times of peak drug levels, respectively, and appropriate expansions of these expressions following repeated doses:

$$C = \frac{k_0 F}{Vk_{el}}\left[1 - e^{-k_{el}(t-t_{lag})}\right] \qquad t \leq t_{max} \qquad \text{(Eq. 2)}$$

$$C = \frac{k_0 F}{Vk_{el}}\left[1 - e^{-k_{el}(t_{max}-t_{lag})}\right]e^{-k_{el}(t-t_{max})} \qquad t > t_{max} \qquad \text{(Eq. 3)}$$

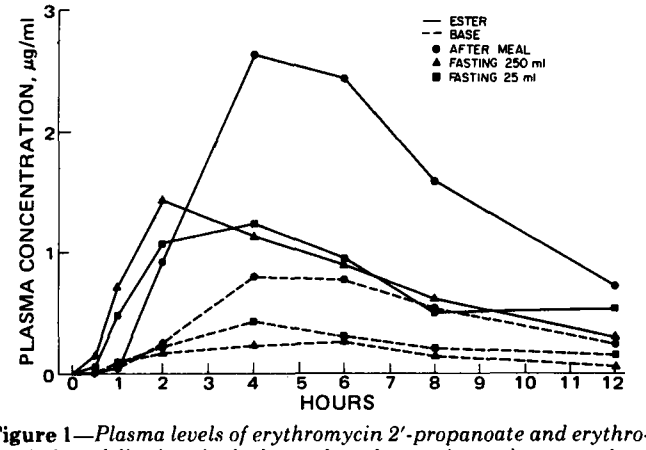

Figure 1—*Plasma levels of erythromycin 2′-propanoate and erythromycin base following single doses of erythromycin estolate capsules.*

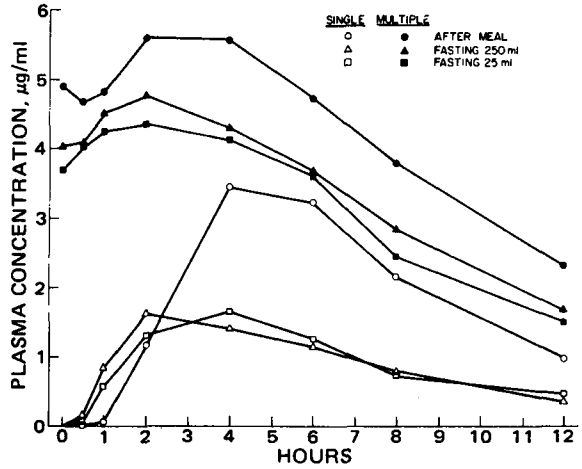

Figure 2—*Plasma levels of total erythromycin activity following single and repeated doses of erythromycin estolate capsules.*

[6] Bacto Antibiotic Medium No. 11, Difco Laboratories, Detroit, Mich.

Table III—Results of Statistical Comparison of Drug Levels in Plasma following Repeated Doses [a]

Drug Level Compared	0 hr	0.5 hr	1 hr	2 hr	4 hr	6 hr	8 hr	12 hr
Ester	1 > 2-4	NSD	NSD	NSD	1 > 2-4	1 > 2-4	1 > 3,4	1 > 3
Base	NSD	NSD	NSD	5-7 > 1-4	5-7 > 1-4	6,7 > 1-4 6 > 5	6,7 > 3	1 > 2-7
Total	1-4 > 5-7	1-4 > 5-7	1-4 > 5-7	1-4 > 5-7	1-3 > 5-7 4 > 5,7	1 > 2-7 2-4 > 5-7 6 > 5	1 > 3-7 2-4 > 5-7	1 > 3-7 2-4 > 5-7

[a] Data were analyzed as in Table II. Comparisons of ester, base, and total drug levels were carried out as in Table II.

where k_0 is the zero-order rate constant for erythromycin absorption into the circulation, t_{max} is the time of observed peak drug level in plasma, and other symbols are as defined for Eq. 1.

In the first-order absorption case, initial estimates of k_a,k_{el}, and FD/V were obtained by standard graphical methods. Improved estimates of parameter values, together with statistical analysis, were obtained using the program NREG on a digital computer[7] (23). The value of t_{lag} was held constant. The value of k_{el} also was held constant during computer fitting to prevent it from converging to the same value as k_a.

Convergence of these constants during computer-fitting procedures was reported previously (24, 25) and can be explained in terms of the nature of Eq. 1. When k_a and k_{el} converge, usually due to data variance or insufficient data points, the function $FD/V[k_a/(k_a - k_{el})]$ becomes a large number while the function $[e^{-k_{el}(t-t_{lag})} - e^{-k_a(t-t_{lag})}]$ becomes very small. Owing to the long word length of the computer, the product of the two functions becomes a very flexible term for data fitting, but meaningless values of k_a and k_{el} are obtained. To avoid this analytical artifact, the more reliable of the two constants, k_{el}, was fixed at the graphical values.

Improved parameter estimates from single doses were used as initial estimates when computer fitting the repeated dose–plasma levels. In this case, both t_{lag} and k_{el} again were held constant.

In the zero-order absorption case, initial estimates of the value k_0F/V were obtained by dividing computer estimates of FD/V, obtained from the first-order case, by the value $t_{max} - t_{lag}$, *i.e.*, the apparent drug absorption time. Since there were only two variables, k_0F/V and k_{el}, both were allowed to float during computer analysis.

Plasma drug levels were compared between treatments by an analysis of variance and between particular treatments by a paired t test. Pharmacokinetic constants were similarly compared between treatments, between single and repeated doses, and, where appropriate, between pharmacokinetic models.

RESULTS

Plasma Levels—Mean plasma levels of erythromycin 2′-propanoate, erythromycin base, and total drug following single doses are summarized in Figs. 1–4. Statistical comparisons are given in Table II. Mean plasma levels and statistical comparisons following repeated doses are summarized in Figs. 5–7, and statistical comparisons are given in Table III.

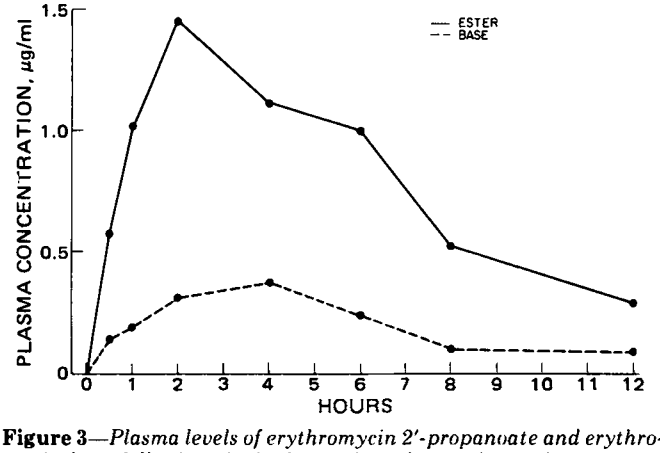

Figure 3—*Plasma levels of erythromycin 2′-propanoate and erythromycin base following single doses of erythromycin estolate suspension.*

From the single-dose data, it can be seen that the absorption of both erythromycin estolate and erythromycin stearate was delayed by food. In Treatment 1, antibiotic was not observed in plasma until 1 hr after dosing; levels were observed within 0.5 hr with all other treatments.

Whereas postprandial dosing of the stearate caused plasma erythromycin levels to be lower compared to an equivalent fasting treatment, circulating levels of the propanoate ester and also of the free base were higher when erythromycin estolate was dosed to nonfasted subjects.

Although plasma levels of total drug tended to be higher from Treatments 1–4 compared to Treatments 5–7, higher levels of erythromycin base were obtained from the stearate dosage form regardless of how the drug was administered. While water volumes had little influence on the absorption of erythromycin estolate, plasma levels of erythromycin base were inhibited by low fluid volume after doses of erythromycin stearate to the same extent as by food. These latter results are consistent with those reported previously with a different brand of erythromycin stearate (16).

Plasma levels of both the propanoate and the base from the suspension dosage were somewhat higher than those obtained from equivalent capsule doses (Treatment 2), despite the somewhat lower dose of the suspension.

From Tables II and III and the figures, it is clear that the trends observed following single doses continued with repeated dosing, although differences between treatments tended to be less significant. Following repeated doses of erythromycin estolate capsules, Treatment 1 continued to yield high levels of propanoate and, to a lesser extent, free base. In fact, plasma levels of free base were consistent at about 1.0 μg/ml, declining slowly throughout the sampling period. Levels of erythromycin base were again uniformly higher from the stearate doses than from the estolate doses, and Treatment 6 again resulted in higher erythromycin levels than did Treatments 5 and 7.

The suspension dosage form yielded plasma levels of both the propanoate and the free base similar to those of the capsule doses. No significant lag time of absorption was observed with the suspension.

Plasma Level Ratios—Mean ratios of plasma propanoate ester to free base following estolate doses were somewhat high following Treatment 2 and were generally higher after initial doses than after repeated doses. The overall ratio following repeated doses was 3.5. This value was fairly constant during the sampling period, and there were no trends between treatments. The ratio obtained was consistent with that reported earlier in blood, serum, plasma, and urine of subjects receiving repeated doses of erythromycin estolate (26).

Pharmacokinetic Parameters—Model-independent parameters C_{max}, t_{max}, and areas under plasma level–time curves, are summarized in Table IV; statistical comparisons are given in Table V. The superior

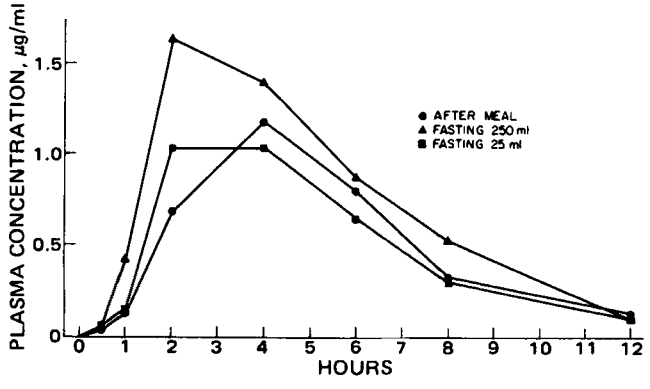

Figure 4—*Plasma levels of erythromycin following single doses of erythromycin stearate tablets.*

[7] Univac model 1108.

Table IV—Mean Peak Plasma Levels (C_{max}), Times of Peak Levels (t_{max}), and Areas[a] under Plasma Profiles (±1 *SD*) following Single and Repeated Doses

Treatment		C_{max}, μg/ml		t_{max}, hr		$AUC_{0\rightarrow 12\ hr}$, μg hr/ml, Single	$AUC_{0\rightarrow 6\ hr}$, μg hr/ml, Repeated
		Single	Repeated	Single	Repeated		
1	Ester	2.8 ± 0.4	4.5 ± 1.1	4.4 ± 1.1	2.4 ± 0.8	17.3 ± 2.9	23.8 ± 6.5
	Base	0.9 ± 0.5	1.8 ± 0.6	5.1 ± 1.5	2.9 ± 1.8	5.6 ± 2.7	7.7 ± 2.3
	Total	3.7 ± 0.8	5.8 ± 1.3	4.7 ± 1.0	2.8 ± 0.9	23.4 ± 5.6	31.5 ± 7.6
2	Ester	1.5 ± 0.7	3.7 ● 1.1	2.8 ± 1.4	1.9 ± 0.9	8.8 ± 4.3	18.2 ± 4.9
	Base	0.4 ± 0.3	1.5 ± 0.6	4.4 ± 1.8	1.9 ± 1.8	2.0 ± 1.2	7.3 ± 3.2
	Total	1.8 ± 0.8	5.0 ± 1.4	2.8 ± 1.4	1.6 ± 0.5	11.2 ± 4.5	25.8 ± 1.2
3	Ester	1.5 ± 0.8	3.5 ± 1.1	3.2 ± 1.4	1.7 ± 1.0	8.4 ± 4.3	17.7 ± 6.4
	Base	0.5 ± 0.5	1.7 ± 0.7	4.2 ± 1.8	2.9 ± 2.8	2.8 ± 2.9	6.6 ± 3.1
	Total	1.9 ± 1.1	4.6 ± 1.2	3.2 ± 1.4	1.6 ± 1.4	11.2 ± 6.7	24.5 ± 7.0
4	Ester	1.6 ± 0.7	3.7 ± 1.3	3.4 ± 1.9	1.5 ± 0.5	9.5 ± 3.2	18.8 ± 7.0
	Base	0.5 ± 0.3	1.9 ± 1.1	3.5 ± 1.7	2.0 ± 1.5	2.6 ± 1.7	8.1 ± 4.8
	Total	1.9 ± 0.9	5.3 ± 2.2	3.6 ± 1.6	2.0 ± 1.3	12.0 ± 4.8	26.3 ± 11.8
5	Base	1.4 ± 0.7	2.9 ± 1.0	4.0 ± 1.3	2.6 ± 1.0	6.3 ± 4.0	11.7 ± 4.6
6	Base	1.7 ± 0.5	3.5 ± 1.0	2.4 ± 0.8	2.9 ± 1.0	9.3 ± 3.5	15.4 ± 4.3
7	Base	1.3 ± 0.4	2.8 ± 0.6	2.8 ± 1.0	2.8 ± 1.0	6.1 ± 2.2	13.1 ± 4.0

[a] Areas measured by trapezoidal rule.

absorption of erythromycin 2′-propanoate from Treatment 1 was reflected in high C_{max} values after single doses and greater area values after both single and repeated doses. Although Treatments 1–4 tended to yield higher C_{max} and area values for total drug than the stearate treatments, values for the free base were generally higher with the stearate. Food gave rise to later t_{max} values compared to fasted treatments in most cases.

Results obtained from pharmacokinetic analysis using the first-order absorption model after single and repeated doses are given in Tables VI and VII. Comparison of the r^2 values shows that this model describes the repeated dose data somewhat better than those from single doses.

Comparison of Tables VI and VII and the results from zero-order analysis in Table VIII indicates that, while the zero-order model may describe single-dose data somewhat better, the first-order model is superior following repeated doses. Using Treatment 2 as an example, the relative accuracy of the two models is indicated in Fig. 8. These curves were obtained from averaged data, but they illustrate the improved fit by the zero-order model to single-dose data and the somewhat better fit by the first-order model to the repeated dose data.

The two models yielded different drug elimination rates. This difference was partially artifactual since the value of k_{el} was held constant in the first-order case. However, the high correlations obtained with the first-order model, particularly after repeated doses, suggest that the visual estimates of k_{el} were quite accurate. The elimination half-lives obtained with the zero-order model were longer than reported values (6, 21, 22) while those from the first-order model were in agreement with previous values.

The comparisons in Table IX are somewhat varied, but the k_a and t_{lag} values indicate relatively slow absorption from Treatment 1 and, to a lesser extent, Treatment 5.

Treatments 5–7 generally resulted in higher k_{el} values than Treatments 1–4, probably due to slow hydrolysis of the propanoate ester to free base in the body. The *FD/V* value, which is a rate-independent measure of relative bioavailability, was higher following Treatment 1 than following other estolate treatments after single doses and following Treatments 2 and 3 after repeated doses. Treatment 1 yielded higher *FD/V* values for total drug activity than Treatments 3, 5, and 7, while Treatments 2, 4, and 6 gave higher values than Treatment 7.

To obtain a more meaningful comparison of plasma drug levels obtained with suspension and capsule doses, C_{max}, *FD/V*, and area values from single doses of the suspension (Treatment 4) were normalized to a dose of 500 mg. There were no significant differences between the normalized values and those obtained from Treatment 2.

DISCUSSION

The results show that, although erythromycin estolate gives rise to higher plasma levels of total antibiotic than equivalent doses of erythromycin stearate, it produces lower, if somewhat more consistent, levels of the free base.

The clinical significance of this finding is uncertain. Esters of erythromycin were found to be antibacterially inactive until hydrolyzed (27), yet *in vivo* studies in animals showed erythromycin 2′-propanoate to be at least as effective as erythromycin base in curing bacterial infections (28). The problem is compounded by the observation that the propanoate ester is more extensively bound to plasma proteins and may penetrate tissues less effectively than the free base, although evidence for this hypothesis is slight (18).

The observation that food and reduced fluid volume both reduce erythromycin stearate absorption is consistent with results of previous studies (16). Increased absorption from erythromycin estolate in the presence of food was unexpected. However, increased estolate absorption from a suspension due to food was reported previously (12).

Reduced absorption of the acid-labile erythromycin stearate due to

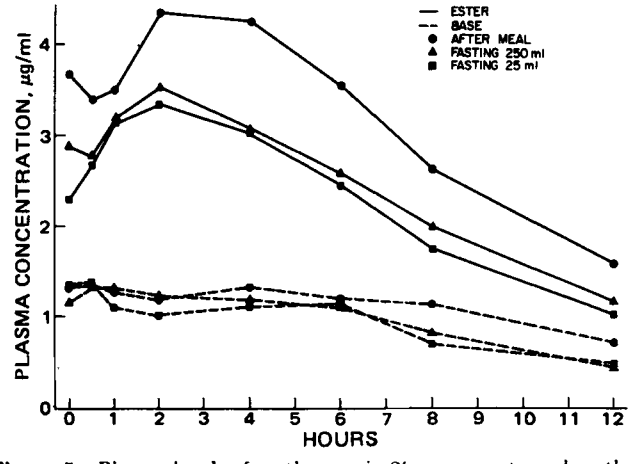

Figure 5—*Plasma levels of erythromycin 2′-propanoate and erythromycin base following repeated doses of erythromycin estolate capsules.*

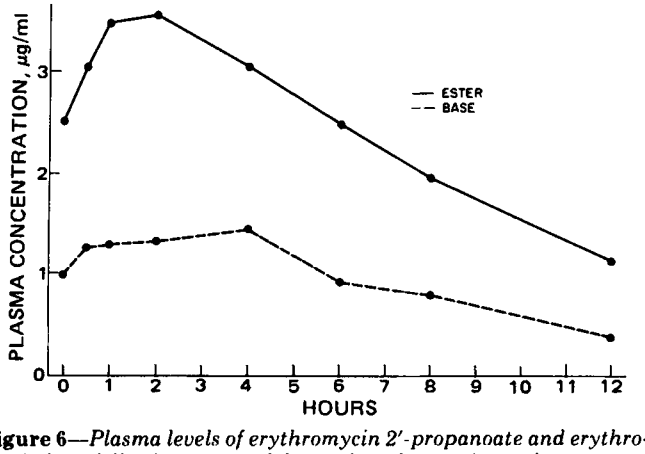

Figure 6—*Plasma levels of erythromycin 2′-propanoate and erythromycin base following repeated doses of erythromycin estolate suspension.*

Table V—Statistical Comparison of C_{max}, t_{max}, and AUC Values between Treatments following Single and Repeated Doses

Compound	C_{max}		t_{max}		$AUC_{0\text{-}12\ hr}$,	$AUC_{0\text{-}6\ hr}$,
	Single	Repeated	Single	Repeated	Single	Repeated
Ester	1 > 2-4	NSD	1 > 2-4	1 > 4	1 > 2-4	1 > 2-4
Base	5-7 > 2-4 6 > 1 > 2,4	5-7 > 1-4 6 > 5	1-3,5 > 6,7	NSD	1,5-7 > 2-4 6 > 5-7	5-7 > 1-3 6,7 > 4 6 > 5
Total	1 > 2-7 4,6 > 7	1-4 > 5-7 6 > 5	1 > 2-7 5 > 6,7	1 > 2-4 5-7 > 2,4	1 > 2-7 3,4,6 > 5,7 2,7	1-4 > 5-7 6 > 5

[a] Comparisons of ester, base, and total drug values were carried out as in Table II.

Table VI—Mean Values (±1 *SD*) of Pharmacokinetic Constants Obtained from Analysis of Individual Single-Dose Data Assuming a One-Compartment Model with First-Order Drug Input and Elimination

Treatment[a]	k_a, hr^{-1}	$t_{1/2}$ (absorbance), hr	k_{el}, hr^{-1}	$t_{1/2}$ (elimination), hr	t_{lag}, hr	FD/V, μg/ml	r^2 [b]
1 Ester	0.34 ± 0.09	2.2 ± 0.7	0.22 ± 0.05	3.3 ± 0.7	0.8 ± 0.26	5.4 ± 1.2	0.94 ± 0.02
Total	0.34 ± 0.10	2.3 ± 0.7	0.22 ± 0.04	3.5 ± 0.9	0.8 ± 0.26	7.2 ± 2.0	0.94 ± 0.02
2 Ester	0.75 ± 0.40	1.2 ± 0.7	0.20 ± 0.05	3.7 ± 1.1	0.2 ± 0.3	2.5 ± 1.1	0.95 ± 0.01
Total	0.69 ± 0.23	1.2 ± 0.5	0.20 ± 0.04	3.7 ± 0.9	0.4 ± 0.4	2.8 ± 1.1	0.95 ± 0.03
3 Ester	0.75 ± 0.39	1.3 ± 1.1	0.21 ± 0.08	3.7 ± 1.4	0.5 ± 0.3	2.4 ± 1.8	0.93 ± 0.05
Total	0.73 ± 0.41	1.6 ± 1.0	0.20 ± 0.05	3.7 ± 0.9	0.5 ± 0.3	3.0 ± 2.1	0.94 ± 0.05
4 Ester	0.67 ± 0.39	1.5 ± 1.0	0.22 ± 0.07	3.6 ± 1.5	0	2.8 ± 1.6	0.96 ± 0.03
Total	0.61 ± 0.32	1.5 ± 0.9	0.24 ± 0.07	3.1 ± 0.7	0	3.5 ± 2.0	0.96 ± 0.05
5 Base	0.61 ± 0.28	1.4 ± 0.5	0.37 ± 0.07	2.0 ± 0.4	1.3 ± 0.6	2.6 ± 1.8	0.87 ± 0.07
6 Base	0.59 ± 0.22	1.4 ± 0.6	0.36 ± 0.09	2.0 ± 0.5	0.6 ± 0.4	3.5 ± 1.2	0.94 ± 0.04
7 Base	0.61 ± 0.19	1.3 ± 0.5	0.30 ± 0.05	2.4 ± 0.4	0.6 ± 0.3	2.1 ± 0.07	0.91 ± 0.05

[a] Plasma erythromycin base levels from Treatments 1-4 were not subjected to pharmacokinetic analysis. [b] Coefficient of determination $(\Sigma^2_{obs} - \Sigma^2_{dev})/\Sigma^2_{obs}$.

Table VII—Mean Values (±1 *SD*) of Pharmacokinetic Constants Obtained from Analysis of Individual Data following Repeated Doses Assuming a One-Compartment Model with First-Order Drug Input and Elimination

Treatment[a]	k_a, hr^{-1}	$t_{1/2}$ (absorbance), hr	k_{el}, hr^{-1}	$t_{1/2}$ (elimination), hr	t_{lag}, hr	FD/V, μg/ml	r^2
1 Ester	0.34 ± 0.17	2.4 ± 1.0	0.22 ± 0.05	3.3 ± 0.7	0.7 ± 0.5	5.2 ± 1.3	0.99 ± 0.01
Total	0.28 ± 0.15	2.9 ± 1.0	0.22 ± 0.05	3.2 ± 0.6	0.6 ± 0.4	7.1 ± 1.6	0.99 ± 0.01
2 Ester	0.46 ± 0.37	2.0 ± 0.8	0.21 ± 0.05	3.6 ± 1.1	0.6 ± 0.6	3.8 ± 0.9	0.99 ± 0.01
Total	0.34 ± 0.10	2.3 ± 0.7	0.20 ± 0.04	3.7 ± 0.9	0.4 ± 0.4	5.6 ± 1.8	0.99 ± 0.01
3 Ester	0.40 ± 0.14	2.0 ± 0.7	0.21 ± 0.08	3.7 ± 1.4	0.1 ± 0.2	4.0 ± 2.2	0.99 ± 0.01
Total	0.37 ± 0.12	2.1 ± 0.7	0.20 ± 0.05	3.7 ± 1.0	0.2 ± 0.3	4.9 ± 1.7	0.99 ± 0.01
4 Ester	0.43 ± 0.16	1.9 ± 0.9	0.22 ± 0.07	3.6 ± 1.5	0	4.2 ± 2.1	0.99 ± 0.1
Total	0.37 ± 0.16	2.3 ± 1.4	0.30 ± 0.18	2.9 ± 1.0	0.2 ± 0.3	5.6 ± 2.0	0.99 ± 0.01
5 Base	0.48 ± 0.24	2.1 ± 1.8	0.37 ± 0.07	2.0 ± 0.4	0.6 ± 0.6	4.4 ± 1.5	0.91 ± 0.06
6 Base	0.49 ± 0.15	1.8 ± 1.1	0.34 ± 0.07	2.1 ± 0.5	0.5 ± 0.4	5.5 ± 1.8	0.93 ± 0.06
7 Base	0.43 ± 0.23	1.4 ± 1.7	0.30 ± 0.05	2.4 ± 0.4	0.3 ± 0.4	3.8 ± 1.3	0.93 ± 0.08

[a] Plasma erythromycin base levels from Treatments 1-4 were not subjected to pharmacokinetic analysis.

Table VIII—Mean Values (±1 *SD*) of Pharmacokinetic Constants Obtained from Analysis of Individual Single- and Multiple-Dose Data Assuming a One-Compartment Model with Zero-Order Input and First-Order Elimination

Treatment[a]	k_0F/V, μg/ml/hr	Single Dose			k_0F/V, μg/ml/hr	Repeated Dose		
		k_{el}, hr^{-1}	$t_{1/2}$ (elimination), hr	r^2		k_{el}, hr^{-1}	$t_{1/2}$ (elimination), hr	r^2
1 Ester	1.1 ± 0.2	0.12 ± 0.05	4.2 ± 1.5	0.98 ± 0.01	1.4 ± 0.5	0.14 ± 0.05	5.7 ± 1.9	0.98 ± 0.02
Total	1.4 ± 0.3	0.18 ± 0.04	4.0 ± 0.1	0.98 ± 0.01	1.3 ± 0.04	0.13 ± 1.0	5.8 ± 1.4	0.99 ± 0.01
2 Ester	0.91 ± 0.50	0.15 ± 0.06	5.5 ± 3.4	0.96 ± 0.03	1.2 ± 0.6	0.13 ± 0.03	5.6 ± 1.1	0.97 ± 0.03
Total	1.1 ± 0.6	0.17 ± 0.07	4.5 ± 1.8	0.96 ± 0.01	1.5 ± 0.7	0.11 ± 0.02	6.9 ● 1.4	0.96 ± 0.04
3 Ester	0.82 ± 0.42	0.22 ± 0.11	3.9 ± 1.9	0.96 ± 0.02	1.0 ± 0.5	0.12 ± 0.03	6.0 ± 1.5	0.95 ± 0.09
Total	0.95 ± 0.45	0.19 ± 0.07	4.2 ± 1.9	0.96 ± 0.02	1.3 ± 0.8	0.13 ± 0.03	5.7 ± 1.3	0.95 ± 0.05
4 Ester	0.98 ± 0.61	0.27 ± 0.11	3.8 ± 4.0	0.96 ± 0.02	1.0 ± 0.6	0.12 ± 0.03	6.1 ± 1.3	0.96 ± 0.04
Total	2.1 ± 1.5	0.29 ± 0.14	2.8 ± 1.2	0.94 ± 0.05	1.4 ± 0.6	0.38 ± 0.51	3.8 ± 1.9	0.95 ± 0.03
5 Base	0.95 ± 0.53	0.31 ± 0.04	2.3 ± 0.3	0.96 ± 0.04	1.6 ± 0.7	0.34 ± 0.17	2.2 ± 1.0	0.95 ± 0.03
6 Base	1.5 ± 0.70	0.22 ± 0.09	3.5 ± 0.9	0.95 ± 0.04	1.9 ± 1.0	0.34 ± 0.18	2.8 ± 2.4	0.95 ± 0.04
7 Base	1.8 ± 1.1	0.24 ± 0.05	2.9 ± 1.1	0.95 ± 0.05	1.1 ± 0.3	0.25 ± 0.16	3.5 ± 1.6	0.94 ± 0.07

[a] Plasma erythromycin base levels from Treatments 1-4 were not subjected to pharmacokinetic analysis.

Table IX—Statistical Comparison between Treatments of Some Pharmacokinetic Constants Described in Tables VI and VII

Compound[a]	k_a		k_{el}		t_{lag}		FD/V	
	Single	Repeated	Single	Repeated	Single	Repeated	Single	Repeated
Ester	2-4 > 1	NSD	NSD	—[b]	1 > 2,3 > 4	1,2 > 4	1 > 2-4	1 > 2,3
Base	NSD	NSD	5 > 7	—	5 > 6,7	NSD	6 > 7	6 > 7
Total	2-7 > 1	NSD	5-7 > 1-4	—	1 > 2-4 2,3,5-7 > 4	1 > 3,4	1 > 2-7 4 > 7	1 > 3,5,7 2,4,6 > 7

[a] Comparison of ester, base, and total drug values were carried out as in Table II, except that erythromycin base values were restricted to Treatments 5-7. [b] k_{el} was fixed at single-dose value.

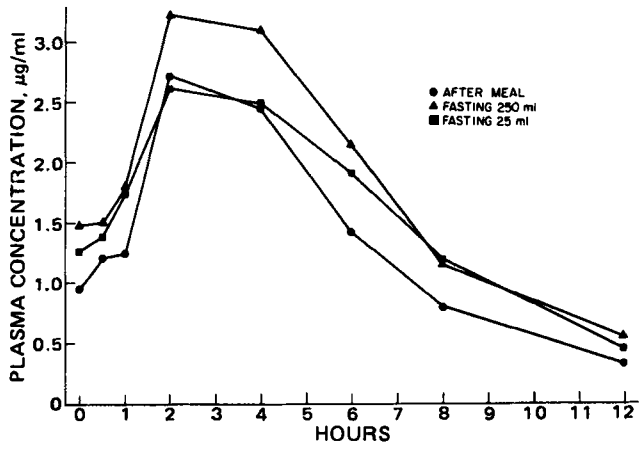

Figure 7—*Plasma levels of erythromycin following repeated doses of erythromycin stearate tablets.*

food and also low fluid volumes may be expected because both factors are likely to delay stomach emptying relative to that occurring after large water volume doses in the fasted state. Increased absorption of erythromycin estolate may be due to a longer stomach residence time increasing the extent of dissolution of this relatively acid-stable drug form. When the drug eventually passes from the stomach into the small intestine, it tends to be in solution form and is, therefore, rapidly and efficiently absorbed.

Results obtained with the erythromycin estolate suspension confirm that this dosage form gives rise to more rapid absorption than capsules. However, overall plasma levels are similar from the two formulations.

This study has not determined the most appropriate model to describe

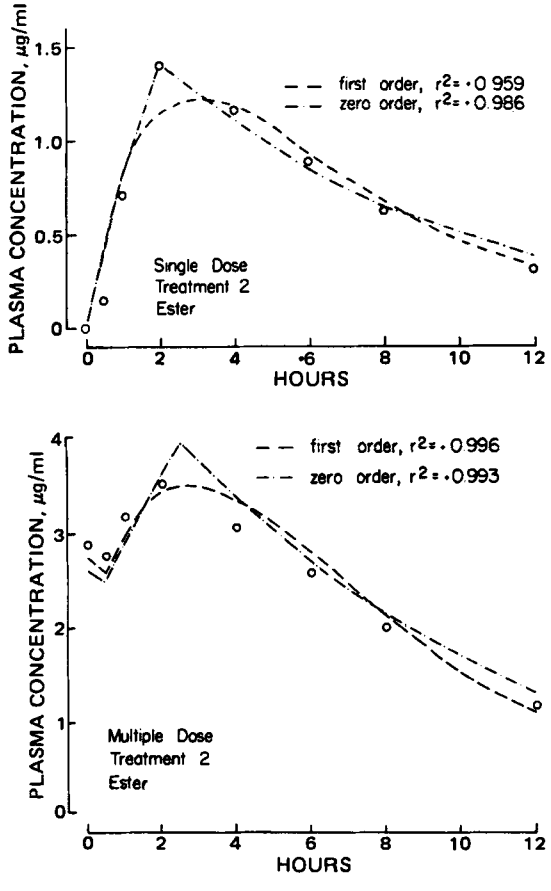

Figure 8—*Plasma curves obtained by fitting averaged data (O) from Treatment 2 following single (top) and repeated (bottom) doses using first- and zero-order absorption models.*

circulating erythromycin levels after oral dosing. After single-dose studies, plasma levels from both the estolate and stearate doses were described better using a zero-order absorption model. However, following repeated doses, the first-order model seemed more appropriate. The equivocal results obtained in this study contrast with those obtained by Colburn *et al.* (17) who presented considerable evidence of zero-order absorption using both enteric-coated erythromycin and film-coated erythromycin stearate tablets.

As indicated by Colburn *et al.* (17), single-dose plasma levels of erythromycin poorly predicted those obtained following repeated doses, with observed C_{max} values exceeding those predicted from single-dose data almost twofold. High drug levels during chronic dosing appear to be due to increased bioavailability, as reflected in *FD/V* values (Tables VI and VII), rather than absorption rates, which were somewhat lower after repeated dosing compared to single-dose values. Despite the poor relationship between single- and multiple-dose plasma levels of erythromycin, any treatment-dependent trends observed following single doses are likely to be maintained with repeated therapy.

REFERENCES

(1) G. A. Hall, C. E. Roberts, D. M. Perry, and W. M. M. Kirby, *Antibiot. Med. Clin. Ther.*, **7**, 231 (1960).

(2) C.-C. Lee, R. C. Anderson, and V. C. Stephens, *Antibiot. Chemother.*, **11**, 110 (1961).

(3) R. S. Griffith, M. Joiner, and H. Kottlowski, *ibid.*, **11**, 555 (1961).

(4) C. Weihl, *J. New Drugs*, **1**, 28 (1961).

(5) B. W. Billow, E. A. Thompson, A. Stern, and A. Florio, *Curr. Ther. Res.*, **6**, 381 (1964).

(6) P. J. McDonald, L. E. Mather, and M. J. Story, *J. Clin. Pharmacol.*, **17**, 601 (1972).

(7) P. G. Welling, *J. Pharmacokinet. Biopharm.*, **5**, 291 (1977).

(8) L. E. Josselyn and J. C. Sylvester, *Antibiot. Chemother.*, **3**, 63 (1952).

(9) J. W. Smith, R. W. Dyke, and R. S. Griffith, *J. Am. Med. Assoc.*, **151**, 805 (1953).

(10) W. E. Clapper, M. Mostyn, and G. H. Meade, *Antibiot. Med. Clin. Ther.*, **7**, 91 (1960).

(11) R. S. Griffith and H. R. Black, *Am. J. Med. Sci.*, **247**, 69 (1964).

(12) R. S. Griffith, M. Joiner, and H. Kottlowski, *Antibiot. Med. Clin. Ther.*, **7**, 320 (1960).

(13) H. A. Hirsch, C. V. Pryles, and M. Finland, *Am. J. Med. Sci.*, **239**, 198 (1960).

(14) Bioavailability Studies 73-190 and 75-103, Abbott Laboratories, North Chicago, Ill., 1976.

(15) J. C. Sylvester and L. E. Josselyn, *Antibiot. Chemother.*, **3**, 930 (1953).

(16) P. G. Welling, H. Huang, P. F. Hewitt, and L. L. Lyons, *J. Pharm. Sci.*, **67**, 764 (1978).

(17) W. A. Colburn, A. R. DiSanto, and M. Gibaldi, *J. Clin. Pharmacol.*, **17**, 592 (1977).

(18) R. G. Wiegand and A. H. C. Chun, *J. Pharm. Sci.*, **61**, 425 (1972).

(19) K.-Y. Tserng and J. G. Wagner, *Anal. Chem.*, **48**, 348 (1976).

(20) C. W. Derrick and H. C. Dillon, *Arch. Am. J. Dis. Child.*, **130**, 125 (1976).

(21) P. G. Welling and W. A. Craig, *J. Pharm. Sci.*, **67**, 1057 (1978).

(22) J. G. Wagner and C. M. Metzler, *ibid.*, **56**, 658 (1967).

(23) P. G. Welling, W. A. Craig, G. L. Amidon, and C. M. Kunin, *J. Infect. Dis., Suppl.*, **128**, S556 (1973).

(24) F. L. S. Tse and P. G. Welling, *J. Pharm. Sci.*, **66**, 1751 (1977).

(25) L. Saunders and T. Natunen, presented at the British Pharmaceutical Conference, London, England, Sept. 1973.

(26) V. C. Stephens, C. T. Pugh, N. E. Davis, M. M. Hochn, S. Ralston, M. C. Sparks, and L. Thompkins, *J. Antibiot.*, **22**, 551 (1970).

(27) P. L. Tardrew, J. C. H. Mao, and D. Kenney, *Appl. Microbiol.*, **18**, 159 (1969).

(28) W. E. Wick and G. E. Mallett, *Antimicrob. Agents Chemother.*, 1968, 410 (1969).

ACKNOWLEDGMENTS

Supported in part by National Institutes of Health Grant GM 20327 and by a grant from Eli Lilly and Co.

Metabolism, Plasma or Serum Levels, and Elimination of Phenformin in Guinea Pigs, Rats, and Dogs

DAVID ALKALAY ˣ, JOSEPH VOLK, WILLIAM ROTH, LAKSHMI KHEMANI, and M. FRED BARTLETT

Received November 2, 1977, from the *Research Department, The Pharmaceuticals Division, Ciba-Geigy Corporation, Ardsley, NY 10502.* Accepted for publication June 28, 1978.

Abstract □ ^{14}C-Phenformin hydrochloride was used for investigating the metabolism, plasma or serum levels, and elimination of the drug following 1.5-mg/kg po or iv doses to guinea pigs, rats, and dogs. The amounts of individual metabolites and unchanged drug were assessed in urine as well as in plasma or serum. The glucuronide of 1-(*p*-hydroxyphenethyl)biguanide was a major metabolite in the blood and urine of all three species. Guinea pig serum and urine contained a sizable quantity of unchanged drug. Dog plasma and urine had significant amounts of nonconjugated 1-(*p*-hydroxyphenethyl)biguanide and of an unidentified major metabolite. In all three species following intravenous drug administration, unchanged drug contributed significantly to the radioactivity found in blood and urine. The apparent half-lives of phenformin elimination were 0.3–0.8 day for guinea pigs and rats and 1–1.5 days for dogs. Urinary excretion data indicate apparent half-lives of approximately 1.3–1.5 days for the elimination of each of the three major metabolites in dogs.

Keyphrases □ Phenformin—metabolism, plasma or serum levels, and elimination in guinea pigs, rats, and dogs, TLC-autoradiographic analysis □ Metabolism—phenformin in guinea pigs, rats, and dogs, TLC-autoradiographic analysis □ Plasma or serum levels—phenformin in guinea pigs, rats, and dogs, TLC-autoradiographic analysis □ Elimination—phenformin in guinea pigs, rats, and dogs, TLC-autoradiographic analysis □ TLC-autoradiography—analysis, phenformin in biological fluids □ Autoradiography-TLC—analysis, phenformin in biological fluids □ Antidiabetic agents—phenformin, metabolism, plasma or serum levels, and elimination in guinea pigs, rats, and dogs, TLC-autoradiographic analysis

The absorption, metabolism, and elimination of phenformin (I) in several animal species and in humans were first investigated when specific and sensitive methods for analysis of this hypoglycemic drug were not available. By relying on the use of ^{3}H-phenformin and various chromatographic techniques, Beckmann (1, 2) demonstrated that 1-(*p*-hydroxyphenethyl)biguanide (II) and its *O*-glucuronide conjugate (III) were the major drug metabolites. He reported that rats excreted II and III in urine; that mice, guinea pigs, and rabbits excreted I, II, and III; and that humans eliminated only I and II. The identities of II and III were confirmed by Murphy and Wick (3).

Recent methodology that permits the determination of trace amounts of phenformin in biological fluids (4, 5) was applied to investigate phenformin pharmacokinetics in humans (6). In the present work, TLC in conjunction with autoradiography was used for investigating the pharmacokinetics, metabolism, and disposition of the drug in guinea pigs, rats, and dogs.

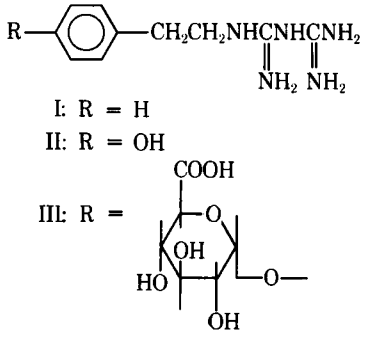

Table I—Percent of Radioactivity Excreted Renally by Three Guinea Pigs during the 24 hr following 1.5 mg of ^{14}C-Phenformin Hydrochloride/kg

Guinea Pig Number	Guinea Pig Weight, g	Drug Administration	Percent of Dose Excreted Renally as I[a]	I[b]	II[a]	III[a]	Unaccounted	Total[c]
28	725	Intravenous	34.3	34.5	3.2	14.9	7.3	59.7
31	745	Oral	17.1	17.0	5.3	8.7	4.8	35.8
34	805	Oral	15.8	14.3	4.8	17.9	6.8	45.3

[a] Determined by quantitative TLC. [b] Determined by GLC. [c] Determined by liquid scintillation counting of urine radioactivity.

EXPERIMENTAL

Chemicals—The reagents and solvents were: 28% ammonium hydroxide[1], reagent grade; 1-butanol[1], reagent grade; chloroform[1], reagent grade; ^{14}C-I and II (as hydrochlorides)[2]; 2,2-dichloro-1,1-difluoroethyl methyl ether[3]; heparin[4]; liquid scintillation counting medium[5]; methane[6], technical grade; phenformin hydrochloride[7]; and 2-propanol[1], reagent grade.

Animal Experiments—Healthy, young, male animals were fasted overnight prior to dosing. Unless otherwise specified, the drug was administered as an aqueous solution. Throughout the experiments, the animals were housed in appropriate metabolism cages. Food and excess water were supplied once daily. Feces and urine were collected and kept frozen until needed.

Guinea pigs[8], ~800 g, were given oral doses by intubation and intravenous doses in the jugular vein following sedation[3]. Blood specimens were withdrawn by heart puncture and stored overnight at 4°. After removal of the clots, the resulting serum samples were frozen until further use.

The rats[9], ~275 g, were given oral doses by intubation and intravenous doses into the tail vein. Blood samples, obtained from the tail, were centrifuged, and the resulting serums were frozen for further use. The total amount of collected blood usually was kept below 2.5 ml/animal.

Purebred beagle dogs, ~12 kg, were given the drug orally in a gelatin capsule[10] and intravenously into the cephalic vein. Blood specimens were withdrawn from the jugular vein with a heparinized syringe. They were centrifuged within 1 hr, and the separated plasma samples were kept frozen until needed.

Quantitative TLC—Prescored 250-μm silica gel plates[11] were divided into 20 parallel bands of 1-cm width each with a scriber[12]. Alternate bands were spotted with samples, in amounts not exceeding 10 μl, using disposable microsampling pipets[13].

Two solvent systems proved suitable. System A contained ammonium

[1] J. T. Baker Chemical Co., Phillipsburg, NJ 08865.
[2] The ^{14}C-radioactivity was associated with the β-carbon atom in the phenethyl moiety of I (18 μCi/mg) and with the two carbon atoms in the biguanide moiety of II (24 μCi/mg).
[3] Metaphane, Pitman-Moore, Inc., Washington Crossing, NJ 07902.
[4] Liquaemin Sodium "10", Organon, Inc., West Orange, N.J.
[5] Scintisol Complete, Isolab, Inc., Akron, OH 44321.
[6] Matheson Gas Products, East Rutherford, NJ 07073.
[7] Ciba-Geigy Corp., Summit, NJ 07901.
[8] Hartley variety, Elm Hill Farms, Chelmsford, MA 01824.
[9] Sprague-Dawley CD variety, Charles River Breeding Laboratories, Wilmington, MA 01887.
[10] Eli Lilly and Co., Indianapolis, IN 46206.
[11] Silica gel GF Uniplates (20 × 20 cm), Analtech, Inc., Newark, DE 19711.
[12] TLC scriber, Applied Science Laboratories, State College, PA 16801.
[13] Corning Glass Works, Corning, NY 14830.

0022-3549/79/0200-0156$01.00/0
© 1979, American Pharmaceutical Association

Table II—Metabolic Profiles of Serum Samples from Three Guinea Pigs after 1.5 mg of ^{14}C-Phenformin Hydrochloride/kg

Guinea Pig	Drug Administration Route	Blood Withdrawal Time, hr	Percent of Radioactivity Attributed to				
			I[a]	I[b]	II[a]	III[a]	Unaccounted
28	Intravenous	0.27	68	84	<3[c]	17[c]	12
28	Intravenous	1	31[c]	35	<3[c]	58	8
31	Oral	1	29[c]	43	7[c]	56[c]	8
31	Oral	3	14[c]	12	≤3[c]	73[c]	10
34	Oral	2	11[c]	14	<3[c]	79	7
34	Oral	3	9[c]	11	<3[c]	79	8

[a] Determined by quantitative TLC. [b] Determined by GLC. [c] Sample radioactivity was less than three times the background level.

hydroxide (10 ml), water (10 ml), 2-propanol (45 ml), 1-butanol (25 ml), and chloroform (20 ml). System B was similar, except that the amounts of water and chloroform were 16 and 14 ml, respectively. At room temperature and in tanks[14] containing 100 ml of the chosen solvent system, the plates required approximately 4 hr for development.

Autoradiograms were obtained in cassettes[15], modified to accept TLC plates, by exposing X-ray film[16] to the radioactivity of the developed plates. The time of exposure (1 week to several months) depended on the amount of radioactivity of the spotted sample. Film development proceeded as recommended by the manufacturer.

Each TLC plate was separated into zones assigned to various metabolites on the basis of the visual appearance of the corresponding autoradiogram. The silica gel material of these zones was carefully scraped into glass vials, and the radioactivity was assessed by liquid scintillation counting. This procedure permitted determination of the relative proportion of different metabolites found on the TLC plate and, consequently, their quantification in the body fluid used for spotting the plate. Thus, quantitative metabolic profiles were obtained for selected serum or plasma samples. By correcting for the volumes of all urine fractions and by adding all individual results, cumulative renal excretion data were obtained both for unchanged drug and for various metabolites.

Enzymatic Hydrolysis of Urine Samples—Selected urine samples were subjected to enzymatic hydrolysis[17,18] in accordance with published procedures (7).

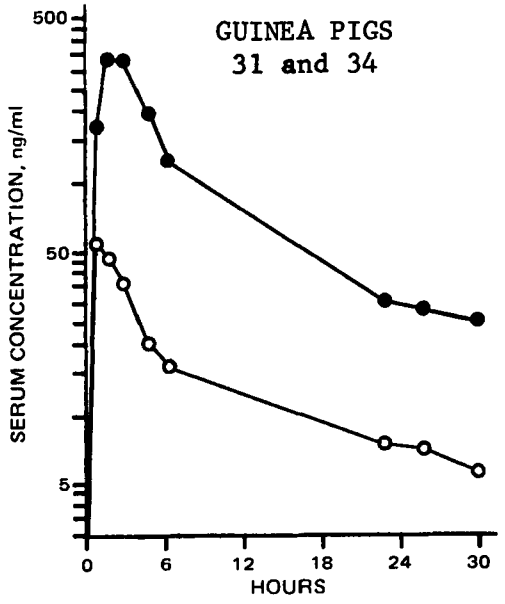

Figure 1—*Average concentration-time plots of phenformin (○) and total radioactivity (●) in serum resulting from 1.5-mg/kg po doses of ^{14}C-phenformin hydrochloride administered to two guinea pigs.*

[14] Desaga TLC tanks, Brinkmann Instruments, Westbury, NY 11590.
[15] Wafer Rigidform cassettes, Halsey X-ray Products, Brooklyn, N.Y.
[16] Blue brand type BB54, Eastman Kodak Co., Rochester, NY 14650.
[17] Glusulase, Endo Laboratories, Garden City, NY 11530.
[18] Ketodase, General Diagnostics Division, Warner-Chilcott, Morris Plains, N.J.

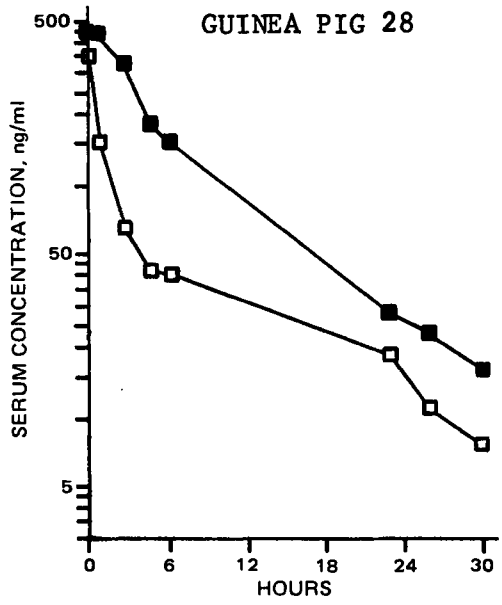

Figure 2—*Concentration-time plots of phenformin (□) and total radioactivity (■) in serum resulting from a 1.5-mg/kg iv dose of ^{14}C-phenformin hydrochloride administered to a guinea pig.*

Fecal Samples—Representative samples were obtained by pretreatment of collected fecal materials.

Rat feces were dried in an oven at 60°. The dry residues were weighed and then ground to a powder with a mortar and pestle.

Preweighed dog feces were homogenized in a blender with a threefold amount of distilled water. Several 10-ml fractions were measured with a pipet and transferred into 20-ml glass vials for lyophilization[19]. The residues were broken up to a powder.

Radioactivity Measurements—A radioscanner[20] was used for scanning developed TLC plates. Operating parameters included ×3 for high voltage, 50-mv sensitivity, 10-counts/sec range, 10-power/time constant, 10-cm/hr scanning speed, 25-ml/min methane quench gas flow, and 2 × 16-mm window slit.

The radioactivity of feces was assessed by placing powdered fecal

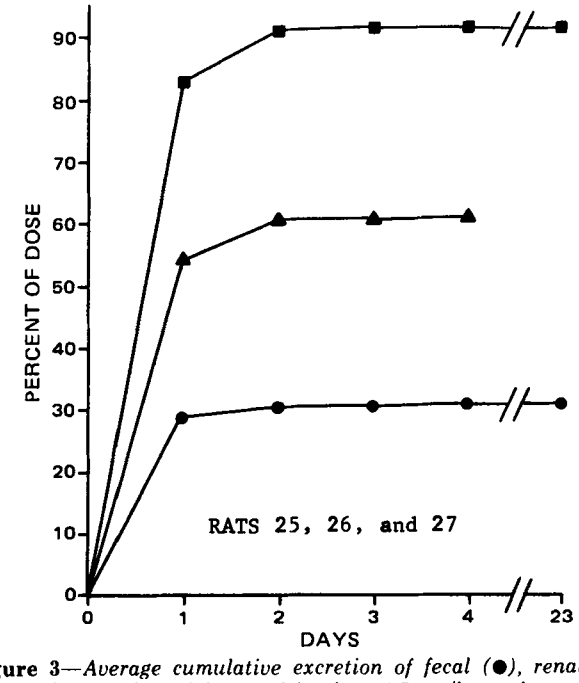

Figure 3—*Average cumulative excretion of fecal (●), renal (▲), and total (■) radioactivity resulting from 1.5-mg/kg po doses of ^{14}C-phenformin hydrochloride administered to three rats.*

[19] Model 10-145 MR-BA lyophilizer, Virtis Co., Gardiner, N.Y.
[20] Model LB 2722, Varian Instrument Division, Palo Alto, CA 94303.

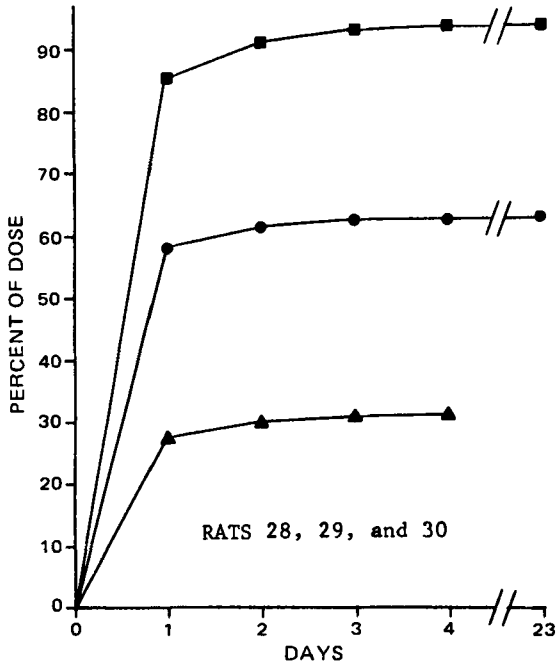

Figure 4—*Average cumulative excretion of fecal (●), renal (▲), and total (■) radioactivity resulting from 1.5-mg/kg iv doses of ^{14}C-phenformin hydrochloride administered to three rats.*

residue samples into size 0 gelatin capsules and burning them in an oxidizer[21]. The resulting $^{14}CO_2$, trapped in ethanolamine, was used for liquid scintillation counting[22]. The latter was done with 10-ml amounts of counting medium[5] for both liquid and silica gel radioactive samples.

GLC Determination of Phenformin—The specific and sensitive method employed is based on the conversion of biguanides into substituted *s*-triazines assayable by GLC and electron-capture detection or selected ion monitoring (4, 5). The gas chromatograph had ^{63}Ni-

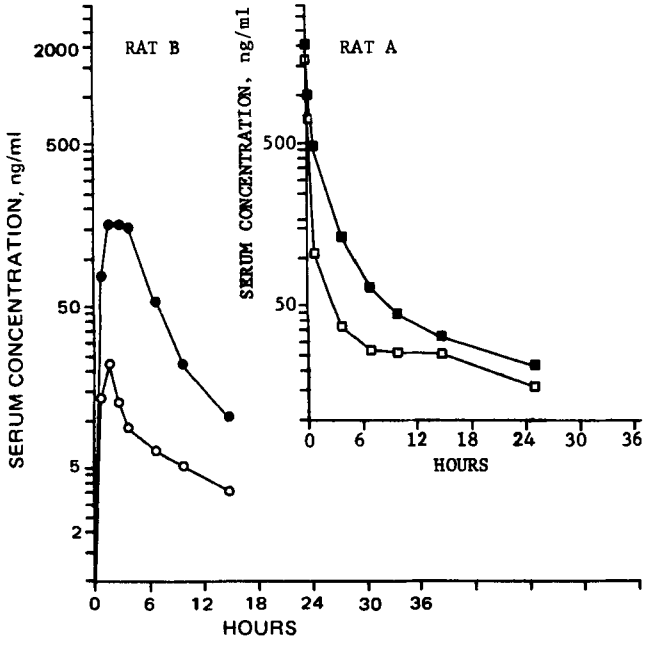

Figure 5—*Concentration–time plots of phenformin (□,○) and total radioactivity (■,●) in serum resulting from 1.5-mg/kg doses of ^{14}C-phenformin hydrochloride administered intravenously to Rat A and orally to Rat B.*

[21] Tri-Carb model 305, Packard Instrument Co., Downers Grove, IL 60515.
[22] Intertechnique model SL-40, Teledyne-Intertechnique, Westwood, NJ 07675.

Table III—Percent of Radioactivity Excreted Renally by Six Rats following 1.5 mg of ^{14}C-Phenformin Hydrochloride/kg

Rat	Drug Administration Route	Percent of Dose Excreted Renally as I[a]	I[b]	II[a]	III[a]	Unaccounted	Total[c]
25	Oral	0.3	0.4	1.0	25.1	2.4	28.7
26	Oral	0.6	0.5	1.9	24.8	2.0	29.2
27	Oral	0.6	0.2	0.7	28.5	3.1	32.9
28	Intravenous	18.6	18.3	9.1	26.6	5.0	59.3
29	Intravenous	16.7	15.5	15.1	25.9	4.4	62.0
30	Intravenous	16.9	12.6	15.2	28.0	4.7	64.8
Mean	Oral	0.5	0.4	1.2	26.1	2.5	30.3
Mean	Intravenous	17.3	15.5	13.2	26.8	4.7	62.1

[a] Determined by quantitative TLC. [b] Determined by GLC. [c] Determined by liquid scintillation counting of urine radioactivity.

electron-capture detection capabilities[23] and was equipped with a silanized glass column, 180 cm × 2 mm i.d., packed with 3% OV-17 on 80–100-mesh Chromosorb W HP[24].

RESULTS AND DISCUSSION

The sensitivity of quantitative TLC was extended significantly by autoradiography. This technique permitted the analysis of biological fluid samples with radioactivity levels undetectable by radioscanning. Its accuracy was estimated by comparison with independent GLC results. Renal phenformin data, representing the excretion of less than 6% of the administered radioactivity, and serum or plasma data, from samples whose phenformin radioactivity was less than three times the background level, were less accurate. They were associated with a relative standard deviation[25] of 26%. The accuracy of all other phenformin data was con-

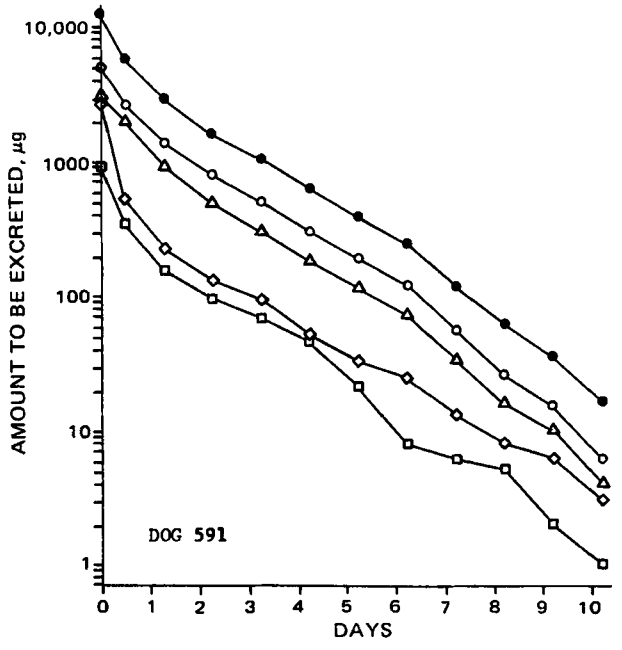

Figure 6—*"Sigma minus" plots for phenformin (□), II (○), III (△), IV (◇), and total radioactivity (●) based on renal data resulting from a 1.5-mg/kg po dose of ^{14}C-phenformin hydrochloride administered to a beagle dog.*

[23] Model 2100 gas chromatograph, Varian, Palo Alto, Calif.
[24] Ohio Valley Specialty Chemicals, Inc., Marietta, OH 45750.
[25] The relative standard deviation was calculated from:

$$S_{rel}(x) = 100\sqrt{\frac{2\Sigma(1/2\, d/m)^2}{n-1}}$$

where d is the difference between duplicates, m is the arithmetic mean of each duplicate determination, and n is the number of determinations.

Table IV—Metabolic Profiles of Serum Samples Obtained from a Rat after 1.5 mg of ^{14}C-Phenformin Hydrochloride/kg iv

Blood Withdrawal Time, min	Percent of Radioactivity Attributed to				
	I[a]	I[b]	II[a]	III[a]	Unaccounted
5	86	83	3	2	9
15	83	73	3[c]	4[c]	13
60	26[c]	23	15[c]	45[c]	14

[a] Determined by quantitative TLC. [b] Determined by GLC. [c] Sample radioactivity was less than three times the background level.

siderably better and was associated with a relative standard deviation of 7%. These values are based on analytical data abstracted from Tables I–VI.

Half-lives were estimated by least-squares fitting of the last five or more data points on the terminal log-linear parts of the concentration–time curves[26].

Guinea Pigs—A single 1.5-mg/kg dose of ^{14}C-phenformin hydrochloride was administered orally to two guinea pigs and intravenously to a third animal. Excretion data were obtained from urine collected for 24 hr (Table I). Phenformin and Metabolites II and III were assessed by quantitative TLC. The amounts of phenformin also were confirmed by GLC determinations.

The identity of phenolic Metabolite II is indicated by the similarity in TLC behavior of an authentic sample. Metabolite III exhibited properties similar to a metabolite in the rat and dog, which, as will be shown, was identified as the glucuronide conjugate of II.

Metabolic profiles were obtained for selected serum samples by use of quantitative TLC (Table II). Glucuronide III was the major radioactive component in all serum samples taken at 1 or more hr after oral or intravenous drug administration.

Serum concentration–time data for phenformin and for total radioactivity are presented graphically in Figs. 1 and 2. The apparent half-lives of elimination were comparable and averaged 11 hr[26].

Rats—Single 1.5-mg/kg doses of ^{14}C-phenformin hydrochloride were given to five rats orally and to five rats intravenously. The resulting five pairs of rats were used as follows.

The rats from one pair were placed individually in metabolism cages[27]. For 24 hr, exhaled carbon dioxide was trapped without detection of any radioactivity.

Excretion data were obtained from three pairs of rats, whose urine and feces were collected for 23 days. About 90% of the administered radioactivity was excreted within 2 days. After the 4th day, the elimination of radioactivity was negligible and amounted to less than 0.05% of the dose. Cumulative radioactivity excretion data for orally and intravenously treated rats are plotted in Figs. 3 and 4, respectively. About 31% of the radioactivity was found in the feces even after intravenous drug administration. Consequently, the biliary route of excretion appears to be significant for rats. Fecal radioactivity amounted to about 61% of the oral dose. This value agrees with data obtained by Beckmann (1), who reported that 5–12% of oral doses were eliminated by the biliary route and concluded that oral absorption was incomplete.

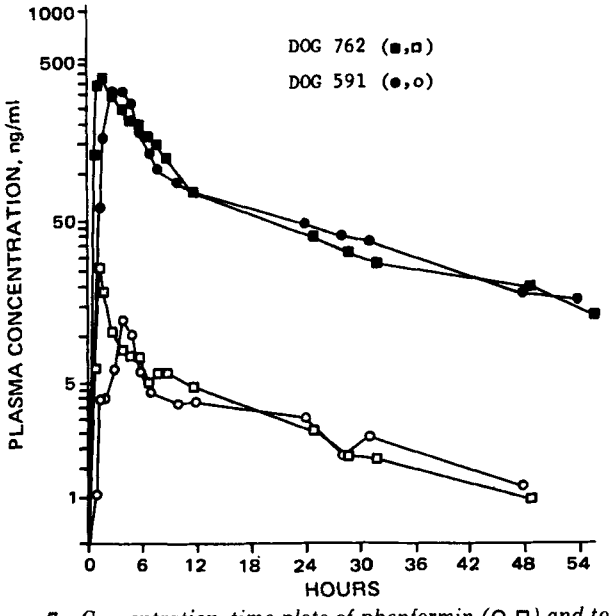

Figure 7—*Concentration–time plots of phenformin (○,□) and total radioactivity (●,■) in plasma resulting from 1.5-mg/kg po doses of ^{14}C-phenformin hydrochloride administered to two beagle dogs.*

[26] Apparent half-lives for the radioactivity elimination data presented in Figs. 1 and 5 (Rat A) were based on the last four data points.
[27] Roth.

Table V—Percent of Radioactivity Excreted Renally by Two Dogs during the Indicated Collection Periods following 1.5 mg of ^{14}C-Phenformin Hydrochloride/kg

Dog	Drug Administration Route	Collection Hours	Percent of Dose Excreted Renally as						
			I[a]	I[b]	II[a]	III[a]	IV[a]	Unaccounted	Total[c]
591	Intravenous	150	26.8	23.0	15.8	13.7	13.9	6.7	77.0
762	Intravenous	270	25.7	23.9	17.4	14.6	12.3	6.6	76.5
591	Oral	270	4.9	2.3	27.5	17.0	14.5	8.1	72.0
762	Oral	150	5.4	2.5	22.3	15.3	14.2	5.9	63.1
Mean	Intravenous		26.3	23.5	16.6	14.2	13.1	6.6	76.7
Mean	Oral		5.2	2.4	24.9	16.1	14.3	7.0	67.5

[a] Determined by quantitative TLC. [b] Determined by GLC. [c] Determined by liquid scintillation counting of urine radioactivity.

Phenformin, II, and III were found in urine and assessed by quantitative TLC. Due to rapidly decreasing radioactivity levels, only samples collected for 2 days after the oral dose and for 3 days after the intravenous dose were analyzed. Phenformin analyses were performed also by GLC (Table III). Independently of the drug administration route, III proved to be the major radioactive component in rat urine. Its identity was established by enzymatic hydrolysis.

Prior to and after hydrolysis, the samples were analyzed by GLC and by quantitative TLC. Only trace amounts of phenformin were found before and after hydrolysis. The radioactivity associated with III was essentially lost during hydrolysis and was replaced by radioactivity associated with II. Considering the experimental conditions, the choice of enzymes[17,18], and the analytical results, it may be concluded that III is a glucuronide conjugate of 1-(*p*-hydroxyphenethyl)biguanide.

A serum metabolic profile was obtained with samples from an intravenously treated rat. Quantitative TLC results (Table IV) indicate that III was the major radioactive component not only in urine but also in blood. The serum concentration–time curve for this animal and the one obtained for an orally dosed rat are plotted in Fig. 5. The intravenous data indicate half-lives for phenformin and for total radioactivity that were comparable and averaged about 17 hr. Oral dose concentrations were too low for estimation of apparent half-lives with a reasonable degree of confidence.

Dogs—Two dogs were given single oral and intravenous ^{14}C-phenformin hydrochloride doses of 1.5 mg/kg. They were treated in a crossover fashion with a 5-week washout period between drug administrations. Unlike rats, the fecal radioactivity excretion of dogs was not very significant, averaging 7% of the intravenous dose and 11% of the oral dose. Most radioactivity was excreted renally.

In analogy with both guinea pigs and rats, dog urine contained significant amounts of phenformin, II, and III. In addition, a radioactive urinary component (Metabolite IV) was also present. In Solvent System B, the R_f values of I, II, III, and IV were 0.39, 0.34, 0.10, and 0.48, respectively. The identities of I and II were confirmed by TLC and radio-

Table VI—Metabolic Profiles of Plasma Samples from Two Dogs following 1.5 mg of ^{14}C-Phenformin Hydrochloride/kg

Dog	Drug Administration Route	Blood Withdrawal Time, hr	Percent of Radioactivity Attributed to					
			I[a]	I[b]	II[a]	III[a]	IV[a]	Unaccounted
591	Oral	3	6[c]	5	28[c]	10[c]	30[c]	26
591	Oral	4	11[c]	4	24[c]	16[c]	27[c]	22
591	Oral	6	6[c]	3	15[c]	23[c]	8[c]	48
762	Intravenous	0.08	77	92	4[c]	2[c]	2[c]	15
762	Intravenous	0.25	48	51	20[c]	3[c]	17[c]	12
762	Intravenous	2	30[c]	20	8[c]	14[c]	17[c]	32

[a] Determined by quantitative TLC. [b] Determined by GLC. [c] Sample radioactivity was less than three times the background level.

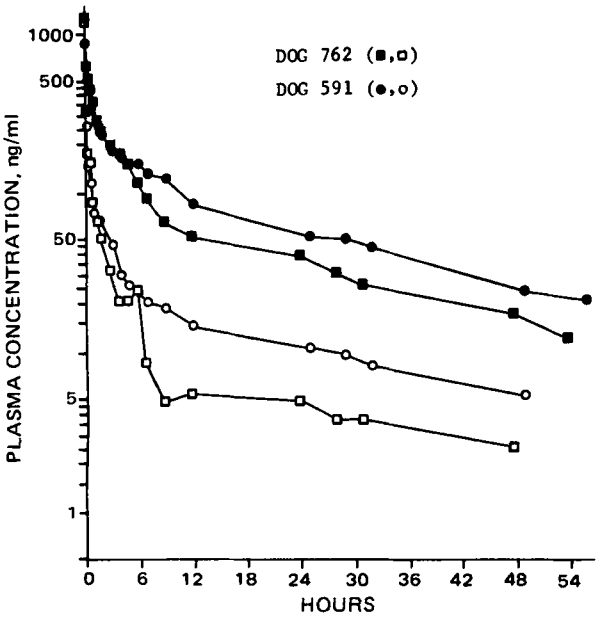

Figure 8—*Concentration-time plots of phenformin (○,□) and total radioactivity (●,■) in plasma resulting from 1.5-mg/kg iv doses of ^{14}C-phenformin hydrochloride administered to two beagle dogs.*

scanning comparisons, and the identity of III was determined by enzymatic hydrolysis experiments similar to those described for rats. Metabolite IV remains to be identified.

The amounts of renally excreted I–IV, as percentages of total administered radioactivity, are presented in Table V. The relatively high urinary radioactivity levels and the lengthy time of collection permitted the preparation of "sigma minus" plots for phenformin, for each metabolite, and for total radioactivity (as apparent drug). These plots allowed the estimation of apparent disposition half-lives for I–IV and total radioactivity. The values averaged 35–37 hr. Figure 6 illustrates the results obtained from one dog after oral drug administration. Similar data were obtained from the second dog after intravenous drug administration. The theoretical considerations and an appraisal of this method were discussed by Martin (8).

Plasma metabolic profiles were obtained after oral and intravenous drug administrations. Quantitative TLC results (Table VI) indicate the presence in plasma of significant amounts of unchanged drug and of each of the three metabolites. Plasma concentration–time curves resulting from single oral and intravenous doses were obtained for both animals (Figs. 7 and 8). The terminal log-linear parts of the curves indicate comparable elimination half-lives for phenformin and for total radioactivity. They averaged about 26 hr.

REFERENCES

(1) R. Beckmann, *Diabetologia*, **3**, 368 (1967).

(2) R. Beckmann, *Ann. N.Y. Acad. Sci.*, **148**, 820 (1968).

(3) P. Murphy and A. Wick, *J. Pharm. Sci.*, **57**, 1125 (1968).

(4) S. Matin, J. Karam, and P. Forsham, *Anal. Chem.*, **47**, 545 (1975).

(5) D. Alkalay, J. Volk, and M. Bartlett, *J. Pharm. Sci.*, **65**, 525 (1976).

(6) D. Alkalay, L. Khemani, W. Wagner, Jr., and M. Bartlett, *J. Clin. Pharmacol.*, **15**, 446 (1975).

(7) W. Conway, H. Minatoya, A. Lands, and J. Shekosky, *J. Pharm. Sci.*, **57**, 1134 (1968).

(8) B. Martin, *Br. J. Pharmacol. Chemother.*, **29**, 181 (1967).

ACKNOWLEDGMENTS

The authors thank Dr. N. Chaudhuri and Mr. T. Ball, who prepared the radioactive compounds.

Fluorocarbon Aerosol Propellants XII: Correlation of Blood Levels of Trichloromonofluoromethane to Cardiovascular and Respiratory Responses in Anesthetized Dogs

YASH M. AMIN, EMMANUEL B. THOMPSON, and WIN L. CHIOU ˣ

Received July 27, 1976, from the *Clinical Pharmacokinetiçs Laboratory and the Department of Pharmacy, Department of Pharmacognosy and Pharmacology, College of Pharmacy, University of Illinois at the Medical Center, Chicago, IL 60612.* Accepted for publication June 28, 1978.

Abstract □ Anesthetized mongrel dogs were exposed to various concentrations of trichloromonofluoromethane. Before, during, and after the inhalation, arterial and venous blood samples were obtained for fluorocarbon analysis. After the cessation of fluorocarbon inhalation, a multiexponential decline from the blood was observed. This finding was similar to that of a previous study in which the fluorocarbon was administered intravenously to unanesthetized dogs. The half-life calculated from the terminal phase was about 280 min, and the pseudodistribution equilibrium was reached about 100 min after dosing. Study of the relationship between blood fluorocarbon levels and effects on the respiration rate and arterial blood pressure indicates that the sites of these pharmacological activities are located in the blood or central compartment rather than in the peripheral compartment. The effect on the heart rate appears to be quite instantaneous after inhalation. These results might shed some light on the fast effect of the fluorocarbon propellants, which caused sudden deaths after inhalation of a large quantity.

Keyphrases □ Trichloromonofluoromethane—blood levels correlated to cardiovascular and respiratory responses in dogs □ Cardiovascular responses—trichloromonofluoromethane, correlated to blood levels in dogs □ Respiratory responses—trichloromonofluoromethane, correlated to blood levels in dogs □ Aerosol propellants—trichloromonofluoromethane, blood levels correlated to cardiovascular and respiratory responses in dogs □ Fluorocarbon aerosol propellants—trichloromonofluoromethane, blood levels correlated to cardiovascular and respiratory responses in dogs

Because of the wide use of fluorocarbon aerosol propellants in various household, cosmetic, and pharmaceutical pressurized packages, the possible adverse effects or toxicities of these compounds have been studied extensively. These studies concerned the effects on the cardiovascular system (1–8), enzyme activities (5, 9–11), muta-

0022-3549/79/0200-0160$01.00/0
© 1979, American Pharmaceutical Association

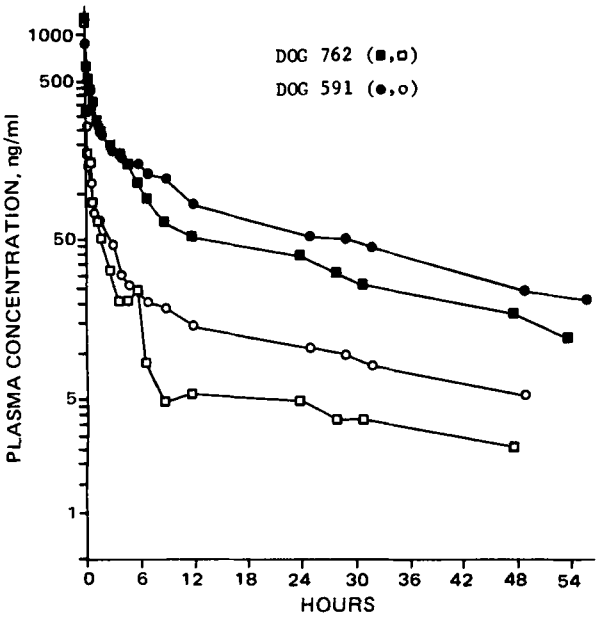

Figure 8—*Concentration-time plots of phenformin (○,□) and total radioactivity (●,■) in plasma resulting from 1.5-mg/kg iv doses of ^{14}C-phenformin hydrochloride administered to two beagle dogs.*

scanning comparisons, and the identity of III was determined by enzymatic hydrolysis experiments similar to those described for rats. Metabolite IV remains to be identified.

The amounts of renally excreted I–IV, as percentages of total administered radioactivity, are presented in Table V. The relatively high urinary radioactivity levels and the lengthy time of collection permitted the preparation of "sigma minus" plots for phenformin, for each metabolite, and for total radioactivity (as apparent drug). These plots allowed the estimation of apparent disposition half-lives for I–IV and total radioactivity. The values averaged 35–37 hr. Figure 6 illustrates the results obtained from one dog after oral drug administration. Similar data were obtained from the second dog after intravenous drug administration. The theoretical considerations and an appraisal of this method were discussed by Martin (8).

Plasma metabolic profiles were obtained after oral and intravenous drug administrations. Quantitative TLC results (Table VI) indicate the presence in plasma of significant amounts of unchanged drug and of each of the three metabolites. Plasma concentration–time curves resulting from single oral and intravenous doses were obtained for both animals (Figs. 7 and 8). The terminal log-linear parts of the curves indicate comparable elimination half-lives for phenformin and for total radioactivity. They averaged about 26 hr.

REFERENCES

(1) R. Beckmann, *Diabetologia*, **3**, 368 (1967).

(2) R. Beckmann, *Ann. N.Y. Acad. Sci.*, **148**, 820 (1968).

(3) P. Murphy and A. Wick, *J. Pharm. Sci.*, **57**, 1125 (1968).

(4) S. Matin, J. Karam, and P. Forsham, *Anal. Chem.*, **47**, 545 (1975).

(5) D. Alkalay, J. Volk, and M. Bartlett, *J. Pharm. Sci.*, **65**, 525 (1976).

(6) D. Alkalay, L. Khemani, W. Wagner, Jr., and M. Bartlett, *J. Clin. Pharmacol.*, **15**, 446 (1975).

(7) W. Conway, H. Minatoya, A. Lands, and J. Shekosky, *J. Pharm. Sci.*, **57**, 1134 (1968).

(8) B. Martin, *Br. J. Pharmacol. Chemother.*, **29**, 181 (1967).

ACKNOWLEDGMENTS

The authors thank Dr. N. Chaudhuri and Mr. T. Ball, who prepared the radioactive compounds.

Fluorocarbon Aerosol Propellants XII: Correlation of Blood Levels of Trichloromonofluoromethane to Cardiovascular and Respiratory Responses in Anesthetized Dogs

YASH M. AMIN, EMMANUEL B. THOMPSON, and WIN L. CHIOU ˣ

Received July 27, 1976, from the *Clinical Pharmacokinetiçs Laboratory and the Department of Pharmacy, Department of Pharmacognosy and Pharmacology, College of Pharmacy, University of Illinois at the Medical Center, Chicago, IL 60612.* Accepted for publication June 28, 1978.

Abstract □ Anesthetized mongrel dogs were exposed to various concentrations of trichloromonofluoromethane. Before, during, and after the inhalation, arterial and venous blood samples were obtained for fluorocarbon analysis. After the cessation of fluorocarbon inhalation, a multiexponential decline from the blood was observed. This finding was similar to that of a previous study in which the fluorocarbon was administered intravenously to unanesthetized dogs. The half-life calculated from the terminal phase was about 280 min, and the pseudodistribution equilibrium was reached about 100 min after dosing. Study of the relationship between blood fluorocarbon levels and effects on the respiration rate and arterial blood pressure indicates that the sites of these pharmacological activities are located in the blood or central compartment rather than in the peripheral compartment. The effect on the heart rate appears to be quite instantaneous after inhalation. These results might shed some light on the fast effect of the fluorocarbon propellants, which caused sudden deaths after inhalation of a large quantity.

Keyphrases □ Trichloromonofluoromethane—blood levels correlated to cardiovascular and respiratory responses in dogs □ Cardiovascular responses—trichloromonofluoromethane, correlated to blood levels in dogs □ Respiratory responses—trichloromonofluoromethane, correlated to blood levels in dogs □ Aerosol propellants—trichloromonofluoromethane, blood levels correlated to cardiovascular and respiratory responses in dogs □ Fluorocarbon aerosol propellants—trichloromonofluoromethane, blood levels correlated to cardiovascular and respiratory responses in dogs

Because of the wide use of fluorocarbon aerosol propellants in various household, cosmetic, and pharmaceutical pressurized packages, the possible adverse effects or toxicities of these compounds have been studied extensively. These studies concerned the effects on the cardiovascular system (1–8), enzyme activities (5, 9–11), muta-

0022-3549/79/0200-0160$01.00/0
© 1979, American Pharmaceutical Association

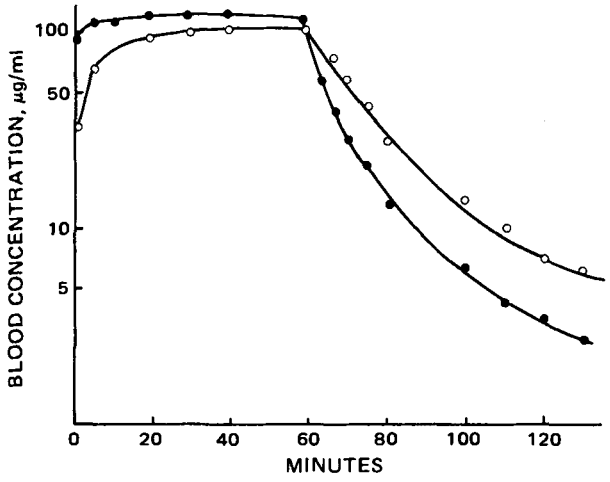

Figure 1—*Arterial (●) and venous (○) blood concentrations of fluorocarbon in a dog inhaling 2% (v/v) of the compound in pure oxygen for 60 min.*

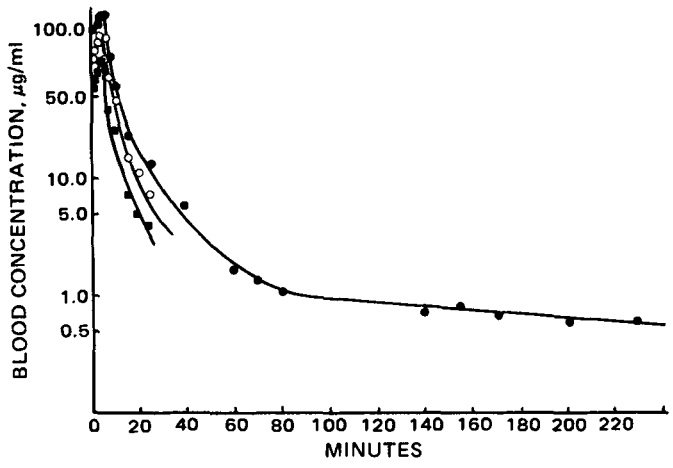

Figure 2—*Arterial blood concentrations of the fluorocarbon in Dog III inhaling 2% (■), 5% (○), and 7.5% (●) of the fluorocarbon in air for 5 min.*

tion (12), and ozone concentrations in the stratosphere (13).

Most investigations of cardiovascular effects predicated the observed cardiotoxicity on the basis of concentrations inhaled rather than blood concentrations of the fluorocarbons. The disposition kinetics of trichloromonofluoromethane, a widely used fluorocarbon, after intravenous administration to unanesthetized dogs are best described by a three-compartment open model (14). The accumulation of the fluorocarbon in the tissue or peripheral compartment following multiple or chronic exposures may have an important bearing on its potential toxicity (14).

The major objective of the present study was to correlate pharmacokinetically blood levels of trichloromonofluoromethane with some cardiovascular and respiratory responses in dogs following brief inhalations of the fluorocarbon.

EXPERIMENTAL

Materials—Trichloromonofluoromethane[1] (bp 23.7°), heparin sodium[2], pentobarbital sodium[3], and normal saline[3] were used.

Method—Mongrel dogs, fasted overnight and weighing 20–25 kg, were anesthetized with 25 mg of pentobarbital sodium/kg iv. The trachea, carotid and femoral arteries, and femoral vein were cannulated. The carotid artery and femoral vein were used for obtaining arterial and venous blood samples, respectively; the femoral artery was used for measuring arterial pressure with a pressure transducer[4] placed two-thirds of the transthoracic distance from the back. The heart rate derived from the ECG (lead II), arterial blood pressure, and respiration were recorded continuously at a paper speed of 25 mm/sec on a polygraph[5]. Some of the data obtained from these measurements were expressed as change or percent change from control values.

The dogs breathed the room air except during exposure to the fluorocarbon when they exhaled into a well-ventilated room but inhaled only the gaseous mixture of the fluorocarbon in air or oxygen contained in a 30-liter plastic bag. The outlet of the bag was connected to the tracheal cannula by a nonrebreathing valve[6]. The fluorocarbon concentration of the content of the bag proximal to its orifice, sampled with a 100-μl syringe[7], was confirmed by GLC (15).

Preliminary studies, in which the dogs were exposed to a 2% (v/v) concentration of fluorocarbon in oxygen, showed that the blood concentration increased rapidly from the time of exposure and approached steady state in less than 5 min. Consequently, following 30–45 min of equilibration after the preparation of the dog, various fluorocarbon concentrations were administered by inhalation through the inlet of the plastic bag for 5 min. An interval of 45 min elapsed before the subsequent concentration of the fluorocarbon was administered.

Dog I was exposed to 2, 5, and 10% (v/v) concentrations of the fluorocarbon in air; Dog II was exposed to 2, 5, 7.5, and 10% (v/v) concentrations in air; and Dog III was exposed to 2, 5, and 7.5% (v/v) concentrations in air. The lower concentration of the fluorocarbon was always studied first. Arterial and venous blood samples (0.5–1.0 ml) were withdrawn at appropriate intervals immediately before, during, and after the end of fluorocarbon inhalation. Blood fluorocarbon concentrations were analyzed by a headspace GLC method (15).

In the early phase of study involving several dogs, mixtures of different concentrations of the fluorocarbon with pure oxygen were used. This approach was considered more unrealistic, and the study was repeated using the fluorocarbon–air mixture. The reported results are based primarily on the fluorocarbon–air mixture study.

RESULTS AND DISCUSSION

Blood Level Profiles following Trichloromonofluoromethane Inhalation—In preliminary studies in which several dogs were exposed to a low concentration mixture of the fluorocarbon in oxygen for 60 min, the fluorocarbon concentrations in the arterial blood increased rapidly after the inhalation and approached steady-state levels in about 3–4 min. The arterial blood level then remained essentially constant throughout the inhalation period. After the cessation of fluorocarbon inhalation, both the arterial and venous blood levels decreased in an apparent triexponential decay pattern. Typical results are shown in Figs. 1 and 2.

In a previous study on four anesthetized dogs, the average terminal half-life of trichloromonofluoromethane after inhalation was 18.34 min (16). This value is in marked contrast with the much longer terminal half-life (average of 92.7 min from four dogs) reported earlier for unanesthetized dogs (7, 14, 15). The difference was attributed to the intravenous administration (7, 14, 15) as compared to the inhalation administration (16). Such reasoning appears to be pharmacokinetically unsound.

The long terminal half-life was again found in the present inhalation study in which blood sampling was continued for about 4 hr following the cessation of inhalation (Fig. 2). The terminal half-life for the anesthetized dog shown in Fig. 2 was approximately 280 min, about 14 times longer than the average half-life reported previously for anesthetized dogs (16).

The fluorocarbon levels in the venous blood always rose more slowly and were also always lower than the corresponding arterial blood levels during inhalation. A similar finding was reported earlier (17). Similar to the earlier intravenous study (14), approximately 100 min was required before a pseudodistribution equilibrium was reached for the fluorocarbon in dogs (Fig. 2). Such a slow equilibrium may be explained by the slow uptake of the fluorocarbon by fatty tissues. Its high solubility in fatty tissues of dogs was reported previously (18). The blood level data shown

[1] E. I. du Pont de Nemours & Co., Wilmington, Del.
[2] Fisher Scientific Co., Fair Lawn, N.J.
[3] Abbott Laboratories, North Chicago, Ill.
[4] Statham Laboratories, Hatorey, Puerto Rico.
[5] Model 7B, Grass Instrument Co., Quincy, Mass.
[6] Rudolph valve, Warren E-Collins, Inc., Braintree, Mass.
[7] Hamilton Co., Reno, Nev.

Table I—Effects of Inhalation of Various Concentrations of the Fluorocarbon on Cardiovascular and Respiratory Parameters at the End of 5 min of Inhalation [a]

Dog	Percent of Fluorocarbon (v/v)	Heart Rate, beats/min		Respiratory Rate, breaths/min		Systolic Pressure, mm Hg		Diastolic Pressure, mm Hg	
		C	R	C	R	C	R	C	R
I	2	144	162	10	14	134	108	77	63
	5	150	150	11	25	129	67	75	38
	10	150	ND	11	ND	129	ND	77	ND
II	2	210	200	14	16	168	132	100	84
	5	212	192	16	21	187	124	115	79
	7.5	216	192	15	20	180	91	109	65
	10	208	198	17	26	153	68	90	43
III	2	174	180	10	16	136	119	105	94
	5	162	156	9	17	117	89	92	69
	7.5	165	162	11	21	122	79	96	60

[a] ND = not determined, C = control, and R = response.

in Fig. 2 are typical of all dog studies using multiple inhalation of various concentrations of the fluorocarbon in air or oxygen.

Cardiovascular and Respiratory Effects following Fluorocarbon Inhalation—In this study, the time-course effects after the fluorocarbon inhalation on the increase of the respiratory rate and the decrease of the systolic and diastolic pressure were evaluated using various concentrations of the fluorocarbon in air or pure oxygen. In more than a dozen dogs, the same general response profiles were observed with either the fluorocarbon-air or the fluorocarbon-oxygen mixture. Since the data from the fluorocarbon-air study were thought to be more relevant, only the results from the more extensive study on three dogs with the air mixture will be presented. Typical results using 5% (v/v) fluorocarbon-95% air are plotted in Fig. 3. The magnitudes of the pharmacological effects were calculated after the correction of their respective control values.

The intensities of all three pharmacological effects evaluated increased with time during inhalation, reached their peaks at the end of inhalation, and dropped quickly afterwards. Such a time course effect is similar to the blood level profile in Fig. 3. Furthermore, the same general pattern was observed during the lower and higher fluorocarbon level studies carried out prior to and after the 5% concentration study on the same day. These results are consistent with the notion that the sites of actions for these pharmacological effects are located in the plasma or central compartment in a multicompartmental open model system (14, 19). However, if the sites of these actions are located in the "peripheral" compartment, the maximum responses should occur some time after the end of inhalation since the concentration in that compartment would continue to rise for a while after inhalation (14). This behavior was postulated for the therapeutic effect of digoxin (20) and theophylline (21).

The composite data showing the relation between the depression of the systolic pressure and the logarithm of the blood fluorocarbon concentrations for Dogs I–III are shown in Fig. 4. Although the data were obtained from three dogs using various fluorocarbon concentrations for each dog study, the same general pattern of correlation prevails. This finding further substantiates the contention that the site of action is located in the blood or central compartment.

A similar plot showing the relation between the depression of the diastolic pressure and the logarithm of the blood fluorocarbon concentrations is shown in Fig. 5. In both Figs. 4 and 5, the plateau effect seen in the conventional logarithm dose or concentration *versus* response plot is absent. Higher blood concentrations in these and other dogs after inhalation of much greater strengths of the fluorocarbon all quickly resulted in their deaths.

The numerical data for the effect on the respiration rate and blood pressure at the end of the 5-min inhalation of various strengths of the fluorocarbon in three dogs are summarized in Table I. These data represent the maximum effect for each inhalation study. A larger dose–response variation usually was seen in the respiratory effect than in the blood pressure effect. For example, after the 5% fluorocarbon inhalation, the percent changes in respiratory rates were +127, +31, and +89% for the three dogs while their corresponding changes were −48, −34, and −24% for systolic pressure, respectively, and −49, −31, and −25% for diastolic pressure, respectively.

During the time course study, the area under the curve for each respiratory cycle was also calculated and compared with the control value. Following inhalation of the fluorocarbon, these values decreased from the control whereas after cessation of the fluorocarbon inhalation, these values returned to the preexposure levels. The observed decrease in the area under the curve, representative of the approximate tidal volume, may have been due to an increase in respiratory rate. The decrease in the systemic arterial blood pressure could have been due to the depression of the myocardial contractile force and/or the relaxant action of the fluorocarbon on the systemic vasculature (22).

The increase in the respiratory rate during inhalation could have been due to the hypoxic drive caused by the lack of oxygen or to the stimulating effect of the fluorocarbon on the chemoreceptors. The possibility of an increase in the respiratory rate due to the lack of oxygen is untenable based on the fact that the studies performed on dogs inhaling various concentrations of the fluorocarbon mixture prepared in pure oxygen also showed a similar increase in the respiratory rate as the concentration of the fluorocarbon in the blood increased.

The effect on the heart rate in all dogs was less consistent and pro-

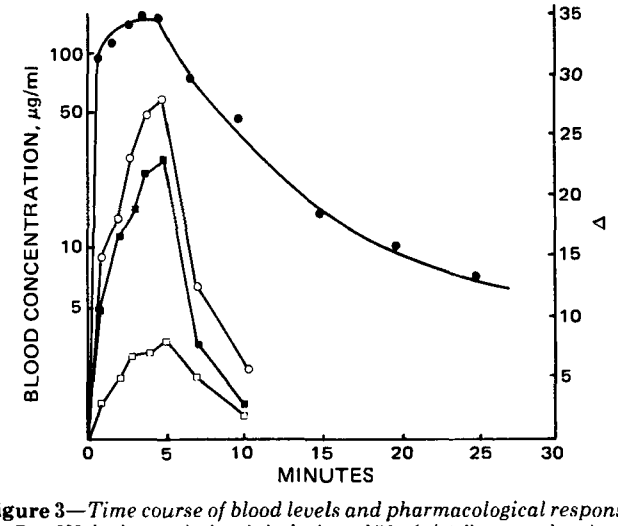

Figure 3—*Time course of blood levels and pharmacological responses for Dog III during and after inhalation of 5% (v/v) fluorocarbon in air. Key: ●, arterial blood concentration; ○, hypotensive effect (systolic pressure, mm Hg); ■, hypotensive effect (diastolic pressure, mm Hg); □, respiratory rate (breaths per minute); and Δ, change in response from control.*

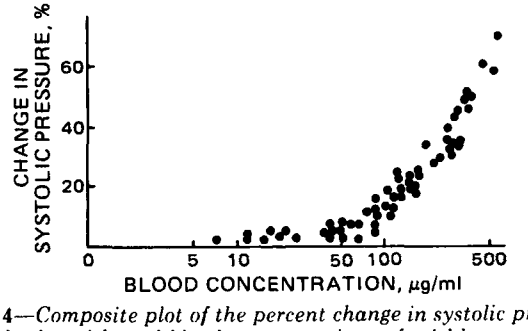

Figure 4—*Composite plot of the percent change in systolic pressure* versus *the logarithm of blood concentrations of trichloromonofluoromethane in three dogs following inhalation of various strengths of the fluorocarbon in air.*

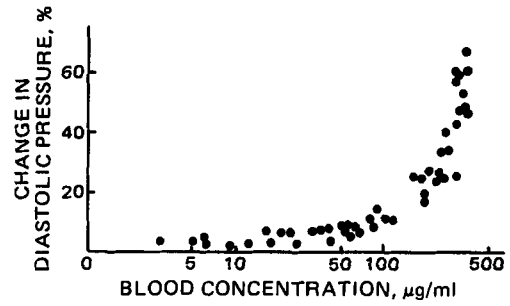

Figure 5—*Composite plot of the percent change in diastolic pressure versus the logarithm of blood concentrations of trichloromonofluoromethane in three dogs following inhalation of various strengths of the fluorocarbon in air.*

nounced. Most dogs showed biphasic responses, with an increase in the heart rate at lower doses and a decrease at higher doses (Table I). The effect on the heart rate in some dogs appeared to be instantaneous and reached a maximum within the 1st min during the inhalation in spite of the fact that the blood level continued to rise in the next few minutes.

The mechanism for such an effect is probably very complex and could not be rationalized by the multicompartmental model proposed for this fluorocarbon in dogs (14). The apparent "instantaneous" effect on the heart rate and the direct correlation between the blood level and the effect on the blood pressure and respiration rate could shed some light on the fast action of the fluorocarbon aerosol propellants, which have caused sudden death of individuals shortly after or during inhalation of large quantities of these propellants (2).

REFERENCES

(1) A. Silverglade, *J. Am. Med. Assoc.*, **222**, 827 (1972).
(2) W. S. Harris, *ibid.*, **223**, 1508 (1973).
(3) D. M. Aviado and M. A. Beles, *Toxicology*, **2**, 31 (1971).
(4) C. T. Dollery, W. M. Faith, G. H. Draffan, G. Wise, H. Sahgoun, J. W. Peterson, and S. R. Walker, *Clin. Pharmacol. Ther.*, **15**, 59 (1974).
(5) G. Marier, H. MacFarland, G. S. Wilberg, H. Buchwald, and P. Dussault, *Can. Med. Assoc. J.*, **111**, 39 (1974).
(6) E. B. Thompson and W. S. Harris, *Toxicol. Appl. Pharmacol.*, **29**, 242 (1974).
(7) W. L. Chiou, *J. Am. Med. Assoc.*, **227**, 658 (1974).
(8) *Ibid.*, **229**, 1722 (1974).
(9) D. B. Lund, *Arch. Biochem. Biophys.*, **129**, 181 (1969).
(10) P. J. Cox, L. J. King, and D. V. Parke, *Biochem. J.*, **130**, 87p (1972).
(11) H. C. Warmkier, O. Fennema, and E. H. Marth, *J. Food Sci.*, **37**, 702 (1972).
(12) V. C. Fohz and R. Fuerst, *Environ. Res.*, **7**, 275 (1974).
(13) R. J. Cicerone, R. S. Stolarski, and S. Walters, *Science*, **185**, 1165 (1974).
(14) S. Niazi and W. L. Chiou, *J. Pharm. Sci.*, **64**, 763 (1975).
(15) W. L. Chiou and S. Niazi, *Res. Commun. Chem. Pathol. Pharmacol.*, **6**, 481 (1973).
(16) J. Adir, D. A. Blake, and G. M. Mergner, *J. Clin. Pharmacol.*, **15**, 760 (1975).
(17) A. Azar, H. J. Trochimowicz, J. B. Terrill, and L. S. Mullin, *Am. Hyg. Assoc. J.*, **34**, 102 (1973).
(18) K. Chang and W. L. Chiou, *J. Pharm. Sci.*, **65**, 53 (1976).
(19) M. Gibaldi and D. Perrier, "Pharmacokinetics," Dekker, New York, N.Y., 1975.
(20) R. H. Reuning, R. A. Sams, and R. E. Notari, *J. Clin. Pharmacol.*, **13**, 127 (1973).
(21) G. Levy and R. Koysook, *J. Pediatr.*, **86**, 789 (1975).
(22) J. A. Simaan and D. M. Avaido, *Toxicology*, **5**, 127 (1975).

ACKNOWLEDGMENTS

Supported in part by Grant PHS-FD 574-03 from the Food and Drug Administration.
The assistance of Mr. Djebra Kasabdji is gratefully acknowledged.

Solution Rate of Crystals at Fluid–Fluid Interface

A. J. M. SCHOONEN ˣ, G. W. de VRIES-NIJBOER, and T. HUIZINGA

Received December 27, 1977, from the *Department of Pharmaceutics, Subfaculty of Pharmacy, University of Groningen, Anthonius Deusinglaan 2, Groningen, The Netherlands.* Accepted for publication June 30, 1978.

Abstract □ A model system was developed in which the dissolution behavior of a single crystal of potassium ferricyanide was studied at a liquid paraffin–water interface. Since the equilibrium position of a crystal at the interface is independent of its size, the lifetime of a crystal dissolving at the interface is determined entirely by its initial size and its dissolution rate in the water phase. The dimensions of every crystal were measured microscopically before dissolution. A continuous-flow recording dissolution apparatus was used to measure spectrophotometrically the mass flow of dissolved potassium ferricyanide. The dissolution cell in this system was mounted in an optical bench, making it possible to follow dissolving crystals visually by projecting them on a screen. The results show that the lifetime of a crystal is proportional to the shortest length of the crystal face in contact with the liquid paraffin and is rather independent of its form. Furthermore, crystal shape changes during dissolution, which is explained partly by the nonisometric dissolution of potassium ferricyanide crystal faces and partly by the nonconstancy of film thickness.

Keyphrases □ Dissolution—potassium ferricyanide crystals at fluid-fluid interface □ Potassium ferricyanide—dissolution of crystals at fluid-fluid interface □ Crystal dissolution—potassium ferricyanide at fluid-fluid interface

The lifetime of a solid particle dissolving in a liquid is governed by its rate of change in surface area. Assuming a constant hydrodynamic boundary layer, Hixson and Crowell (1) derived the cube root law for the dissolution of sodium chloride crystals:

$$w_0^{1/3} - w_t^{1/3} = Kt \qquad \text{(Eq. 1)}$$

where w_0 is the weight of the particle at $t = 0$, w_t is the weight of the particle at time t, and K is a dissolution rate constant also composed of density and a shape factor. Many deviations from the cube root law were found, but it was difficult to explain the results because of the experimental design (in which often a number of particles were employed in a stirred system). In the experiments of Niebergall *et al.* (2) and Hixson and Crowell (3), the rate constant increased as dissolution proceeded. A linear re-

0022-3549/79/0200-0163$01.00/0
© 1979, American Pharmaceutical Association

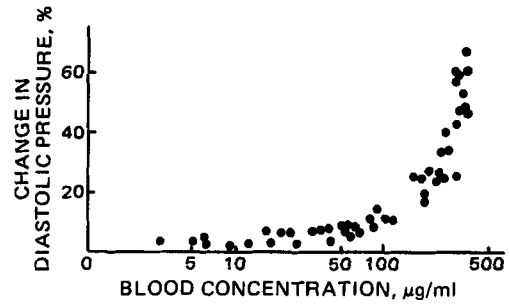

Figure 5—*Composite plot of the percent change in diastolic pressure versus the logarithm of blood concentrations of trichloromonofluoromethane in three dogs following inhalation of various strengths of the fluorocarbon in air.*

nounced. Most dogs showed biphasic responses, with an increase in the heart rate at lower doses and a decrease at higher doses (Table I). The effect on the heart rate in some dogs appeared to be instantaneous and reached a maximum within the 1st min during the inhalation in spite of the fact that the blood level continued to rise in the next few minutes.

The mechanism for such an effect is probably very complex and could not be rationalized by the multicompartmental model proposed for this fluorocarbon in dogs (14). The apparent "instantaneous" effect on the heart rate and the direct correlation between the blood level and the effect on the blood pressure and respiration rate could shed some light on the fast action of the fluorocarbon aerosol propellants, which have caused sudden death of individuals shortly after or during inhalation of large quantities of these propellants (2).

REFERENCES

(1) A. Silverglade, *J. Am. Med. Assoc.*, **222**, 827 (1972).
(2) W. S. Harris, *ibid.*, **223**, 1508 (1973).
(3) D. M. Aviado and M. A. Beles, *Toxicology*, **2**, 31 (1971).
(4) C. T. Dollery, W. M. Faith, G. H. Draffan, G. Wise, H. Sahgoun, J. W. Peterson, and S. R. Walker, *Clin. Pharmacol. Ther.*, **15**, 59 (1974).
(5) G. Marier, H. MacFarland, G. S. Wilberg, H. Buchwald, and P. Dussault, *Can. Med. Assoc. J.*, **111**, 39 (1974).
(6) E. B. Thompson and W. S. Harris, *Toxicol. Appl. Pharmacol.*, **29**, 242 (1974).
(7) W. L. Chiou, *J. Am. Med. Assoc.*, **227**, 658 (1974).
(8) *Ibid.*, **229**, 1722 (1974).
(9) D. B. Lund, *Arch. Biochem. Biophys.*, **129**, 181 (1969).
(10) P. J. Cox, L. J. King, and D. V. Parke, *Biochem. J.*, **130**, 87p (1972).
(11) H. C. Warmkier, O. Fennema, and E. H. Marth, *J. Food Sci.*, **37**, 702 (1972).
(12) V. C. Fohz and R. Fuerst, *Environ. Res.*, **7**, 275 (1974).
(13) R. J. Cicerone, R. S. Stolarski, and S. Walters, *Science*, **185**, 1165 (1974).
(14) S. Niazi and W. L. Chiou, *J. Pharm. Sci.*, **64**, 763 (1975).
(15) W. L. Chiou and S. Niazi, *Res. Commun. Chem. Pathol. Pharmacol.*, **6**, 481 (1973).
(16) J. Adir, D. A. Blake, and G. M. Mergner, *J. Clin. Pharmacol.*, **15**, 760 (1975).
(17) A. Azar, H. J. Trochimowicz, J. B. Terrill, and L. S. Mullin, *Am. Hyg. Assoc. J.*, **34**, 102 (1973).
(18) K. Chang and W. L. Chiou, *J. Pharm. Sci.*, **65**, 53 (1976).
(19) M. Gibaldi and D. Perrier, "Pharmacokinetics," Dekker, New York, N.Y., 1975.
(20) R. H. Reuning, R. A. Sams, and R. E. Notari, *J. Clin. Pharmacol.*, **13**, 127 (1973).
(21) G. Levy and R. Koysook, *J. Pediatr.*, **86**, 789 (1975).
(22) J. A. Simaan and D. M. Avaido, *Toxicology*, **5**, 127 (1975).

ACKNOWLEDGMENTS

Supported in part by Grant PHS-FD 574-03 from the Food and Drug Administration.
The assistance of Mr. Djebra Kasabdji is gratefully acknowledged.

Solution Rate of Crystals at Fluid–Fluid Interface

A. J. M. SCHOONEN ˣ, G. W. de VRIES-NIJBOER, and T. HUIZINGA

Received December 27, 1977, from the *Department of Pharmaceutics, Subfaculty of Pharmacy, University of Groningen, Anthonius Deusinglaan 2, Groningen, The Netherlands.* Accepted for publication June 30, 1978.

Abstract □ A model system was developed in which the dissolution behavior of a single crystal of potassium ferricyanide was studied at a liquid paraffin–water interface. Since the equilibrium position of a crystal at the interface is independent of its size, the lifetime of a crystal dissolving at the interface is determined entirely by its initial size and its dissolution rate in the water phase. The dimensions of every crystal were measured microscopically before dissolution. A continuous-flow recording dissolution apparatus was used to measure spectrophotometrically the mass flow of dissolved potassium ferricyanide. The dissolution cell in this system was mounted in an optical bench, making it possible to follow dissolving crystals visually by projecting them on a screen. The results show that the lifetime of a crystal is proportional to the shortest length of the crystal face in contact with the liquid paraffin and is rather independent of its form. Furthermore, crystal shape changes during dissolution, which is explained partly by the nonisometric dissolution of potassium ferricyanide crystal faces and partly by the nonconstancy of film thickness.

Keyphrases □ Dissolution—potassium ferricyanide crystals at fluid-fluid interface □ Potassium ferricyanide—dissolution of crystals at fluid-fluid interface □ Crystal dissolution—potassium ferricyanide at fluid-fluid interface

The lifetime of a solid particle dissolving in a liquid is governed by its rate of change in surface area. Assuming a constant hydrodynamic boundary layer, Hixson and Crowell (1) derived the cube root law for the dissolution of sodium chloride crystals:

$$w_0^{1/3} - w_t^{1/3} = Kt \qquad \text{(Eq. 1)}$$

where w_0 is the weight of the particle at $t = 0$, w_t is the weight of the particle at time t, and K is a dissolution rate constant also composed of density and a shape factor. Many deviations from the cube root law were found, but it was difficult to explain the results because of the experimental design (in which often a number of particles were employed in a stirred system). In the experiments of Niebergall *et al.* (2) and Hixson and Crowell (3), the rate constant increased as dissolution proceeded. A linear re-

0022-3549/79/0200-0163$01.00/0
© 1979, American Pharmaceutical Association

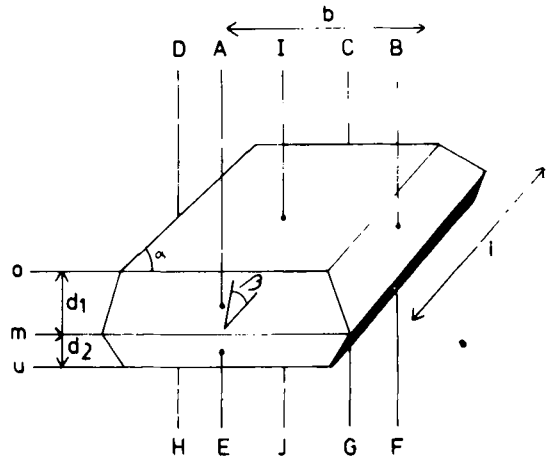

Figure 1—*Shape of a potassium ferricyanide crystal.*

lationship between the film thickness and the square root of particle weight was postulated (2), assuming a constant shape factor, which gives:

$$w_0^{1/2} - w_t^{1/2} = Kt \qquad \text{(Eq. 2)}$$

Wilhelm *et al.* (4), working with crystals of sodium chloride, reported the opposite effect: a decreasing rate during dissolution.

McCabe and Stevens (5) investigated crystal growth of copper sulfate and found a decrease in the growth rate for smaller particles in a stirred system; under conditions of constant shear, however, the growth rate was constant. The influence of the shape factor was recognized, and conditions were chosen such that it was practically constant (5).

Veng Pedersen and Brown (6, 7) developed equations for nonspherical particles, assuming a constant dissolution rate. By using a spherical approximation, they examined a 60–85-mesh fraction of tolbutamide in a system under conditions of constant shear. In spite of the fact that a changing shape factor was taken into account, it was difficult to discriminate between Eqs. 1 and 2 as the best fit for the experimental data.

Clearly, particle dissolution is still not very well explained. In the present study, single crystals of potassium ferricyanide were investigated by employing a dissolution cell in which the crystals dissolve at a liquid paraffin–water interface, enabling simultaneous measurement of the mass flow and particle size.

THEORETICAL

The simplest case of particle dissolution is that of an isometrically shaped crystal (length = width = height) that is dissolving isotropically; *i.e.*, each point on each crystal face is retreating at the same rate.

For a cube with a linear diameter, b, it can be written:

$$-\frac{db}{dt} = 2\sigma \qquad \text{(Eq. 3)}$$

where σ is the retreat rate of one crystal face.

Equation 3 integrates to:

$$b_0 - b_t = 2\sigma t \qquad \text{(Eq. 4)}$$

where b_0 is the dimension at $t = 0$ and b_t is the dimension at time t.

If each crystal face is retreating at the same rate at any time t, a cube is dissolving isometrically; *i.e.*, there is a constant relationship between b, the surface, S, and the volume or weight, W, of the cube throughout the dissolution process:

$$b_t = (\tfrac{1}{6} S_t)^{1/2} = (W/\rho)^{1/3} \qquad \text{(Eq. 5)}$$

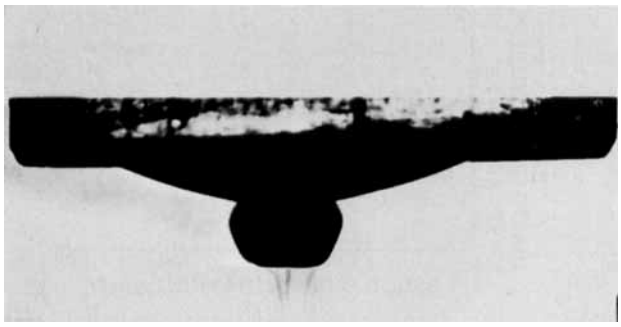

Figure 2—*Photograph of the projection of a potassium ferricyanide crystal in the equilibrium position at a liquid paraffin–water interface.*

where ρ is density. Substitution of Eq. 5 in Eq. 4 yields the cube root law (Eq. 1) or its equivalent:

$$S_0^{1/2} - S_t^{1/2} = 2\sqrt{6}\sigma t \qquad \text{(Eq. 6)}$$

According to Eq. 6, a plot of $S_t^{1/2}$ *versus* time should be a straight line when the cube root law is valid.

Since the mass flow, Q_t, at time t is proportional to the surface at that time for every heterogeneous reaction, it can be written:

$$Q_t = \rho\sigma_t S_t \qquad \text{(Eq. 7)}$$

where σ_t is the retreat rate at time t. Therefore, a plot of $Q_t^{1/2}$ *versus* time also yields a straight line when the cube root law is valid.

Dissolution at an Interface—At an interface, the simplest case of particle dissolution is that for half a cube ($b \times b \times \frac{1}{2}b$) dissolving isotropically. With the assumption that only one face of the cube ($b \times b$) is in contact with the upper fluid and does not take part in the dissolution process, the surface area exposed to the solvent phase is, at any time t:

$$S_t = 4(b_t \tfrac{1}{2} b_t) + b_t^2 = 3b_t^2 \qquad \text{(Eq. 8)}$$

Substitution of Eq. 8 in Eq. 4 gives:

$$S_0^{1/2} - S_t^{1/2} = 2\sqrt{3}\sigma t \qquad \text{(Eq. 9)}$$

Therefore, when half a cube dissolves isotropically at an interface, a plot of $S_t^{1/2}$ or $Q_t^{1/2}$ *versus* time also is linear.

Although Eq. 2 assumes an increasing dissolution rate, at any time t the rate is equal for each crystal face, which means that Eq. 5 is valid in this case. Therefore, substitution of Eq. 5 in Eq. 2 yields:

$$S_0^{3/4} - S_t^{3/4} = Kt \qquad \text{(Eq. 10)}$$

The mass flow, Q_t, at any time t for half a cube at an interface is obtained with Eqs. 4, 7, and 8:

$$Q_t = 3\rho\sigma(b_0 - 2\sigma t)^2 \qquad \text{(Eq. 11)}$$

where σ is a constant if Eq. 1 is valid and $\sigma = f(1/b)^{1/2}$ if Eq. 2 is valid.

Dissolution of a Crystal of Potassium Ferricyanide—The shape

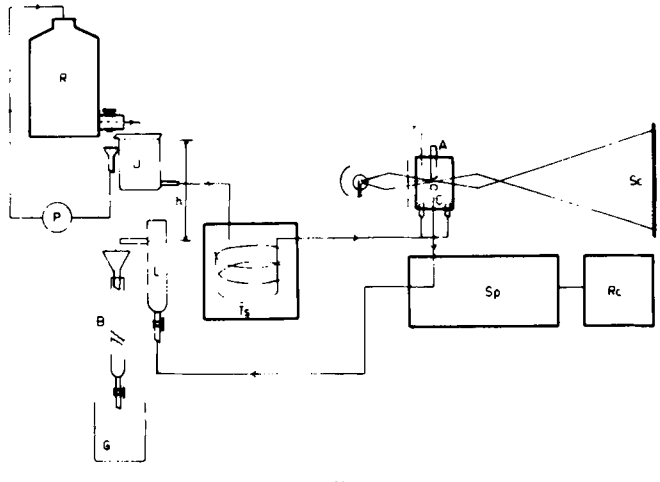

Figure 3—*Continuous-flow recording apparatus.*

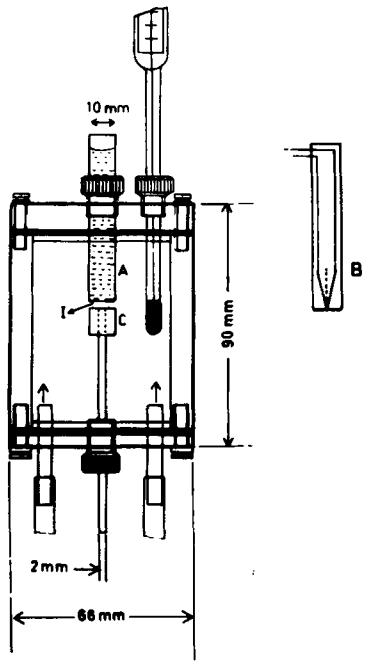

Figure 4—*Dissolution cell. Tube A contains liquid paraffin, forming an interface at I. For calibration, tube B is inserted instead of tube A and is connected with a microburet.*

of a potassium ferricyanide crystal with surfaces S_A, S_B, S_C, *etc.*, is shown in Fig. 1. If crystal face I is in contact with the upper fluid at a fluid–fluid interface, the total area, S, in contact with the solvent is given by:

$$S = S_J + (S_E + S_F + S_G + S_H) + (S_A + S_B + S_C + S_D) \quad \text{(Eq. 12)}$$

Assume that Eq. 4 is valid for some points on the "vertical" faces (A–I). The parameter σ is defined as the rate of retreat directed parallel to the interface and in a plane perpendicular to the retreating crystal face. In this way, σ has the same direction as it would have if the crystal were half a cube. Also assume that a point on the "horizontal" face J is retreating according to Eq. 4 but at a different rate τ.

To eliminate "rounding off" effects at the edges of the crystal faces and a different thickness of the hydrodynamic boundary layer for one face, it is necessary to assume that all points on a certain face are retreating with the same velocity: σ for faces A–I and τ for face J. Since $S_E = S_G$, $S_F = S_H$, $S_A = S_C$, $S_B = S_D$, and α is assumed to equal 90°, the mass flow of a potassium ferricyanide crystal at time t is given by:

$$Q_t = \rho[(S_J)_t\tau + (2S_E + 2S_F)_t\,\sigma \sin\beta + (2S_A + 2S_B)_t\sigma \sin\beta] \quad \text{(Eq. 13)}$$

Crystal faces A–I are trapezoids, whose areas may be expressed in linear dimensions:

$$(S_A)_t = \tfrac{1}{2}(b_{0_t} + b_{m_t})d_{1_t}/\sin\beta \quad \text{(Eq. 14)}$$

$$(S_B)_t = \tfrac{1}{2}(l_{0_t} + l_{m_t})d_{1_t}/\sin\beta \quad \text{(Eq. 15)}$$

$$(S_E)_t = \tfrac{1}{2}(b_{u_t} + b_{m_t})d_{2_t}/\sin\beta \quad \text{(Eq. 16)}$$

$$(S_F)_t = \tfrac{1}{2}(l_{u_t} + l_{m_t})d_{2_t}/\sin\beta \quad \text{(Eq. 17)}$$

Crystal face J may be expressed as:

$$(S_J)_t = (b_{u_t})(l_{u_t}) \quad \text{(Eq. 18)}$$

Due to the shape of a potassium ferricyanide crystal, the retreat rate for dimensions b_u and l_u is also influenced by the rate of decrease of d_2; so for b_{u_t}:

$$(b_{m_t} - b_{u_t})/(b_m - b_u) = d_{2_t}/d_2 \quad \text{(Eq. 19)}$$

With the aid of Eq. 4, it can be written:

$$b_{u_t} = b_u - 2\sigma t + \tau t(b_m - b_u)/d_2 \quad \text{(Eq. 20)}$$

Also:

$$l_{u_t} = l_u - 2\sigma t + \tau t(l_m - l_u)/d_2 \quad \text{(Eq. 21)}$$

By substituting Eq. 4 for the dimensions b_{m_t}, b_{0_t}, l_{m_t}, and l_{0_t} and the relation for b_{u_t} and l_{u_t} in Eqs. 14–18, expressions are obtained in which the area of the crystal in contact with the solvent phase can be calculated at any time t, if σ, τ, and the initial dimensions of the crystal are known.

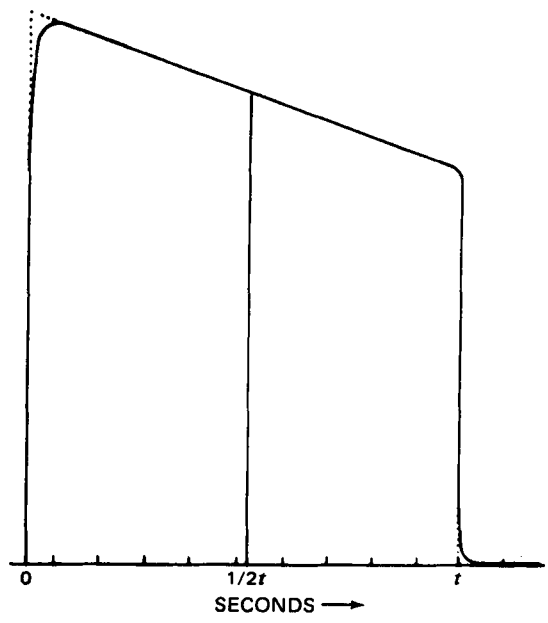

Figure 5—*Calibration curve.*

Finally, the following equation is obtained for the mass flow at time t by substitution of Eqs. 14–19 in Eq. 13:

$$Q_t = \rho\{[l_u - 2\sigma t + \tau t(l_m - l_u)/d_2][b_u - 2\sigma t + \tau t(b_m - b_u)/d_2]\tau + [b_u + \tau t(b_m - b_u)/d_2 + b_m + l_u + \tau t(l_m - l_u)/d_2 + l_m - 8t\sigma] \times (d_2 - \tau t)\sigma + [b_0 + b_m + l_0 + l_m - 8\sigma t]d,\sigma\} \quad \text{(Eq. 22)}$$

Equation 22 can be used to describe the dissolution of a potassium ferricyanide crystal until $d_2 = 0$ or $b_u = 0$. If a potassium ferricyanide crystal can be idealized to half a cube with a rate of decrease of σ for the vertical faces and τ for the horizontal face, Eq. 22 simplifies to:

$$Q_t = \rho[4\sigma(\tfrac{1}{2}b - \tau t)(b - 2\sigma t) + (b - 2\sigma t)^2\tau] \quad \text{(Eq. 23)}$$

EXPERIMENTAL

Crystals of potassium ferricyanide were obtained by recrystallization in an isothermal fashion from distilled water. The fluid–fluid system was liquid paraffin and distilled water. A single crystal was allowed to fall through the upper fluid. When it approached the lower fluid, distilled water, it was oriented by the interface in such a way that crystal face I or J (Fig. 1) was usually the lower face that was wetted first.

It is advantageous to use the notation described in Fig. 1, with the interface as a plane of reference. Therefore, face I is defined now as the upper crystal face.

During the wetting process, one of two things can happen. If the crystal has a size greater than its "critical size" ($b_0 > 2.5$ mm in this system), it is wetted completely and falls away from the interface. If the crystal is smaller than its critical size, it takes up an equilibrium position at the interface as is shown in Fig. 2. Since the edges of the upper crystal face I present a barrier in the wetting process, the equilibrium position is independent of particle size. Therefore, the area of surface in contact with the solvent is known accurately and can be calculated readily.

Apparatus—Figure 3 shows the continuous flow recording system. Reservoir R, together with pump P, maintains a constant height of dissolution liquid, distilled water, in vessel U. The liquid passes through thermostat Ts, which adjusts the liquid temperature when it reaches the dissolution cell. This cell is mounted in an optical bench, which makes it possible to project the dissolving crystal on screen Sc.

Liquid from the dissolution cell passes through a flowcell[1] in spectrophotometer[2] Sp, fitted with a chart recorder[3], and maintains a constant height of liquid in vessel L. The difference in height, h, between vessels

[1] Hellema; 80 μl.
[2] Beckman model DB-GT.
[3] Servogor.

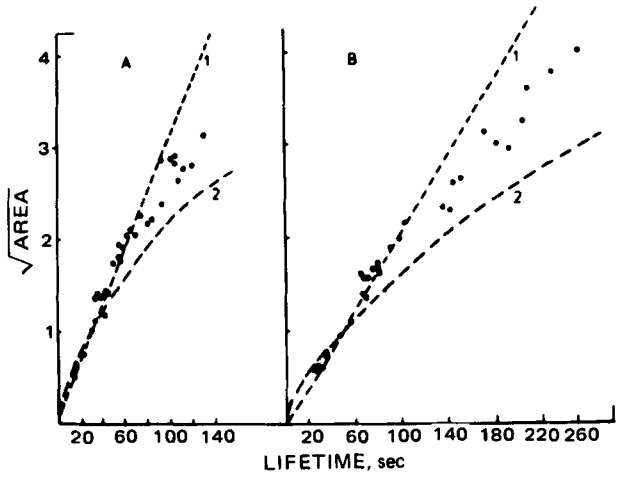

Figure 6—*Lifetime of crystals* versus *square root of area to the water phase. Each symbol represents a crystal. Key: A, streamline flow (slit width of 1.6 mm); B, free convection (slit width of 8 mm); curve 1, theoretical curve if Eq. 1 is valid; and curve 2, theoretical curve if Eq. 2 is valid. For reasons of comparison, this last curve was transformed to an (area)$^{1/2}$ axis and should be linear in an (area)$^{3/4}$* versus T *plot.*

U and L causes a pressure difference that governs the flow rate and keeps the column of liquid paraffin A in place. The interface is a sensitive detector itself for pressure differences that may develop during an experiment. The water flow is measured in buret B and finally accumulates in collection vessel G.

The dissolution cell (Fig. 4) is made of methacrylate polymer[4] and is filled with distilled water entering *via* four stainless steel tubes in every corner of the bottom to minimize turbulency. The solvent leaves the cell *via* tube C, which has a small inner diameter (2 mm), so that the solvent is transported rapidly to the spectrophotometer.

The distance between interface I and tube C (slit width) was 1.6 mm for the experiments in which the lifetime of a crystal was measured at different flow rates. The slit width was 8 mm for the experiments in which the mass flow was measured for the free convection case. At this distance, the influence of the solvent flow used (1 ml/sec) on the dissolution rate of the crystals at the interface was negligible, as was easily checked by comparing the dissolution rates obtained under these conditions and those obtained with zero solvent velocity.

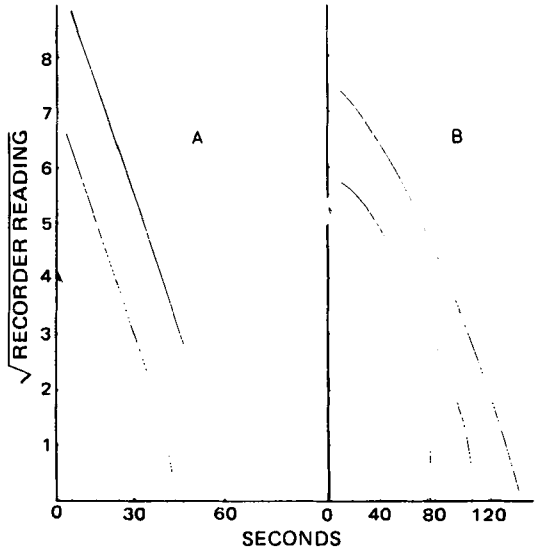

Figure 7—*Dissolution of single crystals of potassium ferricyanide. If the cube root law is valid, a straight line (broken line) should be obtained in this plot. Recorder reading = constant × mass flow at time t measured spectrophotometrically. Key: A, streamline flow (slit width of 1.6 mm); and B, free convection (slit width of 8 mm).*

[4] Perspex.

Table I—Mean Values of Height ($\bar{d}$), Length ($\bar{l}$), and Width ($\bar{b}$) for Crystals of Potassium Ferricyanide Measured Individually[a]

Size Group $(\bar{l} \times \bar{b})^{1/2}$, mm	$\bar{d}$, mm	$\bar{l}$, mm	$\bar{b}$, mm	Shape Factor, $j = (\bar{l} \times \bar{b} \times \bar{d})^{1/3}/\bar{b}$
0.20–0.39	0.18	0.35	0.30	0.888
0.39–0.59	0.23	0.49	0.42	0.861
0.59–0.78	0.25	0.75	0.58	0.823
0.78–0.98	0.33	1.01	0.79	0.811
0.98–1.18	0.39	1.23	0.89	0.846
1.18–1.37	0.49	1.36	1.19	0.778
1.37–1.57	0.56	1.58	1.39	0.771
1.57–1.76	0.54	1.80	1.57	0.773
1.76–1.96	0.60	1.95	1.76	0.723

[a] The mean value of a dimension of the crystal is the arithmetic mean for that dimension of all crystals in the given size group.

At the same time, the acceleration of the dissolved mass began close enough to the crystal surface to prevent differences in transportation time to tube C due to differences in density. This was checked by comparing the lifetime of a crystal as measured by eye using a stopwatch and the total dissolution time as recorded spectrophotometrically. The difference between these two values was never more than 2 sec.

The temperature in the dissolution cell was maintained at 20 ± 0.1°. Crystal sizes were measured microscopically. The projections of a crystal on the screen were photographed at regular time intervals to determine the retreat rate of some points on its circumference.

Calibration—The apparatus was calibrated with the aid of a microburet fixed at a certain height and connected with tube B, which was installed instead of tube A (Fig. 4). Before every measurement, the buret was filled with 0.03% potassium ferricyanide to the exact same height. A 5-ml volume of this solution was allowed to flow into the dissolution cell, and the time needed was measured. The density difference between this concentration and pure water is small, so convection through the orifice of tube B was negligible.

Figure 5 shows a registration of a particular measurement. The mass flow decreased linearly as the meniscus of the solution in the buret was losing height. Ideally, the registration should follow the dotted line. The deviation was caused mainly by a velocity gradient inside the hose connecting the dissolution cell with the flowcell. The value at half-time measured from the end-point at t was used as the mean scale reading. The calibration constant, F, was calculated as follows:

$$F = \frac{\text{mass flow recorded}}{\text{mass flow from buret}} = \frac{uy/a}{cv/t} \qquad \text{(Eq. 24)}$$

where u is the recorder reading, y is the solvent flow rate measured during calibration, a is the scale expansion factor, c is the concentration of potassium ferricyanide in the buret, and v is the volume of solution that has flowed out of the buret in time t.

As a check on the accuracy of the instrument, y was varied. If the mass flow from the buret is constant, u should be inversely proportional to y and F should be constant. The value of F was calculated 14 times at four

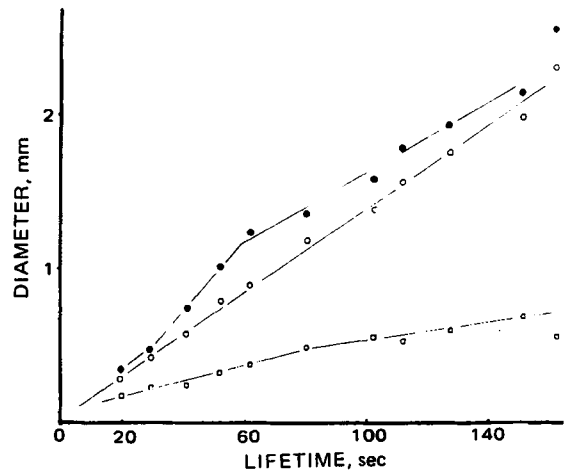

Figure 8—*Plot illustrating the relationship between the mean dimensions of crystals of potassium ferricyanide and lifetime (values from Table I). Key: ●, length; ○, width; and □, height.*

Table II—Accuracy of Measurements ($\Delta G\%$), Size Data, Dissolution Rate Constants, and Deviation in Prediction of $t = T$ by Eqs. 11 and 23 for Eight Crystals ($\Delta T\%$) [a]

Crystal	$\Delta G\%$	b_0, mm	b_{calc}, mm	d/b_0	d/l_0	σ, $\times 10^{-3}$ mm/sec	τ, $\times 10^{-3}$ mm/sec	ΔT, %
1	−1.4	0.72	0.71	0.51	0.47	5.5	2.3 → 2.3	2.-
2	+0.3	0.93	0.78	0.32	0.28	6.0	2.4 → 3.7	16.2
3	−10.2	1.15	1.13	0.60	0.50	5.6	2.7 → 6.8	1.4
4	−5.3	1.59	1.30	0.21	0.16	6.4	1.8 → 3.8	18.4
5	−5.5	0.74	0.91	0.82	0.72	4.9	3.1 → 6.7	22.8
6	+3.4	1.50	1.37	0.42	0.36	6.2	2.2 → 5.3	9.1
7	+1.3	0.98	0.73	0.34	0.32	6.6	3.1 → 3.1	25.7
8	+2.1	1.33	1.04	0.25	0.23	6.3	2.2 → 3.6	22.-

[a] The abbreviations used are: ΔG = (area under experimental curve − area under calculated curve) × 100%/(area under experimental curve) (Fig. 11), b_0 = microscopically measured width of crystal face I (Fig. 1), b_{calc} = dimension of half a cube with the same weight as the crystal: b_{calc} = (weight of crystal/0.5ρ)$^{1/3}$, d = microscopically measured height of the crystal (shortest distance between faces I and J), l_0 = microscopically measured length of crystal face I, σ = rate of retreat of "vertical" crystal faces A–I, and τ = rate of retreat of "horizontal" crystal face J.

different flow rates, ranging from 0.5 to 1 ml/sec. The variation coefficient was 1.3%.

RESULTS AND DISCUSSION

In the first series of experiments, results for single-crystal dissolution were compared with the results for monosized particles obtained by Niebergall *et al.* (2). Therefore, the dimensions of a number of crystals were measured. The length and width of the crystals were defined as the mean values of the dimensions of crystal faces I and J, respectively (Fig. 1).

A plot of the square root of the area exposed to the water phase *versus* the lifetime of the crystal is shown in Fig. 6. If the cube root law is valid, a plot of $S_0^{1/2}$ *versus* lifetime should yield a straight line according to Eq. 9. Also a plot of $S_0^{3/4}$ *versus* T (Eq. 10) is included to compare Eqs. 1 and 2. Although neither of these equations describes the dissolution process accurately, it is clear that the dissolution rate increases with decreasing particle size. The dissolution curves of individual crystals measured spectrophotometrically also show an increasing rate constant.

Figure 7 was obtained by plotting the square root of the recorder reading (= constant × mass flow) *versus* t. As shown in the *Theoretical* section (Eqs. 6 and 7), a plot of $Q_t^{1/2}$ or (recorder reading)$^{1/2}$ *versus* time should be linear if the cube root law is valid.

Although the method of measurement is different from that of Niebergall *et al.* (2), the same questions can be asked:

1. Is there a nonlinear retreat of the surface caused, for instance, by a dependency of the hydrodynamic boundary layer on particle size?
2. Is the shape factor changing because of a nonisometric shape of the crystal or because of a different hydrodynamic boundary layer for different crystal faces?

A first indication that a changing shape factor might be important can be seen in Fig. 7, where the curvature is more pronounced for the crystals dissolving under conditions of free convection (slit width of 8 mm). By visual examination of the projected crystal during dissolution, it became clear that the crystal was changing its form when a solvent flow rate of more than 0.15 ml/sec was applied with a slit width of 1.6 mm. Then the solvent entering the slit radially accelerated to a high velocity, especially attacking the edges of crystal face J if I were in contact with the liquid paraffin. The crystal rapidly changed until a pyramid formed. These differences in form could very well explain the differences in curvature.

A second indication is provided by Table I. All of the measured crystals were classified in groups, and the mean diameters were determined to obtain a shape factor for each size group. This factor changed with particle size. Since approximately the same amount of crystals was used in the same size group for every flow rate measured, it was possible to calculate a mean dissolution time for each size group.

Figure 8 is a plot of the mean diameters of the size classes *versus* the mean dissolution time. These data show that the cube root law is not valid for these crystals due to the dependency of shape on particle size and also that there is a linear relationship between the width, b, of a crystal and its lifetime. When, however, the width of individual crystals was plotted *versus* dissolution time, the results varied widely, making it impossible to explain this relationship.

One reason for this variation could be that only the width of face I or J exhibited the constant rate of decrease while the mean value of the width of both faces was measured. It was assumed that the dimensions of face I in contact with the liquid paraffin probably showed linear dissolution behavior because the circumference of that crystal face was the leading edge and, therefore, independent of the dissolution behavior of other points on the crystal surface. Moreover, the lifetime of a crystal at the interface is determined by the shortest dimension of that face; when it is zero, either the crystal is completely dissolved or it is falling from the interface. Therefore, in a new series of experiments, the actual value of b_0 was measured, as was the lifetime of the crystals at different flow rates.

Figure 9 clearly shows that the rate of decrease of b_0 is independent of particle size. The linear retreat of points on the circumference of crystal face I is affirmed by measurements on the projected diameter of that face (Fig. 10). It can be concluded, therefore, that all diameters of face I decrease with about the same rate. The shortest of these, b_0, terminates the dissolution process by forcing the other parameters to zero. For this diameter, independent of the shape of the crystal, Eq. 4 is valid.

Due to the changing shape of the crystals during dissolution, the cube root law cannot be used to calculate the mass flow of dissolved potassium

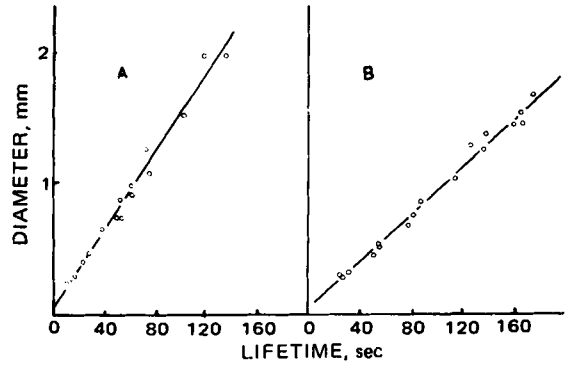

Figure 9—*Plot showing the proportionality between the width, b_0, of crystals of potassium ferricyanide and their lifetime. Key: A, streamline flow (slit width of 1.6 mm); and B, free convection (slit width of 8 mm).*

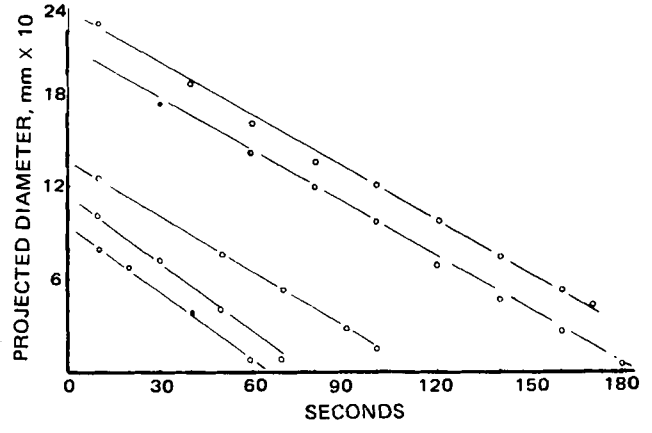

Figure 10—*Decrease of the projected width of crystal face I as a function of time. Only the shortest diameter, b_0, decreases linearly to zero; the others also decrease at about the same rate but are forced to zero at the end of the dissolution process.*

Table III—Percent Deviation of Q_t Values Predicted by Eqs. 22, 11, and 23 from the Measured Value at $t = 0.25T$, $0.5T$, and $0.75T$ for Eight Crystals from Table II [a]

Crystal	Eq. 22			Eq. 11			Eq. 23		
	$0.25T$	$0.5T$	$0.75T$	$0.25T$	$0.5T$	$0.75T$	$0.25T$	$0.5T$	$0.75T$
1	−4	−4	−3	+2	−1	−13	−3	−5	−5
2	0	−1	−2	+6	−16	−14	+3	−7	−10
3	−6	−5	−3	+9	−12	−15	+5	−5	−10
4	−5	−8	−3	+8	−19	−17	+5	−6	−12
5	−6	−6	−6	+3	−7	−10	−2	−5	−5
6	−6	−2	0	+5	−13	−12	+1	−3	−5
7	−5	−3	0	−25	−26	−15	−25	−21	−15
8	−1	−6	−2	+2	−22	−15	+1	−12	−13

[a] The percentages deviation were calculated according to the following equation: [Q_t (measured curve) − Q_t (calculated curve of Eq. 22)] × 100%/Q at $t = 0$ from the calculated curve of Eq. 22 (Fig. 11).

ferricyanide. Therefore, Eq. 22 was derived in which the mass flow, Q_t, is expressed in the linear dimensions of the crystal. Under conditions of free convection (slit width of 8 mm), crystal face J does not deform and can be identified as a separate face during the entire process. Therefore, this case was investigated further.

Numerous crystals were measured accurately; photographs were taken during dissolution, and the total dissolution time was measured. It was assumed that all crystal faces but face J were retreating linearly at a rate of σ mm/sec into a direction parallel to the interface. Crystal face J retreated with a lower velocity and in a nonlinear fashion as measured from the photographs, so these variable values for τ were used in the calculation of the dissolution curve from Eq. 22.

The weight of the crystal was calculated by comparing the area under the curve of the crystal with the area under a calibration curve for which the corresponding amount of potassium ferricyanide was exactly known. Since the area under the curve should be the same for the measured curve and the one calculated with the aid of Eq. 22, the difference in weight, ΔG (Table II), was calculated as a measure of accuracy. Then the mass flow was calculated for half a cube obeying the cube root law, which had the same weight as the crystal (Eq. 11). Here b was calculated from $b = (W/0.5\rho)^{1/3}$ (where W = weight of the crystal). Also the mass flow was calculated for half a cube in which the actual values of τ were inserted, according to Eq. 23.

The percentage deviation of the mass flow calculated according to Eqs. 11, 22, and 23 from the mass flow measured spectrophotometrically is shown in Table III.

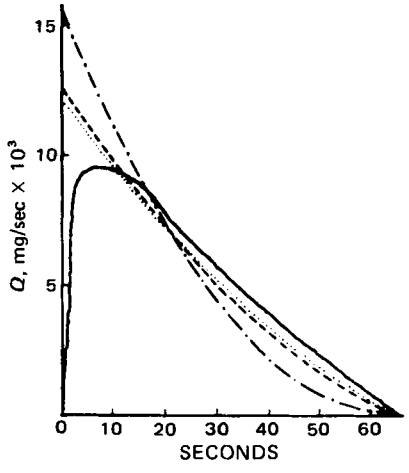

Figure 11—*Comparison of the ability of Eqs. 11, 22, and 23 to describe the dissolution of Crystal 1 (Tables II and III). Key: —, experimental line; ···, Eq. 22; -·-·, Eq. 11; and ---, Eq. 23.*

Two different cases can be identified:

1. The calculated value of b is about the same as the measured value for b_0. The ratios d/b_0 and d/l_0 then are roughly 1/2 (Crystal 1, Tables II and III), as is the ratio of the particle obeying the cube root law, so the effect of shape is minimal. Therefore, Eq. 23 describes the dissolution process almost as accurately as Eq. 22. The difference between Eqs. 11 and 23 is significant (Fig. 11). This difference is caused only by the slower and nonlinear dissolution rate of crystal face J.

2. Especially when b is smaller than b_0, a large deviation can be expected due to the combined effects of shape and the retreat rate of face J. A representative crystal of this class is Crystal 2 (Tables II and III). Since the lifetime of a crystal of potassium ferricyanide is determined by b_0, the slower and nonlinear dissolution rate of face J has no influence on crystal lifetime. Therefore, the deviation in prediction of $t = T$ (ΔT, Table II) is the same for Eqs. 11 and 23 and illustrates purely the effect of shape, which can be quite substantial (up to 25% for these crystals).

Results of this investigation can be summarized as follows. The close agreement between the measured curve and the one calculated with Eq. 22 usually justifies the use of a constant and equal retreat rate for all crystal faces except one. If there is a relative motion between a dissolving crystal and the solvent, there is always a face at the rear side of the crystal at which the flow pattern is different. This situation makes it necessary to use a lower value for this face for the retreat rate, which, according to the present measurements, increases as dissolution proceeds. This effect has a bearing on nonisometric as well as isometric particles.

Furthermore, the effect of shape is important. An apparent increase in the rate constant will be measured if isometric dissolution behavior is postulated for particles that have the shortest diameter terminating the dissolution process.

REFERENCES

(1) A. W. Hixson and J. H. Crowell, *Ind. Eng. Chem.*, **23**, 923 (1931).

(2) P. J. Niebergall, G. Milosovich, and J. E. Goyan, *J. Pharm. Sci.*, **52**, 236 (1963).

(3) A. W. Hixson and J. H. Crowell, *Ind. Eng. Chem.*, **23**, 1160 (1931).

(4) R. H. Wilhelm, L. H. Conklin, and T. C. Sauer, *ibid.*, **33**, 453 (1941).

(5) W. L. McCabe and R. P. Stevens, *Chem. Eng. Proc.*, **47**, 168 (1951).

(6) P. Veng Pederson and H. F. Brown, *J. Pharm. Sci.*, **65**, 1437 (1976).

(7) *Ibid.*, **65**, 1442 (1976).

ACKNOWLEDGMENTS

The authors thank F. Stuurman and P. Plouvier for their valuable contribution to the design of the continuous-flow recording apparatus.

Flupenthixol Dihydrochloride Decomposition in Aqueous Solution

R. P. ENEVER ˣ, A. LI WAN PO, and E. SHOTTON

Received June 22, 1977, from the *Department of Pharmaceutics, School of Pharmacy, University of London, London, WC1N 1AX, England.* Accepted for publication June 30, 1978.

Abstract □ Flupenthixol dihydrochloride in aqueous solution oxidized to trifluoromethylthioxanthone, ethanol, and piperazine *via* aldehydic and epoxidic intermediates in the presence of air. The formation rate of trifluoromethylthioxanthone increased with increases in pH and oxygen concentration. Buffer ions also affected the decomposition rate. Micelle formation by the drug markedly influenced its oxidation rate.

Keyphrases □ Flupenthixol dihydrochloride—decomposition in aqueous solution □ Decomposition—flupenthixol dihydrochloride in aqueous solution □ Tranquilizers—flupenthixol dihydrochloride, decomposition in aqueous solution

The neuroleptic compound flupenthixol dihydrochloride is unstable to light and heat (1). The drug is closely related chemically to phenothiazines, which are susceptible to oxidative decomposition (2). Many phenothiazines also form micelles in aqueous solution (3), and there is evidence that the degradation kinetics of promethazine are influenced by micelle formation (4).

The objectives of the present work with flupenthixol dihydrochloride were to identify its decomposition products, to establish the degradation pathway in aqueous solution, and to examine some factors influencing the appearance rate of the main decomposition product trifluoromethylthioxanthone. The effect of drug concentration on the decomposition kinetics is also reported and related to the observed micelle-forming properties of flupenthixol dihydrochloride.

EXPERIMENTAL

At all times, flupenthixol dihydrochloride solutions were protected from light to prevent photodecomposition.

Identification of Decomposition Products—The decomposition products were prepared by sealing 2-ml volumes of aqueous solutions (pH 6.8) of flupenthixol dihydrochloride[1] in 10-ml ampuls and autoclaving at 115–116° for up to 6 hr. This procedure ensured that air was present in the ampuls. The decomposition products were isolated by TLC using the methods and materials previously described for amitriptyline hydrochloride (5). The physicochemical techniques used to characterize the isolated products were also identical to those reported for amitriptyline hydrochloride (5).

Rate Studies of Flupenthixol Dihydrochloride Decomposition—*Flupenthixol Dihydrochloride Assay*—Direct absorbance measurements can be used for assaying decomposing solutions of flupenthixol dihydrochloride at <pH 4 since the decomposition products do not interfere. There was no change in the general shape or shift in the absorption maximum of the UV absorption curve with drug decomposition. In addition, results obtained from absorbance measurements were identical with those obtained using a specific colorimetric assay involving extraction of the base and reaction with palladium chloride (6).

A calibration curve was constructed using solutions of flupenthixol dihydrochloride ranging in concentration from 0.5 to 2.5 mg/ml in McIlvaine citric acid–phosphate pH 3.0 buffer (7). The drug was stable in this buffer at room temperature since no decomposition could be detected even after 1 month of storage. Each solution was diluted by a factor of 100 with 0.1 *N* HCl prior to the absorbance[2] reading at 230 nm. For assay, the test solutions were diluted to within the concentration range of the calibration curve.

Trifluoromethylthioxanthone Assay—The formation rate of trifluoromethylthioxanthone[1] was followed by GLC[3]. A 1.5-m (5-ft) × 0.6-cm (0.25-in.) i.d. glass column was packed with 3% (w/w) OV-25 on Chromosorb W AW/DCMS[4]. The flow rates of hydrogen, air, and nitrogen were 83, 450, and 28.5 ml/min, respectively.

Calibration solutions of trifluoromethylthioxanthone ranging in concentration from 0.2 to 3.0 mg/ml were prepared in ether[5]. A 1-ml aliquot of each solution was added to a 10-ml ampul[6] containing 2 ml of the buffer used in the experiment. A 1-ml aliquot of a 0.5-mg/ml solution of dibenzosuberone[7] in ether was added to each ampul to act as an internal standard, and the contents of each ampul were shaken and rotated for 10 min. Subsequently, 2 μl of the ethereal extract from each ampul was injected into the chromatograph. A calibration plot of the peak height ratio of trifluoromethylthioxanthone to dibenzosuberone against the trifluoromethylthioxanthone concentration was constructed.

Trifluoromethylthioxanthone was stable in the buffers used for the preparation of the calibration curve since there was no detectable decomposition even after 1 month of storage at room temperature. Test solutions were treated by extracting the contents of an ampul with 2 ml of the dibenzosuberone internal standard solution and assaying the resultant ethereal extract.

Formation Rate of Trifluoromethylthioxanthone—The influence of pH, buffer ions, and oxygen concentration on the formation rate of trifluoromethylthioxanthone was investigated. For all experiments, 2 ml of the appropriate solutions was pipetted into 10-ml clear glass ampuls[6] prior to storage at 70° in water baths covered to protect the contents from light. The trifluoromethylthioxanthone concentration was then determined at various intervals by the GLC method.

Decomposition Rate of Flupenthixol Dihydrochloride—The effect of concentration on the decomposition rate of flupenthixol dihydrochloride was investigated by storing a series of solutions ranging in concentration from 0.5 to 10.0 mg/ml in McIlvaine citric acid–phosphate pH 3.0 buffer at 80° in water baths covered to protect the contents from light. The residual flupenthioxol dihydrochloride in the solution then was assayed by the spectrophotometric method.

Critical Micelle Concentration (CMC) of Flupenthixol—The CMC of flupenthixol dihydrochloride in distilled water was determined at 18° by the du Nouy tensiometer[8] method (8), the specific conductance method[9], and pH measurements[10] (9). CMC measurement of flupenthixol dihydrochloride at 25, 40, and 50° in pH 3.0 McIlvaine citric acid–phosphate buffer was carried out by the du Nouy tensiometer method using a water circulator[11] for temperature control of the dish.

RESULTS AND DISCUSSION

With carbon tetrachloride–benzene (3:7 v/v) and silica gel[12] plates, seven compounds, including flupenthixol, were separated. The R_f values were: I, 0.79; II, 0.63; III, 0.55; IV, 0.40; V, 0.20; VI, 0.13; and VII, 0.00. Flupenthixol dihydrochloride did not move off the baseline during the separation and corresponded to VII. With the same system, trifluoromethylthioxanthone was shown to have an R_f value identical to that of IV. Comparison of their mass fragmentation patterns, as well as UV, IR, and NMR spectra, confirmed that the two compounds were identical.

[1] Lundbeck Ltd., Luton, Bedfordshire, England.
[2] Pye Unicam SP1800 recording spectrophotometer. Pye Unicam, Cambridge, England.
[3] Pye Unicam 105 gas chromatograph equipped with flame-ionization detector.
[4] Perkin-Elmer Ltd., Beaconsfield, Bucks, England.
[5] B.D.H. Ltd., Poole, Dorset, England.
[6] Aldelphi Tubes Ltd., London, England.
[7] Koch Light Ltd., Colnbrook, Bucks, England.
[8] Cambridge Instrument Co., Cambridge, England.
[9] Zeta Meta Inc., New York, N.Y.
[10] Pye 290 Mk 2 pH meter, Pye Unicam, Cambridge, England.
[11] Gallenkamp Compenstat, Gallenkamp Ltd., London, England.
[12] Camag DSF-5 grade, Camag, Switzerland.

0022-3549/79/0200-0169$01.00/0
© 1979, American Pharmaceutical Association

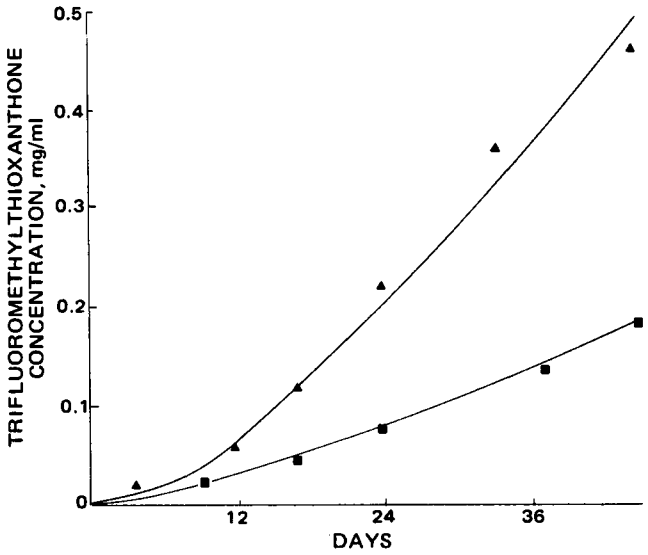

Figure 1—*Influence of oxygen on the formation rate of trifluoromethylthioxanthone from 2 mg of flupenthixol dihydrochloride/ml in pH 5.4 Sorensen citrate buffer at 70°. Key: ▲, under oxygen; and ■, under air.*

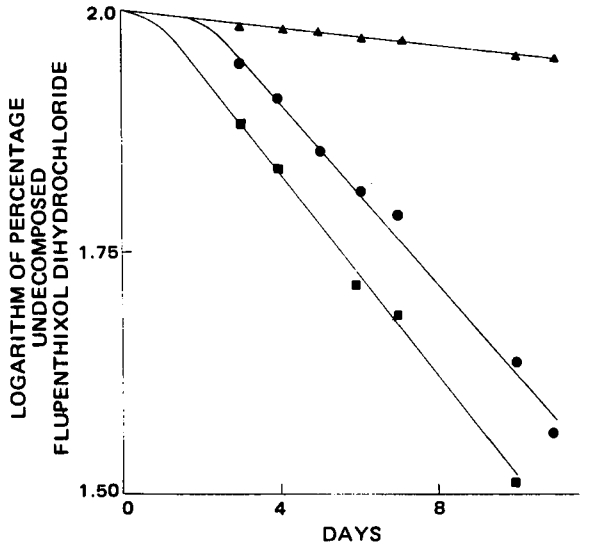

Figure 2—*Effect of drug concentration on the decomposition rate of 5 (▲), 1 (●), and 0.5 (■) mg of flupenthixol dihydrochloride/ml in pH 3.0 McIlvaine citric acid–phosphate buffer at 80°.*

Product V reacted with 2,4-dinitrophenylhydrazine spray reagent to produce a bright-yellow color, indicating the presence of an active carbonyl group. The mass spectrum showed a molecular ion peak at *m/e* 306, corresponding to the molecular formula $C_{16}H_9F_3OS$. The base peak was at *m/e* 305, suggesting a ready loss of proton probably from an aldehyde. A major peak at *m/e* 278, which can be interpreted as β-cleavage accompanied by the loss of an aldehydic function, was observed. Therefore, Structure V was postulated.

The IR spectrum confirmed the presence of a carbonyl function by exhibiting a sharp and intense peak at 1665 cm^{-1}, indicative of a conjugated aldehyde. On exposure to air, TLC showed that the compound was broken down to trifluoromethylthioxanthone.

The mass spectrum of VI showed a molecular ion peak with an *m/e* of 336 and a base peak at *m/e* 265, corresponding to one peak in the mass spectrum of V. The greater relative intensity of the latter peak in the spectrum of VI indicated that the side chain attached to the tricyclic nucleus must be more labile than in V. TLC data showed that the compound was more strongly adsorbed than the aldehydic Compound V (R_f 0.13 compared to 0.20) in the nonpolar benzene–carbon tetrachloride system.

From a knowledge of IV and V, the presence of an oxygen atom or an alkene linkage seemed likely. The higher molecular weight relative to IV and V and the lower R_f value indicate the presence of an oxidized alkene linkage. No carbonyl absorption band could be detected in the IR spectrum. Therefore, Structure VI was postulated.

Such a structure would be expected to be very unstable, and exposure to air did indeed lead to the formation of trifluoromethylthioxanthone. Epoxides of similar compounds have been isolated (10).

The mass spectra of I–III showed them to be high molecular weight compounds, which may be dimers of smaller molecules. Such dimerization was described for phenothiazines, which are structurally closely related to flupenthixol dihydrochloride (11).

Piperazine and ethanol were also identified as products of side-chain decomposition. Methods developed by Uda *et al.* (1) were used for identifying piperazine, while ethanol was detected by GLC[3] with a Porapak Q column[13].

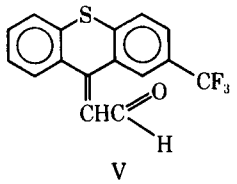

V

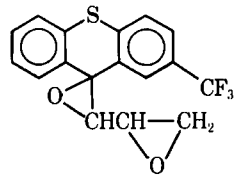

VI

[13] Waters Associates.

The decomposition pathway shown in Scheme I is postulated for flupenthixol dihydrochloride (VII) and is similar to that determined for amitriptyline hydrochloride (5). Oxidation of the parent compound to the corresponding ketone *via* several intermediates was observed with both drugs. The isolation of an epoxidic intermediate (VI) from the decomposed solution of flupenthixol dihydrochloride, but not from amitriptyline hydrochloride solution, is possibly due to the greater instability of such an intermediate in the latter case. Isolation of V and VI indicates that, in flupenthixol dihydrochloride as with amitriptyline hydrochloride, the alkene bond linking the side chain to the tricyclic nucleus is not the only labile center in the molecule.

The ketone, trifluoromethylthioxanthone (IV), was the major product of decomposition; its formation rate was affected by several factors. When 5 mg of flupenthixol dihydrochloride/ml at 70° in Sorensen citrate buffer solutions (7), adjusted to an ionic strength of 0.3, was used, the formation of the ketone obeyed zero-order kinetics. The rate constants were 3.4 at pH 2.4, 5.95 at pH 3.4, 7.37 at pH 4.4, and 15.3 μg/ml/day at pH 5.4. Thus, an increase in pH markedly accelerated the rate.

The type of buffer system employed also affected the process. With the same drug concentration in pH 4.4 buffers (ionic strength adjusted to 0.2) at 70°, the zero-order rate constants were 9.86 in McIlvaine citric acid–phosphate buffer, 3.99 in Walpole acetate buffer, and 7.37 μg/ml/day in Sorensen citrate buffer again.

Storage of 2-mg/ml solutions of flupenthixol dihydrochloride in pH 5.4 Sorensen citrate buffer under air and oxygen showed, as expected, that the formation rate of trifluoromethylthioxanthone was significantly increased in the presence of oxygen (Fig. 1). Zero-order kinetics were not obeyed at this drug concentration.

The effect of flupenthixol dihydrochloride concentration on its degradation rate is shown in Fig. 2. The process was slowest at the highest

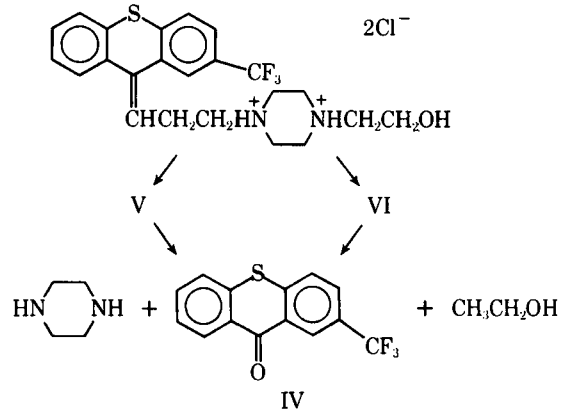

IV

Scheme I

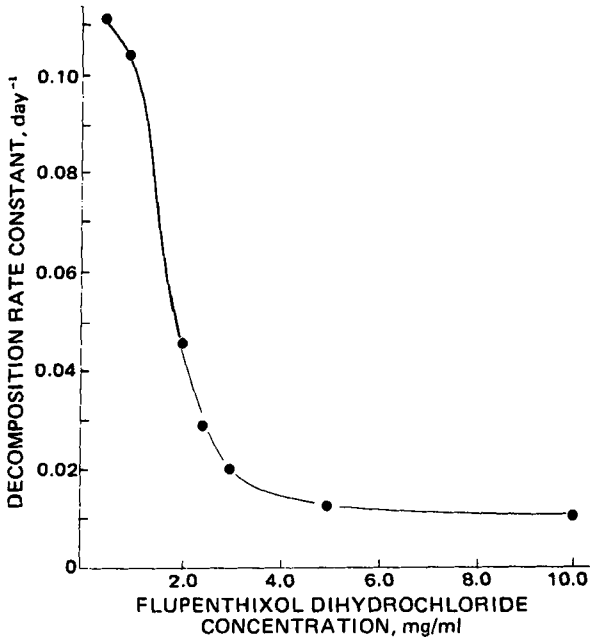

Figure 3—*Relation between first-order rate constant and drug concentration for flupenthixol dihydrochloride in pH 3.0 McIlvaine citric acid–phosphate buffer at 80°.*

concentration and obeyed first-order kinetics. At the lowest concentration, the decomposition also approximated this order of reaction; at intermediate concentrations, *e.g.*, 1 mg/ml, an initial slow rate preceded the more rapid decomposition phase. A control experiment was also carried out by sealing the 1-mg/ml solution under nitrogen and storing it at 80°. There was no detectable decomposition, even after 2 weeks of storage, which confirmed the oxidative nature of the decomposition.

The micelle-forming properties of the drug were investigated in an attempt to explain the phenomenon portrayed in Fig. 2. The three methods used for determining the CMC of the drug in double-distilled water at 18° all gave comparable results (mean value of 3 mg/ml). Thus, the du Nouy method was chosen as the most convenient for determining the effect of temperature on the CMC in buffer solution. The CMC's of flupenthixol dihydrochloride at 25, 40, and 50° in pH 3.0 McIlvaine citric acid–phosphate buffer were 1.25, 1.12, and 1.00 mg/ml, respectively. There was a linear relationship between the logarithm of the CMC and the reciprocal of absolute temperature, and the extrapolated value of the CMC at 80° was estimated to be 0.80 ± 0.05 mg/ml.

The relationship between micelle formation and decomposition can best be seen by plotting the rate constants of flupenthixol dihydrochloride decomposition, calculated from the linear sections of each curve, against initial concentrations (Fig. 3). Where two reaction rate constants were observed for a particular solution, the faster final rate was used in plotting the results. The highest decomposition rate occurred for drug concentrations below the CMC. Thus, micelle formation protected the drug from oxidation; as the drug concentration increased above the CMC, there was a corresponding rise in the relative proportions of the micellar to monomeric forms of the drug and enhancement of this protective effect. Above approximately 3 mg/ml, the rate remained essentially constant (Fig. 3) since the monomeric form of the drug became negligible relative to the total.

The biphasic nature of the data for the decomposition process observed at concentrations between the CMC and 3 mg/ml also can be attributed to micelle formation. Initially, with most of the drug in the micellar form, a slow decomposition rate was observed. As decomposition proceeded, the drug concentration fell below the CMC and the rate was accelerated. Above 3 mg/ml, a single rate of decomposition was observed because, within the time of study, the drug concentration did not fall below the CMC.

The data presented for this class of oxygen-sensitive compounds show that not only pH, oxygen concentration, and buffer composition influence the decomposition rate but also that the ability of the drug to form micellar structures can have a marked effect.

REFERENCES

(1) Y. Uda, E. Mizuta, and T. Yashiki, *J. Takeda Res. Lab.*, **29**, 701 (1970).

(2) J. Stevens, B. J. Meakin, and D. J. Davies, *J. Pharm. Pharmacol.*, **24**, 133 P (1972).

(3) A. T. Florence, *Adv. Colloid Interface Sci.*, **2**, 115 (1968).

(4) J. Stevens, B. J. Meakin, and D. J. Davies, *J. Pharm. Pharmacol.*, **25**, 119 P (1973).

(5) R. P. Enever, A. Li Wan Po, B. Millard, and E. Shotton, *J. Pharm. Sci.*, **64**, 1497 (1975).

(6) A. Li Wan Po, Ph.D thesis, University of London, London, England, 1976.

(7) "Documenta Geigy," 7th ed., K. Diem and C. Lentner, Eds., J. R. Geigy, Basel, Switzerland, 1970, p. 208.

(8) W. D. Harkins and J. F. Jordan, *J. Am. Chem. Soc.*, **52**, 1751 (1930).

(9) K. Thoma and E. Siemer, *Pharm. Acta Helv.*, **51**, 50 (1976).

(10) E. Belvedere, C. Pontarotto, V. Rovei, and A. Frigerio, *J. Pharm. Sci.*, **65**, 815 (1976).

(11) R. Yamamato and S. Fujisawa, *Kongr. Pharm. Wiss. Vortr. Originalmitt.*, **23**, 509 (1963).

ACKNOWLEDGMENTS

Presented in part at the British Pharmaceutical Conference, St. Andrews, Scotland, 1976.

The authors thank Lundbeck Ltd. for the gift of flupenthixol dihydrochloride and trifluoromethylthioxanthone. Dr. A. Li Wan Po thanks the School of Pharmacy for a research grant.

High-Performance Liquid Chromatographic Analysis of Cyclophosphamide

TERRY T. KENSLER ˣ, ROBERT J. BEHME, and DANA BROOKE

Received May 1, 1978, from the *Pharmaceutical Product Development Department, Mead Johnson Pharmaceutical Division, Evansville, IN 47721.* Accepted for publication July 10, 1978.

Abstract □ A reversed-phase high-performance liquid chromatographic technique is described for the analysis of cyclophosphamide in the presence of its hydrolysis products. The drug was quantified using a UV detector at a low wavelength. A single band was observed for the intact drug, which was well separated from its hydrolysis product(s). Quantification was obtained with adequate precision by the use of an injector loop or a suitable internal standard (hydrocortisone). The technique requires no extraction of the drug from aqueous solution or derivatization for analysis. The method was applied to partially hydrolyzed and to known solutions of cyclophosphamide. With suitable modification, the method may be useful for analysis of dosage forms but probably lacks the sensitivity necessary for analysis of the drug in biological samples.

Keyphrases □ Cyclophosphamide—high-performance liquid chromatographic analysis in prepared samples □ High-performance liquid chromatography—analysis, cyclophosphamide in prepared samples □ Antineoplastics—cyclophosphamide, high-performance liquid chromatographic analysis in prepared samples

Cyclophosphamide[1] is widely used in cancer treatment. A stability-indicating method for analyzing the drug directly in aqueous solution was needed. GLC (1) and other analytical methods (2–6) are available. The GLC method of Boughton *et al.* (1) was adopted, essentially unchanged, as the official USP assay (7).

The GLC method was shown to be more acceptable than the other methods, which lacked specificity, reproducibility, accuracy, or convenience. However, in its application to tablets, the GLC method requires a great deal of sample handling (*e.g.*, as extractions) for both standards and samples. No derivatization is required, but the drug decomposes on the column to give several peaks. A GLC method reported by Pantarotto *et al.* (8) gives a single peak but requires derivatization of the drug before injection. A GLC method has also been reported for the analysis of cyclophosphamide recovered from sheep tissues (9).

This paper reports a new analytical method that takes advantage of the inherent convenience, specificity, precision, and accuracy of reversed-phase high-performance liquid chromatography (HPLC). Reversed-phase HPLC allows direct analysis of aqueous solutions of the water-soluble drug without extraction into an organic liquid. An analytical method that requires no sample extraction and minimizes the number of manipulations is obviously desirable.

Presumably, HPLC has not been used to analyze cyclophosphamide because fixed wavelength UV detectors operating at 254 nm cannot detect the drug. Cyclophosphamide has a low molar absorptivity even at its λ_{max}, which occurs at a low wavelength. However, with modern variable wavelength detectors that can monitor effectively in the 190–200-nm region, this limitation can be overcome.

[1] Cytoxan, Mead Johnson Laboratories. Cyclophosphamide and cyclophosphamide monohydrate are often used interchangably; in this report, both refer to the monohydrate.

EXPERIMENTAL

Reagents and Solvents—Cyclophosphamide and hydrocortisone were drawn from laboratory stock. Chemicals used for buffers were reagent grade.

House-distilled water was redistilled in a glass apparatus[2]. Acetonitrile[3], UV grade, was used as received.

Apparatus—For the kinetic study, a reciprocating pump[4] was used. Samples were injected by the use of a 25-μl loop[5]. The detector[6] was set at 200 nm. The chromatograms were recorded on a strip-chart recorder[7], and the band areas were integrated with an electronic integrator[8].

The chromatogram of cyclophosphamide plus hydrocortisone was obtained with a different pumping system[9], injector[10], detector[11], and recorder–integrator[12].

A pH meter[13] and two UV–visible spectrophotometers[14] also were used.

Columns—Bonded reversed-phase[15] HPLC columns were obtained commercially.

Samples—A stock solution for the kinetic study was prepared by adding 28 g of cyclophosphamide to 700 ml of 0.1 *M* (pH 7.0) phosphate buffer. The resulting solution was filtered through filter paper and divided into four stoppered flasks. The flasks were placed in three constant-temperature ovens (40, 50, and 60°), and the temperature of the fourth flask was brought rapidly to 80° by immersing it in boiling water. When the temperature had reached 80°, the flask was transferred to an 80° water bath[16].

Samples were taken from all solutions at appropriate intervals. The sample size was large enough (~12–25 ml) to allow quantitative dilution of an accurately measured aliquot at a later time. All samples were chilled in an ice-water bath immediately after they were withdrawn and then were stored in a refrigerator until analysis. All samples were analyzed on 1 day and compared to an external standard (curve) prepared on that day. The standard solutions were prepared by dissolving weighed amounts (51.9–221.8 mg) of cyclophosphamide in water and diluting to 50.0 ml.

Other drug solutions were prepared by dissolving weighed amounts of cyclophosphamide in water. The solution containing both hydrocortisone and cyclophosphamide was prepared by dissolving the two drugs in acetonitrile and then diluting that solution quantitatively with water.

Analysis—Accurately measured aliquots of the samples from the kinetic study were diluted quantitatively with water, and a 25-μl portion of each was injected onto the column using a 25-μl injector loop. No internal standard was used. A 25-μl portion of each standard was also analyzed using the same chromatographic conditions.

The chromatographic conditions were: column, 30 cm × 3.9 mm i.d.; flow rate, 1.5 ml/hr; mobile phase, 30% acetonitrile–70% water; detector wavelength, 200 nm; detector scale, 0–1.0; and recorder, 0.64 aufs. The same chromatographic conditions were used to check reproducibility of the band areas at 200 nm. The wavelength was changed to 190 and 254 nm for the analysis of certain samples.

The solution containing cyclophosphamide and hydrocortisone was

[2] Corning water distillation apparatus model AG-2.
[3] Burdick & Jackson Laboratories, Muskegon, Mich.
[4] Constametric II G, Laboratory Data Control.
[5] Valco Instruments Co., Houston, Tex.
[6] Vari-Chrom, Varian Instruments.
[7] Varian model 9176.
[8] Minigrator, Spectra-Physics.
[9] Varian model 8500 dual pump.
[10] Rheodyne model 70-10 100-μl loop.
[11] Variscan, model 635, Varian Instruments.
[12] Hewlett-Packard model 3380A.
[13] Corning model 12.
[14] Acta III, Beckman Instruments; Cary 17, Varian Instruments.
[15] μBondapak C_{18}, Waters Associates.
[16] Haake F.J.

0022-3549/79/0200-0172$01.00/0
© 1979, American Pharmaceutical Association

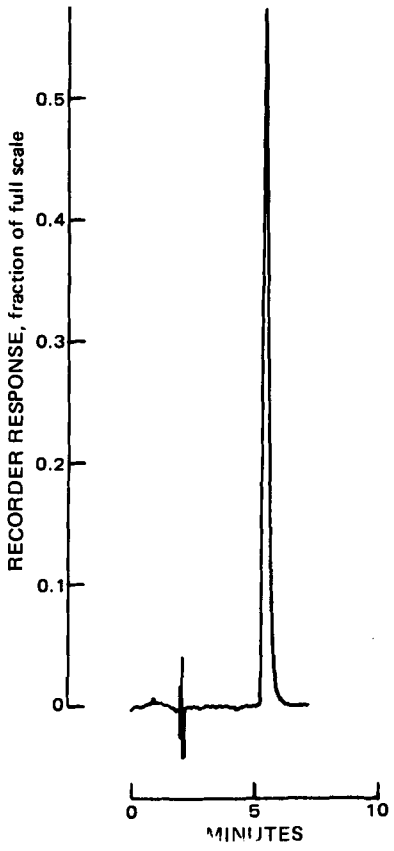

Figure 1—*High-performance liquid chromatogram of cyclophosphamide. Operating conditions were: flow rate, 1.5 ml/min; detector, 200 nm; scale, 0.64 aufs; and sample size, 39 μg (25 μl of 1.56 μg/μl).*

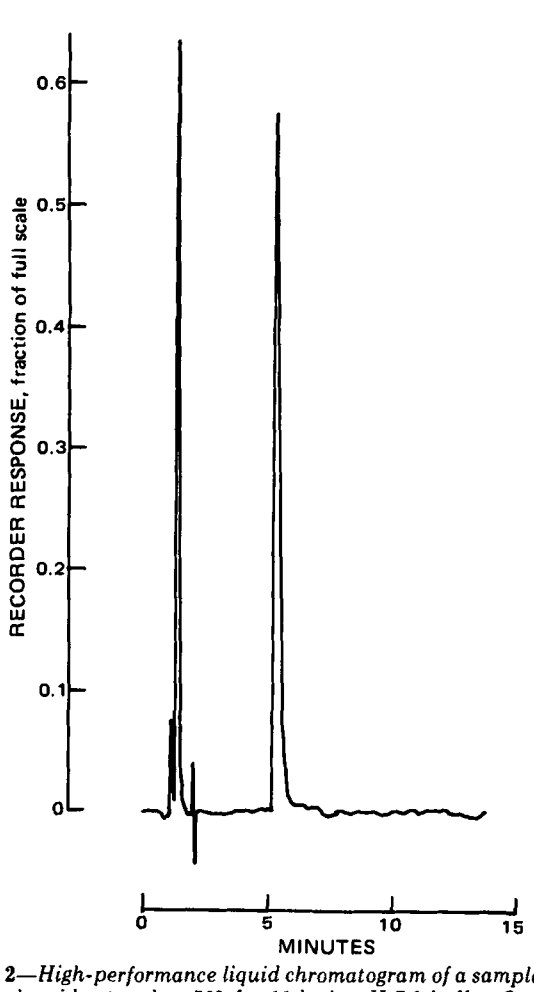

Figure 2—*High-performance liquid chromatogram of a sample of cyclophosphamide stored at 50° for 11 hr in pH 7.0 buffer. Operating conditions were: flow rate, 1.5 ml/min; detector, 200 nm; scale, 0.64 aufs; and sample size, 25 μl of a 1:20 dilution of the reaction mixture that originally contained 40 mg of cyclophosphamide/ml.*

analyzed without further dilution using a 100-μl injector loop. The chromatographic conditions were: column, 30 cm × 3.9 mm i.d.; flow rate, 1.5 ml/hr; mobile phase, 23% acetonitrile–77% 0.1 *M* (pH 7.0) phosphate buffer; detector wavelength, 211 nm; detector scale, 0–0.5; and recorder, 0.4 aufs.

RESULTS AND DISCUSSION

A high-performance liquid chromatogram of a freshly prepared aqueous solution of cyclophosphamide appears in Fig. 1. The drug was eluted in a single band at 325 sec. The fluctuations in the baseline at about 2 min were due to injection anomalies and were not compound related. The single peak illustrated in Fig. 1 gave approximately 60% of a full-scale deflection (0.64 aufs) and was due to about 39 μg of the drug. This result is in contrast with the USP GLC method (7) in which decomposition on the column gives multiple peaks.

The UV absorbance spectrum of cyclophosphamide, in water and in a solvent (25% acetonitrile–75% water) approximating the HPLC mobile phase, was recorded. A local maximum occurred in both solvents at or below 190 nm, but even at this wavelength the drug had a low molar absorptivity (ϵ = 1020 in water). At 200 nm, ϵ equaled 550. The compound had no absorbance at 254 nm, where fixed wavelength detectors operate at maximum sensitivity.

The chromatogram depicted in Fig. 1 was recorded using a variable wavelength detector[6] set at 200 nm. The choice of this wavelength allowed quantification of the chromatographic band due to intact drug, which would not have been observed at 254 nm. The greatest sensitivity was obtained using the lowest wavelength compatible with the detector, flowcell, and solvent used. The chromatograms from the brief kinetic study to be described also were recorded at 200 nm. However, it was possible to operate the same detector at wavelengths as low as 190 nm if the column was equilibrated thoroughly with the eluant (water and UV grade acetonitrile). The cyclophosphamide band area (from an 86-μg sample) was 1.8 times greater at 190 nm than at 200 nm, as expected from the UV spectrum. The ability to monitor at wavelengths as low as 190 nm is not critical for the accurate measurement of cyclophosphamide concentrations, however.

The detector was set at 254 nm for the same 86-μg sample to test the hypothesis that no HPLC absorbance band should be seen. As expected, no band was seen even with the sensitivity increased 100-fold to 0.0064 aufs. A sample 10 times as large (*i.e.*, 855 μg) also gave no chromatographic band (due to absorbance) at this increased sensitivity. However, this concentrated sample did give a deflection in the baseline (first negative and then positive), which was attributed to a refractive index change in the eluant as the drug passed through the detector. This deflection was not suitable for quantification of samples.

Figure 2 illustrates the chromatogram of a buffered (pH 7.0) aqueous sample of cyclophosphamide in which a portion of the drug had been hydrolyzed. Drug solutions buffered at pH 7.0 and stored at 40, 50, 60, and 80° gave chromatograms that were all qualitatively like the one shown in Fig. 2. All injections were made with the same 25-μl loop without an internal standard. Each chromatogram contained a band due to the remaining intact drug at about 325 sec and only one other band (at about 90 sec) due to the degradation product(s). More than one product can result from cyclophosphamide hydrolysis. The band near 90 sec may have been due to more than one product, but no attempts were made to resolve the possible components.

Plots of the natural log of the area of the band due to intact cyclophosphamide *versus* time, for solutions stored at each of the four temperatures, appear in Fig. 3. The plots are linear, and the rate constants calculated from the slopes of the regression lines agree well with those that can be predicted from the Arrhenius equation and data published previously (10) (Table I). The linearity of the plots and agreement with the predicted values indicate that the HPLC technique can provide specific and reliable stability data for the intact drug in the presence of its hydrolysis products. The activation energy of 26.8 kcal/mole/deg calculated from the HPLC data also is in general agreement with the value (~24.5 kcal/mole/deg) previously determined (4).

The brief kinetic study described here was conducted only to show the

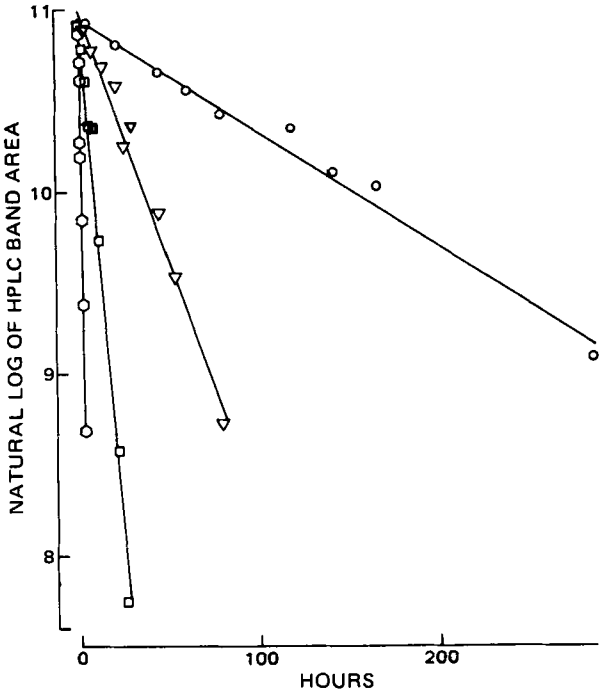

Figure 3—*Semilogarithmic plots of the cyclophosphamide HPLC band area* versus *time for pH 7.0 solutions stored at 40° (○), 50° (▽), 60° (□), and 80° (○).*

possible utility of an HPLC method for analyzing the drug in the presence of its hydrolysis products. No internal standard was used because the precision using an injector loop was considered adequate for the desired results. Of course, each HPLC column and instrument is unique; variations in mobile phase, flow rate, and detector settings for optimum performance are to be expected.

The standard calibration curve used to determine sample concentration was prepared by three or more injections of four standard solutions (1.038–4.436 mg/ml). A least-squares analysis of integrator counts *versus* concentration defined a straight line ($r^2 = 0.9987$) with a slope of 1.305×10^5 counts/(mg/ml), a y-intercept of 1.646×10^4 counts, and a relative standard deviation of the slope of 1.05%. The highest relative standard deviation of the areas (within the group) at any one concentration was 2.1% (at 1.563 mg/ml, three injections). Ten replicate 25-μl injections of a 3.42-mg/ml solution with no internal standard gave band areas with a relative standard deviation of ±1.5%.

While this degree of reproducibility was deemed adequate here, an internal standard may be desirable or necessary for precise kinetic measurements or for accurate day-to-day control of the potency of a drug product. An internal standard would also be useful if the drug were to be analyzed in biological samples. (However, the techniques outlined here probably would not provide the sensitivity, without a drug concentrating step, necessary for the analysis of the small amounts of intact drug in biological samples.) Nevertheless, for the analysis of drug products or relatively concentrated solutions, the sensitivity is adequate, and hydrocortisone is a suitable internal standard.

Table I—Rate Constants for the Hydrolysis of Cyclophosphamide at pH 7.0

T	k[a], min^{-1}	r^2	$k_{expected}$[b,c]
40°	1.04×10^{-4}	0.986	1.48×10^{-4}
50°	4.62×10^{-4}	0.982	5.12×10^{-4}
60°	1.94×10^{-3}	0.995	1.65×10^{-3}
80°	1.37×10^{-2}	0.992	1.40×10^{-2}

[a] Plot of log k *versus* $1/T$ gives a value of $E_a = 26.8$ kcal/mole/deg ($r^2 = 0.994$). [b] These values were calculated from the constants given in Ref. 8 and the Arrhenius equation $k = Ae^{-E_a/RT}$, where $A = 4.22 \times 10^{-13}$ min^{-1} and $E_a = 25.0$ kcal/mole/deg. [c] These values are expected to be nearly independent of pH in the pH 3–10 region, as evidenced by the work of Hirata *et al.* (4).

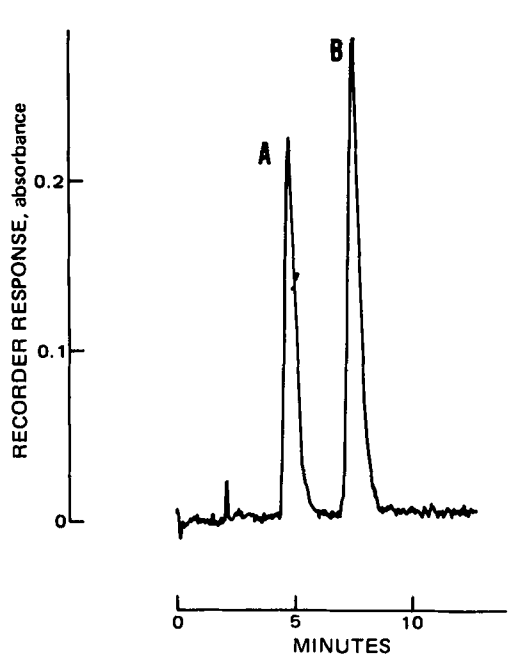

Figure 4—*High-performance liquid chromatogram of cyclophosphamide (A) (4.85 min) and hydrocortisone (B) (7.71 min). Operating conditions were: flow rate, 1.5 ml/min; detector, 211 nm; scale, 0.4 aufs; and sample size, 100 μl of a solution containing 12.5 mg of cyclophosphamide/ml and 0.2 mg of hydrocortisone/ml.*

A chromatogram of a solution containing hydrocortisone and cyclophosphamide is shown in Fig. 4. Since hydrocortisone elutes after the drug, it does not overlap with either the drug or hydrolysis products. Its use in biological samples would require further experimentation. The detector was set at 211 nm for this chromatogram because this detector[11] would not operate below that wavelength with the indicated mobile phase. For this reason, the sensitivity was lower than before, as expected.

Detectors other than UV types (*e.g.*, refractive index) may also be useful for the analysis of cyclophosphamide in certain instances. Although a degree of specificity might be lost in going from a UV to a refractive index detector, advantage might be gained in detecting hydrolysis products or impurities that do not absorb UV light. The data indicate that reversed-phase HPLC is ideal for the analysis of cyclophosphamide when the appropriate detector is employed. Specific methods for the analysis of the drug in solid or liquid dosage forms should easily be developed based on the chromatographic system given.

REFERENCES

(1) O. D. Boughton, R. D. Brown, R. Bryant, F. J. Burger, and C. M. Combs, *J. Pharm. Sci.*, **61**, 97 (1972).

(2) V. Egerts, N. Ozolins, M. V. Schimanskaya, and A. Cebere, *Akad. Nauk Latv. SSR, Inst. Org. Sin., Sb. Statei*, **1965**, 12; through *Chem. Abstr.*, **64**, 1040a (1966).

(3) O. M. Friedman and E. Boger, *Anal. Chem.*, **33**, 906 (1961).

(4) M. Hirata, H. Kagawa, and M. Baba, *Ann. Dept. Shionogi Res. Lab.*, **17**, 107 (1967).

(5) "The British Pharmacopoeia," Pharmaceutical Press, London, England, 1968.

(6) "The National Formulary," 12th ed., Mack Publishing Co., Easton, Pa., 1965. "The United States Pharmacopeia," 18th rev., Mack Publishing Co., Easton, Pa., 1970.

(7) "The United States Pharmacopeia," 19th rev., 2nd Suppl., Mack Publishing Co., Easton, Pa., 1976.

(8) C. Pantarotto, A. Bossi, G. Belvedere, A. Martini, M. G. Donelli, and A. Frigerio, *J. Pharm. Sci.*, **63**, 1554 (1974).

(9) C. Jackson, Jr., and P. J. Reynolds, *J. Agr. Food Chem.*, **20**, 972 (1972).

(10) D. Brooke, R. J. Bequette, and R. E. Davis, *Am. J. Hosp. Pharm.*, **30**, 134 (1973).

Thermodynamic Relationship between α- and β-Forms of Crystalline Progesterone

MITSUO MURAMATSU ˣ, MAKIO IWAHASHI, and USHIO TAKEUCHI

Received October 17, 1977, from the *Faculty of Science, Tokyo Metropolitan University, Setagaya-Ku, Tokyo, Japan 158.* Accepted for publication July 11, 1978.

Abstract □ Thermodynamic properties such as the latent heat of fusion, aqueous solubility, heat of solution, and interchange energy with water were determined for single crystals of progesterone in α- and β-forms. The differences in the properties between the polymorphic crystals arise from a dissimilar mode of molecular packing, rather than of molecular conformation, in the unit cell, as reflected in the IR spectral and X-ray crystallographic results.

Keyphrases □ Thermodynamic properties, various—determined for α- and β-forms of crystalline progesterone □ Progesterone—α- and β-forms of crystals, various thermodynamic properties determined □ Crystals—α- and β-forms of progesterone, various thermodynamic properties determined □ Steroids—progesterone, α- and β-forms of crystals, various thermodynamic properties determined

In addition to its pharmaceutical and pharmacological role (1, 2), the importance of crystalline polymorphism has been recognized in understanding thermodynamic properties of solid substances (3). Some thermodynamic differences between polymorphic crystals are revealed in orientational changes of the molecules in insoluble monolayers at air–solution interfaces when polymorphic transformation is associated essentially with a conformational change of the molecules in the two-dimensional film (4–6).

Progesterone has at least two polymorphic forms in its crystalline state (7–13). Little has been reported on the physicochemical properties to clarify the thermodynamic relationship between them. In the present experiments, an attempt was made to provide information about the thermodynamic and relevant properties of the steroid in different polymorphic states. Such information is necessary not only for establishing criteria of crystallographical and pharmacological purities for quality control of the steroid but also for the quantitative understanding of its surface chemical properties.

EXPERIMENTAL

Identification of the polymorphic crystals was achieved with an X-ray diffraction unit[1], an IR spectrometer[2] (resolving power of 0.5 cm^{-1}), and a differential scanning calorimeter[3] with a temperature range from −150 to +300° (accuracy of ±2.5 mJ/sec). For all experiments, a commercially available sample (pure grade) of crystalline progesterone[4] was used after repeated recrystallization from aqueous ethanol (1:1 v/v).

The solubility in water was determined by the radiotracer method (14) with a radiochemically pure sample of 1,2-^{3}H-progesterone[5] (specific activity of 410 μCi/mmole). The techniques used were similar to those reported previously (6).

RESULTS AND DISCUSSION

Single Crystals of Progesterone—The sample, when recrystallized without seeding from an ethanolic mixture (1:1 v/v) with water or *n*-hexane, was identified as the α-form (9, 10) or Form A (12, 13), which gave only one peak at 128° on the differential scanning calorimetric chart. After equilibrium melting in air at 85 ± 2° for a few hours, it had turned to the 122° melting crystal, which corresponded to the β-form (9, 10) or Form B (12, 13). When such a crude sample of the α- or β-form was used for seeding, upon slow cooling of a progesterone solution, a single crystal (~1 mm × ~2 mm average) was always obtained and was identified as the α-crystal or a mixture of α- and β-crystals, respectively; the latter permitted manipulative separation with the unaided eye.

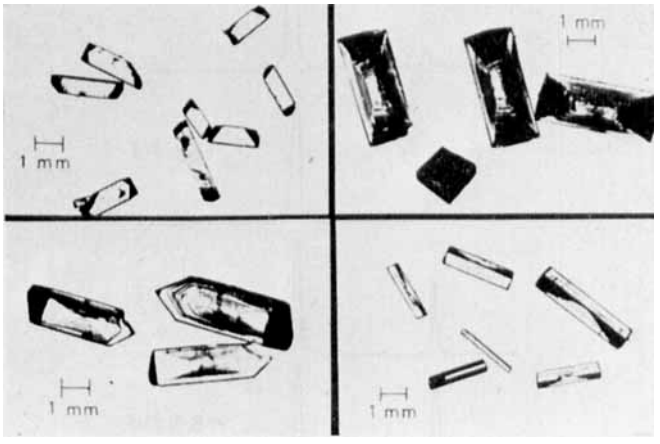

Figure 1—*Single crystals in α- (left) and β- (right) forms obtained by seeding–recrystallization from ethanolic mixtures (1:1 v/v) with water (top) and n-hexane (bottom).*

Figure 1 shows the microphotographs of these single crystals. Those in the left figures were identified as pure samples of the α-form from crystallographical (15, 16) and IR spectral (12, 13) aspects. No definitive data have been established for identification of the β-form.

Crystalline Transformation—When molten liquid underwent equilibrium melting at 85° in air, nitrogen, or helium, β-crystals always were formed; in a vacuum (2–3 mm Hg), α-crystallization took place. At room temperature, both crystals seemed to be so stable that apparently no polymorphic transformation occurred for several months or longer. At a higher temperature, a unilateral transformation, $\beta \rightarrow \alpha$, occurred spontaneously (Fig. 2). The β-form apparently is thermodynamically unstable. Heating at 122 and 128° returned the β- and α- forms, respectively, to the molten state.

Differential scanning calorimetry (−100 ⇄ +150°) of the steroid in air showed that the molten specimen was crystallized at a cooling rate of −1°/min; −10°/min was so fast that the specimen remained supercooled throughout the cooling processes. In such a case, crystallization

Table I—Aqueous Solubilities of Progesterone in α- and β-Forms

Temperature	Solubility, 10^{-5} M	
	α-Form	β-Form
21.7°	2.60	—
24.0°	—	3.72
25.3°	2.81	—
30.2°	3.80	—
30.5°	—	4.52
35.5°	—	5.39
36.4°	4.69	—
40.7°	—	6.75
41.3°	6.37	—
46.1°	6.50	—

[1] Rigaku Denki model 2001.
[2] Hitachi Perkin-Elmer model 225.
[3] Shimadzu model DSC-30 equipped with model LTC-30 cooling unit.
[4] Nakarai Pharmaceutical Co., Kyoto, Japan.
[5] The Radiochemical Centre, Amersham, England.

0022-3549/79/0200-0175$01.00/0
© 1979, American Pharmaceutical Association

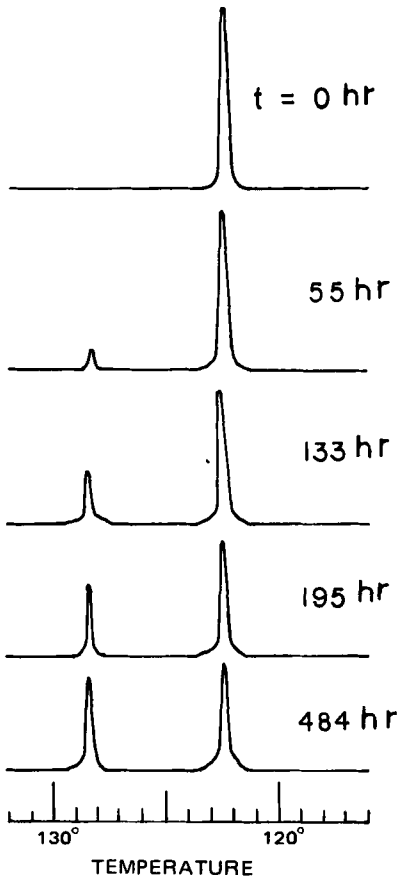

Figure 2—*Differential scanning calorimeter diagrams for β-crystal kept standing in a vacuum (2–3 mm Hg) at 99 ± 1° for the indicated time. Five samples of single β-crystals were split into two half-portions for the high temperature and control tests. No change was observed with the control portion, which had been kept in a vacuum at room temperature. With the α-crystal, no change was observed on the differential scanning calorimetric chart throughout several weeks, regardless of the pressure (2–760 mm Hg) and temperature (25–99°).*

usually took place in the subsequent heating processes. In all cases, the crystallization temperature was from 37 to ~120°, depending on the experimental conditions. All of these crystals proved to be of the β-form regardless of the solidification conditions. Forms III–V, reported by Brändstatter-Kuhnert and coworkers (9–11), seem to represent metastable states that change commonly to the β-form.

Recrystallization from an organic solvent such as ethanol, benzene, acetone, or ether always yielded the α-form, as did any binary mixture of these solvents.

Thermodynamic Relationship—The dissolution processes of progesterone in water obey the first-order rate law (6, 14). The solubility, C_s, at a temperature, T, was determined by extrapolating the rate equation to infinite time (Table I). Table II gives the heat of solution, ΔH_s, based on the linearity of the $C_s \sim 1/T$ relationship, the latent heat

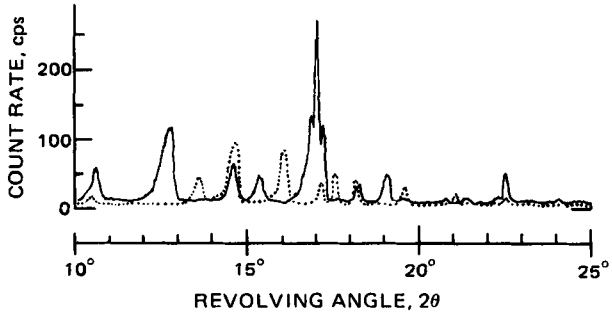

Figure 3—*X-ray diffraction patterns for pulverized samples in α- (—) and β- (. . . .) forms.*

Table II—Heat of Solution, ΔH_s, Latent Heat of Fusion, ΔH_f, and Molar Interchange Energy, Φ, for Progesterone in α- and β-Forms

Parameter, kcal/mole	α-Form	β-Form	Difference
ΔH_s	8.41	7.27	$\delta\Delta H_s = 1.14$
ΔH_f	6.68	5.60	$\delta\Delta H_f = 1.08$
Φ	+1.73	+1.67	$\delta\Phi = 0.06$

Table III—Lattice Constants of Progesterone in α- and β-Forms (Orthorhombic Crystalline System)

Sample	α-Form, Å	β-Form, Å
a	12.62	12.65
b	13.84	22.65
c	10.38	6.36

of fusion, ΔH_f, obtained from the differential scanning calorimetric chart with crystalline potassium nitrate as the reference, and the molar interchange energy, Φ, defined as:

$$\Phi = \Delta H_s - \Delta H_f \qquad \text{(Eq. 1)}$$

This term can, in turn, be expressed (6) as:

$$\Phi = pzN\phi \qquad \text{(Eq. 2)}$$

where N is Avogadro's number, p is the fraction of progesterone–water linkage to all z linkages around a progesterone molecule in the solution, and ϕ is the pair hydrophilicity defined as:

$$\phi = \epsilon_{12} - (\epsilon_{11} + \epsilon_{22})/2 \qquad \text{(Eq. 3)}$$

in terms of the bond energies for the pairs of progesterone–water (ϵ_{12}), water–water (ϵ_{11}), and progesterone–progesterone (ϵ_{22}).

The interchange energy, Φ, or the pair hydrophilicity, ϕ, is rationalized under the assumption that the molecular conformation in a polymorphic crystal remains unchanged throughout the dissolution processes since the solubility is determined by extrapolating the rate equation to infinite time. In Table II, therefore, the small $\delta\Phi$ value is indicative of almost the same conformation of the progesterone molecules in between α- and β-crystals. The $\delta\Delta H_s$ is contributed largely by $\delta\Delta H_f$ and negligibly by $\delta\Phi$, suggesting that the crystalline polymorphism is characterized by the dissimilarity in the packing mode of the molecules without a significant difference in their conformation. In fact, the IR spectral difference appeared only as the shift at ~870 cm^{-1}, which Mesley (13) ascribed to the difference in CH out-of-plane vibration. The X-ray diffraction patterns for pulverous samples (Fig. 3) and the lattice constants thereby obtained (Table III) are in good agreement with the reported values (15–18).

Campsteyn *et al.* (17) reported that the intermolecular cohesion in α-crystalline progesterone is due mainly to van der Waals attraction. Foresti-Serantoni *et al.* (18) indicated that the molecular conformation in the α-crystal is similar to that in the β-crystal and, accordingly, that the packing forces in these crystals have little correlation to the molecular conformation. All these aspects are in accord with the consideration that the thermodynamic difference comes solely from a different mode of molecular packing, rather than the molecular conformation, in the unit cell.

REFERENCES

(1) J. Haleblian and W. McCrone, *J. Pharm. Sci.*, **58**, 911 (1969).

(2) S. Rosenstein and P. P. Lamy, *Am. J. Hosp. Pharm.*, **26**, 598 (1969).

(3) A. R. Verma and P. Krishna, "Polymorphism and Polytypism in Crystals," Wiley, New York, N.Y., 1966, p. 16.

(4) M. Iwahashi, K. Aruga, O. Hirata, T. Horiuchi, and M. Muramatsu, *J. Colloid Interface Sci.*, **42**, 349 (1973).

(5) M. Iwahashi, *ibid.*, **50**, 532 (1975).

(6) M. Muramatsu, M. Iwahashi, and K. Masumoto, *J. Chem. Eng. Data*, **20**, 6 (1975).

(7) K. H. Slotta, H. Ruschig, and E. Blanke, *Chem. Ber.*, **67**, 1974 (1934).

(8) A. Butenandt and J. Schmidt, *ibid.*, **67**, 2088 (1934).

(9) M. Brändstatter-Kuhnert and A. Kofler, *Mikrochim. Acta*, **1959**, 847.

(10) M. Brändstatter-Kuhnert, E. Junger, and A. Kofler, *Microchem. J.*, **9**, 105 (1965).
(11) M. Brändstatter-Kuhnert, *Oesterr. Apoth.-Ztg.*, **13**, 297 (1959).
(12) R. J. Mesley and C. A. Johnson, *J. Pharm. Pharmacol.*, **17**, 329 (1965).
(13) R. J. Mesley, *Spectrochim. Acta*, **22**, 889 (1966).
(14) C. H. Bovington and B. Dacre, in "Radiotracer Techniques and Applications," vol. 1, E. A. Evans and M. Muramatsu, Eds., Dekker, New York, N.Y., 1977, p. 457.
(15) B. A. Haner and D. A. Norton, *Acta Crystallogr.*, **17**, 1610 (1964).
(16) O. Dideberg and L. Dupont, *J. Appl. Crystallogr.*, **4**, 80 (1971).
(17) P. H. Campsteyn, L. Dupont, and O. Dideberg, *Acta Crystallogr.*, **B28**, 3032 (1972).
(18) E. Foresti-Serantoni, A. Krajewski, R. Mongiorgi, L. Riva di Sanseverino, and R. Cameroni, *Cryst. Struct. Commun.*, **4** (1), 189 (1975).

ACKNOWLEDGMENTS

Supported by grants from the Ministry of Education and from Fujisawa Pharmaceutical Co., Osaka, Japan.
The authors are indebted to Dr. Teruo Temma and Dr. Mitsuo Deki, Central Customs Laboratory, Matsudo, Chiba-Ken, for assistance.

New *In Vitro* Dissolution Test Apparatus

S. S. NASIR *[x], L. O. WILKEN, Jr., and S. M. NASIR

Received May 4, 1976, from the *Industrial Pharmacy Laboratories, School of Pharmacy, Auburn University, Auburn, AL 36830.* Accepted for publication July 3, 1978. *Present address: Aspro-Nicholas (Pakistan) Ltd., C/36, Estate Avenue, S.I.T.E., Karachi, Pakistan.

Abstract □ A new *in vitro* dissolution test apparatus was designed and evaluated. Compressed tablets of drugs representing different solubility characteristics were tested at various air pressures and compared to dissolution patterns of similar tablets by the Levy beaker and USP methods. Air pressure of 46 mm generally was suitable for determining the dissolution rates of tablets. This new dissolution tester possibly can be useful in determining drug release from solid dosage forms and correlating it with *in vivo* bioavailability because dissolution rate can be controlled easily with the adjustment of air pressure without complicated changes in the apparatus, there is no excessive settling of particles, and complete drug dissolution can be achieved with no clogging of the screen.

Keyphrases □ Dissolution test apparatus—designed, evaluated with various drugs at various air pressures, compared to other methods □ Apparatus, dissolution test—designed, evaluated with various drugs at various air pressures, compared to other methods

Determination of *in vitro* dissolution rates is important in the design, evaluation, and quality control of solid dosage forms. The USP and NF dissolution tests suffer from a number of technical problems (1, 2).

Various other methods generally involve induced agitation. The Levy beaker method (3) is the most commonly used method and is generally recommended as a standard. Other reported methods (4–7) have the commonly encountered problem of mound formation of particles at the bottom of the container due to poor particle dispersion. Mound formation may affect apparent dissolution characteristics (8). In this study, a better correlation was observed with a rotating flask that allowed good dispersion at low agitation. Another problem is the degree of agitation, which is usually greater than what the dosage form will encounter in the GI tract.

The USP and NF methods also are subject to poor dispersion. In these methods, the screen acts as an interfacial barrier at moderate stirring rates. In addition, the fine mesh screen is clogged by undissolved particles (9).

An apparatus will be most suitable for *in vitro* testing of solid dosage forms if it achieves a thorough dispersion of particles with minimum agitation, similar to the agitation in the GI tract. With these factors under consideration, an *in vitro* dissolution tester was designed and evaluated.

EXPERIMENTAL

Description of Apparatus—The apparatus (Figs. 1 and 2) consists of two cylindrical glass tubes: tube A, 28.4 cm long × 3.4 cm i.d.; and tube B, 29.4 cm high × 2.8 cm i.d. Tube B is connected to tube A at the base and at a length of 17.3 cm by tubes with an identical diameter of 1.0 cm and a length of 4.7 cm.

A stainless steel basket and an air tube are suspended in tube A. The bottom of the basket is approximately 15.7 cm from the bottom of tube A, and the air tube just protrudes from the stopper.

The basket consists of a solid metal top with a small vent and is fitted

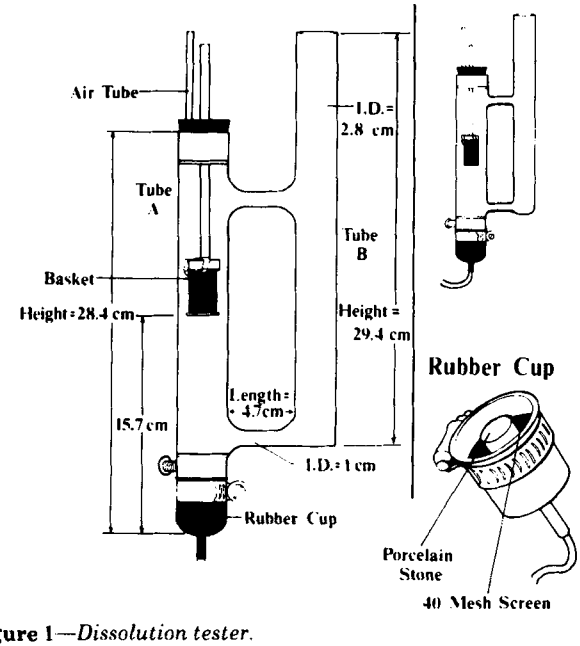

Figure 1—*Dissolution tester.*

© 1979, American Pharmaceutical Association

(10) M. Brändstatter-Kuhnert, E. Junger, and A. Kofler, *Microchem. J.*, **9**, 105 (1965).
(11) M. Brändstatter-Kuhnert, *Oesterr. Apoth.-Ztg.*, **13**, 297 (1959).
(12) R. J. Mesley and C. A. Johnson, *J. Pharm. Pharmacol.*, **17**, 329 (1965).
(13) R. J. Mesley, *Spectrochim. Acta*, **22**, 889 (1966).
(14) C. H. Bovington and B. Dacre, in "Radiotracer Techniques and Applications," vol. 1, E. A. Evans and M. Muramatsu, Eds., Dekker, New York, N.Y., 1977, p. 457.
(15) B. A. Haner and D. A. Norton, *Acta Crystallogr.*, **17**, 1610 (1964).
(16) O. Dideberg and L. Dupont, *J. Appl. Crystallogr.*, **4**, 80 (1971).
(17) P. H. Campsteyn, L. Dupont, and O. Dideberg, *Acta Crystallogr.*, **B28**, 3032 (1972).
(18) E. Foresti-Serantoni, A. Krajewski, R. Mongiorgi, L. Riva di Sanseverino, and R. Cameroni, *Cryst. Struct. Commun.*, **4** (1), 189 (1975).

ACKNOWLEDGMENTS

Supported by grants from the Ministry of Education and from Fujisawa Pharmaceutical Co., Osaka, Japan.
The authors are indebted to Dr. Teruo Temma and Dr. Mitsuo Deki, Central Customs Laboratory, Matsudo, Chiba-Ken, for assistance.

New *In Vitro* Dissolution Test Apparatus

S. S. NASIR *[x], L. O. WILKEN, Jr., and S. M. NASIR

Received May 4, 1976, from the *Industrial Pharmacy Laboratories, School of Pharmacy, Auburn University, Auburn, AL 36830.* Accepted for publication July 3, 1978. *Present address: Aspro-Nicholas (Pakistan) Ltd., C/36, Estate Avenue, S.I.T.E., Karachi, Pakistan.

Abstract □ A new *in vitro* dissolution test apparatus was designed and evaluated. Compressed tablets of drugs representing different solubility characteristics were tested at various air pressures and compared to dissolution patterns of similar tablets by the Levy beaker and USP methods. Air pressure of 46 mm generally was suitable for determining the dissolution rates of tablets. This new dissolution tester possibly can be useful in determining drug release from solid dosage forms and correlating it with *in vivo* bioavailability because dissolution rate can be controlled easily with the adjustment of air pressure without complicated changes in the apparatus, there is no excessive settling of particles, and complete drug dissolution can be achieved with no clogging of the screen.

Keyphrases □ Dissolution test apparatus—designed, evaluated with various drugs at various air pressures, compared to other methods □ Apparatus, dissolution test—designed, evaluated with various drugs at various air pressures, compared to other methods

Determination of *in vitro* dissolution rates is important in the design, evaluation, and quality control of solid dosage forms. The USP and NF dissolution tests suffer from a number of technical problems (1, 2).

Various other methods generally involve induced agitation. The Levy beaker method (3) is the most commonly used method and is generally recommended as a standard. Other reported methods (4–7) have the commonly encountered problem of mound formation of particles at the bottom of the container due to poor particle dispersion. Mound formation may affect apparent dissolution characteristics (8). In this study, a better correlation was observed with a rotating flask that allowed good dispersion at low agitation. Another problem is the degree of agitation, which is usually greater than what the dosage form will encounter in the GI tract.

The USP and NF methods also are subject to poor dispersion. In these methods, the screen acts as an interfacial barrier at moderate stirring rates. In addition, the fine mesh screen is clogged by undissolved particles (9).

An apparatus will be most suitable for *in vitro* testing of solid dosage forms if it achieves a thorough dispersion of particles with minimum agitation, similar to the agitation in the GI tract. With these factors under consideration, an *in vitro* dissolution tester was designed and evaluated.

EXPERIMENTAL

Description of Apparatus—The apparatus (Figs. 1 and 2) consists of two cylindrical glass tubes: tube A, 28.4 cm long × 3.4 cm i.d.; and tube B, 29.4 cm high × 2.8 cm i.d. Tube B is connected to tube A at the base and at a length of 17.3 cm by tubes with an identical diameter of 1.0 cm and a length of 4.7 cm.

A stainless steel basket and an air tube are suspended in tube A. The bottom of the basket is approximately 15.7 cm from the bottom of tube A, and the air tube just protrudes from the stopper.

The basket consists of a solid metal top with a small vent and is fitted

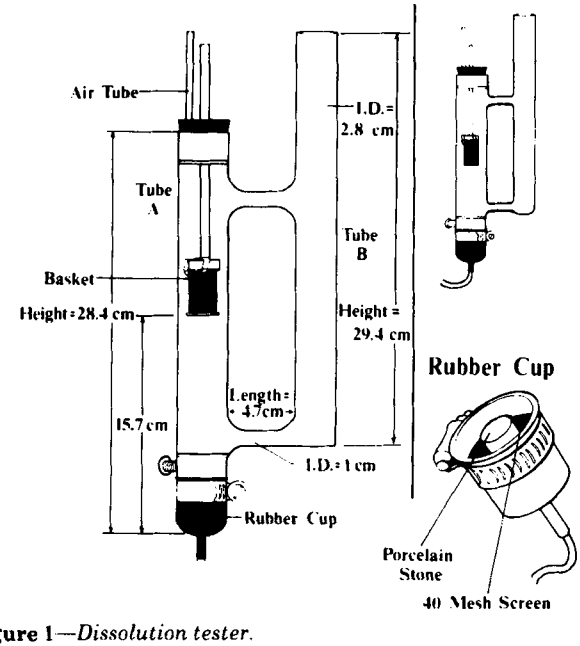

Figure 1—*Dissolution tester.*

© 1979, American Pharmaceutical Association

Table I—Levels of Significance (t Values) of Dissolution Rates of Piperazine Citrate and Isoniazid Tablets at Various Times with the New Tester at Various Air Pressures, the Levy Tester, and the USP Dissolution Tester at $p = 0.05$

	Piperazine Citrate Tablets				Isoniazid Tablets				
	5 min	10 min	20 min	30 min	5 min	10 min	20 min	30 min	40 min
Levy *versus* new tester at various air pressures									
40 mm Hg	2.8982	2.6963	2.2218[a]	2.58888[a]	5.2981	4.2100	3.8107	3.4330	4.5120
43 mm Hg	2.0600[a]	1.5716[a]	1.4132[a]	1.4258[a]	3.5750	3.8300	3.7600[a]	2.7791	3.7850
46 mm Hg	0.5891[a]	0.4715[a]	0.4761[a]	0.3158[a]	1.4100[a]	0.8455[a]	1.8530[a]	1.0100[a]	0.6740[a]
50 mm Hg	3.3870	3.4576	—	—	6.2040	4.2700	4.4131	5.6340	1.6752[a]
55 mm Hg	4.7290	4.9785	—	—	7.8131	5.976	4.738	5.988	2.000[a]
USP *versus* new tester at various air pressures									
40 mm Hg	4.9138	3.5336	3.3733	1.7978	2.6000	9.5890	10.7170	14.2012	14.0258
43 mm Hg	5.7963	4.3974	4.1262	2.5678	4.3340	10.5890	12.1508	15.3370	15.4827
46 mm Hg	8.6940	6.7307	6.0306	4.6922	13.5800	17.7680	21.1520	21.8700	23.8440
50 mm Hg	11.5979	9.5923	—	—	23.8791	23.4086	29.5544	28.0192	25.5271
55 mm Hg	12.4310	10.6009	—	—	29.2345	28.2037	29.7330	28.8143	26.1031
USP *versus* Levy tester					8.7450	16.3810	17.4100	19.1720	22.1480

[a] Statistically not significant.

to the basket with three spring clips. The basket is cylindrical and is made of stainless steel 40-mesh wire cloth, 3.66 cm high and 2.50 cm in diameter.

A cylindrical porcelain stone protruding through a central circular hole in a circular piece of 40-mesh stainless steel screen inside a rubber cup is fixed at the bottom, supported by a stainless steel sleeve. An opening at the bottom of the rubber cup adjacent to the bottom of the porcelain stone is connected by 5.5-mm polyethylene tubing to an air pump through a mercury manometer.

Dissolution Test Procedure—A 350-ml volume of 0.1 N HCl was the dissolution medium. One tablet was added to the basket, and the basket base was adjusted to a distance of 15.7 cm from the tester bottom. The dissolution tester was then immersed in a constant-temperature water bath maintained at 37°.

The dissolution tester was connected to an air pump. The air flow was controlled with a mercury manometer. Tests were conducted at air pressures of 40, 43, 46, 50, and 55 mm. The air pressure created circulation of liquid in the two tubes.

Samples of 5 ml were withdrawn from tube B at specified intervals, and an equal volume of 0.1 N HCl was added after each withdrawal. Each sample was then filtered and assayed by a procedure specified for each drug.

Twenty tablets each of commercial piperazine citrate and isoniazid and six tablets each of aspirin, phenobarbital, and sulfadiazine from various batches were tested. Aspirin (3) and phenobarbital (10) were assayed by the procedures reported previously. Isoniazid (11), piperazine citrate (12), and sulfadiazine (13) were assayed by the USP XVIII procedures.

For comparison, 20 representative tablets of isoniazid and piperazine citrate from the same batches were tested in the USP dissolution test apparatus. Similarly, isoniazid, piperazine citrate, aspirin, phenobarbital, and sulfadiazine were also tested by the Levy method (3), modified by using 350 ml of 0.1 N HCl as the dissolution medium instead of 250 ml. Samples of 5 ml were withdrawn at specified intervals, and equal volumes of 0.1 N HCl were added after each withdrawal. These samples were then assayed for drug concentration.

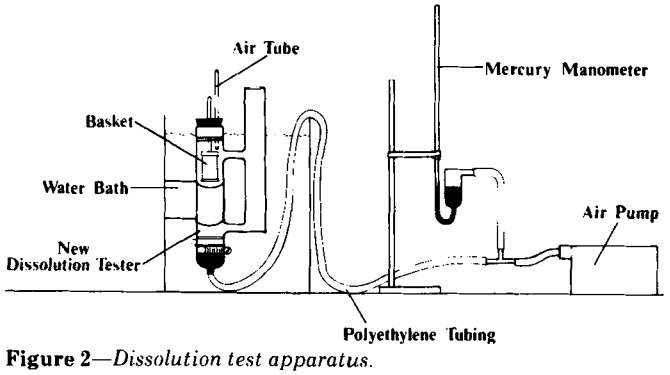

Figure 2—*Dissolution test apparatus.*

RESULTS AND DISCUSSION

The Levy beaker method has been recommended as a standard to compare other dissolution testers (14). This method also showed excellent *in vitro-in vivo* correlation (15, 16) and was used for comparison purposes previously (17, 18).

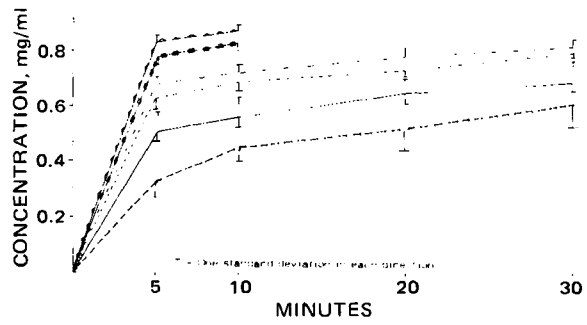

Figure 3—*Comparative dissolution rates of piperazine citrate tablets with the new dissolution tester at various air pressures, the Levy tester, and the USP dissolution tester. Key: HH, USP tester; —, 40 mm Hg; ···, 43 mm Hg; - - -, Levy tester; ·····, 46 mm Hg; □, 50 mm Hg; and △, 55 mm Hg.*

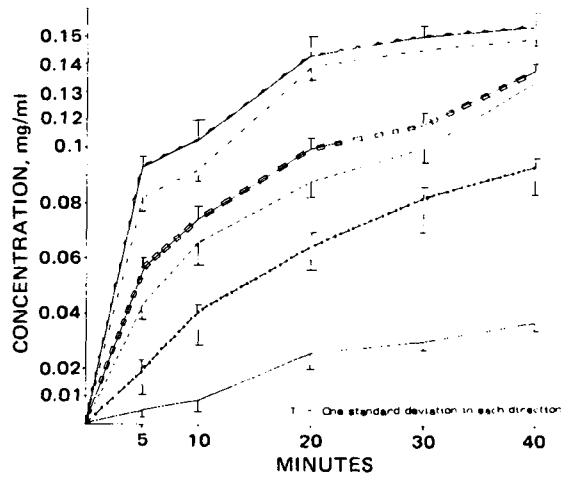

Figure 4—*Comparative dissolution rates of isoniazid tablets with the new dissolution tester at various air pressures, the Levy tester, and the USP dissolution tester. Key: —, USP tester; ····, 40 mm Hg; ●—●, 43 mm Hg; - - -, Levy tester; □, 46 mm Hg; ·····, 50 mm Hg; and △, 55 mm Hg.*

Table II—Levels of Significance (t Values) of Dissolution Rates of Aspirin, Sulfadiazine, and Phenobarbital Tablets at Various Times with the New Tester at Various Air Pressures and the Levy Dissolution Tester at $p = 0.05$

Product	Air Pressure, mm Hg (New Tester)	5 min	10 min	20 min	30 min	55 min	75 min
Aspirin							
Brand I, Batch A	40	1.1050[a]	1.5785[a]	3.6305	4.8932	—	—
Brand I, Batch A	43	0.9866[a]	0.9471[a]	2.5256[a]	4.1040	—	—
Brand I, Batch A	46	0.7893[a]	1.1050[a]	1.2628[a]	2.0677[a]	—	—
Brand I, Batch A	50	4.1438	4.2621	7.8925	7.4187	—	—
Brand I, Batch A	55	7.1037	7.2614	7.4189	7.8923	—	—
Brand I, Batch B	46	1.9930[a]	2.5573[a]	2.5700[a]	0.0159[a]	—	—
Brand II, Batch A	46	0.959[a]	0.732[a]	1.079[a]	0.825[a]	—	—
Brand II, Batch B	46	2.4850[a]	0.6485[a]	2.5600[a]	0.7279[a]	—	—
Sulfadiazine							
Batch A	40	—	30.000	15.930	13.892	16.734	4.908
Batch A	43	—	4.349	5.693	0.999	12.939	5.317
Batch A	46	—	5.480	3.424	6.410	5.899	5.310
Batch A	50	—	0.813[a]	4.962	2.010[a]	2.617	1.694[a]
Batch A	55	—	9.180	24.325	12.808	45.027	12.815
Batch B	46	—	1.602[a]	6.788	4.737	2.292[a]	2.509[a]
Phenobarbital							
Batch A	40	8.776	8.667	4.840	4.840	—	—
Batch A	43	3.112	2.360	4.469	4.469	—	—
Batch A	46	0.846[a]	1.681[a]	0.110[a]	0.110[a]	—	—
Batch B	46	0.533[a]	2.434[a]	2.432[a]	2.432[a]	—	—

[a] Statistically not significant.

Isoniazid, piperazine citrate, aspirin, phenobarbital, and sulfadiazine tablets consisted of 50, 315, 324, 30, and 500 mg of active ingredients/tablet, respectively. The dissolution rate studies with the new apparatus were conducted at 40, 43, 46, 50, and 55 mm of air pressure. All air pressures were sufficient to induce uniform circulation of the liquid in the apparatus. The use of an air tube prevented air bubbles from collecting at the bottom of the stainless steel basket. Any air bubbles at the bottom of the tube immediately combined into a larger bubble and broke off without hindering the movement of solid particles.

Although the circulation of fluid was not violent, it was sufficient at all speeds not to allow settlement of any solid particles at the bottom of the two tubes of the dissolution tester, probably because of the continuous movement of particles and the pattern and path of flow of fluid. There was no clogging of the screen during the test, probably because of the circulation of the dissolution medium through the screen.

Dissolution rates of 20 tablets from the same batch of isoniazid and piperazine citrate were determined. The dissolution rates of these tablets increased with the increase in air pressure. The results (Table I and Figs. 3 and 4) indicate that, for both types of tablets, there was less significant difference in the dissolution rates in the new tester at 46 mm and the Levy tester as compared to 40, 43, 50, and 55 mm of air pressure. Significant differences were observed between dissolution rates in the USP dissolution tester and the new tester at all air pressures. Similar results were obtained for the dissolution in the Levy tester and the USP dissolution tester (Figs. 3 and 4 and Table I).

The dissolution rates of Brand I, Batch A aspirin tablets were determined in the new dissolution tester at air pressures of 40, 43, 46, 50, and 55 mm. The dissolution rate increased with the increase in the air pressure (Fig. 5). The results (Table II and Fig. 5) again indicate less significant difference in the dissolution rate of these aspirin tablets in the new tester at 46 mm and the Levy tester as compared to 40, 43, 50, and 55 mm of air pressure. Therefore, it seemed to be the most appropriate pressure and was used in further investigations of aspirin tablets.

Batch B of Brand I aspirin tablets and Batches A and B of Brand II aspirin tablets also were tested by the Levy tester and the new dissolution tester at 46 mm of air pressure (Figs. 6 and 7, respectively).

Similar studies were conducted on two batches each of one brand of sulfadiazine and phenobarbital tablets at various air pressures (Figs. 8 and 9). Batch A sulfadiazine tablets were tested for dissolution with the

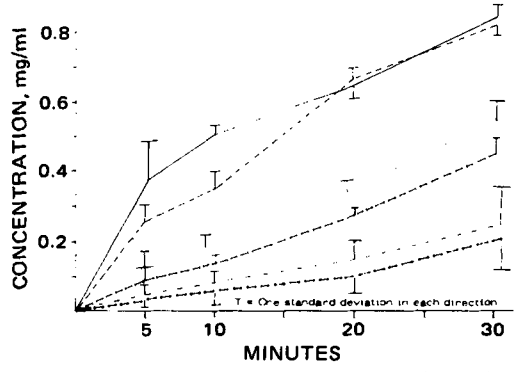

Figure 5—*Comparative dissolution rates of Brand I, Batch A aspirin tablets with the new dissolution rate tester. Key: ·····, 40 mm Hg; -·-·-, 43 mm Hg; ⊢⊣⊢, Levy tester; ····, 46 mm Hg; – – –, 50 mm Hg; and —, 55 mm Hg.*

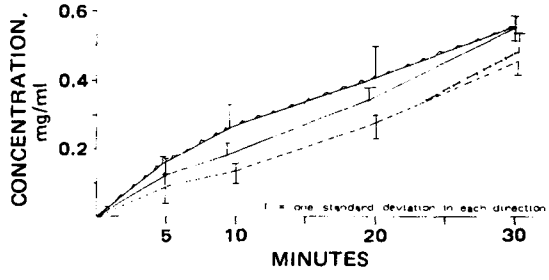

Figure 6—*Comparative dissolution rates of Brand I, Batch B aspirin tablets with the Levy tester and the new dissolution rate tester. Key: Δ, Brand I, Batch B with new tester; —, Brand I, Batch A with new tester; ⊢⊣⊢, Brand I. Batch A with the Levy tester; and - - - -, Brand I, Batch B with the Levy tester.*

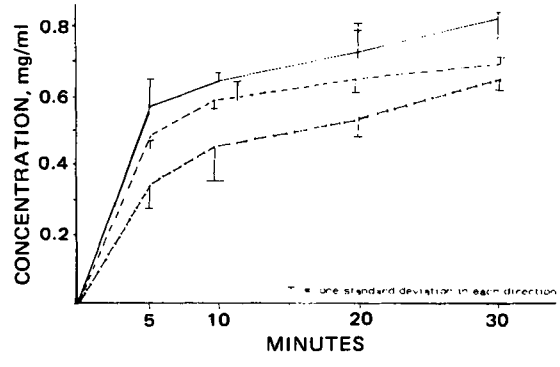

Figure 7—*Comparative dissolution rates of Brand II, Batches A and B aspirin tablets with the Levy tester and the new dissolution rate tester. Key: —, Brand II, Batch A with new tester; ····, Brand II, Batch B with new tester; - - -, Brand II, Batch A with Levy tester; and ⊢⊣⊢, Brand II, Batch B with the Levy tester.*

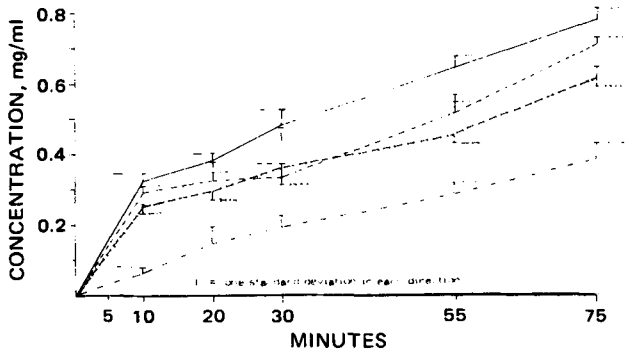

Figure 8—*Comparative dissolution rates of Batch A sulfadiazine tablets with the new dissolution rate tester. Key: ·····, 40 mm Hg; ⊢⊣, 43 mm Hg; ····, 46 mm Hg; - - -, 50 mm Hg; and —, 55 mm Hg.*

new tester at air pressures of 40, 43, 46, 50, and 55 mm. Batch A phenobarbital tablets were not tested at 50 and 55 mm because preliminary studies showed that the tablets went into solution within 5 min, which was less than their disintegration time. The dissolution rate increased with the increase in air pressure. Batch B sulfadiazine tablets were tested at 46 mm of air pressure.

Similar tablets of sulfadiazine and phenobarbital were also tested with the Levy dissolution tester, and the results were compared statistically with the results obtained at various air pressures with the new dissolution tester. There was less significant difference between dissolution rates of sulfadiazine tablets with the Levy tester and the new dissolution tester at 50 mm of pressure as compared to other speeds (Table II). On the other hand, there was a nonsignificant difference between the dissolution rates of phenobarbital tablets with the Levy tester and the new dissolution tester operated at 46 mm of air pressure (Table II).

The results of the dissolution rates of Batches A and B sulfadiazine and phenobarbital tablets with the Levy tester and the new dissolution tester at 46 mm are shown in Figs. 10–13.

Table III—Levels of Significance (t Values) of Dissolution Rates of Various Batches of Tablets at Various Times with the New Tester at 46 mm of Air Pressure at $p = 0.05$

Product	5 min	10 min	20 min	30 min	55 min	75 min
Aspirin Brand I, Batch A *versus* Brand I, Batch B	0.572[a]	1.1087[a]	0.8869[a]	0.1108[a]	—	—
Aspirin Brand II, Batch A *versus* Brand II, Batch B	1.465[a]	0.800[a]	0.526[a]	0.395[a]	—	—
Sulfadiazine Batch A *versus* Batch B	—	0.316[a]	1.517[a]	1.257[a]	0.765[a]	0.607[a]
Phenobarbital Batch A *versus* Batch B	0.667[a]	0.892[a]	0.892[a]	0.892[a]	—	—

[a] Statistically not significant.

Further evaluation of the results by statistically comparing the dissolution rates of two batches of the same brand, each with the Levy tester and with the new dissolution tester at 46 mm of air pressure (Tables III and IV), indicates a nonsignificant difference in the dissolution rates of the two different batches of the same brand when tested with the new tester and the Levy tester, except for sulfadiazine Batches A and B, where the difference was significant with the Levy tester.

Groups of tablets of each product from the same batch were tested individually in the new tester, and the deviations (Figs. 3–13) indicate reproducibility of results within a batch. These results also indicate that this method appears to be as reproducible as the USP or Levy method. In addition, a batch-to-batch nonsignificant difference in the dissolution rates was observed. As shown in Table V, these batches had well-controlled physical properties such as hardness and disintegration time.

An overall reevaluation of the results show that an air pressure of 46 mm generally was suitable in correlating the dissolution rates of various tablets studied with the new tester with the results obtained with the Levy

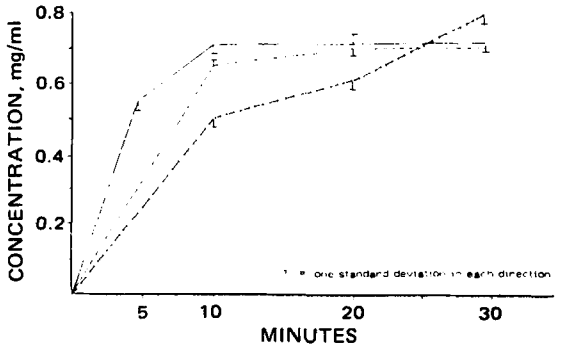

Figure 9—*Comparative dissolution rates of Batch A phenobarbital tablets with the new dissolution rate tester. Key: ⊢⊣, 40 mm Hg; - - -, 43 mm Hg; and —, 46 mm Hg.*

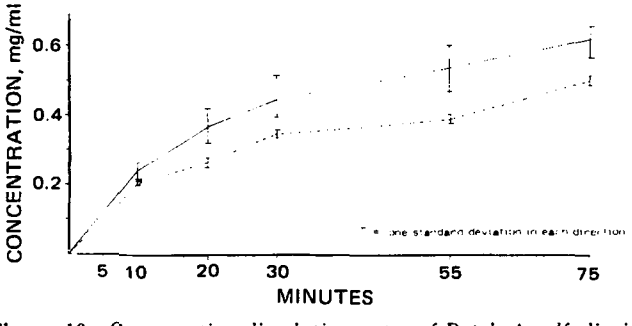

Figure 10—*Comparative dissolution rates of Batch A sulfadiazine tablets with the Levy tester (- - -) and the new dissolution rate tester (—).*

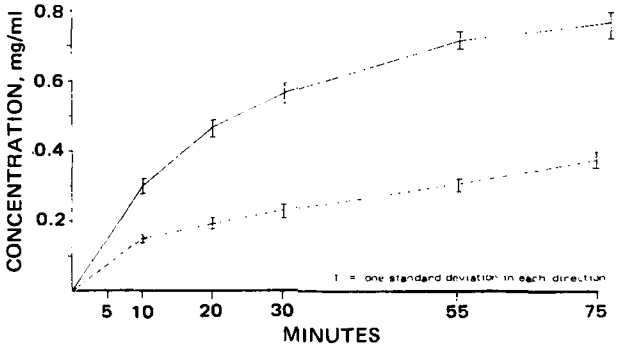

Figure 11—*Comparative dissolution rates of Batch B sulfadiazine tablets with the Levy tester (- - -) and the new dissolution rate tester (—).*

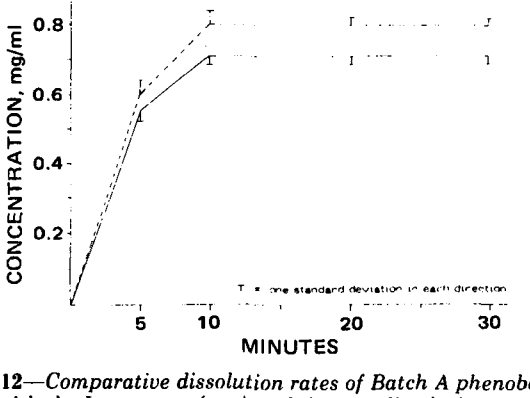

Figure 12—*Comparative dissolution rates of Batch A phenobarbital tablets with the Levy tester (- - -) and the new dissolution rate tester (—).*

Table IV—Levels of Significance (t Values) of Dissolution Rates of Various Batches of Tablets at Various Times with the Levy Tester at $p = 0.05$

Product	5 min	10 min	20 min	30 min	55 min	75 min
Aspirin Brand I, Batch A *versus* Brand I, Batch B	0.000[a]	0.000[a]	0.000[a]	0.2300[a]	—	—
Aspirin Brand II, Batch A *versus* Brand II, Batch B	1.2928[a]	1.3181[a]	1.593[a]	0.4486[a]	—	—
Sulfadiazine Batch A *versus* Batch B	—	4.903	3.531	10.804	61.118	4.302
Phenobarbital Batch A *versus* Batch B	1.123[a]	1.189[a]	0.310[a]	0.310[a]	—	—

[a] Statistically not significant.

tester. On the other hand, less significant differences in the dissolution rate of sulfadiazine tablets with the Levy tester and the new dissolution tester at 50 mm of pressure as compared to other pressures also indicate that other air pressures may be more suitable for some products with considerably different solubility characteristics.

Poor agreement was observed in the dissolution rates of piperazine citrate and isoniazid tablets in the USP dissolution rate tester as compared to the new tester at all pressures and the Levy tester. For better correlation of dissolution rates in the new tester and the USP dissolution tester, other pressures and speeds may be suitable. A detailed study is being conducted.

This new dissolution tester possibly can be useful in determining and correlating *in vitro* drug release from solid dosage forms with *in vivo* bioavailability, because dissolution can be controlled easily with the adjustment of air pressure without complicated changes in the apparatus. Other advantages of this dissolution tester are that, in all systems studied, no excessive settling of solid particles was observed and a complete dissolution of the drugs was achieved with no clogging of the screen. The possibility exists, however, that tablets with significantly different properties may produce contrary results.

Detailed studies also are being conducted to compare *in vitro* dissolution of tablets in the new dissolution tester with *in vivo* availability of various drugs.

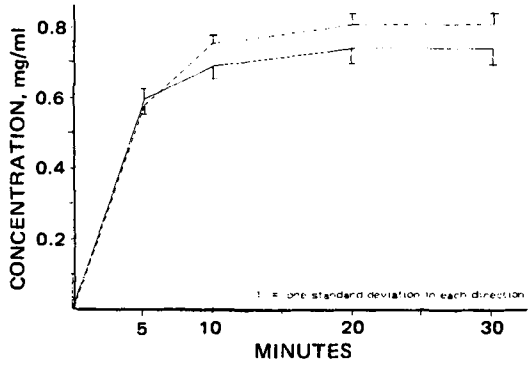

Figure 13—*Comparative dissolution rates of Batch B phenobarbital tablets with the Levy tester (- - -) and the new dissolution rate tester (—).*

Table V—Physical Properties of Various Commercial Tablets Used in the Dissolution Studies

Product	Hardness, kg stokes ± SD	Disintegration Time, sec ± SD
Piperazine citrate	5.5 ± 0.029	55.00 ± 0.030
Isoniazid	4.1 ± 0.004	31.90 ± 0.008
Aspirin Brand I, Batch A	11.333 ± 0.6054	10.833 ± 0.983
Aspirin Brand I, Batch B	11.416 ± 0.4915	11.00 ± 0.8944
Aspirin Brand II, Batch A	5.00 ± 0.5477	9.000 ± 0.8944
Aspirin Brand II, Batch B	5.50 ± 0.6324	9.833 ± 0.7527
Sulfadiazine Batch A	5.333 ± 0.408	283.000 ± 25.976
Sulfadiazine Batch B	8.166 ± 0.605	280.66 ± 25.64
Phenobarbital Batch A	4.083 ± 0.204	387.50 ± 27.522
Phenobarbital Batch B	4.10 ± 0.252	396.00 ± 24.23

REFERENCES

(1) G. L. Mattok and I. J. McGilveray, *J. Pharm. Sci.*, **61**, 460 (1972).

(2) A. M. Rosolia, J. R. O'Connell, J. F. Bavitz, F. A. Restaino, and J. B. Schwartz, *ibid.*, **61**, 1638 (1972).

(3) G. Levy and B. A. Hayes, *N. Engl. J. Med.*, **21**, 1053 (1960).

(4) E. L. Parrot, D. E. Wurster, and T. Higuchi, *J. Am. Pharm. Assoc., Sci. Ed.*, **44**, 269 (1955).

(5) J. H. Wood, J. E. Syarto, and H. Letterman, *J. Pharm. Sci.*, **54**, 1068 (1965).

(6) J. W. Poole, *Drug Inform. Bull.*, **3**, 8 (1969).

(7) H. MacDonald, F. Pisano, J. Burger, A. Dornbush, and E. Pelcak, *ibid.*, **3**, 76 (1969).

(8) M. Gibaldi and H. Weintraub, *J. Pharm. Sci.*, **59**, 725 (1970).

(9) "Bioavailability of Drugs," Proceedings of the Conference on Bioavailability of Drugs, Washington, D.C., 1971, p. 82.

(10) J. T. Jacob and E. M. Plein, *J. Pharm. Sci.*, **57**, 798 (1968).

(11) "The United States Pharmacopeia," 18th rev., Mack Publishing Co., Easton, Pa., 1970, p. 908.

(12) *Ibid.*, p. 509.

(13) *Ibid.*, p. 350.

(14) "Bioavailability of Drugs," Proceedings of the Conference on Bioavailability of Drugs, Washington, D.C., 1971, p. 81.

(15) G. Levy, *Arch. Int. Pharmacodyn. Ther.*, **152**, 59 (1964).

(16) G. Levy, J. R. Leonards, and J. A. Procknal, *J. Pharm. Sci.*, **54**, 1719 (1965).

(17) D. C. Baun and G. C. Walker, *ibid.*, **58**, 611 (1969).

(18) T. E. Needham and L. A. Luzzi, *ibid.*, **63**, 925 (1974).

ACKNOWLEDGMENTS

The authors thank Mr. E. Nelson, Chemistry Department, Auburn University, Auburn, AL 36830, for fabricating the dissolution tester designed by S. S. Nasir.

Synthesis and Antimicrobial Activity of 3*H*-1,2,4-Thiadiazolo Fused Heterocycles

JOHN O. GARDNER ˣ **and COLIN C. BEARD**

Received May 19, 1978, from *Syntex Research, Palo Alto, CA 94304.* Accepted for publication July 12, 1978.

Abstract □ Various fused 3*H*-1,2,4-thiadiazoles were prepared. Significant *in vitro* Gram-positive antibacterial and antifungal activities were observed for certain members of the series.

Keyphrases □ 3*H*-1,2,4-Thiadiazoles, various—synthesized, evaluated for antibacterial and antifungal activities *in vitro* □ Antibacterial activity—various 3*H*-1,2,4-thiadiazoles evaluated *in vitro* □ Antifungal activity—various 3*H*-1,2,4-thiadiazoles evaluated *in vitro* □ Structure-activity relationships—various 3*H*-1,2,4-thiadiazoles evaluated for antibacterial and antifungal activities *in vitro*

Fused ring systems represented by the general formula I are an interesting class of little-studied heterocyclic compounds for which there have been no reports of biological activity. The present report describes the synthesis and antimicrobial activity of a limited number of compounds of this type (Table I).

DISCUSSION

The synthetic sequences are outlined in Scheme I and are essentially those described by Potts and Kane (1). An α-amino *N*-heterocyclic compound (II) was first reacted with perchloromethylsulfur chloride to give the corresponding trichloromethyl sulfenamide (III). Treatment of III with an appropriate amine gave bicyclic compounds (I). While it was possible to isolate and characterize III, this step generally was not performed.

Oxidation of sulfides to the sulfoxides was usually done as a final step on I, using 40% peracetic acid. However, when I corresponded to fusion with a 1,3,4-thiadiazole and R was an aliphatic group, oxidation gave only complex mixtures. Thus, XXXIII was obtained by subjecting IV to the sequence of II to III to I (Scheme II). When I corresponded to fusion with a thiazole, oxidation with an aliphatic R group proceeded smoothly. Initially, the sulfides corresponding to the sulfoxides in Table I were isolated and purified. However, when the sulfides proved to lack biological activity, only the final products were thoroughly characterized.

While no attempt was made to improve yields, steric hindrance and electron-withdrawing groups on the amine adversely affected the III to I reaction. Treatment of III with 2,6-disubstituted anilines gave no reaction.

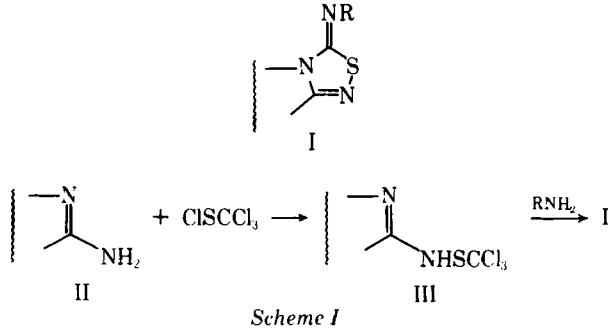

Scheme I

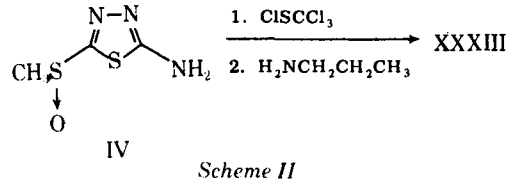

Scheme II

With the exception of V, VI, X, XIII, and XXXIV–XXXVI, the starting materials leading to the compounds in Table I were obtained by alkylation of commercially available 2-amino-5-mercapto-1,3,4-thiadiazole. Reaction of 2-amino-5-bromo-1,3,4-thiadiazole (2) with thiophenol gave 2-amino-5-phenylthio-1,3,4-thiadiazole, which was converted to X.

2-Amino-5-trifluoromethyl-1,3,4-thiadiazole (3), 3-mercapto-5-amino-1,2,4-thiadiazole (4), 2-amino-5-mercaptothiazole (5), and 3-amino-6-mercaptopyridazine (6) were prepared by literature methods and converted into XIII, XXXIV, XXXV, and XXXVI, respectively. Commercially available 2-amino-1,3,4-thiadiazole and 2-amino-5-methyl-1,3,4-thiadiazole were used to prepare V and VI. The amines were either commercially available or were prepared by standard synthetic transformations.

RESULTS

In vitro bacteriostatic and fungistatic activities are presented in Table II along with values for cephalothin sodium[1] and micronazole nitrate[2]. In addition, fungicidal activities are given for XIX, XXII, and XXVII (Table III).

Several generalities emerge. Significant activity within the series was realized only when the 1,2,4-thiadiazole was fused to a 1,3,4-thiadiazole. Replacement of one nitrogen (XXXV) or the sulfur by a vinyl group (XXXVI) of the 1,3,4-thiadiazole resulted in loss of activity. Slight activity was retained in the isomeric 1,2,4-thiadiazole derivative (XXXIV). Furthermore, of all Y groups tested, only the sulfoxides (and to a lesser extent the sulfone IX) were active.

The phenyl sulfoxide seemed to be the most effective Y group but was difficult to make, and the remaining comparisons of R groups were done with methyl sulfoxides. Significant activity was found only when R was an aryl group. Both antifungal and antibacterial activities appeared, at least in part, to be a function of lipophilicity. With the exception of sulfonamide derivatives, no Gram-negative activity was observed.

The most impressive results were antifungal, with *in vitro* fungistatic and fungicidal activities of some compounds at least as high as those of micronazole nitrate.

EXPERIMENTAL[3]

All compounds were prepared in a manner analogous to the synthesis of VII and VIII.

6-Methylthio-3-phenylimino-3*H* - 1,3,4-thiadiazolo[2,3-*c*][1,2,-4]thiadiazole (VII)—To a solution of 8.82 g (60 mmoles) of 2-amino-5-methylthio-1,3,4-thiadiazole in 500 ml of tetrahydrofuran with 6 g of sodium bicarbonate was added 7.2 ml (65 mmoles) of perchloromethylsulfur chloride. After stirring at room temperature for 1 hr, a solution of 6 g (65 mmoles) of aniline and 30 ml (200 mmoles) of triethylamine in 500 ml of tetrahydrofuran was added.

The mixture was stirred for another hour at room temperature and then filtered, and the filtrate was evaporated under reduced pressure. The residue was passed through a 100-g pad of silica gel with methylene chloride. The eluent was evaporated, and the residue was crystallized from methylene chloride–hexane to give 9 g of VII.

6-Methylsulfinyl-3-phenylimino-3*H* - 1,3,4-thiadiazolo[2,3-*c*][1,2,4]thiadiazole (VIII)—To a solution of 9 g (32 mmoles) of VII in 100 ml of chloroform was added 10 ml (~50 mmoles) of 40% peracetic

[1] Keflin, Eli Lilly and Co.
[2] Micatin, Johnson & Johnson.
[3] Melting points were determined in a Thomas-Hoover capillary apparatus and are uncorrected. NMR spectra were obtained in chloroform-d_1 with Varian A-60 and HA-100 instruments, and mass spectra were determined with a Varian-MAT CH4 spectrometer. Elemental analyses were performed by the analytical department of Syntex Research, Institute of Organic Chemistry. Chromatography was done on Merck silica gel 60.

0022-3549/79/0200-0182$01.00/0
© 1979, American Pharmaceutical Association

Table I—Physical Properties of Title Compounds

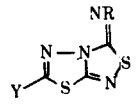

Compound	Y	R	Melting Point	Yield[a], %	Formula	Mass Spectrum, *m/e* (M^+)	Analysis, % Calculated C	H	N	Found C	H	N
V	H	C_6H_5	148–151°[b]	49	$C_9H_6N_4S_2$	234	46.14	2.58	23.91	46.22	2.63	23.69
VI	CH_3	C_6H_5	139–142°[b]	30	$C_{10}H_8N_4S_2$	248	47.98	3.25	22.56	47.98	3.10	22.72
VII	CH_3S	C_6H_5	143–144°[b]	60	$C_{10}H_8N_4S_3$	280	42.84	2.88	19.99	42.50	3.01	19.90
VIII	$CH_3\overset{\uparrow}{S}\!\!\overset{O}{}$	C_6H_5	167–168°[b]	25	$C_{10}H_8N_4OS_3$	296	40.53	2.72	18.90	40.11	2.69	18.82
IX	$CH_3\overset{\uparrow}{S}\!\!\overset{O}{}\!\!\downarrow\!\!O$	C_6H_5	191–192°[b]	22	$C_{10}H_8N_4O_2S_3$	312	38.45	2.58	17.94	38.90	2.56	17.76
X	$C_6H_5\overset{\uparrow}{S}\!\!\overset{O}{}\!\!\downarrow\!\!O$	C_6H_5	133–134°[c]	25	$C_{15}H_{10}N_4OS_3$	358	50.26	2.81	15.63	50.26	2.68	15.79
XI	$C_6H_5CH_2\overset{\uparrow}{S}\!\!\overset{O}{}$	C_6H_5	167–168°[b]	35	$C_{16}H_{12}N_4OS_3$	372	51.59	3.24	15.04	51.47	3.15	15.22
XII	$CH_2CH_2CH_2\overset{\uparrow}{S}\!\!\overset{O}{}$	C_6H_5	122–123°[b]	40	$C_{12}H_{12}N_4OS_3$	324	44.43	3.73	17.27	44.20	3.78	17.28
XIII	CF_3	C_6H_5	90–91°[b]	76	$C_{10}H_5F_3N_4S_2$	302	39.73	1.67	18.53	39.81	1.71	18.36
XIV	$CH_3\overset{\uparrow}{S}\!\!\overset{O}{}$	4-C_6H_4Cl	188–189°[b]	33	$C_{10}H_7ClN_4OS_3$	330–332	36.31	2.13	16.94	36.49	1.81	16.91
XV	$CH_3\overset{\uparrow}{S}\!\!\overset{O}{}$	3-C_6H_4Cl	157–159°[b]	36	$C_{10}H_7ClN_4OS_3$	330–332	36.31	2.13	16.94	36.12	2.06	16.77
XVI	$CH_3\overset{\uparrow}{S}\!\!\overset{O}{}$	2-C_6H_4Cl	181–182°[b]	14	$C_{10}H_7ClN_4OS_3$	330–332	36.31	2.13	16.94	36.56	2.14	16.84
XVII	$CH_3\overset{\uparrow}{S}\!\!\overset{O}{}$	2,4-$C_6H_3Cl_2$	198–199°[b]	4	$C_{10}H_6Cl_2N_4OS_3$	364–368	32.88	1.66	15.34	32.59	1.39	15.27
XVIII	$CH_3\overset{\uparrow}{S}\!\!\overset{O}{}$	4-$C_6H_4OCH_3$	190–192°[b]	20	$C_{11}H_{10}N_4O_2S_3$	326	40.48	3.09	17.17	40.13	3.39	16.77
XIX	$CH_3\overset{\uparrow}{S}\!\!\overset{O}{}$	4-C_6H_4n-C_4H_9	134–135°[b]	32	$C_{14}H_{16}N_4OS_3$	352	47.71	4.58	15.90	47.54	4.86	15.75
XX	$CH_3\overset{\uparrow}{S}\!\!\overset{O}{}$	4-C_6H_4CN	186–189°[b]	15	$C_{11}H_7N_5OS_3$	321	41.11	2.20	21.79	41.16	2.16	21.43
XXI	$CH_3\overset{\uparrow}{S}\!\!\overset{O}{}$	4-$C_6H_4CO_2C_2H_5$	195–197°[b]	18	$C_{13}H_{12}N_4O_3S_3$	368	42.38	3.29	15.21	42.51	3.27	15.01
XXII	$CH_3\overset{\uparrow}{S}\!\!\overset{O}{}$	4-$C_6H_4CF_3$	168–169°[b]	12	$C_{11}H_7F_3N_4OS_3$	364	36.26	1.94	15.38	35.92	1.88	14.99
XXIII	$CH_3\overset{\uparrow}{S}\!\!\overset{O}{}$	4-$C_6H_4O\overset{O}{\overset{\|}{C}}C_6H_5$	186–188°[c]	31	$C_{17}H_{12}N_4O_3S_3$	416	49.03	2.90	13.45	48.68	2.95	13.20
XXIV	$CH_3\overset{\uparrow}{S}\!\!\overset{O}{}$	4-$C_6H_4SO_2NH_2$	212–214°[c]	15	$C_{10}H_9N_5O_3S_4$	375	31.99	2.42	18.65	31.81	2.71	18.47
XXV	$CH_3\overset{\uparrow}{S}\!\!\overset{O}{}$	4-$C_6H_4SO_2N(CH_3)_2$	218–219°[b]	12	$C_{12}H_{13}N_5O_3S_4$	403	35.72	3.25	17.36	35.52	3.31	17.00
XXVI	$CH_3\overset{\uparrow}{S}\!\!\overset{O}{}$	4-$SO_2N\langle\rangle O$	218–219°[c]	15	$C_{14}H_{15}N_5O_4S_4$	445	37.74	3.39	15.79	37.65	3.47	15.49
XXVII	$CH_3\overset{\uparrow}{S}\!\!\overset{O}{}$	4-$C_6H_4OC_6H_5$	152–153°[b]	38	$C_{16}H_{12}N_4O_2S_3$	388	49.47	3.11	14.42	49.48	3.05	14.41
XXVIII	$CH_3\overset{\uparrow}{S}\!\!\overset{O}{}$	4-C_6H_5O-⟨⟩-	121–122°[b]	20	$C_{20}H_{20}N_4O_2S_3$	444	54.03	4.54	12.60	54.18	4.56	12.45

(continued)

Table I—*Continued*

Compound	Y	R	Melting Point	Yield[a], %	Formula	Mass Spectrum, *m/e* (M^+)	Analysis, % Calculated C	H	N	Found C	H	N
XXIX		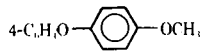	164–165°[b]	21	$C_{17}H_{14}N_4O_3S_3$	418	48.79	3.27	13.39	48.54	3.28	13.03
XXX		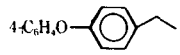	145–147°[b]	39	$C_{18}H_{16}N_4O_2S_3$	416	51.90	3.87	13.45	52.03	3.77	13.18
XXXI		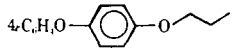	147–149°[b]	36	$C_{20}H_{20}N_4O_3S_3$	460	52.16	4.38	12.16	52.40	4.37	12.13
XXXII		4-$C_6H_4OC_6H_5$	157–158°[b]	50	$C_{17}H_{14}N_4O_2S_3$	402	50.73	3.51	13.92	50.68	3.39	13.81
XXXIII		$CH_2CH_2CH_3$	130–131°[c]	85	$C_7H_{10}N_4OS_3$	262	32.05	3.84	21.36	31.90	3.95	21.30
XXXIV		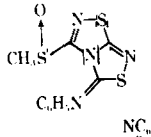	152–154°[b]	40	$C_{10}H_8N_4OS_3$	296	40.53	2.72	18.90	40.25	2.68	18.90
XXXV		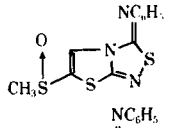	198–200°[b]	33	$C_{11}H_9N_3OS_3$	295	44.73	3.07	14.23	44.51	2.81	13.89
XXXVI		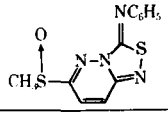	195–196°[b]	24	$C_{12}H_{10}N_4OS_2$	290	49.64	3.47	19.30	49.43	3.66	19.26

[a] Yields are overall values for II → III → I and the oxidation step except where there was no oxidation. [b] Recrystallized from methylene chloride–hexane. [c] Recrystallized from acetone–hexane.

Table II—Antimicrobial Activities[a]

Compound	Bacteriostatic A	B	C	D	E	F	Fungistatic G	H	I	J	K
V	—[b]	—[b]	—[b]	—[b]	—[b]	—[b]	—[c]	—[c]	—[c]	—[d]	—[d]
VI	—[b]	—[b]	—[b]	—[b]	—[b]	—[b]	—[c]	—[c]	—[c]	—[d]	—[d]
VII	—[b]	—[b]	—[b]	—[b]	—[b]	—[b]	—[c]	—[c]	—[c]	—[d]	—[d]
VIII	6.25	25	200	12.5	200	50	3	1	3	100	30
IX	12.5	25	200	200	—[b]	—[b]	3	1	3	30	30
X	0.05	0.8	—[b]	200	200	—[b]	1	1	3	30	10
XI	50	100	—[b]	—[b]	—[b]	—[b]	—[c]	1	—[c]	—[d]	—[d]
XII	6.25	50	—[b]	—[b]	—[b]	—[b]	3	1	3	—[d]	30
XIII	—[b]	—[b]	—[b]	—[b]	—[b]	—[b]	—[c]	—[c]	—[c]	—[d]	—[d]
XIV	3.12	3.12	—[b]	50	—[b]	—[b]	1	0.1	1	10	30
XV	50	50	—[b]	—[b]	—[b]	—[b]	1	1	1	30	10
XVI	6.25	12.5	—[b]	—[b]	—[b]	—[b]	3	1	3	30	30
XVII	1.6	3.12	—[b]	—[b]	—[b]	—[b]	1	0.1	1	10	10
XVIII	6.25	25	—[b]	200	—[b]	—[b]	—	—	—	—	—
XIX	1.6	1.6	—[b]	—[b]	—[b]	—[b]	1	0.1	1	3	3
XX	100	12.5	200	50	—[b]	200	3	3	3	300	30
XXI	25	50	—[b]	—[b]	—[b]	—[b]	1	1	3	—[d]	—[d]
XXII	25	12.5	—[b]	—[b]	—[b]	—[b]	1	0.1	1	10	10
XXIII	50	1.6	—[b]	—[b]	—[b]	—[b]	—[c]	1	—[c]	—[d]	—[d]
XXIV	12.5	12.5	100	25	200	100	—[c]	—[c]	—[c]	—[d]	—[d]
XXV	25	12.5	200	100	—[b]	200	100	10	30	—[d]	—[d]
XXVI	50	12.5	—[b]	—[b]	—[b]	—[b]	100	30	100	—[d]	—[d]
XXVII	0.1	0.8	200	200	—[b]	—[b]	1	0.1	1	3	10
XXVIII	3.12	3.12	—[b]	—[b]	—[b]	—[b]	—[d]	1	—[d]	—[d]	—[d]
XXIX	3.12	3.12	—[b]	—[b]	—[b]	—[b]	1	0.1	1	—[d]	—[d]
XXX	12.5	3.12	—[b]	—[b]	—[b]	—[b]	3	0.1	1	—[d]	—[d]
XXXI	3.12	200	—[b]	200	—[b]	—[b]	100	1	100	—[d]	—[d]
XXXII	1.6	1.6	200	200	200	—[b]	1	0.1	—[d]	—[d]	—[d]
XXXIII	12.5	25	100	25	—[b]	100	30	10	30	300	100
XXXIV	100	25	—[b]	—[b]	—[b]	—[b]	10	3	10	100	30
XXXV	—[b]	—[b]	—[b]	—[b]	—[b]	—[b]	—[c]	—[c]	—[c]	—[d]	—[d]
XXXVI	—[b]	—[b]	—[b]	—[b]	—[b]	—[b]	—[c]	30	—[c]	—[d]	—[d]
Cephalothin sodium	0.05	<0.008	50	0.05	—[b]	—[b]	—	—	—	—	—
Micronazole nitrate	—	—	—	—	—	—	3	0.1	3	30	0.2

[a] Values are minimum inhibitory concentrations in micrograms per milliliter. Assay procedures are described under *Experimental*. A = *Staphylococcus aureus* (ATCC 6538P), B = *Streptococcus pyogenes* (ATCC 8668), C = *Escherichia coli* (ATCC 25922), D = *Klebsiella pneumoniae* (ATCC 10031), E = *Pseudomonas aeruginosa* (ATCC 10145), F = *Proteus vulgaris* (ATCC 9484), G = *Microsporum gypseum* (ATCC 14683), H = *Epidermophyton floccosum* (ATCC 15643), I = *Trichophyton mentagrophytes* (ATCC 11481), J = *Candida albicans* (ATCC 10231), and K = *Cryptococcus neoformans* (ATCC 13690). [b] >200. [c] >100. [d] >300.

Table III—Fungicidal Activities [a]

Compound	Fungicidal G	H	I	J	K
XIX	1	1	1	30	10
XXII	1	1	3	30	10
XXVII	1	0.1	1	—[b]	10
Micronazole nitrate	30	1	30	30	10

[a] See footnotes to Table II. [b] >300.

acid. After stirring at room temperature for 3 hr, a 10% aqueous solution of sodium metabisulfite was added until starch–iodide paper gave a negative result.

Excess saturated potassium bicarbonate solution was then added, and the layers separated. The organic phase was dried (magnesium sulfate) and evaporated under reduced pressure. The residue was chromatographed, using 1% methanol–methylene chloride to elute material that crystallized from methylene chloride–hexane; 4.2 g of VIII was obtained.

Antimicrobial Assays[4]—The bioassays were done by serial broth dilutions in chemically defined media according to the procedure described by Long *et al.* (7).

[4] The bioassays were conducted under the direction of Dr. A. Braemer and Ms. S. Hitt, Institute of Agrisciences, Syntex Research.

REFERENCES

(1) K. T. Potts and J. Kane, *J. Org. Chem.*, **40**, 2600 (1975).

(2) P. Rathgeb, German offen. 2, 156 (1970); through *Chem. Abstr.*, **77**, P12664W (1972).

(3) I. Lalezari and N. Sharghi, *J. Heterocycl. Chem.*, **4**, 336 (1966).

(4) J. Goerdeler and P. Linden, *Chem. Ber.*, **89**, 2742 (1956).

(5) C. D. Hurd and H. L. Wehrmeister, *J. Am. Chem. Soc.*, **71**, 4007 (1949).

(6) T. Horie, K. Kinjo, and T. Ueda, *Chem. Pharm. Bull.*, **10**, 580 (1962).

(7) R. A. Long, T. R. Matthews, and R. K. Robins, *J. Med. Chem.*, **19**, 1072 (1976).

ACKNOWLEDGMENTS

This paper is Contribution No. 504 from the Syntex Institute of Organic Chemistry.

Potential CNS Antitumor Agents VI: Aziridinylbenzoquinones III

JOHN S. DRISCOLL [x], **LEO DUDECK** [*], **GEORGE CONGLETON** [*], and **RUTH I. GERAN** [‡]

Received February 21, 1978, from the *Drug Design and Chemistry Section, Laboratory of Medicinal Chemistry and Biology, Developmental Therapeutics Program, Division of Cancer Treatment, National Cancer Institute, National Institutes of Health, Bethesda, MD 20014.* Accepted for publication June 29, 1978.

*Present address: Hazleton Laboratories, Vienna, VA 22180. ‡Present address: Drug Evaluation Branch, Developmental Therapeutics Program, Division of Cancer Treatment, National Cancer Institute, National Institutes of Health, Bethesda, MD 20014.

Abstract □ Thirty-one aziridinylbenzoquinones were compared against five murine tumor models *in vivo*. Two intracerebral (ependymoblastoma and L-1210 leukemia) and three intraperitoneal (P-388 and L-1210 leukemia and B16 melanoma) systems were utilized. Excellent activity was observed for many compounds. Multiple long-term survivors were produced in the ependymoblastoma, P-388, and intraperitoneal L-1210 systems. Diethyl 2,5-bis(1-aziridinyl)-3,6-dioxo-1,4-cyclohexadiene-1,4-dicarbamate demonstrated superior activity in all five test systems. This compound also was reproducibly active against two colon tumors, a mammary tumor, and the intracerebrally implanted P-388 leukemia model.

Keyphrases □ Aziridinylbenzoquinones—evaluated as potential CNS antitumor agents *in vivo*, various test systems □ CNS antitumor activity—aziridinylbenzoquinones evaluated *in vivo*, various test systems □ Antitumor agents, CNS—aziridinylbenzoquinones evaluated *in vivo*, various test systems □ Structure-activity relationships—aziridinylbenzoquinones evaluated as potential CNS antitumor agents *in vivo*, various test systems

The antitumor activity of aziridinylbenzoquinones in murine model tumor systems has been recognized for almost 25 years (1–5). Recent reports described the activity of two members of this family, trenimon (6–8) and carbazilquinone (8–11), which have had clinical trials.

As part of a program to develop agents that might be effective against neoplasms of the central nervous system (CNS), several series of aziridinylbenzoquinones were prepared and evaluated in murine brain tumor systems (12, 13). Some of these compounds produced long-term survivors in the intracerebral ependymoblastoma tumor model. To determine which aziridinylbenzoquinones might have the greatest potential for clinical trial with emphasis on CNS neoplasms, the 31 analogs available to the National Cancer Institute (NCI) were compared in two intracerebral and three intraperitoneal tumor systems.

EXPERIMENTAL

Materials—Compounds XIV–XXXI (Table I) were synthesized as described previously (12, 13), and I–XIII were obtained from other sources[1].

Tumor Test Systems—The standard NCI protocols for the intracerebral and intraperitoneal tumors are described in Table II and Ref. 14.

Treatment—Treatment was intraperitoneal in all cases. Saline (0.1%) or hydroxypropylcellulose was used as the vehicle. Treatment in all systems other than ependymoblastoma began on Day 1 and continued once daily for 9 days. In a few instances, previous data were available with

[1] Ciba-Geigy, Bayer A. G., Sankyo Co., the U.S. Department of Agriculture, and Dr. H. S. Verter of the Inter American University of Puerto Rico.

0022-3549/79/0200-0185$01.00/0

© 1979, American Pharmaceutical Association

Table III—Fungicidal Activities [a]

Compound	Fungicidal G	H	I	J	K
XIX	1	1	1	30	10
XXII	1	1	3	30	10
XXVII	1	0.1	1	—[b]	10
Micronazole nitrate	30	1	30	30	10

[a] See footnotes to Table II. [b] >300.

acid. After stirring at room temperature for 3 hr, a 10% aqueous solution of sodium metabisulfite was added until starch–iodide paper gave a negative result.

Excess saturated potassium bicarbonate solution was then added, and the layers separated. The organic phase was dried (magnesium sulfate) and evaporated under reduced pressure. The residue was chromatographed, using 1% methanol–methylene chloride to elute material that crystallized from methylene chloride–hexane; 4.2 g of VIII was obtained.

Antimicrobial Assays[4]—The bioassays were done by serial broth dilutions in chemically defined media according to the procedure described by Long *et al.* (7).

[4] The bioassays were conducted under the direction of Dr. A. Braemer and Ms. S. Hitt, Institute of Agrisciences, Syntex Research.

REFERENCES

(1) K. T. Potts and J. Kane, *J. Org. Chem.*, **40**, 2600 (1975).

(2) P. Rathgeb, German offen. 2, 156 (1970); through *Chem. Abstr.*, **77**, P12664W (1972).

(3) I. Lalezari and N. Sharghi, *J. Heterocycl. Chem.*, **4**, 336 (1966).

(4) J. Goerdeler and P. Linden, *Chem. Ber.*, **89**, 2742 (1956).

(5) C. D. Hurd and H. L. Wehrmeister, *J. Am. Chem. Soc.*, **71**, 4007 (1949).

(6) T. Horie, K. Kinjo, and T. Ueda, *Chem. Pharm. Bull.*, **10**, 580 (1962).

(7) R. A. Long, T. R. Matthews, and R. K. Robins, *J. Med. Chem.*, **19**, 1072 (1976).

ACKNOWLEDGMENTS

This paper is Contribution No. 504 from the Syntex Institute of Organic Chemistry.

Potential CNS Antitumor Agents VI: Aziridinylbenzoquinones III

JOHN S. DRISCOLL [x], **LEO DUDECK** [*], **GEORGE CONGLETON** [*], and **RUTH I. GERAN** [‡]

Received February 21, 1978, from the *Drug Design and Chemistry Section, Laboratory of Medicinal Chemistry and Biology, Developmental Therapeutics Program, Division of Cancer Treatment, National Cancer Institute, National Institutes of Health, Bethesda, MD 20014.* Accepted for publication June 29, 1978.

*Present address: Hazleton Laboratories, Vienna, VA 22180. ‡Present address: Drug Evaluation Branch, Developmental Therapeutics Program, Division of Cancer Treatment, National Cancer Institute, National Institutes of Health, Bethesda, MD 20014.

Abstract □ Thirty-one aziridinylbenzoquinones were compared against five murine tumor models *in vivo*. Two intracerebral (ependymoblastoma and L-1210 leukemia) and three intraperitoneal (P-388 and L-1210 leukemia and B16 melanoma) systems were utilized. Excellent activity was observed for many compounds. Multiple long-term survivors were produced in the ependymoblastoma, P-388, and intraperitoneal L-1210 systems. Diethyl 2,5-bis(1-aziridinyl)-3,6-dioxo-1,4-cyclohexadiene-1,4-dicarbamate demonstrated superior activity in all five test systems. This compound also was reproducibly active against two colon tumors, a mammary tumor, and the intracerebrally implanted P-388 leukemia model.

Keyphrases □ Aziridinylbenzoquinones—evaluated as potential CNS antitumor agents *in vivo*, various test systems □ CNS antitumor activity—aziridinylbenzoquinones evaluated *in vivo*, various test systems □ Antitumor agents, CNS—aziridinylbenzoquinones evaluated *in vivo*, various test systems □ Structure-activity relationships—aziridinylbenzoquinones evaluated as potential CNS antitumor agents *in vivo*, various test systems

The antitumor activity of aziridinylbenzoquinones in murine model tumor systems has been recognized for almost 25 years (1–5). Recent reports described the activity of two members of this family, trenimon (6–8) and carbazilquinone (8–11), which have had clinical trials.

As part of a program to develop agents that might be effective against neoplasms of the central nervous system (CNS), several series of aziridinylbenzoquinones were prepared and evaluated in murine brain tumor systems (12, 13). Some of these compounds produced long-term survivors in the intracerebral ependymoblastoma tumor model. To determine which aziridinylbenzoquinones might have the greatest potential for clinical trial with emphasis on CNS neoplasms, the 31 analogs available to the National Cancer Institute (NCI) were compared in two intracerebral and three intraperitoneal tumor systems.

EXPERIMENTAL

Materials—Compounds XIV–XXXI (Table I) were synthesized as described previously (12, 13), and I–XIII were obtained from other sources[1].

Tumor Test Systems—The standard NCI protocols for the intracerebral and intraperitoneal tumors are described in Table II and Ref. 14.

Treatment—Treatment was intraperitoneal in all cases. Saline (0.1%) or hydroxypropylcellulose was used as the vehicle. Treatment in all systems other than ependymoblastoma began on Day 1 and continued once daily for 9 days. In a few instances, previous data were available with

[1] Ciba-Geigy, Bayer A. G., Sankyo Co., the U.S. Department of Agriculture, and Dr. H. S. Verter of the Inter American University of Puerto Rico.

0022-3549/79/0200-0185$01.00/0

© 1979, American Pharmaceutical Association

Table I—Aziridinylbenzoquinone Structures

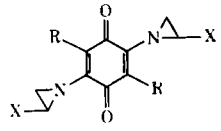

X = H unless specified otherwise

Compound	NSC Number[a]	R
I	17262	$OCH_2CH_2OCH_3$
II	18269	$NHCOCH_3$
III	18270	OCH_2CH_3
IV	18271	$NHCOC_2H_5$
V[b]	18273	$NHCOCH_3$
VI	18274	$NHCOC_3H_7$
VII	29215	
VIII	30705	Cl
IX	31717	
X	51915	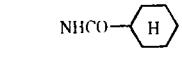
XI	51916	$NHCOC_6H_{13}$
XII	95139	OCH_3
XIII	134679	CH_3, $CH(OCH_3)$-CH_2OCONH_2
XIV	182986	$NHCOOC_2H_5$
XV	220267	$NHCH_3$
XVI[b]	220536	$NHCH_3$
XVII	224066	NHC_2H_5
XVIII	224070	$NHCH_2CH_2OH$
XIX	224071	NHC_3H_7
XX	240026	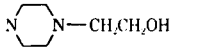
XXI	243037	$NHCH_2CH(OH)$-CH_2OH
XXII	246111	NH_2
XXIII	249009	$N(CH_3)CH_2CH_2OH$
XXIV	249010	NHC_4H_9
XXV	249339	
XXVI	249340	$NHCH_2CONH_2$
XXVII	249989	$N(CH_3)_2$
XXVIII	250433	
XXIX	251727	
XXX	251728	
XXXI	251729	

[a] NCI accession number. [b] X = CH_3.

Table II—Tumor Test Systems

Tumor	Tumor Site	Inoculum, number of cells	Mouse Strain	Mouse Number[a]	Termination Day[b]
Ependymoblastoma	Intracerebral	Fragment (1 mm^3)	C57BL/6	6	60
L-1210 leukemia	Intracerebral	10^4	BDF_1	6	30
L-1210 leukemia	Intraperitoneal	10^5	BDF_1	6	30
P-388 leukemia	Intraperitoneal	10^6	BDF_1	6	30
B16 melanoma	Intraperitoneal	Brei[c]	BDF_1	10	60

[a] Number of mice used per dose tested. [b] Day on which experiment ended and long-term survivors were noted. [c] Using 0.5 ml of a tumor homogenate prepared from 1.0 g of tumor blended with 10 ml of cold balanced salt solution.

treatment starting on Day 1 and continuing until death. This schedule was considered comparable to the Day 1–9 treatment schedule. The ependymoblastoma tumor was treated on the Day 1–5 schedule (14, 15).

Experiments were carried out twice when sufficient compound was available. When conflicting results were obtained, additional experiments were performed. A dose response curve was designed ranging up to toxicity and consisting of four doses, with each dose double the next lower dose. Data from experiments with other than satisfactory controls were not used unless they were the only data available. Data from doses that produced a >4-g weight loss relative to control animals on Day 5 were not used as optimum doses.

The antitumor data in Table III are the highest reproduced values observed (*i.e.*, the highest value confirmed in a separate experiment) for the L-1210, P-388, and B16 systems. The highest two values from separate experiments are reported for the ependymoblastoma system. Intracerebral L-1210 tests were scheduled only if at least one intraperitoneal L-1210 test gave a T/C value[2] $\geq$150%.

RESULTS

Intracerebral Tumor Systems—The ependymoblastoma and intracerebral L-1210 models utilize intracerebral implants of a solid fragment and ascites fluid, respectively. Antitumor activity for standard agents in the ependymoblastoma system was reviewed recently (15).

Compounds III, VI, VII, XIV, XV, XVII, XXII, and XXVII gave multiple long-term (60-day) survivors in more than one experiment. The number of long-term ependymoblastoma survivors is a more meaningful measure of activity for these compounds than the T/C value, because the T/C value is very dependent on the survival time of the control animals when long-term-treated survivors occur.

The most active compounds (T/C > 150%) in the intracerebral L-1210 model were VI, XIII–XV, and XXII. No long-term survivors were produced.

Intraperitoneal Tumor Systems—Activity against two leukemias (intraperitoneal P-388 and L-1210) and one solid tumor (intraperitoneal B16 melanocarcinoma) was evaluated. Of these three intraperitoneally implanted models, the P-388 and B16 models were the most and least sensitive to drug treatment, respectively. All compounds were active in the P-388 system. Indeed, a majority produced T/C values >200%.

Excellent activity was also shown by many compounds in the less sensitive intraperitoneal L-1210 system. Six compounds (II, XIV, XVIII, XX, XXI, and XXIII) gave intraperitoneal L-1210 T/C values >200% and, in some instances, produced long-term (30-day) survivors. In the more refractory B16 melanoma model, the minimum criterion for statistical activity (T/C $\geq$ 140%) was met by six analogs (XII–XIV, XVI, XVIII, and XXI).

DISCUSSION

All 31 compounds met the current minimum statistical criterion for activity in the P-388 (T/C 120%) system, and all except VIII were active in the ependymoblastoma model (T/C 125%). Twenty-five qualified in the intraperitoneal L-1210 (T/C 125%) system and six in the B16 melanoma (T/C 140%) system. Seventeen of the 21 compounds tested against intracerebral L-1210 leukemia were active (T/C 125%). With almost all compounds meeting the minimum statistical criterion for activity in all tumor systems (except B16 melanoma), stricter criteria were devised (Table IV) to differentiate among the compounds.

Table IV lists the compounds that passed at least one of the following stricter criteria for activity: ependymoblastoma, multiple long-term survivors in both experiments; intracerebral L-1210, confirmed T/C 150%; intraperitoneal L-1210, confirmed T/C 200%; and B16 melanoma as previously stated, confirmed T/C 140%. This classification reduced the number of compounds for comparison to 17. When a confirmed T/C $\geq$ 200% criterion in the P-388 system was applied to these 17 compounds, all passed except XV and XXVII. Only one compound, XIV, passed the criterion in all five test systems. Five derivatives passed in three systems. Two of the five (VI and XXII) were active in the intracerebral systems plus P-388; two (XVIII and XXI) were active in the intraperitoneal systems plus P-388; one, carbazilquinone (XIII), which has been studied clinically, was active against one intracerebral (L-1210) plus one intraperitoneal (B16) model as well as the P-388 tumor.

[2] See Table III for definition.

Table III—Aziridinylbenzoquinone Antitumor Activity

Compound	Intracerebral Tumors				Intraperitoneal Tumors[a]					
	Ependymoblastoma		L-1210[a]		P-388		B16		L-1210	
	O.D.[b]	T/C[c]	O.D.	T/C	O.D.	T/C	O.D.	T/C	O.D.	T/C
I	1	138	4	121	2	223 (1)	2	136	2	183
II	0.5	147 (1)[d]	1	146	0.5	270 (1)	1	131	0.5	220
	0.5	150								
III	2	>304 (4)	1	135	2	242	1	136	1	157
	2	211 (2)								
IV	1	193 (1)	1	129	2	225	2	113	1	181
V	2.5	192 (1)	5	120	5	233	1	105	5	184
	5	233								
VI	1	>398 (3)	4	152	1	213	2	118	4	167
	1	>368 (2)								
VII	0.08	>294 (3)	0.02	138	0.02	265 (3)	0.02	126	0.05	145
	0.16	>398 (3)								
VIII	10	123	1	120	5	172	10	124	0.6	128
	2.5	123								
IX	0.04	>361 (3)	—	NT[e]	0.04	268 (1)	0.04	125	0.01	139
	0.02	218								
X	100	218 (1)	400	116	400	170	25	109	175	145
	200	175								
XI	80	253	—	NT	100	245	50	135	115	132
	160	184								
XII	0.5	284 (1)	1	129	2	>252 (5)	2	169	2	136
	2	238								
XIII	1	159	0.05	154	0.25	211	0.5	179	0.25	159
	0.25	148								
XIV	1	>272 (6)	3	179	0.8	212 (1)	3	162	3	213
	2	>376 (5)								
XV	0.2	>319 (5)	0.2	160	0.1	169	0.05	129	0.2	161
	0.4	>318 (4)								
XVI	5	243 (1)	10	125		NT	5	148	2.5	116
	10	394 (1)								
XVII	1.5	287 (2)	3	140	1.5	228	0.75	124	1.5	191 (1)
	1.5	318 (2)								
XVIII	0.75	183	0.75	148	0.4	260 (2)	0.4	161	0.75	234 (3)
	0.75	170								
XIX	5	243 (1)	—	NT	6	208	5	132	6	143
	10	359 (2)								
XX	1	175	1.5	141	1	243 (6)	0.25	122	0.5	214 (1)
	1	175								
XXI	0.5	>288 (6)	4	141	4	241 (4)	6	142	2	233 (2)
	1	199 (1)								
XXII	0.25	277 (6)	0.3	159	0.2	256	0.02	119	0.3	194
	0.2	315 (4)								
XXIII	0.2	175 (1)	2	132	0.8	245	0.8	131	1.5	211 (1)
	0.2	169								
XXIV	3	175 (1)	—	NT	10	149	5	111	5	130
	3	146								
XXV	4	165 (1)	—	NT	1	178	1	137	3	144
	1	129								
XXVI	2	164 (1)	10	116	2	171	0.5	122	10	180
	1	150								
XXVII	1	>315 (5)	—	NT	0.5	137	0.25	112	0.4	116
	1	>290 (4)								
XXVIII	3	201	—	NT	1	155	2	118	2	121
	1.6	147								
XXIX	1.5	149 (1)	—	NT	0.75	147	0.75	117	1.5	120
	1.5	234								
XXX	0.8	149	—	NT	6	154	0.75	109	0.75	114
	1.5	140								
XXXI	12.5	146	—	NT	5	146	2.5	97	5	117
	6	168								

[a] Highest reproduced T/C value; see *Experimental.* [b] Optimum dose (milligrams per kilogram per day). [c] The %T/C = (treated survival/control survival) × 100%. [d] Numbers in parentheses are animals alive on the termination day; see Table II. [e] Not tested.

The relatively low intraperitoneal L-1210 activity found for XIII may be related to the schedule used in this protocol. Other murine test data indicate that XIII may be most active on the Day 1 treatment schedule. It was feasible, however, to compare all compounds only on one schedule. Since chronic treatment (QD 1–9) appeared to give optimum activity for analogs that previously had schedule dependency testing, this schedule was chosen for comparison studies. The two relatively low ependymoblastoma activity values obtained for XIII were checked a third time in light of the active intracerebral L-1210 results obtained with this compound. A comparable third ependymoblastoma value (T/C 143%) was obtained. Trenimon (VII), the other compound with prior clinical studies, possessed excellent ependymoblastoma and P-388 activity but was marginal in the two L-1210 models and inactive against B16 melanoma.

Of the four other compounds with good activity in three of the models (VI, XVIII, XXI, and XXII), the bis(dihydroxypropylamino) analog, XXI, probably comes the closest to XIV in overall superiority. With one more long-term survivor in the second ependymoblastoma experiment and a slightly higher intracerebral L-1210 value, XXI would have met the strict criteria for all five tests. The amino compound, XXII, which is the parent for many of these analogs, almost met the standard in the intraperitoneal L-1210 but was inactive in two B16 tests (T/C 131 and 119%). Compound VI was moderately active against intraperitoneal L-1210 but was inactive against B16 melanoma. Compound XVIII almost met the criterion in the intracerebral L-1210 but was only moderately active in the ependymoblastoma system.

Based on the data shown in Table III, XIV is the superior compound and was tested further against an NCI panel of tumors (16). Compound

Table IV—Aziridinylbenzoquinone Activity Based on Selected Criteria [a]

Compound	Ependymoblastoma	Intracerebral L-1210	P-388	Intraperitoneal L-1210	B16
II			X	X	
III	X		X		
IV	X		X		
VI	X	X	X		
VII	X		X		
XII			X		X
XIII		X	X		X
XIV	X	X	X	X	X
XV	X	X			
XVI			NT[b]		X
XVII	X		X		
XVIII			X	X	X
XX			X	X	
XXI			X	X	X
XXII	X	X	X		
XXIII			X	X	
XXVII	X				

[a] An X indicates a compound that meets the following criterion: ependymoblastoma, multiple long-term survivors in both experiments; intracerebral L-1210, confirmed T/C >150%; P-388, confirmed T/C >200%; intraperitoneal L-1210, confirmed T/C >200%; and B16, confirmed T/C >140%. [b] Not tested.

XIV was inactive against subcutaneous and intracerebral B16 melanocarcinoma as well as subcutaneous and intravenous Lewis lung carcinoma. It had confirmed activity against nine murine models: the five models in Table IV and the four shown in Table V.

Table V—Additional Antitumor Data for XIV [a]

Tumor	O.D.	Treatment Schedule	T/C	Activity Criterion (T/C)
CD mammary (mouse)[b]	12.5	Q7D × 5	23[c]	≤42
Intracerebral P-388[d]	1.5	QD 1–9	151	≥125
C38 colon[b]	25	Q7D × 3	32[c]	≤42
C26 colon[e]	3.1	Q4D × 3	240 (4)	≥130

[a] Highest reproduced T/C; see notes of Table III for definitions. [b] Subcutaneous tumor implantation. [c] Based on mean tumor weights estimated from tumor diameter. [d] Intracerebral tumor implantation. [e] Intraperitoneal tumor implantation.

Pharmacological studies are currently underway with XIV. After development of an acceptable formulation, preclinical toxicological studies will be initiated.

REFERENCES

(1) G. Domagk, S. Petersen, and W. Gauss, *Z. Krebsforsch.*, **59**, 617 (1954).

(2) S. Petersen, W. Gauss, and E. Urbschat, *Angew. Chem.*, **67**, 217 (1955).

(3) Farbenfabriken Bayer A.-G., British pat. 762,723 (Dec. 5, 1956).

(4) Farbenfabriken Bayer A.-G., British pat. 793,796 (Apr. 23, 1958).

(5) Farbenfabriken Bayer A.-G., British pat. 805,518 (Dec. 10, 1958).

(6) J. Mattern, K. Wayss, and M. Volm, *Arch. Gynaekol.*, **216**, 273 (1974).

(7) J. Hartleib, *Z. Krebsforsch.*, **81**, 1 (1974).

(8) J. S. Driscoll, G. F. Hazard, H. B. Wood, and A. Goldin, *Cancer Chemother. Rep., Part 2*, **4**, 1 (1974).

(9) H. Nakao and M. Arakawa, *Chem. Pharm. Bull.*, **20**, 1962 (1972).

(10) H. Nakao, M. Arakawa, T. Nakamura, and M. Fukushima, *ibid.*, **20**, 1968 (1972).

(11) T. Saito, S. Ohira, A. Wakui, M. Yokoyama, *et al.*, *Cancer Chemother. Rep.*, **57**, 447 (1973).

(12) A. H. Khan and J. S. Driscoll, *J. Med. Chem.*, **19**, 313 (1976).

(13) F. Chou, A. H. Khan, and J. S. Driscoll, *ibid.*, **19**, 1302 (1976).

(14) R. I. Geran, N. H. Greenberg, M. M. Macdonald, A. M. Schumacher, and B. J. Abbott, *Cancer Chemother. Rep., Part 3*, **3**, 1 (1972).

(15) P. C. Merker, I. Wodinsky, and R. I. Geran, *Cancer Chemother. Rep.*, **59**, 729 (1975).

(16) S. A. Schepartz, DHEW Publication (NIH) 76-1200, 1976, pp. 13–25.

ACKNOWLEDGMENTS

The authors thank the Ciba-Geigy Co., Bayer A. G., Sankyo Co., H. S. Verter, and the U.S. Department of Agriculture for many of the samples and their permission to report the test results from the compounds they supplied to the National Cancer Institute.

Solubility of Doxycycline in Aqueous Solution

JOSEPH B. BOGARDUS ˣ and ROBERT K. BLACKWOOD, Jr.

Received May 8, 1978, from *Pharmaceutical Research and Development, Pfizer Central Research, Groton, CT 06340.* Accepted for publication July 17, 1978.

Abstract □ The solubility of doxycycline monohydrate and doxycycline hydrochloride dihydrate was investigated in aqueous solution. The hydrochloride dihydrate salt was isolated and identified from solutions initially containing doxycycline hyclate in water. The pKa′ = 3.09 (μ = 0.1 and 25°) for protonation of doxycycline was determined spectrophotometrically. The pH–solubility profiles were determined for doxycycline monohydrate in water and in 1.0 *M* $NaNO_3$–HNO_3 and NaCl–HCl. The pH–solubility profile at 25° for doxycycline in aqueous hydrochloric acid without added salt reached a sharp maximum of 50 mg/ml at pH 2.16. Added chloride ion strongly suppressed the solubility of the hydrochloride dihydrate salt. The apparent solubility product was not constant but decreased as the concentration of added salt increased. A theoretical model was developed involving dimerization of doxycycline and applied to the experimental data. The dimerization constant, K_d = 24 M^{-1}, and true solubility product, $K^0_{sp} = 1.8 \times 10^{-3} M^2$, were calculated. The effect of concentration on NMR and visible spectra indicated that dimerization resulted from intermolecular hydrogen bonding of the phenolic β-diketone portion of the molecule.

Keyphrases □ Doxycycline—monohydrate and hydrochloride dihydrate salts, solubility in aqueous solution, effect of pH □ Solubility—doxycycline monohydrate and hydrochloride dihydrate in aqueous solution, effect of pH □ Antibacterials—doxycycline monohydrate and hydrochloride dihydrate, solubility in aqueous solution, effect of pH

Knowledge of quantitative solubility relationships in purely aqueous solutions is highly important to pharmaceutical research and product development. In water, solute activity is the summation of numerous associative interactions of the drug with other drug molecules and the solvent. These interactions often cause solutions of phar-

0022-3549/79/0200-0188$01.00/0

© 1979, American Pharmaceutical Association

Table IV—Aziridinylbenzoquinone Activity Based on Selected Criteria [a]

Compound	Ependymoblastoma	Intracerebral L-1210	P-388	Intraperitoneal L-1210	B16
II			X	X	
III	X		X		
IV	X		X		
VI	X	X	X		
VII	X		X		
XII			X		X
XIII		X	X		X
XIV	X	X	X	X	X
XV	X	X			
XVI			NT[b]		X
XVII	X		X		
XVIII			X	X	X
XX			X	X	
XXI			X	X	X
XXII	X	X	X		
XXIII			X	X	
XXVII	X				

[a] An X indicates a compound that meets the following criterion: ependymoblastoma, multiple long-term survivors in both experiments; intracerebral L-1210, confirmed T/C >150%; P-388, confirmed T/C >200%; intraperitoneal L-1210, confirmed T/C >200%; and B16, confirmed T/C >140%. [b] Not tested.

XIV was inactive against subcutaneous and intracerebral B16 melanocarcinoma as well as subcutaneous and intravenous Lewis lung carcinoma. It had confirmed activity against nine murine models: the five models in Table IV and the four shown in Table V.

Table V—Additional Antitumor Data for XIV [a]

Tumor	O.D.	Treatment Schedule	T/C	Activity Criterion (T/C)
CD mammary (mouse)[b]	12.5	Q7D × 5	23[c]	≤42
Intracerebral P-388[d]	1.5	QD 1–9	151	≥125
C38 colon[b]	25	Q7D × 3	32[c]	≤42
C26 colon[e]	3.1	Q4D × 3	240 (4)	≥130

[a] Highest reproduced T/C; see notes of Table III for definitions. [b] Subcutaneous tumor implantation. [c] Based on mean tumor weights estimated from tumor diameter. [d] Intracerebral tumor implantation. [e] Intraperitoneal tumor implantation.

Pharmacological studies are currently underway with XIV. After development of an acceptable formulation, preclinical toxicological studies will be initiated.

REFERENCES

(1) G. Domagk, S. Petersen, and W. Gauss, *Z. Krebsforsch.*, **59**, 617 (1954).

(2) S. Petersen, W. Gauss, and E. Urbschat, *Angew. Chem.*, **67**, 217 (1955).

(3) Farbenfabriken Bayer A.-G., British pat. 762,723 (Dec. 5, 1956).

(4) Farbenfabriken Bayer A.-G., British pat. 793,796 (Apr. 23, 1958).

(5) Farbenfabriken Bayer A.-G., British pat. 805,518 (Dec. 10, 1958).

(6) J. Mattern, K. Wayss, and M. Volm, *Arch. Gynaekol.*, **216**, 273 (1974).

(7) J. Hartleib, *Z. Krebsforsch.*, **81**, 1 (1974).

(8) J. S. Driscoll, G. F. Hazard, H. B. Wood, and A. Goldin, *Cancer Chemother. Rep., Part 2*, **4**, 1 (1974).

(9) H. Nakao and M. Arakawa, *Chem. Pharm. Bull.*, **20**, 1962 (1972).

(10) H. Nakao, M. Arakawa, T. Nakamura, and M. Fukushima, *ibid.*, **20**, 1968 (1972).

(11) T. Saito, S. Ohira, A. Wakui, M. Yokoyama, *et al.*, *Cancer Chemother. Rep.*, **57**, 447 (1973).

(12) A. H. Khan and J. S. Driscoll, *J. Med. Chem.*, **19**, 313 (1976).

(13) F. Chou, A. H. Khan, and J. S. Driscoll, *ibid.*, **19**, 1302 (1976).

(14) R. I. Geran, N. H. Greenberg, M. M. Macdonald, A. M. Schumacher, and B. J. Abbott, *Cancer Chemother. Rep., Part 3*, **3**, 1 (1972).

(15) P. C. Merker, I. Wodinsky, and R. I. Geran, *Cancer Chemother. Rep.*, **59**, 729 (1975).

(16) S. A. Schepartz, DHEW Publication (NIH) 76-1200, 1976, pp. 13–25.

ACKNOWLEDGMENTS

The authors thank the Ciba-Geigy Co., Bayer A. G., Sankyo Co., H. S. Verter, and the U.S. Department of Agriculture for many of the samples and their permission to report the test results from the compounds they supplied to the National Cancer Institute.

Solubility of Doxycycline in Aqueous Solution

JOSEPH B. BOGARDUS ˣ and ROBERT K. BLACKWOOD, Jr.

Received May 8, 1978, from *Pharmaceutical Research and Development, Pfizer Central Research, Groton, CT 06340.* Accepted for publication July 17, 1978.

Abstract □ The solubility of doxycycline monohydrate and doxycycline hydrochloride dihydrate was investigated in aqueous solution. The hydrochloride dihydrate salt was isolated and identified from solutions initially containing doxycycline hyclate in water. The pKa′ = 3.09 (μ = 0.1 and 25°) for protonation of doxycycline was determined spectrophotometrically. The pH–solubility profiles were determined for doxycycline monohydrate in water and in 1.0 *M* $NaNO_3$–HNO_3 and NaCl–HCl. The pH–solubility profile at 25° for doxycycline in aqueous hydrochloric acid without added salt reached a sharp maximum of 50 mg/ml at pH 2.16. Added chloride ion strongly suppressed the solubility of the hydrochloride dihydrate salt. The apparent solubility product was not constant but decreased as the concentration of added salt increased. A theoretical model was developed involving dimerization of doxycycline and applied to the experimental data. The dimerization constant, K_d = 24 M^{-1}, and true solubility product, $K^0_{sp} = 1.8 \times 10^{-3} M^2$, were calculated. The effect of concentration on NMR and visible spectra indicated that dimerization resulted from intermolecular hydrogen bonding of the phenolic β-diketone portion of the molecule.

Keyphrases □ Doxycycline—monohydrate and hydrochloride dihydrate salts, solubility in aqueous solution, effect of pH □ Solubility—doxycycline monohydrate and hydrochloride dihydrate in aqueous solution, effect of pH □ Antibacterials—doxycycline monohydrate and hydrochloride dihydrate, solubility in aqueous solution, effect of pH

Knowledge of quantitative solubility relationships in purely aqueous solutions is highly important to pharmaceutical research and product development. In water, solute activity is the summation of numerous associative interactions of the drug with other drug molecules and the solvent. These interactions often cause solutions of phar-

0022-3549/79/0200-0188$01.00/0

© 1979, American Pharmaceutical Association

maceutical interest to deviate from thermodynamic ideality (1).

The complex nature of liquid water and its self-association *via* hydrogen bonding are major complicating factors in the study of aqueous solubility. Another problem is that concentration is usually measured rather than thermodynamic activity (2), except in the case of hydrogen ions. Specific solute–solute and solute–solvent interactions may also be present, such as self-association of drug, hydrogen bonding, and ion pairing.

The effects of pH, drug ionization, salts, solvent (in mixed aqueous systems), and temperature on the solubility of several drugs were studied (1–3). The observed pH–solubility relationships in most cases followed basic mathematical expressions derived from the law of mass action.

An unusual characteristic of aqueous systems leading to nonideal behavior is the existence of common ion effects. Although the concept of solubility product equilibrium originated in inorganic chemistry, this phenomenon also has been observed for organic compounds of pharmaceutical interest. Triamterene exhibited common ion equilibria with hydrochloric, nitric, sulfuric, and phosphoric acids (3). pH–solubility profiles containing maxima at pH 2–3 were reported for chlortetracycline, demeclocycline, and methacycline hydrochlorides in sodium acetate–hydrochloric acid buffers (4). The decrease in solubility at lower pH values was attributed to the common ion effect of chloride on the solubility product equilibrium of the hydrochloride salts. The apparent dissolution rates and solubilities of these hydrochloride salts were less than those of the respective free base forms in chloride-containing media. Tetracycline hydrochloride, however, exhibited a low sensitivity to the chloride ion.

The present paper reports a quantitative study of the solubility properties of doxycycline monohydrate (I*a*) and hydrochloride dihydrate (I*b*) crystal forms. Common ion effects due to chloride and nonideal solubility behavior were investigated.

EXPERIMENTAL

Materials—Doxycycline monohydrate[1] was used as received. Doxycycline hydrochloride dihydrate was prepared from doxycycline hyclate[2] (Ic) by aqueous recrystallization. Doxycycline hyclate was dissolved in warm (40°) water to make a 30% solution. The solution was purged with nitrogen and refrigerated for 4 days. The resulting bright-yellow crystals were isolated and air dried at room temperature. Based on elemental analyses (C, H, N, Cl^-), water content (Karl Fischer method), and neutralization equivalent, the product was identified as the hydrochloride dihydrate salt of doxycycline. Paper chromatography and UV spectrophotometry confirmed that degradation had not occurred.

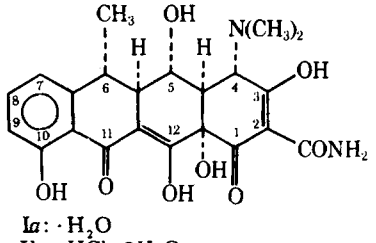

Ia: $\cdot H_2O$
Ib: $\cdot HCl \cdot 2H_2O$
Ic: $\cdot HCl \cdot 0.5H_2O \cdot 0.5C_2H_5OH$

All other chemicals were reagent grade. Water was deionized and double distilled.

Solubility Determination—Equilibration at 25 ± 0.2° was achieved with a vibratory mixer[3] and constant-temperature water bath. Excess amounts of drug were added to amber ampuls containing 5 ml of solution. The sealed ampuls were attached to a plastic holder assembly and vibrated for 18 hr. Preliminary experiments established that this time was sufficient for equilibration. The suspensions at equilibrium were filtered[4], and the first 2 ml of filtrate was discarded.

Apparent binding of doxycycline to the membrane filter caused the concentration in the initial volumes of filtrate to be lower than in later aliquots. This technical artifact has been observed for several other compounds (5). The pH was determined[5] after filtration. Solutions were diluted in 0.1 *N* HCl and assayed spectrophotometrically at 345 nm[6]. Solutions followed Beer's law under these conditions.

pKa′ Determination—The apparent ionization constant, pKa′, for formation of monoprotonated doxycycline was determined spectrophotometrically in citrate buffers at μ = 0.1 (NaCl) and 25°. The absorption spectra of the ionized and nonionized forms indicated that 262 nm was a suitable analytical wavelength. The absorbance of doxycycline was measured at several pH values, and the pKa′ was calculated by the method of Albert and Serjeant (6).

Spectral Studies—NMR spectra were obtained using a 100-MHz spectrometer[7]. Visible absorption measurements were made on a double-beam spectrophotometer[8]. Linearity of detector response over the absorbance range used was verified by constructing a Beer's law plot for FD&C Yellow No. 6 dye in water.

THEORY

Basic pH–Solubility Relationships—Mathematical expressions for the solubility of acid–base forms of weak electrolytes were reported previously (1–3). The terminology of Kramer and Flynn (1) is used here. For weak bases in the pH region where the solubility of the protonated form is limiting, the total solubility is:

$$S_{T,pH<pH_{max}} = [BH^+]_s + [B] = [BH^+]_s(1 + K'_a/[H^+]) \quad \text{(Eq. 1)}$$

where BH^+ is the protonated or salt form, B is the free base, K'_a is the apparent ionization constant, and subscript *s* denotes saturation. The pH_{max} is defined as the pH at which both base and salt species are simultaneously saturated. In a similar manner, the total solubility in the pH region where the free base solubility is limiting may be expressed as:

$$S_{T,pH>pH_{max}} = [BH^+] + [B]_s = [B]_s(1 + [H^+]/K'_a) \quad \text{(Eq. 2)}$$

The present treatment differs from that in Ref. 1 in the theoretical development of pH_{max}. The solubility at this pH is given by:

$$S_{T,pH=pH_{max}} = [BH^+]_s + [B]_s \quad \text{(Eq. 3)}$$

Therefore, Eqs. 1–3 should be sufficient to explain the solubility of a weak base throughout the pH region where pKa′ is applicable. The pH_{max} is defined as:

$$pH_{max} = pKa' + \log \frac{[B]_s}{[BH^+]_s} \quad \text{(Eq. 4)}$$

Application of the Gibbs phase rule to a system at pH_{max} indicates that it is thermodynamically invariant. Therefore, addition of small amounts of acid or base cannot change the equilibrium pH *or* solubility. For example, addition of the conjugate acid, *e.g.*, hydrochloric acid for a hydrochloride salt, temporarily upsets the equilibrium by forming protonated species from base species in solution. Since the concentration of the salt form is then above saturation, precipitation occurs to reestablish its solubility equilibrium. Solid base form also must dissolve to replace the amount "removed" from solution by protonation.

During these events, the pH decreases initially upon addition of acid but then returns to pH_{max} at equilibrium. The net result is that the solid base form is converted to the solid salt form *via* the solution phase. This transformation may proceed until the supply of the solid base form is

[1] Lot 42376, Pfizer.
[2] Lot 55028, Pfizer.
[3] Vibro-Mixer E1, 60 Hz, Chemapec, Woodbury, N.Y.
[4] Millipore, 0.45 μm.
[5] PHM 62, Radiometer, Copenhagen, Denmark.
[6] Model 240, Gilford.
[7] Varian XL-100.
[8] Beckman Acta III.

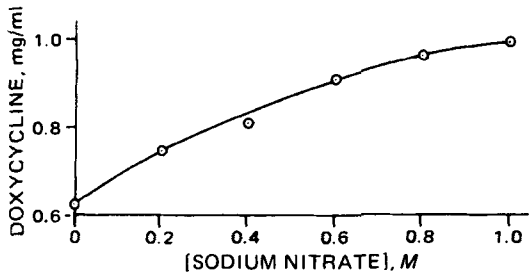

Figure 1—*Solubility of Ia as a function of sodium nitrate concentration in water at 25°. Concentration is expressed as free base equivalent.*

exhausted. The system would then be controlled by Eq. 1 in the normal manner.

A similiar explanation is applicable for addition of hydroxide to convert a salt of a weak base into its free base form. This treatment cannot account for salt effects such as would arise from the generation of sodium chloride from a hydrochloride salt reacting with sodium hydroxide.

The *in situ* salt to base conversion, or its reverse, is often experimentally expedient since both forms of a particular compound are often not available in the pure state. The by-product salt generated must not be neglected in interpretation of the data, however, since the solubility of many compounds is quite dependent on the presence of an electrolyte. This problem may be avoided in some cases by addition of a background electrolyte to maintain ionic strength essentially constant.

Common Ion Effects—The equilibrium for the solubility of a hydrochloride salt of a weak base in water is described by Scheme I and Eq. 5:

$$(BH^+Cl^-)_{solid} \overset{K}{\rightleftharpoons} [BH^+]_s + [Cl^-]$$

Scheme I

$$K = \frac{[BH^+]_s[Cl^-]}{(BH^+Cl^-)_{solid}} \qquad \text{(Eq. 5)}$$

Concentration and activity must be assumed to be equivalent since direct measurement of activity is often not possible for the species of interest other than the hydrogen ion.

If it is assumed that the activity of the solid material is constant, Eq. 5 may be converted to the familiar expression for the solubility product constant:

$$K^0_{sp} = [BH^+]_s[Cl^-] = K(BH^+Cl^-)_{solid} \qquad \text{(Eq. 6)}$$

The apparent solubility product calculated from experimental data is defined by:

$$K'_{sp} = S_T[Cl^-] \qquad \text{(Eq. 7)}$$

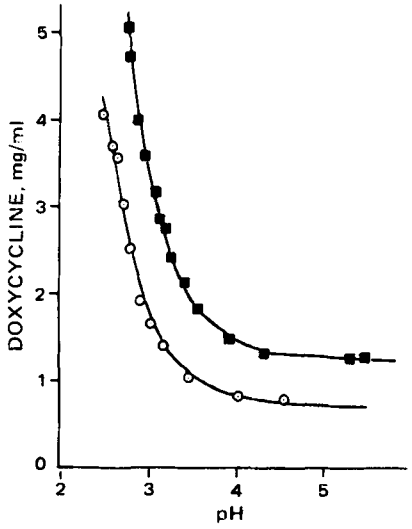

Figure 2—*The pH-solubility profiles for Ia in 1.0 M $NaNO_3$-HNO_3 (■) and 1.0 M NaCl-HCl (⊙) at 25°. The solid lines were calculated according to Eq. 2 using the following constants: $NaNO_3$-HNO_3, pKa' = 3.25, $[B]_s$ = 1.25 mg/ml; and NaCl-HCl, pKa' = 3.20, $[B]_s$ = 0.72 mg/ml. Concentration is expressed as free base equivalent.*

Table I—Effect of Ammonium Chloride and Sodium Chloride on the Solubility of Ib in Water at 25°

[Salt], *M*	S_T, *M*	pH	$[Cl^-]$, *M*[a]	K^0_{sp}, $M^2 \times 10^{-3}$ [b]
0	0.121	2.16	0.121	13.1
Ammonium chloride				
0.02	0.0913	2.16	0.111	9.1
0.05	0.0631	2.26	0.113	6.2
0.1	0.0336	2.44	0.134	3.7
0.2	0.0193	2.57	0.219	3.2
0.4	0.0091	2.76	0.409	2.5
0.8	0.0049	2.89	0.805	2.4
1.0	0.0039	2.93	1.004	2.3
Sodium chloride				
0.02	0.0905	2.16	0.111	8.9
0.05	0.0648	2.25	0.115	6.5
0.1	0.0385	2.40	0.139	4.4
0.2	0.0180	2.58	0.218	3.0
0.4	0.0079	2.75	0.408	2.2
0.8	0.0040	2.89	0.804	2.0
1.0	0.0031	2.95	1.003	1.8

[a] Calculated from Eq. 9. [b] Calculated from Eq. 8 using pKa' = 3.09.

Substitution of Eqs. 1 and 7 into Eq. 6 yields an expression for K^0_{sp} as a function of pH:

$$K^0_{sp} = \frac{K'_{sp}}{(1 + K'_a/[H^+])} \qquad \text{(Eq. 8)}$$

The $[Cl^-]$ in Scheme I and Eqs. 5–8 must be the total chloride ion present in the system. This value is obtained by summation of $[M^+Cl^-]$, where $M^+ = BH^+, H^+, Na^+$, *etc.*, according to:

$$[Cl^-] = \sum_i [M^+Cl^-]_i \qquad \text{(Eq. 9)}$$

When the system is composed of monovalent cations and chloride is the only anion, $[Cl^-]$ is equal to the ionic strength.

RESULTS AND DISCUSSION

Ionization Constant—The pKa' of doxycycline was determined spectrophotometrically. A value of 3.09 ± 0.09 (17 measurements) was calculated at μ = 0.1 and 25°. This pKa' is in agreement with literature values for doxycycline, pKa = 3.4, as well as the pKa = 3.3 reported for oxytetracycline, chlortetracycline, and tetracycline (7, 8).

The microscopic ionization scheme for tetracycline was studied by ^{1}H-NMR (9) and ^{13}C-NMR (10) methods. These studies concluded that protonation of the C-1–C-3 tricarbonylmethane portion of the tetracycline molecule occurred in the pH 1–6 region, forming the corresponding acid salt. The conjugate base species exists predominantly as a zwitterion involving the C-1–C-3 oxyanion and the protonated C-4 dimethylammonium group. Two additional microspecies of the base form, the nonionized neutral molecule and a zwitterion between the C-10–C-12 phenolic diketone anion and the C-4 dimethylammonium group, are present but exist in much lower concentration.

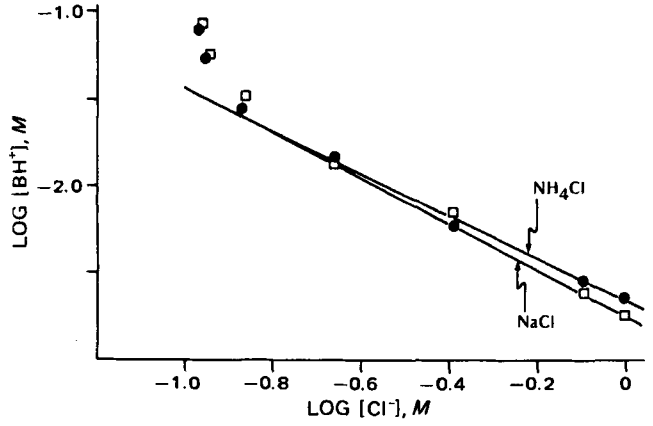

Figure 3—*Logarithmic plot of the relationship between $[BH^+]_s$ calculated from Eq. 1 using pKa' = 3.09 and $[Cl^-]$. The solid lines represent regression slopes of −1.2 (●, NH_4Cl) and −1.3 (□, NaCl).*

Table II—Solubility of I*b* in Aqueous Sodium Chloride and Hydrochloric Acid Solutions at 25°

[HCl], *M*	[NaCl], *M*	pH	S_T, *M*	[Cl⁻], *M*[a]	K'_{sp}, $M^2 \times 10^{-3}$ [b]
0.05	0	1.42	0.0530	0.103	5.3
0.05	0.05	1.41	0.0285	0.128	3.6
0.05	0.15	1.42	0.0128	0.213	2.7
0.05	0.35	1.37	0.0053	0.405	2.1
0.05	0.55	1.35	0.0035	0.603	2.1
0.05	0.75	1.32	0.0026	0.803	2.1
0.05	0.95	1.29	0.0019	1.002	1.9
0.2	0	0.86	0.0128	0.213	2.7
0.2	0.1	0.84	0.0080	0.308	2.5
0.2	0.2	0.82	0.0055	0.407	2.2
0.2	0.3	0.80	0.0044	0.504	2.2
0.2	0.4	0.77	0.0035	0.604	2.1
0.2	0.6	0.75	0.0025	0.803	2.0
0.2	0.8	0.71	0.0020	1.002	2.0
0.01	—	1.92	0.0917	0.102	8.8
0.02	—	1.72	0.0763	0.096	7.0
0.05	—	1.42	0.0530	0.103	5.3
0.10	—	1.11	0.0223	0.122	2.7
0.20	—	0.89	0.0118	0.212	2.5
0.40	—	0.61	0.0056	0.406	2.3
1.0	—	0.21	0.00245	1.002	2.5

[a] Calculated from Eq. 9. [b] Calculated from Eq. 8 using pKa′ = 3.09. $K'_{sp} = K^0_{sp}$ since $K'_a/[H^+] \ll 1$.

Since doxycycline and other tetracyclines are structurally identical in the ionizing functional groups as well as in solution conformation (11), an identical ionization scheme is assumed for these compounds. The chromophore of tetracyclines in the region of 262 nm has been attributed to the $\pi \rightarrow \pi^*$ transition of the C-1–C-3 tricarbonylmethane function (11, 12). The observation that this wavelength exhibited the maximum UV absorptivity change for doxycycline is additional evidence for the assignment of protonation at the C-1–C-3 tricarbonylmethane portion of the molecule.

Salt and pH Effects on Solubility of I*a*.—The effect of sodium nitrate on the solubility of I*a* is shown in Fig. 1. A 65% increase in solubility was found in 1.0 *M* sodium nitrate compared to water. This strong positive salt effect is related to the zwitterionic nature of doxycycline in aqueous solution, which is characteristic of the tetracyclines (13). As a dipolar species, it should be stabilized in an increasingly polar environment. In contrast, uncharged organic species are usually salted out by the addition of an electrolyte.

The pH-solubility profiles for I*a* in the presence of nitrate and chloride ions at μ = 1.0 are shown in Fig. 2. Although the solubility of I*a* was enhanced by nitrate compared to water, it was only slightly affected by chloride ions. Solubility increased uniformly according to Eq. 2 due to protonation of doxycycline. The pKa′ values obtained by curve fitting of these data at μ = 1.0 were in good agreement with those measured spectrophotometrically at μ = 0.1.

The experimental data in Fig. 2 cannot be extended to lower pH values or higher solubility by addition of small increments of acid. Therefore, the systems have reached pH_{max}. By definition, pure base form $[B]_s$ and salt form $[BH^+]_s$ must both be present for the system to be invariant. The maximum solubilities in Fig. 2 are ~10-fold lower than can be attained in purely aqueous solution. This difference is due to the effect of these anions on the solubility product equilibrium of the corresponding acid salt of doxycycline. The existence of doxycycline nitrate was confirmed by dissolving I*a* in water with nitric acid and allowing the product to crystallize. The anhydrous nitrate salt was isolated and identified.

Solubility Product Constant for I*b*.—The stable crystalline form of doxycycline in aqueous hydrochloric acid is I*b*. This salt was isolated from solutions originally prepared with I*c*. Solutions of I*c* can be easily supersaturated by severalfold with respect to the solubility of I*b*. Nucleation and/or crystal growth occur slowly for the interconversion of I*c* → I*b* in water.

The effect of added chloride ion on the solubility of I*b* in water was investigated to determine K^0_{sp}. Ammonium and sodium chlorides were used in the 0.02–1.0 *M* concentration range. Table I summarizes the data from these experiments. The solubility, S_T, decreased strongly with an increasing concentration of either salt. Since the data for the two salts are similar, specific effects due to the cation are considered negligible. The pH increased with an increasing salt concentration due to the lower concentration of I*b*. Since external buffers were not present, the pH of the system was controlled by the concentration of I*b*.

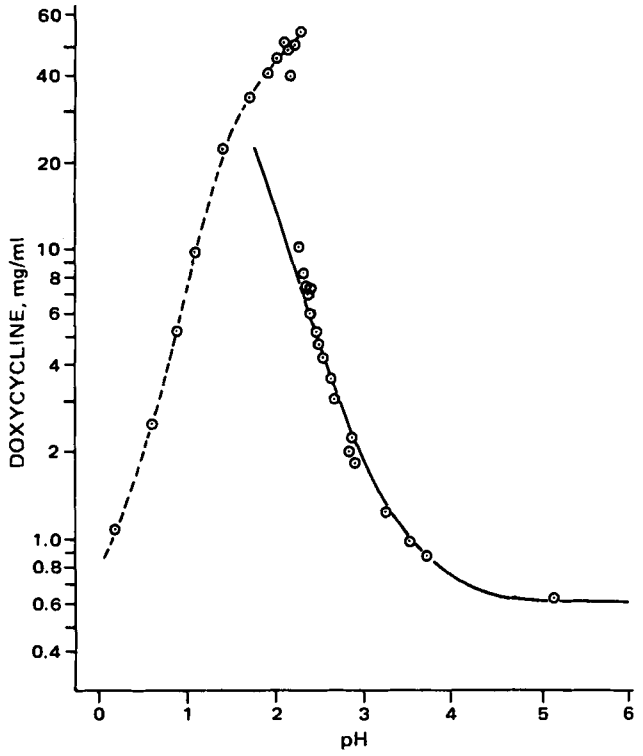

Figure 4—*The pH-solubility profile for I in aqueous hydrochloric acid at 25°. At pH_{max} = 2.16, both I*a *and I*b *were in equilibrium with the solution. Below pH_{max}, I*b *was the solid phase (dashed line). Above this pH, I*a *was in equilibrium with the solution. The solid line is theoretical according to Eq. 2 using $[B]_s$ = 0.625 mg/ml and pKa′ = 3.30. Concentration is expressed as free base equivalent.*

The solubility product, K^0_{sp}, decreased more than fivefold over the concentration range studied. The apparent molecular order of interaction between $[BH^+]$ and $[Cl^-]$ is plotted logarithmically in Fig. 3. A slightly greater than first-order inverse relationship is apparent with strong positive deviation from linearity at low added salt concentrations. A small amount of added salt (0.02–0.05 *M*) caused a much greater than first-order decrease in solubility. The total ionic strength, indicated by $[Cl^-]$ in Table I, was essentially constant at 0.11–0.13 *M* in the region where K^0_{sp} was most sensitive to added salt. In the μ = 0.2–1.0 *M* range, the K^0_{sp} became practically constant.

Since the pH change in these experiments was a complicating factor in data interpretation, the solubility product measurement was repeated under the conditions shown in Table II. Since $K'_a/[H^+]$ was much less than one under these conditions, $K'_{sp} = K^0_{sp}$. Mixtures of sodium chloride and hydrochloric acid, as well as varying concentrations of hydrochloric acid, were used up to 1.0 *M* total added chloride-ion concentration. The downward trend in K'_{sp} with increasing $[Cl^-]$ is again apparent.

The nature of the cation, Na^+ or H^+, had little influence on K'_{sp}. For example, added chloride ion of 0.4 *M* composed of 0.05 *M* HCl + 0.35 *M* NaCl, 0.2 *M* HCl + 0.2 *M* NaCl, or 0.4 *M* HCl resulted in K'_{sp} values of 2.1, 2.2, and 2.3 × 10^{-3} M^2, respectively. These differences were well within experimental error in the value of K'_{sp}. When plotted logarithmically, as in Fig. 3, the data of Table II exhibit linear regression slopes of −1.1 and −1.2.

The K'_{sp} value calculated from a suspension of I*b* in water, *i.e.*, S_T^2, is the most deviant value in the series. Addition of 0.02 *M* NaCl or NH_4Cl (Table I) caused the doxycycline concentration to decrease by 0.03 *M*. This result is impossible according to the principles of common ion equilibria. The solubility cannot decrease by an amount *greater* than the amount of common ion added. Clearly, nonideal behavior was occurring under these conditions. The observed variation in K'_{sp} was not due to changing solution ionic strength. On the contrary, ionic strength (indicated as $[Cl^-]$ in Tables I and II) had little effect on the equilibrium. As already discussed, K'_{sp} varies most under conditions where μ is constant. When μ is changing, K'_{sp} is relatively constant.

pH-Solubility Profile for I*a* and I*b* in Aqueous Hydrochloric Acid—Figure 4 is the pH-solubility profile for I*a* and I*b* in aqueous hydrochloric acid without added salt. Maximum solubility was observed

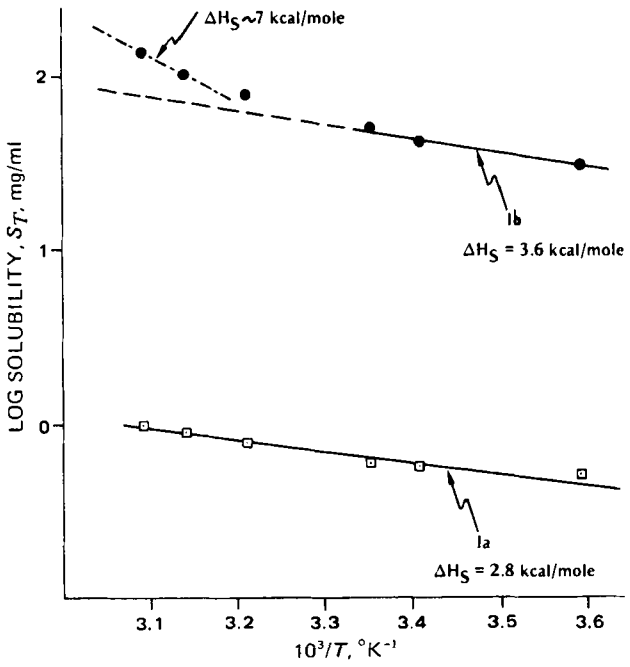

Figure 5—*A van't Hoff-type plot for the solubility of Ia (lower line, ⊡) and Ib (upper line, ●) in water.*

at pH 2.16, which was the result of simultaneous equilibration of crystal forms I*a* and I*b* in water. The ionic strength was not kept constant because of interference of added ions with the solubility equilibria.

A remarkable feature of these data is the approximately fivefold increase in solubility from pH 2.3 to 2.2. Therefore, a much greater than first-order dependence on hydrogen ion would be applicable in this region. Positive deviations of the experimental points from the theoretical line based on Eq. 2 were apparent below pH 2.5. The decrease in solubility below pH_{max} was due to the previously discussed common ion effect of chloride on the solubility product equilibrium.

Solubility-Temperature Relationship—The temperature dependence for solubility of I*a* and I*b* in the 5–50° range is shown graphically in Fig. 5 as van't Hoff-type plots. At the lower temperatures, I*a* and I*b* had similar heats of solution of 2.8 and 3.6 kcal/mole, respectively. At higher temperatures, the slope for I*b* showed upward curvature whereas the slope for I*a* remained linear. In the 45–50° range, ΔH_s for I*b* increased to approximately 7 kcal/mole.

Mechanism of Nonideal Behavior—The data in Figs. 3–5 and Tables I and II clearly show that doxycycline solubility does not follow the expected theoretical relationships given in Scheme I and Eqs. 1–8. All data are consistent with a mechanism involving self-association of doxycycline to form dimeric species such as $(BH^+)_2$, B_2H^+, and, possibly, higher order self-associated forms. The presence of associated species in solution would cause the apparent solubility and, therefore, K'_{sp} to be higher than the values predicted from basic theoretical relationships.

It was previously shown that ionic strength, pH, and specific ion effects (H^+, Na^+, and NH_4^+) were not responsible for the observed changing of K'_{sp}. The absence of crystal transformation during equilibration was verified microscopically and is consistent with the fact that I*a* and I*b* were originally isolated from water. The instability of doxycycline during equilibration could not be a factor affecting solubility since the compound has a half-life of ~100 hr at pH 5 and 50° and shows better stability at lower pH values and temperatures (14).

Scheme II describes the equilibria that would be present if dimerization were to occur forming $(BH^+)_2$ or B_2H^+ species. In this scheme, the solubility of BH^+ is assumed to be limiting.

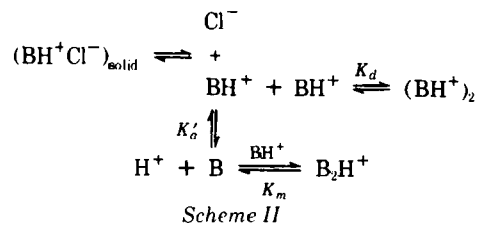

Scheme II

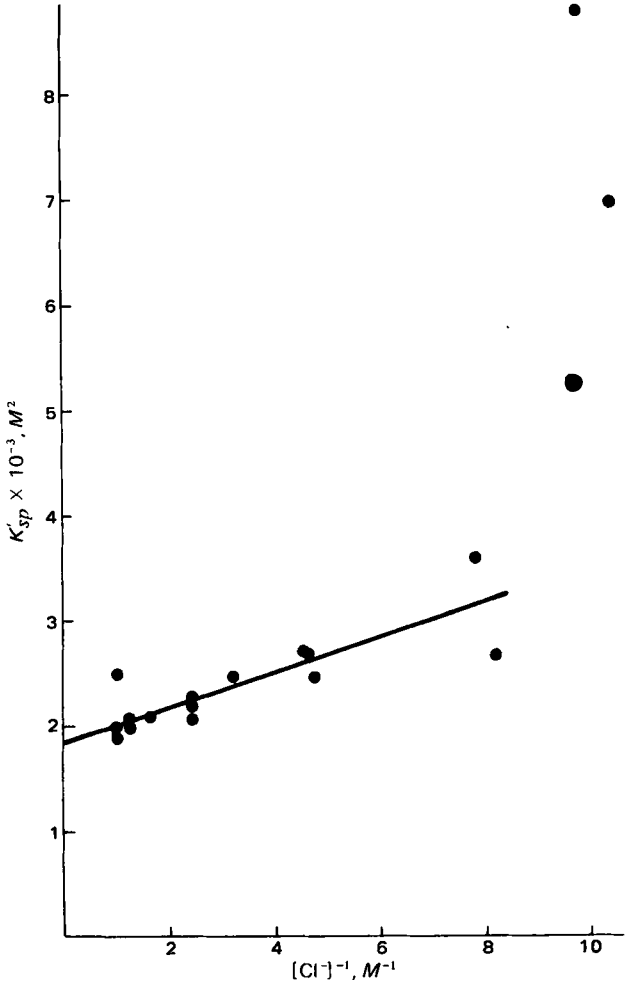

Figure 6—*Apparent solubility product for Ib as a function of the inverse chloride concentration plotted according to Eq. 16.*

The dimerization constants may be defined as:

$$K_d = \frac{[(BH^+)_2]}{[BH^+]^2} \qquad \text{(Eq. 10)}$$

$$K_m = \frac{[B_2H^+]}{[B][BH^+]} \qquad \text{(Eq. 11)}$$

Total solubility is expressed as the sum of the species, taking into account the dimer stoichiometry:

$$S_T = [BH^+]_s(1 + K'_a/[H^+]) + 2[BH^+]_s^2(K_d + K_mK'_a/[H^+]) \qquad \text{(Eq. 12)}$$

Substitution of Eqs. 6 and 12 into Eq. 7 yields an expression for the apparent solubility product:

$$K'_{sp} = K^0_{sp}(1 + K'_a/[H^+]) + \frac{2(K^0_{sp})^2(K_d + K_mK'_a/[H^+])}{[Cl^-]} \qquad \text{(Eq. 13)}$$

The expression analogous to Eq. 12 when the solubility of B is limiting can be shown to be:

$$S_T = [B]_s(1 + [H^+]/K'_a) + 2[B]_s^2(K_d[H^+]^2/K'^2_a + K_m[H^+]/K'_a) \qquad \text{(Eq. 14)}$$

Equation 13 predicts that, at constant pH, K'_{sp} should be an inverse function of the chloride concentration, which is in agreement with the experimental data in Table II. Equation 14 predicts that S_T should first follow Eq. 2 when $[H^+]/K'_a$ is small and then deviate from first-order behavior at lower pH values; these predictions are identical to the solubility data in Fig. 4.

At low pH values, *i.e.*, $K'_a/[H^+] \ll 1$, Eqs. 12 and 13 may be simplified to Eqs. 15 and 16, respectively:

$$S_T = [BH^+]_s(1 + 2K_d[BH^+]_s) \qquad \text{(Eq. 15)}$$

$$K'_{sp} = K^0_{sp} + \frac{2(K^0_{sp})^2K_d}{[Cl^-]} \qquad \text{(Eq. 16)}$$

Table III—Concentration Dependence of ^{1}H-NMR Signals for C-7, C-8, C-9, and C-4 Dimethylamino Protons of I*b* in Deuterium Oxide[a]

[Doxycycline], *M*	Chemical Shift, δ, ppm			
	C-9 H[b]	C-7 H[b]	C-8 H[c]	C-4 $N(CH_3)_2$
0.10	6.67	6.86	7.44	3.04
0.05	6.78	6.99	7.54	3.06
0.017	6.90	7.08	7.64	3.06

[a] Ambient temperature. [b] Doublet, J = 8 Hz. [c] Triplet, J = 8 Hz.

According to Eq. 16, a plot of K'_{sp} *versus* $[Cl^-]^{-1}$ should be linear with slope = $2(K^0_{sp})^2K_d$ and intercept = K^0_{sp}. Figure 6 shows the data of Table II plotted in this manner. Values of K_d = 24 M^{-1} and K^0_{sp} = 1.8×10^{-3} M^2 were calculated from the slope and intercept. Deviation from linear behavior as solubility approaches that of pure I*b* may be due to incomplete equilibrium or existence of higher than second-order association complexes.

It is not possible to prove the existence of the mixed dimer, B_2H^+, with the present data. Under conditions where K_m would be determinable, $(BH^+)_2$ and B_2H^+ species would coexist and separation of the stability constants would be difficult. Attempts to solve Eq. 13 or 14 for K_m did not give reproducible results because of the large error involved in taking the difference between numbers of similar magnitude. Since doxycycline is a large molecule and the site of self-association is remote from the ionizing group, B_2H^+ should have a stability constant at least as large as K_d. The reduced electrostatic interaction in this species indicates that it should be more stable than the dication, $(BH^+)_2$.

The concentration dependence of NMR chemical shifts for certain hydrogens of I*b* in deuterium oxide is shown in Table III. Proton assignments were adapted from those reported for tetracycline (15). An upfield shift in the C-7, C-8, and C-9 aromatic protons of ~0.2 ppm occurred as the concentration was increased from 0.017 to 0.10 *M*. The C-4 dimethylamino protons, however, were essentially unchanged, as were other protons not listed in Table III. Rigler *et al.* (9) found that the chemical shift of the C-8 proton moved 0.28 ppm upfield during ionization of the phenolic β-diketone system (macro pKa = 7.7 and 9.7). The similarity of the concentration-dependent and ionization-induced change in chemical shift of these protons indicates that the phenolic β-diketone moiety is the site of self-association.

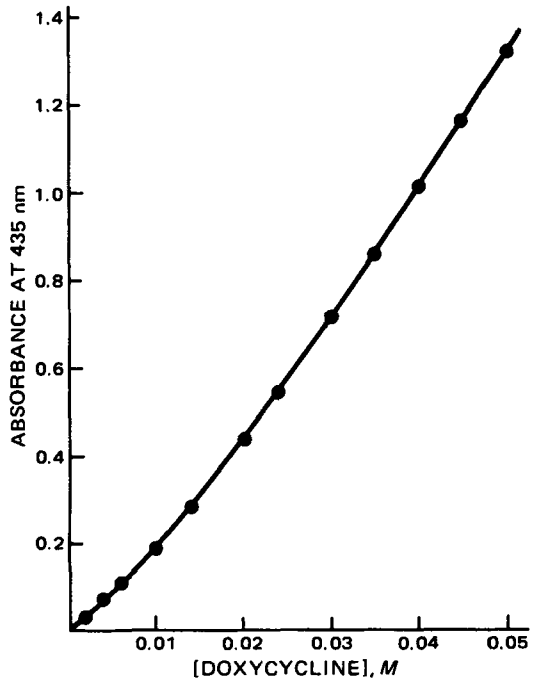

Figure 7—*Absorbance of Ic as a function of concentration in 0.05* M *phosphoric acid buffer (pH 2.0) at 25°. Concentration is expressed as free base equivalent. Points are experimental, and the line is theoretical according to Eq. 18. The theoretical line was constructed using the following constants:* a = *1.0 cm,* E_m = *12* M^{-1} cm^{-1}, E_d = *76* M^{-1} cm^{-1}, *and* K_d = *24* M^{-1}.

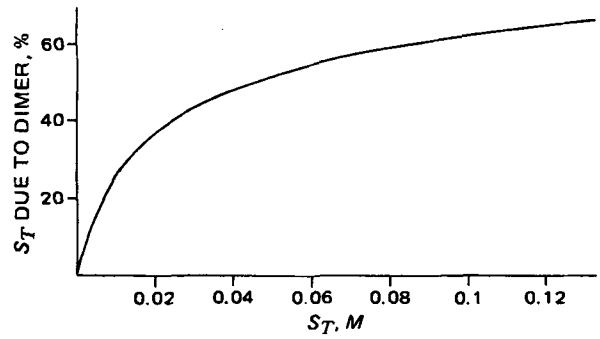

Figure 8—*Theoretical curve of the percent of total solubility contributed by dimer species* $(BH^+)_2$ *as a function of total solubility. Dimerization constant,* K_d = *24* M^{-1}, *was used to calculate the curve.*

Planarity of the aromatic ring with the C-11–C-12 β-diketone groups (12, 16) would allow dimerization to occur *via* multiple intermolecular hydrogen bonds. The C-10 phenol and C-11–C-12 enol–keto groups of one molecule could associate with those of the other molecule, forming an edge-to-edge oriented dimer in solution. In this configuration, the environment of the C-4 methyl protons would not be affected, which is consistent with the data.

Self-association of doxycycline also was observed by visible spectrophotometry (Fig. 7). Absorbance at 435 nm was not linear with concentration but showed an apparent parabolic relationship. The 0–0.05 *M* concentration range was chosen because the solubility product data indicated that dimerization was predominant in this region. The chromophore at this wavelength is a shoulder of the ~350-nm maximum of doxycycline, which is generally attributed to the phenolic β-diketone moiety of tetracyclines (12).

The total concentration, C_T, can be expressed as the sum of the monomer, C_m, and dimer according to:

$$C_T = C_m + 2K_dC_m^2 \qquad \text{(Eq. 17)}$$

The total absorbance, A_T, is defined by:

$$A_T = a(E_mC_m + K_dE_dC_m^2) \qquad \text{(Eq. 18)}$$

where a is the cell path length, E_m is the molar absorptivity of the monomer, and E_d is the molar absorptivity of the dimer.

The theoretical line in Fig. 7 was determined as follows. The value of C_m was calculated from Eq. 17 at various values of C_T, assuming K_d = 24 M^{-1} (determined from the solubility product data). An initial estimate of E_m was taken from the initial slope in Fig. 7, and then E_m and E_d were adjusted to give the best fit of the data according to Eq. 18. The curve was sensitive to changes in constants E_m and E_d, which primarily affected the lower and upper parts of the curve, respectively. The value of the dimerization constant cannot be verified by this procedure, however, because other values of K_d can be fitted to the data as well. For example, assumption of a larger value of K_d will cause the C_m value calculated by Eq. 17 to become smaller. In Eq. 18, however, this decrease can be compensated by adjustment of E_m and E_d to yield an equally good fit of the data.

The molar absorptivity of the dimer species required to fit the data is approximately sixfold larger than that of the monomer. Simple aggregation or hydrophobic association would be expected to yield a ratio nearer twofold. Perturbation of the aromatic system by hydrogen bonding is a possible explanation for the high absorptivity of the dimer.

Figure 8 is a theoretical plot showing the strong effect of dimerization on the apparent solubility of doxycycline. If it is assumed that only the monomer and dimer are present, more than 50% of the total solubility would be contributed by the dimer species at S_T >0.04 *M*. Self-association in solution is probably common to tetracyclines in general because of the similarity of the interacting functional groups.

At concentrations near saturation, all compounds must begin to self-associate. When pushed to slightly higher concentrations, the association complexes become active nuclei for the crystallization process. The lack of suitable analytical methods for the determination of free solute concentrations has limited the investigation of solute properties in saturated or nearly saturated solutions. Analysis of solubility product equilibria was a sensitive indicator of the concentration of unassociated doxycycline cation. This method should be a powerful tool for the study of solution equilibria in general.

REFERENCES

(1) S. F. Kramer and G. L. Flynn, *J. Pharm. Sci.*, **61**, 1896 (1972).

(2) T. Higuchi, M. Gupta, and L. W. Busse, *J. Am. Pharm. Assoc., Sci. Ed.*, **42**, 157 (1953).

(3) L. W. Dittert, T. Higuchi, and D. R. Reese, *J. Pharm. Sci.*, **53**, 1325 (1964).

(4) S. Miyazaki, M. Nakano, and T. Arita, *Chem. Pharm. Bull.*, **23**, 1197 (1975).

(5) S. T. Liu, C. F. Carney, and A. R. Hurwitz, *J. Pharm. Pharmacol.*, **29**, 319 (1977).

(6) A. Albert and E. P. Serjeant, "Ionization Constants of Acids and Bases," Methuen, London, England, 1962, chap. 4.

(7) "The Merck Index," 8th ed., Merck & Co., Rahway, N.J., 1968, p. 398.

(8) C. R. Stephens, K. Murai, K. J. Brunings, and R. B. Woodward, *J. Am. Chem. Soc.*, **78**, 4155 (1956).

(9) N. E. Rigler, S. P. Bag, D. E. Leyden, J. L. Sudmeier, and C. N. Reilley, *Anal. Chem.*, **37**, 872 (1965).

(10) G. L. Asleson and C. W. Frank, *J. Am. Chem. Soc.*, **98**, 4745 (1976).

(11) L. A. Mitscher, A. C. Bonacci, B. Slater-Eng, A. K. Hacker, and T. D. Sokoloski, *Antimicrob. Agents Chemother.*, **1969**, 111.

(12) L. A. Mitscher, A. C. Bonacci, and T. D. Sokoloski, *ibid.*, **1968**, 78.

(13) H. Terada and T. Inagi, *Chem. Pharm. Bull.*, **23**, 1960 (1975).

(14) G. S. Libinson and T. A. Ushakova, *Khim.-Farmatsev. Zh.*, **10**, 91 (1976).

(15) G. L. Asleson, L. J. Stoel, E. C. Newman, and C. W. Frank, *J. Pharm. Sci.*, **63**, 1144 (1974).

(16) M. Schach von Wittenau and R. K. Blackwood, *J. Org. Chem.*, **31**, 613 (1966).

ACKNOWLEDGMENTS

The authors are indebted to Dr. S. J. Desai and Dr. W. I. Higuchi for valuable discussions and encouragement.

R. K. Blackwood, Jr., was a National Pharmaceutical Council Summer Pharmacy Intern, 1977.

Synthesis and Therapeutic Testing of Mono- and Dialkyl Esters of Pentetic (Diethylenetriaminepentaacetic) Acid for Decorporation of Polymeric Plutonium

RAYMOND A. GUILMETTE *, JOHN E. PARKS ‡, and ARTHUR LINDENBAUM ˣ

Received June 17, 1977, from the *Division of Biological and Medical Research, Argonne National Laboratory, Argonne, IL 60439.* Accepted for publication July 13, 1978.

*Present address: Inhalation Toxicology Research Institute, Albuquerque, NM 87115. ‡Present address: Chemical Engineering Division, Argonne National Laboratory, Argonne, IL 60439.

Abstract □ The synthesis, characterization, and therapeutic evaluation of a series of partially esterified derivatives of pentetic (diethylenetriaminepentaacetic) acid are reported. These compounds were prepared in an attempt to promote increased decorporation of insoluble colloidal forms of plutonium, which are not removed by pentetic acid alone. The dimethyl, diethyl, dibutyl, dioctyl, and monoethyl esters were synthesized by reaction of the appropriate alcohol with the dianhydride of pentetic acid. These esters were injected intravenously into mice as their calcium chelates in saline. None of the esters was effective in removing plutonium from the liver. All esters removed approximately 20% of the plutonium in the skeleton. However, when the esters were given together with pentetic acid, only the dioctyl ester showed enhanced removal of plutonium compared to pentetic acid alone. The small increase in effectiveness and the increased acute toxicity make these esters of limited practical interest in plutonium decorporation therapy.

Keyphrases □ Pentetate esters, various—synthesized, evaluated for ability to decorporate polymeric plutonium in mice □ Plutonium, polymeric—decorporation in mice, various pentetate esters evaluated □ Structure-activity relationships—various pentetate esters evaluated for ability to decorporate polymeric plutonium in mice □ Chelating agents—various pentetate esters synthesized, evaluated for ability to decorporate polymeric plutonium in mice

The disposition kinetics of the easily hydrolyzable toxic radiometal plutonium following accidental exposure depend on the physicochemical form to which an individual is exposed as well as the route of exposure. Systemically deposited plutonium (*i.e.*, plutonium that has reached the circulation and is subsequently deposited in the tissues) is generally considered to be soluble ("monomeric") plutonium. However, aggregated insoluble forms of plutonium have been observed at later times in the liver and spleen (1, 2). As a model for insoluble systemically deposited plutonium, a colloidal ("polymeric") plutonium preparation is injected intravenously in animals. A large fraction of this plutonium is rapidly deposited in organs rich in reticuloendothelial elements, particularly the liver (3).

BACKGROUND

Pentetic acid (diethylenetriaminepentaacetic acid or DTPA), *N,N*-bis[2-[bis(carboxymethyl)amino]ethyl]glycine, administered intravenously as the calcium chelate trisodium salt (I), presently is considered the treatment of choice for accidental exposure to certain multivalent lanthanide and actinide radioelements such as plutonium. This drug has also been used for the treatment of lead poisoning, acute iron intoxication, and iron storage disease (4). Although I has been effective in removing soluble plutonium from the liver and, to a lesser extent, from the skeleton (5, 6), this chelating agent has not been successful in decorporating the more insoluble polymeric plutonium (7). Since hepatically deposited polymeric plutonium is primarily associated with lysosomes (8) and I is predominantly distributed in the extracellular space (9) and is rapidly excreted in the urine (10), it was reasoned that increased intracellular uptake of I might place a sufficient concentration of ligand at the site of plutonium deposition to promote increased plutonium decorporation.

Previously, two different approaches were attempted to increase the uptake of I into cells. Markley (11), using the pentaethyl ester of pentetic acid, found that this more lipid-soluble form removed additional plutonium from the mouse liver beyond that removed with I alone. When I and its pentaethyl ester were administered together, their effects in the liver were approximately additive, suggesting that each form was acting on a separate and distinct fraction of hepatic plutonium. However, the pentaethyl ester was much more toxic than I. In the second approach, I encapsulated in phospholipid liposomes was injected intravenously. The encapsulated I deposited intracellularly in the liver (12) to a large

0022-3549/79/0200-0194$01.00/0

© 1979, American Pharmaceutical Association

REFERENCES

(1) S. F. Kramer and G. L. Flynn, *J. Pharm. Sci.*, **61**, 1896 (1972).

(2) T. Higuchi, M. Gupta, and L. W. Busse, *J. Am. Pharm. Assoc., Sci. Ed.*, **42**, 157 (1953).

(3) L. W. Dittert, T. Higuchi, and D. R. Reese, *J. Pharm. Sci.*, **53**, 1325 (1964).

(4) S. Miyazaki, M. Nakano, and T. Arita, *Chem. Pharm. Bull.*, **23**, 1197 (1975).

(5) S. T. Liu, C. F. Carney, and A. R. Hurwitz, *J. Pharm. Pharmacol.*, **29**, 319 (1977).

(6) A. Albert and E. P. Serjeant, "Ionization Constants of Acids and Bases," Methuen, London, England, 1962, chap. 4.

(7) "The Merck Index," 8th ed., Merck & Co., Rahway, N.J., 1968, p. 398.

(8) C. R. Stephens, K. Murai, K. J. Brunings, and R. B. Woodward, *J. Am. Chem. Soc.*, **78**, 4155 (1956).

(9) N. E. Rigler, S. P. Bag, D. E. Leyden, J. L. Sudmeier, and C. N. Reilley, *Anal. Chem.*, **37**, 872 (1965).

(10) G. L. Asleson and C. W. Frank, *J. Am. Chem. Soc.*, **98**, 4745 (1976).

(11) L. A. Mitscher, A. C. Bonacci, B. Slater-Eng, A. K. Hacker, and T. D. Sokoloski, *Antimicrob. Agents Chemother.*, **1969**, 111.

(12) L. A. Mitscher, A. C. Bonacci, and T. D. Sokoloski, *ibid.*, **1968**, 78.

(13) H. Terada and T. Inagi, *Chem. Pharm. Bull.*, **23**, 1960 (1975).

(14) G. S. Libinson and T. A. Ushakova, *Khim.-Farmatsev. Zh.*, **10**, 91 (1976).

(15) G. L. Asleson, L. J. Stoel, E. C. Newman, and C. W. Frank, *J. Pharm. Sci.*, **63**, 1144 (1974).

(16) M. Schach von Wittenau and R. K. Blackwood, *J. Org. Chem.*, **31**, 613 (1966).

ACKNOWLEDGMENTS

The authors are indebted to Dr. S. J. Desai and Dr. W. I. Higuchi for valuable discussions and encouragement.

R. K. Blackwood, Jr., was a National Pharmaceutical Council Summer Pharmacy Intern, 1977.

Synthesis and Therapeutic Testing of Mono- and Dialkyl Esters of Pentetic (Diethylenetriaminepentaacetic) Acid for Decorporation of Polymeric Plutonium

RAYMOND A. GUILMETTE *, JOHN E. PARKS ‡, and ARTHUR LINDENBAUM ˣ

Received June 17, 1977, from the *Division of Biological and Medical Research, Argonne National Laboratory, Argonne, IL 60439.* Accepted for publication July 13, 1978.

*Present address: Inhalation Toxicology Research Institute, Albuquerque, NM 87115. ‡Present address: Chemical Engineering Division, Argonne National Laboratory, Argonne, IL 60439.

Abstract □ The synthesis, characterization, and therapeutic evaluation of a series of partially esterified derivatives of pentetic (diethylenetriaminepentaacetic) acid are reported. These compounds were prepared in an attempt to promote increased decorporation of insoluble colloidal forms of plutonium, which are not removed by pentetic acid alone. The dimethyl, diethyl, dibutyl, dioctyl, and monoethyl esters were synthesized by reaction of the appropriate alcohol with the dianhydride of pentetic acid. These esters were injected intravenously into mice as their calcium chelates in saline. None of the esters was effective in removing plutonium from the liver. All esters removed approximately 20% of the plutonium in the skeleton. However, when the esters were given together with pentetic acid, only the dioctyl ester showed enhanced removal of plutonium compared to pentetic acid alone. The small increase in effectiveness and the increased acute toxicity make these esters of limited practical interest in plutonium decorporation therapy.

Keyphrases □ Pentetate esters, various—synthesized, evaluated for ability to decorporate polymeric plutonium in mice □ Plutonium, polymeric—decorporation in mice, various pentetate esters evaluated □ Structure-activity relationships—various pentetate esters evaluated for ability to decorporate polymeric plutonium in mice □ Chelating agents—various pentetate esters synthesized, evaluated for ability to decorporate polymeric plutonium in mice

The disposition kinetics of the easily hydrolyzable toxic radiometal plutonium following accidental exposure depend on the physicochemical form to which an individual is exposed as well as the route of exposure. Systemically deposited plutonium (*i.e.*, plutonium that has reached the circulation and is subsequently deposited in the tissues) is generally considered to be soluble ("monomeric") plutonium. However, aggregated insoluble forms of plutonium have been observed at later times in the liver and spleen (1, 2). As a model for insoluble systemically deposited plutonium, a colloidal ("polymeric") plutonium preparation is injected intravenously in animals. A large fraction of this plutonium is rapidly deposited in organs rich in reticuloendothelial elements, particularly the liver (3).

BACKGROUND

Pentetic acid (diethylenetriaminepentaacetic acid or DTPA), *N,N*-bis[2-[bis(carboxymethyl)amino]ethyl]glycine, administered intravenously as the calcium chelate trisodium salt (I), presently is considered the treatment of choice for accidental exposure to certain multivalent lanthanide and actinide radioelements such as plutonium. This drug has also been used for the treatment of lead poisoning, acute iron intoxication, and iron storage disease (4). Although I has been effective in removing soluble plutonium from the liver and, to a lesser extent, from the skeleton (5, 6), this chelating agent has not been successful in decorporating the more insoluble polymeric plutonium (7). Since hepatically deposited polymeric plutonium is primarily associated with lysosomes (8) and I is predominantly distributed in the extracellular space (9) and is rapidly excreted in the urine (10), it was reasoned that increased intracellular uptake of I might place a sufficient concentration of ligand at the site of plutonium deposition to promote increased plutonium decorporation.

Previously, two different approaches were attempted to increase the uptake of I into cells. Markley (11), using the pentaethyl ester of pentetic acid, found that this more lipid-soluble form removed additional plutonium from the mouse liver beyond that removed with I alone. When I and its pentaethyl ester were administered together, their effects in the liver were approximately additive, suggesting that each form was acting on a separate and distinct fraction of hepatic plutonium. However, the pentaethyl ester was much more toxic than I. In the second approach, I encapsulated in phospholipid liposomes was injected intravenously. The encapsulated I deposited intracellularly in the liver (12) to a large

0022-3549/79/0200-0194$01.00/0

© 1979, American Pharmaceutical Association

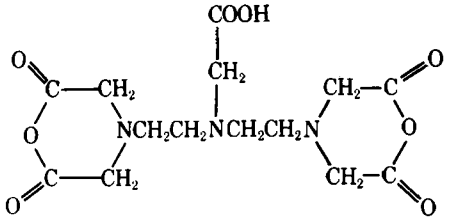

II

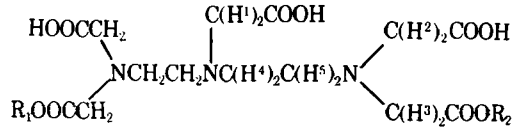

III–VII

extent and removed plutonium from the liver that could not be removed by I alone (13).

The present study was designed to test the possibility that partial esterification of pentetic acid with alcohols of varying chain length might provide compounds less toxic than the pentaethyl ester while retaining effective adjunct potency for removal of polymeric plutonium from the liver. A group of new mono- and diesters of pentetic acid was synthesized for experimental use in plutonium chelation therapy. Preparation of the esters was patterned after the synthesis of corresponding diesters of edetic acid (14, 15). The dianhydride (II) of pentetic acid was used as an intermediate; II reacts smoothly with primary alcohols to provide diesters III–VI (superscript numbers refer to NMR assignments) in good yield.

EXPERIMENTAL

Materials—Methanol and ethanol were purified by distillation from their respective magnesium alkoxides. Reagent grade pyridine and dimethylformamide were dried by storage over freshly activated molecular sieves[1]. Reagent grade pentetic acid[2], 1-butanol, and 1-octanol were used directly.

Methods—Melting points were determined on a hot-stage microscope[3] and are uncorrected. Samples to be characterized by NMR[4] spectroscopy were prepared in 99.5% deuterium oxide at a concentration of 5–10% (w/v); the pD was adjusted to 7.4 by the addition of 1 *M* KOD, Na_2CO_3, or DCl. Shifts are recorded in τ *versus* sodium 3-trimethylsilyl-2,2,3,3-tetradeuteropropionate. Elemental analyses were performed elsewhere[5].

Syntheses—*Dianhydride of Pentetic Acid (II)*—*N,N*-Bis[2-(2,6-dioxo-4-morpholinyl)]ethylglycine was prepared by previously published methods (15, 16).

Dimethyl Ester of Pentetic Acid (III)—A 100-mmole sample of II was refluxed with 250 ml of anhydrous methanol for 4 hr (drying tube), cooled, filtered, washed with 100 ml of methanol, and dried *in vacuo* at 75° overnight to provide 39.1 g (93%) of amorphous white powder, mp 194–195°; NMR: H^1 (6.13, s), H^2 (6.67, s), H^3 (6.37, s), H^4 (6.60, t), H^5 (6.91, t), and OCH_3 (6.17, s) ppm.

Anal.—Calc. for $C_{16}H_{27}N_3O_{10}$: C, 45.50; H, 6.46; N, 9.97. Found: C, 45.50; H, 6.47; N, 9.87.

Diethyl Ester of Pentetic Acid (IV)—A 105-mmole sample of II was refluxed (drying tube) in 250 ml of anhydrous ethanol for 1 hr. The cloudy solution was filtered hot through a medium frit glass filter with pressure. The product crystallized immediately upon cooling the filtrate and was recrystallized from 200 ml of anhydrous ethanol and dried *in vacuo* for 24 hr at 60°. A 39.2-g sample (83%) of white powder, mp 143–144°, was obtained; NMR: H^1 (6.13, s), H^2 (6.67, s), H^3 (6.39, s), H^4 (6.59, t), H^5 (6.90, t), OCH_2 (5.80, q), and CH_3 (8.72, t) ppm.

Anal.—Calc. for $C_{18}H_{31}N_3O_{10}$: C, 48.10; H, 6.95; N, 9.35. Found: C, 47.66; H, 7.11; N, 9.26.

Dibutyl (V) and Dioctyl (VI) Esters of Pentetic Acid—A mixture of 54 mmoles of II, 150 mmoles of the respective 1-alcohol, and 30–50 ml of anhydrous dimethylformamide was stirred at 80° for 4 hr. After precipitating slowly from the cooled clear amber solutions, the products were recrystallized from methanol and dried *in vacuo* to yield white powders: V, 60%, mp 154–156°; and VI, 68%, mp 153–156°; NMR (V): H^1 (6.14, s), H^2 (6.67, s), H^3 (6.39, s), H^4 (6.60, t), H^5 (6.91, t), OCH_2 (5.82); CH_2 (8.35 and 8.63), and CH_3 (9.08, q) ppm; NMR (VI): H^1 (6.13, s), H^2 (6.70, s), H^3 (6.41, s), H^4 (6.56, t), H^5 (6.97, t), OCH_2 (5.91), CH_2 (8.36 and 8.69), and CH_3 (9.12, q) ppm.

Anal.—Calc. for $C_{22}H_{39}N_3O_{10}$ (V): C, 52.26; H, 7.78; N, 8.31. Found: C, 52.16; H, 7.79; N, 8.33. Calc. for $C_{30}H_{55}N_3O_{10}$ (VI): C, 58.32; H, 8.97; N, 6.80. Found: C, 57.86; H, 8.88; N, 7.04.

Monoethyl Ester of Pentetic Acid (VII)—When a sample of IV was refluxed in 95% ethanol, a precipitate appeared. This material, mp 142–144°, was not recrystallized, but elemental analysis and the NMR spectrum showed it to be VII, contaminated with small amounts of pentetic acid; NMR: H^1 (6.15, s), H^3 (6.39, s), H^4 (6.59, t), H^5 (6.85, t), OCH_2 (5.74, q), and CH_3 (8.72, t) ppm. The two H^2 signals in VII were overlapped by corresponding signals from pentetic acid.

Anal.—Calc. for $C_{16}H_{27}N_3O_{10}$: C, 45.60; H, 6.46; N, 9.99. Found: C, 45.96; H, 6.44; N, 9.87.

Solutions for Injection—A quantity of each ester (III–VII) sufficient to give a final concentration of 100 mg/ml (except VI, which gave 50 mg/ml) was weighed into a volumetric flask and slurried with a stoichiometric amount of calcium carbonate and water until foaming subsided; 1.0 *M* Na_2CO_3 then was added dropwise to adjust the pH to 7.00 ± 0.05. The resulting solution was diluted to volume, filtered (fine-glass frit), and refrigerated at 5° until use. Similar solutions were prepared in deuterium oxide and examined by NMR spectroscopy. The results showed that negligible hydrolysis had occurred during preparation and that less than 10% of the esters were hydrolyzed after 60 days.

Biological Studies—Female $B6CF_1$/Anl mice, 80–100 days old, were injected with 1.0 μCi of polymeric plutonium/kg iv, which was 20% ultrafilterable through a cellophane membrane (17). Five days later, groups of five mice each were treated with I (0.25 mmole/kg) intraperitoneally, one of the esters intravenously (0.25 mmole/kg for all esters except VI, which was given at 0.12 mmole/kg), or both. Treatments with I, IV, or VII were continued twice weekly for 4 weeks, with III or V twice weekly for 3 weeks and with VI for 2 weeks. Toxicological considerations dictated the differences in treatment schedules. There were two plutonium control groups. In the first, the mice were treated with saline both intravenously and intraperitoneally. In the second, the mice received saline intravenously and I intraperitoneally.

The mice were sacrificed at 33 days after plutonium injection. Liver, spleen, lungs, and femurs (two per mouse) were removed, weighed, and assayed radiochemically for plutonium activity using published procedures (18). Preliminary toxicity testing of the new compounds was performed to determine a maximum injected dose that should not be acutely lethal to the test animals. This estimated dose was obtained by injecting small groups of animals (generally two to four) initially with a dose corresponding to the intravenous LD_{50} dose for I (*i.e.*, 4 mmoles/kg[6]). If all animals died, the dose was consecutively halved until a dose was reached where all animals survived. This dose was chosen as the initial therapeutic dose.

RESULTS AND DISCUSSION

The diesters III–VI and the monoester VII, reported here for the first time, were obtained as pure crystalline or amorphous compounds and were characterized by elemental analysis and NMR spectroscopy. The NMR spectra were virtually identical, differing only in features assigned to the different alkoxy groups. The monoester VII was prepared from IV. Refluxing IV in 95% ethanol slowly hydrolyzed the diester, resulting in the precipitation of the insoluble VII. The lower esters III, IV, and VII were moderately water soluble as the free acids; upon neutralization, all compounds were soluble to at least 0.1 *M*.

Attempts were made to activate the central carboxyl group of II to prepare symmetrical monoesters or triesters. The conditions employed included a larger excess of acetic anhydride, higher reaction temperatures, and trifluoroacetic anhydride instead of acetic anhydride at room temperature. Extensive decomposition to malodorous tars occurred in each case.

The limited toxicity testing of the synthesized compounds, based on a single intravenous injection, indicates that all of the esterified compounds were more acutely toxic than I. Compared to I, IV was about twice as toxic, III and VII were about three times, V was about six times, and

[1] Linde 4-A, Linde Division, Union Carbide Corp., New York, N.Y.
[2] G. Frederich Smith Chemical Co., Columbus, Ohio.
[3] E. Leitz, Inc., Rockleigh, NJ 07647.
[4] Model HR-220, Varian Associates, Palo Alto, Calif.
[5] Clark Microanalytical Laboratory, Urbana, Ill.

[6] Unpublished data.

Table I—Effect of Pentetic Acid Esters on Plutonium Content of Livers and Femurs of Mice

Compounds Administered[a]	Percent of Controls ± SD[b]		Significance for Femur Comparison[c]
	Liver	Femur	
Saline alone (control)[d]	24.5 ± 3.3	3.18 ± 0.36	
I alone (control)[d]	24.9 ± 1.1	2.29 ± 0.26	
III alone	115 ± 17	81.7 ± 10.8	$p < 0.02$
III + I	106 ± 7	90.5 ± 14.2	N.S.
IV alone	103 ± 4	79.3 ± 8.2	$p < 0.01$
IV + I	102 ± 3	106 ± 10	N.S.
V alone	105 ± 16	81.8 ± 10.9	$p < 0.02$
V + I	97.0 ± 6.7	84.0 ± 12.5	N.S.
VI alone	115 ± 16	82.8 ± 14.8	$p < 0.05$
VI + I	99.8 ± 12.5	84.1 ± 12.1	$p < 0.05$
VII alone	92.2 ± 4.5	79.7 ± 8.7	$p < 0.01$
VII + I	104 ± 5	106 ± 7	N.S.

[a] Compounds III–VII were injected intravenously, and I was given intraperitoneally; comparable saline injections were substituted for I in "alone" groups. [b] Percent figures were obtained by comparison of the ester "alone" groups with saline-treated controls and the ester + I groups with the I alone group. Standard deviations of the ratios were obtained by a propagation of error approximation technique as specified by Deming (20). [c] The test of independent means of treated and control groups (N.S. = no significant difference at $p < 0.05$). [d] Percent of injected dose ± *SD*.

VI was about 10 times as toxic. However, all esters were significantly less toxic than the pentaethyl ester of pentetic acid.

Table I summarizes the results obtained in trials designed to measure removal of polymeric plutonium from mouse liver and skeleton, using each of the esters, either alone or as an adjunct to I. Treatment efficacy is expressed as percent of the respective control level. With respect to the plutonium burden in the liver at 33 days, there was no effect of treatment with any of the esters, whether given alone or with I; nor did treatment with these esters have any significant effect on the plutonium content of the lung or spleen. In the skeleton, however, treatment with III, IV, or VII resulted in about a 20% reduction in the plutonium content of the femurs as compared to saline-treated controls. These reductions were statistically significant. When these esters were given together with I, there was no removal beyond that attributable to I alone. In contrast, treatment with V or VI resulted in a 15–20% reduction of the femur plutonium burden compared to the respective controls whether these esters were given alone or with I.

The objective of this study, removal of polymeric plutonium from the liver, was not achieved using any of the partially esterified compounds III–VII. Since Markley (11) previously demonstrated that the fully esterified pentaethyl ester of pentetic acid could remove a fraction of hepatic plutonium not removed by I, it seems reasonable to assume that the chemical modifications of I to the incompletely esterified forms were not sufficient to achieve the therapeutic action of the pentaethyl ester. This result may be due to the fact that esterification of one or two of the five acid groups does not sufficiently reduce the charge density of the molecule to enhance its cellular membrane transport. On the basis of present evidence, it is assumed that the effectiveness of the neutral pentaethyl ester is due to its increased intracellular uptake by plutonium-bearing liver cells followed by hydrolysis of the ester groups with "reactivation" of the ionic ligand within the vicinity of the target plutonium. This action is followed by chelation and subsequent excretion of the more soluble plutonium chelate.

An unexpected result was the demonstration of adjunct effectiveness of V and VI for removal of skeletal plutonium. The varying effectiveness of the esters tested suggests that partial esterification may have produced differences in their metabolism and/or distribution as compared to the unesterified ligand, I. Compounds III, IV, and VII, when given alone, removed skeletal plutonium; but when given together with I, they exerted no additional effect, suggesting that partial esterification with methyl or ethyl groups did little to alter the therapeutic effect of pentetic acid, at least as related to the removal of skeletal plutonium. Thus, the therapeutic effect noted when the esters were given alone was probably due to a chelating action similar to that of I. If III, IV, and VII behave like the ionic I, then adjunct potency would not be expected since the administered dose of I was shown previously to effect maximum removal of plutonium from the skeleton (19). In effect, the excess ligand, whether as acid or ester, was wasted.

Although the administration of either V or VI, given alone or with I, resulted in increased removal of skeletal plutonium, speculation on the mechanism of action of these esters seems inappropriate, particularly in view of the marginal effect produced. However, these esters are now being tested against other toxic metals, and one of the compounds (V) may be of interest for the decorporation of intracellularly deposited lead.

REFERENCES

(1) H. G. Brugsch, *J. Occup. Med.*, **7**, 394 (1965).

(2) "The Metabolism of Plutonium and Other Actinides," ICRP Publication 19, Pergamon, New York, N.Y., 1972, p. 40.

(3) Y. E. Rahman and A. Lindenbaum, *Radiat. Res.*, **24**, 575 (1964).

(4) G. Boocock, C. J. Danpure, D. S. Popplewell, and D. M. Taylor, *ibid.*, **42**, 381 (1970).

(5) V. H. Smith, *Health Phys.*, **22**, 765 (1972).

(6) D. W. Baxter, M. W. Rosenthal, and A. Lindenbaum, *Radiat. Res.*, **55**, 144 (1973).

(7) M. W. Rosenthal, A. Lindenbaum, D. W. Baxter, G. S. Kalesperis, E. S. Moretti, and J. J. Russell, *ibid.*, **63**, 253 (1975).

(8) A. Catsch and A. Harmuth-Hoene, *Biochem. Pharmacol.*, **24**, 1557 (1975).

(9) F. Bohne, A. Harmuth-Hoene, K. Kurzinger, and F. Havlicek, *Strahlentherapie*, **136**, 609 (1968).

(10) E. Stevens, B. Rosoff, M. Weiner, and H. Spencer, *Proc. Soc. Exp. Biol. Med.*, **111**, 235 (1962).

(11) J. F. Markley, *Int. J. Radiat. Biol.*, **7**, 405 (1963).

(12) Y. E. Rahman and B. J. Wright, *J. Cell Biol.*, **65**, 112 (1965).

(13) M. W. Rosenthal, Y. E. Rahman, E. S. Moretti, and E. A. Cerny, *Radiat. Res.*, **63**, 262 (1975).

(14) W. J. Lennon, U.S. pat. 3,497,535 (1970); through *Chem. Abstr.*, **72**, 120264x (1970).

(15) W. C. Eckelman, S. M. Karesh, and R. C. Reba, *J. Pharm. Sci.*, **64**, 704 (1975).

(16) J. R. Geigy, A.-G. French pat. 1,548,888 (1968); through *Chem. Abstr.*, **71**, 81380q (1969).

(17) A. Lindenbaum and W. Westfall, *Int. J. Appl. Radiat. Isotop.*, **16**, 545 (1965).

(18) A. Lindenbaum and M. A. Smyth, in "Organic Scintillators and Liquid Scintillation Counting," D. L. Horrocks and C. T. Peng, Eds., Academic, New York, N.Y., 1971.

(19) M. W. Rosenthal, J. J. Russell, E. S. Moretti, and A. Lindenbaum, *Health Phys.*, **16**, 806 (1969).

(20) W. E. Deming, "Some Theory of Sampling," Wiley, New York, N.Y., 1950.

ACKNOWLEDGMENTS

Supported by the U.S. Department of Energy.

The authors thank Mrs. E. S. Moretti and Mr. J. J. Russell for their expert assistance in the biological portions of these studies and Mr. Clinton Ainsworth for recording the NMR spectra.

Surface Chemistry of Colloidal Silica and a Possible Application to Stabilize Aspirin in Solid Matrixes

ASHOK Y. GORE * **and GILBERT S. BANKER** ˣ

Received December 1, 1977, from the *Department of Industrial and Physical Pharmacy, School of Pharmacy and Pharmacal Sciences, Purdue University, West Lafayette, IN 47907.* Accepted for publication July 21, 1978. *Present address: Pharmaceutical Technology Department, Squibb Institute for Medical Research, New Brunswick, NJ 08903.

Abstract □ The surface chemistry of colloidal silica was investigated in relation to its application as a stabilizer for a hydrolabile drug, aspirin, in tablets. Water vapor adsorption properties of the selected silicas were studied as a function of vapor pressure at 40°. Silica I, a precipitated colloidal form, exhibited a type IV adsorption isotherm, characteristic of multilayer adsorption with limited pore volume. Therefore, the Brunauer, Emmett, and Teller (BET) theory of multilayer adsorption was employed to quantify the monolayer capacity (X_m) and the specific surface area available for water vapor adsorption (S_w). The surface area and average particle diameter of I, determined by BET nitrogen adsorption, were 714.4 m^2/g and 3.8 nm, respectively. Silica I, which had the greatest moisture adsorption capacity, was then evaluated for its stabilizing effects on aspirin in tablet form. Since silica increased the tablet void space in proportion to its concentration, control (aspirin) and sample (aspirin–silica) tablets with controlled void space (held constant at 20%) were subjected to accelerated stability evaluation. In general, silica enhanced aspirin stability; a concentration of 3% offered maximum stabilization. Tablets with higher silica concentrations (up to 15%) showed poorer stability and approached the control tablets in aspirin content at the end of 120 days.

Keyphrases □ Silica, colloidal—surface chemistry, evaluated for stabilizing effect on aspirin in tablets □ Aspirin—stability in tablets, effect of colloidal silica □ Stability—aspirin in tablets, effect of colloidal silica □ Tablets—aspirin, effect of colloidal silica on stability □ Dosage forms—tablets, effect of colloidal silica on aspirin stability □ Analgesics—aspirin, effect of colloidal silica on stability in tablets

The hydrolytic decomposition of aspirin has been widely studied, especially in the last two decades. While some work concerned the kinetics of the hydrolytic degradation of aspirin in aqueous systems, much of the published work dealt with the stability of aspirin in tablets as influenced by various common excipients.

Aspirin hydrolysis in solid dosage forms can be considered to proceed in the microfilm of moisture at the surface of the aspirin particles. The hydrolysis rate is a function of the available water content, pH, and temperature. The higher the available moisture content, the more rapidly the hydrolysis proceeds. An increase in temperature greatly increases the rate of hydrolysis due to the increased rate constant governing the reaction and the increased amount of aspirin in solution. Furthermore, according to Martin (1), an increase in the surface area of aspirin apparently has no discernible effect on hydrolysis. In the absence of any substance in the tablet that affects the pH of the microenvironment, the aspirin dissolved in the moisture will have the pH at which aspirin exhibits maximum stability. The presence in the tablet of any substance that increases aspirin solubility or modifies the pH will increase the decomposition rate (1).

Byrn (2) suggested a possible mechanism for solid-state aspirin hydrolysis. At elevated temperatures in the presence of moisture, he theorized that the reaction takes place through solution of aspirin from the water vapor adsorbed and in contact with the aspirin surface. The sublimation of salicylic acid observed on the surface of aspirin tablets under stress conditions (3) suggests that other factors than those operating in a pure solution theory must be operable, since it seems unlikely that salicylic acid would sublime out of an aqueous solution. It also was suggested that the degradation reaction may be affected by the dissolution of aspirin in acetic acid as it forms, depending on the rates at which acetic acid volatilizes and is formed by hydrolysis (2).

Colloidal silicas are well known for their large surface area and highly polar silanol surface favorable for water vapor adsorption. Such materials possess a high moisture adsorption capacity and, therefore, are commonly used as desiccants to protect hygroscopic chemicals and pharmaceuticals from atmospheric moisture. Their structural and physicochemical characteristics suggested a possible application for these agents as stabilizers for hydrolabile drugs in solid dosage systems by their acting as local moisture scavengers and by their adsorbing the free moisture within the tablet micropores, rendering it unavailable for interaction with the drug molecules.

The primary objective of this research was to study the moisture adsorption properties and mechanisms of selected silicas, followed by an evaluation of their stabilizing effect for a model hydrolabile drug, aspirin, in solid dosage forms under selected experimental conditions.

EXPERIMENTAL

Surface Chemistry of Colloidal Silicas—An experimental colloidal silica, I[1], and two other commercially available silicas, II[2] (a precipitated silica) and III[3] (a pyrogenically fumed silica), were investigated for their water vapor adsorption properties at selected vapor pressure conditions at 40°.

An adsorption isotherm was established for each material by subjecting a known weight of a preconditioned sample to an atmosphere equilibrated at a selected vapor pressure corresponding to a relative humidity (RH) between 0 and 100%. The amount of moisture adsorbed per gram of silica was thus determined from the total gain in sample weight at the time of equilibrium. This process was then repeated for another preconditioned sample of the same material by subjecting it to the next higher vapor pressure. In this manner, the moisture adsorption data were generated for the entire vapor pressure range at the selected temperature condition, and an adsorption isotherm was constructed by plotting the values of the equilibrium moisture adsorption against the corresponding vapor pressure conditions (Fig. 1).

Apparatus—An electrobalance[4] in conjunction with a recorder[5] was employed to monitor continuously the weight gain of the sample exposed to the selected vapor pressure and temperature conditions. The balance chamber containing the weighing assembly was placed inside an incubator oven[6] maintained at 40 ± 1.0°. The chamber was made air tight, and the selected vapor pressure condition was maintained by inclusion of a suitable saturated salt solution.

[1] Lubrisilk, supplied by Robertshaw Chemical Corp., Phoenix, Ariz.
[2] "Quso" F-2, Philadelphia Quartz Co., Philadelphia, Pa.
[3] "Cabosil" M-5, Cabot Corp., Boston, Mass.
[4] RG, Cahn Instruments Co., Paramount, Calif.
[5] SR, E. H. Sargent and Co., Chicago, Ill.
[6] Thelco, Precision Scientific Co., Evanston, Ill.

0022-3549/79/0200-0197$01.00/0
© 1979, American Pharmaceutical Association

Table I—Control and Sample [a] Tablet Formulations Used in the Stability Study

Tablet Formulation	Aspirin–I Ratio	Weight, mg/tablet		
		Aspirin	I	Starch
Control A (no starch)	100:0	460.0	0.0	0.0
Control B (5% starch)	100:0	460.0	0.0	23.0
Sample 1	99:1	455.4	4.6	23.0
Sample 2	97:3	446.2	13.8	23.0
Sample 3	95:5	437.0	23.0	23.0
Sample 4	90:10	414.0	46.0	23.0
Sample 5	85:15	391.0	69.0	23.0

[a] The sample tablets contained 5% starch equilibrated at 40°. The equilibrated starch contained 5.5% moisture by weight.

The control unit of the electrobalance and the recorder were located outside the oven. The mechanical operation of the electrobalance was not affected by the selected humidity and temperature conditions, as verified during preliminary tests. The change in sample weight, due to adsorption of water vapor, was recorded until an equilibrium was reached under each environmental condition.

Colloidal silicas (such as I) with an active silanol surface desorb any physically bound moisture substantially completely on exposure to temperatures above 110° over 1–2 hr (4, 5). In these experiments, exposure of I to 150° for 2 hr was adequate to ensure complete desorption of the physically bound moisture without alteration of the surface characteristics. Therefore, silica samples used in the adsorption study and later in the preparation of tablets were preconditioned by drying under these conditions to desorb any moisture bound physically under ambient storage.

A known weight of the sample, at room temperature, was transferred to the weighing chamber, which was preequilibrated at the selected vapor pressure condition overnight. The electrobalance was precalibrated for the estimated change in sample weight, and the gain in sample weight was continuously recorded over 3–4 hr or until the sample reached equilibrium. An average of three replicates thus represented the equilibrium weight gain for each material at each vapor pressure level.

Saturated solutions of various salts in contact with an excess of their solid phase (6, 7) were employed to achieve the vapor pressure conditions corresponding to 20–100% RH. For humidity conditions below 20%, appropriate concentrations of sodium hydroxide solutions were used (8). Moisture adsorption properties of aspirin powder USP also were investigated under identical experimental conditions, and equilibrium weights were recorded over the entire vapor pressure range at 40°.

Preparation and Porosity Determination of Aspirin–Silica Tablets—Control (aspirin) and sample (aspirin–I) tablets were prepared according to the formulations listed in Table I. Based on the results of the moisture adsorption study, I, having superior moisture adsorption properties, was chosen for the stability study of aspirin tablets. The ingredients for a batch of about 50 tablets of each formulation were thoroughly mixed in a small laboratory mixer and stored in a vacuum desiccator until ready for compression. The tablets were compressed on a hydraulic press[7] with an 11-mm flat-faced punch and die set.

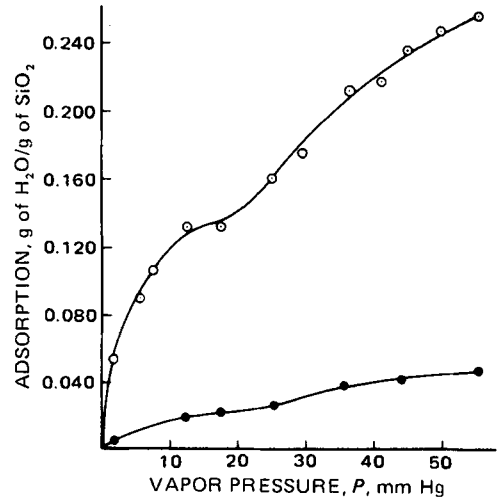

Figure 1—*Adsorption isotherms of I (○) and II (●) at 40°.*

Table II—Compression Conditions, Tablet Thickness, Tablet Hardness, and Percent Void Volume for Various Tablet Formulations

Tablet Formulation[a], Aspirin–I Ratio	Compression Conditions		Tablet Hardness[b], kg	Tablet Thickness[c], mm	Percent Void Volume
	Force, kg	Seconds			
Control A, 100:0	227	1	1.8	3.89	19.66
Control B, 100:0	272	1	1.6	4.10	19.84
Sample 1, 99:1	272	1	4.5	4.06	19.60
Sample 2, 97:3	318	2	6.0	4.04	19.66
Sample 3, 95:5	364	4–5	8.4	4.01	19.52
Sample 4, 90:10	864	3–4	10.6	3.94	19.27
Sample 5, 85:15	1136	12–13	14.9	3.89	19.60

[a] All tablet formulations except Control A contained preequilibrated starch at 5% of the total aspirin–silica content. [b] Average value for five tablets. Measurements were made using the Pfizer hardness tester. [c] Thickness variability was within ± 0.025 mm of the reported mean values.

Initially, tablets of each formulation (Table I) were compressed to a constant hardness using appropriate loading force and time combinations. Porosity (percent void space) determinations were made on each set of tablets by using a method reported earlier (9, 10). This method involved a determination of apparent tablet volume from tablet dimensions measured with a micrometer. The volume occupied by each ingredient in the tablet was estimated from the known values of its weight and true density. The latter values for the three tablet components were obtained by the pycnometer method with petroleum ether as a nonsolvent medium.

Since the porosity determinations on aspirin–I tablets compressed to constant hardness indicated porosity increasing with silica content, it was considered necessary to hold the porosity constant at a selected level to eliminate its effect on the evaluation of aspirin stability. Therefore, the tablets used in the stability study were compressed to a constant porosity by controlling the tablet thickness (and, thus, the tablet volume), using the predetermined values of compression force and loading time for a particular composition. The selected compression conditions and the resultant tablet properties are listed in Table II.

The tablet void space as influenced by the I content also was investigated under constant compression conditions. The sample tablets containing aspirin and I in differing ratios of 3–15% silica content were compressed on the hydraulic press, using a compression force of 454 kg and a compression time of 5 sec. Tablet thickness was determined by means of a thickness gauge[8], and the percent void space was determined by the method described earlier.

The tablets containing 100% aspirin and various combinations of aspirin and I showed poor disintegration properties. Therefore, all test formulations for the stability study were modified to contain 5% corn starch USP to achieve a disintegration time within USP limits. A formulation containing aspirin alone also was included as a primary control in the stability program to determine if the hygroscopic nature of starch interfered with the adsorption properties of silica and, consequently, aspirin stability. The starch powder used was preconditioned to limit its moisture content to an equilibrium level of 5.5%.

Stability Evaluation of Aspirin–Silica Tablets—The stability study was conducted under the conditions of a continuous moisture supply at an elevated temperature (82% RH at 40°). The test samples were placed in a desiccator preequilibrated at 82% RH with a saturated solution of potassium chloride and stored in an incubator oven set for 40°. During the initial period, the gain in weight of the tablets was monitored every 2 hr through the first 12 hr, followed by weighings every 12 hr for 4 days.

Control and sample tablets then were assayed for residual aspirin content at various time intervals during the test period of 120 days by the method reported earlier (3). This method essentially involves simultaneous spectral determination of aspirin and salicylic acid, the hydrolytic degradation product, in a pH 7.4 buffer solution at 262 and 296.5 nm, respectively. The method was modified to exclude the insoluble silica particles from the final dilution before the spectrophotometric measurements. Appropriate corrections for the increased tablet weight due

[7] Fred S. Carver and Co., Summit, N.J.
[8] B. C. Ames Co., Waltham, Mass.

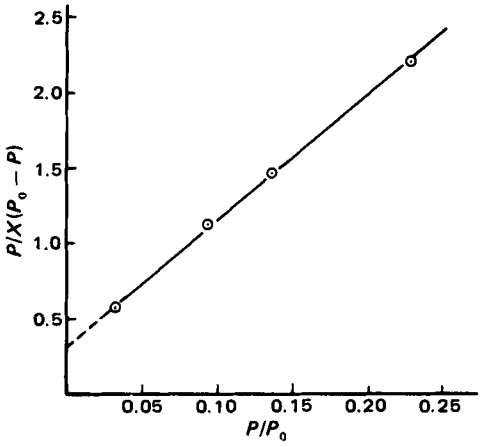

Figure 2—*BET plot for water vapor adsorption isotherm for I at 40°.*

to moisture sorption were made before the residual aspirin content per tablet was determined.

RESULTS

Adsorption Properties of Silicas—Adsorption isotherms, constructed from the data generated in the moisture adsorption study of I and II, are presented in Fig. 1. The isotherm for I showed a close resemblance to the type IV isotherm, typical of adsorbents with limited pore volume and multilayer adsorption. Therefore, the data from the I isotherm were treated according to the Brunauer, Emmett, and Teller (BET) theory of multilayer adsorption to quantify the monomolecular layer capacity (X_m) and the specific surface area (S_w) for I (11–13). This calculation is represented by the equation:

$$\frac{P}{X(P_0 - P)} = \frac{1}{X_m C} + \left(\frac{C-1}{X_m C}\right)\left(\frac{P}{P_0}\right) \qquad \text{(Eq. 1)}$$

where P is the vapor pressure of the adsorbate at the temperature of the experiment, P_0 is the saturation vapor pressure at that temperature, X is the quantity of adsorbate (water) adsorbed per gram of adsorbent, X_m is the quantity of adsorbate required for completion of the monolayer, and C is a constant dependent on the difference between the heat of adsorption for the completion of the monolayer (E_m) and the heat of condensation of successive layers (E_L) and is expressed by the equation:

$$C = e^{(E_m - E_L)/RT} \qquad \text{(Eq. 2)}$$

where R is the gas constant and T is the absolute temperature.

A BET plot of $P/[X(P_0 - P)]$ as a function of P/P_0 yields a straight line, with the slope being equal to $(C-1)/X_mC$ and the y-intercept equal to $1/X_mC$ (Fig. 2). This plot was linear up to a value for P/P_0 (*i.e.*, relative vapor pressure) equal to 0.25, corresponding to the vapor pressure at which the monomolecular layer had been completed. The location of this monolayer depends on the value of C and, therefore, on the heat of adsorption. The slope and y-intercept of the linear portion of this curve were used to calculate the values of X_m and C. From the value of C, the quantity $(E_m - E_L)$, defined earlier, was calculated.

The specific surface area of the adsorbent (S_w) available for adsorption of water vapor as a monolayer can be calculated from a knowledge of X_m and A_m, the area of a single closely packed adsorbate (water) molecule adsorbed in the monolayer, using the following equation (13, 14):

$$S_w = \frac{X_m N A_m}{M/\rho} \qquad \text{(Eq. 3)}$$

where N is Avogadro's number and M/ρ is the molar specific volume of the adsorbate (22,400 ml/mole at standard temperature and pressure).

The value of A_m for water molecules adsorbed on the surface of silica may be calculated from the knowledge of the molecular weight of water (M) and its density in the adsorbed state at the temperature of the experiment (ρ), as given by the relationship (15):

$$A_m = 1.091\left[\frac{M}{N\rho}\right]^{2/3} \qquad \text{(Eq. 4)}$$

The coefficient 1.091 is the appropriate packing factor and involves two assumptions: (*a*) the adsorbate molecules are held in a two-dimensional packing arrangement on the surface, and (*b*) the area occupied by each molecule is the projected cross section of the molecular volume calculated from the density of the condensed adsorbate (12).

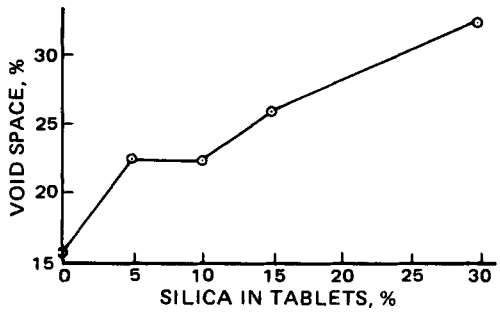

Figure 3—*Percent void space as a function of percent I in tablets of constant hardness (5.5 kg).*

Since the silica surface is covered with silanol groups, the water molecules are adsorbed on the surface through hydrogen bonding. If it is assumed that each water molecule adsorbed on the surface of the silica is held by one hydroxyl group, leading to a closely packed arrangement, and that the adsorbed water is in a liquid state, the value of A_m = 10.6 Å^2 as calculated from Eq. 4 should be accurate.

With this value for A_m, the specific surface area (S_w) for water vapor adsorption was calculated from Eq. 3. The surface area for I calculated from BET nitrogen adsorption data[9] was used to calculate the mean volume surface diameter (d_{vs}) from the relationship (14):

$$d_{vs} = \frac{6}{\rho_s S_w} \qquad \text{(Eq. 5)}$$

where ρ_s is the true density of I. The value of d_{vs} thus calculated was 3.82 nm.

The isotherm for II (Fig. 1) indicates inferior moisture adsorption properties as compared to I at identical vapor pressure conditions. Silica III, a pyrogenic fumed silica, showed little or no moisture adsorption even under saturation vapor pressure conditions and, therefore, is not presented in Fig. 1. The adsorption properties of aspirin, when investigated under identical conditions, also showed no evidence of moisture adsorption at saturation vapor pressure (P/P_0 = 1.0), thus indicating that aspirin has no physical affinity for moisture, although it undergoes hydrolytic degradation at ambient temperature conditions.

On the basis of these results, I was chosen for the study of stabilizing properties for a moisture-sensitive drug (aspirin) in tablet dosage form.

Determination of Tablet Porosity and Effect of Silica on Tablet Voids—Tablets of selected formulations (Table I), compressed to a constant hardness, were evaluated for their total void space by a method described previously (9, 10).

The percent void volume (*i.e.*, porosity), defined as the percent of total volume (V_{tablet}) occupied by the void space (V_v), is given by:

$$\%\ \text{voids} = \left(\frac{V_v}{V_{tablet}}\right) 100 \qquad \text{(Eq. 6)}$$

The volume occupied by the voids is obtained by subtracting the calculated volume occupied by each ingredient within the tablet from the total tablet volume, determined by dimensional measurements.

For the tablet formulations under study, this value of V_v is given by:

$$V_v = V_{tablet} - (V_{aspirin} + V_{silica} + V_{starch}) \qquad \text{(Eq. 7}a\text{)}$$

or:

$$V_v = V_{tablet} - \left[\frac{W_{aspirin}}{\rho_{aspirin}} + \frac{W_{silica}}{\rho_{silica}} + \frac{W_{starch}}{\rho_{starch}}\right] \qquad \text{(Eq. 7}b\text{)}$$

where W and ρ stand for the weight and true density for the components, respectively.

In Fig. 3, the percent void space is plotted against the silica content for tablets having equal hardness. This plot illustrates that I significantly increased the tablet void space. The contributions made by the two tablet components to the tablet void space are illustrated in Fig. 4, which shows

[9] The surface area by BET nitrogen adsorption was determined by the American Instruments Co., Silver Spring, Md., using a model 4-4680 adsorptomat.

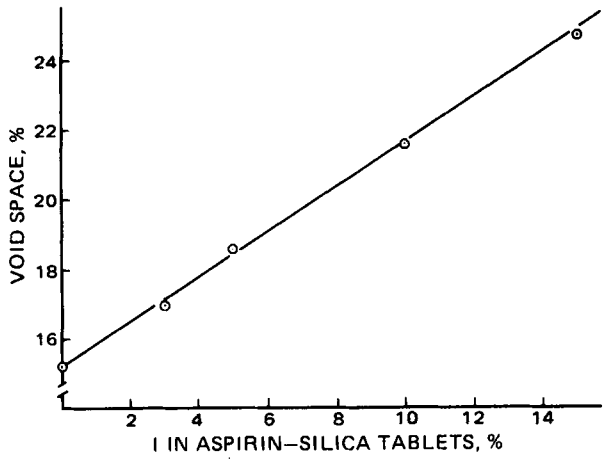

Figure 4—*Percent void space as a function of percent I in aspirin–I tablets under constant compression conditions.*

the relationship between the percent void space and the silica content of tablets compressed under constant compressional forces. A positive linear relationship and a positive y-intercept suggest that the void space contributed by I, on a unit weight basis, remains constant over the range of 0–15% silica content. The relative contributions made by each of the two ingredients to the total void space is estimated from Fig. 5, which represents a plot of the apparent specific volume, *i.e.*, the reciprocal of apparent tablet density, as a function of the weight fraction of silica in the tablets. Equation 8 describes this relationship:

$$\overline{V}_{tablet} = \overline{V}_{aspirin} + m W_{silica} \qquad \text{(Eq. 8)}$$

where $\overline{V}_{tablet}$ and $\overline{V}_{aspirin}$ are the specific volumes of the tablets under test and of tablets containing 100% aspirin, respectively; W_{silica} stands for the weight fraction of silica; and m is the slope of the line (being equal to the difference between the values of $\overline{V}_{silica}$ and $\overline{V}_{aspirin}$). The linearity of this plot suggests that the specific volumes of 100% aspirin and 100% silica tablets remain constant over the range of tablet compositions studied. Since it was not possible to compress tablets containing 100% silica under identical compressional conditions, the value of $\overline{V}_{silica}$ is obtained by extrapolating the line to the right y-intercept or by calculating from the slope.

If reciprocals of true densities of aspirin and silica in their pure crystalline states (*i.e.*, with zero porosity) represent their specific volumes in that state, then the difference between their respective specific volumes of tablet and crystalline states should represent their volume contributions to the void space in a tablet form. The values of $\overline{V}_{void}$ calculated in this manner for aspirin and silica are presented in Table III. These values only represent the data for the set of compressional conditions used in this study and will vary with changes in compressional load.

These data suggest that I increased the tablet void spaces in aspirin–silica tablets to an extent of nearly 600% of that produced by aspirin on an equal weight basis. These results may be explained in terms of the size and geometry of the particles. The needle-shaped aspirin particles, although larger, apparently can pack more tightly than the spherical silica particles. The irregularity of aspirin particles, possibly their deformability

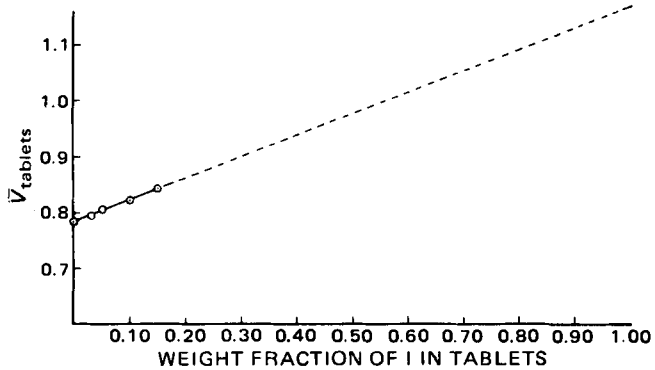

Figure 5—*Specific volume of the tablets as a function of the weight fraction of I in aspirin–I tablets.*

Table III—Specific Volumes of Aspirin and I in Powder and Tablet Form

Component	$\overline{V}_{powder}$, ml/g	$\overline{V}_{tablet}$, ml/g	$\overline{V}_{voids} = \overline{V}_{tablet} - \overline{V}_{powder}$, ml/g
Aspirin powder USP	0.6680	0.7863	0.1183
Silica I	0.4566	1.1700	0.7134

and particle-size distribution, may allow for the interstitial spaces to be filled in a relatively more efficient manner than the nearly spherical and more rigid silica particles with their very narrow size distribution.

Thus, the variable tablet void space as influenced by the silica content could conceivably interfere with an evaluation for any potential stabilizing effect silica may have in aspirin tablets due to variable pore spaces available for water vapor penetration. This possibility necessitated controlling the void space to a constant level of 20% for all aspirin–silica formulations under stability evaluation.

Moisture Sorption by Aspirin–Silica Tablets—The moisture sorption properties of the control and sample tablets subjected to the selected storage conditions (82% RH at 40°) were monitored during the initial test period (Fig. 6). These plots show increasing moisture sorption by the tablets with increased silica content. The tablets containing 0–5% silica adsorbed moisture to their full capacity within the first 8–10 hr, whereas those containing 10 and 15% silica required 24 hr or longer to reach equilibrium. No substantial gain or loss in weight was observed on further exposure up to 72 hr. The control tablets (Formulations A and B) showed no significant weight change over 72 hr. (Formulation B is not presented in Fig. 6.)

Stability of Aspirin–Silica Tablet Systems—The control and sample tablets of the selected formulations (Table I) subjected to the stability study were assayed (3) at selected time intervals for residual aspirin content. The overall variability in the aspirin content for each tablet formulation at a given time was within ±0.5% (Fig. 7). These results clearly demonstrate the stabilizing effect of I, with improved aspirin stability being apparent in tablets containing 1–5% silica as compared to the control tablets. Both controls, with and without starch, showed comparable stability curves.

The decomposition of aspirin in tablets containing 10 and 15% silica, although initially less than that of the control tablets, reached the levels of control tablets by the end of the 120-day test period. The data also indicate that a 3% concentration probably offers maximum aspirin stabilization in these formulations. This conclusion is further demonstrated in Fig. 8, where data are presented as a function of the silica concentration at the end of 30, 60, and 120 days.

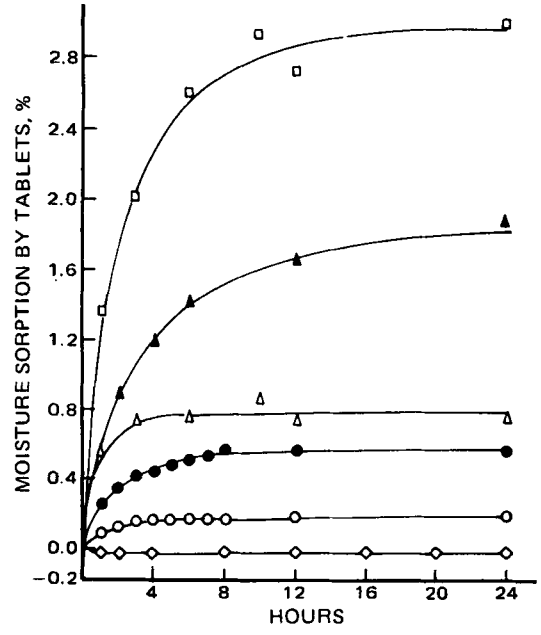

Figure 6—*Percent moisture sorption as a function of time for aspirin and aspirin–I tablets. Key (Formulations in Table I): ◇, A; ○, 1; ●, 2; △, 3; ▲, 4; and □, 5.*

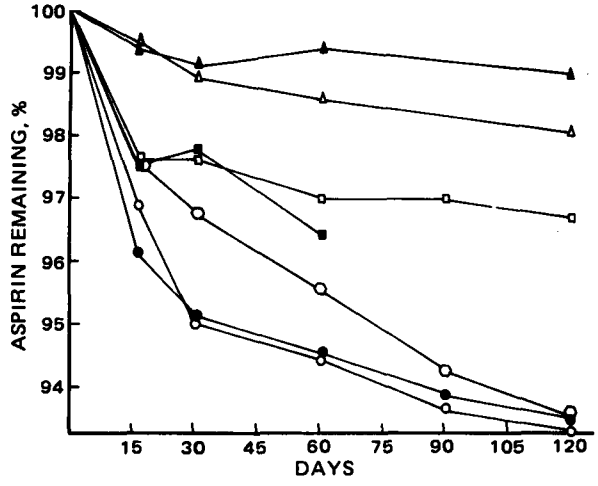

Figure 7—*Stability curves for aspirin in aspirin–I tablets under storage at 81.7% RH and 40°. Key (Formulations in Table I): ○, A; ●, B; △, 1; ▲, 2; □, 3; ■, 4; and ○, 5.*

DISCUSSION

Surface Properties of Silicas—The surface characteristics of I obtained from adsorption isotherm studies are: X_m (monolayer capacity for water vapor adsorption), 0.115 ml of liquid water/g of I; $(E_m - E_L)$, 2.002 kcal/mole of water; S_w (specific surface for water vapor adsorption), 3276 cm^2/g of I; S_w (specific surface from nitrogen adsorption), 714.4 m^2/g of I; and d_{vs} (mean volume surface diameter from nitrogen adsorption), 3.82 nm.

The results for the adsorption of water vapor and nitrogen appear to agree with results reported earlier. Sing and Madeley (16, 17), in a study of the surface properties of certain commercial and laboratory-made silica gels, observed that the value of X_m varied between 0.04 and 0.18 ml/g, depending on the type and method of preparation of the silica gels. The S_w values obtained from nitrogen adsorption isotherms varied within a range of 530–750 m^2/g. Brunauer *et al.* (11), in their original work on the adsorption isotherms of various gases on different adsorbents, reported X_m and S_w values for silica gels to be within 116.2–127.9 ml/g and 534–560 m^2/g, respectively. The specific surface and monolayer capacity of I determined in this study are in agreement with those reported previously.

Based on these results and those of earlier workers, a general hypothesis can be built to suggest a structural configuration of hydrated silica. A finding that the monolayer capacity for water vapor adsorption is significantly lower than that for nitrogen adsorption suggests that the polar water molecules are adsorbed at specific sites on the silica surface. The adsorption of nitrogen gas on the surface of silica gel probably leads to

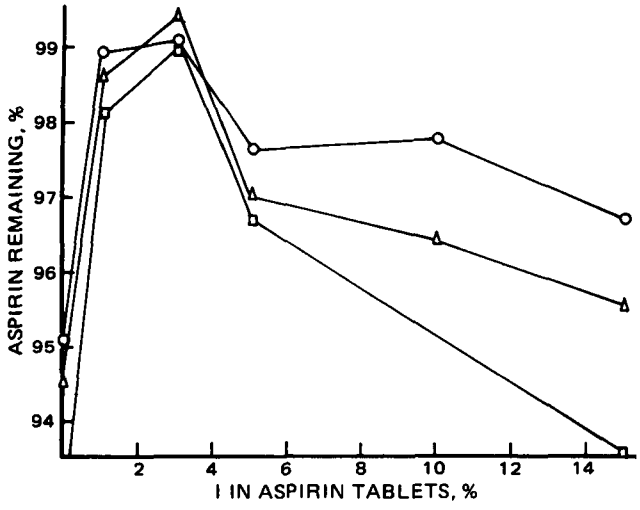

Figure 8—*Percent aspirin remaining as a function of percent I content of tablets at the end of 30 (○), 60 (△), and 120 (□) days of storage at 81.7% RH and 40°.*

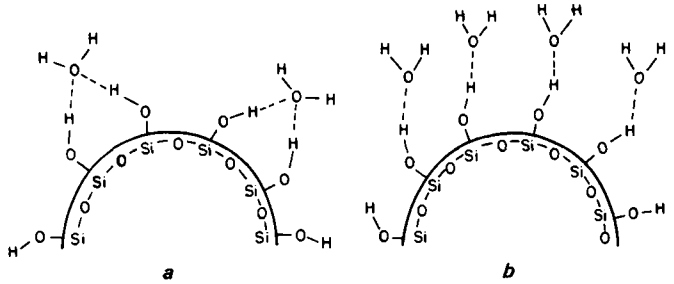

Figure 9—*Two suggested concepts for the adsorption of water on the hydrated surface of I.*

the formation of a continuous monomolecular film and, hence, yields a much higher X_m value. The adsorption of water molecules at the silica surface is thought to be due to hydrogen bonding between the hydrogen of the silanol group and the oxygen of the water molecules, thus leading to adsorption only at silanol sites (4).

Two different theoretical concepts (Fig. 9) were proposed for the adsorption of water vapor on a silica surface. One view (4) implies that adsorption of water and alcohols on the surface of silica may be regarded as a special case since either chemisorption or physisorption may occur, depending on the degree of surface hydration of the silica. This concept (Fig. 9*a*) proposes that a single water molecule is adsorbed by hydrogen bonding to two neighboring silanol groups. If this bonding occurs, a considerably smaller volume of water vapor would suffice for the completion of the monolayer.

According to the second hypothesis (5), the binding of water to the silanol groups on the silica surface in a unimolecular film is in a ratio of 1:1 instead of 1:2, as proposed by Hockey (4) (Fig. 9*b*). Zhdanov (18) quantitatively estimated how surface dehydration affects the adsorption of polar water molecules. Subjecting silica to high temperatures of 600–800° leads to dehydration of silanol groups to siloxane groups. Accordingly, for every silanol group lost from the silica surface, one less water molecule is adsorbed in the monolayer.

However, the data presented in this study are insufficient to suggest which of the two concepts describes the adsorption properties of I.

Stability Evaluation of Aspirin–Silica Tablets—The results of the stability study (Figs. 7 and 8) indicate that the desiccant effect of silica is not the only factor that helps stabilize aspirin in these formulations. The precise mechanism by which this effect occurs is not based on simple retention of water vapor by silica to limit its access to aspirin particles *per se* but probably involves a complex of considerations such as: (*a*) the state of equilibrium between the bound and free water within the microporous structure of the tablets, (*b*) changes in the tablet structure that affect the pore size distribution, and (*c*) the occlusion of pores by silica-bound water or by partial deposition of sublimed salicylic acid on the surfaces of aspirin or silica particles (3, 19).

These phenomena could be explained further by the following hypothesis. Within the micropores of the tablets, the water remaining in association with silica mainly consists of strongly bound water directly bound to the silanol groups in the monolayer and, possibly, in some successive layers. This water probably exists in a polarized oriented form because of its permanent dipole. However, receding from the silica surface, the state of water progressively reaches "liquid water," which is essentially free water, available for the hydrolytic degradation of aspirin.

In a situation of limited moisture supply, an equilibrium is established between the bound and free water within the tablet, and thus, silica effectively stabilizes aspirin after the free moisture within the tablet reaches a negligible level. However, with an essentially unlimited moisture supply, as in the present study, the silica must also limit the access of water to aspirin and/or prevent the release of degradation products. Consequently, the hydrolytic reaction could approach equilibrium and also be diffusion rate limited due to an inability of water to reach the tablet interior. The "strongly bound water" itself may perform this function through occlusion of the tablet pores. However, the possibility of pore occlusion by the subliming salicylic acid cannot be overlooked.

To define these mechanisms, a subsequent study (19) involved the determination of the pore size distribution of aspirin–silica tablets by mercury intrusion porosimetry. The results (19) revealed that, at lower concentrations, silica functioned primarily to reduce the size and volume of coarse pores, presumably representing the spaces between the aggregates of the starch and aspirin particles. This effect was optimum at a concentration of 3% silica, which was also the optimum level of aspirin

stabilization in the present study. At this level, the tablets consistently exhibited the smallest average pore size irrespective of the relative changes in the size and volume of pores resulting from the swelling of starch grains or deposition of salicylic acid in the tablet pores. The role played by subliming salicylic acid and its contribution to the occlusion of the micropores were also evident in this study from the reduction in pore volumes and the size of the pores with increased periods of exposure to water vapor.

SUMMARY AND CONCLUSIONS

Silica I was studied with respect to its physicochemical and surface properties and its ability to stabilize a hydrolabile drug (aspirin) in tablet matrixes. The major findings of the investigation were:

1. Silica I exhibited an adsorption behavior characteristic of adsorbents with limited pore volume. The monolayer capacity and the specific surface area, determined by both water vapor and nitrogen adsorption isotherms employing the BET theory of multilayer adsorption, revealed the superior moisture adsorption capacity of I as compared to the other silicas tested.

2. The void volume of aspirin–silica tablets compressed under constant compressional force was proportional to the silica content of the tablets. Silica contributed approximately six times as much to the void volume as did aspirin on an equal weight basis. Therefore, it was necessary to control the void space of the tablets to eliminate the effect of the void volume variable in the interpretation of stability data.

3. The stability of aspirin tablets containing I at concentration levels of 0–15% was investigated under storage conditions of a continuous moisture supply (82% RH) at 40°. At the end of 120 days, tablets containing up to 5% I exhibited improved aspirin stability in comparison to control tablets. An optimum concentration of 3% silica, however, showed maximum stabilization; the tablets containing 10 and 15% silica showed progressively poorer stability, approaching that of the control tablets at the end of 120 days.

4. Silica I, with superior moisture adsorption properties, proved to be of significant value in enhancing the stability of the hydrolabile test drug (aspirin) by acting as an internal moisture scavenger. This study also demonstrated the importance of controlling the tablet void space in studies involving stability evaluation of drugs prone to moisture hydrolysis in solid drug dosage systems.

REFERENCES

(1) B. K. Martin, in "Advances in Pharmaceutical Sciences," vol. 3, H. S. Bean, A. H. Beckett, and J. E. Carless, Eds., Academic, London, England, 1971, p. 107.

(2) S. R. Byrn, *J. Pharm. Sci.*, **65**, 1 (1976).

(3) A. Y. Gore, K. B. Naik, D. O. Kildsig, G. E. Peck, V. F. Smolen, and G. S. Banker, *ibid.*, **57**, 1850 (1968).

(4) J. A. Hockey, *Chem. Ind. (London)*, **Jan. 9, 1965**, 57.

(5) R. K. Iler, "The Colloid Chemistry of Silica and Silicates," Cornell University Press, Ithaca, N.Y., 1955, pp. 87, 158, 233.

(6) D. S. Carr and B. L. Harris, *Ind. Eng. Chem.*, **41**, 2014 (1949).

(7) R. H. Stokes and R. Robinson, *ibid.*, **41**, 2013 (1949).

(8) "International Critical Tables," 1st ed., vol. III, McGraw-Hill, New York, N.Y., 1928, p. 270.

(9) N. R. Patel and R. E. Hopponen, *J. Pharm. Sci.*, **55**, 1065 (1966).

(10) I. Ingram and W. Lowenthal, *ibid.*, **57**, 393 (1968).

(11) S. Brunauer, P. H. Emmett, and E. Teller, *J. Am. Chem. Soc.*, **60**, 309 (1938).

(12) L. E. Osipow, "Surface Chemistry, Theory and Industrial Applications," Reinhold, New York, N.Y., 1962, p. 26.

(13) S. J. Gregg, "The Surface Chemistry of Solids," 2nd ed., Reinhold, New York, N.Y., 1961, p. 48.

(14) A. N. Martin, J. Swarbrick, and A. Cammarata, "Physical Pharmacy," 2nd ed., Lea & Febiger, Philadelphia, Pa., 1970, p. 482.

(15) P. H. Emmett and S. Brunauer, *J. Am. Chem. Soc.*, **59**, 1553 (1937).

(16) K. S. W. Sing and J. D. Madeley, *J. Appl. Chem.*, **3**, 549 (1953).

(17) *Ibid.*, **4**, 365 (1954).

(18) S. P. Zhdanov, *Dokl. Akad. Nauk, USSR*, **68**, 99 (1949).

(19) H. Gucluyildiz, G. S. Banker, and G. E. Peck, *J. Pharm. Sci.*, **66**, 407 (1977).

ACKNOWLEDGMENTS

Presented at the Industrial Pharmaceutical Technology Section, APhA Academy of Pharmaceutical Sciences, Phoenix meeting, November 1977.

Abstracted in part from a dissertation submitted by A. Y. Gore to Purdue University in partial fulfillment of the Doctor of Philosophy degree requirements.

Supported in part by a research grant from Robertshaw Chemical Corp., Phoenix, Ariz.

Metal-Binding Abilities of Radioprotective Aminoalkyl Disulfides and Thiosulfates

WILLIAM O. FOYE ˣ and JEE-MIN HU

Received June 7, 1978, from the *Samuel M. Best Research Laboratory, Massachusetts College of Pharmacy, Boston, MA 02115.* Accepted for publication July 13, 1978.

Abstract □ Metal-binding stability constants for several heterocyclic aminoalkyl disulfides and thiosulfates with Ni(II) and Al(III) were determined. The data obtained indicated that both classes of compounds were acting as bidentate chelating agents and that the heterocyclic rings apparently prevented tridentate behavior of the disulfides because of steric hindrance. The magnitude of the constants indicated that metal complexes of these compounds could exist in a cellular environment, but no correlation with radiation-protective activity was apparent.

Keyphrases □ Disulfides, aminoalkyl—metal-binding stability constants determined, relation to radiation-protective activity □ Thiosulfates, aminoalkyl—metal-binding stability constants determined, relation to radiation-protective activity □ Metal binding—stability constants determined for various aminoalkyl disulfides and thiosulfates, relation to radiation-protective activity □ Binding, metal—stability constants determined for various aminoalkyl disulfides and thiosulfates, relation to radiation-protective activity □ Radiation-protective activity—various aminoalkyl disulfides and thiosulfates, relation to metal-binding stability constants

Aminoalkyl disulfides and thiosulfates have strong radiation-protective properties in animals (1, 2). The fact that the protective compounds all have a two- or three-carbon distance between the amino and sulfur functions, which confers potential metal-chelating ability to them, suggests that metal binding may be important in their

0022-3549/79/0200-0202$01.00/0

© 1979, American Pharmaceutical Association

stabilization in the present study. At this level, the tablets consistently exhibited the smallest average pore size irrespective of the relative changes in the size and volume of pores resulting from the swelling of starch grains or deposition of salicylic acid in the tablet pores. The role played by subliming salicylic acid and its contribution to the occlusion of the micropores were also evident in this study from the reduction in pore volumes and the size of the pores with increased periods of exposure to water vapor.

SUMMARY AND CONCLUSIONS

Silica I was studied with respect to its physicochemical and surface properties and its ability to stabilize a hydrolabile drug (aspirin) in tablet matrixes. The major findings of the investigation were:

1. Silica I exhibited an adsorption behavior characteristic of adsorbents with limited pore volume. The monolayer capacity and the specific surface area, determined by both water vapor and nitrogen adsorption isotherms employing the BET theory of multilayer adsorption, revealed the superior moisture adsorption capacity of I as compared to the other silicas tested.

2. The void volume of aspirin–silica tablets compressed under constant compressional force was proportional to the silica content of the tablets. Silica contributed approximately six times as much to the void volume as did aspirin on an equal weight basis. Therefore, it was necessary to control the void space of the tablets to eliminate the effect of the void volume variable in the interpretation of stability data.

3. The stability of aspirin tablets containing I at concentration levels of 0–15% was investigated under storage conditions of a continuous moisture supply (82% RH) at 40°. At the end of 120 days, tablets containing up to 5% I exhibited improved aspirin stability in comparison to control tablets. An optimum concentration of 3% silica, however, showed maximum stabilization; the tablets containing 10 and 15% silica showed progressively poorer stability, approaching that of the control tablets at the end of 120 days.

4. Silica I, with superior moisture adsorption properties, proved to be of significant value in enhancing the stability of the hydrolabile test drug (aspirin) by acting as an internal moisture scavenger. This study also demonstrated the importance of controlling the tablet void space in studies involving stability evaluation of drugs prone to moisture hydrolysis in solid drug dosage systems.

REFERENCES

(1) B. K. Martin, in "Advances in Pharmaceutical Sciences," vol. 3, H. S. Bean, A. H. Beckett, and J. E. Carless, Eds., Academic, London, England, 1971, p. 107.

(2) S. R. Byrn, *J. Pharm. Sci.*, **65**, 1 (1976).

(3) A. Y. Gore, K. B. Naik, D. O. Kildsig, G. E. Peck, V. F. Smolen, and G. S. Banker, *ibid.*, **57**, 1850 (1968).

(4) J. A. Hockey, *Chem. Ind. (London)*, **Jan. 9, 1965**, 57.

(5) R. K. Iler, "The Colloid Chemistry of Silica and Silicates," Cornell University Press, Ithaca, N.Y., 1955, pp. 87, 158, 233.

(6) D. S. Carr and B. L. Harris, *Ind. Eng. Chem.*, **41**, 2014 (1949).

(7) R. H. Stokes and R. Robinson, *ibid.*, **41**, 2013 (1949).

(8) "International Critical Tables," 1st ed., vol. III, McGraw-Hill, New York, N.Y., 1928, p. 270.

(9) N. R. Patel and R. E. Hopponen, *J. Pharm. Sci.*, **55**, 1065 (1966).

(10) I. Ingram and W. Lowenthal, *ibid.*, **57**, 393 (1968).

(11) S. Brunauer, P. H. Emmett, and E. Teller, *J. Am. Chem. Soc.*, **60**, 309 (1938).

(12) L. E. Osipow, "Surface Chemistry, Theory and Industrial Applications," Reinhold, New York, N.Y., 1962, p. 26.

(13) S. J. Gregg, "The Surface Chemistry of Solids," 2nd ed., Reinhold, New York, N.Y., 1961, p. 48.

(14) A. N. Martin, J. Swarbrick, and A. Cammarata, "Physical Pharmacy," 2nd ed., Lea & Febiger, Philadelphia, Pa., 1970, p. 482.

(15) P. H. Emmett and S. Brunauer, *J. Am. Chem. Soc.*, **59**, 1553 (1937).

(16) K. S. W. Sing and J. D. Madeley, *J. Appl. Chem.*, **3**, 549 (1953).

(17) *Ibid.*, **4**, 365 (1954).

(18) S. P. Zhdanov, *Dokl. Akad. Nauk, USSR*, **68**, 99 (1949).

(19) H. Gucluyildiz, G. S. Banker, and G. E. Peck, *J. Pharm. Sci.*, **66**, 407 (1977).

ACKNOWLEDGMENTS

Presented at the Industrial Pharmaceutical Technology Section, APhA Academy of Pharmaceutical Sciences, Phoenix meeting, November 1977.

Abstracted in part from a dissertation submitted by A. Y. Gore to Purdue University in partial fulfillment of the Doctor of Philosophy degree requirements.

Supported in part by a research grant from Robertshaw Chemical Corp., Phoenix, Ariz.

Metal-Binding Abilities of Radioprotective Aminoalkyl Disulfides and Thiosulfates

WILLIAM O. FOYE ˣ and JEE-MIN HU

Received June 7, 1978, from the *Samuel M. Best Research Laboratory, Massachusetts College of Pharmacy, Boston, MA 02115.* Accepted for publication July 13, 1978.

Abstract □ Metal-binding stability constants for several heterocyclic aminoalkyl disulfides and thiosulfates with Ni(II) and Al(III) were determined. The data obtained indicated that both classes of compounds were acting as bidentate chelating agents and that the heterocyclic rings apparently prevented tridentate behavior of the disulfides because of steric hindrance. The magnitude of the constants indicated that metal complexes of these compounds could exist in a cellular environment, but no correlation with radiation-protective activity was apparent.

Keyphrases □ Disulfides, aminoalkyl—metal-binding stability constants determined, relation to radiation-protective activity □ Thiosulfates, aminoalkyl—metal-binding stability constants determined, relation to radiation-protective activity □ Metal binding—stability constants determined for various aminoalkyl disulfides and thiosulfates, relation to radiation-protective activity □ Binding, metal—stability constants determined for various aminoalkyl disulfides and thiosulfates, relation to radiation-protective activity □ Radiation-protective activity—various aminoalkyl disulfides and thiosulfates, relation to metal-binding stability constants

Aminoalkyl disulfides and thiosulfates have strong radiation-protective properties in animals (1, 2). The fact that the protective compounds all have a two- or three-carbon distance between the amino and sulfur functions, which confers potential metal-chelating ability to them, suggests that metal binding may be important in their

0022-3549/79/0200-0202$01.00/0

© 1979, American Pharmaceutical Association

Table I—Ionization Constants (25°)

Compound	pKa_1	pKa_2
Bis[2-(*N*-piperidyl)ethyl] disulfide	7.78	6.22
Bis[2-(*N*-3-methylpiperidyl)ethyl] disulfide	7.64	6.13
Bis[2-(*N*-4-methylpiperidyl)ethyl] disulfide	7.63	5.86
Bis[2-(*N*-morpholinyl)ethyl] disulfide	5.50	4.26
2-(*N*-Piperidyl)ethanethiosulfuric acid	8.50	2.00
2-(*N*-Morpholinyl)ethanethiosulfuric acid	6.51	2.38
2-[2-(2-Pyridyl)ethylamino]ethanethiosulfuric acid	9.33	2.28

radioprotective mechanism.

Several postulations have related radiation-protective activity to the ability to bind metals (3, 4), and a correlation between the extent of complexation of catalase, an iron-containing protein, and the protective ability in mice was observed (5). Therefore, it was considered important to ascertain the magnitude of the metal-binding ability of such compounds and to compare it to their radiation-protective properties. The role of metal binding in cellular radiation protection is not clear, but several observations indicated that metal ions are involved in both radiation damage and protection (6).

Both the disulfide group and thiosulfate ion bind metals (7), but there are few examples of the metal-complexing avidities of organic disulfides or thiosulfates. Stability constants for a Cu(II) complex of 2,2′-dithiobis(ethylamine) (8) and for Cu(II), Al(III), and Fe(III) complexes of 2-aminoethanethiosulfuric acid and 3-aminopropanethiosulfuric acid (9) have, however, been reported. Also, an X-ray diffraction study of the nickel complex of bis[2-[2-(2-pyridyl)ethyl]aminoethyl] disulfide revealed an extremely stable complex with five coordinate bonds to the nickel ion from one molecule of disulfide (10).

EXPERIMENTAL

Materials—Analytical reagent grade aluminum chloride hexahydrate and nickel chloride hexahydrate were used. Carbonate-free 0.01 *N* KOH was prepared according to Armstrong (11). Solutions of the metal salts were prepared in boiled distilled water and stored in polyethylene bottles under nitrogen; they were diluted quantitatively with carbon dioxide-free water just prior to use. Normalities were checked against potassium biphthalate.

The organic ligands, isolated as the dihydrochlorides of the disulfides or as the zwitterions of the thiosulfates, were prepared as described previously (12), with one exception. Purity was ascertained by TLC. Chromatogram sheets[1] were spotted with approximately 0.1% solutions of the compounds in ethanol, and the sheets were developed with benzene–methanol (9:1). After the sheets were removed from the chamber and dried, spots were detected by UV light. The presence of one spot confirmed the absence of contaminating compounds.

2-[2-(2-Pyridyl)ethylamino]ethanethiosulfuric Acid—To a solution of 2-[2-(2-pyridyl)ethylamino]ethanethiol (12) (8.35 g, 0.046 mole) in 60 ml of methanol were added potassium metabisulfite (11.1 g, 0.05 mole) and 10 ml of water. The resulting mixture was refluxed overnight, cooled to room temperature, and filtered to remove potassium thiosulfate. The filtrate was flash evaporated, and the residue was treated with boiling methanol and filtered. Evaporation of the methanol left an oil, which was triturated several times with anhydrous ether; 5.4 g (45% yield) of a colorless oil was obtained; n = 1.5523; IR (neat): 3450 (NH), 1590 (pyridine ring), 1235 and 1180 ($S_2O_3^-$), 1020, and 760 (NH) cm^{-1}.

Anal.—Calc. for $C_9H_{14}N_2O_3S_2$: C, 41.20; H, 5.39; N, 10.68; S, 24.44. Found: C, 40.95; H, 5.36; N, 10.34; S, 24.16.

Ionization Constants—The method of Albert and Serjeant (13) consisted of titrations of 0.001 *M* aqueous solutions of the compounds with 0.01 *N* KOH in 0.5-ml portions. The pH was recorded[2] after each addition. Each titration thus yielded 10 pH values, giving 10 values for the pKa, which were averaged (Table I). When pH values fell outside the 5–9 range, corrections were made for hydrogen- or hydroxide-ion concentrations.

Stability Constants—Potentiometric titrations were carried out under nitrogen in 95% ethanol at 25° with the described equipment. Volumes of 50 ml of the 0.001 *M* solutions of the organic ligands were titrated with 0.01 *N* KOH in 0.5-ml portions, first in the absence of metal ions and then in the presence of 0.0005 mole of divalent metal salt or 0.00033 mole of trivalent metal salt.

Volumes of 50 ml of the same quantities of the metal salts also were titrated with 0.01 *N* KOH. The pH readings were recorded 2 min after each addition of titrant to allow equilibrium to be reached. Solvent concentration at the end of the titrations was approximately 72% ethanol.

Calculations were performed as previously described (14) with a computer. The log K_1 values for the Ni(II) complexes and the log K_2 and log K_3 values for the Al(III) complexes are recorded in Table II. Values for K_1, K_2, and K_3 were obtained from Eqs. 1–3, according to Flood and Loras (14) and Albert (15):

$$K_1 = \frac{\bar{n}}{(1-\bar{n})[L^-]} \quad \text{(Eq. 1)}$$

$$K_2 = \frac{(\bar{n}-1)}{(2-\bar{n})[L^-]} \quad \text{(Eq. 2)}$$

$$K_3 = \frac{(\bar{n}-2)}{(3-\bar{n})[L^-]} \quad \text{(Eq. 3)}$$

where $\bar{n}$ is the average number of ligand molecules bound by a metal ion at any stage in complex formation and $[L^-]$ is the concentration of the free chelating species.

The K_1 values for the Al(III) complexes were not uncovered, possibly because of nonstepwise complexation (no values for $\bar{n}$ below 1, and in some cases below 2, were obtained). Representative values for the constants obtained for the Al(III) complex of bis[2-(*N*-4-methylpiperidyl)-ethyl] disulfide are shown in Table III. Values of K_2 for the Ni(II) complexes could not be obtained because of the formation of precipitates. Representative titration data for the Ni(II) complex of bis[2-(*N*-piperidyl)ethyl] disulfide are listed in Table IV.

Table II—Stability Constants for Aminoalkyl Disulfides and Thiosulfates

Compound	Al(III) Complexes, log K_2	Al(III) Complexes, log K_3	Ni(II) Complexes, log K_1
Bis[2-(*N*-piperidyl)ethyl] disulfide	—	13.45	4.21
Bis[2-(*N*-4-methylpiperidyl)ethyl] disulfide	11.34	9.65	3.18
Bis[2-(*N*-3-methylpiperidyl)ethyl] disulfide	—	10.36	2.87
Bis[2-(*N*-morpholinyl)ethyl] disulfide	8.03	5.96	4.46
2-(*N*-Piperidyl)ethanethiosulfuric acid	—	—	4.38
2-(*N*-Morpholinyl)ethanethiosulfuric acid	7.36	4.18	—
2-[2-(2-Pyridyl)ethylamino]ethanethiosulfuric acid	—	11.43	5.50

RESULTS AND DISCUSSION

Both nitrogens of the bis(2-aminoethyl) disulfide molecule, as well as the disulfide function, are capable of simultaneous attachment to the

Table III—Potentiometric Titration of Bis[2-(*N*-4-methylpiperidyl)ethyl] Disulfide Dihydrochloride and Aluminum(III) Chloride

pH	log $[L^-]$	$\bar{n}$	log K_2	log K_3
3.20	$\overline{11}.51$	1.76	11.01	—
3.24	$\overline{11}.56$	1.84	11.16	—
3.30	$\overline{11}.67$	1.87	11.18	—
3.34	$\overline{11}.71$	1.96	11.68	—
3.40	$\overline{11}.80$	2.02	—	8.58
3.46	$\overline{11}.88$	2.09	—	9.16
3.50	$\overline{11}.91$	2.19	—	9.49
3.55	$\overline{11}.95$	2.29	—	9.68
3.59	$\overline{11}.96$	2.41	—	9.91
3.63	$\overline{11}.97$	2.49	—	10.03
	log mean of antilogs		11.34	9.65

[1] Eastman.
[2] Beckman research pH meter with glass and calomel electrodes.

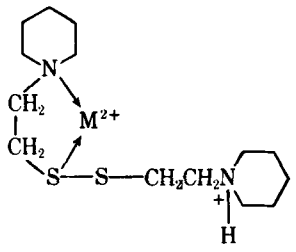

I

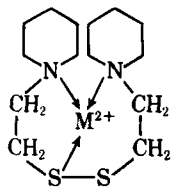

II

same metal ion (8). This molecule, as well as those titrated in this study, is a complex-forming species of type HLRLH and has the added stabilizing factor of the disulfide group, which would provide chelate rings of five or six members. Complex structures of types I and II, with a divalent metal ion (M^{2+}), are theoretically possible.

Steric hindrance between the heterocyclic rings could prevent the formation of II, however; relevant equilibria in acid solution would then be:

$$M^{2+} + {}^{+}HLRLH^{+} \rightleftharpoons {}^{+}HLRLM^{2+} + H^{+}$$

$$M^{2+} + 2{}^{+}HLRLH^{+} \rightleftharpoons ({}^{+}HLRL)_2M^{2+} + 2H^{+}$$

Scheme I

With a metal having hexacoordinate capacity, a 3:1 complex would also be possible:

$$M^{2+} + 3{}^{+}HLRLH^{+} \rightleftharpoons ({}^{+}HLRL)_3M^{2+} + 3H^{+}$$

Scheme II

With these compounds, steric hindrance by the heterocyclic rings might prevent formation of a 3:1 complex.

Titration data for the Ni(II) complexes gave values only for K_1. Precipitation generally took place before values of $\bar{n}$ exceeded 1. For the disulfides, log K_1 values ranged from 2.87 to 4.46; the values for the two thiosulfuric acids where constants were obtained were 4.38 and 5.50. These constants were obtained in the pH 5.75–7.20 range where protonation of the nitrogens should not be extensive. Therefore, both the nitrogen and sulfur functions should participate in complex formation, and structures of type III are proposed for these complexes. The thiosulfates are believed to coordinate through the thiosulfate ion (16), in addition to the amino group, as shown previously for 2-aminoethane- and 3-aminopropanethiosulfuric acids (9).

Complexation of the hydrochlorides of the aminoalkyl disulfides with Al(III) generally occurred in the pH 2.8–3.6 range. At this pH range, one nitrogen may be expected to be protonated; coordination to the metal ion would, therefore, take place only through one nitrogen and sulfur. The fact that values for K_1 for the Al(III) complexes were not found, as well as values for K_2 in some cases, indicates that two or three ligands combine in a nonstepwise fashion. If coordination were taking place through both nitrogens and sulfur, the molecules would act as tridentate ligands, and a total of three ligand molecules would be required to give values for K_3, which would exceed the coordination capacity of Al(III).

The stability constants of the 2:1 and 3:1 complexes obtained appear to be too high for binding to either nitrogen or sulfur alone, so complexes involving one nitrogen and one sulfur are proposed. Log K_1 values for the binding of Ag(I) and Cu(II) to piperidine, for instance, are 3.16 (17) and 2.81 (18), respectively. Where a terdentate chelate is involved, as postulated for bis(2-aminoethyl) disulfide, the K' value for the Cu(II) complex is 5.02×10^6 (8). Comparison of the found constants with these values indicates both nitrogen and sulfur coordination to metal.

From the magnitude and nature of the stability constants, it is apparent that steric hindrance by the heterocyclic rings prevents the compounds from acting as terdentate ligands but does not prevent the formation of 2:1 and 3:1 bidentate complexes. However, the lower values for stability

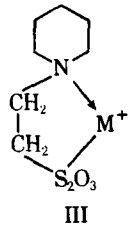

III

Table IV—Potentiometric Titration of Bis[2-(*N*-piperidyl)-ethyl] Disulfide Dihydrochloride with Nickel(II) Chloride

pH	log $[L^-]$	$\bar{n}$	log K_1
6.72	5.81	0.05	2.89
6.78	5.84	0.18	3.50
6.83	5.86	0.31	3.82
6.88	5.85	0.46	4.09
6.92	5.84	0.63	4.41
6.96	5.83	0.76	4.70
	log mean of antilogs		4.21

constants of the morpholine-substituted complexes indicate some interference by the morpholine oxygen. Also, the 3- and 4-methyl groups of the piperidine rings both lower metal-binding avidity, probably sterically. The exceptionally high constant found for 2-[2-(2-pyridyl)ethylamino]ethanethiosulfuric acid in comparison to other organic thiosulfuric acids, *e.g.*, those studied here and in Ref. 9, indicates possible terdentate ligand behavior for Ni(II).

Comparison of the metal-binding strengths of these compounds with the radiation-protective activities in mice (Table V and Ref. 19) showed no apparent correlation. Of the compounds studied here, bis[2-(*N*-morpholinyl)ethyl] disulfide showed the greatest protective effect, giving 50% survival at 30 days, but had the lowest metal-binding constants for Al(III) of the disulfides observed. Its log K_1 for Ni(II) was slightly higher than those values for the other disulfides but did not differ greatly from the log K_1 for 2-(*N*-piperidyl)ethanethiosulfuric acid, which provided only 20% protection to mice. 2-(*N*-Morpholinyl)ethanethiosulfuric acid, however, with somewhat lower binding constants for Al(III), had no radiation-protective ability.

It is unfortunate that radiation-protective data were not obtained for 2-[2-(2-pyridyl)ethylamino]ethanethiosulfuric acid, which had the highest log K_1 for Ni(II). Although a comparison between two different types of compounds, disulfides and thiosulfuric acids, may not be valid, a comparison between the binding ability to catalase and the radiation-protective ability in mice showed a correlation with several varieties of compounds, including dithiocarbamates, trithiocarbonates, and thiols (5).

The magnitude of the metal-binding stability constants observed with these disulfides and thiosulfuric acids is relatively high, particularly for the Al(III) complexes. Since they are equal to or greater than corresponding values for the common amino acids and peptides (15, 20), it may be concluded that these compounds are capable of combining with metal ions in a cellular environment. Since no correlation between the magnitude of the stability constants and radiation-protective ability was evident, any involvement with metal ions in the radiation-protective process would most likely be transient, and formation of relatively stable metal complexes would not be anticipated.

REFERENCES

(1) W. O. Foye, *J. Pharm. Sci.*, **58**, 283 (1969).

Table V—Radiation Protective Activities in Mice [a]

Compound	Dose, mg/kg[b]	Route[c]	Survival, %[d]
Bis[2-(*N*-morpholinyl)-ethyl] disulfide	20	Intraperitoneal	50
	100	Intraperitoneal	20
	300	Oral	20
	600	Oral	40
Bis[2-(*N*-3-methylpiperidyl)-ethyl] disulfide	30	Intraperitoneal	10
	60	Intraperitoneal	10
	100	Oral	20
	300	Oral	22[e]
Bis[2-(*N*-piperidyl)ethyl] disulfide	20	Intraperitoneal	0
	20	Intraperitoneal	10
	100	Oral	10
	200	Oral	20
2-(*N*-Piperidyl)ethanethiosulfuric acid	60	Intraperitoneal	20
	180	Oral	0
2-(*N*-Morpholinyl)ethanethiosulfuric acid	100	Intraperitoneal	0
	400	Oral	0

[a] Carried out at the Walter Reed Army Institute of Research. [b] Radiation dosage was 849 rads from a cesium-137 V irradiator given at a rate of 141.5 rads/min. Ten mice were used at each dosage level. [c] Compounds were administered by the indicated route in water, physiological saline, or 0.3% methylcellulose–0.1% polysorbate 80 (Tween 80) vehicle. [d] Calculated from the number of surviving mice at 30 days postirradiation.

(2) D. L. Klayman and E. S. Copeland, in "Drug Design," vol. VI, E. J. Ariens, Ed., Academic, New York, N.Y., 1975, pp. 81–142.
(3) W. O. Foye and J. Mickles, *Progr. Biochem. Pharmacol.*, **1**, 152 (1965).
(4) W. Lohman, in "Radiation Protection and Sensitization," H. L. Moroson and M. Quintiliani, Eds., Taylor and Francis, London, England, 1970, p. 117.
(5) W. O. Foye and M. C. M. Solis, *J. Pharm. Sci.*, **58**, 352 (1969).
(6) W. O. Foye, *Int. J. Sulfur Chem.*, **8**, 161 (1973).
(7) L. G. Sillén and A. E. Martell, "Stability Constants of Metal-Ion Complexes," Supplement 1, The Chemical Society, London, England, 1971, pp. 131, 338.
(8) C. J. Hawkins and D. D. Perrin, *Inorg. Chem.*, **2**, 843 (1963).
(9) W. O. Foye and C. M. Kim, *J. Pharm. Sci.*, **60**, 151 (1971).
(10) P. E. Riley and K. Seff, *Chem. Commun.*, **1971**, 194.
(11) D. M. G. Armstrong, *Chem. Ind.*, **1955**, 1405.
(12) W. O. Foye, J. J. Lanzillo, Y. H. Lowe, and J. M. Kauffman, *J. Pharm. Sci.*, **64**, 211 (1975).
(13) A. Albert and E. P. Serjeant, "The Determination of Ionization Constants," Chapman and Hall, London, England, 1971.
(14) H. Flood and V. Loras, *Tidsskr. Kjemi Bergv. Met.*, **5**, 83 (1945).
(15) A. Albert, *Biochem. J.*, **47**, 531 (1950).
(16) G. F. Gasparri, A. Musatti, and M. Nardelli, *Chem. Commun.*, **1966**, 602.
(17) J. Bjerrum, *Chem. Rev.*, **46**, 381 (1950).
(18) D. P. Graddon, *Nature*, **183**, 1610 (1959).
(19) W. O. Foye, Y. H. Lowe, and J. J. Lanzillo, *J. Pharm. Sci.*, **65**, 1247 (1976).
(20) A. Albert, *Biochem. J.*, **50**, 690 (1952).

ACKNOWLEDGMENTS

Presented at the Medicinal Chemistry Section, 8th Northeast Regional Meeting, American Chemical Society, Boston, Mass., June 1978.

Abstracted in part from a thesis submitted by J. Hu to the Massachusetts College of Pharmacy in partial fulfillment of the Master of Science degree requirements.

Effect of Microcrystalline Cellulose on Liquid Penetration in and Disintegration of Directly Compressed Tablets

C. F. LERK ˣ, G. K. BOLHUIS, and A. H. de BOER

Received April 25, 1978, from the *Laboratory for Pharmaceutical Technology, University of Groningen, Groningen, The Netherlands.*
Accepted for publication July 31, 1978.

Abstract □ The penetration of isooctane and water into tablets of microcrystalline cellulose, dibasic calcium phosphate dihydrate, spray-crystallized maltose–dextrose, and blends of microcrystalline cellulose with one of the other excipients were studied. The isooctane penetrations occurred according to the Washburn equation and were not affected by the presence of 0.5 or 1.0% magnesium stearate. The inhibition of aqueous penetration into tablets resulting from hydrophobic magnesium stearate was less pronounced for vehicles like dibasic calcium phosphate, which exhibited extensive brittle fracture under compression. Microcrystalline cellulose tablets, both with and without magnesium stearate, exhibited extremely fast aqueous penetration even at low porosities, caused by breaking of the hydrogen bonds and subsequent widening of the pores. Ratios between water uptake and original pore volume up to 20 were obtained for microcrystalline cellulose tablets. This unique property was, however, suppressed by the presence of fast dissolving and highly soluble excipients like dextrose, resulting in an antagonistic disintegration behavior of tablets compressed at pressures over 10,000 N/cm². Improved disintegration properties were obtained by blending microcrystalline cellulose with an insoluble vehicle such as dibasic calcium phosphate dihydrate.

Keyphrases □ Cellulose, microcrystalline—effect on liquid penetration and disintegration of directly compressed tablets □ Penetration, liquid—isooctane and water into directly compressed tablets, effect of microcrystalline cellulose □ Disintegration—directly compressed tablets, effect of microcrystalline cellulose □ Tablets, directly compressed—liquid penetration and disintegration, effect of microcrystalline cellulose □ Excipients, tablet—microcrystalline cellulose, effect on liquid penetration and disintegration of directly compressed tablets

Cellulose was prepared previously in a microcrystalline form having unique properties as a directly compressible tablet vehicle (1). Its disintegration behavior was attributed (2, 3) to the entrance of water into the tablet matrix by capillary forces and subsequent breaking of hydrogen bonds. The hypothesis that hydrogen bonds determine both mechanical strength and disintegration of microcrystalline cellulose tablets was confirmed using a deuterium exchange technique (4).

BACKGROUND

Microcrystalline cellulose was suggested to be useful as a disintegrating agent when used in a proportion of at least 20% (5). One study (6) found that the disintegration properties of microcrystalline cellulose were extremely pressure dependent, and the material was relatively ineffective as a disintegration agent in insoluble, direct compression systems. Microcrystalline cellulose appeared, however, to be a useful complementary disintegrant. The disintegration time of tablets of a cation-exchange resin was reduced significantly in the presence of microcrystalline cellulose (6).

A similar synergistic effect was also reported (7). Tablets containing microcrystalline cellulose and corn starch showed a shorter disintegration time than those containing the disintegrating agent alone. It was suggested that microcrystalline cellulose accelerated water penetration and, thus, swelling of the corn starch.

The penetration rate of a liquid into a porous structure is dependent on the balance between capillary and opposing viscous forces and is given by:

$$L^2 = \frac{2m\,\gamma\cos\theta}{k_0\eta}\,t \qquad \text{(Eq. 1)}$$

where L is the penetrated length at time t, m is the hydraulic pore radius, γ is the surface tension of the liquid, θ is the contact angle between liquid and solid, η is the liquid viscosity, and k_0 is a constant dependent on pore shape. If the total cross-sectional area of the pores does not vary with

0022-3549/79/0200-0205$01.00/0
© 1979, American Pharmaceutical Association

(2) D. L. Klayman and E. S. Copeland, in "Drug Design," vol. VI, E. J. Ariens, Ed., Academic, New York, N.Y., 1975, pp. 81–142.
(3) W. O. Foye and J. Mickles, *Progr. Biochem. Pharmacol.*, **1**, 152 (1965).
(4) W. Lohman, in "Radiation Protection and Sensitization," H. L. Moroson and M. Quintiliani, Eds., Taylor and Francis, London, England, 1970, p. 117.
(5) W. O. Foye and M. C. M. Solis, *J. Pharm. Sci.*, **58**, 352 (1969).
(6) W. O. Foye, *Int. J. Sulfur Chem.*, **8**, 161 (1973).
(7) L. G. Sillén and A. E. Martell, "Stability Constants of Metal-Ion Complexes," Supplement 1, The Chemical Society, London, England, 1971, pp. 131, 338.
(8) C. J. Hawkins and D. D. Perrin, *Inorg. Chem.*, **2**, 843 (1963).
(9) W. O. Foye and C. M. Kim, *J. Pharm. Sci.*, **60**, 151 (1971).
(10) P. E. Riley and K. Seff, *Chem. Commun.*, **1971**, 194.
(11) D. M. G. Armstrong, *Chem. Ind.*, **1955**, 1405.
(12) W. O. Foye, J. J. Lanzillo, Y. H. Lowe, and J. M. Kauffman, *J. Pharm. Sci.*, **64**, 211 (1975).
(13) A. Albert and E. P. Serjeant, "The Determination of Ionization Constants," Chapman and Hall, London, England, 1971.
(14) H. Flood and V. Loras, *Tidsskr. Kjemi Bergv. Met.*, **5**, 83 (1945).
(15) A. Albert, *Biochem. J.*, **47**, 531 (1950).
(16) G. F. Gasparri, A. Musatti, and M. Nardelli, *Chem. Commun.*, **1966**, 602.
(17) J. Bjerrum, *Chem. Rev.*, **46**, 381 (1950).
(18) D. P. Graddon, *Nature*, **183**, 1610 (1959).
(19) W. O. Foye, Y. H. Lowe, and J. J. Lanzillo, *J. Pharm. Sci.*, **65**, 1247 (1976).
(20) A. Albert, *Biochem. J.*, **50**, 690 (1952).

ACKNOWLEDGMENTS

Presented at the Medicinal Chemistry Section, 8th Northeast Regional Meeting, American Chemical Society, Boston, Mass., June 1978.

Abstracted in part from a thesis submitted by J. Hu to the Massachusetts College of Pharmacy in partial fulfillment of the Master of Science degree requirements.

Effect of Microcrystalline Cellulose on Liquid Penetration in and Disintegration of Directly Compressed Tablets

C. F. LERK ˣ, G. K. BOLHUIS, and A. H. de BOER

Received April 25, 1978, from the *Laboratory for Pharmaceutical Technology, University of Groningen, Groningen, The Netherlands.*
Accepted for publication July 31, 1978.

Abstract □ The penetration of isooctane and water into tablets of microcrystalline cellulose, dibasic calcium phosphate dihydrate, spray-crystallized maltose–dextrose, and blends of microcrystalline cellulose with one of the other excipients were studied. The isooctane penetrations occurred according to the Washburn equation and were not affected by the presence of 0.5 or 1.0% magnesium stearate. The inhibition of aqueous penetration into tablets resulting from hydrophobic magnesium stearate was less pronounced for vehicles like dibasic calcium phosphate, which exhibited extensive brittle fracture under compression. Microcrystalline cellulose tablets, both with and without magnesium stearate, exhibited extremely fast aqueous penetration even at low porosities, caused by breaking of the hydrogen bonds and subsequent widening of the pores. Ratios between water uptake and original pore volume up to 20 were obtained for microcrystalline cellulose tablets. This unique property was, however, suppressed by the presence of fast dissolving and highly soluble excipients like dextrose, resulting in an antagonistic disintegration behavior of tablets compressed at pressures over 10,000 N/cm². Improved disintegration properties were obtained by blending microcrystalline cellulose with an insoluble vehicle such as dibasic calcium phosphate dihydrate.

Keyphrases □ Cellulose, microcrystalline—effect on liquid penetration and disintegration of directly compressed tablets □ Penetration, liquid—isooctane and water into directly compressed tablets, effect of microcrystalline cellulose □ Disintegration—directly compressed tablets, effect of microcrystalline cellulose □ Tablets, directly compressed—liquid penetration and disintegration, effect of microcrystalline cellulose □ Excipients, tablet—microcrystalline cellulose, effect on liquid penetration and disintegration of directly compressed tablets

Cellulose was prepared previously in a microcrystalline form having unique properties as a directly compressible tablet vehicle (1). Its disintegration behavior was attributed (2, 3) to the entrance of water into the tablet matrix by capillary forces and subsequent breaking of hydrogen bonds. The hypothesis that hydrogen bonds determine both mechanical strength and disintegration of microcrystalline cellulose tablets was confirmed using a deuterium exchange technique (4).

BACKGROUND

Microcrystalline cellulose was suggested to be useful as a disintegrating agent when used in a proportion of at least 20% (5). One study (6) found that the disintegration properties of microcrystalline cellulose were extremely pressure dependent, and the material was relatively ineffective as a disintegration agent in insoluble, direct compression systems. Microcrystalline cellulose appeared, however, to be a useful complementary disintegrant. The disintegration time of tablets of a cation-exchange resin was reduced significantly in the presence of microcrystalline cellulose (6).

A similar synergistic effect was also reported (7). Tablets containing microcrystalline cellulose and corn starch showed a shorter disintegration time than those containing the disintegrating agent alone. It was suggested that microcrystalline cellulose accelerated water penetration and, thus, swelling of the corn starch.

The penetration rate of a liquid into a porous structure is dependent on the balance between capillary and opposing viscous forces and is given by:

$$L^2 = \frac{2m\,\gamma\cos\theta}{k_0\eta}\,t \qquad \text{(Eq. 1)}$$

where L is the penetrated length at time t, m is the hydraulic pore radius, γ is the surface tension of the liquid, θ is the contact angle between liquid and solid, η is the liquid viscosity, and k_0 is a constant dependent on pore shape. If the total cross-sectional area of the pores does not vary with

0022-3549/79/0200-0205$01.00/0
© 1979, American Pharmaceutical Association

Table I—Compression Force, Tablet Porosity, Calculated Pore Volume, Volumetric Isooctane Uptake, and Ratio of Volumetric Isooctane Uptake and Calculated Pore Volume of the Tablets from Figs. 1 and 2

Formulation	Compression Force, N	Porosity, %	Calculated Pore Volume, cm^3	Volumetric Uptake, cm^3	Ratio of Volumetric Uptake and Calculated Pore Volume
Microcrystalline cellulose	4700	20.3	0.082	0.078	0.95
Dibasic calcium phosphate dihydrate	7900	20.8	0.057	0.053	0.93
Spray-crystallized maltose–dextrose	3400	20.2	0.084	0.068	0.81
Microcrystalline cellulose plus 0.5% magnesium stearate	4700	20.0	0.082	0.078	0.95
Dibasic calcium phosphate dihydrate plus 0.5% magnesium stearate	7900	21.2	0.059	0.055	0.93
Spray-crystallized maltose–dextrose plus 1.0% magnesium stearate	2600	20.4	0.084	0.071	0.85

length, the volume of liquid taken up by a tablet will be proportional to the length of penetration. Therefore, the relationship between the square of volumetric uptake and time is linear (8).

Ganderton and coworkers (9–12) studied liquid penetration of tablets by cyclohexane and water. Highly permeable tablets allowed rapid penetration of the liquid, which isolated a large fraction of the total pore space and resulted in low final degrees of saturation; less permeable tablets became fully saturated. Addition of starch had no significant effect on the pore structure of the tablet but disrupted and altered the structure when penetrated by water (10).

In a study of the effect of magnesium stearate distribution on water penetration, Ganderton (9) reported a large depression of the aqueous penetration rate in the presence of magnesium stearate. The increase in penetration time was roughly proportional to the magnesium stearate concentration and was susceptible to the method of mixing. This finding suggested a proportional increase in the internal surface of the tablet containing magnesium stearate and in the number of capillaries unable to conduct water. The cyclohexane penetration, which freely wets the lubricant, was not inhibited by magnesium stearate.

Previously (13), various excipients were evaluated for tableting by direct compression. The excipients studied could be classified roughly into disintegrating agents with poor flowability (microcrystalline cellulose and directly compressible starch) and into free flowing vehicles exhibiting no disintegration (dibasic calcium phosphate) or disintegration by dissolution (lactose and dextrose). To optimize the characteristics for direct compression, excipients from the group with disintegrant properties were blended with excipients from the group with free flowing properties (14). Blending these excipients resulted, however, in synergism or antagonism in disintegration.

The objectives of the present investigation were to study the effect of microcrystalline cellulose on water penetration into tablets compressed from an insoluble or a soluble directly compressible excipient and to elucidate the difference in disintegration efficiency of this material in different systems.

EXPERIMENTAL

Materials—The directly compressible materials used were microcrystalline cellulose[1], unmilled dibasic calcium phosphate dihydrate[2], and spray-crystallized maltose–dextrose[3]. Dextrose[4] (Ned. Pharm. grade), magnesium stearate[5] (Ph. Ned. grade) (a lubricant), and isooctane[6] (analytical grade) also were used.

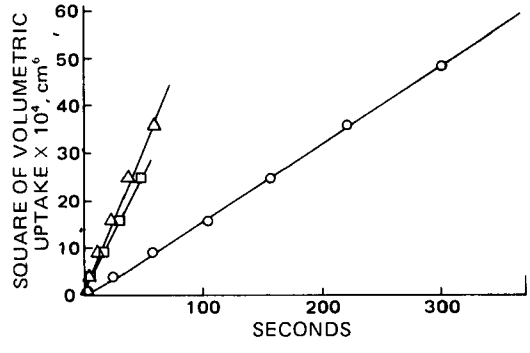

Figure 1—*Isooctane penetration into tablets compressed from dibasic calcium phosphate dihydrate (□), spray-crystallized maltose-dextrose (△), and microcrystalline cellulose (○). Tablet porosity was about 20%.*

Methods—*Mixing*—The excipients were mixed, with (0.5 or 1.0%) or without magnesium stearate, by blending 300 g of material in a 3.4-cubic liter tumbling mixer at 60 rpm for 15 min.

Tablet Compression—Tablets, 9 mm in diameter, were prepared by introducing, manually, 250 or 500 mg of the excipient or blend into the die of a flat-faced punch and die system. The die was prelubricated by careful dusting with magnesium stearate. The punch and die system was mounted between the plattens of an instrumented hydraulic press[7] and loaded at different forces with a compression rate of 2000 N/sec. When the desired force was attained, the crosshead was reversed at the same speed as the compaction process.

The tablets were manually ejected from the die, using a PVC-punch. The porosity and pore volume of a tablet were calculated from its weight and volume and the density of the blend, as measured with an air comparison pycnometer[8].

Crushing Strength—The crushing strength of the tablets was determined immediately after compression by placing the tablets diametrically between the plattens of an instrumented hydraulic press[7] and applying a loading rate of 50 N/sec.

Liquid Penetration—The rate at which liquid penetrated into a tablet was measured by placing the tablet on the glass filter plate of a modified thermostated penetration apparatus, as originally described by Enslin (15). The liquid uptake rate was read from the graduated pipet. Penetrations were carried out with isooctane at 0 ± 0.5° and with water at 37 ± 0.5°. Corrections were made for liquid evaporation. The penetrations and porosity data given are the means of at least five measurements.

Wettability—The wettability of the excipients and blends was characterized by contact angle determinations, as described previously (16).

RESULTS AND DISCUSSION

Figure 1 shows isooctane penetration at 0° into 500-mg tablets of mi-

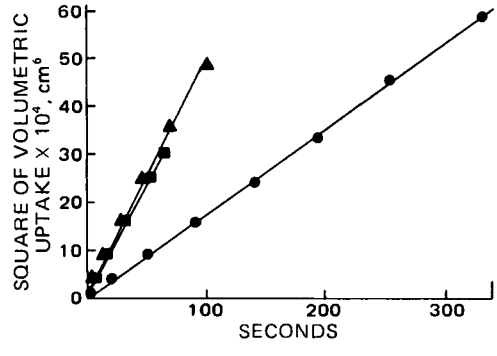

Figure 2—*Isooctane penetration into tablets compressed from dibasic calcium phosphate dihydrate plus 0.5% magnesium stearate (■), spray-crystallized maltose-dextrose plus 1.0% magnesium stearate (▲), and microcrystalline cellulose plus 0.5% magnesium stearate (●). Tablet porosity was about 20%.*

[1] Avicel PH 101, American Viscose Division, FMC Corp., Marcus Hook, Pa.
[2] Emcompress, Edward Mendell Co., New York, N.Y.
[3] Emdex, Edward Mendell Co., New York, N.Y.
[4] Lamers en Indemans, 's-Hertogenbosch, The Netherlands.
[5] Chem. Fabriek Dr. O. Breyer, Venlo, The Netherlands.
[6] E. Merck, Darmstadt, West Germany.
[7] Hydro Mooi, Appingedam, The Netherlands.
[8] Model 930, Beckman Instruments, Fullerton, Calif.

Table II—Compression Force, Tablet Porosity, Calculated Pore Volume, Volumetric Water Uptake, and Ratio of Volumetric Water Uptake and Calculated Pore Volume of the Tablets from Figs. 3–6

Formulation	Compression Force, N	Porosity, %	Calculated Pore Volume, cm^3	Volumetric Uptake, cm^3	Ratio of Volumetric Uptake and Calculated Pore Volume
Microcrystalline cellulose	4,700	20.6	0.042	0.220	5.2
Microcrystalline cellulose plus 0.5% magnesium stearate	4,700	19.7	0.039	0.220	5.6
Microcrystalline cellulose	20,000	5.1	0.009	0.175	19.4
Microcrystalline cellulose plus 0.5% magnesium stearate	20,000	6.1	0.010	0.175	17.5
Microcrystalline cellulose	19,000	5.5	0.010	0.175	17.5
Microcrystalline cellulose plus 0.5% magnesium stearate	30,000	5.5	0.010	0.175	17.5
Dibasic calcium phosphate dihydrate	7,900	20.2	0.056	0.053	0.95
Dibasic calcium phosphate dihydrate plus 0.5% magnesium stearate	7,900	20.9	0.057	0.039	0.68
Dibasic calcium phosphate dihydrate	20,000	15.3	0.039	0.039	1.00
Dibasic calcium phosphate dihydrate plus 0.5% magnesium stearate	20,000	14.9	0.038	0.032	0.84
Spray-crystallized maltose–dextrose	3,400	19.5	0.080	0.140	1.75
Spray-crystallized maltose–dextrose plus 1.0% magnesium stearate	2,600	19.5	0.080	0.030	0.37
Spray-crystallized maltose–dextrose	20,000	2.7	0.005	0	0
Spray-crystallized maltose–dextrose plus 1.0% magnesium stearate	20,000	3.4	0.006	0	0

crocrystalline cellulose, dibasic calcium phosphate dihydrate, or spray-crystallized maltose–dextrose, all having a porosity of about 20%. Table I summarizes compression force, porosity, calculated pore volume, volumetric uptake, and ratio between uptake and pore volume data. A linear relation was obtained between the square of the volumetric uptake and time. This result is in accordance with the Washburn equation, as expected, because isooctane does not loosen bonds between particles, keeping the pore structure constant during penetration.

The dextrose and dibasic calcium phosphate tablets exhibited a higher penetration rate than the microcrystalline cellulose tablets, indicating that the latter had smaller pores. The penetration rate was hardly influenced by magnesium stearate (Fig. 2), because of complete wetting of the excipients and of magnesium stearate by isooctane. Consequently, all tablets became almost saturated (Table I). These results are in agreement with the work of Ganderton (9), who reported that cyclohexane uptake into magnesium carbonate tablets was not affected by magnesium stearate.

Water penetration into tablets containing no lubricant is presented in Fig. 3. A linear relationship existed between the square of volumetric uptake and time only for the dibasic calcium phosphate tablets. The patterns of aqueous penetration into the dextrose and microcrystalline cellulose tablets were quite different. The increased penetration rate of water into dibasic calcium phosphate tablets, compared with the isooctane penetration, was mainly caused by the higher surface tension of water.

The rate at which water entered the dibasic calcium phosphate tablets strongly decreased when the excipient was blended with 0.5% magnesium stearate and compressed to a porosity of about 20% (Fig. 4). Magnesium stearate molecules are sheared off from their crystal surface during a mixing process and are attached to a substrate surface (17, 18). Therefore, a hydrophilic dibasic calcium phosphate surface, exhibiting a contact angle of 0°, can be transformed into a strongly hydrophobic surface, exhibiting a contact angle of about 120°, which corresponds to the contact angle of magnesium stearate (16). This change in surface characteristics can be nullified, however, by fracture of crystalline material during compaction with the creation of clean lubricant-free surfaces. The smaller decrease in the penetration rate found for tablets compressed at a higher compaction force after blending with 0.5% magnesium stearate (Fig. 4) could, therefore, be expected from the compaction behavior of dibasic calcium phosphate, which exhibits an extensive brittle fracture (19).

The ratio between volumetric uptake and calculated pore volume of the tablets is given in Table II. The ratios obtained for the plain dibasic calcium phosphate tablets indicate saturation of the tablets whereas the tablets containing magnesium stearate were less saturated. The observation of an increased saturation with an increase in compaction pressure for the tablets blended prior to compression with magnesium stearate is consistent with the behavior of brittle fracture during compaction.

Spray-crystallized maltose–dextrose tablets showed extremely high penetration rates during the early stages of penetration, but these rates decreased rapidly with time (Fig. 3). The volumetric uptake of the tablets was greater than the calculated pore volume (Table II). The fact that both the initially increased penetration rate and the water uptake were higher than the pore volume was probably caused by the dissolution of the freely soluble dextrose during the penetration process, resulting in wider pores and an increased pore volume. Dissolution, however, sharply increased

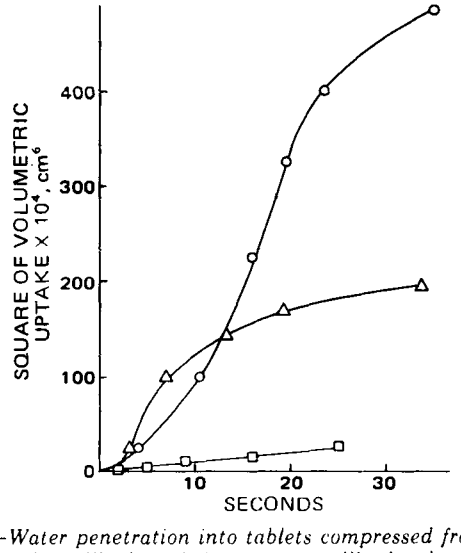

Figure 3—*Water penetration into tablets compressed from dibasic calcium phosphate dihydrate (□), spray-crystallized maltose–dextrose (△), and microcrystalline cellulose (○). Tablet porosity was about 20%.*

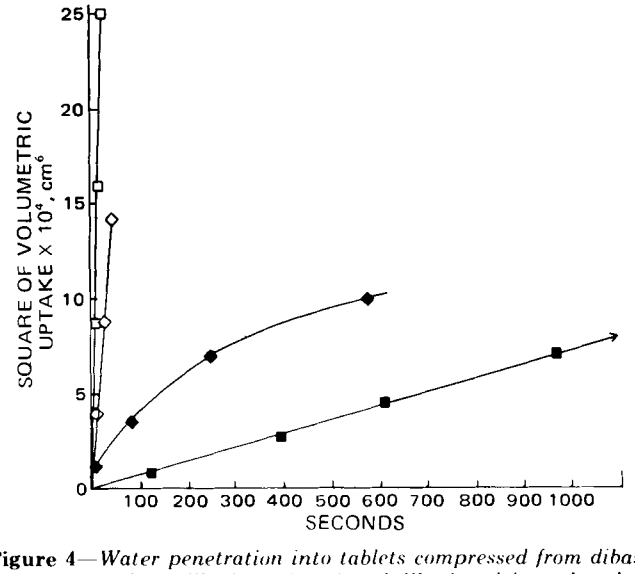

Figure 4—*Water penetration into tablets compressed from dibasic calcium phosphate dihydrate (□, ◇) and dibasic calcium phosphate dihydrate plus 0.5% magnesium stearate (■, ◆). Tablet porosities were about 20% (□, ■) and about 15% (◇, ◆).*

Table III—Compression Force, Tablet Porosity, Calculated Pore Volume, Volumetric Water Uptake, and Ratio of Volumetric Water Uptake and Calculated Pore Volume of the Tablets from Figs. 9 and 10

Formulation[a]	Compression Force, N	Porosity, %	Calculated Pore Volume, cm^3	Volumetric Uptake, cm^3	Ratio of Volumetric Uptake and Calculated Pore Volume
Dibasic calcium phosphate dihydrate (I)	5,000	24.7	0.036	0.015	0.42
I plus 10% microcrystalline cellulose	5,000	23.9	0.036	0.036	1.00
I plus 20% microcrystalline cellulose	5,000	23.7	0.037	0.070	1.90
I plus 40% microcrystalline cellulose	5,000	22.4	0.037	0.120	3.24
Microcrystalline cellulose	5,000	19.7	0.038	0.220	5.3
I	20,000	14.9	0.019	0.018	0.95
I plus 10% microcrystalline cellulose	20,000	12.9	0.017	0.028	1.65
I plus 20% microcrystalline cellulose	20,000	10.5	0.014	0.060	4.28
I plus 40% microcrystalline cellulose	20,000	7.9	0.011	0.100	9.1
Microcrystalline cellulose	20,000	6.1	0.010	0.175	17.5

[a] All formulations contained 0.5% magnesium stearate.

the viscosity of the penetrating liquid, which resulted in a slowdown in the penetration rate.

Water penetration into the dextrose tablets with a porosity of 20% was dramatically inhibited by 1% magnesium stearate and even stopped before saturation of the tablet (Fig. 5 and Table II). Low porosity tablets compressed at 20,000 N, both with and without magnesium stearate, were not penetrated by water at all because of the extremely small pores and dissolution of dextrose.

Microcrystalline cellulose tablets (Fig. 3) showed extremely high penetration rates, which were almost constant (Fig. 6). Furthermore, the tablets, having a porosity of about 20%, exhibited a volumetric uptake about five times higher than the calculated pore volume (Table II); the ratio between uptake and pore volume was about 20 for the tablets with an initial porosity of about 5%. Because of the laminary cracking of 500-mg tablets when penetrated with water, these microcrystalline cellulose tablets were compressed from 250 mg of material, giving lower calculated pore volumes than for the tablets penetrated with isooctane (Table I).

The linearity between the volumetric water uptake and time for the microcrystalline cellulose tablets (Fig. 6) indicates that the capillary force driving the liquid into the tablet is opposed by a constant viscous resistance. A constant viscous resistance can only be realized, however, if the hydraulic radius of the capillaries increases during penetration. Since the binding between microcrystalline cellulose particles is attributed to hydrogen bonds, a fairly constant volumetric penetration rate into these tablets may be explained by the breaking of the hydrogen bonds immediately behind the penetration front and a subsequent increase in the penetrated pore volume. This concept is consistent with the high ratio between water uptake and original pore volume (Table II).

Moreover, observation of the tablet during penetration showed swelling of the penetrated part of the tablet, which was completed when water uptake had finished. In accordance with the findings of Nogami *et al.* (7), swelling of the individual microcrystalline cellulose particles as proposed by Fox *et al.* (2) could not be established. The effect of hydrophobic magnesium stearate on the penetration of water into microcrystalline cellulose tablets is shown in Fig. 6 for different porosities. The 0.5% magnesium stearate decreased the penetration rate into the tablets having a porosity of about 20%. The tablets compressed at a force of 20,000 N exhibited a porosity of 5.1 and 6.1% when compressed without and with 0.5% magnesium stearate, respectively. The increased porosity was caused by an increased relaxation of the tablet when compacted in the presence of magnesium stearate. Because of this relaxation, it was not possible to produce tablets with a porosity of 5.1% from a blend containing 0.5% magnesium stearate. The lowest porosity obtained was 5.5%, and it was reached with a compaction force of 30,000 N or higher. Comparison of lubricated and nonlubricated microcrystalline cellulose tablets with a porosity of 5.5% showed a decreased penetration rate for the lubricated tablets.

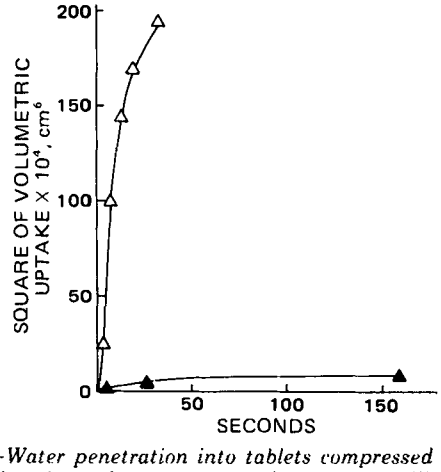

Figure 5—*Water penetration into tablets compressed from spray-crystallized maltose-dextrose (△) and spray-crystallized maltose-dextrose plus 1.0% magnesium stearate (▲). Tablet porosity was about 20%.*

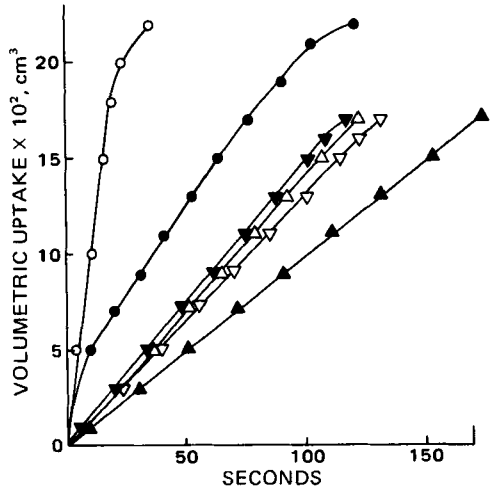

Figure 6—*Water penetration into tablets compressed from microcrystalline cellulose (○,▽,△) and microcrystalline cellulose plus 0.5% magnesium stearate (●,▼,▲). Tablet porosities were about 20% (○,●), 5.5% (△,▲), 5.1% (▽), and 6.1% (▼).*

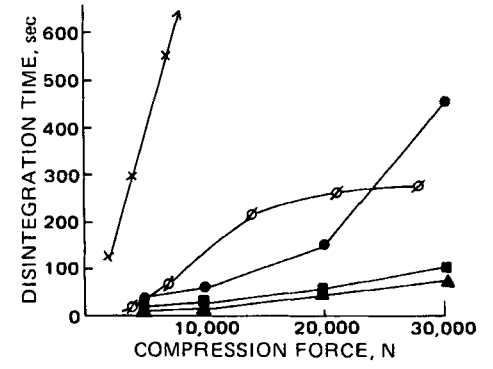

Figure 7—*Disintegration time* versus *applied compression force for tablets compressed from dibasic calcium phosphate dihydrate (×), microcrystalline cellulose (Ø), and blends of dibasic calcium phosphate with 10 (●), 20 (■), and 40% (▲) microcrystalline cellulose. All tablets contained 0.5% magnesium stearate.*

Table IV—Compression Force, Tablet Porosity, Calculated Pore Volume, Volumetric Water Uptake, and Ratio of Volumetric Water Uptake and Calculated Pore Volume of the Tablets from Figs. 11 and 12

Formulation[a]	Compression Force, N	Porosity, %	Calculated Pore Volume, cm^3	Volumetric Uptake, cm^3	Ratio of Volumetric Uptake and Calculated Pore Volume
Spray-crystallized maltose–dextrose (II)	5,000	13.1	0.025	0.014	0.56
II plus 10% microcrystalline cellulose	5,000	13.9	0.026	0.033	1.27
II plus 20% microcrystalline cellulose	5,000	15.9	0.031	0.042	1.35
II plus 40% microcrystalline cellulose	5,000	17.7	0.036	0.163	4.52
Microcrystalline cellulose	5,000	19.7	0.039	0.230	5.9
II	20,000	3.4	0.006	0	0
II plus 10% microcrystalline cellulose	20,000	3.8	0.006	0	0
II plus 20% microcrystalline cellulose	20,000	4.1	0.007	0.005	0.70
II plus 40% microcrystalline cellulose	20,000	5.1	0.009	0.023	2.55
Microcrystalline cellulose	20,000	6.3	0.010	0.190	19.0

[a] All formulations contained 1.0% magnesium stearate.

The penetration measurements presented were performed, as an extension of previous investigations (14), to elucidate the difference in disintegration behavior of the tablets compressed from dibasic calcium phosphate dihydrate–microcrystalline cellulose and from spray-crystallized maltose–dextrose–microcrystalline cellulose blends. Figures 7 and 8 [abstracted from previous work (14)] show a synergistic behavior in disintegration time for the dibasic calcium phosphate–microcrystalline cellulose tablets but an antagonistic behavior for the dextrose–microcrystalline cellulose tablets.

The plain dibasic calcium phosphate tablets, lubricated with 0.5% magnesium stearate, exhibited extremely low penetration rates for compaction forces of 5000 and 20,000 N (Figs. 9 and 10, respectively). When compressed at low compaction forces, the tablets disintegrated because of mechanical damage caused by the disks used for the USP disintegration test. At compaction forces over 10,000 N, the tablets did not disintegrate at all.

Addition of microcrystalline cellulose to the dibasic calcium phosphate strongly increased penetration rates (Figs. 9 and 10). The increased rates were caused by the breaking of the hydrogen bonds between the microcrystalline particles and the subsequent increase in pore volume, expressed by increasing ratios between volumetric water uptake and original pore volume with increasing amounts of microcrystalline cellulose (Table III). This behavior explains the extremely short disintegration time (Fig. 7) for the tablets compressed from dibasic calcium phosphate–microcrystalline cellulose blends. The relatively longer disintegration time for the plain microcrystalline cellulose tablets may be attributed to the maximal number of hydrogen bonds, characterized by a crushing strength of 34 kg for the tablets compacted at a force of 20,000 N in the presence of 0.5% magnesium stearate.

The tablets compressed from dextrose–microcrystalline cellulose blends showed a completely different disintegrating behavior. These tablets were compressed in the presence of 1.0% magnesium stearate to obtain acceptable ejection forces (14). The plain dextrose tablets did not disintegrate but were dissolved by the high solubility of the excipient. The plain tablets compressed at 5000 N exhibited liquid penetration at the early stages of penetration only (Fig. 11). Penetration ceased by fast dissolution of the dextrose, resulting in increasing liquid viscosities in the pores. For these relatively porous tablets, addition of 10% microcrystalline cellulose (w/w) only slightly increased the penetration rate during the early stages. There was, however, a considerable increase in volumetric water uptake (Table IV).

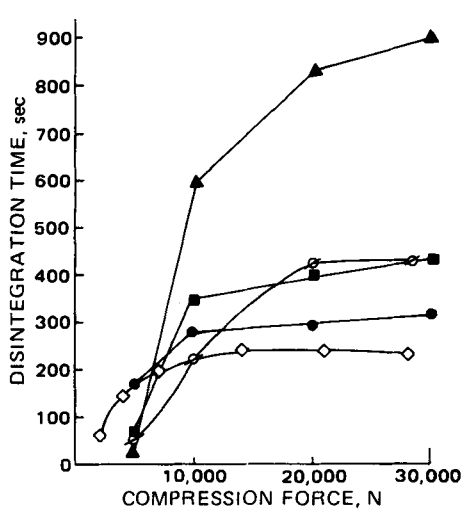

Figure 8—*Disintegration time* versus *applied compression force for tablets compressed from spray-crystallized maltose–dextrose (◇), microcrystalline cellulose (∅), and blends of spray-crystallized maltose–dextrose with 10 (●), 20 (■), and 40% (▲) microcrystalline cellulose. All tablets contained 1.0% magnesium stearate.*

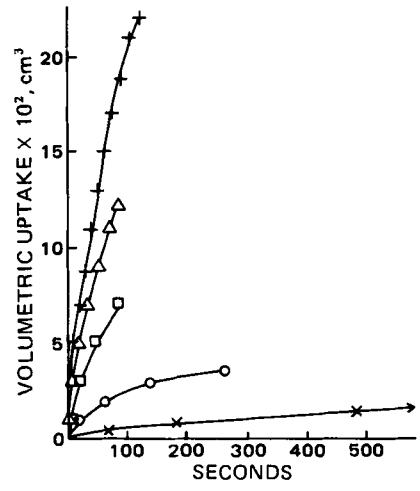

Figure 9—*Water penetration into tablets compressed from dibasic calcium phosphate dihydrate (×), microcrystalline cellulose (+), and blends of dibasic calcium phosphate dihydrate with 10 (○), 20 (□), and 40% (△) microcrystalline cellulose. Compression force was 5000 N. All tablets contained 0.5% magnesium stearate.*

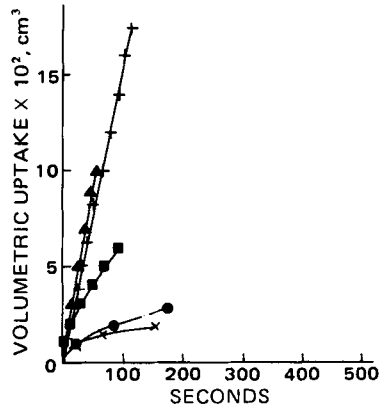

Figure 10—*Water penetration into tablets compressed from dibasic calcium phosphate dihydrate (×), microcrystalline cellulose (+), and blends of dibasic calcium phosphate dihydrate with 10 (●), 20 (■), and 40% (▲) microcrystalline cellulose. Compression force was 20,000 N. All tablets contained 0.5% magnesium stearate.*

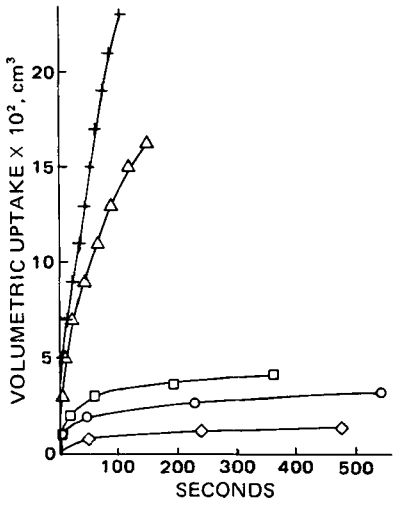

Figure 11—*Water penetration into tablets compressed from spray-crystallized maltose-dextrose (◊), microcrystalline cellulose (+), and from blends of spray-crystallized maltose-dextrose with 10 (○), 20 (□), and 40% (△) microcrystalline cellulose. Compression force was 5000 N. All tablets contained 1.0% magnesium stearate.*

The increase in the ratio between liquid uptake and original pore volume was due to increasing pore volumes during penetration caused by the microcrystalline cellulose. The addition of 40% microcrystalline cellulose resulted in strongly increased penetration rates. These high penetration rates may be attributed to the masking of the dextrose by the microcrystalline cellulose, reducing its dissolution velocity, and the enlargement of the pores. The penetration characteristics obtained were consistent with the disintegration behavior of the tablets compressed at 5000 N. The disintegration time decreased with increasing amounts of microcrystalline cellulose (Fig. 8).

Compaction of the spray-crystallized maltose-dextrose at a force of about 20,000 N gave tablets that exhibited no water penetration at all. Addition of 10% microcrystalline cellulose to the dextrose also resulted in tablets that showed no water penetration. A comparison of the disintegration of plain dextrose tablets with tablets containing 10% microcrystalline cellulose showed slightly longer disintegration times for the latter when compressed at forces over 10,000 N (Fig. 8). Since the dextrose tablets did not really disintegrate but rather dissolved, the increased disintegration time may be ascribed to the masking of the dextrose by the microcrystalline cellulose.

Addition of 20 or even 40% microcrystalline cellulose to the dextrose gave tablets that exhibited only a slight penetration (Fig. 12). The small pores of the tablets, compressed at 20,000 N, indicated low initial penetration rates through which a concentrated dextrose solution was created in the pores by dissolution of the highly soluble excipient. The effect of

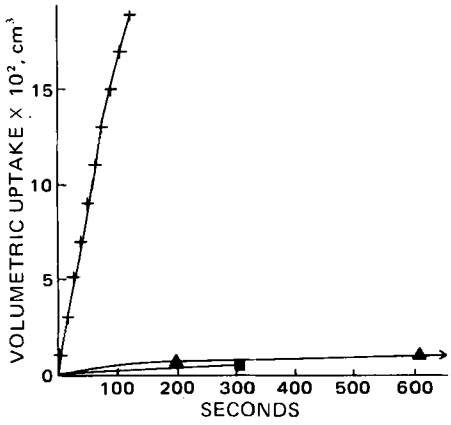

Figure 12—*Water penetration into tablets compressed from microcrystalline cellulose (+) and blends of spray-crystallized maltose-dextrose with 20 (■) and 40% (▲) microcrystalline cellulose. Compression force was 20,000 N. All tablets contained 1.0% magnesium stearate.*

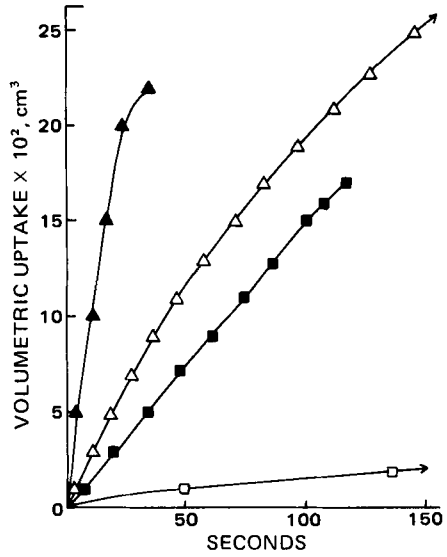

Figure 13—*Penetration into tablets compressed from microcrystalline cellulose using water (▲,■) and a 50% (w/w) dextrose solution (△,□) as the penetrating liquid. Compression forces were 5000 (▲,△) and 20,000 (■,□) N.*

widening of the pores by microcrystalline cellulose during penetration was suppressed, as confirmed by the results shown in Fig. 13. The penetration rate in microcrystalline cellulose tablets was markedly affected by the concentration of the penetrating dextrose solution, especially for the low porosity tablets. Thus, the low porosity dextrose-microcrystalline cellulose tablets exhibited low penetration rates even in the early stages of penetration. The antagonistic behavior of increasing disintegration times (Fig. 8) with increasing amounts of microcrystalline cellulose, when compressed at forces over 10,000 N, can consequently be explained by the masking action of the microcrystalline cellulose on the dissolving dextrose surface and the suppressive action of a dextrose solution on the pore-enlarging effect of the microcrystalline cellulose.

In conclusion, microcrystalline cellulose exhibits, in addition to its high dry binding capacity, extremely fast aqueous penetration into compacts. This behavior is caused by a widening of the pores during penetration. Ratios between water uptake and original pore volume of up to about 20 were obtained for microcrystalline cellulose tablets. This unique property is, however, suppressed by fast dissolving and highly soluble excipients such as dextrose, resulting in an antagonistic disintegration behavior. Improved disintegration properties are obtained by blending microcrystalline cellulose with an insoluble vehicle such as dibasic calcium phosphate dihydrate.

REFERENCES

(1) O. A. Battista and P. A. Smith, *Ind. Eng. Chem.*, **54**, 20 (1962).

(2) D. Fox, M. D. Richman, G. E. Reier, and R. F. Shangraw, *Drug Cosmet. Ind.*, **92**, 161 (1963).

(3) G. E. Reier and R. F. Shangraw, *J. Pharm. Sci.*, **55**, 510 (1966).

(4) R. Hüttenrauch, *Pharmazie*, **26**, 645 (1971).

(5) E. J. Mendell, *Manuf. Chem. Aerosol News*, **43**, 31 (1972).

(6) K. A. Khan and C. T. Rhodes, *Can. J. Pharm. Sci.*, **10**, 62 (1975).

(7) H. Nogami, T. Nagai, E. Fukuoka, and T. Sonobe, *Chem. Pharm. Bull.*, **17**, 1450 (1969).

(8) E. W. Washburn, *Phys. Rev.*, **17**, 273 (1921).

(9) D. Ganderton, *J. Pharm. Pharmacol.*, **21**, 9S (1969).

(10) D. Ganderton and D. R. Fraser, *ibid.*, **22**, 95S (1970).

(11) D. Ganderton and A. B. Selkirk, *ibid.*, **22**, 345 (1970).

(12) D. R. Fraser and D. Ganderton, *ibid.*, **23**, 18S (1971).

(13) G. K. Bolhuis and C. F. Lerk, *Pharm. Weekbl.*, **108**, 469 (1973).

(14) C. F. Lerk and G. K. Bolhuis, *ibid.*, **109**, 945 (1974).

(15) O. Enslin, *Chem. Fabr.*, **6**, 147 (1933).

(16) C. F. Lerk, A. J. M. Schoonen, and J. T. Fell, *J. Pharm. Sci.*, **65**, 843 (1976).

(17) G. K. Bolhuis, C. F. Lerk, H. T. Zijlstra, and A. H. de Boer, *Pharm.*

Weekbl., **110**, 317 (1975).
(18) C. F. Lerk and G. K. Bolhuis, *Pharm. Acta Helv.*, **52**, 39 (1977).
(19) A. H. de Boer, G. K. Bolhuis, and C. F. Lerk, *Powder Technol.*, **20**, 75 (1978).

ACKNOWLEDGMENTS

The authors are indebted to Edward Mendell Co. for the supply of dibasic calcium phosphate dihydrate and spray-crystallized maltose-dextrose. They also thank FMC Corp. for financial support.

Preparation and Evaluation of Microencapsulated Ion-Exchange Resin Beads

S. MOTYCKA * **and J. G. NAIRN** ˣ

Received May 2, 1978, from the *Faculty of Pharmacy, University of Toronto, Toronto, Ontario, Canada, M5S 1A1.* Accepted for publication July 28, 1978. *Present address: Department of Pharmacy, Hospital for Sick Children, Toronto, Ontario, Canada.

Abstract □ Ion-exchange resin beads in the benzoate form were coated by several microencapsulation techniques to alter and improve characteristics, especially the control of drug release, of this type of drug delivery system. The most successful techniques included polymer–polymer interaction, temperature change, and nonsolvent addition. The microencapsulated beads then were studied with respect to the release rate of the organic anion to determine the effects of microencapsulation. The release rate of the organic anion could be controlled over a wide range, depending on the encapsulating material characteristics. Factors affecting the extent and rate of release as a result of microencapsulation are discussed.

Keyphrases □ Microencapsulated ion-exchange resin beads—prepared by various methods, evaluated for release rate □ Ion-exchange microencapsulated resin beads—prepared by various methods, evaluated for release rate □ Delivery systems—microencapsulated ion-exchange resin beads, prepared by various methods, evaluated for release rate □ Dosage forms, potential—microencapsulated ion-exchange resin beads, prepared by various methods, evaluated for release rate

Ion-exchange resins function as effective carriers for prolonging drug release for sustained biological action and for improvement of other pharmacokinetic parameters such as the absorption rate constant (1). In addition, ion-exchange resins are used for binding biological materials such as bile salts and sodium ions within the GI tract (2, 3). While ion-exchange resins form a useful drug delivery system, improvements can be effected in some cases by coating the resin beads with various pharmaceutical adjuvants. Potential improvements are: enhancing the taste of ion-exchange resins (4, 5), decreasing the release rate of drugs from the resins (5, 6), permitting greater saturation of the resin with the drug and a slower elution rate (6), minimizing elution of drug in liquid preparations of ion-exchange resin–drug complexes (6, 7), and minimizing interaction of drugs with resins used as tablet disintegrants (8).

One effective and versatile method of coating small solid particles is microencapsulation, which can be accomplished with various procedures (5, 9, 10). Many researchers discussed the encapsulation of solid particles (11–16), but few applied the process to ion-exchange resins (4, 17). It was deemed appropriate to investigate microencapsulation procedures for the preparation of coated ion-exchange resins to exploit the value of resin beads, such as uniform size and consistent binding of drugs, for improving their pharmaceutical characteristics. Specifically, it was expected that medication with a wide range of prolonged-release characteristics could be prepared. In addition, it was hoped that a uniform coat around the beads could be obtained by various encapsulation methods.

The effect of additives on the characteristics of the film used to coat pharmaceuticals also was investigated. In some cases, additives selected are of such a nature that the rate of transmission or release of drugs is increased (12, 18) or decreased (19). Part of the present research is concerned with employing additives in the preparation of the microencapsulating film to prolong or delay the release so that the coated beads can be considered for other uses in pharmacy besides oral medication.

EXPERIMENTAL

Materials—All experiments were carried out with a 20–50-mesh strongly basic ion-exchange resin[1] in the benzoate form. The resin was screened wet; the beads that passed through a 35-mesh screen but were retained on a 40-mesh screen were used. The resin then was cleaned, conditioned, and converted into the benzoate form by the procedure described previously (20). The average particle size of the resin beads, as determined by microscopic measurement of 30 beads, was 0.366 mm (wet) and 0.325 mm (dry).

Encapsulation Procedures—*Polymer–Polymer Interaction*—The method of Luzzi and Gerraughty (14, 21), adapted from Green and Schleicher (22, 23), was modified for the encapsulation of the resin beads. In this method, the interaction of oppositely charged polyelectrolytes results in the formation of a complex of considerably reduced solubility such that phase separation occurs. The specific procedure used consisted of dissolving 3 g of acacia[2] and 3 g of gelatin[3] separately in 100 ml of distilled water each. The solutions were warmed to 55° and mixed, and the pH was adjusted to 6.5 with 20% NaOH. The resin beads (2 g) then were added, and the pH of the mixture was altered to 4.5 by the dropwise addition of dilute hydrochloric acid with stirring.

The temperature was allowed to drop, and the polymers coalesced around the resin beads. Subsequently, 10 ml of formaldehyde solution USP was added, and the mixture was cooled to 10° by immersion in an ice bath with constant stirring. The pH then was adjusted to 9.0 by the dropwise addition of 20% NaOH. The mixture was diluted to approximately 400 ml with distilled water, left overnight, and then centrifuged for 30 min at 2700 rpm.

The supernate was decanted, and the microencapsulated beads were transferred to a 60-mesh screen and washed with water to remove the empty capsules. The capsules remaining on the screen were poured into a flask along with 100 ml of distilled water. After settling, water was removed by rinsing the capsules with three 50-ml portions of 95% ethanol. The mixture was filtered, washed with ethanol, and dried in a desiccator.

Temperature Change—Five methods of preparation were evaluated.

[1] Dowex 1-X8, Dow Chemical Co., Midland, Mich.
[2] Gum Acacia BP, British Drug Houses (Canada) Ltd., Toronto, Canada.
[3] Gelatin, Pharmagel A., American Agricultural Co., Detroit, Mich.

0022-3549/79/0200-0211$01.00/0
© 1979, American Pharmaceutical Association

Weekbl., **110**, 317 (1975).
(18) C. F. Lerk and G. K. Bolhuis, *Pharm. Acta Helv.*, **52**, 39 (1977).
(19) A. H. de Boer, G. K. Bolhuis, and C. F. Lerk, *Powder Technol.*, **20**, 75 (1978).

ACKNOWLEDGMENTS

The authors are indebted to Edward Mendell Co. for the supply of dibasic calcium phosphate dihydrate and spray-crystallized maltose-dextrose. They also thank FMC Corp. for financial support.

Preparation and Evaluation of Microencapsulated Ion-Exchange Resin Beads

S. MOTYCKA * **and J. G. NAIRN** ˣ

Received May 2, 1978, from the *Faculty of Pharmacy, University of Toronto, Toronto, Ontario, Canada, M5S 1A1.* Accepted for publication July 28, 1978. *Present address: Department of Pharmacy, Hospital for Sick Children, Toronto, Ontario, Canada.

Abstract □ Ion-exchange resin beads in the benzoate form were coated by several microencapsulation techniques to alter and improve characteristics, especially the control of drug release, of this type of drug delivery system. The most successful techniques included polymer–polymer interaction, temperature change, and nonsolvent addition. The microencapsulated beads then were studied with respect to the release rate of the organic anion to determine the effects of microencapsulation. The release rate of the organic anion could be controlled over a wide range, depending on the encapsulating material characteristics. Factors affecting the extent and rate of release as a result of microencapsulation are discussed.

Keyphrases □ Microencapsulated ion-exchange resin beads—prepared by various methods, evaluated for release rate □ Ion-exchange microencapsulated resin beads—prepared by various methods, evaluated for release rate □ Delivery systems—microencapsulated ion-exchange resin beads, prepared by various methods, evaluated for release rate □ Dosage forms, potential—microencapsulated ion-exchange resin beads, prepared by various methods, evaluated for release rate

Ion-exchange resins function as effective carriers for prolonging drug release for sustained biological action and for improvement of other pharmacokinetic parameters such as the absorption rate constant (1). In addition, ion-exchange resins are used for binding biological materials such as bile salts and sodium ions within the GI tract (2, 3). While ion-exchange resins form a useful drug delivery system, improvements can be effected in some cases by coating the resin beads with various pharmaceutical adjuvants. Potential improvements are: enhancing the taste of ion-exchange resins (4, 5), decreasing the release rate of drugs from the resins (5, 6), permitting greater saturation of the resin with the drug and a slower elution rate (6), minimizing elution of drug in liquid preparations of ion-exchange resin–drug complexes (6, 7), and minimizing interaction of drugs with resins used as tablet disintegrants (8).

One effective and versatile method of coating small solid particles is microencapsulation, which can be accomplished with various procedures (5, 9, 10). Many researchers discussed the encapsulation of solid particles (11–16), but few applied the process to ion-exchange resins (4, 17). It was deemed appropriate to investigate microencapsulation procedures for the preparation of coated ion-exchange resins to exploit the value of resin beads, such as uniform size and consistent binding of drugs, for improving their pharmaceutical characteristics. Specifically, it was expected that medication with a wide range of prolonged-release characteristics could be prepared. In addition, it was hoped that a uniform coat around the beads could be obtained by various encapsulation methods.

The effect of additives on the characteristics of the film used to coat pharmaceuticals also was investigated. In some cases, additives selected are of such a nature that the rate of transmission or release of drugs is increased (12, 18) or decreased (19). Part of the present research is concerned with employing additives in the preparation of the microencapsulating film to prolong or delay the release so that the coated beads can be considered for other uses in pharmacy besides oral medication.

EXPERIMENTAL

Materials—All experiments were carried out with a 20–50-mesh strongly basic ion-exchange resin[1] in the benzoate form. The resin was screened wet; the beads that passed through a 35-mesh screen but were retained on a 40-mesh screen were used. The resin then was cleaned, conditioned, and converted into the benzoate form by the procedure described previously (20). The average particle size of the resin beads, as determined by microscopic measurement of 30 beads, was 0.366 mm (wet) and 0.325 mm (dry).

Encapsulation Procedures—*Polymer–Polymer Interaction*—The method of Luzzi and Gerraughty (14, 21), adapted from Green and Schleicher (22, 23), was modified for the encapsulation of the resin beads. In this method, the interaction of oppositely charged polyelectrolytes results in the formation of a complex of considerably reduced solubility such that phase separation occurs. The specific procedure used consisted of dissolving 3 g of acacia[2] and 3 g of gelatin[3] separately in 100 ml of distilled water each. The solutions were warmed to 55° and mixed, and the pH was adjusted to 6.5 with 20% NaOH. The resin beads (2 g) then were added, and the pH of the mixture was altered to 4.5 by the dropwise addition of dilute hydrochloric acid with stirring.

The temperature was allowed to drop, and the polymers coalesced around the resin beads. Subsequently, 10 ml of formaldehyde solution USP was added, and the mixture was cooled to 10° by immersion in an ice bath with constant stirring. The pH then was adjusted to 9.0 by the dropwise addition of 20% NaOH. The mixture was diluted to approximately 400 ml with distilled water, left overnight, and then centrifuged for 30 min at 2700 rpm.

The supernate was decanted, and the microencapsulated beads were transferred to a 60-mesh screen and washed with water to remove the empty capsules. The capsules remaining on the screen were poured into a flask along with 100 ml of distilled water. After settling, water was removed by rinsing the capsules with three 50-ml portions of 95% ethanol. The mixture was filtered, washed with ethanol, and dried in a desiccator.

Temperature Change—Five methods of preparation were evaluated.

[1] Dowex 1-X8, Dow Chemical Co., Midland, Mich.
[2] Gum Acacia BP, British Drug Houses (Canada) Ltd., Toronto, Canada.
[3] Gelatin, Pharmagel A., American Agricultural Co., Detroit, Mich.

0022-3549/79/0200-0211$01.00/0
© 1979, American Pharmaceutical Association

Table I—Data on the Microencapsulation of Ion-Exchange Resins

Abbreviation	Encapsulating Material	Encapsulating Material[a], g / Resin Complex, g	Radius of Encapsulated Bead, mm[b]	B, min^{-1} [c]	D, cm^2 sec^{-1} [d]
I	No coat	—	0.1830	0.0748	4.23×10^{-8}
II	Ethylcellulose standard 20[e]	0.1485	0.1916	0.0417	2.58×10^{-8}
III	Ethylcellulose standard 100	0.1419	0.1913	0.0422	2.60×10^{-8}
IV	Ethylcellulose medium 50	0.1274	0.1905	0.00923	5.65×10^{-9}
V	Ethylcellulose medium 100	0.1198	0.1900	0.00613	3.73×10^{-9}
VI	Gelatin–acacia	0.3963	0.2045	0.0548	3.87×10^{-8}
VII	Cellulose acetate butyrate	0.1289	0.1905	0.00564	3.45×10^{-9}
VIII	II plus butyl stearate	0.1587	0.1922	0.0124	7.73×10^{-9}
IX	II plus castor oil	0.2332	0.1963	0.0393	2.55×10^{-8}
X	II plus polyethylene	0.1334	0.1908	0.0119	7.31×10^{-9}
XI	II plus polyethylene and paraffin	0.2438	0.1968	0.00124	8.11×10^{-10}
XII	III plus butyl stearate	0.1822	0.1935	0.0202	1.27×10^{-8}
XIII	III plus castor oil	0.1988	0.1944	0.0208	1.32×10^{-8}
XIV	III plus polyethylene	0.1185	0.1900	0.00110	6.70×10^{-10}
XV	III plus polyethylene and paraffin	0.3406	0.2018	0.000690	4.74×10^{-10}

[a] Average values of two different preparations, except for cellulose acetate butyrate where three preparations were used. [b] Radius was calculated with the assumptions that the resin bead was wet and the density of the bead and the coating materials in the buffer solution was 1. [c] The values of B were obtained from the initial slopes of the Bt–t plots using observed data of values 2 hr and less and fractional attainment of equilibrium 0.9 or less; see text for discussion. [d] D is the diffusion coefficient. [e] Simple coats are II–VII; complex or mixed coats are VIII–XV.

1. The method of Miller *et al.* (24) utilizes the phase separation coacervation of a binary system of ethylcellulose and cyclohexane. At high temperature, a single homogeneous phase exists; upon cooling, phase separation occurs. The polymer at the appropriate concentration, temperature, and agitation conditions coalesces around the dispersed core particles. Ethylcellulose standard[4], 20 or 100 cps, 0.4 g, with an ethoxyl content of 48–49.5% was dispersed in 25 ml of cyclohexane and heated under reflux at about 80° until the ethylcellulose dissolved. Then 2 g of resin beads was added, and the mixture was refluxed for 2 hr. Throughout the whole procedure, the mixture was stirred with a magnetic stirring bar. The mixture was allowed to cool slowly to room temperature, and the encapsulated beads were separated from the solvent by filtration, air dried, and sieved.

2. A similar procedure was used when ethylcellulose medium[5], 50 or 100 cps, with an ethoxyl content of 45–46.5% was employed as the polymer; however, 5 ml of 95% ethanol was added to improve the solubility characteristics of the solvent.

3. The temperature change technique was modified to alter the film characteristics by using a low molecular weight polyethylene, which was reported to be a phase separation-inducing material (25, 26). Ethylcellulose standard[4], 20 or 100 cps, 0.4 g, and polyethylene[6], 0.4 g, were dispersed in 25 ml of cyclohexane at room temperature and solubilized by raising the temperature to 80°. The procedure was continued as described for Method 1.

4. Method 3 may be modified since the hydrophobic walls can be made more impervious by treating the ethylcellulose capsules with a solution of wax in a solvent capable of swelling, but not dissolving, the capsule wall so that the wax solution penetrates the swollen capsule wall. The capsules are then separated from the solvent and dried so that the wax is entrapped in the polymeric capsule wall (25). The microencapsulated resin beads prepared by Method 3 were dispersed in a 20% solution of hard paraffin in cyclohexane, agitated at room temperature for 30 min, separated from the wax-containing solvent system by suction filtration, and air dried. The dry beads were sieved through a convenient mesh size screen to get rid of dust and broken particles.

5. Ethylcellulose is compatible with many common plasticizers. The plasticizer, when added to the polymer, is capable of forcing the polymer chains apart, thus producing a softening effect. Castor oil and butyl stearate, which produce a considerable softening effect, were employed (27). The ethylcellulose standard[4], 20 or 100 cps, 0.4 g, was dispersed in 25 ml of cyclohexane, and the mixture was refluxed until the polymer dissolved. Then 0.2 g of butyl stearate or 0.2 g of castor oil and 2 g of dry resin were added, and the mixture was refluxed for 2 hr. The mixture was stirred constantly with a magnetic stirring bar during the heating process and for 1 additional hr during cooling. The separation of the beads from the solvent was the same as described for Method 1.

Nonsolvent Addition—This technique is used to induce phase separation by the addition of a liquid that is a nonsolvent for the polymer (28). Cellulose acetate butyrate[7], 0.5 g, was dissolved in 20 ml of methyl ethyl ketone by heating. The dry resin beads (2 g) were then added and dispersed in the solution. The mixture was heated to 55°, and 30 ml of isopropyl ether was added dropwise. The system was allowed to cool slowly to room temperature, and the encapsulated beads were separated by centrifugation, washed with isopropyl ether, and dried in a vacuum.

All microencapsulated beads were stored in a desiccator.

Kinetic Studies—The *in vitro* evaluation of the release rate from the microencapsulated resin beads was carried out by the following procedure. The release pattern of the microencapsulated resin samples was determined by using a centrifugal basket stirrer similar to that used for ion-exchange rate measurements (29). The top and bottom of the cylindrical basket, 1 cm in diameter and 1.5 cm high, were made from 80 wire mesh screen. The basket was enclosed in a cylindrical aluminum body with an opening at the bottom and a series of horizontal holes above the basket. Upon rotation, the water flowed through the bottom of the basket out of the top and then through the holes in the aluminum body as a result of centrifugal force.

About 0.1 g of the microencapsulated resin was weighed accurately and placed into the basket. The basket, in the aluminum body attached to an electric stirrer, was then introduced into a two-neck, round-bottom, 500-ml flask containing 200 ml of a pH 9.2 buffer (containing 12.095 g of dibasic potassium phosphate in 1 liter of solution) previously equilibrated and maintained at 30° with a constant-temperature water bath. The basket was rotated at 1400 rpm. Samples (5 ml) were removed at suitable times and diluted to 50 or 100 ml with the phosphate buffer.

The amount of benzoate released from the resin was determined spectrophotometrically at 224.5 nm from a standard calibration curve for sodium benzoate in the phosphate buffer. The amount released was expressed in terms of sodium benzoate per gram of dry uncoated resin. Each kinetic run, up to 168 hr, was carried out in triplicate. The absorbances of the coating materials at the dilutions used for analysis were negligible.

The amount of material covering the resin beads was determined by dissolving the encapsulating material from a known weight of the encapsulated beads; ethylcellulose and films containing castor oil and butyl stearate dissolved with 95% ethanol; films containing polyethylene, paraffin, and cellulose acetate butyrate dissolved with chloroform; and gelatin–acacia film dissolved with 0.1 N NaOH in water and 95% ethanol. The decapsulated resin was then dried and weighed.

RESULTS AND DISCUSSION

Microscopic examination, a loss of weight upon extraction, and slower rates of release of benzoate ion from the beads indicated that microencapsulation does, in fact, occur and can be accomplished by several methods. Microscopic observation showed that the beads were covered uniformly with the encapsulating material in all cases. Thus, microencapsulation tends to give a more uniform and more consistent coat than other procedures (20).

The ratio of encapsulating material to resin complex was reasonably

[4] Ethocel Standard 20 or Ethocel Standard 100, Dow Chemical Co., Midland, Mich.

[5] Ethocel Medium 50 or Ethocel Medium 100, Dow Chemical Co., Midland, Mich.

[6] Molecular weight 5000, Allied Chemicals, Toronto, Canada.

[7] Cellulose acetate butyrate, Eastman Kodak Co., Rochester, N.Y.

Table II—Elution Data

Encapsulating[d] Material	Amount of Benzoate (Milligrams) Released[a] per Gram of Resin Complex[b] as a Function of Time[c]												
	Minutes						Hours						
	5	10	15	20	25	30	1	2	24	48	72	96	168
I	236	291	320	336	345	352	370	375	379	381	—[e]	—	—
II	130	202	243	273	293	307	348	368	375	377	380	—	—
III	134	206	245	274	293	303	342	359	370	374	—	—	—
IV	46	82	114	139	150	168	234	291	369	—	—	—	—
V	32	60	82	100	114	129	192	255	369	370	—	—	371
VI	134	190	220	237	249	257	273	280	286	291			
VII	46	76	97	112	127	135	179	236	314	315	320	327	348
VIII	61	104	134	158	176	194	271	327	383	—	—	—	384
IX	149	218	261	288	310	325	367	390	398	406	—	—	—
X	80	131	164	190	207	222	268	299	347	—	—	—	349
XI						69	102	135	246	271	368	—	369
XII	82	138	177	207	232	250	313	359	388	—	—	—	—
XIII	85	144	183	217	242	260	330	373	405	—	—	—	—
XIV	3	13	20	28	34	40	67	113	239	274	308	318	329
XV						3	9	15	65	76	152	167	182

[a] Expressed as sodium benzoate. [b] Expressed in terms of resin complex, exclusive of encapsulating material. [c] These are average values of triplicate determinations on a single preparation. [d] See Table I for key. [e] Dashes indicate no further appreciable change.

consistent since the values for individual preparations were within 10% of the average value (Table I), except with cellulose acetate butyrate and ethylcellulose standard 100 when combined with castor oil or butyl stearate where individual values were within 20% of the average value. In general, many ratios were close to a value of 0.12 for the simple encapsulating agents except gelatin, which had a value of 0.39. The addition of butyl stearate, castor oil, and the polyethylene–paraffin combination increased the ratio considerably in conjunction with either cellulose material.

The amount of benzoate, expressed as the sodium salt in milligrams released per gram of resin complex as a function of time, is given in Table II. Samples of the buffer solution were analyzed for benzoate until there was no appreciable change or periodically up to 168 hr; these values were taken to be the equilibrium values. A comparison of the amounts released over this period of 168 hr is useful in terms of the potential use of the encapsulated resin complex as implants or in certain pharmaceutical suspensions.

Table II indicates that, even after 168 hr of elution, a considerable amount of the anion was contained within the resin when it was coated with ethylcellulose standard 100 in combination with polyethylene or both polyethylene and paraffin. The absorbancies of the eluant from the gelatin–acacia-covered resin complex began to decrease after 48 hr, suggesting that some other process such as decomposition or binding was occurring.

The release from the uncoated resin complex was almost complete at 1 hr and had reached an equilibrium within 24 hr; these results are similar to reported findings (20). All coatings decreased the rate of release of the anion from the resin complex. A comparison of the amounts released at the end of the 24-hr period is useful in terms of the potential use of the resin complex as an oral prolonged-release agent where the prolongation of action of the resin itself is further enhanced by the encapsulating material. At the end of 24 hr, two simple coats, cellulose acetate butyrate and gelatin–acacia, and four mixed coats, ethylcellulose standard 20 or 100 in combination with polyethylene or polyethylene and paraffin, prevented the full release of the anion from the resin complex. All ethylcelluloses and the ethylcelluloses in combination with the plasticizers butyl stearate and castor oil released the anion within 24 hr. The plasticizers tended to decrease the initial rate of release and yet permit full release within the 24-hr period.

A comparison of the effect of the encapsulating material on the release of the benzoate during the elution procedure in terms of equilibrium values can be made from the values of the fractional attainment of equilibrium, U, calculated from:

$$U = \frac{R}{R_\infty} \qquad \text{(Eq. 1)}$$

where R is the amount of benzoate released at time t and R_∞ is the amount released at equilibrium as already defined. Representative data (Figs. 1 and 2) clearly indicate the delaying action of the encapsulating materials on the resin complex over a period of time. Ion exchange took place almost immediately, in most cases due to the thin film and the uptake of moisture by the encapsulating materials.

A comparison of the fractional attainment of equilibrium (Fig. 1) of the simple coating material at 1 hr showed that the order of increasing prolongation was as follows: no coat, gelatin–acacia, ethylcellulose standard 20 ~ ethylcellulose standard 100, ethylcellulose medium 50, ethylcellulose medium 100, and cellulose acetate butyrate. All of these coatings had approximately the same ratio of encapsulating material to resin complex except gelatin–acacia; consequently, the properties of the films themselves were primarily responsible for the observed effects rather than the thickness of the coat.

The viscosity numbers (in organic solvents), which are the suffixes of the ethylcellulose compounds listed, are roughly indicative of the size of the ethylcellulose molecule and, within limits, the toughness of the deposited film. In addition, ethylcellulose medium at equivalent molecular weights is reported to be tougher than the standard and have a slightly higher specific gravity (27). The experimental results are in agreement with the concept that tough dense films of large molecular weight compounds delay the release of the anions. For a series of cellulose ester films, water permeability decreased with an increase in the chain length of the nonpolar acid moiety (30). The decrease in the diffusion of ions with an increase of the density of the film also was reported previously (31). The cellulose acetate butyrate film released the anion at a lower rate compared to the cellulose standard, which had a lower specific gravity (32). Thus, the decrease in the exchange rate of phosphate and benzoate ions across the film probably was due to the increase in the molecular weight, the more nonpolar character, and the higher specific gravity of the film, and these properties are related to the decreased water permeability. Gelatin–acacia, the thickest coat, provided the fastest initial rate of release. This effect can be partially explained by the polar character of the film and its ability to swell in water (33).

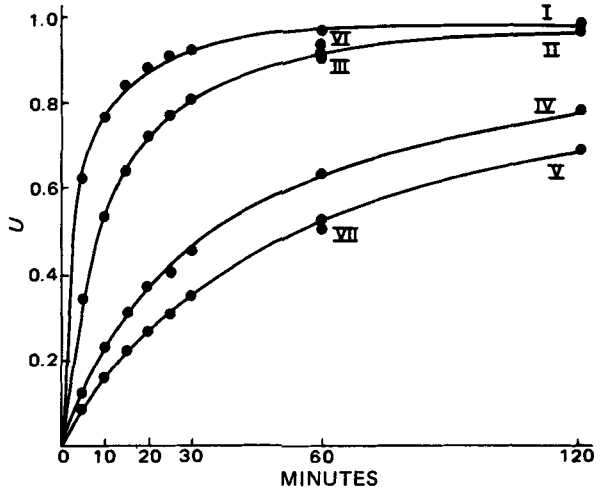

Figure 1—*Typical curves illustrating the effect of simple encapsulating agents on the fractional attainment of equilibrium. Each point is the average of three kinetic experiments at the time indicated. Some curves were omitted for clarity. Key: see Table I.*

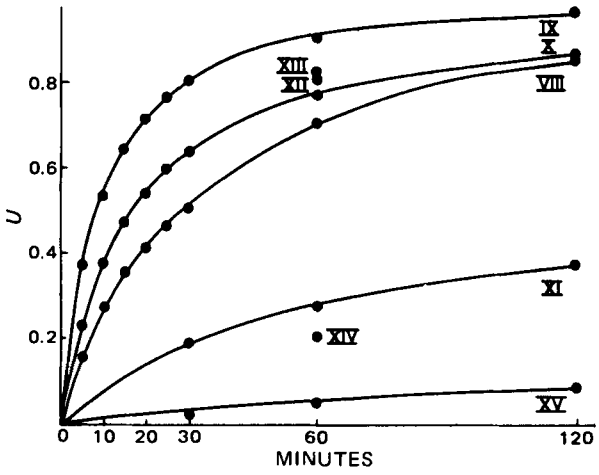

Figure 2—*Typical curves illustrating the effect of complex encapsulating agents on the fractional attainment of equilibrium. Each point is the average of three kinetic experiments at the time indicated. Some curves were omitted for clarity. Key: see Table I.*

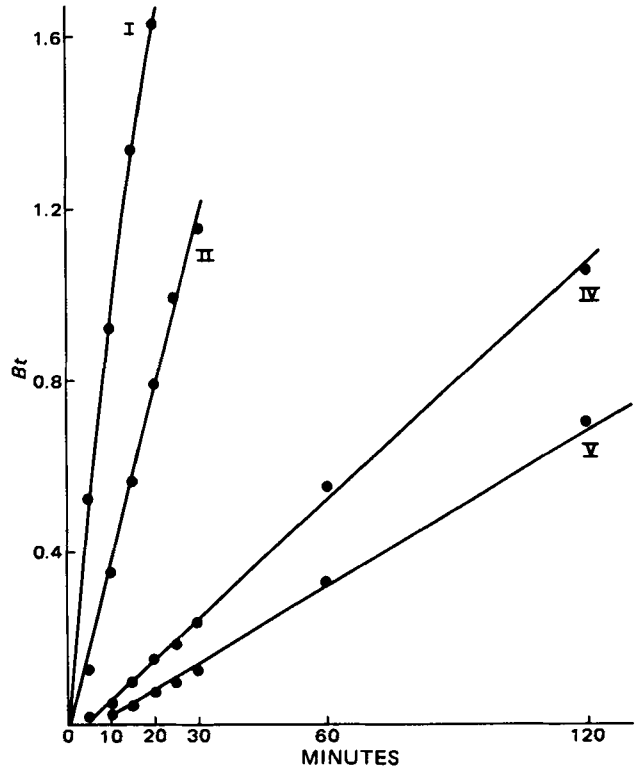

Figure 3—*Typical* Bt-t *plots showing the effect of simple encapsulating agents on the elution of benzoate ion from resin beads. Key: see Table I.*

Figure 2 provides information on the fractional attainment of equilibrium for complex coats. Water probably would be required to permit the transport of ions across the film. Thus, the addition of nonpolar compounds to the ethylcellulose film would decrease the water uptake or water transmission and, hence, lower the rate of anion exchange. Lipophilic films have been found to be less permeable to moisture than hydrophilic systems (19). Other studies indicated that the release rate of water-soluble compounds like neomycin sulfate can be enhanced by increasing the polarity of additives in the films or the celluloses comprising the film (34, 35).

In the present experiments, the additives with the greatest lipophilic character, polyethylene and paraffin, produced the greatest resistance to ion transfer as compared to the not quite so lipophilic compounds castor oil and butyl stearate (Fig. 2). Thus, the release characteristics and water transmission properties of the films depend on the lipophilic and hydrophilic characteristics of the film as influenced by the additives and matrix. In nearly all cases, ethylcellulose standard 100, a tougher film in combination with additives (except butyl stearate), was more effective than ethylcellulose standard 20 in delaying the release of the anion from the resin.

The theoretical treatment of the rate of ion exchange was described (36) and reviewed in detail (37), and the rate equations suitable for sustained release from ion-exchange resins were developed previously (38). The mathematical equation deals with ion exchange within resin beads of spherical shape and uniform diameter in a solution of infinite volume. Some of the experimental conditions did not meet these criteria; for example, the concentration of benzoate ion increased appreciably during the kinetic study, negating the requirement of infinite solution volume. The beads can be regarded as spherical, and diffusion of the benzoate ion probably could take place through all of the encapsulating materials since they or similar films are permeable to water and can absorb water to some extent (27, 32, 39, 40). It is of value to treat the rate of release in this theoretical manner to assist in the interpretation of the effect of the various films.

The method of calculation was described fully (37, 38). The values of the fractional attainment of equilibrium are related to the rate constant B by a summation equation. The rate constant B is defined as:

$$B = \frac{\pi^2 D}{r^2} \qquad \text{(Eq. 2)}$$

where D is the diffusion coefficient and r is the mean particle radius of the resin beads. To calculate the rate constant, values of Bt corresponding to values of fractional attainment of equilibrium (41) are plotted against t; the slope of the line yields the rate constant B. These data are plotted in Figs. 3 and 4. If the line is straight, it can be assumed that ionic diffusion within the resin bead is the rate-controlling step in the diffusion process (41). The rate of release from the uncoated resin beads and most coated beads yields a Bt–t relationship close to linearity over a major portion of the graph (Figs. 3 and 4), suggesting that the diffusion of ions is controlled by a particle diffusion process. Thus, the encapsulating material, while decreasing the rate of release considerably in a number of cases (Figs. 3 and 4), still permits the rate to follow the particle diffusion process of ion exchange.

The Bt–t plots over the complete timespan show deviation from linearity. Materials that rapidly release the anion show a decrease from linearity when the fractional attainment approaches 0.9, possibly as a result of not satisfying the infinite solution volume conditions. Plots of release of encapsulated resins possessing very slow rates of release also show deviations, probably due to a mechanical breakdown of the film as a result of wear or rupture in the rotating basket, thus causing a considerably greater rate of release as the system approaches equilibrium. Two clear examples are the Bt–t plots for ethylcellulose standard 20 and 100 polyethylene paraffin films, which show a very definite jump over the 48–72-hr period.

For discussion purposes, the resin bead and the encapsulating material can be treated as a homogeneous ion-exchange system in view of the linearity of the Bt–t plots and the relatively small increase in the particle diameter caused by the encapsulating material (Table I). The slopes of the Bt–t plots (Figs. 3 and 4 and Table I) were determined from the initial release, using the observed data of 2 hr and less and values of fractional attainment less than 0.9, corresponding to a Bt value of 1.8. To compare the effectiveness of the various coatings on the particle diffusion, values of B were determined from the slope of the Bt–t plots and the diffusion coefficients were determined from Eq. 2 using the radius of the encapsulated beads listed in Table I.

Dissolution and ion exchange, as shown from the Bt–t plots, are important factors governing the rate of drug release. In addition, release of drugs from polymers soluble in the digestive system can be influenced by the permeability of the film and the rate of dissolution of the polymer. Permeability would be a major factor governing the rate of release through a polymer such as ethylcellulose, which is insoluble in water (42). Recent papers (42, 43) indicated that two major mechanisms may be responsible for the diffusion of drugs through films of ethylcellulose, namely, a solubility diffusion process and a transfer through a capillary network. In the present research, both the benzoate and phosphate probably would be transported through the ethylcellulose when the film contains water, thus permitting a greater solubility of the ions.

Previous papers suggest that water vapor transmission and drug release are reduced when the interstices of the film are filled with nonpolar plasticizers such as hexadecyl alcohol, at least over a certain range of concentration of the additive. Somewhat more polar additives like tri-

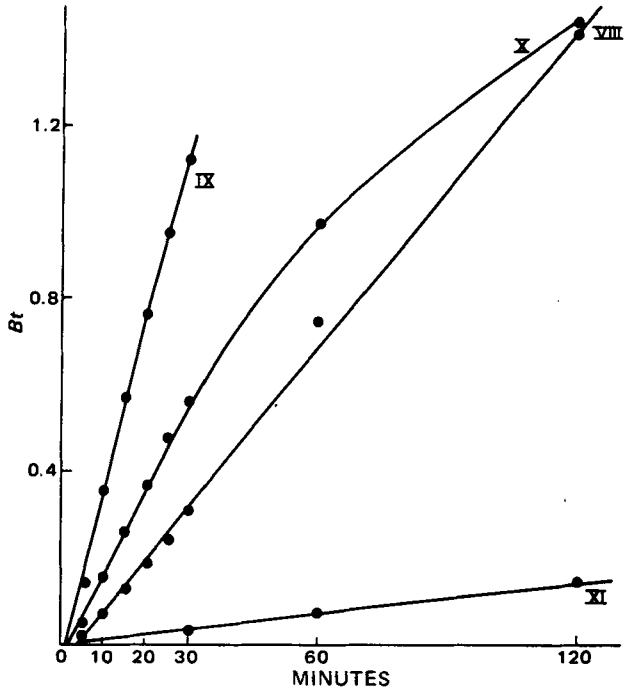

Figure 4—*Typical* Bt-t *plots showing the effect of complex encapsulating agents on the elution of benzoate ion from resin beads. Key: see Table I.*

butyl citrate tend to increase the rate (34, 39). A lipophilic film of *n*-butyl methacrylate was less permeable to moisture than hydrophilic films like hydroxypropylcellulose (19). Large organic ions were released more quickly when the more polar hydroxypropylcellulose content of the cellulose films was increased (44). The permeability of cellulose ester films decreased with the increasing chain length of the acid moiety used, and the plasticizer enhanced or retarded moisture permeation (32).

A review of the rate constants, *B*, or diffusion coefficients, *D*, in Table I supports the suggestion that lipophilic films or the incorporation of lipophilic additives prolongs the release of the anion. The tougher ethylcellulose medium and the nonpolar cellulose acetate butyrate prolonged the release more than the ethylcellulose standard and the polar gelatin films. When additives or plasticizers were added to the ethylcellulose standard 20 and 100 films, the release was further prolonged by the nonpolar compounds. The addition of castor oil to ethylcellulose 20 did not produce appreciable differences but caused almost a 50% decrease in the diffusion coefficient of ethylcellulose standard 100, and butyl stearate provided a generally greater decrease. Polyethylene, especially in conjunction with ethylcellulose standard 100, produced a further reduction; when it was used along with the additive paraffin, the maximum prolongation of release was achieved.

REFERENCES

(1) "The Theory and Practice of Industrial Pharmacy," L. Lachman, H. A. Lieberman, and J. L. Kanig, Eds., Lea & Febiger, Philadelphia, Pa., 1970, p. 427.

(2) H. Ko and M. E. Royer, *J. Pharm. Sci.*, **63**, 1914 (1974).

(3) "Ion Exchangers in Organic and Biochemistry," C. Calmon and T. R. E. Kressman, Eds., Interscience, New York, N.Y., 1957, p. 451.

(4) S. Borodkin and D. P. Sundberg, *J. Pharm. Sci.*, **60**, 1523 (1971).

(5) J. A. Bakan and F. D. Sloan, *Drug Cosmet. Ind.*, **110**, 34 (1972).

(6) P. R. Berg and P. Ostrup, *Dan. Tidsskr. Farm.*, **40**, 33, 55 (1966); through *Int. Pharm. Abstr.*, **3**, 956a (1966).

(7) "Remington's Pharmaceutical Sciences," 13th ed., E. W. Martin, Ed., Mack Publishing Co., Easton, Pa., 1965, p. 620.

(8) S. Borodkin and M. H. Yunker, *J. Pharm. Sci.*, **59**, 481 (1970).

(9) L. A. Luzzi, *ibid.*, **59**, 1367 (1970).

(10) H. Nack, *J. Soc. Cosmet. Chem.*, **21**, 85 (1970).

(11) J. R. Nixon and S. E. Walker, *J. Pharm. Pharmacol.*, **23**, 147S (1971).

(12) L. A. Luzzi and R. J. Gerraughty, *J. Pharm. Sci.*, **56**, 1174 (1967).

(13) H. P. Merkle and P. Speiser, *ibid.*, **62**, 1444 (1973).

(14) L. A. Luzzi and R. J. Gerraughty, *ibid.*, **56**, 634 (1967).

(15) P. L. Madan, L. A. Luzzi, and J. C. Price, *ibid.*, **63**, 280 (1974).

(16) W. Feinstein and J. J. Sciarra, *ibid.*, **64**, 408 (1975).

(17) R. E. Phares, Jr., and G. J. Sperandio, *ibid.*, **53**, 515 (1964).

(18) A. G. Daragan, *Aptechn. Delo*, **15**, 20 (5) (1966); through *Int. Pharm. Abstr.*, **4**, 129e (1967).

(19) G. S. Banker, A. Y. Gore, and J. Swarbrick, *J. Pharm. Pharmacol.*, **18**, 457 (1965).

(20) S. Motycka and J. G. Nairn, *J. Pharm. Sci.*, **67**, 500 (1978).

(21) L. A. Luzzi and R. J. Gerraughty, *ibid.*, **53**, 429 (1964).

(22) B. K. Green and L. Schleicher, U.S. pat. 2,730,456; through Ref. 21.

(23) B. K. Green and L. Schleicher, U.S. pat. 2,730,457; through Ref. 21.

(24) R. E. Miller, G. O. Fanger, and R. G. McNiff, Union of South Africa pat. 4211–66; through Ref. 1, p. 395.

(25) National Cash Register Co., British pat. 1,117,270; through *Chem. Abstr.*, **69**, 46070a (1968).

(26) T. C. Powell and J. L. Anderson, German Offen. 1,917,930; through *Chem. Abstr.*, **72**, 67893y (1970).

(27) "Ethocel for Coatings Applications," Dow Chemical Co., Midland, Mich., 1966.

(28) E. N. Heistand, J. G. Wagner, and E. L. Knoechel, U.S. pat. 3,242,051 (1966); through Ref. 1, p. 396.

(29) F. Helfferich, "Ion Exchange," McGraw-Hill, New York, N.Y., 1962, p. 310.

(30) M. Patel, J. M. Patel, and A. P. Lemberger, *J. Pharm. Sci.*, **53**, 286 (1964).

(31) K. Takamura, M. Koishi, and T. Kondo, *ibid.*, **62**, 610 (1973).

(32) "Modern Plastics Encyclopedia," vol. 53, no. 10A, McGraw-Hill, New York, N.Y., 1976, p. 458.

(33) H. Schott, *Am. J. Pharm. Educ.*, **36**, 104 (1972).

(34) J. Sciarra, S. P. Patel, and M. Luongo, *Drug Dev. Commun.*, **1**, 539 (1974–75).

(35) V. Coletta and H. Rubin, *J. Pharm. Sci.*, **53**, 953 (1964).

(36) G. E. Boyd, A. W. Adamson, and L. S. Myers, Jr., *J. Am. Chem. Soc.*, **69**, 2836 (1947).

(37) F. Helfferich, "Ion Exchange," McGraw-Hill, New York, N.Y., 1962, p. 250.

(38) N. C. Chaudhry and L. Saunders, *J. Pharm. Pharmacol.*, **8**, 975 (1956).

(39) J. J. Sciarra and S. P. Patel, *J. Soc. Cosmet. Chem.*, **23**, 605 (1972).

(40) C. W. Woodruff, G. E. Peck, and G. S. Banker, *J. Pharm. Sci.*, **61**, 1956 (1972).

(41) D. Reichenberg, *J. Am. Chem. Soc.*, **75**, 589 (1953).

(42) M. Donbrow and M. Friedman, *J. Pharm. Pharmacol.*, **26**, 148 (1974).

(43) *Ibid.*, **27**, 633 (1975).

(44) N. B. Shah and B. B. Sheth, *J. Pharm. Sci.*, **61**, 412 (1972).

ACKNOWLEDGMENTS

The authors thank Dr. J. Motycka, Mechanical Engineering Department, University of Toronto, for preparing the rotating-basket apparatus.

GLC Analysis of Loxapine, Amoxapine, and Their Metabolites in Serum and Urine

T. B. COOPER * **and R. G. KELLY** ‡x

Received March 30, 1978, from the *Rockland Research Institute, Orangeburg, NY 10962, and ‡Lederle Laboratories, American Cyanamid Company, Pearl River, NY 10965. Accepted for publication July 18, 1978.

Abstract □ A GLC analysis is presented for loxapine, amoxapine, and their major metabolites in serum and urine. Electron-capture detection is employed for serum analysis, and flame ionization is used for urine analysis. The procedure includes trifluoroacetylation of secondary amine functions, followed by trimethylsilylation of phenolic groups after ethyl acetate extraction of the sample. Urine requires prior enzymatic hydrolysis of conjugates. Data indicating the utility of the procedure in hospitalized patients and normal volunteers are presented.

Keyphrases □ Loxapine—and metabolites, GLC analysis in serum and urine □ Amoxapine—and metabolites, GLC analysis in serum and urine □ GLC—analysis, loxapine, amoxapine, and their metabolites in serum and urine □ Antipsychotics—loxapine and metabolites, GLC analysis in serum and urine □ Antidepressants—amoxapine and metabolites, GLC analysis in serum and urine

Loxapine[1] succinate, 2-chloro-11-(4-methyl-1-piperazinyl)dibenz[*b,f*][1,4]oxazepine succinate, is a new antipsychotic agent effective in the treatment of acute and chronic schizophrenia (1–5). It is the only member of the dibenzoxazepine class currently available in the United States. Amoxapine (*N*-desmethylloxapine), a new drug with antidepressant properties, is currently in advanced clinical evaluation. The metabolic pathways (Scheme I) for these drugs were investigated[2]. This paper describes methods for the quantitation of loxapine, amoxapine, and their 7- and 8-hydroxylated metabolites using GLC following trifluoroacetylation of the secondary amine functions and trimethylsilylation of the phenolic groups.

EXPERIMENTAL

Reagents—Ethyl acetate, ACS reagent grade, was passed through an alumina column or glass distilled immediately prior to use. Carbonate buffer, pH 9.7, was prepared by mixing nine parts of 1 *M* Na_2CO_3 with one part of 1 *M* $NaHCO_3$. Trifluoroacetic anhydride[3], *N*-trimethylsilyldiethylamine[3], β-glucuronidase[4], and 8-methoxyloxapine[5] were used as received.

Apparatus—The gas-liquid chromatograph[6] was equipped with a ^{63}Ni-constant current electron-capture detector and a flame-ionization detector. Glass-stoppered 15- and 5-ml centrifuge tubes were soaked overnight in a concentrated detergent solution and then washed in tap water. The washed tubes were immersed for a minimum of 3 hr in dichromate cleaning fluid and washed again with a final rinse in approximately 1 *M* NH_4OH, followed by three distilled water rinses.

Chromatographic Conditions—Columns were 1.8-m × 2- or 4-mm glass tubes packed with 3% SP 2100 on 100–120-mesh Supelcoport[7]. The temperatures were: oven, 255°; injection port, 280°; and detector, 300°. Argon–methane (95:5) was used as both the carrier and electron-capture detection gas for that mode of detection. Helium was the carrier gas in flame-ionization detection.

Procedure—For the analysis of serum, a sample (1–3 ml) was added to a 15-ml glass-stoppered tube, followed by 0.2 ml of a 500-ng/ml solution of 8-methoxyloxapine (internal standard), 1 ml of 1 *M* pH 9.7 carbonate buffer, and 5 ml of ethyl acetate. The tube was shaken and centrifuged. The organic layer was transferred to a clean 5-ml tube, 1 ml of 0.1 *N* HCl was added, and the contents were shaken and centrifuged. The ethyl acetate was aspirated, and clean ethyl acetate (4 ml) was added to wash the acid extract.

The organic solvent was aspirated, and fresh ethyl acetate (4 ml) was added along with 1 ml of pH 9.7 carbonate buffer. The tube was shaken and centrifuged, the ethyl acetate phase was transferred to a clean 5-ml centrifuge tube, and the solvent was removed by a nitrogen stream. A 0.1-ml aliquot of a solution containing two parts of trifluoroacetic anhydride and five parts of ethyl acetate was added, and the tube was permitted to stand 10 min.

The reagent was removed by evaporation with a nitrogen stream, and 20 μl of *N*-trimethylsilyldiethylamine was added to the residue. The tube was stoppered and heated for 3 hr at 60°. Alternatively, the tube was permitted to stand overnight at room temperature. A 1–2-μl aliquot was injected into the gas chromatograph, and peaks were detected by electron capture.

For urine analysis, a sample (2–5 ml) was added to a tube containing

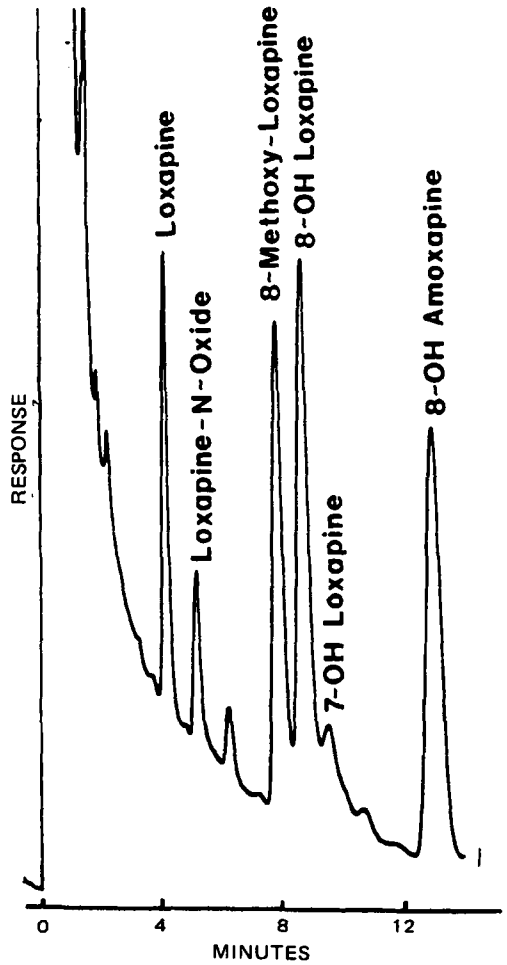

Figure 1—*Chromatogram of serum from a subject receiving loxapine intramuscularly.*

[1] Loxitane, Lederle Laboratories.
[2] Unpublished results.
[3] Pierce Chemical Co., Rockford, Ill.
[4] Glusulase, Endo Laboratories, Garden City, N.Y.
[5] Supplied by Dr. R. A. Hardy, Jr., and Dr. C. F. Howell, Lederle Laboratories, Pearl River, N.Y.
[6] Either a model 900, Perkin Elmer, Norwalk, Conn., or a model 222, Tracor, Austin, Tex.
[7] Supelco, Bellefonte, Pa.

0022-3549/79/0200-0216$01.00/0
© 1979, American Pharmaceutical Association

Table I—Precision Observed on Analysis of 10 Consecutive Standard Curves in Serum Containing Loxapine and Amoxapine Metabolites at the Concentration Indicated

Amount Added, ng/ml	Peak Height Ratio											
	Loxapine		Amoxapine		8-Hydroxyloxapine		7-Hydroxyloxapine		8-Hydroxyamoxapine		7-Hydroxy-amoxapine	
	Mean	*SD*	Mean	*SD*	Mean	*SD*	Mean	*SD*	Mean	*SD*	Mean	*SD*
5	0.128	0.0134	0.249	0.0444	0.132	0.0171	0.141	0.0154	0.275	0.0653	0.302	0.0482
10	0.268	0.0299	0.445	0.0870	0.277	0.0430	0.277	0.0377	0.524	0.0626	0.569	0.0521
15	0.422	0.0457	0.673	0.1298	0.446	0.0723	0.485	0.0415	0.790	0.1097	0.888	0.1083
20	0.585	0.0666	0.964	0.1377	0.604	0.0871	0.700	0.0511	1.056	0.1423	1.207	0.1370
25	0.750	0.1146	1.236	0.2230	0.779	0.1362	0.895	0.0808	1.320	0.3298	1.476	0.3057

10 μg of added 8-methoxyloxapine. (For analysis of urinary loxapine, 10 μg of amoxapine may be used as the internal standard.) The urine pH was adjusted to 5.0 ± 0.2 with 10% acetic acid. Glucuronidase solution, 0.5 ml, was added, and the sample was permitted to incubate for 48 hr at room temperature. A 1-ml aliquot of a 20-mg/ml solution of sodium hydrosulfite in 10% $NaHCO_3$ was added, and the pH was adjusted to 9.0–9.5 with 4 *N* NaOH.

The tube was heated in a boiling water bath for 10 min and cooled, and 6 ml of ethyl acetate was added. It was then stoppered, shaken, and centrifuged. The ethyl acetate phase was transferred to a clean tube, and

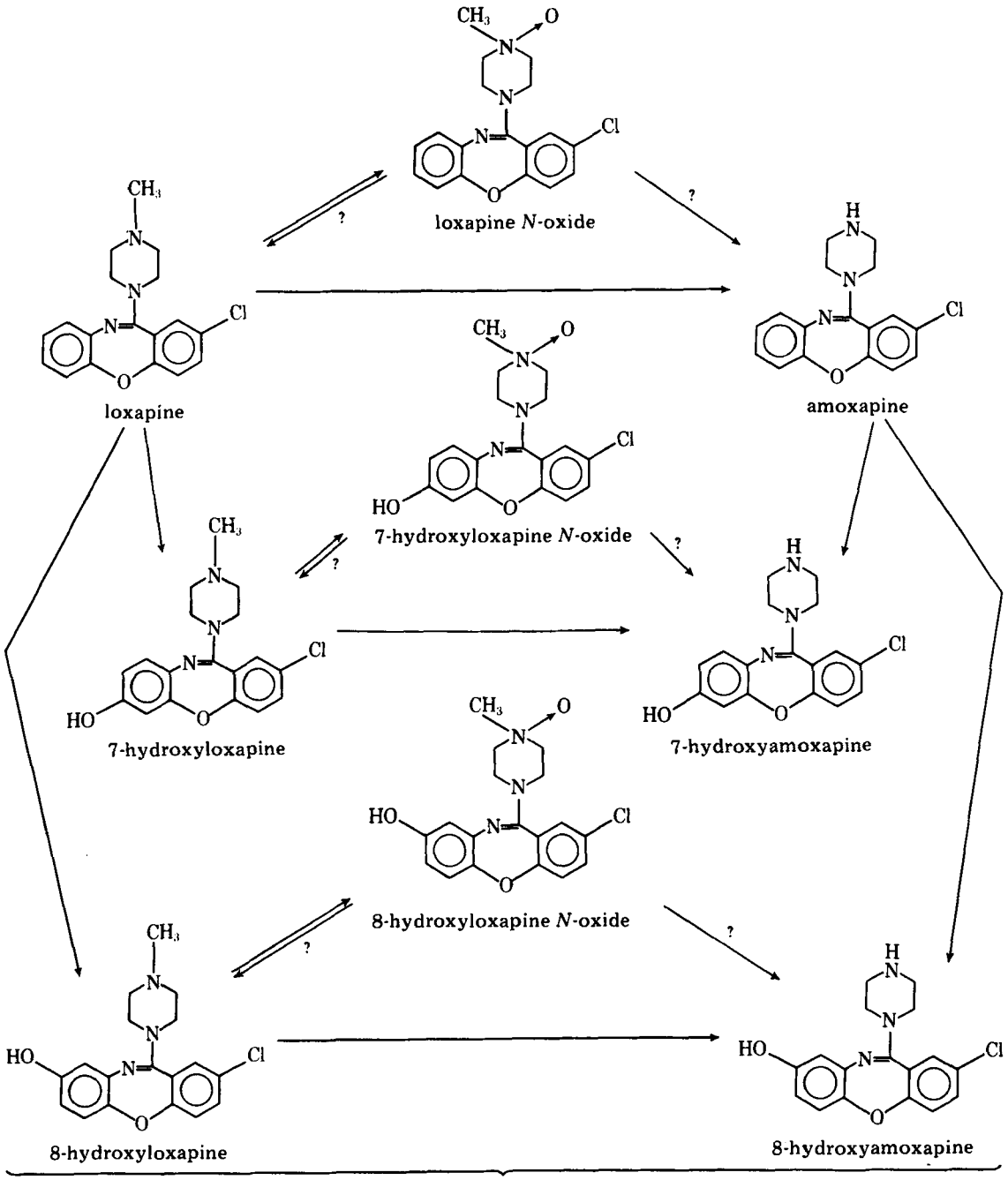

Scheme I

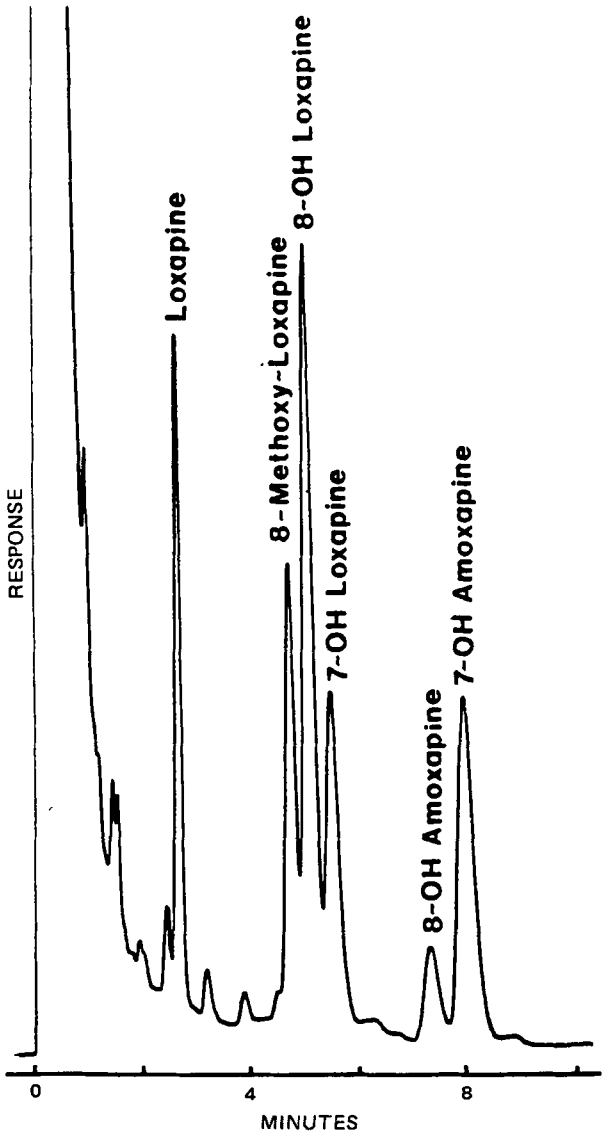

Figure 2—*Chromatogram of the 4–8-hr urine from a subject receiving a single 25-mg dose of loxapine.*

1 ml of 0.1 *N* HCl was added. The contents were mixed and centrifuged, and the ethyl acetate was aspirated. The tube was then covered with a 1.25-cm^2 piece of filter paper, held in place with a rubber band, and lyophilized.

The residue was reacted with a mixture of 0.5 ml of trifluoroacetic anhydride and 0.2 ml of dichloromethane for 30 min, after which the solvent was removed by evaporation. The acylated residue was dissolved in 50 μl of *N*-trimethylsilyldiethylamine and either heated for 3 hr at 60° or permitted to stand overnight at room temperature. A 2-μl aliquot was injected into the gas chromatograph, and peaks were detected by flame ionization.

Standards for analysis of loxapine and its metabolites in serum contained loxapine, 8-hydroxyloxapine, and 8-hydroxyamoxapine at concentrations ranging from 5 to 25 ng/ml. In urine, standards contained loxapine, 7-hydroxyloxapine, 8-hydroxyloxapine, 7-hydroxyamoxapine, and 8-hydroxyamoxapine at concentrations ranging from 5 to 25 μg/analytical sample. For amoxapine analysis, standards contained amoxapine, 7-hydroxyamoxapine, and 8-hydroxyamoxapine in both serum and urine. Serum standards ranged from 20 to 100 ng/ml, and urine standards ranged from 5 to 25 μg/sample.

RESULTS AND DISCUSSION

The chromatogram shown in Fig. 1 demonstrates the separation obtained on an extract of serum from a patient who had been receiving loxapine intramuscularly. A chromatogram from an amoxapine-dosed subject would have shown a peak at approximately 6 min corresponding to amoxapine and would not have peaks due to loxapine or 7- and 8-hydroxyloxapines. As is apparent, it is frequently difficult to measure 7-hydroxyloxapine in serum because of an overwhelmingly large amount of the 8-hydroxy analog. This problem did not occur with urine chromatograms (Fig. 2) where better separations were achieved with the helium carrier gas and where concentrations of these isomers were more nearly the same.

Table II—Plasma Loxapine Metabolites (Steady-State Levels) in 2-ml Aliquots of Serum Analyzed [a]

Patient	Dosage, mg/day	Loxapine, ng/ml	8-Hydroxy-loxapine, ng/ml	8-Hydroxy-amoxapine, ng/ml
1	20	7	18	20
2	25	0	11	11
3	30	1	16	6
4	30	8	12	11
5	40	2	24	14
6	50	1	22	16
7	50	11	36	18
8	60	9	29	23
9	70	4	34	23
10	70	4	37	28
11	80	17	88	29
12	80	7	33	16
13	100	31	72	64
14	100	6	41	31
15	120	2	16	7
16	120	12	40	33
17	150	2	6	4
18	200	12	42	28
19	200	8	47	94
20	250	73	97	114

[a] Samples were obtained just prior to next morning dose.

The precision of the reported procedure for serum analysis was estimated by preparing and running 10 consecutive standard curves containing both loxapine and amoxapine derivatives in serum (Table I). These data indicate a high reproducibility of the technique. An even higher reproducibility was achieved with urine standard curves.

The absolute recoveries of added loxapine, 8-hydroxyloxapine, and 8-hydroxyamoxapine from serum were estimated by comparing results from 10 serum samples to which these compounds had been added and that were carried through the analytical procedure without the internal standard with values from 10 samples prepared from the same stock solution in methanol that were simply derivatized after solvent removal. Extract transfers were measured accurately, and the same amount of the internal standard was added to all of the samples just prior to the trifluoroacetylation step. With an adjustment for extraction volumes, peak height ratio comparisons indicated the recovery of loxapine to be 70% (65–72%); that of 8-hydroxyloxapine was 90% (88–92%), and that of 8-hydroxyamoxapine was 86% (83–90%). These results indicate the desirability of preparing standards for serum analysis in serum.

Concentrations of loxapine, 8-hydroxyloxapine, and 8-hydroxyamoxapine found in the serum of normal volunteers after a single oral dose of 25 mg are illustrated by the curves shown in Fig. 3. Kinetic curves obtained after an amoxapine dosage of 50 mg are shown in Fig. 4. 7-Hydroxyamoxapine is not a metabolite of significance in serum following

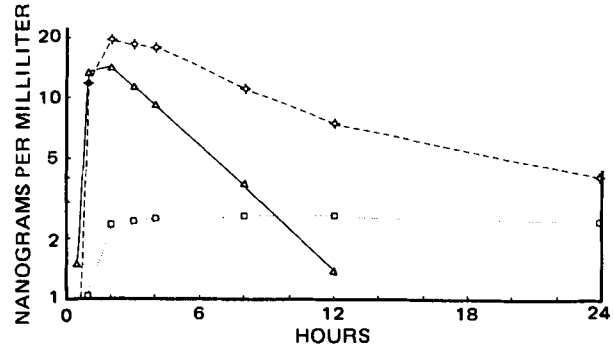

Figure 3—*Serum concentration-time curves of loxapine (△), 8-hydroxyloxapine (○), and 8-hydroxyamoxapine (□) after a single oral 25-mg dose of loxapine (mean values of 23 subjects).*

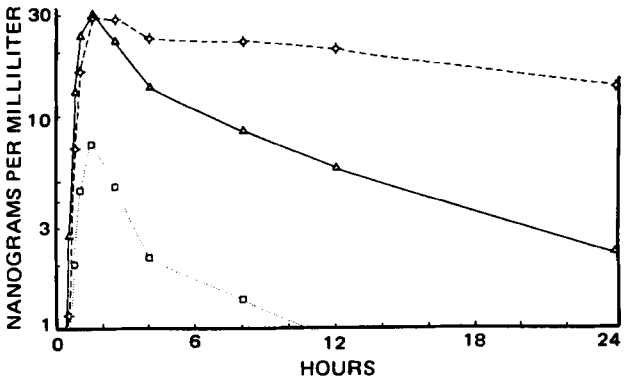

Figure 4—*Serum concentration–time curves of amoxapine (△), 7-hydroxyamoxapine (□), and 8-hydroxyamoxapine (○) after a single oral 50-mg dose of amoxapine (mean values of 26 subjects).*

loxapine dosage; 7-hydroxyloxapine, although present in appreciable quantity, is overwhelmed by the corresponding 8-hydroxy isomer, as previously described.

Observed concentrations of loxapine and its 8-hydroxylated metabolites at steady state following multiple dosage are shown in Table II. The patients under treatment received a twice a day dosage at the level indicated, and serum was obtained for analysis immediately prior to a morning dose. A similar study involving amoxapine dosage was not performed.

The development of the described procedure led to an interesting observation concerning *N*-oxides of loxapine and its *N*-methylated metabolites (7-hydroxyloxapine and 8-hydroxyloxapine). These compounds form stable derivatives with trifluoroacetic anhydride, which survive the described GLC conditions and yield peaks differing in retention time from any of the compounds described. Loxapine *N*-oxide is found in human serum and is a major metabolite in dog serum.

REFERENCES

(1) R. M. Steinbook, B. J. Goldstein, B. Brauzer, S.-S. Moreno, and A. F. Jacobson, *Curr. Ther. Res.*, **15**, 1 (1973).

(2) M. P. Bishop and D. M. Gallant, *ibid.*, **12**, 594 (1970).

(3) C. Z. Moyano, *Dis. Nerv. Syst.*, **36**, 301 (1975).

(4) F. B. Selman, R. F. McClure, and H. Helwig, *Curr. Ther. Res.*, **19**, 645 (1976).

(5) C. D. Van der Velde and H. Kiltie, *ibid.*, **17**, 1 (1975).

ACKNOWLEDGMENTS

The authors thank Mr. K. Douglas Hoyt and Mr. David Allen for their valuable aid and Dr. C. F. Howell and Dr. R. A. Hardy, Jr., for samples of the various metabolites described.

Determination of Guanfacine in Biological Fluids by Electron-Capture GLC

M. GUERRET, D. LAVENE ˣ, J. LONGCHAMPT, and J. L. KIGER

Received February 6, 1978, from the *Centre de Recherches Pharmacocinétiques, Laboratoires Sandoz, 14, Boulevard Richelieu, 92505 Rueil Malmaison, France.* Accepted for publication July 18, 1978.

Abstract □ A quantitative electron-capture GLC method with good sensitivity is described for the determination of guanfacine in human plasma and urine. By condensing its amidino group with hexafluoroacetylacetone, guanfacine is converted to a pyrimidino derivative with better GLC properties than the parent drug. This method allows the determination of guanfacine in plasma and urine at concentrations as low as 0.5 ng/ml and was applied successfully to measurement of plasma levels in humans after therapeutic dosing.

Keyphrases □ Guanfacine—GLC analysis in plasma and urine □ GLC—analysis, guanfacine in plasma and urine □ Antihypertensive agents, potential—guanfacine, GLC analysis in plasma and urine

Guanfacine[1], *N*-amidino-2-(2,6-dichlorophenyl)acetamide hydrochloride (I), is a guanidine derivative showing antihypertensive activity in animals (1) and humans (2, 3). Like clonidine, guanfacine possesses peripheral and central α-adrenoceptor stimulant activity resulting in a reduction in sympathetic nerve activity.

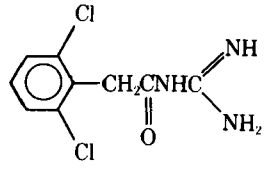

I

This report describes an electron-capture GLC method adapted to the determination of guanfacine in biological fluids. After extraction, the compound is derivatized by condensing the amidino group with hexafluoroacetylacetone to form a pyrimidino compound, as reported[2] for guanido compounds (4, 5).

EXPERIMENTAL

Reagents—Methanol[3] RP, hexafluoroacetylacetone[4], and ethylanthraquinone[4], all analytical grade, were used without further purification. Dichloromethane[5], benzene[3], and methyl isobutyl ketone[5] were freshly distilled under nitrogen.

A standard solution of ethylanthraquinone (internal standard) was prepared by dissolving 100 mg of the product in 50 ml of methanol.

Apparatus—A chromatograph[6] equipped with a ^{63}Ni-electron-capture detector was fitted with a glass column (1.6 m × 3 mm i.d.) packed with 3% OV-225 on 100–120-mesh Gas Chrom Q. The flow rate of the carrier gas, 5% methane in argon, was 60 ml/min. The temperatures of the injection port, column, and detector block were 250, 210, and 300°, respectively.

[1] Clinical code BS 100-141

[2] R. Laplanche, Sandoz-Bale Internal Report, 1976.
[3] E. Merck A. G., Darmstadt, West Germany.
[4] Koch Light Laboratories, Colnbrook, England.
[5] J. T. Baker, Phillipsburg, N.J.
[6] Hewlett-Packard model 5713A.

0022-3549/79/0200-0219$01.00/0
© 1979, American Pharmaceutical Association

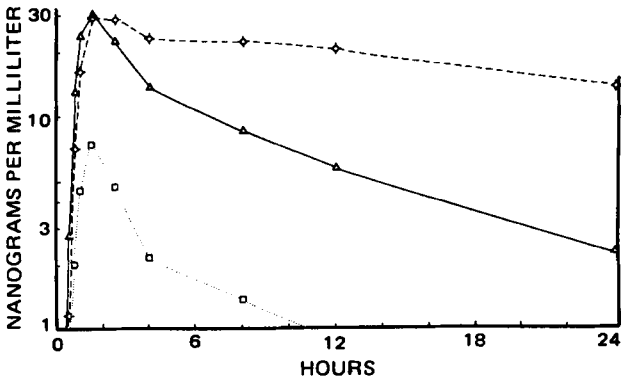

Figure 4—*Serum concentration–time curves of amoxapine (△), 7-hydroxyamoxapine (□), and 8-hydroxyamoxapine (○) after a single oral 50-mg dose of amoxapine (mean values of 26 subjects).*

loxapine dosage; 7-hydroxyloxapine, although present in appreciable quantity, is overwhelmed by the corresponding 8-hydroxy isomer, as previously described.

Observed concentrations of loxapine and its 8-hydroxylated metabolites at steady state following multiple dosage are shown in Table II. The patients under treatment received a twice a day dosage at the level indicated, and serum was obtained for analysis immediately prior to a morning dose. A similar study involving amoxapine dosage was not performed.

The development of the described procedure led to an interesting observation concerning *N*-oxides of loxapine and its *N*-methylated metabolites (7-hydroxyloxapine and 8-hydroxyloxapine). These compounds form stable derivatives with trifluoroacetic anhydride, which survive the described GLC conditions and yield peaks differing in retention time from any of the compounds described. Loxapine *N*-oxide is found in human serum and is a major metabolite in dog serum.

REFERENCES

(1) R. M. Steinbook, B. J. Goldstein, B. Brauzer, S.-S. Moreno, and A. F. Jacobson, *Curr. Ther. Res.*, **15**, 1 (1973).

(2) M. P. Bishop and D. M. Gallant, *ibid.*, **12**, 594 (1970).

(3) C. Z. Moyano, *Dis. Nerv. Syst.*, **36**, 301 (1975).

(4) F. B. Selman, R. F. McClure, and H. Helwig, *Curr. Ther. Res.*, **19**, 645 (1976).

(5) C. D. Van der Velde and H. Kiltie, *ibid.*, **17**, 1 (1975).

ACKNOWLEDGMENTS

The authors thank Mr. K. Douglas Hoyt and Mr. David Allen for their valuable aid and Dr. C. F. Howell and Dr. R. A. Hardy, Jr., for samples of the various metabolites described.

Determination of Guanfacine in Biological Fluids by Electron-Capture GLC

M. GUERRET, D. LAVENE ˣ, J. LONGCHAMPT, and J. L. KIGER

Received February 6, 1978, from the *Centre de Recherches Pharmacocinétiques, Laboratoires Sandoz, 14, Boulevard Richelieu, 92505 Rueil Malmaison, France.* Accepted for publication July 18, 1978.

Abstract □ A quantitative electron-capture GLC method with good sensitivity is described for the determination of guanfacine in human plasma and urine. By condensing its amidino group with hexafluoroacetylacetone, guanfacine is converted to a pyrimidino derivative with better GLC properties than the parent drug. This method allows the determination of guanfacine in plasma and urine at concentrations as low as 0.5 ng/ml and was applied successfully to measurement of plasma levels in humans after therapeutic dosing.

Keyphrases □ Guanfacine—GLC analysis in plasma and urine □ GLC—analysis, guanfacine in plasma and urine □ Antihypertensive agents, potential—guanfacine, GLC analysis in plasma and urine

Guanfacine[1], *N*-amidino-2-(2,6-dichlorophenyl)acetamide hydrochloride (I), is a guanidine derivative showing antihypertensive activity in animals (1) and humans (2, 3). Like clonidine, guanfacine possesses peripheral and central α-adrenoceptor stimulant activity resulting in a reduction in sympathetic nerve activity.

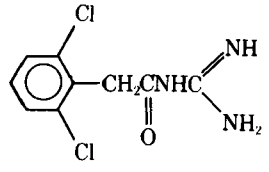

I

This report describes an electron-capture GLC method adapted to the determination of guanfacine in biological fluids. After extraction, the compound is derivatized by condensing the amidino group with hexafluoroacetylacetone to form a pyrimidino compound, as reported[2] for guanido compounds (4, 5).

EXPERIMENTAL

Reagents—Methanol[3] RP, hexafluoroacetylacetone[4], and ethylanthraquinone[4], all analytical grade, were used without further purification. Dichloromethane[5], benzene[3], and methyl isobutyl ketone[5] were freshly distilled under nitrogen.

A standard solution of ethylanthraquinone (internal standard) was prepared by dissolving 100 mg of the product in 50 ml of methanol.

Apparatus—A chromatograph[6] equipped with a ^{63}Ni-electron-capture detector was fitted with a glass column (1.6 m × 3 mm i.d.) packed with 3% OV-225 on 100–120-mesh Gas Chrom Q. The flow rate of the carrier gas, 5% methane in argon, was 60 ml/min. The temperatures of the injection port, column, and detector block were 250, 210, and 300°, respectively.

[1] Clinical code BS 100-141

[2] R. Laplanche, Sandoz-Bale Internal Report, 1976.
[3] E. Merck A. G., Darmstadt, West Germany.
[4] Koch Light Laboratories, Colnbrook, England.
[5] J. T. Baker, Phillipsburg, N.J.
[6] Hewlett-Packard model 5713A.

0022-3549/79/0200-0219$01.00/0
© 1979, American Pharmaceutical Association

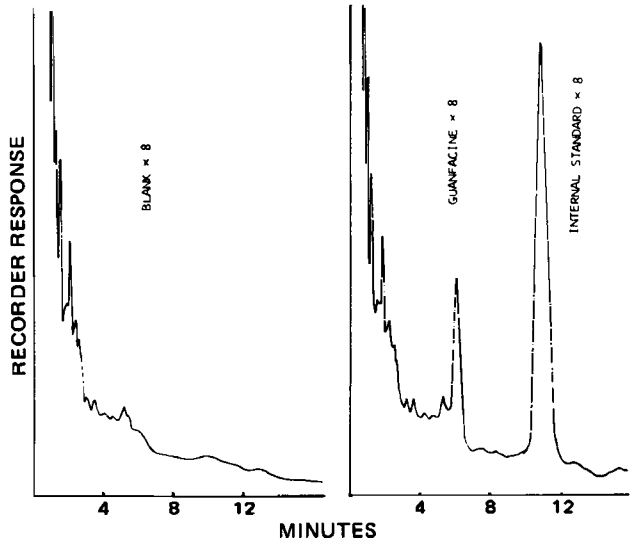

Figure 1—*Gas chromatograms of human plasma assayed as described. Key: left, chromatogram from normal human plasma; and right, chromatogram from normal human plasma containing 2 ng of guanfacine/ml.*

The mass spectrum of the derivative of the parent drug was determined on a mass spectrometer[7] with a multiple ion detector[8] coupled to a gas chromatograph *via* a membrane separator. The source was an electron impact operating at 70 ev and 20 mamp. The source temperature was 220°, and the analyzer temperature was 180°.

Assay—To 4 ml of plasma (or diluted urine) was added 0.5 ml of 1 *N* NaOH. Preliminary extraction was performed by adding 10 ml of methyl isobutyl ketone. After shaking for 20 min and then centrifugation at 2000 rpm for 5 min, the organic phase was transferred to a glass-stoppered tube and shaken for 20 min with 4 ml of 0.1 *N* HCl. After centrifugation (5 min at 2000 rpm), the organic phase was discarded. The acidic phase was alkalinized with 1 ml of 1 *N* NaOH and again extracted with 10 ml of dichloromethane–methyl isobutyl ketone (90:10 v/v).

After centrifugation, an aliquot of the organic phase was evaporated at 40° under nitrogen. The residue was taken up in 1 ml of 10% acetic acid in methanol and dried again. The new residue was dissolved in 200 μl of 10% hexafluoroacetylacetone in methanol. The tubes, stoppered with polytef capsules, were heated in an aluminum heating block at 100° for 1 hr and then evaporated to dryness under nitrogen.

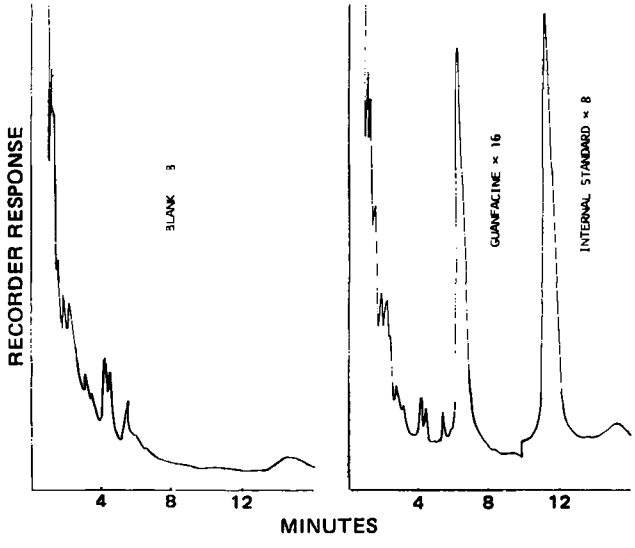

Figure 2—*Gas chromatograms of human urine assayed as described. Key: left, chromatogram from normal human urine; and right, chromatogram from normal human urine containing 50 ng of guanfacine/ml before dilution.*

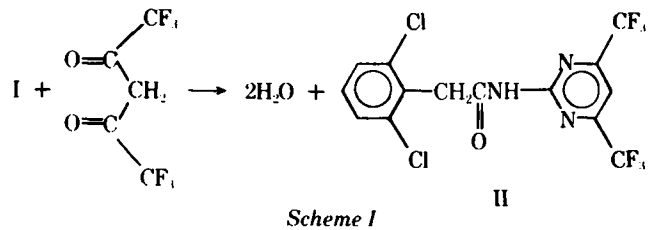

Scheme I

The dry extract was taken up in 400 μl of benzene containing 100 ng of the internal standard (ethylanthraquinone); then 3 ml of 3 *N* NaOH was added to hydrolyze the excess hexafluoroacetylacetone. The samples were vortexed and centrifuged, and 4 μl of the benzene phase was injected into the chromatograph.

RESULTS AND DISCUSSION

To determine the optimal chromatographic extraction and derivatization conditions for the analysis of guanfacine at very low concentrations, various experiments were performed. Initially, the substance was analyzed without derivatization by using a glass column packed with very polar phases[9]. However, due probably to the high polarity of the compound, retention on the column wall led to poor reproducibility.

To reduce this phenomenon and to increase the sensitivity, a pyrimidino derivative was formed by condensing the amidino group with hexafluoroacetylacetone as reported previously (4, 5). The detector response then was stable, and the sensitivity was increased slightly.

Identification of Derivative—A stable derivative, II (Scheme I), was obtained and its structure was confirmed by its mass spectrum[10] (Table I).

Sample Extraction—Various parameters of the procedure were analyzed. Among the different solvents used for extraction, only methyl isobutyl ketone and 10% methyl isobutyl ketone in dichloromethane gave a good yield. Heptane–1.5% isoamyl alcohol, ethyl acetate, ether, benzene, chloroform, hexane, and dichloromethane resulted in less than a 20% yield.

For extraction of the alkalinized acid phase, 10% methyl isobutyl ketone in dichloromethane was substituted for pure methyl isobutyl ketone to minimize the water retention by the residue. Back-extraction into diluted acid removed most of the neutral compounds from the initial methyl isobutyl ketone extract, which may have interfered in the chromatographic analysis. A very clean plasma extract (blank) was thus obtained (Fig. 1). Figure 1 also shows a chromatogram of assayed human plasma with ethylanthraquinone as the internal standard.

The present GLC method also was applied to the determination of guanfacine in urine (Fig. 2).

The data in Table II show that guanfacine transfer from an aqueous into an organic phase was almost complete at pH 11 and that its reextraction into the aqueous phase should occur at pH <3.

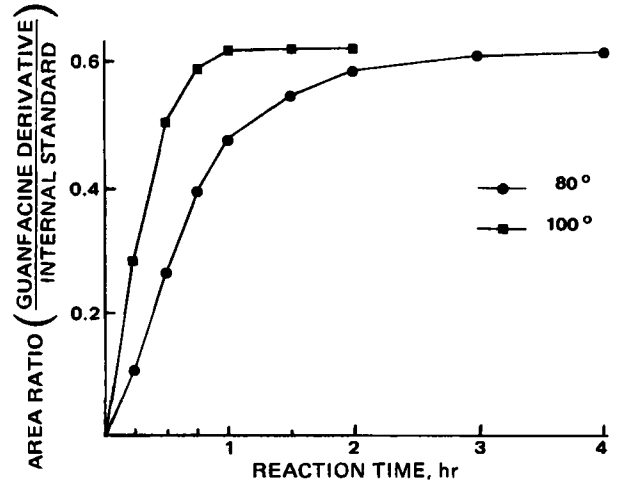

Figure 3—*Influence of temperature and heating time on derivatization kinetics.*

[7] Hewlett-Packard model 5980A.
[8] Hewlett-Packard model 5947A.
[9] Carbowax 20M or neopentylglycolsuccinate from Carlo Erba.
[10] Performed by R. Laplanche.

Table I—Principal Mass Peaks in Mass Spectra of the Compounds

			Guanfacine (Direct Inlet in Ion Source), mol. wt. = 245							
m/e	86	69	123	159	89	100	161	125	87	149
I[a], %	100	(46)[b]	38	35	34	(30)	26	20	15	(15)
			Guanfacine Derivative (GLC–Mass Spectral Coupling), mol. wt. = 417							
m/e	186	159	188	161	101	123	382	238	89	69
I, %	100	88	75	56	(48)	41	27	21	(16)	(16)

[a] Intensity of the mass peak relative to the parent peak = 100. [b] The intensities in parenthesis are possibly too high because of the interference of an impurity or pyrolysis product.

Table II—Influence of pH on Extraction of 8 ng of Guanfacine from 4 ml of Aqueous Phases (*i.e.*, 2 ng/ml)

pH	Recovery[a] ± *SEM*, %
1 (0.1 *N* HCl)	—
3[b] (buffer)	17 ± 1.2
5[b] (buffer)	32 ± 0.9
7[b] (buffer)	55 ± 3.0
9[b] (buffer)	70 ± 1.2
11[b] (buffer)	90 ± 1.5
13 (1 *N* NaOH)	93 ± 1.5

[a] Mean of four determinations. [b] All buffers (Titrisol) were purchased from Merck, Darmstadt, West Germany.

Derivatization—Excess hexafluoroacetylacetone was used for derivatization. A 200-μl aliquot of 10% hexafluoroacetylacetone in methanol afforded complete derivatization over the 1–20-ng/ml range. Urine samples containing more than 20 ng of guanfacine/ml were diluted before analysis.

Figure 3 shows the influence of temperature and heating time on the kinetics of the derivative reaction. At 100°, the reaction was virtually complete after 1 hr; 3 hr was required at 80°.

Initially, toluene was used as the solvent for derivatization[2]. However, the reaction between guanfacine and hexafluoroacetylacetone was more complete with methanol, and the peak area corresponding to II was approximately four times higher than with toluene.

Recovery and Linearity—Guanfacine recovery was determined by adding various known amounts of product to human plasma (Table III) or human urine (Table IV) and analyzing each sample in quadruplicate according to the described procedure. As compared to a similar series of unextracted reference standards of guanfacine, the mean recoveries varied from 73.5 to 84.6% with an average of 79% and were independent of the concentration within the range used for plasma.

The standard curve obtained from plasma spiked with guanfacine was linear in the 0.5–10-ng/ml range as reflected by the values of the correlation coefficient ($y = 0.087x + 0.051$, $r = 0.994$). For urine, a good correlation also was obtained for the 20–400-ng/ml range ($y = 5.46 \times 10^{-3}x + 0.216$, $r = 0.998$). Triplicate assays on different days gave a standard deviation of 3.4% at 10 ng/ml and of 4.2% at 1 ng/ml.

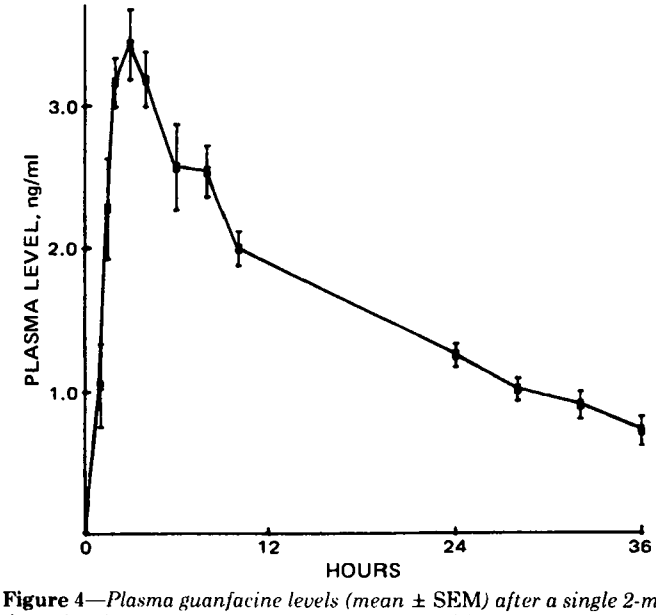

Figure 4—*Plasma guanfacine levels (mean ± SEM) after a single 2-mg dose of active compound in six hypertensive subjects.*

Table III—Recovery of Guanfacine Added to Human Plasma[a] Samples

Guanfacine Added, ng/ml	*n*	Amount Recovered[b], ng/ml	Recovery, mean ± *SEM*, %
0.5	4	0.38	77.0 ± 1.3
1	4	0.85	84.6 ± 2.1
2	4	1.66	83.2 ± 4.0
4	3	3.04	76.1 ± 1.8
8	4	5.88	73.5 ± 1.0

[a] Assays were performed on 4 ml of plasma. [b] Average of *n* determinations.

Table IV—Recovery of Guanfacine Added to Human Urine[a] Samples

Guanfacine Added, ng/ml[b]	*n*	Amount Recovered[c], ng/ml	Recovery, mean ± *SEM*, %
50	2	36.7	73.3 ± 1.4
100	2	76.4	76.4 ± 4.1
200	4	163.4	81.7 ± 1.9
400	4	341.6	85.4 ± 2.3

[a] Assays were performed on 4 ml of diluted urine (1:10). [b] Levels before dilution. [c] Average of *n* determinations.

Sensitivity and Specificity—The detection limit, defined as five times the background level, for guanfacine was 4 pg, corresponding to 0.125 ng/ml of plasma under the assay conditions. Four times this concentration (*i.e.*, 0.5 ng/ml of plasma) was the lowest measurable concentration with an accuracy of ±5%.

The specificity of the method in the presence of other drugs such as diuretics and β-blocking agents, which may be administered concurrently with an antihypertensive drug, was checked. No interfering peak was observed on the chromatogram under the same conditions.

Application to Pharmacokinetic Studies—The suitability of the proposed method for the determination of plasma guanfacine was tested in six hypertensive patients who received 2 mg of guanfacine as a single oral dose. Blood samples (10 ml) were drawn by venipuncture at 0, 1, 1.5, 2, 3, 4, 6, 8, 10, 24, 28, 32, and 36 hr. Plasma was separated, and the samples were frozen until analyzed.

Guanfacine concentrations then were determined by the described method. The mean plasma concentration–time curve (±*SEM*) is shown in Fig. 4. No guanfacine metabolites interfered with the determination of the parent compound.

REFERENCES

(1) K. Saameli, G. Scholtysik, and R. Waite, *Clin. Exp. Pharmacol. Physiol.*, **1975**, Suppl. 207.

(2) A. Jaatela, *Eur. J. Clin. Pharmacol.*, **10**, 69 (1976).

(3) A. S. Turner, VII World Congress of Cardiology, Buenos Aires, Argentina, 1974, Abstract 336.

(4) S. L. Malcom and R. Martent, *Anal. Chem.*, **48**, 807 (1976).

(5) P. Erdmansky and T. J. Goehl, *ibid.*, **47**, 750 (1975).

ACKNOWLEDGMENTS

The authors thank Pr. Safar, Centre de Recherches sur l'Hypertension Artérielle, Hôpital Broussais, Paris, France, for obtaining the plasma samples.

Electrical Conductance of Directly Compressible Materials under Pressure

RAJKUMAR P. BHATIA * **and NICHOLAS G. LORDI** ×

Received May 26, 1978, from the *College of Pharmacy, Rutgers—The State University, Piscataway, NJ 08854.* Accepted for publication July 28, 1978. *Present address: A. H. Robins, Richmond, VA 23220.

Abstract □ An electrometer that allowed direct recording of resistance changes during compression was used to measure the conductances of sodium chloride, potassium chloride, ammonium chloride, and sodium citrate. The effects of initial particle size, lubricant level, moisture content, and compaction pressure were determined. Direct compression tableting diluents also studied were dextrose, sucrose, lactose, microcrystalline cellulose, and dibasic calcium phosphate. Distinctive conductance patterns were observed and are rationalized in terms of previously proposed bonding mechanisms.

Keyphrases □ Electrical conductances—various directly compressible inorganic chlorides and sodium citrate, effects of particle size, lubricant levels, moisture content, and compaction pressure □ Directly compressible materials—various inorganic chlorides and sodium citrate, electrical conductances, effects of particle size, lubricant level, moisture content, and compaction pressure □ Tablets—various directly compressible inorganic chlorides and sodium citrate, electrical conductances, effects of particle size, lubricant level, moisture content, and compaction pressure

This study was designed to evaluate measurement of the electrical conductance of directly compressible materials under pressure as a technique for investigating interparticulate bonding in compacts. The application of electrical resistivity measurements as a tool for studying applied and induced stresses in solid materials has been recognized (1–6) but is still incomplete. This technique has had only limited consideration as a means for investigating tableting.

BACKGROUND

Freshly prepared and aged silver bromide powders were compressed between two silver-plated plungers, which served as electrodes, and specific conductance was measured as a function of applied pressure (1). Specific conductance fell as silver bromide was aged (1). Electrical conductance also was used to describe sintering of powdered metals, and the effects of varying particle size and size distribution on copper powder sintering were noted. A relationship between tensile strength and electrical conductivity was developed and served to evaluate the quality of sintered copper (2).

The bonding in sodium chloride and copper sulfate compacts was studied by measuring electrical conductivity as a function of pressure, using 500–600 v ac (3). The specific conductivity increased with an increase in pressure up to a maximum value and then decreased with further increases in pressure (~1750 kg/cm^2) (3).

In another study (4), a decade bridge was used to measure the electrical resistance of sodium chloride granules containing 8–10% graphite at low pressures (~70 kg/cm^2). It was concluded that an initial packing stage was followed by a brief period during which the granular structure could support the imposed load without breakdown and then, finally, gradual failure of the granules to give a compact mass.

A modified Schering bridge circuit was used to measure the dissipation factor of sodium chloride undergoing compression in a polyester polymer die (5, 6). Hanus (5) correlated physical properties of sodium chloride crystals such as particle size, moisture content, porosity, and hardness of the compacts produced with calculated specific conductances at various pressures. Mohrle (6) studied the effect of addition of magnesium stearate and activated charcoal at a fixed pressure on the specific conductivity of sodium chloride.

In the present study, an electrometer that allowed direct recording of resistance changes during compression was used to measure the conductances of sodium chloride, potassium chloride, ammonium chloride, and sodium citrate. The effects of initial particle size, lubricant level, and moisture content as well as compaction pressure were determined. To establish the value of applying the technique to other than ionic materials, several direct compression tableting diluents and binders also were included.

EXPERIMENTAL

Materials—USP grade sodium, potassium, and ammonium chlorides and sodium citrate (dihydrate) were fractionated using 20-, 30-, 40-, and 50-mesh U.S. standard screens. The sized chlorides were dried at 135° for 16 hr to remove all traces of moisture and other volatile impurities. The samples were stored in sealed containers in a desiccator over silica gel until used.

Moisture was added to samples of dried 30–40-mesh salt by directing moist air at the material tumbling in a coating pan for 15 min. Samples with different moisture levels were prepared by tumbling the damp material in a dry coating pan for varying times. The moisture content was determined gravimetrically.

In experiments where magnesium stearate was added, portions of the dried 30–40-mesh salts were blended with 0.1, 0.2, 0.5, and 0.75% magnesium stearate. The lubricant was dried for 7 days at 65° and passed through a 200-mesh screen before use. The lubricated salts were stored in sealed containers in a desiccator until needed.

The following materials were used as received: spray-dried lactose[1], microcrystalline cellulose[2], anhydrous dextrose[3], polyethylene glycol 4000[4], dibasic calcium phosphate dihydrate[5], and sucrose[5].

Instrumentation—A schematic diagram of the system used to measure the electrical resistance of materials under compression is shown in Fig. 1.

The base of a 2.5-cm diameter tablet punch was cemented to a square acrylic[6] block with an epoxy adhesive. A steel collar placed over the base of the punch was fastened to the acrylic block for added support. A banana plug was welded perpendicularly to the middle of the tablet punch shaft. A cylindrical steel shield, 12.5 cm in diameter, was fastened to the acrylic block with metal brackets so that the banana plug was positioned opposite to a circular window in the shielding. This upper punch unit was fastened to the upper stage of a hydraulic press[7] by large C clamps.

A 15 × 5 × 1-cm polished stainless steel plate resting on the lower stage of the hydraulic press served as the lower punch. The die was fabricated from a 5-cm diameter, 2-cm thick piece of polyethylene terephthalate[8] ring, containing a 2.5-cm diameter cavity. It was positioned in the center of the steel plate to accommodate the sample. The acrylic block and polyethylene terephthalate die served to insulate the compacts from the grounded hydraulic press.

A motorization unit[7] was used to control the application of pressure and the movement of the ram, whose speed could be varied from 0.1 to 0.9 cm/sec. The unit, when activated, drove the press to a preset pressure. If a fall in pressure occurred during the experimental run, the motorized unit was automatically activated to maintain the required pressure.

The shield and steel base plate were connected to the grounded hydraulic press. A shielded cable connected the punch to an electrometer[9]. The output of the electrometer was monitored continuously throughout the experimental run by a recorder[10].

[1] Foremost-McKesson, Appleton, Wis.
[2] Avicel Ph-101, FMC Corp., Philadelphia, Pa.
[3] J. T. Baker Chemical Co., Phillipsburg, N.J.
[4] Ruger, New Brunswick, N.J.
[5] Fisher Scientific Co., Springfield, N.J.
[6] Lucite.
[7] Model C, Fred S. Carver, Menomonee Falls, Wis.
[8] Mylar.
[9] Model 610 C, Keithley Instruments, Cleveland, Ohio.
[10] Model 620, Leeds and Northrup, North Wales, Pa.

0022-3549/79/0200-0222$01.00/0
© 1979, American Pharmaceutical Association

Table I—Reproducibility of Results Showing the Effect of Compression Time on the Conductivity of Dried 30–40-Mesh Sodium Chloride at 2700-kg Applied Load

Minutes	Apparent Specific Conductivity, $ohms^{-1}\ cm^{-1} \times 10^7$ Run 1	Run 2	Run 3
0	7.01	7.21	7.09
2	6.60	6.56	6.63
5	6.07	6.14	6.16
10	5.18	5.38	5.28
15	4.45	4.52	4.64
20	3.82	3.63	3.70
25	3.28	3.08	3.21
30	2.81	2.83	2.88

Procedures—A weighed quantity of material was transferred into the die resting on the steel plate. The lower stage of the hydraulic press was raised manually so that the tablet punch was positioned in the die cavity to rest on the surface of the granulation. The sample thickness was determined with a cathetometer[11], which was set to follow the movement of the base plate. The motorized unit was activated, and the electrometer and recorder were turned on.

The resistance at the moment the pressure reached its maximum value was designated as the zero-time reading. The thickness of the sample was again determined after 30 min, and corrections were made for elastic deformation of the insulating acrylic block. The specific conductance was calculated from resistances recorded at selected times during the run by:

$$\text{specific conductance} = \frac{\text{compact thickness}}{(\text{resistance})\ (\text{punch area})} \qquad \text{(Eq. 1)}$$

The accuracy of the measurements was checked by connecting standard resistors (1–100 megohm ± 1%) between the punch and plate. Resistances in excess of 10^{12} ohms were recorded in the empty die, depending on the distance set between the punch and plate. The range of measurement of the present equipment was limited to a maximum of 10^{10} ohms. All results reported are averages of replicated runs.

All reported results are for experiments run by operating the motorized unit at the lowest practical speed of 0.1 cm/sec with 6-g samples. Preliminary experiments indicated that initial observed conductance values were higher at lower operating speeds but approached the same values at 30 min. The observed specific conductances increased with an increase in weight up to 6 g; a further increase in weight resulted in a decline in specific conductance. Six grams was the maximum weight possible for most materials owing to the limitation imposed by the size of the die.

The reproducibility of experimental data is illustrated by the data summarized in Table I, which shows observed changes in specific conductance of sodium chloride compacts held at an intermediate pressure for three separate runs.

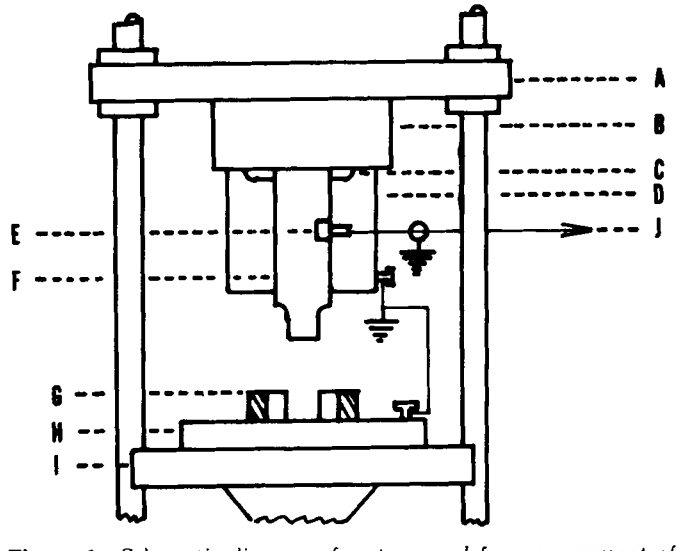

Figure 1—*Schematic diagram of system used for measurement of conductance under load. Key: A, upper stage of hydraulic press; B, acrylic block; C, steel collar; D, steel shield; E, connection to electrometer; F, punch; G, polyethylene terephthalate die; H, steel base plate; I, lower stage of press; and J, shielded cable to electrometer.*

[11] Central Scientific Co., Chicago, Ill.

Table II—Effect of Reduction in Applied Load (3600 kg) on Specific Conductances ($ohms^{-1}\ cm^{-1} \times 10^7$) and Thicknesses of Compacts Produced from 30–40-Mesh Salts

Salt	Initial Specific Conductance at 3600 kg	Specific Conductance at ~50 kg, 0 min	Specific Conductance at ~50 kg, 30 min	Increase in Thickness, %
Sodium chloride	4.9	0.65	0.35	4.1
Potassium chloride	12.2	5.5	6.5	4.3
Ammonium chloride	1.9	0.9	1.2	2.7
Sodium citrate	0.1	0.2	0.3	0.67

RESULTS AND DISCUSSION

The specific conductance of a pure sodium chloride crystal was reported to be 3.4×10^{-17} $ohm^{-1}\ cm^{-1}$ at room temperature (7). Most of this ionic conductance arises from valence vacancies. Although crystals possessing perfect lattices would conduct no current (8), all crystalline materials possess some electrical conductivity due to structural defects and impurities.

The conductance of a polycrystalline mass is the result of a complex interaction of factors, including the kind and concentration of impurities, lattice defects, structural defects such as cracks and fractures, and contact area. Most of the current flow takes place at the interface between the particles making up the mass. Thus, the greater the number of contact points, the greater the observed conductance.

Particles in a compact are forced into intimate contact under pressure, resulting in extensive areas of true contact. Particle rearrangements, fracturing, and plastic and elastic deformations take place. Consolidation processes predominate at low pressures, whereas deformations predominate at high pressures (9). The net effect of pressure during the compaction process should be an increase in conductivity up to the point where plastic deformation becomes significant. Interparticulate bonding reduces the interfacial contact area and, thus, the number of paths for current flow. The observed decrease in conductance is a consequence of healing and stress relaxations as well as bonding.

Interpretation of the conductances measured under the experimental conditions is further complicated by differences arising from ion character, variations in impurity content, and local temperature changes during compaction.

Conductivity at Constant Pressure—Studies of bonding in sodium

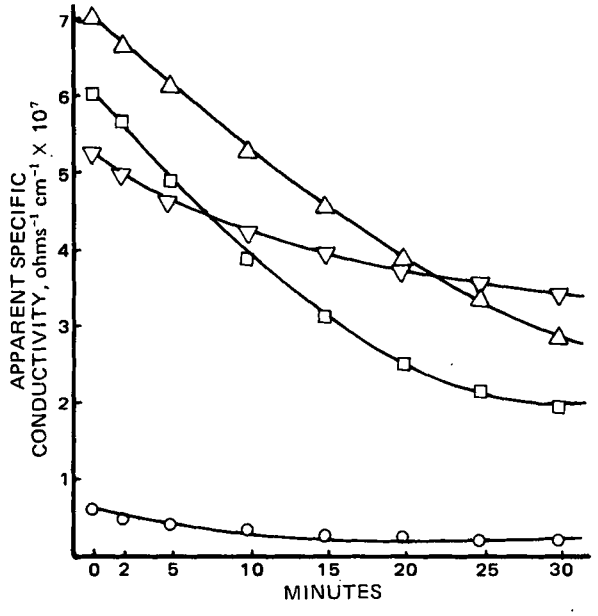

Figure 2—*Specific conductivity of dried 30–40-mesh sodium chloride at 900 (○), 1800 (□), 2700 (△), and 3600 (▽) kg.*

Table III—Effect of Initial Particle Size on Specific Conductances ($ohms^{-1}\ cm^{-1} \times 10^7$) and Densities of Salt Compacts

Salt	Mesh	900 kg			2700 kg		
		Density	Specific Conductance		Density	Specific Conductance	
			0	30 min		0	30 min
Sodium chloride	30–40	1.65	0.62	0.22	1.865	7.0	2.8
	40–50	1.596	3.0	0.05	1.835	4.7	0.93
Potassium chloride	20–30	1.60	5.7	1.5	1.865	17.2	9.8
	30–40	1.59	3.1	1.6	1.84	13.3	8.6
	40–50	1.58	1.6	0.08	1.85	7.9	6.5
Ammonium chloride	20–30	1.40	0.44	4.1	1.53	2.7	0.46
	30–40	1.39	0.05	0.4	1.52	1.3	0.87
	40–50	1.38	0.14	0.29	1.50	0.28	1.16
Sodium citrate	20–30	1.41	0.008	0.038	1.51	0.009	0.033
	30–40	1.40	0.006	0.038	1.49	0.009	0.03

and potassium chloride in contrast to potassium citrate compacts suggest that consolidation occurs primarily by elastic and plastic deformation in the former case and by fragmentation and particle rearrangement in the latter case (10). Figures 2–5 show specific conductivity–time plots for 30–40-mesh sodium, potassium, and ammonium chlorides and sodium citrate at gauge pressures of 900–3600 kg. Zero time on these plots represents the point at which the applied pressure was maintained at a constant value.

Distinctive patterns were observed for each material. In both sodium and potassium chloride compacts, the conductance decreased with time, and the decrease was proportionally less for low, as compared to high, pressures. Cole *et al.* (10) reported that potassium chloride deformed at lower loads than did sodium chloride. This behavior was evident from the fact that the maximum initial conductance was approached at lower pressures with potassium chloride. The decrease in conductance at lower pressures suggests that more complete deformation, fracture, and bonding of crystals take place and that more pathways for current flow are destroyed in potassium chloride. The order of magnitude of observed conductances was potassium > sodium > ammonium chloride > sodium citrate.

Unlike sodium and potassium chlorides, the conductance of ammonium chloride (Fig. 4) increased with time under constant load except at the highest pressure. At the intermediate pressure, a distinct maximum was observed. It was suggested that ammonium chloride deforms by plastic flow (11), with little evidence of fracture and fragmentation. The increase in conductance is likely due to an increase in the number of interparticulate contact points as material flows into interparticulate space.

Sodium citrate (Fig. 5) showed a constant initial conductance, irrespective of the pressure employed to form the compact. Unlike ammonium chloride, the rate of increase in conductance with time was greatest at lower pressures. Consolidation of sodium citrate is the result of fragmentation, which takes place on the initial application of the minimal load necessary to exceed the yield value of the salt. A constant initial conductance value is observed since a fixed number of contact points is made in the powder bed. The results suggest that the degree of fragmentation is constant, irrespective of the applied load. The observed trend to increased conductance with time probably reflects particle rearrangements resulting in increased numbers of contact points.

Table II summarizes data obtained in experiments in which the applied load was relaxed from its initial value to about 45 kg. The load was held at the initial value for 1 min. If compacts show significant elastic recovery, which results in a reduction in stress bonds and the effective area of contact, a reduction in conductance is observed. This reduction was evident with the chlorides; however, an order of magnitude increase in conductance was noted for sodium citrate. Sodium chloride showed a significant decrease in conductance, which further drifted downward with time. The proportionally smaller decreases observed with potassium and ammonium chlorides tended to increase with time. Increases in compact thickness were observed upon release of load. These increases were not significant for the citrate salt, while the sodium and potassium chlorides showed a significantly greater elastic recovery than ammonium chloride. The results reported for sodium chloride are in agreement with observations on sodium chloride tablets (12).

Potassium chloride showed intermediate characteristics, resembling sodium chloride at low loads and ammonium chloride at high loads. Unlubricated ammonium chloride produced translucent compacts even at the lowest applied loads, indicative of plastic deformation. At the

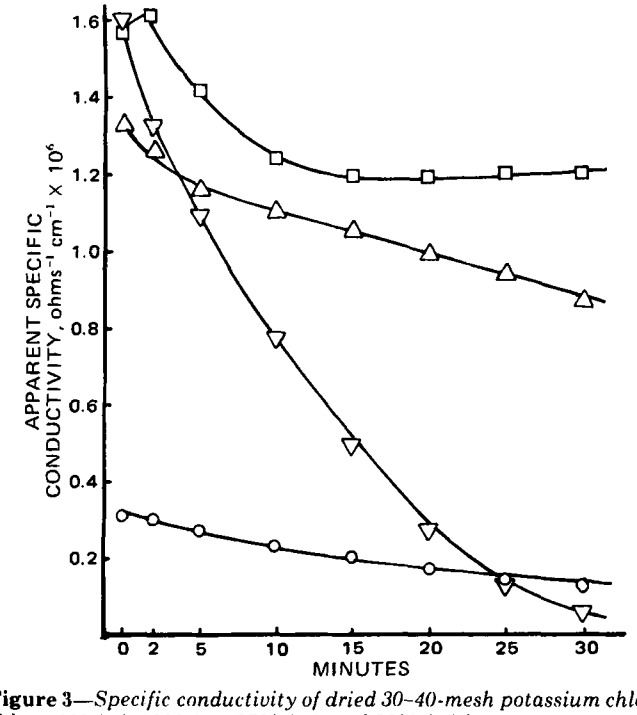

Figure 3—*Specific conductivity of dried 30–40-mesh potassium chloride at 900 (○), 1800 (□), 2700 (△), and 3600 (▽) kg.*

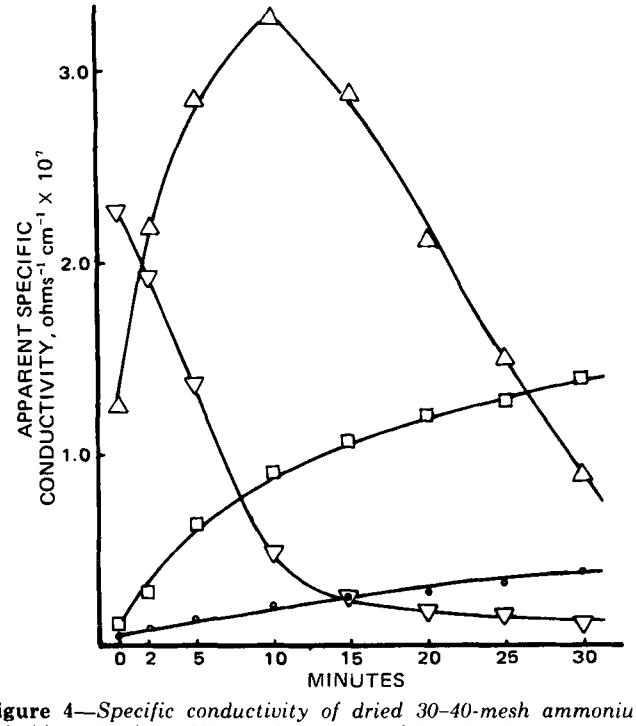

Figure 4—*Specific conductivity of dried 30–40-mesh ammonium chloride at 900 (○), 1800 (□), 2700 (△), and 3600 (▽) kg.*

Table IV—Effect of Magnesium Stearate on Specific Conductances (ohms^{-1} cm^{-1} × 10^7) of Compacts Produced from 30–40-Mesh Salts

Salt	Magnesium Stearate, %	1800 kg		3600 kg	
		0	20 min	0	20 min
Sodium chloride	0	6.0	2.5	5.2	3.7
	0.1	1.35	0.05	1.9	0.96
	0.75	1.40	0.22	1.63	0.65
Potassium chloride	0	15.8	12.1	16.0	2.8
	0.1	0.77	2.03	28.6	16.9
	0.75	0.38	1.13	4.96	0.61
Ammonium chloride	0	0.11	1.22	2.3	0.17
	0.1	0.01	0.07	0.02	0.014
	0.75	0.007	0.05	0.01	0.015

highest loads, potassium chloride compacts tended to resemble more closely the ammonium chloride compact at low pressure than the more granular-like structure of the sodium chloride compact. Sodium citrate compacts produced at even the highest loads crumbled under mild stress, indicating a lack of significant bonding.

Effect of Initial Granule Size—Huffine (3) and Hanus (5) previously reported that the specific conductance of sodium chloride compacts under pressure tended to increase as the initial granule size was increased. These observations were generally confirmed by the data summarized in Table III, except for sodium chloride at low loads and sodium citrate, where conductance was independent of initial granule size. Differences in observed compact densities were not significant except for sodium chloride at the low load, where a less dense compact was attained with 30–40-mesh sodium chloride as compared to the 40–50-mesh granules. Larger granules are subject to greater deformation, resulting in more fractures and defects and, consequently, more paths for current flow.

Effect of Added Magnesium Stearate—Table IV summarizes the observed conductances of compacts containing added magnesium stearate. Figure 6 shows the anomalous results observed in potassium chloride compacts at 3600-kg applied load. In all other cases, additon of magnesium stearate reduced the specific conductance, with the greatest reduction seen at the lowest lubricant level studied. These results are in agreement with those reported by Mohrle (6) for sodium chloride compacts. The addition of even the lowest level of magnesium stearate significantly reduced bonding in salts at the lower applied loads. Compacts produced from lubricated ammonium chloride lacked the translucent-fused structure characteristic of the unlubricated material.

Magnesium stearate potentially has two effects in compacts that can influence conductance. Principally, particles are coated with an insulating layer of the lubricant, which acts to decrease the effective conductance and to reduce bonding. In addition, the lubricant permits easier packing, producing compacts of maximum density with a minimum of particle deformation. The thickness of the lubricated compacts under pressure was somewhat smaller than the thickness of the unlubricated compacts but independent of the magnesium stearate level.

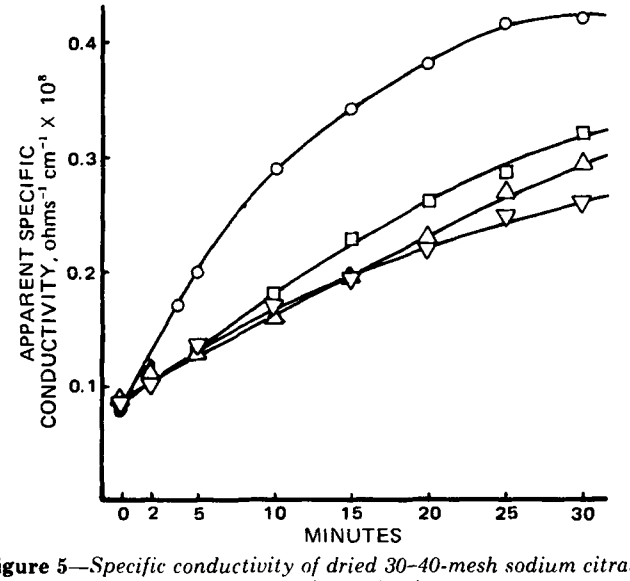

Figure 5—*Specific conductivity of dried 30–40-mesh sodium citrate at 900 (○), 1800 (□), 2700 (△), and 3600 (▽) kg.*

Table V—Effect of Added Moisture on Specific Conductances (ohms^{-1} cm^{-1} × 10^7) of Compacts Produced from 30–40-Mesh Salts

Salt	Water, %	1800 kg		3600 kg	
		0	20 min	0	20 min
Sodium chloride	0	6.0	2.5	5.2	3.7
	0.023	4.74	0.73	5.0	2.48
	0.074	7.94	1.4	7.5	3.1
Potassium chloride	0	15.8	12.1	16.0	2.8
	0.035	3.7	5.5	5.1	4.3
	0.126	4.2	4.7	6.7	3.9
Ammonium chloride	0	0.11	1.22	2.3	0.17
	0.056	0.09	0.16	0.06	0.04
	0.158	0.06	0.09	0.09	0.06

The anomalous behavior evidenced by potassium chloride at the high loads, in which significant conductance increases were observed upon addition of 0.1% stearate, suggests that better packing, which resulted in more contact points, had the greater effect. Thus, a higher concentration of lubricant was necessary to sustain a conductance decrease. At the low pressures, while a decreased conductance was observed, the conductances increased rather than decreased with time.

Effect of Added Moisture—Table V summarizes observed conductances of compacts produced at 1800- and 3600-kg compressional forces from granulations containing low levels of added moisture. Figure 7 shows a representative run for ammonium chloride. The data indicate that as water is added, the conductance decreases and reaches a minimum value, after which an increase is observed. Similar conductance–time patterns were noted with sodium chloride. However, the large shifts in conductance observed with dry potassium and ammonium chlorides were absent after moisture was added.

Rees and Shotton (13), in their study of sodium chloride compaction, demonstrated that added moisture exerted a boundary lubricant effect, which facilitated consolidation. Dissolution of salts in moisture films resulting in "electrolyte solution" pathways should increase conductance. At the moisture levels studied, this increase was observed only in sodium chloride compacts. However, crystallization under pressure, which promotes the formation of salt bridges and the healing of defects, would lead to reduced conductance, an effect that should be most pronounced at the lowest moisture levels. The presence of salt bridges produced in this

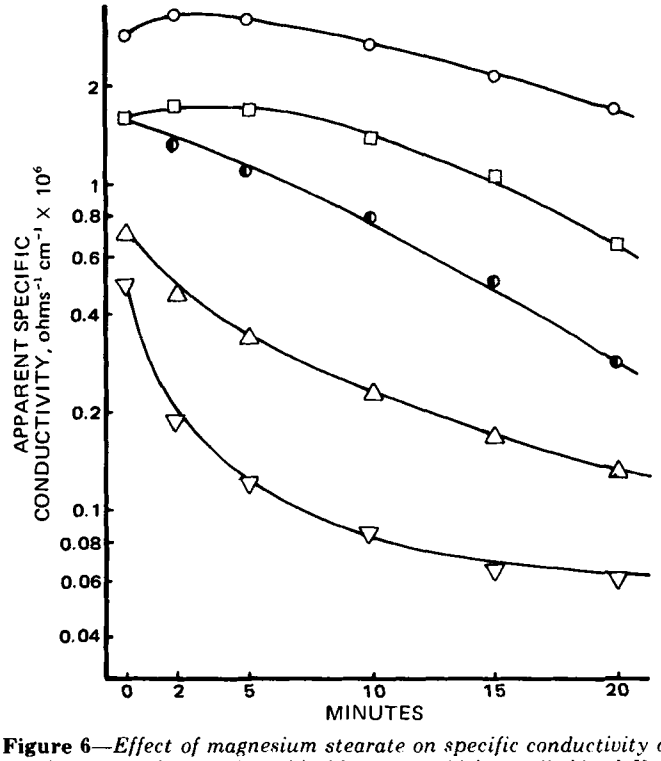

Figure 6—*Effect of magnesium stearate on specific conductivity of dried 30–40-mesh potassium chloride under 3600-kg applied load. Key: ◐, 0.0%; ○, 0.1%; □, 0.2%; △, 0.5%; and ▽, 0.75% magnesium stearate.*

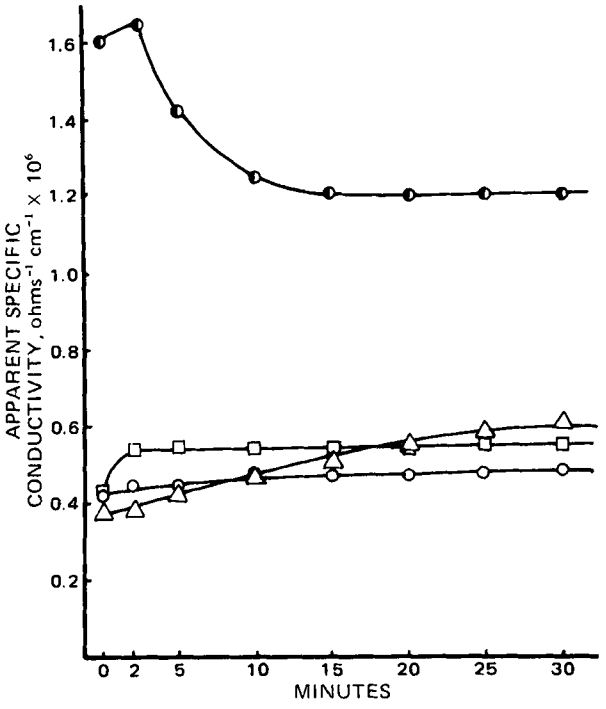

Figure 7—*Effect of added moisture on specific conductivity of dried 30–40-mesh ammonium chloride under 1800-kg applied load. Key:* ◐, *0.0%;* ○, *0.056%;* □, *0.095%; and* △, *0.158%.*

fashion would result in a stable compact under pressure. This result seems to occur with the potassium and ammonium chloride compacts, since these salts are significantly more water soluble than sodium chloride.

Hanus (5) reported that the addition of moisture raised the conductance of sodium chloride at even the lowest levels added. However, sodium chloride compacts were viewed as leaky capacitors. The capacitance effects were more pronounced after the addition of moisture. In the present work, compacts are viewed as resistors—significant capacitance effects were absent under the conditions of measurement.

Direct Compression Tablet Diluents—Large changes in conductance characteristics of the chlorides were not observed except in the case of dibasic calcium phosphate dihydrate at 3600-kg pressure, which may have been the result of release of water of hydration (Table VI). Observed conductances were two to three orders of magnitude lower than the values obtained for the salts.

Compacts prepared from these diluents generally show stable physical characteristics on storage. For example, Horhota *et al.* (14) reported that dibasic calcium phosphate tablets stored under various conditions showed no changes in physical characteristics such as hardness. On the other hand, sodium chloride compacts showed considerable hardness increases on storage (5). A correlation between conductance and hardness was established (15). The data suggest that compacts that reach stable internal states rapidly are not affected by continuous application of pressure.

David and Augsburger (16) reported that in the times prevalent on a tablet press, plastic deformation was more predominant in microcrystalline cellulose as compared to dibasic calcium phosphate. Fracture, with the creation of new surfaces under compression, was more important with lactose and other sugars. No clear distinction could be made in interpreting the conductance patterns since polyethylene glycol, which bonds largely by plastic deformation, reached a stable conductance within 5 min whereas microcrystalline cellulose showed conductance increases at both high and low pressures and lactose showed increases in conductance at 1800-kg and decreases in conductance at 2700-kg loads. The lactose data

Table VI—Apparent Specific Conductances (ohms^{-1} cm^{-1} × 10^{10}) of Direct Compression Diluents under Pressure

Diluent	Minutes	1800 kg	2700 kg	3600 kg
Dibasic calcium phosphate	0	7.0	9.1	1.2
	5	7.5	1.1	1.7
	30	6.7	1.1	2.3
Microcrystalline cellulose[a]	0	1.1	1.6	1.67
	5	1.16	1.6	1.7
	30	1.3	1.87	1.9
Spray-dried lactose	0	0.5	0.4	—
	5	0.38	0.5	—
	30	0.27	0.6	—
Sucrose	0	—	7.5	—
	5	—	7.53	—
	30	—	9.2	—
Dextrose	0	—	7.0	—
	5	—	7.3	—
	30	—	8.6	—
Polyethylene glycol 4000	0	—	67.6	—
	5	—	62.5	—
	30	—	62.0	—

[a] Three-gram compacts.

are consistent with the view that fragmentation is the principal effect at low pressures while deformation resulting in increased bonding dominates at the higher loads. It should be emphasized that unlubricated materials of differing initial particle size are being compared.

REFERENCES

(1) I. Shapiro and I. M. Kolthoff, *J. Phys. Colloid Chem.*, **52**, 1319 (1948).

(2) A. Duffield and P. Grootenhuis, *J. Inst. Met.*, **87**, 33 (1958–59).

(3) C. L. Huffine, Ph.D. thesis, Columbia University, New York, N.Y., 1953.

(4) K. Marshall, *J. Pharm. Pharmacol.*, **15**, 413 (1963).

(5) E. J. Hanus, Ph.D. thesis, Rutgers—The State University, New Brunswick, N.J., 1967.

(6) R. L. Mohrle, M.S. thesis, Rutgers—The State University, New Brunswick, N.J., 1969.

(7) P. F. Weller, "Solid State Chemistry and Physics," vol. 1, 1st ed., Dekker, New York, N.Y., 1973, p. 289.

(8) I. Kovacs and L. Zsoldos, "Dislocations and Plastic Deformations," 1st ed., Pergamon, Oxford, England, 1973, p. 246.

(9) J. A. Hersey, *Aust. J. Pharm. Sci.*, **NS2**, 47 (1973).

(10) E. T. Cole, J. E. Rees, and J. A. Hersey, *Pharm. Acta Helv.*, **50**, 28 (1975).

(11) S. Shlanta and G. Milosovich, *J. Pharm. Sci.*, **53**, 562 (1964).

(12) P. York and E. D. Baily, *J. Pharm. Pharmacol.*, **29**, 70 (1977).

(13) J. E. Rees and E. Shotton, *ibid.*, **22**, *Suppl.*, 17S (1970).

(14) S. T. Horhota, J. Burgio, L. Lonski, and C. T. Rhodes, *J. Pharm. Sci.*, **65**, 1746 (1976).

(15) R. P. Bhatia, Ph.D. thesis, Rutgers—The State University, Piscataway, N.J., 1976.

(16) S. T. David and L. L. Augsburger, *J. Pharm. Sci.*, **66**, 155 (1977).

ACKNOWLEDGMENTS

Presented at the Industrial Pharmaceutics Section, APhA Academy of Pharmaceutical Sciences, New York meeting, May 1977.

Abstracted in part from a thesis submitted by R. P. Bhatia to the Graduate School, Rutgers University, in partial fulfillment of the Doctor of Philosophy degree requirements.

Supported in part by a Gillette and Bevier Fellowship.

Cinoxacin in Female Mongrel Dogs: Effect of Urine pH on Urinary Drug Excretion and Correlation of *In Vitro* Characteristics of Oral Dosage Forms with Bioavailability

J. F. QUAY ˣ, R. F. CHILDERS, D. W. JOHNSON, J. F. NASH, and J. F. STUCKY, II

Received March 8, 1978, from the *Divisions of Pharmacological Research, Analytical Development, and Scientific Information Services, Lilly Research Laboratories, Eli Lilly and Company, Indianapolis, IN 46206.* Accepted for publication July 28, 1978.

Abstract □ Cinoxacin was measured in plasma and in urine of female mongrel dogs after single 10-mg/kg iv doses. The terminal half-life of plasma cinoxacin was 0.873 hr in dogs whose urine had been alkalinized by oral administration of sodium bicarbonate, 3.79 hr in normal dogs, and 15.8 hr in dogs whose urine had been acidified by oral administration of ammonium chloride. Dogs with alkalinized urine were chosen for cinoxacin bioavailability studies to minimize interanimal variability and to maximize recovery of unaltered cinoxacin in the urine. Four lots of crystalline cinoxacin with widely different particle sizes were prepared and characterized with respect to their specific surface areas, particle-size distributions, and dissolution profiles *in vitro*. Capsules of cinoxacin from these lots and aqueous solutions of cinoxacin were administered as single oral doses to dogs with alkalinized urine. Four aspects of the bioavailabilities of the oral preparations, peak plasma cinoxacin concentration, time of peak plasma cinoxacin concentration, area under the plasma cinoxacin concentration–time curve, and urinary excretion of cinoxacin, were determined and found to follow rank-order relationships with the characteristics of the same preparations *in vitro*. Linear relationships were observed between the reciprocal of the dissolution rate constant and the area under the plasma cinoxacin concentration–time curve, between the reciprocal of specific surface area and the reciprocal of the time of peak plasma cinoxacin concentration, and between the reciprocal of specific surface area and the amount of cinoxacin excreted in urine in 24 hr.

Keyphrases □ Cinoxacin—effect of urine pH on urinary excretion, bioavailability correlated with physical characteristics of oral dosage forms, dogs □ Excretion, urinary—cinoxacin, effect of urine pH, dogs □ Bioavailability—cinoxacin, correlated with physical characteristics of oral dosage forms, dogs □ Antibacterials—cinoxacin, effect of urine pH on urinary excretion, bioavailability correlated with physical characteristics of oral dosage forms, dogs

Cinoxacin[1], 1-ethyl-1,4-dihydro-4-oxo[1,3]dioxolo[4,5-*g*]cinnoline-3-carboxylic acid, is a new synthetic compound with an antibacterial spectrum similar to the spectra of nalidixic acid and oxolinic acid (1). Cinoxacin is a weak organic acid[2] with limited solubility under acid conditions[3]. The drug is effective when administered orally to patients with urinary tract infections (2, 3).

BACKGROUND

Nelson (4) and Levy (5) reviewed the literature on the relationship between particle size or surface area of drug preparations and their rates of solution and GI absorption. Smaller particle size (greater surface area) favored rapid dissolution and rapid oral absorption for many drugs. This relationship was demonstrated in human studies of slightly soluble weak organic acids such as sulfadiazine (6), phenytoin (7), aspirin (8), dicumarol (9), and tolbutamide (10).

Moore *et al.* (11) found that the lag time for absorption increased and the absorption rate decreased in the series: sodium nalidixate; nalidixic acid, 4–12 μm; and nalidixic acid, 177–250 μm. The dissolution rates of the same preparations showed rank-order correlation with biological parameters.

The excretion and renal clearance rates of some weak acids and bases are influenced by urinary pH (12, 13). Organic acids with pKa values as widely different as 3.0 (salicylic acid) and 7.0 (phenobarbital) underwent elevated renal clearance in subjects whose urine was alkalinized by sodium bicarbonate administration (14, 15).

Therefore, it appeared likely that, following oral administration, the cinoxacin absorption rate would depend on the surface area or particle size of the preparation. Furthermore, it was expected that the peak blood cinoxacin concentration as well as the rate and extent of excretion of the drug into the urine would depend on both the absorption rate and the renal excretion rate as influenced by the pH of the tubular urine.

The purposes of the present investigation were to establish the relationship between urinary pH and cinoxacin excretion in the dog and then to utilize the appropriate set of experimental conditions in this species to evaluate the relationships between the surface area and dissolution rate of different cinoxacin preparations and their bioavailability.

EXPERIMENTAL

Materials—Samples from one lot of cinoxacin were recrystallized from dimethylformamide at various temperatures and stirring rates to yield three lots of crystals, B, C, and D, with different median particle sizes. Another sample of cinoxacin was sheared in a comminuting mill[4] to prepare the smallest median particle-size material, Lot A. The pure drug substance was assayed by high-pressure liquid chromatography[5] and found to be 100.4, 101.6, 101.7, and 98.4% pure for Lots A, B, C, and D, respectively.

Cinoxacin from each lot was hand filled, without excipients, into No. 2 gelatin capsules. Solutions for oral and intravenous administration consisted of sterile-filtered aqueous solutions of the sodium salt, pH 7.5, containing 100 mg of cinoxacin acid equivalent/ml.

***In Vitro* Characterization of Cinoxacin Preparations**—Specific surface areas of Lots A–D were determined by two Brunauer, Emmett, and Teller (BET) (16) gas adsorption techniques. Surface areas calculated from static volumetric[6] and GC[7] measurements were comparable. Particle-size distributions were determined with an automated counter[8]. The X-ray powder pattern[9] of each lot was identical to that of a reference standard.

Dissolution profiles for 150 mg of each lot in gelatin capsules were generated using a modified[10] USP rotating-basket apparatus (17) at 100 rpm. The medium for dissolution tests was 300 ml of pH 6.5 phosphate buffer USP at 37°. Under these conditions, cinoxacin solubility was 3 mg/ml. During the test, 5-ml aliquots were collected with filter-tipped pipets at 5, 10, 15, 20, 25, 30, 45, and 60 min and at t_∞[11]. The aliquots were diluted by automated analysis equipment[12], and the absorbance due to cinoxacin was measured at 270 nm[13].

[1] Cinobac, Eli Lilly and Co., Indianapolis, Ind.
[2] Aqueous pKa 4.9 at 37°.
[3] The aqueous solubility at 37° is 0.03 mg/ml at pH 1.2, 0.07 mg/ml at pH 4.5, and 1.0 mg/ml at pH 6.0.

[4] Model UD, Fitzpatrick Co., Elmhurst, Ill.
[5] Model 8500 liquid chromatograph, Varian Instrument Division, Palo Alto, Calif.
[6] Micromeritics Instrument Corp., Norcross, Ga.
[7] Quantachrome Corp., Greenvale, N.Y.
[8] Model TA II, Coulter Electronics, Hialeah, Fla.
[9] Cu radiation was used with a Ni filter and diffractometer, North American Phillips Corp., Mt. Vernon, N.Y.
[10] Modifications consisted of the use of a flat-bottom vessel, uncovered.
[11] The t_∞ sample was collected after homogenization of the remaining vessel contents.
[12] Technicon Industrial Systems, Tarrytown, N.Y.
[13] Coleman model 101, Perkin-Elmer Corp., Norwalk, Conn.

0022-3549/79/0200-0227$01.00/0
© 1979, American Pharmaceutical Association

Table I—*In Vitro* Characteristics of Cinoxacin Preparations

Lot	SSA[b], m^2/g	Particle Size[a], μm			K_d[d], min^{-1}
		90%[c]	50%	10%	
A	0.466	15	32	64	0.082
B	0.139	52	83	110	0.045
C	0.0751	84	190	420	0.032
D	0.0259	—	~1000[e]	—	0.016

[a] Equivalent spherical diameter. [b] Specific surface area. [c] Volume percentile, greater than. [d] First-order dissolution rate constant. [e] Visual estimation.

***In Vivo* Evaluation of Cinoxacin**—To prepare dogs with acid urine, female mongrel dogs, 14–20 kg, were treated orally for 2 days preceding the day of the experiment with 2 g of ammonium chloride in gelatin capsules at 7 am, 12 noon, and 4 pm. On the day of the experiment, 2 g was given at 6 am, 7:30 am, and 12 noon.

To prepare dogs with alkaline urine, the same doses of sodium bicarbonate were given on the same schedule. Dogs with unperturbed urine pH were given no premedication but otherwise were treated in an identical manner.

On the night preceding the day of the experiment, the dogs were fasted in their home cages but allowed free access to water. On the day of the experiment, they were transferred to stocks in which they could stand or sit comfortably. Thirty minutes before drug administration, a Foley retention catheter[14] was inserted into the urinary bladder of each dog and secured by inflation of the balloon with 5 ml of water. The dog was then given 500 ml of tap water through a temporarily placed stomach tube.

After 30 min, immediately before the dose of cinoxacin, the bladder was emptied and the urine volume and pH[15] were recorded. The sample was chilled in an ice bath until the end of the experiment and then was frozen and stored at −10° until assayed. Immediately following the collection of the urine sample, a blood sample was withdrawn from one cephalic vein into a heparinized vacuum tube[16]. The plasma fraction was removed, chilled, frozen, and stored in the same manner as the urine sample.

For intravenous studies, 10 mg of cinoxacin/kg as a sterile solution was administered to alkalotic, normal, or acidotic dogs as a bolus by syringe into one cephalic vein. For oral studies, 10 mg of cinoxacin/kg was administered to alkalotic dogs as a sterile solution by stomach tube or as a sample of crystalline powder from Lot A, B, C, or D in a gelatin capsule over the tongue. Both types of oral preparations were followed by 25 ml of water given by the same route as the medication. At specified times, blood and urine samples were collected and treated as described.

On the day of assay, plasma and urine were thawed. A portion of each sample was acidified with 0.1 *N* HCl. Cinoxacin was extracted from the acidified sample into chloroform and then from the chloroform fraction into borate buffer, pH 9.0. The resulting solution was made strongly acidic with concentrated sulfuric acid, and the fluorescence due to cinoxacin was read at 445 nm during excitation at 356 nm[17]. Fluorescence readings were converted to cinoxacin concentrations by use of a calibration curve constructed from extracted plasma samples containing known concentrations of cinoxacin.

Cinoxacin concentrations determined in freshly drawn plasma samples by a fluorometric method (18) were not changed by several months of frozen storage. In addition, several days of cyclic freezing and thawing of plasma samples gave no indication of cinoxacin decomposition. The extraction efficiency of cinoxacin from plasma by this method was determined using ^{14}C-*carboxylic*-cinoxacin.

The radioactive cinoxacin was added to drug-free human plasma in concentrations of 2, 5, 10, 20, and 40 μg/ml, and the samples were analyzed in quintuplicate. The data showed 92–96% recovery of drug in the borate buffer. The fluorescence spectrum of cinoxacin in this buffer coincided with that of extracts (by the described procedure) from both standard spiked plasma and experimentally derived plasma samples of cinoxacin. Furthermore, this method is specific for the parent cinoxacin in either plasma or urine. The principal metabolite, 1-ethyl-1,4-dihydro-7-hydroxy-6-methoxy-4-oxocinnoline-3-carboxylic acid, had 0.1% of the fluorescence of cinoxacin at 445 nm.

Table II—Results of Duncan's Test[a] on the Intravenous Data

t, min	Plasma Cinoxacin, μg/ml		
	Alkalinized	Untreated	Acidified
1.5	86.4[a] (4.9)	83.5[a] (8.4)	103[b] (5.6)
10	52.4[a] (1.4)	1.3[a] (2.0)	54.2[a] (2.0)
20	42.9[a] (1.6)	45.5[ab] (1.7)	51.8[b] (2.4)
30	36.2[a] (1.5)	43.6[b] (1.9)	47.9[b] (1.9)
40	30.8[a] (1.7)	41.6[b] (2.1)	47.3[b] (1.9)
60	24.3[a] (1.6)	39.2[b] (2.3)	46.8[c] (1.9)
80	17.8[a] (1.6)	34.5[b] (2.2)	45.1[c] (2.1)
120	10.6[a] (1.5)	31.4[b] (2.4)	43.3[c] (1.8)
180	3.60[a] (0.40)	25.7[b] (2.9)	41.2[c] (1.9)
240	1.41[a] (0.19)	21.7[b] (3.5)	40.3[c] (2.3)
300	0.53[a] (0.08)	17.7[b] (3.8)	37.0[c] (2.0)
360	0.16[a] (0.05)	15.0[b] (3.6)	36.2[c] (2.1)
420	0.09[a] (0.04)	12.8[b] (3.1)	34.5[c] (1.8)
480	0.07[a] (0.03)	10.1[b] (2.5)	34.1[c] (2.0)
AUC (0–480 min), μg-min/ml	4030[a] (240)	11,600[b] (1300)	19,500[c] (900)
ΣU_{24}, %	98.5[a] (2.7)	81.9[b] (5.7)	7.8[c] (1.1)[b]

[a] Means of the variables within a row are statistically different ($\alpha = 0.05$) if they do not have a superscript letter in common. Numbers in parentheses are standard errors of the mean for eight dogs unless otherwise indicated. [b] Four dogs only.

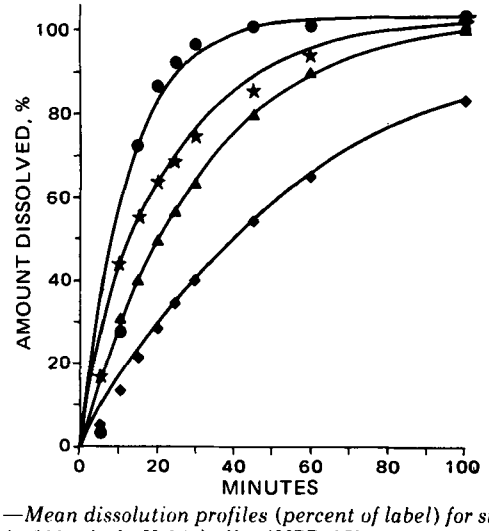

Figure 1—*Mean dissolution profiles (percent of label) for six 150-mg capsules in 300 ml of pH 6.5 buffer (USP, 37°) at 100 rpm (rotating basket). Key: ●, Lot A; ★, Lot B; ▲, Lot C; and ♦, Lot D. Curves were calculated from Eq. 1 using the rate constants of Table I.*

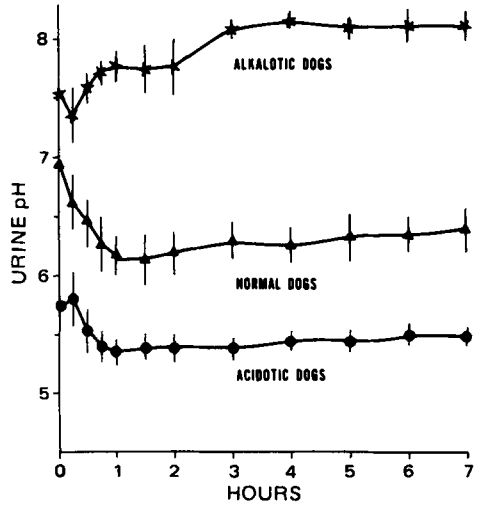

Figure 2—*Mean urine pH (±SEM) in eight dogs following intravenous administration of 10 mg of cinoxacin/kg. Key: ★, alkalotic dogs; ▲, normal dogs; and ●, acidotic dogs.*

[14] French No. 14.
[15] Model 7 pH meter, Corning Scientific Instruments, Medfield, Mass.
[16] Vacutainer, Becton-Dickinson and Co., Rutherford, N.J.
[17] Aminco SPF-125 spectrophotofluorometer, American Instrument Co., Silver Spring, Md.

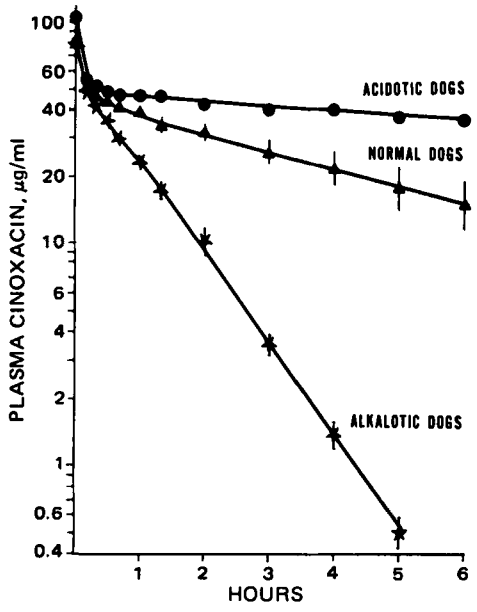

Figure 3—*Mean plasma concentration* (±SEM) *of cinoxacin in eight dogs following 10 mg/kg iv. Key:* ★, *alkalotic dogs;* ▲, *normal dogs; and* ●, *acidotic dogs.*

Eight dogs received 10 mg of cinoxacin/kg by all eight described treatments (five oral preparations and three intravenous protocols). No particular order was followed in the administration sequence of different dosage forms. However, at least 7 days (equivalent to 12 half-lives for cinoxacin in dogs with acidified urine) elapsed between experiments with any given dog. Because only two dogs were used on any given day, the series of experiments required an extended period. Therefore, day effects that may be present in the data are assumed not to influence the evaluation of the bioavailability of the different preparations.

RESULTS AND DISCUSSION

***In Vitro* Characteristics of Cinoxacin Preparations**—Mean dissolution profiles of cinoxacin from capsules of Lots A–D are shown in Fig. 1. Points in Fig. 1 represent the experimentally determined values; the solid lines represent the best fit (weighted nonlinear least-squares regression) to the following equation:

$$D_t = D_\infty(1 - e^{-K_d t}) \qquad \text{(Eq. 1)}$$

where D_t is the amount dissolved at time t in minutes, K_d is the dissolution rate constant in reciprocal minutes, and D_∞ is the amount dissolved at t_∞.

Although Eq. 1 is only rigorously valid for an idealized single-particle system (19), it was chosen to represent the *in vitro* dissolution profiles for its simplicity and because other models sometimes used to describe

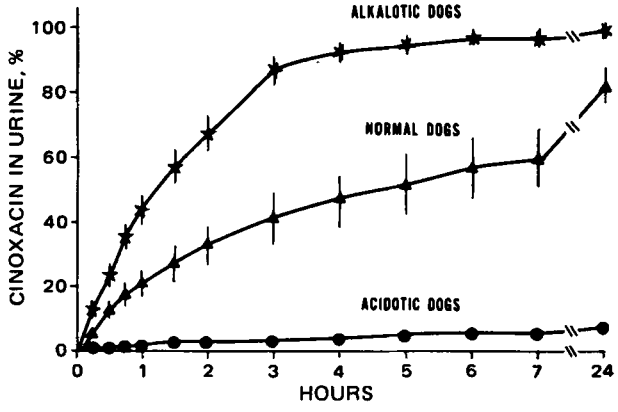

Figure 4—*Mean cumulative cinoxacin* (±SEM) *in the urine of eight dogs following 10 mg/kg iv. Key:* ★, *alkalotic dogs;* ▲, *normal dogs; and* ●, *acidotic dogs.*

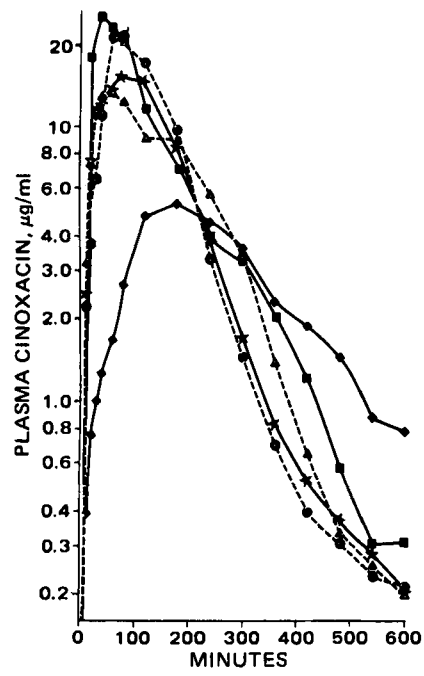

Figure 5—*Mean plasma concentration of cinoxacin in eight alkalotic dogs following 10 mg/kg po. Key:* ■, *solution;* ●, *Lot A;* ★, *Lot B;* ▲, *Lot C; and* ♦, *Lot D.*

dissolution from a multiparticulate system under nonsink conditions, such as the negative two-thirds root law (20), failed to provide a better fit. Best estimates of K_d for the four lots of cinoxacin, along with their specific surface areas and particle-size distributions, are listed in Table I. The observed decrease in surface area in Lots A–D is clearly reflected by the decline in dissolution rate constants calculated for the corresponding lots.

Effect of Urinary pH Perturbations on Cinoxacin Excretion in Dogs—*Urine pH*—The time course of urine pH observed in alkalotic, normal, and acidotic dogs after intravenous administration of 10 mg of cinoxacin/kg is given in Fig. 2. For female dogs rendered alkalotic with sodium bicarbonate, the mean urine pH during the experimental period ranged from 7.4 to 8.2 (overall mean of 7.9).

In normal dogs, the mean urine pH ranged from 6.1 to 6.9 (overall mean of 6.4). For dogs rendered acidotic with ammonium chloride, the mean urine pH ranged from 5.4 to 5.8 (overall mean of 5.5). As shown in Fig.

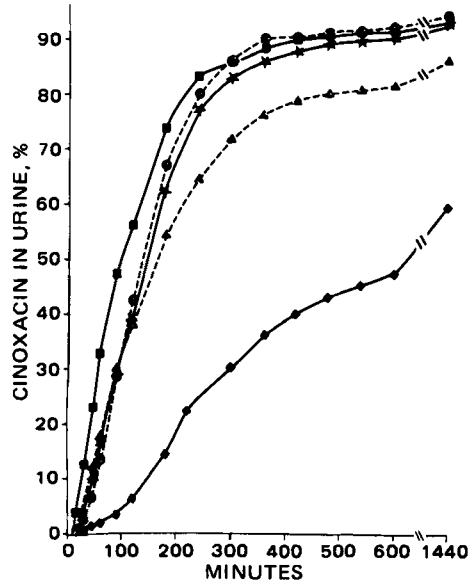

Figure 6—*Mean cumulative cinoxacin in the urine of eight alkalotic dogs following 10 mg/kg po. Key:* ■, *solution;* ●, *Lot A;* ★, *Lot B;* ▲, *Lot C; and* ♦, *Lot D.*

Table III—Results of Duncan's Test [a] on the Oral Data

t, min	Plasma Cinoxacin, μg/ml				
	Lot S	Lot A	Lot B	Lot C	Lot D
10	2.1[a,c]	2.33[a] (2.1)	2.43[a] (1.2)	3.19[a] (1.4)	0.39[a] (0.21)
20	17.6[a] (4.8)	3.72[b] (2.0)	8.41[b] (3.1)	7.39[b] (3.2)	0.75[b] (0.28)
30	18.0[a,c]	6.41[ab] (1.6)	11.5[a] (4.0)	10.8[a] (3.7)	1.02[b] (0.34)
40	24.8[a] (1.8)	10.9[b] (2.3)	12.6[b] (3.9)	12.4[b] (3.3)	1.25[c] (0.42)
60	22.5[a] (1.9)	21.0[ab] (4.0)	14.3[b] (2.5)	13.3[b] (2.9)	1.67[c] (0.47)
80	20.2[a] (3.4)	21.5[a] (2.4)	16.6[ab] (2.0)	12.0[b] (2.2)	2.64[c] (0.62)
120	13.0[ab] (3.0)	17.0[a] (0.86)	15.1[a] (1.8)	8.90[bc] (1.5)	4.71[c] (0.86)
180	6.93[a] (2.0)	9.69[a] (2.1)	8.55[a] (1.9)	8.88[a] (2.8)	5.19[a] (0.85)
240	3.99[a] (1.5)	3.29[a] (0.88)	3.73[a] (0.86)	5.61[a] (1.9)	4.45[a] (1.1)
300	3.20[a] (1.5)	1.44[a] (0.31)	1.70[a] (0.43)	3.38[a] (1.6)	3.59[a] (0.94)
360	2.01[a] (1.1)	0.689[a] (0.14)	0.830[a] (0.15)	1.36[a] (0.59)	2.28[a] (0.57)
420	1.05[ab] (0.51)	0.395[b] (0.046)	0.516[b] (0.11)	0.636[ab] (0.22)	1.86[a] (0.74)
480	0.565[ab] (0.24)[d]	0.306[b] (0.039)	0.373[b] (0.052)	0.327[b] (0.069)	1.42[a] (0.51)
540	0.306[a] (0.12)[d]	0.229[a] (0.025)	0.275[a] (0.041)	0.253[a] (0.040)	0.864[b] (0.20)
600	0.303[a] (0.098)[d]	0.210[a] (0.035)	0.206[a] (0.041)	0.209[a] (0.035)	0.770[b] (0.13)
AUC (0–600 min), μg-min/ml	3460[a] (520)	3160[a] (150)	2910[a] (210)	2690[a] (220)	1580[b] (200)
C_{max}, μg/ml	30.1[a] (2.2)	25.1[ab] (2.5)	20.8[b] (1.7)	20.8[b] (1.9)	7.33[c] (0.65)
T_{max}, min	42.5[a]	75.0[a]	80.0[a]	92.5[a]	173[b]
ΣU_{24}, %	93.4[a] (3.7)	95.0[a] (3.9)	93.1[a] (2.1)	86.2[a] (2.9)	59.8[b] (8.5)

[a] Means of the variables within a row are statistically different ($\alpha = 0.05$) if they do not have a superscript letter in common. Numbers in parentheses are standard errors of the mean for eight dogs unless otherwise indicated. [b] Aqueous solution. [c] Two dogs only. [d] Five dogs only.

2, the variation of urine pH between dogs for individual time points was generally smaller for alkalotic and acidotic dogs than for normals.

Persistence of Cinoxacin in Plasma after Intravenous Administration—The cinoxacin concentrations in the plasma of alkalotic, normal, and acidotic dogs as a function of time after intravenous administration of 10 mg/kg are shown in Fig. 3. As indicated by analysis of variance, significant differences in plasma cinoxacin concentrations appeared among the three groups of dogs at 20 min. At 60 min, the results of all three protocols were different from each other [Duncan's test (21), Table II].

In addition, the rate of decline of mean plasma cinoxacin concentration approximated a first-order decay process, as judged by the apparent linearity of the semilogarithmic plots of the data after 60 min. Therefore, the slopes of the linear regression lines were calculated through the points after 60 min. For alkalotic dogs, the slope was -0.345 ± 0.030 (SD) hr^{-1} with a corresponding half-life of 0.873 hr. For normal dogs, the slope was -0.0795 ± 0.0013 hr^{-1} with a corresponding half-life of 3.79 hr. For acidotic dogs, the slope was -0.0190 ± 0.0011 hr^{-1} with a half-life of 15.8 hr. The correlation coefficients associated with the linear regression of the log mean plasma values on time were 0.978, 0.999, and 0.989 for alkalotic, normal, and acidotic dogs, respectively.

Urinary Excretion of Cinoxacin after Intravenous Administration—The amounts of cinoxacin, expressed as percent of the administered dose, recovered in the urine of alkalotic, normal, and acidotic female mongrel dogs after 10 mg/kg iv are illustrated in Fig. 4. Alkalotic dogs rapidly excreted essentially all of the dose in the urine. Ninety-five percent of the dose appeared in the urine within 5 hr and 98.5% of the dose appeared within 24 hr. Normal dogs excreted appreciably less, 51.7% of the dose, in the same 5 hr. By 24 hr, normal dogs had excreted 81.9% of the dose.

Dogs maintained in the acidotic state excreted very little cinoxacin in the urine, reaching a mean of 4.5% of the dose in 5 hr and 7.8% in 24 hr. However, urinary excretion in six acidotic dogs followed for 72 hr increased to 39.1% as they began to recover from the acidotic state. Variation between dogs in the recovery of cinoxacin in the urine was larger for normal dogs than for either acidotic or alkalotic dogs.

From the results of the preceding intravenous studies, it is clear that, judged by the interanimal variability in urine pH, plasma cinoxacin concentration, and urinary cinoxacin excretion, either acidified or alkalinized dogs would provide a more reproducible test system than would normal dogs. The alkalinized dogs also excreted essentially all of the dose unchanged in the urine within 24 hr, thus minimizing any uncertainty associated with interanimal differences in metabolic degradation. Moreover, the cinoxacin elimination half-life from the blood of the alkalotic dog (0.873 hr) was more representative of that of normal humans (0.96 hr) (22) than was the elimination half-life of either normal or acidotic dogs.

In addition, comparative metabolism studies showed that both humans and dogs excrete primarily unchanged drug in the urine[18]. Although fewer metabolites are formed in dogs than in humans, those found in dogs generally coincide with those formed in humans. Therefore, the alkalinized dog was selected as an animal model to evaluate the bioavailability of different orally administered cinoxacin preparations.

***In Vivo* Characterization of Cinoxacin Oral Preparations in Alkalotic Dogs**—The plasma cinoxacin concentrations of alkalotic dogs at various times after oral administration of a single 10-mg/kg dose as an aqueous solution or as a capsule of Lot A, B, C, or D are shown in Fig. 5. Oral administration of the solution produced the earliest and highest peak mean plasma cinoxacin concentration, 24.8 μg/ml at 40 min. Progressively lower peak mean concentrations were produced by administration of a Lot A, B, C, or D capsule. The most striking difference for most time points was between Lot D, the lot with the smallest surface area (largest particle size), and all of the other preparations.

Analyses of variance were performed on the data represented in Fig. 5. Significant differences in plasma concentrations existed among the five preparations from 20 min to 2 hr and from 8 to 10 hr. Significant differences also existed among the given preparations in urinary recovery, area under the plasma cinoxacin concentration–time curve, peak plasma cinoxacin concentration, and time of peak plasma cinoxacin concentration.

Table III lists the results of Duncan's test applied to the data to ascertain which individual comparisons between groups yield significant differences. As these results indicate, for 24-hr urinary recovery of cinoxacin (ΣU_{24}), for observed area under the plasma cinoxacin con-

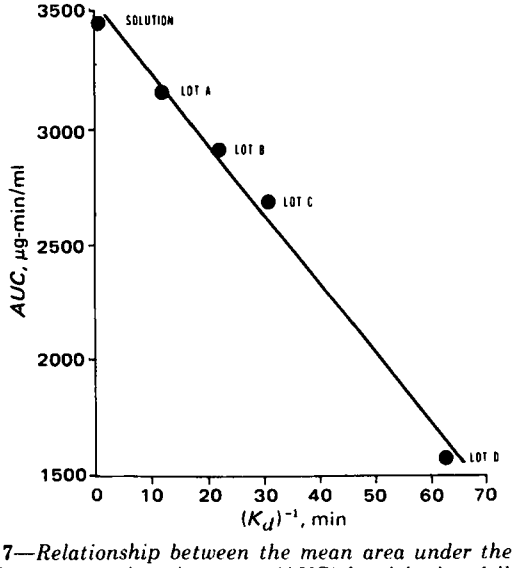

Figure 7—*Relationship between the mean area under the plasma cinoxacin concentration–time curve* (AUC) *for eight dogs following 10 mg/kg po and the mean dissolution rate constant* (K_d) *with a linear correlation coefficient of −0.995.*

[18] Dr. R. L. Wolen, Eli Lilly and Co., Indianapolis, Ind., personal communication.

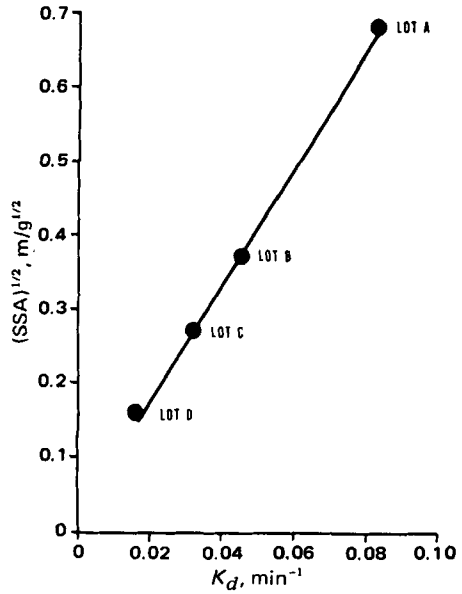

Figure 8—*Relationship between specific surface area (SSA) and the mean dissolution rate constant* (K_d) *for cinoxacin with a linear correlation coefficient of 0.999.*

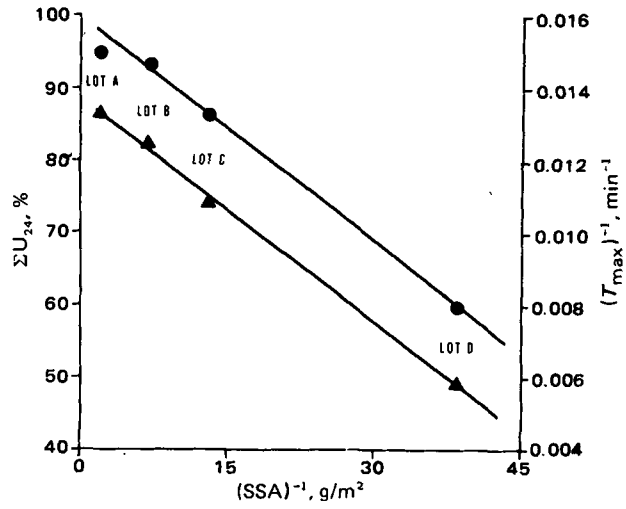

Figure 9—*Relationships between specific surface area (SSA) and both the mean cumulative cinoxacin in the urine after 24 hr* (ΣU_{24}) *and the mean time of peak plasma cinoxacin concentration* (T_{max}) *in eight dogs following 10 mg/kg po. Key:* ▲, T_{max}^{-1} *and* SSA^{-1} *with a linear correlation coefficient of −0.999; and* ●, ΣU_{24} *and* SSA^{-1} *with a linear correlation coefficient of −0.996.*

centration–time curve (*AUC*, 0–10 hr), and for time of peak plasma cinoxacin concentration (T_{max}), the only significant differences ($\alpha = 0.05$) were those between Lot D and the other four preparations. For peak plasma cinoxacin concentration (C_{max}), Lot D was again distinct from the other four preparations. Additionally, the solution was different from Lots B and C. Further comparisons at specific time points can be made by reference to Table III.

The amounts of cinoxacin recovered in the urine of individual alkalotic dogs at various times after administration of a single 10-mg/kg dose as an aqueous solution or as a capsule of Lot A, B, C, or D are shown in Fig. 6.

Correlations of *In Vivo* and *In Vitro* Cinoxacin Data—Numerous correlations for the oral cinoxacin preparations can be formed from the pairwise treatment of the *in vitro* (Table I) and *in vivo* (Table III) data. Even though statistically significant differences did not exist among all *in vivo* parameters for the five different oral preparations, near perfect rank-order correlations (23) existed between the mean values of these *in vivo* and *in vitro* parameters. For predictive purposes, functional relationships were derived from pairs of these parameters. Four such relationships are presented in Figs. 7–9.

The relationship between *AUC* and K_d was linearized (Fig. 7) by plotting the reciprocal of the mean K_d *versus* the mean *AUC*, with a resulting correlation coefficient of −0.995. The dissolution rate constant, K_d, for the oral solution, was assumed to be large relative to that for Lot A, so its reciprocal was assigned a value of zero. This *in vivo–in vitro* correlation relates two parameters, each of which is a function of the entire dose response *versus* time curve. Therefore, the relationship should be a more valid predictor of the performance of formulations over a broader range (24) than any correlation between single points taken from the dose response *versus* time curves. In this case, *AUC* is a measure of the extent of drug absorption and K_d represents the *in vitro* drug dissolution rate. The relationship depicted in Fig. 7 has been used in the generation of a dissolution test specification for cinoxacin formulations.

In Fig. 8, an *in vitro–in vitro* relationship is quantitated for cinoxacin. The dissolution rate constant is correlated with the square root of the specific surface area as measured by the BET gas adsorption technique. In general, specific surface areas generated by the BET method are more accurate measures of the bulk sample surface, independent of either assumed particle geometry or size distribution, than are various sieve, particle-size, or permeametric measurements (25–27). The correlation coefficient associated with the linear regression of K_d on the square root of the specific surface area is 0.999. This relationship is useful in the selection of bulk raw material lots of cinoxacin to help assure that the finished product will have suitable dissolution characteristics.

Relationships between two measures of the absorption of cinoxacin, *i.e.*, the mean T_{max} and the mean ΣU_{24}, and the specific surface area of the drug are presented in Fig. 9. Linear regression of the reciprocal of the specific surface area with ΣU_{24} and with the reciprocal of T_{max} yielded correlation coefficients of −0.996 and −0.999, respectively. This pair of correlations quantitatively relates measures of both the rate and extent of absorption of cinoxacin to a physical property of the raw material.

These correlations have been used to help establish product specifications for the finished dosage forms, 250- and 500-mg capsules. A comparative bioavailability study of these two capsule formulations and an oral solution is being conducted in humans.

REFERENCES

(1) W. E. Wick, D. A. Preston, W. A. White, and R. S. Gordee, *Antimicrob. Agents Chemother.*, **4**, 415 (1973).

(2) A. P. Panwalker, H. Giamarellou, and G. G. Jackson, *ibid.*, **9**, 502 (1976).

(3) A. H. Bennett, "Chemotherapy (Penicillins and Cephalosporins)," vol. 5, Plenum, New York, N.Y., 1975, pp. 417, 418.

(4) E. Nelson, *Clin. Pharmacol. Ther.*, **3**, 673 (1962).

(5) G. Levy, *Am. J. Pharm.*, **135**, 78 (1963).

(6) J. G. Reinhold, F. J. Phillips, and H. F. Flippin, *Am. J. Med. Sci.*, **210**, 141 (1945).

(7) W. A. Dill, A. Kazenko, L. M. Wolf, and A. J. Glazko, *J. Pharmacol. Exp. Ther.*, **118**, 270 (1956).

(8) G. Levy and B. A. Hayes, *N. Engl. J. Med.*, **262**, 1053 (1960).

(9) E. Lozinski, *Can. Med. Assoc. J.*, **83**, 177 (1960).

(10) E. Nelson, S. Long, and J. G. Wagner, *J. Pharm. Sci.*, **53**, 1224 (1964).

(11) W. E. Moore, G. A. Portmann, H. Stander, and E. W. McChesney, *ibid.*, **54**, 36 (1965).

(12) M. D. Milne, B. H. Scribner, and M. A. Crawford, *Am. J. Med.*, **24**, 709 (1958).

(13) I. M. Weiner and G. H. Mudge, *ibid.*, **36**, 743 (1964).

(14) A. B. Gutman, T. F. Yu, and J. H. Sirota, *J. Clin. Invest.*, **34**, 711 (1955).

(15) W. J. Waddell and T. C. Butler, *ibid.*, **36**, 1217 (1957).

(16) S. Brunauer, P. H. Emmett, and E. Teller, *J. Am. Chem. Soc.*, **60**, 309 (1938).

(17) "The United States Pharmacopeia," 19th rev., Mack Publishing Co., Easton, Pa., 1975, p. 651.

(18) K. E. Anderson, S. Colleen, and P. A. Mardh, *J. Antimicrob. Chemother.*, **3**, 417 (1977).

(19) J. T. Carstensen, in "Dissolution Technology," L. J. Leeson and J. T. Carstensen, Eds., APhA Academy of Pharmaceutical Sciences, Washington, D.C., 1974, p. 3.

(20) L. Z. Benet, in *ibid.*, p. 43.

(21) D. B. Duncan, *Biometrics*, **11**, 1 (1955).

(22) K. S. Israel, H. R. Black, G. L. Brier, and J. P. Wolny, presented

at the 17th Interscience Conference on Antimicrobial Agents and Chemotherapy, 1977 (Abstract A167).
(23) "Handbook of Mathematical Tables," R. C. Weast, Ed., Chemical Rubber Co., Cleveland, Ohio, 1964, p. 532.
(24) V. F. Smolen and R. J. Erb, *J. Pharm. Sci.*, **66**, 297 (1977).
(25) D. T. Wasan, *Powder Technol.*, **14**, 209, 229 (1976).
(26) R. L. Grob, M. A. Kaiser, and M. J. O'Brien, *Am. Lab.*, **7**, 13 (1975).
(27) C. Orr, Jr., *Anal. Chem.*, **39**, 834 (1967).

ACKNOWLEDGMENTS

Presented in part at the American Society for Experimental Therapeutics, 1977 fall meeting, Columbus, Ohio, August 1977, and at the 17th Interscience Conference on Antimicrobial Agents and Chemotherapy, New York, N.Y., October 1977.

The authors thank Mr. W. R. Brown and Ms. M. K. Brunson for assaying cinoxacin in biological fluids and Dr. J. M. Indelicato for preparing lots of cinoxacin with different crystal sizes.

Rapid High-Performance Liquid Chromatographic Determination of Bleomycin A_2 in Plasma

GERALD K. SHIU *, THOMAS J. GOEHL *x, and WILLIAM H. PITLICK ‡

Received April 10, 1978, from the **Department of Medicinal Chemistry and the* ‡*Department of Pharmaceutics, School of Pharmacy, University of Pittsburgh, Pittsburgh, PA 15261.* Accepted for publication July 26, 1978.

Abstract □ A rapid and specific method for the determination of bleomycin A_2 is described. A 50-μl aliquot of 20% trichloroacetic acid was added to 200 μl of plasma. The sample was vortexed and centrifuged, and 50 μl of the clear supernate was injected into a liquid chromatograph equipped with a microparticulate reversed-phase column and a fixed wavelength detector. Elution was carried out using methanol–acetonitrile–0.0085 *M* heptanesulfonic acid–acetic acid. A linear calibration curve was found in the 0.05–5-μg/ml range with an estimated precision of ±6% (*CV*). Preliminary pharmacokinetic data in the rabbit also are reported.

Keyphrases □ Bleomycin A_2—high-performance liquid chromatographic analysis in plasma □ High-performance liquid chromatography—analysis, bleomycin A_2 in plasma □ Antineoplastic agents—bleomycin A_2, high-performance liquid chromatographic analysis in plasma

The antibiotic–antineoplastic agent bleomycin is actually a mixture of cationic polypeptides. The complex was isolated from fermentation products of *Streptomyces verticillus* (1). It is effective against human neoplasms, particularly squamous cell carcinoma, lymphoma, and testicular carcinoma (2–4). The most common toxic side effects are minor cutaneous reactions. However, about 10% of the patients develop pulmonary toxicity, occurring as pneumonitis and pulmonary fibrosis (5).

BACKGROUND

Crude bleomycin has been purified by chromatographic methods into two large fractions, A and B (6). Further fractionation provided six bleomycin A fractions and five bleomycin B fractions. Of the various highly hydrophilic polypeptides, 11 components have been completely purified. Each component consists of a carboxy terminal glycopeptide (~1300 daltons), designated as bleomycinic acid, which is substituted in an amide-type linkage with 3-(dimethylthionium)propylamine (bleomycin A_2, II), agmantine (bleomycin B_2, III), or 3-(methylsulfinyl)propylamine (bleomycin A_1, I).

The bleomycin administered clinically consists of, by weight, 55–70% bleomycin A_2, 25–32% bleomycin B_2, and the remaining percentage divided among the other subfractions (7). In all cases, at least 65% is from the bleomycin A group and less than 35% is from the bleomycin B group. The most commonly used regimen has been 15 mg/m^2 iv twice weekly (8).

Although almost all clinical work has been done using this formulation, there are indications that the individual bleomycin fractions should be studied. For example, bleomycin A_5 was more toxic to *Escherichia coli* than the more abundant bleomycin A_2 present in the formulation currently in use (9). Bleomycin acid was devoid of activity against *E. coli* (9). The possible effectiveness of bleomycin A_5 was reported by others (10, 11). Bleomycin B_4 caused kidney damage in dogs and had weak antitumor activity (12). However, few studies on individual components of the bleomycin mixture have been presented (12–14).

To elucidate the pharmacokinetics of individual bleomycins, a specific and sensitive assay must be available. Analytical techniques to estimate plasma levels of the bleomycin mixture include microbiological assays (11, 12, 15, 16), radioactive labeling assays (2, 17–19), and radioimmunoassays (20, 21). Unfortunately, all of these methods do not distinguish between the various components of the bleomycin mixture or their metabolites. Thus, specificity is a problem with all presently available techniques. In this report, a sensitive and specific paired-ion high-performance liquid chromatographic (HPLC) assay for one component of the bleomycin mixture, bleomycin A_2, is presented.

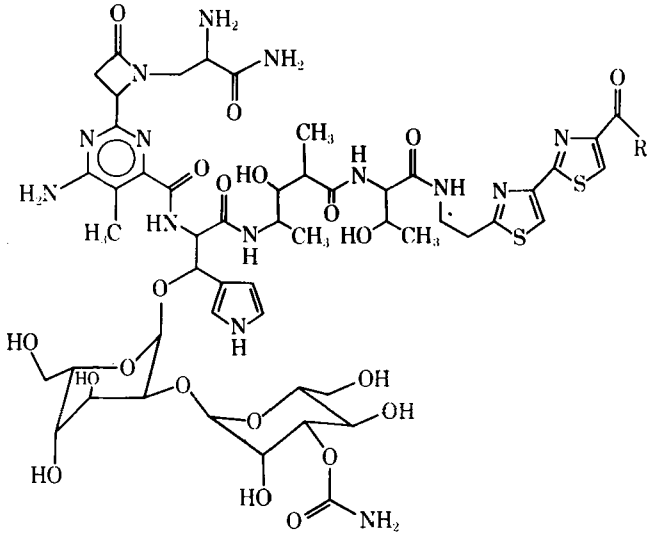

I: R = $NH(CH_2)_3SOCH_3$
II: R = $NH(CH_2)_3\overset{+}{S}{=}(CH_3)_2$
III: R = $NH(CH_2)_4NHC(=NH)NH_2$

0022-3549/79/0200-0232$01.00/0
© 1979, American Pharmaceutical Association

at the 17th Interscience Conference on Antimicrobial Agents and Chemotherapy, 1977 (Abstract A167).
(23) "Handbook of Mathematical Tables," R. C. Weast, Ed., Chemical Rubber Co., Cleveland, Ohio, 1964, p. 532.
(24) V. F. Smolen and R. J. Erb, *J. Pharm. Sci.*, **66**, 297 (1977).
(25) D. T. Wasan, *Powder Technol.*, **14**, 209, 229 (1976).
(26) R. L. Grob, M. A. Kaiser, and M. J. O'Brien, *Am. Lab.*, **7**, 13 (1975).
(27) C. Orr, Jr., *Anal. Chem.*, **39**, 834 (1967).

ACKNOWLEDGMENTS

Presented in part at the American Society for Experimental Therapeutics, 1977 fall meeting, Columbus, Ohio, August 1977, and at the 17th Interscience Conference on Antimicrobial Agents and Chemotherapy, New York, N.Y., October 1977.

The authors thank Mr. W. R. Brown and Ms. M. K. Brunson for assaying cinoxacin in biological fluids and Dr. J. M. Indelicato for preparing lots of cinoxacin with different crystal sizes.

Rapid High-Performance Liquid Chromatographic Determination of Bleomycin A_2 in Plasma

GERALD K. SHIU *, THOMAS J. GOEHL *x, and WILLIAM H. PITLICK ‡

Received April 10, 1978, from the **Department of Medicinal Chemistry and the* ‡*Department of Pharmaceutics, School of Pharmacy, University of Pittsburgh, Pittsburgh, PA 15261.* Accepted for publication July 26, 1978.

Abstract □ A rapid and specific method for the determination of bleomycin A_2 is described. A 50-μl aliquot of 20% trichloroacetic acid was added to 200 μl of plasma. The sample was vortexed and centrifuged, and 50 μl of the clear supernate was injected into a liquid chromatograph equipped with a microparticulate reversed-phase column and a fixed wavelength detector. Elution was carried out using methanol–acetonitrile–0.0085 *M* heptanesulfonic acid–acetic acid. A linear calibration curve was found in the 0.05–5-μg/ml range with an estimated precision of ±6% (*CV*). Preliminary pharmacokinetic data in the rabbit also are reported.

Keyphrases □ Bleomycin A_2—high-performance liquid chromatographic analysis in plasma □ High-performance liquid chromatography—analysis, bleomycin A_2 in plasma □ Antineoplastic agents—bleomycin A_2, high-performance liquid chromatographic analysis in plasma

The antibiotic–antineoplastic agent bleomycin is actually a mixture of cationic polypeptides. The complex was isolated from fermentation products of *Streptomyces verticillus* (1). It is effective against human neoplasms, particularly squamous cell carcinoma, lymphoma, and testicular carcinoma (2–4). The most common toxic side effects are minor cutaneous reactions. However, about 10% of the patients develop pulmonary toxicity, occurring as pneumonitis and pulmonary fibrosis (5).

BACKGROUND

Crude bleomycin has been purified by chromatographic methods into two large fractions, A and B (6). Further fractionation provided six bleomycin A fractions and five bleomycin B fractions. Of the various highly hydrophilic polypeptides, 11 components have been completely purified. Each component consists of a carboxy terminal glycopeptide (~1300 daltons), designated as bleomycinic acid, which is substituted in an amide-type linkage with 3-(dimethylthionium)propylamine (bleomycin A_2, II), agmantine (bleomycin B_2, III), or 3-(methylsulfinyl)propylamine (bleomycin A_1, I).

The bleomycin administered clinically consists of, by weight, 55–70% bleomycin A_2, 25–32% bleomycin B_2, and the remaining percentage divided among the other subfractions (7). In all cases, at least 65% is from the bleomycin A group and less than 35% is from the bleomycin B group. The most commonly used regimen has been 15 mg/m^2 iv twice weekly (8).

Although almost all clinical work has been done using this formulation, there are indications that the individual bleomycin fractions should be studied. For example, bleomycin A_5 was more toxic to *Escherichia coli* than the more abundant bleomycin A_2 present in the formulation currently in use (9). Bleomycin acid was devoid of activity against *E. coli* (9). The possible effectiveness of bleomycin A_5 was reported by others (10, 11). Bleomycin B_4 caused kidney damage in dogs and had weak antitumor activity (12). However, few studies on individual components of the bleomycin mixture have been presented (12–14).

To elucidate the pharmacokinetics of individual bleomycins, a specific and sensitive assay must be available. Analytical techniques to estimate plasma levels of the bleomycin mixture include microbiological assays (11, 12, 15, 16), radioactive labeling assays (2, 17–19), and radioimmunoassays (20, 21). Unfortunately, all of these methods do not distinguish between the various components of the bleomycin mixture or their metabolites. Thus, specificity is a problem with all presently available techniques. In this report, a sensitive and specific paired-ion high-performance liquid chromatographic (HPLC) assay for one component of the bleomycin mixture, bleomycin A_2, is presented.

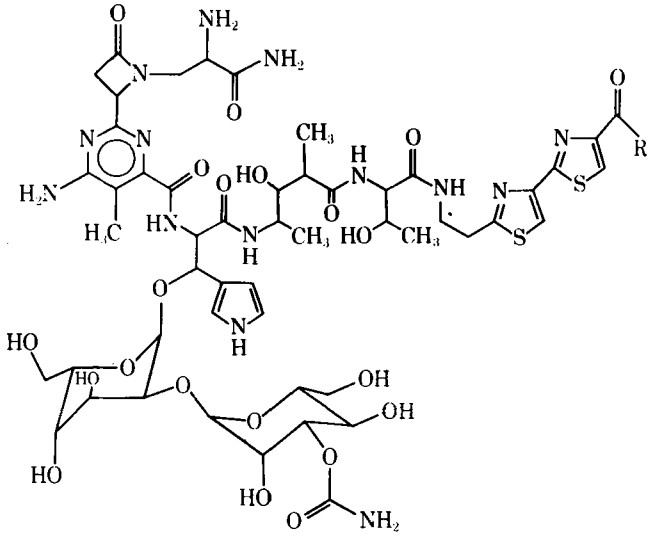

I: R = $NH(CH_2)_3SOCH_3$
II: R = $NH(CH_2)_3\overset{+}{S}{=}(CH_3)_2$
III: R = $NH(CH_2)_4NHC(=NH)NH_2$

0022-3549/79/0200-0232$01.00/0
© 1979, American Pharmaceutical Association

EXPERIMENTAL

Apparatus—A modular high-pressure liquid chromatograph consisting of a constant-flow pump[1], a valve-type injector[2], a fixed wavelength (254-nm) UV detector[3], and a strip-chart recorder[4] was used. A stainless steel column (3.9 mm × 30 cm) packed with fully porous 10-μm silica particles with a chemically bonded monomolecular layer of octadecylsilane[5] was obtained commercially. A guard column (3.9 mm × 6 cm) filled with pellicular reversed-phase packing[6] was used to prolong column life.

Chromatographic Conditions—The mobile phase consisted of methanol–acetonitrile–0.0085 *M* heptanesulfonic acid–acetic acid (30:10:59:1). A flow rate of 2.0 ml/min was established (2500 psi).

Reagents and Materials—Bleomycin[7], bleomycin A_2[8], and sodium 1-heptanesulfonate[9] were used as received. Solvents were of HPLC grade. All other materials were reagent grade. Stock solutions of bleomycin and bleomycin A_2 were prepared by dissolving 10 mg of bleomycin and bleomycin A_2 in 100 ml of deionized water. Plasma standards were prepared by taking appropriate small volumes of stock solutions and adding them to control plasma.

HPLC Assay and Calculations—To 0.2 ml of plasma in a 12-ml glass-stoppered conical centrifuge tube was added 50 μl of a 20% trichloroacetic acid solution. The samples were mixed[10] and then centrifuged[11] at 3000 rpm for 10 min. A 50-μl aliquot of the clear supernate was then injected onto the column, and peak heights were determined. Calibration curves were constructed daily from results obtained from spiked control plasma samples containing 0.5–5 μg/ml by plotting peak heights *versus* bleomycin A_2 concentration.

Pharmacokinetics in Rabbits—Four female New Zealand White rabbits, 1.5–3 kg, received 4 units of bleomycin/kg iv in the marginal ear vein. Fifteen blood samples were withdrawn over 3 hr from the opposite marginal ear vein.

RESULTS AND DISCUSSION

In preliminary studies with methanol–0.01 *M* heptanesulfonic acid–acetic acid (48:51:1), reasonable separations of the major components were obtained, yielding three major fractions. By using TLC methods in which relative R_f values of the HPLC-separated components were compared with literature values, these fractions were determined to be bleomycins A_2, B_2, and A_1. Only bleomycin A_2 was available for direct comparison by TLC and HPLC.

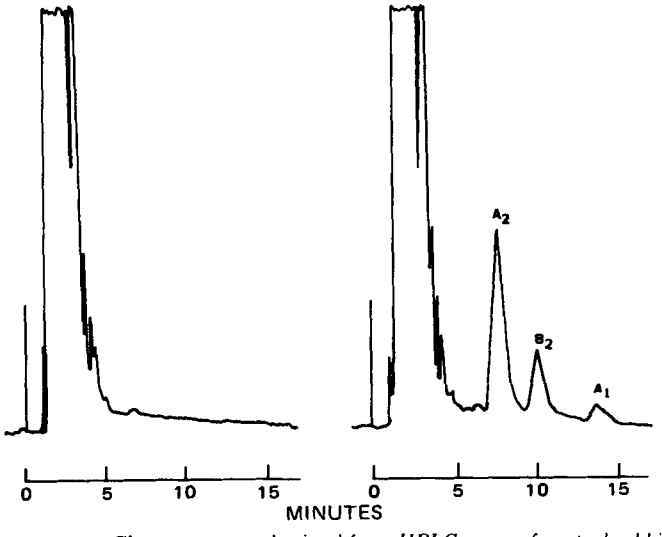

Figure 1—*Chromatogram obtained from HPLC assay of control rabbit plasma (left) and plasma from a rabbit administered a single intravenous dose of bleomycin (right). Peak for bleomycin A_2 corresponded to a concentration of 2.6 μg/ml.*

[1] Model M 6000A, Waters Associates, Milford, Mass.
[2] Model SVOV-6-1, Glenco Scientific, Houston, Tex.
[3] Model 440, Waters Associates, Milford, Mass.
[4] Model 255, Linear Instruments Corp., Irvine, Calif.
[5] Prepacked μBondapak C_{18}, Waters Associates, Milford, Mass.
[6] Co:Pell ODS, Whatman, Inc., Clifton, N.J.
[7] Blenoxane, lot E4095, supplied by Bristol Laboratories, Syracuse, N.Y.
[8] Supplied by Bristol Laboratories, Syracuse, N.Y.
[9] Eastman Kodak Co.
[10] Vortex-Genie, Fisher Scientific Industries, Springfield, Mass.
[11] IEC EXD centrifuge 460G, Damon/IEC Division, Needham Heights, Mass.

Table I—Stability of Bleomycin A_2 in Rabbit Plasma

Days	Concentration[a], μg/ml Sample A	Sample B
0	4.3 ● 0.1	3.0 ± 0.1
1	4.2 ± 0.2	3.1 ± 0.2
4	4.3 ± 0.2	3.0 ± 0.2
8	4.4 ± 0.1	3.1 ± 0.2

[a] Mean ± *SD*, $n = 3$.

Since the bleomycins are very water soluble, separation from normal plasma constituents was considered to be a major obstacle prior to the quantitation of bleomycin A_2. However, a simplistic approach was attempted. The proteins were removed by trichloroacetic acid precipitation, and then an aliquot of the supernate was injected onto a reversed-phase column. This approach proved to be very satisfactory, with no interfering peaks being found in the chromatograms. Comparison between spiked plasma samples and direct aqueous injections gave identical results, indicating complete recovery of the bleomycins.

Resolution between bleomycins A_2 and B_2 was good ($R = 1.2$) on the original HPLC column with the three-component system. However, resolution began to decrease after a relatively short time. After this same experience was noted on two other identical columns, attempts were made to prolong the useful lifetime of columns for this assay. Changing to the four-component system solved the problem. Since this system has been used, column life has been very satisfactory and resolution has been improved ($R = 1.7$).

Previously reported work on the HPLC separation of the bleomycins required long elution times (22, 23). With this ion-pairing technique, elution times were considerably reduced. This method is based on the ability to force drugs into their ionic forms by pH adjustment and then the addition of counterions to form ion-pair complexes. This lipophilicity allows for retention on the reversed-phase column.

Bleomycins reportedly are unstable in biological fluids and tissues. Since all assays could not be performed on the same day that the samples were obtained, a stability study in plasma was begun. The bleomycin mixture (3 units/kg) was injected into a rabbit, and two large blood samples (A and B) were withdrawn 10 and 20 min, respectively, after the intravenous infusion. Aliquots of these samples were assayed immediately, and then other aliquots were assayed after 1, 4, and 8 days. Samples were kept frozen prior to assay. No significant decrease in plasma concentration was noted over the period of study (Table I). In a previously reported study (16) that had shown instability of the drug in plasma, the microbiological assay was used. Since that method exhibited a very large standard deviation and reported decreases in concentration were relatively small, the conclusion is open to question.

Because of the convenience of using plasma as opposed to serum, it was necessary to consider the effect of anticoagulants on the assay. Heparin was used as the anticoagulant in most studies, although citrate also was used. Neither anticoagulant interfered with the method.

Chromatograms obtained on the analysis of control rabbit plasma and plasma containing 2.6 μg of bleomycin A_2/ml are shown in Fig. 1. The chromatogram of control plasma showed no interfering peaks. In the other chromatogram, peaks corresponding to bleomycin A_2 (7.8 min), B_2 (10.2 min), and A_1 (13.8 min) were observed. No internal standard was used because of the simple nature of the assay and the large sample volume injected.

To verify that the peak designated as bleomycin A_2 was indeed that

Table II—Precision and Accuracy for Assay of Bleomycin A_2 in Plasma

Actual Concentration, μg/ml	Experimental Concentration, μg/ml, Mean[a] (Range)	*CV*	Mean Relative Percent Error
Control	<MDL[b]	—	—
0.32	0.30 (0.28–0.34)	9.4	9.4
0.63	0.64 (0.59–0.70)	7.3	5.2
1.2	1.2 (1.1–1.3)	6.8	4.2
2.3	2.3 (2.1–2.4)	6.2	3.8
4.1	4.2 (4.1–4.3)	2.8	2.4
	Overall	(6.0)	(4.9)

[a] $n = 4$. [b] MDL = minimum detectable level (0.08 μg/ml); twice blank value.

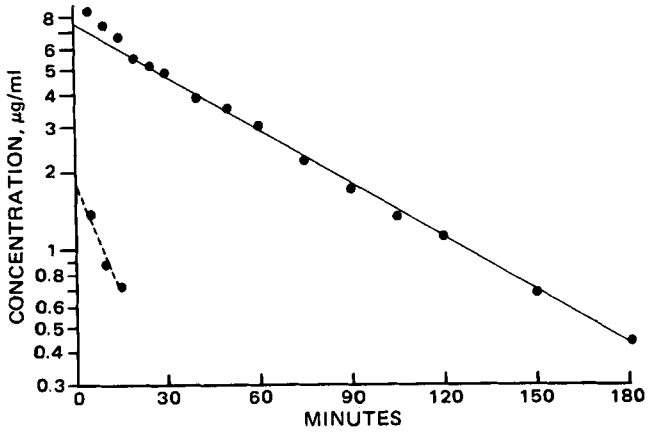

Figure 2—*Plot of plasma concentrations of bleomycin A_2 versus time obtained after a single intravenous dose of the commercially available bleomycin mixture.*

compound, the retention times and peak widths at half-height were compared to the standard. In addition, the standard addition technique was used. These methods confirmed that bleomycin A_2 was present in the rabbit plasma samples and that no interfering peaks were hidden under that bleomycin A_2 peak.

The standard curve for the assay was linear over the 0.5–5-μg/ml range. All samples were diluted to bring them within this range. To study the precision and accuracy of the method, known amounts of the drug were added to control plasma. These samples were assayed subsequently in quadruplicate as described. The coefficient of variation and relative error for the assay of bleomycin A_2 are reported in Table II.

The utility of this method was shown by studying the pharmacokinetics of bleomycin A_2 in rabbits. Since the activity of the commercially available bleomycin mixture varied from batch to batch, all reported data were obtained from a single batch. A dose of 4 units of bleomycin/kg iv was given to each rabbit in the marginal ear vein. The activity of this batch was reported to be approximately 2 units/mg. Blood samples were drawn from the opposite marginal ear vein over 3 hr; plasma was then separated by centrifugation and assayed as described.

The data, plotted on semilog coordinates, are shown in Fig. 2. A biphasic curve was noted, suggesting the data should be fit to a two-compartment model: a central plasma compartment and a peripheral tissue compartment. The elimination half-life was calculated to be about 40 min for the β-phase. The volume of distribution for the central compartment was about 0.2 liter/kg.

In mice, the decrease in plasma levels of the bleomycin mixture did not follow first-order kinetics (16). Samples in that study, however, were assayed by a nonspecific microbiological method. In the present study, preliminary findings indicate that first-order kinetics are followed. This result suggests that each component of the bleomycin mixture may have a different clearance.

Further studies on bleomycin A_2 pharmacokinetics are in progress. With this simple HPLC method for bleomycin A_2 as a model, it is hoped that assays for the other major components may be developed and their pharmacokinetics studied.

REFERENCES

(1) H. Umezawa, K. Maeda, T. Takeuchi, and Y. Okami, *J. Antibiot.*, **19**, 200 (1966).

(2) H. Umezawa, T. Takeuchi, S. Hori, T. Sawa, M. Ishizuka, T. Ichikawa, and T. Komai, *ibid.*, **25**, 409 (1972).

(3) C. D. Haas, C. A. Coltman, Jr., J. A. Gottlieb, A. Haut, J. K. Luce, R. W. Talley, B. Samal, H. E. Wilson, and B. Hoogstraten, *Cancer*, **38**, 8 (1976).

(4) M. H. Cohen, S. J. Pocock, E. D. Savlov, H. J. Lerner, J. Colsky, W. Regelson, and P. P. Carbone, *Eur. J. Cancer*, **13**, 49 (1977).

(5) S. K. Carter and R. H. Blum, *Can. Med. J.*, **24**, 322 (1974).

(6) H. Umezama, Y. Suhora, T. Takita, and K. Maeda, *J. Antibiot.*, **19**, 210 (1966).

(7) Blenoxane, *New Drug Application*, vol. 1, 1971.

(8) R. H. Blum, S. K. Carter, and K. Agre, *Cancer*, **31**, 903 (1973).

(9) S. S. Cohen and J. I. Cohen, *Cancer Res.*, **36**, 2768 (1976).

(10) T. Terasima, Y. Takabe, T. Katsumata, M. Watanabe, and H. Umezawa, *J. Natl. Cancer Inst.*, **49**, 1093 (1972).

(11) M. Ishizuka, H. Takayawa, T. Takeuchi, and H. Umezawa, *J. Antibiot.*, **20**, 15 (1967).

(12) H. Umezawa, M. Ishizuka, K. Kimura, J. Iwanagar, and T. Takeuchi, *ibid.*, **21**, 592 (1968).

(13) H. Umezawa, *Pure Appl. Chem.*, **28**, 665 (1971).

(14) I. Shirakawa, M. Azegami, S. Ishii, and H. Umezawa, *J. Antibiot.*, **24**, 761 (1971).

(15) T. Ichikawa, A. Matsuda, K. Miyamoto, M. Tsubosaki, T. Kaihara, K. Sakamoto, and H. Umezawa, *ibid.*, **20**, 149 (1967).

(16) T. Ohnuwa, J. Holland, H. Masuda, J. Waligunda, and G. Goldberg, *Cancer*, **33**, 1230 (1974).

(17) P. J. Robbins, E. B. Silberstein, and D. L. Fortman, *J. Nucl. Med.*, **15**, 273 (1974).

(18) K. Bitter, *J. Max.-Fac. Surg.*, **4**, 226 (1976).

(19) T. Konikowski, T. P. Haynie, and H. J. Glenn, *J. Nucl. Med.*, **16**, 738 (1975).

(20) A. Broughton and J. E. Strong, *Cancer Res.*, **36**, 1418 (1976).

(21) M. K. Elson, M. M. Oken, and R. B. Shafer, *J. Nucl. Med.*, **18**, 296 (1977).

(22) W. C. Eckelman, W. J. Rzeszotarski, B. A. Siegel, H. Kubota, M. Chelliah, J. Stevenson, and R. C. Reba, *ibid.*, **16**, 1033 (1975).

(23) W. J. Rzeszotarski, W. C. Eckelman, and R. C. Reba, *J. Chromatogr.*, **124**, 88 (1976).

ACKNOWLEDGMENTS

The authors thank Mr. Jack Korpi, Waters Associates, Milford, Mass., for helpful suggestions.

Effect of Hydroxyl Group Substituents on Pyran Ring on Hydrolysis Rate of Benzoates: 2-Tetrahydropyranyl Benzoate

ANWAR HUSSAIN ˣ **and JAMES TRUELOVE**

Received April 7, 1978, from the *College of Pharmacy, University of Kentucky, Lexington, KY 40506.* Accepted for publication June 22, 1978.

Abstract □ The hydrolysis of 2-tetrahydropyranyl benzoate was followed spectrophotometrically at 240 nm and was first order with respect to the compound, independent of pH, and very sensitive to solvent polarity and had an isotope effect (k_{D_2O}/k_{H_2O}) near unity. The pH-independent hydrolysis rate was about 1×10^6 times faster than that of the corresponding glucosyl benzoate. The results suggest that the presence of hydroxyl groups on the pyran ring has tremendous effect on the hydrolysis rate of these compounds.

Keyphrases □ Hydrolysis kinetics—2-tetrahydropyranyl benzoate, effect of pH □ Kinetics, hydrolysis—2-tetrahydropyranyl benzoate, effect of pH □ 2-Tetrahydropyranyl benzoate—hydrolysis kinetics, effect of pH

Various enzyme-catalyzed glycosyl transfer reactions are thought to involve intermediate formation of an acyl linkage (1). Brown and Bruice (2) showed that the hydrolysis of glucosyl benzoate (I) is catalyzed by hydrogen and hydroxide ion and at pH 4 and 25°. The I hydrolysis rate was 4.4×10^{-8} sec^{-1}.

In view of the importance of the acyl linkage in enzymatic reactions and of the possible utility of such linkage as a blocking group for carboxylic acids (3), the hydrolysis kinetics of 2-tetrahydropyranyl benzoate (II) were studied over a wide pH range. The data indicate that the presence of hydroxyl groups on the tetrahydropyran ring has a dramatic effect on the hydrolysis rate of these compounds.

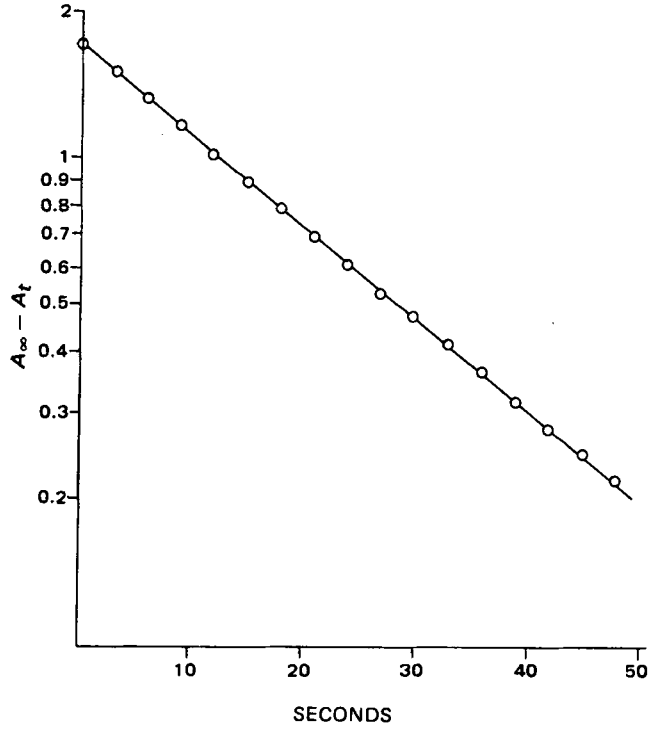

Figure 1—*Semilog plot of* $A_\infty - A_t$ versus *time for the hydrolysis of 2-tetrahydropyranyl benzoate.*

EXPERIMENTAL

Syntheses of II—Compound II was prepared according to the following procedure. To 3.0 g of benzoic acid in 50 ml of freshly distilled

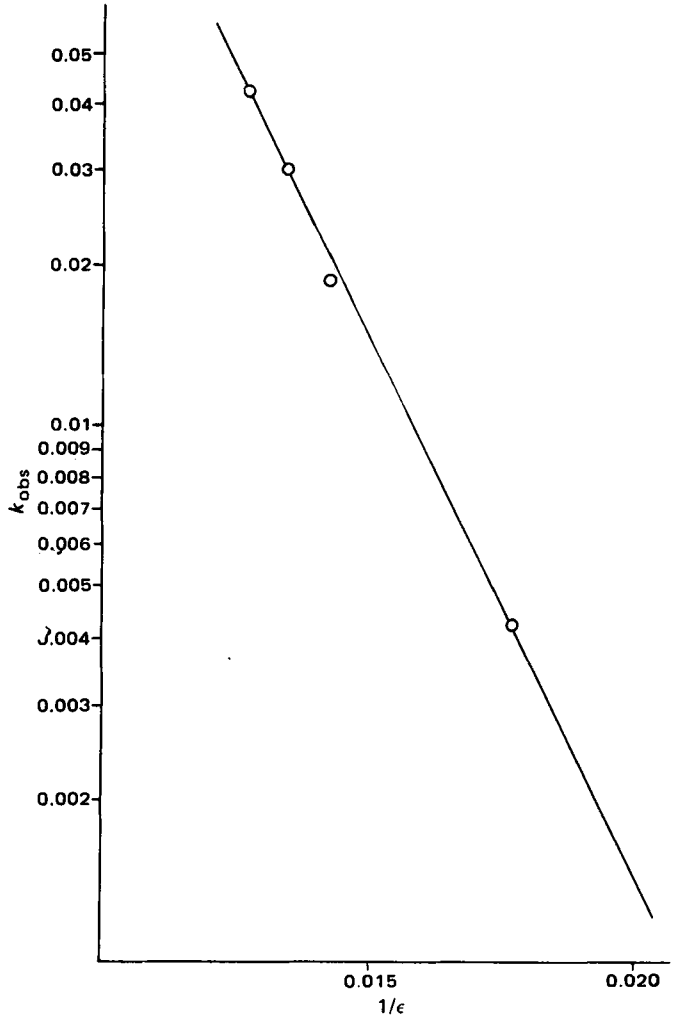

Figure 2—*Plot of log* k_{obs} *for the hydrolysis of 2-tetrahydropyranyl benzoate* versus *the reciprocal of the dielectric constant of the solution [log* $k_{obs} = -(199.7/\epsilon) + 1.164$*].*

0022-3549/79/0200-0235$01.00/0
© 1979, American Pharmaceutical Association

Table I—Half-Lives for II Hydrolysis at 25° and Ionic Strength of 0.1

pH	$t_{1/2}$, sec[a]
2.04	11.8
3.05	15.5
4.00	16.0
5.23	16.2
6.28	16.0
8.80	16.2
10.25	16.8
12.00	16.8

[a] Each half-life is an average of four determinations.

Table II—Effect of Buffer Concentration on the II Hydrolysis Rate at 25° and Ionic Strength of 0.7

Total Acetate Buffer, pH 4.6, *M*	$t_{1/2}$[a], sec	Total Phosphate Buffer, *M*	$t_{1/2}$[a], sec
0.01	15.8	0.01	15.8
0.05	15.8	—	—
0.20	15.9	0.2	16.0

[a] Each half-life is an average of three determinations.

Table III—Dependency of First-Order Constants for II Hydrolysis on the Dielectric Constant of the Solution

Dioxane, %	Dielectric Constant, ϵ
0	78.6
5	74
10	70
25	56.3
50	34.3

dihydropyran[1], 10 ml of 0.4% *p*-toluenesulfonic acid in benzene and 30 ml of freshly distilled dihydropyran were added. The reaction mixture was stirred at room temperature for 3 hr. At the completion of the reaction, the remaining *p*-toluenesulfonic acid was neutralized with 1 equivalent of pyridine. The solvents were then removed at 40° with a rotary evaporator, leaving a viscous liquid.

The NMR spectra and the elemental analysis were consistent with the structure of II; NMR ($CDCl_3$): δ 7.23–8.30 (m, 5H, ArH), 6.30 (m, 1H, 2-CH), 3.10–4.23 (m, 2H, 6-CH_2), and 1.0–2.2 (m, 6H, 3-, 4-, and 5-CH_2).

Anal.—Calc. for $C_{12}H_{14}O_3$: C, 70.20; H, 6.38. Found: C, 72.15; H, 6.30.

The purity of the derivative also was determined spectrophotometrically and was found to be 99% when a known amount of the derivative was hydrolyzed to the parent compound at room temperature with 0.01 *N* HCl and the concentration in solution was calculated from a standard Beer's law plot.

Kinetic Measurements—A stock solution containing 0.02 *M* II was prepared freshly in spectral grade dioxane. A 12-μl aliquot of this stock solution was placed in a 5-cm cell, and 12 ml of a buffer at the desired pH and an ionic strength of 0.1 was added. After rapid mixing, the appearance of benzoic acid was followed at 240 nm with a recording spectrophotometer[2]. Buffer species and concentrations to obtain the desired pH were similar to those employed by Garrett and Won (4).

The effect of acetate and phosphate buffers on the II hydrolysis rate was determined at a constant ionic strength of 0.7.

The effect of the dielectric constant on the II hydrolysis rate was determined in pH 6.28, 0.01 *M* phosphate buffer with an ionic strength of

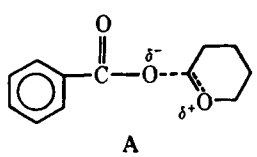

A

[1] Aldrich Chemical Co.
[2] Cary 15.

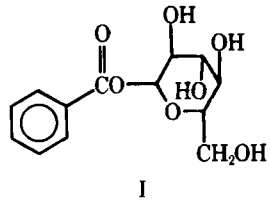

I

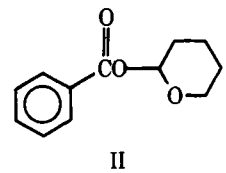

II

0.1. The dielectric constant of these solutions was varied by the addition of spectral grade dioxane to the aqueous buffer solutions (5).

The hydrolysis rate of II also was determined in deuterium oxide and water containing 1 mg of anhydrous sodium carbonate/ml.

RESULTS

The hydrolysis rate of II to benzoic acid was first order with respect to the concentration of the compound over a wide pH range. Figure 1 shows a typical semilog plot of $(A_\infty - A_t)$ *versus* time.

Table I illustrates the dependency of the hydrolysis rate of II on the solution pH. The hydrolysis rates were independent of the hydroxide-ion concentration.

The rate constants for II hydrolysis were determined as a function of acetate and phosphate buffer concentrations (Table II). The hydrolysis rate was independent of the buffer concentration.

The effect of the dielectric constant on the II hydrolysis rate is reported in Table III. Figure 2 shows a typical plot of the logarithms of these rate constants *versus* the reciprocal of the dielectric constant $1/\epsilon$ (6). As is seen in Table III and Fig. 2, the II hydrolysis rates were influenced markedly by the dielectric constant of the medium.

To determine the solvent kinetic isotope effect, the hydrolysis rate of II was determined in deuterium oxide and water containing 1 mg of anhydrous sodium carbonate/ml. The ratio of the two rates of hydrolysis, k_{D_2O}/k_{H_2O}, was 1[3].

DISCUSSION

Compound I hydrolyzes at a much slower rate than II. For example, in the pH 3–5 range and at 25°, I hydrolyzed by a factor of 2×10^{-6} times slower than II. Furthermore, the pH rate profile of I hydrolysis was characterized by three distinct regions: a hydrogen-ion-catalyzed region at low pH, a pH-independent region at pH 3–5, and a hydroxide-ion-catalyzed region at pH > 7, whereas the hydrolysis of II was independent of pH over a wide range (Table I). This result, coupled with the facts that the hydrolysis rate of II was markedly dependent on the dielectric constant of the medium (Table III and Fig. 2) and independent of the buffer concentration (Table II) and that the ratio of k_{D_2O}/k_{H_2O} was unity, strongly suggests that II hydrolysis proceeds by a classical S_N1 mechanism. The rate-limiting step in the hydrolysis reaction is probably the C–O bond cleavage, as shown in Structure A.

The hydrolysis of I in the pH-independent region was postulated (2) to proceed *via* an S_N1 mechanism. In that case, the dramatic difference in the hydrolysis rate of the two compounds apparently is due to the differences in the stability and ease of formation of the carbonium-ion intermediate. This finding indicates that the presence of the hydroxyl group substituent on the pyran ring has a significant effect on the formation of the carbonium ion.

Preliminary studies on the hydrolysis of esters of aspirin[4] strongly suggest that the number, as well as the position, of the hydroxyl group substituents on the pyran ring influences the cleavage rate of these compounds.

REFERENCES

(1) B. Capon, *Chem. Rev.*, **69**, 407 (1969).

(2) A. Brown and J. Bruice, *J. Am. Chem. Soc.*, **95**, 1593 (1977).

(3) A. Hussain, M. Yamuzaki, and J. Truelove, *J. Pharm. Sci.*, **63**, 627 (1974).

(4) E. R. Garrett and C. M. Won, *ibid.*, **60**, 1801 (1971).

(5) C. A. Kraus and R. M. Fuoss, *J. Am. Chem. Soc.*, **55**, 21 (1933).

(6) A. A. Frost and R. G. Pearson, "Kinetics and Mechanism," 2nd ed., Wiley, New York, N.Y., 1961, p. 145.

[3] The half-lives in seconds for II hydrolysis in deuterium oxide and water were 17.0, 16.9, and 16.9 and 16.2, 16.3, and 16.2, respectively.

[4] A. Hussain, J. Truelove, and H. Kostenbauder, unpublished work.

Specific High-Performance Liquid Chromatographic Assay for Nitroglycerin in Dosage Forms

WILLIAM G. CROUTHAMEL *x and BARBARA DORSCH

Received March 1, 1978, from the *Department of Pharmacy, School of Pharmacy, University of Maryland at Baltimore, Baltimore, MD 21201.* Accepted for publication June 28, 1978. *Present address: Department of Biochemistry and Drug Metabolism, Hoffmann-La Roche, Nutley, NJ 07110.

Abstract □ A specific assay for nitroglycerin in dosage forms using high-performance liquid chromatography was developed. Sublingual nitroglycerin tablets are dissolved in 25 ml of water and injected directly into the chromatograph. Chromatographic conditions are: mobile phase, 60% methanol in water; flow rate, 2 ml/min; column, microparticulate reversed phase; and detection, 200 nm. The glyceryl mononitrate and dinitrate degradation products of nitroglycerin are separated from nitroglycerin and can be identified by altering the mobile phase composition of methanol.

Keyphrases □ Nitroglycerin—high-performance liquid chromatographic analysis in various dosage forms □ High-performance liquid chromatography—analysis, nitroglycerin in various dosage forms □ Vasodilators, coronary—nitroglycerin, high-performance liquid chromatographic analysis in various dosage forms

Nitroglycerin (glyceryl trinitrate) is one of the oldest drugs presently in use. It was synthesized in 1846 and was reported to produce a "migraine" when ingested (1). Initial clinical pharmacology research was begun in 1849 when Hering (2) tested nitroglycerin on several medical students.

BACKGROUND

Virtually every analytical method available has been used in an attempt to quantitate nitroglycerin. One of the earliest reported analytical methods dates from 1901 when nitroglycerin was identified by exploding it with a hammer on an anvil following its extraction from the stomach of a cadaver (3). While relatively specific for nitroglycerin, quantitation with this assay was probably a problem. Other methods utilized include colorimetry (4), polarography (5), kinetic methods (6, 7), and, more recently, TLC (8) and GLC (9).

Many early methods lacked specificity and sensitivity, while the later methods are generally more complex and time consuming. The official USP content uniformity assay (10) of Bell (4) is based on alkaline hydrolysis of the nitrate ester to nitrate ion, followed by coupling with *N*-(1-naphthyl)ethylenediamine dihydrochloride to produce a purple compound with absorbance at 545 nm.

The automated version of this assay(11) has a sensitivity of approximately 5 μg/ml. While this assay may be specific for nitroglycerin and, therefore, stability indicating[1], supporting documentation has not been reported. Recent GLC methods are specific for nitroglycerin (9, 12, 13) but require extraction into organic solvents, evaporation, and detection by flame ionization or electron capture. Therefore, they are not applicable if rapid in-process quality control data are required. Analytical methods used to quantitate nitroglycerin were reviewed recently (14).

Significant changes in the potency of nitroglycerin tablets can occur with time, depending on tablet formulation and storage conditions (15). With the advent of the extemporaneous preparation of nitroglycerin injection in many medical centers, a rapid, specific, sensitive assay for nitroglycerin in dosage forms is needed.

EXPERIMENTAL

Equipment and Supplies—All reagents were analytical grade unless indicated otherwise. Methanol[2] was glass distilled. A high-performance liquid chromatograph[3] with a variable wavelength UV detector[4] was used. A C_{18} microparticulate[5] column was used in the separation.

Standard solutions of nitroglycerin were made from nitroglycerin spirit standardized against potassium nitrite using the phenoldisulfonic acid procedure (16). Samples of glyceryl mononitrate and glyceryl dinitrate were used as received. The two test formulations[6] were 400-μg sublingual tablets, Products A[7] and B[8].

Automated Assay—The procedure described in the USP (10) was modified. The concentration of *N*-(1-naphthyl)ethylenediamine dihydrochloride was reduced to 0.25%, the number of samples run per hour was reduced to 20 to allow better separation between samples, and the ratio of sample to wash was 1:4. Three standards were run at the beginning of each series, and one standard was run after every 10 samples.

High-Performance Liquid Chromatographic (HPLC) Assay—Individual tablets for analysis were placed in 25 ml of distilled water and shaken to ensure complete solution of the nitroglycerin. A 10-μl aliquot of the aqueous solution was injected directly into the chromatograph under the following conditions: mobile phase, 60% methanol in distilled water; flow rate, 2 ml/min; column, C_{18} microparticulate[5]; and detection, 200 nm UV. Under these conditions, nitroglycerin had a retention time of 4 min.

Nitroglycerin injection, 50 μg/ml, prepared in a local hospital pharmacy, was assayed as described after appropriate dilution. No interfering peaks were found in the chromatograms of any sample. When identifying glyceryl mononitrate and dinitrate, the mobile phase methanol concentration was decreased to 40% but the procedure was otherwise unchanged.

Because of variability between manufacturers and even between columns for the same manufacturer, different C_{18} microparticulate columns should be evaluated before the one best suited to the HPLC system is selected. Good results were obtained without an internal standard, and one was not routinely used. However, diazepam in a concentration of 20 μg/ml can be utilized as an internal standard; under the conditions described, it has a retention time of 8 min.

RESULTS

Figure 1 shows a typical chromatogram of nitroglycerin from a 400-μg sublingual tablet dissolved in 25 ml of water. The retention time with 60% methanol in water was about 4 min. No interference was found from the constituents of the tablet. The standard curve for nitroglycerin was linear from 3 to 22 μg/ml, passed through the origin, and had a lower limit of detection of approximately 30 ng injected in the column (equivalent to a 3-μg/ml solution).

To determine the precision of this method as compared to the official USP content uniformity assay, a standard solution of nitroglycerin containing 18.3 μg/ml was assayed 10 consecutive times by both methods. The estimated concentration of the solution was 18.3 ± 0.48 μg/ml (mean ± *SD*) by HPLC and 18.3 ± 0.34 μg/ml by the USP method. The relative standard deviation of approximately 2.5% for HPLC is reasonable considering the low dose of the drug; under these conditions, about 183 ng was injected onto the column.

To compare the HPLC assay with the USP content uniformity assay under more realistic assay conditions, 10 tablets were individually dissolved in 25 ml of water as outlined under *Experimental.* Both Products A and B were tested since they contained different excipients (15) to

[1] S. A. Fusari, Parke-Davis and Co., Detroit, Mich., personal communication.
[2] Burdick & Jackson, Muskegon, Mich.
[3] Model 711.
[4] Spectromonitor II, Laboratory Data Control, Riviera Beach, Fla.
[5] μBondapak C_{18}, Waters Associates, Milford, Mass., or Datasorb ODS, Laboratory Data Control, Riviera Beach, Fla.
[6] Purchased in unopened bottles at a local pharmacy.
[7] Lot 0FT97A, Eli Lilly and Co., Indianapolis, Ind.
[8] Lot T L176, Parke-Davis and Co., Detroit, Mich.

0022-3549/79/0200-0237$01.00/0
© 1979, American Pharmaceutical Association

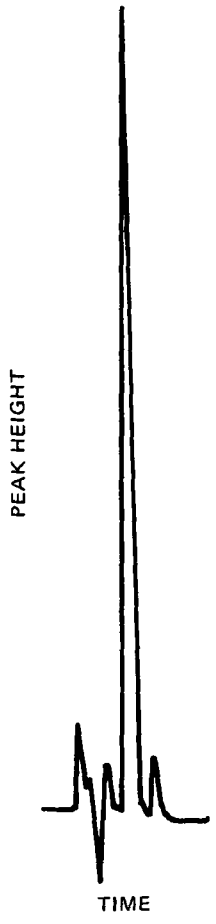

Figure 1—*Typical chromatogram for nitroglycerin from a 400-μg sublingual tablet.*

stabilize the nitroglycerin against volatilization. The results (mean ± *SD*) for Product A were 421.7 ± 25.6 and 420.1 ± 30.8 μg by the HPLC and USP methods, respectively. For Product B, the results were 398.0 ± 22.6 and 412.5 ± 24.5 μg, respectively.

No statistically significant differences were found between the two analytical methods with either product, although the mean concentration obtained with the USP assay was slightly higher for Product B. This same result was found when the experiment was repeated and may be due to a slight interaction with an excipient (such as the polyethylene glycol 400 stabilizer) in the product. No difference in weight variation or content uniformity was found between Products A and B.

The described method is capable of separating nitroglycerin from the glyceryl 1- and 2-mononitrate and glyceryl 1,2- and 1,3-dinitrate degradation products. Since the glyceryl mononitrates and dinitrates are more polar than nitroglycerin, they travel through the reversed-phase column faster than nitroglycerin and are eluted soon after the solvent front, making identification of the glyceryl mononitrates and dinitrates difficult. To separate these degradation products from nitroglycerin, the methanol concentration of the mobile phase must be decreased, thereby increasing the retention time of all nitrate esters. With a mobile phase of 40% methanol in water, the glyceryl mononitrate esters have retention times of approximately 2.00 and 2.75 min, the glyceryl dinitrates have retention times of approximately 3.5 and 3.75 min, and nitroglycerin has a retention time of approximately 11 min.

Although the tablets contained only small amounts of the glyceryl mononitrates and dinitrates, nitroglycerin solutions that were purposely degraded had much larger quantities of these degradation products.

DISCUSSION

During the development of this assay, a number of variations were tried. Methanol and acetonitrile performed equally well as the mobile phase; methanol was chosen because it is less expensive, even though it must be used in higher concentration than acetonitrile. Because of the lower UV cutoff, acetonitrile may be a better mobile phase with a single-beam detector.

The effect of changes in mobile phase pH were studied to determine if pH changes could alter the nitroglycerin retention time. As might be expected for a neutral molecule, chromatographic characteristics were independent of mobile phase pH. As columns age, the retention times of these compounds tend to become shorter, so the methanol concentration may need to be modified when columns are changed or with time of use. Several variable wavelength UV detectors were evaluated, and the one used in this study provided the most stable baseline and the greatest absorbance. Since many compounds absorb UV light at 200 nm, relatively pure organic solvents should be used to minimize extraneous peaks in the chromatogram.

The problem of content uniformity of nitroglycerin tablets is perhaps best indicated by the large limits (75–135%) of potency established by the USP (10). The addition of polyethylene glycol 400 (Product B) or povidone (Product A) as a stabilizer in nitroglycerin tablets has reduced the nitroglycerin volatility problem, so the tablets presently available are usually well within the USP limits. Nevertheless, variations in nitroglycerin potency can still occur even with the stabilized formulations (15).

With the emergence of new nitroglycerin dosage forms with unknown stabilities, it will become increasingly important to monitor product performance. For example, nitroglycerin intravenous injection is presently extemporaneously compounded in many major medical centers due to its lack of commercial availability. No information is presently available on its stability under various storage conditions or in different intravenous solutions. Similarly, little information is available on the ointment dosage forms of nitroglycerin.

Although this HPLC assay is approximately equal to the automated USP content uniformity assay in precision, it has several features that may make it more desirable under certain circumstances. Since the assay specifically detects intact nitroglycerin and utilizes no chemical reactions, there is no likelihood of alterations in the assay due to interference with the reaction or its reagents. Since the assay physically separates nitroglycerin from its primary degradation products, no interference from these compounds should occur. In addition, the glyceryl mononitrate and dinitrate degradation products can be identified with this assay. Thus, much more stability information can be obtained than with the USP assay. Since the USP assay is subject to variations in color development with time, it is difficult to use when it is not automated.

In summary, this assay provides a rapid, precise, sensitive, and specific method for the analysis of nitroglycerin dosage forms, and it can be modified to provide information on the nitroglycerin degradation products as well. In stability studies, this assay provides more information than the conventional USP content uniformity method and is likely to be the analytical method of choice.

REFERENCES

(1) A. Sobrero, *CR Acad. Sci.*, **25**, 274 (1847).

(2) C. Hering, *Kirby's No. Am. J. Homeopathy*, **May 1849.**

(3) G. G. Pond, *J. Am. Chem. Soc.*, **24**, 18 (1902).

(4) F. K. Bell, *J. Pharm. Sci.*, **53**, 752 (1964).

(5) B. C. Flann, *ibid.*, **58**, 122 (1969).

(6) F. Fung, P. Dalecki, E. Tse, and C. T. Rhodes, *ibid.*, **62**, 696 (1973).

(7) T. Woaler, H. Gundersen, I. Kvaleid, and R. Shangraw, *Pharm. Acta Helv.*, **52**, 17 (1977).

(8) M. C. Crew and F. J. DiCarlo, *J. Chromatogr.*, **35**, 506 (1968).

(9) M. T. Rosseel and M. G. Bogaert, *ibid.*, **64**, 364 (1972).

(10) "The United States Pharmacopeia," 19th rev., Mack Publishing Co., Easton, Pa., 1975, p. 674.

(11) S. A. Fusari, *J. Pharm. Sci.*, **62**, 122 (1973).

(12) I. W. F. Davidson, F. J. DiCarlo, and E. I. Szabo, *J. Chromatogr.*, **57**, 345 (1971).

(13) G. B. Neurath and M. Dunger, *Arzneim.-Forsch.*, **27**, 416 (1977).

(14) F. J. DiCarlo, *Drug Metab. Rev.*, **4**, 1 (1975).

(15) B. Dorsch and R. Shangraw, *Am. J. Hosp. Pharm.*, **32**, 795 (1975).

(16) "The United States Pharmacopeia," 19th rev., Mack Publishing Co., Easton, Pa., 1975, p. 343.

ACKNOWLEDGMENTS

Presented at the APhA Academy of Pharmaceutical Sciences, Phoenix meeting, November 1977.

The authors thank Dr. Salvatore Fusari, Parke-Davis and Co., Detroit, Mich., for the glyceryl mononitrates and dinitrates and for information on the specificity of the USP assay.

Quantitation of Sodium in Human Albumin Solutions

PAUL K. NG ˣ and JOHN L. LUNDBLAD

Received March 20, 1978, from *Biochemical Development, Cutter Laboratories, Inc., Berkeley, CA 94710.* Accepted for publication July 7, 1978.

Abstract □ An osmolality method is described for quantitating sodium in isotonic solutions of diafiltered albumin and diafiltered plasma protein fractions. The proposed method shows comparable results with a reference procedure based on atomic absorption spectrometry.

Keyphrases □ Sodium—osmolality method for analysis in isotonic solutions of human albumin and plasma protein fractions □ Osmolality method—analysis of sodium in isotonic solutions of human albumin and plasma protein fractions □ Albumin, isotonic solutions—osmolality method for analysis of sodium □ Plasma protein fractions—osmolality method for analysis of sodium

Preparations of normal serum albumin and plasma protein fraction are clinically useful in plasma volume expansion under similar conditions. The sodium ion in these preparations does not cross vascular membranes instantaneously and, therefore, exerts a transient fluid-drawing or fluid-retaining effect (1). To avoid such a noncolloid osmotic pressure, the sodium content is adjusted to the isotonic range of 130–160 × 10^{-3} *M*.

Accurate measurement of the total sodium and tonicity thus become important criteria for consideration before intravenous administration. This paper reports the sodium quantitation by an osmolality procedure and compares the results with those obtained by atomic absorption spectrometry.

EXPERIMENTAL

Preparations of albumin and plasma protein fraction were obtained by alcohol fractionation according to Cohn *et al.* (2). Removal of alcohol and salt was accomplished by procedures described previously (3, 4). Each solution was adjusted to 5.0 ± 0.3% protein in 0.004 *M* sodium caprylate and 0.004 *M* acetyldetryptophan. The final pH of the protein solution was 6.9 ± 0.5.

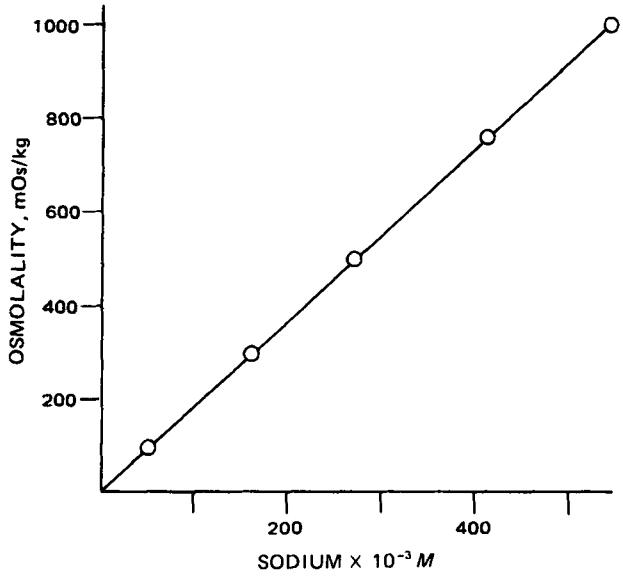

Figure 1—*Correlation of sodium concentration to osmolality.*

Table I—Sodium as Measured by Osmolality Correlation and Atomic Absorption Spectrometry

Sample	Protein, 5.0 ± 0.3%	Osmolality, ±4 mOs/kg	From Correlation, 10^{-3} *M*	From Atomic Absorption Spectrometry, 10^{-3} *M*
1658-64	Albumin	259	140	145
1658-99	Plasma protein fraction	272	147	147
PR2558	Albumin	258	139	142
PR2568	Albumin	248	134	136
PR2589	Plasma protein fraction	280	152	153
1715-13	Plasma protein fraction	269	145	146
1715-16	Plasma protein fraction	266	144	145
1715-41	Plasma protein fraction	282	153	145
1715-48	Plasma protein fraction	269	145	147

The sodium content was assayed by atomic absorption spectrometry[1]. A vapor pressure osmometer[2] measured the solution osmolality. Sodium stock standards were prepared by dissolving reagent grade sodium chloride in water for injection. Osmolality standards of 100, 290, 500, 750, and 1000 mOs/kg were obtained commercially[3].

RESULTS AND DISCUSSION

For the five standard solutions, osmolality *versus* molarity was plotted (Fig. 1). A correlation was obtained by linear regression:

$$\text{sodium} \times 10^{-3}\,M = 0.554 \times \text{osmolality (mOs/kg)} - 3.58 \quad \text{(Eq. 1)}$$

Nine individual samples were tested. Comparison with a reference method based on atomic absorption spectrometry is shown in Table I. The osmolality results were within 10% of the results by atomic absorption spectrometry.

As shown in Table I, interference due to the presence of proteins did not seem to affect the correlation significantly. This result was expected since the albumin solution (at least 96% albumin) or the plasma protein fraction solution (at least 83% albumin) accounted for less than 1 mmole/liter of the total molecules or an osmotic pressure equivalent to less than 25 mm Hg by physical meausrements (5, 6). For an isotonic solution, this value is only 0.5% of the calculated osmotic pressure (~5200 mm Hg).

The electrolytes are the main contributors to the total osmolality. Other ions such as potassium, if present at high enough levels, are interferences and will give erroneous correlation of sodium. In all studied samples, the potassium content did not exceed 2 mmoles/liter and, therefore, had an insignificant influence on the results.

Theoretically, atomic absorption spectrometry measures the total concentration of sodium in a solution and the osmolality procedure measures the total concentration of dissolved particles in a solution without regard for the homogeneity or nonhomogeneity of the molecular species, the molecular weights, the particle sizes, or the densities. By a linear correlation relationship, the osmolality gives a direct reading of sodium content. Since contribution of protein to the total osmolality is

[1] Model 306A, Perkin-Elmer, Norwalk, Conn.
[2] Model 5100B, Wescor, Logan, Utah.
[3] Wescor, Logan, Utah.

0022-3549/79/0200-0239$01.00/0
© 1979, American Pharmaceutical Association

minor, application of the present approach could be extended to other protein species.

The method has been used in conjunction with an existing analytical method. Some advantages are that the reagents are stable and that the method requires no special equipment other than the osmometer and it is efficient. Above all, its accuracy is comparable to that achieved by atomic absorption spectrometry.

REFERENCES

(1) "Rules and Regulations," *Fed. Regist.*, **42**, 27575 (1977).

(2) E. J. Cohn, E. L. Strong, W. L. Hughes, D. J. Mulford, J. N. Ashworth, M. Mein, and H. L. Taylor, *J. Am. Chem. Soc.*, **68**, 459 (1946).

(3) P. K. Ng, J. L. Lundblad, and G. Mitra, *Sep. Sci.*, **11**, 499 (1976).

(4) P. K. Ng, G. Mitra, and J. L. Lundblad, *J. Pharm. Sci.*, **67**, 531 (1978).

(5) G. Scatchard, A. C. Batchelder, and A. J. Brown, *Clin. Invest.*, **23**, 458 (1944).

(6) B. W. Zweifach and M. Intaglietta, *Microvasc. Res.*, **3**, 83 (1971).

Quantitative Determination of Hexylresorcinol in Commercial Antiseptic Solution by High-Pressure Liquid Chromatography

JOSEPH D. MUSTO, JAYANT N. SANE, and VICTOR D. WARNER ˣ

Received July 5, 1977, from the *Department of Medicinal Chemistry and Pharmacology, College of Pharmacy and Allied Health Professions, Northeastern University, Boston, MA 02115.* Accepted for publication June 21, 1978.

Abstract □ High-pressure liquid chromatography was used with a 5-μm silica gel column to quantitate hexylresorcinol in a commercial antiseptic solution following extraction with methylene chloride. This method shows linearity to at least 0.025% hexylresorcinol. A mobile phase consisting of 63% heptane, 34% chloroform, and 5% methanol was used with a UV detector (254 nm) and a flow of 3 ml/min. No interfering substances were observed.

Keyphrases □ Hexylresorcinol—high-pressure liquid chromatographic analysis in commercial preparations □ High-pressure liquid chromatography—analysis, hexylresorcinol in commercial preparations

Methods for the quantitative analysis of phenolic derivatives utilize bromination (1, 2), GLC (3, 4), NMR spectroscopy (5), and high-pressure liquid chromatography (HPLC) (6). This report describes a rapid, quantitative HPLC method for the analysis of hexylresorcinol in a commercial antiseptic solution[1].

EXPERIMENTAL

Chemicals and Reagents—All chemicals and reagents were USP, NF, ACS, or chromatographic grade.

Chromatography—The high-pressure liquid chromatograph[2] was equipped with a UV detector (254 nm) and a recorder. Septum injection was utilized. The column[3] (15 cm × 6.3 mm o.d.) was packed with 5-μm silica.

The chromatographic solvent consisted of 63% heptane, 34% chloroform, and 3% methanol. The temperature was ambient, and the solvent flow rate was 3.0 ml/min (at an inlet pressure of ~70.3 kg/cm²). The detector was set at a sensitivity of 0.08 aufs, and the chart speed was 5.08 cm/min (30.48 cm/hr). The elution order was phenol (2.7 min) and hexylresorcinol (4.7 min); total analysis time was 6 min.

Preparation of Solutions—All solutions of hexylresorcinol and phenol (internal standard) were prepared (weight per volume) in methylene chloride by a simple solution method. An aqueous solution of hexylresorcinol was prepared and used as a primary standard. This aqueous standard was run with each group of samples analyzed. The commercial antiseptic solution was purchased from a local pharmacy.

[1] ST 37 (Calgon).
[2] Waters ALC 202 equipped with a separation injector.
[3] Hi Eff Micropart column (0.5-μm silica), Applied Science Laboratories.

Preparation of Linearity Curve—A 1% hexylresorcinol solution was prepared using methylene chloride containing phenol (0.025%) as the internal standard. Aliquots of this solution were diluted with the methylene chloride containing phenol (0.025%) to yield five standard solutions consisting of 0.025, 0.05, 0.07, 0.10, and 0.125% hexylresorcinol with phenol (0.025%) as the internal standard. A volume of 5–10 μl of each standard was injected, and the peak height ratio of hexylresorcinol to phenol was calculated and plotted *versus* the hexylresorcinol concentration.

The plotted data (Table I) indicated that the hexylresorcinol concentration *versus* the peak height ratio (y) was linear from 0.025 to 0.125% hexylresorcinol (x) ($y = 8.960x + 0.011$; $r = 0.999$), and the straight line intersected zero. Three data points were determined for each concentration. The standard deviations are given in parentheses.

Assay—A 5-ml aliquot of the commercial antiseptic solution was extracted by adding 1 ml of 1 *N* HCl, 0.5 ml of internal standard (0.5% phenol in methylene chloride), and 4.5 ml of methylene chloride. The mixture was hand shaken for 1–2 min and centrifuged; the aqueous supernate was discarded by aspiration with a Pasteur pipet. A 10-μl sample of the extract was injected into the chromatograph. The aqueous standard containing 0.05% hexylresorcinol was carried through the same extraction procedure at the same time as the sample. A 0.1% hexylresorcinol solution in methylene chloride containing phenol (0.025%) was regularly injected during analysis to monitor instrument stability.

Calculation—The following formula was used for calculating concentrations:

$$\% \text{ sample} = \frac{R_s}{R_{std}} \times \% \text{ std} \qquad \text{(Eq. 1)}$$

where % sample is the percent hexylresorcinol in the sample, % std is the percent hexylresorcinol in the standard, R_{std} is the ratio of the peak heights of hexylresorcinol to phenol in the standard, and R_s is the ratio of the peak heights of hexylresorcinol to phenol in the commercial antiseptic.

Table I—Data for Linearity Curve

Hexylresorcinol Standard, %	Peak Height Ratios
0.025	0.232 (0.009)
0.050	0.463 (0.015)
0.070	0.637 (0.014)
0.100	0.905 (0.019)
0.125	1.130 (0.010)

0022-3549/79/0200-0240$01.00/0

© 1979, American Pharmaceutical Association

minor, application of the present approach could be extended to other protein species.

The method has been used in conjunction with an existing analytical method. Some advantages are that the reagents are stable and that the method requires no special equipment other than the osmometer and it is efficient. Above all, its accuracy is comparable to that achieved by atomic absorption spectrometry.

REFERENCES

(1) "Rules and Regulations," *Fed. Regist.*, **42**, 27575 (1977).

(2) E. J. Cohn, E. L. Strong, W. L. Hughes, D. J. Mulford, J. N. Ashworth, M. Mein, and H. L. Taylor, *J. Am. Chem. Soc.*, **68**, 459 (1946).

(3) P. K. Ng, J. L. Lundblad, and G. Mitra, *Sep. Sci.*, **11**, 499 (1976).

(4) P. K. Ng, G. Mitra, and J. L. Lundblad, *J. Pharm. Sci.*, **67**, 531 (1978).

(5) G. Scatchard, A. C. Batchelder, and A. J. Brown, *Clin. Invest.*, **23**, 458 (1944).

(6) B. W. Zweifach and M. Intaglietta, *Microvasc. Res.*, **3**, 83 (1971).

Quantitative Determination of Hexylresorcinol in Commercial Antiseptic Solution by High-Pressure Liquid Chromatography

JOSEPH D. MUSTO, JAYANT N. SANE, and VICTOR D. WARNER ˣ

Received July 5, 1977, from the *Department of Medicinal Chemistry and Pharmacology, College of Pharmacy and Allied Health Professions, Northeastern University, Boston, MA 02115.* Accepted for publication June 21, 1978.

Abstract □ High-pressure liquid chromatography was used with a 5-μm silica gel column to quantitate hexylresorcinol in a commercial antiseptic solution following extraction with methylene chloride. This method shows linearity to at least 0.025% hexylresorcinol. A mobile phase consisting of 63% heptane, 34% chloroform, and 5% methanol was used with a UV detector (254 nm) and a flow of 3 ml/min. No interfering substances were observed.

Keyphrases □ Hexylresorcinol—high-pressure liquid chromatographic analysis in commercial preparations □ High-pressure liquid chromatography—analysis, hexylresorcinol in commercial preparations

Methods for the quantitative analysis of phenolic derivatives utilize bromination (1, 2), GLC (3, 4), NMR spectroscopy (5), and high-pressure liquid chromatography (HPLC) (6). This report describes a rapid, quantitative HPLC method for the analysis of hexylresorcinol in a commercial antiseptic solution[1].

EXPERIMENTAL

Chemicals and Reagents—All chemicals and reagents were USP, NF, ACS, or chromatographic grade.

Chromatography—The high-pressure liquid chromatograph[2] was equipped with a UV detector (254 nm) and a recorder. Septum injection was utilized. The column[3] (15 cm × 6.3 mm o.d.) was packed with 5-μm silica.

The chromatographic solvent consisted of 63% heptane, 34% chloroform, and 3% methanol. The temperature was ambient, and the solvent flow rate was 3.0 ml/min (at an inlet pressure of ~70.3 kg/cm²). The detector was set at a sensitivity of 0.08 aufs, and the chart speed was 5.08 cm/min (30.48 cm/hr). The elution order was phenol (2.7 min) and hexylresorcinol (4.7 min); total analysis time was 6 min.

Preparation of Solutions—All solutions of hexylresorcinol and phenol (internal standard) were prepared (weight per volume) in methylene chloride by a simple solution method. An aqueous solution of hexylresorcinol was prepared and used as a primary standard. This aqueous standard was run with each group of samples analyzed. The commercial antiseptic solution was purchased from a local pharmacy.

[1] ST 37 (Calgon).
[2] Waters ALC 202 equipped with a separation injector.
[3] Hi Eff Micropart column (0.5-μm silica), Applied Science Laboratories.

Preparation of Linearity Curve—A 1% hexylresorcinol solution was prepared using methylene chloride containing phenol (0.025%) as the internal standard. Aliquots of this solution were diluted with the methylene chloride containing phenol (0.025%) to yield five standard solutions consisting of 0.025, 0.05, 0.07, 0.10, and 0.125% hexylresorcinol with phenol (0.025%) as the internal standard. A volume of 5–10 μl of each standard was injected, and the peak height ratio of hexylresorcinol to phenol was calculated and plotted *versus* the hexylresorcinol concentration.

The plotted data (Table I) indicated that the hexylresorcinol concentration *versus* the peak height ratio (y) was linear from 0.025 to 0.125% hexylresorcinol (x) ($y = 8.960x + 0.011$; $r = 0.999$), and the straight line intersected zero. Three data points were determined for each concentration. The standard deviations are given in parentheses.

Assay—A 5-ml aliquot of the commercial antiseptic solution was extracted by adding 1 ml of 1 *N* HCl, 0.5 ml of internal standard (0.5% phenol in methylene chloride), and 4.5 ml of methylene chloride. The mixture was hand shaken for 1–2 min and centrifuged; the aqueous supernate was discarded by aspiration with a Pasteur pipet. A 10-μl sample of the extract was injected into the chromatograph. The aqueous standard containing 0.05% hexylresorcinol was carried through the same extraction procedure at the same time as the sample. A 0.1% hexylresorcinol solution in methylene chloride containing phenol (0.025%) was regularly injected during analysis to monitor instrument stability.

Calculation—The following formula was used for calculating concentrations:

$$\% \text{ sample} = \frac{R_s}{R_{std}} \times \% \text{ std} \qquad \text{(Eq. 1)}$$

where % sample is the percent hexylresorcinol in the sample, % std is the percent hexylresorcinol in the standard, R_{std} is the ratio of the peak heights of hexylresorcinol to phenol in the standard, and R_s is the ratio of the peak heights of hexylresorcinol to phenol in the commercial antiseptic.

Table I—Data for Linearity Curve

Hexylresorcinol Standard, %	Peak Height Ratios
0.025	0.232 (0.009)
0.050	0.463 (0.015)
0.070	0.637 (0.014)
0.100	0.905 (0.019)
0.125	1.130 (0.010)

0022-3549/79/0200-0240$01.00/0

© 1979, American Pharmaceutical Association

Table II—Assay Results on Commercial Antiseptic (Percent Concentration of Hexylresorcinol) [a]

Assay[b]	Percent Found	Percent Reported[c]
1	0.097	0.1
2	0.107	0.1
3	0.106	0.1
4	0.107	0.1

[a] Average deviation = 0.004, *SD* = 0.005, and coefficient of variation = 4.8%. [b] Replicate assays of same sample. [c] Data from "Handbook of Nonprescription Drugs," 5th ed., American Pharmaceutical Association, Washington, D.C., 1977, p. 263.

DISCUSSION

The results (Table II) show that a commercial antiseptic solution can be assayed for hexylresorcinol by using a simple HPLC method. No interfering peaks were observed from the other listed component (glycerin) in the commercial product analyzed. Recovery studies were performed on the aqueous hexylresorcinol solution (0.05%), and the extraction efficiency was 74.9%. The extraction and HPLC analyses of aqueous standard solutions gave a linear response with hexylresorcinol concentrations between 0.025 and 0.125%.

This analysis utilized an aqueous standard carried through the exact procedure as the samples. Since the aqueous standard closely simulated the samples, the concentrations were calculated by comparing peak heights of the aqueous standard and the unknown sample. Extraction efficiency affects both samples and standards equally and, therefore, need not be considered in the calculation of concentrations.

A control also was run with each batch to monitor instrument conditions. This procedure minimizes assay errors due to technique. The total analysis time was less than 10 min/sample.

REFERENCES

(1) "The National Formulary," 14th ed., Mack Publishing Co., Easton, Pa., 1975, p. 317.

(2) D. G. Garrett, "The Quantitative Analysis of Drugs," 3rd ed., Chapman and Hall Ltd., London, England, 1964, pp. 513–518, 550.

(3) P. A. Hedin, J. P. Minyard, Jr., and A. C. Thompson, *J. Chromatogr.*, **30**, 43 (1967).

(4) V. Kusy, *ibid.*, **57**, 132 (1971).

(5) V. D. Gupta and L. A. Cates, *J. Pharm. Sci.*, **63**, 93 (1974).

(6) V. D. Gupta, *ibid.*, **65**, 1706 (1976).

ACKNOWLEDGMENTS

Supported in part by National Institutes of Health Grant RR07143.

High-Pressure Liquid Chromatographic Assay of Folic Acid: A Collaborative Study

WILLIAM O. McSHARRY ˣ **and FRANK P. MAHN**

Received April 17, 1978, from the *Quality Control Department, Hoffmann-La Roche, Inc., Nutley, NJ 07110.* Accepted for publication June 28, 1978.

Abstract □ A collaborative study of the USP high-pressure liquid chromatographic assay for folic acid was performed. Two samples were analyzed in duplicate by 14 participating laboratories. Relative standard deviations for a single determination (*RSDS*) ranged from ±0.40 to ±2.39%. Based on an analysis of variance, it was concluded that the method of peak measurement was a major determinant of reproducibility and that graphical measurement was associated with a high standard deviation. Adequate resolution was obtained using a variety of columns and operating conditions. The interlaboratory *RSDS* was ±1.8%.

Keyphrases □ Folic acid—high-pressure liquid chromatographic analysis in prepared samples, collaborative study □ High-pressure liquid chromatography—analysis, folic acid in prepared samples, collaborative study □ Vitamins—folic acid, high-pressure liquid chromatographic analysis in prepared samples, collaborative study

A recently developed high-pressure liquid chromatographic (HPLC) method (1) for the assay of folic acid bulk substance was introduced into the USP (2) to replace the spectrophotometric method (3). In a subsequent supplement (4), the new method was revised slightly.

The HPLC method is more specific and accurate than the previous one. A collaborative study[1] was undertaken to validate the precision and practical applicability of this HPLC method on a wide scale.

EXPERIMENTAL

Four vials containing 100 mg each of two folic acid test samples (A and B), 75 mg of folic acid USP reference standard, and 20 mg of leucovorin calcium[2] (calcium formyltetrahydrofolate) were sent to 19 collaborators, along with a copy of the method (5) and auxiliary instructions for performing the determination and reporting results. Collaborators were requested to make duplicate injections of each of two weighings of Samples A and B and the folic acid reference standard and to report raw data and results, calculated on the dry basis, using the average response from the duplicate injections in the calculation.

The method as written allowed the individual collaborator considerable latitude in choice of column and operating conditions. However, a system suitability test required that the operator obtain a resolution factor of at least 3.6 between folic acid and leucovorin and a relative standard deviation no greater than ±2% in the responses from six to 10 replicate injections of the standard preparation.

The amounts of folic acid provided were sufficient for two 30-mg weighings by each collaborator plus equipment optimization and checkout. The water content of the folic acid was determined (duplicate 50-mg samples in methanol) before subdivision by the titrimetric method and reported to the collaborators (reference standard, 7.7%; Sample A, 7.6%; and Sample B, 7.8%). Collaborators were requested to report, in addition to raw data and assay results, results of the system suitability test and certain information about instrument and operating conditions.

Raw data from all collaborators were entered into a time-shared computer, and results were calculated by a user-written program.

[1] A subcommittee of the PMA-QC Section, appointed by Dr. H. Hammer and chaired by Dr. J. Sheridan, was responsible for carrying out this study.

[2] Provided by Lederle Laboratories.

0022-3549/79/0200-0241$01.00/0

© 1979, American Pharmaceutical Association

Table II—Assay Results on Commercial Antiseptic (Percent Concentration of Hexylresorcinol) [a]

Assay[b]	Percent Found	Percent Reported[c]
1	0.097	0.1
2	0.107	0.1
3	0.106	0.1
4	0.107	0.1

[a] Average deviation = 0.004, *SD* = 0.005, and coefficient of variation = 4.8%. [b] Replicate assays of same sample. [c] Data from "Handbook of Nonprescription Drugs," 5th ed., American Pharmaceutical Association, Washington, D.C., 1977, p. 263.

DISCUSSION

The results (Table II) show that a commercial antiseptic solution can be assayed for hexylresorcinol by using a simple HPLC method. No interfering peaks were observed from the other listed component (glycerin) in the commercial product analyzed. Recovery studies were performed on the aqueous hexylresorcinol solution (0.05%), and the extraction efficiency was 74.9%. The extraction and HPLC analyses of aqueous standard solutions gave a linear response with hexylresorcinol concentrations between 0.025 and 0.125%.

This analysis utilized an aqueous standard carried through the exact procedure as the samples. Since the aqueous standard closely simulated the samples, the concentrations were calculated by comparing peak heights of the aqueous standard and the unknown sample. Extraction efficiency affects both samples and standards equally and, therefore, need not be considered in the calculation of concentrations.

A control also was run with each batch to monitor instrument conditions. This procedure minimizes assay errors due to technique. The total analysis time was less than 10 min/sample.

REFERENCES

(1) "The National Formulary," 14th ed., Mack Publishing Co., Easton, Pa., 1975, p. 317.

(2) D. G. Garrett, "The Quantitative Analysis of Drugs," 3rd ed., Chapman and Hall Ltd., London, England, 1964, pp. 513–518, 550.

(3) P. A. Hedin, J. P. Minyard, Jr., and A. C. Thompson, *J. Chromatogr.*, **30**, 43 (1967).

(4) V. Kusy, *ibid.*, **57**, 132 (1971).

(5) V. D. Gupta and L. A. Cates, *J. Pharm. Sci.*, **63**, 93 (1974).

(6) V. D. Gupta, *ibid.*, **65**, 1706 (1976).

ACKNOWLEDGMENTS

Supported in part by National Institutes of Health Grant RR07143.

High-Pressure Liquid Chromatographic Assay of Folic Acid: A Collaborative Study

WILLIAM O. McSHARRY ˣ **and FRANK P. MAHN**

Received April 17, 1978, from the *Quality Control Department, Hoffmann-La Roche, Inc., Nutley, NJ 07110.* Accepted for publication June 28, 1978.

Abstract □ A collaborative study of the USP high-pressure liquid chromatographic assay for folic acid was performed. Two samples were analyzed in duplicate by 14 participating laboratories. Relative standard deviations for a single determination (*RSDS*) ranged from ±0.40 to ±2.39%. Based on an analysis of variance, it was concluded that the method of peak measurement was a major determinant of reproducibility and that graphical measurement was associated with a high standard deviation. Adequate resolution was obtained using a variety of columns and operating conditions. The interlaboratory *RSDS* was ±1.8%.

Keyphrases □ Folic acid—high-pressure liquid chromatographic analysis in prepared samples, collaborative study □ High-pressure liquid chromatography—analysis, folic acid in prepared samples, collaborative study □ Vitamins—folic acid, high-pressure liquid chromatographic analysis in prepared samples, collaborative study

A recently developed high-pressure liquid chromatographic (HPLC) method (1) for the assay of folic acid bulk substance was introduced into the USP (2) to replace the spectrophotometric method (3). In a subsequent supplement (4), the new method was revised slightly.

The HPLC method is more specific and accurate than the previous one. A collaborative study[1] was undertaken to validate the precision and practical applicability of this HPLC method on a wide scale.

EXPERIMENTAL

Four vials containing 100 mg each of two folic acid test samples (A and B), 75 mg of folic acid USP reference standard, and 20 mg of leucovorin calcium[2] (calcium formyltetrahydrofolate) were sent to 19 collaborators, along with a copy of the method (5) and auxiliary instructions for performing the determination and reporting results. Collaborators were requested to make duplicate injections of each of two weighings of Samples A and B and the folic acid reference standard and to report raw data and results, calculated on the dry basis, using the average response from the duplicate injections in the calculation.

The method as written allowed the individual collaborator considerable latitude in choice of column and operating conditions. However, a system suitability test required that the operator obtain a resolution factor of at least 3.6 between folic acid and leucovorin and a relative standard deviation no greater than ±2% in the responses from six to 10 replicate injections of the standard preparation.

The amounts of folic acid provided were sufficient for two 30-mg weighings by each collaborator plus equipment optimization and checkout. The water content of the folic acid was determined (duplicate 50-mg samples in methanol) before subdivision by the titrimetric method and reported to the collaborators (reference standard, 7.7%; Sample A, 7.6%; and Sample B, 7.8%). Collaborators were requested to report, in addition to raw data and assay results, results of the system suitability test and certain information about instrument and operating conditions.

Raw data from all collaborators were entered into a time-shared computer, and results were calculated by a user-written program.

[1] A subcommittee of the PMA-QC Section, appointed by Dr. H. Hammer and chaired by Dr. J. Sheridan, was responsible for carrying out this study.

[2] Provided by Lederle Laboratories.

0022-3549/79/0200-0241$01.00/0

© 1979, American Pharmaceutical Association

Table I—Summary of Operating Information

Collaborator	Column Length × i.d., cm	Stationary Phase[a]	Mobile Phase, % methanol	Pressure, psi	Flow Rate, ml/min	Injection Device	Injection Volume, μl	Amount Injected, μg	Measurement Method[b]	Retention Time[c], min	Resolution Factor	RSD[d], %
1	30 × 0.4	B	5	590	1	20-μl loop	20	NR[e]	E	22.6	3.7	0.96
2	30 × 0.4	B	4	2300	2.0	10-μl loop	10	30	H × W	13.8	3.7	1.12
3	30 × 0.4	B	3	1000	1.5	20-μl loop	20	NR	E	18.2	4.7	0.7
4	25 × 0.4	B	3	1750	1.7	25-μl syringe	5	NR	H × W	11.0	3.1	2.0
5	30 × 0.4	B	6	1300	1	20-μl loop	20	10	E	9.7	3.7	0.21
6	25 × 0.5	P	10	600	1	20-μl loop	20	30	E	14.0	3.9	0.95
7	30 × 0.4	B	4	1500	1.0	10-μl loop	10	NR	H	15.0	3.0	1.17
8	25 × 0.5	P	6.5	1690	2.5	25-μl loop	25	6	E	9.5	3.8	0.58
9	25 × 0.5	P	2	1000	1.5	20-μl loop	20	6	H	32.7	5.0	1.22
10	25 × 0.3	S	8	2700	1.2	20-μl loop	20	1	E	7.7	3.9	0.92
11	33 × 0.4	B	5	1000	1.5	25-μl syringe	20	4	H × W	8.8	2.0	0.78
12	30 × 0.2	B	4	2500	2	10-μl loop	10	30	H	25	3.7	1.1
13	30 × 0.4	B	6	1400	1	10-μl loop	10	0.6	H	53.5	4.6	1.4
14	30 × 0.4	B	4	1500	2	10-μl loop	10	30	E	13.1	3.8	0.36

[a] B = μBondapak C_{18}, P = Partisil ODS, and S = Spherisorb ODS. [b] E means electronic, H means peak height only, and H × W means height times width. [c] Typical or average retention time of folic acid. [d] Relative standard deviation obtained in system suitability test. [e] NR means collaborator did not specifically report any deviation from the recommended amount of 30 μg.

RESULTS

Fourteen collaborators (including this laboratory) reported results. Operational information is summarized in Table I. Although a few laboratories were unable to achieve the separation and precision required, a wide range of instrumental conditions can be used to obtain adequate separation between folic acid and leucovorin.

Results for all collaborators are shown in Table II. Collaborators 4, 7, and 11 should not be considered representative of the method because the minimum resolution factor was not obtained. However, even these cases are in good agreement with the other collaborators, presumably because, with the low content of impurity present, poor separation did not change the result very much.

To determine more specifically the sources of error in the method, an analysis of variance was performed. The reproducibility of the chromatographic portion of the procedure (*i.e.*, injection and peak measurement) was evaluated for each collaborator from the relative differences between responses for duplicate injections of samples and standard (*i.e.*, six pairs of numbers). The reproducibility of the overall procedure was evaluated by comparing results obtained for the duplicate weighing of Samples A and B, using the average of instrument responses for two injections. From these data, the variance of the preparation steps alone can be calculated. The equation is derived as follows.

The formula for calculation of results is:

$$\frac{W_s/d}{W_x/d} \times \frac{R'_x/i}{R'_s/i} \times 100 = \% \qquad \text{(Eq. 1)}$$

where W is the weight of the sample (x) or standard (s); R' is the average peak response of the sample (x) or standard (s); and d and i are the dilution volume and injection volume, respectively, and are the same for the sample and standard.

The first term in this expression represents the preparation of material for injection while the second term represents the injection and peak measurements. In multiplication and division, the squares of the relative standard deviations are additive; therefore:

$$2RSD_p^2 + 2RSD_{c'}^2 = RSD_o^2 \qquad \text{(Eq. 2)}$$

where p, c', and o refer to preparative, chromatographic, and overall relative standard deviation, respectively. Since responses from duplicate injections were averaged to obtain R', the $RSD_{c'}^2$ is equal to half of RSD_c^2 (RSD for a single injection) and the expression reduces to:

$$0.5(RSD)_o^2 - RSD_c^2) = RSD_p^2 \qquad \text{(Eq. 3)}$$

Table II—Summary of Results

Collaborator	A_1	A_2	$\bar{A}$	B_1	B_2	$\bar{B}$
1	100.5	99.6	100.1	100.8	99.2	100.0
2	98.5	101.3	99.9	98.2	99.1	98.7
3	100.5	98.6	99.6	97.9	99.1	98.5
4	96.9	101.5	99.2	97.2	98.4	97.8
5	99.9	97.6	98.8	100.4	100.5	100.5
6	99.3	98.9	99.1	99.7	98.5	99.1
7	98.4	96.3	97.3	95.9	94.5	95.2
8	96.0	95.2	95.6	97.9	96.3	97.1
9	99.4	98.3	98.9	96.4	98.8	97.6
10	101.5	99.3	100.4	98.3	98.3	98.3
11	101.8	99.8	100.8	100.3	99.7	100.0
12	100.0	101.1	100.6	103.9	100.0	101.9
13	98.5	99.0	98.8	100.5	99.9	100.2
14	98.8	100.3	99.5	97.9	99.1	98.5
Average	99.3	99.0	99.2	98.9	98.7	98.8
±*RSD*, %	1.7	1.8	1.4	2.1	1.6	1.7

Table III—Precision of the Method

Collaborator	Overall *RSD* (σ_o)	Chromatographic *RSD* (σ_c)	Preparation Relative Variance (σ_p^2)
1	0.93	0.25	0.40
2	1.47	0.51	0.95
3	1.17	0.79	0.37
4	2.39	2.50	−0.26
5	1.15	0.32	0.61
6	0.67	0.36	0.16
7	1.30	1.28	0.03
8	0.91	0.88	0.03
9	1.34	2.17	−1.46
10	1.11	0.86	0.24
11	1.07	0.58	0.41
12	1.99	1.87	0.24
13	0.40	0.60	−0.10
14	0.96	0.36	0.39

The variance of the preparation step for each collaborator was calculated with this equation (Table III). Except for the extreme negative value for Collaborator 9, the results are more uniform than the chromatographic variance. The average variance for the preparation step (excluding Collaborator 9) is 0.27, equivalent to an *RSD* of ±0.5%.

A possible explanation for the poorer chromatographic precision by some collaborators is the apparent correlation between a high *RSD* and graphical peak measurements (Table I). This correlation suggests that electronic area measurements are more precise than either height or height × width measurements.

One collaborator arranged for biological assays of the folic acid samples and reported 10 results on each sample. The average and standard deviation of these results were calculated and compared to the average results obtained by the chromatographic method, using the t test for significance of difference between two averages.

The results seem to indicate that the biological assay result for Sample A differ significantly from both the biological result for Sample B and the chromatographic result for Sample A. However, in view of the limited nature of the biological testing, the real significance of this difference is not known. In any case, the question was not pursued further since it was not the purpose of this collaborative study.

Upon discussion with collaborators, some recommendations concerning the description of the method were formulated:

1. The exact manner of preparation and degassing of the mobile phase should be left to the operator as long as the final solution has the proper pH.

2. The preparation and injection of folic acid solutions should be made more flexible to allow for smaller amounts of folic acid and larger injection volumes. The former change may be necessary to prevent overloading of some detectors while the latter change permits better reproducibility of manual injections.

3. The particle base may be nonspherical since its shape is not critical to the determination.

These recommendations have been incorporated in the latest USP supplement (4).

The majority of collaborators were able to achieve acceptable separation and precision with the chromatographic method in spite of the variety of instrumental and operating conditions used, indicating that the method should be widely applicable.

REFERENCES

(1) V. D. Reif, J. T. Reamer, and L. T. Grady, *J. Pharm. Sci.*, **66**, 1112 (1977).

(2) "Third Supplement to USP XIX and NF XIV," United States Pharmacopeial Convention, Rockville, Md., 1977, p. 71.

(3) "The United States Pharmacopeia," 19th rev., Mack Publishing Co., Easton, Pa., 1975, pp. 211, 212, 624.

(4) "Fourth Supplement to USP XIX and NF XIV," United States Pharmacopeial Convention, Rockville, Md., 1978, p. 86.

(5) *Pharmacopeial Forum*, **2**, 371 (1976).

ACKNOWLEDGMENTS

The authors thank the following persons for their cooperation: J. Bodenmiller, Merrell-National Laboratories; M. D. Bray, Eli Lilly and Co.; F. Cioffi, E. R. Squibb and Sons; R. Elkas, Lederle Laboratories; S. A. Fusari, Parke-Davis & Co.; L. T. Grady, United States Pharmacopeial Convention; W. S. Hardesty, Beecham Laboratories; D. Heuring, Mead Johnson & Co.; R. Kirchmeier, Pfizer Inc.; G. Krol, Ayerst Laboratories; R. S. Lenkiewicz, Stuart Pharmaceuticals; E. Pratt, Sterling Winthrop Research Institute; and E. Townley, Schering Corp.

The authors are also grateful to A. Greene and J. Van Antwerp of Hoffmann-La Roche for characterization and subdivision of the materials for distribution to the collaborators.

Potential Antineoplastics I: Substituted 3,5-Dioxo- and 3-Thioxo-5-oxo-2,3,4,5-tetrahydro-1,2,4-triazines

EL SEBAI A. IBRAHIM, S. A. SHAMS EL DINE, FARID S. G. SOLIMAN ˣ, and IBRAHIM M. LABOUTA

Received April 24, 1978, from the *Department of Pharmaceutical Chemistry, Faculty of Pharmacy, University of Alexandria, Alexandria, A.R. Egypt.* Accepted for publication July 10, 1978.

Abstract □ The synthesis of some 6-substituted 3,5-dioxo- and 3-thioxo-5-oxo-2,3,4,5-tetrahydro-1,2,4-triazines for possible antineoplastic activity is reported. The assigned structures were substantiated by IR, NMR, and mass spectral studies of representative members of the series. Four compounds were tested against P-388 lymphocytic leukemia and were inactive.

Keyphrases □ 1,2,4-Triazines, substituted—synthesized, antineoplastic activity evaluated in mice □ Antineoplastic activity—various substituted 1,2,4-triazines evaluated in mice □ Structure–activity relationships—substituted 1,2,4-triazines evaluated for antineoplastic activity in mice

Of the different 6-aza analogs of pyrimidines screened for anticancer potency, 6-(3,4-methylenedioxystyryl)-3-thioxo-5-oxo-2,3,4,5-tetrahydro-1,2,4-triazine (IV, R = 3,4-$CH_2O_2C_6H_3$ and X = S, Scheme I) was more active than mercaptopurine and fluorouracil in animals (1, 2).

In a search for novel antineoplastic agents, it was of interest to prepare 6-styryl-3,5-dioxo- and 3-thioxo-5-oxo-2,3,4,5-tetrahydro-1,2,4-triazines with new substituents

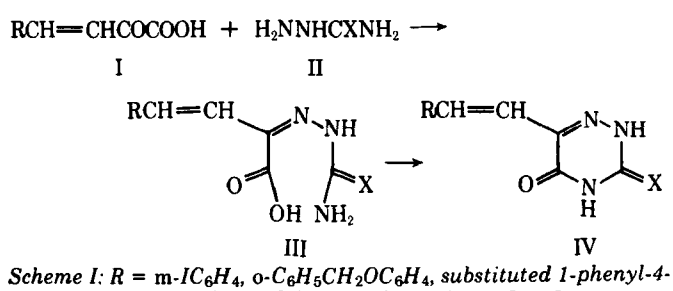

Scheme I: R = m-IC_6H_4, o-$C_6H_5CH_2OC_6H_4$, *substituted 1-phenyl-4-pyrazolyl, or* $C_6H_5CH{=}CH$ *and* X = *O or S*

on the phenyl ring (IV*a*–IV*c*, Table I). The diverse biological activities of the pyrazole nucleus suggested the synthesis of two new *as*-triazines in which a substituted 1-phenyl-4-pyrazolyl moiety replaced the phenyl ring: 6-[β-(3,5-dimethyl-1-phenyl-4-pyrazolyl)vinyl]- and 6-[β-(1,5-diphenyl-3-methyl-4-pyrazolyl)vinyl]-3-thioxo-5-oxo-2,3,4,5-tetrahydro-1,2,4-triazines (IV*d* and IV*e*, Table I). It was also of interest to prepare and screen *as*-triazines having the phenyl ring separated from position 6 by a 1,3-butadiene instead of the vinyl side chain: 6-(4-phenyl-1,3-butadienyl)-3,5-dioxo- and 3-thioxo-5-oxo-2,3,4,5-tetrahydro-1,2,4-triazines (IV*f* and IV*g*, Table I).

RESULTS AND DISCUSSION

Chemistry—For the synthesis of the new triazines, the reactions shown in Scheme I were followed. Condensation of arylidenepyruvic acids (I) with semicarbazide (II, X = O) hydrochloride or thiosemicarbazide (II, X = S) yielded semicarbazono- or thiosemicarbazonoarylidenepyruvic acids (III*a*–III*g*, Table I). Subsequently, III*a*–III*g* were cyclized to the corresponding 1,2,4-triazines (IV*a*–IV*g*, Table I) in the presence of sodium hydroxide. Compound IV*g* previously was synthesized by heating thiosemicarbazonocinnamylidenepyruvic acid (III*g*) with aqueous sodium carbonate for 3 hr (3). Conversion of IV*g* to IV*f* was reported to take place when IV*g* was heated with aqueous alkaline potassium permanganate solution followed by acidification of the reaction mixture (3).

The IR spectra of the triazines showed multiple bands in the 3500–2900-cm^{-1} region (NH stretching) and strong bands at 1720–1680 (C=O stretching) and 1560–1520 (amide II) cm^{-1}. In addition, the spectra of the 3-thio derivatives revealed a band of medium intensity between 1300 and 1270 cm^{-1} (C=S stretching) but lacked the band characteristic of the SH group of a thiol tautomer. These data indicate the existence of

0022-3549/79/0200-0243$01.00/0
© 1979, American Pharmaceutical Association

1. The exact manner of preparation and degassing of the mobile phase should be left to the operator as long as the final solution has the proper pH.

2. The preparation and injection of folic acid solutions should be made more flexible to allow for smaller amounts of folic acid and larger injection volumes. The former change may be necessary to prevent overloading of some detectors while the latter change permits better reproducibility of manual injections.

3. The particle base may be nonspherical since its shape is not critical to the determination.

These recommendations have been incorporated in the latest USP supplement (4).

The majority of collaborators were able to achieve acceptable separation and precision with the chromatographic method in spite of the variety of instrumental and operating conditions used, indicating that the method should be widely applicable.

REFERENCES

(1) V. D. Reif, J. T. Reamer, and L. T. Grady, *J. Pharm. Sci.*, **66**, 1112 (1977).

(2) "Third Supplement to USP XIX and NF XIV," United States Pharmacopeial Convention, Rockville, Md., 1977, p. 71.

(3) "The United States Pharmacopeia," 19th rev., Mack Publishing Co., Easton, Pa., 1975, pp. 211, 212, 624.

(4) "Fourth Supplement to USP XIX and NF XIV," United States Pharmacopeial Convention, Rockville, Md., 1978, p. 86.

(5) *Pharmacopeial Forum*, **2**, 371 (1976).

ACKNOWLEDGMENTS

The authors thank the following persons for their cooperation: J. Bodenmiller, Merrell-National Laboratories; M. D. Bray, Eli Lilly and Co.; F. Cioffi, E. R. Squibb and Sons; R. Elkas, Lederle Laboratories; S. A. Fusari, Parke-Davis & Co.; L. T. Grady, United States Pharmacopeial Convention; W. S. Hardesty, Beecham Laboratories; D. Heuring, Mead Johnson & Co.; R. Kirchmeier, Pfizer Inc.; G. Krol, Ayerst Laboratories; R. S. Lenkiewicz, Stuart Pharmaceuticals; E. Pratt, Sterling Winthrop Research Institute; and E. Townley, Schering Corp.

The authors are also grateful to A. Greene and J. Van Antwerp of Hoffmann-La Roche for characterization and subdivision of the materials for distribution to the collaborators.

Potential Antineoplastics I: Substituted 3,5-Dioxo- and 3-Thioxo-5-oxo-2,3,4,5-tetrahydro-1,2,4-triazines

EL SEBAI A. IBRAHIM, S. A. SHAMS EL DINE, FARID S. G. SOLIMAN ˣ, and IBRAHIM M. LABOUTA

Received April 24, 1978, from the *Department of Pharmaceutical Chemistry, Faculty of Pharmacy, University of Alexandria, Alexandria, A.R. Egypt.* Accepted for publication July 10, 1978.

Abstract □ The synthesis of some 6-substituted 3,5-dioxo- and 3-thioxo-5-oxo-2,3,4,5-tetrahydro-1,2,4-triazines for possible antineoplastic activity is reported. The assigned structures were substantiated by IR, NMR, and mass spectral studies of representative members of the series. Four compounds were tested against P-388 lymphocytic leukemia and were inactive.

Keyphrases □ 1,2,4-Triazines, substituted—synthesized, antineoplastic activity evaluated in mice □ Antineoplastic activity—various substituted 1,2,4-triazines evaluated in mice □ Structure–activity relationships—substituted 1,2,4-triazines evaluated for antineoplastic activity in mice

Of the different 6-aza analogs of pyrimidines screened for anticancer potency, 6-(3,4-methylenedioxystyryl)-3-thioxo-5-oxo-2,3,4,5-tetrahydro-1,2,4-triazine (IV, R = 3,4-$CH_2O_2C_6H_3$ and X = S, Scheme I) was more active than mercaptopurine and fluorouracil in animals (1, 2).

In a search for novel antineoplastic agents, it was of interest to prepare 6-styryl-3,5-dioxo- and 3-thioxo-5-oxo-2,3,4,5-tetrahydro-1,2,4-triazines with new substituents

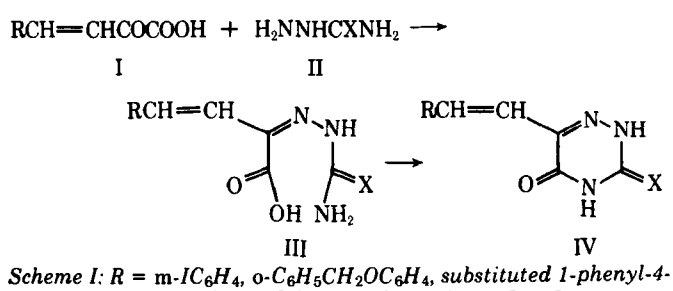

Scheme I: R = m-IC_6H_4, o-$C_6H_5CH_2OC_6H_4$, *substituted 1-phenyl-4-pyrazolyl, or* $C_6H_5CH{=}CH$ *and* X = *O or S*

on the phenyl ring (IV*a*–IV*c*, Table I). The diverse biological activities of the pyrazole nucleus suggested the synthesis of two new *as*-triazines in which a substituted 1-phenyl-4-pyrazolyl moiety replaced the phenyl ring: 6-[β-(3,5-dimethyl-1-phenyl-4-pyrazolyl)vinyl]- and 6-[β-(1,5-diphenyl-3-methyl-4-pyrazolyl)vinyl]-3-thioxo-5-oxo-2,3,4,5-tetrahydro-1,2,4-triazines (IV*d* and IV*e*, Table I). It was also of interest to prepare and screen *as*-triazines having the phenyl ring separated from position 6 by a 1,3-butadiene instead of the vinyl side chain: 6-(4-phenyl-1,3-butadienyl)-3,5-dioxo- and 3-thioxo-5-oxo-2,3,4,5-tetrahydro-1,2,4-triazines (IV*f* and IV*g*, Table I).

RESULTS AND DISCUSSION

Chemistry—For the synthesis of the new triazines, the reactions shown in Scheme I were followed. Condensation of arylidenepyruvic acids (I) with semicarbazide (II, X = O) hydrochloride or thiosemicarbazide (II, X = S) yielded semicarbazono- or thiosemicarbazonoarylidenepyruvic acids (III*a*–III*g*, Table I). Subsequently, III*a*–III*g* were cyclized to the corresponding 1,2,4-triazines (IV*a*–IV*g*, Table I) in the presence of sodium hydroxide. Compound IV*g* previously was synthesized by heating thiosemicarbazonocinnamylidenepyruvic acid (III*g*) with aqueous sodium carbonate for 3 hr (3). Conversion of IV*g* to IV*f* was reported to take place when IV*g* was heated with aqueous alkaline potassium permanganate solution followed by acidification of the reaction mixture (3).

The IR spectra of the triazines showed multiple bands in the 3500–2900-cm^{-1} region (NH stretching) and strong bands at 1720–1680 (C=O stretching) and 1560–1520 (amide II) cm^{-1}. In addition, the spectra of the 3-thio derivatives revealed a band of medium intensity between 1300 and 1270 cm^{-1} (C=S stretching) but lacked the band characteristic of the SH group of a thiol tautomer. These data indicate the existence of

0022-3549/79/0200-0243$01.00/0
© 1979, American Pharmaceutical Association

Table I—Semicarbazono- and Thiosemicarbazonoarylidenepyruvic Acids and 6-Substituted 3,5-Dioxo- and 3-Thioxo-5-oxo-2,3,4,5-tetrahydro-1,2,4-triazines

Compound	R	X	Melting Point	Recrystallization Solvent[a]	Molecular Formula	Analysis, %	Calc.	Found
IIIa	*m*-IC_6H_4	O	219–220°	EW	$C_{11}H_{10}IN_3O_3$	C	36.8	36.8
						H	2.8	2.8
						N	11.7	11.6
IIIb	*m*-IC_6H_4	S	194–195°	EW	$C_{11}H_{10}IN_3O_2S$	C	35.2	34.8
						H	2.7	3.1
						N	11.2	10.7
IIIc	*o*-$C_6H_5CH_2OC_6H_4$	S	175–177°	E	$C_{18}H_{17}N_3O_3S$	N	11.8	12.3
						S	9.0	9.2
IIId	3,5-Dimethyl-1-phenyl-4-pyrazolyl	S	193°	EB	$C_{16}H_{17}N_5O_2S$	C	55.95	55.8
						H	5.0	5.2
						S	9.3	8.9
IIIe	1,5-Diphenyl-3-methyl-4-pyrazolyl	S	216°	EW	$C_{21}H_{19}N_5O_2S$	C	62.2	62.5
						H	4.7	5.0
						S	7.9	7.9
IIIf	C_6H_5CH=CH	O	196–197°	E	$C_{13}H_{13}N_3O_3$	C	60.2	59.8
						H	5.05	5.5
						N	16.2	16.1
IIIg	C_6H_5CH=CH	S	193–194°	E	$C_{13}H_{13}N_3O_2S$ (3)		—	—
IVa	*m*-IC_6H_4	O	215–217°	E	$C_{11}H_8IN_3O_2$[b]	C	38.7	38.3
						H	2.4	2.5
						N	12.3	12.3
IVb	*m*-IC_6H_4	S	237–238°	E	$C_{11}H_8IN_3OS$[c]	C	37.0	37.0
						H	2.3	2.2
						N	11.8	11.6
IVc	*o*-$C_6H_5CH_2OC_6H_4$	S	222°	E	$C_{18}H_{15}N_3O_2S$	C	64.1	63.6
						H	4.5	4.3
						N	12.45	12.0
						S	9.5	9.8
IVd	3,5-Dimethyl-1-phenyl-4-pyrazolyl	S	302–305°	A	$C_{16}H_{15}N_5OS$	C	59.05	58.5
						H	4.65	5.0
						S	9.85	10.4
IVe	1,5-Diphenyl-3-methyl-4-pyrazolyl	S	290–292°	EW	$C_{21}H_{17}N_5OS \cdot H_2O$	C	62.2	62.4
						H	4.7	5.1
						S	7.9	7.9
IVf	C_6H_5CH=CH	O	300–303°	E	$C_{13}H_{11}N_3O_2$ (3)	C	64.7	64.8
						H	4.9	4.8
						N	17.2	16.8
IVg	C_6H_5CH=CH	S	257°	E	$C_{13}H_{11}N_3OS$ (3)		—	—

[a] A = acetic acid, E = ethanol, EB = ethanol–benzene, and EW = ethanol–water. [b] Mass spectrum: *m/e* (relative intensity) 341 (18) (M^+), 340 (9) (M − 1), 316 (14), 315 (25), 300 (11), 298 (5), 297 (11), 272 (13), 271 (21), 270 (14), 256 (29), 255 (100), 241 (7), 230 (7), 156 (11), 145 (7), 144 (26), 143 (8), 129 (18), 128 (50), 127 (7), 117 (16), 116 (14), 115 (38), 114 (19), 113 (32), 102 (16), 101 (21), 95 (21), 89 (11), and 77 (16). [c] Mass spectrum: *m/e* (relative intensity) 357 (100) (M^+), 314 (4), 281 (27), 269 (4), 254 (15), 253 (50), 240 (9), 229 (17), 128 (5), 127 (17), 114 (5), and 113 (8).

these triazines in the 3,5-dioxo- or 3-thioxo-5-oxo form (IV) in the solid state.

In the ^{1}H-NMR spectra, the aromatic and vinyl protons were in the range of δ 6.4–8.0 ppm (multiplet) for IV*a* and IV*b* and the two NH protons were at δ 11.0 ppm (singlet) for IV*a* and at δ 12.8 (singlet) and 13.2 (singlet) ppm for IV*b*. The mass spectrum of IV*a* involved the sequential loss of two molecules of HNCO from the molecular ion (*m/e* 341, 18%), giving *m*-iodocinnamonitrile (*m/e* 255, 100%) (V). The spectrum of IV*b* was characterized by an intense molecular ion, which successively lost HNCO and SH, leading to *m/e* 314 (4%) (VI) and *m/e* 281 (27%) (VII), respectively. A loss of HCS from VI yielded the species *m/e* 269 (4%) (VIII).

Antineoplastic Activity—Compounds IV*a*, IV*b*, IV*f*, and IV*g*[1] were screened against P-388 lymphocytic leukemia in mice according to a standard protocol[2] (4). Median survival time was taken as the activity parameter for tumor evaluation. A compound is considered active in this system if the ratio of the median survival times for treated to control mice (T/C) is ≥125%. None of the compounds reached this value when tested by a three-dose assay at 400, 200, and 100 mg/kg/injection.

EXPERIMENTAL[3]

Arylidenepyruvic Acids (I)—The required acids were prepared by the base-catalyzed condensation of pyruvic acid with the appropriate aldehyde, as previously reported (5).

Semicarbazono- and Thiosemicarbazonoarylidenepyruvic Acids (IIIa–IIIg, Table I)—A solution of I (0.002 mole) in ethanol (20 ml) was heated for 15 min with a solution of semicarbazide (II, X = O) hydrochloride or thiosemicarbazide (II, X = S) (0.002 mole) in a mixture of water (10 ml) and acetic acid (0.5 ml). Most of the alcohol was evaporated; the yellow product was filtered, washed with water, dried, and recrystallized from the proper solvent. The yields were 80–90%.

6-Substituted 3,5-Dioxo- and 3-Thioxo-5-oxo-2,3,4,5-tetrahydro-1,2,4-triazines (IVa–IVg, Table I)—A solution of the appropriate IIIa–IIIg (0.01 mole) in 1 *N* NaOH (15 ml) and water (5 ml) was refluxed for 15 min. After cooling, the yellow clear solution was acidified with dilute hydrochloric acid to pH 6. Then the yellow product was filtered, washed with water, and dried. It was recrystallized from the appropriate solvent as yellow crystals in almost quantitative yields.

[1] NSC 275892, 275891, 275894, and 275893, respectively.

[2] Drug Evaluation Branch, Drug Research and Development, Division of Cancer Treatment, National Cancer Institute, National Institutes of Health, Department of Health, Education, and Welfare, Bethesda, MD 20014.

[3] Melting points were determined in open glass capillaries and are uncorrected. IR spectra were recorded on a Perkin-Elmer 421 spectrometer with potassium bromide. ^{1}H-NMR spectra were determined on a Varian A60A spectrometer with deuterated dimethyl sulfoxide as the solvent. Mass spectra were obtained using an Organic MS 20 AEI (70 ev) instrument. Microanalysis, for samples dried over phosphorus pentoxide at 70° under reduced pressure, was carried out at the Microanalytical Unit, University of Cairo, Cairo, A.R. Egypt.

REFERENCES

(1) SPOFA United Pharmaceutical Works, Netherlands appl. 6,505,411 (Oct. 29, 1965) and Czech. appl. (Apr. 28, 1964); through *Chem. Abstr.*, **64**, 9748c (1966).

(2) M. Semonsky, M. Beran, J. Neumannova, H. Skvorova, and V. Jelinek, *Coll. Czech. Chem. Commun.*, **32**, 4439 (1967); through *Chem. Abstr.*, **68**, 29683q (1968).

(3) J. Slouka, *J. Prakt. Chem.*, **16**, 220 (1962); through *Chem. Abstr.*, **58**, 2453c (1963).

(4) R. I. Geran, N. H. Greenberg, M. M. MacDonald, A. M. Schumacher, and B. J. Abbott, *Cancer Chemother. Rep., Part 3*, **3**, 1 (1972). "Screening Data Summary Interpretation and Outline of Current Screen," Instruction Booklet 14, National Cancer Institute, Bethesda, Md., 1977.

(5) I. M. Roushdi, E. S. A. Ibrahim, R. M. Shafik, and F. S. G. Soliman, *Pharmazie*, **12**, 731 (1972).

ACKNOWLEDGMENTS

The authors thank Dr. Harry B. Wood, Jr., Chief, Drug Synthesis and Chemistry Branch, Developmental Therapeutics Program, Division of Cancer Treatment, National Cancer Institute, National Institutes of Health, Silver Spring, MD 20910, and Dr. Omar C. Yoder, Institute Jules Bordet, 1000 Brussels, Belgium, for the anticancer test reports and Dr. Wolfgang Stadlbauer, Institut für Organische Chemie der Karl-Franzens-Universität Graz, Graz, Austria, for the spectral determinations.

Antihypercholesterolemic Studies with Sterols: β-Sitosterol and Stigmasterol

R. F. CHANDLER ˣ, S. N. HOOPER, and H. A. ISMAIL

Received October 20, 1977, from the *College of Pharmacy, Dalhousie University, Halifax, Nova Scotia, Canada, B3H 3J5.* Accepted for publication August 1, 1978.

Abstract □ Stigmasterol, which differs from β-sitosterol by unsaturation at C_{22}, was tested for antihypercholesterolemic activity under an experimental protocol that gave the results expected with β-sitosterol and cholestyramine. In terms of serum cholesterol, stigmasterol had a barely significant antihypercholesterolemic effect while exhibiting no obvious effect on the heart or liver. It was concluded that saturation of the side chain, at least at C_{22}, is important in conferring antihypercholesterolemic activity on a sterol.

Keyphrases □ β-Sitosterol—antihypercholesterolemic activity evaluated in chickens □ Stigmasterol—antihypercholesterolemic activity evaluated in chickens □ Antihypercholesterolemic activity—β-sitosterol and stigmasterol evaluated in chickens □ Structure–activity relationships—β-sitosterol and stigmasterol evaluated for antihypercholesterolemic activity in chickens

There is no conclusive evidence that lowering plasma cholesterol levels can either reverse or prevent certain cardiovascular diseases. Nevertheless, many antiatherosclerotic studies have been performed with compounds that reduce plasma cholesterol.

Currently, cholestyramine is the only antihypercholesterolemic agent that is relatively free of adverse reactions and reasonably effective in reducing plasma cholesterol levels in type II hyperlipemia (1–3). Unfortunately, it is not always effective (4); therefore, more toxic agents must often be employed.

Niacin and clofibrate, the agents most widely used, have been generally considered effective in reducing cholesterol and triglyceride levels (5). Although their effect on blood triglyceride levels is pronounced, they produce only modest reductions in blood cholesterol levels (6). Both are associated with unpleasant or hazardous side effects.

β-Sitosterol also lowers cholesterol levels in humans (1, 7–11). Reductions in plasma cholesterol levels of the same order of magnitude as those with cholestyramine have been observed (7, 12–14); however, the drug has little effect on plasma triglycerides (10). β-Sitosterol is free of detectable toxicity, and there is no evidence that it accumulates in tissues (2, 15, 16).

The value of these nontoxic agents in the treatment and prevention of such diseases as atherosclerosis, myocardial infarction, and stroke could be significant. Consequently, it was decided to study the structure–activity relationships of sterols related to cholesterol for their antihypercholesterolemic activity. The selection of the White Leghorn cockerel as the animal model was discussed previously (17), as was the use of GLC for sterol analysis (18).

EXPERIMENTAL

General—Day-old White Leghorn cockerels were fed *ad libitum* for 14 days. They were then weighed, banded, and randomly assigned to one of five groups: pretest group, sacrificed on the 1st day of the experiment; Group A, basic diet; and Groups B, C, and D, basic diet supplemented with 1% cholesterol, 1% cholesterol plus 1% test compound, and 1% test compound, respectively. Drinking water was always present.

Serum cholesterol levels were determined (blood collected *via* the brachial vein) at least once during the 4-week experiment. On the final day of the experiment, the chicks were weighed and killed; the hearts and livers were weighed, photographed, and frozen until analyzed. Serum samples also were collected.

Assays were performed by GLC with cholestane as an internal standard (18). Separation of β-sitosterol, campesterol, and stigmasterol from cholesterol was accomplished on columns packed with 3% SE-30 or 3% OV-17 on 100–120-mesh Gas Chrom Q (18). Commercially available laboratory control samples were used routinely to ensure day-to-day reproducibility (18).

Cholestyramine Experiment—In this experiment, the "test compound" was the anion-exchange resin cholestyramine. Only 35 chicks were employed (seven per group); otherwise, the details followed the general procedure described.

β-Sitosterol Experiment—Day-old chicks (White Leghorn cockerels) were fed *ad libitum* for 25 days. On Day 25, blood samples were collected from each chick in the four groups (11 chicks each) of weighed chicks. The chicks were then put on the special diets for 19 days; during this time, blood was collected every 4th day. On Day 19, they were killed.

Stigmasterol Experiment—In this experiment, 44 chicks were used (nine per group, except the pretest group which consisted of eight). The experiment was terminated on Day 24, following the general procedure.

RESULTS AND DISCUSSION

The selection of agents for these experiments was based largely on the knowledge that β-sitosterol and cholestyramine are antihypercholesterolemic agents. These agents were used as standards for comparison of relative activities. Since stigmasterol differs from β-sitosterol only by unsaturation at C_{22}, the results of these experiments should allow the influence of that function on antihypercholesterolemic activity to be determined.

In all experiments, the chicks tolerated their diets well, as indicated by their healthy appearance and consistent weight gain (Table I). The

0022-3549/79/0200-0245$01.00/0
© 1979, American Pharmaceutical Association

(5) I. M. Roushdi, E. S. A. Ibrahim, R. M. Shafik, and F. S. G. Soliman, *Pharmazie*, **12**, 731 (1972).

ACKNOWLEDGMENTS

The authors thank Dr. Harry B. Wood, Jr., Chief, Drug Synthesis and Chemistry Branch, Developmental Therapeutics Program, Division of Cancer Treatment, National Cancer Institute, National Institutes of Health, Silver Spring, MD 20910, and Dr. Omar C. Yoder, Institute Jules Bordet, 1000 Brussels, Belgium, for the anticancer test reports and Dr. Wolfgang Stadlbauer, Institut für Organische Chemie der Karl-Franzens-Universität Graz, Graz, Austria, for the spectral determinations.

Antihypercholesterolemic Studies with Sterols: β-Sitosterol and Stigmasterol

R. F. CHANDLER ˣ, S. N. HOOPER, and H. A. ISMAIL

Received October 20, 1977, from the *College of Pharmacy, Dalhousie University, Halifax, Nova Scotia, Canada, B3H 3J5.* Accepted for publication August 1, 1978.

Abstract □ Stigmasterol, which differs from β-sitosterol by unsaturation at C_{22}, was tested for antihypercholesterolemic activity under an experimental protocol that gave the results expected with β-sitosterol and cholestyramine. In terms of serum cholesterol, stigmasterol had a barely significant antihypercholesterolemic effect while exhibiting no obvious effect on the heart or liver. It was concluded that saturation of the side chain, at least at C_{22}, is important in conferring antihypercholesterolemic activity on a sterol.

Keyphrases □ β-Sitosterol—antihypercholesterolemic activity evaluated in chickens □ Stigmasterol—antihypercholesterolemic activity evaluated in chickens □ Antihypercholesterolemic activity—β-sitosterol and stigmasterol evaluated in chickens □ Structure–activity relationships—β-sitosterol and stigmasterol evaluated for antihypercholesterolemic activity in chickens

There is no conclusive evidence that lowering plasma cholesterol levels can either reverse or prevent certain cardiovascular diseases. Nevertheless, many antiatherosclerotic studies have been performed with compounds that reduce plasma cholesterol.

Currently, cholestyramine is the only antihypercholesterolemic agent that is relatively free of adverse reactions and reasonably effective in reducing plasma cholesterol levels in type II hyperlipemia (1–3). Unfortunately, it is not always effective (4); therefore, more toxic agents must often be employed.

Niacin and clofibrate, the agents most widely used, have been generally considered effective in reducing cholesterol and triglyceride levels (5). Although their effect on blood triglyceride levels is pronounced, they produce only modest reductions in blood cholesterol levels (6). Both are associated with unpleasant or hazardous side effects.

β-Sitosterol also lowers cholesterol levels in humans (1, 7–11). Reductions in plasma cholesterol levels of the same order of magnitude as those with cholestyramine have been observed (7, 12–14); however, the drug has little effect on plasma triglycerides (10). β-Sitosterol is free of detectable toxicity, and there is no evidence that it accumulates in tissues (2, 15, 16).

The value of these nontoxic agents in the treatment and prevention of such diseases as atherosclerosis, myocardial infarction, and stroke could be significant. Consequently, it was decided to study the structure–activity relationships of sterols related to cholesterol for their antihypercholesterolemic activity. The selection of the White Leghorn cockerel as the animal model was discussed previously (17), as was the use of GLC for sterol analysis (18).

EXPERIMENTAL

General—Day-old White Leghorn cockerels were fed *ad libitum* for 14 days. They were then weighed, banded, and randomly assigned to one of five groups: pretest group, sacrificed on the 1st day of the experiment; Group A, basic diet; and Groups B, C, and D, basic diet supplemented with 1% cholesterol, 1% cholesterol plus 1% test compound, and 1% test compound, respectively. Drinking water was always present.

Serum cholesterol levels were determined (blood collected *via* the brachial vein) at least once during the 4-week experiment. On the final day of the experiment, the chicks were weighed and killed; the hearts and livers were weighed, photographed, and frozen until analyzed. Serum samples also were collected.

Assays were performed by GLC with cholestane as an internal standard (18). Separation of β-sitosterol, campesterol, and stigmasterol from cholesterol was accomplished on columns packed with 3% SE-30 or 3% OV-17 on 100–120-mesh Gas Chrom Q (18). Commercially available laboratory control samples were used routinely to ensure day-to-day reproducibility (18).

Cholestyramine Experiment—In this experiment, the "test compound" was the anion-exchange resin cholestyramine. Only 35 chicks were employed (seven per group); otherwise, the details followed the general procedure described.

β-Sitosterol Experiment—Day-old chicks (White Leghorn cockerels) were fed *ad libitum* for 25 days. On Day 25, blood samples were collected from each chick in the four groups (11 chicks each) of weighed chicks. The chicks were then put on the special diets for 19 days; during this time, blood was collected every 4th day. On Day 19, they were killed.

Stigmasterol Experiment—In this experiment, 44 chicks were used (nine per group, except the pretest group which consisted of eight). The experiment was terminated on Day 24, following the general procedure.

RESULTS AND DISCUSSION

The selection of agents for these experiments was based largely on the knowledge that β-sitosterol and cholestyramine are antihypercholesterolemic agents. These agents were used as standards for comparison of relative activities. Since stigmasterol differs from β-sitosterol only by unsaturation at C_{22}, the results of these experiments should allow the influence of that function on antihypercholesterolemic activity to be determined.

In all experiments, the chicks tolerated their diets well, as indicated by their healthy appearance and consistent weight gain (Table I). The

0022-3549/79/0200-0245$01.00/0
© 1979, American Pharmaceutical Association

Table I—Summary of the Antihypercholesterolemic Studies with Cholestyramine, Stigmasterol, and β-Sitosterol

Group[a]	Number in Group	Body: Final Weight, g	Body: Weight Gain, g	Liver: Final Weight, g	Liver: Cholesterol, mg/100 g of lipid	Heart: Final Weight, g	Heart: Cholesterol, mg/100 g of lipid	Serum Cholesterol, mg/100 ml
				Cholestyramine				
A	7	399 ± 17	296 ± 18	13.37 ± 0.79	4894 ± 652	2.84 ± 0.16	926 ± 248	138 ± 16[b]
B	7	462 ± 22	363 ± 16	14.99 ± 0.71	14852 ± 1087[c]	3.12 ± 0.13	2462 ± 416	331 ± 40[c]
C	7	437 ± 18	333 ± 16	12.75 ± 0.29	8368 ± 487[c,d]	2.79 ± 0.10	1938 ± 411	114 ± 5[b,d]
D	7	457 ± 17	352 ± 17	13.64 ± 0.91	7633 ± 464[c]	2.96 ± 0.11	1990 ± 463	98 ± 7[d]
				Stigmasterol				
A	9	511 ± 25	366 ± 20	12.74 ± 0.73	7522 ± 425	3.21 ± 0.13	1232 ± 145	122 ± 6
B	9	504 ± 14	355 ± 12	13.69 ± 0.23[b]	11909 ± 960[b,c]	3.35 ± 0.21	1656 ± 282	538 ± 76[c]
C	9	515 ± 17	373 ± 14	13.48 ± 0.55	10820 ± 844[c]	3.52 ± 0.15	1501 ± 149	343 ± 36[c,d]
D	9	535 ± 17	395 ± 16	13.85 ± 0.61	6822 ± 383[c]	3.25 ± 0.13	1186 ± 80	134 ± 13[d]
				β-Sitosterol				
A	11	353 ± 12	187 ± 9	9.28 ± 0.42[b]	6082 ± 526[b]	1.94 ± 0.13[b]	833 ± 67[b]	108 ± 6[b]
B	11	350 ± 15	190 ± 12	10.10 ± 0.47[b]	16231 ± 726[b,c]	1.92 ± 0.10[e]	1459 ± 258[e]	349 ± 24[c,e]
C	11	401 ± 11	219 ± 9	11.60 ± 0.61[b,c]	8360 ± 746[b,d]	2.02 ± 0.07[b]	1257 ± 184[b]	150 ± 5[d,e]
D	11	376 ± 13	211 ± 14	11.42 ± 0.24[b,c]	6560 ± 908[b,d]	2.18 ± 0.08[b]	767 ± 88[b,d]	126 ± 8[d,e]

[a] Group mean values ± *SE*. [b] Number in group is one less than stated value. [c] Significant at the 95% confidence level when compared to Group A by analysis of variance. [d] Significant at the 95% confidence level when compared to Group B by analysis of variance. [e] Number in group is two less than stated value.

final mean weights and mean weight gains were not significantly different among the groups in any experiment.

Serum collected from the chicks during the experiments showed a significant increase in the cholesterol level in Group B animals (Table I and Figs. 1–3). Group C animals in the stigmasterol experiment, but not the others, also exhibited significantly elevated serum cholesterol levels, although the mean value was still significantly lower than that of Group B as in the other experiments. Neither of the test sterols was detected in any of the tissues studied.

Macroscopic examination of the hearts revealed no apparent differences among the four groups in any experiment. Differences in mean weights, percentage lipid, and mean cholesterol levels of the hearts were not significant, except in the β-sitosterol experiment where the Group D mean cholesterol level was significantly lower than that of Group B.

The livers of all chicks in Group B and in the stigmasterol experiment were a distinct yellow, especially when compared to the healthy red color of the remaining groups. There were no significant differences in percentage lipid and mean liver weights, except for Groups C and D in the β-sitosterol experiment in which the mean weights of the livers were significantly greater than those of Group A. This observation, however, is in keeping with the greater mean body weight of these two groups.

Analysis of the livers for cholesterol demonstrated the highly significant hypercholesterolemia induced in Group B (Table I).

In the experiment with β-sitosterol, the mean liver cholesterol was significantly greater in Group B than in the other groups, which did not differ significantly from each other. With cholestyramine, levels were significantly greater in Group B than in all other groups. Group C was significantly lower than Group B. These results clearly show the antihypercholesterolemic effect of the two compounds on liver cholesterol content.

In the stigmasterol experiment, however, the mean liver cholesterol levels of Groups B and C, although significantly greater than the control level, were not different from each other (Table I). This result shows the relative ineffectiveness of stigmasterol as an antihypercholesterolemic agent.

SUMMARY AND CONCLUSIONS

In summary, the chicks in all experiments tolerated their diets well and gained weight steadily. All Group B animals showed significantly elevated

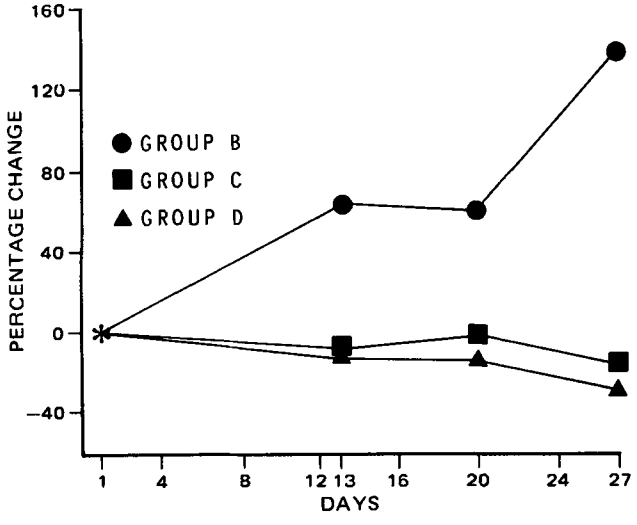

Figure 1—*Percentage change from Group A in mean serum cholesterol of chicks in cholestyramine experiment.*

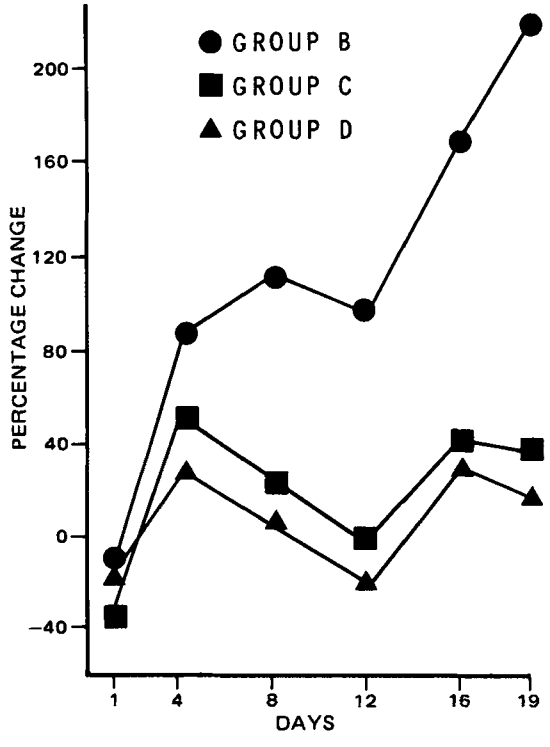

Figure 2—*Percentage change from Group A in mean serum cholesterol of chicks in β-sitosterol experiment.*

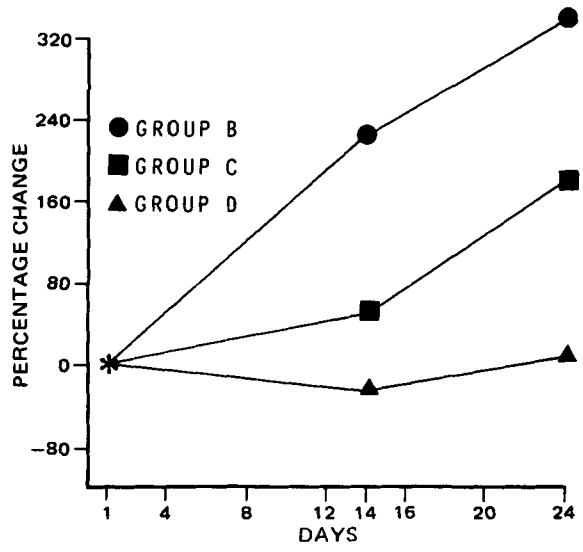

Figure 3—*Percentage change from Group A in mean serum cholesterol of chicks in stigmasterol experiment.*

serum and liver cholesterol values. The coloration of livers closely paralleled the serum cholesterol concentration.

Consistent with the literature (1–3, 7–11), the results of these experiments illustrate the potent antihypercholesterolemic activity of cholestyramine and β-sitosterol. Furthermore, the antihypercholesterolemic activity of these two compounds appears to be of the same order of magnitude, as reported previously (7, 12–14).

Although present in the diet of Groups C and D, neither β-sitosterol nor campesterol (which represents about 40% of the β-sitosterol NF employed) could be detected in the serum. This finding supports the theory that their action is due to their competitive inhibition of cholesterol absorption.

In contrast to the literature (19), the results indicate that stigmasterol, while apparently not exhibiting any deleterious effects, is ineffective as an antihypercholesterolemic agent. It appears, therefore, that unsaturation at C_{22} (the only structural difference between β-sitosterol and stigmasterol) is an undesirable factor in effecting antihypercholesterolemic activity.

REFERENCES

(1) R. I. Levy, D. S. Fredrickson, R. Shulman, D. W. Bilheimer, J. L. Breslow, N. J. Stone, S. E. Lux, H. R. Sloan, R. M. Krauss, and P. N. Herbert, *Ann. Intern. Med.*, **77**, 267 (1972).

(2) R. I. Levy, J. Morganroth, and B. M. Rifkind, *N. Engl. J. Med.*, **290**, 1295 (1974).

(3) *Med. Lett.*, **17**, 49 (1975).

(4) R. S. Lees and D. E. Wilson, *N. Engl. J. Med.*, **284**, 186 (1971).

(5) J. L. Marx, *Science*, **187**, 526 (1975).

(6) The Coronary Drug Project Research Group, *J. Am. Med. Assoc.*, **231**, 360 (1975).

(7) R. I. Levy and B. M. Rifkind, *Drugs*, **6**, 12 (1973).

(8) M. T. R. Subbiah, *Am. J. Clin. Nutr.*, **26**, 219 (1973).

(9) R. Reiser, *ibid.*, **26**, 524 (1973).

(10) M. J. Karvonen, *Practitioner*, **212**, 518 (1974).

(11) N. B. Myant, *ibid.*, **211**, 188 (1973).

(12) O. J. Pollak, *Circulation*, **7**, 702 (1953).

(13) M. M. Best, C. H. Duncan, E. J. Van Loon, and J. D. Wathen, *ibid.*, **10**, 201 (1954).

(14) R. E. Shipley, *Trans. N.Y. Acad. Sci.*, **18**, 111 (1955).

(15) G. A. Braun and J. L. Rabinowitz, in "Topics in Medicinal Chemistry," vol. 3, J. L. Rabinowitz and R. M. Myerson, Eds., Wiley-Interscience, Toronto, Canada, 1970, p. 91.

(16) P. Weiss, *Ration. Drug Ther.*, **6**, 1 (1972).

(17) R. F. Chandler, S. N. Hooper, and H. A. Ismail, *Can. J. Pharm. Sci.*, in press.

(18) S. N. Hooper and R. F. Chandler, *J. Pharm. Sci.*, **67**, 1157 (1978).

(19) D. W. Peterson, E. A. Shneour, N. F. Peek, and H. W. Gaffey, *J. Nutr.*, **50**, 191 (1953).

ACKNOWLEDGMENTS

Presented in part at the Medicinal Chemistry Section, APhA Academy of Pharmaceutical Sciences, Orlando meeting, November 1976.

Supported by Medical Research Council of Canada Grant MA-5424.

The authors thank Dr. J. A. Love, Director, Animal Care Centre, Dalhousie University, for valuable assistance; and Dr. C. A. Field, Mathematics Department, Dalhousie University, for assistance with the statistical components of this project. They also thank Eli Lilly and Co. for supplying the β-sitosterol NF and the cholesterol employed and Mead Johnson Canada for the cholestyramine (Questran).

Chemical Constituents of *Echites hirsuta* (Apocynaceae)

M. M. CHIEN *§, G. H. SVOBODA ‡, P. L. SCHIFF, Jr. *, D. J. SLATKIN *, and J. E. KNAPP *x

Received June 8, 1978, from the **Department of Pharmacognosy, School of Pharmacy, University of Pittsburgh, Pittsburgh, PA 15261*, and the ‡*Lilly Research Laboratories, Eli Lilly and Company, Indianapolis, IN 46206.* Accepted for publication July 28, 1978. §Present address: College of Pharmacy, University of Iowa, Iowa City, IA 52240.

Abstract □ A phytochemical investigation of an ethanolic extract of the whole plant of *Echites hirsuta* (Apocynaceae) resulted in the isolation and identification of the flavonoids naringenin, aromadendrin (dihydrokaempferol), and kaempferol; the coumarin fraxetin; the triterpene ursolic acid; and the sterol glycoside sitosteryl glucoside.

Keyphrases □ *Echites hirsuta*—whole plant ethanolic extract, various flavonoids and sterol glycoside isolated and identified □ Flavonoids, various—isolated and identified in whole plant ethanolic extract of *Echites hirsuta* □ Sitosteryl glucoside—isolated from whole plant ethanolic extract of *Echites hirsuta*

Echites hirsuta (Apocynaceae) (1), also known as *Mandevilla hirsuta* Malme (2), is a woody vine indigenous to the subtropics and tropics (3). Although no medicinal uses have been reported for this genus, the total absence of any phytochemical studies on *Echites* species and the established toxicity of many Apocynaceous plants prompted a phytochemical investigation of this plant.

DISCUSSION

The plant material was extracted by percolation with ethanol to ex-

0022-3549/79/0200-0247$01.00/0
© 1979, American Pharmaceutical Association

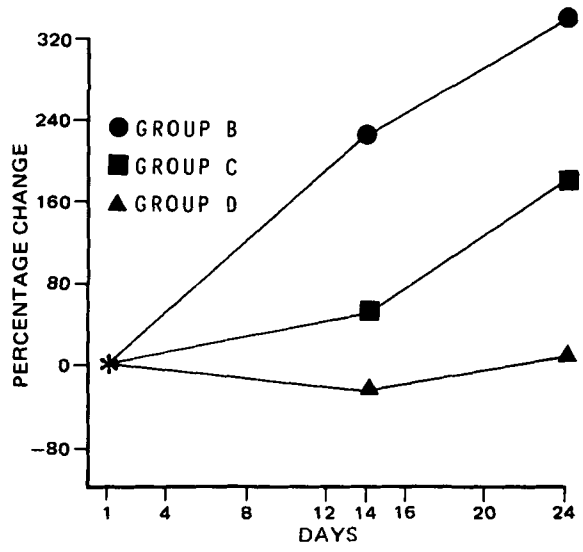

Figure 3—*Percentage change from Group A in mean serum cholesterol of chicks in stigmasterol experiment.*

serum and liver cholesterol values. The coloration of livers closely paralleled the serum cholesterol concentration.

Consistent with the literature (1–3, 7–11), the results of these experiments illustrate the potent antihypercholesterolemic activity of cholestyramine and β-sitosterol. Furthermore, the antihypercholesterolemic activity of these two compounds appears to be of the same order of magnitude, as reported previously (7, 12–14).

Although present in the diet of Groups C and D, neither β-sitosterol nor campesterol (which represents about 40% of the β-sitosterol NF employed) could be detected in the serum. This finding supports the theory that their action is due to their competitive inhibition of cholesterol absorption.

In contrast to the literature (19), the results indicate that stigmasterol, while apparently not exhibiting any deleterious effects, is ineffective as an antihypercholesterolemic agent. It appears, therefore, that unsaturation at C_{22} (the only structural difference between β-sitosterol and stigmasterol) is an undesirable factor in effecting antihypercholesterolemic activity.

REFERENCES

(1) R. I. Levy, D. S. Fredrickson, R. Shulman, D. W. Bilheimer, J. L. Breslow, N. J. Stone, S. E. Lux, H. R. Sloan, R. M. Krauss, and P. N. Herbert, *Ann. Intern. Med.*, **77**, 267 (1972).

(2) R. I. Levy, J. Morganroth, and B. M. Rifkind, *N. Engl. J. Med.*, **290**, 1295 (1974).

(3) *Med. Lett.*, **17**, 49 (1975).

(4) R. S. Lees and D. E. Wilson, *N. Engl. J. Med.*, **284**, 186 (1971).

(5) J. L. Marx, *Science*, **187**, 526 (1975).

(6) The Coronary Drug Project Research Group, *J. Am. Med. Assoc.*, **231**, 360 (1975).

(7) R. I. Levy and B. M. Rifkind, *Drugs*, **6**, 12 (1973).

(8) M. T. R. Subbiah, *Am. J. Clin. Nutr.*, **26**, 219 (1973).

(9) R. Reiser, *ibid.*, **26**, 524 (1973).

(10) M. J. Karvonen, *Practitioner*, **212**, 518 (1974).

(11) N. B. Myant, *ibid.*, **211**, 188 (1973).

(12) O. J. Pollak, *Circulation*, **7**, 702 (1953).

(13) M. M. Best, C. H. Duncan, E. J. Van Loon, and J. D. Wathen, *ibid.*, **10**, 201 (1954).

(14) R. E. Shipley, *Trans. N.Y. Acad. Sci.*, **18**, 111 (1955).

(15) G. A. Braun and J. L. Rabinowitz, in "Topics in Medicinal Chemistry," vol. 3, J. L. Rabinowitz and R. M. Myerson, Eds., Wiley-Interscience, Toronto, Canada, 1970, p. 91.

(16) P. Weiss, *Ration. Drug Ther.*, **6**, 1 (1972).

(17) R. F. Chandler, S. N. Hooper, and H. A. Ismail, *Can. J. Pharm. Sci.*, in press.

(18) S. N. Hooper and R. F. Chandler, *J. Pharm. Sci.*, **67**, 1157 (1978).

(19) D. W. Peterson, E. A. Shneour, N. F. Peek, and H. W. Gaffey, *J. Nutr.*, **50**, 191 (1953).

ACKNOWLEDGMENTS

Presented in part at the Medicinal Chemistry Section, APhA Academy of Pharmaceutical Sciences, Orlando meeting, November 1976.

Supported by Medical Research Council of Canada Grant MA-5424.

The authors thank Dr. J. A. Love, Director, Animal Care Centre, Dalhousie University, for valuable assistance; and Dr. C. A. Field, Mathematics Department, Dalhousie University, for assistance with the statistical components of this project. They also thank Eli Lilly and Co. for supplying the β-sitosterol NF and the cholesterol employed and Mead Johnson Canada for the cholestyramine (Questran).

Chemical Constituents of *Echites hirsuta* (Apocynaceae)

M. M. CHIEN *§, G. H. SVOBODA ‡, P. L. SCHIFF, Jr. *, D. J. SLATKIN *, and J. E. KNAPP *x

Received June 8, 1978, from the **Department of Pharmacognosy, School of Pharmacy, University of Pittsburgh, Pittsburgh, PA 15261*, and the ‡*Lilly Research Laboratories, Eli Lilly and Company, Indianapolis, IN 46206.* Accepted for publication July 28, 1978. §Present address: College of Pharmacy, University of Iowa, Iowa City, IA 52240.

Abstract □ A phytochemical investigation of an ethanolic extract of the whole plant of *Echites hirsuta* (Apocynaceae) resulted in the isolation and identification of the flavonoids naringenin, aromadendrin (dihydrokaempferol), and kaempferol; the coumarin fraxetin; the triterpene ursolic acid; and the sterol glycoside sitosteryl glucoside.

Keyphrases □ *Echites hirsuta*—whole plant ethanolic extract, various flavonoids and sterol glycoside isolated and identified □ Flavonoids, various—isolated and identified in whole plant ethanolic extract of *Echites hirsuta* □ Sitosteryl glucoside—isolated from whole plant ethanolic extract of *Echites hirsuta*

Echites hirsuta (Apocynaceae) (1), also known as *Mandevilla hirsuta* Malme (2), is a woody vine indigenous to the subtropics and tropics (3). Although no medicinal uses have been reported for this genus, the total absence of any phytochemical studies on *Echites* species and the established toxicity of many Apocynaceous plants prompted a phytochemical investigation of this plant.

DISCUSSION

The plant material was extracted by percolation with ethanol to ex-

0022-3549/79/0200-0247$01.00/0
© 1979, American Pharmaceutical Association

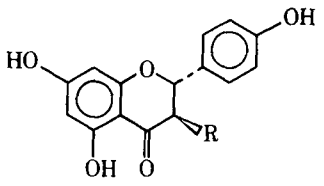

I: R = H
III: R = OH

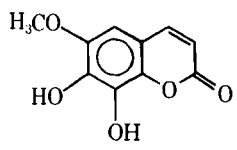

II

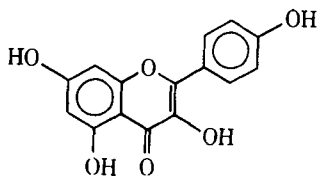

IV

haustion. The ethanol was evaporated under reduced pressure, and the resulting extract was partitioned between chloroform and water. The aqueous layer was further partitioned with ethyl acetate to afford Fractions A (ethyl acetate) and B (water). The chloroform layer was evaporated, and the resulting residue was partitioned between petroleum ether and aqueous methanol to give Fractions C (petroleum ether) and D (aqueous methanol).

Fractions A and D were subsequently combined because of TLC similarities, and the resulting fraction was chromatographed (Column I) over silicic acid. Rechromatography of selected fractions from Column I over silicic acid (Column II) afforded ursolic acid, naringenin (I), fraxetin (II), and sitosteryl glucoside. Further chromatography of selected fractions from Column II yielded aromadendrin (dihydrokaempferol) (III) and kaempferol (IV).

The occurrence of sterols and triterpenes in higher plants is rather common (4); therefore, the isolation of the pentacyclic triterpene ursolic acid and the sterol glycoside sitosteryl glucoside is not unusual. Naringenin (I) is a commonly occurring flavanone (5) in genera of the Rutaceae (6) but also has been found in genera of the Anacardiaceae, Acanthaceae, Balanophoraceae, Compositae, Cruciferae, Fagaceae, Leguminosae, and Myrtaceae (6). However, this paper is the first reported isolation of naringenin from a member of the Apocynaceae. Naringenin may also be obtained by the hydrolysis of the glycoside naringin (naringenin 7-rhamnoglucoside), commonly found in the flowers and fruits of grapefruit and citrus species (6).

Fraxetin (II) is an aglucone of the coumarin glycoside fraxin (8-β-D-glucopyranosyl-7-hydroxy-6-methoxycoumarin), and both are commonly found in species of the genus *Fraxinus* (Oleaceae) (7). This report appears to be the first isolation of fraxetin from a genus of the Apocynaceae. Aromadendrin (III), also known as dihydrokaempferol, is a widely distributed dihydroflavonol (flavanonol), being found in genera of the families Cercidiphyllaceae, Cupressaceae, Ericaceae, Fagaceae, Leguminosae, Moraceae, Myrtaceae, Pinaceae, Platanaceae, Podocarpaceae, and Rosaceae (8). This dihydroflavonol also commonly exists as its 3-*O*-rhamnoside and 7-*O*-glucoside (8). Kaempferol (IV) is a very commonly occurring flavonol, being nearly ubiquitous in woody angiosperms (9) and occurring as glycosides of many kinds.

This paper is the first reported isolation of any constituents from *E. hirsuta* and, apparently, the first reported isolation of naringenin, fraxetin, and aromadendrin from a genus of the family Apocynaceae.

EXPERIMENTAL[1]

Plant Material—The whole plant of *E. hirsuta* (Apocynaceae) was used[2].

Extraction—Air-dried ground whole plant (11 kg) was extracted by percolation with ethanol (55 liters). The extract was evaporated *in vacuo* at 40° and left a dark-green sirupy residue (1.79 kg).

Fractionation—The residue was partitioned between chloroform (5 liters) and water (5 liters). The aqueous layer was further partitioned with ethyl acetate (5 liters), and the solvent was removed from each layer to afford Fractions A (ethyl acetate) (142 g) and B (water) (562 g). The chloroform layer was evaporated to leave a dark residue (787 g), which was further partitioned between petroleum ether (4 liters) and 10% aqueous methanol (4 liters).

The solvent was removed from each layer to afford Fractions C (petroleum ether) (305 g) and D (aqueous methanol) (418 g). TLC on silica gel G[3] using chloroform–ethyl acetate (1:3) showed a very similar chromatographic pattern between Fractions A and D after spraying with vanillin–sulfuric acid reagent (11). Therefore, Fractions A and D were combined for further chromatographic separation.

Chromatography (Column I)—Fractions A and D (560 g) were dissolved in methanol (2 liters), combined, and adsorbed onto silicic acid[4] (100 mesh) (1 kg). The adsorbed mixture was triturated to a fine, dry powder in a mortar and sifted on top of a column of silicic acid[4] (1 kg) (Column I) in petroleum ether. Elution was carried out with petroleum ether, petroleum ether–chloroform mixtures, chloroform, and chloroform–methanol mixtures.

Elution with petroleum ether (4 liters) and petroleum ether–chloroform mixtures (10 liters) afforded lipophilic fractions (192.3 g), which were placed aside. Elution with chloroform (2 liters) and then chloroform–methanol mixtures (99:1, 95:5, 4:1, 7:3, and 1:1) (2 liters each) afforded fractions, which were combined according to TLC similarity [silica gel G[3]; chloroform–ethyl acetate (1:3) and chloroform–methanol (1:1); vanillin–sulfuric acid detecting reagent (10)].

Isolation of Ursolic Acid—Combination of the chloroform through chloroform–methanol (4:1) eluents gave a residue (57.35 g). On treatment with methanol, this residue afforded fine white needles of ursolic acid (230 mg), mp 235° [lit. (11) mp 242° (petroleum ether–methanol)], $[\alpha]_D^{27}$ +73.3° (c 0.3, chloroform) [lit. (11) $[\alpha]_D$ +70° (c 0.4, chloroform)]; IR: ν_{max} (potassium bromide) 3420, 2960, 1700, 1460, and 1040 cm^{-1}; mass spectrum (M^+): *m/e* 456 (4%), 248 (100), 207 (25), 203 (33), and 133 (14). The triterpene was identified as ursolic acid by direct comparison (11) (IR and mass spectra, melting point, mixed melting point, optical rotation, and co-TLC).

Chromatography (Column II)—Combination of the chloroform–methanol 7:3 and 1:1 fractions from Column I gave a residue (310 g). A portion (30 g) of this residue was adsorbed onto silicic acid[4] (67 g) and chromatographed over silicic acid[4] (300 g) in chloroform. Elution with chloroform (5 liters) and chloroform–methanol (95:5) (3 liters) afforded additional ursolic acid (520 mg), while elution with chloroform–methanol (9:1) (1 liter) yielded a residue (5.72 g).

Isolation of Naringenin (I)—Chromatography of this residue over silica gel[3] (100 g) and elution with chloroform–ethyl acetate (1:5) (500 ml) yielded a solid. On treatment with hot methanol, this solid afforded white needles of naringenin (256 mg), mp 260° [lit. (13) mp 255–256°], $[\alpha]_D^{27}$ −15.7° (c 0.7, methanol) [lit. (12) $[\alpha]_D^{20}$ −28.1° (c 1.82, ethanol)]; UV: λ_{max} (methanol) 230 (log ε 3.83), 290 (3.69), and 333 (3.04) nm; IR: ν_{max} (potassium bromide) 3250 (br), 1630, 1605, 1520, 1500, 1460, 1312, 1250, 1182, 1160, 1085, 1065, 1015, 890, 845, and 835 cm^{-1}; mass spectrum (M^+): *m/e* 272 (100%), 179 (30), 166 (30), 153 (100), 124 (11), 119 (12), 107 (19), 91 (13), and 69 (14). This compound was identified as naringenin by direct comparison[5] (UV, IR, and mass spectra, melting point, mixed melting point, optical rotation, and co-TLC).

Isolation of Fraxetin (II)—Continued elution with chloroform–ethyl acetate (1:5) (500 ml) afforded a yellow residue. On crystallization from methanol, this residue gave light-yellow plates of fraxetin (150 mg), mp 240° [lit. (13) mp 228° (ethanol)]; UV: λ_{max} (methanol) 218 (log ε 3.34), 260 (sh) (2.54), and 341 (307) nm; IR: ν_{max} (potassium bromide) 3540 (br), 1690, 1615, 1580, 1510, 1470, 1420, 1325, 1280, 1165, 1120, 1082, 1025, 930, and 835 cm^{-1}; mass spectrum (M^+): *m/e* 208 (100%), 193 (35), 180 (14), 165 (14), 137 (15), 109 (14), and 81 (13). This coumarin was found to be identical to fraxetin[6] by direct comparison (UV, IR, and mass spectra and melting point).

Isolation of Sitosteryl Glucoside—Continued elution of Column II with chloroform–methanol (85:15) (1 liter) gave a light-green residue (7.30

[1] Melting points were taken on a Thomas-Hoover Uni-Melt capillary apparatus and are corrected. IR spectra were determined on a Perkin-Elmer model 257 spectrometer in potassium bromide pellets. UV spectra were obtained on a Perkin-Elmer model 202 recording spectrometer. Optical rotations were measured on a Perkin-Elmer 241 automatic polarimeter. Mass spectra were taken with a LKB-9000 mass spectrometer.

For GLC analysis, an F&M Biomedical gas chromatograph, model 400, was operated isothermally at 255°. The column was 0.31-cm (0.125-in.), 1.84-m (6-ft) stainless steel, packed with 0.8% OV-17 (phenyl methyl silicone) on 80–100-mesh Gas Chrom Q. Helium was the carrier gas at a flow rate of 30 ml/min.

[2] Collected in Trinidad and identified by F. J. Simmonds. A voucher specimen (No. 375-303) is on deposit at Eli Lilly and Co., Indianapolis, IN 46206.

[3] Camag, New Berlin, Wis.

[4] Mallinckrodt Chemical Works, St. Louis, Mo.

[5] K & K Laboratories, Plainview, N.Y.

[6] Professor M. Terazawa, Obihiro University of Agricultural and Veterinary Medicine, Obihiro City, Japan.

g). On treatment with methanol, this residue deposited white granules of sitosteryl glucoside (50 mg), mp 255°. The identity was confirmed by hydrolysis (dilute hydrochloric acid) of the glycoside to afford the aglycone sitosterol, mp 135–137° (methanol) (GLC–mass spectrometry), and glucose (TLC and co-TLC). Finally, a direct comparison with authentic sitosteryl glucoside[7] showed them to be identical (IR spectrum, melting point, mixed melting point, and co-TLC).

Chromatography (Column III)—The mother liquors from the crystallization of naringenin, fraxetin, and sitosteryl glucoside were combined (11.27 g), adsorbed onto silicic acid[4] (30 g), and chromatographed over silicic acid[4] (300 g) in chloroform. Elution with chloroform–methanol (9:1) gave a fraction (3.01 g), which was treated with methanol (100 ml). The methanol-soluble portion (1.69 g) was chromatographed over silica gel[3] (40 g) in chloroform–ethyl acetate (1:3).

Isolation of Aromadendrin (III)—Elution with chloroform–ethyl acetate (1:3) (1 liter) afforded a residue. On treatment with methanol, this residue gave white granules of aromadendrin (dihydrokaempferol) (14 mg), mp 246° [lit. (14) mp 248°], $[\alpha]_D^{27}$ +22.0° (c 0.5, methanol) [lit. (14) $[\alpha]_D^{27}$ +26°]; UV: λ_{max} (methanol) 228 (log ϵ 3.93) and 293 (3.80) nm; IR: ν_{max} (potassium bromide) 1640, 1590, 1518, 1470, 1440, 1410, 1360, 1288, 1255, 1190, 1170, 1128, 1110, 1088, 1022, 995, 958, 935, 865, 850, 835, 810, 760, and 735 cm^{-1}; mass spectrum (M^+): *m/e* 288 (43%), 259 (55), 165 (22), 153 (100), 136 (36), 134 (41), 107 (51), 77 (12), and 69 (18). This compound was identified as aromadendrin (dihydrokaempferol) by direct comparison[8] (UV, IR, and mass spectra, optical rotation, melting point, mixed melting point, and co-TLC).

Isolation of Kaempferol (IV)—Continued elution with chloroform–ethyl acetate (1:3) (1 liter) gave a residue. On treatment with chloroform–methanol, this residue afforded yellow crystals of kaempferol (20 mg), mp 285° [lit. (15) mp 280°]; UV: λ_{max} (methanol) 215 (log ϵ 4.06), 268 (4.00), and 370 (4.09) nm; IR: ν_{max} (potassium bromide) 3320 (br), 1655, 1615, 1570, 1505, 1385, 1320, 1255, 1225, 1175, 1088, 1008, 972, 880, 845, 830, 815, and 795 cm^{-1}; mass spectrum (M^+): *m/e* 286 (100%), 258 (11), 229 (8), 153 (18), 136 (8), 134 (8), 121 (16), 69 (12), and 65 (8). A direct comparison (UV, IR, and mass spectra, melting point, mixed melting point, and co-TLC) with an authentic sample[5] confirmed the identity.

[7] Dr. D. J. Slatkin, Department of Pharmacognosy, School of Pharmacy, University of Pittsburgh, Pittsburgh, PA 15261.
[8] Dr. W. E. Hillis, CSIRO, Melbourne, Australia.

REFERENCES

(1) B. D. Jackson, "Index Kewensis," vol. I, University Press, Oxford, England, 1895, p. 818.
(2) *Ibid.*, Supplement II, 1904, p. 112.
(3) G. H. M. Lawrence, "Taxonomy of Vascular Plants," Macmillan, New York, N.Y., 1951, pp. 672, 673.
(4) T. Robinson, "The Organic Constituents of Higher Plants," 3rd ed., Cordus Press, North Amherst, Mass., 1975, pp. 107–111, 151–157.
(5) J. B. Harborne, T. J. Mabry, and H. Mabry, "The Flavonoids," Academic, London, England, 1975, pp. 573, 574.
(6) *Ibid.*, pp. 564, 600–617.
(7) W. Karrer, "Konstitution und Vorkommen der Organischen Pflanzenstoffe," Birkhäuser Verlag, Basel, Switzerland, 1958, p. 541.
(8) J. B. Harborne, T. J. Mabry, and H. Mabry, "The Flavonoids," Academic, London, England, 1975, pp. 588–590, 600–617.
(9) *Ibid.*, p. 321.
(10) K. Randerath, "Thin-Layer Chromatography," 2nd ed., Academic, New York, N.Y., 1968, p. 132.
(11) J. A. Lopez, D. J. Slatkin, M. Theiner, P. L. Schiff, Jr., and J. E. Knapp, *Phytochemistry*, **13**, 300 (1974).
(12) R. Stevens, "Dictionary of Organic Compounds," 4th ed., 5th and Cumulative Supplement, Oxford University Press, Oxford, England, 1969, p. 677.
(13) T. K. Devon and A. I. Scott, "Naturally Occurring Compounds," vol. I, Academic, New York, N.Y., 1975, p. 65.
(14) *Ibid.*, p. 165.
(15) *Ibid.*, p. 126.

ACKNOWLEDGMENTS

The mass spectrometer facility was supported by Research Grant 5S01RR05455-10 from the National Institutes of Health. The authors are grateful to Mr. John Naworal, Graduate School of Public Health, University of Pittsburgh, for determining the mass spectra; to Professor M. Terazawa, Obihiro University of Agricultural and Veterinary Medicine, Obihiro City, Japan, for UV and IR spectra of fraxetin; and to Dr. W. E. Hillis, CSIRO, Melbourne, Australia, for a sample of aromadendrin.

Fluorescamine Use in High-Performance Liquid Chromatographic Determination of Aminocaproic Acid in Serum

NAGY A. FARID

Received May 15, 1978, from the *Clinical Laboratories, Methodist Hospital of Indiana, Inc., Indianapolis, IN 46202.* Accepted for publication July 13, 1978.

Abstract □ A sensitive and specific high-performance liquid chromatographic determination of aminocaproic acid in serum is described. ω-Aminocaprylic acid is used as an internal standard. To 10 μl of serum, 10 μl of the internal standard solution and 50 μl of ethanol are added. After centrifugation, a portion of the supernate is evaporated. The residue is dissolved in 750 μl of 50 m*M* dibasic sodium phosphate, and then 250 μl of fluorescamine in acetonitrile (35 mg/100 ml) is added. The reaction mixture is chromatographed using a column of octadecylsilane bonded to silica and 44% acetonitrile in 0.5 m*M* phosphoric acid as the eluent. Quantitation is achieved by monitoring either the absorbance of the effluent at 405 nm or the fluorescence of the compounds with a fluorometer equipped with a flowcell. The method is reproducible, simple, and fast and has a precision of 4.4%.

Keyphrases □ Aminocaproic acid—high-performance liquid chromatographic analysis in serum □ High-performance liquid chromatography—analysis, aminocaproic acid in serum □ Hemostatic agents—aminocaproic acid, high-performance liquid chromatographic analysis in serum

Aminocaproic acid[1] (I), an antifibrinolytic agent, inhibits the conversion of plasminogen to plasmin (1, 2). The chemistry, pharmacological properties, and mechanism of action of I were reviewed earlier (3). Several methods for the determination of I in biological fluids were reported (4–14). Most of these methods were either indirect or required a large sample volume and elaborate extraction and purification steps.

[1] Amicar, Lederle, Pearl River, N.Y.

0022-3549/79/0200-0249$01.00/0

© 1979, American Pharmaceutical Association

g). On treatment with methanol, this residue deposited white granules of sitosteryl glucoside (50 mg), mp 255°. The identity was confirmed by hydrolysis (dilute hydrochloric acid) of the glycoside to afford the aglycone sitosterol, mp 135–137° (methanol) (GLC–mass spectrometry), and glucose (TLC and co-TLC). Finally, a direct comparison with authentic sitosteryl glucoside[7] showed them to be identical (IR spectrum, melting point, mixed melting point, and co-TLC).

Chromatography (Column III)—The mother liquors from the crystallization of naringenin, fraxetin, and sitosteryl glucoside were combined (11.27 g), adsorbed onto silicic acid[4] (30 g), and chromatographed over silicic acid[4] (300 g) in chloroform. Elution with chloroform–methanol (9:1) gave a fraction (3.01 g), which was treated with methanol (100 ml). The methanol-soluble portion (1.69 g) was chromatographed over silica gel[3] (40 g) in chloroform–ethyl acetate (1:3).

Isolation of Aromadendrin (III)—Elution with chloroform–ethyl acetate (1:3) (1 liter) afforded a residue. On treatment with methanol, this residue gave white granules of aromadendrin (dihydrokaempferol) (14 mg), mp 246° [lit. (14) mp 248°], $[\alpha]_D^{27}$ +22.0° (c 0.5, methanol) [lit. (14) $[\alpha]_D^{27}$ +26°]; UV: λ_{max} (methanol) 228 (log ϵ 3.93) and 293 (3.80) nm; IR: ν_{max} (potassium bromide) 1640, 1590, 1518, 1470, 1440, 1410, 1360, 1288, 1255, 1190, 1170, 1128, 1110, 1088, 1022, 995, 958, 935, 865, 850, 835, 810, 760, and 735 cm^{-1}; mass spectrum (M^+): *m/e* 288 (43%), 259 (55), 165 (22), 153 (100), 136 (36), 134 (41), 107 (51), 77 (12), and 69 (18). This compound was identified as aromadendrin (dihydrokaempferol) by direct comparison[8] (UV, IR, and mass spectra, optical rotation, melting point, mixed melting point, and co-TLC).

Isolation of Kaempferol (IV)—Continued elution with chloroform–ethyl acetate (1:3) (1 liter) gave a residue. On treatment with chloroform–methanol, this residue afforded yellow crystals of kaempferol (20 mg), mp 285° [lit. (15) mp 280°]; UV: λ_{max} (methanol) 215 (log ϵ 4.06), 268 (4.00), and 370 (4.09) nm; IR: ν_{max} (potassium bromide) 3320 (br), 1655, 1615, 1570, 1505, 1385, 1320, 1255, 1225, 1175, 1088, 1008, 972, 880, 845, 830, 815, and 795 cm^{-1}; mass spectrum (M^+): *m/e* 286 (100%), 258 (11), 229 (8), 153 (18), 136 (8), 134 (8), 121 (16), 69 (12), and 65 (8). A direct comparison (UV, IR, and mass spectra, melting point, mixed melting point, and co-TLC) with an authentic sample[5] confirmed the identity.

[7] Dr. D. J. Slatkin, Department of Pharmacognosy, School of Pharmacy, University of Pittsburgh, Pittsburgh, PA 15261.
[8] Dr. W. E. Hillis, CSIRO, Melbourne, Australia.

REFERENCES

(1) B. D. Jackson, "Index Kewensis," vol. I, University Press, Oxford, England, 1895, p. 818.
(2) *Ibid.*, Supplement II, 1904, p. 112.
(3) G. H. M. Lawrence, "Taxonomy of Vascular Plants," Macmillan, New York, N.Y., 1951, pp. 672, 673.
(4) T. Robinson, "The Organic Constituents of Higher Plants," 3rd ed., Cordus Press, North Amherst, Mass., 1975, pp. 107–111, 151–157.
(5) J. B. Harborne, T. J. Mabry, and H. Mabry, "The Flavonoids," Academic, London, England, 1975, pp. 573, 574.
(6) *Ibid.*, pp. 564, 600–617.
(7) W. Karrer, "Konstitution und Vorkommen der Organischen Pflanzenstoffe," Birkhäuser Verlag, Basel, Switzerland, 1958, p. 541.
(8) J. B. Harborne, T. J. Mabry, and H. Mabry, "The Flavonoids," Academic, London, England, 1975, pp. 588–590, 600–617.
(9) *Ibid.*, p. 321.
(10) K. Randerath, "Thin-Layer Chromatography," 2nd ed., Academic, New York, N.Y., 1968, p. 132.
(11) J. A. Lopez, D. J. Slatkin, M. Theiner, P. L. Schiff, Jr., and J. E. Knapp, *Phytochemistry*, **13**, 300 (1974).
(12) R. Stevens, "Dictionary of Organic Compounds," 4th ed., 5th and Cumulative Supplement, Oxford University Press, Oxford, England, 1969, p. 677.
(13) T. K. Devon and A. I. Scott, "Naturally Occurring Compounds," vol. I, Academic, New York, N.Y., 1975, p. 65.
(14) *Ibid.*, p. 165.
(15) *Ibid.*, p. 126.

ACKNOWLEDGMENTS

The mass spectrometer facility was supported by Research Grant 5S01RR05455-10 from the National Institutes of Health. The authors are grateful to Mr. John Naworal, Graduate School of Public Health, University of Pittsburgh, for determining the mass spectra; to Professor M. Terazawa, Obihiro University of Agricultural and Veterinary Medicine, Obihiro City, Japan, for UV and IR spectra of fraxetin; and to Dr. W. E. Hillis, CSIRO, Melbourne, Australia, for a sample of aromadendrin.

Fluorescamine Use in High-Performance Liquid Chromatographic Determination of Aminocaproic Acid in Serum

NAGY A. FARID

Received May 15, 1978, from the *Clinical Laboratories, Methodist Hospital of Indiana, Inc., Indianapolis, IN 46202.* Accepted for publication July 13, 1978.

Abstract □ A sensitive and specific high-performance liquid chromatographic determination of aminocaproic acid in serum is described. ω-Aminocaprylic acid is used as an internal standard. To 10 μl of serum, 10 μl of the internal standard solution and 50 μl of ethanol are added. After centrifugation, a portion of the supernate is evaporated. The residue is dissolved in 750 μl of 50 m*M* dibasic sodium phosphate, and then 250 μl of fluorescamine in acetonitrile (35 mg/100 ml) is added. The reaction mixture is chromatographed using a column of octadecylsilane bonded to silica and 44% acetonitrile in 0.5 m*M* phosphoric acid as the eluent. Quantitation is achieved by monitoring either the absorbance of the effluent at 405 nm or the fluorescence of the compounds with a fluorometer equipped with a flowcell. The method is reproducible, simple, and fast and has a precision of 4.4%.

Keyphrases □ Aminocaproic acid—high-performance liquid chromatographic analysis in serum □ High-performance liquid chromatography—analysis, aminocaproic acid in serum □ Hemostatic agents—aminocaproic acid, high-performance liquid chromatographic analysis in serum

Aminocaproic acid[1] (I), an antifibrinolytic agent, inhibits the conversion of plasminogen to plasmin (1, 2). The chemistry, pharmacological properties, and mechanism of action of I were reviewed earlier (3). Several methods for the determination of I in biological fluids were reported (4–14). Most of these methods were either indirect or required a large sample volume and elaborate extraction and purification steps.

[1] Amicar, Lederle, Pearl River, N.Y.

0022-3549/79/0200-0249$01.00/0

© 1979, American Pharmaceutical Association

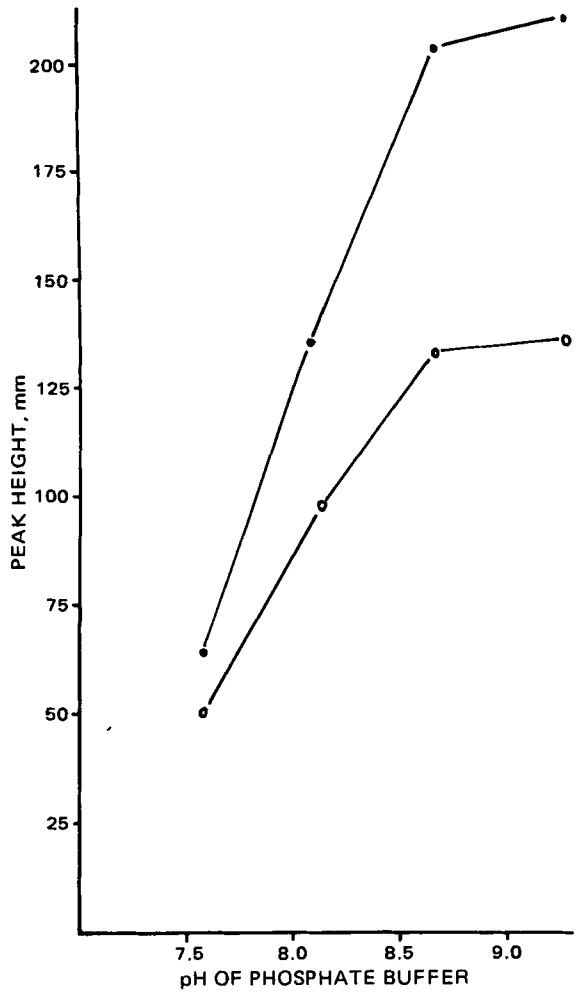

Figure 1—*Effect of change in the pH of phosphate buffer, used in the derivatization of aminocaproic acid (●) and ω-aminocaprylic acid (○) with fluorescamine, on resultant peak heights.*

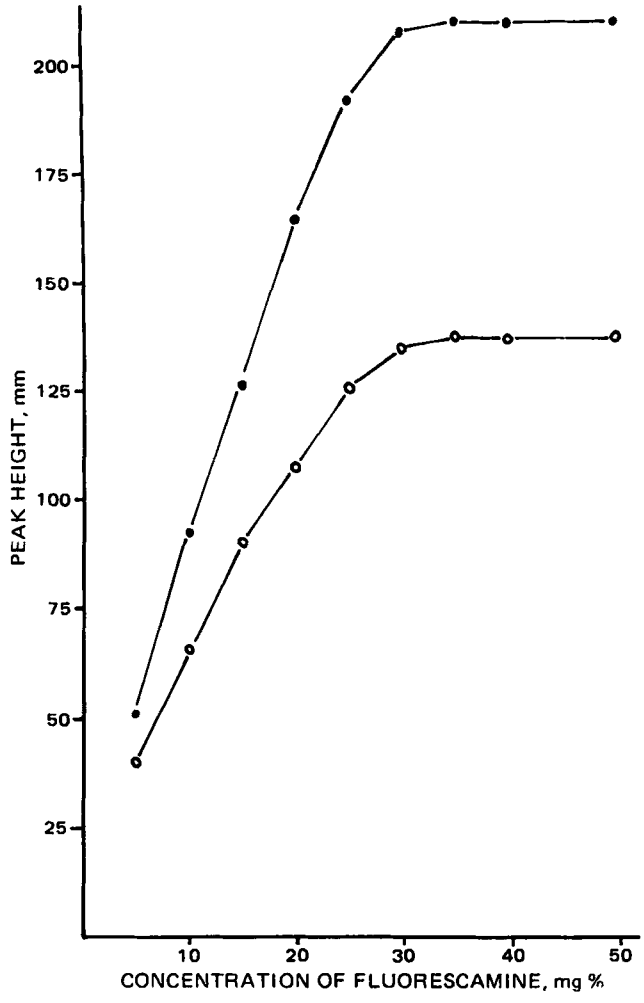

Figure 2—*Effect of change in the concentration of fluorescamine, used in the derivatization of aminocaproic acid (●) and ω-aminocaprylic acid (○), on resultant peak heights.*

Two high-performance liquid chromatographic (HPLC) methods for I in physiological fluids were reported (15, 16). One method (15) utilized postcolumn derivatization of I with ninhydrin and required 2 hr/sample. The fluorometric determination of dansylated I by HPLC (16) required heating for the derivatization reaction and heating of the column to 60°, which is inconvenient in a clinical laboratory.

Fluorescamine[2], a nonfluorescent compound, reacts very rapidly with primary amines to form highly fluorescent pyrrolinone derivatives. While fluorescamine reacts with other nucleophilic functional groups, only primary amines form fluorescent products. These fluorescent derivatives exhibit an absorption maximum at 390 nm and a fluorescence maximum at 475 nm (17). The use of fluorescamine for the formation of fluorescent derivatives of peptides and amines and its use in chromatography were reviewed recently (18). Only three preliminary publications dealt with the HPLC separation of fluorophores formed using fluorescamine. Two reports (19, 20) discussed the separation of the fluorescamine derivatives of dopamine and norepinephrine. The third article (21) was on the separation of some aliphatic diamines.

[2] Fluram, Hoffmann-La Roche, Nutley, N.J.

The need for a rapid, simple, and accurate procedure for the routine determination of I in biological samples and the favorable properties of the reaction of primary amines with fluorescamine led to the present study. The preparation of the fluorescamine derivative of I and the elution and quantitation of the fluorophore by HPLC are described.

EXPERIMENTAL

Apparatus—A modular liquid chromatograph was equipped with an injector[3], a pump[4], a single-wavelength (405-nm) absorbance detector[5], and a filter fluorometer[6]. The fluorometer had a primary filter[7], a secondary filter[8], and a quartz flowcell. The stainless steel column, 3.9 mm i.d. × 300 mm, was packed with octadecylsilane bonded to 10-μm silica[9]. A stainless steel precolumn, 2.1 mm i.d. × 75 mm, contained octadecylsilane bonded to pellicular silica[10].

Reagents—Dibasic sodium phosphate, monobasic potassium phosphate, and phosphoric acid were reagent grade. Acetonitrile was distilled in glass[11].

Fluorescamine Solution—Fluorescamine, 35 mg, was dissolved in

[3] Model U6K, Waters Associates, Milford, Mass.
[4] Model 6000A, Waters Associates, Milford, Mass.
[5] Model 440, Waters Associates, Milford, Mass.
[6] Fluoro-Monitor analyzer, American Instrument Co., Silver Spring, Md.
[7] Corning No. 7-51.
[8] Wratten No. 8.
[9] μBondapak C_{18}, Waters Associates, Milford, Mass.
[10] Co:Pell-ODS, Whatman Inc., Clifton, N.J.
[11] Burdick & Jackson Laboratories, Muskegon, Mich.

Table I—Comparison of Serum Aminocaproic Acid Levels of Patients Determined by HPLC and GLC

Patient[a]	Level, mg/liter HPLC[b]	GLC[c]	Patient[d]	Level, mg/liter HPLC[e]	HPLC[b]
1	84	84	16	ND[f]	ND
2	99	95	17	43	42
3	106	106	18	84	81
4	133	113	19	107	97
5	143	143	20	210	195
6	158	142	21	244	235
7	203	195	22	283	283
8	208	202	23	379	379
9	218	214	24	381	381
10	227	231	25	381	390
11	249	225	26	389	403
12	258	256			
13	263	272			
14	333	356			
15	550	554			

[a] For Patients 1–15 (n = 15), slope = 1.04, r = 0.996, and intercept = −10.7. [b] Using absorbance detector, 405 nm. See text for details. [c] Analyzed by the method of Keucher *et al.* (14). [d] For Patients 16–26 (n = 11), slope = 1.03, r = 0.999, and intercept = −7.1. [e] Using fluorescence detector. See text for details. [f] None detected.

100 ml of acetonitrile. Other concentrations of fluorescamine needed to study the derivatization conditions also were prepared in acetonitrile.

Internal Standard Solution—ω-Aminocaprylic acid[12] (II), 40 mg, was dissolved in 100 ml of water.

Reference Standards—Individual solutions containing 5, 10, 20, 40, and 60 mg of I[12] in 100 ml of water were prepared. Similar concentrations of I in human serum also were prepared.

Procedure—The internal standard solution, 10 μl, was added to 10 μl of serum followed by 50 μl of ethanol. The contents were mixed and centrifuged. A portion of the supernate was transferred to another tube and evaporated under nitrogen at room temperature. The residue was dissolved in 750 μl of 0.05 *M* Na_2HPO_4 (pH 9.3), and 250 μl of the fluorescamine solution was added with mixing.

Chromatographic Conditions—The column temperature was ambient. The mobile phase consisted of 44% acetonitrile in 0.5 m*M* H_3PO_4. The flow rate was 1.8 ml/min. The volume of sample injected was 10–25 μl. The absorbance of the eluted fluorophores was measured at 405 nm with the electrometer set at 0.005 aufs. The fluorescence of the fluorophores was measured using the fluorometer with the relative intensity scale set at 0–10.

RESULTS AND DISCUSSION

Various factors affecting the elution profile were studied. The composition and molarity of the eluting solvent were established first. The optimum concentration of fluorescamine and the pH of the phosphate buffer used in the derivatization of I and II also were determined. These determinations were achieved by injecting equal volumes of solutions containing identical concentrations of I and II prepared under various conditions and then measuring the corresponding peak heights (Figs. 1 and 2). Accordingly, the conditions detailed under *Experimental* for the preparation and elution of the fluorophores were chosen. Under these conditions, the retention times for I and II were 5.0 and 7.8 min, respectively. The fluorophores were stable for several hours. Figure 3 shows typical chromatograms obtained using the absorbance and fluorescence detectors from serum of two patients receiving I and two that did not.

Recovery of known concentrations of I in serum ranging from 50 to 600 mg/liter was studied by using II as a reference standard and comparing peak height ratios to those obtained with aqueous standards of I. The recovery for the concentration range specified was 98.4 ± 2.3% (mean ± *SD*) with a range of 95.1–101.6%.

Triplicate 10-μl samples of serum standards containing 50–600 mg of I/liter were analyzed. The relationship between the concentration of I and the peak height ratio of I to II was linear by either detection method. As little as 10 pg of I injected onto the column could be detected by the fluorescence detector whereas the detection limit for the absorbance detector was 3 ng.

To determine the precision of the method, 20 mg of I was dissolved in 50 ml of serum, divided in small portions, and frozen. Seven analysts

[12] Sigma Chemical Co., St. Louis, Mo.

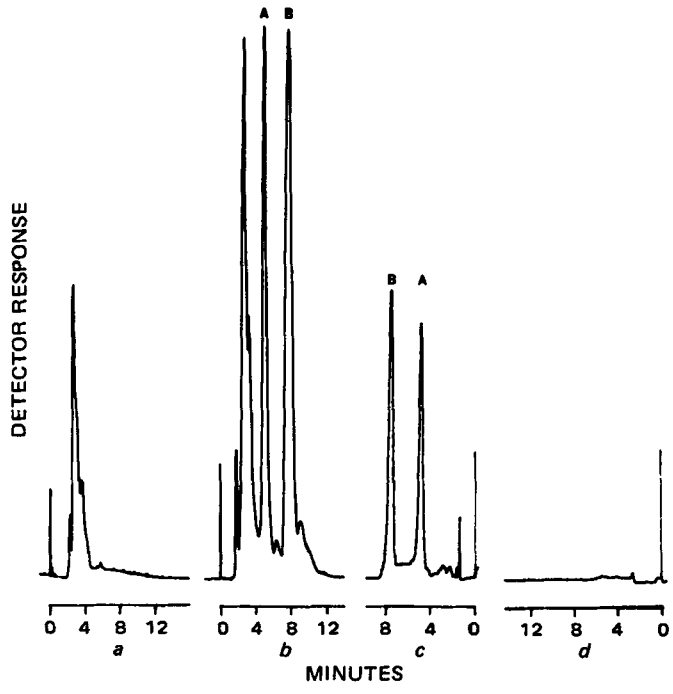

Figure 3—*Chromatograms of serum samples from patients receiving aminocaproic acid (b and c) and patients that were not (a and d), using fluorescence (a and b) and absorbance (c and d) detection systems. Key: A, aminocaproic acid; and B, ω-aminocaprylic acid.*

analyzed 10-μl aliquots of this solution over 75 days. The mean (±*SD*) was 404.3 ± 17.8 mg/liter. This result shows a day-to-day precision of 4.4%. The within-day variation was determined by analyzing one sample five times. The mean was 403.6 ± 4.4 mg/liter.

Fifteen clinical samples were analyzed for I as already detailed and by the method of Keucher *et al.* (14). The results (Table I) indicate an excellent correlation between the two methods. A comparison between the absorbance and fluorescence detectors of the HPLC procedure showed an equally good correlation (Table I).

Serum samples containing several drugs (phenobarbital, phenytoin, ethosuximide, methsuximide, phensuximide, primidone, and theophylline) were analyzed by this procedure to check for possible interference. None of these compounds was detected with either the absorbance or fluorescence detector.

The proposed method for the analysis of I in serum is rapid, sensitive, and easily applied to routine therapeutic monitoring for patients. Five samples of serum can be analyzed in 1 hr. As expected, fluorescence detection is more sensitive than absorbance detection. However, the results indicate that either method could be used satisfactorily in the clinical laboratory.

REFERENCES

(1) N. Alkjaersig, A. P. Fletcher, and S. Sherry, *J. Biol. Chem.*, **234**, 832 (1959).

(2) F. B. Ablondi, J. J. Hagan, M. Philips, and E. C. deRenzo, *Arch. Biochem.*, **82**, 153 (1959).

(3) W. M. Sweeney, *Am. J. Med. Sci.*, **249**, 576 (1965).

(4) A. Sjoerdsma and E. A. Hanson, *Acta Chem. Scand.*, **13**, 2150 (1959).

(5) G. P. McNichol, A. P. Fletcher, N. Alkjaersig, and S. Sherry, *J. Clin. Lab. Med.*, **59**, 7 (1962).

(6) *Ibid.*, **59**, 15 (1962).

(7) Y. Takada, A. Takada, and U. Okamoto, *Keio J. Med.*, **13**, 115 (1964).

(8) N. Wolosowicz, S. Niewiarowski, and K. Czerepko, *Thromb. Diath. Haemorrh.*, **10**, 309 (1964).

(9) N. Wolosowicz and S. Niewiarowski, *Clin. Chim. Acta*, **12**, 555 (1965).

(10) N. Ikekawa, O. Hoshino, R. Watanuki, H. Orimo, T. Fujita, and M. Yoshikawa, *Anal. Biochem.*, **17**, 16 (1966).

(11) F. Markwardt, H. P. Klöcking, and M. Richter, *Pharmazie*, **22**, 83 (1967).

(12) R. W. Zumwalt, K. C. Kuo, and C. W. Gehrke, *J. Chromatogr.*, **55**, 267 (1971).
(13) C. W. Gehrke, K. C. Kuo, and R. W. Zumwalt, *ibid.*, **57**, 209 (1971).
(14) T. R. Keucher, E. B. Solow, J. Metaxas, and R. L. Campbell, *Clin. Chem.*, **22**, 806 (1976).
(15) J. A. Shepherd, D. W. Nibbelink, and L. D. Stegink, *J. Chromatogr.*, **86**, 173 (1973).
(16) R. F. Adams, G. J. Schmidt, and F. L. Vandemark, *Clin. Chem.*, **23**, 1226 (1977).
(17) S. deBernardo, M. Weigele, V. Toome, K. Manhart, W. Leimgruber, P. Böhlen, S. Stein, and S. Udenfriend, *Arch. Biochem. Biophys.*, **163**, 390 (1974).
(18) N. Seiler and L. Demisch, in "Handbook of Derivatives for Chromatography," K. Blau and G. S. King, Eds., Heyden & Sons, Bellmawr, N.J., 1977, pp. 372–376.
(19) K. Imai, *J. Chromatogr.*, **105**, 135 (1975).
(20) G. Schwedt, *ibid.*, **118**, 429 (1976).
(21) K. Samejima, *ibid.*, **96**, 250 (1974).

ACKNOWLEDGMENTS

Presented in part at the APhA Academy of Pharmaceutical Sciences, Montreal meeting, May 1978.

The author thanks Dr. J. R. Mackenzie, Director of the Clinical Laboratories, for his interest and helpful discussions and Mrs. E. B. Solow, Division of Neurological Surgery, Indiana University School of Medicine, for performing the GLC assays.

Theophylline Protein Binding in Humans

K. J. SIMONS *, F. E. R. SIMONS ‡x, C. J. BRIGGS *, and L. LO *

Received May 2, 1978, from the **Faculty of Pharmacy and the* ‡*Section of Allergy and Clinical Immunology, Department of Pediatrics, Faculty of Medicine, University of Manitoba, Winnipeg, Manitoba, Canada R3T 2N2.* Accepted for publication August 1, 1978.

Abstract □ Theophylline protein binding was 58–82% in serum from six normal adults and 42 asthmatic patients, 1–25 years old, who were given 5 mg of theophylline/kg. The binding range was greatest in young patients, but the proportion of protein-bound drug did not correlate with age. Theophylline protein binding was higher than previously reported. The effect of binding should be considered in patients who do not have optimal bronchodilation from theophylline despite total serum theophylline concentrations of 10–20 μg/ml.

Keyphrases □ Theophylline—protein binding in humans □ Protein binding—theophylline in humans □ Relaxants, smooth muscle—theophylline, protein binding in humans

Drug-protein interactions may influence drug distribution, metabolism, and excretion (1). The extent of theophylline binding to plasma proteins is said to be negligible (2) and is not usually considered when theophylline clearance rates are calculated or when total serum theophylline concentrations are measured.

In this study, theophylline protein binding was measured in serum samples from normal adults and patients with asthma.

EXPERIMENTAL

After informed consent was obtained, six normal adult volunteers not previously treated with theophylline and 42 patients with asthma, 1–25 years old, who had received long-term treatment with theophylline, were given 5 mg/kg po of the drug[1]. Venipuncture was performed 2 hr later. Serum was separated and frozen at −10° for up to 1 month.

Protein binding studies were carried out at room temperature (22°). Serum, 2 ml, was placed in each membrane cone[2]. The cones were centrifuged three times at 1500 rpm for 8–10 min to produce 100 μl of filtrate each time. Theophylline concentrations in the last two ultrafiltrate samples and in an aliquot of retentate were measured by high-performance liquid chromatography[3] (HPLC) (3).

[1] Quibron Elixir, Mead Johnson Canada, Candiac, Quebec, Canada.
[2] Amicon Centriflo cones (CF50), Amicon Corp., Lexington, MA 02173.
[3] Model 8500, Varian Instrument Division, Palo Alto, CA 94303.

Table I—Serum Theophylline Concentrations and Protein Binding Values

Subjects Age, years	*n*	Serum Theophylline Concentration ± *SD*, μg/ml	Theophylline Protein Binding ± *SD*, %	Range, %
Asthmatics, 1–5	10	9.9 ± 4.4	72.1 ± 7.9	58–82
Asthmatics, 6–11	16	9.0 ± 5.2	70.3 ± 4.0	64–76
Asthmatics, 12–25	16	13.4 ± 3.2	70.3 ± 3.2	65–74
Normal adult volunteers, 26–37	6	13.3 ± 2.2	71.8 ± 5.9	66–79

The extent of theophylline protein binding was calculated using:

$$\beta = \frac{D_b}{D_t} = \frac{D_t - D_f}{D_t} \qquad \text{(Eq. 1)}$$

where β represents the fraction of total drug bound to protein, D_b is the amount of drug bound, D_f is the amount of free drug (protein-free filtrate), and D_t is the total amount of drug present (bound plus free). Drug binding was expressed as β%. No corrections for volume change or membrane adsorption were required.

RESULTS AND DISCUSSION

Serum theophylline concentrations and theophylline protein binding values are summarized in Table I. Theophylline protein binding was similar in patients with asthma and in normal adults. The range of binding was greatest in young children, but the proportion of protein-bound drug did not correlate with age.

Previously reported theophylline protein binding values are summarized in Table II. Theophylline was 42–69% bound in plasma from normal adults and in serum from asthmatic mothers who had ingested the drug (4, 5). A similar range was found when theophylline was added to plasma from normal adults who had not received the drug (6). The extent of binding found in both normal adults and patients in the present study was higher, being 58–82%. This result may be due to the various methods of measuring protein binding and theophylline and because either serum or plasma was used, both from dosed patients and from subjects to whose serum drug was added *in vitro* (4–6).

Protein binding has been assumed to be insignificant as far as theophylline distribution, metabolism, and excretion are concerned. Jenne

0022-3549/79/0200-0252$01.00/0
© 1979, American Pharmaceutical Association

(12) R. W. Zumwalt, K. C. Kuo, and C. W. Gehrke, *J. Chromatogr.*, **55**, 267 (1971).
(13) C. W. Gehrke, K. C. Kuo, and R. W. Zumwalt, *ibid.*, **57**, 209 (1971).
(14) T. R. Keucher, E. B. Solow, J. Metaxas, and R. L. Campbell, *Clin. Chem.*, **22**, 806 (1976).
(15) J. A. Shepherd, D. W. Nibbelink, and L. D. Stegink, *J. Chromatogr.*, **86**, 173 (1973).
(16) R. F. Adams, G. J. Schmidt, and F. L. Vandemark, *Clin. Chem.*, **23**, 1226 (1977).
(17) S. deBernardo, M. Weigele, V. Toome, K. Manhart, W. Leimgruber, P. Böhlen, S. Stein, and S. Udenfriend, *Arch. Biochem. Biophys.*, **163**, 390 (1974).
(18) N. Seiler and L. Demisch, in "Handbook of Derivatives for Chromatography," K. Blau and G. S. King, Eds., Heyden & Sons, Bellmawr, N.J., 1977, pp. 372–376.
(19) K. Imai, *J. Chromatogr.*, **105**, 135 (1975).
(20) G. Schwedt, *ibid.*, **118**, 429 (1976).
(21) K. Samejima, *ibid.*, **96**, 250 (1974).

ACKNOWLEDGMENTS

Presented in part at the APhA Academy of Pharmaceutical Sciences, Montreal meeting, May 1978.

The author thanks Dr. J. R. Mackenzie, Director of the Clinical Laboratories, for his interest and helpful discussions and Mrs. E. B. Solow, Division of Neurological Surgery, Indiana University School of Medicine, for performing the GLC assays.

Theophylline Protein Binding in Humans

K. J. SIMONS *, F. E. R. SIMONS ‡x, C. J. BRIGGS *, and L. LO *

Received May 2, 1978, from the **Faculty of Pharmacy and the* ‡*Section of Allergy and Clinical Immunology, Department of Pediatrics, Faculty of Medicine, University of Manitoba, Winnipeg, Manitoba, Canada R3T 2N2.* Accepted for publication August 1, 1978.

Abstract □ Theophylline protein binding was 58–82% in serum from six normal adults and 42 asthmatic patients, 1–25 years old, who were given 5 mg of theophylline/kg. The binding range was greatest in young patients, but the proportion of protein-bound drug did not correlate with age. Theophylline protein binding was higher than previously reported. The effect of binding should be considered in patients who do not have optimal bronchodilation from theophylline despite total serum theophylline concentrations of 10–20 μg/ml.

Keyphrases □ Theophylline—protein binding in humans □ Protein binding—theophylline in humans □ Relaxants, smooth muscle—theophylline, protein binding in humans

Drug-protein interactions may influence drug distribution, metabolism, and excretion (1). The extent of theophylline binding to plasma proteins is said to be negligible (2) and is not usually considered when theophylline clearance rates are calculated or when total serum theophylline concentrations are measured.

In this study, theophylline protein binding was measured in serum samples from normal adults and patients with asthma.

EXPERIMENTAL

After informed consent was obtained, six normal adult volunteers not previously treated with theophylline and 42 patients with asthma, 1–25 years old, who had received long-term treatment with theophylline, were given 5 mg/kg po of the drug[1]. Venipuncture was performed 2 hr later. Serum was separated and frozen at −10° for up to 1 month.

Protein binding studies were carried out at room temperature (22°). Serum, 2 ml, was placed in each membrane cone[2]. The cones were centrifuged three times at 1500 rpm for 8–10 min to produce 100 μl of filtrate each time. Theophylline concentrations in the last two ultrafiltrate samples and in an aliquot of retentate were measured by high-performance liquid chromatography[3] (HPLC) (3).

[1] Quibron Elixir, Mead Johnson Canada, Candiac, Quebec, Canada.
[2] Amicon Centriflo cones (CF50), Amicon Corp., Lexington, MA 02173.
[3] Model 8500, Varian Instrument Division, Palo Alto, CA 94303.

Table I—Serum Theophylline Concentrations and Protein Binding Values

Subjects Age, years	*n*	Serum Theophylline Concentration ± *SD*, μg/ml	Theophylline Protein Binding ± *SD*, %	Range, %
Asthmatics, 1–5	10	9.9 ± 4.4	72.1 ± 7.9	58–82
Asthmatics, 6–11	16	9.0 ± 5.2	70.3 ± 4.0	64–76
Asthmatics, 12–25	16	13.4 ± 3.2	70.3 ± 3.2	65–74
Normal adult volunteers, 26–37	6	13.3 ± 2.2	71.8 ± 5.9	66–79

The extent of theophylline protein binding was calculated using:

$$\beta = \frac{D_b}{D_t} = \frac{D_t - D_f}{D_t} \qquad \text{(Eq. 1)}$$

where β represents the fraction of total drug bound to protein, D_b is the amount of drug bound, D_f is the amount of free drug (protein-free filtrate), and D_t is the total amount of drug present (bound plus free). Drug binding was expressed as β%. No corrections for volume change or membrane adsorption were required.

RESULTS AND DISCUSSION

Serum theophylline concentrations and theophylline protein binding values are summarized in Table I. Theophylline protein binding was similar in patients with asthma and in normal adults. The range of binding was greatest in young children, but the proportion of protein-bound drug did not correlate with age.

Previously reported theophylline protein binding values are summarized in Table II. Theophylline was 42–69% bound in plasma from normal adults and in serum from asthmatic mothers who had ingested the drug (4, 5). A similar range was found when theophylline was added to plasma from normal adults who had not received the drug (6). The extent of binding found in both normal adults and patients in the present study was higher, being 58–82%. This result may be due to the various methods of measuring protein binding and theophylline and because either serum or plasma was used, both from dosed patients and from subjects to whose serum drug was added *in vitro* (4–6).

Protein binding has been assumed to be insignificant as far as theophylline distribution, metabolism, and excretion are concerned. Jenne

0022-3549/79/0200-0252$01.00/0
© 1979, American Pharmaceutical Association

Table II—Summary of Theophylline Protein Binding Studies

Source	n	Procedure	Assay	Percent Bound	Reference
Rabbit plasma	—	Equilibrium dialysis: cellophane membrane	UV spectrophotometry	5–10	11
Bovine serum albumin (2%) solutions	—	Equilibrium dialysis: cellophane membrane	UV spectrophotometry	20	7
Plasma of normal dosed volunteers	7	Equilibrium dialysis: cellophane membrane	UV spectrophotometry	59 ± 3	4
Serum from dosed nursing mothers	4	Ultrafiltration: cellophane membrane	HPLC	42–69	5
"Spiked" normal adult plasma	21	Ultrafiltration: membrane cones[a]	LSC[b]	56.4 ± 3.8	6
"Spiked" cord plasma of full-term infants	21	Ultrafiltration: membrane cones[a]	LSC	36.4 ± 3.8	6
"Spiked" plasma of cirrhotic patients	4	Ultrafiltration: membrane cones[a]	LSC	32.3–40.2	8

[a] Amicon Centriflo cones (CF-50), Amicon Corp., Lexington, MA 02173. [b] LSC = liquid scintillation counting of ^{14}C-theophylline.

et al. (2) concluded that, since only 20% theophylline was protein bound (7), binding need not be considered when the volume of distribution was measured. However, Aranda *et al.* (6) reported decreased binding, which might be important when determining effective serum theophylline concentrations in premature infants with apnea. Piafsky *et al.* (8) found reduced binding in cirrhotic patients but did not determine if greater availability of free drug in the liver increased plasma clearance. In the present study, theophylline protein binding did not increase with age. Therefore, it is unlikely that it contributes to the decreased clearance rates found in older patients (9, 10).

Considerable variation in unbound serum theophylline could be possible in patients, based on the 29% range of protein binding found in this study. The effect of binding should possibly be considered in patients who do not have optimal bronchodilation from theophylline despite total serum theophylline concentrations of 10–20 μg/ml.

REFERENCES

(1) J. J. Vallner, *J. Pharm. Sci.*, **66**, 447 (1977).

(2) J. W. Jenne, E. Wyze, F. S. Rood, and F. M. MacDonald, *Clin. Pharmacol. Ther.*, **13**, 349 (1972).

(3) D. S. Sitar, K. M. Piafsky, R. E. Rangno, and R. I. Ogilvie, *Clin. Chem.*, **21**, 1774 (1975).

(4) R. Koysooko, E. F. Ellis, and G. Levy, *Clin. Pharmacol. Ther.*, **15**, 454 (1974).

(5) A. M. Yurchak and W. J. Jusko, *Pediatrics*, **53**, 518 (1976).

(6) J. V. Aranda, D. S. Sitar, W. D. Parsons, P. M. Loughnan, and A. H. Neims, *N. Engl. J. Med.*, **295**, 413 (1976).

(7) M. L. Eichman, D. E. Guttman, Q. van Winkle, and E. P. Guth, *J. Pharm. Sci.*, **51**, 66 (1962).

(8) K. M. Piafsky, D. S. Sitar, R. E. Rangno, and R. I. Ogilvie, *N. Engl. J. Med.*, **296**, 1495 (1977).

(9) E. F. Ellis, R. Koysooko, and G. Levy, *Pediatrics*, **58**, 542 (1976).

(10) E. Ginchansky and M. Weinberger, *J. Pediatr.*, **91**, 655 (1977).

(11) J. A. Shack and S. H. Waxler, *J. Pharmacol. Exp. Ther.*, **97**, 283 (1949).

ACKNOWLEDGMENTS

Supported by a grant from The Children's Hospital of Winnipeg Research Foundation, Inc.

F. E. R. Simons is a Queen Elizabeth II Scientist. L. Lo was the recipient of a Medical Research Council Summer Studentship.

Liquid Chromatography in Pharmaceutical Analysis X: Determination of Chlorzoxazone and Hydroxy Metabolite in Plasma

I. L. HONIGBERG ˣ, J. T. STEWART, and J. W. COLDREN

Received September 13, 1977, from the *Department of Medicinal Chemistry, School of Pharmacy, University of Georgia, Athens, GA 30602.* Accepted for publication July 26, 1978.

Abstract □ A method for the high-pressure liquid chromatographic determination of chlorzoxazone and its hydroxy metabolite in human plasma samples is presented. The separation of the compounds is achieved on an octadecylsilane column with a mobile phase of absolute methanol–distilled water (40:60) at a flow rate of 2.0 ml/min (3100 psig). The chromatographic separation is achieved within 10 min. The overall analysis time is about 45 min, which includes extraction of the drug and metabolite from plasma followed by high-pressure liquid chromatographic separation and quantification. The accuracy of the procedure is in the 1–5% range.

Keyphrases □ Chlorzoxazone and hydroxy metabolite—high-pressure liquid chromatographic analysis in plasma □ High-pressure liquid chromatography—analysis, chlorzoxazone and hydroxy metabolite in plasma □ Relaxants, skeletal muscle—chlorzoxazone and hydroxy metabolite, high-pressure liquid chromatographic analysis in plasma

Chlorzoxazone (I) is one of the most useful agents in the treatment of painful muscle spasms, especially in combination with acetaminophen. It can be used as a potent long-acting central muscle relaxant (1, 2). Clinical studies (3) indicated its therapeutic utility and showed no significant side effects (4). Its metabolism was studied (5, 6), and the major metabolite was 6-hydroxychlorzoxazone (II). Chlorzoxazone is rapidly and completely absorbed from the GI tract. The intact drug essentially disappears from the human body in 7 hr, with less than 1% found in urine. Synthesis of II was reported previously (7).

Analytical methods previously reported for I in biological fluids are scarce. The initial and most commonly used method is a spectrophotometric assay (5), involving extraction of drug from biological fluid and reextraction into basic solution with the absorbance read at 289 nm. Other titrimetric (8), GLC (9, 10), and TLC (11) methods were reported for I but were not adapted to the analysis of the intact drug or metabolites in biological samples.

In continuing efforts to apply high-pressure liquid

0022-3549/79/0200-0253$01.00/0

© 1979, American Pharmaceutical Association

Table II—Summary of Theophylline Protein Binding Studies

Source	n	Procedure	Assay	Percent Bound	Reference
Rabbit plasma	—	Equilibrium dialysis: cellophane membrane	UV spectrophotometry	5–10	11
Bovine serum albumin (2%) solutions	—	Equilibrium dialysis: cellophane membrane	UV spectrophotometry	20	7
Plasma of normal dosed volunteers	7	Equilibrium dialysis: cellophane membrane	UV spectrophotometry	59 ± 3	4
Serum from dosed nursing mothers	4	Ultrafiltration: cellophane membrane	HPLC	42–69	5
"Spiked" normal adult plasma	21	Ultrafiltration: membrane cones[a]	LSC[b]	56.4 ± 3.8	6
"Spiked" cord plasma of full-term infants	21	Ultrafiltration: membrane cones[a]	LSC	36.4 ± 3.8	6
"Spiked" plasma of cirrhotic patients	4	Ultrafiltration: membrane cones[a]	LSC	32.3–40.2	8

[a] Amicon Centriflo cones (CF-50), Amicon Corp., Lexington, MA 02173. [b] LSC = liquid scintillation counting of ^{14}C-theophylline.

et al. (2) concluded that, since only 20% theophylline was protein bound (7), binding need not be considered when the volume of distribution was measured. However, Aranda *et al.* (6) reported decreased binding, which might be important when determining effective serum theophylline concentrations in premature infants with apnea. Piafsky *et al.* (8) found reduced binding in cirrhotic patients but did not determine if greater availability of free drug in the liver increased plasma clearance. In the present study, theophylline protein binding did not increase with age. Therefore, it is unlikely that it contributes to the decreased clearance rates found in older patients (9, 10).

Considerable variation in unbound serum theophylline could be possible in patients, based on the 29% range of protein binding found in this study. The effect of binding should possibly be considered in patients who do not have optimal bronchodilation from theophylline despite total serum theophylline concentrations of 10–20 μg/ml.

REFERENCES

(1) J. J. Vallner, *J. Pharm. Sci.*, **66**, 447 (1977).

(2) J. W. Jenne, E. Wyze, F. S. Rood, and F. M. MacDonald, *Clin. Pharmacol. Ther.*, **13**, 349 (1972).

(3) D. S. Sitar, K. M. Piafsky, R. E. Rangno, and R. I. Ogilvie, *Clin. Chem.*, **21**, 1774 (1975).

(4) R. Koysooko, E. F. Ellis, and G. Levy, *Clin. Pharmacol. Ther.*, **15**, 454 (1974).

(5) A. M. Yurchak and W. J. Jusko, *Pediatrics*, **53**, 518 (1976).

(6) J. V. Aranda, D. S. Sitar, W. D. Parsons, P. M. Loughnan, and A. H. Neims, *N. Engl. J. Med.*, **295**, 413 (1976).

(7) M. L. Eichman, D. E. Guttman, Q. van Winkle, and E. P. Guth, *J. Pharm. Sci.*, **51**, 66 (1962).

(8) K. M. Piafsky, D. S. Sitar, R. E. Rangno, and R. I. Ogilvie, *N. Engl. J. Med.*, **296**, 1495 (1977).

(9) E. F. Ellis, R. Koysooko, and G. Levy, *Pediatrics*, **58**, 542 (1976).

(10) E. Ginchansky and M. Weinberger, *J. Pediatr.*, **91**, 655 (1977).

(11) J. A. Shack and S. H. Waxler, *J. Pharmacol. Exp. Ther.*, **97**, 283 (1949).

ACKNOWLEDGMENTS

Supported by a grant from The Children's Hospital of Winnipeg Research Foundation, Inc.

F. E. R. Simons is a Queen Elizabeth II Scientist. L. Lo was the recipient of a Medical Research Council Summer Studentship.

Liquid Chromatography in Pharmaceutical Analysis X: Determination of Chlorzoxazone and Hydroxy Metabolite in Plasma

I. L. HONIGBERG ˣ, J. T. STEWART, and J. W. COLDREN

Received September 13, 1977, from the *Department of Medicinal Chemistry, School of Pharmacy, University of Georgia, Athens, GA 30602.* Accepted for publication July 26, 1978.

Abstract □ A method for the high-pressure liquid chromatographic determination of chlorzoxazone and its hydroxy metabolite in human plasma samples is presented. The separation of the compounds is achieved on an octadecylsilane column with a mobile phase of absolute methanol–distilled water (40:60) at a flow rate of 2.0 ml/min (3100 psig). The chromatographic separation is achieved within 10 min. The overall analysis time is about 45 min, which includes extraction of the drug and metabolite from plasma followed by high-pressure liquid chromatographic separation and quantification. The accuracy of the procedure is in the 1–5% range.

Keyphrases □ Chlorzoxazone and hydroxy metabolite—high-pressure liquid chromatographic analysis in plasma □ High-pressure liquid chromatography—analysis, chlorzoxazone and hydroxy metabolite in plasma □ Relaxants, skeletal muscle—chlorzoxazone and hydroxy metabolite, high-pressure liquid chromatographic analysis in plasma

Chlorzoxazone (I) is one of the most useful agents in the treatment of painful muscle spasms, especially in combination with acetaminophen. It can be used as a potent long-acting central muscle relaxant (1, 2). Clinical studies (3) indicated its therapeutic utility and showed no significant side effects (4). Its metabolism was studied (5, 6), and the major metabolite was 6-hydroxychlorzoxazone (II). Chlorzoxazone is rapidly and completely absorbed from the GI tract. The intact drug essentially disappears from the human body in 7 hr, with less than 1% found in urine. Synthesis of II was reported previously (7).

Analytical methods previously reported for I in biological fluids are scarce. The initial and most commonly used method is a spectrophotometric assay (5), involving extraction of drug from biological fluid and reextraction into basic solution with the absorbance read at 289 nm. Other titrimetric (8), GLC (9, 10), and TLC (11) methods were reported for I but were not adapted to the analysis of the intact drug or metabolites in biological samples.

In continuing efforts to apply high-pressure liquid

0022-3549/79/0200-0253$01.00/0

© 1979, American Pharmaceutical Association

Table I—Effect of Mobile Phase Composition on Retention Times Using Octadecylsilane Column [a]

Mobile Phase[b]	Chlorzoxazone	Phenacetin	Hydroxy-chlorzoxazone
A	292 (32)[c]	220 (24)	139 (23)
	Rs[d] = 2.57	Rs = 3.45	
B	514 (50)	359 (38)	196 (27)
	Rs = 3.52	Rs = 5.02	
C	271 (22)	208 (22)	130 (18)
	Rs = 2.86	Rs = 3.90	

[a] Retention time expressed as seconds measured as elapsed time between injection and attainment of the chromatographic peak maximum. The eluted peaks were monitored using UV detection. [b] Solvent composition: A, absolute methanol–distilled water (50:50); B, absolute methanol–distilled water (40:60); and C, acetonitrile–distilled water (35:65). [c] Base peak width expressed as seconds. [d] See Ref. 13.

chromatography (HPLC) in pharmaceutical analysis[1], an HPLC procedure for the separation and quantification of I and II in human plasma is reported. The chromatographic separation takes approximately 10 min. The overall analysis time is about 45 min, which includes extraction of the drug and its metabolite from plasma followed by HPLC separation and quantification.

EXPERIMENTAL[2]

Reagents and Chemicals—Powdered samples of chlorzoxazone[3] and 6-hydroxychlorzoxazone[3] were used in the analytical procedure and in the preparation of standard curves. All other chemicals and solvents were the highest purity of the commercially available materials.

Mobile Phase—Absolute methanol–distilled water (40:60) was used as the mobile phase and was degassed before use.

Internal Standard Stock Solution—Powdered phenacetin[4] was dissolved in absolute methanol to give a stock internal standard solution of 100 μg/ml.

Preparation of Stock Solutions for Calibration Curve—Separate stock solutions (5 μg/ml) of chlorzoxazone and 6-hydroxychlorzoxazone were prepared by dissolving 5 mg of each powder in 100 ml of absolute methanol followed by a 1:10 dilution of the resulting solution with methanol.

Determination of Calibration Curves for Plasma Levels—Into individual 15-ml centrifuge tubes were placed accurately pipetted volumes of 0.2, 0.5, and 1.0 ml of both chlorzoxazone and hydroxychlorzoxazone stock solutions. Then 0.1 ml of internal standard stock solution was added to each tube, and the contents were evaporated to dryness on a steam bath with a nitrogen stream.

Unspiked human plasma (1.0 ml) was added, and the mixture was shaken[5] for 1 min followed by the addition of 1 ml of 0.1 N H_2SO_4. Ammonium sulfate (0.5 g) was then added to each sample in four evenly divided portions, with shaking[5] and heating on a steam bath after each addition. Ether (5 ml) was added, and the mixture was shaken[5] and centrifuged at 5000 rpm for 5 min. The mixture was quick frozen with the aid of a dry ice–acetone solution in a Dewar flask. The ether layer was decanted and filtered through a 0.5-μm filter[6] into a clean 15-ml centrifuge tube and evaporated to dryness on a steam bath under a nitrogen stream. Absolute methanol (100 μl) was added to dissolve the residue, and a 20-μl aliquot was injected into the liquid chromatograph.

Determination of Chlorzoxazone and Hydroxychlorzoxazone in Human Plasma—Into individual 15-ml centrifuge tubes were placed accurately pipetted volumes of 0.25, 0.7, and 1.0 ml of both chlorzoxazone and hydroxychlorzoxazone stock solution. Then 0.1 ml of internal standard stock solution was added to each mixture. Each sample was then treated in the same manner as described under *Determination of Calibration Curves for Plasma Levels*. A control blank with unspiked human plasma also was performed. Replicate injections of 20 μl were made for each sample.

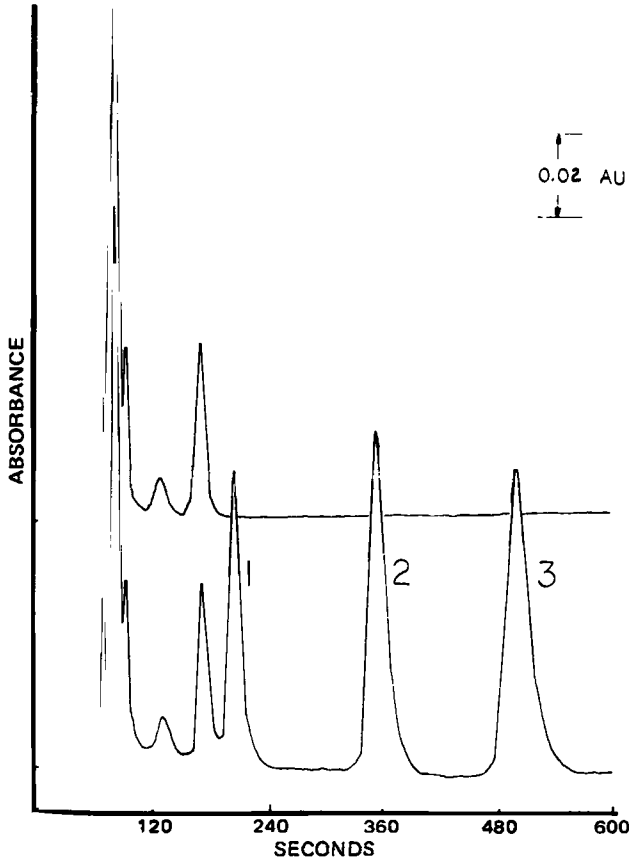

Figure 1—*Liquid chromatogram of chlorzoxazone and 6-hydroxychlorzoxazone from a spiked plasma sample at a flow rate of 2.0 ml/min on an octadecylsilane column. The mobile phase was absolute methanol–distilled water (40:60). The initial drug and metabolite concentration in plasma was 5 μg/ml. Key: A, plasma blank; and B, spiked plasma sample containing 6-hydroxychlorzoxazone (1), phenacetin (2) (internal standard), and chlorzoxazone (3).*

Chromatographic Separation and Quantification—The degassed mobile phase was pumped through an octadecylsilane column[7] at a flow rate of 2.0 ml/min (3100 psig) at room temperature (23 ± 2°) until a stable baseline was obtained. Replicate 20-μl injections of sample and standard solutions were made using a 100-μl syringe[8]. A record of drug elution from the column as peaks on a chromatogram was provided by a chart recorder. The wavelength of the UV detector was set at 280 nm. Each solute was measured by digital integration of the peak area[1].

RESULTS AND DISCUSSION

The HPLC analysis of a chlorzoxazone–hydroxychlorzoxazone mixture and its application to plasma extracts necessitated the examination of three separate problems: (*a*) the development of a set of HPLC operating parameters that would separate the two compounds without peak overlap, (*b*) the detection and quantification of each compound at the levels found in plasma (1–10 μg/ml), and (*c*) the determination of the contribution of the extracted plasma blank to the chromatograms.

Initial chromatographic separation was attempted using a cyanopropylsilane[9] column and the Snyder concept (12) of solvent selectivity and polarity index (PI) as two measurable parameters for the selection of a proper solvent mixture in HPLC. Preliminary data revealed that the polarity index of the solvent mixture should be in the 1.9–2.3 range to obtain a k' for each component between 3 and 10. Various solvents in Snyder's nine solvent categories were intermixed to give the same PI value but change solvent selectivity and maximize resolution of the solute

[1] For other papers in this series, see I. L. Honigberg, J. T. Stewart, and M. Smith, *J. Pharm. Sci.*, 67, 675 (1978).

[2] A Waters Associates liquid chromatograph (model ALC 202) equipped with an M-6000 pump and a U6K injector, a Perkin-Elmer model LC-55 variable wavelength UV–visible detector, a Spectra-Physics autolab minigrator with digital printout, and Waters packed columns (30 cm × 4 mm i.d.) were used.

[3] A. H. Robins, Richmond, Va.

[4] Matheson, Coleman and Bell, East Rutherford, N.J.

[5] Vortex Genie mixer, Scientific Industries, Bohemia, N.Y.

[6] Catalog No. FHLP01300, Millipore Corp., Bedford, MA 01730.

[7] Waters packed <10-μm μBondapak C_{18} columns, Waters Associates, Milford, Mass.

[8] Model B-110, Precision Sampling Corp., Baton Rouge, La.

[9] μBondapak CN, <10 μm, Waters Associates, Milford, Mass.

Table II—Typical Calibration Data for Standard Solutions

Compound	Final Concentration, μg[a]	D/IS Ratio[b]	Slope[c]	Intercept	$r \pm s_{yx}$[d]
Chlorzoxazone	1.0	0.2097 ± 0.0179			
	2.5	0.5159 ± 0.0341	0.2613	−0.0846	0.9962 ± 0.0377
	5.0	1.2417 ± 0.0032			
6-Hydroxychlorzoxazone	1.0	0.1036 ± 0.0088			
	2.5	0.2438 ± 0.0122	0.1128	−0.0203	0.9977 ± 0.0126
	5.0	0.5502 ± 0.0100			

[a] Total micrograms per 100 μl of solution. [b] Data represent triplicate injections of duplicate samples of standard solutions. D/IS is the ratio of the area of the drug at some concentration divided by the area of phenacetin at a concentration of 100 μg/100 μl. [c] Repetition of calibration curve data on different days ($n = 4$) revealed that relative standard deviations of the slope for chlorzoxazone and hydroxychlorzoxazone were 1.25 and 4.3%, respectively. [d] The r is the correlation coefficient calculated from regression analysis, and s_{yx} is the standard error of the estimate of y (D/IS) on x (concentration).

Table III—Determination of Chlorzoxazone and Hydroxy Metabolite in Human Plasma

Mixture	Components	Amount Added, μg	Amount Found, μg[a]	*RSD*, %	Accuracy, %
A	Chlorzoxazone	1.25	1.30 ± 0.06	4.6	4.0
	Hydroxychlorzoxazone	1.25	1.22 ± 0.06	4.9	2.4
B	Chlorzoxazone	3.5	3.47 ± 0.05	1.4	0.86
	Hydroxychlorzoxazone	3.5	3.52 ± 0.04	1.1	0.57
C	Chlorzoxazone	5.0	4.78 ± 0.13	2.7	4.4
	Hydroxychlorzoxazone	5.0	5.08 ± 0.28	5.5	1.6

[a] Based on triplicate injections of duplicate plasma samples.

mixture. This approach was unsuccessful because of the lack of satisfactory resolution of the mixture caused by band spreading of II on the column.

Further investigations revealed that reversed-phase chromatography on an octadecyl column was a more successful approach to the separation of I and II. The effect of mobile phase composition on the retention time of each component on the column is shown in Table I. Although adequate separation could be achieved using any of the solvent systems studied, as evidenced by the resolution (*Rs*) values (13), the compounds were most propitiously separated with absolute methanol–distilled water (40:60). This solvent mix allowed the separation of drugs from endogenous plasma components (Fig. 1) as well as the use of phenacetin as a suitable internal standard.

A flow rate of 2.0 ml/min (3100 psig at room temperature) was the most satisfactory since separations could be obtained in less than 10 min. The void volume of the column was 2.4 ml. UV detection at 280 nm was employed since both I and II have UV absorption maxima close to this value and the detector would, therefore, provide maximum sensitivity for the low concentration levels present in the plasma. Acetaminophen does not interfere with the assay since it elutes close to the solvent front in the mobile phase employed.

The solutions used in the determination of the standard curves as well as the plasma samples were extracted with ether. The percent recoveries for I and II using the described procedure were 96.1 ± 3.0 and 83.2 ± 5.2%, respectively[10] (mean ± *SD*). The internal standard (percent recovery was 83.2 ± 2.6%) was added to the original samples prior to extraction to improve precision. The drug concentrations used in the preparation of the standard curve and plasma were in the range of those reported for plasma (6). The minimum detectability of both the drug and its metabolite with the chromatographic procedure was 80 ng at two times the noise level.

Calibration curves for plasma of I and II were obtained as follows. Digital integration of the area under the curve for each peak on the chromatograms was performed. The ratios of each compound to the area of the internal standard were calculated for each chromatogram. Regression analysis of these data at the various concentrations of each component gave the slope, intercept, and correlation coefficient for the plasma calibration curve (Table II).

A liquid chromatogram of I and II from a spiked plasma sample is shown in Fig. 1. No interference from blank plasma was noted. The ratios of drug peak areas to internal standard peak areas (D/IS) were calculated for both components. The constants (slope and intercept) shown in Table II for the linear regression equations were used to solve for drug concentration in the plasma sample: [D/IS = (slope × concentration) + intercept]. Calculations were performed on a programmable calculator[11].

The data in Table III demonstrate the utility of HPLC in the analysis of I and II at plasma concentration levels.

REFERENCES

(1) D. F. Marsh and A. P. Roszkowski, "Abstracts," American Society for Pharmacology and Experimental Therapeutics, Ann Arbor, Mich., Fall 1958, p. 24.

(2) A. P. Roszkowski, *J. Pharmacol. Exp. Ther.*, **129**, 75 (1960).

(3) S. D. Olinger, R. D. Currier, and R. N. DeJong, *Univ. Mich. Med. Bull.*, **24**, 259 (1958).

(4) E. Settel, *Clin. Med.*, **6**, 1371 (1890).

(5) A. H. Conney, N. Trousof, and J. J. Burns, *J. Pharmacol. Exp. Ther.*, **128**, 333 (1960).

(6) A. H. Conney and J. J. Burns, *ibid.*, **128**, 340 (1060).

(7) J. N. Plampin and C. K. Cain, *J. Med. Chem.*, **6**, 247 (1963).

(8) H. Beral, V. Gamentzy, and I. Bucur, *Rev. Chim. (Bucharest)*, **16**, 322 (1965).

(9) K. D. Parker, C. R. Fontan, and P. L. Kirk, *Anal. Chem.*, **34**, 757 (1962).

(10) B. Kaempe, *Arch. Pharm. Chem., Sci. Ed.*, **2**, 145 (1974).

(11) I. Ullah, D. E. Cadwallader, and I. L. Honigberg, *J. Chromatogr.*, **46**, 211 (1970).

(12) L. Snyder, *ibid.*, **92**, 233 (1974).

(13) B. L. Karger, L. R. Snyder, and C. Horvath, "An Introduction to Separation Science," Wiley, New York, N.Y., 1973, pp. 146–150.

[10] Percent recoveries of chlorzoxazone and the hydroxy metabolite were determined by comparing the HPLC peak area ratios of equivalent quantities of extracted and unextracted compound to unextracted internal standard. Triplicate injections of three individual samples of drug and metabolite were performed.

[11] Olivetti-Underwood Programma 101.

Antimicrobial Activity of Chlormerodrin

V. N. PANDEY, KUM. P. S. RAO, K. M. PATEL, and N. G. S. GOPAL ˣ

Received October 17, 1977, from the *Isotope Group, Bhabha Atomic Research Centre, Trombay, Bombay 400 085, India.* Accepted for publication August 2, 1978.

Abstract □ A radiochemical study for antimicrobial activity of chlormerodrin was performed using some commonly occurring nonpathogenic and pathogenic microorganisms. Chlormerodrin concentrations of 15–35 and 20–45 μg/ml of the culture medium were microbiostatic and microbicidal, respectively. The microbiostatic effect was reversible in the presence of cysteine, an amino acid containing a sulfhydryl group.

Keyphrases □ Chlormerodrin—antimicrobial activity evaluated *in vitro* □ Antimicrobial activity—chlormerodrin evaluated *in vitro* □ Diuretics—chlormerodrin, antimicrobial activity evaluated *in vitro*

Chlormerodrin, an organomercurial compound, is classified as a diuretic and not as an antimicrobial agent like phenylmercuric nitrate and thimerosal (1).

When sterility testing is performed on solutions containing organomercurials such as thimerosal and phenylmercuric salts (0.01 and 0.002%, respectively) as preservatives, the inoculum is recommended to be diluted at least 10-fold with fluid thioglycolate medium (I), even though 5 ml of this medium can inactivate the mercurial preservatives in 1 ml of the solution (2). Medium I contains 0.03% (v/v) thioglycolic acid to neutralize the organomercurials.

This paper reports a study of the degree of antimicrobial activity of chlormerodrin using a variety of microorganisms and cysteine as a binding agent. To evaluate the microbiostatic and microbicidal doses of chlormerodrin, a radiochemical sensitivity test (3–5) against some commonly occurring nonpathogenic and pathogenic microorganisms was performed.

EXPERIMENTAL

Apparatus—A semiautomatic radioactive detection system[1] measured, in terms of the growth index reading (1 division = 0.25 μCi), $^{14}CO_2$ released from ^{14}C-glucose metabolized by microorganisms.

Preparation of Double-Strength Glucose-Free Medium with ^{14}C-Glucose—The medium consisted of 3.4% Bacto Tryptone[2], 0.6% Bacto Soytone[2], 1% NaCl, 0.5% K_2HPO_4, and 100 μCi of *U*-^{14}C-glucose[3] (specific activity of 1.39 μCi/mg)/liter. Aliquots of 10 ml of the medium were distributed into 50-ml culture vials, and the vials were autoclaved at 1.05 kg/cm² for 20 min.

Table I—Microbiostatic and Microbicidal Effects of Chlormerodrin

Test Culture	Hours of Incubation	Growth Index Reading at Chlormerodrin Concentration, μg/ml of medium							MMID, μg/ml	MLD, μg/ml
		Nil	10	15	20	25	30	35		
E. coli	24	100	35	15	10	No growth			25	35
	48	100	80	40	50					
	72	100	100	100	100					
	96	100	100	100	100					
S. typhosa	24	100	38	30	25	25	20	No growth	35	45
	48	100	85	80	80	83	80			
	72	100	100	100	100	100	100			
	96	100	100	100	100	100	100			
S. aureus	24	100	40	45	—	No growth			25	30
	48	100	90	50	15					
	72	100	100	100	40					
	96	100	100	100	70					
B. subtilis	24	100	40	40	35	30	No growth		25	25
	48	100	95	70	55	50				
	72	100	100	100	100	100				
	96	100	100	100	100	100				
B. cereus	24	100	35	30	25	No growth			25	40
	48	100	100	90	70					
	72	100	100	100	100					
	96	100	100	100	100					
Cl. sporogenes	24	100	35	30	35	25	25	No growth	35	40
	48	100	100	70	65	70	50			
	72	100	100	100	100	100	100			
	96	100	100	100	100	100	100			
C. albicans	24	100	40	40	35	20	20	No growth	35	40
	48	100	100	80	60	45	48			
	72	100	100	100	100	100	100			
	96	100	100	100	100	100	100			
Flavobacterium sp.	24	100	25	No growth					15	20
	48	100	60							
	72	100	80							
	96	100	100							

Sample Preparation—Chlormerodrin[4] (125 mg) was dissolved in 250 ml of freshly distilled water and sterilized by filtration[5] (pore size of 0.45 μm).

L-(−)-Cysteine[6] (1 g) was dissolved in 50 ml of freshly distilled water and sterilized by autoclaving at 1.05 kg/cm² for 15 min.

Preparation of Test Cultures—These cultures were standardized cell suspensions containing 3 × 10⁴ viable cells/ml and were prepared from a 24-hr-old culture of *Escherichia coli* (ATCC 9637), *Staphylococcus aureus* (ATCC 9144), *Bacillus cereus* (C. 1448), *Bacillus subtilis*

[1] Bactec-301, Johnston Laboratories, Cockeysville, Md.
[2] Difco Laboratories, Detroit, Mich.
[3] Isotope Division, BARC, Bombay, India.
[4] Neohydrin, Lakeside Laboratories, Milwaukee, Wis.
[5] Millipore Corp., Bedford, Mass.
[6] E. Merck, Darmstadt, West Germany.

0022-3549/79/0200-0256$01.00/0
© 1979, American Pharmaceutical Association

Table II—Influence of Cysteine on the Antimicrobial Effect of Chlormerodrin

	Vial					
	1	2	3	4	5	6
Volume of double-strength medium, ml	10	10	10	10	10	10
Chlormerodrin solution, ml	2.4	2.4	1.2	1.2	1.2	1.2
Test column of *E. coli* cell, ml	0.2	0.2	0.1	0.1	0.1	0.1
Mixed well and allowed to stand at room temperature for 4 hr						
Cysteine solution, ml	0.0	3.0	0.0	0.5	1.0	3.0
Sterile water, ml	7.4	4.4	8.7	8.2	7.7	5.7
Mixed well and incubated at 30–34°						
Incubation period, hr	Growth index reading					
24	Nil	Nil	Nil	Nil	Nil	70
48	Nil	Nil	Nil	Nil	25	90
72	Nil	Nil	Nil	10	60	100
96	Nil	Nil	Nil	35	100	100

(ATCC 6633), *Clostridium sporogenes* (ATCC 19404), *Salmonella typhosa*, *Candida albicans*, and *Flavobacterium* sp. isolated and identified according to a literature method (6).

Antimicrobial Activity of Chlormerodrin—All operations were carried out on a laminar flow bench. Twelve culture vials, each containing 10 ml of double-strength medium, were arranged in duplicate for each test organism. Then 0.4, 0.6, 0.8, . . . , 2.2, and 2.4 ml of chlormerodrin solution were added to the vials serially marked 2–12. Sterile water was added to each vial to a volume of 20 ml so that the concentration of ^{14}C-glucose was 0.05 μCi/ml of the culture medium.

The test cultures, 50 μl, were added to each vial, and the vials were capped and incubated at 30–34°. The growth index reading was measured at the end of every 24 hr for 4 days. After the last observation, a 0.1-ml aliquot from each culture vial (showing no growth index reading) was transferred to soybean–casein digest medium (15 ml) and incubated for 5 days at 30–34° to confirm the microbiostatic and microbicidal doses of chlormerodrin for each test culture (Table I).

Antimicrobial Activity of Chlormerodrin in Presence of Cysteine—Six culture vials, each containing 10 ml of double-strength medium, were taken. Chlormerodrin solution was added to the vials as follows: 2.4 ml to vials 1 and 2 and 1.2 ml to vials 3–6. Then 0.1–0.2 ml of test culture of *E. coli* was added to each of the six vials (Table II). The vials stood at room temperature for 4 hr to allow sufficient time for inactivation of the microbial cells.

Vials 1 and 3 were kept aside as controls. To vials 2, 4, 5, and 6, 3.0, 0.5, 1.0, and 3.0 ml of cysteine solution were added, respectively. The mixture was diluted to 20 ml with sterile distilled water and then incubated at 30–34°. The growth index reading was measured at the end of every 24 hr for 4 days (Table II).

RESULTS AND DISCUSSION

Preliminary tests for sterility on aqueous solutions of chlormerodrin showed that visible growth did not occur in the control tube containing 1–2.5 mg of chlormerodrin in 15 ml of fluid thioglycolate and soybean–casein digest media (7) with *B. subtilis* or *C. albicans* as the challenging microorganism, even after 10 days of incubation. Therefore, eight different microorganisms were tested for their sensitivity to chlormerodrin.

The microbiostatic or minimum metabolic inhibition dose (MMID), *i.e.*, the minimum dose at which there is no growth index reading but growth occurs on subculturing, is in the range of 15–30 μg/ml of the culture medium. The microbicidal dose or minimum lethal dose (MLD), *i.e.*, the minimum dose at which there is neither a growth index reading nor growth on subculturing, is in the range of 20–45 μg/ml (Table I). The microbiostatic effect was reversed by the addition of cysteine (0.3% w/v final concentration) but not the microbicidal effect (Table II). This result indicates that the microbiostatic and microbicidal effects of chlormerodrin, like other organomercurials, may result from its strong binding capacity with the sulfhydryl group of microbial enzymes involved in the cellular metabolic cycle.

The chlormerodrin concentration in chlormerodrin Hg 203 injection may sometimes be in the range of 1–2.5 mg/ml, which would be 20–125 times higher than the microbicidal dose. Hence, the chances of survival of viable cells are almost negligible in the radiopharmaceutical preparation. If 1 ml of such a solution is diluted to 20 ml as described earlier, the final concentration of chlormerodrin becomes 50–150 μg/ml, which would still be 1–8 times higher than the microbicidal dose. If any surviving microorganisms are in a "shock-state," the chances of their growth would be very poor.

In view of this finding, the sterility test on this radiopharmaceutical preparation should be carried out either by dilution of the injection with sufficient sterility test medium to bring the final concentration in the medium to not more than 10 μg/ml, which is below the range of its microbiostatic effect, or by aseptic filtration through a bacteria-retaining filter and then performance of the sterility test on the filter.

REFERENCES

(1) "The United States Pharmacopeia," 19th rev., Mack Publishing Co., Easton, Pa., 1975, p. 622.

(2) "Difco Manual," 9th ed., Difco Laboratories, Detroit, Mich., 1971, pp. 196, 197.

(3) F. H. Deland and H. N. Wagner, Jr., *J. Lab. Clin. Med.*, **75**, 529 (1970).

(4) F. H. Deland and H. N. Wagner, Jr., *Radiology*, **92**, 154 (1969).

(5) F. H. Deland, *J. Nucl. Med.*, **13**, 424 (1972).

(6) R. S. Breed, E. G. D. Murray, and N. R. Smith, "Bergey's Manual of Determinative Bacteriology," Williams & Wilkins, Baltimore, Md., 1957.

(7) "The United States Pharmacopeia," 19th rev., Mack Publishing Co., Easton, Pa., 1975, pp. 592, 593.

ACKNOWLEDGMENTS

The authors thank BARC authorities for their encouragement and interest.

Determination of Iodide in Metabolic Studies of ^{125}I-Labeled Compounds

Y. Y. SHUM * **and J. E. SINSHEIMER** ˣ

Received January 18, 1978, from the *College of Pharmacy, University of Michigan, Ann Arbor, MI 48109.* Accepted for publication August 7, 1978. *Present address: Warner-Lambert/Parke-Davis Pharmaceutical Research Division, Ann Arbor, MI 48106.

Abstract □ Methods capable of measuring inorganic iodide in the presence of other highly polar metabolites were developed in support of studies concerning the metabolism of ^{125}I-labeled compounds. The methods included separation of iodine on a weakly basic resin paper followed by γ-counting, methyl iodide exchange, and reverse isotopic dilution.

Keyphrases □ Iodide—analyzed in urine by paper chromatography–γ-counting, methyl iodide exchange, and reverse isotopic dilution □ Chromatography, paper—followed by γ-counting, analysis of iodide in urine □ Methyl iodide exchange—analysis of iodide in urine □ Reverse isotopic dilution—analysis of iodide in urine

Methods for the measurement of inorganic iodide were required in studies concerning the metabolism of ^{125}I-labeled compounds. It was desired to have chromatographic separation procedures followed by γ-counting and also independent chemical confirmation of such chromatographic results. For example, these methods had to be capable of measuring iodide in the presence of other highly polar metabolites such as the glucuronides, sulfates, and mercapturic acid derivatives formed during the metabolism of 4-iodobiphenyl (1).

Chemical determinations of iodide in biological systems appeared not to be applicable to these studies. The limit of detection of the electrometric titration method (2) is 25 μg/50 ml of urine in systems containing relatively large amounts of organically bound iodide. In several procedures, the iodide was oxidized to iodine, followed by colorimetric determination (3), γ-counting (4), or titration with sodium thiosulfate (5). Iodine in urine or filtrates of incubation mixtures containing iodine-131 in the presence of organically bound iodine also was measured by passing such a solution through a silver chloride column (6–8). The activity of the silver iodide formed at the top of the column was counted with excellent recovery, but the presence of easily oxidizable iodo compounds could be a problem.

Several acidic and basic alcohol–water solvent systems were applied to paper chromatographic separations of iodide in biological systems (4, 6, 9–16). The 1-butanol–0.5 *N* ammonia–ethanol–water system (16) was found to be applicable to metabolic studies. In addition, a resin paper separation, a methyl iodide exchange procedure, and a reverse isotopic dilution method were developed. This paper describes these three procedures for iodide measurements in biological systems. These procedures are being applied for metabolism studies of ^{125}I-4-iodobiphenyl in rats in which the daily yield of iodide in urine represents a maximum of 3% of the radioactivity of an original dose of 400 mg/kg (400 μCi).

EXPERIMENTAL

Resin Paper Chromatography—Weakly basic resin papers[1] were developed to 16.0 cm by an ascending method in tanks lined with filter paper and saturated with butanol–acetone–concentrated ammonium hydroxide–water (65:20:10:5). Radioactivity was detected by γ-counting[2] 0.5-cm strips of the chromatogram. In urine samples showing multiple peak activity, the resin paper chromatogram corresponding to inorganic iodide was extracted with methanol. The extract was concentrated and redeveloped in the same system for improved separation of the inorganic iodide.

Methyl Iodide Exchange—A volume of 50.0 μl of rat urine was transferred with a microliter pipet to a 10 × 75-cm screw-capped culture tube and dried under a gentle nitrogen stream. To the residue were added 100 μl of acetone and 100 μl of methyl iodide, both freshly distilled before use. The tube was capped, and the sample was allowed to exchange overnight at room temperature. The exchanged radioactive methyl iodide was removed along with acetone by a slow nitrogen stream, which had passed through a solution trap containing 2.0 ml of 5% NaOH.

The dried residue was dissolved in 200 μl of acetone and counted in a γ-counting system. The difference in radioactivity before and after exchange was used to calculate the inorganic iodide concentration in the urine (17). The amount of ^{125}I-label present in a sample was calculated by dividing the difference in activity before and after methyl iodide exchange by the factor 0.926, as established from known concentrations of iodine-125.

Reverse Isotopic Dilution—To 3.0 ml of rat sample urine was added about 1 g of carrier sodium iodide, accurately weighed, to give a homogeneous solution. An excess volume of saturated lead nitrate was added to the solution to precipitate iodide as lead ^{125}I-iodide, which was filtered and recrystallized in large volumes of boiling water. The radioactive lead iodide was oxidized to elemental iodine by addition of a slight excess of sodium nitrite (~0.5 g) in a 2.5 × 20.3-cm test tube. Concentrated nitric acid was added dropwise until the release of nitrous acid ceased.

The iodine crystals were trapped on the inside wall of the test tube, which had a cooling coil around the outside. Purification of the radioactive iodine crystals was by repeated sublimations until a constant specific activity was obtained.

RESULTS AND DISCUSSION

To develop a rapid analytical method to separate inorganic iodide from other highly polar metabolites, a number of reported TLC systems (18, 19) were tested and found to be unsatisfactory. Separation by paper electrophoresis in various buffer systems could be achieved, but quantification of the results was poor. In pH 3 phthalate buffer, even at the minimal constant voltage (15 v) or current (15 mamp) required for satisfactory iodide-ion mobility (0.25 cm/hr), there was appreciable oxidation of the iodide.

With a weakly basic polyamine anion-exchange resin[3] (0.2 g dry weight), it was possible to separate iodide from polar metabolites. The ^{125}I-ions in urine samples (10,000 cpm) from rats dosed with ^{125}I-4-iodobiphenyl were retained at the top of the resin column while all other radioactive compounds from the hydroxylation of the iodobiphenyl and their conjugates were removed by elution with 0.8% HCl in methanol. γ-Counting of iodide activity bound to the resin particles, however, did not give consistent results, probably because of the difficulty in controlling the geometry of counting the resin particles.

The information gained from this resin column led to the use of chromatography on resin-loaded papers. A single-phase solvent system of butanol–acetone–concentrated ammonium hydroxide–water (65:20:10:5) was used with a weakly basic resin paper. It was speculated that an ammonia–iodide interaction (20) would be useful to separate iodide from other polar urinary metabolites. In urine sample chromatograms, a peak

[1] WB 2 resin paper, Reeve Angel, Clifton, N.J.

[2] Model 1185 γ-counting system, Searle, Chicago, Ill. The limit of counting was set for 10,000 cpm or 1 min, and the counting efficiency for iodine-125 was 76%.

[3] IR-45, Mallinckrodt, St. Louis, Mo.

0022-3549/79/0200-0258$01.00/0
© 1979, American Pharmaceutical Association

at R_f 0.39 corresponded to the single peak appearing in the ^{125}I-control chromatograms. The presence of iodide in the peak was confirmed by methanol extraction of the peak and rechromatography in the USP paper system (21) used to determine the purity of the ^{125}I-label. Both a reference sample of sodium ^{125}I-iodide[4] and the concentrated extracted material had R_f values of 0.71 in the paper system.

The resin paper system in the metabolism study of iodobiphenyl in rats (1) provided a satisfactory separation of inorganic iodide (R_f 0.39) from other urinary metabolites (polar conjugates, R_f 0.16; iodobiphenyl and 2- and 4-hydroxy-4′-iodobiphenyl, R_f 0.73). The same system failed when it was used for liver homogenate studies of the biodehalogenation of 4-iodobiphenyl, 4-iodonitrobenzene, and 4-iodoaniline (22). The system was incapable of separating iodide after the addition of trichloroacetic acid, which was required for the workup of these *in vitro* samples. However, a reported paper partition system (16) was used for this purpose and also provided excellent separations for iodide in the presence of other metabolites in urine samples.

The results of the analysis of six urine samples by both the resin paper and partition systems differed by less than 3% in total urinary activity. In general, while the paper partition system gave better defined separations in complex mixtures of polar metabolites, the resin paper system was less time consuming and results could be achieved in the time required for conventional TLC systems.

To confirm further the accuracy of iodide determinations by the paper and resin paper chromatographic systems, alternative quantitative techniques were sought. Existing methods with adequate sensitivity all involve quantitations of total iodide concentrations after chemical manipulations, including electrometric titrations, oxidations, adsorption, and extractions, of the original biological samples, which may introduce artifacts. Limitations due to these artifacts have been discussed (3, 6, 23).

A reverse isotopic dilution method was one of two procedures devised to avoid these artifacts. Since isotopic dilution methods depend on specific activity as the criterion for quantitation instead of on total content in the processed samples, any loss of iodide resulting from multistep handling would not affect the final determination. After addition of cold sodium iodide to radioactive urine samples, precipitation with lead nitrate was used to provide an initial isolation of inorganic iodide. The lead iodide formed could not be reproducibly counted directly because of the apparent quenching effect of lead, so the lead ^{125}I-iodide was oxidized to iodine. The iodine crystals were purified by repeated sublimations to a constant specific activity. This specific activity, multiplied by the weight of cold iodide added, was used as a measure of the ^{125}I-label in the urine sample.

Evaluation of this procedure with duplicate samples of sodium ^{125}I-iodide (73,000 and 80,000 cpm) content gave an average of 95.6% recovery with a difference of 0.6%. A constant specific activity was obtained after three sublimations and remained constant for the additional three sublimations tested. The method also was applied to urine samples (243,000–1,000,000 cpm/5 ml) from rats dosed with ^{125}I-4-iodobiphenyl (400 mg/kg; 400 μCi), with a constant specific activity being obtained after three or four sublimations and remaining constant for at least the three additional sublimations tested.

[4] New England Nuclear (17 Ci/mg); used within 6 months of calibration.

A second chemical analytical method used an exchange reaction between methyl iodide and the ^{125}I-label and was based on studies (17, 24) of rates of exchange of organic iodides with radioactive inorganic iodide. In the present studies, when the exchange procedure was applied to iodide in urine samples, it was important to establish anhydrous conditions; acetone was an excellent solvent for the exchange. Thirty exchange experiments with known quantities (500–14,000 cpm) of sodium ^{125}I-iodide (17 Ci/mg) added to control rat urine indicated that 92.6 ± 2.23% of added activity was removed after methyl iodide exchange.

A comparison of the exchange and reverse isotopic procedures for iodide determination was made for the first 4-day urine excretion after the administration of ^{125}I-4-iodobiphenyl (400 mg/kg; 400 μCi) to rats. The two procedures agreed within 3.4% of the total daily urinary radioactivity and were equally effective in measuring iodide in metabolic systems.

REFERENCES

(1) Y. Y. Shum, Ph.D. thesis, University of Michigan, Ann Arbor, Mich., 1977.

(2) J. H. Wilkinson, W. E. Sprott, C. H. Browden, and N. F. Maclagan, *Biochem. J.*, **56,** 215 (1954).

(3) M. K. Johnson, *ibid.*, **98,** 44 (1966).

(4) J. R. Tata, J. E. Rall, and R. W. Rawson, *Endocrinology*, **60,** 83 (1957).

(5) H. G. Bray, J. C. Caygill, S. P. James, and P. B. Wood, *Biochem. J.*, **90,** 127 (1964).

(6) L. G. Plaskett, *ibid.*, **78,** 652 (1961).

(7) K. Fletcher, *ibid.*, **67,** 136 (1957).

(8) *Ibid.*, **67,** 140 (1957).

(9) D. W. Slingerland and R. K. Josephs, *Endocrinology*, **62,** 853 (1958).

(10) J. B. Stanbury, *J. Biol. Chem.*, **228,** 801 (1957).

(11) E. Yamazaki and D. W. Slingerland, *Endocrinology*, **64,** 126 (1959).

(12) F. C. Larson and E. D. Albright, *J. Clin. Invest.*, **40,** 1132 (1961).

(13) J. R. Tata, *Biochem. J.*, **77,** 214 (1960).

(14) J. Gross, C. P. Leblond, A. E. Franklin, and J. H. Quastel, *Science*, **111,** 605 (1950).

(15) J. Roche, M. Jutisz, S. Lissitzky, and R. Michel, *Biochim. Biophys. Acta*, **7,** 257 (1951).

(16) R. Grasbeck, B. A. Lamberg, and F. Bjorkstén, *Acta Endocrinol.*, **34,** 113 (1960).

(17) P. Beronius and A.-B. Gabrielsson, *Anal. Chem. Acta*, **40,** 352 (1968).

(18) C. E. Mellish, *Panel Anal. Control Radiopharm.*, **1970,** 115.

(19) V. Shen, K. R. Hetzel, and R. D. Ice, in "Technical Bulletin 32," Gelman Instrument Co., Ann Arbor, Mich., 1974.

(20) "Thin-Layer Chromatography," E. Stahl, Ed., Springer-Verlag, New York, N.Y., 1965.

(21) "The United State Pharmacopeia," 19th rev., Mack Publishing Co., Easton, Pa., 1975, p. 462.

(22) J. E. Sinsheimer, T. Wang, S. Röder, and Y. Y. Shum, *Biochem. Biophys. Res. Commun.*, in press.

(23) J. D. Acland, *Nature*, **170,** 32 (1952).

(24) P. Beronius, *Acta Chem. Scand.*, **15,** 1151 (1961).

Equations for Estimation of First-Pass Effect and Apparent Distribution Volume of Drug with Incomplete Oral Absorption and Partial Renal Excretion

Keyphrases □ First-pass effect—estimation and distribution volume, drugs with incomplete oral absorption and partial renal excretion □ Distribution volume—estimation and first-pass effect, drugs with incomplete oral absorption and partial renal excretion □ Absorption, GI, incomplete—estimation of first-pass effect and distribution volume □ Excretion, renal, partial—estimation of first-pass effect and distribution volume

To the Editor:

Equations assuming complete absorption have been used to estimate the degree of pulmonary (1) and hepatic (2, 3) first-pass effect and the apparent distribution volume (1, 3) after oral dosing of drugs having partial pulmonary and renal excretion. The purpose of this communication is to present general equations that can be used when a drug is known to be absorbed only partially from the dosage form.

Based on the previously derived equations (1), the extent of the first-pass effect or the hepatic extraction ratio, designated as f_m, is:

$$f_m = \frac{(F_m)(F)(\text{dose})}{(F)(\text{dose}) + (HFR)(AUC_\infty)} \qquad \text{(Eq. 1)}$$

where F_m is the hepatically metabolized drug fraction after intravenous administration or after entry into the general circulation through other routes of administration, F is the dose fraction available for GI absorption from the dosage form, HFR is the hepatic blood flow rate, and AUC_∞ is the total area under the blood concentration *versus* time curve at infinite time.

The apparent volume of distribution, V_d, based on the area method can be estimated by:

$$V_d = \frac{(F)(1 - f_m)(\text{dose})}{(K_t)(AUC_\infty)} \qquad \text{(Eq. 2)}$$

where K_t is the first-order rate constant of the terminal postabsorption and postdistribution phase.

Similar equations can be derived for drugs that are partially absorbed and partially excreted from the lung and kidney.

(1) W. L. Chiou, *J. Pharmacokin. Biopharm.*, **3**, 193 (1975).
(2) W. L. Chiou, *J. Pharm. Sci.*, **64**, 1734 (1975).
(3) D. C. Hobbs, T. M. Twomey, and R. F. Palmer, *J. Clin. Pharmacol.*, 18, 402 (1978).

Win L. Chiou
Clinical Pharmacokinetics Laboratory
and Department of Pharmacy
University of Illinois
at the Medical Center
Chicago, IL 60612

Received November 2, 1978.
Accepted for publication December 4, 1978.
Presented in part at the APhA Academy of Pharmaceutical Sciences, Chicago meeting, 1974.

N-Benzoyl Derivatives of Amino Acids and Amino Acid Analogs as Inhibitors in Microbial Antitumor Screen

Keyphrases □ Antineoplastic agents, potential—amino acids, *N*-benzoyl derivatives, microbial screen □ Amino acids, *N*-benzoyl derivatives—potential antineoplastic agents, microbial screen

To the Editor:

For some time, we have been studying the *N*-acylated derivatives of amino acids and amino acid analogs as possible antitumor agents (1–3). Certain chloroacetylated (1, 3) and trifluoroacetylated (4) amino acids and amino acid analogs were found to be active inhibitors of the growth of a microbial system selected for antitumor screening. The degree of inhibition ranged from about 20 to 50%.

With the hope of increasing the activity of these compounds by giving them more lipophilic character, the benzoyl and ring-substituted benzoyl derivatives were prepared. The acylation was accomplished by the conventional Schotten–Baumann procedure (5). The purity of these compounds was ascertained by elemental analysis, melting-point determination, optical rotation determination where applicable, and Van Slyke nitrous acid determination of the primary amino nitrogen (6). The microbiological assay system utilized was *Lactobacillus casei* (7469) in a riboflavin-supplemented riboflavin assay system (3).

Mercaptopurine, a known and accepted antitumor agent, assayed concurrently with the test compounds, showed an inhibition of about 54% at a final concentration of 0.1 mg (0.6 μmole)/ml in this test system. Growth was determined turbidimetrically (3). Initially, the activity was determined at 1 mg/ml, in accord with the screening protocol (7), and the nine most active compounds were compared on an equimolar basis at 4.47 μmoles/ml, the final concentration. This concentration is equivalent to 1 mg of chloroacetyl-β-hydroxy-D-norleucine B/ml, the compound previously found to be the most active in these studies (2).

Of the 28 benzoyl compounds tested, the nine listed in Table I showed pronounced activity, greater than that

Table I—Effect of Equimolar Concentrations of *N*-Benzoyl Derivatives of Amino Acids and Amino Acid Analogs on the Growth of *L. casei* 7469 [a]

Compound	Inhibition[b], %
N-Benzoyl-*o*-fluoro-DL-phenylalanine	82
N-Benzoyl-*m*-fluoro-DL-phenylalanine	96
N-Benzoyl-*p*-fluoro-DL-phenylalanine	72
N-Benzoyl-β-2-thienyl-DL-alanine	76
N-Benzoyl-β-3-thienyl-DL-alanine	56
N^{α}-Benzoyl-L-tryptophan	74
N-Benzoyl-*p*-chloro-DL-phenylalanine	94
N^{α}-Benzoyl-*p*-nitro-L-phenylalanine	78
N^{α}-*p*-Nitrobenzoyl-L-phenylalanine	78

[a] Maximum growth in inoculated control tubes containing no test compound, measured turbidimetrically, was 166-173 Klett units. [b] Concentration was 4.47 μmoles/ml and was the final concentration in the assay system.

0022-3549/79/0200-0260$01.00/0
© 1979, American Pharmaceutical Association

Equations for Estimation of First-Pass Effect and Apparent Distribution Volume of Drug with Incomplete Oral Absorption and Partial Renal Excretion

Keyphrases □ First-pass effect—estimation and distribution volume, drugs with incomplete oral absorption and partial renal excretion □ Distribution volume—estimation and first-pass effect, drugs with incomplete oral absorption and partial renal excretion □ Absorption, GI, incomplete—estimation of first-pass effect and distribution volume □ Excretion, renal, partial—estimation of first-pass effect and distribution volume

To the Editor:

Equations assuming complete absorption have been used to estimate the degree of pulmonary (1) and hepatic (2, 3) first-pass effect and the apparent distribution volume (1, 3) after oral dosing of drugs having partial pulmonary and renal excretion. The purpose of this communication is to present general equations that can be used when a drug is known to be absorbed only partially from the dosage form.

Based on the previously derived equations (1), the extent of the first-pass effect or the hepatic extraction ratio, designated as f_m, is:

$$f_m = \frac{(F_m)(F)(\text{dose})}{(F)(\text{dose}) + (HFR)(AUC_\infty)} \qquad \text{(Eq. 1)}$$

where F_m is the hepatically metabolized drug fraction after intravenous administration or after entry into the general circulation through other routes of administration, F is the dose fraction available for GI absorption from the dosage form, HFR is the hepatic blood flow rate, and AUC_∞ is the total area under the blood concentration *versus* time curve at infinite time.

The apparent volume of distribution, V_d, based on the area method can be estimated by:

$$V_d = \frac{(F)(1 - f_m)(\text{dose})}{(K_t)(AUC_\infty)} \qquad \text{(Eq. 2)}$$

where K_t is the first-order rate constant of the terminal postabsorption and postdistribution phase.

Similar equations can be derived for drugs that are partially absorbed and partially excreted from the lung and kidney.

(1) W. L. Chiou, *J. Pharmacokin. Biopharm.*, **3**, 193 (1975).
(2) W. L. Chiou, *J. Pharm. Sci.*, **64**, 1734 (1975).
(3) D. C. Hobbs, T. M. Twomey, and R. F. Palmer, *J. Clin. Pharmacol.*, 18, 402 (1978).

Win L. Chiou
Clinical Pharmacokinetics Laboratory
and Department of Pharmacy
University of Illinois
at the Medical Center
Chicago, IL 60612

Received November 2, 1978.
Accepted for publication December 4, 1978.
Presented in part at the APhA Academy of Pharmaceutical Sciences, Chicago meeting, 1974.

N-Benzoyl Derivatives of Amino Acids and Amino Acid Analogs as Inhibitors in Microbial Antitumor Screen

Keyphrases □ Antineoplastic agents, potential—amino acids, *N*-benzoyl derivatives, microbial screen □ Amino acids, *N*-benzoyl derivatives—potential antineoplastic agents, microbial screen

To the Editor:

For some time, we have been studying the *N*-acylated derivatives of amino acids and amino acid analogs as possible antitumor agents (1–3). Certain chloroacetylated (1, 3) and trifluoroacetylated (4) amino acids and amino acid analogs were found to be active inhibitors of the growth of a microbial system selected for antitumor screening. The degree of inhibition ranged from about 20 to 50%.

With the hope of increasing the activity of these compounds by giving them more lipophilic character, the benzoyl and ring-substituted benzoyl derivatives were prepared. The acylation was accomplished by the conventional Schotten–Baumann procedure (5). The purity of these compounds was ascertained by elemental analysis, melting-point determination, optical rotation determination where applicable, and Van Slyke nitrous acid determination of the primary amino nitrogen (6). The microbiological assay system utilized was *Lactobacillus casei* (7469) in a riboflavin-supplemented riboflavin assay system (3).

Mercaptopurine, a known and accepted antitumor agent, assayed concurrently with the test compounds, showed an inhibition of about 54% at a final concentration of 0.1 mg (0.6 μmole)/ml in this test system. Growth was determined turbidimetrically (3). Initially, the activity was determined at 1 mg/ml, in accord with the screening protocol (7), and the nine most active compounds were compared on an equimolar basis at 4.47 μmoles/ml, the final concentration. This concentration is equivalent to 1 mg of chloroacetyl-β-hydroxy-D-norleucine B/ml, the compound previously found to be the most active in these studies (2).

Of the 28 benzoyl compounds tested, the nine listed in Table I showed pronounced activity, greater than that

Table I—Effect of Equimolar Concentrations of *N*-Benzoyl Derivatives of Amino Acids and Amino Acid Analogs on the Growth of *L. casei* 7469 [a]

Compound	Inhibition[b], %
N-Benzoyl-*o*-fluoro-DL-phenylalanine	82
N-Benzoyl-*m*-fluoro-DL-phenylalanine	96
N-Benzoyl-*p*-fluoro-DL-phenylalanine	72
N-Benzoyl-β-2-thienyl-DL-alanine	76
N-Benzoyl-β-3-thienyl-DL-alanine	56
N^{α}-Benzoyl-L-tryptophan	74
N-Benzoyl-*p*-chloro-DL-phenylalanine	94
N^{α}-Benzoyl-*p*-nitro-L-phenylalanine	78
N^{α}-*p*-Nitrobenzoyl-L-phenylalanine	78

[a] Maximum growth in inoculated control tubes containing no test compound, measured turbidimetrically, was 166-173 Klett units. [b] Concentration was 4.47 μmoles/ml and was the final concentration in the assay system.

0022-3549/79/0200-0260$01.00/0
© 1979, American Pharmaceutical Association

observed for any acyl compounds previously tested. These compounds exhibited inhibition greater than 50% at 1 mg/ml, thus meeting the criterion of positivity set in the microbiological assay protocol (7). Therefore, these compounds have been submitted for antitumor test in mammalian systems.

Most of the active compounds were derivatives of phenylalanine analogs. Their activity was tested against melanomas, in which phenylalanine metabolism is believed to be intimately involved.

Detailed description of these findings will be reported elsewhere.

(1) T. T. Otani, *Cancer Chemother. Rep.*, **38**, 25 (1964).
(2) T. T. Otani and M. R. Briley, *J. Pharm. Sci.*, **65**, 534 (1976).
(3) *Ibid.*, **67**, 520 (1978).
(4) *Ibid.*, in press.
(5) J. P. Greenstein and M. Winitz, in "Chemistry of the Amino Acids," Wiley, New York, N.Y., 1961, p. 1267.
(6) D. D. Van Slyke, *J. Biol. Chem.*, **83**, 425 (1929).
(7) G. E. Foley, R. E. McCarthy, V. M. Binns, E. E. Snell, B. M. Guirard, G. W. Kidder, V. C. Dewey, and P. S. Thayer, *Ann. N.Y. Acad. Sci.*, **76**, 413 (1958).

Theodore T. Otani ˣ
Mary R. Briley
Nucleic Acids Section
Laboratory of Pathophysiology
National Cancer Institute
Bethesda, MD 20014

Received September 8, 1978.
Accepted for publication November 28, 1978.

Chlordiazepoxide: A New, More Sensitive and Specific Radioimmunoassay

Keyphrases □ Chlordiazepoxide—radioimmunoassay, in blood, plasma, saliva □ Radioimmunoassay—chlordiazepoxide in blood, plasma, saliva □ Tranquilizers—chlordiazepoxide, radioimmunoassay in blood, plasma, saliva

To the Editor:

In 1975, we reported (1) in detail the development of the first radioimmunoassay (RIA) for the widely used antianxiety agent chlordiazepoxide. Since that time, the radioimmunoassay has been used extensively here for studies involving the pharmacokinetic and biopharmaceutical evaluation of different formulations of the drug. Recently, however, we directed our attention toward measuring chlordiazepoxide in microsamples of whole blood, which can be simply obtained by a fingerstick, and in saliva, which offers a noninvasive approach. Simultaneous determination of chlordiazepoxide in blood/plasma and saliva might also allow us to evaluate both the pharmacokinetics and extent of *in vivo* drug protein binding as reflected by its concentrations in the two media. However, since the original radioimmunoassay procedure employed relatively low specific activity 2-^{14}C-chlordiazepoxide as the radioligand, it lacked the necessary sensitivity to achieve these aims.

We now wish to report the development of a radioimmunoassay for chlordiazepoxide that incorporates both a new radioligand and an antiserum.

The new hapten, 5-(4-aminophenyl)-7-chloro-2-methylamino-3*H*-1,4-benzodiazepine-4-oxide, was diazotized with 0.9 equivalents of nitrous acid and coupled to bovine serum albumin essentially as described by Peskar and Spector (2). The excess hapten was removed by exhaustive dialysis, and the conjugate was isolated by lyophilization as a brick-red powder. Rabbits were immunized with the conjugate as previously described (1), and the antiserum with the highest titer (1:15,000) of antibodies to chlordiazepoxide was used for all further studies.

The new radioligand, 8-^{3}H-chlordiazepoxide, was prepared by selective reduction of 2-amino-4,5-dichlorobenzophenone with tritium over Lindlar catalyst to yield 4-^{3}H-2-amino-5-chlorobenzophenone, which was converted to the desired product as previously described (3, 4). The 8-^{3}H-chlordiazepoxide was crystallized as its hydrochloride salt from methanol–ether to yield material with a specific activity of 17.8 Ci/mmole.

The radioimmunoassay procedure was identical with that recently described by Dixon and Crews (5) for diazepam. A logit–log calibration curve for chlordiazepoxide was linear between 50 and 5000 pg/tube, which represents a 40-fold increase in sensitivity over the original procedure (1). Routinely, 10 μl of blood or plasma was diluted to 1 ml with assay buffer and a 100-μl aliquot was taken for analysis. Saliva (100 μl) was assayed without dilution. Under these conditions, the working limits of sensitivity for blood/plasma and saliva were 50 and 0.5 ng/ml of chlordiazepoxide, respectively.

The new antiserum exhibited a fortuitously improved specificity toward chlordiazepoxide in that the cross-reactivity of a major metabolite, *N*-desmethylchlordiazepoxide, was <1% as opposed to 5% with the original antiserum (1). Other metabolites found in plasma, demoxepam and *N*-desmethyldiazepam, still cross-reacted less than 1%. A similar lack of cross-reactivity was found with all other benzodiazepines marketed in the United States. Amitriptyline and its metabolite, nortriptyline, showed no interference in the determination of chlordiazepoxide. The latter finding is particularly relevant in view of the recent introduction of a chlordiazepoxide–amitriptyline combination drug.

Preliminary studies using the new radioimmunoassay have indicated a chlordiazepoxide saliva to plasma concentration ratio of about 0.03, which is in close agreement with the ratio of unbound to bound chlordiazepoxide in plasma that we determined by equilibrium dialysis.

(1) W. R. Dixon, J. Earley, and E. Postma, *J. Pharm. Sci.*, **64**, 937 (1975).
(2) B. Peskar and S. Spector, *J. Pharmacol. Exp. Ther.*, **186**, 167 (1973).
(3) G. Field and L. Sternbach, U.S. pat. 3,515,724 (1970).
(4) G. Field and L. Sternbach, U.S. pat. 3,398,139 (1968).
(5) R. Dixon and T. Crews, *J. Anal. Toxicol.*, **2**, 210 (1978).

Ross Dixon ˣ
Rudolph Lucek
James Earley
Clark Perry
Research Division
Hoffmann-La Roche Inc.
Nutley, NJ 07110

Received October 27, 1978.
Accepted for publication November 28, 1978.

0022-3549/79/0200-0261$01.00/0
© 1979, American Pharmaceutical Association

observed for any acyl compounds previously tested. These compounds exhibited inhibition greater than 50% at 1 mg/ml, thus meeting the criterion of positivity set in the microbiological assay protocol (7). Therefore, these compounds have been submitted for antitumor test in mammalian systems.

Most of the active compounds were derivatives of phenylalanine analogs. Their activity was tested against melanomas, in which phenylalanine metabolism is believed to be intimately involved.

Detailed description of these findings will be reported elsewhere.

(1) T. T. Otani, *Cancer Chemother. Rep.*, **38**, 25 (1964).
(2) T. T. Otani and M. R. Briley, *J. Pharm. Sci.*, **65**, 534 (1976).
(3) *Ibid.*, **67**, 520 (1978).
(4) *Ibid.*, in press.
(5) J. P. Greenstein and M. Winitz, in "Chemistry of the Amino Acids," Wiley, New York, N.Y., 1961, p. 1267.
(6) D. D. Van Slyke, *J. Biol. Chem.*, **83**, 425 (1929).
(7) G. E. Foley, R. E. McCarthy, V. M. Binns, E. E. Snell, B. M. Guirard, G. W. Kidder, V. C. Dewey, and P. S. Thayer, *Ann. N.Y. Acad. Sci.*, **76**, 413 (1958).

Theodore T. Otani ˣ
Mary R. Briley
Nucleic Acids Section
Laboratory of Pathophysiology
National Cancer Institute
Bethesda, MD 20014

Received September 8, 1978.
Accepted for publication November 28, 1978.

Chlordiazepoxide: A New, More Sensitive and Specific Radioimmunoassay

Keyphrases □ Chlordiazepoxide—radioimmunoassay, in blood, plasma, saliva □ Radioimmunoassay—chlordiazepoxide in blood, plasma, saliva □ Tranquilizers—chlordiazepoxide, radioimmunoassay in blood, plasma, saliva

To the Editor:

In 1975, we reported (1) in detail the development of the first radioimmunoassay (RIA) for the widely used antianxiety agent chlordiazepoxide. Since that time, the radioimmunoassay has been used extensively here for studies involving the pharmacokinetic and biopharmaceutical evaluation of different formulations of the drug. Recently, however, we directed our attention toward measuring chlordiazepoxide in microsamples of whole blood, which can be simply obtained by a fingerstick, and in saliva, which offers a noninvasive approach. Simultaneous determination of chlordiazepoxide in blood/plasma and saliva might also allow us to evaluate both the pharmacokinetics and extent of *in vivo* drug protein binding as reflected by its concentrations in the two media. However, since the original radioimmunoassay procedure employed relatively low specific activity 2-^{14}C-chlordiazepoxide as the radioligand, it lacked the necessary sensitivity to achieve these aims.

We now wish to report the development of a radioimmunoassay for chlordiazepoxide that incorporates both a new radioligand and an antiserum.

The new hapten, 5-(4-aminophenyl)-7-chloro-2-methylamino-3*H*-1,4-benzodiazepine-4-oxide, was diazotized with 0.9 equivalents of nitrous acid and coupled to bovine serum albumin essentially as described by Peskar and Spector (2). The excess hapten was removed by exhaustive dialysis, and the conjugate was isolated by lyophilization as a brick-red powder. Rabbits were immunized with the conjugate as previously described (1), and the antiserum with the highest titer (1:15,000) of antibodies to chlordiazepoxide was used for all further studies.

The new radioligand, 8-^{3}H-chlordiazepoxide, was prepared by selective reduction of 2-amino-4,5-dichlorobenzophenone with tritium over Lindlar catalyst to yield 4-^{3}H-2-amino-5-chlorobenzophenone, which was converted to the desired product as previously described (3, 4). The 8-^{3}H-chlordiazepoxide was crystallized as its hydrochloride salt from methanol–ether to yield material with a specific activity of 17.8 Ci/mmole.

The radioimmunoassay procedure was identical with that recently described by Dixon and Crews (5) for diazepam. A logit–log calibration curve for chlordiazepoxide was linear between 50 and 5000 pg/tube, which represents a 40-fold increase in sensitivity over the original procedure (1). Routinely, 10 μl of blood or plasma was diluted to 1 ml with assay buffer and a 100-μl aliquot was taken for analysis. Saliva (100 μl) was assayed without dilution. Under these conditions, the working limits of sensitivity for blood/plasma and saliva were 50 and 0.5 ng/ml of chlordiazepoxide, respectively.

The new antiserum exhibited a fortuitously improved specificity toward chlordiazepoxide in that the cross-reactivity of a major metabolite, *N*-desmethylchlordiazepoxide, was <1% as opposed to 5% with the original antiserum (1). Other metabolites found in plasma, demoxepam and *N*-desmethyldiazepam, still cross-reacted less than 1%. A similar lack of cross-reactivity was found with all other benzodiazepines marketed in the United States. Amitriptyline and its metabolite, nortriptyline, showed no interference in the determination of chlordiazepoxide. The latter finding is particularly relevant in view of the recent introduction of a chlordiazepoxide–amitriptyline combination drug.

Preliminary studies using the new radioimmunoassay have indicated a chlordiazepoxide saliva to plasma concentration ratio of about 0.03, which is in close agreement with the ratio of unbound to bound chlordiazepoxide in plasma that we determined by equilibrium dialysis.

(1) W. R. Dixon, J. Earley, and E. Postma, *J. Pharm. Sci.*, **64**, 937 (1975).
(2) B. Peskar and S. Spector, *J. Pharmacol. Exp. Ther.*, **186**, 167 (1973).
(3) G. Field and L. Sternbach, U.S. pat. 3,515,724 (1970).
(4) G. Field and L. Sternbach, U.S. pat. 3,398,139 (1968).
(5) R. Dixon and T. Crews, *J. Anal. Toxicol.*, **2**, 210 (1978).

Ross Dixon ˣ
Rudolph Lucek
James Earley
Clark Perry
Research Division
Hoffmann-La Roche Inc.
Nutley, NJ 07110

Received October 27, 1978.
Accepted for publication November 28, 1978.

0022-3549/79/0200-0261$01.00/0
© 1979, American Pharmaceutical Association

Stable Solutions for Marijuana Analysis

Keyphrases □ Marijuana—GLC analysis, stability of cannabinoids in chloroform and ethanol solutions □ Cannabinoids—GLC analysis, stability in chloroform and ethanol solutions □ GLC—analysis, marijuana, stability of cannabinoids in chloroform and ethanol solutions

To the Editor:

Research on the stability of synthetic and naturally occurring cannabinoids in chloroform solution resulted in conflicting reports by Parker *et al.* (1) and Turner and Henry (2). Greater decomposition of synthetic cannabidiol stored in spectrograde chloroform over an 8-day period was reported relative to its stability in ethanol (1). However, in a subsequent 3-month stability study (2), chloroform solutions of synthetic cannabidiol were stable for 21 days, despite daily exposure to both ambient temperature and a combination of natural and artificial light under normal laboratory conditions.

This discrepancy was of interest because of our current involvement with marijuana analyses; our past experience with such analyses seemed to be midway between these two conflicting reports. Observations made during the development of our methods led us to the conclusion that chloroform solutions of cannabinoids should be refrigerated at all times (3).

Since the authors of the cited articles had used differing commercial brands of chloroform, we repeated the Parker *et al.* (1) study, replacing their brand of spectrograde chloroform[1] with the one[2] used by Turner and Henry (2). The GLC analysis was performed using a gas chromatograph[3] equipped with a hydrogen flame-ionization detector and a glass column packed with 3% OV-17 on 100–120-mesh Supelcoport[4]. The experimental conditions were: column temperature, 210°; injector temperature, 250°; detector temperature, 250°; and internal standard, *dl*-methadone hydrochloride.

Our results were nearly identical to those reported by Parker *et al.* (1); the ratio of the areas of the cannabidiol[5] *versus* internal standard peaks decreased an average of 16%/day for the chloroform solutions as compared to an average decrease of only 0.6%/day for the ethanol solutions. Solutions were stored in darkness at room temperature in well-sealed vials. We also tried 4-androsten-3,17-dione[6] as an internal standard since it was used by the previous researchers. No quantitative differences were found between 4-androsten-3,17-dione and *dl*-methadone hydrochloride. Methadone hydrochloride was preferred for our studies since it gave a sharper, more easily quantified GLC peak than did 4-androsten-3,17-dione.

Dr. Turner informed us that the cannabidiol used for analysis in his laboratories is first purified using column chromatography. In addition, the solute concentration used was 10 times greater than that used by Parker. Since either of these factors might affect solution stability, we tried to attain a stable solution of the column-purified material at both concentrations. Again, the solutions were unstable overnight and strongly discolored by the 3rd day. Thus, although the chloroform solutions of synthetic cannabidiol stored in darkness showed less than a 1% decrease on the day they were prepared, significant decomposition occurred by the 2nd day and continued steadily thereafter (Table I).

Table I—Decomposition of Synthetic Cannabidiol in Chloroform Solution

Conditions	Ratio of Cannabidiol to Methadone Peak Areas		
	Initially	After 3 hr	After 24 hr
Constant exposure to ambient temperature and fluorescent light	1.2	1.1	0.62
Constant exposure to ambient temperature and darkness	1.4	1.4	1.3

The stability of cannabinoid constituents in various solvents during analysis of actual plant material is of forensic importance. For this reason, we studied extracts from plant material, continuing to investigate cannabidiol stability but giving primary consideration to the stability of the active constituent, tetrahydrocannabinol. Turner and Henry (2) also included plant material in their study.

Our procedure was as follows. For the chloroform solution, 1 g of plant material was placed in a stoppered flask containing 20 ml of chloroform and 17.4 mg of methadone hydrochloride. The flask was placed in the refrigerator and shaken at 10-min intervals for 1 hr; then the plant material was filtered off and discarded. This chloroform solution was used directly for injection. To prepare the ethanol solutions, 1 g of plant material was extracted with pure chloroform as already described. After filtration, the chloroform was evaporated and the residue was redissolved in 20 ml of ethanol containing 17.4 mg of methadone hydrochloride.

Standard chloroform and ethanol extraction solutions were refrigerated at all times, and peak area ratios for cannabidiol to methadone and tetrahydrocannabinol to methadone were obtained daily. Both solutions were stable for several weeks under these conditions.

Preliminary degradation studies were done to determine the effect of sunlight, fluorescent light, and temperature on cannabinoid stability. The standard ethanol and chlo-

Table II—Effect of Sunlight and Laboratory Conditions on the Stability of Chloroform and Ethanol Solutions of Plant Material

Conditions	Total Exposure Time	Ratio of Δ^9-Tetrahydrocannabinol[a] to Methadone Peak Areas	Ratio of Cannabidiol[a] to Methadone Peak Areas
	Chloroform Solution		
Sunlight	30 min	0.63	0.20
Ambient laboratory	Overnight	0.68	0.12
Control	—	1.00	0.27
	Ethanol Solution		
Sunlight	30 min	0.63	0.26
Ambient laboratory	Overnight	0.81	0.26
Control	—	0.81	0.28

[a] The identities of the Δ^9-tetrahydrocannabinol and cannabidiol peaks were confirmed by mass spectrometry.

[1] Fisher Scientific.
[2] Mallinckrodt nanograde.
[3] Perkin-Elmer model 900.
[4] Supelco.
[5] Applied Science Laboratories (purity of 93%).
[6] Applied Science Laboratories.

0022-3549/79/0200-0262$01.00/0
© 1979, American Pharmaceutical Association

Table III—Effect of Sunlight on Chloroform Solutions with and without Added Stabilizers

Parameter	Total Exposure Time, min	Ratio of Δ^9-Tetrahydrocannabinol to Methadone Peak Areas	Ratio of Cannabidiol to Methadone Peak Areas
With stabilizers	30	1.1	0.32
Control	—	1.1	0.31
Without stabilizers	30	0.63	0.20
Control	—	1.0	0.27

roform extraction solutions (100-μl portions) were exposed to these conditions for controlled periods. Stability was tested by comparison of ratios from the exposed solutions to daily ratios from the standard solutions (Table II).

Thirty minutes of exposure to sunlight caused rapid decomposition and decolorization in the chloroform solution and a significant, although lesser, amount of decomposition in the ethanol solution. Overnight exposure to a combination of fluorescent light and room temperature, an approximation of normal ambient laboratory conditions, caused a marked decomposition in the chloroform solution; the ethanol solution remained stable within experimental error after more than 18 hr of exposure to these conditions.

Decomposition in chloroform solution is not significant for our current method, which limits solution exposure to ambient laboratory conditions to 30–45 min. For other laboratories, handling and sampling procedures may make lengthy exposure to normal ambient laboratory conditions unavoidable. In such cases, the demonstrated cannabinoid stability in ethanol suggests that the most reliable procedure for analysis would be extraction with chloroform, flash evaporation of the solvent, and redissolution in ethanol. This procedure is still inconvenient, however, for any analyst who does not do such work on a routine basis or who has a large number of samples to analyze. The convenience of maintaining the cannabinoids in the extracting solvent is often desirable, so a means of stabilizing the chloroform solution would be useful.

Since cannabinoid degradation by chloroform is thought to be a free radical reaction (4), a combination of free radical inhibitors was added to portions of the chloroform solutions immediately subsequent to the extraction procedure. To each 5-ml aliquot, 2.6 μl of mercaptoethanol and enough sodium diethyldithiocarbamate to saturate the solution were added. Portions of this solution (100 μl) were removed for timed exposures to sunlight or normal laboratory conditions. Control solutions were refrigerated routinely, and stability was measured by comparison of peak area ratios from these 100-μl portions with those from the control solutions.

After 30 min of exposure to sunlight, there was no evidence of decomposition in the stabilized solution, as compared to 25–35% decreases in the cannabinoid–methadone ratios for the solution without added stabilizers (Table III). In addition, the solution containing the stabilizers remained stable for up to 10 hr of exposure to normal ambient laboratory conditions. Therefore, we suggest that chloroform solutions of naturally occurring cannabinoids either be refrigerated at all times or, if substantial exposure to fluorescent or natural light cannot be avoided, that the combination of stabilizers, sodium diethyldithiocarbamate and mercaptoethanol, be added as a protective measure.

(1) M. J. Parker, M. L. Borke, L. M. Block, and T. G. Cochran, *J. Pharm. Sci.*, **63**, 970 (1974).
(2) C. E. Turner and J. T. Henry, *ibid.*, **64**, 357 (1975).
(3) P. Lerner, *Bull. Narcotics*, **21**, 39 (1969).
(4) E. R. Garrett, A. J. Gouyette, and H. Roseboom, *J. Pharm. Sci.*, **67**, 27 (1978).

Catherine M. Bonuccelli
U.S. Customs Service
Washington, DC 20229

Received June 28, 1978.
Accepted for publication December 1, 1978.
The author thanks Dr. Carlton E. Turner for providing the column-purified cannabidiol, which Dr. Turner assayed at 95.47% pure.

Selectivity of Silicone Rubber toward Prostaglandin Permeability

Keyphrases □ Silicone rubber membranes—selectivity toward transport of E and F prostaglandins □ Prostaglandins, E and F—transport selectivity of silicone rubber membranes □ Delivery systems, potential—silicone rubber membranes, selectivity toward transport of E and F prostaglandins

To the Editor:

Considerable interest is being focused on the design of controlled-release drug delivery systems (1, 2). Their rational development requires a basic understanding of the physical–chemical parameters that control drug transport through the delivery module. The type of polymer matrix and the chemical form of the drug must provide a delivery rate in phase with the pharmacological potency of the therapeutic agent.

In the field of fertility regulation, several prostaglandins in various vaginal dosage forms have been studied to optimize bioavailability, reduce side effects, eliminate mul-

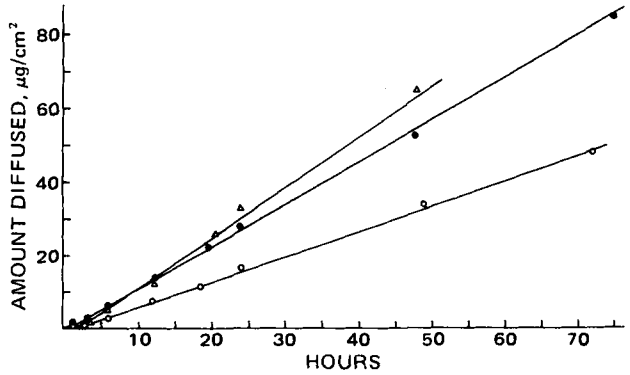

Figure 1—*Amount of prostaglandin transported across a silicone rubber membrane as a function of time. The donor compartment was maintained saturated with drug, and the membrane thickness was 0.05 cm. Key:* △, *dinoprost isopropyl ester;* ●, *dinoprost ethyl ester; and* ○, *dinoprost methyl ester.*

0022-3549/79/0200-0263$01.00/0
© 1979, American Pharmaceutical Association

Table III—Effect of Sunlight on Chloroform Solutions with and without Added Stabilizers

Parameter	Total Exposure Time, min	Ratio of Δ^9-Tetrahydrocannabinol to Methadone Peak Areas	Ratio of Cannabidiol to Methadone Peak Areas
With stabilizers	30	1.1	0.32
Control	—	1.1	0.31
Without stabilizers	30	0.63	0.20
Control	—	1.0	0.27

roform extraction solutions (100-μl portions) were exposed to these conditions for controlled periods. Stability was tested by comparison of ratios from the exposed solutions to daily ratios from the standard solutions (Table II).

Thirty minutes of exposure to sunlight caused rapid decomposition and decolorization in the chloroform solution and a significant, although lesser, amount of decomposition in the ethanol solution. Overnight exposure to a combination of fluorescent light and room temperature, an approximation of normal ambient laboratory conditions, caused a marked decomposition in the chloroform solution; the ethanol solution remained stable within experimental error after more than 18 hr of exposure to these conditions.

Decomposition in chloroform solution is not significant for our current method, which limits solution exposure to ambient laboratory conditions to 30–45 min. For other laboratories, handling and sampling procedures may make lengthy exposure to normal ambient laboratory conditions unavoidable. In such cases, the demonstrated cannabinoid stability in ethanol suggests that the most reliable procedure for analysis would be extraction with chloroform, flash evaporation of the solvent, and redissolution in ethanol. This procedure is still inconvenient, however, for any analyst who does not do such work on a routine basis or who has a large number of samples to analyze. The convenience of maintaining the cannabinoids in the extracting solvent is often desirable, so a means of stabilizing the chloroform solution would be useful.

Since cannabinoid degradation by chloroform is thought to be a free radical reaction (4), a combination of free radical inhibitors was added to portions of the chloroform solutions immediately subsequent to the extraction procedure. To each 5-ml aliquot, 2.6 μl of mercaptoethanol and enough sodium diethyldithiocarbamate to saturate the solution were added. Portions of this solution (100 μl) were removed for timed exposures to sunlight or normal laboratory conditions. Control solutions were refrigerated routinely, and stability was measured by comparison of peak area ratios from these 100-μl portions with those from the control solutions.

After 30 min of exposure to sunlight, there was no evidence of decomposition in the stabilized solution, as compared to 25–35% decreases in the cannabinoid–methadone ratios for the solution without added stabilizers (Table III). In addition, the solution containing the stabilizers remained stable for up to 10 hr of exposure to normal ambient laboratory conditions. Therefore, we suggest that chloroform solutions of naturally occurring cannabinoids either be refrigerated at all times or, if substantial exposure to fluorescent or natural light cannot be avoided, that the combination of stabilizers, sodium diethyldithiocarbamate and mercaptoethanol, be added as a protective measure.

(1) M. J. Parker, M. L. Borke, L. M. Block, and T. G. Cochran, *J. Pharm. Sci.*, **63**, 970 (1974).
(2) C. E. Turner and J. T. Henry, *ibid.*, **64**, 357 (1975).
(3) P. Lerner, *Bull. Narcotics*, **21**, 39 (1969).
(4) E. R. Garrett, A. J. Gouyette, and H. Roseboom, *J. Pharm. Sci.*, **67**, 27 (1978).

Catherine M. Bonuccelli
U.S. Customs Service
Washington, DC 20229

Received June 28, 1978.
Accepted for publication December 1, 1978.
The author thanks Dr. Carlton E. Turner for providing the column-purified cannabidiol, which Dr. Turner assayed at 95.47% pure.

Selectivity of Silicone Rubber toward Prostaglandin Permeability

Keyphrases □ Silicone rubber membranes—selectivity toward transport of E and F prostaglandins □ Prostaglandins, E and F—transport selectivity of silicone rubber membranes □ Delivery systems, potential—silicone rubber membranes, selectivity toward transport of E and F prostaglandins

To the Editor:

Considerable interest is being focused on the design of controlled-release drug delivery systems (1, 2). Their rational development requires a basic understanding of the physical–chemical parameters that control drug transport through the delivery module. The type of polymer matrix and the chemical form of the drug must provide a delivery rate in phase with the pharmacological potency of the therapeutic agent.

In the field of fertility regulation, several prostaglandins in various vaginal dosage forms have been studied to optimize bioavailability, reduce side effects, eliminate mul-

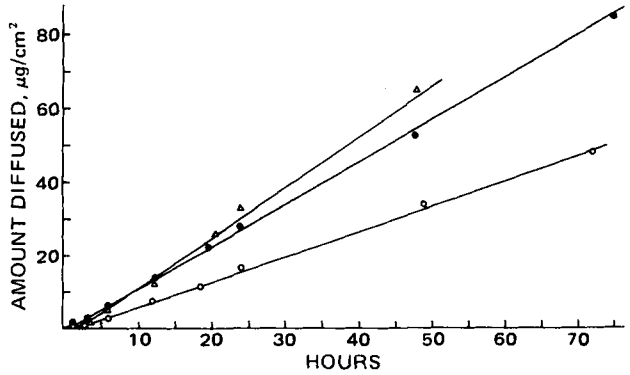

Figure 1—*Amount of prostaglandin transported across a silicone rubber membrane as a function of time. The donor compartment was maintained saturated with drug, and the membrane thickness was 0.05 cm. Key:* △, *dinoprost isopropyl ester;* ●, *dinoprost ethyl ester; and* ○, *dinoprost methyl ester.*

0022-3549/79/0200-0263$01.00/0
© 1979, American Pharmaceutical Association

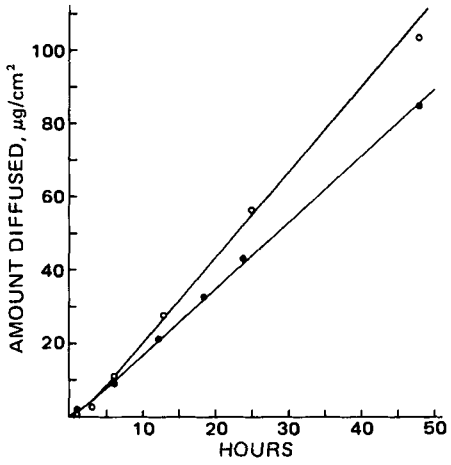

Figure 2—*Amount of prostaglandin transported across a silicone rubber membrane as a function of time. The donor compartment was maintained saturated with drug, and the membrane thickness was 0.05 cm. Key:* ○, *(15S)-15-methylprostaglandin $F_{2\alpha}$ ethyl ester; and* ●, *(15S)-15-methylprostaglandin $F_{2\alpha}$ methyl ester.*

tiple dosing regimens, and allow for self-administration (3, 4). This communication reports on the selectivity of silicone rubber toward the transport of E and F prostaglandins and its potential as a controlled-release delivery system.

Figures 1–3 show the diffusion profiles[1] of certain prostaglandins[2] across fillerless silicone rubber[3] membranes mounted in a diffusion cell (5). The free acid forms of dinoprost (prostaglandin $F_{2\alpha}$) and (15*S*)-15-methylprostaglandin $F_{2\alpha}$ did not permeate the membrane and are not presented on the graphs.

The presence of an ester linkage at the C-1 position markedly enhanced the permeation of dinoprostone (prostaglandin E_2) and the two F prostaglandins. Substitution of the C-9 hydroxyl group in dinoprost with a ketone moiety (*i.e.*, forming dinoprostone) also substantially increased the transport rate. Under saturation conditions

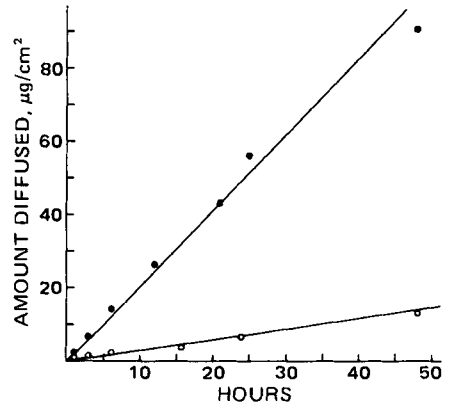

Figure 3—*Amount of prostaglandin transported across a silicone rubber membrane as a function of time. The donor compartment was maintained saturated with drug, and the membrane thickness was 0.05 cm. Key:* ●, *dinoprostone methyl ester; and* ○, *dinoprostone.*

[1] A GLC assay was used for prostaglandins of the F series while a UV assay was employed for the E series. Stability of E prostaglandins was verified by TLC, and stability of F prostaglandins was confirmed by GLC or TLC.

[2] The Upjohn Co., Kalamazoo, MI 49001.

[3] Dimethylpolysiloxane, Dow Corning Medical Products Division, Midland, Mich.

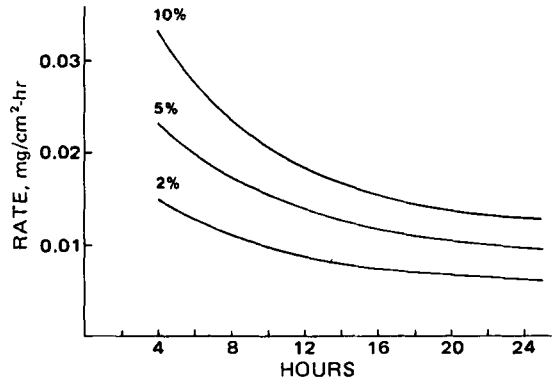

Figure 4—*Theoretical release rate profiles of (15S)-15-methylprostaglandin $F_{2\alpha}$ methyl ester from monolithic devices as a function of concentration.*

in the donor compartment, the steady-state flux, F, is given by (6):

$$F = \frac{C_s D_s}{h} \qquad \text{(Eq. 1)}$$

where C_s and D_s are the solubility and diffusivity in the membrane, respectively, and h is the membrane thickness. The dependence of flux on the chain length of alkyl esters of *p*-aminobenzoic acid was reported previously (7). For short chain lengths, $d \log F_n/dn = 0.19$, where F_n is the flux for a homolog with n carbons in the alkyl chain. Although sufficient data are not available to derive rigorously a dependence of F_n on n for prostaglandins, the flux of prostaglandins apparently is less sensitive to changes in ester chain length.

Release rate profiles of drugs from planar monolithic devices are given by the following time- (t) dependent equation when the total drug concentration, A, is much greater than C_s (8):

$$\text{rate} = \left(\frac{AC_s D_s}{2t}\right)^{1/2} \qquad \text{(Eq. 2)}$$

Normalizing the flux times distance given by Eq. 1 to unit thickness (*i.e.*, F_h) and substitution into Eq. 2 give:

$$\text{rate} = \left(\frac{AF_h}{2t}\right)^{1/2} \qquad \text{(Eq. 3)}$$

where F_h has the units of milligrams per centimeter-hour.

Equation 3 states that the drug release rate from polymer matrixes can be predicted once the steady-state flux across a membrane is determined (9). Theoretical release rate curves are shown in Fig. 4 for (15*S*)-15-methylprostaglandin $F_{2\alpha}$ methyl ester. A forthcoming publication will consider, in further detail, the applicability of Eq. 3 and the influence of membrane diffusivity and solubility on prostaglandin transport.

(1) "Controlled Release of Biologically Active Agents," Advances in Experimental Medicine and Biology, vol. 47, A. C. Tanquary and R. E. Lacey, Eds., Plenum, New York, N.Y., 1974.

(2) "Controlled Release Polymeric Formulations," ACS Symposium Series 33, D. R. Paul and F. W. Harris, Eds., American Chemical Society, Washington, D.C., 1976.

(3) "Prostaglandins and Reproduction," S. M. M. Karim, Ed., MPT Press, St. Leonard's House, Great Britain, 1975.

(4) C. H. Spilman, D. C. Beuving, A. D. Forbes, T. J. Roseman, and L. J. Larion, *Prostaglandins, Suppl.*, **12**, 1 (1976).

(5) G. L. Flynn and E. W. Smith, *J. Pharm. Sci.*, **60**, 1713 (1971).

(6) W. Jost, "Diffusion in Solids, Liquids, Gases," Academic, New York, N.Y., 1960.

(7) G. L. Flynn and S. H. Yalkowsky, *J. Pharm. Sci.*, **61**, 838 (1972).
(8) T. Higuchi, *ibid.*, **52**, 1145 (1963).
(9) D. R. Paul and S. K. McSpadden, *J. Membrane Sci.*, **1**, 33 (1976).

Theodore J. Roseman
The Upjohn Company
Kalamazoo, MI 49001

Received August 28, 1978.
Accepted for publication October 4, 1978.

BOOKS

REVIEWS

Psychopharmacology: From Theory To Practice. Edited by JACK D. BARCHAS, PHILIP A. BERGER, ROLAND D. CIARANELLO, and GLEN R. ELLIOTT. Oxford University Press, 200 Madison Ave., New York, NY 10016. 1977. xxiii + 557 pp. 15 × 23 cm. Price $17.95 cloth, $10.95 paper.

Although the treatment of mental and emotional diseases still leaves much to be desired, some of the most dramatic accomplishments have occurred in the area of pharmacotherapy. A quarter of a century has elapsed since the introduction of the new psychotropic drugs. During this generation of progress, the number of patients in mental hospitals has steadily decreased by about 360,000 from 559,000 in 1955 to the current estimate of less than 200,000. Attitudes have also changed toward mental and emotional disorders, with the recognition that these disorders are treatable and affect people of all ages. The economic cost of mental illness to this nation is estimated at more than $50 billion annually.

This book discusses recent developments in the study of neurotransmitters and neuromodulators (neuroregulators) and evidence indicating that behavioral events alter neurochemical function and that altered neurochemical function also can change behavior. Its central theme is the importance of neuroregulators and how they are affected by drugs. Thus, the interrelationships of drugs, neuroregulators, and behavior become the essence of psychopharmacology.

The text is fundamentally concerned with "the major psychiatric disorders and the manner in which the science of pharmacology may be applied, either immediately or ultimately, to their amelioration." The authors attempt to integrate the basic science and clinical aspects of psychopharmacology for those who will be responsible for the treatment of psychiatric patients. The scientific principles behind psychopharmacology are explained first, and then their relevance to the use of psychotropic drugs in good patient care is demonstrated. The text does not delve deeply into patient management, provide detailed descriptions of drug classes, summarize drug efficacy studies, or review classifications of psychiatric illnesses. Its coverage of pharmacotherapy is not very detailed.

"Psychopharmacology" is divided into five parts. Part I reviews, very nicely, the basic fields of study in psychopharmacology dealing with biochemical information on neuroregulators and the presumed mechanism of action of psychotropic drugs. Part I also includes chapters on the psychological and sociological aspects of psychopharmacology. Part II describes disorders that affect most patients who require psychiatric care, while Part III deals with drug abuse. Part IV discusses the pharmacotherapy of the young and the elderly, and Part V discusses specific topics important to psychopharmacology such as the use of placebos, the psychiatric effects of nonpsychiatric drugs, and the relationship of psychotherapy and pharmacotherapy.

The authors tried to make the treatment sections as practical as possible, providing information on normal dose ranges and side effects. They caution physicians that "the act of prescribing requires knowledge, care and clinical judgment," but omit a warning about individual human variability.

This book was written by 27 contributors, mostly physicians from Stanford University and the Palo Alto Veterans Administration Hospital, who have drawn upon their cumulative research and clinical experience to provide a useful guide, from theory to practice, of the major psychiatric disorders in the "new territory of psychopharmacology." It provides a knowledge base in psychopharmacology that will permit its readers to be informed practitioners and enable them to evaluate new information as it becomes available. Although "Psychopharmacology" is not a comprehensive survey of the generation of progress in this field, it is a good book and should be useful to clinicians, pharmacists, researchers, teachers, and students alike. Those interested in neuroregulators and their relation to behavioral disorders should buy a copy.

Reviewed by George J. Cosmides
National Institutes of Health
Bethesda, MD 20014

Drugs. How They Act and Why. By ALEX GRINGAUZ. C. V. Mosby, 11830 Westline Industrial Drive, St. Louis, MO 63141. 1978. 344 pp. 18 × 26 cm. Price $14.95.

This book is intended to serve as an aid to continuing education of pharmacists and other health professionals, particularly those who completed their formal academic training several years ago, before the advent of modern medicinal chemistry and molecular pharmacology. Accordingly, the level of presentation is elementary, and the discussions should be easily understood by the reader who has only minimal recollection of undergraduate biochemistry and medicinal chemistry.

The first chapter is a general introduction of some fundamentals of biochemistry. Chapters 2–4 consist of a review of some important characteristics of drug action, with emphasis on physicochemical principles, *e.g.*, factors affecting bioactivity, theories of drug action, selective toxicity, drug–receptor interactions, some stereochemistry and topography, some enzymology, antimetabolites, and chelation.

Thereafter, the book discusses some major classes of medicinal agents from the standpoint of biochemical mechanisms of action and clinical pharmacology. As the author emphasizes in the preface, not all categories of drugs are included because the book is not intended to be encyclopedic. Thus, the author selected the following topics: anticancer agents, antibiotics, adrenergic drugs, cholinergic drugs, analgesics, psychotherapeutics, and cardiovascular agents. Considering the objective of the book, most discussions seem to be adequate; however, in some cases extreme brevity leads to incomplete characterizations of important structure–activity relationships and mechanisms of action.

(7) G. L. Flynn and S. H. Yalkowsky, *J. Pharm. Sci.*, **61**, 838 (1972).
(8) T. Higuchi, *ibid.*, **52**, 1145 (1963).
(9) D. R. Paul and S. K. McSpadden, *J. Membrane Sci.*, **1**, 33 (1976).

Theodore J. Roseman
The Upjohn Company
Kalamazoo, MI 49001

Received August 28, 1978.
Accepted for publication October 4, 1978.

BOOKS

REVIEWS

Psychopharmacology: From Theory To Practice. Edited by JACK D. BARCHAS, PHILIP A. BERGER, ROLAND D. CIARANELLO, and GLEN R. ELLIOTT. Oxford University Press, 200 Madison Ave., New York, NY 10016. 1977. xxiii + 557 pp. 15 × 23 cm. Price $17.95 cloth, $10.95 paper.

Although the treatment of mental and emotional diseases still leaves much to be desired, some of the most dramatic accomplishments have occurred in the area of pharmacotherapy. A quarter of a century has elapsed since the introduction of the new psychotropic drugs. During this generation of progress, the number of patients in mental hospitals has steadily decreased by about 360,000 from 559,000 in 1955 to the current estimate of less than 200,000. Attitudes have also changed toward mental and emotional disorders, with the recognition that these disorders are treatable and affect people of all ages. The economic cost of mental illness to this nation is estimated at more than $50 billion annually.

This book discusses recent developments in the study of neurotransmitters and neuromodulators (neuroregulators) and evidence indicating that behavioral events alter neurochemical function and that altered neurochemical function also can change behavior. Its central theme is the importance of neuroregulators and how they are affected by drugs. Thus, the interrelationships of drugs, neuroregulators, and behavior become the essence of psychopharmacology.

The text is fundamentally concerned with "the major psychiatric disorders and the manner in which the science of pharmacology may be applied, either immediately or ultimately, to their amelioration." The authors attempt to integrate the basic science and clinical aspects of psychopharmacology for those who will be responsible for the treatment of psychiatric patients. The scientific principles behind psychopharmacology are explained first, and then their relevance to the use of psychotropic drugs in good patient care is demonstrated. The text does not delve deeply into patient management, provide detailed descriptions of drug classes, summarize drug efficacy studies, or review classifications of psychiatric illnesses. Its coverage of pharmacotherapy is not very detailed.

"Psychopharmacology" is divided into five parts. Part I reviews, very nicely, the basic fields of study in psychopharmacology dealing with biochemical information on neuroregulators and the presumed mechanism of action of psychotropic drugs. Part I also includes chapters on the psychological and sociological aspects of psychopharmacology. Part II describes disorders that affect most patients who require psychiatric care, while Part III deals with drug abuse. Part IV discusses the pharmacotherapy of the young and the elderly, and Part V discusses specific topics important to psychopharmacology such as the use of placebos, the psychiatric effects of nonpsychiatric drugs, and the relationship of psychotherapy and pharmacotherapy.

The authors tried to make the treatment sections as practical as possible, providing information on normal dose ranges and side effects. They caution physicians that "the act of prescribing requires knowledge, care and clinical judgment," but omit a warning about individual human variability.

This book was written by 27 contributors, mostly physicians from Stanford University and the Palo Alto Veterans Administration Hospital, who have drawn upon their cumulative research and clinical experience to provide a useful guide, from theory to practice, of the major psychiatric disorders in the "new territory of psychopharmacology." It provides a knowledge base in psychopharmacology that will permit its readers to be informed practitioners and enable them to evaluate new information as it becomes available. Although "Psychopharmacology" is not a comprehensive survey of the generation of progress in this field, it is a good book and should be useful to clinicians, pharmacists, researchers, teachers, and students alike. Those interested in neuroregulators and their relation to behavioral disorders should buy a copy.

Reviewed by George J. Cosmides
National Institutes of Health
Bethesda, MD 20014

Drugs. How They Act and Why. By ALEX GRINGAUZ. C. V. Mosby, 11830 Westline Industrial Drive, St. Louis, MO 63141. 1978. 344 pp. 18 × 26 cm. Price $14.95.

This book is intended to serve as an aid to continuing education of pharmacists and other health professionals, particularly those who completed their formal academic training several years ago, before the advent of modern medicinal chemistry and molecular pharmacology. Accordingly, the level of presentation is elementary, and the discussions should be easily understood by the reader who has only minimal recollection of undergraduate biochemistry and medicinal chemistry.

The first chapter is a general introduction of some fundamentals of biochemistry. Chapters 2–4 consist of a review of some important characteristics of drug action, with emphasis on physicochemical principles, *e.g.*, factors affecting bioactivity, theories of drug action, selective toxicity, drug–receptor interactions, some stereochemistry and topography, some enzymology, antimetabolites, and chelation.

Thereafter, the book discusses some major classes of medicinal agents from the standpoint of biochemical mechanisms of action and clinical pharmacology. As the author emphasizes in the preface, not all categories of drugs are included because the book is not intended to be encyclopedic. Thus, the author selected the following topics: anticancer agents, antibiotics, adrenergic drugs, cholinergic drugs, analgesics, psychotherapeutics, and cardiovascular agents. Considering the objective of the book, most discussions seem to be adequate; however, in some cases extreme brevity leads to incomplete characterizations of important structure–activity relationships and mechanisms of action.

(7) G. L. Flynn and S. H. Yalkowsky, *J. Pharm. Sci.*, **61**, 838 (1972).
(8) T. Higuchi, *ibid.*, **52**, 1145 (1963).
(9) D. R. Paul and S. K. McSpadden, *J. Membrane Sci.*, **1**, 33 (1976).

Theodore J. Roseman
The Upjohn Company
Kalamazoo, MI 49001

Received August 28, 1978.
Accepted for publication October 4, 1978.

BOOKS

REVIEWS

Psychopharmacology: From Theory To Practice. Edited by JACK D. BARCHAS, PHILIP A. BERGER, ROLAND D. CIARANELLO, and GLEN R. ELLIOTT. Oxford University Press, 200 Madison Ave., New York, NY 10016. 1977. xxiii + 557 pp. 15 × 23 cm. Price $17.95 cloth, $10.95 paper.

Although the treatment of mental and emotional diseases still leaves much to be desired, some of the most dramatic accomplishments have occurred in the area of pharmacotherapy. A quarter of a century has elapsed since the introduction of the new psychotropic drugs. During this generation of progress, the number of patients in mental hospitals has steadily decreased by about 360,000 from 559,000 in 1955 to the current estimate of less than 200,000. Attitudes have also changed toward mental and emotional disorders, with the recognition that these disorders are treatable and affect people of all ages. The economic cost of mental illness to this nation is estimated at more than $50 billion annually.

This book discusses recent developments in the study of neurotransmitters and neuromodulators (neuroregulators) and evidence indicating that behavioral events alter neurochemical function and that altered neurochemical function also can change behavior. Its central theme is the importance of neuroregulators and how they are affected by drugs. Thus, the interrelationships of drugs, neuroregulators, and behavior become the essence of psychopharmacology.

The text is fundamentally concerned with "the major psychiatric disorders and the manner in which the science of pharmacology may be applied, either immediately or ultimately, to their amelioration." The authors attempt to integrate the basic science and clinical aspects of psychopharmacology for those who will be responsible for the treatment of psychiatric patients. The scientific principles behind psychopharmacology are explained first, and then their relevance to the use of psychotropic drugs in good patient care is demonstrated. The text does not delve deeply into patient management, provide detailed descriptions of drug classes, summarize drug efficacy studies, or review classifications of psychiatric illnesses. Its coverage of pharmacotherapy is not very detailed.

"Psychopharmacology" is divided into five parts. Part I reviews, very nicely, the basic fields of study in psychopharmacology dealing with biochemical information on neuroregulators and the presumed mechanism of action of psychotropic drugs. Part I also includes chapters on the psychological and sociological aspects of psychopharmacology. Part II describes disorders that affect most patients who require psychiatric care, while Part III deals with drug abuse. Part IV discusses the pharmacotherapy of the young and the elderly, and Part V discusses specific topics important to psychopharmacology such as the use of placebos, the psychiatric effects of nonpsychiatric drugs, and the relationship of psychotherapy and pharmacotherapy.

The authors tried to make the treatment sections as practical as possible, providing information on normal dose ranges and side effects. They caution physicians that "the act of prescribing requires knowledge, care and clinical judgment," but omit a warning about individual human variability.

This book was written by 27 contributors, mostly physicians from Stanford University and the Palo Alto Veterans Administration Hospital, who have drawn upon their cumulative research and clinical experience to provide a useful guide, from theory to practice, of the major psychiatric disorders in the "new territory of psychopharmacology." It provides a knowledge base in psychopharmacology that will permit its readers to be informed practitioners and enable them to evaluate new information as it becomes available. Although "Psychopharmacology" is not a comprehensive survey of the generation of progress in this field, it is a good book and should be useful to clinicians, pharmacists, researchers, teachers, and students alike. Those interested in neuroregulators and their relation to behavioral disorders should buy a copy.

Reviewed by George J. Cosmides
National Institutes of Health
Bethesda, MD 20014

Drugs. How They Act and Why. By ALEX GRINGAUZ. C. V. Mosby, 11830 Westline Industrial Drive, St. Louis, MO 63141. 1978. 344 pp. 18 × 26 cm. Price $14.95.

This book is intended to serve as an aid to continuing education of pharmacists and other health professionals, particularly those who completed their formal academic training several years ago, before the advent of modern medicinal chemistry and molecular pharmacology. Accordingly, the level of presentation is elementary, and the discussions should be easily understood by the reader who has only minimal recollection of undergraduate biochemistry and medicinal chemistry.

The first chapter is a general introduction of some fundamentals of biochemistry. Chapters 2–4 consist of a review of some important characteristics of drug action, with emphasis on physicochemical principles, *e.g.*, factors affecting bioactivity, theories of drug action, selective toxicity, drug–receptor interactions, some stereochemistry and topography, some enzymology, antimetabolites, and chelation.

Thereafter, the book discusses some major classes of medicinal agents from the standpoint of biochemical mechanisms of action and clinical pharmacology. As the author emphasizes in the preface, not all categories of drugs are included because the book is not intended to be encyclopedic. Thus, the author selected the following topics: anticancer agents, antibiotics, adrenergic drugs, cholinergic drugs, analgesics, psychotherapeutics, and cardiovascular agents. Considering the objective of the book, most discussions seem to be adequate; however, in some cases extreme brevity leads to incomplete characterizations of important structure–activity relationships and mechanisms of action.

The last chapter is on drug interactions, and its purpose is to survey mechanisms and factors involved in drug interactions.

Finally, the book contains two appendixes: drug metabolism and inactivation, and drug-induced effects on laboratory diagnostic tests.

The author succeeded in accomplishing his objective in the preparation of this book. Moreover, this book will prove to be beneficial not only to practicing pharmacists but also to other professionals who need updating in medicinal chemistry.

Reviewed by Jaime N. Delgado
College of Pharmacy
University of Texas
Austin, TX 78712

Drug Fate and Metabolism: Methods and Techniques, Vol. 2. Edited by EDWARD R. GARRETT and JEAN L. HIRTZ. Dekker, 270 Madison Ave., New York, NY 10016. 1978. 382 pp. 14 × 23 cm. Price $39.50.

This volume is the second in a series dealing with drug fate and metabolism, including such topics as spectroscopy, stereochemistry, and the mechanisms of drug action. Emphasis is placed on methods rather than on theory. The book is divided into six chapters, each of which is authored by scientists having expertise in a specific area of drug methodology.

Chapter 1 emphasizes the application of voltammetric methods to drug analysis. Chapter 2 discusses the use of derivatization, detection, and metabolic transformation in GLC. The authors include an excellent literature reference list of various drugs analyzed by GLC. Chapter 3 describes stereochemical methodology, especially the discrimination of diastereoisomers and enantiomers. Chapter 4 reviews the physicochemical, instrumental, and experimental features of fluorescence spectroscopy. Chapter 5 describes the use of nonradioactive immunoassays, including viroimmunoassay and enzymoimmunoassay. Chapter 6 discusses the isolation, separation, and assay methods for the analysis of glucuronic acid conjugates.

Although the main emphasis of this book is geared toward the research scientist, it is a valuable supplement for students interested in toxicology, analytical chemistry, and pharmacology.

Reviewed by Gerald W. A. Slywka
School of Pharmacy
Ferris State College
Big Rapids, MI 49307

NOTICES

Thrombosis. Animal and Clinical Models. Vol. 102 of Advances in Experimental Medicine and Biology. Edited by H. JAMES DAY, BASIL A. MOLONY, EDWARD E. NISHIZAWA, and RONALD H. RYNBRANDT. Plenum, 227 W. 17th St., New York, NY 10011. 1978. 337 pp. 16 × 25 cm. Price $35.00.

Prevention and Detection of Cancer. Part II. Detection. Vol. 1. High Risk Markers. Detection Methods and Management. Edited by HERBERT E. NIEBURGS. Dekker, 270 Madison Ave., New York, NY 10016. 1978. 1299 pp. 18 × 25 cm. Price $62.50.

Etiology, Pathophysiology, and Treatment of Acute Gastroenteritis. Report of the 74th Ross Conference on Pediatric Research. Ross Laboratories, Columbus, OH 43216. 1978. 125 pp. 14× 22 cm.

Manual of Dermatologic Therapeutics With Essentials of Diagnosis, 2nd Edition. By KENNETH A. ARNDT. Little, Brown, 34 Beacon St., Boston, MA 02106. 1978. 377 pp. 13 × 23 cm. Price $10.95.

Journal of Veterinary Pharmacology and Therapeutics. Vol. 1, No. 1. Edited by ANDREW YOXALL and CHARLES SHORT. Blackwell Scientific Publications, Osney Mead, Oxford OX20EL, England. 1978. 92 pp. 16 × 25 cm.

Drugs and the Inheritance of Behavior. A Survey of Comparative Psychopharmacogenetics. By P. L. BROADHURST. Plenum, 227 W. 17th St., New York, NY 10011. 1978. 206 pp. 15 × 23 cm. Price $19.50.

Biosynthetic Products for Cancer Chemotherapy. Vol. 2. By GEORGE R. PETTIT and GORDON M. CRAGG. Plenum, 227 W. 17th St., New York, NY 10011. 1978. 150 pp. 14 × 23 cm. Price $35.00.

Discovery, Development and Delivery of New Drugs. By KARL H. BEYER, Jr. Spectrum, 175-20 Wexford Terrace, Jamaica, NY 11432. 1978. 238 pp. 15 × 12 cm. Price $20.00.

An Introduction to Microscopy by Means of Light, Electrons, X-Rays, or Ultrasound. By THEODORE GEORGE ROCHOW and EUGENE GEORGE ROCHOW. Plenum, 227 W. 17th St., New York, NY 10011. 1978. 367 pp. 15 × 23 cm. Price $29.50.

Acetylcholine Synthesis in Neurons. By S. TUCEK. Wiley, 605 Third Ave., New York, NY 10016. 1978. 259 pp. 15 × 24 cm. Price $37.50.

Reviews of Physiology, Biochemistry and Pharmacology. 81. (Formerly *Ergebnisse der Physiologie, Biologischen Chemie und Experimentellen Pharmackologie.*) Edited by R. H. ADRIAN *et al.* Springer-Verlag New York Inc., 175 Fifth Ave., New York, NY 10016. 1978. 214 pp. 16 × 25 cm. Price $43.00.

Scientific Foundations of Clinical Biochemistry. Vol. 1: Analytical Aspects. Edited by DAVID L. WILLIAMS, RONALD F. NUNN, and VINCENT MARKS. William Heinemann Medical Books Ltd., 23 Bedford Square, London WC1B3HH, England. 1978. 490 pp. 21 × 28 cm. Price 25.00 Fr.

The last chapter is on drug interactions, and its purpose is to survey mechanisms and factors involved in drug interactions.

Finally, the book contains two appendixes: drug metabolism and inactivation, and drug-induced effects on laboratory diagnostic tests.

The author succeeded in accomplishing his objective in the preparation of this book. Moreover, this book will prove to be beneficial not only to practicing pharmacists but also to other professionals who need updating in medicinal chemistry.

Reviewed by Jaime N. Delgado
College of Pharmacy
University of Texas
Austin, TX 78712

Drug Fate and Metabolism: Methods and Techniques, Vol. 2. Edited by EDWARD R. GARRETT and JEAN L. HIRTZ. Dekker, 270 Madison Ave., New York, NY 10016. 1978. 382 pp. 14 × 23 cm. Price $39.50.

This volume is the second in a series dealing with drug fate and metabolism, including such topics as spectroscopy, stereochemistry, and the mechanisms of drug action. Emphasis is placed on methods rather than on theory. The book is divided into six chapters, each of which is authored by scientists having expertise in a specific area of drug methodology.

Chapter 1 emphasizes the application of voltammetric methods to drug analysis. Chapter 2 discusses the use of derivatization, detection, and metabolic transformation in GLC. The authors include an excellent literature reference list of various drugs analyzed by GLC. Chapter 3 describes stereochemical methodology, especially the discrimination of diastereoisomers and enantiomers. Chapter 4 reviews the physicochemical, instrumental, and experimental features of fluorescence spectroscopy. Chapter 5 describes the use of nonradioactive immunoassays, including viroimmunoassay and enzymoimmunoassay. Chapter 6 discusses the isolation, separation, and assay methods for the analysis of glucuronic acid conjugates.

Although the main emphasis of this book is geared toward the research scientist, it is a valuable supplement for students interested in toxicology, analytical chemistry, and pharmacology.

Reviewed by Gerald W. A. Slywka
School of Pharmacy
Ferris State College
Big Rapids, MI 49307

NOTICES

Thrombosis. Animal and Clinical Models. Vol. 102 of Advances in Experimental Medicine and Biology. Edited by H. JAMES DAY, BASIL A. MOLONY, EDWARD E. NISHIZAWA, and RONALD H. RYNBRANDT. Plenum, 227 W. 17th St., New York, NY 10011. 1978. 337 pp. 16 × 25 cm. Price $35.00.

Prevention and Detection of Cancer. Part II. Detection. Vol. 1. High Risk Markers. Detection Methods and Management. Edited by HERBERT E. NIEBURGS. Dekker, 270 Madison Ave., New York, NY 10016. 1978. 1299 pp. 18 × 25 cm. Price $62.50.

Etiology, Pathophysiology, and Treatment of Acute Gastroenteritis. Report of the 74th Ross Conference on Pediatric Research. Ross Laboratories, Columbus, OH 43216. 1978. 125 pp. 14× 22 cm.

Manual of Dermatologic Therapeutics With Essentials of Diagnosis, 2nd Edition. By KENNETH A. ARNDT. Little, Brown, 34 Beacon St., Boston, MA 02106. 1978. 377 pp. 13 × 23 cm. Price $10.95.

Journal of Veterinary Pharmacology and Therapeutics. Vol. 1, No. 1. Edited by ANDREW YOXALL and CHARLES SHORT. Blackwell Scientific Publications, Osney Mead, Oxford OX20EL, England. 1978. 92 pp. 16 × 25 cm.

Drugs and the Inheritance of Behavior. A Survey of Comparative Psychopharmacogenetics. By P. L. BROADHURST. Plenum, 227 W. 17th St., New York, NY 10011. 1978. 206 pp. 15 × 23 cm. Price $19.50.

Biosynthetic Products for Cancer Chemotherapy. Vol. 2. By GEORGE R. PETTIT and GORDON M. CRAGG. Plenum, 227 W. 17th St., New York, NY 10011. 1978. 150 pp. 14 × 23 cm. Price $35.00.

Discovery, Development and Delivery of New Drugs. By KARL H. BEYER, Jr. Spectrum, 175-20 Wexford Terrace, Jamaica, NY 11432. 1978. 238 pp. 15 × 12 cm. Price $20.00.

An Introduction to Microscopy by Means of Light, Electrons, X-Rays, or Ultrasound. By THEODORE GEORGE ROCHOW and EUGENE GEORGE ROCHOW. Plenum, 227 W. 17th St., New York, NY 10011. 1978. 367 pp. 15 × 23 cm. Price $29.50.

Acetylcholine Synthesis in Neurons. By S. TUCEK. Wiley, 605 Third Ave., New York, NY 10016. 1978. 259 pp. 15 × 24 cm. Price $37.50.

Reviews of Physiology, Biochemistry and Pharmacology. 81. (Formerly *Ergebnisse der Physiologie, Biologischen Chemie und Experimentellen Pharmackologie.*) Edited by R. H. ADRIAN *et al.* Springer-Verlag New York Inc., 175 Fifth Ave., New York, NY 10016. 1978. 214 pp. 16 × 25 cm. Price $43.00.

Scientific Foundations of Clinical Biochemistry. Vol. 1: Analytical Aspects. Edited by DAVID L. WILLIAMS, RONALD F. NUNN, and VINCENT MARKS. William Heinemann Medical Books Ltd., 23 Bedford Square, London WC1B3HH, England. 1978. 490 pp. 21 × 28 cm. Price 25.00 Fr.

The last chapter is on drug interactions, and its purpose is to survey mechanisms and factors involved in drug interactions.

Finally, the book contains two appendixes: drug metabolism and inactivation, and drug-induced effects on laboratory diagnostic tests.

The author succeeded in accomplishing his objective in the preparation of this book. Moreover, this book will prove to be beneficial not only to practicing pharmacists but also to other professionals who need updating in medicinal chemistry.

Reviewed by Jaime N. Delgado
College of Pharmacy
University of Texas
Austin, TX 78712

Drug Fate and Metabolism: Methods and Techniques, Vol. 2. Edited by EDWARD R. GARRETT and JEAN L. HIRTZ. Dekker, 270 Madison Ave., New York, NY 10016. 1978. 382 pp. 14 × 23 cm. Price $39.50.

This volume is the second in a series dealing with drug fate and metabolism, including such topics as spectroscopy, stereochemistry, and the mechanisms of drug action. Emphasis is placed on methods rather than on theory. The book is divided into six chapters, each of which is authored by scientists having expertise in a specific area of drug methodology.

Chapter 1 emphasizes the application of voltammetric methods to drug analysis. Chapter 2 discusses the use of derivatization, detection, and metabolic transformation in GLC. The authors include an excellent literature reference list of various drugs analyzed by GLC. Chapter 3 describes stereochemical methodology, especially the discrimination of diastereoisomers and enantiomers. Chapter 4 reviews the physicochemical, instrumental, and experimental features of fluorescence spectroscopy. Chapter 5 describes the use of nonradioactive immunoassays, including viroimmunoassay and enzymoimmunoassay. Chapter 6 discusses the isolation, separation, and assay methods for the analysis of glucuronic acid conjugates.

Although the main emphasis of this book is geared toward the research scientist, it is a valuable supplement for students interested in toxicology, analytical chemistry, and pharmacology.

Reviewed by Gerald W. A. Slywka
School of Pharmacy
Ferris State College
Big Rapids, MI 49307

NOTICES

Thrombosis. Animal and Clinical Models. Vol. 102 of Advances in Experimental Medicine and Biology. Edited by H. JAMES DAY, BASIL A. MOLONY, EDWARD E. NISHIZAWA, and RONALD H. RYNBRANDT. Plenum, 227 W. 17th St., New York, NY 10011. 1978. 337 pp. 16 × 25 cm. Price $35.00.

Prevention and Detection of Cancer. Part II. Detection. Vol. 1. High Risk Markers. Detection Methods and Management. Edited by HERBERT E. NIEBURGS. Dekker, 270 Madison Ave., New York, NY 10016. 1978. 1299 pp. 18 × 25 cm. Price $62.50.

Etiology, Pathophysiology, and Treatment of Acute Gastroenteritis. Report of the 74th Ross Conference on Pediatric Research. Ross Laboratories, Columbus, OH 43216. 1978. 125 pp. 14× 22 cm.

Manual of Dermatologic Therapeutics With Essentials of Diagnosis, 2nd Edition. By KENNETH A. ARNDT. Little, Brown, 34 Beacon St., Boston, MA 02106. 1978. 377 pp. 13 × 23 cm. Price $10.95.

Journal of Veterinary Pharmacology and Therapeutics. Vol. 1, No. 1. Edited by ANDREW YOXALL and CHARLES SHORT. Blackwell Scientific Publications, Osney Mead, Oxford OX20EL, England. 1978. 92 pp. 16 × 25 cm.

Drugs and the Inheritance of Behavior. A Survey of Comparative Psychopharmacogenetics. By P. L. BROADHURST. Plenum, 227 W. 17th St., New York, NY 10011. 1978. 206 pp. 15 × 23 cm. Price $19.50.

Biosynthetic Products for Cancer Chemotherapy. Vol. 2. By GEORGE R. PETTIT and GORDON M. CRAGG. Plenum, 227 W. 17th St., New York, NY 10011. 1978. 150 pp. 14 × 23 cm. Price $35.00.

Discovery, Development and Delivery of New Drugs. By KARL H. BEYER, Jr. Spectrum, 175-20 Wexford Terrace, Jamaica, NY 11432. 1978. 238 pp. 15 × 12 cm. Price $20.00.

An Introduction to Microscopy by Means of Light, Electrons, X-Rays, or Ultrasound. By THEODORE GEORGE ROCHOW and EUGENE GEORGE ROCHOW. Plenum, 227 W. 17th St., New York, NY 10011. 1978. 367 pp. 15 × 23 cm. Price $29.50.

Acetylcholine Synthesis in Neurons. By S. TUCEK. Wiley, 605 Third Ave., New York, NY 10016. 1978. 259 pp. 15 × 24 cm. Price $37.50.

Reviews of Physiology, Biochemistry and Pharmacology. 81. (Formerly *Ergebnisse der Physiologie, Biologischen Chemie und Experimentellen Pharmackologie.*) Edited by R. H. ADRIAN *et al.* Springer-Verlag New York Inc., 175 Fifth Ave., New York, NY 10016. 1978. 214 pp. 16 × 25 cm. Price $43.00.

Scientific Foundations of Clinical Biochemistry. Vol. 1: Analytical Aspects. Edited by DAVID L. WILLIAMS, RONALD F. NUNN, and VINCENT MARKS. William Heinemann Medical Books Ltd., 23 Bedford Square, London WC1B3HH, England. 1978. 490 pp. 21 × 28 cm. Price 25.00 Fr.

A publication of the
American Pharmaceutical Association—
the National Professional Society
of Pharmacists

JOURNAL OF PHARMACEUTICAL SCIENCES

INDEX TO AUTHORS
INDEX TO SUBJECTS

VOLUME 68
JANUARY TO DECEMBER, 1979

Published monthly under the supervision of the Board of Trustees

MARY H. FERGUSON
Editor

SHELLY ELLIOTT
Production Editor

MARCIA GARTRELL
Copy Editor

NICOLETTE TRIANTAFELLU
Copy Editor

EDWARD G. FELDMANN
Contributing Editor

SAMUEL W. GOLDSTEIN
Contributing Editor

BELLE R. BECK
Editorial Secretary

DAVID BOHARDT
Director of Publications

L. LUAN CORRIGAN
Assistant Director of Publications

EDITORIAL ADVISORY BOARD

John Autian
Norman R. Farnsworth
William O. Foye
William J. Jusko
Herbert A. Lieberman
David E. Mann, Jr.
Gerald J. Papariello
Edward G. Rippie

MARCH 1979
VOLUME 68 NUMBER 3

JOURNAL OF PHARMACEUTICAL SCIENCES

(ISSN 0022-3549)

MARY H. FERGUSON
Editor

SHELLY ELLIOTT
Production Editor

JANIS KELLY
Copy Editor

EDWARD G. FELDMANN
Contributing Editor

SAMUEL W. GOLDSTEIN
Contributing Editor

BELLE R. BECK
Editorial Secretary

DAVID BOHARDT
Director of Publications

L. LUAN CORRIGAN
Assistant Director of Publications

EDITORIAL ADVISORY BOARD

JOHN AUTIAN
HERBERT A. LIEBERMAN
NORMAN R. FARNSWORTH
DAVID E. MANN, JR.
WILLIAM O. FOYE
GERALD J. PAPARIELLO
WILLIAM J. JUSKO
EDWARD G. RIPPIE

The *Journal of Pharmaceutical Sciences* is published monthly by the American Pharmaceutical Association (APhA) at 2215 Constitution Ave., N.W., Washington, DC 20037. Second-class postage paid at Washington, D.C., and at additional mailing office.

All expressions of opinion and statements of supposed fact appearing in articles or editorials carried in this journal are published on the authority of the writer over whose name they appear and are not to be regarded as necessarily expressing the policies or views of APhA.

Offices—Editorial, Advertising, and Subscription: 2215 Constitution Ave., N.W., Washington, DC 20037. Printing: 20th & Northampton Streets, Easton, PA 18042.

Annual Subscriptions—United States and foreign, industrial and government institutions $50, educational institutions $50, individuals *for personal use only* $30; single copies $5. All foreign subscriptions add $5 for postage. Subscription rates are subject to change without notice. Members of APhA may elect to receive the *Journal of Pharmaceutical Sciences* as a part of their annual $70 (foreign $75) APhA membership dues.

Claims—Missing numbers will not be supplied if dues or subscriptions are in arrears for more than 60 days or if claims are received more than 60 days after the date of the issue, or if loss was due to failure to give notice of change of address. APhA cannot accept responsibility for foreign delivery when its records indicate shipment has been made.

Change of Address—Members and subscribers should notify at once both the Post Office and APhA of any change of address.

Photocopying—The code at the foot of the first page of an article indicates that APhA has granted permission for copying of the article beyond the limits permitted by Sections 107 and 108 of the U.S. Copyright Law provided that the copier sends the per copy fee stated in the code to the Copyright Clearance Center, Inc., P.O. Box 8891, Boston, MA 02114. Copies may be made for personal or internal use only and not for general distribution.

Microfilm—Available from University Microfilms International, 300 N. Zeeb Road, Ann Arbor, MI 48106.

© Copyright 1979, American Pharmaceutical Association, 2215 Constitution Ave., N.W., Washington, DC 20037; all rights reserved.

RISKING PUBLIC CREDIBILITY

"Wolf! Wolf!" they cried, and the fattened calves no longer came to market. This resulted because of fear that hormone-supplemented animal feed might lead to residues in meat and, upon consumption, such residues would induce cancer in those people ingesting such products.

"Wolf! Wolf!" they cried, and food store shelves were swept clean of cyclamate sweetener products, also out of fear of their alleged carcinogenicity.

"Wolf! Wolf!" they cried, and we witnessed the ludicrous sight of state highway crews in Maryland digging up roads in an effort to eliminate asbestos-containing gravel which also has been suspected of having carcinogenic properties.

And so on, we have witnessed a whole host of products indicted as cancer-causing agents that must be eliminated from the marketplace at any and all costs.

Initially, such accusations were made carefully, and only after reasonable proof was produced, as in the case with smoking as a causative factor with regard to lung, throat, and mouth cancer. But the movement rapidly has escalated in more recent years to the point where reckless charges are leveled and corrective actions are quickly initiated on the basis of only the most meager evidence. It is almost as if the political excesses of the French Revolution, or of the Senator McCarthy era in the United States, had been revived in the guise of misdirected science and runaway regulation.

Smoked bacon, charcoal-grilled steaks, chlorine-treated drinking water, plastic soft drink bottles, fire-resistant treated sleepwear, hair dyes, and saccharin are just a few of the many other familiar products which have been tarred with the broad brush of "carcinogenic" often on the flimsiest of grounds.

But recently there are signs that the broad swing of the pendulum may have reached its zenith and that it is returning toward reasonableness.

"Regulation" in its general sense appears to be growing less popular with President Carter and his White House advisors. The President's economic report to Congress in late January suggested that compliance with overzealous environmental, health, and safety regulations represents a big drag on productivity. Although regulation is certainly worthwhile, the report went on to declare that "regulation is very costly; benefits should be closely compared with costs."

But even more targeted to the cancer-scare phobia discussed above, we were gratified to read some words of sanity coming from a very unexpected source—the Consumer Product Safety Commission, a relative new-comer agency on the federal scene, and one that on other matters has generated a rather deserved label of being "an extremist in the pursuit of safety."

No less than the vice-chairman of the CPSC, Commissioner Barbara Hackman Franklin, has been telling a variety of public and private groups such down-to-earth things as: "You can't just ban things because they cause cancer. That's too simple."

Our scientist-readers may not be impressed with this statement, but in politically-sensitive Washington to speak such truths is seen as career-suicide or even heresy. Heads have been known to roll for much less reason.

But as Commissioner Franklin wisely has pointed out in a series of speeches she has delivered over the past year: *Consumers are confused and being increasingly "turned off" by the bombardment of warnings about the cancer-causing potential of many products. People want answers about causes of cancer, but they are frustrated by the proliferation of cancer warnings.*

She has been preaching a message in her talks across the country that we need to generate a unified, thoughtful, and well-reasoned approach to regulatory actions intended to protect the public against real cancer threats. She has even addressed President Carter on several occasions with specific proposals to *"plot an effective course of action which would make sense for industry, government, and most of all, for consumers—those who feel increasingly confused or cynical."*

Commissioner Franklin appears to be saying to all who will listen that we can only tell people "Wolf! Wolf!" so often before both scientists and political leaders lose their credibility on the subject. Then the public will not believe us even when something comes along with a 100% fatality rate in submicro quantities!

—EGF

Phytochemists Aren't Perfect—But Almost

Janzen[1] has expressed an opinion that phytochemists and others reporting on the isolation of secondary chemical compounds from plants often fail to indicate the specific plant part from which the compounds originate. This omission appears to be hindering biologists interested in relating plant and animal biology, more specifically, herbivore-eating habits.

We have been computerizing the world literature on natural products since before 1975 in a system referred to as NAPRALERT. We include the specific plant part(s) from which chemical compounds are isolated and/or identified (including percentage yields when they are stated or can be calculated). It was thought to be of interest to query the computer to determine all publications that have been computerized since 1975 in which the authors failed to specify the plant part from which compounds were isolated. We did not determine the total number of papers involved; but from experience, it can be presumed that about 50% of the papers we computerize involve the isolation and/or identification of secondary principles from plants. For purposes of determining this information, we considered all gymnosperms, angiosperms, pteridophytes, bryophytes, and lichens to constitute "plants." The results are presented in the accompanying table. None of the "organless" reports appeared in *J. Pharm. Sci.*

In 1975–1978, the 73 papers in which plant parts were not indicated when results of isolation studies were reported were derived from a total estimated number of papers published on this subject of about 5000. Since about one-third of the data in the 73 "organless" papers was computerized from abstracts rather than from original manuscripts, it cannot be said with certainty that those original reports failed to include the plant part(s).

Unless Janzen has found a source of phytochemical papers that has eluded us, he does not have much of a case relative to the aforementioned criticism.

Norman R. Farnsworth
William D. Loub
Department of Pharmacognosy and Pharmacology
College of Pharmacy
University of Illinois at the Medical Center
Chicago, IL 60612

Received January 29, 1979.

[1] D. H. Janzen, *J. Pharm. Sci.*, 68 (1), VIII (1979).

Numbers of Publications Reporting Isolation of Secondary Constituents from Plants in which the Plant Part Studied Was Not Reported (1975–1978)

Country	Year of Publication			
	1975	1976	1977	1978[a]
Bangladesh	0	0	1	0
Brazil	0	1	0	0
Bulgaria	0	0	1	0
China (People's Republic)	0	0	2	0
Czechoslovakia	0	1	1	0
England	0	1	1	0
Finland	0	0	1	0
France	1	1	2	1
Germany (West)	1	3	2	1
Hungary	0	0	2	0
India	1	2	0	1
Japan	2	1	4	0
Nigeria	0	2	0	0
Pakistan	0	0	0	1
Philippines	0	1	0	0
Poland	0	1	0	0
Sweden	0	0	1	0
Taiwan	1	0	0	0
Republic of South Africa	0	0	1	0
United States	1	6	3	0
Russia	10	8	2	0
Total	17	28	24	4

[a] Incomplete for 1978.

Senior Research Pharmacist

Does the milder climate of a southern metropolitan atmosphere (seldom any snow) appeal to you?

Immediate opening in our Pharmacy Research Department for a Ph.D. Pharmacist with 0–3 years of formulation experience. Responsibilities include formulation of solids and liquids and scale up to manufacturing.

Pleasant and professional working environment with excellent benefits and competitive salary based on background and experience.

Send resume and salary requirements in confidence to:

Manager of Personnel Placement
A·H·ROBINS
1407 Cummings Drive
Richmond, Virginia 23220

See our representative in Anaheim in April.

EOE M/F

PHARMACEUTICAL PROFESSIONALS

We are a 13 million dollar division of an international conglomerate with 26 divisions throughout the nation. The technical division of Wells Recruiting Systems specializes in the placement of pharmaceutical professionals. Our consultants are degreed technical specialists compensated on a salary basis to assure permanent relationships with discriminating professionals in the pharmaceutical industry. Our Fortune 500 clients seek degreed candidates from the B.S. to Ph.D. level with exposure to any of the following areas.

Pharmaceutical Product Development
Ph.D. with experience in all phases of product development. Familiarity with process and pilot plant scale up a must. Should have good exposure to GMP and FDA regulations.

Senior Research Pharmacist
Ph.D. with 2 to 5 years industrial experience in the development of pharmaceutical solids, liquids, and semi-solids. Should have some supervisory experience.

Research Pharmacist
B.S. to Ph.D. with 1 to 3 years industrial experience in percutaneous absorption, skin permeation and semi-solids and solids.

Pathology
Requires a M.D. or D.V.M. with 2 to 5 years experience in the area of complete pharmaceutical pathological studies. Will be responsible for development and expansion of present facilities. Pathology board certification a plus.

Toxicology
Requires a Ph.D. and 2+ years industrial experience in the areas of mutagenicity testing. Should be familiar with Ames, DNA repair and kill testing. Ability to supervise a group of 5 or more professionals.

Clinical Research Associate
M.S. to Ph.D. with 2 to 3 years experience in the Phase II, III, IV testing of C-V, CNS, Anti-Inflams, Anti-Infectives and Antibiotics.

Analytical Ph.D.
1 to 5 years experience in the area of Methods Development. Should be familiar with assay development and should have good experience in HPLC techniques.

Any inquiries will be treated with the strictest confidence and are fee paid by our clients.

Phil Sanford M.T. (ASCP)—Pharmaceutical Division
WELLS RECRUITING SYSTEMS
1620 Route 22, Union, N.J. 07083 (201)-964-9100

JOURNAL OF PHARMACEUTICAL SCIENCES

MARCH 1979
VOLUME 68 NUMBER 3

RESEARCH ARTICLES

Individualizing Gentamicin Dosage Regimens in Burn Patients with Gram-Negative Septicemia: A Cost–Benefit Analysis

J. LYLE BOOTMAN *x, ALBERT I. WERTHEIMER ‡, DARWIN ZASKE §, and CLAYTON ROWLAND ‡

Received June 9, 1978, from the *College of Pharmacy, University of Arizona, Tucson, AZ 85721, the ‡College of Pharmacy, University of Minnesota, Minneapolis, MN 55455, and the §Clinical Pharmacy Services, St. Paul-Ramsey Medical Center, St. Paul, MN 55101. Accepted for publication July 31, 1978.

Abstract □ Services provided by a clinical pharmacokinetics laboratory were evaluated in terms of an accepted cost–benefit model, and a model to evaluate clinical services provided by the pharmacist is presented. A retrospective study was conducted to evaluate the impact, in terms of patient outcomes, of individualizing gentamicin dosage regimens in severely burned patients. Analysis was conducted using multivariate statistical techniques and appropriate nonparametric and parametric tests to determine significant differences. This analysis provided the necessary data to quantify the impact of the pharmacokinetic service. The findings suggest that significant differences do exist in comparing individually dosed patients against those who were not, based upon discriminant and multiple regression analyses and/or nonparametric tests. Furthermore, the results will be useful for insurance companies, third-party payers, and government agencies in deciding which innovative clinical services should be reimbursed.

Keyphrases □ Gentamicin—dosage regimens individualized in burn patients, cost–benefit analysis □ Cost–benefit—analysis, gentamicin dosage regimens individualized in burn patients □ Dosage regimens—gentamicin, individualized in burn patients, cost–benefit analysis □ Antibacterials—gentamicin, dosage regimens individualized in burn patients, cost–benefit analysis

The new roles of the pharmacist go beyond the distribution function and center around optimal utilization of drug knowledge. The main thrust of clinical pharmacy is aimed at enhancing the benefits of drug therapy and correcting detected deficiencies in drug use. The ultimate goal of the clinical pharmacist is to be recognized as a drug therapy specialist who provides judgmental services (1, 2).

BACKGROUND

The expanded role of the pharmacist includes offering new services such as counseling patients with respect to drug therapy, conducting drug histories, providing therapeutic advice to physicians, and applying pharmacokinetic principles in monitoring and adjusting dosage regimens (3).

Few pharmacists would argue that these additional clinical services do not provide added benefit to the treatment of patients and the cure of disease. However, health administrators and other policy decision makers emphasize that innovative health services that further expand the health-care system must be sufficiently evident to the buyer that he/she is willing to pay the increased price over that in which the service is not provided. Unfortunately, furnishing this information has been a serious problem that may partially explain the slow acceptance of the clinical pharmacy concept by the consumer and other health-care providers.

In the past few years, the health-care system has been faced with the growing rate of inflation and the reality that resources for medical care are clearly finite. It was suggested (4, 5) that future medical innovations be evaluated in terms of social and medical priorities relative to costs incurred. The ever increasing problem of rising costs and limited resources has led many leaders in pharmacy to the realization that innovative clinical services must be cost justified (6).

Economists have suggested that cost–benefit or cost–effectiveness analyses are necessary to evaluate rationally innovative health services that result in increased costs to the system. This analysis is often necessary to gain acceptance from the health-care sector (7–9). It was proposed that the utilization of such a valuable tool in evaluating the benefits and costs of clinical pharmacy services may be one solution to increasing acceptance of such services by the medical profession, third-party payers, and consumers (10–15).

In examining the scope of services provided by the clinical pharmacists, the application of clinical pharmacokinetic principles to individualize drug dosage regimens has the greatest potential for directly affecting patient outcome with respect to drug therapy. Burn patients treated with gentamicin often receive subtherapeutic doses, theoretically leading to a decrease in a positive therapeutic effect and, thus, altering the chances for positive patient outcome (18–20).

The present study attempted to evaluate whether a clinical pharmacokinetic service staffed by clinical pharmacists has a measurable and positive impact on the care and outcome of burn patients with Gram-negative septicemia. A cost–benefit method was employed for this evaluation.

EXPERIMENTAL

A retrospective cohort study was conducted to evaluate the impact, in terms of patient outcomes, of individualizing gentamicin dosages for burn patients with Gram-negative septicemia. Data were abstracted[1]

[1] To avoid bias, data were abstracted by hospital auditors unconnected with the project. The abstractors had prior experience in chart review and medical care audits.

0022-3549/79/0300-0267$01.00/0
© 1979, American Pharmaceutical Association

Table I—Comparison between Nonkinetics and Kinetics Study Groups of Selected Independent Variables

Patient Variable	Nonkinetics (Mean ± *SD*)	Kinetics (Mean ± *SD*)
Age, years	34.1 ± 22.1	39.1 ± 24.1
Weight, kg	62.1 ± 25.4	67.5 ± 25.5
Percent body surface area burned	47.0 ± 19.8	50.7 ± 21.1
Delay in admission, hr	6.8 ± 6.7	4.9 ± 4.7
Onset of sepsis, days	9.4 ± 2.1	9.3 ± 2.2
Percent of females	23.1	27.3

Table II—Gentamicin Dosage Regimen Comparison for the First Septic Episode

Dosage Variable	Nonkinetics Group (Mean ± *SD*)	Kinetics Group (Mean ± *SD*)	Test Value	Significance Level
Dosage, mg/kg/day	4.4 ± 4.5	7.4 ± 2.8	$t_{(103)} = 4.13$	0.001
Dosage interval, hr	8.1 ± 2.9	5.3 ± 1.7	$t_{(103)} = 5.24$	0.001
Duration of therapy[a], days	8.3 ± 2.3	10.3 ± 4.8	$t_{(53)} = 2.28$	0.05

[a] Determined for surviving patients only.

from the medical charts of patients admitted to the burn center[2] during 1972–1976.

Based on a predetermined set of criteria, the "treatment" group was selected from burn victims whose gentamicin dosage regimens were individualized by the pharmacokinetic service from the second half of 1974 through 1976. The comparison group (serving as the "control") consisted of burn patients admitted to the burn care center prior to the implementation of the pharmacokinetic service, during 1972 through the first half of 1974. Their gentamicin dosage regimens were determined *via* traditional recommendations.

For admission to the study, patients must have had:

1. At least one Gram-negative septic episode (documented by either a blood culture or clinical observation).
2. Gentamicin treatment for at least 3 days.
3. At least a third-degree burn or a combination of second- and third-degree burns.
4. Less than 24 hr between time of burn and time of admission (patient must not have been a referral case).
5. No prior renal disease.
6. An internally consistent and complete data base on the relevant variables.

Analysis Design—As previously mentioned, this study consisted of a retrospective cohort design in which many of the variables that could potentially affect patient outcome were not controlled as would be the case in an experimental design approach. In other words, this epidemiological approach affords no way of knowing that the two groups were equivalent before the implementation of the pharmacokinetics service. As a result, various multivariate statistical techniques, such as multiple regression and discriminant analyses, were utilized to measure adequately the impact of the pharmacokinetics service while treating the independent variables as covariates.

Independent Variables—When using a multivariate technique, independent variables for the multivariate model must be selected carefully. Variables were selected on the basis of support from the literature in terms of their impact on patient outcome in burn wound victims. The variables collected in this study were: type of burn, sex, age, total body surface area burned (percent), delay between injury and admission (hours), onset of sepsis (days from burn injury), disease complications (*e.g.*, pulmonary and cardiovascular), preexisting disease, blood culture, type of topical treatment, pharmacokinetic protocol (yes or no), gentamicin dosage (interval and duration), and carbenicillin dosage and interval.

Patient Outcome Variables—Several dependent variables were chosen to detect significant differences between patients whose gentamicin dosages were pharmacokinetically determined and those for which the dosage regimen was determined *via* traditional mechanisms. The patient "outcome" variables were: survival, length of infection, length of stay, number of adverse drug reactions, and number of septic episodes.

Cost–Benefit Model—The mathematical statement of the cost–benefit model used in this study was:

$$BC_{pv} = \frac{\sum_{t=1}^{n} B_t/(1+r)^t}{\sum_{t=1}^{n} C_t/(1+r)^t} \qquad \text{(Eq. 1)}$$

where B_t is the total economic value of all benefits (Σb_i) that accrue to a program in time period t, C_t is the total economic value of all costs (Σc_j) that are incurred by a program in time period t, r is the annual opportunity cost or discount rate, n is the economic life of the proposal, and BC_{pv} is the benefit-to-cost ratio at present value.

With this model, programs under evaluation would be socially valuable or would be considered a desirable use of resources as long as the BC_{pv} is greater than 1.0.

Pharmacokinetics Service Costs—Two major types of costs, the fixed and operating costs, were incurred in the implementation and operation of the pharmacokinetics service. The fixed costs included the cost of the physical facility based on the size in square feet, the annual maintenance expenditures, and equipment costs that were depreciated over a 20-year straight line.

The operating costs measured in this project included: administrative, professional staff, and supportive personnel salaries; equipment leasing fees; subscription fees for professional journals and miscellaneous references; and medical supplies (*e.g.*, drug assay kits, syringes, and needles).

The total annual cost was determined by the simple addition of the fixed and operational costs. However, the cost per gentamicin serum determination was computed by dividing the total costs by the number of gentamicin samples obtained and analyzed for the period in which the costs were incurred.

Direct and Indirect Benefits—Direct benefits were regarded as the incremental reduction in the direct costs associated with the particular program. In this study, direct benefits were estimated based on significant changes observed in the two study groups. The relative contribution of the pharmacokinetics service to explaining observed changes was estimated using both regression and discriminant analyses. The variables measured to estimate the direct benefits were: length of hospital stay, length of infection, number of septic episodes, and number of adverse drug reactions.

A reduction in one or more dependent variables provided an estimate of the benefits derived by the burn patient in this study. The following formula was used to determine the dollar value associated with the direct benefits accrued:

$$DB = IX_1LOS + JX_2LOI + KX_3NSEP + LX_4ADR \qquad \text{(Eq. 2)}$$

where:

DB = direct benefits in dollar value
LOS = observed change (days) in length of stay between the two study groups
LOI = observed change (days) in length of infection between the two study groups
$NSEP$ = observed change in the number of septic episodes between the two study groups
ADR = observed change in the number of adverse drug reactions between the two study groups
X_1, X_2, X_3, X_4 = relative contribution of the pharmacokinetics service in explaining the observed change in the respective dependent variables, estimated using multivariate techniques
I = medical and hospitalization costs per day of hospitalization
J = incremental medical and hospitalization costs per day of infection
K = incremental medical and hospitalization costs per septic episode
L = incremental medical and hospitalization costs per adverse drug reaction

Indirect benefits were regarded as a measure of the productivity losses attributed to an increased length of hospital stay and/or to persons who would have died if the pharmacokinetics service were not in effect.

[2] The burn care center at St. Paul-Ramsey Medical Center is a 24-bed facility, one of the largest in the upper midwest of the United States and the major center in Minnesota. Approximately 190 patients are admitted annually.

Table III—Stepwise Summary of Discriminant Analysis for Mortality during the Study Period, 1972–1976

Step	Variable	Wilks Lambda	Significance Level	Change in r^2	Rao's V	Change in Rao's V	Significance Level
1	Age	0.87	0.001	0.13	15.81	15.81	0.001
2	Percent body surface area burned	0.76	0.001	0.12	29.88	14.07	0.001
3	Pharmacokinetics	0.63	0.001	0.13	44.73	14.85	0.001
4	Disease complications	0.60	0.000	0.03	49.03	4.30	0.007
5	Blood culture	0.56[a]	0.000	0.03	53.15	4.12	0.009

[a] χ^2 (5 df) = 47.1; $p < 0.0001$.

Morbidity savings (MBS) were calculated using:

$$MBS = X_1(E_a)LOS \quad \text{(Eq. 3)}$$

where X_1 is the relative contribution of the pharmacokinetics service in explaining the observed change in the length of stay between the two study groups, LOS is the observed change (days) in the length of stay between the two study groups, and E_a is the average earnings at age group a. Morbidity savings were calculated separately for males and females.

The following formula was used to compute the mortality savings (the average per capita income was adjusted for sex):

$$L_t = \sum_{t=i}^{n} Y_n(1 + r)^{-(t-i)} \quad \text{(Eq. 4)}$$

where L_t is the expected total earnings up to time t, Y is the average per capita income in the age group where the midpoint of the group is age i, n is the number of years of expected earnings, and r is the discount rate. The measure of output loss for an individual was the year-round, full-time earnings, which include wages and salaries before deduction of the proposed measure of expected earnings in the arithmetic average or mean.

The discount rates were chosen from those studies conducted in recent years. A sensitivity analysis approach was used. The rates used were 1, 6, and 10%.

RESULTS AND DISCUSSION

Data were abstracted from the medical charts of 832 burn patients; 105 patients met the criteria for admission to the study, representing approximately 12.6% of the burn patients admitted to the sponsoring hospital. The nonkinetics group consisted of 39 patients, whereas 66 patients were in the kinetics study group.

Comparison of Independent Variables between Kinetics and Nonkinetics Study Groups—In terms of the independent variables collected, few significant differences were detected. There were no significant differences in the demographic factors, percent body surface area burned, delay in admission, or the number of days for onset of sepsis. Table I shows that over 90% of the patients in both groups were inflicted with a flame injury. The incidence of preexisting diseases was 21.1 and 22.7% in the nonkinetics and kinetics groups, respectively, and was not significantly different. The predominant preexisting diseases were hypertension, diabetes mellitus, and emphysema.

In terms of disease complications, no significant differences between the groups were detected. Twenty-three (60.5%) nonkinetics patients had one or more complications, whereas 40 (62.5%) kinetics patients developed at least one disease complication. The various complications detected were pneumonia, cardiovascular problems, GI disorders, and renal failure. The number of patients having a positive blood culture was 23 (59%) for the nonkinetics group and 37 (56.1%) for those patients whose gentamicin dosage regimen was individualized by the pharmacokinetics service. This difference was not significant using χ^2 analysis.

Table IV—Discriminant Analysis Coefficients for the Mortality-Dependent Variable during the Study Period, 1972–1976

Independent Variable	Standardized Coefficient	Unstandardized Coefficient
Age	−0.92	−0.04
Percent body surface area burned	−0.60	−0.03
Pharmacokinetics	−0.63	−1.3
Disease complications	−0.42	−0.53
Blood culture	−0.40	−0.80
Constant		+3.21

Table II shows significant differences in the dosage, interval, and duration of gentamicin therapy between the two study groups, supporting the hypothesis that burn patients may require higher dosages to obtain therapeutic serum levels. The mean dosage in the nonkinetics group fell within the manufacturer's recommended dosage; patients in the pharmacokinetics group were given higher dosages at significantly shorter intervals. These findings further support those of Zaske *et al.* (17), which suggest the measurement of serum gentamicin levels in all burn patients with life-threatening infections.

The antibiotic carbenicillin is often used in conjunction with gentamicin for patients with *Pseudomonas* infections. In the nonkinetics group, 51% of the patients received carbenicillin and 58% of the kinetics patients received the drug. The average doses were 410 and 439 mg/kg/day in the nonkinetics and kinetics groups, respectively. These differences were not statistically significant (t = 1.12; 56 df; n.s.). In terms of topical therapy, no significant differences were observed. All patients received silver sulfadiazine with either povidone-iodine or mafenide.

Finally, the antibiotic sensitivity patterns were examined for the study period to detect any significant changes in susceptibility of the bacterial organisms to gentamicin. The results indicated nonsignificant changes over the 6-year period.

Pharmacokinetics Service Annual Costs—*Fixed Costs*—The annual fixed costs of $778.00 were relatively small compared to the other costs. The fixed costs for the pharmacokinetics office facility and equipment were depreciated in accordance with the depreciation schedules used by the sponsoring hospital.

Operating Costs—The total annual cost to operate the pharmacokinetics service was approximately $73,915. Salaries accounted for the largest percentage, but the costs of the gentamicin blood sample assays were similar. A breakdown of the laboratory costs showed that the average cost to assay a blood sample of gentamicin was $7.72.

Total Annual Costs—The total annual costs, $74,693, included the fixed and operating costs associated with operating the pharmacokinetics service. The total annual costs divided by the total annual number of gentamicin blood samples (4305) provided an estimate of $17.35 for the cost per gentamicin blood sample[3].

Total Cost per Burn Patient—The cost per burn patient whose gentamicin dosage regimen was determined by the pharmacokinetics service was approximated by multiplying the total cost per blood sample ($17.35) by the mean number of gentamicin samples (6.8) obtained per burn patient in the study. Rounding the 6.8 to 7.0 yielded a cost of approximately $122.00/patient for individualized gentamicin dosage. Since the total number of patients was 66, the total costs for individualizing the gentamicin dosages was approximately $8052. This figure represented the denominator in the cost–benefit model.

Benefit Determinations—Each patient outcome variable was analyzed using the appropriate multivariate analytical techniques to determine the relative contribution of the pharmacokinetics service.

Prior to multivariate analysis, Kendall's tau correlation coefficients were obtained for the independent variables collected. If any two variables had a correlation greater than 0.40, then one was deleted to help minimize the problems of multicollinearity.

After the elimination of those variables, which were highly intercorrelated, the following multivariate linear model was developed:

$$Y = B_1(\text{type of burn}) + B_2(\text{sex}) + B_3(\text{age}) + B_4(\text{percent of body surface area burned}) + B_5(\text{delay before admission}) + B_6(\text{onset of sepsis}) + B_7(\text{disease complications}) + B_8(\text{preexisting diseases}) + B_9(\text{blood culture}) + B_{10}(\text{topical therapy}) + B_{11}(\text{carbenicillin dose}) + B_{12}(\text{pharmacokinetics}) + \text{constant} \quad \text{(Eq. 5)}$$

[3] St. Paul-Ramsey Medical Center currently charges the patient $21.00/sample.

Table V—Mortality Rates between the Two Study Groups [a]

	Nonkinetics Group	Percent	Kinetics Group	Percent
Survived	13	33.3	42	63.6
Died	26	66.7	24	36.4
Total	39	100	66	100

[a] χ^2 (1 *df*) = 7.85; $p < 0.005$.

Variables not included were gentamicin dosage and interval, weight, and carbenicillin interval.

Mortality—Discriminant analysis was used to determine the relative influence of the various independent variables on explaining observed changes in those patients who died and those who survived Gram-negative sepsis secondary to the burn injury. In addition, it allowed the quantification of the relative contribution of the pharmacokinetics service to explain the observed differences between the two study groups.

Table III summarizes the discriminant analysis for mortality. As specified in the model, all variables were included in the analysis. The step-down analysis was repeated until the change in Rao's V was not significant. This procedure was followed for all multivariate analyses. The final model was significant ($p < 0.0001$), as indicated by the overall significance of Wilks lambda. The canonical correlation was 0.66. Examination of the standardized coefficients (Table IV) shows that the pharmacokinetics service was positively correlated with survival, whereas age, percent body surface area burned, disease complications, and blood cultures were negatively correlated with survival.

The findings also suggest a significant impact of the pharmacokinetics service in terms of reducing mortality. Pharmacokinetics explained 13% of the variance in the observed mortality rates between the two study groups. As predicted, age and percent of body surface area burned were also good predictors in explaining this variance. The findings support the hypothesis that a significant reduction in the mortality rate between the two study groups can be attributed to the pharmacokinetics service.

The observed change in the percentage of patients that died between the nonkinetics and kinetics study groups was approximately 30.3% (Table V). This percentage represents a difference of 20 lives saved between the two groups. The results of the discriminant analysis indicated that the pharmacokinetics service accounted for approximately 13% of the variance, equivalent to 2.6 lives saved. In terms of sex differences, the ratio of male to female in the kinetics population was 8 to 3. The 2.6 lives saved can then be transformed into 1.9 males and 0.7 females for the purposes of estimating dollar value of lives saved. This information was incorporated into the cost–benefit formula using the average earnings[4] for both the male and female wage earners.

These estimates were based on the mean ages of the males and females in the kinetics study group, 35 and 27 years, respectively. Table VI provides a summary of the mortality savings for the respective discount rates.

Length of Stay and Length of Infection—Table VII shows that the mean length of hospital stay and the mean length of infection were greater for the kinetics group. The mean length of infection was 10.3 days for the kinetics group and 8.1 days for the nonkinetics group. The mean length of stay was 72.3 days for the nonkinetics group and 93.2 days for the kinetics group. These findings were significantly different and contradict the hypotheses that the pharmacokinetics service would reduce the lengths of infection and hospital stay. A possible explanation is that the increased probability of survival, as described earlier, may have affected the ratio of severe patients in the kinetics group as compared to the nonkinetics group, which may have ultimately affected the length of stay and the length of infection. This decrease may be reflected by the survival of patients who would have normally died if their gentamicin dosages were not individualized by the clinical pharmacokinetics service.

In addition, the mean length of stay of patients who died was greater for those in the kinetics group *versus* the nonkinetics group. However, this difference was not statistically significant. The mean length of infection for patients that died was 5.7 and 11.2 days for patients in the nonkinetics and kinetics groups, respectively. This difference was significantly different (Table VII). These findings give further support to the explanation given with regard to the stated hypotheses. In other words, this finding, which is opposite to the stated hypothesis, may be a reflection of patients who would have normally died if their gentamicin dosages were not individualized by the clinical pharmacokinetics service.

[4] Source: U.S. Bureau of the Census, "Incomes in 1975 of Families and Persons in the United States," *Current Population Reports*, Series P-60, No. 102, U.S. Government Printing Office, Washington, D.C., 1977.

Table VI—Cost–Benefit Ratios for Selected Discount Rates

Parameter	Discount Rate 1%	Discount Rate 6%	Discount Rate 10%
Mortality savings, dollars	911,520	331,068	171,931
Morbidity losses, dollars	29,798	29,798	29,798
Pharmacokinetics service costs, dollars	8,052	8,052	8,052
Total costs, dollars	37,850	37,850	37,850
Benefit-to-cost ratio	24.0	8.7:1	4.5:1

Multiple regression analysis was used to determine the relative contribution of the independent variables identified earlier to explaining variances in the length of infection and the length of stay between the study groups. Patients who died were analyzed separately from those who survived.

In examining the regression analysis in the length of infection for those patients that survived, the significance of the *F* statistic was not significant at any level of the analysis. In other words, none of the variables entered in the model were significant contributors to explaining variance between the study groups.

Table VIII provides a summary of the regression analysis for the length of infection in those patients that died. The pharmacokinetics service accounted for approximately 32% of the variance. The significance of the *F* statistic shows that the model was significant to $p < 0.001$. Examination of the sign of the standardized coefficients showed that the pharmacokinetics variable was positive, indicating that patients whose gentamicin dosage regimen was determined by the pharmacokinetics service experienced longer periods of infection before they actually died (Table IX).

In summary, the contribution of the pharmacokinetics service for those patients who survived was not significant using multiple regression. However, regression analysis for those patients that died indicates that a significant portion (32%) of the observed change can be attributed to the pharmacokinetics service. As noted earlier, however, this change was not in the direction hypothesized. Table VII shows that the mean length of infection was greater for the kinetics group. The mean difference in the length of infection for those patients that died was 5.5 days. Multiplying this observed change by 32% yields the increase in the length of infection attributable to the pharmacokinetics service. Rounded to the nearest day, approximately 2 days/patient that died can be attributed to the pharmacokinetics service. If this number is multiplied by the number of patients in the kinetics group (24), the total number of additional days of infection was approximately 48 days. The incremental cost per day of infection over and above the normal daily medical and hospitalization charges was estimated to be $531.00, using the records supplied by the sponsoring hospital. If this figure is multiplied by 48 days, the additional cost attributed to the pharmacokinetics service was $24,488.

Finally, in examining the regression analyses for the length of hospital stay, the pharmacokinetics service did not contribute significantly to explaining the variance observed between the two study groups and was not included in the cost–benefit model as a result of the analyses.

Number of Septic Episodes per Patient—In examining the number of septic episodes per patient, there was a significant difference between the two study groups (Table X). In the nonkinetics group, three (7.7%)

Table VII—Length of Infection and Length of Stay Comparisons for Patients Who Died and Survived in Study Groups

Patient Outcome Variable	Nonkinetics Group (Mean ± *SD*)	Kinetics Group (Mean ± *SD*)	Test Value	Significance Level
Length of stay, days				
Survived	72.3 ± 24.3	93.2 ± 32.4	$t_{(53df)} = 2.11$	0.05
Died	26.3 ± 31.2	36.1 ± 30.4	$t_{(48df)} = 1.12$	n.s.
Length of infection, days				
Survived	8.1 ± 2.3	10.3 ± 4.8	$t_{(53df)} = 2.28$	0.05
Died	5.7 ± 3.2	11.2 ± 4.9	$t_{(48df)} = 4.64$	0.001

Table VIII—Stepwise Summary for Regression Analysis for Length of Infection in Patients Who Died [a]

Step	Variable	Significance Level	Multiple R	r^2	Change in r^2	Overall F	Significance Level
1	Pharmacokinetics	0.000	0.56	0.32	0.32	22.23	0.001
2	Preexisting diseases	0.003	0.66	0.44	0.12	18.20	0.001
3	Topical therapy	0.081	0.69	0.47	0.03	13.72	0.001
4	Carbenicillin dose	0.152	0.73	0.53	0.03	9.93	0.001
5	Sex	0.152	0.73	0.53	0.03	9.93	0.001
6	Age	0.459	0.73	0.54	0.01	8.28	0.001
7	Disease complications	0.576	0.74	0.54	0.001	7.03	0.001
8	Percent body surface area burned	0.640	0.74	0.54	0.001	6.07	0.001
9	Onset of sepsis	0.756	0.74	0.54	0.001	5.28	0.001
10	Blood culture	0.806	0.74	0.54	0.001	4.65	0.001
11	Delay in admission	0.812	0.74	0.54	0.001	4.13	0.001

[a] The F level for "type" was insufficient to be included in the analysis.

patients had more than one spetic episode. One of the three patients had three septic episodes. All three of these patients died as a result of the Gram-negative sepsis.

In the kinetics group, 15 (22.7%) patients had at least two septic episodes, which was significantly different from the nonkinetics group ($\chi^2 = 3.91, p < 0.05$). Twelve patients had two septic episodes while the remaining patients experienced three septic episodes. Also, seven of the 15 patients died as a result of the sepsis.

These findings do not support the main hypothesis that fewer patients in the kinetics group would experience more than one septic episode as compared to the nonkinetics group. A possible explanation parallels that given for the unexpected findings associated with the length of infection and the length of stay. That is, the survival of patients who would have normally died if the pharmacokinetics service were not in effect significantly offset this patient outcome variable.

The relative contribution of the pharmacokinetics service to explaining observed changes in the number of septic episodes per patient between the two study groups was determined using discriminant analysis. The dependent variable was separated for those patients who had one septic episode *versus* those patients experiencing more than one septic episode. This analysis was conducted separately for those patients that survived and those that died.

Table XI provides a summary of the multivariate analysis for patients that survived. Age contributed the most to explaining variance, with a 0.87 Wilks lambda. The pharmacokinetics service was second, explaining approximately 9% of the variance as indicated by the change in Wilks lambda. The canonical correlation was 0.55.

Examination of the standardized coefficients showed that age and the time at which the patient developed sepsis were negatively associated with the increase in the number of septic episodes between the two study populations (Table XII). In other words, the older the patient and the later the patient developed sepsis from the time of admission, the fewer were the number of septic episodes. The pharmacokinetics service, however, was positively related to the number of septic episodes.

The results of the discriminant analysis indicate that the pharmacokinetics service contributed significantly (9%) to explaining the variance between the two study groups in the number of septic episodes for those patients that survived (Table XI). The regression analysis was not significant for those patients that died.

Multiplying the mean length per septic episode (10.3 days) by the increase in the number of septic episodes (0.25) per kinetics patient that survived provided an estimate of the increase in the number of days of infection per patient between the two study groups (2.6 days). The number of patients that survived in the kinetics group was 42; thus, the increase in the total number of days of infection due to patients having more than one septic episode was approximately 110 days. Multiplying this number by the relative contribution of the pharmacokinetics service (9%) showed that the increase in the total number of days of infection attributable to the service was 10 days. Multiplying this number by the incremental cost per day due to the infection ($531.00) showed that the total cost due to the increase in the number of septic episodes attributable to the pharmacokinetics service was $5310.00.

Table IX—Regression Coefficients for Length of Infection in Patients Who Died

Independent Variable	Standardized Coefficient	Unstandardized Coefficient
Pharmacokinetics	0.43	4.17
Preexisting disease	0.34	2.16
Topical therapy	−0.18	−1.02
Carbenicillin dose	0.26	0.01
Sex	−0.18	−1.94
Age	−0.04	−0.01
Disease complications	0.06	0.46
Percent body surface area burned	−0.05	−0.01
Onset of sepsis	−0.05	−0.23
Blood culture	−0.03	−0.32
Delay in admission	−0.03	−0.03
Constant		6.13

Incidence of Adverse Drug Reactions—The reported incidence of nephrotoxicity and ototoxicity ranges from 5 to 10% (20). Three (7.7%) patients in the nonkinetics group possibly had renal complications secondary to gentamicin therapy. It is difficult to distinguish renal toxicity due to gentamicin and that due to a secondary complication of the burn injury or to other underlying conditions following the burn injury. There was no evidence of nephrotoxicity in the pharmacokinetics group.

In reviewing the medical charts, no patient complaints of any hearing deficit could be found. Also, for those patients whose hearing was tested, no impairment of auditory function was detected. A possible explanation for the low incidence of detected ototoxicity could be the difficulty in abstracting this information from medical charts. In addition, it was apparent that few patients (0.8%) were given auditory examinations; thus, an accurate estimate of the incidence of ototoxicity could not be obtained.

In summary, evidence was insufficient to conclude that the incidence of gentamicin-related adverse drug reactions was significantly reduced by the pharmacokinetics service and was deleted from the cost–benefit model. However, the frequency of nephrotoxicity observed with the nonkinetics group was similar to the reported incidence of from 5 to 10%.

Benefit-to-Cost Ratio—Table VI provides a summary of the costs and benefits. The ratios were calculated for the respective discount rates. The morbidity losses due to the increase in the length of infection and the number of septic episodes per patient were added to the pharmacokinetics service costs.

The benefit-to-cost ratios were greater than one for each discount rate. The 6% discount rate was the mean of those rates previously reported. The ratio (8.7:1) for this discount rate may represent the most reasonable estimate of worth for the pharmacokinetics service. These findings indicate that the benefits associated with the pharmacokinetics dosage intervention for burn patients with secondary Gram-negative septicemia outweigh the costs associated with operating the service.

CONCLUSION

The objectives of this study were accomplished. It was undertaken

Table X—Number of Septic Episodes per Patient between Study Groups [a]

Number of Septic Episodes per Patient	Nonkinetics Group	Percent	Kinetics Group	Percent
1	36	92.3	51	77.3
2	2	5.1	12	18.2
3	1	2.6	3	4.5
Total	39	100	66	100

[a] χ^2 (1 df) = 3.91; $p < 0.05$.

Table XI—Stepwise Summary of Discriminant Analysis for Number of Septic Episodes in Patients Who Survived [a]

Step	Variable	Wilks Lambda	Significance Level	Change in r^2	Rao's V	Change in Rao's V	Significance Level
1	Age	0.87	0.002	0.13	7.37	7.37	0.007
2	Pharmacokinetics	0.78	0.002	0.09	14.22	6.86	0.009
3	Onset of sepsis	0.70[a]	0.002	0.08	18.01	3.79	0.050

[a] χ^2 (3 *df*) = 15.35; $p < 0.002$.

partially to apply a practical cost–benefit decision model that could be used by the decision maker to determine the desirability of establishing and operating a clinical pharmacokinetics service within the hospital environment. Beginning with a considerable volume of theoretical, economic, and mathematical literature, this work set out to bridge the gap between the theoretical discussion of cost–benefit analysis and its practical application to evaluating clinical pharmacy services.

Cost–benefit analysis proved to be a satisfactory technique in evaluating the use of clinical pharmacokinetics in the treatment of burn patients. A major contribution of cost–benefit analysis was identifying the specific costs and benefits associated with the pharmacokinetics program. This step is important if one is ultimately interested in making the operation more efficient in terms of maximizing the cost–benefit ratio.

The major conclusion to be made from this study is that the pharmacokinetics service evaluated may be beneficial not only to the burn patient who develops Gram-negative infections secondary to a third-degree burn wound but also to society. In other words, this study demonstrated that the ability of the pharmacist to provide services related to the application of pharmacokinetics in the treatment of burn wound infections may improve the quality, as well as the cost–benefit, of patient care as related to drug therapy.

As stated by McLeod (3), the continued success of clinical pharmacy will be proportional to its contribution to patient care and public welfare. It appears that cost–benefit analysis can be a mechanism to document successfully and accurately the contributions of the clinical pharmacist.

Table XII—Discriminant Analysis Coefficients for Number of Septic Episodes in Patients Who Survived

Variable	Standardized Coefficient	Unstandardized Coefficient
Age	−0.99	−0.05
Pharmacokinetics	0.70	1.63
Onset of sepsis	−0.47	−0.05
Constant		0.76

REFERENCES

(1) D. C. McLeod, *Am. J. Hosp. Pharm.*, **33**, 29 (1976).

(2) D. C. Brodie and R. A. Benson, *Drug Intell. Clin. Pharm.*, **10**, 506 (1976).

(3) D. C. McLeod, *Am. J. Hosp. Pharm.*, **33**, 912 (1976).

(4) W. J. Feely, *Hosp. Pharm.*, **8**, 1 (1973).

(5) A. I. Wertheimer, and J. L. Bootman, *Drug Dev. Ind. Pharm.*, **3**, 219 (1977).

(6) M. R. Cohen, S. Turco, and A. J. Weltmann, *Hosp. Pharm.*, **12**, 9 (1977).

(7) W. Smith, *Public Health Rep.*, **83**, 899 (1968).

(8) R. Crystal and A. Brewster, *Inquiry*, **1966**, 3.

(9) H. E. Klarman, *Am. J. Public Health*, **57** (Nov. 1967).

(10) P. Parker, presented at the American Health Congress, Chicago, Ill., Aug. 22, 1973.

(11) D. Sorby, K. Kelly, and R. Elenbaas, "Evaluation of Clinical Pharmacy Programs, Proceedings of the First International Congress on Clinical Pharmacy Education," Minneapolis, Minn., July 13–16, 1976.

(12) W. Smith, HEW Publication No. HSM 72-3019, Washington, D.C., 1971.

(13) A. Cheung and R. Kayne, *Calif. Pharmacist* (Sept. 1975).

(14) W. F. McGhan, C. R. Rowland, and J. L. Bootman, *Am. J. Hosp. Pharm.*, **35**, 133 (1978).

(15) R. J. Plumridge, *Aust. J. Hosp. Pharm.*, **7**, 86 (1977).

(16) R. Sawchuk and D. Zaske, *J. Pharmacokinet. Biopharm.*, 4, 2 (1976).

(17) D. Zaske, R. J. Sawchuk, D. Gerding, and R. G. Strate, *J. Trauma*, **16**, 10 (1976).

(18) P. Noone, T. M. C. Parsons, J. R. Pattison, R. C. B. Slack, D. Garfield-Davies, and K. Hughes, *Br. J. Med.*, **1**, 477 (1974).

(19) A. Andersen, G. R. Hodges, and W. G. Barnes, *Arch. Intern. Med.*, **136** (July 1976).

(20) P. Noone, J. R. Pattison, and D. G. Davies, *Post Grad. Med. J.*, **50**, 9 (1974).

Effect of Obtrusive Measures on Antibiotic Compliance

ROBERT H. HUNTER *x and JEFFREY A. KOTZAN

Received May 30, 1978, from the *School of Pharmacy, University of Georgia, Athens, GA 30602.* Accepted for publication August 2, 1978.

*Present address: College of Pharmacy, University of Cincinnati, Cincinnati, OH 45267.

Abstract □ The influence of compliance measurement activities on patient behavior was studied. The project measured the relationship among physical capsule counts, patient interviews, and the amounts of excreted ampicillin. The capsule counts and patient interviews were conducted in a manner that disguised their intent. Sixty college-age patients were assigned to one of three experimental groups: a telephone interview, a personal interview and capsule count, or a control group. Stimulation (interviews) occurred on the 2nd day of the prescribed regimen, and urine was collected on random days thereafter. Results indicated that both stimulation types were associated with more positive compliance rates. The influence diminished rapidly. The reactive influence of experimentor intervention associated with personal and phone communication was demonstrated.

Keyphrases □ Compliance—effect of measurement activities on patient behavior □ Dosage regimens—effect of compliance measurement activities on patient behavior

Since 1954, when Jenkins (1) reported that the "average patient" consumed only about half of the total number of prescribed doses, members of the health community have responded with increased interest in the prevalence, associated factors, and methods of improving medication compliance. Most published research studies regarding

0022-3549/79/0300-0272$01.00/0

© 1979, American Pharmaceutical Association

Table XI—Stepwise Summary of Discriminant Analysis for Number of Septic Episodes in Patients Who Survived [a]

Step	Variable	Wilks Lambda	Significance Level	Change in r^2	Rao's V	Change in Rao's V	Significance Level
1	Age	0.87	0.002	0.13	7.37	7.37	0.007
2	Pharmacokinetics	0.78	0.002	0.09	14.22	6.86	0.009
3	Onset of sepsis	0.70[a]	0.002	0.08	18.01	3.79	0.050

[a] χ^2 (3 *df*) = 15.35; $p < 0.002$.

partially to apply a practical cost–benefit decision model that could be used by the decision maker to determine the desirability of establishing and operating a clinical pharmacokinetics service within the hospital environment. Beginning with a considerable volume of theoretical, economic, and mathematical literature, this work set out to bridge the gap between the theoretical discussion of cost–benefit analysis and its practical application to evaluating clinical pharmacy services.

Cost–benefit analysis proved to be a satisfactory technique in evaluating the use of clinical pharmacokinetics in the treatment of burn patients. A major contribution of cost–benefit analysis was identifying the specific costs and benefits associated with the pharmacokinetics program. This step is important if one is ultimately interested in making the operation more efficient in terms of maximizing the cost–benefit ratio.

The major conclusion to be made from this study is that the pharmacokinetics service evaluated may be beneficial not only to the burn patient who develops Gram-negative infections secondary to a third-degree burn wound but also to society. In other words, this study demonstrated that the ability of the pharmacist to provide services related to the application of pharmacokinetics in the treatment of burn wound infections may improve the quality, as well as the cost–benefit, of patient care as related to drug therapy.

As stated by McLeod (3), the continued success of clinical pharmacy will be proportional to its contribution to patient care and public welfare. It appears that cost–benefit analysis can be a mechanism to document successfully and accurately the contributions of the clinical pharmacist.

Table XII—Discriminant Analysis Coefficients for Number of Septic Episodes in Patients Who Survived

Variable	Standardized Coefficient	Unstandardized Coefficient
Age	−0.99	−0.05
Pharmacokinetics	0.70	1.63
Onset of sepsis	−0.47	−0.05
Constant		0.76

REFERENCES

(1) D. C. McLeod, *Am. J. Hosp. Pharm.*, **33**, 29 (1976).

(2) D. C. Brodie and R. A. Benson, *Drug Intell. Clin. Pharm.*, **10**, 506 (1976).

(3) D. C. McLeod, *Am. J. Hosp. Pharm.*, **33**, 912 (1976).

(4) W. J. Feely, *Hosp. Pharm.*, **8**, 1 (1973).

(5) A. I. Wertheimer, and J. L. Bootman, *Drug Dev. Ind. Pharm.*, **3**, 219 (1977).

(6) M. R. Cohen, S. Turco, and A. J. Weltmann, *Hosp. Pharm.*, **12**, 9 (1977).

(7) W. Smith, *Public Health Rep.*, **83**, 899 (1968).

(8) R. Crystal and A. Brewster, *Inquiry*, **1966**, 3.

(9) H. E. Klarman, *Am. J. Public Health*, **57** (Nov. 1967).

(10) P. Parker, presented at the American Health Congress, Chicago, Ill., Aug. 22, 1973.

(11) D. Sorby, K. Kelly, and R. Elenbaas, "Evaluation of Clinical Pharmacy Programs, Proceedings of the First International Congress on Clinical Pharmacy Education," Minneapolis, Minn., July 13–16, 1976.

(12) W. Smith, HEW Publication No. HSM 72-3019, Washington, D.C., 1971.

(13) A. Cheung and R. Kayne, *Calif. Pharmacist* (Sept. 1975).

(14) W. F. McGhan, C. R. Rowland, and J. L. Bootman, *Am. J. Hosp. Pharm.*, **35**, 133 (1978).

(15) R. J. Plumridge, *Aust. J. Hosp. Pharm.*, **7**, 86 (1977).

(16) R. Sawchuk and D. Zaske, *J. Pharmacokinet. Biopharm.*, 4, 2 (1976).

(17) D. Zaske, R. J. Sawchuk, D. Gerding, and R. G. Strate, *J. Trauma*, **16**, 10 (1976).

(18) P. Noone, T. M. C. Parsons, J. R. Pattison, R. C. B. Slack, D. Garfield-Davies, and K. Hughes, *Br. J. Med.*, **1**, 477 (1974).

(19) A. Andersen, G. R. Hodges, and W. G. Barnes, *Arch. Intern. Med.*, **136** (July 1976).

(20) P. Noone, J. R. Pattison, and D. G. Davies, *Post Grad. Med. J.*, **50**, 9 (1974).

Effect of Obtrusive Measures on Antibiotic Compliance

ROBERT H. HUNTER *x and JEFFREY A. KOTZAN

Received May 30, 1978, from the *School of Pharmacy, University of Georgia, Athens, GA 30602.* Accepted for publication August 2, 1978.

*Present address: College of Pharmacy, University of Cincinnati, Cincinnati, OH 45267.

Abstract □ The influence of compliance measurement activities on patient behavior was studied. The project measured the relationship among physical capsule counts, patient interviews, and the amounts of excreted ampicillin. The capsule counts and patient interviews were conducted in a manner that disguised their intent. Sixty college-age patients were assigned to one of three experimental groups: a telephone interview, a personal interview and capsule count, or a control group. Stimulation (interviews) occurred on the 2nd day of the prescribed regimen, and urine was collected on random days thereafter. Results indicated that both stimulation types were associated with more positive compliance rates. The influence diminished rapidly. The reactive influence of experimentor intervention associated with personal and phone communication was demonstrated.

Keyphrases □ Compliance—effect of measurement activities on patient behavior □ Dosage regimens—effect of compliance measurement activities on patient behavior

Since 1954, when Jenkins (1) reported that the "average patient" consumed only about half of the total number of prescribed doses, members of the health community have responded with increased interest in the prevalence, associated factors, and methods of improving medication compliance. Most published research studies regarding

0022-3549/79/0300-0272$01.00/0

© 1979, American Pharmaceutical Association

Table I—Design of the Experiment

Experimental Group	Day of Regimen 2	3	4	5	6	7
1	S1[a]	0[b]				
	S1		0			
	S1			0		
	S1				0	
	S1					0
2	S2[c]	0				
	S2		0			
	S2			0		
	S2				0	
	S2					0
3	NS[d]	0				
	NS		0			
	NS			0		
	NS				0	
	NS					0

[a] S1 = patients subjected to a telephone interview. [b] 0 = day on which patient provided urine sample. [c] S2 = patients subjected to a personal interview and capsule count. [d] NS = patients not subjected to either stimulus (control group).

drug compliance utilized the basic measurement techniques of personal interviews, dosage unit counts, and body fluid analyses.

Different measurement techniques were utilized jointly, but comparative results were often lacking (2, 3). Experimentor intervention was unavoidable in many situations. The act of counting capsules or obtaining fluid samples in itself is stimulation. Unfortunately, a conscious effort to avoid experimental intervention has been undocumented in patient compliance literature or it has been little recognized as a potential source of error.

The objective of this project was to identify the influence of measurement activities on compliance behavior patterns. The assumption of noninfluence on patient behavior in previous studies was evaluated. Two obtrusive measures of patient compliance, telephone interviews and physical capsule counts, and the amount of excreted ampicillin were studied. By isolating the effects of the obtrusive stimulations from the dependent variable measure, the results validly described the influence of experimentor bias.

EXPERIMENTAL

A quantitative urinalysis for ampicillin utilizing UV spectrophotometry (4, 5) was tested and found applicable to the project. A Beer's law equation for concentrations in the 5.0–1250.0-μg/ml range was developed. The coefficient of correlation (r) was 0.9998.

Operational Definition of Compliant Behavior—The objective of the first phase of the study was to define compliant behavior based on excreted quantities of ampicillin. Twenty college-age students each consumed a single 250-mg capsule of ampicillin trihydrate from the same lot. The administration time was recorded, and the subjects were instructed to conduct normal patterns of food and beverage consumption and urine excretion. Urine samples were collected from each subject at 12 and 24 hr following consumption.

Collected urine samples were analyzed, and concentrations of excreted ampicillin were recorded. A paired t test was calculated to determine if the mean values for the two periods differed significantly. The 12-hr data were selected as a reference standard, and a 70% confidence interval ($\alpha = 0.30$, $df = 19$) was calculated for the 12-hr mean concentration. The 70% confidence interval was chosen to reduce the probability of a type II error. A type II error is accepting the hypothesis that an individual is a member of the same population from which the 12-hr sample members were drawn when, in fact, that individual is not a member of the same population.

After the confidence interval was calculated, the operational definition of compliant behavior was formulated. Individuals who consumed at least a single 250-mg dose of ampicillin less than 12 hr before sampling were expected to excrete larger quantities of ampicillin than the noncompliant reference group.

Compliant behavior was then defined by urinalysis quantities greater than the upper tail of the 70% confidence interval.

Table II—Analysis of Variance (Two Factor, 5 × 3)

Source	df	Sum of Squares	Mean Square	F Value	PF
Experimental group	2	203817.78	101908.89	2.31	0.11
Day of regimen	4	296935.84	74233.96	1.68	0.17
Interaction	8	534769.27	66846.16	0.52	0.18
Error	45	1983014.92	44067.00		
Corrected total	59	3018537.80			

Experimental Design and Procedures—The project separated the urine collection procedure from the other measurement techniques by treating the interview and capsule count as stimuli rather than as measurement procedures. The experimental design is given in Table I. Four subjects were randomly assigned to each experimental cell.

The experimental groups were those patients who were subjected to a telephone interview (S1), those patients who were subjected to a personal interview and capsule count (S2), and those patients who were not subjected to either stimulus (NS) on the 2nd day of the drug regimen. The control received no stimulation.

College age student patients[1] for whom a normal ampicillin regimen was prescribed were eligible for the study. Subjects were selected if:

1. The ampicillin prescription was written for a 250-mg capsule to be taken four times a day for 7–10 days.
2. The brand dispensed when the patient received the prescription matched the selected brand and lot number of ampicillin.
3. The patient did not receive any other confounding medication, particularly penicillin, during the ampicillin regimen.
4. The patient was seen only on an out-patient basis during the ampicillin regimen.
5. The patient agreed to release his/her pharmaceutical information by signing the release form at the time the ampicillin prescription was received. The release forms were collected daily and were designed to minimize association with the compliance study.

Subject stimulation took place the day after the patient received the prescription. The primary researcher, posing as a graduate student currently enrolled in a sociology course, conducted both the telephone and personal interviews. Subjects, told that they were randomly selected from the University's telephone directory, were administered the "Survey of Self-Medication Habits of College Age Adults."

The subjects assigned to the experimental group receiving a personal interview were asked to show the interviewer all medication they were currently taking; the interviewer pretended not to know how to spell the names of the medications and requested to see the containers. Patients in the second experimental group were administered the questionnaire by telephone. They also were asked if they were currently taking any medication and the name(s) of the medication(s).

All subjects were contacted by telephone on the evening prior to the randomly assigned day for sampling of the student's urine and were requested to present themselves at the College of Pharmacy to provide "data" for the Northeast Georgia Drug Study. The nature of the data was not specifically identified. The subjects were promised $10 for their cooperation.

If the subject agreed to provide data and did appear at the College, he/she was then informed of the exact nature and purpose of the data collection. Upon receipt of the urine sample, the researcher analyzed the sample spectrophotometrically.

RESULTS

Urine samples collected from the 20 selected subjects at 12 and 24 hr following dosing yielded mean concentrations of excreted ampicillin equal to 89.72 and 26.92 μg/mg, respectively. The standard deviations were 52.53 and 24.42 for the 12- and 24-hr periods, respectively. The paired comparison t test, using a pooled standard deviation of 9.79, yielded a calculated value of 6.41. Therefore, it was concluded that excretion of ampicillin decreased in concentration between the two time periods.

The 70% confidence interval calculated for the 12-hr sample was

[1] At the University of Georgia Gilbert Health Center.

Table III—Experimental Cell Means

Experimental Group	Day of Regimen				
	3	4	5	6	7
1	107.50	133.13	290.69	588.75	121.13
2	137.56	228.75	143.81	122.50	78.06
3	57.50	75.63	22.69	200.00	206.50

76.86–102.58 μg/ml. Therefore, sampled patients who exhibited urine concentrations of ampicillin less than 102.58 μg/ml were defined as noncompliant. They were defined as having consumed not more than a single 250-mg dose, 12 hr prior to urine sampling.

A total of 92 students released their pharmaceutical information to the Northeast Georgia Drug Compliance Study between July 1 and October 18, 1976. Thirty-two students were not included because some could not be contacted while others failed to comply with one or more of the selection criteria.

A two-factor analysis of variance was conducted utilizing the SAS ANOVA computer program (6). The analysis of variance table and F values calculated by this procedure are found in Table II.

The analysis of variance demonstrated that neither the main effects (experimental group and day of regimen) nor the two-way interaction contributed significantly to the total variation in the data.

For Days 6 and 7 of the regimen, the mean cell values of excreted ampicillin concentration of the control group increased dramatically from the three previous regimen days (Table III). This observation prompted a second two-factor analysis of variance utilizing the day-of-regimen factor with only three levels. The remaining two levels (Days 6 and 7) were deleted from this analysis.

A series of three two-factor analysis of variance procedures, each utilizing levels 3, 4, and 5 of the day-of-regimen factor, and all pair comparisons of the experimental group factor levels was conducted (Table IV). A significant difference was found among the experimental group levels, personal interview, and control and among experimental group levels, telephone interview, and control. The respective p values were 0.00 and 0.01, with 1 degree of freedom associated with each F value. No significant difference was found among the experimental group factor levels, telephone interview, and personal interview at $\alpha = 0.05$ with 1 degree of freedom.

Thus far, the analysis conducted utilized the raw measure of micrograms of excreted ampicillin per milliliter as the dependent variable. Comparisons between the marginal mean values of excreted ampicillin that denote compliant behavior were then conducted to determine if significant differences found between experimental groups based on the raw data corresponded to actual differences in compliance. The results indicated that the significant differences found, based on quantities of excreted ampicillin, were similar to expected differences based on the operationally defined standard of compliant behavior (Table V).

Table IV—Analysis of Variance (Two Factor, 3 × 3)

Source	df	Sum of Squares	Mean Square	F Value	PF
Experimental group	2	118660.67	59330.4	7.14	0.00[a]
Day of regimen	2	18890.94	9445.5	1.14	0.36
Interaction	4	86377.92	21594.5	2.60	0.06
Error	27	224420.44	8311.9		
Corrected total	35	448349.97			

[a] Significant at $\alpha = < 0.05$.

Table V—Comparison of Experimental Group Marginal Values to Operational Defined Level Indicative of Compliant Behavior

Experimental Group	Day of Regimen			Marginal	Compliant Marginal (≥102.58)
	3	4	5		
1	107.5	133.13	290.69	177.11	Yes
2	137.56	288.75	143.81	170.04	Yes
3	57.50	75.63	22.69	51.94	No

DISCUSSION

Patients subjected to either physical capsule counts *via* a personal interview or to a telephone interview differed in compliance rates from patients who received no stimulation. Stimuli were associated with more positive compliance. The influence of both stimuli diminished after the 5th day of the regimen. This conclusion was based on the results of the 3 × 5 two-factor analysis of variance, which included Days 6 and 7.

Patients subjected to a personal interview differed in compliance rates from those subjected to a telephone interview. No significant difference between the two stimuli was found.

As the duration of time increased between the point of stimulation and the measurement of compliance, the medication compliance rate decreased. Based on the analysis of variance procedures, a significant day-of-regimen effect was not verified. However, the excreted quantities of ampicillin increased on the 6th and 7th regimen days for the experimental group that received no stimulation (control). The experimental group that received the telephone interview maintained high levels of excreted ampicillin throughout the last 2 regimen days measured. For the experimental group that received the personal interview, excretion levels decreased dramatically on the 7th day.

This project demonstrated that the act of measurement was of interest to the patient. Being so, it elicited more positive compliance rates. Health care personnel can benefit from this and other projects that have demonstrated the association between improved compliance habits and increased interest in the patient population.

This project has impact on the validity of previous studies that utilized either a patient interview or dosage unit count to generate a dependent measure of compliance. The act of measurement does influence resultant compliance rates to a degree that must be accounted for if accurate measures are to be achieved. Past reports of patient compliance must be weighted with the intrinsic bias isolated.

REFERENCES

(1) B. W. Jenkins, *Gen. Pract.*, **9**, 66 (1954).

(2) L. C. Park and R. S. Lipman, *Psychopharmacologia*, **6**, 299 (1964).

(3) A. M. W. Porter, *Br. Med. J.*, **1**, 218 (1969).

(4) J. W. G. Smith, G. E. DeGrey, and V. J. Patel, *Analyst*, **92**, 247 (1967).

(5) L. Angelucci and M. Baldieri, *J. Pharm. Pharmacol.*, **23**, 471 (1971).

(6) "Statistical Analysis System," Institute of Statistics, Raleigh, N.C., 1972.

ACKNOWLEDGMENTS

The authors express their appreciation for the cooperation received from the Gilbert Health Center and the School of Pharmacy at the University of Georgia.

Effects of Polyoxypropylene 15 Stearyl Ether and Propylene Glycol on Percutaneous Penetration Rate of Diflorasone Diacetate

JOSEPH S. TURI *x, DOUGLAS DANIELSON ‡, and J. WILLIAM WOLTERSOM *

Received May 8, 1978, from *Pharmacy Research, The Upjohn Company, Kalamazoo, MI 49001, and the ‡School of Pharmacy, University of Minnesota, Minneapolis, MN 55418. Accepted for publication June 14, 1978.

Abstract □ Theoretical models for percutaneous penetration are described, and a diffusion apparatus useful in the evaluation of transport kinetics of drugs applied to skin is discussed. Experimental data are presented for: (*a*) the flux of diflorasone diacetate through hairless mouse skin, (*b*) the percutaneous penetration profile of propylene glycol, (*c*) the effects of vehicle concentrations of polyoxypropylene 15 stearyl ether and propylene glycol on the percutaneous flux of diflorasone diacetate, (*d*) skin-vehicle partition coefficients of diflorasone diacetate, (*e*) the solubility profile of diflorasone diacetate as a function of solvent concentration, and (*f*) the alteration of the skin's resistance to the penetration of diflorasone diacetate due to propylene glycol. Excess solvent in a vehicle caused a decrease in the percutaneous flux of diflorasone diacetate. Formulations containing 0.05 and 0.1% diflorasone diacetate had similar penetration rates when the solvent concentration was optimized for each percentage of diflorasone diacetate.

Keyphrases □ Diflorasone diacetate—percutaneous absorption rate, effect of polyoxypropylene 15 stearyl ether and propylene glycol □ Absorption, percutaneous—diflorasone diacetate, effect of polyoxypropylene 15 stearyl ether and propylene glycol □ Vehicles—polyoxypropylene 15 stearyl ether and propylene glycol, effect on percutaneous absorption rate of diflorasone diacetate □ Anti-inflammatory agents—diflorasone diacetate, percutaneous absorption rate, effect of polyoxypropylene 15 stearyl ether and propylene glycol

Various theoretical relationships (1–11) as well as experimental findings (12–27) concerning the diffusion of substances through heterogeneous barriers, such as skin, have been published. Three potential rate-determining barriers to percutaneous penetration are: (*a*) the dissolution rate of the drug in the vehicle, (*b*) the diffusion rate of solubilized drug through the vehicle to the skin, and (*c*) the permeation rate of drug through the stratum corneum. The slowest step determines the percutaneous penetration rate of the drug.

In the design of topical formulations, it is usually simple to eliminate the dissolution rate of the drug in a vehicle as a potential barrier through the incorporation of a suitable solvent. Factors such as vehicle ingredients, the chemical structure of the active component, and the condition of the skin determine if the rate-limiting step is in the vehicle diffusion layer or in permeation through the stratum corneum.

The importance of the vehicle in determining topical bioavailability is well documented (17–19, 21–23, 27). Nevertheless, vehicle design is often ignored in the biological evaluation of series of related compounds, in dose–response studies of a given drug, and, eventually, in marketed products. It is not generally recognized that the improper selection of the vehicle leads to biased biological results, because the chosen vehicle can have a different influence on each drug and even on different concentrations of a given drug.

In this study, the influence of propylene glycol in an aqueous base and polyoxypropylene 15 stearyl ether[1] in a mineral oil base on the percutaneous penetration rate of diflorasone diacetate (6α,9α-difluoro-11β,17α,21-trihydroxy-16β-methylpregna-1,4-diene-3,20-dione 17,21-diacetate) was investigated.

Table I—Buffered Balanced Salt Solution

Ingredient	Percent (w/v)
Sodium chloride	0.8
Potassium chloride	0.04
Magnesium chloride	0.0075
Dibasic sodium phosphate	0.0154
Monobasic potassium phosphate	0.015
Glucose	0.11
Thimerosal	0.02
Sodium hydroxide *qs ad*	pH 7.0
Deionized water *qs ad*	100.00

THEORETICAL

The important physical factors in the penetration of a substance through a membrane are the concentration of dissolved drug in the vehicle, the partition coefficient of the drug between the skin and the vehicle, and the diffusion coefficients of the drug in the various barriers. The concentration of dissolved drug is important, because the percutaneous penetration rate is directly proportional to the concentration. The partition coefficient is an index of the relative affinity of the drug for the vehicle and the skin. The diffusion coefficient is an indication of the resistance to movement through a barrier. The relative magnitude of the

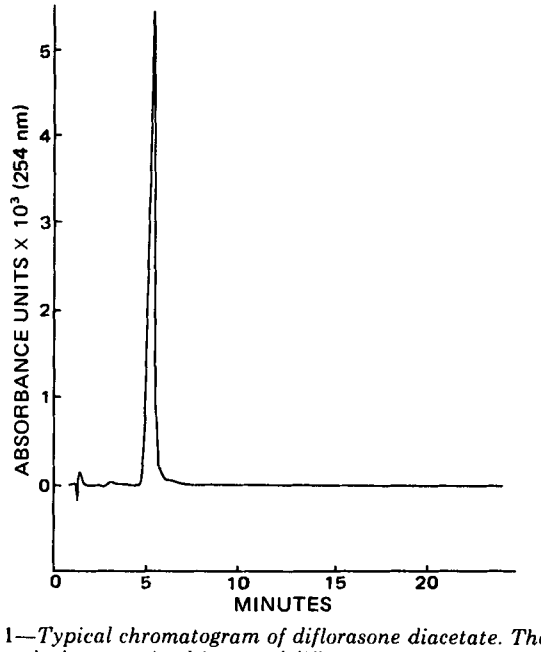

Figure 1—*Typical chromatogram of diflorasone diacetate. The acetonitrile solution contained 0.1 mg of diflorasone diacetate/ml.*

[1] ICI United States.

0022-3549/79/0300-0275$01.00/0
© 1979, American Pharmaceutical Association

Table II—^{3}H-Diflorasone Diacetate Topical Formulations [a]

Ingredient	Formulations												
	1	2	3	4	5	6	7	8	9	10	11	12	13
^{3}H-Diflorasone diacetate	0.05	0.05	0.05	0.05	0.05	0.05	0.05	0.05	0.05	0.05	0.05	0.05	0.10
Propylene glycol	10.0	30.0	50.0	70.0	99.95	—	—	—	—	—	—	—	—
Polyoxypropylene 15 stearyl ether	—	—	—	—	—	—	5	15	20	30	40	60	40
Mineral oil (85 viscosity)	—	—	—	—	—	99.95	94.95	84.95	79.95	69.95	59.95	39.95	59.95
Deionized water	89.95	69.95	49.95	29.95	—	—	—	—	—	—	—	—	—

[a] Values are percent (w/w).

diffusion coefficients in the vehicle and skin determines if penetration is rate limited by release from the vehicle or by the skin.

Relationships of these important parameters to drug transport were discussed previously (10). The influence of diffusion layer resistance and membrane resistance on the flux-determining properties of barrier and solute was quantified (10). The resistance to transport of a solute across a silicone membrane was shown to be not only within the membrane but also within the regions adjacent to its surface. The conditions needed for "membrane control of flux" and "diffusion layer control of flux" were explained (10).

The data obtained for the *in vitro* percutaneous penetration kinetics of diflorasone diacetate in vehicles consisting of propylene glycol–water and polyoxypropylene 15 stearyl ether–mineral oil suggest that the skin is the rate-determining barrier for this compound. In this case, the appropriate relationship is represented by:

$$\frac{-dC_F}{dt} = \frac{AK_sC_FD_s}{V_Fh_s} \qquad \text{(Eq. 1)}$$

where:

A = surface area of application (square centimeters)
C_F = concentration of dissolved diflorasone diacetate in the vehicle (micrograms per cubic centimeters)
D_s = diffusion coefficient of diflorasone diacetate through the skin (square centimeters per second)
h_s = thickness of the skin barrier (centimeters)
K_s = diflorasone diacetate skin–vehicle partition coefficient
V_F = volume of formulation applied (cubic centimeters)

The thickness of the skin barrier and the diffusion coefficient are combined and defined as a resistance, $R_s = h_s/D_s$. The resistance has units of time per length. Equation 1 can be simplified to:

$$\frac{-dC_F}{dt} = \frac{AK_sC_F}{V_FR_s} \qquad \text{(Eq. 2)}$$

The concentration of dissolved diflorasone diacetate, C_F, the partition coefficient, K_s, and, possibly, the resistance, R_s, are influenced by the quantity of solvent in a given vehicle. Under certain conditions, the solubility of a drug in a cosolvent system can be represented by the following expression (10):

$$C_F = C_0e^{\alpha(fs)} \qquad \text{(Eq. 3)}$$

where C_0 is the solubility of the drug in the formulation when the weight fraction of the solvent is zero, α is a constant, and fs is the weight fraction of the solvent.

In a similar manner, the partition coefficient of a drug between the skin and the vehicle can be expressed as:

$$K_s = K_{0}e^{-\beta(fs)} \qquad \text{(Eq. 4)}$$

where K_0 is the partition coefficient of the drug between the skin and the vehicle when the weight fraction of the solvent is zero and β is a constant. Inserting Eqs. 3 and 4 into Eq. 2 leads to the following expression:

$$\frac{-dC_F}{dt} = \frac{A[K_0e^{-\beta(fs)}][C_0e^{\alpha(fs)}]}{V_FR_s} \qquad \text{(Eq. 5)}$$

During the steady-state period of penetration, the following relationship is valid:

$$V_R\frac{dC_R}{dt} = \frac{-V_F\,dC_F}{dt} \qquad \text{(Eq. 6)}$$

where C_R is the concentration of diflorasone diacetate in the receptor compartment of the diffusion apparatus and V_R is the volume of the receptor compartment.

Equation 6 states that the amount of diflorasone diacetate leaving the vehicle per unit time is equal to the amount entering the receptor solution of the diffusion apparatus. With this relationship, Eq. 5 can be written as:

$$V_R\frac{dC_R}{dt} = \frac{a[K_0e^{-\beta(fs)}][C_0e^{\alpha(fs)}]}{R_s} \qquad \text{(Eq. 7)}$$

Integration of Eq. 7 yields:

$$Q_R = \frac{A}{R_s}[K_0e^{-\beta(fs)}][C_0e^{\alpha(fs)}]t \qquad \text{(Eq. 8)}$$

where Q_R is the amount of diflorasone diacetate in the receptor compartment at time t. Equation 8 predicts that the addition of a solvent to a formulation could increase, decrease, or have no effect on the amount of drug diffusing through the skin. The result depends on the magnitudes of α and β and whether or not the drug solution is saturated or unsaturated.

EXPERIMENTAL

Diflorasone Diacetate Solubility—The solubility of diflorasone diacetate was determined in mixtures of polyoxypropylene 15 stearyl ether–mineral oil and propylene glycol–water at 23°. A reversed-phase high-performance liquid chromatographic (HPLC) procedure was used to analyze diflorasone diacetate in these mixtures.

A moderate excess of diflorasone diacetate and 10 ml of the appropriate mixtures were placed in 20-ml vials and shaken for 1 week with a wrist-action shaker. The samples were then filtered, and an appropriate amount of the filtrate was transferred to another vial, extracted, and analyzed by HPLC. The extraction system for the polyoxypropylene 15 stearyl ether–mineral oil mixtures was equal volumes of acetonitrile and hexane. It was not necessary to extract the diflorasone diacetate from the propylene glycol–water mixtures. These samples were diluted with acetonitrile[2] and analyzed.

Extraction Mixture—Acetonitrile and hexane[3], each saturated with the other, were used to extract diflorasone diacetate from the polyoxypropylene 15 stearyl ether–mineral oil mixtures.

Standard Solutions—Standard solutions containing 0.0002, 0.001, 0.002, 0.01, 0.1, and 0.5 mg of diflorasone diacetate/ml of acetonitrile were used to generate a calibration curve. The slope obtained with linear regression of the absorbance data was 0.057 (±0.00012 *SD*).

Sample Solution—An appropriate amount of the diflorasone diacetate polyoxypropylene 15 stearyl ether–mineral oil solution was weighed accurately into 20-ml vials, and 7.0 ml each of acetonitrile and hexane were added. The mixture was shaken for 20 min and centrifuged at 2000 rpm for 15 min. After centrifugation, a portion of the acetonitrile layer was transferred to another vial and held for assay. The diflorasone diacetate propylene glycol–water solutions were filtered, and an appropriate weight of the solubility solution was diluted with acetonitrile and held for assay.

HPLC Procedure—A high-performance liquid chromatograph[4], operated at ambient temperature, was equipped with a UV detector[5] for monitoring the column effluent at 254 nm. The stainless steel column, 30 cm × 3.9 mm (i.d.), was packed with a bonded-phase nonpolar surface[6]. A 20-μl loop injection valve[7] was used to introduce samples into the chromatographic system.

Mobile Phase—The mobile phase, deionized water–acetonitrile (45:55 v/v), was degassed prior to use.

Chromatography—A flow rate of 2.0 ml/min and a chart speed of 0.051 cm/min were used. The detector sensitivity was adjusted as needed

[2] Distilled in glass, Burdick and Jackson.
[3] Spectroquality, Matheson, Coleman & Bell.
[4] Altex model 110 solvent pump.
[5] Altex model 153.
[6] μBondapak C_{18}, Waters Associates.
[7] Rheodyne model 70-10.

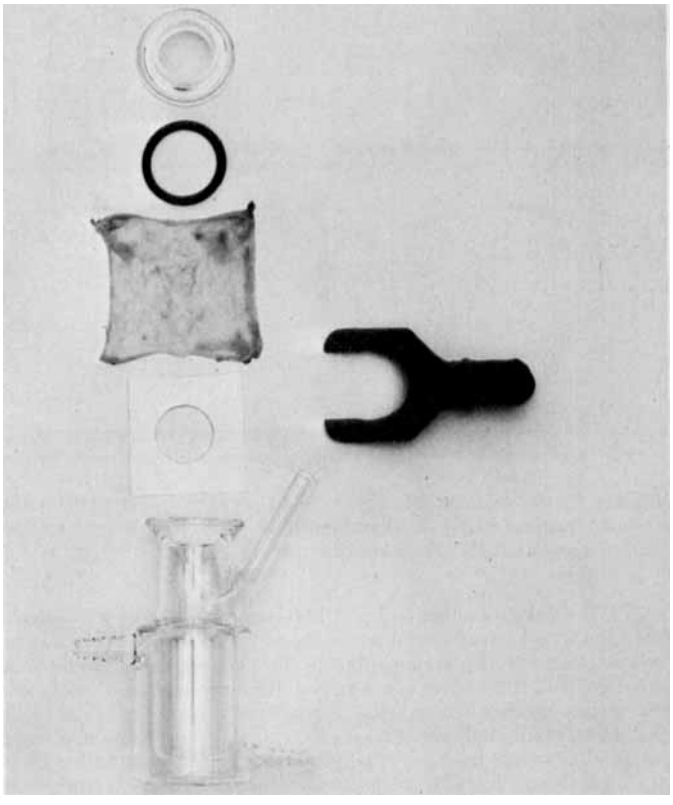

Figure 2—*Component parts of the percutaneous diffusion apparatus (bottom to top): the receptor compartment, waxed film gasket, clamp, hairless mouse skin section, rubber "O" ring, and donor compartment.*

for each sample. Aliquots of 20 μl of the sample solutions and standard solutions were injected, the absorbance (AU) was measured at 254 nm, and the solubility of diflorasone diacetate was calculated using:

$$S_{d.d.} = \frac{AU \times D.F.}{0.057 \times W} \qquad \text{(Eq. 9)}$$

where $S_{d.d.}$ is the solubility of diflorasone diacetate in milligrams per gram, $D.F.$ is the dilution factor, 0.057 is the slope of the calibration curve, and W is sample weight (grams) of solubility solution. A typical chromatogram is shown in Fig. 1.

Partition Coefficient Determination—The partition coefficients between hairless mouse skin and the various vehicles were determined as follows. Skin sections, 1.35 cm in diameter, were placed in 20.0-ml vials and weighed. Then 10 ml of each vehicle containing ^{3}H-diflorasone diacetate[8] was added. The vials were shaken with a wrist-action shaker for 3 and 5 days, and the skin sections and vehicles were assayed for ^{3}H-diflorasone diacetate. The partition coefficients, K_s, were calculated using:

$$K_s = \frac{\text{dpm/mg of skin}}{\text{dpm/mg of vehicle}} \qquad \text{(Eq. 10)}$$

Equilibrium was reached in 3 days.

Percutaneous Transport Procedures—*Preparation of Hairless Mouse Skin*—Female hairless mice[9] were sacrificed, and the skin was removed just prior to use. The skin sections were assembled in the percutaneous diffusion apparatus shown in Figs. 2 and 3. The following procedure was used to assemble the percutaneous diffusion apparatus.

The lower portion (receptor compartment) of the glass diffusion cell was clamped over the magnetic stirring motors and connected to the water bath set at 37°. The degassed, buffered balanced salt solution (Table I) was added, and a waxed film[10] gasket was placed on the top of the receptor compartment. The skin section was placed over the gasket (care was taken to exclude air bubbles under the skin). Then a rubber "O" ring, coated with white wax, was placed over the skin section. The upper

[8] Synthesized by R. S. P. Hsi, The Upjohn Co.
[9] Jackson Laboratories, Bar Harbor, Me.
[10] Parafilm, American Can Co.

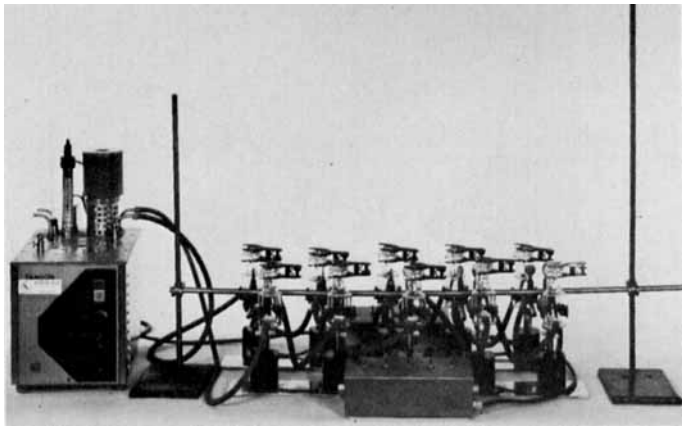

Figure 3—*Assembled percutaneous diffusion apparatus. Included are a water bath, 10 diffusion cells, and a magnetic stirrer.*

portion (donor compartment) of the glass diffusion cell was clamped in place, an additional 3 ml of buffered balanced salt solution was added through the side arm, and 1.0 ml of formulation was applied to the skin.

Receptor Compartment Analysis—At various times, 2.0 ml of the receptor solution was withdrawn and placed in scintillation vials. Scintillation cocktail[11], 15 ml, was added, and the samples were assayed using a liquid scintillation spectrometer[12]. Quench corrections were made with a calibration curve.

^{3}H-Diflorasone Diacetate Formulations—The formulations used in the transport experiments are shown in Table II.

RESULTS

An attempt was made to optimize diflorasone diacetate release from aqueous and lipid vehicle systems. Propylene glycol was selected as the

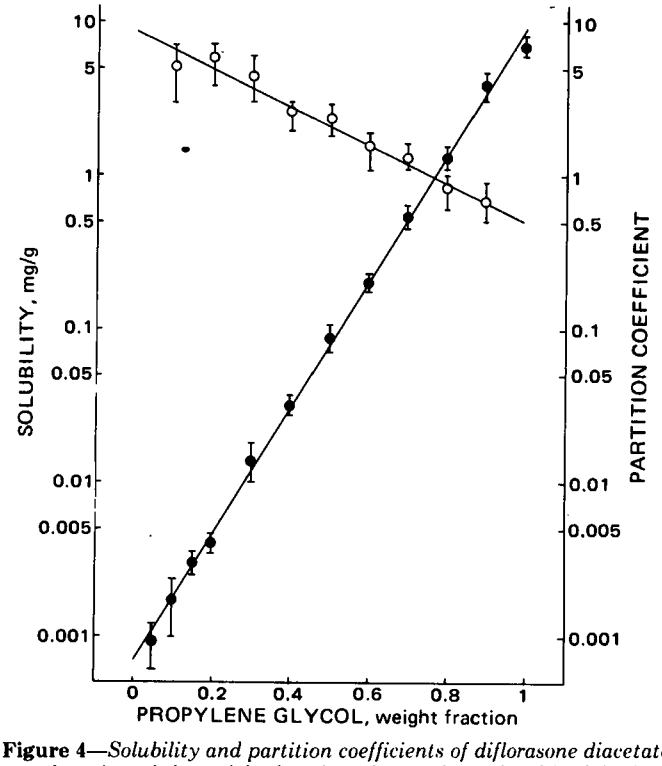

Figure 4—*Solubility and partition coefficients of diflorasone diacetate as a function of the weight fraction of propylene glycol in deionized water; average (± SD) of four determinations. Key: ●, solubility; and ○, partition coefficient.*

[11] PCS, Amersham/Searle.
[12] Searle Mark III.

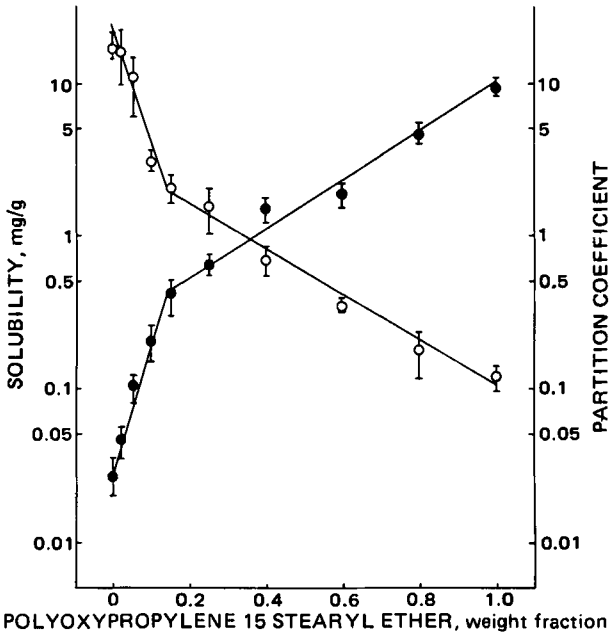

Figure 5—*Solubility and partition coefficients of diflorasone diacetate as a function of the weight fraction of polyoxypropylene 15 stearyl ether in mineral oil (85 viscosity); average* (± SD) *of four determinations. Key:* ●, *solubility; and* ○, *partition coefficient.*

aqueous miscible solvent since it is a satisfactory solvent for steroids and is commonly used in many topical steroid formulations. A fairly new solvent, polyoxypropylene 15 stearyl ether, also was selected because of its good solvent capacity for diflorasone diacetate. It is a nonirritating emollient miscible with mineral oil.

Solubility and Partition Coefficients of Diflorasone Diacetate in Propylene Glycol–Water Mixtures—The solubility and partition coefficients (defined by Eq. 10) of diflorasone diacetate, as a function of the weight fraction of propylene glycol, are shown in Fig. 4. The increase in solubility and the decrease in the partition coefficient as the weight fraction of propylene glycol is increased can be described by Eqs. 3 and 4, respectively. From these data, α and β were calculated to be 9.4 and 2.9, respectively. Since α is larger than β, Eq. 8 predicts that an increase in the percutaneous penetration rate of diflorasone diacetate should result when the weight fraction of propylene glycol is increased, provided a saturated solution is maintained.

Solubility and Partition Coefficients of Diflorasone Diacetate in Polyoxypropylene 15 Stearyl Ether–Mineral Oil Mixtures—The solubility and partition coefficients of diflorasone diacetate in the polyoxypropylene 15 stearyl ether–mineral oil solvent systems are shown in Fig. 5. Both the solubility and partition coefficient curves are biphasic with the transition at a point where the weight fraction of polyoxypropylene 15 stearyl ether is approximately 0.15. The reason for this biphasic solubility and partitioning is not known. However, each portion of these curves can be described by Eqs. 3 and 4. Since there are two slopes each for the solubility and partition coefficient, there are two α and two β values. For weight fractions of polyoxypropylene 15 stearyl ether up to 0.15, α and β are 20 and 17, respectively; for weight fractions larger than 0.15, α and β are 3.7 and 3.5, respectively.

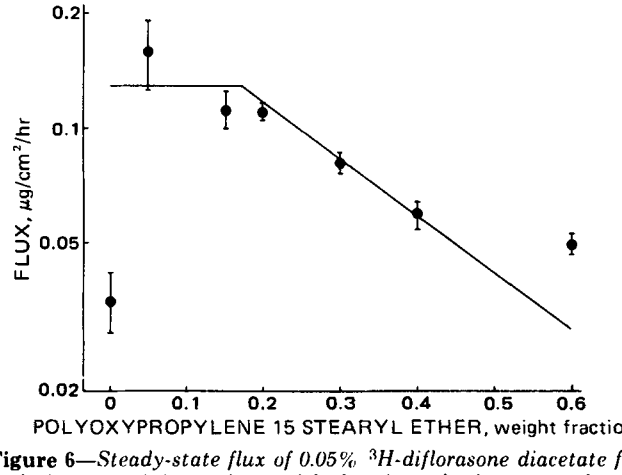

Figure 6—*Steady-state flux of 0.05% ^{3}H-diflorasone diacetate formulations containing various weight fractions of polyoxypropylene 15 stearyl ether in mineral oil (85 viscosity). The solid line was generated using Eq. 8. The points are experimental values obtained from penetration studies.*

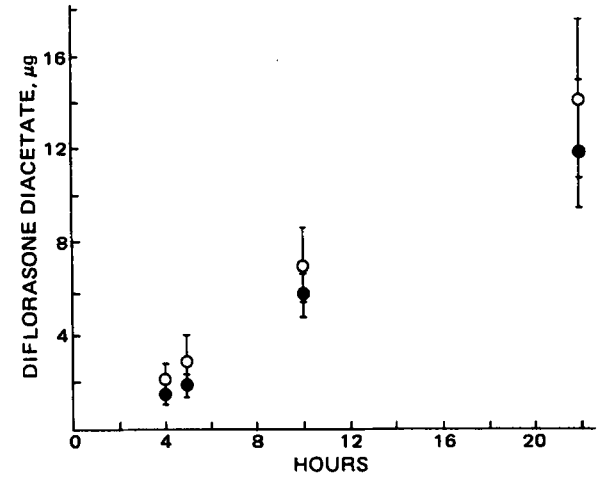

Figure 7—*Cumulative amount of ^{3}H-diflorasone diacetate diffusing through hairless mouse skin as a function of time. Key:* ●, *0.05% (Formula 9); and* ○, *0.1% (Formula 13).*

Since α and β are comparable in both cases, the percutaneous penetration rate of diflorasone diacetate should be independent of the weight fraction of polyoxypropylene 15 stearyl ether, as predicted by Eq. 8. This hypothesis should be true, provided a saturated solution of diflorasone diacetate is maintained and the solvent does not affect the barrier properties of the skin. An excess of solvent should result in a decreased flux since the partition coefficient declines while the concentration of dissolved drug remains constant.

Percutaneous Penetration of Diflorasone Diacetate Formulated in Polyoxypropylene 15 Stearyl Ether–Mineral Oil—The steady-state flux of ^{3}H-diflorasone diacetate as a function of the weight fraction of polyoxypropylene 15 stearyl ether is shown in Fig. 6. The solid line was generated using the theoretical Eq. 8. Experimental values for the solubility and partition coefficients and a skin resistance of 6666 hr/cm were

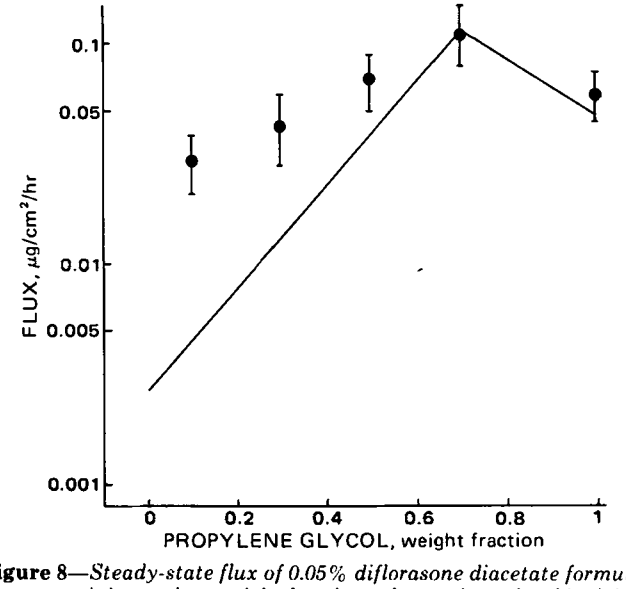

Figure 8—*Steady-state flux of 0.05% diflorasone diacetate formulations containing various weight fractions of propylene glycol in deionized water. The solid line was generated using Eq. 8. The points are experimental values obtained from penetration studies.*

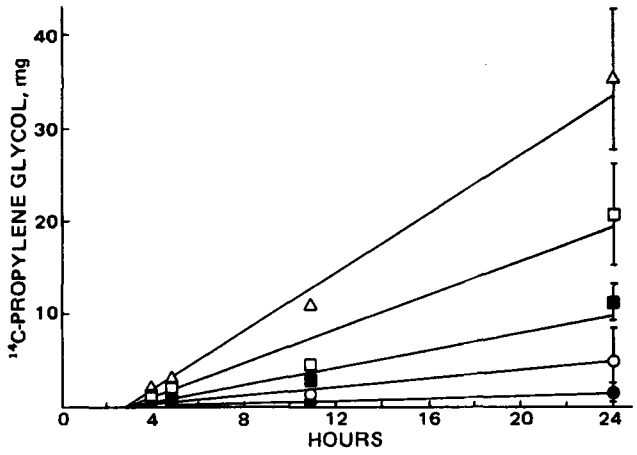

Figure 9—*Cumulative amount of ^{14}C-propylene glycol diffusing through hairless mouse skin as a function of time. Key (^{14}C-propylene glycol in deionized water): ●, 10%; ○, 30%; ■, 50%; □, 70%; and △, 90%.*

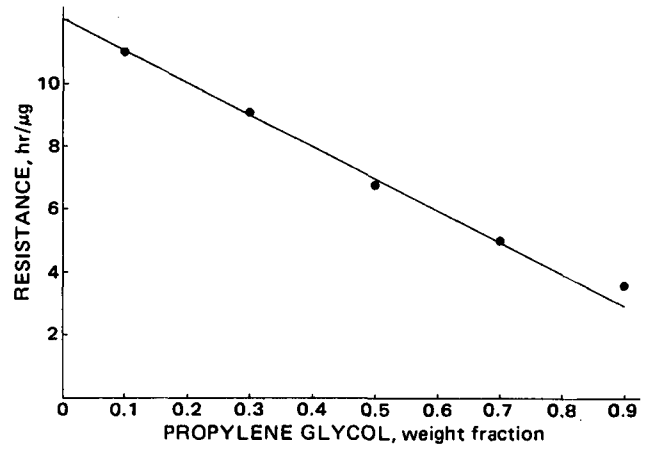

Figure 10—*Resistance of hairless mouse skin to the penetration of ^{14}C-propylene glycol as a function of the weight fraction ^{14}C-propylene glycol in deionized water.*

used in the calculations. The data points are the experimental values obtained from the penetration studies.

The low value obtained in the vehicle without polyoxypropylene 15 stearyl ether could be attributable to the low solubility and slow dissolution rate of diflorasone diacetate in mineral oil. The other data points agree with the theoretical line. The decrease in flux of the 0.05% diflorasone diacetate solutions obtained for vehicles containing greater than 0.15 weight fraction of polyoxypropylene 15 stearyl ether is expected. This result occurs because the partition coefficient is reduced while the concentration of dissolved diflorasone diacetate remains constant.

The theoretical model also predicts that the steady-state flux will be maintained as long as saturation of the drug in the vehicle exists. Therefore, increasing the amount of diflorasone diacetate in a formulation should not result in a greater steady-state flux. This will be true for a given period of time if the drug and solvent do not affect the skin barrier and if the vehicle is saturated with drug since the skin is the rate-limiting barrier. Figure 7 shows the comparison of two percentages of diflorasone diacetate in the polyoxypropylene 15 stearyl ether–mineral oil system. The steady-state penetration rates obtained with 0.05 and 0.1% diflorasone diacetate were similar. These data suggest that no additional therapeutic benefit will result from the use of a 0.1% formulation.

Percutaneous Penetration of Diflorasone Diacetate Formulated in Propylene Glycol–Water Mixture—The influence of propylene glycol on the penetration rate of 0.05% diflorasone diacetate formulations is shown in Fig. 8. The solid line was generated as described previously. The penetration rate should increase as the propylene glycol weight fraction is increased to 0.7 and should decrease beyond this point. The experimental values are greater than the predicted values according to the theoretical model. One feasible explanation for the deviation is supersaturation, which would result in larger penetration rates. These formulations were prepared by dissolving the diflorasone diacetate in propylene glycol and then adding water. Up to 5 days was required to reach equilibrium solubility when this method was used.

Differential scanning calorimetry of diflorasone diacetate crystals obtained from propylene glycol–water mixtures indicated a change in the polymorphic form, which might explain the prolonged equilibration time. These high experimental values could also be attributed to the loss of some water from the vehicle due to evaporation. Even though the donor compartment was sealed in these experiments, some water could evaporate and condense on the stopper, which would cause an increase in the weight fraction of solvent and result in a larger flux.

Percutaneous Penetration of ^{14}C-Propylene Glycol—Figure 9 shows the percutaneous penetration data of ^{14}C-propylene glycol[13] through hairless mouse skin. Propylene glycol penetrated the skin rather easily, and the skin resistance to propylene glycol decreased as the weight fraction of propylene glycol increased (Fig. 10). Further evidence that propylene glycol decreases the diffusional resistance of skin was obtained by pretreating skin sections in propylene glycol for 18 hr (Fig. 11). The skin sections treated with propylene glycol were very dry and without supple characteristics. The penetration rate of diflorasone diacetate through the propylene glycol-pretreated skin was twice the rate without pretreatment.

[13] ICN Isotope and Nuclear Division.

SUMMARY

An important factor affecting topical bioavailability is the release rate of the drug from the vehicle. The development of topical formulations should include the use of theoretical models and appropriate experimental procedures to quantify drug–vehicle interactions and topical bioavailability. This procedure should be used in early biological screening as well as in the design of final marketed products. In biological tests of topical drugs, the vehicle and its effects on the release rates of test compounds must be considered to avoid biased results due to vehicle–drug interactions.

The data presented demonstrate the effects of two solvents on the *in vitro* penetration rate of diflorasone diacetate. Incorporation of too much solvent in the vehicle resulted in a decreased penetration rate. In the polyoxypropylene 15 stearyl ether–mineral oil systems, it was possible to obtain similar penetration rates with 0.05 and 0.1% diflorasone diacetate formulations by selection of the optimum weight fraction of the solvent for the given percentage of diflorasone diacetate. Selection of a common vehicle with too high a solvent composition would have given a larger flux for the 0.1% formulation. Another observation was that the steady-state flux for both concentrations was maintained during the time

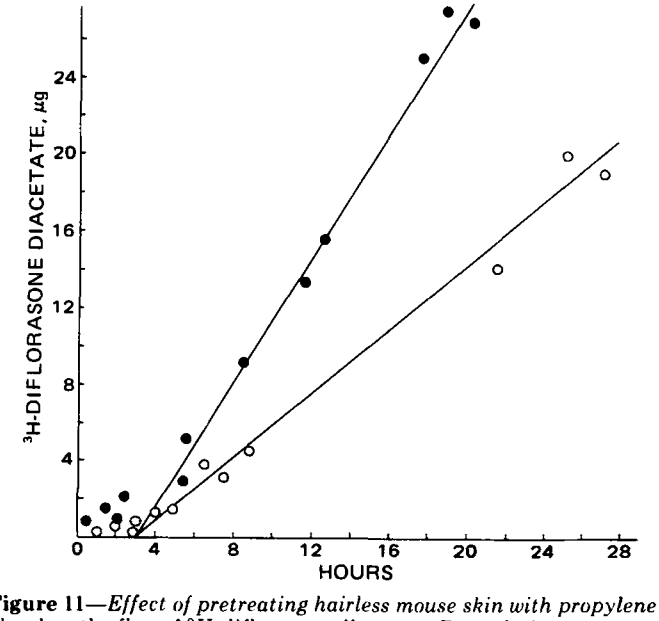

Figure 11—*Effect of pretreating hairless mouse skin with propylene glycol on the flux of ^{3}H-diflorasone diacetate. Formulation 8 was applied to the skin sections. Key: ●, skin pretreated with propylene glycol; and ○, untreated skin.*

of the experiment (approximately 24 hr).

Based on these results, one could hypothesize that one daily application would be sufficient for the optimal therapeutic effect, provided the formulation is not washed or rubbed off by the patient. The results also show that the formulation with 0.1% diflorasone diacetate offers no therapeutic advantage over the 0.05% formulation. Recent clinical studies comparing the therapeutic benefit of diflorasone diacetate 0.05 and 0.1% ointments (28) support this hypothesis.

REFERENCES

(1) T. Higuchi, *J. Pharm. Sci.*, **50**, 874 (1961).

(2) W. I. Higuchi, *ibid.*, **51**, 802 (1962).

(3) T. Higuchi and W. I. Higuchi, *J. Am. Pharm. Assoc., Sci. Ed.*, **49**, 598 (1960).

(4) T. Higuchi, *J. Soc. Cosmet Chem.*, **11**, 85 (1960).

(5) T. Higuchi, *J. Pharm. Sci.*, **52**, 1145 (1963).

(6) G. L. Flynn and T. J. Roseman, *ibid.*, **60**, 1788 (1971).

(7) G. L. Flynn, O. S. Carpenter, and S. H. Yalkowsky, *ibid.*, **61**, 312 (1972).

(8) G. L. Flynn and S. H. Yalkowsky, *ibid.*, **61**, 838 (1972).

(9) S. H. Yalkowsky and G. L. Flynn, *ibid.*, **62**, 210 (1973).

(10) *Ibid.*, **63**, 1276 (1974).

(11) J. W. Ayres and F. T. Lindstrom, *J. Pharm. Sci.*, **66**, 654 (1977).

(12) R. J. Scheuplein and L. W. Ross, *J. Invest. Dermatol.*, **62**, 353 (1974).

(13) R. J. Scheuplein, *ibid.*, **48**, 79 (1967).

(14) R. J. Scheuplein, I. H. Blank, G. J. Brauner, and D. J. McFarland, *ibid.*, **52**, 63 (1969).

(15) R. J. Scheuplein, *ibid.*, **45**, 334 (1965).

(16) M. K. Polano and M. Ponec, *Arch. Dermatol.*, **112**, 675 (1976).

(17) T. Malone, J. K. Haleblian, B. J. Poulsen, and K. H. Burdick, *Br. J. Dermatol.*, **90**, 187 (1974).

(18) B. J. Poulsen, E. Young, V. Coquilla, and M. Katz, *J. Pharm. Sci.*, **57**, 928 (1968).

(19) J. Oishi, Y. Ushio, K. Narobara, M. Takebara, and T. Nakagawa, *Chem. Pharm. Bull.*, **24**, 1765 (1976).

(20) R. J. Scheuplein, *J. Invest. Dermatol.*, **67**, 672 (1976).

(21) J. Ostrenga, C. Steinmetz, and B. Poulsen, *J. Pharm. Sci.*, **60**, 1175 (1971).

(22) J. Ostrenga, C. Steinmetz, B. Poulsen, and S. Yett, *ibid.*, **60**, 1180 (1971).

(23) M. F. Coldman, B. J. Poulsen, and T. Higuchi, *ibid.*, **58**, 1098 (1969).

(24) R. J. Scheuplein and I. H. Blank, *J. Invest. Dermatol.*, **60**, 286 (1973).

(25) T. J. Franz, *ibid.*, **64**, 190 (1975).

(26) M. I. Foreman and I. Kelly, *Br. J. Dermatol.*, **95**, 265 (1976).

(27) W. M. Ponec and M. K. Polano, *Ned. Tijdschr. Geneesk.*, **119**, 172 (1975).

(28) M. M. Cahn, J. H. Hall, M. B. Kerschenbaum, L. Klein, E. Kiebsohn, V. T. Peng, H. L. Roth, T. C. Savin, and C. A. Schlagel, *Curr. Ther. Res.*, **22**, 297 (1977).

ACKNOWLEDGMENTS

The authors thank Dr. S. H. Yalkowsky and Dr. W. Morozowich for valuable discussions, Dr. R. S. P. Hsi for the radiolabeled diflorasone diacetate, and Ms. S. L. Matteson for technical assistance.

High-Pressure Liquid Chromatographic Assay of Benzoyl Peroxide in Dermatological Gels and Lotions

FREDERICK W. BURTON, R. RAO GADDE, and WALTER L. McKENZIE ˣ

Received April 3, 1978, from the *Pharmaceutical Development Department, Westwood Pharmaceuticals Inc., Buffalo, NY 14213.* Accepted for publication August 3, 1978.

Abstract □ A high-pressure liquid chromatographic method for the assay of benzoyl peroxide in dermatological preparations is described. Degradation products such as benzoic acid and perbenzoic acid do not interfere. The method is simple, precise, accurate, and stability indicating.

Keyphrases □ Benzoyl peroxide—high-pressure liquid chromatographic analysis in pharmaceutical preparations □ High-pressure liquid chromatography—analysis, benzoyl peroxide in pharmaceutical preparations □ Keratolytics—benzoyl peroxide, high-pressure liquid chromatographic analysis in pharmaceutical preparations

Benzoyl peroxide is inherently a very reactive compound, and its chemical stability has been studied extensively. Depending on the experimental conditions (temperature, pH, solvent, *etc.*), the degradation of benzoyl peroxide may lead to benzoic acid, biphenyl, phenyl benzoate, benzene, and carbon dioxide. In alcoholic solutions, the degradation products were carbon dioxide, benzoic acid, and alcohol esters of benzoic acid (1). In pharmaceutical lotions, benzoic acid was the significant product (2).

BACKGROUND

The existing stability assays for benzoyl peroxide in pharmaceutical preparations have used spectrophotometric, iodometric, polarographic, and TLC techniques (3–6). Controversial claims of superiority of one method over the others have been made. Gruber and Klein (4) reported that the polarographic method is superior to the spectrophotometric method which, in turn, is much better than the iodometric method. Simmons *et al.* (6) compared the iodometric method with a combination TLC–spectrophotometric method and reported good agreement in assay results, suggesting that the iodometric method is stability indicating.

Daly *et al.* (5) reported "fair agreement" between the assay results by the iodometric method and a combination TLC–iodometric method. Furthermore, the results were reported to be lower than the corresponding assay results by the iodometric and spectrophotometric methods of Gruber and Klein (4). From these observations, Daly *et al.* (5) concluded that the described iodometric method is a stability-indicating procedure. This iodometric procedure has been accepted as the USP method for benzoyl peroxide in lotions (7).

In evaluating the stability-indicating nature of the methods, one or both of the following criteria were used:

1. The results obtained by the method should agree with those obtained by a separate and inherently stability-indicating "reference" method (*e.g.*, chromatographic methods).
2. The results obtained by the method should be lower than those obtained by other methods.

0022-3549/79/0300-0280$01.00/0

© 1979, American Pharmaceutical Association

of the experiment (approximately 24 hr).

Based on these results, one could hypothesize that one daily application would be sufficient for the optimal therapeutic effect, provided the formulation is not washed or rubbed off by the patient. The results also show that the formulation with 0.1% diflorasone diacetate offers no therapeutic advantage over the 0.05% formulation. Recent clinical studies comparing the therapeutic benefit of diflorasone diacetate 0.05 and 0.1% ointments (28) support this hypothesis.

REFERENCES

(1) T. Higuchi, *J. Pharm. Sci.*, **50**, 874 (1961).

(2) W. I. Higuchi, *ibid.*, **51**, 802 (1962).

(3) T. Higuchi and W. I. Higuchi, *J. Am. Pharm. Assoc., Sci. Ed.*, **49**, 598 (1960).

(4) T. Higuchi, *J. Soc. Cosmet Chem.*, **11**, 85 (1960).

(5) T. Higuchi, *J. Pharm. Sci.*, **52**, 1145 (1963).

(6) G. L. Flynn and T. J. Roseman, *ibid.*, **60**, 1788 (1971).

(7) G. L. Flynn, O. S. Carpenter, and S. H. Yalkowsky, *ibid.*, **61**, 312 (1972).

(8) G. L. Flynn and S. H. Yalkowsky, *ibid.*, **61**, 838 (1972).

(9) S. H. Yalkowsky and G. L. Flynn, *ibid.*, **62**, 210 (1973).

(10) *Ibid.*, **63**, 1276 (1974).

(11) J. W. Ayres and F. T. Lindstrom, *J. Pharm. Sci.*, **66**, 654 (1977).

(12) R. J. Scheuplein and L. W. Ross, *J. Invest. Dermatol.*, **62**, 353 (1974).

(13) R. J. Scheuplein, *ibid.*, **48**, 79 (1967).

(14) R. J. Scheuplein, I. H. Blank, G. J. Brauner, and D. J. McFarland, *ibid.*, **52**, 63 (1969).

(15) R. J. Scheuplein, *ibid.*, **45**, 334 (1965).

(16) M. K. Polano and M. Ponec, *Arch. Dermatol.*, **112**, 675 (1976).

(17) T. Malone, J. K. Haleblian, B. J. Poulsen, and K. H. Burdick, *Br. J. Dermatol.*, **90**, 187 (1974).

(18) B. J. Poulsen, E. Young, V. Coquilla, and M. Katz, *J. Pharm. Sci.*, **57**, 928 (1968).

(19) J. Oishi, Y. Ushio, K. Narobara, M. Takebara, and T. Nakagawa, *Chem. Pharm. Bull.*, **24**, 1765 (1976).

(20) R. J. Scheuplein, *J. Invest. Dermatol.*, **67**, 672 (1976).

(21) J. Ostrenga, C. Steinmetz, and B. Poulsen, *J. Pharm. Sci.*, **60**, 1175 (1971).

(22) J. Ostrenga, C. Steinmetz, B. Poulsen, and S. Yett, *ibid.*, **60**, 1180 (1971).

(23) M. F. Coldman, B. J. Poulsen, and T. Higuchi, *ibid.*, **58**, 1098 (1969).

(24) R. J. Scheuplein and I. H. Blank, *J. Invest. Dermatol.*, **60**, 286 (1973).

(25) T. J. Franz, *ibid.*, **64**, 190 (1975).

(26) M. I. Foreman and I. Kelly, *Br. J. Dermatol.*, **95**, 265 (1976).

(27) W. M. Ponec and M. K. Polano, *Ned. Tijdschr. Geneesk.*, **119**, 172 (1975).

(28) M. M. Cahn, J. H. Hall, M. B. Kerschenbaum, L. Klein, E. Kiebsohn, V. T. Peng, H. L. Roth, T. C. Savin, and C. A. Schlagel, *Curr. Ther. Res.*, **22**, 297 (1977).

ACKNOWLEDGMENTS

The authors thank Dr. S. H. Yalkowsky and Dr. W. Morozowich for valuable discussions, Dr. R. S. P. Hsi for the radiolabeled diflorasone diacetate, and Ms. S. L. Matteson for technical assistance.

High-Pressure Liquid Chromatographic Assay of Benzoyl Peroxide in Dermatological Gels and Lotions

FREDERICK W. BURTON, R. RAO GADDE, and WALTER L. McKENZIE ˣ

Received April 3, 1978, from the *Pharmaceutical Development Department, Westwood Pharmaceuticals Inc., Buffalo, NY 14213.* Accepted for publication August 3, 1978.

Abstract □ A high-pressure liquid chromatographic method for the assay of benzoyl peroxide in dermatological preparations is described. Degradation products such as benzoic acid and perbenzoic acid do not interfere. The method is simple, precise, accurate, and stability indicating.

Keyphrases □ Benzoyl peroxide—high-pressure liquid chromatographic analysis in pharmaceutical preparations □ High-pressure liquid chromatography—analysis, benzoyl peroxide in pharmaceutical preparations □ Keratolytics—benzoyl peroxide, high-pressure liquid chromatographic analysis in pharmaceutical preparations

Benzoyl peroxide is inherently a very reactive compound, and its chemical stability has been studied extensively. Depending on the experimental conditions (temperature, pH, solvent, *etc.*), the degradation of benzoyl peroxide may lead to benzoic acid, biphenyl, phenyl benzoate, benzene, and carbon dioxide. In alcoholic solutions, the degradation products were carbon dioxide, benzoic acid, and alcohol esters of benzoic acid (1). In pharmaceutical lotions, benzoic acid was the significant product (2).

BACKGROUND

The existing stability assays for benzoyl peroxide in pharmaceutical preparations have used spectrophotometric, iodometric, polarographic, and TLC techniques (3–6). Controversial claims of superiority of one method over the others have been made. Gruber and Klein (4) reported that the polarographic method is superior to the spectrophotometric method which, in turn, is much better than the iodometric method. Simmons *et al.* (6) compared the iodometric method with a combination TLC–spectrophotometric method and reported good agreement in assay results, suggesting that the iodometric method is stability indicating.

Daly *et al.* (5) reported "fair agreement" between the assay results by the iodometric method and a combination TLC–iodometric method. Furthermore, the results were reported to be lower than the corresponding assay results by the iodometric and spectrophotometric methods of Gruber and Klein (4). From these observations, Daly *et al.* (5) concluded that the described iodometric method is a stability-indicating procedure. This iodometric procedure has been accepted as the USP method for benzoyl peroxide in lotions (7).

In evaluating the stability-indicating nature of the methods, one or both of the following criteria were used:

1. The results obtained by the method should agree with those obtained by a separate and inherently stability-indicating "reference" method (*e.g.*, chromatographic methods).
2. The results obtained by the method should be lower than those obtained by other methods.

0022-3549/79/0300-0280$01.00/0

© 1979, American Pharmaceutical Association

In applying the first criterion, it is essential that the chosen reference method be truly stability indicating. Simmons *et al.* (6) and Daly *et al.* (5) chose TLC as the reference. However, certain TLC conditions (6) do not appear to be capable of separating benzoyl peroxide from its polar degradation products (*e.g.*, benzoic acid). The more polar degradation products also would migrate with benzoyl peroxide and appear as one spot at the solvent front. Hence, the TLC method of Simmons *et al.* (6) is not truly stability indicating and the conclusions reached regarding its reliability (6) are subject to question.

The second criterion was applied by Gruber and Klein (4), who concluded that the iodometric method is not a good stability-indicating method. Similar reasoning by Daly *et al.* (5) led them to conclude that their iodometric method is better than the iodometric and the spectrophotometric methods of Gruber and Klein. Although Daly *et al.* (5) reported fair agreement between the results by the iodometric method and the reference TLC method, the reported results indicate that the agreement was good only for four of seven cream and lotion samples.

Clearly, the existing methods for benzoyl peroxide are either stability indicating only when applied to certain formulations or only partially stability indicating.

This paper describes the development of a new high-pressure liquid chromatographic (HPLC) method for benzoyl peroxide and compares its performance with that of the USP iodometric method (7). The HPLC method is inherently stability indicating and is simple, accurate, and precise.

EXPERIMENTAL

Apparatus—Column 1 was a stainless steel column (50 cm long, 2.6 mm i.d.) dry packed with macroparticulate (37–50-μm range) bonded octadecylsilane material[1]. The HPLC unit[2] had a syringe-type pump, a septum injector, and a 254-nm absorbance detector.

Stability samples were analyzed using Column 2, a commercial column[3] (30 cm long, 3.9 mm i.d.) prepacked with microparticulate (10 μm) bonded octadecylsilane material. The HPLC unit[4] used with this column had a low volume positive displacement pump[5], a universal injector[6], and a 254-nm absorbance detector[7]. This change from Column 1 to Column 2, with a corresponding change in HPLC units, became necessary when the former column did not provide adequate separation of benzoic acid (a degradation product) from the solvent front.

Reagents—Hydrous benzoyl peroxide[8] (~70% benzoyl peroxide) was used after assaying within the week by the USP procedure (8). Perbenzoic acid was synthesized by the procedure described by Brown (9). Ethyl benzoate[9] was purified by distillation and used as the internal standard. All other reagents used were ACS grade. Water used for preparing HPLC eluents and solutions was distilled from an all-glass still[10].

Samples—The method was developed utilizing samples of two products: a gel formulation containing 5% benzoyl peroxide, polyethylene glycol lauryl ether, carboxypolymethylene, diisopropanolamine, ethylenediaminetetraacetic acid, and water; and a lotion containing 4% benzoyl peroxide, sodium octoxynol-3-sulfonate, water, dioctyl sodium sulfosuccinate, sodium lauryl sulfoacetate, magnesium aluminum silicate, methylcellulose, and ethylenediaminetetraacetic acid.

Control blanks were produced in the same manner as the commercial products, except that the benzoyl peroxide was not added. Synthetic samples of the gel and lotion formulations were made by adding an exactly known aliquot of freshly prepared benzoyl peroxide solution in a suitable solvent (acetone or acetonitrile) to the corresponding control blank. Each synthetic sample was made independently from the control blank and benzoyl peroxide stock solution, and the entire sample was assayed by the chosen method.

Synthetic samples prepared as described are close approximations to commercial products but have an exactly known amount of benzoyl peroxide; the only difference was that benzoyl peroxide was added as a solution. To study the effect of relative amounts of control blank and benzoyl peroxide, some synthetic samples with various ratios of benzoyl peroxide to control blank also were prepared by a similar procedure.

[1] Bondapak C_{18}/Corasil, Waters Associates.
[2] Model 1220, Perkin-Elmer.
[3] μBondapak C_{18}, Waters Associates.
[4] Model ALC/GPC 204, Waters Associates.
[5] Model 6000A, Waters Associates.
[6] Model U6K, Waters Associates.
[7] Model 440, Waters Associates.
[8] Aztec Chemicals.
[9] Eastman Chemicals.
[10] F1-Still 4, Barnstead.

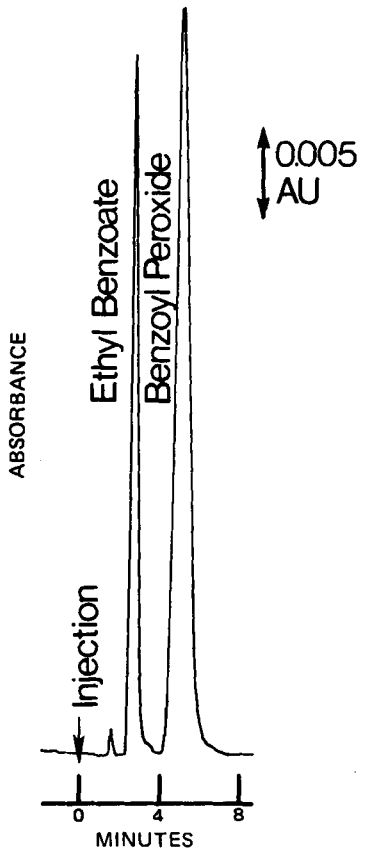

Figure 1—*HPLC separation of ethyl benzoate and benzoyl peroxide using Column 1, 50% acetonitrile in water, and a flow rate of 1 ml/min.*

HPLC Method—A sample containing about 40 mg of benzoyl peroxide was shaken with 50 ml of acetonitrile until the sample was dislodged from the sides and dispersed in solution. The sample solution was then sonicated for 5 min and clarified by centrifugation. The solution for HPLC analysis was made by mixing 10 ml of the clear centrifugate with 5 ml of ethyl benzoate (~18 mg) solution in acetonitrile and then diluting to 25 ml with acetonitrile. Unless otherwise mentioned, the following HPLC parameters were used: eluent, 50% acetonitrile in water; flow rate, 1 ml/min; optical density setting, 0.05 unit; recorder, 10 mv full scale; and chart speed, 5 mm/min.

USP Iodometric Titration Method (5)—Benzoyl peroxide in the sample was extracted into acetone, phenyl sulfide was added, and the solution was titrated iodometrically.

RESULTS AND DISCUSSION

HPLC Method Development—Preliminary TLC studies of benzoyl peroxide formulations showed that the excipients of the formulations are more polar than benzoyl peroxide. Based on this observation, a reversed-phase column was an obvious choice because it permitted the elution of excipients before benzoyl peroxide. Furthermore, dermatological creams and lotions are generally soluble in polar solvents (*e.g.*, methanol and acetonitrile), and these solvents are compatible with the packing of the reversed-phase column. Sample preparation prior to HPLC analysis is simply dissolution and filtration. Acetonitrile was selected as the solvent for sample dissolution because the samples dissolved easier in acetonitrile than in methanol and because benzoyl peroxide is much more soluble in acetonitrile.

The separation of benzoyl peroxide on Column 1 was studied with different acetonitrile–water mixtures as eluents. A reasonably symmetrical (gaussian) benzoyl peroxide peak was observed at a retention time of about 6 min using 50% acetonitrile in water as the eluent at a flow rate of 1 ml/min. With the same HPLC parameters, ethyl, butyl, and phenyl benzoates were evaluated as possible internal standards. Phenyl and butyl benzoates gave peaks that were not fully resolved from the benzoyl peroxide peak. Ethyl benzoate was fully resolved and was chosen as the internal standard. A typical chromatogram of the benzoyl peroxide and ethyl benzoate mixture is shown in Fig. 1.

Table I—HPLC Determination of Benzoyl Peroxide in Synthetic Gel Samples [a]

Synthetic Sample: Control Blank, g	Synthetic Sample: Benzoyl Peroxide, mg	Benzoyl Peroxide Found, mg	Recovery, %
2	71.6	71.1, 71.1, 71.4	99.3, 99.3, 99.7
2	95.5	95.3, 94.8, 93.4	99.8, 99.3, 97.8
2	119.5	121.8, 120.3, 119.1	101.9, 100.7, 99.7

[a] Benzoyl peroxide was added to the control blank as its solution in acetonitrile. A sample containing 2 g (control blank) and 100 mg of benzoyl peroxide approximates the normal gel containing 5% benzoyl peroxide.

Table II—HPLC Determination of Benzoyl Peroxide in Synthetic Lotion Samples [a]

Synthetic Sample: Control Blank, g	Synthetic Sample: Benzoyl Peroxide, mg	Benzoyl Peroxide Found, mg	Recovery, %
0.9	48.3	48.5, 48.6, 48.9	100.4, 100.6, 101.2
1.2	48.3	48.9, 48.2, 48.4	101.2, 99.8, 100.2
1.5	48.3	47.9, 47.4, 47.7	99.2, 98.1, 98.7

[a] Benzoyl peroxide was added to the control blank as its solution in acetonitrile. A sample containing 1.2 g (control blank) and 48 mg of benzoyl peroxide approximates the normal lotion containing 4% benzoyl peroxide.

Likely degradation products of benzoyl peroxide are benzoic acid (2) and perbenzoic acid (5). With the same HPLC system as that used to obtain Fig. 1, benzoic acid gave a peak at the solvent front, thereby causing no interference in the benzoyl peroxide assay. Since it is desirable to determine benzoic acid also, particularly in stability studies, the more efficient Column 2 was tested to effect the separation of benzoic acid from the solvent front. Adequate separation was observed with 50% acetonitrile in water as the eluent at a flow rate of 1 ml/min. Under the same HPLC conditions, the separation of ethyl benzoate and benzoyl peroxide was also adequate, suggesting that both benzoyl peroxide and benzoic acid may be determined by a single HPLC method using Column 2. A typical chromatogram of a mixture of the three compounds is shown in Fig. 2. The use of Column 1 permits only the determination of benzoyl peroxide and not benzoic acid.

The HPLC characteristics of perbenzoic acid were studied using both columns. When 50% acetonitrile in water was the eluent, perbenzoic acid eluted with the solvent front in both cases. With Column 2 and 20% acetonitrile in water as the eluent, perbenzoic acid could be separated from both the solvent front and benzoic acid. A typical chromatogram of the benzoic acid and perbenzoic acid mixture is shown in Fig. 3. When the development of an HPLC method to include the determination of perbenzoic acid was investigated, it was found that perbenzoic acid degraded significantly to benzoic acid in dilute solutions.

In refining and optimizing the HPLC method for the benzoyl peroxide assay, commercial samples of benzoyl peroxide gel and lotion were used. The conditions for extraction of benzoyl peroxide into solution (dispersion, sonication, and centrifugation) were selected such that the percentage of benzoyl peroxide found in these samples by the HPLC method was maximum and further increases in dispersion time or sonication time had no effect on the assay values.

Analysis of the control blanks for the benzoyl peroxide gel and lotion by the proposed HPLC method showed no chromatographic peaks at the retention times for benzoyl peroxide and ethyl benzoate (internal standard). Thus, the control blanks caused no direct interference in the benzoyl peroxide assay with either column.

The results obtained in the analysis of nine synthetic samples representing benzoyl peroxide gel (control blank to benzoyl peroxide ratio altered in some cases) with Column 1 are shown in Table I. The method yielded accurate results (average recovery of 99.7%), and the control blank to benzoyl peroxide ratio had no noticeable effect on the recovery values. Similar data obtained with nine synthetic lotion samples (Table II) suggest that the method gave accurate results for the lotion also. Again, the ratio of control blank to benzoyl peroxide had no noticeable effect on the recovery values.

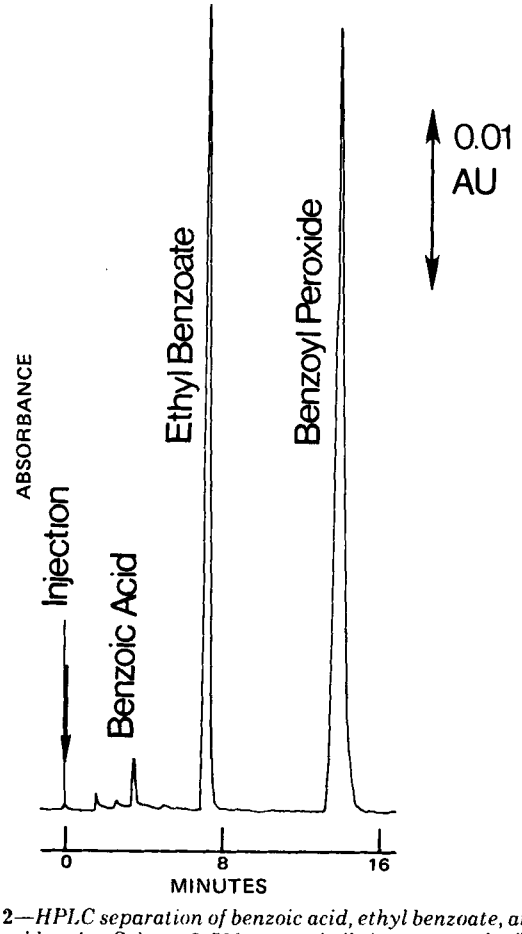

Figure 2—*HPLC separation of benzoic acid, ethyl benzoate, and benzoyl peroxide using Column 2, 50% acetonitrile in water, and a flow rate of 1 ml/min.*

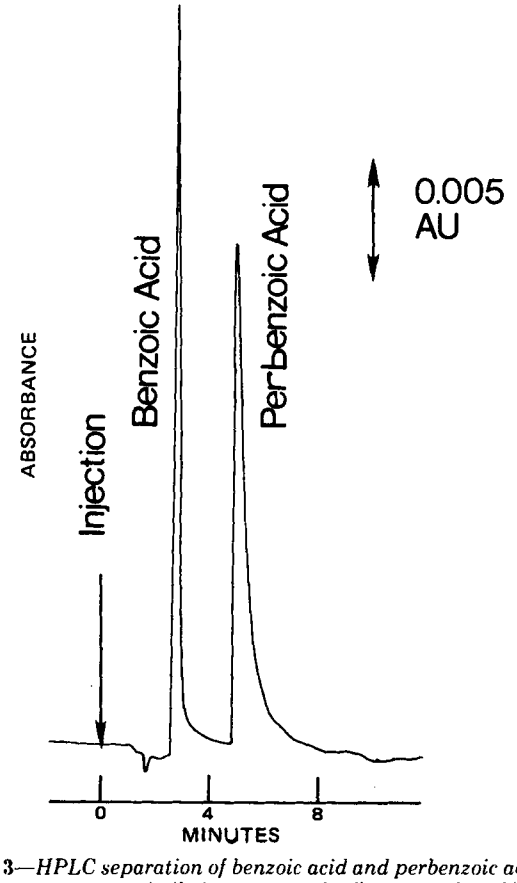

Figure 3—*HPLC separation of benzoic acid and perbenzoic acid using Column 2, 20% acetonitrile in water, and a flow rate of 1 ml/min.*

Table III—Benzoyl Peroxide Assay of Stability Samples of Benzoyl Peroxide Gel by HPLC and USP Methods

Stability Parameters	HPLC Method			USP Iodometric Method[a]	
	Benzoyl Peroxide, %	Percent Initial	Benzoic Acid, %	Benzoyl Peroxide, %	Percent Initial
Initial	5.77	—	—	5.39	—
60°, 2 days	5.64	97.7	0.20	5.38	99.8
60°, 4 days	5.48	95.0	0.27	5.20	96.5
60°, 7 days	5.34	92.5	0.44	5.00	92.8
60°, 9 days	5.30	91.9	0.48	4.90	90.9

[a] Recommended method for benzoyl peroxide lotions (5).

Nine analyses of a product sample[11] of gel containing 10% benzoyl peroxide by the HPLC method with Column 1 gave results with a relative standard deviation of 0.82%. Similarly, three analyses of the gel containing 5% benzoyl peroxide gave a relative standard deviation of 1.2%. Analysis of the lotion samples containing 4% benzoyl peroxide led to assay values with a relative standard deviation of 0.67%.

Although the precision and accuracy data of the HPLC method were collected using Column 1, the method was as good or better with Column 2. Five analyses of synthetic benzoyl peroxide gel samples using Column 2 gave recoveries of 99.9, 99.5, 99.1, 100.7, and 99.7% (average of 99.8%). Similarly, five analyses of the gel containing 5% benzoyl peroxide gave results with a relative standard deviation of 0.65%.

Application to Stability Studies—Samples of benzoyl peroxide gel were force degraded at 60°. Samples were taken at different time intervals and assayed by the HPLC method with Column 2. For comparison, the samples were also assayed by the USP iodometric method for benzoyl peroxide lotions (Table III).

Both the HPLC and the USP iodometric methods were stability indicating (Table III). Judging from the percent initial values of benzoyl peroxide obtained by both methods, the HPLC method showed only slightly higher degradation of samples. Excellent agreement between the amount of benzoyl peroxide degraded and the amount of benzoic acid formed was obtained with the HPLC method, which suggests that benzoic acid is the only, or the major, degradation product of benzoyl peroxide under the experimental conditions.

Comparison of the HPLC and USP iodometric methods (Table III) showed that the results (percent benzoyl peroxide) obtained by the USP method were consistently lower. To explain this difference, the accuracy of the USP method was evaluated using synthetic benzoyl peroxide gel samples. Analysis of three samples gave recovery values of 90.9, 90.1, and 86.6%. Evidently, the USP iodometric method for benzoyl peroxide lotion is not suitable for the benzoyl peroxide gel tested. Although the USP method appeared to be stability indicating, as judged from the percent initial values, its poor accuracy makes its use questionable for this gel.

Assay of five synthetic samples of benzoyl peroxide lotion by the USP method gave an average recovery value of 99.8%. Similar assay of five commercial benzoyl peroxide lotion samples gave a relative standard deviation of 0.83%. These results showed that the USP iodometric method for benzoyl peroxide lotions was accurate and precise. Limited comparative assay data of benzoyl peroxide lotion samples by the USP iodometric method and the HPLC method suggest that both methods are stability indicating when applied to lotions.

In summary, the HPLC method described is stability indicating for both gel and lotion formulations of benzoyl peroxide products; furthermore, the most likely degradation products or impurities, benzoic acid and perbenzoic acid, do not interfere in the assay. The method may be used with either type of octadecylsilane column. The more efficient Column 2, however, permits the simultaneous determination of benzoic acid.

[11] Similar composition to 5% benzoyl peroxide gel.

REFERENCES

(1) H. Gelissen and P. Hermans, *Chem. Ber.*, **58**, 765 (1925).

(2) M. Gruber, R. Klein, and M. Foxx, *J. Pharm. Sci.*, **58**, 566 (1969).

(3) A. J. Martin, in "Organic Analysis," vol. 4, J. Mitchell, Jr., I. M. Kolthoff, E. S. Proskauer, and A. Weissberger, Eds., Interscience, New York, N.Y., 1960, chap. 1.

(4) M. P. Gruber and R. W. Klein, *J. Pharm. Sci.*, **56**, 1505 (1967).

(5) R. E. Daly, J. J. Lommer, and L. Chafetz, *ibid.*, **64**, 1999 (1975).

(6) D. L. Simmons, H. S. L. Woo, J. J. Liston, and R. J. Ranz, *Can. J. Pharm. Sci.*, **3**, 101 (1967).

(7) "Third Supplement to the United States Pharmacopeia, 19th Rev.," Mack Publishing Co., Easton, Pa., 1975, p. 22.

(8) "The United States Pharmacopeia," 19th rev., Mack Publishing Co., Easton, Pa., 1975, p. 51.

(9) G. Brown, in "Organic Synthesis," coll. vol. 1, A. H. Blatt, Ed., Wiley, New York, N.Y., 1941, p. 431.

ACKNOWLEDGMENTS

The authors thank Dr. M. Bhambhani and Dr. B. Patel for their comments and suggestions, Ms. K. Burke for technical assistance, and Ms. E. Brown for assistance in manuscript preparation.

Identification and Synthesis of a Methylated Catechol Metabolite of Glutethimide Isolated from Biological Fluids of Overdose Victims

BRIAN D. ANDRESEN ˣ, FRANK T. DAVIS, and MICHAEL D. LONG

Received May 30, 1978, from the *Analytical Toxicology Laboratory, College of Pharmacy, University of Florida, Gainesville, FL 32610.* Accepted for publication August 3, 1978.

Abstract □ Urine samples from victims severely intoxicated by glutethimide were hydrolyzed enzymatically. TLC, GLC, and mass spectral analyses revealed a methylated catechol metabolite of the parent drug. Two synthetic pathways are described for the preparation of 2-ethyl-2-(3-methoxy-4-hydroxyphenyl)glutarimide and 2-ethyl-2-(3-hydroxy-4-methoxyphenyl)glutarimide. Comparisons of GLC and mass spectral data to a compound isolated from the body fluids of glutethimide overdose victims conclusively identified a new 3-methoxy-4-hydroxyphenyl metabolite of glutethimide in humans.

Keyphrases □ Glutethimide—metabolites identified in human urine, synthesized □ Metabolites—of glutethimide, identified in human urine, synthesized □ Sedatives—glutethimide, metabolites identified in human urine, synthesized

Since the introduction of glutethimide, (±)-2-ethyl-2-phenylglutarimide, in 1954 (1), it has been the subject of considerable study. Originally assumed to be a nonbarbiturate and sedative–hypnotic with few side effects

0022-3549/79/0300-0283$01.00/0

© 1979, American Pharmaceutical Association

Table III—Benzoyl Peroxide Assay of Stability Samples of Benzoyl Peroxide Gel by HPLC and USP Methods

Stability Parameters	HPLC Method			USP Iodometric Method[a]	
	Benzoyl Peroxide, %	Percent Initial	Benzoic Acid, %	Benzoyl Peroxide, %	Percent Initial
Initial	5.77	—	—	5.39	—
60°, 2 days	5.64	97.7	0.20	5.38	99.8
60°, 4 days	5.48	95.0	0.27	5.20	96.5
60°, 7 days	5.34	92.5	0.44	5.00	92.8
60°, 9 days	5.30	91.9	0.48	4.90	90.9

[a] Recommended method for benzoyl peroxide lotions (5).

Nine analyses of a product sample[11] of gel containing 10% benzoyl peroxide by the HPLC method with Column 1 gave results with a relative standard deviation of 0.82%. Similarly, three analyses of the gel containing 5% benzoyl peroxide gave a relative standard deviation of 1.2%. Analysis of the lotion samples containing 4% benzoyl peroxide led to assay values with a relative standard deviation of 0.67%.

Although the precision and accuracy data of the HPLC method were collected using Column 1, the method was as good or better with Column 2. Five analyses of synthetic benzoyl peroxide gel samples using Column 2 gave recoveries of 99.9, 99.5, 99.1, 100.7, and 99.7% (average of 99.8%). Similarly, five analyses of the gel containing 5% benzoyl peroxide gave results with a relative standard deviation of 0.65%.

Application to Stability Studies—Samples of benzoyl peroxide gel were force degraded at 60°. Samples were taken at different time intervals and assayed by the HPLC method with Column 2. For comparison, the samples were also assayed by the USP iodometric method for benzoyl peroxide lotions (Table III).

Both the HPLC and the USP iodometric methods were stability indicating (Table III). Judging from the percent initial values of benzoyl peroxide obtained by both methods, the HPLC method showed only slightly higher degradation of samples. Excellent agreement between the amount of benzoyl peroxide degraded and the amount of benzoic acid formed was obtained with the HPLC method, which suggests that benzoic acid is the only, or the major, degradation product of benzoyl peroxide under the experimental conditions.

Comparison of the HPLC and USP iodometric methods (Table III) showed that the results (percent benzoyl peroxide) obtained by the USP method were consistently lower. To explain this difference, the accuracy of the USP method was evaluated using synthetic benzoyl peroxide gel samples. Analysis of three samples gave recovery values of 90.9, 90.1, and 86.6%. Evidently, the USP iodometric method for benzoyl peroxide lotion is not suitable for the benzoyl peroxide gel tested. Although the USP method appeared to be stability indicating, as judged from the percent initial values, its poor accuracy makes its use questionable for this gel.

Assay of five synthetic samples of benzoyl peroxide lotion by the USP method gave an average recovery value of 99.8%. Similar assay of five commercial benzoyl peroxide lotion samples gave a relative standard deviation of 0.83%. These results showed that the USP iodometric method for benzoyl peroxide lotions was accurate and precise. Limited comparative assay data of benzoyl peroxide lotion samples by the USP iodometric method and the HPLC method suggest that both methods are stability indicating when applied to lotions.

In summary, the HPLC method described is stability indicating for both gel and lotion formulations of benzoyl peroxide products; furthermore, the most likely degradation products or impurities, benzoic acid and perbenzoic acid, do not interfere in the assay. The method may be used with either type of octadecylsilane column. The more efficient Column 2, however, permits the simultaneous determination of benzoic acid.

[11] Similar composition to 5% benzoyl peroxide gel.

REFERENCES

(1) H. Gelissen and P. Hermans, *Chem. Ber.*, **58**, 765 (1925).

(2) M. Gruber, R. Klein, and M. Foxx, *J. Pharm. Sci.*, **58**, 566 (1969).

(3) A. J. Martin, in "Organic Analysis," vol. 4, J. Mitchell, Jr., I. M. Kolthoff, E. S. Proskauer, and A. Weissberger, Eds., Interscience, New York, N.Y., 1960, chap. 1.

(4) M. P. Gruber and R. W. Klein, *J. Pharm. Sci.*, **56**, 1505 (1967).

(5) R. E. Daly, J. J. Lommer, and L. Chafetz, *ibid.*, **64**, 1999 (1975).

(6) D. L. Simmons, H. S. L. Woo, J. J. Liston, and R. J. Ranz, *Can. J. Pharm. Sci.*, **3**, 101 (1967).

(7) "Third Supplement to the United States Pharmacopeia, 19th Rev.," Mack Publishing Co., Easton, Pa., 1975, p. 22.

(8) "The United States Pharmacopeia," 19th rev., Mack Publishing Co., Easton, Pa., 1975, p. 51.

(9) G. Brown, in "Organic Synthesis," coll. vol. 1, A. H. Blatt, Ed., Wiley, New York, N.Y., 1941, p. 431.

ACKNOWLEDGMENTS

The authors thank Dr. M. Bhambhani and Dr. B. Patel for their comments and suggestions, Ms. K. Burke for technical assistance, and Ms. E. Brown for assistance in manuscript preparation.

Identification and Synthesis of a Methylated Catechol Metabolite of Glutethimide Isolated from Biological Fluids of Overdose Victims

BRIAN D. ANDRESEN ˣ, FRANK T. DAVIS, and MICHAEL D. LONG

Received May 30, 1978, from the *Analytical Toxicology Laboratory, College of Pharmacy, University of Florida, Gainesville, FL 32610.* Accepted for publication August 3, 1978.

Abstract □ Urine samples from victims severely intoxicated by glutethimide were hydrolyzed enzymatically. TLC, GLC, and mass spectral analyses revealed a methylated catechol metabolite of the parent drug. Two synthetic pathways are described for the preparation of 2-ethyl-2-(3-methoxy-4-hydroxyphenyl)glutarimide and 2-ethyl-2-(3-hydroxy-4-methoxyphenyl)glutarimide. Comparisons of GLC and mass spectral data to a compound isolated from the body fluids of glutethimide overdose victims conclusively identified a new 3-methoxy-4-hydroxyphenyl metabolite of glutethimide in humans.

Keyphrases □ Glutethimide—metabolites identified in human urine, synthesized □ Metabolites—of glutethimide, identified in human urine, synthesized □ Sedatives—glutethimide, metabolites identified in human urine, synthesized

Since the introduction of glutethimide, (±)-2-ethyl-2-phenylglutarimide, in 1954 (1), it has been the subject of considerable study. Originally assumed to be a nonbarbiturate and sedative–hypnotic with few side effects

0022-3549/79/0300-0283$01.00/0

© 1979, American Pharmaceutical Association

(2), the drug rapidly gained popularity. However, reports of acute intoxication indicated that glutethimide possessed abuse potential (3). This drug is toxic in humans at doses considerably lower than those values previously determined from animal experiments (4).

BACKGROUND

Currently, toxicology studies as well as analyses of metabolites in both humans and animals are actively conducted to ascertain the reasons for the toxicity of glutethimide. A metabolite, 2-ethyl-2-phenyl-4-hydroxyglutarimide, was identified (5) in the blood of dogs (6) and patients intoxicated by glutethimide. This metabolite contributed to the morbidity and mortality of overdose victims (7); through biological assays in mice, the synthetic metabolite was shown to be as active as the parent drug in its sedative-hypnotic properties (8). Many other unusual metabolites of the parent drug also have been isolated and identified (8–10).

The existence of a previously unobserved human metabolite, 2-ethyl-2-(3-methoxy-4-hydroxyphenyl)glutarimide (XII), was proposed, and it was isolated (11). The designation of a substituted methylated catechol ring system was based initially on reports of similar metabolic pathways for aromatic rings (12) and on interpretation of mass spectral and NMR data. The information obtained from 100 μg of material isolated from the urine of an overdose victim was initially uncertain because of the other impurities and metabolites present. Interpretation of mass spectral data of the material revealed a tentative molecular ion at *m/e* 263, pointing to the addition of two oxygen atoms and one methylene group to the parent drug.

Initially, only a tentative conclusion could be reached from the NMR data. An NMR spectrum of the crude mixture revealed a singlet at δ 3.84 ppm, pointing to the presence of a methoxy group in the sample. From these limited data, a methylated catechol metabolite was proposed. Therefore, it was necessary to synthesize XII and 2-ethyl-2-(3-hydroxy-4-methoxyphenyl)glutamide (IV) to prove the structure of the proposed metabolite. The work reported here conclusively confirms the identity of a unique positional isomer as a new methylated catechol metabolite of glutethimide in humans.

EXPERIMENTAL

Sample Procurement—Urine samples were collected from three patients, soon after their admission to the hospital, who had taken large doses of glutethimide. The urine samples were collected and stored at −10° until the enzymatic hydrolysis.

Enzymatic Hydrolysis—Urine, 500-ml portions, was acidified to pH 5.5 with 1 *N* HCl. Citrate buffer, pH 5.5, was added to a total volume of 700 ml. An aqueous solution[1] of sulfatase and glucuronidase, 1.5 ml, then was added, and the mixture was incubated with shaking for 24 hr at 37°. The entire incubation mixture was shielded from light. The mixture then was extracted with 3 × 500 ml of ether[2]. After solvent evaporation, the dark extract was stored at 0° prior to preparative GLC.

GLC—After extraction, each enzymatically hydrolyzed sample was evaporated to a small volume. Then repetitive aliquots were injected into a preparative gas chromatograph[3], using a 1.5-m × 6.3-mm 15% OV-17 column[4] at 200°. Helium carrier gas at 40 ml/min yielded a variety of peaks which were individually collected. The purity of each collected fraction was monitored with an analytical gas chromatograph[5], using a 1.8-m × 3.1-mm 7% OV-17 glass column[4] at 200° with the flow rate of nitrogen carrier gas at 40 ml/min.

TLC—A small aliquot from each collected GLC peak was spotted on a 5 × 20-cm TLC plate[6] and developed with a standard drug-screening solvent system (ethyl acetate–methanol–ammonium hydroxide, 85:10:5). After the plate had developed 12 cm, it was removed and sprayed with mercuric sulfate and diphenylcarbazone[7] (0.5 g of mercuric oxide in 20 ml of concentrated sulfuric acid, diluted with 200 ml of water; 0.05% diphenylcarbazone in chloroform) to detect glutethimide-related materials as violet spots.

[1] Glusulase, Endo Laboratories, Garden City, NY 11530.
[2] Mallinckrodt Chemical Works, Montreal, Quebec, Canada.
[3] Model 90-P, Varian Aerograph, Walnut Creek, CA 94598.
[4] Applied Science Laboratories, State College, PA 16801.
[5] Model 2100, Varian Aerograph, Walnut Creek, CA 94598.
[6] Silica gel 60, E.M. Laboratories, Elmsford, NY 10523.
[7] Aldrich Chemical Co., Milwaukee, WI 53233.

Table I—Comparison of GLC Retention Times of Synthetic Intermediates and Analogs of Glutethimide on Various Columns Relative to Straight Chain Hydrocarbons as Methylene Units

Synthetic Compound	OV-1[a]	OV-17[b]	OV-210[c]
III	20.3	25.4	29.1
IV	24.0	29.2	32.1
VI	21.5	25.7	26.0
VII	21.1	25.1	25.4
VIII	22.3	26.9	29.5
IX	22.8	27.4	30.3
X	26.2	32.4	35.0
XI	28.5	34.5	35.5
XII	22.0	27.0	31.5

[a] Five percent on Gas Chrom Q (100–200 mesh); column, 1.8-m × 3.1-mm glass; temperature programmed, 6°/min from 175 to 260°; detector and injector temperature, 285°; nitrogen flow, 60 ml/min; hydrogen flow, 40 ml/min; and air flow, 300 ml/min. [b] Seven percent on Gas Chrom Q (100–200 mesh); column, 1.8-m × 3.1-mm glass; temperature programmed, 6°/min from 175 to 260°; detector and injector temperature, 285°; nitrogen flow, 60 ml/min; hydrogen flow, 40 ml/min; and air flow, 300 ml/min. [c] Three percent on Gas Chrom Q (100–200 mesh); column, 1.8-m × 3.1-mm glass; temperature, 200° isothermal; detector and injector temperature, 285°; nitrogen flow, 60 ml/min; hydrogen flow, 40 ml/min; and air flow, 300 ml/min.

Iodine vapor also was used to determine the total organics present on the plates. Synthetic materials were analyzed using silica gel plates. The solvent systems for development are noted with each sample.

NMR—Individual GLC fractions were dissolved in 75 μl of deuterated chloroform[8] (containing 1% tetramethylsilane) and placed in an NMR microbulb[9] sample holder. Each NMR spectrum was recorded on a medium-resolution NMR instrument[10].

Mass Spectrometry—A small aliquot of the analytically pure GLC fractions was subjected to 70-ev electron-impact mass spectrometry, using a single-focusing, magnetic sector[11], mass spectrometer interfaced to an analytical gas chromatograph[12]. Each collected GLC peak was either volatilized directly into the source of the mass spectrometer by probe distillation or analyzed directly by combined GLC–mass spectral techniques with a jet separator.

General Synthetic Methods—Melting points (uncorrected) were determined on a capillary apparatus[13]. IR spectra were recorded with a medium-resolution IR spectrophotometer[14] with sodium chloride cells and pressed potassium bromide pellets. Solutions were concentrated under reduced pressure using rotary evaporators[15]. GLC identification of synthetic materials utilized an analytical instrument[5] with a 1.8-m × 3.1-mm 3% OV-210 (Chromsorb W) column[4], a 3.05-m × 3.1-mm 3% Dexil-300 column[4], or a 1.8-m × 3.1-mm 7% OV-17 column[4]. Retention times were compared to straight chain hydrocarbon methylene units (Table I). Solvents were chromatographic grade.

2-Ethyl-2-(4-methoxyphenyl)glutarimide (III)—A solution of 2.0 g (8.6 mmoles) of 2-ethyl-2-(4-aminophenyl)glutarimide[16] (I) in 50 ml of 2 *N* H_2SO_4 was cooled to 5° in an ice water bath. To this solution was added slowly 1.2 g (17 mmoles) of sodium nitrite in 20 ml of water at 5°. The reaction mixture was stirred for 30 min until a clear solution developed. Then 0.54 g (8.8 mmoles) of urea was added to eliminate residual sodium nitrite in the reaction mixture. The diazonium salt, II, was added dropwise by a cannula to 250 ml of boiling methanol and then allowed to reflux for an additional 30 min.

The solution then was evaporated to dryness to yield an amber oil. Column chromatographic isolation [15 × 2.5-cm silica gel–cellulose (3:1) column, eluted with 160 ml of chloroform] yielded white crystals after solvent evaporation. Recrystallization from boiling ethanol and water yielded 1.2 g (54%) of III, mp 105–106°; TLC: R_f 0.70 [silica gel; chloroform–acetone (80:20), diphenylcarbazone–mercuric sulfate positive[6]]; IR (NaCl film): 3200 (NH), 1700, and 1680 (C=O, imide) cm^{-1}; mass spectrum: *m/e* 218 (100%), M^+ = 247 (75%).

2-Ethyl-2-(3-hydroxy-4-methoxyphenyl)glutarimide (IV)—A solution containing 0.15 g (0.61 mmole) of III and 5.8 ml of 30% H_2O_2[17]

[8] Silanor-C, Merck & Co., Rahway, NJ 07065.
[9] Wilmad Glass Co., Buena, NJ 08310.
[10] Model A-60, Varian Aerograph, Walnut Creek, CA 94598.
[11] Model 490-F, DuPont Instrument Product Division, Wilmington, DE 19898.
[12] Model 2700, Varian Aerograph, Walnut Creek, CA 94598.
[13] A. H. Thomas Co., Philadelphia, PA 19090.
[14] Model 4210, Beckman Instruments, Fullerton, CA 92634.
[15] Model RE/A, Brinkmann Instruments, Westbury, NY 11590.
[16] Generously supplied by Ciba-Geigy.
[17] Fisher Scientific Co., Fair Lawn, NJ 07410.

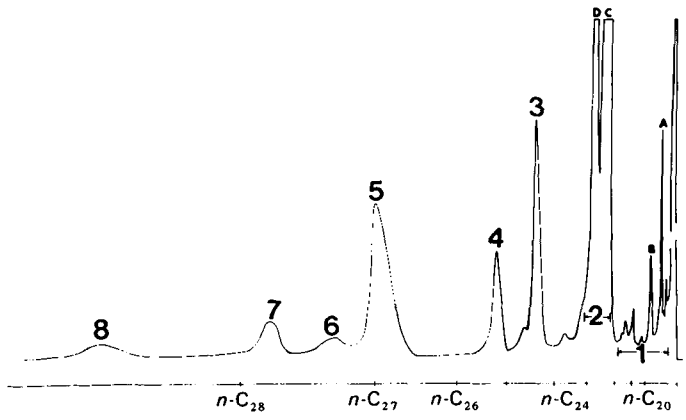

Figure 1—*Preparative GLC trace of an enzymatically hydrolyzed urine sample obtained from a glutethimide overdose victim after oral ingestion of 14 g of the parent drug. The ether extract of the sample was analyzed on a 1.8-m × 6.3-mm 7% OV-17 column at 200° with helium as the carrier gas (40 ml/min). The relative GLC retention times of* n-C_{20}-n-C_{28} *are indicated. Samples designated fractions 1–8 were collected for more complete characterization by other analytical techniques.*

dissolved in 30 ml of acetonitrile[18] was irradiated with 254-nm UV light[19] in a 50° water bath overnight. To the reaction mixture was added 10 ml of an aqueous solution saturated with sodium bisulfite to decompose the hydrogen peroxide. The phases were separated, and the aqueous layer was extracted with 3 × 50 ml of ether. The combined extracts were concentrated under reduced pressure, and the residue was streaked onto a 20 × 20-cm silica gel 60 TLC plate[6].

The residue was developed undisturbed to a distance of 15 cm. After solvent evaporation, 90% of the TLC plate was covered; only the edge (10%) was sprayed with diphenylcarbazone–mercuric sulfate[7] to reveal the imide positive band. The position of this band was extrapolated across the TLC plate, and then the remaining unreacted product was scraped off and extracted into methanol to yield IV; TLC: R_f 0.52 [silica gel; chloroform–acetone (80:20)]; IR (KBr): 3400 (NH), 1700 and 1600 (CO, imide), and 1200 (phenyl O) cm^{-1}; mass spectrum: M^+ = 263 (100%).

3-Methoxy-4-benzoxybenzyl Alcohol (VI)—A mixture of 10 g (65 mmoles) of vanillin alcohol[7] (V), 10 g (73 mmoles) of potassium carbonate, and 8.8 g (70 mmoles) of benzyl chloride[7] in 200 ml of ethanol was refluxed 12 hr. This solution was filtered hot. The filtrate was evaporated to dryness, yielding a brown oil, which solidified on cooling. Sublimation[20] resulted in 13.0 g (82.3%) of white crystals, mp 66–67°; IR (KBr): 3400 (OH), 3030, 1600, 1500 (phenyl), 1270, and 1130 (aromatic ether) cm^{-1}; mass spectrum: *m/e* 91 (100%), M^+ = 244 (12%); TLC: R_f 0.56 [silica gel; chloroform–acetone (80:20), sulfuric acid–char[21]].

3-Methoxy-4-benzoxybenzyl Chloride (VII)—Anhydrous hydrogen chloride gas[22] was bubbled through a solution of 11.5 g (47.1 mmoles) of VI in 150 ml of methylene chloride for 2 hr with stirring. The solvent was evaporated, yielding an amber oil, which solidified on cooling. Sublimation[20] produced 12 g (98%) of white crystals, mp 72–73°; IR (KBr): 3030, 1600, 1500 (phenyl), 1270, 1130 (aromatic ether), and 735 (chloride) cm^{-1}; mass spectrum: *m/e* 91 (100%), M^+ = 262/264 (3:1)(6%); TLC: R_f 0.84 [silica gel; chloroform–acetone (80:20), sulfuric acid–char[21]].

3-Methoxy-4-benzoxybenzylnitrile (VIII)—A solution of 6.5 g (25 mmoles) of VII and 10 g (154 mmoles) of potassium cyanide in 75 ml of dry dimethylformamide was stirred at room temperature for 12 hr. The solvent was evaporated, and the residue was partitioned between water and methylene chloride. Then the solvent was evaporated, producing a solid, which, upon recrystallization from hexane, yielded 3.9 g (62%) of white crystals, mp 69–70°; IR (KBr): 3030, 1600, 1500 (phenyl), 2230 (nitrile), 1270, and 1130 (aromatic ether) cm^{-1}; mass spectrum: *m/e* 91 (100%), M^+ = 253 (10%); TLC: R_f 0.38 (silica gel; benzene, sulfuric acid–char[21]).

2-(3-Methoxy-4-benzoxyphenyl)butyronitrile (IX)—This intermediate was generated when 10.5 g (41.5 mmoles) of VIII was added to a solution of 1.9 g (79 mmoles) of sodium hydride in dry toluene and stirred at room temperature for 2 hr. To this solution was added, dropwise, 4.6 g (42 mmoles) of ethyl bromide[7], and the resulting solution was refluxed for 17 hr. GLC peak area integrator[23] analysis of the resulting yellow oil showed 82% of IX, 10% of unreacted VIII, and 6% of a dialkylated product. This mixture was used without further purification; mass spectrum: *m/e* 91 (100%), M^+ = 281 (8%); TLC: R_f 0.5 (silica gel; benzene, sulfuric acid–char[21]).

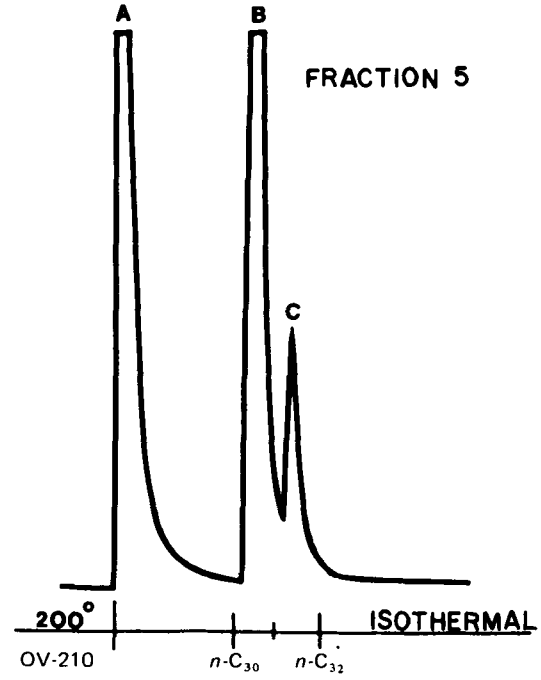

Figure 2—*Analytical GLC trace of metabolites (fraction 5) collected by preparative GLC. Although a single GLC peak was shown on OV-17, the OV-210 phase revealed two components: A, solvent; B, 2-ethyl-2-(4-hydroxyphenyl)glutarimide; and C, new metabolite, which was analyzed mass spectrometrically.*

2-Ethyl-2-(3-methoxy-4-benzoxyphenyl)glutarodinitrile (X)—To a solution of 4.7 g of the products from the previous reaction and 0.94 g (18 mmoles) of acrylonitrile[7] in dry dioxane[7] was added slowly, with stirring, 2.0 ml of 40% base[24]. The resulting solution was refluxed for 21 hr. The solvent was then evaporated, and the residue was extracted with ether to yield 4.6 g (82%) of X as white crystals, mp 125–126°; IR (KBr): 3030, 1600, 1500 (phenyl), 2230 (nitrile), 1270, and 1130 (aromatic ether) cm^{-1}; mass spectrum: *m/e* 91 (100%), M^+ = 334 (9%); TLC: R_f 0.08 (silica gel; benzene, sulfuric acid–char[21]).

2-Ethyl-2-(3-methoxy-4-hydroxyphenyl)glutarimide (XII)—A solution of 1.5 g (4.5 mmoles) of X and 7 ml of concentrated sulfuric acid in 25 ml of acetic acid was heated in a water bath for 6 hr. The resulting dark-brown liquid was poured onto 100 ml of crushed ice and extracted with methylene chloride. This organic fraction was washed well with saturated sodium carbonate (100 ml). The organic layer was extracted with ether and evaporated to dryness, yielding XI; TLC: R_f 0.67 [silica gel; chloroform–acetone (80:20), diphenylcarbazone–mercuric sulfate positive]; mass spectrum: *m/e* 91 (37%), 296 (53), 324 (62), and 353 (M^+, 100).

Compound XI was finally reduced with 10% palladium-on-charcoal[25] at 1 atmosphere in a Parr hydrogenator[26] to yield XII; TLC: R_f 0.52 [silica gel; chloroform–acetone (80:20), diphenylcarbazone–mercuric sulfate positive]; mass spectrum: *m/e* 91 (10%), 131 (30), 206 (53), 234 (100), and 263 (M^+, 85).

RESULTS AND DISCUSSION

In many acute drug intoxications, the analysis of biological fluids is of paramount importance for the identification of the causative toxic

[18] Mallinckrodt Chemical Co., St. Louis, MO 63147.
[19] Quartz pencil lamp, Edmund Scientific Co., Barrington, NJ 08007.
[20] Model 8027, Ace Glass Inc., Vineland, NJ 08360.
[21] Sulfuric acid–char indicates that the TLC plate was sprayed with 5% H_2SO_4–H_2O and heated to 100° for 2 min to reveal brown spots.
[22] Generated from concentrated sulfuric acid and sodium chloride.
[23] Model 480, Varian Aerograph, Walnut Creek, CA 94598.
[24] Triton B as the methoxy salt (40% in methanol), Baker Chemical Co., Phillipsburg, NJ 08865.
[25] Matheson, Coleman and Bell, Norwood, OH 45212.
[26] Parr Instrument Co., Moline, IL 61265.

agent. Routinely, body fluids from overdose victims can be extracted and the compounds of interest can be screened by TLC (13), analyzed by GLC (14), or quantitated by combined GLC–mass spectrometric techniques (15). Once the drugs responsible for the severe intoxication have been identified, proper supportive techniques for the patient can be administered.

Severe glutethimide intoxication in drug overdose victims is easily identified because the levels of the intoxicant are usually high. Extractions and analysis of urine samples typically reveal the parent drug, which is easily identified by standard TLC and GLC methods (13). However, recent questions have been raised (6) concerning the impact of metabolites in the body fluids of overdose victims and their contribution to the morbidity and mortality associated with glutethimide overdose.

The preparative GLC trace of an enzymatically hydrolyzed urine extract obtained from a glutethimide overdose victim, identified as having taken 14 g of glutethimide, is seen in Fig. 1. From the diagram, eight major fractions were designated. Each fraction was collected repeatedly to obtain sizable quantities for complete characterization. By comparison of GLC retention times to authentic glutethimide, peak C of fraction 2 was considered initially to be the parent drug. However, following mass spectral analysis, peak C was determined to be glutethimide and α-phenylglutarimide, a known metabolite.

Because fraction 5 appeared to be reasonably pure and in high concentrations, it was next analyzed completely. However, mass spectral analyses revealed two components, which were easily separated when the GLC liquid support phase was changed from OV-17 to OV-210 (Fig. 2). The major component was identical in all respects to *p*-hydroxyphenylglutethimide, a known metabolite of the parent drug (16). The minor component appeared to be new and unique. The mass spectrum obtained from this compound is seen in Fig. 3A. A molecular ion at *m/e* 263, an intense ion at *m/e* 234 (indicating loss of an ethyl side chain), and the very polar GLC characteristics compared to the parent drug suggested a methylated catechol. Confirmation of a methoxy group was made by NMR analysis of fraction 5, a mixture, which revealed a signal at δ 3.84 ppm, often indicative of methoxy groups.

With this information, 10 possible isomeric methylated catechol metabolites of glutethimide could be proposed. However, in most metabolic pathways, 3-OH and 4-OCH_3, 3-OCH_3, or 4-OH phenyl substitution patterns predominate. For example, the methylated catechol metabolites of levodopa (17), phenacetylurea (18), and phenytoin (12) in humans have been identified and synthesized to confirm that the 3-OCH_3 and 4-OH phenyl metabolites are the rule and not the exception. Therefore, to make direct analytical comparisons, both 3,4-monomethylated catechol isomers of glutethimide were prepared. Schemes I and II reveal the synthetic pathway leading to IV and XII, respectively.

In Scheme I, I was converted to the diazonium salt, II, and hydrolyzed in absolute methanol (19) to yield a new *p*-methoxy analog, III. Following a modification of a known procedure (20), the new methylated catechol, IV, was conveniently prepared by photochemical oxidation of III in hydrogen peroxide.

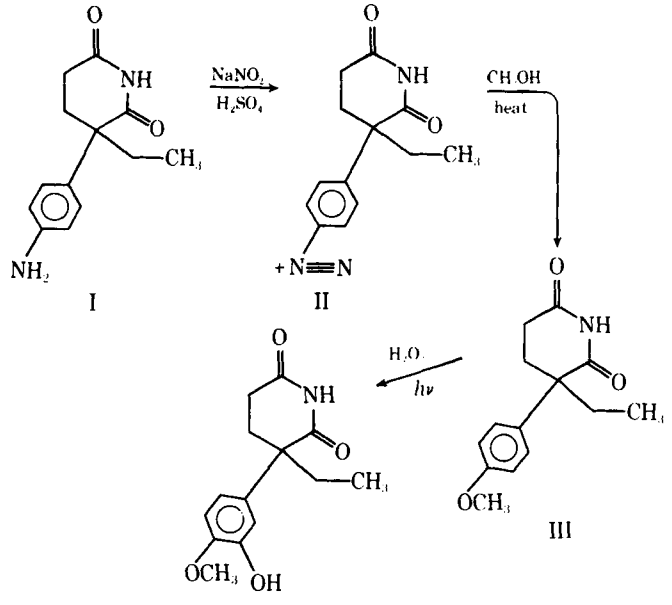

Scheme I

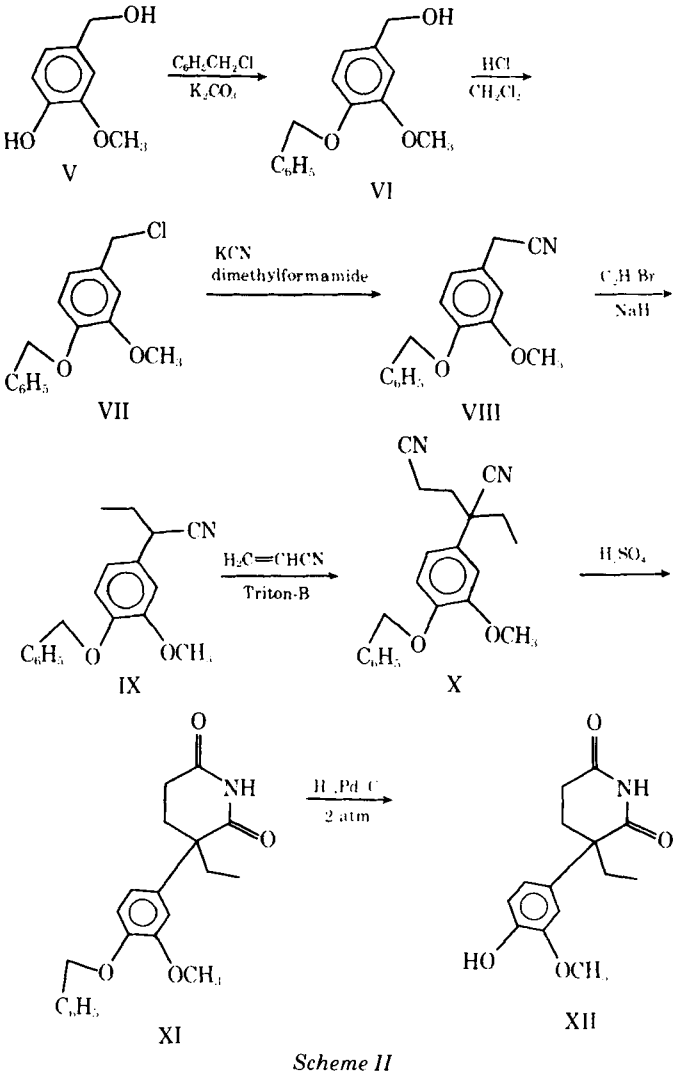

Scheme II

To prepare XII, partial methylation of the catechol metabolite (21) of glutethimide was attempted. However, complex mixtures of products were obtained (with either diazomethane or methyl iodide in base) and were difficult to characterize accurately. Therefore, a total synthesis of XII was needed to assure the isomeric purity of the final product.

Scheme II reveals the complete synthesis leading to the desired compound. Protection of vanillin alcohol, V, with benzyl chloride yielded VI in high purity and in an excellent yield. Conversions of the alcohol, VI, to the chloride, VII, and then to the nitrile, VIII, were accomplished following procedures (22) similar to those described for the preparation of the parent drug. The monoethylated intermediate, IX, was generated by reacting ethyl bromide with VIII in a suspension of sodium hydride and refluxing toluene. The reaction was analyzed frequently by GLC to monitor the formation of IX as the ethyl bromide was added slowly to the reaction mixture. This procedure reduced the generation of excessive amounts of a diethylated product.

Conversion of IX to the dinitrile, X, was accomplished following known procedures (23). It was next determined that cyclization of X to the protected glutethimide analog, XI, could be performed in either strong acid or strong base. Base hydrolysis of X yielded a purer product, XI, which required only the addition of acid to the reaction mixture to precipitate the desired compound. However, the yields by this method were lower then those obtained by acid hydrolysis. Finally, catalytic hydrogenation of XI generated XII, which was isolated and characterized by standard methods (23).

Figures 3B and 3C show the mass spectra of IV and XII, respectively. The compound isolated from the enzymatically hydrolyzed glutethimide urine sample apparently produces a mass spectrum virtually identical to the spectrum in Fig. 3C. Whereas the base peak (100%) is *m/e* 263 (the

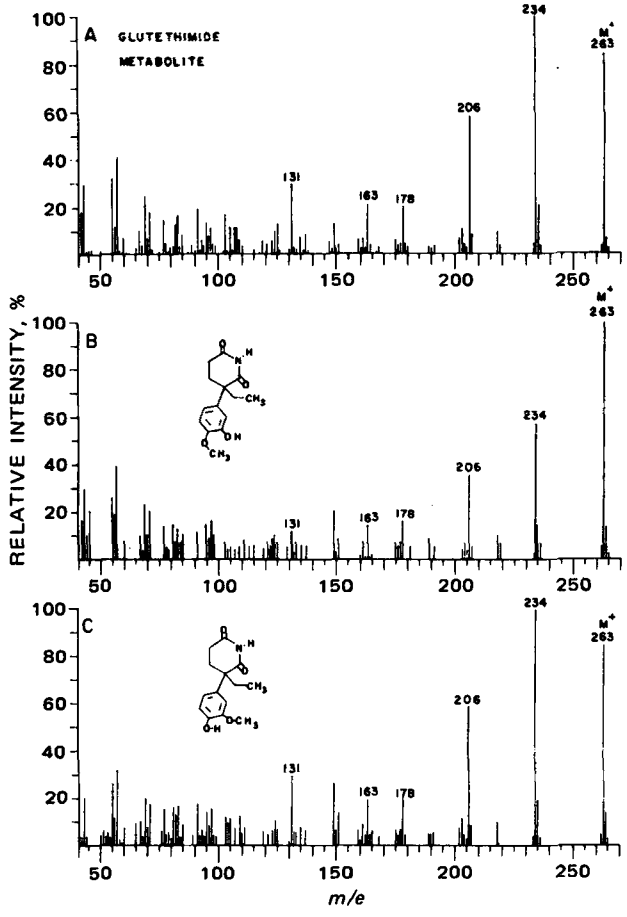

Figure 3—*Mass spectral comparison of the minor component (C in Fig. 2) to two methylated catechol analogs of glutethimide. The mass spectral data of the glutethimide metabolite (A) agree favorably with 2-ethyl-2-(3-methoxy-4-hydroxyphenyl)glutarimide (C).*

molecular ion) for IV, the glutethimide metabolite and the synthetic XII reveal a base peak (100%) for *m/e* 234 (loss of the ethyl side chain). The *p*-hydroxyphenyl compound more strongly favors stabilization of the benzyl cation (XIII, Scheme III) and is clearly an aid in differentiating the isomers.

These findings were confirmed by comparisons of GLC retention times. The metabolite (collected preparatively on OV-210 and reanalyzed) revealed methylene unit hydrocarbon retention values (24) of 22.0, 27.0, and 31.5 on OV-1, OV-17, and OV-210, respectively. Compound XII revealed exactly the same values. However, IV revealed methylene unit values of 24.0, 29.2, and 32.1 on OV-1, OV-17, and OV-210, respectively. Therefore, the monomethylated catechol metabolite of glutethimide is XII.

In Fig. 1, it can be seen that many other fractions were collected; each is currently in different phases of characterization. Fraction 1 possessed

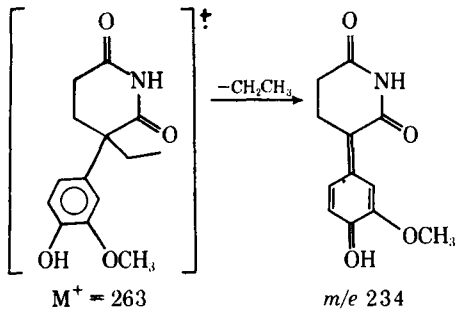

$M^+ = 263$ *m/e* 234

XII XIII

Scheme III

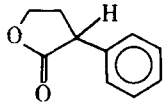

XIV

two major components, A and B, which were initially identified by mass spectrometric techniques (25) and finally synthesized (26) to confirm *p*-hydroxymethylbenzoate and α-phenyl-γ-butyrolacetone (XIV), respectively. The former may be a metabolite of glutethimide, but the latter clearly was associated (25) with new metabolites of the parent drug.

Fraction 2-D revealed a compound whose mass spectral and GLC properties were identical to data previously reported (6) for 2-ethyl-2-phenyl-4-hydroxyglutarimide, an active metabolite of the parent drug.

Fractions 3 and 4 both possessed different chromatographic properties than the known hydroxylated metabolite, 2-ethyl-2-phenyl-4-hydroxyglutarimide, fraction 2-D. However, both compounds also revealed a molecular ion at *m/e* 233, indicative of a single O added to glutethimide, suggesting new hydroxylated metabolites. Currently, synthetic hydroxylated analogs of glutethimide are in preparation to confirm the exact structure of each compound.

Due to the limited amount of material present in fraction 6, only preliminary characterization was attempted. However, fraction 7 was shown by mass spectral analysis to possess a molecular weight of 233 and to produce a much different spectrum than that of the parent drug or metabolites. NMR data revealed the complete loss of the ethyl side chain, and TLC revealed a very polar compound. Thus, a new and very polar metabolite is proposed for peak 7.

The preliminary data obtained concerning peak 8 revealed a compound with a molecular weight of 279 (characterized by mass spectrometry), one methoxy group by NMR, and a compound more polar by TLC analysis than the 2-ethyl-2-(4-hydroxyphenyl)glutarimide (16) (fraction 5) and active toward mercuric sulfate–diphenylcarbazone (indicative of imide systems). Consequently, a dihydroxymethoxy metabolite of glutarimide is proposed. The exact substitution on the parent drug is not known, but synthetic work is in progress.

In conclusion, the glutethimide overdose victims described provided many new metabolites of the parent drug. Further characterization and synthesis of each individual metabolite are currently in progress. The results may uncover new and active metabolites that contribute to the toxicity associated with an overdose of the parent compound.

REFERENCES

(1) Ciba Pharmaceutical Products, U.S. pat. 2,673,205 (1954).

(2) N. Burnstein, *South. Med. J.*, **4**, 174 (1956).

(3) J. L. Graeme, *Clin. Toxicol.*, **1**, 135 (1968).

(4) A. J. McBay and G. G. Katsas, *N. Engl. J. Med.*, **257**, 97 (1957).

(5) J. J. Ambre and L. J. Fischer, *Res. Commun. Chem. Pathol. Pharmacol.*, **4**, 307 (1972).

(6) J. J. Ambre and L. J. Fischer, *Drug Metab. Dispos.*, **2**, 151 (1974).

(7) A. R. Hanse, K. A. Kennedy, J. J. Ambre, and L. J. Fischer, *N. Engl. J. Med.*, **292**, 250 (1975).

(8) H. Y. Aboul-Enein, C. W. Schanberger, A. R. Hansen, and L. J. Fischer, *J. Med. Chem.*, **18**, 736 (1975).

(9) W. G. Stillwell, *Res. Commun. Chem. Pathol. Pharmacol.*, **12**, 25 (1975).

(10) B. D. Andresen, J. L. Templeton, R. H. Hammer, H. L. Panzik, and M. J. Moldowan, *ibid.*, **10**, 443 (1975).

(11) *Ibid.*, **13**, 193 (1976).

(12) T. Chang, R. H. Okesholm, and A. J. Glazko, *Res. Commun. Chem. Pathol. Pharmacol.*, **4**, 13 (1972).

(13) B. Davidow, N. LiPetre, and B. Quame, *J. Clin. Pathol.*, **50**, 714 (1968).

(14) J. MacGee, *Clin. Chem.*, **17**, 587 (1971).

(15) R. F. Skinner, E. J. Gallagher, J. B. Knight, and E. J. Bornelli, *J. Forensic Sci.*, **17**, 189 (1972).

(16) B. D. Andresen, J. L. Templeton, R. H. Hammer, H. L. Panzik, and M. J. Moldowan, *Res. Commun. Chem. Pathol. Pharmacol.*, **12**, 627 (1975).

(17) N. S. Sharpless, G. M. Tyce, M. D. Muenter, and R. P. Dinapoli, *Clin. Pharmacol. Ther.*, **16**, 770 (1974).

(18) K. Tatsumi, H. Yoshimura, and H. Tsukamoto, *Biochem. Phar-*

macol., **16**, 1941 (1967).
(19) D. F. DeTar and M. N. Turetyky, *J. Am. Chem. Soc.*, **77**, 1745 (1955).
(20) K. Omura and T. Matsura, *Tetrahedron*, **26**, 255 (1970).
(21) B. D. Andresen, J. L. Templeton, R. H. Hammer, and H. L. Panzik, *Res. Commun. Chem. Pathol. Pharmacol.*, **14**, 259 (1976).
(22) E. Tegmann, E. Sury, and K. Hoffmann, *Helv. Chim. Acta*, **35**, 1235 (1952).
(23) S. Kukolja, D. Grguric, and L. Lopina, *Croat. Chem. Acta*, **33**, 41 (1961).
(24) E. von Kovates, *Helv. Chim. Acta*, **41**, 1915 (1958).
(25) B. D. Andresen, F. T. Davis, J. L. Templeton, R. H. Hammer, and H. L. Panzik, *Res. Commun. Chem. Pathol. Pharmacol.*, **15**, 21 (1976).
(26) B. D. Andresen, F. T. Davis, J. L. Templeton, H. L. Panzik, and R. H. Hammer, *ibid.*, **18**, 439 (1977).

ACKNOWLEDGMENTS

Supported in part by a Cottrell Starter Grant administered by Research Corporation.

The authors thank Dr. Harold L. Panzik and Mr. James L. Templeton for assistance.

Hydrolysis and Dissolution Behavior of a Prolonged-Release Prodrug of Theophylline: 7,7′-Succinylditheophylline

H. K. LEE *x, H. LAMBERT *, V. J. STELLA ‡, D. WANG ‡, and T. HIGUCHI ‡

Received June 14, 1978, from **Pharmaceutical Research and Development, Searle Laboratories, Skokie, IL 60076*, and the ‡*Department of Pharmaceutical Chemistry, University of Kansas, Lawrence, KS 66045.* Accepted for publication August 11, 1978.

Abstract □ The physicochemical characteristics of 7,7′-succinylditheophylline, a slow dissolving prodrug of theophylline, were investigated at 25°. One molecule of 7,7′-succinylditheophylline hydrolyzed to give two molecules of theophylline and one molecule of succinic acid. At 25° in aqueous solution, constant ionic strength, and zero buffer concentration, the pH profile for the hydrolysis of 7,7′-succinylditheophylline could be described adequately by a spontaneous constant, k_0, of 8.15×10^{-2} sec^{-1} and a hydroxide catalytic constant, k_{OH^-}, of 1.46×10^5 M^{-1} sec^{-1}. No specific acid catalysis was seen at pH values as low as 1. This dissolution rate of 7,7′-succinylditheophylline from a constant surface area pellet was independent of pH below 8. However, at pH values greater than 8, the dissolution rate was accelerated by a base. This behavior was consistent with the dissolution rate being catalyzed by the simultaneous chemical reaction of 7,7′-succinylditheophylline with hydroxide ion at a rate such that substantial hydrolysis of the substrate was occurring in the dissolution film. Dissolution with simultaneous chemical reaction for 7,7′-succinylditheophylline was analyzed theoretically on the basis of a film theory model. Excellent correlation between the theoretical and observed dissolution behavior was found. At pH values less than 8, the dissolution of 7,7′-succinylditheophylline was 35 times slower than that of theophylline. Based on this result, the aqueous solubility of 7,7′-succinylditheophylline was estimated to be 1.63×10^{-3} M.

Keyphrases □ 7,7′-Succinylditheophylline—hydrolysis and dissolution, effect of pH □ Prodrugs, theophylline—7,7′-succinylditheophylline, hydrolysis and dissolution, effect of pH □ Hydrolysis—7,7′-succinylditheophylline, effect of pH □ Dissolution—7,7′-succinylditheophylline, effect of pH □ Theophylline prodrugs—7,7′-succinylditheophylline, hydrolysis and dissolution, effect of pH

Theophylline is an effective bronchodilator used widely for the treatment of asthma. The improvement of pulmonary function in asthmatic patients was related to the plasma theophylline concentration (1–4). An optimal serum concentration range of 10–20 μg/ml was reported (5), although ranges from 5 to 20 μg/ml are often quoted. Theophylline levels greater than 16 μg/ml were associated with toxicity (5). For a drug with this narrow therapeutic index, it is difficult to maintain the optimum blood level for the desired time period; higher concentrations frequently result in toxicity and lower values appear less likely to provide maximal therapeutic benefit. Those problems suggest that modification of pharmaceutical properties are necessary to maintain the optimum blood level by the prodrug approach.

One main objective of a prodrug is to influence the plasma drug concentration–time profile with known pharmacological activity. This effect is achieved conveniently when the prodrug is much less soluble in water and has a slower dissolution rate in aqueous fluid than the parent drug. Under these circumstances, the appearance of the parent drug in the body is slowed by the slow dissolution of the prodrug in the GI tract (6–8). The purpose of this study was to investigate some physicochemical properties of 7,7′-succinylditheophylline as a potential prolonged-release theophylline prodrug.

THEORETICAL

The dissolution of 7,7′-succinylditheophylline will be shown to be pH dependent above pH 8. At pH values greater than 8, the hydrolysis of 7,7′-succinylditheophylline to theophylline occurs so rapidly that it takes place in the diffusion layer film. That is, the dissolution of 7,7′-succinylditheophylline occurs with a simultaneous irreversible chemical reaction.

Theoretical predictions of the dissolution rate with simultaneous irreversible chemical reactions have been treated previously (9, 10). The experimental data for the dissolution rate of 7-acetyltheophylline agreed with theoretical predictions based on the film theory model under steady-state conditions. This theoretical treatment also may be applied to 7,7′-succinylditheophylline.

The problem to be considered is that in which a solid phase, A, dissolves into the liquid phase and then reacts irreversibly with a species, B, already present in the liquid phase: $A + B \rightarrow C + D$. The intermediate species, D, then reacts irreversibly with B to form the final products: $D + (n-1)B \rightarrow$ products, where n is the number of molecules of B. If A is 7,7′-succinylditheophylline and B is hydroxide ion, n is equal to 2 below pH 8 and to 4 above pH 9. The first step, disappearance of A by reaction with B, would be considered a rate-determining step.

Let A be the concentration of 7,7′-succinylditheophylline at a distance X within the liquid film, t the time, k_0 the first-order rate constant of a

0022-3549/79/0300-0288$01.00/0
© 1979, American Pharmaceutical Association

macol., **16**, 1941 (1967).
(19) D. F. DeTar and M. N. Turetyky, *J. Am. Chem. Soc.*, **77**, 1745 (1955).
(20) K. Omura and T. Matsura, *Tetrahedron*, **26**, 255 (1970).
(21) B. D. Andresen, J. L. Templeton, R. H. Hammer, and H. L. Panzik, *Res. Commun. Chem. Pathol. Pharmacol.*, **14**, 259 (1976).
(22) E. Tegmann, E. Sury, and K. Hoffmann, *Helv. Chim. Acta*, **35**, 1235 (1952).
(23) S. Kukolja, D. Grguric, and L. Lopina, *Croat. Chem. Acta*, **33**, 41 (1961).
(24) E. von Kovates, *Helv. Chim. Acta*, **41**, 1915 (1958).
(25) B. D. Andresen, F. T. Davis, J. L. Templeton, R. H. Hammer, and H. L. Panzik, *Res. Commun. Chem. Pathol. Pharmacol.*, **15**, 21 (1976).
(26) B. D. Andresen, F. T. Davis, J. L. Templeton, H. L. Panzik, and R. H. Hammer, *ibid.*, **18**, 439 (1977).

ACKNOWLEDGMENTS

Supported in part by a Cottrell Starter Grant administered by Research Corporation.

The authors thank Dr. Harold L. Panzik and Mr. James L. Templeton for assistance.

Hydrolysis and Dissolution Behavior of a Prolonged-Release Prodrug of Theophylline: 7,7′-Succinylditheophylline

H. K. LEE *x, H. LAMBERT *, V. J. STELLA ‡, D. WANG ‡, and T. HIGUCHI ‡

Received June 14, 1978, from **Pharmaceutical Research and Development, Searle Laboratories, Skokie, IL 60076*, and the ‡*Department of Pharmaceutical Chemistry, University of Kansas, Lawrence, KS 66045.* Accepted for publication August 11, 1978.

Abstract □ The physicochemical characteristics of 7,7′-succinylditheophylline, a slow dissolving prodrug of theophylline, were investigated at 25°. One molecule of 7,7′-succinylditheophylline hydrolyzed to give two molecules of theophylline and one molecule of succinic acid. At 25° in aqueous solution, constant ionic strength, and zero buffer concentration, the pH profile for the hydrolysis of 7,7′-succinylditheophylline could be described adequately by a spontaneous constant, k_0, of 8.15×10^{-2} sec^{-1} and a hydroxide catalytic constant, k_{OH^-}, of 1.46×10^5 M^{-1} sec^{-1}. No specific acid catalysis was seen at pH values as low as 1. This dissolution rate of 7,7′-succinylditheophylline from a constant surface area pellet was independent of pH below 8. However, at pH values greater than 8, the dissolution rate was accelerated by a base. This behavior was consistent with the dissolution rate being catalyzed by the simultaneous chemical reaction of 7,7′-succinylditheophylline with hydroxide ion at a rate such that substantial hydrolysis of the substrate was occurring in the dissolution film. Dissolution with simultaneous chemical reaction for 7,7′-succinylditheophylline was analyzed theoretically on the basis of a film theory model. Excellent correlation between the theoretical and observed dissolution behavior was found. At pH values less than 8, the dissolution of 7,7′-succinylditheophylline was 35 times slower than that of theophylline. Based on this result, the aqueous solubility of 7,7′-succinylditheophylline was estimated to be 1.63×10^{-3} M.

Keyphrases □ 7,7′-Succinylditheophylline—hydrolysis and dissolution, effect of pH □ Prodrugs, theophylline—7,7′-succinylditheophylline, hydrolysis and dissolution, effect of pH □ Hydrolysis—7,7′-succinylditheophylline, effect of pH □ Dissolution—7,7′-succinylditheophylline, effect of pH □ Theophylline prodrugs—7,7′-succinylditheophylline, hydrolysis and dissolution, effect of pH

Theophylline is an effective bronchodilator used widely for the treatment of asthma. The improvement of pulmonary function in asthmatic patients was related to the plasma theophylline concentration (1–4). An optimal serum concentration range of 10–20 μg/ml was reported (5), although ranges from 5 to 20 μg/ml are often quoted. Theophylline levels greater than 16 μg/ml were associated with toxicity (5). For a drug with this narrow therapeutic index, it is difficult to maintain the optimum blood level for the desired time period; higher concentrations frequently result in toxicity and lower values appear less likely to provide maximal therapeutic benefit. Those problems suggest that modification of pharmaceutical properties are necessary to maintain the optimum blood level by the prodrug approach.

One main objective of a prodrug is to influence the plasma drug concentration–time profile with known pharmacological activity. This effect is achieved conveniently when the prodrug is much less soluble in water and has a slower dissolution rate in aqueous fluid than the parent drug. Under these circumstances, the appearance of the parent drug in the body is slowed by the slow dissolution of the prodrug in the GI tract (6–8). The purpose of this study was to investigate some physicochemical properties of 7,7′-succinylditheophylline as a potential prolonged-release theophylline prodrug.

THEORETICAL

The dissolution of 7,7′-succinylditheophylline will be shown to be pH dependent above pH 8. At pH values greater than 8, the hydrolysis of 7,7′-succinylditheophylline to theophylline occurs so rapidly that it takes place in the diffusion layer film. That is, the dissolution of 7,7′-succinylditheophylline occurs with a simultaneous irreversible chemical reaction.

Theoretical predictions of the dissolution rate with simultaneous irreversible chemical reactions have been treated previously (9, 10). The experimental data for the dissolution rate of 7-acetyltheophylline agreed with theoretical predictions based on the film theory model under steady-state conditions. This theoretical treatment also may be applied to 7,7′-succinylditheophylline.

The problem to be considered is that in which a solid phase, A, dissolves into the liquid phase and then reacts irreversibly with a species, B, already present in the liquid phase: $A + B \rightarrow C + D$. The intermediate species, D, then reacts irreversibly with B to form the final products: $D + (n-1)B \rightarrow$ products, where n is the number of molecules of B. If A is 7,7′-succinylditheophylline and B is hydroxide ion, n is equal to 2 below pH 8 and to 4 above pH 9. The first step, disappearance of A by reaction with B, would be considered a rate-determining step.

Let A be the concentration of 7,7′-succinylditheophylline at a distance X within the liquid film, t the time, k_0 the first-order rate constant of a

0022-3549/79/0300-0288$01.00/0
© 1979, American Pharmaceutical Association

spontaneous hydrolysis reaction, k_B the second-order rate constant for the reaction between solute A and component B, D_A the diffusion coefficient of A in the medium, and D_B the diffusion coefficient of B in the medium.

If the chemical reaction is fast enough, it takes place in a thin zone within the diffusional film; the concentration distribution that establishes the diffusional film is sketched in Fig. 1. The diffusion rate in an element of unit area can be expressed by:

$$W_A = -D_A \frac{dA}{dX} \qquad \text{(Eq. 1)}$$

The diffusion rate out of the element at the point $X + dX$ will be:

$$W'_A = -D_A \left(\frac{dA}{dX} + \frac{d^2A}{dX^2} dX\right) \qquad \text{(Eq. 2)}$$

The consumption rate of A within the element is, therefore:

$$W_A - W'_A = D_A \frac{d^2A}{dX^2} dX \qquad \text{(Eq. 3)}$$

For component B, the analogous expression is:

$$-(W'_B - W_B) = D_B \frac{d^2B}{dX^2} dX \qquad \text{(Eq. 4)}$$

Per unit time, the consumption of A and B is expressed also by the reaction rate:

$$-\frac{dA}{dt} = -\frac{1}{n}\frac{dB}{dt} = (k_0 + k_B B)A \qquad \text{(Eq. 5a)}$$

So that the number of molecules A and B disappearing within the volume element will be:

$$-\frac{dA}{dt} dX = -\frac{1}{n}\frac{dB}{dt} dX = (k_0 + k_B B)A\, dX \qquad \text{(Eq. 5b)}$$

Combining Eqs. 3, 4, and 5b yields:

$$D_A \frac{d^2A}{dX^2} = \frac{D_B}{n}\frac{d^2B}{dX^2} = (k_0 + k_B B)A \qquad \text{(Eq. 6)}$$

A general solution of this equation by exact mathematical methods is not possible. However, one important conclusion can immediately be drawn from the equation since:

$$D_A \frac{d^2A}{dX^2} - \frac{D_B}{n}\frac{d^2B}{dX^2} = 0 \qquad \text{(Eq. 7)}$$

After two integrations, the constants of integration are evaluated to give Eq. 8 by use of boundary conditions:

$$-D_A \left(\frac{dA}{dX}\right)_{x=0} = \frac{D_A}{X_L}(A_0 - A_L) + \frac{D_B}{nXL}(B_L - B_0) \qquad \text{(Eq. 8)}$$

where $X = 0$, $A = A_0$, and $B = B_0$ at the interface and $X = X_L$, $A = A_L$, and $B = B_L$ at the film edge.

Although Eq. 8 represents the dissolution rate of A per unit area of film, it cannot be determined directly from this relationship since the B_0 concentration is unknown. However, it is possible to find a solution for B_0 in specific cases by a numerical integration of Eq. 6.

A mathematical solution of Eq. 6 was described previously (11, 12) for some special cases when the concentration of B (or liquid phase reactants) is constant throughout the liquid film:

$$D_A \left(\frac{d^2A}{dX^2}\right) = (k_0 + k_B B_L)A \qquad \text{(Eq. 9a)}$$

The solution of the equation is given by:

$$A = \frac{A_L \sinh(aX) + A_0 \sinh[a(X_L - X)]}{\sinh(aX_L)} \qquad \text{(Eq. 9b)}$$

where:

$$a = \sqrt{\frac{k_0 + k_B B_L}{D_A}} \qquad \text{(Eq. 9c)}$$

The slope of the concentration curve is obtained by differentiating Eq. 9b. The diffusion rate of A into the solution phase, N_A, is obtained by multiplying the slope at $X = 0$ by the diffusivity, D_A:

$$N_A = -D_A \left(\frac{dA}{dX}\right)_{x=0} = \frac{D_A a\,[A_0 \cosh(aX_L) - A_L]}{\sinh(aX_L)} \qquad \text{(Eq. 10)}$$

and:

$$N_A = \frac{D_A}{X_L}\left(A_0 \frac{Y}{\tanh Y} - A_L \frac{Y}{\sinh Y}\right) \qquad \text{(Eq. 11)}$$

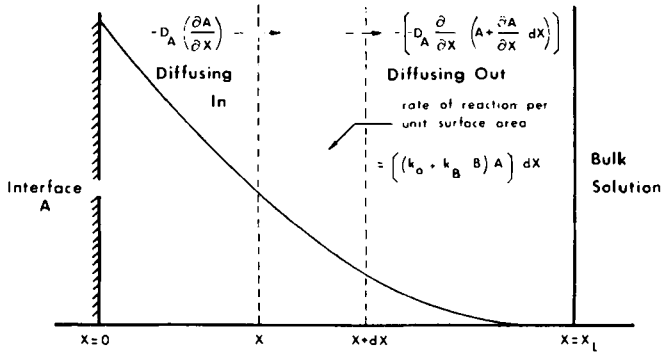

Figure 1—*Schematic illustration of concentration profiles during the dissolution of solid* A *in reactive media. Key:* X, *distance from* A; *and* L, *diffusion layer thickness.*

where $Y = aX_L$.

Consider the following conditions:

1. When the reaction rate is practically zero, Y is nearly equal to sinh Y and tanh Y. Equation 11 is reduced to:

$$N_A = \frac{D_A}{X_L}(A_0 - A_L) \qquad \text{(Eq. 12a)}$$

For the special case where $A_L = 0$:

$$N_A = M_1 = \frac{D_A}{X_L} A_0 \qquad \text{(Eq. 12b)}$$

this value must be considered as the limiting rate of diffusion; *i.e.*, when the reaction proceeds entirely within the bulk of the liquid, diffusion through the liquid film is the rate-determining step.

2. When the reaction rate is large, tanh $Y = 1$ and sinh Y tends toward infinity so Eq. 11 reduces to:

$$N_A = \left(\frac{D_A}{X_L} A_0\right) Y = A_0 \sqrt{(k_0 + k_B B_L) D_A} \qquad \text{(Eq. 13)}$$

At a high reaction rate, the reaction proceeds completely within the liquid film and the overall appearance rate of product (theophylline), R_1, is:

$$R_1 = A_0 \sqrt{(k_0 + k_B B_L) D_A} \qquad \text{(Eq. 14)}$$

EXPERIMENTAL

Measurement of Hydrolysis Rates—Reactions were performed in the cell of a UV spectrophotometer[1]. Appropriate portions (0.5 and 2.5 ml) of 4×10^{-4} *M* 7,7′-succinylditheophylline in dioxane were placed in a 2-cm cell, and buffer solutions (5 and 3 ml) were injected from a syringe into the cell at 25° at the same time as the chart motor was started.

Measurements of the absorbance change at 300 nm were taken. The apparent first-order rate constants were obtained by plotting the net absorbance change against time on semilogarithmic paper and calculating the first-order constant from the equation $k_{app} = 0.693/t_{0.5}$.

Dissolution Rate Determination—Pellets of 7,7′-succinylditheophylline were prepared by directly compressing 200 mg of the material in a die (1.3 cm i.d.) under a force of 454 kg with a laboratory press[2]. The pellet was held firmly in the die by covering the inside surface with melted paraffin (exposed surface area of 1.130 cm^2).

A 500-ml volume of the selected buffer solution was placed in 1-liter, three-necked, round-bottom flasks and kept at 25° in a constant-temperature water bath. A semicircular stirring blade (width of 4.8 cm and maximum depth of 1.4 cm) was positioned in the dissolution medium so that the top of the blade was maintained at the same level as the dissolution medium surface.

The pellet was placed in the medium by guiding it through the side neck of the flask, and it remained at the bottom of the flask without moving during agitation. A stirring rate of 50 rpm was initiated immediately after the pellet was introduced into the flask. At the same time, a sample of the solution was circulated continuously, at a flow rate of 43 ml/min, with a peristaltic pump[3] to a UV spectrophotometer. Absorbances were recorded at 270 nm using a 1-cm flowcell.

[1] Model 14, Cary, Monrovia, CA 91016.
[2] Model C, Fred S. Carver, Menomonee Falls, WI 53051.
[3] Model 7016, Cole-Palmer, Chicago, IL 60648.

Table I—Apparent First-Order Rate Constants (k_{app}, seconds^{-1}) for Hydrolysis of 7,7-Succinylditheophylline in Various Buffer Concentrations and pH Values

Buffer[a]			pH[b]	$k_{app}^{45.5\%}$[c], sec^{-1}	$k_{app}^{9\%}$[d], sec^{-1}
	0.1 N HCl		1.10	3.01×10^{-2}	8.04×10^{-2}
	1×10^{-2} N HCl		2.05	2.95×10^{-2}	
	1×10^{-3} N HCl		3.07	2.95×10^{-2}	8.15×10^{-2}
$[CH_3COOH]$	$[CH_3COONa]$	[NaCl]			
6.0×10^{-4}	1.4×10^{-3}	9.86×10^{-2}	5.05 ± 0.03	2.95×10^{-2}	
1.2×10^{-3}	2.8×10^{-3}	9.72×10^{-2}	5.05 ± 0.03	2.95×10^{-2}	
2.4×10^{-3}	5.6×10^{-3}	9.44×10^{-2}	5.05 ± 0.03	3.01×10^{-2}	
3.6×10^{-3}	8.4×10^{-3}	9.16×10^{-2}	5.05 ± 0.03	2.95×10^{-2}	
			5.05 ± 0.03	2.95×10^{-2} [e]	8.15×10^{-2} [e]
$[Na_2HPO_4]$	$[NaH_2PO_4]$	[NaCl]			
1.4×10^{-3}	1.0×10^{-2}	8.58×10^{-2}	6.0 ± 0.01	3.01×10^{-2}	8.66×10^{-2}
2.8×10^{-3}	2.0×10^{-2}	7.16×10^{-2}	6.0 ± 0.01	3.38×10^{-2}	9.00×10^{-2}
4.2×10^{-3}	3.0×10^{-2}	5.74×10^{-2}	6.0 ± 0.01	3.55×10^{-2}	9.24×10^{-2}
5.7×10^{-3}	4.0×10^{-2}	4.28×10^{-2}	6.0 ± 0.01	3.85×10^{-2}	9.50×10^{-2}
7.0×10^{-3}	5.0×10^{-2}	2.80×10^{-2}	6.0 ± 0.01	4.08×10^{-2}	
			6.0 ± 0.01	2.79×10^{-2} [e]	8.34×10^{-2} [e]
4.88×10^{-3}	3.12×10^{-3}	8.22×10^{-2}	6.95 ± 0.05	4.47×10^{-2}	9.90×10^{-2}
7.32×10^{-3}	4.68×10^{-3}	7.34×10^{-2}	6.95 ± 0.05	4.62×10^{-2}	10.27×10^{-2}
9.76×10^{-3}	6.24×10^{-3}	6.45×10^{-2}	6.95 ± 0.05	5.33×10^{-2}	10.66×10^{-2}
12.20×10^{-3}	7.80×10^{-3}	5.56×10^{-2}	6.95 ± 0.05	5.54×10^{-2}	11.19×10^{-2}
			6.95 ± 0.05	3.62×10^{-2} [e]	9.02×10^{-2} [e]
1.0×10^{-2}	2.34×10^{-3}	1.68×10^{-1}	7.40 ± 0.05	7.70×10^{-2}	
2.0×10^{-2}	4.70×10^{-3}	1.35×10^{-1}	7.40 ± 0.05	8.35×10^{-2}	
4.0×10^{-2}	9.38×10^{-3}	9.06×10^{-2}	7.40 ± 0.05	9.90×10^{-2}	
5.0×10^{-2}	11.72×10^{-3}	3.83×10^{-2}	7.40 ± 0.05	10.83×10^{-2}	
			7.40 ± 0.05	6.85×10^{-2} [e]	
1.88×10^{-2}	3.12×10^{-2}	11.20×10^{-2}	6.46	4.62×10^{-2}	
2.45×10^{-2}	2.55×10^{-2}	10.10×10^{-2}	6.07	4.78×10^{-2}	
3.05×10^{-2}	1.95×10^{-2}	8.90×10^{-2}	6.89	6.93×10^{-2}	
3.60×10^{-2}	1.40×10^{-2}	7.80×10^{-2}	7.12	7.70×10^{-2}	
4.05×10^{-2}	9.50×10^{-3}	6.90×10^{-2}	7.35	9.90×10^{-2}	
4.35×10^{-2}	6.50×10^{-3}	6.30×10^{-2}	7.54	10.66×10^{-2}	
4.58×10^{-2}	4.20×10^{-3}	5.81×10^{-2}	7.74	14.66×10^{-2}	

[a] Values in the aqueous medium without dioxane. [b] All pH values were measured in aqueous buffers at 25° before mixing with dioxane. [c] The apparent first-order rate constant (seconds^{-1}) for the reaction in 45.5% dioxane–54.5% aqueous buffer solution. [d] The apparent first-order rate constant (seconds^{-1}) for the reaction in 9% dioxane–91% aqueous buffer solution. [e] Values obtained by extrapolation to zero buffer concentration.

The total amount of compound in solution as a function of time was determined. The total dissolution rate of 7,7′-succinylditheophylline, $(dA/dt)_{t=0}$, was obtained from the initial slope of the concentration–time curve, and the dissolution rate per unit area of the pellet was obtained from the value of $(V/S)(dA/dt)_{t=0}$, where V is the dissolution medium volume of 500 ml and S is the pellet surface area of 1.13 cm^2. 7,7′-Succinylditheophylline was measured in solution as theophylline since, as will be shown later, 7,7′-succinylditheophylline rapidly and quantitatively reverted to theophylline at all pH values studied.

RESULTS AND DISCUSSION

Spectral Change and Molar Absorptivity—The spectra of 7,7′-succinylditheophylline showed a λ_{max} at 300 nm in dioxane (Fig. 2, curve 1). After 3 ml of 1×10^{-4} M 7,7′-succinylditheophylline in dioxane was mixed with 0.5 ml of water, the spectra were taken at appropriate time intervals (4–10 min, Fig. 2, curves 2–6); the initial absorbance at 300 nm in dioxane (λ_{max} of 7,7′-succinylditheophylline) decreased with time. A new band appeared at 274 nm (λ_{max} of theophylline). The λ_{max} at 300 nm completely disappeared within 1.5 hr (Fig. 2, curve 7). Maintenance of an apparent isosbestic point at 287 nm was evident for the transformation of 7,7′-succinylditheophylline.

Appropriate volumes of 7,7′-succinylditheophylline stock solution (1×10^{-4} M) in dioxane were diluted with 0.1 N HCl to give a 4×10^{-5}–1×10^{-5} M range, and spectra were taken with a 5-cm silica cell after overnight standing at room temperature. Molar absorptivities of degraded 7,7′-succinylditheophylline and theophylline at 270 nm were 2.025×10^4 and 1.003×10^4 liters/mole-cm, respectively. These data showed that molar absorptivity of degraded 7,7′-succinylditheophylline in 0.1 N HCl was two times greater than that of theophylline. This information, coupled with the spectral change (from 300 to 270 nm), demonstrated that 1 mole of 7,7′-succinylditheophylline degraded to produce 2 moles of theophylline.

Catalytic Hydrolysis Rate Constants—No significant buffer catalysis was observed in the acetate buffer and dioxane mixture with an ionic strength of 0.1 (Table I). However, a small, but significant, buffer effect was observed with phosphate buffer. The apparent first-order rate constant at zero phosphate buffer concentration was obtained from plots of the apparent first-order rate constants, k_{app}, against the phosphate buffer concentration (Table I and Fig. 3).

No specific acid catalysis was observed (Fig. 4). The important contribution to hydrolysis of 7,7′-succinylditheophylline at the pH-independent region below pH 6 would be water catalysis. The apparent first-order rate constant for a 9% dioxane–91% aqueous system below pH 6 was $k_{app}^{9\%} = 8.15 \times 10^{-2}$ sec (Table I and Fig. 4). The extrapolated value, k_0, agreed reasonably with the $k_0^{9\%}$ value. It was based on the premise that the results in a 9% dioxane–water system are very similar to those in pure water systems (13). Above pH 7, the hydrolysis kinetics in a 9% dioxane–buffer system were difficult to follow by conventional UV spectrophotometry because of the rapid hydrolytic reaction.

The specific base catalytic constant, $k_{OH^-}^{45.5\%}$, in a 45.5% dioxane–55.5% aqueous buffer system was obtained from plots of k_{app} against $[OH^-]$ (where pH was measured in pure aqueous buffer with ionic strength 0.2); $k_{OH^-}^{45.5\%}$ was 1.46×10^5 liters/mole-sec (Fig. 5). Because the value of $k_{OH^-}^{45.5\%}$ was obtained from the apparent hydroxide-ion concentration, ranging from 10^{-6} to 10^{-8} M, the activity coefficient of OH^- in a 45.5% dioxane–water system, $\gamma_{OH^-}^{45.5\%}$, as well as the activity coefficient of OH^- in water, $\gamma_{OH^-}^{0\%}$, can be assumed to be unity, so the value of $k_{OH^-}^{45.5\%}$ can be treated as that of the specific base catalytic constant in water, k_{OH^-}.

Based on those values of k_0 and k_{OH^-}, the theoretical log k_{app}–pH profiles were constructed as shown in Fig. 4.

Hydrolytic Reactivity and Mechanisms—7-Acetyltheophylline (I) and 7,7′-succinylditheophylline have half-lives of 40 and 8 sec, respec-

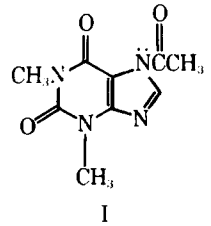

I

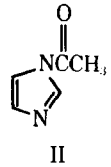

II

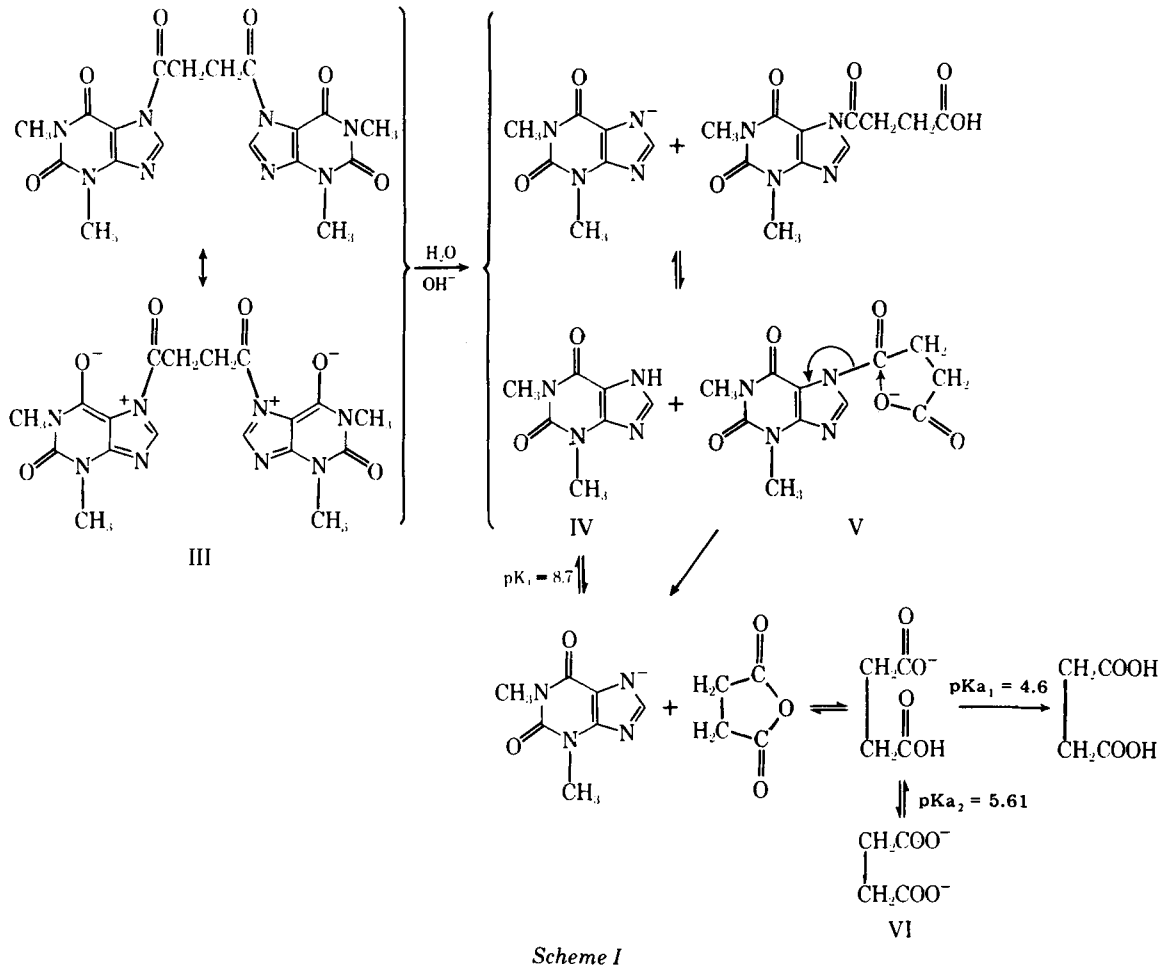

Scheme I

tively, in water at room temperature. The high degree of reactivity of *N*-acylated theophylline compounds compared with the low reactivity of normal amides may be related to the quasiaromatic character of the theophylline ring. As a result of the participation of the electron pair on the 7-nitrogen in the π-electron system, this nitrogen becomes more positive, exerting attraction toward the ring. This electron attraction increases the rate of nucleophilic reactions involving the carbonyl group.

N-Acetylimidazole (II) is hydrolyzed with a half-life of 40 min at room temperature in water (14). The difference in reactivity between *N*-acylated theophylline compounds and *N*-acetylimidazole can be explained by the greater delocalization of the lone electron pair of the imide nitrogen in the theophylline ring (I) than in the imidazole ring (II). Higher reactivity of 7,7′-succinylditheophylline over 7-acetyltheophylline was expected since the theophylline hemisuccinate group is much better as a leaving group than is the acetyl group.

The overall hydrolytic degradation of 7,7′-succinylditheophylline is illustrated in Scheme I. It is assumed that 7,7′-succinylditheophylline (III) hydrolyzes to theophylline (IV) and theophylline hemisuccinate (V); then the latter degrades to theophylline and the succinate ion (VI) as a consecutive first-order process as shown in Scheme II:

$$A \xrightarrow{k_1} C + D$$

$$D \xrightarrow{k_2} C + E$$

Scheme II

In this study, the kinetics were followed by the disappearance of 7,7′-succinylditheophylline under pseudo-first-order conditions. Experimentally, k_1 and k_2 were inseparable, given by a single exponential decrease in starting material as a function of time. The intermediate, V, could not be isolated by the chromatographic method. It suggested that k_2 is much larger than k_1, so the first step is rate determining.

The hydrolysis of hemisuccinate is catalyzed powerfully by a suitably spaced, neighboring ionized carboxyl group (15, 16). The intramolecular hydrolysis rate of phenyl succinate (VII) at 25° is 1.42×10^{-3} sec^{-1} at neutral pH (16). However, the intermolecular reaction rate of phenyl acetate (VIII) with acetate ion at 63° is 1.02×10^{-5} liter/mole-sec (14).

The intermolecular reaction of phenyl acetate with acetate ion requires more than 100 *M* acetate ion for the hydrolysis rate to be equivalent to the rate of the intramolecular hydrolysis of phenyl succinate. Furthermore, under favorable conditions, the effect of the carboxylate attack is much larger than the effect of hydrogen- and hydroxide-ion-catalyzed ester hydrolysis (16). Therefore, the hydrolysis rate of 7,7′-succinylditheophylline can be expected to be no less than 100-fold of that of 7-acetyltheophylline (1.6×10^{-2} sec), so $k_2 \gg k_1$ (first step is rate determining).

Estimation of Diffusion Coefficient—The values of the diffusion coefficient for 7,7′-succinylditheophylline and hydroxide ion were estimated using the Stokes–Einstein equation (17):

$$D = \frac{RT}{6\pi\mu N}\sqrt[3]{\frac{4\pi N}{3M\nu}} \qquad \text{(Eq. 15)}$$

where M is the molecular weight, ν is the partial specific volume, T is the absolute temperature, R is the molar gas constant, N is Avogadro's number, and μ is the solvent viscosity.

When $\nu = 1$ and $\mu = 0.01$ poise, the values of the diffusion coefficient of 7,7′-succinylditheophylline, D_A, and hydroxide ion, D_B, at 25° were 3.90×10^{-6} and 1.15×10^{-5} cm^2/sec, respectively.

Estimations of Film Thickness, X_L, and Saturation Solubility, A_0—The dissolution rate of A per unit area of film is represented by Eq. 8. The value of A_L is assumed to be zero under the steady-state condition,

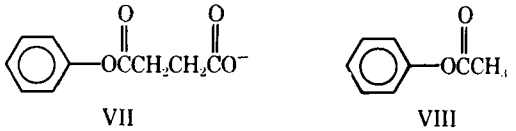

Table II—Comparison of Reaction Time (t_r) and Diffusion Time[a] (t_D = 2 sec) with Respect to Various pH Values

pH	[OH⁻], mole/cm³	k_{app}[b], sec⁻¹	t_r[c], sec
1.0	1×10^{-16}	8.15×10^{-2}	12.27
3.0	1×10^{-14}	8.15×10^{-2}	12.27
5.0	1×10^{-12}	8.16×10^{-2}	12.25
7.0	1×10^{-10}	9.61×10^{-2}	10.41
9.0	1×10^{-8}	1.54	6.49×10^{-1}
10.14	1.38×10^{-7}	2.02×10^{1}	4.94×10^{-2}
11.0	1.0×10^{-6}	1.46×10^{2}	6.85×10^{-3}
11.7	5.0×10^{-6}	7.30×10^{2}	1.37×10^{-3}
12.0	1.0×10^{-5}	1.46×10^{3}	6.85×10^{-4}
12.48	3.0×10^{-5}	4.38×10^{3}	2.28×10^{-4}
12.70	5.0×10^{-5}	7.30×10^{3}	1.37×10^{-4}
13.0	1.0×10^{-4}	1.46×10^{4}	6.85×10^{-5}
13.3	2.0×10^{-4}	2.92×10^{4}	3.42×10^{-5}
13.48	3.0×10^{-4}	4.38×10^{4}	2.28×10^{-5}

[a] $t_D = (X_L^2)/(2D_A)$, where $X_L = 3.87 \times 10^{-3}$ cm and $D_A = 3.90 \times 10^{-6}$ cm²/sec. [b] $k_{app} = k_0 + k_{OH^-}[OH^-]$, where $k_0 = 8.15 \times 10^{-2}$ sec⁻¹ and $k_{OH^-} = 1.46 \times 10^8$ cm³/mole-sec. [c] $t_r = 1/k_{app}$.

and rearrangement of Eq. 8 gives:

$$D_A\left(\frac{dA}{dX}\right)_{x=0} = \left(\frac{D_A}{X_L}A_0 - \frac{D_B}{nB_L}B_0\right) + \frac{D_B}{nX_L}B_L \qquad \text{(Eq. 16)}$$

When the chemical reaction takes place mainly in the film, film thickness X_L can be obtained from the slope of the plot of $D_A(dA/dX)_{x=0}$, which is equal to $(V/S)(dc/dt)_{t=0}$, against $[OH^-]$ (Fig. 6). The value of X_L obtained from this plot is 3.87×10^{-3} cm.

The value of X_L also can be obtained under the same hydrodynamic conditions as those for theophylline. With the values of the total dissolution rate of theophylline (1.43×10^{-10} mole/cm³-sec), the saturation solubility (4×10^{-5} mole/cm³), and the diffusion coefficient of theophylline estimated from the Stokes-Einstein equation (5.26×10^{-6} cm²-sec), the value of X_L, 3.33×10^{-3} cm, was obtained from the Noyes-Nernst equation in an analogous manner to previous work (9). Those two estimated values of X_L agreed reasonably well with each other within experimental error.

Direct measurement of the solubility of 7,7′-succinylditheophylline (III) was impossible because of its high reactivity in water ($t_{0.5}$ = 8.0 sec below pH 6). However, with the values of the initial dissolution rate at the pH-independent region, $(V/S)(dc/dt)_{t=0} = 1.78 \times 10^{-9}$ mole/cm²-sec, k_{app} below pH 6 (8.15×10^{-2} sec), D_A, and X_L, the saturation solubility can be estimated from Eqs. 11 and 13, assuming that A_L is equal to zero, so that:

$$A_0 = \frac{X_L}{D_A}\left(\frac{\tanh Y}{Y}\right)N_A \qquad \text{(Eq. 17a)}$$

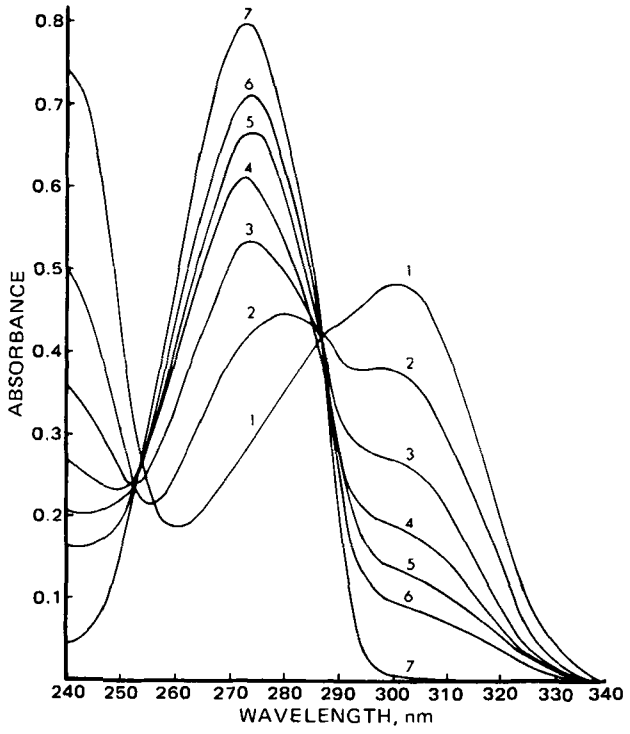

Figure 2—*UV spectral changes for the hydrolysis of 7,7′-succinylditheophylline (1×10^{-4} M) in an 85.7% dioxane and 14.3% water system at 25°.*

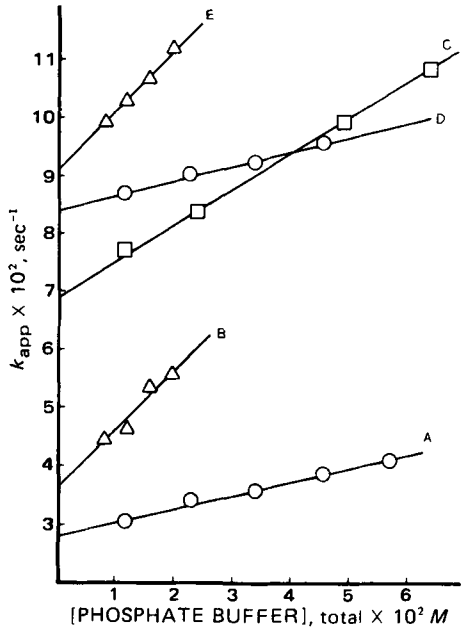

Figure 3—*Plots of apparent first-order rate constants (k_{app}) against various concentrations of phosphate buffer at a constant pH and an ionic strength of 0.1. Curves I, II, and III show the reactions in a 45.5% dioxane-54.5% aqueous buffer system at pH 6.0, 7.0, and 7.4, respectively. Intercept values were: I, 2.79×10^{-2} sec; II, 2.62×10^{-2} sec⁻¹; and III, 6.85×10^{-2} sec⁻¹. Curves IV and V show the reactions in a 9% dioxane-91% aqueous buffer system at pH 6.0 and 7.0, respectively. Their intercept values were: IV, 8.34×10^{-2} sec⁻¹; and V, 9.20×10^{-2} sec⁻¹.*

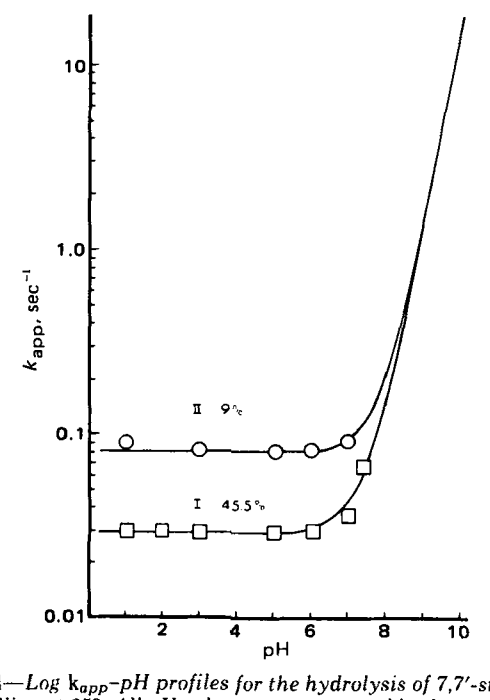

Figure 4—*Log k_{app}-pH profiles for the hydrolysis of 7,7′-succinylditheophylline at 25°. All pH values were measured in the pure aqueous system before the reaction started. Curves I and II show the reactions in 45.5 and 9% dioxane systems, respectively.*

Table III—Dissolution Rates, $(V/S)(dL/dt)_{t=0}$, as a Function of the Buffer Concentration at Various pH Values

Buffer			pH[a]	$V/S(dL/dt)_{t=0}$, mole/cm²-sec
	0.1 *N* HCl		1.0	1.78×10^{-9}
[HCOOH]	[NaOH]	[Buffer]total		
0.05	0.01	0.06	3.1	1.90×10^{-9}
CH_3COOH	$[CH_3COONa]$	[Buffer]total		
1.12×10^{-2}	4.80×10^{-3}	1.60×10^{-2}	5.0 ± 0.05	1.98×10^{-9}
2.24×10^{-2}	9.60×10^{-3}	3.20×10^{-2}	5.0 ± 0.05	1.82×10^{-9}
3.36×10^{-2}	14.40×10^{-3}	4.80×10^{-2}	5.0 ± 0.05	1.75×10^{-9}
6.40×10^{-2}	19.20×10^{-3}	6.40×10^{-2}	5.0 ± 0.05	1.95×10^{-9}
			5.0 ± 0.05	1.88×10^{-9} [b]
$[KH_2PO_4]$	[NaOH]	[Buffer]total		
3.0×10^{-2}	1.78×10^{-2}	4.78×10^{-2}	7.0 ± 0.07	2.09×10^{-9}
4.0×10^{-2}	2.37×10^{-2}	6.37×10^{-2}	7.0 ± 0.07	2.21×10^{-9}
5.0×10^{-2}	2.96×10^{-2}	7.95×10^{-2}	7.0 ± 0.07	2.26×10^{-9}
6.0×10^{-2}	3.55×10^{-2}	9.55×10^{-2}	7.0 ± 0.07	2.27×10^{-9}
			7.0 ± 0.07	1.78×10^{-9} [c]
[Glycine]	[NaOH]	[Buffer]total		
2.0×10^{-2}	3.52×10^{-3}	2.35×10^{-2}	9.0 ± 0.05	3.05×10^{-9}
3.0×10^{-2}	5.29×10^{-3}	3.53×10^{-2}	9.0 ± 0.05	3.50×10^{-9}
3.0×10^{-2}	5.29×10^{-3}	3.53×10^{-2}	9.0 ± 0.05	3.50×10^{-9}
4.0×10^{-2}	7.04×10^{-3}	4.70×10^{-2}	9.0 ± 0.05	3.93×10^{-9}
5.0×10^{-2}	8.80×10^{-3}	5.88×10^{-2}	9.0 ± 0.05	4.39×10^{-9}
6.0×10^{-2}	10.55×10^{-3}	7.06×10^{-2}	9.0 ± 0.05	4.83×10^{-9}
			9.0 ± 0.05	2.18×10^{-9} [c]
$[K_2CO_3]$	$[KHCO_3]$	[Buffer]total		
1.2×10^{-2}	0.8×10^{-2}	2.0×10^{-2}	10.14 ± 0.01	5.03×10^{-9}
2.4×10^{-2}	1.6×10^{-2}	4.0×10^{-2}	10.14 ± 0.01	7.79×10^{-9}
3.6×10^{-2}	2.4×10^{-2}	6.0×10^{-2}	10.14 ± 0.01	9.51×10^{-9}
4.8×10^{-2}	3.2×10^{-2}	8.0×10^{-2}	10.14 ± 0.01	12.24×10^{-9}
6.0×10^{-2}	4.0×10^{-2}	10.0×10^{-2}	10.14 ± 0.01	14.50×10^{-9}
			10.14 ± 0.01	2.77×10^{-9} [c]
	1×10^{-3} *N* NaOH		11.0	3.42×10^{-9}
	5×10^{-3} *N* NaOH		11.7	5.69×10^{-9}
	1×10^{-2} *N* NaOH		12.0	9.21×10^{-9}
	3×10^{-2} *N* NaOH		12.5	2.55×10^{-8}
	5×10^{-2} *N* NaOH		12.7	4.24×10^{-8}
	0.1 *N* NaOH		13.0	7.08×10^{-8}
	0.2 *N* NaOH		13.3	1.45×10^{-7}
	0.3 *N* NaOH		13.5	2.30×10^{-7}

[a] The pH values in hydrochloric acid and sodium hydroxide were calculated under the assumption that activity coefficient of hydrochloric acid and sodium hydroxide was unity. [b] Average value at constant pH. [c] Values obtained by extrapolation to zero buffer concentration.

where:

$$Y = X_L \sqrt{\frac{k_{app}}{D_A}} \qquad \text{(Eq. 17b)}$$

and:

$$A_0 = \frac{X_L}{D_A} \frac{V}{S} \left(\frac{dA}{dt}\right)_{t=0} \qquad \text{(Eq. 17c)}$$

where:

$$\frac{V}{S}\left(\frac{dA}{dt}\right)_{t=0} = D_A \left(\frac{dA}{dt}\right)_{t=0} \qquad \text{(Eq. 17d)}$$

The value of A_0 at 25° was found to be 1.61×10^{-6} mole/cm³ from Eq. 17a and 1.67×10^{-6} mole/cm³ from Eq. 17c.

Another way of estimating solubility is from the intercept value, $(D_A/X_L)A_0 - (D_B/nX_L)B_0 = 1.242 \times 10^{-9}$ mole/cm², of the plots of $D_A (dA/dX)_{x=0}$ *versus* $[OH^-]$ (Fig. 6). With the assumption that B_0 was equal to zero, A_0 was estimated to be 1.21×10^{-6} mole/cm³ from Eq. 17c, and best fit the experimental values according to:

$$R = \frac{D_A}{X_L} A_0 + \frac{D_B}{nX_L} B_L \qquad \text{(Eq. 18)}$$

Estimations of Diffusion Time and Reaction Time—The diffusion time, t_D, for steady state was derived previously (8, 9):

$$t_D = \frac{X_L^2}{2D_A} \qquad \text{(Eq. 19)}$$

The physical meaning of the diffusion time is the average lifetime for element A to travel through distance X_L, and it depends on the hydrodynamic conditions. According to Eq. 19, the estimated value of the diffusion time of III was 2 sec.

A useful concept in the analysis of a chemical reaction is the reaction time, t_r, defined (18) as A/r, where r is the chemical reaction rate and A is the actual initial concentration of the reactant. For a simple first-order reaction with a kinetic constant k_{app}:

$$t_r = \frac{1}{k_{app}} \qquad \text{(Eq. 20)}$$

Thus, at the end of the reaction time, 63% of III will have undergone reaction with first-order kinetics. The reaction times under various pH conditions are shown in Table II. These times are useful in analyzing dissolution kinetics.

Comparison of Estimated and Measured Dissolution Rates—The dissolution rates at various pH values were obtained by extrapolating to zero buffer concentration (Table III and Fig. 7). At pH values below

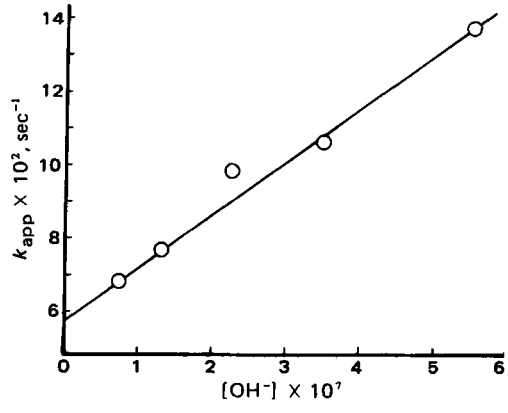

Figure 5—*Plot of apparent first-order rate constants* (k_{app}) *for the hydrolysis of 7,7'-succinylditheophylline in 45.5% dioxane–54.5% aqueous buffer system at pH 6.89–7.74 with a constant phosphate buffer concentration (0.1 M) and an ionic strength of 0.2 at 25°. The value of the slope* ($k_{OH}^{45.5\%}$) *was 1.45 × 10⁻⁵ liter/mole-sec.*

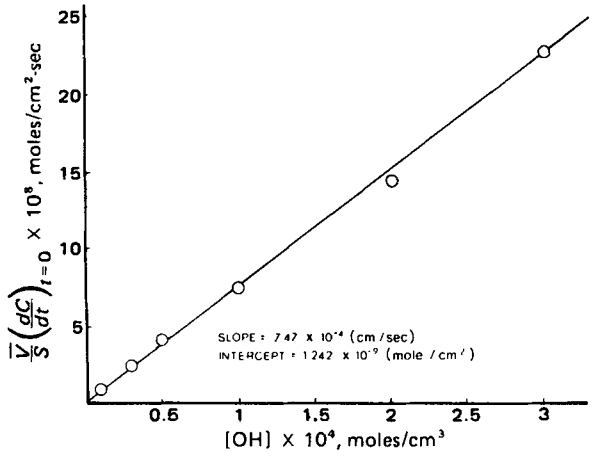

Figure 6—*Plots of the initial dissolution rate,* $(V/S)(dC/dt)_{t=0}$, *against the hydroxide-ion concentration. The slope of the plot* (D_B/nXL) *was* 7.4×10^{-4} *cm/sec.*

7, the reaction times were about sixfold greater than the diffusion time of 2 sec under these experimental conditions. The observed dissolution rate depends on the diffusion time rather than reaction time. The rate-determining factor is the diffusion rate of III from the solid–liquid interface into the bulk of the solution. The theoretical dissolution rates in these cases were estimated from the simplified equations and all led to Eq. 21 when A_L and B_0 were assumed to be zero under the sink conditions, respectively:

$$N_A = \frac{D_A}{X_L} A_0 \left(\frac{Y}{\tanh Y}\right) \qquad \text{(Eq. 21)}$$

Also, in Eq. 18, the second term, $(D_B/nX_L)B_L$, can be neglected in comparison with the first term, $M_1 = (D_A/X_L)A_0$, so that the overall dissolution rate is independent of pH and governed by M_1. The results obtained experimentally agreed fairly well with analytical solutions to Eqs. 18 and 21 (Table IV and Fig. 8).

At pH 9–11, the reaction times, t_r, were small compared to the diffusion time, t_0, of 2 sec. Thus, the chemical reactions were fast enough to proceed in the diffusion layer so that the dissolution rate was affected by $[OH^-]$.

The estimated values from Eq. 18 and the observed values at pH 9, 10, 11, and 14 were reached within experimental error (Table IV and Fig. 8).

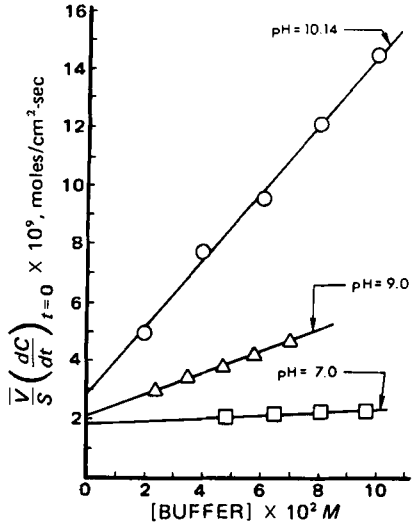

Figure 7—*Plots of the initial dissolution rate,* $(V/S)(dC/dt)_{t=0}$, *against buffer concentrations. The buffer systems were monobasic potassium phosphate–sodium hydroxide (pH 7.0), glycine–sodium hydroxide (pH 9.0), and potassium carbonate–potassium bicarbonate (pH 10.14). The intercepts were* 1.78×10^{-9}, 2.18×10^{-9}, *and* 2.77×10^{-9}, *respectively.*

Table IV—Comparison of Theoretical and Experimental Dissolution Rates at Each pH

pH	$M_2 = (D_B/nX_L)BL$[a], mole/cm²-sec	$R = M_1 + M_2$[b], mole/cm²-sec	$V/S(dC/dt)_{t=0}$[c], mole/cm²-sec
1.0	—	1.78×10^{-9}	1.78×10^{-9}
3.0	—	1.78×10^{-9}	1.78×10^{-9}
5.0	1.49×10^{-15}	1.78×10^{-9}	1.69×10^{-9}
7.0	1.49×10^{-13}	1.78×10^{-9}	1.78×10^{-9}
9.0	7.45×10^{-12}	1.79×10^{-9}	2.18×10^{-9}
10.14	1.03×10^{-10}	1.88×10^{-9}	2.77×10^{-9}
11.0	7.47×10^{-10}	2.53×10^{-9}	3.42×10^{-9}
11.7	3.73×10^{-9}	5.51×10^{-9}	5.69×10^{-9}
12.0	7.46×10^{-9}	9.24×10^{-9}	9.21×10^{-9}
12.48	2.24×10^{-8}	2.42×10^{-8}	2.55×10^{-8}
12.70	3.73×10^{-8}	3.91×10^{-8}	4.24×10^{-8}
13.0	7.46×10^{-8}	7.64×10^{-8}	7.08×10^{-8}
13.3	1.49×10^{-7}	1.51×10^{-7}	1.40×10^{-7}
13.48	2.24×10^{-7}	2.26×10^{-7}	2.30×10^{-7}

[a] Below pH 7, $n = 2$; above pH 9, $n = 4$; $D_B = 1.155 \times 10^{-5}$ cm²/sec; $X_L = 3.87 \times 10^{-3}$ cm. [b] Theoretically estimated values according to Eq. 19, where $M_1 = (DA)/(X_L)A_0 = 1.78 \times 10^{-9}$. [c] Experimentally measured values.

From these data, it is apparent that the dissolution rate is controlled by the diffusion rate of A as well as that of B $[OH^-]$, resulting in curvature of the logarithmic dissolution rate–pH rate profile (Fig. 8).

At pH >11.7, the reactions were sufficiently fast to take place in a diffusion layer, because the reaction times were extremely small (10^{-3}–10^{-5}-fold) compared with the diffusion time of 2 sec (Table II). The observed values of the dissolution rates agreed with the estimated values from Eq. 18. Thus, the rate-controlling phenomenon is the diffusion rate of hydroxide ion from the bulk solution to the solid–liquid interface, and the dissolution rate is greatly increased with a rise in the hydroxide-ion concentration; *i.e.*, the dissolution rate is linearly dependent on the pH in this region (Fig. 8).

Log Dissolution Rate–pH Profile—The log dissolution rate–pH profile (Fig. 8) exhibits a break point at pH 11 between the pH-independent and pH-dependent regions, whereas the log k_{app}–pH profile (Fig. 4) has a break point at pH 7. The ascending slope for the hydrolytic reaction is theoretically unity; however, that observed for the dissolution rate is 0.94 (theoretically estimated value, 0.94). These two differences in the dissolution plot can be rationalized adequately on the basis of a model system.

From the mathematical model, a general solution of Eq. 8 for the dissolution rate was obtained. The dissolution rate increased with a rise in the value of the second term of the equation, $(D_B/nX_L)(B_L - B_0)$, *i.e.*, with the value of B_L. The dissolution rate at the ascending part of the profile (above pH 12) was slightly influenced by the first term of the equation, $(D_A/X_L)(A_0 - A_L)$, where A_L was assumed to be zero under

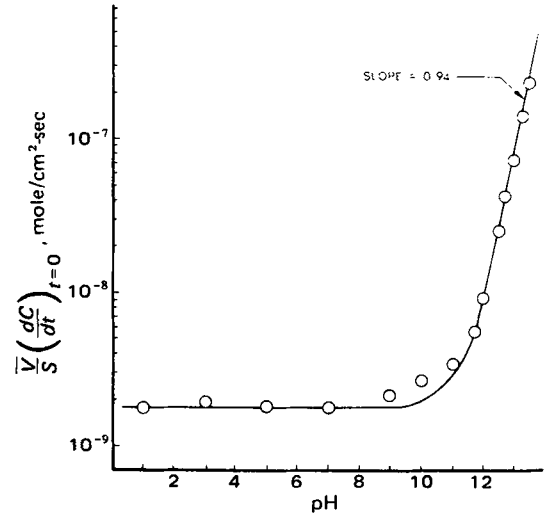

Figure 8—*Plots of the logarithmic dissolution rate against pH at 25°, where the values at pH 7, 9, and 10.14 were obtained by extrapolation to zero buffer concentration and the pH values in sodium hydroxide were calculated under the assumption that the activity coefficient of sodium hydroxide was unity.*

the sink condition (compared with M_1 and M_2 in Table IV). The deviation from the slope of unity existed as long as some degree of the first term, $(D_A/X_L)A_0$, affected the dissolution rate. The break point difference can be explained by the differences between $k_{OH^-}[OH^-] - k_0$ and $(D_B/nX_L)B_L - (D_A/X_L)A_0$.

SUMMARY AND CONCLUSION

The prodrug, 7,7′-succinylditheophylline, was hydrolyzed with a half-life of about 10 sec in the physiological pH range. These hydrolysis studies suggested that the prodrug would hydrolyze very rapidly and release the parent molecule, theophylline, once it was dissolved.

The dissolution rate of 7,7′-succinylditheophylline was 35 times slower than that of theophylline under the same conditions, and its dissolution rate was independent of pH within the physiological pH range. Dissolution rate studies coupled with hydrolysis rate studies suggested that the dissolution process would be the rate-determining step to keep the steady-state release into solution (Scheme III).

$$\text{prodrug in solid} \xrightarrow[\text{slow process}]{\text{dissolution}} \text{prodrug in solution} \xrightarrow[\text{rapid process}]{\text{hydrolysis}} \text{parent drug in solution}$$

Scheme III

The saturation solubility of 7,7′-succinylditheophylline at 25° in water was estimated to be 1.63×10^{-3} M from the rate dissolution data. Under the same conditions, theophylline solubility was 4×10^{-2} M. From these results, it appears that 7,7′-succinylditheophylline might be a valuable candidate as a prolonged-release theophylline prodrug.

REFERENCES

(1) R. Maselli, G. L. Casal, and E. F. Ellis, *J. Pediatr.*, **76**, 777 (1970).

(2) R. H. Jackson, J. I. McHenry, F. B. Moreland, W. J. Raymer, and R. L. Etter, *Dis. Chest*, **45**, 75 (1974).

(3) D. P. Nicholson and T. W. Chick, *Am. Rev. Respir. Dis.*, **108**, 241 (1973).

(4) P. A. Mitenko and R. I. Ogilvie, *N. Engl. J. Med.*, **289**, 600 (1973).

(5) J. W. Jenne, E. Wyze, B. S. Rood, and R. M. MacDonald, *Clin. Pharmacol. Ther.*, **13**, 349 (1972).

(6) R. E. Notari, *J. Pharm. Sci.*, **62**, 865 (1973).

(7) A. A. Sinkula and S. H. Yalkowsky, *ibid.*, **64**, 3259 (1975).

(8) T. Higuchi and V. Stella, "Pro-drugs as Novel Drug Delivery Systems," ACS Symposium Series 14, American Chemical Society, Washington, D.C., 1975.

(9) H. K. Lee, Ph.D. thesis, University of Kansas, Lawrence, Kans., 1970.

(10) T. Higuchi, H. K. Lee, and I. H. Pitman, *Farm. Aikak.*, **80**, 55 (1971).

(11) D. W. Van Krevelen and P. J. Hoftijer, *Rec. Trav. Chim. Pays-Bas*, **67**, 563 (1948).

(12) T. K. Sherwood and R. L. Pigford, "Absorption and Extraction," McGraw-Hill, New York, N.Y., 1952, p. 327.

(13) H. S. Harnetand and B. B. Owen, "The Physical Chemistry of Electrolytic Solutions," 3rd ed., Reinhold, New York, N.Y., 1958, p. 453.

(14) T. C. Bruice and S. J. Benkovic, "Bioorganic Mechanisms," vol. I, Benjamin, New York, N.Y., 1966, p. 61.

(15) M. L. Bender, F. Chloupek, and M. C. Neven, *J. Am. Chem. Soc.*, **80**, 5384 (1958).

(16) E. Gaetigens and H. Morawetz, *ibid.*, **82**, 5328 (1960).

(17) A. N. Martin, J. Swarbrick, and A. Cammarata, "Physical Pharmacy," 2nd ed., Lea & Febiger, Philadelphia, Pa., 1969, p. 452.

(18) G. Astarita, "Mass Transfer with Chemical Reaction," Elsevier, New York, N.Y., 1967, p. 9.

ACKNOWLEDGMENTS

Supported jointly by G. D. Searle and Co. and INTERx Research Corp. Some of the work at the University of Kansas was supported by National Institutes of Health Grant GM 22357.

The authors deeply appreciate the cooperation of Dr. N. Bodor, Dr. K. B. Slaon, and Dr. Y. N. Kuo of INTERx Research Corp. and Mr. C. Kim of G. D. Searle & Co. for providing the 7,7′-succinylditheophylline. Thanks are also extended to Dr. Y. W. Chien, Searle Laboratories, for reviewing this manuscript.

Beneficial Effects of Methionine and Histidine in Aspirin Solutions on Gastric Mucosal Damage in Rats

JAMES K. LIM ˣ, PREM K. NARANG *, DENNIS O. OVERMAN, and ARTHUR I. JACKNOWITZ

Received March 10, 1978, from the *School of Pharmacy and Department of Anatomy, Medical Center, West Virginia University, Morgantown, WV 26506.* Accepted for publication August 3, 1978. *Present address: School of Pharmacy, University of Maryland, Baltimore, MD 21201.

Abstract □ Amino acids methionine and histidine, which are soluble in propylene glycol, were investigated for their purported beneficial effects on aspirin-induced gastric mucosal damage in the rat. The pathognomonic changes observed microscopically in the fundic region of the stomach of animals administered daily doses (100 mg/kg), for up to 15 days, of aspirin solutions (0.36 M) in propylene glycol incorporated with the amino acids were compared with those of animals given equivalent quantities of aspirin in an aqueous suspension combined with an aluminum hydroxide antacid. A "delayed" onset of aspirin-induced cellular damage due to the presence of amino acids, analogous to that associated with the use of antacids, was found as determined partly by differences in the staining ability of injured cells with hematoxylin and eosin.

Keyphrases □ Methionine—effect on aspirin-induced gastric mucosal damage in rats □ Histidine—effect on aspirin-induced gastric mucosal damage in rats □ Aspirin—induction of gastric mucosal damage in rats, effect of methionine and histidine □ Amino acids—methionine and histidine, effect of aspirin-induced gastric mucosal damage in rats □ Gastric mucosal damage—induced by aspirin in rats, effect of methionine and histidine

GI bleeding in normal subjects, but especially in patients afflicted with chronic GI lesions, can accompany aspirin ingestion (1, 2). Several mechanisms reported for the pathogenesis of these lesions involve aspirin administration by the intra- or extragastric route (3–5). Among the more significant factors in aspirin-induced gastric hem-

0022-3549/79/0300-0295$01.00/0
© 1979, American Pharmaceutical Association

the sink condition (compared with M_1 and M_2 in Table IV). The deviation from the slope of unity existed as long as some degree of the first term, $(D_A/X_L)A_0$, affected the dissolution rate. The break point difference can be explained by the differences between $k_{OH^-}[OH^-] - k_0$ and $(D_B/nX_L)B_L - (D_A/X_L)A_0$.

SUMMARY AND CONCLUSION

The prodrug, 7,7′-succinylditheophylline, was hydrolyzed with a half-life of about 10 sec in the physiological pH range. These hydrolysis studies suggested that the prodrug would hydrolyze very rapidly and release the parent molecule, theophylline, once it was dissolved.

The dissolution rate of 7,7′-succinylditheophylline was 35 times slower than that of theophylline under the same conditions, and its dissolution rate was independent of pH within the physiological pH range. Dissolution rate studies coupled with hydrolysis rate studies suggested that the dissolution process would be the rate-determining step to keep the steady-state release into solution (Scheme III).

$$\text{prodrug in solid} \xrightarrow[\text{slow process}]{\text{dissolution}} \text{prodrug in solution} \xrightarrow[\text{rapid process}]{\text{hydrolysis}} \text{parent drug in solution}$$

Scheme III

The saturation solubility of 7,7′-succinylditheophylline at 25° in water was estimated to be 1.63×10^{-3} M from the rate dissolution data. Under the same conditions, theophylline solubility was 4×10^{-2} M. From these results, it appears that 7,7′-succinylditheophylline might be a valuable candidate as a prolonged-release theophylline prodrug.

REFERENCES

(1) R. Maselli, G. L. Casal, and E. F. Ellis, *J. Pediatr.*, **76**, 777 (1970).

(2) R. H. Jackson, J. I. McHenry, F. B. Moreland, W. J. Raymer, and R. L. Etter, *Dis. Chest*, **45**, 75 (1974).

(3) D. P. Nicholson and T. W. Chick, *Am. Rev. Respir. Dis.*, **108**, 241 (1973).

(4) P. A. Mitenko and R. I. Ogilvie, *N. Engl. J. Med.*, **289**, 600 (1973).

(5) J. W. Jenne, E. Wyze, B. S. Rood, and R. M. MacDonald, *Clin. Pharmacol. Ther.*, **13**, 349 (1972).

(6) R. E. Notari, *J. Pharm. Sci.*, **62**, 865 (1973).

(7) A. A. Sinkula and S. H. Yalkowsky, *ibid.*, **64**, 3259 (1975).

(8) T. Higuchi and V. Stella, "Pro-drugs as Novel Drug Delivery Systems," ACS Symposium Series 14, American Chemical Society, Washington, D.C., 1975.

(9) H. K. Lee, Ph.D. thesis, University of Kansas, Lawrence, Kans., 1970.

(10) T. Higuchi, H. K. Lee, and I. H. Pitman, *Farm. Aikak.*, **80**, 55 (1971).

(11) D. W. Van Krevelen and P. J. Hoftijer, *Rec. Trav. Chim. Pays-Bas*, **67**, 563 (1948).

(12) T. K. Sherwood and R. L. Pigford, "Absorption and Extraction," McGraw-Hill, New York, N.Y., 1952, p. 327.

(13) H. S. Harnetand and B. B. Owen, "The Physical Chemistry of Electrolytic Solutions," 3rd ed., Reinhold, New York, N.Y., 1958, p. 453.

(14) T. C. Bruice and S. J. Benkovic, "Bioorganic Mechanisms," vol. I, Benjamin, New York, N.Y., 1966, p. 61.

(15) M. L. Bender, F. Chloupek, and M. C. Neven, *J. Am. Chem. Soc.*, **80**, 5384 (1958).

(16) E. Gaetigens and H. Morawetz, *ibid.*, **82**, 5328 (1960).

(17) A. N. Martin, J. Swarbrick, and A. Cammarata, "Physical Pharmacy," 2nd ed., Lea & Febiger, Philadelphia, Pa., 1969, p. 452.

(18) G. Astarita, "Mass Transfer with Chemical Reaction," Elsevier, New York, N.Y., 1967, p. 9.

ACKNOWLEDGMENTS

Supported jointly by G. D. Searle and Co. and INTERx Research Corp. Some of the work at the University of Kansas was supported by National Institutes of Health Grant GM 22357.

The authors deeply appreciate the cooperation of Dr. N. Bodor, Dr. K. B. Slaon, and Dr. Y. N. Kuo of INTERx Research Corp. and Mr. C. Kim of G. D. Searle & Co. for providing the 7,7′-succinylditheophylline. Thanks are also extended to Dr. Y. W. Chien, Searle Laboratories, for reviewing this manuscript.

Beneficial Effects of Methionine and Histidine in Aspirin Solutions on Gastric Mucosal Damage in Rats

JAMES K. LIM ˣ, PREM K. NARANG *, DENNIS O. OVERMAN, and ARTHUR I. JACKNOWITZ

Received March 10, 1978, from the *School of Pharmacy and Department of Anatomy, Medical Center, West Virginia University, Morgantown, WV 26506.* Accepted for publication August 3, 1978. *Present address: School of Pharmacy, University of Maryland, Baltimore, MD 21201.

Abstract □ Amino acids methionine and histidine, which are soluble in propylene glycol, were investigated for their purported beneficial effects on aspirin-induced gastric mucosal damage in the rat. The pathognomonic changes observed microscopically in the fundic region of the stomach of animals administered daily doses (100 mg/kg), for up to 15 days, of aspirin solutions (0.36 M) in propylene glycol incorporated with the amino acids were compared with those of animals given equivalent quantities of aspirin in an aqueous suspension combined with an aluminum hydroxide antacid. A "delayed" onset of aspirin-induced cellular damage due to the presence of amino acids, analogous to that associated with the use of antacids, was found as determined partly by differences in the staining ability of injured cells with hematoxylin and eosin.

Keyphrases □ Methionine—effect on aspirin-induced gastric mucosal damage in rats □ Histidine—effect on aspirin-induced gastric mucosal damage in rats □ Aspirin—induction of gastric mucosal damage in rats, effect of methionine and histidine □ Amino acids—methionine and histidine, effect of aspirin-induced gastric mucosal damage in rats □ Gastric mucosal damage—induced by aspirin in rats, effect of methionine and histidine

GI bleeding in normal subjects, but especially in patients afflicted with chronic GI lesions, can accompany aspirin ingestion (1, 2). Several mechanisms reported for the pathogenesis of these lesions involve aspirin administration by the intra- or extragastric route (3–5). Among the more significant factors in aspirin-induced gastric hem-

0022-3549/79/0300-0295$01.00/0
© 1979, American Pharmaceutical Association

Table I—Composition of Various Aspirin Formulations Administered to Rats

Formulation	Aspirin, 6.5% (w/v) (0.36 *M*)	Histidine, 0.32% (w/v) (0.02 *M*)	Methionine, 0.30% (w/v) (0.02 *M*)	Propylene Glycol	Water	Antacid
I	+			+		
II	+	+		+		
III	+		+	+		
IV	+				+	
V[a]					+	+

[a] Contained 3.63% aspirin with 10 ml of antacid (60 mg/ml) and 1 ml of water.

orrhages were area and duration of contact of solid drug particles with mucosal cells (6). Consequently, efforts toward reducing these undesirable effects with solid or crystalline aspirin frequently have led to the concomitant use of buffering agents (7, 8) and the administration of freshly prepared solutions of aspirin in water (9).

The objective of the present study was to determine the advantages of a solution form of aspirin with and without "buffers" on experimentally induced gastric lesions in the rat. For stability reasons, a nonaqueous medium, propylene glycol[1], was used as the solvent. Methionine[2] and histidine[1] were investigated because of their solubility in propylene glycol. Furthermore, encouraging results have been ascribed to amino acids generally for reducing aspirin-induced gastric lesions (10–12).

The extent of gastric mucosal damage was examined carefully by light microscopy similar to that previously

Figure 1—*Fundic region of stomach of rat dosed daily with 100 mg of aspirin/kg in Formulation III for 15 days. Shown are intact epithelial lining cells (a), chief cells (b), and parietal cells (p). Overall gastric histology appears normal.*

[1] Fisher Scientific Co.
[2] Mann Research Laboratory.

Table II—Pharmacokinetic Parameters Estimated from Blood Plasma Salicylate Levels following Intubation of a Single Aspirin Dose (100 mg/kg) to Fasting Rats

Formulation	Peak Concentration, mg/ml	Peak Time, min	K_a, hr^{-1}	K_e, hr^{-1}	$t_{1/2}$, min	$AUC_{0-\infty}$, mg hr/ml
I	0.271	30	5.94	0.3080	135	0.6960
II	0.246	30	5.21	0.3035	137	0.6871
III	0.286	30	5.54	0.1979	210	1.0450
IV	0.126	45	3.78	0.3465	120	0.2828
V	0.120	48	2.19	0.2665	156	0.3560

described for the loss of staining intensity by the cytoplasmic matrix of injured epithelial cells with hematoxylin and eosin (13). For comparison, freshly prepared suspensions of aspirin[3] in water and of aspirin combined with a commercially available antacid, aluminum hydroxide suspension[4], were administered.

EXPERIMENTAL

Fifty-four male Wistar rats[5], 300–350 g, were divided into six groups of nine animals. Five groups each received one of the five formulations (Table I), and one group served as the control. At the outset, three animals were randomly selected from within a group and staggered for blood withdrawals to study the rate and extent of aspirin absorption following administration of only a single dose of each formulation. These partially bled animals were then returned to their original groups for further daily dosing with the respective aspirin formulations.

The pathognomonic changes resultant from the daily oral intubation

Figure 2—*Fundic region of stomach of control rat dosed daily with 0.5 ml of water/0.3 kg for 15 days. Shown are intact epithelial lining cells (a), chief cells (b), and parietal cells (p).*

[3] Amend Drugs and Chemicals, Irvington, N.J.
[4] Amphojel Suspension, Wyeth Laboratories, Philadelphia, Pa.
[5] Hilltop Laboratories, Scotsdale, Pa.

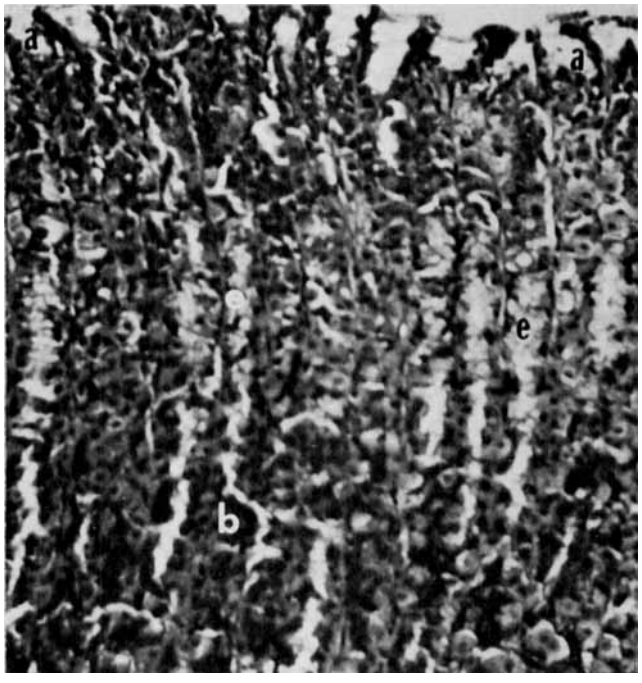

Figure 3—*Fundic region of stomach of rat dosed daily with 100 mg of aspirin/kg in Formulation II for 12 days. Shown are normal epithelial cells (a) and chief cells (b) but very few pale, unstained cells (e). General histology appears normal.*

of single doses of aspirin (100 mg/kg) for 7, 12, or 15 consecutive days (arbitrarily chosen) were derived from three animals sacrificed from each group, including controls, at the end of these designated periods. Routinely, all animals were lightly anesthetized with ether before intubation with the aspirin formulations and also prior to blood withdrawals by the orbital sinus puncture method (14). Animals were kept on regular chow diet and fasted 20–24 hr before the absorption experiment or prior to their sacrifice with a lethal dose of ether; they were allowed access to drinking water at all times.

At autopsy, after both the pylorus and esophagus were securely tied, a fixative solution was injected into the gastric cavity to prevent excessive wrinkling of tissues. With the stomach completely removed, small sections of its lesser and greater curvatures were obtained and dehydrated to be imbedded in paraffin. Sections from these tissues, 5–7 μm thick, subsequently were prepared for microscopic examination.

In the absorption studies, approximately 1 ml of blood was collected in heparinized centrifuge tubes from animals staggered at 10–180 min after oral intubation. These samples were stored at refrigeration temperature. For the analysis of aspirin, 0.5 ml of thawed blood was mixed with 6 ml of Trinder's reagent (15) and immediately centrifuged at 3000 rpm for 10 min to remove the precipitated proteins. A sufficient volume of the clear supernate was used for the absorbance measurement at 540 nm. The respective aspirin concentrations then were derived from a calibration graph prepared with 0.05–0.80 mg of sodium salicylate[1]/ml of deproteinized blood. All aspirin solution formulations were prepared by continuous agitation for 4–6 hr on a mechanical shaker[6] at ambient room temperatures until complete solution of the drug.

RESULTS

Histology of Gastric Mucosa—Figure 1 presents the typical normal appearance of a section in the fundic region of the stomach of rats dosed daily with Formulation III (Table I) for 15 consecutive days. It shows intact gastric epithelial lining cells, chief cells, and parietal cells analogous to those observed for control animals fed plain water (Fig. 2). Similarly, the general histology of animals given Formulation II daily for 12 days appeared normal, with only a few cells losing the ability to pick up the hematoxylin and eosin stain (Fig. 3).

In contrast, the fundic region of stomachs of animals dosed daily with IV for 7 (Fig. 4) and 15 (Figs. 5 and 6) days exhibited not only numerous pale cells but also engorged capillaries containing blood cells, rupturing lining epithelial cells and gastric glands in the later stages. A vast improvement was observed in the general histology of animals administered V. Numerous pale cells remained, but the lining gastric epithelial cells generally appeared intact (Fig. 7). A careful examination of corresponding sites in animals fed a single daily dose of a simple solution of aspirin in propylene glycol (I) for up to 12 days showed generally intact epithelial lining cells and some pale cells, closely analogous to those of Fig. 3.

[6] Model S3, Gyrotory, New Brunswick, N.J.

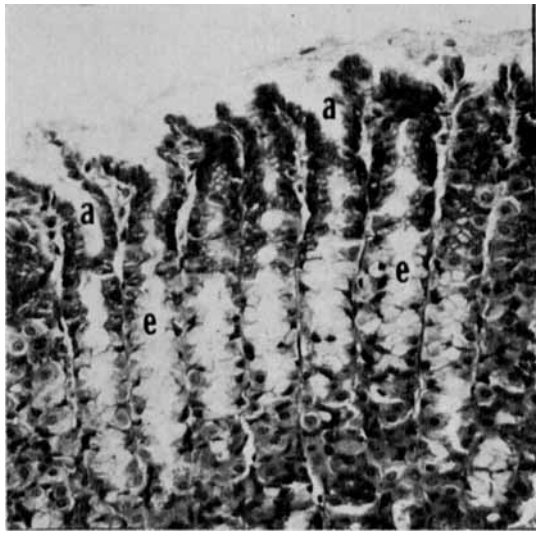

Figure 4—*Fundic region of stomach of rat dosed daily with 100 mg of aspirin/kg in Formulation IV for 7 days. Shown are normal epithelial lining cells (a) and numerous pale cells (e) that did not pick up the stain.*

Aspirin Absorption—Figure 8 illustrates the blood plasma salicylate concentrations reached at 10–180 min following administration of a single dose of aspirin in Formulations I–V. With solutions I–III, the salicylate levels peaked at about 30 min after oral intubation. In comparison, the salicylate peaks occurred after approximately 45–50 min with ingestion of suspensions IV and V.

On the basis of the area under the curve, *AUC*, the amounts of drug absorbed appeared significantly different between solutions and suspensions. The total amounts of aspirin "apparently" absorbed with I–III were three to four times greater than those obtained with IV and V. Again, the *AUC* of III, about 1.5 times greater than those of I and II, was relatively the largest because of a low elimination rate (Table II).

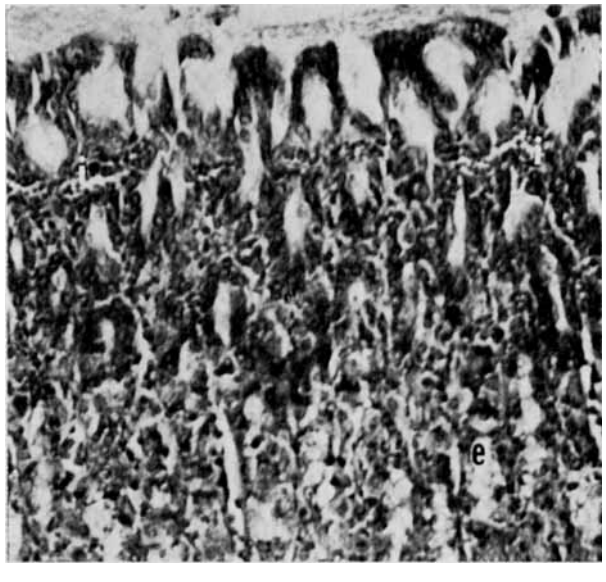

Figure 5—*Fundic region of stomach of rat dosed daily with 100 mg of aspirin/kg in Formulation IV for 15 days. Shown are pale cells (e) and numerous capillaries engorged with blood cells (i).*

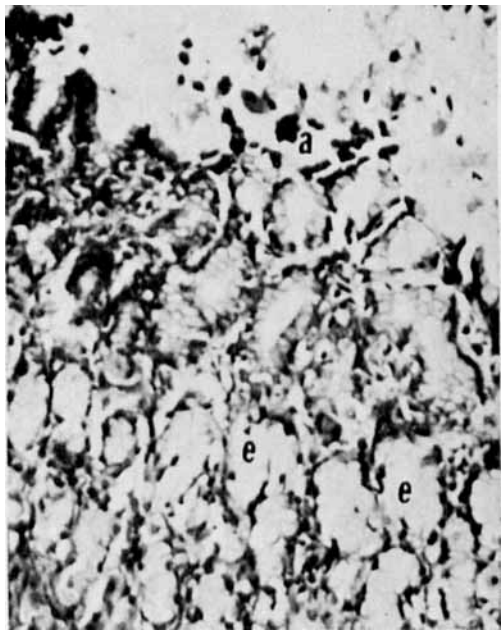

Figure 6—*Fundic region of stomach of rat dosed daily with 100 mg of aspirin/kg in Formulation IV for 15 days. Shown are broken and ruptured lining epithelial cells and gastric glands (a) and also pale cells (e).*

DISCUSSION

On the basis of the loss of staining ability by injured epithelial cells, described by Hingson and Ito (13) as the preliminary diagnostic stage leading to gastric ulceration, a histologic examination of the gastric mucosa tissue sections revealed that the daily oral administration for up to 15 days of single doses of an aspirin solution, aqueous or nonaqueous, produced comparatively less damage than the same dose given as a suspension in the rat. An enhanced beneficial effect due to the incorporation of methionine or histidine was seen with the solutions of aspirin in propylene glycol. This result parallels the observation of Aron *et al.* (16) on reduced fecal blood loss in humans and rats following ingestion of aspirin

Figure 7—*Fundic region of stomach of rat dosed daily with 100 mg of aspirin/kg in Formulation V for 15 days. Shown are intact epithelial lining cells (a), numerous pale cells (e), and an engorged capillary (i).*

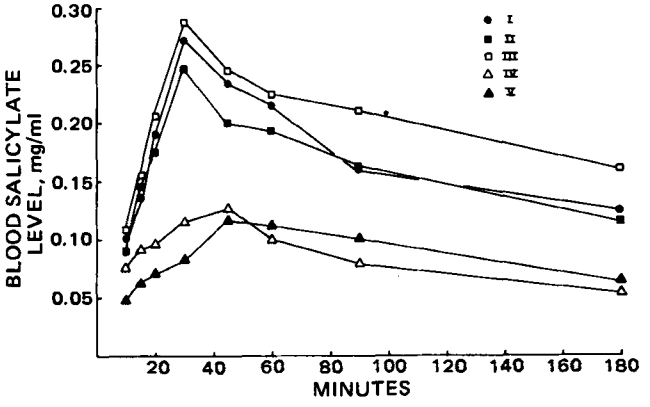

Figure 8—*Single-point plasma salicylate levels obtained at 10–180 min after administration of aspirin Formulations I–V.*

with another amino acid, lysine, as soluble lysine acetylsalicylate.

No data are available at present to elucidate the probable mechanism associated with the use of these amino acids. However, since amino acids represent "weak buffers," an analogous process attributed to the general use of antacids (8) probably occurred. Cooke (17) recently strongly suggested that hydrogen ions from unbuffered aspirin were responsible for the breakdown of the gastric mucosal barrier. A decrease in transmucosal potential difference attributed to an increase in the net passive fluxes of both hydrogen and sodium ions (18) was observed following aspirin-induced gastric mucosal damage. The present data support previous findings (19, 20) that the unionized aspirin molecule, not its ionized or salt form, is mainly responsible for these gastric injuries. In addition, the apparent "delay" in the onset of gastric damage in the rat from administration of an aspirin suspension with an antacid (≃2 mEq) resembles results with humans.

REFERENCES

(1) P. N. Wood, S. E. A. Harvey, and A. S. J. Dixon, *Br. Med. J.*, **1**, 669 (1962).

(2) M. I. Grossman, K. K. Matsumoto, and R. J. Lichter, *Gastroenterology*, **40**, 383 (1961).

(3) A. Weiss, E. R. Pitman, and E. C. Graham, *Am. J. Med.*, **31**, 266 (1961).

(4) A. Muir and I. A. Cossar, *Br. Med. J.*, **2**, 7 (1955).

(5) R. Bugat, M. R. Thompson, D. Aures, and M. I. Grossman, *Gastroenterology*, **71**, 754 (1976).

(6) J. R. Leonards and G. Levy, *Clin. Pharmacol. Ther.*, **8**, 400 (1967).

(7) *Ibid.*, **10**, 571 (1969).

(8) J. R. Leonards and G. Levy, *Drug Ther.*, **2**, 78 (1972).

(9) J. R. Leonards and G. Levy, *J. Pharm. Sci.*, **58**, 1277 (1969).

(10) S. Okabe, K. Takeuchi, K. Honda, and K. Takagi, *Digestion*, **14**, 85 (1976).

(11) W. H. Steinberg, H. H. Hastings, P. G. Pick, and J. S. Lazar, *J. Pharm. Sci.*, **54**, 625 (1965).

(12) Frohlich, *Med. Klin.*, **33**, 933 (1937); through "United States Dispensatory," 25th ed., Lippincott, Philadelphia, Pa., 1960, p. 650.

(13) D. J. Hingson and S. Ito, *Gastroenterology*, **61**, 156 (1971).

(14) D. A. Sorg and B. Buckner, *Proc. Soc. Exp. Biol. Med.*, **115**, 1131 (1964).

(15) P. Trinder, *Biochem. J.*, **57**, 301 (1954).

(16) E. Aron, B. Delbarre, and J. C. Besnard, *Therapie*, **31**, 247 (1976).

(17) A. R. Cooke, *Aust. N.Z. J. Med. Suppl.*, **6**, 26 (1976).

(18) A. R. Cooke, *Am. J. Dig. Dis.*, **21**, 155 (1976).

(19) J. R. Leonards, *Gastroenterology*, **44**, 617 (1963).

(20) J. R. Leonards and G. Levy, *Arch. Intern. Med.*, **129**, 457 (1972).

ACKNOWLEDGMENTS

Abstracted in part from a thesis submitted by P. K. Narang to the Graduate School, West Virginia University, in partial fulfillment of the Master of Science degree requirements.

Kinetics and Mechanism of Hydrolysis of 1-(2′-Acetoxybenzoyl)-2-deoxy-α-D-glucopyranose, a Novel Aspirin Prodrug

ANWAR HUSSAIN ˣ, J. TRUELOVE, and H. KOSTENBAUDER

Received May 1, 1978, from the *College of Pharmacy, University of Kentucky, Lexington, KY 40506.* Accepted for publication August 7, 1978.

Abstract □ The formation rate of aspirin from the prodrug was determined as a function of the pH, temperature, and dielectric constant of the solvent spectrophotometrically and was confirmed by high-pressure liquid chromatography. Aspirin formation was first order with respect to the prodrug and zero order with respect to the hydroxide-ion concentrations. The hydrolysis rate was independent of buffer concentration but very sensitive to the dielectric constant of the solvents. The half-life for the formation of aspirin at 37° was 7 min. The activation energy for the hydrolysis was 23.7 kcal/mole. The results suggest that the hydrolysis of the prodrug to aspirin proceeds by an S_N1-type mechanism.

Keyphrases □ 1-(2′-Acetoxybenzoyl)-2-deoxy-α-D-glucopyranose—aspirin prodrug, kinetics and mechanism of hydrolysis, effect of pH, temperature, and dielectric constant □ Aspirin prodrug—kinetics and mechanism of hydrolysis, effect of pH, temperature, and dielectric constant □ Prodrugs, aspirin—kinetics and mechanism of hydrolysis, effect of pH, temperature, and dielectric constant □ Hydrolysis—aspirin prodrug, kinetics and mechanism, effect of pH, temperature, and dielectric constant

Oral administration of aspirin induces gastric irritation and bleeding (1–3) because of local irritation of the gastric mucosal membrane by the very acidic aspirin particles. One approach to minimizing this side effect is to mask the acidic carboxyl group of aspirin reversibly *via* a prodrug. Upon administration, the neutral derivative dissolves first and then hydrolyzes, generating aspirin in solution.

Classical esterification of the carboxyl group of aspirin results in nonirritating but insoluble species, which do not revert to aspirin. For example, the methyl ester of aspirin hydrolyzes to methyl salicylate (4). Another neutral aspirin derivative, aspirin anhydride, was absorbed slowly and incompletely (5) and was highly immunogenic (6).

An acylal-type derivative can lead to a prodrug that cleaves rapidly to aspirin (7). This report describes the hydrolysis kinetics of 1-(2′-acetoxybenzoyl)-2-deoxy-α-D-glucopyranose (I).

EXPERIMENTAL

Material and Equipment—Compound I was synthesized and characterized in this laboratory[1]. Prodrug I was characterized by elemental analysis.

Anal.—Calc. for $C_{15}H_{18}O_8$: C, 55.20; H, 5.57. Found: C, 55.35; H, 5.59.

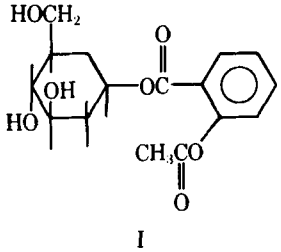

I

In addition, the ^{13}C-NMR, ^1H-NMR, and IR spectra are consistent with the structure of I. All reagents were of high quality; aspirin USP, spectral grade dioxane, deuterium chloride, and deuterium oxide were used without further purification.

A recording spectrophotometer[2] and a high-pressure liquid chromatograph[3] with a detector[4] were used. The instrument and column conditions for high-pressure liquid chromatographic (HPLC) analysis were: column, 2.6 mm i.d. × 3 × 0.5 m long, packed with pellicular polyamide adsorbent[5]; detector, UV at 254 or 280 nm; mobile phase, 1.7% phosphoric acid in water; flow rate, 1.5 ml/min; pressure, 1000–1100 psi; and internal standard, benzoic acid.

The concentration of aspirin generated from the prodrug was calculated from the peak height using a standard solution of aspirin. The pH of the solutions was measured using a research pH meter, and the temperature was maintained constant at the desired value using a circulating water bath.

Kinetic Measurements—The I hydrolysis rate was determined by the spectrophotometric method. Solutions of about 5 mg of com-

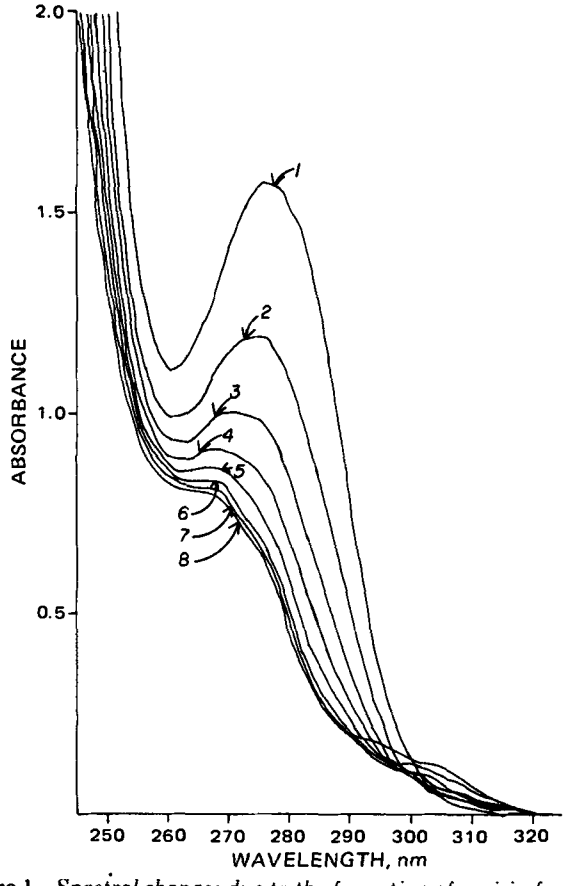

Figure 1—*Spectral changes due to the formation of aspirin from the prodrug as a function of time at 28° and pH 6. Key (elapse time from t_0 in minutes): 1, 0; 2, 20; 3, 40; 4, 60; 5, 80; 6, 100; 7, 120; and 8, 140.*

[1] A. Hussain, J. Truelove, and H. Kostenbauder, unpublished work.

[2] Cary model 15.
[3] Elmer model 1220.
[4] DuPont model 835.
[5] Pellamidon, Catalog No. A008, ReeveAngel Co., Clifton, N.J.

0022-3549/79/0300-0299$01.00/0
© 1979, American Pharmaceutical Association

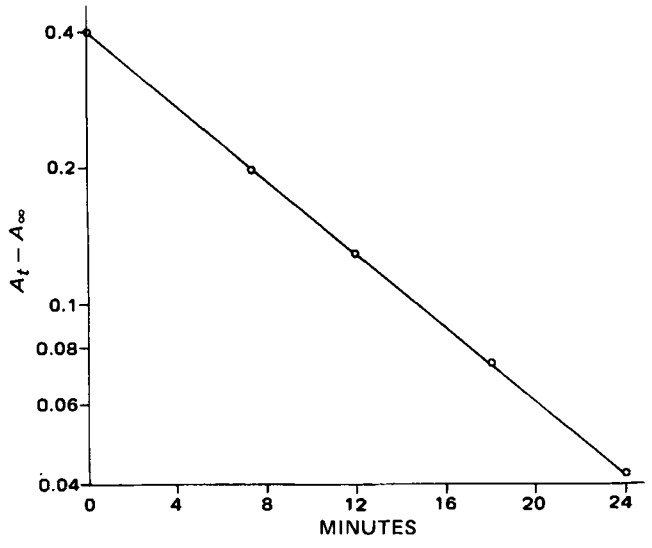

Figure 2—*First-order plot for the hydrolysis of the prodrug to aspirin at pH 6 and 28°.*

pounds/ml were prepared and maintained at 25, 27, 30, or 37° in a circulating water bath. At appropriate time intervals, 200 μl of the reaction mixture was added to 3 ml of buffer at the desired pH in a 1-cm path length spectrophotometer cell; after inverting the cell several times to ensure a uniform mixture, the absorbance was observed at 285 nm against a blank consisting of the buffer only.

Observed first-order rate constants were obtained by linear regression analysis of log $[A_t - A_\infty] = k/2.303(t) + b$[6]. In some cases, where the absorbance value at time infinity (seven half-lives) was not available due to conversion of aspirin to salicylic acid, rate constants were obtained by linear regression analysis of log $[\Delta A/\Delta t] = k/2.303(t) + b$.

To verify that the decreasing absorbances observed in the spectrophotometric method were indeed the result of generation of aspirin from the prodrug, an HPLC experiment was performed.

A solution of the prodrug at the desired pH was maintained at 22°, and 4-μl aliquots were injected periodically onto the column. The aspirin appearance rate was then estimated from the slope of the line of points generated by plotting log aspirin [peak height ($t = \infty$) − peak height (t)] *versus* time.

Buffers employed were hydrochloric acid (pH 1–2), citrate (pH 3), acetate (pH 4–6), and phosphate (pH 7–9). Ionic strength was adjusted with potassium chloride (usually to 0.1). In addition, a buffer dilution experiment was carried out with acetate buffers at pH 4.75 and a constant ionic strength (1 *M*) over a 10-fold concentration range.

Solvent dielectric effects were determined at 37° with solutions of dioxane in acetate buffer (pH 4.75) at concentrations of 0, 10, 20, and 25% (v/v) dioxane. The dielectric constants of the mixtures were taken to be those of Akerlof and Short (8). Solvent deuterium isotope effects were determined at 25° and pD values of 5.2 and 1.35 utilizing acetate–deuterium chloride and deuterium chloride buffers, respectively.

All pH measurements were made with a research pH meter with a glass

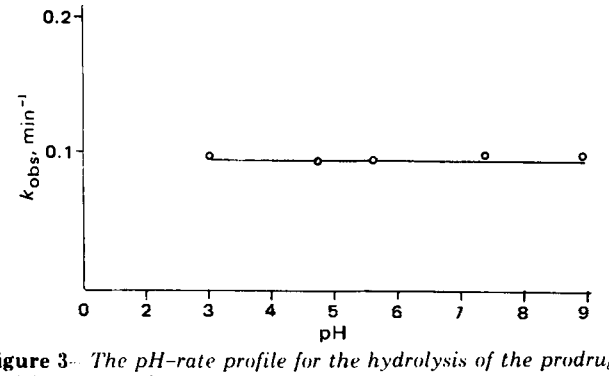

Figure 3—*The pH–rate profile for the hydrolysis of the prodrug to aspirin at 37° and μ = 0.1.*

[6] Wang program 1000-2-ST3.

Table I—Half-Lives of Hydrolysis of I to Aspirin as a Function of pH at 37°

pH	$t_{1/2}$[a], min
3	7
4.6	7.1
6.4	7.0
8	7.02
9	7.0

[a] Each value is the average of three determinations.

electrode[7]. The glass electrode gives the correct pH reading in dioxane–water mixtures. For deuterium oxide solutions, the relationship pD = pH meter reading +0.4 was employed (9).

RESULTS

The hydrolysis rate of the prodrug to aspirin was followed spectrophotometrically at 285 nm. Figure 1 shows the change in absorbance as a function of time at pH 6 and 28°. Figure 2 shows a first-order plot of $A_t - A_\infty$ *versus* time. To obtain an independent check on the spectrophotometric data, the hydrolysis rate also was determined by HPLC by measuring aspirin appearance as a function of time.

A semilog plot of aspirin [peak height ($t = \infty$) − peak height (t)] *versus* time resulted in a straight line. Furthermore, at the completion of the reaction, 1 mole of aspirin was formed from every mole of the prodrug. Figure 3 and Table I show the effect of pH on the prodrug hydrolysis rate. Figure 4 shows the effect of the dielectric constant of the solvent on the I hydrolysis rate.

The effect of temperature also was determined at pH 5.6 (Fig. 5). The activation energy was 23.7 kcal/mole, and the entropy of activation was +5 eu. The solvent deuterium isotope effect, determined at 25° and pD 5.2, gave a ratio of 0.86 for k_{D_2O}/k_{H_2O}[8].

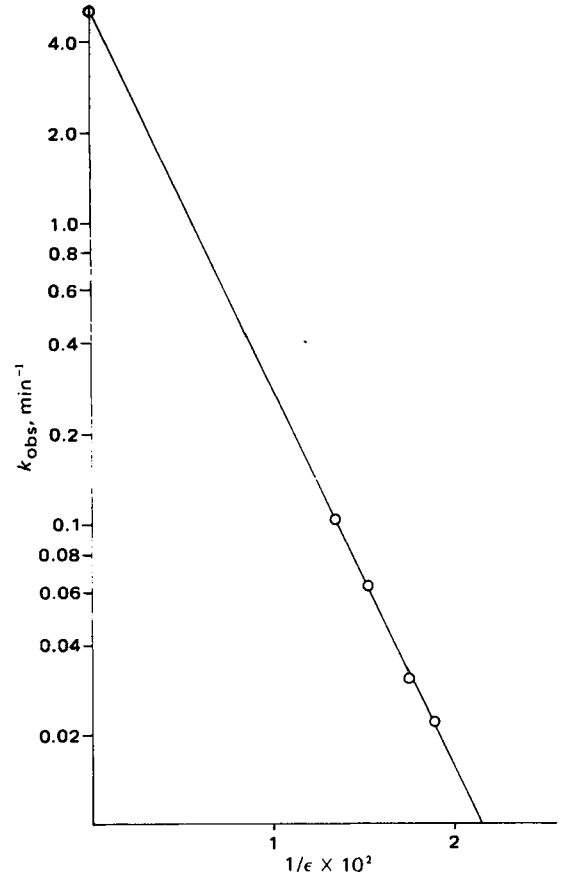

Figure 4—*Plot of the log of the observed rate of hydrolysis of the prodrug at pH 4.75, 37°, and μ = 1 as a function of 1/ε of the solvent.*

[7] Beckman model 1019.

[8] The observed first-order rates of hydrolysis of I at 25° in acetate-buffered deuterium chloride and water are 0.0170 and 0.0198 min^{-1}, respectively.

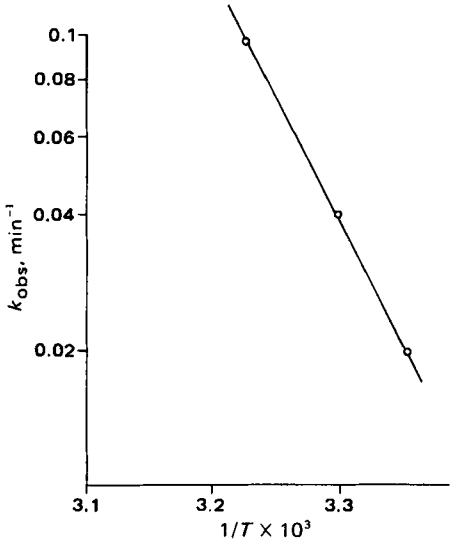

Figure 5—*Arrhenius plot for the hydrolysis of the prodrug at pH 5.6.*

Buffer concentrations of up to 1 *M* acetate buffer at pH 5.4 did not affect the hydrolysis rate.

DISCUSSION

The hydrolysis of the prodrug to aspirin followed first-order kinetics. The most likely mechanism occurring in the pH 3–9 range is an uncatalyzed unimolecular decomposition. The absence of buffer catalysis and the slightly positive entropy of activation make catalysis by water unlikely (10). Additionally, the pronounced effect of the solvent dielectric constant on the hydrolysis rate provides evidence for increasing separation of changes in the transition state. Finally, the absence of a significant solvent deuterium isotope effect provides evidence that specific acid catalysis is not occurring at this pH range.

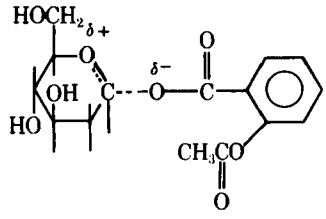

II

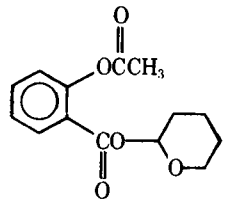

III

Based on these data, it is possible that I hydrolysis proceeds *via* the formation of the charged intermediate (II), which then undergoes simple CO bond cleavage, generating aspirin. In the same pH range, the hydrolysis rate of the corresponding pyran derivative (III) proceeds by a factor of 60 times faster than prodrug I[1].

The data presented show that the transient blocking of the acidic carboxylic group of aspirin by formation of deoxyglucose acylal-linked derivatives can result in a prodrug that regenerates aspirin at an acceptable rate independent of pH. Such a compound could potentially reduce the GI liability of aspirin by presenting a neutral molecule to the gastric membrane. Plans are underway to test this concept *in vivo*.

REFERENCES

(1) J. P. Leonards and G. Levy, *J. Pharm. Sci.*, **59**, 1511 (1970).

(2) K. W. Anderson, *Arch. Int. Pharmacodyn. Ther.*, **152**, 379 (1964).

(3) C. Davison, D. H. Hertig, and R. DeVine, *Clin. Pharmacol. Ther.*, **7**, 329 (1966).

(4) T. S. Pierre and W. P. Jencks, *J. Am. Chem. Soc.*, **90**, 3817 (1968).

(5) G. Levy and B. A. Gagliardi, *J. Pharm. Sci.*, **52**, 730 (1963).

(6) A. DeWeck, *Int. Arch. Allergy*, **41**, 393 (1971).

(7) A. Hussain, M. Yamasaki, and J. E. Truelove, *J. Pharm. Sci.*, **63**, 627 (1974).

(8) G. Akerlof and O. Short, *J. Am. Chem. Soc.*, **58**, 1241 (1936).

(9) R. G. Bates, "Determination of pH Theory and Practice," Wiley, New York, N.Y., 1967.

(10) A. Brown and T. C. Bruice, *J. Am. Chem. Soc.*, **95**, 1593 (1973).

Kinetics and Mechanism of Reaction of *m*-Nitrobenzhydrazide and Other Hydrazines with Acetic Acid

THOMAS MEDWICK ˣ **and HAMED M. ABDOU** *

Received June 20, 1977, from the *College of Pharmacy, Rutgers—the State University of New Jersey, New Brunswick, NJ 08903.* Accepted for publication August 31, 1978. * Present address: E. R. Squibb & Sons, New Brunswick, NJ 08903.

Abstract □ A comprehensive kinetic study was conducted of the reactions of *m*-nitrobenzhydrazide and some other hydrazines with acetic acid. The overall reaction rate for all of the compounds studied followed pseudo-first-order kinetics. The temperature dependence of the *m*-nitrobenzhydrazide degradation reaction was determined. The reaction rate dependence on the acetic acid concentration was found to be close to first order. High-pressure liquid chromatography was used extensively in identifying and measuring the appearance or disappearance rates of *m*-nitrobenzhydrazide degradation products in acetous solution. With *m*-nitrobenzhydrazide, the major degradation products were *N,N'*-bis(*m*-nitrobenzoyl)hydrazine, *N*-acetyl-*N'*-*m*-nitrobenzoylhydrazine, diacetylhydrazine, and hydrazine. The concentration profiles of these products in solution suggested a complex mechanism by which hydrazides react with acetic acid. All eight rate constants at 61° in the suggested mechanism were calculated by an approximation method based on experimental data. The findings in the present study indicate that acetic acid is to be avoided as a solvent for hydrazine derivatives.

Keyphrases □ *m*-Nitrobenzhydrazide—kinetics and mechanism of reaction with acetic acid □ Hydrazine derivatives—kinetics and mechanism of reaction with acetic acid □ Kinetics—reactions of hydrazines with acetic acid

Hydrazides and other hydrazine derivatives constitute a large and important class of organic compounds and have long been used in the chemical and pharmaceutical fields. In analytical chemistry, they are used as good quantitative carbonyl reagents. Although hydrazides are weaker bases than other hydrazine derivatives and, therefore, possess

0022-3549/79/0300-0301$01.00/0
© 1979, American Pharmaceutical Association

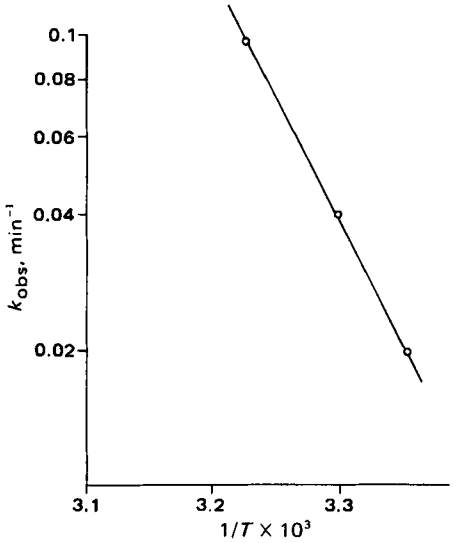

Figure 5—*Arrhenius plot for the hydrolysis of the prodrug at pH 5.6.*

Buffer concentrations of up to 1 *M* acetate buffer at pH 5.4 did not affect the hydrolysis rate.

DISCUSSION

The hydrolysis of the prodrug to aspirin followed first-order kinetics. The most likely mechanism occurring in the pH 3–9 range is an uncatalyzed unimolecular decomposition. The absence of buffer catalysis and the slightly positive entropy of activation make catalysis by water unlikely (10). Additionally, the pronounced effect of the solvent dielectric constant on the hydrolysis rate provides evidence for increasing separation of changes in the transition state. Finally, the absence of a significant solvent deuterium isotope effect provides evidence that specific acid catalysis is not occurring at this pH range.

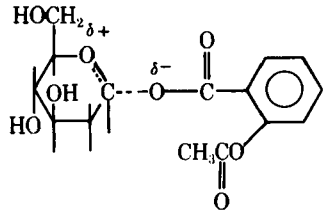

II

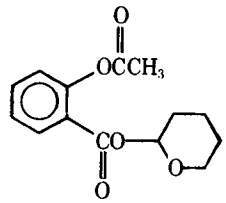

III

Based on these data, it is possible that I hydrolysis proceeds *via* the formation of the charged intermediate (II), which then undergoes simple CO bond cleavage, generating aspirin. In the same pH range, the hydrolysis rate of the corresponding pyran derivative (III) proceeds by a factor of 60 times faster than prodrug I[1].

The data presented show that the transient blocking of the acidic carboxylic group of aspirin by formation of deoxyglucose acylal-linked derivatives can result in a prodrug that regenerates aspirin at an acceptable rate independent of pH. Such a compound could potentially reduce the GI liability of aspirin by presenting a neutral molecule to the gastric membrane. Plans are underway to test this concept *in vivo*.

REFERENCES

(1) J. P. Leonards and G. Levy, *J. Pharm. Sci.*, **59**, 1511 (1970).

(2) K. W. Anderson, *Arch. Int. Pharmacodyn. Ther.*, **152**, 379 (1964).

(3) C. Davison, D. H. Hertig, and R. DeVine, *Clin. Pharmacol. Ther.*, **7**, 329 (1966).

(4) T. S. Pierre and W. P. Jencks, *J. Am. Chem. Soc.*, **90**, 3817 (1968).

(5) G. Levy and B. A. Gagliardi, *J. Pharm. Sci.*, **52**, 730 (1963).

(6) A. DeWeck, *Int. Arch. Allergy*, **41**, 393 (1971).

(7) A. Hussain, M. Yamasaki, and J. E. Truelove, *J. Pharm. Sci.*, **63**, 627 (1974).

(8) G. Akerlof and O. Short, *J. Am. Chem. Soc.*, **58**, 1241 (1936).

(9) R. G. Bates, "Determination of pH Theory and Practice," Wiley, New York, N.Y., 1967.

(10) A. Brown and T. C. Bruice, *J. Am. Chem. Soc.*, **95**, 1593 (1973).

Kinetics and Mechanism of Reaction of *m*-Nitrobenzhydrazide and Other Hydrazines with Acetic Acid

THOMAS MEDWICK ˣ **and HAMED M. ABDOU** *

Received June 20, 1977, from the *College of Pharmacy, Rutgers—the State University of New Jersey, New Brunswick, NJ 08903.* Accepted for publication August 31, 1978. * Present address: E. R. Squibb & Sons, New Brunswick, NJ 08903.

Abstract □ A comprehensive kinetic study was conducted of the reactions of *m*-nitrobenzhydrazide and some other hydrazines with acetic acid. The overall reaction rate for all of the compounds studied followed pseudo-first-order kinetics. The temperature dependence of the *m*-nitrobenzhydrazide degradation reaction was determined. The reaction rate dependence on the acetic acid concentration was found to be close to first order. High-pressure liquid chromatography was used extensively in identifying and measuring the appearance or disappearance rates of *m*-nitrobenzhydrazide degradation products in acetous solution. With *m*-nitrobenzhydrazide, the major degradation products were *N,N'*-bis(*m*-nitrobenzoyl)hydrazine, *N*-acetyl-*N'*-*m*-nitrobenzoylhydrazine, diacetylhydrazine, and hydrazine. The concentration profiles of these products in solution suggested a complex mechanism by which hydrazides react with acetic acid. All eight rate constants at 61° in the suggested mechanism were calculated by an approximation method based on experimental data. The findings in the present study indicate that acetic acid is to be avoided as a solvent for hydrazine derivatives.

Keyphrases □ *m*-Nitrobenzhydrazide—kinetics and mechanism of reaction with acetic acid □ Hydrazine derivatives—kinetics and mechanism of reaction with acetic acid □ Kinetics—reactions of hydrazines with acetic acid

Hydrazides and other hydrazine derivatives constitute a large and important class of organic compounds and have long been used in the chemical and pharmaceutical fields. In analytical chemistry, they are used as good quantitative carbonyl reagents. Although hydrazides are weaker bases than other hydrazine derivatives and, therefore, possess

0022-3549/79/0300-0301$01.00/0
© 1979, American Pharmaceutical Association

less carbonyl affinity, they are still preferred as carbonyl reagents because of their stability when present as a free base.

In many cases, these reactions of hydrazides with carbonyls were carried out in an acetic acid medium (1–3) because of its enhancement of their basicity. In some instances, assays of hydrazides and other hydrazine derivatives were also performed in acetic acid (4, 5). A serious limitation of this solvent system, however, is the tendency of these compounds to lose their basicity and to degrade rapidly in acetous solution. This degradation process was reported earlier (2, 3, 6), but its mechanism and the degradation products involved have not been studied. In recent work (7) in these laboratories, the reaction kinetics of hydrazine (I) and monoacetylhydrazine (II) with acetic acid were found to behave according to a complex mechanism in which diacetylhydrazine (III) was the main degradation product.

In the present study, the reaction kinetics of some other hydrazines and hydrazides with acetic acid were thoroughly investigated to establish a general mechanism by which most of these compounds degrade. The disappearance rate of a group of compounds in acetous solution was determined by potentiometric titration. However, potentiometric titrations are limited because of their inability to measure the quantities of each degradation product. Thus, potentiometry was used together with TLC and high-pressure liquid chromatography (HPLC) to study a representative compound, *m*-nitrobenzhydrazide (IV).

The degradation of IV was studied in solutions of different acetic acid concentrations in chloroform to establish the rate order with respect to acetic acid. The temperature dependence of the reaction was established. The degradation products were identified, and their disappearance or appearance rates were measured using HPLC. On this basis, a complex kinetic mechanism is suggested to account for the various rates. Approximation methods were used to calculate all rate constants.

EXPERIMENTAL

Reagents, Chemicals, and Solutions—All chemicals were reagent grade unless otherwise specified.

Benzenesulfonylhydrazine[1], 4-phenyl-3-thiosemicarbazide[2], *p*-nitrophenylhydrazine[2], and *p*-bromophenylhydrazine[2] were used as received. Phenylhydrazine[2] was distilled under reduced pressure and nitrogen prior to use.

Semicarbazide (mp 91–95°) was formed by reacting the hydrochloride[2] with sulfuric acid, removing the water under reduced pressure, and reacting the resultant, dried sulfate salt with anhydrous liquid ammonia. The formed ammonium sulfate precipitated and was filtered off; the filtrate was allowed to stand in the hood so that the ammonia would evaporate. The crude semicarbazide was recrystallized from absolute ethanol.

4-Phenylsemicarbazide[1] (mp 124–126°), *m*-nitrobenzhydrazide[2] (mp 153–155°), and *p*-nitrobenzhydrazide[2] (mp 210°) were recrystallized from water.

o-Nitrobenzhydrazide (mp 117–120°) was prepared by refluxing ethyl *o*-nitrobenzoate[1] with hydrazine[2] (97+%, anhydrous) in ethanol for 3 hr (ester to hydrazine molar ratio of 1:2). On cooling the solution, the hydrazide separated and was filtered off. The crude product was recrystallized from water.

Benzhydrazide (mp 110–112°) and *p*-bromobenzhydrazide (mp 165–166°) were prepared using ethyl benzoate[1] and methyl *p*-bromobenzoate[1], respectively, in the procedure described for *o*-nitrobenzhydrazide.

The hydrazine, acetic acid, salicylaldehyde, and solvents used and the syntheses of acethydrazide and diacetylhydrazine were described previously (7).

Synthesis of N-*Acetyl*-N′-m-*nitrobenzoylhydrazine* (*V*)—A mixture of 2.78 g of IV (0.015 mole) and 15 ml of acetic anhydride (0.18 mole) was refluxed for 2 hr. Then 15 ml of pyridine was added, and the reflux was continued for 4 more hr. The solution was evaporated under reduced pressure, and the remaining solid was dissolved in alcohol. The solution was kept in a refrigerator overnight, and brownish-yellow crystals precipitated. Light-yellow crystals (mp 192°), dried overnight *in vacuo*, were obtained by recrystallization from alcohol and then methanol.

The purity of V was corroborated by both TLC (100-μm silica, 7.5% isopropanol in chloroform, R_f 0.62) and HPLC (described later).

Synthesis of N,N′-*Bis*(m-*nitrobenzoyl*)*hydrazine* (*VI*)—To a 100-ml low actinic volumetric flask containing 50 ml of acetic acid, 5.45 g (0.03 mole) of IV was transferred. After the solid had dissolved, the flask was stoppered, the stopper closure was covered with aluminum foil, and the flask was left at room temperature in a closed cabinet. A flaky precipitate appeared on the 2nd day, and the quantity increased rapidly with time. After 10 days, the white precipitate was filtered off and recrystallized twice from hot acetic acid. After drying for 48 hr *in vacuo*, the dried crystals had a melting point of 242.2° [lit. (2) mp 242.0°].

The purity of VI was checked by HPLC (described later).

Acetous perchloric acid, about 0.1 *N*, was prepared according to Fritz (8).

α-Naphtholbenzein indicator solution was prepared by dissolving about 0.1000 g of the dye in enough acetic acid to make 100 ml.

Salicylaldehyde Reagent Solution—Exactly 50 ml of salicylaldehyde[1] was diluted to 100 ml with isopropanol.

Standard solutions for I, II, and IV–VI were prepared at concentration levels such as those encountered in the analysis for the respective compound, using the chromatographic mobile phase as the solution solvent. Except for I and II, all other solutions were used directly. Standard Solutions I and II were diluted as necessary and subjected to salicylaldehyde derivatization concomitantly with the kinetic samples undergoing analysis for I–III.

HPLC Mobile Phases and Columns—All mobile phases were filtered and degassed prior to use. The normal phase system for measurement of IV–VI consisted of 7.5% (v/v) isopropanol in chloroform and a 100-cm × 2-mm i.d. stainless steel tube packed manually with a pellicular silica gel[3] adsorbent.

The reversed-phase system for measurement of I–III consisted of 47% (v/v) acetonitrile in 0.14 *M* aqueous potassium dihydrogen phosphate and a 30-cm × 4-mm i.d. stainless steel tube packed with spherical siliceous microbeads, 5–10 μm, chemically bonded to a monomolecular layer of octadecyltrichlorosilane[4].

Instrumentation—The potentiometric titrations were carried out using the electrode system and the automatic potentiometric titrator (as used for IV) described by Medwick and Kirschner (9).

The modular HPLC instrument was described previously (7). All mobile phases were pumped at a flow rate of 1 ml/min.

Solutions were kept at a desired constant temperature in a water bath whose temperature was thermostatically controlled[5] to ±0.01° of the nominal setting.

Procedures—Throughout the described procedures, low actinic glass volumetric flasks and erlenmeyer flasks were used. For HPLC analysis, the appropriate standard solutions were run concomitantly with sample solutions.

Kinetic Studies—All kinetic runs were conducted in duplicate.

Solution Preparation and Sampling Acetous solutions (usually 0.06 *M*) of the hydrazine derivative were prepared by weighing accurately an appropriate quantity and dissolving it in and bringing to volume with acetic acid. The solution, usually kept at the temperature of the kinetic study in a water bath, was sampled at desired times, and the aliquots were transferred to suitable glassware for the analytical procedure.

For indicator titration or potentiometric titration, two 10.00-ml aliquots in separate 250-ml beakers were used. For the HPLC normal phase system (IV–VI analysis), two 2.00-ml aliquots in separate 10-ml volumetric flasks were used. For the HPLC reversed-phase system (I–III analysis), four 2.00-ml aliquots in separate 10-ml volumetric flasks were

[1] Eastman White Label.
[2] Matheson, Coleman and Bell.
[3] HC Pellosil, Whatman, Inc., Clifton, N.J.
[4] μBondapak C_{18}, Waters Associates, Milford, Mass.
[5] Lauda/Brinkmann circulator model K-2/RD.

Table I—Degradative Behavior of Some Aryl-, Carbamyl-, and Aroylhydrazines

Compound	Apparent First-Order Rate Constant, $sec^{-1} \times 10^6$
Arylhydrazines	
Phenylhydrazine	3.65
p-Bromophenylhydrazine	8.75
Carbamylhydrazines	
Semicarbazide	8.75
4-Phenylsemicarbazide	4.46
4-Phenyl-3-thiosemicarbazide	2.97
Aroylhydrazines (hydrazides)	
Benzhydrazide	2.01
o-Nitrobenzhydrazide	2.11
m-Nitrobenzhydrazide	1.67
p-Nitrobenzhydrazide	1.51
p-Bromobenzhydrazide	1.87

used. The aliquots were kept at 0.0° until sample collection for a particular run was completed and analyses were to be performed.

In the study of acetic acid dependence, six different 0.06 *M* IV solutions were prepared in solutions of varying pure acetic acid concentration in chloroform: 8.74, 5.25, 3.5, 1.75, and 0.874 *M*. The procedure was as described for the general case.

For analysis by indicator titration or potentiometric titration, the beakers were removed from the freezer, and 75 ml of acetic acid was added. The aliquots were titrated using α-naphtholbenzein indicator or according to the potentiometric titration procedure described by Medwick and Kirschner (9).

For HPLC analysis of IV–VI, the normal phase system was used for measurement. After the aliquots were removed from the freezer and brought to volume with the corresponding mobile phase, the solutions were analyzed by HPLC. Calculations were performed using:

$$W_u = \frac{H_u}{H_s} W_s p \qquad \text{(Eq. 1)}$$

where W_u is the weight, in grams, of the specified component in the sample solution; H_u is the peak height of the specified component in the sample chromatogram; H_s is the peak height of the specified component in the standard chromatogram; W_s is the weight, in grams, of the corresponding standard; and p is the purity of the standard, expressed as a decimal.

For HPLC analysis of I–III, the reversed-phase system was used for measurement. After the aliquots were removed from the freezer, 1.00 ml of isopropanol was added to each flask. The solutions were divided into two equal parts. The first half was used for measuring the amount of I and II in solution as follows. To each flask, 0.05 ml of the salicylaldehyde reagent was added (calculated to be an approximate 50% stoichiometric excess), and the flasks were then transferred to a 55° water bath for 5 min to ensure complete derivatization. The flasks were then removed, and 4.00 ml of chloroform was added to each. Finally, all solutions were brought to volume with methanol and analyzed.

The second half of the solution was used for the determination of III in solution as follows. To each flask, 2.00 ml of aqueous alcoholic hydrochloric acid was added, and the flasks were then immersed in a 60° water bath for 5 min. The flasks were then removed, and 0.05 ml of the salicylaldehyde reagent was added to each. The flasks were treated afterward in the same manner as for I and II analysis. The quantity of III in solution was calculated as the difference between the total amount of I after hydrolysis and the amount of I and II obtained from a nonhydrolyzed sample.

RESULTS AND DISCUSSION

Kinetic Studies—Because of its accuracy and simplicity, potentiometric titration was used to determine the apparent overall pseudo-first-order rate constants (Table I) for the reactions of several hydrazine derivatives with acetic acid. These data establish the nature of the reaction and show, as expected, that hydrazides are generally more stable than other hydrazines, probably due to their weak basicity. Within hydrazides as a separate group, stability increased as the acidity of the parent acid increased, so *p*-bromobenzhydrazide (pKa 3.97) had a faster rate of degradation than *p*-nitrobenzhydrazide (pKa 3.42).

Since the potentiometric analysis cannot identify or measure the different degradation products, TLC was explored. A partially degraded solution of IV was spotted on a TLC plate (100-μm silica) with 7.5% isopropanol in chloroform as a mobile phase. The following compounds were identified after spraying with Ehrlich's reagent: I (R_f 0.05), II (R_f 0.40), V (R_f 0.62), VI (R_f 0.65), and IV (R_f 0.50). After spraying the plate with aqueous alcoholic hydrochloric acid, another spot was identified as III (R_f 0.58). Attempts to use TLC quantitatively were unsuccessful because of the incomplete resolution of the spots and the rapid volatilization of hydrazine from the plate.

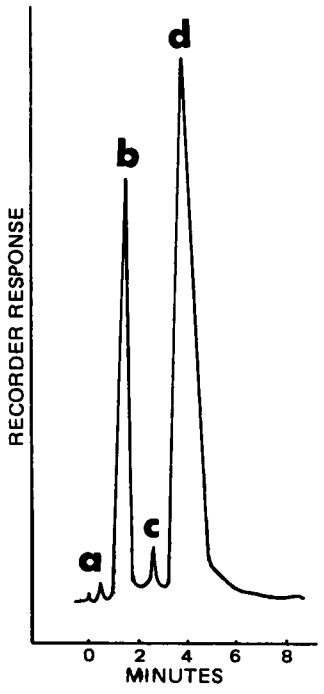

Figure 1—*HPLC analysis of* m-*nitrobenzhydrazide (IV) acetous solution at room temperature (after 6 hr) on pellicular silica with 7.5% isopropanol in chloroform as the mobile phase. Key: a, solvent; b,* N,N′-*bis*(m-*nitrobenzoyl)hydrazine (VI); c,* N-*acetyl*-N′-m-*nitrobenzoylhydrazine (V); and d,* m-*nitrobenzhydrazide (IV).*

HPLC was used successfully to quantitiate every component in solution. An HPLC system in the normal phase was developed to quantitate IV–VI. Figure 1 is a typical chromatogram. The chromatographic response for every compound was linear with a linear regression correlation coefficient of 0.999. The minimum limits of detectability were 6.1×10^{-5} *M* for VI, 1.79×10^{-4} *M* for V, and 2.8×10^{-4} *M* for IV. This system, however, can neither detect nor quantitate I–III because these compounds do not absorb UV radiation, as is required by the 254-nm detector. A refractive index detector was also inadequate for the trace analysis required in this study.

For these reasons, another system was developed whereby the salicylaldehyde derivatives of I and II (and of III after hydrolysis) were formed and separated on an HPLC reversed-phase column. The salicylaldehyde derivative of IV plus V and VI (both do not react with salicylaldehyde) also was resolved completely from the I and II derivatives, but the behavior of IV–VI did not allow their determination with this HPLC system. Figure 2 is a chromatogram showing the separation achieved using the reversed-phase system. The chromatographic response for both I and II was linear with concentration since both responses gave linear regression correlation coefficients of 0.9999; the minimum detectable quantities for I and II were 5×10^{-5} and 4.85×10^{-4} *M*, respectively.

Table II shows the temperature dependence of the IV reaction with acetic acid using HPLC analysis. HPLC analysis is specific in measuring a single compound whereas potentiometric analysis measures the total basicity of the solution; *i.e.*, any basic degradation product such as I or II would be titrated along with IV, so values of the rate constants would be inaccurate.

Table III describes the role of acetic acid concentration in the degradation of IV in acetous solution. Although the degradation reaction overall kinetics in excess acetic acid were pseudo-first order with respect to IV, the rate increased with the increase in the acetic acid concentration. An expression involving dependence on the acetic acid concentration may be written as:

$$\text{rate} = k'[\text{IV}] = k[\text{IV}][\text{HOAc}]^n \qquad \text{(Eq. 2)}$$

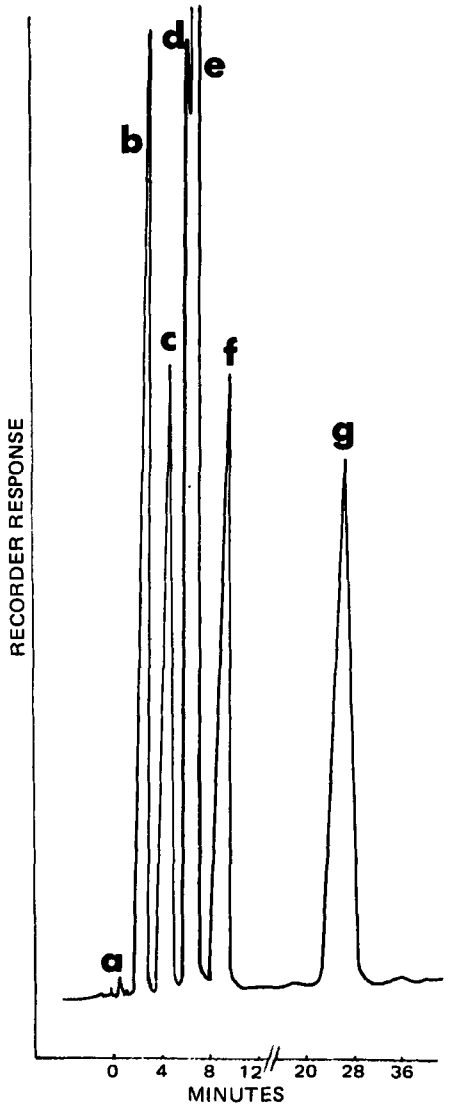

Figure 2—*Chromatogram of a synthetic mixture of the compounds to be found in a degraded acetous solution of* m-*nitrobenzhydrazide after derivatization with salicylaldehyde and using a reversed-phase column and acetonitrile (47%)-0.14 M potassium dihydrogen phosphate (53%) as the mobile phase. Key: a, solvent; b,* N-*acetyl-*N′-m-*nitrobenzoylhydrazine (V); c, salicylaldehyde acethydrazone; d,* N,N′-*bis*(m-*nitrobenzoyl)hydrazine (VI); e, salicylaldehyde (excess); f, salicylaldehyde* m-*nitrobenzhydrazone; and g, salicylaldazine.*

It is noticed that $k' = k[\text{HOAc}]^n$. Taking the logarithm results in:

$$\log k' = \log k + n \log [\text{HOAc}] \qquad \text{(Eq. 3)}$$

where k' = pseudo-first-order rate constant, k = true bimolecular rate constant, and n = relative order with respect to acetic acid.

When log k' was plotted *versus* log [HOAc], the linear least-squares parameters calculated were correlation coefficient 0.995 and intercept of 1.74×10^{-7} sec^{-1} (after taking the antilog). The calculated bimolecular rate constant was 2.90×10^{-6} liter mole^{-1} sec^{-1}. The slope value of n, the order relative to acetic acid, was calculated to be 0.82 by HPLC and 1.3 by potentiometric titration analysis; both values were close to first order.

The HPLC determination of the appearance and/or disappearance rates of the IV degradation products in acetic acid was conducted at 61°. This temperature was chosen since the I and II reaction with salicylaldehyde is very rapid at 60°. Thus, no temperature disturbance is introduced during analytical manipulations.

The reaction profiles of IV, I, V, and III are presented in Fig. 3. Although VI appeared almost instantaneously in acetous solutions of IV and increased regularly with time, it started to precipitate after about 3 hr due to its insolubility in acetic acid. Therefore, no accurate plot could be constructed for its appearance rate. Compound II, on the other hand, was not detected at any time in solution, even though the lower limit for its detection by the HPLC system was 4.85×10^{-4} *M*. As shown in Fig. 3, the IV concentration decreased regularly whereas I decreased after an initial increase. Both V and III increased monotonically with time.

Table II—Temperature Dependence of Degradation of IV in Acetic Acid Using HPLC Analysis

Temperature	First Order[a], $k \times 10^6$ sec^{-1}	E_a[b], kcal/mole
25.0°	2.06 (0.99)	
32.0°	3.39 (0.98)	14.7
42.2°	8.93 (0.999)	
61.0°	38.63 (0.999)	

[a] Values represent the rate constant and, in parentheses, the linear regression correlation coefficient. [b] For this Arrhenius plot, the linear least-squares parameters are: correlation coefficient, 0.999; slope, −3200 degree sec^{-1}; and intercept, +3.93 sec^{-1}.

The shape of the concentration profile of III in Fig. 3 is a consequence of the complicated reaction sequence, as will be seen later, in that III is formed in Schemes III, VII, and VIII but Scheme VIII gives rise to I, which subsequently appears as III. The same shape curve was observed in the study of the reaction of I and II with acetic acid (7).

The mechanism to be proposed for the reactions of IV with acetic acid must account for the presence of each degradation product and explain its concentration profile.

Although VI was reported (2) to form as an oxidation product of IV, an oxidation mechanism was disregarded in the present study because the degradation rate of the hydrazine derivative did not differ significantly when its acetous solution was kept in a nitrogen atmosphere in sealed ampuls or in air. Sealed ampuls filled with an acetous solution of IV under reduced pressure were analyzed by GC for any released nitrogen gas (as an oxidation by-product); no excess nitrogen gas was found, again indicating that no oxidation was operative. Photocatalyzed degradation was also eliminated because the degradation study was conducted in the dark and with solutions in low actinic glassware. The dependence of degradation on the acetic acid concentration suggested a mechanism in which acetic acid plays an active role.

Proposed Mechanism—After fitting different mechanisms to the experimental data, one scheme was arrived at as the most plausible mechanism consistent with the findings in the present study.

In the proposed mechanism (Schemes I–VIII), eight elementary reactions occur in the reaction of IV with acetic acid:

$$\text{IV} + \text{HOAc} \xrightarrow{k_0} \text{IV}^*$$
Scheme I

$$\text{IV}^* \xrightarrow{k_1} \text{V} + \text{H}_2\text{O}$$
Scheme II

$$2\,\text{IV}^* \xrightarrow{k_2} \text{VI} + \text{III}$$
Scheme III

$$\text{IV} + \text{IV}^* \xrightarrow{k_3} \text{VI} + \text{II}$$
Scheme IV

$$2\,\text{IV} \xrightarrow{k_4} \text{VI} + \text{I}$$
Scheme V

$$\text{I} + \text{HOAc} \xrightarrow{k_5} \text{II} + \text{H}_2\text{O}$$
Scheme VI

$$\text{II} + \text{HOAc} \xrightarrow{k_6} \text{III} + \text{H}_2\text{O}$$
Scheme VII

$$2\,\text{II} \xrightarrow{k_7} \text{III} + \text{I}$$
Scheme VIII

(k_5 + HOAc)

In this sequence, IV* is an intermediate and acetic acid is present in large excess.

Rate equations consistent with the elementary equations and that reflect overall system stoichiometry are:

$$\frac{d\text{IV}}{dt} = -k_0[\text{IV}] - k_3[\text{IV}][\text{IV}^*] - 2k_4[\text{IV}]^2 \qquad \text{(Eq. 4)}$$

$$\frac{d\text{IV}^*}{dt} = k_0[\text{IV}] - k_1[\text{IV}^*] - k_2[\text{IV}^*]^2 - k_3[\text{IV}][\text{IV}^*] \qquad \text{(Eq. 5)}$$

$$\frac{dV}{dt} = k_1[IV^*] \quad \text{(Eq. 6)}$$

$$\frac{dVI}{dt} = \tfrac{1}{2}k_2[IV^*]^2 + k_3[IV][IV^*] + k_4[IV]^2 \quad \text{(Eq. 7)}$$

$$\frac{dIII}{dt} = \tfrac{1}{2}k_2[IV^*]^2 + 2k_6[II] + k_7[II]^2 \quad \text{(Eq. 8)}$$

$$\frac{dII}{dt} = k_3[IV][IV^*] + 2k_5[I] - 2k_6[II] - 2k_7[II]^2 \quad \text{(Eq. 9)}$$

$$\frac{dI}{dt} = k_4[IV]^2 - 2k_5[I] + k_7[II]^2 \quad \text{(Eq. 10)}$$

The solution of this complex reaction pattern is presented in the *Appendix*. Table IV lists calculated rate constants. The reactions using actual structures are presented in Scheme IX.

The k_4 reaction was included to explain the rapid appearance of I in solution, which could not be accounted for by the k_7 reaction alone.

The reason for suggesting an intermediate or a transition state as an alternative route for the formation of VI was dictated by the fact that the rapid appearance rate of III and its high concentration were too large to be coming only from I in an indirect manner. Compound III had to be formed directly. Another possible route was the reaction of 2 moles of V to give VI plus III; however, this possibility was eliminated when V was found to be stable in acetic acid and no significant amount of VI formed in acetous solutions of V. The k_3 reaction in the mechanism was found necessary for the quantities of VI calculated to be present.

The nature of the intermediate has to be related to both IV and acetic acid, and its intrinsic structure has to have the ability of yielding either V or VI and III very rapidly. To understand the chemical nature of the intermediate, experiments were carried out in which solutes were introduced to disturb the acetic acid autoprotolysis to observe the effect, if any, on the reaction kinetics.

Table III—Dependence of IV Degradation on Acetic Acid Concentration at 25.0° by HPLC Analysis

Acetic Acid in Chloroform, *N*	Pseudo-First Order[a], $k \times 10^7$ sec^{-1}
17.4 (pure acetic acid)	20.60 (0.99)
8.740	9.61 (0.99)
5.250	5.90 (0.998)
3.500	4.72 (0.98)
1.750	2.83 (0.97)
0.874	1.63 (0.99)

[a] Values represent the rate constant and, in parentheses, the linear regression correlation coefficient.

Sodium acetate, triphenylguanidine, strong bases, and benzoic acid, a weak acid, had no significant effect on the reaction rate of IV with acetic acid. Perchloric acid, a strong acid, decreased the rate sharply, depending on its concentration. This finding may be explained if it is recognized that perchloric acid ties up an equivalent amount of IV in the protonated form and thus decreases the effective concentration of unprotonated IV available for the degradation reaction with acetic acid.

Although the details of the kinetic calculations are given in the *Appendix*, the agreement between the experimental data and the proposed mechanism should be discussed, particularly in light of the approximations used to solve this complex system. If $k = 38.63 \times 10^{-6}$ at 61.0° is used from Table II together with the experimental value for [IV] of 0.0315 at 5 hr (Fig. 3), the time chosen for the calculations, the experimental value for the disappearance of IV may be calculated using:

$$\frac{dIV}{dt} = -k[IV] = 12.2 \times 10^{-7} \text{ mole sec}^{-1} \quad \text{(Eq. 11)}$$

Equation 4 reduces to first-order form since $-2k_4[IV]^2$ is small when

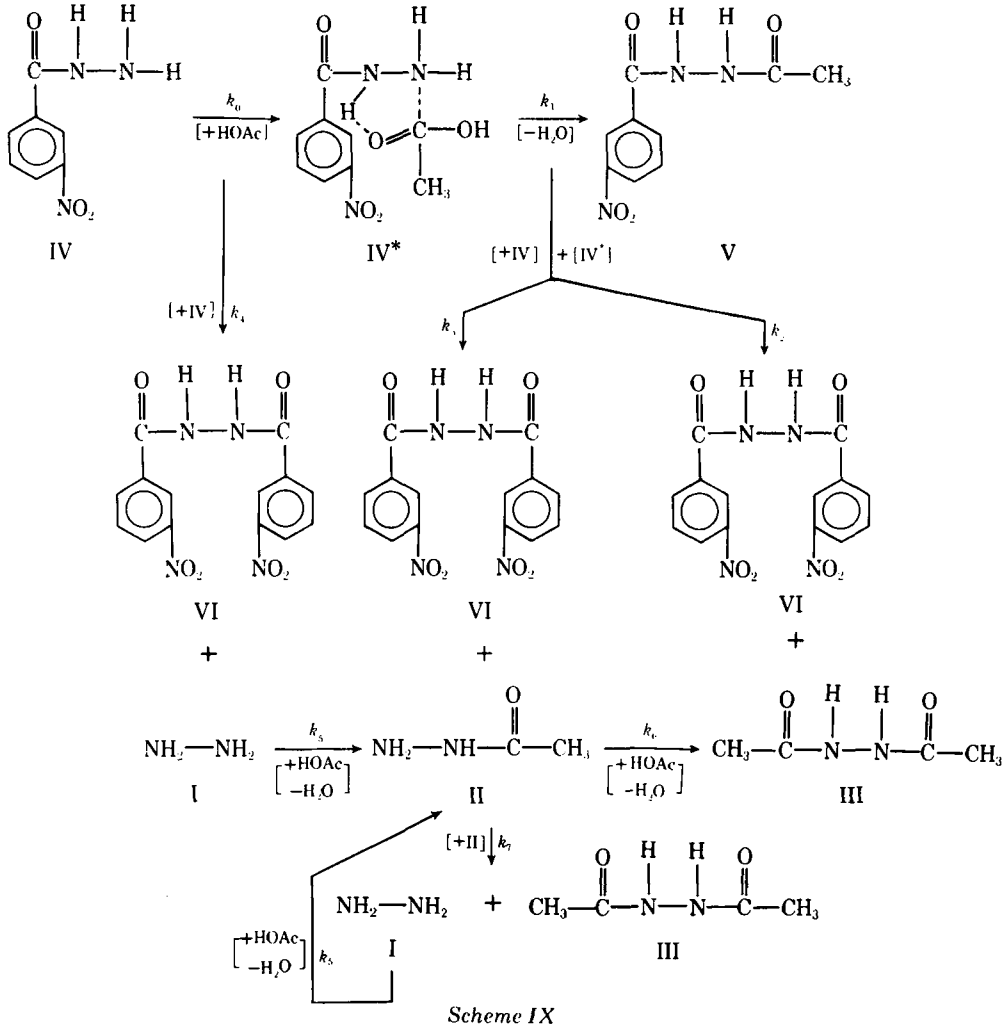

Scheme IX

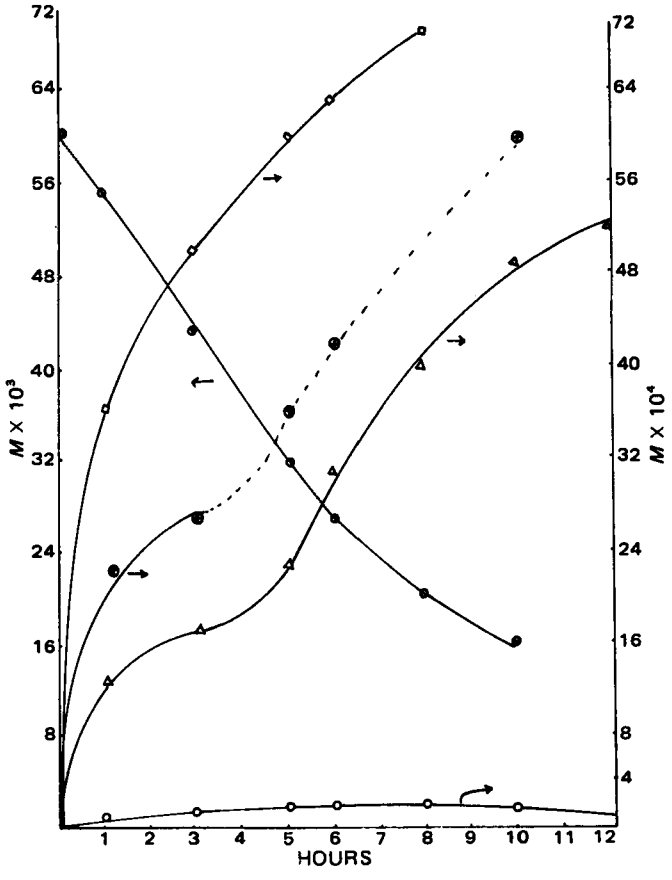

Figure 3—*Concentration profiles of* m-*nitrobenzhydrazide and its degradation products in acetic acid solution at 61°. Key:* ○, *I*, M × 10^{-4}; △, *III*, M × 10^{-4}; □, *V*, M × 10^{-4}; ⊘, *IV*, M × 10^{-3}; *and* ⊕, *VI*, M × 10^{-4}. *Compound VI precipitated from solution after 3 hr.*

the k values from Table IV, the linear least-squares line concentration at 5 hr from Fig. 3 for [IV] of 0.0345, and the [IV*] value of 2.52×10^{-3} M from Table V are used as in:

$$\frac{d\text{IV}}{dt} = -7.176 \times 10^{-7} - 3.558 \times 10^{-7} - 1.42 \times 10^{-7}$$

$$\cong -10.732 \times 10^{-7} \text{ mole sec}^{-1} \qquad \text{(Eq. 12)}$$

The value of $-2k_4[\text{IV}]^2$ constitutes only 13% of the total value of $d\text{IV}/dt$. Thus, since [IV*] is invariant owing to its steady state, the approximate form of Eq. 4 as a first-order rate equation may be written as:

$$\frac{d\text{IV}}{dt} = -[\text{IV}](k_0 + k_3[\text{IV}^*]) \qquad \text{(Eq. 13)}$$

When the least-squares value for [IV] from Fig. 3, the k_0 and k_3 values from Table IV, and the [IV*] value from Table V are substituted into Eq. 13, the result is 10.73×10^{-7} mole sec^{-1}. This calculated result agrees with the experimental value of Eq. 11 within 12%.

Another test of the agreement between predicted values and experimental data may be carried out for V. Equation 14 may be evaluated using $k_1 = 4.64 \times 10^{-5}$ sec^{-1} from Table IV and [IV*] = 2.52×10^{-3} M from Table V:

$$\frac{d\text{V}}{dt} = k_1[\text{IV}^*] = 1.17 \times 10^{-7} \text{ mole sec}^{-1} \qquad \text{(Eq. 14)}$$

If the experimental concentrations for [V] are plotted *versus* time in a first-order fashion, a straight line results (correlation coefficient = 0.987, excluding the first point) and gives a first-order rate constant of 1.60×10^{-5} sec^{-1}. When this rate constant is used with the experimental value for [V] at 5 hr, the point chosen for use in the approximation, Eq. 15 results:

$$\frac{d\text{V}}{dt} = k''[\text{V}] = 0.954 \times 10^{-7} \text{ mole sec}^{-1} \qquad \text{(Eq. 15)}$$

The predicted rate of Eq. 14 is within 18% of the experimental rate seen in Eq. 15. This good agreement adds credence to the approximations used to interpret the observed kinetics. The k'' (Eq. 15) is not the same as k_1 since the appearance rate of [V] is actually a function of the processes described in Schemes I and II.

Table IV—Rate Constants Calculated for Reactions Occurring in Acetous Solution of IV at 61°

Rate Constant	Value
k_0	2.08×10^{-5} sec^{-1}
k_1	4.64×10^{-5} sec^{-1}
k_2	3.90×10^{-2} liter mole^{-1} sec^{-1}
k_3	4.09×10^{-3} liter mole^{-1} sec^{-1}
k_4	5.89×10^{-5} liter mole^{-1} sec^{-1}
k_5	2.09×10^{-5} sec^{-1}
k_6	8.89×10^{-6} sec^{-1}
k_7	2.03×10^{-3} liter mole^{-1} sec^{-1}

Another convenient index of the rationality of a proposed mechanism is the calculated mass balance and its agreement with experimental values. Attempts to establish the mass balance relationship in this case were hampered by the insolubility of VI and the fact that II was beyond the limit of detection. With these limitations, calculation accounted for about 80% of the initial concentration of IV. This amount is reasonable and expected.

APPENDIX

The following symbols will be used: I, hydrazine; II, acetylhydrazine; III, diacetylhydrazine; IV, *m*-nitrobenzhydrazide; V, *N*-acetyl-*N'*-*m*-nitrobenzoylhydrazine; and VI, *N,N'*-bis(*m*-nitrobenzoyl)hydrazine.

The rate constants specified in Schemes I–VIII and found in the differential equations (Eqs. 4–10) that describe the reaction rates of the six hydrazine compounds in the IV–acetic acid system were evaluated.

Preliminary Considerations—Before the solution is described, several assumptions should be considered.

1. Due to the presence of both consecutive and parallel bimolecular reactions in the suggested mechanism, difficulties were encountered in integrating the differential rate equations. Mathematical treatments reported by Chien (10) and by Pearson *et al.* (11) for less complicated mechanisms, which involved either consecutive or parallel bimolecular reactions using transforms and introduction of Bessel functions, were investigated; however, the solution was complicated in this case because of the presence of the hydrazine loop (Scheme VIII, k_7, and Scheme VI, k_5). Although an exact solution for this complicated mechanism may be possible, an approximation was used.

Since the concentration–time profiles for each compound over the timespan studied (Fig. 3) are obviously not linear, some points were neglected to obtain linear least-squares lines for each profile. To indicate the nature of the lines, the points neglected are mentioned, together with the linear correlation coefficient of the resulting straight line: IV, all points used, 0.984; V, first point neglected, 0.993; I, first point neglected, 0.999; and III, last two points neglected, 0.983. This approach permitted use of slopes for derivatives, *e.g.*, $d\text{IV}/dt = \Delta\text{IV}/\Delta t$.

When the concentration of a reactant or product was required, the value on the least-squares line at 5 hr, approximately the midpoint representing a point where deviation of the least-squares point from experimental values would be the least, was chosen in solving the rate equations. In some cases, these solutions were compared with the solution obtained using actual experimental concentrations at 5 hr.

2. In a separate study of I and II reactions with acetic acid at 61° (7), k_5, k_6, and k_7 were determined. The average value for each rate constant was: k_5, 7.53×10^{-2} hr^{-1}; k_6, 3.20×10^{-2} hr^{-1}; and k_7, 7.32 liters mole^{-1} hr^{-1}.

3. Because II was not detected in solution during the study (lower limit of detectability was 4.8×10^{-4} M), its concentration was considered small enough so that when it or its square was multiplied by k_6 or k_7, respectively, the [II] and $[\text{II}]^2$ terms in Eqs. 8 and 10 were negligible and Eqs. A1 and A2, respectively, resulted:

$$\frac{d\text{III}}{dt} = \tfrac{1}{2}k_2[\text{IV}^*]^2 \qquad \text{(Eq. A1)}$$

$$\frac{d\text{I}}{dt} = k_4[\text{IV}]^2 - 2k_5[\text{I}] \qquad \text{(Eq. A2)}$$

Equation A1 is valid after about 3.5 hr. Prior to this point, the disproportionation of II and the production of I cause the unusual saddle region seen in the profile for III in Fig. 3.

4. A steady-state approximation can be used for Eq. 5, *i.e.*, $\Delta\text{IV}^*/\Delta t$

Table V—Calculated Values for k_3, k_2, k_1, and [IV*]

Reaction Variable	Set 1	Set 2
k_3, liters mole^{-1} hr^{-1}	14.74	7.66
k_2, liters mole^{-1} hr^{-1}	140.4	37.91
k_1, hr^{-1}	1.67×10^{-1}	8.67×10^{-2}
[IV*], M	2.52×10^{-3}	4.9×10^{-3}

= 0. This assumption was supported by the fact that k_0 can be considered significantly smaller than both k_2 and k_3, as was proven to be true in both I and II studies (7). This condition allows very small changes in [IV*] during the short period between its formation and degeneration to the final products. If the steady-state approximation is used, Eq. 5 may be written as:

$$k_0[\text{IV}] = k_1[\text{IV*}] + k_2[\text{IV*}]^2 + k_3[\text{IV}][\text{IV*}] \qquad \text{(Eq. A3)}$$

Calculation of Rate Constants—Substituting the experimental value of $\Delta\text{III}/\Delta t$ from Fig. 3 into Eq. A1 gives:

$$[\text{IV*}]^2 = 8.92 \times 10^{-4}\, k_2^{-1} \qquad \text{(Eq. A4)}$$

The experimental value for $\Delta V/\Delta t$ from Fig. 3 is substituted into Eq. 6 and yields Eq. A5:

$$\Delta V/\Delta t = k_1[\text{IV*}] = 4.324 \times 10^{-4}\, M\ \text{hr}^{-1} \qquad \text{(Eq. A5)}$$

Substitution of Eqs. A4 and A5 into Eq. A3 results in:

$$k_0[\text{IV}] = 0.0004324 + 0.000892 + k_3[\text{IV}][\text{IV*}] \qquad \text{(Eq. A6)}$$

Approximating $d\text{IV}/dt$ as $\Delta\text{IV}/\Delta t$ in Eq. 4 and adding this modified equation to Eq. A6 produces:

$$2k_0[\text{IV}] + (\Delta\text{IV}/\Delta t) = 0.0013244 - 2k_4[\text{IV}]^2 \qquad \text{(Eq. A7)}$$

From Fig. 3, values are introduced for $\Delta\text{I}/\Delta t$ and [I] into Eq. A2:

$$\Delta\text{I}/\Delta t = 0.000212 = k_4[\text{IV}]^2 - 2(0.0753)(0.00017) \qquad \text{(Eq. A8)}$$

$$k_4[\text{IV}]^2 = 0.000240 \qquad \text{(Eq. A9)}$$

Substitution of the Fig. 3 linear least-squares (at 5 hr) value of IV = 0.0345 M into Eq. A9 yields:

$$k_4 = 2.1 \times 10^{-1}\ \text{liter mole hr}^{-1} \qquad \text{(Eq. A10)}$$

Substitution for k_4 from Eq. A10 and for [IV] and $\Delta\text{IV}/\Delta t$ from Fig. 3 in Eq. A7 produces:

$$2k_0(0.0345) - 0.004364 = 0.0008245 \qquad \text{(Eq. A11)}$$

The value for k_0 is thus 7.51×10^{-2} hr^{-1}. Substitution of the values for k_0 and k_4 in Eq. 4, where $d\text{IV}/dt$ is approximated as $\Delta\text{IV}/\Delta t$, yields:

$$-0.004364 = -0.0751(0.0345) - k_3(0.0345)[\text{IV*}] - 2(0.212)(0.0345)^2 \qquad \text{(Eq. A12)}$$

$$[\text{IV*}] = 0.0371k_3^{-1} \qquad \text{(Eq. A13)}$$

If the values for [IV*] and [IV*]^2 are substituted into Eq. A3, Eq. A14 results:

$$(0.0751)(0.0345) = 0.0371k_1k_3^{-1} + (0.0345)(0.0371) + k_2(0.0371)^2k_3^{-2} \qquad \text{(Eq. A14)}$$

Multiplying Eq. A14 by k_3^2 and rearranging result in:

$$0.00131k_3^2 = 0.0371k_1k_3 + 0.00138k_2 \qquad \text{(Eq. A15)}$$

Equations A14 and A13 are equated to yield:

$$k_2 = 0.646k_3^2 \qquad \text{(Eq. A16)}$$

Substituting this value for k_2 into Eq. A15 yields:

$$0.00131k_3^2 = 0.0371k_1k_3 + 0.00138(0.646)k_3^2 \qquad \text{(Eq. A17)}$$

$$k_3 = 88.31k_1 \qquad \text{(Eq. A18)}$$

Substitution for k_3 from Eq. A18 into Eq. A16 results in:

$$k_2 = (88.31)^2k_1^2/1.547 \qquad \text{(Eq. A19)}$$

At this point, values for k_0, k_4, k_5, k_6, and k_7 are known. However, it is necessary to obtain values for k_1, k_2, and k_3 with Eqs. A4, A18, and A19 such that the range of values of [IV*] satisfies mass balance restrictions. The mass balance statement based on [IV] (initial) = 0.06 M is only approximate since [II] is small and below the limit of detectability and [VI] can be determined only approximately since it precipitates from solution.

The values at 5 hr of [IV], [V], [I], and [III] were obtainable from Fig. 3. The amount of [VI] that had precipitated was estimated by gravimetric analysis following simple filtration of a solution aliquot, and this value was added to the [VI] in solution at 5 hr. The approximate sum of all [IV]-derived species was 0.056, exclusive of [IV*]; thus, to satisfy the [IV] (initial) of 0.06 M, the [IV*] must be less than 0.004 M.

The solution of Eqs. A4, A18, and A19 for k_1, k_2, k_3, and [IV*], the latter still being unknown even though a range of values is known to be acceptable, is not possible by usual means since four unknowns cannot be calculated from three equations. Empirical trials were carried out to discover an additional relationship between [IV*] and the unknown constants. By assuming values for k_1, values for k_2, k_3, and [IV*] were computed using computer calculation. For [IV*] to be less than 0.004 M as required, it was found that k_1 had to be larger than 0.08.

A number of plots of [IV*] *versus* k_2 and k_3 in different forms showed that useful relationships exist when [IV*]^2 was plotted against k_3/k_2 or $1/k_3$. In both instances, a straight-line relationship was obtained (correlation coefficient of 0.993) in the valid range of k_1, *i.e.*, k_1 larger than 0.08. Equation A20 is written using the slope and intercept values from the linear plot of k_3/k_2 *versus* [IV*]^2:

$$k_3/k_2 = 0.0691 + 5643[\text{IV*}]^2 \qquad \text{(Eq. A20)}$$

Substituting for [IV*]^2 from Eq. A4 into Eq. A20 gives:

$$k_3 = 0.0691k_2 + 5.04 \qquad \text{(Eq. A21}a\text{)}$$

or:

$$k_2 = 14.47k_3 - 72.94 \qquad \text{(Eq. A21}b\text{)}$$

Equation A16 is used to substitute into Eqs. A21a and A21b, yielding a quadratic equation for k_3:

$$k_3 = \frac{14.47 \pm \sqrt{209.38 - 4(0.646)(72.94)}}{2(0.646)} \qquad \text{(Eq. A22)}$$

which may be solved to yield two values of k_3. The existence of two values for k_3 leads to pairs of values for k_2, k_1, and [IV*] (Table V). A decision between the acceptability of data of Sets 1 and 2 in Table V was based on the requirements of the mass balance of all species arising from [IV] (initial). If the values from Set 2 of [IV*] are included in the mass balance, then the total IV-derived species concentration is larger than the experimental [IV] (initial); however, use of [IV*] from Set 1 makes the total IV-derived species concentration agree well with the known experimental value for [IV] (initial), 0.06 M.

REFERENCES

(1) B. Camber, *Clin. Chim. Acta*, **2**, 188 (1957).

(2) H. Strain, *J. Am. Chem. Soc.*, **57**, 758 (1935).

(3) L. Stattler and F. W. Zerban, *ibid.*, **70**, 873 (1948).

(4) H. E. Malone, "The Determination of Hydrazino-Hydrazide Groups," Pergamon, New York, N.Y., 1970.

(5) M. L. Blake, D. Bode, and H. J. Rhodes, *J. Pharm. Sci.*, **63**, 1303 (1974).

(6) W. C. Harris and K. G. Stone, *J. Org. Chem.*, **23**, 2032 (1958).

(7) H. M. Abdou and T. Medwick, *J. Org. Chem.*, **43**, 15 (1978).

(8) J. S. Fritz, "Acid-Base Titrations in Nonaqueous Solvents," G. Frederick Smith Chemical Co., Columbus, Ohio, 1952, p. 13.

(9) T. Medwick and E. Kirschner, *J. Pharm. Sci.*, **55**, 1296 (1966).

(10) J. Chien, *J. Am. Chem. Soc.*, **70**, 2256 (1948).

(11) R. G. Pearson, L. C. King, and S. H. Langer, *J. Am. Chem. Soc.*, **73**, 4149 (1951).

ACKNOWLEDGMENTS

Adapted in part from a thesis submitted by H. M. Abdou to the Graduate School, Rutgers University, in partial fulfillment of the Doctor of Philosophy degree requirements.

Thanks are extended to Dr. Takeru Higuchi, University of Kansas, for advice and encouragement and to the Wisconsin Alumni Research Foundation for aid. Gratitude is expressed to Dr. F. J. Cioffi and Mr. Robert Lanza, E. R. Squibb and Sons, for help with the calculations. Mr. Donald Martone is thanked for technical aid.

Physicochemical Properties of Amphoteric β-Lactam Antibiotics II: Solubility and Dissolution Behavior of Aminocephalosporins as a Function of pH

AKIRA TSUJI, EMI NAKASHIMA, and TSUKINAKA YAMANA ˣ

Received June 16, 1978, from the *Faculty of Pharmaceutical Sciences, Kanazawa University, Takara-machi, Kanazawa 920, Japan.* Accepted for publication August 9, 1978.

Abstract □ The solubility of aminocephalosporins in aqueous solution at 37° and an ionic strength of 0.5 exhibited U-shaped curves against pH. At their isoelectric pH, cephradine monohydrate was the most soluble, followed by cephalexin monohydrate and cephaloglycin dihydrate, with intrinsic solubilities of 26.0, 17.2, and 14.8 mg/ml, respectively. The dissolution rate constants from the rotating disk were also determined as a function of the pH of the dissolution medium and interpreted reasonably by the simultaneous dissociation equilibrium reaction and the diffusion kinetics model. Energies for the solubility and dissolution were determined for these three aminocephalosporins.

Keyphrases □ β-Lactam antibiotics—various aminocephalosporins, solubility and dissolution, effect of pH □ Aminocephalosporins, various—solubility and dissolution, effect of pH □ Solubility—various aminocephalosporins, effect of pH □ Dissolution—various aminocephalosporins, effect of pH □ Antibacterials—various aminocephalosporins, solubility and dissolution, effect of pH

The solubility and dissolution rate of drugs ingested orally are important physicochemical properties for understanding their bioavailability and the rate-limiting step in absorption. Previously (1), the dissolution behavior of aminopenicillins such as ampicillin, amoxicillin, and cyclacillin, which are used therapeutically by the oral route, was described. It was concluded that the dissolution of these antibiotics follows diffusion-controlled kinetics over the entire pH range and cannot become the rate-limiting step of their GI absorption, consistent with the previous claim (2) given for ampicillin.

The present paper describes the solubility and kinetics of the dissolution rate of some orally effective aminocephalosporins, cephalexin, cephradine, and cephaloglycin, as a function of the dissolution medium pH.

EXPERIMENTAL

Materials—Cephalexin monohydrate[1] (925 μg/mg), cephradine monohydrate[2] (952 μg/mg), and cephaloglycin dihydrate[1] (962 μg/mg) were used as supplied. All chemicals were the highest grade available commercially.

Procedure—Procedures for the determination of pKa values, diffusion coefficients, solubility, and dissolution rates were described previously (1). Aminocephalosporins were determined by UV spectrophotometric measurement[3] at 260 nm. All experimental conditions were chosen from previously published kinetic data (3) so that the degradation of antibiotics was within 5%.

RESULTS AND DISCUSSION

Solubility–pH Profile—The solubility of aminocephalosporins was determined as a function of the solution pH at 37° and $\mu = 0.5$ (Scheme I). The relationship between the solubility and pH showed U-shaped curves with the minimum solubility near the respective isoelectric point (Fig. 1), similar to those of aminopenicillins (1, 4).

Table I—Intrinsic Solubility and Dissociation Constants of Aminocephalosporins and Aminopenicillins[a] at 37° and $\mu = 0.5$

Antibiotic	Molecular Weight	Solubility[b], $10^2 \times C_0$, M (mg/ml)	Dissociation Constants[c] pK_1	pK_2
Cephradine monohydrate	367.4	7.08 (26.0)	2.63	7.35
Cephalexin monohydrate	365.4	4.72 (17.2)	2.67	6.96
Cephaloglycin dihydrate	441.4	3.36 (14.8)	2.03	6.89
Ampicillin trihydrate	403.4	2.23 (9.0)	2.67	6.95
Ampicillin anhydrate	349.4	3.97 (13.9)		
Amoxicillin trihydrate	419.4	1.30 (5.4)	2.67	7.11
Cyclacillin anhydrate	341.4	8.90 (30.4)	2.64	7.18

[a] Values determined previously (1). [b] Defined by Eq. 1. [c] Determined by the potentiometric method.

The total solubility, C_T, as a function of the solution pH can be expressed as:

$$C_T = C_0\left(\frac{a_{H^+}}{K_1} + 1 + \frac{K_2}{a_{H^+}}\right) \qquad \text{(Eq. 1)}$$

where C_0 is the intrinsic solubility of amphoteric cephalosporins with the electrically neutral zwitterion, a_{H^+} is the hydrogen-ion activity of the solution, and K_1 and K_2 are dissociation constants for 4-carboxylic acid and the conjugated acid of the α-amino group, respectively. The C_0 values estimated from the solubility near the isoelectric point, $pI = \frac{1}{2}(pK_1 + pK_2)$, and the dissociation constants determined by a potentiometric method (1) under the same experimental conditions are listed in Table I. As seen in Fig. 1, the theoretical curves generated from Eq. 1 fit rea-

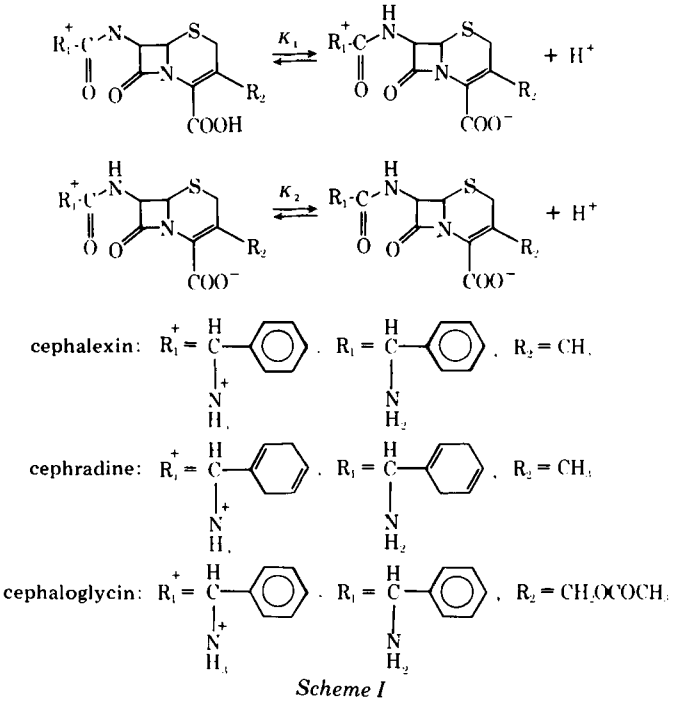

Scheme I

[1] Shionogi & Co., Osaka, Japan.
[2] Sankyo Co., Tokyo, Japan.
[3] Model UV-200S double-beam recording spectrophotometer, Shimadzu Seisakusho, Kyoto, Japan.

0022-3549/79/0300-0308$01.00/0
© 1979, American Pharmaceutical Association

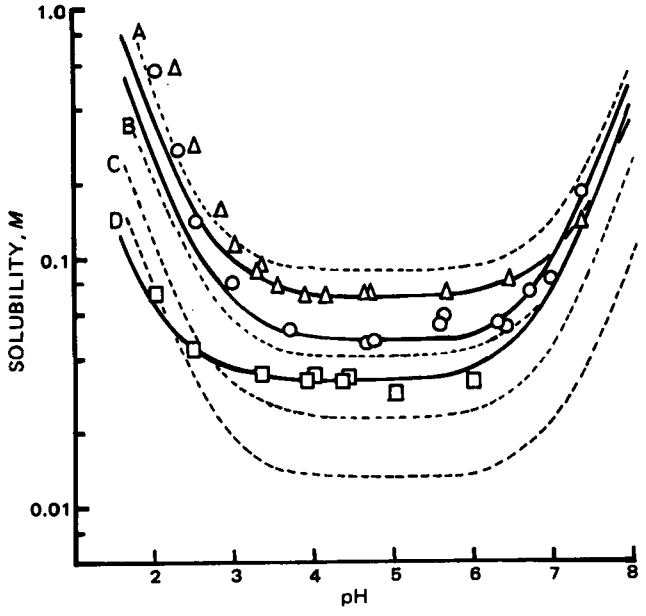

Figure 1—*Solubility–pH profiles of aminocephalosporins at 37° and μ = 0.5. The points are experimental values. The solid curves were generated from Eq. 1 and the parameters listed in Table I. Key: ○, cephalexin monohydrate; △, cephradine monohydrate; and □, cephaloglycin dihydrate. The dotted lines are theoretical curves (1) for the solubility of aminopenicillins at 37° and μ = 0.5. Key: A, cyclacillin anhydrate; B, ampicillin anhydrate; C, ampicillin trihydrate; and D, amoxicillin trihydrate.*

sonably well with experimental points for all aminocephalosporins.

In the pH range below 7, cephradine monohydrate was the most soluble, followed by cephalexin monohydrate; cephaloglycin dihydrate exhibited the lowest solubility. For comparison, the solubilities of several aminopenicillins determined under the same conditions (1) are also shown in Fig. 1 and Table I.

The apparent equilibrium solubility observed over the temperature range of 25–60°, when plotted in the classical van't Hoff fashion, gave a reasonably good linear relationship (Fig. 2). The values of the heat of solution, ΔH_{sol}, for cephalexin monohydrate, cephradine monohydrate, and cephaloglycin dihydrate were calculated from the slopes in Fig. 2 to be 1.39, 1.58, and 1.87 kcal/mole, respectively.

Dissolution Rate–pH Profile—The dissolution rate of an antibiotic solid in aqueous solution can be represented by Eq. 2 at an earlier stage of dissolution (1):

$$\left(\frac{dC}{dt}\right)_0 = \frac{S}{V} k_T \qquad \text{(Eq. 2)}$$

where C is the concentration of the drug dissolved at time t, S is the area of the solid surface exposed to the solvent, V is the volume of the dissolution medium, and k_T is the dissolution rate constant in units of molar centimeters per second.

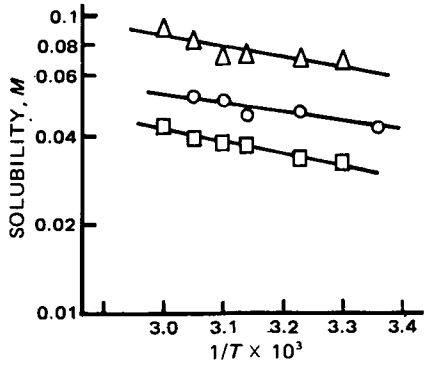

Figure 2—*Plots of solubilities of aminocephalosporins in 0.5 M KCl versus reciprocal of absolute temperature. Key: ○, cephalexin monohydrate; △, cephradine monohydrate; and □, cephaloglycin dihydrate.*

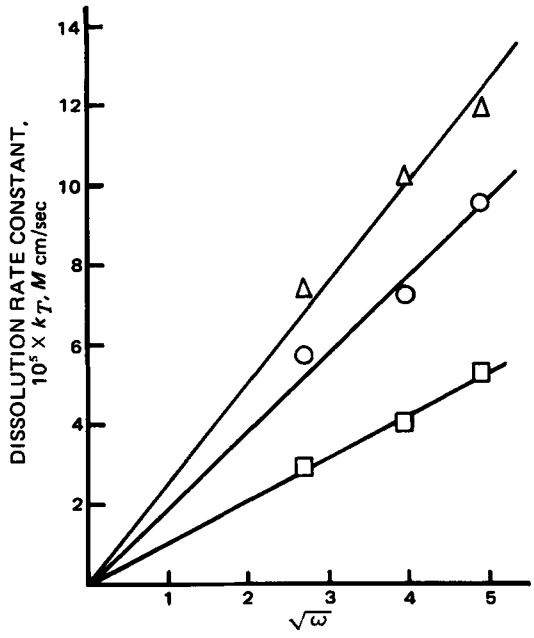

Figure 3—*Effect of stirring speed, $\sqrt{\omega}$, on the dissolution rate of aminocephalosporins in 0.5 M KCl at 37°. Key: ○, cephalexin monohydrate; △, cephradine monohydrate; and □, cephaloglycin dihydrate.*

If dissolution of aminocephalosporins from the rotating disk follows the rate-limiting diffusion, the dissolution rate constants at their isoelectric pH values can be predicted theoretically (5) as:

$$k_T = 0.620 D^{2/3} \nu^{-1/6} \omega^{1/2} C_0 \qquad \text{(Eq. 3)}$$

where D is the diffusion coefficient of a drug, ν is the kinematic viscosity of dissolution medium, and ω is the angular velocity of rotation. The dissolution rate constants, k_T, measured in 0.5 M KCl at 70, 150, and 228 rpm, were on the straight line against $\sqrt{\omega}$ (Fig. 3), apparently obeying

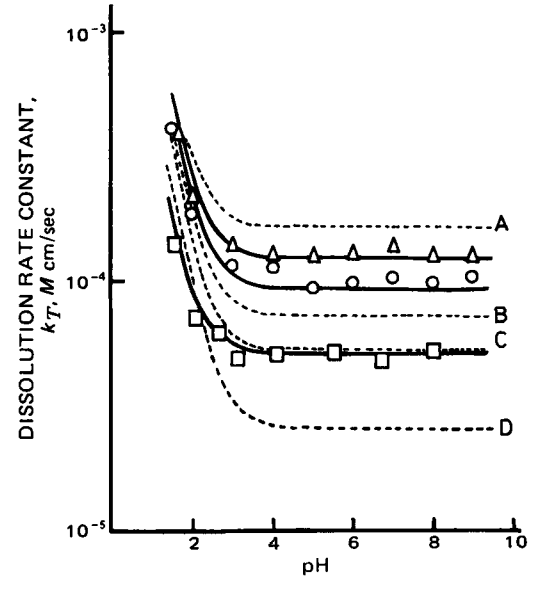

Figure 4—*Log k_T–pH profiles for the dissolution of aminocephalosporins at 228 rpm, 37°, and μ = 0.5. The points are experimental values, and the solid curves were generated from the theoretical equations listed in Table II. Key: ○, cephalexin monohydrate; △, cephradine monohydrate; and □, cephaloglycin dihydrate. The dotted lines are theoretical curves (1) for the dissolution rate constants of aminopenicillins at 228 rpm and μ = 0.5. Key: A, cyclacillin anhydrate; B, ampicillin anhydrate; C, ampicillin trihydrate; and D, amoxicillin trihydrate.*

Table II—Theoretical Equations[a] for the Dissolution Rate Constants at 228 rpm and Diffusion Coefficients of Aminocephalosporins at 37° and μ = 0.5

Aminocephalosporin	Theoretical Equation[b], k_T(theor.), M cm/sec	Diffusion Coefficients, $10^6 \times D$, cm²/sec: Dissolution Rate[c]	Diffusion Cell[d]
Cephradine monohydrate	$1.35 \times 10^{-2}(a_{H^+})_h + 1.24 \times 10^{-4} + 1.5 \times 10^{-2}(a_{OH^-})_h$	3.98	3.33
Cephalexin monohydrate	$1.22 \times 10^{-2}(a_{H^+})_h + 9.43 \times 10^{-5} + 1.5 \times 10^{-2}(a_{OH^-})_h$	4.90	3.23
Cephaloglycin dihydrate	$4.31 \times 10^{-3}(a_{H^+})_h + 5.19 \times 10^{-5} + 1.5 \times 10^{-2}(a_{OH^-})_h$	3.32	3.44

[a] Equation 4. [b] Calculated from Eqs. 4 and 5 with the parameters listed in Table I and those cited in the text. [c] Determined in 0.5 M KCl aqueous solution and used for the calculation of Eqs. 4 and 5. [d] Determined in 0.5 M KCl aqueous solution by means of a diffusion cell apparatus described previously (1) at the initial concentration of 0.01 M.

Eq. 3. Therefore, the diffusion coefficients of these antibiotics can be calculated from the slopes in Fig. 3 according to Eq. 3 by using the corresponding values of C_0 (Table I) and the viscosity of the solution, ν = 6.99×10^{-3} cm²/sec (6). The D values thus evaluated (Table II) are in good agreement with those determined by the diffusion cell method (1).

The dissolution rate constants, k_T, were determined as a function of the bulk solution pH maintained with a pH-stat. For comparison with the previous study on aminopenicillins (1), the experimental conditions were fixed at 228 rpm, 37°, and μ = 0.5 (Fig. 4).

The overall dissolution rate constants can be expressed theoretically as (1):

$$k_T = \frac{1}{h}\left[D_{H^+}\frac{D_{A^+}C_0}{D_{H^+}K_1 + D_{A^+}C_0}(a_{H^+})_h + D_{A^\pm}C_0 + D_{OH^-}\frac{D_{A^-}K_2C_0}{D_{OH^-}K_w + D_{A^-}K_2C_0}(a_{OH^-})_h \right] \quad \text{(Eq. 4)}$$

where subscripts A^+, $A^\pm$, and A^- represent the cationic, zwitterionic, and anionic species of amphoteric cephalosporins, respectively; D is the diffusion coefficient of the species indicated by the subscript; $(a_{H^+})_h$ and $(a_{OH^-})_h$ are the hydrogen-ion and hydroxide-ion activities, respectively, in the bulk solution; and h is the diffusion layer thickness calculated from (5):

$$h = 1.612 D^{1/3} \nu^{1/6} \omega^{-1/2} \quad \text{(Eq. 5)}$$

By assuming $D_{A^+} = D_{A^\pm} = D_{A^-}$ and employing $D_{H^+} = 4.12 \times 10^{-5}$ cm²/sec (7), $D_{OH^-} = 3.43 \times 10^{-5}$ cm²/sec (8, 9), $K_w = 2.38 \times 10^{-14}$ (10), and the parameters determined in this study (Table I), the theoretical dissolution rate constants, k_T (theor.), for the present experimental conditions can be derived from Eqs. 4 and 5 (Table II).

The theoretical curves calculated from these equations (Fig. 4) indicate reasonably good agreement with the experimental points for all aminocephalosporins. Figure 4 includes theoretical curves for the aminopenicillins from the previous report (1), showing almost similar dissolution rate behavior between aminopenicillins and aminocephalosporins with respect to the change in pH of the bulk dissolution medium.

Figure 5 shows plots of the logarithm of the apparent dissolution rate constants of aminocephalosporins in 0.5 M KCl at 228 rpm against the reciprocal of the absolute temperature. The heats of dissolution, ΔH_{dis}, calculated from the slope of these lines were 4.36, 4.76, and 6.09 kcal/mole for cephalexin monohydrate, cephradine monohydrate, and cephaloglycin dihydrate, respectively. These values are smaller than the 9.09 kcal/mole for ampicillin trihydrate (11) and the 9.67 kcal/mole for amoxicillin trihydrate (1) but higher than the 2.54 kcal/mole for ampicillin anhydrate (11).

By subtracting the heat of solubility, ΔH_{sol}, from that of dissolution, the intrinsic energy concerned with diffusion and viscosity of the solution can be obtained. The calculated energies, $\Delta H_{dis} - \Delta H_{sol}$, were 2.97, 3.18, and 4.22 kcal/mole for cephalexin monohydrate, cephradine monohydrate, and cephaloglycin dihydrate, respectively, comparable to the values of 3–4 kcal/mole (1, 11) obtained for amoxicillin trihydrate, ampicillin trihydrate, and ampicillin anhydrate. These energies are in the reasonable range of 3–5 kcal/mole reported (11) for diffusion processes.

The evidence obtained from the pH and temperature dependence of the dissolution rate constant strongly indicates that the dissolution of aminocephalosporins as well as aminopenicillins follows diffusion-controlled kinetics.

The dissolution rate of ampicillin anhydrate significantly decreased (1) with an increase in the ionic strength of the solution, probably as a result of the decrease in solubility (4). As seen in Fig. 6, the dissolution

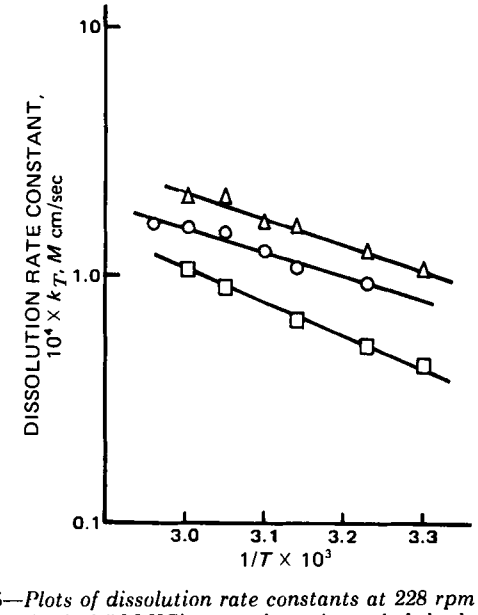

Figure 5—*Plots of dissolution rate constants at 228 rpm of aminocephalosporins in 0.5 M KCl versus the reciprocal of absolute temperature. Key: ○, cephalexin monohydrate; △, cephradine monohydrate; and □, cephaloglycin dihydrate.*

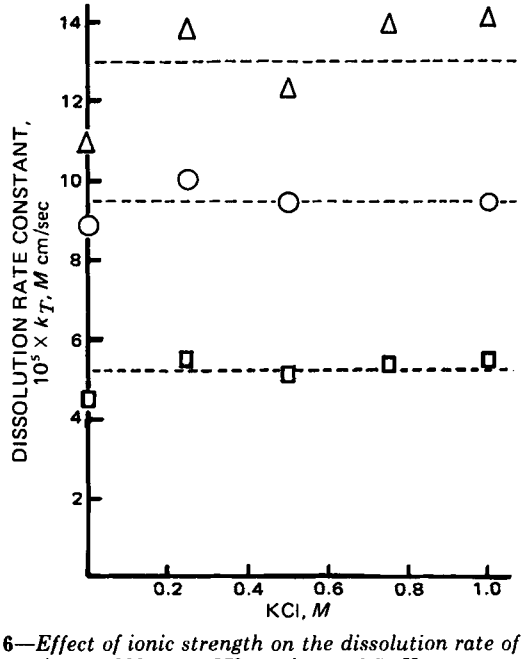

Figure 6—*Effect of ionic strength on the dissolution rate of aminocephalosporins at 228 rpm, 37°, and μ = 0.5. Key: ○, cephalexin monohydrate; △, cephradine monohydrate; and □, cephaloglycin dihydrate. The dotted lines are mean values of the data.*

rate of all types of aminocephalosporins was not significantly affected by a salt concentration.

From the present results, it is suggested that the dissolution of the aminocephalosporins studied cannot be a rate-limiting step in their absorption when they are ingested with sufficient water, as concluded previously (1) for aminopenicillins. The reduced bioavailability reported (12) for the least soluble cephaloglycin may be the result of the instability of the antibiotic at gastric and intestinal pH (3, 12) and of relatively slow GI membrane permeability of the dissolved cephaloglycin itself (13).

REFERENCES

(1) A. Tsuji, E. Nakashima, S. Hamano, and T. Yamana, *J. Pharm. Sci.*, **67**, 1059 (1978).

(2) S. A. Hill, K. H. Jones, H. Seager, and C. B. Taskis, *J. Pharm. Pharmacol.*, **27**, 594 (1975).

(3) T. Yamana and A. Tsuji, *J. Pharm. Sci.*, **65**, 1563 (1976).

(4) J. P. Hou and J. W. Poole, *ibid.*, **58**, 1510 (1969).

(5) V. G. Levich, "Physicochemical Hydrodynamics," Prentice-Hall, Englewood Cliffs, N.J., 1962, p. 69.

(6) H. Nogami, T. Nagai, and A. Suzuki, *Chem. Pharm. Bull.*, **14**, 329 (1966).

(7) R. H. Stokes, *J. Am. Chem. Soc.*, **72**, 2243 (1950).

(8) R. N. Bhatia, K. E. Gubbins, and R. D. Walker, *Trans. Faraday Soc.*, **64**, 2091 (1968).

(9) H. R. Bruins, in "International Critical Tables," vol. 5, E. W. Washburn, Ed., McGraw-Hill, New York, N.Y., 1929, p. 68.

(10) H. S. Harned and W. J. Hammer, *J. Am. Chem. Soc.*, **55**, 2194 (1933).

(11) D. A. Wadke and G. E. Reier, *J. Pharm. Sci.*, **61**, 868 (1972).

(12) C. H. Nightingale, D. S. Greene, and R. Quintiliani, *ibid.*, **64**, 1899 (1975).

(13) J. L. DeYoung, H. G. H. Tan, H. E. Huber, and M. A. Zoglio, *ibid.*, **67**, 320 (1978).

ACKNOWLEDGMENTS

The authors acknowledge the gift of aminocephalosporins from Shionogi & Co. and Sankyo Co., Japan. They also thank Miss H. Yamazaki and Miss S. Omura for assistance.

Separation and Quantitation of Esterified Estrogens in Bulk Mixtures and Combination Drug Preparations Using High-Performance Liquid Chromatography

G. CAPITANO ˣ **and R. TSCHERNE**

Received March 15, 1978, from the *Quality Control Department, Hoffmann-La Roche, Inc., Nutley, NJ 07110.* Accepted for publication August 21, 1978.

Abstract □ A high-performance liquid chromatographic method for esterified estrogens is described. By using a facile acid hydrolysis extraction procedure for the sample preparation, the compounds are chromatographed as their free phenolic forms. The separation of structurally similar compounds, such as equilenin, equilin, estrone, and estradiol, was achieved with a reversed-phase column and a methanol–water mobile phase. Several samples of bulk mixtures and tablets were assayed; the results compared favorably with those obtained using the USP XIX method. The method was rapid, and the detector response was linear over a wide concentration range. A relative standard deviation of ±5% indicates the reliability and accuracy of the proposed method.

Keyphrases □ Estrogens, esterified—high-performance liquid chromatographic analysis in prepared solutions □ High-performance liquid chromatography—analysis, esterified estrogens in prepared solutions □ Hormones—esterified estrogens, high-performance liquid chromatographic analysis in prepared solutions

A combination drug preparation containing chlordiazepoxide base and esterified estrogens[1] is assayed for estrone and equilin by the USP colorimetric procedure. This modified Kober reaction procedure is quite lengthy (1) and complicated. Quantitation is concerned mainly with the proper ratio of the sulfate esters of estrone and equilin, calculated on the basis of the total estrogen content.

BACKGROUND

The present compendial analytical technique is remiss in that minor constituents of these complex estrogenic substances, such as equilenin, dihydroequilenin, dihydroequilin, and estradiol, are not differentiated readily (2–4). In an attempt to replace the cumbersome USP assay, many steroid separations have been reported.

In TLC, emphasis is placed on the use of silver nitrate-impregnated silica gel plates and a variety of solvent systems for resolution of the equine estrogens and their sulfates (5, 6).

Reversed-phase partition liquid chromatographic separation of estrone and equilin was achieved (7) by using an argentated mobile phase. The presence of small amounts of silver ion produced well-resolved equilin and estrone peaks (7).

Reported GLC determinations of urinary estrogens require preliminary purification and isolation on adsorption columns (8) and/or thin-layer plates (9, 10). These isolated free estrogens are derivatized subsequently to a more stable form amenable to the high temperatures encountered in GLC. Since these compounds are heat-labile substances, conversion to their silyl ethers is mandatory (11–13). It is this particular characteristic that makes open-column liquid chromatographic (14–16) and high-performance liquid chromatographic (HPLC) applications more practical and less time consuming (17–25).

Published HPLC determinations of conjugated and esterified estrogens in commercial dosage formulations are few (20, 22, 24). Most described methods are not applicable to this product because derivatizations with heat are used prior to the final chromatographic analysis (22–25).

These problems motivated the development of the assay described in this report. An analytical separation of the hydrolyzed esterified estrogens in various dosages was obtained by HPLC *via* a reversed-phase column and a methanol–water mobile phase.

Data obtained from statistical evaluations show that reliability and precision are attained using the method; the total estrogen content is easily quantitated by adding the individual estrogens.

EXPERIMENTAL

Apparatus—A constant pressure pump[2] was used in conjunction with

[1] Menrium, Hoffmann-La Roche, Nutley, N.J.

[2] Haskel pump in Dupont Instruments model 830 liquid chromatograph.

0022-3549/79/0300-0311$01.00/0

© 1979, American Pharmaceutical Association

rate of all types of aminocephalosporins was not significantly affected by a salt concentration.

From the present results, it is suggested that the dissolution of the aminocephalosporins studied cannot be a rate-limiting step in their absorption when they are ingested with sufficient water, as concluded previously (1) for aminopenicillins. The reduced bioavailability reported (12) for the least soluble cephaloglycin may be the result of the instability of the antibiotic at gastric and intestinal pH (3, 12) and of relatively slow GI membrane permeability of the dissolved cephaloglycin itself (13).

REFERENCES

(1) A. Tsuji, E. Nakashima, S. Hamano, and T. Yamana, *J. Pharm. Sci.*, **67**, 1059 (1978).

(2) S. A. Hill, K. H. Jones, H. Seager, and C. B. Taskis, *J. Pharm. Pharmacol.*, **27**, 594 (1975).

(3) T. Yamana and A. Tsuji, *J. Pharm. Sci.*, **65**, 1563 (1976).

(4) J. P. Hou and J. W. Poole, *ibid.*, **58**, 1510 (1969).

(5) V. G. Levich, "Physicochemical Hydrodynamics," Prentice-Hall, Englewood Cliffs, N.J., 1962, p. 69.

(6) H. Nogami, T. Nagai, and A. Suzuki, *Chem. Pharm. Bull.*, **14**, 329 (1966).

(7) R. H. Stokes, *J. Am. Chem. Soc.*, **72**, 2243 (1950).

(8) R. N. Bhatia, K. E. Gubbins, and R. D. Walker, *Trans. Faraday Soc.*, **64**, 2091 (1968).

(9) H. R. Bruins, in "International Critical Tables," vol. 5, E. W. Washburn, Ed., McGraw-Hill, New York, N.Y., 1929, p. 68.

(10) H. S. Harned and W. J. Hammer, *J. Am. Chem. Soc.*, **55**, 2194 (1933).

(11) D. A. Wadke and G. E. Reier, *J. Pharm. Sci.*, **61**, 868 (1972).

(12) C. H. Nightingale, D. S. Greene, and R. Quintiliani, *ibid.*, **64**, 1899 (1975).

(13) J. L. DeYoung, H. G. H. Tan, H. E. Huber, and M. A. Zoglio, *ibid.*, **67**, 320 (1978).

ACKNOWLEDGMENTS

The authors acknowledge the gift of aminocephalosporins from Shionogi & Co. and Sankyo Co., Japan. They also thank Miss H. Yamazaki and Miss S. Omura for assistance.

Separation and Quantitation of Esterified Estrogens in Bulk Mixtures and Combination Drug Preparations Using High-Performance Liquid Chromatography

G. CAPITANO ˣ **and R. TSCHERNE**

Received March 15, 1978, from the *Quality Control Department, Hoffmann-La Roche, Inc., Nutley, NJ 07110.* Accepted for publication August 21, 1978.

Abstract □ A high-performance liquid chromatographic method for esterified estrogens is described. By using a facile acid hydrolysis extraction procedure for the sample preparation, the compounds are chromatographed as their free phenolic forms. The separation of structurally similar compounds, such as equilenin, equilin, estrone, and estradiol, was achieved with a reversed-phase column and a methanol–water mobile phase. Several samples of bulk mixtures and tablets were assayed; the results compared favorably with those obtained using the USP XIX method. The method was rapid, and the detector response was linear over a wide concentration range. A relative standard deviation of ±5% indicates the reliability and accuracy of the proposed method.

Keyphrases □ Estrogens, esterified—high-performance liquid chromatographic analysis in prepared solutions □ High-performance liquid chromatography—analysis, esterified estrogens in prepared solutions □ Hormones—esterified estrogens, high-performance liquid chromatographic analysis in prepared solutions

A combination drug preparation containing chlordiazepoxide base and esterified estrogens[1] is assayed for estrone and equilin by the USP colorimetric procedure. This modified Kober reaction procedure is quite lengthy (1) and complicated. Quantitation is concerned mainly with the proper ratio of the sulfate esters of estrone and equilin, calculated on the basis of the total estrogen content.

BACKGROUND

The present compendial analytical technique is remiss in that minor constituents of these complex estrogenic substances, such as equilenin, dihydroequilenin, dihydroequilin, and estradiol, are not differentiated readily (2–4). In an attempt to replace the cumbersome USP assay, many steroid separations have been reported.

In TLC, emphasis is placed on the use of silver nitrate-impregnated silica gel plates and a variety of solvent systems for resolution of the equine estrogens and their sulfates (5, 6).

Reversed-phase partition liquid chromatographic separation of estrone and equilin was achieved (7) by using an argentated mobile phase. The presence of small amounts of silver ion produced well-resolved equilin and estrone peaks (7).

Reported GLC determinations of urinary estrogens require preliminary purification and isolation on adsorption columns (8) and/or thin-layer plates (9, 10). These isolated free estrogens are derivatized subsequently to a more stable form amenable to the high temperatures encountered in GLC. Since these compounds are heat-labile substances, conversion to their silyl ethers is mandatory (11–13). It is this particular characteristic that makes open-column liquid chromatographic (14–16) and high-performance liquid chromatographic (HPLC) applications more practical and less time consuming (17–25).

Published HPLC determinations of conjugated and esterified estrogens in commercial dosage formulations are few (20, 22, 24). Most described methods are not applicable to this product because derivatizations with heat are used prior to the final chromatographic analysis (22–25).

These problems motivated the development of the assay described in this report. An analytical separation of the hydrolyzed esterified estrogens in various dosages was obtained by HPLC *via* a reversed-phase column and a methanol–water mobile phase.

Data obtained from statistical evaluations show that reliability and precision are attained using the method; the total estrogen content is easily quantitated by adding the individual estrogens.

EXPERIMENTAL

Apparatus—A constant pressure pump[2] was used in conjunction with

[1] Menrium, Hoffmann-La Roche, Nutley, N.J.

[2] Haskel pump in Dupont Instruments model 830 liquid chromatograph.

0022-3549/79/0300-0311$01.00/0

© 1979, American Pharmaceutical Association

Table I—Linearity Range of Detector Response and Retention Times of Estrogen Compounds

Compound	Linear Range, μg injected	Retention Time, min	Relative Retention Time
2,3,6-Trimethylphenol	—	17.0	1.00
Equilinen	0.02–0.09	23.8	1.40
Equilin	0.09–0.45	26.4	1.55
Estrone	0.06–0.30	29.1	1.71
Estradiol (17β-isomer)	0.03–0.12	32.6	1.92

a septumless injector[3], a variable wavelength detector[4] set at 280 nm, and a 30-cm × 4-mm i.d. partition column containing silica permanently bonded with octadecylsilane[5].

Reagents and Standards—The mobile phase was methanol–water (60:40). Methanol and anhydrous sodium sulfate were reagent grade. The four estrogens used in the standard preparation were reference grade (99%+), as was the internal standard, 2,3,6-trimethylphenol.

Chromatographic Separation—The procedure was run at ambient temperature with a solvent flow of 0.6 ml/min. The UV monitor was set at 280 nm with a sensitivity of 0.04 absorbance unit. Standards and samples were injected with a 10-μl syringe.

Standard Solution Preparations—*Internal Standard*—Weigh accurately 20 mg of 2,3,6-trimethylphenol into a 100-ml volumetric flask. Dissolve and dilute to volume with methanol (internal standard stock solution).

Estrone Reference Standard—Weigh accurately 32 mg of reference standard into a 25-ml volumetric flask. Dissolve and dilute to volume with methanol.

Equilin Reference Standard—Weigh accurately 12.5 mg of reference standard into a 100-ml volumetric flask. Dissolve and dilute to volume with methanol.

Equilenin Reference Standard—Weigh accurately 12 mg of reference standard into a 25-ml volumetric flask. Dissolve and dilute to volume with methanol. Subdilute by pipetting 2 ml into a 25-ml volumetric flask and bring to volume with methanol.

Estradiol Reference Standard—Weigh accurately 10 mg of reference standard into a 25-ml volumetric flask. Dissolve and dilute to volume with methanol. Subdilute by pipetting 3 ml into a 25-ml volumetric flask and bring to volume with methanol.

Combined Reference Standard Solution—Into a 50-ml glass-stoppered erlenmeyer flask, pipet the following amounts of the previously prepared individual reference standards: 2 ml of estrone solution, 3 ml of equilin solution, 2 ml of subdiluted equilenin solution, and 3 ml of subdiluted estradiol solution.

Evaporate the methanolic mixture of estrogens to dryness under a nitrogen stream. To the dried residue, add 10 ml of the internal standard stock solution. Stopper the flask and mix thoroughly for complete dissolution (working standard solution).

Sample Preparation—Perform this preparation in duplicate. Into a 50-ml glass-stoppered centrifuge tube, accurately weigh a portion of either the bulk substance or finely ground tablet mass equivalent to 4 mg of esterified estrogens. Add 10 ml of 1 *N* HCl and swirl the tube contents until the powder is completely dispersed; then shake mechanically for approximately 5 min. After removal from the shaker, extract the acidified sample with five 20-ml portions of ether, shaking each extract mechanically for 5 min. (A gel-like emulsion is formed upon shaking but clears up immediately on standing; centrifuging hastens the process.) Withdraw the ether layer with a syringe, passing each extract through a layer of anhydrous sodium sulfate, and collect the combined extracts in an appropriately sized (~200 ml) amber, glass-stoppered erlenmeyer flask.

After the final extraction, rinse the sodium sulfate with additional ether, add to the combined extracts, and then evaporate to dryness with a nitrogen stream. Do not use heat! Dissolve the completely dried residue in 10 ml of the internal standard stock solution (working sample solution).

Procedure—Alternately inject 10 μl of the working standard and sample solutions into the liquid chromatograph to evaluate the retention times and condition of the column and to ensure constant response.

[3] Model U6K injector, Waters Associates, Milford, Mass.

[4] Model 770 spectroflow monitor, Schoeffel Instruments Corp., Westwood, N.J.

[5] μBondapak C_{18}, Waters Associates, Milford, Mass.

Table II—Analytical Results for a Typical Lot of Esterified Estrogens Bulk Substance

Estrogen Quantitated	HPLC Assay	Colorimetric Assay[a]
Equilenin, mg/g	0.83	—
Equilin, mg/g	5.11	3.20
Estrone, mg/g	28.88	28.28
Estradiol (17β-isomer), mg/g	0.72	—
Total estrogen content, mg/g	35.54	34.89
Percent claim	103	101.1
Equilin to estrone ratio	0.177	0.113

[a] Results as reported by the vendor *via* protocol.

Chromatograph duplicate standards and samples, and determine the respective responses using integration or peak height measurements.

Calculations—The response ratio for any particular estrogen, RR_E, may be determined as follows:

$$RR_E = \frac{P_E(\text{std})C_{IS}}{P_{IS}(\text{std})C_E} \qquad \text{(Eq. 1)}$$

where P_E is the peak height of the estrogen in the working standard, P_{IS} is the peak height of the internal standard in the working standard, C_{IS} is the concentration of the internal standard (milligrams per milliliter) in the working standard, and C_E is the concentration of the estrogen (milligrams per milliliter) in the working standard.

The amount of each esterified estrogen per gram of sample may be calculated as follows:

$$\text{mg of esterified estrogen/g of sample} = \frac{P_E(\text{spl})C_{IS}F}{P_{IS}(\text{spl})RR_E \text{ sample weight (g)}} \qquad \text{(Eq. 2)}$$

where P_E is the peak height of the estrogen in the working sample, P_{IS} is the peak height of the internal standard in the working sample, RR_E is the response ratio for the estrogen as described, C_{IS} is the concentration of the internal standard (milligrams per milliliter) in the working sample, and F is the dilution factor multiplied by the factor for converting free estrogen to the esterified estrogen = 10 × 1.38[6].

The amount of each esterified estrogen per tablet may be calculated by multiplying the milligrams of esterified estrogen per gram by the average unit weight.

After each component has been quantitated, the total esterified estrogen content of a bulk powder or tablet formulation may be determined by adding the amounts found for equilenin, equilin, estrone, and estradiol.

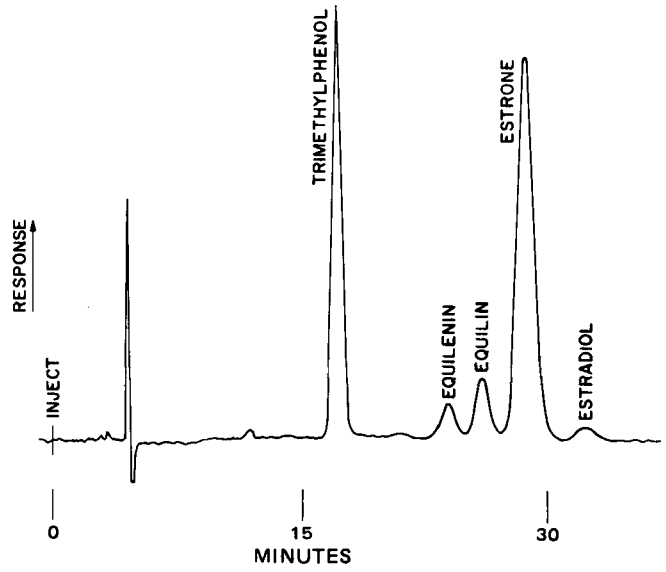

Figure 1—*Typical standard chromatogram for estrogen and internal standard compounds.*

[6] The molecular weight of sodium salt of the esterified estrogen divided by the molecular weight of the free estrogen is 1.38.

Table III—Estrogen Content (Milligrams per Tablet) of Various Sample Lots by HPLC and the Spectrophotometric Procedure

Lot	Equilenin	Equilin	Estrone	Estradiol	Total[a] Equilin + Estrone	Total Four Estrogens	Spectro-photometric[b]
A-1	0.005	0.035	0.172	0.003	0.207	0.215	0.197
A-2	0.004	0.032	0.167	0.004	0.199	0.206	0.206
A-3	0.005	0.035	0.176	0.005	0.211	0.221	0.208
A-4	0.005	0.038	0.179	0.004	0.217	0.226	0.197
A-5	0.005	0.038	0.178	0.004	0.216	0.225	0.196
B-1	0.010	0.072	0.356	0.007	0.427	0.444	0.419
B-2	0.010	0.072	0.352	0.009	0.424	0.442	0.404
C-K[c]-1	0.011	0.070	0.332	0.010	0.402	0.412	0.417
C-C[d]-1	0.012	0.057	0.316	0.008	0.373	0.392	0.411
C-K[c]-2	0.011	0.050	0.324	0.009	0.374	0.408	0.406
C-C[d]-2	0.013	0.062	0.329	0.010	0.391	0.414	0.391

[a] HPLC determination. [b] Equilin + estrone content. [c] Kernels or uncoated tablets. [d] Coated tablets.

RESULTS AND DISCUSSION

The determination of esterified estrogens in bulk substrates and combination dosage tablets presents many analytical problems. The time-consuming sample preparation prior to the colorimetric assay has too many steps where errors can be introduced, making final results questionable.

After a simple hydrolysis procedure, the converted free estrogens are extracted readily with ether. The evaporated extract residues, reconstituted in a methanolic solution containing the internal standard, are chromatographed; a run is completed in approximately 35 min. Typical standard and sample chromatograms are shown in Figs. 1 and 2.

With a flow rate of 0.6 ml/min, theoretical plates were calculated to range between 2100 and 3700 for the estrogens. Linearity of detector response and relative retention time data of each quantifiable estrogen are listed in Table I.

To verify noninterference of tablet excipients with estrogen elutions, placebo tablets were pulverized, extracted, reconstituted in methanol, and chromatographed. A baseline run was obtained, clearly showing no interference. Another portion of the powdered placebo mass was spiked with an equivalent amount of the bulk sodium estrone sulfate; upon extraction and chromatography, the recovery of 99+% was achieved.

A mixture of chlordiazepoxide base and ground placebo tablets, in the proportion found in the particular dosage form, was subjected to the extraction procedure and chromatography; no extraneous peaks were evident in any areas of the estrogen elutions.

To assure completeness of the extraction procedure, five individual extracts of 20 ml of ether were evaporated to dryness, dissolved in 2 ml of methanol, and chromatographed. This procedure was performed on two lots of tablets and on a bulk lot of the esterified estrogen mixture. The component percentages found per individual estrogens averaged 45.5 and 43.8 for the first and second extractions, respectively. The remaining extracts contained 5–20% for the third, 2–6% for the fourth, and 1% for the fifth. These data substantiated the need for more than three extractions.

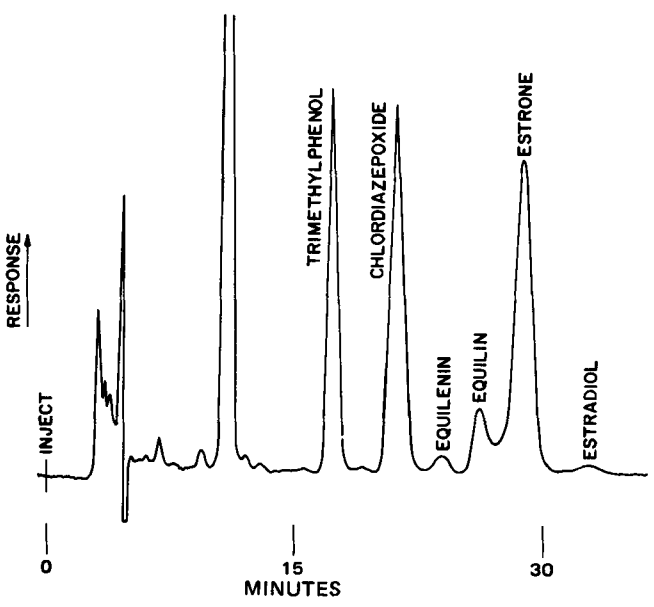

Figure 2—*Typical sample chromatogram for a tablet formulation.*

Results obtained for a typical lot of esterified estrogen bulk substance using the proposed HPLC method and the current spectrophotometric procedure are presented in Table II; data obtained from analyses of various dosage forms are compiled in Table III.

Statistical evaluations performed on six samples per lot of uncoated and coated tablets produced the following results (milligrams per tablet) for total estrogens: Lot C-K-1, 0.442, 0.429, 0.380, 0.390, and 0.423 (mean ± SD = 0.41 ± 0.02); Lot C-C-1, 0.375, 0.380, 0.379, 0.391, 0.396, and 0.411 (mean ± SD = 0.39 ± 0.02); Lot C-K-2, 0.391, 0.398, 0.411, 0.418, 0.412, and 0.418 (mean ± SD = 0.42 ± 0.01); and Lot C-C-2, 0.405, 0.414, 0.445, 0.398, 0.411, and 0.408 (mean ± SD = 0.41 ± 0.02).

The data presented affirm that this method is more acceptable than the procedure currently used because it is a rapid analytical technique of high precision and specificity.

REFERENCES

(1) "The United States Pharmacopeia," 19th rev., Mack Publishing Co., Easton, Pa., 1975, pp. 181–183.

(2) L. E. Fieser and M. Fieser, "Steroids," Reinhold, New York, N.Y., 1959, pp. 477, 478.

(3) J. Carol, F. M. Kunze, D. Banes, and J. H. Graham, *J. Pharm. Sci.*, **50**, 550 (1961).

(4) G. F. Krol, G. R. Boyden, R. H. Moody, J. C. Comeau, and B. T. Kho, *J. Chromatogr.*, **61**, 187 (1971).

(5) F. A. Isherwood, *Br. Med. Bull.*, **10**, 202 (1954).

(6) L. Hough and J. K. N. Jones, in "Methods in Carbohydrate Chemistry," vol. I, R. L. Whistler and M. L. Wolfrom, Eds., Academic, New York, N.Y., 1962, p. 21.

(7) R. J. Tscherne and G. Capitano, *J. Chromatogr.*, **136**, 337 (1977).

(8) S. Maglione, A. Bellastella, R. Gasbarro, A. Ghionini, and G. Iacono, *Biochim. Appl.*, **15**, 542 (1968).

(9) J. H. H. Thijssen and W. Veeman, *Steroids*, **11**, 369 (1968).

(10) J. C. Touchstone, T. Murawec, O. Brual, and M. Breckwolt, *ibid.*, **17**, 285 (1971).

(11) R. Johnson, R. Masserano, R. Haring, B. Kho, and G. Schilling, *J. Pharm. Sci.*, **64**, 1007 (1975).

(12) R. Roman, C. H. Yates, J. F. Millar, and W. J. A. VandenHeuvel, *Can. J. Pharm. Sci.*, **10**, 8 (1975).

(13) *Ibid.*, **10**, 12 (1975).

(14) H. Van Baelen, W. Heyns, and P. DeMoor, *J. Chromatogr.*, **30**, 226 (1967).

(15) A. R. Hurwitz, H. J. Burke, and R. A. Marra, *J. Pharm. Sci.*, **56**, 1509 (1967).

(16) G. J. Krol, R. P. Masserano, J. F. Carney, and B. T. Kho, *ibid.*, **59**, 1483 (1970).

(17) R. A. Dishman, Ph.D. thesis, University of Massachusetts, Amherst, Mass., 1970.

(18) J. A. Schmit, in "Modern Practice of Liquid Chromatography," J. J. Kirkland, Ed., Wiley–Interscience, New York, N.Y., 1971, pp. 393–397.

(19) R. J. Dolphin, *J. Chromatogr.*, **83**, 421 (1973).

(20) "Application Highlight," AH 336, Waters Associates, Milford, Mass., 1974.
(21) W. C. Landgraf and E. C. Jennings, *J. Pharm. Sci.*, **62**, 278 (1973).
(22) R. A. Henry, J. A. Schmit, and J. F. Dieckman, *J. Chromatogr. Sci.*, **9**, 513 (1971).
(23) A. G. Butterfield, B. A. Lodge, and N. J. Pound, *ibid.*, **2**, 401 (1973).
(24) R. W. Roos, *J. Pharm. Sci.*, **63**, 594 (1974).
(25) R. W. Roos, *J. Chromatogr. Sci.*, **14**, 505 (1976).

Surface Activities of Procaine, Lidocaine, and Tetracaine and Their Interaction Energies with Phospholipid Monolayers

FEDERICO A. VILALLONGA ˣ **and EDWARD W. PHILLIPS**

Received November 7, 1977, from the *College of Pharmacy, University of Florida, Gainesville, FL 32610.* Accepted for publication August 7, 1978.

Abstract □ The free energies of adsorption of procaine, lidocaine, and tetracaine at the air–water interface were estimated from plots of surface pressure ($\pi \leq 5$ dynes/cm) against bulk concentration. Their interaction energies with dipalmitoylphosphatidylethanolamine and dipalmitoyllecithin monolayers, previously spread at the air–water interface, were estimated from the increase of surface pressure with increasing concentrations of the subphase-injected anesthetic. Free energies of adsorption and the interaction energies were in the order procaine < lidocaine < tetracaine and correlate with relative anesthetic potencies and the blocking of nerve conduction.

Keyphrases □ Anesthetics, local—free energies of adsorption at air–water interface and interaction energies with phospholipid monolayers correlated with pharmacological activity □ Adsorption, free energies—various local anesthetics at air–water interface, correlated with pharmacological activity □ Interaction energies—various local anesthetics with phospholipid monolayers, correlated with pharmacological activity □ Phospholipid monolayers—interaction energies with various local anesthetics correlated with pharmacological activity □ Surface activities—various local anesthetics, correlated with pharmacological activity

The correlation between the potency of local anesthetics in blocking nerve conduction and their penetrations into lipidic monolayers has been demonstrated (1–5). More recently, it was shown by NMR (6, 7) and spin-labeled local anesthetics (8) that they do penetrate into zwitterionic phospholipid bilayers of liposomes.

The present work examines the surface activities of procaine, lidocaine, and tetracaine at the air–aqueous interface and estimates their interaction energies with dipalmitoylphosphatidylethanolamine and dipalmitoyllecithin monolayers, previously spread at the air–aqueous interface.

EXPERIMENTAL

Reagents—Procaine hydrochloride[1], lidocaine hydrochloride[2], and tetracaine hydrochloride[2] were used without further purification. Dipalmitoyllecithin[3], dipalmitoylphosphatidylethanolamine[4], hexane[5] used for the preparation of the spreading solutions, and distilled water used for the preparation of the solutions fulfilled the requirements previously specified (9, 10). Analytical reagent sodium chloride[6] was roasted for 6 hr at 700° prior to the preparation of the aqueous solutions to remove surface-active organic impurities.

Instruments and Methods—Surface tension was measured with a Wilhelmy platinum plate attached to an electrobalance[7] whose output was fed into a recorder[8]. The methods for the measurement of the surface tension of aqueous solutions, γ, and the change of the surface pressure, $\Delta\pi$, of the phospholipid monolayer as a function of time after drug injection in the subphase were described previously (9–11). All experiments were performed in 0.15 *M* NaCl at 20 ± 1°.

In the injection experiments, the initial surface pressure of the phospholipid monolayer spread at the air–0.15 *M* NaCl interface was 5 ± 0.1 dynes/cm. The surface pressure, π, of the drug solution is the difference between the previously determined surface tension of the 0.15 *M* NaCl, γ_{NaCl}, and the surface tension of the drug solution in this saline solution, γ_d. The surface pressure, π, was fitted to a function of the drug concentration, *C*, by digital computerized nonlinear regression to exponential equations of the form:

$$\pi = \gamma_{NaCl} - \gamma_d = B_1 e^{[B_2(\log C)^2 + B_3 \log C]} \qquad \text{(Eq. 1)}$$

where the B_i values were adjustable parameters (9).

Densities of the drug solutions were determined with 10-ml specific gravity bottles previously calibrated with water. The precision of the weighing was ± 0.1 mg.

RESULTS

Adsorption at Air–Aqueous Interface—Typical plots of the surface pressure against the logarithm of the concentration (moles per liter) for procaine hydrochloride, lidocaine hydrochloride, and tetracaine hydrochloride in 0.15 *M* NaCl are given in Fig. 1.

A simple expression for the free energy of adsorption was derived (12) from thermodynamic and molecular kinetic considerations:

$$\Delta G^\circ = -RT \ln \frac{\pi}{X_2^*} \qquad \text{(Eq. 2)}$$

where ΔG° is the change in standard free energy associated with the adsorption of the solute at an air–water interface, π is the surface pressure, X_2^* is the activity of the solute, and R and T are the universal gas constant and the absolute temperature, respectively. Thus, the numerical value of ΔG can be calculated from the slope, π/X_2^*, of a linear plot of π against the mole fraction, X_2, of the solute in bulk solution when $X_2 \to 0$ and $X_2 \to X_2^*$ at low mole fractions. This expression was used recently for the estimation of the free energy of adsorption of alkanols from C_1 to C_{14} at the air–aqueous interface (11).

The plots (Fig. 2) of π against X_2 for the three compounds were reasonably linear in the region $\pi \leq 5$ dynes/cm under the experimental

[1] Sigma Chemical Co., St. Louis, Mo.
[2] Pfaltz and Bauer, Stamford, Conn.
[3] Applied Science Laboratories, State College, Pa.
[4] Schwarz-Mann Research Laboratories, Orangeburg, N.Y.
[5] J. H. Baker Chemical Co., Phillipsburg, N.J.
[6] Mallinckrodt Chemical Works, St. Louis, Mo.
[7] Cahn Division, Ventron Instrumental Corp., Paramount, Calif.
[8] Leeds Northrup, North Wales, Pa.

0022-3549/79/0300-0314$01.00/0
© 1979, American Pharmaceutical Association

(20) "Application Highlight," AH 336, Waters Associates, Milford, Mass., 1974.
(21) W. C. Landgraf and E. C. Jennings, *J. Pharm. Sci.*, **62**, 278 (1973).
(22) R. A. Henry, J. A. Schmit, and J. F. Dieckman, *J. Chromatogr. Sci.*, **9**, 513 (1971).
(23) A. G. Butterfield, B. A. Lodge, and N. J. Pound, *ibid.*, **2**, 401 (1973).
(24) R. W. Roos, *J. Pharm. Sci.*, **63**, 594 (1974).
(25) R. W. Roos, *J. Chromatogr. Sci.*, **14**, 505 (1976).

Surface Activities of Procaine, Lidocaine, and Tetracaine and Their Interaction Energies with Phospholipid Monolayers

FEDERICO A. VILALLONGA ˣ **and EDWARD W. PHILLIPS**

Received November 7, 1977, from the *College of Pharmacy, University of Florida, Gainesville, FL 32610.* Accepted for publication August 7, 1978.

Abstract □ The free energies of adsorption of procaine, lidocaine, and tetracaine at the air–water interface were estimated from plots of surface pressure ($\pi \leq 5$ dynes/cm) against bulk concentration. Their interaction energies with dipalmitoylphosphatidylethanolamine and dipalmitoyllecithin monolayers, previously spread at the air–water interface, were estimated from the increase of surface pressure with increasing concentrations of the subphase-injected anesthetic. Free energies of adsorption and the interaction energies were in the order procaine < lidocaine < tetracaine and correlate with relative anesthetic potencies and the blocking of nerve conduction.

Keyphrases □ Anesthetics, local—free energies of adsorption at air–water interface and interaction energies with phospholipid monolayers correlated with pharmacological activity □ Adsorption, free energies—various local anesthetics at air–water interface, correlated with pharmacological activity □ Interaction energies—various local anesthetics with phospholipid monolayers, correlated with pharmacological activity □ Phospholipid monolayers—interaction energies with various local anesthetics correlated with pharmacological activity □ Surface activities—various local anesthetics, correlated with pharmacological activity

The correlation between the potency of local anesthetics in blocking nerve conduction and their penetrations into lipidic monolayers has been demonstrated (1–5). More recently, it was shown by NMR (6, 7) and spin-labeled local anesthetics (8) that they do penetrate into zwitterionic phospholipid bilayers of liposomes.

The present work examines the surface activities of procaine, lidocaine, and tetracaine at the air–aqueous interface and estimates their interaction energies with dipalmitoylphosphatidylethanolamine and dipalmitoyllecithin monolayers, previously spread at the air–aqueous interface.

EXPERIMENTAL

Reagents—Procaine hydrochloride[1], lidocaine hydrochloride[2], and tetracaine hydrochloride[2] were used without further purification. Dipalmitoyllecithin[3], dipalmitoylphosphatidylethanolamine[4], hexane[5] used for the preparation of the spreading solutions, and distilled water used for the preparation of the solutions fulfilled the requirements previously specified (9, 10). Analytical reagent sodium chloride[6] was roasted for 6 hr at 700° prior to the preparation of the aqueous solutions to remove surface-active organic impurities.

Instruments and Methods—Surface tension was measured with a Wilhelmy platinum plate attached to an electrobalance[7] whose output was fed into a recorder[8]. The methods for the measurement of the surface tension of aqueous solutions, γ, and the change of the surface pressure, $\Delta\pi$, of the phospholipid monolayer as a function of time after drug injection in the subphase were described previously (9–11). All experiments were performed in 0.15 *M* NaCl at 20 ± 1°.

In the injection experiments, the initial surface pressure of the phospholipid monolayer spread at the air–0.15 *M* NaCl interface was 5 ± 0.1 dynes/cm. The surface pressure, π, of the drug solution is the difference between the previously determined surface tension of the 0.15 *M* NaCl, γ_{NaCl}, and the surface tension of the drug solution in this saline solution, γ_d. The surface pressure, π, was fitted to a function of the drug concentration, *C*, by digital computerized nonlinear regression to exponential equations of the form:

$$\pi = \gamma_{NaCl} - \gamma_d = B_1 e^{[B_2(\log C)^2 + B_3 \log C]} \qquad \text{(Eq. 1)}$$

where the B_i values were adjustable parameters (9).

Densities of the drug solutions were determined with 10-ml specific gravity bottles previously calibrated with water. The precision of the weighing was ± 0.1 mg.

RESULTS

Adsorption at Air–Aqueous Interface—Typical plots of the surface pressure against the logarithm of the concentration (moles per liter) for procaine hydrochloride, lidocaine hydrochloride, and tetracaine hydrochloride in 0.15 *M* NaCl are given in Fig. 1.

A simple expression for the free energy of adsorption was derived (12) from thermodynamic and molecular kinetic considerations:

$$\Delta G^\circ = -RT \ln \frac{\pi}{X_2^*} \qquad \text{(Eq. 2)}$$

where ΔG° is the change in standard free energy associated with the adsorption of the solute at an air–water interface, π is the surface pressure, X_2^* is the activity of the solute, and R and T are the universal gas constant and the absolute temperature, respectively. Thus, the numerical value of ΔG can be calculated from the slope, π/X_2^*, of a linear plot of π against the mole fraction, X_2, of the solute in bulk solution when $X_2 \to 0$ and $X_2 \to X_2^*$ at low mole fractions. This expression was used recently for the estimation of the free energy of adsorption of alkanols from C_1 to C_{14} at the air–aqueous interface (11).

The plots (Fig. 2) of π against X_2 for the three compounds were reasonably linear in the region $\pi \leq 5$ dynes/cm under the experimental

[1] Sigma Chemical Co., St. Louis, Mo.
[2] Pfaltz and Bauer, Stamford, Conn.
[3] Applied Science Laboratories, State College, Pa.
[4] Schwarz-Mann Research Laboratories, Orangeburg, N.Y.
[5] J. H. Baker Chemical Co., Phillipsburg, N.J.
[6] Mallinckrodt Chemical Works, St. Louis, Mo.
[7] Cahn Division, Ventron Instrumental Corp., Paramount, Calif.
[8] Leeds Northrup, North Wales, Pa.

0022-3549/79/0300-0314$01.00/0
© 1979, American Pharmaceutical Association

Table I—Free Energies of Adsorption at the Air-Water Interface (ΔG), Interaction Energies with Phospholipid Monolayers (Ψ), and Free Energies of Transfer (ΔG_{tr}) from Water to Octanol of Procaine, Lidocaine, and Tetracaine

Local Anesthetic	Interface: Air–0.15 *M* NaCl, $\Delta G°$, kcal/mole	Interface: I[a]–0.15 *M* NaCl, Ψ, kcal/mole	Interface: II[b]–0.15 *M* NaCl, Ψ, kcal/mole	Octanol-Water[c], $\Delta G°_{tr}$, kcal/mole	Relative[a] Anesthetic Potency	Relative[e] Blocking Potency
Procaine	3.9	3.5	4.2	2.5	1	1
Lidocaine	4.9	3.6	5.1	—	3.8	—
Tetracaine	7.3	6.5	6.5	5.0	36.5	460

[a] I = dipalmitoyllecithin monolayer. [b] II = dipalmitoylphosphatidylethanolamine monolayer. [c] Calculated from Ref. 17. [d] Reference 2. [e] Reference 13.

conditions. The intercepts were close to the limits of the reproducibility of the surface tension measurements (±0.2 dyne/cm). The estimated values of $\Delta G°$ (±0.2 kcal/mole) from such plots are given in Table I. The free energies of adsorption, $\Delta G°$ (kilocalories per mole), were in the order tetracaine > lidocaine > procaine and correlate with their blocking potencies on the decapitated frog sciatic nerve (2) and their anesthetic potencies obtained with the frog sciatic nerve trunk (13).

Interaction with Phospholipid Monolayers—The interaction of the subphase-injected drugs with dipalmitoylphosphatidylethanolamine and dipalmitoyllecithin monolayers was virtually complete in the first 15 min after the injection. The criterion of equilibrium was the constancy (±0.1 dyne/cm) of the surface pressure increment, $\Delta\pi$, during 30 min. The interaction energies, Ψ, were estimated (9–11, 14) from the slopes of the linear plots of the reciprocals of the equilibrium surface pressures, $\Delta\pi_{eq}$, after the injection against the reciprocals of the final concentrations, n (molecules per cubic centimeter), of the subphase-injected drug. In both cases, such energies (Table I) were in the order procaine < lidocaine < tetracaine.

DISCUSSION

Adsorption at Air–Aqueous Interface—Even for nonideal solutions, the amount of surfactant ion present in an adsorbed monolayer at the air–aqueous interface can be estimated directly from measurements of the variation of the surface tension with surfactant bulk concentration at constant counterion concentration using the equation:

$$-\Gamma_2^m = \frac{1}{RT}\left(\frac{d\sigma}{d\ln m_2}\right)_{m_3} \qquad \text{(Eq. 3)}$$

where Γ_2^m is the amount of surfactant ion in the monolayer (moles per square centimeter), R is the universal gas constant (ergs per degree per mole), T is the absolute temperature (degrees Kelvin), σ is the surface tension of the surfactant solution (dynes per centimeter), and m_2 and m_3 are the molalities (moles per kilogram) of the surfactant ion and of the counterion, respectively, in the bulk solution (15).

Equation 3 can be conveniently transformed into:

$$\Gamma_2^m = \frac{1}{RT}\left(\frac{d\pi}{d\ln m_2}\right)_{m_3} \qquad \text{(Eq. 4)}$$

where π is the surface pressure (dynes per centimeter) of the surfactant solution containing a constant (m_3) molal counterion concentration.

The derivative $[d\pi/(d\ln C_2)]$ of the exponential equation (Eq. 1) that characterized the dependence of the surface pressure on the concentration was computed with respect to the logarithm of the concentration (moles per kilogram) of the anesthetic compound. Substitution of these values into Eq. 4 permitted the calculation of the amount of anesthetic ion in the monolayer, Γ_2^m (moles per square centimeter), at any bulk concentration.

Space-filling molecular models and molecular volume calculations performed using group increments (16) indicate that the molecular dimensions of these anesthetic ions are such that they can be accommodated into a thin interfacial region 10–20 Å thick. On the premise that the anesthetic ions that form the adsorbed monolayer at the air–aqueous interface are completely immersed in the aqueous phase and on the assumption of an average thickness of 15 Å, the volume, V_s, of the interfacial region containing the number of anesthetic ions, Γ_2^m (moles per square centimeter), can reasonably be estimated for comparative purposes.

Plots of the concentration of such a thin interfacial region [$\Gamma_2' = (\Gamma_2^m/V_s)$ in moles per liter] estimated from these volumes and from the surface concentration, Γ_2^m (moles per square centimeter), against the bulk concentration, C (moles per liter), are given in Fig. 3 for procaine, lidocaine, and tetracaine and indicate that the concentration of adsorbed tetracaine at the thin interfacial region could be up to 10^3 times greater than that of procaine or lidocaine with the same experimental conditions.

Interaction with Phospholipid Monolayers—Dipalmitoylphosphatidylethanolamine forms a condensed liquid monolayer. The strong $P^- \sim N^+$ electrostatic interaction of the zwitterionic hydrophilic polar groups jointly with the attractive forces between the hydrocarbon chains of neighboring molecules produce a rigid structuring where any net electrical charge is essentially negligible (14).

Dipalmitoyllecithin forms a relatively less condensed monolayer at the air–water interface, because the shielding effect of the positively charged amino group by the three methyl groups decreases the attractive potential between neighboring molecules (14).

Partition coefficients have been measured between octanol–aqueous solution for procaine (17) and tetracaine (18). On the assumptions that the given numerical values of the interaction energies of procaine and tetracaine are valid estimates (*i.e.*, the entropies are invariant) and that the same energies are operative under the conditions in which partition coefficients were measured, the changes in free energies that correspond

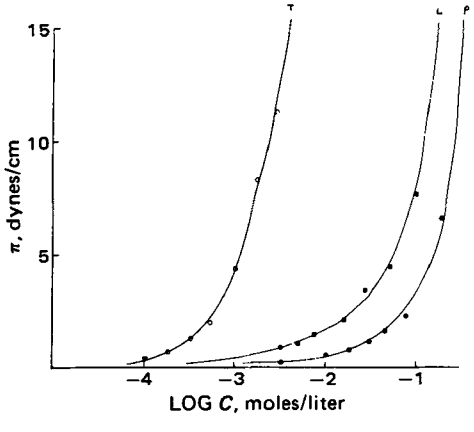

Figure 1—*Plots of surface pressure, π, against the logarithm of the bulk concentration, C (moles per liter), for tetracaine (T), lidocaine (L), and procaine (P). The lines drawn through the experimental points were the "best fit" to Eq. 1 obtained from the computer.*

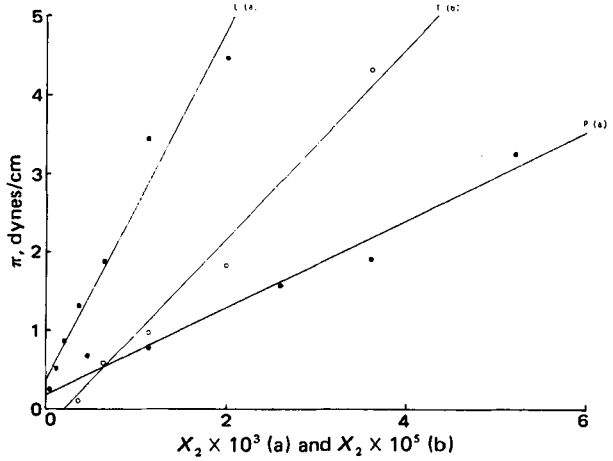

Figure 2—*Plots of surface pressure, π (≤5 dynes/cm), against the mole fraction, X_2, for tetracaine (T), lidocaine (L), and procaine (P).*

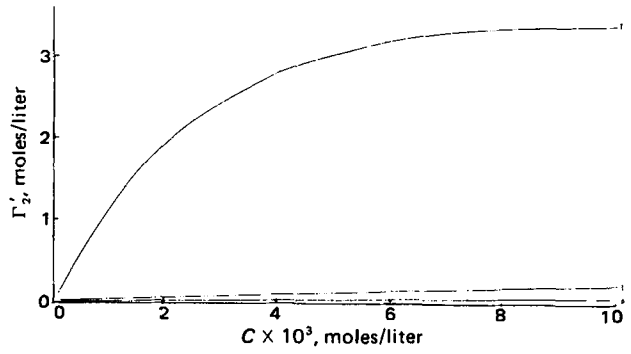

Figure 3—*Plots of concentration at the interfacial region* (Γ'_2, *moles per liter*) *against bulk concentration* (C, *moles per liter*) *for tetracaine* (*T*), *lidocaine*, (*L*), *and procaine* (*P*).

to octanol–water partition coefficients of procaine and tetracaine were calculated from the literature data (17) using:

$$\Delta G^\circ_{tr} = RT \ln P \qquad \text{(Eq. 5)}$$

where P is the partition coefficient and ΔG°_{tr} is the standard free energy of transfer of the solute. Such energies (ΔG°_{tr}) (Table I) correlate with the interaction energies with phospholipid monolayers.

NMR evidence for the hydrophobic interaction of tetracaine, lidocaine, and procaine with egg yolk phospholipid liposomes indicates that the aromatic protons of procaine are affected more drastically than those between the aromatic side of the molecule and the quaternary amine. The less affected protons are those of the CH_2N groups, which suggests that they face the aqueous phase. For tetracaine, the less affected protons are those of the CH_2N groups; the more affected are those of the butylene groups at the nonpolar side of the molecule. These findings indicate that the property of penetrating the liposome membrane is dependent on the nonpolar side of the molecules (6, 7).

The results show that the interaction energies of tetracaine with dipalmitoylphosphatidylethanolamine and dipalmitoyllecithin monolayers are higher than those of lidocaine and procaine. This fact seems to confirm that the enhanced hydrophobicity of the nonpolar end of this molecule due to the presence of the butylene group favors the penetration of the tetracaine nonpolar moiety through the liposome bilayers. This facilitated penetration and the observed increase of the relative anesthetic and blocking potencies may be the results of the comparatively greater interfacial concentration of tetracaine.

REFERENCES

(1) J. C. Skou, *Acta Pharmacol. Toxicol.*, **10**, 325 (1954).

(2) *Ibid.*, **10**, 281 (1954).

(3) A. M. Shanes and N. L. Gershfeld, *J. Gen. Physiol.*, **44**, 345 (1960).

(4) N. L. Gershfeld, *J. Phys. Chem.*, **66**, 1923 (1962).

(5) H. S. Hendrickson, *J. Lipid Res.*, **17**, 393 (1976).

(6) J. Cerbon, *Biochim. Biophys. Acta*, **290**, 51 (1973).

(7) M. S. Fernandez and J. Cerbon, *ibid.*, **298**, 8 (1973).

(8) G. J. Giotta, D. S. Chan, and H. H. Wang, *Arch. Biochem. Biophys.*, **163**, 453 (1974).

(9) F. A. Vilallonga, E. R. Garrett, and M. Cereijido, *J. Pharm. Sci.*, **61**, 1720 (1972).

(10) F. A. Vilallonga and E. R. Garrett, *ibid.*, **62**, 1605 (1973).

(11) F. A. Vilallonga, E. R. Garrett, and J. S. Hunt, *ibid.*, **66**, 1226 (1977).

(12) J. H. Clint, J. M. Corkill, J. F. Goodman, and J. R. Tate, *J. Colloid Interface Sci.*, **28**, 522 (1968).

(13) M. P. Blaustein and D. E. Goldman, *Science*, **153**, 429 (1966).

(14) F. A. Vilallonga and E. W. Phillips, *J. Pharm. Sci.*, **67**, 773 (1978).

(15) D. G. Hall, B. A. Pethica, and K. Shinoda, *Bull. Chem. Soc. Jpn.*, **48**, 324 (1975).

(16) A. Bondi, "Physical Properties of Molecular Crystals, Liquids and Glasses," Wiley, New York, N.Y., 1968, p. 453.

(17) A. Leo, C. Hansch, and D. Elkins, *Chem. Rev.*, **71**, 525 (Table XVII) (1971).

(18) A. Brandstrom, *Acta Pharm. Suec.*, **1**, 159 (1966).

Synthesis of Substituted 2-Aminopyrrole Analogs of Lidocaine I

RONALD W. JOHNSON *, THOMAS H. KEENAN ‡, JOSEPH W. KOSH, and J. WALTER SOWELL, Sr. ˣ

Received June 1, 1978, from the *College of Pharmacy, University of South Carolina, Columbia, SC 29208.* Accepted for publication August 28, 1978. *Present address: Medical University of South Carolina, Charleston, S.C. ‡Present address: Purdue University, West Lafayette, Ind.

Abstract □ The synthesis, local anesthetic, and antiarrhythmic properties of nine 2-diethylaminoacetamido-3-cyano-4-methyl-5-substituted pyrroles are described. All compounds showed local anesthetic activity by the guinea pig wheal test and antiarrhythmic activity for chloroform-induced ventricular arrhythmias in mice.

Keyphrases □ 2-Aminopyrrole analogs of lidocaine, various—synthesized, evaluated for local anesthetic activity in guinea pigs and antiarrhythmic activity in mice □ Structure–activity relationships—various 2-aminopyrrole analogs of lidocaine evaluated for local anesthetic activity in guinea pigs and antiarrhythmic activity in mice □ Lidocaine analogs—2-aminopyrroles synthesized

The use of lidocaine (I) as a local anesthetic is well documented. In recent years, lidocaine has also gained popularity for the treatment of ventricular arrhythmia. Due to its rapid metabolic rate (1), lidocaine is normally given by continuous intravenous administration in the treatment of ventricular arrhythmia. Plasma and tissue lidocaine levels fall rapidly (1) when intravenous administration is discontinued. The limited extent of plasma protein binding coupled with rapid metabolic transformations (2–4) accounts for the relatively short biological half-life.

Numerous analogs and homologs of lidocaine have been synthesized and evaluated. The major research thrust has been directed at modification of the aminoacyl portion of the lidocaine structure. The effect of these structural modifications on activity has been well established. The replacement of the benzenoid ring system in lidocaine by the heteroaromatic pyrrole ring system, however, has not been studied.

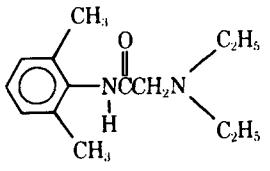

I

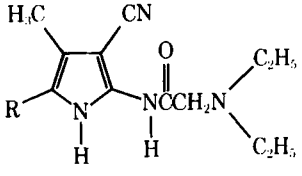

II

A series of 2-diethylaminoacetamido-3-cyano-4-methyl-5-substituted pyrrole (II) analogs of lidocaine was synthesized to compare the effects of this nuclear modification on both the local anesthetic and antiarrhythmic activities.

DISCUSSION

Chemistry—The synthesis of 2-amino-3-cyano-4-methyl-5-substituted pyrroles (III*a*–III*i*) (Scheme I) was reported previously (5–7). Comparatively few simple 2-aminopyrroles are known, and the majority of those are substituted with an electron-withdrawing group on the pyrrole ring (8). The nitrile at the 3-position of III*a*–III*i* stabilizes the 2-aminopyrroles from decomposition. The substituent at the 5-position corresponds to the R group of various α-amino acids utilized as precursors to III*a*–III*i*. The choice of these compounds as starting materials for the synthesis of the lidocaine analogs was made on the basis of their availability in good yields from commercially available L- or DL-α-amino acids.

The synthetic route to the 2-aminopyrrole analogs (II) of lidocaine parallels the original synthesis of lidocaine by Löfgren and Lundgvist (9). Acylation of III*a*–III*i* with chloroacetyl chloride in acetone with an equivalent amount of pyridine gave the corresponding 2-chloroacetamides (IV*a*–IV*i*) in excellent yields (Table I). These amides were high melting, stable, and relatively insoluble. The IR and NMR spectra were

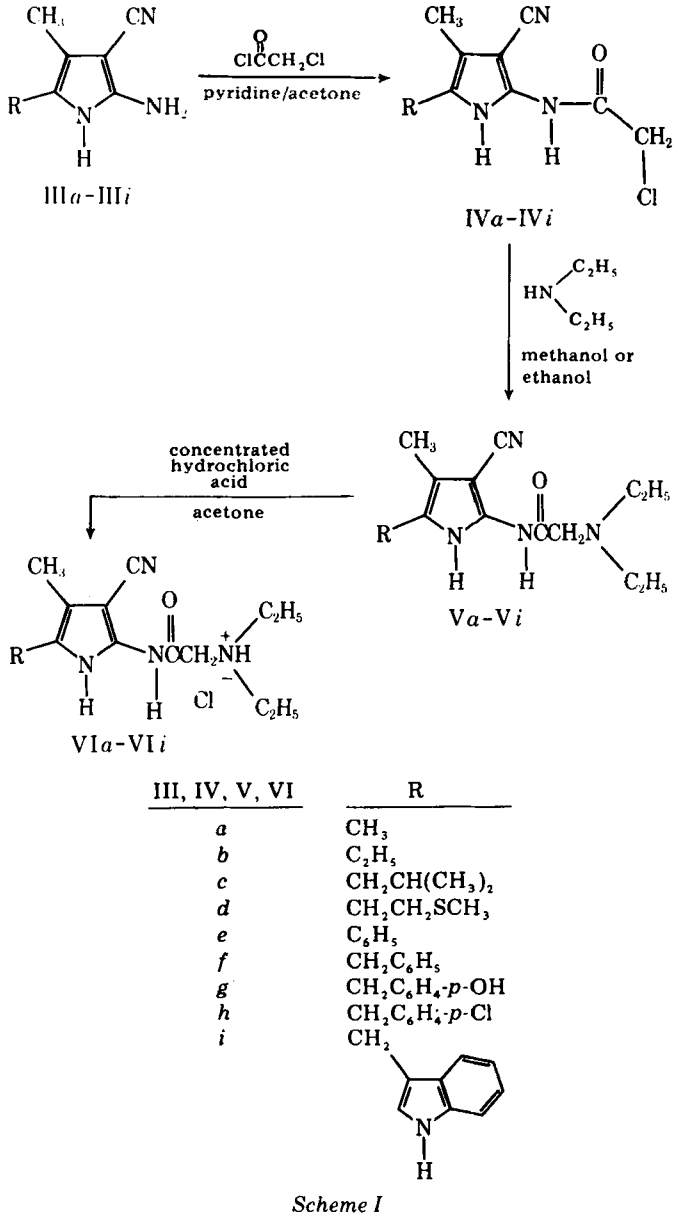

III, IV, V, VI	R
a	CH_3
b	C_2H_5
c	$CH_2CH(CH_3)_2$
d	$CH_2CH_2SCH_3$
e	C_6H_5
f	$CH_2C_6H_5$
g	$CH_2C_6H_4$-*p*-OH
h	$CH_2C_6H_4$-*p*-Cl
i	CH_2

Scheme I

0022-3549/79/0300-0317$01.00/0
© 1979, American Pharmaceutical Association

Table I—Data for 2-Chloroacetamido-3-cyano-4-methyl-5-substituted Pyrroles

Compound	Yield, %	Melting Point	R_f[a]	Recrystallization Solvent	Formula	Analysis, %	Calc.	Found
IV*a*	90.0	240–241.5° dec.	0.57	Ethanol	$C_9H_{10}ClN_3O$	C	51.07	51.04
						H	4.76	4.76
						Cl	16.75	16.74
						N	19.85	19.89
IV*b*	94.2	208–209° dec.	0.56	Ethanol	$C_{10}H_{12}ClN_3O$	C	53.22	53.28
						H	5.36	5.39
						Cl	15.71	15.80
						N	18.62	18.61
IV*c*	94.1	160–161°	0.57	Ethanol	$C_{12}H_{16}ClN_3O$	C	56.80	56.85
						H	6.36	6.37
						Cl	13.97	13.93
						N	16.56	16.54
IV*d*	81.6	166–167°	0.46	Ethanol	$C_{11}H_{14}ClN_3OS$	C	48.61	48.67
						H	5.19	5.19
						Cl	13.05	13.03
						N	15.46	15.45
						S	11.80	11.77
IV*e*	95.6	246–247.5° dec.	0.55	Ethanol	$C_{14}H_{12}ClN_3O$	C	61.43	61.38
						H	4.42	4.46
						Cl	12.95	13.05
						N	15.35	15.32
IV*f*	100	183.5–184°	0.57	Ethanol–2-propanol–water	$C_{15}H_{14}ClN_3O$	C	62.61	62.62
						H	4.90	4.91
						Cl	12.32	12.38
						N	14.60	14.63
IV*g*	80	218–219° dec.	0.57	Ethanol–water	$C_{15}H_{14}ClN_3O_2$	C	59.31	59.21
						H	4.65	4.66
						Cl	11.67	11.66
						N	13.83	13.82
IV*h*	91.7	188–189°	0.58	Ethanol	$C_{15}H_{13}Cl_2N_3O$	C	55.92	55.96
						H	4.07	4.09
						Cl	22.01	22.14
						N	13.04	13.02
IV*i*	73.5	200–201° dec.	0.56	Ethanol–water	$C_{17}H_{15}ClN_4O$	C	62.48	62.55
						H	4.63	4.66
						Cl	10.85	10.75
						N	17.14	17.17

[a] Ethyl acetate.

Table II—Data for 2-Diethylaminoacetamido-3-cyano-4-methyl-5-substituted Pyrroles

Compound	Yield, %	Melting Point	Reaction Solvent[a]	Recrystallization Solvent	Formula
V*a*	83.9	88–89°	Methanol	—[b]	$C_{13}H_{20}N_4O$
V*b*	98.0	84–85°	Ethanol	—[b]	$C_{14}H_{22}N_4O$
V*c*	95.8	86.5–87.5°	Ethanol	Methanol–water (4:1)	$C_{16}H_{26}N_4O$
V*d*	97.5	95–96°	Ethanol	Methanol–water (4:1)	$C_{15}H_{24}N_4OS$
V*e*	88.7	84.5–86°	Methanol	Methanol–water (4:1)	$C_{18}H_{22}N_4O$
V*f*	83.7	133–134°	Methanol	—[b]	$C_{19}H_{24}N_4O$
V*g*	64.7	149–150.5°	Methanol	—[b]	$C_{19}H_{24}N_4O_2$
V*h*	90.0	99–99.5°	Ethanol	Methanol–water (4:1)	$C_{19}H_{23}ClN_4O$
V*i*[c]	86.3	141–142.5°	Methanol	Methanol–water (4:1)	$C_{21}H_{25}N_5O$

[a] Absolute. [b] Free amine suitable for hydrochloride salt formation without recrystallization. [c] Calc. for: C, 69.40; H, 6.93; N, 19.27. Found: C, 69.45; H, 6.97; N, 19.22.

consistent with the assigned structures. The purity of the chloroacetamides was determined by TLC and elemental analysis (Table I).

The 2-diethylaminoacetamido-3-cyano-4-methyl-5-substituted pyrroles (V*a*–V*i*) were obtained by refluxing a suspension of the corresponding chloroacetamides (IV*a*–IV*i*) in absolute methanol or ethanol with excess diethylamine. During these reactions, solutions were achieved within 1–4 hr. The solvent and excess diethylamine were removed *in vacuo*, the amine residues were dissolved in 10% HCl, and the solutions were filtered to remove unreacted chloroacetamides. The amines were precipitated by the addition of 5% aqueous sodium hydroxide. Yields, melting points, and purification data are given in Table II.

All amine hydrochlorides, except VI*c* and VI*d*, were conveniently prepared by treating an acetone solution of the free amines with concentrated hydrochloric acid (Method A in *Experimental*). Compounds VI*c* and VI*d* were prepared in excellent yields by treating a solution of the amines in anhydrous ether with a saturated solution of hydrogen chloride in absolute ethanol (Method B in *Experimental*).

The IR spectra of the amine hydrochlorides (VI*a*–VI*h*) exhibited the expected N–H stretching absorption bands between 3400 and 3100 cm^{-1} and broad absorption in the 2800–2300-cm^{-1} region for the amine salts. The spectra contained intense, sharp absorption bands in the 2220–2210-cm^{-1} region for the nitrile and carbonyl absorption bands at 1630–1610 cm^{-1}. The NMR spectra of the amine hydrochlorides in dimethyl sulfate-d_6 contained a singlet at 1.84–2.12 ppm, integrating for three protons, which was assigned to the methyl group of the C-4 position. The protons of the diethylamino moiety appeared as a typical triplet and quartet for the methyl and methylene, respectively. The chemical shift for the triplet ranged from 1.16 to 1.30 ppm, and that for the quartet ranged from 3.10 to 3.28 ppm. The triplet and quartet integrated for three protons and two protons, respectively.

The methylene, alpha to the carbonyl, appeared as a singlet, integrating for two protons, at 3.89–4.20 ppm. The NH proton of the salt appeared as a broad singlet at 10.0–10.8 ppm. The NH protons of the amide and the pyrrole ring appeared as two broad singlets at 11.15–11.90 ppm.

Table III—Data for 2-Diethylaminoacetamido-3-cyano-4-methyl-5-substituted Pyrrole Hydrochlorides

Compound	Method	Yield, %	Recrystallization Solvent	R_f[a]	Melting Point	Formula	Analysis, %	Calc.	Found
VI*a*	A	84.7	Methanol–acetone	0.52	237.5–239° dec.	$C_{13}H_{21}ClN_4O$	C	54.82	54.77
							H	7.43	7.45
							Cl	12.45	12.54
							N	19.67	19.66
VI*b*	A	96.2	—[b]	0.48	221–222° dec.	$C_{14}N_{23}ClN_4O$	C	56.27	56.26
							H	7.76	7.76
							Cl	11.87	11.88
							N	18.75	18.74
VI*c*	B	94.5	Acetone–ether	0.50	156.5–157°	$C_{16}H_{27}ClN_4O$	C	58.79	58.68
							H	8.33	8.35
							Cl	10.85	10.85
							N	17.14	17.13
VI*d*	B	89.3	Acetone–ether	0.48	133–133.5°	$C_{15}H_{25}ClN_4OS$	C	52.23	52.18
							H	7.31	7.34
							Cl	10.28	10.24
							N	16.25	16.22
VI*e*	A	55.6[c]	Acetone–ether	0.51	199–201° dec.	$C_{18}H_{23}ClN_4O$	C	62.33	62.20
							H	6.68	6.72
							Cl	10.22	10.14
							N	16.15	16.12
VI*f*	A	51.5[c]	Methanol–acetone	0.56	221–222° dec.	$C_{19}H_{25}ClN_4O$	C	63.23	63.27
							H	6.98	6.98
							Cl	9.83	9.80
							N	15.53	15.54
VI*g*	A	46.7[c]	Ethanol–acetone	0.50	74–76°	$C_{19}H_{25}ClN_4O_2 \cdot H_2O$	C	57.78	57.78
							H	6.89	6.89
							Cl	8.98	8.99
							N	14.19	14.18
VI*h*	A	37.4[c]	—[b]	0.49	229–231° dec.	$C_{19}H_{24}Cl_2N_4O$	C	57.72	57.75
							H	6.12	6.12
							Cl	17.94	17.93
							N	14.17	14.17
VI*i*[d]	A and B	—	—	—	Oil	—		—	—

[a] Ethyl acetate. [b] Salt obtained was analytically pure. [c] Near quantitative yields obtained upon concentration of mother liquor. [d] Hydrochloride salt was a red oil, which would not solidify with several techniques employed. Elemental analysis was determined on the free base (V*i*).

Miscellaneous absorptions for the various members were consistent with their structures. The purity of the amine hydrochlorides (VI*a*–VI*h*) was determined by TLC and elemental analysis (Table III).

Pharmacology—*Antiarrhythmic Activity*—Cardiac rates of less than 200 beats/min were used as an index of protection from arrhythmia at 70 mg/kg. Compounds VI*a*, VI*b*, and VI*d*–VI*g* (Table IV) all showed activity at this dosage. The most active agent (VI*f*) was only slightly less potent than lidocaine.

Local Anesthetic Activity—All lidocaine analogs (VI*a*–VI*i*) possessed varying degrees of local anesthetic action (Table V). Compound VI*h* appeared to have the least activity while VI*e* and VI*f* were the most active. The latter compounds were more active than lidocaine at all three solution concentrations.

EXPERIMENTAL[1]

Chemistry—*2-Chloroacetamido-3-cyano-4,5-dimethylpyrrole (IVa)*—The procedure for the synthesis of IV*a* is given as representative for IV*b*–IV*i*. A solution of 2-amino-3-cyano-4,5-dimethylpyrrole (III*a*) (20.3 g, 0.15 mole) (5) in 300 ml of absolute acetone with pyridine (12.0 g, 0.15 mole) was prepared in a 500-ml erlenmeyer flask equipped with a drying tube. This solution was stirred in an acetone–ice bath for 10 min, followed by the dropwise addition of chloroacetyl chloride (17.4 g, 0.18 mole). The solution was stirred in the acetone–ice bath for 10 min and then at room temperature for 20 min. The reaction mixture was poured over 400 g of crushed ice.

After the ice had melted, the crude product was collected by filtration, resuspended in cold 95% methanol, filtered, and air dried. Two grams of the pale-yellow product (28.6 g, 90.0%) was recrystallized twice from absolute ethanol to yield white needle-shaped crystals (homogeneous on TLC, ethyl acetate, R_f 0.57), mp 240–241.5° dec.; IR (KBr): 3345, 3300, 3280, 3180, 2230, 1675, 1635, 1480, 1335, 1250, 1220, 755, 730, 680, and 640 cm^{-1}; NMR ((dimethyl sulfate-d_6): δ 1.85 (s, 3H, CH_3 at C_4), 1.95 (s, 3H, CH_3 at C_5), 4.12 (s, 2H, CH_2), 10.41 (broad s, 1H, NH of amide at C_2 or N_1H), and 10.95 (broad s, 1H, N_1H or NH of amide at C_2) ppm. (See Table I for analyses.)

2-Diethylaminoacetamido-3-cyano-4,5-dimethylpyrrole (Va)—The procedure for the synthesis of V*a* is given as representative for V*b*–V*i*.

[1] IR spectral data were determined on a Beckman IR-20A grating spectrophotometer using the potassium bromide technique. NMR spectra were determined on a Hitachi Perkin-Elmer R24 high-resolution spectrometer with tetramethylsilane as the internal reference. Melting points were obtained using a Thomas-Hoover capillary apparatus and are uncorrected. Carbon, hydrogen, chlorine, and nitrogen values were obtained from analyses performed by Atlantic Microlab, Inc., Atlanta, Ga. TLC was performed using Eastman Chromatogram sheets, type 6060 (silica gel), and the plates were developed in an iodine chamber.

Table IV—Antiarrhythmic Activity of 2-Aminopyrrole Analogs of Lidocaine[a]

Compound	40 mg/kg	70 mg/kg	100 mg/kg
Lidocaine	242 ± 13	141 ± 23	116 ± 6
VI*a*	206 ± 16	182 ± 14	140 ± 12
VI*b*	198 ± 19	186 ± 3	148 ± 18
VI*c*	196 ± 10	202 ± 6	186 ± 13
VI*d*	219 ± 8	175 ± 12	167 ± 13
VI*e*	249 ± 15	162 ± 7	140 ± 5
VI*f*	193 ± 16	153 ± 5	147 ± 7
VI*g*	220 ± 6	200 ± 7	183 ± 14
VI*h*	227 ± 4	233 ± 10	211 ± 12
VI*i*	278 ± 14	243 ± 8	197 ± 9
Control	351 ± 8	—	—

[a] Data represent arrhythmias induced in mice by exposure to chloroform vapor (n = 6).

Table V—Local Anesthetic Activity of 2-Aminopyrrole Analogs of Lidocaine[a]

Compound	1%	0.5%	0.2%
VI*a*	72	27	10
VI*b*	45	25	6
VI*c*	63	32	7
VI*d*	41	13	—
VI*e*	72	60	20
VI*f*	72	72	50
VI*g*	72	19	14
VI*h*	25	8	—
VI*i*	50	17	8
Lidocaine	68	41	17
0.9% NaCl	0	0	0

[a] Data represent the number of pricks failing to elicit a response following intradermal injection in guinea pigs (n = 2).

A suspension of IV*a* (21.2 g, 0.10 mole) in 300 ml of absolute methanol and diethylamine (36.6 g, 0.5 mole) was refluxed, with stirring, until complete solution was achieved (1–4 hr). The deep-orange-colored solution was refluxed for an additional 1 hr, the solvent and excess diethylamine were removed *in vacuo*, and the residue was dissolved in 100 ml of 10% HCl.

The acidic solution was filtered, 400 g of ice was added, and the amine was precipitated by the addition of 5% aqueous sodium hydroxide. The product was collected by filtration, washed with water, and air dried. The light-tan product (20.8 g, 83.9%), mp 88–89°, was suitable for formation of the hydrochloride salt. (See Table II for analogs.)

2-Diethylaminoacetamido-3-cyano-4-methyl-5-substituted Pyrrole Hydrochlorides (VIa–VIh)—Method A, as illustrated for 2-diethylaminoacetamido-3-cyano-4,5-dimethylpyrrole hydrochloride (VI*a*), is representative for the synthesis of VI*b* and VI*e*–VI*h*. To a solution of the free amine (V*a*) (9.9 g, 0.04 mole) in 150 ml of cold absolute acetone, 8 ml of concentrated hydrochloric acid (dissolved in 15 ml of acetone) was added. After 3 min of stirring, a heavy white precipitate formed. The white powder was collected, washed with acetone, and air dried.

Four grams of the crude product (9.6 g, 84.2%) was recrystallized from methanol–acetone to yield white flakes (homogeneous on TLC, ethyl acetate, R_f 0.52), mp 237.5–239° dec.; IR (KBr): broad absorption between 3300 and 2500 (with peaks at 3140, 3050, 2960, 2840, 2800, 2790, and 2690), 2220, 1695, 1610, 1565, 1470, 1430, 1420, 1340, 1300, 1280, 1265, 1215, 960, 740, 715, and 690 cm^{-1}; NMR (dimethyl sulfate-d_6): δ 1.19 (t, 6H, CH_3's of diethylamine), 1.84 (s, 3H, CH_3 at C_4), 1.95 (s, 3H, CH_3 at C_5), 3.10 (q, 4H, CH_2's of diethylamine), 3.89 (s, 2H, $COCH_2$), 10.10–10.70 (broad s, 1H, N^+H), 11.18 (broad s, 1H, NH of amide at C_2 or N_1H), and 11.30 (broad s, 1H, N_1H or NH of amide at C_2) ppm. (See Table III for analyses.)

2 - Diethylaminoacetamido - 3 - cyano-4-methyl-5-isobutylpyrrole Hydrochloride (VIc)—Method B was used for the synthesis of VI*c* and VI*d*. For VI*c*, a solution of V*c* (7.8 g, 0.027 mole) in 150 ml of anhydrous ether was treated with 4 ml of absolute ethanol, which had been saturated with hydrogen chloride gas. After 15 min in the freezer, the solvents were decanted from the gummy residue. The residue was triturated with 40 ml of anhydrous acetone, the acetone solution was diluted with 40 ml of anhydrous ether, and the powder was collected by filtration and dried over phosphorus pentoxide.

The white powder (8.3 g, 94.5%) was analytically pure (homogeneous on TLC, ethyl acetate, R_f 0.50), mp 156.5–157°; IR (KBr): 3400, 3120, 3020, 2960, broad absorption between 2800 and 2300, 2215, 1700, 1610, 1560, 1460, 1270, 1210, 980, and 960 cm^{-1}; NMR (dimethyl sulfate-d_6): δ 0.82 (d, 6H, gem dimethyls of isobutyl), 0.8–1.2 (m, 1H, methine of isobutyl), 1.28 (t, 6H, CH_3's of diethylamino), 1.95 (s, 3H, CH_3 at C_4), 2.3 (d, 2H, methylene of isobutyl at C_5), 3.28 (q, 4H, methylenes of diethylamino), 4.15 (s, 2H, $COCH_2$), 10.5–11.0 (broad s, 1H, N^+H), and 11.47 (s, 2H, N_1H and NH of amide at C_2) ppm. (See Table III for analyses.)

Pharmacology—*Antiarrhythmic Activity*—With the method of Lawson (10), fibrillations were induced in 20–30-g male mice by exposure to chloroform vapor until respiration ceased. The heart was then exposed, and the cardiac rate was determined with the aid of a binocular microscope. Mice with cardiac rates in excess of 200 beats/min were considered unprotected (Table IV).

Local Anesthetic Activity—The guinea pig wheal method of Bülbring and Wajda (11) was used to determine the activity. The back of the guinea pig was shaved 1 day prior to the test, and 0.25 ml of the aqueous drug solution was administered intradermally at two sites along the midline. The resulting wheals were tested by pricking the area six times with a pin at 5-min intervals for 1 hr. Local anesthesia was present if the pinprick did not elicit a skin twitch. The number of pinpricks that failed to elicit a response was then recorded at each time interval (Table V).

REFERENCES

(1) C.-Y. Sung and A. P. Truant, *J. Pharmacol. Exp. Ther.*, **112**, 432 (1954).

(2) G. Hollunger, *Acta Pharmacol.*, **17**, 356 (1960).

(3) *Ibid.*, **17**, 365 (1960).

(4) R. N. Boyes, D. B. Scott, P. J. Jebson, M. H. Godman, and D. G. Julian, *Clin. Pharmacol. Ther.*, **12**, 105 (1971).

(5) R. Gewald, *Z. Chem.*, **1**, 349 (1961).

(6) R. W. Johnson, R. J. Mattson, and J. W. Sowell, Sr., *J. Heterocycl. Chem.*, **14**, 383 (1977).

(7) V. I. Shvedov, M. V. Mezentseva, and A. N. Grinev, *Khim. Geterotsikl. Soedin.*, **9**, 1219 (1975); through *Chem. Abstr.*, **84**, 59299 (1976).

(8) R. M. Acheson, "An Introduction to the Chemistry of Heterocyclic Compounds," 2nd ed., Wiley, New York, N.Y., 1967, pp. 78, 79.

(9) N. M. Löfgren and B. J. Lundgvist, *Chem. Abstr.*, **42**, 6378g (1948).

(10) J. W. Lawson, *J. Pharmacol. Exp. Ther.*, **160**, 22 (1968).

(11) E. Bülbring and I. Wajda, *ibid.*, **85**, 78 (1945).

ACKNOWLEDGMENTS

Adapted in part from theses submitted by R. W. Johnson and T. H. Keenan to the Graduate School, University of South Carolina, in partial fulfillment of the Master of Science degree requirements.

The authors thank Mr. Charles Devlin for assistance in the synthesis of some starting materials and Ms. Myra Montjoy for manuscript typing.

Indolizine Derivatives with Biological Activity IV: 3-(2-Aminoethyl)-2-methylindolizine, 3-(2-Aminoethyl)-2-methyl-5,6,7,8-tetrahydroindolizine, and Their *N*-Alkyl Derivatives

IPPOLITO ANTONINI, FRANCESCO CLAUDI ˣ, UGO GULINI, LUIGI MICOSSI *, and FABRIZIO VENTURI *

Received June 9, 1978, from the *Istituto di Chimica Farmaceutica e di Chimica Organica, Università di Camerino, 62032 Camerino (MC), Italy.* Accepted for publication August 21, 1978. *Istituto di Farmacologia, Farmacognosia e Tecnica Farmaceutica della Università di Camerino, 62032 Camerino (MC), Italy.

Abstract □ In a continuing search for new biologically active agents derived from indolizine, 3-(2-aminoethyl)-2-methylindolizine, 3-(2-aminoethyl)-2-methyl-5,6,7,8-tetrahydroindolizine, and some mono- and di-*N*-substituted derivatives were prepared. Initial pharmacological screening showed that these compounds possess anti-5-hydroxytryptamine, antihistamine, antiacetylcholine, and CNS-depressant activities.

Keyphrases □ Indolizines, substituted—series synthesized, evaluated for pharmacological activity □ Anti-5-hydroxytryptamine activity—series of substituted indolizines evaluated □ Antihistaminic activity—series of substituted indolizines evaluated □ Antiacetylcholine activity—series of substituted indolizines evaluated □ CNS activity—series of substituted indolizines evaluated □ Structure–activity relationships—series of substituted indolizines evaluated

A previous paper (1) reported the synthesis of 3-(3-aminopropyl)-2-methylindolizine, 3-(3-aminopropyl)-2-methyl-5,6,7,8-tetrahydroindolizine, and some *N*-alkyl derivatives. These compounds showed anti-5-hydroxytryptamine, antihistamine, antiacetylcholine, and central nervous system (CNS)-depressant activities.

To explore further the structure–activity relationships of indolizine compounds, 3-(2-aminoethyl)-2-methylindolizine, 3-(2-aminoethyl)-2-methyl-5,6,7,8-tetrahydroindolizine, and some *N*-substituted derivatives were synthesized. The *in vitro* anti-5-hydroxytryptamine, antihistamine, and antiacetylcholine activities, as well as the *in vivo* effect on the CNS, were studied.

EXPERIMENTAL

Chemistry—The 3-(2-alkylaminoethyl)indolizine derivatives (Table I) were prepared as shown in Scheme I.

2-Methyl-3-(2-nitroethyl)indolizine (II) was obtained by the reaction of 2-methylindolizine (I) with nitroethylene. The structure of II was established on the basis of its NMR spectrum, which showed a singlet at δ 6.22 (1-H) ppm and signals at δ 7.85–7.55 (m, 5-H), 7.45–7.07 (m, 8-H), and 6.85–6.37 (m, 7-H and 6-H) ppm.

Reduction of II with lithium aluminum hydride gave 3-(2-aminoethyl)-2-methylindolizine (III). Treatment of III with ethyl chloroformate, followed by reduction of the 3-ethoxycarbonylaminoethyl derivative (IV), afforded 3-(2-methylaminoethyl)-2-methylindolizine (V). It was converted into the dimethyl derivative (VII) by the same reaction.

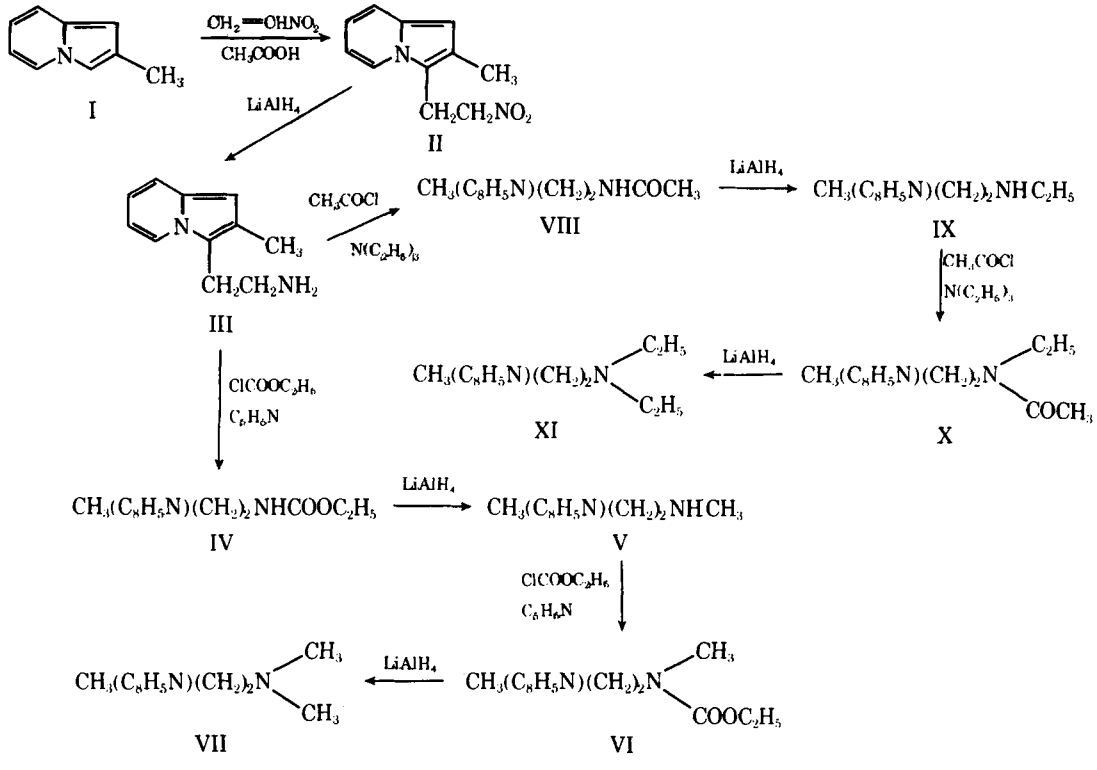

Scheme I

0022-3549/79/0300-0321$01.00/0
© 1979, American Pharmaceutical Association

Table I—Characteristics of 3-(2-Aminoethyl)-2-methylindolizines

Compound	Boiling Point/mm or Melting Point	Yield, %	Maleate Melting Point	Formula		Analysis, % Calc.	Found		Maleate Analysis, % Calc.	Found
III	81°/0.05	84	163–164°[a]	$C_{11}H_{14}N_2$	C	75.82	76.03	C	62.05	62.09
					H	8.10	8.21	H	6.25	6.22
					N	16.08	16.07	N	9.65	9.57
IV	65–66°[b]	83	—	$C_{14}H_{18}N_2O_2$	C	68.27	68.13	—	—	
					H	7.37	7.19			
					N	11.37	11.34			
V	85°/0.05	90	163–164°[c]	$C_{12}H_{16}N_2$	C	76.55	76.48	C	63.14	63.22
					H	8.57	8.51	H	6.62	6.59
					N	14.88	14.92	N	9.21	9.17
VI	122°/0.05	80	—	$C_{15}H_{20}N_2O_2$	C	69.20	69.26	—	—	
					H	7.74	7.71			
					N	10.76	10.69			
VII	84°/0.05	86	131–132°[a]	$C_{13}H_{18}N_2$	C	77.18	77.13	C	64.13	64.05
					H	8.97	8.90	H	6.97	6.88
					N	13.85	13.81	N	8.80	8.73
VIII	124–125°[d]	47	—	$C_{13}H_{16}N_2O$	C	72.19	72.14	—	—	
					H	7.46	7.40			
					N	12.95	12.89			
IX	105°/0.05	81	148–149°[c]	$C_{13}H_{18}N_2$	C	77.18	77.21	C	64.13	64.21
					H	8.97	8.86	H	6.97	6.84
					N	13.85	13.77	N	8.80	8.86
X	124°/0.1	88	—	$C_{15}H_{20}N_2O$	C	73.73	73.69	—	—	
					H	8.25	8.27			
					N	11.47	11.46			
XI	88°/0.1	83	94–95°[c]	$C_{15}H_{22}N_2$	C	78.21	78.15	C	65.87	65.72
					H	9.63	9.58	H	7.57	7.49
					N	12.16	12.19	N	8.09	8.12

[a] Recrystallized from ethanol. [b] Recrystallized from *n*-hexane. [c] Recrystallized from isopropanol. [d] Recrystallized from benzene.

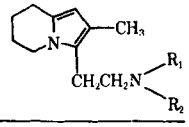

Table II—Characteristics of 3-(2-Aminoethyl)-2-methyl-5,6,7,8-tetrahydroindolizines

Compound	R_1	R_2	Boiling Point/mm	Yield, %	Maleate Melting Point	Formula		Analysis, % Calc.	Found		Maleate Analysis, % Calc.	Found
XII	H	H	77°/0.03	72	135–137°[a]	$C_{11}H_{18}N_2$	C	74.11	74.02	C	61.20	61.18
							H	10.18	10.15	H	7.53	7.47
							N	15.71	15.73	N	9.52	9.56
XIII	H	C_2H_5	86°/0.1	78	143–145°[b]	$C_{13}H_{22}N_2$	C	75.67	75.61	C	63.33	63.37
							H	10.75	10.77	H	8.13	8.18
							N	13.58	13.56	N	8.69	8.62
XIV	H	CH_3	73°/0.05	78	170–172°[c]	$C_{12}H_{20}N_2$	C	74.95	74.98	C	62.31	62.30
							H	10.48	10.44	H	7.85	7.79
							N	14.57	14.53	N	9.09	9.12
XV	C_2H_5	C_2H_5	90°/0.1	73	—[d]	$C_{15}H_{26}N_2$	C	76.86	76.89	C	65.11	65.13
							H	11.18	11.10	H	8.63	8.61
							N	11.95	11.93	N	7.99	7.94
XVI	CH_3	CH_3	83°/0.1	75	153–155°[b]	$C_{13}H_{22}N_2$	C	75.67	75.62	C	63.33	63.38
							H	10.75	10.79	H	8.13	8.17
							N	13.58	13.51	N	8.69	8.63

[a] Recrystallized from ethanol and anhydrous ether. [b] Recrystallized from isopropanol. [c] Recrystallized from anhydrous ethanol. [d] The maleate decomposed when heated in solution and is highly hygroscopic.

Again, acetylation of III gave the *N*-acetyl derivative (VIII), which was converted by reduction into 3-(2-ethylaminoethyl)-2-methylindolizine (IX).

Compound IX, again by acetylation followed by reduction, yielded 3-(2-diethylaminoethyl)-2-methylindolizine (XI). The 5,6,7,8-tetrahydroindolizines (XII–XVI, Table II) were prepared by catalytic hydrogenation of the corresponding indolizines III, V, VII, IX, and XI. All NMR spectra showed the signal of the 1-proton as a singlet whose position varied between δ 5.27 and 5.94 ppm. Moreover, the typical signals of the pyridine moiety protons, between δ 7.9 and 5.8 ppm in the unreduced products, had disappeared. All amines were converted to maleates.

Syntheses[1]—*2-Methyl-3-(2-nitroethyl)indolizine (II)*—Nitroethylene (0.06 mole) in dry benzene (25 ml) was added dropwise to a stirred and cooled (0–5°) solution of I (0.057 mole) (2) in acetic acid (5 ml) and dry benzene (50 ml). Stirring was continued for 2 days at room temperature. The solution was filtered on silica gel and then carefully made alkaline with 2 *N* NaOH; the solvent layer was separated and dried. Solvent evaporation gave a dark oily residue from which a solid product was precipitated by ethanol.

The solid was filtered and recrystallized from ethanol, mp 78–80°, in a 57% yield; IR: ν_{max} (mineral oil) 1535 and 1350 (NO_2) cm^{-1}; NMR ($CDCl_3$): δ 7.85–7.55 (m, 1H, 5-H), 7.45–7.07 (m, 1H, 8-H), 6.85–6.37 (m, 2H, 6,7-H), 6.22 (s, 1H, 1-H), 4.42 (t, 2H, CH_2NO_2), 3.52 (t, 2H, $ArCH_2$), and 2.25 (s, 3H, 2-CH_3) ppm.

Anal.—Calc. for $C_{11}H_{12}N_2O_2$: C, 64.69; H, 5.92; N, 13.71. Found: C, 64.37; H, 5.79; N, 13.83.

3-(2-Aminoethyl)-2-methylindolizine (III)—Slowly, with stirring, a solution of II (0.01 mole) in dry ether (70 ml) was added to a suspension of lithium aluminum hydride (0.031 mole) in dry ether (25 ml). After the solution was stirred for 24 hr at room temperature, the lithium aluminum hydride excess was destroyed with aqueous ethanol, and 2 *N* NaOH (15

[1] Boiling points are uncorrected. Melting points were determined on a Buchi apparatus and are uncorrected. IR spectra were obtained with a Perkin-Elmer 257 spectrophotometer. NMR spectra were recorded on a Jeol C-60 HL instrument.

ml) was added. The solid was filtered off; after drying, the ethereal solution was evaporated.

The oil residue was distilled; IR: ν_{max} (liquid film) 3350 and 3280 (NH_2) cm^{-1}; NMR (CCl_4): δ 7.8–7.5 (m, 1H, 5-H), 7.3–6.97 (m, 1H, 8-H), 6.6–6.15 (m, 2H, 6,7-H), 6.05 (s, 1H, 1-H), 3.07–2.7 (m, 4H, CH_2CH_2), 2.22 (s, 3H, 2-CH_3), and 0.82 (s, 2H, NH_2) ppm.

3-(2-Ethoxycarbonylaminoethyl)-2-methylindolizine (IV) and 3-(N-Ethoxycarbonyl-2-methylaminoethyl)-2-methylindolizine (VI)—With stirring, a solution of ethyl chloroformate (0.05 mole) in chloroform (10 ml) was added dropwise to an ice-cooled solution of III or V (0.048 mole) in chloroform (50 ml). After 1 hr, water (20 ml) was added; stirring was continued for 3 hr. The chloroform layer was recovered, washed with 2 *N* NaOH, dried, and evaporated. Compound III yielded a solid, which was crystallized; V gave an oil residue, which was distilled.

3-(2-Methylaminoethyl)-2-methylindolizine (V) and 3-(2-Dimethylaminoethyl)-2-methylindolizine (VII)—To a suspension of lithium aluminum hydride (0.05 mole) in dry ether (20 ml) was slowly added 0.024 mole of IV or VI in dry ether (50 ml). The mixture was heated under reflux for 14 hr. Aqueous ethanol was added to destroy excess lithium aluminum hydride, and then 2 *N* NaOH (20 ml) was added. After filtration, the solution was dried and evaporated, and the residue was distilled.

3-(2-Acetylaminoethyl)-2-methylindolizine (VIII) and 3-(N-Acetyl-2-ethylaminoethyl)-2-methylindolizine (X)—With stirring, acetyl chloride (0.038 mole) in dry ether (10 ml) was slowly added to a solution of III or IX (0.038 mole). Triethylamine (0.038 mole) in dry ether (20 ml) was added, and then the ether was separated off. The aqueous solution was again extracted with ether. The extracts were dried, and the solvent was driven off. Compound III afforded a solid, which was recrystallized from benzene. The liquid obtained from IX was distilled.

3-(2-Ethylaminoethyl)-2-methylindolizine (IX)—A solution of VIII (0.025 mole) in dry tetrahydrofuran (90 ml) was added to a suspension of lithium aluminum hydride (0.050 mole) in dry tetrahydrofuran. The mixture was refluxed for 6 hr; then aqueous ethanol and 2 *N* NaOH (30 ml) were added. After filtration, the solution was dried and evaporated. The residue was distilled.

3-(2-Dimethylaminoethyl)-2-methylindolizine (XI)—To a suspension of lithium aluminum hydride (0.04 mole) in anhydrous ether (20 ml) was added a solution of X (0.019 mole) in dry ether (50 ml). The mixture was refluxed for 12 hr; aqueous ethanol and 2 *N* NaOH (25 ml) were added. After filtration, the ethereal solution was dried and evaporated. The residue was distilled.

3-(2-Aminoethyl)-2-methyl-5,6,7,8-tetrahydroindolizine (XII) and N-Alkyl Derivatives (XIII–XVI)—A mixture of the suitable indolizine, III, V, VII, IX, or XI (0.023 mole), in absolute ethanol (100 ml), 1 g of 5% palladium-on-charcoal, and a few drops of acetic acid was hydrogenated at room temperature at 0.027 atm. Hydrogenation was stopped when 2 moles of hydrogen/mole of compound had been absorbed (7 days). The catalyst was filtered off, and the solution was made alkaline with 3 *N* NaOH and extracted with ether.

The ethereal extract was dried and evaporated, and the residue was distilled. For XII, the IR spectrum showed ν_{max} (liquid film) 3350 and 3280 (NH_2) cm^{-1}; NMR (CCl_4): δ 5.3 (s, 1H, 1-H), 3.7 (t, 2H, 5-CH_2), 2.8–2.2 (m, 6H, 8-CH_2, CH_2CH_2), 2–1.6 (m, 7H, 2-CH_3, 7-CH_2, 6-CH_2), and 0.93 (s, 2H, NH_2) ppm.

Maleates of Indolizines III, V, VII, IX, and XI–XVI—The suitable base in dry ether was added slowly to a stirred equimolar solution of maleic acid in dry ether. After cooling, the solid was collected and recrystallized. The maleate of base XV is highly hygroscopic and uncrystallizable; it was used in the pharmacological test after drying under vacuum. All compounds, with the exception of II, are unstable to light and air but can be stored for several months in an inert atmosphere in a refrigerator.

Biological Activities—*In vitro*, the anti-5-hydroxytryptamine, antihistamine, and antiacetylcholine activities of compounds were determined on the isolated guinea pig ileum or the isolated uterus of estrous rats. A previously described technique (1) was employed without any modification.

As comparison standards, tryptamine hydrochloride[2] and specific inhibitors of 5-hydroxytryptamine (metergoline maleate[3]), histamine (diphenhydramine[4]), and acetylcholine (atropine sulfate[5]) were used. In addition, the following agonists and doses were used: 5-hydroxytryptamine (creatinine sulfate[5]), 0.011 μg/ml; histamine dihydrochloride[6], 0.016 μg/ml; and acetylcholine chloride[7], 0.043 μg/ml. The synthesized products were used as maleates.

For each substance, the agonist to antagonist ratio was calculated. It was the ratio between a constant dose of the agonist and the dose of the antagonist that reduced by 50% the response evoked by the agonist.

In vivo experiments were carried out on Swiss male albino mice. The LD_{50} values and the effects on the CNS were determined after intravenous administration. The LD_{50} value was calculated by the Weil (3) method 14 days after treatment.

To study the CNS effects, the following tests were employed: potentiation of the hypnotic effect of barbiturates (4), grip strength (5), grooming (6), and exploratory activity both in an open field (7) and in a hole board (8). For this last test, the number of rearing reactions (open field) or of holes explored (hole board) during a 3-min period was considered. In these experiments, mice that received simple saline solution acted as controls.

Since this work investigated the effect of replacement of the indole with the indolizine system on pharmacological activity, tryptamine was employed as reference indole derivative.

Table III—*In Vitro* ID_{50} Values on Guinea Pig Ileum Smooth Muscle Preparation [a]

Compound	Acetylcholine	Histamine
Atropine	0.0027 (15.9)	
Diphenhydramine		0.0072 (2.22)
Tryptamine	86.8 (0.0005)	10.83 (0.0014)
III	9.99 (0.0043)	11.19 (0.0014)
V	10.3 (0.0041)	2.88 (0.0055)
VII	15.24 (0.0028)	0.16 (0.1)
IX	17.34 (0.0024)	2.54 (0.0062)
XI	8.84 (0.0048)	0.43 (0.037)
XII	64.56 (0.0006)	32.28 (0.0005)
XIII	38.39 (0.0011)	25.59 (0.0006)
XIV	37.41 (0.0011)	17.83 (0.0008)
XV	89.14 (0.0004)	4.45 (0.0035)
XVI	34.12 (0.0012)	1.49 (0.01)

[a] All concentrations (micrograms per milliliter) refer to the free base. The numbers in parentheses are the antagonistic activity rates (agonist concentration/antagonist concentration ratio).

RESULTS AND DISCUSSION

The results of the *in vitro* experiments are summarized in Table III. All substances tested possessed anti-5-hydroxytryptamine, antihistamine, and antiacetylcholine activities.

The antihistamine effect was clearly more intense in the indolizine than in the tetrahydroindolizine derivatives. In both series of compounds, the activity increased in the following order: unalkylated, monoalkylated, and dialkylated amines. In some instances, the antihistamine activity was compared to that of 3-(3-aminopropyl)-2-methylindolizine derivatives, whose synthesis and pharmacological properties were described previously (1).

In these experiments, all compounds except XIII appeared less effective than the corresponding 3-(3-aminopropyl)-2-methylindolizines in inhibiting the spasmogenic effect of histamine on the isolated guinea pig ileum. The agonist to antagonist ratios of diphenhydramine and

Table IV—Acute Toxicity [a]

Compound	LD_{50} (Confidence Limits), mg/kg
Tryptamine	228.6 (203.4–246.2)
III	89.3 (104–76)
V	126 (144–111)
VII	138 (155–122)
IX	70.8 (79–63)
XI	102.9 (114–92)
XII	52.1 (60–45)
XIII	40 (47–33)
XIV	96.9 (103–90)
XV	100 (109–91)
XVI	66.5 (76–58)

[a] All values refer to the free base.

[2] Fluka.
[3] Farmitalia, Milan, Italy.
[4] Parke-Davis.
[5] Merck.
[6] Ibis, Florence, Italy.
[7] Roche, Milan, Italy.

Table V—Effects on the CNS [a]

Compound	Dose, mg/kg[b]	Grip Strength[c]	Grooming[d]	Behavior in Open Field[e]	Barbiturate Narcosis Potentiation[f]	Hole Board[g]
Controls		208.3 ± 9.3	15.1 ± 3.5	20.6 ± 3.1	0	26.6 ± 2.9
Tryptamine	76.2	181.2 ± 6.9	131.2 ± 21.5	0.12 ± 0.1	90	3.25 ± 0.63
III	30	120 ± 9.3	146.5 ± 19.5	0	90	0.4 ± 0.34
V	42	178.3 ± 9.3	59.4 ± 19.5	0.3 ± 0.34	50	9.7 ± 3.1
VII	46	173.3 ± 9.3	110.7 ± 19.5	0.1 ± 0.1	70	3 ± 1.1
IX	23.5	160 ± 9.3	63.2 ± 19.2	2.7 ± 1.65	0	16.6 ± 4.1
XI	34.5	205 ± 9.3	49.2 ± 19.5	0.4 ± 0.34	20	5.1 ± 1
XII	17.6	190.7 ± 13	85.3 ± 20.5	0	60	2.2 ± 0.6
XIII	13.4	212.5 ± 10.4	13 ± 3.1	6.75 ± 1.65	10	8.12 ± 1.5
XIV	32.4	175 ± 3.5	30.7 ± 10	0.75 ± 0.75	0	3.37 ± 1.25
XV	33.4	220.8 ± 10.4	14.3 ± 4.6	2.37 ± 0.88	0	7.6 ± 1.64
XVI	22.2	220.8 ± 10.4	13.25 ± 5	1.75 ± 1.14	10	6.37 ± 1.14

[a] Figures are the mean ± *SE* of the results obtained on 10–15 mice. [b] All values refer to the free base. [c] Arbitrary units. [d] Latency time of the reflex. [e] Rearing reaction (during a 3-min observation). [f] Percentage of mice that lost the righting reflex. [g] Number of holes explored (during a 3-min observation).

tryptamine were 2.22 and 0.0014, respectively. The agonist to antagonist ratios of VII and XVI were 0.1 and 0.01, respectively; for the other compounds, this ratio ranged between 0.037 (XI) and 0.0005 (XII). Thus, the antihistamine activity of VII and XVI was about 20 and 200 times less, respectively, than that of diphenhydramine while that of the other compounds was up to about 4500 times inferior.

The antiacetylcholine effect of the indolizine derivatives was generally larger than that of the corresponding tetrahydroindolizines. All compounds except XV were up to about eight to 10 times (III, V, and XI) more effective antiacetylcholine agents than tryptamine, but their antiacetylcholine effect proved to be negligible when compared to that of atropine. In fact, the agonist to antagonist ratio of atropine was 15.9 while that of the other compounds ranged between 0.0048 (XI) and 0.0004 (XV). Thus, the substances tested were about 3000–40,000 times less active than atropine in inhibiting acetylcholine activity.

The anti-5-hydroxytryptamine activity of the compounds was negligible and was evident only at doses that irreversibly damaged the isolated uterus.

The results of *in vivo* experiments are summarized in Tables IV and V. The LD_{50} value of tryptamine was 228.6 mg/kg. All other compounds were more toxic than the reference standard, with the LD_{50} value ranging between 40 (XIII) and 138 (VII) (Table IV).

All compounds showed a more or less intense depressive effect on the CNS. Exploratory activity in a open field or in a hole board was strongly depressed by all substances tested except IX, which reduced rearing reactions but did not significantly alter the number of holes explored by mice.

Grooming was inhibited by III, VII, and, to a lesser extent, XII, V, and IX but was not reduced significantly or was left unmodified by the remaining substances.

The hypnotic action of barbiturates was strongly potentiated by III, XII, V, and VII but was only slightly increased or was left unmodified by the others.

Muscular strength was practically never altered.

Among the tested substances, III and, to a lesser extent, V, VII, and XII proved to be very effective CNS depressants, but their effects could not be considered specific since they inhibited all of the central activities studied to the same extent. However, XV could be considered a more specific inhibitor of the CNS since its effect was limited to the inhibition of exploratory activity.

On the whole, the indolizine derivatives proved to be more effective in inhibiting CNS activity than the corresponding tetrahydroindolizines. The effect of the latter appeared to be more specific, however, since these compounds mainly affected explorative behavior and practically did not modify grip strength, grooming, and the hypnotic action of barbiturates.

REFERENCES

(1) I. Antonini, M. Cardellini, F. Claudi, P. Franchetti, U. Gulini, G. De Caro, and F. Venturi, *J. Pharm. Sci.*, **66**, 1692 (1977).

(2) D. O. Holland and J. H. C. Nayler, *J. Chem. Soc.*, **1955**, 1657.

(3) C. S. Weil, *Biometrics*, **8**, 249 (1952).

(4) K. Morita, I. Yamamoto, and H. Iwata, *Biochem. Pharmacol.*, **22**, 1115 (1973).

(5) H. Van Riezen and L. Boersma, *Eur. J. Pharmacol.*, **6**, 353 (1969).

(6) M. G. Hansen and I. Q. Whishaw, *Psychopharmacologia*, **29**, 33 (1973).

(7) D. F. Smith and H. B. Smith, *ibid.*, **30**, 83 (1973).

(8) S. E. File and A. G. Wardill, *ibid.*, **44**, 47 (1975).

ACKNOWLEDGMENTS

Supported by a grant from the Consiglio Nazionale delle Ricerche, Rome, Italy.

The authors are indebted to Professor M. Cardellini and Professor G. De Caro for helpful discussions.

Sustained Release of Drugs from Ethylcellulose–Polyethylene Glycol Films and Kinetics of Drug Release

Y. SAMUELOV, M. DONBROW ˣ, and M. FRIEDMAN

Received April 11, 1978, from the *Pharmacy Department, School of Pharmacy, Hebrew University, Jerusalem, Israel.* Accepted for publication August 22, 1978.

Abstract □ Cast films composed of different ratios of polyethylene glycol and ethylcellulose containing salicylic acid, caffeine, and tripelennamine as model dispersed drugs were prepared and exhibited sustained release. The drug content of the film declined at an apparent first-order rate initially, whereas the drug quantity released was proportional to the square root of time. Data analysis validated the latter treatment, which is in accordance with the diffusional matrix model, and disproved the validity of the apparent first-order conformity. The release rates were independent of film thickness and proportional to drug concentration in pure ethylcellulose films; in polyethylene glycol–ethylcellulose films, a positive deviation from linearity was observed. The logarithm of the rate constant was proportional to the fraction of polyethylene glycol in the film. Unlike in pure ethylcellulose films, the release rate in mixed films was altered by a change in the external fluid pH.

Keyphrases □ Ethylcellulose–polyethylene glycol films—containing model dispersed drugs, drug release kinetics □ Polyethylene glycol–ethylcellulose films—containing model dispersed drugs, drug release kinetics □ Films—ethylcellulose–polyethylene glycol containing model dispersed drugs, drug release kinetics □ Sustained-release films—ethylcellulose–polyethylene glycol, containing model dispersed drugs, drug release kinetics □ Dosage forms, potential—ethylcellulose–polyethylene glycol films, containing model dispersed drugs, drug release kinetics

Incorporation of drugs in inert polymer films during their manufacture affords a possible method of achieving controlled release. Such products can be adapted to topical, oral, and other routes of administration by utilizing them directly or in the form of coatings (1–3). Drug release rates may be altered by variations of the dimensional parameters of the film, the polymer matrix material, and the drug concentration in the film.

Greater changes may be obtained by the use of additive polymers selected on the basis of hydrophilicity properties, such as hydroxypropylcellulose in polyvinyl acetate films (3). Polyethylene glycol 4000 was recently studied in connection with barrier films and drastically increased the permeability of ethylcellulose films in proportion to the amount added (4). Unlike hydroxypropylcellulose, the polyethylene glycol is leachable, introducing porosity and, hence, solvent-occupied regions into the films without loss of barrier properties.

The objective of the present work was to study the influence of polyethylene glycol as a film component on the release of drugs dispersed in ethylcellulose films. While such films might behave diffusionally (5) like ethylcellulose films containing caffeine and salicylic acid (1), the loss of polyethylene glycol could give rise to either homogeneous or heterogeneous release (6).

In the design of controlled-release products, the combination of drug and permeabilizing agent in different quantities has an important influence on the release rate and membrane structure. The presence of two leachable components, one tending to form isolated pores and the other of undetermined pore-forming and plasticizing properties, could give rise to more than one kinetic pattern and could increase the release rate abruptly at a critical porosity value. Films heavily loaded with drugs or permeabilizers might be expected ultimately to show structure breakdown, leading to rapid dissolution-controlled drug release.

The effects of composition on the consistency of release behavior were explored utilizing salicylic acid and caffeine. Their permeabilities were studied in the corresponding barrier film systems. Films containing the basic drug tripelennamine were also included for comparison. Preliminary work showed that these combinations had satisfactory film-forming and release properties (7). The general approach followed that of Borodkin and Tucker (3) in their study on mixed film composition.

EXPERIMENTAL

Materials—Ethylcellulose (N-type) had an ethoxyl content of 47.5–49.0%. The viscosity of a 5% (w/w) solution in toluene–ethanol (80:20 w/w) was 100 cps[1]. Polyethylene glycol 4000[2] was BPC grade. Caffeine, salicylic acid, and tripelennamine hydrochloride were USP grade. The pH 7.00 and 2.00 buffers were USP buffer mixtures.

Film Preparation—The films were cast from a chloroform solution containing 10% (w/w) total drug and polymers on polytef-coated plates, using the techniques of Kanig and Goodman (8). The solvent was allowed to evaporate for 24 hr, the film was removed from the plate and air dried for 24 hr, and the drug content was calculated from the weight ratio of drug and polymers used.

Tripelennamine was added as an oily liquid, prepared from an aqueous solution of the salt by addition of 5 *N* NaOH, extraction with chloroform, and evaporation of the solvent. Spectrophotometric determination of the drug content after solution of specimen films in chloroform gave results that accorded with the weight ratios used in all three systems.

Determination of Release Rate—Films were cut to a circular form 36 cm^2 in area and were weighed accurately. Film thickness was measured in 10 different places with a micrometer[3]. The thickness used did not vary by more than 5% over the film surface. The membranes were attached to glass plates with a silicone pressure-sensitive adhesive[4] and immersed in 500 ml of buffer solution preheated to 37°. (The quantities used afforded sink conditions.) The solution was mixed with a polystaltic pump[5] at a flow rate of 31 ml/min. To avoid water evaporation, the vessels were covered with aluminum foil during the experiments.

Aliquots (5 ml) were withdrawn at various times and replaced by fresh solvent, with corrections being applied in the calculations. The amount of drug released was determined spectrophotometrically[6] at the maximum: salicylic acid at 296 nm, caffeine at 273 nm (both in pH 7 buffer), and tripelennamine at 246 nm in 0.1 *N* HCl.

Experiments were duplicated or triplicated, and mean results were reported. Reproducibility was within 5% of the mean.

THEORETICAL

The release of drugs dispersed in thin films can be treated using the Higuchi (5, 6) equations for diffusion-controlled transport in a polymer matrix. In a planar homogeneous system, the following relationship holds:

$$Q = [D(2A - C_s)C_s t]^{1/2} \quad \text{(Eq. 1)}$$

[1] Hercules, Wilmington, Del.
[2] B.D.H. Ltd., Poole, England.
[3] Tesa Master, Tesa, Switzerland.
[4] Dow Corning Corp., Midland, Mich.
[5] Model MHRK, Watson-Marlow, Falmouth, England.
[6] Unicam SP 1800, Pye Unicam Ltd., Cambridge, England.

0022-3549/79/0300-0325$01.00/0
© 1979, American Pharmaceutical Association

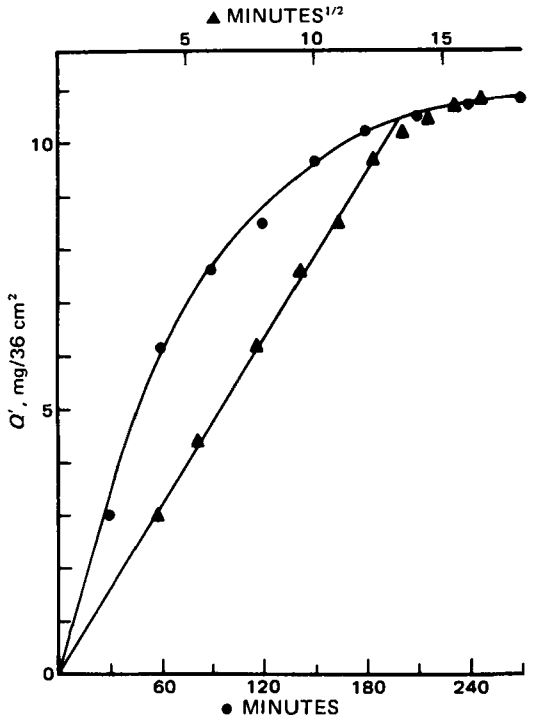

Figure 1—*Drug release into pH 7 buffer from film containing 5% (w/w) caffeine in 4:6 polyethylene glycol–ethylcellulose. (The total drug content was 12 mg.) Key:* ●, Q′ versus t; *and* ▲, Q′ versus $t^{1/2}$.

where Q is the amount of drug released per unit area exposed after time t; and D, A, and C_s are the diffusivity, initial concentration, and solubility of the drug in the matrix, respectively. Where the matrix is granular and the drug is removed from a planar slab by leaching through a capillary network, Q, the amount of drug liberated per unit surface area of matrix into the external medium in time t is given by:

$$Q = \left[\frac{\epsilon}{\tau} D(2A - \epsilon C_s)C_s t\right]^{1/2} \quad \text{(Eq. 2)}$$

where C_s is the solubility and D is the diffusion coefficient of the drug in the leaching medium and ϵ is the porosity and τ is the tortuosity of the matrix.

In the homogeneous case, drug release is directly proportional to the square root of time. Equation 1 then reduces to:

$$Q' = k' t^{1/2} \quad \text{(Eq. 3)}$$

If Q' is the amount of drug released from an area of film S, $Q' = QS$ and $k' = kS$, where k is the release rate constant given by:

$$k = [D(2A - C_s)C_s]^{1/2} \quad \text{(Eq. 4)}$$

Equation 3 also describes the case of the granular matrix if the value of k remains constant throughout the leaching process. Then k is given by:

$$k = \left[\frac{\epsilon}{\tau} D(2A - \epsilon C_s)C_s\right]^{1/2} \quad \text{(Eq. 5)}$$

RESULTS AND DISCUSSION

From each film composition studied, the drugs were released at a rate that decreased with time. Treatment of the experimental data on the basis of the diffusion-controlled model indicated that the drug concentration increased linearly with the square root of time in all systems. Figure 1 shows typical Q'–t and Q'–$t^{1/2}$ plots obtained from films containing 5% caffeine with polyethylene glycol 4000 and ethylcellulose in a 4:6 ratio. All of the drugs and films used gave this type of release pattern.

The data also appeared to fit a first-order equation (Eq. 6), used to describe the release from certain polymer films (2, 9):

$$\log A' = \log A - \frac{Kt}{2.303} \quad \text{(Eq. 6)}$$

where A' is the drug content of the film at time t.

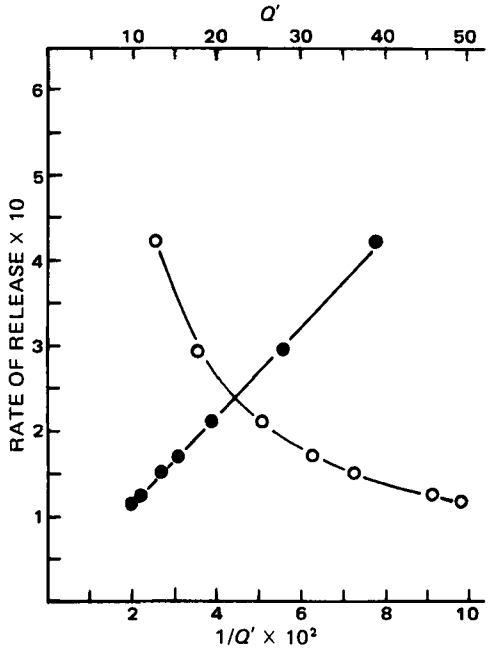

Figure 2—*Plots of release rate into pH 7 buffer of 20% (w/w) salicylic acid from 4:6 polyethylene glycol–ethylcellulose film against the amount of drug release* (Q′) (○) *and the reciprocal of the amount of drug release* (1/Q′) (●).

Table I—Comparison between Linearizations of Release Rate Data [a] by First-Order and Diffusion Treatments for a 20% (w/w) Salicylic Acid in Polyethylene Glycol–Ethylcellulose Film

Polyethylene Glycol–Ethylcellulose Ratio	First Order		Diffusion Control	
	t_{lag}, min	Correlation Coefficient	t_{lag}, min	Correlation Coefficient
0:10	−173	0.987	0.11	0.999
1:9	−174	0.986	0.22	0.999
2:8	−209	0.991	0	0.999
4:6	−141	0.989	0.16	0.998
5:5	−65	0.989	0.32	0.997

[a] Release into pH 7 buffer.

Some typical evaluations of the best statistical lines obtained using the two equations with release data from salicylic acid films are listed in Table I. The diffusion equation gave consistently higher values for the correlation coefficient (0.997–0.999) than did the first-order equation (0.986–0.991).

Lag times for establishment of the apparent linear relations in the two treatments also are included in Table I. They were negligibly short in the diffusion model and unreasonable in the first-order model.

Further evidence bearing upon the relative validity of these two models was obtained by utilizing the differential forms of their rate equations (1, 10). For diffusion control, the rate dQ'/dt is proportional to the reciprocal $1/Q'$, where Q' is the total drug released at a given time:

$$\frac{dQ'}{dt} = \frac{k'^2}{2Q'} \quad \text{(Eq. 7)}$$

For first-order release, the rate is related directly to Q':

$$\frac{dQ'}{dt} = KA - KQ' \quad \text{(Eq. 8)}$$

Release rates were determined by measurement of the slopes of Q' *versus* time curves. When the release rates from a typical film of high leachable content (52%) were plotted as a function of Q' and $1/Q'$, linearity was obtained only in the latter case (Fig. 2), indicating that the process is diffusional.

Similar results were obtained with films containing other drugs and concentrations; some representative data are included in Table II.

Final evidence is provided by plots of log Q' against log t, based on the logarithmic form of the diffusional Eq. 3 (Fig. 3). All film compositions studied gave slopes of 0.5.

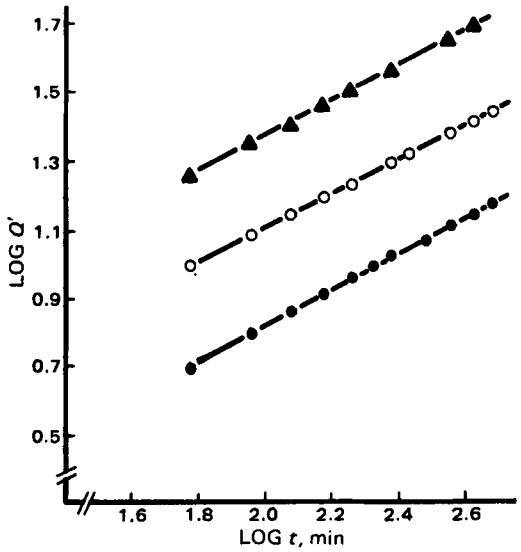

Figure 3—*Relationship of log Q′ to log t. Key: ▲, 20% (w/w) salicylic acid in 4:6 polyethylene glycol—ethylcellulose film (slope = 0.514, r = 0.999); ○, 20% (w/w) salicylic acid in 2:8 polyethylene glycol—ethylcellulose film (slope = 0.499, r = 0.999); and ●, 20% (w/w) tripelennamine in 2:8 polyethylene glycol-ethylcellulose film (slope = 0.526, r = 0.999). (Release was into pH 7 buffer.)*

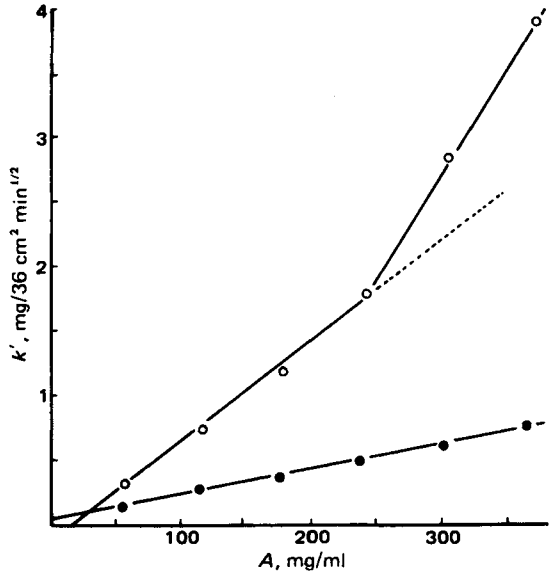

Figure 4—*Relationship of k′ to the initial salicylic acid concentration. Key: ●, ethylcellulose film; and ○, 3:7 polyethylene glycol–ethylcellulose film. (Release was into pH 7 buffer.)*

Experimentally, the linear diffusion model held up to 80–90% drug release, after which the rate decreased progressively. This deviation would be explained by the total exhaustion of solid drug phase from the film, subsequent to which the diffusion gradient would show first-order dependence on drug content. The experimental conditions used ensured that, with all three drugs, ultimate sink concentrations were insignificant compared to drug solubilities in the external buffer solutions. Therefore, the deviation was not the result of an external concentration gradient.

Film Thickness—As expected from Higuchi's equation, film thickness had no influence on the release rate constant (Table III). However, the time for release of half of the drug content of the film, termed the product half-life ($t_{1/2}$), is related to the film thickness. This relationship is indicated conveniently by Eq. 9, derived from Eq. 3, and shows the direct relationship between $t_{1/2}$ and the square of film thickness, h:

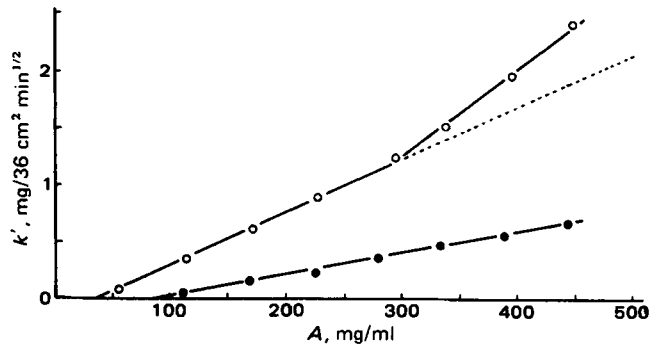

Figure 5—*Relationship of k′ to the initial tripelennamine concentration. Key: ●, ethylcellulose film; and ○, 3:7 polyethylene glycol–ethylcellulose film. (Release was into pH 7 buffer.)*

Table II—Comparison of Parameters of Linearity Obtained from Plots of Release Rate [a] against the Reciprocal Amount ($1/Q'$) and the Amount (Q') of Drug Released

Drug	Concentration[b], % (w/w)	Polyethylene Glycol–Ethylcellulose Ratio	Correlation Coefficient Rate *versus* $1/Q'$	Correlation Coefficient Rate *versus* Q'
Salicylic acid	20	4:6	0.999	0.919
Salicylic acid	20	2:8	0.999	0.959
Tripelennamine	20	4:6	0.991	0.960
Tripelennamine	20	2:8	0.999	0.938
Caffeine	5	4:6	0.993	0.970

[a] Release into pH 7 buffer. [b] Drug in dry film.

$$t_{1/2} = \left(\frac{Ah}{2k}\right)^2 \qquad \text{(Eq. 9)}$$

where A is the initial drug concentration in the film (milligrams per milliliter) and k is the release rate constant (*cf.*, Ref. 3).

The calculated and measured times for 50% drug release from membranes containing 20% salicylic acid and tripelennamine in polyethylene

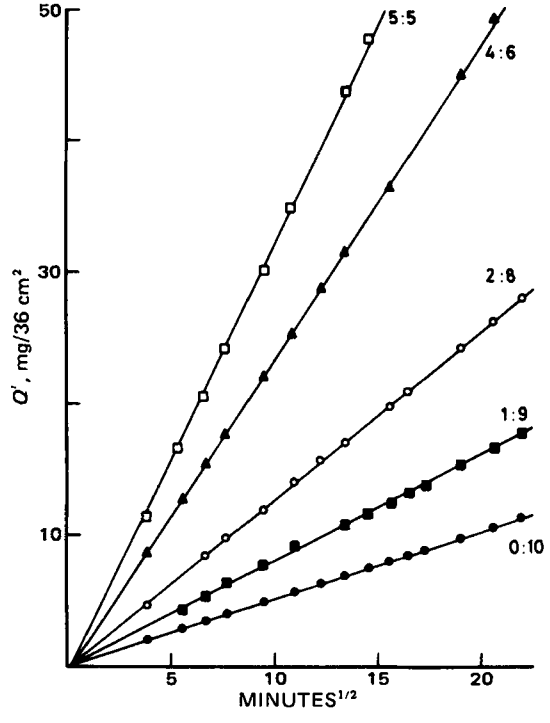

Figure 6—*Drug release into pH 7 buffer from films containing 20% (w/w) salicylic acid at different polyethylene glycol–ethylcellulose ratios. Key: □, 5:5; ▲, 4:6, ○, 2:8; ■, 1:9; and ●, 0:10.*

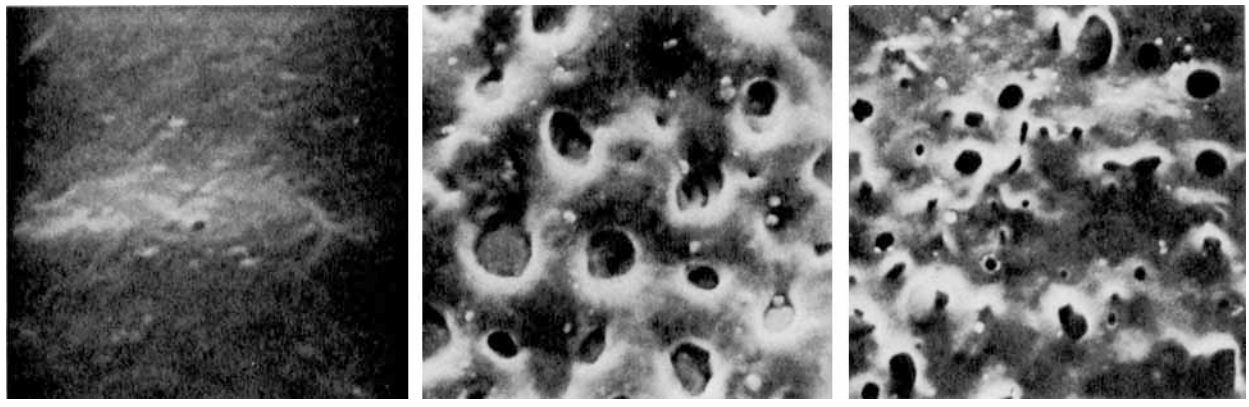

A B C

Figure 7—*Scanning electron micrographs of films (×5000): Key: A, 20% (w/w) salicylic acid in pure ethylcellulose after release of most of the drug; B, 30% (w/w) polyethylene glycol in ethylcellulose film after leaching out of the hydrophilic component (no drug present); and C, 20% (w/w) salicylic acid in 3:7 polyethylene glycol–ethylcellulose film after release of the drug.*

Table III—Effect of Film Thickness (h) on the Drug Release Rate Constant (k') and Half-Life ($t_{1/2}$) for 1:1 Polyethylene Glycol–Ethylcellulose Films Containing Drugs

System[a]	Film Thickness, mm	k', mg/36 cm^2 min$^{1/2}$	$t_{1/2}$, min Calculated[b]	$t_{1/2}$, min Measured[c]	Correlation Coefficient
Salicylic acid, 20%, pH 7	0.072	3.85	55	58	0.995
	0.100	3.83	107	105	0.997
	0.133	3.90	183	192	0.997
Tripelennamine, 20%, pH 7	0.071	2.38	153	162	0.997
	0.104	2.46	305	299	0.998
	0.128	2.45	466	454	0.996
Tripelennamine, 20%, pH 2	0.069	3.65	61	59	0.999
	0.097	3.57	126	133	0.995
	0.125	3.62	203	212	0.997

[a] Drug concentration by weight in dry film; pH of external solution. [b] Calculated according to Eq. 9. [c] Measured from the experimental graphs at the point corresponding to the release of exactly 50% of the initial drug content of the film.

Table IV—Effect of Polyethylene Glycol–Ethylcellulose Ratio and pH on the Release Rate Constant (k') for Films Containing 20% (w/w) Tripelennamine

Polyethylene Glycol–Ethylcellulose Ratio	Film Thickness, mm	k' (pH 7)[a], mg/36 cm^2 min$^{1/2}$	Film Thickness, mm	k' (pH 2)[a], mg/36 cm^2 min$^{1/2}$
0:10	0.098	0.219	0.087	0.229
1:9	0.089	0.346	0.099	0.405
2:8	0.117	0.723	0.125	0.748
3:7	0.117	0.900	0.124	1.30
4:6	0.071	1.48	0.091	2.39
5:5	0.128	2.45	0.125	3.62
6:4	0.106	4.41	0.097	6.15

[a] Correlation coefficient: 0.995–0.999.

Table V—Effect of Polyethylene Glycol–Ethylcellulose Ratio on the Drug Release Rate Constant (k') for 20% (w/w) Salicylic Acid and 10% (w/w) Caffeine Films

System[a]	Polyethylene Glycol–Ethylcellulose Ratio	Film Thickness, mm	k', mg/36 cm^2 min$^{1/2}$	Correlation Coefficient
Salicylic acid, 20%	0:10	0.057	0.518	0.999
	1:9	0.057	0.793	0.999
	2:8	0.073	1.24	0.999
	3:7	0.087	1.80	0.998
	4:6	0.082	2.69	0.999
	5:5	0.133	3.90	0.997
Caffeine, 10%	0:10	0.085	0.301	0.997
	1:9	0.069	0.491	0.999
	2:8	0.106	0.851	0.995
	3:7	0.102	1.44	0.998
	4:6	0.130	2.51	0.999

[a] Drug concentration by weight in dry film using pH 7 external solutions.

glycol–ethylcellulose (1:1) films are included in Table III and are in excellent agreement.

Drug Concentration—The effect of drug concentration on the release rate constant was tested using eight concentrations of tripelennamine (5–40%) and six concentrations of salicylic acid (5–30%) in pure ethylcellulose and polyethylene glycol 4000–ethylcellulose (3:7) films (Figs. 4 and 5). There was a linear relationship between the release rate constant and the drug concentration in a pure ethylcellulose film. Both diffusion-controlled release models (Eqs. 4 and 5) indicate that the release rate constant should be proportional to the square root of the initial drug concentration, A[7]. However, in systems where the drug is the only extractable component and the initial porosity of the film is negligible, increasing the amount of drug dispersed in the film would increase the porosity by the same factor but would not affect the other parameters. Thus, for these systems, the release rate constants should increase in direct proportion to the drug concentration (6).

Different results were obtained for films composed of ethylcellulose and polyethylene glycol 4000 (Figs. 4 and 5). Although there was a linear relationship between k and A when the drug content was low, a positive deviation was observed at elevated drug concentrations in both drug systems. This result may indicate that other factors are changing with the amount of drug in the film. In particular, leaching out of the polyethylene glycol 4000 and pore formation increase the external film area exposed to the solvent, increase the internal porosity, and decrease the tortuosity. The added contribution of leaching out of the drug to these factors is most significant at high drug concentrations. A similar phenomenon was observed (11, 12) in studies on the release of chlorpheniramine and sodium salicylate from a hydrophilic matrix.

Polyethylene Glycol Content—The effect of an increasing polyethylene glycol content at constant drug concentration was a marked increase in the release rate for all three drugs. Some examples are shown in Fig. 6 for salicylic acid; the other drugs gave a similar pattern.

The slopes of the linear Q–$t^{1/2}$ plots give the diffusional release rate constants (k', Eq. 3) for the individual drug film systems (Tables IV and V).

[7] Subject to the condition that $2A \gg C_s$ or ϵC_s.

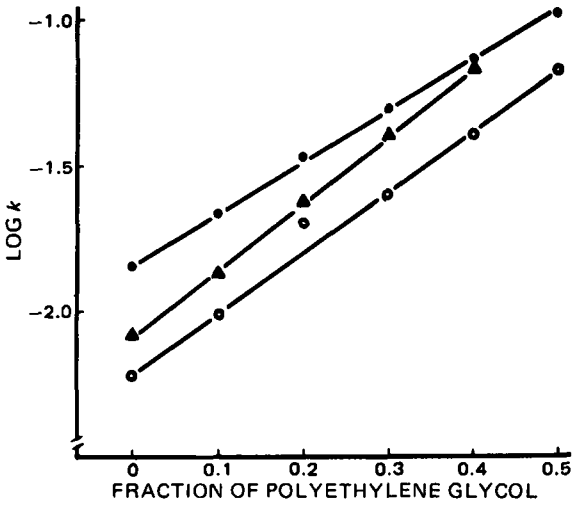

Figure 8—*Relationship of log* k *(release rate constant) to the fraction of polyethylene glycol in the polymer matrix. Key:* ●, *20% (w/w) salicylic acid films;* ○, *20% (w/w) tripelennamine films; and* ▲, *10% (w/w) caffeine films. (Release was into pH 7 buffer.)*

The polyethylene glycol 4000 underwent rapid leaching out, with about 90% being recovered from the water within 15 min for 35-μm film containing 30% of the polyethylene glycol. Scanning electron microscopy (Fig. 7) demonstrated that the loss of polyethylene glycol from polyethylene glycol–ethylcellulose films on leaching with water resulted in the formation of large pores (Fig. 7B) that were not formed in films of the drug in pure ethylcellulose (Fig. 7A). The presence of drug and polyethylene glycol together in ethylcellulose films gave pores on leaching (Fig. 7C) that were indistinguishable from those given by polyethylene glycol–ethylcellulose alone.

With an increase in porosity, the void volume would be expected to be occupied by external solvent diffusing into the film. In most compositions studied, the release rate constants increased drastically with an elevation of the polyethylene glycol content of the film. A plot of the release rate constant, k, against the fraction of polyethylene glycol in the polymer mixture demonstrated a positive deviation. On the other hand, plots of log k against the polyethylene glycol fraction were linear, following Borodkin and Tucker's equation (3):

$$\log k = k_D f_{PEG} + \log k_{EC} \qquad \text{(Eq. 10)}$$

where k_D is a constant specific for each drug and polymer system and drug concentration, f is the fraction of polyethylene glycol, and k_{EC} is the value of the release rate constant in ethylcellulose film. Figure 8 shows graphically the linear relationship of log k to the fraction of polyethylene glycol 4000 in ethylcellulose film for salicylic acid, tripelennamine, and caffeine. The same relation was obtained with hydroxypropylcellulose–polyvinyl acetate films (3).

pH Effects—In films containing polyethylene glycol, the release rate of tripelennamine was altered by a change in the pH of the external fluid. Release was more rapid at pH 2 than at pH 7 (Table IV). The same phenomenon, but in the reverse direction with respect to pH, was observed with salicylic acid; at an ethylcellulose–polyethylene glycol ratio of 6:4, it gave significantly faster release at pH 7 than at pH 1 (Table VI). These drugs would be expected to be converted into their salts or into mixtures of the salts and unionized forms when dissolved in the leaching solvent, according to their pKa values and the buffer pH values.

Table VI—Effect of pH on the Drug Release Rate from Films Containing 20% (w/w) Salicylic Acid

Polyethylene Glycol–Ethylcellulose Ratio	k' (pH 7), mg/36 cm^2 min$^{1/2}$	Correlation Coefficient	k' (pH 1), mg/36 cm^2 min$^{1/2}$	Correlation Coefficient
0:10	0.518	0.999	0.525	0.998
4:6	2.69	0.999	1.85	0.999

With tripelennamine, the salt form would predominate in the test buffers, but the ratio of unionized to ionized drug and, hence, the solubility of the drug in the leaching fluid would be reduced at pH 7 compared to pH 2. Similarly, salicylic acid would be less ionized and less soluble at pH 1. Evidently, ionizable drugs are released at rates related to their solubilities in the leaching solvent.

As the polyethylene glycol–ethylcellulose ratio increases, the differential pH effect becomes more significant. These mixed films behave as granular matrixes in which the solubility and diffusivity of the drug in the permeating fluid determine the release rate. In contrast, pure ethylcellulose films behave as homogeneous matrixes, with drug release being controlled by transport through the ethylcellulose and unaffected by the external pH. This behavior is clearly shown by the identical release rate constants of tripelennamine at pH 2 and 7 and of salicylic acid at pH 1 and 7 in pure ethylcellulose films (Tables IV and VI).

REFERENCES

(1) M. Donbrow and M. Friedman, *J. Pharm. Sci.*, **64**, 76 (1975).
(2) J. J. Sciarra and R. N. Gidwani, *ibid.*, **61**, 754 (1972).
(3) S. Borodkin and F. E. Tucker, *ibid.*, **63**, 1359 (1974).
(4) M. Donbrow and M. Friedman, *J. Pharm. Pharmacol.*, **27**, 633 (1975).
(5) T. Higuchi, *J. Pharm. Sci.*, **50**, 874 (1961).
(6) *Ibid.*, **52**, 1145 (1963).
(7) M. Donbrow and Y. Samuelov, *J. Pharm. Pharmacol., Suppl.*, **28**, 23P (1976).
(8) J. L. Kanig and H. Goodman, *J. Pharm. Sci.*, **51**, 77 (1962).
(9) J. J. Sciarra and R. N. Gidwani, *J. Cosmet. Chem.*, **21**, 667 (1970).
(10) J. B. Schwartz, A. P. Simonelli, and W. I. Higuchi, *J. Pharm. Sci.*, **57**, 274 (1968).
(11) H. Lapidus and N. G. Lordi, *ibid.*, 55, 840 (1966).
(12) *Ibid.*, **57**, 1292 (1968).

ACKNOWLEDGMENTS

Abstracted in part from work submitted by Y. Samuelov to the Hebrew University in partial fulfillment of the Doctor of Philosophy degree requirements.

The authors thank the family of the late Mr. Jack Bogush of London, England, for the presentation of a Unicam SP 1800 recording spectrophotometer.

Structure–Activity Studies on Tetrahydro- and Hexahydrocannabinol Derivatives

W. A. SKINNER ˣ, GERHARD RACKUR *, and EDWARD UYENO

Received July 6, 1978, from the *Life Sciences Division, SRI International, Menlo Park, CA 94025.* Accepted for publication August 17, 1978. *Present address: F. Hoechst, Frankfurt, West Germany.

Abstract □ A series of tetrahydro- and hexahydrocannabinol derivatives was prepared in which the substituents at position 9 were varied. These compounds were evaluated in mice for their effects on locomotor activity, body temperature, muscle tone, and analgesia. Depression of body temperature and locomotor function was demonstrated by several compounds, but all were devoid of any significant analgesic activity.

Keyphrases □ Tetrahydrocannabinol derivatives, various—synthesized, pharmacological activity evaluated in mice □ Hexahydrocannabinol derivatives, various—synthesized, pharmacological activity evaluated in mice □ Structure–activity relationships—various tetrahydrocannabinol and hexahydrocannabinol derivatives, pharmacological activity evaluated in mice

Numerous synthetic tetrahydrocannabinol derivatives have been prepared and tested since the accidental discovery that synthetic $\Delta^{6a,10a}$-tetrahydrocannabinol caused ataxia in dogs and corneal areflexia in rabbits (1, 2). Reviews of those studies have been published (3, 4).

The purpose of this study was to examine the structure–activity relationships in some synthetic tetrahydro- and hexahydrocannabinol derivatives with variations in ring C, especially at position 9. A modified primary mouse screening test, developed in this laboratory, was used for the bioassay.

RESULTS AND DISCUSSION

Chemistry—The key intermediate in the synthesis of most of the compounds was the ketone, 9-nor-9-oxohexahydrocannabinol (I, Scheme I). It was prepared either as a racemic mixture according to the procedure of Fahrenholtz *et al.* (5) or as an optically active compound with the natural configuration according to a slightly improved procedure (6). (−)-$\Delta^{9,11}$-Tetrahydrocannabinol acetate[1] was treated with osmium tetroxide and sodium periodate in tetrahydrofuran–water to give the ketone after saponification of the acetate in an overall yield of 75%.

Compound I was converted to the dithioketal (II) by treatment with ethanedithiol–boron trifluoride etherate (7), and it gave 9-norhexahydrocannabinol (III) after reduction with Raney nickel in refluxing methanol (8). The optically active I afforded an approximate 1:1 mixture of the two isomeric 9-nor-9-hydroxyhexahydrocannabinols (IV) in almost quantitative yield by reduction with sodium borohydride in methanol (6).

Grignard reaction with the I acetate and propylmagnesium bromide gave, after treatment with acid, *dl*-Δ^{8}-9-nor-9-*n*-propyltetrahydrocannabinol (VI).

Hydrogenation of (−)-Δ^{9}-tetrahydrocannabinol[1] (VII, Scheme II) with palladium-on-charcoal (10%) yielded an approximately 1:1 mixture of the two isomeric (−)-hexahydrocannabinols (VIII) (9).

Reaction of (−)-$\Delta^{9,11}$-tetrahydrocannabinol acetate (IX, Scheme III) with borohydride–tetrahydrofuran–diglyme and subsequent oxidation of the resulting organoborane with trimethylamine *N*-oxide dihydrate (10) gave, after saponification of the acetate (X), an approximately 1:1 mixture of the two isomeric (−)-11-hydroxyhexahydrocannabinols (XI).

Pharmacology—A primary mouse screening test was applied to bioassay Δ^{9}-tetrahydrocannabinol and its analogs. A battery of 11 relatively objective subtests was administered successively to each mouse in a systematic order. The assessment began by observing the undisturbed behavior and the eyes of the animal to detect any gross abnormality. Then the mouse was put in an open-field box (11) to record its locomotor activity. Postural arrest was noted when the mouse stopped abruptly and remained still for more than 10 sec.

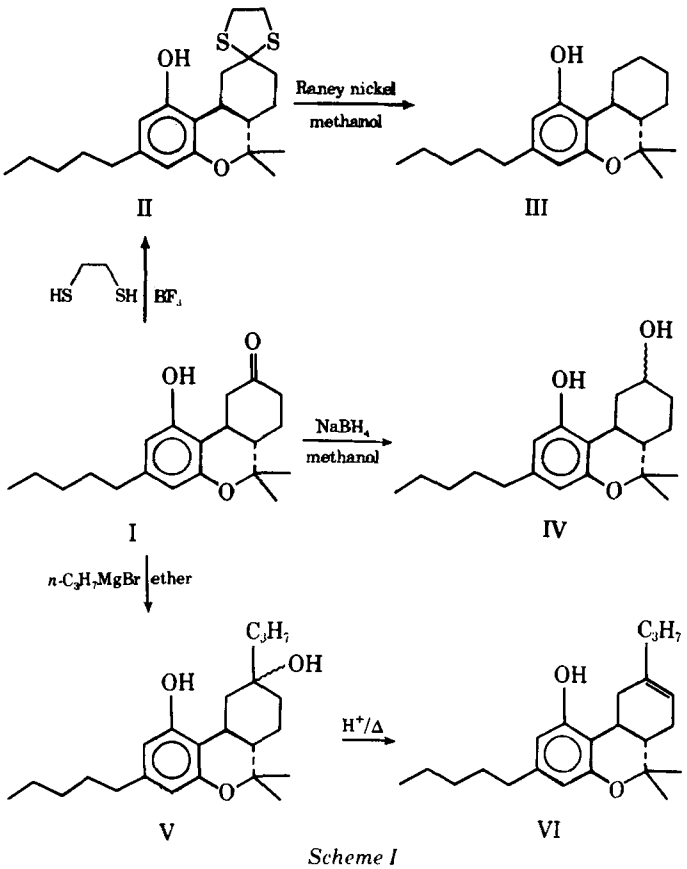

Scheme I

Touch response was evaluated by watching the "popcorn" reaction of the animal when its thorax was touched with the tip of a long forceps. A sharp sound was emitted by means of a metal clicker to score the startle response. To test for the biting response, the animal was held at the nape and a small wooden dowel was brought near its mouth (12). Body temperature was registered by inserting a rectal probe connected to a telethermometer.

Muscle tone was assayed by allowing the animal to suspend from a tiny bar fixed to a 0.5-kg push–pull strain gauge and slowly pulling the mouse down by its tail. The amount of force required to compel the subject to release its grip was read from the gauge. Neuromuscular coordination

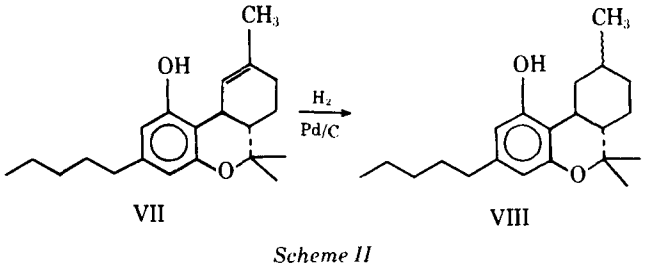

Scheme II

[1] Supplied by the Center for Studies of Narcotics and Drug Abuse, Alcohol, Drug Abuse, and Mental Health Adminstration.

0022-3549/79/0300-0330$01.00/0
© 1979, American Pharmaceutical Association

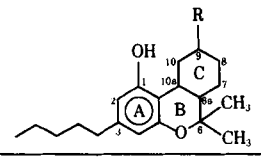

Table I—Structure–Activity Relationships of Δ^9-Tetrahydrocannabinol (VII) and Its Synthetic Analogs in Primary Mouse Screen

Compound	R	Δ	ED_{50}, μm/kg Locomotor Activity	Postural Arrest	Body Temperature	Pain Sensitivity
VII	CH_3	9 (1)	0.8	1.3	1.7	3.2
III	H	—	0.4	1.5	0.9	—
VI	$CH_2CH_2CH_3$	8 (6)	1.6	1.5	17.6	—
VIII	CH_3	—	27.1	21.0	12.7	—
IV	OH	—	0.4	1.1	0.7	—
XI	CH_2OH	—	0.8	1.0	2.0	—

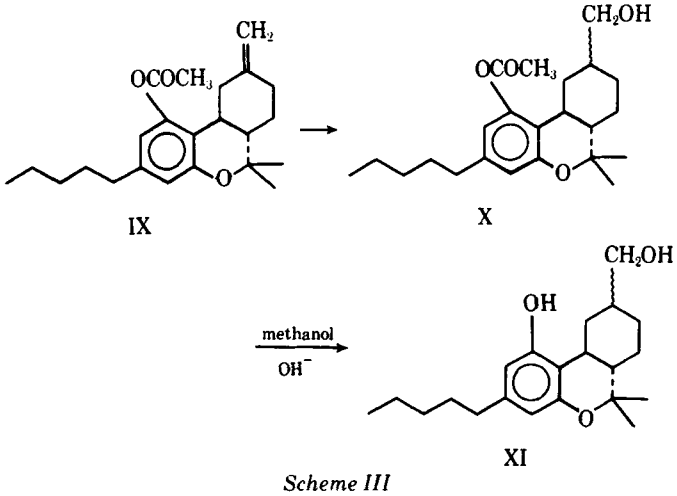

Scheme III

was measured by a rotarod (13). In the analgesic test, the animal was placed on a hot plate (14) regulated at 55 ± 0.5°. The interval of time during which the animal remained on the plate without showing any obvious reaction to heat was recorded.

Swiss–Webster male mice, 18–22 g, were used. Baseline scores for several subtests, *i.e.*, locomotor activity, postural arrest, touch response, biting response, and neuromuscular coordination, were obtained as a basis of comparison between predrug and postdrug responses. Initially, a series of dose range studies was conducted using a $\frac{1}{2}$ $\log_{10}$ interval scale. After a minimum effective dose range was established and a probable slope was estimated for each compound, dose–response studies were performed. The compounds were dissolved in polyethylene glycol 400 and administered at the rate of 2.4 ml/kg ip in a manner similar to the procedure reported by Uliss *et al.* (15).

Three appropriate doses of each compound were selected, and 10 animals were tested at each dose level. Each time a compound was evaluated, a control group of 10 mice injected with polyethylene glycol 400 also was observed. The bioassay was conducted 30 min after treatment.

The predrug baseline scores and the data obtained by assessing the physiological and behavioral states of the control subjects were analyzed to establish a control or criterion value for each subtest. The subtest score of each treated animal was considered to show a decrease, no change, or an increase in response relative to the control value.

The data showed that all compounds decreased locomotor activity and body temperature and increased postural arrest in a substantial number of animals. Although most compounds had no analgesic effects, Δ^9-tetrahydrocannabinol reduced pain sensitivity in some subjects. On other physiological states and behavioral responses, the compounds produced no appreciable effects. The percentages of mice showing a decrease in locomotor activity were computed at each dose level and plotted against dose (in micromoles per kilogram) on logarithmic probability paper. Similarly, the percentages of subjects manifesting a decrease in body temperature and the percentages revealing an increase in postural arrest were plotted against dose.

The dose–response curves indicated that the effects were dose related. From the curves, the median effective doses (ED_{50}'s) were calculated according to the method of Litchfield and Wilcoxon (16). The ED_{50} is the estimated dose at which 50% of the animals are expected to show a decrease (or an increase) in response to a given subtest. The ED_{50} values are listed in Table I, depicting the structure–activity relationships of the most active compounds.

EXPERIMENTAL

Boiling points are uncorrected. Melting points[2], determined in open glass capillaries, are uncorrected. Analytical results for the elements were within ±0.4% of the theoretical values.

***dl*-9-Norhexahydrocannabinol (III)**—Ethanedithiol (3 ml), I (4 g), and 3 ml of boron trifluoride etherate were mixed and stirred until they were homogeneous. After standing for an additional 10 min, this solution was chromatographed on silica gel with methylene chloride–ether. The methylene chloride–2% ether and methylene chloride–5% ether fractions were evaporated to give 4.7 g (95%) of the dithioketal as a colorless oil, which soon started to crystallize. Recrystallization from pentane gave colorless crystals, mp 84–87°.

These crystals were dissolved in 1100 ml of methanol and refluxed for 30 hr with 70 g of Raney nickel. The solution was then filtered over diatomaceous earth[3], and the solvent was evaporated to give 3.4 g (94%) of a yellow oil. Chromatography on silica gel with benzene and subsequent distillation at reduced pressure yielded 2.3 g of a slightly yellow oil, bp 160–180°/0.25 mm.

Anal.—Calc. for $C_{20}H_{30}O_2$: C, 79.42; H, 10.00. Found: C, 79.53; H, 10.32.

***dl*-Δ^8-9-*n*-Propyltetrahydrocannabinol (VI)**—Compound I acetate (800 mg, 2.25 mmoles) was treated with propylmagnesium bromide according to the standard Grignard reaction procedure to afford 600 mg of the mixture of carbinols (V) as a semisolid oil (74%). This crude product was treated with *p*-toluenesulfonic acid in refluxing benzene and chromatographed on silica gel with benzene to give 430 mg (55% overall yield) of VI as a nearly colorless oil.

Anal.—Calc. for $C_{23}H_{34}O_2$: C, 80.65; H, 10.01. Found: C, 80.51; H, 9.75.

11-Hydroxyhexahydrocannabinol (XI)—(−)-$\Delta^{9,11}$-Tetrahydrocannabinol acetate (456 mg, 1 mmole), prepared from (−)-$\Delta^{9,11}$-tetrahydrocannabinol by reaction with acetic anhydride–pyridine, was dissolved in 4 ml of dry diglyme and hydroborated with 0.44 ml of 1 *N* borohydride–tetrahydrofuran solution in tetrahydrofuran at 0° for 1 hr. Then the reaction was refluxed for 2 hr, and trimethylamine *N*-oxide dihydrate was added. The reaction mixture was gently refluxed with stirring for 2 hr. Then the contents of the reaction flask were transferred to a separator, diluted with methylene chloride, and washed once with 10% HCl and three times with saturated sodium chloride solution.

The organic layer was dried (magnesium sulfate) and evaporated to afford 400 mg of a brownish, viscous oil. Saponification of the acetate with methanolic 2% KOH at room temperature overnight and repeated chromatography of the product on silica gel with petroleum ether–40% ether gave 80 mg (25% overall yield) of an approximately 1:1 mixture of the two isomeric carbinols as a yellow oil.

Anal.—Calc. for $C_{21}H_{32}O_3$: C, 75.86; H, 9.70. Found: C, 75.76; H, 9.53.

REFERENCES

(1) R. Adams and B. R. Baker, *J. Am. Chem. Soc.*, **62**, 2405 (1940).

(2) R. Ghosh, A. R. Todd, and S. Wilkinson, *J. Chem. Soc.*, **1940**, 1121.

[2] Thomas-Hoover Uni-Melt apparatus.
[3] Celite.

(3) J. L. Neumeyer and R. A. Shagoury, *J. Pharm. Sci.*, **60**, 1433 (1971).
(4) R. Mechoulam, "Marijuana," Academic, New York, N.Y., 1973.
(5) K. E. Fahrenholtz, M. Lurie, and R. W. Kierstead, *J. Am. Chem. Soc.*, **89**, 5934 (1967).
(6) R. S. Wilson and E. L. May, *J. Med. Chem.*, **18**, 700 (1975).
(7) K. E. Fahrenholtz, *J. Org. Chem.*, **37**, 2204 (1972).
(8) T. Petrzilka, W. Kawfliger, and C. Sikemeier, *Helv. Chim. Acta*, **52**, 1102 (1969).
(9) R. A. Archer, D. B. Boyd, P. V. Demarco, I. J. Tyminski, and N. L. Allinger, *J. Am. Chem. Soc.*, **92**, 5200 (1970).
(10) G. W. Kabalka and H. C. Hedgecock, Jr., *J. Org. Chem.*, **40**, 1776 (1975).
(11) P. L. Broadhurst, *Br. J. Pharmacol.*, **48**, 1 (1957).
(12) S. Irwin, *Psychopharmacologia*, **13**, 222 (1968).
(13) W. J. Kinnard, Jr., and C. J. Carr, *J. Pharmacol. Exp. Ther.*, **121**, 354 (1957).
(14) N. B. Eddy, C. F. Touchberry, and J. E. Lieberman, *ibid.*, **98**, 121 (1950).
(15) D. B. Uliss, H. C. Dalzell, G. R. Handrick, J. F. Howes, and R. K. Razdan, *J. Med. Chem.*, **18**, 213 (1975).
(16) J. T. Litchfield, Jr., and F. Wilcoxon, *J. Pharmacol. Exp. Ther.* **96**, 99 (1949).

ACKNOWLEDGMENTS

Supported by SRI Institute Research and Development Program.

Synthesis of 4-Substituted Aminobenzoate Quaternary Salts as Potent Antispasmodic Agents

EL SEBAI A. IBRAHIM, RAAFAT SOLIMAN ˣ, and MOHAMED GABR

Received May 30, 1978, from the *Department of Pharmaceutical Chemistry, Faculty of Pharmacy, University of Alexandria, Alexandria, Egypt.* Accepted for publication August 24, 1978.

Abstract □ *N*-(Diethylaminoethyl)-4-substituted aminobenzoate quaternary salts, *N*-(diethylaminoethyl)-4-substituted aminobenzamide quaternary salts, 4-substituted acylaminobenzamide quaternary salts, and 4-substituted acylaminosalicylamide derivatives were prepared and tested for antispasmodic activity. Preliminary pharmacological tests on isolated guinea pig ileum revealed that the new compounds possess nonspecific inhibitory action on smooth muscles.

Keyphrases □ Aminobenzoic acid derivatives—quaternary salts synthesized, antispasmodic activity evaluated □ Quaternary salts—of aminobenzoic acid derivatives synthesized, antispasmodic activity evaluated □ Antispasmodic activity—quaternary salts of various aminobenzoic acid derivatives evaluated □ Structure–activity relationships—quaternary salts of aminobenzoic acid derivatives evaluated for antispasmodic activity

Studies based on the empirical structural scission of the atropine molecule indicated that it did not have a highly specific action. The tropine moiety is a complex amino alcohol that can be simplified but still retain the antispasmodic activity.

Many parasympatholytic drugs possess potent antispasmodic activity and show some structural resemblance to acetylcholine; at least a tertiary nitrogen atom is needed for activity. Moreover, quaternization of some antispasmodics resulted in significant variations in activity, including enhancement, duration, and toxicity.

The discovery of smooth muscle relaxant properties among many *N*-substituted 4-aminobenzoate esters and amides (1, 2) inspired the preparation of some analogs derived from 4-aminobenzoic and 4-aminosalicylic acids.

The present paper reports the synthesis of some *N*-(diethylaminoethyl)-4-substituted aminobenzoate quaternary salts, *N*-(diethylaminoethyl)-4-substituted aminobenzamide quaternary salts, 4-substituted acylaminobenzamide quaternary salts, and 4-substituted acylaminosalicylamide derivatives and their evaluation for antispasmodic and/or cardiovascular effects.

RESULTS AND DISCUSSION

Synthesis—The key intermediates, 4-substituted acylaminobenzoyl chlorides (I*a*–I*d*, Table I), were prepared by the classical method using thionyl chloride and the appropriate acid. *N*-(Diethylaminoethyl)-4-substituted aminobenzoate derivatives (III*a*–III*o*, Scheme I and Table II) were prepared by: Method A, condensation of the appropriate acid

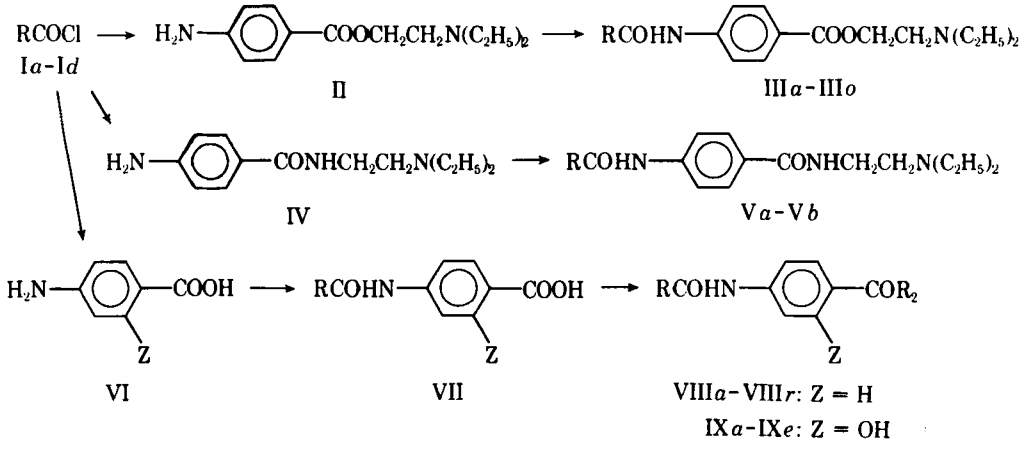

Scheme I

0022-3549/79/0300-0332$01.00/0
© 1979, American Pharmaceutical Association

(3) J. L. Neumeyer and R. A. Shagoury, *J. Pharm. Sci.*, **60**, 1433 (1971).
(4) R. Mechoulam, "Marijuana," Academic, New York, N.Y., 1973.
(5) K. E. Fahrenholtz, M. Lurie, and R. W. Kierstead, *J. Am. Chem. Soc.*, **89**, 5934 (1967).
(6) R. S. Wilson and E. L. May, *J. Med. Chem.*, **18**, 700 (1975).
(7) K. E. Fahrenholtz, *J. Org. Chem.*, **37**, 2204 (1972).
(8) T. Petrzilka, W. Kawfliger, and C. Sikemeier, *Helv. Chim. Acta*, **52**, 1102 (1969).
(9) R. A. Archer, D. B. Boyd, P. V. Demarco, I. J. Tyminski, and N. L. Allinger, *J. Am. Chem. Soc.*, **92**, 5200 (1970).
(10) G. W. Kabalka and H. C. Hedgecock, Jr., *J. Org. Chem.*, **40**, 1776 (1975).
(11) P. L. Broadhurst, *Br. J. Pharmacol.*, **48**, 1 (1957).
(12) S. Irwin, *Psychopharmacologia*, **13**, 222 (1968).
(13) W. J. Kinnard, Jr., and C. J. Carr, *J. Pharmacol. Exp. Ther.*, **121**, 354 (1957).
(14) N. B. Eddy, C. F. Touchberry, and J. E. Lieberman, *ibid.*, **98**, 121 (1950).
(15) D. B. Uliss, H. C. Dalzell, G. R. Handrick, J. F. Howes, and R. K. Razdan, *J. Med. Chem.*, **18**, 213 (1975).
(16) J. T. Litchfield, Jr., and F. Wilcoxon, *J. Pharmacol. Exp. Ther.* **96**, 99 (1949).

ACKNOWLEDGMENTS

Supported by SRI Institute Research and Development Program.

Synthesis of 4-Substituted Aminobenzoate Quaternary Salts as Potent Antispasmodic Agents

EL SEBAI A. IBRAHIM, RAAFAT SOLIMAN ˣ, and MOHAMED GABR

Received May 30, 1978, from the *Department of Pharmaceutical Chemistry, Faculty of Pharmacy, University of Alexandria, Alexandria, Egypt.* Accepted for publication August 24, 1978.

Abstract □ *N*-(Diethylaminoethyl)-4-substituted aminobenzoate quaternary salts, *N*-(diethylaminoethyl)-4-substituted aminobenzamide quaternary salts, 4-substituted acylaminobenzamide quaternary salts, and 4-substituted acylaminosalicylamide derivatives were prepared and tested for antispasmodic activity. Preliminary pharmacological tests on isolated guinea pig ileum revealed that the new compounds possess nonspecific inhibitory action on smooth muscles.

Keyphrases □ Aminobenzoic acid derivatives—quaternary salts synthesized, antispasmodic activity evaluated □ Quaternary salts—of aminobenzoic acid derivatives synthesized, antispasmodic activity evaluated □ Antispasmodic activity—quaternary salts of various aminobenzoic acid derivatives evaluated □ Structure–activity relationships—quaternary salts of aminobenzoic acid derivatives evaluated for antispasmodic activity

Studies based on the empirical structural scission of the atropine molecule indicated that it did not have a highly specific action. The tropine moiety is a complex amino alcohol that can be simplified but still retain the antispasmodic activity.

Many parasympatholytic drugs possess potent antispasmodic activity and show some structural resemblance to acetylcholine; at least a tertiary nitrogen atom is needed for activity. Moreover, quaternization of some antispasmodics resulted in significant variations in activity, including enhancement, duration, and toxicity.

The discovery of smooth muscle relaxant properties among many *N*-substituted 4-aminobenzoate esters and amides (1, 2) inspired the preparation of some analogs derived from 4-aminobenzoic and 4-aminosalicylic acids.

The present paper reports the synthesis of some *N*-(diethylaminoethyl)-4-substituted aminobenzoate quaternary salts, *N*-(diethylaminoethyl)-4-substituted aminobenzamide quaternary salts, 4-substituted acylaminobenzamide quaternary salts, and 4-substituted acylaminosalicylamide derivatives and their evaluation for antispasmodic and/or cardiovascular effects.

RESULTS AND DISCUSSION

Synthesis—The key intermediates, 4-substituted acylaminobenzoyl chlorides (I*a*–I*d*, Table I), were prepared by the classical method using thionyl chloride and the appropriate acid. *N*-(Diethylaminoethyl)-4-substituted aminobenzoate derivatives (III*a*–III*o*, Scheme I and Table II) were prepared by: Method A, condensation of the appropriate acid

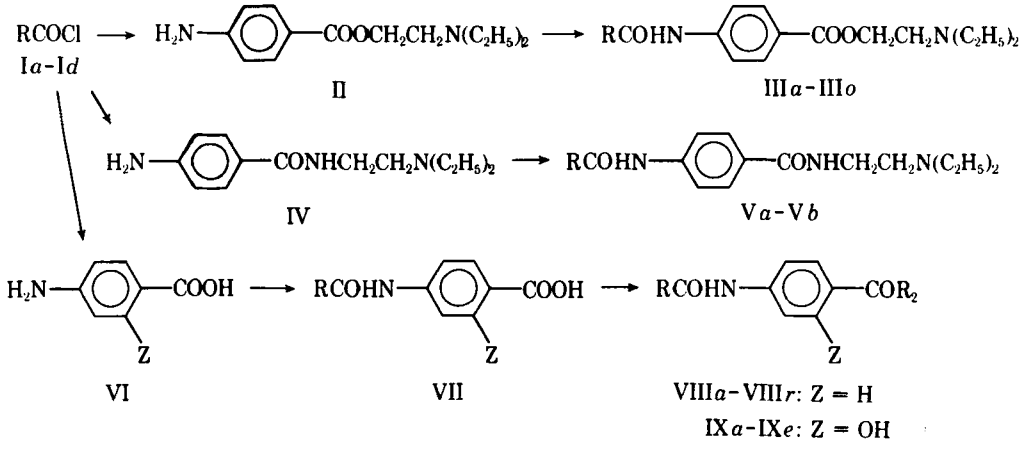

Scheme I

0022-3549/79/0300-0332$01.00/0
© 1979, American Pharmaceutical Association

Table I—Acyl 4-Aminobenzoic Acids

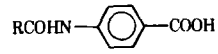

Compound	R	Yield, %	Melting Point[a]	Formula	Analysis, %	Calc.	Found
Ia	2-ClC_6H_4	72	262–263°	$C_{14}H_{10}ClNO_3$	C	61.0	60.6
					H	3.6	3.3
					Cl	12.9	13.1
					N	5.1	5.1
Ib	3-ClC_6H_4	78	267–268°	$C_{14}H_{10}ClNO_3$	C	61.0	61.2
					H	3.6	3.9
					Cl	12.9	13.3
					N	5.1	4.6
Ic	4-ClC_6H_4	76	270–272°	$C_{14}H_{10}ClNO_3$	C	61.0	60.7
					H	3.6	3.4
					N	5.1	4.7
Id	1-Naphthyl	85	275–277°	$C_{18}H_{13}NO_3$	C	74.1	74.1
					H	4.5	5.0
					N	4.8	5.0

[a] All compounds were crystallized from ethanol.

chloride with procaine hydrochloride in cold aqueous sodium carbonate solution; Method B, condensation of the appropriate acid chloride with procaine hydrochloride in dry benzene in the presence of sodium bicarbonate; or Method C, condensation of the appropriate acid with procaine base in chloroform solution using dicyclohexylcarbodiimide.

N-(Diethylaminoethyl)-4-substituted aminobenzamide derivatives (V*a* and V*b*, Scheme I and Table II) were prepared similarly using Methods A, B, and D, which involve treatment of procainamide with the appropriate acid chloride in dry pyridine. 4-Substituted acylaminobenzamide derivatives (VIII*a*–VIII*r*, Scheme I and Table II) were prepared using Methods B and D. The compounds were quaternized using ethyl iodide in dry ether. 4-Substituted acylaminosalicylamide derivatives (IX*a*–IX*e*, Scheme I and Table II) were prepared using Method B.

The structures were substantiated by IR, PMR, and mass spectrometric studies of representative members of the series.

Pharmacology—Testing of the antispasmodic activity (3) of III*c*, III*e*, III*g*, V*a*, V*g*, and IX*c* was carried out on isolated guinea pig ileum. All compounds tested inhibited contraction produced by standard submaximal doses of acetylcholine, histamine, or serotonin, with no specificity toward any of these spasmogens. The results showed that the tested compounds might possess considerable nonspecific inhibitory action on smooth muscles similar to that of procaine hydrochloride.

A comparative study of III*c*, III*e*, III*g*, V*a*, V*g*, and IX*c* with a similar molar concentration of procaine hydrochloride was then conducted. All tested compounds were more potent smooth muscle relaxants than procaine, as shown by their antagonistic effects on acetylcholine-induced contractions (Table III).

Table II—4-Substituted Acylaminobenzoate Derivatives

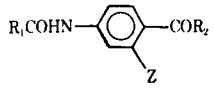

Compound	R_1	R_2	Z	Yield, %	Melting Point	Formula	Analysis, %	Calc.	Found
III*a*	C_6H_5	$OCH_2CH_2N(C_2H_5)_2$	H	65	78° [a]	$C_{20}H_{24}N_2O_3$		—	—
III*b*	C_6H_5	$OCH_2CH_2N(C_2H_5)_3I$	H	55	176–177° [b]	$C_{22}H_{29}IN_2O_3$	C	53.2	53.2
							H	5.9	5.5
							N	5.6	5.7
III*c*	2-ClC_6H_4	$OCH_2CH_2N(C_2H_5)_2$	H	65	130–131° [c]	$C_{20}H_{23}ClN_2O_3$	C	64.1	63.7
							H	6.2	6.3
III*d*	2-ClC_6H_4	$OCH_2CH_2N(C_2H_5)_3I$	H	60	178–179° [d]	$C_{22}H_{28}ClIN_2O_3$	C	49.8	50.2
							H	5.3	5.2
							N	5.3	5.5
III*e*	3-ClC_6H_4	$OCH_2CH_2N(C_2H_5)_2$·HCl	H	70	187–188° [c]	$C_{20}H_{24}Cl_2N_2O_3$	C	58.4	58.6
							H	5.9	5.5
							Cl	17.2	17.6
							N	6.8	6.8
III*f*	3-ClC_6H_4	$OCH_2CH_2N(C_2H_5)_3I$	H	80	180–181° [e]	$C_{22}H_{28}ClIN_2O_3$	C	49.8	49.8
							H	5.3	4.8
							N	5.3	5.0
III*g*	4-ClC_6H_4	$OCH_2CH_2N(C_2H_5)_2$	H	65	145–146° [f]	$C_{20}H_{23}ClN_2O_3$	C	64.1	64.3
							H	6.2	5.8
							Cl	9.5	9.4
							N	7.5	7.9
III*h*	4-ClC_6H_4	$OCH_2CH_2N(C_2H_5)_3I$	H	78	194–196° [e]	$C_{22}H_{28}ClIN_2O_3$	C	49.8	50.2
							H	5.3	5.7
							N	5.3	5.2
III*i*	$C_6H_5CH_2$	$OCH_2CH_2N(C_2H_5)_2$ picrate	H	54	141–142° [g]	$C_{27}H_{29}N_5O_{10}$	C	55.6	55.6
							H	5.0	5.3
							N	12.0	12.2
III*j*	$C_6H_5OCH_2$	$OCH_2CH_2N(C_2H_5)_2$	H	40	86–87° [h]	$C_{21}H_{26}N_2O_4$	C	68.1	68.1
							H	7.1	7.0
							N	7.5	7.3
III*k*	$C_6H_5OCH_2$	$OCH_2CH_2N(C_2H_5)_2$ picrate	H	82	146–147° [g]	$C_{27}H_{29}N_5O_{11}$	C	54.1	54.1
							H	4.9	5.0
							N	11.7	11.8
III*l*	$C_6H_5OCH_2$	$OCH_2CH_2N(C_2H_5)_3I$	H	40	117–118° [e]	$C_{23}H_{31}IN_2O_4$	C	52.4	52.8
							H	6.1	5.7
							N	5.3	5.5
III*m*	1-Naphthyl	$OCH_2CH_2N(C_2H_5)_2$	H	55	147–148° [g]	$C_{24}H_{26}N_2O_3$	C	73.8	73.5
							H	6.7	6.5
							N	7.2	7.4
III*n*	1-Naphthyl	$OCH_2CH_2N(C_2H_5)_2$ picrate	H	80	179–180° [g]	$C_{30}H_{29}H_5O_{10}$	C	58.1	58.3
							H	4.7	4.8
							N	11.3	11.1
III*o*	1-Naphthyl	$OCH_2CH_2N(C_2H_5)_3I$	H	82	157–158° [e]	$C_{26}H_{31}IN_2O_3$	C	57.3	57.0
							H	5.5	5.1
							N	5.1	5.5
V*a*	2-ClC_6H_4	$NHCH_2CH_2N(C_2H_5)_2$	H	65	140–142° [c]	$C_{20}H_{24}ClN_3O_2$	C	64.3	64.7
							H	6.5	6.2
							Cl	9.5	10.0
							N	11.2	11.7

(*continued*)

Table II—*Continued*

Compound	R_1	R_2	Z	Yield, %	Melting Point	Formula		Analysis, % Calc.	Found
V*b*	2-ClC_6H_4	$NHCH_2CH_2N(C_2H_5)_3I$	H	75	Sub. 64° [i]	$C_{22}H_{29}ClIN_3O_2$	N	7.9	8.2
VIII*a*	2-ClC_6H_4	$N(C_2H_5)_2$	H	78	203–204° [j]	$C_{18}H_{19}ClN_2O_2$	C	65.4	65.0
							H	5.8	6.1
							Cl	10.7	10.9
							N	8.5	8.8
VIII*b*	2-ClC_6H_4	Pyrrolidino	H	72	173–175° [g]	$C_{18}H_{17}ClN_2O_2$	C	65.8	65.6
							H	5.2	5.2
							Cl	10.8	11.2
							N	8.5	8.7
VIII*c*	2-ClC_6H_4	Piperidino	H	80	210–211° [j]	$C_{19}H_{19}ClN_2O_2$	C	66.6	66.4
							H	5.6	5.4
							Cl	10.4	10.8
							N	8.2	8.6
VIII*d*	2-ClC_6H_4	Morpholino	H	70	167–168° [j]	$C_{18}H_{17}ClN_2O_3$	C	62.7	63.1
							H	5.0	5.4
							Cl	10.3	10.1
VIII*e*	2-ClC_6H_4	*N*-Methylpiperazino	H	75	130–131° [j]	$C_{19}H_{20}ClN_3O_2$	C	63.8	63.6
							H	5.6	5.8
							Cl	9.9	9.9
VIII*f*	3-ClC_6H_4	$N(C_2H_5)_2$	H	72	217–219° [j]	$C_{18}H_{17}ClN_2O_2$	C	65.4	65.5
							H	5.8	5.4
							Cl	10.7	11.0
							N	8.5	8.2
VIII*g*	3-ClC_6H_4	Piperidino	H	75	186–187° [j]	$C_{19}H_{19}ClN_2O_2$	C	66.6	67.0
							H	5.6	6.0
							Cl	10.3	9.9
							N	8.2	7.8
VIII*h*	3-ClC_6H_4	Morpholino	H	80	179–181° [g]	$C_{18}H_{17}ClN_2O_3$	C	62.7	63.0
							H	5.0	5.0
							Cl	10.3	10.8
							N	8.1	8.0
VIII*i*	3-ClC_6H_4	*N*-Methylpiperazino	H	65	132–133° [h]	$C_{19}H_{20}ClN_3O_2$	C	63.8	63.4
							H	5.6	5.6
							Cl	9.9	10.0
							N	11.7	11.3
VIII*j*	3-ClC_6H_4	*N*-Methylpiperazinoethiodide	H	65	201–202° [i]	$C_{21}H_{25}ClIN_3O_2$	Cl	6.9	7.2
VIII*k*	4-ClC_6H_4	Pyrrolidino	H	78	178–179° [g]	$C_{18}H_{17}ClN_2O_2$	C	65.8	65.7
							H	5.2	4.8
							Cl	10.8	11.3
							N	8.5	8.3
VIII*l*	4-ClC_6H_4	Piperidino	H	82	187–188° [g]	$C_{19}H_{19}ClN_2O_2$	C	66.6	66.5
							H	5.6	6.0
							Cl	10.4	10.7
							N	8.2	7.8
VIII*m*	4-ClC_6H_4	Morpholino	H	76	207–208° [g]	$C_{18}H_{17}ClN_2O_3$	C	62.7	62.4
							H	5.0	5.4
							Cl	10.3	9.8
							N	8.1	8.5
VIII*n*	$C_6H_5OCH_2$	Morpholino	H	56	177–178° [g]	$C_{19}H_{20}N_2O_4$	C	67.1	66.9
							H	5.9	6.1
							N	8.2	7.9
VIII*o*	$C_6H_5OCH_2$	*N*-Methylpiperazino	H	25	196–197° [k]	$C_{20}H_{23}N_3O_3$	C	68.0	68.2
							H	6.6	6.6
							N	11.9	11.7
VIII*p*	1-Naphthyl	Piperidino	H	77	195–196° [c]	$C_{23}H_{22}N_2O_2$	C	77.1	76.9
							H	6.2	6.3
							N	7.8	7.6
VIII*q*	1-Naphthyl	Morpholino	H	66	185–186° [g]	$C_{22}H_{20}N_2O_3$	C	73.3	73.2
							H	5.6	5.6
							N	7.8	8.1
VIII*r*	1-Naphthyl	*N*-Methylpiperazino	H	35	205–206° [h]	$C_{23}H_{23}N_3O_2$	C	74.0	73.6
							H	6.2	6.2
							N	11.3	10.8
IX*a*	C_6H_5	NHC_3H_7	OH	85	168–169° [j]	$C_{17}H_{18}N_2O_3$	C	68.4	68.3
							H	6.1	6.2
							N	9.4	9.0
IX*b*	C_6H_5	NHC_4H_9	OH	80	196–198° [j]	$C_{18}H_{20}N_2O_3$	C	69.2	68.8
							H	6.5	6.7
							N	9.0	8.6
IX*c*	C_6H_5	Piperidino	OH	72	190–192° [g]	$C_{19}H_{20}N_2O_3$	C	70.4	70.1
							H	6.2	5.8
							N	8.6	8.5
IX*d*	C_6H_5	Morpholino	OH	40	224–225° [h]	$C_{18}H_{18}N_2O_4$	C	66.2	66.4
							H	5.6	5.7
							N	8.6	8.8
IX*e*	C_6H_5	*N*-Methylpiperazino	OH	58	237–238° [h]	$C_{19}H_{21}N_3O_3$	C	67.2	66.7
							H	6.2	6.0
							N	12.4	12.4

[a] Known compound (II). [b] Recrystallized from methanol–ether. [c] Recrystallized from benzene. [d] Recrystallized from methanol–acetone. [e] Recrystallized from methanol–benzene. [f] Recrystallized from methanol. [g] Recrystallized from ethanol. [h] Recrystallized from benzene–petroleum ether (bp 40–60°). [i] Recrystallized from ethyl acetate. [j] Recrystallized from dilute ethanol. [k] Recrystallized from ethyl acetate–petroleum ether (bp 40–60°).

Table III—Smooth Muscle Relaxant Activity of Some of the Tested Compounds Compared to Procaine Hydrochloride

Compound[a]	Mean Reduction[b] Response[c], % ± *SE*
Procaine hydrochloride	6.5 ± 1.18
IIIc	60.0 ± 1.30
IIIe	30.3 ± 1.36
IIIg	24.0 ± 1.41
Va	48.6 ± 1.21
Vg	99.6 ± 1.50
IXc	94.0 ± 1.17

[a] The concentration used was 3×10^{-5} mole/ml. Aqueous solutions were used. [b] Average of three experiments. [c] Concentration produced by acetylcholine (0.2 μg/ml).

EXPERIMENTAL[1]

General Method (4) for Preparation of Substituted Acyl-4-aminobenzoic Acids (Ia–Id)—To a solution of 4-aminobenzoic acid (5.5 g, 0.04 mole) in 25% NaOH (100 ml) was added, with stirring, the appropriate acid chloride (Ia–Id) (0.04 mole). The mixture was shaken vigorously for 15 min, cooled, and acidified with hydrochloric acid. The crude product thus obtained was filtered, washed with water, and recrystallized from the proper solvent.

IR spectra of these acids showed peaks at 3300 (NH), 2700–2540 (OH), 1705 (aromatic COOH), and 1680, 1530, and 1260 (amide I, II, and III bands, respectively) cm^{-1}; mass spectrometry of Ia: *m/e* (relative intensity) 275 (M^+, 96), 276 ($M^+ + 1$, 31), 258 (M − OH, 9), 200 (13), 144 (16), 142 (20), 141 (98), 140 (56), 139 ($C_7H_4ClO^+$, 100), 127 (33), 113 (44), 111 ($C_6H_4Cl^+$, 84), 100 (18), 76 ($C_6H_4^+$, 13), and 75 (44).

***N*-(Diethylaminoethyl)-4-substituted Aminobenzoates (IIIa–IIIo)**—*Method A (4)*—To a cold aqueous solution of procaine hydrochloride (II) (0.01 mole) in water (50 ml) was added slowly, with stirring, the appropriate Ia–Id (0.01 mole). The mixture was rendered alkaline with sodium carbonate, and stirring and cooling were continued for 30 min. The semisolid product obtained was extracted with ether, dried, filtered, and recrystallized from the proper solvent or converted to the hydrochloride salt by passing dry hydrogen chloride through the ethereal solution.

Method B—A mixture of II (0.01 mole), the appropriate Ia–Id (0.01 mole), and sodium bicarbonate (0.02 mole) in dry benzene (50 ml) was refluxed for 1–2 hr and filtered. The product was recrystallized from the proper solvent.

Method C (5–8)—A solution of II (0.01 mole) in water (10 ml) was made alkaline with ammonium hydroxide solution, and the liberated procaine base was extracted with chloroform. To the dry chloroform solution, *N,N'*-dicyclohexylcarbodiimide (0.01 mole) and the appropriate acid (0.01 mole) were added with cooling to 0° for 1 hr. Then the reaction mixture was left at room temperature overnight and filtered from the precipitated dicyclohexylurea. The filtrate was concentrated under reduced pressure, and the product was converted to the picrate salt.

***N*-(Diethylaminoethyl)-4-substituted Aminobenzamides (Va and Vb): Method D (9, 10)**—To a cooled, stirred solution of procainamide hydrochloride (IV) (0.005 mole) in dry pyridine (5 ml) was gradually added a cold solution of the appropriate Ia–Id (0.005 mole) in dry pyridine (5 ml) over 15 min. Stirring and cooling were continued for 1 hr, pyridine was removed under reduced pressure, and the residue was treated with ice cold water. The white precipitate thus obtained was collected, washed with water, and recrystallized from the proper solvent.

The IR spectra of Va showed a peak at 3340–3250 cm^{-1} indicative of NH (a secondary amide) and an amide I band at 1680 cm^{-1}. The PMR spectrum of Va ($CDCl_3$) exhibited peaks at δ 0.81–0.96 (t, 6H, $2CH_3$), 2.2–2.5 [q, 6H, $CH_2N(CH_2)_2$], 3.2 (q, 2H, C-2 of ethylenediamine), 6.2 (b, 1H, NH), and 7.0–7.5 (m, 8H, aromatic) ppm.

Quaternary Salts—To a solution of the amino compound (0.01 mole) in dry ether (50 ml) was added ethyl iodide (0.011 mole), and the mixture was stirred at room temperature for 24 hr. Ether was evaporated, and the product was recrystallized from the proper solvent.

4-Substituted Acylaminobenzamides (VIIIa–VIIIr)—These compounds were prepared following Methods B and D. Their IR spectra showed a peak at 3340–3250 cm^{-1} indicative of NH (a secondary amide) and an amide I band at 1680 cm^{-1}.

Mass spectrometry of VIIIe indicated *m/e* (relative intensity) 357 (M^+, 5), 258 ($M^+ - C_5H_{11}N_2^+$, 5), 218 ($C_{12}H_{16}N_3O^+$, 3), 141 (45), 140 (C_7H_5ClO, 14), 139 ($C_7H_4ClO^+$, 100), 113 (12), 111 ($C_6H_4Cl^+$, 38), 100 ($C_5H_{12}N_2$, 20), 99 ($C_5H_{11}N_2^+$, 6), 91 ($C_6H_5N^+$, 8), 76 ($C_6H_4^+$, 12), and 75 ($C_6H_3^+$, 22). The PMR spectrum of VIIIe (dimethyl sulfoxide-d_6) exhibited peaks at δ 2.25 (s, 3H, CH_3N-4), 2.33–2.4 (d, 4H, C_3 and C_5 piperazine), 3.45–3.6 (t, 4H, C_2 and C_6 piperazine), 7.33–7.9 (m, 8H, aromatic), and 10.67 (s, 1H, NH) ppm.

The PMR spectrum of VIIIb ($CDCl_3$) exhibited peaks at δ 1.88 (m, 4H, C_3 and C_4 pyrrolidine), 3.45–3.5 (d, 4H, C_2 and C_5 pyrrolidine), and 7.37–8.16 (m, 8H, aromatic) ppm.

The PMR spectrum of VIIIg ($CDCl_3$) exhibited peaks at δ 1.29–1.65 (t, 6H, C_3 and C_4 piperidine), 3.55 (s, 4H, C_2 and C_6 piperidine), 7.25–8.06 (t, 7H, aromatic), and 9.4 (s, 1H, C_2 of 3-chlorobenzoyl) ppm.

The PMR spectrum of VIIIi ($CDCl_3$) exhibited peaks at δ 2.3 (s, 3H, CH_3N-4), 2.36–2.38 (d, 4H, C_3 and C_5 piperazine), 3.59 (b, s, 4H, C_2 and C_6 piperazine), 7.26–7.94 (m, 7H, aromatic), and 8.57 (s, 1H, C_2 of 3-chlorobenzoyl) ppm.

4-Substituted Acylaminosalicylamides (IXa–IXe)—These compounds were prepared following Method B.

REFERENCES

(1) M. Ghelardoni, V. Pestellini, N. Pisanti, and G. Volterra, *J. Med. Chem.*, **16**, 1063 (1973).

(2) M. Ghelardoni, F. Russo, N. Pisanti, and G. Volterra, U.S. pat. 3,536,723 (1970); through *Chem. Abstr.*, **72**, 100318g (1970).

(3) G. S. Barsoum and J. H. Gaddum, *J. Physiol. (London)*, **85**, 1 (1935).

(4) N. O. V. Sonntag, *Chem. Rev.*, **52**, 272 (1953).

(5) H. O. Khorana, *ibid.*, **67**, 107 (1967).

(6) J. C. Sheehan and G. P. Hess, *J. Am. Chem. Soc.*, **77**, 1067 (1955).

(7) J. C. Sheehan and K. R. Henery, *ibid.*, **81**, 3089 (1959).

(8) H. Brauniger and W. Delzer, *Pharmazie*, **20**, 279 (1965).

(9) A. Einhorn and E. Uhlfrder, *Justus Liebigs Ann. Chem.*, **371**, 131 (1909).

(10) J. A. Mills, *J. Chem. Soc.*, **1951**, 2332.

(11) J. L. Regnier, *Chem. Abstr.*, **32**, 1051 (1938).

ACKNOWLEDGMENTS

The authors thank Mr. S. Mousa, Department of Pharmacology, Faculty of Pharmacy, University of Alexandria, Alexandria, Egypt, for the pharmacological evaluations. They also thank Dr. K. R. L. Mansford, Beecham Pharmaceuticals, United Kingdom, for the spectral determinations.

[1] IR spectra were determined on a Beckman IR-4210 as Nujol mulls. PMR spectra were determined on a Perkin-Elmer R12 spectrometer with tetramethylsilane as the internal standard. Mass spectra were determined using an AEI MS9 spectrometer. Melting points were determined in open glass capillaries and are uncorrected. Microanalyses were performed by the Microanalytical Unit, Faculty of Science, University of Cairo, Cairo, Egypt.

6-Substituted 1-Methylquinolinium-2-dithioacetic Acid Zwitterions: Antileukemia Activity

WILLIAM O. FOYE [x] **and JOEL M. KAUFFMAN**

Received July 12, 1978, from the *Samuel M. Best Research Laboratory, Massachusetts College of Pharmacy, Boston, MA 02115.* Accepted for publication August 16, 1978.

Abstract □ Condensation of the anhydro bases derived from 6-substituted 1-methylquinaldinium iodides with carbon disulfide provided the 2-dithioacetic acid zwitterions. Since 1,6-dimethylquinolinium-2-dithioacetic acid zwitterion previously showed appreciable activity against P-388 lymphocytic leukemia in mice, a series of analogs with other 6-substituents was synthesized to assess the importance of substitution in this position. Both electron-donating and electron-attracting 6-substituents gave compounds with antileukemia activity. The 6-unsubstituted analog had only marginal activity.

Keyphrases □ Dithioacetic acids, quinolinium—zwitterions synthesized, antileukemic activity evaluated in mice □ Zwitterions—quinolinium-2-dithioacetic acids synthesized, antileukemic activity evaluated in mice □ Antileukemic activity—various quinolinium-2-dithioacetic acid zwitterions evaluated in mice □ Structure-activity relationships—quinolinium-2-dithioacetic acid zwitterions evaluated for antileukemic activity in mice

1,6-Dimethylquinolinium-2-dithioacetic acid zwitterion (IV, Scheme I, R = CH_3) showed appreciable activity against P-388 lymphocytic leukemia in mice (1). It was considered that the dithiocarboxylic anion was a necessary function for this activity; but since several other related structures having a dithiocarboxylic anion lacked antileukemic activity, the 6-substituent of the quinoline ring also was regarded as important to this activity.

A similar requirement for a 6-substituent in the quinoline ring was found necessary for antileukemic activity in a series of 6-nitro- and 6-aminobis(4-quinaldinyl)-α,ω-diaminoalkanes (2). Accordingly, a series of 6-substituted *N*-methylquinolinium-2-dithioacetic acid zwitterions was synthesized to assess the importance of the 6-substituent in antileukemic activity. Both electron-donating and electron-attracting groups were included.

DISCUSSION

Chemistry—Synthesis of the quinaldines (I, Scheme I), based on the method of Campbell and Schaffner (3), involved the condensation of the *para*-substituted anilines with crotonaldehyde, using ferric chloride as the oxidizing agent. The free bases rather than the aniline hydrochlorides could be used, and 85% crotonaldehyde gave satisfactory yields. Isolation of the quinaldines was accomplished by addition of toluene to the reaction mixtures, azeotropic distillation of water, and distillation of the resulting toluene solutions. 2,4-Dimethylquinoline was prepared from 3-penten-2-one.

6-Trifluoromethylquinaldine, a new compound, was obtained in 21% yield. The NMR spectrum showed three C-methyl protons at δ 2.71 ppm, unsplit, and the aromatic protons at δ 7.2–8.2 ppm. Yields of the other substituted quinaldines ranged from 40 to 62%.

Preparation of the *N*-methylquinaldines first was attempted with dimethyl sulfate to provide higher yields and to avoid the discoloration associated with methiodides. Reaction of dimethyl sulfate with quinaldine gave an 80% yield of colorless material melting at 156–157° [lit. mp 152° (4) and 220° (5)]. Use of the methylsulfate of quinaldine gave only a 5% yield of the dithioacetic acid zwitterion, so the methiodides were employed.

The methiodides (II) were prepared by heating the quinaldines without solvent in a 25% excess of iodomethane (6). This method worked well for the 4-methyl, 6-methyl, 6-methoxy, and the 6-bromo compounds, but it gave no product with 6-chloroquinaldine. The 6-chloro methiodide was obtained by slow addition of iodomethane to a solution of the quinaldine in toluene at 100°. The only previous method reported for this compound was a sealed-tube reaction (7). The same procedure was used for the 6-trifluoromethyl methiodide, but the yield was only 13%.

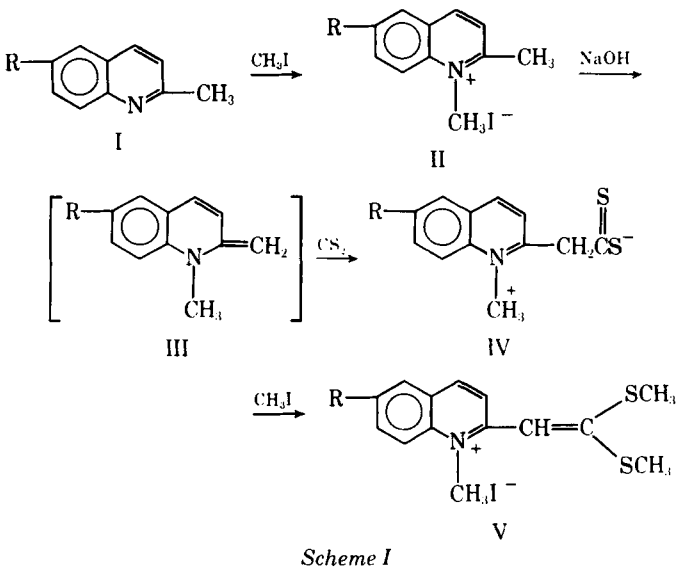

Scheme I

A previous preparation of pyridinium- and quinoliniumdithioacetic acid zwitterions involved the condensation of *N*-methylpicolinium or *N*-methylquinaldinium iodide with carbon disulfide in a solution of sodium hydroxide in aqueous dioxane (1). Rosenhauer (8) reported the preparation of the 1-methylquinolinium-2-dithioacetic acid zwitterion (IV, R = H) by isolation of the intermediate methylene base (III) followed by condensation with carbon disulfide. Repetition of this method gave a green solid melting at 73–75° [lit. mp 195° (8) and 185–187° (1)], which decomposed slowly on standing in a desiccator. Gompper *et al.* (9) also found this preparation to be unstable at −60°. Therefore, the previous procedure (1) was employed, and some improvement in yields was realized by vigorous mechanical stirring, use of less sodium hydroxide, and prevention of overheating of the reaction mixtures. Yields of the dithioacetic acid zwitterions (IV) ranged from 27 to 68%. These compounds were too insoluble in the common solvents for NMR spectra to be taken.

Preparations of the bis(*S*-methyl) derivatives of dithio acids were reported (9, 10). With the 6-bromo-1-methylquinolinium-2-dithioacetic acid zwitterion, treatment with excess iodomethane gave a bis(*S*-methyl) derivative (V, R = Br) whose NMR spectrum showed five ring protons at δ 8.2–9.0 ppm, *N*-methyl protons at δ 4.35 ppm, *S*-methyl protons at δ 2.50 and 2.63 ppm, and a one-proton singlet at δ 6.65 ppm for the olefinic proton.

The dithio acid zwitterion of the 6-unsubstituted 1-methylquinaldinium iodide also was converted to the bis(*S*-methyl) ketene acetal and showed essentially the same NMR spectrum. The *N*-methyl protons appeared at δ 4.40 ppm, the *S*-methyl protons at δ 2.55 and 2.70 ppm, and the olefinic proton at δ 6.80 ppm. Gompper *et al.* (9) reported this compound, but the only physical constant listed was a decomposition point of 203°; in the present preparation, a melting point of 198–201° was obtained.

Antileukemia Test Results—Antileukemia testing was performed[1]

[1] At Lederle Laboratories; results were reported through the courtesy of Dr. Ralph G. Child.

0022-3549/79/0300-0336$01.00/0
© 1979, American Pharmaceutical Association

Table I—Antileukemia Activities in Mice

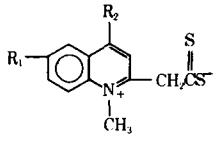

			Median Survival Time, T/C × 100 at					
			300	200	100	50	12.5	3.25
R_1	R_2	Test	mg/kg	mg/kg	mg/kg	mg/kg	mg/kg	mg/kg
H	H	1	—	130	—	110	100	100
		2	130	120	120	—	—	—
H	CH_3	1	—	110	—	110	90	115
		2	110	110	—	—	—	—
CH_3	H	1	—	140	—	120	120	110
Cl	H	1	—	130	—	130	115	110
		2	145	140	130	115	—	—
Br	H	1	—	135	—	120	105	115
		2	145	120	120	—	—	—
CH_3O	H	1	—	135	—	125	110	115
		2	150	140	130	120	—	—
CF_3	H	1	—	105	—	105	100	105
		2	100	100	—	—	—	—

using P-388 lymphocytic leukemia essentially in accordance with the protocol of the National Cancer Institute (11). BDF_1 (C57BL/6 × DBA/2)F_1 hybrid mice, 18–22 g, were inoculated intraperitoneally with 10^6 tumor cells. Test compounds were administered intraperitoneally on Days 1, 5, and 9 following tumor inoculation. Control mice received saline or 0.2% Noble agar[2] in saline. Six mice were used in each test group, and 12–18 mice were in each placebo control group. Animals were observed daily for deaths, and the median survival time was calculated. No weight loss was found at the highest dose used.

Of the seven compounds tested, five showed positive activity (a T/C × 100 ratio of 125 or better) (Table I). Although the 6-unsubstituted compound gave marginal activity, somewhat better results were shown by the 6-substituted derivatives. Little difference in activity appeared between electron-attracting and electron-donating substituents, although the strongly electronegative trifluoro derivative was inactive. It may be concluded that 6-substituents contribute to the antileukemic activity of these compounds; but similarly to the series of 6-nitro- and 6-amino-bis(4-quinaldinyl)-α,ω-diaminoalkanes (2), the relative electronegativities of the substituents seem unimportant.

EXPERIMENTAL[3]

2,4-Dimethylquinoline—This compound was prepared in 38% yield by the method of Campbell and Schaffner (3), bp 81–82° (0.8 torr) [lit. (3) bp 103–105° (2–3 torr)].

6-Methoxyquinaldine—This compound was prepared in 40% yield by the method of Campbell *et al.* (12), bp 95–96° (0.5 torr) [lit. (12) bp 145–146° (8 torr)].

6-Chloroquinaldine—To a stirred solution of 100 g (0.783 mole) of 4-chloroquinoline and 562 ml of 95% ethanol were added 77.5 g (0.781 mole) of 37% hydrochloric acid, 337 g of ferric chloride hexahydrate, and 12.5 g of zinc chloride. The reaction mixture was heated to 60°, and 51.5 g (0.625 mole) of 85% crotonaldehyde was added during 2.75 hr. The mixture was refluxed for 2 hr, and ethanol was distilled until the boiling temperature reached 100°.

After the resulting mixture had cooled, 100 ml of water and 500 ml of toluene were added. Free quinaldine was liberated by addition of 180 ml of 50% sodium hydroxide with stirring, the temperature was maintained below 65°. With a Dean–Stark trap, 200 ml of water was removed azeotropically, 100 ml of toluene was added, and 60 ml more of water was removed. The resulting liquid was decanted through coarse filter paper, and solvent was removed by rotary evaporation at 60° (40 torr).

The residue was extracted with 200 ml of toluene, filtered, and evaporated with the first extract. The resulting dark oil was distilled, with stirring, through a plug of stainless steel wool at 123–145° (9.5 torr) and solidified. The yellow solid was recrystallized twice from hexane at 5° and once from a mixture of 150 ml of methanol and 80 ml of water to give 52.28 g (47%) of white spars, mp 95–98° [lit. (13) mp 91°].

6-Bromoquinaldine—This compound was prepared from 4-bromoaniline in the same manner as the chloro analog, giving a 45% yield of colorless spars, mp 103–104.5° [lit. (13) mp 96–97°].

6-Trifluoromethylquinaldine—This compound was prepared from 4-aminobenzotrifluoride in the same manner as the chloro analog. The crude oil distilled at 50–68° (0.35–0.5 torr). It was freed from solvent by rotary evaporation, dissolved in 50 ml of toluene, and reevaporated. It was then refluxed with 100 ml of toluene and 4.3 g of succinic anhydride for 1 hr, cooled to 20°, and stirred for 0.5 hr with 100 ml of 5% sodium hydroxide. The mixture was heated to 30° to dissolve any solid, and the organic phase was washed with 30 ml of warm water and evaporated.

The resulting oil was crystallized from 50 ml of hexane at −20° and washed with 25 ml of hexane at −20° to give 11.37 g (21%) of colorless plates, mp 62.5–64.5°; NMR (carbon tetrachloride): δ 2.71 (s, 3H, 2-CH_3), 7.20 (d, 1H, 4-H, J = 8 Hz), and 7.5–8.2 (m, 4H, aromatic H) ppm; IR (carbon tetrachloride): 1607, 1573, 1508, 1485 (quinoline ring), 1330, 1170, and 1140 (CF_3) cm^{-1}.

Anal.—Calc. for $C_{11}H_8F_3N$: C, 62.56; H, 3.82; N, 6.63. Found: C, 61.99; H, 3.37; N, 6.81.

The compound was lachrymatory and caused eyelid inflammation.

1,2-Dimethyl-6-methoxyquinolinium Iodide—A solution of 17.3 g (0.1 mole) of 6-methoxyquinaldine and 17.7 g (0.125 mole) of iodomethane was heated to 98° for 23 hr. The resulting solid was refluxed with 150 ml of 95% ethanol for 2 hr, the solvent was decanted, and the extraction was repeated twice. The yellow needles were washed with acetone and dried, giving 25.5 g (81% yield), mp 235–238° dec. [lit. (14) mp 238° dec.].

Anal.—Calc. for $C_{12}H_{14}INO$: I, 40.33. Found: I, 40.27.

1,2-Dimethyl-6-chloroquinolinium Iodide—A solution of 13.23 g (0.0745 mole) of 6-chloroquinaldine and 100 ml of toluene was heated to 100°. Iodomethane (14.2 g, 0.1 mole) was added dropwise in two 7-hr periods on successive days while the temperature was maintained at 100° overnight both during and after the addition. The cooled mixture was filtered, washed with 100 ml of acetone, dried, and recrystallized from 100 ml of 95% ethanol, giving 9.53 g (40% yield) of yellow platelets, mp 223–224° [lit. (7) mp 211–212°].

1,2-Dimethyl-6-bromoquinolinium Iodide—This compound was prepared by the method used for the 6-methoxy derivative, except that 95% ethanol was used for recrystallization. A 75% yield of brown spars was obtained, mp 233–236° dec. [lit. (15) mp 237° dec.].

Anal.—Calc. for $C_{11}H_{11}BrIN$: I, 34.86. Found: I, 34.52.

1,2-Dimethyl-6-(trifluoromethyl)quinolinium Iodide—This compound was prepared by the method used for the 6-chloro analog, except that heating at 100° was continued for 4 days after the addition of iodomethane and the product was not recrystallized. A 13% yield of yellow prisms was obtained, mp 241–242° dec.; IR (KBr): 1320, 1175, and 1130 (CF_3) cm^{-1}.

Anal.—Calc. for $C_{12}H_{11}F_3IN$: C, 40.81; H, 3.14; N, 3.97. Found: C, 40.92; H, 3.08; N, 4.00.

6-Methoxy-1-methylquinolinium-2-dithioacetic Acid Zwitterion—To a solution of 6-methoxy-1-methylquinolinium iodide (12.61 g, 0.04 mole), water (20 ml), dioxane (40 ml), and carbon disulfide (20 ml, 0.233 mole) was added, at 25°, 30 ml of 50% sodium hydroxide at such a rate that the temperature did not exceed 29°. After 6 hr of stirring and addition of 50 ml of water, the mixture was filtered, washed with 400 ml of water, and dried (25°, 0.6 torr) to give 2.82 g (27%) of red-brown solid, mp 181° dec.; IR (KBr): 1315 (C=S) cm^{-1}.

Anal.—Calc. for $C_{13}H_{13}NOS_2 \cdot 2H_2O$: C, 52.14; H, 5.68; N, 4.68; S, 21.42. Found: C, 52.33; H, 4.90; N, 4.49; S, 20.84.

6-Chloro-1-methylquinolinium-2-dithioacetic Acid Zwitterion—This compound was prepared in the same manner as the 6-methoxy-1-methylquinolinium-2-dithioacetic acid zwitterion. An 80% yield of orange-brown solid was obtained, mp 300° dec.; IR (KBr): 1285 (C=S) and 885 (C=S) cm^{-1}.

Anal.—Calc. for $C_{12}H_{10}ClNS_2$: C, 53.82; H, 3.78; N, 5.23. Found: C, 54.02; H, 3.60; N, 5.10.

6-Bromo-1-methylquinolinium-2-dithioacetic Acid Zwitterion—The same procedure was used as for the 6-methoxy analog. A 55% yield of green-brown powder was obtained, mp 210–212° dec.; IR (KBr): 1305 (C=S) and 930 (C=S) cm^{-1}.

Anal.—Calc. for $C_{12}H_{10}BrNS_2 \cdot H_2O$: C, 43.64; H, 3.33; N, 4.24. Found: C, 43.96; H, 3.52; N, 3.86.

6-Trifluoromethyl-1-methylquinolinium-2-dithioacetic Acid

[2] Difco.

[3] Melting points were determined in capillaries with a Mel-Temp block and are uncorrected. IR absorption spectra were obtained with a Perkin-Elmer model 457A grating spectrophotometer and were corrected against polystyrene bands. NMR spectra were measured with a Varian T60 spectrometer with tetramethylsilane as internal standard. Elemental analyses were done by F. B. Strauss, Oxford, England. TLC was carried out using silica gel, and products were detected by exposure to iodine vapor. Organic reagents were supplied by Aldrich Chemical Co. or Eastman Organic Chemicals.

Zwitterion—This compound was prepared in the same manner as the 6-methoxy analog. A 68% yield of red-brown solid was obtained, mp 185° dec.

Anal.—Calc. for $C_{13}H_{10}F_3NS_2$: C, 51.82; H, 3.32; N, 4.65. Found: C, 52.16; H, 3.49; N, 4.35.

6-Bromo-1-methyl-2-bis(2-methylthio)vinylquinolinium Iodide—A mixture of 6-bromo-1-methylquinolinium-2-dithioacetic acid zwitterion (6.81 g, 0.0208 mole), iodomethane (10 ml), and dimethylformamide (40 ml) was allowed to stand at room temperature, with occasional shaking, for 17 hr. The dark-brown solid was filtered, washed with acetone, and dried at 23° (0.2 torr) for 6 days, giving 4.81 g (49% yield), mp 194–197° dec.; NMR (dimethyl sulfoxide-d_6): δ 2.50 (s, 3H, SCH_3), 2.63 (s, 3H, SCH_3), 4.35 (s, 3H, NCH_3), 6.65 (s, 1H, vinyl H), and 8.2–9.0 (m, 5H, ring H) ppm.

Anal.—Calc. for $C_{14}H_{15}BrINS_2$: C, 35.91; H, 3.23; N, 2.99; S, 13.70. Found: C, 35.55; H, 3.08; N, 2.94; S, 13.12.

1-Methyl-2-bis(2-methylthio)vinylquinolinium Iodide—The same procedure was used as the for 6-bromo analog. The resulting dark-yellow solid was washed with ether, recrystallized from water, and dried at 25° (1.5 torr), giving a 15.5% yield of yellow crystals, mp 198–201° dec. [lit. (9) mp 203° dec.]; NMR (dimethyl sulfoxide-d_6): δ 2.55 (s, 3H, SCH_3), 2.70 (s, 3H, SCH_3), 4.40 (s, 3H, NCH_3), 6.80 (s, 1H, vinyl H), and 8.3–9.0 (m, 6H, ring H) ppm.

REFERENCES

(1) W. O. Foye, Y. J. Lee, K. A. Shah, and J. M. Kauffman, *J. Pharm. Sci.*, **67**, 962 (1978).

(2) B. K. Sinha, R. M. Philen, R. Sato, and R. L. Cysyk, *J. Med. Chem.*, **20**, 1528 (1977).

(3) K. N. Campbell and I. J. Schaffner, *J. Am. Chem. Soc.*, **67**, 86 (1945).

(4) L. Horowitz, *ibid.*, **77**, 1687 (1955).

(5) J. Willems and J. Nys, *Bull. Soc. Chim. Belg.*, **66**, 502 (1957). P. Lochon and M. Jambu-Geoffroy, *Bull. Soc. Chim. Fr.*, **1965**, 393.

(6) L. G. S. Booker and L. A. Smith, *J. Am. Chem. Soc.*, **59**, 67 (1937).

(7) R. J. N. Sahay, A. K. Sinha, and J. C. Banerji, *J. Indian Chem. Soc.*, **43**, 255 (1966).

(8) E. Rosenhauer, *Chem. Ber.*, **57**, 1294 (1924).

(9) R. Gompper, B. Wetzel, and W. Elser, *Tetrahedron Lett.*, **1968**, 5519.

(10) K. Mizuyama, Y. Tominaga, J. Matsuda, and G. Kobayashi, *Yakugaku Zasshi*, **94**, 702 (1974).

(11) R. I. Geran, N. H. Greenberg, M. M. MacDonald, A. M. Schumacher, and B. J. Abbott, *Cancer Chemother. Rep., Part 3*, **3**, 1 (1972).

(12) K. N. Campbell, C. H. Helbing, and J. F. Kerwin, *J. Am. Chem. Soc.*, **68**, 1840 (1946).

(13) N. S. Kozlov and O. E. Kostromina, *J. Gen. Chem. USSR*, **25**, 907 (1955).

(14) W. Cocker and D. G. Turner, *J. Chem. Soc.*, **1941**, 143.

(15) K. L. Moudgill, *J. Am. Chem. Soc.*, **43**, 2257 (1921).

ACKNOWLEDGMENTS

Presented at the Medicinal Chemistry Section, 8th Northeast Regional Meeting, American Chemical Society, Boston, Mass., June 1978.

Supported by funds from the John R. and Marie K. Sawyer Memorial Fund, Massachusetts College of Pharmacy.

The authors are indebted to Dr. Ralph G. Child and Lederle Laboratories for the results of the antileukemia testing.

Differential Pulse Polarographic Analysis of Thyroid Hormone: Determination of Iodine, Thyroxine, and Liothyronine

WALTER HOLAK ˣ **and DONALD SHOSTAK**

Received June 30, 1978, from the *Food and Drug Administration, Department of Health, Education, and Welfare, Brooklyn, NY 11232.* Accepted for publication August 24, 1978.

Abstract □ A differential pulse polarographic method for the analysis of thyroid and thyroid tablets for total iodine, thyroxine, and liothyronine is described. The procedure for iodine, which is also applicable to individual tablet assay, consists of ashing the sample, converting iodide to iodate, and analyzing by differential pulse polarography. The procedure for thyroxine and liothyronine involves hydrolysis of the sample with barium hydroxide and isolation and separation of the iodoamino acids using ion exchangers, followed by differential pulse polarographic determination in a supporting electrolyte composed of 0.5 *N* Na_2CO_3 in 20% 2-propanol containing 1% tetrabutylammonium bromide. The differential pulse polarographic results for iodine agree with values obtained using the USP XIX procedure, and the quantities of thyroxine and liothyronine found agree with literature values.

Keyphrases □ Thyroid—differential pulse polarographic analysis of iodine, thyroxine, and liothyronine in hormone and tablets □ Polarography, differential pulse—analysis of iodine, thyroxine, and liothyronine in thyroid hormone and tablets □ Iodine—differential pulse polarographic analysis in thyroid hormone and tablets □ Thyroxine—differential pulse polarographic analysis in thyroid hormone and tablets □ Liothyronine—differential pulse polarographic analysis in thyroid hormone and tablets

The thyroid gland produces various iodoamino acids that are derivatives of thyronine and tyrosine including thyroxine, liothyronine, 3,3′,5′-triiodothyronine, 3,5-diiodothyronine, diiodotyrosine, and monoiodotyrosine (1, 2). The major biological activity is present only in thyroxine and liothyronine. 3,3′,5′-Triiodothyronine and 3,5-diiodothyronine have little or no biological activity and are present in small amounts; diiodotyrosine and monoiodotyrosine have no biological activity.

BACKGROUND

The USP XIX method for the estimation of thyroid potency involves the determination of total iodine. The compendial assay requires ashing the sample with potassium carbonate, which releases iodide ion. The chemical transformations consist of oxidation of iodide to iodate, reduction to iodine, and, finally, titration with sodium thiosulfate.

This titrimetric procedure is not applicable to individual tablet analysis because it lacks sufficient sensitivity. For this reason, a procedure that requires a Schöniger flask oxygen combustion treatment followed by the chemical transformations is used. However, the determination of total iodine is a nonspecific test for thyroid potency since iodine is available from biologically inactive compounds as well as the biologically active hormones. This assay is used because total iodine is relatively simple to determine accurately.

A better indication of thyroid potency would be the determination of the biologically active hormones, thyroxine and liothyronine. The development of a simple and reliable method for their determination has been a challenge. The approach has been to hydrolyze the sample by

0022-3549/79/0300-0338$01.00/0

© 1979, American Pharmaceutical Association

Zwitterion—This compound was prepared in the same manner as the 6-methoxy analog. A 68% yield of red-brown solid was obtained, mp 185° dec.

Anal.—Calc. for $C_{13}H_{10}F_3NS_2$: C, 51.82; H, 3.32; N, 4.65. Found: C, 52.16; H, 3.49; N, 4.35.

6-Bromo-1-methyl-2-bis(2-methylthio)vinylquinolinium Iodide—A mixture of 6-bromo-1-methylquinolinium-2-dithioacetic acid zwitterion (6.81 g, 0.0208 mole), iodomethane (10 ml), and dimethylformamide (40 ml) was allowed to stand at room temperature, with occasional shaking, for 17 hr. The dark-brown solid was filtered, washed with acetone, and dried at 23° (0.2 torr) for 6 days, giving 4.81 g (49% yield), mp 194–197° dec.; NMR (dimethyl sulfoxide-d_6): δ 2.50 (s, 3H, SCH_3), 2.63 (s, 3H, SCH_3), 4.35 (s, 3H, NCH_3), 6.65 (s, 1H, vinyl H), and 8.2–9.0 (m, 5H, ring H) ppm.

Anal.—Calc. for $C_{14}H_{15}BrINS_2$: C, 35.91; H, 3.23; N, 2.99; S, 13.70. Found: C, 35.55; H, 3.08; N, 2.94; S, 13.12.

1-Methyl-2-bis(2-methylthio)vinylquinolinium Iodide—The same procedure was used as the for 6-bromo analog. The resulting dark-yellow solid was washed with ether, recrystallized from water, and dried at 25° (1.5 torr), giving a 15.5% yield of yellow crystals, mp 198–201° dec. [lit. (9) mp 203° dec.]; NMR (dimethyl sulfoxide-d_6): δ 2.55 (s, 3H, SCH_3), 2.70 (s, 3H, SCH_3), 4.40 (s, 3H, NCH_3), 6.80 (s, 1H, vinyl H), and 8.3–9.0 (m, 6H, ring H) ppm.

REFERENCES

(1) W. O. Foye, Y. J. Lee, K. A. Shah, and J. M. Kauffman, *J. Pharm. Sci.*, **67**, 962 (1978).

(2) B. K. Sinha, R. M. Philen, R. Sato, and R. L. Cysyk, *J. Med. Chem.*, **20**, 1528 (1977).

(3) K. N. Campbell and I. J. Schaffner, *J. Am. Chem. Soc.*, **67**, 86 (1945).

(4) L. Horowitz, *ibid.*, **77**, 1687 (1955).

(5) J. Willems and J. Nys, *Bull. Soc. Chim. Belg.*, **66**, 502 (1957). P. Lochon and M. Jambu-Geoffroy, *Bull. Soc. Chim. Fr.*, **1965**, 393.

(6) L. G. S. Booker and L. A. Smith, *J. Am. Chem. Soc.*, **59**, 67 (1937).

(7) R. J. N. Sahay, A. K. Sinha, and J. C. Banerji, *J. Indian Chem. Soc.*, **43**, 255 (1966).

(8) E. Rosenhauer, *Chem. Ber.*, **57**, 1294 (1924).

(9) R. Gompper, B. Wetzel, and W. Elser, *Tetrahedron Lett.*, **1968**, 5519.

(10) K. Mizuyama, Y. Tominaga, J. Matsuda, and G. Kobayashi, *Yakugaku Zasshi*, **94**, 702 (1974).

(11) R. I. Geran, N. H. Greenberg, M. M. MacDonald, A. M. Schumacher, and B. J. Abbott, *Cancer Chemother. Rep., Part 3*, **3**, 1 (1972).

(12) K. N. Campbell, C. H. Helbing, and J. F. Kerwin, *J. Am. Chem. Soc.*, **68**, 1840 (1946).

(13) N. S. Kozlov and O. E. Kostromina, *J. Gen. Chem. USSR*, **25**, 907 (1955).

(14) W. Cocker and D. G. Turner, *J. Chem. Soc.*, **1941**, 143.

(15) K. L. Moudgill, *J. Am. Chem. Soc.*, **43**, 2257 (1921).

ACKNOWLEDGMENTS

Presented at the Medicinal Chemistry Section, 8th Northeast Regional Meeting, American Chemical Society, Boston, Mass., June 1978.

Supported by funds from the John R. and Marie K. Sawyer Memorial Fund, Massachusetts College of Pharmacy.

The authors are indebted to Dr. Ralph G. Child and Lederle Laboratories for the results of the antileukemia testing.

Differential Pulse Polarographic Analysis of Thyroid Hormone: Determination of Iodine, Thyroxine, and Liothyronine

WALTER HOLAK ˣ **and DONALD SHOSTAK**

Received June 30, 1978, from the *Food and Drug Administration, Department of Health, Education, and Welfare, Brooklyn, NY 11232.* Accepted for publication August 24, 1978.

Abstract □ A differential pulse polarographic method for the analysis of thyroid and thyroid tablets for total iodine, thyroxine, and liothyronine is described. The procedure for iodine, which is also applicable to individual tablet assay, consists of ashing the sample, converting iodide to iodate, and analyzing by differential pulse polarography. The procedure for thyroxine and liothyronine involves hydrolysis of the sample with barium hydroxide and isolation and separation of the iodoamino acids using ion exchangers, followed by differential pulse polarographic determination in a supporting electrolyte composed of 0.5 *N* Na_2CO_3 in 20% 2-propanol containing 1% tetrabutylammonium bromide. The differential pulse polarographic results for iodine agree with values obtained using the USP XIX procedure, and the quantities of thyroxine and liothyronine found agree with literature values.

Keyphrases □ Thyroid—differential pulse polarographic analysis of iodine, thyroxine, and liothyronine in hormone and tablets □ Polarography, differential pulse—analysis of iodine, thyroxine, and liothyronine in thyroid hormone and tablets □ Iodine—differential pulse polarographic analysis in thyroid hormone and tablets □ Thyroxine—differential pulse polarographic analysis in thyroid hormone and tablets □ Liothyronine—differential pulse polarographic analysis in thyroid hormone and tablets

The thyroid gland produces various iodoamino acids that are derivatives of thyronine and tyrosine including thyroxine, liothyronine, 3,3′,5′-triiodothyronine, 3,5-diiodothyronine, diiodotyrosine, and monoiodotyrosine (1, 2). The major biological activity is present only in thyroxine and liothyronine. 3,3′,5′-Triiodothyronine and 3,5-diiodothyronine have little or no biological activity and are present in small amounts; diiodotyrosine and monoiodotyrosine have no biological activity.

BACKGROUND

The USP XIX method for the estimation of thyroid potency involves the determination of total iodine. The compendial assay requires ashing the sample with potassium carbonate, which releases iodide ion. The chemical transformations consist of oxidation of iodide to iodate, reduction to iodine, and, finally, titration with sodium thiosulfate.

This titrimetric procedure is not applicable to individual tablet analysis because it lacks sufficient sensitivity. For this reason, a procedure that requires a Schöniger flask oxygen combustion treatment followed by the chemical transformations is used. However, the determination of total iodine is a nonspecific test for thyroid potency since iodine is available from biologically inactive compounds as well as the biologically active hormones. This assay is used because total iodine is relatively simple to determine accurately.

A better indication of thyroid potency would be the determination of the biologically active hormones, thyroxine and liothyronine. The development of a simple and reliable method for their determination has been a challenge. The approach has been to hydrolyze the sample by

0022-3549/79/0300-0338$01.00/0

© 1979, American Pharmaceutical Association

heating in an alkaline medium, followed by isolation of the hormones by extraction into 1-butanol prior to the determinative step. The separation of thyroxine from liothyronine recently was accomplished using ion exchangers (3). Several methods involve TLC (1) and GLC after derivatization (2).

This paper reports an investigation of differential pulse polarography in the analysis of thyroid. Iodine is determined by conventional dc polarography, and thyroxine and tyrosine also have been determined by this method (4–6). Its application to thyroid analysis is not practical, however, because of the lack of sensitivity, which is largely due to the capacitance current contribution to the Faradaic current. In differential pulse polarography, this difficulty is reduced so that this technique is well suited to the analysis of thyroid for total iodine, thyroxine, and liothyronine.

EXPERIMENTAL

Apparatus and Polarographic Conditions—A polarographic analyzer[1] was equipped with a drop timer in conjunction with three electrodes: dropping mercury, saturated calomel, and platinum wire auxiliary. The drop timer was set at 1 sec, and the dropping mercury electrode had a flow rate of 0.80 mg/sec. The height of the mercury column was 70 cm.

Other conditions were: current range, 1–5 μamp; pulse amplitude, 100 mv; and scan rate, 5 mv/sec. The potential range scans, in volts, were: iodate, from −0.9 to −1.50; and iodoamino acids, from −0.6 to −1.7. All polarograms were recorded on an *x–y* recorder[2].

A pH meter[3] was fitted with a combination glass–saturated calomel electrode.

Reagents and Chemicals—All chemicals were reagent grade, unless otherwise specified.

The potassium carbonate was purified to remove iodide. The following procedure was used. Dissolve about 100 g of potassium carbonate in 200 ml of water, add 25 g of 20–50-mesh ion-exchange resin[4], and agitate for 30 min. Filter, evaporate to dryness on a hot plate, and heat at 675° for 25 min. Then cool to room temperature.

The iodoamino acids[5] used were thyroxine (T_4, 3,5,3′,5′-tetraiodothyronine), liothyronine (T_3, 3,5,3′-triiodothyronine), 3,3′,5′-triiodothyronine ($T_{3'}$), 3,5-diiodothyronine (T_2), diiodotyrosine, and monoiodotyrosine. The ion-exchange resins used were 200–400-mesh AG 1 × 2[6], QAE-Sephadex A-25[7], and SP-Sephadex C-25[7].

Preparation of Solutions—*Standard Solutions*—The standard iodate stock solution containing 1000 μg of iodine/ml is prepared by dissolving 1.6860 g of potassium iodate in water and diluting to 1 liter.

The working standard iodate solution contains 1 μg of iodine/ml. Dilute with water, stepwise, aliquots of the standard iodate stock solution to achieve a concentration of 10 μg of iodine/ml. Pipet 10 ml of this solution into a 100-ml volumetric flask containing 8.0 g of potassium carbonate dissolved in about 20 ml of water. Then add 1 ml of bromine water and mix. Add about 10 mg of sodium sulfite to remove the excess bromine, mix, and dilute to volume.

Standard thyroxine and liothyronine solutions are prepared in the same manner. Add 10 mg of compound, accurately weighed, to separate 10-ml volumetric flasks. Add about 5 ml of water, then add dropwise 1 *N* NaOH to dissolve the amino acid salts, dilute to volume with water, and mix. Protect from light.

Supporting Electrolyte for Liothyronine and Thyroxine—Dissolve 5.3 g of sodium carbonate in about 30 ml of water. Then add 20 ml of 2-propanol, 1.0 g of tetrabutylammonium bromide, and 10 ml each of saturated aqueous solutions of sodium sulfite and disodium ethylenediaminetetraacetate. Dilute to 100 ml with water and mix. Adjust the pH to 11.6 with 5 *N* NaOH.

Elution Solutions—Solution A contains 0.02 *M* NaOH in water. For Solution B, dissolve 12.1 g of tris(hydroxymethyl)aminomethane (I) and 11.8 g of succinic acid in 1 liter of water. Adjust the pH to 8.7 with 0.1 *N* NaOH.

To prepare Solution C, dissolve 12.1 g of I and 11.8 g of succinic acid in 1 liter of 30% (v/v) 2-propanol in water. Adjust the apparent pH to 8.7 with a solution of 4 g of sodium hydroxide in 1 liter of 30% (v/v) 2-propanol in water.

For Solution D, dissolve 12.1 g of I and 11.8 g of succinic acid in 1 liter of 30% (v/v) 2-propanol in water. Adjust the apparent pH to 6.3 with a solution of 4 g of sodium hydroxide in 1 liter of 30% (v/v) 2-propanol in water.

Solution E is 2.5 *M* acetic acid in water, and Solution F is 12.0 *M* acetic acid in water.

Preparation of Columns—Plastic, 1-cm diameter[8] columns are packed as follows: Column 1, fill to a depth of 4 cm with QAE-Sephadex A-25 in 0.02 *N* NaOH; Column 2, fill to a depth of 4 cm with a mixed-bed exchanger, 40% SP-Sephadex C-25 and 60% QAE-Sephadex A-25 in Solution B; and Column 3, fill to a depth of 1 cm with 200–400-mesh AG 1 × 2 resin in 7 *M* acetic acid in water. Place a small pledget of glass wool on top of the resin.

Determination of Iodine—*Composite Assay Solution*—Weigh and finely powder not less than 20 tablets. Weigh a portion of powder containing about 60 mg of thyroid into a Vycor crucible, mix with 4 g of potassium carbonate, and overlay with 4 g of potassium carbonate. Place the crucible in a preheated muffle furnace at 675–700° for 25 min. Cool, dissolve the residue in 20 ml of hot water, and filter through a glass wool plug into a 100-ml volumetric flask.

Wash the crucible with two additional 20-ml portions of hot water and add these portions through the glass wool plug to the volumetric flask. Add 1 ml of bromine water, mix, add about 20 mg of sodium sulfite, and mix. Cool to room temperature and dilute to volume.

Individual Tablet Assay Solution—Weigh and finely powder each tablet. Weigh a portion of powder containing about 15 mg of thyroid into a Vycor crucible and mix with 1 g of potassium carbonate. Place into a preheated muffle furnace at 675–700° for 25 min. Cool, dissolve the residue in 10 ml of hot water, and filter through a glass wool plug into a 25-ml volumetric flask.

Wash the crucible with two 5-ml portions of hot water and add these portions through the glass wool plug to the volumetric flask. Add 1 ml of bromine water, mix, add about 20 mg of sodium sulfite, and mix. Cool to room temperature and dilute to volume.

Polarographic Procedure—Polarograph individually the composite assay solution, the individual tablet assay solution, and the working standard iodate solution as follows. Add about 10 ml of the solution to be assayed to the polarographic cell, deaerate for 5 min with nitrogen, and then polarograph using the described conditions. Measure the peak heights of the sample and the standard peaks that occur at approximately −1.18 v *versus* the saturated calomel electrode and calculate the percent iodine in the sample.

Determination of Thyroxine and Liothyronine—Weigh and finely powder not less than 20 tablets. Weigh a portion of powder containing about 0.2 g of thyroid into a 20-ml polyethylene screw-capped vial. Add 1.5 g of barium hydroxide octahydrate and 4 ml of water. Close the vial tightly, shake vigorously to mix the contents, and place in an oven at 95° for 6 hr. Transfer the contents of the vial with the aid of water to a 25-ml volumetric flask, cool to room temperature, dilute to volume, and mix. Allow any precipitate to settle. Label this solution the sample solution.

To another 25-ml flask, add 100 μl each of standard thyroxine and liothyronine solutions, 1.5 g of barium hydroxide, and about 20 ml of water. Mix and then dilute to volume. Label this solution the standard solution. Carry 15 ml of the standard solution through the chromatographic procedure in the same manner as the sample solution.

Feed a 15-ml aliquot of the sample solution to Column 1 and wash the column with 10 ml of Solution B or until the eluate pH is 8.7. Discard this eluate. Arrange the columns so that Column 1 elutes into Column 2, which then elutes into Column 3, which elutes into a waste beaker. Elute with 20 ml of Solution C. Remove Column 3, which now retains liothyronine. Place a new Column 3 under Columns 2 and 1 and elute with 20 ml of Solution D. Remove this second Column 3, which now retains thyroxine. Wash both columns with 5 ml of Solution E and discard the washings.

Elute liothyronine and thyroxine from the individual columns into glass evaporating dishes with 5 ml of Solution F. Evaporate the eluates to dryness at 60° with a current of nitrogen. Reserve the residue obtained from the liothyronine and thyroxine standard solutions for later use. Dissolve the sample residue in 5 ml of supporting electrolyte for liothyronine and thyroxine and transfer to the polarographic cell. Wash the evaporating dish with one 3-ml and one 2-ml portion of the supporting

[1] Princeton Applied Research model 174.
[2] Houston Omnigraphic model 2000.
[3] Beckman Zeromatic 55-3.
[4] Amberlite IRA-400.
[5] Courtesy of Joseph H. Graham, Food and Drug Administration, Washington, D.C.
[6] BioRad Laboratories, Richmond, Calif.
[7] Pharmacia Fine Chemicals, Piscataway, N.J.
[8] Chromaflex disposable columns, Kontes Glass Co., Vineland, N.J.

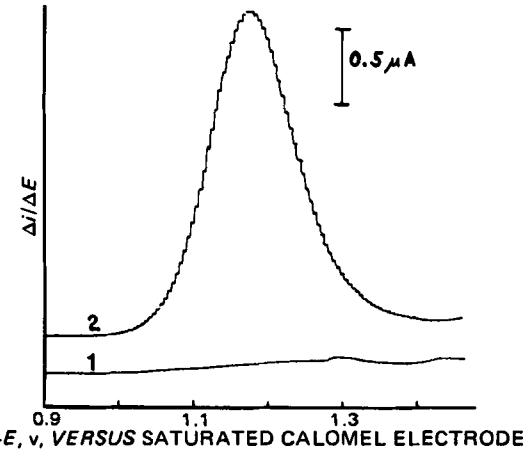

Figure 1—*Differential pulse polarogram of iodate. Key: 1, reagent blank; and 2, thyroid tablets.*

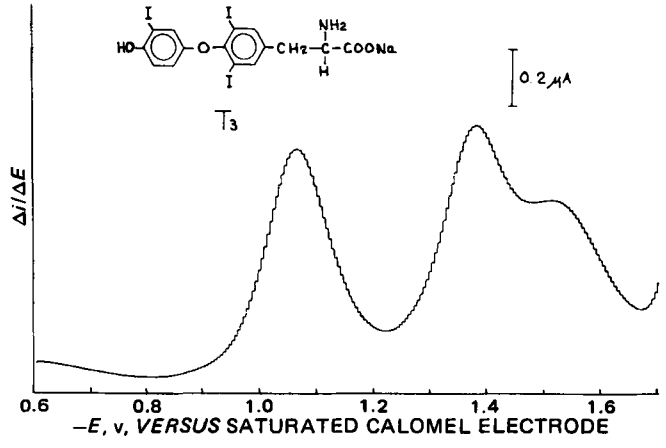

Figure 2—*Differential pulse polarogram of liothyronine standard.*

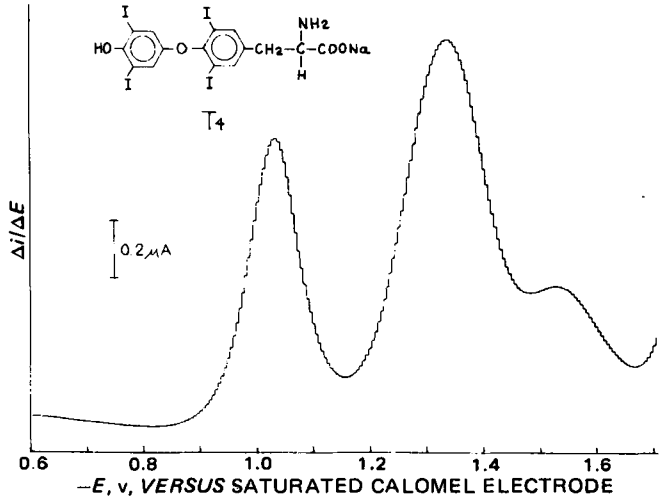

Figure 3—*Differential pulse polarogram of thyroxine standard.*

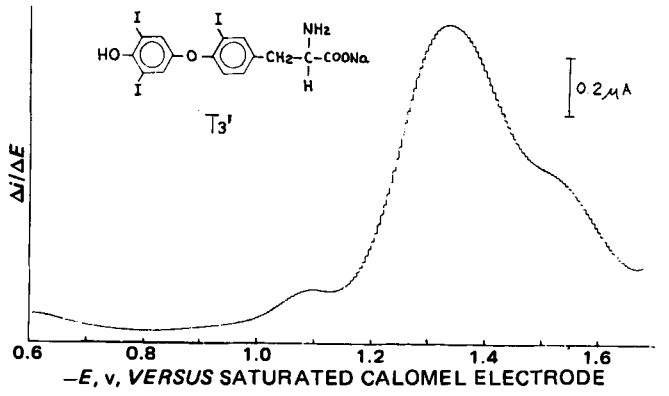

Figure 4—*Differential pulse polarogram of 3,3',5'-triiodothyronine standard. (This standard contained an impurity, probably liothyronine.)*

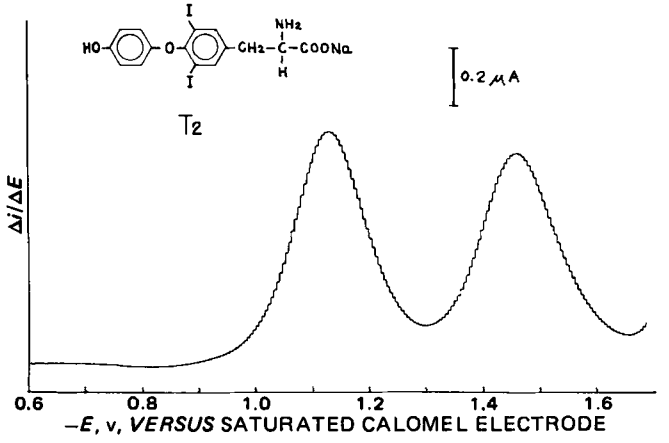

Figure 5—*Differential pulse polarogram of 3,5-diiodothyronine standard.*

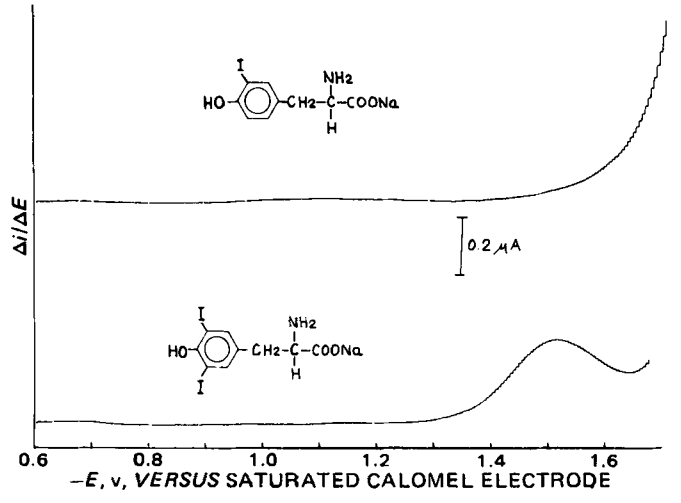

Figure 6—*Differential pulse polarograms of monoiodotyrosine and diiodotyrosine standards.*

electrolyte for liothyronine and thyroxine and transfer to the polarographic cell. Bubble nitrogen through the cell for 5 min and polarograph according to the described conditions.

Add the solution from the polarographic cell containing the sample to the evaporating dish containing the appropriate standard residue (either liothyronine or thyroxine) and swirl to dissolve. Quantitatively transfer the solution to the cell, wash the evaporating dish with solution in the cell, and then transfer back to the cell. Bubble in nitrogen for 3 min and polarograph using the same conditions as before. Calculate the percent of the hormone in the sample by the method of standard additions.

RESULTS AND DISCUSSION

Typical differential pulse polarograms of iodate and the iodoamino acid standards are shown in Figs. 1–6. Although only liothyronine and thyroxine are of interest, 3,3',5'-triiodothyronine, 3,5-diiodothyronine, diiodotyrosine, and monoiodotyrosine also were polarographed for comparison. Apparently, the sequential reduction of organically bound

Table I—Qualitative and Quantitative Differential Pulse Polarographic Behavior of Iodate and Iodoamino Acids Found in Thyroid

Compound	E_p, v, *versus* Saturated Calomel Electrode	Solution Concentration[a], μg/ml					Correlation Coefficient[b]
Iodate	−1.18	0.20 (0.22)	0.70 (0.75)	1.70 (1.66)	3.70 (4.02)	8.70 (9.74)	1.000
Liothyronine[c]	−1.06, −1.38, −1.53	2.34 (0.05)	8.19 (0.18)	19.89 (0.44)	31.59 (0.70)	43.29 (1.02)	0.999
Thyroxine[c]	−1.03, −1.34, −1.53	2.48 (0.06)	8.68 (0.21)	21.08 (0.55)	33.48 (0.95)	45.88 (1.26)	0.999
3,3′,5′-Triiodothyronine	−1.34, −1.53						
3,5-Diiodothyronine	−1.13, −1.46						
Diiodotyrosine	−1.52						
Monoiodotyrosine	N.R.[d]						

[a] Corresponding peak height in microamperes is given in parentheses. [b] Linear correlation coefficient showing relationship between concentration and peak height. [c] First peak used for quantitation. [d] No reduction before the decomposition of supporting electrolyte.

Table II—Analysis of Thyroid Powder for Iodine, Liothyronine, and Thyroxine Using the Differential Pulse Polarographic Method

	Liothyronine, %	Thyroxine, %	Iodine[a], %
	0.017	0.051	0.023
	0.016	0.046	0.200
	0.016	0.052	0.204
	0.015	0.049	0.206
Average	0.016	0.050	0.203
SD	0.001	0.003	0.003

[a] USP XIX method for iodine shows 0.202%.

Table III—Analysis of Thyroid Tablets of Various Strengths Using the Differential Pulse Polarographic Method and the USP XIX Procedure

Strength, mg	Differential Pulse Polarography			USP XIX,
	Liothyronine, %	Thyroxine, %	Iodine, %	Iodine, %
16	0.016	0.040	0.196	0.200
65	0.016	0.043	0.197	0.209
130	0.019	0.040	0.213	0.211
325	0.014	0.018	0.203	0.202

iodine proceeds as follows. The first peak results from reduction of iodine in the 5-position, the second peak results from the reduction of iodine in the 3′- and 5′-positions, and the third peak results from reduction of the iodine atom in the 3-position.

Table I summarizes the differential pulse polarographic behavior of iodate and six iodine-containing compounds found in thyroid. The correlation coefficients given in Table I indicate that a linear relationship exists between concentration and peak height for all three species of interest.

Thyroid is hydrolyzed by heating with barium hydroxide in a polyethylene vial. This procedure is more convenient than the common practice of using bottles or centrifuge tubes fitted with air condensers. After hydrolysis with barium hydroxide, liothyronine and thyroxine usually are isolated by extraction into 1-butanol, after which the alcohol is removed by evaporation. In this work, this time-consuming procedure was eliminated by use of an ion-exchange column that retained liothyronine and thyroxine. Then the two hormones were separated from each other by chromatography on mixed-bed resins and elution with solutions containing 1-propanol adjusted to a desired pH with buffers. The liothyronine and thyroxine standards also were subjected to the chromatographic procedure to compensate for possible adsorption on the columns and light-catalyzed degradation.

The constituents of the eluting solution must not be polarographically active in the region of interest, because traces always coelute with the iodoamino acids and can interfere. For this reason, succinic acid, instead of the polarographically active maleic acid, was used. Furthermore, to eliminate metal impurities such as zinc and to aid in the removal of dissolved oxygen, it was necessary to add disodium ethylenediaminetetraacetate and sodium sulfite to the supporting electrolyte.

The polarograms obtained in the reduction of iodoamino acids vary considerably with minor changes in the composition of the supporting electrolyte and the pH. To compensate for these variables, a quantitation procedure was employed using the method of standard addition. The volume of the supporting electrolyte containing the sample need not be known since a known weight of the standard is dissolved in this solution so that no volume change occurs as a result of the standard addition. This procedure simplifies the analysis and calculations. If several samples are to be analyzed, however, it may be advantageous to perform quantitations based on the calibration curve. In the latter case, accurate dilutions to volumes would be necessary. Figures 7 and 8 are polarograms obtained during the analysis of thyroid powder.

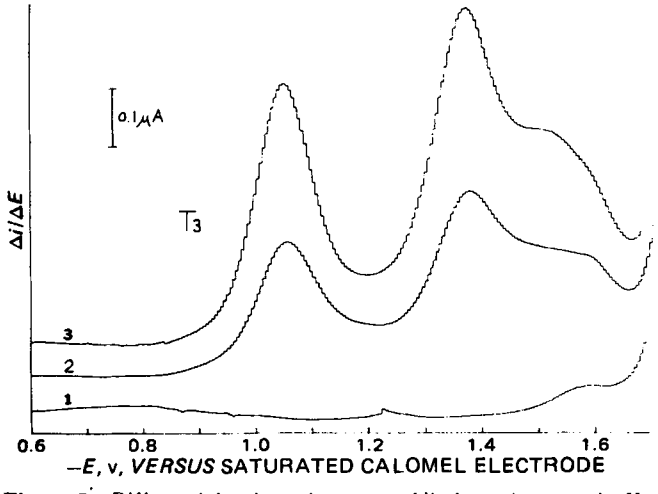

Figure 7—*Differential pulse polarogram of liothyronine sample. Key: 1, reagent blank; 2, liothyronine as derived from thyroid; and 3, after addition of liothyronine standard.*

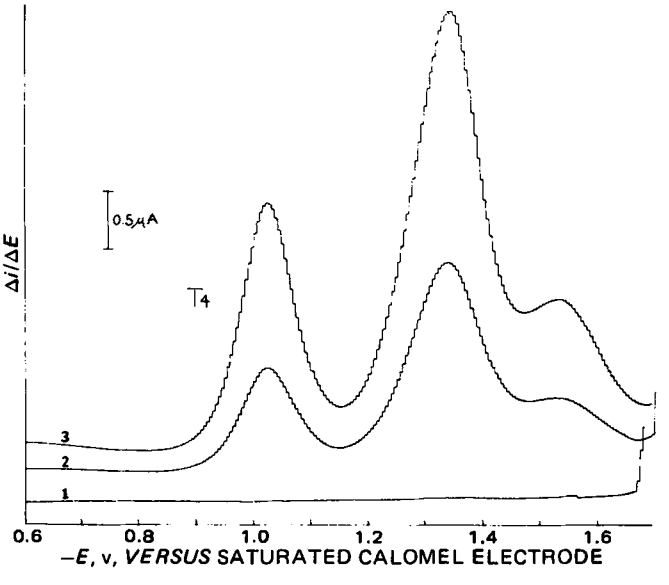

Figure 8—*Differential pulse polarogram of thyroxine sample. Key: 1, reagent blank; 2, thyroxine as derived from thyroid; and 3, after addition of thyroxine standard.*

Thyroid and thyroid tablets ranging in strength from 16 to 325 mg were analyzed for total iodine, liothyronine, and thyroxine by the proposed method. In addition, total iodine was determined by the USP XIX procedure. The results are given in Tables II and III. The iodine results agree with the USP analysis, and the values of liothyronine and thyroxine found in thyroid agree with literature results (1).

The procedures described in this work are relatively straightforward and are specific for the analysis of thyroid since intact liothyronine and thyroxine are determined.

REFERENCES

(1) J. E. Moody, Jr., J. R. Hohmann, Jr., and G. B. Kaplan, *J. Pharm. Sci.*, **57**, 634 (1968).

(2) R. Bilous and J. J. Windheuser, *ibid.*, **62**, 274 (1973).

(3) G. Knapp, H. Spitzy, and H. Leopold, *Anal. Chem.*, **46**, 724 (1974).

(4) I. M. Kolthoff and J. J. Lingane, "Polarography," 2nd ed., vol. II, Interscience, New York, N.Y., 1955, pp. 772–776.

(5) M. Brezina and P. Zuman, "Polarography in Medicine, Biochemistry and Pharmacy," rev. English ed., Interscience, New York, N.Y., 1958, pp. 216–221.

(6) D. C. M. Adamson, A. P. Domleo, J. F. Jeffries, and W. A. C. Shaw, *J. Pharm. Pharmacol.*, **4**, 760 (1952).

ACKNOWLEDGMENTS

The authors thank Dr. Thomas Medwick, Science Advisor, Food and Drug Administration, Brooklyn, N.Y., and Professor of Pharmaceutical Chemistry, Rutgers University, New Brunswick, N.J., for assistance in the preparation of this paper.

Nonlinear Model for Acetazolamide

ROBERT L. KUNKA * and ALBERT M. MATTOCKS ˣ

Received March 20, 1978, from the *School of Pharmacy, University of North Carolina, Chapel Hill, NC 27514.* Accepted for publication August 31, 1978.

*Present address: School of Pharmacy, University of Pittsburgh, Pittsburgh, PA 15261.

Abstract □ Intravenous bolus injections of ^{14}C-labeled acetazolamide were made in rabbits. Plasma, urine, and washed red blood cell concentrations were measured, the latter indicating bound drug. AUTOAN and NONLIN were used to fit the plasma data to a linear two-compartment model. However, utilization of the urine and red blood cell data suggested that a nonlinear model was more appropriate. The developed nonlinear system uses a one-compartment model with two tissue-binding parameters. The system simultaneously fits three equations describing drug in the plasma, in the body, and bound to red blood cells. Six parameters were estimated. The initial plasma concentration and the maximum amount bound to tissue protein (minus red blood cell protein) correlated with dose. The dissociation constant from this protein fraction suggested that it is composed mainly of the enzyme, carbonic anhydrase. The dissociation constant for the red blood cell fraction suggested that the drug binds to other protein in addition to carbonic anhydrase. The elimination constants were quite similar, indicating little variation from one animal to another. Utilization of the concepts of site and mechanism of action in this model should be of considerable help in relating drug concentration to pharmacological response.

Keyphrases □ Acetazolamide—nonlinear pharmacokinetic model, plasma, urine, and red blood cell data, intravenous bolus injection of ^{14}C-acetazolamide □ Pharmacokinetics—nonlinear model proposed for acetazolamide □ Models—nonlinear pharmacokinetic model proposed for acetazolamide

The efficacy and safety of drug therapy are commonly thought to be functions of the drug concentration at the site of action, but measurement of the drug concentration in remote tissues is usually difficult or impossible. Measurement of drug in the plasma is convenient and relatively easy, however, and plasma drug levels, although recognized to be vaguely related to effect, are used to evaluate therapy.

The common utilization of plasma levels to develop pharmacokinetic models and equations describing drug behavior in the body likewise depends largely on plasma measurements and thus yields equations that describe plasma levels quite accurately but that may not give useful estimates of drug concentrations in other tissues.

Recently, attention has been focused on equations that describe the time course of drug effect and that relate effect to plasma or peripheral compartment concentrations (1, 2). Pharmacokinetics must move in this direction to achieve the goal of enhancing effective and safe drug usage. This paper deals with such research on a well-known drug, acetazolamide.

Acetazolamide was selected since it was reported to be excreted entirely by the kidney in unchanged form (3, 4), its activity being uncomplicated by active metabolites. Furthermore, the mechanism of action is the inhibition of carbonic anhydrase (3, 5). The target organs of primary interest are the kidney, where the drug induces diuresis (3, 6), and the eye, where it causes reduction in intraocular pressure (5, 7–9).

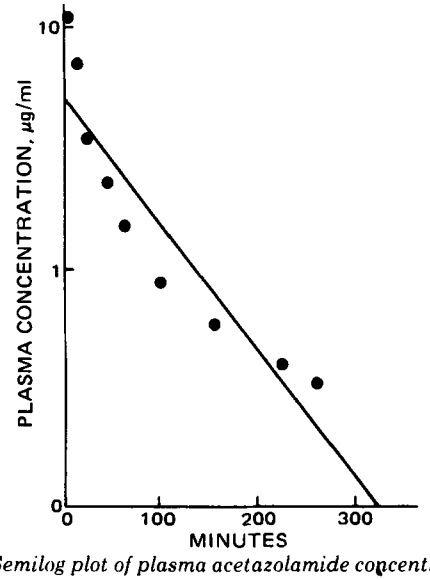

Figure 1—*Semilog plot of plasma acetazolamide concentration* versus *time.*

0022-3549/79/0300-0342$01.00/0

© 1979, American Pharmaceutical Association

Thyroid and thyroid tablets ranging in strength from 16 to 325 mg were analyzed for total iodine, liothyronine, and thyroxine by the proposed method. In addition, total iodine was determined by the USP XIX procedure. The results are given in Tables II and III. The iodine results agree with the USP analysis, and the values of liothyronine and thyroxine found in thyroid agree with literature results (1).

The procedures described in this work are relatively straightforward and are specific for the analysis of thyroid since intact liothyronine and thyroxine are determined.

REFERENCES

(1) J. E. Moody, Jr., J. R. Hohmann, Jr., and G. B. Kaplan, *J. Pharm. Sci.*, **57**, 634 (1968).

(2) R. Bilous and J. J. Windheuser, *ibid.*, **62**, 274 (1973).

(3) G. Knapp, H. Spitzy, and H. Leopold, *Anal. Chem.*, **46**, 724 (1974).

(4) I. M. Kolthoff and J. J. Lingane, "Polarography," 2nd ed., vol. II, Interscience, New York, N.Y., 1955, pp. 772–776.

(5) M. Brezina and P. Zuman, "Polarography in Medicine, Biochemistry and Pharmacy," rev. English ed., Interscience, New York, N.Y., 1958, pp. 216–221.

(6) D. C. M. Adamson, A. P. Domleo, J. F. Jeffries, and W. A. C. Shaw, *J. Pharm. Pharmacol.*, **4**, 760 (1952).

ACKNOWLEDGMENTS

The authors thank Dr. Thomas Medwick, Science Advisor, Food and Drug Administration, Brooklyn, N.Y., and Professor of Pharmaceutical Chemistry, Rutgers University, New Brunswick, N.J., for assistance in the preparation of this paper.

Nonlinear Model for Acetazolamide

ROBERT L. KUNKA * and ALBERT M. MATTOCKS ˣ

Received March 20, 1978, from the *School of Pharmacy, University of North Carolina, Chapel Hill, NC 27514.* Accepted for publication August 31, 1978.

*Present address: School of Pharmacy, University of Pittsburgh, Pittsburgh, PA 15261.

Abstract □ Intravenous bolus injections of ^{14}C-labeled acetazolamide were made in rabbits. Plasma, urine, and washed red blood cell concentrations were measured, the latter indicating bound drug. AUTOAN and NONLIN were used to fit the plasma data to a linear two-compartment model. However, utilization of the urine and red blood cell data suggested that a nonlinear model was more appropriate. The developed nonlinear system uses a one-compartment model with two tissue-binding parameters. The system simultaneously fits three equations describing drug in the plasma, in the body, and bound to red blood cells. Six parameters were estimated. The initial plasma concentration and the maximum amount bound to tissue protein (minus red blood cell protein) correlated with dose. The dissociation constant from this protein fraction suggested that it is composed mainly of the enzyme, carbonic anhydrase. The dissociation constant for the red blood cell fraction suggested that the drug binds to other protein in addition to carbonic anhydrase. The elimination constants were quite similar, indicating little variation from one animal to another. Utilization of the concepts of site and mechanism of action in this model should be of considerable help in relating drug concentration to pharmacological response.

Keyphrases □ Acetazolamide—nonlinear pharmacokinetic model, plasma, urine, and red blood cell data, intravenous bolus injection of ^{14}C-acetazolamide □ Pharmacokinetics—nonlinear model proposed for acetazolamide □ Models—nonlinear pharmacokinetic model proposed for acetazolamide

The efficacy and safety of drug therapy are commonly thought to be functions of the drug concentration at the site of action, but measurement of the drug concentration in remote tissues is usually difficult or impossible. Measurement of drug in the plasma is convenient and relatively easy, however, and plasma drug levels, although recognized to be vaguely related to effect, are used to evaluate therapy.

The common utilization of plasma levels to develop pharmacokinetic models and equations describing drug behavior in the body likewise depends largely on plasma measurements and thus yields equations that describe plasma levels quite accurately but that may not give useful estimates of drug concentrations in other tissues.

Recently, attention has been focused on equations that describe the time course of drug effect and that relate effect to plasma or peripheral compartment concentrations (1, 2). Pharmacokinetics must move in this direction to achieve the goal of enhancing effective and safe drug usage. This paper deals with such research on a well-known drug, acetazolamide.

Acetazolamide was selected since it was reported to be excreted entirely by the kidney in unchanged form (3, 4), its activity being uncomplicated by active metabolites. Furthermore, the mechanism of action is the inhibition of carbonic anhydrase (3, 5). The target organs of primary interest are the kidney, where the drug induces diuresis (3, 6), and the eye, where it causes reduction in intraocular pressure (5, 7–9).

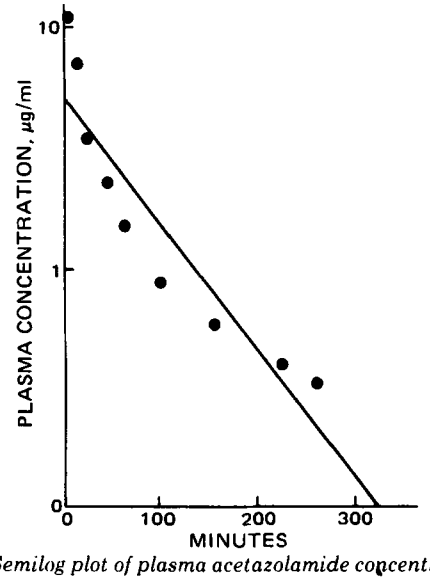

Figure 1—*Semilog plot of plasma acetazolamide concentration* versus *time.*

0022-3549/79/0300-0342$01.00/0

© 1979, American Pharmaceutical Association

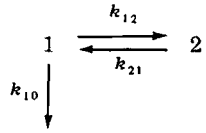

Scheme I

Acetazolamide kinetics have been studied only to describe plasma levels; the plasma data were limited in number, and a one-compartment model was used. These reports (4, 10, 11) reflect the level of interest in kinetics at the time of their publication and are not comparable to a modern detailed pharmacokinetic study.

This paper describes the use of ^{14}C-acetazolamide in rabbits to evaluate its pharmacokinetics, using a model that may be correlated with drug activity. A pharmacokinetic model for acetazolamide was devised using all available data from plasma, urine, and red blood cells. Parameters obtained from this model were later used to relate drug concentration to pharmacological response (12). This paper deals with the development of the nonlinear model.

EXPERIMENTAL

^{14}C-Acetazolamide was synthesized by the deacetylation of acetazolamide[1] and reacetylation with radioactive acetic anhydride[2,3]. TLC was used to test the purity of the radioactive compound. It was demonstrated that essentially all radioactive material was acetazolamide and that the deacetylated intermediate was present in trace amounts. Solutions for injection were prepared by adding appropriate amounts of radioactive and nonradioactive acetazolamide, converting the drug to its sodium salt *via* addition of 0.1 *N* NaOH, and diluting with water to volume. The final pH was 9.0–9.6.

Intravenous bolus acetazolamide doses ranging from 2 to 20 mg/kg were injected into the marginal ear veins of New Zealand White rabbits anesthetized with a 25% urethan[4] solution or sedated with 50 mg of chlorpromazine[5]. Blood and urine samples were collected at intervals up to 6–10 hr after injection; plasma was immediately separated from erythrocytes *via* centrifugation. Plasma samples, 0.5 ml, were mixed with 10 ml of a scintillation cocktail composed of 12 g of 2,5-diphenyloxazole[6] and 300 mg of 1,4-bis[2-(5-phenyloxazolyl)]benzene[6] in a mixture of 1 liter of surfactant[7] and 2 liters of toluene. Samples were counted in a liquid scintillation counter[8] and results were corrected for quenching using the channels ratio method (13).

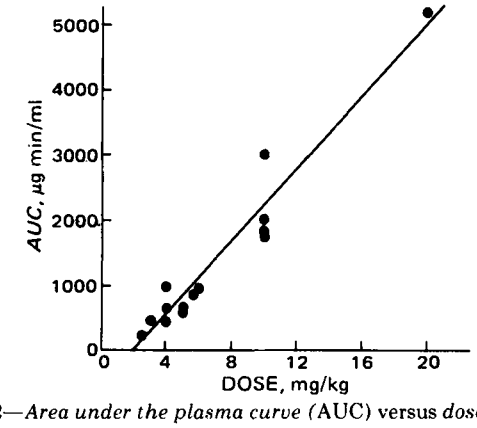

Figure 2—*Area under the plasma curve* (AUC) versus *dose.*

[1] Supplied by Lederle Laboratories, Pearl River, N.Y.
[2] New England Nuclear, Boston, Mass.
[3] R. Kudla, Lederle Laboratories, Pearl River, N.Y., personal communication.
[4] Nutritional Biochemical Co., Cleveland, Ohio.
[5] Thorazine, Smith Kline and French Laboratories, Philadelphia, Pa.
[6] Packard Instruments Co., Downers Grove, Ill.
[7] Triton-X100, Fisher Scientific Co., Raleigh, N.C.
[8] Model 3320 liquid scintillation spectrometer, Packard Instruments Co., Downers Grove, Ill.

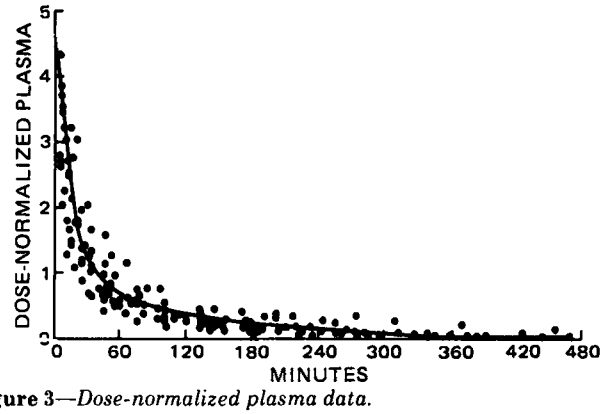

Figure 3—*Dose-normalized plasma data.*

Red blood cells were measured for bound drug by washing approximately 0.5-ml samples with 3 ml of normal saline (4). Accurately pipetted aliquots of packed cells were placed in No. 0 gelatin capsules, dried in a desiccator, and burned in an oxygen flask[9]. A carbon dioxide-capturing cocktail, 10 ml, was used to trap the gas. The solution contained 50 mg of 1,4-bis[2-(5-phenyloxazolyl)]benzene and 2 g of 2,5-diphenyloxazole in a mixture of 135 ml of methanol, 135 ml of phenylethylamine, and 230 ml of toluene. These samples were also measured in a scintillation counter.

Although no metabolites have been reported (3, 4), recoveries of 65–103% during the experiment prompted an examination of the urine for possible metabolites. TLC, involving development of urine samples in chloroform–methanol (80:30), indicated that no metabolism had occurred.

RESULTS AND DISCUSSION

Thirteen animals were tested by the described procedure. In all animals, plasma and red cell samples were collected at suitable intervals, but urine collections were not satisfactory in three animals. Curves of plasma, urine, and red cell concentrations were smooth and judged suitable for evaluation of possible kinetic models.

Since previous workers used a simple one-compartment model for acetazolamide, the data were examined as to fit to a monoexponential equation. When plotted as log plasma concentration *versus* time, systematic deviation from linearity was found invariably (Fig. 1). Obviously, a single-compartment model was not suitable.

Possibly, the best means of deciding on the number of exponentials required to describe the data is use of the computer programs AUTOAN and NONLIN. Plasma data from each animal were tested by computer *via* multiple correlation coefficients. The average coefficients obtained were 0.6425 ± 0.0241 for the monoexponential, 0.9959 ± 0.0026 for the biexponential, and 0.9985 ± 0.0013 for the triexponential equations. From these results, it was decided that the biexponential equation was best. The improvement gained by use of a triexponential equation did not justify the increased complexity.

The fit of the biexponential equation indicated that the plasma acetazolamide data fit a linear two-compartment model (Scheme I) where Compartment 1 is the circulating plasma plus other highly perfused

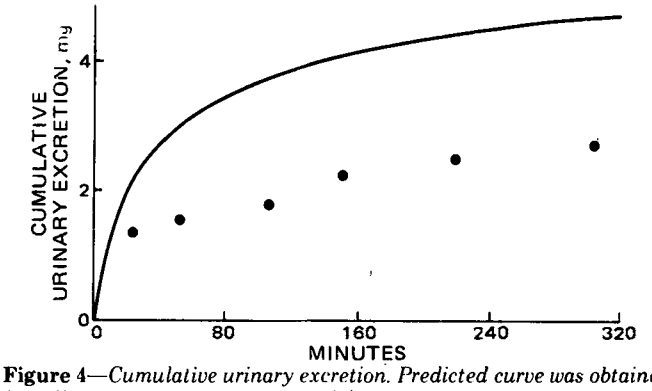

Figure 4—*Cumulative urinary excretion. Predicted curve was obtained from linear two-compartment model.*

[9] Thomas-Ogg model 11, Sargent Instrument Co., Chicago, Ill.

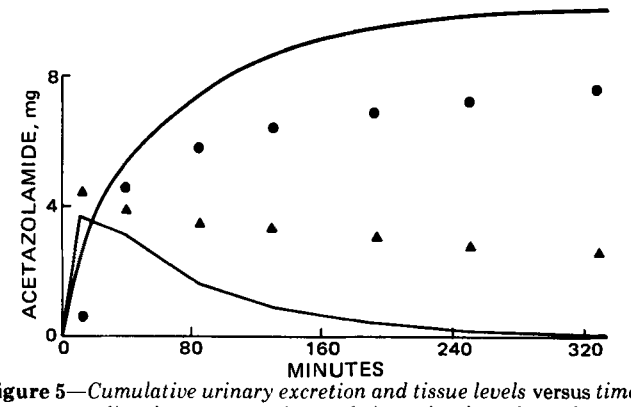

Figure 5—*Cumulative urinary excretion and tissue levels* versus *time. Key: —, predicted curves; ▲, observed tissue level; and ●, observed cumulative urinary excretion.*

tissues, Compartment 2 is less highly perfused tissue, and excretion occurs from Compartment 1 by way of the urine. With NONLIN, the kinetic parameters for this model were obtained for all animals. All plasma curves were fit satisfactorily to the model.

Since the mechanism of action of the drug involves tight binding in a widely distributed enzyme, the model was tested for linearity. Classically, a drug that follows linear kinetics will have a linear relationship between the area under the plasma curve (*AUC*) and dose (14) (Fig. 2). Dose-normalized plasma data obtained from plasma data at various doses should give a satisfactory fit to one superimposable curve if a drug follows linear kinetics. Figure 3 shows excellent agreement from data obtained following doses ranging from 1 to 20 mg/kg. Furthermore, no trends were seen when the individual curves were plotted together. Derived rate constants were also independent of dose and indicated kinetic linearity. In addition to these criteria, acetazolamide excretion was found to follow linear kinetics as judged by the computer program AUTOAN.

While these tests indicated that the linear model was appropriate, further examination utilizing urine and red blood cell data cast doubt on its suitability. Plots of observed and predicted drug elimination showed a consistent and marked overprediction (Fig. 4). Moreover, computed values for plasma concentrations at later time points were consistently below measured values.

The suitability of the linear model was also judged by comparing predicted amounts in the tissue with observed values. These values were determined by:

$$X_2 = D - (CV_1 + X_e) \qquad \text{(Eq. 1)}$$

where X_2 is the observed value, D is the dose, C is the plasma concentration, V_1 is the calculated volume of the central compartment, and X_e is the cumulative amount of acetazolamide measured in the urine. At later times, the value CV_1 becomes very small and the equation effectively reduces to:

$$X_2 = D - X_e \qquad \text{(Eq. 2)}$$

Graphs of the observed and predicted tissue levels showed that the model consistently underpredicted the later points (Fig. 5). While the predicted curve decreased substantially with time, the observed values did not, indicating strong binding to tissue protein. Additional insight was gained

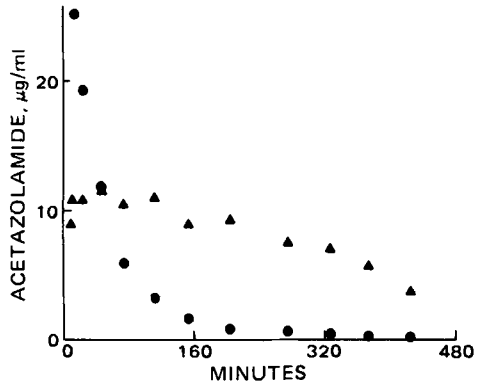

Figure 6—*Acetazolamide concentrations. Key: ●, plasma; and ▲, washed red blood cells.*

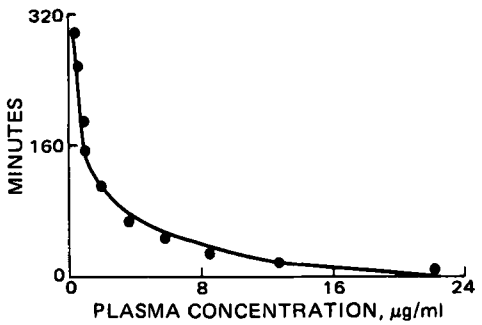

Figure 7—*Plasma curve obtained from nonlinear model with two tissue binding parameters.*

by obtaining the difference between the actual and predicted values of X_2 at later times. A fairly consistent difference of approximately 2.2 mg was found, indicating a nearly constant fraction of drug not accounted for by the model.

Washed red blood cells were also examined for the drug. Following bolus injection, prompt saturation of the cells was attained (Fig. 6). Plateau drug levels in the red cells were consistently above plasma concentrations and were maintained for varying times, again indicating tight binding to protein.

While several classical tests for linearity indicated that the model was satisfactory, utilization of the urine and red blood cell data showed that the linear model did not accurately describe all data. The strong binding suggested that a nonlinear model would be more appropriate than a more complicated linear model.

A nonlinear model system presented by Wagner (15) incorporates the concept of tissue binding. While a linear model gives a linear plot of *AUC versus* dose, a nonlinear model can also give this relationship. Wagner showed that data following the tissue-binding model can also be fitted to a biexponential equation (15). The simplest model in this system, a one-compartment model with one type of tissue binding, was tested first. The model makes two assumptions: that maximum binding occurs instantaneously on injection since the plasma concentration is highest at this time (data from red blood cells indicated that uptake of the drug is sufficiently rapid to make this assumption) and that different types of protein–drug interactions are similar enough to be represented by one binding equation.

The data were fitted to the nonlinear model, and satisfactory fits to plasma and amount of drug in the body were obtained. The tissue curve, however, did not describe red blood cell concentrations well. Therefore, it was decided to expand the model to contain two tissue-binding parameters, one a generalized tissue and the other the red blood cells. The equations for this model (Scheme II) are:

$$\frac{dC}{dt} = \frac{-KC}{1 + \dfrac{A_1B_1}{(B_1 + C)^2} + \dfrac{A_2B_2}{(B_2 + C)^2}} \qquad \text{(Eq. 3)}$$

$$t = \frac{1}{K}\left[\left(1 + \frac{A_1}{B_1} + \frac{A_2}{B_2}\right)\ln\left(\frac{C_0}{C}\right) + \frac{A_1}{B_1}\ln\left(\frac{B_1 + C}{B_1 + C_0}\right) + \frac{A_2}{B_2}\ln\left(\frac{B_2 + C}{B_2 + C_0}\right) + A_1\left(\frac{C - C_0}{(B_1 + C_0)(B_1 + C)}\right) + A_2\left(\frac{C - C_0}{(B_2 + C_0)(B_2 + C)}\right)\right] \qquad \text{(Eq. 4)}$$

$$T_1 + T_2 = \frac{A_1C}{B_1 + C} + \frac{A_2C}{B_2 + C} \qquad \text{(Eq. 5)}$$

where C is the plasma concentration with C_0 its initial value; t is time; K is the elimination constant; A_1 is the maximum concentration of drug bound to the generalized binding tissue, T_1; B_1 is the dissociation constant for the drug–tissue complex; and A_2 and B_2 are corresponding values for red blood cells, T_2.

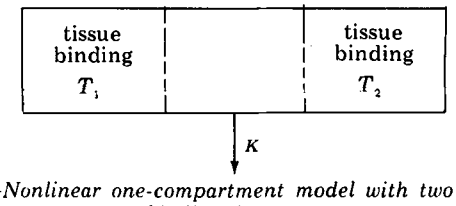

Scheme II—Nonlinear one-compartment model with two types of binding sites.

Table I—Summary of Pharmacokinetic Parameters for Nonlinear Model with Two Binding Parameters

Rabbit	C_0, μg/ml	A_1, μg/ml	B_1, μg/ml	A_2, μg/ml	B_2, μg/ml	K, μg/ml	Volume, ml/kg	R^2 RBC[a]	R^2 X_b	R^2 Plasma	R^2 Total
14	39.38 ± 0.83	11.27 ± 0.49	0.00011 ± 0.00001	4.00 ± 0.47	1.3777 ± 0.4628	0.0165 ± 0.0156	182.98	0.980	0.997	0.963	0.997
15	8.33 ± 0.37	3.22 ± 0.43	0.0137 ± 0.0150	0.77 ± 0.25	0.8331 ± 0.6383	0.0126 ± 0.0062	405.84	0.994	0.996	0.966	0.996
16	15.10 ± 0.46	1.72 ± 0.14	0.00011 ± 0.00004	2.45 ± 0.12	0.0708 ± 0.00094	0.0173 ± 0.0088	259.47	0.994	0.995	0.977	0.995
22	9.23 ± 0.19	1.50 ± 0.09	0.00014 ± 0.00003	1.80 ± 0.0857	0.00014 ± 0.00004	0.0145 ± 0.0091	399.04	0.980	0.999	0.972	0.997
23	5.43 ± 0.02	4.20 ± 0.23	0.0373 ± 0.0040	2.94 ± 0.11	0.00012 ± 0.00001	0.0290 ± 0.0126	198.89	0.981	0.998	0.983	0.994
25	13.58 ± 1.04	6.07 ± 0.83	0.0021 ± 0.0014	4.05 ± 0.63	0.3377 ± 0.1293	0.0251 ± 0.0089	168.78	0.980	0.989	0.998	0.988
26	4.88 ± 0.15	1.30 ± 0.15	0.00011 ± 0.00003	1.10 ± 0.07	0.00022 ± 0.00006	0.0113 ± 0.0058	412.09	0.993	0.998	0.934	0.997
27	5.66 ± 0.09	1.49 ± 0.10	0.00033 ± 0.00013	0.98 ± 0.06	0.1095 ± 0.0397	0.0153 ± 0.0073	492.00	0.987	0.999	0.949	0.999
28	19.74 ± 0.54	9.44 ± 0.47	0.00063 ± 0.00008	4.84 ± 0.28	0.2540 ± 0.0447	0.0222 ± 0.0056	176.37	0.995	0.999	0.997	0.999
29	29.16 ± 0.32	16.29 ± 0.29	0.00016 ± 0.000004	2.84 ± 0.10	0.0826 ± 0.0080	0.0155 ± 0.0446	207.08	0.971	1.000	0.992	0.999
		$\bar{x}$	0.00547 ± 0.0119	2.58 ± 1.42	0.3066 ± 0.4539	0.0179 ± 0.0057	290.25 ± 123.01	Rabbits 18, 19, and 21 were fit using estimates from above data. No urine was taken.			
18	8.39 ± 1.42	31.69 ± 8.72	0.0057 ± 0.0011	3.95 ± 0.76	0.2613 ± 0.0517	0.0151 ± 0.0071	129.00	0.998	—	0.979	0.998
19	121.11 ± 21.04	34.69 ± 15.79	0.0058 ± 0.0026	6.29 ± 0.93	0.3975 ± 0.0924	0.0156 ± 0.0106	123.39	0.996	—	0.970	0.996
21	30.23 ± 2.09	7.28 ± 1.73	0.0025 ± 0.0007	3.20 ± 0.25	0.0583 ± 0.0250	0.0116 ± 0.0031	245.64	1.000	—	0.926	0.999

[a] Red blood cells.

The data were fitted by computer to three equations simultaneously. The first (Eq. 4) is the integrated plasma equation. The equation describing the amount of drug in the body, X_b, as a function of plasma concentration is:

$$X_b = \frac{\text{dose}}{C_0 + A_1 + A_2}\left(C + \frac{A_1 C}{B_1 + C} + \frac{A_2 C}{B_2 + C}\right) \qquad \text{(Eq. 6)}$$

where dose/$(C_0 + A_1 + A_2)$ is the volume of distribution. The equation for the quantity of drug bound to the red cells, T'_2, is:

$$T'_2 = \frac{\text{dose}}{C_0 + A_1 + A_2}\left(\frac{A_2 C}{B_2 + C}\right) \qquad \text{(Eq. 7)}$$

Data for the first equation were observed plasma concentrations, data for the second equation were calculated amounts remaining in the body (dose $- X_e$), and data for the third equation were observed amounts in the red cells. While good initial estimates of C_0 could be obtained from the biexponential fit, estimates of the other parameters proved hard to obtain. The value of A_2 was obtained from a nonlinear fit of the bound red blood cell data, and A_1 was assumed to be larger than A_2. The value of B_2 was also estimated from individual fitting of red blood cell data while the value of B_1 was assumed to be much smaller than B_2. An unsatisfactory estimate resulted in an improbable parameter value, and the fitting procedure was rerun with a new estimate. Excellent fits were obtained for all but one data set with regression coefficients of about 0.99. Figures 7–9 are examples of the types of curves obtained. Table I lists the estimated parameters, calculated volumes, and multiple regression coefficients for the data sets.

The initial plasma concentration, C_0, increased proportionally with dose, as might be expected. The maximum concentration of drug bound to red cells, A_2, was not correlated with dose but was highly variable from one animal to another. The erythrocytes, being readily accessible to drug in plasma and limited in number, might be expected to be saturated readily, but individual variation appeared to mask this effect.

The maximum concentration of drug bound to the undefined binding tissue, T_1, was found to be a function of dose with no evidence of saturation. Since carbonic anhydrase, which is thought to be the major binding component of this tissue, is present in practically all body cells, saturation would not be expected except at extremely large doses. The effect of increasing dose in the normal range probably is the result of the penetration of the drug to less accessible regions.

Insight into the nature of the binding in T_1 is obtained from values of B_1; B_1 represents the dissociation constant of the complex in micrograms per milliliter. Conversion of the average value for B_1, 0.00547 μg/ml, into molar units yields 2.5×10^{-8} M. If acetazolamide binding to plasma

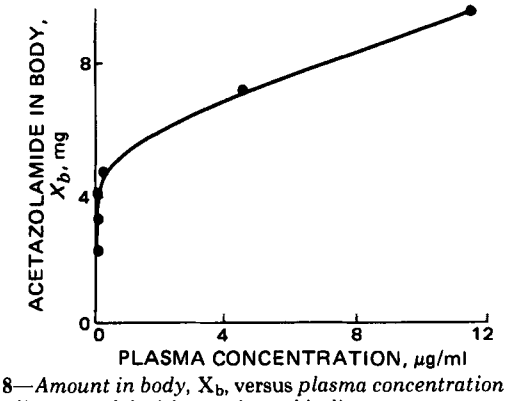

Figure 8—*Amount in body,* X_b, versus *plasma concentration obtained from nonlinear model with two tissue-binding parameters.*

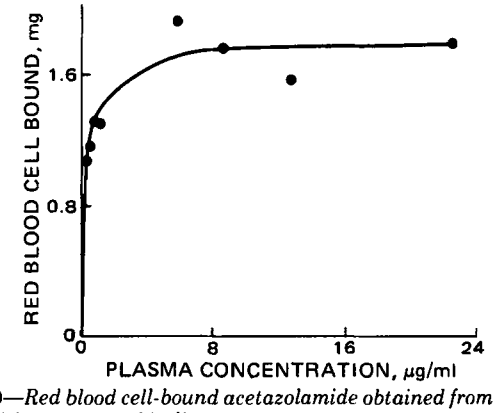

Figure 9—*Red blood cell-bound acetazolamide obtained from nonlinear model with two tissue-binding parameters.*

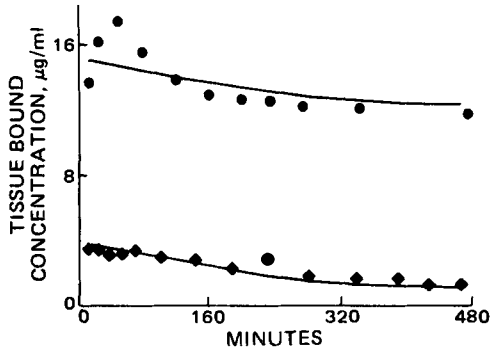

Figure 10—*Tissue-bound acetazolamide from nonlinear model with two tissue-binding parameters. Key:* ●, *observed total bound* ($T_1 + T_2$); *and* ♦, *observed red blood cells bound.*

protein (90% bound at this range of concentration) is considered, this value would be somewhat smaller but still within the limits expected for carbonic anhydrase, $(0.8–8.0) \times 10^{-8} M$ (16). This value agrees with the concept that carbonic anhydrase probably is the major component of binding tissue, T_1. Likewise, the highest value of B_2 probably reflects the larger proportion of binding proteins other than carbonic anhydrase in the red blood cells.

Values obtained for the various data sets for the excretion constant, K, were quite similar, indicating little variation in the excretion rate from one animal to another. The average K, 0.0179 min^{-1}, when multiplied by the average V, 290.25 ml/kg, gives a value of 5.20 ml/min kg as the computed clearance of acetazolamide. Comparison of this value to the average creatinine clearance for rabbits, 3.23 ml/min kg (17), indicates that acetazolamide is partially excreted by an active process.

Although values of R^2 indicate good fit for these data sets, the equation predicts lower values for the early part of the plasma curve than were observed. This finding is reflected in estimates of C_0, some of which are lower than the earliest observed points. This discrepancy is the result of the assumption of instantaneous maximal binding when actual data indicate that maximal binding may not occur for as long as 20 min after injection. This error occurs only in the early portion of the curve, the rest being predicted within experimental error.

An excellent way of determining how well the model fits the data is to compare predicted and observed tissue values. Observed tissue concentration values, T_{obs}, are obtained using the equation:

$$T_{obs} = \frac{X_b - CV}{V} \qquad \text{(Eq. 8)}$$

while predicted values are the sums of $T_i + T_2$ for the same points in time. Figure 10 is a typical plot of predicted and observed values. Predicted and observed values for the red blood cell concentrations, T_2, are also shown. Excellent agreement was seen with all data.

As a result of this work, it is concluded that the nonlinear tissue model is superior to a linear model in describing acetazolamide kinetics. Since it describes the binding of the drug to particular tissues, it appears to be especially suitable for correlation of kinetics of distribution with physiological activity. Such a study is the subject of a subsequent report (12).

REFERENCES

(1) J. G. Wagner, *J. Mond. Pharm.*, **4**, 14 (1971).

(2) J. G. Wagner, *J. Theoret. Biol.*, **20**, 173 (1968).

(3) T. H. Maren, E. Mayer, and B. C. Wadsworth, *Bull. Johns Hopkins Hosp.*, **95**, 199 (1954).

(4) P. Wistrand, *Acta Pharmacol. Toxicol.*, **16**, 171 (1959).

(5) B. Lehmann, E. Linner, and P. J. Wistrand, *Adv. Biosci.*, **5**, 197 (1969).

(6) T. H. Maren, *Physiol. Rev.*, **47**, 595 (1967).

(7) O. I. Nissen, *Acta Ophthalmol.*, **53**, 537 (1957).

(8) B. Becker, *Am. J. Ophthalmol.*, **47**, 342 (1959).

(9) R. P. Thomas and M. W. Riley, *ibid.*, **60**, 240 (1965).

(10) P. Wistrand, J. A. Rawls, Jr., and T. H. Maren, *Acta Pharmacol. Toxicol.*, **17**, 337 (1960).

(11) T. H. Maren and B. Robinson, *Bull. Johns Hopkins Hosp.*, **106**, 1 (1960).

(12) R. L. Kunka and A. M. Mattocks, *J. Pharm. Sci.*, **68**, 347 (1979).

(13) G. A. Brujo and J. E. Christian, *Anal. Chem.*, **33**, 650 (1961).

(14) J. G. Wagner, "Fundamentals of Clinical Pharmacokinetics," Drug Intelligence, Hamilton, Ill., 1975, pp. 271–283.

(15) J. G. Wagner, "Biopharmaceutics and Relevant Pharmacokinetics," Drug Intelligence, Hamilton, Ill., 1971, pp. 302–317.

(16) H. Green, C. A. Bocher, A. F. Calnan, and I. H. Leopold, *Arch. Ophthalmol.*, **53**, 463 (1955).

(17) H. W. Smith, "The Kidney: Structure and Function in Health and Disease," Oxford, New York, N.Y., 1958, p. 536.

ACKNOWLEDGMENTS

Supported in part by a grant from Lederle Laboratories.

R. L. Kunka is a Fellow, American Foundation for Pharmaceutical Education.

Relationship of Pharmacokinetics to Pharmacological Response for Acetazolamide

ROBERT L. KUNKA * **and ALBERT M. MATTOCKS** ˣ

Received March 20, 1978, from the *School of Pharmacy, University of North Carolina, Chapel Hill, NC 27514.* Accepted for publication August 31, 1978. *Present address: School of Pharmacy, University of Pittsburgh, Pittsburgh, PA 15261.

Abstract □ Acetazolamide concentration values derived from a nonlinear model system were related to two pharmacological responses in the rabbit. Kidney response was measured by monitoring urine flow and sodium elimination. Ocular response was followed using an applanation tonometer. Maximum urine flow and sodium elimination occurring immediately after injection correlated with log dose. Urine flow dropped below control values along with a rise in osmolality, suggesting the involvement of antidiuretic hormone. Sodium elimination was correlated with plasma levels. Urine pH is thought to be involved in reducing accessibility of drug to carbonic anhydrase in the kidney. Maximum ocular response also was correlated with log dose. Ocular response was related to a protein fraction, which is believed to be mainly carbonic anhydrase. However, the duration of ocular response was related to the red blood cell protein fraction. Thus, drug activity could conceivably be regulated by monitoring a tissue that is not the site of action and can be sampled readily.

Keyphrases □ Acetazolamide—relationship of pharmacokinetics to pharmacological response, kidney and ocular responses □ Pharmacokinetics—acetazolamide, relationship to two pharmacological responses □ Carbonic anhydrase inhibitors—acetazolamide, relationship of pharmacokinetics to pharmacological responses

Although pharmacokinetic research has been mainly concerned with the time course of a drug and its metabolites in a biological system, the relationship of pharmacokinetics to pharmacological response is now being emphasized. An earlier report (1) described the pharmacokinetics of acetazolamide using a nonlinear model system. This model proposed a single compartment of distribution containing two drug-binding tissues, T_1 and T_2, where T_2 represents binding to red blood cells and T_1 represents binding to other tissues. Binding in the tissues is believed to consist of attachment to carbonic anhydrase (2, 3) following the general concepts of enzyme inhibition. Such a model, incorporating the known mechanism of action of acetazolamide, was thought to offer the most promise for correlation of drug distribution with physiological effect.

The purpose of this study was to determine whether the drug distribution proposed by the model can be related to the measured physiological response of acetazolamide. The drug elicits two major types of response involving well-separated organs, the kidney and the eye, *via* carbonic anhydrase inhibition.

EXPERIMENTAL

At the same time that samples were being collected for plasma, red blood cell, and urine drug level measurements as described previously (1), physiological response was being measured. Additional animals were given acetazolamide, and only physiological response was measured. The New Zealand White rabbit was the experimental animal, and the drug was injected intravenously at several levels.

To evaluate the effect of the drug on renal function, urine samples were examined for flow rate, osmolality, and sodium elimination. Following catheterization of the bladder, urine was collected at 5–15-min intervals at first and then at 1-hr intervals and flow rates were calculated. Osmolality was measured directly with an electronic freezing-point osmometer[1]. Sodium content in urine was measured with a specific ion electrode[2]. This procedure consisted of diluting 1 ml of urine to 100 ml, adding 2 ml of ionic strength adjuster solution (25% ammonium chloride and 4% ammonium hydroxide), mixing, and reading with the sodium electrode. The reading was referred to a curve prepared by reading a series of sodium chloride standards ranging from 10^{-1} to 10^{-5} *M*.

To evaluate the effect of the drug on ocular function, intraocular pressure readings were taken at frequent intervals throughout the experiment using a recording applanation tonometer[3]. Only readings that reflected accurate measurement of intraocular pressure as judged by the shape of the applanation curve were accepted. In most cases, the average of three readings was made. A drop of procaine solution was given at the beginning of the experiment and, if needed, during the experiment.

For 1–2 hr before injection, measurements of urine flow and intraocular pressure were made to assure relatively constant control values. Two rabbits did not respond to acetazolamide and were not used.

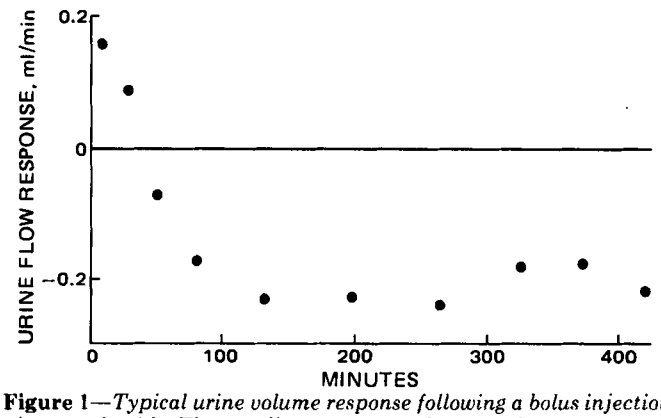

Figure 1—*Typical urine volume response following a bolus injection of acetazolamide. The zero line represents the control rate.*

RESULTS AND DISCUSSION

Kidney Response—Urine flow rate response was calculated as the flow rate, in milliliters per minute, minus the control rate. The urine excretion rate increased dramatically immediately after injection (Fig. 1). This increase was followed by a sharp drop to levels below control

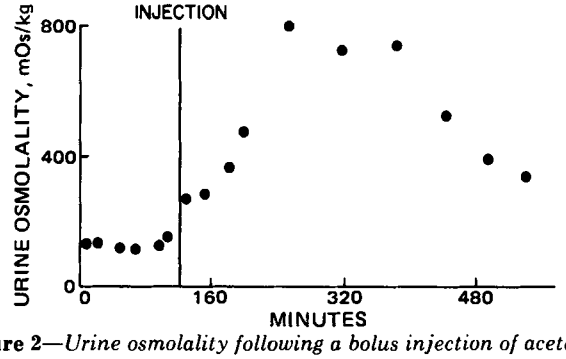

Figure 2—*Urine osmolality following a bolus injection of acetazolamide.*

[1] DigiMatic, Advanced Instruments, Needham Heights, Mass.
[2] Orion 94-11A sodium-ion electrode and 90-01-00 reference electrode, Orion Research, Cambridge, Mass.
[3] Applanation pneumatonograph, Alcon Laboratories, Fort Worth, Tex.

0022-3549/79/0300-0347$01.00/0
© 1979, American Pharmaceutical Association

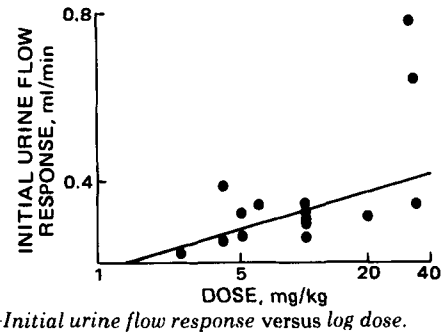

Figure 3—*Initial urine flow response* versus *log dose.*

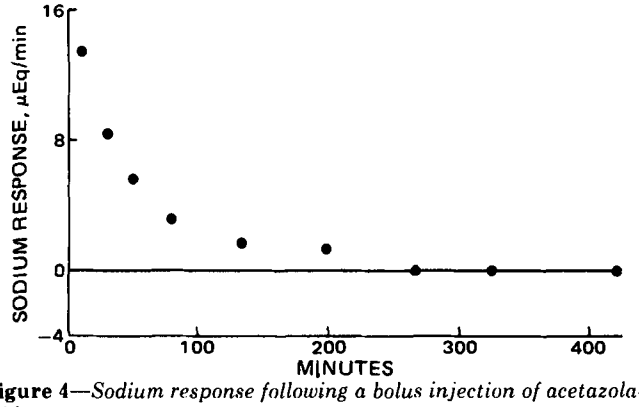

Figure 4—*Sodium response following a bolus injection of acetazolamide.*

values. These subnormal rates were usually maintained for the duration of the experiment.

Urine osmolality increased immediately after drug administration, probably due to the increased sodium and bicarbonate elimination. However, a dramatic rise in osmolality occurred a short time afterward (Fig. 2). High osmolality was maintained for several hours but usually returned to normal during the experimental period. This dramatic increase in osmolality was not correlated with sodium elimination and thus appeared to be due entirely to increased water resorption and concentration of the urine. This effect would most likely result from release of antidiuretic hormone (ADH).

Thus, the drug effect on urine flow seems to be confounded by compensatory mechanisms, and attempts at correlation of flow to acetazolamide concentrations in body compartments are not justified. The earlier responses (points 1 and 2) show a sharp decrease following drug administration and appear to reflect minimum compensatory activity (Fig. 2). This response suggests that urine flow increase is correlated with plasma concentration and not with red cell or general tissue levels since the latter decreased quite slowly. Initial flow increases did show the common log dose relationship (Fig. 3).

Sodium response was calculated as the sodium elimination rate, in microequivalents per minute, minus the control rate. Sodium elimination increased sharply following the bolus injection of acetazolamide (Fig. 4). Maximum sodium elimination occurred within 20 min of injection in

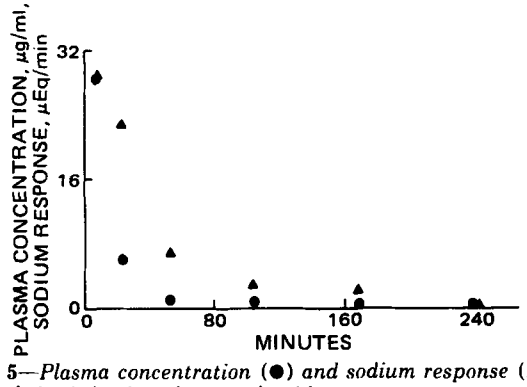

Figure 5—*Plasma concentration* (●) *and sodium response* (▲) *following a bolus injection of acetazolamide.*

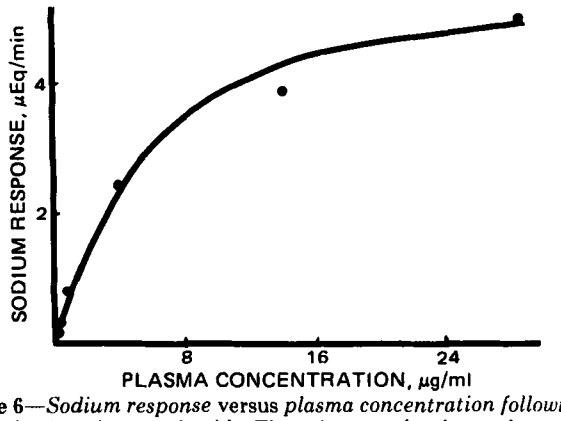

Figure 6—*Sodium response* versus *plasma concentration following a bolus injection of acetazolamide. The points are the observed response. The fitted curve was obtained from the equation: sodium response = 5.98*(C)/(5.60 + C).

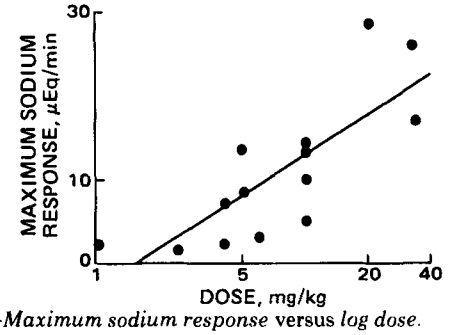

Figure 7—*Maximum sodium response* versus *log dose.*

virtually all experiments. A sharp fall followed, with the level dropping to less than 10% of maximum and remaining at approximately this level for the duration of the experiment. Since the effect of acetazolamide depends on its blocking carbonic anhydrase in the kidney, one might expect this drug action to be related to tissue concentration; but tissue concentrations peak immediately after injection and decrease quite slowly (1), obviously not correlating with kidney response. However, a definite relationship between sodium response and plasma level was seen (Fig. 5).

When response is plotted *versus* plasma concentration, a Langmuir-type curve results (Fig. 6); the response appears to be a linear function of plasma level at low concentrations, to be nonlinear in the intermediate range, and to approach a maximum response at high levels. Eight data sets could be plotted in this manner. Other sets were not suitable since sodium excretion dropped below control levels at later points. Of the eight, seven yielded Langmuir-type curves; the eighth, involving a small dose of 4 mg/kg, was linear throughout. This result was thought to be due to not having achieved high enough plasma levels to demonstrate nonlinearity. A linear relationship was seen between log dose and sodium elimination (Fig. 7).

Closer consideration of the environment in which kidney carbonic anhydrase operates reveals some interesting concepts. Although carbonic anhydrase appears in both the proximal and distal renal tubules, reab-

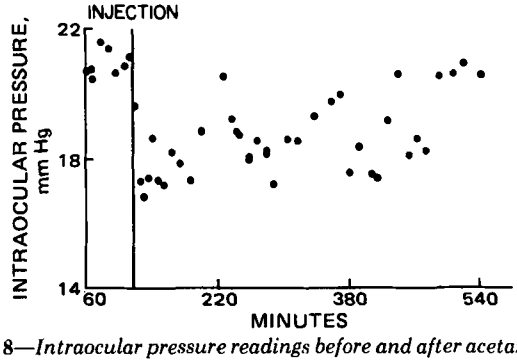

Figure 8—*Intraocular pressure readings before and after acetazolamide injection.*

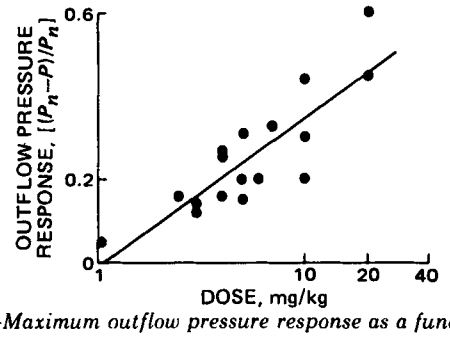

Figure 9—*Maximum outflow pressure response as a function of log dose.*

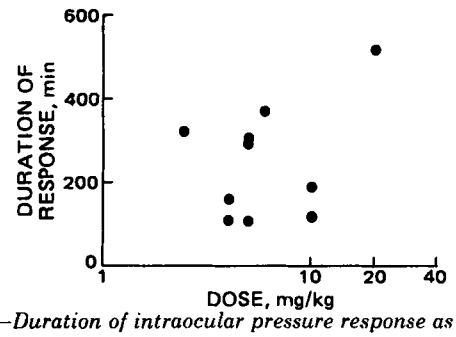

Figure 10—*Duration of intraocular pressure response as a function of log dose.*

sorption of sodium *via* the action of carbonic anhydrase occurs primarily in the luminal membrane of the tubule cell (4). The unique location of enzyme adjacent to a fluid prone to considerable variations in pH may expose these cells to substantial variations in drug transfer not encountered in other regions. Control readings of urine pH in the animals studied ranged from 6.16 to 8.86 with an average value of 7.89. At this pH, acetazolamide, with a pKa of 7.4, would be 24% undissociated. Within 30 min after dosing, urine pH rose to 7.76–8.82 with an average of 8.24, at which pH the drug would be 13% undissociated.

If it is assumed that only the undissociated form of the drug may diffuse across the cell wall, the effective drug concentration within the region of the enzyme may be greatly reduced by the change in urine pH. The effective drug concentration drops to about one-fourth. Thus, the action of the drug to increase the pH of the tubular fluid probably increases its own removal from the site of action, hence decreasing its duration of activity. These assumptions also suggest that the dynamics of drug activity in the kidney will differ from those in other regions.

Ocular Response—Shortly after an intravenous dose of acetazolamide, the intraocular pressure began to drop. It reached a minimum in 15–20 min, cycled up to nearly normal and back down to the minimum, and eventually returned to normal where it remained. The wave-like variation in intraocular pressure, which was more pronounced during drug activity, may reflect a muscular resistance to outflow of intraocular fluid.

The variation in pressure (Fig. 8) makes assignment of a single value to drug response difficult. It was decided to characterize effect as the average drop, $\Delta P/P_n$, where ΔP is the change in outflow pressure and P_n is the normal outflow pressure. Outflow pressure was taken in the usual manner as the intraocular pressure minus 9 mm Hg (5–7). As well as can be determined by experimental measurement, each dose of acetazolamide gave an early minimum pressure (maximum response), which did not change significantly until it returned to normal.

Obviously, the ocular response shows no correlation with plasma level. Data from all animals studied, however, indicated that the ocular response terminates before the tissue-bound concentration, T_1, approaches 99% of maximum. This finding agrees with the theoretical concept that more than 99% of the carbonic anhydrase in the ciliary body must be inhibited for physiological response to occur. When the enzyme of the ciliary body is considered to be a part of a large mass of tissue called T_1, a drop to 99% of the maximum bound value would be expected to result in loss of activity. Thus, the pharmacokinetic model apparently does predict the effective drug concentration, T_1, with reasonable accuracy whereas a predicted plasma level, except for the peak concentration, would be of no use in assessing drug effect.

Correlation of the results of this study with those of the kinetic report (1) indicated that the acetazolamide is rapidly taken up by the binding tissue, T_1, at which time maximum intraocular pressure response occurs. Beyond this point, the tissue concentration is practically independent of plasma level, being primarily dependent upon drug–tissue dissociation.

The magnitude of intraocular response was a function of T_1 and correlated with log dose (Fig. 9). However, no correlation was found between the duration of response and dose (Fig. 10). This finding suggests that duration of activity is dependent on the dissociation rate of the drug from its tissue attachment. Response terminated when the red cell concentration fell to 6–9 μg/ml. In four animals, intraocular pressure did not return to normal during the experiment; in three of these animals, the red cell drug level did not fall below 6 μg/ml.

It has been reported that metabolic and respiratory acidosis lowers intraocular pressure (8, 9). Therefore, acetazolamide might offset, to some degree, intraocular pressure *via* action on erythrocyte enzymes in this manner. This concept suggests that red cell drug concentrations may be used as a means of selecting intervals for drug administration.

The common concepts of maximum drug action *via* enzyme inhibition are that the enzyme is present in limited quantity and that the drug is given in quantities sufficient to saturate all enzyme. Thus, a maximum effect is obtained and then decreases as drug slowly dissociates from the enzyme–drug complex. In this case, the enzyme is present throughout the body, and the amount of drug is not sufficient to saturate all enzyme. Yet, the enzyme in a given organ, such as the eye, may be nearly saturated, causing a drug response. Moreover, because of the large amount of enzyme present in the body, a substantially larger dose would be distributed to a variety of organs and the eye would only receive a small fraction of the additional drug, thus giving a higher response but not yet its maximum response. This concept explains how each dose above 1 mg/kg gave an ocular response, yet a maximum response was not elicited at 20 mg/kg. From literature reports (3, 10), 10–20 mg/kg is expected to be near the level yielding maximum effect.

The results of this study and the previous report (1) demonstrate the need to use an unusual model system to describe the kinetics of a drug in a manner suitable for correlation with pharmacological response. Since acetazolamide acts by enzyme inhibition, it is representative of a rather large class of therapeutic agents, so a much wider application of this tissue-binding model is anticipated. Advantages of this model are that it takes into account the mechanism of drug action and simultaneously describes the concentrations in different tissues. Ultimately, as the technique is refined, one of these tissues may be the site of action.

REFERENCES

(1) R. L. Kunka and A. M. Mattocks, *J. Pharm. Sci.*, **68**, 342 (1979).

(2) T. H. Maren, E. Mayer, and B. C. Wadsworth, *Bull. Johns Hopkins Hosp.*, **95**, 199 (1954).

(3) B. Lehmann, E. Linner, and P. J. Wistrand, *Adv. Biosci.*, **5**, 197 (1969).

(4) F. C. Rector, Jr., N. W. Carter, and D. W. Seldin, *J. Clin. Invest.*, **44**, 278 (1965).

(5) E. Seidel, *XX Mitt., Albrecht von Graefes Arch. Ophthalmol.*, **112**, 252 (1923).

(6) W. D. Kornbluth and E. Linner, *Arch. Ophthalmol.*, **54**, 717 (1955).

(7) P. Wistrand, *Acta Pharmacol. Toxicol.*, **16**, 171 (1959).

(8) P. Wistrand and T. H. Maren, *Am. J. Ophthalmol.*, **50**, 291 (1960).

(9) D. M. Travis, C. Wiley, and T. H. Maren, *J. Pharmacol. Exp. Ther.*, **151**, 464 (1966).

(10) P. Wistrand, *Acta Pharmacol. Toxicol.*, **17**, 337 (1960).

ACKNOWLEDGMENTS

Abstracted from a thesis submitted by R. L. Kunka to the University of North Carolina in partial fulfillment of the Doctor of Philosophy degree requirements.

Supported in part by a grant from Lederle Laboratories.

R. L. Kunka is a Fellow, American Foundation for Pharmaceutical Education.

Synthesis of α-Methylenebutyrolactams as Potential Antitumor Agents

MILTON J. KORNET

Received June 12, 1978, from the *Division of Medicinal Chemistry, College of Pharmacy, University of Kentucky, Lexington, KY 40506.*
Accepted for publication August 30, 1978.

Abstract □ A series of 1-aryl-3-methylene-2-pyrrolidinones was synthesized *via* a three-step reaction sequence. 1,4-Bis-[*N*-(3-methylene-2-oxopyrrolidino)]benzene, which can undergo alkylation at two sites, was also prepared. These compounds are related to the known antitumor agents α-methylenebutyrolactones. Attempts to prepare bis-α-methylenelactams, in which the heterocyclic rings are joined through their nitrogen atoms by an alkylene bridge, were unsuccessful. All of the α-methylenelactams were screened in B16 melanocarcinoma and P-388 lymphocytic leukemia tumor systems but failed to show significant activity.

Keyphrases □ α-Methylenebutyrolactams—synthesized as potential antitumor agents and screened □ Pyrrolidinones, substituted—synthesized as potential antitumor agents, screened □ Antitumor agents, potential—synthesis and screening of α-methylenebutyrolactams

Investigations (1–3) on sesquiterpene lactones possessing cytotoxic and antitumor activities have shown that biological activity is largely dependent on the presence of an α-methylene-γ-lactone moiety. This activity has been ascribed to a rapid and essentially irreversible 1,4-addition reaction between the α,β-unsaturated lactone and the SH group of L-cysteine, either as the free amino acid or, more likely, as part of a protein molecule (4). Other biological nucleophiles may also be involved. Recent work has concentrated on the synthesis of simple α-methylenelactones (5–8) and has produced some active new compounds. Compounds that contain more than one alkylating group appear to enhance cytotoxicity significantly (5, 9).

This report is concerned with the synthesis of mono- and bis-α-methylenelactam systems (III, VI, and IX) as potential antitumor agents. These investigations were prompted by the facts that an *N*-aryl-3-methylene-2-pyrrolidinone readily adds nucleophiles, such as cyanide ion and thiophenol (10), and that isosteric replacement of oxygen by nitrogen often leads to improved drugs. Moreover, there is a dearth of literature information on the antitumor properties of α-methylenelactams. Also noteworthy is the recent proposal (11) that the oncolytic actions of camptothecin may occur as a consequence of its bioreduction to an α-methylenevalerolactam intermediate, which then functions as an alkylating agent.

DISCUSSION

Chemistry—The synthesis of the mono-α-methylenelactam compounds (III) was achieved by a three-step reaction sequence similar to that used by Seidel and Cook (10) (Scheme I). Modifications of these

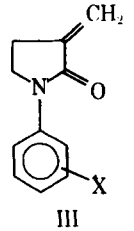

III

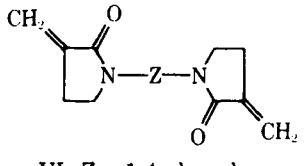

VI: Z = 1,4-phenylene
IX: Z = alkylene

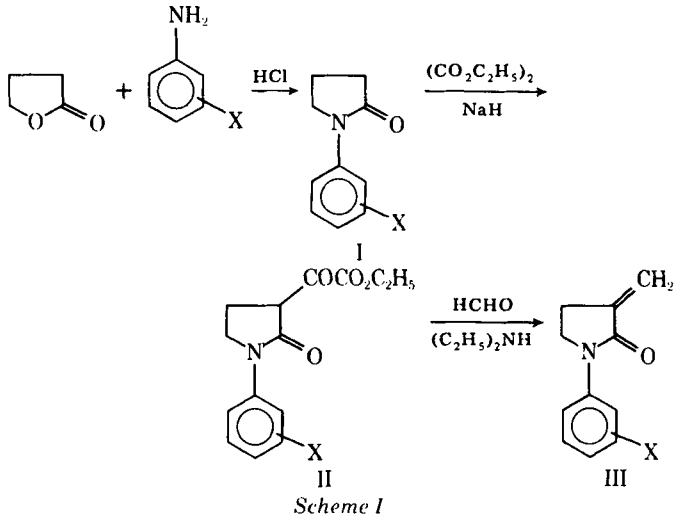

Scheme I

procedures have been described (12). The physical properties of the intermediates and final products are listed in Tables I–III.

The last two steps used in the synthesis of the bis-α-methylenelactams

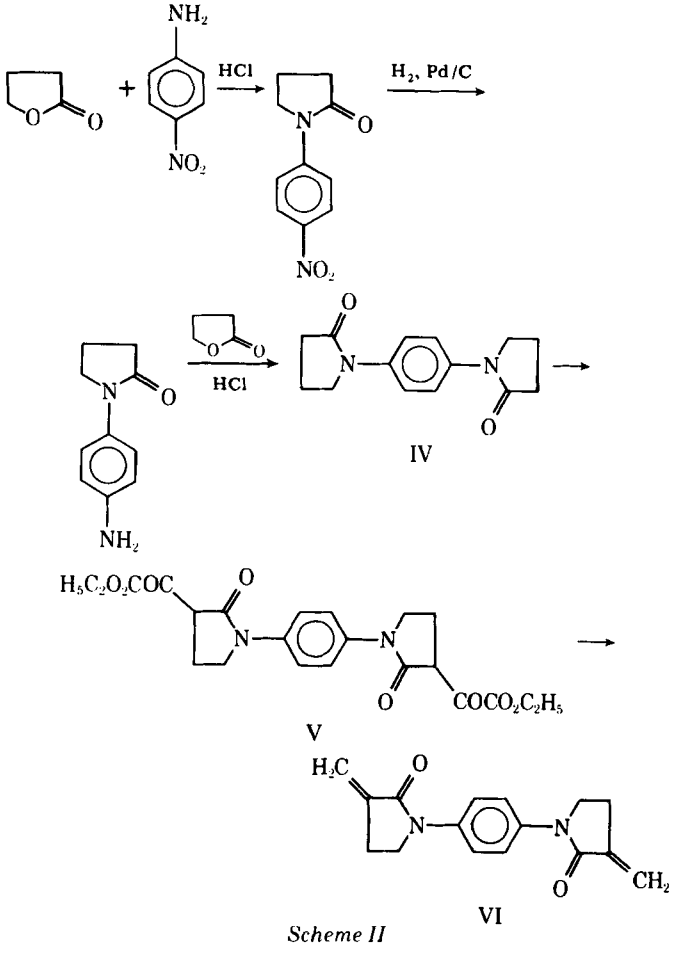

Scheme II

0022-3549/79/0300-0350$01.00/0
© 1979, American Pharmaceutical Association

Table I—Physical Properties of 1-Aryl-2-pyrrolidinones (I)

Compound	X	Melting Point	Yield, %	Recrystallization Solvent[a]	Formula	Analysis, % Calc.	Found
I*a*	H	65.5–66.5°[b]	78	A	$C_{10}H_{11}NO$	— —	—
I*b*	*p*-Br	97.5–98.5°[c]	61	B	$C_{10}H_{10}BrNO$	— —	—
Ic	*o*-Cl	55–57°[d]	73	—	$C_{10}H_{10}ClNO$	— —	—
I*d*	*m*-Cl	64–65.5°[e]	85	C	$C_{10}H_{10}ClNO$	C 61.39	61.41
						H 5.15	5.24
						N 7.16	7.23
I*e*	*p*-F	54–55.5°	61	D	$C_{10}H_{10}FNO$	C 67.02	66.95
						H 5.63	5.62
						N 7.82	7.81
I*f*	*p*-OC_2H_5	111–113°	59[f]	B	$C_{12}H_{15}NO_2$	C 70.22	70.34
						H 7.37	7.38
						N 6.82	6.91
I*g*	*p*-NO_2	125.5–127°[g]	77[h]	E	$C_{10}H_{10}N_2O_3$	C 58.25	58.23
						H 4.89	4.85
						N 13.59	13.69
I*h*	*p*-CH_3	86–87.5°[i]	36	B	$C_{11}H_{13}NO$	— —	—
I*i*	*p*-NH_2	129–131°[j,k]	100	E	$C_{10}H_{12}N_2O$	C 68.16	68.19
						H 6.86	6.75
						N 15.90	15.86

[a] A = 35% aqueous ethanol, B = 50% aqueous ethanol, C = 70% aqueous ethanol, D = 25% aqueous ethanol, and E = 95% ethanol. [b] Lit. mp 65–66°; M. S. Manhas and S. J. Jeng, *J. Org. Chem.*, **32**, 1246 (1967). [c] Lit. mp 97–98°; see footnote *b* for reference. [d] Lit. mp 62–63°; S. S. Kukalenko and N. A. Gracheva, *Khim. Geterotsikl. Soedin.*, **1971**, 773. [e] Lit. mp 66–68°; D. Ludsteck and O. Kaufmann, German pat. 1,301,314 (1969); through *Chem. Abstr.*, **71**, 124226p (1969). [f] The corresponding phenol occurred as a by-product and was separated by washing the organic phase with 5% aqueous sodium carbonate solution. [g] Lit. mp 131°; W. Reppe *et al.*, *Justus Liebigs Ann. Chem.*, **596**, 158 (1955). [h] Reaction time of 48 hr. [i] Lit. mp 87.5°; J. T. Braunholtz and F. G. Mann, *J. Chem. Soc.*, **1957**, 4174. [j] Lit. mp 127°; see footnote *g* for reference. [k] Obtained by catalytic reduction of I*g*; see *Experimental*.

Table II—Physical Properties of 1-Aryl-3-ethoxalyl-2-pyrrolidinones (II)

Compound	X	Melting Point	Yield, %	Reflux Time, hr	Recrystallization Solvent[a]	Formula	Analysis, % Calc.	Found
II*a*	H	110–111°	76	3	A	$C_{14}H_{15}NO_4$	C 64.36	64.37
							H 5.79	5.81
							N 5.36	5.47
II*b*	*p*-Br	152.5–154°	80	7	B	$C_{14}H_{14}BrNO_2$	C 49.43	49.43
							H 4.15	4.22
							N 4.12	4.19
II*c*	*o*-Cl	123–125°	51	4	A	$C_{14}H_{14}ClNO_4$	C 56.86	56.81
							H 4.77	4.93
							N 4.74	4.87
II*d*	*m*-Cl	115–116°	50	3	A	$C_{14}H_{14}ClNO_4$	C 56.86	56.83
							H 4.77	4.86
							N 4.74	4.82
II*e*	*p*-F	121–122°	66	6	A	$C_{14}H_{14}FNO_4$	C 60.21	60.33
							H 5.05	5.16
							N 5.02	5.09
II*f*	*p*-OC_2H_5	126–130°	81	6.5	A	$C_{16}H_{19}NO_5$	C 62.94	62.97
							H 6.27	6.34
							N 4.59	4.61
II*g*	*p*-NO_2	185–186°	93	6	C	$C_{14}H_{14}N_2O_6$	C 54.90	55.00
							H 4.61	4.72
							N 9.15	9.16
II*h*	*p*-CH_3	127–128°	72	6	A	$C_{15}H_{17}NO_4$	C 65.44	65.56
							H 6.22	6.31
							N 5.09	5.19

[a] A = 95% ethanol, B = benzene, and C = tetrahydrofuran.

(VI and IX) are identical to those used for the mono compounds (Scheme I). The reaction sequence used for the preparation of the precursor dilactam (IV) containing an arylene bridge is shown in Scheme II. The reaction employed for the synthesis of the precursor dilactams (VII) containing an alkylene bridge is shown in Scheme III.

All attempts to convert the bis-ethoxalyllactams (VIII*a* and VIII*b*) containing an alkylene bridge into the corresponding bis-α-methylenelactams gave intractable mixtures. In contrast, the conversion of the bis-ethoxalyllactam (V) containing a 1,4-phenylene bridge into the corresponding bis-α-methylenelactam (VI) succeeded.

Biological Results—Antineoplastic activity for III*a*–III*h* and VI was determined under the auspices of the National Cancer Institute, National Institutes of Health, according to general screening procedures (13). Both B16 melanocarcinoma and P-388 lymphocytic leukemia tumor systems were employed. Although initial assays of Ic, I*e*, and I*f* with P-388 leukemia indicated marginal activity (%T/C = 125–136), these results were not reproducible. The compounds also failed to show reproducible activity in the B16 melanocarcinoma assay. Because of insufficient material, VI was not assayed against B16 melanocarcinoma.

The apparent conclusion from these studies is that *N*-aryl nitrogen is not a beneficial replacement for the oxygen of α-methylenebutyrolactones. Further investigations are necessary to determine whether this result is due to steric or electronic factors in the reaction with biological

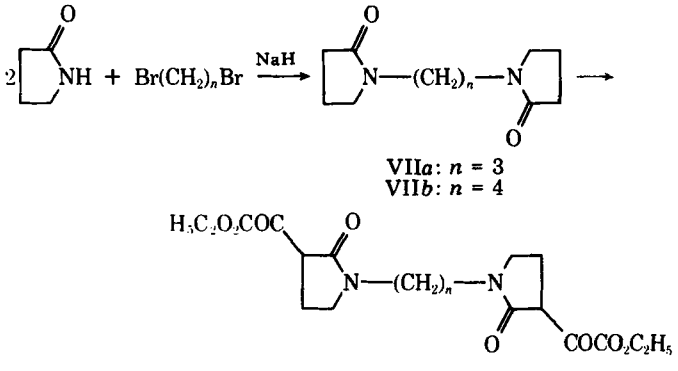

Scheme III

Table III—Physical Properties of 1-Aryl-3-methylene-2-pyrrolidinones (III)

Compound	X	Melting Point	Yield, %	Recrystallization Solvent[a]	Formula	Analysis, %	Calc.	Found
III*a*	H	77.5–78.5°	21	A	$C_{11}H_{11}NO$	C	76.28	76.44
						H	6.40	6.42
						N	8.09	8.17
III*b*	*p*-Br	125–126.5°	33	B	$C_{11}H_{10}BrNO$	C	52.40	52.36
						H	4.00	4.49
						N	5.56	5.67
III*c*	*o*-Cl	83–84°	32	A	$C_{11}H_{10}ClNO$	C	63.62	63.68
						H	4.85	4.86
						N	6.75	6.85
III*d*	*m*-Cl	78.5–80°	40	A	$C_{11}H_{10}ClNO$	C	63.62	63.71
						H	4.85	4.85
						N	6.75	6.90
III*e*	*p*-F	90–91.5°	29	A	$C_{11}H_{10}FNO$	C	69.09	69.13
						H	5.27	5.35
						N	7.33	7.40
III*f*	*p*-OC_2H_5	89–90.5°	23	A	$C_{13}H_{15}NO_2$	C	71.87	71.82
						H	6.96	7.01
						N	6.45	6.47
III*g*	*p*-NO_2	175–176°	41	C	$C_{11}H_{10}N_2O_3$	C	60.55	60.64
						H	4.62	4.76
						N	12.84	12.88
III*h*	*p*-CH_3	92–93°	32	A	$C_{12}H_{13}NO$	C	76.98	77.09
						H	7.00	7.11
						N	7.48	7.52

[a] A = cyclohexane, B = benzene–cyclohexane, and C = isopropyl alcohol.

nucleophiles or to poor transport of the compounds across cell membranes.

EXPERIMENTAL[1]

1-Aryl-2-pyrrolidinones (I)—A typical reaction is described: that for the preparation of 1-(*m*-chlorophenyl)-2-pyrrolidinone (I*d*) (Table I). A mixture of 34.4 g (0.40 mole) of butyrolactone, 56.1 g (0.44 mole) of *m*-chloroaniline, and 10.7 ml of concentrated hydrochloric acid was heated under a water-cooled reflux condenser for 2.5 hr in an oil bath at 150°. After changing to an air-cooled condenser, heating was continued at 180–190° for 17 hr. The reaction mixture was cooled and treated with 100 ml of 2 *N* HCl. The resulting tan solid was filtered and recrystallized to afford 66.5 g of off-white crystals.

1-Aryl-3-ethoxalyl-2-pyrrolidinones (II)—A typical reaction is described: that for the preparation of 1-(*p*-ethoxyphenyl)-3-ethoxalyl-2-pyrrolidinone (II*f*) (Table II). To a stirred, refluxing mixture of 8.43 g (0.20 mole) of a 57% mineral oil dispersion of sodium hydride in 100 ml of dry tetrahydrofuran, protected by a nitrogen atmosphere, was added dropwise a solution of 20.5 g (0.10 mole) of 1-(*m*-chlorophenyl)-2-pyrrolidinone and 29.2 g (0.20 mole) of diethyl oxalate in 300 ml of dry tetrahydrofuran.

Hydrogen gas was evolved during the addition as well as during the subsequent reflux period of 6.5 hr. The reaction mixture was then cooled and treated dropwise with 12 ml of acetic acid. After stirring for 10 min, the mixture was poured into 1.5 liters of ice water, and the precipitated solid was filtered and dried. The dry solid was triturated with petroleum ether to remove mineral oil. Recrystallization from 95% ethanol afforded 24.5 g of product.

1-Aryl-3-methylene-2-pyrrolidinones (III)—A typical reaction is described: that for the preparation of 1-(*p*-tolyl)-3-methylene-2-pyrrolidinone (III*h*) (Table III). To a magnetically stirred mixture of 21.8 g (0.079 mole) of 1-(*p*-tolyl)-3-ethoxalyl-2-pyrrolidinone, 26.5 ml of 48% aqueous diethylamine, and 135 ml of distilled water was added dropwise 26.5 ml of 40% aqueous formaldehyde while the temperature was maintained at 25–30°. After stirring at room temperature for 22.5 hr, the mixture was acidified with 10% HCl to pH ~ 4 and extracted three times with 100-ml portions of chloroform.

The combined extracts were dried (magnesium sulfate), filtered, and concentrated. The oily residue (16.9 g) was chromatographed on 130 g of silica gel 60. Elution with benzene and benzene–ethyl acetate solutions of increasing polarity gave 4.79 g of white solid; IR (potassium bromide): 5.93 μm (C=O); NMR ($CDCl_3$): δ 2.30 (s, 3, CH_3), 2.50–3.10 (m, 2, NCH_2CH_2), 3.73 (t, 2, NCH_2CH_2), 5.28–5.50 (m, 1, $C{=}CH_2$), 5.98–6.22 (m, 1, $C{=}CH_2$), 7.15 (d, 2, ArH), and 7.62 (d, 2, ArH) ppm.

1-(*p*-Aminophenyl)-2-pyrrolidinone (I*i*)—A suspension of 10.3 g (0.05 mole) of 1-(*p*-nitrophenyl)-2-pyrrolidinone (II*g*) and 0.6 g of 5% palladium-on-charcoal in 150 ml of 95% ethanol was shaken on the Parr hydrogenator for 1.25 hr. The reaction mixture was filtered, and the filtrate was evaporated under reduced prssure. The remaining white solid amounted to a quantitative yield, mp 124–126°. Recrystallization from 95% ethanol gave an analytically pure product.

1,4-Bis-[*N*-(2-oxopyrrolidino)]benzene (IV)—This compound was obtained from 8.8 g (0.05 mole) of I*i*, 6.45 g (0.075 mole) of butyrolactone, and 2.5 ml of concentrated hydrochloric acid by the identical procedure used for the preparation of I. Workup and recrystallization from 95% ethanol afforded 5.72 g (47%) of crystals, mp 251–253°.

Anal.—Calc. for $C_{14}H_{16}N_2O_2$: C, 68.83; H, 6.60; N, 11.47. Found: C, 68.91; H, 6.60; N, 11.47.

1,4-Bis-[*N*-(3-ethoxalyl-2-oxopyrrolidino)]benzene (V)—This compound was obtained from 4.47 g (0.018 mole) of IV, 10.5 g (0.072 mole) of ethyl oxalate, and 3.0 g (0.072 mole) of a 57% mineral oil dispersion of sodium hydride according to the same procedure used for the preparation of II. Workup gave 7.65 g (96%) of solid, mp 260–264°. Recrystallization from dimethylformamide gave an analytically pure product, mp 276–278°.

Anal.—Calc. for $C_{22}H_{24}N_2O_8$: C, 59.46; H, 5.44; N, 6.30. Found: C, 59.80; H, 5.13; N, 6.27.

1,4-Bis-[*N*-(3-methylene-2-oxopyrrolidino)]benzene (VI)—This compound was obtained from 6.51 g (0.0147 mole) of V, 9.87 ml of 48% aqueous diethylamine, 9.87 ml of 40% aqueous formaldehyde, and 60 ml of distilled water according to the procedure used for the preparation of III. Workup gave 2.9 g of crude product. Purification was effected by preparative TLC on silica gel[2], employing multiple development (10 developments were required) with benzene–ethyl acetate (4:1). The progress of the purification was followed visually at 254 nm.

Chromatography of 1.5 g of the crude product on six 20 × 20-cm glass plates, followed by extraction of the product band with chloroform–methanol (1:1), afforded 312 mg of solid; this material moved as one spot in several solvent systems. Recrystallization from methanol gave an analytically pure material, mp 475° dec. (sealed tube); IR (KBr): 5.93 μm (C=O); NMR (trifluoroacetic acid): δ 2.35–2.93 (m, 4, NCH_2CH_2), 3.42–3.93 (m, 4, NCH_2CH_2), 5.23–5.53 (m, 2, $C{=}CH_2$), 5.73–6.01 (m, 2, $C{=}CH_2$), and 7.26 (s, 4, ArH) ppm; mass spectrum: *m/e* 268 (M^+).

Anal.—Calc. for $C_{16}H_{16}N_2O_2$: C, 71.62; H, 6.01; N, 10.44. Found: C, 71.61; H, 5.95; N, 10.45.

1,4-Bis-[*N*-(2-oxopyrrolidino)]butane (VII*b*)—Sodium hydride (57% mineral oil dispersion), 27.36 g (0.65 mole), was rapidly weighed, washed three times with hexane and twice with xylene, suspended in 400

[1] Melting points were determined on a Thomas-Hoover apparatus and are uncorrected. IR spectra were taken on a Perkin-Elmer 700 spectrophotometer as liquid films or potassium bromide pellets. NMR spectra were recorded on a Varian A-60A spectrometer with tetramethylsilane as the internal reference. Elemental analyses were performed by Dr. Kurt Eder, Geneva, Switzerland.

[2] Merck F-254 precoated TLC plates, 2-mm thick layer.

ml of xylene, and charged into a reaction flask. To this stirred mixture, 51.06 g (0.60 mole) of 2-pyrrolidinone in 125 ml of xylene was added dropwise at 60–80°. The initial vigorous evolution of hydrogen abated after 1 hr. The mixture was heated to 140–150°, and 53.98 g (0.25 mole) of 1,4-dibromobutane in 100 ml of xylene was added dropwise.

The mixture was then heated to reflux and refluxed for 17 hr. After cooling to 60°, 8.6 ml of acetic acid was added, and stirring was continued for 10 min. The mixture was filtered using glass filter paper, and the solids were washed with 150 ml of benzene. The filtrate was concentrated under reduced pressure (water pump). Vacuum distillation (bath temperature of 140–190°, 0.4 mm Hg) removed unreacted starting materials. Upon cooling, the product solidified in the distillation flask. Recrystallization from benzene–cyclohexane afforded 35.1 g (63%) of product, mp 69–77°. A second recrystallization gave analytically pure material, mp 82.5–85°; IR (potassium bromide): 6.0 μm (C=O).

Anal.—Calc. for $C_{12}H_{20}N_2O_2$: C, 64.26; H, 8.99; N, 12.49. Found: C, 64.28; H, 8.91; N, 12.61.

1,3-Bis-[*N*-(2-oxopyrrolidino)]propane (VII*a*)—This compound was obtained from 21.3 g (0.25 mole) of 2-pyrrolidinone, 20.2 g (0.10 mole) of trimethylene bromide, and 16.8 g (0.40 mole) of a 57% mineral oil dispersion of sodium hydride according to the procedure for VII*b*. Workup and distillation gave 16.5 g (79%) of liquid, bp 177°/0.36 mm; IR (film): 5.97 μm (C=O).

Anal.—Calc. for $C_{11}H_{18}N_2O_2$: C, 62.83; H, 8.63; N, 13.32. Found: C, 62.95; H, 8.72; N, 13.28.

1,3-Bis-[*N*-(3-ethoxalyl-2-oxopyrrolidino)]propane (VIII*a*)—A suspension of 16.8 g (0.40 mole) of a 57% mineral oil dispersion of sodium hydride in 140 ml of dry tetrahydrofuran was heated to reflux. To it was added a solution of 58.5 g (0.40 mole) of diethyl oxalate and 21.0 g (0.10 mole) of VII*a* in 260 ml of dry tetrahydrofuran dropwise with stirring. Hydrogen evolution was monitored with a mercury bubbler.

After completion of the addition, the mixture was refluxed for 15 hr. After cooling to room temperature, 23 ml of acetic acid was added, and stirring was continued for 15 min. The mixture was poured into 1500 ml of ice water with stirring, and the precipitate was filtered and dried in a vacuum desiccator. Trituration with 50 ml of petroleum ether (bp 30–60°) and filtration gave 19.8 g (48%) of product, mp 121–123°. Recrystallization from 95% ethanol led to the pure compound, mp 124.5–126°.

Anal.—Calc. for $C_{19}H_{26}N_2O_8$: C, 55.60; H, 6.39; N, 6.83. Found: C, 55.63; H, 6.42; N, 6.58.

1,4-Bis-[*N*-(3-ethoxalyl-2-oxopyrrolidino)]butane (VIII*b*)—This compound was obtained from 11.2 g (0.05 mole) of VII*b*, 29.2 g (0.20 mole) of diethyl oxalate, and 8.42 g (0.20 mole) of a 57% mineral oil dispersion of sodium hydride according to the procedure for VIII*a*. Workup gave 13.0 g (61%) of solid, mp 142–147°. Recrystallization produced an analytically pure product, mp 146–148°.

Anal.—Calc. for $C_{20}H_{28}N_2O_8$: C, 56.60; H, 6.65; N, 6.60. Found: C, 56.42; H, 7.14; N, 6.69.

Pharmacological Testing—*P-388 Assay*—Ascitic fluid containing about 6×10^6 cells was inoculated intraperitoneally into male CDF_1 mice. In this assay, median survival times of %T/C ≥ 125 are considered significant. The compounds were administered by the intraperitoneal route in a saline plus alcohol vehicle. Nine daily doses were given, starting 24 hr after tumor inoculation.

B16 Melanocarcinoma Assay—B16 melanocarcinoma homogenate (dilution 1:10) was inoculated intraperitoneally into male BDF_1 mice. In this assay, median survival times of %T/C ≥ 125 are considered significant. Administration and dosing of compounds were the same as for the P-388 testing.

REFERENCES

(1) K.-H. Lee, E.-S. Huang, C. Piantadosi, J. S. Pagano, and T. A. Geissman, *Cancer Res.*, **31**, 1649 (1971).

(2) S. M. Kupchan, M. A. Eakin, and A. M. Thomas, *J. Med. Chem.*, **14**, 1147 (1971).

(3) P. A. Grieco, J. A. Noguez, Y. Masaki, K. Hiroi, M. Nishizawa, A. Rosowsky, S. Oppenheim, and H. Lazarus, *ibid.*, **20**, 71 (1977).

(4) S. M. Kupchan, D. C. Fessler, M. A. Eakin, and T. J. Giacobbe, *Science*, **168**, 376 (1970).

(5) A. Rosowsky, N. Papathanasopoulos, H. Lazarus, G. E. Foley, and E. J. Modest, *J. Med. Chem.*, **17**, 672 (1974).

(6) K.-H. Lee, T. Ibuka, S.-H. Kim, B. R. Vestal, I. H. Hall, and E.-S. Huang, *ibid.*, **18**, 812 (1975).

(7) P. A. Grieco, J. A. Noguez, Y. Masaki, K. Hiroi, M. Nishizawa, A. Rosowsky, S. Oppenheim, and H. Lazarus, *ibid.*, **20**, 71 (1977).

(8) I. K. Stamos, S. Evans, A. McKenzie, S. R. Byrn, and J. M. Cassady, Abstracts of 174th ACS Meeting, Medi 56, Chicago, Ill., 1977.

(9) K.-H. Lee, S.-H. Kim, C. Piantadosi, E.-S. Huang, and T. A. Geissman, *J. Pharm. Sci.*, **63**, 1162 (1974).

(10) M. C. Seidel and R. S. Cook, *J. Heterocycl. Chem.*, **3**, 311 (1966).

(11) H. W. Moore, *Science*, **197**, 527 (1977).

(12) M. J. Kornet, A. M. Crider, and E. O. Magarian, *J. Med. Chem.*, **20**, 1210 (1977).

(13) R. I. Geran, N. H. Greenberg, M. M. MacDonald, A. M. Schumacher, and B. J. Abbott, *Cancer Chemother. Rep., Part 3*, **3** (2), 1 (1972).

ACKNOWLEDGMENTS

The author is indebted to Mr. Marshall Davis, Mr. George Piltz, and Mr. James Swencki for the syntheses of some of the compounds.

Facile *In Vitro* Method for Screening Inhibitors of IgE Binding to Mast Cells

STEPHEN M. COUTTS ˣ, DOROTHY M. REID, and IRA WEINRYB

Received July 6, 1978, from the *Department of Biochemistry and Drug Disposition, USV Pharmaceutical Corporation, Tuckahoe, NY 10707.* Accepted for publication August 28, 1978.

Abstract □ A method for rapidly testing large numbers of chemical structures as potential modulators of the interaction between immunoglobulin E (IgE) and its specific receptors on rat peritoneal mast cells is described. IgE, isolated from the ascitic fluid of a transplantable rat IgE immunocytoma, is labeled with iodine-125 under mild conditions employing the Bolton–Hunter reagent. The antibody is incubated with mixed peritoneal cells at 37°, and the cell-bound IgE is separated from unbound label by sedimentation through an 8% sucrose–polymer solution in microsediment tubes. Optimal conditions for the interaction of 3 n*M* IgE with 3×10^5 mast cells in 150 μl are: incubation time, 2 hr; pH, 6.5–7.0; and ionic strength, equivalent to 150 m*M* NaCl. Mixed peritoneal cells bind IgE with an affinity equal to that of purified mast cells. Human IgE pentapeptide III and several antiallergic agents do not compete with rat IgE in this assay.

Keyphrases □ Immunoglobulin E—binding to mast cells, *in vitro* method for screening inhibitors □ Binding—immunoglobulin E to mast cells, *in vitro* method for screening inhibitors □ Inhibitors—immunoglobulin E to rat peritoneal mast cells, *in vitro* screening method

The immunologically induced secretion of mediators of anaphylaxis by sensitized rat or human mast cells exposed to the appropriate antigen triggers a series of intracellular events that require Ca^{2+}, involve an activatable

0022-3549/79/0300-0353$01.00/0

© 1979, American Pharmaceutical Association

ml of xylene, and charged into a reaction flask. To this stirred mixture, 51.06 g (0.60 mole) of 2-pyrrolidinone in 125 ml of xylene was added dropwise at 60–80°. The initial vigorous evolution of hydrogen abated after 1 hr. The mixture was heated to 140–150°, and 53.98 g (0.25 mole) of 1,4-dibromobutane in 100 ml of xylene was added dropwise.

The mixture was then heated to reflux and refluxed for 17 hr. After cooling to 60°, 8.6 ml of acetic acid was added, and stirring was continued for 10 min. The mixture was filtered using glass filter paper, and the solids were washed with 150 ml of benzene. The filtrate was concentrated under reduced pressure (water pump). Vacuum distillation (bath temperature of 140–190°, 0.4 mm Hg) removed unreacted starting materials. Upon cooling, the product solidified in the distillation flask. Recrystallization from benzene–cyclohexane afforded 35.1 g (63%) of product, mp 69–77°. A second recrystallization gave analytically pure material, mp 82.5–85°; IR (potassium bromide): 6.0 μm (C=O).

Anal.—Calc. for $C_{12}H_{20}N_2O_2$: C, 64.26; H, 8.99; N, 12.49. Found: C, 64.28; H, 8.91; N, 12.61.

1,3-Bis-[*N*-(2-oxopyrrolidino)]propane (VII*a*)—This compound was obtained from 21.3 g (0.25 mole) of 2-pyrrolidinone, 20.2 g (0.10 mole) of trimethylene bromide, and 16.8 g (0.40 mole) of a 57% mineral oil dispersion of sodium hydride according to the procedure for VII*b*. Workup and distillation gave 16.5 g (79%) of liquid, bp 177°/0.36 mm; IR (film): 5.97 μm (C=O).

Anal.—Calc. for $C_{11}H_{18}N_2O_2$: C, 62.83; H, 8.63; N, 13.32. Found: C, 62.95; H, 8.72; N, 13.28.

1,3-Bis-[*N*-(3-ethoxalyl-2-oxopyrrolidino)]propane (VIII*a*)—A suspension of 16.8 g (0.40 mole) of a 57% mineral oil dispersion of sodium hydride in 140 ml of dry tetrahydrofuran was heated to reflux. To it was added a solution of 58.5 g (0.40 mole) of diethyl oxalate and 21.0 g (0.10 mole) of VII*a* in 260 ml of dry tetrahydrofuran dropwise with stirring. Hydrogen evolution was monitored with a mercury bubbler.

After completion of the addition, the mixture was refluxed for 15 hr. After cooling to room temperature, 23 ml of acetic acid was added, and stirring was continued for 15 min. The mixture was poured into 1500 ml of ice water with stirring, and the precipitate was filtered and dried in a vacuum desiccator. Trituration with 50 ml of petroleum ether (bp 30–60°) and filtration gave 19.8 g (48%) of product, mp 121–123°. Recrystallization from 95% ethanol led to the pure compound, mp 124.5–126°.

Anal.—Calc. for $C_{19}H_{26}N_2O_8$: C, 55.60; H, 6.39; N, 6.83. Found: C, 55.63; H, 6.42; N, 6.58.

1,4-Bis-[*N*-(3-ethoxalyl-2-oxopyrrolidino)]butane (VIII*b*)—This compound was obtained from 11.2 g (0.05 mole) of VII*b*, 29.2 g (0.20 mole) of diethyl oxalate, and 8.42 g (0.20 mole) of a 57% mineral oil dispersion of sodium hydride according to the procedure for VIII*a*. Workup gave 13.0 g (61%) of solid, mp 142–147°. Recrystallization produced an analytically pure product, mp 146–148°.

Anal.—Calc. for $C_{20}H_{28}N_2O_8$: C, 56.60; H, 6.65; N, 6.60. Found: C, 56.42; H, 7.14; N, 6.69.

Pharmacological Testing—*P-388 Assay*—Ascitic fluid containing about 6×10^6 cells was inoculated intraperitoneally into male CDF_1 mice. In this assay, median survival times of %T/C ≥ 125 are considered significant. The compounds were administered by the intraperitoneal route in a saline plus alcohol vehicle. Nine daily doses were given, starting 24 hr after tumor inoculation.

B16 Melanocarcinoma Assay—B16 melanocarcinoma homogenate (dilution 1:10) was inoculated intraperitoneally into male BDF_1 mice. In this assay, median survival times of %T/C ≥ 125 are considered significant. Administration and dosing of compounds were the same as for the P-388 testing.

REFERENCES

(1) K.-H. Lee, E.-S. Huang, C. Piantadosi, J. S. Pagano, and T. A. Geissman, *Cancer Res.*, **31**, 1649 (1971).

(2) S. M. Kupchan, M. A. Eakin, and A. M. Thomas, *J. Med. Chem.*, **14**, 1147 (1971).

(3) P. A. Grieco, J. A. Noguez, Y. Masaki, K. Hiroi, M. Nishizawa, A. Rosowsky, S. Oppenheim, and H. Lazarus, *ibid.*, **20**, 71 (1977).

(4) S. M. Kupchan, D. C. Fessler, M. A. Eakin, and T. J. Giacobbe, *Science*, **168**, 376 (1970).

(5) A. Rosowsky, N. Papathanasopoulos, H. Lazarus, G. E. Foley, and E. J. Modest, *J. Med. Chem.*, **17**, 672 (1974).

(6) K.-H. Lee, T. Ibuka, S.-H. Kim, B. R. Vestal, I. H. Hall, and E.-S. Huang, *ibid.*, **18**, 812 (1975).

(7) P. A. Grieco, J. A. Noguez, Y. Masaki, K. Hiroi, M. Nishizawa, A. Rosowsky, S. Oppenheim, and H. Lazarus, *ibid.*, **20**, 71 (1977).

(8) I. K. Stamos, S. Evans, A. McKenzie, S. R. Byrn, and J. M. Cassady, Abstracts of 174th ACS Meeting, Medi 56, Chicago, Ill., 1977.

(9) K.-H. Lee, S.-H. Kim, C. Piantadosi, E.-S. Huang, and T. A. Geissman, *J. Pharm. Sci.*, **63**, 1162 (1974).

(10) M. C. Seidel and R. S. Cook, *J. Heterocycl. Chem.*, **3**, 311 (1966).

(11) H. W. Moore, *Science*, **197**, 527 (1977).

(12) M. J. Kornet, A. M. Crider, and E. O. Magarian, *J. Med. Chem.*, **20**, 1210 (1977).

(13) R. I. Geran, N. H. Greenberg, M. M. MacDonald, A. M. Schumacher, and B. J. Abbott, *Cancer Chemother. Rep., Part 3*, **3** (2), 1 (1972).

ACKNOWLEDGMENTS

The author is indebted to Mr. Marshall Davis, Mr. George Piltz, and Mr. James Swencki for the syntheses of some of the compounds.

Facile *In Vitro* Method for Screening Inhibitors of IgE Binding to Mast Cells

STEPHEN M. COUTTS ˣ, DOROTHY M. REID, and IRA WEINRYB

Received July 6, 1978, from the *Department of Biochemistry and Drug Disposition, USV Pharmaceutical Corporation, Tuckahoe, NY 10707.* Accepted for publication August 28, 1978.

Abstract □ A method for rapidly testing large numbers of chemical structures as potential modulators of the interaction between immunoglobulin E (IgE) and its specific receptors on rat peritoneal mast cells is described. IgE, isolated from the ascitic fluid of a transplantable rat IgE immunocytoma, is labeled with iodine-125 under mild conditions employing the Bolton–Hunter reagent. The antibody is incubated with mixed peritoneal cells at 37°, and the cell-bound IgE is separated from unbound label by sedimentation through an 8% sucrose–polymer solution in microsediment tubes. Optimal conditions for the interaction of 3 n*M* IgE with 3×10^5 mast cells in 150 μl are: incubation time, 2 hr; pH, 6.5–7.0; and ionic strength, equivalent to 150 m*M* NaCl. Mixed peritoneal cells bind IgE with an affinity equal to that of purified mast cells. Human IgE pentapeptide III and several antiallergic agents do not compete with rat IgE in this assay.

Keyphrases □ Immunoglobulin E—binding to mast cells, *in vitro* method for screening inhibitors □ Binding—immunoglobulin E to mast cells, *in vitro* method for screening inhibitors □ Inhibitors—immunoglobulin E to rat peritoneal mast cells, *in vitro* screening method

The immunologically induced secretion of mediators of anaphylaxis by sensitized rat or human mast cells exposed to the appropriate antigen triggers a series of intracellular events that require Ca^{2+}, involve an activatable

0022-3549/79/0300-0353$01.00/0

© 1979, American Pharmaceutical Association

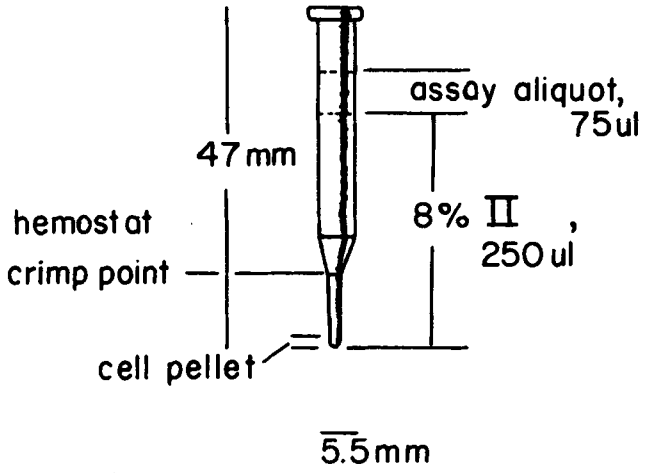

Figure 1—*Diagram of the polyethylene microsediment tube. The capillary is cut between the crimp point and the cell pellet.*

serine protease, can be blocked by metabolic inhibitors, and are modulated by cyclic nucleotides (1). Sensitization of the mast cells is accomplished by the binding of immunoglobulin E (IgE) to specific receptors on the cell's surface and is long lived, a reflection of the high affinity of the process (2).

Little attention has been paid to the possibility of altering the IgE–mast cell interaction, although this approach is potentially one of the most specific ways of interfering with the release of mediators. This paper describes the development and optimization of an assay to measure directly IgE binding to mast cells. This procedure is a modification of previously reported assays (3, 4) and permits the rapid study of large numbers of potential modulators. Also included is an evaluation of the putative inhibitor, human myeloma IgE pentapeptide III (5), and several antiallergic agents.

EXPERIMENTAL

Materials—Ethyleneglycol-bis(β-aminoethyl ether)-*N,N'*-tetraacetic acid (I), a copolymer of sucrose and epichlorohydrin (II, mol. wt. ~40,000), and zwitterionic buffers 2-(*N*-morpholino)ethanesulfonic acid (III), piperazine-*N,N'*-bis(2-ethanesulfonic acid) (IV), and *N*-2-hydroxyethylpiperazine-*N'*-2-ethanesulfonic acid (V) were used as obtained[1]. Calfskin gelatin[2] was warmed to aid in its dissolution in buffers.

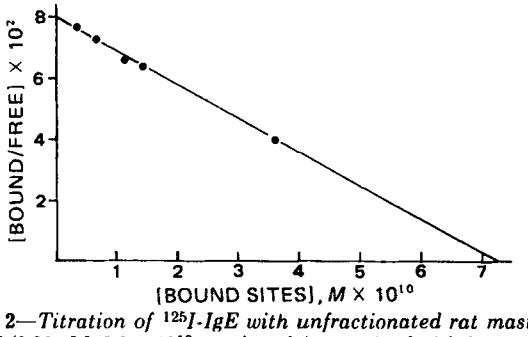

Figure 2—*Titration of ^{125}I-IgE with unfractionated rat mast cells. ^{125}I-IgE (0.89 nM, 3.0 × 10^{10} cpm/μmole) was mixed with from 2 × 10^5 to 4 × 10^6 mast cells in a total volume of 210 μl. Blank values, determined with a 100-fold excess of unlabeled IgE, were subtracted from test values. The least-squares line, having a correlation coefficient of 0.99, extrapolated to a value of 0.72 nM sites bound at infinite cell concentration. A value of 3 × 10^5 sites/cell was assumed in the calculation, although the actual number of sites per cell influenced only the slope of the line calculated* (i.e., K_a) *and not the value of the concentration of bound sites at infinite cell concentration (x-intercept). The molecular weight of IgE was assumed to be 183,000 (7).*

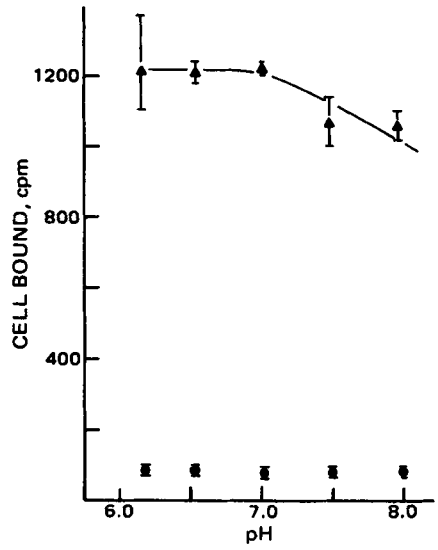

Figure 3—*pH-binding profile of ^{125}I-IgE with unfractionated mast cells. Assays were run in triplicate, with the standard error of the mean indicated by vertical bars. Cell-bound counts of 1000 are equivalent to 2 × 10^{-8} μmole of ^{125}I-IgE. Key: ▲, ^{125}I-IgE; and ●, ^{125}I-IgE plus a 100-fold excess of unlabeled IgE.*

The following antiallergic compounds were tested: theophylline[1], 1-methyl-3-isobutylxanthine[3], 7-(2-hydroxyethoxy)-9-oxoxanthene-2-carboxylic acid sodium salt (VI)[4], 5,5-dimethyl-11-oxo-5*H*,11*H*-(2)-benzpyrano[4,3-*g*](1)benzopyran-9-carboxylic acid ethanolamine salt (VII)[5], doxantrazole[6], disodium cromoglycate[7], etazolate hydrochloride[8], and the prostaglandins[1] E_1, A_1, and $F_{2\alpha}$. Pentapeptide III (aspartyl-seryl-aspartyl-prolyl-arginine[9]) was subjected to amino acid analysis after a 22-hr hydrolysis and yielded the following molar ratios of aminio acid to proline: aspartic acid, 2.08; serine, 0.91; arginine, 1.01; proline, 1.0; and lysine, 0.01. Less than 10 nmoles/mg of peptide was detected for the amino acids.

Bolton-Hunter reagent[10] was purchased in vials of 500 μCi with a specific activity of 1500 Ci/mmole. Polyethylene capillary microsediment tubes[11] were selected to fit the adapted rotor holes of a small centrifuge[12]. Collodion bags for protein dialysis[13] had an exclusion limit of 25,000 daltons. Dimethyl sulfoxide[14] (grade 1) and other solvents[1] were ACS grade.

Buffers—The buffer generally employed in isolating and washing cells (cell isolation buffer) had the following composition: 150 m*M* NaCl, 2.7 m*M* KCl, 0.1 m*M* I, 0.1% gelatin, and 1 m*M* NaH_2PO_4; it was adjusted to pH 7.0 with sodium hydroxide. The buffer utilized in the assay solution (assay buffer) consisted of 500 m*M* NaCl, 9 m*M* KCl, 0.3 m*M* I, 0.32% gelatin, and 50 m*M* IV; it also was adjusted to pH 7.0 with sodium hydroxide.

The assay contained 50 μl of cells in cell isolation buffer, 30 μl of assay buffer, test compound, and labeled and unlabeled IgE in a total of 150 μl. The final salt concentrations were 150 m*M* NaCl, 2.7 m*M* KCl, 0.1 m*M* I, 0.1% gelatin, and 10 m*M* IV (pH 7.0).

Cells—Mast cells were obtained by peritoneal lavage of male Sprague-Dawley rats[15] (250–350 g). The animals were anesthetized with

[1] Sigma Chemical Co., St. Louis, Mo. The trade name of II is Ficoll; supplier's designations of other compounds are: I, EGTA; III, MES; IV, PIPES; and V, HEPES.
[2] Eastman Chemical Corp., Rochester, N.Y.
[3] Aldrich Chemical Co., Milwaukee, Wis.
[4] AH 7725, Allen and Hanburys Research Ltd., Hertfordshire, England.
[5] PR-D92-EA, Pharma-Research Canada Ltd., Pointe Claire, Quebec, Canada.
[6] Wellcome Research Laboratories, Triangle Park, N.C.
[7] Fisons Corp., Bedford, Mass.
[8] SQ 20,009, Squibb, Princeton, N.J.
[9] Peninsula Laboratories, San Carlos, Calif.
[10] New England Nuclear, Boston, Mass.
[11] No. 47/7, W. Sarstedt, Inc., Princeton, N.J.
[12] Eppendorf 3200 microfuge, Bio-Rad Laboratories, Richmond, Calif.
[13] Schleicher and Schuell, Keene, N.H.
[14] Fisher Scientific, Springfield, N.J.
[15] Charles River Laboratories, Cambridge, Mass.

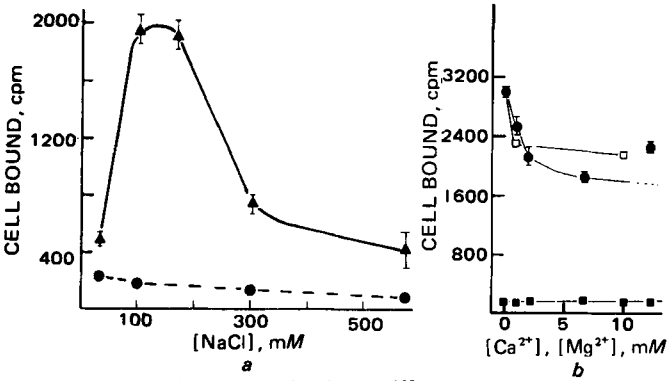

Figure 4—*Dependence of the binding of ^{125}I-IgE to mast cells on ionic strength and divalent metal ions. (a) Each assay tube contained, in a total volume of 150 µl, 1.5 µmoles of III (pH 7.0), 0.4 µmole of potassium chloride, 0.015 µmole of I, 150 µg of gelatin, 5.4–86 µmoles of sodium chloride, 3 × 10^5 unfractionated mast cells, and 6.4 × 10^{-7} µmole of ^{125}I-IgE (specific activity of 2.8 × 10^5 cpm/µg). Cell-bound counts of 1000 are equivalent to 2 × 10^{-8} µmole of ^{125}I-IgE. Contributions from III and I to the sodium-ion concentration were calculated according to the Henderson–Hasselbach equation. Key: ▲, ^{125}I-IgE; and ●, ^{125}I-IgE plus a 100-fold excess of unlabeled IgE (blanks). Vertical bars represent error of the means. (b) Each assay tube contained, in a total volume of 150 µl, 1.5 µmoles of III (pH 7.0), 0.4 µmole of potassium chloride, 22.5 µmoles of sodium chloride, 0.015 µmole of I, 150 µg of gelatin, 3 × 10^5 unfractionated mast cells, and 6.7 × 10^{-7} µmole of ^{125}I-IgE (specific activity of 2.8 × 10^5 cpm/µg). Calcium chloride (0.15–2.0 µmoles) or magnesium chloride (0.3–1.5 µmoles) was added to the various tubes. Key: ●, calcium; □, magnesium; and ■, blanks.*

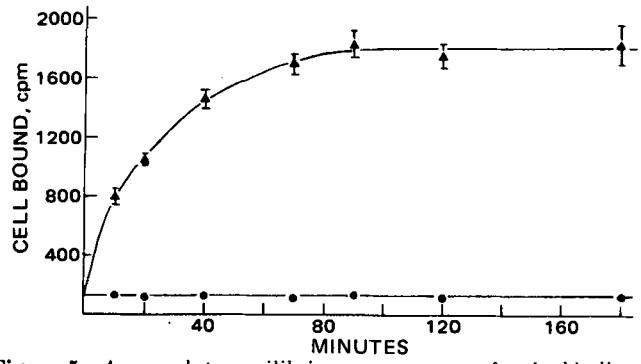

Figure 5—*Approach to equilibrium measurement for the binding of ^{125}I-IgE to unfractionated rat mast cells at 37°. Each assay tube contained, in a total volume of 150 µl, 3 × 10^5 unfractionated mast cells, 6.7 × 10^{-7} µmole of ^{125}I-IgE (specific activity of 2.7 × 10^5 cpm/µg; 1000 cpm is equivalent to 2 × 10^{-8} µmole of antibody), 1.5 µmoles of III (pH 7.0), 22.5 µmoles of sodium chloride, 0.4 µmole of potassium chloride, 0.015 µmole of I, and 150 µg of gelatin. Key: ▲, ^{125}I-IgE; and ●, ^{125}I-IgE plus a 100-fold excess of unlabeled IgE.*

ether, decapitated, and exsanguinated before the injection of cold cell isolation buffer (~7 ml/animal) into the peritoneal cavity. Combined peritoneal washes were harvested by sedimentation at 160×*g* for 10 min, and the cell pellet was washed three times with cell isolation buffer (mixed cells). The final pellet was suspended in 1 ml of cell isolation buffer, an aliquot was stained with 0.1% toluidine blue in phosphate-buffered saline, and the mast cell concentration was determined with a hemocytometer.

Purified mast cells were obtained by the method of Ishizaka *et al.* (6), except that cell isolation buffer was employed. The cells were kept at 0° except during centrifugation, which was done at room temperature. Mixed peritoneal cells generally contained 5–10% mast cells, with a yield of 1–2 × 10^6 mast cells/rat. Cells fractionated over II were generally 50–80% mast cells, with a yield of 0.5–1 × 10^6 mast cells/rat. Cells were diluted with cell isolation buffer such that 50 µl contained 2–3 × 10^5 mast cells.

IgE—Pure IgE was isolated from the ascitic fluid of a transplantable IgE immunocytoma (IR-162) grown in rats (7). The IgE-containing ascites[16] was treated according to Kulczycki and Metzger (3), with certain modifications[17], to yield a preparation of IgE that showed just two bands on 10% polyacrylamide gels subjected to electrophoresis under denaturing conditions (sodium lauryl sulfate and β-mercaptoethanol) (8). The purified IgE was stored as a dry lyophilized powder[17] at −80° after dialysis against 15 m*M* Na_2HPO_4.

^{125}I-Labeling of IgE—The Bolton–Hunter reagent was used according to the manufacturer's directions (*cf.*, 9); the charcoal filter was employed to trap volatile iodine compounds. The combination vial containing the dried reagent (500 µCi, 0.33 nmole) was chilled at −18° for 2 hr and then placed in ice for 30 min to ensure that the insulated inner vessel was at 0°. A solution of 500 µg of IgE (3.3 nmoles) in 100–200 µl of ice-cold 0.1 *M* sodium borate buffer, pH 8.5, was injected into the vial, which was then mixed, centrifuged briefly, and set aside at 0° overnight.

The vial's contents were transferred with two rinses of 100 µl of 0.1 *M* sodium borate buffer (pH 8.0) into a collodion bag, and the combined solutions were dialyzed against the same buffer (for a total dilution factor of 10^6) at 4°. The dialyzed solution was diluted to 2.0 ml with the pH 8.0 borate buffer, and the specific activity was determined, using a value of 1.36 for $E^{0.1\%}_{280\,nm}$ (3). Specific activities ranged between 4 and 5 × 10^5 cpm/µg of protein, 95–97% of which could be precipitated by 10% trichloroacetic acid in the presence of a 40-fold excess of bovine serum albumin. These values corresponded to ~60% of radiochemical incorporation of iodine-125 into protein.

The solution of ^{125}I-IgE was stored at 4° and was stable in borate buffer for at least 3 months.

Binding Assay—Rat peritoneal mast cells (2–3 × 10^5 cells/tube) were incubated with assay buffer. If desired, the test compound was added at this time to preincubate at 37° for 5 min prior to the addition of ^{125}I-IgE. The labeled antibody was then added; incubation was continued for 2 hr in a shaking water bath, which was adjusted to 150 cpm to keep the cells evenly suspended. The total volume of the assay was 150 µl, and the final concentrations of ^{125}I-IgE and the test compound were generally 3 n*M* and 100 µ*M*, respectively. Other components present were 150 m*M* NaCl, 2.7 m*M* KCl, 0.1 m*M* I, 0.1% (w/v) gelatin, and 10 m*M* IV (pH 7.0).

After the incubation was completed, 75 µl was withdrawn from each tube, after first evenly distributing the cells, and layered over 250 µl of an 8% solution of II (made up in cell isolation buffer, with a final refractive index of ~1.3455) in a polyethylene microsediment tube. Cell-bound radioactivity was separated from unbound ^{125}I-IgE by centrifuging the cells at 8000×*g* for 2 min. The cell pellet then resided in the capillary tip of the microsediment tube and was collected by cutting the tip off with a hot wire after first crimping, with a hemostat, the top of the capillary beneath the cell cushion of II (Fig. 1).

The tip was dropped into a plastic vial and was counted in a γ-spectrometer. If the effect of a test compound was measured, the control consisted of adding solvent (in which the test compound was added) alone to the mast cells and ^{125}I-IgE and treating the tubes in the same manner (*e.g.*, with 5-min preincubation). The blank was obtained by adding a 100-fold excess of unlabeled IgE to an additional three tubes to check for nonspecific binding, entrainment of labeled antibody in the cell pellet, and background radiation.

Many test compounds of interest were not soluble in aqueous buffers. Then the choice was to disperse them in a more or less homogeneous suspension by physical means (*e.g.*, sonication) or to dissolve them in an organic solvent. It was convenient to dissolve most compounds in dimethyl sulfoxide, to dilute them with buffer, and to add them to the assay mixture such that the final dimethyl sulfoxide concentration was 0.17%. This low concentration of dimethyl sulfoxide did not affect the binding parameters of IgE to mast cells, nor did it affect the spontaneous release of histamine from the same cells. Cell viability after the assay under these conditions was about 60–80% in control samples, as measured by trypan blue exclusion.

pH Profile—Labeled antibody was incubated with mast cells under standard ionic strength conditions (150 m*M* NaCl, 2.7 m*M* KCl, 0.1 m*M* I, and 0.1% gelatin) in the presence of different buffers at 10 m*M*. Buffers utilized for the different pH values were III (pH 6.0), IV (pH 6.5 and 7.0), and V (pH 7.5 and 8). The buffers were made up in stock solutions of 100 m*M*, and the pH was checked for each sample after the buffer had been diluted to the same concentration and ionic strength as used in the assay.

[16] Gift of Dr. H. Metzger, National Institutes of Health.

[17] Dr. H. Metzger, National Institute of Arthritis, Metabolism, and Digestive Diseases, National Institutes of Health, Bethesda, MD 20014, personal communication.

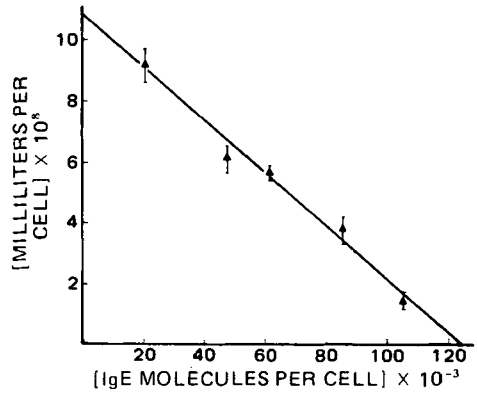

Figure 6—*Scatchard plot of the binding of ^{125}I-IgE to unpurified rat mast cells. Each assay tube contained 3 × 10^5 mast cells and 0.4–13 n*M *^{125}I-IgE (specific activity of 1.65 × 10^5 cpm/μg) in a total volume of 150 μl. The points were run in triplicate, with a blank (100-fold excess unlabeled IgE added to labeled IgE) subtracted from each point. The standard error of the mean is indicated by bars. The least-squares line yielded values of 125,000 IgE receptor sites/cell with an affinity constant of 5 × 10^8 M^{-1}. The correlation coefficient for the plot is 0.99.*

RESULTS

Binding Assay—The IgE isolated from IR-162 ascites had a high degree of purity as judged by sodium lauryl sulfate gel electrophoresis. Autoradiography of the IgE labeled with Bolton-Hunter reagent after electrophoresis yielded a pattern identical to the stained bands. Over 95% of the labeled antibody could be precipitated with trichloroacetic acid, and approximately 80% of the iodinated IgE could be bound by mast cells as assessed from the intercept value of a Scatchard analysis of the binding data (Fig. 2) in which bound and free *receptor sites* were the variables.

The interaction of ^{125}I-IgE with rat peritoneal mast cells was measured in an assay utilizing a facile, one-step separation of cell-bound labeled IgE from unbound antibody. In general, 6–12% of the total counts was bound to cells under the assay conditions. Optimal conditions for the interaction between IgE and its mast cell receptors on both purified and unfractionated mast cells were pH 6.5–7.0 (Fig. 3), about 150 m*M* NaCl (in the presence of 2.7 m*M* KCl, 0.1 m*M* I, and 10 m*M* buffer) (Fig. 4*a*), no magnesium or calcium (Fig. 4*b*), and 37°. Kinetic experiments at 37° under the optimized conditions indicated that, at the IgE and mast cell concentrations employed in the assay (3–5 n*M* and 1–2 × 10^6 cells/ml, respectively), less than 2 hr was sufficient to establish equilibrium (Fig. 5).

A number of experimental observations with this system supported the conclusion that the binding equilibrium of ^{125}I-labeled IgE was to a finite number of receptors on mast cells, *i.e.*, was specific:

1. A 100-fold excess of unlabeled IgE blocked the binding of labeled IgE by greater than 95%.

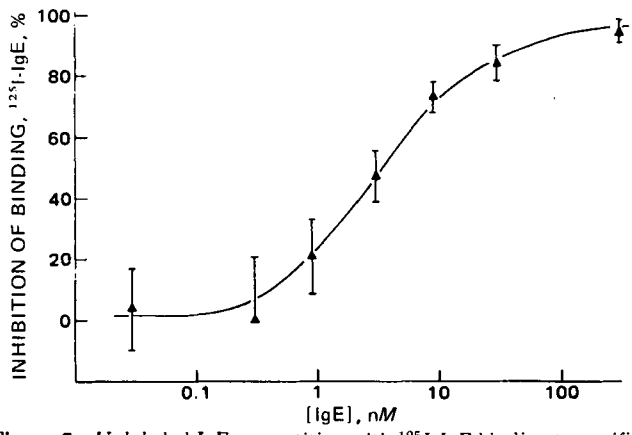

Figure 7—*Unlabeled IgE competition with ^{125}I-IgE binding to purified rat mast cells. Each assay tube contained 2 × 10^5 mast cells and 3 n*M *^{125}I-IgE (specific activity of 2.7 × 10^5 cpm/μg); 9.7% of the total counts was bound to cells in the control. The I_{50} for unlabeled IgE obtained from this plot is 3.5 n*M.

Table I—Effects of Standard Antiallergic Agents on ^{125}I-IgE Binding to Rat Mast Cells [a]

Agent	Cell Bound, cpm ± *SEM*		Inhibition of IgE Binding, % ± *SEM*
	Control	100 μ*M* of Compound	
Theophylline (10)	1843 ± 47	1717 ± 17	7 ± 3
Methylisobutylxanthine (11)	1843 ± 47	1746 ± 98	5 ± 8
Doxantrazole (10)	1843 ± 47	1589 ± 156	15 ± 11
VI (10)	1843 ± 47	1886 ± 41	0 ± 5
VII (12)	1843 ± 47	1743 ± 78	6 ± 7
Etazolate hydrochloride (10)	1843 ± 47	1982 ± 180	−5 ± 8
Disodium cromoglycate (10)	1703 ± 35	1622 ± 108	5 ± 12

[a] These assays were performed using unfractionated cells. The final dimethyl sulfoxide concentration was 0.67%, and a 100-fold excess of unlabeled IgE inhibited labeled IgE binding by 93%. Greater than 25% inhibition is regarded as significant.

2. Greater than 98% of the binding activity of ^{125}I-IgE could be eliminated by heating the antibody preparation at 56° for 4 hr.

3. Scatchard plots, according to Conrad *et al.* (4) (Fig. 6), on both purified mast cells and mixed peritoneal cells yielded the same binding parameters for both cell preparations. An average of eight experiments gave the number of binding sites per cell ± *SEM* as 2 ± 0.4 × 10^5, the affinity constant K_a ± *SEM* as 6.4 ± 0.9 × 10^8 M^{-1}, and the correlation coefficient ± *SEM* as 0.96 ± 0.01. These data were *not* corrected for the apparent inability of 20% of the labeled IgE to bind to mast cells. Conrad *et al.* (4) obtained values of 3 × 10^5 for sites per cell and about 10^9 M^{-1} for K_a.

4. A dose-response inhibition curve obtained by adding variable amounts of unlabeled IgE to a constant amount of ^{125}I-IgE (Fig. 7) gave a normal dose-response with an I_{50} value equal to the concentration of labeled antibody.

The extent of antibody binding was not affected by 10 m*M* NaN_3, suggesting that cellular ATP is not required for receptor-antibody interaction.

Anaphylactic Agents—Several compounds with demonstrated antiallergic activities were assayed at 100 μ*M* as inhibitors of IgE binding. However, none demonstrated significant inhibition (Table I). Since prostaglandins are known to interact with mast cell membranes (13), three representatives (A_1, E_1, and $F_{2\alpha}$) were tested at 10 μ*M* for their ability to inhibit the antibody receptor formation. All were inactive.

Pentapeptide—Experiments to test the inhibition of binding of ^{125}I-IgE to mast cells by unlabeled peptide were performed (Table II). The data demonstrate that a 100-fold excess of unlabeled IgE inhibited labeled IgE binding by 95% and that, within experimental error, a large excess of pentapeptide did not affect antibody binding to the receptor.

DISCUSSION

Desirable features for an assay for measuring the binding of ^{125}I-labeled IgE to rat peritoneal mast cells are the availability of a pure antibody preparation and a gentle labeling procedure that yields a native product of high specific activity. The first condition was fulfilled by the existence of rodent immunocytoma lines from which IgE could be readily isolated (7). The preparation reported here showed two major bands on sodium lauryl sulfate and β-mercaptoethanol gel electrophoresis, with apparent molecular weights corresponding to the heavy and light chains of IgE (~76,000 and 20,000 daltons, respectively).

Table II—Ability of Pentapeptide to Compete for IgE Binding Sites on Rat Mast Cells

Inhibitor	Inhibitor-^{125}I-IgE Ratio[a]	cpm_{bound}^{I}/cpm_{bound}^{C} [b]
IgE	100	0.05 ± 0.02
Pentapeptide	1.2 × 10^4	0.93 ± 0.22
	1.2 × 10^5	1.10 ± 0.16
	4.8 × 10^5	1.07 ± 0.29
	1.2 × 10^6	1.12 ± 0.28

[a] Inhibitor-^{125}I-IgE is the molar ratio of the particular inhibitor investigated to ^{125}I-labeled IgE, whose concentration in these experiments was between 0.1 and 1 n*M*. There were about 2 × 10^5 rat mast cells/aliquot counted. [b] cpm_{bound}^{I} and cpm_{bound}^{C} are cell-bound counts in the presence (*I*) and absence (*C*) of inhibitor, respectively.

The second condition can be fulfilled by one of several methods. For example, ^{14}C-phenylisothiocyanate can be used under nondenaturing conditions to label antibodies without loss of activity (14). However, because of its high specific activity, iodine-125 is still most often the isotope of choice, although the labeling procedures frequently utilize oxidizing agents such as chloramine-T or hydrogen peroxide. Conrad *et al.* (4) found that less than 50% of the IgE labeled with chloramine-T oxidation could be bound to rat mast cells. However, Kulczycki and Metzger (3) found that up to 80% of the IgE labeled by the same method bound to rat basophilic leukemia cells. The findings reported here indicate that 80% of the IgE reacted with Bolton–Hunter reagent could be bound to mixed peritoneal cells (Fig. 2), even after 3 months of storage at 4° in borate buffer. The fact that unlabeled IgE inhibited with an I_{50} equal to the concentration of ^{125}I-IgE (Fig. 7) provided additional support that the labeled antibody is native and that its binding is not affected by the reaction with Bolton–Hunter reagent.

The assay reported here incorporates the approach of Kulczycki and Metzger (3) with certain significant modifications. The use of an 8% solution of II as a cell cushion and of microsediment tubes in the isolation of cell-bound radioactivity provided a more facile and reproducible assay. Considerable savings of time and animals were made possible by the use of mixed peritoneal cells. A protocol with optimal ionic strength, pH, and time of incubation conditions for the interaction of myeloma IgE with rat mast cells has been elaborated in this paper. Although high concentrations (10 m*M*) of calcium and magnesium appeared to inhibit the binding of IgE to mast cells, the inclusion of low amounts of Ca^{2+} (0.1–1 m*M*) may be desirable to maintain membrane and cell integrity. Adequate shaking during the incubation was important for reproducible results.

Compounds that lyse mast cells, making them incapable of penetrating the sucrose–polymer (II) cushion in the microsediment tube (Fig. 1), show up as apparent inhibitors of IgE binding. Therefore, active compounds should be examined for their ability to release cytoplasmic enzymes. In these inhibition studies, concentrations of test compound and ^{125}I-IgE of 100 μM and 3 n*M*, respectively, were generally employed. The cytolytic activity of some agents may be circumvented by decreasing the concentrations of compounds and antibody (keeping the ratio constant) and by increasing the specific activity of IgE by reacting less protein (see *Experimental*) with Bolton–Hunter reagent.

The insensitivity of the assay system to low concentrations of dimethyl sulfoxide has facilitated the testing of lipophilic compounds. A concentration of solvent that not only does not affect the binding parameters of IgE to its receptor but also does not affect the interaction of the drug with the cells must be used. Dimethyl sulfoxide was found to be more suitable than dimethylformamide, acetone, or ethanol, both as a solvent for dissolving compounds and for its lack of interaction with the biological system (data not shown). To avoid solvent–drug artifacts, however, dimethyl sulfoxide should be used at a final concentration below 0.2% (v/v).

This assay to quantitate cell-bound ligand appeared more convenient than the micromethod suggested by Davis *et al.* (15), which employed a two-tube assembly with a quartz-wool filter to trap the cells. Whereas the method described here had a one-step sedimentation procedure for separating cell-bound counts, the method described by Davis *et al.* required three washing steps.

Pentapeptide III, Asp-Ser-Asp-Pro-Arg, was reported by Hamburger (5) to inhibit the Prausnitz–Küstner (P.–K.) reaction. This finding implied that the pentapeptide could block the binding of IgE to its mast cell receptors. Direct binding studies (16) of pentapeptide III, as well as the competition experiments reported here, failed to indicate strong ($K_a < 5 \times 10^5\ M^{-1}$) or specific binding. This finding was supported by the report (17) that the pentapeptide did not affect the binding of human IgE to human basophils, nor did it block antigen-induced histamine release.

Two recent communications (18, 19), however, supported Hamburger's (5) original results. One article stated that the pentapeptide could inhibit antigen-induced degranulation of rat mast cells in several models, as assessed by the estimation of the number of degranulated mast cells in a mixed peritoneal cell sample (18). These researchers suggested that the pentapeptide could interfere with both IgE–mast cell interactions and IgE–antigen combination. The other article reported the inhibition of wheal and flare reactions by the pentapeptide when used against certain antigens in the human Prausnitz–Küstner and baboon passive cutaneous anaphylaxis systems (19). The experiments reported here, however, failed to show any evidence of a specific interaction between pentapeptide III and the IgE receptors on rat mast cells.

This assay should facilitate the discovery and characterization of modulators of the binding of IgE to its mast cell receptor.

REFERENCES

(1) K. F. Austen, *Fed. Proc.*, **33,** 2256 (1974).

(2) S. Newman, G. Rossi, and H. Metzger, *Proc. Natl. Acad. Sci. USA*, **74,** 869 (1977).

(3) A. Kulczycki, Jr., and H. Metzger, *J. Exp. Med.*, **140,** 1676 (1974).

(4) D. Conrad, H. Bazin, A. Sehon, and A. Froese, *J. Immunol.*, **144,** 1688 (1975).

(5) R. N. Hamburger, *Science*, **189,** 389 (1975).

(6) T. Ishizaka, T. Adachi, T.-H. Chang, and K. Ishizaka, *J. Immunol.* **118,** 211 (1977).

(7) H. Bazin, P. Querinjean, A. Beckers, J. F. Heremans, and F. Dessy, *Immunology*, **26,** 713 (1974).

(8) U. K. Laemmli, *Nature*, **227,** 680 (1970).

(9) A. E. Bolton and W. M. Hunter, *Biochem. J.*, **133,** 529 (1973).

(10) C. J. Coulson, R. E. Ford, S. Marshall, J. L. Walker, K. R. Wooldridge, K. Bowden, and T. J. Coombs, *Nature*, **265,** 545 (1977).

(11) J. A. Beavo, N. L. Rogers, O. B. Crofford, J. G. Hardman, E. W. Sutherland, and E. V. Newman, *Mol. Pharmacol.*, **6,** 597 (1970).

(12) P. B. Stewart, J. P. Devlin, and K. R. Freter, *Fed. Proc.*, **33,** 762 (1974).

(13) I. Tauber, M. Kaliner, D. J. Stechschulte, and K. F. Austen, *J. Immunol.*, **111,** 27 (1973).

(14) N. Levy and J. Dawson, *ibid.*, **116,** 1526 (1976).

(15) E. Davis, D. Tsay, M. Schlamowitz, and E. Walborg, Jr., *Anal. Biochem.*, **80,** 416 (1977).

(16) S. Coutts, D. Reid, and I. Weinryb, *Fed. Proc.*, **36,** 743 (1977).

(17) H. Bennich, U. Ragnarsson, S. Johansson, K. Ishizaka, T. Ishizaka, D. Levy, and L. Lichtenstein, *Int. Arch. Allergy Appl. Immunol.*, **53,** 459 (1977).

(18) N. Vardinon, Z. Spirer, M. Fridkin, J. Schwartz, and S. Ben-Efraim, *Acta Allergol.*, **32,** 291 (1977).

(19) D. Stanworth, M. Kings, P. Roy, and D. Moran, *Int. Arch. Allergy Appl. Immunol.*, **56,** 409 (1978).

ACKNOWLEDGMENT

The authors thank Dr. H. Bazin (Louvain) for furnishing a sample of IgE-containing ascitic fluid. They also acknowledge helpful comments from Dr. Metzger and Dr. Bazin during preliminary work.

Interaction of Digoxin and Montmorillonite: Mechanism of Adsorption and Degradation

LINDA S. PORUBCAN *, GORDON S. BORN ‡, JOE L. WHITE §, and STANLEY L. HEM *x

Received June 23, 1978, from the *Departments of *Industrial and Physical Pharmacy, ‡Bionucleonics, and §Agronomy, Purdue University, West Lafayette, IN 47907.* Accepted for publication August 31, 1978.

Abstract □ IR, X-ray diffraction, and adsorption studies showed that digoxin is adsorbed onto montmorillonite by a reversible adsorption mechanism at pH 2 and 6. Degradation studies indicated abnormally high acid hydrolysis rates for digoxin interacted with montmorillonite. Accelerated digoxin degradation is attributed to the ability of the clay surface to concentrate both digoxin and protons. The effective pH at the clay surface appeared to be 1.5 pH units lower than the bulk suspension pH. Bisdigoxigenin was the major adsorbed degradation product. A similar catalytic effect also may occur with other neutral drugs that degrade by acid hydrolysis and should be considered in the formulation of clay-containing drug products or their coadministration with other drugs.

Keyphrases □ Digoxin—interaction with montmorillonite, mechanism of adsorption and degradation, IR, X-ray diffraction, and adsorption studies □ Montmorillonite—interaction with digoxin, mechanism of adsorption and degradation, IR, X-ray diffraction, and adsorption studies □ Interactions—digoxin and montmorillonite, mechanism of adsorption and degradation, IR, X-ray diffraction, and adsorption studies

The adsorption mechanism of the cationic drugs clindamycin and tetracycline by montmorillonite was elucidated recently using IR and X-ray analysis (1). Both drugs were adsorbed by cation exchange under pH conditions favoring the cationic form of the drug. Tetracycline also was found to complex with certain interlayer cations at higher pH conditions where the zwitterionic or anionic forms were present.

The application of IR spectroscopy and X-ray diffraction to the study of drug–clay interactions was extended to neutral compounds using digoxin as the model drug. Interaction was possible since many neutral molecules are known to interact with clays by physical adsorption (2) and hydrogen bonding (3). In addition, a number of saccharides similar to digitoxose have been shown to interact with montmorillonite (4).

Montmorillonite was used as a model clay because it possesses the highest surface area and exchange capacity of the clays commonly used in pharmacy. Since these properties are related directly to clay adsorption mechanisms, the results obtained with montmorillonite should be useful in predicting the adsorption behavior of clay minerals having lower adsorptive capacities such as kaolinite and attapulgite.

EXPERIMENTAL

Materials—All chemicals were either official or reagent grade. An X-ray diffractogram of bentonite USP indicated that it was composed of montmorillonite and a small quantity of quartz. To study the clay component responsible for the adsorptive properties observed in bentonite USP, the <2-μm clay fraction was separated by sedimentation and collected (1).

The cation-exchange capacity of the purified montmorillonite was 102 mEq/100 g as determined by the ammonium saturation method (5). Of this total, metal-ion analysis by atomic absorption spectrometry[1] showed that 7.1% of the cation-exchange capacity was satisfied by calcium ions, 2.7% by magnesium ions, and the balance by sodium ions.

Table I—Changes (in Angstroms) of Interlayer Spacing of Montmorillonite Interacted with Digoxin

	pH 2.0		pH 6.0	
Washings	Digoxin–Clay	Clay Control	Digoxin–Clay	Clay Control
1	4.6, 0.2–3.0	0.9	4.6	1.4
5	1.3	1.3	5.4	1.2
10	1.3, 2.5	1.2	4.9	1.3

Adsorption Mechanism—One milliliter of digoxin stock solution [60 mg/ml in chloroform–ethanol (1:1)] was added to clay aliquots and adjusted with hydrochloric acid or sodium hydroxide to pH 2.0 or 6.0 to yield 100 ml of a 1% montmorillonite suspension. After mixing and correcting for any pH change, the clay–drug system was equilibrated for 1 hr at 37°. Aliquots were then centrifuged at 6000 rpm, the supernate was decanted, and the solids were resuspended in water adjusted to the initial mixture pH.

To each washing was added enough chloroform–ethanol to achieve the original 1% (v/v) ratio of solvent to suspension. After 15 min of equilibration, this procedure was repeated to give samples washed 1, 5, and 10 times. For these samples, clay–drug solids were resuspended in water to yield a 2% suspension. IR and X-ray analyses of these clay–drug samples were then performed (1).

Effect of pH on Adsorption—Three adsorbate solutions containing 0.2 mg of digoxin were prepared from a digoxin stock solution (0.02 mg/ml in 50% ethanol) and labeled with 2.0 μCi of ^{3}H-digoxin[2] (specific activity of 12.8 mCi/mmole) in 100 μl of benzene–ethanol (1:9). These solutions were then added to clay suspensions containing 1 g of montmorillonite. The drug–clay mixtures were diluted to 1% clay suspensions and adjusted to pH 2, 4, and 6. Interaction occurred at 37° over a 5-hr period.

Aliquots were centrifuged for 30 min at 6000 rpm. Supernatant liquids were decanted into a second test tube to which a few crystals of sodium chloride were added to facilitate separation of the clay. The equilibrium concentration of the supernate was determined by quantitating the radioactivity using liquid scintillation counting[3] techniques. The counting efficiency was established using an external standard, and all samples were counted to a preset counting error of ±2.0%.

Effect of Montmorillonite on Digoxin Degradation—Montmorillonite and digoxin samples were prepared as already described except that pH adjustments were made to 2.0, 3.0, 4.0, and 5.0, and 40 μCi (2.0 ml) of the ^{3}H-digoxin stock solution was incorporated into each unlabeled digoxin solution. After immediate centrifugation for 30 min at 6000 rpm, each sample was decanted, the solids were washed twice with chloroform–methanol (1:1), and the two wash supernates were combined.

This double extraction, together with the first supernate, showed 99 ± 9% recovery of the tritium label. Subsequent evaporation under a dry nitrogen stream to the aliquot volume yielded a concentrated radioactive solution representing adsorbed digoxin and any adsorbed degradation products.

Labeled digoxin control samples were prepared without clay at pH 1.0, 1.5, 2.0, 2.5, and 3.0. Degradation was halted in each aliquot by adding 1 *N* NaOH to bring the pH above 3.0.

Twenty microliters of the desorbed (extracted) solutions and the control aliquots were spotted on precoated silica gel TLC plates[4] and developed in ethyl acetate–chloroform–acetic acid (90:5:5) (6). A chlo-

[1] Model 290B, Perkin-Elmer Corp., Norwalk, Conn.

[2] ^{3}H-Digoxin, Amersham Corp., Arlington Heights, Ill.

[3] Isocap/300 liquid scintillation system (Searle Analytical, Des Plaines, Ill.) with Riafluor (New England Nuclear, Boston, Mass.) as the scintillant.

[4] E. Merck AG, Darmstadt, West Germany.

0022-3549/79/0300-0358$01.00/0
© 1979, American Pharmaceutical Association

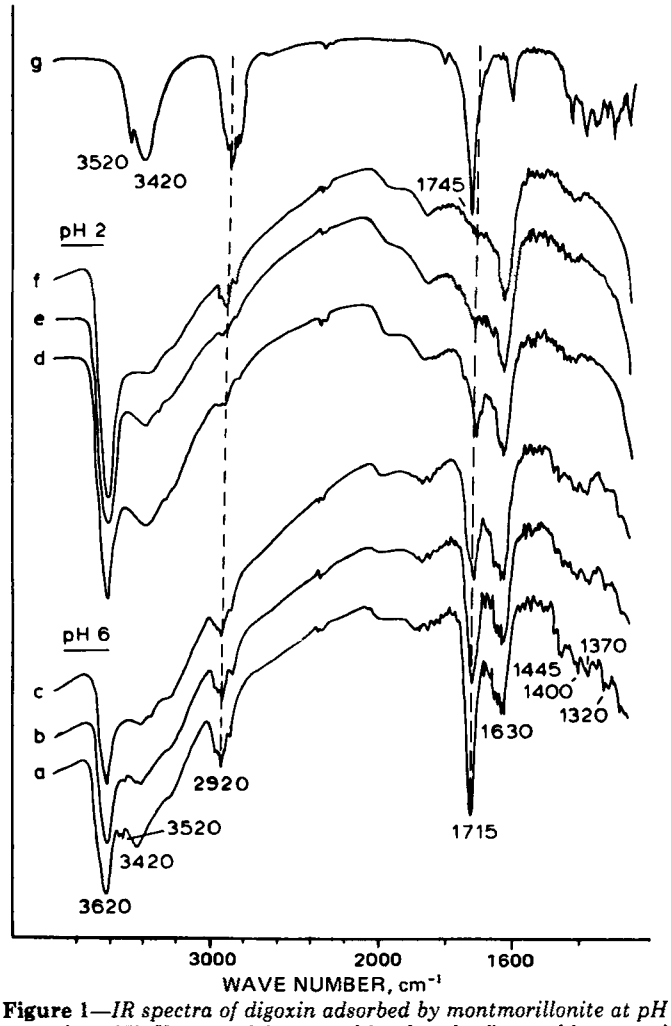

Figure 1—*IR spectra of digoxin adsorbed by montmorillonite at pH 2.0 and 6.0, 37°. Key: a and d, one washing; b and e, five washings; c and f, 10 washings; and g, digoxin in potassium bromide.*

roform–isopropanol–acetone (80:5:15) system (6) confirmed that total separation of digoxin and its degradation products was attained with the first system.

The concentration of each component was determined by measuring the radioactivity level in 5-mm sections of the TLC plates. Each zone was scraped into a scintillation vial, mixed with scintillant, and counted. The components were identified by matching experimental R_f values with those of standard compounds.

RESULTS

X-Ray—The X-ray diffraction d_{001} spacing for montmorillonite in the absence of drug under the dehydration conditions used in this study was 9.6 Å, indicating that no interlayer molecules (*i.e.*, water or drug) were present in the control sample. Adsorption of drug molecules between the layers of montmorillonite increased the d_{001} spacing; the difference between the d_{001} spacing of the expanded montmorillonite–drug system and the d_{001} spacing of the collapsed montmorillonite–control system is designated as the Δd_{001} value. The Δd_{001} values for digoxin–montmorillonite samples at pH 2.0 and 6.0 are listed in Table I.

The minimum dimension of the drug was calculated to be 5.6 Å from a Corey–Pauling–Kolton (CPK) molecular model. Keying of the digoxin molecule in the oxygen surface of the montmorillonite layers may result in an apparent contact distance that is 1 Å less than the true molecular dimension (7). This foreshortening agrees well with the experimental values reported in Table I.

The Δd_{001} values due to digoxin interaction at pH 2.0 (Table I) differ from those at pH 6.0. Although a Δd_{001} of 4.6 Å was observed after one washing for both pH 6.0 and 2.0, the pH 2.0 peak contained a shoulder indicating additional Δd_{001} values in the 0.2–3.0-Å range. After five washings, only a Δd_{001} value of 1.3 Å was detected. This Δd_{001} value was due most likely to nonaqueous solvent adsorption and was verified by an identical spacing in the control sample (Table I) where chloroform–methanol (1:1) was added without digoxin. This 1.3-Å value is considerably less than the thickness of a single layer of solvent molecules and was probably due to irregular surface coverage. A Δd_{001} of 1.3 Å was again observed after 10 washings and was accompanied by a large shoulder indicating a concomitant Δd_{001} value of 2.5 Å. This result can be attributed to more complete and uniform solvent adsorption.

The decrease in the Δd_{001} value from 4.6 to 1.3 Å as a result of washing indicated that digoxin was no longer present between the clay layers and that simple washing facilitated desorption. Such behavior implies physical adsorption or hydrogen bonding as the means of digoxin–montmorillonite interaction. X-ray diffraction patterns of samples at pH 2.0 were more broad and of lower intensity than those observed at pH 6.0. This finding suggests irregularly expanded clay sheets due to incomplete adsorption. The diffraction peaks of samples at pH 6.0 were very sharp and indicated a high degree of intercalation.

IR—IR spectra for digoxin adsorbed by montmorillonite at pH 2.0 and 6.0 are shown in Fig. 1. The absorption band at 3620 cm^{-1} was assigned to the OH-stretching vibration of the clay; water displayed an OH-asymmetric stretching band at 3420 cm^{-1} and an OH-bending vibration at 1630 cm^{-1}. Digoxin absorption bands were evident at 3520, 3420, 2920, and 1715 cm^{-1} and in the 1445–1320-cm^{-1} region. With repeated washings, all drug band intensities decreased (Fig. 1, curves b, c, e, and f), indicating that desorption occurred readily. This reversible behavior is characteristic of weak bonding forces (8).

The IR spectra of digoxin–montmorillonite support weak adsorption mechanisms. Generally, adsorption due to hydrogen bonding can be detected by shifts in the absorption bands of participating functional groups. Numerous hydroxyl groups, especially those in the digitoxoside portion of the digoxin molecule, might be expected to take part in hydrogen bonding with the clay surface. Although these OH-stretching vibrations at 3520 and 3420 cm^{-1} were readily apparent in the pH 6.0 clay–drug sample, no shifts in frequency were noted (Fig. 1, curve a).

Physical adsorption would be expected to result in isolated molecules of digoxin on the clay surface, thus reducing intermolecular hydrogen bonding between digoxin molecules (9, 10). Decreased hydrogen bonding causes stretching vibrations to shift to a higher frequency. Since this was not observed for the drug hydroxide bands (Fig. 1, curve a), it is suggested that hydrogen bonding between digoxin and the clay surface occurs but that the energy levels involved are comparable to intermolecular bonding in digoxin (Fig. 1, curve g). The digoxin carbonyl-stretching vibration shifted from 1745 to 1715 cm^{-1} as a result of interaction with montmorillonite. This shift to lower frequency further indicates hydrogen bonding as the principal adsorption mechanism, although van der Waals' forces also may contribute.

At pH 2.0, the low concentration of adsorbed digoxin and the interference from the OH-stretching frequency of water obscured any possible shifts in the OH-stretching vibrations of the drug as a result of interaction with montmorillonite. However, a shift in the carbonyl vibration from 1745 to 1715 cm^{-1} was apparent (Fig. 1, curve d).

Although the adsorption mechanism seemed to be the same for samples at pH 2.0 and 6.0, their relative intensities were quite different; the pH 2.0 bands were substantially smaller than the corresponding ones at pH 6.0. Since digoxin degrades by acid hydrolysis with the apparent first-order rate constant increasing below pH 3.0 (11–14), the smaller amount of adsorbate observed by IR and X-ray analysis at pH 2.0 was thought to be due to digoxin degradation. Therefore, the effect of pH on adsorption and degradation was investigated.

Effect of pH on Adsorption—Adsorption studies of tritiated digoxin were run at pH 6.0, 4.0, and 2.0 (Table II). The nearly complete adsorption seen at pH 6.0 was expected based on the high ratio of adsorbent to adsorbate. At this pH, no acid hydrolysis occurred and the percent digoxin adsorbed remained essentially constant at 90%.

At pH 4.0, the initial adsorption of 87% decreased to 51% after 5 hr.

Table II—Effect of pH on Adsorption of Digoxin and Digoxin Degradation Products

Hours	Tritium Label Adsorbed, %		
	pH 6	pH 4	pH 2
0	91	87	81
0.5	91	83	24
1	90	80	24
2	91	70	25
5	92	51	22

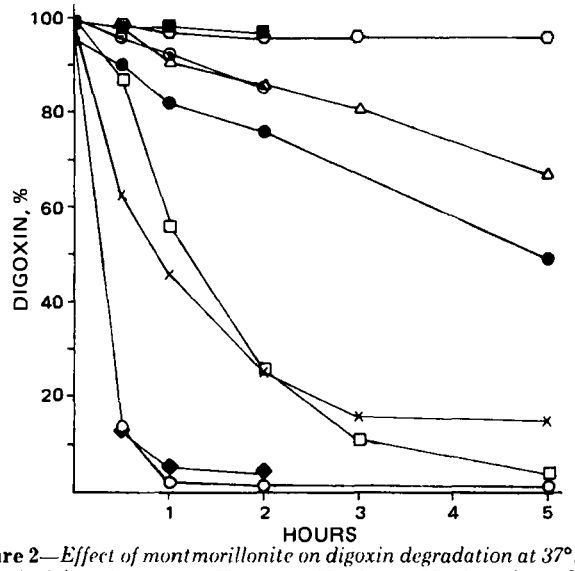

Figure 2—*Effect of montmorillonite on digoxin degradation at 37°. Key (adsorbed digoxin at): ○, pH 2.0; □, pH 3.0; △, pH 4.0; and ○, pH 5.0. Key (digoxin control at): ♦, pH 1.0; ×, pH 1.5; ●, pH 2.0; ⊙, pH 2.5; and ■, pH 3.0.*

This result was unexpected since minimal degradation has been reported at pH 4.0 (11–14) and no desorption was expected under the experimental conditions.

Interaction at pH 2.0 showed the immediate adsorption of 81% of the tritium label. This amount decreased rapidly to 24% within 30 min. The observed decrease in adsorption may have been due to digoxin degradation at this pH, although the apparent rate of change in adsorption was greater than would be predicted from the published digoxin hydrolysis rate at pH 2.0 (11–14). Because of this unexpected catalysis at pH 2.0 and 4.0, digoxin degradation in the presence of montmorillonite was examined in more detail.

Effect of Montmorillonite on Digoxin Degradation—Tritiated digoxin and montmorillonite were interacted at pH 2.0, 3.0, 4.0, and 5.0 and sampled over 5 hr. The adsorbed species (digoxin and its degradation products) were extracted from the montmorillonite, separated, and quantified by TLC and liquid scintillation counting. The percent digoxin in the adsorbate is presented in Fig. 2; the percent bisdigoxigenin, the initial digoxin degradation product, is shown in Fig. 3.

The bisdigoxigenin formation rate at pH 2.0, 3.0, and 4.0 indicates accelerated digoxin degradation. Montmorillonite did not alter the kinetics of digoxin degradation, as evidenced by the first-order relationship obtained at each pH. However, the degradation rate was significantly

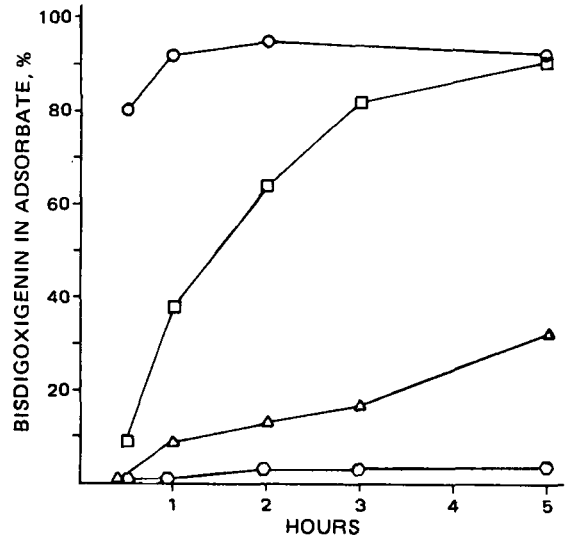

Figure 3—*Effect of montmorillonite on bisdigoxigenin formation at 37°. Key (adsorbed digoxin at): ○, pH 2.0; □, pH 3.0; △, pH 4.0; and ○, pH 5.0.*

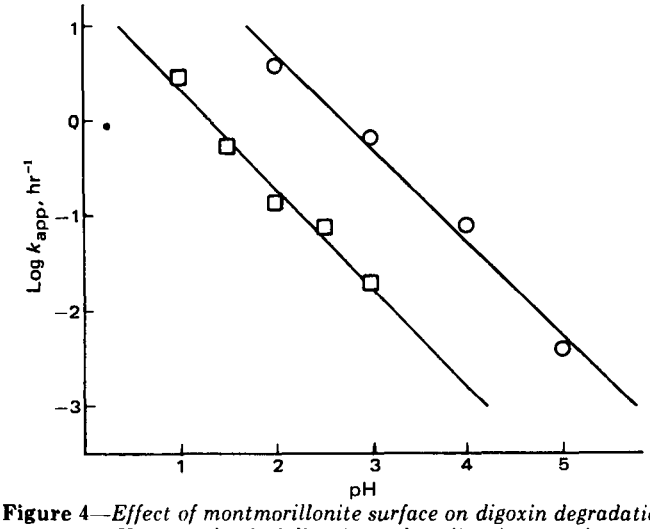

Figure 4—*Effect of montmorillonite surface on digoxin degradation rate at 37°. Key: ○, adsorbed digoxin; and □, digoxin control.*

increased (Fig. 4). The rate constants for the controls (Fig. 2) agreed well with previous studies (12–14).

DISCUSSION

After 1 hr of interaction with montmorillonite at pH 2.0, the adsorbed digoxin had degraded 98% (Fig. 2). However, 24% of the labeled compound remained adsorbed (Table II). Clearly, this latter adsorbate contains more than digoxin, probably a digoxin degradation product similar to digoxin in structure and thus accounting for the apparent digoxin bands in the IR spectra (Fig. 1, curve d). This suggestion is possible since the degradation pathway for digoxin acid hydrolysis involves cleavage of digitoxose molecules, yielding bisdigoxigenin, monodigoxigenin, and the digoxin aglycone, digoxigenin.

To identify the adsorbed degradation product responsible for the IR spectra at pH 2.0, relative quantities of all degradation products were obtained from the TLC and liquid scintillation counting analysis of digoxin adsorption. Figure 3 shows that bisdigoxigenin was the principal adsorbed component at pH 2.0. The smaller adsorption of bisdigoxigenin compared to that of digoxin at pH 6.0 was probably due to loss of a digitoxose unit, similar to other sugars known to be adsorbed by clays (4). Monodigoxigenin and digoxigenin also are generated under these conditions but have an even lower affinity for the clay due to digitoxose cleavage.

The lower degree of bisdigoxigenin adsorption by montmorillonite is illustrated by the X-ray diffraction data at pH 2.0 (Table I). After one washing, a Δd_{001} value of 4.6 Å was observed; however, the pattern was broader and of lower intensity than that observed at pH 6.0. Since the minimum molecular dimension of bisdigoxigenin is the same as digoxin, the Δd_{001} value would be unaffected by digoxin degradation. Collapse of the clay layers after five washings was a direct result of the weaker bonding between bisdigoxigenin and montmorillonite. With desorption facilitated by bisdigoxigenin formation, the nonaqueous solvent was then free to penetrate the clay layers to form a more complete and uniform solvent layer, ultimately resulting in a Δd_{001} value of 2.5 Å.

In the presence of montmorillonite, the hydrolysis rate suggests that the microenvironment of the clay is more acidic than the bulk solution. For example, Fig. 4 shows that the apparent rate constant at pH 4.0 for adsorbed digoxin was the same as the rate constant for a digoxin solution at pH 2.5. Although clays have been reported to catalyze the acid hydrolysis of esters such as ethyl acetate, the inversion of sucrose, and the protonation and hydrolysis of *s*-triazine herbicides (15, 16), the catalytic effect of clays on drugs is generally unrecognized.

This catalytic effect of montmorillonite on the acid-catalyzed digoxin degradation is due to the ability of the clay surface to serve as a site where digoxin molecules and protons are concentrated by adsorption and cation exchange, respectively. Therefore, the probability of reaction is enhanced, and an increased hydrolysis rate is observed. This effect was noted most dramatically at pH 2.0 (Table I) where 82% of the digoxin in the control remained after 1 hr at 37° while only 2% intact digoxin was found when interacted with montmorillonite.

A recent report suggested that some variation in the bioavailability

of orally administered digoxin may be due to variation in gastric pH, which would modify the composition of digoxin species available for absorption (12). The catalytic effect of montmorillonite will accentuate this problem. Therefore, the concomitant administration of drug products containing digoxin and montmorillonite should be avoided.

A similar catalytic effect may also occur with other neutral drugs that degrade by acid hydrolysis and should be considered in the formulation of clay-containing drug products or their coadministration with other drugs.

REFERENCES

(1) L. S. Porubcan, C. J. Serna, J. L. White, and S. L. Hem, *J. Pharm. Sci.*, **67**, 1081 (1978).

(2) W. F. Bradley, *J. Am. Chem. Soc.*, **67**, 975 (1945).

(3) D. M. C. MacEwan, *Trans. Faraday Soc.*, **44**, 349 (1948).

(4) B. K. G. Theng, "The Chemistry of Clay-Organic Reactions," Adam Hilger, London, England, 1974, pp. 206–210.

(5) D. D. Evans, in "Methods of Soil Analysis, Part 2," C. A. Black, Ed., American Society of Agronomy, Madison, Wis., 1965, chap. 57.

(6) M. L. Carvalhas and M. A. Figueira, *J. Chromatogr.*, **86**, 254 (1973).

(7) R. Greene-Kelley, *Trans. Faraday Soc.*, **51**, 412 (1955).

(8) J. L. White, *ACS Symp. Ser.*, **29**, 208 (1976).

(9) M. Cruz, J. L. White, and J. D. Russell, *Isr. J. Chem.*, **6**, 315 (1968).

(10) R. L. Ledoux and J. L. White, *J. Colloid Interface Sci.*, **21**, 127 (1966).

(11) K. Kasahara and A. Ruily-Torres, *Klin. Wochenschr.*, **47**, 1109 (1969).

(12) J. Kuhlmann, U. Abshagen, and N. Rietbrock, *Naunyn-Schmiedebergs Arch. Pharmacol.*, **276**, 149 (1973).

(13) M. H. Gault, J. D. Charles, D. L. Sugden, and D. C. Kepkay, *J. Pharm. Pharmacol.*, **29**, 27 (1977).

(14) L. A. Sternson and R. D. Shaffer, *J. Pharm. Sci.*, **67**, 327 (1978).

(15) N. T. Coleman and C. McAuliffe, in "Proceedings of the Third National Conference on Clays and Clay Minerals," W. V. Milligan, Ed., National Academy of Sciences–National Research Council, Washington, D.C., 1955, pp. 282–289.

(16) J. D. Russell, M. Cruz, J. L. White, G. W. Bailey, W. R. Payne, Jr., J. D. Pope, Jr., and J. I. Teasley, *Science*, **160**, 1340 (1968).

ACKNOWLEDGMENTS

Supported in part by The Upjohn Co.

This report is Journal Paper 7215, Purdue University Agricultural Experiment Station, West Lafayette, IN 47907.

Digoxin was kindly supplied by the Burroughs-Wellcome Co.

NOTES

Crystal Structure of 1:1 Complex of Barbital with 1-Methylimidazole

ALBERT WANG and B. M. CRAVEN ×

Received May 8, 1978, from the *Crystallography Department, University of Pittsburgh, Pittsburgh, PA 15260.* Accepted for publication August 9, 1978.

Abstract □ The prediction of a strong hydrogen-bonding interaction between barbital and 1-methylimidazole was confirmed. Two crystal complexes were obtained, 1:1 and 2:1, and the X-ray structure was determined for the 1:1 complex, which is monoclinic, space group $P2_1/c$, with a = 12.236(3) Å, b = 11.332(4) Å, c = 12.495(4) Å, and β = 120.67(1)°. The structure contains disk-shaped hydrogen-bonded tetramers with two molecules of each kind. There is a short NH···N hydrogen bond (2.82 Å) in which barbiturate provides the NH donor.

Keyphrases □ Barbital—complex with 1-methylimidazole, crystal structure determined □ 1-Methylimidazole—complex with barbital, crystal structure determined □ Complexes—barbital with 1-methylimidazole, crystal structure determined □ Crystal structure—determined for complex of barbital with 1-methylimidazole

Barbiturate drugs behave as strong hydrogen-bonding donors through their two NH groups but are weak acceptors through their three carbonyl oxygen atoms. These conclusions were derived from the hydrogen-bonding arrangements and interatomic distances observed in the crystal structures of a series of complexes of barbital with other small molecules representative of biological systems (1, 2). Thus, barbiturate drug receptor sites are likely to involve strongly electronegative hydrogen-bonding acceptor groups, such as the nitrogen atoms of adenine (3, 4), the imidazole ring in histidine or histamine (2), or the phosphoryl oxygen atoms of phospholipids (5).

These studies indicated that a strong hydrogen-bonding interaction would occur between barbital (5,5-diethylbarbituric acid) and 1-methylimidazole (Fig. 1), which might lead to crystal complexation. Indeed, 1-methylimidazole was a powerful solvent for barbital. The high viscosity of this solution made direct crystallization impractical. However, two crystal complexes were obtained from an ethanol solution; in one complex (1:1), crystal structure determination confirmed a short hydrogen bond NH···N (2.82 Å) in which barbital is the donor and 1-methylimidazole is the acceptor.

EXPERIMENTAL

Crystals of the 1:1 and 2:1 complexes were obtained from the same ethanolic solution, which was saturated at 60° with respect to both barbital and 1-methylimidazole, and slowly cooled in a sealed vial. Space groups and approximate cell data for these complexes were determined from X-ray precession photographs[1].

Crystals of the 1:1 complex, which dissociate at 96°, are monoclinic, space group $P2_1/c$, with a = 12.236(3) Å, b = 11.332(4) Å, c = 12.495(4) Å, and β = 120.67(1)°. The crystal density (1.190 g/cm^3) determined by

[1] No further work is planned on the 2:1 complex of barbital and 1-methylimidazole. These crystals are monoclinic, space group $P2_1/c$, with a = 16.7 Å, b = 12.1 Å, c = 12.4 Å, and β = 102°. There are eight barbital and four 1-methylimidazole molecules per unit cell.

0022-3549/79/0300-0361$01.00/0

© 1979, American Pharmaceutical Association

of orally administered digoxin may be due to variation in gastric pH, which would modify the composition of digoxin species available for absorption (12). The catalytic effect of montmorillonite will accentuate this problem. Therefore, the concomitant administration of drug products containing digoxin and montmorillonite should be avoided.

A similar catalytic effect may also occur with other neutral drugs that degrade by acid hydrolysis and should be considered in the formulation of clay-containing drug products or their coadministration with other drugs.

REFERENCES

(1) L. S. Porubcan, C. J. Serna, J. L. White, and S. L. Hem, *J. Pharm. Sci.*, **67**, 1081 (1978).

(2) W. F. Bradley, *J. Am. Chem. Soc.*, **67**, 975 (1945).

(3) D. M. C. MacEwan, *Trans. Faraday Soc.*, **44**, 349 (1948).

(4) B. K. G. Theng, "The Chemistry of Clay-Organic Reactions," Adam Hilger, London, England, 1974, pp. 206–210.

(5) D. D. Evans, in "Methods of Soil Analysis, Part 2," C. A. Black, Ed., American Society of Agronomy, Madison, Wis., 1965, chap. 57.

(6) M. L. Carvalhas and M. A. Figueira, *J. Chromatogr.*, **86**, 254 (1973).

(7) R. Greene-Kelley, *Trans. Faraday Soc.*, **51**, 412 (1955).

(8) J. L. White, *ACS Symp. Ser.*, **29**, 208 (1976).

(9) M. Cruz, J. L. White, and J. D. Russell, *Isr. J. Chem.*, **6**, 315 (1968).

(10) R. L. Ledoux and J. L. White, *J. Colloid Interface Sci.*, **21**, 127 (1966).

(11) K. Kasahara and A. Ruily-Torres, *Klin. Wochenschr.*, **47**, 1109 (1969).

(12) J. Kuhlmann, U. Abshagen, and N. Rietbrock, *Naunyn-Schmiedebergs Arch. Pharmacol.*, **276**, 149 (1973).

(13) M. H. Gault, J. D. Charles, D. L. Sugden, and D. C. Kepkay, *J. Pharm. Pharmacol.*, **29**, 27 (1977).

(14) L. A. Sternson and R. D. Shaffer, *J. Pharm. Sci.*, **67**, 327 (1978).

(15) N. T. Coleman and C. McAuliffe, in "Proceedings of the Third National Conference on Clays and Clay Minerals," W. V. Milligan, Ed., National Academy of Sciences–National Research Council, Washington, D.C., 1955, pp. 282–289.

(16) J. D. Russell, M. Cruz, J. L. White, G. W. Bailey, W. R. Payne, Jr., J. D. Pope, Jr., and J. I. Teasley, *Science*, **160**, 1340 (1968).

ACKNOWLEDGMENTS

Supported in part by The Upjohn Co.

This report is Journal Paper 7215, Purdue University Agricultural Experiment Station, West Lafayette, IN 47907.

Digoxin was kindly supplied by the Burroughs-Wellcome Co.

NOTES

Crystal Structure of 1:1 Complex of Barbital with 1-Methylimidazole

ALBERT WANG and B. M. CRAVEN ×

Received May 8, 1978, from the *Crystallography Department, University of Pittsburgh, Pittsburgh, PA 15260.* Accepted for publication August 9, 1978.

Abstract □ The prediction of a strong hydrogen-bonding interaction between barbital and 1-methylimidazole was confirmed. Two crystal complexes were obtained, 1:1 and 2:1, and the X-ray structure was determined for the 1:1 complex, which is monoclinic, space group $P2_1/c$, with a = 12.236(3) Å, b = 11.332(4) Å, c = 12.495(4) Å, and β = 120.67(1)°. The structure contains disk-shaped hydrogen-bonded tetramers with two molecules of each kind. There is a short NH···N hydrogen bond (2.82 Å) in which barbiturate provides the NH donor.

Keyphrases □ Barbital—complex with 1-methylimidazole, crystal structure determined □ 1-Methylimidazole—complex with barbital, crystal structure determined □ Complexes—barbital with 1-methylimidazole, crystal structure determined □ Crystal structure—determined for complex of barbital with 1-methylimidazole

Barbiturate drugs behave as strong hydrogen-bonding donors through their two NH groups but are weak acceptors through their three carbonyl oxygen atoms. These conclusions were derived from the hydrogen-bonding arrangements and interatomic distances observed in the crystal structures of a series of complexes of barbital with other small molecules representative of biological systems (1, 2). Thus, barbiturate drug receptor sites are likely to involve strongly electronegative hydrogen-bonding acceptor groups, such as the nitrogen atoms of adenine (3, 4), the imidazole ring in histidine or histamine (2), or the phosphoryl oxygen atoms of phospholipids (5).

These studies indicated that a strong hydrogen-bonding interaction would occur between barbital (5,5-diethylbarbituric acid) and 1-methylimidazole (Fig. 1), which might lead to crystal complexation. Indeed, 1-methylimidazole was a powerful solvent for barbital. The high viscosity of this solution made direct crystallization impractical. However, two crystal complexes were obtained from an ethanol solution; in one complex (1:1), crystal structure determination confirmed a short hydrogen bond NH···N (2.82 Å) in which barbital is the donor and 1-methylimidazole is the acceptor.

EXPERIMENTAL

Crystals of the 1:1 and 2:1 complexes were obtained from the same ethanolic solution, which was saturated at 60° with respect to both barbital and 1-methylimidazole, and slowly cooled in a sealed vial. Space groups and approximate cell data for these complexes were determined from X-ray precession photographs[1].

Crystals of the 1:1 complex, which dissociate at 96°, are monoclinic, space group $P2_1/c$, with a = 12.236(3) Å, b = 11.332(4) Å, c = 12.495(4) Å, and β = 120.67(1)°. The crystal density (1.190 g/cm^3) determined by

[1] No further work is planned on the 2:1 complex of barbital and 1-methylimidazole. These crystals are monoclinic, space group $P2_1/c$, with a = 16.7 Å, b = 12.1 Å, c = 12.4 Å, and β = 102°. There are eight barbital and four 1-methylimidazole molecules per unit cell.

0022-3549/79/0300-0361$01.00/0

© 1979, American Pharmaceutical Association

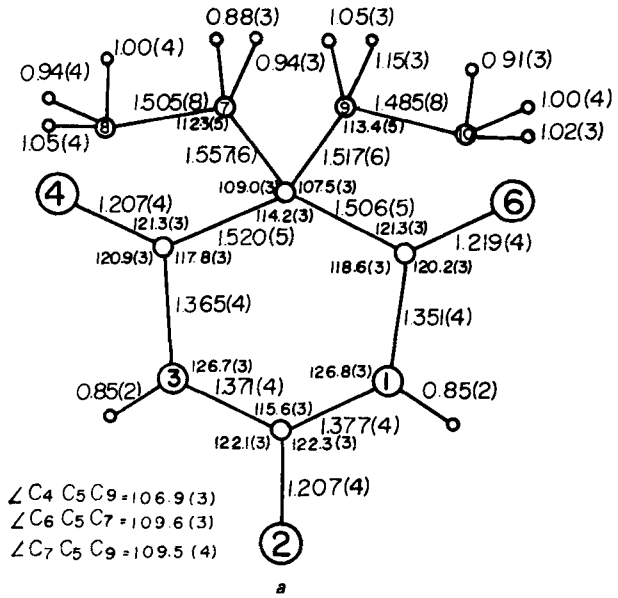

Figure 1 —*Bond lengths (angstroms) and angles (degrees) for barbital* (a) *and 1-methylimidazole* (b). *Estimated standard deviations are given in brackets. Circles of decreasing size represent oxygen, nitrogen, carbon, and hydrogen atoms, in that order.*

flotation in carbon tetrachloride–benzene agrees with the calculated density (1.187 g/cm^3), assuming that the unit cell contains four molecules of each kind.

The cell data and the X-ray intensities were measured at room temperature using a four-circle computer-controlled diffractometer[2] with graphite-monochromated MoKα-radiation (λ = 0.7093 Å). The crystal (0.32 × 0.22 × 0.20 mm) was mounted with the c-axis almost along the diffractometer Φ-axis. Integrated intensities for 2625 nonsymmetry related reflections were measured by $\theta/2\theta$ scans. The variance in an integrated intensity was assumed to be $\sigma^2(I) = \sigma^2 + (0.02I)^2$, where σ^2 is the variance due to counting statistics. There were 1887 reflections with an intensity greater than $2\sigma(I)$. No corrections were made for X-ray absorption or extinction.

The phase problem was solved by direct methods, using symbolic addition and tangent refinement procedures (6). The nonhydrogen atomic parameters obtained from an E-map were refined initially by block-diagonal least-squares methods. Nine of the 18 hydrogen atoms were readily found in a difference Fourier map. The remainder, which consisted mostly of terminal methyl hydrogen atoms, were found near the end of a full matrix least-squares refinement.

The function minimized by least squares was $\Sigma w_H \Delta_H^2$, where $\Delta_H = |F_{obs}| - |F_{calc}|$ and $w_H = 1/\sigma^2(F_{obs})$. Atomic scattering factors were those of Cromer and Waber (7) for nonhydrogen and of Stewart *et al.* (8) for hydrogen. The data were suspected to be subject to X-ray extinction since reflections with strong intensities and large d-spacings gave calculated structure amplitudes systematically larger than the observed values. In the final refinement, seven such reflections were omitted. The final R-

[2] Enraf-Nonius CAD-4.

Table I—Atomic Positional Parameters for the 1-Methylimidazole–Barbital Complex [a]

	x	y	z
	Nonhydrogen Atoms[b]—Barbital		
N(1)	5936 (2)	4106 (2)	6423 (2)
C(2)	4719 (3)	4016 (2)	6211 (3)
O(2)	3818 (2)	4452 (2)	5313 (2)
N(3)	4602 (2)	3424 (2)	7104 (2)
C(4)	5557 (3)	2909 (3)	8153 (3)
O(4)	5346 (2)	2439 (2)	8896 (2)
C(5)	6881 (3)	2908 (3)	8328 (3)
C(6)	6995 (3)	3611 (3)	7367 (3)
O(6)	8013 (2)	3727 (2)	7421 (2)
C(7)	7843 (4)	3384 (6)	9651 (4)
C(8)	7617 (5)	4663 (6)	9802 (4)
C(9)	7199 (4)	1635 (5)	8222 (5)
C(10)	6312 (5)	1093 (4)	6997 (5)
	Nonhydrogen Atoms[b]—1-Methylimidazole		
NI(1)	1138 (2)	2571 (2)	7773 (2)
CI(1)	807 (4)	1866 (4)	8538 (4)
CI(2)	2204 (3)	2479 (3)	7728 (3)
NI(3)	2230 (2)	3217 (2)	6957 (2)
CI(4)	1116 (3)	3825 (3)	6476 (3)
CI(5)	443 (3)	3436 (3)	6974 (3)
	Hydrogen Atoms[c]—Barbital		
H(1)	595 (2)	453 (2)	587 (2)
H(3)	386 (2)	340 (2)	700 (2)
H(71)	870 (3)	335 (3)	984 (2)
H(72)	773 (3)	301 (2)	1020 (3)
H(81)	786 (3)	519 (3)	931 (3)
H(82)	827 (4)	491 (3)	1059 (4)
H(83)	675 (3)	481 (3)	977 (3)
H(91)	715 (3)	118 (3)	893 (3)
H(92)	819 (3)	158 (3)	834 (3)
H(101)	659 (3)	34 (3)	701 (3)
H(102)	609 (3)	145 (3)	618 (3)
H(103)	535 (3)	100 (3)	653 (3)
	Hydrogen Atoms[c]—1-Methylimidazole		
HI(11)	0 (3)	165 (3)	814 (3)
HI(12)	84 (3)	242 (3)	913 (3)
HI(13)	140 (3)	127 (3)	903 (3)
HI(2)	283 (2)	192 (2)	821 (2)
HI(4)	92 (2)	446 (2)	583 (2)
HI(5)	966 (2)	363 (2)	684 (2)

[a] Positional parameters are given as fractions of the lattice translations. Estimated standard deviations given in parentheses refer to the least-significant figures in parameter values. [b] Positional parameters × 10^4. [c] Positional parameters × 10^3.

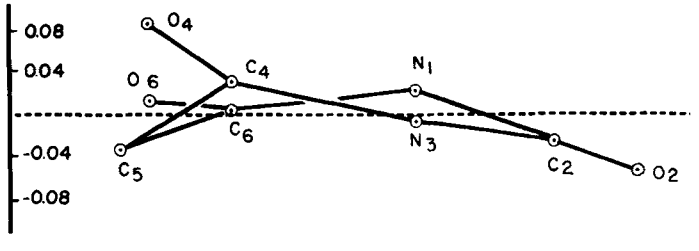

Figure 2—*Barbital ring. The dashed line is the trace of the best least-squares plane through the ring atoms. Atomic displacements from this plane (angstroms) are shown on a vertical scale eight times greater than the horizontal scale.*

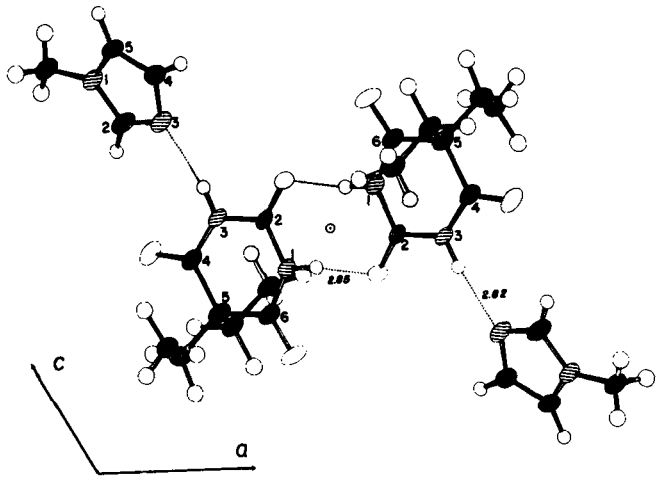

Figure 3—*Hydrogen-bonded tetramer. Thermal ellipsoids are shown that have 50% probability of enclosing each vibrating atom. Nitrogen atom ellipsoids are hatched, and carbon atom ellipsoids are cross-hatched. Hydrogen-bonded N···O and N···N distances (angstroms) are shown.*

factors were $R = \Sigma_H|\Delta_H|/\Sigma_H F_{obs} = 0.077$ and $R_w = [\Sigma_H(w\Delta_H)^2/\Sigma_H(wF_{obs})^2]^{1/2} = 0.034$. A list of observed and calculated structure factors and a table of anisotropic temperature factors for nonhydrogen atoms were compiled[3]. Final atomic positional parameters are given in Table I.

DISCUSSION

Bond lengths and angles (Fig. 1) agree with those in the barbital–imidazole complex (2) within the limits of experimental error. The barbital ring atoms are in an almost coplanar conformation (Fig. 2) similar to that observed in a number of other barbiturate crystal structures (Fig. 3 in Ref. 9). The ethyl group carbon atoms and the ring atom C(5) in barbital are almost coplanar, with atom C(2) having the largest displacement (0.065 Å) from the least-squares plane. This coplanar group and the ring plane make a dihedral angle of 91.7°. In 1-methylimidazole, the imidazole ring atoms and the 1-methyl carbon atom are coplanar.

The most interesting feature in the structure is the formation of hydrogen-bonded tetramers consisting of two molecules of each kind (Fig. 3). Two barbital molecules related by a crystallographic center of symmetry form N(1)H···O(2) hydrogen bonds with N···O distance (2.85 Å). This distance is within the range (2.8–3.0 Å) observed for other hydrogen bonds between barbiturates (1). The other barbital N(3)H donor group forms a very short hydrogen bond (N···N, 2.82 Å) with the nitrogen acceptor atom of 1-methylimidazole (2). The NH···N angle is 172°. The barbiturate and imidazole rings of molecules that form a tetramer are at dihedral angles of 19.1°. The tetramers are thus disk shaped, with nonpolar groups forming most of the outer surface. There is an unusual CH···O interaction between tetramers (C···O distance, 3.31 Å; CH···O angle 154.1°) involving the 1-methylimidazole C(5)–H(5) group and barbiturate atom O(6). This interaction is not considered to be a hydrogen bond because the C···O distance is too long.

The hydrogen-bonding arrangement is quite different from that of the imidazole complex with barbital. In that complex, barbitals dimerize through NH···O hydrogen bonds involving O(6) rather than O(2). These dimers are cross-linked by hydrogen bonds formed at opposite sides of imidazole molecules to make infinite ribbons through the crystal structure. The important feature common to both crystal complexes is the short NH···N hydrogen bond (N···N distance, 2.78 Å in the imidazole complex) in which barbiturate is the donor.

Thus, the present crystal structure fits a pattern of behavior in which barbiturate NH groups form strong hydrogen bonds with acceptor groups in other molecules.

[3] Available on request from authors.

REFERENCES

(1) G. L. Gartland and B. M. Craven, *Acta Crystallogr.*, **B30**, 980 (1974).

(2) I. N. Hsu and B. M. Craven, *ibid.*, **B30**, 988 (1974).

(3) S. H. Kim and A. Rich, *Proc. Natl. Acad. Sci. USA*, **60**, 402 (1968).

(4) D. Voet, *J. Am. Chem. Soc.*, **94**, 8213 (1972).

(5) I. N. Hsu and B. M. Craven, *Acta Crystallogr.*, **B30**, 1299 (1974).

(6) J. Karle and I. L. Karle, *ibid.*, **21**, 849 (1966).

(7) D. T. Cromer and J. T. Waber, *ibid.*, **18**, 104 (1965).

(8) R. F. Stewart, E. R. Davidson, and W. T. Simpson, *J. Chem. Phys.*, **43**, 3175 (1965).

(9) B. M. Craven, C. Cusatis, G. L. Gartland, and E. A. Vizzini, *J. Mol. Struct.*, **16**, 331 (1973).

ACKNOWLEDGMENTS

Supported by Grant GM-22548 from the U.S. Public Health Service, National Institutes of Health.

TLC Determination of Biotin in a Lyophilized Multivitamin Preparation

KERSTIN GRÖNINGSSON ˣ **and LARS JANSSON**

Received December 12, 1977, from the *Analytical Chemistry Research Department, AB Kabi, S-112 87 Stockholm, Sweden.* Accepted for publication August 7, 1978.

Abstract □ A TLC method for the determination of biotin was developed. The method is selective and sensitive and permits the determination of biotin in the presence of all water-soluble vitamins as well as glycine, edetate sodium, and methylparaben. The main steps are: dissolution of the lyophilized multivitamin preparation in water, addition of the internal standard, application on a thin-layer plate, separation from interfering components, visualization by spraying with 4-dimethylaminocinnamaldehyde, and *in situ* determination by reflectance measurements. Spraying the plate with paraffin after the coloring procedure increases the sensitivity of the method. The coefficient of variation is 2.3% with 0.15 μg of biotin/spot. Quantities as low as 10 ng/spot can be determined.

Keyphrases □ Biotin—TLC analysis in lyophilized multivitamin preparation □ TLC—analysis, biotin in lyophilized multivitamin preparation □ Vitamins—biotin, TLC analysis in lyophilized multivitamin preparation

Microbiological methods generally are used to determine biotin in small amounts (1–5), but bioassays also have been used (6). The chemical and physicochemical methods are spectrophotometric assays based on the binding of a dye by avidin (7), oxidation with potassium iodate (8), or reaction with 4-dimethylaminocinnamaldehyde (9, 10). GLC after silylation with bis(trimethylsilyl)acetamide (11–14), polarography (15, 16), and isotope dilution (9, 17, 18) also are used.

None of the chemical and physicochemical methods was applicable to a lyophilized multivitamin preparation because of a lack of sensitivity or interference from other components. However, the use of 4-dimethylaminocinnamaldehyde as a spray reagent for biotin after separation by TLC or paper chromatography has been proposed (9, 19). This paper reports the conditions for *in situ* quantitation of biotin in a complex mixture after TLC separation and coloration with 4-dimethylaminocinnamaldehyde.

EXPERIMENTAL

Apparatus—A dual-wavelength chromatogram scanner[1] was used in the *in situ* reflection measurements. Sample and reference wavelengths were 530 and 400 nm, respectively. The scanning was performed in the zig-zag mode at 10 mm/min with a 1.25 × 1.25-mm slit. A two-channel[2] recorder, range 10–20 mv, also was used.

Silica gel 60 precoated plates[3] (20 × 20 cm) were developed in a sealed chromatographic chamber, lined with filter paper to obtain a saturated atmosphere. A polytef-tipped 10-μl syringe[4] and a home-made precision device were used to obtain reproducible spotting of the sample and standard solutions on the plates.

The coloring reagent and paraffin solution were applied with all-glass sprayers.

Substances and Reagents—The biotin[5] (I) standard solution contained 0.12 mg/ml of water, and the 2-imidazolidone[5] (II) internal standard solution contained 0.15 mg/ml of water. The eluent was chloroform[3]–methanol[3]–formic acid[3] (70:40:2, v/v/v).

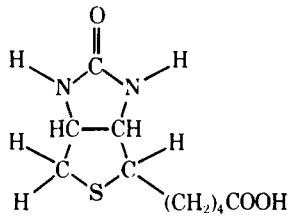

I

The reagent spray solution contained a mixture of 0.1% (w/v) 4-dimethylaminocinnamaldehyde[6] and 1% (v/v) sulfuric acid in ethanol. The paraffin spray solution contained 10% (v/v) liquid paraffin USP in chloroform[3].

Preparation of Sample and Standard Solutions—To separate 10-ml volumetric flasks were transferred 1.00, 2.00, 3.00, and 4.00 ml of biotin standard solution. Then 0.50 ml of internal standard solution was added to each flask, and the contents were diluted to the mark with water.

To the sample bottle containing the lyophilized multivitamin powder, 0.50 ml of internal standard solution and 9.50 ml of water were added. The bottle was shaken to dissolve the powder.

TLC—Aliquots of 5 μl of sample and standard solutions were applied to the TLC plate, 2 cm from the lower edge, and the spots were dried carefully. The chromatogram was developed in a saturated atmosphere (saturation overnight), and the solvent front migrated 15 cm above the application line.

After removal of the plate from the chamber, it was dried in a stream of cold air for about 5 min and then sprayed homogeneously with reagent solution until the spots appeared distinct red to red-violet. After the plate was again blown with a stream of cold air for about 5 min, it was sprayed homogeneously with paraffin solution until there was no visual increase in color intensity. ("Wet" layers were avoided.) Chloroform was removed from the plate with a stream of cold air. The chromatogram was scanned

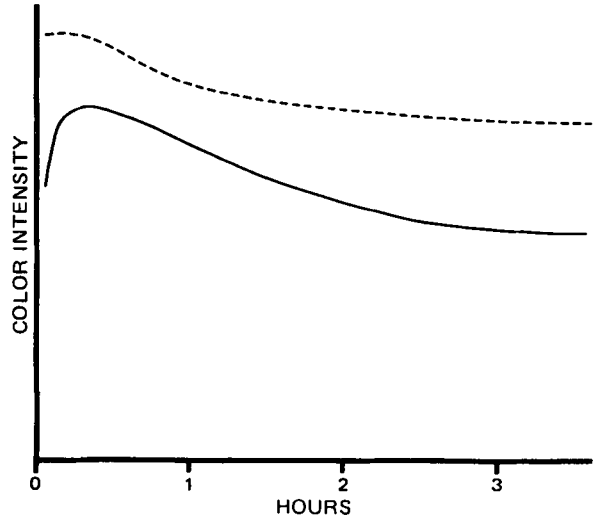

Figure 1—*Color development after spraying with 4-dimethylaminocinnamaldehyde. The color intensity was measured as the peak area at 530 nm. Key: —, biotin; and - - -, 2-imidazolidone.*

[1] Model CS-900, equipped with a background correction unit (BCU-1), Shimadzu, Tokyo, Japan.
[2] Servogor 320, Goerz Electro G.m.b.H., Vienna, Austria.
[3] E. Merck, Darmstadt, West Germany.
[4] Unimetrics Corp., Anaheim, Calif.
[5] Fluka AG., Buchs, Switzerland.
[6] Sigma Chemical Co., St. Louis, Mo.

0022-3549/79/0300-0364$01.00/0
© 1979, American Pharmaceutical Association

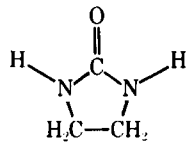

II

in the direction of the development 4 hr after spraying with paraffin solution.

A standard graph was plotted with the peak area ratio of biotin to the internal standard as the ordinate against the total amount of biotin in the standard solutions. By using the peak area ratio of the sample, the amount of biotin in the sample bottle was obtained directly from this standard graph.

RESULTS AND DISCUSSION

Color Reaction—Biotin (I) and other cyclic ureido compounds react with 4-dimethylaminocinnamaldehyde in nonaqueous media (or on dry chromatograms) to form Schiff bases (9). This reaction is stereospecific and involves the less sterically hindered N_1 of the ureido portion of biotin. The monocyclic ureide, 2-imidazolidone (II), used as an internal standard, is less hindered sterically and gives a more intense color than biotin.

The composition of the lyophilized multivitamin preparation is given in Table I. A colorimetric determination of biotin with 4-dimethylaminocinnamaldehyde added directly to the sample mixture, as described by Shimada *et al.* (9), failed because of interference from the other components. However, 4-dimethylaminocinnamaldehyde appeared to be an excellent reagent for visualization of biotin and 2-imidazolidone after separation from interfering components on silica gel thin-layer plates, where they were seen as red and red-violet spots, respectively. Attempts to perform the reaction before chromatography and subsequent separation of the products failed because of color instability and nonhomogeneous spots.

Figure 1 shows the color development of TLC spots after spraying with 4-dimethylaminocinnamaldehyde and paraffin. Maximum color intensity was reached after 20–25 min for biotin and after 5–10 min for 2-imidazolidone. The relation between color intensities of equimolar amounts of 2-imidazolidone and biotin was about 3:2. The color faded with time but seemed to stabilize after about 3–4 hr. In fact, spots scanned after more than 24 hr showed about the same intensity as after 3–4 hr. Spraying with paraffin increased the color intensity measured at 530 nm about three times and stabilized (prevented discoloration of) the background.

Table I—Composition of the Lyophilized Multivitamin Preparation

Compound	Milligrams per Flask
Thiamine mononitrate	1.24
Riboflavin phosphate (sodium)	2.47
Niacinamide	10
Pyridoxine hydrochloride	2.43
Sodium pantothenate	11
Sodium ascorbate	34
Biotin	0.3
Folic acid	0.2
Cyanocobalamin	0.002
Glycine	100
Edetate sodium	0.5
Methylparaben	0.5

Table II—Quantitative Results from Repeated Determinations of a Lyophilized Vitamin Sample

Number[a]	Milligrams of Biotin per Flask[b]
1	0.356
2	0.339
3	0.345
4	0.350
5	0.350
6	0.335
7	0.346
8	0.354
9	0.340
10	0.332
Mean	0.345
CV, %	2.3
Recovery, %[c]	101

[a] Different thin-layer plates. [b] Mean of two sample spots per plate. [c] Obtained by addition of biotin to a standard vitamin mixture (see Table I).

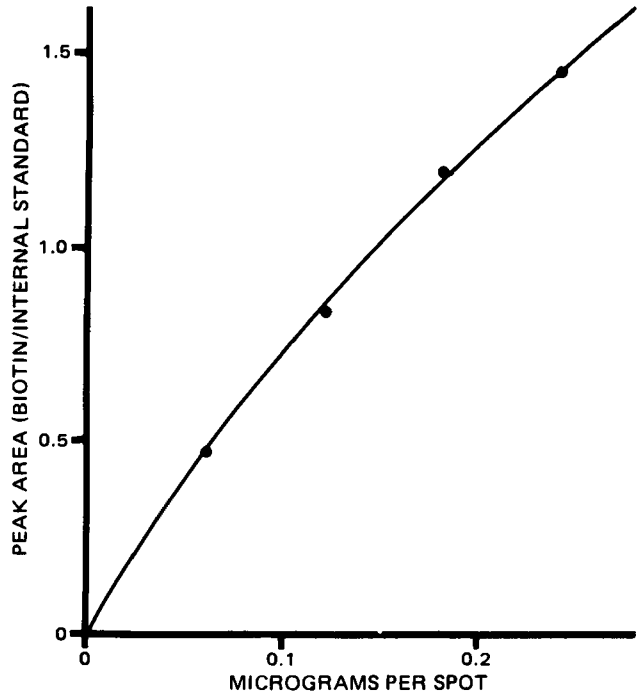

Figure 2—*Standard graph of biotin after spraying with 4-dimethylaminocinnamaldehyde and liquid paraffin;* λ_{sample} = *530 nm and* $\lambda_{reference}$ = *400 nm. Scanning was in the zig-zag mode.*

TLC Procedure—The atmosphere in the chromatographic chamber must be carefully saturated. It was convenient to saturate overnight. Incomplete saturation caused tailing (or at least asymmetrical) spots and incomplete separation between biotin and the internal standard. Furthermore, the composition of the eluent was critical for the separation.

The relative R_f (biotin to internal standard) was about 1.2, with the R_f values of biotin and internal standard being approximately 0.55 and 0.45, respectively. Separation was somewhat reduced in the presence of the sample components because of a slight change in shape of the biotin spot. The addition of glycine (Table I) to the standard solutions did not affect the spot shape remarkably. Niacinamide migrated between biotin and the internal standard, and sodium pantothenate migrated closely above the biotin spot in the chromatogram. However, they did not interfere in the determinations since they did not react with 4-dimethylaminocinnamaldehyde.

***In Situ* Quantitation**—Quantitation was performed by scanning in the reflectance mode. Because of the differences in spot shape already mentioned, zig-zag scanning yielded the most accurate results (20). Measurements in the transmission mode increased the sensitivity by a factor of about two; but due to higher background disturbances, the reflectance mode was chosen.

The standard graph (Fig. 2) is slightly curved. The reason for this nonlinearity was discussed previously (20–22).

The recovery of the method was determined by addition of a known amount of biotin to a standard vitamin mixture. The precision was calculated from repeated determinations of a sample solution. The results are presented in Table II. Biotin was recovered completely and could be determined with good precision without interference from the other components.

REFERENCES

(1) G. G. Villela and A. Cury, *Proc. Soc. Exp. Biol. Med.*, **76**, 341 (1951).

(2) L. D. Wright and H. R. Skeggs, *ibid.*, **56**, 95 (1944).

(3) M. Landy and D. M. Dicken, *J. Lab. Clin. Med.*, **27**, 1086 (1942).

(4) L. Atkin, A. S. Schultz, W. L. Williams, and C. N. Frey, *Ind. Eng. Chem. Anal. Ed.*, **15**, 141 (1943).
(5) J. G. Bell, *Lab. Pract.*, **23**, 235 (1974).
(6) C. I. Bliss and P. György, in "Vitamin Methods," vol. 1, P. György, Ed., Academic, New York, N.Y., 1951, p. 228.
(7) N. M. Green, *Biochem. J.*, **94**, 23 C (1965).
(8) C. Plinton, F. P. Mahn, M. Hawrylyshyn, V. S. Venturella, and B. Z. Senkowski, *J. Pharm. Sci.*, **58**, 875 (1969).
(9) K. Shimada, Y. Naganese, and U. Matsumoto, *Yakugaku Zasshi*, **89**, 436 (1969).
(10) D. B. McCormick and J. A. Roth, *Anal. Biochem.*, **34**, 226 (1970).
(11) M. C. Horning, E. A. Boucher, and A. M. Moos, *J. Gas Chromatogr.*, **5**, 297 (1967).
(12) V. Viswanathan, F. P. Mahn, V. S. Venturella, and B. Z. Senkowski, *J. Pharm. Sci.*, **59**, 400 (1970).
(13) H. Janecke and H. Voege, *Naturwissenschaften*, **55**, 447 (1968).
(14) H. Janecke and H. Voege, *Fresenius Z. Anal. Chem.*, **254**, 355 (1971).
(15) A. Serna, J. Vera, and D. Marin, *J. Electroanal. Chem. Interfacial Electrochem.*, **45**, 156 (1973).
(16) J. Davídek, *Naturwissenschaften*, **48**, 403 (1961).
(17) K. Shimada, U. Matsumoto, and Y. Nagase, *Yakugaku Zasshi*, **92**, 575 (1972).
(18) K. Dakshinamurti, A. D. Landman, L. Ramamurti, and R. J. Constable, *Anal. Biochem.*, **61**, 225 (1974).
(19) L. Reio, *J. Chromatogr.*, **47**, 60 (1970).
(20) H. Yamamoto, T. Kurita, J. Suzuki, R. Hira, K. Nakano, and H. Makabe, *ibid.*, **116**, 29 (1976).
(21) L. Treiber, *ibid.*, **100**, 123 (1974).
(22) L. Treiber, *ibid.*, **123**, 23 (1976).

Determination of Ketoprofen by Direct Injection of Deproteinized Body Fluids into a High-Pressure Liquid Chromatographic System

R. BALLERINI, A. CAMBI, P. DEL SOLDATO, F. MELANI, and A. MELI ˣ

Received April 24, 1978, from *"A. Menarini" Pharmaceuticals, Via Sette Santi 1, 50131 Florence, Italy.* Accepted for publication August 11, 1978.

Abstract □ A rapid, sensitive, and specific determination of ketoprofen in human and animal deproteinized body fluids by reversed-phase high-pressure liquid chromatography is presented. The acid is detectable in amounts as low as 0.1 μg/ml. Limits of error are in the range of ±5.1% of the sample mean.

Keyphrases □ Ketoprofen—high-pressure liquid chromatographic analysis in various body fluids □ High-pressure liquid chromatography—analysis, ketoprofen in various body fluids □ Anti-inflammatory agents—ketoprofen, high-pressure liquid chromatographic analysis in various body fluids

A TLC procedure (1) for the determination of ketoprofen, 2-(3-benzoylphenyl)propionic acid, in body fluids overcame most limitations of other procedures (2). The search for new methods to shorten the time required to perform analyses and to improve sensitivity led to the present high-pressure liquid chromatographic (HPLC) procedure.

EXPERIMENTAL

Apparatus and Operating Conditions—A high-pressure liquid chromatograph[1] was equipped with two independent pumps, a reversed-phase column[2] (0.25 m × 4 mm), a variable wavelength spectrophotometer[3] to monitor the column effluent, and a liquid chromatograph terminal[4] to program chromatography conditions and record and integrate peak areas. Operating conditions were adjusted to give a mobile phase flow rate of 0.8 ml/min (operating resulting pressure of 32–38 atm). The column oven temperature was set at 40°. The detector wavelength was 255 nm (for quantitative evaluation) or 205 nm (for qualitative evaluation of metabolites).

Table I—Recovery of Ketoprofen Added to Human Plasma as Compared to Ketoprofen Dissolved in Phosphate Buffer (255 nm)

Ketoprofen Added, μg/ml	Relative Area		Recovery, %
	Buffer	Plasma	
1	16.760	13.946	83.9
	16.500	13.685	
	17.040	13.750	
	15.500	13.800	
	16.450	13.795	
2	33.000	31.822	90.4
	34.590	29.370	
	35.670	29.582	
	32.730	32.103	
	33.998	30.719	
4	68.700	64.428	90.3
	72.400	63.862	
	71.500	61.596	
	71.100	65.844	
	70.800	63.933	
8	140.320	127.430	90.7
	139.570	128.010	
	139.870	127.100	
	142.010	126.750	
	140.443	127.323	

Reagents—Methanol[5] for HPLC was used as received. Double-distilled water was filtered through a 0.2-μm pore size membrane filter[6]. The mobile phase was double-distilled water–methanol (85:15).

Preparation of Standards—Ketoprofen was dissolved in 96% ethanol or 0.15 *M* phosphate buffer at pH 8. Aliquots of ethanolic solutions equivalent to 1, 2, 4, and 8 μg were placed in glass-stoppered centrifuge tubes and evaporated to dryness under a gentle nitrogen stream. Then 1 ml of untreated body fluid was added to each tube and mixed well.

[1] Hewlett-Packard 1084A.
[2] Hewlett-Packard RP8-79918A.
[3] Hewlett-Packard 1030B.
[4] Hewlett-Packard 79850A.
[5] Merck.
[6] Sartorius type SM 11307.

0022-3549/79/0300-0366$01.00/0
© 1979, American Pharmaceutical Association

(4) L. Atkin, A. S. Schultz, W. L. Williams, and C. N. Frey, *Ind. Eng. Chem. Anal. Ed.*, **15**, 141 (1943).
(5) J. G. Bell, *Lab. Pract.*, **23**, 235 (1974).
(6) C. I. Bliss and P. György, in "Vitamin Methods," vol. 1, P. György, Ed., Academic, New York, N.Y., 1951, p. 228.
(7) N. M. Green, *Biochem. J.*, **94**, 23 C (1965).
(8) C. Plinton, F. P. Mahn, M. Hawrylyshyn, V. S. Venturella, and B. Z. Senkowski, *J. Pharm. Sci.*, **58**, 875 (1969).
(9) K. Shimada, Y. Naganese, and U. Matsumoto, *Yakugaku Zasshi*, **89**, 436 (1969).
(10) D. B. McCormick and J. A. Roth, *Anal. Biochem.*, **34**, 226 (1970).
(11) M. C. Horning, E. A. Boucher, and A. M. Moos, *J. Gas Chromatogr.*, **5**, 297 (1967).
(12) V. Viswanathan, F. P. Mahn, V. S. Venturella, and B. Z. Senkowski, *J. Pharm. Sci.*, **59**, 400 (1970).
(13) H. Janecke and H. Voege, *Naturwissenschaften*, **55**, 447 (1968).
(14) H. Janecke and H. Voege, *Fresenius Z. Anal. Chem.*, **254**, 355 (1971).
(15) A. Serna, J. Vera, and D. Marin, *J. Electroanal. Chem. Interfacial Electrochem.*, **45**, 156 (1973).
(16) J. Davídek, *Naturwissenschaften*, **48**, 403 (1961).
(17) K. Shimada, U. Matsumoto, and Y. Nagase, *Yakugaku Zasshi*, **92**, 575 (1972).
(18) K. Dakshinamurti, A. D. Landman, L. Ramamurti, and R. J. Constable, *Anal. Biochem.*, **61**, 225 (1974).
(19) L. Reio, *J. Chromatogr.*, **47**, 60 (1970).
(20) H. Yamamoto, T. Kurita, J. Suzuki, R. Hira, K. Nakano, and H. Makabe, *ibid.*, **116**, 29 (1976).
(21) L. Treiber, *ibid.*, **100**, 123 (1974).
(22) L. Treiber, *ibid.*, **123**, 23 (1976).

Determination of Ketoprofen by Direct Injection of Deproteinized Body Fluids into a High-Pressure Liquid Chromatographic System

R. BALLERINI, A. CAMBI, P. DEL SOLDATO, F. MELANI, and A. MELI ˣ

Received April 24, 1978, from *"A. Menarini" Pharmaceuticals, Via Sette Santi 1, 50131 Florence, Italy.* Accepted for publication August 11, 1978.

Abstract □ A rapid, sensitive, and specific determination of ketoprofen in human and animal deproteinized body fluids by reversed-phase high-pressure liquid chromatography is presented. The acid is detectable in amounts as low as 0.1 μg/ml. Limits of error are in the range of ±5.1% of the sample mean.

Keyphrases □ Ketoprofen—high-pressure liquid chromatographic analysis in various body fluids □ High-pressure liquid chromatography—analysis, ketoprofen in various body fluids □ Anti-inflammatory agents—ketoprofen, high-pressure liquid chromatographic analysis in various body fluids

A TLC procedure (1) for the determination of ketoprofen, 2-(3-benzoylphenyl)propionic acid, in body fluids overcame most limitations of other procedures (2). The search for new methods to shorten the time required to perform analyses and to improve sensitivity led to the present high-pressure liquid chromatographic (HPLC) procedure.

EXPERIMENTAL

Apparatus and Operating Conditions—A high-pressure liquid chromatograph[1] was equipped with two independent pumps, a reversed-phase column[2] (0.25 m × 4 mm), a variable wavelength spectrophotometer[3] to monitor the column effluent, and a liquid chromatograph terminal[4] to program chromatography conditions and record and integrate peak areas. Operating conditions were adjusted to give a mobile phase flow rate of 0.8 ml/min (operating resulting pressure of 32–38 atm). The column oven temperature was set at 40°. The detector wavelength was 255 nm (for quantitative evaluation) or 205 nm (for qualitative evaluation of metabolites).

Table I—Recovery of Ketoprofen Added to Human Plasma as Compared to Ketoprofen Dissolved in Phosphate Buffer (255 nm)

Ketoprofen Added, μg/ml	Relative Area		Recovery, %
	Buffer	Plasma	
1	16.760	13.946	83.9
	16.500	13.685	
	17.040	13.750	
	15.500	13.800	
	16.450	13.795	
2	33.000	31.822	90.4
	34.590	29.370	
	35.670	29.582	
	32.730	32.103	
	33.998	30.719	
4	68.700	64.428	90.3
	72.400	63.862	
	71.500	61.596	
	71.100	65.844	
	70.800	63.933	
8	140.320	127.430	90.7
	139.570	128.010	
	139.870	127.100	
	142.010	126.750	
	140.443	127.323	

Reagents—Methanol[5] for HPLC was used as received. Double-distilled water was filtered through a 0.2-μm pore size membrane filter[6]. The mobile phase was double-distilled water–methanol (85:15).

Preparation of Standards—Ketoprofen was dissolved in 96% ethanol or 0.15 *M* phosphate buffer at pH 8. Aliquots of ethanolic solutions equivalent to 1, 2, 4, and 8 μg were placed in glass-stoppered centrifuge tubes and evaporated to dryness under a gentle nitrogen stream. Then 1 ml of untreated body fluid was added to each tube and mixed well.

[1] Hewlett-Packard 1084A.
[2] Hewlett-Packard RP8-79918A.
[3] Hewlett-Packard 1030B.
[4] Hewlett-Packard 79850A.
[5] Merck.
[6] Sartorius type SM 11307.

0022-3549/79/0300-0366$01.00/0
© 1979, American Pharmaceutical Association

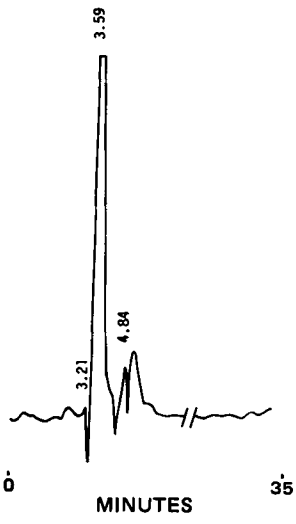

Figure 1—*Chromatogram of untreated deproteinized human plasma. The attenuation was 2^6 (64×10^{-4}/aufs), and the slope sensitivity was 0.45. UV monitoring was at 255 nm.*

These standards and the appropriate blanks were handled in the same manner as body specimens. For recovery determination, the same aliquots of standard dissolved in phosphate buffer were injected into the chromatograph without any manipulation.

Preparation of Sample—A 1-ml aliquot of human or rat plasma or rat inflammatory exudate [prepared according to Fukuhara and Tsurufuji (3)] was mixed with 10 ml of absolute ethanol and centrifuged at 2000 rpm for approximately 10 min. The supernate was flash evaporated to dryness and taken up with 1 ml of 0.15 *M* phosphate buffer at pH 8. The sample was shaken for 20 min at 37°, cooled, and filtered through a 0.2-μm pore size membrane filter. A 50-μl aliquot of the filtrate was injected in the chromatograph.

Increased sensitivity could be obtained by taking up the sample with 0.5 ml of phosphate buffer and filtering it through a homemade filter having a dead volume of only 100 μl and/or injecting 200 μl of the filtrate into the chromatograph instead of the customary 50 μl.

Calculation—Calibration curves were prepared by plotting the integrated areas of standards against the relative concentrations. Values for unknown concentrations of ketoprofen in biological specimens were calculated from the slope of the standard curve.

Column Purge—To preserve column efficiency daily after analyses, it was advantageous to set the oven temperature at 55° and to wash the column with double-distilled water for 10 min, with water–methanol (1:1) for 10 min, and with methanol for 10 min.

Precision Parameter Determination—To assess the precision of the assay, 10 complete determinations were carried out on the same day on one rat plasma sample collected 1 hr after oral ketoprofen.

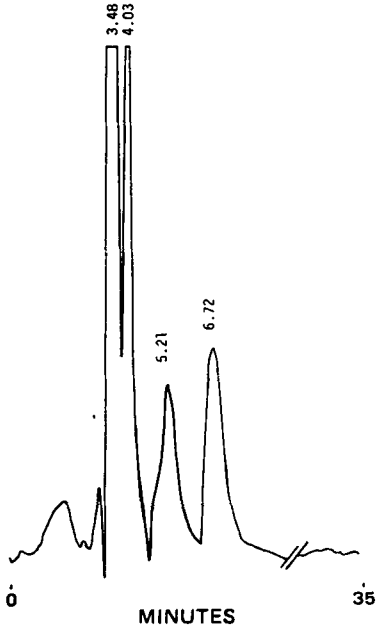

Figure 2—*Chromatogram of untreated deproteinized human plasma. UV monitoring was at 205 nm.*

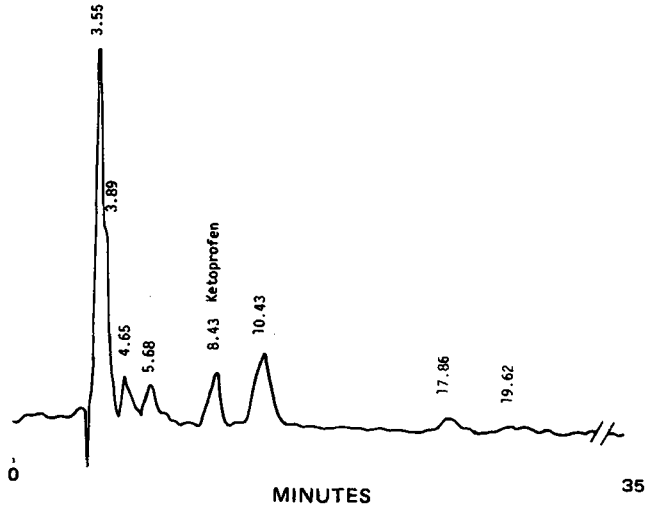

Figure 3—*Chromatogram of deproteinized human plasma 1 hr after oral administration of ketoprofen. UV monitoring was at 255 nm.*

Limits of error of the sample mean were calculated from the relative standard deviation according to Saunders and Fleming (4).

Clinical Utility of Assay—To evaluate the clinical utility of the present procedure, plasma samples from five patients receiving ketoprofen at 40 mg po were assayed.

RESULTS AND DISCUSSION

Percent recoveries of known amounts of ketoprofen added to plasma are shown in Table I. Chromatograms of untreated human plasma at 255 and 205 nm are shown in Figs. 1 and 2, respectively. In Figs. 3 and 4, chromatograms obtained at 255 and 205 nm, respectively, show typical profiles of ketoprofen in human plasma 1 hr following administration.

The method is sensitive enough to reveal ketoprofen in concentrations as low as 0.1 μg/ml of body fluids. Limits of error were in the range of ±5.1% of the sample mean. Human plasma levels (mean ± *SE*) of ketoprofen at 1 and 2 hr following administration were 3.2 ± 0.4 and 2.8 ± 0.3 μg/ml, respectively.

Reversed-phase HPLC is particularly useful for the analysis of body fluids because endogenous polar components elute first and column efficiency is preserved. These characteristics permitted the development of an analytical procedure without time-consuming purification and extraction. In fact, it was sufficient to remove plasma protein that could subsequently interfere with the efficiency of the analytical system.

Body fluids other than plasma and inflammatory exudate were examined including human synovial fluid and rat bile, feces, and urine for which, however, further extraction and purifications steps were necessary.

Although 255 nm was used for quantitative evaluation, examination

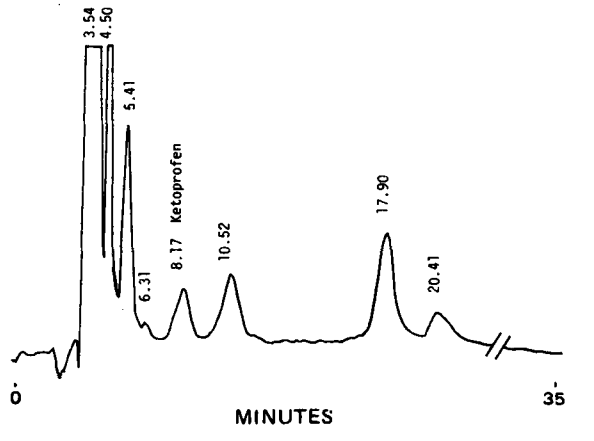

Figure 4—*Chromatogram of deproteinized human plasma 1 hr after oral administration of ketoprofen. UV monitoring was at 205 nm.*

of samples at 205 nm gave interesting qualitative information on the presence of metabolites of ketoprofen. In fact, at 205 nm, the number of metabolites detected was greater than at 255 nm. Such metabolites show a kinetic behavior quite dissimilar from that of ketoprofen. Previous work (5) supports the assumption that area peaks (detected at 205 and 255 nm) having a retention time longer than that of ketoprofen can be referred to hydroxylated metabolites whereas area peaks detectable only at 205 nm can be referred to compounds with modified unsaturated system.

This procedure appears to be useful for studies of separation and characterization of these metabolites. It also has the advantage of rapidity since a technician can process 20–30 samples in 1 day with an automatic sampler and a minimum of active involvement. In conclusion, high sensitivity, specificity, and rapidity, coupled with the ability to separate unchanged ketoprofen from its metabolites, make this procedure particularly suitable for study of the pharmacokinetics of ketoprofen in humans.

REFERENCES

(1) R. Ballerini, A. Cambi, and P. Del Soldato, *J. Pharm. Sci.*, **66**, 281 (1977).

(2) P. Populaire, B. Terlain, S. Pascal, B. Decouvelaere, G. Lebreton, A. Renard, and J. P. Thomas, *Ann. Pharm. Fr.*, **31**, 679 (1973).

(3) M. Fukuhara and S. Tsurufuji, *Biochem. Pharmacol.*, **18**, 475 (1969).

(4) L. Saunders and R. Fleming, "Mathematics and Statistics," Pharmaceutical Press, London, England, 1971, p. 179.

(5) P. Populaire, B. Terlain, S. Pascal, B. Decouvelaere, A. Renard, and J. P. Thomas, *Ann. Pharm. Fr.*, **31**, 735 (1973).

ACKNOWLEDGMENTS

The authors are indebted to Mr. A. Stocchi for assistance.

Light Stability of Norethindrone and Ethinyl Estradiol Formulated with FD&C Colorants

E. E. KAMINSKI ˣ, R. M. COHN, J. L. McGUIRE, and J. T. CARSTENSEN *

Received August 18, 1977, from the *Research Laboratories, Ortho Pharmaceutical Corporation, Raritan, NJ 08869.* Accepted for publication August 4, 1978. *Present address: School of Pharmacy, University of Wisconsin, Madison, WI 53706.

Abstract □ In general, light-sensitive tablets exhibit discoloration in the surface layer(s) only. A case is discussed where a quantitative interaction between a drug, ethinyl estradiol (in a combination tablet containing norethindrone and ethinyl estradiol), and a dye (FD&C Red No. 3) occurs, and discoloration exists throughout the tablet. The data suggest that accelerated light studies should be carried further than those dictated by predictive periods so that equilibrium levels can be deduced.

Keyphrases □ Norethindrone—stability in tablets, effect of FD&C dyes □ Ethinyl estradiol—stability in tablets, effect of FD&C dyes □ Dyes, FD&C—effect on stability of norethindrone and ethinyl estradiol in tablets □ Stability—norethindrone and ethinyl estradiol in tablets, effect of FD&C dyes □ Tablets—norethindrone and ethinyl estradiol, effect of FD&C dyes on stability

Drug stability in solution can be affected adversely by the presence of a colorant (1). Since colors are used routinely to identify solid dosage forms, a study was initiated to determine whether such reactions could occur with compressed tablets. Although there are no compendial or regulatory procedures to evaluate the effect of light, previous reports (2) correlated accelerated light studies with ordinary room light exposure.

Reported interactions between light and substances in solid dosage forms usually were confined to the top layer(s) of the tablet (3–5) and occurred when a single component was photosensitive. Photo-induced drug interactions in solid form have not been reported.

This report presents results of studies on the stability of norethindrone and ethinyl estradiol in uncolored compressed tablets as well as in tablets containing selected FD&C colorants when exposed to accelerated light stress.

EXPERIMENTAL

Tablets—All tablets contained 0.5 mg of norethindrone and 0.035 mg of ethinyl estradiol and were prepared with the same excipients by classical granulation techniques. Three formulas were prepared: pink, containing 4.5 μg of erythrosine (FD&C Red No. 3)/tablet; white, containing no colorant; and orange, containing 30 μg of the disodium salt of 1-*p*-sulfophenylazo-2-naphthol-6-sulfonic acid (FD&C Yellow No. 6)/tablet.

The dyes were added in a methanolic solution to the basic excipient system. The uncolored tablets were processed with the same amount of methanol as used in the tablets containing a colorant. All tablets were then dried, screened, lubricated, blended, and compressed in similar fashions.

Analytical Methods—Single tablets were disintegrated and then dissolved in a homogenizer with methanol as the solvent. The solution containing the dissolved steroids was filtered and divided into two

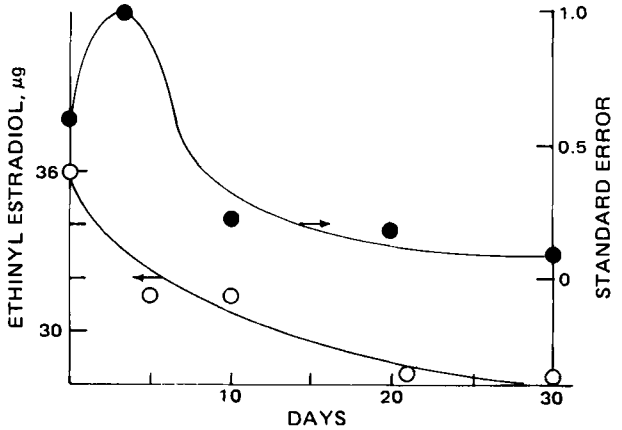

Figure 1—*Ethinyl estradiol assays as a function of time (left scale, open circles) and standard error of the assay mean as a function of time (right scale, closed circles).*

0022-3549/79/0300-0368$01.00/0

© 1979, American Pharmaceutical Association

of samples at 205 nm gave interesting qualitative information on the presence of metabolites of ketoprofen. In fact, at 205 nm, the number of metabolites detected was greater than at 255 nm. Such metabolites show a kinetic behavior quite dissimilar from that of ketoprofen. Previous work (5) supports the assumption that area peaks (detected at 205 and 255 nm) having a retention time longer than that of ketoprofen can be referred to hydroxylated metabolites whereas area peaks detectable only at 205 nm can be referred to compounds with modified unsaturated system.

This procedure appears to be useful for studies of separation and characterization of these metabolites. It also has the advantage of rapidity since a technician can process 20–30 samples in 1 day with an automatic sampler and a minimum of active involvement. In conclusion, high sensitivity, specificity, and rapidity, coupled with the ability to separate unchanged ketoprofen from its metabolites, make this procedure particularly suitable for study of the pharmacokinetics of ketoprofen in humans.

REFERENCES

(1) R. Ballerini, A. Cambi, and P. Del Soldato, *J. Pharm. Sci.*, **66**, 281 (1977).

(2) P. Populaire, B. Terlain, S. Pascal, B. Decouvelaere, G. Lebreton, A. Renard, and J. P. Thomas, *Ann. Pharm. Fr.*, **31**, 679 (1973).

(3) M. Fukuhara and S. Tsurufuji, *Biochem. Pharmacol.*, **18**, 475 (1969).

(4) L. Saunders and R. Fleming, "Mathematics and Statistics," Pharmaceutical Press, London, England, 1971, p. 179.

(5) P. Populaire, B. Terlain, S. Pascal, B. Decouvelaere, A. Renard, and J. P. Thomas, *Ann. Pharm. Fr.*, **31**, 735 (1973).

ACKNOWLEDGMENTS

The authors are indebted to Mr. A. Stocchi for assistance.

Light Stability of Norethindrone and Ethinyl Estradiol Formulated with FD&C Colorants

E. E. KAMINSKI ˣ, R. M. COHN, J. L. McGUIRE, and J. T. CARSTENSEN *

Received August 18, 1977, from the *Research Laboratories, Ortho Pharmaceutical Corporation, Raritan, NJ 08869.* Accepted for publication August 4, 1978. *Present address: School of Pharmacy, University of Wisconsin, Madison, WI 53706.

Abstract □ In general, light-sensitive tablets exhibit discoloration in the surface layer(s) only. A case is discussed where a quantitative interaction between a drug, ethinyl estradiol (in a combination tablet containing norethindrone and ethinyl estradiol), and a dye (FD&C Red No. 3) occurs, and discoloration exists throughout the tablet. The data suggest that accelerated light studies should be carried further than those dictated by predictive periods so that equilibrium levels can be deduced.

Keyphrases □ Norethindrone—stability in tablets, effect of FD&C dyes □ Ethinyl estradiol—stability in tablets, effect of FD&C dyes □ Dyes, FD&C—effect on stability of norethindrone and ethinyl estradiol in tablets □ Stability—norethindrone and ethinyl estradiol in tablets, effect of FD&C dyes □ Tablets—norethindrone and ethinyl estradiol, effect of FD&C dyes on stability

Drug stability in solution can be affected adversely by the presence of a colorant (1). Since colors are used routinely to identify solid dosage forms, a study was initiated to determine whether such reactions could occur with compressed tablets. Although there are no compendial or regulatory procedures to evaluate the effect of light, previous reports (2) correlated accelerated light studies with ordinary room light exposure.

Reported interactions between light and substances in solid dosage forms usually were confined to the top layer(s) of the tablet (3–5) and occurred when a single component was photosensitive. Photo-induced drug interactions in solid form have not been reported.

This report presents results of studies on the stability of norethindrone and ethinyl estradiol in uncolored compressed tablets as well as in tablets containing selected FD&C colorants when exposed to accelerated light stress.

EXPERIMENTAL

Tablets—All tablets contained 0.5 mg of norethindrone and 0.035 mg of ethinyl estradiol and were prepared with the same excipients by classical granulation techniques. Three formulas were prepared: pink, containing 4.5 μg of erythrosine (FD&C Red No. 3)/tablet; white, containing no colorant; and orange, containing 30 μg of the disodium salt of 1-*p*-sulfophenylazo-2-naphthol-6-sulfonic acid (FD&C Yellow No. 6)/tablet.

The dyes were added in a methanolic solution to the basic excipient system. The uncolored tablets were processed with the same amount of methanol as used in the tablets containing a colorant. All tablets were then dried, screened, lubricated, blended, and compressed in similar fashions.

Analytical Methods—Single tablets were disintegrated and then dissolved in a homogenizer with methanol as the solvent. The solution containing the dissolved steroids was filtered and divided into two

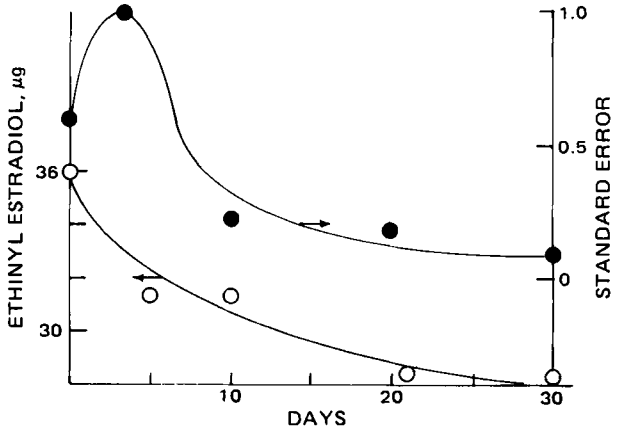

Figure 1—*Ethinyl estradiol assays as a function of time (left scale, open circles) and standard error of the assay mean as a function of time (right scale, closed circles).*

0022-3549/79/0300-0368$01.00/0

© 1979, American Pharmaceutical Association

Table I—Norethindrone Assays after Storage in Light Cabinet [a]

Formula	Initial Assay	*SEM*	5-Day Assay	*SEM*	10-Day Assay	*SEM*	21-Day Assay	*SEM*	30-Day Assay	*SEM*
White:										
Exposed	504	4.6	506	3.5	491	4.6	488	3.2	474	2.6
Control			511	4.8	501	5.4	500	5.2	507	3.8
Pink:										
Exposed	500	4.4	503	3.7	494	3.3	489	2.4	484	2.8
Control			511	6.8	507	4.6	509	3.6	495	2.1
Orange:										
Exposed	499	5.3	509	6.2	489	7.3	495	5.2	495	5.0
Control			513	6.6	500	5.6	532	3.3	506	2.6

[a] Assay and standard error of the mean are expressed in micrograms per tablet. The standard deviation may be calculated by multiplying the standard error of the mean $\times \sqrt{10}$, where 10 is the number of tablets analyzed.

Table II—Ethinyl Estradiol Assays after Storage in Light Cabinet [a]

Formula	Initial Assay	*SEM*	5-Day Assay	*SEM*	10-Day Assay	*SEM*	21-Day Assay	*SEM*	30-Day Assay	*SEM*
White:										
Exposed	35.7	0.24	36.1	0.24	35.0	0.44	34.2	0.21	34.3	0.22
Control			36.2	0.33	34.5	0.54	35.1	0.25	35.8	0.56
Pink:										
Exposed	36.0	0.60	31.3	1.01	31.3	0.21	28.4	0.18	28.4	0.09
Control			35.4	0.74	35.5	0.67	35.9	0.29	34.9	0.26
Orange:										
Exposed	35.1	0.11	35.0	0.34	34.6	0.22	34.6	0.36	34.9	0.36
Control			35.3	0.28	34.6	0.53	37.0	0.38	36.3	0.37

[a] Assay and standard error of the mean are expressed in micrograms per tablet. The standard deviation may be calculated by multiplying the standard error of the mean $\times \sqrt{10}$, where 10 is the number of tablets analyzed.

Table III—Regression Values for Assays: Slope (*b*), Intercept (*a*), and Correlation Coefficient (γ)

	Norethindrone						Ethinyl Estradiol					
	Exposed			Control			Exposed			Control		
Formula	*a*	*b*	γ	*a*	*b*	γ	*a*	*b*	γ	*a*	*b*	γ
White	506	−1.01	−0.95	505	−0.04	−0.13	35.9	−0.06	−0.89	35.5	−0.005	−0.100
Pink	502	−0.61	−0.95	507	−0.21	−0.39	34.0	−0.22	−0.88	35.8	−0.021	−0.595
Orange	501	−0.25	−0.41	504	. 0.43	0.39	35.0	−0.008	−0.43	34.9	0.059	0.737

streams. The first stream was mixed with isonicotinic acid-hydrolyzed reagent, which produced a chromophore absorbing in the 380-nm region (6). The second stream was mixed with 90% sulfuric acid, which produced a chromophore in the presence of ethinyl estradiol. The acid-induced fluorescence determination can be traced to the work of Khoury and Cali (7).

Test Conditions—All samples were subjected to accelerated conditions by placing them in a light cabinet containing both incandescent and fluorescent bulbs operated at an approximate light intensity of 1000 footcandles. The selection of the light source was designed to approximate the spectral energy curve of sunlight.

Two samples of each formula were exposed: A, in an open dish; and B, in a light-transparent container. Two samples (controls) were stored in the light cabinet in light-protecting containers; C, in a folding box; and D, in a foil overwrap. Five units of each sample were tested at the intervals shown in Tables I and II.

RESULTS AND DISCUSSION

Table I summarizes the accelerated light stability data for norethindrone and Table II summarizes the data for ethinyl estradiol from the three formulations. In no case were there significant differences ($p = 0.05$) between means or variances from Groups A and B. Therefore, the data for these two groups were pooled to give one mean and standard error for the exposed group. The same held true for Groups C and D, which were combined and listed as the control group. In several cases, however, there were significant differences between the exposed group and the control. Each number in the table represents an average of 10 assays.

The linear regression parameters for the data are given in Table III. With the white and pink tablets, there was a slight but significant regression in the data of the exposed samples for norethindrone. Rank testing of the data and the correlation coefficient are obvious indicators of this regression. This correlation was not demonstrated with significance for the orange tablets. There was no indication of light sensitivity regarding norethindrone (in fact, the colored tablets appeared to be better than the uncolored control), so the interaction in the system probably occurred between the dye and ethinyl estradiol only. The largest loss for norethindrone amounted to only 6%.

With ethinyl estradiol, the white formula showed slight but significant regression (loss), but the pink formula showed substantial losses. This latter result is shown graphically in Fig. 1. The orange formula was significantly more stable than the white, and the yellow colorant seemed to stabilize the ethinyl estradiol while the red dye seemed to interact with it.

Erythrosine is a fluorescein derivative and is thus in a class of compounds that are known sensitizing agents for photooxygenation and photorearrangement reactions (8, 9). The disodium salt of 1-*p*-sulfophenylazo-2-naphthol-6-sulfonic acid is, however, an azo dye and not considered a sensitizer for such reactions. Thus, based on the experimental results obtained from the 30-day accelerated light stability study, it appears that erythrosine can induce photochemical changes in ethinyl estradiol-containing tablets. Removal of this dye or its replacement with a nonsensitizing dye results in tablets with superior ethinyl estradiol light stability.

The 21% loss of ethinyl estradiol (mol. wt. 296) was on the order of 8 μg, *i.e.*, 27 nmoles, whereas the amount of red dye (mol. wt. 880) present (4.5 μg) was only 5 nmoles, which suggests a possible stoichiometric reaction. In the tablets containing the red dye, the entire tablet discolored, as opposed to the conventional type of light sensitivity that leads to a surface fading only (3–5).

The data in Table II seem to imply a trend: the standard error at the onset is small (and comparable to that derived from content uniformity data) but increases with time as the reaction comes to completion. This increase is by no means demonstrated with statistical confidence, but the chemical implication that the rate of reaction has either not started or has come to an end is not contradicted by the data.

Accelerated light studies should be carried further than those dictated by predictive periods so that "equilibrium" levels can be deduced.

REFERENCES

(1) R. Baugh, R. T. Calvert, and J. T. Fell, *J. Pharm. Sci.*, **66**, 733 (1977).

(2) L. Lachman, C. J. Swartz, and J. Cooper, *J. Am. Pharm. Assoc., Sci. Ed.*, **49**, 213 (1960).

(3) C. J. Swartz, T. Urbanyi, and J. Cooper, *ibid.*, **49**, 165 (1960).

(4) L. Lachman, S. Weinstein, C. Swartz, T. Urbanyi, and J. Cooper, *J. Pharm. Sci.*, **50**, 141 (1961).

(5) J. T. Carstensen, "Theory of Pharmaceutical Systems," vol. II, Academic, New York, N.Y., 1972, p. 347.

(6) R. A. Umberger, *Anal. Chem.*, **27**, 768 (1955).

(7) A. J. Khoury and L. J. Cali, *J. Pharm. Sci.*, **56**, 1485 (1967).

(8) J. M. Talmage, M. H. Penner, and M. Geller, *ibid.*, **54**, 1194 (1965).

(9) J. A. Waters, Y. Kondo, and B. Witkop, *ibid.*, **61**, 321 (1972).

ACKNOWLEDGMENTS

The authors thank Dr. Tom Norwood for his review and comments on the statistical content of the presentation.

Quantitative Structure–Activity Relationships and Carminative Activity II: Steric Considerations

BRIAN K. EVANS *, KENNETH C. JAMES ˣ, and DAVID K. LUSCOMBE

Received January 10, 1978, from the *Welsh School of Pharmacy, University of Wales Institute of Science and Technology, Cardiff, CF1 3NU, United Kingdom.* Accepted for publication August 9, 1978.

*Present address: Department of Pharmacy, University Hospital of Wales, Cardiff, United Kingdom.

Abstract □ The unexplained variation in the relationships between carminative activities and octanol–water distribution coefficients of various classes of compounds was explained. The steric substituent constant (E_s) value, van der Waals volume, and molecular connectivity were introduced into a previously derived correlation. Each parameter brought about an improvement, and molecular connectivity was the most successful. Correlations containing molecular connectivity terms explained the excess variation. The results were in agreement with a mechanism in which carminative activity depended on the availability of the oxygen atom in the functional group of the molecule and was reduced when the substituent attached to the oxygen hindered the interaction between the oxygen atom and the receptor.

Keyphrases □ Carminative activities—various oxygen-containing compounds, related to solubility, steric considerations □ Solubility—various oxygen-containing compounds, related to carminative activities, steric considerations □ Structure–activity relationships—carminative activities of various oxygen-containing compounds related to solubility, steric considerations

Recently, the carminative activities of 34 alcohols, esters, ethers, phenols, and carbonyl compounds were described (1). Carminative activity was expressed as the ability to produce a 50% inhibition (ID_{50}) of a standard response to carbachol in the guinea pig isolated ileum preparation. Regression analysis revealed a significant rectilinear relationship between log $1/ID_{50}$ and the logarithms of the octanol–water distribution coefficients (log P), but the correlation equation explained only 50% of the variation.

However, each chemical class of compounds, in isolation, produced more precise correlations, indicating the influence of factors other than solubility on carminative activity. Electronic distributions were unimportant, and it was suggested that the variation was due to the oxygen atom being shielded by the group attached to it. Consequently, the bulkier the group, the lower would be the carminative activity. Therefore, the hypothesis was tested by introducing steric parameters into the correlation equation between log P and log $1/ID_{50}$.

EXPERIMENTAL

The ID_{50} results and octanol–water distribution coefficients were reported previously (1). The compounds examined and other data are listed in Table I. All compounds consist of an oxygen joined to two chemical groups, one of which may be hydrogen. In choosing the groups to which to assign steric parameters, the decision was unambiguous with four of the five ethers since they each had two identical groups linked to oxygen. The vinyl group was chosen for the fifth compound, ethyl vinyl ether, since it was the smaller group. Similarly, values for hydrogen were given to all of the alcohols and phenols. The smaller groups were chosen because it was considered that interaction between oxygen and the receptor site would take place along the path of least resistance.

In each compound, the groups are located on opposite sides of the oxygen atom so that it is unlikely that both groups would interfere at once. Therefore, the probability of interaction through the bulkier group would be low. No logical way of allocating steric parameters to the carbonyl compounds, in accord with these assignments, was possible, so this class of compounds was omitted from the correlations. It was suggested previously (1) that the carbonyl oxygen of the esters, and not the ether oxygen, was responsible for carminative activity. Parameters for $CH_3C=$ were assigned, therefore, to the esters (since they are all acetates).

RESULTS AND DISCUSSION

Taft (2) assigned substituent constants (E_s), which are a measure of steric effects on reaction rates, to a range of substituent groups. The best correlation of log $1/ID_{50}$ against log P, reported previously (1), and the E_s value is:

$$\log 1/ID_{50} = 0.128 + \underset{8.8}{0.521(0.059)} \log P + \underset{4.7}{0.360(0.077)} E_s \quad \text{(Eq. 1)}$$

$$n = 22 \quad r = 0.915 \quad s = 0.220 \quad F_{2,19} = 49\alpha(0.001) = 10.2$$

where n represents the number of results considered (reduced from 26 to 22 because an E_s value for $CH_3C=$ was not available), r is the correlation coefficient, and s is the standard deviation. The figures in parenthesis following the coefficient in log P and E_s represent their standard errors ($p = 0.05$), and the figures below the coefficients are the ratios of the coefficients to their standard errors. Comparison of these values with t values obtained from statistical tables indicated that both physical parameters are related to log $1/ID_{50}$ ($p < 0.001$).

Equation 1 explains 84% of the variation and is a significant improvement on the corresponding equation containing log P alone. The relationship is confirmed by the figures shown below the equation, which are the results of analysis of variance of the observed results about the regression, followed by an F test.

Kier and coworkers (3, 4) developed a range of parameters, collectively termed molecular connectivity (χ), related to the topological structure of organic groups. The simplest term, the zero-order connectivity, is designated ${}^0\chi^v$ and is calculated from:

$${}^0\chi^v = \sum (\delta_i)^{-1/2} \quad \text{(Eq. 2)}$$

where δ_i is a number assigned to each nonhydrogen atom and reflects the

0022-3549/79/0300-0370$01.00/0

© 1979, American Pharmaceutical Association

REFERENCES

(1) R. Baugh, R. T. Calvert, and J. T. Fell, *J. Pharm. Sci.*, **66**, 733 (1977).

(2) L. Lachman, C. J. Swartz, and J. Cooper, *J. Am. Pharm. Assoc., Sci. Ed.*, **49**, 213 (1960).

(3) C. J. Swartz, T. Urbanyi, and J. Cooper, *ibid.*, **49**, 165 (1960).

(4) L. Lachman, S. Weinstein, C. Swartz, T. Urbanyi, and J. Cooper, *J. Pharm. Sci.*, **50**, 141 (1961).

(5) J. T. Carstensen, "Theory of Pharmaceutical Systems," vol. II, Academic, New York, N.Y., 1972, p. 347.

(6) R. A. Umberger, *Anal. Chem.*, **27**, 768 (1955).

(7) A. J. Khoury and L. J. Cali, *J. Pharm. Sci.*, **56**, 1485 (1967).

(8) J. M. Talmage, M. H. Penner, and M. Geller, *ibid.*, **54**, 1194 (1965).

(9) J. A. Waters, Y. Kondo, and B. Witkop, *ibid.*, **61**, 321 (1972).

ACKNOWLEDGMENTS

The authors thank Dr. Tom Norwood for his review and comments on the statistical content of the presentation.

Quantitative Structure–Activity Relationships and Carminative Activity II: Steric Considerations

BRIAN K. EVANS *, KENNETH C. JAMES ˣ, and DAVID K. LUSCOMBE

Received January 10, 1978, from the *Welsh School of Pharmacy, University of Wales Institute of Science and Technology, Cardiff, CF1 3NU, United Kingdom.* Accepted for publication August 9, 1978.

*Present address: Department of Pharmacy, University Hospital of Wales, Cardiff, United Kingdom.

Abstract □ The unexplained variation in the relationships between carminative activities and octanol–water distribution coefficients of various classes of compounds was explained. The steric substituent constant (E_s) value, van der Waals volume, and molecular connectivity were introduced into a previously derived correlation. Each parameter brought about an improvement, and molecular connectivity was the most successful. Correlations containing molecular connectivity terms explained the excess variation. The results were in agreement with a mechanism in which carminative activity depended on the availability of the oxygen atom in the functional group of the molecule and was reduced when the substituent attached to the oxygen hindered the interaction between the oxygen atom and the receptor.

Keyphrases □ Carminative activities—various oxygen-containing compounds, related to solubility, steric considerations □ Solubility—various oxygen-containing compounds, related to carminative activities, steric considerations □ Structure–activity relationships—carminative activities of various oxygen-containing compounds related to solubility, steric considerations

Recently, the carminative activities of 34 alcohols, esters, ethers, phenols, and carbonyl compounds were described (1). Carminative activity was expressed as the ability to produce a 50% inhibition (ID_{50}) of a standard response to carbachol in the guinea pig isolated ileum preparation. Regression analysis revealed a significant rectilinear relationship between log $1/ID_{50}$ and the logarithms of the octanol–water distribution coefficients (log P), but the correlation equation explained only 50% of the variation.

However, each chemical class of compounds, in isolation, produced more precise correlations, indicating the influence of factors other than solubility on carminative activity. Electronic distributions were unimportant, and it was suggested that the variation was due to the oxygen atom being shielded by the group attached to it. Consequently, the bulkier the group, the lower would be the carminative activity. Therefore, the hypothesis was tested by introducing steric parameters into the correlation equation between log P and log $1/ID_{50}$.

EXPERIMENTAL

The ID_{50} results and octanol–water distribution coefficients were reported previously (1). The compounds examined and other data are listed in Table I. All compounds consist of an oxygen joined to two chemical groups, one of which may be hydrogen. In choosing the groups to which to assign steric parameters, the decision was unambiguous with four of the five ethers since they each had two identical groups linked to oxygen. The vinyl group was chosen for the fifth compound, ethyl vinyl ether, since it was the smaller group. Similarly, values for hydrogen were given to all of the alcohols and phenols. The smaller groups were chosen because it was considered that interaction between oxygen and the receptor site would take place along the path of least resistance.

In each compound, the groups are located on opposite sides of the oxygen atom so that it is unlikely that both groups would interfere at once. Therefore, the probability of interaction through the bulkier group would be low. No logical way of allocating steric parameters to the carbonyl compounds, in accord with these assignments, was possible, so this class of compounds was omitted from the correlations. It was suggested previously (1) that the carbonyl oxygen of the esters, and not the ether oxygen, was responsible for carminative activity. Parameters for $CH_3C=$ were assigned, therefore, to the esters (since they are all acetates).

RESULTS AND DISCUSSION

Taft (2) assigned substituent constants (E_s), which are a measure of steric effects on reaction rates, to a range of substituent groups. The best correlation of log $1/ID_{50}$ against log P, reported previously (1), and the E_s value is:

$$\log 1/ID_{50} = 0.128 + \underset{8.8}{0.521(0.059)} \log P + \underset{4.7}{0.360(0.077)} E_s \quad \text{(Eq. 1)}$$

$$n = 22 \quad r = 0.915 \quad s = 0.220 \quad F_{2,19} = 49\alpha(0.001) = 10.2$$

where n represents the number of results considered (reduced from 26 to 22 because an E_s value for $CH_3C=$ was not available), r is the correlation coefficient, and s is the standard deviation. The figures in parenthesis following the coefficient in log P and E_s represent their standard errors ($p = 0.05$), and the figures below the coefficients are the ratios of the coefficients to their standard errors. Comparison of these values with t values obtained from statistical tables indicated that both physical parameters are related to log $1/ID_{50}$ ($p < 0.001$).

Equation 1 explains 84% of the variation and is a significant improvement on the corresponding equation containing log P alone. The relationship is confirmed by the figures shown below the equation, which are the results of analysis of variance of the observed results about the regression, followed by an F test.

Kier and coworkers (3, 4) developed a range of parameters, collectively termed molecular connectivity (χ), related to the topological structure of organic groups. The simplest term, the zero-order connectivity, is designated ${}^0\chi^v$ and is calculated from:

$${}^0\chi^v = \sum (\delta_i)^{-1/2} \quad \text{(Eq. 2)}$$

where δ_i is a number assigned to each nonhydrogen atom and reflects the

0022-3549/79/0300-0370$01.00/0

© 1979, American Pharmaceutical Association

Table I—Steric Parameters

Compound	Hindering Group	E_s	V_w, nm^3 × 10^{-1}	Molecular Connectivity $^0\chi^v$	Molecular Connectivity $^1\chi^v$
Isobutyl alcohol	H	1.24	0.022	0.000	0.000
n-Butyl acetate	$CH_3C=$	—	0.364	1.500	0.704
1,2-Dihydroxybenzene	H	1.24	0.022	0.000	0.000
1,3-Dihydroxybenzene	H	1.24	0.022	0.000	0.000
1,4-Dihydroxybenzene	H	1.24	0.022	0.000	0.000
o-Cresol	H	1.24	0.022	0.000	0.000
m-Cresol	H	1.24	0.022	0.000	0.000
p-Cresol	H	1.24	0.022	0.000	0.000
Dibutyl ether	$CH_3(CH_2)_3$	−0.39	0.651	3.121	1.996
Diethyl ether	CH_3CH_2	−0.07	0.343	1.707	0.996
3,4-Dimethylphenol	H	1.24	0.022	0.000	0.000
Diisopropyl ether	$(CH_3)_2CH$	−0.47	0.497	2.577	1.390
Dipropyl ether	$CH_3(CH_2)_2$	−0.36	0.497	2.414	1.495
Ethyl acetate	$CH_3C=$	—	0.364	1.500	0.704
Ethyl vinyl ether	$CH_3C=$	—	0.301	1.284	0.644
Eugenol	H	1.24	0.022	0.000	0.000
Hexanol	H	1.24	0.022	0.000	0.000
Menthol	H	1.24	0.022	0.000	0.000
2-Methoxyphenol	H	1.24	0.022	0.000	0.000
4-Methoxyphenol	H	1.24	0.022	0.000	0.000
1-Pentanol	H	1.24	0.022	0.000	0.000
2-Phenoxyethanol	H	1.24	0.022	0.000	0.000
Isopropyl acetate	$CH_3C=$	—	0.364	1.500	0.704
n-Propyl acetate	$CH_3C=$	—	0.364	1.500	0.704
Salicylaldehyde	H	1.24	0.022	0.000	0.000
Thymol	H	1.24	0.022	0.000	0.000

number of atoms bonded to it. A similar term is derived for each bond by calculating the product of the numbers associated with the two atoms of the bond. These values are summed to give the first-order connectivity, $^1\chi^v$. In general, extended terms of χ ($^m\chi_p^v$) are computed for linear paths, p, of m bonds by:

$$^m\chi_p^v = \sum_{j=1}^{N_s} \left[\prod_{i=1}^{m+1} (\delta_i)_j \right]^{-1/2} \quad \text{(Eq. 3)}$$

where N_s is the number of distinct paths with m edges. Detailed information on the significance and calculation of connectivities was reported previously (4, 5). Murray (6) demonstrated relationships between E_s values and connectivity. Therefore, correlations similar to Eq. 1 were attempted with connectivity terms in place of E_s. This substitution provided the advantage that a steric parameter could be allocated to the esters. Connectivities are given in Table I. The best correlations obtained are represented by Eqs. 4–6:

$$\log 1/ID_{50} = 0.563 + 0.537(0.048) \log P - 0.242(0.039)\,{}^0\chi^v \quad \text{(Eq. 4)}$$
$$\qquad\qquad 11.3 \qquad\qquad 6.2$$
$$r = 0.937 \quad n = 26 \quad s = 0.186 \quad F_{2,23} = 83.0\alpha(0.001) = 9.47$$
$$t(\phi = 24; p = 0.001) = 3.75$$

$$\log 1/ID_{50} = 0.531 + 0.553(0.045) \log P - 0.433(0.064)\,{}^1\chi^v \quad \text{(Eq. 5)}$$
$$\qquad\qquad 12.3 \qquad\qquad 6.8$$
$$r = 0.944 \quad n = 26 \quad s = 0.056 \quad F_{2,23} = 9.46\alpha(0.001) = 9.47$$

$$\log 1/ID_{50} = 0.478 + 0.577(0.048) \log P + 0.351(0.284)\,{}^0\chi^v$$
$$\qquad\qquad 12.0 \qquad\qquad 1.2$$
$$-1.036(0.493)\,{}^1\chi^v \quad \text{(Eq. 6)}$$
$$\qquad 2.1$$
$$r = 0.948 \quad n = 26 \quad s = 0.054 \quad F_{3,22} = 65.0\alpha(0.001) = 7.80$$
$$t(\phi = 23; p = 0.03) = 1.06$$

There is no significant difference between the equations with regard to goodness of fit ($p > 0.05$), but all are better than Eq. 1 ($p < 0.01$). Therefore, $^0\chi^v$ and $^1\chi^v$ are more suitable than E_s for assessing the steric hindrance presented by groups bonded to oxygen in the carminative molecules. There is nothing to choose between the two connectivity terms ($p > 0.05$), and the fit is not improved either by combining them or by incorporating higher order connectivity parameters. No combination of connectivities alone gave a satisfactory correlation with log $1/ID_{50}$. A term involving the distribution coefficient was always essential for a good predictive relationship.

The E_s values are linear functions of van der Waals radii (6–8). Moriguchi *et al.* (9) published a list of van der Waals volumes, V_w, for substituent groups and used them as a measure of steric effects on biological activities. Multiple regression analysis of log P and V_w against the carminative activities of the alcohols, esters, ethers, and phenols produced Eq. 7:

$$\log 1/ID_{50} = 0.576 + 0.529(0.057) \log P - 0.893(0.201)V_w \quad \text{(Eq. 7)}$$
$$\qquad\qquad 9.3 \qquad\qquad 4.5$$
$$r = 0.909 \quad n = 26 \quad s = 0.222 \quad F_{2,23} = 55\alpha(0.001) = 9.47$$

It is a significant improvement on the corresponding equation containing log P as the only independent variable, but it is not as good a correlation as Eqs. 4–6.

The E_s values are defined by:

$$E_s = \log \frac{k}{k_0} \quad \text{(Eq. 8)}$$

where k and k_0 represent rate constants for the acid hydrolysis of esters (R_1COOR_2); k_0 is the rate constant when R_1 is methyl, and k is the corresponding constant when R_1 is the substituent group of interest. The underlying principle of the concept is that acid hydrolysis of esters is not influenced by polar effects and is dependent exclusively on the stereochemistry of the transition state.

In the present work, the groups are attached to oxygen, rather than to carbon, representing a different environment from that used to calculate the parameters. Nevertheless, it can be argued that since the groups are all bonded to the same element, any errors involved in using E_s values would be constant. A more serious objection is that the second group attached to the oxygen varies from compound to compound, although the same criticism can be leveled at Taft's calculations (2) in which a range of alkyl groups (R_2) was used. Furthermore, since the second group in each carminative is remote from the first, significant steric interaction on the other side of the oxygen atom would be unlikely. An exception is possible with substituents containing bulky groups alpha to the oxygen; but the only candidate for this situation was 2-methoxyphenol, and its carminative activity is predicted reasonably well by Eq. 1. The principal effect brought about by the second group attached to oxygen would be expected to be polar rather than steric.

The E_s values may give better predictions than van der Waals volumes, which are calculated geometrically, because they are based on chemical considerations. Molecular connectivity was the most successful approach. This method of expressing the stereochemistry of substituent groups is more sophisticated than the van der Waals volume, and the results obtained with carminatives suggest that they are more representative of steric hindrance than either E_s or V_w. The failure of the E_s values to match the success achieved with connectivities could be due to inherent errors in their derivation, particularly the assumption that the reaction constants (ρ_A and ρ_B) are equal. Taft (2) described E_s values as "nearly quantitative measures of steric factors."

The most important conclusion is that correlations between carminative activity and the distribution coefficient are improved by consideration of a parameter that is a measure of steric factors. All three parameters examined brought about such an improvement. Molecular connectivities were the best parameters and are easily calculated. Previously (1), correlation of the log $1/ID_{50}$ for all compounds against log P gave a relationship that explained only 50% of the variation. But when only one chemical class, hydroxy compounds, was considered, 90% of the variation was accounted for. Inclusion of molecular connectivity terms in the first correlation increased the explained variation from 50 to 88–90%, as shown in Eqs. 4–6. The inference is that steric factors are the sole cause of biological variation resulting from changing the functional groups in the carminatives investigated.

REFERENCES

(1) B. K. Evans, K. C. James, and D. K. Luscombe, *J. Pharm. Sci.*, **67**, 277 (1978).

(2) R. W. Taft, *J. Am. Chem. Soc.*, **74**, 3120 (1952).

(3) L. H. Hall, L. B. Kier, and W. J. Murray, *J. Pharm. Sci.*, **64**, 1974 (1975).

(4) L. B. Kier and L. H. Hall, "Molecular Connectivity in Chemistry and Drug Research," Academic, New York, N.Y., 1976.

(5) T. D. Paolo, L. B. Kier, and L. H. Hall, *Mol. Pharmacol.*, **13**, 31 (1977).

(6) W. J. Murray, *J. Pharm. Sci.*, **66**, 1352 (1977).

(7) M. Charton, *J. Am. Chem. Soc.*, **91**, 615 (1969).

(8) E. Kutter and C. Hansch, *J. Med. Chem.*, **12**, 647 (1969).

(9) I. Moriguchi, Y. Kanada, and K. Komatsu, *Chem. Pharm. Bull.*, **24**, 1799 (1976).

Metabolic Studies with Nonnutritive Sweeteners Cyclooctylsulfamate and 4-Methylcyclohexylsulfamate

WILLIAM J. SPILLANE ˣ, G. ANTHONY BENSON, and GRAINNE McGLINCHEY

Received September 12, 1977, from the *Department of Chemistry, University College, Galway, Ireland.* Accepted for publication August 21, 1978.

Abstract □ The nonnutritive sweeteners cyclooctylsulfamate and 4-methylcyclohexylsulfamate were fed separately to female Wistar albino rats, and the urine was examined for the possible metabolites cyclooctylamine, cyclooctanone, cyclooctanol, 4-methylcyclohexylamine, 4-methylcyclohexanone, and *cis*- and *trans*-4-methylcyclohexanols. The average percent conversions to cyclooctylamine, cyclooctanone, and cyclooctanol were 0.127, 0.08, and 0.092, respectively. The average percent conversions to 4-methylcyclohexylamine and 4-methylcyclohexanone were 0.007 and 0.0013, respectively. No *cis*- or *trans*-4-methylcyclohexanol metabolites were found. With cyclooctylsulfamate, 42% was recovered unchanged from the urine. Cyclooctyl- and cycloheptylsulfamates were metabolized to a greater extent than cyclopentylsulfamate, which, in turn, was metabolized to a greater extent than cyclohexylsulfamate (cyclamate) and 4-methylcyclohexylsulfamate.

Keyphrases □ Cyclooctylsulfamate—metabolism in rats □ 4-Methylcyclohexylsulfamate—metabolism in rats □ Metabolism—cyclooctylsulfamate and 4-methylcyclohexylsulfamate in rats □ Sweeteners, nonnutritive—cyclooctylsulfamate and 4-methylcyclohexylsulfamate, metabolism in rats

Previously, sodium cyclopentylsulfamate (1), cycloheptylsulfamate (2), and cyclopentylmethylsulfamate (3) were administered to rabbits and/or rats. Cyclopentylsulfamate also was administered over a prolonged period to rats (3). The purpose of these studies was to probe the effect of structural modification of the cyclamate, *i.e.*, cyclohexyl, nucleus on the stability of these compounds in the body. Metabolism to the amine and other metabolites was determined by GLC, and the percent of recovered sulfamate in the urine was determined by hydrolyzing to the corresponding amine, coupling with *p*-benzoquinone, and measuring the absorbance of the colored product.

The remaining sweet, unsubstituted, reduced ring sulfamate not studied previously is cyclooctylsulfamate. Since this compound, first prepared in 1954 (4), is of the same order of sweetness as cyclamate[1], it was included in the *in vivo* feeding experiments. 4-Methylcyclohexylsulfamate also is of comparable sweetness to cyclamate[2]; since no substituted cyclamates have been screened metabolically, it too was included. This paper describes the feeding of these two sulfamates to rats and the subsequent screening of urine for metabolites.

EXPERIMENTAL

Reagents and Chemicals—The sodium salts of cyclooctylsulfamate and 4-methylcyclohexylsulfamate were synthesized by reaction of the appropriate amines in dry chloroform with chlorosulfonic acid according to the method of Audrieth and Sveda (7). Each compound was recrystallized twice from 95% ethanol.

Anal.—Calc. for $C_8H_{16}NNaO_3S \cdot H_2O$: C, 38.86; H, 7.28; N, 5.66. Found: C, 38.72; H, 7.86; N, 5.43. Calc. for $C_7H_{14}NNaO_3S$: C, 39.06; H, 6.5; N, 6.5. Found: C, 39.02; H, 6.46; N, 6.74.

[1] The order of relative sweetness is cyclamate > cycloheptyl > cyclooctyl > cyclopentyl (5, 6).

[2] Unpublished results.

Table I—Percent Recovery of Cyclooctylamine, Cyclooctanone, and Cyclooctanol from Urine

Amine		Ketone		Alcohol	
μg	%	μg	%	μg	%
90.2	80.20	199.9	78.05	97.4	80.84
150.4	85.40	299.8	78.03	162.3	85.82
210.6	88.20	399.8	72.70	227.2	95.94
300.9	97.68	499.8	87.63	324.6	87.6
601.9	98.67	599.7	98.03	649.3	97.92
902.8	79.74	—	—	974.0	92.64
Mean ± *SE*	88.28 ± 6.59		82.88 ± 7.94		90.12 ± 5.37

Cyclooctylamine[3] and dichloromethane[4] were redistilled. Cyclooctanone[5], cyclooctanol[5], 4-methylcyclohexylamine[6], 4-methylcyclohexanone[6], *cis*- and *trans*-4-methylcyclohexanols[6], *n*-dodecane[7], sulfosalicylic acid[8], chloroform, ethanol, and dioxane (reagent grade) were used as obtained. *p*-Benzoquinone[4,7] was sublimed before use.

Feeding Experiments—Female Wistar albino rats, ~300 g, were kept on solid food and water in special rat metabolism cages[9]. Prior to sulfamate feeding, the urine of each rat was collected and monitored for metabolites by GLC. The samples of sodium cyclooctylsulfamate and sodium 4-methylcyclohexylsulfamate to be used for feeding were tested for occluded amines by dissolving 20 mg in water, extracting with dichloromethane, concentrating the extracts to dryness, and resuspending the residues in dichloromethane containing the internal standard, *n*-dodecane. No occluded amine was observed when these samples were chromatographed.

Sodium cyclooctylsulfamate (1450 mg/kg) was administered orally in 25–30 ml of water in calibrated drinking bottles. One rat refused to take the solution until it was diluted twice. Sodium 4-methylcyclohexylsulfamate (960 mg/kg) was administered orally in 20 ml of water.

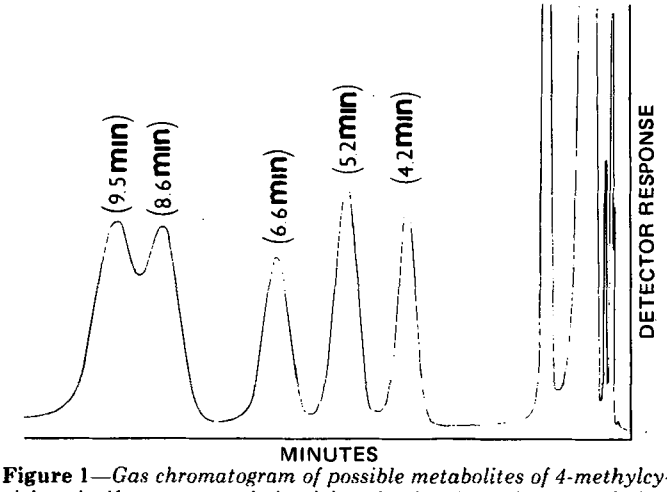

Figure 1—*Gas chromatogram of possible metabolites of 4-methylcyclohexylsulfamate: 4-methylcyclohexylamine (4.2 min), 4-methylcyclohexanone (6.6 min), and* cis- *(8.6 min) and* trans- *(9.5 min) 4-methylcyclohexanols. The internal standard was* n-*dodecane (5.2 min).*

[3] Aldrich Chemical Co.
[4] May & Baker.
[5] Ralph Emanuel.
[6] Fluka.
[7] British Drug Houses.
[8] May & Baker, AnalaR grade.
[9] NKP, Kent, England.

0022-3549/79/0300-0372$01.00/0
© 1979, American Pharmaceutical Association

Table II—Percent Recovery of 4-Methylcyclohexylamine, 4-Methylcyclohexanone, and *cis*- and *trans*-4-Methylcyclohexanols

Amine		Ketone		*cis*-Alcohol		*trans*-Alcohol	
μg	%	μg	%	μg	%	μg	%
0.15	106.7	0.07	105.714	0.03	93.33	0.100	102.000
0.15	108.0	0.5	96.00	0.04	100.00	0.250	91.200
0.2	84.0	0.5	91.50	0.20	96.000	0.912	98.710
0.25	92.0	1.097	101.730	0.917	94.220	—	—
0.44	97.7	1.83	83.680	0.917	100.109	2.740	94.525
0.44	100.0	6.396	92.250	2.75	102.109	6.380	112.850
6.09	111.475	10.97	107.468	6.42	112.149	10.942	98.702
9.57	97.806	10.97	113.843	8.25	99.49	10.942	96.219
13.92	100.862	—	—	11.00	99.91	8.210	94.714
17.4	100.144	—	—	11.00	99.873	8.210	100.868
30.45	100.493	—	—	16.51	101.756	16.410	98.964
Mean ± *SE*	99.925 ± 5.1		99.02 ± 8.16		99.9 ± 3.0		98.875 ± 3.8

Table III—Metabolism of Sodium Cyclooctylsulfamate in Rats

Animal	Parent Drug[a]		Cyclooctanol[b]		Cyclooctanone[b]		Cyclooctylamine[b]		Total Metabolites
	mg	%	mg	%	mg	%	mg	%	
1	256.1	51.2	0.100	0.035	0.082	0.029	0.115	0.041	0.105
2	333.0	66.6	None	—	None	—	None	—	—
3	136.8	27.2	0.487	0.174	0.410	0.147	0.623	0.224	0.545
4	128.3	25.6	0.721	0.250	0.598	0.215	1.026	0.37	0.835
5	35.2	17.6	None	—	None	—	None	—	—
Mean ± *SE*	213.6 ± 81.17	42.6 ± 16.2	0.261 ± 0.169	0.092 ± 0.075	0.22 ± 0.141	0.08 ± 0.051	0.353 ± 0.116	0.127 ± 0.085	0.297 ± 0.196

[a] Determined using visible spectrophotometry. [b] Determined by GLC.

Table IV—Metabolites of Sodium 4-Methylcyclohexylsulfamate[a] in Rats

Animal	4-Methylcyclohexylamine[b]		4-Methylcyclohexanone[b]	
	mg	%	mg	%
1[c]	0.009	0.006	None	—
2	0.005	0.003	None	—
3[c]	0.009	0.006	None	—
4	0.003	0.004	None	—
5[c]	0.008	0.005	0.0012	0.008
6	0.029	0.019	None	—
Mean ± *SE*	0.0106 ± 0.007	0.0073 ± 0.0045	0.0002	0.0013

[a] Rat 4 received only approximately half the amount of sulfamate, *i.e.*, 500 mg/kg. [b] Determined by GLC. [c] Urine was collected for 5 days after feeding, because these rats had excreted small volumes of urine after 3 days.

Table V—Metabolism of Sulfamates in Rats

Cyclic Sulfamate	Percent Metabolites			Reference
	Amine	Ketone	Alcohol	
Pentyl	0.057	0.016	0.008	1
Pentylmethyl	0.007	—	0.07	3
Hexyl	0.03	0.002	0.003	11
Hexyl	0.0063	0.0004	0.0004	12
4-Methylhexyl	0.007	0.0013	—	This work
Heptyl	0.051	0.009	0.003	2
Octyl	0.127	0.08	0.092	This work

Urine was collected for 3 days (for 5 days in some cases) after feeding and was refrigerated as described previously (1). The stability of sodium cyclooctylsulfamate in urine was checked as described previously (1).

GLC and Visible Spectrophotometric Analysis—Cyclooctylamine, cyclooctanone, and cyclooctanol were determined in urine by a reported GLC method (8). The percent sodium cyclooctylsulfamate in urine was determined by coupling, with *p*-benzoquinone, the amine produced on hydrolysis (9). Table I gives the percent recovery from urine of three metabolites of cyclooctylsulfamate.

Four metabolites of 4-methylcyclohexylsulfamate could be determined by GLC from a single injection. The details of the column and the general method were described previously (8, 10). The column temperature was 120°, and the gas flow rates were: nitrogen (carrier), 60 ml/min; hydrogen, 80 ml/min; and overall, 500 ml/min. Under these conditions, the retention times of 4-methylcyclohexylamine, *n*-dodecane, 4-methylcyclohexanone, and *cis*- and *trans*-4-methylcyclohexanols were 4.2, 5.2, 6.6, 8.6, and 9.5, min, respectively (Fig. 1). Table II gives the percent recoveries from urine of these metabolites.

RESULTS AND DISCUSSION

To test the efficiency of the extraction from urine, the percent recovery of varying amounts of the amine, the ketone, and the alcohol was determined by GLC (Tables I and II). The results from the analysis of rat urine for unchanged cyclooctylsulfamate and various metabolites are given in Table III. The average percentage of unchanged cyclooctylsulfamate in rat urine was 42%. Three of the five rats excreted metabolites of cyclooctylsulfamate, and the average percent conversions were 0.127, 0.08, and 0.092 for the amine, the ketone, and the alcohol, respectively (Table III).

Only two metabolites were detected in the urine of rats fed 4-methylcyclohexylsulfamate (Table IV). The percent conversions to the amine and the ketone were 0.0073 and 0.0013, respectively. Only one of the six rats gave the ketone, and none excreted the alcohol. From a single injection, it was possible to determine the amine, the ketone, and the *cis*- and *trans*-alcohol compounds of 4-methylcyclohexylsulfamate (Fig. 1).

Table V lists the average percent conversions to metabolites for the various sulfamates. The most obvious point to emerge from a comparison of the data in Table V is that the conversion of cyclooctylsulfamate to metabolites was somewhat greater than the conversion of cycloheptylsulfamate or cyclopentylsulfamate to metabolites. The conversion of the latter compound into its metabolites was, in turn, greater than the conversions of cyclamate to cyclohexylamine, cyclohexanone, and cyclohexanol. Furthermore, 4-methylcyclohexylsulfamate appeared to be metabolized to about the same extent as cyclamate. Thus, cyclamate and its ring-substituted derivatives apparently are more stable to metabolic cleavage than any of their neighboring reduced ring sulfamates.

REFERENCES

(1) G. A. Benson and W. J. Spillane, *J. Pharm Sci.*, **65**, 1841 (1976).

(2) *Ibid.*, **66**, 881 (1977).

(3) *Ibid.*, **67**, 226 (1978).

(4) F. F. Blicke, H. E. Millson, Jr., and N. J. Doorenbos, *J. Am. Chem. Soc.*, **76**, 2498 (1954).

(5) B. Unterhalt and L. Böschemeyer, *Z. Lebensm.-Unters.-Forsch.*, **145**, 93 (1971).

(6) G. A. Benson and W. J. Spillane, *J. Med. Chem.*, **19**, 869 (1976).

(7) L. F. Audrieth and M. Sveda, *J. Org. Chem.*, **9**, 89 (1944).
(8) G. A. Benson and W. J. Spillane, *J. Chromatogr.*, **136**, 318 (1977).
(9) G. A. Benson and W. J. Spillane, *Anal. Chem.*, **48**, 2149 (1976).
(10) P. H. Derse and R. J. Daun, *J. Assoc. Offic. Anal. Chem.*, **49**, 1090 (1966).
(11) H. Ichibagase, S. Kojima, K. Inoue, and A. Suenaga, *Chem. Pharm. Bull.*, **20**, 175 (1972).
(12) A. Suenaga, S. Kojima, and H. Ichibagase, *ibid.*, **20**, 1357 (1972).

ACKNOWLEDGMENTS

The authors thank the Department of Education (Ireland) for grants to G. A. Benson and G. McGlinchey. The Van't Hoff Fund (Amsterdam, The Netherlands) and the Chemical Society (London, England) are thanked for grants.

GLC Determination of Purity of Schiff Bases Bakrine and Saddamine

STUART G. WOOD, MAJEED R. AL-ANI *, and ALEXANDER LAWSON ˣ

Received May 31, 1978, from the *Department of Biochemistry, Charing Cross Hospital Medical School, University of London, London 6 8RF, England.* Accepted for publication August 18, 1978. *Present address: Department of Biochemistry, College of Medicine, University of Baghdad, Baghdad, Iraq.

Abstract □ GLC methods were developed for the investigation of impurities in bakrine and saddamine. The method used for bakrine was unsuitable for saddamine since two possible saddamine impurities, benzylamine and salicylaldehyde, reacted very readily in solution to form saddamine, thus giving a false low value for the original concentration of these impurities. The method devised for saddamine involved silylation, which greatly reduced the possibility of saddamine formation from its precursors and also enabled the detection of another possible impurity, salicylic acid. The method described has an obvious application to the determination of other Schiff bases.

Keyphrases □ Bakrine and impurities—GLC analysis in prepared samples □ Saddamine and impurities—GLC analysis in prepared samples □ Anti-inflammatory agents, potential—bakrine and saddamine, GLC analysis in prepared samples

Bakrine, *N*-[1-(*o*-hydroxyphenyl)ethylidine]benzylamine (I), and saddamine, *N*-[*o*-hydroxyphenylmethylidine]benzylamine (II), are novel Schiff bases (1) with promising anti-inflammatory properties (2). These compounds are currently undergoing clinical trials in Iraq.

During the development of a method for the determination of the purity of bakrine and saddamine samples, spectrophotometric and TLC procedures were shown to lack specificity; GLC was the method of choice because of its speed, sensitivity, and specificity. However, although a solution of bakrine containing expected impurities could be analyzed satisfactorily by direct injection onto the GLC column, a similar procedure for saddamine gave inconsistent results. Therefore, the possibility that saddamine could be reformed from any salicylaldehyde and benzylamine present as impurities in the final product was investigated.

EXPERIMENTAL

Reagents and Materials—Bakrine[1], saddamine[1], and bis(trimeth-

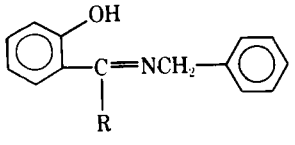

I: R = CH_3
II: R = H

[1] Maybridge Chemical Co., Cornwall, England.

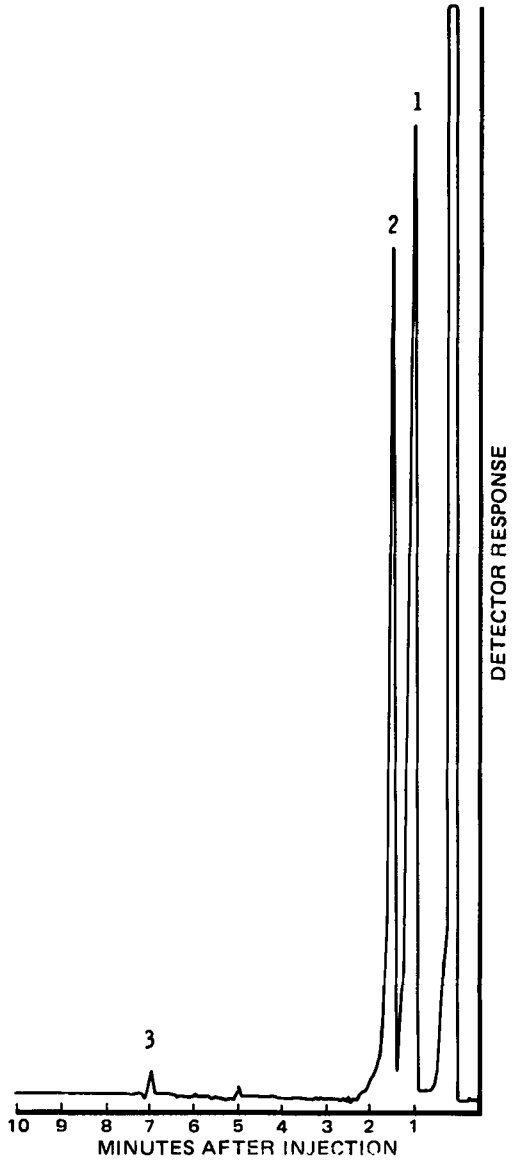

Figure 1—*Gas chromatogram of benzylamine (peak 1) and 2-hydroxyacetophenone (peak 2) in 1,2-dichloroethane. Very little bakrine (peak 3) was formed.*

0022-3549/79/0300-0374$01.00/0
© 1979, American Pharmaceutical Association

(7) L. F. Audrieth and M. Sveda, *J. Org. Chem.*, **9**, 89 (1944).
(8) G. A. Benson and W. J. Spillane, *J. Chromatogr.*, **136**, 318 (1977).
(9) G. A. Benson and W. J. Spillane, *Anal. Chem.*, **48**, 2149 (1976).
(10) P. H. Derse and R. J. Daun, *J. Assoc. Offic. Anal. Chem.*, **49**, 1090 (1966).
(11) H. Ichibagase, S. Kojima, K. Inoue, and A. Suenaga, *Chem. Pharm. Bull.*, **20**, 175 (1972).
(12) A. Suenaga, S. Kojima, and H. Ichibagase, *ibid.*, **20**, 1357 (1972).

ACKNOWLEDGMENTS

The authors thank the Department of Education (Ireland) for grants to G. A. Benson and G. McGlinchey. The Van't Hoff Fund (Amsterdam, The Netherlands) and the Chemical Society (London, England) are thanked for grants.

GLC Determination of Purity of Schiff Bases Bakrine and Saddamine

STUART G. WOOD, MAJEED R. AL-ANI *, and ALEXANDER LAWSON ˣ

Received May 31, 1978, from the *Department of Biochemistry, Charing Cross Hospital Medical School, University of London, London 6 8RF, England.* Accepted for publication August 18, 1978. *Present address: Department of Biochemistry, College of Medicine, University of Baghdad, Baghdad, Iraq.

Abstract □ GLC methods were developed for the investigation of impurities in bakrine and saddamine. The method used for bakrine was unsuitable for saddamine since two possible saddamine impurities, benzylamine and salicylaldehyde, reacted very readily in solution to form saddamine, thus giving a false low value for the original concentration of these impurities. The method devised for saddamine involved silylation, which greatly reduced the possibility of saddamine formation from its precursors and also enabled the detection of another possible impurity, salicylic acid. The method described has an obvious application to the determination of other Schiff bases.

Keyphrases □ Bakrine and impurities—GLC analysis in prepared samples □ Saddamine and impurities—GLC analysis in prepared samples □ Anti-inflammatory agents, potential—bakrine and saddamine, GLC analysis in prepared samples

Bakrine, *N*-[1-(*o*-hydroxyphenyl)ethylidine]benzylamine (I), and saddamine, *N*-[*o*-hydroxyphenylmethylidine]benzylamine (II), are novel Schiff bases (1) with promising anti-inflammatory properties (2). These compounds are currently undergoing clinical trials in Iraq.

During the development of a method for the determination of the purity of bakrine and saddamine samples, spectrophotometric and TLC procedures were shown to lack specificity; GLC was the method of choice because of its speed, sensitivity, and specificity. However, although a solution of bakrine containing expected impurities could be analyzed satisfactorily by direct injection onto the GLC column, a similar procedure for saddamine gave inconsistent results. Therefore, the possibility that saddamine could be reformed from any salicylaldehyde and benzylamine present as impurities in the final product was investigated.

EXPERIMENTAL

Reagents and Materials—Bakrine[1], saddamine[1], and bis(trimeth-

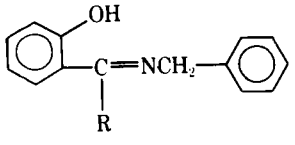

I: R = CH_3
II: R = H

[1] Maybridge Chemical Co., Cornwall, England.

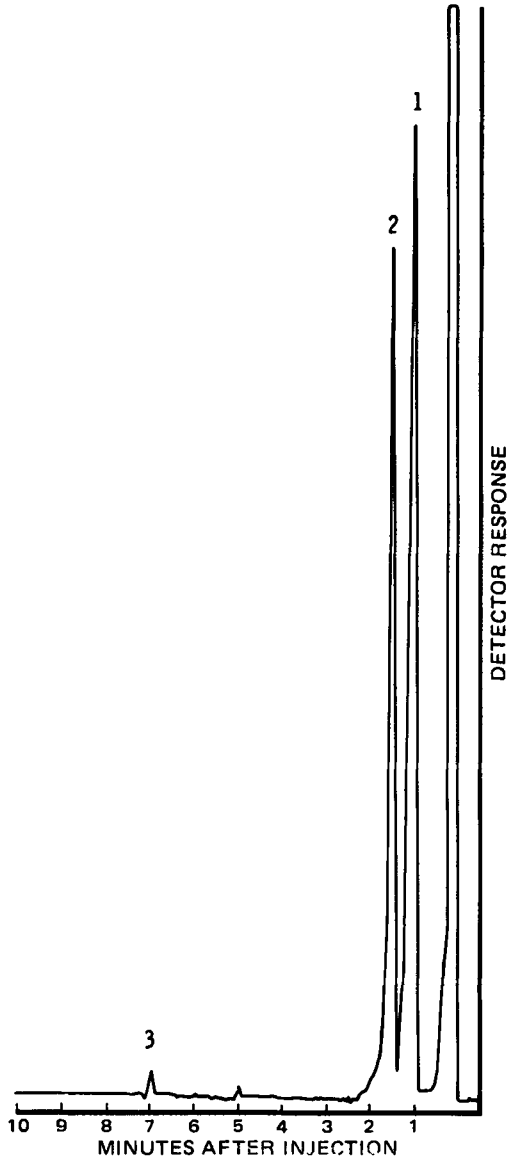

Figure 1—*Gas chromatogram of benzylamine (peak 1) and 2-hydroxyacetophenone (peak 2) in 1,2-dichloroethane. Very little bakrine (peak 3) was formed.*

0022-3549/79/0300-0374$01.00/0
© 1979, American Pharmaceutical Association

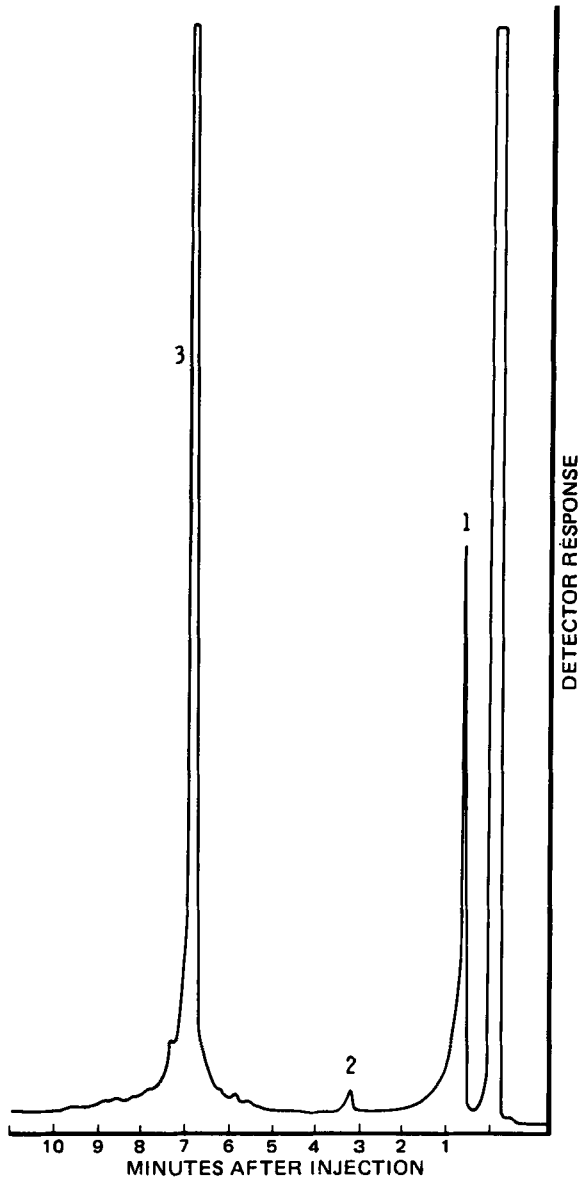

Figure 2—*Gas chromatogram of benzylamine (peak 1) and salicylaldehyde (peak 2) in 1,2-dichloroethane. Saddamine (peak 3) formation was almost quantitative.*

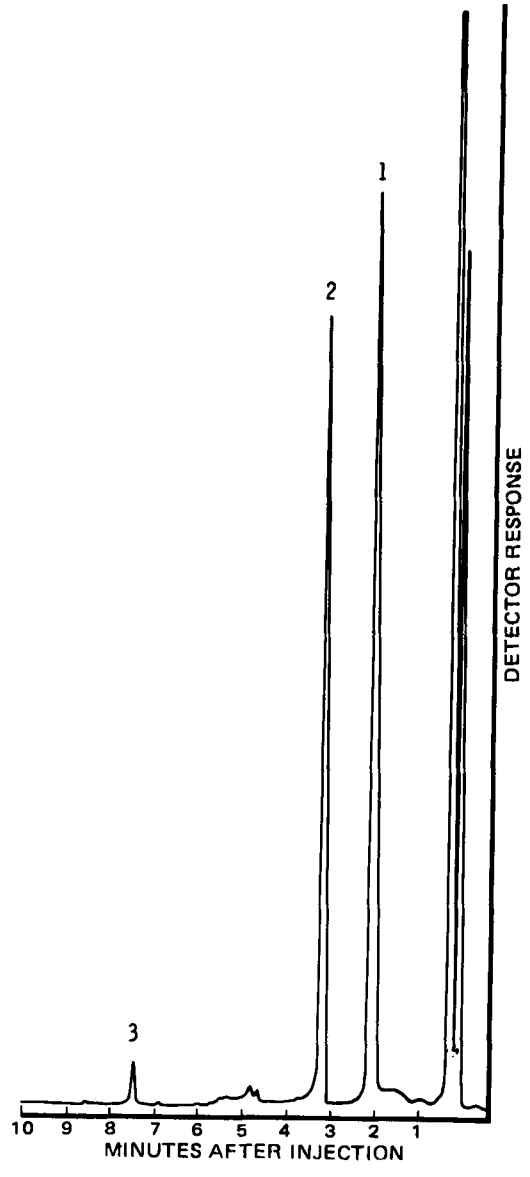

Figure 3—*Gas chromatogram of derivatized benzylamine (peak 1) and salicylaldehyde (peak 2). The formation of saddamine (peak 3), in this case derivatized, was greatly reduced.*

ylsilyl)trifluoroacetamide[2] were used as supplied. All other solvents and reagents were analytical reagent grade. Screw-capped 1-ml tapered reaction vials, fitted with polytef-faced rubber seals[3], were used for silylation.

Apparatus—A gas chromatograph[4] was equipped with a flame-ionization detector and a 2-m × 2.5-mm i.d. stainless steel column packed with 5% OV-1 on 100–120-mesh Gas Chrom Q[5]. The column was conditioned before use at 275° for 24 hr with the carrier gas (nitrogen) at a flow rate of 35 ml/min. The chromatograph was operated under the following conditions: column and injection port temperature, 275°; detector temperature, 275°; carrier gas flow, 30 ml/min; air flow, 300 ml/min; and hydrogen flow, 40 ml/min. The oven temperature was initially 130° for 2 min and was then increased to 260° at a rate of 20°/min.

Silylation Procedure—Trimethylsilyl derivatives were prepared by the addition of 250 μl of silylating reagent to 5 mg of the test compounds in separate reaction vials. The vials were capped immediately and left for 2 hr at room temperature (20°). The silylation reaction went to completion after 2 hr for all compounds tested, and the derivatives were stable for at least 24 hr when kept in the sealed vials.

[2] Regisil, Regis Chemical Co., Chicago, Ill.
[3] Regis Chemical Co., Chicago, Ill.
[4] Perkin-Elmer model F33.
[5] Phase Separations, Clwyd, Wales.

For the chromatography of derivatives, suitable volumes of solutions of the individual silylated compounds were mixed and diluted with silylating reagent to give a final concentration of 2 mg/ml for each component in the mixture. Aliquots of 1 μl were injected onto the column.

RESULTS AND DISCUSSION

GLC determination of the purities of bakrine and saddamine was first attempted by separate injections of 1,2-dichloroethane solutions of the two compounds and mixtures of their carbonyl and amino precursors, respectively. This procedure was satisfactory for bakrine; as shown in Fig. 1, a mixture of benzylamine (0.1 ml) and 2-hydroxyacetophenone (0.1 ml) in 1,2-dichloroethane (10 ml) reacted to produce less than 1% of the theoretical yield of bakrine after 2 hr at room temperature. With benzylamine and salicylaldehyde under the same conditions, however, almost quantitative conversion to saddamine took place (Fig. 2). If these compounds had been present in the original saddamine, the purity determination would have been invalidated.

Since it was necessary to eliminate this source of error, trimethylsilyl derivatives of the two saddamine precursors were used to reduce their reactivity. Such derivatization had a further advantage in that salicylic acid, another potential impurity that cannot be chromatographed directly, may be determined successfully under these conditions (3–5). Chromatography of a mixture of the trimethylsilyl derivatives of benzylamine and salicylaldehyde left at room temperature for 2 hr showed

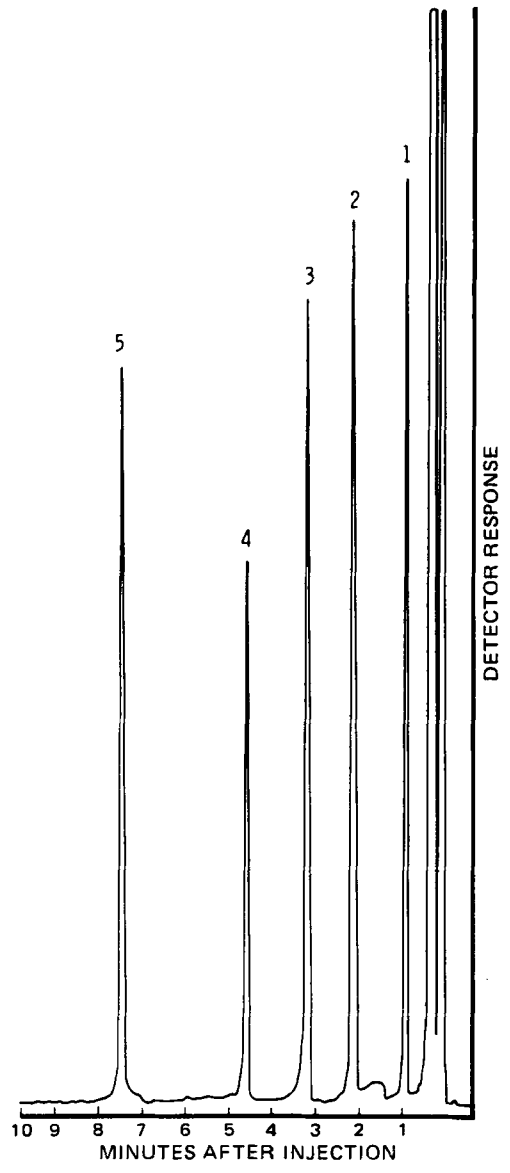

Figure 4—*Gas chromatogram of derivatized phenol (peak 1), benzylamine (peak 2), salicylaldehyde (peak 3), salicylic acid (peak 4), and saddamine (peak 5), each present at a concentration of 2 mg/ml of silylating solution.*

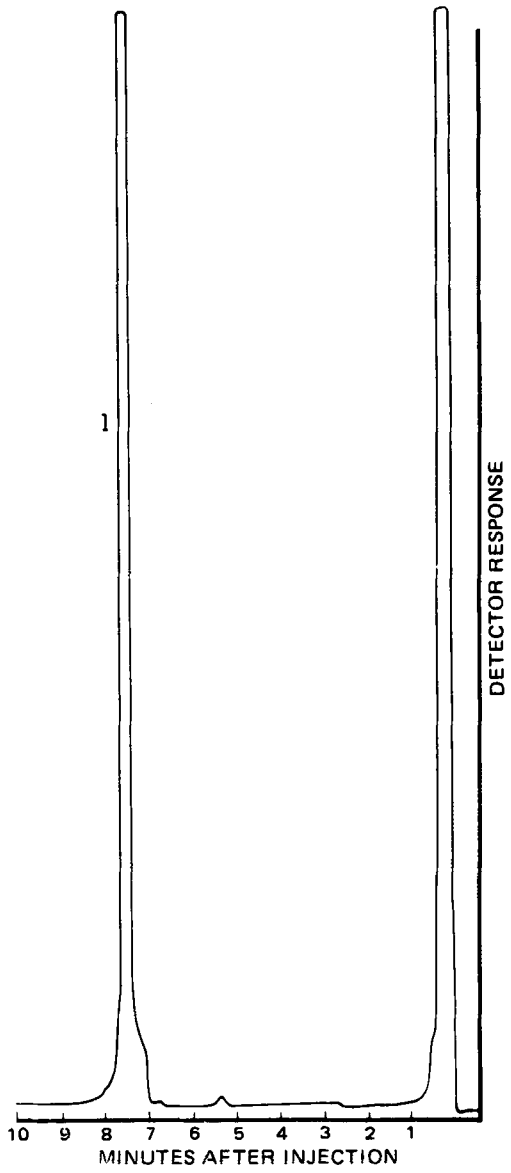

Figure 5—*Typical gas chromatogram of saddamine (peak 1) purity determination.*

that formation of the trimethylsilyl derivative of saddamine amounted to less than 5% of the total theoretical yield (Fig. 3). Thus, with this method, benzylamine and salicylaldehyde would be easily detected should they occur together as saddamine impurities.

Chromatography of a mixture of the trimethylsilyl derivatives of phenol, benzylamine, salicylaldehyde, salicylic acid, and saddamine (Fig. 4) indicated that there was good separation of the saddamine derivative from the derivatives of the potential impurities. The impurities present in many samples of saddamine were investigated using this method, and the chromatogram shown in Fig. 5 is typical of those obtained after on-column injection of 1 μl of a 20-mg/ml solution of the trimethylsilyl derivative of saddamine. Each potential impurity shown in Fig. 4 was absent down to a level of less than 0.5%.

The described method has an obvious application to the determination of other Schiff bases.

REFERENCES

(1) A. F. Al-Sayyab, A. Lawson, and J. O. Stevens, *J. Chem. Soc. C*, **1968**, 411.

(2) A. Lawson and A. F. Al-Sayyab, *Chem. Abstr.*, **84**, 70 (1976).

(3) B. H. Thomas, G. Solomonraj, and B. B. Coldwell, *J. Pharm. Pharmacol.*, **25**, 201 (1973).

(4) M. J. Rance, B. J. Jordan, and J. D. Nichols, *ibid.*, **27**, 425 (1975).

(5) J. P. Tischio, *J. Pharm. Sci.*, **65**, 1530 (1976).

ACKNOWLEDGMENTS

The authors are grateful to the Government of the Republic of Iraq, who completely financed this study, and to the University of Baghdad, who granted a leave of absence for M. R. Al-Ani.

Synthesis of 1-Phenyl-2-(phenylcarbamoyl)pyrazolidines as Potential Anticonvulsant Agents

MILTON J. KORNET [x] **and R. JOYCE GARRETT**

Received July 10, 1978, from the *College of Pharmacy, University of Kentucky, Lexington, KY 40506.* Accepted for publication August 17, 1978.

Abstract □ Twelve 1-phenyl-2-(phenylcarbamoyl)pyrazolidines were synthesized from 1-arylpyrazolidines and aryl isocyanates. These adducts showed little anticonvulsant activity in the maximal electroshock seizure and pentylenetetrazol seizure assays.

Keyphrases □ Pyrazolidines, substituted—synthesized, anticonvulsant activity evaluated □ Anticonvulsant activity—various substituted pyrazolidines evaluated □ Structure-activity relationships—substituted pyrazolidines evaluated for anticonvulsant activity

The synthesis and evaluation of a series of 1-methyl-2-(phenylcarbamoyl)pyrazolidines (I) as anticonvulsant agents revealed good activity for at least three compounds (1). In the most active compounds, R_1 = Cl or CH_3 and R_2 = H or CH_3. To study compounds of this type further, the *N*-methyl group of the pyrazolidine ring was replaced by phenyl. Such a substitution changes the basicity of the molecule and is thereby expected to affect the absorption, distribution, and metabolism of the resultant compounds. This report describes the synthesis and anticonvulsant activity of such compounds, *i.e.*, the 1-phenyl-2-(phenylcarbamoyl)pyrazolidines (III*a*–III*l*, Table I).

DISCUSSION

Chemistry—1-Phenylpyrazolidine has been prepared from trimethylene bromide and a large excess of the sodium salt of phenylhydrazine (2, 3). The latter reagent was obtained from sodium metal and phenylhydrazine. To avoid the tedious procedure employed to make the sodium salt of phenylhydrazine, a modified procedure was developed with sodium hydride as the base. Isolation of the sodium salt of phenylhydrazine also was eliminated; after its formation from phenylhydrazine and sodium hydride in benzene *in situ*, it was reacted directly with the dibromide. In this way, a much smaller excess of phenylhydrazine was required and 1-phenylpyrazolidine (II*a*) was obtained in an 86% yield. With a similar procedure, 1-*p*-(chlorophenyl)pyrazolidine (II*b*) (4) and 1-*p*-tolylpyrazolidine (II*c*) (5) were synthesized in moderate yields (Scheme I).

Table I—Physical Properties of 1-Phenyl-2-phenylcarbamoylpyrazolidines

Compound	X	Y	Melting Point	Yield, %	Formula	Analysis, %	Calc.	Found
III*a*	H	H	116.5–118° [a]	52	$C_{16}H_{17}N_3O$	C	71.89	71.98
						H	6.41	6.50
						N	15.72	15.70
III*b*	*m*-Cl	H	121–123°	90	$C_{16}H_{16}ClN_3O$	C	63.63	63.77
						H	5.34	5.48
						N	13.92	13.85
III*c*	*p*-Cl	H	110–112°	58	$C_{16}H_{16}ClN_3O$	C	63.68	63.79
						H	5.34	5.46
						N	13.92	13.90
III*d*	*p*-F	H	109–111°	68	$C_{16}H_{16}FN_3O$	C	67.35	67.58
						H	5.65	5.59
						N	14.73	14.70
III*e*	*p*-CH_3O	H	117–118.5°	54	$C_{17}H_{19}N_3O_2$	C	68.67	68.41
						H	6.44	6.91
						N	14.13	13.95
III*f*	*p*-C_2H_5O	H	142–143°	42	$C_{18}H_{21}N_3O_2$	C	69.43	69.00
						H	6.80	6.24
						N	13.49	13.35
III*g*	*o*-CH_3	H	110–113°	50	$C_{17}H_{18}N_3O$	C	72.83	72.78
						H	6.47	6.81
						N	14.99	15.05
III*h*	*p*-CH_3	H	97–98°	38	$C_{17}H_{18}N_3O$	C	72.83	72.61
						H	6.47	6.61
						N	14.99	14.91
III*i*	2-Cl,6-CH_3	H	100–101°	32	$C_{17}H_{18}ClN_3O$	C	64.66	64.70
						H	5.74	5.83
						N	13.31	13.47
III*j*	2,6-$(CH_3)_2$	H	125–127°	29	$C_{18}H_{21}N_3O$	C	73.19	73.26
						H	7.17	7.05
						N	14.22	14.29
III*k*	H	Cl	130–133°	54	$C_{16}H_{16}ClN_3O$	C	63.68	63.82
						H	5.34	5.39
						N	13.92	14.01
III*l*	*m*-Cl	CH_3	89.5–91°	13	$C_{17}H_{18}ClN_3O$	C	64.66	64.68
						H	5.74	5.85
						N	13.31	13.32

[a] Lit. (3) mp 114°.

0022-3549/79/0300-0377$01.00/0
© 1979, American Pharmaceutical Association

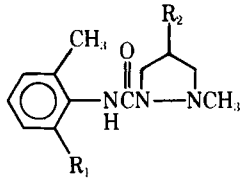

I

Reaction of these 1-arylpyrazolidines with aryl-substituted isocyanates occurred readily to give the adducts IIIa–IIIl. In most cases, these adducts were accompanied by the corresponding ureas derived from the starting isocyanates. The unwanted urea by-products were insoluble in benzene and could be removed by trituration of the crude reaction mixture followed by filtration. The physical properties of IIIa–IIIl are given in Table I.

Biological Activity—Compounds IIIa–IIIl were examined in the maximal electroshock seizure and pentylenetetrazol seizure threshold tests for anticonvulsant activity and neurotoxicity in mice by reported procedures (1). With one exception, all compounds were devoid of anticonvulsant activity at the highest dose tested (300 mg/kg). Compound IIIh showed activity in the pentylenetetrazol seizure test at 300 mg/kg (0.5 hr). None of the compounds showed toxicity at the three doses tested (30, 100, and 300 mg/kg).

This study indicates that replacement of *N*-methyl by phenyl in I results in a loss of anticonvulsant activity. Solubility tests in 5% HCl revealed that the *N*-methyl series of compounds (I) (1) is soluble whereas the *N*-phenyl series (IIIa–IIIl) is insoluble. Perhaps the inactivity of IIIa–IIIl results from a failure in absorption caused by poor solubility.

EXPERIMENTAL[1]

1-Phenylpyrazolidine (IIa)—To a stirred suspension of 40.42 g (0.960 mole) of a 57% mineral oil dispersion of sodium hydride in 500 ml of dry benzene, protected by a nitrogen atmosphere, was added dropwise a solution of 64.8 g (0.60 mole) of phenylhydrazine in 100 ml of dry benzene. The reaction mixture was warmed on an oil bath until hydrogen evolution (monitored by mercury bubbler) occurred. After 30 min, gas evolution had slowed; then 40.40 g (0.20 mole) of 1,3-dibromopropane was added in one portion to the reaction mixture, which had been cooled to room temperature. Upon heating, hydrogen was evolved over 1.5 hr.

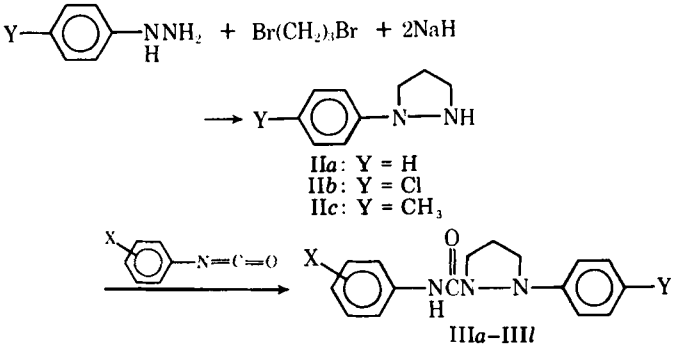

Scheme I

The mixture was then refluxed for 1.5 hr. A second portion of 40.40 g (0.20 mole) of 1,3-dibromopropane was added dropwise to the refluxing reaction mixture, and refluxing was continued overnight (17–18 hr). After cooling, the reaction mixture was washed twice with 100-ml portions of water, and the benzene layer was dried (magnesium sulfate). After removal of the benzene under reduced pressure, the residue separated into two distinct layers. The top mineral oil layer was separated off. The lower product layer was distilled and afforded 50.6 g (86%) of liquid, bp 81–86°/0.25 mm [lit. (3) bp 160°/20 mm]; IR (film): 3300 (NH) cm^{-1}.

1-*p*-(Chlorophenyl)pyrazolidine (IIb) (4)—This compound was obtained from 11.8 g (0.083 mole) of *p*-chlorophenylhydrazine, 12.93 g (0.064 mole) of 1,3-dibromopropane, and 6.48 g (0.154 mole) of a 57% mineral oil dispersion of sodium hydride according to the same procedure used for the preparation of IIa. Distillation gave 6.03 g (52%) of product, bp 110–115°/0.25 mm; IR (film): 3295 (NH) cm^{-1}.

1-*p*-Tolylpyrazolidine (IIc) (5)—This compound was prepared from 12.5 g (0.102 mole) of *p*-tolylhydrazine, 15.9 g (0.0786 mole) of 1,3-dibromopropane, and 8.0 g (0.190 mole) of a 57% mineral oil dispersion of sodium hydride according to the same procedure used for the synthesis of IIa. Distillation afforded 6.42 g (50%) of the pyrazolidine, bp 94°/0.15 mm; IR (film): 3300 (NH) cm^{-1}.

1-Phenyl-2-(phenylcarbamoyl)pyrazolidines (III)—A typical reaction is described, that for the preparation of 1-phenyl-2-*p*-tolylcarbamoylpyrazolidine (IIIh). A mixture of 4.56 g (0.0308 mole) of IIa, 3.72 g (0.028 mole) of *p*-tolyl isocyanate, and 40 ml of dry toluene was refluxed for 6 hr. The mixture was cooled, and the solvent was evaporated under reduced pressure.

The remaining thick oily residue was triturated with petroleum ether and produced 8.0 g of solid crude product. The latter was triturated with benzene and filtered. Evaporation of the benzene solution gave a product uncontaminated with the urea by-product. Recrystallization from 95% ethanol gave 3.0 g (38%) of analytically pure material, mp 97–98°; IR (KBr): 1650 (C=O) and 3260 (NH) cm^{-1}; NMR ($CDCl_3$): δ 2.23 (s, 3, CH_3), 1.67–4.5 (m, 6, aliphatic ring H), 6.68–7.57 (m, 9, ArH), and 7.95 (broad s, 1, CONH) ppm.

[1] Melting points were determined on a Thomas-Hoover apparatus and are uncorrected. IR spectra were taken on a Perkin-Elmer 700 spectrophotometer as either liquid films or potassium bromide pellets. NMR spectra were recorded on a Varian A-60A spectrometer with tetramethylsilane as the internal reference. Elemental analyses were performed by Dr. Kurt Eder, Geneva, Switzerland.

REFERENCES

(1) M. J. Kornet, *J. Pharm. Sci.*, **67**, 1471 (1978).

(2) A. Michaelis, *Justus Liebigs Ann. Chem.*, **252**, 266 (1871).

(3) A. Michaelis and O. Lampe, *ibid.*, **274**, 316 (1893).

(4) G. A. Golubeva, Y. N. Portnov, A. N. Kost, and L. A. Sviridova, *Khim. Geterotsikl. Soedin.*, **7**(1), 118 (1971).

(5) H. Gysling and H. J. Peterli, U.S. pat. 2,936,290 (1960); through *Chem. Abstr.*, **54**, P24804f (1960).

ACKNOWLEDGMENTS

The authors are indebted to Mr. Gill D. Gladding, ADD Program, National Institutes of Health, for providing the anticonvulsant activity data and to Mrs. Kelly Filo for technical assistance in the syntheses.

Sensitive High-Pressure Liquid Chromatographic Determination of Propranolol in Plasma

GLORIA NYGARD, WILLIAM H. SHELVER ˣ, and S. K. WAHBA KHALIL

Received June 19, 1978, from the *College of Pharmacy, North Dakota State University, Fargo, ND 58105.* Accepted for publication August 16, 1978.

Abstract □ A high-pressure liquid chromatographic method is presented for the determination of propranolol in human plasma. A reversed-phase cyanopropylsilane column was utilized with a liquid phase consisting of 70% acetonitrile and 30% 0.02 *M* acetate buffer, pH 7.0. A spectrofluorometric detector with an excitation wavelength of 276 nm and an emission filter with a 340-nm cutoff provided a detectable peak for 0.8 ng of propranolol/injection with this system. The reproducibility and precision of the method are shown from the analyses of samples containing 10–150 ng/ml of plasma.

Keyphrases □ Propranolol—high-pressure liquid chromatographic analysis in plasma □ High-pressure liquid chromatography—analysis, propranolol in plasma □ Cardiac depressants—propranolol, high-pressure liquid chromatographic analysis in plasma

Propranolol is used in the treatment of hypertension, angina pectoris, and cardiac arrhythmias and is used experimentally for several other conditions. Because of differences in both the pharmacokinetics and the response to the drug, the dosage regimen must be individualized. Clinical determination of plasma levels provides the most efficient and precise aid in adjusting dosage.

Plasma levels encountered during therapy with propranolol may range from a low of 20 to >100 ng/ml (1–3), a concentration range that prohibits the use of many common analytical techniques. Several methods for the quantitative determination of propranolol in plasma use electron-capture GLC, which involves derivatization of the compound (4–6). Radioimmunology (7), in spite of high sensitivity and specificity, is seldom used because of limitations in availability of antiserums. Direct fluorometric determination (8–10) is popular but lacks specificity.

This paper describes a rapid method for the determination of propranolol involving high-pressure liquid chromatographic (HPLC) separation and fluorometric detection. The combination of HPLC and fluorometry provides the needed specificity and sensitivity for the drug. Conditions are discussed for the extraction, separation, and detection of propranolol. The applicability of this procedure was demonstrated by the analysis of plasma from patients taking propranolol.

EXPERIMENTAL

Instrumentation—A high-pressure liquid chromatograph[1] was equipped with a fluorometric detector[2] and a cyanopropylsilane[3] column, 300 mm long × 4 mm i.d. The degassed mobile phase was pumped through the column at 2.0 ml/min (1100–1200 psi) at ambient temperature until a stable baseline was obtained. The fluorometer was set at an excitation wavelength of 276 nm, and an emission cutoff filter (type 340) was used.

Chemicals and Reagents—Sodium acetate, sodium phosphate, acetic acid, phosphoric acid, dichloromethane, benzene, chloroform, and ethyl acetate were reagent grade. HPLC grade methanol and acetonitrile were used. Propranolol hydrochloride[4], 4-hydroxypropranolol[4], and cyclomethycaine sulfate[5] were obtained commercially.

Mobile Phase—Sodium acetate solutions (0.01, 0.02, and 0.04 *M*) were prepared in distilled water. The pH was adjusted to 4, 5, 6, or 7 with acetic acid. The mobile phase was prepared by adding an appropriate amount of acetonitrile to the aqueous buffer and degassing under vacuum. The effect on the retention time of various buffer concentrations and buffer pH was studied.

Extraction Conditions—The extraction of propranolol and the internal standard (cyclomethycaine) from plasma at pH 7.4 and 12 was studied using dichloromethane. The relative extractability of solutes from spiked plasma samples at pH 7.4 was compared using four solvents: benzene, hexane, ethyl acetate, and dichloromethane.

Analytical Procedure—To 0.5 ml of heparinized plasma (in a 15-ml screw-capped centrifuge tube) were added 0.5 ml of phosphate buffer (pH 7.4 and 0.1 *M*), 5 ml of solvent containing 0.16 μg of cyclomethycaine

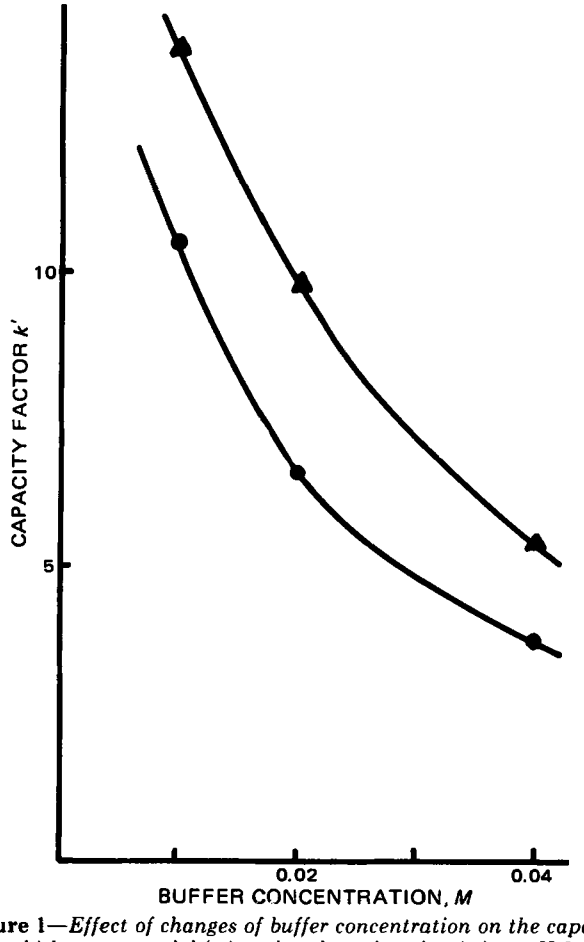

Figure 1—*Effect of changes of buffer concentration on the capacity factor k' for propranolol (●) and cyclomethycaine (▲) at pH 6 using 75% acetonitrile.*

[1] Model 202 chromatograph, M 600 pump, and U6K Universal injector, Waters Associates, Milford, Mass.
[2] FS-970, Schoeffel, Westwood, N.J.
[3] μBondapak CN, Waters Associates, Milford, Mass.
[4] Ayerst Laboratories, New York, N.Y.
[5] Eli Lilly and Co., Indianapolis, Ind.

0022-3549/79/0300-0379$01.00/0
© 1979, American Pharmaceutical Association

Table I—Evaluation of Assay Precision and Accuracy for Propranolol

Propranolol Hydrochloride Added, ng/ml	n	Mean Propranolol Hydrochloride Measured, ng/ml	Percent Recovered	CV
10	5	10.56	105.6	13.7
25	4	24.19	96.8	5.6
50	4	54.51	109.0	5.7
75	5	73.38	97.8	1.3
100	3	100.69	100.7	4.5
150	3	149.20	99.5	2.6
Average			101.6	

sulfate/ml as the internal standard, and an aliquot of the propranolol hydrochloride solution containing 5.0–75.0 ng (10–150 μl of a methanolic solution). The tubes were then vortexed for 10 sec and centrifuged for 5 min at 900×*g*. A 4.0-ml volume of the organic phase was transferred to special concentration tubes[6] and evaporated to dryness at ambient temperature under a gentle stream of nitrogen.

The residue was dissolved in 100 μl of methanol, and replicate 50-μl injections were made using a 50-μl syringe[7]. A standard curve was constructed by injecting plasma extracts simulating concentrations of propranolol hydrochloride from 10 to 150 ng/ml. The chromatograms were recorded[8] at a chart speed of 5 mm/min. The peak heights were measured, and the ratios (propranolol to cyclomethycaine) were calculated and plotted *versus* the propranolol concentrations expressed as nanograms per milliliter.

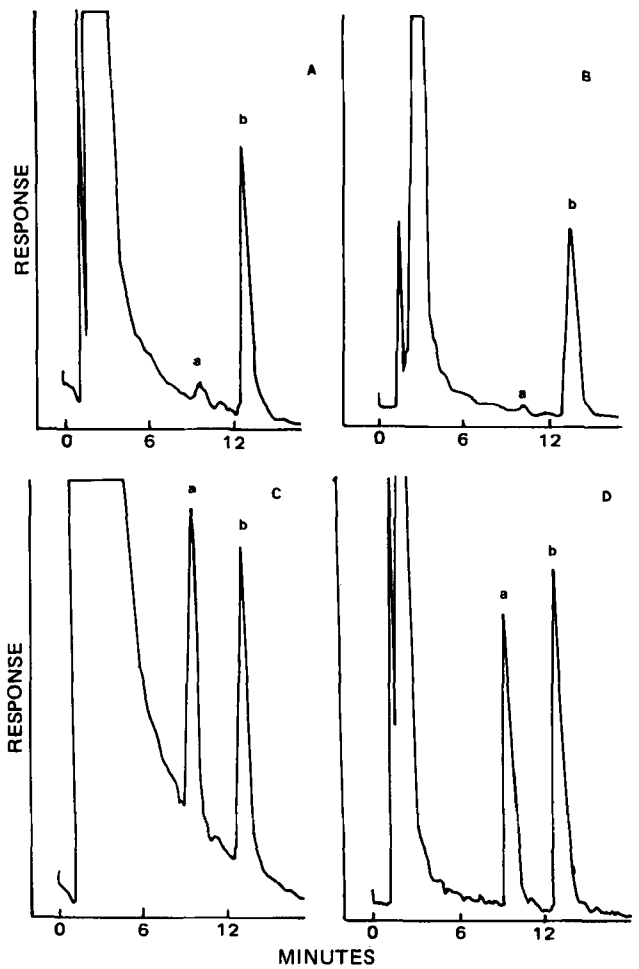

Figure 2—*Chromatograms of plasma extracts containing propranolol hydrochloride (a) and cyclomethycaine sulfate (b). Key: A, hexane; B, benzene; C, ethyl acetate; and D, dichloromethane.*

Interferences—The possible interferences from normal plasma constituents and the major metabolite (4-hydroxypropranolol) (11), as well as other drugs, were studied by adding therapeutic concentrations of these drugs to plasma containing propranol and the internal standard and then performing the analysis.

Sample Preparation and Assay—Heparinized plasma samples from patients receiving oral propranolol therapy were processed in duplicate as described under *Analytical Procedure*. The amount of propranolol was calculated by comparison with standards prepared daily.

RESULTS AND DISCUSSION

Increasing the buffer molar concentration shortened the capacity factor in a nonlinear fashion (Fig. 1). The capacity factor of the compounds also was affected by pH change. A mobile phase of 70% acetonitrile and 30% acetate buffer (pH 7.0 and 0.02 *M*) gave well-resolved sharp peaks for propranolol, 4-hydroxypropranolol, and cyclomethycaine with retention times of 10.0, 7.7, and 13.5 min, respectively. Quinidine, lidocaine, procainamide, and disopyramide, commonly utilized cardiac drugs, were eluted at different retention times and thus did not interfere with the analysis under the experimental conditions. The choice of fluorometer parameters allowed a concentration of propranolol as low as 0.8 ng on-column to give a peak clearly distinguishable from baseline noise. After the study was completed, a cyanopropylsilane column from a different manufacturer[9] was utilized with only minor changes in solvent conditions.

Dichloromethane was selected as the solvent for extraction of propranolol from plasma at pH 7.4. This selection was based on the highest amount of propranolol and/or the lowest amount of interfering fluorescent material being extracted. Hexane and benzene were inefficient in the extraction of propranolol, while ethyl acetate extracted excessive fluorescent substances from plasma (Fig. 2). Dichloromethane produced excellent recovery of propanolol and minimum extraction of interfering constituents from plasma and was evaporated easily.

A high recovery of propranolol (90%) from spiked plasma samples was obtained with dichloromethane at pH 7.4. When 0.1 *N* NaOH was used as an alkalinizing agent, the ratio of the propranolol peak height to the internal standard peak height dropped appreciably. Extraction at pH 7.4 with dichloromethane using a ratio of the organic phase to the aqueous phase of 5 gave satisfactory recoveries of propanolol and the internal standard; a second extraction yielded only trace quantities of the two compounds.

The ratio of the peak height of propranolol to the peak height of the internal standard was calculated. Statistical analyses (Table I) by linear regression indicated excellent linearity and reproducibility with a correlation coefficient of 0.994, a slope of 0.00297, and an intercept of 0.000302 in the range of 1.8–26.4 ng of propranolol on-column. This range corresponds to 10–150 ng of propranolol hydrochloride/1.0 ml of plasma and includes the therapeutic range of the drug.

The method was applied to the determination of free propranolol in patient plasma before and after administration of a dose. No interference was noted, and the method proved to be sensitive even to the trace amount of propranolol present before dosing. The method can be recommended for the pharmacokinetic studies of propranolol in the presence or absence of other simultaneously prescribed cardiovascular drugs.

REFERENCES

(1) M. Esler, A. Zweifler, O. Rindall, and V. DeQuattro, *Clin. Pharmacol. Ther.*, **22**, 299 (1977).

(2) E. Vervlaet, B. F. M. Pluym, J. Cilissen, K. Kohlen, and F. W. H. M. Merkus, *ibid.*, **22**, 853 (1977).

(3) D. M. Kornhausen, A. J. J. Wood, R. E. Vestal, G. R. Wilkinson, R. A. Branch, and D. G. Shend, *ibid.*, **23**, 165 (1978).

(4) E. DiSalle, K. M. Baker, S. R. Bareggi, W. D. Watkins, C. A. Chidsey, A. Frigerio, and P. L. Morselli, *J. Chromatogr.*, **84**, 347 (1973).

(5) T. Walle, *J. Pharm. Sci.*, **63**, 1885 (1974).

(6) T. Walle, J. Morrison, K. Walle, and E. Conradi, *J. Chromatogr.*, **114**, 351 (1975).

[6] Concentratubes, Laboratory Research Co., Los Angeles, Calif.
[7] Hamilton Co., Reno, Nev.
[8] Model 56, Perkin-Elmer, Norwalk, Conn.
[9] DuPont, Wilmington, Del.

(7) K. Kawashima, A. Levy, and S. Spector, *J. Pharmacol. Exp. Ther.*, **196**, 517 (1976).
(8) M. Kraml and W. T. Robinson, *Clin. Chem.*, **24**, 169 (1978).
(9) P. K. Ambler, B. N. Singh, and M. Lever, *Clin. Chim. Acta*, **54**, 373 (1974).
(10) L. Offerhaus and J. R. Van Der Vecht, *Br. J. Clin. Pharmacol.*, **3**, 1061 (1976).
(11) C. R. Cleveland and D. G. Shand, *Clin. Pharmacol. Ther.*, **13**, 181 (1972).

ACKNOWLEDGMENTS

The authors thank the Veterans Administration Center, Fargo, N.D., for assistance in this project.

Electron-Capture GLC Assay of Dichlorphenamide

C. SCHMITT *x, W. J. A. VANDENHEUVEL ‡, R. W. WALKER ‡, and B. PLAZONNET *

Received June 14, 1978, from the **Institut Merck Sharp & Dohme-Chibret, 63018 Clermont-Ferrand, France*, and the ‡*Merck Sharp & Dohme Research Laboratories, Rahway, NJ 07065.* Accepted for publication August 22, 1978.

Abstract □ GLC with electron-capture detection was applied to the assay of the carbonic anhydrase inhibitor dichlorphenamide and demonstrated a sensitivity of 10 ng in 0.5 ml of rabbit serum or whole aqueous humor (≃0.25 ml) from one rabbit eye. After extraction of the drug and internal standard (monochlorphenamide) from the biological fluid, these compounds were converted to their tetramethyl derivatives by a nucleophilic alkylation method. Dichlorphenamide contents of aqueous humor and serum of rabbits treated with this drug are reported.

Keyphrases □ Dichlorphenamide—GLC analysis in biological fluids □ GLC—analysis, dichlorphenamide in biological fluids □ Carbonic anhydrase inhibitors—dichlorphenamide, GLC analysis in biological fluids

Dichlorphenamide (I), 4,5-dichloro-1,3-disulfamoylbenzene, is an orally effective carbonic anhydrase [carbonate dehydratase EC 4.2.1.1 (1)] inhibitor[1] (2). This drug possesses diuretic activity (3, 4) and decreases intraocular pressure in rabbits (5) and in normal (2) and glaucomatous (2, 6, 7) humans. Assay of dichlorphenamide in biological fluids, especially aqueous humor, requires a very sensitive method. GLC with electron-capture detection is useful for the determination of submicrogram quantities of compounds in small volumes of body fluids. However, direct GLC of polar compounds is usually not possible; derivatization techniques must be used to convert these compounds to less polar derivatives.

This paper describes a GLC technique combined with electron-capture detection for the assay of dichlorphenamide and its application to the determination of aqueous humor and serum drug levels following dichlorphenamide administration to rabbits by different routes.

EXPERIMENTAL

Reagents and Chemicals—The following were used: dichlorphenamide[2] (I), 4-chloro-1,3-disulfamoylbenzene[2] (II) as the internal standard, toluene[3] (pesticide quality), ethyl acetate[3] (pesticide quality), *N,N*-dimethylacetamide[4] for synthesis, acetic acid[4] for analysis, sodium bicarbonate[4], anhydrous sodium sulfate[4], 10% aqueous tetramethylammonium hydroxide[4], methanol[4], and methyl iodide[5] (purum). A half-saturated solution of sodium bicarbonate and 0.1 *N* NH_4OH were prepared with deionized water. The tetramethylammonium hydroxide was diluted fourfold with methanol.

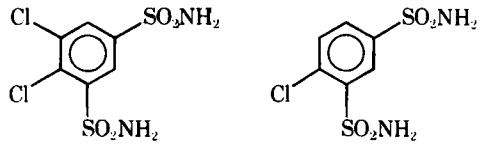

I II

Instrumentation—The gas chromatograph[6] was equipped with a ^{63}Ni (10-mCi) electron-capture detector. A 1.5-m × 3-mm i.d. glass column containing 3% OV-17 on 100–120-mesh Gas Chrom Q[7] was used. The carrier gas was argon–methane (90:10) with a flow rate of 60 ml/min and <5 ml/min detector scavenge. Temperatures were 265° for the column and 290° for the injector and detector.

GLC–mass spectrometry of the derivative was carried out with a mass spectrometer[8] operated in the electron-impact (70 ev) mode and equipped with a 1.5-m × 3-mm column packed with 2% SE-30 on 80–100-mesh Gas Chrom Q[7] (250°).

Drug Extraction—The extraction method was based on that described by VandenHeuvel *et al.* (8) for hydrochlorothiazide in human plasma. An appropriate, known volume of aqueous humor or serum (containing less than 100 ng of dichlorphenamide) was diluted with water to 0.5 ml in a 7-ml disposable, silanized, glass-stoppered tube to which 75 ng of II in 0.1 ml of ethyl acetate (taken to dryness with a nitrogen

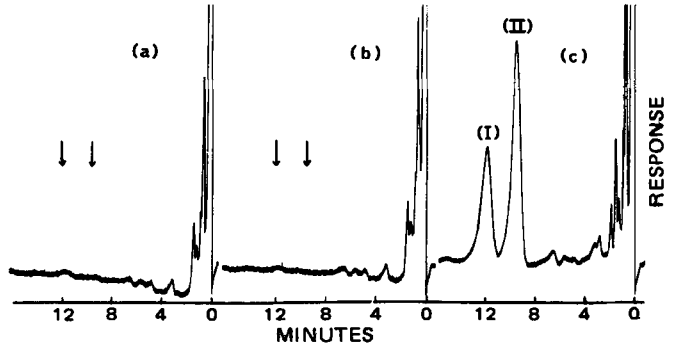

Figure 1—*Chromatograms (1 × 10^{-9} afs at 1 mv) from control aqueous humor (a), control serum (b), and control aqueous humor spiked with 50 ng of dichlorphenamide (I) and 75 ng of the internal standard (II) (c).*

[1] Daranide, Merck Sharp & Dohme.
[2] Merck Sharp & Dohme.
[3] Carlo Erba.
[4] E. Merck.
[5] Fluka.
[6] Girdel 75.
[7] Altech Associates.
[8] Finnigan 3200.

0022-3549/79/0300-0381$01.00/0
© 1979, American Pharmaceutical Association

(7) K. Kawashima, A. Levy, and S. Spector, *J. Pharmacol. Exp. Ther.*, **196**, 517 (1976).
(8) M. Kraml and W. T. Robinson, *Clin. Chem.*, **24**, 169 (1978).
(9) P. K. Ambler, B. N. Singh, and M. Lever, *Clin. Chim. Acta*, **54**, 373 (1974).
(10) L. Offerhaus and J. R. Van Der Vecht, *Br. J. Clin. Pharmacol.*, **3**, 1061 (1976).
(11) C. R. Cleveland and D. G. Shand, *Clin. Pharmacol. Ther.*, **13**, 181 (1972).

ACKNOWLEDGMENTS

The authors thank the Veterans Administration Center, Fargo, N.D., for assistance in this project.

Electron-Capture GLC Assay of Dichlorphenamide

C. SCHMITT *x, W. J. A. VANDENHEUVEL ‡, R. W. WALKER ‡, and B. PLAZONNET *

Received June 14, 1978, from the **Institut Merck Sharp & Dohme-Chibret, 63018 Clermont-Ferrand, France*, and the ‡*Merck Sharp & Dohme Research Laboratories, Rahway, NJ 07065.* Accepted for publication August 22, 1978.

Abstract □ GLC with electron-capture detection was applied to the assay of the carbonic anhydrase inhibitor dichlorphenamide and demonstrated a sensitivity of 10 ng in 0.5 ml of rabbit serum or whole aqueous humor (≃0.25 ml) from one rabbit eye. After extraction of the drug and internal standard (monochlorphenamide) from the biological fluid, these compounds were converted to their tetramethyl derivatives by a nucleophilic alkylation method. Dichlorphenamide contents of aqueous humor and serum of rabbits treated with this drug are reported.

Keyphrases □ Dichlorphenamide—GLC analysis in biological fluids □ GLC—analysis, dichlorphenamide in biological fluids □ Carbonic anhydrase inhibitors—dichlorphenamide, GLC analysis in biological fluids

Dichlorphenamide (I), 4,5-dichloro-1,3-disulfamoylbenzene, is an orally effective carbonic anhydrase [carbonate dehydratase EC 4.2.1.1 (1)] inhibitor[1] (2). This drug possesses diuretic activity (3, 4) and decreases intraocular pressure in rabbits (5) and in normal (2) and glaucomatous (2, 6, 7) humans. Assay of dichlorphenamide in biological fluids, especially aqueous humor, requires a very sensitive method. GLC with electron-capture detection is useful for the determination of submicrogram quantities of compounds in small volumes of body fluids. However, direct GLC of polar compounds is usually not possible; derivatization techniques must be used to convert these compounds to less polar derivatives.

This paper describes a GLC technique combined with electron-capture detection for the assay of dichlorphenamide and its application to the determination of aqueous humor and serum drug levels following dichlorphenamide administration to rabbits by different routes.

EXPERIMENTAL

Reagents and Chemicals—The following were used: dichlorphenamide[2] (I), 4-chloro-1,3-disulfamoylbenzene[2] (II) as the internal standard, toluene[3] (pesticide quality), ethyl acetate[3] (pesticide quality), *N,N*-dimethylacetamide[4] for synthesis, acetic acid[4] for analysis, sodium bicarbonate[4], anhydrous sodium sulfate[4], 10% aqueous tetramethylammonium hydroxide[4], methanol[4], and methyl iodide[5] (purum). A half-saturated solution of sodium bicarbonate and 0.1 *N* NH_4OH were prepared with deionized water. The tetramethylammonium hydroxide was diluted fourfold with methanol.

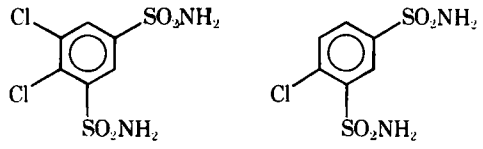

I II

Instrumentation—The gas chromatograph[6] was equipped with a ^{63}Ni (10-mCi) electron-capture detector. A 1.5-m × 3-mm i.d. glass column containing 3% OV-17 on 100–120-mesh Gas Chrom Q[7] was used. The carrier gas was argon–methane (90:10) with a flow rate of 60 ml/min and <5 ml/min detector scavenge. Temperatures were 265° for the column and 290° for the injector and detector.

GLC–mass spectrometry of the derivative was carried out with a mass spectrometer[8] operated in the electron-impact (70 ev) mode and equipped with a 1.5-m × 3-mm column packed with 2% SE-30 on 80–100-mesh Gas Chrom Q[7] (250°).

Drug Extraction—The extraction method was based on that described by VandenHeuvel *et al.* (8) for hydrochlorothiazide in human plasma. An appropriate, known volume of aqueous humor or serum (containing less than 100 ng of dichlorphenamide) was diluted with water to 0.5 ml in a 7-ml disposable, silanized, glass-stoppered tube to which 75 ng of II in 0.1 ml of ethyl acetate (taken to dryness with a nitrogen

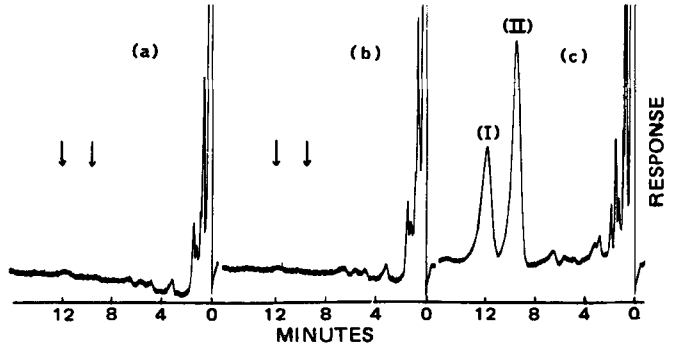

Figure 1—*Chromatograms (1 × 10^{-9} afs at 1 mv) from control aqueous humor (a), control serum (b), and control aqueous humor spiked with 50 ng of dichlorphenamide (I) and 75 ng of the internal standard (II) (c).*

[1] Daranide, Merck Sharp & Dohme.
[2] Merck Sharp & Dohme.
[3] Carlo Erba.
[4] E. Merck.
[5] Fluka.
[6] Girdel 75.
[7] Altech Associates.
[8] Finnigan 3200.

0022-3549/79/0300-0381$01.00/0
© 1979, American Pharmaceutical Association

Table I—Recovery of Dichlorphenamide from Biological Fluids

Amount Added, ng		Amount Recovered[a]								Mean ± *SD*
					From Aqueous Humor					
10	A	4.2	7.7	7.7	—	7.7	3.1	7.7	10.0	6.9 ± 2.4
	B	42	77	77	—	77	31	77	100	69 ± 24
20	A	20.5	21.7	17.00	20.5	20.5	10.00	21.7	25.1	19.6 ± 4.5
	B	103	108	85	103	103	50	108	126	98 ± 22
50	A	43.8	55.4	44.9	34.4	50.7	46.1	49.6	43.8	46.1 ± 6.2
	B	88	111	90	69	101	92	99	88	92 ± 12
100	A	101.9	104.2	71.7	77.5	93.8	84.4	85.6	79.8	87.4 ± 11.6
	B	102	104	72	77	94	84	86	80	87 ± 12
					From Serum					
10	A	6.5	10.0	4.2	5.4	6.5	5.4	8.9	8.9	7.0 ± 2.0
	B	65	100	42	54	65	54	89	89	70 ± 21
20	A	18.2	19.3	25.1	13.5	21.7	27.5	20.6	21.7	21.0 ± 4.3
	B	91	97	126	68	108	137	102	108	105 ± 21
50	A	57.7	61.2	41.4	42.6	48.4	57.7	55.4	49.6	51.8 ± 7.4
	B	115	122	82	85	97	115	111	99	103 ± 15
100	A	120.5	120.50	90.3	85.6	81.0	92.6	—	72.8	94.7 ± 18.7
	B	121	120	90	86	81	93	—	73	95 ± 19

[a] Values in the A rows represent nanograms recovered; values in the B rows represent percent recovery.

stream) had been added. The tube was agitated to ensure dissolution of the internal standard. Toluene (0.5 ml) was added to this sample, and, after agitation[9] and centrifugation, the organic phase was discarded; this step was repeated.

The remaining aqueous phase was extracted twice with 0.5 ml of ethyl acetate, and the organic phases were transferred to another tube. A 0.5-ml aliquot of 0.1 *N* NH_4OH was added to the combined ethyl acetate phases, the tube was agitated (vortex mixer) and centrifuged, and the upper organic phase was discarded. Acetic acid (50 μl) was added to the aqueous phase to give a pH between 3.5 and 4, and this solution was extracted twice with 0.5 ml of ethyl acetate. The extracts were combined and taken to dryness under a nitrogen stream.

Derivatization—Dichlorphenamide methylation was carried out using a procedure similar to that used by Least *et al.* (9) for the butylation of ethosuximide. Purification of the derivative prior to GLC analysis was carried out as described by Greeley (10). *N,N*-Dimethylacetamide (40 μl), 10 μl of methanolic tetramethylammonium hydroxide, and 10 μl of methyl iodide were added to the dry residue. The stoppered tube was allowed to stand for 10 min at room temperature, 0.5 ml of toluene was added, and the tube was agitated[9] and centrifuged.

The upper phase was transferred to another tube, and the extraction was repeated. The combined toluene phases were washed sequentially with 0.5 ml of water, 0.5 ml of bicarbonate, and 0.5 ml of water. After drying over anhydrous sodium sulfate, the organic phase was taken to dryness under a nitrogen stream. The residue was dissolved in 50 μl of toluene, and 2 μl was injected into the gas chromatograph.

Assay—Peak heights for derivatized dichlorphenamide and the internal standard were measured. A standard curve was constructed by derivatization and GLC assay of known amounts of dichlorphenamide added to 75 ng of monochlorphenamide. The ratio obtained by dividing the dichlorphenamide peak height by the internal standard peak height was plotted against the amount of dichlorphenamide used.

Known amounts of dichlorphenamide and 75 ng of the internal standard were added to either 0.2 ml of aqueous humor or 0.5 ml of serum. These spiked samples were extracted, derivatized, and analyzed to obtain standard curves from both biological fluids. Concentrations of dichlorphenamide in biological samples were determined by referring to the corresponding standard curve.

Treatment of Rabbits and Collection of Samples—Dichlorphenamide was used as either a 5% suspension in distilled water or a 5% solution of the potassium salt in saline (all concentrations are expressed as dichlorphenamide). Unanesthetized rabbits in restraining boxes were used throughout this study. Agents were administered as follows: (*a*) a 1-ml/kg dose of the suspension of dichlorphenamide or of the potassium salt solution was given by stomach tube (50 mg/kg); and (*b*) a 1-ml/kg dose of the potassium salt solution was injected intravenously into the marginal ear vein (50 mg/kg).

All rabbits were fasted for 16 hr. At the end of experiments, rabbits were anesthetized by intravenous injection of pentobarbital sodium[10], the aqueous humor of each eye was withdrawn using a needle gun (11), and ≃7 ml of blood was sampled by intracardiac puncture. Blood was allowed to clot for ≃2 hr and then centrifuged, and the serum was pipetted for the assay.

[9] Maxi Mix, Thermolyne.
[10] Nembutal, Abbott.

RESULTS AND DISCUSSION

Chromatograms resulting from assay of control aqueous humor and serum and aqueous humor spiked with dichlorphenamide and the internal standard (50 and 75 ng, respectively) are shown in Fig. 1. The retention times were ≃9 and 12 min for the tetramethyl derivatives of the internal standard and dichlorphenamide, respectively.

A linear response should be obtained with monochlorphenamide to validate its use as an internal standard. By plotting the peak height of the derivative of monochlorphenamide against the quantity of monochlorphenamide used, it was demonstrated that a linear response was obtained between 1.6 and 8 ng injected.

A calibration curve prepared by derivatization of known amounts of dichlorphenamide indicated that a linear relation existed in the 10–100-ng range between the peak height ratio of dichlorphenamide to the internal standard and the amount of derivatized dichlorphenamide. The parameters of this linear relationship, calculated according to Carstensen (12), were: slope, 0.009 ± 0.001; intercept, 0.154 ± 0.034; and coefficient of regression, 0.995. Eight values were obtained for each concentration.

Recovery was calculated by referring to the previous standard curve for samples of serum or aqueous humor spiked with known amounts of dichlorphenamide. The recoveries were 87 ± 13% (*SD*) for aqueous humor and 93 ± 16% for serum (Table I).

By plotting the peak height ratio of dichlorphenamide to the internal standard of these spiked samples against the amount of added dichlorphenamide, it was demonstrated that the relationship was statistically linear in aqueous humor ($r = 0.998$) and serum ($r = 0.997$). The standard curves thus obtained were used for assays.

The electron-impact (70 ev) mass spectrum of the derivative of dichlorphenamide was obtained by GLC–mass spectrometry. The characteristic dichloro molecular ion (*m/e* 360/362) demonstrated the formation of the tetramethyl derivative. Other dichloro ions with their characteristic pattern (13) were: ($M - SO_2NC_2H_5$) (*m/e* 253/255) and $[M - [SO_2N(CH_3)_2]_2]$ (*m/e* 144/146). The base peak (*m/e* 108) was not chlorine containing and could have been $[SO_2N(CH_3)_2]^+$. The mass spectrum of the derivatized internal standard was obtained using similar conditions. The molecular ion (*m/e* 326/328) demonstrated the formation

Table II—Dichlorphenamide Selective Ion Monitoring

Sample	Intensity Ratios *m/e* 255/253	*m/e* 362/360
Standard tetramethyldichlorphenamide	0.61	0.72
Serum spiked with dichlorphenamide	0.62	0.74
Aqueous humor spiked with dichlorphenamide	0.61 0.62	0.74 0.73

Table III—Biolevels of Dichlorphenamide after Administration to Rabbits [a]

Hours	Group A [b] Aqueous Humor Level, ng/100 mg	Group A [b] Serum Level, ng/100 μl	Group B [c] Aqueous Humor Level, ng/100 mg	Group B [c] Serum Level, ng/100 μl	Group C [d] Aqueous Humor Level, ng/100 mg	Group C [d] Serum Level, ng/100 μl
0.5	19.9 ± 31	1.8 ± 1.2	27.8 ± 34.1	468.9 ± 409.7	315.4 ± 145.0	2176.3 ± 732.8
1	14.8 ± 22	54.1 ± 8.9	117.4 ± 43.2	41.7 ± 13.2	344.3 ± 98.9	1915.7 ± 583.8
2	41.8 ± 31.5	118.3 ± 86.3	86.1 ± 58.6	460.0 ± 319.8	277.0 ± 41.7	1580.0 ± 47.2
4	41.6 ± 24.1	148.8 ± 63.9	119.8 ± 75.2	709.7 ± 408.8	192.5 ± 109.3	2370.2 ± 669.2
8	50.1 ± 35.8	164.8 ± 44.6	58.6 ± 39.2	135.6 ± 79.1	58.3 ± 29.2	— [e]
16	28.4 ± 12.1	129.8 ± 60.2	7.3 ± 8.3	31.2 ± 14.6	13.3 ± 3.7	— [e]
24	7.7 ± 5.6	9.3 ± 14	2.1 ± 2.7	24 ± 11.1	— [e]	— [e]

[a] Results are means ± *SD* (12 samples for aqueous humor and six samples for serum). [b] Rabbits received dichlorphenamide suspension orally (50 mg/kg). [c] Rabbits received dichlorphenamide potassium salt orally (50 mg/kg). [d] Rabbits received dichlorphenamide potassium salt intravenously (50 mg/kg). [e] Amount under the limit of detection.

of the tetramethyl derivative; the base peak was ($M - SO_2NC_2H_5$) (*m/e* 219/221).

To confirm that the drug is converted to the tetramethyl derivative in biological extracts at the submicrogram level, selective ion monitoring was carried out after derivatization of extracts from aqueous humor or serum spiked with dichlorphenamide. The ion intensity ratios for *m/e* 253/255 ($M - SO_2NC_2H_5$) and *m/e* 360/362 (M) from these isolates and a sample of tetramethyldichlorphenamide are presented in Table II. Clearly, the values from the isolates were the same as those from the reference standard. The ions of *m/e* 346/348 (M) of the trimethyl derivative also were monitored, but no signals were observed, demonstrating the absence of a detectable amount (1%) of this derivative in the injected sample. Unquestionably, the tetramethyl derivative was formed in each case.

The levels of dichlorphenamide in the aqueous humor and the serum of rabbits receiving this drug are reported in Table III. Usually, the sensitivity of the method was sufficient to determine levels in these two biological fluids. The solubilization of dichlorphenamide as its potassium salt tremendously enhanced the bioavailability in both fluids.

The use of an internal standard eliminated any errors in quantitation as a result of sample manipulation (14). The sensitivity of this method is such that 10 ng of drug/sample (~4 ng/100 μl of aqueous humor or 2 ng/100 μl of serum) can be quantitated.

REFERENCES

(1) "Enzyme Nomenclature: Recommendations (1964) of the International Union of Biochemistry," Elsevier, New York, N.Y., 1965, p. 166.

(2) E. Gonzales-Jimenez and I. H. Leopold, *Arch. Ophthalmol.*, **60,** 427 (1958).

(3) J. B. Rochelle, J. H. Moyer, and R. V. Ford, *Am. J. Med. Sci.*, **235,** 168 (1958).

(4) P. J. Talso, A. P. Rememchick, C. E. Miller, and E. O. Willoughby, *Circulation*, **24,** 1054 (1961).

(5) J. E. Harris, O. Beaubreau, and G. Hoskinson, *Am. J. Ophthalmol.*, **45,** 120 (1958).

(6) M. H. Luntz, *Br. J. Ophthalmol.*, **45,** 125 (1961).

(7) H. Bleckmann, *Albrecht von Graefes Arch. Klin. Exp. Ophthalmol.*, **201,** 69 (1976).

(8) W. J. A. VandenHeuvel, V. F. Gruber, R. W. Walker, and F. J. Wolf, *J. Pharm. Sci.*, **64,** 1309 (1975).

(9) C. J. Least, Jr., G. F. Johnson, and H. M. Solomon, *Clin. Chim. Acta*, **60,** 285 (1975).

(10) R. H. Greeley, *J. Chromatogr.*, **88,** 229 (1974).

(11) M. L. Sears, *Arch. Ophthalmol.*, **63,** 707 (1960).

(12) J. T. Carstensen, "Theory of Pharmaceutical Systems, Vol. 1: General Principles," Academic, New York, N.Y., 1972, pp. 14–18.

(13) H. C. Hill, "Introduction to Mass Spectrometry," 2nd ed., Heyden & Son, London, England, 1972, pp. 14–17.

(14) H. M. McNair and E. J. Bonelli, "Basic Gas Chromatography," 5th ed., Varian Aerograph, Walnut Creek, Calif., 1969, pp. 150, 151.

ACKNOWLEDGMENTS

The authors are grateful to Dr. J. C. Le Douarec for his continuing interest in this work and to Dr. V. J. Lotti for reviewing the manuscript. They also thank Mrs. M. J. Gonin, N. Ducroux, and Mrs. V. F. Gruber for their skilled technical assistance and Ms. N. Chabry and Mrs. N. Forest for the preparation of the figure and manuscript.

Comparison of *In Vitro* Activity of Undecylenic Acid and Tolnaftate against Athlete's Foot Fungi

LEWIS P. AMSEL [x], **LEO CRAVITZ** [*], **RAYMOND VANDERWYK** [‡], **and SAFWAT ZAHRY**

Received July 17, 1978, from the *Pharmaceutical Division, Pennwalt Corporation, Rochester, NY 14623.* Accepted for publication August 28, 1978. [*]Present address: Rochester General Hospital, Rochester, N.Y. [‡]Pharmaceutical Research Associates, Waltham, Mass.

Abstract □ Undecylenic acid and tolnaftate were tested in an *in vitro* test system to evaluate their relative "killing time" efficacy against *Trichophyton mentagrophytes, Trichophyton rubrum,* and *Epidermophyton floccosum.* Commercial products containing these active agents were tested similarly. The pure active agents were equivalent in activity. The commercial product containing undecylenic acid appeared to be more effective against the test organisms than did the product containing tolnaftate.

Keyphrases □ Undecylenic acid—*in vitro* comparison to tolnaftate against athlete's foot fungi, drugs and formulations □ Tolnaftate—*in vitro* comparison to undecylenic acid against athlete's foot fungi, drugs and formulations □ Athlete's foot—*in vitro* comparison of effectiveness of undecylenic acid and tolnaftate as pure drug and commercial formulations

Athlete's foot or *Tinea pedis* is probably the most common superficial fungus infection in humans. A number of causative agents are usually present, including *Trichophyton mentagrophytes,* which normally infects the interdigital spaces of the toes, *Trichophyton rubrum,* which resides on the plantar surface, and *Epidermophyton floccosum* (1).

Numerous preparations are available for the treatment of *T. pedis.* Underwood *et al.* (2) estimated that over 100 proprietary products were available in 1946. The latest estimate (1977) shows more than 50 products available on a nonprescription basis (3). Oral and topical prescription products raise this number significantly. However, relatively few active ingredients are used in these products. Typically, a product contains a keratolytic, an antifungal agent, and, perhaps, an antibacterial agent.

Fatty acids and their salts possess antifungal activity. The antifungal activity of products containing undecylenic acid and its salts was demonstrated some time ago (4). Until the 1960's, it was probably the therapy of choice. Recent human efficacy studies confirmed this earlier work (5). Since 1960, other compounds have been synthesized for topical relief of athlete's foot. Among these is tolnaftate.

To evaluate the relative efficacy of the undecylenates and tolnaftate, a series of clinical studies was performed[1]. The current study was designed to evaluate *in vitro* the relative "killing time" of undecylenic acid and tolnaftate as well as commercial products incorporating these active ingredients.

EXPERIMENTAL

Fresh cultures of *Trichophyton mentagrophytes* (ATCC 9533), *Trichophyton rubrum* (ATCC 10218), and *Epidermophyton floccosum* (ATCC 10227) were used. After 1 month of culturing and subculturing on Mycosel agar, a sufficient quantity of mycelial growth was obtained to begin testing. Plugs of agar containing mycelial growth were cut out using a sterile No. 2 cork borer with an outside diameter of 7 mm. Plugs were cut for replicate experiments and controls. The cut plugs were placed in sterile plastic petri dishes (60 × 15 mm). Each dish contained the necessary number of plugs for one replicate study. All excess agar was trimmed away from the mycelium using a sterile transfer loop and was discarded.

Table I—Comparison of Times Required to Kill Three Fungi by Suspensions of Undecylenic Acid (2%) and Tolnaftate (1%)—First Study

Organism	Contact Time, min	Number Killed of Seven Replicates: Undecylenic Acid	Tolnaftate
T. mentagrophytes	5	0	0
	10	0	0
	15	0	0
	20	0	1
	30	3	2
	60	7	7
T. rubrum	5	0	0
	10	0	1
	15	0	0
	20	4	3
	30	7	6
	60	7	7
E. floccosum	5	0	0
	10	0	0
	15	0	0
	20	0	0
	30	1	0
	60[a]	7	0

[a] Values significantly different ($p = 0.0003$); all others not significant.

Materials tested for antifungal activity included undecylenic acid[2], tolnaftate[3], and commercial powders containing these active ingredients[4]. The commercial powders were prepared and tested as 20% aqueous suspensions. Undecylenic acid was tested at a 2% concentration (aqueous suspension), and tolnaftate was tested at a 1% suspension concentration. All suspensions contained 0.1% polysorbate 20 as a dispersant.

All test mycelial plugs were immersed in the test product contained in a covered sterile dish. The positive control replicate was removed almost immediately, and the beaker was then placed on a mechanical rotator to keep the product in suspension and in good contact with the plugs. At each predetermined contact time (5, 10, 15, 20, 30, and 60 min for the pure actives and 60, 90, 120, 180, and 240 min for the commercial products), a set of seven replicate plugs was removed and the beaker was replaced on the rotator.

The treated plugs were carried through the following rinse cycle:

1. Placed in a culture tube containing 20 ml of the "first rinse" sterile solution, vortexed for 1 min, and allowed to remain in the rinse solution for 1 hr.
2. Transferred to the "second rinse" tube (10 ml), vortexed for 1 min, and soaked for an additional 30 min.
3. Transferred to the "third rinse" tube (10 ml), vortexed for 1 min, and allowed to soak overnight.

The rinsing solutions were prepared as follows. The first rinse was 1% peptone, 0.1% polysorbate 20, and sodium bicarbonate and distilled water

[1] To be published.

[2] Pennwalt receiving No. 05294.

[3] Code 56500, received from Schering Co.

[4] Desenex Powder, lot 3107 (also contains 20% zinc undecylenate), Pennwalt. Aftate Powder, lot 5VY, Plough.

0022-3549/79/0300-0384$01.00/0
© 1979, American Pharmaceutical Association

Table II—Comparison of Times Required to Kill Three Fungi by Suspensions of Commercial Antifungal Products—First Study

Organism	Contact Time, min	Number Killed of Seven Replicates: Product A[a]	Product B[b]	Statistical Conclusion
T. mentagrophytes	60	3	1	N.S.[c]
	90	6	0	Significant ($p = 0.002$)
	120	7	2	Significant ($p = 0.01$)
	180	7	5	N.S.
	240	7	7	N.S.
T. rubrum	60	5	0	Significant ($p = 0.01$)
	90	7	4	Significant ($p = 0.09$)
	120	7	7	N.S.
	180	7	7	N.S.
	240	7	7	N.S.
E. floccosum	60	0	0	N.S.
	90	1	0	N.S.
	120	6	0	Significant ($p = 0.002$)
	180	7	2	Significant ($p = 0.01$)
	240	7	3	Significant ($p = 0.03$)

[a] A 20% aqueous suspension of Desenex powder. [b] A 20% aqueous suspension of Aftate powder. [c] Not significantly different.

to volume, with the pH adjusted to 7.6. The second and third rinses were 1% peptone, 0.1% polysorbate 20, and distilled water. On the following day, the plugs were resuspended by vortexing and aseptically transferred to the surface of Mycosel agar (BBL) plates. All seven replicates were placed in a single agar plate. The plates were incubated at ambient room temperature (24–28°) for 7 days for *T. mentagrophytes*, 10 days for *T. rubrum*, and 12 days for *E. floccosum*, and the number of replicate plugs showing growth in each set was recorded.

The described studies (seven replicates for each organism, test product, and time interval) were performed twice by different investigators approximately 1 year apart. The second investigator, however, utilized test dermatophytes that were recent clinical isolates maintained in his laboratory culture collection rather than the ATCC cultures.

RESULTS AND DISCUSSION

The results of the *in vitro* testing are shown in Tables I–IV. Tables I and III and II and IV compare the results obtained for the pure material and commercial products, respectively, by the two investigators. When the activity of pure undecylenic acid was compared to that of pure tolnaftate, no significant differences were found (except for one organism, at one time, and by only one investigator and not deemed experimentally significant) in the time required to kill the test fungi. All analyses were conducted using Fisher's Exact Test (6). Comparison of commercial powders containing these active agents showed interesting results. The first investigator (Table II) showed equivalence between both products in about half of the test instances and superiority of the undecylenate-containing product in the other half. These significant differences indicate that the undecylenate product (as tested by this investigator) killed the test organisms more rapidly than the tolnaftate-containing product.

Table III—Comparison of Times Required to Kill Three Fungi by Suspensions of Undecylenic Acid (2%) and Tolnaftate (1%) —Second Study

Organism	Contact Time, min	Number Killed of Seven Replicates[a]: Undecylenic Acid	Tolnaftate
T. mentagrophytes	5	0	0
	10	0	0
	15	0	0
	20	0	0
	30	2	2
	60	7	7
T. rubrum	5	0	0
	10	0	0
	15	0	0
	20	0	2
	30	2	2
	60	6	5
E. floccosum	5	0	0
	10	0	0
	15	0	0
	20	0	0
	30	1	0
	60	2	2

[a] Values not significantly different.

Table IV—Comparison of Times Required to Kill Three Fungi by Suspensions of Commercial Antifungal Products—Second Study

Organism	Contact Time, min	Number Killed of Seven Replicates: Product A[a]	Product B[b]
T. mentagrophytes	60	0	0
	90	0	0
	120	0	0
	180	1	0
	240[c]	5	0
T. rubrum	60	0	0
	90	0	0
	120	0	0
	180	1	0
	240	3	0
E. floccosum	60	0	0
	90	0	0
	120	5	2
	180	7	5
	240	7	7

[a] A 20% aqueous suspension of Desenex powder. [b] A 20% aqueous suspension of Aftate powder. [c] Values significantly different ($p = 0.01$); all others not significant.

The data in Tables III and IV are the results of the equivalent study by another investigator. No significant differences were found between the two active ingredients, essentially confirming the first study. When the two commercial products were tested, results were again essentially equivalent to the first study. There was a different time interval where statistical significance was observed compared to the initial study. However, on a global basis, one can conclude that undecylenates are possibly more effective in *in vitro* killing time than tolnaftate alone. Moreover, this finding would probably apply to the commercial powders containing these active agents.

The concentrations of active ingredients used differed for the two agents tested to simulate the commercial products available. Thus, undecylenic acid was used in a concentration of 2% and tolnaftate was used at 1%. Although the concentrations of active agents varied in the commercial products tested, the undecylenates are probably more effective (as determined by killing time) than tolnaftate.

REFERENCES

(1) "Merck Manual," 12th ed., D. N. Holvey, Ed., Merck Sharp & Dohme Research Laboratories, Rahway, N.J., 1972, pp. 1450 *ff.*

(2) G. B. Underwood, L. E. Gual, E. Collins, and M. Mosby, *J. Am. Med. Assoc.*, **130,** 249 (1946).

(3) "Handbook of Nonprescription Drugs," 5th ed., American Pharmaceutical Association, Washington, D.C., 1977.

(4) H. C. Shaw, M. B. Sulzberger, and A. Kanof, *J. Am. Med. Assoc.*, **129,** 1170 (1945).

(5) A. B. Smith, R. F. Powell, J. L. Graham, and J. A. Ulrich, *Int. J. Dermatol.*, **16,** 52 (1977).

(6) C. I. Bliss, "Statistics in Biology," vol. 1, McGraw-Hill, New York, N.Y., 1967, p. 63.

Rapid, Sensitive GLC Determination of Pentobarbital and Other Barbiturates in Serum Using Nitrogen-Specific Detector

SY-RONG SUN [x] **and D. J. HOFFMAN**

Received May 1, 1978, from the *Pharmaceutical Product Division, Abbott Laboratories, North Chicago, IL 60064.* Accepted for publication August 23, 1978.

Abstract □ A GLC method for the analysis of pentobarbital in serum was developed. After extraction from serum, a methyl derivative was prepared and quantitated by nitrogen-specific detection. The method has a sensitivity of 0.08 μg/ml for pentobarbital with only 0.1 ml of serum. Secobarbital was the internal standard. Derivatives of other barbiturates also were prepared.

Keyphrases □ Pentobarbital—GLC analysis in serum □ Barbiturates, various—GLC analysis in serum □ GLC—analysis, pentobarbital and various barbiturates in serum □ Sedatives—pentobarbital and various barbiturates, GLC analysis in serum

The GLC determination of pentobarbital and other barbiturates in biological fluids using flame-ionization detection has been reported extensively (1–11). The compounds are not readily gas chromatographed without derivatization and require carefully prepared columns, especially when nanogram amounts are injected. Recently, Sun and Chun (12) reported a sensitive GLC procedure, using electron-capture detection on the pentafluorobenzyl derivative of pentobarbital after serum extraction. However, it required numerous cleanup steps before GLC analysis. Brochmann-Hanssen and Oke (13) methylated the barbiturates by the flash-heater methylation technique with trimethylanilinium hydroxide.

Dunges and Bergheim-Irps (14) used methyl iodide for derivative formation with some barbiturates in pure drug form (the unformulated barbiturates) with subsequent flame-ionization detection. This paper reports a modification of their procedure (14) for the determination of pentobarbital in serum, using a nitrogen-specific detector to achieve selectivity and sensitivity.

EXPERIMENTAL

Reagents and Materials—Pentobarbital[1], secobarbital[2] (the internal standard), and methyl iodide[3] were used as supplied. Ether[4] and other chemicals were analytical reagent grade.

Apparatus—A mixer[5] and refrigerated centrifuge[6] at 10° were used. Methyl derivative formation at 56° was carried out on a heating block[7].

GLC—A reporting gas chromatograph[8] equipped with a dual nitrogen–phosphorus flame-ionization detector[9], a computing integrator[10], and an automatic sampler[11] were used. The glass column, 1.22 m × 2 mm (i.d.), was packed with 2% OV-101[12] on 100–120-mesh Chromosorb WHP.

The operating conditions were: column oven temperature, 140°; detector temperature, 250°; injection port temperature, 160°; helium carrier gas flow rate, 40 ml/min; hydrogen flow rate, 3 ml/min; air flow rate, 50 ml/min; and recorder attenuation, 16.

Preparation of Standards—The pentobarbital serum standard of 15 μg/ml was prepared from a standard solution of 500 μg/ml in methanol. Other serum standards at 0.1, 0.25, 0.5, 1.0, 2.5, 5.0, 7.0, and 10.0 μg/ml were prepared from serial dilutions of this standard with serum. For human studies, serum standards up to 2.5 μg/ml were used; this range covered the human serum pentobarbital levels expected after oral administration of a 100-mg dose of pentobarbital sodium (12).

The internal standard of 8 μg/ml in distilled water was prepared from a standard solution of 200 μg/ml in methanol.

Extraction and Derivatization Procedure—To a 15-ml conical glass centrifuge tube were added 0.1 ml of the internal standard solution, 0.1 ml of serum sample, 0.1 ml of 0.2 *N* HCl, and 5 ml of ether. After mixing for 15 sec twice and centrifuging at 2500 rpm for 3 min at 10°, 4 ml of organic layer was transferred into a conical tube and evaporated to dryness at 45° with filtered air. To the dry residue were added 0.5 ml of acetone, 0.1 ml of methyl iodide, and about 5 mg of sodium carbonate.

The mixture was capped, agitated, heated at 56° for 30 min, and then

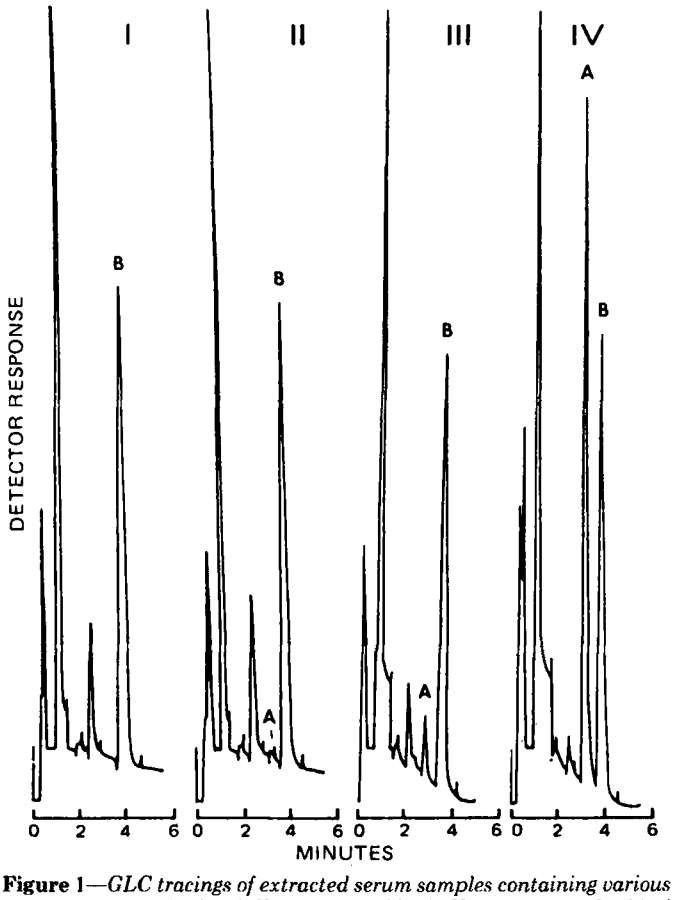

Figure 1—*GLC tracings of extracted serum samples containing various amounts of pentobarbital. Key: I, serum blank; II, serum pentobarbital standard at 0.1 μg/ml; III, serum pentobarbital standard at 1.0 μg/ml; IV, serum pentobarbital standard at 10.0 μg/ml; A, pentobarbital; and B, internal standard (secobarbital).*

[1] Abbott Laboratories, North Chicago, Ill.
[2] Eli Lilly Co., Indianapolis, Ind.
[3] J. T. Baker Chemical Co., Phillipsburg, N.J.
[4] Mallinckrodt Chemicals, St. Louis, Mo.
[5] Vortex Genie model K-550-GT, Scientific Industries, Springfield, Mass.
[6] Model RC-3, Sorvall, Newtown, Conn.
[7] Dri-block DB-3, Techne, Princeton, N.J.
[8] Model 5830A, Hewlett-Packard, Avondale, Pa.
[9] Model 18789, Hewlett-Packard, Avondale, Pa.
[10] Model 18850A, Hewlett-Packard, Avondale, Pa.
[11] Model 7671A, Hewlett-Packard, Avondale, Pa.
[12] Hewlett-Packard, Avondale, Pa.

0022-3549/79/0300-0386$01.00/0
© 1979, American Pharmaceutical Association

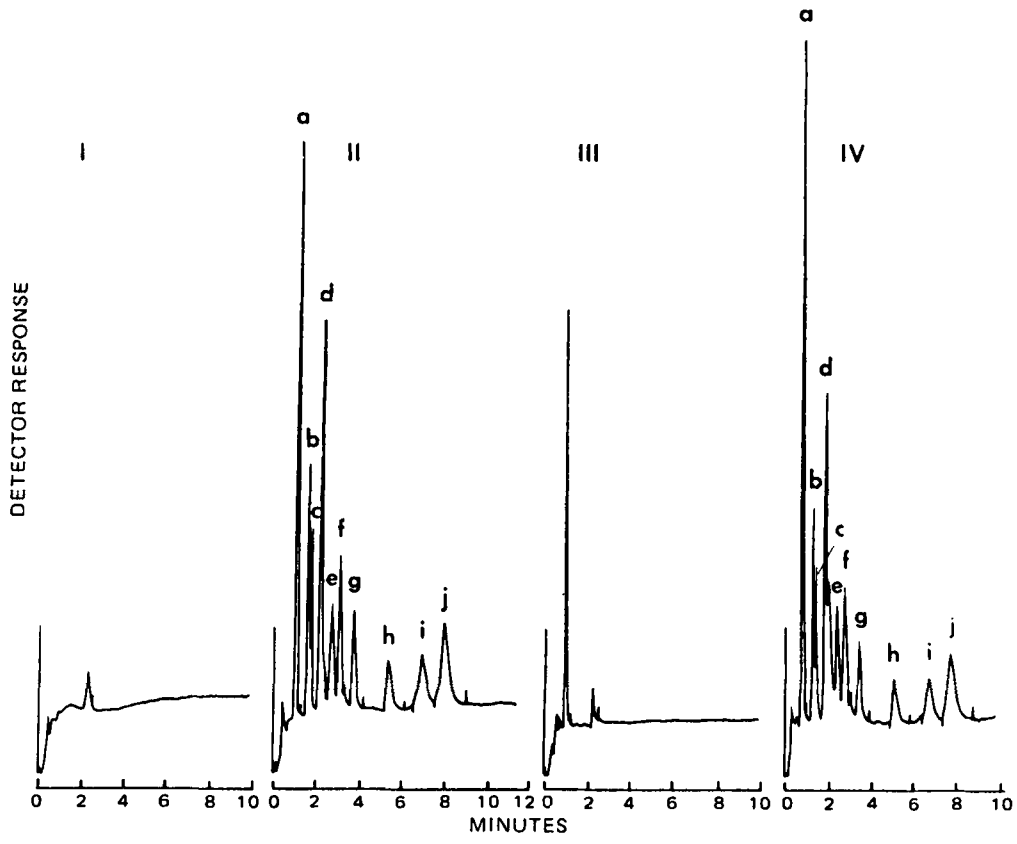

Figure 2—*GLC tracings of N,N′-dimethyl derivatives of barbiturate mixtures. Key: I, reagent blank (composed of 0.5 ml of acetone, 0.1 ml of methyl iodide, and 5 mg of sodium carbonate); II, pure drug reacted (as N,N′-dimethyl derivatives of barbiturates injected as 5 μl of the completed reaction solution); III, serum blank extract; IV, serum extract containing different barbiturate derivatives; a, barbital and metharbital; b, allobarbital; c, aprobarbital; d, butabarbital, butethal, and butalbital; e, amobarbital; f, pentobarbital and thiopental; g, secobarbital; h, hexethal; i, hexobarbital; and j, mephobarbital and phenobarbital.*

Table I—Assay Reproducibility: Serum Pentobarbital Concentration (Micrograms per Milliliter)

Theoretical	Observed Mean[a] ± *SD*	*RSD*, %
0	0	—
0.10	0.100 ± 0.0100	10.0
0.25	0.227 ± 0.0153	6.7
0.50	0.487 ± 0.0379	7.8
1.00	1.033 ± 0.0493	4.8
2.50	2.490 ± 0.0173	0.7
5.00	4.987 ± 0.2021	4.0
7.50	7.590 ± 0.0529	0.7
10.00	9.957 ± 0.0907	0.9
15.00	14.973 ± 0.4822	3.2
Average		4.3

[a] Mean of three determinations at each concentration.

cooled to room temperature. The supernate was transferred into a GLC microvial[12], and 5 μl was injected into the GLC column with the automatic sampler[11].

RESULTS AND DISCUSSION

The peak area ratio of pentobarbital to the internal standard was plotted against known standards of pentobarbital, expressed as micrograms per milliliter in serum. Values for unknown concentrations of pentobarbital in serum were calculated from this standard curve using a least-squares regression method.

Under the assay conditions, pentobarbital and the internal standard had retention times of 3.11 and 3.80 min, respectively (Fig. 1).

The precision of the assay is reported in Table I. Relative standard deviations ranged from 0.7 to 10.0%, with an average relative standard deviation of 4.3%. Statistical evaluation of the peak area ratio at 0.1 μg/ml, using a one-sided tolerance limit test, showed that the sensitivity was less than 0.1 μg/ml. The calculated sensitivity of the assay was about 0.08 μg/ml, calculated by least-squares linear regression for concentrations from 0 to 0.5 μg/ml (Table II). Sensitivity was defined as the concentration calculated by linear regression analysis to give any response greater than zero in 95% of the samples.

The accuracy of this assay was tested by analyzing 18 unknown serum samples spiked with pentobarbital sodium under blind conditions (Table

Table II—Sensitivity of Serum Pentobarbital Assay[a]

Serum Pentobarbital Concentration, μg/ml	Peak Area Ratio[b]
0	0
	0
	0
0.10	0.005
	0.007
	0.006
0.25	0.021
	0.018
	0.022
0.5	0.055
	0.047
	0.048

[a] Least-squares linear regression calculation: number of points, 12; slope, 0.1019 ± 0.0089; *y*-intercept ± 95% confidence limit, −0.00258 ± 0.00637; correlation coefficient, 0.988; and calculated sensitivity, 0.080 (μg/ml). [b] Pentobarbital to the internal standard.

Table III—Accuracy of Serum Pentobarbital Assay

Unknown	Serum Pentobarbital Concentration, μg/ml			Difference, %
	Theoretical	Observed	Difference	
1	0	0	0	0
2	0.10	0.11	0.01	10.0
3	0.18	0.16	−0.02	11.1
4	0.25	0.23	−0.02	8.0
5	0.38	0.36	−0.02	5.3
6	0.50	0.53	0.03	6.0
7	0.75	0.72	−0.03	4.0
8	1.00	1.01	0.01	1.0
9	1.75	1.72	−0.03	1.7
10	2.50	2.44	−0.06	2.4
11	3.75	3.62	−0.13	3.5
12	5.00	5.22	0.22	4.4
13	6.25	6.17	−0.08	1.3
14	7.50	7.53	0.03	0.4
15	8.75	8.46	−0.29	3.3
16	10.00	9.95	−0.05	0.5
17	12.50	12.28	−0.22	1.8
18	15.00	15.14	0.14	0.9

III). The assay error exceeded 5% for all samples containing 0.50 μg/ml or less of pentobarbital. The assay error was below 5% for all samples containing pentobarbital between 0.75 and 15.0 μg/ml of serum.

The method is specific for pentobarbital. Except for thiopental, it was resolved from 13 other barbiturates (Fig. 2). A similar quantitative determination for these barbiturates should be applicable.

This rapid assay can be used to conduct single oral dose pentobarbital bioavailability studies in adult and pediatric patients using only 0.1 ml of serum. This procedure also is applicable to the general screening of some other barbiturates in biological fluids.

REFERENCES

(1) H. F. Martin and J. L. Driscoll, *Anal. Chem.*, **38**, 345 (1966).

(2) E. A. Fiereck and N. W. Tietz, *Clin. Chem.*, **17**, 1024 (1971).

(3) M. Ehrnebo, S. Agurell, and L. O. Boreus, *Eur. J. Clin. Pharmacol.*, **4**, 191 (1972).

(4) J. MacGee, *Clin. Chem.*, **17**, 587 (1971).

(5) R. C. Driscoll, F. S. Barr, B. J. Gragg, and G. W. Moore, *J. Pharm. Sci.*, **60**, 1492 (1971).

(6) R. G. Cooper, M. S. Greaves, and G. Oaen, *Clin. Chem.*, **18**, 1343 (1972).

(7) R. J. Flanagan and G. Withers, *J. Clin. Pathol.*, **25**, 899 (1972).

(8) R. B. Smith, L. W. Dittert, W. O. Griffen, Jr., and J. T. Doluisio, *J. Pharmacokinet. Biopharm.*, **1**, 5 (1973).

(9) D. J. Berry, *J. Chromatogr.*, **86**, 89 (1973).

(10) L. T. Sennello and F. E. Kohn, *Anal. Chem.*, **46**, 752 (1974).

(11) D. D. Breimer and J. M. Van Rossum, *J. Chromatogr.*, **88**, 235 (1974).

(12) S. Sun and A. H. C. Chun, *J. Pharm. Sci.*, **66**, 477 (1977).

(13) E. Brochmann-Hanssen and T. O. Oke, *ibid.*, **58**, 370 (1969).

(14) W. Dunges and E. Bergheim-Irps, *Anal. Lett.*, **6**, 185 (1973).

ACKNOWLEDGMENTS

The authors thank Ms. M. Leveque for technical assistance and Dr. S. Borodkin for helpful discussions.

Separation, Identification, and Quantitation of Anthralin and Its Decomposition Products

HASSAN M. ELSABBAGH *, CLYDE W. WHITWORTH ˣ, and LEE C. SCHRAMM

Received May 19, 1978, from the *Department of Pharmacy, School of Pharmacy, University of Georgia, Athens, GA 30602.* Accepted for publication August 24, 1978. *Present address: School of Pharmacy, University of Mansoura, Mansoura, Egypt.

Abstract □ Anthralin and its decomposition products were separated by both column chromatographic and TLC techniques. Two decomposition products were characterized by TLC, melting-point data, and UV and IR spectroscopy. Pure anthralin and its decomposition products also were determined quantitatively.

Keyphrases □ Anthralin—column chromatographic and TLC analysis and separation from decomposition products □ Chromatography, column—analysis and separation of anthralin from decomposition products □ TLC—analysis and separation of anthralin from decomposition products □ Decomposition products, anthralin—column chromatographic and TLC analysis and separation □ Antipsoriatic agents—anthralin, column chromatographic and TLC analysis and separation from decomposition products

The first use of anthralin (1,8,9-anthracenetriol) for topical therapy of psoriasis was noted in a report on chrysarobin, a related compound, in 1878 (1). Psoriasis is a skin disease characterized in part by epidermal hyperplasia and, therefore, should be controllable with antimetabolic drugs. It has been assumed that anthralin acts by blocking cell division (2). Although local treatment of psoriasis vulgaris with corticosteroid creams under plastic occlusion is accepted widely, psoriasis is still treated with anthralin pastes (USP XIX) (3–6).

In treating psoriatic lesions with commercial anthralin, two side effects were documented: staining of skin and clothing and irritation of surrounding normal skin. Anthralin is relatively unstable in the presence of air, light, and heat (7). Since commercial anthralin samples contain degradation products, it was not clear what relationship existed between anthralin and its degradation products with regard to therapeutic effectiveness and side effects. It was reported (2, 8, 9) that any therapeutic effect in psoriasis results from anthralin and not its decomposition products. These findings supported that of Comaish *et al.* (10), who noted that discolored anthralin pastes (possibly containing large amounts of the quinone) are ineffective in treating psoriasis.

Table I—R_f Values for Anthralin and Its Decomposition Products

Solvent System	Plates	R_f (×100) Anthralin	Danthron	Dianthrone
Benzene–cyclohexane–methanol (15:15:0.25)	Silica	42	35	21
Benzene–cyclohexane–acetic acid (15:15:0.5)	Silica	31	20	11
Benzene–cyclohexane–methanol (15:15:0.25)	Compound I-treated silica	54	41	27
Benzene–cyclohexane–acetic acid (15:15:0.5)	Compound I-treated silica	32	20	7

The aims of the present research were to investigate the purity of a commercial anthralin sample and to separate, identify, and determine any decomposition products in order to judge the stability and the potency of preparations of the drug as an antipsoriatic agent.

EXPERIMENTAL

Materials—Commercial anthralin NF and reference samples of anthralin, danthron, and dianthrone were used as received[1]. All solvents

[1] Pfaltz and Bauer, Stanford, Conn.

0022-3549/79/0300-0388$01.00/0

© 1979, American Pharmaceutical Association

III). The assay error exceeded 5% for all samples containing 0.50 μg/ml or less of pentobarbital. The assay error was below 5% for all samples containing pentobarbital between 0.75 and 15.0 μg/ml of serum.

The method is specific for pentobarbital. Except for thiopental, it was resolved from 13 other barbiturates (Fig. 2). A similar quantitative determination for these barbiturates should be applicable.

This rapid assay can be used to conduct single oral dose pentobarbital bioavailability studies in adult and pediatric patients using only 0.1 ml of serum. This procedure also is applicable to the general screening of some other barbiturates in biological fluids.

REFERENCES

(1) H. F. Martin and J. L. Driscoll, *Anal. Chem.*, **38**, 345 (1966).

(2) E. A. Fiereck and N. W. Tietz, *Clin. Chem.*, **17**, 1024 (1971).

(3) M. Ehrnebo, S. Agurell, and L. O. Boreus, *Eur. J. Clin. Pharmacol.*, **4**, 191 (1972).

(4) J. MacGee, *Clin. Chem.*, **17**, 587 (1971).

(5) R. C. Driscoll, F. S. Barr, B. J. Gragg, and G. W. Moore, *J. Pharm. Sci.*, **60**, 1492 (1971).

(6) R. G. Cooper, M. S. Greaves, and G. Oaen, *Clin. Chem.*, **18**, 1343 (1972).

(7) R. J. Flanagan and G. Withers, *J. Clin. Pathol.*, **25**, 899 (1972).

(8) R. B. Smith, L. W. Dittert, W. O. Griffen, Jr., and J. T. Doluisio, *J. Pharmacokinet. Biopharm.*, **1**, 5 (1973).

(9) D. J. Berry, *J. Chromatogr.*, **86**, 89 (1973).

(10) L. T. Sennello and F. E. Kohn, *Anal. Chem.*, **46**, 752 (1974).

(11) D. D. Breimer and J. M. Van Rossum, *J. Chromatogr.*, **88**, 235 (1974).

(12) S. Sun and A. H. C. Chun, *J. Pharm. Sci.*, **66**, 477 (1977).

(13) E. Brochmann-Hanssen and T. O. Oke, *ibid.*, **58**, 370 (1969).

(14) W. Dunges and E. Bergheim-Irps, *Anal. Lett.*, **6**, 185 (1973).

ACKNOWLEDGMENTS

The authors thank Ms. M. Leveque for technical assistance and Dr. S. Borodkin for helpful discussions.

Separation, Identification, and Quantitation of Anthralin and Its Decomposition Products

HASSAN M. ELSABBAGH *, CLYDE W. WHITWORTH ˣ, and LEE C. SCHRAMM

Received May 19, 1978, from the *Department of Pharmacy, School of Pharmacy, University of Georgia, Athens, GA 30602.* Accepted for publication August 24, 1978. *Present address: School of Pharmacy, University of Mansoura, Mansoura, Egypt.

Abstract □ Anthralin and its decomposition products were separated by both column chromatographic and TLC techniques. Two decomposition products were characterized by TLC, melting-point data, and UV and IR spectroscopy. Pure anthralin and its decomposition products also were determined quantitatively.

Keyphrases □ Anthralin—column chromatographic and TLC analysis and separation from decomposition products □ Chromatography, column—analysis and separation of anthralin from decomposition products □ TLC—analysis and separation of anthralin from decomposition products □ Decomposition products, anthralin—column chromatographic and TLC analysis and separation □ Antipsoriatic agents—anthralin, column chromatographic and TLC analysis and separation from decomposition products

The first use of anthralin (1,8,9-anthracenetriol) for topical therapy of psoriasis was noted in a report on chrysarobin, a related compound, in 1878 (1). Psoriasis is a skin disease characterized in part by epidermal hyperplasia and, therefore, should be controllable with antimetabolic drugs. It has been assumed that anthralin acts by blocking cell division (2). Although local treatment of psoriasis vulgaris with corticosteroid creams under plastic occlusion is accepted widely, psoriasis is still treated with anthralin pastes (USP XIX) (3–6).

In treating psoriatic lesions with commercial anthralin, two side effects were documented: staining of skin and clothing and irritation of surrounding normal skin. Anthralin is relatively unstable in the presence of air, light, and heat (7). Since commercial anthralin samples contain degradation products, it was not clear what relationship existed between anthralin and its degradation products with regard to therapeutic effectiveness and side effects. It was reported (2, 8, 9) that any therapeutic effect in psoriasis results from anthralin and not its decomposition products. These findings supported that of Comaish *et al.* (10), who noted that discolored anthralin pastes (possibly containing large amounts of the quinone) are ineffective in treating psoriasis.

Table I—R_f Values for Anthralin and Its Decomposition Products

Solvent System	Plates	R_f (×100) Anthralin	Danthron	Dianthrone
Benzene–cyclohexane–methanol (15:15:0.25)	Silica	42	35	21
Benzene–cyclohexane–acetic acid (15:15:0.5)	Silica	31	20	11
Benzene–cyclohexane–methanol (15:15:0.25)	Compound I-treated silica	54	41	27
Benzene–cyclohexane–acetic acid (15:15:0.5)	Compound I-treated silica	32	20	7

The aims of the present research were to investigate the purity of a commercial anthralin sample and to separate, identify, and determine any decomposition products in order to judge the stability and the potency of preparations of the drug as an antipsoriatic agent.

EXPERIMENTAL

Materials—Commercial anthralin NF and reference samples of anthralin, danthron, and dianthrone were used as received[1]. All solvents

[1] Pfaltz and Bauer, Stanford, Conn.

0022-3549/79/0300-0388$01.00/0

© 1979, American Pharmaceutical Association

Table II—UV Spectroscopy Data for Anthralin and Its Decomposition Products

Compound	Maximum Absorbance (λ_{max}), nm	Molar Absorptivity (ϵ)
Anthralin	356	1.03×10^4
Danthron	432	1.19×10^4
Dianthrone	368	3.13×10^4 [a]

[a] The molar absorptivity of dianthrone was calculated on the basis of the molecular weight 450.4 found by Segal *et al.* (17).

were reagent grade and distilled before use. TLC was accomplished on 0.25-mm layers of silica gel 60 GF_{254}[2], precoated plates of the same material, and 0.25-mm layers of silica gel 60 H containing ethylenediaminetetraacetic acid (I) prepared by the method of Arends (11). Column chromatography was accomplished on specially purified silica gel containing 2% I prepared according to the method of Arends (11).

Separation by Column Chromatography—A 500-mg sample of commercial anthralin NF was applied to a column containing 100 g of specially purified silica gel containing I and chromatographed with benzene–cyclohexane–methanol (15:15:0.25). The resulting fractions were examined by TLC. A brown-violet zone, which remained at the top of the column, was eventually eluted with methanol.

Identification of Fractions—*TLC*—Routinely, 5 μl of each fraction was applied to both silica gel TLC plates and I-treated silica gel layers on glass plates, and all plates were developed with either benzene–cyclohexane–methanol (15:15:0.25) or benzene–cyclohexane–acetic acid (15:15:0.5). The plates were air dried, and the spots were identified by color, fluorescence, and R_f values compared with reference samples (Table I).

Melting Point—The three separated compounds were recrystallized from benzene–cyclohexane–methanol, yielding pure characteristic crystals for each compound. The melting points of the obtained compounds were determined[3].

UV Spectroscopy—Solutions (0.001% w/v) of the three isolated compounds in chloroform were prepared. The UV spectra of the solutions were examined[4] from 750 to 350 nm (scan speed of 5 nm/sec), and the absorption maxima (λ_{max}) as well as the molar absorptivity (ϵ) of each compound were determined (Table II).

IR Spectroscopy—IR spectra were obtained for anthralin, danthron, and dianthrone using potassium bromide pellets[5].

Quantitation of Anthralin and Its Decomposition Products—Three random samples of commercial anthralin NF, 50 mg each, were dissolved in chloroform, and the volume of the solution obtained was adjusted to 25 ml in a volumetric flask. A 0.5-ml sample of each solution was diluted to 50 ml with chloroform to give a concentration of 20 μg/ml. These solutions were measured at 356, 432, and 368 nm, corresponding to anthralin, danthron, and dianthrone, respectively. Since the absorption maximum of anthralin interfered with that of dianthrone because of their closeness, it was not possible to determine dianthrone in the presence of anthralin. However, because dianthrone was present in low concentration compared to anthralin, dianthrone did not interfere with the determination of anthralin in the commercial form. It was necessary to separate the mixture into its components by TLC prior to quantitation. A standard absorbance–concentration curve was determined for each compound and was used to estimate its percentage content in the commercial anthralin sample (Table III).

RESULTS AND DISCUSSION

Anthralin is official in the USP and NF. In ointment form at concentrations of 0.1, 0.2, 0.25, 0.4, 0.5, and 5%, it is categorized as a topical antipsoriatic. Topically applied anthralin not only provides a proven efficaceous treatment for psoriasis but is also free from systemic toxicity when used in low concentrations (4, 12–14). Anthralin is preferred over drugs such as steroids, because the prolonged use of steroids commonly induces a facial erythema. Systemic steroids for psoriasis treatment should be avoided whenever possible because they may induce a more severe form of the disease (15).

The degradation products of anthralin constitute one of the most objectionable aspects of anthralin treatment because they are responsible for staining of skin and clothing and irritation of surrounding normal skin

[2] E. Merck and Co.
[3] Thomas-Hoover capillary melting-point apparatus.
[4] Cary model 118 recording spectrophotometer.
[5] Perkin-Elmer 437 grating spectrophotometer.

Table III—Percent of Anthralin and Its Decomposition Products in a Commercial Anthralin Sample

Compound	Amount Found, %	
	TLC Method	Direct Spectrophotometric Method
Anthralin	93.83	95.00
Danthron	4.25	3.75
Dianthrone	1.38	1.25

(2, 8, 16). Few reports deal with the separation and identification of anthralin decomposition products (2, 17, 18), and none deals with the quantitation of these products in anthralin. Segal *et al.* (17) claimed that a commercial quality material of anthralin was purified by TLC on silica gel with benzene. However, since impure anthralin is soluble in benzene, its decomposition products probably are not separated from anthralin with benzene alone as an eluant (19, 20). Thielemann (18) used TLC on silica gel with heptane–benzene–chloroform (1:1:1) as the eluent for separation and identification of anthrarobin and anthralin. The same solvent system also was used by Fisher and Maibach (2) for separation of purified anthralin from its decomposition products, and they identified these products according to the method of Segal *et al.* (17).

TLC—In this study, anthralin and two decomposition products were separated from commercial anthralin (Table I). The two decomposition products were identified as danthron (1,8-dihydroxy-9-anthrone) and dianthrone after matching with reference samples. A very small spot of a violet-colored artifact was noted at the origin on the thin-layer plate. This spot may have resulted from the reaction of traces of iron present in commercial silica gel with anthralin. With column chromatography, a violet-colored zone remained at the top of the column.

The formation of this artifact was prevented either by using salicylic acid-treated silica plates (0.2% w/v in methanol) or by adding salicylic acid to anthralin in a ratio of two parts of salicylic acid to one part of anthralin. The quantity of the artifact was also greatly reduced when I-treated silica gel was used. The salicylic acid may have prevented the formation of the violet-colored artifact by the formation of an iron salicylate, thus effectively removing iron from the presence of anthraquinones. Compound I chelated most of the iron in the I-treated silica, but small quantities of the artifact were observed.

Melting Point—Anthralin was separated as lemon-yellow crystals, mp 181–182° [lit. (21) mp 175–181°]. Danthron was obtained as orange-yellow crystals, mp 193.5–195° [lit. (20) mp 193–197°]. Dianthrone was crystallized as yellow platelets, mp 233–234° [lit. (17) mp 235–237°].

UV Spectroscopy—Table II shows the maximum absorbance (λ_{max}) and the molar absorptivity (ϵ) of anthralin, danthron, and dianthrone in chloroform.

IR Spectroscopy—The IR spectra (potassium bromide) of all three compounds were similar. In the 4000–1700-cm^{-1} region, all three were identical. Minor differences were found in the fingerprint region. All compounds exhibited peaks in the 1635–1640-cm^{-1} region, characteristic of H-bonded C=O conjugated to an aromatic nucleus.

Quantitation of Anthralin and Its Decomposition Products—USP XIX considers danthron as a common constituent of anthralin and offers an equation for the calculation of both compounds in powder or in ointment form. However, danthron reportedly is inactive as an antipsoriatic agent (2, 8, 9) and is partly responsible for the objectionable side effects of anthralin (2, 9, 15).

In this study, two decomposition products for anthralin were found. Therefore, it was necessary to determine each one to judge the potency and, thereby, the therapeutic effectiveness of the drug. Accordingly, a precise determination of anthralin and its decomposition products was accomplished by separating the mixture by TLC prior to the quantitation of each component spectrophotometrically at its own wavelength (Table III). By this method, it was possible to determine quantitatively anthralin, danthron, and dianthrone without any interference or overlapping.

If the original concentration of the commercial anthralin sample is known, it is possible to determine the concentration of the components by direct spectrophotometric measurement. These determinations were made by observing the absorbance at two wavelengths (356 and 432 nm) for anthralin and danthron and then obtaining the amount of dianthrone by algebraic difference (Table III).

REFERENCES

(1) B. Squire, *Dermatologica*, **144**, 115 (1972).

(2) L. B. Fisher and H. I. Maibach, *J. Invest. Dermatol.*, **64**, 338 (1975).

(3) J. T. Ingram, *Br. Med. J.*, **2**, 591 (1953).
(4) S. Comaish, *Arch. Dermatol.*, **92**, 26 (1965).
(5) R. H. Seville, *Br. J. Dermatol.*, **78**, 269 (1966).
(6) E. Young, *ibid.*, **82**, 516 (1970).
(7) W. P. Raab and B. M. Gmeiner, *Dermatologica*, **150**, 267 (1975).
(8) H. J. Hulsebosch and M. Ponec-Waelsch, *ibid.*, **144**, 287 (1972).
(9) M. Ponec-Waelsch and H. J. Hulsebosch, *Arch. Dermatol. Forsch.*, **249**, 141 (1974).
(10) S. Comaish, J. Smith, and R. H. Seville, *Br. J. Dermatol.*, **84**, 282 (1971).
(11) P. Arends, *J. Chromatogr.*, **47**, 550 (1970).
(12) H. Beerman, G. V. Kulchar, and D. M. Pillsbury, *J. Am. Med. Assoc.*, **104**, 26 (1935).
(13) E. M. Farber and D. R. Harris, *Arch. Dermatol.*, **101**, 381 (1970).
(14) M. W. Gay, W. J. Moore, J. M. Morgan, and L. F. Montes, *ibid.*, **105**, 213 (1972).
(15) H. Baker and T. J. Ryan, *Br. J. Dermatol.*, **80**, 771 (1968).
(16) M. Whitefield, *Arzneim.-Forsch.*, **20**, 137 (1970).
(17) A. Segal, C. Kutz, and B. L. Van Duuren, *J. Med. Chem.*, **14**, 394 (1971).
(18) H. Thielemann, *Sci. Pharm.*, **42**, 55 (1974).
(19) E. G. Clarke, "Isolation and Identification of Drugs," vol. 2, Pharmaceutical Press, London, England, 1975, p. 1025.
(20) "The Merck Index," 9th ed., Merck and Co., Rahway, N.J., 1976, p. 3394.
(21) "The United States Pharmacopeia," 19th rev., Mack Publishing Co., Easton, Pa., 1975, p. 33.

ACKNOWLEDGMENTS

The authors thank Ms. Yanee Pongpaibul for technical assistance.

Topical Mosquito Repellents XI: Carbamates Derived from *N,N'*-Disubstituted Diamines

W. A. SKINNER ˣ, H. T. CRAWFORD, L. C. RUTLEDGE *, and M. A. MOUSSA ‡

Received May 26, 1978, from the *Life Sciences Division, SRI International, Menlo Park, CA 94025.* Accepted for publication August 17, 1978. *Present address: Letterman Army Institute of Research, Presidio of San Francisco, CA 94129. ‡Present address: Medical Entomology Consultant, Office of the Surgeon General, Washington, DC 20310.

Abstract □ Carbamates derived from various *N,N'*-disubstituted diamines were synthesized and evaluated as repellents for *Aedes aegypti* mosquitoes with an *in vitro* blood-feeding test system. Several compounds were more effective than diethyltoluamide.

Keyphrases □ Carbamates from *N,N'*-disubstituted amines—synthesized and evaluated as mosquito repellents □ Repellents, mosquito—various carbamates derived from *N,N'*-disubstituted diamines synthesized and evaluated □ Structure–activity relationships—various carbamates derived from *N,N'*-disubstituted diamines evaluated as mosquito repellents

Carbamates as mosquito repellents were discussed previously (1). Substituted 2-oxazolidones were synthesized and found to possess repellent activity (1). However, improvement of their repellency was desired, and a new synthetic effort was initiated to prepare carbamates from *N,N'*-disubstituted diamines.

To vary the boiling-point ranges of the proposed repellents, syntheses were concentrated on ethylenediamine, diethylenediamine, and triethylenediamine derivatives. Previous studies (1) showed that repellency duration is a function of boiling points or volatility of repellents.

These compounds were evaluated in the *in vitro* mosquito blood-feeding test system reported previously (2). Mosquitoes used for these evaluations were female *Aedes aegypti* (yellow fever mosquito).

Table I—Physical and Biological Properties of Carbamates Derived from *N,N'*-Disubstituted Diamines

$R_1N(CH_2CH_2)_nNR_3$ (R_2, R_4)

Compound	R_1	R_2	R_3	R_4	n	Boiling Point (0.5 mm Hg)	Repellency ED_{50}	Repellency ED_{90}	r
I[a]	C_3H_7	H	C_3H_7	CO_2CH_3	1	90°	2.8	79	−0.97
II[b]	C_4H_9	H	C_4H_9	CO_2CH_3	1	102°	0.12	0.59	−0.88
III[c]	C_3H_7	CO_2CH_3	C_3H_7	CO_2CH_3	1	110°	0.049	0.13	−0.92
IV[b]	C_4H_9	CO_2CH_3	C_4H_9	CO_2CH_3	1	130°	0.014	0.072	−0.87
V[d]	C_6H_{13}	H	C_6H_{13}	CO_2CH_3	1	146°	0.028	0.083	−0.79
VI[e]	C_6H_{13}	CO_2CH_3	C_6H_{13}	CO_2CH_3	1	160°	0.036	0.21	−0.84
VII[f]	C_3H_7	H	C_3H_7	CO_2CH_3	2	112°	0.25	2.5	−0.68
VIII[g]	C_3H_7	CO_2CH_3	C_3H_7	CO_2CH_3	2	141°	0.020	0.073	−0.96
IX[h]	C_3H_7	H	C_3H_7	CO_2CH_3	3	131°	0.23	4.0	−0.68
X[i]	C_3H_7	CO_2CH_3	C_3H_7	CO_2CH_3	3	155°	0.018	0.10	−0.82
Diethyltoluamide						100°	0.031	0.10	−0.81
N,N'-Dihexamethylenecarbamide						130°	0.00081	0.056	−0.83

[a] *Anal.*—Calc. for $C_{10}H_{22}N_2O$: C, 59.37; H, 10.98; N, 13.85. Found: C, 58.84; H, 11.03; N, 13.76. [b] See *Experimental.* [c] *Anal.*—Calc. for $C_{12}H_{24}N_2O_4$: C, 55.36; H, 9.29; N, 10.76. Found: C, 55.15; H, 9.23; N, 10.70. [d] *Anal.*—Calc. for $C_{16}H_{34}N_2O_2$: C, 67.08; H, 11.96; N, 9.78. Found: C, 66.99; H, 11.87; N, 9.66. [e] *Anal.*—Calc. for $C_{18}H_{36}N_2O_4$: C, 62.75; H, 10.53; N, 8.13. Found: C, 63.05; H, 10.74; N, 8.23. [f] *Anal.*—Calc. for $C_{12}H_{26}N_2O_2$: C, 62.57; H, 11.38; N, 12.16. Found: C, 62.44; H, 11.54; N, 12.05. [g] *Anal.*—Calc. for $C_{14}H_{28}N_2O_4$: C, 58.30; H, 9.79; N, 9.72. Found: C, 57.99; H, 9.85; N, 9.68. [h] *Anal.*—Calc. for $C_{14}H_{30}N_2O_2$: C, 65.07; H, 11.70; N, 10.84. Found: C, 65.07; H, 11.74; N, 10.66. [i] *Anal.*—Calc. for $C_{16}H_{32}N_2O_4$: C, 60.73; H, 10.19; N, 8.85. Found: C, 60.65; H, 10.39; N, 8.66.

0022-3549/79/0300-0390$01.00/0
© 1979, American Pharmaceutical Association

(3) J. T. Ingram, *Br. Med. J.*, **2**, 591 (1953).
(4) S. Comaish, *Arch. Dermatol.*, **92**, 26 (1965).
(5) R. H. Seville, *Br. J. Dermatol.*, **78**, 269 (1966).
(6) E. Young, *ibid.*, **82**, 516 (1970).
(7) W. P. Raab and B. M. Gmeiner, *Dermatologica*, **150**, 267 (1975).
(8) H. J. Hulsebosch and M. Ponec-Waelsch, *ibid.*, **144**, 287 (1972).
(9) M. Ponec-Waelsch and H. J. Hulsebosch, *Arch. Dermatol. Forsch.*, **249**, 141 (1974).
(10) S. Comaish, J. Smith, and R. H. Seville, *Br. J. Dermatol.*, **84**, 282 (1971).
(11) P. Arends, *J. Chromatogr.*, **47**, 550 (1970).
(12) H. Beerman, G. V. Kulchar, and D. M. Pillsbury, *J. Am. Med. Assoc.*, **104**, 26 (1935).
(13) E. M. Farber and D. R. Harris, *Arch. Dermatol.*, **101**, 381 (1970).
(14) M. W. Gay, W. J. Moore, J. M. Morgan, and L. F. Montes, *ibid.*, **105**, 213 (1972).
(15) H. Baker and T. J. Ryan, *Br. J. Dermatol.*, **80**, 771 (1968).
(16) M. Whitefield, *Arzneim.-Forsch.*, **20**, 137 (1970).
(17) A. Segal, C. Kutz, and B. L. Van Duuren, *J. Med. Chem.*, **14**, 394 (1971).
(18) H. Thielemann, *Sci. Pharm.*, **42**, 55 (1974).
(19) E. G. Clarke, "Isolation and Identification of Drugs," vol. 2, Pharmaceutical Press, London, England, 1975, p. 1025.
(20) "The Merck Index," 9th ed., Merck and Co., Rahway, N.J., 1976, p. 3394.
(21) "The United States Pharmacopeia," 19th rev., Mack Publishing Co., Easton, Pa., 1975, p. 33.

ACKNOWLEDGMENTS

The authors thank Ms. Yanee Pongpaibul for technical assistance.

Topical Mosquito Repellents XI: Carbamates Derived from *N,N'*-Disubstituted Diamines

W. A. SKINNER ˣ, H. T. CRAWFORD, L. C. RUTLEDGE *, and M. A. MOUSSA ‡

Received May 26, 1978, from the *Life Sciences Division, SRI International, Menlo Park, CA 94025.* Accepted for publication August 17, 1978. *Present address: Letterman Army Institute of Research, Presidio of San Francisco, CA 94129. ‡Present address: Medical Entomology Consultant, Office of the Surgeon General, Washington, DC 20310.

Abstract □ Carbamates derived from various *N,N'*-disubstituted diamines were synthesized and evaluated as repellents for *Aedes aegypti* mosquitoes with an *in vitro* blood-feeding test system. Several compounds were more effective than diethyltoluamide.

Keyphrases □ Carbamates from *N,N'*-disubstituted amines—synthesized and evaluated as mosquito repellents □ Repellents, mosquito—various carbamates derived from *N,N'*-disubstituted diamines synthesized and evaluated □ Structure–activity relationships—various carbamates derived from *N,N'*-disubstituted diamines evaluated as mosquito repellents

Carbamates as mosquito repellents were discussed previously (1). Substituted 2-oxazolidones were synthesized and found to possess repellent activity (1). However, improvement of their repellency was desired, and a new synthetic effort was initiated to prepare carbamates from *N,N'*-disubstituted diamines.

To vary the boiling-point ranges of the proposed repellents, syntheses were concentrated on ethylenediamine, diethylenediamine, and triethylenediamine derivatives. Previous studies (1) showed that repellency duration is a function of boiling points or volatility of repellents.

These compounds were evaluated in the *in vitro* mosquito blood-feeding test system reported previously (2). Mosquitoes used for these evaluations were female *Aedes aegypti* (yellow fever mosquito).

Table I—Physical and Biological Properties of Carbamates Derived from *N,N'*-Disubstituted Diamines

$R_1N(CH_2CH_2)_nNR_3$ (R_2, R_4)

Compound	R_1	R_2	R_3	R_4	n	Boiling Point (0.5 mm Hg)	Repellency ED_{50}	Repellency ED_{90}	r
I[a]	C_3H_7	H	C_3H_7	CO_2CH_3	1	90°	2.8	79	−0.97
II[b]	C_4H_9	H	C_4H_9	CO_2CH_3	1	102°	0.12	0.59	−0.88
III[c]	C_3H_7	CO_2CH_3	C_3H_7	CO_2CH_3	1	110°	0.049	0.13	−0.92
IV[b]	C_4H_9	CO_2CH_3	C_4H_9	CO_2CH_3	1	130°	0.014	0.072	−0.87
V[d]	C_6H_{13}	H	C_6H_{13}	CO_2CH_3	1	146°	0.028	0.083	−0.79
VI[e]	C_6H_{13}	CO_2CH_3	C_6H_{13}	CO_2CH_3	1	160°	0.036	0.21	−0.84
VII[f]	C_3H_7	H	C_3H_7	CO_2CH_3	2	112°	0.25	2.5	−0.68
VIII[g]	C_3H_7	CO_2CH_3	C_3H_7	CO_2CH_3	2	141°	0.020	0.073	−0.96
IX[h]	C_3H_7	H	C_3H_7	CO_2CH_3	3	131°	0.23	4.0	−0.68
X[i]	C_3H_7	CO_2CH_3	C_3H_7	CO_2CH_3	3	155°	0.018	0.10	−0.82
Diethyltoluamide						100°	0.031	0.10	−0.81
N,N'-Dihexamethylenecarbamide						130°	0.00081	0.056	−0.83

[a] *Anal.*—Calc. for $C_{10}H_{22}N_2O$: C, 59.37; H, 10.98; N, 13.85. Found: C, 58.84; H, 11.03; N, 13.76. [b] See *Experimental.* [c] *Anal.*—Calc. for $C_{12}H_{24}N_2O_4$: C, 55.36; H, 9.29; N, 10.76. Found: C, 55.15; H, 9.23; N, 10.70. [d] *Anal.*—Calc. for $C_{16}H_{34}N_2O_2$: C, 67.08; H, 11.96; N, 9.78. Found: C, 66.99; H, 11.87; N, 9.66. [e] *Anal.*—Calc. for $C_{18}H_{36}N_2O_4$: C, 62.75; H, 10.53; N, 8.13. Found: C, 63.05; H, 10.74; N, 8.23. [f] *Anal.*—Calc. for $C_{12}H_{26}N_2O_2$: C, 62.57; H, 11.38; N, 12.16. Found: C, 62.44; H, 11.54; N, 12.05. [g] *Anal.*—Calc. for $C_{14}H_{28}N_2O_4$: C, 58.30; H, 9.79; N, 9.72. Found: C, 57.99; H, 9.85; N, 9.68. [h] *Anal.*—Calc. for $C_{14}H_{30}N_2O_2$: C, 65.07; H, 11.70; N, 10.84. Found: C, 65.07; H, 11.74; N, 10.66. [i] *Anal.*—Calc. for $C_{16}H_{32}N_2O_4$: C, 60.73; H, 10.19; N, 8.85. Found: C, 60.65; H, 10.39; N, 8.66.

0022-3549/79/0300-0390$01.00/0
© 1979, American Pharmaceutical Association

EXPERIMENTAL[1]

To prepare *N,N'*-dibutyl-*N*-methoxycarbonylethylenediamine (II) and *N,N'*-dibutyl-*N,N'*-di(methoxycarbonyl)ethylenediamine (IV), a 1-liter, three-necked flask was fitted with a thermometer, an addition funnel, a magnetic stirrer, a reflux condenser, and a heating mantle. The diamine (25 g, 0.145 mole) was dissolved in anhydrous methanol (800 ml) and placed in the flask. As this solution was slowly heated to 60°, a solution of methyl chloroformate (13.7 g, 0.145 mole) in anhydrous methanol (50 ml) was added dropwise over 1 hr. The reaction mixture was stirred at 60° for an additional 3 hr and then overnight at room temperature.

The methanol was removed *in vacuo*, and the residue was taken up in methylene chloride (300 ml), filtered to remove the hydrochloride salt of the starting material, and concentrated *in vacuo*. The residue was dissolved in distilled water, acidified (pH 3), and extracted with ether (three times) to yield Fraction E_1. The aqueous solution was made basic with 10% NaOH and reextracted with ether (three times), affording Fraction E_2.

Distillation of E_1 yielded 12.1 g of IV, bp 123°/0.35 mm Hg.

Anal.—Calc. for $C_{14}H_{28}N_2O_4$: C, 58.31; H, 9.79; N, 9.72. Found: C, 58.17; H, 9.92; N, 9.69.

Fraction E_2 was dried, evaporated *in vacuo*, and distilled to yield 17.1 g of II, bp 96–98°/0.4 mm Hg.

Anal.—Calc. for $C_{12}H_{26}N_2O_2$: C, 62.57; H, 11.38; N, 12.16. Found: C, 62.25; H, 11.43; N, 12.09.

[1] Boiling points were determined using a short path distillation apparatus and are uncorrected. Elemental analyses were performed by the Microanalytical Laboratory, Department of Chemistry, Stanford University, Stanford, Calif.

RESULTS AND DISCUSSION

Table I gives the structures, boiling points, and repellency data of the tested carbamates.

Compounds IV–VI, VIII, and X had ED_{50} values equal to or less than that of diethyltoluamide. The ED_{90} values of III–V, VII, and X were outstanding. These values indicate that all of these compounds should be considered as candidate repellents to replace diethyltoluamide, and advanced repellency and preliminary toxicity tests are planned.

With these compounds, the boiling range for effective repellency in this test system is considerably higher that of diethyltoluamide (100°/0.5 mm Hg), being 110–160°/0.5 mm Hg. These less volatile repellents may have an increased duration of effectiveness when applied to human skin.

Future studies will depend on the results of human skin tests of the best compounds of the series.

REFERENCES

(1) W. A. Skinner, H. T. Crawford, D. Skidmore, and H. I. Maibach, *J. Pharm. Sci.*, **66**, 587 (1977).

(2) L. C. Rutledge, M. A. Moussa, and C. J. Belletti, *Mosquito News*, **36**, 283 (1976).

ACKNOWLEDGMENTS

Supported by U.S. Army Medical Research and Development Command Contract DADA 17-70-C-0112.

Topical Mosquito Repellents XII: *N*-Substituted Ureas and Cyclic Ureas

W. A. SKINNER ˣ, H. T. CRAWFORD, L. C. RUTLEDGE *, and M. A. MOUSSA ‡

Received June 5, 1978, from the *Life Sciences Division, SRI International, Menlo Park, CA 94025.* Accepted for publication August 17, 1978. *Present address: Letterman Army Institute of Research, Presidio of San Francisco, CA 94129. ‡Present address: Medical Entomology Consultant, Office of the Surgeon General, Washington, DC 20310.

Abstract □ Various *N*-substituted urea and cyclic urea derivatives were synthesized and evaluated as repellents for *Aedes aegypti* mosquitoes with an *in vitro* blood-feeding test system. Several compounds were superior to diethyltoluamide.

Keyphrases ◻ Ureas and cyclic ureas, *N*-substituted—synthesized and evaluated as mosquito repellents □ Repellents, mosquito—various *N*-substituted ureas and cyclic ureas synthesized and evaluated □ Structure–activity relationships—various *N*-substituted ureas and cyclic ureas evaluated as mosquito repellents

In continuing efforts to find improved mosquito repellents, various *N*-substituted ureas and cyclic ureas were synthesized for evaluation in an *in vitro* blood-feeding test system using *Aedes aegypti* mosquitoes as described previously (1).

N,N'-Dihexamethylenecarbamide[1], a urea derivative, was reported (2) to be effective as a repellent for mosquitoes and black flies. The minimum effective dosage was 0.04 mg/cm^2 for mosquitoes (*A. hexodontus* and *A. punctor*) and 0.12 mg/cm^2 for black flies (*Simulium venustum*) when evaluated on human skin. The minimum effective dosages obtained for *N,N'*-dihexamethylenecarbamide were lower than those for diethyltoluamide (0.14 mg/cm^2) for the same mosquitoes.

In view of the interesting effectiveness of this *N*-substituted urea, it was decided to explore the structure–repellent activity relationships of *N*-substituted ureas and cyclic ureas. To vary the boiling-point ranges, both open chain and cyclic ureas were synthesized. For the same reason, substituents on the nitrogens were varied in alkyl chain lengths.

EXPERIMENTAL[2]

Preparation of *N,N'*-Dibutylurea (IV)—A 1-liter, three-necked flask was charged with 200 ml of benzene, and phosgene was bubbled

[1] Carboxide.

[2] Boiling points were determined using a short path distillation apparatus and are uncorrected. Elemental analyses were performed by the Microanalytical Laboratory, Department of Chemistry, Stanford University, Stanford, Calif.

0022-3549/79/0300-0391$01.00/0
© 1979, American Pharmaceutical Association

EXPERIMENTAL[1]

To prepare *N,N'*-dibutyl-*N*-methoxycarbonylethylenediamine (II) and *N,N'*-dibutyl-*N,N'*-di(methoxycarbonyl)ethylenediamine (IV), a 1-liter, three-necked flask was fitted with a thermometer, an addition funnel, a magnetic stirrer, a reflux condenser, and a heating mantle. The diamine (25 g, 0.145 mole) was dissolved in anhydrous methanol (800 ml) and placed in the flask. As this solution was slowly heated to 60°, a solution of methyl chloroformate (13.7 g, 0.145 mole) in anhydrous methanol (50 ml) was added dropwise over 1 hr. The reaction mixture was stirred at 60° for an additional 3 hr and then overnight at room temperature.

The methanol was removed *in vacuo*, and the residue was taken up in methylene chloride (300 ml), filtered to remove the hydrochloride salt of the starting material, and concentrated *in vacuo*. The residue was dissolved in distilled water, acidified (pH 3), and extracted with ether (three times) to yield Fraction E_1. The aqueous solution was made basic with 10% NaOH and reextracted with ether (three times), affording Fraction E_2.

Distillation of E_1 yielded 12.1 g of IV, bp 123°/0.35 mm Hg.

Anal.—Calc. for $C_{14}H_{28}N_2O_4$: C, 58.31; H, 9.79; N, 9.72. Found: C, 58.17; H, 9.92; N, 9.69.

Fraction E_2 was dried, evaporated *in vacuo*, and distilled to yield 17.1 g of II, bp 96–98°/0.4 mm Hg.

Anal.—Calc. for $C_{12}H_{26}N_2O_2$: C, 62.57; H, 11.38; N, 12.16. Found: C, 62.25; H, 11.43; N, 12.09.

[1] Boiling points were determined using a short path distillation apparatus and are uncorrected. Elemental analyses were performed by the Microanalytical Laboratory, Department of Chemistry, Stanford University, Stanford, Calif.

RESULTS AND DISCUSSION

Table I gives the structures, boiling points, and repellency data of the tested carbamates.

Compounds IV–VI, VIII, and X had ED_{50} values equal to or less than that of diethyltoluamide. The ED_{90} values of III–V, VII, and X were outstanding. These values indicate that all of these compounds should be considered as candidate repellents to replace diethyltoluamide, and advanced repellency and preliminary toxicity tests are planned.

With these compounds, the boiling range for effective repellency in this test system is considerably higher that of diethyltoluamide (100°/0.5 mm Hg), being 110–160°/0.5 mm Hg. These less volatile repellents may have an increased duration of effectiveness when applied to human skin.

Future studies will depend on the results of human skin tests of the best compounds of the series.

REFERENCES

(1) W. A. Skinner, H. T. Crawford, D. Skidmore, and H. I. Maibach, *J. Pharm. Sci.*, **66**, 587 (1977).

(2) L. C. Rutledge, M. A. Moussa, and C. J. Belletti, *Mosquito News*, **36**, 283 (1976).

ACKNOWLEDGMENTS

Supported by U.S. Army Medical Research and Development Command Contract DADA 17-70-C-0112.

Topical Mosquito Repellents XII: *N*-Substituted Ureas and Cyclic Ureas

W. A. SKINNER ˣ, H. T. CRAWFORD, L. C. RUTLEDGE *, and M. A. MOUSSA ‡

Received June 5, 1978, from the *Life Sciences Division, SRI International, Menlo Park, CA 94025.* Accepted for publication August 17, 1978. *Present address: Letterman Army Institute of Research, Presidio of San Francisco, CA 94129. ‡Present address: Medical Entomology Consultant, Office of the Surgeon General, Washington, DC 20310.

Abstract □ Various *N*-substituted urea and cyclic urea derivatives were synthesized and evaluated as repellents for *Aedes aegypti* mosquitoes with an *in vitro* blood-feeding test system. Several compounds were superior to diethyltoluamide.

Keyphrases ◻ Ureas and cyclic ureas, *N*-substituted—synthesized and evaluated as mosquito repellents □ Repellents, mosquito—various *N*-substituted ureas and cyclic ureas synthesized and evaluated □ Structure–activity relationships—various *N*-substituted ureas and cyclic ureas evaluated as mosquito repellents

In continuing efforts to find improved mosquito repellents, various *N*-substituted ureas and cyclic ureas were synthesized for evaluation in an *in vitro* blood-feeding test system using *Aedes aegypti* mosquitoes as described previously (1).

N,N'-Dihexamethylenecarbamide[1], a urea derivative, was reported (2) to be effective as a repellent for mosquitoes and black flies. The minimum effective dosage was 0.04 mg/cm^2 for mosquitoes (*A. hexodontus* and *A. punctor*) and 0.12 mg/cm^2 for black flies (*Simulium venustum*) when evaluated on human skin. The minimum effective dosages obtained for *N,N'*-dihexamethylenecarbamide were lower than those for diethyltoluamide (0.14 mg/cm^2) for the same mosquitoes.

In view of the interesting effectiveness of this *N*-substituted urea, it was decided to explore the structure–repellent activity relationships of *N*-substituted ureas and cyclic ureas. To vary the boiling-point ranges, both open chain and cyclic ureas were synthesized. For the same reason, substituents on the nitrogens were varied in alkyl chain lengths.

EXPERIMENTAL[2]

Preparation of *N,N'*-Dibutylurea (IV)—A 1-liter, three-necked flask was charged with 200 ml of benzene, and phosgene was bubbled

[1] Carboxide.

[2] Boiling points were determined using a short path distillation apparatus and are uncorrected. Elemental analyses were performed by the Microanalytical Laboratory, Department of Chemistry, Stanford University, Stanford, Calif.

0022-3549/79/0300-0391$01.00/0
© 1979, American Pharmaceutical Association

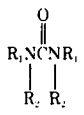

I-VIII

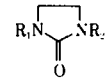

IX-XI

Table I—Physical and Biological Properties of *N*-Substituted Ureas and Cyclic Ureas

Compound	R_1	R_2	Boiling Point (0.5 mm Hg)	Repellency ED_{50}	Repellency ED_{90}	Repellency r
I[a]	C_3H_7	C_3H_7	81°	0.075	0.25	−0.92
II[b]	C_4H_9	C_2H_5	95°	0.027	0.10	−0.76
III[c]	C_3H_7	C_4H_9	103°	0.0028	0.024	−0.85
IV[d]	C_4H_9	C_4H_9	119°	0.0073	1.5	−0.99
V[e]	C_3H_7	$CH(CH_3)_2$	74°	0.11	0.80	−0.91
VI[f]	C_4H_9	CH_3	83°	0.039	0.30	−0.69
VII[g]	C_2H_5	$CH(CH_3)_2$	60°	0.30	1.4	−0.70
VIII[h]	C_3H_7	CH_3	59°	0.045	0.22	−0.88
IX[d]	C_3H_7	C_3H_7	92°	0.049	0.23	−0.99
X[i]	C_4H_9	C_4H_9	110°	0.041	0.14	−0.97
XI[j]	C_6H_{13}	C_6H_{13}	145°	0.0052	0.074	−0.68
Diethyltoluamide			100°	0.031	0.10	−0.81
N,N'-Dihexamethylenecarbamide			130°	0.00081	0.056	−0.83

[a] *Anal.*—Calc. for $C_7H_{14}N_2O$: C, 68.37; H, 12.37; N, 12.32. Found: C, 68.32; H, 12.56; N, 12.24. [b] *Anal.*—Calc. for $C_{13}H_{28}N_2O$: C, 68.37; H, 12.36; N, 12.27. Found: C, 68.22; H, 12.55; N, 12.12. [c] *Anal.*—Calc. for $C_{15}H_{32}N_2O$: C, 70.25; H, 12.58; N, 10.93. Found: C, 70.36; H, 12.74; N, 10.96. [d] See *Experimental*. [e] *Anal.*—Calc. for $C_{13}H_{28}N_2O$: C, 68.37; H, 12.36; N, 12.27. Found: C, 68.17; H, 12.41; N, 12.37. [f] *Anal.*—Calc. for $C_{11}H_{24}N_2O$: C, 65.95; H, 12.08; N, 13.99. Found: C, 65.95; H, 12.19; N, 14.00. [g] *Anal.*—Calc. for $C_{11}H_{24}N_2O$: C, 65.95; H, 12.08; N, 13.99. Found: C, 65.72; H, 12.33; N, 13.87. [h] *Anal.*—Calc. for $C_9H_{20}N_2O$: C, 62.74; H, 11.70; N, 16.27. Found: C, 62.66; H, 11.94; N, 16.08. [i] *Anal.*—Calc. for $C_{11}H_{22}N_2O$: C, 66.62; H, 11.18; N, 14.13. Found: C, 66.43; H, 11.29; N, 14.07. [j] *Anal.*—Calc. for $C_{15}H_{30}N_2O$: C, 70.81; H, 11.89; N, 11.01. Found: C, 70.43; H, 11.73; N, 10.87.

through the stirred solution until approximately 9 g had been collected (0.039 *M*). Potassium carbonate (25.6 g, 0.186 mole) was then added, and the flask was fitted with a nitrogen inlet–outlet, a reflux condenser, and an addition funnel. The stirrer was started, and dibutylamine (15.6 ml, 0.093 mole) was added dropwise over 30 min. Occasional cooling was necessary to ensure that the temperature did not rise above 35°. After the addition was complete, the solution was stirred at room temperature for 3 hr. Another 15.65 ml of dibutylamine was then added, and the solution was refluxed for 3 hr.

The cooled reaction mixture then was filtered to remove potassium carbonate–potassium chloride, evaporated *in vacuo*, and distilled. Redistillation after stripping off benzene after ethanol was added gave a liquid, bp 119°/0.5 mm Hg.

Anal.—Calc. for $C_{17}H_{36}N_2O$: C, 77.77; H, 12.76; N, 9.85. Found: C, 77.92; H, 12.88; N, 9.84.

Preparation of *N,N'*-Dipropylmethoxycarbonylethylenediamine—Preparation of *N,N'*-dipropyl-1,3-diaza-2-cyclopentanone (IX) was *via* the carbamate *N,N'*-dipropylmethoxycarbonylethylenediamine, which was prepared as follows. A 1-liter, three-necked, round-bottom flask was fitted with a thermometer, an addition funnel, a magnetic stirrer, a reflux condenser, and a heating mantle. The diamine (25 g, 0.174 mole) was dissolved in anhydrous methanol (800 ml) and placed in the flask. As this solution was slowly heated to 60°, a solution of methyl chloroformate (16.4 g, 0.174 mole) in anhydrous methanol (50 ml) was added dropwise over 1 hr. The reaction mixture was stirred at 60° for an additional 3 hr and then at room temperature overnight. The methanol was removed at reduced pressure, and the residue was taken up in methylene chloride (300 ml), filtered to remove the hydrochloride salt of the starting material (4.71 g), and evaporated *in vacuo*.

The residue was dissolved in distilled water, acidified (pH 3), and extracted with ether (three times) to yield Fraction E_1. The aqueous solution was basified with 10% NaOH and reextracted with ether (three times), affording Fraction E_2. Fraction E_1 was dried over sodium sulfate and evaporated *in vacuo*. After distillation, 7.25 g of the dicarbamate was obtained. Fraction E_2, after removal of the solvent *in vacuo*, yielded the monocarbamate intermediate.

Preparation of *N,N'*-Dipropyl-1,3-diaza-2-cyclopentanone (IX)—A 500-ml, three-necked flask was fitted with a Y-tube nitrogen inlet, an ammonia inlet, a dry ice condenser, a gas bubbler, and a magnetic stirrer. The nitrogen was started, and the apparatus flamed out. After cooling under nitrogen, the condenser was charged with dry ice, and ammonia (1) (150 ml) was collected in the flask. Ferric nitrate nonahydrate (50 mg) was added, and the ammonia solution turned light brown. A small piece of sodium (50 mg) was added, and the solution was stirred at −33° until the blue color had disappeared and a black precipitate of catalyst formed.

The remainder of the sodium (0.93 g, 0.04 mole) was then added in portions over 10 min. After the blue color was discharged (0.5 hr), a solution of the carbamate (4.0 g, 0.02 mole) in anhydrous ether (10 ml) was added dropwise from the addition funnel over 30 min. The black solution was then stirred at −33° for 4 hr, and the ammonia was allowed to evaporate overnight under nitrogen.

The residue was dissolved in a water–ether slurry and transferred to a separator. The layers were separated, and the organic phase was washed with ether twice. The combined ether layers were dried (magnesium sulfate), evaporated *in vacuo*, and distilled to afford the desired product, 3.0 g, bp 63–66°/0.08 mm Hg.

Anal.—Calc. for $C_9H_{18}N_2O$: C, 63.49; H, 10.65; N, 16.46. Found: C, 61.97; H, 10.68; N, 16.04.

RESULTS AND DISCUSSION

Table I gives the structures, boiling points, and repellency data for the compounds. Those repellents for *A. aegypti* (yellow fever mosquito) having ED_{50} and ED_{90} values lower than the standard repellent (diethyltoluamide) are candidates for further evaluation in other tests for repellency. However, prior to application to human skin, preliminary toxicology studies must be performed.

Compared to diethyltoluamide, II–IV, VI, and XI had lower or comparable ED_{50} values and II, III, and XI had lower or comparable ED_{90} values. Compared to *N,N'*-hexamethylenecarbamide, III and XI had as good or better ED_{90} values.

The relationship between boiling point and repellency in this test is not as clear as in prior studies (3), but maximum effectiveness in terms of ED_{50} or ED_{90} values appeared to peak with the *N*-substituted ureas around 100° at 0.5 mm Hg, which is very similar to the value found with analogs of diethyltoluamide by skin testing (3). With the cyclic urea derivatives, the peak activity was found around 145° at 0.5 mm Hg, closer to that of *N,N'*-dihexamethylenecarbamide.

Further study of the most active of these compounds may yield improved topical repellents for mosquitoes and point the way to improved compounds in this series by variation of their volatility.

REFERENCES

(1) L. C. Rutledge, M. A. Moussa, and C. J. Belletti, *Mosquito News*, **36**, 283 (1976).

(2) V. P. Dremova, V. V. Markina, and N. A. Kamennov, *Int. Pest Control*, **Sept./Oct. 1971**, 13.

(3) H. L. Johnson, W. A. Skinner, T. R. Pearson, and H. I. Maibach, *J. Econ. Entomol.*, **60**, 173 (1966).

ACKNOWLEDGMENTS

Supported by U.S. Army Medical Research and Development Command Contract DADA 17-70-C-0112.

Ticrynafen Effect on Warfarin Protein Binding in Human Serum

Keyphrases □ Ticrynafen—effect on warfarin protein binding, human serum □ Protein binding—warfarin to serum protein, effect of ticrynafen, humans □ Warfarin—serum protein binding, effect of ticrynafen, humans □ Antihypertensive agents—ticrynafen, effect on warfarin protein binding, human serum □ Anticoagulants—warfarin, serum protein binding, effect of ticrynafen, humans

To the Editor:

Ticrynafen[1] [2,3-dichloro-4-(2-thienylcarbonyl)-phenoxyacetic acid] is a new antihypertensive, diuretic, and uricosuric agent (1). About 99.5% of this weak acid is bound to human serum proteins in the therapeutic drug concentration range (2). Serious drug interactions between ticrynafen and the coumarin anticoagulants ethyl biscoumacetate and acenocoumarol have been reported, with anticoagulant potentiation and hemorrhages (3–5). It has been suggested that these interactions resulted from anticoagulant displacement from serum protein binding sites by ticrynafen and that this might also occur with warfarin (2–5).

We determined the ticrynafen effect on warfarin protein binding in human serum over a wide range of ticrynafen concentrations. Blood was obtained from two healthy adult male donors, serum was separated and pooled, and racemic ^{14}C-warfarin (2 μg/ml) was added. Ticrynafen[2] was dissolved in 50 μl of ethanol, and pH 7.4 sodium phosphate buffer (0.134 *M*) was added to yield 5 ml of solution containing 10–200 μg of ticrynafen/ml. Ticrynafen-free buffer solutions contained the same concentration of ethanol. Plasma containing warfarin was dialyzed at 37° to equilibrium against these solutions. Warfarin was then extracted from both phases, separated from impurities and degradation products by TLC, and assayed by scintillation spectrometry as previously described (6, 7).

The results are shown in Table I. Warfarin, in the absence of ticrynafen, was 99.288% bound (results of three dialysis experiments were 99.265, 99.297, and 99.301%). Ticrynafen (10–200 μg/ml) had no apparent effect on warfarin serum protein binding. Essentially identical results were obtained when both warfarin and ticrynafen were added to serum (without ethanol), and these serums were dialyzed against buffer only. The warfarin concentration used in this study was in the upper therapeutic concentration range (8, 9); the concentrations of ticrynafen ranged from therapeutic (~10–40 μg/ml) to far above therapeutic concentrations (1, 2). Since both drugs are extensively protein-bound weak acids, displacement effects may occur at even higher concentrations of either compound or in diluted plasma or diluted albumin solutions.

The results indicate that warfarin will not be significantly displaced from serum protein binding sites by ticrynafen under the usual therapeutic conditions. They do not rule out other interactions such as inhibition of warfarin metabolism, direct effects of ticrynafen on the blood coagulation process, and effects of ticrynafen metabolites.

Table I—Effect of Ticrynafen on Warfarin Protein Binding in Human Serum [a]

Ticrynafen Concentration, μg/ml	Warfarin Free Fraction[b] × 100	Warfarin Free Fraction Ratio[c]
0	0.712	1.00
10	0.688	0.97
20	0.655	0.92
30	0.710	1.00
40	0.771	1.08
50	0.695	0.98
100	0.751	1.05
200	0.725	1.02

[a] Determined by equilibrium dialysis at 37°. Initial warfarin concentration was 2 μg/ml. [b] Mean of two or three determinations. [c] Free fraction divided by free fraction in the absence of ticrynafen.

(1) R. Okun and M. Beg, *Clin. Pharmacol. Ther.*, **23**, 703 (1978).
(2) A. J. Wood, P. Bolli, H. J. Waal-Manning, and F. O. Simpson, *ibid.*, **23**, 697 (1978).
(3) M. Detilleux, R. Caquet, and C. Laroche, *Nouv. Presse Med.*, **5**, 2395 (1976).
(4) H. Portier, F. Destaing, and L. Chauve, *ibid.*, **6**, 468 (1977).
(5) A. Grand, B. Drouin, and G. J. Arche, *ibid.*, **6**, 2691 (1977).
(6) A. Yacobi and G. Levy, *J. Pharm. Sci.*, **64**, 1660 (1975).
(7) A. Yacobi, L. B. Wingard, Jr., and G. Levy, *ibid.*, **63**, 868 (1974).
(8) A. Yacobi, J. A. Udall, and G. Levy, *Clin. Pharmacol. Ther.*, **19**, 552 (1976).
(9) A. Jain, F. G. McMahon, J. T. Slattery, and G. Levy, *ibid.*, in press.

John T. Slattery
Gerhard Levy ˣ
Department of Pharmaceutics
School of Pharmacy
State University of New York at Buffalo
Amherst, NY 14260

Received November 15, 1978.
Accepted for publication December 27, 1978.
Supported in part by Grant GM 20852 from the National Institute of General Medical Sciences, National Institutes of Health, Bethesda, MD 20014.

Comparison of Antineoplastic Activity of Aminoethylaminoanthraquinones and Anthracycline Antibiotics

Keyphrases □ Antineoplastic activity—aminoethylaminoanthraquinones, doxorubicin, daunorubicin, and cardiotoxicity □ Antineoplastic agents—aminoethylaminoanthraquinones, doxorubicin, daunorubicin, and cardiotoxicity □ Aminoethylaminoanthraquinones—antineoplastic activity and cardiotoxicity, compared to doxorubicin and daunorubicin □ Cardiotoxicity—evaluated, aminoethylaminoanthraquinones, doxorubicin, daunorubicin

To the Editor:

The anthracycline antibiotics doxorubicin and daunorubicin are among the most important antineoplastic agents studied in recent years. Both antibiotics demon-

[1] SKF-62698, Selacryn.
[2] Supplied by Smith Kline & French Laboratories, Philadelphia, Pa.

0022-3549/79/0300-0393$01.00/0
© 1979, American Pharmaceutical Association

Ticrynafen Effect on Warfarin Protein Binding in Human Serum

Keyphrases □ Ticrynafen—effect on warfarin protein binding, human serum □ Protein binding—warfarin to serum protein, effect of ticrynafen, humans □ Warfarin—serum protein binding, effect of ticrynafen, humans □ Antihypertensive agents—ticrynafen, effect on warfarin protein binding, human serum □ Anticoagulants—warfarin, serum protein binding, effect of ticrynafen, humans

To the Editor:

Ticrynafen[1] [2,3-dichloro-4-(2-thienylcarbonyl)-phenoxyacetic acid] is a new antihypertensive, diuretic, and uricosuric agent (1). About 99.5% of this weak acid is bound to human serum proteins in the therapeutic drug concentration range (2). Serious drug interactions between ticrynafen and the coumarin anticoagulants ethyl biscoumacetate and acenocoumarol have been reported, with anticoagulant potentiation and hemorrhages (3–5). It has been suggested that these interactions resulted from anticoagulant displacement from serum protein binding sites by ticrynafen and that this might also occur with warfarin (2–5).

We determined the ticrynafen effect on warfarin protein binding in human serum over a wide range of ticrynafen concentrations. Blood was obtained from two healthy adult male donors, serum was separated and pooled, and racemic ^{14}C-warfarin (2 μg/ml) was added. Ticrynafen[2] was dissolved in 50 μl of ethanol, and pH 7.4 sodium phosphate buffer (0.134 *M*) was added to yield 5 ml of solution containing 10–200 μg of ticrynafen/ml. Ticrynafen-free buffer solutions contained the same concentration of ethanol. Plasma containing warfarin was dialyzed at 37° to equilibrium against these solutions. Warfarin was then extracted from both phases, separated from impurities and degradation products by TLC, and assayed by scintillation spectrometry as previously described (6, 7).

The results are shown in Table I. Warfarin, in the absence of ticrynafen, was 99.288% bound (results of three dialysis experiments were 99.265, 99.297, and 99.301%). Ticrynafen (10–200 μg/ml) had no apparent effect on warfarin serum protein binding. Essentially identical results were obtained when both warfarin and ticrynafen were added to serum (without ethanol), and these serums were dialyzed against buffer only. The warfarin concentration used in this study was in the upper therapeutic concentration range (8, 9); the concentrations of ticrynafen ranged from therapeutic (~10–40 μg/ml) to far above therapeutic concentrations (1, 2). Since both drugs are extensively protein-bound weak acids, displacement effects may occur at even higher concentrations of either compound or in diluted plasma or diluted albumin solutions.

The results indicate that warfarin will not be significantly displaced from serum protein binding sites by ticrynafen under the usual therapeutic conditions. They do not rule out other interactions such as inhibition of warfarin metabolism, direct effects of ticrynafen on the blood coagulation process, and effects of ticrynafen metabolites.

Table I—Effect of Ticrynafen on Warfarin Protein Binding in Human Serum [a]

Ticrynafen Concentration, μg/ml	Warfarin Free Fraction[b] × 100	Warfarin Free Fraction Ratio[c]
0	0.712	1.00
10	0.688	0.97
20	0.655	0.92
30	0.710	1.00
40	0.771	1.08
50	0.695	0.98
100	0.751	1.05
200	0.725	1.02

[a] Determined by equilibrium dialysis at 37°. Initial warfarin concentration was 2 μg/ml. [b] Mean of two or three determinations. [c] Free fraction divided by free fraction in the absence of ticrynafen.

(1) R. Okun and M. Beg, *Clin. Pharmacol. Ther.*, **23**, 703 (1978).
(2) A. J. Wood, P. Bolli, H. J. Waal-Manning, and F. O. Simpson, *ibid.*, **23**, 697 (1978).
(3) M. Detilleux, R. Caquet, and C. Laroche, *Nouv. Presse Med.*, **5**, 2395 (1976).
(4) H. Portier, F. Destaing, and L. Chauve, *ibid.*, **6**, 468 (1977).
(5) A. Grand, B. Drouin, and G. J. Arche, *ibid.*, **6**, 2691 (1977).
(6) A. Yacobi and G. Levy, *J. Pharm. Sci.*, **64**, 1660 (1975).
(7) A. Yacobi, L. B. Wingard, Jr., and G. Levy, *ibid.*, **63**, 868 (1974).
(8) A. Yacobi, J. A. Udall, and G. Levy, *Clin. Pharmacol. Ther.*, **19**, 552 (1976).
(9) A. Jain, F. G. McMahon, J. T. Slattery, and G. Levy, *ibid.*, in press.

John T. Slattery
Gerhard Levy ˣ
Department of Pharmaceutics
School of Pharmacy
State University of New York at Buffalo
Amherst, NY 14260

Received November 15, 1978.
Accepted for publication December 27, 1978.
Supported in part by Grant GM 20852 from the National Institute of General Medical Sciences, National Institutes of Health, Bethesda, MD 20014.

Comparison of Antineoplastic Activity of Aminoethylaminoanthraquinones and Anthracycline Antibiotics

Keyphrases □ Antineoplastic activity—aminoethylaminoanthraquinones, doxorubicin, daunorubicin, and cardiotoxicity □ Antineoplastic agents—aminoethylaminoanthraquinones, doxorubicin, daunorubicin, and cardiotoxicity □ Aminoethylaminoanthraquinones—antineoplastic activity and cardiotoxicity, compared to doxorubicin and daunorubicin □ Cardiotoxicity—evaluated, aminoethylaminoanthraquinones, doxorubicin, daunorubicin

To the Editor:

The anthracycline antibiotics doxorubicin and daunorubicin are among the most important antineoplastic agents studied in recent years. Both antibiotics demon-

[1] SKF-62698, Selacryn.
[2] Supplied by Smith Kline & French Laboratories, Philadelphia, Pa.

0022-3549/79/0300-0393$01.00/0
© 1979, American Pharmaceutical Association

Table I—Antineoplastic Activity of Anthracycline Antibiotics and 1,4-Bis(substituted aminoethylamino)anthraquinones in Mice

Agent	NSC Number	L-1210 Leukemia			P-388 Leukemia			B16 Melanoma			C6 Colon			P-388/Doxorubicin (PA)		P-388/Daunorubicin (PB)	
		Dose, mg/kg	T/C, %	Cures	Dose, mg/kg	T/C, %	Cures	Dose, mg/kg	T/C, %	Cures	Dose, mg/kg	T/C, %	Cures	Dose, mg/kg	T/C, %	Dose, mg/kg	T/C, %
Doxorubicin hydrochloride	123127	4	291	2/8	2	254	2/8	6	189	3/10	10.5	205		10	87	6	92
		2	251	1/8	1	250		3	412	5/10	8.1	148	1/10	6	106	3.6	105
		1	129		0.5	177		1.5	412	9/10	6.3	197	1/10	3	102	2.16	105
		0.5	134					0.75	210	3/10							
								0.5	158	1/10							
Daunorubicin hydrochloride	82151	2	145		4	105		1	285	4/6	4	128		8	107	4.8	117
		1	126		2	224		0.5	285	3/6	2	124		4.8	121	2.88	117
		0.5	120		1	234		0.25	188					2.88	114		
					0.5	191		0.13	142								
					0.25	194											
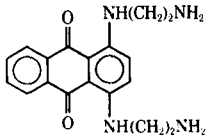	281246	25	272		16	243	1/8	8	218	4/10	16	227	1/10	21.6	87	21.6	87
		12.5	227		8	203		4	210	2/10	8	213	1/10	13	106	13	93
		6	156		4	194					4	175					
					2	185											
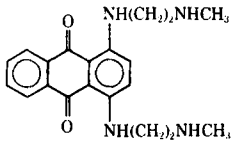	291923	8	185		12.5	200	2/6	8	231	1/10	8	225	2/10	13	93	13	90
		4	150		4	175	1/6	2	230	2/10	4	215	2/10				
		2	146		2	183	1/6	1	150	1/10	2	219	1/10				
		1	134														
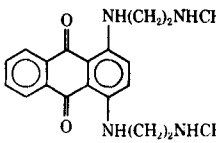	276740	16	130		16	166	1/6	16	158		16	169		21.6	100	21.6	101
		8	128		8	174		8	157	1/10	8	166		13	93	13	102
		4	122		4	157		4	127		4	145	1/10				
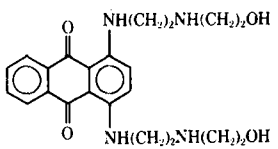	196473	16	250	3/6	25	517	7/8	8	280	6/10	8	286		21.6	104		
		8	220	2/6	16	416		4	248		4	215	2/10	13	105		
		4	157		6.25	189	2/8	2	186		2	139					
					3.2	239	3/8										
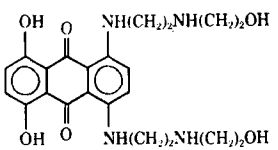	279836	18	308	5/8	2	280	5/6	8	303	7/10	6	305	4/10	3.6	150	3.6	131
		10.8	261	1/8	1	450		2	317	7/10	3	324	7/10	2.16	135	2.16	134
		4	230	2/6	0.5	351	3/8	1	222	3/10	1	365	8/10			1.3	131
		2	223	2/6	0.25	280	2/6	0.5	262	8/10	0.5	365	6/10				
		1	274	2/6							0.25	359	4/10				
		0.25	196														

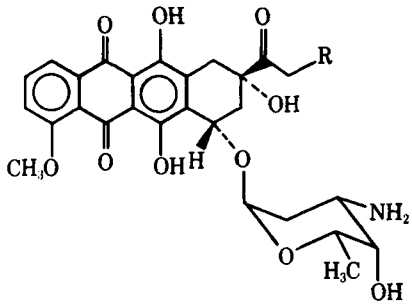

doxorubicin: R = OH
daunorubicin: R = H

strated inhibitory activity against a wide spectrum of experimental animal neoplasms and human cancers, including leukemias, lymphomas, and several solid tumors. These drugs possess some serious toxicities, of which the most troublesome is cardiotoxicity. The latter is characterized by a delayed and insidious cardiomyopathy with ECG abnormalities, cyanosis, dyspnea, and, in some cases, irreversible congestive heart failure (1). In spite of some studies indicating that preadministration of vitamin E, edetate disodium, 1,2-di(3,5-dioxopiperazin-1-yl)propane, *cis*-diamminedichloroplatinum, or ubiquinone$_{10}$ may relieve the cardiotoxicity (1–6), it remains a grave concern.

In 1970, the presence of a common N—O—O triangular feature among a number of antileukemic compounds, including doxorubicin and daunorubicin, was postulated (7). Based on this report, Adamson (8) proposed replacing the amino sugar portion of these antibiotics, believed to cause their cardiotoxicity, with amino-containing functions having the nitrogen atom placed at a proper spatial distance from the oxygen atoms of the aglycone portion. This arrangement would, hopefully, produce antineoplastic compounds with minimal cardiotoxicity.

In connection with a study of various amino- and hydroxyquinones as potential antineoplastic agents (9–12), Adamson's suggestion prompted the synthesis and structure–activity analysis of a number of bis(substituted aminoalkylamino)anthraquinones (13). Recent test data (14, 15) revealed that the biological activity profile of these compounds resembles that of doxorubicin and daunorubicin. In addition, most of these aminoanthraquinones were cross-resistant to the doxorubicin- and daunorubicin-resistant leukemia P-388 sublines (Table I), indicating antineoplastic action similar to the naturally occurring antibiotics. Perhaps due to a lipophilicity change of the ring-hydroxylated derivative, 1,4-dihydroxy-5,8-bis[[2-(hydroxyethyl)amino]ethyl]amino-9,10-anthracenedione, which may modify the cellular transport mechanism, a low level of antileukemic activity of this anthracenedione against the doxorubicin- and daunorubicin-resistant P-388 sublines was retained.

Table II—Minimum Cumulative Cardiotoxic Dose

Agent	NSC Number	P-388 Leukemia Optimum Dose in Mice, QD 1–9, mg/kg ip	Minimum Cumulative Cardiotoxic Dose in Rats, mg/kg ip/duration	Ratio
Daunorubicin	82151	9.73	14	1.44
Doxorubicin	123127	10.69	11	1.03
1,4-Bis[2-[(2-hydroxyethyl)amino]ethyl]amino-9,10-anthracenedione diacetate	287513	137.5	300	2.18
1,4-Dihydroxy-5,8-bis[[(2-hydroxyethyl)amino]ethyl]amino-9,10-anthracenedione	279836	8.3	18	2.17

Preliminary evaluation of the cardiotoxicity of the anthracenedione was conducted in rats (16, 17). The minimal cumulative cardiotoxic dose of this anthracenedione was 18 mg/kg. (It was somewhat less cardiotoxic than doxorubicin, whose minimal cumulative cardiotoxic dose was ~11 mg/kg.) The margin of safety (Table II) of the two anthracenediones, 1,4-bis[2-[(2-hydroxyethyl)amino]ethyl]amino-9,10-anthracenedione diacetate and 1,4-dihydroxy-5,8-bis[[(2-hydroxyethyl)amino]ethyl]amino-9,10-anthracenedione, was slightly larger than that of the two anthracyclines (daunorubicin hydrochloride and doxorubicin hydrochloride). The margin of safety is the ratio of the minimal cumulative cardiotoxic dose to the optimum therapeutic cumulative dose in the P-388 leukemia model.

Even though some interesting investigations on the syntheses of daunorubicin and doxorubicin have been conducted, the main supplies of these antineoplastic drugs still come from natural sources. The ease of synthesis of the aminoanthraquinones, their relatively low cardiotoxicity level, and their biological activity resemblance to the anthracycline antibiotics indicate that 1,4-dihydroxy-5,8-bis[[2-(hydroxyethyl)amino]ethyl]amino-9,10-anthracenedione and related compounds merit further oncological studies.

(1) "Adriamycin: New Drug Seminar," N. R. Bachur, R. S. Benjamin, and T. C. Hall, Eds., San Francisco, Calif., Jan. 1975. *Cancer Chemother. Rep.*, Part 3, **6**, 83 (1975).

(2) R. J. Woodman, I. Kline, and J. M. Venditti, *Proc. Am. Assoc. Cancer Res.*, **13**, 31 (1972).

(3) C. E. Myers, W. McGuire, and R. Young, *Cancer Treat. Rep.*, **60**, 961 (1976).

(4) A. B. Combs, D. Acosta, and K. Folkers, *ICRS Med. Sci. Libr. Compend.*, **4**, 403 (1976).

(5) E. H. Herman, R. M. Mhatre, I. P. Lee, and V. S. Waravdekar, *Proc. Soc. Exp. Biol. Med.*, **140**, 234 (1972).

(6) R. C. Mills, L. H. Maurer, R. J. Forcier, W. R. Grace, G. P. Burke, D. D. Karp, R. C. Smith, O. R. McIntyre, and C. Bean, *Cancer Treat. Rep.*, **61**, 477 (1977).

(7) K. Y. Zee-Cheng and C. C. Cheng, *J. Pharm. Sci.*, **59**, 1630 (1970).

(8) R. H. Adamson, *Cancer Chemother. Rep.*, **58**, 293 (1974).

(9) T. K. Liao, W. H. Nyberg, and C. C. Cheng, *Angewandte Chem.*, **79**, 100 (1967).

(10) E. G. Podrebarac and C. C. Cheng, *J. Org. Chem.*, **35**, 281 (1970).

(11) K. Y. Zee-Cheng and C. C. Cheng, *J. Med. Chem.*, **13**, 264 (1970).

(12) K. D. Paull, R. K. Y. Zee-Cheng, and C. C. Cheng, *J. Med. Chem.*, **19**, 337 (1976).

(13) R. K. Y. Zee-Cheng and C. C. Cheng, *J. Med. Chem.*, **21**, 291 (1978).

(14) R. I. Geren, N. H. Greenberg, M. M. MacDonald, A. M. Schumacher, and B. J. Abbott, *Cancer Chemother. Rep.*, Part 3, **3**, 1 (1972).

(15) "Screening Data Summary Interpretation and Outline of Current

Screen," Instruction Booklet 14, Drug Evaluation Branch, Division of Cancer Treatment, National Cancer Institute, Bethesda, Md., 1977.

(16) G. Zbinden and E. Brändle, *Cancer Chemother. Rep.*, Part 1, **59**, 707 (1975).

(17) G. Zbinden, E. Bachmann, and C. H. Hoderegger, *Antibiot. Chemother.*, **23**, 255 (1978).

C. C. Cheng *x
Midwest Research Institute
Kansas City, MO 64110

G. Zbinden
Institute of Toxicology
Federal Institute of Technology
and University of Zurich
Zurich, Switzerland

Robert K. Y. Zee-Cheng
Midwest Research Institute
Kansas City, MO 64110

Received October 16, 1978.

Accepted for publication December 14, 1978.

Supported by Contract N01-CM-33743 from the Division of Cancer Treatment, National Cancer Institute, National Institutes of Health.

The authors thank Dr. Harry B. Wood and Mr. Robert B. Ing of the National Cancer Institute for their interest and encouragement.

*Present address: Mid-America Cancer Center Program, University of Kansas Medical Center, Kansas City, KS 66103.

Conformation, Partition, and Drug Design

Keyphrases □ Conformations—drug, biological activity, fraction of conformer and partition coefficient □ Structure-activity relationships—drug conformers, biological activity, fraction of conformer and partition coefficient □ Partition coefficients—drug conformers, structure-activity relationships, biological activity

To the Editor:

Current interest in drug conformation rests on the postulate that a single preferred conformer binds to the receptor productively. If this conformer can be identified, it can then be fixed, or at least its population can be enhanced, by chemical means. In most areas of interest in drug design, however, drug–receptor complexes are not available for detailed molecular study, so the active conformation must be inferred. The usual procedure has been to seek correlations between conformation, determined experimentally or theoretically for a drug series, and biological response.

Until recently, the dominant conformer was assumed to be the biologically active agent (1). While there have been problems of agreement on the form of the dominant conformer (2), the widely variable responses that can occur even when the physical conformation is unambiguous (3) have encouraged the idea that a minor conformer may sometimes be responsible for activity (4–7). Thus, besides an interest in the nature of the active conformation, there is an interest in the fraction of active conformer in solution and in how it varies with chemical structure (5, 6).

An entirely different approach to drug design is based on multiparameter correlations of biological response with partition coefficients and other physical properties. This

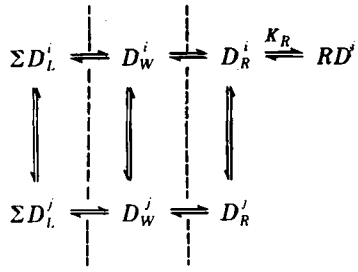

Scheme I—Distribution of drug D *as active conformer* D^i *and inactive conformer(s)* D^j *between the aqueous phase* W, *the lipoidal loss phases* L, *the receptor phase* R, *and the receptor surface.*

quantitative structure–activity relationship approach (8) is used routinely by medicinal chemists in drug design (9). These two different approaches are almost invariably pursued in isolation. The purpose of this paper is to discuss the relation between them.

A flexible molecule behaves as many different molecules, depending on conformation. Different conformations have their own physical, chemical, biological, and thermodynamic properties. Of particular use is the concept of the micropartition coefficient, defined as the partition coefficient attaching to an individual conformer.

Consider a drug supplied as a single dose to a multiphase system (Scheme I). Regions of similar partition coefficient constitute a single phase even if anatomically separate. The model comprises an aqueous phase (volume V_W) and a receptor phase (volume V_R), together with N nonaqueous loss phases (devoid of receptors) with volumes V_L (L = 1–N). If biological activity resides in a single conformer D^i, its equilibrium concentrations in the various phases are $[D_W^i]$, $[D_R^i]$, and $[D_L^i]$, giving fractions of active conformer:

$$f_W^i = \frac{[D_W^i]}{[D_W]} \qquad \text{(Eq. 1a)}$$

$$f_R^i = \frac{[D_R^i]}{[D_R]} \qquad \text{(Eq. 1b)}$$

$$f_L^i = \frac{[D_L^i]}{[D_L]} \qquad \text{(Eq. 1c)}$$

Equilibration of the drug between the receptors and the receptor phase is defined by a binding constant:

$$K_R = \frac{[RD^i]}{[R][D_R^i]} \qquad \text{(Eq. 2)}$$

where $[R]$ and $[RD^i]$ are the concentrations of free receptors and productive drug–receptor complexes, respectively.

Suppose that drug distribution is much faster than degradation or elimination. Suppose also that the biological response is directly proportional to receptor coverage $[RD^i]$, that receptors are identical and independent, and that a negligible fraction of the total drug is bound to receptors. Receptor flexibility and the mechanism and kinetics of drug binding are outside the scope of this discussion. If the total dose is S, then:

$$S = V_W[D_W] + V_R[D_R] + \sum_{L=1}^{L=N} V_L[D_L] \qquad \text{(Eq. 3)}$$

$$S = [D_W]\left\{V_W + V_R P_R + \sum_{L=1}^{L=N} V_L P_L\right\} \qquad \text{(Eq. 4)}$$

where P_R and P_L are partition coefficients. The relationship $[D_W] = [D_R]/P_R$, taken with Eqs. 1 and 2, allows $[D_W]$ to be substituted, giving:

0022-3549/79/0300-0396$01.00/0
© 1979, American Pharmaceutical Association

Screen," Instruction Booklet 14, Drug Evaluation Branch, Division of Cancer Treatment, National Cancer Institute, Bethesda, Md., 1977.

(16) G. Zbinden and E. Brändle, *Cancer Chemother. Rep.*, Part 1, **59**, 707 (1975).

(17) G. Zbinden, E. Bachmann, and C. H. Hoderegger, *Antibiot. Chemother.*, **23**, 255 (1978).

C. C. Cheng *x
Midwest Research Institute
Kansas City, MO 64110

G. Zbinden
Institute of Toxicology
Federal Institute of Technology
and University of Zurich
Zurich, Switzerland

Robert K. Y. Zee-Cheng
Midwest Research Institute
Kansas City, MO 64110

Received October 16, 1978.

Accepted for publication December 14, 1978.

Supported by Contract N01-CM-33743 from the Division of Cancer Treatment, National Cancer Institute, National Institutes of Health.

The authors thank Dr. Harry B. Wood and Mr. Robert B. Ing of the National Cancer Institute for their interest and encouragement.

*Present address: Mid-America Cancer Center Program, University of Kansas Medical Center, Kansas City, KS 66103.

Conformation, Partition, and Drug Design

Keyphrases □ Conformations—drug, biological activity, fraction of conformer and partition coefficient □ Structure-activity relationships—drug conformers, biological activity, fraction of conformer and partition coefficient □ Partition coefficients—drug conformers, structure-activity relationships, biological activity

To the Editor:

Current interest in drug conformation rests on the postulate that a single preferred conformer binds to the receptor productively. If this conformer can be identified, it can then be fixed, or at least its population can be enhanced, by chemical means. In most areas of interest in drug design, however, drug–receptor complexes are not available for detailed molecular study, so the active conformation must be inferred. The usual procedure has been to seek correlations between conformation, determined experimentally or theoretically for a drug series, and biological response.

Until recently, the dominant conformer was assumed to be the biologically active agent (1). While there have been problems of agreement on the form of the dominant conformer (2), the widely variable responses that can occur even when the physical conformation is unambiguous (3) have encouraged the idea that a minor conformer may sometimes be responsible for activity (4–7). Thus, besides an interest in the nature of the active conformation, there is an interest in the fraction of active conformer in solution and in how it varies with chemical structure (5, 6).

An entirely different approach to drug design is based on multiparameter correlations of biological response with partition coefficients and other physical properties. This

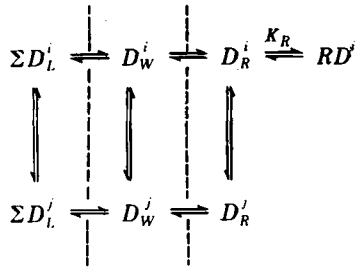

Scheme I—Distribution of drug D *as active conformer* D^i *and inactive conformer(s)* D^j *between the aqueous phase* W, *the lipoidal loss phases* L, *the receptor phase* R, *and the receptor surface.*

quantitative structure–activity relationship approach (8) is used routinely by medicinal chemists in drug design (9). These two different approaches are almost invariably pursued in isolation. The purpose of this paper is to discuss the relation between them.

A flexible molecule behaves as many different molecules, depending on conformation. Different conformations have their own physical, chemical, biological, and thermodynamic properties. Of particular use is the concept of the micropartition coefficient, defined as the partition coefficient attaching to an individual conformer.

Consider a drug supplied as a single dose to a multiphase system (Scheme I). Regions of similar partition coefficient constitute a single phase even if anatomically separate. The model comprises an aqueous phase (volume V_W) and a receptor phase (volume V_R), together with N nonaqueous loss phases (devoid of receptors) with volumes V_L (L = 1–N). If biological activity resides in a single conformer D^i, its equilibrium concentrations in the various phases are $[D_W^i]$, $[D_R^i]$, and $[D_L^i]$, giving fractions of active conformer:

$$f_W^i = \frac{[D_W^i]}{[D_W]} \qquad \text{(Eq. 1a)}$$

$$f_R^i = \frac{[D_R^i]}{[D_R]} \qquad \text{(Eq. 1b)}$$

$$f_L^i = \frac{[D_L^i]}{[D_L]} \qquad \text{(Eq. 1c)}$$

Equilibration of the drug between the receptors and the receptor phase is defined by a binding constant:

$$K_R = \frac{[RD^i]}{[R][D_R^i]} \qquad \text{(Eq. 2)}$$

where $[R]$ and $[RD^i]$ are the concentrations of free receptors and productive drug–receptor complexes, respectively.

Suppose that drug distribution is much faster than degradation or elimination. Suppose also that the biological response is directly proportional to receptor coverage $[RD^i]$, that receptors are identical and independent, and that a negligible fraction of the total drug is bound to receptors. Receptor flexibility and the mechanism and kinetics of drug binding are outside the scope of this discussion. If the total dose is S, then:

$$S = V_W[D_W] + V_R[D_R] + \sum_{L=1}^{L=N} V_L[D_L] \qquad \text{(Eq. 3)}$$

$$S = [D_W]\left\{V_W + V_R P_R + \sum_{L=1}^{L=N} V_L P_L\right\} \qquad \text{(Eq. 4)}$$

where P_R and P_L are partition coefficients. The relationship $[D_W] = [D_R]/P_R$, taken with Eqs. 1 and 2, allows $[D_W]$ to be substituted, giving:

0022-3549/79/0300-0396$01.00/0
© 1979, American Pharmaceutical Association

Table I—Conformer Populations in Furfuraldehyde

Medium	ϵ	$\Delta G_{cis} - \Delta G_{trans}$, kcal/mole	Ratio *trans/cis*	Reference
Vapor	1.0	1.0 (25°)	5	11
		2.0 (25°)	31	12
		2.0 (37°)	26	13
1,1-Difluoro-2,2-dichloroethylene	2.9	0.34 (37°)	1.7	13
Dimethyl sulfoxide	45	−0.84 (37°)	0.22	13

$$\frac{1}{S} = \frac{K_R[R]f^i_R P_R}{[RD^i]\left\{V_W + V_R P_R + \sum_{L=1}^{L=N} V_L P_L\right\}} \quad \text{(Eq. 5)}$$

For a constant biological response (*i.e.*, constant $[RD^i]$), $1/S$ is a measure of the potency of any drug within a series. If all nonaqueous loss phases can be considered collectively with P_N as a net coefficient for partition into phases of total volume $V_N = \Sigma_{L=1}^{L=N} V_L$, then:

$$\frac{1}{S} = \frac{K_R[R]f^i_R P_R}{[RD^i]\{V_W + V_R P_R + V_N P_N\}} \quad \text{(Eq. 6)}$$

Three special cases exist, depending on which phase is dominant (contains most of the drug).

Case 1—If $V_R P_R \gg V_W + V_N P_N$, then $1/S \propto K_R f^i_R$. Potency increases with the fraction of drug in the active conformation and with increasing affinity constant. This case is trivial.

Case 2—If $V_W \gg V_R P_R + V_N P_N$, then $1/S \propto K_R f^i_R P_R$. If most of the drug is lost in the aqueous phase, potency becomes a mixed function of partition coefficient and active conformer fraction; neither alone can be expected to correlate directly with biological data.

Case 3—If $V_N P_N \gg V_W + V_R P_R$, then $1/S \propto K_R f^i_R P_R / P_N$.

Attention concentrates on Case 2, which is simpler than Case 3 but demonstrates the main principles and is applicable equally to steady-state models (7).

The micropartition coefficient, P^i_R, for the active conformer may be defined by analogy with the overall or macropartition coefficient, P_R:

$$P^i_R = \frac{[D^i_R]}{[D^i_W]} P_R = \frac{[D_R]}{[D_W]} \quad \text{(Eq. 7)}$$

By combining Eqs. 1 and 7, it may be seen that:

$$f^i_R P_R = f^i_W P^i_R \quad \text{(Eq. 8)}$$

so an alternative form for Case 2 is $1/S \propto K_R f^i_W P^i_R$.

Equation 8 demonstrates a necessary interdependence between the conformer balance and partition coefficient. Variations in the active conformer fraction between phases must be accompanied by variations in macro- and micropartition coefficients. This result has consequence only to the extent that shifts in conformer balance actually occur. Conformer populations can vary substantially with solvent (10–14) (Tables I and II), and this must mean that micropartition coefficients can vary sharply with conformation. Further evidence comes from recent work on hydroxyureas (15). Similarly, the 4.3-fold increase in the octanol–water partition coefficient between *p*- and *ortho*-hydroxybenzoic acids is almost certainly due to internally hydrogen-bonded species in the latter having greater micropartition coefficients than the open forms (16).

In real tissues, drugs distribute themselves among the different biological phases in a complex manner. The two forms for Case 2 show the effects of partition and conformation to be complementary variables in any model of such behavior. In our idealized situation (Case 2), the biological potency is related to the usual macropartition coefficient, P, and the active conformer fraction in the receptor phase. Alternatively, a relation could be sought involving the active aqueous phase conformer fraction and the micropartition coefficient, P^i_R. Either relation in logarithmic form takes on a quantitative structure–activity relationship appearance (9). The choice between them is a matter of experimental convenience. The utility of $1/S \propto K_R f^i_W P^i_R$ is limited by experimental difficulties in determining the micropartition coefficient, P^i, but such values may become more accessible as methods for theoretical calculation improve. Some measure of the active conformer fraction will be required in any comprehensive study of the relation between structure and activity.

This complementary relationship has implications for toxicity and pharmacodynamics.

Table II—Conformer Populations in 1-Fluoro-2-chloroethane[a]

Medium	ϵ	$\Delta G_{gauche} - \Delta G_{trans}$, kcal/mole	Ratio *trans/gauche*	Reference
Vapor	1.0	0.90	2.3	14
Cyclohexane	2.0	0.31	0.85	14
Methyl iodide	7.0	−0.16	0.38	14
Acetone	20.7	−0.64	0.17	14
Pure liquid	21.1	−0.67	0.16	14

[a] These values assume that the intensity of the C—Cl stretching band is independent of conformation. The relative values of the *trans–gauche* ratio and $\delta\,\Delta G$ are unaffected by this assumption.

(1) L. B. Kier, "Molecular Orbital Theory in Drug Research," Academic, New York, N.Y., 1971.

(2) B. Pullman, *Trends Biochem. Sci.*, **1976**, N130.

(3) H. C. Mautner, in "Molecular and Quantum Pharmacology," E. D. Bergman and B. Pullman, Eds., Reidel, Dordrecht, The Netherlands, 1974.

(4) G. C. K. Roberts, *Trends Biochem. Sci.*, **1976**, N80.

(5) W. G. Richards, R. Clarkson, and C. R. Ganellin, *Phil. Trans. Roy. Soc. (B)*, **272**, 75 (1975).

(6) C. R. Ganellin, *J. Med. Chem.*, **16**, 620 (1973).

(7) R. H. Davies, *Int. J. Quant. Chem.*, **QBS4**, 413 (1977).

(8) C. Hansch and T. Fujita, *J. Am. Chem. Soc.*, **86**, 1616 (1964).

(9) C. Hansch, in "Drug Design," vol. 1, E. J. Ariens, Ed., Academic, New York, N.Y., 1971.

(10) R. J. Abraham and E. Bretschneider, in "Internal Rotation in Molecules," W. J. Orville-Thomas and M. Redshaw, Eds., Wiley, New York, N.Y., 1974.

(11) F. Moennig, H. Freitzler, and H. D. Rudolph, *Z. Naturforsch.*, **20a**, 1323 (1965).

(12) F. A. Miller, W. G. Fateley, and R. E. Witkowski, *Spectrochim. Acta*, **23A**, 891 (1967).

(13) R. J. Abraham and T. M. Siverns, *Tetrahedron*, **28**, 3015 (1972).

(14) M. F. El Bermani, A. J. Woodward, and N. Jonathan, *J. Am. Chem. Soc.*, **92**, 6750 (1970).

(15) G. R. Parker, T. L. Lemke, and E. C. Moore, *J. Med. Chem.*, **20**, 1221 (1977).

(16) A. Leo, C. Hansch, and D. Elkins, *Chem. Rev.*, **71**, 525 (1971).

Robin H. Davies [x]
Brian Sheard
Peter J. Taylor
Pharmaceuticals Division
I.C.I.
Alderley Park
Macclesfield, Cheshire SK10 4TG
England

Received July 31, 1978.
Accepted for publication December 6, 1978.

Time-Dependent Kinetics IV: Pharmacokinetic Theory of Enzyme Induction

Keyphrases □ Kinetics, time dependent—enzyme induction, pharmacokinetic theory □ Enzyme induction—drug induced, time-dependent kinetics, pharmacokinetic theory

To the Editor:

The phenomenon of enzyme induction by drugs and foreign chemicals is well established. Many drugs stimulate their own metabolism (autoinduction) as well as that of other drugs administered concurrently (heteroinduction) (1). These phenomena have serious therapeutic implications.

In humans, experimental evidence for the enzyme-inducing abilities of a drug is generally based on decreases in plasma concentrations of the induced species. However, it is our observation that no general theory or quantitative approach has been proposed to describe the time course of plasma drug concentrations in conjunction with the phenomenon of auto- or heteroinduction. We have developed a pharmacokinetic theory able to predict the rate and extent of auto- or heteroinduction during chronic drug administration. This theory is based on biochemical models governing changes in enzyme levels in the body.

Berlin and Schimke (2) first proposed a model to describe the change in intracellular enzyme concentration following induction. They showed that when an inducer causes an increase in the rate of synthesis from S to S' and/or a decrease in the rate constant of degradation from k to k', the kinetics of the shift in enzyme level, $E(t)$, are governed by k':

$$E(t) = \frac{S'}{k'} - \left(\frac{S'}{k'} - \frac{S}{k}\right)e^{-k't} \qquad \text{(Eq. 1)}$$

where S/k and S'/k' represent the basal and induced steady-state enzyme concentrations, respectively, and $S/k \leq E(t) \leq S'/k'$ (Fig. 1). This model assumes that enzyme synthesis is zero order, that degradation is first order, and that the increase from S to S' and/or the decrease from k to k' are rapid relative to the enzyme half-life, $\ln 2/k'$.

By using the Michaelis–Menten model with steady-state approximation (3), an expression similar to Eq. 1 can be obtained to describe the change in maximum velocity, V_m, during induction:

$$V_m(t) = V'_m - (V'_m - V_m)e^{-k't} \qquad \text{(Eq. 2)}$$

where $V_m = k_2S/k$, $V'_m = k_2S'/k'$, and k_2 is the rate constant for dissociation of the enzyme–substrate complex to product and free enzyme. Equation 2 can be extended to describe drug disposition in the whole body during induction. Metabolic clearance, Cl, was defined by Rane *et al.* (4) as:

$$Cl = V_m/K_m \qquad \text{(Eq. 3)}$$

where V_m (amount time^{-1}) is a macroscopic maximal rate of metabolism, K_m (amount volume^{-1}) is a macroscopic Michaelis constant, and the substrate concentration is less than 0.1 K_m. If it is assumed that the inducer has no effect on K_m and free fraction and that clearance is not blood-flow limited, induction will result in an exponential increase in metabolic clearance. In the case of metabolism by one enzyme (single enzymatic site), the increase in Cl is given by:

$$Cl(t) = Cl' - (Cl' - Cl)e^{-k't} \qquad \text{(Eq. 4)}$$

Let us assume that the drug under consideration is also eliminated from the body through other metabolic pathways controlled by noninducible enzymes (each with its first-order clearance, M_j) and through excretion of unchanged drug by several routes (each with its first-order clearance, R_k). Prior to induction, total body clearance is given by:

$$Q = Cl + \sum M_j + \sum R_k \qquad \text{(Eq. 5)}$$

After induction, overall drug elimination from the body is controlled by a time-dependent clearance, $Q(t)$:

$$Q(t) = Q' - (Q' - Q)e^{-k't} \qquad \text{(Eq. 6)}$$

where:

$$Q' = Cl' + \sum M_j + \sum R_k \qquad \text{(Eq. 7)}$$

Equation 6 shows that the rate of change of clearance is also governed by k', the induced enzyme degradation rate constant (Fig. 1).

In the case of multiple-enzyme induction, Eq. 4 can be written for each induced enzyme. For the general case of a drug eliminated from the body by metabolism through inducible ($Cl_i \rightarrow Cl'_i$) as well as noninducible pathways (M_j), simultaneous with first-order unchanged drug excretion (R_k), $Q(t)$ is given by:

$$Q(t) = Q' - \sum_{i=1}^{n} (Cl'_i - Cl_i)e^{-k't} \qquad \text{(Eq. 8)}$$

where:

$$Q' = \sum_{i=1}^{n} Cl'_i + \sum M_j + \sum R_k \qquad \text{(Eq. 9)}$$

and n represents the number of induced enzymes.

Equation 6 (or Eq. 8) can be incorporated into the differential equations of a one-compartment pharmacokinetic model with appropriate input conditions to derive equations for the drug level time course during induction. The effect of an increase in clearance on drug levels is best illustrated (Fig. 1) when the induced species is administered by constant-rate intravenous infusion (Scheme I).

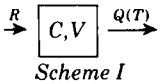

Scheme I

where C represents the plasma concentration of the induced agent, V is its apparent volume of distribution, R is its infusion rate, $T = t - \lambda$, λ is the time from the commencement of the induced agent infusion to the beginning of the increase in clearance, $Q(T)$ is as given in Eq. 6 where t is replaced by T, and the other terms are as previously defined. A solution[1] of the differential equation for Scheme I is:

$$C = \frac{R}{Q(T)} - \frac{R}{Q}\exp\left[\frac{-Q'}{V}(t - \lambda) + \frac{Q' - Q}{Vk'}\{1 - \exp[-k'(t - \lambda)]\}\right]\exp\left(\frac{-Q\lambda}{V}\right) \qquad \text{(Eq. 10)}$$

where all of the terms are as previously defined. In Fig. 1,

[1] A derivation of this equation is available from the corresponding author.

0022-3549/79/0300-0398$01.00/0
© 1979, American Pharmaceutical Association

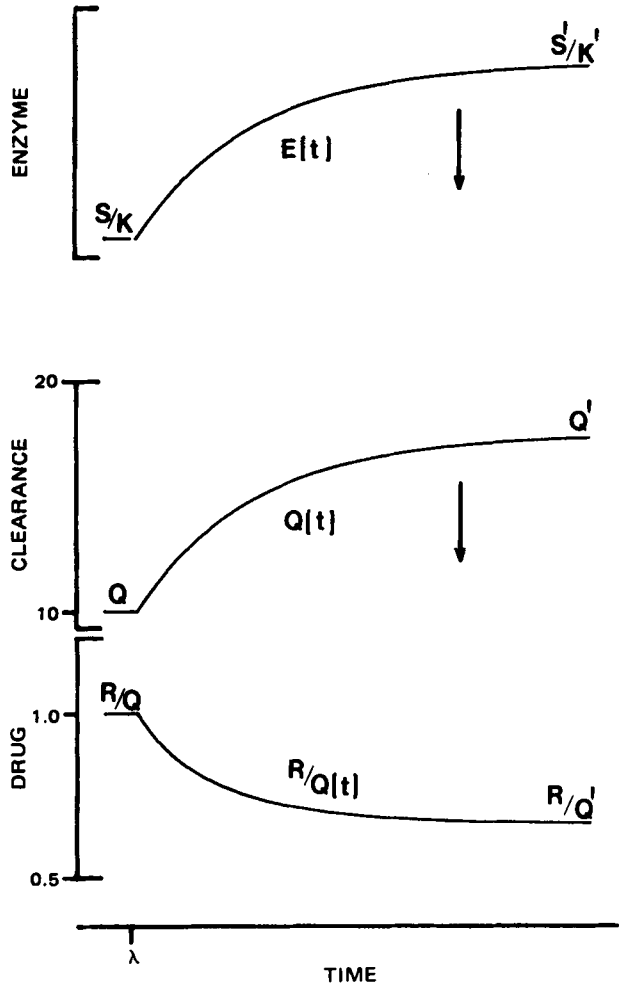

Figure 1—*Relationship between increase in enzyme level, E(t), and the corresponding increase in clearance, Q(t), and decrease in blood concentration. The drug administered by constant rate intravenously reached a steady state R/Q prior to the beginning of the increase in clearance, λ, since λ > 5 ln 2V/Q. The following parameter values were used:* S'/k' = *1.66* S/k, k' = *0.0577 hr*$^{-1}$, Q = *10.69 liters/hr*, Q' = *17.72 liters/hr, and* R = *12.4 mg/hr.*

it was assumed that $\lambda > 5[(\ln 2V)/Q]^2$ and, therefore, C is at a steady state (R/Q) prior to the beginning of induction. For $t > \lambda$, drug concentration decreases and reaches a lower steady state given by R/Q'.

The applicability of this theory is supported by a series of experimental observations:

1. In preliminary studies, three rhesus monkeys were given carbamazepine by intravenous infusion as an inducer and two other antiepileptic drugs, valproic acid and ethosuximide, as the induced agents (5, 6). Following addition of carbamazepine, plasma levels of these two drugs decreased exponentially to a lower steady state, as predicted from Eq. 10. Computer regression analysis of experimental data to Eq. 10 gave correlation coefficients (r) ranging from 0.886 to 0.996.

2. Follow-up studies in four rhesus monkeys with clonazepam (7) as the induced agent showed that the experimental decrease in clonazepam levels was consistent with model predictions (least-squares fit to Eq. 10, r = 0.924–0.993).

3. The model of Berlin and Schimke (2) also predicts that, following removal of an inducer, the return of the enzyme level to basal conditions is described by Eq. 1[3]. According to Eq. 6[4], this decrease in enzyme level should be mirrored by an exponential increase in body level of the induced agent. This hypothesis was verified by following the increase in plasma clonazepam level upon withdrawal of carbamazepine in four monkeys (7). The experimental data points and predicted concentrations were in excellent agreement ($0.905 < r < 0.964$).

4. Validation of this pharmacokinetic theory in humans was also realized (8). Seven healthy normal volunteers received (orally) clonazepam for 29 days and carbamazepine from Day 7 to 29. Least-squares fit of experimental data points to the corresponding model equation were adequate ($0.904 < r < 1.000$ in six subjects).

A priori, Eqs. 1 and 6 should also apply to autoinduction. This postulate was verified with published data from this laboratory on carbamazepine autoinduction in humans (9).

The proposed pharmacokinetic theory has broad implications. In biochemical pharmacology, it suggests a possibility of measuring enzyme turnover half-lives *in vivo* under experimental conditions that respect the integrity of the enzyme system(s). In clinical pharmacology, this theory provides a rational understanding of drug interactions caused by enzyme induction.

(1) A. H. Conney, *Pharmacol. Rev.*, **19**, 317 (1967).
(2) C. M. Berlin and R. T. Schimke, *Mol. Pharmacol.*, **1**, 149 (1965).
(3) G. E. Briggs and J. B. S. Haldane, *Biochem. J.*, **19**, 388 (1975).
(4) A. Rane, G. R. Wilkinson, and D. G. Shand, *J. Pharmacol. Exp. Ther.*, **200**, 420 (1977).
(5) P. H. Corbisier and R. H. Levy, *APhA Academy of Pharmaceutical Sciences Abstracts*, **7** (1), 163 (1977).
(6) *Ibid.*, **7** (2), 134 (1977).
(7) A. A. Lai and R. H. Levy, *J. Pharm. Sci.*, in press.
(8) A. A. Lai, R. H. Levy, and R. E. Cutler, *Clin. Pharmacol. Ther.*, **24**, 316 (1978).
(9) W. H. Pitlick, R. H. Levy, A. S. Troupin, and J. R. Green, *J. Pharm. Sci.*, **65**, 462 (1976).

R. H. Levy ˣ
A. A. Lai *
M. S. Dumain
Departments of Pharmaceutical Sciences and Neurological Surgery
Schools of Pharmacy and Medicine
University of Washington
Seattle, WA 98195

Received September 7, 1978.
Accepted for publication December 7, 1978.
Supported by National Institutes of Health research contracts N01-NS-1-2282 and N01-NS-6-2341.
The authors acknowledge the assistance of Ms. B. Teri Ludwick.
* Present address: Department of Clinical Research, Medical Division, Burroughs Wellcome, Research Triangle Park, NC 27709.

[2] When $\lambda \gg (\ln 2V/Q)$, the second term in Eq. 10 becomes negligible.

[3] In this case, S and k refer to the induced state and S' and k' refer to the non-induced (basal) state; thus, $S' < S$ and $k' > k$.

[4] Similarly, in this case, $Q' < Q$.

NOTICES

Practical Antimicrobial Therapy. By HERBERT L. DUPONT. Program in Infectious Diseases and Clinical Microbiology. The University of Texas Health Science Center at Houston Medical School, Houston, Tex. Appleton-Century-Crofts, 292 Madison Ave., New York, NY 10017. 1978. 122 pp. 14 × 22 cm.

Infertility: An Interdisciplinary Journal for the Rapid Communication of Clinical Aspects of Human Infertility. Vol. 1. No. 1. Edited by WAYNE H. DECKER, M.D. Dekker, 260 Madison Ave., New York, NY 10016. 1978. 135 pp. 15 × 23 cm. Price $20.00/vol.

Phosphorus in the Environment: Its Chemistry and Biochemistry. Ciba Foundation Symposium 57 (new series). Elsevier/North-Holland Inc., 52 Vanderbilt Ave., New York, NY 10017. 1978. 320 pp. 16 × 24 cm.

Vitamins: Synthesis, Production and Use. Advances Since 1970. By CHARLES S. SODANO. Noyes Data Corp., Mill Road at Grand Ave., Park Ridge, NJ 07656. 1978. 305 pp. 15 × 23 cm. Price $42.00.

Serotonin in Health and Disease. Vol. 1: Availability, Localization and Disposition. Edited by WALTER B. ESSMAN. Spectrum, 175-20 Wexford Terrace, Jamaica, NY 11432. 1978. 409 pp. 15 × 23 cm. Price $37.50.

The Influenza Virus Hemagglutinin. Topics in Infectious Diseases Vol. 3. Symposium, Baden near Vienna, 3-21-23,77. Edited by W. G. LAVER, H. BACHMAYER, and R. WEIL. Springer-Verlag, 175 Fifth Ave., New York, NY 10010. 1978. 259 pp. 15 × 24 cm. Price $24.90.

Psychiatric Aspects of Opiate Dependence. By ALBERT A. KURLAND. CRC Press, 2255 Palm Beach Lakes Blvd., West Palm Beach, FL 33409. 1978. 273 pp. 18 × 25 cm. Price $59.95.

Nuclear Magnetic Resonance Spectroscopy in Molecular Biology. The Jerusalem Symposia On Quantum Chemistry & Biochemistry. Vol. II. Edited by BERNARD PULLMAN. D. Reidel Publishing Co., 306 Dartmouth St., Boston, MA 02116. 1978. 537 pp. 16 × 24 cm. Price $56.00.

Recent Development in Mass Spectrometry in Biochemistry and Medicine, Vol. 1. Edited by ALBERTO FRIGERIO. Plenum, 227 W. 17th St., New York, NY 10011. 1978. 655 pp. 16 × 25 cm. Price $55.00.

Europaisches Arzneibuch. Band III. Amtliche Ausgabe. Deutscher Apotheker Verlag Stuttgart, Postach 40, Birkenwaldsrafe 44, 7000 Stuttgart 1, Germany. 1978. 394 pp. 16 × 24 cm.

Deutsches Arzneibuch. 8. Augsgabe 1978. Amtliche Augsgabe. Deutscher Apotheker Verlag Stuttgart, Postach 40, Birkenwaldsrafe 44, 7000 Stuttgart 1, Germany. 1978. 680 pp. 16 × 24 cm.

Functions of the Septo-Hippocampal System. Ciba Foundation Symposium 58 (new series). Elsevier/North-Holland Inc., 52 Vanderbilt Ave., New York, NY 10017. 1978. 438 pp. 16 × 24 cm.

Major Mental Handicap: Methods and Costs of Prevention. Ciba Foundation Symposium 59 (new series). Elsevier/North-Holland Inc., 52 Vanderbilt Ave., New York, NY 10017. 1978. 226 pp. 16 × 24 cm.

Schizophrenia. Theory, Diagnosis, and Treatment. Edited by HERMAN C. B. DENBER. Dekker, 270 Madison Ave., New York, NY 10016, 1978. 242 pp. 15 × 23 cm. Price $14.95.

Les essais des nouveaux médicaments chez l'homme. Problemes juridiques et éthiques. By J.-M. ROUZIOUX. Masson et Cie, 120 Boulevard Saint-Germain, Paris, France. 1978. 183 pp. 15 × 24 cm. Price 70F.

A Study Guide to Epidemiology and Biostatistics. Including 100 multiple-choice questions. By RICHARD F. MORTON and J. RICHARD HEBEL. University Park Press, 233 E. Redwood St., Baltimore, MD 21202. 1978. 153 pp. 15 × 23 cm. Price $8.95.

Abrégé De Droit Et Déontologie Pharmaceutiques. Notions Generales. By MONIQUE BERRY-TISSEYRE. Masson, 120 Boulevard Saint-German, 75280 Paris, Cedex 06, France. 1978. 285 pp. 13 × 21 cm.

Homöopathisches Arzneibuch. 8. Ausgabe 1978. Deutscher Apotheker-Verlag, 7000 Stuttgart, Postfach 40, Germany. 1978. 95 pp. 16 × 24 cm. Price DM 19.

The Living State and Cancer. Workshop of the National Foundation for Cancer Research, Marine Biological Laboratory, Woods Hole, MA. By ALBERT SZENT-GYORGYI. Dekker, 270 Madison Ave., New York, NY 10016. 86 pp. 12 × 16 cm. Price $7.50.

Manual of Neurologic Therapeutics With Essentials of Diagnosis. Edited by MARTIN A. SAMUELS. Little, Brown, 34 Beacon St., Boston, MA 02106. 1978. 436 pp. 13 × 22 cm. Price $12.50.

A publication of the
American Pharmaceutical Association—
the National Professional Society
of Pharmacists

JOURNAL OF PHARMACEUTICAL SCIENCES

INDEX TO AUTHORS
INDEX TO SUBJECTS

VOLUME 68
JANUARY TO DECEMBER, 1979

Published monthly under the supervision of the Board of Trustees

MARY H. FERGUSON
Editor

SHELLY ELLIOTT
Production Editor

MARCIA GARTRELL
Copy Editor

NICOLETTE TRIANTAFELLU
Copy Editor

EDWARD G. FELDMANN
Contributing Editor

SAMUEL W. GOLDSTEIN
Contributing Editor

BELLE R. BECK
Editorial Secretary

DAVID BOHARDT
Director of Publications

L. LUAN CORRIGAN
Assistant Director of Publications

EDITORIAL ADVISORY BOARD

John Autian
Norman R. Farnsworth
William O. Foye
William J. Jusko
Herbert A. Lieberman
David E. Mann, Jr.
Gerald J. Papariello
Edward G. Rippie

APRIL 1979
VOLUME 68 NUMBER 4

JOURNAL OF PHARMACEUTICAL SCIENCES

MARY H. FERGUSON
Editor

SHELLY ELLIOTT
Production Editor

JANIS KELLY
Copy Editor

EDWARD G. FELDMANN
Contributing Editor

SAMUEL W. GOLDSTEIN
Contributing Editor

BELLE R. BECK
Editorial Secretary

DAVID BOHARDT
Director of Publications

L. LUAN CORRIGAN
Assistant Director of Publications

EDITORIAL ADVISORY BOARD

JOHN AUTIAN
NORMAN R. FARNSWORTH
WILLIAM O. FOYE
WILLIAM J. JUSKO
HERBERT A. LIEBERMAN
DAVID E. MANN, JR.
GERALD J. PAPARIELLO
EDWARD G. RIPPIE

The *Journal of Pharmaceutical Sciences* (ISSN 0022-3549) is published monthly by the American Pharmaceutical Association (APhA) at 2215 Constitution Ave., N.W., Washington, DC 20037. Second-class postage paid at Washington, D.C., and at additional mailing office.

All expressions of opinion and statements of supposed fact appearing in articles or editorials carried in this journal are published on the authority of the writer over whose name they appear and are not to be regarded as necessarily expressing the policies or views of APhA.

Offices—Editorial, Advertising, and Subscription: 2215 Constitution Ave., N.W., Washington, DC 20037. Printing: 20th & Northampton Streets, Easton, PA 18042.

Annual Subscriptions—United States and foreign, industrial and government institutions $50, educational institutions $50, individuals *for personal use only* $30; single copies $5. All foreign subscriptions add $5 for postage. Subscription rates are subject to change without notice. Members of APhA may elect to receive the *Journal of Pharmaceutical Sciences* as a part of their annual $70 (foreign $75) APhA membership dues.

Claims—Missing numbers will not be supplied if dues or subscriptions are in arrears for more than 60 days or if claims are received more than 60 days after the date of the issue, or if loss was due to failure to give notice of change of address. APhA cannot accept responsibility for foreign delivery when its records indicate shipment has been made.

Change of Address—Members and subscribers should notify at once both the Post Office and APhA of any change of address.

Photocopying—The code at the foot of the first page of an article indicates that APhA has granted permission for copying of the article beyond the limits permitted by Sections 107 and 108 of the U.S. Copyright Law provided that the copier sends the per copy fee stated in the code to the Copyright Clearance Center, Inc., P.O. Box 8891, Boston, MA 02114. Copies may be made for personal or internal use only and not for general distribution.

Microfilm—Available from University Microfilms International, 300 N. Zeeb Road, Ann Arbor, MI 48106.

© Copyright 1979, American Pharmaceutical Association, 2215 Constitution Ave., N.W., Washington, DC 20037; all rights reserved.

APhA PERSPECTIVE ON "LANNETT"

When the so-called "Lannett decision" was handed down by the courts last fall, an acquaintance in the pharmaceutical industry commented to us, "Well, I guess this will make APhA happy, since you people think all generic drug products are equivalent and don't need to be tested or checked for their quality!"

He was surprised when I informed him that, "No, I can't say that we were happy about it; and, in fact, the decision appears to run contrary to official APhA policy."

This exchange seems to suggest that a brief review of the Association's position, in the context of the litigation situation, may be beneficial for all of our readers.

APhA has long and consistently held: (*a*) that judgment should enter into drug product selection; (*b*) that by training and experience, pharmacists are generally best equipped to fill the role of exercising drug product selection; and (*c*) that only quality pharmaceutical products should be dispensed in all situations—whether or not the pharmacist is selecting the source of the product.

The question then moves to: "What is a quality product?" and at this point the problem becomes much more sticky, if not downright difficult.

There is not sufficient space in this column to delineate all that the Association has offered by way of advice, suggestions, and information on this subject, but a few such examples include evaluating drug company recall records, physically examining the drug product itself, and reviewing information in APhA's *The Bioavailability of Drug Products.*

But beyond such suggestions, APhA has taken the position that—if three basic conditions prevail—drug products can generally be considered as being of acceptable quality and as being interchangeable irrespective of their source of manufacture. "Interchangeable" here is synonymous with therapeutically or clinically equivalent.

In APhA's view, the three requisite conditions are: (*a*) premarket approval of the product by the Food and Drug Administration; (*b*) manufacture of the product in a manufacturing facility that is in compliance with FDA's Good Manufacturing Practice regulations; and (*c*) the resultant product passes all applicable official compendium standards and specifications.

As long as these conditions prevail as the minimum hurdle for drug products to move legally into the marketplace, we could have a reasonable level of confidence in the quality of the drug supply.

This past fall, however, a court decision was handed down that significantly undercut the first of these three requisites. In the celebrated "Lannett decision," the court basically ruled against what FDA has chosen to define as constituting a "new drug."

The court decision goes on to lay out the crux of the case: The FDA "*maintains that for each specific drug product there must be general recognition of its safety and efficacy. This, the FDA contends, is especially true if applied to the bioavailability, the bioequivalence, and the quality control problems of specific drugs such as Lannett's.*" Hence, the FDA has required premarketing approval of each manufacturer's product in the form of a full or abbreviated new drug application.

Lannett, however, challenged this requirement, and the significance of the decision was that the court decided against FDA.

As noted above, this decision also appears to run contrary to the APhA policy position—a position that has contributed in great measure to the confidence that we feel regarding the general high quality of marketed drugs.

In November 1969, the APhA House of Delegates met in a special session, and one action taken during that meeting was to adopt an amended preamble statement on "Drug Product Quality," submitted by the APhA Academy of Pharmaceutical Sciences. That statement specified the need for every manufacturer to conduct appropriate and sufficient tests prior to the initial distribution of a drug product or modifications of an existing product in order to demonstrate its clinical safety and efficacy. This is the same policy that FDA has been following in its drug approval process, and which the Lannett decision would seem to overturn.

FDA has vowed to battle the Lannett decision, and in mid-January of this year an important court ruling was announced in the "Pharmadyne case." In this U.S. District Court decision, the judge denied Pharmadyne's suit to block FDA from seizing certain drug products that the company began to market without specific FDA preapproval. In handing down his ruling, the judge recognized that he was contradicting the Lannett decision.

It is apparent that the matter has not yet been fully settled, and appeals will be probably entered by several of the parties. But whatever the outcome, we wish to clarify that APhA continues to support a system that provides for appropriate premarket testing and approval as a basic requisite before the initial distribution of any manufacturer's drug products. On such a foundation, confidence in product quality is both logical and warranted.

—EGF

JOURNAL OF PHARMACEUTICAL SCIENCES

APRIL 1979
VOLUME 68 NUMBER 4

RESEARCH ARTICLES

Effect of Lidocaine and Derivatives on Time of Death and Overturn in Goldfish

PETER J. CASCELLA * and STUART FELDMAN ×

Received June 24, 1977, from the *Department of Pharmaceutics, University of Houston, Houston, TX 77004.* Accepted for publication September 22, 1978. *Present address: College of Pharmacy, South Dakota State University, Brookings, SD 57006.

Abstract □ The effect of lidocaine and five derivatives on the time of overturn and time of death was examined in goldfish. A relationship between the minimum effective concentration of drug necessary to produce the pharmacological response and the partition coefficient between *n*-heptane or *n*-octanol and pH 7.4 buffer was found. Further investigations confirmed that, in goldfish, the nonionized local anesthetic agent is solely responsible for the observed effects on overturn time and time of death. Experiments performed to determine the amount of drug in the goldfish at the time of pharmacological response indicated that, for five of the six compounds studied, the same concentration of drug was found in the fish at the time of response. This finding supports the observation that, for the compounds studied, the critical concentration of drug in the goldfish necessary to produce a given response is identical, the difference in time of response being due to differences in absorption rate. The relationship between overturn time and time of death in goldfish was examined, and linear regression of 1/time of death *versus* 1/overturn time yielded $1/T_D = 0.2860(1/T_O) + 0.0001$ ($r = 0.9648$). The relationship between overturn and death may simply be a function of the amount of drug in the fish at the time of the pharmacological response, and the relationship between the amounts of the drug in the fish at the two end-points may be constant regardless of the derivative evaluated.

Keyphrases □ Lidocaine—effect on time of death in goldfish, effect on time of overturn in goldfish, derivatives, ionization, absorption □ Goldfish—effect of lidocaine and derivatives on times of death and overturn, effect of pH on times of death and overturn □ Toxicity—lidocaine and derivatives, use of goldfish as biological models

Goldfish may be used as biological models for the assessment of absorption and toxicity of chemical compounds and for the elucidation of the physical-chemical parameters of a pharmacological response (1–6). Goldfish were used as a model for the assessment of structure–toxicity relationships between substituted phenothiazines (4); differences in toxicity may have been due to differences in absorption. Goldfish also were used to study the effects of alkyl chain length on biological activity for *n*-alkyl esters of *p*-aminobenzoic acid (5). The activity of local anesthetic agents was studied using goldfish, and a possible relationship between the minimum effective concentration (MEC) of drug in the bathing solution and the minimum blocking concentration of the same anesthetic agent on isolated nerve and muscle fibers was observed (6).

Whenever goldfish are used as biological models, the investigator has the choice of two common pharmacological end-points: the overturn time, defined as the loss of the righting reflex, or the time of death, defined as the complete cessation of gill and mouth movements. This report evaluates the activity of lidocaine and a series of lidocaine derivatives in producing overturn and death and examines the relationship between these two end-points.

EXPERIMENTAL

Goldfish of the variety *Carassius auratus*, 2–4 g, were used initially. The overturn and death times of individual goldfish in 200 ml of a solution of lidocaine and its derivatives[1] in pH 7.4 phosphate buffer (0.05 *M*) were determined. All solutions were freshly prepared before each experiment. The goldfish tank and test solutions were maintained at 22 ± 2°.

The overturn and death times of individual goldfish in 200 ml of various concentrations of lidocaine and benzocaine[2] in 0.05 *M* phosphate buffer in solutions of varying pH were also determined.

Partition coefficients of lidocaine (I) and each derivative (II–VI) were determined between *n*-octanol and pH 7.4 phosphate buffer (0.05 *M*). Various volumes of organic phase and 20 ml of aqueous phase containing

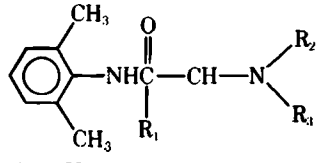

I: $R_1 = H$, $R_2 = R_3 = C_2H_5$
II: $R_1 = H$, $R_2 = R_3 = CH_3$
III: $R_1 = R_2 = R_3 = CH_3$
IV: $R_1 = H$, $R_2 = CH_3$, $R_3 = C_2H_5$
V: $R_1 = CH_3$, $R_2 = R_3 = C_2H_5$
VI: $R_1 = CH_3$, $R_2 = C_2H_5$, $R_3 = C_3H_7$

[1] Supplied by Astra Pharmaceuticals, Worcester, Mass.
[2] Eastman Organic Chemicals, Rochester, N.Y.

0022-3549/79/0400-0401$01.00/0
© 1979, American Pharmaceutical Association

Table I—Average Overturn Time of Goldfish in Solutions of Local Anesthetic Agents in pH 7.4 Buffer

Compound	Concentration, m*M*	Number of Fish	Mean Overturn Time, min	*SD*	Reciprocal of Mean Overturn Time, min^{-1}
I	0.2	5	93.11	10.21	0.0107
	0.3	5	53.36	8.26	0.0187
	0.5	13	16.26	8.19	0.0615
	0.7	5	17.33	1.51	0.0577
	0.8	3	3.34	0.77	0.2977
	0.9	5	4.26	2.09	0.2347
	1.0	26	4.16	3.62	0.2402
	1.1	6	2.62	1.40	0.3817
	1.2	6	1.56	0.54	0.6397
II[a]	0.8	3	70.86	22.69	0.0141
	1.0	3	44.69	11.26	0.0224
	1.1	3	31.98	12.38	0.0313
	1.2	3	16.22	4.66	0.0616
	1.5	3	13.22	7.44	0.0757
III[b]	0.5	5	25.46	5.79	0.0393
	0.8	5	19.02	4.62	0.0526
	1.0	8	12.48	3.57	0.0801
	1.2	6	11.43	2.96	0.0875
	1.4	3	10.80	5.59	0.0926
	1.5	3	13.53	4.31	0.0739
IV[c]	0.5	3	22.61	9.61	0.0442
	0.8	3	12.22	0.19	0.0819
	1.0	3	9.54	4.35	0.1048
	1.1	3	9.85	3.97	0.1016
	1.2	6	7.78	5.89	0.1285
V[d]	0.3	3	20.50	16.02	0.0488
	0.5	3	3.30	0.65	0.3028
	0.8	6	2.96	1.35	0.3384
	1.0	3	2.66	0.66	0.3759
	1.2	3	1.15	0.49	0.8673
VI[e]	0.1	8	9.42	5.28	0.1062
	0.3	9	3.09	1.75	0.3233
	0.5	11	1.24	0.51	0.8097
	0.8	6	1.17	0.36	0.8562
	1.0	6	0.70	0.21	1.4389

[a] W36017. [b] W36024. [c] W36004. [d] W36023. [e] W36032.

Table II—Average Death Time of Goldfish in Solutions of Local Anesthetic Agents in pH 7.4 Buffer

Compound	Concentration, m*M*	Number of Fish	Mean Death Time, min	*SD*	Reciprocal of Mean Death Time, min^{-1}
I	0.2	5	138.22	33.52	0.0072
	0.3	5	86.35	16.27	0.0115
	0.5	13	38.64	15.90	0.0259
	0.7	5	40.43	5.99	0.0247
	0.8	3	15.48	6.59	0.0646
	0.9	5	12.58	3.88	0.0795
	1.0	26	13.20	8.91	0.0758
	1.1	6	9.96	4.28	0.1004
	1.2	6	7.31	1.56	0.1369
II	0.8	3	216.77	11.82	0.0046
	1.0	3	132.55	43.29	0.0075
	1.1	3	46.68	14.47	0.0214
	1.2	3	69.07	20.71	0.0145
	1.5	3	34.85	2.86	0.0287
III	0.5	5	130.59	96.62	0.0077
	0.8	4	67.55	45.29	0.0148
	1.0	6	73.33	3.48	0.0136
	1.2	6	40.02	14.61	0.0250
	1.4	3	36.08	21.45	0.0277
	1.5	3	36.92	7.31	0.0271
IV	0.5	3	73.82	22.97	0.0136
	0.8	3	33.03	13.82	0.0302
	1.0	3	30.87	5.94	0.0324
	1.1	3	20.18	6.73	0.0496
	1.2	6	19.68	13.55	0.0508
V	0.3	3	41.33	23.46	0.0242
	0.5	3	16.55	2.88	0.0604
	0.8	6	9.91	3.82	0.1010
	1.0	3	9.68	2.52	0.1033
	1.2	3	4.85	0.33	0.2061
VI	0.1	8	40.65	7.48	0.0246
	0.3	9	10.55	5.66	0.0948
	0.5	11	6.73	1.60	0.1485
	0.8	6	3.28	1.22	0.3049
	1.0	6	2.11	0.73	0.4735

the local anesthetics were placed in glass bottles and shaken[3] for a minimum of 16 hr at 100 oscillations/min. Equilibrium was established by repetitive sampling. Assay for each drug in the aqueous phase was performed spectrophotometrically[4] at 262 nm. All determinations were performed at room temperature (22 ± 2°).

The amounts of drug in individual fish at the pharmacological endpoints (overturn and death) also were determined. Fish weighing 4–6 g were placed in 200 ml of 0.5, 1.0, or 1.5 m*M* solutions of lidocaine or 1.0 m*M* solutions of derivatives buffered to pH 7.4 with a 0.05 *M* phosphate buffer. All experiments were performed at room temperature (22 ± 2°). At the time of overturn, fish were removed from solution and washed with 100 ml of distilled water.

Whole fish were then sectioned and placed in vials, and 5 ml of distilled water and 2.0 ml of a 2 *N* NaOH solution were added; the fish were homogenized[5] and the vial was rinsed with 5 ml of distilled water, which was added to the homogenate. Samples were centrifuged[6] at 10,000 rpm for 10 min, and the supernate was added to 20 ml of carbon tetrachloride and shaken[7] for 5 min. The aqueous layer was aspirated, and the organic layer was filtered. The sample was added to 10 ml of distilled water as a wash and shaken for 5 min.

The aqueous layer was removed, and 10 ml of the organic layer was added to an equal volume of a 0.004% bromthymol blue solution buffered to pH 6.0 with a 0.05 *M* phosphate buffer. This mixture was shaken for 5 min and centrifuged[8] at 4000 rpm for 6 min. The aqueous layer was aspirated, and 5 ml of the organic layer was added to 5 ml of a 0.1 *N* NaOH solution. Then this mixture was shaken for 5 min and centrifuged[9] at 2000 rpm for 5 min. The top layer was read at 615 nm[4].

Calibration plots were obtained by adding known amounts of each drug and 5 ml of distilled water to vials containing a sectioned fish and 1 ml of 2 *N* NaOH. Blanks were run for each experiment and consisted of 5 ml of distilled water added to a sectioned fish and 1 ml of 2 *N* NaOH. Although nonlinearity was observed at some high drug concentrations, all determinations were made in the linear portion of the absorbance *versus* concentration plots.

[3] Precision water bath shaker model 25, Precision Scientific Co.
[4] Perkin-Elmer model 124.
[5] Brinkmann Polytron.
[6] Sorvall RC-5 superspeed refrigerated centrifuge.
[7] Eberbach shaker unit, model 6000.
[8] Damon/IEC Division model HN-S centrifuge.
[9] Clay Adams Dynac centrifuge.

THEORETICAL

The Levy–Gucinski (7) model assumes that the absorption rate of drug into the fish is proportional to the drug concentration in the bathing solution:

$$R = KC \qquad \text{(Eq. 1)}$$

where R is the absorption rate into the fish, K is the relative absorption rate constant, and C is the drug concentration in the bathing solution.

If the drug concentration in the aqueous medium is high enough to elicit the pharmacological response before any appreciable amount undergoes biotransformation or elimination, then the drug concentration in the fish is equal to:

$$C_B^* = Rt^* \qquad \text{(Eq. 2)}$$

where C_B^* is the drug concentration in the fish at the time (t^*) of the pharmacological response. Substituting for the absorption rate in Eq. 2 yields:

$$C_B^* = KCt^* \qquad \text{(Eq. 3)}$$

which, upon rearrangement, is equivalent to:

$$1/t^* = (K/C_B^*)C \qquad \text{(Eq. 4)}$$

Therefore, plots of reciprocal time of response as a function of drug concentration in the aqueous medium should be linear, pass through the origin, and have a slope equal to the absorption rate constant divided by the drug concentration in the fish necessary to produce the desired pharmacological response.

The Nightingale–Gibaldi (8) model extends the previous model to

Table III—Linear Least-Squares Regression of Reciprocal Time of Response as a Function of Concentration

Compound	Least-Squares Equation—Overturn	r	r^2	Least-Squares Equation—Death	r	r^2
I	$1/T = 0.5191C - 0.1704$	0.8761	0.7676	$1/T = 0.1190C - 0.0301$	0.9408	0.8851
II	$1/T = 0.0965C - 0.0670$[a]	0.9456	0.8942	$1/T = 0.0345C - 0.0233$[b]	0.9031	0.8156
III	$1/T = 0.0461C + 0.0217$	0.8360	0.6989	$1/T = 0.0211C - 0.0032$	0.9536	0.9094
IV	$1/T = 0.1112C - 0.0101$[b]	0.9791	0.9586	$1/T = 0.0532C - 0.0136$[b]	0.9591	0.9199
V	$1/T = 0.7221C - 0.1622$	0.8844	0.7822	$1/T = 0.1742C - 0.0334$[b]	0.9322	0.8690
VI	$1/T = 1.3680C - 0.0318$	0.9616	0.9247	$1/T = 0.4841C - 0.0521$	0.9799	0.9602

[a] Intercept significant, $p < 0.05$. [b] Intercept significant, $p < 0.01$.

include the minimum effective concentration (MEC) of drug in the bathing solution below which no pharmacological response occurs and in the vicinity of which there is a disproportionate increase in the time of the pharmacological response. With the assumption that the occurrence of the pharmacological response is absorption rate limited, Scheme I has been proposed:

$$A \underset{K_{21}}{\overset{K_{12}}{\rightleftharpoons}} B$$

Scheme I

where A is the drug solution bathing the fish, B represents the fish, K_{12} is the absorption rate constant into the fish, and K_{21} is the exsorption rate constant out of the fish. Therefore, the rate of change of drug in the bathing solution can be written as:

$$dX_A/dt = K_{21}X_B - K_{12}X_A \qquad \text{(Eq. 5)}$$

and the rate of change of drug in the fish is:

$$dX_B/dt = K_{12}X_A - K_{21}X_B \qquad \text{(Eq. 6)}$$

Integration of Eq. 6 yields:

$$X_B = \frac{K_{12}X_A^0}{(K_{12} + K_{21})}[1 - e^{-(K_{12}+K_{21})t}] \qquad \text{(Eq. 7)}$$

where X_B is the amount of drug in the fish at any time (t) and X_A^0 is the initial amount of drug in the bathing solution. Changing the amounts to concentrations and rearranging yield:

$$e^{-(K_{12}+K_{21})t} = \frac{KC_A^0 - C_B}{KC_A^0} \qquad \text{(Eq. 8)}$$

where C represents the drug concentration in the respective compartments, $K = [K_{12}V_A/(K_{12} + K_{21})V_B]$, V_A is the volume of the drug solution in the bathing solution, and V_B is the volume of the fish.

If the concentration of drug in the fish, C_B, reaches the level necessary to produce the C_B^* effect at time t^*, then Eq. 9 or 10 is applicable:

$$e^{-(K_{12}+K_{21})t} = \frac{KC_A^0 - C_B^*}{KC_A^0} \qquad \text{(Eq. 9)}$$

$$1/t^* = \frac{K_{12} + K_{21}}{\ln \dfrac{KC_A^0}{KC_A^0 - C_B^*}} \qquad \text{(Eq. 10)}$$

Equation 10 can be approximated by (8):

$$1/t^* = \frac{K(K_{12} + K_{21})C_A^0}{C_B^*} - \frac{K_{12} + K_{21}}{2} \qquad \text{(Eq. 11)}$$

which is equivalent to:

$$1/t^* = \frac{K_{12}V_A(K_{12} + K_{21})C_A^0}{(K_{12} + K_{21})V_BC_B^*} - \frac{K_{12} + K_{21}}{2} \qquad \text{(Eq. 12)}$$

It follows that:

$$1/t^* = \frac{K_{12}V_AC_A^0}{V_BC_B^*} - \frac{K_{12} + K_{21}}{2} \qquad \text{(Eq. 13)}$$

and:

$$1/t^* = \frac{K_{12}V_AC_A^0}{X_B^*} - \frac{K_{12} + K_{21}}{2} \qquad \text{(Eq. 14)}$$

where X_B^* is the amount of drug in the fish at the time of the pharmacological response. Therefore, a plot of $1/t^*$ as a function of the initial drug concentration in the bathing solution should be linear with a slope equal to $K_{12}V_A/X_B^*$ and an intercept equal to $-(K_{12} + K_{21})/2$.

RESULTS AND DISCUSSION

The concentrations of drugs employed in the study, number of fish used at each concentration, mean time of response, standard deviation, and reciprocal of the mean time of response are listed in Tables I and II for overturn and death, respectively. The data were analyzed by least-squares linear regression according to the relationship expressed in Eqs. 11–14; the values for the slope, intercept, correlation coefficient, and coefficient of determination are listed in Table III.

Figures 1 and 2 illustrate the relationship between the reciprocal of the mean time of response and the concentration of drug in the bathing solutions for overturn and death times, respectively. Table III indicates a strong relationship between the reciprocal time of response and the drug concentration in the bathing medium. Unexplained variability may have been due to variations in goldfish from different suppliers.

To investigate the effect of pH on overturn and death time, goldfish were placed in various concentrations of lidocaine solutions buffered to various pH values with 0.05 M phosphate buffers (Table IV). Goldfish were also placed in a pH 6.0 phosphate buffer (0.05 M) containing either a 1.0 or 1.2 mM lidocaine solution. No death responses were evident after 4 hr. Responses for overturn were elicited at the 1.2 mM concentration, but only three of five fish demonstrated overturn at the end of 4 hr at 1.0 mM.

Figure 3 is a plot of the reciprocal time of response as a function of pH for the 0.8 mM concentration of lidocaine. As the pH of the bulk solution decreased, the reciprocal time of response increased. At pH 6.0, 7.0, 7.4, and 8.0, lidocaine existed approximately as 2, 16, 32, and 65% unionized species, respectively. Plots of the reciprocal time of response as a function of the fraction unionized species present for lidocaine at the 0.8 mM

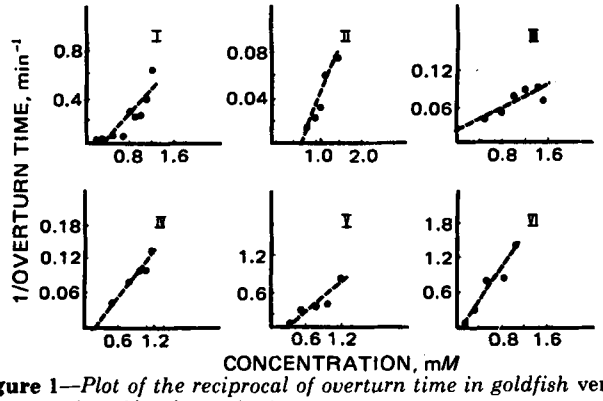

Figure 1—*Plot of the reciprocal of overturn time in goldfish* versus *concentration of local anesthetic.*

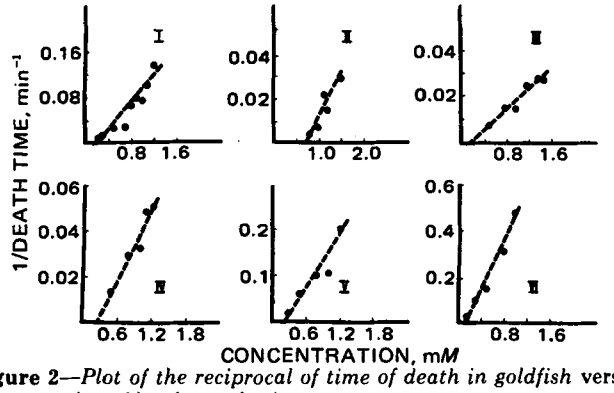

Figure 2—*Plot of the reciprocal of time of death in goldfish* versus *concentration of local anesthetic.*

Table IV—Effects of pH on Time of Response of Goldfish in Lidocaine Solutions

Concentration, m*M*	pH 7 Mean Overturn Time, min	*n*	*SD*	pH 7 Reciprocal Overturn Time, min^{-1}	pH 7.4 Mean Overturn Time, min	*n*	*SD*	pH 7.4 Reciprocal Overturn Time, min^{-1}	pH 8.0 Mean Overturn Time, min	*n*	*SD*	pH 8.0 Reciprocal Overturn Time, min^{-1}
0.5	—	—	—	—	16.26	13	8.19	0.0615	2.48	5	1.01	0.4033
0.8	6.96	5	1.78	0.1437	3.34	3	0.77	0.2994	1.82	5	0.84	0.5495
1.0	9.84	5	3.27	0.1016	4.16	26	3.62	0.2402	1.26	5	0.18	0.7937
1.2	8.52	5	3.01	0.1174	1.56	6	0.54	0.6397	3.55	5	2.62	0.2817

Concentration, m*M*	pH 7 Mean Death Time, min	*n*	*SD*	pH 7 Reciprocal Death Time, min^{-1}	pH 7.4 Mean Death Time, min	*n*	*SD*	pH 7.4 Reciprocal Death Time, min^{-1}	pH 8.0 Mean Death Time, min	*n*	*SD*	pH 8.0 Reciprocal Death Time, min^{-1}
0.5	—	—	—	—	38.64	13	15.90	0.0259	11.59	5	3.86	0.0863
0.8	30.23	5	1.85	0.0331	15.48	3	6.59	0.0646	7.35	5	1.36	0.1361
1.0	25.96	5	7.99	0.0385	13.20	26	8.91	0.0758	6.00	5	0.53	0.1667
1.2	16.15	5	2.34	0.0619	7.31	6	1.56	0.1369	5.24	5	0.77	0.1908

concentration (Fig. 4) suggest that the unionized drug may be responsible for producing the observed effects. Plots of the reciprocal time of response as a function of the concentration of unionized species present are shown in Fig. 5. The least-squares linear regression for the overturn data[10] is: 1/overturn time = 1.388 [concentration unionized] + 0.0949 ($r = 0.9334$, $p < 0.01$); that for death is: 1/death time = 0.2550 [concentration unionized] + 0.0025 ($r = 0.9689$, $p < 0.01$). To rule out the possibility that the observed effects were a result of pH-induced changes in membrane permeability rather than of unionized drug species, experiments were performed utilizing various concentrations of benzocaine over a pH 6–8 range (Table V and Fig. 6). Benzocaine exists virtually 100% as the unionized species in this pH range. No apparent trend exists in the data for the reciprocal time of response for equal concentrations of drug as a function of pH. This result indicates that pH changes are not affecting membrane permeability and that the unionized species is responsible for the effects observed.

The concentrations of drug found in the fish from three different bathing concentrations at the times of overturn and death are listed in Table VI. There was no significant difference ($p > 0.05$) in concentrations of drug in the fish at the time of the pharmacological response, regardless of the concentrations of lidocaine employed as the bathing solution.

The concentrations of derivatives found in the fish at the time of the pharmacological response to 1 m*M* concentrations of the derivatives are presented in Table VII. A significant difference ($p < 0.05$) existed between the amounts in the fish at overturn and death. Compound VI was the only drug whose concentration was significantly different from the others at the time of the pharmacological response. Compound VI differed significantly from all of the other compounds at the dosage causing overturn and from I, II, and III at the lethal dose.

The minimum effective concentration (MEC) of the bulk solution is the concentration below which no response will occur. Theoretically, this value should be the abscissa intercept of a reciprocal time of response as a function of concentration plot. The MEC of the bulk solution was calculated by setting the ordinate value to zero and calculating what the concentration of the bulk solution would be at that point. If the unionized drug molecule is responsible for the effects observed, then the MEC thus calculated are incorrect; the derivatives have different pKa values and, therefore, different fractions unionized at pH 7.4.

Table VIII contains the apparent MEC, the pKa of the compounds, the fraction unionized of the compounds at pH 7.4, and the MEC of unionized species. Some obvious discrepancies are apparent. The least-

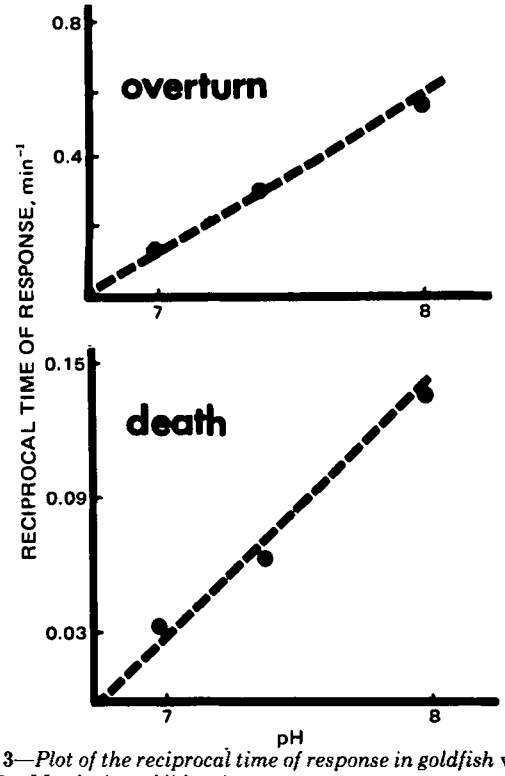

Figure 3—*Plot of the reciprocal time of response in goldfish* versus *pH for a 0.8 m*M *solution of lidocaine.*

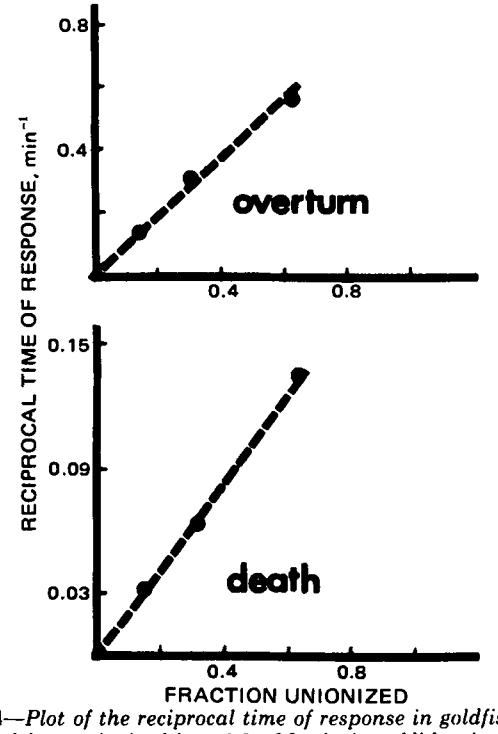

Figure 4—*Plot of the reciprocal time of response in goldfish* versus *fraction of drug unionized for a 0.8 m*M *solution of lidocaine.*

[10] The data point for the 0.78 m*M* concentration of unionized drug was omitted from the regression analysis.

Table V—Reciprocal of Overturn and Death Times for Benzocaine as a Function of Concentration [a] and pH

Concentration, m*M*	pH 6.0 Mean Overturn Time, min	*SD*	pH 6.0 Reciprocal Overturn Time, min^{-1}	pH 7.0 Mean Overturn Time, min	*SD*	pH 7.0 Reciprocal Overturn Time, min^{-1}	pH 8.0 Mean Overturn Time, min	*SD*	pH 8.0 Reciprocal Overturn Time, min^{-1}
0.1	31.63	4.16	0.0316	18.09	6.32	0.0553	23.83	8.57	0.0420
0.2	8.66	0.80	0.1155	10.12	2.54	0.0988	10.32	1.87	0.0920
0.3	5.79	0.99	0.1727	5.18	2.25	0.1931	5.86	2.63	0.1718
0.4	3.33	1.11	0.3003	1.98	0.53	0.5051	2.43	0.73	0.4115

Concentration, m*M*	pH 6.0 Mean Death Time, min	*SD*	pH 6.0 Reciprocal Death Time, min^{-1}	pH 7.0 Mean Death Time, min	*SD*	pH 7.0 Reciprocal Death Time, min^{-1}	pH 8.0 Mean Death Time, min	*SD*	pH 8.0 Reciprocal Death Time, min^{-1}
0.1	—[b]	—	—	—[b]	—	—	—[b]	—	—
0.2	28.58	9.26	0.0350	43.40	12.44	0.0230	39.43	9.25	0.0254
0.3	12.30	2.07	0.0813	15.20	4.92	0.0658	14.08	1.60	0.0710
0.4	9.68	1.80	0.1033	9.21	3.26	0.1086	8.50	2.31	0.1176

[a] Five fish used at each concentration. [b] No response at end of 4 hr.

Table VI—Concentration (C_B^*)[a] of Lidocaine in Goldfish at Time of Pharmacological Response

Concentration, m*M*	Overturn C_B^*, μm/g	*SD*	Number of Fish	Time of Response, min	*SD*	Death C_B^*, μm/g	*SD*	Number of Fish	Time of Response, min	*SD*
0.5	0.3072	0.0781	5	6.89	1.69	0.5664	0.1030	4	20.58	2.21
1.0	0.4984	0.1448	5	2.01	0.36	0.6545	0.3082	5	7.74	2.03
1.5	0.3395	0.1323	4	2.05	0.26	0.7185	0.3162	4	8.14	2.11

Analysis of Variance for Unequal Data Sets

Source of Variation	Overturn *df*	*SS*	*MS*	*F*	Significance	Death *df*	*SS*	*MS*	*F*	Significance
Between concentrations	2	0.1028	0.0514	3.52	NS ($p > 0.05$)	2	0.0468	0.0234	0.3297	
Within concentrations	11	0.1609	0.0146			10	0.7118	0.0718		NS ($p > 0.05$)
Total	13	0.2637				12	0.7586			

[a] $C_B^* = X_B^*/V_B$, where X_B^* is the amount of drug in the fish at the pharmacological end-point and V_B is the weight (grams) of the fish.

Table VII—Concentration of Derivatives (C_B^*) in Goldfish at Time of Pharmacological Response

Compound	Overturn C_B^*, μm/g	*SD*	Number of Fish	Time of Response, min	*SD*	Death C_B^*[a], μm/g	*SD*	Number of Fish	Time of Response, min	*SD*
I	0.4984	0.1448	5	2.01	1.69	0.6545	0.3082	5	7.75	2.03
II	0.2981	0.1460	5	61.82	8.92	0.5466	0.2583	5	94.08	38.02
III	0.3757	0.0974	5	16.68	6.71	0.6418	0.1047	4	42.80	10.46
IV	0.3235	0.0765	5	10.14	2.24	0.4975	0.1647	5	30.24	5.90
V	0.3805	0.1900	3	2.97	0.50	0.6689	0.1909	4	9.27	1.02
VI	0.0634	0.0513	4	0.75	0.14	0.2324	0.0812	5	2.19	0.53

Analysis of Variance for Unequal Data Sets[b]

Source of Variation	Overturn *df*	*SS*	*MS*	*F*	Significance[c]	Death *df*	*SS*	*MS*	*F*	Significance
Between drugs	5	0.4495	0.0899	6.07	$p < 0.05$	5	0.6537	0.13074	3.11	$p < 0.05$
Within drugs	21	0.3109	0.0148			22	0.9248	0.04201		
Total	26	0.7604				27	1.5785			

[a] $C_B^* = X_B^*/V_B$, where X_B^* is the amount of drug in the fish at the pharmacological end-point and V_B is the weight (grams) of the fish. [b] Homogeneity of variance tested using $F_{max} = S^2$ largest/Si^2 smallest at the 95% confidence level. For overturn, $F_{max} = 14.5$ ($p > 0.05$); for death, $F_{max} = 13.57$ ($p > 0.05$). [c] Newman-Keuls method with a harmonic mean to compensate for unequal data sets (9).

Table VIII—Minimum Effective Concentration (MEC) in Goldfish for Lidocaine and Derivatives

Compound	pKa	Fraction Unionized at pH 7.4	MEC, m*M*—Overturn	MEC, m*M*—Overturn, Unionized Species	MEC, m*M*—Death	MEC, m*M*—Death, Unionized Species
I	7.72	0.3246	0.328	0.106	0.253	0.082
II	7.22	0.6015	0.694	0.417	0.675	0.406
III	7.26	0.5798	—	—	0.152	0.088
IV	7.53	0.4273	0.091	0.039	0.256	0.109
V	7.98	0.2083	0.225	0.047	0.192	0.029
VI	7.88	0.2487	0.023	0.006	0.108	0.027

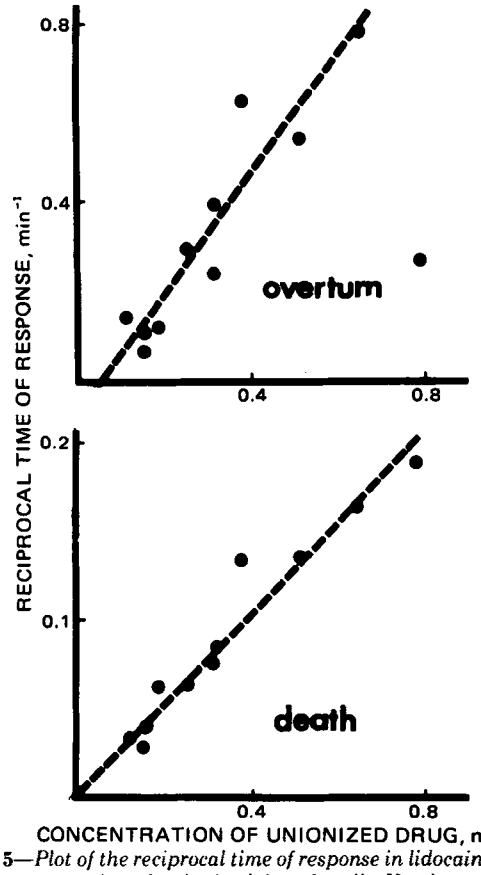

Figure 5—*Plot of the reciprocal time of response in lidocaine in goldfish versus concentration of unionized drug for all pH values studied.*

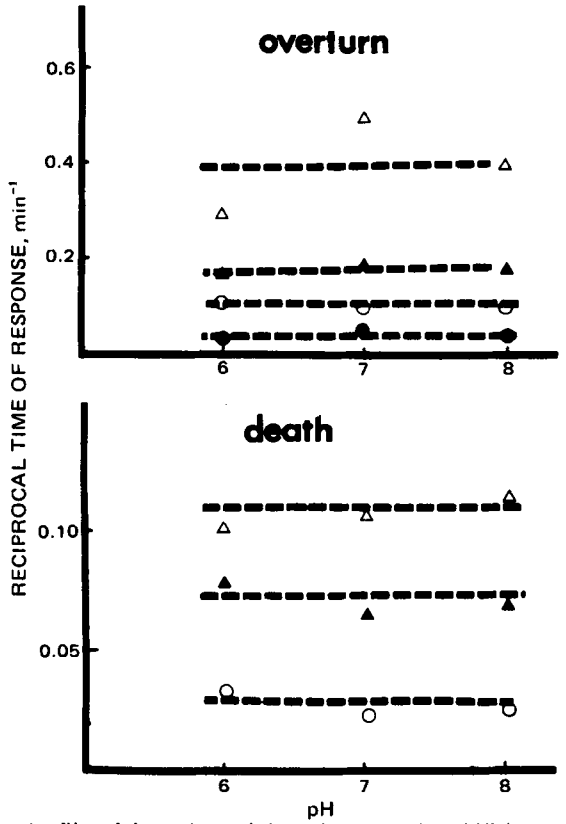

Figure 6—*Plot of the reciprocal time of response in goldfish versus pH for varying concentrations of benzocaine. Key: ●, 0.1 mM; ○, 0.2 mM; ▲, 0.3 mM; and △, 0.4 mM.*

Table IX—Least-Squares Analysis Reciprocal Time of Death as a Function of Reciprocal Time of Overturn

Compound	Least-Squares Equation	r	Significance
I	$1/T_D = 0.2077\ 1/T_O + 0.0136$	0.9732	$p < 0.01$
II	$1/T_D = 0.2944\ 1/T_O + 0.0032$	0.7852	N.S.
III	$1/T_D = 0.3205\ 1/T_O - 0.0034$	0.7975	N.S.
IV	$1/T_D = 0.4414\ 1/T_O - 0.0053$	0.9029	$p < 0.05$
V	$1/T_D = 0.2242\ 1/T_O + 0.0124$	0.9837	$p < 0.01$
VI	$1/T_D = 0.2309\ 1/T_O - 0.0246$	0.9528	$p < 0.05$

squares estimate of the MEC for III was omitted since it produced a physically impossible negative MEC. Furthermore, the MEC for overturn was apparently greater than that for death for I, II, and V, which again is physically impossible. And, finally, the MEC values calculated for overturn and death for I and for death for VI were larger than concentrations that produced a pharmacological response in the fish in this study. Thus, the MEC values of the drugs calculated in the present investigation are simply statistically generated numbers with high variability and questionable physical significance.

Overturn and death times were investigated to determine whether a relationship exists between the two end-points such that selection of one over the other would change the interpretation of the data. The possibility exists that these responses are mediated at physically and chemically distinct effective receptor sites. Overturn might be mediated by local muscle paralysis while death might be a result of central nervous system (CNS) depression.

Linear regression analysis was performed on individual data for the reciprocal of overturn time (Table IX). Reasonable predictions of the reciprocal of time of death can be obtained from the reciprocal of overturn

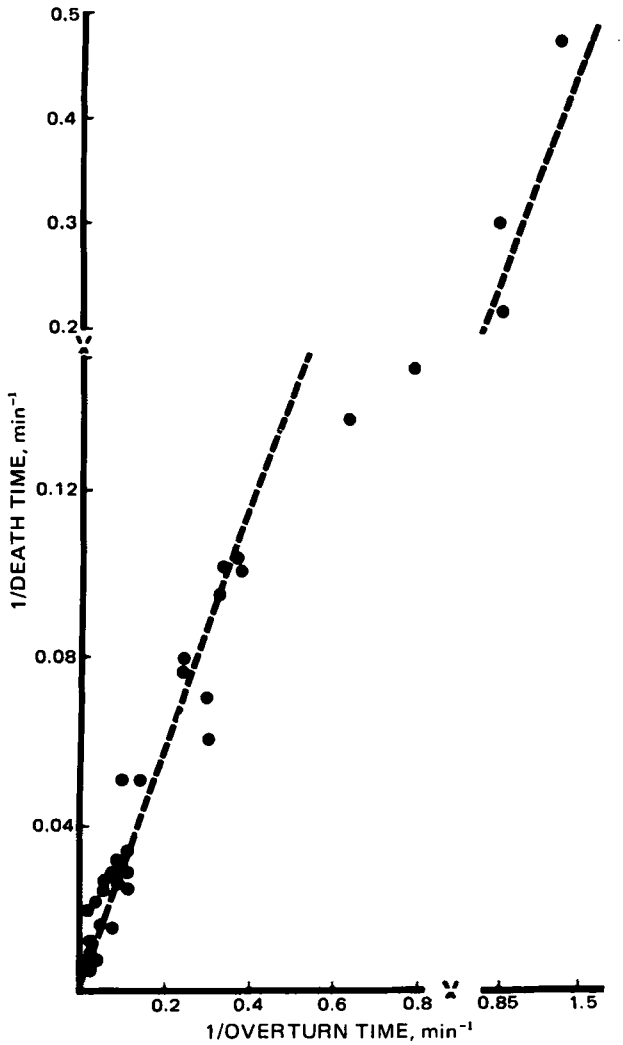

Figure 7—*Plot of the reciprocal of time of death in goldfish versus the reciprocal time of overturn in goldfish for all compounds studied.*

Table X—Ratio of Amounts in Fish at Overturn and Death

Compound	Ratio (X^*_{BO}/X^*_{BD})
I	0.590
II	0.545
III	0.585
IV	0.650
V	0.569
VI	0.273
Mean	0.535

time at that concentration. The apparent slopes do not differ much, and the intercepts are scattered about zero, indicating that all of the data may be grouped together. Linear regression of the combined data gave: $1/T_D = 0.2860(1/T_O) + 0.0001$ ($r = 0.9648$, $p < 0.01$), where T_D and T_O are the lethal and overturn times, respectively. A plot of $1/T_D$ *versus* $1/T_O$ is presented in Fig. 7.

For all data, there appears to be a linear relationship between the reciprocals of the time of response end-points at each concentration (Fig. 7). Pharmacologically, this finding suggests a simple relationship between the concentrations inducing narcosis and death. Where bulk solution concentrations are sufficiently high to make the MEC values negligible, the slope of $1/T_D$ *versus* $1/T_O$ is approximately equal to:

$$m = \frac{K_{12}V_AC^0_A}{X^*_{B_{death}}} \Big/ \frac{K_{12}V_AC^0_A}{X^*_{B_{overturn}}} \qquad \text{(Eq. 15)}$$

and:

$$m = \frac{X^*_{B_{overturn}}}{X^*_{B_{death}}} \qquad \text{(Eq. 16)}$$

Table X contains the ratio of the amount of each drug in the fish at the time of response, which may be regarded as a direct estimate of the narcosis to death ratio. The average value of the ratios is approximately 0.54. However, the value of the slope in Fig. 7, a second estimate, is only 0.29. The agreement between these two independent estimates is rough at best. The direct estimate assumes that the total fish concentration reflects the concentration in the critical CNS tissues at the moment the fish are removed from the drug solution, which may not be the case. Therefore, the pharmacological ratio would be the better estimate of the turnover to death concentration ratio. This fundamental point is worthy of more research.

REFERENCES

(1) G. Levy, K. E. Miller, and R. H. Reuning, *J. Pharm. Sci.*, **55**, 394 (1966).

(2) G. Levy and J. A. Anello, *ibid.*, **57**, 101 (1968).

(3) J. A. Anello and G. Levy, *ibid.*, **58**, 721 (1969).

(4) C. H. Nightingale, M. Tse, and E. I. Stupak, *ibid.*, **61**, 149 (1972).

(5) S. H. Yalkowsky, T. G. Slunick, and G. L. Flynn, *ibid.*, **63**, 691 (1974).

(6) S. Feldman, M. DeFrancisco, and P. J. Cascella, *ibid.*, **64**, 1713 (1975).

(7) G. Levy and S. P. Gucinski, *J. Pharmacol. Exp. Ther.*, **146**, 80 (1964).

(8) C. H. Nightingale and M. Gibaldi, *J. Pharm. Sci.*, **60**, 1360 (1971).

(9) B. J. Winer, "Statistical Principles in Experimental Design," McGraw-Hill, New York, N.Y., 1962, chap. 3.

Synthesis and Antimicrobial Evaluation of Quaternary Salts of 4-Phenyl-1,2,3,6-tetrahydropyridine and 3,6-Dimethyl-6-phenyltetrahydro-2*H*-1,3-oxazine

NATHANIEL GRIER

Received July 21, 1978, from the *Merck Sharp & Dohme Research Laboratories, Merck & Co., Inc., Rahway, NJ 07065.* Accepted for publication September 5, 1978.

Abstract □ Fifteen predominantly alkyl bromide quaternary salts of 1-substituted 4-phenyl-1,2,3,6-tetrahydropyridine and 10 from 3,6-dimethyl-6-phenyltetrahydro-2*H*-1,3-oxazine were synthesized. None was effective against the parasitic protozoan *Eimeria tenella* and the helminth trichostrongyle nematode. Nearly all inhibited Gram-positive and Gram-negative bacteria; maximum efficiency was obtained with nonyl through dodecyl bromide salt derivatives. Antifungal effectiveness paralleled these results. The oxazinium salt analogs were inhibitory in an *in vitro* peridontal microorganism screen. The decyl bromide derivative at 0.05% in drinking water prevented dental plaque and reduced calculus deposition in rats but not in hamsters fed cariogenic diets. A 0.01% concentration of the tetrahydropyridinium analog caused increased plaque in rats compared to nonmedicated control animals.

Keyphrases □ 4-Phenyl-1,2,3,6-tetrahydropyridine quaternary salts—synthesis and antimicrobial evaluation □ 3,6-Dimethyl-6-phenyltetrahydro-2*H*-1,3-oxazine quaternary salts—synthesis and antimicrobial evaluation □ Antimicrobial activity—quaternary salts of 4-phenyl-1,2,3,6-tetrahydropyridine and 3,6-dimethyl-6-phenyltetrahydro-2*H*-1,3-oxazine

Two heterocyclic nitrogen bases, 1-methyl-4-phenyl-1,2,3,6-tetrahydropyridine and 3,6-dimethyl-6-phenyltetrahydro-2*H*-1,3-oxazine, are readily accessible from the reaction of α-methylstyrene, formaldehyde, and methylamine salts (1) among other processes. Both compound types have served as moieties of synthetic drugs, *e.g.*, analgesics (2) and antineoplastic agents (3). Quaternary *N*-alkyl salt derivatives of the two bases appeared attractive as potential antimicrobials; in addition to the microbial cell wall degradative capability of the widely used cationic quaternary ammonium compounds (4), such novel products could have a possible mechanism for formaldehyde release initiated by Hofmann elimination. The inhibitory action of some preservatives, disinfectants, and antiseptics such as 1,3,5-trisubstituted hexahydro-*s*-triazines and methenamine compounds is considered attributable in part to a latent source of formaldehyde (5).

RESULTS AND DISCUSSION[1]

Thirteen quaternary salts of the tetrahydropyridine (Table I) were synthesized by alkylation with C-1–C-18 alkyl halides, decamethylene

[1] Tests for biological activities were carried out by divisions of Merck & Co., Rahway, N.J.

0022-3549/79/0400-0407$01.00/0

© 1979, American Pharmaceutical Association

Table X—Ratio of Amounts in Fish at Overturn and Death

Compound	Ratio (X^*_{BO}/X^*_{BD})
I	0.590
II	0.545
III	0.585
IV	0.650
V	0.569
VI	0.273
Mean	0.535

time at that concentration. The apparent slopes do not differ much, and the intercepts are scattered about zero, indicating that all of the data may be grouped together. Linear regression of the combined data gave: $1/T_D = 0.2860(1/T_O) + 0.0001$ ($r = 0.9648$, $p < 0.01$), where T_D and T_O are the lethal and overturn times, respectively. A plot of $1/T_D$ *versus* $1/T_O$ is presented in Fig. 7.

For all data, there appears to be a linear relationship between the reciprocals of the time of response end-points at each concentration (Fig. 7). Pharmacologically, this finding suggests a simple relationship between the concentrations inducing narcosis and death. Where bulk solution concentrations are sufficiently high to make the MEC values negligible, the slope of $1/T_D$ *versus* $1/T_O$ is approximately equal to:

$$m = \frac{K_{12}V_AC^0_A}{X^*_{B_{death}}} \Big/ \frac{K_{12}V_AC^0_A}{X^*_{B_{overturn}}} \qquad \text{(Eq. 15)}$$

and:

$$m = \frac{X^*_{B_{overturn}}}{X^*_{B_{death}}} \qquad \text{(Eq. 16)}$$

Table X contains the ratio of the amount of each drug in the fish at the time of response, which may be regarded as a direct estimate of the narcosis to death ratio. The average value of the ratios is approximately 0.54. However, the value of the slope in Fig. 7, a second estimate, is only 0.29. The agreement between these two independent estimates is rough at best. The direct estimate assumes that the total fish concentration reflects the concentration in the critical CNS tissues at the moment the fish are removed from the drug solution, which may not be the case. Therefore, the pharmacological ratio would be the better estimate of the turnover to death concentration ratio. This fundamental point is worthy of more research.

REFERENCES

(1) G. Levy, K. E. Miller, and R. H. Reuning, *J. Pharm. Sci.*, **55**, 394 (1966).

(2) G. Levy and J. A. Anello, *ibid.*, **57**, 101 (1968).

(3) J. A. Anello and G. Levy, *ibid.*, **58**, 721 (1969).

(4) C. H. Nightingale, M. Tse, and E. I. Stupak, *ibid.*, **61**, 149 (1972).

(5) S. H. Yalkowsky, T. G. Slunick, and G. L. Flynn, *ibid.*, **63**, 691 (1974).

(6) S. Feldman, M. DeFrancisco, and P. J. Cascella, *ibid.*, **64**, 1713 (1975).

(7) G. Levy and S. P. Gucinski, *J. Pharmacol. Exp. Ther.*, **146**, 80 (1964).

(8) C. H. Nightingale and M. Gibaldi, *J. Pharm. Sci.*, **60**, 1360 (1971).

(9) B. J. Winer, "Statistical Principles in Experimental Design," McGraw-Hill, New York, N.Y., 1962, chap. 3.

Synthesis and Antimicrobial Evaluation of Quaternary Salts of 4-Phenyl-1,2,3,6-tetrahydropyridine and 3,6-Dimethyl-6-phenyltetrahydro-2*H*-1,3-oxazine

NATHANIEL GRIER

Received July 21, 1978, from the *Merck Sharp & Dohme Research Laboratories, Merck & Co., Inc., Rahway, NJ 07065.* Accepted for publication September 5, 1978.

Abstract □ Fifteen predominantly alkyl bromide quaternary salts of 1-substituted 4-phenyl-1,2,3,6-tetrahydropyridine and 10 from 3,6-dimethyl-6-phenyltetrahydro-2*H*-1,3-oxazine were synthesized. None was effective against the parasitic protozoan *Eimeria tenella* and the helminth trichostrongyle nematode. Nearly all inhibited Gram-positive and Gram-negative bacteria; maximum efficiency was obtained with nonyl through dodecyl bromide salt derivatives. Antifungal effectiveness paralleled these results. The oxazinium salt analogs were inhibitory in an *in vitro* peridontal microorganism screen. The decyl bromide derivative at 0.05% in drinking water prevented dental plaque and reduced calculus deposition in rats but not in hamsters fed cariogenic diets. A 0.01% concentration of the tetrahydropyridinium analog caused increased plaque in rats compared to nonmedicated control animals.

Keyphrases □ 4-Phenyl-1,2,3,6-tetrahydropyridine quaternary salts—synthesis and antimicrobial evaluation □ 3,6-Dimethyl-6-phenyltetrahydro-2*H*-1,3-oxazine quaternary salts—synthesis and antimicrobial evaluation □ Antimicrobial activity—quaternary salts of 4-phenyl-1,2,3,6-tetrahydropyridine and 3,6-dimethyl-6-phenyltetrahydro-2*H*-1,3-oxazine

Two heterocyclic nitrogen bases, 1-methyl-4-phenyl-1,2,3,6-tetrahydropyridine and 3,6-dimethyl-6-phenyltetrahydro-2*H*-1,3-oxazine, are readily accessible from the reaction of α-methylstyrene, formaldehyde, and methylamine salts (1) among other processes. Both compound types have served as moieties of synthetic drugs, *e.g.*, analgesics (2) and antineoplastic agents (3). Quaternary *N*-alkyl salt derivatives of the two bases appeared attractive as potential antimicrobials; in addition to the microbial cell wall degradative capability of the widely used cationic quaternary ammonium compounds (4), such novel products could have a possible mechanism for formaldehyde release initiated by Hofmann elimination. The inhibitory action of some preservatives, disinfectants, and antiseptics such as 1,3,5-trisubstituted hexahydro-*s*-triazines and methenamine compounds is considered attributable in part to a latent source of formaldehyde (5).

RESULTS AND DISCUSSION[1]

Thirteen quaternary salts of the tetrahydropyridine (Table I) were synthesized by alkylation with C-1–C-18 alkyl halides, decamethylene

[1] Tests for biological activities were carried out by divisions of Merck & Co., Rahway, N.J.

0022-3549/79/0400-0407$01.00/0

© 1979, American Pharmaceutical Association

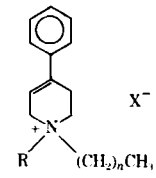

Table I—1-Substituted 1-Alkyl-4-phenyl-1,2,3,6-tetrahydropyridinium Salt Derivatives

Compound	R	n	X	Melting Point	Yield, %	Recrystallization Solvent	Empirical Formula	Analysis, %	Calc.	Found
Ia	H	9	Br	197–198.5°	36	Acetone	$C_{21}H_{35}BrN$	C	66.12	66.39
								H	9.25	9.62
								Br	20.71	20.95
								N	3.62	3.63
Ib	Methyl	0	I	266–268°	55	Ethanol	$C_{13}H_{18}IN$	C	49.54	49.67
								H	5.75	6.04
								N	4.44	4.45
Ic	Methyl	7	Br	199–201°	65	Acetone	$C_{20}H_{32}BrN$	C	65.55	65.08
								H	8.80	8.83
								Br	21.81	21.50
								N	3.82	3.80
Id	Methyl	8	Br	199–201°	51	Acetone	$C_{21}H_{34}BrN$	C	66.28	66.08
								H	9.01	8.93
								Br	20.99	20.49
								N	3.68	3.61
Ie[a]	Methyl	9	Br	200–202°	89	Acetone	$C_{22}H_{36}BrN$	C	66.97	66.91
								H	9.20	9.46
								N	3.55	3.61
If	Methyl	9	Dodecyl sulfate	152–156°	31	—[b]	$C_{34}H_{61}NO_4S$	C	70.42	69.96
								H	10.60	10.64
								N	2.42	2.30
Ig	Methyl	9	2-(Dodecyloxy)-ethyl sulfate	156–162°	51	—[b]	$C_{36}H_{65}NO_5S$	C	69.29	69.65
								H	10.50	10.57
								N	2.24	2.28
								S	5.14	5.13
Ih	Methyl	9	o-Sulfobenz-imide	190–190.5°	95	Acetonitrile–ether	$C_{29}H_{40}N_2O_3S$	C	70.13	69.66
								H	8.12	8.13
								N	5.64	5.55
								S	6.46	6.20
Ii	Methyl	10	Br	199–201°	37	Acetone	$C_{23}H_{38}BrN$	C	67.63	67.20
								H	9.38	9.57
								N	3.43	3.23
Ij	Methyl	11	Br	202–205°	59	Acetone	$C_{24}H_{40}BrN$	C	68.24	68.67
								H	9.54	9.67
								Br	18.91	19.20
								N	3.30	3.35
Ik	Methyl	13	Br	204–207°	49	Acetone	$C_{26}H_{44}BrN$	C	69.31	69.43
								H	9.84	9.86
								Br	17.74	18.09
								N	3.11	3.13
Il	Methyl	15	Br	211–214°	49	Acetone	$C_{28}H_{48}BrN$	C	70.27	70.43
								H	10.11	10.31
								Br	16.69	16.95
								N	2.93	2.86
Im	Methyl	17	Br	218–222°	39	Acetone	$C_{30}H_{52}BrN$	C	71.12	71.27
								H	10.35	10.34
								Br	15.77	16.12
								N	2.77	2.61
In	Ethyl	9	Br	168.5–169.5°	38	Acetone	$C_{23}H_{38}BrN$	C	67.63	67.47
								H	9.38	9.58
								Br	19.56	19.57
								N	3.48	3.41
Io	Decamethylene-bis	0	Br	259–260.5°	84	Ethanol	$C_{34}H_{50}Br_2N_2$	C	63.17	63.47
								H	7.79	8.11
								Br	24.73	24.74
								N	4.33	4.48
Ip	Phenylmethyl	0	Cl	204–206.5°	76	2-Propanol–ether	$C_{19}H_{22}ClN \cdot \frac{1}{2}H_2O$	C	73.86	73.80
								H	7.50	7.59
								Cl	11.48	11.57
								N	4.53	4.50

[a] Prepared by F. Waksmunski, Merck Sharp and Dohme Research Laboratories, Rahway, NJ 07065. [b] Not recrystallized.

dibromide, or phenylmethyl chloride in refluxing acetone. The normethyl and 1-ethyl base homologs (1) were reacted with decyl bromide to provide nonquaternary 1-decyl-4-phenyl-1,2,3,6-tetrahydropyridinium hydrobromide (Ia) and 1-decyl-1-ethyl-4-phenyl-1,2,3,6-tetrahydropyridinium bromide (In). Ten oxazinium salts (Table II) were similarly prepared; the properties of several of these compounds were reported previously (6).

All compounds were evaluated for antimicrobial and antiparasitic potencies. None was active in the parasitology screen, which included *in vitro* and *in vivo* helminthiasis assays with trichostrongyle nematode, ova and larvae, and coccidiosis (*Eimeria tenella*) in chickens. The methods for these tests and the *in vitro* antibacterial and antifungal studies (Tables III and IV) were described previously (7).

The eight C-8–C-18 alkyl oxazinium bromide salts (IIb–IId and IIf–IIj) were additionally tested in an *in vitro* microbial periodontal disease screen (Table V). The decyl derivative, IId, was further studied in an *in vivo* experiment (rat and hamster) for the prevention of dental calculus and plaque.

An *in vitro* chemotherapy assay (Table III) utilized Gram-positive and Gram-negative bacteria; fungi associated with industrial and agricultural

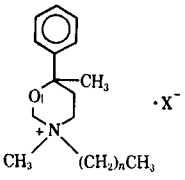

Table II—3-Alkyl-3,6-dimethyl-6-phenyltetrahydro-2*H*-1,3-oxazinium Salt Derivatives

Compound	*n*	X	Melting Point	Yield, %	Recrystallization Solvent	Empirical Formula	Analysis, %	Calc.	Found
II*a*	0	I	205–207°	76	Ethanol	$C_{13}H_{20}INO$	C	46.85	46.85
							H	6.05	6.36
							I	38.09	38.34
							N	4.21	4.28
II*b*	7	Br	199–200°	40	Acetone	$C_{20}H_{34}BrNO$	C	62.48	62.49
							H	8.91	8.86
							Br	20.79	20.51
							N	3.64	3.38
II*c*	8	Br	192–193.5°	34	Acetone	$C_{21}H_{36}BrNO$	C	63.30	63.64
							H	9.11	9.40
							Br	20.05	20.16
							N	3.52	3.28
II*d*	9	Br	194–195.5°	34	Acetone	$C_{22}H_{38}BrNO$	C	64.07	63.80
							H	9.29	9.33
							Br	19.37	19.13
							N	3.48	3.32
II*e*	9	*o*-Benzo-sulfimide	115–116°	64	Acetonitrile–ether	$C_{29}H_{42}N_2O_4S$	C	67.64	67.68
							H	8.23	8.52
							N	5.45	5.36
							S	6.23	6.18
II*f*	10	Br	186–187°	30	Acetone	$C_{23}H_{40}BrNO$	C	64.77	64.96
							H	9.45	9.50
							Br	18.74	18.32
							N	3.28	3.58
II*g*	11	Br	190–191.5°	32	Acetone	$C_{24}H_{42}BrNO$	C	65.48	65.29
							H	9.61	9.69
							Br	18.13	18.10
							N	3.18	3.20
II*h*	13	Br	183–184.5°	36	Acetone	$C_{26}H_{46}BrNO$	C	66.62	67.16
							H	9.90	10.05
							Br	17.05	17.41
							N	2.99	2.88
II*i*	15	Br	174–176°	67	Acetone	$C_{28}H_{50}BrNO$	C	67.62	67.99
							H	10.15	10.17
							N	2.82	2.75
II*j*	17	Br	171.5–173°	55	Acetone	$C_{30}H_{54}BrNO$	C	68.69	69.15
							H	10.38	10.60
							N	2.67	2.64

Table III—*In Vitro* Antibacterial and Antifungal Assay

Compound	Minimal Inhibitory Concentration, μg/ml							
	S. aureus[a]	*S. pyogenes*[b]	*B. bronchiseptica*[c]	*K. pneumoniae*[d]	*E. aerogenes*[e]	*E. coli*[f]	*A. pullulans*[g]	*A. niger*[h]
I*a*	60	20	—[i]	—	—	—	200	200
I*c*	60	60	200	200	100	200	—	200
I*d*	10	10	100	100	100	200	60	200
I*e*	10	10	20	60	10	60	20	10
I*h*	60	60	60	60	60	100	20	200
I*i*	1	10	10	20	60	60	—	—
I*j*	1	20	20	10	60	200	10	10
I*k*	1	1	10	10	—	—	20	60
I*l*	10	10	—	—	—	—	—	—
I*m*	10	10	—	—	—	—	—	—
I*n*	20	20	60	60	60	200	100	—
I*o*	10	10	100	—	—	200	20	—
II*b*	10	100	—	200	100	—	—	—
II*c*	10	20	60	100	60	200	200	200
II*d*	10	10	20	60	10	100	100	—
II*e*	10	10	60	60	100	—	60	200
II*f*	1	1	1	60	60	100	10	100
II*g*	20	20	20	20	20	100	10	200
II*h*	20	20	20	100	—	—	—	—
II*i*	1	10	10	20	60	60	—	—
II*j*	10	60	—	—	—	—	—	—
Cetylpyridinium bromide[j]	1	10	20	60	—	—	60	—
Benzalkonium chloride[k]	10	10	20	10	10	200	60	—

[a] Merck Bacteria (MB) 2865. [b] MB 2874. [c] MB 3551. [d] MB 3123. [e] MB 1503. [f] MB 2884. [g] MF 4341. [h] MF 442. [i] Greater than 200 μg/ml. [j] K & K Laboratories, New York, N.Y. [k] Hyamine 3500, Rohm & Haas, which contains alkyl (50% C-14, 40% C-12, 10% C-16) dimethylbenzylammonium chloride as an 80% solution in ethanol.

Table IV—Antimicrobial Evaluation of Decyl Bromide Quaternary Salts

Compound	Minimal Inhibitory Concentration[a], μg/ml										
	S. aureus[b]	*B. mycoides*[c]	*E. aerogenes*[d]	*P. aeruginosa*[e]	*A. pullulans*[f]	*A. niger*[g]	*P. luteum*[h]	*R. solani*[i]	*C. globosum*[j]	*T. viride*[k]	*V. alboatrium*[l]
Ie	10	10	50	—[m]	—	—	—	50	100	—	50
IId	10	50	50	100	100	100	100	50	50	100	100
Hexahydro-1,3,5-triethyl-*s*-triazine	100	100	100	100	100	100	100	100	100	100	100

[a] Tested at 1, 10, 50, and 100 μg/ml. [b] ATCC 6538. [c] Institute of Paper Chemistry 509. [d] Institute of Paper Chemistry 500. [e] ATCC 10145. [f] ATCC 9348. [g] ATCC 6275. [h] ATCC 10466. [i] ATCC 16115. [j] ATCC 6205. [k] ATCC 8678. [l] V3H. [m] Greater than 100 μg/ml.

Table V—Microbial Periodontal Disease Screen for 3-(C-8–C-18)-Alkyl Bromide Salts of 3-Methyl-6-phenyltetrahydro-2*H*-1,3-oxazine

Compound	Zone of Inhibition, mm diameter[a]				
	O. viscosus[b]	*Bacteroides* sp.[c]	*Strep.* SL-1[d]	*S. aureus*[e]	*E. coli*[f]
IIb	26	17	15	11	21
IIc	34	22	20	13	20
IId	32	27	21	13	20
IIf	32	23	20	10	18
IIg	25	20	17	8	13
IIh	17	12	10	0	9
IIi	10	9	0	0	8
IIj	15	0	0	0	0
Control A[g]	17	14	20	8	9
Control B[h]	28	35	24	15	23

[a] For all compounds, a concentration of 50 μg/6.35-mm diameter assay disk was used. [b] MB 2065. [c] MB 2022. [e] ATCC 9637. [f] ATCC 6538. [g] 1,1′-Hexamethylenebis[5-(2-ethylhexyl)biguanide]·2HCl, 50 μg/disk. [h] Chlortetracycline, 5 μg/disk.

Table VI—*In Vivo* Rat Dental Plaque and Calculus Inhibition

Compound	Concentration in Drinking Water, % (w/w)	Percent of Control	
		Plaque	Calculus
Ie	0.01	200	80
IId	0.01	30	65
Control A[a]	0.01	20	125
Quaternary salt[b]	0.01	15	65
IId	0.05	0	15
Quaternary salt[b]	0.05	0	30

[a] 1,1′-Hexamethylenebis[5-(2-ethylhexyl)biguanide]·2HCl. [b] Cinnamyldimethyldodecyl ammonium chloride.

economic losses were included. Method details were reported (7); concentrations of 200, 100, 60, 20, 10, 5, and 1 μg/ml of test compound in brain heart infusion agar culture medium[2] were run in duplicate as outlined.

Broad spectrum antimicrobial efficiency appeared to peak and approximate that of benzalkonium chloride in both series of compounds when the quaternary alkyl methyl bromide salts were of C-10–C-12 chain length. The higher alkyl derivatives, Il, Im, and IIj, proved effective only for Gram-positive bacteria, similar to the nonquaternary salt Ia. Failure to inhibit any microorganisms was observed with Ib, If, Ig, and Ip with *Staphylococcus aureus, Streptococcus pyogenes, Bordetella bronchiseptica, Klebsiella pneumoniae, Enterobacter aerogenes, Escherichia coli, Aureobasidium pullulans,* and *Aspergillus niger.* Additionally, no inhibitory action was obtained at the maximum concentration, 200 μg/ml, for all compounds against *Pseudomonas aeruginosa* (MB 418 and MB 2245), *Proteus mirabilis* (MB 3549), *Fusarium* sp. (MF 4648), and *Cephalosporium* sp. (MF 4641).

Two representatives of the more active compounds, Ie and 1-decyl-1,6-dimethyl-6-phenyltetrahydro-2*H*-1,3-oxazinium bromide (IId), were compared *in vitro* (Table IV) with a commercial antimicrobial, hexahydro-1,3,5-triethyl-*s*-triazine, using microorganisms relevant to biodeterioration and the noted procedure (7). Compound IId was at least equipotent to the triazine; Ie had a significantly narrower antifungal spectrum than both but was markedly superior against Gram-positive bacteria.

The suspected periodontal disease organisms, *Odontomyces viscosus, Bacteroides* sp., and the cariogenic *Streptococcus* SLI strain, along with a general Gram-positive type, *S. aureus,* and a Gram-negative bacteria, *E. coli,* were studied for sensitivity to the oxazinium salts (Table V). Brain heart infusion agar, enriched with 5% sucrose for the *Streptococcus,* was used as the culture medium. A paper disk, medicated by wetting with 0.025 ml of compound stock solution, was placed on the surface. Five milligrams of compound was dissolved in 0.1 ml of dimethylformamide and diluted to 2.5 ml with distilled water to provide 50 μg/0.025 ml. All inoculum cultures were 16–24 hr old, and 5 ml was added to 200 ml of medium (10 ml/200 ml of medium for *O. viscosus*); 10 ml of each mixture was used per plate.

Incubation was overnight at 37° in anaerobe jars under nitrogen–carbon dioxide, and diameters of inhibition zones were measured. Antibacterial efficiencies appeared maximal with the nonyl, decyl, and undecyl bromides (IIc–IIe) and were much higher than with the bisbiguanide (Table V) control across the spectrum of microorganisms. The bacterial efficacy and structural requirements for *in vitro* dental antiplaque activity of this compound and 15 related guanide and biguanide derivatives were studied previously (8). The second control, chlortetracycline, at one-tenth the dosage was appreciably more effective against *Bacteroides* sp. and approximately matched the best compounds for the other four bacteria.

Compounds Ie and IId were further evaluated as inhibitors *in vivo* of dental plaque and calculus in rats (Table VI) and hamsters. Ten male weanling rats, Holtzmann strain, in each group were given a high sucrose diet, NIH 2000 (9), *ad libitum* and drinking water medicated with each compound at 0.01% concentration. After 14 days and then at weekly intervals, the upper six molar teeth were scored for plaque and calculus. Control animals on the same diet were given nondosed distilled drinking water.

Data were averaged over the 5–10-week test period and compared with the bisbiguanide (Control A) and cinnamyldimethyldodecyl ammonium chloride. Compound Ie-treated animals appeared to have twice the surface deposition of plaque as compared to those without medication. In similar studies, antimicrobials such as subtilin and nalidixic acid caused increased caries over untreated controls; one mechanism postulated is the selective removal of competing noncariogenic microflora (10).

The cinnamyl quaternary salt derivative and IId at 0.05% concentration in drinking water prevented plaque completely and reduced calculus to less than one-third of the control. Corresponding tests in hamsters indicated both compounds to be ineffective. Differences in dental plaque properties and treatment responses between the two species (11) and methods for caries prevention assay in hamsters (9) were reported previously.

EXPERIMENTAL[3]

Table I compounds were prepared as halide salts according to the method described for Ic; the normethyl and 1-ethyl base homologs were intermediates for Ia and In, respectively. Other salts were synthesized from the bromide as outlined for Ih. The same procedures were employed for Table II compounds, and 3,6-dimethyl-6-phenyltetrahydro-2*H*-1,3-oxazine (1) served as the base for all. No effort was made to improve yields or to separate isomers.

IR spectra appeared consistent with the structures assigned. Halide salts were characterized by PMR spectra in methanol-d_4, except for Io which required trifluoroacetic acid for solubilization. The 4-phenyl group of I compounds appeared as a multiplet (5H) between 7.2 and 7.6 ppm

[2] Difco.

[3] Melting points were taken in open capillary tubes with a Thomas-Hoover apparatus and are uncorrected. IR spectra were obtained from mineral oil mulls with a Perkin-Elmer model 137 spectrophotometer, and NMR spectra were obtained with a Varian T-60 (60 MHz) spectrometer. Chemical shifts (δ) are reported in parts per million relative to tetramethylsilane.

[the phenylmethyl derivative, Ip, 7.1–7.8 ppm (10H)], and the vinyl proton (1H) appeared as a broad singlet at 6.0–6.3 ppm. The 6-phenyl group of II compounds was in the same range downfield, and the 2-methylene group (OCH_2N) appeared as a doublet of doublet, 4.41 and 4.58 ppm and 4.80 and 4.95 ppm, probably corresponding to the axial and equatorial protons, respectively[4].

1-Methyl-1-octyl-4-phenyl-1,2,3,6-tetrahydropyridinium Bromide (Ic)—A solution of 3.5 g (0.02 mole) of 1-methyl-4-phenyl-1,2,3,6-tetrahydropyridine (1) and 10 g (0.05 mole) of 1-bromooctane in 50 ml of anhydrous acetone was heated on a steam bath for 12 hr. The mixture obtained upon final cooling in an ice bath was filtered. Then the crystalline solid was washed with cold acetone and diethyl ether and purified by recrystallization, 1 g/50 ml of acetone, to provide colorless needles.

1-Decyl-1-methyl-4-phenyl-1,2,3,6-tetrahydropyridinium *o*-Sulfobenzimide (Ih)—One gram (0.0025 mole) of 1-decyl-1-methyl-4-phenyl-1,2,3,6-tetrahydropyridinium bromide (Ie) was suspended in 100 ml of warm (35°) deionized water with stirring, and a solution of 3.0 g (0.012 mole) of sodium *o*-sulfobenzimide dihydrate in 10 ml of deionized water was dripped in (10 min). The product separated initially as a colorless oil and solidified upon mixing an additional 2 hr, followed by cooling in an ice bath. The water-washed and air-dried colorless solid was recrystallized by solution of 1 g in 2 ml of acetonitrile and addition of approximately 18 ml of ether until incipient turbidity. The colorless plates obtained were washed with cold acetonitrile–ether (1:9 v/v).

REFERENCES

(1) C. J. Schmidle and R. C. Mansfield, *J. Am. Chem. Soc.*, **78**, 425, 1702 (1956). *Ibid.*, **77**, 5698 (1955). C. J. Schmidle and R. C. Mansfield, U.S. pats. 2,847,414 (1958) and 2,750,385 (1956).

(2) M. Rajšner, E. Adlerová, and M. Protiva, *Coll. Czech. Chem. Commun.*, **28**, 1031 (1963).

(3) T. Urbański, D. Guene, S. Šlopek, H. Modarska, and M. Modarska, *Nature*, **187**, 426 (1960).

(4) A. N. Petrocci, in "Disinfection, Sterilization, and Preservation," 2nd ed., S. S. Block, Ed., Lea & Febiger, Philadelphia, Pa., 1977, p. 325.

(5) J. DeMare, H. W. Rossmore, and T. H. F. Smith, *Dev. Ind. Microbiol.*, **13**, 341 (1972).

(6) N. Grier, U.S. pat. 3,920,642 (Nov. 18, 1975).

(7) N. Grier and R. Strelitz, *J. Pharm. Sci.*, **65**, 616 (1976).

(8) J. M. Tanzer, A. M. Slee, and B. A. Kamay, *Antimicrob. Agents Chemother.*, **12**, 721 (1977).

(9) P. L. Block, C. L. Dooley, and E. E. Howe, *J. Periodont.*, **40**, 41 (1969).

(10) R. J. Fitzgerald, *Antimicrob. Agents Chemother.*, **1**, 296 (1972).

(11) H. B. Woodruff, K. H. Nollstadt, R. B. Walton, and T. H. Stoudt, *Dev. Ind. Microbiol.*, **17**, 405 (1976).

(12) Y. E. Kazantsev, I. P. Boiko, Y. F. Malina, O. I. Zhuk, Y. Y. Samitov, and B. V. Unkovskii, *Zh. Org. Khim.*, **9**, 2616 (1972) (in English).

(13) H. Booth and R. U. Lemieux, *Can. J. Chem.*, **49**, 777 (1971).

ACKNOWLEDGMENTS

The author thanks Microanalytical Services for the elemental analyses, the Basic Microbiology Department for the *in vitro* antimicrobial assays, Dr. R. B. Walton for the *in vitro* periodontal disease screen, and Dr. E. E. Howe and associates for the *in vivo* dental study.

[4] Detailed NMR studies of the tetrahydro-1,3-2*H*-oxazine ring system were reported (12, 13).

Plasma Naltrexone Kinetics after Intravenous Bolus Administration in Dogs and Monkeys

R. H. REUNING *x, V. K. BATRA *§, T. M. LUDDEN *¶, M. Y. JAO *, B. E. MORRISON *, D. A. McCARTHY ‡†, S. E. HARRIGAN ‡, S. B. ASHCRAFT *, R. A. SAMS *‖, M. S. BATHALA *•, A. E. STAUBUS *, and L. MALSPEIS *

Received April 14, 1978, from the **College of Pharmacy, Ohio State University, Columbus, OH 43210,* and the ‡*Pharmaceutical Research Division, Warner-Lambert/Parke-Davis, Ann Arbor, Mich.* Accepted for publication September 6, 1978.

§Present address: Lederle Laboratories, Pearl River, NY 10965. ¶Present address: University of Texas Health Science Center, San Antonio, TX 78284. ‖Present address: Department of Veterinary Clinical Sciences, Ohio State University, Columbus, OH 43210. •Present address: A. H. Robins Research Laboratories, Richmond, VA 23220. †Deceased.

Abstract □ This investigation generated data characterizing a specific electron-capture GLC assay reported previously for naltrexone and applied the method to a determination of naltrexone pharmacokinetics. Extraction efficiencies are reported for the assay, and mass spectral evidence indicates that naltrexone forms a triester when derivatized for electron-capture GLC with pentafluoropropionic anhydride and a base catalyst. Plasma level–time data for intravenous naltrexone at two dose levels in monkeys yielded no evidence of dose-dependent kinetics. A two-compartment open pharmacokinetic model was fitted to plasma level–time data for naltrexone in two dogs and yielded a total body clearance of 51–55 ml/min/kg. Urine collected for 0–24 hr contained 36% of the dose as naltrexone conjugates with less than 1% as unchanged naltrexone. Plasma level–time data for intravenous naltrexone in six monkeys yielded an average terminal half-life of 7.8 hr and a total body clearance of 64 ml/min/kg. The total body clearance for naltrexone was greater than the hepatic plasma or blood flow in both dogs and monkeys. This finding, together with the extremely low renal excretion of naltrexone, suggests the existence of elimination mechanisms besides liver metabolism and renal excretion.

Keyphrases □ Naltrexone—plasma kinetics after intravenous bolus administration, dogs and monkeys, electron-capture GLC assay □ Pharmacokinetics—naltrexone after intravenous bolus administration, dogs and monkeys, electron-capture GLC assay □ GLC, electron capture—specific assay for naltrexone □ Narcotic antagonists—naltrexone, pharmacokinetics after intravenous bolus administration, dogs and monkeys, electron-capture GLC assay

Naltrexone, a narcotic antagonist, has been investigated for use in the treatment of opioid dependence (1). In humans, most of the typical responses to a heroin challenge (25 mg iv) are blocked by naltrexone for 48–72 hr after a 100-mg oral dose (2). Because the duration of action of naltrexone is short in relation to that considered optimal

0022-3549/79/0400-0411$01.00/0

© 1979, American Pharmaceutical Association

[the phenylmethyl derivative, Ip, 7.1–7.8 ppm (10H)], and the vinyl proton (1H) appeared as a broad singlet at 6.0–6.3 ppm. The 6-phenyl group of II compounds was in the same range downfield, and the 2-methylene group (OCH_2N) appeared as a doublet of doublet, 4.41 and 4.58 ppm and 4.80 and 4.95 ppm, probably corresponding to the axial and equatorial protons, respectively[4].

1-Methyl-1-octyl-4-phenyl-1,2,3,6-tetrahydropyridinium Bromide (Ic)—A solution of 3.5 g (0.02 mole) of 1-methyl-4-phenyl-1,2,3,6-tetrahydropyridine (1) and 10 g (0.05 mole) of 1-bromooctane in 50 ml of anhydrous acetone was heated on a steam bath for 12 hr. The mixture obtained upon final cooling in an ice bath was filtered. Then the crystalline solid was washed with cold acetone and diethyl ether and purified by recrystallization, 1 g/50 ml of acetone, to provide colorless needles.

1-Decyl-1-methyl-4-phenyl-1,2,3,6-tetrahydropyridinium *o*-Sulfobenzimide (Ih)—One gram (0.0025 mole) of 1-decyl-1-methyl-4-phenyl-1,2,3,6-tetrahydropyridinium bromide (Ie) was suspended in 100 ml of warm (35°) deionized water with stirring, and a solution of 3.0 g (0.012 mole) of sodium *o*-sulfobenzimide dihydrate in 10 ml of deionized water was dripped in (10 min). The product separated initially as a colorless oil and solidified upon mixing an additional 2 hr, followed by cooling in an ice bath. The water-washed and air-dried colorless solid was recrystallized by solution of 1 g in 2 ml of acetonitrile and addition of approximately 18 ml of ether until incipient turbidity. The colorless plates obtained were washed with cold acetonitrile–ether (1:9 v/v).

REFERENCES

(1) C. J. Schmidle and R. C. Mansfield, *J. Am. Chem. Soc.*, **78**, 425, 1702 (1956). *Ibid.*, **77**, 5698 (1955). C. J. Schmidle and R. C. Mansfield, U.S. pats. 2,847,414 (1958) and 2,750,385 (1956).

(2) M. Rajšner, E. Adlerová, and M. Protiva, *Coll. Czech. Chem. Commun.*, **28**, 1031 (1963).

(3) T. Urbański, D. Guene, S. Šlopek, H. Modarska, and M. Modarska, *Nature*, **187**, 426 (1960).

(4) A. N. Petrocci, in "Disinfection, Sterilization, and Preservation," 2nd ed., S. S. Block, Ed., Lea & Febiger, Philadelphia, Pa., 1977, p. 325.

(5) J. DeMare, H. W. Rossmore, and T. H. F. Smith, *Dev. Ind. Microbiol.*, **13**, 341 (1972).

(6) N. Grier, U.S. pat. 3,920,642 (Nov. 18, 1975).

(7) N. Grier and R. Strelitz, *J. Pharm. Sci.*, **65**, 616 (1976).

(8) J. M. Tanzer, A. M. Slee, and B. A. Kamay, *Antimicrob. Agents Chemother.*, **12**, 721 (1977).

(9) P. L. Block, C. L. Dooley, and E. E. Howe, *J. Periodont.*, **40**, 41 (1969).

(10) R. J. Fitzgerald, *Antimicrob. Agents Chemother.*, **1**, 296 (1972).

(11) H. B. Woodruff, K. H. Nollstadt, R. B. Walton, and T. H. Stoudt, *Dev. Ind. Microbiol.*, **17**, 405 (1976).

(12) Y. E. Kazantsev, I. P. Boiko, Y. F. Malina, O. I. Zhuk, Y. Y. Samitov, and B. V. Unkovskii, *Zh. Org. Khim.*, **9**, 2616 (1972) (in English).

(13) H. Booth and R. U. Lemieux, *Can. J. Chem.*, **49**, 777 (1971).

ACKNOWLEDGMENTS

The author thanks Microanalytical Services for the elemental analyses, the Basic Microbiology Department for the *in vitro* antimicrobial assays, Dr. R. B. Walton for the *in vitro* periodontal disease screen, and Dr. E. E. Howe and associates for the *in vivo* dental study.

[4] Detailed NMR studies of the tetrahydro-1,3-2*H*-oxazine ring system were reported (12, 13).

Plasma Naltrexone Kinetics after Intravenous Bolus Administration in Dogs and Monkeys

R. H. REUNING *x, V. K. BATRA *§, T. M. LUDDEN *¶, M. Y. JAO *, B. E. MORRISON *, D. A. McCARTHY ‡†, S. E. HARRIGAN ‡, S. B. ASHCRAFT *, R. A. SAMS *‖, M. S. BATHALA *•, A. E. STAUBUS *, and L. MALSPEIS *

Received April 14, 1978, from the **College of Pharmacy, Ohio State University, Columbus, OH 43210,* and the ‡*Pharmaceutical Research Division, Warner-Lambert/Parke-Davis, Ann Arbor, Mich.* Accepted for publication September 6, 1978.

§Present address: Lederle Laboratories, Pearl River, NY 10965. ¶Present address: University of Texas Health Science Center, San Antonio, TX 78284. ‖Present address: Department of Veterinary Clinical Sciences, Ohio State University, Columbus, OH 43210. •Present address: A. H. Robins Research Laboratories, Richmond, VA 23220. †Deceased.

Abstract □ This investigation generated data characterizing a specific electron-capture GLC assay reported previously for naltrexone and applied the method to a determination of naltrexone pharmacokinetics. Extraction efficiencies are reported for the assay, and mass spectral evidence indicates that naltrexone forms a triester when derivatized for electron-capture GLC with pentafluoropropionic anhydride and a base catalyst. Plasma level–time data for intravenous naltrexone at two dose levels in monkeys yielded no evidence of dose-dependent kinetics. A two-compartment open pharmacokinetic model was fitted to plasma level–time data for naltrexone in two dogs and yielded a total body clearance of 51–55 ml/min/kg. Urine collected for 0–24 hr contained 36% of the dose as naltrexone conjugates with less than 1% as unchanged naltrexone. Plasma level–time data for intravenous naltrexone in six monkeys yielded an average terminal half-life of 7.8 hr and a total body clearance of 64 ml/min/kg. The total body clearance for naltrexone was greater than the hepatic plasma or blood flow in both dogs and monkeys. This finding, together with the extremely low renal excretion of naltrexone, suggests the existence of elimination mechanisms besides liver metabolism and renal excretion.

Keyphrases □ Naltrexone—plasma kinetics after intravenous bolus administration, dogs and monkeys, electron-capture GLC assay □ Pharmacokinetics—naltrexone after intravenous bolus administration, dogs and monkeys, electron-capture GLC assay □ GLC, electron capture—specific assay for naltrexone □ Narcotic antagonists—naltrexone, pharmacokinetics after intravenous bolus administration, dogs and monkeys, electron-capture GLC assay

Naltrexone, a narcotic antagonist, has been investigated for use in the treatment of opioid dependence (1). In humans, most of the typical responses to a heroin challenge (25 mg iv) are blocked by naltrexone for 48–72 hr after a 100-mg oral dose (2). Because the duration of action of naltrexone is short in relation to that considered optimal

0022-3549/79/0400-0411$01.00/0

© 1979, American Pharmaceutical Association

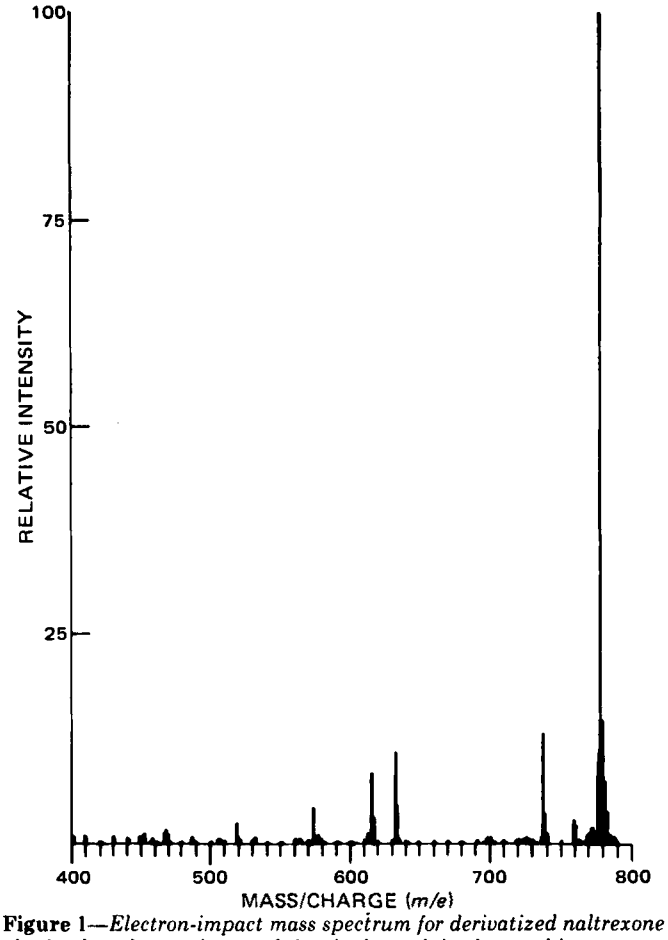

Figure 1—*Electron-impact mass spectrum for derivatized naltrexone obtained at the maximum of the single peak in the total ion current* versus *scan number plot.*

from a treatment standpoint, an effort to develop and evaluate sustained-release delivery systems for naltrexone was initiated (3). One prerequisite to a pharmacokinetic evaluation of *in vivo* release rates of naltrexone from such delivery systems is a knowledge of its distribution and elimination kinetics in the species of interest.

Cone *et al.* (4) were the first to report kinetic data on naltrexone in humans. Their data on urinary naltrexone excretion after a single 50-mg po dose indicated a urinary excretion half-life of 1.1 hr (mean of six subjects). However, since the urinary excretion data were obtained after oral administration, it is not possible to ascertain whether the half-life observed is representative of absorption or elimination (5). In addition, the half-life estimate appears to be based on only two time points (4).

Another study (2) reported the plasma level and urinary excretion kinetics of naltrexone in four postaddict human volunteers. The plasma naltrexone data indicated a half-life of 10 hr for the time period up to 24 hr and a half-life of 96 hr from 24 to 72 hr after an oral naltrexone dose. In the absence of intravenous data, however, it is difficult to ascertain the meaning of these half-life values.

The values reported by Verebey *et al.* (2) were much longer than those of Cone *et al.* (4). It is possible that kinetic parameters measured over the first 24 hr are influenced by continuing naltrexone absorption over part or all of this time period. The subsequent 96-hr half-life at very low drug levels probably represents either slow

Table I—Efficiency of Extraction of Naltrexone from Plasma [a]

Naltrexone Added, ng	Blank Plasma, ml	Percent Extracted with Benzene[b] Dog Plasma[c]	Percent Extracted with Benzene[b] Monkey Plasma[c]	Percent Extracted with Ethyl Acetate[b] Dog Plasma[d]	Percent Extracted with Ethyl Acetate[b] Monkey Plasma[c]
5[e]	0.5	70	82	—	—
10[e]	0.5	—	—	107	78
50[e]	0.5	68	76	96	90
100[e]	0.5	72	81	95	92
2[f]	2.0	64	64	—	—
10[f]	2.0	71	76	—	—
20[f]	2.0	77	67	—	—
Mean (*SD*)	—	70 (4)	74 (7)	99 (7)	87 (8)

[a] Blank plasma samples containing the added naltrexone were basified and supplemented with sodium chloride, extracted with either benzene or ethyl acetate, back-extracted into 0.1 *N* H_2SO_4, basified and supplemented with sodium chloride, and then reextracted into the same organic solvent. For the controls, naltrexone was added after the complete extraction procedure. [b] Results are for the entire extraction procedure and are corrected for volume losses. [c] Single determinations. [d] Mean of duplicate determinations. [e] Internal standard, naloxone (60 ng), added after extraction. [f] Internal standard, naloxone (12 ng), added before extraction because inconsistent results were obtained when it was added after extraction.

mobilization of a small amount of naltrexone from a tissue depot or assay interference at very low naltrexone concentrations. Thus, past studies have provided important data and raised pertinent questions regarding naltrexone kinetics in humans. No studies have been published on naltrexone pharmacokinetics in animals.

To understand naltrexone pharmacokinetics, it is necessary to measure its pharmacokinetic parameters after intravenous administration as well as to perform quantitative studies of naltrexone absorption, distribution, excretion, and metabolism. This paper reports the results of the initial stage of a comprehensive investigation of naltrexone pharmacokinetics in animals and humans. The plasma level kinetics determined after intravenous administration in monkeys and dogs were obtained using an assay previously developed in these laboratories[1] (6).

EXPERIMENTAL

Reagents—Naltrexone hydrochloride[2], naltrexone reference standard[2], naloxone reference standard[2], GLC–spectrophotometric quality methanol[3], and benzene[4] were used without further treatment. Pentafluoropropionic anhydride[5] was distilled prior to use, and 4-dimethylaminopyridine[6] was recrystallized. All other chemicals were reagent grade.

Extraction—An appropriate amount of a solution of naloxone (internal standard) in methanol was placed in each siliconized, screw-capped test tube. Samples of plasma or urine, 0.05–2.0 ml, were added and then extracted according to a reported procedure (7) with either benzene (dog study and initial study in four monkeys) or ethyl acetate (final study in six monkeys) as the organic solvent.

The efficiency of extraction of naltrexone from plasma was determined by assaying samples in which known amounts of naltrexone were added before and after extraction. Expression of the assayed amount in samples in which naltrexone was added prior to extraction as a percentage of the assayed amount in samples in which an equal amount of naltrexone was added after extraction yielded the extraction efficiency.

Derivatization and GLC—The residue obtained after extraction was dried by storage for at least 16 hr in a vacuum desiccator. Derivatization with pentafluoropropionic anhydride and subsequent electron-capture GLC were carried out according to the procedure described by Sams and Malspeis (6) with several modifications. The derivatization was done in

[1] Hopefully, similar studies in humans will be carried out when naltrexone is approved for intravenous use.
[2] Endo Laboratories, Garden City, N.Y.
[3] J. T. Baker Chemical Co., Phillipsburg, N.J.
[4] Burdick & Jackson, Muskegon, Mich.
[5] Pierce Chemical Co., Rockford, Ill.
[6] Aldrich Chemical Co., Milwaukee, Wis.

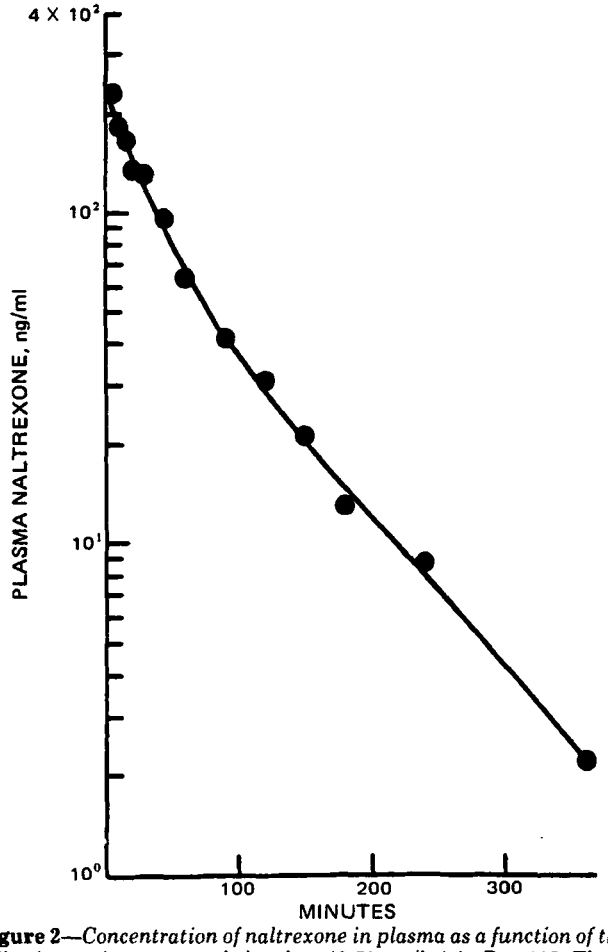

Figure 2—*Concentration of naltrexone in plasma as a function of time following an intravenous bolus dose (0.72 mg/kg) in Dog 105. The regression line was obtained by a nonlinear least-squares method using all data points. The fitting procedure and equations were described previously (12).*

benzene at 68–70° for 1 hr with 1% 4-dimethylaminopyridine as the catalyst (8).

The derivatives were chromatographed on a gas chromatograph equipped with a ^{63}Ni-electron-capture detector[7]. The coiled glass column was 2 mm i.d., either 1.8 m (6 ft) or 2.4 m (8 ft) in length, and was packed with 3% OV-17 on 100–120-mesh support[8]. The oven temperatures were 205° for the 1.8-m column (dog study and initial study in four monkeys) and 203° for the 2.4-m column (final study in six monkeys). The argon–methane (95:5) carrier gas flow rates were 40 ml/min for the 1.8-m column and 24–30 ml/min for the 2.4-m column.

Mass Spectrometry—The derivatization of naltrexone was done on a much larger scale than that described for assay purposes. Naltrexone base (2.0 mg) was placed in a siliconized culture tube with a polytef-lined cap and derivatized with 100 μl of pentafluoropropionic anhydride, using 200 μl of 1% dimethylaminopyridine in benzene as a catalyst. The mixture was heated at 68° for 1 hr and then cooled in an ice bath. The excess pentafluoropropionic anhydride was removed by washing the mixture with 10 ml of aqueous saturated sodium tetraborate.

A sample of the organic phase was transferred to another siliconized tube, and 2 μl of the organic phase was injected into a gas chromatograph[9] that had been interfaced through a glass jet separator to a mass spectrometer[10]. The gas chromatograph contained a 1.8-m coiled glass column, 2 mm i.d., packed with 3% OV-17 on 100–120-mesh support[8]. The carrier gas was helium. The spectrometer was operated in the electron-impact mode at 70 ev. A plot of total ion current *versus* scan number revealed only one peak, and mass spectra were recorded at the maximum of this peak.

[7] Model 5700A, Hewlett-Packard, Palo Alto, Calif.
[8] Gas Chrom Q, Applied Science Laboratories, State College, Pa.
[9] Model 2700, Varian Instrument Division, Palo Alto, Calif.
[10] Model 21-491, Dupont Instruments, Wilmington, Del.

Pharmacokinetic Studies in Animals—Two male foxhound dogs, 20 kg, were fasted for 24 hr prior to drug administration. Naltrexone hydrochloride was dissolved in normal saline and administered *via* the cephalic vein at 0.72 mg of naltrexone/kg over 30 sec. Blood was obtained at frequent intervals by venipuncture using a heparinized syringe. Total 0–24-hr urine was collected either by catheterization of the dog or by use of a metabolism cage.

Monkeys were supplied with a polyethylene venous catheter, which extended into the inferior vena cava *via* the saphenous vein. Naltrexone, 1.0 or 10.0 mg/kg, was administered through the catheter as a bolus dose followed by a saline rinse. At predetermined times after dosing, blood samples were drawn from the catheter into heparinized syringes.

Plasma was separated from dog and monkey blood samples by centrifugation, and all plasma and urine samples were stored frozen prior to analysis. Total body clearance was calculated by dividing the dose by the area under the plasma naltrexone level–time curve from time zero to infinity. The area was estimated from the macroconstants of a biexponential equation (9).

Enzymatic Hydrolysis and Dilution of Urine—After thawing and mixing the urine samples, a 0.5-ml aliquot of each sample was mixed with 1 ml of a 1:10 dilution of a commercial enzymatic mixture[11] of β-glucuronidase (~177,000 units/ml) and sulfatase (~35,000 units/ml) in 0.2 *M* acetate buffer, pH 5.0. Each sample was incubated in a water bath at 37° for 24 hr. These conditions result in a maximal degree of enzymatic hydrolysis of naltrexone conjugates (10). Hydrolyzed and unhydrolyzed urine samples were diluted 10–1000-fold with 0.9 *M* NaCl prior to extraction.

RESULTS

Analytical Aspects—Derivatization and chromatography of naltrexone, either at the nanogram level for assay purposes or at the milli-

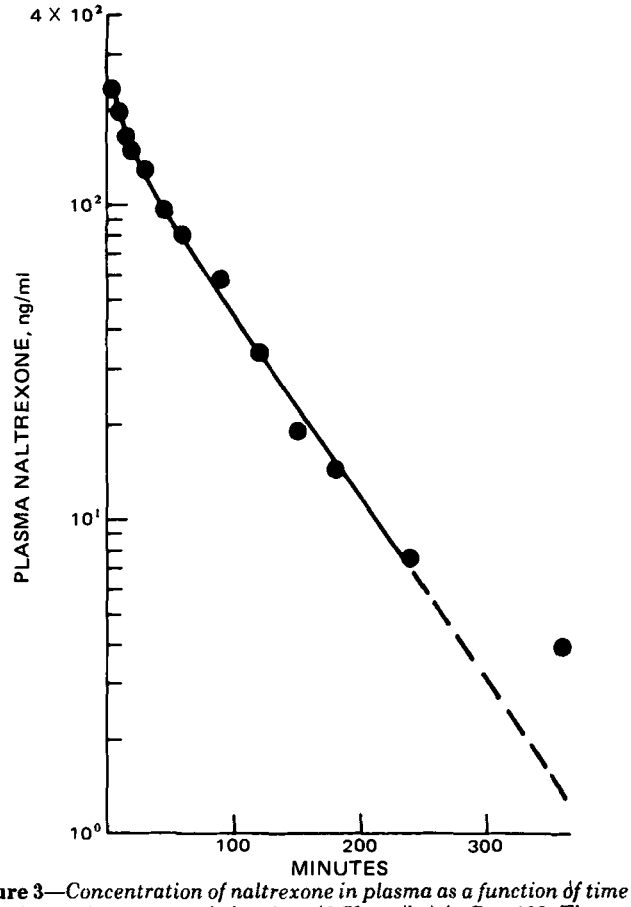

Figure 3—*Concentration of naltrexone in plasma as a function of time following an intravenous bolus dose (0.72 mg/kg) in Dog 103. The regression line was obtained by a nonlinear least-squares method using the data from 5 to 240 min.*

[11] Glusulase, Endo Laboratories, Garden City, N.Y.

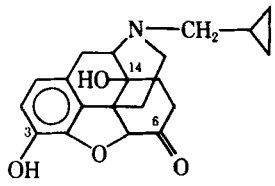

I

gram level for mass spectrometry studies, yielded a single peak with the same retention time in each case. Thus, the GLC results indicate that the same derivative was formed at either level. The mass spectrum, obtained at the maximum of the single peak in the plot of total ion current *versus* scan number, is illustrated in Fig. 1. The base peak at *m/e* 779 corresponds to the molecular ion of the pentafluoropropionyl triester derivative of naltrexone. This finding is consistent with formation of a completely derivatized naltrexone molecule esterified at the 3-, 6-, and 14-positions (I). The only significant fragment ions observed were at *m/e* 738 (12.9% of base peak), corresponding to a loss of a C_3H_5 moiety from the *N*-cyclopropylmethyl group, *m/e* 632 (10.8% of base peak), corresponding to a loss of a CF_3CF_2CO moiety, and *m/e* 616 (8.3% of base peak), corresponding to a loss of a CF_3CF_2COO moiety from the molecular ion.

The efficiency of benzene extraction of naltrexone from plasma averaged 70% in the dog (range of 64–77%) and 74% in the monkey (range of 64–82%) (Table I). There was no discernible concentration dependence of the extraction efficiency over the concentration ranges encountered in routine assays of plasma samples. These extraction efficiencies compare favorably to the 72.5% reported previously for extraction of naltrexone from dog urine with this procedure (7). When ethyl acetate was substituted for benzene, these efficiencies increased to an average of 99% for dog plasma and 87% for monkey plasma (Table I).

Standard curves for the assay were obtained by: (*a*) adding varying known amounts of naltrexone and a constant amount of naloxone (internal standard) to a series of blank plasma samples, (*b*) measuring the chromatographic peak heights after completion of the extraction, derivatization, and GLC assay, and (*c*) plotting the peak height ratio, naltrexone to naloxone, as a function of the amount of added naltrexone. Linear standard curves were obtained and a new standard curve covering the range of expected concentrations was prepared on each day of analysis.

Pharmacokinetic Studies—The plasma naltrexone concentration–time curves obtained after administration of an intravenous bolus dose to each of two foxhound dogs are illustrated in Figs. 2 and 3. Because the plasma naltrexone levels declined with time in a biexponential manner, the classical two-compartment open model (Scheme I) was chosen for initial attempts at fitting a model to the data (5). The results of the nonlinear least-squares fit (11, 12) are indicated in Figs. 2 and 3. The terminal half-life values of the fitted curves averaged 1.0 hr (range of 52–67 min), and the total body clearance was in the range of 51–55 ml/min/kg.

Assay of both enzymatically hydrolyzed and unhydrolyzed 0–24-hr urine collections provided an estimate of the urinary excretion of naltrexone and its conjugates. An average of 37% of the dose was excreted as total (unconjugated plus conjugated) naltrexone during the first 24 hr after the intravenous dose with less than 1% excreted as unconjugated naltrexone (Table II). No attempt was made to analyze for the small amounts of other metabolites that may have been present (7).

The initial experiment on naltrexone pharmacokinetics in the monkey was designed to determine the concentration ranges in plasma encountered at various intravenous dosage levels and to detect any pronounced dose dependence of naltrexone pharmacokinetics. The limited data obtained (Table III) indicate that, at each point in time, a 10-fold increase in dosage yielded about a 10-fold increase in the average plasma level.

Table II—Naltrexone and Conjugates in Dog Urine Collected 0–24 hr following an Intravenous Bolus of Naltrexone

	Percent of Dose		
Dog	Naltrexone[a]	Naltrexone Conjugates[b]	Total[c]
103	0.90	35.7	36.6
105	0.73	37.2	37.9

[a] Determined by assay of unhydrolyzed urine samples. [b] The difference between total and unchanged naltrexone. [c] Determined by assay of urine samples subsequent to enzymatic hydrolysis of naltrexone conjugates.

Table III—Initial Study of Naltrexone Levels in Monkey Plasma as a Function of Time after an Intravenous Bolus Dose

	Plasma Level, ng/ml			
	10 mg/kg		1 mg/kg	
Minutes	6715[a]	6700[b]	6705[c]	6719[d]
10	2275[e]	3440	244	252
20	1880	2075	166	167
40	1280	1447	150	120
80	666	810	91.5	46.7
160	212	288	44.8	11.8
320	31.2	52.8	11.8	—
AUC[f]	171	224	23.0	13.8

[a] Monkey 6715 was a 3.8-kg female. [b] Monkey 6700 was a 6.4-kg male. [c] Monkey 6705 was a 4.7-kg female. [d] Monkey 6719 was a 3.6-kg male. [e] Each value is the mean of duplicate assays. [f] Area under the plasma naltrexone level–time curve from zero time to the last data point (μg min/ml) determined by the trapezoidal method.

When plotted as a function of time, the plasma levels declined in a biexponential manner. The average area under the plasma level–time curve for the 10-mg dose was 10.7 times that for the 1-mg dose.

Following completion of this initial experiment, another investigation was carried out in six monkeys at the 10-mg/kg dosage. Blood samples were obtained at more frequent intervals over 48 hr. The results of the nonlinear least-squares fit (11, 12) of the two-compartment open model (Scheme I) to the plasma level–time data are shown in Figs. 4 and 5 for two monkeys. The close proximity of the data points to the regression curve indicate that an excellent fit was obtained whether measurable levels were found over 24 hr (Fig. 4, representative of four monkeys) or over 48 hr (Fig. 5, representative of two monkeys). The pharmacokinetic parameters obtained from the nonlinear least-squares fit of the data for all six monekys are summarized in Table IV. The terminal half-life of the plasma naltrexone level–time curve averaged 7.8 hr, and the total body clearance averaged 64 ml/min/kg.

DISCUSSION

Mass spectral evidence that the base peak of the derivative formed during the assay corresponds to the molecular weight of the pentafluoropropionyl triester of naltrexone indicates that the completely derivatized naltrexone moiety is the compound being chromatographed. The fragmentation pattern is also consistent with this conclusion. Sams and Malspeis (6) presented mass and IR spectral evidence that naltrexone reacted with heptafluorobutyric anhydride in the presence of a base catalyst forms the analogous heptafluorobutyryl triester. Although derivatization of an aliphatic enol such as that at the 6-position of naltrexone is unusual (13), Cone *et al.* (14) presented evidence consistent with the formation of a similar acyl derivative of hydromorphone. This complete degree of derivatization in the presence of a base catalyst in the present assay permits maximal sensitivity and avoids any variability due to an inconsistent degree of partial derivatization.

With benzene as the organic solvent for extraction, possible interference from the blank and from unknown polar naltrexone metabolites is minimized. However, when ethyl acetate is used, the extraction efficiency of naltrexone is close to 100% and the extraction and chromatographic assay of certain polar metabolites may also be possible. It was previously shown that this procedure is specific for naltrexone (7) and that the known metabolites, *i.e.*, α-naltrexol and β-naltrexol, as well as the potential metabolite noroxymorphone do not interfere. Thus, the evidence on specificity indicates that the analytical method is suitable for pharmacokinetic studies.

The fit of the two-compartment open model to the plasma naltrexone level–time data was excellent for both dogs (Figs. 2 and 3), with the exception of the last sample in one dog (Fig. 3). The deviation of this last point from the extrapolation of the curve fitted to the other data points could be due to experimental error or may indicate a very slow terminal phase for a small fraction of the dose. Because of the limitation of assay sensitivity, it was not possible in this experiment to investigate further

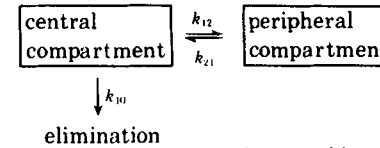

Scheme I—Two-compartment open pharmacokinetic model. The k's *are rate constants for the transfer processes indicated.*

Table IV—Pharmacokinetic Parameters [a] for Intravenous Naltrexone in the Monkey

Monkey[b]	k_{12}, min^{-1}	k_{21}, min^{-1}	k_{10}, min^{-1}	$t_{1/2}$, min	V_{d_β}, liters/kg	Total Body Clearance, ml/min/kg
6726 (4.36 kg)	0.00109 (0.00011)[c]	0.00095 (0.00018)	0.01278 (0.00043)	797	63	55
6695 (5.26 kg)	0.00102 (0.00025)	0.00184 (0.00040)	0.01104 (0.00070)	418	61	101
6763 (5.76 kg)	0.00111 (0.00025)	0.00085 (0.00026)	0.00984 (0.00078)	910	94	71
428 (5.55 kg)	0.00060 (0.00009)	0.00211 (0.00022)	0.01089 (0.00029)	351	26	50
6706 (5.08 kg)	0.00117 (0.00020)	0.00110 (0.00018)	0.01302 (0.00079)	691	68	69
6761 (4.90 kg)	0.00111 (0.00011)	0.00308 (0.00014)	0.00886 (0.00016)	265	15	41
Mean	0.00102	0.00166	0.01107	468[d]	54 (29)	64 (21)

[a] The parameters k_{12}, k_{21}, and k_{10} are the rate constants defined in Scheme I and were obtained by nonlinear least-squares regression (9, 10). The $t_{1/2}$ is the half-life of the terminal exponential phase of the plasma naltrexone level–time curve; V_{d_β}, the apparent volume of distribution, was calculated by an accepted method. [b] Monkeys were all female. [c] Standard deviation in parentheses. [d] Harmonic mean. The coefficient of variation of the mean of the reciprocal $t_{1/2}$ values was 50%.

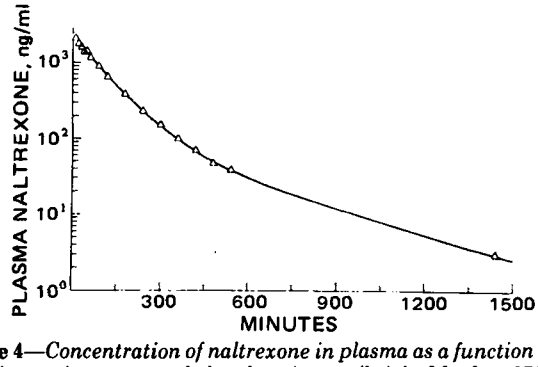

Figure 4—*Concentration of naltrexone in plasma as a function of time following an intravenous bolus dose (10 mg/kg) in Monkey 6761. The regression line was obtained by a nonlinear least-squares method.*

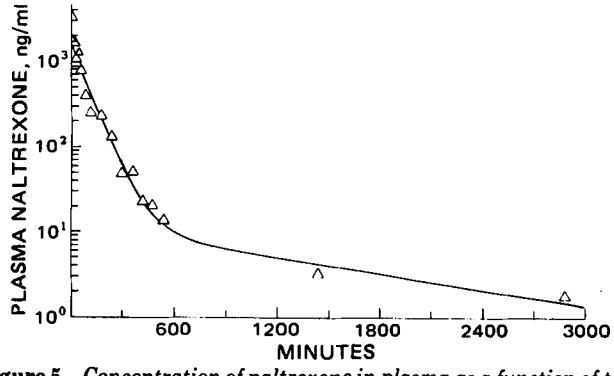

Figure 5—*Concentration of naltrexone in plasma as a function of time following an intravenous bolus dose (10 mg/kg) in Monkey 6763. The regression line was obtained by a nonlinear least-squares method.*

the possible existence of a terminal phase of the plasma level–time curve having a much longer half-life. This possibility will be examined in the dog using alternative experimental designs.

The recovery of 37% of the naltrexone dose from 0 to 24 hr in dog urine, mostly as conjugated naltrexone, is consistent with literature data. Malspeis *et al.* (7) found only small amounts of β-naltrexol in enzyme[11]-hydrolyzed dog urine after intravenous administration and could not detect any α-naltrexol. Only 38% of an oral dose was accounted for in humans as unchanged drug and metabolites in 0–24-hr urine (2), and 53% was accounted for in 0–6-day urine (4). Thus, there is incomplete recovery of naltrexone in the urine in both humans and dogs. Possible additional modes of elimination include fecal excretion of naltrexone and/or its metabolites, formation of unknown metabolites, and urinary excretion of conjugates not hydrolyzed by the enzyme preparation[11]. The relative importance of these potential elimination pathways is currently under investigation.

The initial experiment on plasma naltrexone level kinetics at two different dose levels in the monkey did not yield any evidence of nonlinear pharmacokinetics since plasma naltrexone levels and areas under the curve were approximately proportional to dose (Table III) even though the experiment was not done in crossover fashion. However, this evidence is not conclusive and will be investigated in a more definitive manner.

The experiment designed to determine the pharmacokinetic parameters of naltrexone in the monkey from plasma level–time data yielded evidence of a very long terminal half-life in comparison to that found in the dog. However, when the terminal data point for Dog 103 was included in the data analysis, a half-life of 356 min for the terminal phase was obtained; this value is within the range of the terminal half-life values observed in the six monkeys (Table IV). Thus, these findings suggest that the terminal half-life for naltrexone is at least several hours in duration in both the dog and monkey. This result agrees with the results of Verebey *et al.* (2) obtained after oral administration of naltrexone in humans. A more accurate quantitation of this long half-life will require more plasma samples at various times in the terminal phase and perhaps either a more sensitive assay for plasma naltrexone or the inclusion of urinary excretion data in the pharmacokinetic analysis. This terminal phase probably represents a rather small, slowly equilibrating compartment for naltrexone.

The total body clearance of naltrexone was in the range of 51–55 ml/min/kg in the dog and 40–100 ml/min/kg in the monkey. The calculation of total body clearance was influenced mainly by the contribution of the initial (alpha) phase of the plasma level–time curve (Figs. 2–5) to the area under the curve and thus was not appreciably affected by the uncertainty of the estimation of the terminal phase half-life in the dog. Each of these values is higher than the respective liver plasma flow of 15–25 ml/min/kg in the dog and 11–17 ml/min/kg in the monkey as well as the liver blood flow of 29–45 ml/min/kg in the dog and about 25 ml/min/kg in the monkey (15).

The fact that the total body clearance of naltrexone is greater than the liver plasma flow or blood flow in both species, coupled with the extremely low renal excretion of unchanged drug in monkeys (16) and dogs (Table II), suggests the existence of elimination pathways besides liver metabolism and renal excretion. If such alternative eliminating organs are quantitatively important in humans, the calculations by Kogan *et al.* (17) of total body clearance and extent of first-pass metabolism of naltrexone (based on plasma level data after oral administration of naltrexone in humans) are erroneous since the calculation method is applicable only to drugs eliminated exclusively by renal excretion and hepatic metabolism (18).

REFERENCES

(1) W. R. Martin, D. R. Jasinski, and P. A. Mansky, *Arch. Gen. Psychiatry*, **28**, 784 (1973).

(2) K. Verebey, J. Volavka, S. J. Mule, and R. B. Resnick, *Clin. Pharmacol. Ther.*, **20**, 315 (1976).

(3) "Narcotic Antagonists: The Search for Long-Acting Preparations," R. Willette, Ed., Monograph Series 4, National Institute on Drug Abuse, Rockville, Md., 1975.

(4) E. J. Cone, C. W. Gorodetzky, and S. Y. Yeh, *Drug Metab. Dispos.*, **2**, 506 (1974).

(5) M. Gibaldi and D. Perrier, "Pharmacokinetics," Dekker, New York, N.Y., 1975, pp. 41, 42, 48–55.

(6) R. A. Sams and L. Malspeis, *J. Chromatogr.*, **125**, 409 (1976).

(7) L. Malspeis, M. S. Bathala, T. M. Ludden, H. B. Bhat, S. G. Frank, T. D. Sokoloski, B. E. Morrison, and R. H. Reuning, *Res. Commun. Chem. Pathol. Pharmacol.*, **12**, 43 (1975).
(8) K. A. Connors and K. S. Albert, *J. Pharm. Sci.*, **62**, 845 (1973).
(9) J. G. Wagner, "Fundamentals of Clinical Pharmacokinetics," Drug Intelligence Publications, Hamilton, Ill., 1975, p. 83.
(10) T. M. Ludden, M. S. Bathala, L. Malspeis, M. A. Drum, and R. H. Reuning, *Drug Metab. Dispos.*, **6**, 321 (1978).
(11) C. M. Metzler, NONLIN, Technical Report 7292/68/7292/005, The Upjohn Co., Kalamazoo, Mich., 1969.
(12) W. G. Kramer, R. P. Lewis, T. C. Cobb, W. F. Forester, Jr., J. A. Visconti, L. A. Wanke, H. G. Boxenbaum, and R. H. Reuning, *J. Pharmacokinet. Biopharm.*, **2**, 299 (1974).
(13) C. F. Poole, in "Handbook of Derivatives for Chromatography," K. Blau and G. S. King, Eds., Heyden, London, England, 1977, pp. 160–163.
(14) E. J. Cone, B. A. Phelps, and C. W. Gorodetzky, *J. Pharm. Sci.*, **66**, 1709 (1977).
(15) "Biology Data Book," vol. III, 2nd ed., P. L. Altman and D. S. Dittmer, Eds., Federation of American Societies for Experimental Biology, Bethesda, Md., 1974, pp. 1702–1705.
(16) H. E. Dayton and C. E. Inturrisi, *Drug Metab. Dispos.*, **4**, 474 (1976).
(17) M. J. Kogan, K. Verebey, and S. J. Mulé, *Res. Commun. Chem. Pathol. Pharmacol.*, **18**, 29 (1977).
(18) D. P. Vaughan, *J. Pharm. Pharmacol.*, **27**, 458 (1975).

ACKNOWLEDGMENTS

Supported by Contract HSM 42-73-182 (Ohio State), Grant DA-00473 (Ohio State), and Contract HSM-72-72-167 (Warner-Lambert/Parke-Davis) from the National Institute on Drug Abuse, U.S. Department of Health, Education, and Welfare, Rockville, Md.

The authors thank Dr. E. H. Fairchild for the mass spectrum.

Pharmacokinetic Description of Drug Interactions by Enzyme Induction: Carbamazepine–Clonazepam in Monkeys

ALLEN A. LAI * and RENÉ H. LEVY ˣ

Received April 24, 1978, from the *Departments of Pharmaceutical Sciences and Neurological Surgery, Schools of Pharmacy and Medicine, University of Washington, Seattle, WA 98195.* Accepted for publication September 6, 1978. *Present address: Clinical Research Department, Medical Division, Burroughs Wellcome Co., Research Triangle Park, NC 27709.

Abstract □ The applicability of a pharmacokinetic model for drug interactions by enzyme induction was tested in rhesus monkeys using a design in which both the inducer (carbamazepine) and the induced agent (clonazepam) were infused chronically. Two types of studies were conducted. Studies I and II examined the kinetic behavior of plasma clonazepam levels during induction and postinduction, respectively. The addition of carbamazepine (Study I) caused the preinduction clonazepam steady-state level to decrease exponentially to a lower (induced) steady state after lag times of 14.0–60.5 hr, and the removal of carbamazepine (Study II) caused induced clonazepam steady-state levels to climb exponentially to a higher steady state after lag times of 34.0–81.0 hr. The extent of induction ranged between 23 and 54%. The time course of clonazepam levels was described in terms of a one-compartment induction model with zero-order input and a metabolic clearance that increased (Study I) or decreased (Study II) exponentially with time. In both studies, induced clonazepam half-lives (3.7–7.7 hr) were significantly shorter ($p < 0.0005$) than control values (5.2–12.2 hr). Apparent enzyme turnover half-lives were shorter in Study II (2.7–19.3 hr) than in Study I (6.9–66.4 hr). A two- to threefold increase in urinary excretion of D-glucaric acid during carbamazepine administration provided additional evidence that the present interaction was due to enzyme induction.

Keyphrases □ Interactions—carbamazepine and clonazepam in monkeys by enzyme induction, pharmacokinetic description □ Carbamazepine—interaction with clonazepam by enzyme induction, pharmacokinetic description, monkeys □ Clonazepam—interaction with carbamazepine by enzyme induction, pharmacokinetic description, monkeys □ Enzyme induction—pharmacokinetic description of carbamazepine–clonazepam interaction, monkeys □ Pharmacokinetics—description of carbamazepine–clonazepam interaction by enzyme induction, monkeys □ Models—drug interactions by enzyme induction, carbamazepine–clonazepam, monkeys

Many drugs possess enzyme-inducing properties and thereby stimulate their own metabolism (autoinduction) and/or that of other drugs (heteroinduction). In humans and animals, experimental evidence for enzyme induction is often associated with decreases in plasma concentrations of the induced agent. Recently, a pharmacokinetic theory was proposed to describe the kinetics of plasma drug levels during auto- and heteroinduction (1). This theory proposes that the metabolic clearance of the induced species increases exponentially during induction. The time course of this increase in clearance is governed by the apparent turnover half-life of the induced metabolic enzyme(s).

The simplest and most critical experimental validation of this theory entails administration of both an inducer and an induced agent by constant rate intravenous infusion. Preliminary studies with this design were performed in monkeys using carbamazepine as the inducer and valproic acid and ethosuximide as the induced agents (2, 3). Following addition of carbamazepine, plasma levels of these two drugs decreased in an exponential fashion to a lower steady state, as expected.

The present study, in addition to investigating shifts of steady-state levels during induction, focused on determining control and induced half-lives of clonazepam. Furthermore, the hypothesis that removal of an inducer causes a return of metabolic clearance from an induced state to the basal state was tested by following increases in plasma clonazepam levels upon removal of carbamazepine.

EXPERIMENTAL

Animal Preparation—Five healthy male rhesus (*Macaca mulatta*) monkeys, 4.0–5.6 kg, were chair adapted for 1 month prior to surgical implantation of catheters at two different sites. The jugular and femoral veins were catheterized for drug infusion and blood sampling, respectively. Each monkey was maintained in a three-level restraining chair during individual studies and was given cage rest at appropriate intervals. Patency of catheters was assured by a slow, continuous saline infusion (1 ml/hr). The daily diet consisted of fresh fruit (bananas, oranges, and apples) and monkey chow.

0022-3549/79/0400-0416$01.00/0
© 1979, American Pharmaceutical Association

(7) L. Malspeis, M. S. Bathala, T. M. Ludden, H. B. Bhat, S. G. Frank, T. D. Sokoloski, B. E. Morrison, and R. H. Reuning, *Res. Commun. Chem. Pathol. Pharmacol.*, **12**, 43 (1975).
(8) K. A. Connors and K. S. Albert, *J. Pharm. Sci.*, **62**, 845 (1973).
(9) J. G. Wagner, "Fundamentals of Clinical Pharmacokinetics," Drug Intelligence Publications, Hamilton, Ill., 1975, p. 83.
(10) T. M. Ludden, M. S. Bathala, L. Malspeis, M. A. Drum, and R. H. Reuning, *Drug Metab. Dispos.*, **6**, 321 (1978).
(11) C. M. Metzler, NONLIN, Technical Report 7292/68/7292/005, The Upjohn Co., Kalamazoo, Mich., 1969.
(12) W. G. Kramer, R. P. Lewis, T. C. Cobb, W. F. Forester, Jr., J. A. Visconti, L. A. Wanke, H. G. Boxenbaum, and R. H. Reuning, *J. Pharmacokinet. Biopharm.*, **2**, 299 (1974).
(13) C. F. Poole, in "Handbook of Derivatives for Chromatography," K. Blau and G. S. King, Eds., Heyden, London, England, 1977, pp. 160–163.
(14) E. J. Cone, B. A. Phelps, and C. W. Gorodetzky, *J. Pharm. Sci.*, **66**, 1709 (1977).
(15) "Biology Data Book," vol. III, 2nd ed., P. L. Altman and D. S. Dittmer, Eds., Federation of American Societies for Experimental Biology, Bethesda, Md., 1974, pp. 1702–1705.
(16) H. E. Dayton and C. E. Inturrisi, *Drug Metab. Dispos.*, **4**, 474 (1976).
(17) M. J. Kogan, K. Verebey, and S. J. Mulé, *Res. Commun. Chem. Pathol. Pharmacol.*, **18**, 29 (1977).
(18) D. P. Vaughan, *J. Pharm. Pharmacol.*, **27**, 458 (1975).

ACKNOWLEDGMENTS

Supported by Contract HSM 42-73-182 (Ohio State), Grant DA-00473 (Ohio State), and Contract HSM-72-72-167 (Warner-Lambert/Parke-Davis) from the National Institute on Drug Abuse, U.S. Department of Health, Education, and Welfare, Rockville, Md.

The authors thank Dr. E. H. Fairchild for the mass spectrum.

Pharmacokinetic Description of Drug Interactions by Enzyme Induction: Carbamazepine–Clonazepam in Monkeys

ALLEN A. LAI * and RENÉ H. LEVY ˣ

Received April 24, 1978, from the *Departments of Pharmaceutical Sciences and Neurological Surgery, Schools of Pharmacy and Medicine, University of Washington, Seattle, WA 98195.* Accepted for publication September 6, 1978. *Present address: Clinical Research Department, Medical Division, Burroughs Wellcome Co., Research Triangle Park, NC 27709.

Abstract □ The applicability of a pharmacokinetic model for drug interactions by enzyme induction was tested in rhesus monkeys using a design in which both the inducer (carbamazepine) and the induced agent (clonazepam) were infused chronically. Two types of studies were conducted. Studies I and II examined the kinetic behavior of plasma clonazepam levels during induction and postinduction, respectively. The addition of carbamazepine (Study I) caused the preinduction clonazepam steady-state level to decrease exponentially to a lower (induced) steady state after lag times of 14.0–60.5 hr, and the removal of carbamazepine (Study II) caused induced clonazepam steady-state levels to climb exponentially to a higher steady state after lag times of 34.0–81.0 hr. The extent of induction ranged between 23 and 54%. The time course of clonazepam levels was described in terms of a one-compartment induction model with zero-order input and a metabolic clearance that increased (Study I) or decreased (Study II) exponentially with time. In both studies, induced clonazepam half-lives (3.7–7.7 hr) were significantly shorter ($p < 0.0005$) than control values (5.2–12.2 hr). Apparent enzyme turnover half-lives were shorter in Study II (2.7–19.3 hr) than in Study I (6.9–66.4 hr). A two- to threefold increase in urinary excretion of D-glucaric acid during carbamazepine administration provided additional evidence that the present interaction was due to enzyme induction.

Keyphrases □ Interactions—carbamazepine and clonazepam in monkeys by enzyme induction, pharmacokinetic description □ Carbamazepine—interaction with clonazepam by enzyme induction, pharmacokinetic description, monkeys □ Clonazepam—interaction with carbamazepine by enzyme induction, pharmacokinetic description, monkeys □ Enzyme induction—pharmacokinetic description of carbamazepine–clonazepam interaction, monkeys □ Pharmacokinetics—description of carbamazepine–clonazepam interaction by enzyme induction, monkeys □ Models—drug interactions by enzyme induction, carbamazepine–clonazepam, monkeys

Many drugs possess enzyme-inducing properties and thereby stimulate their own metabolism (autoinduction) and/or that of other drugs (heteroinduction). In humans and animals, experimental evidence for enzyme induction is often associated with decreases in plasma concentrations of the induced agent. Recently, a pharmacokinetic theory was proposed to describe the kinetics of plasma drug levels during auto- and heteroinduction (1). This theory proposes that the metabolic clearance of the induced species increases exponentially during induction. The time course of this increase in clearance is governed by the apparent turnover half-life of the induced metabolic enzyme(s).

The simplest and most critical experimental validation of this theory entails administration of both an inducer and an induced agent by constant rate intravenous infusion. Preliminary studies with this design were performed in monkeys using carbamazepine as the inducer and valproic acid and ethosuximide as the induced agents (2, 3). Following addition of carbamazepine, plasma levels of these two drugs decreased in an exponential fashion to a lower steady state, as expected.

The present study, in addition to investigating shifts of steady-state levels during induction, focused on determining control and induced half-lives of clonazepam. Furthermore, the hypothesis that removal of an inducer causes a return of metabolic clearance from an induced state to the basal state was tested by following increases in plasma clonazepam levels upon removal of carbamazepine.

EXPERIMENTAL

Animal Preparation—Five healthy male rhesus (*Macaca mulatta*) monkeys, 4.0–5.6 kg, were chair adapted for 1 month prior to surgical implantation of catheters at two different sites. The jugular and femoral veins were catheterized for drug infusion and blood sampling, respectively. Each monkey was maintained in a three-level restraining chair during individual studies and was given cage rest at appropriate intervals. Patency of catheters was assured by a slow, continuous saline infusion (1 ml/hr). The daily diet consisted of fresh fruit (bananas, oranges, and apples) and monkey chow.

0022-3549/79/0400-0416$01.00/0
© 1979, American Pharmaceutical Association

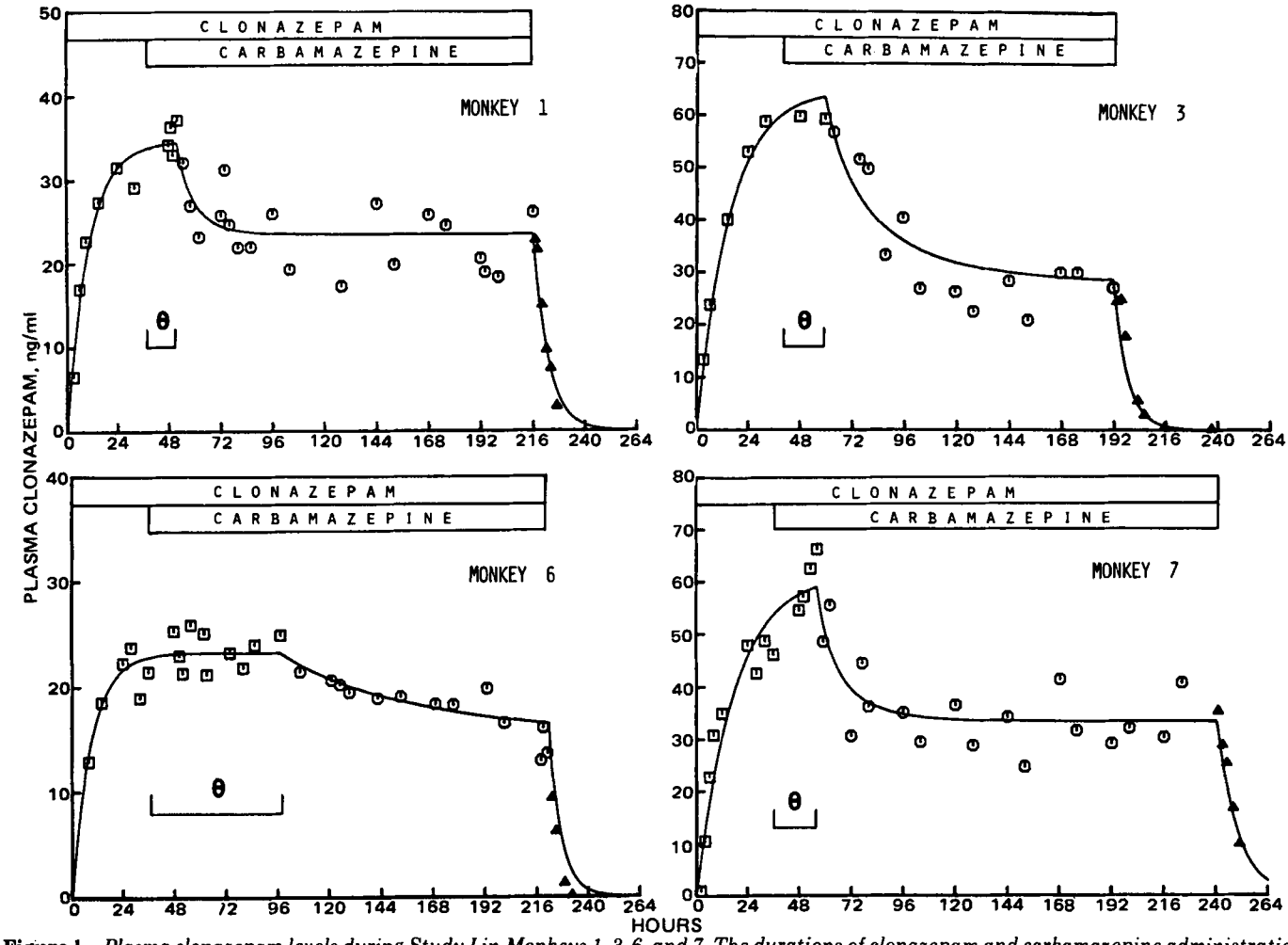

Figure 1—*Plasma clonazepam levels during Study I in Monkeys 1, 3, 6, and 7. The durations of clonazepam and carbamazepine administration are illustrated at the top of individual plots. The continuous lines were simulated with parameters obtained from curve fitting of experimental data to Eqs. 3, 4, and 6.*

Protocol and Analytical Procedures—All intravenous solutions were polyethylene glycol 400–water mixtures (60:40). Three types of intravenous solutions were prepared: Solution A, clonazepam only (80–130 μg/ml); Solution B, both clonazepam and carbamazepine (80–130 μg/ml and 10 mg/ml, respectively); and Solution C, carbamazepine only (10 mg/ml).

Two types of studies were conducted. In Study I, clonazepam was infused in four monkeys (Monkeys 1, 3, 6, and 7) at a constant rate for 8–9 days to achieve and maintain steady-state levels; carbamazepine was added to the infusion after 2 days. (Solution A was used for Days 1–2 and Solution B for Days 3–9.) In Study II, carbamazepine was infused in four monkeys (Monkeys 3, 4, 6, and 7) from Days 1 to 6; clonazepam was infused from Days 4 to 12. (Solution C was used for Days 1–3, Solution B for Days 4–6, and Solution A for Days 7–12.) In both studies, 30–34 blood samples (1.2 ml each) were collected. The plasma of these samples was separated and frozen until assay. Four to six 24-hr urine samples also were collected during each study.

Plasma levels of clonazepam were measured by the electron-capture GLC method of de Silva and Bekersky (4), and those of carbamazepine were measured by the GLC–chemical-ionization mass spectrometric method of Trager *et al.* (5). Urinary excretion of D-glucaric acid was determined using the spectrophotometric procedure of Ishidate *et al.* (6).

Data Analysis—Experimental plasma concentration–time data were fitted to appropriate pharmacokinetic model equations using the BMDX85 nonlinear least-squares program. All data points were assigned equal weights. A one-tailed paired t-test was used in all statistical comparisons.

Table I—Daily Urinary Excretion of D-Glucaric Acid from Monkeys during Carbamazepine–Clonazepam Interaction Studies

Monkey	Control Period, mg/day	Clonazepam Infusion Period[a], mg/day	Induction Period[b], mg/day
6[c]	30.8	34.1	70.7
7[c]	16.9	13.3	23.3
3[d]	18.1	16.0	45.3
4[d]	18.3	23.2	50.5
7[d]	9.3	11.7	25.5

[a] Animals during this period received only clonazepam. [b] Animals during this period received both clonazepam and carbamazepine. [c] Study I. [d] Study II.

RESULTS AND DISCUSSION

Plasma Clonazepam Levels during Studies I and II—Figure 1 shows experimental plasma clonazepam levels as a function of time in Monkeys 1, 3, 6, and 7 during Study I. The entire time course can be divided into three phases (I-A, I-B, and I-C), as illustrated by the three different symbols representing the experimental data points. In Phase I-A, plasma clonazepam concentrations increased exponentially and steady-state plasma levels (preinduction steady state, C_0) were essentially achieved within 36–48 hr. In Phase I-B, the addition of carbamazepine caused clonazepam levels to decrease to lower steady-state levels (induced steady state, C_∞).

Lag times (θ = 14.0, 17.5, 60.5, and 19.0 hr in Monkeys 1, 3, 6, and 7, respectively) were observed between the addition of carbamazepine and the start of the decrease of clonazepam levels. Upon termination of both clonazepam and carbamazepine infusions, clonazepam levels decayed to less than 5% of C_∞ within 24–36 hr (Phase I-C). The scatter in exper-

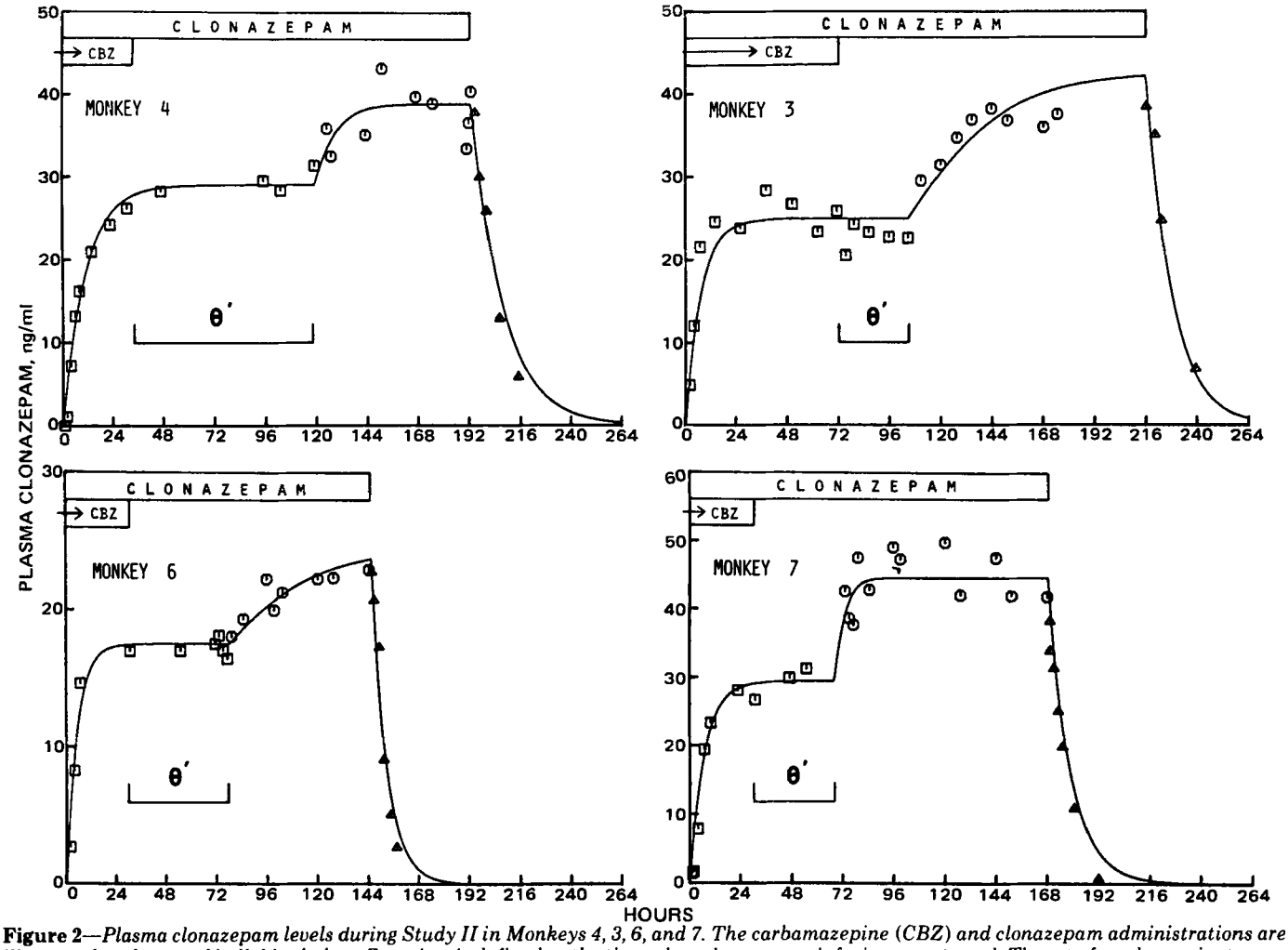

Figure 2—*Plasma clonazepam levels during Study II in Monkeys 4, 3, 6, and 7. The carbamazepine (CBZ) and clonazepam administrations are illustrated at the top of individual plots. Zero time is defined as the time when clonazepam infusion was started. Three to four days prior to zero time, animals were started on the carbamazepine infusion (indicated by an arrow starting prior to zero time in the carbamazepine bar). The continuous lines were simulated with parameters obtained from curve fitting of experimental data to Eqs. 7–9.*

imental data points during both steady states (C_0 and C_∞) was probably due to diurnal oscillations (7).

Figure 2 shows experimental clonazepam levels as a function of time in Monkeys 4, 3, 6, and 7 during Study II. The time course of this study can also be divided into three phases. As noted earlier, animals were pretreated with an infusion of carbamazepine (for 3–4 days) prior to initiation of clonazepam administration (at $t = 0$). Carbamazepine administration was continued during clonazepam infusion for 33.5, 72.0, 31.0, and 31.0 hr in Monkeys 4, 3, 6, and 7, respectively.

In Phase II-A, plasma clonazepam levels increased exponentially and reached an induced steady state, C_∞, within 24 hr in all monkeys. Upon removal of carbamazepine and after variable lag times (θ' = 81.0, 34.0, 47.0, and 37.0 hr in Monkeys 4, 3, 6, and 7, respectively), clonazepam levels increased to a higher postinduction steady state, C_0' (Phase II-B). Clonazepam infusion was terminated (at 215.5, 193.0, 144.5, and 168.0 hr in Monkeys 4, 3, 6, and 7, respectively), and experimental plasma levels declined to less than 5% of C_0' within 48 hr (Phase II-C).

Urinary Excretion of D-Glucaric Acid—Control urinary excretion of D-glucaric acid in four monkeys (Monkeys 3, 4, 6, and 7) ranged from 9.3 to 30.8 mg/day with a mean (±*SD*) of 20.1 ± 7.5 mg/day (Table I). Values obtained during intravenous infusion of clonazepam *alone* were not significantly different, ranging from 11.7 to 34.1 mg/day with a mean (±*SD*) of 21.5 ± 9.5 mg/day. However, urinary excretion of D-glucaric acid increased two- to threefold when carbamazepine was added to the infusion ($p < 0.005$). The values obtained during this induction period ranged from 23.3 to 70.7 mg/day with a mean (±*SD*) of 47.7 ± 19.1 mg/day.

Plasma Levels of Carbamazepine—Since most plasma samples were needed for the determination of clonazepam levels, it was not possible to document the entire time course of carbamazepine autoinduction (8–16) during the present interaction study. However, occasional plasma samples assayed for carbamazepine concentrations showed that the preinduction steady-state levels (1.22–2.84 μg/ml) were significantly higher ($p > 0.0005$) than the induced steady-state levels (0.79–1.97 μg/ml).

Pharmacokinetic Modeling—In the analysis of experimental data, the induction theory recently developed by Levy *et al.* (1) was applied. This theory describes body levels of an induced agent during induction and postinduction in terms of changes in total body clearance. The time course of these changes is governed by an induction rate constant, K_I or K_I'. In single-enzyme induction, K_I and K_I' represent the degradation rate constants of the induced enzyme in the presence and absence of the inducing agent, respectively. In multienzyme induction, K_I or K_I' becomes a hybrid of the degradation rate constant of all induced enzymes. Upon induction, total body clearance, $Q(T)$, of the induced agent increases exponentially from Q to Q' according to (1)[1]:

$$Q(T) = Q' - (Q' - Q) \exp(-K_I t) \qquad \text{(Eq. 1)}$$

Conversely, in the postinduction period, $Q(T)$ decreases from Q' to Q as given by (1):

$$Q(T) = Q - (Q - Q') \exp(-K_I' t) \qquad \text{(Eq. 2)}$$

The distinction between K_I and K_I' allows for the possibility that the inducer may cause induction not only by increasing the enzyme synthesis rate but also by decreasing the degradation rate constant from K_I' to K_I.

[1] A derivation of this equation will be published and is available upon request.

Changes in plasma clonazepam levels during Studies I and II can be described in terms of the pharmacokinetic model shown in Scheme I:

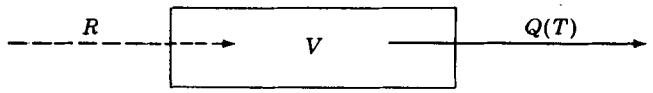

Scheme I—Model I

where V is a single-compartment volume of distribution for clonazepam, R is the zero-order infusion rate, and $Q(T)$ is as defined in Eq. 1 (Study I) or Eq. 2 (Study II).

During Phase I-A, clonazepam levels at any time, t, simply follow the one-compartment infusion equation with constant clearance, Q:

$$C = \frac{R}{Q}(1 - e^{-Qt/V}) \qquad \text{(Eq. 3)}$$

During Phase I-B, the decrease in clonazepam levels is given by the following previously reported (1) equation[2]:

$$C = \frac{R}{Q^{t-\tau_1}} + \frac{R}{Q}\exp\left\{\frac{-Q'}{V}(t-\tau_1) + \frac{Q'-Q}{VK_1}[1-\exp(-K_I(t-\tau_1))]\right\}\exp\left(\frac{-Q\tau_1}{V}\right) \qquad \text{(Eq. 4)}$$

where τ_1 is the time from commencement of Study I to the decrease in clonazepam "steady-state" levels (inclusive of lag time θ), $Q^{t-\tau_1}$ is given in Eq. 1 where t is replaced by $t - \tau_1$, and other terms are as previously defined. If induction commences after plasma clonazepam levels have achieved C_0, the last term in Eq. 4 approaches zero and Eq. 4 can be approximated by its first term:

$$C = \frac{R}{Q^{t-\tau_1}} \qquad \tau_1 \geq 5V \ln 2/Q \qquad \text{(Eq. 5)}$$

During Phase I-C, the decrease in clonazepam levels from C_∞ is simply described by:

$$C = \frac{R}{Q'}e^{-Q'(t-\tau_2)/V} \qquad \text{(Eq. 6)}$$

where τ_2 is the time at which clonazepam infusion is stopped.

Conversely, plasma clonazepam levels during Phases II-A, II-B, and II-C can be described by the following three equations, respectively:

$$C = \frac{R}{Q'}(1 - e^{-Q't/V}) \qquad \text{(Eq. 7)}$$

$$C = \frac{R}{Q^{t-\tau_3}} + \frac{R}{Q'}\exp\left\{\frac{-Q}{V}(t-\tau_3) + \frac{Q-Q'}{VK_I'}[1-\exp(-K_I'(t-\tau_3))]\right\}\exp\left(\frac{-Q'\tau_3}{V}\right) \qquad \text{(Eq. 8)}$$

$$C = \frac{R}{Q}e^{-Q(t-\tau_4)/V} \qquad \text{(Eq. 9)}$$

where τ_3 is the time from the start of clonazepam infusion to the increase in clonazepam steady-state levels inclusive of the lag time θ', $Q^{t-\tau_3}$ is as given in Eq. 2 where t is replaced by $t - \tau_3$, and τ_4 is the time at which clonazepam infusion is stopped. A simple and accurate approximation of Eq. 8 (analogous to Eq. 5) is:

$$C = \frac{R}{Q^{t-\tau_3}} \qquad \tau_3 \geq 5V \ln 2/Q' \qquad \text{(Eq. 10)}$$

A computer subroutine was developed for use in conjunction with the BMDX85 nonlinear least-squares regression analysis program to determine the four pharmacokinetic parameters (Q, Q', K_I or K_I', and V) of Model I. This subroutine yields a single set of best values for the four parameters by fitting experimental data points from the three phases of each study simultaneously to appropriate model equations. This subroutine was tested using generated data without and with 5–10% random error.

Curve fitting of generated data without error yielded the input values. For data with 5 and 10% random error, the program yielded values for Q, Q', and V that deviated from input values by 6–8%. However, the values obtained for K_I (or K_I') deviated more, by as much as 20–25% in a few cases. This behavior of K_I (or K_I') can be attributed in part to the fact that its value is determined only from data in Phase I-B (or Phase II-B) of the interaction study. Also, the value of K_I (or K_I') can be easily affected by slight changes in the value of Q' (or Q).

Analysis of Experimental Data—The approach used in the present study was to fit experimental data from Studies I and II to Eqs. 3, 4, and 6 and Eqs. 7–9, respectively (Method A) as well as to Eqs. 3, 5, and 6 and Eqs. 7, 10, and 9, respectively (Method B). The continuous lines in Figs. 1 and 2 represent the results of curve fitting with Method A. A measure of the fit of experimental data to model equations can be given by the correlation coefficient. The mean correlation coefficient ($\pm SD$) for Method A was 0.938 ± 0.030 (Table II); for Method B, it was 0.900 ± 0.116. Thus, the induction theory proposed by Levy *et al.* (1) adequately describes the present interaction between clonazepam and carbamazepine.

A comparison of Methods A and B in terms of the four parameters (Q, Q', K_I or K_I', and V) shows negligible differences, indicating that Eqs. 5 and 10 are accurate approximations of Eqs. 4 and 8 under the present experimental conditions. A summary of pharmacokinetic parameters determined with Method A, along with values for θ and θ' (obtained directly from clonazepam level *versus* time plots), are given in Table II. For ease of interpretation, control and induced elimination half-lives of clonazepam are listed. Similarly, apparent turnover half-lives of induced enzyme(s) [ratio between ln 2 and K_I (or K_I')] are shown in place of induction rate constants.

In Study I, the mean value ($\pm SD$) for the control (preinduction) half-life of clonazepam was 9.0 ± 2.4 hr; for the volume of distribution, it was 8.2 ± 2.1 liters/kg. These parameters were comparable but slightly larger than those reported previously (7). The mean induced half-life of clonazepam ($\pm SD$) was shorter (4.9 ± 1.1 hr) than the control value. Statistical comparison showed that the difference was significant ($p \leq 0.005$). Apparent turnover half-lives of the induced enzyme(s) were 6.9, 27.2, 66.4, and 11.4 hr for Monkeys 1, 3, 6, and 7, respectively. The extent of induction, f_i, as measured by the fractional decrease in C_0 was calculated using:

$$f_i = \frac{C_0 - C_\infty}{C_0} \qquad \text{(Eq. 11)}$$

Values for f_i ranged from 0.32 to 0.54.

Table II—Pharmacokinetic Parameters Determined from Clonazepam–Carbamazepine Interaction Studies in Monkeys

Monkey	Volume of Distribution, liters/kg	Control Half-Life of Clonazepam, hr	Induced Half-Life of Clonazepam, hr	Apparent Turnover Half-Life of Induced Enzyme(s), hr	Extent of Induction	Lag Time, hr	Correlation Coefficient from Curve Fitting
			Study I				
1[a]	8.5 (12)[b]	7.0[c] (14)	4.7 (11)	6.9 (53)	0.23	14.0[d]	0.924
3	10.8 (13)	10.5[c] (17)	4.6 (13)	27.2 (29)	0.54	17.5[d]	0.993
6	7.7 (12)	6.2[c] (13)	4.0 (11)	66.4 (36)	0.37	60.5[d]	0.936
7	5.8 (12)	12.2[c] (17)	6.6 (12)	11.4 (38)	0.45	19.0[d]	0.953
			Study II				
4	9.6 (14)	8.4[e] (15)	5.0 (12)	18.2 (25)	0.31	81.0[f]	0.964
3	11.2 (9)	10.2[e] (11)	7.7 (8)	5.7 (54)	0.25	34.0[f]	0.923
6	8.1 (10)	5.2[e] (10)	3.7 (8)	19.3 (33)	0.28	47.0[f]	0.909
7	7.9 (10)	7.3[e] (12)	4.8 (9)	2.7 (35)	0.34	37.0[f]	0.905

[a] Replaced by Monkey 4 in Study II. [b] Numbers in parentheses are the standard deviations in percent. [c] Preinduction half-life. [d] Value for θ. [e] Postinduction half-life. [f] Value for θ'.

For Study II, the mean value ($\pm SD$) for the control (postinduction) half-life of clonazepam was 7.8 ± 2.1 hr; for the volume of distribution, it was 9.2 ± 1.5 liters/kg. These two parameters were in agreement with those found in Study I and comparable to those reported earlier (7). The mean induced half-life of clonazepam was 5.2 ± 1.7 hr. This parameter was significantly shorter ($p \leq 0.005$) than the control value. The extent of induction, f_i, was of the same order of magnitude as that of Study I. Values for f_i ranged from 0.25 to 0.41.

Apparent turnover half-lives of induced enzymes in Study II ranged from only 2.7 to 19.3 hr as compared to 6.9–66.4 hr in Study I. There was also a difference in lag time values between Studies I and II. Values for θ' (Study II) were longer than corresponding θ values (Study I). These differences (in apparent turnover half-lives of induced enzymes and lag times) will be discussed further.

Mechanistic Considerations—The observed reduction in plasma clonazepam levels and half-lives was attributed to enzyme induction with carbamazepine as the inducing agent. The two- to threefold increase in urinary D-glucaric acid excretion supports this contention. Several major anticonvulsants (phenytoin and phenobarbital) that are potent enzyme inducers increase urinary excretion of D-glucaric acid in humans (17, 18). Although the exact mechanism whereby both the drug-metabolizing system and the glucuronic acid pathway are stimulated remains unknown, urinary excretion of D-glucaric acid is commonly used as an index of induction (19, 20).

The long lag times (both θ and θ') are also consistent with an interaction due to enzyme induction. Recent investigations of the molecular mechanism of enzyme induction have accumulated sufficient information to allow a detailed description of events leading to enzyme induction (21–23). The facts that the effect of carbamazepine (reduction in plasma clonazepam levels) was not elicited until 14.0–60.5 hr after its addition to the infusion and that its effect did not dissipate until 34.0–81.0 hr after withdrawal fit within the time frame of the sequence of molecular events leading to increased protein synthesis.

The observed decreases in plasma clonazepam levels during carbamazepine induction are also compatible with a number of reports indicating that carbamazepine is able to induce the metabolism of a variety of drugs (2, 3, 24, 25). In rats, repeated oral doses of carbamazepine enhanced cytochrome P-450 and NADPH cytochrome C-reductase activity (26).

Two alternative explanations for the present interaction between clonazepam and carbamazepine were considered: (*a*) displacement of clonazepam from its plasma protein binding sites by carbamazepine with a resulting modification of the pharmacokinetics of the former, and (*b*) enzyme activation by carbamazepine with enhanced activity in the metabolism of clonazepam. A recent study (27) on the pharmacokinetics of tolbutamide displacement by sulfadimethoxine from protein binding sites in sheep showed that the lag time for sulfadimethoxine to cause a change in plasma tolbutamide concentration was essentially nil. The long lag times (θ and θ') observed in the present study exclude an interaction due to competitive binding. Furthermore, *in vitro* equilibrium dialysis experiments showed that carbamazepine did not displace clonazepam from its protein binding sites (28). To date, the literature contains little or no information on the pharmacokinetic implications of enzyme activation. However, it is unlikely that carbamazepine continues enzyme activation 27.0–74.0 hr[2] after elimination (Study II).

In the present study, values of K_I obtained in Study I were three to five times less than values of K'_I determined in Study II for the three monkeys (Monkeys 3, 6, and 7) in which both interaction studies were conducted. Therefore, enzyme turnover during Study I was apparently three to five times slower than during Study II. Such behavior was most unusual and warranted further explanation.

In studies of mechanism of induction (29) designed to distinguish between increased enzyme synthesis and decreased enzyme breakdown[3], the half-life of the initial shift from the basal to induced enzyme level is the degradation half-life of the enzyme in the presence of the inducer. The half-life of return to the basal enzyme level after the inducer is withdrawn is the degradation half-life of the enzyme in the absence of the inducer.

Such an approach was used to analyze the mechanism whereby continuous administration of phenobarbital to rats increased the amount of liver microsomal barbiturate-oxidizing enzyme (30). The half-life of the upward shift in enzyme level was 2.2 days, and that of the downward shift was 2.6 days. Thus, enzyme turnover was essentially unaffected by phenobarbital, and the main cause of the increase in enzyme level was an increase in its synthesis rate. If similar reasoning is applied to the data of Studies I and II, it is suggested that carbamazepine and/or its metabolites acted by causing an increased enzyme synthesis rate as well as by stabilizing some enzymes[4].

Therapeutic Implications—Clonazepam is a new anticonvulsant and, therefore, is often added to therapeutic regimens of other anticonvulsants. Thus, a thorough understanding of potential interactions between clonazepam and these agents is essential. Knop *et al.* (31) reported that the clearances of clonazepam in four epileptic patients also receiving other antiepileptic drugs (phenytoin, phenobarbital, carbamazepine, *etc.*) were considerably larger than the values in healthy subjects. Another report documented the interaction between clonazepam and phenytoin (32). More recently, Bekersky *et al.* (33) found that phenobarbital increased the total plasma clearance of clonazepam by 102% in dogs.

The results of the present studies prompted an investigation of the interaction between carbamazepine and clonazepam in normal volunteers. It was found that steady-state clonazepam levels decreased by 19–37% in seven subjects following addition of a daily dose of carbamazepine (28).

REFERENCES

(1) R. H. Levy, A. A. Lai, and M. S. Dumain, *J. Pharm. Sci.*, **68**, 398 (1979).

(2) P. H. Corbisier and R. H. Levy, *APhA/Academy of Pharmaceutical Sciences Abstracts*, **7** (1), 163 (1977).

(3) *Ibid.*, **7** (2), 134 (1977).

(4) J. A. F. de Silva and I. Bekersky, *J. Chromatogr.*, **99**, 447 (1974).

(5) W. F. Trager, R. H. Levy, I. H. Patel, and J. M. Neal, *Anal. Lett.*, **B11** (2), 119 (1978).

(6) M. Ishidate, M. Matsui, and M. Okada, *Anal. Chem.*, **11**, 176 (1965).

(7) A. A. Lai and R. H. Levy, *J. Pharm. Sci.*, **67**, 295 (1978).

(8) P. L. Morselli, P. Biandrate, A. Frigerio, and S. Garattini, *Eur. J. Clin. Invest.*, **2**, 297 (1972).

(9) M. Eichelbaum, K. Ikbom, L. Bertilsson, V. A. Ringberger, and A. Rane, *Eur. J. Clin. Pharmacol.*, **8**, 337 (1975).

(10) P. L. Morselli, in "Advances in Neurology," vol. 11, J. K. Penry and D. D. Daly, Eds., Raven, New York, N.Y., 1975, pp. 279–294.

(11) P. L. Morselli, M. Gerna, D. DeMaio, G. Zanda, F. Viani, and S. Garattini, in "Clinical Pharmacology of Anti-Epileptic Drugs," H. Schneider, D. Janz, C. Gardner-Thorpe, H. Meinardi, and A. L. Sherwin, Eds., Springer-Verlag, New York, N.Y., 1975, pp. 166–180.

(12) W. H. Pitlick and R. H. Levy, *J. Pharm. Sci.*, **65**, 462 (1976).

(13) A. P. Gerardin, F. V. Abadie, J. A. Campestrini, and W. Theobald, *J. Pharmacokinet. Biopharm.*, **4**, 521 (1976).

(14) P. L. Morselli, L. Bussi, and M. Gerna, in "Epileptic Seizures—Behavior—Pain," W. Birkmayer, Ed., Hans Huber, Bern, Switzerland, 1976, pp. 141–150.

(15) J. W. Faigle, S. Brechbuhler, K. F. Feldmann, and W. J. Richter, in *ibid.*, pp. 159–165.

(16) W. H. Pitlick and R. H. Levy, *J. Pharm. Sci.*, **66**, 647 (1977).

(17) A. G. Hildebrandt, I. Roots, M. Speck, K. Saalfrank, and H. Kewitz, *Eur. J. Clin. Pharmacol.*, **8**, 327 (1975).

(18) A. Richens and G. W. Houghton, in "Clinical Pharmacology of Anti-Epileptic Drugs," H. Schneider, D. Janz, C. Gardner-Thorpe, H. Meinardi, and A. L. Sherwin, Eds., Springer-Verlag, New York, N.Y., 1975, pp. 89–110.

(19) E. M. Aarts, *Biochem. Pharmacol.*, **14**, 359 (1965).

(20) J. Hunter, J. D. Maxwell, M. Carrella, and D. A. Stewart, *Lancet*, **1**, 572 (1971).

(21) T. D. Gelehrter, *N. Engl. J. Med.*, **294**, 522 (1976).

(22) *Ibid.*, **294**, 589 (1976).

(23) *Ibid.*, **294**, 646 (1976).

(24) J. Hansen, K. Siersbaek-Nielsen, and L. Skovsted, *Clin. Pharmacol. Ther.*, **12**, 539 (1971).

(25) O. Penttila, P. J. Neuvonen, K. Aho, and R. Lehtovaara, *Br. Med. J.*, **2**, 470 (1974).

(26) J. W. Faigle, S. Brechbuhler, K. F. Feldmann, and W. J. Richter, in "Epileptic Seizures—Behavior—Pain," W. Birkmayer, Ed., Hans Huber, Bern, Switzerland, 1976, pp. 127–140.

(27) J. Thiessen and M. Rowland, *J. Pharm. Sci.*, **66**, 1063 (1977).

(28) A. A. Lai, R. H. Levy, and R. E. Cutler, *Clin. Pharmacol. Ther.*,

[2] Obtained by subtracting five to seven elimination half-lives of carbamazepine (16) from θ'.

[3] Assuming that enzyme activation has been ruled out.

[4] Inhibition of degradation of hepatic enzymes.

23, 117 (1978).
(29) H. L. Segal and Y. S. Kim, *Proc. Natl. Acad. Sci. USA*, **50**, 912 (1963).
(30) I. M. Arias and A. deLeon, *Mol. Pharmacol.*, **3**, 216 (1967).
(31) H. J. Knop, E. Van der Kleijn, and L. C. Edmunds, in "Clinical Pharmacology of Anti-Epileptic Drugs," H. Schneider, D. Janz, C. Gardner-Thorpe, H. Meinardi, and A. L. Sherwin, Eds., Springer-Verlag, New York, N.Y., 1975, pp. 247–260.
(32) O. Sjo, E. F. Hvidberg, J. Naestoft, and M. Lund, *Eur. J. Clin. Pharmacol.*, **8**, 249 (1975).
(33) I. Bekersky, A. C. Maggio, V. Mattaliano, Jr., H. G. Boxenbaum, D. E. Maynard, P. D. Cohn, and S. A. Kaplan, *J. Pharmacokinet. Biopharm.*, **5**, 507 (1977).

ACKNOWLEDGMENTS

Presented at the Basic Pharmaceutics Section, APhA Academy of Pharmaceutical Sciences, New York meeting, May 1977.

Supported in part by NIH Research Contract N01-NS-1-2282 and Research Grant NS-4053 awarded by the National Institute of Neurological and Communicative Disorders and Stroke, U.S. Public Health Service.

The authors thank Dr. William Trager for helpful discussion and James Cook, Douglas Ng, Raina Hanson, John Hokanson, Kenneth Lee, Jennifer Andrews, and John Neal for technical assistance. They also thank Hoffmann-La Roche for the generous supply of clonazepam and nitrazepam.

Analysis of Fludrocortisone Acetate and Its Solid Dosage Forms by High-Performance Liquid Chromatography

THERESE M. AST and HAMED M. ABDOU ˣ

Received May 25, 1978, from *E. R. Squibb & Sons, Inc., New Brunswick, NJ 08902.* Accepted for publication September 8, 1978.

Abstract □ A newly developed reversed-phase high-performance liquid chromatographic assay and test method for determining content uniformity are described for fludrocortisone acetate. The method is stability indicating and separates most known degradation products and impurities. In addition, the method is simple, sensitive, accurate, and relatively free of interferences. The coefficient of variation for multiple weight assays is between 0.3 and 1.8%.

Keyphrases □ Fludrocortisone acetate—and solid dosage forms, high-performance liquid chromatographic analysis □ High-performance liquid chromatography—analysis, fludrocortisone acetate and solid dosage forms □ Steroids—fludrocortisone acetate and solid dosage forms, high-performance liquid chromatographic analysis

Fludrocortisone acetate (9-fluoro-11β,17,21-trihydroxypregn-4-ene-3,20-dione 21-acetate) (I) is a powerful synthetic adrenocortical steroid. As an unsaturated 3-keto steroid, it may be analyzed by the isoniazid method (1) or with 4-aminoantipyridine hydrochloride reagent (2). The latter is used in the USP procedure for content uniformity. As a 17α-ketol steroid, fludrocortisone acetate is analyzed by the blue tetrazolium method (1), the official USP assay. A colorimetric assay in fermentation broths (3) and an automated colorimetric method for assaying single tablets of fludrocortisone acetate (4) also were reported.

Since none of these methods is selective for fludrocortisone acetate, it was the purpose of this study to develop a specific, stability-indicating, high-performance liquid chromatographic (HPLC) assay that would circumvent any excipient interferences. The HPLC method described here is capable of separating fludrocortisone acetate from its known degradation products and possible impurities. Norethindrone was used as an internal standard. The HPLC data were in excellent agreement with results obtained by the isoniazid assay. The method is simple, selective, and highly reliable.

EXPERIMENTAL

Reagents and Materials—Fludrocortisone acetate and norethindrone USP reference standards and acetonitrile[1] (UV grade and distilled in glass) were used. The mobile phase was 42 ± 2% acetonitrile in water.

The internal standard solution was prepared by dissolving norethindrone in acetonitrile to concentrations of 65 μg/ml for assay and 10 μg/ml for content uniformity analysis.

Standard Solutions and Calibration Curves—Fludrocortisone acetate solutions were prepared to contain 50, 70, 100, and 120 μg of fludrocortisone acetate/ml for assay and 15, 20 and 25 μg/ml for content uniformity analysis.

Sample Preparation—*Assay*—A portion of ground tablets equivalent to 2.5 mg of fludrocortisone acetate was transferred to a 50-ml low actinic centrifuge tube, and 5 ml of distilled water was added by pipet. After the suspension was mixed[2] for 1 min, 20 ml of internal standard solution was added, and the resulting mixture was transferred to a mechanical shaker for 40 min. The tablet extract was then centrifuged, and the clear liquid was injected into the HPLC system. The ratio of the peak heights of fludrocortisone acetate to the internal standard was determined, and the quantity of fludrocortisone acetate in the sample was calculated using the assay calibration curve.

Content Uniformity Analysis—One tablet (containing 0.1 mg of fludrocortisone acetate) was transferred to a 10-ml low actinic centrifuge tube, and 1 ml of distilled water was added. A vortex mixer[2] was used to effect complete disintegration, and then 4 ml of the internal standard solution was added. The mixture was then treated as in the assay.

Apparatus and Operating Conditions—The liquid chromatograph consisted of a reciprocating pump[3], a 20-ml loop injector[4], and a UV detector[3] equipped with a 254-nm filter. The analytical column was 30-cm × 4-mm i.d. stainless steel, packed with porous siliceous microbeads to which a stationary phase of octadecyltrichlorosilane was chemically bonded[3]. A flow rate of 1.8–2.0 ml/min, maintained at about 800–1000 psi, was used at ambient temperature. The output of the detector was displayed on a recorder having a full-scale range of 10 mv[5].

System Suitability Test—The standard preparation, 100 μg/ml, was chromatographed five or six times, and the peak response was measured as the ratio of resulting peak heights of fludrocortisone acetate to the internal standard. The relative standard deviation was less than 2%. The resolution factor between fludrocortisone acetate and the internal standard was more than three. For a particular column, resolution may be increased by decreasing the amount of acetonitrile in the mobile phase.

Placebo Analysis—A placebo of the sample commercial tablets used in this study was prepared and extracted in parallel with the sample. The placebo chromatogram was checked for interfering peaks near fludrocortisone acetate or norethindrone.

Recovery Studies—The efficiency of the recovery was checked by

[1] Burdick & Jackson Laboratories, Muskegon, Mich.

[2] Vortex-Genie mixer, Scientific Industries, Springfield, Mass.
[3] μBondapak-C_{18}, Waters Associates, Milford, Mass.
[4] Chromatronix HPSV-20, Spectra-Physics, Santa Clara, Calif.
[5] Model 410, Pharmacia Fine Chemicals, Piscataway, N.J.

0022-3549/79/0400-0421$01.00/0
© 1979, American Pharmaceutical Association

23, 117 (1978).
(29) H. L. Segal and Y. S. Kim, *Proc. Natl. Acad. Sci. USA*, **50**, 912 (1963).
(30) I. M. Arias and A. deLeon, *Mol. Pharmacol.*, **3**, 216 (1967).
(31) H. J. Knop, E. Van der Kleijn, and L. C. Edmunds, in "Clinical Pharmacology of Anti-Epileptic Drugs," H. Schneider, D. Janz, C. Gardner-Thorpe, H. Meinardi, and A. L. Sherwin, Eds., Springer-Verlag, New York, N.Y., 1975, pp. 247–260.
(32) O. Sjo, E. F. Hvidberg, J. Naestoft, and M. Lund, *Eur. J. Clin. Pharmacol.*, **8**, 249 (1975).
(33) I. Bekersky, A. C. Maggio, V. Mattaliano, Jr., H. G. Boxenbaum, D. E. Maynard, P. D. Cohn, and S. A. Kaplan, *J. Pharmacokinet. Biopharm.*, **5**, 507 (1977).

ACKNOWLEDGMENTS

Presented at the Basic Pharmaceutics Section, APhA Academy of Pharmaceutical Sciences, New York meeting, May 1977.

Supported in part by NIH Research Contract N01-NS-1-2282 and Research Grant NS-4053 awarded by the National Institute of Neurological and Communicative Disorders and Stroke, U.S. Public Health Service.

The authors thank Dr. William Trager for helpful discussion and James Cook, Douglas Ng, Raina Hanson, John Hokanson, Kenneth Lee, Jennifer Andrews, and John Neal for technical assistance. They also thank Hoffmann-La Roche for the generous supply of clonazepam and nitrazepam.

Analysis of Fludrocortisone Acetate and Its Solid Dosage Forms by High-Performance Liquid Chromatography

THERESE M. AST and HAMED M. ABDOU ˣ

Received May 25, 1978, from *E. R. Squibb & Sons, Inc., New Brunswick, NJ 08902.* Accepted for publication September 8, 1978.

Abstract □ A newly developed reversed-phase high-performance liquid chromatographic assay and test method for determining content uniformity are described for fludrocortisone acetate. The method is stability indicating and separates most known degradation products and impurities. In addition, the method is simple, sensitive, accurate, and relatively free of interferences. The coefficient of variation for multiple weight assays is between 0.3 and 1.8%.

Keyphrases □ Fludrocortisone acetate—and solid dosage forms, high-performance liquid chromatographic analysis □ High-performance liquid chromatography—analysis, fludrocortisone acetate and solid dosage forms □ Steroids—fludrocortisone acetate and solid dosage forms, high-performance liquid chromatographic analysis

Fludrocortisone acetate (9-fluoro-11β,17,21-trihydroxypregn-4-ene-3,20-dione 21-acetate) (I) is a powerful synthetic adrenocortical steroid. As an unsaturated 3-keto steroid, it may be analyzed by the isoniazid method (1) or with 4-aminoantipyridine hydrochloride reagent (2). The latter is used in the USP procedure for content uniformity. As a 17α-ketol steroid, fludrocortisone acetate is analyzed by the blue tetrazolium method (1), the official USP assay. A colorimetric assay in fermentation broths (3) and an automated colorimetric method for assaying single tablets of fludrocortisone acetate (4) also were reported.

Since none of these methods is selective for fludrocortisone acetate, it was the purpose of this study to develop a specific, stability-indicating, high-performance liquid chromatographic (HPLC) assay that would circumvent any excipient interferences. The HPLC method described here is capable of separating fludrocortisone acetate from its known degradation products and possible impurities. Norethindrone was used as an internal standard. The HPLC data were in excellent agreement with results obtained by the isoniazid assay. The method is simple, selective, and highly reliable.

EXPERIMENTAL

Reagents and Materials—Fludrocortisone acetate and norethindrone USP reference standards and acetonitrile[1] (UV grade and distilled in glass) were used. The mobile phase was 42 ± 2% acetonitrile in water.

The internal standard solution was prepared by dissolving norethindrone in acetonitrile to concentrations of 65 μg/ml for assay and 10 μg/ml for content uniformity analysis.

Standard Solutions and Calibration Curves—Fludrocortisone acetate solutions were prepared to contain 50, 70, 100, and 120 μg of fludrocortisone acetate/ml for assay and 15, 20 and 25 μg/ml for content uniformity analysis.

Sample Preparation—*Assay*—A portion of ground tablets equivalent to 2.5 mg of fludrocortisone acetate was transferred to a 50-ml low actinic centrifuge tube, and 5 ml of distilled water was added by pipet. After the suspension was mixed[2] for 1 min, 20 ml of internal standard solution was added, and the resulting mixture was transferred to a mechanical shaker for 40 min. The tablet extract was then centrifuged, and the clear liquid was injected into the HPLC system. The ratio of the peak heights of fludrocortisone acetate to the internal standard was determined, and the quantity of fludrocortisone acetate in the sample was calculated using the assay calibration curve.

Content Uniformity Analysis—One tablet (containing 0.1 mg of fludrocortisone acetate) was transferred to a 10-ml low actinic centrifuge tube, and 1 ml of distilled water was added. A vortex mixer[2] was used to effect complete disintegration, and then 4 ml of the internal standard solution was added. The mixture was then treated as in the assay.

Apparatus and Operating Conditions—The liquid chromatograph consisted of a reciprocating pump[3], a 20-ml loop injector[4], and a UV detector[3] equipped with a 254-nm filter. The analytical column was 30-cm × 4-mm i.d. stainless steel, packed with porous siliceous microbeads to which a stationary phase of octadecyltrichlorosilane was chemically bonded[3]. A flow rate of 1.8–2.0 ml/min, maintained at about 800–1000 psi, was used at ambient temperature. The output of the detector was displayed on a recorder having a full-scale range of 10 mv[5].

System Suitability Test—The standard preparation, 100 μg/ml, was chromatographed five or six times, and the peak response was measured as the ratio of resulting peak heights of fludrocortisone acetate to the internal standard. The relative standard deviation was less than 2%. The resolution factor between fludrocortisone acetate and the internal standard was more than three. For a particular column, resolution may be increased by decreasing the amount of acetonitrile in the mobile phase.

Placebo Analysis—A placebo of the sample commercial tablets used in this study was prepared and extracted in parallel with the sample. The placebo chromatogram was checked for interfering peaks near fludrocortisone acetate or norethindrone.

Recovery Studies—The efficiency of the recovery was checked by

[1] Burdick & Jackson Laboratories, Muskegon, Mich.

[2] Vortex-Genie mixer, Scientific Industries, Springfield, Mass.
[3] μBondapak-C_{18}, Waters Associates, Milford, Mass.
[4] Chromatronix HPSV-20, Spectra-Physics, Santa Clara, Calif.
[5] Model 410, Pharmacia Fine Chemicals, Piscataway, N.J.

0022-3549/79/0400-0421$01.00/0
© 1979, American Pharmaceutical Association

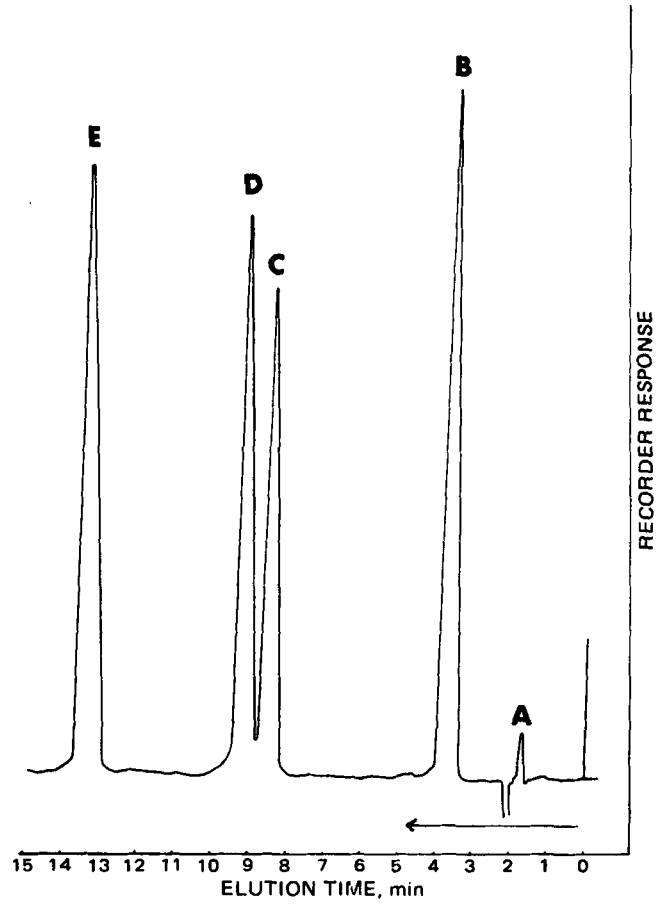

Figure 1—*HPLC separation of fludrocortisone acetate (I) and its impurities and degradation products. Key: A, solvent front; B, II and IV; C, III; D, I; and E, norethindrone acetate (internal standard).*

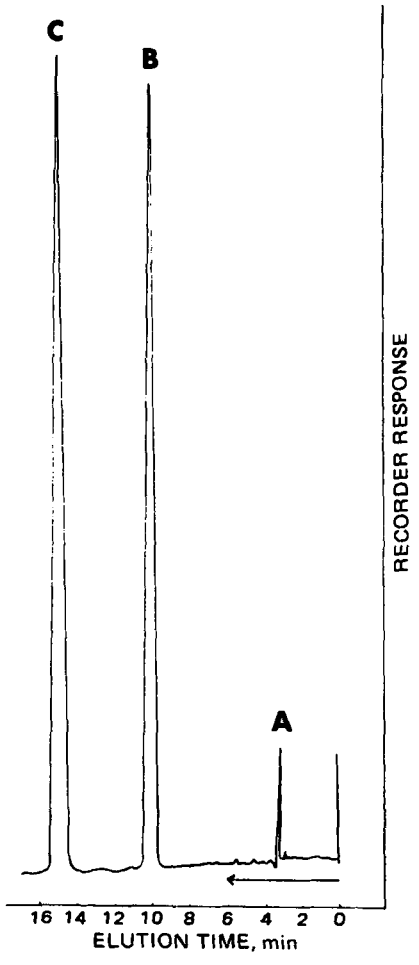

Figure 2—*HPLC assay of fludrocortisone acetate "tablet extract." Key: A, solvent front and tablet excipients; B, fludrocortisone acetate; and C, norethindrone acetate (internal standard).*

spiking both the placebo and tablets with known amounts of fludrocortisone acetate and norethindrone reference standards. The spiked samples were extracted and chromatographed in parallel with the sample.

Stress Test—To demonstrate the stability-indicating ability of the HPLC procedure, fludrocortisone acetate tablets were assayed by HPLC and then were intentionally degraded by elevated temperature for an extended period. The fludrocortisone acetate content was then determined by both HPLC and the blue tetrazolium procedures (compendial assay).

RESULTS AND DISCUSSION

Fludrocortisone acetate (I) is stable as a solid, especially when stored in closed brown bottles (5). However, II–IV may be present either as impurities or as degradation products. The presence of $\Delta^{1,4}$-diene system (III and IV) can be attributed to the fact that it is a possible precursor in the preparation of fludrocortisone acetate. The presence of the 21-hydroxyl analogs (I and II) are expected as hydrolytic products of the acetate esters, especially in hydrolytic solvents. Moreover, these hydrolytic degradation products can be formed on storage for long periods. The reliability of the HPLC method is best shown by its ability to resolve fludrocortisone acetate from all of II–IV (Fig. 1). Furthermore, no interfering peaks were noticed in the placebo chromatogram.

The linearity of both fludrocortisone acetate and norethindrone chromatographic responses was checked by a separate calibration curve for each compound. The correlation coefficient for a straight-line equation was higher than 0.999 (concentration range of 45–120 μg/ml) in both cases. A representative chromatogram for the fludrocortisone acetate commercial tablet is shown in Fig. 2. Recoveries of fludrocortisone acetate and norethindrone were 100.7 and 99.1%, respectively. There was no significant difference between recoveries from spiked placebo or spiked tablets.

The stability-indicating ability of the HPLC procedure was demonstrated by the results of the stress test. Fludrocortisone acetate tablets, which assayed at 95.2% of "label claim" by HPLC before being subjected to elevated temperatures, assayed at only 72.2% of label claim, and 10.1% of the 21-hydroxyl analog (II) was found. However, no $\Delta^{1,4}$-diene derivatives (III and IV) were detected. When the same degraded sample was analyzed by the blue tetrazolium procedure (compendial assay), the

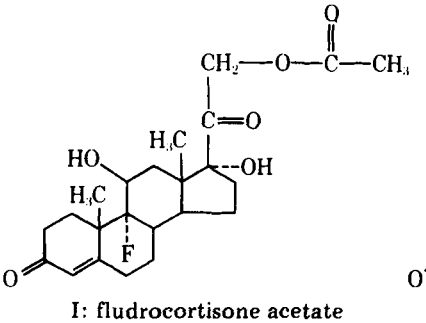

I: fludrocortisone acetate

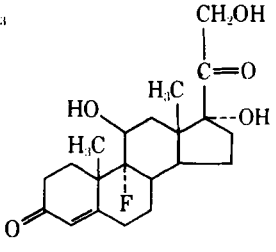

II: fludrocortisone

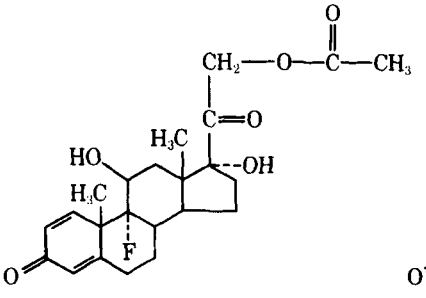

III: $\Delta^{1,4}$-diene system of fludrocortisone acetate

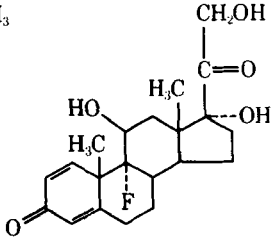

IV: $\Delta^{1,4}$-diene system of fludrocortisone

Table I—HPLC Assay (Milligrams per Tablet) of 0.1-mg Fludrocortisone Acetate Tablets

Lot	First Weight: Average of Two Injections	First Weight: *RSD*, %	Second Weight: Average of Two Injections	Second Weight: *RSD*, %	Total Average: Total Average of Two Weights	Total Average: Overall *RSD*, %	Isoniazid Assay, mg/tablet
1	0.0948	0.1	0.0930	0.6	0.0939	1.8	0.094
2	0.0970	0.2	0.0976	1.0	0.0973	0.3	0.095
3	0.0952	0.4	0.0953	0.7	0.0953	0.4	0.0947
4	0.0908	0.6	0.0924	0.6	0.0916	0.9	0.094

Table II—HPLC Content Uniformity Analysis (Milligrams per Tablet) of 0.1-mg Fludrocortisone Acetate Tablets

	Lot 1	Lot 2
Tablet 1	0.0966	0.0975
Tablet 2	0.0933	0.1012
Tablet 3	0.0907	0.0946
Tablet 4	0.0875	0.0989
Tablet 5	0.0976	0.0951
Tablet 6	0.0952	0.0991
Tablet 7	0.0932	0.0994
Tablet 8	0.0927	0.0963
Tablet 9	0.0941	0.1009
Tablet 10	0.0928	0.0994
Average	0.0933	0.0982
RSD, %	0.3	2.3
HPLC assay	0.0939	0.0970
Isoniazid assay[a]	0.0940	0.0947
4-AAP content uniformity[b]	0.0966	0.0967

[a] Average of three sets of runs, 10 tablets each. [b] 4-Aminoantipyrine method, average of 10 tablets.

fludrocortisone acetate content was 88.3% of label value. This high result compared to that obtained by the HPLC method (72.2%) may be attributed to the fact that the blue tetrazolium method does not differentiate between the 21-hydroxyl analog and fludrocortisone acetate.

To identify other possible degradation products in the degraded sample, which may explain the other 6% loss unaccounted for by the HPLC procedure, a foreign peak that eluted just before III in the degraded sample chromatogram was collected from 40 runs. Mass spectral and NMR analyses showed that the compound was not a steroid but probably a fatty acid formed by hydrolysis of excipients. The UV spectrum of that foreign peak showed a maximum at 259 nm. Other foreign peaks eluted very close to the solvent front, and their separation and identification were not attempted.

Results of the HPLC analysis of four lots of a commercial tablet preparation are shown in Table I. Fludrocortisone acetate content varied between 91.6 and 97.3% of label claim. The average relative standard deviation for multiple weights of the same lot was 0.85% (range of 0.3–1.8%) while that for duplicate injections of the same weight was 0.5% (range of 0.1–1.0%). Table I also shows a comparison between the HPLC results and the isoniazid assay values for the same lots. No significant differences were found.

For content uniformity analysis, 10 individual tablets of two lots were analyzed by the HPLC method (Table II). The relative standard deviation between individual tablets of the same lot was 2–3% compared to 2–5% with the compendial content uniformity method. This result was probably due to the elimination of excipient interferences, especially from impurities present in lactose, which caused up to 7% bias on the high side with the official procedure.

In conclusion, the reversed-phase HPLC assay developed for fludrocortisone acetate is suitable for batching, content uniformity, and stability assays. The method is more selective than the blue tetrazolium and isoniazid assays because it separates most of the expected impurities and degradation products. The method is simple, sensitive, accurate, and virtually free from interferences.

REFERENCES

(1) T. Higuchi and E. Brochmann-Hanssen, "Pharmaceutical Analysis," Interscience, New York, N.Y., 1961, pp. 72, 80.

(2) E. P. Shulz, M. A. Diaz, G. Lopez, L. M. Guerrero, H. Barrera, A. L. Pereda, and A. Aguilera, *Anal. Chem.*, **36**, 1625 (1964).

(3) E. Ivashkiv, *ibid.*, **33**, 1051 (1961).

(4) F. M. Russo-Alesi, *Ann. N.Y. Acad. Sci.*, **153**, 511 (1968).

(5) "Analytical Profiles of Drug Substances," vol. 3, K. Florey, Ed., Academic, New York, N.Y., 1974, p. 293.

ACKNOWLEDGMENTS

The authors are grateful to Dr. F. J. Cioffi, E. R. Squibb & Sons, for advice about the analytical system and to Dr. C. M. Cimarusti, Squibb Institute for Medical Research, for counsel involving impurities and degradation products of fludrocortisone acetate.

Dielectric Constants of Solid–Liquid and Liquid–Liquid Systems as a Function of Composition

G. CAVÉ, F. PUISIEUX ˣ, and J. T. CARSTENSEN *

Received March 13, 1978, from the *Faculté de Pharmacie, Laboratoire de Pharmacie Galénique, Université de Paris-Sud, Rue J. B. Clément, 92290 Châtenay-Malabry, France.* Accepted for publication September 11, 1978. *School of Pharmacy, University of Wisconsin, Madison, WI 53706 (on sabbatical at the University of Paris-Sud, 1977–1978).

Abstract □ The dielectric constant of a solid substance in the dissolved state may be found by using a solvent with a dielectric constant that remains invariable when the solid substance is dissolved. The slope values obtained from dielectric constant *versus* concentration plots of the solid substance in two solvents with different dielectric constants are extrapolated or interpolated. The dielectric constant of a solid substance in the dissolved state also can be found directly from the dielectric constants of solutions of the solid in one solvent at two concentrations. The dielectric constants are converted to polarizations, and the two values allow calculations of the polarizations of the solvent and solute separately. From the polarization of the solute, one can calculate its dielectric constant (in dissolved state). Such a procedure is correct only if the dielectric constant is concentration independent.

Keyphrases □ Dielectric constants—solid-liquid and liquid-liquid systems, as a function of composition, polarizations, monoethyl ether, diethylene glycol, propylene glycol, methylparaben □ Solid-liquid systems—dielectric constants determined as a function of composition □ Liquid-liquid systems—dielectric constants determined as a function of composition

Dielectric constants (ϵ) are used in pharmaceutics for a variety of correlations, particularly concerning solubility (1–5) and hydrophobic–lyophobic balance (6, 7). Since binary or larger component number systems are frequently involved in basic investigations in pharmaceutics, the behavior of ϵ as a function of composition is important.

In a binary system, ϵ is a function of the content (x) of one of the components (A or B). For two pure liquids, A and B, one can introduce the respective dielectric constants ϵ_A and ϵ_B and can estimate the dielectric constant, ϵ, of a mixture of the two *via* a weight-averaging formula:

$$\epsilon = x_A\epsilon_A + x_B\epsilon_B \qquad \text{(Eq. 1)}$$

Whether x should be a volume or a weight fraction has been discussed previously (7, 8) and will be addressed in a subsequent article.

If one component (A) is a solid, then Eq. 1 cannot be used directly unless one knows ϵ_A in a dissolved state (ϵ_A^l). Thus, there is a need for establishing ϵ_A^l for substances that are solid at room temperature (or other temperatures of investigation). This requirement is particularly important (9) if one evaluates macroscopic properties (*e.g.*, hydrophile–lipophile balance) for a series of compounds where one or more are solid and the remainder liquid at room temperature. In such a case, one would be forced to work at temperatures above the melting point of the highest melting substance in the series, and this can introduce other problems, both experimental and theoretical.

This article deals with two methods of obtaining ϵ^l for a substance that is solid at the temperature of investigation.

EXPERIMENTAL

Materials—Analytical grade materials were used as received. As shown in Table I, various dielectric constants were obtained by mixing the monoethyl ether of diethylene glycol[1] with either propylene glycol or water in various proportions. Other dielectric constants were obtained by use of other solvents (as a check for solvent nonspecificity)—*viz.*, polyethylene glycol 400[2], triethylene glycol[3], and mixed mono- and diglycerides of saturated C_{16-18} fatty acids[4]. Methylparaben USP[5] was used as the solute.

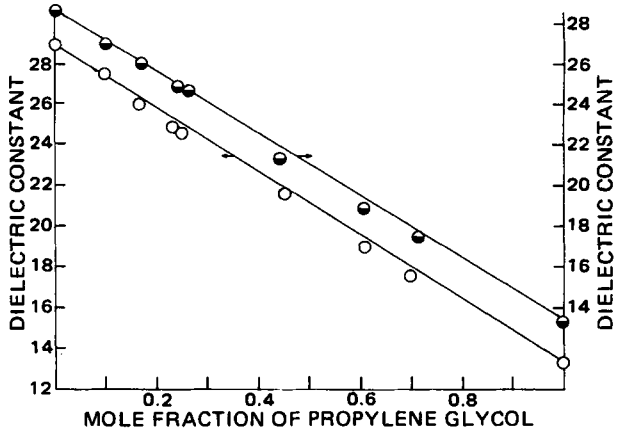

Figure 1—*Dielectric constant of monoethyl ether of diethylene glycol with various amounts of propylene glycol (Table I). These values are expressed as volume fractions (◒) and weight fractions (○).*

Determination of Dielectric Constant—The solutions were prepared without volume adjustment, equilibrated thermally in a thermostatic bath at 25°, and brought to volume with solvent. After their densities were determined (to allow concentration conversions), the solutions were placed in the cell of a Q-meter[6] to measure dielectric constants. The cell was thermostated at 25 ± 0.1°, and the dielectric constant was determined at 1340 kHz. The apparatus was equipped with a "powder cell," which, in a similar fashion, allows measurement of the dielectric constant of a solid.

Determinations were made at nine different concentrations in each

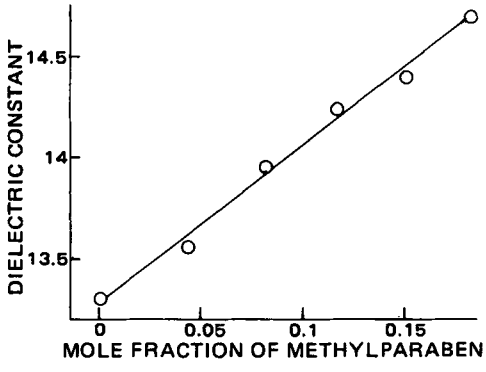

Figure 2—*Effect of mole fraction of methylparaben on the dielectric constant in solutions in monoethyl ether of diethylene glycol.*

[1] Gattefosse, SFPA, St. Priest, France.
[2] Hoechst Chemical Co., Hoechst, West Germany.
[3] Rhone-Poulenc Chemical Co., Paris, France.
[4] Labrasol Solvent, Gattefoss, SPFA, St. Priest, France.
[5] Merck & Co., Rahway, N.J.
[6] Q-metre Ferisol T 803 A, Geffroy et Cie, Paul-Vaillant-Couturier, 78 Trappes, France.

0022-3549/79/0400-0424$01.00/0
© 1979, American Pharmaceutical Association

Table I—Solvents Used in Mixtures for Dielectric Constant Measurements

Solvent	Solvent A	Solvent B	Volume Fraction	Mole Fraction	Weight Fraction	Dielectric Constant, 25°
1	Monoethyl ether of diethylene glycol	—	1.0	1.0	1.0	13.3
2	Monoethyl ether of diethylene glycol	Propylene glycol	0.715	0.928	0.709	17.6
3	Monoethyl ether of diethylene glycol	Propylene glycol	0.617	0.899	0.606	18.9
4	Monoethyl ether of diethylene glycol	Propylene glycol	0.454	0.321	0.443	21.3
5	Monoethyl ether of diethylene glycol	Propylene glycol	0.240	0.144	0.231	24.9
6	Monoethyl ether of diethylene glycol	Propylene glycol	0.170	0.100	0.163	26.1
7	Monoethyl ether of diethylene glycol	Propylene glycol	0.100	0.050	0.096	27.5
8	—	Propylene glycol	0.000	0.000	0.000	28.5
9	Monoethyl ether of diethylene glycol	Water	0.909	0.571	0.908	20.8
10	Monoethyl ether of diethylene glycol	Water	0.869	0.471	0.868	23.9
11	Monoethyl ether of diethylene glycol	Water	0.823	0.386	0.821	26.6
12	Monoethyl ether of diethylene glycol	Water	0.792	0.337	0.791	29.6
13	Polyethylene glycol 400	—	1.00	1.00	1.00	14.0
14	Triethylene glycol	—	1.00	1.00	1.00	23.5
15	Mono- and diglycerides of saturated C_{16-18} fatty acids	—	1.00	1.00	1.00	9.9

of the 15 solvents listed in Table I. Measurement of the dielectric constant of solid methylparaben also was carried out by measuring the dielectric constant of a suspension in a mixture of chloroform and the monoethyl ether of diethylene glycol[1] having a density matching that of methylparaben. This was done to minimize settling during the dielectric constant determination.

RESULTS AND DISCUSSION

A typical set of dielectric constants plotted *versus* composition of a liquid–liquid binary mixture is shown in Fig. 1. Plotting is carried out as a function of both weight and volume fractions. The line shown is not a least-squares fit line but connects the terminal experimental points, This line shows that all of the experimental points lie on one side of the chord, indicating that there is some curvature in either case. If one includes $x = 0$, this curvature becomes more evident.

When one component is a solid, linearity is retained, as in the case studied here (Fig. 2). These plots cannot be made over the entire concentration range because of the limiting solubility. Good linearity of such plots was observed with all solvents in Table I, the correlation coefficients being above 0.98 for all plots with six to nine data points. Therefore, one can write for the dielectric constant of the solution (ϵ):

$$\epsilon = \gamma N_A + \zeta \qquad \text{(Eq. 2)}$$

where N_A is mole fraction of methylparaben and where the slope, γ, and the intercept, ζ, are functions of the solvent used, *i.e.*, are functions of the solvent dielectric constant, ϵ_B.

With a solvent for which $\gamma = 0$, addition of methylparaben to the solvent will not change the dielectric constant, and the dielectric constant of the solvent and solute will be identical. If such a procedure is adopted, the dielectric constant of methylparaben in the dissolved state, ϵ_A^I, can be found as the value of ϵ_B where γ becomes zero. The least-squares fit values of γ (slopes) from the solvents in Table I are shown in Fig. 3 as a function of the solvent dielectric constant. This plot is linear, and the least squares fit of the line is given by $\epsilon_B = -20.75\gamma + 21.0$. The ordinate intercept occurs at 21.0 ± 0.6. At this dielectric constant, the solution will have a dielectric constant that is concentration independent.

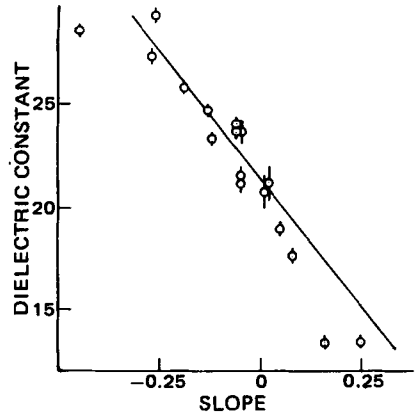

Figure 3—*Slopes, γ, of data plotted according to Eq. 2 as the abscissa with the dielectric constant of the pure solvent, ϵ_B, as the ordinate.*

For accuracy, it should be noted that the rationale for weighted averaging (Eq. 1) is based on polarizations, P (10), rather than on dielectric constants. Polarizations of molecules in the condensed states are usually determined in the following fashion. The substance (with a molecular weight of M_A) is dissolved in a solvent of molecular weight M_B. The mole fractions of the solute and solvent are N_A and N_B, respectively. The dielectric constant, ϵ, of this binary mixture is then measured. This procedure allows calculation of the composite polarization, P:

$$P = \frac{\epsilon - 1}{\epsilon + 2} \frac{N_A M_A + N_B M_B}{\rho} \qquad \text{(Eq. 3)}$$

where ρ is the mixture density. The composite polarization is assumed to be related to the individual polarizations, P_A and P_B (8), by the relation:

$$P = N_A P_A + N_B P_B = (P_A - P_B)N_A + P_B \qquad \text{(Eq. 4)}$$

since:

$$N_A + N_B = 1 \qquad \text{(Eq. 5)}$$

If ϵ is not composition dependent, then Eqs. 3 and 4 can be combined to:

$$P = \frac{Q}{\rho}(N_A M_A + N_B M_B) = N_A P_A + N_B P_B \qquad \text{(Eq. 6)}$$

where $Q = (\epsilon - 1)/(\epsilon + 2)$. Equation 6 has the unique solution:

$$P_A = QM_A/\rho \qquad \text{(Eq. 7}a\text{)}$$

and:

$$P_B = QM_B/\rho \qquad \text{(Eq. 7}b\text{)}$$

allowing direct evaluation of P_A from ϵ. If ϵ is concentration dependent, then the direct transition from Eq. 5 to Eq. 7*a* is not necessarily valid. For this reason, the dielectric constant of methylparaben in various solvent mixtures was determined. When conversions to polarization values are carried out according to Eq. 3, plots such as Fig. 4 result and Eq. 4 is

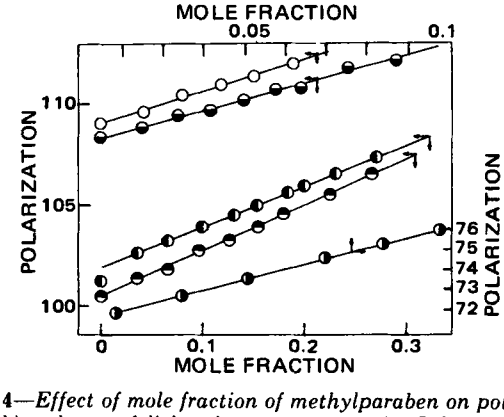

Figure 4—*Effect of mole fraction of methylparaben on polarization observed in solvents of dielectric constants: 13.4 (○, Solvent 1), 20.8 (◒, Solvent 9), 23.9 (◐, Solvent 10), 27.5 (◓, Solvent 7), and 29.6 (◑, Solvent 12). The solvent numbers correspond to designations in Table I.*

Table II—Slopes and Intercepts of Graphs Plotted According to Eq. 4 for Methylparaben

Dielectric Constant, 25°[a]	R[b]	n[c]	Intercept	Slope	$P(1)$ at N_A = 1
17.6	0.985	8	98.8	27.7	121.4
18.9	1.000	8	94.8	26.8	121.5
21.3	1.000	8	88.4	32.6	121.0
23.5	0.998	9	106.1	16.8	122.8
21.3	1.000	7	78.6	42.7	121.3
28.5	1.000	5	51.7	69.7	121.4
23.5	0.986	8	117.6	3.33	120.9
13.3	0.994	7	109.2	15.3	124.5
23.9	1.000	9	101.7	21.0	122.7
20.8	0.998	9	108.4	13.8	122.2
29.6	0.999	9	100.5	22.7	123.2
24.9	0.999	6	73.6	48.3	122.0
26.1	1.000	5	71.4	49.8	121.2
27.5	1.000	5	69.4	51.5	120.7

[a] Solvents are listed in Table I. [b] Correlation coefficient. [c] Number of points from which the least-squares parameters were determined.

obeyed. The least-squares statistics for these lines are shown in Table II.

According to Eq. 4, if extrapolation is carried out to $N_A = 1$, a value is obtained for the polarization of the solute, *i.e.*, $P_A = P(1)$, where the latter is the extrapolated value. These values are listed in Table II; even though the extrapolation is long, there is good agreement. By inserting the average of these values (122.7), the density of methylparaben (1.09 g/cm^3), and its molecular weight (152) into Eq. 7*a*, one obtains:

$$Q = \frac{\epsilon - 1}{\epsilon + 2} = P_A\rho/M_A = 1.09(122.7/152) = 0.88 \qquad \text{(Eq. 8)}$$

This equation gives $\epsilon = 21.8$, which coincides with the previously quoted value $\gamma = 21.0 \pm 0.6$. This value may rationally be denoted ϵ_A^l, *i.e.*, the dielectric constant of the methylparaben in the dissolved state. This result differs significantly from values obtained by using a solids cell in the Q-meter [ϵ_A (solid) = 2.70] and suspension techniques ($\epsilon = 5.8$).

REFERENCES

(1) A. N. Paruta, *J. Pharm. Sci.*, **56**, 1565 (1967).

(2) A. N. Paruta and S. A. Irani, *ibid.*, **54**, 1334 (1965).

(3) *Ibid.*, **55**, 1055 (1966).

(4) A. N. Paruta and B. B. Sheth, *J. Pharm. Sci.*, **55**, 1208 (1966).

(5) N. Lordi, B. Sciarrone, T. Ambroisio, and A. N. Paruta, *ibid.*, **53**, 463 (1964).

(6) W. G. Gorman and G. D. Hall, *ibid.*, **52**, 442 (1963).

(7) J. T. Carstensen, "Theory of Pharmaceutical Systems," vol. I, Academic, New York, N.Y., 1972, p. 134.

(8) W. Moore, *J. Am. Pharm. Assoc., Sci. Ed.*, **47**, 855 (1958).

(9) F. Mouazen, F. Puisieux, M. Seiller, and J. T. Carstensen, *Int. J. Pharm.*, **1**, 275 (1978).

(10) S. H. Maron and C. F. Prutton, "Principles of Physical Chemistry," 4th ed., Macmillan, New York, N.Y., 1965, p. 698.

Acid Dissociation and Metal Complex Formation Constants of Penicillamine, Cysteine, and Antiarthritic Gold Complexes at Simulated Biological Conditions

T. D. ZUCCONI, G. E. JANAUER ˣ, S. DONAHE, and C. LEWKOWICZ

Received April 13, 1978, from the *Department of Chemistry, State University of New York at Binghamton, Binghamton, NY 13901.* Accepted for publication September 11, 1978.

Abstract □ Ionization constants for acid functions of D-penicillamine, L-cysteine, thiomalic acid, and thioglucose were measured by pH titration at 37° and 0.15 *M* ionic strength. Chelate formation constants for these ligands with calcium(II), iron(III), and gold(I) were then determined under the same conditions chosen to approximate the *in vivo* situation. Only iron(III) formed both 1:1 and 1:2 chelates with D-penicillamine, L-cysteine, and thiomalate; calcium formed weak and gold strong 1:1 complexes with all ligands studied. Because of precipitate formation, the stability constants for the systems thioglucose-iron(III), D-penicillamine-gold(I), and L-cysteine-gold(I) had to be determined indirectly with thiomalic acid as the competing ligand. The *in vivo* fate of antiarthritic gold(I) compounds remained uncertain, but gold(I) chelates probably persist as such for extended periods.

Keyphrases □ Penicillamine—acid dissociation and metal complex formation constants with calcium(II), iron(III), and gold(I), simulated biological conditions □ Cysteine—acid dissociation and metal complex formation constants with calcium(II), iron(III), and gold(I), simulated biological conditions □ Thiomalic acid—acid dissociation and metal complex formation constants with calcium(II), iron(III), and gold(I), simulated biological conditions □ Thioglucose—acid dissociation and metal complex formation constants with calcium(II), iron(III), and gold(I), simulated biological conditions □ Gold complexes—stability constants of antiarthritic gold(I) complexes and penicillamine and cysteine, simulated biological conditions □ Iron(III) and calcium(II) complexes—with penicillamine, cysteine, thiomalic acid, and thioglucose, simulated biological conditions

D-Penicillamine (I), 3-mercapto-D-valine, is the accepted therapeutic agent for the treatment of Wilson's disease (1, 2) and cystinuria (3, 4). Compound I is also a well-known antidote in lead and mercury poisoning (5–7) and has been investigated as a protective agent against radiation (8). It has been approved for rheumatoid arthritis therapy (9) in several countries but not in the United States because of some potentially severe side reactions. However, I success rates in rheumatoid arthritis treatment are at least as high as those with the established drugs aurothioglucose (II) and aurothiomalate (III), and dangerous toxic side effects can largely be avoided by careful monitoring of the patient's blood (10).

The mode of action of I in cystinuria is well understood—the mixed disulfide (IV) formed with cysteine (V) is more soluble than cystine (VI) (11). The therapeutic value in Wilson's disease as well as in the treatment of heavy metal poisoning results from its strong *in vivo* metal

0022-3549/79/0400-0426$01.00/0

© 1979, American Pharmaceutical Association

Table II—Slopes and Intercepts of Graphs Plotted According to Eq. 4 for Methylparaben

Dielectric Constant, 25°[a]	R[b]	n[c]	Intercept	Slope	$P(1)$ at N_A = 1
17.6	0.985	8	98.8	27.7	121.4
18.9	1.000	8	94.8	26.8	121.5
21.3	1.000	8	88.4	32.6	121.0
23.5	0.998	9	106.1	16.8	122.8
21.3	1.000	7	78.6	42.7	121.3
28.5	1.000	5	51.7	69.7	121.4
23.5	0.986	8	117.6	3.33	120.9
13.3	0.994	7	109.2	15.3	124.5
23.9	1.000	9	101.7	21.0	122.7
20.8	0.998	9	108.4	13.8	122.2
29.6	0.999	9	100.5	22.7	123.2
24.9	0.999	6	73.6	48.3	122.0
26.1	1.000	5	71.4	49.8	121.2
27.5	1.000	5	69.4	51.5	120.7

[a] Solvents are listed in Table I. [b] Correlation coefficient. [c] Number of points from which the least-squares parameters were determined.

obeyed. The least-squares statistics for these lines are shown in Table II.

According to Eq. 4, if extrapolation is carried out to $N_A = 1$, a value is obtained for the polarization of the solute, *i.e.*, $P_A = P(1)$, where the latter is the extrapolated value. These values are listed in Table II; even though the extrapolation is long, there is good agreement. By inserting the average of these values (122.7), the density of methylparaben (1.09 g/cm^3), and its molecular weight (152) into Eq. 7*a*, one obtains:

$$Q = \frac{\epsilon - 1}{\epsilon + 2} = P_A\rho/M_A = 1.09(122.7/152) = 0.88 \qquad \text{(Eq. 8)}$$

This equation gives $\epsilon = 21.8$, which coincides with the previously quoted value $\gamma = 21.0 \pm 0.6$. This value may rationally be denoted ϵ_A^l, *i.e.*, the dielectric constant of the methylparaben in the dissolved state. This result differs significantly from values obtained by using a solids cell in the Q-meter [ϵ_A (solid) = 2.70] and suspension techniques ($\epsilon = 5.8$).

REFERENCES

(1) A. N. Paruta, *J. Pharm. Sci.*, **56**, 1565 (1967).

(2) A. N. Paruta and S. A. Irani, *ibid.*, **54**, 1334 (1965).

(3) *Ibid.*, **55**, 1055 (1966).

(4) A. N. Paruta and B. B. Sheth, *J. Pharm. Sci.*, **55**, 1208 (1966).

(5) N. Lordi, B. Sciarrone, T. Ambroisio, and A. N. Paruta, *ibid.*, **53**, 463 (1964).

(6) W. G. Gorman and G. D. Hall, *ibid.*, **52**, 442 (1963).

(7) J. T. Carstensen, "Theory of Pharmaceutical Systems," vol. I, Academic, New York, N.Y., 1972, p. 134.

(8) W. Moore, *J. Am. Pharm. Assoc., Sci. Ed.*, **47**, 855 (1958).

(9) F. Mouazen, F. Puisieux, M. Seiller, and J. T. Carstensen, *Int. J. Pharm.*, **1**, 275 (1978).

(10) S. H. Maron and C. F. Prutton, "Principles of Physical Chemistry," 4th ed., Macmillan, New York, N.Y., 1965, p. 698.

Acid Dissociation and Metal Complex Formation Constants of Penicillamine, Cysteine, and Antiarthritic Gold Complexes at Simulated Biological Conditions

T. D. ZUCCONI, G. E. JANAUER ˣ, S. DONAHE, and C. LEWKOWICZ

Received April 13, 1978, from the *Department of Chemistry, State University of New York at Binghamton, Binghamton, NY 13901.* Accepted for publication September 11, 1978.

Abstract □ Ionization constants for acid functions of D-penicillamine, L-cysteine, thiomalic acid, and thioglucose were measured by pH titration at 37° and 0.15 *M* ionic strength. Chelate formation constants for these ligands with calcium(II), iron(III), and gold(I) were then determined under the same conditions chosen to approximate the *in vivo* situation. Only iron(III) formed both 1:1 and 1:2 chelates with D-penicillamine, L-cysteine, and thiomalate; calcium formed weak and gold strong 1:1 complexes with all ligands studied. Because of precipitate formation, the stability constants for the systems thioglucose-iron(III), D-penicillamine-gold(I), and L-cysteine-gold(I) had to be determined indirectly with thiomalic acid as the competing ligand. The *in vivo* fate of antiarthritic gold(I) compounds remained uncertain, but gold(I) chelates probably persist as such for extended periods.

Keyphrases □ Penicillamine—acid dissociation and metal complex formation constants with calcium(II), iron(III), and gold(I), simulated biological conditions □ Cysteine—acid dissociation and metal complex formation constants with calcium(II), iron(III), and gold(I), simulated biological conditions □ Thiomalic acid—acid dissociation and metal complex formation constants with calcium(II), iron(III), and gold(I), simulated biological conditions □ Thioglucose—acid dissociation and metal complex formation constants with calcium(II), iron(III), and gold(I), simulated biological conditions □ Gold complexes—stability constants of antiarthritic gold(I) complexes and penicillamine and cysteine, simulated biological conditions □ Iron(III) and calcium(II) complexes—with penicillamine, cysteine, thiomalic acid, and thioglucose, simulated biological conditions

D-Penicillamine (I), 3-mercapto-D-valine, is the accepted therapeutic agent for the treatment of Wilson's disease (1, 2) and cystinuria (3, 4). Compound I is also a well-known antidote in lead and mercury poisoning (5–7) and has been investigated as a protective agent against radiation (8). It has been approved for rheumatoid arthritis therapy (9) in several countries but not in the United States because of some potentially severe side reactions. However, I success rates in rheumatoid arthritis treatment are at least as high as those with the established drugs aurothioglucose (II) and aurothiomalate (III), and dangerous toxic side effects can largely be avoided by careful monitoring of the patient's blood (10).

The mode of action of I in cystinuria is well understood—the mixed disulfide (IV) formed with cysteine (V) is more soluble than cystine (VI) (11). The therapeutic value in Wilson's disease as well as in the treatment of heavy metal poisoning results from its strong *in vivo* metal

0022-3549/79/0400-0426$01.00/0

© 1979, American Pharmaceutical Association

chelating properties (1, 6, 7). The mechanism of action of I in rheumatic disease is not yet understood, although theories have been advanced (12). A striking similarity between side effects in rheumatoid arthritis patients caused by gold treatment (with II or III) and I therapy has been observed (13).

In vivo metal chelation by I and similar sulfur-containing amino acids has been studied (14–21), and stability constants for many biologically important metal ions were determined at standard conditions and varying ionic strengths. However, the formation constants of gold(I) and iron(III) complexes with I and V were never measured. Furthermore, the stability constants of II and III, the gold salts most widely used in rheumatoid arthritis treatment, were not known before this study. Acid dissociation constants (pKa) were measured previously for I, V, and thiomalic acid (VII), but not for thioglucose (VIII), at standard conditions (14, 18). So far, none has been determined at simulated biological conditions, *i.e.*, 37° and 0.15 ionic strength.

The technique chosen for this study was potentiometric titration of the acid protons (on the thiol, amino, and carboxylic functions), a method used previously with excellent success in a similar system (14, 16, 17). Titrations of the free ligands yield the pKa values, while titration after addition of the metal ions allows calculation of the metal complex formation constants from the respective curves. This method also permits the indirect determination of K_f values for inaccessible complexes by titration of the metal ion in the presence of two competing ligands (22, 23). A precipitation reaction with the systems thioglucose–iron(III) and cysteine–gold(I) and the unavailability of I and V complexes with gold(I) necessitated the use of this indirect technique.

EXPERIMENTAL

Materials—D-Penicillamine[1], L-cysteine[2], thioglucose[3], thiomalic acid[3], sodium aurothiomalate[4], and aurothioglucose[5] were standardized by potentiometric titration and characterized by optical rotatory dispersion, NMR, and IR spectra and melting points.

Metal-ion solutions were prepared from reagent grade nitrates[6] and were standardized according to routine procedures (24).

Potentiometric Measurements—The pH measurements were carried out in a 100-ml jacketed titration cell fitted with a magnetic stirrer and rubber stopper through which were inserted nitrogen and buret delivery tubes and glass and calomel electrodes. A research pH meter[7] was used; the system was calibrated at pH 4 and 9.22. The ionic strength was 0.15 in all cases (potassium nitrate). The temperature was held to ±0.05° of the desired value.

Acid Dissociation Constants—Each acid function was titrated with increments of 0.1000 *M* KOH, carbonate free[8].

Chelate Formation Constants—The stepwise chelate formation constants were determined according to the procedure of Doornbos and Faber (14). The calcium(II) or iron(III) solution was added to that of the ligand, except for the thioglucose–iron(III) system which was unstable. Solutions of aurothioglucose and sodium aurothiomalate were prepared from the salts and used as such. The thioglucose–iron(III), I–gold(I), and V–gold(I) formation constants were determined by ligand competition with the thiomalate complexes.

[1] Merck Sharp and Dohme, New Brunswick, N.J.
[2] Sigma Chemical, St. Louis, Mo.
[3] Eastman Organic, Rochester, N.Y.
[4] Aldrich, Milwaukee, Wis.
[5] Schering-Plough, Bloomfield, N.J.
[6] Baker Chemical Co., Phillipsburg, N.J.
[7] Radiometer M52-b.
[8] Calculations were performed with an APL program written by T. D. Zucconi based on the equations of Doornbos (19).

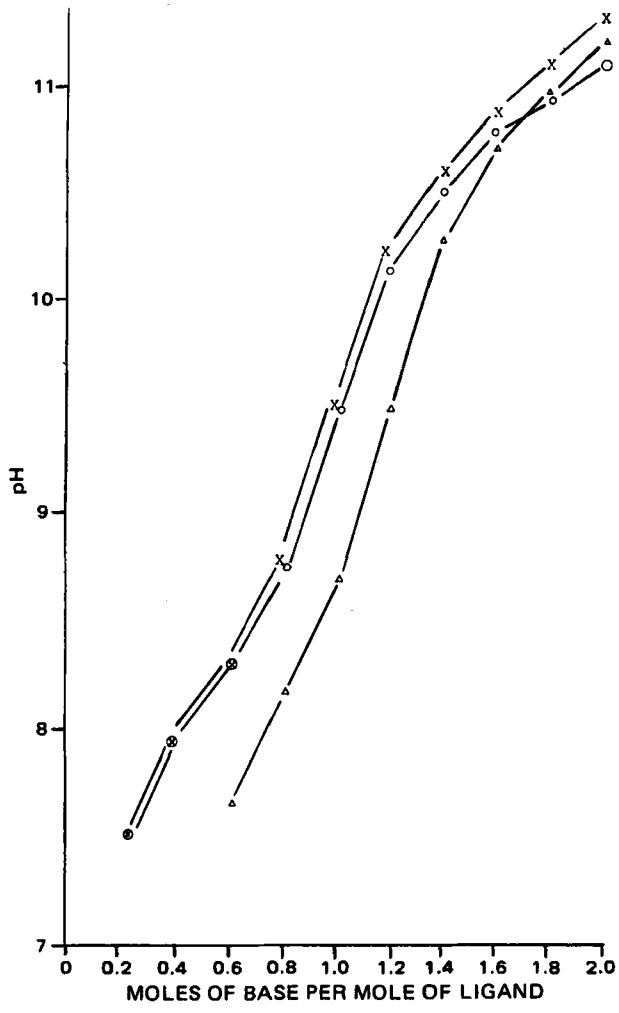

Figure 1—*Formation curves of penicillamine with calcium(II) (○), iron(III) (△), and free ligand (×) at 20°.*

Calculations—Calculations for K_1 and β_2 (*i.e.*, K_1K_2) were made with the FORTRAN IV program SCOGS[9] developed by Perrin and Sayce (25).

The validity of the experimental procedures and apparatus was tested as a whole by determination of the pKa of benzoic acid at 25°. The determined value of 4.25 ± 0.02 compared exactly with the literature value of 4.25.

RESULTS

Acid Dissociation Constants—Table I shows the values obtained for the ligands studied and available literature values. These values were used in calculating the stability constants because both sets of determinations were done under the same conditions. Some well-known pKa values were also redetermined to evaluate the precision and accuracy of the experimental technique and procedures.

Metal Complex Formation Constants—The values of the formation constants K_1 and β_2 are listed in Table II. These constants were calculated from the curves of the number of equivalents of base added *versus* pH (Figs. 1–8). The constants for some systems could not be determined directly. The VII–iron(III) system gave a precipitate under all conditions studied. It was evaluated as VII–VIII–iron(III) indirectly.

Compounds I, V, and VII gave precipitates at high values (≥9), but sufficient data points were available at lower pH values to permit calculation of the constants. No point where a precipitate existed was used in finding the reported values in Table II. The I- and V-gold(I) systems were determined by ligand competition with aurothiomalate because of the unavailability of the I- and V-gold(I) salts.

[9] Modified for use on the campus computer, IBM 370-158.

Table I—Acid Dissociation Constants

	$\overset{O}{\overset{\|}{C}}OH$	NH_3^+	SH
	pKa at 20°, μ = 0.15 (Literature Values)		
Penicillamine	(2)[a]	8.11 ± 0.02 (8.03)[a]	10.82 ± 0.04 (10.83)[a]
Cysteine	(1.88)[a]	8.38 ± 0.02 (8.32)[a]	10.60 ± 0.03 (10.48)[a]
Thiomalic acid	4.68 ± 0.03 (4.68)[b]	—	10.51 ± 0.03 (10.55)[b]
Thioglucose	—	—	11.67 ± 0.05
	pKa at 37°, μ = 0.15		
Penicillamine	—	7.83 ± 0.01	10.34 ± 0.04
Cysteine	—	8.04 ± 0.02	10.21 ± 0.06
Thiomalic acid	4.68 ± 0.04	—	10.24 ± 0.02
Thioglucose	—	—	11.51 ± 0.03
	pKa at 25°		
Benzoic acid	—	4.25 ± 0.02	(4.25)[c]

[a] According to D. A. Doornbos, *Pharm. Weekbl.*, **102**, 269 (1967). [b] According to J. Bjerrum, G. Schwarzenbach, and L. G. Sillén, "Stability Constants of Complex Compounds," Chemical Society, London, England, Special Publication 6, 1957. [c] Standard material used for evaluating equipment performance.

DISCUSSION

Values obtained for acid dissociation constants of I, V, and VII at 20° (Table I) were in excellent agreement with previously published values (14–18), allowing for differences in ionic strength. The precision of all pKa values determined ranged from ±0.01 to ±0.06 unit, well within acceptable limits. The pKa found for VIII was significantly higher than the pKa values of both I and V. It was of a magnitude typical for isolated thiol groups.

The increase in temperature from 20 to 37° decreased most pKa values. However, the magnitude of the change was quite different for different functions and different compounds. The carboxyl group of thiomalic acid was unaffected while the pKa values of the amino groups of all four ligands were reduced by 0.3 unit. The thiol group showed the greatest variation in its decrease of pKa: 0.16 unit for thioglucose, 0.27 for thiomalic acid, 0.29 for V, and 0.48 for I. Because the pKa values for the functional groups of interest were far enough apart, the groups could be treated as monoprotic acids.

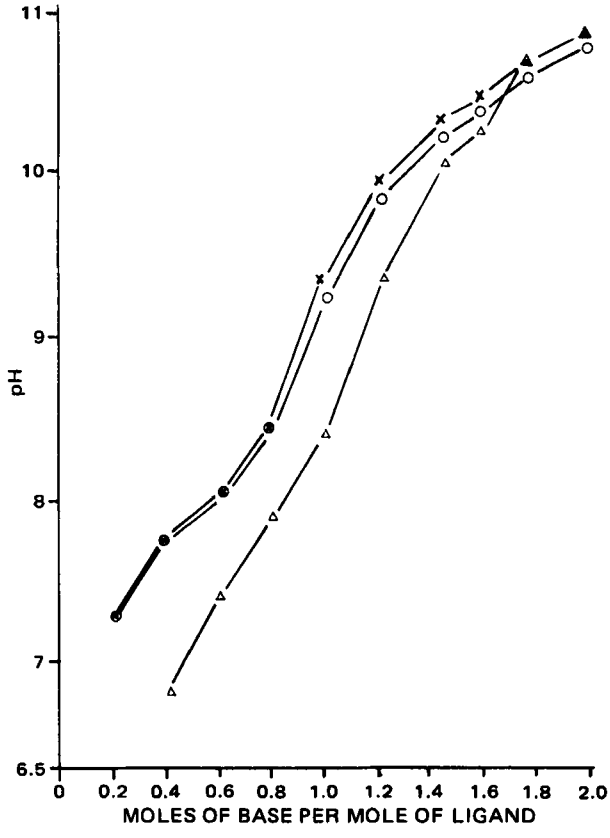

Figure 2—*Formation curves of penicillamine with calcium(II) (○), iron(III) (△), and free ligand (×) at 37°.*

The ionic strength, μ, was 0.15 (potassium nitrate) in all experiments to approximate *in vivo* conditions, although this value was not high enough to guarantee a completely constant ionic strength medium. Changes in K values with changing ionic strength can sometimes be appreciable for sulfur-containing amino acids (26). However, no attempt was made to correct for changes in ionic strength due to changes in species distribution as a function of pH or different concentrations of metal ions and ligands used. The maximal change was estimated as 0.024. Like most other authors (14–21), we neglected these small changes since the main emphasis of this work was not on their effect.

The formation constant for the I chelate with calcium was determined at 20° to permit comparison and correlation of results with those of previous investigators. The 3.15 value for log K_f compared well with the 2.7 obtained by Doornbos and Faber (19), considering the difference in ionic strength and the usual variance among laboratories. The stabilities of the iron(III) complexes were also determined at 20° with I, V, and VII (Table II) because no literature data were available although the iron(II) complexes had been studied earlier (14). The stability constants for both calcium(II) and iron(III) with all four ligands were determined at 37° (Table II).

The formation curves (Figs. 1 and 2) do not reveal anything unexpected for the interaction of I with calcium, which forms a rather weak complex. Actually, there was no deviation of the curves with calcium present until after addition of 1 mole equivalent of base. This finding may indicate that bonding occurs at the thiol group. The complex may be with the thiol group alone or with it and one of the other two functions. The carboxyl site seems less likely than the amino group, however, because of its greater distance from the thiol group.

Table II—Formation Constants Determined

System	log K_1	log β_2[a]
	20°, μ = 0.15	
I-Calcium(II)	3.15	—
VII-Calcium(II)	2.84	—
I-Iron(III)	—	—
I-Iron(III)	11.27	16.25
V-Iron(III)	10.85	14.49
VII-Iron(III)	9.18	11.98
I-Gold(I)	12.50[b]	—
V-Gold(I)	11.11[b]	—
VII-Gold(I)	10.27	—
VIII-Gold(I)	8.51	—
	37°, μ = 0.15	
I-Calcium(II)	3.01	—
V-Calcium(II)	2.98	—
VII-Calcium(II)	2.79	—
VIII-Calcium	1.58	—
I-Iron(III)	11.02	15.79
V-Iron(III)	10.63	14.01
VII-Iron(III)	9.01	12.52
VIII-Iron(III)	—	7.25[b]
I-Gold(I)	13.50[b]	—
V-Gold(I)	12.04[b]	—
VII-Gold(I)	11.23	—
VIII-Gold(I)	8.87	—

[a] $\beta_2 = K_1K_2$. [b] Determined by ligand competition.

Comparison of the iron(III) curves for I and V (Figs. 5–8) revealed a larger deviation from the free ligand curve for I–iron(III). Above pH 10.5, the curve of V–iron(III) actually was higher than that for the free ligand. Moreover, a precipitate began to form above pH 9 with V–iron(III). The fact that this phenomenon was not seen with I may be taken as evidence for a stronger complex. Values of pH in regions where a precipitate formed were not used to calculate K_f.

The rather large deviation at pH 6 (I, 37°) may not have been due to chelate formation but, perhaps, to a weaker association with the ionized acid group and was definitely in part due to the formation of some hydroxide compounds. The presence of an iron hydroxide–V complex was investigated by Tanaka (27), although Gruenwedel and Hsien-Chung (28) concluded that the onset of precipitation would not allow its investigation.

The VII–iron system and the I–iron system both turned purple as soon as iron was added, but the color disappeared upon mixing. When base was added to VII–iron, the color formed at pH 5, much lower than with I–iron. This result is expected because of the two comparatively strong acid groups in VII. The color at a pH well below the pKa of the thiol group indicated a chelation through the two carboxyl groups and no involvement of the thiol. The meter reading became unstable at about pH 7 and, again, a precipitate formed at pH 9. The thiol group could not play an important role in this complex unless its acidity were greatly enhanced by complex formation. The VIII–iron system was not stable at any ratio of ligand to metal. Therefore, the K_f values were determined by titrating VIII together with VII and iron(III), followed subsequently by resolution of the data by a computer. Thus, no formation curve is shown.

Comparison of the K_f values at 20 *versus* 37° revealed a decreasing tendency to complex at the higher temperature for calcium(II) and iron(III) while the opposite was true for gold(I). The difference was large enough to be considered real. The same value of gold hydroxide formation (29) was used for calculation of K_f at both temperatures. This procedure probably introduced only a small error between the K_f values obtained at different temperatures and may not account for the total observed difference.

A larger error at any given temperature could be caused by the use of a "wrong" value for the formation of gold hydroxide; literature values for equilibrium constants of metal-ion protolysis equilibria often range over many orders of magnitude as obtained by research workers using different techniques in different laboratories. Quantitative information concerning gold(I) hydrolysis is particularly scarce (30). Of course, certain hydrolysis equilibria might themselves be strongly affected by temperature changes. Earlier work on thiomalic acid chelation of silver(I) as a function of temperature (31) showed an increase of K_f with increasing temperature in that system.

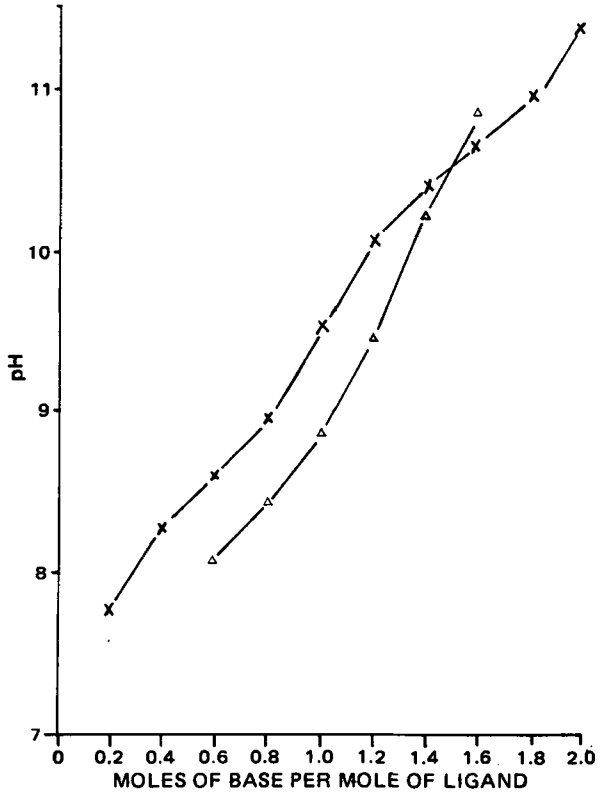

Figure 3—*Formation curves of cysteine with iron(III) (△) and free ligand (×) at 20°.*

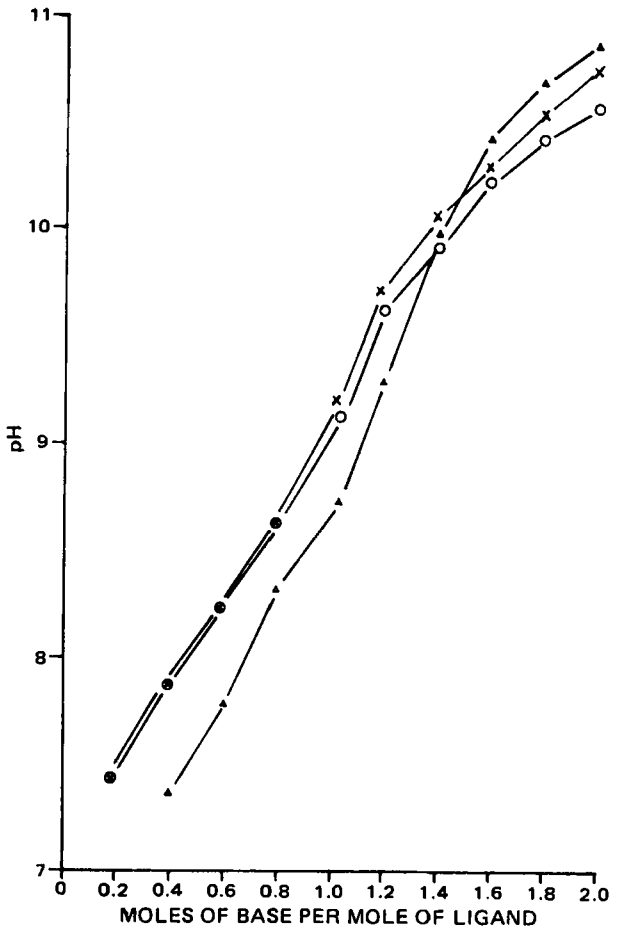

Figure 4—*Formation curves of cysteine with calcium(II) (○), iron(III) (△), and free ligand (×) at 37°.*

The ligand effect on the order of stabilities was the same with all three metal ions studied: I > V > VII > VIII. This order was also found in the literature for complexes of three of these ligands with other metals (14–17). No data were available for VIII.

In all cases, I formed a more stable complex than did V. Obviously, steric hindrance by the two added methyl groups in I is not a destabilizing factor but may have a small stabilizing effect on the chelate ring formed, thus giving rise to a higher K_f value of the I complex relative to the corresponding V complex. The lower stability of complexes with VII was probably due to the weaker interaction of the metal ions with the carboxyl group. Compound VIII was the weakest ligand. This finding is easily explained by the presence of only one strongly interacting group and the geometry that precludes the formation of a stable ring structure. The effects of structure and various substituents on the biochemical properties and the activity of I derivatives were studied previously (32–34), and chelate formation tendency was only one of a number of factors investigated.

Major differences between the V and I complexes existed that are not evident from the data shown. It was reported (17, 18, 26) that V tends to form precipitates with some metal ions, especially copper. This tendency was found with gold(I) as well. When V was added to II, a white precipitate formed immediately. The insoluble matter became slowly soluble after addition of some base [this same phenomenon was observed by Perrin and Sayce (15) for the V–zinc system]. The precipitate formed even when a large excess of V was added. Compound I also gave a precipitate with II in a 1:1 ratio but did not precipitate in a 4:1 ratio mixture.

No precipitate developed with V or I when added in excess to aurothiomalate.

Both ligands formed a dark precipitate with iron(III). The V system,

however, did precipitate at lower pH values (10 *versus* 11). At the same concentration, the solution of I–iron was a darker purple, indicating a stronger complex.

The V–gold(I) system was the most troublesome. Additions of the ligand to aurothioglucose resulted in immediate formation of a white precipitate. The precipitate very gradually became soluble with additions of base. However, this compound was not used to calculate K_f because of its unknown fate after the solid formation. The reaction may be analogous to the well-known copper–V oxidation–reduction reaction (26).

The iron(III)-V system was more stable, especially when some base was added to the solution before V. This system was used to calculate the K_f value of the V–gold complex.

The bonding in silver amino acid complexes was previously (17) postulated to occur through the amino nitrogen with very little, if any, contribution from the sulfur. These gold complexes were linear, as can be expected for all gold complexes studied. However, in the case of gold(I) complexes, the main bonding site is the thiol group. The K_f value for VIII–gold is about 75% of that with I or V. This value is quite high considering the absence of the amine group, since increased stability of the I and V complexes is due to the formation of a chelate through the nitrogen. The lower value obtained with thiomalic acid is attributed to a smaller affinity of gold for the carboxyl group, reaffirming the role of the sulfur.

The results of this study have some limited implications for the possible fate of I *in vivo*. Thus, the lower pKa values at physiological temperature will change somewhat the fraction of protonated, neutral species. While I sorption from the stomach will remain virtually unaffected (because the pH of the gastric solution is below the pKa of all acid groups present), the bioavailability of I *via* colonic absorption will be even smaller than would be predicted from pKa values at lower temperatures (20–25°). Similarly, the fraction of ionized I species in blood will be increased. As is generally recognized, oral administration is the only logical route for I, even though I has been given by injection (35, 36). Different therapeutic results with oral administration *versus* injection should have been expected.

While I has significantly greater *in vitro* complex formation constants with all metal ions than V, as exemplified again in this work, the *in vivo* *stability* of I, especially against L-amino acid hydrase, is the overriding factor (37). Enhanced excretion of metal ions induced by I (but not by V) may be much more a consequence of the relative biological stability of the thiol group in I than of higher *in vitro* K_f values. Even so, a correlation exists between the actual values of K_f (largest for the most toxic heavy metals mercury and lead) and metal-ion removal from the body, the excretion of copper having been studied most thoroughly.

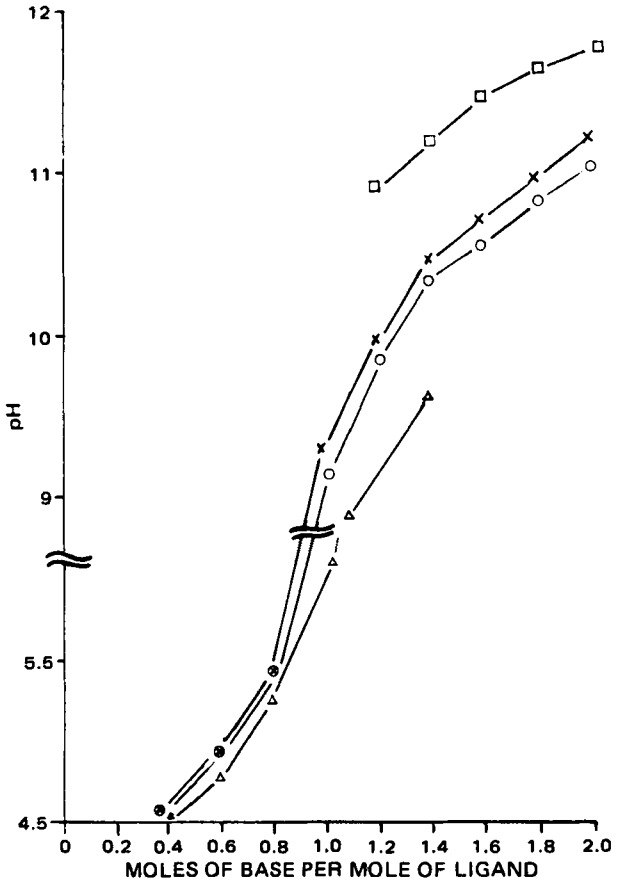

Figure 5—*Formation curves of thiomalic acid with calcium(II) (○), iron(III) (△), gold(I) (□), and free ligand (×) at 20°.*

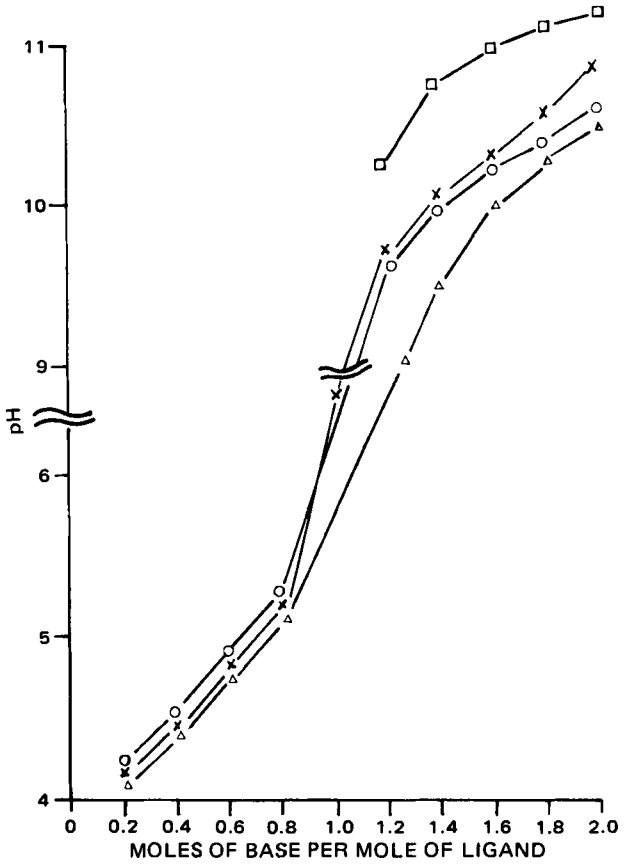

Figure 6—*Formation curves of thiomalic acid with calcium(II) (○), iron(III) (△), gold(I) (□), and free ligand (×) at 37°.*

The complex formation constants determined for gold(I) complexes in the present study are relatively high. While these values might be taken as evidence that I can remove previously deposited gold from the body of rheumatoid arthritis patients, they are not sufficient proof that that effect is important *in vivo*. In fact, some experts on I treatment of rheumatoid arthritis do not believe that I is beneficial in cases of gold poisoning[10].

For gold removal to occur, some, if not most, of the gold would have to be present in ionic form since I could obviously not complex directly with the free metal. It seems that an equilibrium between gold metal and gold ions is very unlikely (kinetically) *in vivo*. Conclusions concerning the oxidation state of gold species after injection in the body are hard to draw. In aqueous solutions, gold(I) has a tendency to disproportionate into gold metal and gold(III) (30), which is enhanced by increasing the temperature.

Furthermore, I would have to remain in a form that complexes the gold. Gold is supposed to be removed from areas where it is deposited. It is not circulating in the blood. Therefore, the I may have to circulate through the entire body before it reaches eventually the sites of gold deposition. During this time, it would be subject to many other reactions that can reduce the amount of I available for complex formation with gold. Only with extended administration of I could this condition be expected to occur. A one-time I dose for gold intoxication seems very unlikely to be effective.

Yet another consideration concerns the fact that the very strong 2:1 chelates formed with mercury, lead, nickel, copper, zinc, *etc.*, have significantly greater overall stabilities than the gold(I)–I complex, which has a 1:1 stoichiometry. The efficient removal of such heavy metal ions

[10] I. A. Jaffe, New York Medical College, New York, NY 10029, personal communication.

from the human body possibly is aided by the formation of "mixed chelates" *in vivo* (*e.g.*, I–metal ion–V). Mixed ligand chelates are believed to play an important role in biological systems (38) and are often significantly stronger than corresponding homoligand chelates. Gold(I) cannot enter into mixed ligand chelates and, therefore, would not be complexed as effectively *in vivo*.

Gold therapy is useful in a significant fraction of rheumatoid arthritis patients. The assumption is that the metal is the active agent of the gold compounds administered. The following observations, when considered together, may encourage speculation that this assumption need not necessarily be true:

1. Patients respond quite differently to different gold preparations (39).
2. Colloidal gold and gold compounds other than VII and VIII have been discontinued as ineffective or too toxic (40).
3. Ligands now used in rheumatoid arthritis therapy [with gold(I)] have a thiol group.
4. The biochemical activity of the only alternative drug to gold, I, is attributed to its thiol function (41).
5. Toxic side effects with I resemble those seen with patients receiving gold therapy (13).

The therapeutic effect of gold(I) compounds currently in use may be partly or entirely due to the thiol-containing ligand, *i.e.*, thioglucose or thiomalate. Apparently, this possibility has not been studied (42).

The relatively high K_f values for I with many metals also raise questions about the effect of I therapy on the balance of essential metals in the body. It will be remembered that the removal of metals is the basis of major accepted therapeutic uses of I.

The loss of taste due to a reduced zinc level has been reported by subjects during I therapy (43). Zinc supplements were given and normal taste sensitivity was restored, but normal taste returned by itself as well (44). The effect of I on body calcium levels is probably very small because of the small K_f and the large amount of the metal ion present in the body (10 mg/100 ml of blood). The amount of I complexed with iron might be expected to be quite high due to the relatively large K_f values determined in this study. However, most iron in the body is strongly tied up in hemoglobin. The actual ligand that chelates this iron *in vivo* is porphyrin, which is specific for iron; the complex has the very large K_f of $\sim 10^{30}$. Still, the fact that iron deposits are removed from synovial tissue by I (45) is in accord with iron complexing by I *in vivo*.

Similar considerations for some other trace metals in the body have not revealed extensive depletion of essential metals, although there have been no systematic studies except with copper and zinc. Certainly, the possibility of depleting metal ions such as cobalt(II) or chrome(III) needs further study.

Such studies as well as investigations into the pharmacokinetics of I and just patient monitoring would be considerably facilitated by reliable and rapid separation/analysis procedures for I and its complexes, metabolites, and derivatives. Current efforts are directed toward developing such methodology[11].

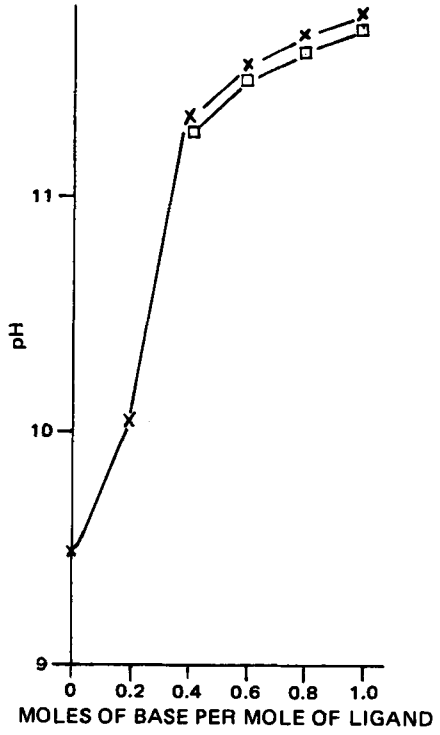

Figure 7—*Formation curves of thioglucose with gold(I) (□) and free ligand (×) at 20°.*

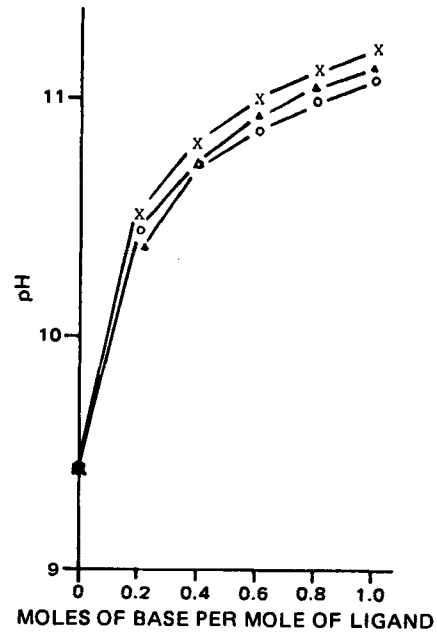

Figure 8—*Formation curves of thioglucose with calcium(II) (○), gold(I) (△), and free ligand (×) at 37°.*

REFERENCES

(1) J. M. Walshe, *Lancet*, **2**, 775 (1968).
(2) *Ibid.*, **4**, 1401 (1969).
(3) F. C. Bartter, M. Lotz, F. Thier, L. E. Rosenberg, and J. T. Potts, *Ann. Intern. Med.*, **62**, 796 (1965).
(4) J. C. Crawhall, E. F. Scowen, and R. W. Watts, *Br. Med. J.*, **1**, 588 (1963).
(5) J. E. Boulding and R. A. Baker, *Lancet*, **2**, 985 (1957).
(6) S. Selander, *Br. J. Ind. Med.*, **24**, 272 (1967).
(7) K. F. Swaiman and D. G. Flagler, *Pediatrics*, **48**, 639 (1971).
(8) H. Langendorff, M. Langendorff, and R. Koch, *Strahlentherapie*, **107**, 212 (1958).
(9) I. A. Jaffe, *Ann. Rheum. Dis.*, **22**, 71 (1963).
(10) Multi-Centre Trial Group, *Lancet*, **1**, 275 (1973).
(11) M. D. Milne, *Br. Med. J.*, **1**, 327 (1964).
(12) I. A. Jaffe, *Arthritis Rheum.*, **13**, 436 (1970).
(13) E. C. Cribson, *Ann. Rheum. Dis.*, **33**, 532 (1974).
(14) D. A. Doornbos and J. Faber, *Pharm. Weekbl.*, **99**, 289 (1964).
(15) D. Perrin and G. Sayce, *J. Chem. Soc., A*, **1968**, 53.
(16) *Ibid.*, **1967**, 82.
(17) A. Martell and G. Lenz, *Biochemistry*, **3**, 745 (1961).
(18) E. Kuchinskas and Y. Rosen, *Arch. Biochem. Biophys.*, **47**, 370 (1962).
(19) D. A. Doornbos and J. Faber, *Pharm. Weekbl.*, **103**, 1221 (1968).
(20) N. Li and N. Manning, *J. Am. Chem. Soc.*, **77**, 5225 (1955).
(21) A. Albert, *Biochem. J.*, **50**, 690 (1952).
(22) S. Fronaeus, *Acta Chem. Scand.*, **4**, 72 (1950).
(23) G. Schwarzenbach and G. Anderegg, *Helv. Chim. Acta*, **40**, 1773 (1957).
(24) F. J. Welcher, "The Analytical Uses of EDTA," Van Nostrand, New York, N.Y., 1957.
(25) D. Perrin and I. Sayce, *Talanta*, **15**, 1397 (1968).
(26) H. Sigel, "Metal Ions in Biological Systems," vol. 6, Dekker, New York, N.Y., 1973.

[11] S. Donahe, G. E. Janauer, and T. D. Zucconi, to be published. C. Lewkowicz, T. D. Zucconi, G. E. Janauer, and S. Donahe, to be published.

(27) K. Tanaka, *J. Am. Chem. Soc.*, **77**, 1996 (1955).
(28) D. W. Gruenwedel and H. Hsien-Chung, *J. Agr. Food Chem.*, **21**, 246 (1973).
(29) K. B. Yatsimirskii, "Ion Stability Constants of Complex Compounds," Consultants Bureau, New York, N.Y., 1960.
(30) J. C. Bailar, "Comprehensive Inorganic Chemistry," Pergamon, New York, N.Y., 1973.
(31) R. S. Saxena, K. C. Gupta, and M. L. Mittal, *J. Inorg. Nucl. Chem.*, **30**, 189 (1968).
(32) H. V. Aposhian, *Ann. N.Y. Acad. Sci.*, 481 (1972).
(33) L. Field, W. S. Hanley, P. L. Kelly, W. J. Sanders, J. E. White, I. A. Jaffe, and P. Merryman, *J. Med. Chem.*, **16**, 1152 (1973).
(34) B. J. Sweetman, M. M. Vestling, S. T. Ticaric, P. L. Kelly, L. Field, P. Merryman, and I. A. Jaffe, *ibid.*, **14**, 868 (1971).
(35) F. Planas-Bohne, *Naturforscher*, **28**, 774 (1973).
(36) K. Gibbs, *Q. J. Med.*, **40**, 275 (1971).
(37) "The Pharmacological Basis of Therapeutics," L. S. Goodman and A. G. Gilman, Eds., Macmillan, New York, N.Y., 1975.
(38) H. Sigel, "Metal Ions in Biological Systems," vol. 2, Dekker, New York, N.Y., 1973.
(39) R. Eberl, *Wien Klin. Wochenschr.*, **86** (15), Suppl. 25 (1974).
(40) H. Conn, "Current Therapy, 1976," Saunders, Philadelphia, Pa., 1976.
(41) I. A. Jaffe, in "Proceedings of Symposium on Penicillamine Treatment of Rheumatoid Arthritis," Spatind, Norway, Mar. 1976, pp. 11–24.
(42) I. A. Jaffe, in "3rd Annual Arthritis Teaching Day," Binghamton, N.Y., Apr. 13, 1977. See also Ref. 41, p. 79.
(43) R. Henkin and D. Bradley, *Life Sci.*, **9**, 701 (1970).
(44) "Proceedings of Symposium on Penicillamine Treatment of Rheumatoid Arthritis," Spatind, Norway, Mar. 1976, p. 92.
(45) E. Munthe and S. Refsum, in "Proceedings of Symposium on Penicillamine Treatment of Rheumatoid Arthritis," Spatind, Norway, Mar. 1976, pp. 41–44.

ACKNOWLEDGMENTS

Presented in part at the Division of Medicinal Chemistry, American Chemical Society, Chicago meeting, August 28–September 2, 1977.

The authors thank Dr. Vincent Maddi and Dr. John Baum for helpful advice and Dr. Israeli Jaffe for informative discussions as well as important literature references. A grant from the National Institutes of Health-Biomedical Research Support Grant fund of the State University of New York at Binghamton has enabled G. E. Janauer to continue this project.

Predictability of Warfarin Dose Requirements: Theoretical Considerations

WILLIAM T. SAWYER

Received June 19, 1978, from the *Division of Pharmacy Practice, School of Pharmacy, University of North Carolina, Chapel Hill, NC 27514* and the *Charlotte Area Health Education Center, Charlotte Memorial Hospital and Medical Center, Charlotte, NC 28232* (where inquiries should be directed). Accepted for publication September 7, 1978.

Abstract □ The theoretical basis of the predictability of warfarin maintenance dose requirements was evaluated using computer-generated hypothetical patient responses to a 10-mg/day "loading" dose regimen. Correlations between these responses and projected maintenance dose requirements were evaluated statistically, and a significant relationship was identified.

Keyphrases □ Warfarin—predictability of dose requirements, theoretical considerations, correlations between hypothetical patient responses and projected maintenance dose requirements □ Doses—predictability of warfarin requirements, theoretical considerations □ Maintenance dose requirements—predicting warfarin levels, theoretical considerations

Problems encountered in selecting an appropriate warfarin dosing regimen continue to represent a major obstacle to improvements in the quality and efficiency of oral anticoagulant therapy (1). Although the daily maintenance warfarin dose usually falls between 5.0 and 7.5 mg in large patient populations studied (2), wider variations in daily dose requirements are seen clinically, and the dose titration process used to determine this maintenance dose may be time consuming and relatively inefficient. The cost of added days of patient hospitalization required to select the maintenance dose may be significant.

Efforts to improve the efficiency of warfarin therapy have proceeded in two areas: (*a*) mathematical treatments describing the time course of warfarin's anticoagulant effects (3–5), and (*b*) clinical studies evaluating the predictability of steady-state warfarin dose requirements based on initial patient drug response (6–8). Two clinical investigations suggested a degree of predictability of anticoagulant maintenance dose requirements. A correlation was observed between the time required to achieve therapeutic anticoagulation (using a 15-mg/day "loading" dose regimen) and the maintenance warfarin dose finally required (6). Recently, a significant correlation between patient response to a specific loading dose regimen (10 mg/day for 3 days) and the maintenance dose required to achieve a desired steady-state degree of anticoagulation was demonstrated (7).

To evaluate the potential of these findings, the theoretical basis of observed correlations between loading and maintenance warfarin doses was investigated, using a previously described mathematical model for warfarin effect. The results of this evaluation and their clinical implications are described here.

BACKGROUND

Warfarin pharmacokinetics have been extensively investigated and are considered to be first order (3). They are described by:

$$C_p(t) = C_p^0 e^{-k_r t} \qquad \text{(Eq. 1)}$$

where $C_p(t)$ is the plasma drug concentration at any time t during a dosing interval, C_p^0 is the initial plasma concentration, and k_r is the first-order warfarin degradation constant.

0022-3549/79/0400-0432$01.00/0
© 1979, American Pharmaceutical Association

(27) K. Tanaka, *J. Am. Chem. Soc.*, **77**, 1996 (1955).
(28) D. W. Gruenwedel and H. Hsien-Chung, *J. Agr. Food Chem.*, **21**, 246 (1973).
(29) K. B. Yatsimirskii, "Ion Stability Constants of Complex Compounds," Consultants Bureau, New York, N.Y., 1960.
(30) J. C. Bailar, "Comprehensive Inorganic Chemistry," Pergamon, New York, N.Y., 1973.
(31) R. S. Saxena, K. C. Gupta, and M. L. Mittal, *J. Inorg. Nucl. Chem.*, **30**, 189 (1968).
(32) H. V. Aposhian, *Ann. N.Y. Acad. Sci.*, 481 (1972).
(33) L. Field, W. S. Hanley, P. L. Kelly, W. J. Sanders, J. E. White, I. A. Jaffe, and P. Merryman, *J. Med. Chem.*, **16**, 1152 (1973).
(34) B. J. Sweetman, M. M. Vestling, S. T. Ticaric, P. L. Kelly, L. Field, P. Merryman, and I. A. Jaffe, *ibid.*, **14**, 868 (1971).
(35) F. Planas-Bohne, *Naturforscher*, **28**, 774 (1973).
(36) K. Gibbs, *Q. J. Med.*, **40**, 275 (1971).
(37) "The Pharmacological Basis of Therapeutics," L. S. Goodman and A. G. Gilman, Eds., Macmillan, New York, N.Y., 1975.
(38) H. Sigel, "Metal Ions in Biological Systems," vol. 2, Dekker, New York, N.Y., 1973.
(39) R. Eberl, *Wien Klin. Wochenschr.*, **86** (15), Suppl. 25 (1974).
(40) H. Conn, "Current Therapy, 1976," Saunders, Philadelphia, Pa., 1976.
(41) I. A. Jaffe, in "Proceedings of Symposium on Penicillamine Treatment of Rheumatoid Arthritis," Spatind, Norway, Mar. 1976, pp. 11–24.
(42) I. A. Jaffe, in "3rd Annual Arthritis Teaching Day," Binghamton, N.Y., Apr. 13, 1977. See also Ref. 41, p. 79.
(43) R. Henkin and D. Bradley, *Life Sci.*, **9**, 701 (1970).
(44) "Proceedings of Symposium on Penicillamine Treatment of Rheumatoid Arthritis," Spatind, Norway, Mar. 1976, p. 92.
(45) E. Munthe and S. Refsum, in "Proceedings of Symposium on Penicillamine Treatment of Rheumatoid Arthritis," Spatind, Norway, Mar. 1976, pp. 41–44.

ACKNOWLEDGMENTS

Presented in part at the Division of Medicinal Chemistry, American Chemical Society, Chicago meeting, August 28–September 2, 1977.

The authors thank Dr. Vincent Maddi and Dr. John Baum for helpful advice and Dr. Israeli Jaffe for informative discussions as well as important literature references. A grant from the National Institutes of Health-Biomedical Research Support Grant fund of the State University of New York at Binghamton has enabled G. E. Janauer to continue this project.

Predictability of Warfarin Dose Requirements: Theoretical Considerations

WILLIAM T. SAWYER

Received June 19, 1978, from the *Division of Pharmacy Practice, School of Pharmacy, University of North Carolina, Chapel Hill, NC 27514* and the *Charlotte Area Health Education Center, Charlotte Memorial Hospital and Medical Center, Charlotte, NC 28232* (where inquiries should be directed). Accepted for publication September 7, 1978.

Abstract □ The theoretical basis of the predictability of warfarin maintenance dose requirements was evaluated using computer-generated hypothetical patient responses to a 10-mg/day "loading" dose regimen. Correlations between these responses and projected maintenance dose requirements were evaluated statistically, and a significant relationship was identified.

Keyphrases □ Warfarin—predictability of dose requirements, theoretical considerations, correlations between hypothetical patient responses and projected maintenance dose requirements □ Doses—predictability of warfarin requirements, theoretical considerations □ Maintenance dose requirements—predicting warfarin levels, theoretical considerations

Problems encountered in selecting an appropriate warfarin dosing regimen continue to represent a major obstacle to improvements in the quality and efficiency of oral anticoagulant therapy (1). Although the daily maintenance warfarin dose usually falls between 5.0 and 7.5 mg in large patient populations studied (2), wider variations in daily dose requirements are seen clinically, and the dose titration process used to determine this maintenance dose may be time consuming and relatively inefficient. The cost of added days of patient hospitalization required to select the maintenance dose may be significant.

Efforts to improve the efficiency of warfarin therapy have proceeded in two areas: (*a*) mathematical treatments describing the time course of warfarin's anticoagulant effects (3–5), and (*b*) clinical studies evaluating the predictability of steady-state warfarin dose requirements based on initial patient drug response (6–8). Two clinical investigations suggested a degree of predictability of anticoagulant maintenance dose requirements. A correlation was observed between the time required to achieve therapeutic anticoagulation (using a 15-mg/day "loading" dose regimen) and the maintenance warfarin dose finally required (6). Recently, a significant correlation between patient response to a specific loading dose regimen (10 mg/day for 3 days) and the maintenance dose required to achieve a desired steady-state degree of anticoagulation was demonstrated (7).

To evaluate the potential of these findings, the theoretical basis of observed correlations between loading and maintenance warfarin doses was investigated, using a previously described mathematical model for warfarin effect. The results of this evaluation and their clinical implications are described here.

BACKGROUND

Warfarin pharmacokinetics have been extensively investigated and are considered to be first order (3). They are described by:

$$C_p(t) = C_p^0 e^{-k_r t} \qquad \text{(Eq. 1)}$$

where $C_p(t)$ is the plasma drug concentration at any time t during a dosing interval, C_p^0 is the initial plasma concentration, and k_r is the first-order warfarin degradation constant.

0022-3549/79/0400-0432$01.00/0
© 1979, American Pharmaceutical Association

Mathematical expressions describing the time course of the warfarin effect on coagulation after single or multiple doses were reported (5):

$$PCA(t) = P^0 e^{-k_d t} - \frac{mk_r}{(k_d)^2}(1 - e^{-k_d t} - k_d t) - \frac{m}{k_d}(1 - e^{-k_d t}) \ln \frac{C_p^0}{C_p^{max}} \quad \text{(Eq. 2)}$$

where PCA represents prothrombin complex activity, k_d is a first-order rate constant for prothrombin complex activity degradation, m is a constant relating the plasma warfarin concentration to clotting factor synthesis, and C_p and C_p^{max} are the actual plasma warfarin concentration and the plasma drug level at which the clotting factor synthesis rate reduces to zero, respectively.

In addition, the equation describing steady-state drug effects during uniform dosing schedules was derived (5):

$$PCA_{ss}(\tau) = [1 - k_d\tau/(1 - e^{-k_d\tau})]\frac{mk_r}{k_d{}^2} - \frac{m}{k_d} \ln C_p^0(m)/[C_p^{max}(1 - e^{-k_r\tau})] \quad \text{(Eq. 3)}$$

where $PCA_{ss}(\tau)$ is the prothrombin complex activity at steady state at the beginning of a dosing interval, $C_p^0(m)$ is the plasma level at the beginning of a dosing interval at steady state after a maintenance dose, C_p^{max} is the plasma warfarin concentration above which all clotting factor synthesis ceases, and τ is the dosing interval. All other constants are as previously described.

Rearrangement of Eq. 3 produces an expression for the estimation of required maintenance doses needed to produce desired steady-state anticoagulant effects:

$$\text{dose} = \exp\left[-PCA_{ss}(\tau) + \frac{mk_r}{k_d{}^2}[1 - k_d\tau/(1 - e^{-k_d\tau})]\frac{k_d}{m}\right] \times [C_p^{max}(1 - e^{-k_r\tau})]V_d \quad \text{(Eq. 4)}$$

where V_d is the volume of distribution.

For calculation purposes, warfarin absorption after oral administration can be considered to be instantaneous and complete, obviating the need for a biexponential expression. The volume of distribution is considered to be 0.13 liter/kg (5).

EXPERIMENTAL

Equation 2 was used to generate a series of hypothetical patient responses to the administration of five consecutive daily 10-mg warfarin doses. A patient weight of 70 kg was arbitrarily selected. The case responses were produced by iterative substitution of sets of parameter values (k_r, k_d, m, and C_p^{max}) into the equations. The parameter ranges and increment sizes used in the computations are listed in Table I.

Estimated prothrombin complex activity levels were calculated at 18-hr intervals after each 10-mg dose. Projected maintenance doses required to achieve a desired therapeutic steady-state prothrombin complex activity level of 20% were calculated using Eq. 3.

After initial calculations, only parameter sets producing projected daily maintenance doses between 2.0 and 15.0 mg were used for correlation analyses with the patient response data.

The statistical correlations between the projected maintenance doses and the calculated prothrombin complex activity values after each 10-mg dose were computed[1]. All calculations were performed on a digital computer[2] using the PL/I language.

RESULTS AND DISCUSSION

A total of 914 hypothetical cases was evaluated. The mean prothrombin complex activity values observed after each dose and the respective ranges and standard deviations are shown in Table II. The mean projected maintenance dose was 6.9 mg/day (range of 2.0–15.0). This value is consistent with average daily doses reported previously (2).

Statistically significant linear correlations ($p < 0.0001$) were observed between calculated responses after each dose, or their logarithmic transforms, and the projected maintenance doses. These correlations, although significant, were relatively poor after the first dose ($r = 0.28$) but improved considerably. After the second dose ($r = 0.79$), this improvement was relatively asymptotic up to the fifth dose ($r = 0.92$). The values of the correlation coefficient, r, are given in Table III. There appears to be little difference in the correlations obtained using raw coagulation data or the logarithmic transform.

The observed correlation coefficient between the projected daily maintenance dose and the logarithm of the prothrombin complex activity, calculated 18 hr after the third 10-mg dose, was 0.89. This value is in very close agreement with the coefficient, 0.90, recently reported in a clinical investigation using experimental data for 34 patients. The clinical findings contained in that report may have sound theoretical support. Graphical illustration of the relationships between the projected maintenance doses and the responses observed after the third dose is provided in Fig. 1.

Another report (6) proposed a relationship between the number of days required to reach minimal therapeutic levels of anticoagulant effect (PCA ≤ 35%), using a fixed loading regimen (15 mg/day), and the maintenance warfarin dose finally required. This concept was evaluated using the hypothetical data generated from a 10-mg dosing regimen. The mean projected maintenance doses were calculated for three groups of response cases where: (*a*) a prothrombin complex activity of 35% was achieved after one or two doses, (*b*) a 35% level was achieved after the third or fourth dose, and (*c*) a 35% level was not achieved until at least the fifth dose (Table IV). As can be expected, the mean projected maintenance dose increased as the time required to achieve a therapeutic effect increased.

Many facilities currently assess warfarin effect by measurement of the prothrombin time and calculation of the prothrombin ratio (PR). To bring these findings into perspective in relation to the prothrombin ratio,

Table I—Parameter Range and Increment Values Used in the Iterative Data Generation

Parameter	Upper Limit	Lower Limit	Increment Value
k_d, day^{-1}	3.5	0.5	0.5
k_r, day^{-1}	0.6	0.3	0.1
m	60.0	10.0	5.0
C_p^{max}, μg/ml	15.0	5.0	1.0

Table II—Mean Values and Ranges of Prothrombin Complex Activity as a Function of the Number of 10-mg Warfarin Doses Administered

Dose	Prothrombin Complex Activity, %		
	Mean	*SD*	Range
1	90.2	6.4	73.1–100.0
2	42.8	11.2	21.8–84.1
3	32.4	9.4	16.2–70.9
4	28.2	8.2	14.2–60.4
5	26.1	7.6	11.9–52.4

Table III—Correlation Coefficients between Projected Maintenance Dose Requirements and Predicted Loading Dose Response as a Function of the Number of Doses Administered

Dose	Correlation Coefficient *r*	
	Dose *versus* Prothrombin Complex Activity	Dose *versus* $\log_{10}$ Prothrombin Complex Activity
1	0.28	0.28
2	0.78	0.80
3	0.87	0.89
4	0.92	0.92
5	0.92	0.92

Table IV—Mean Projected Maintenance Dose as a Function of the Time Required to Achieve Therapeutic Prothrombin Complex Activity Levels (≤35%)

Days	Dose, mg/day	Dose Range, mg/day	Cases
0–2	3.4	2.0–6.6	255
3–4	6.7	2.0–13.1	464
5 or more	12.0	5.0–15.1	195

[1] Statistical Analysis System, Version 76.5, GLM Procedure.
[2] IBM 370/155, Triangle University Computation Center, Research Triangle Park, N.C.

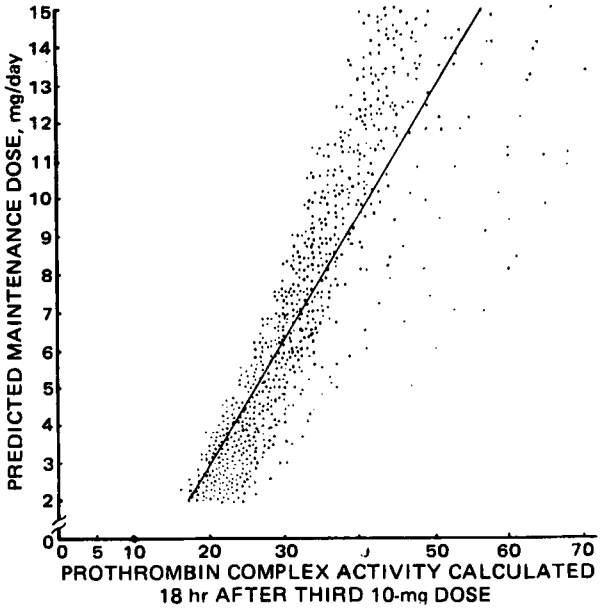

Figure 1—*Relation between projected maintenance warfarin dose and prothrombin complex activity value estimated 18 hr after the third 10-mg dose* [$y = 0.332\ (PCA - 11.60)$, $r = 0.89$, *and* $n = 914$]. *The solid line represents the best statistical fit line.*

a conversion between prothrombin complex activity and the prothrombin ratio proposed previously (4) can be used:

$$PR = \frac{(100/PCA) + 2.636}{3.636} \qquad \text{(Eq. 5)}$$

With this expression, a stratified description of the relationship between ratio values observed after the third 10-mg dose and mean projected maintenance doses was produced (Table V). In addition, rough clinical approximations of maintenance dose requirements can be derived from Table IV. If a prothrombin ratio of 1.5 is achieved after the first or second dose, the daily maintenance dose required might approximate 4–5 mg. If three or four doses are required to achieve this ratio, 7.5 mg/day would be required. If five or more doses are needed, 10–15 (12.5) mg/day would be needed.

Any evaluation of these results must be considered carefully until more clinical data are available. Application of the mathematical concepts described here to individual patient situations should ideally be based on additional results of clinical studies. It has been shown that oral anticoagulants such as warfarin exert their pharmacological effects on prothrombin synthesis through inhibition of the regeneration of vitamin K_1 from its epoxide metabolite (8). Therefore, the anticoagulant action of warfarin depends not only on the drug concentration at its site of action but also on the concentrations of vitamin K_1 and vitamin K_1 epoxide in the body. Factors such as diet and concomitant drug therapy can influence these concentrations and coagulation, independently of warfarin concentration. Certainly, these results are based on conditions where

Table V—Projected Maintenance Dose Requirements as a Function of the Estimated Response to Three Daily 10-mg Doses

Prothrombin Ratio[a]	Mean Projected Maintenance Dose, mg/day	Maintenance Dose Range, mg/day
1.00–1.20	12.3	8.4–15.0
1.21–1.30	11.8	5.0–14.9
1.31–1.40	12.0	6.0–15.1
1.41–1.50	9.5	4.8–13.6
1.51–1.60	7.6	3.7–11.3
1.61–1.70	5.8	3.0–8.3
1.71–1.80	4.7	2.2–6.8
1.81–1.90	3.7	2.0–5.6
1.91–2.00	3.2	2.0–4.5
>2.00	2.6	2.0–3.8

[a] Ratio value estimated 18 hr after third 10-mg dose.

nonlinear alterations in warfarin effects do not influence patient response. Drug or dietary influences that might alter usual patient response are still relatively difficult to quantitate, and the need for routine measurement of the prothrombin ratio as a definitive indicator of warfarin effects is not in any way affected by these findings.

With further assessment and confirmation of the potential clinical validity of these results, more efficient, less time-consuming methods for initiating warfarin therapy might be developed. Previous clinical studies (6, 7) showed that adequate anticoagulation can be achieved with the use of a standardized loading dose regimen. In light of the results of those investigations and the data presented in this paper, there seems to be little justification for use of the erratic dosing patterns followed in the past when the initial administration of a relatively simple 10-mg/day regimen can provide a reasonably reliable indicator of maintenance drug needs. Any regimen used, however, should include daily monitoring of clinical coagulation parameters.

REFERENCES

(1) S. Husted and F. Andreasen, *Acta Med. Scand.*, **200**, 379 (1976).

(2) J. H. Hull and W. Murray, presented at the Seventy-Eighth Annual Meeting of the American Society for Clinical Pharmacology and Therapeutics, Dallas, Tex., 1977.

(3) R. Nagashima, R. A. O'Reilly, and G. Levy, *Clin. Pharmacol. Ther.*, **10**, 22 (1969).

(4) L. B. Sheiner, *Comp. Biomed. Res.*, **2**, 507 (1969).

(5) T. G. Theofanous and R. G. Barile, *J. Pharm. Sci.*, **62**, 261 (1973).

(6) R. A. O'Reilly and P. M. Aggeler, *Circulation*, **38**, 169 (1968).

(7) P. A. Routledge, D. M. Davies, S. M. Bell, J. S. Cavanagh, and M. D. Rawlins, *Lancet*, **2**, 854 (1977).

(8) P. Ren, P. Y. Stark, R. L. Johnson, and R. G. Bell, *J. Pharmacol. Exp. Ther.*, **201**, 541 (1977).

ACKNOWLEDGMENTS

The author thanks J. Hull for helpful comments and advice and J. Bryant for expert secretarial assistance.

Pharmacokinetics of Topically Applied Pilocarpine in the Albino Rabbit Eye

MICHAEL C. MAKOID * and JOSEPH R. ROBINSON ˣ

Received February 23, 1978, from the *School of Pharmacy, University of Wisconsin, Madison, WI 53706.* Accepted for publication October 4, 1978. *Present address: College of Pharmacy, University of Nebraska Medical Center, Omaha, NB 68105.

Abstract □ The temporal and spatial pattern of [^{3}H]-pilocarpine nitrate distribution in the albino rabbit eye following topical administration was determined. A four-compartment caternary chain model describing this disposition corresponds to the precorneal area, the cornea, the aqueous humor, and the lens and vitreous. Simultaneous computer fitting of data from tissue corresponding to some compartments in the model supported the proposed model. Additional support was provided by the excellent correlation between predicted and observed values in multiple-dosing studies. Several important aspects of ocular drug disposition are evident from the model. The extensive parallel elimination at the absorption site gives rise to an apparent absorption rate constant that is one to two orders of magnitude larger than the true absorption rate constant. In addition, aqueous flow accounts for most of the drug removal. Thus, major effects on absorption and elimination, independent of the drug structure, suggest the possibility of similar pharmacokinetics for vastly different drugs.

Keyphrases □ Pilocarpine—distribution following topical administration, precorneal area, cornea, aqueous humor, lens, vitreous humor, rabbits, models □ Eye—pilocarpine distribution following topical administration, rabbits, models □ Models, pharmacokinetic—pilocarpine distribution following topical administration, eye

Until recently, the ocular disposition of topically applied pilocarpine was described with a one-compartment model. This model was satisfactory for short-term drug levels, but studies over longer times revealed significant deviation from the model (Fig. 1) (1–3).

Many ocular drugs of different physicochemical properties have strikingly similar pharmacokinetic profiles (4–8). The peak times and the absorption and elimination rate constants for these drugs are remarkably similar in view of the differences in drug properties and the complexity of the eye. Most drugs, when analyzed with a simple one-compartment model, appear to penetrate the cornea very rapidly. This rapid penetration from single doses differs from levels from multiple dosing of short duration and from sustained-release products. Maintenance of a high drug concentration in the lacrimal fluid for extended periods should significantly increase the amount of drug penetrating the eye if the penetration rate is rapid. This effect was found not to be the case (9).

The present study was designed to examine the disposition of topically administered pilocarpine in an attempt to clarify previous observations.

EXPERIMENTAL

Materials—Water was double distilled from alkaline permanganate solution in an all-glass apparatus.

Pilocarpine nitrate USP[1] was used without further purification. Tritiated pilocarpine nitrate[2], specific activity 4.1–6.95 Ci/mmole, was purified as previously described (10). Purity was established by paper chromatography and TLC. All other chemicals and reagents were either analytical or reagent grade and were used as received.

Male New Zealand albino rabbits[3], 1.8–2.4 kg, were used. Animals were individually housed in standard laboratory cages and were fed a regular diet with no restrictions on food or water.

Methods—*Solution Preparation*—Pilocarpine nitrate solutions, 5×10^{-4}–10^{-1} *M*, were prepared in 0.067 *M* Sorensen pH 6.24 phosphate buffer to which a small quantity of radioactive pilocarpine had been added. Solutions were made isoosmotic with tears by addition of sodium chloride, except in the 10^{-1} *M* case, which was already slightly hyperosmotic. In preparing the 5×10^{-4} *M* solutions, the amount of tritiated pilocarpine added was included when calculating the final solution molarity. For the remaining solutions, the small amount of tritiated pilocarpine did not influence the molarity of the final solution.

No attempt was made to induce or to maintain the sterility of the solutions, which were freshly prepared and discarded immediately after use. The final activity of the labeled tracer solutions varied depending on the duration of the experiment. The activity ranged from 0.025 mCi/ml (4×10^5 cpm/25 μl) in the short time periods to 1 mCi/ml (1.6×10^7 cpm/25 μl) in experiments lasting over 6 hr. Raw data in counts per minute were converted to micrograms of drug per milliliter of aqueous humor or per gram of tissue by use of an internal standard and standard radioisotope techniques.

Sampling Techniques—Pilocarpine solution, 25 μl, was instilled onto the animal cornea and collected in the cul-de-sac. For instillation, the lower lid was gently pulled away from the eye globe to form a pocket but was immediately returned to the normal position after drug instillation. In the multiple-dose study, this procedure was repeated at 30-min intervals for five doses. The animals were dosed upright in minimum restraining cages and were returned to their cages for the longer time periods.

At various postinstillation times, rabbits were sacrificed by rapid injection of an overdose of pentobarbital sodium into the marginal ear vein. A single puncture was then made, with a 27-gauge 1.25-cm needle, through the corneal-scleral junction into the anterior chamber. Aqueous humor, 100–200 μl, was aspirated from the anterior chamber and allowed to remain in the syringe until completion of the surgery, at which time

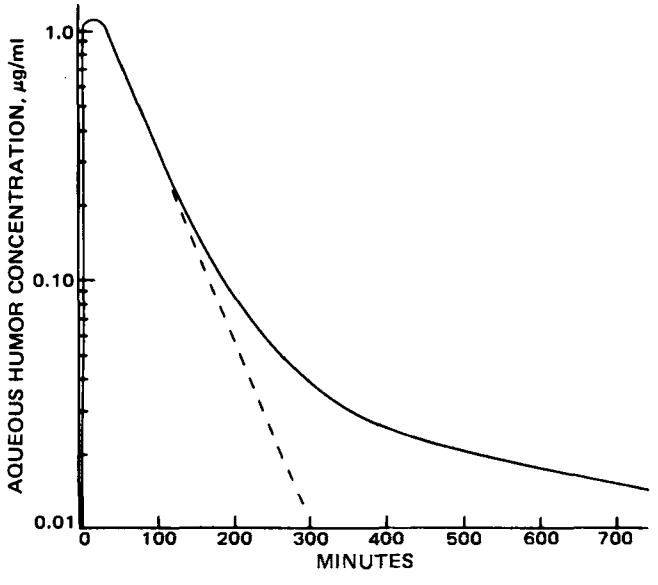

Figure 1—*Aqueous humor drug concentration* versus *time profile following topical administration of 25 μl of 10^{-2} M pilocarpine nitrate. The initial apparent one-compartment kinetics are shown as a dashed line, and deviations at longer time points are shown with a continuous line.*

[1] Merck & Co., Rahway, N.J.
[2] New England Nuclear, Boston, Mass.
[3] Klubertanz Rabbitry, Edgerton, Wis.

0022-3549/79/0400-0435$01.00/0
© 1979, American Pharmaceutical Association

a 100-μl aliquot was transferred quantitatively by micropipet[4] from a planchet to a scintillation counting vial[5] containing 5 ml of scintillation fluid[6]. To minimize chemiluminescence, the liquid scintillation cocktail was refrigerated for at least 24 hr at 4° prior to transfer and counting. Solutions were read on a liquid scintillation counter[7].

After removal of aqueous humor, the eye was proptosed by inserting the handle of a scalpel behind the orb at the lateral (outer) canthus, and a straight Kelly clamp was placed under the orb at the medial (inner) canthus. A perilimbal incision was then made to a depth sufficient to sever the iris from the ciliary body. The cornea and iris were removed as a single unit, placed on a small filter paper, and gently blotted to remove excess fluid. The tissues were then separated and placed in preweighed combustion cones[8] for subsequent assay. The lens extruded during this procedure and was also placed in a preweighed combustion cone for analysis. The ciliary body was extracted from the sclera with vitreous humor attached.

By drawing the ciliary body between two sets of forceps, it was possible to remove the gel-like vitreous humor. Both tissues were then placed in preweighed combustion cones. All tissues were immediately weighed and allowed to air dry to facilitate oxidation. No significant difference could be detected between samples allowed to air dry prior to oxidation or oxidized wet. The tissue samples were introduced into a sample oxidizer[9] for analysis. Tritium was trapped as tritiated water in 10 ml of solvent[10]. These solutions were then equilibrated at 13° in the refrigerated scintillation counter for 6 hr prior to tritium assay.

The time between animal sacrifice and sampling should be minimal, especially at the earlier time points. Time for total surgery ranged from 1.5 to 2 min/eye.

At least eight determinations were made at each time point for each tissue. The various tissue–drug concentration *versus* time data fit a multicompartment model. After initial graphical estimates of the associated parameters, the profiles were subjected to computer analysis[11]. To determine the amount of pilocarpine in the various compartments, the data were converted to micrograms by multiplying the concentration in micrograms per milliliter by the estimated compartment size. The average cornea weighed 50 mg, the average iris and ciliary body weighed 20 mg each, the lens weighed 250 mg, the vitreous weighed 1 g, and the aqueous humor contained 250 μl. The absolute values of these compartments may vary by as much as 20%.

Stability Studies on Pilocarpine—*Chemical Analysis*—Intact pilocarpine was determined by the ferric hydroxamate method (11): 200 μl of 2.7 *N* NaOH, together with 200 μl of 2.5 *N* hydroxylamine hydrochloride, was spiked with 500 μl of the pilocarpine solution to be assayed. The solutions were allowed to react for 1 hr at room temperature or 4 min at 75°. Then 1.5 ml of 1.7 *M* ferric perchlorate in 0.8 *M* perchloric acid was added, and the resultant solution was allowed to react in the dark for 30 min. Finally, the solutions were brought to a volume of 7 ml with distilled water and read on a spectrophotometer[12] at 515 nm. The molar absorptivity of the solutions was 1.1×10^3 liters mole^{-1} cm^{-1}. This method produced a more stable color than previously reported, with an estimated fading rate of 15% in 24 hr.

Paper Chromatography—To determine the degradation and metabolic products of pilocarpine, various solutions and extracts were subjected to two-dimensional paper chromatography. The stationary phase was Whatman No. 4 paper; mobile phase one was *n*-butanol saturated with 0.1 *N* NH_4OH; mobile phase two was *n*-butanol saturated with 0.1 *N* HCl. The solvent front was allowed to proceed 10 cm in both directions, followed by drying of the paper and subsequent sectioning into 100 uniformly spaced squares. Each square was assayed for radioactivity, and the resulting R_f values were compared to known standards. Pilocarpic acid was prepared from intact pilocarpine by heating at 100° at pH 12 for 1 hr (12). In each case, only pilocarpine or pilocarpic acid could be shown to be present.

This procedure did not permit the detection of isopilocarpine, shown to be present by Sendelbeck *et al.* (13) using GLC. Tritiated pilocarpine was judged to contain 0.8% pilocarpic acid as a contaminant and to be stable with respect to lactone hydrolysis during the experiments. *In vitro* determinations of metabolites were carried out by incubating the iris and cornea in 1.0 ml of pilocarpine, 500 μg/ml, for various times and analyzing the solution for total pilocarpine by radioactive tracer analysis and for intact pilocarpine by spectral analysis.

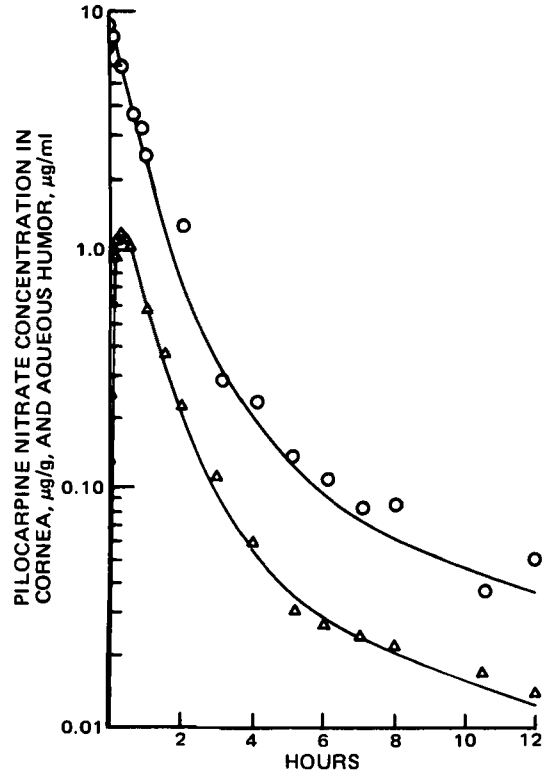

Figure 2—*Comparison of cornea* (○) *and aqueous humor* (△) *concentration data following instillation of 25 μl of* 10^{-2} M *pilocarpine nitrate with best-fit line generated by computer analysis.*

RESULTS

Degradation Studies—Intact pilocarpine was measured colorimetrically, and radioactive tracer analysis was used for total pilocarpine in determining the extent of pilocarpine degradation. Chromatography on *in vitro* incubates and *in vivo* ocular tissue homogenates identified degradation products. The metabolic rate was about 10^{-4} min^{-1}, in good agreement with the work of Sendelbeck *et al.* (13). The magnitude of this rate constant indicates significant differences between intact and total drug over time, *i.e.*, approximately 10–20% degradation over the 10–12 hr of the present study.

Drug Disposition Studies—*Tissue Drug Concentration* versus *Time Profiles from Single Dose*—Table I shows single-dose pilocarpine concentrations in various ocular tissues. The data for the 10^{-2} *M* pilocarpine were used for the primary analysis, with the results of other concentrations used as support. Cornea, C_c, and aqueous humor, C_{AH}, data from the 10^{-2} *M* dose were computer fitted to the four-compartment model equations (Fig. 2):

$$C_c = Ae^{-\alpha t} + Be^{-\beta t} + Ce^{-\Gamma t} + De^{-\Delta t} = \sum_{i=1}^{4} A_i e^{-\alpha_i t} \quad \text{(Eq. 1)}$$

$$C_{AH} = Ee^{-\alpha t} + Fe^{-\beta t} + Ge^{-\Gamma t} + He^{-\Delta t} = \sum_{i=1}^{4} A_i e^{-\alpha_i t} \quad \text{(Eq. 2)}$$

(Equation parameters are explained in the *Appendix*.)

Tissue Drug Concentrations versus *Time Profiles from Multiple Doses*—The multiple-dose tissue drug concentration *versus* time profiles are presented in Table II. The cornea and aqueous humor data were fitted to the four-compartment model multiple-dosing equations:

$$C_c = M\left[\sum_{i=1}^{4} \frac{A_i e^{-\alpha_i t}(1 - e^{-n\alpha_i \tau})}{(1 - e^{-\alpha_i \tau})}\right] \quad \text{(Eq. 3)}$$

$$C_{AH} = M\left[\sum_{i=1}^{4} \frac{A_i e^{-\alpha_i t}(1 - e^{-n\alpha_i \tau})}{(1 - e^{-\alpha_i \tau})}\right] \quad \text{(Eq. 4)}$$

where t equals the time since the last dose, τ is the time between doses, and M represents the lacrimal concentration buildup as explained pre-

[4] Biopette, Schwarz/Mann, Orangeburg, N.Y.
[5] Minivials, I.C.N., Irvine, Calif.
[6] Aquasol, New England Nuclear, Boston, Mass.
[7] Tri-Carb, Packard Instrument Co., Downers Grove, Ill.
[8] Combusto-Cones, Packard Instrument Co., Downers Grove, Ill.
[9] Packard model 306, Packard Instrument Co., Downers Grove, Ill.
[10] Monophase-40, Packard Instrument Co., Downers Grove, Ill.
[11] MACC subroutine NREG.
[12] Cary 16.

Table I—Tissue Drug Concentrations at Various Times following a Single Instillation of 25 μl of Pilocarpine Nitrate of Various Concentrations [a]

	Cornea				Aqueous Humor				Iris			
Minutes	10^{-1} M [b]	10^{-2} M	5×10^{-3} M	5×10^{-4} M	10^{-1} M [b]	10^{-2} M	5×10^{-3} M	5×10^{-4} M	10^{-1} M [b]	10^{-2} M	5×10^{-3} M	5×10^{-4} M
0.5		3.1 (11)				0.018 (16.7)						
2		7.0 (6)				0.017 (29)						
4		9.0 (5)				0.25 (8)				0.45 (12.4)		
6		8.8 (10)				0.6 (10)				0.67 (15)		
10		7.8 (16)				0.95 (4.7)				0.65 (20)		
20	21.2 (11)	6.0 (13)	2.2 (10)	0.29 (11)	5.7 (9.8)	1.2 (4.4)	0.71 (11)	0.076 (7.9)	4.8 (20)	1.1 (19)	0.54 (18)	0.129 (13)
30			0.87 (10)			1.1 (4.6)	0.46 (7.8)				0.16 (18)	
40		3.7 (13)										
50		3.2 (19)										
60	5.8 (8.2)	2.5 (9)	0.59 (11)	0.11 (12)	2.3 (8.8)	0.56 (7.7)	0.41 (6.6)	0.033 (12)	1.57 (6.4)	0.54 (20)	0.058 (9)	0.032 (16)
90						0.37 (8.6)						
120	3.8 (34)	1.2 (10)	0.25 (8)	0.025 (20)	1.3 (5.3)	0.22 (8.6)	0.13 (10)	0.0079 (8.9)	0.9 (30)	0.31 (9.7)	0.11 (11.5)	0.018 (22)
180		0.27 (10)				0.12 (11.3)				0.12 (11)		
240	0.5 (11)	0.22 (12)	0.15 (13)		1.6 (1.6)	0.059 (11.9)	0.022 (9.1)		0.32 (12.5)	0.073 (8.2)	0.029 (14)	
300		0.13 (9)				0.031 (22.8)				0.028 (14)		
360		0.10 (10)	0.098 (20)	0.0048 (17)	0.08 (6.3)	0.027 (7.9)	0.015 (13.3)	0.001 (10)	0.35 (22)	0.03 (33)	0.029 (21)	0.0015 (27)
420		0.075 (13)				0.024 (4.2)				0.026 (38)		
480	0.38 (20)	0.076 (12)		0.0038 (13)		0.022 (9.1)		0.00072 (10)	0.32 (29)	0.021 (19)		0.0007 (29)
600				0.0031 (16)				0.00065 (7.7)				0.0006 (21)
630		0.032 (3)				0.017 (5.9)						
720	0.27 (22)	0.043 (14)	0.029 (17)		0.09 (7.8)	0.014 (7.1)	0.008 (3.8)		0.22 (19)	0.016 (12.5)	0.022 (64)	

	Ciliary Body				Lens				Vitreous Humor			
Minutes	10^{-1} M [b]	10^{-2} M	5×10^{-3} M	5×10^{-4} M	10^{-1} M [b]	10^{-2} M	5×10^{-3} M	5×10^{-4} M	10^{-1} M [b]	10^{-2} M	5×10^{-3} M	5×10^{-4} M
0.5												
2						0.016 (25)				0.017 (23)		
4		0.3 (12)				0.017 (12)				0.024 (17)		
6		0.56 (21)				0.024 (8)				0.018 (28)		
10		0.50 (22)				0.017 (24)				0.029 (14)		
20	3.7 (13.5)	1.2 (19)	0.37 (12)	0.031 (16)	0.32 (15)	0.04 (12)	0.025 (8)	0.005 (16)	0.38 (29)	0.040 (18)	0.044 (27)	0.003 (37)
30							0.022 (14)				0.12 (17)	
40												
50												
60	1.1 (12)	0.38 (13)	0.11 (14)	0.036 (42)	0.22 (10)	0.058 (14)	0.012 (8.3)	0.005 (10)	0.26 (18)	0.028 (14)	0.004 (25)	0.0027 (37)
90												
120	0.64 (28)	0.19 (27)	0.071 (14)	0.01 (15)	0.19 (31)	0.047 (11)	0.024 (17)	0.003 (16)	0.078 (22)	0.032 (28)	0.0077 (39)	0.0005 (40)
180		0.09 (11.1)				0.039 (13)				0.021 (24)		
240	0.39 (21)	0.11 (18)	0.049 (63)		0.2 (9)	0.051 (16)	0.014 (11)		0.047 (30)	0.010 (20)	0.0067 (49)	
300		0.033 (30)				0.016 (6)				0.005 (20)		
360	0.24 (11)	0.033 (24)	0.043 (81)	0.0008 (36)	0.072 (20)	0.033 (9)	0.011 (9)	0.0011 (9)	0.035 (17)	0.015 (40)	0.006 (25)	0.00033 (21)
420		0.016 (13)				0.02 (20)				0.006 (33)		
480	0.19 (21)	0.029 (28)			0.14 (14)	0.021 (9)		0.00015 (7)	0.032 (9)	0.016 (31)		0.0005 (41)
600				0.0004 (29)				0.00010 (9)				0.00048 (8)
630		0.013 (62)				0.01 (10)				0.01 (20)		
720	0.091 (37)	0.014 (29)	0.014 (64)		0.061 (23)	0.01 (10)	0.0077 (14)		0.030 (23)	0.005 (20)	0.0027 (22)	

[a] Calculations are based on pilocarpine nitrate, although it is probable that pilocarpine is being measured. Concentrations are defined as micrograms of pilocarpine nitrate per gram of wet tissue or per milliliter of aqueous humor. Standard error of the mean is expressed as a percent of the value determined and is shown in parentheses. The number of eyes ranged between eight and 37 per time point. [b] Toxic manifestations, *e.g.*, copious lacrimation, occurred at this level. Accuracy of the numbers is, therefore, questionable.

Table II—Drug Concentration during Multiple Dosing of 25 μl of 10^{-2} *M* Pilocarpine Nitrate Every 0.5 hr for a Total of Five Doses [a]

Minutes	Cornea	Aqueous Humor	Ciliary Body	Iris	Lens	Vitreous Humor
45	8.4 (5.1)	2.4 (7.4)	0.91 (9.1)	1.4 (2.2)	0.13 (2.2)	0.033 (12)
60	3.8 (6.3)	2.0 (14.7)	0.74 (21)	1.0 (17)	0.10 (15)	0.039 (24)
75	19.0 (1.1)	1.9 (4.6)	2.4 (12)	2.9 (7.8)	0.18 (9)	0.12 (23)
90	5.9 (6.3)	3.3 (21)	1.9 (22)	2.9 (7.2)	0.16 (16)	0.13 (21)
105	15.0 (11)	5.8 (12)	2.7 (25)	3.0 (13)	0.27 (42)	0.10 (81)
120	15.0 (6.1)	5.1 (12)	2.2 (15)	3.6 (8.1)	0.27 (6)	0.11 (20)
135	14.0 (10)	3.4 (23)	2.9 (13)	5.2 (8.9)	0.26 (15)	0.26 (20)
150	14.0 (10)	2.5 (24)	2.2 (14)	2.6 (20)	0.19 (14)	0.090 (18)
165	7.0 (10)	3.0 (6.6)	1.7 (14)	1.9 (6.8)	0.18 (12)	0.051 (12)
180	4.4 (16)	1.9 (16)	1.1 (28)	1.4 (15)	0.22 (19)	—
240	2.1 (32)	0.64 (16)	0.4 (39)	0.73 (15)	0.13 (16)	0.051 (34)
300	2.1 (24)	0.38 (9.3)	0.45 (25)	0.68 (12)	0.16 (17)	0.070 (26)
360	0.82 (29)	0.23 (10)	0.13 (11)	0.15 (22)	0.12 (22)	0.030 (13)
480	0.52 (28)	0.14 (412)	0.10 (23)	0.11 (26)	0.08 (25)	0.033 (24)

[a] Concentrations are micrograms of drug per gram of wet tissue. Standard error of the mean is expressed as a percent of the value determined and is shown in parentheses; $n \geq 8$.

viously (14, 15). A more complete program is currently under investigation. The results of the equation fitting are shown in Figs. 3 and 4.

DISCUSSION

Drug Disposition Studies—Only the model shown in Scheme I gave simultaneous fit to both cornea and aqueous data ($r > 0.99$). The pharmacokinetic parameters generated by computer fitting are shown in Table III.

Two- or three-compartment caternary models gave reasonable correlation coefficients ($r \approx 0.9$), but major portions of the data had to be ignored in the fitting process. More complex models also gave good fit to the data, but there was no compelling reason to adopt them. The four-compartment model was selected partly because anatomical significance could be attributed to the various compartments.

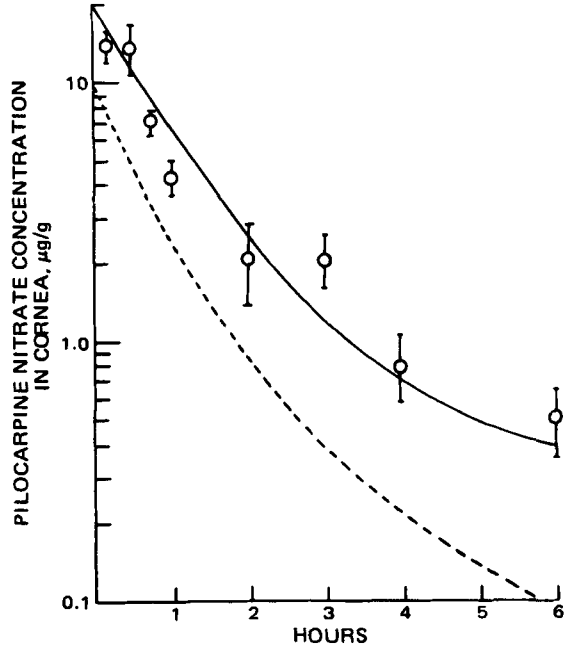

Figure 3—*Concentration of pilocarpine nitrate in the cornea (O) as a function of time after the last dose as compared with the calculated (—) multiple-dose line using Eq. 3. The single-dose line (– –) generated by the four-compartment model is drawn in for comparison.*

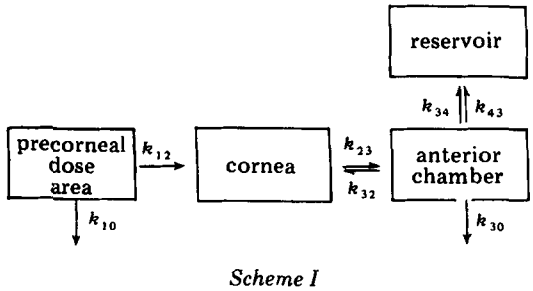

Scheme I

These data and the proposed model explain some previously anomalous findings. The observations that many drugs are rapidly absorbed across the cornea and that drugs with dissimilar physical-chemical properties show similar corneal absorption profiles (4–8) can be explained by recognizing the importance of the precorneal elimination pathway, k_{10}, on corneal absorption. Several investigators (1–3) commented recently that the cornea is not a simple semipermeable membrane. Aqueous humor drug studies of short duration frequently produced a biphasic curve of drug level *versus* time, which led to a simplistic view of the cornea. The idea that drugs diffused from lacrimal fluid through the "membrane" of the cornea into the aqueous humor led to the erroneous conclusion that the absorption rate constant obtained from such studies represented drug transfer from the tears to the aqueous humor. Studies of longer duration showed the disposition pattern of drug in both the cornea and aqueous humor to be more complex.

Drug contact time from 0 to 5 min postinstillation has been shown to be critical for drug absorption into the cornea and aqueous humor (16). The early peak time in the cornea led to the assumption of an erroneously large absorption rate constant of 0.5–0.7 min^{-1}. The early peak times in the cornea and aqueous humor are due to rapid elimination from the precorneal area and a rapid decrease in the concentration gradient between the tears and the cornea surface.

The influence of parallel elimination from an absorption site on the pharmacokinetic parameters obtained has been described (17–20). The simplest pharmacokinetic model for the eye is the single-compartment model (Scheme II). A more appropriate model, incorporating the parallel elimination step from the precorneal area, is shown in Scheme III.

Table III—Pharmacokinetic Parameters [a] Obtained by Fitting Data Generated from a Single 25-μl Dose of 10^{-2} *M* Pilocarpine Nitrate to Four-Compartment Model Equations [b] for Cornea and Aqueous Humor

Parameter	Cornea		Aqueous Humor	
	Concentration	Amount	Concentration	Amount
A_1[c]	−12	−0.61	0.41	0.10
A_2[c]	+0.20	+0.01	0.077	0.019
A_3[c]	4.3	0.22	−2.4	0.6
A_4[c]	7.7	0.39	1.9	0.47
α_1, min^{-1}	0.58	0.58	0.58	0.58
α_2, min^{-1}	0.0026	0.0026	0.0026	0.0026
α_3, min^{-1}	0.11	0.11	0.11	0.11
α_4, min^{-1}	0.019	0.019	0.019	0.019
AUC[d]	510	25.9	210	27
Peak time, min	4	4	20	20
r^2	0.99+	0.99+	0.99+	0.99+
r	0.99+	0.99+	0.99+	0.99+

[a] All parameters were allowed to float free to obtain best fit by nonlinear regression analysis of simultaneous aqueous humor and corneal data. [b] $C_C = Ae^{-\alpha t} + Be^{-\beta t} + Ce^{-\Gamma t} + De^{-\Delta t}$, and $C_{AH} \approx Ee^{-\alpha t} + Fe^{-\beta t} + Ge^{-\Gamma t} + He^{-\Delta t}$. Derivation of these equations are shown in the *Appendix*. [c] Corneal concentration equals micrograms per gram, aqueous humor concentration equals micrograms per milliliter, and amount equals micrograms. [d] Area under the curve in concentration (or amount units) × minutes.

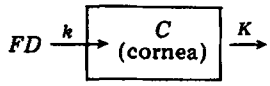

Scheme II

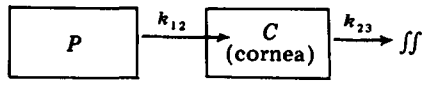

Scheme III

The equations describing these processes in terms of drug amounts are:

$$C = (FD)\left(\frac{k}{k-K}\right)(e^{-Kt} - e^{-kt}) \qquad \text{(Eq. 5)}$$

for Scheme II, where F is the fraction of the dose absorbed and D is the dose, and:

$$C = \left(\frac{Dk_{12}}{k_{12}+k_{10}-k_{23}}\right)[e^{-k_{23}t} - e^{-(k_{12}+k_{10})t}] \qquad \text{(Eq. 6)}$$

for Scheme III.

Since $F = k_{12}/(k_{12}+k_{10})$, it is obvious that $K = k_{23}$ and $k = k_{12}+k_{10}$; or, in other words, the absorption rate constant into the compartment monitored (Scheme II) is the summation of the elimination rate constants from the previous compartments. The first implication of this analysis is that the fraction of drug absorbed bears directly on the apparent absorption rate constant. Since the apparent rate constant is proportional to $1/F$, multiplication of the apparent rate constant by F should result in an approximation of the true rate constant; *i.e.*, $F \times k_{apparent} = k_{true}$. This is borne out by analysis of the initial corneal data, *i.e.*, less than 2 hr. The apparent absorption rate constant in this case is 0.62 min^{-1}, which, when multiplied by $F \approx 1$–2%, yields 6–12 $\times 10^{-3}$ min^{-1}. Computer estimate of k_{12} is 6.2 $\times 10^{-3}$ min^{-1}, in excellent agreement with the proposed model.

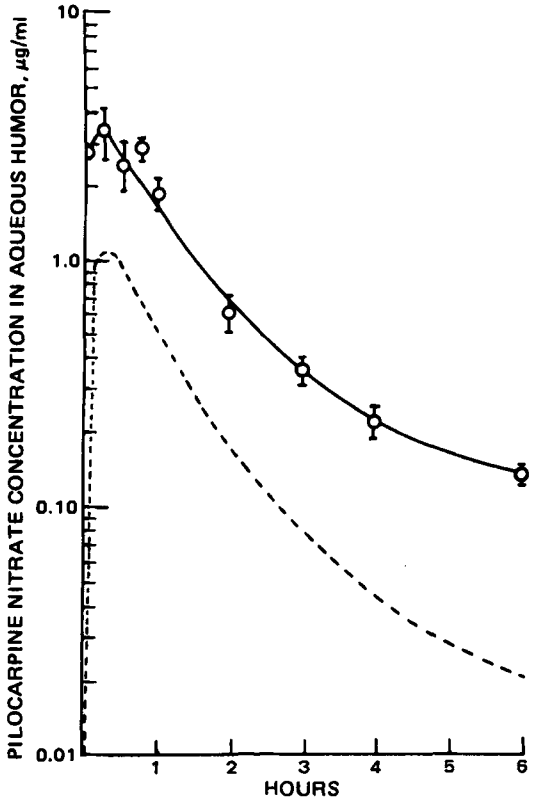

Figure 4—*Concentration of pilocarpine nitrate in the aqueous humor (○) as a function of time after the last dose as compared with the calculated (—) multiple-dose line using Eq. 4. The single-dose line (– –) generated by the four-compartment model is drawn in for comparison.*

Table IV—Bioavailabilities of Drug in the Aqueous Humor and Cornea after Rinsing at Various Times

Rinse Time Postinstillation, min	Percent Bioavailable[a]	Aqueous[b] Humor	Cornea[c]
0.5	33	33	34
1	—	55	—
2	75	80	78
3	—	91	—
4	—	100	100
5	100	100	100
No rinse	100	100	100

[a] Percent maximum miosis peak height (14). [b] Percent maximum area under the curve (16). [c] Percent maximum concentration.

The second implication is that peak time is:

$$T_p = \frac{\ln\left(\frac{k_{12}+k_{10}}{k_{23}}\right)}{k_{12}+k_{10}-k_{23}} \qquad \text{(Eq. 7)}$$

If $k_{10} \gg k_{12}$, then:

$$T_p = \frac{\ln\left(\frac{k_{10}}{k_{23}}\right)}{k_{10}-k_{23}} \qquad \text{(Eq. 8)}$$

This means that F approaches zero, k_{10} approaches infinity, and T_p approaches zero. The T_p value is relatively insensitive to k_{23} and k_{12}; *e.g.*, at small F, a 100-fold change in k_{23} results in a threefold change in T_p, and k_{12} must approach k_{10} to have a significant effect on T_p. Consequently, T_p would be similar even for dissimilar drugs because of the overshadowing of k_{12} and k_{23} by k_{10}.

This analysis also explains aqueous humor drug concentrations observed by Patton (9), who blocked the drainage ducts of rabbits, thus effectively reducing k_{10}. He observed a modest shift in peak time and a two- to threefold increase in the area under the curve (*AUC*), both of which are consistent with this model.

Corneal drug absorption ceases at 4–5 min postinstillation due to a very

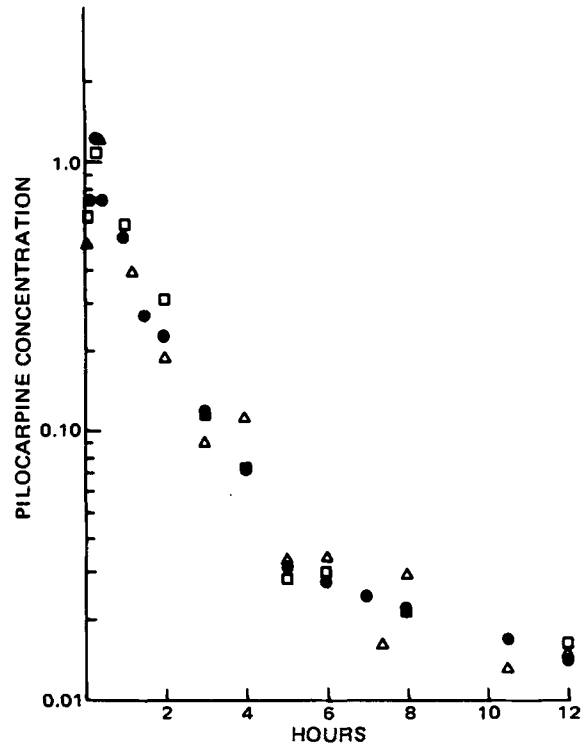

Figure 5—*Comparison of iris (□) and ciliary body (△) concentrations following a single dose of 25 μl of 10^{-2} M pilocarpine nitrate with aqueous humor data (●). Aqueous humor drug concentrations are in micrograms per milliliter; for the other tissues, drug concentration is in micrograms per gram wet weight tissue. Error bars are omitted for clarity.*

Table V—Pilocarpine in All Tissues Based on Area under the Curve Calculations and Estimated Tissue Size

Observed Parameter	Cornea	Aqueous Humor	Ciliary Body	Iris	Lens	Vitreous
Model size, mg	50	250	20	20	250	1000
Observed size, mg ($\bar{x} \pm SEM$, $n = 100$)	53.1 ± 0.8	300	20.7 ± 6.2	19.7 ± 7.3	257 ± 48	1077 ± 9.3
AUC, μg-min	25.4	27.2	2.17	2.17	6.4	11.82
Amount, μg	0.75	0.8	0.064	0.064	0.19	0.35
Instilled dose, %	1.1	1.2	0.1	0.1	0.28	0.52
Relative absorbed dose, %	100	110	8.8	8.8	26	48

large precorneal elimination rate constant and substantial drug accumulation at the corneal surface, as shown by the drug levels in the tears and the cornea at 4–5 min.

The cornea consists of two main tissue types, the lipophilic epithelium and the hydrophilic stroma, which have considerably different drug absorption and transport characteristics (16). The principal barrier and depot for pilocarpine, and presumably many ocular drugs, is in the epithelium. Movement of water-soluble drug through the stroma is usually rapid, with diffusion coefficients similar to those in water. Consequently, the cornea can be treated as two subcompartments, the epithelium and the stroma, assuming that the endothelium, a single layer of cells intermediate in properties between the lipophilic epithelium and hydrophilic stroma, is not rate limiting. Because of the facility of pilocarpine movement through the stroma, it can be combined with the aqueous humor, effectively reducing the cornea to a single compartment, the epithelium.

Since most of the drug present in the cornea is in the epithelial layer, the drug concentration at the cornea–tear interface is considerably higher than the average drug level in the cornea would indicate (16). At 5–6 hr postinstillation, the drug concentration in the cornea is three times that in the aqueous humor (stroma) (Fig. 2). Stated differently, the lipophilic epithelium contains 75% of the drug in approximately 10% of the corneal volume whereas the hydrophilic stroma contains 25% of the drug in 90% of the corneal volume. Use of this ratio to examine the 9-μg/g peak corneal drug concentration from a 10^{-2} *M* pilocarpine nitrate solution gives the ratio of drug between the epithelium and stroma:

$$\frac{\text{epithelium}}{\text{stroma}} = \left(\frac{75\% \times 9\ \mu g/g}{10\%}\right) \Big/ \left(\frac{25\% \times 9\ \mu g/g}{90\%}\right) = \frac{67.5\ \mu g/g}{2.5\ \mu g/g} \quad \text{(Eq. 9)}$$

Since the 3:1 ratio was obtained at 5–6 hr postinstillation while the corresponding ratio was much higher (~30–50:1) at times before the peak corneal drug level, these figures must be multiplied by 10–15 to give an average drug concentration in the epithelium of between 675 and 1000 μg/g. To average between 675 and 1000 μg/g in the epithelium during the first few minutes postinstillation, the drug concentration at the epithelial–tear surface would have to be twice that at the epithelial–stroma surface or between 1300 and 2000 μg/g.

Similarly, one can calculate the tear drug concentration. The following equation was modified from earlier work (14, 15):

$$C_L = \left(\frac{A_0}{V_0 + V_A}\right) \exp\left[-\left(\frac{0.66}{V_L + V_0 e^{-kt}} + k_n\right)t\right] \quad \text{(Eq. 10)}$$

where:

C_L = lacrimal concentration
A_0 = amount instilled
V_0 = volume instilled
V_L = resident lacrimal volume
V_A = apparent lacrimal volume due to volume of drop drained out undiluted
k_d = volume-dependent drainage rate constant
k_n = rate constant for nonproductive absorption

Solving Eq. 10 for a 25-μl drop gives a lacrimal drug concentration at 4 min of 1400 μg/ml, *i.e.*, approximately equal to that at the epithelial–tear interface at the same time (1300–2000 μg/ml). This explains the apparently large k_{10}, when no other process in the eye is of the magnitude necessary to shut down around 4 min. This apparent discrepancy is because flux is concentration dependent whereas present models are built on amount relationships.

On the basis of this analysis, flux should stop at about 4 min postinstillation and actually reverse at later times. Since this reverse flux is dependent not only on a small concentration difference but also on a very small first-order rate constant, the actual transfer rate out of the cornea should be very small. In fact, studies designed to show lacrimal drug concentration after dosing and subsequent flushing with saline failed to show detectable amounts of drug coming out of the cornea. Although the transfer between the precorneal fluid and the cornea is depicted as irreversible, it is probably reversible but not enough to interfere with the accuracy of the model.

The rapid decline in the lacrimal fluid–corneal surface concentration gradient results in apparent nonsink kinetics onto or into the cornea, as was demonstrated by initial corneal uptake studies (16). These studies, which determine relative pilocarpine bioavailability, correspond nicely with data from miosis studies (14) and with corneal absorption (Table IV). Thus, inclusion of the cornea as a component in the scheme of drug movement from the precorneal fluid into the anterior chamber explains the large apparent k_a and accounts for drug absorption into the aqueous humor even after the drug has been removed from the precorneal area. The corneal epithelium acts as a depot for drugs because it has significant volume and is not a simple semipermeable membrane.

Once the drug penetrates the cornea and enters the aqueous humor, it distributes throughout the eye. The anterior chamber is in intimate contact with the cornea, iris, ciliary body, lens, and vitreous. Rapid drug distribution to these areas is apparent from the iris and ciliary body data. Because of the lack of barrier epithelium and the open meshwork of connective tissue making up the iris and ciliary body, the drug concentration in these tissues mirrors that in the aqueous humor (Fig. 5). For pilocarpine disposition in albino rabbits, where pigment binding is absent, the anterior chamber compartment consists of the aqueous humor, iris, and ciliary body. Further work using pigmented strains will determine whether the iris and ciliary body drug disposition profiles also follow aqueous humor levels. Pigmentation is expected to significantly affect the amount of drug present in the iris (21).

The data show ~75% of the absorbed drug passing into the lens and vitreous reservoirs, as predicted by the model (Table V). The lens and vitreous data are fitted to a biexponential curve for preliminary treatment (Table VI). These preliminary data show that a portion of the drug becomes associated with the lens. The concentration gradient of drug within the lens has yet to be determined. Initial studies indicated that a substantial concentration gradient exists between the interior and exterior portions of the lens. Since the drug first penetrates the anterior chamber, the ventral surface of the lens should have a high drug concentration unless there is facile transport of drug around the lens. Thus, a critical examination of drug disposition in the lens needs to be conducted.

Transport into the vitreous humor also should be considered. The discrete anatomical tissue, the fibrils, comprising approximately 2% of the vitreous humor, should not hinder diffusion of relatively small molecules through the fluid space. Thus, microviscosity, rather than macroviscosity, should determine the diffusion rate. If this were the case, diffusion throughout the vitreous would be relatively rapid and the concentration gradient within the vitreous would be relatively shallow. Moreover, the peak time of drug in the vitreous would correspond closely to the aqueous humor peak time, which appears to be the case (Tables III and VI).

Table VI—Pharmacokinetic Parameters [a] Obtained by Fitting Lens and Vitreous Data to the Single-Compartment Model Equation, $Y = Ae^{-\alpha t} - Be^{\beta t}$, following a Single Instillation of 25 μl of 10^{-2} *M* Pilocarpine Nitrate

Parameter	Lens		Vitreous
	Concentration	Amount	Concentration [b]
A [c]	0.075	0.019	0.036
B [b]	0.071	0.018	0.037
α, min^{-1}	0.0027	0.0027	0.003
β, min^{-1}	0.037	0.037	0.21
AUC [d]	25	6.4	12
Peak time, min	76 min	76 min	21
r^2	0.96+	0.96+	0.97+
r	0.98+	0.98+	0.93+

[a] All parameters were allowed to float free to obtain best fit by nonlinear regression analysis. [b] The equation for the amount data is numerically identical because vitreous is 1 g; however, the units differ. [c] Lens and vitreous concentration equal micrograms per gram, and amount equals micrograms. [d] Area under the curve units: area concentration (or amount units) × minutes.

Table VII—Pharmacokinetic Parameters of Biphasic Decline of Aqueous Humor and Corneal Concentration Data Fit to the Equation $C = Ae^{-\alpha t} + Be^{-\beta t}$ following Instillation of 25 μl of Various Concentrations of Pilocarpine Nitrate

Parameter	Cornea				Aqueous Humor			
	10^{-1} M	10^{-2} M	5×10^{-3} M	5×10^{-4} M	10^{-1} M	10^{-2} M	5×10^{-3} M	5×10^{-4} M
Best Fit: All Parameters Allowed to Float Free								
A, μg/g	39.0	9.3	4.5	0.48	8.0	1.7	0.86	0.12
B, μg/g	1.1	0.48	0.070	0.0070	0.087	0.053	0.0083	0.0013
α, min^{-1}	0.034	0.24	0.016	0.026	0.02	0.019	0.016	0.023
β, min^{-1}	0.0030	0.0040	0.0060	0.0010	—	0.0039	—	0.0045
$A + B$, μg/g	40	9.8	4.6	0.49	8.1	1.8	0.87	0.12
AUC, μg/g min	1500	500	290	25	—	120	—	6.3
r^2	0.98+	0.99+	0.99+	0.99+	0.99+	0.99+	0.98+	0.99+
r	0.99+	0.99+	0.99+	0.99+	0.99+	0.99+	0.98+	0.99+
Constrained Fit: α and β Fixed to 10^{-2} M Exponents								
A, μg/g	28	9.3	4.6	0.43	7.6	1.7	0.92	0.1
B, μg/g	1.1	0.48	0.26	0.016	0.17	0.053	0.28	0.012
α, min^{-1}	0.024	0.024	0.024	0.024	0.019	0.019	0.019	0.019
β, min^{-1}	0.0040	0.0040	0.0040	0.0040	0.0039	0.0039	0.0039	0.0039
$A + B$, μg/g	29	9.8	4.8	0.45	7.7	1.8	0.95	0.1
AUC, μg/g min	3000	500	250	25	496	122	64.0	6.0
r^2	0.97+	0.99+	0.88+	0.99+	0.99+	0.99+	0.98+	0.99+
r	0.99−	0.99+	0.91+	0.99+	0.99+	0.99+	0.98+	0.99+

Most drug removal from the internal eye is *via* bulk flow of aqueous humor, although systemic loss *via* the vascular bed also occurs. Metabolism of the drug by ocular enzymes will be considered more fully in a subsequent publication.

This picture of drug removal is consistent with previous observations that the elimination rate for pilocarpine is significantly smaller than the aqueous flow rate (3), suggesting that:

1. Permeation from the cornea to the aqueous is slow so that the cornea becomes a depot for the drug, or
2. Iris tissue and its pigments bind the drug, forming a deep depot, or
3. Receptor dissociation occurs at a slow rate.

The fact that the data from albino rabbits without pigmented irides showed similar kinetics to the data from pigmented irides (3) indicates that tissue pigments may not be the dominant cause of deviation from simple one-compartment kinetics. The amounts of drug in the iris are not sufficient to maintain aqueous humor levels for an extended time. The cornea may modify pilocarpine penetration (22). Lazare and Horlington (1) showed an elimination phase in tissue samples that does not fit a simple biexponential equation, but they rejected the cornea as a drug reservoir. The deviation from simple kinetics may be due to distributive aspects, as in the present findings.

Both the corneal reservoir and drug equilibration from the vitreous humor are viable explanations of the pharmacokinetics, and both approaches are mathematically necessary to reproduce the curves simultaneously generated by the cornea and aqueous humor data. The "absorption and elimination rate constants" previously generated from the simple one-compartment model were only part of the story. They are a compilation of the various ongoing processes in the whole system (see *Appendix*), dominated by an apparent parallel elimination in the precorneal area and a distribution in the aqueous humor, with neither process especially dependent on the drug structure.

Testing the Model—*Concentration Dependence*—Consistency of the concentration-independent model would be evident if various concentrations of a drug generated a family of curves with similar slopes. The peak concentrations, AUC, and the intercept of the concentration axis in a semilogarithmic plot should be proportional to concentrations. Since the data collection for the absorption phase was complete only for the 10^{-2} M study, only the elimination phase was compared in all studies, using the 10^{-2} M study as the reference.

The results of these calculations (Tables VII and VIII) bear out the hypothesis ($r > 0.98$). The 10^{-1} M solution caused excessive lacrimation and a larger k_{10}, which was reflected in the decrease in drug uptake. This result is consistent with previous findings that aqueous humor drug concentrations over a large instilled fluid concentration range produce a linear relationship over several orders of magnitude (10).

Multiple-Dose Studies—Multiple-dosing studies were conducted at 0.5-hr dosing intervals to ensure integrity of the label and to get a sufficient amount in the reservoirs to show significant differences.

The model predicts a certain amount of drug buildup in ocular tissues due to deposition and equilibration of the drug in the aqueous humor with these tissues. There is excellent correlation between prediction and observation (Figs. 3 and 4) for both the cornea and aqueous humor. What the model does not predict, however, is the buildup of the precorneal concentration due to the previous dose. When the concentration in the precorneal area drops to that of the corneal epithelium, flux into the cornea ceases, even though there is still a significant amount of drug in the cul-de-sac. Upon addition of a second dose within a short period, dilution with tears does not have as much effect on incoming drug due to the presence of drug remaining from the previous dose. This buildup has been incorporated into the mathematics for multiple dosing of short τ.

The stepwise buildup of drug in all tissues is clear from Table II. The peak drug level shifted to longer times, which is normal in dosing intervals

Table VIII—Pharmacokinetic Parameters of Monophasic Decline of Lens and Vitreous Concentration Data Fit to the Equation $C = Ae^{-\alpha t}$ following Instillation of 25 μl of Various Concentrations of Pilocarpine Nitrate

Parameter	Lens				Vitreous Humor			
	10^{-1} M	10^{-2} M	5×10^{-3} M	5×10^{-4} M	10^{-1} M	10^{-2} M	5×10^{-3} M	5×10^{-4} M
Best Fit: All Parameters Allowed to Float Free								
A, μg/g	0.17	0.073	0.020	0.005	0.14	0.036	0.0099	0.0039
α, min^{-1}	0.0016	0.0027	0.0011	0.0033	0.0013	0.0031	0.0019	0.013
AUC, μg/g min	110	27	17	1.6	110	12	5.2	0.30
r^2	0.88	0.98	0.79	0.96	0.47	0.93	0.45	0.91
r	0.94	0.99	0.89	0.98	0.64	0.98	0.53	0.94
Constrained Fit: α Fixed to 10^{-2} M Exponent								
A, μg/g	0.21	0.073	0.032	0.0046	0.19	0.036	0.012	0.0025
α, min^{-1}	0.0027	0.0027	0.0027	0.0027	0.0031	0.0031	0.0031	0.0031
AUC, μg/g min	79	27	12	1.8	60	12	4.0	8.0
r^2	0.78	0.98	0.50	0.95	0.44	0.93	0.48	0.84
r	0.92	0.99	0.78	0.97	0.63	0.98	0.56	0.85

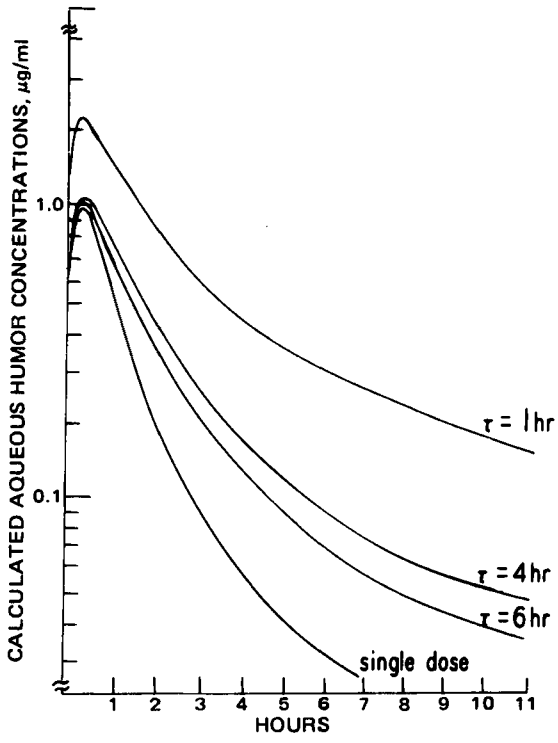

Figure 6—*Calculated aqueous humor levels* (n = ∞) *based on different dosing intervals* (τ).

of a short duration. Continuation of the dosage regimen would eventually cause a plateauing effect at a higher level than the original. Once drug in the reservoirs became significant, the overall shape of the curve changed (Fig. 6).

After a sufficient number of doses, the term $1 - e^{-n\alpha_i\tau}$ in Eqs. 3 and 4 goes to one. Consequently, at long-term maintenance:

$$C = M\left[\sum_{i=1}^{4}\frac{A_i e^{-\alpha_i\tau}}{(1-e^{-\alpha_i\tau})}\right] \qquad \text{(Eq. 11)}$$

With this equation, it is possible to generate the family of curves for varying dosing intervals (Fig. 6).

The model predicts a negligible increase in peak height at $n \to \infty$ for large τ (dosing intervals of 4–6 hr are normal) but significant increases in the amount remaining at the end of the dosing interval, showing an apparent reduction in the elimination rate constant. The increase in drug concentration is two to three times higher than the single-dose information in a properly designed experimental model (quadexponential) and several orders of magnitude higher in the biexponential model, which is currently being used in ocular pharmacokinetics.

APPENDIX

The mathematical derivation of the pharmacokinetic model for pilocarpine in the rabbit eye is as follows. Drug distribution in the eye can be compartmentalized as shown in Scheme IV:

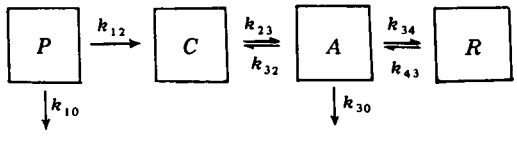

Scheme IV

where P is the precorneal area, C is the cornea, A is the anterior segment (excluding lens and cornea), R is the reservoir consisting of the lens and vitreous, and k_{ij} is the rate constant for drug transport into and out of the various areas.

By using standard matrix theory, it can be shown that the equations for concentrations in cornea, aqueous, and reservoirs are:

$$\text{cornea} = C_c = Ae^{-\alpha t} + Be^{-\beta t} + Ce^{-\Gamma t} + De^{-\Delta t} \qquad \text{(Eq. A1)}$$

$$\text{aqueous} = C_a = Ee^{-\alpha t} + Fe^{-\beta t} + Ge^{-\Gamma t} + He^{-\Delta t} \qquad \text{(Eq. A2)}$$

$$\text{reservoir} = C_R = Ie^{-\alpha t} + Je^{-\beta t} + Ke^{-\Gamma t} + Le^{-\Delta t} \qquad \text{(Eq. A3)}$$

where:

$$A = [(\text{dose/volume})k_{12}(XA-\alpha)(XB-\alpha)]\div[(\Gamma-\alpha)(\Delta-\alpha)(\beta-\alpha)]$$
$$B = [(\text{dose/volume})k_{12}(XA-\beta)(XB-\beta)]\div[(\Gamma-\beta)(\Delta-\beta)(\alpha-\beta)]$$
$$C = [(\text{dose/volume})k_{12}(XA-\Gamma)(XB-\Gamma)]\div[(\beta-\Gamma)(\Delta-\Gamma)(\alpha-\Gamma)]$$
$$D = [(\text{dose/volume})k_{12}(XA-\Delta)(XB-\Delta)]\div[(\beta-\Delta)(\Gamma-\Delta)(\alpha-\Gamma)]$$
$$E = [(\text{dose/volume})(k_{12}k_{23})(k_{43}-\alpha)]\div[(\beta-\alpha)(\Gamma-\alpha)(\Delta-\alpha)]$$
$$F = [(\text{dose/volume})(k_{12}k_{23})(k_{43}-\beta)]\div[(\alpha-\beta)(\Gamma-\beta)(\Delta-\beta)]$$
$$G = [(\text{dose/volume})(k_{12}k_{23})(k_{43}-\Gamma)]\div[(\alpha-\Gamma)(\beta-\Gamma)(\Delta-\Gamma)]$$
$$H = [(\text{dose/volume})(k_{12}k_{23})(k_{43}-\Delta)]\div[(\alpha-\Delta)(\beta-\Delta)(\Gamma-\Delta)]$$
$$I = (E)(k_{34})\div(k_{43}-\alpha)$$
$$J = (F)(k_{34})\div(k_{43}-\beta)$$
$$K = (G)(k_{34})\div(k_{43}-\Gamma)$$
$$L = (H)(k_{34})\div(k_{43}-\Delta)$$
$$XA = \tfrac{1}{2}\{(k_{43}+k_{32}+k_{34}+k_{30}) + [(k_{43}+k_{32}+k_{34}+k_{30})^2 - 4(k_{43})(k_{32}+k_{30})]^{1/2}\}$$
$$XB = \tfrac{1}{2}\{(k_{43}+k_{32}+k_{34}+k_{30}) - [(k_{43}+k_{32}+k_{34}+k_{30})^2 - 4(k_{43})(k_{32}+k_{30})]^{1/2}\}$$
$$\alpha = k_{12} + k_{10}$$
$$\beta = S - T + P/3$$
$$\Gamma = \frac{S+T}{2} - \frac{S-T}{2}\sqrt{-3} + (P/3)$$
$$\Delta = \frac{S+T}{2} + \frac{S-T}{2}\sqrt{-3} + (P/3)$$
$$P = k_{23} + k_{32} + k_{34} + k_{43} + k_{30}$$
$$Q = 2(k_{43}k_{23}) + (k_{43}k_{30}) + (k_{23}k_{34}) + (k_{23}k_{30})$$
$$R = (k_{23}k_{43}k_{30})$$
$$S = \left[-b/2 + \left(\frac{b^2}{4} + \frac{a^3}{27}\right)^{1/2}\right]^{1/3}$$
$$T = \left[-b/2 - \left(\frac{b^2}{4} + \frac{a^3}{27}\right)^{1/2}\right]^{1/3}$$
$$a = (1/3)(3Q - P^2)$$
$$b = (1/27)(2P^3 - 9PQ + 27R)$$

The magnitude of the first-order constants associated with drug disposition in the eye are:

microconstants	minutes^{-1}
k_{10}	5.71×10^{-1}
k_{12}	6.2×10^{-3}
k_{23}	4.85×10^{-2}
k_{32}	4.03×10^{-2}
k_{34}	8.89×10^{-3}
k_{43}	3.39×10^{-3}
k_{30}	3.49×10^{-2}

REFERENCES

(1) R. Lazare and H. Horlington, *Exp. Eye Res.*, **21**, 281 (1975).

(2) M. D. Van Hoose and F. E. Leaders, *Invest. Ophthalmol.*, **13**, 377 (1974).

(3) S. Yoshida and S. Mishima, *Jpn. J. Ophthalmol.*, **19**, 121 (1975).

(4) J. W. Sieg and J. R. Robinson, *J. Pharm. Sci.*, **64**, 931 (1975).

(5) K. Green and D. L. MacKeen, *Invest. Ophthalmol.*, **15**, 220 (1976).

(6) H. Beasley, J. J. Boltralik, and H. A. Baldwin, *Arch. Ophthalmol.*, **93**, 184 (1975).

(7) J. Y. Massey, C. Hanna, R. Goodart, and T. Wallace, *Am. J. Ophthalmol.*, **81**, 151 (1976).

(8) R. E. Hardberger, C. Hanna, and R. Goodart, *ibid.*, **80**, 133 (1975).

(9) T. F. Patton, Ph.D. thesis, University of Wisconsin, Madison, Wis., 1975.

(10) S. S. Chrai and J. R. Robinson, *Am. J. Ophthalmol.*, **77**, 735 (1974).

(11) K. A. Connors, "A Textbook of Pharmaceutical Analysis," Wiley, New York, N.Y., 1967, p. 502.

(12) P. Chung, T. Chin, and J. Lach, *J. Pharm. Sci.*, **59**, 1300 (1970).

(13) L. Sendelbeck, D. Moore, and J. Urquhart, *Am. J. Ophthalmol.*, **80**, 214 (1975).
(14) S. S. Chrai, M. C. Makoid, S. P. Eriksen, and J. R. Robinson, *J. Pharm. Sci.*, **63**, 333 (1974).
(15) S. S. Chrai, T. F. Patton, A. Mehta, and J. R. Robinson, *ibid.*, **62**, 1112 (1973).
(16) J. W. Sieg and J. R. Robinson, *ibid.*, **65**, 1816 (1976).
(17) R. E. Notari, J. E. DeYoung, and R. H. Reuning, *ibid.*, **61**, 135 (1972).
(18) D. Perrier and M. Gibaldi, *ibid.*, **62**, 225 (1973).
(19) L. J. Leeson and H. Weintraub, *ibid.*, **62**, 1936 (1973).
(20) M. C. Makoid, J. W. Sieg, and J. R. Robinson, *ibid.*, **65**, 150 (1976).
(21) J. S. Lyons and D. L. Krohn, *Am. J. Ophthalmol.*, **75**, 885 (1973).
(22) D. M. Maurice, *The Sight Saving Review*, **42**, 42 (1972).

ACKNOWLEDGMENTS

Supported by a grant from Allergan Pharmaceuticals, Irvine, CA 92664, and by Grant EY-01332 from the National Institutes of Health.
The authors thank Mr. Arthur Welnitz for technical assistance.

Rapid Determination of Theophylline in Serum by Electron-Capture GLC

SY-RONG SUN

Received July 13, 1978, from the *Pharmaceutical Products Division, Abbott Laboratories, North Chicago, IL 60064.* Accepted for publication September 11, 1978.

Abstract □ A rapid and sensitive GLC procedure was developed for the determination of theophylline in serum. After extraction from serum with ethyl acetate, theophylline and the internal standard were derivatized with pentafluorobenzyl bromide under alkaline conditions. The derivatives were quantitated by electron-capture detection. The method has a sensitivity of 0.1 μg/ml with a 0.1-ml serum sample.

Keyphrases □ Theophylline—electron-capture GLC determination of serum levels □ GLC, electron capture—analysis, theophylline in serum □ Relaxants, smooth muscle—electron-capture GLC analysis of theophylline in serum

Methods for the determination of theophylline in biological fluids are based on spectrophotometry (1–3), GLC (4–8), TLC (9), and high-pressure liquid chromatography (10–14). Recently, an electron-capture GLC procedure was reported (15) that involves the extraction of theophylline and the internal standard, theobromine, into methylene chloride by elution through a cellulose column. The compounds are then back-extracted into an alkaline aqueous phase and derivatized with pentafluorobenzyl bromide by extractive alkylation. The derivatives are separated from excess reagent by solvent extraction and finally determined by electron-capture GLC. This method is tedious, and the use of theobromine as an internal standard is not a good choice because it is present in beverages such as tea and cocoa and is a metabolite of caffeine (16–18).

The present, rapid method requires only 0.1-ml serum sample. It involves one-step extraction of the serum sample with ethyl acetate, followed by derivatization with pentafluorobenzyl bromide under alkaline conditions at 100°. Excess reagent is removed by evaporation. A chemical isomer of theophylline, which is not present in beverages and is not a metabolite of caffeine, is used as the internal standard. The sensitivity of the assay is 0.1 μg/ml with a 0.1-ml serum sample.

EXPERIMENTAL

Reagents and Materials—Theophylline[1], the internal standard (5,7-dimethyl-2*H*-pyrazolo[3,4-*d*]pyrimidine-4,6-(5*H*,7*H*)-dione, I)[2], and pentafluorobenzyl bromide[3] were used as supplied. The other chemicals were analytical reagent grade.

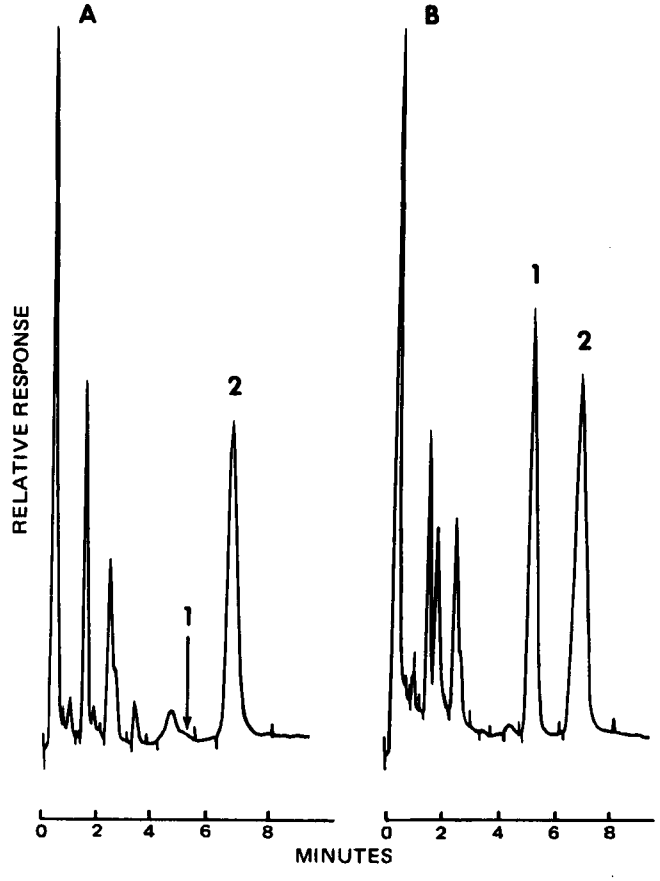

Figure 1—*GLC tracings of extracted serum samples. Key: A, serum blank containing the internal standard; B, serum standard containing the internal standard and theophylline at 5 μg/ml serum; 1, theophylline; and 2, internal standard.*

[1] Theophylline USP ($C_7H_8N_4O_2 \cdot H_2O$).

[2] Nippons Shinyaku Co., Kyoto, Japan.
[3] Pentafluorobenzyl bromide, Pierce Chemical Co., Rockford, Ill.

0022-3549/79/0400-0443$01.00/0
© 1979, American Pharmaceutical Association

(13) L. Sendelbeck, D. Moore, and J. Urquhart, *Am. J. Ophthalmol.*, **80**, 214 (1975).
(14) S. S. Chrai, M. C. Makoid, S. P. Eriksen, and J. R. Robinson, *J. Pharm. Sci.*, **63**, 333 (1974).
(15) S. S. Chrai, T. F. Patton, A. Mehta, and J. R. Robinson, *ibid.*, **62**, 1112 (1973).
(16) J. W. Sieg and J. R. Robinson, *ibid.*, **65**, 1816 (1976).
(17) R. E. Notari, J. E. DeYoung, and R. H. Reuning, *ibid.*, **61**, 135 (1972).
(18) D. Perrier and M. Gibaldi, *ibid.*, **62**, 225 (1973).
(19) L. J. Leeson and H. Weintraub, *ibid.*, **62**, 1936 (1973).
(20) M. C. Makoid, J. W. Sieg, and J. R. Robinson, *ibid.*, **65**, 150 (1976).
(21) J. S. Lyons and D. L. Krohn, *Am. J. Ophthalmol.*, **75**, 885 (1973).
(22) D. M. Maurice, *The Sight Saving Review*, **42**, 42 (1972).

ACKNOWLEDGMENTS

Supported by a grant from Allergan Pharmaceuticals, Irvine, CA 92664, and by Grant EY-01332 from the National Institutes of Health.
The authors thank Mr. Arthur Welnitz for technical assistance.

Rapid Determination of Theophylline in Serum by Electron-Capture GLC

SY-RONG SUN

Received July 13, 1978, from the *Pharmaceutical Products Division, Abbott Laboratories, North Chicago, IL 60064.* Accepted for publication September 11, 1978.

Abstract □ A rapid and sensitive GLC procedure was developed for the determination of theophylline in serum. After extraction from serum with ethyl acetate, theophylline and the internal standard were derivatized with pentafluorobenzyl bromide under alkaline conditions. The derivatives were quantitated by electron-capture detection. The method has a sensitivity of 0.1 μg/ml with a 0.1-ml serum sample.

Keyphrases □ Theophylline—electron-capture GLC determination of serum levels □ GLC, electron capture—analysis, theophylline in serum □ Relaxants, smooth muscle—electron-capture GLC analysis of theophylline in serum

Methods for the determination of theophylline in biological fluids are based on spectrophotometry (1–3), GLC (4–8), TLC (9), and high-pressure liquid chromatography (10–14). Recently, an electron-capture GLC procedure was reported (15) that involves the extraction of theophylline and the internal standard, theobromine, into methylene chloride by elution through a cellulose column. The compounds are then back-extracted into an alkaline aqueous phase and derivatized with pentafluorobenzyl bromide by extractive alkylation. The derivatives are separated from excess reagent by solvent extraction and finally determined by electron-capture GLC. This method is tedious, and the use of theobromine as an internal standard is not a good choice because it is present in beverages such as tea and cocoa and is a metabolite of caffeine (16–18).

The present, rapid method requires only 0.1-ml serum sample. It involves one-step extraction of the serum sample with ethyl acetate, followed by derivatization with pentafluorobenzyl bromide under alkaline conditions at 100°. Excess reagent is removed by evaporation. A chemical isomer of theophylline, which is not present in beverages and is not a metabolite of caffeine, is used as the internal standard. The sensitivity of the assay is 0.1 μg/ml with a 0.1-ml serum sample.

EXPERIMENTAL

Reagents and Materials—Theophylline[1], the internal standard (5,7-dimethyl-2*H*-pyrazolo[3,4-*d*]pyrimidine-4,6-(5*H*,7*H*)-dione, I)[2], and pentafluorobenzyl bromide[3] were used as supplied. The other chemicals were analytical reagent grade.

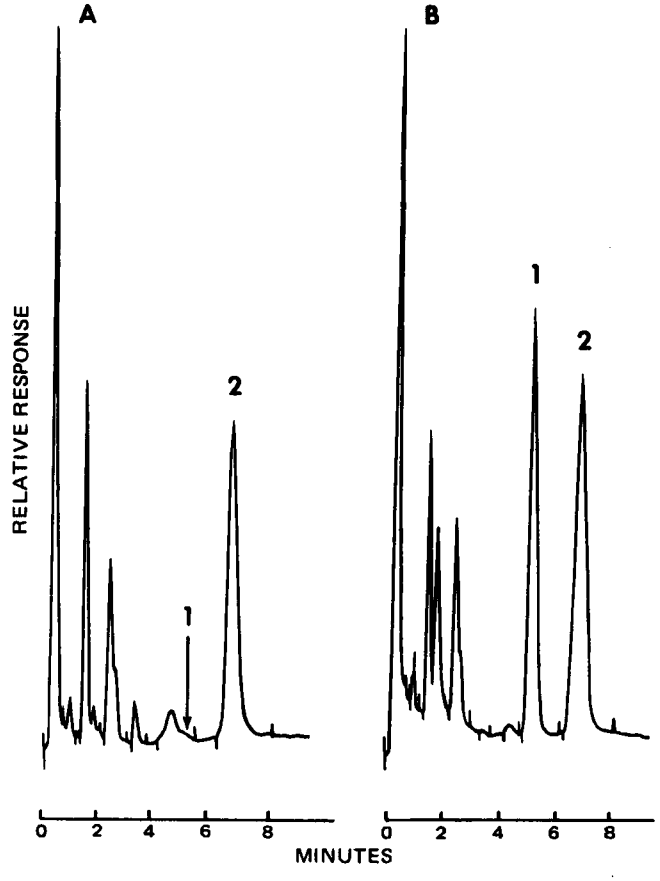

Figure 1—*GLC tracings of extracted serum samples. Key: A, serum blank containing the internal standard; B, serum standard containing the internal standard and theophylline at 5 μg/ml serum; 1, theophylline; and 2, internal standard.*

[1] Theophylline USP ($C_7H_8N_4O_2 \cdot H_2O$).

[2] Nippons Shinyaku Co., Kyoto, Japan.
[3] Pentafluorobenzyl bromide, Pierce Chemical Co., Rockford, Ill.

0022-3549/79/0400-0443$01.00/0
© 1979, American Pharmaceutical Association

Table I—Assay Reproducibility

Serum Theophylline Concentration, μg/ml		
Theoretical	Observed Mean[a] ± *SD*	*RSD*, %
0.10	0.115 ± 0.026	22.2
0.25	0.189 ± 0.029	15.3
0.50	0.489 ± 0.027	5.5
1.00	1.034 ± 0.070	6.8
2.50	2.567 ± 0.219	8.5
5.00	4.942 ± 0.386	7.8
10.00	10.001 ± 0.345	3.4

[a] Mean of three determinations at each concentration.

Table II—Assay Sensitivity

Serum Theophylline Concentration, μg/ml	Peak Area Ratio, Theophylline/Internal Standard
0.25	0.039
	0.046
	0.046
0.50	0.090
	0.084
	0.083
1.0	0.162
	0.174
	0.154
2.5	0.423
	0.393
	0.356
5.0	0.705
	0.836
	0.783

Least-Squares Linear Regression Calculation (19)

Number of points	15
Slope	0.1540
y-Intercept ± 95% confidence limit	0.00551 ± 0.01466
Correlation coefficient	0.996
Calculated sensitivity[a], μg/ml	0.095 μg/ml

[a] The calculated sensitivity was the *x* value (in concentration) corresponding to the upper part of the 95% confidence interval of the *y* intercept (in peak area ratio).

Apparatus—A refrigerated centrifuge[4] was used. Sample solutions were mixed[5] in the test tubes. Pentafluorobenzyl derivative formation at high temperature was carried out on a heating block[6].

GLC—A reporting gas chromatograph[7] equipped with a computing integrator[8] and a ^{63}Ni constant current electron-capture detector[9] was used. The 1.21-m × 4-mm (i.d.) glass column was packed with 5% OV-225[10] on 80–100-mesh Gas Chrom Q[10]. The column was conditioned at 250° for 16 hr with a carrier gas [argon–methane[11] (95:5)] at 20 ml/min before connection to the detector. The carrier gas cylinder was fitted with an oxygen trap filter[12].

The operating conditions were: column oven temperature, 250°; electron-capture detector temperature, 320°; injection port temperature, 270°; and carrier gas flow rate, 45 ml/min. Under these conditions, the pentafluorobenzyl derivatives for theophylline and the internal standard had retention times of 5.3 and 7.1 min, respectively (Fig. 1).

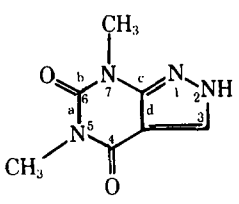

I

[4] Model RC-3, Sorvall, Newton, Conn.
[5] Vortex Genie model K-550-GT mixer, Scientific Industries, Springfield, Mass.
[6] Dri-block DB-3, Techne, Princeton, N.J.
[7] Hewlett-Packard model 5830A.
[8] Hewlett-Packard model 18850A.
[9] Hewlett-Packard model 18803A.
[10] Applied Science Laboratories, State College, Pa.
[11] Matheson Gas Products, Elk Grove Village, Ill.
[12] Altech Associates, Arlington Heights, Ill.

Table III—Assay Accuracy

Serum Theophylline Concentration, μg/ml		
Theoretical	Observed	Difference
10.00	9.60	−0.40
5.00	4.85	−0.15
2.50	2.76	0.26
1.00	1.09	0.09
0.50	0.36	−0.14
0.25	0.16	−0.09
0.10	0.14	0.04
0	0	0
7.50	6.92	−0.58
3.75	3.66	−0.09
1.75	1.79	0.04
0.75	0.79	0.04
0.38	0.52	0.14
6.25	6.26	0.01
3.0	2.76	−0.24

Preparation of Standards—A 200-μg/ml stock solution of theophylline was prepared by dissolving 22.0 mg of theophylline in a 100-ml volumetric flask with distilled water and bringing the mixture to volume. A working serum theophylline standard at 10 μg/ml was prepared by adding 5.0 ml of the stock solution to a 100-ml volumetric flask and bringing the mixture to volume with drug-free serum. Drug-free serum was obtained from volunteers that did not drink coffee, tea, or cocoa. Other serum standards were prepared from serial dilutions (with serum) of the 10-μg/ml serum standard.

The internal standard stock solution (100 μg/ml) was prepared by dissolving 20.0 mg of the internal standard in a 200-ml volumetric flask with methanol and bringing the mixture to volume. A working internal standard solution (3 μg/ml) was prepared by diluting 3 ml of the internal standard stock solution to 100 ml with distilled water.

Assay—To 0.1 ml of serum in a 15-ml conical test tube were added 0.1 ml of 0.1 *N* HCl, 0.1 ml of the internal standard solution, and 1 ml of ethyl acetate. The tube was vortexed for 15 sec and centrifuged at 3000 rpm for 3 min at 10°. Then 0.7 ml of the organic phase was transferred into a 15-ml screw-capped conical test tube and evaporated to dryness at 50° with filtered air.

To the dry residue were added 0.1 ml of sodium carbonate solution (250 μg/ml of water) and 0.1 ml of pentafluorobenzyl bromide in alcohol (2 mg/ml). The mixture was capped, vortexed for 15 sec, reacted at 100° for 20 min on the heating block, and cooled to room temperature. Then 0.5 ml of water and 1.3 ml of benzene were added, followed by vortexing for 15 sec.

One milliliter of the benzene extract was separated and evaporated to dryness at 50° with filtered air. The clear residue was reconstituted with 1.5 ml of benzene by vortexing for 15 sec, and 5 μl of the solution was injected into the GLC column by the automatic sampler[13].

Calculations—The peak area ratios of theophylline to the internal standard were plotted against known standards of theophylline expressed as micrograms per milliliter of serum. The curve was linear in the 0.25–5.0-μg/ml region. Values for unknown serum theophylline concentrations were obtained from the calibration curve.

RESULTS AND DISCUSSION

Figure 1 shows a chromatogram of an extract from 0.1 ml of serum spiked with theophylline. Peak shapes were symmetrical. Theophylline and the internal standard were resolved from coextractive peaks.

The reproducibility of the assay is shown in Table I. Relative standard deviations ranged from 3.4 to 8.5% for serum concentrations from 0.5 to 10.0 μg/ml. Larger deviations were observed at lower serum concentrations. The calculated sensitivity of the assay was 0.095 μg/ml (Table II).

The accuracy of this assay was tested by analyzing 15 unknown spiked serum samples under blind conditions (Table III). The assay is specific for theophylline; the retention times for pentafluorobenzyl derivatives of theophylline, the internal standard, and theobromine were 5.31, 7.09, and 4.74 min, respectively.

Recoveries averaged 104.0 ± 3.1% (mean ± *SD*) for triplicate serum theophylline samples at 10 μg/ml. This value was calculated by comparing the peak area ratios between the extracted serum sample and the water sample.

This method is specific and sensitive and can be used to conduct single

[13] Hewlett-Packard model 7671A.

oral dose theophylline bioavailability studies in human adults and pediatric patients.

REFERENCES

(1) J. A. Schack and S. H. Waxler, *J. Pharmacol. Exp. Ther.*, **97**, 283 (1949).

(2) J. W. Jenne, E. Wyze, B. S. Rood, and F. M. MacDonald, *Clin. Pharmacol. Ther.*, **14**, 349 (1972).

(3) R. C. Gupta and G. D. Lundberg, *Anal. Chem.*, **45**, 2403 (1973).

(4) V. P. Shah and S. Riegelman, *J. Pharm. Sci.*, **63**, 283 (1974).

(5) B. Wesley-Hadzija, *Br. J. Clin. Pharmacol.*, **1**, 516 (1974).

(6) A. Arbin and P. O. Edlund, *Acta Pharm. Suec.*, **11**, 249 (1974).

(7) J. D. Lowry, L. J. Williamson, and V. A. Raisys, *J. Chromatogr.*, **143**, 83 (1977).

(8) G. F. Johnson, W. A. Dechtiaruk, and H. M. Solomon, *Clin. Chem.*, **21**, 144 (1974).

(9) B. Wesley-Hadzija and A. M. Mattocks, *J. Chromatogr.*, **115**, 501 (1975).

(10) R. D. Thompson, H. T. Nagasawa, and J. W. Jenne, *J. Lab. Clin. Med.*, **84**, 584 (1974).

(11) D. S. Sitar, K. M. Piafsky, and R. E. Rangao, *Clin. Res.*, **22**, 726A (1974).

(12) G. W. Peng, V. Smith, A. Peng, and W. L. Chiou, *Res. Commun. Chem. Pathol. Pharmacol.*, **15**, 341 (1976).

(13) R. E. Hill, *J. Chromatogr.*, **135**, 419 (1977).

(14) J. J. Orcutt, P. P. Kozak, Jr., S. A. Gillman, and L. H. Cummins, *Clin. Chem.*, **23**, 599 (1977).

(15) A. Arbin and P. Edlund, *Acta Pharm. Suec.*, **12**, 119 (1975).

(16) G. Schmidt and R. Schoyere, *Dtsch. Z. Gesamte Gerichtl. Med.*, **57**, 402 (1966).

(17) A. W. Burg, *Drug Metab. Rev.*, **4**, 199 (1975).

(18) K. K. Midha, S. Sved, R. D. Hossie, and I. J. McGilveray, *Biomed. Mass Spectrom.*, **4**, 172 (1977).

(19) A. Goldstein, "Biostatistics: An Introductory Test," Macmillan, New York, N.Y., 1967.

ACKNOWLEDGMENTS

The author thanks M. Leveque for technical assistance and Dr. Mario Gonzalez of Purdue University and Dr. S. Borodkin for helpful discussions.

Sensitive GLC Assay for Pemoline in Biological Fluids Using Nitrogen-Specific Detection

DANIEL J. HOFFMAN

Received May 31, 1978, from the *Pharmaceutical Products Division, Abbott Laboratories, North Chicago, IL 60064.* Accepted for publication September 9, 1978.

Abstract □ Extractive alkylation was used to determine intact pemoline in serum and urine. Pemoline was extracted into methylene chloride as an ion-pair with tetrapentylammonium hydroxide under alkaline conditions. Evaporation of the solvent at 70° in the presence of methyl iodide yielded the *N,N*-dimethylpemoline derivative. GLC analysis was performed on a 5% FFAP column with nitrogen-specific detection. Sensitivity was 0.05 μg/ml with 1 ml of urine or serum. Calibration curves were linear to at least 4 μg/ml with serum and 15 μg/ml with urine. Precision was excellent with a pooled relative standard deviation of ±7.5% for serum samples in a 0.1–4-μg/ml range.

Keyphrases □ Pemoline—GLC assay using nitrogen-specific detection, biological fluids □ GLC—analysis, pemoline in biological fluids □ Stimulants—pemoline, GLC assay in biological fluids

Several methods to determine pemoline (2-amino-5-phenyl-2-oxazolin-4-one) in biological fluids have been published. In one method (1), pemoline is hydrolyzed to mandelic acid with subsequent oxidation to benzaldehyde. The benzaldehyde is then determined spectrophotometrically. Benzaldehyde generated from pemoline has also been determined by GLC (2). Large sample volumes are required, and the method is tedious and nonspecific. High-pressure liquid chromatography has been applied to urine samples and pharmaceutical preparations (3). However, this method and a TLC method (4) lack the sensitivity for plasma samples.

A GLC method (5) using flame-ionization detection involves hydrolysis of pemoline to 5-phenyl-2,4-oxazolidinedione with subsequent methylation using diazomethane. Extensive cleanup procedures are needed with blood samples, and 60% of the final extract is injected into the chromatograph to achieve sensitivity. A similar approach was recently taken by Libeer and Schepens (6).

A recent GLC method using electron-capture detection determined 5-phenyl-2,4-oxazolidinedione without methylation (7). The method is sensitive but requires careful column preparation and preservation to minimize tailing and to maximize resolution from coextractives.

This paper describes the application of extractive alkylation (8, 9) and nitrogen-specific detection for the analysis of pemoline in biological fluids.

Table I—Precision of Serum and Urine Pemoline Assay

Pemoline Concentration, μg/ml	Peak Area Ratio[a]	*RSD*, %
	Serum	
0	0	—
0.05	0.015 ± 0.0006	4.0
0.10	0.029 ± 0.0040	13.8
0.25	0.097 ± 0.0038	3.9
0.50	0.17 ± 0.023	13.5
1.0	0.33 ± 0.011	3.3
2.0	0.68 ± 0.013	1.9
3.0	1.0 ± 0.025	2.5
4.0	1.4 ± 0.076	5.4
	Urine	
0	0	—
1.0	0.25 ± 0.0050	2.0
5.0	1.4 ± 0.047	3.4
15.0	4.4 ± 0.095	2.2

[a] Mean ± *SD* of triplicate standards.

0022-3549/79/0400-0445$01.00/0

© 1979, American Pharmaceutical Association

oral dose theophylline bioavailability studies in human adults and pediatric patients.

REFERENCES

(1) J. A. Schack and S. H. Waxler, *J. Pharmacol. Exp. Ther.*, **97**, 283 (1949).

(2) J. W. Jenne, E. Wyze, B. S. Rood, and F. M. MacDonald, *Clin. Pharmacol. Ther.*, **14**, 349 (1972).

(3) R. C. Gupta and G. D. Lundberg, *Anal. Chem.*, **45**, 2403 (1973).

(4) V. P. Shah and S. Riegelman, *J. Pharm. Sci.*, **63**, 283 (1974).

(5) B. Wesley-Hadzija, *Br. J. Clin. Pharmacol.*, **1**, 516 (1974).

(6) A. Arbin and P. O. Edlund, *Acta Pharm. Suec.*, **11**, 249 (1974).

(7) J. D. Lowry, L. J. Williamson, and V. A. Raisys, *J. Chromatogr.*, **143**, 83 (1977).

(8) G. F. Johnson, W. A. Dechtiaruk, and H. M. Solomon, *Clin. Chem.*, **21**, 144 (1974).

(9) B. Wesley-Hadzija and A. M. Mattocks, *J. Chromatogr.*, **115**, 501 (1975).

(10) R. D. Thompson, H. T. Nagasawa, and J. W. Jenne, *J. Lab. Clin. Med.*, **84**, 584 (1974).

(11) D. S. Sitar, K. M. Piafsky, and R. E. Rangao, *Clin. Res.*, **22**, 726A (1974).

(12) G. W. Peng, V. Smith, A. Peng, and W. L. Chiou, *Res. Commun. Chem. Pathol. Pharmacol.*, **15**, 341 (1976).

(13) R. E. Hill, *J. Chromatogr.*, **135**, 419 (1977).

(14) J. J. Orcutt, P. P. Kozak, Jr., S. A. Gillman, and L. H. Cummins, *Clin. Chem.*, **23**, 599 (1977).

(15) A. Arbin and P. Edlund, *Acta Pharm. Suec.*, **12**, 119 (1975).

(16) G. Schmidt and R. Schoyere, *Dtsch. Z. Gesamte Gerichtl. Med.*, **57**, 402 (1966).

(17) A. W. Burg, *Drug Metab. Rev.*, **4**, 199 (1975).

(18) K. K. Midha, S. Sved, R. D. Hossie, and I. J. McGilveray, *Biomed. Mass Spectrom.*, **4**, 172 (1977).

(19) A. Goldstein, "Biostatistics: An Introductory Test," Macmillan, New York, N.Y., 1967.

ACKNOWLEDGMENTS

The author thanks M. Leveque for technical assistance and Dr. Mario Gonzalez of Purdue University and Dr. S. Borodkin for helpful discussions.

Sensitive GLC Assay for Pemoline in Biological Fluids Using Nitrogen-Specific Detection

DANIEL J. HOFFMAN

Received May 31, 1978, from the *Pharmaceutical Products Division, Abbott Laboratories, North Chicago, IL 60064.* Accepted for publication September 9, 1978.

Abstract □ Extractive alkylation was used to determine intact pemoline in serum and urine. Pemoline was extracted into methylene chloride as an ion-pair with tetrapentylammonium hydroxide under alkaline conditions. Evaporation of the solvent at 70° in the presence of methyl iodide yielded the *N,N*-dimethylpemoline derivative. GLC analysis was performed on a 5% FFAP column with nitrogen-specific detection. Sensitivity was 0.05 μg/ml with 1 ml of urine or serum. Calibration curves were linear to at least 4 μg/ml with serum and 15 μg/ml with urine. Precision was excellent with a pooled relative standard deviation of ±7.5% for serum samples in a 0.1–4-μg/ml range.

Keyphrases □ Pemoline—GLC assay using nitrogen-specific detection, biological fluids □ GLC—analysis, pemoline in biological fluids □ Stimulants—pemoline, GLC assay in biological fluids

Several methods to determine pemoline (2-amino-5-phenyl-2-oxazolin-4-one) in biological fluids have been published. In one method (1), pemoline is hydrolyzed to mandelic acid with subsequent oxidation to benzaldehyde. The benzaldehyde is then determined spectrophotometrically. Benzaldehyde generated from pemoline has also been determined by GLC (2). Large sample volumes are required, and the method is tedious and nonspecific. High-pressure liquid chromatography has been applied to urine samples and pharmaceutical preparations (3). However, this method and a TLC method (4) lack the sensitivity for plasma samples.

A GLC method (5) using flame-ionization detection involves hydrolysis of pemoline to 5-phenyl-2,4-oxazolidinedione with subsequent methylation using diazomethane. Extensive cleanup procedures are needed with blood samples, and 60% of the final extract is injected into the chromatograph to achieve sensitivity. A similar approach was recently taken by Libeer and Schepens (6).

A recent GLC method using electron-capture detection determined 5-phenyl-2,4-oxazolidinedione without methylation (7). The method is sensitive but requires careful column preparation and preservation to minimize tailing and to maximize resolution from coextractives.

This paper describes the application of extractive alkylation (8, 9) and nitrogen-specific detection for the analysis of pemoline in biological fluids.

Table I—Precision of Serum and Urine Pemoline Assay

Pemoline Concentration, μg/ml	Peak Area Ratio[a]	*RSD*, %
	Serum	
0	0	—
0.05	0.015 ± 0.0006	4.0
0.10	0.029 ± 0.0040	13.8
0.25	0.097 ± 0.0038	3.9
0.50	0.17 ± 0.023	13.5
1.0	0.33 ± 0.011	3.3
2.0	0.68 ± 0.013	1.9
3.0	1.0 ± 0.025	2.5
4.0	1.4 ± 0.076	5.4
	Urine	
0	0	—
1.0	0.25 ± 0.0050	2.0
5.0	1.4 ± 0.047	3.4
15.0	4.4 ± 0.095	2.2

[a] Mean ± *SD* of triplicate standards.

0022-3549/79/0400-0445$01.00/0

© 1979, American Pharmaceutical Association

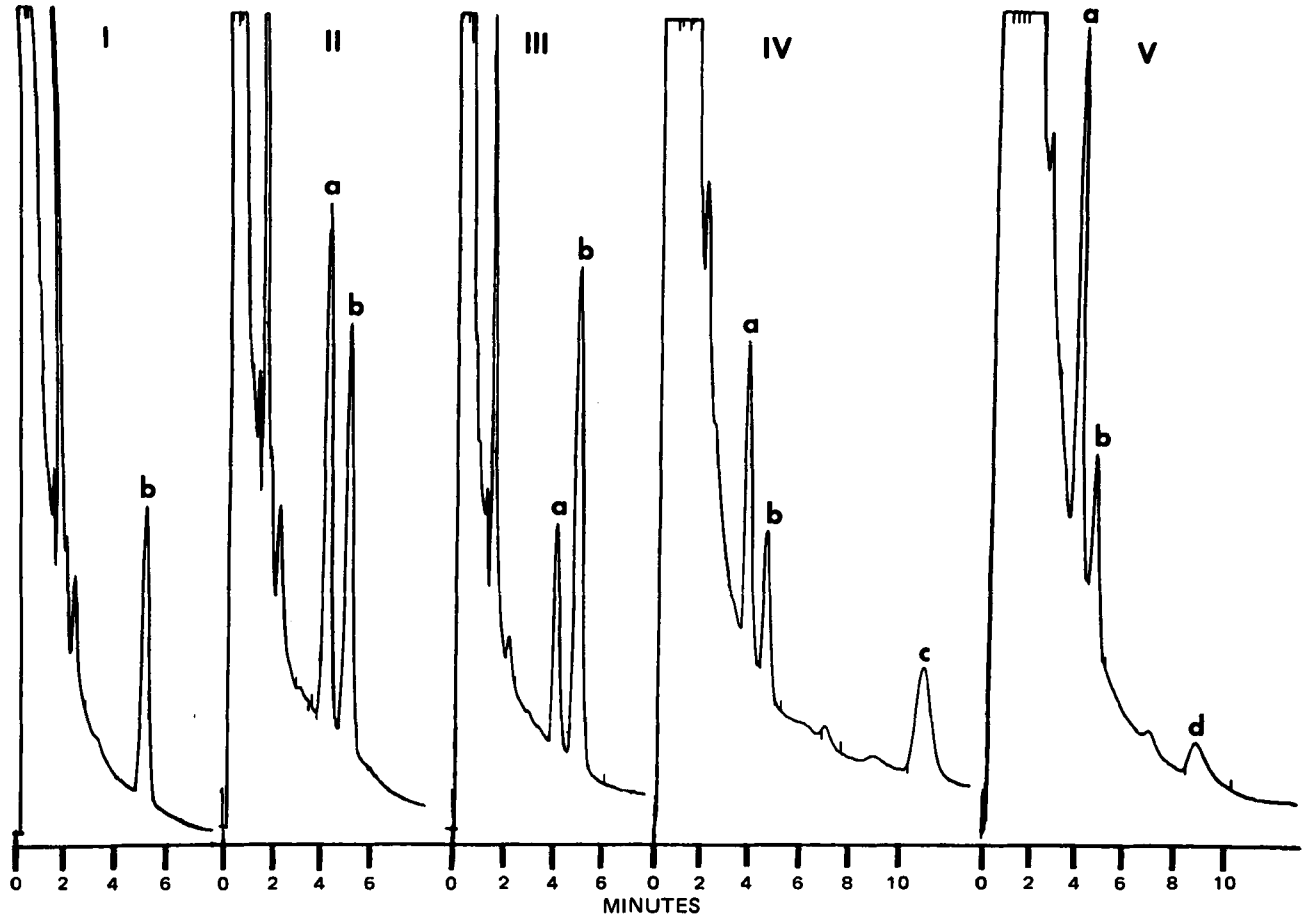

Figure 1—*GLC tracings of serum and urine samples containing pemoline. Key: I, serum blank with internal standard; II, serum standard containing 3 μg of pemoline/ml; III, human serum sample 8 hr after 50-mg oral dose of pemoline; IV, urine standard containing 4 μg of pemoline/ml and 8 μg of* p*-methoxypemoline/ml; V, human urine sample 8 hr after 50-mg oral dose of pemoline; a, pemoline; b, internal standard; c, 5-(*p*-hydroxyphenyl)-2-amino-2-oxazolin-4-one (possible metabolite, although not observed in humans); and d, 5-phenyl-2,4-oxazolidinedione (metabolite).*

EXPERIMENTAL

Reagents—All solvents were analytical reagent grade[1]. Tetrapentylammonium hydroxide[2], pemoline, 2-(*N,N*-dimethylamino)-5-phenyl-2-oxazolin-4-one, 5-phenyl-2,4-oxazolidinedione, and the internal standard 2-amino-5-(2′-methylphenyl)-2-oxazolin-4-one were used as supplied[3].

Instrumentation—A gas chromatograph[4] equipped with a dual nitrogen–phosphorus flame-ionization detector, an automatic sampler[5], and a computing integrator was used. The chromatograph was fitted with a 1.2-m × 2-mm i.d. coiled glass column packed with 5% FFAP[6] on Chromosorb W-HP[7] (80–100 mesh). The column was conditioned overnight at 255° with a helium gas flow rate of 35 ml/min.

Normal operating temperatures were 250, 245, and 280° for the injection port, oven, and detector, respectively. The helium carrier gas flow rate was 38 ml/min. The hydrogen and air flow rates were 3.0 and 50 ml/min, respectively. An attenuation of 2^3 or 2^4 was used.

Preparation of Standards—Standard stock solutions of 1 mg/ml of pemoline and the internal standard were prepared in methanol. A working internal standard solution at 0.5 μg/ml was prepared by diluting 0.5 ml of the 1-mg/ml solution to 1 liter with distilled water. A 4-μg/ml pemoline serum standard was prepared by adding exactly 400 μl of the 1-mg/ml pemoline stock solution to a 100-ml volumetric flask and adjusting to volume with drug-free serum.

Other serum standards were prepared by serial dilutions with serum. Urine standards were prepared in a similar manner using fresh urine. All standards were kept in a freezer until used.

[1] Mallinckrodt.
[2] Eastman.
[3] Abbott Laboratories.
[4] Hewlett-Packard model 5830A.
[5] Hewlett-Packard model 7671A.
[6] Varian Aerograph.
[7] Applied Science Laboratories.

Table II—Accuracy of Serum and Urine Pemoline Assay

Pemoline Concentration, μg/ml		Percent
Actual	Calculated	Difference
	Serum	
1.0	0.97	−3.0
0.24	0.28	+16.7
3.8	3.9	+2.6
2.6	2.5	−3.8
0.12	0.10	−16.7
0.84	0.77	−8.3
1.9	1.9	0
2.5	2.5	0
4.1	4.0	−2.4
3.3	3.1	−6.1
3.4	3.6	+5.9
	Urine	
4.5	4.3	−4.4
10.7	10.8	+0.9
15.2	15.5	+2.0
5.6	5.5	−1.8
1.8	1.6	−11.1
7.7	8.0	+3.9

Extraction Procedure—Serum and urine sample volumes were adjusted, if necessary, to the 0.1–4-μg of pemoline/sample range.

To a 15-ml screw-capped polytef (lined) conical test tube containing 6 ml of 0.5 *M* methyl iodide in methylene chloride were added exactly 1 ml of the internal standard solution and 1 ml of serum or urine sample. Then 0.5 ml of 0.5 *N* NaOH and 100 μl of 0.05 *M* tetrapentylammonium hydroxide were added, and the tube was capped, shaken[8] on a reciprocal

[8] Eberbach Corp.

shaker at about 150 cpm for 10 min, and centrifuged at 20° for 10 min at 3000 rpm.

The upper aqueous phase was discarded, and 5 ml of the organic phase was transferred to a 15-ml conical screw-capped test tube. This separation could also be accomplished using phase separation paper[9]. The extract was evaporated to dryness at 70° plus an additional 10 min after reaching dryness with a stream of filtered air or nitrogen. The residue was reconstituted with 0.3 ml of benzene and mixed for 5 sec. Samples were centrifuged for 5 min at 2500 rpm and then stood at room temperature at least 1 hr before 2 μl was injected into the chromatograph.

Total urinary pemoline levels were determined by incubating 1 ml of an adjusted urine sample[10] with 1000 units of a glucuronidase–sulfatase[11] preparation in 0.2 ml of 0.2 *M* acetate buffer (pH 4.5) for 20 hr at 37°. After incubation, 1 ml of the internal standard solution, 0.6 ml of 0.5 *N* NaOH, 100 μl of 0.05 *M* tetraphenylammonium hydroxide, and 6 ml of 0.5 *M* methyl iodide in dichloromethane were added. Extractive methylation was performed as described for serum samples.

Calculations—A linear calibration curve was constructed by plotting peak area ratios (pemoline/internal standard) against the serum or urine pemoline concentration of pemoline spiked standards. Unknowns were calculated using a computing integrator programmed with the slope of the calibration curve. The slope was obtained by a least-squares linear regression analysis of the pemoline standards.

RESULTS AND DISCUSSION

Under the conditions of alkylative extraction, pemoline was methylated with methyl iodide to 2-(*N,N*-dimethylamino)-5-phenyl-2-oxazolin-4-one

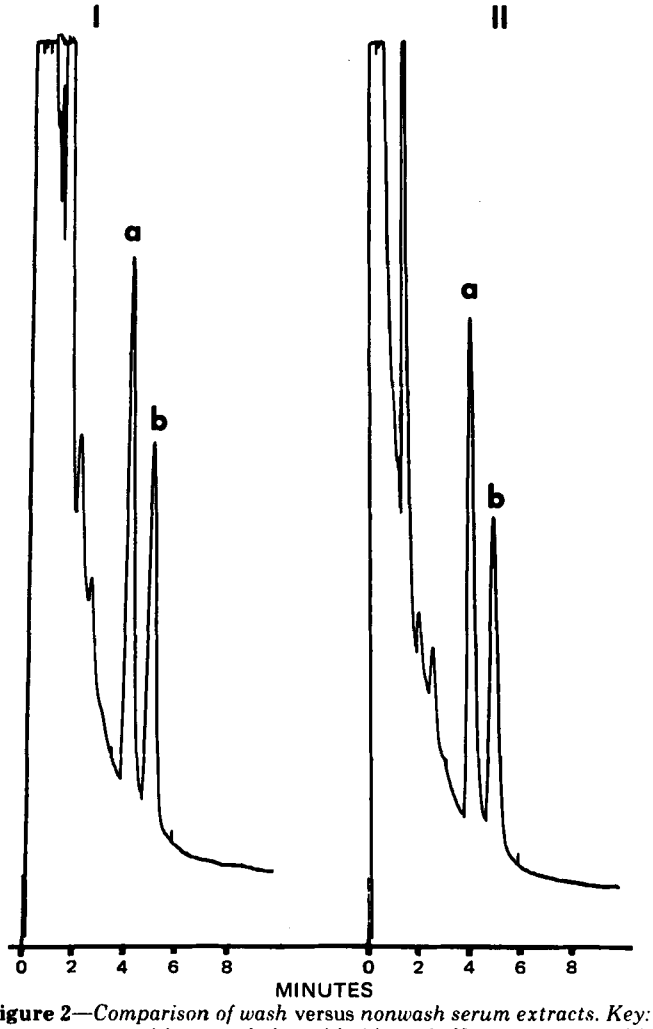

Figure 2—*Comparison of wash* versus *nonwash serum extracts. Key: I, serum extract without methylene chloride wash; II, serum extract with methylene chloride wash; a, pemoline; and b, internal standard.*

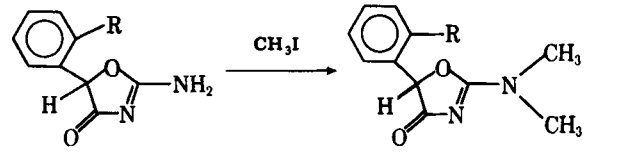

pemoline: R = H 2-*N,N*-dimethylamino derivative
internal standard: R = CH_3

Scheme I

(Scheme I). Identification was made by comparison of the GLC–mass spectral properties with those of an authentic sample of 2-(*N,N*-dimethylamino)-5-phenyl-2-oxazolin-4-one. Pemoline (R_T 4.2 min) and the internal standard (R_T 5.0 min) peak shapes were symmetrical and well resolved from coextractives (Fig. 1). The 5-phenyl-2,4-oxazolidinedione metabolite had a retention time of 9.4 min (Fig. 1).

The choice of tetrapentylammonium hydroxide was based on preliminary experiments with radioactive pemoline[3] (1-^{14}C-pemoline). Recoveries from serum (0.5 μg/ml) averaged 63 ± 1.2% using the tetrapentylammonium counterion. Recoveries from serum using tetramethyl-, tetrahexyl-, and tetraheptylammonium counterions were 1.7, 57, and 27%, respectively.

The assay precision was good for both serum and urine samples (Table I). Relative standard deviations ranged from ±1.9 to ±13.8% with a pooled value of ±7.5% for serum samples. Relative standard deviations for urine samples ranged from ±2.0 to ±3.4% with a pooled value of ±2.5%. The assay sensitivity was less than 0.05 μg/sample. Calibration curves were linear over the range of 0.05–4 μg of pemoline/sample. Correlation coefficients were >0.99 with *y*-intercepts not significantly different from zero.

Accuracy was evaluated by analyzing serum and urine samples spiked with pemoline. As shown in Table II, the accuracy was excellent, especially for samples containing more than 0.5 μg of pemoline.

Inclusion of a methylene chloride wash step prior to the addition of tetrapentylammonium hydroxide reduced the amount of coextractives in the solvent front (Fig. 2) with only a slight improvement in precision. Triplicate serum standards at 4 μg/ml were assayed with and without the methylene chloride wash. The relative standard deviation with the methylene chloride wash was ±1.7%; without the wash (described procedure), it was ±2.5%. The additional step may be necessary with highly contaminated serum, plasma, or urine samples.

The efficiency of the FFAP column is maintained at a high level by repacking the first 10 cm of the column every 100–150 sample injections.

Since pemoline is assayed without prior hydrolysis, this method is useful for the analysis of pemoline metabolites. 5-Phenyl-2,4-oxazolidinedione, which is a metabolite in rabbits[12], can be determined, as can the possible metabolite 5-(*p*-hydroxyphenyl)-2-amino-2-oxazoline-4-one (R_T 10.5 min in Fig. 2). The degree of pemoline conjugation in urine also can be determined from the difference between enzymatically hydrolyzed and nonhydrolyzed samples.

Its sensitivity, precision, and specificity make this method desirable for bioavailability and pharmacokinetic studies. Ease of performance allows for the rapid screening of biological samples for pemoline in drug abuse cases.

REFERENCES

(1) L. M. Cummins and J. E. Perry, *J. Pharm. Sci.*, **58**, 762 (1969).
(2) F. DeSio, C. Marena, and E. Bertol, *Med. Sport*, **26**, 23 (1975).
(3) G. P. Cartoni and F. Natalizia, *J. Chromatogr.*, **123**, 474 (1976).
(4) H. Eberhardt and M. Debackere, *Arzneim.-Forsch.*, **15**, 929 (1965).
(5) M. Van Boven and P. Daenens, *J. Chromatogr.*, **134**, 415 (1977).
(6) J. Libeer and P. Schepens, *J. Pharm. Sci.*, **67**, 419 (1978).
(7) S.-Y. Chu and L. T. Sennello, *J. Chromatogr.*, **137**, 343 (1977).
(8) B. Lindström, M. Molander, and M. Groschinsky, *ibid.*, **114**, 459 (1975).
(9) H. Ehrsson, *Anal. Chem.*, **46**, 922 (1974).

ACKNOWLEDGMENTS

The author is grateful to Dr. S. Sun and Dr. S.-Y. Chu for helpful discussions and to Mr. G. Thomas and Ms. M. Leveque for technical assistance.

[9] Whatman 1 PS.
[10] Urine samples from a fasted subject administered a single 75-mg oral dose of pemoline.
[11] Glusulase, Endo Laboratories.
[12] R. Sonders, Abbott Laboratories, North Chicago, Ill., personal communication.

Quinidine and Dihydroquinidine Interactions in Human Plasma

CLARENCE T. UEDA ˣ and MICHAEL C. MAKOID

Received December 20, 1977, from the *Department of Pharmaceutics and Clinical Pharmacokinetics Laboratory, College of Pharmacy and Cardiovascular Center, University of Nebraska Medical Center, Omaha, NE 68105.* **Accepted for publication September 11, 1978.**

Abstract □ The protein-binding characteristics of dihydroquinidine, a known impurity in drug grade quinidine, in human plasma and the effects of dihydroquinidine on quinidine interactions with these plasma constituents were studied by equilibrium dialysis. In the plasma concentration range of 1.75–23.0 mg/liter, dihydroquinidine binding was similar to the binding observed with quinidine. The data suggested the presence of a single class of binding sites for both compounds in the plasma drug concentration range and samples studied. The mean values for the association constant, K, and the total concentration of binding sites, nP_t, for dihydroquinidine were $4.75 \pm 0.67 \times 10^4\ M^{-1}$ and $5.78 \pm 0.17 \times 10^{-5}\ M$, respectively. The corresponding values for quinidine were $4.78 \pm 1.00 \times 10^4\ M^{-1}$ and $5.65 \pm 0.48 \times 10^{-5}\ M$. In the presence of 5 and 10% (of total alkaloid content) dihydroquinidine, the plasma concentration of unbound quinidine did not change significantly. At a 20% level of dihydroquinidine, however, an increase in unbound quinidine was observed ($p < 0.05$). The elevations in free quinidine concentrations were directly related to the level of dihydroquinidine present. The results of this study indicate that the interactions between dihydroquinidine and quinidine for binding sites on human plasma proteins are competitive.

Keyphrases □ Quinidine—interactions with plasma constituents, effects of dihydroquinidine on binding □ Dihydroquinidine—protein binding, effects on quinidine interactions with plasma constituents □ Interactions—quinidine and dihydroquinidine in human plasma □ Protein binding—quinidine and dihydroquinidine, interactions in plasma

It is well known that by effectively retarding drug movement out of the vascular system, interactions of a drug with plasma proteins can greatly affect the drug's disposition behavior and pharmacological activity (1–3). Quinidine (I), a widely used cardiac antiarrhythmic agent, interacts with various protein components of human plasma. In its therapeutic plasma concentration range of 2–5 μg/ml (4), approximately 80% of the drug is reportedly bound to plasma proteins (5–7). Many studies demonstrated that quinidine interacts with serum albumin (5, 8–11). Nilsen and Jacobsen (12) showed that the drug binds to low and high density plasma lipoproteins. In addition, Skuterud *et al.* (7) suggested the possible interaction of quinidine with α_1- and α_2-serum globulins. Quinidine binding to γ-globulin is reportedly negligible (5).

Although data are available on quinidine binding to plasma proteins, the binding properties of dihydroquinidine (II, a common impurity in drug grade quinidine) to these plasma constituents as well as the effects of dihydroquinidine on quinidine binding in the vascular compartment are not known. The USP (13) presently allows dihydroquinidine levels of up to 20% of the total alkaloidal content in quinidine preparations. In addition, the disposition kinetics of dihydroquinidine and quinidine were similar after intravenous administration of quinidine gluconate containing relatively low levels of the impurity (14).

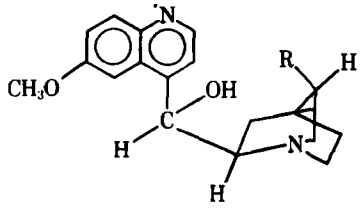

I: R = CH_2=CH
II: R = CH_3—CH_2

These observations suggest that substantial quantities of the impurity can be present in the blood after quinidine administration. More important, the structural similarities between the two compounds suggest that dihydroquinidine can potentially affect the disposition and activity of quinidine through alterations in drug binding to plasma proteins.

This paper discusses the protein-binding characteristics of dihydroquinidine in human plasma and the effects of this impurity on quinidine interactions with these plasma constituents.

EXPERIMENTAL

Materials—Quinidine base, free of dihydroquinidine, was prepared from quinidine sulfate USP[1] according to the method of Thron and Dirscherl (15).

The dihydroquinidine base, which was separated from the quinidine base, was used after catalytic reduction of the trace levels of quinidine to the dihydro derivative. The hydrogenation method described by Heidelberger and Jacobs (16) was used for reduction. A pure sample of dihydroquinidine was obtained after separation on a silica gel[2] chromatographic column and recrystallization with hot methanol and ether (1:1). This material was identical in its melting point, specific rotation in chloroform, NMR, IR, and fluorescence spectra, and chromatographic behavior in various thin-layer systems to those of a pure dihydroquinidine reference sample[3].

Aqueous solutions of quinidine and dihydroquinidine were prepared with sulfuric acid to facilitate drug solution.

Fresh plasma[4] was obtained from 12 healthy and drug-free adult volunteers after separation of the red blood cell fraction.

Methods—The binding of quinidine and dihydroquinidine to plasma proteins was studied by equilibrium dialysis. The apparatus[5] used consisted of 20 polytef cells, each of which was divided into two 1-ml compartments (half-cells) by cellulose tubing[6]. Plasma, 1 ml, was dialyzed against 1 ml of pH 7.4 Krebs–Ringer bicarbonate buffer at 37 ± 0.5° for 3.5 hr. Preliminary investigations indicated that the distribution equilibrium was reached in 3 hr and that the binding of quinidine or dihydroquinidine to the dialysis membrane and/or cell surfaces was less than 7%.

After time for equilibration, the solutions in the buffer and plasma half-cells were removed and assayed for their drug content. The unbound drug fraction was determined by dividing the concentration of drug in the buffer half-cell, which contained unbound drug only, by the drug concentration in the corresponding plasma half-cell.

[1] New York Quinine and Chemical Works, New York, N.Y.
[2] EM Reagents, Brinkmann Instruments, Westbury, N.Y.
[3] Supplied by Fluka AG, Buch SC, Switzerland. This material can be purchased commercially from this company.
[4] Blood Bank, University Hospital, Omaha, Neb.
[5] Dianorm equilibrium dialyzing system, Innovati-Medizin AG, CH-Esslingen, Switzerland.
[6] Spectrapor 1 membrane tubing, Spectrum Medical Instruments, Los Angeles, Calif.

0022-3549/79/0400-0448$01.00/0
© 1979, American Pharmaceutical Association

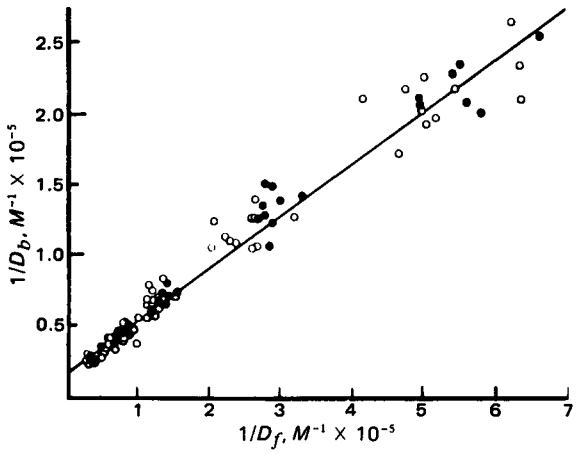

Figure 1—*Relationship between the reciprocal of the bound drug concentration, $1/D_b$, and the reciprocal of the free drug concentration, $1/D_f$, of dihydroquinidine (●) and quinidine (○). Slope and intercept values were 0.36 ± 0.04 and 1.73 ± 0.17 × 10^4 M^{-1} for dihydroquinidine and 0.37 ± 0.05 and 1.77 ± 0.29 × 10^4 M^{-1} for quinidine, respectively.*

Dihydroquinidine binding to plasma proteins was studied with predialysis plasma drug concentrations in the range of 9.2 × 10^{-3}–9.2 × 10^{-2} mM. These concentrations correspond to 3–30 mg/liter of plasma. Double reciprocal plots (17) in the form of Eq. 1 were used to evaluate the binding data:

$$\frac{1}{D_b} = \frac{1}{nKP_t}\frac{1}{D_f} + \frac{1}{nP_t} \qquad \text{(Eq. 1)}$$

where D_b and D_f are the molar concentrations of bound and unbound drug, respectively; n is the number of binding sites on each protein molecule; K is the association constant for the drug–protein complex; and P_t is the total protein concentration.

Equation 1, which assumes the existence of a single class of binding sites, shows that a linear graph is obtained when $1/D_b$ is plotted as a function of $1/D_f$. Therefore, the binding parameters (K and nP_t) can be obtained from the slope and $1/D_b$ axis intercept values of the line. In this way, no direct knowledge of the total protein concentration is required for the analysis of the binding data; the product nP_t reflects the total concentration of binding sites in the plasma sample.

Two types of binding experiments were performed to investigate the competitive influences of dihydroquinidine on the interactions of quinidine with plasma proteins. In the first series, the effects of 0, 5, 10, and 20% (of the total alkaloidal content) dihydroquinidine on quinidine binding were examined. The data were evaluated by assessing the unbound quinidine fraction as a function of the total plasma drug concentration in the 1.2–23.7-mg/liter range.

To evaluate the potential for competitive binding interactions, constant dihydroquinidine concentrations of 2.25 × 10^{-6}, 4.5 × 10^{-6}, and 6.0 × 10^{-6} M were used in the second series with predialysis plasma quinidine concentrations varying between 9.2 × 10^{-3} and 9.2 × 10^{-2} mM. The results were analyzed as previously reported (11, 18, 19).

Dihydroquinidine and quinidine (in the absence of the impurity) in buffer and plasma were assayed by the double-extraction method of Cramer and Isaksson (20). In the presence of the impurity, quinidine concentrations were determined with the previously reported TLC–fluorometric procedure (21).

The data are reported as the mean ± SD. Statistical evaluations were performed using the Student t test.

RESULTS AND DISCUSSION

Dihydroquinidine Binding Studies—Figure 1 summarizes the binding of dihydroquinidine in human plasma when the observed drug concentration ranged from 1.75 to 23.0 mg/liter and the bound drug fraction varied between 0.75 and 0.45. The linearity of this double reciprocal plot supported the assumption of a single class of binding sites for dihydroquinidine in the plasma drug concentration range and samples studied and, hence, the appropriateness of Eq. 1 to describe the binding data. After linear regression analysis of the data obtained for each individual plasma sample, the best values of K and nP_t were 4.75 ± 0.67 × 10^4 M^{-1} and 5.78 ± 0.17 × 10^{-5} M, respectively. The corresponding values for quinidine were 4.78 ± 1.00 × 10^4 M^{-1} and 5.65 ± 0.48 × 10^{-5} M.

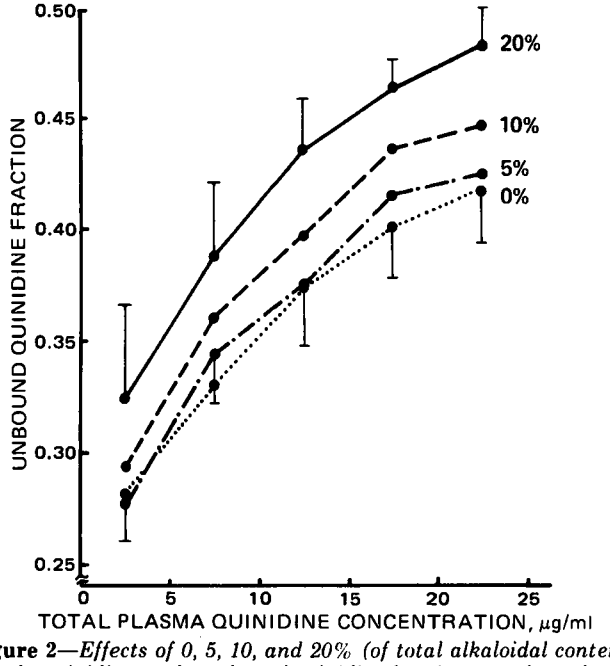

Figure 2—*Effects of 0, 5, 10, and 20% (of total alkaloidal content) dihydroquinidine on the unbound quinidine fraction at various plasma quinidine concentrations.*

The binding characteristics of dihydroquinidine and quinidine in human plasma were virtually identical (Fig. 1). Furthermore, no differences in the binding parameters were observed between the two drugs. The data suggest that both compounds interact with the same sites and protein fractions in plasma. Moreover, these observations suggest that the free plasma quinidine concentration could be elevated in the presence of dihydroquinidine and that the increases would be directly related to the levels of impurity in the initial quinidine sample (*e.g.*, tablet or capsule).

Competitive Binding Studies—The effects of 0, 5, 10, and 20% (of total alkaloid content) dihydroquinidine on the interactions of quinidine with plasma proteins are presented in Fig. 2. Plasma quinidine concentrations in the ranges of 0–4.99, 5–9.99, 10–14.99, 15–19.99, and 20–24.99 mg/liter were graphed as 2.5, 7.5, 12.5, 17.5, and 22.5 mg/liter, respectively.

In the drug concentration range of 2–23 mg/liter and in the absence of impurity, the free, unbound quinidine fraction varied between 0.28 ± 0.02 and 0.42 ± 0.02. In the presence of 5 and 10% dihydroquinidine, although the unbound quinidine fraction was generally slightly greater,

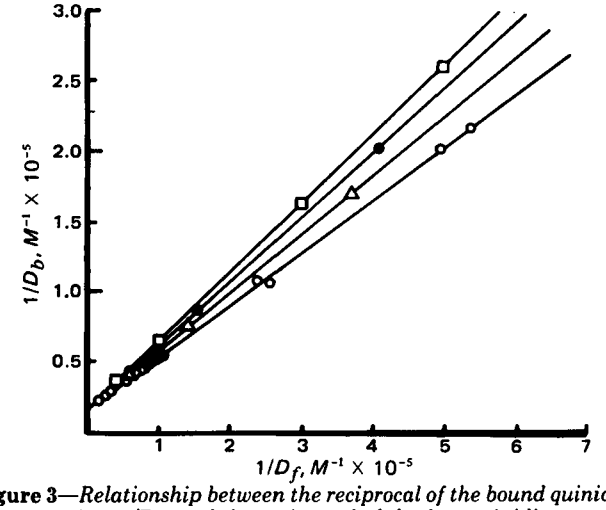

Figure 3—*Relationship between the reciprocal of the bound quinidine concentration, $1/D_b$, and the reciprocal of the free quinidine concentration, $1/D_f$, in the absence (○) and presence of 2.25 × 10^{-6} (△), 4.5 × 10^{-6} (●), and 6.0 × 10^{-6} (□) M of dihydroquinidine.*

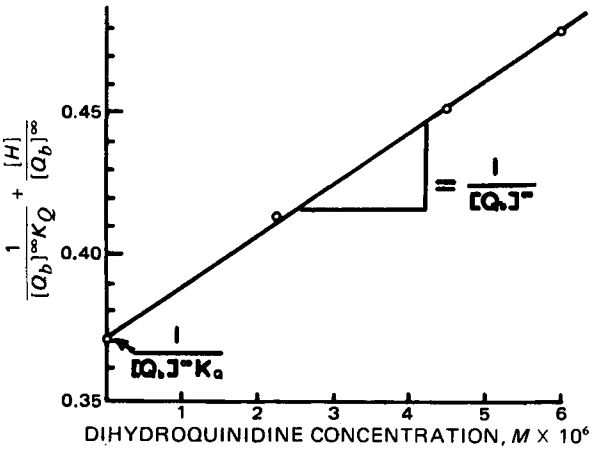

Figure 4—*Relationship between the slope of the individual $1/D_b$ versus $1/D_f$ curves in Fig. 3, obtained by linear regression analysis, and the corresponding dihydroquinidine concentration. See text for discussion.*

the differences were not significant. At the 20% level of the impurity, however, the free quinidine concentrations were increased ($p < 0.05$). Moreover, these increases were approximately those that would have been predicted assuming equivalent affinities and competitive interactions. For example, at a concentration of 23 mg/liter and in the absence of dihydroquinidine, approximately 60% of the total plasma quinidine concentration was present in the bound form. The presence of 20% dihydroquinidine produced an additional 6% (0.5 × 20% × 60%) increase in the free quinidine fraction (from 0.42 to 0.48).

The results of the second series of experiments are summarized in Figs. 3 and 4. In the presence of constant levels of dihydroquinidine of 2.25×10^{-6}, 4.5×10^{-6}, and 6.0×10^{-6} M, the quinidine fraction bound to plasma proteins decreased with increasing dihydroquinidine concentrations. Furthermore, all double reciprocal graphs of the binding data for quinidine at each impurity level were shown (Fig. 3) to intercept the $1/D_b$ coordinate at essentially the same point (approximately 1.75×10^4 M^{-1}). These observations support the conclusion that dihydroquinidine and quinidine interactions for human plasma protein are competitive (11, 18, 19).

Additional evidence was obtained in the following manner. If the interactions of dihydroquinidine and quinidine for binding to human plasma proteins are competitive, the process can be described by:

$$[Q_b] = \frac{[Q_b]^\infty K_Q [Q_f]}{1 + K_Q[Q_f] + K_H[H]} \qquad \text{(Eq. 2)}$$

Rewritten in its reciprocal form, Eq. 2 becomes:

$$\frac{1}{[Q_b]} = \frac{1}{[Q_b]^\infty K_Q [Q_f]} + \frac{K_H[H]}{[Q_b]^\infty K_Q [Q_f]} + \frac{1}{[Q_b]^\infty} \qquad \text{(Eq. 3)}$$

where K_Q and K_H are the affinity constants for plasma proteins of quinidine and dihydroquinidine, respectively; $[Q_b]$ and $[Q_f]$ are the bound and free plasma quinidine concentrations, respectively; $[Q_b]^\infty$ is the maximum concentration of bound quinidine at saturation; and $[H]$ is the plasma concentration of dihydroquinidine.

If it is assumed that dihydroquinidine and quinidine have equivalent affinities for the plasma proteins as the data suggest, then $K_H = K_Q$ and Eq. 3 reduces to:

$$\frac{1}{[Q_b]} = \left[\frac{1}{[Q_b]^\infty K_Q} + \frac{[H]}{[Q_b]^\infty}\right]\frac{1}{[Q_f]} + \frac{1}{[Q_b]^\infty} \qquad \text{(Eq. 4)}$$

It can be seen from Eq. 4 that the slope of the line for each quinidine-binding curve in the presence of dihydroquinidine is a linear function of the competitor concentration. Therefore, a plot of

$$\frac{1}{[Q_b]^\infty K_Q} + \frac{[H]}{[Q_b]^\infty}$$

the slope of each regression line obtained by a given concentration of dihydroquinidine, *versus* $[H]$ should be a straight line with a slope of $1/[Q_b]^\infty$ and an intercept of $1/[Q_b]^\infty K_Q$ if the interactions are competitive.

A plot of this relationship is shown in Fig. 4; a linear relationship, indicative of competitive binding interactions between dihydroquinidine and quinidine, was obtained. Furthermore, by using the slope (1.82×10^4 M^{-1}) and intercept (0.37) values obtained by regression analysis of this curve, a value of 4.92×10^4 M^{-1} was computed for K_Q, which is in excellent agreement with the previous studies using quinidine alone ($K_Q = 4.78 \pm 1.00 \times 10^4$ M^{-1}).

Although the binding of quinidine and dihydroquinidine in human plasma might have been suspected to be similar and their interactions competitive because of their structural similarities, this study presents definitive evidence to support these conclusions. The observed competitive effects of dihydroquinidine on quinidine binding suggest that they are directly related to the levels of impurity in the initial quinidine sample. The therapeutic importance of these observations, however, is presently not known. *A priori*, it appears that they are of little or no clinical significance in view of the generally low levels (<7%) of dihydroquinidine in commercial quinidine preparations.

REFERENCES

(1) M. C. Meyer and D. E. Guttman, *J. Pharm. Sci.*, **57**, 895 (1968).

(2) P. T. Schoenemann, D. W. Yesair, J. J. Coffey, and F. J. Bullock, *Ann. N.Y. Acad. Sci.*, **226**, 162 (1973).

(3) P. G. Dayton, Z. H. Israili, and J. M. Perel, *ibid.*, **226**, 172 (1973).

(4) H. Warner, *Med. Clin. North Am.*, **58**, 995 (1974).

(5) H. L. Conn and R. Luchi, *J. Clin. Invest.*, **40**, 509 (1961).

(6) J. Koch-Weser, in "Basis of Drug Therapy in Man," Fifth International Congress of Pharmacology, San Francisco, Calif., 1972, p. 56.

(7) B. Skuterud, E. Enger, S. Halvorsen, S. Jacobsen, and P. K. M. Lunde, in *ibid.*, p. 79.

(8) O. G. Nilsen and S. Jacobsen, *Biochem. Pharmacol.*, **25**, 1261 (1976).

(9) O. G. Nilsen, *ibid.*, **25**, 1007 (1976).

(10) R. F. Mais, S. Keresztes-Nagy, J. F. Zaroslinski, and Y. T. Oester, *J. Pharm. Sci.*, **63**, 1423 (1974).

(11) Y. W. Chien, H. J. Lambert, and A. Karim, *ibid.*, **63**, 1877 (1974).

(12) O. G. Nilsen and S. Jacobsen, *Biochem. Pharmacol.*, **24**, 995 (1975).

(13) "The United States Pharmacopeia," 19th rev., Mack Publishing Co., Easton, Pa., 1975, p. 434.

(14) C. T. Ueda, B. J. Williamson, and B. S. Dzindzio, *Res. Commun. Chem. Pathol. Pharmacol.*, **14**, 215 (1976).

(15) H. Thron and W. Dirscherl, *Justus Liebigs Ann. Chem.*, **515**, 252 (1935).

(16) M. Heidelberger and W. Jacobs, *J. Am. Chem. Soc.*, **41**, 817 (1919).

(17) I. M. Klotz, *Arch. Biochem.*, **9**, 109 (1946).

(18) H. M. Solomon, J. J. Schrogie, and D. Williams, *Biochem. Pharmacol.*, **17**, 143 (1968).

(19) R. I. Nazareth, T. D. Sokoloski, D. T. Witiak, and A. T. Hopper, *J. Pharm. Sci.*, **63**, 199 (1974).

(20) G. Cramer and B. Isaksson, *J. Clin. Lab. Invest.*, **15**, 553 (1963).

(21) C. T. Ueda, B. E. Ballard, and M. Rowland, *J. Pharmacol. Exp. Ther.*, **200**, 459 (1977).

ACKNOWLEDGMENTS

Supported by a grant-in-aid from the Nebraska Heart Association, an affiliate of the American Heart Association.

The authors are grateful to Dr. Theodore Sokoloski of the College of Pharmacy, Ohio State University, for providing a copy of a computer program used in some preliminary evaluations of the binding data and to Ms. Sherry E. Hinze, Ms. Terri J. Lanham, and Ms. Mary Ann Strong for assistance.

Improved Delivery of Methoxsalen

JÖRG KREUTER * **and TAKERU HIGUCHI** *

Received May 2, 1978, from the *Department of Pharmaceutical Chemistry, University of Kansas, Lawrence, KS 66044.* Accepted for publication September 11, 1978. *Present address: School of Pharmacy, Federal Institute of Technology, Clausiusstr. 25, CH-8092 Zürich, Switzerland.

Abstract □ Significant improvement in the effective bioavailability of methoxsalen was achieved when it was administered to rats and dogs in a solution as compared to a suspension. Much earlier and higher peak levels were observed for the solution in both animals. The possible impact of these observations on current use of this agent for psoriasis treatment is discussed.

Keyphrases □ Methoxsalen—solution formulated for improved delivery, bioavailability characteristics, rats and dogs □ Bioavailability—methoxsalen, improved delivery, rats and dogs □ Formulations—improved delivery of methoxsalen using solution form □ Dosage forms—methoxsalen solution compared to suspension, bioavailability characteristics evaluated, rats and dogs

Methoxsalen (I) is commercially available as hard gelatin powder capsules[1]. Because of the poor water solubility of this drug (1), its bioavailability was suspected to be rather poor. This study aimed at developing both a simple, yet sensitive, method for its analysis in blood samples and a drug formulation that would permit more rapid and effective drug absorption. Such a dosage form would permit more optimal exposure to a UV source and significantly reduce the required amount of the rather toxic drug substance.

BACKGROUND

Plants containing furocoumarins (psoralens) have been used to produce skin pigmentation for at least 3000 years (2). Modern usage of psoralens for repigmenting vitiligo began in the early 1950's (3–5). Methoxsalen (xanthotoxin) proved to be one of the most potent photosensitizers of this group of compounds (6, 7). Over the past few years, this drug has been shown to be effective in the treatment of psoriasis (8–10), a chronic, intractable skin disease common in 1–3% of the world's population.

Methoxsalen, together with longwave UV irradiation, leads to the formation of a thicker and denser stratum corneum and, therefore, to enhanced pigmentation (2, 11). Its mechanism of action seems to be a photoreaction with the thymine bases of the body DNA (7, 8, 12). UV light (365 nm) induces formation of C_4-cycloadducts between the 5,6-double bond of thymine and the 4′,5′- or 3,4-double bond of methoxsalen. Acting as a bifunctional reagent, it forms interstrand cross-linkages between pyrimidine bases in opposite strands of the DNA double helix.

Only limited information is available regarding the pharmacokinetics of methoxsalen and related compounds. Two studies investigated the elimination of radioactivity after oral (13, 14) and topical (14) application of psoralen (13), trimethylpsoralen (13), and methoxsalen (14). Approximately 80% of the radioactivity was excreted within 8 hr. After application of methoxsalen, 80% of the radioactivity appeared in the urine and 20% in the feces. Urine analysis showed that methoxsalen was totally metabolized (14). Gazith and Schaefer (15) followed plasma levels of unchanged methoxsalen in two humans for 5 hr after oral application of 50 mg (15).

The reason for the very limited information on methoxsalen biopharmaceutics was the lack of sufficiently sensitive analytical methods. Lerman and Borkman (16) recently detected methoxsalen concentrations of 10^{-5} *M* (2.2 μg/ml) in intact rat lenses. Gazith and Schaefer (15) detected 0.1 μg/ml in serum using a combined TLC–GLC method. Since their procedure is rather complicated, it is not suitable for extensive investigations. Moreover, these two methods are not sensitive enough for analysis of low plasma or blood levels.

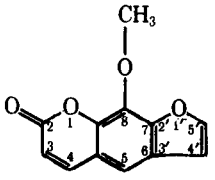

I

In a recent study with nine patients, Steiner *et al.* (17) found enormous variations of peak plasma levels, ranging from 0.15 to 4.58 μg/ml after administration of commercial methoxsalen powder capsules. The time required to reach maximal plasma levels also differed significantly from patient to patient. These variations suggest great differences in the absorption rate, probably largely caused by poor solubility.

The present article reports results of a biopharmaceutical study on the furocoumarin in two oral dosage forms. Data are presented for experiments conducted on rats and dogs based on the high-pressure liquid chromatographic (HPLC) determination of the parent drug.

EXPERIMENTAL

Materials—Methylene chloride[2], methanol[2], 2-propanol[2], ethylene chloride[3], and heptane[3] were all HPLC grade. All other materials were reagent grade.

Calibration Curve—Methoxsalen[4], 20 mg, was dissolved in 100 ml of methylene chloride. This solution was twice diluted 1:10 with methylene chloride to give a solution containing 2.0×10^{-3} mg/ml (Solution I). Blood sample blanks were spiked with different amounts (2.5–100.0 μl) of a solution containing 20.0 mg of drug in 1000 ml of distilled water (Solution II); after mixing with a vortex mixer for 1 min and standing for 4 hr at room temperature, the spiked blood samples were assayed as described later.

Methoxsalen standards prepared by further dilution of Solution I with methylene chloride served as a comparison. All standard solutions were freshly prepared before usage.

Assay—The blood samples of rats were extracted with 2 ml of a mixture of 20% methylene chloride and 80% heptane by agitation with a vortex mixer for 1 min. The blood samples of dogs were weighed and then extracted with 5 ml of the same mixture (20% methylene chloride and 80% heptane) by the same procedure. After separation by centrifugation with a laboratory centrifuge for 15 min, the organic layer was transferred into a stoppered tube with a disposable pipet[2].

The organic solvents were then evaporated under nitrogen by heating in a water bath (60°), and the residue was stored in a vacuum desiccator for 12 hr. The residue was then redissolved in 1 ml of methylene chloride, containing 3.0 μg of griseofulvin/ml as an internal standard, by agitation with a vortex mixer for 30 sec. Replicate 10-μl injections were made for each sample using the HPLC method described later. Control blanks for each biological fluid were also included.

Chromatographic Procedure—A high-pressure liquid chromatograph[5] equipped with a fixed wavelength (254 nm) detector and recorder[6] was used. The mobile phase was 4% methanol, 20% ethylene chloride, and 76% heptane. The degassed mobile phase was pumped through the column[7] at a flow rate of 2 ml/min at room temperature until a stable baseline was reached. Replicate 10-μl injections of samples or standard solutions were made with a 10-μl syringe. The column had to be flushed with 2-propanol for 45 min after 15–20 injections.

[1] Oxsoralen, Paul B. Elder Co., Hamilton, Ind.

[2] Fisher Scientific Co., Fair Lawn, N.J.
[3] Burdick & Jackson Laboratories, Muskegon, Mich.
[4] Sigma Chemical Co., St. Louis, Mo.
[5] Waters ALC 202 equipped with a U6K universal injector.
[6] Omniscribe, Houston Instruments, Austin, Tex.
[7] μBondapak CN, Waters Associates, Milford, Mass.

0022-3549/79/0400-0451$01.00/0
© 1979, American Pharmaceutical Association

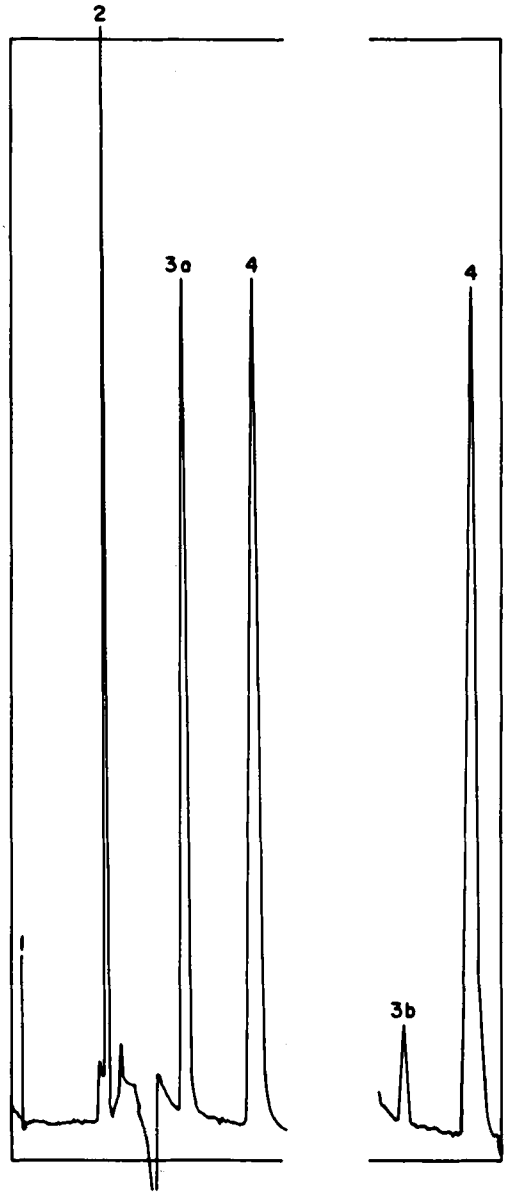

Figure 1—*Liquid chromatogram of rat blood extracts. Key: 1, injection marker; 2, solvent front; 3a, 800 ng of methoxsalen/ml of blood; 3b, 100 ng of methoxsalen/ml of blood; 4, internal standard, 3.0 μg of griseofulvin/ml.*

During the first run of both the rat and dog experiments, samples with the solution resembling the methoxsalen zone (Fig. 1, peak 3) were collected after HPLC separation and investigated with TLC using silica gel 60 F-254 plates[8] (0.2 mm thick). Benzene[2] was the mobile phase. After drying, the plates were examined with UV light.

Rat Experiments—Male rats[9], 250–300 g, were deprived of food, but not water, 12 hr prior to dosing. Five groups of three rats were formed, and three rats per day received one of three formulations. For Formulation A, 10.0 mg of methoxsalen[4] was dissolved in 2 ml of ethanol[2]; 100 μl of this solution (0.5 mg of drug) was administered into the penal dorsal vein.

For Formulation B, 100.0 mg of methoxsalen[4] was dissolved in 1 ml of 2,2,2-trichloroethanol[10]. This solution was mixed with 4 ml of peanut oil[11]. For Formulation C, one capsule was suspended in 5 ml of distilled water by agitation with a vortex mixer. One hundred microliters of Formulation B and 1 ml of Formulation C, both containing 2.0 mg of drug, were administered with an oral syringe.

A 200-μl blood sample was taken by tail clipping with a graded pipet[2] after 5, 10, and 30 min and 1, 1.5, 3, 4, 6, and 8 hr. The blood samples were assayed as already described.

Dog Experiments—The dog experiments were designed as a 3 × 3 crossover study with a latent time of 2 weeks between each run. Three beagle dogs were used: Dog A, 9 kg; Dog B, 10 kg; and Dog C, 7 kg. The dogs were deprived of food, but not water, 24 hr prior to and 12 hr after dosing.

For Formulation D, 5.0 mg of methoxsalen[4] was dissolved in 1 ml of ethanol[2] and mixed with 1 ml of 5% dextrose solution in water[12]. For Formulation E, 100.0 mg of methoxsalen[4] was dissolved in 1 ml of 2,2,2-trichloroethanol[10] and mixed with 4 ml of peanut oil[11]. A hard gelatin capsule[13], size 000, was filled with 1 ml of this solution (20.0 mg of drug). Formulation F was two capsules[1] containing a total of 20 mg of drug.

Formulation D was administered intravenously. Formulations E and F were administered orally with 100 ml of water. Blood samples of 1.0–1.5 ml were drawn before dosing and after 10, 20, 40, and 90 min and 3, 6, 12, and 25 hr and assayed as already described.

RESULTS AND DISCUSSION

Analysis of trace substances in a biological system is often limited by method sensitivity. In previous studies on methoxsalen in biological systems, a fluorometric (15) or a combined TLC–GLC (14) method was used. Neither method was sensitive enough for analysis of low plasma or blood levels.

In the present work, HPLC was used. Figure 1 shows the chromatogram of spiked rat blood samples. The method allows the detection of 10 ng of methoxsalen/ml of blood. Thus, it is 10 times more sensitive than the method of Gazith and Schaefer (15) and 100 times more sensitive than the method of Lerman and Borkman (16). The sensitivity of this HPLC method can be extended by increasing the volume injected into the liquid chromatograph and the amount of serum taken for extraction.

The specificity of the HPLC separation was tested by further investigation of the methoxsalen fraction (peak 3, Fig. 1) with TLC. TLC using

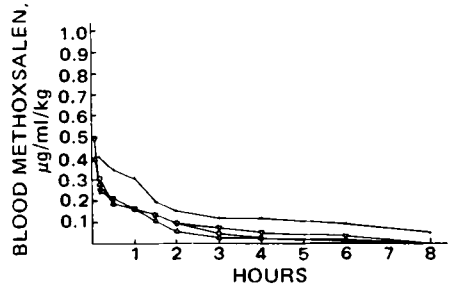

Figure 2—*Blood levels in rats after intravenous administration of 0.5 mg of methoxsalen (Formulation A). Key: ●, Rat 1A; ○, Rat 2A; △, Rat 3A; and ▽, Rat 4A.*

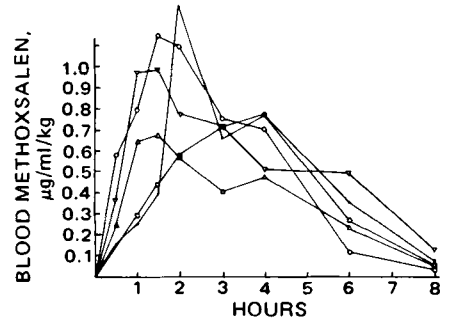

Figure 3—*Blood levels in rats after oral administration of 2.0 mg of methoxsalen in a trichloroethanol–peanut oil formulation (Formulation B). Key: ●, Rat 1B; ○, Rat 2B; △, Rat 3B; ▽, Rat 4B; and □, Rat 5B.*

[8] E. Merck, Darmstadt, West Germany.
[9] Sprague-Dawley, Madison, Wis.
[10] Aldrich Chemical Co., Milwaukee, Wis.
[11] Planters Manufacturing Co., New York, N.Y.
[12] Abbott Laboratories, North Chicago, Ill.
[13] Eli Lilly and Co., Indianapolis, Ind.

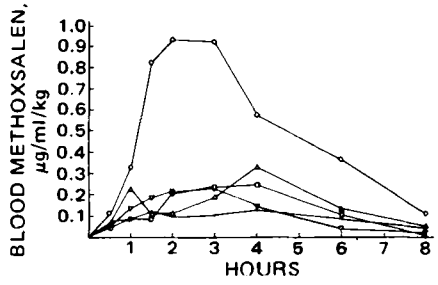

Figure 4—*Blood levels in rats after oral administration of 2.0 mg of methoxsalen as a suspension of a commercial capsule formulation (Formulation C). Key: ●, Rat 1C; ○, Rat 2C; □, Rat 3C; △, Rat 4C; and ▽, Rat 5C.*

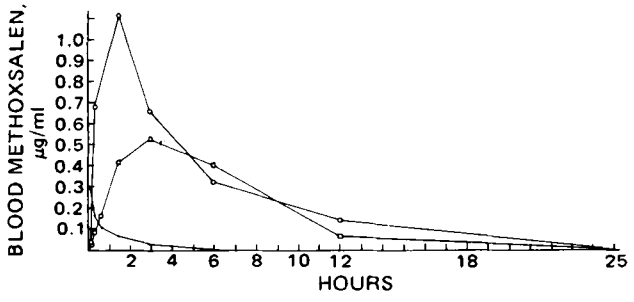

Figure 5—*Blood levels of methoxsalen in Dog A. Key: ●, intravenous administration (5.0 mg), Formulation D; ○, oral administration (20.0 mg), Formulation E; and □, oral administration (20.0 mg), Formulation F.*

the mobile phase from HPLC resulted in only one spot with the same R_f value as methoxsalen.

The assay presented is uncomplicated. A single extraction led to a reproducible 96% recovery of drug from blood samples. A second extraction yielded an additional 4%.

Because of the good reproducibility, only one extraction is required for routine analysis. The chromatogram is characterized by short retention times. With a flow rate of 2 ml/min, the methoxsalen peak appeared after 3 min; griseofulvin, the internal standard, appeared after 4 min 15 sec. Thus, total assay time is less than 5 min for each sample.

The blood level data (Figs. 2–7) are characterized by broad individual variations. Nevertheless, the oral liquid formulations (Formulations B and E) generally gave higher blood levels (Figs. 3 and 5–7) and better bioavailability (area under the concentration–time curve) (Tables I and II) than the powder formulations (Formulations C and F) (Figs. 4–7), which were administered as suspensions to the rats and as intact capsules to the dogs. Exceptions to these findings were Rat 2C and Dog C (Tables I and II) in whom the powder formulations were equivalent in bioavailability to the oral liquid formulations.

The intravenous data suggest that methoxsalen pharmacokinetics follow a two-compartment model with a rapid α-phase, significant for only 10 min in rats and for about 30 min in dogs. The intravenous bioavailability data (Tables I and II) calculated from the concentration–time curves were, however, unexpectedly low in comparison to the oral formulations. Since the intravenous dose was one-fourth of the oral doses, the expected bioavailability should be at least one-fourth of the oral bioavailability.

With two exceptions (Rat 1A and Dog B), the bioavailability of several oral formulations was significantly higher than four times the intravenous bioavailability. There may be two reasons for this finding. Either

Table I—Bioavailability [(µg min/ml)/kg] of Methoxsalen in Rats

Rat	Formulation A	Rat	Formulation B	Rat	Formulation C
1A	75	1B	238	1C	42
2A	34	2B	249	2C	238
3A	28	3B	171	3C	66
4A	38	4B	260	4C	78
		5B	201	5C	54

Table II—Bioavailability [(µg min)/ml] of Methoxsalen in Dogs

Dog	Formulation D	Formulation E	Formulation F
A	38	382	252
B	64	183	93
C	51	257	239

methoxsalen does not show linear pharmacokinetics or the drug precipitates after intravenous administration due to its poor water solubility and then is redissolved very slowly over a long period with blood levels below the detection limit. Occasional inflammation at the injection site of the rats may support the latter hypothesis. The smaller dose was used to limit the injection volume because of separate effects of the vehicle.

In the blood level curves of rats, a second peak, or at least a shoulder, was observed about 4 hr after application of most oral formulations (Figs. 3 and 4). It may possibly be caused by analytical errors, by variations in the absorption rate, or by enterohepatic recycling. Analytical errors are unlikely, however, because the rat experiments and the assay procedures were carried out on different days. The occurrence of enterohepatic recycling seems questionable since no second peaks are observable after intravenous administration. Enterohepatic recycling would have to be determined by analysis of unchanged drug and metabolites after bile cannulation.

Comparison of the bioavailabilities, measured by the area under the concentration–time curves, is of only limited value if nonlinear pharmacokinetics exist because the area under the curve is then not only dependent on the drug formulation but to a great extent also dosage dependent. For the therapeutic use of methoxsalen, bioavailability is of limited relevance because it is used as a "hit-and-run" (18) drug. The desired photoreaction of this drug occurs only if the patient is exposed to UV irradiation. Therefore, the effectiveness of the drug is dependent on the drug concentration in the epidermis. For this reason, blood levels shortly before or at the time of irradiation are of main interest. To avoid a prolonged photosensitivity of the patient (8), prolonged absorption is not desirable.

The UV treatment (irradiation time of about 10 min) is normally carried out 2 hr after drug administration. Gazith and Schaefer (15) reported maximal serum methoxsalen levels 1.5 hr after administration (drug formulation not specified). In the present study, maximal blood levels were observed in rats 2–4 hr and in dogs 3 hr after administration of the oral powder formulations (C and F). After administration of the oral liquid formulations (B and E), the time for the appearance of the maximal blood levels was reduced in both rats (1.5–2 hr) and dogs (20–90 min). In addition, the maximal blood levels in both species were increased significantly ($2p < 0.05$ according to the Student t-test) relative to the powder formulations. Therefore, the oral liquid formulations considerably enhanced the absorption rate and the maximal blood levels.

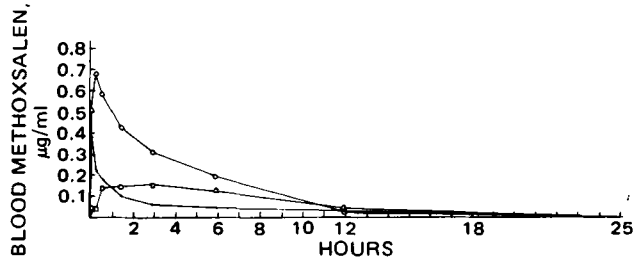

Figure 6—*Blood levels of methoxsalen in Dog B. Key: see Fig. 5.*

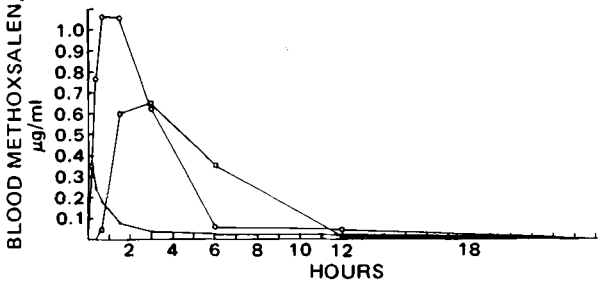

Figure 7—*Blood levels of methoxsalen in Dog C. Key: see Fig. 5.*

REFERENCES

(1) *Drug Stand.*, **25**, 89 (1957).
(2) S. W. Becker, Jr., *J. Am. Med. Assoc.*, **173**, 1483 (1960).
(3) E. Sidi and J. Bourgeous-Gavardin, *J. Invest. Dermatol.*, **18**, 391 (1952).
(4) A. B. Lerner, C. R. Denton, and T. B. Fitzpatrick, *ibid.*, **20**, 299 (1953).
(5) E. W. Kelly, Jr., and H. Pinkus, *ibid.*, **25**, 453 (1955).
(6) M. A. Pathak and T. B. Fitzpatrick, *ibid.*, **32**, 255 (1959).
(7) G. Rodighiero, L. Musajo, F. Dall'Acqua, S. Marciani, G. Carporale, and L. Ciavatta, *Biochim. Biophys. Acta*, **217**, 40 (1970).
(8) J. F. Walter, J. J. Voorhees, W. H. Kelsey, and E. A. Duell, *Arch. Dermatol.*, **107**, 861 (1973).
(9) J. A. Parrish, T. B. Fitzpatrick, L. Tanenbaum, and M. A. Pathak, *N. Engl. J. Med.*, **291**, 1207 (1974).
(10) J. W. Melski, L. Tanenbaum, J. A. Parrish, T. B. Fitzpatrick, and H. L. Bleich, *J. Invest. Dermatol.*, **68**, 328 (1977).
(11) S. W. Becker, Jr., *Science*, **127**, 878 (1958).
(12) F. Dall'Acqua, S. Marciani, L. Ciavatta, and G. Rodighiero, *Z. Naturforsch.*, **26b**, 561 (1971).
(13) M. A. Pathak, F. Dall'Acqua, G. Rodighiero, and J. A. Parrish, *J. Invest. Dermatol.*, **62**, 347 (1974).
(14) W. Schalla, H. Schaefer, B. Kammerau, and A. Zesch, *ibid.*, **66**, 258 (1976).
(15) J. Gazith and H. Schaefer, *Biochem. Med.*, **18**, 102 (1977).
(16) S. Lerman and R. F. Borkman, *Science*, **197**, 1287 (1977).
(17) I. Steiner, T. Prey, F. Gschnait, J. Washüttl, and I. Greiter, *Arch. Derm. Res.*, **259**, 299 (1977).
(18) J. G. Wagner, "Fundamentals of Clinical Pharmacokinetics," 1st ed., Drug Intelligence, Hamilton, Ill., p. 45.

ACKNOWLEDGMENTS

Supported in part by funds provided by INTERx Research Corp.

High-Pressure Liquid Chromatographic Determination of Amoxicillin in Urine

TEH LO LEE ˣ, LUCIUS D'ARCONTE †, and MARVIN A. BROOKS

Received June 23, 1978, from the *Department of Biochemistry and Drug Metabolism, Hoffmann-La Roche Inc., Nutley, NJ 07110.* Accepted for publication September 12, 1978. †Deceased.

Abstract □ A rapid and specific high-pressure liquid chromatographic (HPLC) assay was developed for the simultaneous determination of amoxicillin and its penicilloic acid metabolite in urine. The two compounds, assayed directly in urine or after dilution with water–methanol (85:15), are separated by reversed-phase chromatography and quantitated spectrofluorometrically following postcolumn derivatization with fluorescamine. Linear calibration curves were measured in the ranges of 25–250 and 50–400 ng injected for amoxicillin and the penicilloic acid metabolite, respectively. The sensitivity limit of the assay is 2.5–5.0 μg/ml of urine for amoxicillin and the penicilloic acid metabolite. Urine samples (0–8 hr) taken from six subjects following single 250-mg po doses and assayed by HPLC showed ranges of cumulative percent of the dose excreted as amoxicillin and the penicilloic acid metabolite (reported as amoxicillin equivalents) of 50.2–68.0 and 21.6–30.0%, respectively. An excellent correlation (r = 0.985) was demonstrated for the measurement of amoxicillin concentrations by the HPLC and microbiological assays.

Keyphrases □ Amoxicillin—high-pressure liquid chromatographic determination in urine □ Antibacterials—amoxicillin and penicilloic acid metabolite, high-pressure liquid chromatographic determination in urine □ High-pressure liquid chromatography—analysis, amoxicillin and penicilloic acid metabolite in urine

Amoxicillin[1] (I) [D-(−)-α-amino-*p*-hydroxybenzylpenicillin trihydrate], synthesized from 6-aminopenicillanic acid, is an orally absorbed, acid-stable, semisynthetic, broad-spectrum antimicrobial agent (1–3). Studies on its biotransformation demonstrate that it is excreted in urine intact and as the penicilloic acid of amoxicillin (II) [6-D-(−)-α-amino-*p*-hydroxyphenylpenicilloic acid] (4, 5).

BACKGROUND

Routine determinations of I in biological fluids are usually performed by microbiological assay using one of a variety of sensitive bacterial strains

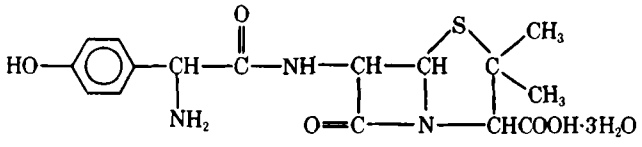

I

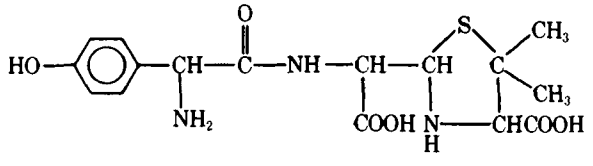

II

(6). Since the metabolic cleavage of the β-lactam ring to II inactivates this compound toward microbiological activity, the microbiological assays are specific for I in the presence of II. The analysis of II has been reported using a separate aliquot of the sample by iodometric titration (7) and by TLC, followed by formation of an ammonium–molybdate complex and spectrophotometry (5).

Spectrofluorometric methods are capable of measuring ampicillin (8–10) and amoxicillin (11–14) in serum, plasma, or urine following therapeutic doses. The spectrofluorometric assays are based on the formation of strongly fluorescent products by heating either in the presence of formaldehyde (8, 11–13) or uranylacetate in acid solution (10) or at room temperature in the presence of mercuric chloride in neutral solution (9, 14). Jusko (8) postulated that the fluorescent product formed is a 3,6-disubstituted diketopiperazine and demonstrated that ampicillin levels measured by the spectrofluorometric assay were appreciably higher than those measured in identical samples by a microbiological assay. This result was attributed to the formation of the identical fluorophore by both the penicilloic acid and the penicillin.

Thus, the spectrofluorometric methods described using formaldehyde (8, 11–13) or uranylacetate (10) are "total" assays, which measure the sum of the penicillin and penicilloic acid. The spectrofluorometric methods using mercuric chloride described for ampicillin (9) and amoxicillin (14) differ from the other methods employing formaldehyde (8, 11–13) in that

[1] Larotid, Hoffmann-La Roche Inc., Nutley, NJ 07110.

0022-3549/79/0400-0454$01.00/0

© 1979, American Pharmaceutical Association

REFERENCES

(1) *Drug Stand.*, **25**, 89 (1957).
(2) S. W. Becker, Jr., *J. Am. Med. Assoc.*, **173**, 1483 (1960).
(3) E. Sidi and J. Bourgeous-Gavardin, *J. Invest. Dermatol.*, **18**, 391 (1952).
(4) A. B. Lerner, C. R. Denton, and T. B. Fitzpatrick, *ibid.*, **20**, 299 (1953).
(5) E. W. Kelly, Jr., and H. Pinkus, *ibid.*, **25**, 453 (1955).
(6) M. A. Pathak and T. B. Fitzpatrick, *ibid.*, **32**, 255 (1959).
(7) G. Rodighiero, L. Musajo, F. Dall'Acqua, S. Marciani, G. Carporale, and L. Ciavatta, *Biochim. Biophys. Acta*, **217**, 40 (1970).
(8) J. F. Walter, J. J. Voorhees, W. H. Kelsey, and E. A. Duell, *Arch. Dermatol.*, **107**, 861 (1973).
(9) J. A. Parrish, T. B. Fitzpatrick, L. Tanenbaum, and M. A. Pathak, *N. Engl. J. Med.*, **291**, 1207 (1974).
(10) J. W. Melski, L. Tanenbaum, J. A. Parrish, T. B. Fitzpatrick, and H. L. Bleich, *J. Invest. Dermatol.*, **68**, 328 (1977).
(11) S. W. Becker, Jr., *Science*, **127**, 878 (1958).
(12) F. Dall'Acqua, S. Marciani, L. Ciavatta, and G. Rodighiero, *Z. Naturforsch.*, **26b**, 561 (1971).
(13) M. A. Pathak, F. Dall'Acqua, G. Rodighiero, and J. A. Parrish, *J. Invest. Dermatol.*, **62**, 347 (1974).
(14) W. Schalla, H. Schaefer, B. Kammerau, and A. Zesch, *ibid.*, **66**, 258 (1976).
(15) J. Gazith and H. Schaefer, *Biochem. Med.*, **18**, 102 (1977).
(16) S. Lerman and R. F. Borkman, *Science*, **197**, 1287 (1977).
(17) I. Steiner, T. Prey, F. Gschnait, J. Washüttl, and I. Greiter, *Arch. Derm. Res.*, **259**, 299 (1977).
(18) J. G. Wagner, "Fundamentals of Clinical Pharmacokinetics," 1st ed., Drug Intelligence, Hamilton, Ill., p. 45.

ACKNOWLEDGMENTS

Supported in part by funds provided by INTERx Research Corp.

High-Pressure Liquid Chromatographic Determination of Amoxicillin in Urine

TEH LO LEE ˣ, LUCIUS D'ARCONTE †, and MARVIN A. BROOKS

Received June 23, 1978, from the *Department of Biochemistry and Drug Metabolism, Hoffmann-La Roche Inc., Nutley, NJ 07110.* Accepted for publication September 12, 1978. †Deceased.

Abstract □ A rapid and specific high-pressure liquid chromatographic (HPLC) assay was developed for the simultaneous determination of amoxicillin and its penicilloic acid metabolite in urine. The two compounds, assayed directly in urine or after dilution with water–methanol (85:15), are separated by reversed-phase chromatography and quantitated spectrofluorometrically following postcolumn derivatization with fluorescamine. Linear calibration curves were measured in the ranges of 25–250 and 50–400 ng injected for amoxicillin and the penicilloic acid metabolite, respectively. The sensitivity limit of the assay is 2.5–5.0 μg/ml of urine for amoxicillin and the penicilloic acid metabolite. Urine samples (0–8 hr) taken from six subjects following single 250-mg po doses and assayed by HPLC showed ranges of cumulative percent of the dose excreted as amoxicillin and the penicilloic acid metabolite (reported as amoxicillin equivalents) of 50.2–68.0 and 21.6–30.0%, respectively. An excellent correlation (r = 0.985) was demonstrated for the measurement of amoxicillin concentrations by the HPLC and microbiological assays.

Keyphrases □ Amoxicillin—high-pressure liquid chromatographic determination in urine □ Antibacterials—amoxicillin and penicilloic acid metabolite, high-pressure liquid chromatographic determination in urine □ High-pressure liquid chromatography—analysis, amoxicillin and penicilloic acid metabolite in urine

Amoxicillin[1] (I) [D-(−)-α-amino-*p*-hydroxybenzylpenicillin trihydrate], synthesized from 6-aminopenicillanic acid, is an orally absorbed, acid-stable, semisynthetic, broad-spectrum antimicrobial agent (1–3). Studies on its biotransformation demonstrate that it is excreted in urine intact and as the penicilloic acid of amoxicillin (II) [6-D-(−)-α-amino-*p*-hydroxyphenylpenicilloic acid] (4, 5).

BACKGROUND

Routine determinations of I in biological fluids are usually performed by microbiological assay using one of a variety of sensitive bacterial strains

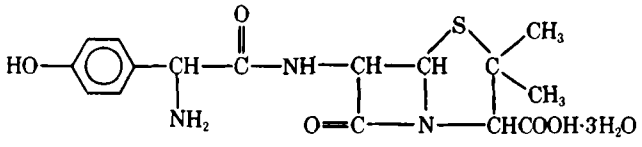

I

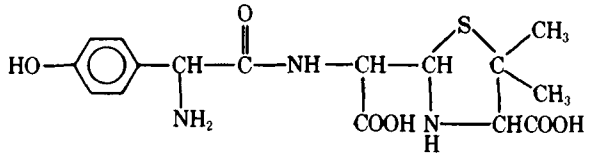

II

(6). Since the metabolic cleavage of the β-lactam ring to II inactivates this compound toward microbiological activity, the microbiological assays are specific for I in the presence of II. The analysis of II has been reported using a separate aliquot of the sample by iodometric titration (7) and by TLC, followed by formation of an ammonium–molybdate complex and spectrophotometry (5).

Spectrofluorometric methods are capable of measuring ampicillin (8–10) and amoxicillin (11–14) in serum, plasma, or urine following therapeutic doses. The spectrofluorometric assays are based on the formation of strongly fluorescent products by heating either in the presence of formaldehyde (8, 11–13) or uranylacetate in acid solution (10) or at room temperature in the presence of mercuric chloride in neutral solution (9, 14). Jusko (8) postulated that the fluorescent product formed is a 3,6-disubstituted diketopiperazine and demonstrated that ampicillin levels measured by the spectrofluorometric assay were appreciably higher than those measured in identical samples by a microbiological assay. This result was attributed to the formation of the identical fluorophore by both the penicilloic acid and the penicillin.

Thus, the spectrofluorometric methods described using formaldehyde (8, 11–13) or uranylacetate (10) are "total" assays, which measure the sum of the penicillin and penicilloic acid. The spectrofluorometric methods using mercuric chloride described for ampicillin (9) and amoxicillin (14) differ from the other methods employing formaldehyde (8, 11–13) in that

[1] Larotid, Hoffmann-La Roche Inc., Nutley, NJ 07110.

0022-3549/79/0400-0454$01.00/0

© 1979, American Pharmaceutical Association

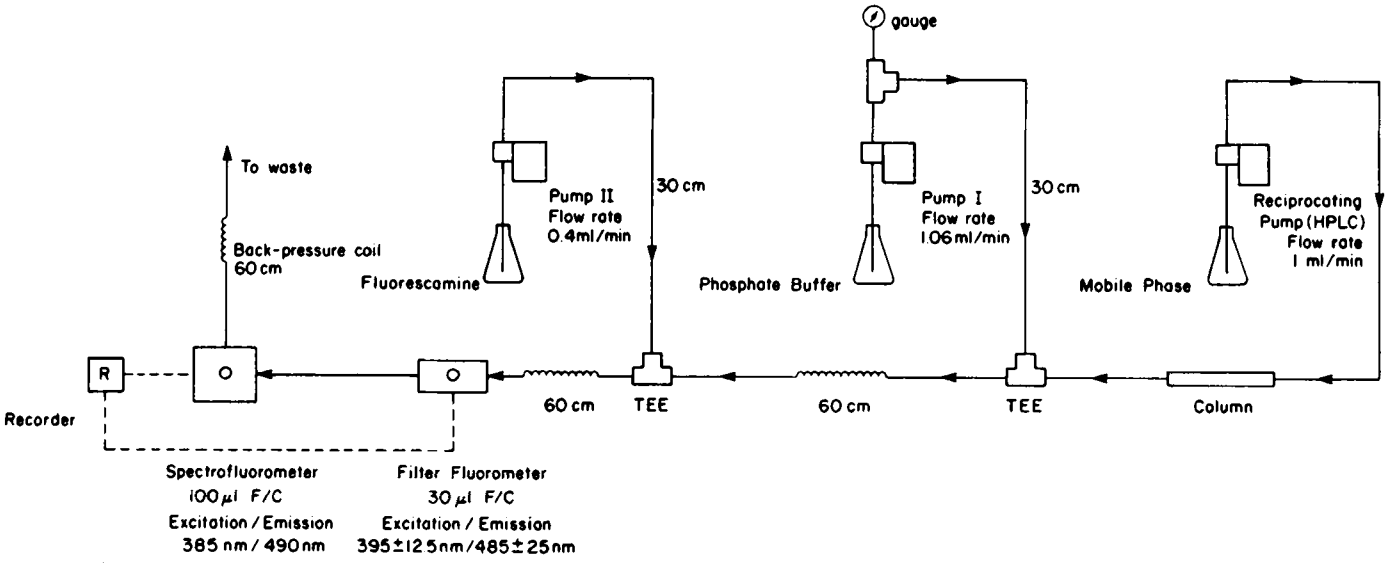

Figure 1—*Schematic diagram of equipment used for HPLC determination of I and II.*

only the penicilloic acid forms the fluorophore. Two aliquots of the same sample are required for the measurement of the penicillin and its penicilloic acid (9, 14). The first sample is required for the direct measurement of the "free" penicilloic acid fraction. The second sample is used to measure "total" penicilloic acid after alkaline hydrolysis of the penicillin to the penicilloic acid. The measurement of free penicillin is based on the difference between the "total" and "free" penicilloic acid fractions.

The aim of the present study was to develop a routine chemical assay capable of the simultaneous and specific measurement of both I and II without multiple assays and differential measurement. High-pressure liquid chromatography (HPLC) using spectrophotometric detection was recently described for the analysis of penicillins in pure forms (15–17). Utilization of HPLC separation followed by postcolumn derivatization with fluorescamine is a facile and reproducible procedure and has been used successfully for the determination of peptides (18) and kanamycin (19). The method described permits the rapid, simultaneous measurement of I and II in urine without extraction and with minimal sample cleanup. The method was successfully applied following the administration of therapeutic doses of amoxicillin and can be used in biopharmaceutical and pharmacokinetic studies.

EXPERIMENTAL

Column—The 30-cm × 4-mm i.d. stainless steel column contained octadecyltrichlorosilane chemically bonded (10% by weight) to 10-μm silica gel[2]. The column generated 10,000 plates/m.

Instrumental Parameters—The HPLC separation was performed using the column together with a reciprocating piston pump[3] and loop injector[4]. The isocratic mobile phase was a mixture of water–methanol–acetic acid (85:15:0.5) at a column head pressure of 1.6×10^3 psi and a constant flow rate of 1.0 ml/min. Two pumps[5] were used to add the 0.2 *M* phosphate buffer (pH 11.4) and fluorescamine reagent at flow rates of 1.06 and 0.4 ml/min, respectively. All connections from the effluent to the detectors were made with 1.5-mm o.d. × 0.3-mm i.d.[6] polytef[7] tubing, with the exception of the tubing from the buffer reagent and fluorescamine reservoir which was 3.0 mm o.d. × 1.5 mm i.d.[8]. All mixing tees, tube end fittings, couples, and gauges were obtained from a commercial source[9] (Fig. 1). The total flow rate through the system was 2.46 ml/min.

Fluorometric measurement was made with a filter fluorometer[10] using a polytef tube flowcell[11] of 32 μl and interference filters at 395 ± 12.5 and 485 ± 25 nm for excitation and emission, respectively. The excitation source was a 4-w fluorescent lamp[12], and detection was made with a nine-stage photomultiplier[13] powered by a regulated 700-v dc power supply[10]. In series with this detector was a spectrofluorometer[14] with a rectangular 0.1-ml quartz flowcell[15]. This instrument contains a 150-w xenon lamp[16] for excitation at 385 nm and measures the resultant emission at 490 nm using a photomultiplier tube[17]. A back-pressure coil (approximately 60 cm of polytef tubing) was attached to the exit line of the second detector to eliminate the formation of air bubbles in the flowcell. The filter fluorometer and spectrofluorometer were connected to a recorder[18] with input voltages of 1 v and 10 mv, respectively, with a chart speed of 2.54 cm/2 min.

A schematic diagram of the instrumentation used for determination of I and II is shown in Fig. 1. Under the described conditions, the retention times of the fluorescamine derivatives of I and II was 7.0 and 5.2 min, respectively (Fig. 2*a*). The injection of 250 ng of I and 400 ng of II/10 μl yielded peaks of nearly full-scale response at an attenuation of ×32 using the filter fluorometric detector. The injection of the same amounts of I and II using the spectrofluorometer with the selector at 1 and sensitivity at 7 yielded peaks of nearly full-scale deflection.

Reagents—All inorganic reagents were analytical grade and were prepared in deionized, distilled water.

Stock Buffer Solution—Phosphate buffer (1.0 *M*, pH 11.4) was prepared by mixing 530 ml of 1 *M* potassium phosphate dibasic (trihydrate)[19] and 470 ml of saturated tribasic sodium phosphate (Na_3PO_4)[19]. The mixture was adjusted to pH 11.4 with 1 *M* potassium phosphate monobasic ($KH_2PO_4 \cdot 3H_2O$) or saturated tribasic sodium phosphate.

Reagent Buffer Solution—The stock buffer solution was diluted with deionized, distilled water to yield 0.2 *M* phosphate buffer (pH 11.4). This solution was pumped into the effluent stream by Pump I at a rate of 1.06 ml/min (Fig. 1) to adjust the pH of the effluent of the liquid chromatographic column to 8–8.5 for optimum yield of the fluorescamine derivative.

Fluorescamine Reagent—A solution containing 20 mg of fluorescamine[20]/100 ml of acetone[21] was prepared. The reagent was pumped into the effluent stream by Pump II (Fig. 1) at a rate of 0.4 ml/min.

Mobile Phase—The mobile phase for HPLC separation was a mixture

[2] No. 27324, μBondapak C_{18}, Waters Associates, Milford, MA 01757.
[3] Model 6000, Waters Associates, Milford, MA 01757.
[4] Model U6K, Waters Associates, Milford, MA 01757.
[5] Model 396-31, Part 19-60006-001, Milton Roy mini-pump (16–160 ml/hr), Laboratory Data Control, Englewood Cliffs, NJ 07636.
[6] No. 200-34, Rainin Instrument Co., Fort Lee, NJ 07024.
[7] Teflon, du Pont.
[8] No. 200-32, Rainin Instrument Co., Fort Lee, NJ 07024.
[9] Tees No. 200-22, tube end fittings No. 200-00, couples No. 200-16, and gauges (0–1000 psi) No. 904-01, Rainin Instrument Co., Fort Lee, NJ 07024.
[10] Models 500-D and 500-C fluorometer detectors, Cambridge Bioengineering Inc., Cambridge, MA 02142.
[11] Cambridge Bioengineering Inc., Cambridge, MA 02142. (An 8-μl flowcell with filter accessory recently became available.)
[12] Cambridge lamp, F4T5/212/60°.
[13] RCA IP28 or equivalent.
[14] Model 204, Perkin-Elmer Corp., Norwalk, CT 06856.
[15] No. 22-0275, Perkin-Elmer Corp., Norwalk, CT 06856. (A 10-μl flowcell accessory kit; No. 010-0137, recently became available.)
[16] No. 350-1646 (OSR AM), Perkin-Elmer Corp., Norwalk, CT 06856.
[17] RCA R212 or equivalent.
[18] Speedomax, XL, 625 series dual-pen recorder, Leeds and Northrup, North Wales, PA 19454.
[19] Mallinckrodt Inc., St. Louis, MO 63160.
[20] Fluram, Hoffmann–La Roche Inc., Nutley, NJ 07110.
[21] Spectrograde, Eastman Chemical Co.

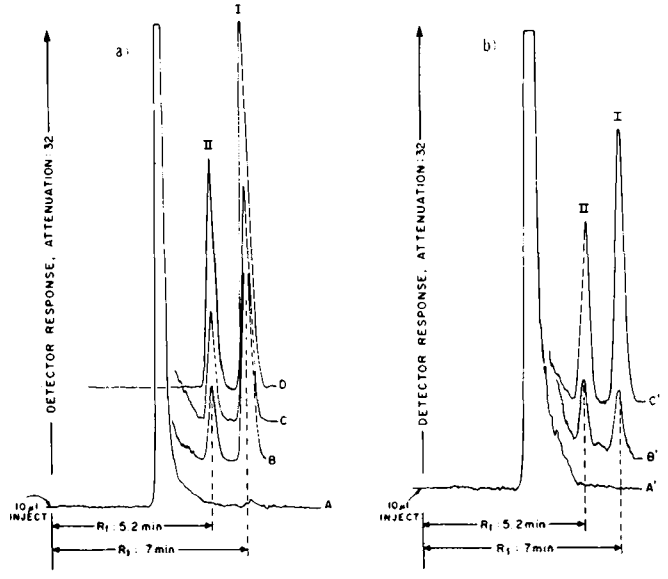

Figure 2—*Chromatograms of HPLC assay using a filter fluorometric detector. Key:* (a) *A, diluted control urine; B, human subject diluted urine after an oral dose; C, diluted control urine containing added standards; D, authentic standards;* (b) *A′, control urine; B′, human subject urine after an oral dose; and C′, control urine containing added standards.*

of water–methanol[22]–acetic acid[23] (85:15:0.5), which was deaerated in an ultrasonic bath prior to use.

Standard Solutions—First, 11.78 mg of I, 6-[(*R*)-2-amino-2-(*p*-hydroxyphenyl)acetamido]-3,3-dimethyl-7-oxo-4-thia-1-azabicyclo-[3.2.0]heptane-2-carboxylic acid trihydrate ($C_{16}H_{19}O_5N_3S{\cdot}3H_2O$, mol. wt. 419.45 corrected for 84.9% potency), was weighed out into a 10-ml volumetric flask and dissolved in deionized, distilled water. This stock solution contained 1.0 mg of I/ml. Then 11.15 mg of II, (α *R*, 2*R*, 4*S*)-α-[(*R*)-2-amino-2-(*p*-hydroxyphenyl)acetamido]-4-carboxy-5,5-dimethyl-2-thiazolidineacetic acid disodium salt ($C_{16}H_{19}O_5N_3Na_2S$, mol. wt. 427.38), equivalent to 10.00 mg of the free acid of II, was weighed out into a 10-ml volumetric flask and dissolved in deionized, distilled water. This stock solution contained 1.0 mg of II/ml.

These stock solutions were used to prepare the following six mixed standard solutions (A–F) containing 25, 50, 100, 150, 200, and 250 µg of I/ml and 50, 100, 150, 200, 300, and 400 µg of II/ml, respectively, by dilution with water–methanol (85:15). The mixed standards (A–F) were diluted further (1:10) with water–methanol (85:15) to yield a series of mixed working solutions containing 2.5, 5, 10, 15, 20, or 25 µg of I/ml and 5, 10, 15, 20, 30, or 40 µg of II/ml, respectively. A 10-µl aliquot of these mixed working solutions equivalent to 25, 50, 100, 150, 200, or 250 ng of I and 50, 100, 150, 200, 300, or 400 ng of II was injected onto the HPLC column to establish an external calibration curve of peak height *versus* concentration injected of I and II.

One-milliliter aliquots of Standards A–F were added directly to 1 ml of control urine and diluted to 10 ml with water–methanol (85:15) as internal standards for the construction of an internal standard curve. The internal standard calibration curve of peak height *versus* concentration injected was used to determine the concentration of the unknowns by interpolation.

All external standards and internal standards of I and II should be prepared fresh daily.

Urine Analysis—A 5-ml urine sample was placed into a 15-ml conical tube and centrifuged to spin down the suspended materials. A 1-ml aliquot of this supernate was transferred to another 15-ml centrifuge tube, and 9 ml of water–methanol (85:15) was added. A 10-µl aliquot of this supernate was injected into the chromatograph (Fig. 2*a*). For higher sensitivity, a 10-µl aliquot of the supernate could be assayed directly by HPLC (Fig. 2*b*).

Upon completion of a day's analysis, it was necessary to flush the phosphate reagent line with distilled water and the fluorescamine reagent line with acetone to avoid plugging.

Calculations—Quantitation was based on a linear relationship between peak heights of the fluorescamine derivatives and the concentrations of material added to the control urines. The peak heights of I and II in the respective internal standards and unknowns were determined. The absolute amount injected in the unknowns was obtained by interpolation from the internal standard curve. These values were corrected for the appropriate dilution and calculated as micrograms per milliliter of urine.

Precision and Sensitivity Limit—The efficiencies of postcolumn derivatization of I and II to their respective fluorescent derivatives from a urine sample as compared to a water (control) sample were 92.2 ± 5.6 and 100.4 ± 3.3% (*SD*), respectively. These calculations were based on the analysis of 10-µl aliquots of mixtures of 1 ml of urine or water to which were added 1 ml of Solutions A–F and 8 ml of water–methanol (85:15). Experiments demonstrated that the efficiencies of fluorophore formation of I and II were essentially identical using the direct injection of the urine supernate.

The sensitivity limits of detection were 25.0 and 50.0 µg/ml of urine for I and II, respectively, using the 10:1 dilution with water–methanol (85:15). Sensitivity limits of 2.5 and 5.0 µg/ml of urine for I and II, respectively, were obtained without dilution of the urine supernate. The specificity of the assay against endogenous interferences was demonstrated by the absence of peaks with retention volumes similar to I and II in the chromatograms of the control urines.

RESULTS AND DISCUSSION

The original goal of this work was to develop a rapid, straightforward HPLC assay suitable for the simultaneous analysis of I and II in both plasma and urine. Studies on the extractability of these compounds showed that, due to their amphoteric nature, recoveries were very poor. Therefore, investigations were undertaken to assay these compounds after derivatization in the biological specimen and extraction of the derivatives or to assay the biological specimens directly.

The first approach met with partial success using the technique of fluorophore formation (8) with minor modifications. The assay required the formation of a protein-free filtrate of plasma with metaphosphoric acid and heating to 70° for 15 min. The filtrate was washed twice with 2 × 10-ml portions of ether and then made strongly acidic with concentrated hydrochloric acid. This solution was heated (100°) in the presence of formaldehyde to yield an extractable yellow fluorophore, which was quantitated by HPLC using filter fluorometric detection with a low pressure mercury lamp excitation source (excitation of 365 and emission of >451 nm). Analysis was performed using a silica gel[24] column with an

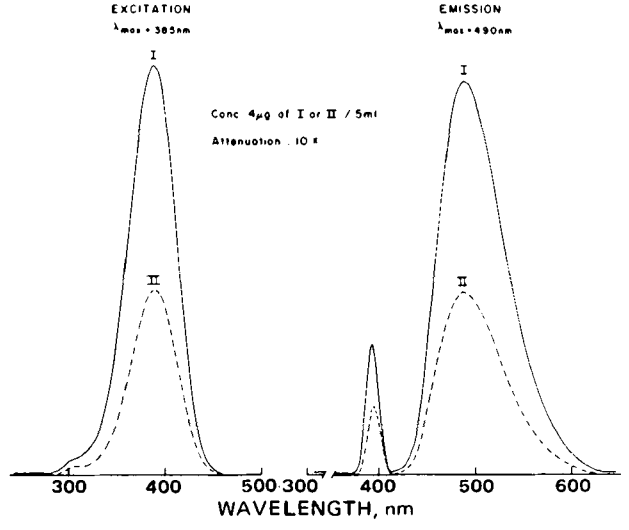

Figure 3—*Uncorrected excitation–emission spectra of a solution containing 4 µg of I and II, 0.4 ml of 1 M phosphate buffer (pH 8), and 0.2 ml of 20 mg fluorescamine/100 ml of acetone, diluted to 5 ml with water–methanol (85:15).*

[22] Fisher Scientific, Springfield, NJ 07081.
[23] J. T. Baker Chemical Co., Phillipsburg, NJ 08865.
[24] A 0.25-m × 4.6-mm i.d. Partisil silica gel 10-µm stainless steel column, Whatman, Clifton, NJ 07014.

Table I—Comparison of the HPLC Assay Using a Filter Fluorometer and a Spectrofluorometer as Detectors

Compound I, μg/ml			Compound II, μg/ml		
Filter Fluorometer (a)[a]	Spectrofluorometer (b)[a]	Ratio (a/b)	Filter Fluorometer (a)[a]	Spectrofluorometer (b)[a]	Ratio (a/b)
136.5	133.4	1.02	57.8	46.0	1.25
217.5	210.3	1.03	80.6	86.0	0.94
145.7	159.1	0.92	64.4	58.6	1.09
213.5	221.7	0.96	71.5	71.4	1.00
270.9	283.4	0.96	118.7	120.0	0.99
118.0	129.3	0.99	50.8	50.0	0.92
r = 0.989			r = 0.982		
Mean ± *SD*		0.98 ± 0.04			1.03 ± 0.11

[a] Filter fluorometer attenuation at ×32; spectrofluorometer selector at 1 and sensitivity at 7.

Table II—Urinary Excretion of I and II over 0–8 hr following Single 250-mg po Doses in Six Human Subjects

	Microbiological Assay—Excreted as Unchanged I		HPLC Assay[a]					
			Excreted as Unchanged I		Excreted as II[b]			
Subject	μg/ml (a)	% of Dose Recovered	μg/ml (b)	% of Dose Recovered	μg/ml	% of Dose Recovered	Total Dose Recovered, %	Ratio (a/b)
1	135.0	54.0	136.5	54.6	57.8	23.1	77.7	0.99
2	222.6	63.2	217.5	61.8	80.6	22.9	84.7	1.02
3	158.2	73.8	145.7	68.0	64.4	30.0	98.1	1.08
4	223.3	69.2	213.5	66.2	71.5	22.2	88.3	1.05
5	264.5	59.6	270.9	61.0	118.7	26.7	87.7	0.98
6	100.9	44.3	118.0	50.2	50.8	21.6	71.8	0.85
Range		44.3–73.8		50.2–68.0		21.6–30.0		
Mean		60.7		60.3		24.4		
Mean ± *SD*								1.00 ± 0.07

[a] Using filter fluorometer. [b] Reported as I equivalent. Factor = (419.45/383.38) = 1.09.

isocratic mobile phase of methylene chloride–methanol (95:5) at a flow rate of 1.6 ml/min on a commercially available liquid chromatograph.

Under these conditions, both I and II yielded the identical derivative (R_t 5.6 min) with a limit of sensitivity of 200 ng/ml of plasma. Comparison of the fluorescent properties of the yellow derivative of I and II (excitation/emission maxima: 363/452 nm) with those of the colorless authentic standard of the 3,6-disubstituted diketopiperazine (excitation/emission maxima: 280/305 nm) demonstrated that the 3,6-disubstituted diketopiperazine was not produced upon heating I and II in acid in the presence of formaldehyde, as suggested by Jusko (8). When the 3,6-disubstituted diketopiperazine itself was reacted under the conditions described, it produced a compound with the identical fluorescent properties as the derivative of I and II. The chemical structure was recently identified as 2-hydroxy-3-phenyl-6-methylpyrazine (20).

The assay was applied to the analysis of I in plasma and urine of a dog following a 500-mg dose of a commercial formulation[1]. The levels obtained were compared to those measured by the microbiological assay using *Staphylococcus aureus* (ATCC 6538P) as the test organism. Over a 6-hr period, plasma levels measured by the HPLC tecnhique were as much as 15 times higher than those measured by the microbiological assay. The large difference was attributed to the formation of the identical fluorophore by II, the nonmicrobiologically active metabolite of I. The possibility of other unidentified inactive metabolites of I yielding the same fluorophore cannot be discounted. Thus, in plasma, this procedure is only useful for the measurement of total levels of amoxicillin (I) and its metabolites. Due to the lack of specificity, this approach was discontinued. Modification of the reaction conditions for this procedure (8) as well as that of Miyazaki *et al.* (9, 14) did not yield two derivatives that were separable by HPLC for quantitation. Attempts to form fluorescamine derivatives prior to HPLC of plasma samples were also unsuccessful due to formation of multiple products upon derivatization.

HPLC separation of I and II followed by a highly specific reaction with fluorescamine under alkaline condition permitted the direct determination of these compounds in urine. The limitation of this procedure is its inability to measure levels of I and II in the protein-free filtrates of plasma due to a lack of sensitivity.

The fluorescamine derivatives of I and II were examined by spectrofluorometry prior to HPLC analysis to establish reaction conditions to maximize the yield of the fluorophore. The optimum reaction pH was 8–8.5 with excitation and emission maxima for the fluorescamine derivatives at 385 and 490 nm, respectively (Fig. 3). The quantum yield of fluorescence for II was approximately half that of I and was probably related to the structural differences. A concentration of 20 mg of fluorescamine/100 ml of acetone was determined to be optimal for postcolumn derivatization. A concentration of 10 mg/100 ml of acetone resulted in a 50% loss in response, while concentrations greater than 20 mg/100 ml resulted in precipitation of the reagent in the polytef tubing.

The main criteria for the choice of the detector were its high energy output for excitation at approximately 390 nm and its selectivity for monitoring the fluorescence emission at approximately 490 nm. Both a filter fluorometer[12] and a spectrofluorometer[13] were evaluated as postcolumn detectors for fluorescence measurement. The data indicated that both instruments gave comparable results (r = 0.989 and r = 0.982) for I and II, respectively (21) (Table I). Since the two instruments evaluated met both these criteria, either can be employed for pharmacokinetic studies.

Urinary Excretion in Humans—The HPLC assay was applied to the measurement of the urinary excretion of I in six human subjects following administration of a single oral 250-mg dose. Urine samples were collected prior to administration (control) and for 8 hr thereafter. Levels of unchanged I and II were determined by HPLC. The percent of dose recovered as I within the 8-hr period ranged from 50 to 68% of the ad-

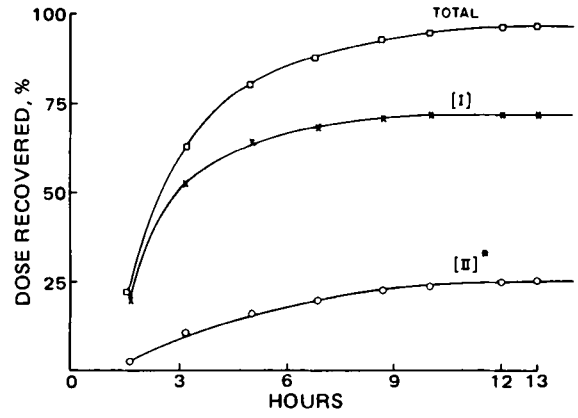

Figure 4—*Percent of dose of I and II recovered in the urine at intervals over 13.00 hr from a human subject following a single 250-mg po dose (* = reported as I equivalent).*

Table III—HPLC Measurement [a] of the Urinary Excretion of I and II at Various Time Intervals in One Human Subject following a 250-mg po Dose

Hours at Conclusion of Excretion Interval	Unchanged I			II [b]			Total Dose Accumulated, %
	Total Excreted, mg	% of Dose Recovered	% of Dose Accumulated	Total Excreted, mg	% of Dose Recovered	% of Dose Accumulated	
1.58	48.6	19.4	19.4	6.2	2.5	2.5	21.9
3.17	82.6	33.0	52.4	20.4	8.2	10.7	63.1
5.00	29.1	11.7	64.1	14.1	5.6	16.3	80.4
6.83	10.4	4.2	68.3	8.5	3.4	19.7	88.0
8.67	5.9	2.4	70.7	7.1	2.8	22.5	93.2
10.00	1.6	0.6	71.3	3.0	1.2	23.7	95.0
12.00	1.1	0.4	71.7	2.8	1.1	24.8	96.5
13.00	0.4	0.1	71.8	1.0	0.4	25.2	97.1
21.50	n.m. [c]			n.m. [c]			
24.50	n.m. [c]			n.m. [c]			

[a] Using filter fluorometer. [b] Reported as I equivalent. [c] Not measurable.

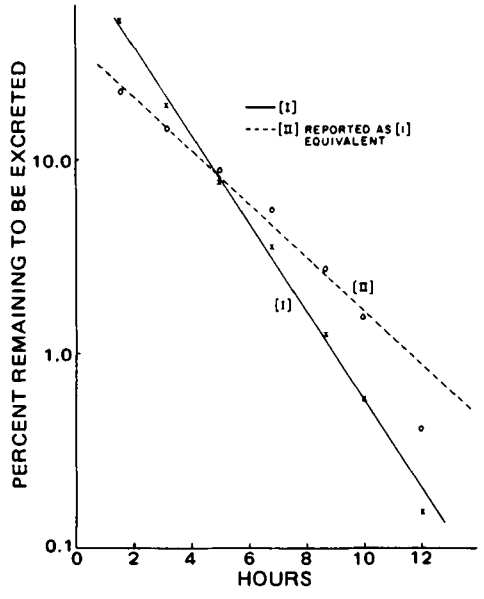

Figure 5—*Plot of the percent of dose remaining to be excreted as I and II in the urine of a human subject following a single 250-mg po dose.*

ministered dose (Table II). The recoveries of II, calculated as equivalents of I, excreted within the same period ranged from 22 to 30%. The I levels also were measured by the microbiological assay using *S. aureus* (ATCC 6538P) as a test organism (22) (Table II). An excellent correlation (r = 0.985) (21) was obtained for the determination of I by HPLC and bioassay, demonstrating that the two procedures were equivalent. These data are in good agreement with previously reported (4) recoveries of 72 ± 15 and 19 ± 12.6% for I and II, respectively, in a 12-hr period following a single 500-mg po dose.

The urinary excretion of I and II also was measured in another subject following a single 250-mg po dose. Ten urine samples were collected at intervals over 24.5-hr, the volume voided was measured, and the specimens were assayed by HPLC only. Approximately 100% of the drug was recovered in the urine as I and II (Table III and Fig. 4). A semilogarithmic plot of percent of intact I remaining to be excreted *versus* time (Fig. 5) yielded a linear plot with a slope equivalent to a half-life for I of 1.3 hr. The half-life value for I calculated for this subject was in good agreement with half-life values reported in the literature ($t_{1/2}$ = 1.1–3.2 hr) (23). The penicilloic acid metabolite (II) also exhibited linear elimination characteristics (Fig. 5). These findings demonstrate the utility of this method for clinical pharmacokinetic evaluation.

REFERENCES

(1) S. J. Faigenbaum, G. L. Boyle, A. S. Prywes, R. Abel, Jr., and I. H. Leopold, *Am. J. Ophthamol.*, **82,** 598 (1976).

(2) E. A. P. Croydon and R. Sutherland, *Antimicrob. Agents Chemother.*, **1970,** 427.

(3) H. C. Neu and E. B. Winshell, *ibid.*, **1970,** 423.

(4) F. Miki, *Proc. Eur. Soc. Study Drug Toxic (Int. Congr. Ser. 326, Symp. Amoxicillin, London, Sept. 3–4, 1973)*, 25 (1974).

(5) H. Graber, T. Perenyi, M. Arr, and E. Ludwig, *Int. J. Clin. Pharmacol.*, **14,** 284 (1976).

(6) R. Sutherland and G. N. Robinson, *Antimicrob. Agents Chemother.*, **1970,** 411.

(7) T. Murakawa, Y. Yokota, Y. Kono, M. Nishida, S. Goto, and S. Kuwahara, *Chemotherapy (Tokyo)*, **21,** 1399 (1973).

(8) W. J. Jusko, *J. Pharm. Sci.*, **60,** 728 (1971).

(9) K. Miyazaki, O. Ogino, and T. Arita, *Chem. Pharm. Bull.*, **22,** 1910 (1974).

(10) A. Dürr and H. J. Schatzmann, *Experientia*, **31,** 503 (1975).

(11) D. F. Davidson, *Clin. Chim. Acta*, **69,** 67 (1976).

(12) E. Puigdellival, G. Obiols, and J. Moreno Dalman, *Afinidad*, **30,** 749 (1973).

(13) R. H. Barhaiya, P. Turner, and E. Shaw, *Clin. Chim. Acta*, **77,** 373 (1977).

(14) K. Miyazaki, O. Ogino, H. Sato, M. Nakano, and T. Arita, *Chem. Pharm. Bull.*, **25,** 253 (1977).

(15) E. R. White, M. A. Carroll, J. E. Zarembo, and D. Bender, *J. Antibiot.*, **28,** 205 (1975).

(16) E. R. White, M. A. Carroll, and J. E. Zarembo, *ibid.*, **30,** 811 (1977).

(17) J. M. Blaha, A. M. Knevel, and S. L. Hem, *J. Pharm. Sci.*, **64,** 1384 (1975).

(18) R. W. Frei, L. Michel, and W. Santi, *J. Chromatogr.*, **126,** 665 (1976).

(19) D. L. Mays, R. J. Van Apeldoorm, and R. G. Lauback, *ibid.*, **120,** 93 (1976).

(20) R. H. Barbhaiya, R. C. Brown, D. W. Payling, and P. Turner, *J. Pharm. Pharmacol.*, **30,** 224 (1978).

(21) M. G. Kendall and A. Stuart, "The Advanced Theory of Statistics," Hafner, New York, N.Y., 1961, chap. 29, sections 29.37–29.41.

(22) J. V. Bennett, J. L. Brodie, E. J. Benner, and W. M. M. Kirby, *Appl. Microbiol.*, **14,** 170 (1966).

(23) P. G. Welling, H. Huang, P. A. Koch, W. A. Craig, and P. O. Madsen, *J. Pharm. Sci.*, **66,** 549 (1977).

ACKNOWLEDGMENTS

The authors thank Mr. T. Daniels for the drawings of the figures and Mrs. K. M. Catala for the preparation of the manuscript.

Antibacterial and Antifungal Activities of Isatin *N*-Mannich Bases

MIRJANA KUPINIĆ *, MARICA MEDIĆ-ŠARIĆ ‡, MARIJA MOVRIN ‡, and DUŠICA MAYSINGER ‡x

Received January 4, 1978, from the **Institute for the Control of Drugs, Zagreb, Yugoslavia*, and the ‡*Faculty of Pharmacy and Biochemistry, University of Zagreb, Zagreb, Yugoslavia.* Accepted for publication September 14, 1978.

Abstract □ The antimicrobial and antifungal activities of 29 congeneric isatin *N*-Mannich bases were investigated by testing against standard test microorganisms and 21 pathogenic Gram-negative microorganisms. Considerable growth inhibition of Gram-negative bacteria and yeasts and slight inhibition of Gram-positive bacteria resulted when they were treated with the various *N*-Mannich bases of isatin and 5-nitroisatin, respectively.

Keyphrases □ Isatin *N*-Mannich bases—screened for antimicrobial and antifungal activities □ Nitroisatin *N*-Mannich bases—screened for antimicrobial and antifungal activities □ Antimicrobial activity—series of isatin and 5-nitroisatin *N*-Mannich bases screened □ Antifungal activity—series of isatin and 5-nitroisatin *N*-Mannich bases screened

Interest in biologically active isatin (indole-2,3-dione) derivatives, particularly hydrazones, is increasing (1, 2). The biological activities of isatin-3-*o*-nitrophenylhydrazones against the Walker carcinosarcoma 256 were reported (3). Results indicated that all compounds except the parent compound, *i.e.*, isatin-3-*o*-nitrophenylhydrazone, were inactive. Methyl and ethyl derivatives of some isatin-3-thiosemicarbazones, however, were more active biologically than the parent compound (4).

Preliminary screening results for antiviral, antibacterial, and antifungal activities of some isatin *N*-Mannich bases were reported (5). Isatin *N*-Mannich bases with morpholine and piperidine moieties as amino components showed some activity against certain Gram-negative bacteria but were inactive against tested fungi and yeasts.

This study concerns a series of structurally related *N*-Mannich bases of isatin that have not been tested for antimicrobial and antifungal activities. This series includes a group of compounds substituted in position 1 (Mannich bases) and a group substituted in positions 1 and 3 (Mannich base hydrazones)[1] (6). All compounds were tested against various microorganisms.

EXPERIMENTAL

Materials—Isatin *N*-Mannich bases (Table I) were prepared according to the previously described procedure[1] (6).

Test Microorganisms—Compounds I–XXIX were subjected to antibacterial and antifungal screening procedures against the following test microorganisms[2]: *Micrococcus flavus* (ATCC 10240), *Sarcina lutea* (FDA 1001), *Sarcina lutea* (ATCC 9341), *Staphylococcus albus*, *Staphylococcus aureus* (ATCC 209-P), *Staphylococcus aureus* (ATCC 6538-P), *Staphylococcus epidermidis* (ATCC 12228), *Streptococcus faecalis* (ATCC 8043), *Brucella bronchiseptica* (ATCC 4617), *Escherichia coli* (99-1), *Escherichia coli* (ATCC 10536), *Klebsiella pneumoniae* (ATCC 10031), *Mycobacterium smegmatis*, *Candida albicans*, and *Candida monosa*.

The following pathogenic microorganisms were used[3]: *Aerobacter aerogenes* (two strains), *Escherichia coli* (13 strains), *Klebsiella* sp. (one strain), *Proteus mirabilis* (two strains), *Proteus morganii* (one strain), and *Pseudomonas aeruginosa* (two strains).

Assay—Preliminary assays were performed with 15 Gram-negative and Gram-positive microorganisms grown on agar[4]. The diffusion technique generally used for antibiotic screening was adopted both for growth inhibition studies and determination of the minimum inhibitory concentration. Stock solutions (1 mg/ml) of the compounds were prepared in 96% ethanol (I–XIII and XVI–XXV) or dimethylformamide (XIV, XV, and XXVI–XXIX). Working solutions of 0.5 and 0.25 mg/ml were prepared by dilution of stock solution with pH 7.4 phosphate buffer. Paper disks were immersed into these solutions, drained, and placed onto the nutrient surface.

The cup–plate technique was used to determine minimum inhibitory concentrations. Several dilutions containing 0.06, 0.125, 0.25, 0.50, 1.0, 2.5, 5.0, 10.0, 20.0, 40.0, 62.5, 125, and 250 μg of compounds/ml were prepared, and 100-μl portions were transferred to 9-mm diameter holes cut into the agar plates with a micropipet. Compounds that had a strong inhibitory effect in preliminary testing were retested against the second group of microorganisms. These tests were made at two concentration levels, 10.0 and 0.125 μg/ml, respectively. In all tests, the cultures were incubated at 37° for 16–18 hr before the diameters of inhibition zones surrounding each disk or hole were measured.

RESULTS AND DISCUSSION

Preliminary values for growth inhibition of different microorganisms treated with isatin and nitroisatin derivatives are given in Tables II and III. Most isatin *N*-Mannich bases strongly inhibited Gram-negative bacteria and fungi but only moderately inhibited the growth of Gram-positive bacteria (Table II). Compounds V, VI, and XIII were more active against *M. flavus*, a Gram-positive microorganism, than against some Gram-negative bacteria, as evidenced by the relative size of the inhibition zones. Compound XIII was particularly active against all test organisms, and VII was active against all test organisms but *M. flavus*.

In several instances, the diameters of the inhibition zones with various concentrations of the test compounds did not differ markedly, *e.g.*, for X against *E. coli* (99-1), *K. pneumoniae*, and *C. monosa*; for XI against *C. monosa*; and for XIII against *M. flavus* and *S. lutea* (ATCC 9341). The inhibition zones increased with a decrease in concentration for some compounds, *e.g.*, V against *E. coli* (ATCC 10536 and 99-1), *B. bronchiseptica*, and *C. albicans*; VII against *S. lutea* (ATCC 9341), *E. coli* (ATCC 10536), *C. albicans*, and *C. monosa*; X against *M. smegmatis* and *C. albicans*; XI against *M. flavus* and *K. pneumoniae*; XIII against *S. lutea* (ATCC 9341), *E. coli* (99-1); and XV against *E. coli* (ATCC 10536 and 99-1).

Table II also shows that most isatin nitrogen mustards (IV, VIII, XII, and XVII) were least active against all tested microorganisms. Compound IV showed slight inhibition against *K. pneumoniae* except at the highest concentration (1 mg/ml). Compounds VIII, XII, and XVII were active at the highest concentrations against the acid-fast *M. smegmatis*. Furthermore, XII showed some activity against *B. bronchiseptica* at both 0.5 and 1 mg/ml. *C. monosa* was inhibited at the lowest concentration by XVII.

Compound III, closely related structurally to nitrogen mustards, showed some activity against *K. pneumoniae* at the maximum concentration, but XVI was inactive. Compound IX was active against Gram-positive *M. flavus* at two concentrations. The observed dependencies of inhibition zones on the concentration of the test compounds could be attributed to effects of solvent interaction with test compounds and/or limiting solubility of the test compounds in agar, as was found with XVI and XVIII, which partially precipitated.

[1] See M. Movrin and M. Medić-Šarić, *Eur. J. Med. Chem.*, **13**, 309 (1978).

[2] Obtained from ATCC, FDA, and the Institute for the Control of Drugs.

[3] Obtained from the Microbiological Laboratory at the hospital "Dr. Ozren Novosel," Zagreb, Yugoslavia.

[4] Difco.

0022-3549/79/0400-0459$01.00/0
© 1979, American Pharmaceutical Association

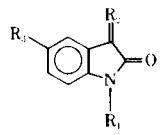

Table I—Synthesized Isatin *N*-Mannich Bases

Compound	R_1	R_2	R_3	Reference
I		O	H	7
II		O	H	7
III	$CH_2N(CH_2CH_2OH)_2$	O	H	—[a]
IV	$CH_2N(CH_2CH_2Cl)_2$	O	H	8
V	H	$NNHCOCH_3$	H	6
VI		$NNHCOCH_3$	H	6
VII		$NNHCOCH_3$	H	6
VIII	$CH_2N(CH_2CH_2Cl)_2$	$NNHCOCH_3$	H	6
IX	H	$NNHCH_3$	H	6
X		$NNHCH_3$	H	6
XI		$NNHCH_3$	H	6
XII	$CH_2N(CH_2CH_2Cl)_2$	$NNHCH_3$	H	6
XIII	H	$NNHCSNH_2$	H	10
XIV		$NNHCSNH_2$	H	5
XV		$NNHCSNH_2$	H	5
XVI	$CH_2N(CH_2CH_2OH)_2$	$NNHCSNH_2$	H	—[a]
XVII	$CH_2N(CH_2CH_2Cl)_2$	$NNHCSNH_2$	H	8
XVIII	H	O	NO_2	9
XIX		O	NO_2	—[a]
XX		O	NO_2	—[a]
XXI	$CH_2N(CH_2CH_2Cl)_2$	O	NO_2	—[a]
XXII	H	$NNHCH_3$	NO_2	—[a]
XXIII		$NNHCH_3$	NO_2	—[a]
XXIV		$NNHCH_3$	NO_2	—[a]
XXV	$CH_2N(CH_2CH_2Cl)_2$	$NNHCH_3$	NO_2	—[a]
XXVI	H	$NNHCSNH_2$	NO_2	—[a]
XXVII		$NNHCSNH_2$	NO_2	—[a]
XXVIII		$NNHCSNH_2$	NO_2	—[a]
XXIX	$CH_2N(CH_2CH_2Cl)_2$	$NNHCSNH_2$	NO_2	—[a]

[a] M. Movrin and M. Medić-Šarić, *Eur. J. Med. Chem.*, 13, 309 (1978).

Table III shows that of 12 5-nitroisatin derivatives, only XXVI–XXIX inhibited considerably the acid-fast bacteria, the Gram-negative bacteria except *B. bronchiseptica*, and the test fungi. The same compounds, except XXVII and XXVIII, were inactive against the Gram-positive bacteria; XXVII and XXVIII showed some activity against *S. aureus* (ATCC 6538-P) and *S. epidermidis*. Compounds XVIII–XXV did not show any inhibition except XVIII, which affected the growth of *K. pneumoniae*. Compounds XX and XXV were completely inactive in all concentrations against any tested microorganism.

The diameter of inhibition zones increased with a decrease in concentration with XXVI against *K. pneumoniae* and *C. monosa*, with XXVII against *E. coli* (ATCC 10536), and with XXVIII against *E. coli* (99-1), *K. pneumoniae*, *C. albicans*, and *C. monosa*. Compounds XXII–XXV did not show any effect against the test microorganisms, except XXII and XXIV very slightly inhibited *B. bronchiseptica* and XXIII inhibited *S. lutea* (ATCC 9341).

Compounds XVIII–XXI did not show any inhibition against *M. smegmatis*, *E. coli*, and fungi. These compounds showed the strongest resistance with *S. lutea* (ATCC 9341), *S. aureus* (ATCC 209-P), *S. albus*, *S. faecalis*, and *M. flavus*.

Based on the results presented in Tables II and III, the 12 most biologically active substances, *i.e.*, V–VII, X, XI, XIII–XVIII, and XXIX, were further tested to determine their minimum inhibitory concentrations. Three Gram-negative bacteria, *i.e.*, *E. coli* (99-1), *E. coli* (ATCC 10536), and *K. pneumoniae*, which were maximally inhibited in the presence of these substances, were used for minimum inhibitory concentration determinations. The results obtained are depicted in Fig. 1.

E. coli (99-1) was inhibited by all compounds at 0.125 μg/ml. The demonstration of strong antibacterial activity by the 12 compounds included in Fig. 1 stimulated interest to test some pathogenic strains of the Gram-negative bacteria. Of the 13 pathogenic *E. coli* strains, seven were strongly inhibited by all compounds (I–XXIX). Five other strains were

Table II—Antibacterial and Antifungal Activities of Isatin *N*-Mannich Bases [a]

Compound	Diameter of Inhibition Zones, mm × 10											
	M. flavus			*S. lutea* (ATCC 9341)			*M. smegmatis*			*E. coli* (ATCC 10536)		
I	–	–	–	–	–	170	–	–	–	–	–	–
II	–	–	–	–	–	–	–	–	–	–	–	–
III	–	–	–	–	–	–	–	–	–	–	–	–
IV	–	–	–	–	–	–	–	–	–	–	–	–
V	190	210	225	–	–	–	240	210	240	155	160	148
VI	223	–	–	–	–	–	170	170	180	–	140	156
VII	–	–	–	148	150	145	210	210	220	158	155	152
VIII	–	–	–	–	–	–	–	–	158	–	–	–
IX	135	142	–	–	–	–	–	–	–	–	–	–
X	179	182	188	–	–	–	220	223	210	170	161	248
XI	272	250	132	–	–	–	200	160	220	±	±	145
XII	–	–	–	–	–	–	–	–	170	–	–	–
XIII	182	180	181	148	145	145	210	220	260	140	147	150
XIV	–	–	–	–	–	–	–	180	201	185	160	180
XV	–	–	–	–	–	–	–	–	302	178	172	155
XVI	–	–	–	–	–	–	–	–	–	–	–	–
XVII	–	–	–	–	–	–	–	–	180	–	–	–
Concentration [b]	T_1	T_2	T_3	T_1	T_2	T_3	T_1	T_2	T_3	T_1	T_2	T_3

Compound	Diameter of Inhibition Zones, mm × 10														
	E. coli (99-1)			*K. pneumoniae*			*B. bronchiseptica*			*C. monosa*			*C. albicans*		
I	–	–	–	–	–	142	–	–	–	–	–	–	–	–	–
II	158	153	159	–	–	149	–	–	162	–	–	–	–	–	–
III	–	–	–	–	–	161	–	–	–	–	–	–	–	–	–
IV	–	–	–	–	–	146	–	–	–	–	–	–	–	–	–
V	300	158	147	181	175	189	180	170	170	195	200	210	180	180	178
VI	208	245	310	177	151	162	–	–	–	177	190	240	148	198	211
VII	>300	300	>300	162	161	182	179	181	190	250	220	212	248	202	160
VIII	–	–	–	–	–	–	–	–	–	–	–	–	–	–	–
IX	–	–	–	–	–	–	–	–	–	–	–	–	–	–	–
X	>300	300	>300	185	182	185	145	160	162	200	201	202	205	202	192
XI	238	208	290	212	192	171	±	162	±	198	190	198	158	160	212
XII	–	–	–	–	–	–	–	170	172	–	–	–	–	–	–
XIII	190	168	148	158	181	175	170	175	180	188	210	210	198	198	180
XIV	280	250	248	201	212	203	–	–	–	200	210	215	170	185	205
XV	255	220	217	201	205	201	–	–	–	–	–	218	–	–	210
XVI	–	–	–	–	–	–	–	–	–	165	170	172	–	–	–
XVII	–	–	–	–	–	–	–	–	–	168	–	–	–	–	–
Concentration [b]	T_1	T_2	T_3	T_1	T_2	T_3	T_1	T_2	T_3	T_1	T_2	T_3	T_1	T_2	T_3

[a] ± = minimally observable inhibition, and – = no inhibition. [b] T_1 = 0.25 mg/ml, T_2 = 0.5 mg/ml, and T_3 = 1 mg/ml.

Table III—Antibacterial and Antifungal Activities of 5-Nitroisatin *N*-Mannich Bases[a]

Compound	Diameter of Inhibition Zones, mm × 10														
	S. lutea (FDA 1001)			*S. aureus* (ATCC 6538-P)			*S. epidermidis*			*M. smegmatis*			*E. coli* (ATCC 10536)		
XVIII	–	–	–	–	165	200	–	–	138	–	–	–	–	–	148
XIX	–	–	–	–	–	–	–	–	–	–	–	–	–	–	–
XX	–	–	–	–	–	–	–	–	–	–	–	–	–	–	–
XXI	–	–	160	–	–	–	–	–	–	–	–	–	–	–	–
XXII	–	–	–	–	–	–	–	–	–	–	–	–	–	–	–
XXIII	–	–	268	–	–	–	–	–	–	–	–	–	–	–	–
XXIV	–	–	–	–	–	–	–	–	–	–	–	–	–	–	–
XXV	–	–	–	–	–	–	–	–	–	–	–	–	–	–	–
XXVI	–	–	–	–	–	–	–	–	–	160	185	215	168	162	181
XXVII	–	–	–	–	160	180	±	±	148	235	290	310	168	163	151
XXVIII	–	–	–	153	–	–	158	–	–	280	–	–	140	152	171
XXIX	–	–	–	–	–	–	–	–	–	160	192	210	153	160	165
Concentration[b]	T_1	T_2	T_3	T_1	T_2	T_3	T_1	T_2	T_3	T_1	T_2	T_3	T_1	T_2	T_3

Compound	*E. coli* (99-1)			*K. pneumoniae*			*B. bronchiseptica*			*C. monosa*			*C. albicans*		
XVIII	–	–	–	141	162	187	–	–	–	–	–	–	–	–	–
XIX	–	–	–	–	–	150	–	152	158	–	–	–	–	–	–
XX	–	–	–	–	–	–	–	–	–	–	–	–	–	–	–
XXI	–	–	–	–	–	151	–	–	159	–	–	–	–	–	–
XXII	–	–	–	–	–	–	170	162	–	–	–	–	–	–	–
XXIII	–	–	–	–	–	–	–	–	–	–	–	–	–	–	–
XXIV	–	–	–	–	–	–	–	168	180	–	–	–	–	–	–
XXV	–	–	–	–	–	–	–	–	–	–	–	–	–	–	–
XXVI	160	180	185	203	202	196	–	–	–	201	195	188	170	185	202
XXVII	170	190	195	208	212	220	–	–	–	245	260	260	202	220	238
XXVIII	180	175	165	212	191	191	–	–	–	228	168	165	215	160	160
XXIX	148	170	190	206	200	298	–	–	–	188	205	210	170	175	–
Concentration[b]	T_1	T_2	T_3	T_1	T_2	T_3	T_1	T_2	T_3	T_1	T_2	T_3	T_1	T_2	T_3

[a] ± = minimally observable inhibition, and – = no inhibition. [b] T_1 = 0.25 mg/ml, T_2 = 0.5 mg/ml, and T_3 = 1 mg/ml.

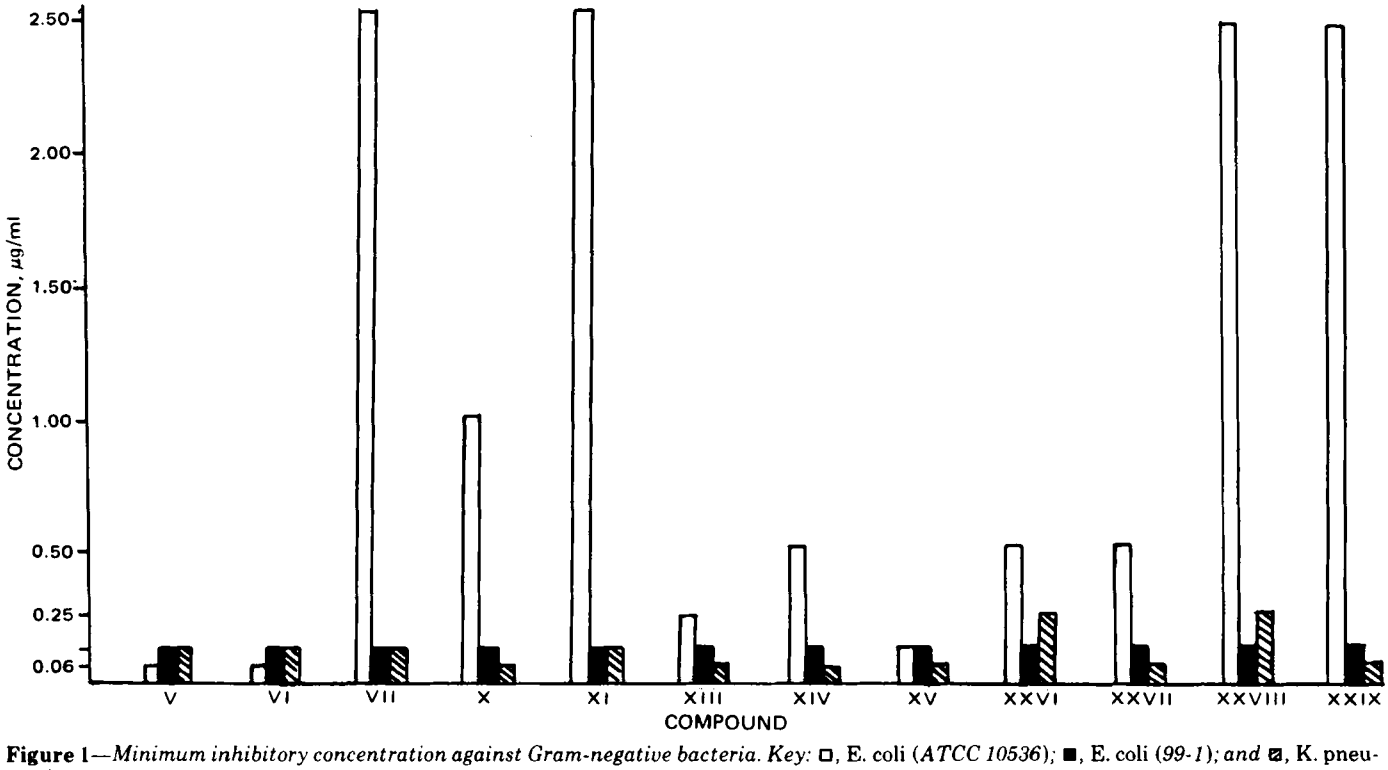

Figure 1—*Minimum inhibitory concentration against Gram-negative bacteria. Key:* □, E. coli (*ATCC 10536*); ■, E. coli (*99-1*); *and* ▨, K. pneumoniae.

moderately resistant and one *E. coli* strain was highly resistant to the action of any isatin derivative at 1 mg/ml.

Compounds I–XXIX also were tested against *P. mirabilis* but antimicrobial activity was not observed at 1 mg/ml or less.

REFERENCES

(1) R. S. Varma and W. L. Nobles, *J. Pharm. Sci.*, **64**, 881 (1975).

(2) R. S. Varma, *Pol. J. Pharmacol. Pharm.*, **26**, 641 (1975).

(3) F. D. Popp, *J. Med. Chem.*, **12**, 182 (1969).

(4) D. J. Bauer and P. W. Sadler, *Br. J. Pharmacol.*, **15**, 101 (1960).

(5) R. S. Varma and W. L. Nobles, *J. Med. Chem.*, **10**, 972 (1967).

(6) M. Movrin, M. Jakševac, and M. Medić-Šarić, *Acta Pharm. Jugosl.*, **26**, 67 (1976).

(7) H. Hellmann and J. Löschmann, *Chem. Ber.*, **87**, 1684 (1954).

(8) G. R. Pettit and J. A. Settepani, *J. Org. Chem.*, **27**, 1714 (1962).

(9) H. Rupe and E. Stocklin, *Helv. Chim. Acta*, **7**, 566 (1924).

(10) A. B. Tomchin and V. S. Dimitrukha, *Zh. Org. Khim.*, **11**, 184 (1975).

Quantitative Structure–Activity Relationships and Dipole Moments of Anticonvulsants and CNS Depressants

ERIC J. LIEN [x], **RICHARD C. H. LIAO, and H. G. SHINOUDA** [1]

Received June 12, 1978, from the *Section of Biomedicinal Chemistry, School of Pharmacy, University of Southern California, Los Angeles, CA 90033.* Accepted for publication September 14, 1978.

Abstract □ The anticonvulsant and CNS-depressant activities of 16 commercially available antiepileptics were subjected to regression analysis. For the maximal electroshock seizure test and pentylenetetrazol seizure threshold test, good correlations were obtained only after diazepam, clonazepam, and carbamazepam were deleted; for the median toxic dose (rotorod ataxia), all 16 compounds can be included in one single equation using log *MW*, log *P*, and dipole moment (μ) terms. For the anticonvulsant activities of 7-substituted 1,4-benzodiazepinones, a parabolic equation of π combined with the Hammett σ constant gave fair correlations for most derivatives examined in three different tests. Based upon the correlations obtained, further molecular modifications are suggested. The dipole moments of seven clinically used antiepileptic drugs were measured in 1,4-dioxane for the first time.

Keyphrases □ Anticonvulsants—quantitative structure–activity relationships and dipole moments □ CNS depressants—quantitative structure–activity relationships and dipole moments □ Structure–activity relationships—anticonvulsants and CNS depressants □ Dipole moments—anticonvulsants and CNS depressants

According to a literature survey in 1970, no more than 50% of epileptic patients were controlled by available antiepileptic drugs (1). Unfortunately, because of the limited market, relatively few pharmaceutical companies are actively pursuing antiepileptic drug research and development. To stimulate interest, a screening program was initiated in 1975 by the Antiepileptic Drug Development Program. Standardized testing methods have been used to evaluate new as well as 16 marketed antiepileptic drugs (1). This evaluation provides uniform sets of data suitable for quantitative structure–activity analysis.

The main purpose of this report is to analyze the structure–activity relationships of various anticonvulsant drugs (Tables I and II) in quantitative terms. The results obtained may be helpful to medicinal chemists in designing new antiepileptic drugs.

EXPERIMENTAL

The first set of data was from the recent publication (1) on 16 marketed antiepileptic drugs, using three anticonvulsant screening methods: the maximal electroshock seizure (MES) test, the subcutaneous pentylenetetrazol seizure threshold (MET) test, and the median toxic dose (TD_{50}) test. The biological data were all converted to log $1/C$, where C is the ED_{50} or LD_{50} value in moles per kilogram. The octanol–water partition coefficients (log *P*) were taken from the literature (2–4). The dipole moments were either from the literature (2, 5) or were experimentally determined in this study (Table III) using the published method of Halverstadt and Kumler (6, 7). The method of least squares was used in deriving the equations listed in Tables IV and V.

The second set of data, on anticonvulsant activities of 7-substituted 1,4-benzodiazepinones (Table II), was taken from the work of Sternbach *et al.* (8). The results of the regression analysis are given in Table V.

RESULTS AND DISCUSSION

Equations correlating the anticonvulsant activities of 16 clinically used antiepileptics are summarized in Table IV. For the maximal electroshock seizure test, a fair correlation with log *P* was obtained when all 16 compounds were included (Eq. 1). Addition of the nonlinear term [(log *P*)^2] or dipole moment term (μ) did not improve the correlation significantly, as judged by the correlation coefficients (r) and standard deviations (s).

A recent study (9) suggested that benzodiazepines appeared to occupy specific receptors. This led the authors to delete diazepam, clonazepam, and carbamazepine from the regression. When these structurally quite different compounds were eliminated, much better correlations were obtained (Eqs. 6–10). Not only were the correlation coefficients increased, but the standard deviations were decreased. Surprisingly, log *MW* gave the best correlation (Eq. 7). Similar dependence of biological activity on the log *MW* term and its implications were reported previously[2].

Table I—Anticonvulsant Activities and Physicochemical Constants of Various Drugs Used in the Regression Analysis

Compound	log $1/C$ MES Obs.[a]	log $1/C$ MES Calc.[b]	log $1/C$ MET Obs.[a]	log $1/C$ MET Calc.[c]	log $1/C$ TD_{50} Obs.[a]	log $1/C$ TD_{50} Calc.[d]	log *MW*	log P^e, Octanol–Water	μ^e, debeyes
Phenytoin	4.42	4.22	—	—	3.58	3.62	2.40	2.47	1.74
Ethotoin	3.38	3.52	3.63	3.64	3.08	3.10	2.31	1.53	1.74
Mephenytoin	3.56	3.76	3.86	3.51	3.15	3.03	2.34	2.09	1.74
Phenobarbital	4.03	3.99	4.25	4.20	3.44	3.69	2.37	1.42	0.87
Metharbital	3.19	3.45	4.30	4.02	3.47	2.92	2.30	1.21	1.13
Mephobarbital	3.86	4.15	4.02	4.10	3.10	3.46	2.39	1.98	0.87
Primidone	4.28	3.76	3.57	3.76	<2.56[f]	2.80	2.34	2.10	1.35[g]
Trimethadione	2.36	2.36	2.68	2.69	2.24	2.56	2.16	−0.37	1.74
Paramethadione	2.82	2.67	3.40	3.18	2.73	2.68	2.20	0.13	1.69
Ethosuximide	<2.15[f]	2.28	3.04	3.22	2.50	1.88	2.15	0.01	1.47
Methsuximide	3.43	3.52	3.48	3.73	3.03	3.02	2.31	1.54	1.61
Phensuximide	3.23	3.29	3.58	3.73	2.91	2.68	2.28	1.40	1.61
Phenacemide	3.31	3.06	3.19	3.23	2.63	3.25	2.25	0.57	2.06[g]
Diazepam	(4.17)[h]	(4.61)	(6.24)[h]	(1.94)	4.59	4.58	2.45	2.82	2.65[g]
Clonazepam	(3.56)[h]	(5.08)	(7.55)[h]	(2.98)	6.24	5.76	2.51	2.41[i]	2.33[g]
Carbamazepine	(4.40)[h]	(3.99)	—	—	3.52	3.79	2.37	2.18[j]	2.41[g]

[a] From Ref. 1. [b] Calculated from Eq. 7. [c] Calculated from Eq. 19. [d] Calculated from Eq. 23. [e] From Refs. 2 and 5 unless stated otherwise. [f] Exclusion of this data point does not affect the correlation significantly. [g] From this study. [h] Not included in the regression. [i] From Ref. 3. [j] Calculated from log $P_{(C_6H_5)_2NCONH_2} + \frac{1}{2}\pi(C_6H_5) = 1.53 + 0.65 = 2.18$.

[1] On leave from the Department of Chemistry, University of Cairo, Cairo, Egypt.

[2] E. J. Lien, presented at the APhA Academy of Pharmaceutical Sciences, Orlando meeting, November 1976.

0022-3549/79/0400-0463$01.00/0
© 1979, American Pharmaceutical Association

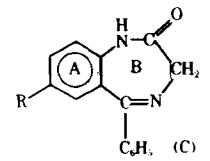

Table II—Anticonvulsant Activities and Physicochemical Constants of 7-Substituted 1,4-Benzodiazepinones

R	log 1/C: MET Obs.[a]	MET Calc.[b]	Maximum Obs.[a]	Maximum Calc.[c]	Minimum Obs.[a]	Minimum Calc.[d]	log *MW*	$\pi_{(R)}$[e]	$\sigma_{(R)}$[e]
H	<2.47[f]	(4.56)[f]	3.89	3.66	3.49	3.26	2.37	0.00	0.00
F	<2.50[f]	(4.65)[f]	2.92[f]	(3.76)[f]	3.40	3.33	2.40	0.14	0.06
Cl	4.65	4.80	4.03	4.01	3.32	3.43	2.43	0.71	0.23
Br	5.20	4.81	4.90[f]	(4.00)[f]	3.20	3.39	2.50	0.86	0.23
CN	5.31	5.23	3.89	4.00	2.59[f]	(3.79)	2.42	−0.57	0.66
NO_2	5.60	5.50	3.97	4.28	2.90[f]	(3.99)	2.45	−0.28	0.78
CF_3	5.48	5.14	4.78	4.29	4.16	3.69	2.48	0.88	0.54
CH_3	3.16[f]	(4.32)	3.22	3.66	<2.54[f]	(3.07)	2.40	0.56	−0.17
$N(CH_3)_2$	3.85	3.50	2.88	2.93	2.62	2.45	2.45	0.18	−0.83
SCH_3	4.15	4.53	3.93	3.78	2.97	3.23	2.45	0.61	0.00
SC_2H_5	3.57	4.40	3.07[f]	(3.78)	2.69	3.13	2.47	1.07	0.03
SC_4H_9	3.81	3.58	3.21	3.33	2.66	2.52	2.51	2.07	0.03
$SOCH_3$	4.07	4.20	3.52	2.91	2.99	3.07	2.47	−1.58	0.49
SO_2CH_3	2.72[f]	(4.44)	2.60	3.07	<2.60[f]	(3.25)	2.50	−1.63	0.72
C_6H_5	<2.60[f]	(3.65)	<2.59[f]	(3.27)	<2.59[f]	(2.57)	2.49	1.96	−0.01

[a] From Ref. 8. [b] Calculated from Eq. 25. [c] Calculated from Eq. 27. [d] Calculated from Eq. 29. [e] From Ref. 14. [f] Not included in the regression.

Table III—Dipole Moments (Debyes ● *SE*) of Some CNS Acting Drugs

Compound	In Dioxane	In Benzene
Chlordiazepoxide	2.15 ± 0.02	1.99 ± 0.01
Diazepam	2.65 ± 0.02	2.62 ± 0.01
Clonazepam	2.33 ± 0.02	—
Flurazepam	3.75 ± 0.02	3.11 ± 0.01
Phenacemide	2.06 ± 0.02	(Insoluble)
Primidone	1.34 ± 0.02	(Insoluble)
Carbamazepine	2.41 ± 0.01	(Insoluble)

Although the dependence on the dipole moment (μ) was not statistically significant, the negative sign of the coefficient was in agreement with previous findings (2, 10). The fact that diazepam and clonazepam had relatively high dipole moments (2.82 and 2.41 debyes, respectively) and were still active as antiepileptics, together with the finding that much better correlations were obtained when they were excluded, appears to support the contention that benzodiazepines probably occupy different receptors (9).

Improvements in correlation after deletion of diazepam and clonazepam were even more striking in the pentylenetetrazol seizure threshold test (Eqs. 11–19). Equation 19 was the best. The optimum lipophilicity (log P_0) for maximum activity was 1.42 with a 95% confidence interval of 1.06–9.61[3]. The dependence on μ was negative. The dipole moment term is statistically significant at the 97.5 percentile level as indicated by an F-test ($F_{1,8} = 9.83$, $F_{1,8_{0.975}} = 7.57$).

[3] The 95% confidence interval is skewed toward the upper limit as dictated by the equation used. For more details, see C. Hansch, A. R. Steward, S. M. Anderson, and D. Bentley, *J. Med. Chem.* **11**, 1 (1968).

Table IV—Equations Correlating Anticonvulsant Activities with Physicochemical Constants

Equation	*n*	*r*	*s*
Maximal Electroshock Seizure Test (MES)			
1. $\log 1/C = 0.627 \log P + 2.588$	16	0.874	0.342
2. $\log 1/C = 5.554 \log MW - 9.379$	16	0.806	0.417
3. $\log 1/C = -0.064 (\log P)^2 + 0.781 \log P + 2.554$	16	0.877	0.351
4. $\log 1/C = 0.647 \log P - 0.133\mu + 2.785$	16	0.879	0.348
5. $\log 1/C = -0.030 (\log P)^2 + 0.714 \log P - 0.105\mu + 2.727$	16	0.880	0.362
(Without Diazepam, Clonazepam, and Carbamazepine)			
6. $\log 1/C = 0.681 \log P + 2.544$	13	0.896	0.314
7. $\log 1/C = 7.776 \log MW - 14.438$	13	0.941	0.241
8. $\log 1/C = 0.028 (\log P)^2 + 0.624 \log P + 2.551$	13	0.897	0.328
9. $\log 1/C = 0.669 \log P - 0.112\mu + 2.727$	13	0.898	0.326
10. $\log 1/C = 0.043 (\log P)^2 + 0.580 \log P - 0.130\mu + 2.768$	13	0.899	0.342
Subcutaneous Pentylenetetrazol Seizure Threshold Test (MET)			
11. $\log 1/C = 0.967 \log P + 2.755$	14	0.704	0.967
12. $\log 1/C = 6.105 \log MW - 10.185$	14	0.654	1.029
13. $\log 1/C = 0.502 (\log P)^2 - 0.206 \log P + 3.002$	14	0.779	0.890
14. $\log 1/C = 4.925 \log MW + 0.335 \log P + 1.257\mu - 9.934$	14	0.864	0.750
15. $\log 1/C = 4.817 \log MW + 0.256 (\log P)^2 - 0.222 \log P + 0.971\mu - 9.145$	14	0.875	0.762
16. $\log 1/C = 0.408 \log P + 3.121$	12	0.719	0.350
17. $\log 1/C = 2.676 \log MW - 2.594$	12	0.756	0.330
18. $\log 1/C = -0.302 (\log P)^2 + 0.960 \log P + 3.082$	12	0.799	0.319
19. $\log 1/C = -0.301 (\log P)^2 + 0.852 \log P - 0.629\mu + 4.139$; $\log P_0 = 1.42$ (1.06–9.61)	12	0.915	0.227
Median Toxic Dose (Rotorod Ataxia) TD_{50}			
20. $\log 1/C = 0.647 \log P + 2.348$	16	0.637	0.769
21. $\log 1/C = 8.030 \log MW - 15.336$	16	0.823	0.566
22. $\log 1/C = 0.265 (\log P)^2 + 0.010 \log P + 2.490$	16	0.677	0.761
23. $\log 1/C = 15.939 \log MW - 0.972 \log P + 0.549\mu - 33.187$; $F_{2,12} = 8.88$, $F_{2,12_{0.995}} = 8.51$	16	0.933	0.388

Table V—Equations Correlating Anticonvulsant and CNS-Depressant Activities of 1,4-Benzodiazepinones with Their Physicochemical Properties

Equation	n	r	s
Pentylenetetrazol Test			
24. $\log 1/C = -0.257\pi^2 - 0.082\pi + 4.869$	10	0.489	0.764
25. $\log 1/C = -0.307\pi^2 + 0.144\pi + 1.291\sigma + 4.558$	10	0.867	0.470
$\pi_0 = 0.23$ (−2.86–3.75)[a]			
Maximal Electroshock Test			
26. $\log 1/C = -0.188\pi^2 + 0.171\pi + 3.816$	11	0.513	0.592
27. $\log 1/C = -0.258\pi^2 + 0.361\pi + 0.954\sigma + 3.660$	11	0.824	0.418
$\pi_0 = 0.70$ (0.08–5.35)[a]			
Minimal Electroshock Test			
28. $\log 1/C = -0.132\pi^2 + 0.002\pi + 3.286$	10	0.379	0.497
29. $\log 1/C = -0.220\pi^2 + 0.081\pi + 0.984\sigma + 3.262$	10	0.827	0.326
$\pi_0 = 0.18$ (−2.82–2.37)[a]			

[a] For the derivation of these 95% confidence intervals, see C. Hansch, A. R. Steward, S. M. Anderson, and D. Bentley, *J. Med. Chem.*, **11**, 1 (1968).

For the more nonspecific toxic dose (rotorod ataxia), all 16 compounds were well correlated with a three-parameter equation (Eq. 23). Furthermore, the dependence on the dipole moment was positive, in contrast with the anticonvulsant tests. Log *MW* gave better correlation than log *P*, with or without the quadratic term (compare Eq. 20 with 22). The positive dependence on log *MW* in Eqs. 21 and 23 suggests that van der Waals forces with nonspecific receptor sites are more important than hydrophobic interactions in the rotorod ataxia test.

The negative coefficient associated with the log *P* term in Eq. 23 is intriguing. Whether or not it represents interaction with somewhat hydrophilic sites remains to be studied. In any event, it is *not* parabolically dependent on log *P* as seen in many other cases of central nervous system (CNS) acting drugs (2, 10, 11).

The squared correlation matrix of the four parameters used for the 16 compounds in Eqs. 20–23 is shown here:

	log *MW*	$(\log P)^2$	log *P*	μ
log *MW*	1	0.785	0.861	0.071
$(\log P)^2$		1	0.882	0.193
log *P*			1	0.073
μ				1

It is apparent that log *MW* and log *P* are not independent while μ is practically independent of either log *MW* or log *P*. Therefore, the exact physical meaning of the log *MW* term can not be ascertained. A better selection of compounds with a wider range of log *MW* independent of log *P* is needed to delineate its contribution to the activity.

For the anticonvulsant activities of 1,4-benzodiazepinones with substitution at the 7-position of ring A, a parabolic equation of π_R combined with the Hammett σ constant appeared to give fair correlations for the results of all three tests (Table V). The ideal lipophilicity of the substituent (π_0) for the maximal electroshock test appears to be higher than those for the pentylenetetrazol test and the minimal electroshock test, although the 95% confidence intervals do overlap. Two or three compounds had to be excluded to obtain a correlation coefficient (r) of 0.82 or higher. Whether this result was due to experimental error or solubility problems (*e.g.*, the C_6H_5-derivative) could not be ascertained.

The importance of the electronic character was clearly reflected by the high coefficient associated with σ (0.95–1.29). In addition to the lipophilic and electronic characters, steric and directional factors also appear to be quite critical since substitutions at position 6, 8, or 9 of ring A reduced activity (12). Steinman *et al.* (13) reported that 7-Cl-9-NO_2- and 7,9-$(NO_2)_2$-derivatives of 1,4-benzodiazepine had weak activity (>100 mg/kg) as compared to diazepam (1 mg/kg) in pentylenetetrazol tests. Whether or not the same trend exists in the 1,4-benzodiazepinone series remains to be studied.

Clonazepam, one of the most potent compounds against pentylenetetrazol seizures, has a nitro group in ring A and a chloro atom in ring C. With regard to substitutions in ring C, Sternbach (12) showed that only the *ortho*-positions can be substituted and still maintain high activity. The 2′,6′-difluoro and dichloro derivatives had "high activity," while *meta*- and *para*-substituents decreased the activity almost to zero. It would be interesting to investigate combinations of Cl and NO_2, Br and NO_2, and CF_3 and NO_2 in the 2′,6′-positions of ring C.

REFERENCES

(1) Epilepsy Branch, Neurological Disorder Program, National Institute of Neurological and Communicative Disorder and Stroke, "Anticonvulsant Screening Project, Antiepileptic Drug Development Program," U.S. Department of Health, Education, and Welfare, Public Health Service, National Institutes of Health, Publication No. (NIH) 78-1093, Bethesda, Md., 1978.

(2) E. J. Lien, G. L. Tong, J. T. Chou, and L. L. Lien, *J. Pharm. Sci.*, **62**, 246 (1973).

(3) W. Muller and U. Wollert, *Arch. Pharmacol.*, **278**, 301 (1973).

(4) A. Leo, C. Hansch, and D. Elkins, *Chem. Rev.*, **71**, 525 (1971).

(5) A. L. McClellan, "Tables of Experimental Dipole Moments," vol. 2, Rahara Enterprises, El Cerrito, Calif., 1974.

(6) I. F. Halverstadt and W. D. Kumler, *J. Am. Chem. Soc.*, **64**, 2988 (1942).

(7) E. J. Lien and W. D. Kumler, *J. Med. Chem.*, **11**, 214 (1968).

(8) L. H. Sternbach, L. O. Randall, R. Banziger, and H. Lehr, in "Drugs Affecting the Central Nervous System," vol. 2, A. Burger, Ed., Dekker, New York, N.Y., 1968, pp. 237–264.

(9) H. Möhler and T. Okuda, *Science*, **198**, 849 (1977).

(10) E. J. Lien, *J. Med. Chem.*, **13**, 1189 (1970).

(11) C. Hansch and J. M. Clayton, *J. Pharm. Sci.*, **62**, 1 (1973).

(12) L. H. Sternbach, in "The Benzodiazepines," S. Garattini, E. Mussini, and L. O. Randall, Eds., Raven, New York, N.Y., 1973.

(13) M. Steinman, J. G. Topliss, R. Alekel, Y. S. Wong, and E. E. York, *J. Med. Chem.*, **16**, 1354 (1973).

(14) C. Hansch, A. Leo, S. H. Unger, K. H. Kim, D. Nikaitani, and E. J. Lien, *ibid.*, **16**, 1207 (1973).

ACKNOWLEDGMENTS

Presented in part at the 176th National American Chemical Society Meeting, Miami Beach, Fla., September 1978.

The authors thank Dr. W. E. Scott and Mr. J. I. Boyland of Hoffmann-La Roche for generous samples of diazepam, clonazepam, flurazepam, and chlordiazepoxide. Phenacemide was obtained from Dr. A. O. Geiszler of Abbott Laboratories, and primidone was obtained from Dr. G. R. Goetchins of Ayerst Laboratories. Carbamazepine was an analytical sample obtained from Ciba-Geigy Corp. through Dr. J. Cohen of the School of Pharmacy, University of Southern California.

Pharmacokinetic and Clinical Implications of Quinidine Protein Binding

ELAINE WOO and DAVID J. GREENBLATT ˣ

Received June 28, 1978, from the *Clinical Pharmacology Unit, Massachusetts General Hospital, Boston, MA 02114.* Accepted for publication September 21, 1978.

Abstract □ Equilibrium dialysis was used to assess factors influencing quinidine binding to serum proteins. Binding was not influenced by prolonged storage at −20° or by variation in total serum quinidine concentrations over a clinically relevant range. Protein binding decreased with increasing temperature between 24 and 37° ($p < 0.001$) and when total serum protein concentrations were decreased from 6.0 to 2.6 g/100 ml by dilution with phosphate buffer. The addition of therapeutic concentrations of salicylic acid, phenylbutazone, and tolbutamide significantly reduced quinidine binding ($p < 0.025$), but 10 other commonly coadministered drugs did not. Displacement of quinidine by salicylic acid was nonlinear; the extent of displacement increased with increasing total quinidine concentrations. The unbound quinidine fraction among 12 healthy subjects varied almost twofold and was partly explained by differences in serum albumin concentrations within the usual range of normal (3.9–4.8 g/100 ml). Pharmacokinetic analysis was performed on simultaneous total and unbound serum quinidine concentrations in 12 volunteers who received single intravenous doses of quinidine lactate. The mean elimination half-lives of total and unbound quinidine were not significantly different. However, the mean volume of distribution and total metabolic clearance of unbound quinidine were considerably greater than those determined using total drug concentrations. Renal clearance of free quinidine exceeded creatinine clearance, consistent with tubular secretion of the unbound fraction. Between-subject variability in elimination half-life and metabolic clearance of quinidine was less when free rather than total serum concentrations were analyzed. Acute ECG changes due to intravenous quinidine correlated better with unbound than with total drug concentrations. Thus, measurement of unbound as well as total serum quinidine concentrations may provide additional understanding of variations between individuals in pharmacokinetics and clinical effects of quinidine.

Keyphrases □ Quinidine—pharmacokinetic and clinical implications of protein binding, equilibrium dialysis □ Protein binding—quinidine, clinical implications □ Pharmacokinetics—quinidine, clinical implications of protein binding, equilibrium dialysis □ Cardiac depressants—quinidine, pharmacokinetic and clinical implications of protein binding

The measurement of plasma or serum levels of drugs as a means of monitoring and titrating clinical response is widely accepted (1); but for many drugs, serum concentrations and clinical effects are not well correlated. A major factor may be variability in protein binding of the drug in serum. The degree of protein binding of extensively bound drugs is a major determinant of the intensity and duration of pharmacological action (2–7). Only unbound or free drug can diffuse across membrane barriers to the sites of pharmacological activity or of metabolic alteration or excretion from the body. Since quinidine is approximately 70–80% bound to serum proteins (8, 9), alterations in quinidine binding may contribute to the variability in clinical response (10, 11).

An equilibrium dialysis technique was used to assess protein binding of quinidine. Some factors that contribute to alterations in binding are identified. The potential clinical significance of individual differences in protein binding was assessed in a study relating the acute ECG effects of intravenous quinidine to the pharmacokinetics of total and unbound drug.

EXPERIMENTAL

Determination of Total and Unbound Quinidine—*Dialysis*—Equilibrium dialysis as described by Hughes *et al.* (12) was used with modifications. Plasma or serum was incubated with quinidine sulfate and other drugs at room temperature for at least 30 min prior to dialysis. Serum specimens from volunteers receiving quinidine were kept frozen at −20° and thawed just prior to dialysis.

Equilibrium dialysis of 2 ml of plasma or serum was carried out with 15-cm strips of cellulose dialysis tubing[1] that were treated with distilled water at 100° for 4 hr and then rinsed with cold distilled water. The integrity of all bags was checked, and they were used immediately after preparation. The tubing ends were sealed by double knots, and the bags were then suspended in 7.5 ml of pH 7.4 phosphate buffer (14.11 g of K_2HPO_4/liter, 2.59 g of KH_2PO_4/liter, and 1.99 g of NaCl/liter) and dialyzed for 20 hr at 37° with gentle agitation.

Quantitation of Quinidine—A modification of the method of Cramer and Isaksson (13) was used to assay quinidine in all specimens. Serum or dialysate (0.5–1.0 ml) was alkalinized with 1 ml of 0.1 *N* NaOH and extracted with 7.5 ml of toluene (containing 1.5% isoamyl alcohol). After shaking (5 min) and centrifugation (10 min at 3000 rpm), 5 ml of the organic layer was removed and back-extracted with 5 ml of 0.1 *N* H_2SO_4. The toluene layer was discarded, and the fluorescence of an aliquot of the acidic aqueous phase was measured using a spectrophotofluorometer[2] at an excitation of 350 nm and an emission of 450 nm. This method has a sensitivity limit of 0.03 μg/ml and is linear through concentrations of at least 20 μg/ml. The coefficient of variation of replicate samples was less than 3%.

Recent studies assessed the specificity of the extraction-fluorescence technique. In a number of reports, serum quinidine concentrations determined by extraction-fluorescence were essentially identical to those determined by more specific chromatographic methods (14–18). In two other studies, the fluorescence assay yielded concentrations 5–20% higher than chromatographically determined levels (19, 20). The difference is apparently due to fluorescent quinidine metabolites that are not entirely excluded by the extraction. Additional alkaline washing of extracts prior to quantitation by fluorescence improves specificity (21).

In any case, overestimation of quinidine concentrations by the assay method used in the present study, if it did occur, would be relatively small and unlikely to introduce important errors in pharmacokinetic calculations. This is particularly true for plasma concentration determinations following single doses of quinidine since accumulation of metabolites would be minimal.

***In Vitro* Studies**—*Method Assessment*—The following studies employed blood bank plasma to which indicated amounts of quinidine sulfate and other drugs were added.

1. Recovery was assessed in replicate samples containing quinidine sulfate, 0.5–10 μg/ml ($n = 12$).
2. Reproducibility was determined in multiple specimens containing quinidine sulfate, 0.5–20 μg/ml, and the coefficient of variation (CV = standard deviation divided by the mean, expressed in percent) at each drug concentration was calculated.
3. The time necessary to reach equilibrium was determined by dialyzing replicate plasma specimens containing 5 μg of quinidine sulfate/ml at 37° for 6, 12, 18, 20, 22, and 26 hr.
4. Dialysis of replicate specimens at both room temperature (24°) and at 37° was compared.
5. Concentration dependence of protein binding of quinidine was determined by dialyzing replicate specimens containing 0.5, 1.0, 5.0, and 10 μg of quinidine sulfate/ml.
6. Protein concentration was varied by diluting plasma with phosphate

[1] Size 20, 25225-226, VWR Scientific Inc., Newton Upper Falls, Mass.
[2] American Instrument Co., Silver Spring, Md.

0022-3549/79/0400-0466$01.00/0
© 1979, American Pharmaceutical Association

Table I—Effects of Drugs on Quinidine Protein Binding

Added Drug	Concentration, μg/ml	Quinidine Protein Binding[a], Mean (±SD) Percent Unbound		Value of Student's Independent *t*	Level of Significance (Two-Tailed) Test)
		Without Added Drug	With Added Drug		
Propranolol	0.1	28.9 (±1.3)	29.0 (±3.1)	0.07	NS[b]
Warfarin	5.0	27.2 (±1.2)	28.6 (±1.5)	1.81	NS
Salicylic acid	200.0	27.8 (±1.5)	30.5 (±0.9)	3.86	$p < 0.005$
Phenylbutazone	100.0	28.8 (±2.1)	31.7 (±1.4)	2.85	$p < 0.025$
Phenytoin	20.0	28.7 (±1.4)	30.0 (±2.0)	1.28	NS
Tolbutamide	75.0	29.4 (±2.6)	34.0 (±1.1)	3.97	$p < 0.005$
Diazepam	1.0	31.4 (±2.7)	29.8 (±1.1)	1.35	NS
Sulfisoxazole	100.0	30.6 (±0.5)	29.4 (±3.0)	0.99	NS
Pentobarbital	3.0	30.2 (±0.9)	29.9 (±1.7)	0.38	NS
Trichloroacetic acid	100.0	30.4 (±2.1)	29.4 (±1.4)	0.93	NS
Digoxin	0.002	29.3 (±1.8)	29.9 (±1.5)	0.59	NS
Acetaminophen	10.0	30.7 (±2.3)	31.0 (±1.0)	0.32	NS
Chlordiazepoxide	1.0	28.8 (±0.8)	28.5 (±0.5)	0.73	NS

[a] Quinidine sulfate concentration in all samples was 5 μg/ml; $n = 6$ except for chlordiazepoxide where $n = 5$. [b] Not significant.

buffer at pH 7.4. Replicate specimens (with a quinidine sulfate concentration of 5 μg/ml) at each dilution were dialyzed.

7. The effect of storage of serum samples at −20° on protein binding of quinidine was examined by comparing binding in a fresh specimen of plasma to binding after freezing overnight and thawing to room temperature.

8. The effect of blood collection methods on quinidine protein binding was determined by transferring aliquots of a freshly drawn blood sample into: (*a*) a glass tube, (*b*) an additive-free (red-top) evacuated blood collecting tube[3] without contact with the rubber stopper, and (*c*) an evacuated tube with the sample contacting the rubber stopper.

In Vitro Drug Interactions—The effect of the following drugs, prepared in the therapeutically relevant concentrations (Table I) using absolute ethanol and distilled water, on quinidine protein binding was tested in replicate blood bank plasma samples containing 5 μg of quinidine sulfate/ml: phenylbutazone, digoxin, pentobarbital, phenytoin, tolbutamide, salicylic acid, acetaminophen, propranolol, warfarin, sulfisoxazole, chlordiazepoxide, diazepam, and trichloroacetic acid.

All drugs were added to plasma specimens and incubated at room temperature for at least 30 min prior to dialysis. The diluate for the added drugs (absolute ethanol and water) did not influence quinidine binding. Control samples containing 5 μg of quinidine sulfate/ml alone were analyzed in parallel.

The interaction of salicylic acid and quinidine was studied in detail in freshly obtained human plasma. A series of samples containing 5 μg of quinidine sulfate/ml with salicylic acid concentrations varying from 20 to 400 μg/ml was dialyzed. A series of replicate samples containing 200 μg of salicylic acid/ml with quinidine sulfate concentrations varying from 0.5 to 20 μg/ml also was dialyzed.

Clinical Studies—Intravenous (5 mg/kg) quinidine base as the lactate salt was administered by 15-min infusion to 12 healthy young volunteers who gave written informed consent (22). Free and total quinidine concentrations in multiple serum samples drawn in the 30 hr after each dose were measured as already described and analyzed by iterative weighted nonlinear least-squares regression techniques (22). All urine was collected in divided samples for 48 hr. Urinary excretion of quinidine over 48 hr and the apparent excretion rate constant were used to determine the projected cumulative urinary excretion of quinidine. The following pharmacokinetic variables were then determined for total and free quinidine: elimination half-life, total volume of distribution, total metabolic clearance, and renal clearance.

Acute ECG effects immediately following the intravenous infusion were analyzed by a blind observer. Changes in ventricular rate, corrected QT, and QRS intervals were quantitated. The relation of these changes to free and total drug levels was assessed by linear regression analysis.

Within-subject variability in quinidine protein binding was assessed in seven patients who received quinidine on more than one occasion separated by at least 2 weeks.

RESULTS

Method Evaluation—Mean (±*SD*) recovery was 99.4 ± 1.6% ($n = 12$) when dialysis bags were used immediately after preparation.

[3] Vacutainer, Becton-Dickinson and Co., Rutherford, N.J.

The coefficient of variation for replicate specimens of quinidine sulfate concentrations ranging from 0.5 to 20 μg/ml was always less than 5%. Protein binding was not altered by freezing and storage of serum samples. Contact with rubber stoppers resulted in a small increase in the unbound quinidine fraction (19.0 *versus* 22.4% unbound). Equilibrium was complete by 18 hr of dialysis, and no further changes in protein binding were seen through 26 hr of dialysis. At 24°, quinidine was 25.1 ± 0.8% unbound ($n = 7$) as compared to 29.6 ± 0.6% ($n = 5$) at 37° ($t = 10.18$, $p < 0.001$).

Serial dilution of plasma to 40% of the original concentration increased the unbound fraction from 32 to 44% (Fig. 1). Total protein concentrations of progressively diluted samples ranged from 6.0 to 2.6 g/100 ml, and albumin concentrations ranged from 3.9 to 1.5 g/100 ml.

At normal concentrations of serum proteins, there was no saturability in protein binding as quinidine sulfate concentrations were increased through the therapeutically relevant range from 0.5 to 10.0 μg/ml.

Drug Interactions—Salicylic acid, phenylbutazone, and tolbutamide significantly reduced quinidine protein binding (Table I). Other drugs had no significant effect.

Binding of quinidine in the presence of salicylic acid (200 μg/ml) decreased from 82.5 to 69.0% as the quinidine concentration was increased from 0.25 to 20 μg/ml. Quinidine binding at 5.0 μg/ml decreased from 83.0 to 72.5% as the salicylic acid concentration was increased from 20 to 400 μg/ml (Fig. 2).

Clinical Studies—The mean percent of unbound quinidine among the 12 volunteers ranged from 18.7 to 30.3% (Fig. 3). This variability was partly related to differences in the serum albumin concentrations ($r = -0.569$, $p < 0.05$) (Fig. 3). Pharmacokinetic data for free and total quinidine are summarized in Fig. 4. Use of total rather than unbound quinidine concentrations in pharmacokinetic analyses does not influence the half-life estimation but results in substantially lower values for the volume of distribution and total clearance.

Renal clearance of quinidine based upon total serum levels (1.44 ml/min/kg) averaged slightly less than creatinine clearance (1.58 ml/min/kg), but renal clearance of unbound quinidine—the fraction available

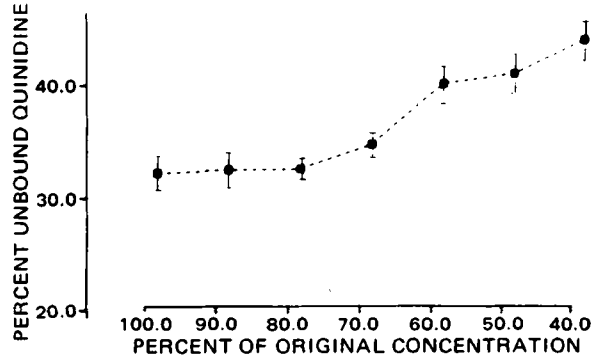

Figure 1—*Effect of plasma dilution on quinidine protein binding. Blood bank plasma was diluted with phosphate buffer, decreasing total protein concentration from 6.0 to 2.6 g/100 ml. The quinidine sulfate concentration was 5 μg/ml in all samples, and each point is the mean* (±SE) *of five determinations.*

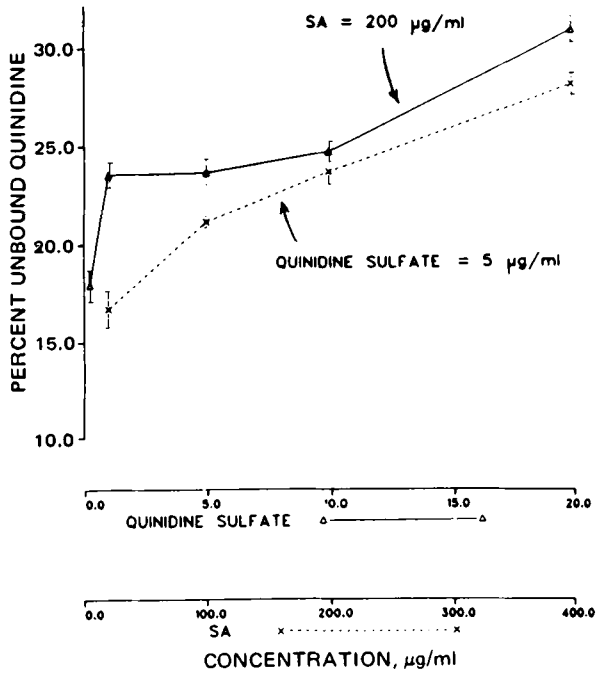

Figure 2—*Effect of salicylic acid (SA) on quinidine binding. The solid line represents the effect of a therapeutic serum concentration of salicylic acid (200 μg/ml) on the saturability of quinidine protein binding where the quinidine sulfate concentration was increased from 0.5 to 20 μg/ml. The dashed line shows the progressive increase in the unbound fraction of quinidine sulfate (5 μg/ml) as the salicylic acid concentration was increased from 20 to 400 μg/ml. Each point is the mean (±SE) of three or four determinations.*

for filtration—averaged 5.97 ml/min/kg. This amount exceeds creatinine clearance and suggests that the unbound fraction undergoes tubular secretion. Figure 5 shows representative serum concentration curves for free and total quinidine.

Individual differences in protein binding partly explained the differences between subjects in pharmacokinetic variables and in acute clinical effects as determined by acute ECG changes. The percent unbound quinidine was significantly correlated with total clearance ($r = 0.68$, $p < 0.05$). Correlations of percent unbound with elimination half-life ($r = 0.48$) and volume of distribution ($r = 0.24$) did not reach significance. Two of the three ECG changes correlated better with free than with total quinidine concentration (Table II).

In contrast to the substantial between-subject differences in protein binding, within-subject variation from time to time was minimal in six of seven subjects and varied by less than 20% in the seventh. Differences were not related to minor changes over time in serum albumin concentration.

DISCUSSION

Equilibrium dialysis for determination of quinidine protein binding utilizes a well-validated approach (23) and has proved to be reliable and reproducible. The method has a sensitivity limit of 0.25 μg of total quinidine/ml of the original serum sample, which incorporates the lower

Table II—Relation of Total and Unbound Serum Quinidine Concentrations to Acute ECG Effects

ECG Change[b]	Number of Data Pairs	Correlation Coefficients for ECG Changes *versus* Peak Serum Quinidine Concentration[a] Total	Unbound
QRS duration	12	0.279	0.536[c]
Corrected QT interval	10[d]	0.626[c]	0.581[c]
Ventricular rate	12	0.050	0.648[c]

[a] Peak concentrations reached at the end of the 15-min infusion. [b] Changes over prequinidine baseline values. [c] $p < 0.05$. [d] Corrected QT interval could not be determined for two subjects.

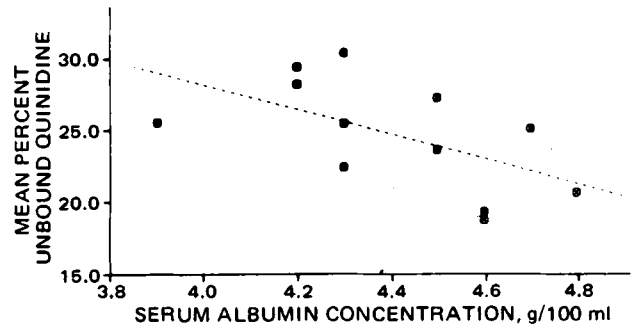

Figure 3—*Variation of quinidine protein binding with serum albumin in 12 healthy young volunteers. Each point is the mean of two or more determinations. The dashed line was determined from least-squares regression analysis ($r = -0.57$, $p < 0.05$).*

limit of the therapeutic range for this drug. When dialysis bags are prepared and used immediately, recovery is essentially 100% complete. Delay in using the dialysis bags increases variability and decreases recovery, presumably due to binding of quinidine by the cellulose tubing. Although some investigators added bactericidal agents to their dialysis solutions (12), this step is generally not necessary. Some turbidity of the phosphate buffer dialysate is observed after 24 hr of dialysis, but protein binding is unchanged between 18 hr of dialysis, when the solution is clear, and 24 hr.

Since quinidine protein binding may be influenced by collection of blood into heparinized tubes (24), all of the blood samples were collected into nonheparinized tubes. Contact of the sample with the red rubber stopper of collection tubes slightly reduced the extent of binding, but the difference was small and unlikely to be of clinical importance.

Increased temperature, decreased protein concentration, and the presence of certain drugs that are highly protein bound can increase the unbound or free fraction of quinidine within the therapeutic range. With salicylic acid, the displacement effect was nonlinear. Salicylic acid not only decreased quinidine protein binding at any given quinidine concentration, but the displacement effect was greater at higher quinidine concentrations. This interaction might cause a disparity between total blood level and expected clinical effect in the therapeutic range and disproportionately greater toxicity at higher blood levels.

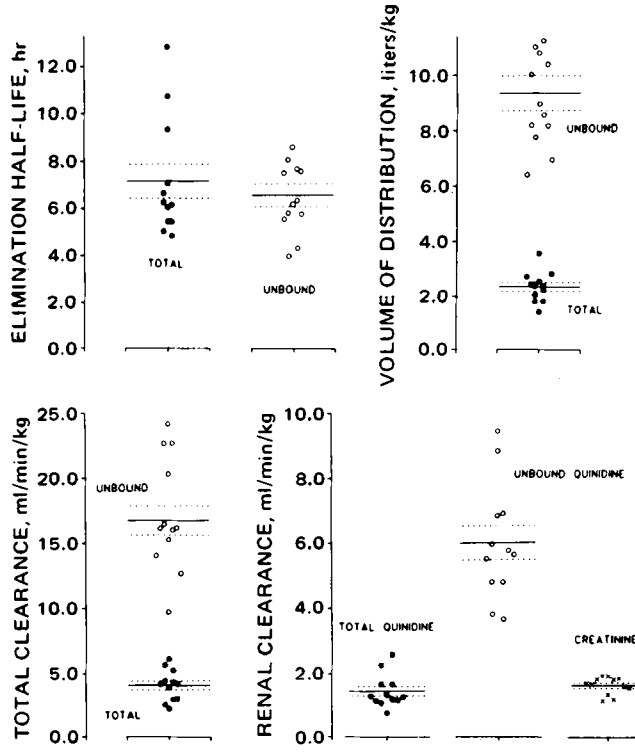

Figure 4—*Comparison of pharmacokinetics of unbound and total quinidine. Individual and mean (±SE) values of pharmacokinetic variables are shown for all 12 healthy volunteers.*

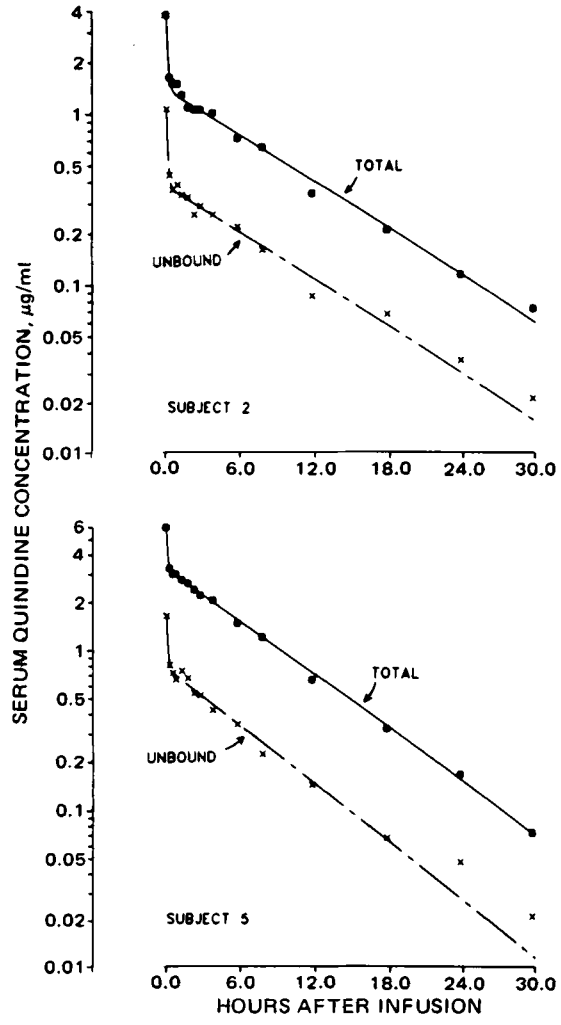

Figure 5—*Serum concentration curves for free and unbound quinidine in two volunteers who received a single intravenous dose of 5 mg of quinidine base/kg. Also shown are pharmacokinetic functions determined by iterative least-squares regression analysis.*

Quinidine binding by blood bank plasma was frequently less extensive than with fresh serum or plasma. Preservative and/or anticoagulants added to bank specimens may explain this result. Protein concentrations of donors also may vary. Since some of the *in vitro* studies required large volumes of plasma, use of bank specimens was unavoidable. Although the same plasma pool was used for any given set of studies, the use of bank plasma with its higher baseline unbound fraction might minimize observed displacement effects. For example, the use of a freshly obtained plasma specimen during the detailed quinidine–salicylic acid interaction study resulted in a much larger displacement effect (from 17 to 24% unbound) than did the same concentrations of both drugs in bank plasma (from 27 to 30% unbound). Thus, the observations of protein-binding displacement interactions in the *in vitro* study probably are a conservative reflection of such interactions during actual drug therapy in humans.

Quinidine protein binding among the healthy volunteers on no other medication varied almost twofold. Some of this variability was related to differences in serum albumin concentrations, even though all albumin concentrations were in the normal range and did not vary greatly (3.9–4.8 g/100 ml). α-Lipoprotein concentrations were not measured but may also contribute to differences in binding. These clinical findings confirm the *in vitro* data and suggest that hypoalbuminemic patients are at greater risk from quinidine toxicity even at total serum quinidine levels within the therapeutic range.

Pharmacokinetic studies of free quinidine yield values of volume of distribution and total clearance that are much larger than those determined using total (free plus bound) quinidine levels. Although these calculations do not identify the precise sites of drug distribution (25), the findings suggest that quinidine distribution is more extensive than that predicted by total drug concentrations. In addition, renal clearance of unbound quinidine exceeds creatinine clearance, consistent with renal tubular secretion of the unbound drug.

Measurement of free quinidine decreased the between-subject variability in some pharmacokinetic variables. The coefficient of variation for elimination half-life was 35% when total drug data were used and 24% when free drug data were used. Likewise, the coefficient of variation of total metabolic clearance decreased from 30 to 23% when free drug data were used. Variability in protein binding appears to contribute to variability in both clearance and elimination half-life values.

Differences in protein binding also contributed to variability in the clinical response. Peak free drug levels ranged from 0.64 to 1.6 μg/ml following a 5-mg/kg iv infusion, and these levels correlated significantly with changes in the heart rate, QRS duration, and corrected QT interval. Peak levels of total quinidine ranged from 1.7 to 5.0 μg/ml, and only the corrected QT interval was significantly related to total serum levels.

Many factors can influence protein binding of quinidine. Two such factors analyzed in the present study—hypoalbuminemia and coadministration of other drugs—commonly occur among patients receiving quinidine. Other potential sources of variability need to be identified. These alterations in protein binding contribute importantly to variability in critical pharmacokinetic parameters as well as to the clinical response to this drug.

REFERENCES

(1) J. Koch-Weser, *N. Engl. J. Med.*, **287**, 227 (1972).

(2) H. E. Booker and B. Darcy, *Epilepsia*, **14**, 177 (1973).

(3) R. Gugler, D. W. Shoeman, D. H. Huffman, J. B. Cohlmia, and D. L. Azarnoff, *J. Clin. Invest.*, **55**, 1182 (1975).

(4) D. W. Shoeman and D. L. Azarnoff, *J. Pharmacol. Exp. Ther.*, **195**, 84 (1975).

(5) W. J. Jusko and M. Gretch, *Drug Metab. Rev.*, **5**, 43 (1976).

(6) J. Koch-Weser and E. M. Sellers, *N. Engl. J. Med.*, **294**, 311, 526 (1976).

(7) A. Yacobi, J. A. Udall, and G. Levy, *Clin. Pharmacol. Ther.*, **19**, 552 (1976).

(8) S. I. Cohen, in "Drugs in Cardiology," vol. 1, E. Donoso, Ed., Stratton Intercontinental Medical Book, New York, N.Y., 1975, p. 17.

(9) O. G. Nilson and S. Jacobsen, *Biochem. Pharmacol.*, **24**, 995 (1975).

(10) T. F. Blaschke, *Clin. Pharmacokinet.*, **2**, 32 (1977).

(11) G. R. Wilkinson and D. G. Shand, *Clin. Pharmacol. Ther.*, **18**, 377 (1975).

(12) I. E. Hughes, K. F. Ilett, and L. B. Jellett, *Br. J. Clin. Pharmacol.*, **2**, 521 (1975).

(13) G. Cramer and B. Isaksson, *Scand. J. Clin. Lab. Invest.*, **15**, 553 (1963).

(14) K. K. Midha, I. J. McGilveray, C. Charette, and M. L. Rose, *Can. J. Pharm. Sci.*, **12**, 41 (1977).

(15) K. K. Midha and C. Charette, *J. Pharm. Sci.*, **63**, 1244 (1974).

(16) J. L. Valentine, P. Driscoll, E. L. Hamburg, and E. D. Thompson, *ibid.*, **65**, 96 (1976).

(17) W. G. Crouthamel, B. Kowarski, and P. M. Narang, *Clin. Chem.*, **23**, 2030 (1977).

(18) D. H. Huffman and C. E. Hignite, *ibid.*, **22**, 810 (1976).

(19) R. E. Kates, D. W. McKennon, and T. J. Comstock, *J. Pharm. Sci.*, **67**, 269 (1978).

(20) D. E. Drayer, K. Restivo, and M. M. Reidenberg, *J. Lab. Clin. Med.*, **90**, 816 (1977).

(21) T. Huynh-Ngoc and G. Sirois, *J. Pharm Sci.*, **66**, 591 (1977).

(22) D. J. Greenblatt, H. J. Pfeifer, H. R. Ochs, K. Franke, D. S. MacLaughlin, T. W. Smith, and J. Koch-Weser, *J. Pharmacol. Exp. Ther.*, **202**, 365 (1977).

(23) H. Kurz, H. Trunk, and B. Weitz, *Arzneim.-Forsch.*, **27**, 1373 (1977).

(24) D. Fremstad and K. Bergerud, *Clin. Pharmacol. Ther.*, **20**, 120 (1976).

(25) D. J. Greenblatt, *Anesthesiology*, **47**, 405 (1977).

ACKNOWLEDGMENTS

Presented in part at the 79th Annual Meeting of the American Society for Clinical Pharmacology and Therapeutics, Atlanta, March 29, 1978.

Dr. E. Woo was the recipient of a research fellowship (HL-05723) from the U.S. Public Health Service. Dr. D. J. Greenblatt was supported in part

by Grant MH-12279 from the U.S. Public Health Service. Dr. D. S. MacLaughlin was supported by U.S. Public Health Service Grant GM-23430 to the Boston Collaborative Drug Surveillance Program. This work was done in part during the tenure of the following research-in-aid awards (to D. J. Greenblatt): 13-056-756 from the American Heart Association, Western Massachusetts Division and the American Heart Association, Massachusetts Affiliate, Inc.; and 13-512-767 from the American Heart Association, Central Massachusetts Division.

The authors are grateful for the assistance and collaboration of Kate Franke, Dr. Jan Koch-Weser, Dr. Dean S. MacLaughlin, Lawrence J. Moschitto, Dr. Hermann R. Ochs, Henry J. Pfeifer, Dr. Thomas W. Smith, and Ann Werner.

Fourier Transform Carbon-13 NMR Spectra of Ampyrone and Aminopyrine

SHIVA P. SINGH, SYLVIA A. FARNUM, VIRGIL I. STENBERG, and SURENDRA S. PARMAR ˣ

Received February 13, 1978, from the *Departments of Physiology and Chemistry, University of North Dakota, Grand Forks, ND 58202.* Accepted for publication September 11, 1978.

Abstract □ The natural abundance ^{13}C-NMR spectra of ampyrone and aminopyrine were obtained using the pulse Fourier transform technique. The chemical shifts were assigned with the help of the chemical shift theory, multiplicity generated in single-frequency off-resonance decoupled spectra, relaxation time, and comparison with structurally related compounds.

Keyphrases □ Ampyrone—Fourier transform carbon-13 NMR spectra □ Aminopyrine—Fourier transform carbon-13 NMR spectra □ NMR spectroscopy—ampyrone and aminopyrine

The assignments of ^{13}C-NMR chemical shifts of synthetic and natural therapeutic agents (1–6) initiated the carbon-13 analysis of 4-amino-1,5-dimethyl-2-phenyl-3*H*-pyrazol-3-one (I, ampyrone) and 4-dimethylamino-1,5-dimethyl-2-phenyl-3*H*-pyrazol-3-one (II, aminopyrine), both of which possess antipyretic and analgesic properties. The natural abundance ^{13}C-NMR spectra, both proton noise decoupled and single frequency off-resonance decoupled (SFORD), of ampyrone and aminopyrine were recorded using the Fourier transform technique. The proton noise-decoupled spectra gave the chemical shift of various carbon resonances of I and II while the SFORD spectra differentiated the methyl, methine, and quaternary carbons.

The assignments of carbon-13 signals are based on the chemical shift theory, multiplicity generated in SFORD spectra, percent intensity of signals, and carbon chemical shifts of the model compounds. These studies could possibly contribute toward the understanding of the biotransformation of I and II.

EXPERIMENTAL

The ^{13}C-NMR spectra of ampyrone, aminopyrine, and 1,5-dimethyl-2-phenyl-3*H*-pyrazol-3-one were obtained on a spectrometer[1] operating at 15.00 kHz. The samples were run in a 10-mm tube with deuterochloroform (30% w/v) as an internal lock and solvent and tetramethylsilane as a reference. The spectrometer settings during the experiment were: spectral width, 4 kHz; pulse width, 18 msec (90°); repetition rates, 5, 15, and 45 sec; and data points, 4 K.

The T_1 measurements of these two compounds were carried out in undegassed solution and were automatically calculated[2] by least-squares analysis (10) of the plot of ln $(I_\infty - I_T)$ *versus* T.

[1] Jeol FX 60 spectrometer.
[2] By FX-60 computer.

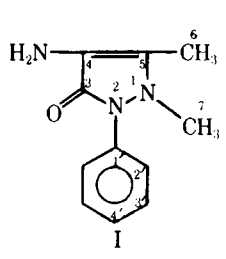

I

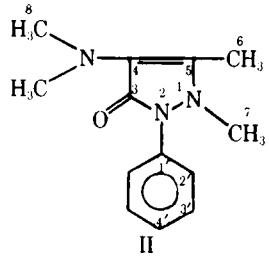

II

Ampyrone, aminopyrine, and antipyrine were obtained from commercial sources[3].

DISCUSSION

Ampyrone (I)—The carbon-13 chemical shifts of I are recorded in Table I, and its carbon resonances are illustrated in Fig. 1. The proton noise-decoupled spectrum of I gave seven signals in the lower field region and two signals in the higher field region. The quartets centered at δ 36.7 and 9.0 ppm could be easily assigned to C-7 and C-6, respectively, on the basis of chemical shift theory (7).

Feeney *et al.* (8) obtained the ^{13}C-NMR spectrum of 1,5-dimethyl-2-phenyl-3*H*-pyrazol-3-one (III, antipyrine) in dimethyl sulfoxide and reported the chemical shift of the ring carbon resonances relative to the upfield of carbon disulfide. To check the chemical shift of the carbons of two methyl groups present at positions 1 and 5 of the pyrazole ring in III, the proton noise-decoupled and SFORD spectra of III were recorded in deuterochloroform. The chemical shifts of the carbon signals of III obtained are represented on the structure of III while the figures in parenthesis indicate the chemical shifts reported earlier (8).

Table I—Carbon-13 Chemical Shifts of Ampyrone

Assignment[a]	Multiplicity[b]	Chemical Shift[c]	Relaxation Time[d], T_1, sec
C-3	s	160.7	27.4
C-5	s	136.3	18.9
C-1′	s	134.2	17.8
C-3′	d	127.8	1.08
C-4′	d	124.4	0.77
C-2′	d	121.4	1.11
C-4	s	118.0	13.8
C-7	q	36.7	1.55
C-6	q	9.0	2.90

[a] Numbering of carbons are shown in the structure. [b] Signal multiplicity obtained from SFORD; s = singlet, d = doublet, and q = quartet. [c] Chemical shifts are expressed in parts per million relative to tetramethylsilane. [d] The relaxation time was obtained in undegassed solution.

[3] Sigma Chemical Co., St. Louis, Mo.

0022-3549/79/0400-0470$01.00/0
© 1979, American Pharmaceutical Association

by Grant MH-12279 from the U.S. Public Health Service. Dr. D. S. MacLaughlin was supported by U.S. Public Health Service Grant GM-23430 to the Boston Collaborative Drug Surveillance Program. This work was done in part during the tenure of the following research-in-aid awards (to D. J. Greenblatt): 13-056-756 from the American Heart Association, Western Massachusetts Division and the American Heart Association, Massachusetts Affiliate, Inc.; and 13-512-767 from the American Heart Association, Central Massachusetts Division.

The authors are grateful for the assistance and collaboration of Kate Franke, Dr. Jan Koch-Weser, Dr. Dean S. MacLaughlin, Lawrence J. Moschitto, Dr. Hermann R. Ochs, Henry J. Pfeifer, Dr. Thomas W. Smith, and Ann Werner.

Fourier Transform Carbon-13 NMR Spectra of Ampyrone and Aminopyrine

SHIVA P. SINGH, SYLVIA A. FARNUM, VIRGIL I. STENBERG, and SURENDRA S. PARMAR ˣ

Received February 13, 1978, from the *Departments of Physiology and Chemistry, University of North Dakota, Grand Forks, ND 58202.* Accepted for publication September 11, 1978.

Abstract □ The natural abundance ^{13}C-NMR spectra of ampyrone and aminopyrine were obtained using the pulse Fourier transform technique. The chemical shifts were assigned with the help of the chemical shift theory, multiplicity generated in single-frequency off-resonance decoupled spectra, relaxation time, and comparison with structurally related compounds.

Keyphrases □ Ampyrone—Fourier transform carbon-13 NMR spectra □ Aminopyrine—Fourier transform carbon-13 NMR spectra □ NMR spectroscopy—ampyrone and aminopyrine

The assignments of ^{13}C-NMR chemical shifts of synthetic and natural therapeutic agents (1–6) initiated the carbon-13 analysis of 4-amino-1,5-dimethyl-2-phenyl-3*H*-pyrazol-3-one (I, ampyrone) and 4-dimethylamino-1,5-dimethyl-2-phenyl-3*H*-pyrazol-3-one (II, aminopyrine), both of which possess antipyretic and analgesic properties. The natural abundance ^{13}C-NMR spectra, both proton noise decoupled and single frequency off-resonance decoupled (SFORD), of ampyrone and aminopyrine were recorded using the Fourier transform technique. The proton noise-decoupled spectra gave the chemical shift of various carbon resonances of I and II while the SFORD spectra differentiated the methyl, methine, and quaternary carbons.

The assignments of carbon-13 signals are based on the chemical shift theory, multiplicity generated in SFORD spectra, percent intensity of signals, and carbon chemical shifts of the model compounds. These studies could possibly contribute toward the understanding of the biotransformation of I and II.

EXPERIMENTAL

The ^{13}C-NMR spectra of ampyrone, aminopyrine, and 1,5-dimethyl-2-phenyl-3*H*-pyrazol-3-one were obtained on a spectrometer[1] operating at 15.00 kHz. The samples were run in a 10-mm tube with deuterochloroform (30% w/v) as an internal lock and solvent and tetramethylsilane as a reference. The spectrometer settings during the experiment were: spectral width, 4 kHz; pulse width, 18 msec (90°); repetition rates, 5, 15, and 45 sec; and data points, 4 K.

The T_1 measurements of these two compounds were carried out in undegassed solution and were automatically calculated[2] by least-squares analysis (10) of the plot of ln $(I_\infty - I_T)$ *versus* T.

[1] Jeol FX 60 spectrometer.
[2] By FX-60 computer.

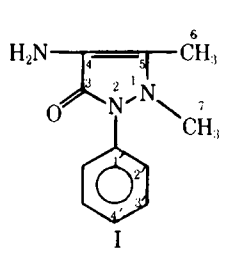

I

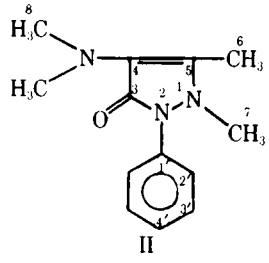

II

Ampyrone, aminopyrine, and antipyrine were obtained from commercial sources[3].

DISCUSSION

Ampyrone (I)—The carbon-13 chemical shifts of I are recorded in Table I, and its carbon resonances are illustrated in Fig. 1. The proton noise-decoupled spectrum of I gave seven signals in the lower field region and two signals in the higher field region. The quartets centered at δ 36.7 and 9.0 ppm could be easily assigned to C-7 and C-6, respectively, on the basis of chemical shift theory (7).

Feeney *et al.* (8) obtained the ^{13}C-NMR spectrum of 1,5-dimethyl-2-phenyl-3*H*-pyrazol-3-one (III, antipyrine) in dimethyl sulfoxide and reported the chemical shift of the ring carbon resonances relative to the upfield of carbon disulfide. To check the chemical shift of the carbons of two methyl groups present at positions 1 and 5 of the pyrazole ring in III, the proton noise-decoupled and SFORD spectra of III were recorded in deuterochloroform. The chemical shifts of the carbon signals of III obtained are represented on the structure of III while the figures in parenthesis indicate the chemical shifts reported earlier (8).

Table I—Carbon-13 Chemical Shifts of Ampyrone

Assignment[a]	Multiplicity[b]	Chemical Shift[c]	Relaxation Time[d], T_1, sec
C-3	s	160.7	27.4
C-5	s	136.3	18.9
C-1′	s	134.2	17.8
C-3′	d	127.8	1.08
C-4′	d	124.4	0.77
C-2′	d	121.4	1.11
C-4	s	118.0	13.8
C-7	q	36.7	1.55
C-6	q	9.0	2.90

[a] Numbering of carbons are shown in the structure. [b] Signal multiplicity obtained from SFORD; s = singlet, d = doublet, and q = quartet. [c] Chemical shifts are expressed in parts per million relative to tetramethylsilane. [d] The relaxation time was obtained in undegassed solution.

[3] Sigma Chemical Co., St. Louis, Mo.

0022-3549/79/0400-0470$01.00/0
© 1979, American Pharmaceutical Association

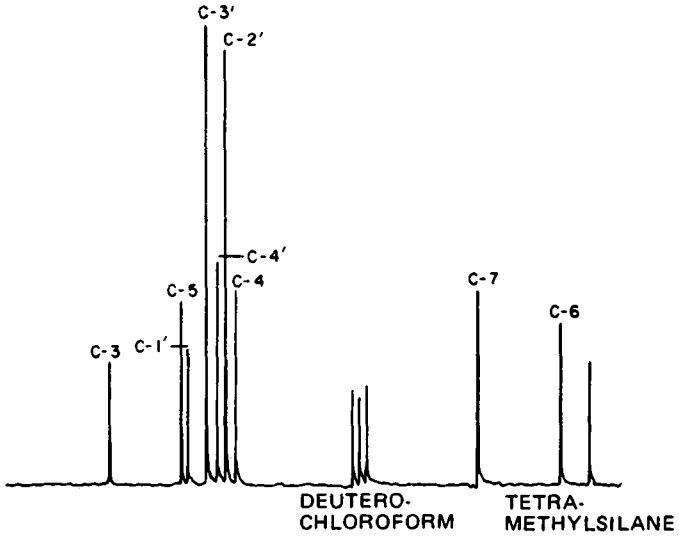

Figure 1—*Proton noise-decoupled spectrum of ampyrone.*

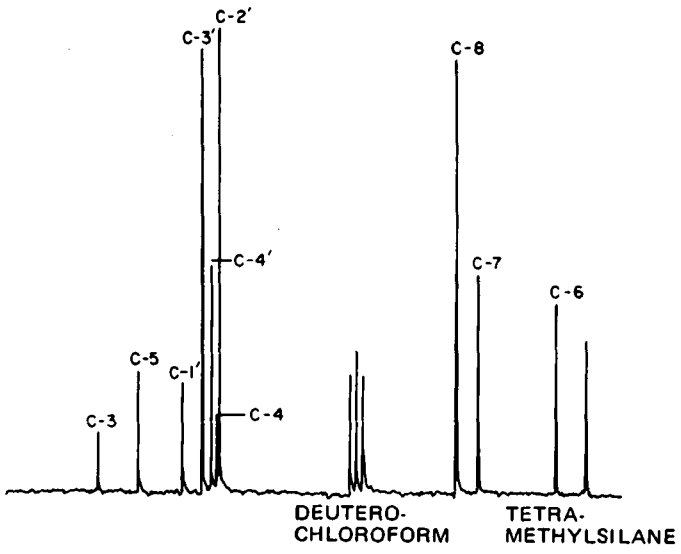

Figure 3—*Proton noise-decoupled spectrum of aminopyrine.*

The two quartets centered at δ 33.8 and 11.2 ppm were assigned to the carbon of methyl groups present at positions 1 and 5 of the pyrazoline ring, respectively, on the basis of chemical shift theory and comparison with the carbon signal of the methyl group of IV. These assignments further support the assignments of C-7 and C-6 of I. The chemical shifts of the ring carbons of III in the present study are in agreement with the chemical shifts of III (8) under the experimental limit due to the solvent effect (7). However, the assignments of C-2′ (122.4 ppm) and C-3′ (127.4 ppm) differ from the assignments of C-2′ (130.8 ppm) and C-3′ (124.8 ppm) reported earlier for III (8). The electronic effect of the nitrogen atom attached to the benzene nucleus produces an upfield shift to its *ortho*- and *para*-carbons, and the former appears at a higher field than the latter (7). On this basis and by comparison with the chemical shift of the corresponding carbons of V (9) and VI (4), the signals at δ 127.4 (reported earlier at 124.8 ppm) and 122.4 (reported earlier at 130.8 ppm) were assigned to C-3′ and C-2′, respectively.

The SFORD spectrum of I showed four singlets, which could be assigned to C-3, C-4, C-5, and C-1′. These quaternary carbons were also distinguished, as compared to methine carbons, by running the proton noise-decoupled spectrum of I at three different pulsing sequences of 5, 15, and 45 sec (Fig. 2). The longer relaxation time for quaternary carbons as compared to other carbons indicated that the increase in time between pulsing sequences provides these carbons more time to relax, which consequently results in their larger peaks (Fig. 2). Furthermore, the chemical shift of the quaternary carbons, C-3, C-4, C-5, and C-1′, were separated from methine carbons based on their longer relaxation times (Table I). Since the carbon signal of the carbonyl group in various amides was in the δ 160–180-ppm region (7), the singlet at δ 160.7 ppm was assigned to C-3.

An electronegative group attached to vinylic carbon causes a pronounced paramagnetic shift to the directly bonded carbon and a dimagnetic shift to the next carbon of the vinyl group. The dimagnetic shift decreases with the steric bulk of the electronegative group (7). On this basis and by comparison with the chemical shifts of III and VI, the singlets at δ 136.3, 134.2, and 118.0 ppm were assigned to C-5, C-1′, and C-4, respectively.

The chemical shift of C-4′ could be differentiated from the chemical shift of C-2′ and C-3′ by its shorter relaxation time (T_1). Since C-4′ is *para* to the phenyl ring, it should have a shorter T_1 value compared to C-2′ and C-3′ due to the motion along the C-1′–C-4′ axis where C-2′ and C-3′ can rotate, resulting in longer T_1 values due to less favored dipole–dipole interactions. As is evident from Table I, C-4′ has a shorter T_1 value than C-2′ and C-3′. The doublets centered at δ 127.8, 124.4, and 121.4 ppm were assigned to C-3′, C-4′, and C-2′, respectively, by comparing the percent integration of the signals in the proton noise-decoupled spectrum of I, relaxation time (T_1), and chemical shift theory (7). These assignments were supported by the chemical shifts observed for III, V (9), and VI (4).

Aminopyrine (II)—The proton noise-decoupled spectrum of II is shown in Fig. 3, and the chemical shifts of the carbon resonances with their relaxation times are shown in Table II. There were seven signals in the downfield and three signals in the upfield region. The three quartets

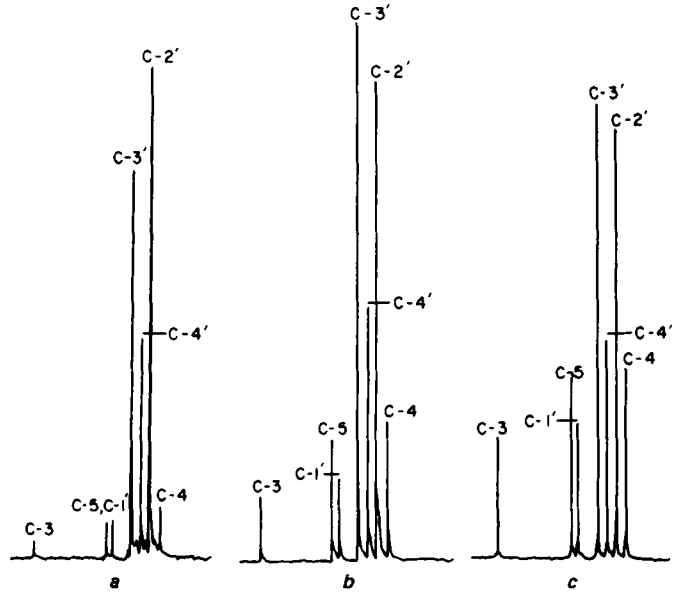

Figure 2—*Pulse repetition. Key:* a, *5 sec;* b, *15 sec; and* c, *45 sec.*

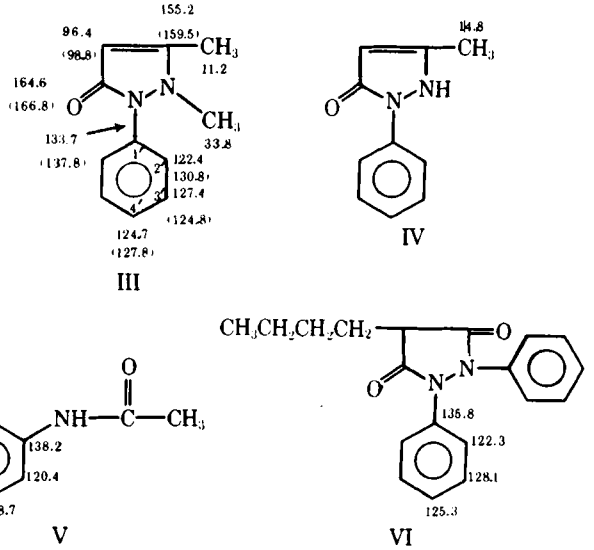

Table II—Carbon-13 Chemical Shifts of Aminopyrine

Assignment[a]	Multiplicity[b]	Chemical Shift[c]	Relaxation Time[d], T_1, sec
C-3	s	163.6	48.9
C-5	s	150.2	30.7
C-1′	s	135.4	32.7
C-3′	d	128.9	2.54
C-4′	d	125.7	1.28
C-4	s	123.9	41.4
C-2′	d	123.0	2.32
C-8	q	43.8	2.37
C-7	q	36.6	3.23
C-6	q	10.2	4.40

[a,b,c,d] See corresponding footnotes in Table I.

centered at δ 43.8, 36.6, and 10.2 ppm were assigned to C-8, C-7, and C-6, respectively, on the basis of chemical shift theory (7), percent intensity of the signals, and comparison with the chemical shifts of I and III. The four singlets at δ 163.6, 150.2, 135.4, and 123.9 ppm observed in the SFORD spectrum of II were assigned to C-3, C-5, C-1′, and C-4, respectively, on the basis of chemical shift theory (7), relaxation time, and comparison of the assignments of the corresponding carbons of I and III.

The chemical shifts of C-4 and C-5 in II were at a lower field as compared to the chemical shift of the coresponding carbons in I. This shift was due to the dimethyl amino group present at position 4 in II, which is more electronegative and bulky than the amino group present at position 4 in I. Earlier studies indicated that the electronegative group produces a downfield shift to the attached carbon of the vinyl group and an upfield shift to the next carbon of the vinyl group. The upfield shift decreases with an increase in the bulkiness of the electronegative group (7). The three doublets centered at δ 128.9, 125.7, and 123.0 ppm were attributed to C-3′, C-4′, and C-2′, respectively, on the basis of chemical shift theory, relaxation time, and comparison with the chemical shift of structurally related compounds I, III, V, and VI.

REFERENCES

(1) V. I. Stenberg, N. K. Narain, and S. P. Singh, *J. Heterocycl. Chem.*, **14**, 225 (1977).

(2) V. I. Stenberg, N. K. Narain, S. P. Singh, R. H. Obenauf, and M. J. Albright, *ibid.*, **14**, 407 (1977).

(3) S. P. Singh, S. S. Parmar, and V. I. Stenberg, *ibid.*, **15**, 9 (1978).

(4) S. P. Singh, S. S. Parmar, V. I. Stenberg, and S. A. Farnum, *ibid.*, **15**, 13 (1978).

(5) S. P. Singh, S. S. Parmar, V. I. Stenberg, and T. K. Akers, *ibid.*, **15**, 53 (1978).

(6) S. P. Singh, S. S. Parmar, V. I. Stenberg, and S. A. Farnum, *Spectrosc. Lett.*, **11**, 59 (1978).

(7) G. C. Levy and G. L. Nelson, "Carbon-13 Nuclear Magnetic Resonance for Organic Chemists," Wiley-Interscience, New York, N.Y., 1972, pp. 47, 62, 63, 91, 120.

(8) J. Feeney, G. A. Newman, and P. J. S. Pauwels, *J. Chem. Soc. C*, **1970**, 1842.

(9) L. F. Johnson and W. C. Jankowski, "Carbon-13 NMR Spectra," Wiley-Interscience, New York, N.Y., 1972, p. 295.

(10) K. Mullen and P. S. Pregosin, "Fourier Transform NMR Techniques: A Practical Approach," Academic, New York, N.Y., 1976, p. 65.

ACKNOWLEDGMENTS

Supported in part by National Institute on Drug Abuse Grant 7-R01-DA01893-01, National Institutes of Health Grant 5-T01-HL05930-03, and National Science Foundation Grant CHE 76-05678 for the partial purchase of the ^{13}C-NMR spectrometer.

Grateful acknowledgment is made to the North West Area Foundation, St. Paul, Minn., for providing a Hill professorship to S. S. Parmar.

Evaluation of Adsorption from Dispersion Charge Profile

A. ATILLA HINCAL * and BHOGI B. SHETH ‡x

Received October 3, 1977, from the *Division of Drug Product Technology, College of Pharmacy, University of Tennessee Center for the Health Sciences, Memphis, TN 38163.* Accepted for publication September 14, 1978.

*Present address: Faculty of Pharmacy, University of Hacettepe, Ankara, Turkey. ‡Present address: Vick Divisions Research and Development, Mt. Vernon, NY 10553.

Abstract □ The evaluation of adsorption behavior from the charge profile of an adsorbent dispersion determined as a function of the adsorbate concentration was investigated by the streaming current measurement, using methylene blue and erythrosine as adsorbates and activated charcoal, microcrystalline cellulose, and polyvinylpolypyrrolidone as adsorbents. Adsorption capacity was evaluated using streaming current *versus* solute concentration plots of dye solutions and of corresponding dye solutions equilibrated with the adsorbent. It was also determined by adsorption isotherm measurement and application of the Langmuir equation. Good agreement was obtained between the adsorption capacity values from streaming current data and adsorption isotherm measurements for microcrystalline cellulose, suggesting that adsorption here was a surface phenomenon without water-soluble extractives affecting particle charge. Similar agreement was not obtained for charcoal adsorption, and this result was attributed to the unusual adsorption behavior of charcoal. Since polyvinylpolypyrrolidone gave a dispersion with high particle charge, the streaming current method could not be used with this system. The charge profile could be useful in characterizing powders for unusual adsorption behavior and possible water-soluble extractives as well as for surface area estimation in the absence of these factors.

Keyphrases □ Adsorption—evaluated from charge profile, streaming current measurement □ Charge profile—used to evaluate adsorption of dispersion, streaming current measurement □ Powders—application of charge profile for characterizing unusual adsorption behavior

New methods for screening powders for adsorption behavior are of significant pharmaceutical interest. Reports deal with the adsorption of drugs by excipients (1–3), the use of adsorbents in the treatment of accidental poisoning (4, 5), the estimation of surface area by solute adsorption (6, 7), and the control of particle charge by polyelectrolytes (8, 9).

The initial inflection point of a charge profile may be considered to represent monolayer adsorption capacity (10). Therefore, it is potentially feasible to estimate the monolayer adsorption capacity from charge profiles. This approach was utilized in systems involving chemical adsorption in an industrial application requiring surface area control of a fine particle dispersion. However, it should also

0022-3549/79/0400-0472$01.00/0

© 1979, American Pharmaceutical Association

Table II—Carbon-13 Chemical Shifts of Aminopyrine

Assignment[a]	Multiplicity[b]	Chemical Shift[c]	Relaxation Time[d], T_1, sec
C-3	s	163.6	48.9
C-5	s	150.2	30.7
C-1′	s	135.4	32.7
C-3′	d	128.9	2.54
C-4′	d	125.7	1.28
C-4	s	123.9	41.4
C-2′	d	123.0	2.32
C-8	q	43.8	2.37
C-7	q	36.6	3.23
C-6	q	10.2	4.40

[a,b,c,d] See corresponding footnotes in Table I.

centered at δ 43.8, 36.6, and 10.2 ppm were assigned to C-8, C-7, and C-6, respectively, on the basis of chemical shift theory (7), percent intensity of the signals, and comparison with the chemical shifts of I and III. The four singlets at δ 163.6, 150.2, 135.4, and 123.9 ppm observed in the SFORD spectrum of II were assigned to C-3, C-5, C-1′, and C-4, respectively, on the basis of chemical shift theory (7), relaxation time, and comparison of the assignments of the corresponding carbons of I and III.

The chemical shifts of C-4 and C-5 in II were at a lower field as compared to the chemical shift of the coresponding carbons in I. This shift was due to the dimethyl amino group present at position 4 in II, which is more electronegative and bulky than the amino group present at position 4 in I. Earlier studies indicated that the electronegative group produces a downfield shift to the attached carbon of the vinyl group and an upfield shift to the next carbon of the vinyl group. The upfield shift decreases with an increase in the bulkiness of the electronegative group (7). The three doublets centered at δ 128.9, 125.7, and 123.0 ppm were attributed to C-3′, C-4′, and C-2′, respectively, on the basis of chemical shift theory, relaxation time, and comparison with the chemical shift of structurally related compounds I, III, V, and VI.

REFERENCES

(1) V. I. Stenberg, N. K. Narain, and S. P. Singh, *J. Heterocycl. Chem.*, **14**, 225 (1977).

(2) V. I. Stenberg, N. K. Narain, S. P. Singh, R. H. Obenauf, and M. J. Albright, *ibid.*, **14**, 407 (1977).

(3) S. P. Singh, S. S. Parmar, and V. I. Stenberg, *ibid.*, **15**, 9 (1978).

(4) S. P. Singh, S. S. Parmar, V. I. Stenberg, and S. A. Farnum, *ibid.*, **15**, 13 (1978).

(5) S. P. Singh, S. S. Parmar, V. I. Stenberg, and T. K. Akers, *ibid.*, **15**, 53 (1978).

(6) S. P. Singh, S. S. Parmar, V. I. Stenberg, and S. A. Farnum, *Spectrosc. Lett.*, **11**, 59 (1978).

(7) G. C. Levy and G. L. Nelson, "Carbon-13 Nuclear Magnetic Resonance for Organic Chemists," Wiley-Interscience, New York, N.Y., 1972, pp. 47, 62, 63, 91, 120.

(8) J. Feeney, G. A. Newman, and P. J. S. Pauwels, *J. Chem. Soc. C*, **1970**, 1842.

(9) L. F. Johnson and W. C. Jankowski, "Carbon-13 NMR Spectra," Wiley-Interscience, New York, N.Y., 1972, p. 295.

(10) K. Mullen and P. S. Pregosin, "Fourier Transform NMR Techniques: A Practical Approach," Academic, New York, N.Y., 1976, p. 65.

ACKNOWLEDGMENTS

Supported in part by National Institute on Drug Abuse Grant 7-R01-DA01893-01, National Institutes of Health Grant 5-T01-HL05930-03, and National Science Foundation Grant CHE 76-05678 for the partial purchase of the ^{13}C-NMR spectrometer.

Grateful acknowledgment is made to the North West Area Foundation, St. Paul, Minn., for providing a Hill professorship to S. S. Parmar.

Evaluation of Adsorption from Dispersion Charge Profile

A. ATILLA HINCAL * and BHOGI B. SHETH ‡x

Received October 3, 1977, from the *Division of Drug Product Technology, College of Pharmacy, University of Tennessee Center for the Health Sciences, Memphis, TN 38163.* Accepted for publication September 14, 1978.

*Present address: Faculty of Pharmacy, University of Hacettepe, Ankara, Turkey. ‡Present address: Vick Divisions Research and Development, Mt. Vernon, NY 10553.

Abstract □ The evaluation of adsorption behavior from the charge profile of an adsorbent dispersion determined as a function of the adsorbate concentration was investigated by the streaming current measurement, using methylene blue and erythrosine as adsorbates and activated charcoal, microcrystalline cellulose, and polyvinylpolypyrrolidone as adsorbents. Adsorption capacity was evaluated using streaming current *versus* solute concentration plots of dye solutions and of corresponding dye solutions equilibrated with the adsorbent. It was also determined by adsorption isotherm measurement and application of the Langmuir equation. Good agreement was obtained between the adsorption capacity values from streaming current data and adsorption isotherm measurements for microcrystalline cellulose, suggesting that adsorption here was a surface phenomenon without water-soluble extractives affecting particle charge. Similar agreement was not obtained for charcoal adsorption, and this result was attributed to the unusual adsorption behavior of charcoal. Since polyvinylpolypyrrolidone gave a dispersion with high particle charge, the streaming current method could not be used with this system. The charge profile could be useful in characterizing powders for unusual adsorption behavior and possible water-soluble extractives as well as for surface area estimation in the absence of these factors.

Keyphrases □ Adsorption—evaluated from charge profile, streaming current measurement □ Charge profile—used to evaluate adsorption of dispersion, streaming current measurement □ Powders—application of charge profile for characterizing unusual adsorption behavior

New methods for screening powders for adsorption behavior are of significant pharmaceutical interest. Reports deal with the adsorption of drugs by excipients (1–3), the use of adsorbents in the treatment of accidental poisoning (4, 5), the estimation of surface area by solute adsorption (6, 7), and the control of particle charge by polyelectrolytes (8, 9).

The initial inflection point of a charge profile may be considered to represent monolayer adsorption capacity (10). Therefore, it is potentially feasible to estimate the monolayer adsorption capacity from charge profiles. This approach was utilized in systems involving chemical adsorption in an industrial application requiring surface area control of a fine particle dispersion. However, it should also

0022-3549/79/0400-0472$01.00/0

© 1979, American Pharmaceutical Association

be feasible in systems showing physical adsorption where the dispersion is clean so that there are no interferences with charge measurements either by soluble contaminants of the adsorbent or by unusual adsorption behavior.

This study was concerned with the evaluation of adsorption behavior of dispersions from charge profiles obtained by the streaming current measurement using a streaming current detector. This detector provides a relatively rapid method for determination of charge profiles.

EXPERIMENTAL

The estimation of adsorption capacity from charge profiles was evaluated for the adsorption of two model solutes, an anionic dye, erythrosine[1] (I), and a cationic dye, methylene blue[2] (II), by activated charcoal[3] (III), microcrystalline cellulose[4] (IV), and polyvinylpolypyrrolidone[5] (V). Charge profiles were determined by streaming current measurements. Adsorption capacity also was determined by adsorption isotherm measurements.

Streaming Current Titrations—Streaming current titrations were done using a streaming current detector[6]. Test samples for streaming current titrations were increasing concentration dye solutions and aqueous dispersions of adsorbents in the same concentration dye solutions.

The samples were prepared as follows. Weighed amounts of the adsorbent were placed in a 250-ml conical screw-capped flask (0.1 g for III and 1 g for IV). Increasing concentration dye solutions, 250 ml, were added to each flask. The flasks were closed with a parafilm liner and screw cap. The dispersions were shaken mechanically for at least 4 hr to reach equilibrium.

Streaming current values of dye solutions and adsorbent dispersions were measured. The procedure used for the titrations was essentially similar to that reported by Shah and Sheth (11). In a typical measurement, the instrument surfaces were cleaned adequately and the sample (solution or dispersion) contained in a tall 400-ml beaker was placed in the instrument. The values were recorded after the instrument ran for 5 min to allow the reading to stabilize. Since the streaming current value is obtained in arbitrary units, it was necessary to establish a point of reference for measurement indicating that the boot and piston surfaces were clean with no solute on them. The reference point was a streaming current value of deionized water ranging from −51 to −60.

The profile for the test samples was obtained by plotting the streaming current as a function of increasing dye concentration. The profile for the solution was referred to as the solution curve, and that for the dispersion was referred to as the dispersion curve. Profiles were determined by this procedure for test systems with III and IV. Similar profiles for systems with V could not be determined because of the presence of soluble extractive that resulted in dispersions of V with a high particle charge.

Adsorption Isotherm Measurement—Weighed amounts of the adsorbent were placed in a 250-ml conical screw-capped flask (0.1 g for III and 1 g for the other two adsorbents). Increasing concentration dye solutions, 100 ml, were added to each flask, and each flask was closed with a parafilm liner and a screw cap. Then the dispersions were shaken mechanically for a sufficient time to reach equilibrium. After equilibration, the samples were centrifuged and the supernate was analyzed at room temperature (25 ± 1°) for dye concentration spectrophotometrically[7] at 526 nm for I and at 664.5 nm for II.

RESULTS AND DISCUSSION

Adsorption Isotherms—The adsorption behavior of both solutes on III and IV and of I on V essentially followed the Type I adsorption isotherm. However, the adsorption of II on V was greatly reduced and did not follow the Type I adsorption isotherm. The results of adsorption

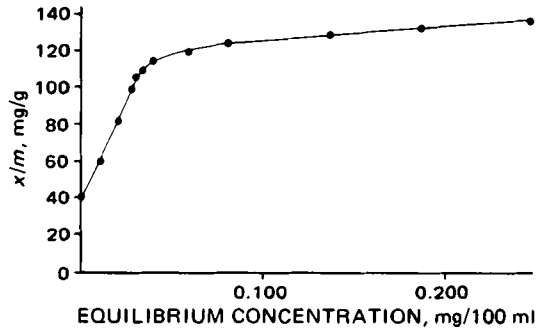

Figure 1—*Adsorption isotherm of methylene blue on activated charcoal.*

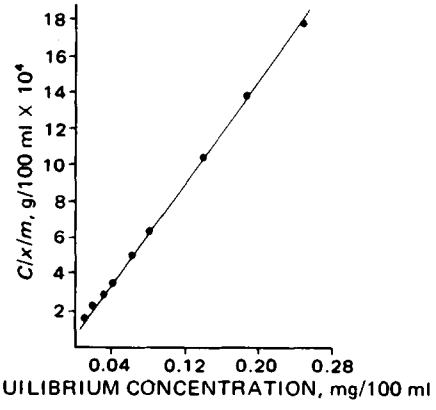

Figure 2—*Langmuir isotherm for the adsorption of methylene blue on activated charcoal.*

studies were evaluated by the application of the Langmuir equation as follows:

$$\frac{x}{m} = \frac{k_1 k_2 C}{1 + k_1 C} \qquad \text{(Eq. 1)}$$

where C is the solute concentration at equilibrium; k_1 and k_2 are constants; x/m is the amount of solute adsorbed per gram of adsorbent; and k_2 is equivalent to $(x/m)_{max}$, the monolayer adsorption capacity.

Figure 1 shows the adsorption of II on III, and Fig. 2 shows the Langmuir plot for this system. Figures 3 and 4 show the same data for the adsorption of II by IV. Plots of $C/x/m$ *versus* C were linear for these systems. The Langmuir constants, k_1 and k_2, are given in Table I.

The value of k_2 may be considered as the monolayer adsorption capacity of the adsorbent for the solute. Compound III had a higher adsorption capacity for both solutes than the other two adsorbents (Table I). There was essentially no adsorption of I by IV, and II was essentially not adsorbed by V. These two adsorbents were selective adsorbents.

The adsorption of I on III was lower than that of II on the molar basis. An explanation may be found in the report of Giles and D'Silva (6), who classified the pores of finely divided III by average width into three groups on an arbitrary basis: micropores with less than 20 Å width, transitional pores between 20 and 200 Å width, and macropores that are larger than transitional pores and difficult to distinguish from the external surface.

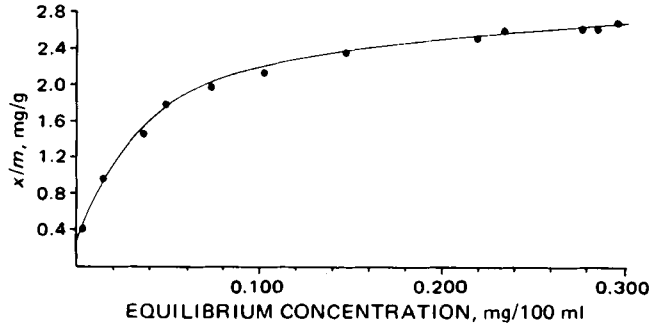

Figure 3—*Adsorption isotherm of methylene blue on microcrystalline cellulose.*

[1] Lot 96294, KSK Laboratories, Plainview, N.Y.
[2] Eastman Kodak Corp., Rochester, N.Y.
[3] Activated charcoal USP, American Norit Co., Jacksonville, Fla.
[4] Avicel PH-101, lot 1-90768, FMC Corp., Marcus Hook, Pa.
[5] Polyclar-AT, lot 125, GAF Corp., New York, N.Y.
[6] Hydroscan streaming current detector, Leeds & Northrup Co., North Wales, Pa.
[7] Coleman model 124 double-beam recording spectrophotometer, Perkin-Elmer, Coleman Instrument Division, Maywood, Ill.

Table I—Langmuir Constants for Adsorption of Methylene Blue and Erythrosine by Activated Charcoal, Microcrystalline Cellulose, and Polyvinylpolypyrrolidone

Adsorbate	Langmuir Constant	Activated Charcoal	Microcrystalline Cellulose	Polyvinyl-polypyrrolidone
Methylene blue	k_1, 100 ml/mole	3.403×10^7	1.110×10^7	1.169×10^6
	k_2, mole/g	3.804×10^{-4}	7.924×10^{-6}	2.249×10^{-6}
Erythrosine	k_2, mole/g	1.149×10^{-4}	4.651×10^{-8}	7.987×10^{-6}
	k_1, 100 ml/mole	1.88×10^7	8.488×10^5	2.577×10^6

Table II—Comparison of Adsorption Capacity (Moles per Gram $\times 10^6$) Determined by Adsorption Isotherm Method and Streaming Current Titration for Adsorption of Methylene Blue

Adsorbent	Adsorption Isotherm	Streaming Current
Microcrystalline cellulose	7.92	7.22
Activated charcoal	380	80.2

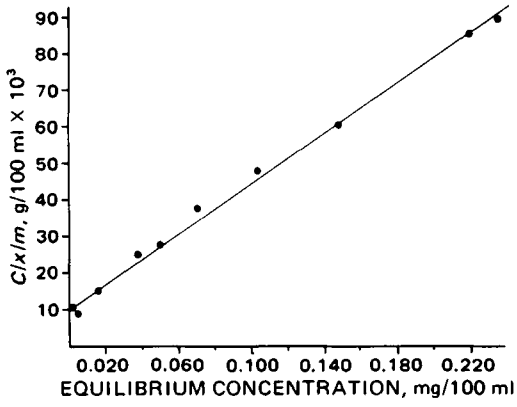

Figure 4—*Langmuir isotherm for the adsorption of methylene blue on microcrystalline cellulose.*

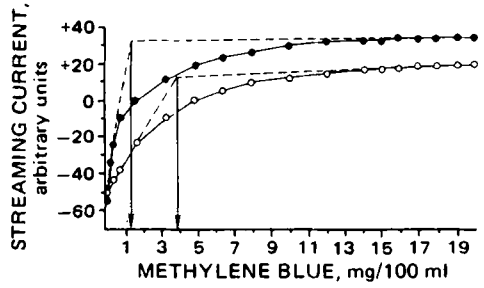

Figure 5—*Solution (●) and dispersion (○) streaming current curves for the microcrystalline cellulose–methylene blue system.*

These authors proposed that micropores were significant in the adsorption of small molecules such as nitrogen. Larger molecules would be excluded from micropores but reach some or all of the transitional pores and all of the macropores. Transitional pores were considered to have their most important influence in the adsorption of organic solutes. Therefore, the difference in adsorption behavior of I and II may be due to the difference in their molecular size, the molecule of I being much larger than II.

It was also observed that the adsorption of II caused a drop in the pH of III–II dispersions. Such behavior was noted by Bartel and Miller (12) and by Giles *et al.* (3). This effect was attributed to the release of hydrogen ion to the solution phase on adsorption of the dye cation.

Adsorption from Charge Profile—No literature reports were found dealing with estimation of adsorption capacity from the charge profile of a dispersion. Surface area was estimated from the charge profile in an industrial application for a system involving chemical adsorption by taking the first inflection point as the point of monolayer adsorption (13). In a chemical adsorption situation, the slope changes greatly in the streaming current charge profile at this point so that the inflection point can be determined reasonably. However, such an inflection point cannot be identified readily in a physical adsorption situation. Therefore, a method was developed for the estimation of adsorption capacity in physical adsorption situations by utilizing the solution and dispersion curves of the system, and the adsorption capacity of II by IV and of I and II by III was evaluated.

The method is based on the determination of the inflection points of the solution and dispersion curves by regression analysis. Adsorption capacity is calculated from the difference in solute concentration at the inflection points of the two curves. Figure 5 shows the solution and dispersion curves for the IV–II system. The adsorption capacity was calculated as follows. The concentration of II at the streaming current solution curve inflection point = C_s = 1.2 mg/100 ml. The concentration of II at the streaming current dispersion curve inflection point = C_d = 3.9 mg/100 ml. Then the adsorption capacity of IV for II, milligrams of II per gram of IV, is $C_d - C_s = 3.9 - 1.2 = 2.7$ mg/g = 7.22×10^{-6} mole/g.

The streaming current curve for the III–II system is shown in Fig. 6. This curve is not similar to that of the IV–II system. The adsorption capacities estimated from the streaming current curves for both of these systems are given in Table II.

The type of data in Fig. 5 for the IV–II system is to be expected when there are no interferences or other complications in the streaming current measurement. The value obtained for the aqueous dispersion of IV in water without dye was −52, which was very close to the streaming current value for water. This value may be taken to indicate the absence of water-extractable material in IV. There was good agreement between the adsorption capacity values obtained by both methods (Table II). These results indicate that the developed method is applicable for physical adsorption systems where there is no interference from extractable electrolytes and the adsorption behavior is not unusual.

The estimate of adsorption capacity for the III–II system from the charge profile was also much lower than the value obtained from the adsorption isotherm. Hence, for this system, the value determined from the streaming current charge profile cannot be interpreted as representing adsorption capacity. The data for the III–II system in Fig. 6 differ from what might be expected in that the dispersion curve is higher than the

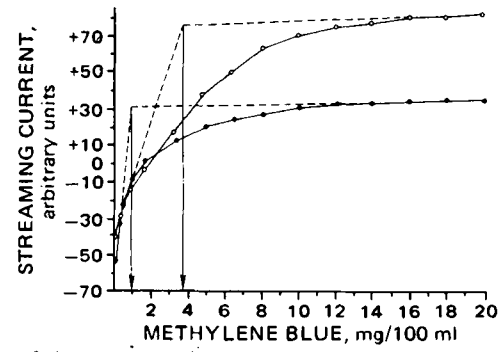

Figure 6—*Solution (●) and dispersion (○) streaming current curves for the activated charcoal–methylene blue system.*

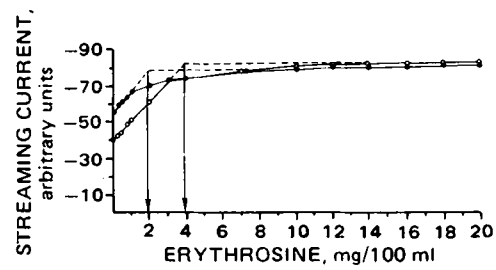

Figure 7—*Solution (●) and dispersion (○) streaming current curves for the activated charcoal–erythrosine system.*

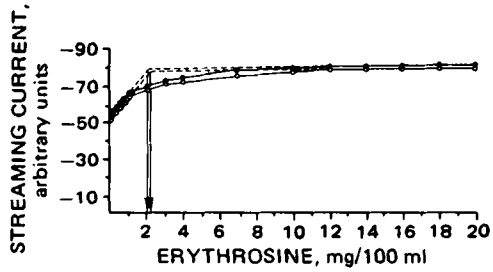

Figure 8—*Solution (●) and dispersion (○) streaming current curves for the microcrystalline cellulose–erythrosine system.*

solution curve. Typically, the dispersion curve would be below the solution curve. The reasons for this behavior are not clear, but a number of aspects of the adsorption behavior of II by III might be contributing factors. There was a drop in the aqueous dispersion pH at higher II concentrations, as discussed previously. The amount of adsorption was quite high. In measurements with the detector, the streaming current values for dispersions represent the net effect of the shearing of the double layers formed on the boot and piston surfaces as well as the double layers surrounding the dispersed particles. The contribution to the measured streaming current values from the double layers surrounding the dispersed particles may be substantially higher for dispersions with high adsorption capacity. Furthermore, higher dye concentrations were used for streaming current measurements than for adsorption isotherm measurements. At these concentrations, the dye would be expected to be in the dimer and trimer forms, with a corresponding effect on the nature of the double layer.

For the III–I system, the dispersion curve was only slightly different from the solution curve (Fig. 7). The adsorption capacity calculated from the streaming current data was also substantially lower than that estimated from the value of k_2, the Langmuir constant for the system. Where there was no adsorption, the solution and dispersion curves were similar, as shown in Fig. 8 for the IV–I system.

REFERENCES

(1) H. Nogami, T. Nagai, and S. Wada, *Chem. Pharm. Bull.*, **18**, 342 (1970).

(2) A. L. Thakkar, W. L. Wilham, and G. Zografi, *J. Pharm. Sci.*, **59**, 1467 (1970).

(3) C. H. Giles, I. A. Easton, R. B. McKay, C. C. Patel, N. B. Shah, and D. Smith, *Trans. Faraday Soc.*, **62**, 1963 (1966).

(4) R. H. Fiser, H. M. Maetz, J. J. Treuting, and W. J. Decker, *J. Pediatr.*, **78**, 1045 (1971).

(5) A. L. Picchioni, L. Chin, and H. E. Laird, *Clin. Toxicol.*, **7**, 97 (1974).

(6) C. H. Giles and A. P. D'Silva, *Trans. Faraday Soc.*, **65**, 1943 (1969).

(7) P. T. Hang and G. W. Brindley, *Clay Clays Minerals*, **18**, 203 (1970).

(8) B. A. Matthews and C. T. Rhodes, *J. Pharm. Pharmacol.*, **20**, 204S (1968).

(9) A. N. Martin, *J. Pharm. Sci.*, **50**, 513 (1961).

(10) R. A. Nash and R. E. Haeger, *ibid.*, **55**, 829 (1966).

(11) D. G. Shah and B. B. Sheth, *Drug. Dev. Ind. Pharm.*, in press.

(12) F. E. Bartel and E. J. Miller, *J. Am. Chem. Soc.*, **44**, 1866 (1922).

(13) W. E. Gray and M. Manning, "Preprints of the Society of Photographic Scientists and Engineers Meeting," Los Angeles, Calif., 1969, p. 179.

Microencapsulation of Bitolterol for Controlled Release and Its Effect on Bronchodilator and Heart Rate Activities in Dogs

PHILLIP M. JOHN ˣ, HIROAKI MINATOYA, and FRANKLIN J. ROSENBERG

Received July 6, 1978, from the *Sterling-Winthrop Research Institute, Rensselaer, NY 12144.* Accepted for publication September 25, 1978.

Abstract □ Spheronized cores produced by extrusion and marumerization were microencapsulated with ethylcellulose by organic phase separation to produce beads exhibiting controlled-release characteristics. *In vitro* dissolution studies indicated that the drug was released as a first-order model and that the release rates were proportional to the amount of film on the bead. The bronchodilator activity in the anesthetized dog and the heart rate effect in the unanesthetized trained dog were evaluated. Microencapsulated beads were prepared which produced controlled release as assayed by bronchodilation. The heart rate increases induced by the controlled-release formulations were gradual in onset, and the total increase in heart rate over a 6-hr period was less than that associated with the plain drug powder.

Keyphrases □ Bitolterol—microencapsulation for controlled release, effects on bronchodilator and heart rate activities, dogs □ Microencapsulation—bitolterol, controlled-release characteristics assessed, effects on bronchodilator and heart rate activities, dogs □ Dosage forms—controlled-release bitolterol formulations prepared by microencapsulation, effects on bronchodilator and heart rate activities, dogs

The properties of bitolterol, an ester of *N-tert*-butylarterenol, as a long-acting bronchodilator with reduced cardiac effects, were recently reported (1, 2). Additional improvement in the duration of action and in the reduction of side effects was sought by preparing material exhibiting a controlled release.

Microencapsulation has been applied successfully to many areas of pharmaceutical interest. Microencapsulation as a unit operation was described and reviewed (3), as was the patent literature (4). An informative history of microencapsulation and its uses was presented (5). Most pharmaceutical work has been with irregularly shaped granules of powders or dispersed liquids, crystals, or sized granulations (6–16). This study concerns regular spherical cores in the 500–1000-μm range, encapsulated by organic phase separation.

Spherical particles were prepared (17) using an extrusion technique followed by spheronization in a marumerizer. Briefly, the drug and suitable excipients are moistened thoroughly with granulating agents and water until a damp mass is formed. The material is then passed through an extruder to produce strands of uniform diameter. The extruded material is introduced into the chamber

0022-3549/79/0400-0475$01.00/0
© 1979, American Pharmaceutical Association

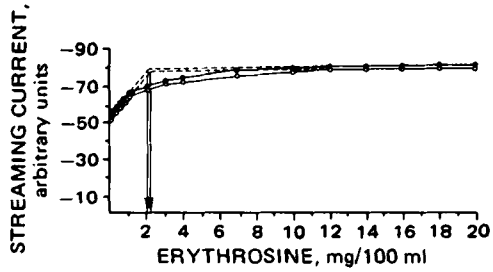

Figure 8—*Solution (●) and dispersion (○) streaming current curves for the microcrystalline cellulose–erythrosine system.*

solution curve. Typically, the dispersion curve would be below the solution curve. The reasons for this behavior are not clear, but a number of aspects of the adsorption behavior of II by III might be contributing factors. There was a drop in the aqueous dispersion pH at higher II concentrations, as discussed previously. The amount of adsorption was quite high. In measurements with the detector, the streaming current values for dispersions represent the net effect of the shearing of the double layers formed on the boot and piston surfaces as well as the double layers surrounding the dispersed particles. The contribution to the measured streaming current values from the double layers surrounding the dispersed particles may be substantially higher for dispersions with high adsorption capacity. Furthermore, higher dye concentrations were used for streaming current measurements than for adsorption isotherm measurements. At these concentrations, the dye would be expected to be in the dimer and trimer forms, with a corresponding effect on the nature of the double layer.

For the III–I system, the dispersion curve was only slightly different from the solution curve (Fig. 7). The adsorption capacity calculated from the streaming current data was also substantially lower than that estimated from the value of k_2, the Langmuir constant for the system. Where there was no adsorption, the solution and dispersion curves were similar, as shown in Fig. 8 for the IV–I system.

REFERENCES

(1) H. Nogami, T. Nagai, and S. Wada, *Chem. Pharm. Bull.*, **18**, 342 (1970).

(2) A. L. Thakkar, W. L. Wilham, and G. Zografi, *J. Pharm. Sci.*, **59**, 1467 (1970).

(3) C. H. Giles, I. A. Easton, R. B. McKay, C. C. Patel, N. B. Shah, and D. Smith, *Trans. Faraday Soc.*, **62**, 1963 (1966).

(4) R. H. Fiser, H. M. Maetz, J. J. Treuting, and W. J. Decker, *J. Pediatr.*, **78**, 1045 (1971).

(5) A. L. Picchioni, L. Chin, and H. E. Laird, *Clin. Toxicol.*, **7**, 97 (1974).

(6) C. H. Giles and A. P. D'Silva, *Trans. Faraday Soc.*, **65**, 1943 (1969).

(7) P. T. Hang and G. W. Brindley, *Clay Clays Minerals*, **18**, 203 (1970).

(8) B. A. Matthews and C. T. Rhodes, *J. Pharm. Pharmacol.*, **20**, 204S (1968).

(9) A. N. Martin, *J. Pharm. Sci.*, **50**, 513 (1961).

(10) R. A. Nash and R. E. Haeger, *ibid.*, **55**, 829 (1966).

(11) D. G. Shah and B. B. Sheth, *Drug. Dev. Ind. Pharm.*, in press.

(12) F. E. Bartel and E. J. Miller, *J. Am. Chem. Soc.*, **44**, 1866 (1922).

(13) W. E. Gray and M. Manning, "Preprints of the Society of Photographic Scientists and Engineers Meeting," Los Angeles, Calif., 1969, p. 179.

Microencapsulation of Bitolterol for Controlled Release and Its Effect on Bronchodilator and Heart Rate Activities in Dogs

PHILLIP M. JOHN ˣ, HIROAKI MINATOYA, and FRANKLIN J. ROSENBERG

Received July 6, 1978, from the *Sterling-Winthrop Research Institute, Rensselaer, NY 12144.* Accepted for publication September 25, 1978.

Abstract □ Spheronized cores produced by extrusion and marumerization were microencapsulated with ethylcellulose by organic phase separation to produce beads exhibiting controlled-release characteristics. *In vitro* dissolution studies indicated that the drug was released as a first-order model and that the release rates were proportional to the amount of film on the bead. The bronchodilator activity in the anesthetized dog and the heart rate effect in the unanesthetized trained dog were evaluated. Microencapsulated beads were prepared which produced controlled release as assayed by bronchodilation. The heart rate increases induced by the controlled-release formulations were gradual in onset, and the total increase in heart rate over a 6-hr period was less than that associated with the plain drug powder.

Keyphrases □ Bitolterol—microencapsulation for controlled release, effects on bronchodilator and heart rate activities, dogs □ Microencapsulation—bitolterol, controlled-release characteristics assessed, effects on bronchodilator and heart rate activities, dogs □ Dosage forms—controlled-release bitolterol formulations prepared by microencapsulation, effects on bronchodilator and heart rate activities, dogs

The properties of bitolterol, an ester of *N-tert*-butylarterenol, as a long-acting bronchodilator with reduced cardiac effects, were recently reported (1, 2). Additional improvement in the duration of action and in the reduction of side effects was sought by preparing material exhibiting a controlled release.

Microencapsulation has been applied successfully to many areas of pharmaceutical interest. Microencapsulation as a unit operation was described and reviewed (3), as was the patent literature (4). An informative history of microencapsulation and its uses was presented (5). Most pharmaceutical work has been with irregularly shaped granules of powders or dispersed liquids, crystals, or sized granulations (6–16). This study concerns regular spherical cores in the 500–1000-μm range, encapsulated by organic phase separation.

Spherical particles were prepared (17) using an extrusion technique followed by spheronization in a marumerizer. Briefly, the drug and suitable excipients are moistened thoroughly with granulating agents and water until a damp mass is formed. The material is then passed through an extruder to produce strands of uniform diameter. The extruded material is introduced into the chamber

0022-3549/79/0400-0475$01.00/0
© 1979, American Pharmaceutical Association

Table I—Marumerized Core Formulations by Percent Composition

Ingredient	Core A	Core B	Core C
Bitolterol methanesulfonate	5.00	12.08	12.08
Lactose USP, regular, hydrous	57.00	50.38	47.92
Microcrystalline cellulose	19.00	18.67	20.00
Starch USP	16.00	15.87	17.00
Starch as 15% paste	3.00	3.00	3.00
Total	100.00	100.00	100.00
Batch size, g	3000	6500	12,000

of a marumerizer where the strands are broken into short rods and rolled on a spinning friction plate to form spheres.

The effect of the several process variables on the resulting product, such as the rotational speed of the friction plate and the residence time in the spheronizing chamber, was studied (18); in addition, an evaluation was made (19) of the effects of granulation moisture content, extruder screen size, and extruder speed. These studies found that particular physical qualities must be developed during processing to produce uniform solid spheres: the material must be soft enough to extrude, cohesive enough to produce strands, sufficiently friable that the strands break into short rods when placed in the spheronization chamber, and plastic enough that the short rods are converted to regular spheres when rolled.

Preliminary experiments were conducted to develop formulations of bitolterol that could be extruded and spheronized to produce uniform cores. The cores were subsequently microencapsulated with ethylcellulose to prepare coated beads. The dissolution characteristics of several products were evaluated in 0.1 *N* HCl, and relationships between the calculated film thicknesses and corresponding release rates were developed. The bronchodilator activity in the anesthetized dog and the heart rate effects in the unanesthetized trained dog were evaluated for representative products according to an established method reported for isoproterenol (20, 21).

EXPERIMENTAL

Materials—Bitolterol[1] (α-[(*tert*-butylamino)methyl]-3,4-dihydroxybenzyl alcohol 3,4-di-*p*-toluate methanesulfonate) was pharmaceutical grade with a mean particle size of 12 μm. The core formulations were compounded of commonly used excipients including microcrystalline cellulose USP[2], lactose USP[3] (regular, hydrous), and starch USP[4]. The encapsulating medium was composed of ethylcellulose USP[5] (100 cps), polyethylene[6] (pharmaceutical grade), and cyclohexane[7] (practical grade). The dissolutions were conducted in 0.1 *N* HCl[8] (analytical grade).

Core Preparation—The formulations for the core materials are presented in Table I. Powders were passed through an oscillator[9] fitted with a 30-mesh screen and blended in a twin-shell dry blender[10]. The material was transferred to a planetary mixer[11] and granulated with starch paste; sufficient additional water was incorporated to make a very damp mass.

The material was then extruded[12] through 1.0-mm screens and spheronized in a marumerizer[13] operating at 400 ± 50 rpm. The spheronized cores were dried in a hot air oven at 40° until the moisture was no more than 2% as determined by a moisture balance[14]. After drying, the cores were classified to remove particles smaller than 40 mesh (420 μm) or larger than 16 mesh (1190 μm)[15]. About 95% yields were obtained.

Microencapsulation—Compositions of the microencapsulation schemes are shown in Table II. In a typical laboratory batch, ethylcellulose and polyethylene were dissolved in hot cyclohexane in a three-necked, round-bottom flask equipped with a thermometer, stirrer, and reflux condenser. The prepared cores were introduced into the system and suspended by rapid agitation while the temperature was brought to reflux (about 78°) for 5 min. Heating was then discontinued, and the system was allowed to cool; stirring was continued until 40° was reached.

During this cooling period, the ethylcellulose phase separated and coated the suspended particles. The polyethylene was present to limit ethylcellulose solubility in the solvent, thus causing the film to be formed at a higher temperature where its viscosity was low enough to allow each particle to be uniformly coated. The encapsulated beads were washed with three portions of cold cyclohexane to remove residual ethylcellulose and polyethylene. The product was then allowed to air dry at ambient temperature.

Initial studies were made with material encapsulated in small batches in this laboratory using Core A. Later, encapsulations were scaled up[16] to test the feasibility of producing larger lots; a more concentrated core formula, representing 10% bitolterol as the base (120.8 mg of methanesulfonate salt = 100.0 mg of bitolterol base), was used.

Dissolution Studies—A modification of the USP rotating-basket method (22) was used to examine the dissolution patterns of each core and encapsulated bead preparation. A quantity of cores or beads containing 15 mg of bitolterol was placed in the basket and immersed in 250 ml of 0.1 *N* HCl at 37°, with the basket rotating at 100 rpm. Samples, 5 ml, were withdrawn every 15 min for the 1st hr, every 30 min during the 2nd hr, and hourly thereafter. Sample replacement was made with 5 ml of 0.1 *N* HCl to maintain a constant volume.

After appropriate dilutions were made, samples were read at 247 nm using a UV-grating spectrophotometer[17]. A separate analysis for total drug content was made by crushing a sample of beads in a mortar and pestle, extracting the drug with 0.1 *N* HCl, and reading the solution as before.

Ethylcellulose Assay—Ethylcellulose present in the microencapsulated bead products was assayed by a residue weight method. Approximately 5 g of microencapsulated beads was finely powdered in a mortar and weighed into a 250-ml flask to which 100 ml of chloroform[18] was added. The mixture was shaken for 30 min and filtered. Fifty milliliters of filtrate was evaporated to dryness and a constant weight in a 105° oven. A 3-ml sample of the remaining filtrate was assayed for bitolterol to correct for extracted drug present in the ethylcellulose residue.

Particle-Size Analysis—A sample of beads was suspended in a drop of immersion oil[19] on a microscope slide and examined through an image-splitting eyepiece at a magnification of 35×. The horizontal diameters of at least 500 particles from each product were measured and classified into appropriate 50-μm intervals from which the volume–surface distributions were constructed.

Determination of Film Thickness—No direct method of measuring the thickness of the applied films around the hard cores proved satisfactory. The beads shattered or were dislodged from the embedding matrix by all microtome techniques attempted. For purposes of batch characterization, it was possible to estimate the average thickness of the film for the ideal case (assuming perfect sphericity and film uniformity) by calculation. There is good indication (23) that the thickness of an applied film is fairly constant over a broad range of particle sizes simultaneously microencapsulated and is independent of the core diameters within that range.

The film content of many systems can be determined by a direct analysis of the encapsulated beads, either by assaying for the film itself

[1] Winthrop Laboratories, New York, N.Y.
[2] Avicel PH 101, American Viscose Division, FMC Corp., Newark, Del.
[3] Foremost Foods Co., San Francisco, Calif.
[4] Hubinger Co., Keokuk, Iowa.
[5] Hercules Inc., Wilmington, Del.
[6] Epolene Wax, C-10, Eastman Chemical Products, Kingsport, Tenn.
[7] Matheson, Coleman & Bell, Norwood, Ohio.
[8] J. T. Baker Chemical Co., Phillipsburg, N.J.
[9] Model 43B, F. J. Stokes Corp., Philadelphia, Pa.
[10] Patterson-Kelly Co., East Stroudsburg, Pa.
[11] Model A-200, Hobart Manufacturing Co., Troy, Ohio.
[12] Model EXDCS-100, Elanco Products Co., Indianapolis, Ind.
[13] Model Q-400, Elanco Products Co., Indianapolis, Ind.
[14] Model 6000, Ohaus Scale Corp., Union, N.J.
[15] Model 24-444 Dynoscreen separator-classifier, Master Machines, Houston, Tex.
[16] Capsular Products Division, National Cash Register Corp., Dayton, Ohio.
[17] Model DB-G, Beckman Instruments, Fullerton, Calif.
[18] Ashland Chemical Co., Columbus, Ohio.
[19] Type B, R. P. Cargille Labs Inc., Cedar Grove, N.J.

Table II—Microencapsulation Schemes and Analytical Data for Experimental Products

	Product												
	A	A-1	A-2	B	B-1	B-2	B-3	C	C-1	C-2	C-3	C-4	C-5
Core A, g	—	332	280	—	—	—	—	—	—	—	—	—	—
Core B, g	—	—	—	—	150	250	300	—	—	—	—	—	—
Core C, g	—	—	—	—	—	—	—	—	2100	2000	1600	2,000	2,000
Ethylcellulose, g	—	10	10	—	5	10	10	—	70	80	80	100	100
Polyethylene, g	—	29	29	—	20	20	20	—	140	160	160	200	200
Cyclohexane, g	—	2000	2000	—	1000	1000	1000	—	7000	8000	8000	10,000	10,000
Bitolterol content, %	4.9	4.8	4.7	12.4	11.8	11.9	11.6	12.0	12.0	12.0	11.8	11.8	11.7
Film content, %	—	2.6	3.3	—	3.2	4.0	3.1	—	3.2	3.6	4.2	4.6	5.0
Density, g/cm^3	1.37	—	—	1.38	1.31	1.23	—	1.32	—	—	—	—	—
Mean volume-surface diameter, μm	740	782	774	824	861	900	1020	1026	1075	1037	1035	995	1099
SD, μm	200	200	200	225	225	250	225	175	250	225	225	250	225

or for a decrease in the specific activity of the drug species. Where chemical analysis is not possible due to the complexity of the film system or to a low level of drug content, the film may be determined by stripping a weighed sample of beads with a suitable solvent, in which case the film fraction, F, is given by:

$$F = \frac{M_b - M_c}{M_b} \qquad \text{(Eq. 1)}$$

where M_b is the mass of the encapsulated beads and M_c is the mass after stripping, and with suitable corrections for extractables in the core, equivalent to the mass of the cores. Since the number of particles of diameter d per unit weight is equal to $6/\pi d^3\rho$, where ρ is the density of the particles, and the surface area of one particle is πd^2, the total surface area for a sample of cores is:

$$S = \frac{6}{\pi d^3 \rho} \pi d^2 M = \frac{6M_c}{d_{vs}\rho_c} \qquad \text{(Eq. 2)}$$

where d_{vs} represents the mean volume–surface diameter of the sample and ρ_c is the density of the cores. For thin films, the surface of the cores may be considered planar of area S. The film thickness is then given by:

$$h = \frac{\text{volume of film}}{\text{surface of cores}} = \frac{F(M_b)/\rho_f}{6(M_c)/d_{vs}\rho_c} = \frac{Fd_{vs}(M_b)\rho_c}{6(M_c)\rho_f} \qquad \text{(Eq. 3)}$$

where ρ_f is the density of the film material. In the limit as $F \rightarrow 0$, the ratio M_b/M_c approaches unity and Eq. 3 simplifies to:

$$h = \frac{Fd_{vs}\rho_c}{6\rho_f} \qquad \text{(Eq. 4)}$$

It is useful to compare the more exact expression presented previously (23), which, when expressed in the above terms, is:

$$h = \frac{Fd_{vs}\rho_c}{6[(1-F)\rho_f + F\rho_c]} \qquad \text{(Eq. 5)}$$

where again for very small F the denominator becomes $6\rho_f$ and is otherwise equivalent to Eq. 4. For film fractions of 10% or less, the thicknesses estimated by Eqs. 4 and 5 differ by less than 2%. Over the range of film fractions considered, the thicknesses estimated by the two equations differed by less than 1% and were considered directly proportional to the amount of film present. Densities were determined gravimetrically by displacement in n-hexane[20], the ethylcellulose film fraction was determined by residue weight as described, the mean volume–surface diameter was found by microscopic particle-size analysis, and the film thickness was estimated from Eq. 4.

Bronchodilator Activity—The bronchodilator activity of selected formulations was compared to plain bitolterol powder in the intact, anesthetized (pentobarbital sodium, 30 mg/kg iv)[21] open-chest dog maintained under artificial respiration using a constant-volume respirator[22] attached to a tracheal cannula. The chest cavity was opened by sternotomy and kept retracted. The opening was covered loosely with a moist gauze. A specially designed, nonrebreathing Leucite valve was attached to the cannula, regulating the inflow and outflow of air.

Bronchoconstriction was induced by intravenous injections of histamine diphosphate[23] (20–50 μg/kg). The changes in airway pressure were measured by a pressure transducer[24] and recorded on a polygraph[25]. The degree of bronchoconstriction was determined by measuring with a planimeter the area of the airway pressure recordings above the baseline for a 5-min period after the histamine injection. A dose of histamine was chosen that would double the airway pressure. An initial dose of 20 μg/kg was given. If the airway pressure were not approximately doubled by this dose of histamine, a higher dose (30–50 μg/kg) was administered 30 min later. The response to this second dose was then used as the control, against which the bronchodilator effects of the microencapsulated products and the plain powder were measured. Bronchodilation was expressed as the percent inhibition of the control histamine-induced bronchoconstriction.

Bitolterol powder or formulations equivalent to 240 μg/kg as the base were administered directly into the duodenal lumen through a small stab opening and washed in with 2 ml of water. The opening was then closed by suturing. The duodenum had been made accessible through a small midline incision in the abdomen. The first postmedication histamine injection was given at 10 min, with subsequent injections at 0.5 and 1 hr and hourly thereafter for 6 hr.

Intravenous injections of saline (1 ml) were given to three dogs to assay the stability of the histamine response. Under these experimental conditions, the degree of histamine-induced bronchoconstriction remained constant throughout the test.

Heart Rate Effect—In the heart rate study, six trained dogs of both sexes, 10–14 kg, were used repeatedly but not more than once a week. Food was withheld from these dogs 17–18 hr prior to the test. During the experiment, the dogs were placed in sling-stand frames designed to keep the animal still with a minimum of restraint. Heart rate was monitored every 5 min *via* a lead II ECG[26].

The microencapsulated formulations, as well as the plain powder of bitolterol in a dose of 240 μg/kg (base), were placed in a No. 4 hard gelatin

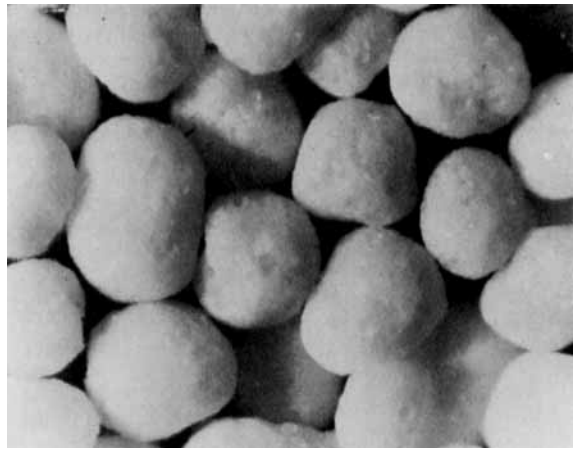

Figure 1—*Marumerized cores prior to microencapsulation containing 12.08% bitolterol mesylate; mean volume–surface diameter = 784 μm.*

[20] Ashland Chemical Co., Columbus, Ohio.
[21] Nembutal Sodium, Abbott Laboratories, North Chicago, Ill.
[22] Model 607, Harvard Apparatus Co., Dover, Mass.
[23] Dickenson & Co., Orangeburg, N.Y.
[24] Model P23B, Statham Instruments, Hatorey, Puerto Rico.
[25] Model 5, Grass Instrument Co., Quincy, Mass.
[26] Model 300 Visette, Sanborn Co., Waltham, Mass.

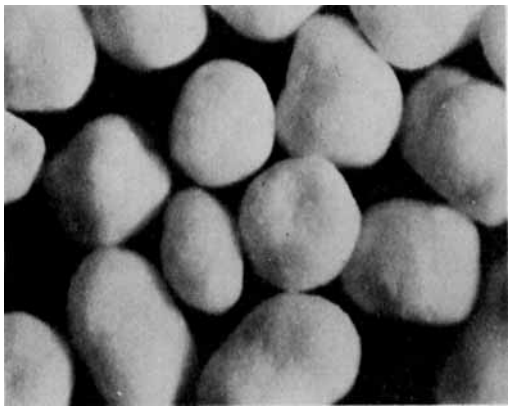

Figure 2—*Microencapsulated beads; calculated film thickness = 6.6 μm.*

capsule and administered to the animal orally, followed by 10 ml of water. Each dog was medicated at weekly intervals with either the microencapsulated formulations or the plain powder until each had received each product twice. Two dogs were used on each test day.

For the evaluation of heart rate effects, baseline pulse rates were analyzed to determine the limits of expected control values. Contrasting baseline values for the different experimental periods, days, dogs, and observation times (20-, 10-, and 0-min pretreatment) produced 95% confidence limits ranging from 83 to 117% of the mean. Consequently, on any one experimental day, the onset of a drug effect was defined as that first point in time where four successive 5-min readings were equal to or greater than 1.17 times the mean of a test animal's pretreatment readings. The end of a drug effect was defined as that first point where either four successive 5-min readings were less than the mean baseline or, in a few instances, the 300-min time period was reached.

The statistic employed in the analysis was the sum of the pulse changes from baseline over the drug effect portion of the time–response curve. The single dog not showing a drug effect was assigned a result of zero for the sum of the pulse changes.

Since all six dogs received, in different order, all possible treatments twice, in six experimental periods, the order effect was assumed to be small relative to other sources of variation.

RESULTS AND DISCUSSION

Appearance of Microencapsulated Products—The uncoated cores appeared to be regular crystalline agglomerates, generally spherical with an occasional rod- or dumbbell-shaped particle (Fig. 1). Microencapsulation with ethylcellulose produced a very glossy surface, free from gross irregularities (Fig. 2). For visualization purposes, the thin film was swelled in Fig. 3 by flooding the field of coated beads with cyclohexane. The frequently reported knobs of film at either end of some ellipsoidal beads, formed when the polymer was still mobile under conditions of high agitation and spinning, appear somewhat exaggerated in this photomicrograph due to light refraction and to the optical advantage of viewing the swelled film through a smaller cross section. The significance of these knobs regarding their possible effects on dissolution or thickness calculations has not been evaluated. The phenomenon appears to be a function of particle shape rather than size and does not affect the usefulness of the correlations obtained among calculated film thickness, release rate, and biological effect.

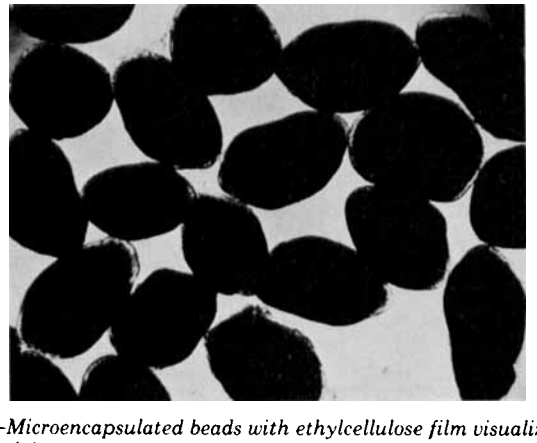

Figure 3—*Microencapsulated beads with ethylcellulose film visualized through cyclohexane perfusion.*

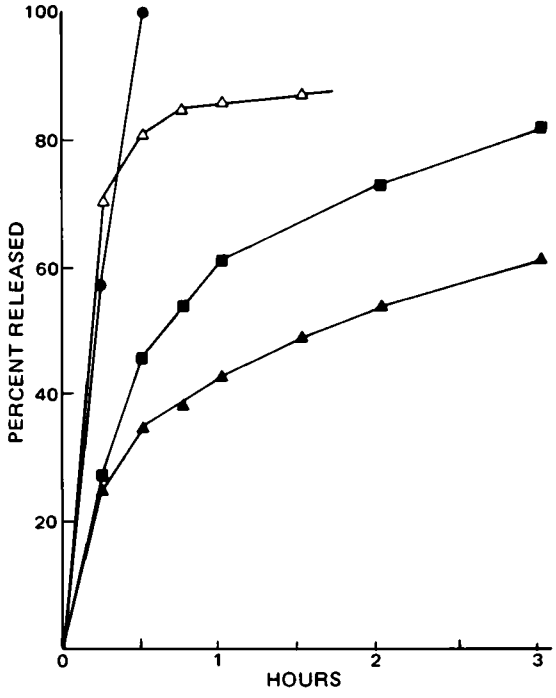

Figure 4—*Release of bitolterol in 0.1 N HCl from various experimental products. Key: ●, conventional hard gelatin capsule; △, Product A, uncoated cores; ■, Product A-1, microencapsulated beads, 2.6% film; and ▲, Product A-2, microencapsulated beads, 3.3% film.*

Dissolution Studies—Formation of the spheronized cores brought about some delay in itself, as shown in Fig. 4 where Core A and Products A-1 and A-2 are compared to the release of a conventional 5-mg capsule of bitolterol containing standard excipients of starch and lactose. The uncoated cores required about 30 min to release half of the dose *in vitro*. Encapsulation with film comprising 2.6% of the total weight of the bead resulted in a $t_{50\%}$ of 40 min. Increasing the film to 3.3% total bead weight further increased the $t_{50\%}$ to about 90 min.

During dissolution, the uncoated cores, as well as the beads, remained essentially intact after several hours of exposure to the dissolution medium in a rotating basket and did not disintegrate. Drug was presumably released by passive diffusion from a relatively unchanging surface. The dissolution of particles encapsulated with insoluble films and releasing their soluble components by diffusive mechanisms has been treated by first-order kinetics (3, 24). The microencapsulated beads prepared for this study could also be characterized by a logarithmic release model (Fig. 5). The effect of increasing the thickness of the film was to reduce the apparent first-order release rate constant. Linearity was found up to and beyond 2 hr under these conditions. The standard errors shown in Fig. 5 were calculated from four replications of the dissolution procedure and indicate the variability seen between samples.

Correlation for the semilog plots of undissolved material against time over the first 120 min was high (r = 0.97–0.99). The slopes of the independent estimates were used to calculate the dissolution rate constants and the corresponding half-lives. The regression lines were not constrained to pass through the point C = 100% at t_0, and the extrapolated t value found for the initial concentration within the bead was taken to be a measure of the penetration time, *i.e.*, the time required for the dissolution medium (0.1 N HCl) to penetrate the bead and to initiate drug release. Thicker films in general led to longer penetration times; therefore, $t_{50\%}$, the time required to release half of the bead content, was equal to the sum of the calculated half-life and the penetration time.

Table II presents the density and particle-size data used to calculate the film thickness of the encapsulating walls. Fick's law of diffusion may be written as:

$$dC/dt = -\frac{SDC}{h} \qquad \text{(Eq. 6)}$$

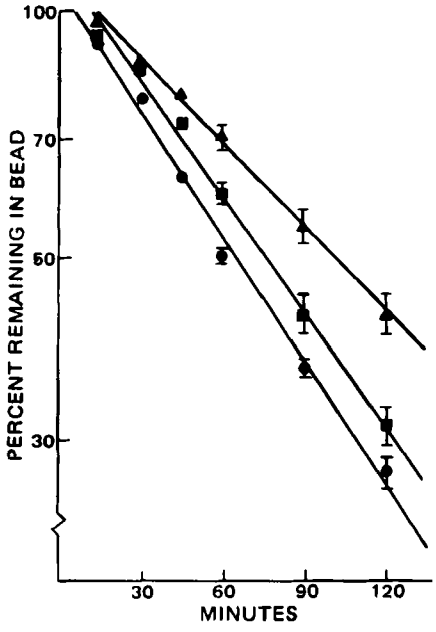

Figure 5—*Release of bitolterol in 0.1 N HCl from a series of microencapsulated beads. Key: ▲, Product B-2, film thickness = 7.3 μm; ■, Product B-3, film thickness = 6.4 μm; and ●, Product B-1, film thickness = 5.6 μm.*

where C is the drug concentration inside the bead, t is time, S is the surface area of the beads, and D is the diffusion coefficient which is inversely proportional to the film thickness h and includes consideration of solute volume, film porosity, and stirring rate. Since these beads remained intact throughout dissolution, the surface area and the diffusion coefficient may be combined:

$$dC/C = -\frac{K}{h}dt \qquad \text{(Eq. 7)}$$

Integration of this expression gives:

$$\ln\frac{C}{C_0} = -\frac{K}{h}t \qquad \text{(Eq. 8)}$$

At $t = t_{1/2}$, Eq. 8 can be rearranged to:

$$h = \frac{Kt_{1/2}}{0.693} \qquad \text{(Eq. 9)}$$

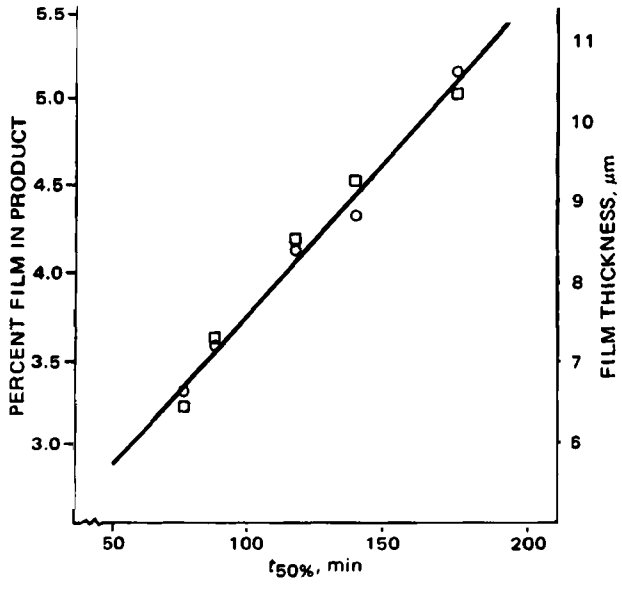

Figure 6—*Time required to release 50% of drug content ($t_{50\%}$) in 0.1 N HCl from a series of microencapsulated products as a function of percent film in sample (left ordinate) and film thickness (right ordinate). Key: □, film content; and ○, calculated film thickness.*

Table III—Heart Rate Prior to Oral Administration of Plain Drug Powder or Microencapsulated Formulations of Bitolterol

Dog	Baseline Means[a], beats/min: Plain Powder	Product B-1	Product B-2
1	53	50	55
2	66	56	62
3	65	62	63
4	54	53	60
5	60	67	58
6	67	62	58
Arithmetic mean	60.9	58.2	59.2

Analysis of Variance[b] — Source of Variation	*df*	*MS*	*F*
Dogs	5	107.69	6.2
Formulations	2	21.78	1.2
Dogs × formulations	10	30.94	1.78
Residual error	18	17.42	

[a] Arithmetic mean of 20-, 10-, and 0-min pretreatment heart rates. [b] Least significant difference at $p = 0.05$ between two treatment means = 3.6.

For large surface area and low film fraction, F was shown to be essentially proportional to the effective thickness of the film in Eq. 4. However, examination of the particle-size distributions of the products before and after microencapsulation revealed that fine particles present in the core material were removed during coating by agglomeration with larger particles. The modes of the distributions were not appreciably changed during microencapsulation, but the removal of the fines caused an upward shift in the mean volume–surface diameters. Accordingly, the d_{vs} of each microencapsulated *product* was considered to be the best measure of the size of the actual *cores* undergoing encapsulation and was used to calculate film thicknesses for the various products.

Agglomeration occurred to a greater extent in systems where the solids-to-solvent ratio was higher, with the effect that the total surface area to be covered by the film was reduced. The phase ratio (core material to film material) of Products B-1 and B-3 was the same (30:1), but Product B-3 was prepared in a system with double the solids content of B-1. The ethylcellulose assay showed virtually no difference between the amount of film present in the two products, but the mean volume–surface diameters indicated that greater agglomeration had taken place in the more concentrated system, leading to a thicker film being deposited on Product B-3.

Confirmation of the thicker film was found in the dissolution rates shown in Fig. 5, where Product B-3 was slower than B-1, although the film content of each product was about the same. Therefore, the film content is only proportional to some measure of the dissolution rate for a series of products encapsulated around identical core material from systems where agglomeration proceeds to the same extent and the mean volume–surface diameters of the microencapsulated products are similar.

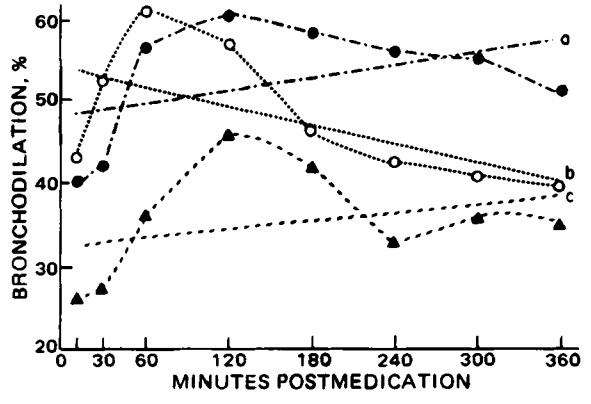

Figure 7—*Bronchodilator activity in anesthetized dogs following a dose of 240 μg of bitolterol (base)/kg administered intraduodenally. Linear effect regression lines are shown for each corresponding time–response curve. Key: ○, plain drug powder (control); ●, microencapsulated Product B-1, 3.2% film; and ▲, microencapsulated Product B-2, 4.0% film. Regression line slopes ± SE are: a, 0.024 ± 0.014; b, −0.039 ± 0.014; and c, 0.015 ± 0.014.*

Table IV—Heart Rate Effect in Unanesthetized Dogs Given 240 μg/kg Bitolterol (Base) Orally

Dog	Sum of Pulse Changes from Baseline (t_0) over Drug Effect Portion of Time–Response Curve, beats/min: Plain Powder	Product B-1	Product B-2
1	1377	1948	1300
2	1070	826	459
3	2423	369	461
4	180	1255	0
5	2940	2053	2127
6	404	266	208
Arithmetic mean	1400	1120	760

Source of Variation	Analysis of Variance[a]: *df*	*MS*	*F*
Dogs	5	3,544,999	12.0
Formulations	2	1,234,469	4.2
Dogs × formulations	10	664,720	2.2
Residual error	18	295,709	

[a] Least significant difference at $p = 0.05$ between two treatment means = 466; at $p = 0.01$, least significant difference = 566.

With allowance for the initial penetration time delays, film fraction was plotted against $t_{50\%}$ for five microencapsulated products (Core C) ranging in film content from 3.2 to 5.0% (Fig. 6). The corresponding calculated film thickness is given on the right-hand scale. Graphs of this type were useful when preparing material with specific release characteristics. The y-intercept in Fig. 6 was thought to represent the minimum amount of film (~2.0% for this series) that must be present before a sufficient number of particles was entirely coated to exhibit a depressed release rate. The significance of the intercept was somewhat obscured since the cores in these experiments were not themselves instantaneously dissolving. However, encapsulated materials carrying less than 2% film showed only slightly slower release rates than the corresponding uncoated cores.

Biological Evaluation—On the basis of *in vitro* dissolution studies, two formulations were selected for biological evaluation: Product B-1 with a $t_{50\%}$ of 65 min representing faster releasing formulations, and Product B-2, with a $t_{50\%}$ of 101 min representing the slower releasing formulations.

Bronchodilator Activity in Anesthetized Dog—The change in bronchodilator activity resulting from the administration of the two microencapsulated formulations over the 6-hr observation period was significantly different from that of plain bitolterol powder, showing delayed release properties at the early time periods and a flatter response decay at the later time periods. Linear regressions calculated for the three dosage forms are shown in Fig. 7 against the actual bronchodilation time–response curves. Both controlled-release formulations exhibited sustained activity with similar positive slopes, while the slope for the plain drug was negative. Bronchodilations ranging from 26 to 43% were obtained within 10 min after medication. A 60% peak effect was obtained at 60 min with the plain powder whereas Products B-1 and B-2 showed peak effects of 60 and 46% at 120 min, respectively.

The bronchodilation appeared prolonged for all treatments, with 35–51% effect still obtained at the 6th hr. After the 1st hr, the bronchodilation by Product B-1 was maintained at a significantly ($p = 0.05$) higher level (50–60%) than that of Product B-2 (32–46%). Bronchodilation following the administration of Product B-2 was significantly less than that from the plain powder through the 1st hr; however, neither microencapsulated formulation was significantly different from the plain powder after the 1st hr.

Heart Rate Effect in Unanesthetized (Trained) Dog—An analysis of baseline mean pulse rates showed no significant differences among the three formulations (Table III). Subsequent analysis of the posttreatment results showed a significant difference ($p = 0.01$) between the slower Product B-2 and the plain powder with respect to the mean sum of the pulse changes from baseline over the drug-effect portion of the time–response curve (Table IV). While the sum of the pulse rate changes was lower after Product B-1 relative to the powder, the difference was not statistically significant. Comparison of the mean pulse rates at 30, 60, 90, and 120 min (Fig. 8) showed significantly lower rates with both microencapsulated formulations at 30 and 60 min, significantly lower pulse rates with the slower formulation (Product B-2) than with both of the other products at 90 min, and equivalent rates for all three forms at 120 min and thereafter.

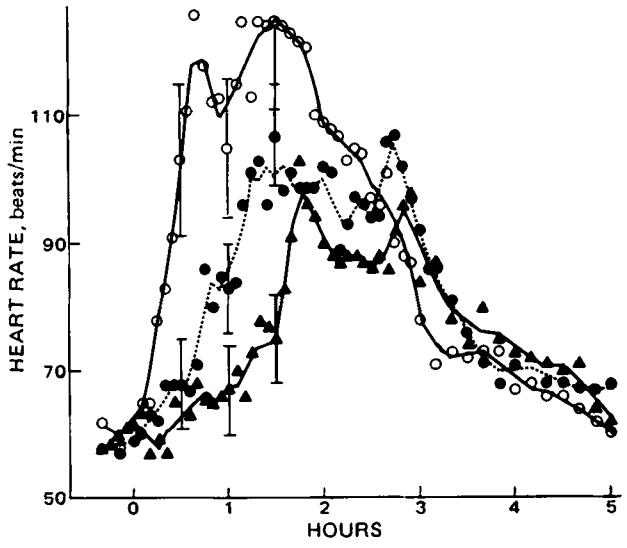

Figure 8—*Heart rate effect in unanesthetized dogs following a single dose of 240 μg of bitolterol (base)/kg administered orally; six dogs received two separate medications of each drug on different days. Key: ○, plain drug powder (control); ●, microencapsulated Product B-1, 3.2% film; and ▲, microencapsulated Product B-2, 4.0% film.*

In both anesthetized and unanesthetized dogs, the microencapsulated products demonstrated controlled-release properties, and effective bronchodilator activity was obtained with an attenuation of the concommitant cardiac stimulation.

REFERENCES

(1) B. F. Tullar, H. Minatoya, and R. R. Lorenz, *J. Med. Chem.*, **19**, 834 (1976).

(2) H. Minatoya, *J. Pharmacol. Exp. Ther.*, **206**, 515 (1978).

(3) J. A. Bakan and J. L. Anderson, in "The Theory and Practice of Industrial Pharmacy," 2nd ed., L. Lachman, H. A. Lieberman, and J. L. Kanig, Eds., Lea & Febiger, Philadelphia, Pa., 1976, p. 420.

(4) L. A. Luzzi, *J. Pharm. Sci.*, **59**, 1367 (1970).

(5) G. O. Fanger, "Microencapsulation, A Brief History and Introduction," (Proceedings of the American Chemical Society Symposium on Microencapsulation, Chicago, 1973) Plenum, New York, N.Y., 1974.

(6) W. Sliwaka, *Angew. Chem. Int. Ed.*, **14**, 593 (1975).

(7) H. G. Bungenberg de Jong and Kass, *Biochem. Z.*, **232**, 338 (1931).

(8) B. K. Green (to National Cash Register Co.), U.S. pat. reissue 24,899 (Nov. 29, 1960).

(9) B. K. Green and L. Schleicher (to National Cash Register Co.), U.S. pat. 2,800,457 (July 23, 1957).

(10) T. C. Powell, M. E. Steinle, and R. A. Yoncoskie (to National Cash Register Co.), U.S. pat. 3,415,758 (Dec. 10, 1968).

(11) J. A. Bakan (to National Cash Register Co.), U.S. pat. 3,436,355 (Apr. 1, 1969).

(12) R. E. Miller and J. L. Anderson (to National Cash Register Co.), U.S. pat. 3,155,590 (Nov. 3, 1964).

(13) J. L. Anderson, G. L. Gardner, and N. H. Yoshida (to National Cash Register Co.), U.S. pat. 3,341,416 (Sept. 12, 1967).

(14) G. O. Fanger, R. E. Miller, and R. G. McNiff (to National Cash Register Co.), U.S. pat. 3,531,481 (Sept. 29, 1970).

(15) M. Gutcho, "Capsule Technology & Microencapsulation," Noyes Data Corp., Park Ridge, N.J., 1972.

(16) T. M. S. Chang, "Artificial Cells," Charles C Thomas, Springfield, Ill., 1972.

(17) J. W. Conine and H. R. Hadley, *Drug Cosmet. Ind.*, **106**, 38 (1970).

(18) C. W. Woodruff and N. H. Nuessle, *J. Pharm. Sci.*, **61**, 787 (1972).

(19) H. J. Malinowski, Ph.D. thesis, Philadelphia College of Pharmacy and Science, Philadelphia, Pa., 1973.

(20) H. Minatoya, A. M. Lands, and G. A. Portmann, *J. Pharm. Sci.*, **54**, 968 (1965).
(21) G. A. Portmann, H. Minatoya, and A. M. Lands, *ibid.*, **54**, 973 (1965).
(22) "The United States Pharmacopeia," 19th rev., Mack Publishing Co., Easton, Pa., 1975, p. 651.
(23) L. Si-Nang, P. F. Carlier, P. Delort, J. Gazzola, and D. Lafont, *J. Clin. Pharmacol.*, **9**, 399 (1969).
(24) A. T. Florence and A. W. Jenkins, in "Microencapsulation," J. R. Nixon, Ed., Dekker, New York, N.Y., 1976, p. 39.

ACKNOWLEDGMENTS

The authors thank Mr. Herbert Stander for statistical analysis and Ms. Mary Gosztyla for technical assistance.

Rapid and Accurate Stability-Indicating Assay for Nitroglycerin

DAVID M. BAASKE ˣ, JAMES E. CARTER, and ANTON H. AMANN

Received July 21, 1978, from the *Department of Pharmaceutical Development, Arnar-Stone Laboratories Inc., McGaw Park, IL 60085.* Accepted for publication September 21, 1978.

Abstract □ A rapid high-pressure liquid chromatographic method for determining the nitroglycerin concentration in liquid dosage forms and intravenous admixture solutions is presented. A coefficient of variation of less than 1.8% was achieved over the concentration range most commonly encountered (50–500 μg/ml). A variable wavelength detector (λ = 218 nm) and a micro-alkyl phenyl column were employed. The mobile phase was acetonitrile–tetrahydrofuran–water (26:10:64). Total analysis time was 12 min.

Keyphrases □ Nitroglycerin—assay of liquid dosage forms and intravenous solutions, stability, degradation products □ Stability—nitroglycerin in intravenous solutions □ High-pressure liquid chromatography—analysis, nitroglycerin liquid dosage forms and intravenous solutions □ Cardiac vasodilators—nitroglycerin, analysis, liquid dosage forms and intravenous solutions

Intravenous nitroglycerin (glyceryl trinitrate) is commonly used for patients with acute myocardial infarction. Several methods of preparing such solutions for human patients have been reported (1–3). Recent reports indicated that intravenous nitroglycerin solutions lose potency when prepared or stored in certain containers (4–6). This loss may be due to degradation or adsorption. Thus, a rapid and accurate assay of nitroglycerin in intravenous solutions is needed.

BACKGROUND

Nitroglycerin is the triester of nitric acid and glycerol. Breakdown occurs by a stepwise loss of nitrate groups (Scheme I).

Spectrophotometric methods require little instrumentation but are time consuming and complex and do not indicate stability (7–10) or differentiate nitroglycerin, mononitroglycerin, dinitroglycerin, and endogenous nitrates. TLC (11–13) is selective but not quantitative. Although polarographic methods (14, 15) offer both selectivity and sensitivity, they require sophisticated instrumentation not available in many laboratories.

A kinetic method of analysis (16) based on the transient appearance of a chromophoric intermediate during base hydrolysis offers speed and specificity but lacks sensitivity. GLC methods (17–21) give sensitivity for nitroglycerin in excess of that required. Some give the desired selectivity. However, all require a time-consuming extraction into an organic solvent.

Two normal phase high-performance liquid chromatographic methods were reported (22, 23). Both reports failed to discuss interference from excipients and breakdown products, and both methods require extraction into an organic solvent. Assay sensitivity is potentially a problem when applying these methods to intravenous nitroglycerin admixture solutions.

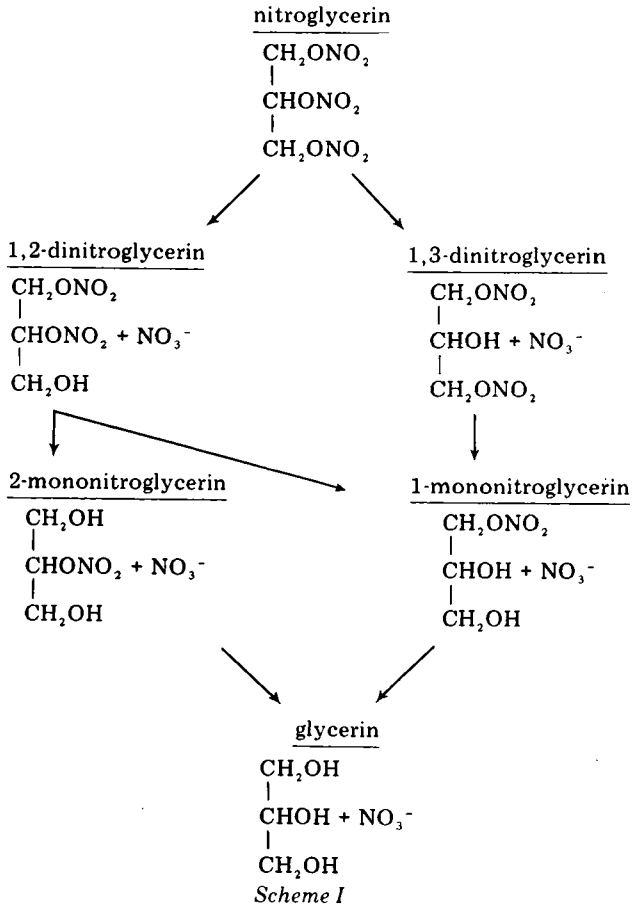

Scheme I

A new method is described here that allows the rapid direct measurement of nitroglycerin in intravenous admixture solutions, offers adequate sensitivity, and provides the potential for measuring breakdown products.

EXPERIMENTAL

Materials—Nitroglycerin[1] [10% in lactose or 1% (v/v) in ethanol], isosorbide dinitrate[2] (25% in lactose), and sublingual nitroglycerin tablets[3]

[1] ICI, Wilmington, Del.
[2] Napp Chemicals, Lodi, N.J.
[3] Eli Lilly and Co., Indianapolis, Ind.

0022-3549/79/0400-0481$01.00/0
© 1979, American Pharmaceutical Association

(20) H. Minatoya, A. M. Lands, and G. A. Portmann, *J. Pharm. Sci.*, **54**, 968 (1965).
(21) G. A. Portmann, H. Minatoya, and A. M. Lands, *ibid.*, **54**, 973 (1965).
(22) "The United States Pharmacopeia," 19th rev., Mack Publishing Co., Easton, Pa., 1975, p. 651.
(23) L. Si-Nang, P. F. Carlier, P. Delort, J. Gazzola, and D. Lafont, *J. Clin. Pharmacol.*, **9**, 399 (1969).
(24) A. T. Florence and A. W. Jenkins, in "Microencapsulation," J. R. Nixon, Ed., Dekker, New York, N.Y., 1976, p. 39.

ACKNOWLEDGMENTS

The authors thank Mr. Herbert Stander for statistical analysis and Ms. Mary Gosztyla for technical assistance.

Rapid and Accurate Stability-Indicating Assay for Nitroglycerin

DAVID M. BAASKE ˣ, JAMES E. CARTER, and ANTON H. AMANN

Received July 21, 1978, from the *Department of Pharmaceutical Development, Arnar-Stone Laboratories Inc., McGaw Park, IL 60085.* Accepted for publication September 21, 1978.

Abstract □ A rapid high-pressure liquid chromatographic method for determining the nitroglycerin concentration in liquid dosage forms and intravenous admixture solutions is presented. A coefficient of variation of less than 1.8% was achieved over the concentration range most commonly encountered (50–500 μg/ml). A variable wavelength detector (λ = 218 nm) and a micro-alkyl phenyl column were employed. The mobile phase was acetonitrile–tetrahydrofuran–water (26:10:64). Total analysis time was 12 min.

Keyphrases □ Nitroglycerin—assay of liquid dosage forms and intravenous solutions, stability, degradation products □ Stability—nitroglycerin in intravenous solutions □ High-pressure liquid chromatography—analysis, nitroglycerin liquid dosage forms and intravenous solutions □ Cardiac vasodilators—nitroglycerin, analysis, liquid dosage forms and intravenous solutions

Intravenous nitroglycerin (glyceryl trinitrate) is commonly used for patients with acute myocardial infarction. Several methods of preparing such solutions for human patients have been reported (1–3). Recent reports indicated that intravenous nitroglycerin solutions lose potency when prepared or stored in certain containers (4–6). This loss may be due to degradation or adsorption. Thus, a rapid and accurate assay of nitroglycerin in intravenous solutions is needed.

BACKGROUND

Nitroglycerin is the triester of nitric acid and glycerol. Breakdown occurs by a stepwise loss of nitrate groups (Scheme I).

Spectrophotometric methods require little instrumentation but are time consuming and complex and do not indicate stability (7–10) or differentiate nitroglycerin, mononitroglycerin, dinitroglycerin, and endogenous nitrates. TLC (11–13) is selective but not quantitative. Although polarographic methods (14, 15) offer both selectivity and sensitivity, they require sophisticated instrumentation not available in many laboratories.

A kinetic method of analysis (16) based on the transient appearance of a chromophoric intermediate during base hydrolysis offers speed and specificity but lacks sensitivity. GLC methods (17–21) give sensitivity for nitroglycerin in excess of that required. Some give the desired selectivity. However, all require a time-consuming extraction into an organic solvent.

Two normal phase high-performance liquid chromatographic methods were reported (22, 23). Both reports failed to discuss interference from excipients and breakdown products, and both methods require extraction into an organic solvent. Assay sensitivity is potentially a problem when applying these methods to intravenous nitroglycerin admixture solutions.

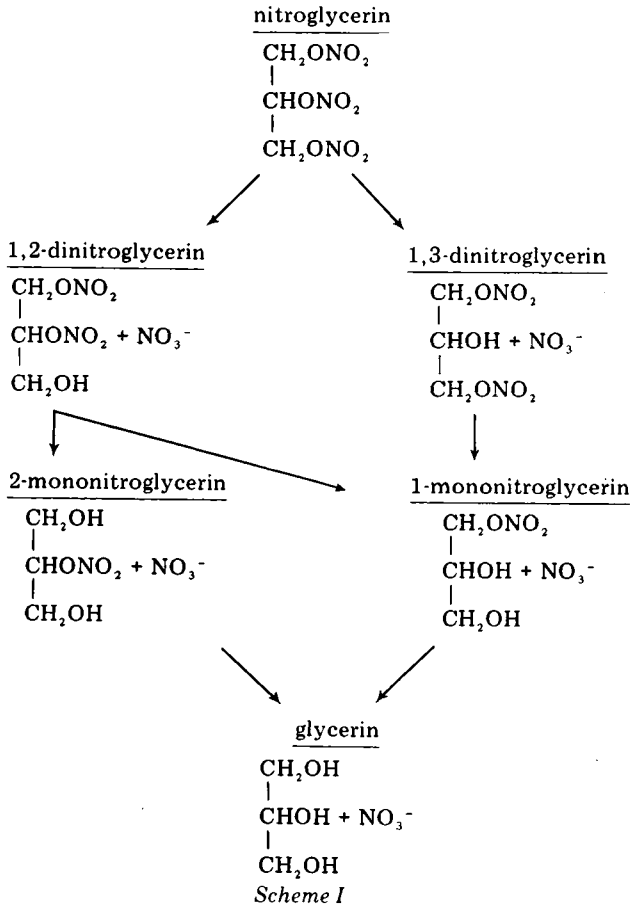

Scheme I

A new method is described here that allows the rapid direct measurement of nitroglycerin in intravenous admixture solutions, offers adequate sensitivity, and provides the potential for measuring breakdown products.

EXPERIMENTAL

Materials—Nitroglycerin[1] [10% in lactose or 1% (v/v) in ethanol], isosorbide dinitrate[2] (25% in lactose), and sublingual nitroglycerin tablets[3]

[1] ICI, Wilmington, Del.
[2] Napp Chemicals, Lodi, N.J.
[3] Eli Lilly and Co., Indianapolis, Ind.

0022-3549/79/0400-0481$01.00/0
© 1979, American Pharmaceutical Association

Table I—Accuracy and Precision Data

Nitroglycerin Concentration, μg/ml	Peak Height Ratios (Nitroglycerin/Isosorbide Dinitrate)				Mean	Adjusted Group Mean	Group *SD*
	Sample 1	Sample 2	Sample 3	Sample 4			
500	3.955	4.028	4.120	4.048	4.047	100.2	1.8
400	3.257	3.242	3.213	3.225	3.234	100.1	0.6
300	2.367	2.393	2.407	2.390	2.392	98.8	0.5
200	1.622	1.598	1.615	1.605	1.610	100.0	0.7
100	0.803	0.811	0.807	0.806	0.807	100.5	0.4
50	0.403	0.400	0.398	0.398	0.400	100.8	0.6
Overall	—	—	—	—	—	100.1	1.5

Table II—Admixture Measurement Data

Intravenous Solution	Theoretical Nitroglycerin Concentration, μg/ml	Measured Concentration, μg/ml				Mean, μg/ml	*SD*
		Bottle A	Bottle B	Bottle C	Bottle D		
Normal saline	50	47.5	51.3	48.5	55.5	50.6	3.4
Dextrose (5%)	50	49.5	50.0	52.0	48.4	50.0	1.5
Normal saline	100	104.1	100.8	101.8	99.3	101.5	2.0
Dextrose (5%)	100	100.5	100.7	98.7	99.4	99.8	0.9

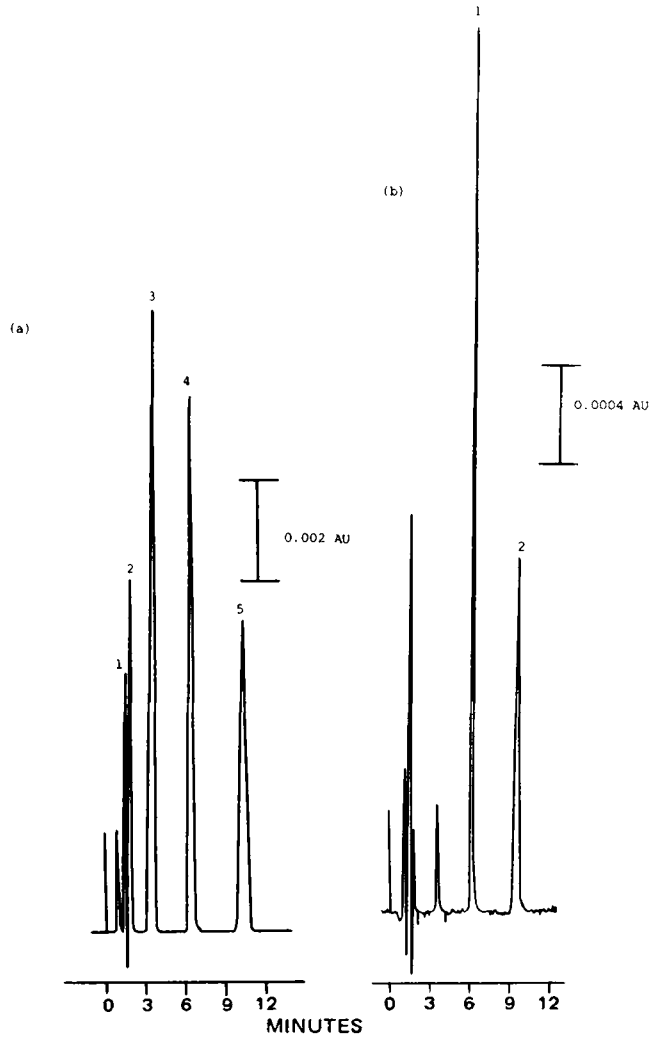

Figure 1—(a) *Chromatogram of a mixture of all the components of interest. Key: 1, glycerin; 2, mixture of the two mononitroglycerins; 3, mixture of the two dinitroglycerins; 4, isosorbide dinitrate; and 5, nitroglycerin. (b) Actual chromatogram of nitroglycerin (50 μg/ml) in 0.9% NaCl using a 40-μl injection. Key: 1, isosorbide dinitrate; and 2, nitroglycerin.*

USP were used as received. 1,2-Dinitroglycerin, 1,3-dinitroglycerin, 1-mononitroglycerin, and 2-mononitroglycerin were synthesized[4] using literature methods (24). Glass-distilled acetonitrile, methanol, and tetrahydrofuran were used for all procedures[5]. Five percent dextrose in water USP (D_5W) and sodium chloride injection USP (0.9% NaCl) in 250-ml glass bottles were used for admixture solutions[6]. Purified water USP was purified[7] further prior to use.

Instrumentation—The liquid chromatographic system consisted of a solvent pumping system[8], a septumless syringe-loading sample injector[9], a variable wavelength detector[10], and a 10-mv recorder[11]. A 30-cm × 3.9-mm column packed with alkyl phenyl bonded to silica gel[12] (10 μm), a detector wavelength of 218 nm, and a chart speed of 20 cm/hr were employed. Sample injections of 10–40 μl were used.

Mobile Phase—Approximately 1 liter of mobile phase was prepared fresh daily by thoroughly mixing 260 ml of acetonitrile, 100 ml of tetrahydrofuran, and 640 ml of water. The mobile phase was filtered through a 0.5-μm filter[13] prior to use and pumped at a constant rate of 2 ml/min, which yielded a pressure of less than 1600 psi.

Standard Curve—An accurately weighed sample of nitroglycerin (or isosorbide dinitrate), equivalent to 100 mg of active ingredient, was placed in a 100-ml volumetric flask and either dissolved in 10 ml of alcohol USP and brought to volume with water or dissolved in approximately 95 ml of water by vigorous agitation and then brought to volume with water. Lower concentrations were obtained by proper dilutions with water, 5% (v/v) ethanol, or appropriate intravenous solutions.

Standard concentrations of 500, 400, 300, 200, 100, and 50 μg/ml were prepared in quadruplicate. To 1.0 ml of each standard or sample was added 150 μl of isosorbide dinitrate (0.5 mg/ml), the internal standard; each was vortexed[14] for 5 sec and chromatographed. Peak heights were measured for nitroglycerin and isosorbide dinitrate. The peak height ratio (nitroglycerin/isosorbide dinitrate) was then plotted *versus* the nitroglycerin concentration to yield a calibration curve.

Admixtures—Admixture solutions were prepared to test the practicality of the method. Either 25 or 50 ml of intravenous solution was withdrawn from the intravenous bottle with a syringe[15], and then 25 or 50 ml of a 0.5-mg/ml nitroglycerin solution was added to the bottle, also with a syringe, to yield a theoretical concentration of 50 or 100 μg/ml. The solutions were thoroughly mixed and then sampled with a syringe.

[4] Midwest Research, Kansas City, Mo.
[5] Burdick & Jackson, Muskegon, Mich.
[6] McGaw Laboratories, Irvine, Calif.
[7] Milli-Q water purification system, Millipore Corp., Bedford, Mass.
[8] Series 2, Perkin-Elmer Corp., Norwalk, Conn.
[9] Model 7105, Rheodyne, Berkeley, Calif.
[10] LC-55A, Perkin-Elmer Corp., Norwalk, Conn.
[11] Model 023, Perkin-Elmer Corp., Norwalk, Conn.
[12] μBondapak phenyl, Waters Associates, Milford, Mass.
[13] Millipore Corp., Bedford, Mass.
[14] Votex Genie mixer, Scientific Products, McGaw Park, Ill.
[15] Becton, Dickinson and Co., Rutherford, N.J.

RESULTS AND DISCUSSION

The direct measurement of nitroglycerin in intravenous solutions in the presence of the anticipated breakdown products, glycerin, 1-mononitroglycerin, 2-mononitroglycerin, 1,2-dinitroglycerin, and 1,3-dinitroglycerin, is achieved for the first time. The potential to quantitate the anticipated breakdown products exists but has not yet been pursued, and no effort to resolve the dinitroglycerins or the mononitroglycerins was made. Other components of a potential intravenous formulation or admixture such as dextrose, sodium chloride, phosphate, and acetate ions or alcohol do not interfere with the quantitation of the nitroglycerin. A chromatogram illustrating the obtainable separations is seen in Fig. 1.

The described procedure, using 1 ml of sample or standard and 150 μl of internal standard, allows an accurate assay of nitroglycerin over the concentration range commonly encountered in nitroglycerin liquid dosage forms and intravenous admixture programs (50–500 μg/ml). Quantitation down to 5 μg/ml is possible with smaller quantities of internal standard, and the detection limit of 0.5 μg/ml is achievable with 100-μl injections. Still greater sensitivities are possible through the use of larger injection volumes or increased percentages of acetonitrile, which brings the peaks closer to the origin of the chromatogram, resulting in sharper peaks. However, this increase in sensitivity is counterbalanced by the decreased resolution of potential breakdown products.

Accuracy and Precision—Four replicate nitroglycerin samples (500, 400, 300, 200, 100, and 50 μg/ml) were chromatographed (Table I). A correlation of better than 0.999 was consistently obtained, as was a coefficient of variation of less than 1.8%.

Applicability—Hospitals presently employ three procedures to make standard nitroglycerin solutions, which are then used to prepare intravenous admixtures. Sublingual tablets are crushed and dissolved in sterile water for injection. Nitroglycerin in lactose is dissolved in a similar manner. Alcoholic nitroglycerin solutions are diluted to the required concentrations. Solutions prepared from each of these nitroglycerin materials were successfully analyzed by the described method, and no interferences were encountered in any instance.

A standard, 0.5 mg/ml, prepared from nitroglycerin in lactose was used to prepare a series of intravenous admixtures. This series was then analyzed to illustrate method practicality (Table II).

Unlike a methanol–water mobile phase, the acetonitrile–tetrahydrofuran–water mobile phase does not precipitate the lactose from the sample. Thus, the rapid pressure increases seen with methanol–water mixtures due to the clogging of column inlet filters are not encountered. The tetrahydrofuran is necessary only to resolve the glycerin and the mononitroglycerins. If this resolution is not required, the tetrahydrofuran portion of the mobile phase can be replaced with an equivalent amount of acetonitrile. The presence or absence of salts (*i.e.*, sodium nitrate and sodium phosphate, monobasic) or a variation of the mobile phase pH (pH 4–7.5) has no effect on resolution or retention times of components.

REFERENCES

(1) J. A. Kaplan, R. W. Dunbar, and E. L. Jones, *Anesthesiology*, **45**, 14 (1976).

(2) H. L. Fung and C. T. Rhodes, *Am. J. Hosp. Pharm.*, **32**, 139 (1975).

(3) T. W. Dean and D. C. Baun, *ibid.*, **32**, 1036 (1975).

(4) H. L. Fung, *ibid.*, **35**, 528 (1978).

(5) J. K. Sturek, T. D. Sokoloski, W. T. Winsley, and P. E. Stach, *ibid.*, **35**, 537 (1978).

(6) D. J. Ludwig and C. T. Veda, *ibid.*, **35**, 541 (1978).

(7) F. K. Bell, *J. Pharm. Sci.*, **53**, 752 (1964).

(8) F. W. Goodhart, H. Gucluyildiz, R. E. Daly, L. Chafetz, and F. C. Ninger, *ibid.*, **65**, 1466 (1976).

(9) J. R. Hohmann and J. Levine, *J. Assoc. Off. Anal. Chem.*, **47**, 471 (1964).

(10) D. P. Page, N. A. Carson, C. A. Buhr, P. E. Flinn, C. E. Wells, and M. T. Randall, *J. Pharm. Sci.*, **64**, 140 (1975).

(11) M. C. Crew and F. J. DiCarlo, *J. Chromatogr.*, **35**, 506 (1968).

(12) G. F. Macke, *ibid.*, **38**, 47 (1968).

(13) M. J. Pikal, D. A. Bibler, and B. Rutherford, *J. Pharm. Sci.*, **66**, 1293 (1977).

(14) B. C. Flann, *ibid.*, **58**, 122 (1969).

(15) A. L. Woodson and L. L. Alber, *J. Assoc. Off. Anal. Chem.*, **52**, 847 (1969).

(16) S. K. Yap, C. T. Rhodes, and H. L. Fung, *Am. J. Hosp. Pharm.*, **32**, 1039 (1973).

(17) E. T. Fossel, *J. Gas Chromatogr.*, **3**, 179 (1965).

(18) A. F. Williams and W. J. Murray, *Nature*, **210**, 816 (1966).

(19) E. Cameia and D. Pravisani, *Anal. Chem.*, **36**, 2108 (1964).

(20) B. J. Alley and H. W. H. Dykes, *J. Chromatogr.*, **72**, 182 (1972).

(21) P. S. K. Yap, E. F. McNiff, and H. L. Fung, *J. Pharm. Sci.*, **67**, 582 (1978).

(22) C. D. Chandler, G. R. Gibson, and W. T. Bolleter, *J. Chromatogr.*, **100**, 185 (1974).

(23) J. O. Doali and A. A. Juhasz, *J. Chromatogr. Sci.*, **12**, 51 (1974).

(24) I. Dunstan, J. V. Griffitho, and S. A. Harvey, *J. Chem. Soc.*, **1965**, 1319.

ACKNOWLEDGMENTS

The authors thank Ms. Deborah Worklan for assistance in the preparation of this manuscript and Ms. Martha Mooers for preparation of admixture solutions.

High-Performance Liquid Chromatographic Determination of Ketoprofen in Blood and Urine

R. FARINOTTI and G. MAHUZIER ˣ

Received April 24, 1978, from the *Laboratoire de Chimie Analytique, Centre d'Etudes Pharmaceutiques, Université de Paris-Sud, rue Jean Baptiste Clément, 92290 Chatenay Malabry, France.* Accepted for publication September 18, 1978.

Abstract □ A rapid, simple determination was developed for ketoprofen in biological fluids using high-performance liquid chromatography. The method requires selective extraction of this antirheumatic medicament and an internal standard with ether from the previously acidified plasma and urine. After evaporation of the ether, the residue is taken up by methanol and analyzed by reversed-phase liquid chromatography with detection at 254 nm. A concentration as low as 0.1 μg/ml can be determined with a 0.5-ml sample.

Keyphrases □ Ketoprofen—high-performance liquid chromatographic determination in blood and urine □ High-performance liquid chromatography—analysis, ketoprofen in blood and urine □ Anti-inflammatory agents—ketoprofen, high-performance liquid chromatographic analysis in blood and urine

Ketoprofen [2-(benzoyl-3-phenyl)propionic acid, I] is widely used in rheumatology because of its analgesic and anti-inflammatory properties. Pharmacokinetic studies of this product in humans and animals require a rapid, sensitive, and specific method. Various colorimetric, polarographic, TLC, and GLC methods have been reported. However, they generally require large test samples, and the operations are lengthy.

High-performance liquid chromatography (HPLC) eliminates these drawbacks and enables the rapid determination of plasma and urine concentrations after normal therapeutic doses.

EXPERIMENTAL

Reagents—Compound I and the internal standard, 2-(benzoyl-3-phenyl)butyric acid (II), were synthesized and obtained analytically pure[1]. The ether, methanol, and other reagents were of analytical quality and were used without prior purification[2].

Apparatus—A high-performance liquid chromatograph[3] was equipped with a spectrophotometer[4]. The plasma and urinary extracts were introduced on a column filled with 10-μm silica particles covered by a monomolecular layer of octadecylsilane[5]. The mobile phase was methanol–distilled water (45:55 v/v). This eluent, previously disengaged by magnetic agitation, crossed the chromatographic column at ambient temperature with a flow of 1.1 ml/min at 1800 psig.

The absorption intensities of I and II were measured at 254 nm using an attenuation of 0.05 unit full scale.

Standard Solutions—All stock and standard solutions of I and II were prepared in methanol and included a 500-μg/ml ketoprofen stock solution, a 500-μg/ml internal standard stock solution, ketoprofen standard solutions (prepared by diluting the stock solution 1:5, 1:10, 3:40, 1:20, 5:200, 1:100, and 1:200), and a 25-μg/ml internal standard solution (prepared by diluting the stock solution 1:20). These solutions were stored in the dark at 4°.

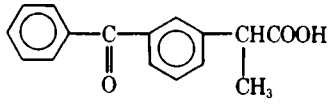

I

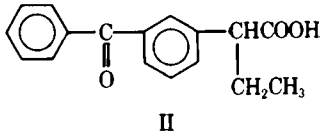

II

Samples—Blood was collected on sodium heparinate and centrifuged to separate the erythrocytes. The plasma was frozen until assayed.

The urinary determinations were carried out on recovered fractions with no special precautions.

Plasma Determinations—One hundred-microliter aliquots of the internal standard solution, at 25 μg/ml, were transferred to 30-ml stoppered centrifuge tubes and evaporated under a nitrogen stream. Then 0.5 ml of plasma, 0.5 ml of distilled water, 100 μl of perchloric acid at 70%, and 10 ml of ether were added to the residue. After mechanical agitation for 15 min, the ether phase extract was removed with 10 ml of ether. The combined ether phases were washed by agitation for 5 min with 5 ml of 1 *N* HCl and then 5 ml of distilled water.

The organic phase was dried by passage over anhydrous sodium sulfate and evaporated to dryness in a nitrogen stream at ambient temperature. Then 100 μl of methanol was added to the residue, and 10 μl of the solution was injected into the chromatograph.

Calibration was achieved by loading the plasma of nontreated subjects with increasing quantities of I and fixed quantities of II.

One hundred microliters of each I standard solution was introduced into 30-ml centrifuge tubes, identical to those used previously, together with 100 μl of the 25-μg/ml internal standard solution. These methanol solutions were evaporated in a nitrogen stream, and then 0.5 ml of plasma from nontreated subjects was added to each tube. The tubes contained quantities of I corresponding to plasma concentrations of 0.5, 2.5, 5, 7.5, 10, and 20 μg/ml. Each loaded plasma was then treated as already described and injected into the chromatograph.

Urinary Determination—Two hundred-microliter aliquots of the internal standard stock solution (500-μg/ml solution) were transferred to similar 30-ml centrifuge tubes together with 1 ml of the urine to be determined, 100 μl of 10 *N* NaOH, and 10 ml of ether. After a contact period of 10 min and mechanical agitation for 10 min, the ether phase was separated and elminated. The aqueous phase was acidified with 1 ml of 3 *N* HCl and then, as with the plasma, ether extraction was performed. The residues of the ether extracts were taken up by 1 ml of methanol, and 5 μl of this methanol solution was injected into the chromatograph.

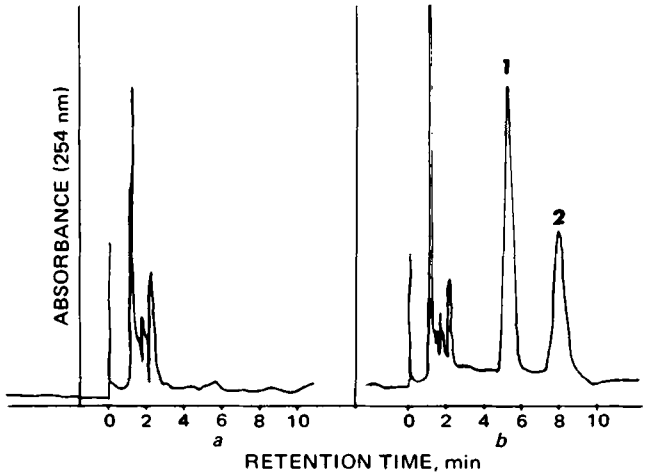

Figure 1—*Chromatogram of human plasma. Key:* a, *control plasma;* b, *plasma of a patient who received 100 mg of ketoprofen orally (2 hr after administration); 1, ketoprofen; and 2, internal standard.*

[1] Laboratories Specia, Paris, France.
[2] Prolabo Normapur.
[3] Model 6000 A pump and U6K injector, Waters Associates.
[4] Varian Varichrom.
[5] μBondapack C_{18} column (4 mm i.d. × 30 cm), Waters Associates.

0022-3549/79/0400-0484$01.00/0
© 1979, American Pharmaceutical Association

Table I—Values of Plasma and Urinary Calibration Curve Points

Biological Medium	Concentration, μg/ml	Peak Height Ratios between I and II	Equation
Plasma	0.5	0.125 ± 0.01	$y = 0.366x + 0.022$
	1	0.33 ± 0.02	
	2.5	0.935 ± 0.03	
	5	1.98 ± 0.04	
	7.5	2.94 ± 0.046	
	10	3.61 ± 0.055	
	15	5.43 ± 0.07	
Urine	10	0.155 ± 0.003	$y = 0.019x - 0.07$
	50	0.91 ± 0.07	
	100	1.73 ± 0.02	
	150	2.67 ± 0.02	
	200	3.80 ± 0.03	

For calibration, 20, 100, 200, and 400 μl of the 500-μg/ml I stock solution were introduced into 30-ml centrifuge tubes. These methanol solutions were then evaporated in a nitrogen stream. To each tube were added 1 ml of urine from a nontreated subject and 200 μl of the internal standard stock solution. The rest of the procedure was as described for plasma.

Calculations—The peak height ratios between the ketoprofen standard and those of the internal standard were plotted as the ordinate, and the corresponding ketoprofen concentrations were plotted on the abscissa. The unknown plasma or urine concentrations were calculated from the calibration curves thus obtained.

RESULTS

Separation—Separation of the ketoprofen and the internal standard was satisfactory since retention times were 5.3 and 8 min, respectively (Figs. 1*b* and 2*b*), under the experimental conditions proposed. Moreover, none of the normal constituents of either plasma or urine appeared on the chromatograms.

Extraction Yield—Extraction yields of I were determined by adding known quantities of I to 10 reference plasma samples. Extractions were performed as already described, and the internal standard was added to the extracts obtained. The average extraction yield was 84.1 ± 5.2%.

Linearity—Peak height ratio values of I and II as a function of the concentration of I are given in Table I. Good linearity was observed both for plasma and urine.

Accuracy and Precision—The accuracy of the method was checked by carrying samples at three concentration levels in replicates of five through the entire method; the detected concentration was calculated from a pooled standard curve. The accuracy is indicated by the mean error between the detected and theoretical values (Table II). The mean errors were −0.054, +0.050, and +0.27 μg/ml for the 1.00-, 2.50-, and 5.00-μg/ml samples, respectively. Their corresponding relative errors were −5.4, +2, and +5.4%.

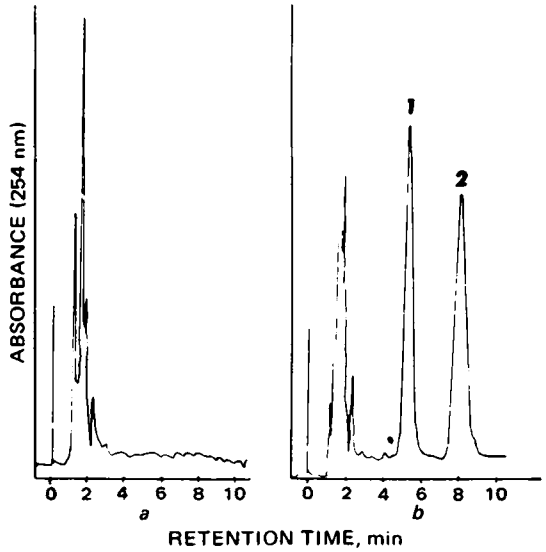

Figure 2—*Chromatogram of human urine. Key:* a, *control urine;* b, *urine of a patient who received 100 mg of ketoprofen orally (24-hr collected urines); 1, ketoprofen; and 2, internal standard.*

Table II—Accuracy and Precision of I Analysis in Plasma by HPLC

I Added to Human Plasma, μg/ml	I Detected μg/ml		Difference, μg/ml	
1		0.92		−0.08
		1.00		0.00
		0.95		−0.05
		1.00		0.00
		0.86		−0.14
	Mean ± *SD*	0.95 ± 0.06	Mean error	−0.054
	RSD	6.2%	Relative error	−5.4%
2.5		2.47		−0.03
		2.50		0.00
		2.50		0.00
		2.52		+0.02
		2.70		+0.20
	Mean ± *SD*	2.54 ± 0.09	Mean error	+0.050
	RSD	3.6%	Relative error	+2.0%
5		5.35		+0.35
		5.20		+0.20
		5.20		+0.20
		5.25		+0.25
		5.35		+0.35
	Mean ± *SD*	5.25 ± 0.07	Mean error	+0.27
	RSD	1.4%	Relative error	+5.4%

The precision of the method was examined similarly by comparing the results between these five replicate samples at each concentration level. The mean detected concentrations were 0.95, 2.54, and 5.25 μg/ml for samples of 1.00, 2.50, and 5.00 μg/ml, respectively. The standard deviations were 0.06, 0.09, and 0.07 μg/ml, respectively, and the corresponding relative standard deviations were 6.2, 3.6, and 1.4%.

DISCUSSION

The presence of two benzene rings in I allows chromatography of this molecule on a nonpolar column and its detection at 254 nm, its absorption maximum. The sensitivity achieved is sufficient for the plasma and urinary contents encountered. However, some substances present in biological media, and equally extractable in an acid medium, could show up if the extraction is not sufficiently selective.

Extraction conditions were chosen after various tests concerned with agitation time and the type and volume of solvents. Of the solvents tested (chloroform, methylene chloride, ethyl acetate, and ether), ether gave the best results. A good baseline was obtained if washing was carried out with 1 *N* HCl and distilled water as previously suggested (1).

No improvement was achieved by purification tests, either by passage through an alkaline medium followed by further extraction or by passage over Amberlite XAD2 resin.

The great affinity of I for plasma proteins (over 90%) (2) required their denaturation, and perchloric acid afforded better yields than hydrochloric acid.

Since most I is eliminated in the urine as the glucuronide, hydrolysis is necessary. In accordance with previous results (3), the addition of 10 *N* NaOH to the urine specimen gave better results after 10 min than enzymatic hydrolysis with *Helix pomatia* juice after 24 hr.

Urine contents, about 10 times those of plasma contents, require the use of more concentrated standards.

The method proposed is simple, sensitive, and rapid for the determinations of I in biological fluids during kinetic studies. It avoids the prior formation of methyl derivatives, a drawback with GLC.

REFERENCES

(1) P. Populaire, B. Terlain, S. Pascal, B. Decouvelaere, G. Lebreton, A. Renard, and J. P. Thomas, *Ann. Pharm. Fr.*, **31**, 679 (1973).

(2) R. Ballerini, A. Cambi, and P. Del Soldato, *J. Pharm. Sci.*, **66**, 282 (1977).

(3) P. Populaire, B. Terlain, S. Pascal, B. Decouvelaere, A. Renard, and J. P. Thomas, *Ann. Pharm. Fr.*, **31**, 735 (1973).

ACKNOWLEDGMENTS

The authors thank Laboratories Specia who supplied the ketoprofen and the internal standard.

Surfactant Solutions as Test Liquids for Measurement of Critical Surface Tension

WEI-CHI LIAO and JOEL L. ZATZ ˣ

Received June 29, 1978, from the *College of Pharmacy, Rutgers—the State University of New Jersey, Piscataway, NJ 08854.* Accepted for publication September 22, 1978.

Abstract □ Contact angles of various liquids and surfactant solutions on polytef and paraffin were measured. Critical surface tension values were obtained by extrapolation of plots of cosine of the contact angles *versus* corresponding surface tension values. Contact angles measured using polyoxyethylene octylphenols produced linear Zisman plots and yielded critical surface tensions that agreed with accepted values. This liquid series provides a reasonable approach to the measurement of critical surface tension for solid drugs that are soluble in organic liquids but relatively insoluble in water.

Keyphrases □ Surfactants, polyoxyethylene octylphenols—test liquids for measurement of critical surface tension □ Surface tensions—analysis, various drugs, solid-liquid mixtures, surfactants □ Structure-activity relationships—surface tension, various surfactants □ Contact angles—wetting of pharmaceutical solids

Critical surface tension, γ_c, was introduced as an empirical index of the wettability of solid surfaces (1) where γ_c represents the liquid surface tension at which liquids just spread over the solid surface. Liquids whose surface tension is below γ_c wet the solid completely, while liquids whose surface tension exceeds γ_c do not. The latter form drops with contact angles greater than 0° on the solid surface.

BACKGROUND

To determine the critical surface tension of a particular solid, a series of liquids with different surface tensions are applied to the surface of the solid and the contact angles, θ, are measured. A plot of cosine of the contact angle *versus* liquid surface tension is often linear. Extrapolation of this plot to where the cosine of the contact angle equals 1 yields the critical surface tension.

The composition of the liquid mixture influences the critical surface tension (2), possibly due to interfacial interaction (3). Anionic, cationic, and nonionic surfactants in aqueous solution have been used to determine the γ_c values of polytef and polyethylene (4). Experiments were carefully done by using diluted surfactant solutions to vary the surface tension. Zisman plots of the surfactants exhibited discontinuities at points that corresponded to the critical micelle concentration (CMC) of the surfactants. When the surfactant concentrations were higher than the CMC, the plots were linear and indicated the correct values of γ_c.

There has been little work on the determination of γ_c values for pharmaceutical substances other than aspirin (5). Such research would be useful because of the importance of wetting in dispersion of powders (6) and dissolution (7). The selection of suitable liquids for the determination of γ_c presents some problems. Hydrocarbons have surface tensions that are too low to be useful with many pharmaceutical powders. Other organic liquids and liquid mixtures may be used, but many drugs

Table I—Properties of Polyoxyethylene Octylphenols

Average Number of Oxyethylene Groups per Molecule	Average Molecular Weight, daltons	γ_L[a], dynes/cm
5	420	28.5
7	514	28.8
9	596	30.0
12	734	31.1
12.5	756	33.0
16	910	34.7
30	1526	38.8
40	1966	40.0

[a] Using 2.5×10^{-3} *M* aqueous solutions.

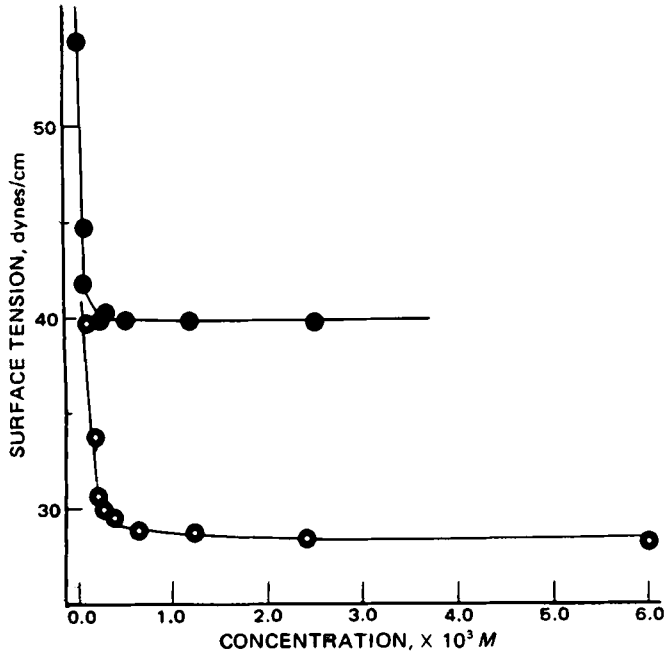

Figure 1—*Surface tension as a function of surfactant concentration. Key:* ○, *polyoxyethylene (5) octylphenol; and* ●, *polyoxyethylene (40) octylphenol.*

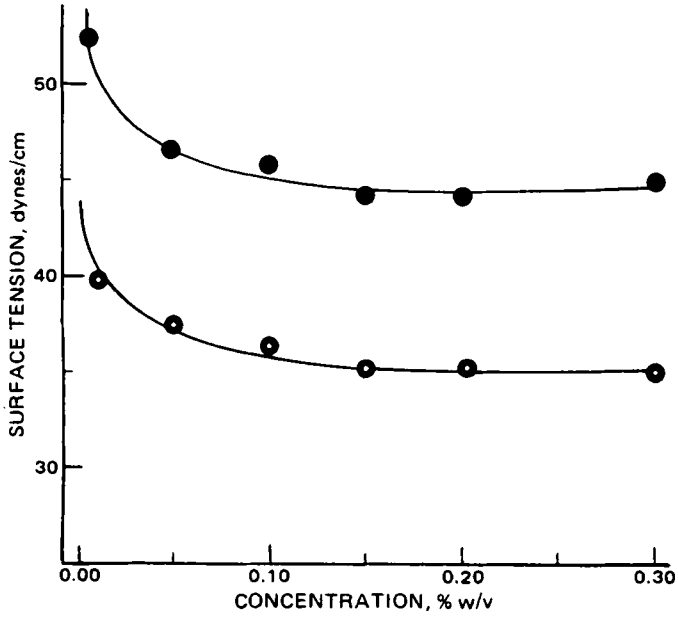

Figure 2—*Surface tension as a function of surfactant concentration. Key:* ○, *polyethylene glycol 600 monostearate; and* ●, *polyethylene glycol 4000 monostearate.*

0022-3549/79/0400-0486$01.00/0
© 1979, American Pharmaceutical Association

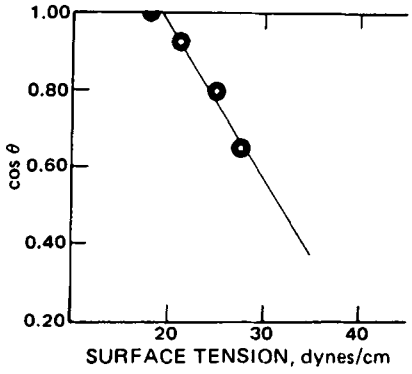

Figure 3—*Cosine of contact angle as a function of surface tension for hydrocarbon liquids on polytef.*

expected to have low energy surfaces are quite soluble in semipolar liquids, and dissolution complicates contact angle measurement. Drugs that present problems in wetting are likely to be poorly water soluble. Aqueous surfactant solutions should function well in studies of critical surface tension because liquid surface tension may be varied (within certain limits) and solubility problems are minimized.

This study investigated the use of surfactant solutions in the determination of critical surface tension. Nonionic surfactants were chosen since this class is least likely to exhibit specific adsorption effects on solid surfaces. A series of solutions graduated in surface tension was prepared without extreme dilution by using a family of surfactants differing only in polyoxyethylene chain length.

EXPERIMENTAL

Materials—The nonionic surfactants, polyoxyethylene octylphenols[1] and polyethylene glycol monostearates[2], were used as received. Polytef film[3] was used after surface cleaning. Paraffin[4] was USP grade. Hexane[5], octane[5], dodecane[5], and hexadecane[5] were reagent grade. Water was double distilled in an all-glass still.

Preparation of Surfaces—Polytef film was cleaned with dichromic acid cleaning solution, rinsed thoroughly with distilled water, and dried. It was then affixed to a glass slide with tape. Molten paraffin was poured onto a clean glass slide on a hot plate. A smooth sheet of cleaned aluminum foil was placed on top of the paraffin, and a plastic scraper was drawn across the covered paraffin film. The slide was allowed to cool, and the foil was removed just prior to use.

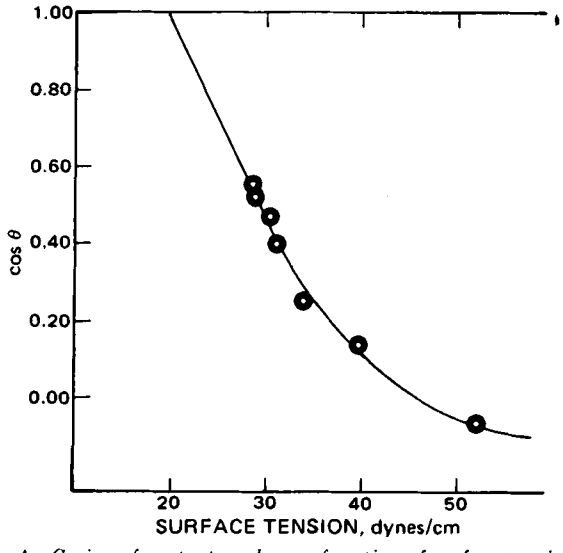

Figure 4—*Cosine of contact angle as a function of surface tension for solutions of polyoxyethylene (5) octylphenol on polytef.*

[1] Igepal CA-520, 620, 630, 720, and 897, GAF Corp., New York, N.Y. Triton X-102, 165, and 305, Rohm & Haas Co., Philadelphia, Pa.
[2] Mapeg 600 MS, 1000 MS, and 4000 MS, Mazer Chemical Inc., Gurnee, Ill.
[3] Teflon, Du Pont Co., Wilmington, Del.
[4] J. T. Baker Chemical Co., Phillipsburg, N.J.
[5] MC & B Co., East Rutherford, N.J.

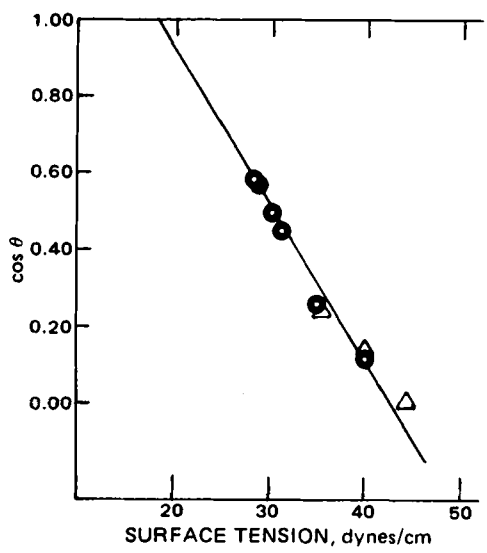

Figure 5—*Cosine of contact angle as a function of surface tension on polytef. Key: ○, polyoxyethylene octylphenols; and △, polyethylene glycol monostearates.*

Methods—Surface tension was measured by the Wilhelmy plate method[6]. Distilled water was used as the standard.

The advancing contact angles of sessile drops on the flat surfaces were measured directly by a goniometer attached to a telemicroscope[7]. Measurements were made at 25 ± 1° without humidity control. A drop containing 20 μl was applied to the surface using a microliter syringe held in place by a supporting rack. After 5 min, more liquid was slowly added (8) and the advancing angle was measured. Contact angle readings were taken from both sides of the drop separately, and at least three individual drops were used for each measurement.

RESULTS AND DISCUSSION

Four different liquid series were used to determine critical surface tensions of paraffin and polytef. The first series consisted of pure liquid hydrocarbons. The second series consisted of aqueous solutions of polyoxyethylene (5) octylphenol in which variations in surface tension

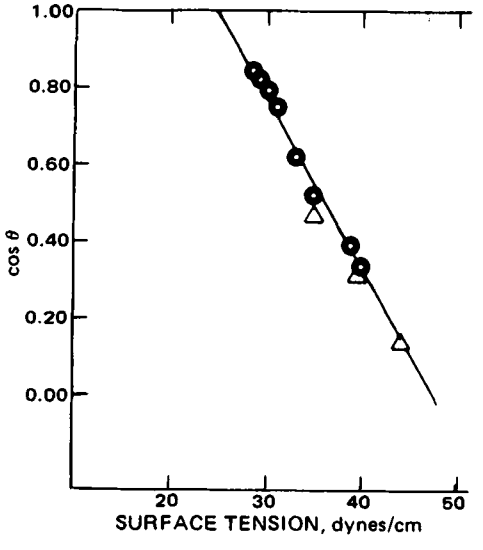

Figure 6—*Cosine of contact angle as a function of surface tension on paraffin. Key: ○, polyoxyethylene octylphenols; and △, polyethylene glycol monostearates.*

[6] Rosano surface tensiometer, Pacific Scientific Co., Newark, N.J.
[7] Gaertner Co., Chicago, Ill.

Table II—Critical Surface Tensions

Material	γ_c Hydrocarbon Series	γ_c Diluted Surfactant Series[a]	γ_c Polyoxyethylene Octylphenols	Literature Value
Polytef	19.2	19.5	17.9	18.5 (Ref. 1)
Paraffin	—	—	24.9	25.5 (Ref. 3)

[a] Polyoxyethylene (5) octylphenol solutions.

were achieved by dilution. Figure 1 shows the relationship between surface tension and solution concentration for this surfactant, which has the shortest hydrophilic group among the octylphenol derivatives. Also included in Fig. 1 are similar data for polyoxyethylene (40) octylphenol, which has the longest hydrophilic group.

The third liquid series contained eight octylphenol derivatives of uniform concentration. From the results in Fig. 1, 2.5×10^{-3} *M* was selected as the concentration to be used because, at that value, small variations in concentration would have a negligible influence on surface tension. Properties of the surfactants in this series are presented in Table I.

The fourth liquid series consisted of some polyethylene glycol monostearates. Only three with sufficient water solubility were available. Figure 2 is a plot of surface tension as a function of concentration for two members of this surfactant family. All solutions for contact angle measurement contained 0.15% (w/v) of the monostearates; γ_L values for polyethylene glycol 600, 1000, and 4000 were 35.3, 39.7, and 44.2 dynes/cm, respectively.

Figure 3 is a Zisman plot for hydrocarbon liquids on polytef. The critical surface tension determined from this plot, 19.2 dynes/cm, is in good agreement with the literature value of 18.5 dynes/cm (1). Results with polytef using the second liquid series, diluted solutions of polyoxyethylene (5) octylphenol, are presented in Fig. 4. The curvature this plot exhibits interfered with the required extrapolation, but γ_c was estimated to be 19.5 dynes/cm.

Contact angles of the two surfactant series on polytef are shown in Fig. 5. A critical surface tension value for the polyethylene glycol stearates was not determined because of the long extrapolation required, but it is evident that results with both sets of surfactants were similar. The plot of $\cos\theta$ *versus* γ_L is linear. The same is true for contact angles on paraffin (Fig. 6).

The critical surface tension values obtained on polytef and paraffin are summarized in Table II. In both cases, γ_c values derived from the use of surfactant solutions are quite close to those found using pure nonpolar liquids. Values of critical surface tension are not independent of the properties of the group of liquids used in their determination (2). The agreement in γ_c found with surfactant solutions and hydrocarbon liquids supports the notion that surfactant solutions above the CMC behave as though the liquid surface were a hydrocarbon (4). In the presence of a low energy surface, the adsorbed surfactant film seems to maintain its orientation and arrangement.

The use of a family of surfactants has several advantages over dilution of a single compound to vary surface tension. Diluted surfactant solutions invariably lead to curved Zisman plots, which make extrapolation to γ_c difficult. This may be because dilution below the CMC causes the solution to lose its compact surface film, and the surface tension acquires a larger polar component. Use of a series of surfactants allows maintenance of the surface film in each solution and leads to linear plots (Figs. 5 and 6).

Furthermore, if adsorption of the surfactant molecules by the solid material or a component of the apparatus should occur, the concentration of surfactant in a highly dilute solution may be changed sufficiently to affect the surface tension in the liquid drop whose contact angle is being measured. Thus, the actual surface tension of the liquid would be different from that ascribed to it. Because concentrations of surfactant solutions are well above the CMC for each member of a surfactant family, some adsorption of surfactant would not cause this problem.

To summarize, critical surface tension values for polytef and paraffin determined using a family of solutions containing nonionic surfactants agree well with reported values. This liquid series provides a reasonable approach to the measurement of γ_c values for solid drugs that are soluble in organic liquids but relatively insoluble in water.

REFERENCES

(1) W. A. Zisman, *Adv. Chem. Ser., No. 43*, **1964**, 1.
(2) J. R. Dann, *J. Colloid Interface Sci.*, **32**, 302 (1970).
(3) F. M. Fowkes, *J. Phys. Chem.*, **66**, 382 (1962).
(4) M. K. Bernett and W. A. Zisman, *ibid.*, **63**, 1241 (1959).
(5) S. W. Harder, D. A. Zuck, and J. A. Wood, *J. Pharm. Sci.*, **59**, 1787 (1970).
(6) E. N. Hiestand, *ibid.*, **53**, 1 (1964).
(7) P. Finholt and S. Solvang, *ibid.*, **57**, 1968 (1968).
(8) E. G. Shafrin and W. A. Zisman, *J. Colloid Sci.*, **7**, 166 (1952).

Critical Surface Tensions of Pharmaceutical Solids

WEI-CHI LIAO and JOEL L. ZATZ ×

Received June 29, 1978, from the *College of Pharmacy, Rutgers—the State University of New Jersey, Piscataway, NJ 08854.* Accepted for publication September 22, 1978.

Abstract □ Advancing contact angles measured on compacts of several drugs by the sessile drop method and also by penetration through a column of drug granules were used to find the critical surface tension of the drugs. After liquid was delivered at a very slow rate, the contact angle of sessile drops decreased with time, but use of a consistent method of timing always led to the same value for critical surface tension. Results from penetration studies and work on compacts were in agreement, provided that the surfaces of the compacts were smooth and highly reflective. Critical surface tension of the six drugs, three analgesics and three sulfonamides, ranged from 31 to 33 dynes/cm. The critical surface tension of mixtures of phenacetin and microcrystalline cellulose was not a linear function of the relative surface fractions of the two materials. If the surface contained 25% or more of phenacetin, the critical surface tension barely differed from that of pure phenacetin.

Keyphrases □ Surface tensions, critical—various pharmaceutical solids analysis, by sessile drop method □ Surfactants, nonionic—used to determine surface tensions of various pharmaceutical solids □ Solids—surface tensions □ Contact angles—wetting of pharmaceutical solids

Wetting of a solid by a liquid is an important step in several pharmaceutical processes including the preparation of suspensions (1) and the adhesion of film coatings to tablets (2). The dissolution rate of powdered phenacetin was sensitive to the surface tension of the dissolution medium because of differences in wetting (3).

As described previously (4), the critical surface tension, γ_c, of a solid is a measure of its wettability and is related

0022-3549/79/0400-0488$01.00/0

© 1979, American Pharmaceutical Association

Table II—Critical Surface Tensions

Material	γ_c Hydrocarbon Series	γ_c Diluted Surfactant Series[a]	γ_c Polyoxyethylene Octylphenols	Literature Value
Polytef	19.2	19.5	17.9	18.5 (Ref. 1)
Paraffin	—	—	24.9	25.5 (Ref. 3)

[a] Polyoxyethylene (5) octylphenol solutions.

were achieved by dilution. Figure 1 shows the relationship between surface tension and solution concentration for this surfactant, which has the shortest hydrophilic group among the octylphenol derivatives. Also included in Fig. 1 are similar data for polyoxyethylene (40) octylphenol, which has the longest hydrophilic group.

The third liquid series contained eight octylphenol derivatives of uniform concentration. From the results in Fig. 1, 2.5×10^{-3} *M* was selected as the concentration to be used because, at that value, small variations in concentration would have a negligible influence on surface tension. Properties of the surfactants in this series are presented in Table I.

The fourth liquid series consisted of some polyethylene glycol monostearates. Only three with sufficient water solubility were available. Figure 2 is a plot of surface tension as a function of concentration for two members of this surfactant family. All solutions for contact angle measurement contained 0.15% (w/v) of the monostearates; γ_L values for polyethylene glycol 600, 1000, and 4000 were 35.3, 39.7, and 44.2 dynes/cm, respectively.

Figure 3 is a Zisman plot for hydrocarbon liquids on polytef. The critical surface tension determined from this plot, 19.2 dynes/cm, is in good agreement with the literature value of 18.5 dynes/cm (1). Results with polytef using the second liquid series, diluted solutions of polyoxyethylene (5) octylphenol, are presented in Fig. 4. The curvature this plot exhibits interfered with the required extrapolation, but γ_c was estimated to be 19.5 dynes/cm.

Contact angles of the two surfactant series on polytef are shown in Fig. 5. A critical surface tension value for the polyethylene glycol stearates was not determined because of the long extrapolation required, but it is evident that results with both sets of surfactants were similar. The plot of $\cos\theta$ *versus* γ_L is linear. The same is true for contact angles on paraffin (Fig. 6).

The critical surface tension values obtained on polytef and paraffin are summarized in Table II. In both cases, γ_c values derived from the use of surfactant solutions are quite close to those found using pure nonpolar liquids. Values of critical surface tension are not independent of the properties of the group of liquids used in their determination (2). The agreement in γ_c found with surfactant solutions and hydrocarbon liquids supports the notion that surfactant solutions above the CMC behave as though the liquid surface were a hydrocarbon (4). In the presence of a low energy surface, the adsorbed surfactant film seems to maintain its orientation and arrangement.

The use of a family of surfactants has several advantages over dilution of a single compound to vary surface tension. Diluted surfactant solutions invariably lead to curved Zisman plots, which make extrapolation to γ_c difficult. This may be because dilution below the CMC causes the solution to lose its compact surface film, and the surface tension acquires a larger polar component. Use of a series of surfactants allows maintenance of the surface film in each solution and leads to linear plots (Figs. 5 and 6).

Furthermore, if adsorption of the surfactant molecules by the solid material or a component of the apparatus should occur, the concentration of surfactant in a highly dilute solution may be changed sufficiently to affect the surface tension in the liquid drop whose contact angle is being measured. Thus, the actual surface tension of the liquid would be different from that ascribed to it. Because concentrations of surfactant solutions are well above the CMC for each member of a surfactant family, some adsorption of surfactant would not cause this problem.

To summarize, critical surface tension values for polytef and paraffin determined using a family of solutions containing nonionic surfactants agree well with reported values. This liquid series provides a reasonable approach to the measurement of γ_c values for solid drugs that are soluble in organic liquids but relatively insoluble in water.

REFERENCES

(1) W. A. Zisman, *Adv. Chem. Ser., No. 43*, **1964**, 1.
(2) J. R. Dann, *J. Colloid Interface Sci.*, **32**, 302 (1970).
(3) F. M. Fowkes, *J. Phys. Chem.*, **66**, 382 (1962).
(4) M. K. Bernett and W. A. Zisman, *ibid.*, **63**, 1241 (1959).
(5) S. W. Harder, D. A. Zuck, and J. A. Wood, *J. Pharm. Sci.*, **59**, 1787 (1970).
(6) E. N. Hiestand, *ibid.*, **53**, 1 (1964).
(7) P. Finholt and S. Solvang, *ibid.*, **57**, 1968 (1968).
(8) E. G. Shafrin and W. A. Zisman, *J. Colloid Sci.*, **7**, 166 (1952).

Critical Surface Tensions of Pharmaceutical Solids

WEI-CHI LIAO and JOEL L. ZATZ ×

Received June 29, 1978, from the *College of Pharmacy, Rutgers—the State University of New Jersey, Piscataway, NJ 08854.* Accepted for publication September 22, 1978.

Abstract □ Advancing contact angles measured on compacts of several drugs by the sessile drop method and also by penetration through a column of drug granules were used to find the critical surface tension of the drugs. After liquid was delivered at a very slow rate, the contact angle of sessile drops decreased with time, but use of a consistent method of timing always led to the same value for critical surface tension. Results from penetration studies and work on compacts were in agreement, provided that the surfaces of the compacts were smooth and highly reflective. Critical surface tension of the six drugs, three analgesics and three sulfonamides, ranged from 31 to 33 dynes/cm. The critical surface tension of mixtures of phenacetin and microcrystalline cellulose was not a linear function of the relative surface fractions of the two materials. If the surface contained 25% or more of phenacetin, the critical surface tension barely differed from that of pure phenacetin.

Keyphrases □ Surface tensions, critical—various pharmaceutical solids analysis, by sessile drop method □ Surfactants, nonionic—used to determine surface tensions of various pharmaceutical solids □ Solids—surface tensions □ Contact angles—wetting of pharmaceutical solids

Wetting of a solid by a liquid is an important step in several pharmaceutical processes including the preparation of suspensions (1) and the adhesion of film coatings to tablets (2). The dissolution rate of powdered phenacetin was sensitive to the surface tension of the dissolution medium because of differences in wetting (3).

As described previously (4), the critical surface tension, γ_c, of a solid is a measure of its wettability and is related

0022-3549/79/0400-0488$01.00/0

© 1979, American Pharmaceutical Association

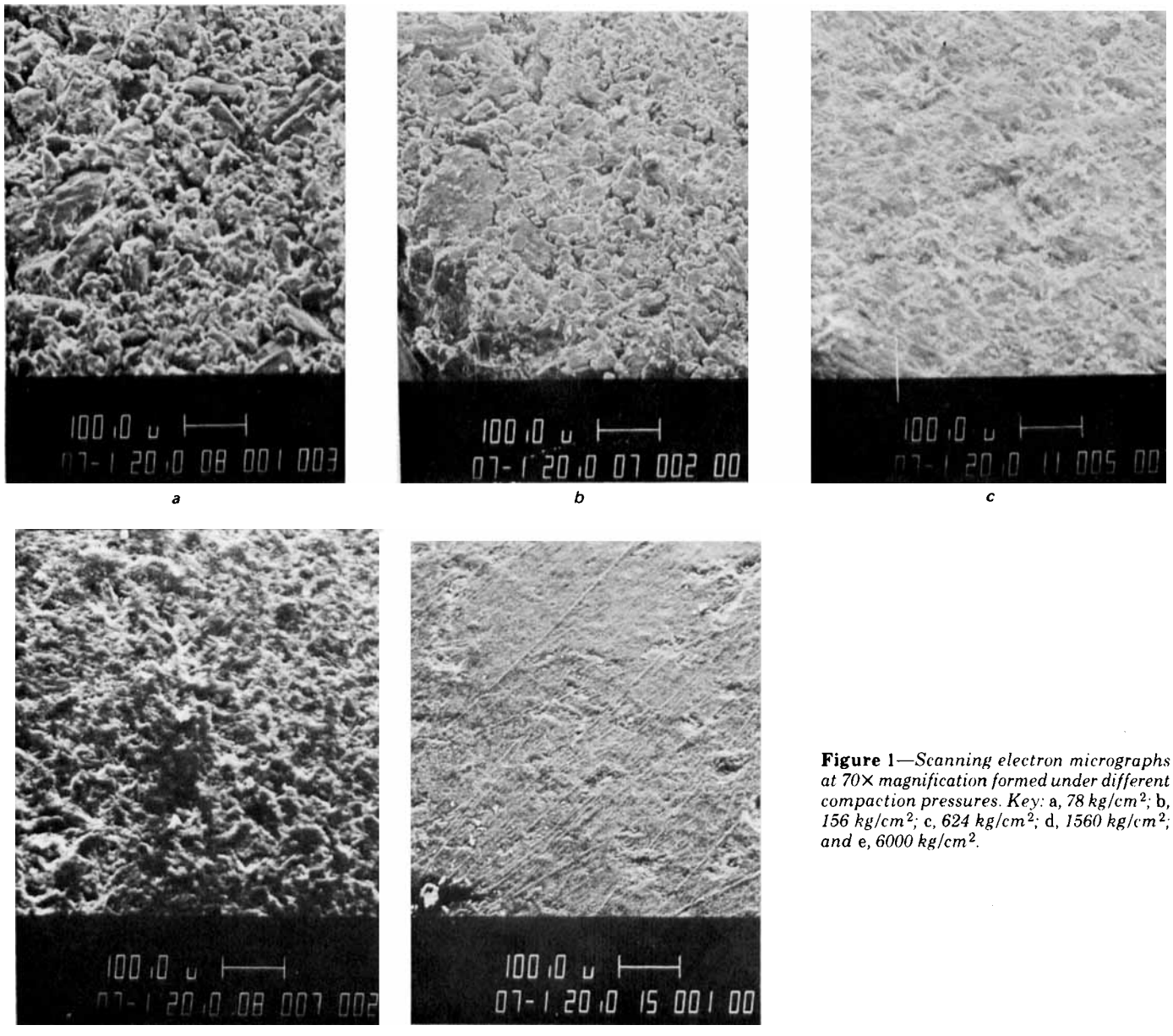

a b c d e

Figure 1—*Scanning electron micrographs at 70× magnification formed under different compaction pressures. Key:* a, *78 kg/cm²*; b, *156 kg/cm²*; c, *624 kg/cm²*; d, *1560 kg/cm²*; *and* e, *6000 kg/cm²*.

to solid surface energy (5–7). If nonpolar liquids are used for the contact angle measurements, γ_c is equal to the dispersion force component of the surface energy of the solid (6). While much work has been done on polymeric solids, comparatively few studies have been concerned with low molecular weight materials (8). Other studies dealt with keratin and skin (9–11).

BACKGROUND

The critical surface tension of aspirin and effects of adjuvants were studied using methanol–water and 1-butanol–formamide solutions to measure the contact angles (12). Contact angles of water and methylene iodide were determined on the surfaces of a number of substances (13). In experiments of this type, contact angles, θ, are used to gain an understanding of the forces acting at the interfaces. The known properties of the liquids are used as tools to explore the nature of the solid surface.

Various approaches have been used to measure contact angles on powdered pharmaceutical solids. Direct angle measurement with a goniometer was used after compression of the powder to obtain a smooth surface (13). The maximum height of a liquid drop on a compact of powder saturated with that liquid was measured (14). Contact angles were also determined from the penetration rate of liquids through the solid material (15–17).

With the sessile drop technique, smooth surfaces yield the most reliable measurements. Surface roughness causes deviation of the measured contact angle from its true value and increases the difference in magnitude between advancing and receding angles (18). Dissolution of the solid can lead to changes in the physical characteristics of the surface and also in the surface tension of the liquid. Both effects lead to biased contact angles. Penetration of the liquid into the solid can cause difficulties as well.

The choice of a suitable series of liquids may also present difficulties. The liquids should exhibit poor solvent power for the solid and a broad range of surface tension values. Previous work in this laboratory showed that homologous nonionic surfactants have suitable properties for contact angle work (4). Each surfactant is used to prepare a single solution well above its critical micelle concentration. In this way, the liquid surface consists of an oriented layer of surfactant molecules, making the surface similar to that of a hydrocarbon. Experiments with polytef and paraffin (4) showed that this liquid series could be used to obtain reliable values of critical surface tension.

In this study, critical surface tensions of several pharmaceutical solids were obtained using the nonionic surfactant series described. The poor solubility of hydrophobic drugs in these surfactant solutions minimizes problems due to dissolution during contact angle measurement. The

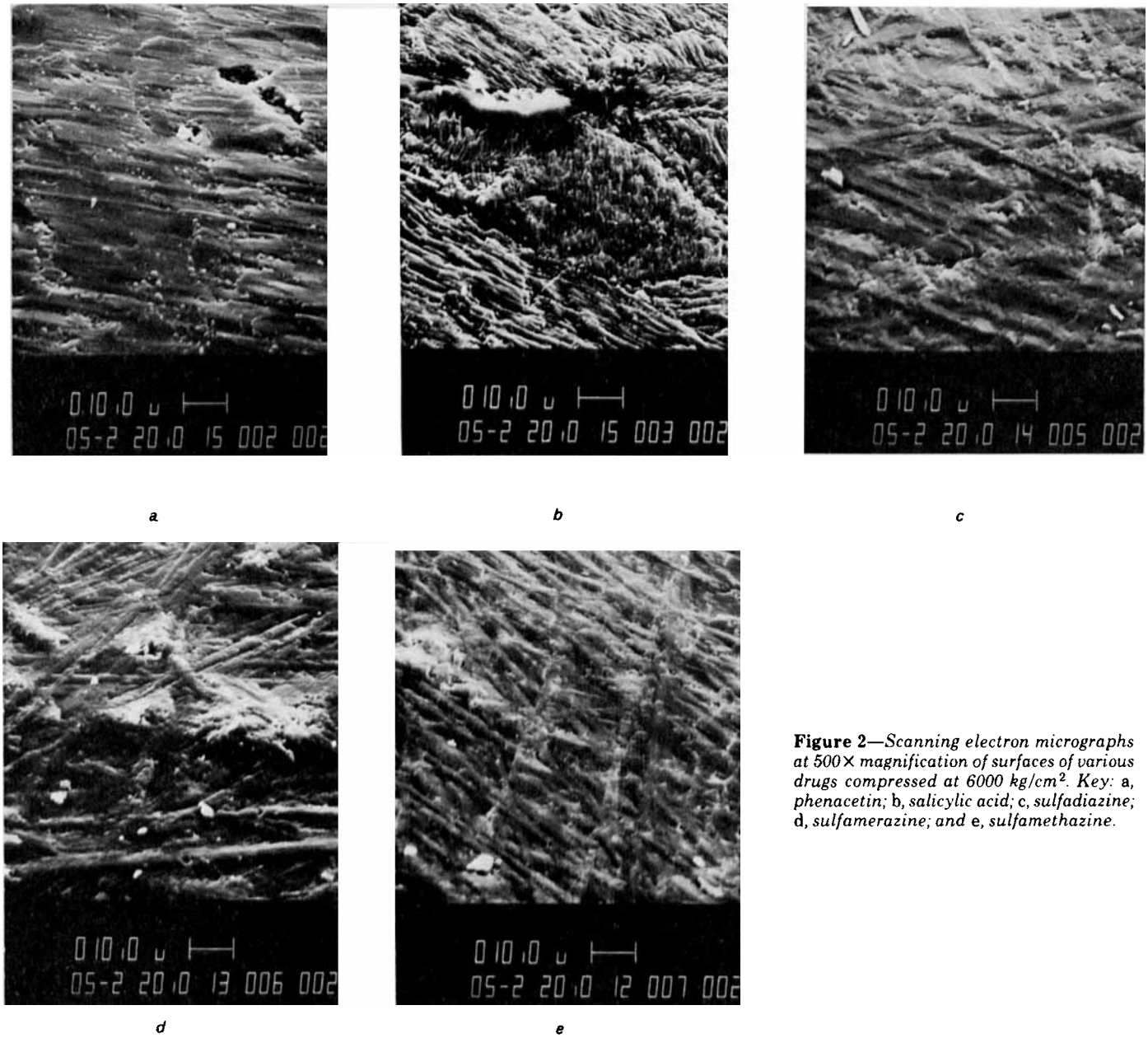

Figure 2—*Scanning electron micrographs at 500× magnification of surfaces of various drugs compressed at 6000 kg/cm². Key:* a, *phenacetin;* b, *salicylic acid;* c, *sulfadiazine;* d, *sulfamerazine; and* e, *sulfamethazine.*

sessile drop method and a penetration rate method were compared. The effects of surface heterogeneity in mixtures of phenacetin and microcrystalline cellulose on contact angles and critical surface tensions were also evaluated.

EXPERIMENTAL

Materials—Aspirin[1], phenacetin[1], salicylic acid[2], sulfadiazine[3], sulfamerazine[3], sulfamethazine[3], and microcrystalline cellulose[4] were the solid drugs studied. The nonionic polyoxyethylene octylphenol series tested previously (4) was used because of its numerous members with adequate water solubility and the relatively wide range of surface tension encompassed. Water was double distilled in an all-glass still. Other materials were reagent or USP grade.

Particle Size—The average particle size of the drugs was determined with a subsieve analyzer[5].

Preparation of Compacts—The solid material was loaded into a 1.27-cm die. A stainless steel block covered with aluminum foil previously cleaned with acetone was used to support the die. The lower punch was not used. Pressure was exerted by a manual press[6] through the upper punch to form the compact. Surfaces of representative compacts were examined by scanning electron microscopy. The specimens were mounted, coated with gold using a sputter coater, and scanned at 45° tilt under an accelerating voltage of 20 kv. Images were recorded on black and white film.

The effect of compaction pressure on the appearance of aspirin surfaces is shown in Fig. 1. Surface irregularities became fainter as the compaction pressure was raised. A standard value of 6000 kg/cm² was chosen, and all contact angle measurements by the sessile drop method were conducted on compacts formed at this pressure. Photomicrographs of other drug surfaces produced at this pressure are shown in Fig. 2.

All surfaces were judged by eye to be sufficiently smooth and reflective except salicylic acid, which exhibited channels. Compacts with smooth, shiny surfaces were used for contact angle measurement. For this purpose, the compacts were formed and retained in the die. Only the smooth lower surface was used.

Preparation of Solids for Penetration Study—Preliminary work showed that the use of powdered drug was unsatisfactory for penetration rate experiments. Anomalous results were obtained and were attributed to clogging of the frit by tiny particles. Consequently, granules were used in the experiments reported here.

The drugs studied by the penetration method, aspirin, phenacetin, and

[1] USP powder, Merck & Co., Rahway, N.J.
[2] Reagent powder, J. T. Baker Chemical Co., Phillipsburg, N.J.
[3] USP powder, American Cyanamid Co., Pearl River, N.Y.
[4] Avicel Ph-102, Fisher Scientific Co., Pittsburgh, Pa.
[5] Fisher Scientific Co., Pittsburgh, Pa.

[6] Model 341-20, Loomis Co., Caldwell, N.J.

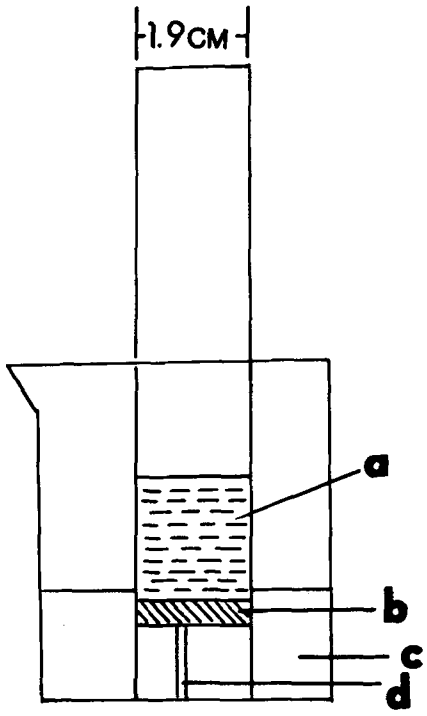

Figure 3—*Apparatus for penetration studies. Key:* a, *packed column in tube;* b, *glass frit;* c, *penetrating liquid; and* d, *slit in tube.*

salicylic acid, were granulated by adding 40 ml of acetone to 400 g of drug powder. Wet granules, obtained by extrusion through a 30-mesh sieve, were collected and dried in an oven for 1 hr with the ventilation air temperature at 26.7°. Dry granules that passed through a 20-mesh sieve but were retained on a 30-mesh sieve were collected and used.

Properties of Nonionic Surfactant Solutions—All of the polyoxyethylene octylphenols were used at 2.5×10^{-3} *M*. The surface tension of these solutions was reported (4). Solution viscosity was measured at 25° by a capillary viscometer[7]. Water was used as a standard. No kinetic energy correction was needed.

Contact Angle Measurements—For the sessile drop method, the instrumentation was the same as that previously employed (4). The total

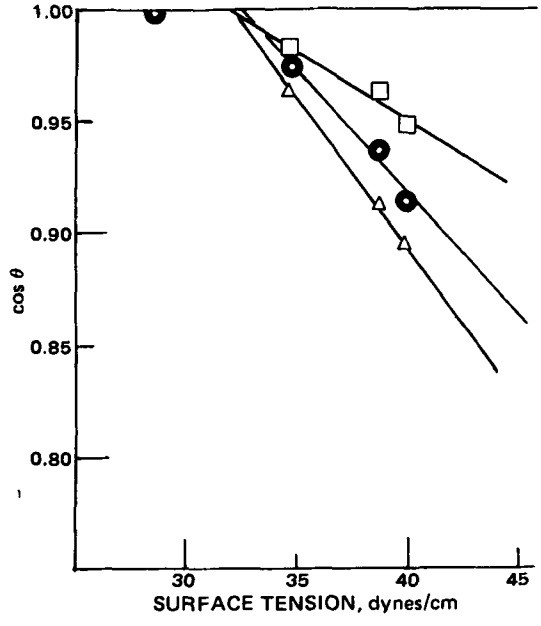

Figure 4—*Cosine of contact angle on sulfamerazine as a function of surface tension. Key:* △, *dynamic angle;* ○, *static angle; and* □, *angle after 5 min.*

[7] Cannon-Fenske.

Table I—Contact Angles of Polyoxyethylene Octylphenol Solutions on Sulfamerazine Compacts by the Sessile Drop Technique

Average Number of Oxyethylene Groups per Molecule	Surface Tension, dynes/cm	θ		
		Dynamic	Static	5 min
5	28.5	Spreads	Spreads	Spreads
9	30.0	Spreads	Spreads	Spreads
12.5	33.0	>10°	>10°	>10°
16	34.7	16°	13°	11°
30	38.8	24°	21°	16°
40	40.0	26°	24°	19°

volume of the drop was about 15 μl. The liquid was slowly placed on the surface (0.5–1.0 μl/sec), and the contact angle of the moving liquid boundary was measured directly. This measure is called the dynamic contact angle. Fifteen seconds following the final addition of liquid, a second measurement, the "static" contact angle (19), was made. A third measurement was made 5 min after the liquid application. Mean values of contact angle were calculated from at least three readings, each on a newly prepared solid surface. Values of θ were reproducible within ±3°.

The apparatus used for penetration rate measurements is shown in Fig. 3. A glass frit (with a pore size of 25–50 μm) was fused into the glass tube about 1.0 cm above the bottom. Two slits were cut in the glass from the frit to the bottom of the tube to permit liquid to reach the cylinder without trapping air bubbles. With aspirin, 2.40 g of the granules was loaded into the tube. The granules were packed to a constant height (1.7 cm) by dropping the tube 60 times from a height of 2.5 cm. Column preparation was the same for phenacetin and salicylic acid, except that 2.50 g of these materials was used.

A very small amount of amaranth was sprinkled on top of the packed column. The tube was then inserted into a 50-ml beaker containing 8.00 ml of the solution whose contact angle was to be measured, and the timer was started. Penetration of the liquid completely through the column caused the appearance of a red color at the center of the top of the column, and this color was used as the end-point. A single beaker was used for all experiments on a particular solid.

RESULTS AND DISCUSSION

The contact angles determined by direct observation on compacted powdered drugs depended on the time lapsed after application of the drop. Table I lists the various contact angles for sulfamarazine. Angles less than 10° were difficult to measure accurately and were not used in Zisman plots to determine critical surface tension.

The pattern seen in Table I was observed for all drugs. As observed previously (19), the dynamic angle was always the largest of the three

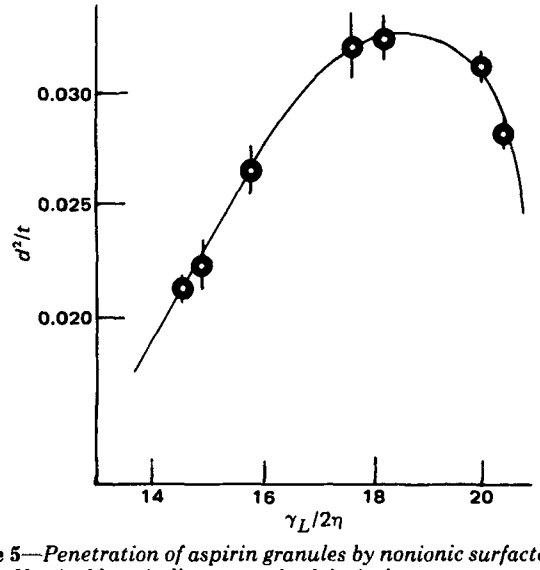

Figure 5—*Penetration of aspirin granules by nonionic surfactant solutions. Vertical bars indicate standard deviation.*

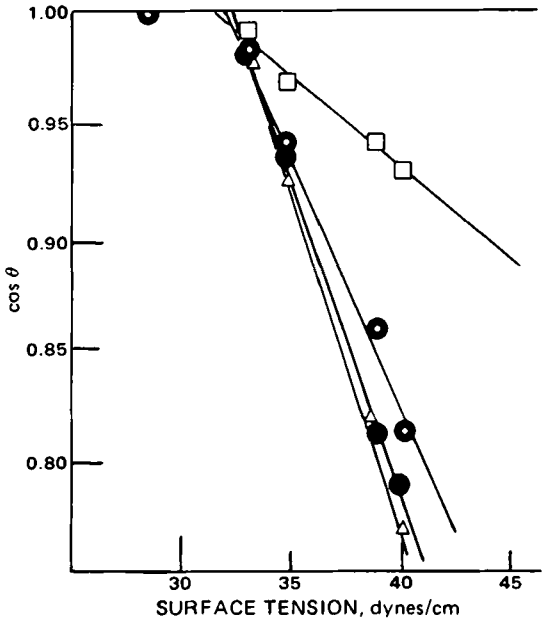

Figure 6—*Cosine of contact angle on aspirin as a function of liquid surface tension. Key: △, dynamic angle; ○, static angle; □, angle after 5 min; and ●, angle from penetration study.*

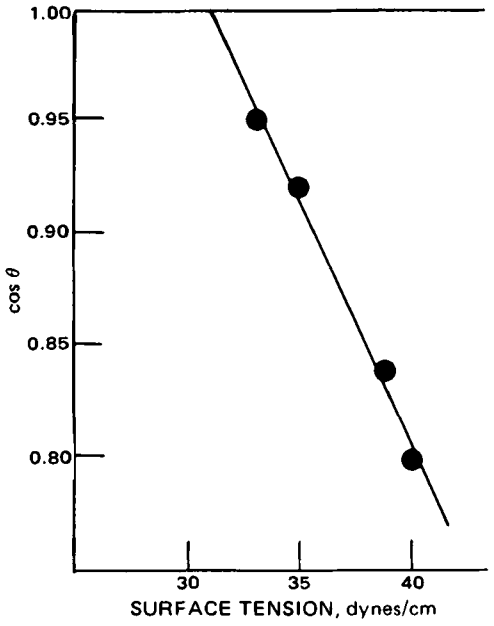

Figure 8—*Cosine of contact angle on salicylic acid as a function of liquid surface tension.*

measured values. The static angle, measured after 15 sec, was always somewhat smaller. The contact angle observed after 5 min was the smallest.

The dynamic angle is based on a measurement made at the edge of a moving liquid boundary in contact with a fresh surface. After addition of liquid has ceased, evaporation and, possibly, penetration cause a decrease in drop volume that leads to a lowering of the contact angle. Under these conditions, the contact angle approaches that of a receding drop (20).

In Fig. 4, $\cos\theta$ for sulfamerazine is plotted against liquid surface tension. The critical surface tension is the surface tension required for the liquid just to spread on the solid. It is found by extrapolation of the curves to a value of $\cos\theta = 1$. Extrapolation of each set of points leads to the same value of critical surface tension for sulfamerazine. This pattern was observed for all solids.

In the penetration studies, there was no evidence of collapse or cracking of the granule columns. The penetration data were analyzed by the Washburn equation (15–17):

$$\frac{d^2}{t} = \frac{\bar{r}\gamma_L \cos\theta}{2\eta} \qquad \text{(Eq. 1)}$$

where d is the distance traveled by the penetrating liquid, t is the time required, $\bar{r}$ is the average pore radius, and η is the viscosity. In these experiments, d was always the same for a particular solid and t was experimentally determined for each liquid.

A typical penetration plot is shown in Fig. 5. Curves with this shape are obtained when the range of liquid surface tensions encompasses both wetting and nonwetting liquids. For the wetting liquids, $\cos\theta = 1$. According to Eq. 1, d^2/t should decrease as γ_L is decreased. This decrease accounts for the shape of the left side of Fig. 5. In this region, a plot of d^2/t *versus* $\gamma_L/2\eta$ is linear and permits determination of $\bar{r}$ from the slope. This plot did not go through the origin as predicted from Eq. 1. Instead, a

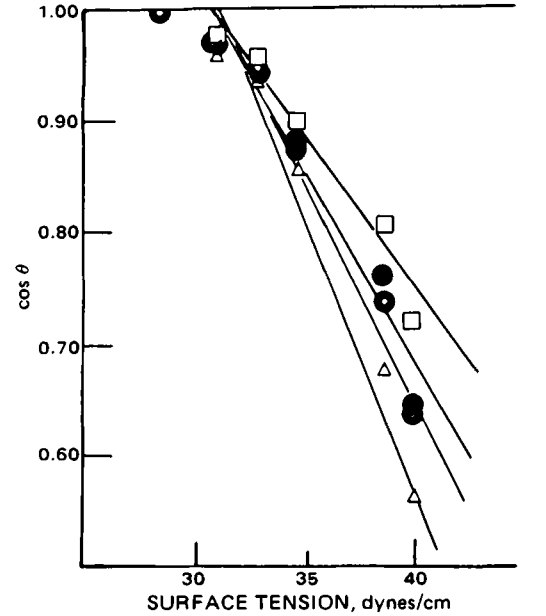

Figure 7—*Cosine of contact angle on phenacetin as a function of liquid surface tension. Key: △, dynamic angle; ○, static angle, □, angle after 5 min; and ●, angle from penetration study.*

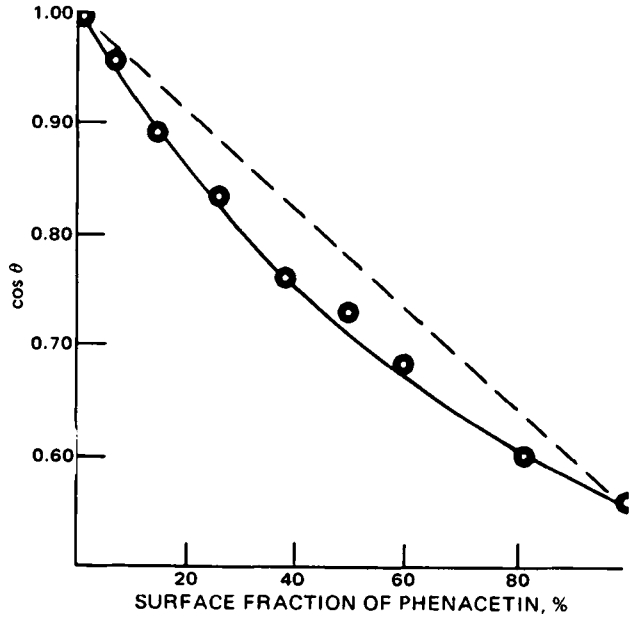

Figure 9—*Contact angles of polyoxyethylene (40) octylphenol solution on mixtures of phenacetin and microcrystalline cellulose. Points are experimental; the theoretical curve is from Eq. 5.*

Table II—Critical Surface Tension Values of Drugs

Substance	γ_c, dynes/cm
Sulfadiazine	33
Sulfamerazine	32
Sulfamethazine	31
Aspirin	32
Phenacetin	31
Salicylic acid	31

constant term, C, had to be added:

$$\frac{d^2}{t} = \frac{\bar{r}\gamma_L}{2\eta} + C \qquad \text{(Eq. 2)}$$

to correct for such effects as the resistance of the glass frit, the effect of the glass walls of the tube on the rate of liquid movement, and possible vapor adsorption on the unwetted granules (21). Equation 1 must be modified to yield:

$$\frac{d^2}{t} = \frac{\bar{r}\gamma_L \cos\theta}{2\eta} + C \qquad \text{(Eq. 3)}$$

Once $\bar{r}$ is known, cos θ for each nonwetting liquid can be calculated from Eq. 3.

Zisman plots were constructed using contact angles from penetration studies and sessile drop measurement. With aspirin (Fig. 6), contact angles determined from penetration data fell between values of the dynamic and static angles of sessile drops. They were within 2° of the dynamic angles. All four sets of values may be extrapolated to yield very nearly the same critical surface tension, 32 dynes/cm. A value of 31 dynes/cm was reported for aspirin (12).

For phenacetin (Fig. 7), the contact angles from penetration experiments were nearly identical to the static angle, differing from the dynamic angles by about 5°. Again, the same critical surface tension was obtained from all extrapolations. Results for salicylic acid are shown in Fig. 8. Contact angles were calculated from the penetration data. Contact angle measurements on these surfaces of compacts by the sessile drop method always yielded angles considerably lower than those from the penetration study. This result may be attributed to the effect of surface roughness of the salicylic acid compacts noted by scanning electron microscopy. When the true contact angle is less than 90°, surface roughness reduces the apparent contact angle (18). Therefore, the angles measured on the compacts were too low and were not used.

Of the two techniques studied, the sessile drop method is faster and less tedious. The penetration method may be applied when compacts with smooth surfaces cannot be obtained.

The values of critical surface tension of the six solid materials investigated are summarized in Table II. They were all rather close to each other, ranging from 31 to 33 dynes/cm. Zisman (18) stated that methylene and phenyl groups in the surface would lead to γ_c values of 31–35. It is possible that γ_c is controlled largely by the hydrophobic groups in the molecule.

The critical surface tension can serve as a useful empirical guide in the selection of a wetting agent in aqueous suspension formulation. Complete wetting will occur spontaneously if the particular agent in the concentration chosen is capable of lowering the surface tension of the medium to correspond to γ_c. Reduction of surface tension much below γ_c has no advantage as far as wetting is concerned. Although the γ_c values reported in Table II were obtained using solutions of a single surfactant family, they are expected to apply with little error to other surfactant systems, provided specific adsorption effects are absent.

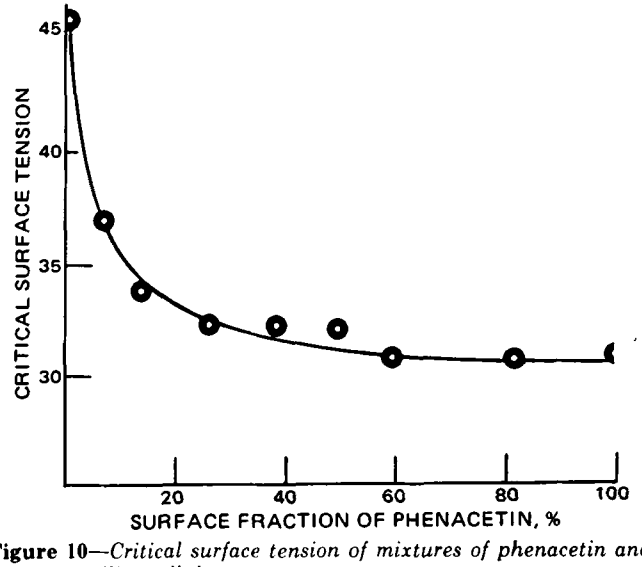

Figure 10—*Critical surface tension of mixtures of phenacetin and microcrystalline cellulose.*

A set of experiments was conducted on mixtures of microcrystalline cellulose and phenacetin. Microcrystalline cellulose was chosen because all surfactant solutions used as test liquids spread on this material. Phenacetin was chosen because, of the six drugs studied, the average particle size of phenacetin (12.0 μm) was closest to that of microcrystalline cellulose (9.7 μm). A series of mixtures of varying composition was prepared in 250-ml erlenmeyer flasks by extensive stirring with a glass rod. This mixing method was used to avoid comminution of the particles. Contact angle measurements by the sessile drop technique were complicated by the rapid penetration of liquid into the compact and disturbance of the surface geometry. Only the dynamic contact angle measurements are considered reliable.

The Cassie and Baxter equation (22) was employed to analyze the contact angles as a function of solid composition:

$$\cos\theta_{obs} = \sigma_P \cos\theta_P + \sigma_A \cos\theta_A \qquad \text{(Eq. 4)}$$

where σ_P and σ_A are the surface area fractions of phenacetin and microcrystalline cellulose, respectively; θ_P is the contact angle on pure phenacetin; θ_A is the contact angle on pure microcrystalline cellulose; and θ_{obs} is the contact angle on the mixture. Since $\sigma_P + \sigma_A = 1$ and cos $\theta_A = 1$ for all test liquids used, substitution in Eq. 4 and rearrangement yield:

$$\cos\theta_{obs} = 1 - \sigma_P(1 - \cos\theta_P) \qquad \text{(Eq. 5)}$$

In calculating area fractions for the mixtures, which were prepared on a weight/weight basis, it was assumed that the particles were spherical, that they were evenly distributed on the surface, and that the area fractions depended only on the relative particle numbers at the surface because the particle sizes were close. Equation 6 is the expression for σ_P:

$$\sigma_P = \frac{n_P 2\pi r_P^2}{n_P 2\pi r_P^2 + n_A 2\pi r_A^2} \qquad \text{(Eq. 6)}$$

where n_A and n_P are the surface particle numbers for microcrystalline cellulose and phenacetin, respectively; and r_A and r_P are the respective particle radii. The particle number, n, is defined by:

$$n = \frac{W}{\rho \frac{4}{3}\pi r^3} \qquad \text{(Eq. 7)}$$

where W is total weight and ρ is true particle density. Substituting Eq. 7 for n_A and n_P in Eq. 6 gives:

$$\sigma_P = \frac{W_P \rho_A r_A}{W_P \rho_A r_A + W_A \rho_P r_P} \qquad \text{(Eq. 8)}$$

Contact angles of polyoxyethylene (40) octylphenol on mixtures are shown in Fig. 9. Included is the curve based on the equation of Cassie and Baxter (22) (Eq. 5). Agreement is poor. Wetting of the solid mixture is apparently dominated by the nonwetting component and is not as good as that predicted by the equation. This result was typical and is similar to the pattern found in the wetting of aspirin–dicalcium phosphate dihydrate mixtures by water (14).

Critical surface tension is plotted against phenacetin surface fraction in Fig. 10. If the surface contained 25% or more of phenacetin, the critical surface tension barely differed from that of pure phenacetin. Wetting of the mixture is largely controlled by the component most resistant to wetting.

REFERENCES

(1) E. N. Hiestand, *J. Pharm. Sci.*, **53**, 1 (1964).

(2) J. A. Wood and S. W. Harder, *Can. J. Pharm. Sci.*, **5**, 18 (1970).

(3) P. Finholt and S. Solvang, *J. Pharm. Sci.*, **57**, 1968 (1968).

(4) W. Liao and J. L. Zatz, *ibid.*, **68**, 486 (1979).

(5) L. A. Girafalco and R. J. Good, *J. Phys. Chem.* **61**, 904 (1957).

(6) F. M. Fowkes, *ibid.*, **66**, 382 (1962).

(7) S. Wu, *J. Polym. Sci. Part C*, **34**, 19 (1971).

(8) S. Wu and K. J. Brozowski, *J. Colloid Interface Sci.*, **37**, 686 (1971).

(9) A. El-Shimi and E. D. Goddard, *ibid.*, **48**, 242 (1974).

(10) M. E. Ginn, C. M. Noyes, and E. Jungermann, *ibid.*, **26**, 146 (1968).
(11) A. Rosenberg, R. Williams, and G. Cohen, *J. Pharm. Sci.*, **62**, 920 (1973).
(12) S. W. Harder, D. A. Zuck, and J. A. Wood, *ibid.*, **59**, 1787 (1970).
(13) G. Zografi and S. S. Tam, *ibid.*, **65**, 1145 (1976).
(14) C. F. Lerk, A. J. M. Shoonen, and J. T. Fell, *ibid.*, **65**, 843 (1976).
(15) E. W. Washburn, *Phys. Rev.*, **1**, 273 (1921).
(16) H. G. Bruil and J. J. Aartsen, *Colloid Polym. Sci.*, **252**, 32 (1974).
(17) K. Miyasaka, T. Manabe, and M. Koishi, *Chem. Pharm. Bull.*, **24**, 330 (1976).
(18) W. A. Zisman, *Adv. Chem. Ser.*, **43**, 1 (1964).
(19) L. Carino, *Colloid Polym. Sci.*, **254**, 108 (1976).
(20) R. H. Ottewill and B. Vincent, *JCS Faraday I*, **68**, 1533 (1972).
(21) R. J. Good, *Chem. Ind.* (May 29, 1971).
(22) A. B. D. Cassie and S. Baxter, *Trans. Faraday Soc.*, **40**, 546 (1944).

Fluorometric Determination of Clobazam, a 1,5-Benzodiazepine, in Human Plasma

J. T. STEWART *, I. L. HONIGBERG *x, A. Y. TSAI *, and P. HAJDU ‡§

Received April 26, 1978, from the **Bioavailability Group Studies, School of Pharmacy, University of Georgia, Athens, GA 30602*, and ‡*Hoechst-Roussel Pharmaceuticals, Inc., Somerville, NJ 08876.* Accepted for publication September 25, 1978. §Present address: Pharma-Forschung, Hoechst, A.G., Frankfurt, West Germany.

Abstract □ A fluorometric procedure for clobazam, a 1,5-benzodiazepine, based on a fluorophore formed upon irradiation of the drug using short wavelength UV light (254 nm) for 35 min is presented. Fluorescence is linear over a 100–6400-ng/ml range using excitation and emission wavelengths of 350 and 400 nm, respectively. Application of the method to the determination of clobazam in spiked human plasma samples revealed that the drug can be determined at nanogram per milliliter levels with an accuracy of 1–5%. The procedure is specific for clobazam in samples containing its major plasma metabolite, *N*-desmethylclobazam, and also in samples containing 1,4-benzodiazepines and other selected drugs. A plasma level–time profile after oral administration of a single 40-mg dose of clobazam to a healthy adult male is also illustrated.

Keyphrases □ Clobazam—fluorometric determination in human plasma □ Benzodiazepines—fluorometric determination of clobazam in human plasma □ Tranquilizers—clobazam, fluorometric determination in human plasma □ Fluorometry—analysis, clobazam in human plasma

Clobazam (I) [7-chloro-1-methyl-5-phenyl-1*H*-1,5-benzodiazepine-2,4(3*H*,5*H*)-dione] is a new antianxiety agent currently under clinical investigation. It has demonstrated relatively low sedation potential (1, 2) and relatively limited effects on normal levels of human performance[1] (3, 4). An effective therapeutic dose of 20–40 mg/day has been suggested (4).

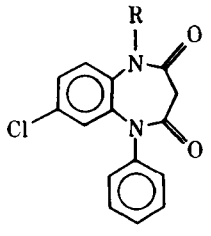

I: R = CH_3
II: R = H

[1] J. A. Kotzan, T. E. Needham, I. L. Honigberg, J. J. Vallner, J. T. Stewart, W. J. Brown, and H. W. Jun, presented at the APhA Academy of Pharmaceutical Sciences, Montreal meeting, May 1978.

Table I—Typical Calibration Data for Clobazam in Human Plasma

Initial Concentration, ng/ml	Fluorescence Intensity[a]	Slope	Intercept	$r \pm s_{y \cdot x}$ [b]
150	4.05 ± 0.07	0.0258	0.2525	0.9998 ± 0.0906
300	8.00 ± 0.01			
600	15.75 ± 0.21			

[a] Based on duplicate samples. [b] s is the standard error of estimate of y (fluorescence intensity) on x (concentration).

This paper presents a fluorometric procedure for the analysis of clobazam in human plasma. The method allows the determination of drug in the presence of *N*-desmethylclobazam (II), its major plasma metabolite, which has also been reported to possess psychosedative and anticonvulsant activities with low toxicity (5). The utilization of fluorescence offers nanogram per milliliter sensitivity along with suitable reproducibility and accuracy.

EXPERIMENTAL

Apparatus and Reagents—Fluorescence measurements were obtained using a spectrophotofluorometer[2] equipped with a corrected spectra accessory and operated in the true emission mode. Excitation and emission slits were set at 7 and 4 nm, respectively, and sample sensitivity for all measurements was set at 1.

Clobazam powder[3] was used for the preparation of a stock solution (1 μg/ml) in plasma. This solution was prepared by the addition of 0.25 ml of an ethanolic clobazam solution (200 μg/ml) to a 50-ml volumetric flask, followed by the addition of the blank human plasma[4] to volume. *N*-Desmethylclobazam, mp 305–307°, was synthesized according to the procedure of Rossi *et al.* (6). All other chemicals were the highest purity available from commercial sources and were utilized as received.

Determination of Calibration Curve—Quantities of 0.15, 0.30, and 0.60 ml of the clobazam stock solution in plasma were each placed in 15-ml ground-glass stoppered centrifuge tubes, followed by the addition of blank human plasma to make 1 ml. The solution was mixed[5] for 1 min.

[2] Model MPF-4, Perkin-Elmer, Norwalk, Conn.
[3] Hoechst-Roussel Pharmaceuticals, Somerville, NJ 08876.
[4] Obtained from a local hospital blood bank.
[5] Vortex-Genie mixer, Scientific Industries, Bohemia, N.Y.

0022-3549/79/0400-0494$01.00/0
© 1979, American Pharmaceutical Association

(10) M. E. Ginn, C. M. Noyes, and E. Jungermann, *ibid.*, **26**, 146 (1968).
(11) A. Rosenberg, R. Williams, and G. Cohen, *J. Pharm. Sci.*, **62**, 920 (1973).
(12) S. W. Harder, D. A. Zuck, and J. A. Wood, *ibid.*, **59**, 1787 (1970).
(13) G. Zografi and S. S. Tam, *ibid.*, **65**, 1145 (1976).
(14) C. F. Lerk, A. J. M. Shoonen, and J. T. Fell, *ibid.*, **65**, 843 (1976).
(15) E. W. Washburn, *Phys. Rev.*, **1**, 273 (1921).
(16) H. G. Bruil and J. J. Aartsen, *Colloid Polym. Sci.*, **252**, 32 (1974).
(17) K. Miyasaka, T. Manabe, and M. Koishi, *Chem. Pharm. Bull.*, **24**, 330 (1976).
(18) W. A. Zisman, *Adv. Chem. Ser.*, **43**, 1 (1964).
(19) L. Carino, *Colloid Polym. Sci.*, **254**, 108 (1976).
(20) R. H. Ottewill and B. Vincent, *JCS Faraday I*, **68**, 1533 (1972).
(21) R. J. Good, *Chem. Ind.* (May 29, 1971).
(22) A. B. D. Cassie and S. Baxter, *Trans. Faraday Soc.*, **40**, 546 (1944).

Fluorometric Determination of Clobazam, a 1,5-Benzodiazepine, in Human Plasma

J. T. STEWART *, I. L. HONIGBERG *x, A. Y. TSAI *, and P. HAJDU ‡§

Received April 26, 1978, from the **Bioavailability Group Studies, School of Pharmacy, University of Georgia, Athens, GA 30602*, and ‡*Hoechst-Roussel Pharmaceuticals, Inc., Somerville, NJ 08876.* Accepted for publication September 25, 1978. §Present address: Pharma-Forschung, Hoechst, A.G., Frankfurt, West Germany.

Abstract □ A fluorometric procedure for clobazam, a 1,5-benzodiazepine, based on a fluorophore formed upon irradiation of the drug using short wavelength UV light (254 nm) for 35 min is presented. Fluorescence is linear over a 100–6400-ng/ml range using excitation and emission wavelengths of 350 and 400 nm, respectively. Application of the method to the determination of clobazam in spiked human plasma samples revealed that the drug can be determined at nanogram per milliliter levels with an accuracy of 1–5%. The procedure is specific for clobazam in samples containing its major plasma metabolite, *N*-desmethylclobazam, and also in samples containing 1,4-benzodiazepines and other selected drugs. A plasma level–time profile after oral administration of a single 40-mg dose of clobazam to a healthy adult male is also illustrated.

Keyphrases □ Clobazam—fluorometric determination in human plasma □ Benzodiazepines—fluorometric determination of clobazam in human plasma □ Tranquilizers—clobazam, fluorometric determination in human plasma □ Fluorometry—analysis, clobazam in human plasma

Clobazam (I) [7-chloro-1-methyl-5-phenyl-1*H*-1,5-benzodiazepine-2,4(3*H*,5*H*)-dione] is a new antianxiety agent currently under clinical investigation. It has demonstrated relatively low sedation potential (1, 2) and relatively limited effects on normal levels of human performance[1] (3, 4). An effective therapeutic dose of 20–40 mg/day has been suggested (4).

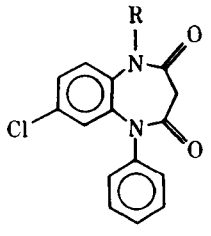

I: R = CH_3
II: R = H

[1] J. A. Kotzan, T. E. Needham, I. L. Honigberg, J. J. Vallner, J. T. Stewart, W. J. Brown, and H. W. Jun, presented at the APhA Academy of Pharmaceutical Sciences, Montreal meeting, May 1978.

Table I—Typical Calibration Data for Clobazam in Human Plasma

Initial Concentration, ng/ml	Fluorescence Intensity[a]	Slope	Intercept	$r \pm s_{y \cdot x}$ [b]
150	4.05 ± 0.07	0.0258	0.2525	0.9998 ± 0.0906
300	8.00 ± 0.01			
600	15.75 ± 0.21			

[a] Based on duplicate samples. [b] s is the standard error of estimate of y (fluorescence intensity) on x (concentration).

This paper presents a fluorometric procedure for the analysis of clobazam in human plasma. The method allows the determination of drug in the presence of *N*-desmethylclobazam (II), its major plasma metabolite, which has also been reported to possess psychosedative and anticonvulsant activities with low toxicity (5). The utilization of fluorescence offers nanogram per milliliter sensitivity along with suitable reproducibility and accuracy.

EXPERIMENTAL

Apparatus and Reagents—Fluorescence measurements were obtained using a spectrophotofluorometer[2] equipped with a corrected spectra accessory and operated in the true emission mode. Excitation and emission slits were set at 7 and 4 nm, respectively, and sample sensitivity for all measurements was set at 1.

Clobazam powder[3] was used for the preparation of a stock solution (1 μg/ml) in plasma. This solution was prepared by the addition of 0.25 ml of an ethanolic clobazam solution (200 μg/ml) to a 50-ml volumetric flask, followed by the addition of the blank human plasma[4] to volume. *N*-Desmethylclobazam, mp 305–307°, was synthesized according to the procedure of Rossi *et al.* (6). All other chemicals were the highest purity available from commercial sources and were utilized as received.

Determination of Calibration Curve—Quantities of 0.15, 0.30, and 0.60 ml of the clobazam stock solution in plasma were each placed in 15-ml ground-glass stoppered centrifuge tubes, followed by the addition of blank human plasma to make 1 ml. The solution was mixed[5] for 1 min.

[2] Model MPF-4, Perkin-Elmer, Norwalk, Conn.
[3] Hoechst-Roussel Pharmaceuticals, Somerville, NJ 08876.
[4] Obtained from a local hospital blood bank.
[5] Vortex-Genie mixer, Scientific Industries, Bohemia, N.Y.

0022-3549/79/0400-0494$01.00/0
© 1979, American Pharmaceutical Association

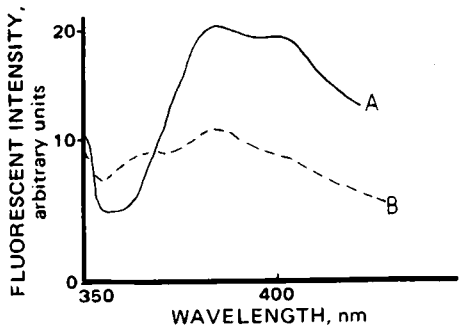

Figure 1—*True emission spectra of clobazam in ethanol before (- -B) and after (—A) irradiation (254 nm) for 35 min. Excitation wavelength was 350 nm.*

Hexane (5 ml) was then added, and the two phases were mixed[5] for an additional 30 sec. After centrifugation for 1 min at 4000 rpm, 4 ml of the hexane phase was transferred to a clean 15-ml centrifuge tube and evaporated to dryness in a water bath (80 ± 1°) using a nitrogen stream.

The residue was then redissolved in 1 ml of ethanol, and a portion of the solution was transferred to a 0.5-ml quartz microcell[6] (pathlength of 5 mm). A fluorometric measurement was obtained using excitation and emission wavelengths of 350 and 400 nm, respectively. The solution was then evenly irradiated at close proximity to the microcell with two short wavelength UV lamps[7] for 35 min, followed by fluorescence measurement at the same excitation and emission wavelengths (E_2).

The final fluorescence value (E) was calculated from $E = E_2 - E_1$. The three concentrations of clobazam used in the calibration curves were then subjected to linear regression analysis; the slope, intercept, and regression coefficient were calculated as shown in Table I.

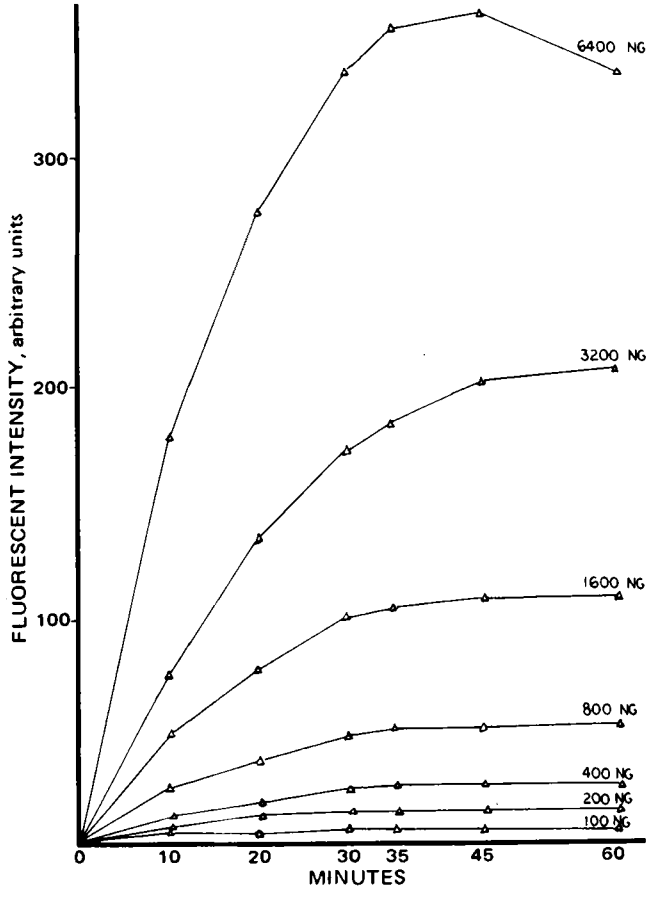

Figure 2—*Plot of fluorescent intensity of clobazam at various concentrations in ethanol after irradiation (254 nm) of the ethanolic solutions for different time periods.*

[6] Part 018-0056, Hitachi Ltd., Tokyo, Japan.
[7] Model UVS-11, Ultraviolet Products, San Gabriel, Calif.

Determination of Clobazam in Human Plasma—A 1.0-ml sample of human plasma containing clobazam was placed in a 15-ml ground-glass stoppered centrifuge tube and treated in the same manner as described under *Determination of Calibration Curve*, starting with: "Hexane (5 ml) was added . . . ." A calibration curve was run concurrently. Slope and intercept data obtained from the regression analysis of the blank and standard plasma samples were utilized to solve for drug concentration in the plasma samples: [fluorescence intensity = (slope × concentration) + intercept][8].

RESULTS AND DISCUSSION

Interest in the development of a procedure to measure therapeutic plasma clobazam levels for a bioavailability study led to the use of fluorescence. The fluorometric procedure for clobazam reported here is based on a fluorophore, formed when an ethanolic solution of the drug is irradiated with short wavelength UV light (254 nm) (7). Examination of corrected emission spectra before and after irradiation (Fig. 1) revealed that the irradiated solution was more fluorescent than the nonirradiated solution at emission wavelengths greater than 370 nm, with maximum intensity occurring around 400 nm. Use of this wavelength in the true emission mode of the spectrophotofluorometer required an excitation wavelength of 350 nm.

A study of fluorescence intensity *versus* irradiation time for varying concentrations of clobazam (Fig. 2) revealed that a 35-min irradiation time was satisfactory for the assay procedure, especially for the anticipated plasma drug levels (100–1000 ng/ml) after a single 20–40-mg dose (4, 8). Drug concentrations in the range of 1000–6400 ng/ml (Fig. 2) would require slightly longer irradiation times to reach the plateau region of the irradiation curve. However, with the 35-min irradiation time, fluorescence was linear over the 100–6400-ng/ml concentration range of clobazam with $r = 0.9995$. The minimum detection limit for the drug is 50 ng/ml (signal/noise = 2) using the calibration curve from a series of spiked plasma samples.

Studies to determine the nature of the fluorophore formed upon drug irradiation are underway. The desmethyl metabolite forms a fluorophore with a similar emission spectrum under the conditions used for clobazam.

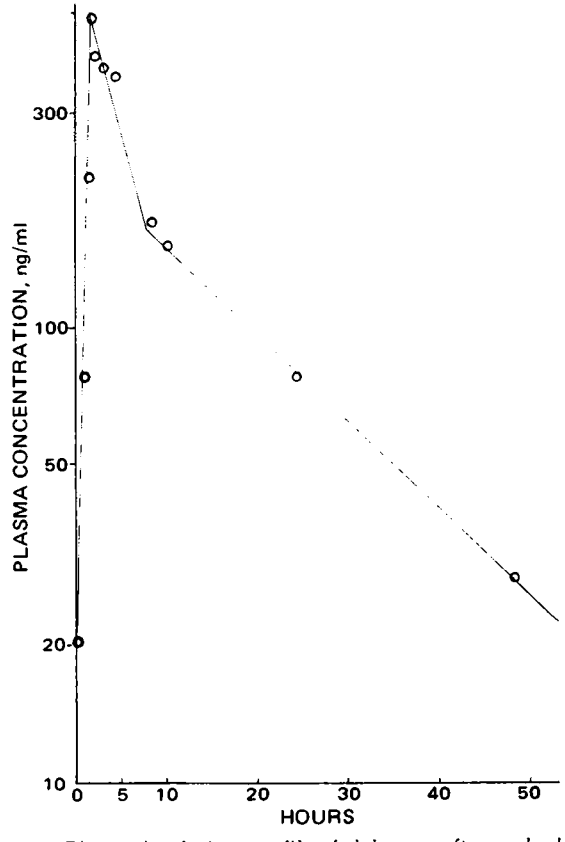

Figure 3—*Plasma level–time profile of clobazam after oral administration of a 40-mg dose to a healthy adult male.*

[8] Olivetti-Underwood programma 101.

Table II—Analysis of Spiked Plasma Samples for Clobazam

Mixture	Concentration Added, ng/ml	Concentration Found[a], ng/ml	Accuracy, %
1 Clobazam	200	196.90 ± 2.30	1.55
2 Clobazam	400	409.75 ± 15.00	2.44
3 Clobazam	600	608.00 ± 28.00	1.33
4 Clobazam	1200	1211.75 ± 29.81	0.98
5 Clobazam	300	285.45 ± 6.43	4.85
N-Desmethylclobazam	300		
6 Clobazam	600	604.00 ± 23.00	0.67
N-Desmethylclobazam	600		
7 Clobazam	400	389.30 ± 2.20	2.68
Diazepam[b]	400		
8 Clobazam	400	373.35 ± 11.35	6.66
Chlordiazepoxide hydrochloride[c]	400		
9 Clobazam	400	368.85 ± 6.85	7.79
Oxazepam[d]	400		
10 Clobazam	400	398.00 ± 29.00	0.50
Clidinium bromide[e]	400		
11 Clobazam	400	376.00 ± 20.00	6.00
Aspirin	400		

[a] Based on duplicate samples. [b] Valium, Hoffmann-La Roche, Nutley, N.J. [c] Librium, Hoffmann-La Roche, Nutley, N.J. [d] Serax, Wyeth Laboratories, Radnor, Pa. [e] Quarzan, Hoffmann-La Roche, Nutley, N.J.

The other known metabolites of clobazam, in which hydroxy and hydroxy and methoxy substituents are present on the drug molecule, have not been shown in these laboratories to form fluorophores and should not interfere with the analysis of clobazam.

Initial extractions of clobazam from spiked plasma samples were performed using ether (9) (percent extraction = 85.58 ± 7.59%). Analysis of a 1-ml plasma sample spiked with 400 ng each of clobazam and *N*-desmethylclobazam with ether as the extraction solvent indicated that the clobazam concentration was 608.95 ± 19.05 ng/ml (n = 2). Assay of a plasma sample containing only the metabolite (400 ng/ml) gave 215.40 ± 0.40 ng/ml (n = 2), expressed as clobazam concentration. These data establish that the fluorophore formed from the desmethyl metabolite interferes with the clobazam analysis because of concurrent extraction of drug and metabolite from the plasma sample. Thus, partitioning studies were performed to find an organic solvent that would selectively extract clobazam from the desmethyl compound.

Chloroform, benzene, hexane, cyclohexane, petroleum ether, heptane, carbon tetrachloride, methylene chloride, and ethyl acetate were investigated. Hexane provided the best selectivity for the extraction of clobazam over that of the *N*-desmethyl metabolite at equimolar concentrations. The percent extraction of clobazam from plasma with hexane was 51.27 ± 2.00%.

Application of the fluorometric assay to the determination of spiked plasma samples containing clobazam and to plasma samples containing mixtures of clobazam and *N*-desmethylclobazam, some 1,4-benzodiazepines, or other drugs is presented in Table II. Determination of clobazam in these samples was achieved with accuracy in the range of 0.50–7.8%.

Figure 3 shows a plasma level–time profile after oral administration of a single 40-mg dose of clobazam to a healthy adult male. The data, obtained by using the described fluorometric procedure, indicate that the method should be applicable to studies where plasma levels of the intact drug are desired.

REFERENCES

(1) A. C. Parrot and I. Hindmarch, *IRCS Med. Sci. Clin. Pharmacol. Ther.*, **3**, 177 (1975).

(2) R. G. Borland and A. N. Nicholson, *Br. J. Clin. Pharmacol.*, **2**, 215 (1975).

(3) P. A. Berry, R. Burtles, D. Grubb, and M. V. Hoare, *ibid.*, **1**, 346 (1974).

(4) Clinical Investigator Literature, Hoechst-Roussel Pharmaceuticals, Somerville, N.J., May 1973.

(5) S. Fielding and I. Hoffman, *Br. J. Clin. Pharmacol.*, in press.

(6) S. Rossi, O. Pinola, and R. Maggi, *Chim. Ind.*, **51**, 479 (1969).

(7) P. Hajdu and D. Damm, *Arzneim.-Forsch.*, **26**, 2141 (1976).

(8) J. J. Vallner, T. E. Needham, I. L. Honigberg, J. T. Stewart, W. J. Brown, J. A. Kotzan, and H. W. Jun, *J. Clin. Pharmacol.*, **18**, 319 (1978).

(9) P. Hajdu, M. Uihlein, and D. Damm, *Arzneim.-Forsch.*, in press.

ACKNOWLEDGMENTS

Presented in part at the Pharmaceutical Analysis and Control Section, APhA Academy of Pharmaceutical Sciences, Phoenix meeting, November 1977.

Effect of *N*-Trifluoroacetyl Derivatives of Amino Acids and Amino Acid Analogs on Microbial Antitumor Screen

THEODORE T. OTANI ˣ and MARY R. BRILEY

Received August 11, 1978, from the *Laboratory of Pathophysiology, National Cancer Institute, Bethesda, MD 20014.* Accepted for publication September 28, 1978.

Abstract □ Eighteen trifluoroacetyl derivatives of amino acids and of amino acid analogs were prepared and tested for growth-inhibitory activity using a *Lactobacillus casei* system as a prescreen for antitumor activity. Of the compounds tested, the trifluoroacetyl derivatives of *o*-, *m*-, and *p*-fluorophenylalanine and of β-3-thienylalanine showed modest activity; trifluoroacetyl derivatives of phenylalanine and of β-2-thienylalanine showed marginal activity. The activity exhibited by the active trifluoroacetyl compounds was equal to that noted for most active chloroacetyl derivatives reported previously, as judged by comparison of their activity with that of chloroacetyl-*m*-fluorophenylalanine. No reversal of inhibition was noted when a representative of these inhibitors was challenged with a corresponding natural metabolite, both as a free amino acid and as a noninhibitory acylated compound.

Keyphrases □ Amino acids and analogs—*N*-trifluoroacetyl derivatives, effect on microbial antitumor screen □ Antitumor activity—18 trifluoroacetyl derivatives of amino acids and amino acid analogs, growth inhibitory activity using *Lactobacillus casei* system

An alteration in the biological behavior of certain amino acids, both the naturally occurring and the "unnatural," as measured by growth-inhibitory capacity in a microbial system, was noted upon acylation (1–3). The extent of such activity varied with the nature of the acyl group and the amino acid moiety (3). While *N*-acetyl and *N*-propionyl derivatives of these amino acids showed no appreciable growth-inhibitory activity, the *N*-chloroacetyl derivatives showed modest activity (3), particularly with those amino acids that are normally considered to be essential for

0022-3549/79/0400-0496$01.00/0

© 1979, American Pharmaceutical Association

Table II—Analysis of Spiked Plasma Samples for Clobazam

Mixture	Concentration Added, ng/ml	Concentration Found[a], ng/ml	Accuracy, %
1 Clobazam	200	196.90 ± 2.30	1.55
2 Clobazam	400	409.75 ± 15.00	2.44
3 Clobazam	600	608.00 ± 28.00	1.33
4 Clobazam	1200	1211.75 ± 29.81	0.98
5 Clobazam	300	285.45 ± 6.43	4.85
N-Desmethylclobazam	300		
6 Clobazam	600	604.00 ± 23.00	0.67
N-Desmethylclobazam	600		
7 Clobazam	400	389.30 ± 2.20	2.68
Diazepam[b]	400		
8 Clobazam	400	373.35 ± 11.35	6.66
Chlordiazepoxide hydrochloride[c]	400		
9 Clobazam	400	368.85 ± 6.85	7.79
Oxazepam[d]	400		
10 Clobazam	400	398.00 ± 29.00	0.50
Clidinium bromide[e]	400		
11 Clobazam	400	376.00 ± 20.00	6.00
Aspirin	400		

[a] Based on duplicate samples. [b] Valium, Hoffmann-La Roche, Nutley, N.J. [c] Librium, Hoffmann-La Roche, Nutley, N.J. [d] Serax, Wyeth Laboratories, Radnor, Pa. [e] Quarzan, Hoffmann-La Roche, Nutley, N.J.

The other known metabolites of clobazam, in which hydroxy and hydroxy and methoxy substituents are present on the drug molecule, have not been shown in these laboratories to form fluorophores and should not interfere with the analysis of clobazam.

Initial extractions of clobazam from spiked plasma samples were performed using ether (9) (percent extraction = 85.58 ± 7.59%). Analysis of a 1-ml plasma sample spiked with 400 ng each of clobazam and *N*-desmethylclobazam with ether as the extraction solvent indicated that the clobazam concentration was 608.95 ± 19.05 ng/ml (n = 2). Assay of a plasma sample containing only the metabolite (400 ng/ml) gave 215.40 ± 0.40 ng/ml (n = 2), expressed as clobazam concentration. These data establish that the fluorophore formed from the desmethyl metabolite interferes with the clobazam analysis because of concurrent extraction of drug and metabolite from the plasma sample. Thus, partitioning studies were performed to find an organic solvent that would selectively extract clobazam from the desmethyl compound.

Chloroform, benzene, hexane, cyclohexane, petroleum ether, heptane, carbon tetrachloride, methylene chloride, and ethyl acetate were investigated. Hexane provided the best selectivity for the extraction of clobazam over that of the *N*-desmethyl metabolite at equimolar concentrations. The percent extraction of clobazam from plasma with hexane was 51.27 ± 2.00%.

Application of the fluorometric assay to the determination of spiked plasma samples containing clobazam and to plasma samples containing mixtures of clobazam and *N*-desmethylclobazam, some 1,4-benzodiazepines, or other drugs is presented in Table II. Determination of clobazam in these samples was achieved with accuracy in the range of 0.50–7.8%.

Figure 3 shows a plasma level–time profile after oral administration of a single 40-mg dose of clobazam to a healthy adult male. The data, obtained by using the described fluorometric procedure, indicate that the method should be applicable to studies where plasma levels of the intact drug are desired.

REFERENCES

(1) A. C. Parrot and I. Hindmarch, *IRCS Med. Sci. Clin. Pharmacol. Ther.*, **3**, 177 (1975).

(2) R. G. Borland and A. N. Nicholson, *Br. J. Clin. Pharmacol.*, **2**, 215 (1975).

(3) P. A. Berry, R. Burtles, D. Grubb, and M. V. Hoare, *ibid.*, **1**, 346 (1974).

(4) Clinical Investigator Literature, Hoechst-Roussel Pharmaceuticals, Somerville, N.J., May 1973.

(5) S. Fielding and I. Hoffman, *Br. J. Clin. Pharmacol.*, in press.

(6) S. Rossi, O. Pinola, and R. Maggi, *Chim. Ind.*, **51**, 479 (1969).

(7) P. Hajdu and D. Damm, *Arzneim.-Forsch.*, **26**, 2141 (1976).

(8) J. J. Vallner, T. E. Needham, I. L. Honigberg, J. T. Stewart, W. J. Brown, J. A. Kotzan, and H. W. Jun, *J. Clin. Pharmacol.*, **18**, 319 (1978).

(9) P. Hajdu, M. Uihlein, and D. Damm, *Arzneim.-Forsch.*, in press.

ACKNOWLEDGMENTS

Presented in part at the Pharmaceutical Analysis and Control Section, APhA Academy of Pharmaceutical Sciences, Phoenix meeting, November 1977.

Effect of *N*-Trifluoroacetyl Derivatives of Amino Acids and Amino Acid Analogs on Microbial Antitumor Screen

THEODORE T. OTANI ˣ and MARY R. BRILEY

Received August 11, 1978, from the *Laboratory of Pathophysiology, National Cancer Institute, Bethesda, MD 20014.* Accepted for publication September 28, 1978.

Abstract □ Eighteen trifluoroacetyl derivatives of amino acids and of amino acid analogs were prepared and tested for growth-inhibitory activity using a *Lactobacillus casei* system as a prescreen for antitumor activity. Of the compounds tested, the trifluoroacetyl derivatives of *o*-, *m*-, and *p*-fluorophenylalanine and of β-3-thienylalanine showed modest activity; trifluoroacetyl derivatives of phenylalanine and of β-2-thienylalanine showed marginal activity. The activity exhibited by the active trifluoroacetyl compounds was equal to that noted for most active chloroacetyl derivatives reported previously, as judged by comparison of their activity with that of chloroacetyl-*m*-fluorophenylalanine. No reversal of inhibition was noted when a representative of these inhibitors was challenged with a corresponding natural metabolite, both as a free amino acid and as a noninhibitory acylated compound.

Keyphrases □ Amino acids and analogs—*N*-trifluoroacetyl derivatives, effect on microbial antitumor screen □ Antitumor activity—18 trifluoroacetyl derivatives of amino acids and amino acid analogs, growth inhibitory activity using *Lactobacillus casei* system

An alteration in the biological behavior of certain amino acids, both the naturally occurring and the "unnatural," as measured by growth-inhibitory capacity in a microbial system, was noted upon acylation (1–3). The extent of such activity varied with the nature of the acyl group and the amino acid moiety (3). While *N*-acetyl and *N*-propionyl derivatives of these amino acids showed no appreciable growth-inhibitory activity, the *N*-chloroacetyl derivatives showed modest activity (3), particularly with those amino acids that are normally considered to be essential for

0022-3549/79/0400-0496$01.00/0

© 1979, American Pharmaceutical Association

Table I—Purity Data of *N*-Trifluoroacetyl Derivatives

N-Trifluoroacetyl Derivative	Melting Point		Optical Rotation $[\alpha]_D^{21-24}$		Van Slyke Nitrous Acid Determination[c], % amino nitrogen		Empirical Formula	Analysis, %[d]		
	Reported	Observed[a]	Reported	Observed[b]	Calc.	Obs.			Calc.	Obs.
L-Alanine	66–68°[e]	62–64°	−60.7° (W)	−54.6° (W)[f]	0	2	$C_5H_6F_3NO_3$	C	32.44	32.03
								H	3.27	3.38
								N	7.57	7.28
L-Aspartic acid	—	164–165°	—	−18.0° (W)	0	0	$C_6H_6F_3NO_5$	C	31.45	31.40
								H	2.64	2.74
								N	6.11	6.19
o-Fluoro-DL-phenylalanine	—	117–119°	—	—	0	7	$C_{11}H_9F_4NO_3$	C	47.32	47.40
								H	3.24	3.45
								N	5.03	5.23
m-Fluoro-DL-phenylalanine	—	117–119°	—	—	0	0	$C_{11}H_9F_4NO_3$	C	47.32	47.26
								H	3.24	3.24
								N	5.01	5.15
p-Fluoro-DL-phenylalanine	—	143°	—	—	0	1	$C_{11}H_9F_4NO_3$	C	47.32	47.64
								H	3.24	3.16
								N	5.01	5.01
Glycine	117–119°[e]	115–117°	—	—	0	0	$C_4H_4F_3NO_3$	C	28.08	28.08
								H	2.36	2.49
								N	8.19	8.32
β-Hydroxy-DL-norleucine AB[g]	—	179–180°	—	—	0	3	$C_8H_{12}F_3NO_4$	C	39.51	38.89
								H	4.98	5.21
								N	5.76	6.25
L-Isoleucine	—	71–72°	—	+4.2° (A)[h]	0	1	$C_8H_{12}F_3NO_3$	C	42.29	42.40
								H	5.32	5.40
								N	6.17	6.40
L-Leucine	72–75°[e]	76–77°	−39.5° (A)	−26.2° (A)[f]	0	0	$C_8H_{12}F_3NO_3$	C	42.29	42.37
								H	5.32	5.41
								N	6.17	6.16
DL-Methionine	95–96°[e]	91–96°	—	—	0	1	$C_7H_{10}F_3NO_3S$	C	34.28	34.32
								H	4.11	4.36
								N	5.71	5.74
DL-Norleucine	79–82.5°[e]	79–81°	—	—	0	1	$C_8H_{12}F_3NO_3$	C	42.29	42.50
								H	5.32	5.34
								N	6.17	6.10
DL-Norvaline	—	62°	—	—	0	0	$C_7H_{10}F_3NO_3$	C	39.44	39.46
								H	4.73	4.54
								N	6.57	6.85
L-Phenylalanine	120–122°[e]	120–121°	+17.4° (A)[e]	+15.8° (A)	0	5	$C_{11}H_{10}F_3NO_3$	C	50.58	49.95
								H	3.86	3.85
								N	5.36	5.46
D-Phenylalanine hemihydrate	120–122°[e]	120–122°	−17.2° (A)[e]	+14.8° (A)[i]	0	3	$C_{11}H_{12}F_3NO_{3\text{-}1/2}$	C	48.89	48.59
								H	4.10	3.86
								N	5.18	5.32
DL-Phenylalanine	127–128°[e]	127–128°	—	—	0	1	$C_{11}H_{10}F_3NO_3$	C	50.58	50.90
								H	3.86	4.01
								N	5.36	5.68
β-2-Thienyl-DL-alanine	—	128–130°	—	—	0	0	$C_9H_8F_3NO_3S$	C	40.45	40.51
								H	3.02	3.04
								N	5.24	5.46
β-3-Thienyl-DL-alanine hemihydrate	—	115–118°	—	—	0	0	$C_9H_9F_3NO_{3\text{-}1/2}S$	C	39.13	39.43
								H	3.28	3.06
								N	5.07	5.15
DL-Tyrosine dihydrate	—	194°	—	—	0	2	$C_{11}H_{14}F_3NO_6$	C	42.18	41.90
								H	4.50	3.92
								N	4.47	4.45
L-Tyrosine	192.5–193.5°	195–198°	+45.0° (WB)	+48.6° (WB)	0	1	$C_{11}H_{10}F_3NO_4$	C	47.66	47.55
								H	3.64	3.76
								N	5.05	5.12
L-Valine	86–88°	85–86°	−15.2° (W)	−15.2° (W)	0	1	$C_7H_{10}F_3NO_3$	C	39.44	39.47
								H	4.73	4.85
								N	6.57	6.82

[a] Melting points (uncorrected) were determined on a Fisher-Johns melting point block (Fisher Scientific Co., Silver Spring, Md.). [b] Optical rotation was determined on a Rudolf polarimeter (Rudolf Research, Fairfield, N.J.), model 80, sodium lamp, using 100-mm tubes (bore size of 3 mm) and a sample capacity of 0.7 ml. (W) = water, (A) = absolute ethanol, (WB) = water and equivalent amount of sodium hydroxide, c = 2. [c] Van Slyke nitrous acid determination of primary amino nitrogen (8) made on a 1-ml sample containing an equivalent of 0.3 mg of amino nitrogen (when hydrolyzed). [d] Elemental analyses were performed by the Microanalytical Laboratory, National Institute of Arthritis, Metabolism, and Digestive Diseases, National Institutes of Health, Bethesda, Md. [e] *Cf.*, Ref. 10. [f] Not optically pure but predominantly the desired enantiomer. [g] Mixture of diastereomers A and B, A being the isomer moving faster and B being the isomer moving slower in a methyl ethyl ketone–1-butanol–ammonia–water system (2). [h] Probable racemization during preparation. [i] Rotation value, measured as hemihydrate.

growth and with those that are analogs of essential amino acids (3).

The ability of fluoro derivatives of metabolites to interfere and disrupt the normal metabolic pathway of analogous metabolites is well known. The fluoroacetates, the fluorocitrates as inhibitors of specific steps in the citric acid cycle, and the interference of nucleic acid metabolism by fluorouracil and its role in cancer chemotherapy are examples. The anomalous behavior of the trifluoroacetyl derivatives of certain amino acids, especially the straight-chain amino acids, as substrates of hog renal acylase where there was no optical specificity in the enzymatic hydrolysis was reported (4, 5).

In view of these observations, coupled with earlier

Table II—Effect of *N*-Trifluoroacetyl Derivatives of Amino Acids and Amino Acid Analogs on Growth of *L. casei* 7469 [a]

N-Trifluoroacetyl Derivative	Concentration Equivalent at 1 mg/ml, m*M*	Inhibition[b], % 0.1 mg/ml[c]	0.5 mg/ml[c]	1.0 mg/ml[c]
L-Alanine	5.40	0	0	+1[d]
L-Aspartic acid	4.36	3	4	2
o-Fluoro-DL-phenylalanine	3.58	3	9	17
m-Fluoro-DL-phenylalanine	3.58	4	10	22
p-Fluoro-DL-phenylalanine	3.58	4	9	19
Glycine	5.84	+4	+3	+3
β-Hydroxy-DL-norleucine AB	4.11	+2	5	+3
DL-Isoleucine	4.40	1	0	0
L-Leucine	4.40	1	1	2
DL-Methionine	4.08	+2	+1	3
DL-Norleucine	4.40	+5	+2	3
DL-Norvaline	4.69	+2	+1	0
DL-Phenylalanine	3.83	+1	8	12
β-2-Thienyl-DL-alanine	3.74	+3	3	13
β-3-Thienyl-DL-alanine hemihydrate	3.62	+2	8	23
DL-Tyrosine dihydrate	3.19	1	6	6
L-Tyrosine	3.61	+2	+1	5
L-Valine	4.69	3	5	4
Trifluoroacetic acid[e]	8.77	4	0	4

[a] For details, see text and Ref. 3. [b] Turbidity readings of the inoculated control tubes (containing no test compound) were 154–194 Klett units. At least three duplicate determinations were made for each compound. The duplicate values in each determination agreed within ±5 Klett units. The extent of variation in these experiments has been discussed (*cf.*, 3). The standard deviation of a compound showing a mean value of 20% inhibition, for example, was 2.7 and the standard error was 0.95. [c] Final concentration in assay system. [d] The + indicates stimulation of growth. [e] Free acid.

findings of the alteration of certain biological properties of amino acids upon chloroacetylation, the trifluoroacetyl derivatives of these amino acids were studied to note their action on the growth of a microbial system selected as a prescreen for antitumor action.

EXPERIMENTAL

The free amino acids, except for the β-hydroxynorleucines which were prepared in this laboratory (6), were obtained commercially and were recrystallized from water–ethanol before use. Their purity was checked by paper chromatography in at least four solvent systems (*cf.*, 2), by elemental analyses, and, where applicable, by optical rotation measurements. The *N*-trifluoroacetyl derivatives were prepared by acylation with freshly distilled trifluoroacetyl chloride[1] in freshly distilled trifluoroacetic acid[1] in an anhydrous system according to the method of Weygand and Geiger (7).

The purity of the products was checked by melting-point determination, elemental analysis, optical rotation measurements, and Van Slyke nitrous acid determination of primary amino nitrogen (8). The acyl compounds liberated no nitrogen upon treatment with nitrous acid, as determined by the Van Slyke nitrous acid determination of primary amino nitrogen, indicating that the compounds contained no appreciable amount of the unacylated amino acids. Chloroacetyl-*m*-fluoro-DL-phenylalanine was prepared in this laboratory (*cf.*, 3). Data on the purity of these compounds are summarized in Table I.

The preparation of the test solution for the microbiological assay and details of the assay were described previously (1). The microorganism, *Lactobacillus casei* 7469[2], was carried on agar[3] as stab cultures and subcultured in broth[3]. The assay medium, as described previously (1), was a riboflavin-supplemented riboflavin assay medium. Growth was determined turbidimetrically after 19 hr as described (1). Inhibition is expressed as the percentage of growth and is 100 times the ratio of the difference of the turbidity readings of the control and experimental tubes to the turbidity reading of the control tube (*cf.*, 1).

Special care was taken to check the final pH of the assay system, the test compounds being neutralized to pH 6 before being added to the test system. The pH of the assay system containing the maximum quantity of the test compound was within 0.05 pH unit of the control system, which contained water in place of the test solution.

In studies where the inhibitors were challenged by the natural metabolite or by the acyl derivative of the natural compounds, the medium was two times the normal concentration so that the final concentration, after the addition of the inhibitor, the challenging compound, and an appropriate volume of water, was equal to that of the normal assay system. Both the inhibitor and the challenging compounds were neutralized with appropriate volumes of 0.1 *N* NaOH to bring the pH of the solutions to 6. The final pH of the system was determined, as before, in a tube containing equivalent amounts of the test solution, the reversing agent, the medium, and water as in the corresponding experimental tubes. The final pH of these tubes was also within 0.05 pH unit of the control tubes.

[1] Eastman Organic Chemicals, Rochester, N.Y.
[2] American Type Culture Collection, Rockville, Md.
[3] Micro assay culture agar (Difco B319) and micro inoculum broth (Difco B320), Difco Laboratories, Detroit, Mich.

Table III—Comparison of the Effect of Equimolar Concentrations of *N*-Acyl Derivatives of Amino Acids and Amino Acid Analogs on Growth of *L. casei* 7469 [a]

N-Acyl Amino Acid	Inhibition[b], %
N-Trifluoroacetyl-*o*-fluoro-DL-phenylalanine	18
N-Trifluoroacetyl-*m*-fluoro-DL-phenylalanine	20
N-Trifluoroacetyl-*p*-fluoro-DL-phenylalanine	23
N-Trifluoroacetyl-DL-phenylalanine	16
N-Trifluoroacetyl-L-phenylalanine	23
N-Trifluoroacetyl-D-phenylalanine	20
N-Trifluoroacetyl-β-2-thienyl-DL-alanine	24
N-Trifluoroacetyl-β-3-thienyl-DL-alanine	26
N-Chloroacetyl-*m*-fluoro-DL-phenylalanine	23
Trifluoroacetic acid[c]	1

[a] Maximum growth in inoculated control tube containing no test compound, measured turbidimetrically, was 166 Klett units. For explanation of extent of variations of values, see footnote of Table II. [b] Concentration was 4.47 μmoles/ml and was the final concentration in the assay system. For details of assay, see text. [c] Free acid.

RESULTS AND DISCUSSION

The trifluoroacetyl derivatives of 18 amino acids and amino acid analogs were prepared and tested for growth-inhibitory activity using a *L. casei* system as a prescreen for possible antitumor activity (9). Such a system was selected because of the rapidity with which the test could be made with a minimal amount of the test compound. Of the compounds tested, four showed moderate, but distinct, activity (Table II): the *N*-trifluoroacetyl derivatives of *o*-fluoro-DL-phenylalanine, *m*-fluoro-DL-phenylalanine, *p*-fluoro-DL-phenylalanine, and β-3-thienyl-DL-alanine. The trifluoroacetyl derivatives of β-2-thienyl-DL-alanine and of DL-phenylalanine showed marginal activity at 1 mg/ml final concentration.

Because of the uncertainty of the Klett readings of about 5%, the inhibition of 1–6% shown by some compounds (Table II) was considered to be insignificant. When the activity of these compounds was tested on an equimolar basis (Table III), the growth-inhibitory activity of these compounds was in the same range. The molar concentration selected was equivalent to 1 mg of *N*-chloroacetyl-β-hydroxy-D-norleucine B/ml (*cf.*, 3). The activity of the trifluoroacetylfluorophenylalanines was about that of the chloroacetyl counterparts (Table III) (*cf.*, 3). Unlike the chloroacetyl derivatives, which showed activity with both the essential amino acids and with analogs of essential amino acids, the activity of the trifluoroacetyl derivatives was confined to the analogs of phenylalanine.

Where the pure enantiomers were tested, neither optical isomer showed greater or lesser activity than the racemic mixture (Table III). Hence, the inhibition at the level of the inhibitor does not appear to involve an enzymatic reaction. The nonspecificity probably is not due to the trifluoroacetyl radical, as it is in the nonspecific hydrolysis of trifluoroacetyl amino acids by hog renal acylase (4, 5), since similar nonspecificity in growth inhibition was observed with the chloroacetyl compounds (*cf.*, 3). The participation of a racemase, however, is not ruled out.

The trifluoroacetyl derivative of a natural amino acid, phenylalanine, showed growth-inhibitory activity, suggesting that the trifluoroacetyl moiety had some function in this activity. Since free *o*-fluorophenylalanine showed little activity in the system used here, the activity probably is not due to the hydrolytic release of the free *o*-fluorophenylalanine (*cf.*, 3). Furthermore, it is unlikely that the hydrolytic release of free trifluoroacetic acid could be a factor since free trifluoroacetic acid present in equimolar quantity exhibited no inhibition (Table III).

Earlier experiments (3) showed that there was no appreciable hydrolysis of the test compounds during incubation with chloroacetyl-DL-norleucine. Apparently, the activity of the trifluoroacetyl derivatives

Table IV—Effect of Phenylalanine and *N*-Acetylphenylalanine on the Inhibition [a] (Percent) by Trifluoroacetyl-*p*-fluoro-DL-phenylalanine

Reversing Agent [b]	*N*-Trifluoroacetyl-*p*-fluoro-DL-phenylalanine			
	0	1.43 m*M*	3.58 m*M*	7.16 m*M*
None	0	6	21	40
L-Phenylalanine (6.05 m*M*)	+4	9	22	41
N-Acetyl-L-phenylalanine (4.82 m*M*)	8	12	25	47

[a] Maximum growth of controls containing no inhibitor was 141 Klett units. [b] Final concentration of 1 mg/ml. Figures in parentheses are molar equivalents.

of these amino acids and amino acid analogs is independent of the activity of the free parent amino acid. While free *p*-fluoro-DL-phenylalanine and β-3-thienyl-DL-alanine showed considerable activity, their corresponding trifluoroacetyl derivatives did not show as much activity; *o*-fluro-DL-phenylalanine, *m*-fluoro-DL-phenylalanine, and β-2-thienyl-DL-alanine, which showed no activity as free amino acids, showed considerable activity as the trifluoroacetyl derivatives (*cf.*, 3).

It is difficult to propose any mechanism of such inhibition. Interference with phenylalanine metabolism may be involved, since all trifluoroacetyl compounds showing activity are analogs of phenylalanine.

A study was made to note if the inhibition could be overcome or reversed by the addition of suitable quantities of the natural metabolite. In a series of experiments, the active trifluoroacetyl derivative was challenged by various levels of a natural metabolite and of a noninhibitory acyl derivative. No significant degree of reversal was observed with either phenylalanine or acetylphenylalanine (Table IV). This observation, however, does not rule out the involvement of phenylalanine because the area of inhibitory action could be beyond the point of participation of these compounds as free amino acids or as simple acyl derivatives in its metabolic pathway. More sophisticated studies are required to learn the mechanism of inhibition.

In view of the involvement of the trifluoroacetyl derivatives of only phenylalanine-related compounds in this screening system, consideration of these compounds as potential inhibitors of melanomas, wherein the metabolism of phenylalanine is believed to be intimately associated, may be of value. These compounds are now being prepared in larger quantities in preparation for testing in mammalian systems, especially in melanomas.

REFERENCES

(1) T. T. Otani, *Cancer Chemother. Rep.*, **38**, 25 (1964).
(2) T. T. Otani and M. R. Briley, *J. Pharm. Sci.*, **65**, 534 (1976).
(3) *Ibid.*, **67**, 520 (1978).
(4) W. S. Fones and M. Lee, *J. Biol. Chem.*, **201**, 847 (1953).
(5) *Ibid.*, **210**, 227 (1954).
(6) T. T. Otani and M. Winitz, *Arch. Biochem. Biophys.*, **102**, 464 (1963).
(7) F. Weygand and R. Geiger, *Chem. Ber.*, **89**, 647 (1956).
(8) D. D. Van Slyke, *J. Biol. Chem.*, **83**, 425 (1929).
(9) G. E. Foley, R. E. McCarthy, V. M. Binns, E. E. Snell, B. M. Guirard, G. W. Kidder, V. C. Dewey, and P. S. Thayer, *Ann. N.Y. Acad. Sci.*, **76**, 413 (1958).
(10) J. P. Greenstein and M. Winitz, "Chemistry of the Amino Acids," Wiley, New York, N.Y., 1961.

Stability-Indicating Assay for Vidarabine

WEN-HAI HONG ˣ and DALE H. SZULCZEWSKI

Received June 12, 1978, from the *Pharmaceutical Research Division, Warner-Lambert/Parke-Davis, Detroit, MI 48232.* Accepted for publication September 29, 1978.

Abstract □ A physicochemical procedure for the analysis of vidarabine in aqueous parenteral formulations was needed to assure potency and to define stability. Concurrent with the development of this method, its decomposition products and route in aqueous solution were determined. A quantitative procedure was developed to determine intact drug in the presence of decomposition products, and the results obtained were validated by microbial assay. Spectral (UV and polarimetric) and TLC evidence indicated that, in aqueous solution, hydrolysis without racemization occurs, yielding adenine and arabinose. The sensitivity of the method to decomposition is improved by ion-exchange separation of adenine and drug before UV measurement. Analysis of partially decomposed solutions of the drug by both ion-exchange and microbiological methods gave comparable results.

Keyphrases □ Vidarabine—stability-indicating assay, analysis in aqueous parenteral formulations, behavior in aqueous solutions, analysis in the presence of decomposition products □ Parenterals—analysis of vidarabine stability □ Stability—vidarabine in aqueous parenteral formulations

Vidarabine (9-β-D-arabinofuranosyladenine, Vira-A or Ara-A) is an antiviral agent with marked activity *in vitro* and *in vivo* against a wide spectra of DNA viruses (1–8). It also inhibits DNA synthesis in bacteria (9), in mouse fibroblasts in cell culture (10), and in experimental tumors in mice (11, 12).

Since the dosage form being developed is essentially aqueous, information pertinent to the drug's chemistry in an aqueous system is of value for predicting characteristics of the finished formulation and designing a stability-indicating assay. This paper presents a physicochemical procedure for the analysis of vidarabine in aqueous parenteral suspension needed to assure potency and define stability.

EXPERIMENTAL

Chemicals and Reagents—All chemicals used in the preparation of 0.2 *M* borate buffer and 0.1 *M* phosphate buffer were reagent grade and were used without further purification. The hydrochloric acid solutions were prepared from a prestandardized volumetric solution[1]. Vidarabine was an experimental batch[2]; adenine[3] was obtained from a commercial source.

Instrumentation—A direct-reading digital pH meter[4] was used. UV spectra were obtained using a recording UV spectrophotometer[5]. The specific rotation was determined using a polarimeter[6].

Degradation of Vidarabine in Acidic Solution—A 1% solution of vidarabine was prepared in 0.1 *N* HCl, and 2-ml aliquots were sealed in glass ampuls. The ampuls were heated at 100°, withdrawn periodically, and cooled to room temperature; then the specific rotation was measured

[1] Acculute, Anachemia Chemicals.
[2] Rx X lot 41020, Warner-Lambert/Parke-Davis, Detroit, MI 48232.
[3] Lot E-1528, Mann Research Laboratories, New York, N.Y.
[4] Sargent, model DR.
[5] Cary model 11 or 14.
[6] Perkin-Elmer model 141.

0022-3549/79/0400-0499$01.00/0

© 1979, American Pharmaceutical Association

Table IV—Effect of Phenylalanine and *N*-Acetylphenylalanine on the Inhibition [a] (Percent) by Trifluoroacetyl-*p*-fluoro-DL-phenylalanine

Reversing Agent [b]	*N*-Trifluoroacetyl-*p*-fluoro-DL-phenylalanine			
	0	1.43 m*M*	3.58 m*M*	7.16 m*M*
None	0	6	21	40
L-Phenylalanine (6.05 m*M*)	+4	9	22	41
N-Acetyl-L-phenylalanine (4.82 m*M*)	8	12	25	47

[a] Maximum growth of controls containing no inhibitor was 141 Klett units. [b] Final concentration of 1 mg/ml. Figures in parentheses are molar equivalents.

of these amino acids and amino acid analogs is independent of the activity of the free parent amino acid. While free *p*-fluoro-DL-phenylalanine and β-3-thienyl-DL-alanine showed considerable activity, their corresponding trifluoroacetyl derivatives did not show as much activity; *o*-fluro-DL-phenylalanine, *m*-fluoro-DL-phenylalanine, and β-2-thienyl-DL-alanine, which showed no activity as free amino acids, showed considerable activity as the trifluoroacetyl derivatives (*cf.*, 3).

It is difficult to propose any mechanism of such inhibition. Interference with phenylalanine metabolism may be involved, since all trifluoroacetyl compounds showing activity are analogs of phenylalanine.

A study was made to note if the inhibition could be overcome or reversed by the addition of suitable quantities of the natural metabolite. In a series of experiments, the active trifluoroacetyl derivative was challenged by various levels of a natural metabolite and of a noninhibitory acyl derivative. No significant degree of reversal was observed with either phenylalanine or acetylphenylalanine (Table IV). This observation, however, does not rule out the involvement of phenylalanine because the area of inhibitory action could be beyond the point of participation of these compounds as free amino acids or as simple acyl derivatives in its metabolic pathway. More sophisticated studies are required to learn the mechanism of inhibition.

In view of the involvement of the trifluoroacetyl derivatives of only phenylalanine-related compounds in this screening system, consideration of these compounds as potential inhibitors of melanomas, wherein the metabolism of phenylalanine is believed to be intimately associated, may be of value. These compounds are now being prepared in larger quantities in preparation for testing in mammalian systems, especially in melanomas.

REFERENCES

(1) T. T. Otani, *Cancer Chemother. Rep.*, **38**, 25 (1964).
(2) T. T. Otani and M. R. Briley, *J. Pharm. Sci.*, **65**, 534 (1976).
(3) *Ibid.*, **67**, 520 (1978).
(4) W. S. Fones and M. Lee, *J. Biol. Chem.*, **201**, 847 (1953).
(5) *Ibid.*, **210**, 227 (1954).
(6) T. T. Otani and M. Winitz, *Arch. Biochem. Biophys.*, **102**, 464 (1963).
(7) F. Weygand and R. Geiger, *Chem. Ber.*, **89**, 647 (1956).
(8) D. D. Van Slyke, *J. Biol. Chem.*, **83**, 425 (1929).
(9) G. E. Foley, R. E. McCarthy, V. M. Binns, E. E. Snell, B. M. Guirard, G. W. Kidder, V. C. Dewey, and P. S. Thayer, *Ann. N.Y. Acad. Sci.*, **76**, 413 (1958).
(10) J. P. Greenstein and M. Winitz, "Chemistry of the Amino Acids," Wiley, New York, N.Y., 1961.

Stability-Indicating Assay for Vidarabine

WEN-HAI HONG ˣ and DALE H. SZULCZEWSKI

Received June 12, 1978, from the *Pharmaceutical Research Division, Warner-Lambert/Parke-Davis, Detroit, MI 48232.* Accepted for publication September 29, 1978.

Abstract □ A physicochemical procedure for the analysis of vidarabine in aqueous parenteral formulations was needed to assure potency and to define stability. Concurrent with the development of this method, its decomposition products and route in aqueous solution were determined. A quantitative procedure was developed to determine intact drug in the presence of decomposition products, and the results obtained were validated by microbial assay. Spectral (UV and polarimetric) and TLC evidence indicated that, in aqueous solution, hydrolysis without racemization occurs, yielding adenine and arabinose. The sensitivity of the method to decomposition is improved by ion-exchange separation of adenine and drug before UV measurement. Analysis of partially decomposed solutions of the drug by both ion-exchange and microbiological methods gave comparable results.

Keyphrases □ Vidarabine—stability-indicating assay, analysis in aqueous parenteral formulations, behavior in aqueous solutions, analysis in the presence of decomposition products □ Parenterals—analysis of vidarabine stability □ Stability—vidarabine in aqueous parenteral formulations

Vidarabine (9-β-D-arabinofuranosyladenine, Vira-A or Ara-A) is an antiviral agent with marked activity *in vitro* and *in vivo* against a wide spectra of DNA viruses (1–8). It also inhibits DNA synthesis in bacteria (9), in mouse fibroblasts in cell culture (10), and in experimental tumors in mice (11, 12).

Since the dosage form being developed is essentially aqueous, information pertinent to the drug's chemistry in an aqueous system is of value for predicting characteristics of the finished formulation and designing a stability-indicating assay. This paper presents a physicochemical procedure for the analysis of vidarabine in aqueous parenteral suspension needed to assure potency and define stability.

EXPERIMENTAL

Chemicals and Reagents—All chemicals used in the preparation of 0.2 *M* borate buffer and 0.1 *M* phosphate buffer were reagent grade and were used without further purification. The hydrochloric acid solutions were prepared from a prestandardized volumetric solution[1]. Vidarabine was an experimental batch[2]; adenine[3] was obtained from a commercial source.

Instrumentation—A direct-reading digital pH meter[4] was used. UV spectra were obtained using a recording UV spectrophotometer[5]. The specific rotation was determined using a polarimeter[6].

Degradation of Vidarabine in Acidic Solution—A 1% solution of vidarabine was prepared in 0.1 *N* HCl, and 2-ml aliquots were sealed in glass ampuls. The ampuls were heated at 100°, withdrawn periodically, and cooled to room temperature; then the specific rotation was measured

[1] Acculute, Anachemia Chemicals.
[2] Rx X lot 41020, Warner-Lambert/Parke-Davis, Detroit, MI 48232.
[3] Lot E-1528, Mann Research Laboratories, New York, N.Y.
[4] Sargent, model DR.
[5] Cary model 11 or 14.
[6] Perkin-Elmer model 141.

0022-3549/79/0400-0499$01.00/0

© 1979, American Pharmaceutical Association

Table I—Observed Specific Rotation as a Function of Time

Hours	$[\alpha]^{25°}$ (1%, 0.1 *N* HCl) 589 nm (sodium D)	436 nm	365[a] nm
0	+5.8	+6.6	−2.3
0.5	−49.7	−96.2	−146.3
1	−54.0	−104.9	−159.0
2	−55.2	−107.3	−162.2
4	−55.2	−107.6	−162.2
Expected rotation[b]	−55.1	−106.0	−160.0

[a] It is advantageous to follow the degradation at 365 nm since the specific rotation of arabinose is greater at this wavelength than at 589 nm. [b] Based on rotation of equimolar solution of D-arabinose.

at 589, 436, and 365 nm. After the polarimetric determination, 1-ml aliquots were diluted 250-fold in 0.1 *N* NaOH (50 times and then five times) for UV determination at 278 and 260 nm. The remaining portions of the solutions were stored at 4° until the run was completed.

Aliquots of 20 μl were spotted sequentially on a 20 × 20-cm thin-layer plate coated with silica gel F-254[7]. The plate was developed in ethanol–acetic acid (98:2) and then viewed under short wavelength UV light (254 nm) for the detection of vidarabine and adenine. The percent of vidarabine remaining at any time during hydrolysis was calculated from the polarimetric data as follows:

$$\%\ \text{vidarabine remaining} = \left(1 - \frac{[\alpha]_t^{25} - [\alpha]_{\text{initial}}^{25}}{-\Delta[\alpha]_{\text{total}}^{25}}\right) \times 100 \quad \text{(Eq. 1)}$$

where $[\alpha]_{\text{initial}}^{25}$ and $[\alpha]_t^{25}$ are the specific rotations obtained initially and at time t at a specified wavelength, respectively, and $\Delta[\alpha]_{\text{total}}^{25}$ is the total change in specific rotation at time zero and at time infinity.

From the UV spectrophotometric data:

$$C_{\text{vidarabine}} = \left(\frac{A_{260} - A_{278} \times 1.291}{10.67}\right) \times 10^{-3} \quad \text{(Eq. 2)}$$

$$C_{\text{adenine}} = \left(\frac{A_{278} - A_{260} \times 0.237}{5.13}\right) \times 10^{-3} \quad \text{(Eq. 3)}$$

$$\%\ \text{vidarabine remaining} = \left(\frac{C_{\text{vidarabine}}}{C_{\text{vidarabine}} + C_{\text{adenine}}}\right) \times 100 \quad \text{(Eq. 4)}$$

where $C_{\text{vidarabine}}$ and C_{adenine} are the molar concentrations of vidarabine and adenine at any time during hydrolysis, and A_{260} and A_{278} are the absorbances at 260 and 278 nm, respectively.

Solubility Studies—An excess amount of vidarabine (or adenine), 30–50 mg, was placed in each of several equilibration vials (21 × 70 mm, 16 ml) containing 10 ml of water or 0.2 *M* borate buffer of a suitable pH.

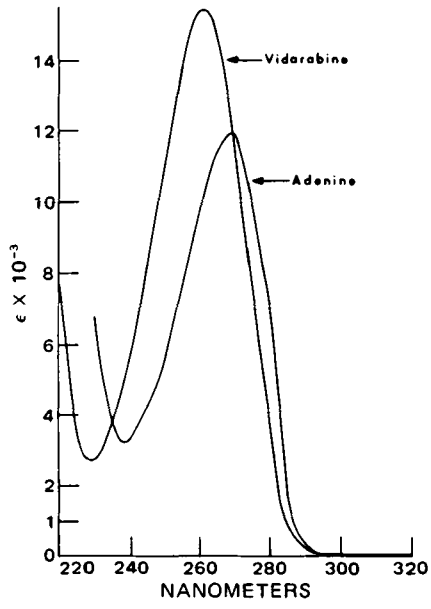

Figure 1—*UV spectra of vidarabine and adenine in 0.1* N *NaOH.*

[7] Merck.

Table II—Recovery Studies

Vidarabine Taken in 20-ml Sample, mg	Adenine Taken in 20-ml Sample, mg	Vidarabine Found, mg	Recovery, %
1.545	0	1.516	98.2
1.545	0	1.524	98.6
1.440	0	1.420	98.6
1.440	0	1.420	98.6
Average			98.5
1.545	0.76	1.499	97.0
1.545	0.76	1.496	96.9
1.413	0.75	1.372	97.2
1.484	1.00	1.473	99.4
Average			97.6

The vials were tumbled end-over-end in a constant-temperature water bath (20°) for at least 24 hr, and then the pH of the mixture was determined. The mixture was then centrifuged, and an aliquot of the clear supernate was diluted 25-fold in 0.1 *M* pH 7 phosphate buffer (further dilution was made if necessary).

The UV spectrum of the diluted solution was recorded using 1-cm silica cells and 0.1 *M* pH 7 phosphate buffer as blank. The solubility of vidarabine (or adenine) was calculated as follows:

$$\text{mg of vidarabine (or adenine)/ml} = \frac{A_{\lambda_{\max}}}{E_1^1} \times 10 \times D \quad \text{(Eq. 5)}$$

where $A_{\lambda_{\max}}$ is the absorbance at $\lambda_{\max}$ (260 nm for vidarabine and 261 nm for adenine), E_1^1 is the absorbance (540 for vidarabine and 981 for adenine) of a 1% solution at $\lambda_{\max}$, and D is the dilution factor.

Recovery Studies—A 250-ml volumetric flask was positioned beneath a glass chromatographic column (1 × 30 cm with polytef stopcock) previously packed with 2 g of 50–100-mesh Dowex 1-X4, chloride form (well soaked in water and washed with 100 ml of water prior to use). A 20-ml aliquot of sample solution in 0.2 *M* pH 10 borate buffer, either a synthetic mixture of vidarabine (75 μg/ml) and adenine (50 μg/ml) or a degraded solution of vidarabine, was charged onto the column. The column was subsequently eluted with 0.2 *M* pH 10 borate buffer until 250 ml was collected.

The UV spectrum of the solution was recorded using 5-cm silica cells

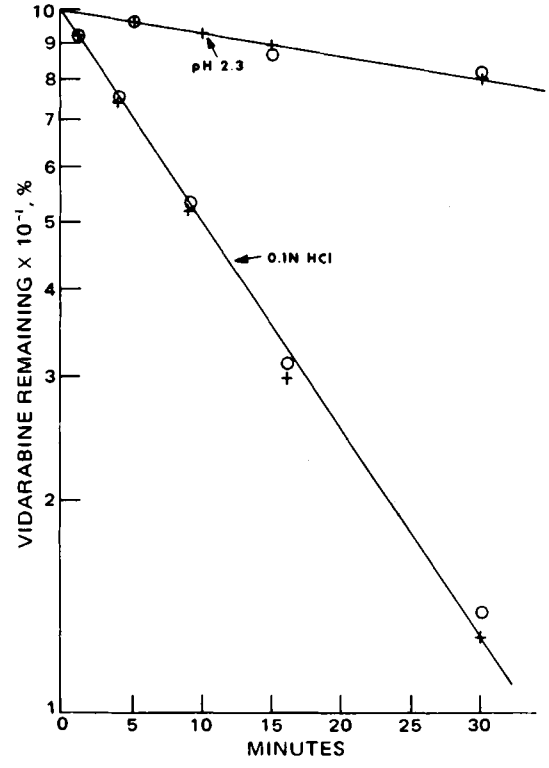

Figure 2—*Hydrolysis of vidarabine at 100°. Key: +, spectrophotometry; and O, polarimetry.*

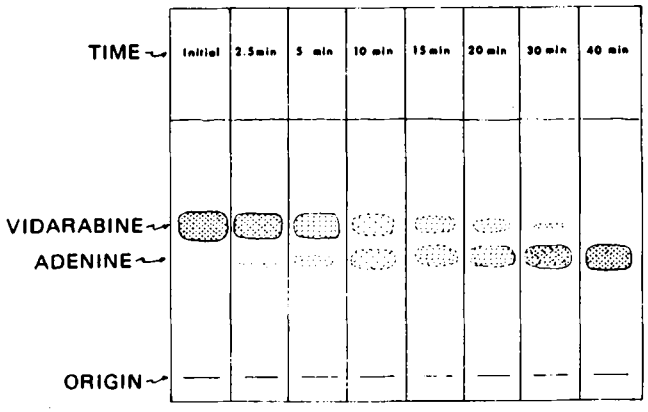

Figure 3—*TLC separation of vidarabine solution degraded in 0.1 N HCl at 100°. The plate was silica gel F-254, the developer was ethanol–acetic acid (98:2), and detection was by shortwave UV light (254 nm).*

and 0.2 *M*, pH 10 borate buffer as the blank. The content of vidarabine was calculated as follows:

$$\text{mg of vidarabine found} = \frac{A_{260}}{540 \times 5} \times 10 \times 250 \qquad \text{(Eq. 6)}$$

Formulation Analysis—*Column Preparation*—A slurry of 0.5 g QAE-Sephadex A-25, chloride form[8], with distilled water was prepared and allowed to hydrate overnight. The hydrated resin slurry was then poured into a chromatographic column[9]. After settling, the resin was converted into borate form by washing the column with 125 ml of 0.1 *M*, pH 10 borate buffer. A layer of solvent was always maintained above the resin bed.

Sample Preparation—Depending on the label claim, 2 ml of the homogeneous suspension was transferred into a volumetric flask with adequate size such that each milliliter contained 0.4 mg of vidarabine. The flask was half-filled with distilled water and heated on a steam bath with occasional shaking until the drug was completely dissolved. The solution was then cooled to room temperature and brought to the mark with distilled water. Twenty milliliters of the resulting solution was further diluted to 25 ml with 0.5 *M*, pH 10 borate buffer and mixed well.

Procedure—A 50-ml volumetric flask was positioned beneath the previously prepared ion-exchange resin column. Three milliliters of the alkaline sample dilution was charged onto the column and allowed to flow through the resin bed at a rate of approximately 1 ml/min. The column was eluted with 0.1 *M*, pH 10 borate buffer until 50 ml was collected.

The UV spectrum of the eluate was determined over the 320–220-nm region using 1-cm silica cells and 0.1 *M*, pH 10 borate buffer as the blank. The content of vidarabine in the sample was calculated as follows:

$$\text{mg of vidarabine/ml} = \frac{A_{260}}{540} \times 10 \times \frac{25}{20} \times \frac{50}{3} \times \frac{V}{2} \qquad \text{(Eq. 7)}$$

where V is the volume (milliliters) of the volumetric flask used for the sample preparation.

RESULTS AND DISCUSSION

Past work showed that vidarabine could be hydrolyzed to yield D-arabinose and adenine according to Scheme I. To determine whether this

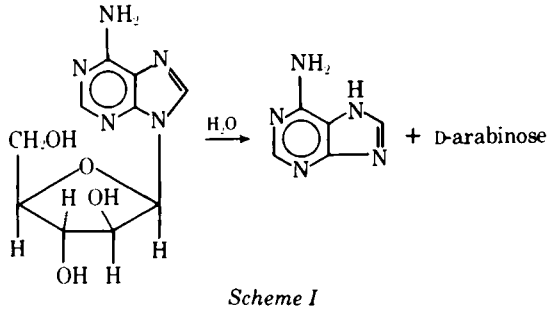

Scheme I

reaction constituted the only likely route of drug decomposition under these environmental conditions, the hydrolytic reaction was monitored by two independent procedures, one sensitive to possible changes in the optically active pentose moiety and the other sensitive to change in the adenine part of the molecule. Correlation of results by either method provides strong evidence for the occurrence of only one reaction and identifies degradation products that could interfere.

The specific rotation of vidarabine is rather small while that of D-arabinose is substantial. Any process that yields D-arabinose changes the observed specific rotation. If D-arabinose is the only carbohydrate product of the reaction, *e.g.*, if racemization of either drug or D-arabinose does not occur, then the rotation of a completely hydrolyzed drug sample could be predicted based on the known rotation of the sugar. Comparison of observed results from a spent reaction mixture with those expected indicates whether or not racemization occurs.

Polarimetric data obtained on drug solutions subjected to hydrolytic conditions are given in Table I. The observed specific rotation changed with time for up to 2 hr. The rotation after completion of the reaction was that expected for an equimolar solution of D-arabinose.

Change in the adenine portion is conveniently monitored spectrophotometrically. The UV spectra of vidarabine and adenine differ maximally (Fig. 1) when determined in 0.1 *N* NaOH. This spectral difference, although not great, is adequate for the analysis of mixtures containing both where decomposition is in the 20–80% range. The composition of such mixtures can be determined by using observed absorbancy readings at 278 and 260 nm (wavelengths of maximum difference) and application of the conventional mixture formula.

Table III—Comparison of Results by Ion-Exchange and Microbiological Assays

Residence Time of Vidarabine in 0.1 *N* HCl in Steam Bath, min	Vidarabine Found, mg	
	Microbiological	Ion Exchange-UV
0	288[a]	302[a]
4	260	232
7	189	178
10	153	139
13	109	112

[a] 300.9 mg of vidarabine was initially taken.

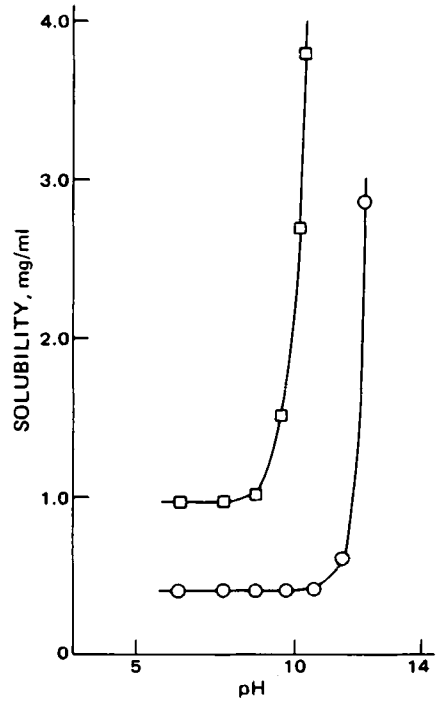

Figure 4—*Solubility profiles of vidarabine (○) and adenine (□) in borate buffer at 20°.*

[8] Pharmacia Fine Chemicals, Piscataway, NJ 08854. This resin was preferable because it produced less extraneous absorption at analytical wavelengths.
[9] Sephadex column, k9/15, Pharmacia Fine Chemicals, Piscataway, NJ 08854.

Table IV—Analysis of Vidarabine Parenteral Suspension Stored at Various Temperatures

Storage Time, weeks	Percent of Label Claim					
	25°[a] or 5°[b]		38°[a] or 25°[b]		45°	
	Upright[c]	Invert	Upright	Invert	Upright	Invert
Batch A						
Initial	100.3	—	—	—	—	—
78	100.8	97.7	—	—	102.2	102.3
156	100.3	99.4	100.9	101.7	—	—
Batch B						
Initial	100.2	—	—	—	—	—
39	—	—	100.9	99.9	98.4	102.9
104	100.8	99.0	100.3	100.4	101.7	102.4

[a] Batch A. [b] Batch B. [c] Vial position.

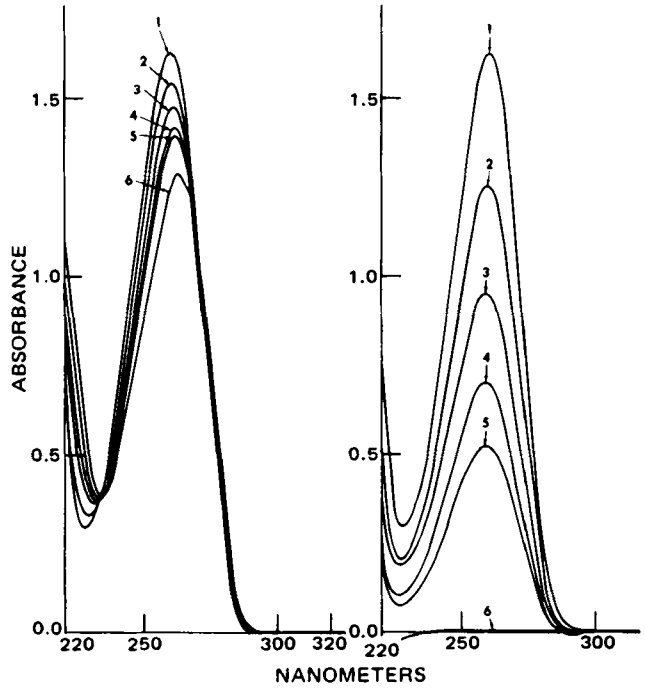

Figure 5—*Sequential spectra of vidarabine maintained at 100° in 0.1 N HCl. Left: Spectra obtained after diluting 12.5-fold into 0.2 M, pH 10 borate buffer. Right: Spectra obtained after passing solution through ion-exchange resin column. Residence times in 0.1 N HCl at 100° were: initial (1), 4 min (2), 7 min (3), 10 min (4), 13 min (5), and 2.5 hr (6).*

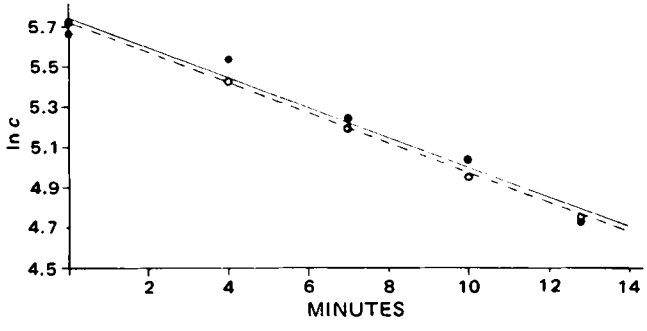

Figure 6—*Least-squares best fits for microbiological (●) and ion-exchange-UV (○) data.*

Internal consistency requires that analysis of partially degraded solutions of vidarabine by polarimetric and UV methods yield the same result. Therefore, 1% solutions of vidarabine were prepared, subdivided in sealed ampuls, and heated at 100°. Samples were withdrawn periodically, diluted in 0.1 *N* NaOH for UV determination, and used directly for optical activity determination.

The results obtained (Fig. 2) demonstrate that the only process occurring is uncomplicated hydrolysis of the *N*-glycoside linkage without racemization or other side reactions. This result was also confirmed by TLC analysis (Fig. 3).

While more complete information is now available concerning the route of decomposition in an aqueous system, work is still necessary to provide analysis of the dosage form. The specific rotation of the drug is too low to have analytical utility, and the UV spectral properties of vidarabine and adenine are such to preclude sensitive analysis. Drug analysis requires that the experimentally determined quantity be a direct measure of drug content and that information regarding identity be obtained simultaneously. A method that separates drug from likely decomposition products would have value.

Results obtained from a study of solubility as a function of pH (Fig. 4) show that vidarabine is a weaker acid than adenine by a difference of approximately 2 pKa units. This difference in acidity should make feasible their separation *via* ion exchange. Adenine at pH 10 is roughly 50% ionized and would be expected to be retained on an anion-exchange resin. Vidarabine would exist as a neutral molecule and should not be retained. Known solutions of vidarabine alone and admixed with adenine were run through an anion-exchange column, giving the results summarized in Table II.

Sequential UV spectra (Fig. 5) were obtained on a hydrolyzed solution of vidarabine after (*a*) direct dilution and (*b*) passage through the ion-exchange column. The spectra obtained by direct dilution change from those produced by vidarabine to those that arise from adenine. The spectra obtained after ion-exchange separation are those from vidarabine only. Results calculated from these spectra plot well as a first-order reaction and compare favorably with microbiological results.

Since this drug is an antiviral agent, any physicochemical method used for assay should reflect potency in the same manner as would microbiological analysis. Therefore, samples were analyzed microbiologically for comparison with results obtained by the ion-exchange procedure (Table III). Intuitively, after allowance for the anticipated variance of the microbiological method, the results appear in good agreement.

Statistically, both sets of data yielded information that, when plotted as a first-order reaction, gave straight lines with the same slope (Fig. 6). The "scatter," as measured by the correlation coefficient, was significantly less for ion-exchange results than microbiological results (0.9988 *versus* 0.9775).

Table IV summarizes the data obtained from two batches of vidarabine parenteral suspensions during stability evaluation. The data are in good agreement with the label claim. The overall average recovery was 100.6%, with a standard deviation of 1.5%.

In summary, a physicochemical stability-indicating procedure was developed for vidarabine parenteral formulations. The procedure is simple and yields results consistent with the microbiological method.

REFERENCES

(1) "Adenine Arabinoside: An Antiviral Agent," D. Pavan-Langston, R. A. Buchanan, and C. A. Alford, Eds., Raven, New York, N.Y., 1975.

(2) W. M. Shannon, in *ibid.*, pp. 7–43.

(3) B. J. Sloan, in *ibid.*, pp. 45–94.

(4) F. A. Miller, G. J. Dixon, J. Ehrlich, B. J. Sloan, and I. W. McLean, Jr., in "Antimicrobial Agents and Chemotherapy—1968," G. L. Hubby, Ed., American Society for Microbiology, Bethesda, Md., 1969, pp. 136–147.

(5) R. E. Keeney and R. A. Buchanan, *Ann. N.Y. Acad. Sci.*, **225**, 185 (1975).

(6) L. T. Ch'ien, N. J. Cannon, L. J. Charamella, R. J. Dismakes, R. J. Whitney, R. A. Buchanan, and C. A. Alford, Jr., *J. Infect. Dis.*, **128**, 658 (1973).

(7) L. T. Ch'ien, F. M. Schabel, Jr., and C. A. Alford, Jr., in "Selective Inhibitors of Viral Function," W. A. Carter, Ed., CRC Press, Cleveland, Ohio, 1973, pp. 227–256.

(8) F. M. Schabel, Jr., *Chemotherapy (Basel)*, **13**, 321 (1968).
(9) M. Hubert-Habart and S. S. Cohen, *Biochim. Biophys. Acta*, **59**, 468 (1962).
(10) A. M. Doering, J. Keller, and S. S. Cohen, *Cancer Res.*, **26**, 2444 (1966).
(11) J. J. Brink and G. A. LePage, *ibid.*, **24**, 312 (1964).
(12) *Ibid.*, **24**, 1042 (1964).

ACKNOWLEDGMENTS

The authors are indebted to Ms. C. Johnston for assistance, to Dr. H. Dion for microbiological analysis, to Dr. L. M. Wheeler for encouragement and support, and to Ms. J. Pohl for assistance in preparing this manuscript.

GLC Determination of Trihexyphenidyl Hydrochloride Dosage Forms

EILEEN BARGO

Received July 18, 1978, from the *U.S. Food and Drug Administration, Baltimore District, Baltimore, MD 21201.* Accepted for publication September 28, 1978.

Abstract □ A rapid, sensitive, and specific GLC method for the quantitation of trihexyphenidyl hydrochloride in various pharmaceutical dosage forms is described. The procedure involves chloroform extraction of the active ingredient from a weakly acidic solution, followed by GLC determination using a 3% methyl silicone column. The specificity of the system in relation to several compendial drug analogs also is reported.

Keyphrases □ Trihexyphenidyl hydrochloride—GLC analysis in various pharmaceutical dosage forms, analogs □ GLC—analysis, trihexyphenidyl hydrochloride, in various pharmaceutical dosage forms, analogs □ Antiparkinsonism agents—GLC analysis of trihexyphenidyl hydrochloride in various pharmaceutical dosage forms

Several methods for quantitating the antiparkinsonism drug trihexyphenidyl hydrochloride (I) in toxicological samples and dosage forms have been published. These procedures include nonaqueous titration (1–3), colorimetric determination (4–6), polarography (7), and fluorescence (8). The USP procedures for assaying I in elixirs (9) and tablets (10) consist of dye–complex formation with bromcresol purple, chloroform extraction, and colorimetric measurement. All of these analytical procedures are relatively nonspecific and may measure any similarly structured compounds present, leading to erroneous results. Although the more specific technique of GLC has been employed to quantitate I (11–17), little work has been reported on its use in assaying I in dosage forms. In addition, variable results have been encountered in this laboratory with the compendial methods.

The purpose of this work was to develop a rapid, sensitive, reproducible, and discriminating method for the determination of I in pharmaceutical formulations. The procedure presented involves the chloroform extraction of the active ingredient from weakly acidic sample solutions of elixirs, tablets, and sustained-release capsules, followed by GLC determination using a 3% methyl silicone column. The method is an adaption of the GLC procedure developed by Clark[1] for assaying phencyclidine hydrochloride in sample matrixes. This GLC system also permits the differentiation of I from several compendial analogs based on differing retention times.

[1] Charles C. Clark, U.S. Drug Enforcement Administration, Miami, Fla. Method and collaborative study results are currently in press.

EXPERIMENTAL

Reagents and Chemicals—All chemicals and reagents were USP, NF, ACS, or chromatographic grade.

Instrumentation—A pH meter[2] was fitted with a glass–calomel electrode system. The gas chromatograph[3] was equipped with a flame-ionization detector connected to an electronic integrator[4]. The glass column, 4 mm i.d. × 1.8 m long, was packed with 3% OV-1 on 100–120-mesh Chromosorb WHP[5] and conditioned at 260° for 24 hr under nitrogen at a flow rate of 30 ml/min. The instrument parameters were: injected quantity of sample solution, 4–5 μl; injector temperature, 240°; detector temperature, 240°; column temperature, 210° (isothermal); carrier gas (nitrogen) flow rate, 60 ml/min; hydrogen flow rate, 60 ml/min; and air flow rate, 240 ml/min, or according to manufacturer's recommendations.

Column temperature and flow rate were adjusted to elute I in about 7 min and the internal standard in about 8.8 min. (The relative retention time of I *versus* the internal standard is about 0.8.) Electrometer sensitivity was adjusted so that 4–6 μl of the standard solution gave a suitable recorder response, *i.e.*, 40–80% of full-scale deflection.

Preparation of Solutions—The dosage forms[6] studied were an elixir, 2 mg/5 ml; tablets, 2 mg; and sustained-release capsules, 5 mg. The stock solution of 1 mg of *n*-tricosane (II)/ml, the internal standard, was prepared by directly dissolving 100 mg of II in 100 ml of chloroform. The standard solution of I, 0.2 mg/ml, was prepared by treating 10 mg of the standard in the same way as the elixir but with 1% K_2HPO_4 for pH adjustment.

The standard mixture solution of I and its analogs, 1 mg/ml, was prepared by dissolving 10 mg each of cycrimine hydrochloride, biperidin hydrochloride, procyclidine hydrochloride, tridihexethyl chloride, and I in 10 ml of the internal standard solution and mixing.

Sample Preparation—*Elixir*—An amount of sample equivalent to 10 mg of I was pipetted into a 100-ml beaker. Volume was adjusted to about 50 ml with water. The pH was adjusted to 6 ± 0.5 by dropwise addition of 10% K_2HPO_4 (~1 ml) using a pH meter. The sample was then transferred quantitatively with water into a 125-ml separator.

Tablets—Not less than 20 tablets were weighed and finely ground. An accurately weighed portion of the powder, equivalent to about 10 mg of I, was transferred into a 125-ml separator. Twenty-five milliliters of hydrochloric acid (1 in 1000) was added, and the mixture was shaken vigorously mechanically for about 30 min. Then the contents were transferred to a 100-ml beaker, and the pH was adjusted to 6 ± 0.5 with dropwise addition of 1% K_2HPO_4 using a pH meter. The sample was transferred quantitatively with water back into the 125-ml separator.

Capsules (Sustained Release)—The contents of not less than 20 capsules were weighed and finely ground. An accurately weighed portion

[2] Orion model 701A.
[3] Hewlett-Packard model 5830A.
[4] Hewlett-Packard model 18850A.
[5] Applied Science Laboratories, State College, Pa.
[6] Artane, Lederle Laboratories, Pearl River, N.Y.

0022-3549/79/0400-0503$01.00/0
© 1979, American Pharmaceutical Association

(8) F. M. Schabel, Jr., *Chemotherapy (Basel)*, **13**, 321 (1968).
(9) M. Hubert-Habart and S. S. Cohen, *Biochim. Biophys. Acta*, **59**, 468 (1962).
(10) A. M. Doering, J. Keller, and S. S. Cohen, *Cancer Res.*, **26**, 2444 (1966).
(11) J. J. Brink and G. A. LePage, *ibid.*, **24**, 312 (1964).
(12) *Ibid.*, **24**, 1042 (1964).

ACKNOWLEDGMENTS

The authors are indebted to Ms. C. Johnston for assistance, to Dr. H. Dion for microbiological analysis, to Dr. L. M. Wheeler for encouragement and support, and to Ms. J. Pohl for assistance in preparing this manuscript.

GLC Determination of Trihexyphenidyl Hydrochloride Dosage Forms

EILEEN BARGO

Received July 18, 1978, from the *U.S. Food and Drug Administration, Baltimore District, Baltimore, MD 21201.* Accepted for publication September 28, 1978.

Abstract □ A rapid, sensitive, and specific GLC method for the quantitation of trihexyphenidyl hydrochloride in various pharmaceutical dosage forms is described. The procedure involves chloroform extraction of the active ingredient from a weakly acidic solution, followed by GLC determination using a 3% methyl silicone column. The specificity of the system in relation to several compendial drug analogs also is reported.

Keyphrases □ Trihexyphenidyl hydrochloride—GLC analysis in various pharmaceutical dosage forms, analogs □ GLC—analysis, trihexyphenidyl hydrochloride, in various pharmaceutical dosage forms, analogs □ Antiparkinsonism agents—GLC analysis of trihexyphenidyl hydrochloride in various pharmaceutical dosage forms

Several methods for quantitating the antiparkinsonism drug trihexyphenidyl hydrochloride (I) in toxicological samples and dosage forms have been published. These procedures include nonaqueous titration (1–3), colorimetric determination (4–6), polarography (7), and fluorescence (8). The USP procedures for assaying I in elixirs (9) and tablets (10) consist of dye–complex formation with bromcresol purple, chloroform extraction, and colorimetric measurement. All of these analytical procedures are relatively nonspecific and may measure any similarly structured compounds present, leading to erroneous results. Although the more specific technique of GLC has been employed to quantitate I (11–17), little work has been reported on its use in assaying I in dosage forms. In addition, variable results have been encountered in this laboratory with the compendial methods.

The purpose of this work was to develop a rapid, sensitive, reproducible, and discriminating method for the determination of I in pharmaceutical formulations. The procedure presented involves the chloroform extraction of the active ingredient from weakly acidic sample solutions of elixirs, tablets, and sustained-release capsules, followed by GLC determination using a 3% methyl silicone column. The method is an adaption of the GLC procedure developed by Clark[1] for assaying phencyclidine hydrochloride in sample matrixes. This GLC system also permits the differentiation of I from several compendial analogs based on differing retention times.

[1] Charles C. Clark, U.S. Drug Enforcement Administration, Miami, Fla. Method and collaborative study results are currently in press.

EXPERIMENTAL

Reagents and Chemicals—All chemicals and reagents were USP, NF, ACS, or chromatographic grade.

Instrumentation—A pH meter[2] was fitted with a glass–calomel electrode system. The gas chromatograph[3] was equipped with a flame-ionization detector connected to an electronic integrator[4]. The glass column, 4 mm i.d. × 1.8 m long, was packed with 3% OV-1 on 100–120-mesh Chromosorb WHP[5] and conditioned at 260° for 24 hr under nitrogen at a flow rate of 30 ml/min. The instrument parameters were: injected quantity of sample solution, 4–5 μl; injector temperature, 240°; detector temperature, 240°; column temperature, 210° (isothermal); carrier gas (nitrogen) flow rate, 60 ml/min; hydrogen flow rate, 60 ml/min; and air flow rate, 240 ml/min, or according to manufacturer's recommendations.

Column temperature and flow rate were adjusted to elute I in about 7 min and the internal standard in about 8.8 min. (The relative retention time of I *versus* the internal standard is about 0.8.) Electrometer sensitivity was adjusted so that 4–6 μl of the standard solution gave a suitable recorder response, *i.e.*, 40–80% of full-scale deflection.

Preparation of Solutions—The dosage forms[6] studied were an elixir, 2 mg/5 ml; tablets, 2 mg; and sustained-release capsules, 5 mg. The stock solution of 1 mg of *n*-tricosane (II)/ml, the internal standard, was prepared by directly dissolving 100 mg of II in 100 ml of chloroform. The standard solution of I, 0.2 mg/ml, was prepared by treating 10 mg of the standard in the same way as the elixir but with 1% K_2HPO_4 for pH adjustment.

The standard mixture solution of I and its analogs, 1 mg/ml, was prepared by dissolving 10 mg each of cycrimine hydrochloride, biperidin hydrochloride, procyclidine hydrochloride, tridihexethyl chloride, and I in 10 ml of the internal standard solution and mixing.

Sample Preparation—*Elixir*—An amount of sample equivalent to 10 mg of I was pipetted into a 100-ml beaker. Volume was adjusted to about 50 ml with water. The pH was adjusted to 6 ± 0.5 by dropwise addition of 10% K_2HPO_4 (~1 ml) using a pH meter. The sample was then transferred quantitatively with water into a 125-ml separator.

Tablets—Not less than 20 tablets were weighed and finely ground. An accurately weighed portion of the powder, equivalent to about 10 mg of I, was transferred into a 125-ml separator. Twenty-five milliliters of hydrochloric acid (1 in 1000) was added, and the mixture was shaken vigorously mechanically for about 30 min. Then the contents were transferred to a 100-ml beaker, and the pH was adjusted to 6 ± 0.5 with dropwise addition of 1% K_2HPO_4 using a pH meter. The sample was transferred quantitatively with water back into the 125-ml separator.

Capsules (Sustained Release)—The contents of not less than 20 capsules were weighed and finely ground. An accurately weighed portion

[2] Orion model 701A.
[3] Hewlett-Packard model 5830A.
[4] Hewlett-Packard model 18850A.
[5] Applied Science Laboratories, State College, Pa.
[6] Artane, Lederle Laboratories, Pearl River, N.Y.

0022-3549/79/0400-0503$01.00/0
© 1979, American Pharmaceutical Association

Table I—Assay Results [a] of I in Pharmaceutical Preparations following the USP, NDA, and GLC Methods

Dosage Form	USP/NDA	GLC
Elixir (2 mg/5 ml)	98.5	102.0
	105.2	103.5
	108.0	101.0
	102.5	98.9
SD	4.05	1.93
CV, %	3.91	1.90
Tablets (2 mg)	104.0	104.0
	103.6	105.5
	111.0	104.0
	107.5	104.5
	100.6	103.6
	103.7	
SD	3.64	0.73
CV, %	3.46	0.70
Sustained-release capsules (5 mg)	94.0	97.6
	93.4	96.4
	84.6	96.4
	94.2	95.2
	91.2	
	93.4	
SD	3.69	0.98
CV, %	4.02	1.02

[a] Shown in percent declared.

of the well-mixed powder, equivalent to about 10 mg of I, was transferred into a 125-ml separator.

Fifty milliliters of hydrochloric acid (1 in 1000) was added, and the mixture was shaken vigorously mechanically for about 30 min. Then the contents were transferred to a 100-ml beaker, and the pH was adjusted to 6 ± 0.5 by dropwise addition of 10% K_2HPO_4 (~1 ml) using a pH meter. The sample was transferred quantitatively with water back into the 125-ml separator.

Extraction—The standard, elixir, tablet, and capsule solutions were extracted with five 25-ml portions of chloroform. The extracts were filtered through a chloroform-washed cotton pledget into a 150-ml beaker. All extracts were evaporated carefully on a steam bath with a gentle current of air to about 25 ml. The residue was transferred quantitatively with chloroform to a 50-ml volumetric flask, to which had been added 10.0 ml of internal standard solution. The solution was diluted to volume with chloroform and mixed. Aliquots of 4–5 μl of the sample and standard solutions were injected into the gas chromatograph using a 10-μl syringe.

Table II—Recovery Results of I in Spiked Pharmaceutical Preparations with the GLC Method

Dosage Form	Added, mg	Found, mg	Recovery, %
Elixir	9.98	10.10	101.2
Tablets	9.98	10.15	101.7
Capsules	9.98	9.90	99.2

Calculations—The following formulas were used to calculate the I concentrations:

$$\text{mg/5 ml} = \left(\frac{A}{A'}\right)\left(\frac{I'}{I}\right)(CDF)\left(\frac{5}{S}\right) \qquad \text{(Eq. 1)}$$

$$\text{mg}\Big/\frac{\text{tablet or}}{\text{capsule}} = \left(\frac{A}{A'}\right)\left(\frac{I'}{I}\right)(CDF)\left(\frac{T}{W}\right) \qquad \text{(Eq. 2)}$$

where A and A' are the peak heights or areas of the sample and standard, respectively; I and I' are the peak heights or areas of the internal standard for the sample and standard, respectively; C is the concentration of standard (milligrams per milliliter); DF is the dilution factor; S is the sample aliquot (milliliters) taken; W is the weight of sample used (grams); and T is the average tablet or capsule net contents weight.

RESULTS AND DISCUSSION

Each dosage form studied was assayed by both the official USP (elixirs and tablets) or manufacturer's New Drug Application (NDA) (capsules) procedures and the proposed method. The results (Table I) show good correlation between the methods. The standard deviations and coefficients of variation obtained indicate that the proposed method is more precise than the USP and NDA methods for all forms analyzed.

Results of recovery studies for standard I added to each formulation are shown in Table II. The recoveries obtained were complete and consistent from product to product.

Gas chromatograms for the extracted standard and samples are presented in Fig. 1. Good peak symmetry, absence of interfering sample peaks, and short retention times for trihexyphenidyl (6.8 min) and II (8.8 min) were obtained. The GLC responses for trihexyphenidyl and II were linear over at least a range of 0.6–1.4 μg of drug injected. The minimum detectable level was 0.4 ng of trihexyphenidyl.

A study was conducted to determine the effect of pH on the extractability of the active ingredient in each type of formulation. A range between pH 5 and 7 was optimum for the total extraction of I in all dosage forms studied. Dibasic potassium phosphate or hydrochloric acid (1 in

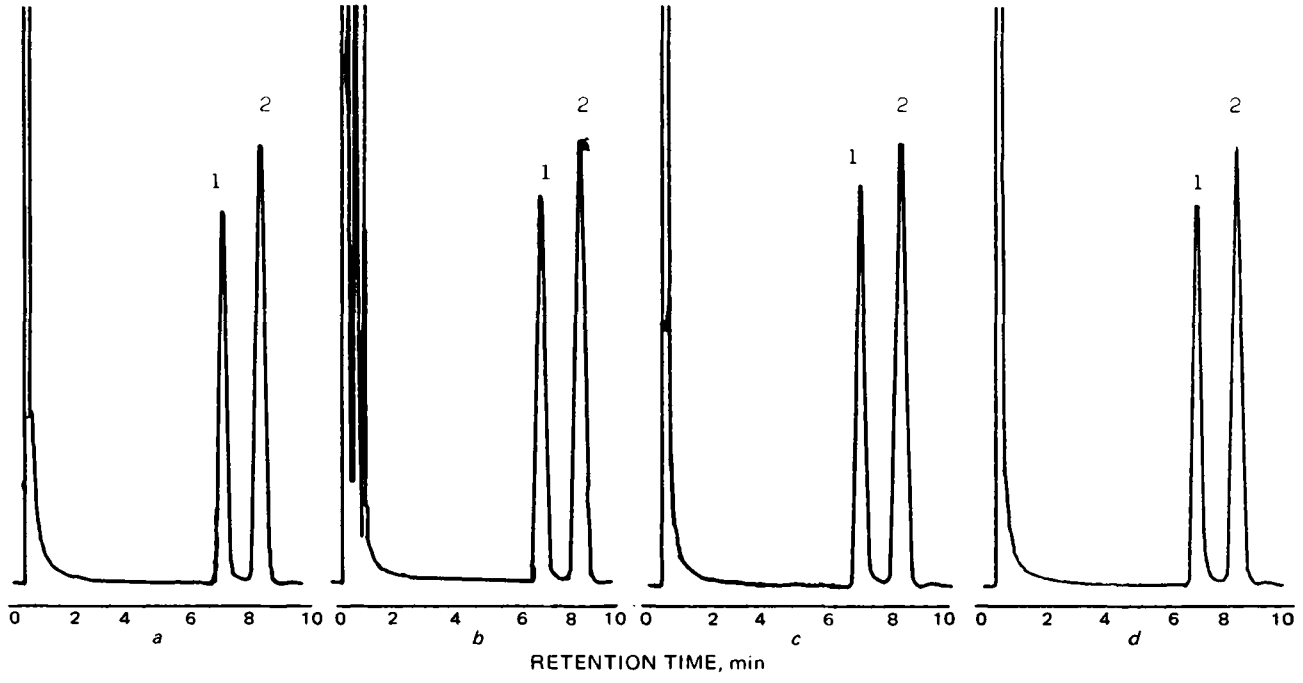

Figure 1—*Chromatograms of extracted solutions of:* (a) *standard I,* (b) *elixir (2 mg of I/5 ml),* (c) *tablets (2 mg of I), and* (d) *capsules (5 mg of I). Key: 1, trihexyphenidyl; and 2,* n-*tricosane.*

Table III—Chemical Structures and Relative GLC Retention Times of I and Compendial Drug Analogs

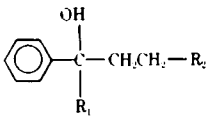

Compound	R_1	R_2	*RRT*[a]
Tridihexethyl		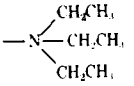	0.46
Cycrimine			0.56
Procyclidine			0.64
Trihexyphenidyl			0.80
Biperiden			0.88

[a] Relative retention time *versus* II, the internal standard.

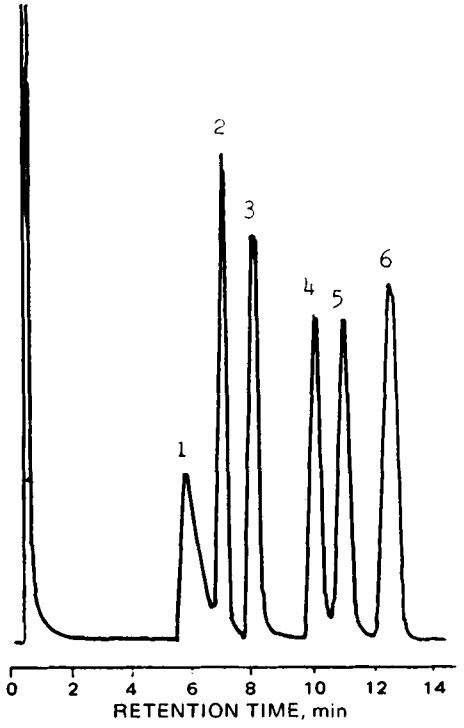

Figure 2—*Chromatogram of standard mixture of tridihexethyl chloride (1), cycrimine hydrochloride (2), procyclidine hydrochloride (3), I (4), biperiden hydrochloride (5), and II (6). Instrumental parameters and column conditions were as described under* Experimental, *except that the column temperature was 200°. All mixture components were at 1-mg/ml concentrations.*

1000) solutions were used to keep the sample and standard solutions within this pH range.

A literature search and discussions with various sources indicated that I is a stable compound under normal storage conditions. Little information was obtained on I degradation products, but the search for such reports continues. If degradation products are discovered, standards of such compounds will be obtained and their behavior in the proposed method will be tested. It is believed that chloroform-extractable degradation products would be detected by the proposed procedure, based on differing GLC retention times. Chromatograms obtained by the proposed method of 3-year-old elixir products stored at room temperature, of 3-month-old refrigerated I standard solutions, and of solutions from dissolution experiments involving blending of the capsule product for several minutes at high revolutions per minute in boiling water showed no extraneous peaks.

NF XIV contains monographs for procyclidine hydrochloride (18), tridihexethyl chloride (19), cycrimine hydrochloride (20), and biperiden hydrochloride (21), which are structurally related to I (Table III) and have similar pharmacological actions. The NF assays for these analogs all employ the bromcresol purple colorimetric procedure used in the USP assay for I. Thus, a study was undertaken to determine if these drugs could also be chromatographed successfully with the same GLC system developed for I. As indicated in Fig. 2, all compounds except tridihexethyl chloride exhibited excellent GLC peak shapes, short retention times (Table III), and near-baseline resolution from each other and from I and II.

This method may be used to differentiate I and its compendial analogs from one another and offers better specificity and precision than do the current compendial assays for I-containing formulations.

REFERENCES

(1) L. G. Chatten and W. J. Racy, *J. Pharm. Sci.*, **57**, 137 (1968).

(2) E. Papke, *Pharmazie*, **23**, 362 (1968).

(3) R. Simionovici, H. Aftalion, and F. Albert, *Rev. Chim.*, **18**, 498 (1967).

(4) E. Papke, *Pharmazie*, **23**, 449 (1968).

(5) L. Nyberg, *J. Pharm. Pharmacol.*, **22**, 500 (1970).

(6) E. O. Gryaznova and T. K. Vergeichik, *Farm. Zh. (Kiev)*, **27**, 82 (1972).

(7) G. Bonpai and G. Vastagh, *Pharm. Zentralh.*, **103**, 403 (1964).

(8) M. Gelbcke, *J. Pharm. Belg.*, **31**, 397 (1976).

(9) "The United States Pharmacopeia," 19th rev., Mack Publishing Co., Easton, Pa., 1975, p. 519.

(10) *Ibid.*, p. 520.

(11) D. J. Lovejoy, *J. Chromatogr.*, **57**, 139 (1971).

(12) F. L. Fricke, *J. Assoc. Off. Anal. Chem.*, **55**, 1162 (1972).

(13) B. S. Finkle, E. J. Cherry, and D. M. Taylor, *J. Chromatogr. Sci.*, **9**, 393 (1971).

(14) E. Marozzi, V. Gambaro, F. Lodi, and A. Pariali, *Farmaco, Ed. Prat.*, **31**, 180 (1976).

(15) *Ibid.*, **31**, 253 (1976).

(16) J. Wells, G. Cinbura, and E. Koves, *J. Forensic Sci.*, **20**, 382 (1975).

(17) A. C. Moffat, *J. Chromatogr.*, **113**, 69 (1975).

(18) "The National Formulary," 14th ed., Mack Publishing Co., Easton, Pa., 1975, p. 609.

(19) *Ibid.*, pp. 733, 734.

(20) *Ibid.*, pp. 166, 167.

(21) *Ibid.*, p. 94.

ACKNOWLEDGMENTS

The author thanks Richard L. Everett and William M. Ment, U.S. Food and Drug Administration, Baltimore District, for assistance.

Simultaneous GLC Determination of Methyl Salicylate and Menthol in a Topical Analgesic Formulation

JOSEPH P. SAPIO ˣ, KRISH SETHACHUTKUL, and JOSEPH E. MOODY

Received August 25, 1978, from the *USV Pharmaceutical Corporation, Tuckahoe, NY 10707.* Accepted for publication October 5, 1978.

Abstract □ A simultaneous GLC determination for methyl salicylate and menthol in a topical analgesic formulation is reported. *n*-Nonadecane is used as the internal standard. The method is rapid, accurate, precise, and selective in the presence of salicylic acid and ethyl salicylate.

Keyphrases □ Methyl salicylate—GLC analysis, topical analgesic formulation □ Menthol—GLC analysis, topical analgesic formulation □ GLC—analysis, methyl salicylate and menthol, topical analgesic formulation □ Analgesics, topical—methyl salicylate and menthol, GLC analysis

Combinations of methyl salicylate and menthol are used in several commercially available topical analgesic products (1). Official analytical methods for the quantitation of each of these active ingredients have been published (2). Other GLC determinations of methyl salicylate and menthol also have been published (3–5).

Simultaneous quantitation of methyl salicylate and menthol involved separating camphor, menthol, and methyl salicylate within 16 min on a 2-m × 2-mm i.d. stainless steel column containing 10% (w/w) polyethylene glycol on silanized Chromosorb W (5). Prior to GLC analysis, each sample was steam distilled and each distillate was extracted with chloroform. The amounts of camphor, menthol, and methyl salicylate were quantitated by peak area normalization. The reported precision was not greater than ±4%.

The described method is more rapid, more accurate, and more precise than the method described by Bruno (5) for the simultaneous determination of methyl salicylate and menthol in a topical analgesic formulation.

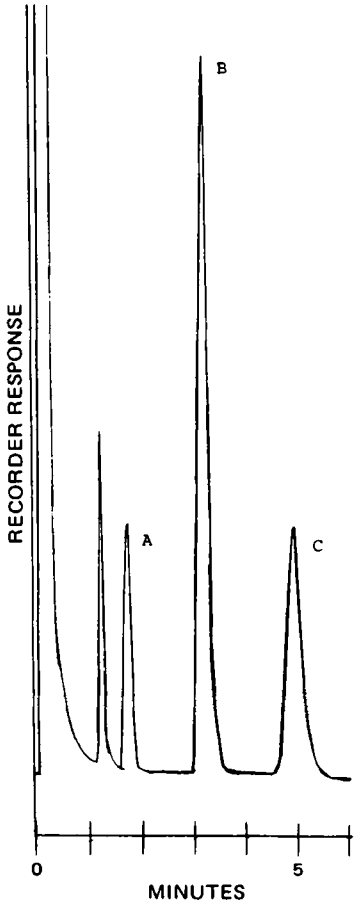

Figure 1—*Typical GLC separation of menthol (A), methyl salicylate (B), and* n*-nonadecane (C).*

EXPERIMENTAL

Chemicals and Reagents—Glass-distilled hexane[1], chloroform[1], and methanol[1] were used. Methyl salicylate[2], menthol[2], salicylic acid[2], and ethyl salicylate[3] were used as received. The internal standard was *n*-nonadecane[4].

GLC—A gas chromatograph[5] with a flame-ionization detector was used. A glass column, 180 cm × 3 mm i.d., was packed with 20% (w/w) polyethylene glycol[6] on 80–100-mesh Gas Chrom Q[6]. The carrier gas was helium[7] at a flow rate of 55 ml/min.

Analyses were carried out under the following conditions: injection port temperature, 200°; column oven temperature, 155°; and detector temperature, 220°. An electronic integrator[8] was used to determine peak areas.

Procedure—Approximately 1 g of the formulation was accurately weighed into a 100-ml volumetric flask. Then 10.0 ml of the internal standard solution [13 mg/ml in hexane–chloroform–methanol (50:50:3)] was pipetted into the flask, and the solution was diluted to volume with the same solvent. A standard solution was prepared similarly by accurately weighing proportional amounts of reference standard methyl salicylate and menthol. One microliter of the sample and standard preparations was injected into the gas chromatograph. Figure 1 shows a typical GLC separation.

Sensitivity—Calibration curves were determined for methyl salicylate and menthol in spiked placebo mixtures over the concentration ranges of interest.

Accuracy and Precision—The accuracy and precision of the GLC determination were evaluated from the recovery data for methyl salicylate (Table I) and menthol (Table II) from 10 spiked placebo mixtures.

The precision of injection for the GLC determination was evaluated from 20 injections of a placebo mixture spiked with methyl salicylate and menthol (Table III).

Selectivity—The selectivity of the GLC determination in the presence of salicylic acid and ethyl salicylate was evaluated by injecting standard mixtures containing these two compounds (Figs. 2 and 3).

RESULTS AND DISCUSSION

The calibration curves for methyl salicylate and menthol in this formulation were linear from 70 to 700 and 10 to 120 mg/g, respectively. No interference from a placebo mixture was observed.

The accuracy of this method, as measured from the recovery data, was 98.4 and 98.7% for methyl salicylate (Table I) and menthol (Table II), respectively. The precision, as measured from the standard deviations

[1] Burdick & Jackson Laboratories, Muskegon, Mich.
[2] USP reference standard.
[3] Aldrich Chemical Co., Milwaukee, Wis.
[4] Pfaltz & Bauer, Stamford, Conn.
[5] Model 3920 B, Perkin-Elmer Corp., Norwalk, Conn.
[6] Carbowax 20M, Alltech Associates, Arlington Heights, Ill.
[7] Liquid Carbonic Co., Chicago, Ill.
[8] Minigrator, Spectra-Physics, Piscataway, N.J.

0022-3549/79/0400-0506$01.00/0
© 1979, American Pharmaceutical Association

Table I—Recovery Data for the GLC Determination of Methyl Salicylate

Mixture	Theory, mg/g	Found, mg/g[a]	Recovery, %
1	300.06	297.92	99.3
2	299.25	292.48	97.7
3	306.00	300.26	98.1
4	305.09	302.56	99.2
5	300.06	295.55	98.5
6	303.23	295.12	97.3
7	304.40	296.06	97.3
8	303.08	297.28	98.1
9	300.07	296.11	98.7
10	300.50	298.79	99.4
Mean			98.4
SD, %			0.79

[a] Each value represents the average of duplicate sample injections.

Table II—Recovery Data for the GLC Determination of Menthol

Mixture	Theory, mg/g	Found, mg/g[a]	Recovery, %
1	51.15	50.98	99.7
2	31.78	31.34	98.6
3	49.97	49.24	98.5
4	50.06	49.92	99.7
5	49.24	48.63	98.8
6	50.83	49.66	97.7
7	50.53	49.18	97.3
8	51.78	51.16	98.8
9	48.94	48.56	99.2
10	51.09	50.60	99.0
Mean			98.7
SD, %			0.77

[a] Each value represents the average of duplicate sample injections.

of the recovery data, was ±0.79 and ±0.77% for methyl salicylate (Table I) and menthol (Table II), respectively.

The precision of injection (Table III), as measured from the standard deviations of the peak area ratios of the sample to the internal standard, was 1.428 ± 0.0201 and 0.356 ± 0.0048 for methyl salicylate and menthol, respectively. Such precision was obtained by filling the injection syringe in the following order: 0.5 μl of the solvent mixture, 0.5 μl of air, and 1 μl of the sample solution. This procedure assures that the sample will not be lost by volatilization through the rear seal of the syringe.

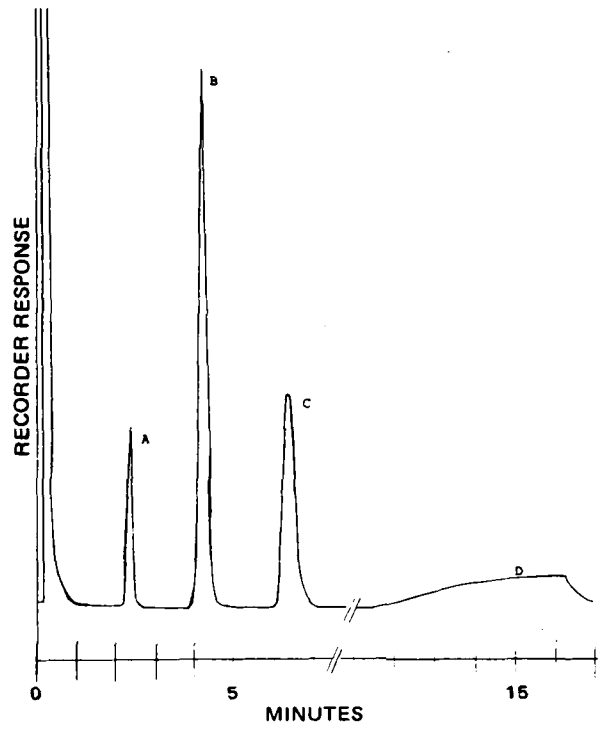

Figure 2—*GLC separation of menthol (A), methyl salicylate (B), n-nonadecane (C), and salicylic acid (D).*

Table III—Precision of Injection for the GLC Determination of Methyl Salicylate and Menthol

Injection	Area Methyl Salicylate / Area *n*-Nonadecane	Area Menthol / Area *n*-Nonadecane
1	1.443	0.359
2	1.431	0.356
3	1.431	0.357
4	1.399	0.351
5	1.447	0.361
6	1.431	0.357
7	1.409	0.351
8	1.415	0.353
9	1.451	0.363
10	1.405	0.352
11	1.419	0.354
12	1.404	0.350
13	1.421	0.355
14	1.454	0.363
15	1.421	0.355
16	1.475	0.367
17	1.426	0.355
18	1.408	0.351
19	1.452	0.362
20	1.423	0.354
Mean	1.428	0.356
SD, %	0.0201	0.0048

The selectivity of this method in the presence of salicylic acid (Fig. 2) and ethyl salicylate (Fig. 3) has been demonstrated. Such selectivity became important from the standpoint of product stability studies. The major hydrolysis product of methyl salicylate in this formulation would be salicylic acid. The major product from the transesterification between methyl salicylate and ethanol, a solvent used in the formulation, would be ethyl salicylate.

Prior sample preparations, such as steam distillation or solvent extraction, were not necessary for the analysis of this formulation. Elimination of these steps saved considerable analysis time and produced a chromatographic separation within 7 min. Column performance was maintained by periodically programming the column temperature to 220° to bleed off less volatile sample components.

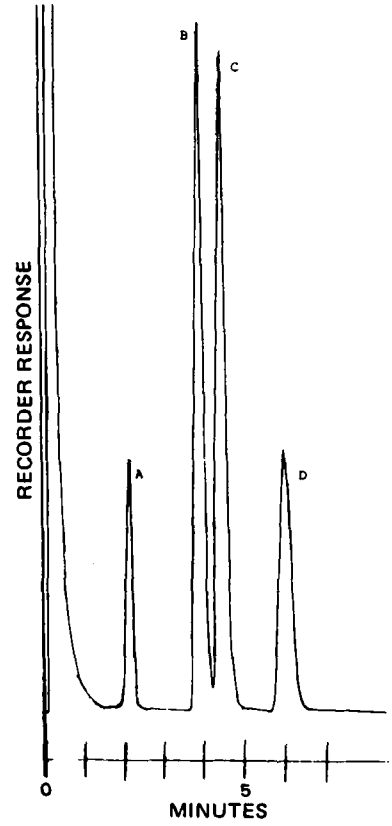

Figure 3—*GLC separation of menthol (A), methyl salicylate (B), ethyl salicylate (C), and n-nonadecane (D).*

REFERENCES

(1) "Handbook of Nonprescription Drugs," 5th ed., American Pharmaceutical Association, Washington, D.C., 1977, p. 293.

(2) "Official Methods of Analysis of the Association of Official Analytical Chemists," 12th ed., Association of Official Analytical Chemists, Washington, D.C., 1975, pp. 696, 753.

(3) S. Collings and R. Sinar, *J. Assoc. Public Anal.*, **4**, 59 (1966).

(4) W. Groebel, *Arch. Pharm.*, **300**, 226 (1967).

(5) E. Bruno, *Atti Congr. Qual.*, **6**, 121 (1967).

ACKNOWLEDGMENTS

The authors thank Ms. Rose Lancellotti and Ms. Theresia Mueller for assistance in the preparation of this manuscript.

Analysis of Dienestrol and Its Dosage Forms by High-Performance Liquid Chromatography

LEONARD C. BAILEY ˣ **and CAROLE A. BAILEY**

Received September 22, 1977, from the *Department of Pharmaceutical Chemistry, College of Pharmacy, Rutgers—the State University of New Jersey, Piscataway, NJ 08854.* Accepted for publication October 3, 1978.

Abstract □ A high-performance liquid chromatographic (HPLC) analysis is described for dienestrol as a drug substance and in cream, foam, and tablet dosage forms. After incorporation of the drug or dosage form into a solvent mixture containing an internal standard, biphenyl, an aliquot was chromatographed using a reversed-phase medium, followed by UV spectrophotometric detection at 254 nm. The response of the chromatographic system was linear over a concentration range corresponding to 50–200% of the labeled amount of dienestrol. Satisfactory accuracy and precision were confirmed by analyzing cream by the standard addition method. The advantages of the HPLC method are its simplicity, speed, and sensitivity, which permit direct analysis of single-dose quantities of dienestrol.

Keyphrases □ Dienestrol—analysis by high-performance liquid chromatography, in various dosage forms □ High-performance liquid chromatography—analysis, dienestrol in various dosage forms □ Estrogens, synthetic—high-performance liquid chromatographic analysis in various dosage forms

Dienestrol [4,4′-(1,2-diethylidene-1,2-ethanediyl)bisphenol, I] is a synthetic estrogenic compound used for the treatment of osteoporosis and estrogen deficiency. Because of its high level of potency, the dose used is very small. Therefore, analysis of pharmaceutical preparations requires not only separation of the compound from the dosage form matrix but also detection of microgram quantities of drug.

BACKGROUND

Separation of dienestrol from associated interfering substances has been accomplished by TLC (1), solvent extraction (2), open column chromatography (2, 3), and reversed-phase high-performance liquid chromatography (HPLC) at elevated temperatures (4). Quantitation has been obtained by UV spectrophotomety of dienestrol itself or of the indene formed by acid-induced isomerization (2). A recent publication (5) discussed the optimization of a normal-phase HPLC separation of dienestrol but not its applicability to pharmaceutical dosage forms.

The method of analysis official in NF XIV (6) for dienestrol cream requires a preliminary solvent extraction followed by lengthy column chromatography. The isolated phenolic fraction is then reacted with nitrous acid, and the nitrosophenols are determined polarographically (7). Although the method is sensitive, it is time consuming and subject to wide variation due to the number of manipulations required.

The purpose of this study was to use the inherent speed and sensitivity of HPLC to develop a simple, direct, accurate, and sensitive enough method for dienestrol to determine single-dose quantities. Such an analysis would be particularly applicable in quality assurance and stability testing situations.

The proposed method involves only dissolution of the sample, addition of the internal standard, and introduction of an aliquot of the resulting mixture onto a liquid chromatograph with a reversed-phase column and a UV detector operated at 254 nm. The accuracy and precision are comparable to those reported for other methods, but the time required is significantly less.

EXPERIMENTAL

Reagents and Chemicals—Dienestrol NF reference standard was used as received. Biphenyl[1] was recrystallized twice from ethanol, dried *in vacuo*, and stored in a vacuum desiccator, mp 69–71°.

Solvents—Acetonitrile[2] (99 mole % pure) was used as received.

Apparatus—The HPLC system consisted of a pump[3] and a UV monitor[4] operated at 254 nm. Samples were introduced using a loop injector[5] with a fixed volume of 20 μl. The loop injector was equipped with a sample prefilter (8). The output of the detector was displayed on a recorder[6] having a full-scale range of 10 mv. The output signal was integrated, and results were calculated using an electronic integrator[7]. The 25-cm × 4.6-mm i.d. stainless steel column contained reversed-phase packing material[8]. The mobile phase was pumped at a pressure of about 1600 psig, which resulted in a flow rate of 3.0 ml/min.

A mechanical shaker[9] was used in the extraction of samples.

Mobile Phase—The mobile phase, a mixture of acetonitrile and water (40:60), was degassed *in vacuo* prior to use.

Standard Solutions—*Dienestrol Standard Solution*—An accurately weighed 0.0500-g sample of dienestrol was transferred to a 100-ml volumetric flask and diluted to volume with acetonitrile.

Internal Standard Solution—An accurately weighed 0.0500-g sample of biphenyl was transferred to a 100-ml volumetric flask and diluted to volume with acetonitrile.

Diluted Internal Standard Solution—Exactly 5.0 ml of internal standard solution was transferred to a 250-ml volumetric flask and diluted to volume with acetonitrile.

Dienestrol Drug Substance—*Standard Preparation*—Exactly 2.0 ml of dienestrol standard solution and 2.0 ml of internal standard solution were transferred to a 100-ml volumetric flask and diluted to volume with acetonitrile. A 20-μl sample was introduced into the liquid chromatograph. The areas under the two peaks were measured, and the ratio, R_s, was calculated by dividing the area of the dienestrol peak by the area of the internal standard peak.

Assay Preparation—About 50 mg of dienestrol was weighed and transferred to a 100-ml volumetric flask and diluted to volume with ac-

[1] Eastman Kodak Co., Rochester, N.Y.
[2] Fisher Scientific Co., Fair Lawn, N.J.
[3] Constametric IIG, Laboratory Data Control, Riviera Beach, Fla.
[4] Model 1203, Laboratory Data Control.
[5] Model HPSV-20, Spectra-Physics.
[6] Omniscribe model 521I-151, Houston Instruments, Austin, Tex.
[7] Model 3380A, Hewlett-Packard, Avondale, Pa.
[8] Partisil PXS-1025 ODS, Whatman, Clifton, N.J.
[9] Eberbach Corp., Ann Arbor, Mich.

0022-3549/79/0400-0508$01.00/0

© 1979, American Pharmaceutical Association

REFERENCES

(1) "Handbook of Nonprescription Drugs," 5th ed., American Pharmaceutical Association, Washington, D.C., 1977, p. 293.

(2) "Official Methods of Analysis of the Association of Official Analytical Chemists," 12th ed., Association of Official Analytical Chemists, Washington, D.C., 1975, pp. 696, 753.

(3) S. Collings and R. Sinar, *J. Assoc. Public Anal.*, **4**, 59 (1966).

(4) W. Groebel, *Arch. Pharm.*, **300**, 226 (1967).

(5) E. Bruno, *Atti Congr. Qual.*, **6**, 121 (1967).

ACKNOWLEDGMENTS

The authors thank Ms. Rose Lancellotti and Ms. Theresia Mueller for assistance in the preparation of this manuscript.

Analysis of Dienestrol and Its Dosage Forms by High-Performance Liquid Chromatography

LEONARD C. BAILEY ˣ **and CAROLE A. BAILEY**

Received September 22, 1977, from the *Department of Pharmaceutical Chemistry, College of Pharmacy, Rutgers—the State University of New Jersey, Piscataway, NJ 08854.* Accepted for publication October 3, 1978.

Abstract □ A high-performance liquid chromatographic (HPLC) analysis is described for dienestrol as a drug substance and in cream, foam, and tablet dosage forms. After incorporation of the drug or dosage form into a solvent mixture containing an internal standard, biphenyl, an aliquot was chromatographed using a reversed-phase medium, followed by UV spectrophotometric detection at 254 nm. The response of the chromatographic system was linear over a concentration range corresponding to 50–200% of the labeled amount of dienestrol. Satisfactory accuracy and precision were confirmed by analyzing cream by the standard addition method. The advantages of the HPLC method are its simplicity, speed, and sensitivity, which permit direct analysis of single-dose quantities of dienestrol.

Keyphrases □ Dienestrol—analysis by high-performance liquid chromatography, in various dosage forms □ High-performance liquid chromatography—analysis, dienestrol in various dosage forms □ Estrogens, synthetic—high-performance liquid chromatographic analysis in various dosage forms

Dienestrol [4,4′-(1,2-diethylidene-1,2-ethanediyl)bisphenol, I] is a synthetic estrogenic compound used for the treatment of osteoporosis and estrogen deficiency. Because of its high level of potency, the dose used is very small. Therefore, analysis of pharmaceutical preparations requires not only separation of the compound from the dosage form matrix but also detection of microgram quantities of drug.

BACKGROUND

Separation of dienestrol from associated interfering substances has been accomplished by TLC (1), solvent extraction (2), open column chromatography (2, 3), and reversed-phase high-performance liquid chromatography (HPLC) at elevated temperatures (4). Quantitation has been obtained by UV spectrophotomety of dienestrol itself or of the indene formed by acid-induced isomerization (2). A recent publication (5) discussed the optimization of a normal-phase HPLC separation of dienestrol but not its applicability to pharmaceutical dosage forms.

The method of analysis official in NF XIV (6) for dienestrol cream requires a preliminary solvent extraction followed by lengthy column chromatography. The isolated phenolic fraction is then reacted with nitrous acid, and the nitrosophenols are determined polarographically (7). Although the method is sensitive, it is time consuming and subject to wide variation due to the number of manipulations required.

The purpose of this study was to use the inherent speed and sensitivity of HPLC to develop a simple, direct, accurate, and sensitive enough method for dienestrol to determine single-dose quantities. Such an analysis would be particularly applicable in quality assurance and stability testing situations.

The proposed method involves only dissolution of the sample, addition of the internal standard, and introduction of an aliquot of the resulting mixture onto a liquid chromatograph with a reversed-phase column and a UV detector operated at 254 nm. The accuracy and precision are comparable to those reported for other methods, but the time required is significantly less.

EXPERIMENTAL

Reagents and Chemicals—Dienestrol NF reference standard was used as received. Biphenyl[1] was recrystallized twice from ethanol, dried *in vacuo*, and stored in a vacuum desiccator, mp 69–71°.

Solvents—Acetonitrile[2] (99 mole % pure) was used as received.

Apparatus—The HPLC system consisted of a pump[3] and a UV monitor[4] operated at 254 nm. Samples were introduced using a loop injector[5] with a fixed volume of 20 μl. The loop injector was equipped with a sample prefilter (8). The output of the detector was displayed on a recorder[6] having a full-scale range of 10 mv. The output signal was integrated, and results were calculated using an electronic integrator[7]. The 25-cm × 4.6-mm i.d. stainless steel column contained reversed-phase packing material[8]. The mobile phase was pumped at a pressure of about 1600 psig, which resulted in a flow rate of 3.0 ml/min.

A mechanical shaker[9] was used in the extraction of samples.

Mobile Phase—The mobile phase, a mixture of acetonitrile and water (40:60), was degassed *in vacuo* prior to use.

Standard Solutions—*Dienestrol Standard Solution*—An accurately weighed 0.0500-g sample of dienestrol was transferred to a 100-ml volumetric flask and diluted to volume with acetonitrile.

Internal Standard Solution—An accurately weighed 0.0500-g sample of biphenyl was transferred to a 100-ml volumetric flask and diluted to volume with acetonitrile.

Diluted Internal Standard Solution—Exactly 5.0 ml of internal standard solution was transferred to a 250-ml volumetric flask and diluted to volume with acetonitrile.

Dienestrol Drug Substance—*Standard Preparation*—Exactly 2.0 ml of dienestrol standard solution and 2.0 ml of internal standard solution were transferred to a 100-ml volumetric flask and diluted to volume with acetonitrile. A 20-μl sample was introduced into the liquid chromatograph. The areas under the two peaks were measured, and the ratio, R_s, was calculated by dividing the area of the dienestrol peak by the area of the internal standard peak.

Assay Preparation—About 50 mg of dienestrol was weighed and transferred to a 100-ml volumetric flask and diluted to volume with ac-

[1] Eastman Kodak Co., Rochester, N.Y.
[2] Fisher Scientific Co., Fair Lawn, N.J.
[3] Constametric IIG, Laboratory Data Control, Riviera Beach, Fla.
[4] Model 1203, Laboratory Data Control.
[5] Model HPSV-20, Spectra-Physics.
[6] Omniscribe model 521I-151, Houston Instruments, Austin, Tex.
[7] Model 3380A, Hewlett-Packard, Avondale, Pa.
[8] Partisil PXS-1025 ODS, Whatman, Clifton, N.J.
[9] Eberbach Corp., Ann Arbor, Mich.

0022-3549/79/0400-0508$01.00/0

© 1979, American Pharmaceutical Association

etonitrile. Exactly 2.0 ml of this solution and 2.0 ml of internal standard solution were transferred to a 100-ml volumetric flask and diluted to volume with acetonitrile.

Assay—A 20-μl sample was introduced into the liquid chromatograph. The areas under the two peaks were measured, and the ratio, R_u, was calculated by dividing the area of the dienestrol peak by the area of the internal standard peak. The quantity, in micrograms of dienestrol present in the sample, was calculated by the formula:

$$\text{dienestrol } (\mu g) = W_s(R_u/R_s) \qquad \text{(Eq. 1)}$$

where R_u and R_s are as defined previously and W_s is the weight, in micrograms, of dienestrol present in 10.0 ml of the standard preparation.

Dienestrol Cream—*Standard Preparation*—The procedure was as given under *Dienestrol Drug Substance.*

Assay Preparation—An accurately weighed quantity of the cream, equivalent to not less than 100 μg of dienestrol, was transferred to a 25-ml glass-stoppered flask, and 10.0 ml of diluted internal standard solution was added and agitated on a mechanical shaker for 15 min. The resulting suspension was poured into a 15-ml conical centrifuge tube and centrifuged at high speed for 5 min.

Assay—The procedure was as given under *Dienestrol Drug Substance.*

Dienestrol Foam—*Standard Preparation*—The procedure was as given under *Dienestrol Drug Substance.*

Assay Preparation—The dienestrol container was shaken vigorously, the actuator was depressed, and a portion of the contents was discharged into a 125-ml glass-stoppered flask. The flask was immersed in a 60° water bath, and the contents were swirled until the entrapped propellant was dispelled and there was no further reduction in volume. Then the procedure was as given under *Dienestrol Cream Assay Preparation.*

Assay—The procedure was as given under *Dienestrol Drug Substance.*

Dienestrol Tablets—*Diluted Biphenyl Solution*—Exactly 5.0 ml of internal standard solution was transferred to a 250-ml volumetric flask and diluted to volume with mobile phase.

Standard Preparation—Exactly 2.0 ml of dienestrol standard solution and 2.0 ml of internal standard solution were transferred to a 100-ml volumetric flask and diluted to volume with mobile phase. The preparation continued as directed under *Dienestrol Drug Substance Standard Preparation,* beginning with: "A 20-μl sample was introduced . . . ."

Assay Preparation—A single dienestrol tablet was weighed and transferred to a glass-stoppered flask. An exactly measured quantity of diluted biphenyl solution was added such that the final concentration of dienestrol was nominally 10 μg/ml. The solution was agitated on a mechanical shaker for 15 min or until the tablet had completely disintegrated. The resulting suspension was poured into a 15-ml conical centrifuge tube and centrifuged at high speed for 5 min.

Assay—The procedure was as given under *Dienestrol Drug Substance.*

System Suitability Test—Five injections of the standard preparation were chromatographed as directed under *Dienestrol Cream.* In a suitable system, dienestrol exhibits one major peak with a retention time of about 0.71 relative to the internal standard and the resolution factor (9) between dienestrol and the internal standard is not less than 2.5. The relative standard deviation of the ratio of the peak areas of dienestrol to the peak areas of the internal standard should be not more than 2%.

RESULTS AND DISCUSSION

Mobile Phase—The suggested mobile phase, acetonitrile–water (40:60), was used for most of the work reported here. However, when new columns or those from manufacturers[10] other than the one cited under *Experimental* were used, adjustments were necessary in the relative proportions of the mobile phase components to achieve acceptable separations. Mobile phases containing as much as 55% acetonitrile were used with some columns with satisfactory results.

Higher proportions of acetonitrile reduced the retention times and, consequently, the time for each analysis, but an undesirable reduction in the resolution of dienestrol and the internal standard may result if the amount of acetonitrile is excessive. The suggested mobile phase should be used when required for sample dissolution because of the limited solubility of dienestrol in aqueous media.

Chromatographic Response—The typical response of dienestrol and the internal standard to the chromatographic system is shown in Fig. 1. This chromatogram was obtained from the analysis of dienestrol cream containing 80.1 μg/g of dienestrol.

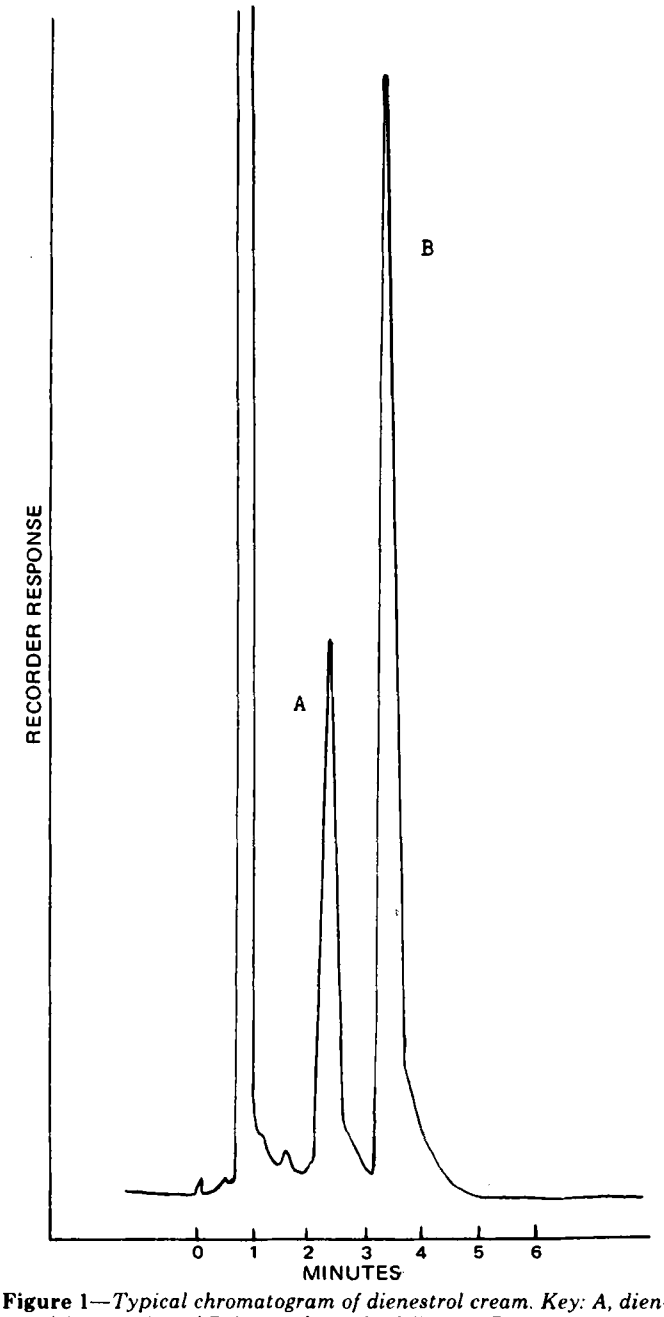

Figure 1—*Typical chromatogram of dienestrol cream. Key: A, dienestrol (0.160 μg); and B, internal standard (0.2 μg). Detector range was 0.032 aufs.*

To determine the linearity of the chromatographic response, a calibration curve was run in which the internal standard concentration was maintained constant while the dienestrol concentration was varied. The resulting response was linear (r = 0.999) over a range corresponding to quantities of dienesterol that would be obtained in the analysis of dosage forms containing 50–200% of the label claim. The intercept was essentially zero. The limit of sensitivity, defined as that quantity of dienestrol which, when injected on the column, gave a symmetrical peak with a height at least twice that of the noise level, was 1 ng.

No degradation of column performance was noted even after hundreds of injections. As a precautionary measure, the column was rinsed thoroughly with acetonitrile at the end of each day and kept filled with acetonitrile.

Analysis of Dosage Forms—Table I gives the results obtained from the analysis of some commercially available dosage forms containing dienestrol. In all cases except that of the cream, the amount recovered was essentially that claimed to be present by the manufacturer. The precision was also satisfactory, as indicated by the standard deviations

[10] μBondapak C18, Waters Associates, Milford, MA 01757; Datasorb ODS, 10 mm × 25 cm, Laboratory Data Control.

Table I—Determination of Dienestrol by HPLC

Drug Entity	Label Claim	Mean	*SD*	n^a
Powder	—	99.91[b]	1.02	4
Cream	100 μg/g	78.46	1.52	9
Foam	100 μg/g	104.83	0.50	6
Tablet	100 μg/tablet	100.07	4.48	10

[a] Number of samples analyzed. [b] Percent of label claim.

Table II—Single-Tablet Analysis of 0.1-mg Dienestrol Tablets

	Tablet Weight, g	Dienestrol Found, % of claim
	0.1614	101.71
	0.1499	103.83
	0.1395	97.08
	0.1722	100.88
	0.1487	97.23
	0.1550	99.83
	0.1626	106.47
	0.1546	90.53
	0.1626	99.35
	0.1606	103.80
Mean	0.1567	100.07
RSD, %	5.87	4.48

Table III—Analysis of Dienestrol Cream by HPLC with Standard Addition

Dienestrol Added[a], μg/g	Dienestrol Found	Standard Recovered[a]
0	78.46	—
25	24.59	98.4
50	50.44	100.9

[a] Percent of amount added.

of 1.52% or less except with tablets. Since all analyses of tablets were done on single tablets (Table II), the variation in tablet weight, which was 5.87 (% *RSD*) for the samples taken, was superimposed on the usual analytical variation due to weighing, pipetting, and diluting. If the results were corrected to a constant tablet weight or if a composite sample were analyzed, the variability would probably be less than that reported.

The low recoveries obtained from cream samples were assumed initially to be the result of incomplete extraction of dienestrol from the cream base. Various techniques, including heat, longer extraction times, and different mixtures of solvents, were employed to improve recoveries, but none increased the quantity of dienestrol recovered. Therefore, it was decided to verify the accuracy of the results by the method of standard addition (10). Three sets of samples of dienestrol cream were weighed and extracted in the usual manner with acetonitrile containing 10 μg/ml of internal standard and 0, 25, and 50 μg of dienestrol/10 ml.

The results obtained on the cream samples containing no added dienestrol confirmed the earlier analyses (Table III). Recovery of the added dienestrol was 98.4% for the 25-μg samples and 100.9% for the 50-μg samples. Therefore, it was concluded that the analytical results accurately reflected the true content of dienestrol in the sample used.

Because of the proven photochemical instability of synthetic estrogens of similar chemical structure (4), samples should be analyzed promptly after dissolution. A sample of dienestrol standard solution that had been left exposed to ambient light for 4 days showed no chromatographic peak at the dienestrol retention time. Instead, three smaller peaks with lower retention times were observed. They did not interfere with the dienestrol or internal standard peaks and, therefore, did not detract from the specificity of the method.

Other UV-absorbing ingredients in several formulations were benzoic acid, methylparaben, propylparaben, and nonoxynol. Qualitative analysis of these compounds showed no interference with dienestrol or the internal standard.

REFERENCES

(1) H. Neuninger, *Sci. Pharm.*, **40**, 12 (1972); through *Chem. Abstr.*, **76**, 15842r.

(2) J. H. Graham, D. Banes, and J. B. Proctor, *J. Assoc. Off. Anal. Chem.*, **55**, 190 (1972).

(3) R. E. Graham and C. T. Kenner, *J. Pharm. Sci.*, **62**, 1845 (1973).

(4) R. W. Roos, *ibid.*, **63**, 594 (1974).

(5) C. Hesse, K. Pietrzid, and D. Hotzel, *Chromatographia*, **10**, 256 (1977).

(6) "The National Formulary," 14th ed., Mack Publishing Co., Easton, Pa., 1975, p. 201.

(7) A. F. Summa and J. H. Graham, *J. Pharm. Sci.*, **54**, 612 (1965).

(8) L. C. Bailey, *J. Chem. Educ.*, **54**, 428 (1977).

(9) "The United States Pharmacopeia," 19th rev., Mack Publishing Co., Easton, Pa., 1975, p. 640.

(10) D. A. Skoog and D. M. West, "Fundamentals of Analytical Chemistry," 3rd ed., Holt, Rinehart and Winston, New York, N.Y., 1976, p. 588.

ACKNOWLEDGMENTS

The authors express their appreciation to Dr. Thomas Medwick for helpful discussions and to Theresa A. Folinusz for technical assistance.

Improved Electron-Capture GLC Determination of Alprenolol and Oxprenolol in Serum Using a Wall-Coated Open Tubular Column

D. DeBRUYNE, H. KINSUN ˣ, M. A. MOULIN, and M. C. BIGOT

Received March 31, 1978, from the *Laboratory of Pharmacology, Faculty of Medicine, Functional Explorations B Department, University Hospital Center of Caen, 14032 Caen Cedex, France.* Accepted for publication September 5, 1978.

Abstract □ An accurate, rapid, and sensitive GLC determination of alprenolol and oxprenolol in serum is described. This method combines an electron-capture detector with a wall-coated open tubular column. The lowest detectable amount of the halogenated (heptafluoroacyl) derivatives of alprenolol and oxprenolol is 2 pg. The high resolving power and the rapid elution time of the wall-coated open tubular column dramatically improve the performance (accuracy and sensitivity) of the conventional electron-capture detector and packed column system in these determinations. This method allows the use of small volumes of sample (100–200 μl), does not require redistilled reagents, and has a simplified extraction procedure.

Keyphrases □ Alprenolol—electron-capture GLC determination of serum levels, wall-coated open tubular column □ Oxprenolol—electron-capture GLC determination of serum levels, wall-coated open tubular column □ GLC—determination of alprenolol and oxprenolol in serum using wall-coated open tubular column and electron-capture detection

Because of their lower therapeutic serum levels [10–100 ng/ml (1, 2)], the β-blocking agents alprenolol and oxprenolol have been determined by electron-capture GLC (3–7) as their halogenated derivatives. Unfortunately, these methods require a large blood sample (1–4 ml), involve a time-consuming extraction step, and sometimes have poor reproducibility (3).

The purpose of this work was to develop a fast and more convenient GLC determination for alprenolol and oxprenolol in blood by the simultaneous use of an electron-capture detector and a wall-coated open tubular column.

EXPERIMENTAL

Instrumentation—The gas chromatograph[1], equipped with a ^{63}Ni electron-capture detector[2] and a splitter injector[3], was connected to a recorder[4] with a scale range of 1 mv.

The 0.3-μm OV-101 phase thickness glass capillary column[5] (25 m × 0.25 mm) was pretreated and tested by the manufacturer. According to the spot test, it had an effective number of theoretical plates (N) of 38,000 (endrin[6]) at 200° for a carrier gas (nitrogen) with a velocity of 16 cm/sec and a capacity factor of 6.08.

The test conditions were: sample injected, 1 μl; injector temperature, 270°; column temperature, 205° (assay of alprenolol) or 185° (assay of oxprenolol); split ratio, 1:12; linear velocity of carrier gas, 34 (assay of alprenolol) or 58 (assay of oxprenolol) cm/sec; makeup gas (nitrogen) flow rate, 30 ml/min; detector temperature, 280°; duration and interval of pulsed mode, 0.8–4 and 100–200 μsec, respectively; sensitivity and attenuation, 0.1 × 64 and 1 × 32; and chart speed, 10 mm/min.

Standard Solutions—The standard stock solutions (0.2 μg/ml) of pure alprenolol[7] and oxprenolol[8] were prepared by dissolving them directly in 0.2 N HCl; these solutions were stored at 4° in a cold chamber. Chemical purity of standards was checked by high-resolution (wall-coated open tubular column) GLC.

Extraction and Preparation of Derivatives—To 200 μl of normal human serum[9] in glass test tubes (polytef-lined screw cap) were added, successively, 5–30 ng of alprenolol, 40 ng of oxprenolol from stock solutions as the internal standard, 25 μl of 1 N NaOH, and 5 ml of ether. The mixture was shaken for 5 min. After washing with 0.5 ml of distilled water and centrifugation (5 min at 15° and 3500 rpm), the ethereal phase was evaporated to dryness on a water bath at 50°. Then 100 μl of heptafluorobutyryl anhydride[10] solution in ethyl acetate (1:3 v/v) was added as the acylating reagent (8), and the temperature was raised to 60° for 15 min. Excess heptafluorobutyryl anhydride was eliminated by evaporation in a rapid current of air. After it was completely discharged, 100 μl of hexane was added and the mixture was evaporated once again.

The same procedure was used for the standardization of oxprenolol with 5 ng of alprenolol as the internal standard.

The residue was dissolved in 50 μl of hexane, and 1 μl of the mixture was injected into the chromatograph.

RESULTS AND DISCUSSION

Figure 1 illustrates the chromatographic responses of the alprenolol (α) and oxprenolol (β) heptafluorobutyryl derivatives. The chromatogram (Fig. 1a) obtained from 3% OV-1 on a 100–120-mesh Gas Chrom Q packed stainless steel column[3] (2.17 mm × 2 m) with the back-extraction procedure of Di Salle *et al.* (8) for propranolol clearly shows fewer peaks than that obtained from the wall-coated open tubular column (Fig. 1b). Figure 1b shows retention times relative to the solvent of 6 min for alprenolol and 7.5 min for oxprenolol. The lowest detectable amount was 2 pg.

Comparison of the two chromatograms obtained with equivalent nonpolar phases depicts the poor separation of interfering substances from alprenolol and oxprenolol owing to the insufficient resolving power of the packed column (9). This result could constitute a source of error in the accuracy and reproducibility of any method.

The high efficiency (10–12) of the wall-coated open tubular column is substantiated by Fig. 1c. It was obtained after using the described simple extraction procedure with reagents that had not been redistilled (ether and heptafluorobutyryl anhydride). Interfering substances were completely absent from drug peaks. Under these conditions, the calibration curve of alprenolol (with oxprenolol as the internal standard) (13) was linear over a range of 0–150 ng/ml. The slope of the regression line was 0.014 with a correlation coefficient of 0.999. The standard deviation varied from 3% at 25 ng/ml to 1.5% at 150 ng/ml over 2–3 months. The calibration curve of oxprenolol (with alprenolol as the internal standard) was linear over a range of 0–150 ng/ml. The slope of the regression line was 0.012 with a correlation coefficient of 0.999. The standard deviation varied from 3% at 25 ng/ml to 2% at 150 ng/ml over 2–3 months. The recovery was 97 ± 4.5% for both drugs.

[1] Girdel model 3000 FC 1 ERPT, Suresnes, France.
[2] Girdel model 3000, Suresnes, France.
[3] Girdel, Suresnes, France.
[4] Servotrace PU Sefram, Paris, France.
[5] Catalog No. 2101-201, LKB, Bromma, Sweden.
[6] Applied Sciences, Inglewood, CA 90304.
[7] Aptine, Lematte Boinot, Paris, France.
[8] Trasicor, Ciba-Geigy, Rueil Malmaison, France.
[9] Biotrol 00A, Biotrol, Paris, France.
[10] Pierce Chemical Co., Rockford, IL 61105.

0022-3549/79/0400-0511$01.00/0
© 1979, American Pharmaceutical Association

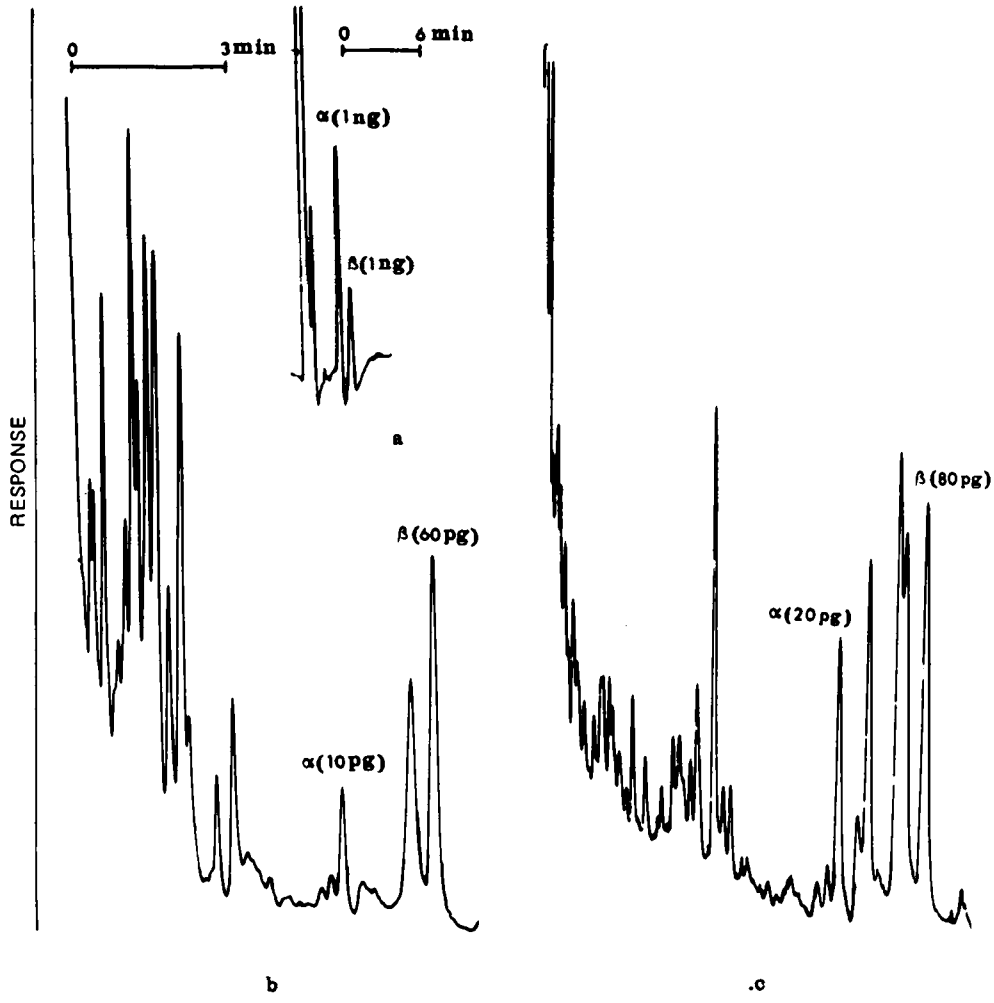

Figure 1—*(a) Chromatogram according to the extraction procedure of Di Salle* et al. *(8) but with a 3% OV-1 packed column. The test conditions were: injector temperature, 260°; detector temperature; 280°; column temperature, 185°; nitrogen pressure, 2 bar; duration and pulse interval, 0.8 and 100 μsec; sensitivity and attenuation, 1 × 32; and chart speed, 2.5 mm/min. (b) Chromatogram according to the extraction procedure described in Fig. 1a but with the wall-coated open tubular column and chromatographic conditions described under* Experimental. *(c) Chromatogram according to the single extraction procedure with chromatographic conditions similar to those used for Fig. 1b. The α and β are peaks of alprenolol and oxprenolol, respectively.*

The most troublesome interference from endogenous substances coextracted with the drugs, such as amines and alcohols that react with heptafluorobutyryl anhydride or aromatic and oxygen derivatives, was not found under the test conditions because of the high efficiency of the wall-coated open tubular column. Exogenous substances such as clonazepam[11], flunitrazepam[11], diazepam[11], endrin[6], dicophane[6], and propranolol[12] do not coelute with alprenolol and oxprenolol.

The method has been used in clinical pharmacology and pharmacokinetic studies. In monitoring blood oxprenolol levels, patients receiving an oral oxprenolol dose of 0.66–1.5 mg/kg/8 hr from tablets[8] showed blood concentrations of 100–385 ng/ml. In dogs, blood alprenolol levels reached 448 ± 13.5 ng/ml 1.5 hr after a single oral dose of 15 mg of alprenolol/kg from tablets[7] and decreased rapidly to 148 ± 4.5 ng/ml 3 hr after administration. The chromatograms obtained in both cases, *i.e.*, alprenolol in dogs and oxprenolol in humans, were of the same form as in Figs. 1*b* and 1*c*.

The high resolving power and sensitivity (14) of the wall-coated open tubular column relative to the conventional packed column (in which the number of theoretical plates is limited by the length of the column) led to the development of a fast, accurate, and convenient electron-capture GLC method for alprenolol and oxprenolol determinations in blood. The small volume of working sample (100–200 μl instead of 1–4 ml) and the simplified extraction procedure are desirable in the analysis of β-blockers (15–18).

REFERENCES

(1) P. Collste, K. Haglund, M. Frisk-Holmberg, and M. D. Rawlins, *Eur. J. Clin. Pharmacol.*, **10**, 85 (1976).

(2) W. D. Mason and N. Winer, *Clin. Pharmacol. Ther.*, **20**, 401 (1976).

(3) M. Erwik, *Acta Pharm. Suec.*, **6**, 393 (1969).

(4) T. Nambara, S. Akiyama, and M. Kurata, *Yakugaku Zasshi*, **93**, 439 (1973).

(5) D. B. Jack and W. Riess, *J. Chromatogr.*, **88**, 173 (1974).

(6) T. Walle, *J. Pharm. Sci.*, **63**, 1885 (1974).

(7) P. H. Degen and W. Riess, *J. Chromatogr.*, **121**, 71 (1976).

(8) E. Di Salle, K. M. Baker, S. R. Bareggi, W. D. Watkins, C. A. Chidsey, A. Frigerio, and P. L. Morselli, *ibid.*, **84**, 347 (1973).

(9) M. G. Horning, E. C. Chambaz, C. J. Brooks, A. M. Moss, E. A. Boucher, E. C. Horning, and R. M. Hill, *Anal. Biochem.*, **31**, 512 (1969).

(10) J. De Graeve and J. Vanroy, *J. Chromatogr.*, **129**, 171 (1976).

(11) F. Berthou, D. Picart, L. Bardou, and H. H. Floch, *ibid.*, **118**, 135 (1976).

(12) H. Kinsun, M. A. Moulin, R. Venezia, D. Laloum, and M.-C. Bigot, *Clin. Chim. Acta*, **84**, 315 (1978).

(13) D. A. Saelens, T. Walle, and P. J. Privitera, *J. Chromatogr.*, **123**, 185 (1976).

(14) J. Macloue, M. Rigaud, J. Durand, and P. Chebroux, *Prostaglandins*, **6**, 999 (1976).

(15) M. D. Rawlins, P. Collste, M. Frisk-Holmberg, M. Lind, J. Ostman, and F. Sjoqvist, *Eur. J. Clin. Pharmacol.*, **7**, 353 (1974).

(16) B. Ablad, K. O. Borg, G. Johnsson, C. G. Regardh, and L. Solvell, *Life Sci.*, **14**, 693 (1974).

(17) M. J. West, M. J. Kendall, M. Mitchard, and E. B. Faragher, *Br. J. Clin. Pharmacol.*, **3**, 439 (1976).

(18) M. J. Kendall, M. J. Mitchard, M. West, W. A. John, and A. F. Faragher, *Eur. J. Drug Metab. Pharmacokinet.*, **3**, 155 (1976).

[11] Roche, France.
[12] Sigma, St. Louis, MO 63178.

ACKNOWLEDGMENTS

The authors thank A. Berra, E. Come, V. Liard, and M. Perault for their help in preparing this manuscript.

New Spectrophotometric Determination of Inorganic Bromide and Chloride Salts in Aqueous Solutions

ANWAR HUSSAIN [x] **and R. BAWARSHI**

Received April 28, 1978, from the *College of Pharmacy, University of Kentucky, Lexington, KY 40506.* Accepted for publication September 7, 1978.

Abstract □ A new method for the determination of inorganic salts of chloride and bromide is described. The method is based on the facts that iodine forms complexes with the anions and that these complexes absorb strongly in the UV region. The molar absorptivities of I_2Br^- at 265 nm and I_2Cl^- at 245 nm were calculated to be 3.27×10^4 and 2.3×10^4 M^{-1} cm^{-1}, respectively.

Keyphrases □ Inorganic salts—spectrophotometric determination of aqueous solutions □ Salts—spectrophotometric determination of inorganic bromide and chloride salts in aqueous solutions □ Complexes—iodine with inorganic bromide and chloride salts, spectrophotometric determination

Various methods are available for the quantitative determination of chloride and bromide ions in aqueous solutions. Some of these methods are volumetric and gravimetric (1–4) and, therefore, are laborious, time consuming, and expensive to do routinely. Relatively newer methods (5) based on the use of ion selective electrodes are excellent. However, in view of their lack of selectivity, it is necessary to have an electrode for each ion and its reagent (6).

This report describes a sensitive and simple spectrophotometric method for the determination of these halides. The method is based on the fact that both chloride and bromide ions interact with iodine in solution to form complexes that absorb strongly in the UV region.

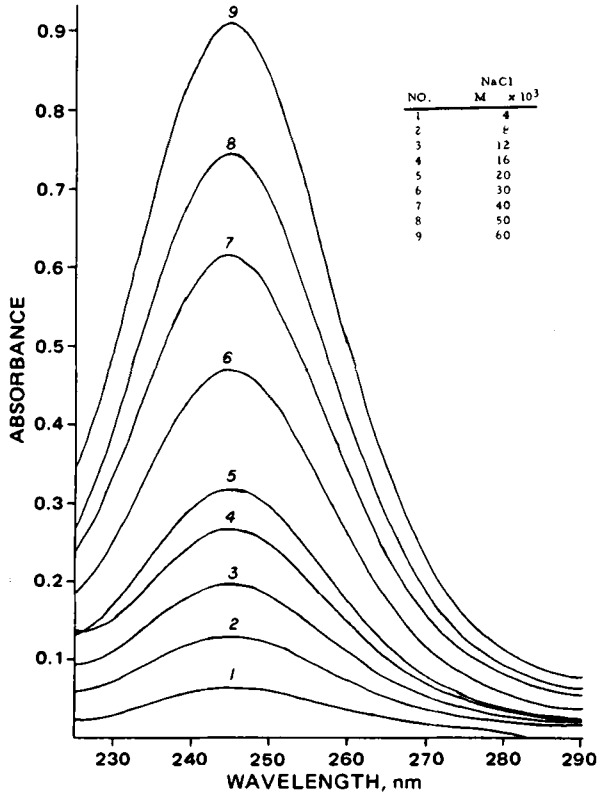

Figure 1—*UV spectra of solutions containing 3 × 10⁻⁴ M I_2 and varying amounts of sodium chloride (NaCl).*

BACKGROUND

Iodide, bromide, and chloride ions are known to interact with iodine in solution to form complexes of the type I_2X^- (7) (Schemes I–III).

$$I_2 + I^- \rightleftharpoons I_2I^-$$

Scheme I

$$I_2 + Br^- \rightleftharpoons I_2Br^-$$

Scheme II

$$I_2 + Cl^- \rightleftharpoons I_2Cl^-$$

Scheme III

The equilibrium constants, defined as:

$$K = \frac{(I_2X^-)_{eq}}{(I_2)_{eq}(X^-)_{eq}} \qquad \text{(Eq. 1)}$$

for Schemes I–III have been reported to be 702, 11.0, and 2.1, respectively (7). These values were confirmed in this study using a different technique based on phase solubility.

Although iodide absorbs rather strongly at 238 nm and can be determined spectrophotometrically, chloride and bromide ions have no UV absorbance in this region. However, when chloride or bromide salts are added to an aqueous iodine solution to form I_2Br^- and I_2Cl^-, these solutions absorb light strongly in the UV region. The maximum absorbances for I_2Br^- and I_2Cl^- are at 265 and 245 nm, respectively, whereas iodine at the same concentration absorbs insignificantly (Figs. 1 and 2). Furthermore, the absorbance of solutions containing fixed amounts of iodine and varying amounts of the halides increases linearly as a function of the concentration of the halides (Figs. 3 and 4).

In view of this information, it would be possible to determine quantitatively both chloride and bromide in aqueous solutions.

EXPERIMENTAL

Reagents and Equipment—A saturated stock iodine solution was prepared by adding 2 liters of double-distilled water to 5 g of iodine. The solution was left overnight on a shaker to reach saturation. The saturated solubility of iodine in water at 25° was found by titration to be 7.5×10^{-4}

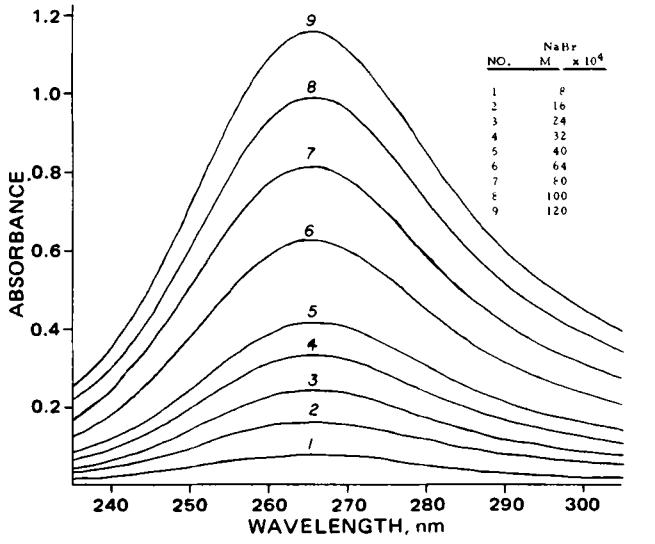

Figure 2—*UV spectra of solutions containing 3 × 10⁻⁴ M I_2 and varying amounts of sodium bromide (NaBr).*

0022-3549/79/0400-0513$01.00/0
© 1979, American Pharmaceutical Association

Table I—Concentration of I_2Br^- Calculated from Eq. 1 as a Function of Added Sodium Bromide and the Corresponding UV Absorbance at 265 nm [a]

Sodium Bromide Added, $M \times 10^4$	I_2Br^- Calculated, $M \times 10^6$	UV Absorbance at 265 nm
8	2.54	0.080
16	5.08	0.160
24	7.42	0.240
32	9.81	0.530
40	12.2	0.420
64	19.0	0.620
80	23.4	0.820
100	28.6	0.990
120	33.8	1.150

[a] All samples contained 3×10^{-4} M I_2.

M, in good agreement with the reported value (8). Sodium iodide, sodium chloride, and sodium bromide were analytical reagent grades.

A recording spectrophotometer[1] was used.

Phase Solubility Study—Into a 25-ml screw-capped vial with a polytef lining, 0.1 g of iodine was placed. Then 12 ml of sodium chloride or sodium bromide solution of known concentration was added. The vials were left in the shaker for 24 hr, and 10 ml of the supernatant liquid was titrated with 1×10^{-3} M sodium thiosulfate. The iodine concentration was calculated and plotted against the concentration of the halide added.

Spectrophotometric Analysis—To each 20 ml of the saturated iodine solution (7.5×10^{-4} M) placed in 50-ml volumetric flasks, different volumes of 0.01 M NaBr or 0.1 M NaCl were added to obtain halide concentrations ranging from 8×10^{-4} to 1.2×10^{-2} M for sodium bromide and 4×10^{-3} to 6×10^{-2} M for sodium chloride. The volumes were completed to 50 ml with double-distilled water. The UV spectra of the solutions were then measured spectrophotometrically against a blank iodine solution prepared as already described. Common impurities normally found in these salts such as phosphate, sulfate, and carbonate have no effect on the absorbance of these solutions.

Stability of Solutions—The UV spectra of the solutions were determined immediately after their preparation and 3 hr later. No change in the UV absorbance was observed.

Comparison between USP and Spectrophotometric Analyses of Sodium Chloride Tablets USP—To compare the reliability of this method for analyzing dosage forms, three tablets[2] were weighed individually and dissolved in 100 ml of double-distilled water. Then 25 ml of each solution was titrated according to the USP method (1). The same solutions were analyzed spectrophotometrically by pipetting 10 ml into a 50-ml volumetric flask. To this solution, 10 ml of the saturated iodine solution was added. The solutions were analyzed spectrophotometrically, and the concentration of sodium chloride was calculated by comparing the absorbance of these solutions to that of a standard sodium chloride solution treated similarly.

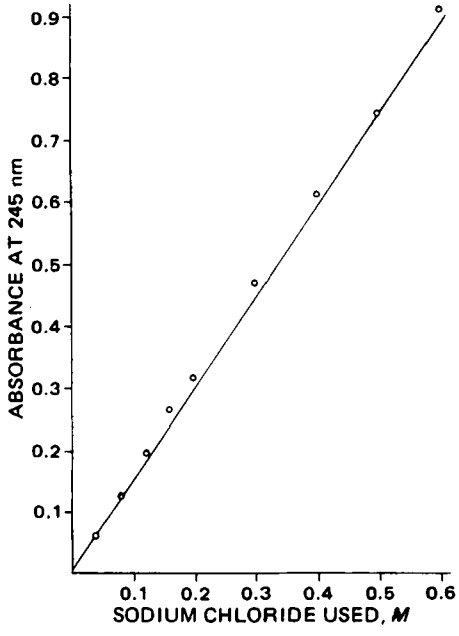

Figure 3—*Plot showing a linear increase in the absorbance at 245 nm of solutions containing the same concentration of iodine, 3×10^{-4} M, and varying concentrations of sodium chloride (NaCl).*

[1] Varian model 118.
[2] Eli Lilly lot IFB50A.

Table II—Concentration of I_2Cl^- Calculated from Eq. 1 as a Function of Added Sodium Chloride and the Corresponding UV Absorbance at 245 nm [a]

Sodium Chloride Added, $M \times 10^3$	I_2Cl^- Calculated, $M \times 10^6$	UV Absorbance at 245 nm
4	2.85	0.065
8	5.65	0.130
12	8.39	0.198
16	11.1	0.265
20	13.7	0.320
30	20.1	0.470
40	26.3	0.615
50	32.1	0.742
60	37.7	0.910

[a] All samples contained 3×10^{-4} M I_2.

Table III—Results and Comparisons of the USP and Spectrophotometric Methods Using Commercial Sodium Chloride Tablets USP

Weight of Tablet, g	USP Method, g	Spectrophotometric Method, g
1.015	1.016	1.018
1.010	1.014	1.015
1.020	1.021	1.020

RESULTS AND DISCUSSION

Figure 5 shows the results of the phase solubility studies between iodine and chloride and bromide ions. The equilibrium constants determined

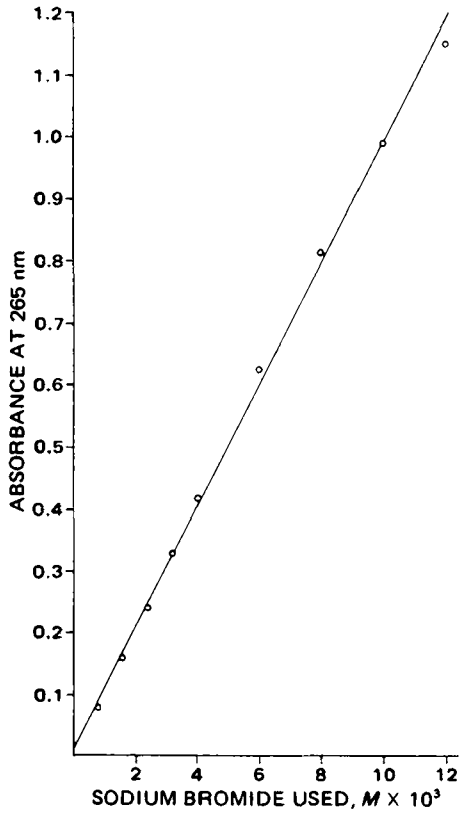

Figure 4—*Plot showing a linear increase in the absorbance at 265 nm of solutions containing the same concentration of iodine, 3×10^{-4} M, and varying concentrations of sodium bromide (NaBr).*

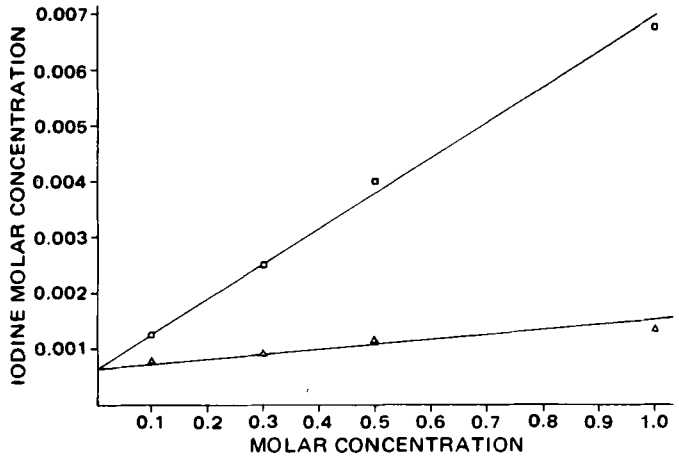

Figure 5—*Plot showing the increase in the solubility of iodine as a function of added sodium chloride (△) and sodium bromide (□).*

from the slope of the lines of Fig. 5 were 10.6 and 2.4 for bromide and chloride, respectively, in good agreement with reported values (7).

Figures 1 and 2 show the UV absorbances of solutions containing 3×10^{-4} *M* I_2 and varying concentrations of sodium bromide and sodium chloride. A linear relationship between the absorbance at the corresponding wavelengths and the concentration of the added halide salts was observed. It is apparent from the data of Figs. 1 and 2 that the change in the magnitude of the absorbance as a function of the added halide was due to changes in the concentration of the complexes formed in solution.

The concentrations of I_2Br^- and I_2Cl^- can be calculated as a function of added halides using Eq. 1 (Tables I and II). The calculated molar absorptivities were 3.27×10^4 and 2.3×10^4 M^{-1} cm^{-1} for I_2Br^- and I_2Cl^-, respectively.

Table III shows the results obtained for the determination of sodium chloride tablets by the USP and spectrophotometric methods. The agreement between the two methods was excellent. In practice, it is advisable to determine the unknown together with a known sample using the same iodine concentration in both samples.

REFERENCES

(1) "The United States Pharmacopeia," 19th rev., Mack Publishing Co., Easton, Pa., 1975, p. 457.

(2) W. M. MacNevin, B. B. Baker, and R. D. McIver, *Anal. Chem.*, **25**, 274 (1953).

(3) I. M. Kolthoff and V. A. Stenger, "Volumetric Analysis," 2nd ed., Interscience, New York, N.Y., 1947.

(4) R. Belcher, A. M. MacDonald, and E. Parry, *Anal. Chim. Acta*, **16**, 524 (1957).

(5) R. Rechnitz, *Chem. Eng. News*, **45**, 146 (1967).

(6) G. A. Rechnitz, M. R. Kresz, and A. Sloan, *Anal. Chem.*, **38**, 1786 (1966).

(7) P. J. Durrant and B. Durrant, "Introduction to Advanced Inorganic Chemistry," Wiley, New York, N.Y., 1962, p. 933.

(8) "Remington's Pharmaceutical Sciences," 14th ed., Mack Publishing Co., Easton, Pa., 1970, p. 1180.

Stability of 10-Acetylphenothiazine

H. ROSEBOOM ˣ **and A. D. FÖRCH**

Received April 7, 1978, from the *Farmaceutisch Laboratorium Rijksuniversiteit Utrecht, Catharijnesingel 60, Utrecht, The Netherlands.* Accepted for publication August 30, 1978.

Abstract □ The degradation kinetics of 10-acetylphenothiazine were studied after isolation and identification of its degradation products, phenothiazine, phenothiazine-5-oxide, 3*H*-phenothiazine-3-one, and 7-(10′-phenothiazinyl)-3*H*-phenothiazine-3-one. The acetyl group was not present in any degradation product. The degradation rate was independent of oxygen but highly pH dependent, indicating a specific hydrogen-ion-catalyzed hydrolysis of 10-acetylphenothiazine to give phenothiazine, which was oxidized. The experimental values for the phenothiazine concentration were in good agreement with values calculated on the basis of this assumption, both in the presence and absence of oxygen.

Keyphrases □ 10-Acetylphenothiazine—stability and degradation kinetics, pH dependency □ Phenothiazines—10-acetylphenothiazine, stability and degradation kinetics, pH dependency □ Degradation—10-acetylphenothiazine, kinetics, effect of pH

The kinetics and mechanism of the oxidative degradation of phenothiazine and its 10-methyl derivative were described previously (1, 2). In this paper, the influence of the introduction of an acetyl group on stability is investigated. The 10-acetyl derivative can be considered as a model compound for the phenothiazines having a carbonyl function next to the nitrogen atom; these compounds possess antiarrhythmic properties (3). The electron-withdrawing properties of the acetyl group could possibly have a strong stabilizing effect on the phenothiazine ring system.

EXPERIMENTAL

Materials—10-Acetylphenothiazine[1] (I) was recrystallized from 96% ethanol, mp 204°, and had a molar absorptivity at 257 nm of 10,194. TLC of the recrystallized product in various systems showed only one spot, so no further purification was performed.

All other materials were as previously described (1).

Isolation and Identification of Degradation Products—Compound I was dissolved in 52.5% ethanol, buffered to an apparent pH of 2.8 with sodium acetate–hydrochloric acid (4), and stored in the dark at 85° for 3 days after saturation with oxygen. The degradation products were extracted with carbon tetrachloride and isolated by TLC and column chromatography. Silica gel and aluminum oxide were used as adsorbents, and the solvents were ether, petroleum ether, chloroform, acetone, and their mixtures. The best separation was obtained with aluminum oxide and ether and silica gel and chloroform, both giving five zones. When the degradation was carried out at pH 1.7, the same products were found by TLC as at pH 2.8.

To isolate the degradation products, the carbon tetrachloride extract was evaporated to dryness under reduced pressure at room temperature and the residue was dissolved in ether. This solution was put onto a silica gel column, and the column was then eluted with ether until the colored products had left the column. Because one degradation product was not eluted with ether, the elution was continued with acetone, giving a solution that contained only one degradation product.

The ether eluate was evaporated to dryness under reduced pressure at room temperature, and the residue was dissolved in ether–petroleum ether (1:3). This solution was put onto an aluminum oxide column, and

[1] 10-Acetylphenothiazine was a gift from Dr. C. D. M. ten Berge, Farmaceutisch Laboratorium, Groningen, The Netherlands.

0022-3549/79/0400-0515$01.00/0
© 1979, American Pharmaceutical Association

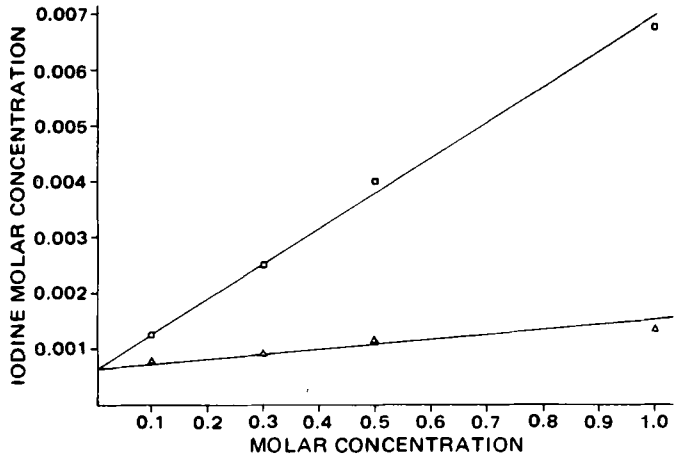

Figure 5—*Plot showing the increase in the solubility of iodine as a function of added sodium chloride (△) and sodium bromide (□).*

from the slope of the lines of Fig. 5 were 10.6 and 2.4 for bromide and chloride, respectively, in good agreement with reported values (7).

Figures 1 and 2 show the UV absorbances of solutions containing 3×10^{-4} *M* I_2 and varying concentrations of sodium bromide and sodium chloride. A linear relationship between the absorbance at the corresponding wavelengths and the concentration of the added halide salts was observed. It is apparent from the data of Figs. 1 and 2 that the change in the magnitude of the absorbance as a function of the added halide was due to changes in the concentration of the complexes formed in solution.

The concentrations of I_2Br^- and I_2Cl^- can be calculated as a function of added halides using Eq. 1 (Tables I and II). The calculated molar absorptivities were 3.27×10^4 and 2.3×10^4 M^{-1} cm^{-1} for I_2Br^- and I_2Cl^-, respectively.

Table III shows the results obtained for the determination of sodium chloride tablets by the USP and spectrophotometric methods. The agreement between the two methods was excellent. In practice, it is advisable to determine the unknown together with a known sample using the same iodine concentration in both samples.

REFERENCES

(1) "The United States Pharmacopeia," 19th rev., Mack Publishing Co., Easton, Pa., 1975, p. 457.

(2) W. M. MacNevin, B. B. Baker, and R. D. McIver, *Anal. Chem.*, **25**, 274 (1953).

(3) I. M. Kolthoff and V. A. Stenger, "Volumetric Analysis," 2nd ed., Interscience, New York, N.Y., 1947.

(4) R. Belcher, A. M. MacDonald, and E. Parry, *Anal. Chim. Acta*, **16**, 524 (1957).

(5) R. Rechnitz, *Chem. Eng. News*, **45**, 146 (1967).

(6) G. A. Rechnitz, M. R. Kresz, and A. Sloan, *Anal. Chem.*, **38**, 1786 (1966).

(7) P. J. Durrant and B. Durrant, "Introduction to Advanced Inorganic Chemistry," Wiley, New York, N.Y., 1962, p. 933.

(8) "Remington's Pharmaceutical Sciences," 14th ed., Mack Publishing Co., Easton, Pa., 1970, p. 1180.

Stability of 10-Acetylphenothiazine

H. ROSEBOOM ˣ **and A. D. FÖRCH**

Received April 7, 1978, from the *Farmaceutisch Laboratorium Rijksuniversiteit Utrecht, Catharijnesingel 60, Utrecht, The Netherlands.* Accepted for publication August 30, 1978.

Abstract □ The degradation kinetics of 10-acetylphenothiazine were studied after isolation and identification of its degradation products, phenothiazine, phenothiazine-5-oxide, 3*H*-phenothiazine-3-one, and 7-(10′-phenothiazinyl)-3*H*-phenothiazine-3-one. The acetyl group was not present in any degradation product. The degradation rate was independent of oxygen but highly pH dependent, indicating a specific hydrogen-ion-catalyzed hydrolysis of 10-acetylphenothiazine to give phenothiazine, which was oxidized. The experimental values for the phenothiazine concentration were in good agreement with values calculated on the basis of this assumption, both in the presence and absence of oxygen.

Keyphrases □ 10-Acetylphenothiazine—stability and degradation kinetics, pH dependency □ Phenothiazines—10-acetylphenothiazine, stability and degradation kinetics, pH dependency □ Degradation—10-acetylphenothiazine, kinetics, effect of pH

The kinetics and mechanism of the oxidative degradation of phenothiazine and its 10-methyl derivative were described previously (1, 2). In this paper, the influence of the introduction of an acetyl group on stability is investigated. The 10-acetyl derivative can be considered as a model compound for the phenothiazines having a carbonyl function next to the nitrogen atom; these compounds possess antiarrhythmic properties (3). The electron-withdrawing properties of the acetyl group could possibly have a strong stabilizing effect on the phenothiazine ring system.

EXPERIMENTAL

Materials—10-Acetylphenothiazine[1] (I) was recrystallized from 96% ethanol, mp 204°, and had a molar absorptivity at 257 nm of 10,194. TLC of the recrystallized product in various systems showed only one spot, so no further purification was performed.

All other materials were as previously described (1).

Isolation and Identification of Degradation Products—Compound I was dissolved in 52.5% ethanol, buffered to an apparent pH of 2.8 with sodium acetate–hydrochloric acid (4), and stored in the dark at 85° for 3 days after saturation with oxygen. The degradation products were extracted with carbon tetrachloride and isolated by TLC and column chromatography. Silica gel and aluminum oxide were used as adsorbents, and the solvents were ether, petroleum ether, chloroform, acetone, and their mixtures. The best separation was obtained with aluminum oxide and ether and silica gel and chloroform, both giving five zones. When the degradation was carried out at pH 1.7, the same products were found by TLC as at pH 2.8.

To isolate the degradation products, the carbon tetrachloride extract was evaporated to dryness under reduced pressure at room temperature and the residue was dissolved in ether. This solution was put onto a silica gel column, and the column was then eluted with ether until the colored products had left the column. Because one degradation product was not eluted with ether, the elution was continued with acetone, giving a solution that contained only one degradation product.

The ether eluate was evaporated to dryness under reduced pressure at room temperature, and the residue was dissolved in ether–petroleum ether (1:3). This solution was put onto an aluminum oxide column, and

[1] 10-Acetylphenothiazine was a gift from Dr. C. D. M. ten Berge, Farmaceutisch Laboratorium, Groningen, The Netherlands.

0022-3549/79/0400-0515$01.00/0
© 1979, American Pharmaceutical Association

Table I—Apparent First-Order Rate Constants, $k_1 \times 10^3$ hr^{-1}, for the Degradation of 10-Acetylphenothiazine in 52.5% Ethanol at 85° at Various pH Values

pH	Oxygen-Saturated Medium	Oxygen-Free Medium
1.9	17.9	17.7
2.1	11.1	—
2.4	5.5	—
2.8	2.4	2.3

the products were then eluted successively with 150 ml of ether–petroleum ether (1:3), 150 ml of ether–petroleum ether (1:1), and 100 ml of ether–acetone (1:1). The eluate was collected in eight fractions of 50 ml, and the fractions were analyzed by TLC as already described.

Since none of the fractions gave spots with R_f values different from those of the products in the carbon tetrachloride extract, the products appeared to be stable in the isolation procedure. Fractions that contained more than one product were purified further by TLC. The isolated products were then identified by comparing their TLC properties and their UV, IR, and mass spectra with those of known compounds.

Quantitative Analysis of I and Its Degradation Products—Phenothiazine (II), 3*H*-phenothiazine-3-one (III), and 7-(10′-phenothiazinyl)-3*H*-phenothiazine-3-one (IV) were determined spectrophotometrically after they were separated on an aluminum oxide column as described previously (5) with the following modification. Since the expected phenothiazine concentrations were much lower than in the previous studies, the eluate containing phenothiazine was not diluted with ethanol but was evaporated to dryness under reduced pressure. Then the residue was dissolved in 50 ml of ethanol, and the absorbance was measured at 254 nm in a 1-cm cell with ethanol as a blank.

Compound I, which eluted at the same time as III in the system used, was determined by measuring the absorbance at 257 nm of the solution containing I and III after a 10-fold dilution with ethanol. The absorbance of this solution at 504 nm is directly proportional to the concentration of III. Therefore, by multiplying this concentration by the molar absorptivity of III at 257 nm and dividing by the dilution factor, the absorbance at 257 nm caused by III can be calculated and subtracted from the measured absorbance at this wavelength. This difference is directly proportional to the I concentration.

This method is reasonably accurate when the I concentration is much larger than the III concentration, as in these studies. With higher III concentrations, a different procedure would be necessary. Recovery studies with samples containing the various products in various concentrations showed good results: 92.7 ± 1.3% for I, 94 ± 2% for II, 91 ± 2% for III, and 92 ± 2% for IV.

Kinetic Studies—Solutions of I were prepared by dissolving 200 mg in 400 ml of a mixture of ethanol and sodium acetate–hydrochloric acid buffers (4). The pH of these buffers was measured at 85°. The solution was placed in small, screw-capped bottles, saturated with oxygen or oxygen-free nitrogen, and kept in the dark at 85°. The influence of pH on the kinetics was studied in the presence and absence of oxygen.

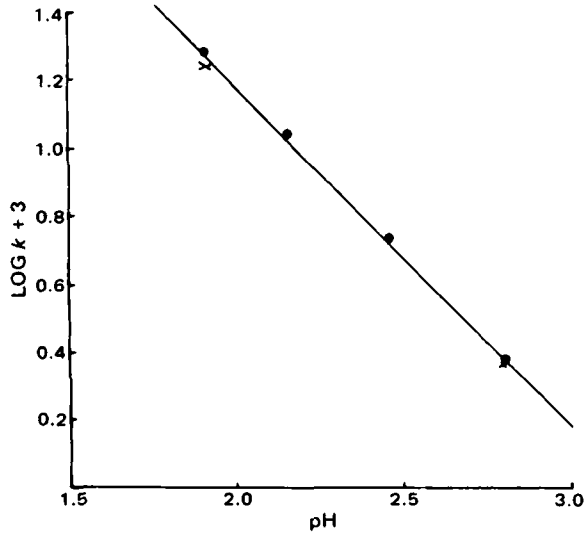

Figure 1—*Plot of log* k versus *pH for the degradation of 10-acetylphenothiazine in 52.5% ethanol at 85° in the presence* (●) *and absence* (×) *of oxygen.*

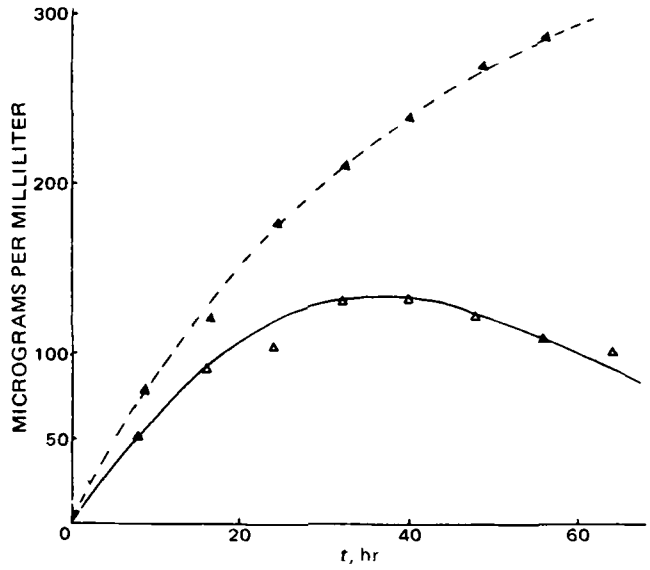

Figure 2—*Plot of the formation of phenothiazine* versus *time in the degradation of 10-acetylphenothiazine in 52.5% ethanol, pH 1.9, at 85°. The solid line was calculated according to Eq. 1 (oxygen saturated), and the dashed line was calculated according to Eq. 2 (oxygen free). The points are experimental values obtained in the presence* (△) *or absence* (▲) *of oxygen.*

RESULTS AND DISCUSSION

Identification of Degradation Products—In the silica gel and chloroform system, the R_f values of the five products were 0.05, 0.12, 0.19, 0.40, and 0.73; in the aluminum oxide and ether system, the R_f values were 0.03, 0.10, 0.24, 0.30, and 0.46, respectively. One product had a very low R_f value in both systems, so its isolation by column chromatography in one of these systems would require a long time and a large volume of solvent. Therefore, this product was separated from the other products by eluting them from a silica gel column with ether and then eluting this compound with acetone.

The product was compared with phenothiazine-5-oxide in various TLC systems, and the same R_f values were obtained for both compounds. Furthermore, their UV, IR, and mass spectra were similar, indicating that the product with the lowest R_f value was phenothiazine-5-oxide. Although phenothiazine-5-oxide and 10-acetylphenothiazine-5-oxide could possibly have the same chromatographic properties and similar spectra, the fact that the parent peak in the mass spectrum was at *m/e* 215, in agreement with the empirical formula $C_{12}H_9NOS$, shows that this product did not have the acetyl group present.

Comparison of the other products with I–IV, as described previously (1), showed that the compound with R_f 0.12 in silica gel and chloroform was identical with IV; the product with R_f 0.19 was identical with III, the product with R_f 0.40 was identical with I, and the one with R_f 0.70 was identical with II.

Kinetic Studies—Under all circumstances, the degradation was first order with respect to 10-acetylphenothiazine. Table I gives the observed rate constants for the degradation at various pH values in 52.5% ethanol saturated with oxygen. The plot of log *k versus* pH (Fig. 1) gives a straight line with a slope equal to −1, indicating that the degradation is a specific hydrogen-ion-catalyzed reaction. Solutions of I with pH 6.9, stored at 85° in an oxygen atmosphere, showed no significant degradation over 11 days.

Table I also lists the observed rate constants for the degradation under the same conditions but in an oxygen-free medium. The rate constants were essentially the same in the presence and absence of oxygen. This result indicates that the degradation of 10-acetylphenothiazine is a specific hydrogen-ion-catalyzed hydrolysis, giving phenothiazine and acetic acid; the phenothiazine is then oxidized. This pattern was also indicated by the fact that no other degradation products were found than those that were obtained in the oxidative degradation of phenothiazine.

If the first step in the degradation is a hydrolytic cleavage, then the

phenothiazine concentration should change with time in the presence of oxygen according to:

$$P = aP_0 \frac{k_1}{k_1 - k_2} (e^{-k_2 t} - e^{-k_1 t}) \quad \text{(Eq. 1)}$$

where P is the phenothiazine concentration, aP_0 is the initial concentration of I, k_1 is the rate constant for I degradation, and k_2 is the rate constant for phenothiazine degradation. At the various pH values, the phenothiazine concentrations were calculated using the values for k_1 given in Table I and the value of 19.7×10^{-3} hr^{-1} for k_2 (1). The calculated curves were in good agreement with the observed ones; a typical example is given in Fig. 2. The small differences were probably due to the experimental conditions being not exactly the same as in the previous studies.

In the absence of oxygen, the phenothiazine concentration can be calculated from the equation:

$$P = aP_0(1 - e^{-k_1 t}) \quad \text{(Eq. 2)}$$

With the evaluated k_1 values, the phenothiazine concentration was calculated as a function of time. Values in good agreement with the experimental ones were obtained (Fig. 2).

From these findings, it can be concluded that the first step in the degradation of I is its hydrolytic cleavage, giving II, which is degraded further by oxidation. This increase in stability of the phenothiazine ring system is probably caused by two factors: the steric effect of the introduction of a side chain at the nitrogen atom (1) and the electron-withdrawing properties of the acetyl group, which decrease the electron density in the ring system.

Interpretation of the data obtained for the formation of III and IV is difficult. Their formation proceeds *via* a number of consecutive reactions (2), their concentrations are rather small so they cannot be measured accurately, and they are unstable at the pH values used. There is, however, no reason to assume that their formation proceeds *via* pathways different from the ones elucidated previously.

REFERENCES

(1) H. Roseboom and J. H. Perrin, *J. Pharm. Sci.*, **66**, 1392 (1977).

(2) *Ibid.*, **66**, 1395 (1977).

(3) P. Danilo, Jr., W. B. Langan, M. R. Rosen, and B. F. Hoffman, *Eur. J. Pharmacol.*, **45**, 127 (1977).

(4) H. T. S. Britton, "Hydrogen Ions," 4th ed., vol. 1, Chapman and Hall, London, England, 1955, p. 357.

(5) H. Roseboom and J. A. Fresen, *Pharm. Acta Helv.*, **50**, 64 (1975).

Drug Absorption from *In Situ* Rat Small Intestine during Metoclopramide Administration

VESA M. K. VENHO

Received May 22, 1978, from the *Department of Pharmacology, University of Helsinki, Siltavuorenpenger 10, SF-00170 Helsinki 17, Finland.* Accepted for publication August 30, 1978.

Abstract □ The effect of metoclopramide on the absorption of drugs in solution in the small intestinal lumen of rats *in situ* was studied. Metoclopramide in doses up to 50 mg/kg sc did not significantly modify the disappearance of isoniazid and quinidine from the small intestinal lumen. At the end of the absorption experiments, quinidine in the whole blood of the experimental animals was increased after metoclopramide. The blood level did not correlate to the drug disappearance from the intestinal lumen. The results probably differ from those obtained when drugs are given orally to subjects treated with metoclopramide.

Keyphrases □ Metoclopramide—effect on absorption of other drugs, *in situ* rat small intestine preparation □ Absorption—drugs from *in situ* rat small intestine, effect of metoclopramide administration □ Isoniazid—absorption from rat small intestinal lumen, effect of metoclopramide administration □ Quinidine—absorption from rat small intestinal lumen, effect of metoclopramide administration

Metoclopramide modifies the absorption of orally administered drugs (1, 2). Its effects are mainly due to changes in gastric emptying, resulting in an accelerated, but not necessarily totally increased, absorption when measured by urinary drug excretion (1). Decreased intestinal drug absorption, probably due to rapid GI transit, also was reported (3).

EXPERIMENTAL

To study whether metoclopramide has effects on the absorption of drugs already in solution in the small intestinal lumen, experiments were carried out in urethan-anesthetized (1–1.5 g/kg im) rats using an *in situ* absorption technique (4, 5) whereby the drug disappearance from a buffer (pH 6.0) in the small intestinal lumen can be measured. Depending on the weight of the rats (200–250 g), 10–15 ml of warm (37°) buffer was introduced into the intestinal lumen through a polyethylene cannula in the proximal duodenum.

Samples were taken from this "intestinal fluid," expelled at 10-min intervals, either through the other cannula in the distal ileum or through the proximal cannula in the duodenum. At the end of the 40-min experiment, whole blood was drawn by heart puncture and the whole small intestine was removed as a sample.

Metoclopramide[1], 50 mg/kg sc, was administered to the anesthetized rats 30 min before the absorption experiment; isoniazid (neutral drug) and quinidine sulfate (basic drug) were used as the test drugs. Smaller doses of metoclopramide (5–10 mg/kg) also were used.

Isoniazid was assayed spectrophotometrically (6), and quinidine was assayed fluorometrically (7).

RESULTS AND DISCUSSION

Figure 1 shows the disappearance of quinidine from the small intestinal lumen in control and metoclopramide-treated (50 mg/kg) rats. A similar plot was made for isoniazid. The absorption half-lives of isoniazid and quinidine, measured from the semilogarithmic plot of drug concentration in the intestinal lumen (intestinal fluid) *versus* time, are presented in Table I.

No statistically significant differences in absorption half-lives could be demonstrated, although the quinidine absorption half-life seemed to be somewhat longer after metoclopramide than in controls. However, in spite of an unchanged absorption half-life, the blood level of quinidine, but not of isoniazid, at the end of the 40-min experiment was statistically significantly increased by metoclopramide, 50 mg/kg (Table I). After 5–10 mg of metoclopramide/kg, the blood quinidine level (0.62 ± 0.03 μg/ml, two experiments) seemed to be also higher than in controls, but blood isoniazid level was the same as in controls.

With solids, a decreased intestinal motility allows more time for the drugs to be dissolved, tending to increase absorption and vice versa (8).

[1] Primperan, H. Lundbeck & Co., Copenhagen, Denmark.

0022-3549/79/0400-0517$01.00/0

© 1979, American Pharmaceutical Association

phenothiazine concentration should change with time in the presence of oxygen according to:

$$P = aP_0 \frac{k_1}{k_1 - k_2} (e^{-k_2 t} - e^{-k_1 t}) \quad \text{(Eq. 1)}$$

where P is the phenothiazine concentration, aP_0 is the initial concentration of I, k_1 is the rate constant for I degradation, and k_2 is the rate constant for phenothiazine degradation. At the various pH values, the phenothiazine concentrations were calculated using the values for k_1 given in Table I and the value of 19.7×10^{-3} hr^{-1} for k_2 (1). The calculated curves were in good agreement with the observed ones; a typical example is given in Fig. 2. The small differences were probably due to the experimental conditions being not exactly the same as in the previous studies.

In the absence of oxygen, the phenothiazine concentration can be calculated from the equation:

$$P = aP_0(1 - e^{-k_1 t}) \quad \text{(Eq. 2)}$$

With the evaluated k_1 values, the phenothiazine concentration was calculated as a function of time. Values in good agreement with the experimental ones were obtained (Fig. 2).

From these findings, it can be concluded that the first step in the degradation of I is its hydrolytic cleavage, giving II, which is degraded further by oxidation. This increase in stability of the phenothiazine ring system is probably caused by two factors: the steric effect of the introduction of a side chain at the nitrogen atom (1) and the electron-withdrawing properties of the acetyl group, which decrease the electron density in the ring system.

Interpretation of the data obtained for the formation of III and IV is difficult. Their formation proceeds *via* a number of consecutive reactions (2), their concentrations are rather small so they cannot be measured accurately, and they are unstable at the pH values used. There is, however, no reason to assume that their formation proceeds *via* pathways different from the ones elucidated previously.

REFERENCES

(1) H. Roseboom and J. H. Perrin, *J. Pharm. Sci.*, **66**, 1392 (1977).

(2) *Ibid.*, **66**, 1395 (1977).

(3) P. Danilo, Jr., W. B. Langan, M. R. Rosen, and B. F. Hoffman, *Eur. J. Pharmacol.*, **45**, 127 (1977).

(4) H. T. S. Britton, "Hydrogen Ions," 4th ed., vol. 1, Chapman and Hall, London, England, 1955, p. 357.

(5) H. Roseboom and J. A. Fresen, *Pharm. Acta Helv.*, **50**, 64 (1975).

Drug Absorption from *In Situ* Rat Small Intestine during Metoclopramide Administration

VESA M. K. VENHO

Received May 22, 1978, from the *Department of Pharmacology, University of Helsinki, Siltavuorenpenger 10, SF-00170 Helsinki 17, Finland.* Accepted for publication August 30, 1978.

Abstract □ The effect of metoclopramide on the absorption of drugs in solution in the small intestinal lumen of rats *in situ* was studied. Metoclopramide in doses up to 50 mg/kg sc did not significantly modify the disappearance of isoniazid and quinidine from the small intestinal lumen. At the end of the absorption experiments, quinidine in the whole blood of the experimental animals was increased after metoclopramide. The blood level did not correlate to the drug disappearance from the intestinal lumen. The results probably differ from those obtained when drugs are given orally to subjects treated with metoclopramide.

Keyphrases □ Metoclopramide—effect on absorption of other drugs, *in situ* rat small intestine preparation □ Absorption—drugs from *in situ* rat small intestine, effect of metoclopramide administration □ Isoniazid—absorption from rat small intestinal lumen, effect of metoclopramide administration □ Quinidine—absorption from rat small intestinal lumen, effect of metoclopramide administration

Metoclopramide modifies the absorption of orally administered drugs (1, 2). Its effects are mainly due to changes in gastric emptying, resulting in an accelerated, but not necessarily totally increased, absorption when measured by urinary drug excretion (1). Decreased intestinal drug absorption, probably due to rapid GI transit, also was reported (3).

EXPERIMENTAL

To study whether metoclopramide has effects on the absorption of drugs already in solution in the small intestinal lumen, experiments were carried out in urethan-anesthetized (1–1.5 g/kg im) rats using an *in situ* absorption technique (4, 5) whereby the drug disappearance from a buffer (pH 6.0) in the small intestinal lumen can be measured. Depending on the weight of the rats (200–250 g), 10–15 ml of warm (37°) buffer was introduced into the intestinal lumen through a polyethylene cannula in the proximal duodenum.

Samples were taken from this "intestinal fluid," expelled at 10-min intervals, either through the other cannula in the distal ileum or through the proximal cannula in the duodenum. At the end of the 40-min experiment, whole blood was drawn by heart puncture and the whole small intestine was removed as a sample.

Metoclopramide[1], 50 mg/kg sc, was administered to the anesthetized rats 30 min before the absorption experiment; isoniazid (neutral drug) and quinidine sulfate (basic drug) were used as the test drugs. Smaller doses of metoclopramide (5–10 mg/kg) also were used.

Isoniazid was assayed spectrophotometrically (6), and quinidine was assayed fluorometrically (7).

RESULTS AND DISCUSSION

Figure 1 shows the disappearance of quinidine from the small intestinal lumen in control and metoclopramide-treated (50 mg/kg) rats. A similar plot was made for isoniazid. The absorption half-lives of isoniazid and quinidine, measured from the semilogarithmic plot of drug concentration in the intestinal lumen (intestinal fluid) *versus* time, are presented in Table I.

No statistically significant differences in absorption half-lives could be demonstrated, although the quinidine absorption half-life seemed to be somewhat longer after metoclopramide than in controls. However, in spite of an unchanged absorption half-life, the blood level of quinidine, but not of isoniazid, at the end of the 40-min experiment was statistically significantly increased by metoclopramide, 50 mg/kg (Table I). After 5–10 mg of metoclopramide/kg, the blood quinidine level (0.62 ± 0.03 μg/ml, two experiments) seemed to be also higher than in controls, but blood isoniazid level was the same as in controls.

With solids, a decreased intestinal motility allows more time for the drugs to be dissolved, tending to increase absorption and vice versa (8).

[1] Primperan, H. Lundbeck & Co., Copenhagen, Denmark.

0022-3549/79/0400-0517$01.00/0

© 1979, American Pharmaceutical Association

Table I—Isoniazid and Quinidine Absorption Half-Lives *In Situ* and Their Levels in the Whole Blood and Intestinal Wall at the End of the Experiments [a]

Drugs and Treatment	Absorption Half-Life, min	Correlation Coefficient	Drug Levels at 40 min	
			Whole Blood, μg/ml	Intestinal Wall, μg/g
Isoniazid, 100 μg/ml				
Metoclopramide, 50 mg/kg (6)	17	0.96	3.6 ± 1.1 / 5.9 ± 0.8	1.8 ± 0.8 / 2.4 ± 1.1
Control (7)	17	0.98	2.8 ± 1.1 / 6.7 ± 1.1	0.7 ± 0.7 / 3.9 ± 0.4
Quinidine sulfate, 100 μg/ml				
Metoclopramide, 50 mg/kg (6)	32	0.91	0.63 ± 0.05[b]	19.0 ± 2.8
Control (8)	24	0.84	0.26 ± 0.02	20.4 ± 2.1

[a] Means ± *SE*. Number of experiments is in parentheses. Isoniazid in the whole blood and intestinal wall refers to unacetylated isoniazid divided by total isoniazid hydrazides. [b] $p < 0.001$.

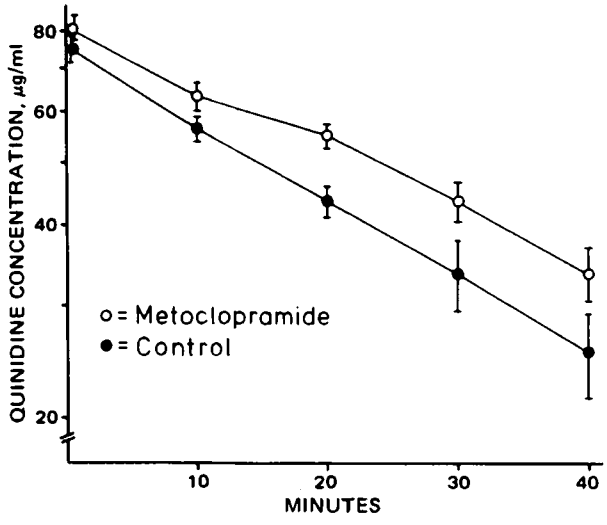

Figure 1—*Disappearance of quinidine sulfate from the rat small intestine* in situ *in control rats (n = 8) and rats treated with metoclopramide (n = 6), 50 mg/kg sc, 30 min before the start of the absorption experiment (means ± SE).*

In humans, metoclopramide reduces the transit time of fluid in the intestinal lumen and may induce an increased water and electrolyte secretion into the intestinal lumen (9), an effect that might be expected to decrease drug absorption. The reduced transit time of fluid both in humans and in animals seems to be associated with a reduction in the diameter of the small intestinal lumen (1). In spite of a relatively large dose (50 mg/kg) of metoclopramide, it did not clearly affect absorption half-lives in the present experiments. This result is understandable since the drugs were in solution in the intestinal lumen and in a better absorbable state than solid drugs.

The increased blood quinidine concentration at the end of the experiment did not correlate with the slightly decreased or unchanged drug disappearance from the intestinal lumen. Because the drugs in blood were measured only at the end of the experiments, these concentrations cannot be regarded as important indexes of drug absorption. The reason for the increased blood quinidine level cannot be found with this experimental setup. The present results indicate that, at least with metoclopramide, the *in situ* rat small intestine is not the best technique of studying its effect on drug absorption; the results do not seem to reflect the eventual absorption changes when drugs are administered orally.

REFERENCES

(1) R. M. Pinder, R. N. Brogden, P. R. Sawyer, T. M. Speight, and G. S. Avery, *Drugs*, **12**, 81 (1976).

(2) L. F. Prescott, in "Drug Interactions," P. L. Morselli, S. Garattini, and S. N. Cohen, Eds., Raven, New York, N.Y., 1974, p. 11.

(3) V. Manninen, A. Apajalahti, J. Melin, and M. Karesoja, *Lancet*, **1**, 398 (1973).

(4) J. T. Doluisio, N. F. Billups, L. W. Dittert, E. T. Sugita, and J. V. Swintosky, *J. Pharm. Sci.*, **58**, 1196 (1969).

(5) V. M. K. Venho, *Acta Pharmacol. Toxicol.*, **39**, 321 (1976).

(6) H. Tiitinen, M. J. Mattila, and A. W. Eriksson, *Am. Rev. Resp. Dis.*, **108**, 375 (1973).

(7) G. Cramer and B. Isaksson, *Scand. J. Clin. Lab. Invest.*, **15**, 553 (1963).

(8) R. R. Levine, *Am. J. Dig. Dis.*, **15**, 171 (1970).

(9) C. Matuchansky, P. M. Huet, J. Y. Mary, J. C. Rambaud, and J. J. Bernier, *Eur. J. Clin. Invest.*, **2**, 169 (1972).

Synthesis of 3-Hydroxy-3-phenacyloxindole Analogs

F. D. POPP ˣ and B. E. DONIGAN

Received April 24, 1978, from the *Department of Chemistry, University of Missouri–Kansas City, Kansas City, MO 64110.* Accepted for publication September 11, 1978.

Abstract □ Substituted isatins and substituted acetophenones were condensed to give analogs of 3-hydroxy-3-phenacyloxindole. These alcohols were dehydrated, and the alkene was reduced. None of the products had the level of anticonvulsant activity exhibited by the parent compound.

Keyphrases □ 3-Hydroxy-3-phenacyloxindole analogs—synthesized as potential anticonvulsants □ Isatins, substituted—condensed with substituted acetophenones to give 3-hydroxy-3-phenacyloxindole analogs, screened for anticonvulsant activity □ Acetophenones, substituted—condensed with substituted isatins to give 3-hydroxy-3-phenacyloxindole analogs, screened for anticonvulsant activity □ Anticonvulsant activity—screening of 3-hydroxy-3-phenacyloxindole analogs

3-Hydroxy-3-phenacyloxindole (I) (1) and the related Compound II (2) were synthesized by condensation of isatin with the appropriate methyl ketones. Both I and II exhibited anticonvulsant activity in the maximal electroshock seizure test[1]. This paper reports on the synthesis and screening of various analogs of I.

DISCUSSION

With the procedure of Lindwall and coworkers (1, 2), a number of isatin derivatives were condensed with a number of acetophenones to give 3-hydroxy-3-phenacyloxindoles (Table I) of type III. Dehydration of III gave 3-phenacylidene-2-indolinones (Table II) of type IV, which were reduced to 3-phenacyl-2-indolinones (Table III) of type V.

Although I (1 in Table I) was active at both 100 and 300 mg/kg in the maximal electroshock seizure test, all other compounds in Tables I–III, except 3 and 14, were inactive at 300 mg/kg in both that screen and the pentylenetetrazol seizure threshold test[1]. Compounds 14, formed from isatin and 2-acetylpyridine, and 3, formed from 1-piperidylmethylisatin and acetophenone were both active at 300 mg/kg in the maximal electroshock seizure test.

The Schiff base (VI) derived from isatin and 4-aminoacetophenone was also inactive as an anticonvulsant.

Some of the compounds submitted for other screening were found to be inactive[1]. Compounds 2, 5, 6, and 18 were inactive at 640 mg/kg in an antimalarial screen; 1 and 25 were inactive in an antitrypansomiasis

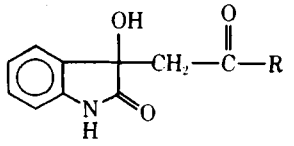

I: R = C_6H_5
II: R = CH_3

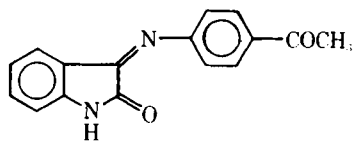

VI

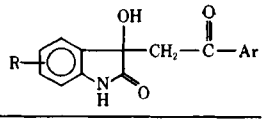

[1] Anticonvulsant and anticancer screenings were carried out through the National Institutes of Health and antimalarial and antitrypansomiasis screenings were carried out through the Walter Reed Army Medical Center. The standard protocols of these groups were followed.

Table I—Reaction of Isatins with Methyl Aryl Ketones (Type III)

Compound	R	Ar	Melting Point[a]	Yield, %	Formula		Analysis, % Calc.	Found	IR (KBr), cm^{-1}
1	H	C_6H_5	173–175°[b]	80	$C_{16}H_{13}NO_3$		—	—	3350, 1710, 1680
2	1-CH_3	C_6H_5	173–175°[c]	84	$C_{17}H_{15}NO_3$	N	4.98	4.84	—
3	1-$CH_2C_5H_{10}N$	C_6H_5	143–145°	71	$C_{22}H_{24}N_2O_3$	C	72.50	72.19	3300, 1685–1695
						H	6.64	6.45	
4	5-Br	C_6H_5	220–221°	79	$C_{16}H_{12}BrNO_3$	N	4.05	4.02	3250, 1680–1705
5	5-CH_3	C_6H_5	189–190°	81	$C_{17}H_{15}NO_3$	N	4.98	4.92	3325, 1710, 1670
6	5-NO_2	C_6H_5	230–232°	63	$C_{16}H_{12}N_2O_5$	N	8.97	8.91	3250, 1705, 1675
7	5,7-$(CH_3)_2$	C_6H_5	181–182°	68	$C_{18}H_{17}NO_3$	N	4.74	4.67	3300, 1705, 1665
8	6-Cl	C_6H_5	209–211°	48	$C_{16}H_{12}ClNO_3$	C	63.69	63.63	3300, 1710, 1680
						H	4.01	4.07	
9	H	4-$NO_2C_6H_4$	185–186°	68	$C_{16}H_{12}N_2O_5$	C	61.54	61.41	3200–3400, 1720, 1690
						H	3.87	3.74	
10	H	4-$C_5H_{10}NC_6H_4$	209–211°	90	$C_{21}H_{22}N_2O_3$	C	71.98	71.95	3375, 1700, 1660
						H	6.33	6.37	
11	H	4-$CH_3C_6H_4$	189–192°[d]	88	$C_{17}H_{15}NO_3$		—	—	3350, 1710, 1670
12	H	4-$CH_3OC_6H_4$	184–186°[e]	94	$C_{17}H_{15}NO_4$		—	—	3360, 1700, 1665
13	H	4-ClC_6H_4	197–199°[f]	97	$C_{16}H_{12}ClNO_3$		—	—	3350, 1665–1700
14	H	2-Pyridyl	159–160°	57	$C_{15}H_{12}N_2O_3$	C	67.17	67.01	3250, 1680–1710
						H	4.51	4.55	
15	H	3-Pyridyl	144–146°	17	$C_{15}H_{12}N_2O_3$	C	67.15	67.20	3275, 1705, 1690
						H	4.51	4.42	
16	H	3-Indolyl	180°	61	$C_{18}H_{14}N_2O_3$	C	70.58	70.65	3250–3300, 1695–1710
						H	4.61	4.65	
						N	9.15	8.88	
17	H	Ferrocenyl	190°	93	$C_{20}H_{17}FeNO_3$	C	64.02	64.01	3350, 1700, 1650
						H	4.57	4.65	
						N	3.73	3.66	

[a] Recrystallized from ethanol. [b] Lit. (1) mp 169–172°. [c] Lit. (1) mp 168–170°. [d] Lit. (1) mp 185–186°. [e] Lit. (1) mp 186–187°. [f] Lit. (1) mp 175–176° (material softens at 175° and melts at 197–199°).

0022-3549/79/0400-0519$01.00/0
© 1979, American Pharmaceutical Association

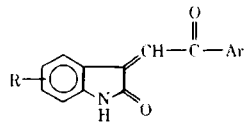

Table II—Dehydration of Dioxindoles (Type IV)

Compound	R	Ar	Melting Point[a]	Yield, %	Formula		Analysis, % Calc.	Found	IR (KBr), cm^{-1}
18	H	C_6H_5	192–194°[b]	81	$C_{16}H_{11}NO_2$		—	—	1710, 1660
19	5-Br	C_6H_5	204–205°	92	$C_{16}H_{10}BrNO_2$	C	58.56	58.72	1710, 1665
						H	3.07	3.15	
20	5-CH_3	C_6H_5	174–175°	67	$C_{17}H_{13}NO_2$	C	77.55	77.52	1705, 1655
						H	4.98	5.04	
21	5-NO_2	C_6H_5	230–231°	85	$C_{16}H_{10}N_2O_4$	C	65.30	65.36	1705, 1655
						H	3.42	3.42	
22	5,7-$(CH_3)_2$	C_6H_5	225–226°	92	$C_{18}H_{15}NO_2$	C	77.96	77.91	1705, 1670
						H	5.45	5.44	
23	6-Cl	C_6H_5	250–251°	95	$C_{16}H_{10}ClNO_2$	C	67.73	67.89	1710, 1660
						H	3.55	3.47	
24	H	3-Indolyl	294–295°	92	$C_{18}H_{12}N_2O_2$	C	74.99	74.85	1705
						H	4.20	4.31	
						N	9.72	9.65	

[a] Recrystallized from ethanol. [b] Lit. (1) mp 193–194°.

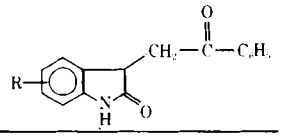

Table III—Reduction to Oxindoles (Type V)

Compound	R	Melting Point[a]	Yield, %	Formula		Analysis, % Calc.	Found	IR (KBr), cm^{-1}
25	H	173–175°[b]	90	$C_{16}H_{13}NO_2$		—	—	1695, 1670
26	5-Br	253–254°	74	$C_{16}H_{12}BrNO_2$	C	58.20	58.21	1700, 1670
					H	3.66	3.69	
27	5-CH_3	210–211°	82	$C_{17}H_{15}NO_2$	C	76.96	76.94	1670–1700
					H	5.70	5.62	
28	6-Cl	171–172°	90	$C_{16}H_{12}ClNO_2$	C	67.25	67.08	1700, 1675
					H	4.23	4.18	

[a] Recrystallized from ethanol. [b] Lit. (1) mp 177°.

screen; 1, 4, 16–19, 22, 24, and 25 were all inactive at 400 mg/kg in the L-1210 lymphoid leukemia screen; and 2–5, 11–14, 21, and VI were all inactive at 200 mg/kg in the P-388 lymphocytic leukemia screen.

Preliminary studies on analogs of II appear more promising and will be reported in detail at a later date.

EXPERIMENTAL

Preparation of 3-Hydroxy-3-phenacyloxindoles (III)—Equimolar amounts (0.01 mole) of the isatin and acetophenone in 30–50 ml of absolute ethanol, containing 3–4 drops of diethylamine, were heated at reflux on the steam bath for 30–60 min. After standing for several days at room temperature, the products (Table I) were collected by filtration.

Conversion of III to 3-Phenacylidene-2-indolinones (IV)—A mixture of 0.01 mole of III, 0.5 ml of concentrated hydrochloric acid, and 17 ml of acetic acid was heated at 95° on the steam bath for 15–30 min. Ethanol (17 ml) was added, and the mixture was allowed to stand at room temperature. The products listed in Table II were obtained.

Conversion of IV to 3-Phenacyl-2-indolinones (V)—To 1 g of IV in 25 ml of ethanol was added 2 g of sodium hyposulfite in 7 ml of water. The mixture was heated at 95° until the color disappeared and then was heated for 7 min more. After filtration, the products listed in Table III were obtained.

Synthesis of Schiff Base VI—Equimolar quantities of isatin and 4-aminoacetophenone in absolute ethanol were heated at reflux on the steam bath for 30 min. After cooling, filtration gave a 90% yield of VI, mp 257–258° (from ethanol).

Anal.—Calc. for $C_{16}H_{12}N_2O_2$: C, 72.71; H, 4.58. Found: C, 72.69; H, 4.54.

REFERENCES

(1) H. G. Lindwall and J. S. Maclennan, *J. Am. Chem. Soc.*, **54**, 4739 (1932).

(2) F. Brande and H. G. Lindwall, *ibid.*, **55**, 325 (1933).

GLC Analysis of Theophylline, Hydroxyethyltheophylline, and Diphenylpyraline Hydrochloride Syrup

FABRIZIO DE FABRIZIO

Received June 15, 1978, from *Adcock Ingram Laboratories Limited, P.O. Box 2368, Johannesburg, 2000 South Africa.* Accepted for publication September 21, 1978.

Abstract □ A GLC method for determining theophylline, hydroxyethyltheophylline, and diphenylpyraline hydrochloride is presented. The method permits the separation and quantitative determination of the therapeutically active ingredients with a single injection in an overall time of approximately 2.5 hr.

Keyphrases □ Theophylline—GLC analysis, in syrup □ Hydroxyethyltheophylline—GLC analysis, in syrup □ Diphenylpyraline hydrochloride—GLC analysis, in syrup □ GLC—analyses, theophylline, hydroxyethyltheophylline, diphenylpyraline hydrochloride

Analysis of theophylline (I), hydroxyethyltheophylline (II), and diphenylpyraline hydrochloride (III) by spectrophotometry and a titrimetric procedure (1) or a combination of ion-exchange chromatography and spectrophotometry was not applicable because of large amounts of ammonium chloride (24 mg/ml) and sodium citrate (10 mg/ml) contained as ingredients in the syrup formulation. This paper presents a uniform and simple GLC method.

Compounds I–III have been determined by GLC singly and in combination (2, 3), but their simultaneous quantitative analysis has never been recorded. The polar nature of certain xanthines causes absorption and tailing peaks, which complicate quantitative determination. In the present study, this problem was resolved by methylating the xanthine bases in the flash heater of a gas chromatograph with a methanolic solution of their trimethylanilinium salts (4).

EXPERIMENTAL

Apparatus—A gas chromatograph[1] with a flame-ionization detector was fitted with a 1.8-m × 2-mm i.d. glass column packed with 10% OV-101 on 80–100-mesh Chromosorb W.

Reagents[2]—A commercially prepared 0.2 *M* trimethylanilinium hydroxide solution[3] was used for methylating the xanthine bases. The pH 3.8 buffer was prepared as follows. Monobasic potassium phosphate, 6.805 g, was dissolved in 900 ml of water, and the pH was adjusted to 3.8 with 1% (v/v) phosphoric acid in water. Then the solution was diluted to 1000 ml with water. The mixed solvent system was chloroform–isopropanol (3:1).

Standard Solutions—To prepare the theophylline standard solution, 100 mg of anhydrous theophylline USP reference standard was weighed and dissolved in 50 ml of pH 3.8 buffer (2 mg/ml). Hydroxyethyltheophylline (Austria P. grade), 100 mg, was dissolved in 50 ml of pH 3.8 buffer (2 mg/ml). Diphenylpyraline hydrochloride, 80 mg, was dissolved in 50 ml of pH 3.8 buffer (1.6 mg/ml). The internal standard, pyrilamine maleate, 100 mg, was dissolved in 100 ml of pH 3.8 buffer (1 mg/ml).

Chromatography—The oven was programmed at 215–230° at 2°/min, the injection port was set at 275°, and the detector was set at 280°. The nitrogen carrier flow rate was 15 ml/min. Hydrogen and air flow rates were adjusted to give maximum response. An attenuation of 10 was reduced to 7 after 4.8 min.

Standard Preparation—Standard solutions of I (10 ml), II (1 ml), III (1 ml), and pyrilamine maleate (1 ml) were pipetted into a 150-ml separator and extracted with two 25-ml and two 15-ml portions of mixed solvent. Each organic extract was filtered through anhydrous sodium sulfate into a 250-ml conical flask. The aqueous phase was made alkaline with 10% NaOH, and the extraction was continued with two 20-ml and two 10-ml portions of chloroform.

Organic phases were pooled, and the sodium sulfate was rinsed with two 10-ml aliquots of chloroform. Then the combined extracts were evaporated in a rotating evaporator at 45°. The residue was redissolved in 5 ml of mixed solvent and then pipetted in 20-μl aliquots into vials for evaporation at room temperature. The residue in each vial was redissolved in 30 μl of reagent and then injected[4] in 1-μl samples into the chromatograph.

Sample Preparation—The weight per milliliter was determined, and an amount of syrup[5] equivalent to about 6 ml was weighed in a 50-ml beaker. The pH was adjusted to 3.8 after addition of 10 ml of pH 3.8 buffer. Then the solution was transferred into a 150-ml separator, and the beaker was rinsed with small portions of pH 3.8 buffer. Internal standard solution, 1 ml, was pipetted into a 150-ml separator and extracted according to the *Standard Preparation* procedure previously described.

RESULTS AND DISCUSSION

Well-resolved chromatographic peaks were obtained for the three active ingredients and the internal standard (Fig. 1). The retention times of I–III and pyrilamine maleate were 3.52, 5.64, 7.56, and 9.97, respectively, based on freshly prepared solutions. The solution was analyzed six times (Table I).

Precision was also examined by analyzing a production lot of the syrup. Each of three replicate extractions was chromatographed five times (Table II). Precision and accuracy data indicate good reproducibility. The precision with which diphenylpyraline hydrochloride was determined was less than expected when compared to that of theophylline and

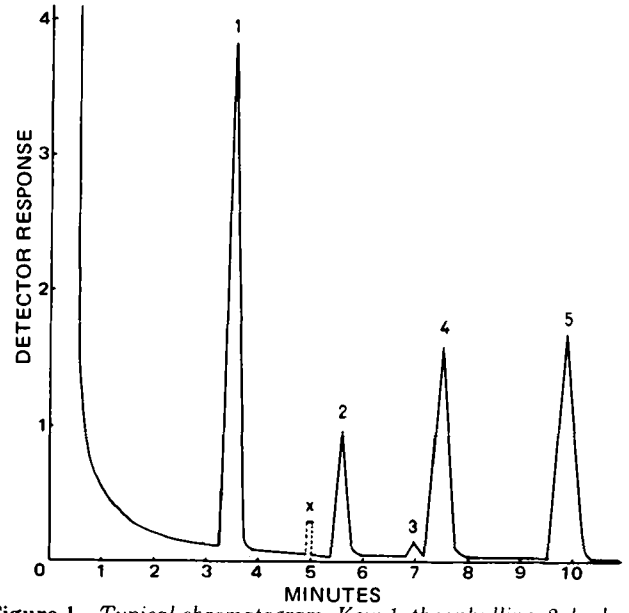

Figure 1—*Typical chromatogram. Key: 1, theophylline; 2, hydroxyethyltheophylline; 3, precursor peak; 4, diphenylpyraline hydrochloride; and 5, pyrilamine maleate.*

[1] Hewlett-Packard 5840-A.
[2] All reagents were Analar grade by BDH.
[3] Pierce Chemical Co., Rockford, Ill.
[4] Microliter syringe, 10 μl, Hamilton Co., Reno, Nev.
[5] The commercial syrup contained (per 30 ml): theophylline, 100 mg; hydroxyethyltheophylline, 10 mg; and diphenylpyraline hydrochloride, 8 mg.

0022-3549/79/0400-0521$01.00/0
© 1979, American Pharmaceutical Association

Table I—Standard Solution

Trial	Theophylline		Hydroxyethyltheophylline		Diphenylpyraline Hydrochloride	
	Sample, mg	Recovery, %	Sample, mg	Recovery, %	Sample, mg	Recovery, %
1	100.7	97.9	9.3	98.9	8.6	104.7
2	99.3	99.1	10.7	98.1	7.9	101.3
3	101.5	100.8	11.1	97.3	8.1	97.5
4	98.9	101.2	9.8	98.0	8.3	97.6
5	99.2	102.1	10.5	100.0	7.9	102.5
6	99.1	99.4	10.5	98.1	8.4	97.2
Mean relative error, %	1.26		1.43		2.63	
$\bar{X}$	100.1		98.4		100.1	
SD, %	±1.55		±0.93		±3.4	
RSD, %	1.55		0.95		3.4	

Table II—Production Lot of Syrup

	Theophylline	Hydroxyethyltheophylline	Diphenylpyraline Hydrochloride
Theoretical concentration, mg/30 ml	100.0	10.0	8.0
$\bar{X}$ of 15 samples	99.3	10.5	8.3
RSD, %	1.87	1.20	3.50

hydroxyethyltheophylline. Diphenylpyraline hydrochloride appeared not to undergo any chemical reaction in methanol and reaction mixtures as shown by the retention time. A preliminary 1-μl injection of reagent alone showed a small precursor peak just before the diphenylpyraline hydrochloride peak. This peak may insignificantly affect measurement of diphenylpyraline hydrochloride.

Linearity was also determined. Linear curves passing through the origin were obtained for solutions containing 40–100% of the quantities of drug ingredients being sought. These curves related the peak area and drug concentration.

The initial pH 3.8 of the sample and standard solutions was necessary to ensure the extraction of theophylline and hydroxyethyltheophylline.

REFERENCES

(1) T. Kanieuska and W. Zyzynski, *Zaklad Chemii Analitycznej Instytutu Lekou Warszawie, Poland;* through *Int. Pharm. Abstr.*, **4**, 499b (1967).

(2) A. C. Celeste and M. V. Polito, *J. Assoc. Off. Anal. Chem.*, **49**, 541 1966.

(3) J. Reisch and H. Walker, *Farmazie*, **21**, 467 (1966); through *Anal. Abstr.*, **14**, 7784 (1967).

(4) E. Brochmann-Hanssen and T. O. Oke, *J. Pharm. Sci.*, **58**, 370 1969.

Stereochemical Preferences for Curarimimetic Neuromuscular Junction Blockade IV: Monoquaternary Ammonium Probes Possessing Carbon and Nitrogen Asymmetry

PAUL W. ERHARDT *x and TAITO O. SOINE †

Received May 19, 1978, from the *Medicinal Chemistry Department, College of Pharmacy, University of Minnesota, Minneapolis, MN 55455.* Accepted for publication August 17, 1978.

*Present address: Arnar-Stone Laboratories, McGaw Park, IL 60085. †Deceased.

Abstract □ Two enantiomeric pairs of neuromuscular junction blocking agents were prepared in which an asymmetric carbon atom is adjacent to an asymmetric quaternized nitrogen moiety. The blocking agents were obtained from the enantiomers of laudanosine by stereoselective quaternization with benzyl and ethyl iodides. Curarimimetic potencies were measured with an *in vivo* cat hypoglossal nerve–tongue muscle preparation. The studies suggest that the asymmetry present in these structures does not lead to significant differences in blocking potency between enantiomers.

Keyphrases □ Enantiomers—benzyl- and ethyllaudanosinium iodides synthesized, curarimimetic potencies compared □ Neuromuscular junction blocking agents—enantiomers of benzyl- and ethyllaudanosinium iodides synthesized, curarimimetic potencies compared □ Curarimimetic potency—compared in enantiomers of benzyl- and ethyllaudanosinium iodides □ Quaternary ammonium probes—enantiomers of benzyl- and ethyllaudanosinium iodides synthesized, curarimimetic potencies compared □ Structure–activity relationships—enantiomers of benzyl- and ethyllaudanosinium iodides, curarimimetic potencies compared

Previous reports (1–4) described stereochemical preferences exhibited by the neuromuscular junction toward nondepolarizing blocking agents having carbon asymmetry alpha to quaternary ammonium functionality. Initial studies (1) employed monoquaternary structures (hemicurares) as probes and indicated a modest blocking preference for the (*S*)-enantiomers; subsequent investigations (2, 3) employed bisquaternary probes and indicated that the order of blocking preference is (*R*) > (*S*) for these structures. Since the quaternary ammonium function is the most distinguishing pharmacophore of this pharmacological class, structures having nitrogen asymmetry could possess larger enantiomeric potency differences that might also be independent of other, more remote structural modification.

An early example of variation in curarimimetic potency due to nitrogen asymmetry is the report (5) that the diastereomers derived from asymmetric quaternization of coniine show small potency differences. Larger potency differences were reported for the stereoisomers resulting from quaternization of canadine (6, 7). Similarly, certain optically active inorganic onium ions also showed small

0022-3549/79/0400-0522$01.00/0

© 1979, American Pharmaceutical Association

Table I—Standard Solution

Trial	Theophylline		Hydroxyethyltheophylline		Diphenylpyraline Hydrochloride	
	Sample, mg	Recovery, %	Sample, mg	Recovery, %	Sample, mg	Recovery, %
1	100.7	97.9	9.3	98.9	8.6	104.7
2	99.3	99.1	10.7	98.1	7.9	101.3
3	101.5	100.8	11.1	97.3	8.1	97.5
4	98.9	101.2	9.8	98.0	8.3	97.6
5	99.2	102.1	10.5	100.0	7.9	102.5
6	99.1	99.4	10.5	98.1	8.4	97.2
Mean relative error, %	1.26		1.43		2.63	
$\bar{X}$	100.1		98.4		100.1	
SD, %	±1.55		±0.93		±3.4	
RSD, %	1.55		0.95		3.4	

Table II—Production Lot of Syrup

	Theophylline	Hydroxyethyltheophylline	Diphenylpyraline Hydrochloride
Theoretical concentration, mg/30 ml	100.0	10.0	8.0
$\bar{X}$ of 15 samples	99.3	10.5	8.3
RSD, %	1.87	1.20	3.50

hydroxyethyltheophylline. Diphenylpyraline hydrochloride appeared not to undergo any chemical reaction in methanol and reaction mixtures as shown by the retention time. A preliminary 1-μl injection of reagent alone showed a small precursor peak just before the diphenylpyraline hydrochloride peak. This peak may insignificantly affect measurement of diphenylpyraline hydrochloride.

Linearity was also determined. Linear curves passing through the origin were obtained for solutions containing 40–100% of the quantities of drug ingredients being sought. These curves related the peak area and drug concentration.

The initial pH 3.8 of the sample and standard solutions was necessary to ensure the extraction of theophylline and hydroxyethyltheophylline.

REFERENCES

(1) T. Kanieuska and W. Zyzynski, *Zaklad Chemii Analitycznej Instytutu Lekou Warszawie, Poland;* through *Int. Pharm. Abstr.*, **4**, 499b (1967).

(2) A. C. Celeste and M. V. Polito, *J. Assoc. Off. Anal. Chem.*, **49**, 541 1966.

(3) J. Reisch and H. Walker, *Farmazie*, **21**, 467 (1966); through *Anal. Abstr.*, **14**, 7784 (1967).

(4) E. Brochmann-Hanssen and T. O. Oke, *J. Pharm. Sci.*, **58**, 370 1969.

Stereochemical Preferences for Curarimimetic Neuromuscular Junction Blockade IV: Monoquaternary Ammonium Probes Possessing Carbon and Nitrogen Asymmetry

PAUL W. ERHARDT *x and TAITO O. SOINE †

Received May 19, 1978, from the *Medicinal Chemistry Department, College of Pharmacy, University of Minnesota, Minneapolis, MN 55455.* Accepted for publication August 17, 1978.

*Present address: Arnar-Stone Laboratories, McGaw Park, IL 60085. †Deceased.

Abstract □ Two enantiomeric pairs of neuromuscular junction blocking agents were prepared in which an asymmetric carbon atom is adjacent to an asymmetric quaternized nitrogen moiety. The blocking agents were obtained from the enantiomers of laudanosine by stereoselective quaternization with benzyl and ethyl iodides. Curarimimetic potencies were measured with an *in vivo* cat hypoglossal nerve–tongue muscle preparation. The studies suggest that the asymmetry present in these structures does not lead to significant differences in blocking potency between enantiomers.

Keyphrases □ Enantiomers—benzyl- and ethyllaudanosinium iodides synthesized, curarimimetic potencies compared □ Neuromuscular junction blocking agents—enantiomers of benzyl- and ethyllaudanosinium iodides synthesized, curarimimetic potencies compared □ Curarimimetic potency—compared in enantiomers of benzyl- and ethyllaudanosinium iodides □ Quaternary ammonium probes—enantiomers of benzyl- and ethyllaudanosinium iodides synthesized, curarimimetic potencies compared □ Structure–activity relationships—enantiomers of benzyl- and ethyllaudanosinium iodides, curarimimetic potencies compared

Previous reports (1–4) described stereochemical preferences exhibited by the neuromuscular junction toward nondepolarizing blocking agents having carbon asymmetry alpha to quaternary ammonium functionality. Initial studies (1) employed monoquaternary structures (hemicurares) as probes and indicated a modest blocking preference for the (*S*)-enantiomers; subsequent investigations (2, 3) employed bisquaternary probes and indicated that the order of blocking preference is (*R*) > (*S*) for these structures. Since the quaternary ammonium function is the most distinguishing pharmacophore of this pharmacological class, structures having nitrogen asymmetry could possess larger enantiomeric potency differences that might also be independent of other, more remote structural modification.

An early example of variation in curarimimetic potency due to nitrogen asymmetry is the report (5) that the diastereomers derived from asymmetric quaternization of coniine show small potency differences. Larger potency differences were reported for the stereoisomers resulting from quaternization of canadine (6, 7). Similarly, certain optically active inorganic onium ions also showed small

0022-3549/79/0400-0522$01.00/0

© 1979, American Pharmaceutical Association

Table I—Neuromuscular Junction Blocking Potency Data for the Pharmacological Probes

Probe	Stereochemistry	ED_{50}, mg/kg	ED_{50} Potency Ratio to (+)-Tubocurarine (1/N)	Slope Comparison[a], F_{slope} (dF', dF)	Potency Ratio of Enantiomers	Elevation Comparison[b], $F_{elevation}$ (dF', dF)
(+)-Tubocurarine		0.09	1			
I	C-1 (*S*); N (*R*)	1.81	24	0.38 (2, 20)	2:1 (I:II)	5.79 (1, 19)
II	C-1 (*R*); N (*S*)	3.64	48	+		+
III	(*S,S*)	5.33	79	0.65 (2, 15)	1:1 (III:IV)	0.06 (1, 15)
IV	(*R,R*)	5.23	78	+		−

[a] Statistical comparisons were made between the regression line slopes of the probes and (+)-tubocurarine (+ indicates that the slopes are not statistically dissimilar). [b] Statistical comparisons were made between the line elevations of enantiomeric pairs to evaluate the significance of the difference in ED_{50} values (+ indicates a statistically significant difference, and − indicates that the difference is not statistically significant).

enantiomeric differences in curariform activity (8). More recent reports considered nitrogen asymmetry present in bisquaternary isomers related to tubocurarine (9) and in monoquaternary structures derived from norcoralydine (10).

DISCUSSION

Chemistry—Simple hemicurare structures (1) having a single asymmetric nitrogen were sought as probes. Stereoselective quaternization (11–14), exploiting carbon asymmetry alpha to a tertiary amine to direct an incoming alkyl halide, provided a ready method for the synthesis of structures containing the requisite features of the desired probes. The enantiomeric laudanosines were chosen as candidates for stereoselective quaternization with a large (benzyl iodide) and small (ethyl iodide) alkylating agent. Preparation of the laudanosine racemate and enantiomers was as previously described (1). Stereoselective quaternization of these materials followed the method reported by Kobor *et al.* (12), who synthesized the racemic derivatives of these compounds.

When (±)-laudanosine was quaternized with benzyl iodide, the *trans*-material represented 95% of the initial reaction product mixture and crystallization of the pure *trans*-material could be effected from either ethanolic or aqueous solutions. When (±)-2-benzyl-1,2,3,4-tetrahydropapaverine (VI) [prepared *via* benzylation of papaverine to give V followed by sodium borohydride reduction (1)] was quaternized with methyl iodide, the reaction product mixture showed a substantial increase in the *cis*-material. Repetition of this latter process with methyl iodide-d_3 supported the NMR chemical shift assignments of Kobor *et al.* (12) for the *trans*-(δ 3.43) and *cis*-(δ 3.09) N^+CH_3 protons since the resonances at these locations were decreased. Finally, when chloroformic solutions of either the pure *trans*-product or the increased *cis*-product mixture were subjected to heated bomb conditions, the same equilibrium relationship between *cis*- and *trans*-products was obtained, as predicted previously (12).

When each of the enantiomeric laudanosines was quaternized with benzyl iodide, the initial product mixtures again showed 95% *trans*-material. Precipitates obtained from aqueous ethanol were taken up in acetone and, after evaporation of this solvent, the resulting amorphous powders gave acceptable elemental analyses, showed only the *trans*-spot on thin-layer chromatograms, and yielded identical NMR spectra corresponding to the *trans*-diastereomer. These compounds represent pharmacological probes (1*S*,2*R*)-*N*-benzyllaudanosinium iodide (I) and (1*R*,2*S*)-*N*-benzyllaudanosinium iodide (II). Probes (1*S*,2*S*)-*N*-ethyllaudanosinium iodide (III) and (1*R*,2*R*)-*N*-ethyllaudanosinium iodide (IV) were prepared similarly by quaternization with ethyl iodide and yielded crystalline materials from 95% ethanol.

Biology—In addition to their ready chemical accessibility, the selection of I–IV as probes for preliminary study was based on prior investigations (1, 15) where closely related structures were shown to possess modest curarimimetic activity. Also, biological comparison between probes alkylated with both large and small groups could provide additional information about the importance of steric parameters associated with any stereochemical features related to the anionic site of the neuromuscular junction receptor.

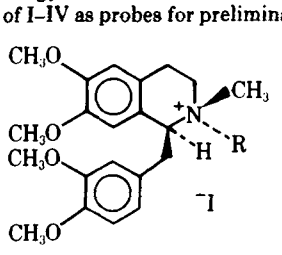

I: R = CH_2—⬡

III: R = CH_2CH_3

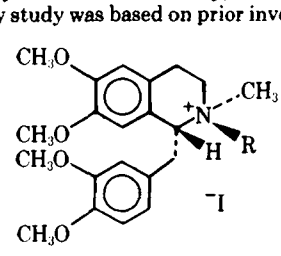

II: R = CH_2—⬡

IV: R = CH_2CH_3

The cat hypoglossal nerve–tongue muscle procedure was employed to assess the blocking potencies of I–IV. Probes were tested in three animals at a minimum of three concentrations. Probit values of the percent decrease from control response levels due to inhibition by the probes were plotted against log dose *via* a linear regression program (1).

As expected, I–IV possessed only modest blocking activity. That the nature of this blockade was curarimimetic was established by the observation that a characteristic relief of the blockade could be effected by subsequent administration of edrophonium and by a statistically nonsignificant difference of linear regression slopes between I–IV and (+)-tubocurarine (performed by analysis of covariance). The enantiomeric potency relationships for I and II and III and IV are presented in Table I. Based on previous studies (1), it seems reasonable to assume that the tabulated potencies reflect differences in interaction with neuromuscular junction receptors rather than differences in distribution patterns or in interactions with acetylcholinesterase.

Since III and IV did not show a significant potency difference and I and II showed only a small difference with the same trend [C-1 (*S*) > C-1 (*R*)] obtained for related probes having carbon asymmetry only (1), these preliminary results suggest that the effect of nitrogen asymmetry on neuromuscular junction receptor interaction with these structural types is not significant. However, relatively few compounds were studied; a more generalized conclusion would require a wider range of candidate compounds, which are currently being prepared.

EXPERIMENTAL[1]

Laudanosine Bases—The preparation and resolution of racemic laudanosine followed published methods (1).

***N*-Benzylpapaverinium Iodide (V)**—Papaverine (24 g, 0.0695 mole) was added in portions, with stirring, to a solution of benzyl iodide in acetone[2] (0.278 mole in 400 ml). The mixture was refluxed for 4 hr, and then the volume was reduced to 200 ml. After standing at room temperature, yellow crystals separated; they were collected and washed with ether to give 25 g (67%), mp 202–204°.

(±)-2-Benzyl-1,2,3,4-tetrahydropapaverine (VI)—Compound V (10 g, 0.018 mole) was suspended in methanol (250 ml); 2 ml of water was added, and the mixture was cooled in an ice bath. Sodium borohydride (10 g, 0.263 mole) was added in small portions, with vigorous stirring, after which the mixture was gently refluxed for 2 hr. Water (40 ml) was then added, the mixture was cooled, and the resulting precipitate was collected and recrystallized in a similar fashion to give 7.0 g (90%), mp 84–86° [lit. (13) mp 91–92° (from ether)].

Quaternization with Benzyl Iodide—Racemic, (*S*)-, or (*R*)-laudanosine (1.87 g, 0.0052 mole) was dissolved in acetone (50 ml). Benzyl iodide (0.0052 mole) in acetone (25 ml) was added, and the combined solutions were refluxed gently for 3 days under nitrogen while protected

[1] Melting points were determined on a Thomas-Hoover apparatus. Optical rotations were measured on a Perkin-Elmer 141 polarimeter. Analyses were performed by M-H-W Laboratories, Garden City, Mich. TLC was conducted on Eastman chromatogram sheet 6060 silica gel developed in butanol–water–acetic acid (7:2:1), and visualization was by a UV lamp and iodine vapor. NMR spectra were measured with a Varian Associates model A-60 D NMR spectrometer with tetramethylsilane as an internal standard.

[2] Acetone solutions of benzyl iodide (0.7 *M*) were prepared by quantitative Finkelstein conversion of benzyl bromide plus sodium iodide.

Table II—Physical and Analytical Data for Probe Molecules and New Compounds [a]

Compound	Melting Point	Optical Rotation [b], $[\alpha]_D^{25}$	Formula		Analysis, % Calc.	Found
I	112–114° [c]	+29°	$C_{28}H_{34}INO_4$	C	58.4	58.16
				H	5.9	6.12
				I	22.1	21.90
				N	2.4	2.11
II	116–118° [c]	−30°	$C_{28}H_{34}INO_4$	C	58.4	58.20
				H	5.9	5.77
				I	22.1	22.46
				N	2.4	2.34
III	166–168°	+74°	$C_{23}H_{32}INO_4 \cdot H_2O$	C	52.0	51.78
				H	6.4	6.24
				I	23.9	24.19
				N	2.6	2.47
IV	164–168° [c]	−72°	$C_{23}H_{32}INO_4 \cdot H_2O$	C	52.0	51.83
				H	6.4	6.57
				I	23.9	23.73
				N	2.6	2.49
V	202–204°	0°	$C_{27}H_{28}INO_4$	C	58.2	58.21
				H	5.0	4.99
				I	22.8	22.66
				N	2.5	2.25
VI	84–86°	0°	$C_{27}H_{31}NO_4$	C	74.8	74.57
				H	7.2	7.33
				N	3.2	3.03

[a] Reported only for new compounds and for VI because of a discrepancy in melting-point data for this compound. [b] All rotations determined as (c 0.5, ethanol). [c] Obtained as amorphous solids.

from light. The solvent was then removed under reduced pressure, and the racemic derivative was crystallized from either ethanol or water while enantiomeric derivatives yielded soft, tar-like materials. The enantiomeric tars were taken up in acetone, which was then evaporated to produce fine amorphous powders. Final yields were: racemic material, 75%; I, 67%; and II, 17%. Physical data for probe compounds are recorded in Table II.

Quaternization with Ethyl Iodide—Either (*S*)- or (*R*)-laudanosine (3.57 g, 0.01 mole) was dissolved in ethanol (100 ml), ethyl iodide (1.6 ml, 0.02 mole) was added, and the mixture was refluxed gently for 12 hr. The solution was evaporated, and the residue was recrystallized (six times) from ethanol until its NMR spectrum and TLC showed only the *trans*-product. Final yields were: III, 14%; and IV, 10%.

Quaternization of VI—To a solution of VI (2.17 g, 0.005 mole) in methanol (50 ml) was added methyl iodide or methyl iodide-d_3 (0.01 mole). The mixtures were refluxed gently for 6 hr under nitrogen while protected from light. The solvent was removed by evaporation, and the initial reaction product mixture residues were used for NMR studies.

***cis–trans*-Equilibration Reactions**—A chloroformic solution of *trans*-(±)-*N*-benzyllaudanosinium iodide or of the residue obtained from quaternization of VI was subjected to the conditions specified previously (12, 16), except that reactions were carried out in a stainless steel bomb apparatus. Residues obtained after solvent evaporation were utilized for NMR studies.

REFERENCES

(1) P. W. Erhardt and T. O. Soine, *J. Pharm. Sci.*, **64**, 53 (1975).

(2) A. A. Genenah, T. O. Soine, and N. A. Shaath, *ibid.*, **64**, 62 (1975).

(3) T. O. Soine, W. S. Hanley, N. A. Shaath, and A. A. Genenah, *ibid.*, **64**, 67 (1975).

(4) T. O. Soine and J. Naghaway, *ibid.*, **63**, 1643 (1974).

(5) M. Scholtz, *Chem. Ber.*, **38**, 595 (1905).

(6) H. A. D. Jowett and F. L. Pyman, *J. Chem. Soc.*, **103**, 290 (1913).

(7) P. P. Laidlaw, *J. Pharmacol. Exp. Ther.*, **4**, 461 (1913).

(8) F. P. Dwyer, E. C. Gyarfas, R. D. Wright, and A. Shulman, *Nature (London)*, **179**, 425 (1957).

(9) I. G. Marshall, J. B. Murray, G. A. Smail, and J. B. Stenlake, *J. Pharm. Pharmacol.*, **19**, 535 (1967).

(10) J. C. Craig, M. Martin-Smith, S. K. Roy, and J. B. Stenlake, *ibid.*, **25**, 154-P (1973).

(11) G. Bernath, K. Koczka, J. Kobor, L. Radics, and M. Kajtar, *Acta Chim. Acad. Sci. Hung.*, **55**, 331 (1968).

(12) J. Kobor, G. Bernath, L. Radics, and M. Kajtar, *ibid.*, **60**, 255 (1969).

(13) L. Radics, M. Kajtar, J. Kobor, and G. Bernath, *ibid.*, **60**, 381 (1969).

(14) J. Volford, G. Toth, G. Bernath, and J. Kobor, *Tetrahedron Lett.*, **1971**, 4019.

(15) L. E. Craig and D. S. Tarbell, *J. Am. Chem. Soc.*, **70**, 2783 (1948).

(16) J. McKenna, J. M. McKenna, and J. White, *J. Chem. Soc.*, **1965**, 1733.

Phenazines with Two Cationic Side Chains as Potential Antimalarials

SHANTI N. SAWHNEY and DAVID W. BOYKIN ˣ

Received July 12, 1978, from the *Department of Chemistry, Georgia State University, Atlanta, GA 30303.* Accepted for publication September 13, 1978.

Abstract □ 1,9-Phenazine-bis(dialkylaminocarboxamides) were prepared for screening as potential antimalarials. No significant activity against *Plasmodium berghei* was observed. The phenazine targets were prepared from 1,9-phenazinedicarboxylic acid by standard methods. The reaction between 1,9-phenazinedicarboxylic acid and thionyl chloride in the presence of dimethylformamide unexpectedly gave 4-chloro-1,9-phenazinedicarbonyl chloride.

Keyphrases □ Phenazines—with two cationic side chains, synthesized and screened as potential antimalarials □ Antimalarials, potential—synthesis and screening of phenazines with two cationic side chains

As part of a research program to develop new antimalarials (1), some selected phenazine derivatives were synthesized because of indications of antimalarial activity for several phenazine types. Clofazimine, which has proven safe for human use against leprosy, has been reported to suppress parasitemia completely in mice infected with *Plasmodium berghei* (2). Modest activity against *P. berghei* in mice has been observed for several simple phenazines, including 7-chloro-2-phenazinenitrile, methylene violet/Bernthsen, and diazine black[1].

While the mode of antimalarial action of these compounds is unknown, the fact that phenazine antibiotics such as myxin and iodimin (3), as well as other phenazines (4, 5), related phenoxazines (6) (actinomycins), and related

[1] Dr. E. A. Steck, Walter Reed Army Institute of Research, Washington, D.C., personal communication.

0022-3549/79/0400-0524$01.00/0

© 1979, American Pharmaceutical Association

Table II—Physical and Analytical Data for Probe Molecules and New Compounds [a]

Compound	Melting Point	Optical Rotation [b], $[\alpha]_D^{25}$	Formula		Analysis, % Calc.	Found
I	112–114° [c]	+29°	$C_{28}H_{34}INO_4$	C	58.4	58.16
				H	5.9	6.12
				I	22.1	21.90
				N	2.4	2.11
II	116–118° [c]	−30°	$C_{28}H_{34}INO_4$	C	58.4	58.20
				H	5.9	5.77
				I	22.1	22.46
				N	2.4	2.34
III	166–168°	+74°	$C_{23}H_{32}INO_4 \cdot H_2O$	C	52.0	51.78
				H	6.4	6.24
				I	23.9	24.19
				N	2.6	2.47
IV	164–168° [c]	−72°	$C_{23}H_{32}INO_4 \cdot H_2O$	C	52.0	51.83
				H	6.4	6.57
				I	23.9	23.73
				N	2.6	2.49
V	202–204°	0°	$C_{27}H_{28}INO_4$	C	58.2	58.21
				H	5.0	4.99
				I	22.8	22.66
				N	2.5	2.25
VI	84–86°	0°	$C_{27}H_{31}NO_4$	C	74.8	74.57
				H	7.2	7.33
				N	3.2	3.03

[a] Reported only for new compounds and for VI because of a discrepancy in melting-point data for this compound. [b] All rotations determined as (c 0.5, ethanol). [c] Obtained as amorphous solids.

from light. The solvent was then removed under reduced pressure, and the racemic derivative was crystallized from either ethanol or water while enantiomeric derivatives yielded soft, tar-like materials. The enantiomeric tars were taken up in acetone, which was then evaporated to produce fine amorphous powders. Final yields were: racemic material, 75%; I, 67%; and II, 17%. Physical data for probe compounds are recorded in Table II.

Quaternization with Ethyl Iodide—Either (*S*)- or (*R*)-laudanosine (3.57 g, 0.01 mole) was dissolved in ethanol (100 ml), ethyl iodide (1.6 ml, 0.02 mole) was added, and the mixture was refluxed gently for 12 hr. The solution was evaporated, and the residue was recrystallized (six times) from ethanol until its NMR spectrum and TLC showed only the *trans*-product. Final yields were: III, 14%; and IV, 10%.

Quaternization of VI—To a solution of VI (2.17 g, 0.005 mole) in methanol (50 ml) was added methyl iodide or methyl iodide-d_3 (0.01 mole). The mixtures were refluxed gently for 6 hr under nitrogen while protected from light. The solvent was removed by evaporation, and the initial reaction product mixture residues were used for NMR studies.

***cis–trans*-Equilibration Reactions**—A chloroformic solution of *trans*-(±)-*N*-benzyllaudanosinium iodide or of the residue obtained from quaternization of VI was subjected to the conditions specified previously (12, 16), except that reactions were carried out in a stainless steel bomb apparatus. Residues obtained after solvent evaporation were utilized for NMR studies.

REFERENCES

(1) P. W. Erhardt and T. O. Soine, *J. Pharm. Sci.*, **64**, 53 (1975).

(2) A. A. Genenah, T. O. Soine, and N. A. Shaath, *ibid.*, **64**, 62 (1975).

(3) T. O. Soine, W. S. Hanley, N. A. Shaath, and A. A. Genenah, *ibid.*, **64**, 67 (1975).

(4) T. O. Soine and J. Naghaway, *ibid.*, **63**, 1643 (1974).

(5) M. Scholtz, *Chem. Ber.*, **38**, 595 (1905).

(6) H. A. D. Jowett and F. L. Pyman, *J. Chem. Soc.*, **103**, 290 (1913).

(7) P. P. Laidlaw, *J. Pharmacol. Exp. Ther.*, **4**, 461 (1913).

(8) F. P. Dwyer, E. C. Gyarfas, R. D. Wright, and A. Shulman, *Nature (London)*, **179**, 425 (1957).

(9) I. G. Marshall, J. B. Murray, G. A. Smail, and J. B. Stenlake, *J. Pharm. Pharmacol.*, **19**, 535 (1967).

(10) J. C. Craig, M. Martin-Smith, S. K. Roy, and J. B. Stenlake, *ibid.*, **25**, 154-P (1973).

(11) G. Bernath, K. Koczka, J. Kobor, L. Radics, and M. Kajtar, *Acta Chim. Acad. Sci. Hung.*, **55**, 331 (1968).

(12) J. Kobor, G. Bernath, L. Radics, and M. Kajtar, *ibid.*, **60**, 255 (1969).

(13) L. Radics, M. Kajtar, J. Kobor, and G. Bernath, *ibid.*, **60**, 381 (1969).

(14) J. Volford, G. Toth, G. Bernath, and J. Kobor, *Tetrahedron Lett.*, **1971**, 4019.

(15) L. E. Craig and D. S. Tarbell, *J. Am. Chem. Soc.*, **70**, 2783 (1948).

(16) J. McKenna, J. M. McKenna, and J. White, *J. Chem. Soc.*, **1965**, 1733.

Phenazines with Two Cationic Side Chains as Potential Antimalarials

SHANTI N. SAWHNEY and DAVID W. BOYKIN ˣ

Received July 12, 1978, from the *Department of Chemistry, Georgia State University, Atlanta, GA 30303.* Accepted for publication September 13, 1978.

Abstract □ 1,9-Phenazine-bis(dialkylaminocarboxamides) were prepared for screening as potential antimalarials. No significant activity against *Plasmodium berghei* was observed. The phenazine targets were prepared from 1,9-phenazinedicarboxylic acid by standard methods. The reaction between 1,9-phenazinedicarboxylic acid and thionyl chloride in the presence of dimethylformamide unexpectedly gave 4-chloro-1,9-phenazinedicarbonyl chloride.

Keyphrases □ Phenazines—with two cationic side chains, synthesized and screened as potential antimalarials □ Antimalarials, potential—synthesis and screening of phenazines with two cationic side chains

As part of a research program to develop new antimalarials (1), some selected phenazine derivatives were synthesized because of indications of antimalarial activity for several phenazine types. Clofazimine, which has proven safe for human use against leprosy, has been reported to suppress parasitemia completely in mice infected with *Plasmodium berghei* (2). Modest activity against *P. berghei* in mice has been observed for several simple phenazines, including 7-chloro-2-phenazinenitrile, methylene violet/Bernthsen, and diazine black[1].

While the mode of antimalarial action of these compounds is unknown, the fact that phenazine antibiotics such as myxin and iodimin (3), as well as other phenazines (4, 5), related phenoxazines (6) (actinomycins), and related

[1] Dr. E. A. Steck, Walter Reed Army Institute of Research, Washington, D.C., personal communication.

0022-3549/79/0400-0524$01.00/0

© 1979, American Pharmaceutical Association

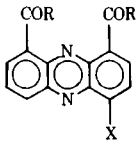

Table I—1,9-Substituted Phenazines

Number	R	X	Melting Point	Yield, %	Recrystallization Solvent	Formula	Analysis, %	Calc.	Found
IX	$CONH(CH_2)_3N(CH_3)_2$	H	179–180°	60	Benzene	$C_{24}H_{32}N_6O_2$	C	66.03	65.88
							H	7.29	7.42
							N	19.25	19.17
X	$CONH(CH_2)_3N(C_2H_5)_2$	H	149–150°	84	Benzene–*n*-hexane	$C_{28}H_{40}N_6O_2$	C	68.26	68.43
							H	8.18	8.25
							N	17.06	17.08
XI	$CONH(CH_2)_3\underset{\displaystyle CH_3}{\underset{\vert}{N}}(CH_2)_2N(CH_3)_2$	H	105–107°	66	Cyclohexane	$C_{30}H_{46}N_8O_2$	C	65.42	65.19
							H	8.42	8.49
							N	20.35	20.29
XII	$CONH(CH_2)_3\underset{\displaystyle C_2H_5}{\underset{\vert}{N}}(CH_2)_2N(C_2H_5)_2$	H	88–90°	87	Cyclohexane	$C_{36}H_{58}N_8O_2$	C	68.10	68.00
							H	9.21	9.22
							N	17.65	17.64
XIII	$CONH(CH_2)_3N(CH_3)_2$	Cl	210–211°	65	Benzene	$C_{24}H_{31}ClN_6O_2$	C	61.20	60.88
							H	6.65	7.05
							Cl	7.53	7.52
							N	17.84	17.69
XIV	$CONH(CH_2)_3\underset{\displaystyle C_2H_5}{\underset{\vert}{N}}(CH_2)_2N(C_2H_5)_2$	Cl	88–90°	65	*n*-Hexane	$C_{36}H_{57}ClN_8O_2$	C	64.60	64.57
							H	8.58	8.61
							N	16.74	16.81

thiaxantenones (6), intercalate with DNA permits the working hypothesis that DNA binding might be involved in their antimalarial action. Recent work (7) on other antimalarials, however, emphasized the need for caution in such speculations. Nevertheless, in the absence of necessary biochemical information, it was decided to make phenazines with cationic side chains at the 1- and 9-positions for evaluation as possible antimalarials. This approach appeared promising in view of the reports (8–10) of the enhancement of DNA binding brought about by attachment of cationic side chains to planar aromatic rings that intercalate with DNA.

RESULTS AND DISCUSSION

The synthesis of the phenazines (VI) was achieved by employing known approaches to the phenazine ring system, followed by side-chain attachment in a conventional manner (Scheme I). The first step was an Ullman-type condensation between 2-bromo-3-nitrobenzoic acid and anthranilic acid to produce 2-nitrodiphenylamine-6,2′-dicarboxylic acid. The reductive cyclization of 2-nitrodiphenylamines by sodium borohydride is a well-established phenazine synthesis (11, 12). Decarboxylation occurred during this reaction since, in addition to IV, 1-phenazinecarboxylic acid was isolated.

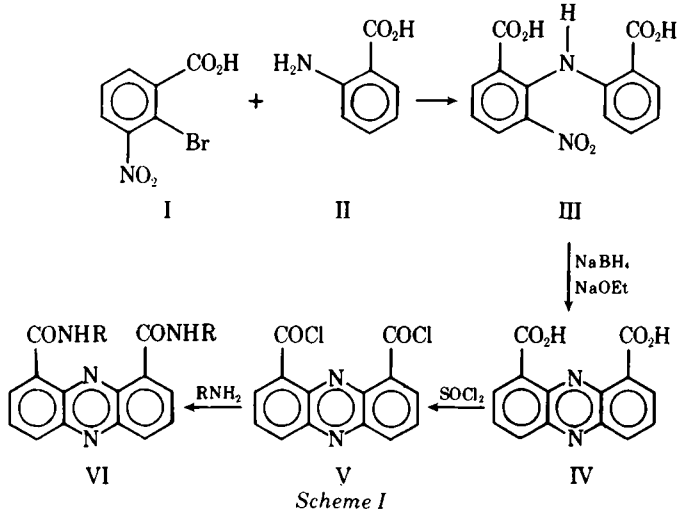

Scheme I

The subsequent steps in the synthesis of VI involved classical amide preparation procedures. One aliphatic diamine employed to make the side chains was a new compound, but it was prepared by standard methods and the details are given under *Experimental*.

In the conversion of 1,9-phenazinedicarboxylic acid into its diacid chloride, when dimethylformamide was added as a catalyst, aromatic ring chlorination unexpectedly occurred in addition to conversion into the dicarbonyl chloride. The product of the dimethylformamide–thionyl chloride reaction was 4-chloro-1,9-phenazinedicarbonyl chloride. This structural assignment was based on hydrolysis of the dicarbonyl chloride to 4-chloro-1,9-phenazinedicarboxylic acid. The latter structure was demonstrated by decarboxylation of the dicarboxylic acid to the known 1-chlorophenazine (13). This heteroaromatic ring chlorination reaction by dimethylformamide–thionyl chloride appears to be unreported and is being investigated. Because of the availability of 4-chloro-1,9-phenazinedicarboxylic acid, it was decided to make target compounds from it for evaluation as antimalarials as well.

The targets (IX–XIV) shown in Table I were screened against *P. berghei* by the method of Osdene *et al.* (14). These compounds exhibited only very limited activity. The maximum observed increase in mean survival time of test animals over controls was less than 1 day. Preliminary viscosity studies with IX and XIII indicate that these compounds bind very strongly to DNA, and these results will be reported elsewhere.

EXPERIMENTAL[2]

Melting points under 300° were taken using an oil bath melting-point apparatus; melting points above 300° were obtained using a solid block apparatus. All melting points are uncorrected. Satisfactory IR spectra were recorded on all new compounds. The expected carbon and PMR spectra were recorded on selected compounds in ^{2}H-chloroform and ^{2}H-dimethyl sulfoxide using tetramethylsilane as the standard.

The amines used in side-chain preparation were commercially available (*N,N*-dimethylpropanediamine and *N,N*-diethylpropanediamine), previously reported [*N*-(2-dimethylaminoethyl)-*N*-methyl-1,3-propanediamine] (15), or synthesized as described here.

[2] Elemental analyses were performed by Atlantic Microlab, Atlanta, Ga.

N - (2 - Diethylaminoethyl) - N - ethyl - 1,3 - propanediamine—*N,N,N'*-Triethylethylenediamine (36 g, 0.25 mole) was added gradually to acrylonitrile (26.5 g, 0.4 mole) with stirring at room temperature. The mixture was left at room temperature for 1 hr and then heated under reflux on a steam bath for 22 hr. Acrylonitrile was distilled off at reduced pressure, and the residual liquid was fractionally distilled under vacuum. The fraction of bp 81–83°/0.2 mm was collected in a 45-g yield (90%). The picrate of *N,N,N'*-triethyl-*N'*-(2-cyanoethyl)-ethylenediamine was prepared in alcohol and crystallized from acetone, mp 188–189°.

Anal.—Calc. for dipicrate $C_{23}H_{29}N_9O_{14}$: C, 42.14; H, 4.46; N, 19.23. Found: C, 42.05; H, 4.44; N, 19.16.

A solution of this cyanoamine (19.7 g, 0.1 mole) in dry ether (50 ml) was added slowly, with vigorous stirring, to a suspension of lithium aluminum hydride (4 g) in dry ether (200 ml) and was then cooled in an ice bath. The addition took about 30 min. Stirring was continued for 2 hr with cooling in ice. Water (5 ml), 20% NaOH (5 ml), and water (15 ml) were added successively. The ether layer was decanted, and the residual white solid was washed twice with ether by decantation. The combined ether extracts were dried over potassium hydroxide, and the ether was removed under reduced pressure. The residual liquid was distilled under vacuum, and the fraction of bp 76–77°/0.2 mm was collected in a 14.5-g yield (72%). The picrate was prepared in alcohol and crystallized from methyl ethyl ketone, mp 211–212°.

Anal.—Calc. for tripicrate $C_{29}H_{36}N_{12}O_{21}$: C, 39.19; H, 4.08; N, 18.91. Found: C, 39.14; H, 4.12; N, 18.96.

2-Nitrodiphenylamine-6,2'-dicarboxylic Acid (III)—2-Bromo-3-nitrobenzoic acid (I) (24.6 g, 0.1 mole), anthranilic acid (II) (15.1 g, 0.11 mole), potassium carbonate (50 g), and copper powder (0.5 g) were mixed throughly and added to isoamyl alcohol (27.5 ml). The mixture was heated gradually with stirring until the bath temperature reached 150°, when it melted and the alcohol began to reflux. Heating was continued for 1 hr at 160–170°, and the alcohol was removed by steam distillation. The residue was dissolved in water and filtered. The filtrate was shaken with chloroform, and the aqueous layer was added gradually to stirred 1 *N* HCl (1 liter); stirring was continued for 0.5 hr. The yellow solid was filtered, washed with water, dried, and crystallized from acetic acid in a 16-g yield (53%), mp 283–285° [lit. (12) mp 285–290°].

1,9-Phenazinedicarboxylic Acid (IV)—The diphenylamine (III) (9.1 g, 0.03 mole) was added with stirring to absolute ethanol (250 ml) containing dissolved sodium (8.9 g) and sodium borohydride (6.3 g). The mixture was refluxed, with vigorous stirring, for 16 hr when a greenish-brown suspension resulted. Water (50 ml) was added, and the solid was filtered and washed with a small volume of water. The residue on the filter was dissolved in water (800 ml) by heating, cooled in ice, and acidified with concentrated hydrochloric acid. The precipitated acid was filtered, washed with water, dried, boiled with ethylene glycol monomethyl ether (50 ml), and filtered hot. The residual product was crystallized from dimethylformamide in a 3-g yield (38%), mp 362°.

Anal.—Calc. for $C_{14}H_8N_2O_4$: C, 62.68; H, 3.00; N, 10.44. Found: C, 62.52; H, 3.01; N, 10.42.

After removal of the greenish-brown suspension, the alkaline filtrate was diluted with water. Ethanol was removed by distillation under reduced pressure. On acidification, the aqueous solution gave an acid which, after crystallization from ethylene glycol monomethyl ether, melted at 238–239°. Some of this material was also obtained from the ethylene glycol monomethyl ether filtrate during purification of IV. The total yield was 1.6 g. This compound was found to be 1-carboxyphenazine [lit. (16) mp 239°]. Its mixed melting point with an authentic sample remained undepressed, and the IR spectra of two samples were superimposable.

Phenazine-1,9-dicarboxylic Acid Chloride (V)—Compound IV (3 g) was suspended in dry benzene (60 ml), and thionyl chloride (5 ml) was added. The mixture was refluxed for 1 hr. Thionyl chloride (1 ml) was added, and refluxing was continued for 1 hr more when a clear solution resulted. On cooling, the acid chloride crystallized. It was filtered, washed with a small amount of dry ether, and crystallized from benzene in a 3-g yield (89%), mp 193–194°.

Anal.—Calc. for $C_{14}H_6Cl_2N_2O_2$: C, 55.10; H, 1.98; N, 9.18. Found: C, 55.33; H, 2.02; N, 9.08.

4-Chlorophenazine-1,9-dicarboxylic Acid Chloride (VIII)—To IV (2 g) suspended in dry benzene (10 ml) were added thionyl chloride (2 ml) and dimethylformamide (0.4 g), and the mixture was refluxed gently for 3 hr. The solution was allowed to stand at room temperature, and the acid chloride crystallized. It was filtered, washed with cold benzene, and crystallized from benzene in a 1.3-g yield (50%), mp 188–190°.

Anal.—Calc. for $C_{14}H_5Cl_3N_2O_2$: C, 49.51; H, 1.48; Cl, 31.32; N, 8.25. Found: C, 49.65; H, 1.49; Cl, 31.24; N, 8.23.

4-Chlorophenazine-1,9-dicarboxylic Acid (VII)—The acid chloride (VIII) (1 g) was boiled with water (20 ml) for 3 hr and then allowed to stand overnight. The solid was separated, dissolved in a 5% $NaHCO_3$ solution by heating, and precipitated by acidification with hydrochloric acid. Then it was filtered, washed with water, and crystallized twice from acetic acid in a 0.5-g yield (57%), mp 298°.

Anal.—Calc. for $C_{14}H_7ClN_2O_4$: C, 55.55; H, 2.32; N, 9.25. Found: C, 55.70; H, 2.34; N, 9.22.

Decarboxylation of VII—The acid (VII) (1.5 g), copper powder (0.4 g), and dry redistilled quinoline (10 ml) were heated at 175–185° under nitrogen for 2 hr. After cooling, the mixture was added to an excess of 1 *N* HCl, and a dark-brown solid separated. It was filtered, washed with 1 *N* HCl and water, and dried. This material was vacuum sublimed at 125–130°/3 mm. The sublimate was dissolved in chloroform and chromatographed over alumina. Then it was eluted with benzene, and the yellow band that eluted first was collected. The solvent was removed, and the light-yellow residue was crystallized from methanol in a 0.3-g yield (30%), mp 119–120° [lit. (13) mp 122–123°].

Anal.—Calc. for $C_{14}H_7ClN_2$: C, 67.14; H, 3.29; N, 13.05. Found: C, 67.09; H, 3.30; N, 13.03.

Target Compounds (IX–XIV)—The synthesis of XI is given as a typical example of the synthesis of all target amides. A solution of V (1.3 g, 0.004 mole) in hot dry benzene (100 ml) was added gradually to a stirred solution of *N*-methyl-*N*-(2-dimethylaminoethyl)-1,3-propanediamine (3 g, 0.019 mole) in benzene (30 ml), and the mixture was stirred at room temperature for 1 hr. The mixture was then refluxed on a steam bath for 2 hr.

After cooling, the benzene solution was washed with 10% Na_2CO_3 solution (4 × 25 ml). The aqueous layer was then extracted with hot benzene. The combined benzene extracts were dried (calcium sulfate), the benzene was distilled off, the residual semisolid mass was triturated with hexane, and a greenish-yellow solid was obtained. It was filtered, washed with a small amount of hexane, dried, and crystallized from cyclohexane in a 1.6-g yield (66%), mp 105–107°.

REFERENCES

(1) B. P. Das and D. W. Boykin, *J. Med. Chem.*, **20,** 531 (1977).

(2) J. N. Sheagren, *J. Parasitol.*, **54,** 1250 (1968).

(3) U. Hollstein and R. J. Van Germert, Jr., *Biochemistry*, **10,** 497 (1971).

(4) W. Müller and D. M. Crothers, *Eur. J. Biochem.*, **54,** 267 (1975).

(5) W. Müller, H. Bünemann, and N. Dattaguta, *ibid.*, **54,** 279 (1975).

(6) V. A. Bloomfield, M. Crothers, and J. Tinoco, Jr., "Physical Chemistry of Nucleic Acids," Harper and Row, New York, N.Y., 1974, p. 469.

(7) M. W. Davidson, B. G. Griggs, D. W. Boykin, and W. D. Wilson, *J. Med. Chem.*, **20,** 1117 (1977).

(8) W. Müller and D. M. Crothers, *J. Mol. Biol.*, **35,** 251 (1978).

(9) R. A. Carchman, E. Hirschberg, and I. B. Weinstein, *Biochim. Biophys. Acta*, **179,** 158 (1969).

(10) S. N. Cohen and K. L. Yielding, *J. Biol. Chem.*, **240,** 3123 (1965).

(11) S. R. Challand, R. B. Herbert, and F. G. Holliman, *Chem. Commun.*, **1970,** 1423.

(12) E. Breitmaier and U. Hollstein, *J. Org. Chem.*, **41,** 2104 (1976).

(13) I. J. Pachter and M. C. Kloetzel, *J. Am. Chem. Soc.*, **74,** 971 (1952).

(14) T. S. Osdene, P. B. Russell, and L. Rane, *J. Med. Chem.*, **10,** 431 (1967).

(15) I. N. Somin, *Zh. Org. Khim.*, **4,** 128 (1968); through *Chem. Abstr.*, **68,** 86833 (1968).

(16) F. Kogl and J. J. Postowsky, *Ann.*, **480,** 280 (1930).

ACKNOWLEDGMENTS

Supported in part by the U.S. Army Medical Research and Development Command under Contract DADA17-68-C-8035.

This report is Contribution 1492 from the Army Research Program on Malaria.

The authors thank Dr. Edgar A. Steck for helpful discussions and advice.

Determination of Oxycodone in Plasma and Identification of a Major Metabolite

STEPHEN H. WEINSTEIN ˣ **and JANET C. GAYLORD**

Received July 10, 1978, from the *Pharmaceuticals Division, Biochemicals Department, E. I. du Pont de Nemours & Co., Wilmington, DE 19898.* Accepted for publication September 25, 1978.

Abstract □ An electron-capture GLC method is described for oxycodone and its major metabolite, noroxycodone, in plasma and urine. The method involves extraction of the two substances into benzene–isopropanol at pH 10.4, followed by back-extraction into 0.1 *N* HCl. The acid phase is washed with hexane and made alkaline prior to reextraction into benzene–isopropanol. The solvent is removed by evaporation, and the heptafluorobutyryl derivatives of the test substances are formed. After removal of excess reagent, oxycodone and noroxycodone are quantitated by GLC. The characteristics of both substances, with respect to plasma levels in dogs and analgesic activity in mice, are reported. Isolation of noroxycodone from human urine and its identification by TLC, GLC, and mass spectrometry are described.

Keyphrases □ Oxycodone—analysis in plasma and urine, metabolites, electron-capture GLC method □ GLC, electron capture—analysis, oxycodone and noroxycodone in plasma and urine □ Noroxycodone—analysis in plasma and urine, electron-capture GLC method

Oxycodone (4,5α-epoxy-14-hydroxy-3-methoxy-17-methylmorphinan-6-one) has pharmacological properties similar to those of codeine and is used in combination with aspirin, phenacetin, and caffeine[1] and with acetaminophen[2] in the treatment of moderate to moderately severe pain (1). Existing methods (2, 3) for the determination of oxycodone in biological materials, while useful as screening procedures for forensic purposes, are not sufficiently sensitive to determine the drug in plasma after clinical doses.

This report describes a specific, sensitive analytical method for plasma oxycodone and noroxycodone, its major metabolite.

EXPERIMENTAL

Extraction of Oxycodone and Noroxycodone from Plasma—A 2-ml plasma sample containing oxycodone and noroxycodone was placed in a 25-ml screw-capped centrifuge tube[3], and 25 ng of naltrexone hydrochloride[4] (in 0.1 ml of aqueous solution), the internal standard, was added followed by 1 ml of distilled water. The pH was adjusted to 10 with 1 *N* NaOH, and 1.5 ml of pH 10.4 phosphate buffer[5] was added, followed by 1.5 g of sodium chloride.

This mixture was extracted with 10 ml of benzene[6] containing 1% (v/v) isopropanol by shaking on a wrist-action shaker for 30 min. After centrifugation for 15 min at 2200×*g*, 9 ml of the upper organic layer was transferred into a 15-ml glass-stoppered centrifuge tube containing 1 ml of 0.1 *N* HCl. The tube was agitated on a mixer[7] for 1 min and then centrifuged for 10 min at 1240×*g*.

The upper organic phase was discarded, and the remaining aqueous layer was washed with 5 ml of hexane[6]. After the hexane was discarded, the aqueous phase was adjusted to pH 10 with 0.1 *N* NaOH, and 1.5 ml of pH 10.4 phosphate buffer was added. The alkaline aqueous phase was extracted into 6 ml of benzene containing 1% isopropanol by shaking for 30 min on a wrist-action shaker. After centrifugation at 1240×*g* for 10 min, 5 ml of the upper benzene phase was transferred, 2.5 ml at a time, to a 5-ml glass-stoppered centrifuge tube and evaporated to dryness[8].

Preparation of Plasma Standards—Aqueous solutions of oxycodone hydrochloride in the concentration range from 100 to 6.25 ng/ml were prepared by serial dilution. Aliquots of these solutions were added to control plasma samples such that the concentrations of oxycodone hydrochloride in plasma ranged from 10.0 to 0.625 ng/ml. The internal standard was added, and extraction and quantitation were performed as already described.

Expired human plasma obtained from blood banks and dog plasma were both used for oxycodone plasma standards.

Derivatization and GLC—The heptafluorobutyryl derivatives of oxycodone, noroxycodone, and naltrexone (the internal standard) were prepared by treating the dried residue of the extract with heptafluorobutyrylimidazole[9] (I). Ten microliters each of benzene and I were added to the dried residue. The mixture was agitated on a mixer for 3 sec and incubated at 85° for 45 min in a heating block[10]. After cooling, 50 μl of toluene was added to the reaction mixture. The toluene solution was washed once with 1 ml of 2.5% aqueous NH_4OH and then three times with distilled water. After each washing, the mixture was centrifuged and the lower aqueous phase was removed with a Pasteur pipet.

A 2- or 4-μl aliquot of the toluene solution was injected into the gas chromatograph[11], which was equipped with a 15-mCi ^3H-electron-capture detector. The 1.8-m glass column, packed with 3.8% methyl phenyl silicon gum rubber[12], had been previously conditioned for 48 hr at 250° with a helium flow rate of 12 ml/min. The oven, detector, and injection port temperatures were 215, 220, and 220°, respectively. The pulse interval setting was 15. The carrier was helium, 75 ml/min; 10% methane in argon, 100 ml/min, was the purge gas.

The peak height ratios of oxycodone and naltrexone heptafluorobutyrates and of noroxycodone and naltrexone heptafluorobutyrates were determined and were proportional to the amounts of oxycodone and noroxycodone injected.

Extraction of Oxycodone and Noroxycodone from Urine—Urine samples were extracted for oxycodone or noroxycodone analysis by diluting 0.1 ml of urine with 2.9 ml of distilled water. The pH of the diluted urine was adjusted to 1.0 with 5 *N* H_2SO_4. The diluted, acidified urine was washed with 10 ml of benzene on a mixer for 1–2 min. Then the benzene wash was discarded, and the aqueous phase pH was adjusted to 10 with 5 *N* NaOH. The extraction was then performed as already described for plasma.

After formation of the heptafluorobutyryl derivatives, the samples were reconstituted in 100 μl of toluene and washed as described for plasma extracts. Then 1-μl aliquots were injected. The oxycodone or noroxycodone concentration in urine was determined using an external standard consisting of control urine with known amounts of oxycodone added. Control urine samples with oxycodone hydrochloride added to yield concentrations between 100 and 2500 ng/ml were appropriate standards. The internal standard used in plasma was obscured by an interfering peak in urine extracts.

Metabolite Isolation and Identification—For TLC and subsequent mass spectrometry, 10 ml of urine containing oxycodone and noroxycodone (spiked control urine containing 10 μg/ml of each was used as a standard) was adjusted to pH 1.0 with 5 *N* H_2SO_4. The acidified urine was washed with benzene and readjusted to pH 10 with 5 *N* NaOH. After addition of 1.5 ml of pH 10.4 phosphate buffer and 2 g of sodium chloride, the urine sample was extracted with 6.0 ml of benzene. Then the benzene extract was evaporated to dryness.

[1] Percodan, Endo Laboratories.
[2] Percocet-5, Endo Laboratories.
[3] Corex tube with Teflon-lined cap.
[4] Naltrexone hydrochloride, oxycodone hydrochloride, and noroxycodone hydrochloride were obtained from Endo Laboratories.
[5] Potassium phosphate buffer is prepared by adding 5% aqueous K_3PO_4-H_2O to 35% aqueous K_2HPO_4 until pH 10.4 is attained. Both phosphate salts are "Baker analyzed" reagent grade.
[6] All organic solvents used are Burdick & Jackson, distilled in glass.
[7] Vortex.
[8] Evaporation was performed with a Buchler Evapo-Mix attached to a water aspirator.
[9] Pierce Chemicals, Rockford, Ill.
[10] Temp-Blok, Lab Line Instruments, Melrose Park, Ill.
[11] Hewlett-Packard model 7610A.
[12] OV-17 on 80–100-mesh Gas Chrom Q.

0022-3549/79/0400-0527$01.00/0
© 1979, American Pharmaceutical Association

Table I—Plasma Concentrations (Nanograms per Milliliter) of Oxycodone and Noroxycodone in Dogs

Minutes	Dog 1, 0.5 mg/kg po		Dog 2, 0.1 mg/kg po	
	Oxycodone	Noroxycodone[a]	Oxycodone	Noroxycodone[a]
0	ND[b]	ND	ND	ND
5	3.0	11.5	...[c]	—[c]
7	—[c]	—[c]	ND	ND
15	6.5	34.5	1.1	1.7
30	5.8	34.7	2.3	7.5
45	5.3	38.3	4.4	—[d]
60	3.8	28.4	2.6	4.2
90	2.7	31.5	1.6	3.2
120	4.8	23.7	1.5	7.4
180	2.1	17.5	0.8	7.0
240	ND	21.3	ND	4.9
420	ND	14.7	—[c]	—[c]
24 hr	ND	ND	—[c]	—[c]

[a] Calculated as oxycodone equivalents. [b] ND = not detectable. [c] No sample. [d] Quantitation impossible due to interfering peaks.

Table II—Effects of Oxycodone Hydrochloride and Noroxycodone Hydrochloride in Mouse Phenylquinone Writhing Test

Route	ED_{50}[a], mg/kg	
	Oxycodone	Noroxycodone
Oral	0.74	26
Subcutaneous	0.16	22

[a] See text for details.

The residue was reconstituted with 100 μl of methanol, and 20 μl was spotted on a 0.25-mm silica gel thin-layer plate[13]. The developing solvent was chloroform–ethanol (absolute)–concentrated ammonium hydroxide (50:50:1 v/v). Oxycodone and its metabolite were detected with Dragendorf spray reagent oversprayed with 5% aqueous $NaNO_2$ (4).

The area of the thin-layer plate corresponding to the R_f of standard noroxycodone was scraped from the plate, and the metabolite was eluted from the silica with 1 ml of methanol. Then the eluate was evaporated to dryness.

The mass spectrum of the isolated metabolite in the dried residue was determined with a high-resolution mass spectrometer[14]. The mass spectrum of noroxycodone was also determined for comparison.

Animal Studies—One male beagle dog was given oxycodone hydrochloride by gavage, 0.5 mg/kg in 100 ml of water. Blood samples were collected from the jugular vein into heparinized tubes[15] at 0, 5, 15, 30, 45, 60, 90, 120, 180, and 240 min and 24 hr after dosing.

To determine plasma concentrations at a dose approximating the clinical dose, another male beagle dog was given, by gavage, 0.1 mg of oxycodone hydrochloride/kg in 100 ml of water. Blood samples were collected as already described at 0, 7, 15, 30, 45, 60, 90, 120, 180, and 240 min.

Plasma was extracted and derivatized, and oxycodone and noroxycodone concentrations were determined as already described. Noroxycodone is reported quantitatively as oxycodone equivalents.

Oral and parenteral activities of the metabolite were compared with that of the parent compound in a modification of the mouse phenylquinone writhing test described by Siegmund *et al.* (5) Twenty mice were used for oxycodone evaluations, and 10 were used for noroxycodone. Noroxycodone values were determined at the peak time observed for oxycodone by the oral (20 min) and subcutaneous (5 min) routes.

Metabolite Identification—A urine sample obtained from a patient being treated with high doses of oxycodone by his personal physician (*i.e.*, approximately 700 mg/day) was processed as already described for isolation and identification of the metabolite. The urine extract was subjected to analysis by GLC, TLC, and mass spectrometry.

[13] Brinkmann silica gel 60.
[14] Du Pont model 21-492.
[15] Vacutainer.

RESULTS

GLC and Extractions—Under the described chromatographic conditions, the heptafluorobutyryl derivatives of oxycodone and naltrexone had retention times of 3.5 and 5.7 min, respectively. There were no interfering peaks from either human or dog plasma extracts; however, an interfering peak from urine prevented the use of naltrexone with urine samples. The recovery of oxycodone was 90% of an unextracted standard. There was a linear, reproducible relationship betwen the electron-capture GLC response and the plasma or urine oxycodone concentration.

Reproducibility of peak height ratios for quadruplicate samples with oxycodone hydrochloride added to contain 10.0 and 1.0 ng/ml was 6.0 and 17.0% (percent standard deviation), respectively.

When urine and plasma samples were analyzed by this method, a peak with a retention time of 4.8 min was consistently observed. This peak did not appear in any zero-time, blank, or control samples, and evidence is presented here for its identity with noroxycodone.

Metabolite Identification—The heptafluorobutyryl derivative of noroxycodone was prepared under the same conditions used for dog plasma and human urine analysis. The derivative of noroxycodone had a retention time of 4.8 min when subjected to the GLC conditions identical to those used for the metabolite.

TLC yielded R_f values of 0.15 for both the metabolite isolated from human urine and standard noroxycodone and 0.73 for oxycodone. The concentrations, determined by GLC, of oxycodone and noroxycodone in the human urine sample were 12.9 and 18.3 μg/ml, respectively.

Mass spectral data confirmed that the metabolite isolated by TLC from human urine was noroxycodone. The mass spectrum showed a strong molecular ion peak at m/e 301 and a characteristic fragment pattern that agreed well with the pattern obtained for the standard noroxycodone.

Animal Studies—In dogs given 0.1 and 0.5 mg/kg of oxycodone po, plasma noroxycodone levels were higher than those of the parent compound (Table I). In mice, results of the phenylquinone writhing test (Table II) indicated that noroxycodone is considerably less active than oxycodone, both orally and parenterally. Moreover, in contrast to observations of mice given oxycodone, the Straub tail response was not observed following noroxycodone administration.

REFERENCES

(1) "AMA Drug Evaluations," 2nd ed., Publishing Sciences Group, Acton, Mass., 1973, p. 272.
(2) S. J. Mulé, *Anal. Chem.*, **36**, 1907 (1964).
(3) S. J. Mulé, *J. Chromatogr. Sci.*, **10**, 275 (1972).
(4) W. W. Fike, *Anal. Chem.*, **38**, 1967 (1966).
(5) E. Siegmund, R. Cadmus, and G. Lee, *Proc. Soc. Exp. Biol. Med.*, **95**, 729 (1957).

ACKNOWLEDGMENTS

The authors are indebted to the following members of the Biochemicals Department, E. I. du Pont de Nemours & Co.: Dr. D. H. Smith, for pharmacological testing of noroxycodone; and R. W. Reiser, for the mass spectrometric data.

Synthesis of Methyl 1-(3,4-Dichlorobenzyl)-hexahydro-2,3-dioxo-4-pyridinecarboxylate

THOMAS J. SCHWAN ˣ, JOSEPH E. GRAY, and GEORGE C. WRIGHT

Received May 23, 1978, from the *Research Department, Norwich-Eaton Pharmaceuticals, Division of Morton-Norwich Products, Inc., Norwich, NY 13815.* Accepted for publication September 18, 1978.

Abstract □ Methyl 1-(3,4-dichlorobenzyl)-hexahydro-2,3-dioxo-4-pyridinecarboxylate was prepared by alkylation of methyl hexahydro-2,3-dioxo-4-pyridinecarboxylate with α,3,4-trichlorotoluene. The compound showed significant antifungal activity when challenged by a spectrum of pathogenic yeast species in a minimum inhibitory concentration test. It was active against some dermatophytic fungi and *Aspergillus niger.*

Keyphrases □ Methyl 1-(3,4-dichlorobenzyl)-hexahydro-2,3-dioxo-4-pyridinecarboxylate—synthesized and screened for antifungal activity □ Antifungal activity—synthesis and screening of methyl 1-(3,4-dichlorobenzyl)-hexahydro-2,3-dioxo-4-pyridinecarboxylate

The literature contains no reports of *N*-substituted benzyl hexahydro-2,3-dioxo-4-pyridinecarboxylates. Such a compound was desired for antifungal evaluation. Accordingly, the methyl ester (I) was treated with α,3,4-trichlorotoluene (II) in toluene in the presence of 1 *M* equivalent of sodium hydride. No crystalline product resulted, and it is possible that a mixture of products was obtained by C- or *O*-alkylation of the monoanion (III) (Scheme I).

For this reason, I was treated with 2 *M* equivalents of sodium hydride, presumably to generate the dianion (IV). Alkylation of IV with 1 *M* equivalent of II generated the 1-benzyl enolate ion (V). Acidification of V gave rise to VI (Scheme II).

Alkylation of I in this manner gave VI in yields ranging from 9 to 21% (Scheme II). The structural assignment of VI is based on IR spectral evidence, elemental analysis, and the NMR spectrum, which is highlighted by a singlet at δ 4.61 ppm, indicative of the *N*-benzyl moiety.

DISCUSSION

The antifungal activity of VI was challenged by a spectrum of yeast species in a minimum inhibitory concentration procedure (1) in Sabouraud's liquid medium BBL. *Candida albicans* (Eaton Code Nos. VM-71, VM-81, and M-3), *Candida krusei* (VM-29B), *Candida guilliermondi* (VM-42), and *Torulopsis glabrata* (VM-22) were inhibited at 20 μg/ml; *Candida tropicalis* (VM-25) was inhibited at 30 μg/ml. The fungistatic activity of VI was determined by an agar dilution procedure (2) using Sabouraud's dextrose agar BBL.

Plates inoculated with *Microsporum canis* (M-4) and *Aspergillus niger* (M-29) were incubated at 25°. Complete inhibition of growth for 10 days was the criterion for activity. Under these conditions, *M. canis* was inhibited by 10 μg/ml and *A. niger* was inhibited by 100 μg/ml.

Fungicidal activity of VI was determined by exposing viable cultures

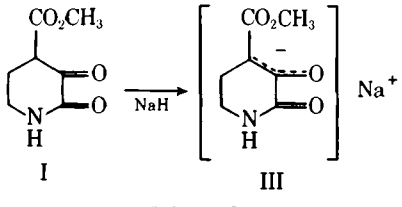

I III

Scheme I

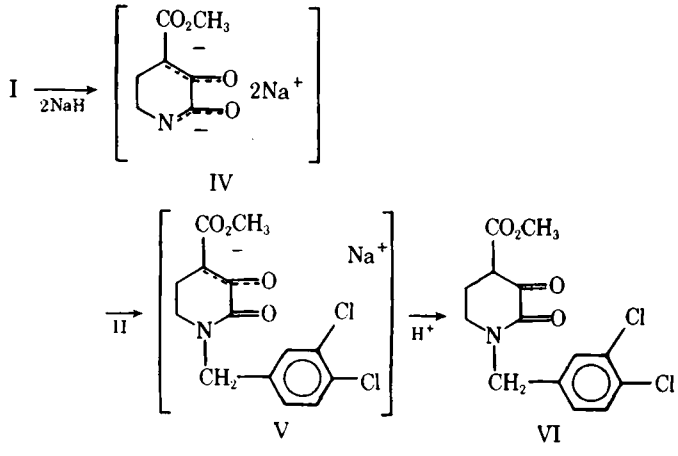

Scheme II

of dermatophytic organisms in agar plugs to a 2% solution of VI in polyethylene glycol 400 for specific time intervals (3). After exposure, the plugs were rinsed and subcultured. Cultures of *M. canis* (M-4), *Microsporum audouini* (M-17), *Trichophyton mentagrophytes* (M-93), and *Trichophyton tonsurans* (M-76) were sterilized by exposure of 15 min or less. Compound VI was significantly active against yeast and mold species.

EXPERIMENTAL[1]

Methyl hexahydro-2,3-dioxo-4-pyridinecarboxylate (I) was prepared by transesterification of ethyl hexahydro-2,3-dioxo-4-pyridinecarboxylate (4), using sodium methoxide in methanol. Recrystallization from methanol gave an analytical sample, mp 155–156°; IR: 3.05 (NH), 5.91 (C=O ester), 6.02 (C=O amide), and 8.05–8.15 (COC ester) μm.

Anal.—Calc. for $C_{11}H_{18}N_2O_5$: C, 49.12; H, 5.30; N, 8.18. Found: C, 49.02; H, 5.53; N, 8.07.

Methyl 1-(3,4-dichlorobenzyl)-hexahydro-2,3-dioxo-4-pyridinecarboxylate (VI) was prepared as follows. To a mixture of 51.3 g (0.30 mole) of I in 1000 ml of toluene was added 24 g of sodium hydride (60%) in mineral oil (*i.e.*, 14.4 g, 0.60 mole). The mixture was stirred and refluxed for 1.5 hr and cooled to room temperature, and 58.5 g (0.30 mole) of II was added rapidly. Then the mixture was stirred and refluxed for 18 hr and cooled to 15–20°, and 2.0 ml of methanol and 30 ml of acetic acid were added. With the temperature maintained at 10–15°, the mixture was diluted with 800 ml of water.

The toluene layer was separated, and the aqueous layer was extracted with 300 ml of toluene. The combined organic layers were washed with 500 ml of water, dried (magnesium sulfate), and concentrated to dryness *in vacuo*. The oily residue was washed with 3 × 100 ml of cold hexane and crystallized from 125 ml of toluene to give 9.40 g (9.5%) of the product, mp 94–99°.

Further recrystallization from toluene gave the analytical sample, mp 99–101°; IR: 5.92 (ester C=O), 6.00 (amide C=O), 8.00 (COC ester), and no NH at 3.00–3.30 μm; NMR (deuterochloroform): δ 2.56 (t, 2, pyridine, 5-CH_2), 3.36 (t, 2, pyridine, 6-CH_2), 3.86 (s, 3, OCH_3), 4.61 (s, 2, NCH_2Ar), 7.01–7.20 (m, 3, phenyl CH), and 11.10 (m exchanges with D_2O, 1, pyridine, 4-CH) ppm.

[1] Melting points were determined on a Mel-Temp apparatus, and those below 230° are corrected. IR spectra were determined as mineral oil mulls with a Perkin-Elmer 137B spectrophotometer. NMR spectra were obtained on a Varian A-60A instrument with tetramethylsilane as an internal standard.

0022-3549/79/0400-0529$01.00/0
© 1979, American Pharmaceutical Association

Anal.—Calc. for $C_{14}H_{13}Cl_2NO_4$: C, 50.93; H, 3.98; N, 4.24. Found: C, 51.10; H, 4.02; N, 4.27.

REFERENCES

(1) D. C. Grove and W. A. Randall, "Assay Methods of Antibiotics: A Laboratory Manual," Medical Encyclopedia, New York, N.Y., 1955.

(2) G. F. Reddish, "Antiseptics, Fungicides and Chemical and Physical Sterilization," 1st ed., Lea & Febiger, New York, N.Y., 1954, pp. 135, 136.

(3) M. J. Golden and K. A. Oster, *J. Am. Pharm. Assoc., Sci. Ed.*, **36**, 359 (1947).

(4) K. Hasse and A. Weiland, *Chem. Ber.*, **93**, 1686 (1960).

ACKNOWLEDGMENTS

The authors are indebted to Mr. Frederick Abbott and Mr. R. C. Finch for the large-scale synthesis of intermediates, Ms. Connie Lloyd for the NMR spectra, Ms. Cora Jeffrey for the microanalysis, and Mr. Ralph Bush and Mr. Larry Wood for technical assistance.

Rapid, Stability-Indicating, High-Pressure Liquid Chromatographic Determination of Theophylline, Guaifenesin, and Benzoic Acid in Liquid and Solid Pharmaceutical Dosage Forms

D. R. HEIDEMANN

Received August 21, 1978, from the *Analytical Research Department, Dorsey Laboratories (Division of Sandoz, Inc.), Lincoln, NE 68501.* Accepted for publication September 29, 1978.

Abstract □ Theophylline, guaifenesin, and benzoic acid were determined by reversed-phase high-pressure liquid chromatography without interference from active and/or vehicle decomposition. A degradation product of sucrose, 5-hydroxymethylfurfural, can be identified and quantified in liquid samples simultaneously.

Keyphrases □ Theophylline—analysis, high-pressure liquid chromatography, in liquid and solid pharmaceutical dosage forms, stability □ Guaifenesin—analysis, high-pressure liquid chromatography, in liquid and solid pharmaceutical dosage forms, stability □ Benzoic acid—analysis, high-pressure liquid chromatography, in liquid and solid pharmaceutical dosage forms, stability □ High-pressure liquid chromatography—analysis of theophylline, guaifenesin, benzoic acid in liquid and solid pharmaceutical dosage forms

Determination of active components and preservatives in pharmaceutical products subjected to aging and stress requires a highly specific method. The actives and preservatives must be determined in the presence of vehicle degradation as well as their degradation products.

Vehicle degradation is particularly critical in syrups, where the decomposition of hexose sugars results in a series of complex reaction products (1–3). Resulting UV-absorbing species, such as 5-hydroxymethylfurfural, can interfere with some assays (4).

Theophylline and guaifenesin, widely used in asthmatic preparations, have been assayed by various methods. Spectrophotometric determinations are rapid but nonspecific unless the actives are separated from interfering species adequately (5–7).

While GLC methods demonstrate greater specificity, derivatization is generally required to avoid excessive tailing due to the polar nature of theophylline and guaifenesin (8–15). In addition, theophylline sodium glycinate, a commonly used water-soluble form of theophylline, is not readily soluble in organic solvents required by GLC methods.

Determination of theophylline and guaifenesin by high-pressure liquid chromatography (HPLC) in biological

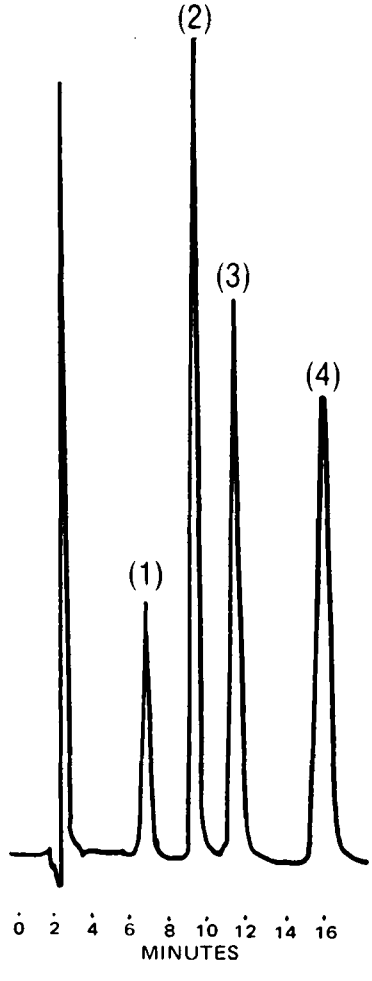

Figure 1—*Representative chromatogram of an elixir. The concentrations of components in the sample were: (1), benzoic acid, 0.01 mg/ml; (2), theophylline sodium glycinate, 0.2 mg/ml; (3), guaifenesin, 0.067 mg/ml; and (4), methylparaben internal standard, 0.1 mg/ml.*

0022-3549/79/0400-0530$01.00/0

© 1979, American Pharmaceutical Association

Anal.—Calc. for $C_{14}H_{13}Cl_2NO_4$: C, 50.93; H, 3.98; N, 4.24. Found: C, 51.10; H, 4.02; N, 4.27.

REFERENCES

(1) D. C. Grove and W. A. Randall, "Assay Methods of Antibiotics: A Laboratory Manual," Medical Encyclopedia, New York, N.Y., 1955.

(2) G. F. Reddish, "Antiseptics, Fungicides and Chemical and Physical Sterilization," 1st ed., Lea & Febiger, New York, N.Y., 1954, pp. 135, 136.

(3) M. J. Golden and K. A. Oster, *J. Am. Pharm. Assoc., Sci. Ed.*, **36**, 359 (1947).

(4) K. Hasse and A. Weiland, *Chem. Ber.*, **93**, 1686 (1960).

ACKNOWLEDGMENTS

The authors are indebted to Mr. Frederick Abbott and Mr. R. C. Finch for the large-scale synthesis of intermediates, Ms. Connie Lloyd for the NMR spectra, Ms. Cora Jeffrey for the microanalysis, and Mr. Ralph Bush and Mr. Larry Wood for technical assistance.

Rapid, Stability-Indicating, High-Pressure Liquid Chromatographic Determination of Theophylline, Guaifenesin, and Benzoic Acid in Liquid and Solid Pharmaceutical Dosage Forms

D. R. HEIDEMANN

Received August 21, 1978, from the *Analytical Research Department, Dorsey Laboratories (Division of Sandoz, Inc.), Lincoln, NE 68501.* Accepted for publication September 29, 1978.

Abstract □ Theophylline, guaifenesin, and benzoic acid were determined by reversed-phase high-pressure liquid chromatography without interference from active and/or vehicle decomposition. A degradation product of sucrose, 5-hydroxymethylfurfural, can be identified and quantified in liquid samples simultaneously.

Keyphrases □ Theophylline—analysis, high-pressure liquid chromatography, in liquid and solid pharmaceutical dosage forms, stability □ Guaifenesin—analysis, high-pressure liquid chromatography, in liquid and solid pharmaceutical dosage forms, stability □ Benzoic acid—analysis, high-pressure liquid chromatography, in liquid and solid pharmaceutical dosage forms, stability □ High-pressure liquid chromatography—analysis of theophylline, guaifenesin, benzoic acid in liquid and solid pharmaceutical dosage forms

Determination of active components and preservatives in pharmaceutical products subjected to aging and stress requires a highly specific method. The actives and preservatives must be determined in the presence of vehicle degradation as well as their degradation products.

Vehicle degradation is particularly critical in syrups, where the decomposition of hexose sugars results in a series of complex reaction products (1–3). Resulting UV-absorbing species, such as 5-hydroxymethylfurfural, can interfere with some assays (4).

Theophylline and guaifenesin, widely used in asthmatic preparations, have been assayed by various methods. Spectrophotometric determinations are rapid but nonspecific unless the actives are separated from interfering species adequately (5–7).

While GLC methods demonstrate greater specificity, derivatization is generally required to avoid excessive tailing due to the polar nature of theophylline and guaifenesin (8–15). In addition, theophylline sodium glycinate, a commonly used water-soluble form of theophylline, is not readily soluble in organic solvents required by GLC methods.

Determination of theophylline and guaifenesin by high-pressure liquid chromatography (HPLC) in biological

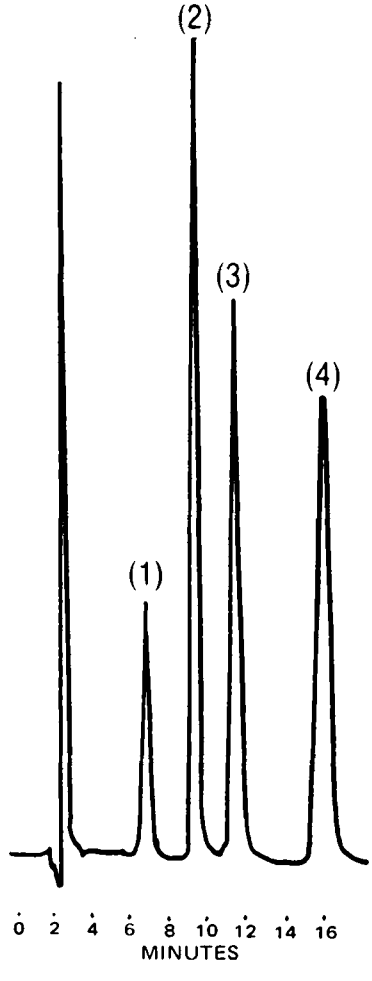

Figure 1—*Representative chromatogram of an elixir. The concentrations of components in the sample were: (1), benzoic acid, 0.01 mg/ml; (2), theophylline sodium glycinate, 0.2 mg/ml; (3), guaifenesin, 0.067 mg/ml; and (4), methylparaben internal standard, 0.1 mg/ml.*

0022-3549/79/0400-0530$01.00/0

© 1979, American Pharmaceutical Association

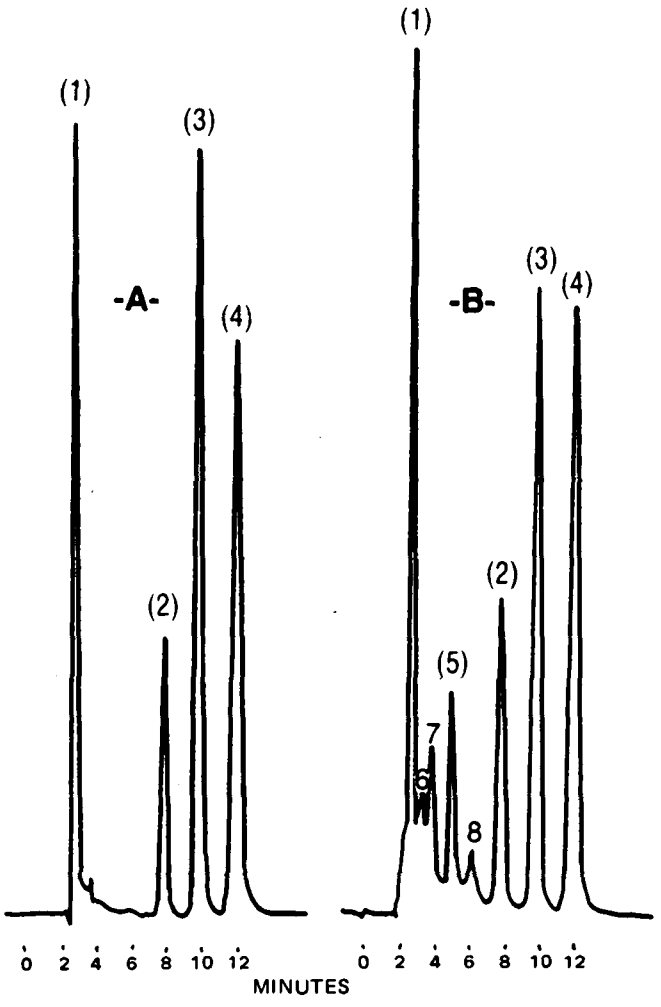

Figure 2—*Chromatograms of a liquid product. Key: A, fresh sample; B, after 50° storage for 9 months; (1), excipients; (2), benzoic acid; (3), theophylline; (4), guaifenesin; (5), 5-hydroxymethylfurfural; and (6, 7, and 8), unidentified decomposition products.*

fluids is highly specific for both actives in the presence of dietary metabolites and various other drugs (16–23). In this study using stability-indicating HPLC methods, theophylline, guaifenesin, and benzoic acid were determined in the presence of both active and vehicle degradation in liquid and solid pharmaceutical dosage forms. 5-Hydroxymethylfurfural, resulting from the degradation of sucrose, can also be measured by this method.

EXPERIMENTAL

Reagents—Acetonitrile[1], theophylline sodium glycinate[2], guaifenesin[3], methylparaben[4], benzoic acid[5], 5-hydroxymethylfurfural[6], guaiacol[6], and 1,3-dimethyluric acid[7] were used as obtained. All other chemicals were reagent grade and were used without further purification.

Apparatus—A constant-flow, high-pressure liquid chromatograph[8] was used in conjunction with a variable wavelength detector[9]. Effluents were monitored at 230 nm. Peak areas were determined using an electronic digital integrator[10]. The stainless steel column, 4.6 mm i.d. × 25 cm, was obtained prepacked with 10-μm reversed-phase material[11]. A sample injection valve was used to introduce the samples into the column inlet[12]. The mobile phase was 10^{-3} *M* sodium citrate–citric acid buffer adjusted to pH 4.15 and acetonitrile in the ratio of 9:1 (v/v). The flow rate was 2 ml/min.

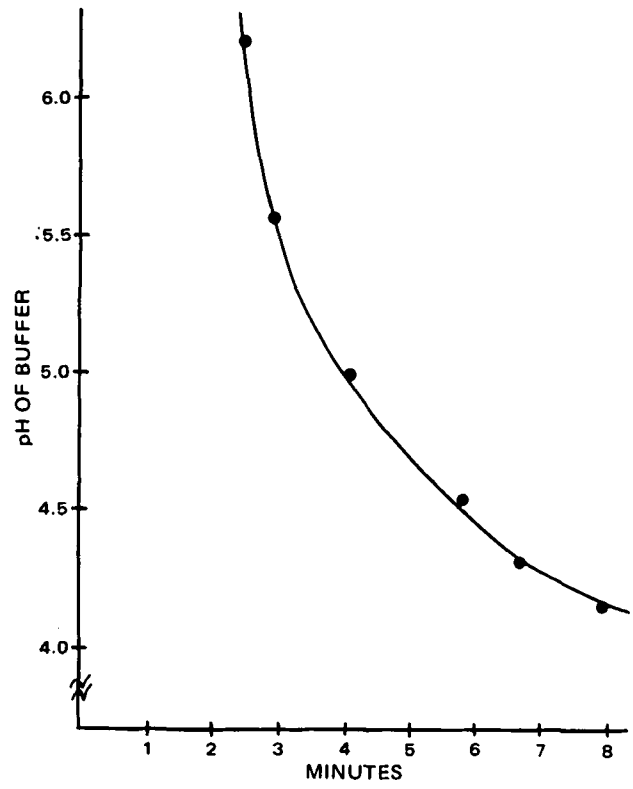

Figure 3—*Relationship of retention time of benzoic acid to the pH of the buffer in the mobile phase.*

Samples—The following formulations were investigated: tablet, elixir, and syrup containing theophylline sodium glycinate and tablet and elixir containing theophylline sodium glycinate and guaifenesin[13]. The preservative in the liquid products was benzoic acid. Samples were assayed initially and after storage at 30, 40, 50, and 65° for varying periods.

Liquid preparations were diluted with water and an internal standard. Solid dosage forms were ground, wetted with alcohol, diluted with water, and stirred automatically for 1 hr. A filtered portion of the solution was diluted with water and an internal standard. Methylparaben was the internal standard for products containing both theophylline and guaifenesin. The internal standard for single-entity theophylline products was guaifenesin.

Assay—Standard and sample preparations, 20 μl, were injected into the chromatograph, and the peak areas were determined. The quantity of actives and preservative present was determined by comparing the peak area ratio of the sample to the respective peak area ratio of the standard of known concentration, where the ratio was component peak area divided by internal standard peak area.

All standards demonstrated linearity over a region ±20% of theoretical product content. The addition of sample blank to the standard did not alter the peak areas of interest.

Figure 1 represents a typical chromatogram for elixir containing the active components theophylline sodium glycinate and guaifenesin and the preservative benzoic acid.

RESULTS AND DISCUSSION

Jensen (24) reported the hydrolysis of guaifenesin to guaiacol and glycerol by boiling guaifenesin with hydrochloric acid and the oxidation

[1] Burdick & Jackson Laboratories, Muskegon, MI 49440.
[2] Chattem Chemicals, c/o Austin Chemical Co., Chicago, IL 60631.
[3] Ganes Chemical, New York, NY 10036.
[4] Tenneco Chemicals, Chicago, IL 60630.
[5] Monsanto Co., St. Louis, MO 63166.
[6] Aldrich Chemical Co., Milwaukee, WI 53233.
[7] Adams Chemical Co., Round Lake, IL 60073.
[8] Model 830 with model 833, Du Pont, Wilmington, DE 19898.
[9] Model 837, Du Pont, Wilmington, DE 19898.
[10] Autolab System IV, Spectra-Physics Corp., Mountain View, CA 94040.
[11] Partisil-10-ODS, Whatman, Inc., Clifton, NJ 07014.
[12] Model 7105, Rheodyne, Berkeley, CA 94710.
[13] Dorsey Laboratories, Lincoln, NE 68501.

of guaifenesin with periodic acid to o-methoxyphenoxy acetaldehyde and formaldehyde. The extreme conditions required to degrade guaifenesin indicate that its decomposition is highly unlikely in pharmaceutical products subjected to several years of aging at normal conditions or several months at 50–70°. The present study supports this assumption in that no significant loss in guaifenesin was observed for the products assayed.

Cohen (25) stated that theophylline solutions subjected to strongly alkaline pH showed decomposition and apparent ring opening after several weeks and that theophylline was also susceptible to oxidation, resulting in the formation of 1,3-dimethyluric acid.

Significant loss of theophylline was observed in liquid products subjected to 50–70° for several months. A comparison of the chromatograms from fresh liquid products and high stress samples showed a loss in theophylline as well as increases in the 5-hydroxymethylfurfural peak and several additional unidentified peaks (Fig. 2). Sample blanks subjected to similar stress contained corresponding unidentified peaks. If 1,3-dimethyluric acid is present, it is well removed from the peaks of interest.

The degradation of sucrose solutions results in a highly complex series of decomposition products, including 5-hydroxymethylfurfural. Because of the quasistable state of this strongly UV-absorbing species in solution, it is frequently regarded as an indication of vehicle decomposition (1).

The amount of 5-hydroxymethylfurfural present in the sample can readily be quantified by the addition of this component to the standard. A study conducted on a liquid theophylline product indicated that decreasing the pH over the 6–5 range decreased theophylline stability and increased the amounts of 5-hydroxymethylfurfural and a second unidentified vehicle decomposition product.

The retention time of benzoic acid was highly sensitive to the mobile phase pH (Fig. 3). When the pH of the buffer in the mobile phase was adjusted to 4.15, the benzoic acid eluted between the last vehicle decomposition product peak and the theophylline peak.

REFERENCES

(1) K. R. Heimlich and A. N. Martin, *J. Am. Pharm. Assoc., Sci. Ed.*, **49**, 592 (1960).

(2) C. J. Moye, *Pure Appl. Chem.*, **14**, 161 (1964).

(3) R. N. Duvall, K. T. Koshy, and J. W. Pyles, *J. Pharm. Sci.*, **54**, 607 (1965).

(4) D. Woo, J. K. C. Yen, and K. R. Heimlich, *ibid.*, **62**, 1993 (1973).

(5) H. Wullen, *Arch. Pharm. Chemi*, **68**, 197 (1961).

(6) E. Haberli and E. Beguin, *Pharm. Acta Helv.*, **34**, 65 (1959).

(7) Y. S. Chae and W. H. Shelver, *J. Pharm. Sci.*, **65**, 1179 (1976).

(8) B. R. Rader and E. S. Aranda, *ibid.*, **57**, 847 (1968).

(9) J. Hudanick, *ibid.*, **59**, 238 (1970).

(10) W. R. Maynard, Jr., and R. B. Bruce, *ibid.*, **59**, 1346 (1970).

(11) E. Mario and L. G. Meehan, *ibid.*, **59**, 538 (1970).

(12) H. A. Schwertner, T. M. Ludden, and J. E. Wallace, *Anal. Chem.*, **48**, 1875 (1976).

(13) D. G. Bailey, H. L. Davis, and G. E. Johnson, *J. Chromatogr.*, **121**, 263 (1976).

(14) M. Sheehan and P. Haythorn, *ibid.*, **117**, 393 (1976).

(15) G. F. Johnson, W. A. Dechtiaruk, and H. M. Solomon, *Clin. Chem.*, **21**, 1038 (1975).

(16) J. W. Nelson, A. L. Cordry, C. G. Aron, and R. A. Bartell, *ibid.*, **23**, 124 (1977).

(17) G. W. Peng, V. Smith, A. Peng, and W. L. Chiou, *Res. Commun. Chem. Pathol. Pharmacol.*, **15**, 341 (1976).

(18) A. G. Maijub, D. T. Stafford, and R. T. Chamberlain, *J. Chromatogr. Sci.*, **14**, 521 (1976).

(19) L. C. Franconi, G. L. Hawk, B. J. Sandmann, and W. G. Haney, *Anal. Chem.*, **48**, 372 (1976).

(20) D. S. Sitar, K. M. Piafsky, R. E. Rangno, and R. I. Ogilvie, *Clin. Chem.*, **21**, 1774 (1975).

(21) O. H. Weddle and W. D. Mason, *J. Pharm. Sci.*, **65**, 865 (1976).

(22) R. D. Thompson, H. T. Nagasawa, and J. W. Jenne, *J. Lab. Clin. Med.*, **84**, 584 (1974).

(23) R. K. Desiraju, E. T. Sugita, and R. L. Mayock, *J. Chromatogr. Sci.*, **15**, 563 (1977).

(24) F. Jensen, *Medd. Norsk. Farm. Selskap.*, **39**, 38 (1977).

(25) J. L. Cohen, *Anal. Profiles Drug Subst.*, **4**, 466 (1975).

ACKNOWLEDGMENTS

The author acknowledges the support of Dr. Eugene Brockemeyer, Director of Research, Development and Quality Assurance of Dorsey Laboratories. She also thanks Dr. Robert D. Hargens for advice during this project and Dr. V. K. Olson for guidance in the preparation of this article.

COMMUNICATIONS

Precaution in Use of High-Pressure Liquid Chromatographic Simultaneous Plasma Procainamide and *N*-Acetylprocainamide Determination

Keyphrases □ Procainamide—analysis, plasma, high-pressure liquid chromatography deproteinization *versus* extraction methods □ *N*-Acetylprocainamide—analysis, plasma, high-pressure liquid chromatography, deproteinization *versus* extraction methods □ High-pressure liquid chromatography—analysis, procainamide and *N*-acetylprocainamide in plasma, deproteinization *versus* extraction methods

To the Editor:

A high-pressure liquid chromatographic (HPLC) method for the simultaneous plasma procainamide and *N*-acetylprocainamide determination was reported recently from this laboratory (1). The method involved microvolume acetonitrile plasma protein precipitation and injection of an aliquot of the resultant supernatant solution onto a cation-exchange column. Detection was by UV absorption at 274 nm. *N*-Acetylprocainamide and procainamide eluted from the system with retention times of 4 and 5 min, respectively, and appeared to be symmetrical peaks that were satisfactorily resolved from each other and other plasma components. Total analysis time per sample was ~7 min. The method required extremely simple sample preparation and short analysis time. The purpose of this communication is to report some precautions in the use of this method.

Due to an irreversible loss of column performance, a new cation-exchange column obtained from the same manufacturer[1] was used as previously reported (1). This new column demonstrated that the peak in patient samples

[1] Partisil PXS 10/25 SCX, Whatman, Clifton, N.J.

0022-3549/79/0400-0532$01.00/0

© 1979, American Pharmaceutical Association

of guaifenesin with periodic acid to o-methoxyphenoxy acetaldehyde and formaldehyde. The extreme conditions required to degrade guaifenesin indicate that its decomposition is highly unlikely in pharmaceutical products subjected to several years of aging at normal conditions or several months at 50–70°. The present study supports this assumption in that no significant loss in guaifenesin was observed for the products assayed.

Cohen (25) stated that theophylline solutions subjected to strongly alkaline pH showed decomposition and apparent ring opening after several weeks and that theophylline was also susceptible to oxidation, resulting in the formation of 1,3-dimethyluric acid.

Significant loss of theophylline was observed in liquid products subjected to 50–70° for several months. A comparison of the chromatograms from fresh liquid products and high stress samples showed a loss in theophylline as well as increases in the 5-hydroxymethylfurfural peak and several additional unidentified peaks (Fig. 2). Sample blanks subjected to similar stress contained corresponding unidentified peaks. If 1,3-dimethyluric acid is present, it is well removed from the peaks of interest.

The degradation of sucrose solutions results in a highly complex series of decomposition products, including 5-hydroxymethylfurfural. Because of the quasistable state of this strongly UV-absorbing species in solution, it is frequently regarded as an indication of vehicle decomposition (1).

The amount of 5-hydroxymethylfurfural present in the sample can readily be quantified by the addition of this component to the standard. A study conducted on a liquid theophylline product indicated that decreasing the pH over the 6–5 range decreased theophylline stability and increased the amounts of 5-hydroxymethylfurfural and a second unidentified vehicle decomposition product.

The retention time of benzoic acid was highly sensitive to the mobile phase pH (Fig. 3). When the pH of the buffer in the mobile phase was adjusted to 4.15, the benzoic acid eluted between the last vehicle decomposition product peak and the theophylline peak.

REFERENCES

(1) K. R. Heimlich and A. N. Martin, *J. Am. Pharm. Assoc., Sci. Ed.*, **49**, 592 (1960).

(2) C. J. Moye, *Pure Appl. Chem.*, **14**, 161 (1964).

(3) R. N. Duvall, K. T. Koshy, and J. W. Pyles, *J. Pharm. Sci.*, **54**, 607 (1965).

(4) D. Woo, J. K. C. Yen, and K. R. Heimlich, *ibid.*, **62**, 1993 (1973).

(5) H. Wullen, *Arch. Pharm. Chemi*, **68**, 197 (1961).

(6) E. Haberli and E. Beguin, *Pharm. Acta Helv.*, **34**, 65 (1959).

(7) Y. S. Chae and W. H. Shelver, *J. Pharm. Sci.*, **65**, 1179 (1976).

(8) B. R. Rader and E. S. Aranda, *ibid.*, **57**, 847 (1968).

(9) J. Hudanick, *ibid.*, **59**, 238 (1970).

(10) W. R. Maynard, Jr., and R. B. Bruce, *ibid.*, **59**, 1346 (1970).

(11) E. Mario and L. G. Meehan, *ibid.*, **59**, 538 (1970).

(12) H. A. Schwertner, T. M. Ludden, and J. E. Wallace, *Anal. Chem.*, **48**, 1875 (1976).

(13) D. G. Bailey, H. L. Davis, and G. E. Johnson, *J. Chromatogr.*, **121**, 263 (1976).

(14) M. Sheehan and P. Haythorn, *ibid.*, **117**, 393 (1976).

(15) G. F. Johnson, W. A. Dechtiaruk, and H. M. Solomon, *Clin. Chem.*, **21**, 1038 (1975).

(16) J. W. Nelson, A. L. Cordry, C. G. Aron, and R. A. Bartell, *ibid.*, **23**, 124 (1977).

(17) G. W. Peng, V. Smith, A. Peng, and W. L. Chiou, *Res. Commun. Chem. Pathol. Pharmacol.*, **15**, 341 (1976).

(18) A. G. Maijub, D. T. Stafford, and R. T. Chamberlain, *J. Chromatogr. Sci.*, **14**, 521 (1976).

(19) L. C. Franconi, G. L. Hawk, B. J. Sandmann, and W. G. Haney, *Anal. Chem.*, **48**, 372 (1976).

(20) D. S. Sitar, K. M. Piafsky, R. E. Rangno, and R. I. Ogilvie, *Clin. Chem.*, **21**, 1774 (1975).

(21) O. H. Weddle and W. D. Mason, *J. Pharm. Sci.*, **65**, 865 (1976).

(22) R. D. Thompson, H. T. Nagasawa, and J. W. Jenne, *J. Lab. Clin. Med.*, **84**, 584 (1974).

(23) R. K. Desiraju, E. T. Sugita, and R. L. Mayock, *J. Chromatogr. Sci.*, **15**, 563 (1977).

(24) F. Jensen, *Medd. Norsk. Farm. Selskap.*, **39**, 38 (1977).

(25) J. L. Cohen, *Anal. Profiles Drug Subst.*, **4**, 466 (1975).

ACKNOWLEDGMENTS

The author acknowledges the support of Dr. Eugene Brockemeyer, Director of Research, Development and Quality Assurance of Dorsey Laboratories. She also thanks Dr. Robert D. Hargens for advice during this project and Dr. V. K. Olson for guidance in the preparation of this article.

COMMUNICATIONS

Precaution in Use of High-Pressure Liquid Chromatographic Simultaneous Plasma Procainamide and *N*-Acetylprocainamide Determination

Keyphrases □ Procainamide—analysis, plasma, high-pressure liquid chromatography deproteinization *versus* extraction methods □ *N*-Acetylprocainamide—analysis, plasma, high-pressure liquid chromatography, deproteinization *versus* extraction methods □ High-pressure liquid chromatography—analysis, procainamide and *N*-acetylprocainamide in plasma, deproteinization *versus* extraction methods

To the Editor:

A high-pressure liquid chromatographic (HPLC) method for the simultaneous plasma procainamide and *N*-acetylprocainamide determination was reported recently from this laboratory (1). The method involved microvolume acetonitrile plasma protein precipitation and injection of an aliquot of the resultant supernatant solution onto a cation-exchange column. Detection was by UV absorption at 274 nm. *N*-Acetylprocainamide and procainamide eluted from the system with retention times of 4 and 5 min, respectively, and appeared to be symmetrical peaks that were satisfactorily resolved from each other and other plasma components. Total analysis time per sample was ~7 min. The method required extremely simple sample preparation and short analysis time. The purpose of this communication is to report some precautions in the use of this method.

Due to an irreversible loss of column performance, a new cation-exchange column obtained from the same manufacturer[1] was used as previously reported (1). This new column demonstrated that the peak in patient samples

[1] Partisil PXS 10/25 SCX, Whatman, Clifton, N.J.

0022-3549/79/0400-0532$01.00/0

© 1979, American Pharmaceutical Association

Table I—Apparent Concentration of *N*-Acetylprocainamide and Procainamide in Plasma Collected from Patients as Determined by the Deproteinization Method and the Extraction Method [a]

Sample	*N*-Acetylprocainamide Concentration, μg/ml		Percent Deviation [b]	Procainamide Concentration, μg/ml		Percent Deviation [b]
	Deproteinization	Extraction		Deproteinization	Extraction	
1	1.44	1.28	12.5	20.11	— [c]	—
2	1.59	1.18	34.8	6.87	6.74	1.93
3	1.55	1.16	33.6	5.20	5.02	3.60
4	1.42	1.13	25.7	4.87	4.97	−2.00

[a] The HPLC column did not resolve the interference peak from the *N*-acetylprocainamide peak. Detection was at 254 nm with the fixed-wavelength detector. [b] (Concentration by deproteinization method − concentration by extraction method/concentration by extraction method) × 100. [c] Above the upper limit of the calibration curve.

Table II—Concentration of *N*-Acetylprocainamide and Procainamide in Plasma Collected from Patients and Analyzed by the Deproteinization Method and the Extraction Method with UV Detection at 254 and 274 nm [a]

Sample	*N*-Acetylprocainamide Concentration, μg/ml				Procainamide Concentration, μg/ml			
	Deproteinization		Extraction		Deproteinization		Extraction	
	254 nm [b]	274 nm [c]	254 nm	274 nm	254 nm	274 nm	254 nm	274 nm
5	0.24	0.22	0.28	0.28	6.72	6.70	6.67	7.00
6	0.47	0.47	0.43	0.43	4.09	4.25	3.57	3.91
7	2.50	2.77	2.31	2.58	2.55	2.81	2.29	2.56
8	3.67	3.93	3.75	3.94	5.57	5.82	5.60	5.98
9	3.07	3.26	3.13	3.29	2.24	2.21	2.14	2.28
10	1.52	1.40	1.40	1.43	5.44	5.50	5.45	5.79
11	1.28	1.31	1.24	1.17	3.87	4.08	3.68	3.76
12	0.68	0.63	0.63	0.70	3.61	3.62	3.51	3.70
13	1.70	1.80	1.74	1.90	4.69	5.09	4.66	4.90

[a] The HPLC column resolved the interference peak from the *N*-acetylprocainamide peak. [b] Fixed-wavelength detector. [c] Variable-wavelength detector.

formerly attributed entirely to *N*-acetylprocainamide was not homogeneous since its leading edge was deformed. Other cation-exchange columns of the same make demonstrated various degrees of peak resolution from the *N*-acetylprocainamide peak. This resolution was achieved with the mobile phase as originally reported (1) or with slightly modified acetonitrile or salt concentrations so that *N*-acetylprocainamide and procainamide eluted with retention times less than 6 min. The interference peak was not present in plasma samples collected just prior to initial procainamide dose administration, suggesting that the compound responsible may have been another procainamide metabolite.

Patient plasma samples were also prepared for chromatography by a solvent extraction method. The extraction sequence used was as follows. A mixture of 0.1 ml of plasma, 0.5 ml of water, and 0.1 ml of 1 *M* NaOH was vortexed for 1 min with 3 ml of ethyl acetate. After centrifugation, most of the organic layer was transferred to a tapered tube and vortexed (1 min) with 0.1 ml of 0.5% phosphoric acid. The tube was centrifuged, and an aliquot (20–40 μl) of the aqueous phase was injected. With this sample preparation, the *N*-acetylprocainamide and procainamide peaks appeared as symmetrical peaks with no interference.

Therefore, plasma samples were prepared for quantitative chromatography by the extraction method. The internal standard was *p*-amino-*N*-(2-dipropylaminoethyl)benzamide hydrochloride[2]; 0.2 ml of an aqueous solution (2 μg/ml) was included in the first sample preparation step described in place of water. To resolve procainamide and the internal standard, the mobile phase acetonitrile concentration was reduced. The mobile phase was composed of 18 parts of acetonitrile and 82 parts of 0.1 *M* ammonium phosphate (monobasic), which had been acidified with 0.2% phosphoric acid. The percentage of phosphoric acid (0.05%) in the mobile phase reported previously (1) was in error. With a 3-ml/min flow rate, the *N*-acetylprocainamide, procainamide, and internal standard retention times were 5.1, 7.1, and 8.7 min, respectively.

The mobile phase composition may need some adjustment when different columns are used due to column differences in chromatographic behavior. An increased salt or acetonitrile concentration in the mobile phase decreased resolution of the interference peak from the *N*-acetylprocainamide peak and vice versa.

Table I summarizes a comparison between the deproteinization method published previously (1) and the method described here, which involves solvent extraction prior to HPLC. The column used on this occasion did not resolve the interference peak from the *N*-acetylprocainamide peak. The plasma samples were collected from inpatients who were receiving procainamide intravenously. The *N*-acetylprocainamide concentration was substantially overestimated by the deproteinization method.

A column that did resolve the interference from the *N*-acetylprocainamide peak in deproteinized samples was used in another experiment. The column effluent was passed through a fixed-wavelength UV detector[3] (254 nm) and a variable-wavelength UV detector[4] (274 nm), which were connected in series. Plasma samples collected from inpatients who were receiving oral or intravenous procainamide were prepared for analysis by both deproteinization and solvent extraction (Table II). There was general good agreement among the four concentration estimates for each compound quantitated. Therefore, the deproteinization method appears to be suitable for rapidly quantitating plasma *N*-acetylprocainamide and procainamide provided that an efficient HPLC column is used.

[2] E. R. Squibb & Sons, Princeton, N.J.

[3] Model 440, Waters Associates, Milford, Mass.

[4] Model LC55, Perkin-Elmer Corp., Norwalk, Conn.

The interference peak–*N*-acetylprocainamide peak height ratio in the deproteinized samples was 0.12–1.0 at 254 nm and 0.18–1.78 at 274 nm. The ratio was higher at the longer wavelength.

UV absorption maxima occur at 282 and 268 nm for procainamide and *N*-acetylprocainamide, respectively (1). However, monitoring the column effluent at 254 nm with a fixed-wavelength detector[3] is suitable for detecting these compounds because of the superior signal-to-noise ratio of that detector relative to the variable-wavelength detector[4].

The deproteinization sample preparation method produced a number of peaks not present in predose plasma. These peaks elute before the *N*-acetylprocainamide peak and may represent other procainamide metabolites.

Care needs to be exercised with the previously reported deproteinization plasma sample preparation method (1) to avoid overestimation of the pharmacologically active *N*-acetylprocainamide concentration. If a column is used that does not resolve the interference from the *N*-acetylprocainamide peak, the solvent extraction sequence described improves *N*-acetylprocainamide quantitation. A prudent general approach is to use the extraction method.

(1) M. A. F. Gadalla, G. W. Peng, and W. L. Chiou, *J. Pharm. Sci.*, **67**, 869 (1978).

Roger L. Nation
Myung G. Lee
Shiew-Mei Huang
Win L. Chiou ˣ
Clinical Pharmacokinetics Laboratory
and Department of Pharmacy
College of Pharmacy
University of Illinois at the
Medical Center
Chicago, IL 60612

Received September 25, 1978.
Accepted for publication January 10, 1979.

Creatinine VII: Determination of Saliva Creatinine by High-Performance Liquid Chromatography

Keyphrases □ Creatinine—analysis, saliva, high-performance liquid chromatography □ Saliva—analysis, creatinine, high-performance liquid chromatography □ High-performance liquid chromatography—analysis, saliva creatinine

To the Editor:

Measurements of creatinine levels in biological fluids are important to the renal function determination and drug dosage adjustment in patients with renal insufficiency (1–4). Recently, a high-performance liquid chromatographic (HPLC) method for endogenous plasma, serum, and urine creatinine determination was developed (5, 6). This method, however, was not sensitive enough for the assay of saliva creatinine, which might be as low as 0.03 mg %, or about 3% of the plasma or serum levels determined by the less specific colorimetric method (3). Furthermore,

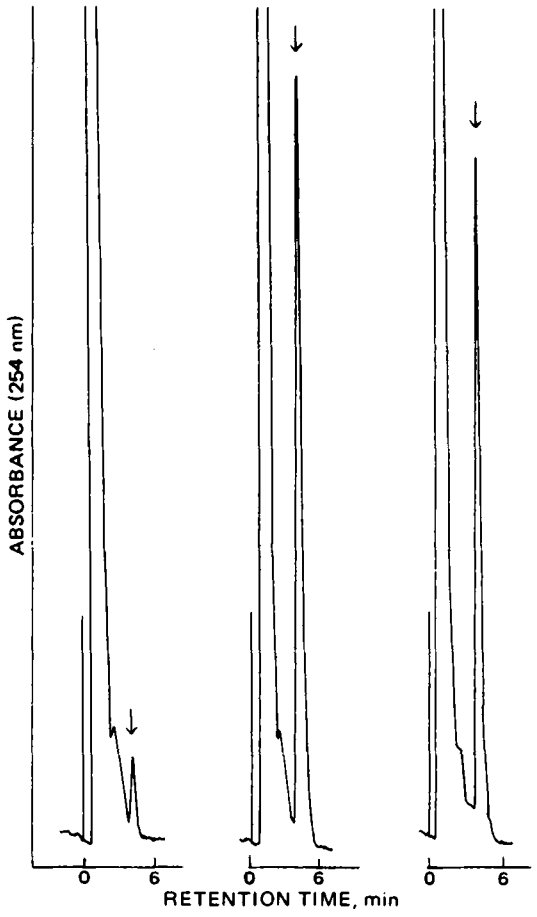

Figure 1—*Chromatograms of creatinine (↓) from various saliva samples. Key: left, pooled saliva from normal subjects; middle, pooled saliva spiked with 0.3 mg % of creatinine; and right, saliva from a normal subject with a creatinine level of 0.256 mg %. Detector sensitivity was at 0.005 A full scale.*

serious interfering peaks from the deproteinized saliva coexisted with the creatinine peak. This result is somewhat ironic because saliva composition is commonly assumed to be less complicated than that of plasma. This communication reports a modified HPLC method that is able to quantify low levels of endogenous saliva creatinine.

Sample preparation included vortex mixing of 0.3 ml of saliva with 2 ml of acetonitrile for about 10 sec in a 13 × 100-mm screw-capped glass culture tube, centrifugation at 2000 rpm for about 1 min, and direct pouring of the clear supernate into another tube containing 2 ml of methylene chloride, followed by vortex mixing and centrifugation. Exactly 100 μl of the upper aqueous layer was then injected into the chromatograph. Essentially all of the acetonitrile was partitioned into the methylene chloride layer.

The HPLC system consisted of a solvent delivery pump[1], a sample injection valve[2], and a fixed wavelength (254 nm) detector[3]. A 25.4-cm linear recorder and a 25-cm cation-exchange column[4] were used. The mobile phase was 0.012 *M* ammonium phosphate solution made basic with 0.4% (v/v) 0.1 *N* NaOH to pH 4.80. The creatinine studied at ambient temperature had an ~4.5-min retention time

[1] Model 6000A, Waters Associates, Milford, Mass.
[2] Model U6K, Waters Associates, Milford, Mass.
[3] Model 440, Waters Associates, Milford, Mass.
[4] Whatman Partisil PXS 10/25 SCX column, Whatman Inc., Clifton, N.J.

0022-3549/79/0400-0534$01.00/0
© 1979, American Pharmaceutical Association

The interference peak–*N*-acetylprocainamide peak height ratio in the deproteinized samples was 0.12–1.0 at 254 nm and 0.18–1.78 at 274 nm. The ratio was higher at the longer wavelength.

UV absorption maxima occur at 282 and 268 nm for procainamide and *N*-acetylprocainamide, respectively (1). However, monitoring the column effluent at 254 nm with a fixed-wavelength detector[3] is suitable for detecting these compounds because of the superior signal-to-noise ratio of that detector relative to the variable-wavelength detector[4].

The deproteinization sample preparation method produced a number of peaks not present in predose plasma. These peaks elute before the *N*-acetylprocainamide peak and may represent other procainamide metabolites.

Care needs to be exercised with the previously reported deproteinization plasma sample preparation method (1) to avoid overestimation of the pharmacologically active *N*-acetylprocainamide concentration. If a column is used that does not resolve the interference from the *N*-acetylprocainamide peak, the solvent extraction sequence described improves *N*-acetylprocainamide quantitation. A prudent general approach is to use the extraction method.

(1) M. A. F. Gadalla, G. W. Peng, and W. L. Chiou, *J. Pharm. Sci.*, **67**, 869 (1978).

Roger L. Nation
Myung G. Lee
Shiew-Mei Huang
Win L. Chiou ˣ
Clinical Pharmacokinetics Laboratory
and Department of Pharmacy
College of Pharmacy
University of Illinois at the
Medical Center
Chicago, IL 60612

Received September 25, 1978.
Accepted for publication January 10, 1979.

Creatinine VII: Determination of Saliva Creatinine by High-Performance Liquid Chromatography

Keyphrases □ Creatinine—analysis, saliva, high-performance liquid chromatography □ Saliva—analysis, creatinine, high-performance liquid chromatography □ High-performance liquid chromatography—analysis, saliva creatinine

To the Editor:

Measurements of creatinine levels in biological fluids are important to the renal function determination and drug dosage adjustment in patients with renal insufficiency (1–4). Recently, a high-performance liquid chromatographic (HPLC) method for endogenous plasma, serum, and urine creatinine determination was developed (5, 6). This method, however, was not sensitive enough for the assay of saliva creatinine, which might be as low as 0.03 mg %, or about 3% of the plasma or serum levels determined by the less specific colorimetric method (3). Furthermore,

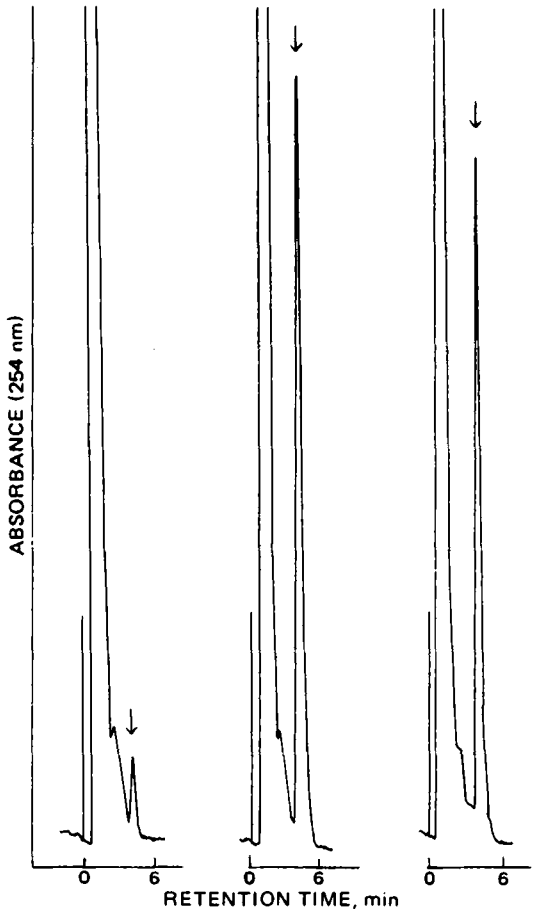

Figure 1—*Chromatograms of creatinine (↓) from various saliva samples. Key: left, pooled saliva from normal subjects; middle, pooled saliva spiked with 0.3 mg % of creatinine; and right, saliva from a normal subject with a creatinine level of 0.256 mg %. Detector sensitivity was at 0.005 A full scale.*

serious interfering peaks from the deproteinized saliva coexisted with the creatinine peak. This result is somewhat ironic because saliva composition is commonly assumed to be less complicated than that of plasma. This communication reports a modified HPLC method that is able to quantify low levels of endogenous saliva creatinine.

Sample preparation included vortex mixing of 0.3 ml of saliva with 2 ml of acetonitrile for about 10 sec in a 13 × 100-mm screw-capped glass culture tube, centrifugation at 2000 rpm for about 1 min, and direct pouring of the clear supernate into another tube containing 2 ml of methylene chloride, followed by vortex mixing and centrifugation. Exactly 100 μl of the upper aqueous layer was then injected into the chromatograph. Essentially all of the acetonitrile was partitioned into the methylene chloride layer.

The HPLC system consisted of a solvent delivery pump[1], a sample injection valve[2], and a fixed wavelength (254 nm) detector[3]. A 25.4-cm linear recorder and a 25-cm cation-exchange column[4] were used. The mobile phase was 0.012 *M* ammonium phosphate solution made basic with 0.4% (v/v) 0.1 *N* NaOH to pH 4.80. The creatinine studied at ambient temperature had an ~4.5-min retention time

[1] Model 6000A, Waters Associates, Milford, Mass.
[2] Model U6K, Waters Associates, Milford, Mass.
[3] Model 440, Waters Associates, Milford, Mass.
[4] Whatman Partisil PXS 10/25 SCX column, Whatman Inc., Clifton, N.J.

0022-3549/79/0400-0534$01.00/0
© 1979, American Pharmaceutical Association

Table I—Typical Response Factors of Creatinine at Various Spiked Concentrations in Saliva Samples

Sample	Spiked Concentration, mg %	Peak Height[a], cm	Response Factor[b]
1	0	1.16	—
2	0.05	3.04	37.60
3	0.10	5.12	39.60
4	0.20	9.10	39.70
5	0.30	12.70	38.47
6	0.50	19.60	36.88
Average ± *SD*			38.45 ± 1.232

[a] The detector sensitivity was set at 0.005 *A* full scale, and a 25.4-cm recorder chart paper was used. [b] Response factor = (peak height from spiked sample—peak height from unspiked sample)/spiked creatinine concentration.

(Fig. 1). The creatinine peak was not as well resolved as that observed in plasma or serum samples using simple deproteinization (5).

Methylene chloride in the sample preparation served two purposes. It removed interfering substances from saliva through extraction. It also concentrated the aqueous supernate as compared to the previous deproteinization procedure (5), since essentially all acetonitrile remained with the methylene chloride layer in the last step. Our preliminary study indicated that most creatinine remains in the upper aqueous layer. In other words, about a threefold increase in sensitivity can be achieved by the present extraction method.

In our previous study (5), a variable wavelength detector set at 215 nm was used for creatinine quantitation. Although creatinine absorption at 254 nm in the mobile phase used here was only ~28% of that at 215 nm, the higher signal-to-noise ratio using the 254-nm fixed wavelength detector as compared to the variable wavelength detector (7) would still make the former detector more sensitive. Based on a criterion of a signal-to-noise ratio of 3, one could estimate the lower limit for quantitation with the present method as 0.0065 mg %.

The satisfactory creatinine peak height linearity with increasing concentrations was demonstrated by the response factor studies (Table I). The coefficient of variation in the range studied was 3.2%. The coefficients of variation for the intraassay and interassay studies (n = 6) using a saliva sample with 0.048 mg % creatinine were 4.2 and 6.7%, respectively. The coefficients of variation were reduced to 2 and 5.5%, respectively, with a 0.248-mg % saliva creatinine sample. Over several months, many hundred saliva samples have been satisfactorily analyzed by the present method.

In most of our saliva creatinine studies, the recorder chart speed was 10 cm/hr. The advantages of such a slow chart speed were discussed previously (8). In the present study, a micrometer[5] with its dial graduated in 0.1-mm increments was used for the measurement of peak heights.

(1) W. L. Chiou and F. H. Hsu, *J. Clin. Pharmacol.*, **15**, 427 (1975).
(2) W. L. Chiou and F. H. Hsu, *Res. Commun. Chem. Pathol. Pharmacol.*, **10**, 315 (1975).
(3) W. L. Chiou, F. H. Hsu, C. Westenfelder, and N. A. Kurtzman, *ibid.*, **16**, 549 (1977).
(4) R. S. Lott and W. L. Hayton, *Drug Intell. Clin. Pharm.*, **12**, 140 (1978).
(5) W. L. Chiou, M. A. F. Gadalla, and G. W. Peng, *J. Pharm. Sci.*, **67**, 182 (1978).
(6) W. L. Chiou, G. W. Peng, M. A. F. Gadalla, and S. T. Nerenberg, *ibid.*, **67**, 292 (1978).
(7) N. K. Athanikar, G. W. Peng, R. L. Nation, S. M. Huang, and W. L. Chiou, *J. Chromatogr. Biomed. Appl.*, in press.
(8) W. L. Chiou, *Clin. Chem.*, **25**, 197 (1979).

[5] Vernier Caliper, Fisher Scientific Co., Chicago, Ill.

Frances S. Pu
Win L. Chiou ˣ
Clinical Pharmacokinetics Laboratory and Department of Pharmacy
College of Pharmacy
University of Illinois at the Medical Center
Chicago, IL 60612

Received November 9, 1978.
Accepted for publication January 9, 1979.
Abstracted from a thesis submitted by F. S. Pu to the Graduate College, University of Illinois at the Medical Center, in partial fulfillment of the Master of Science degree requirements.

Potential Antiarthritic Agents I: Benzoylacetonitriles

Keyphrases □ Antiarthritic agents—benzoylacetonitriles, synthesis, screened in rats, structure–activity relationships □ Benzoylacetonitriles—antiarthritis activity, synthesis, screened in rats, structure–activity relationships

To the Editor:

Rheumatoid arthritis, a chronic inflammatory disorder of unknown etiology, is treated largely with agents useful only in ameliorating the acute inflammatory symptoms, *i.e.*, pain and swelling. Clearly, nontoxic drugs effective in the remission of joint and cartilage destruction are critically needed. We screened compounds in the chronic Freund's adjuvant-induced arthritis model (1) and discovered that benzoylacetonitrile (I) and its monofluorophenyl analogs (II–IV) were highly effective in this assay.

Concurrently, we found this series to be inactive against carrageenan-induced edema in rats and urate synovitis in dogs and only weakly active in suppressing UV-induced erythema in guinea pigs. When tested for the suppression of prostaglandin synthesis *in vitro*, benzoylacetonitrile had only one-third of the potency of aspirin. Additionally, I and IV displayed little or no ulcerogenic potential in rats at total daily doses as high as 800 mg/kg. These facts suggest that prostaglandin synthesis inhibition is unlikely to ac-

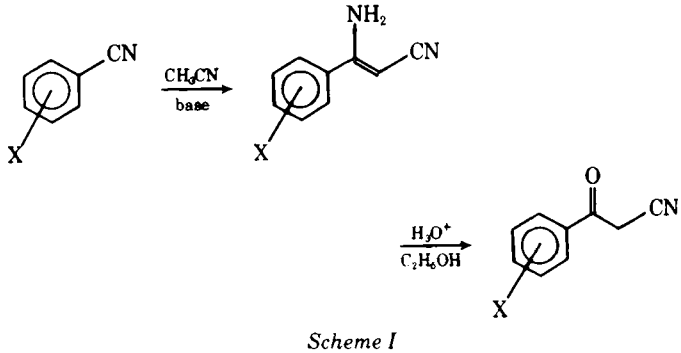

Scheme I

© 1979, American Pharmaceutical Association

Table I—Typical Response Factors of Creatinine at Various Spiked Concentrations in Saliva Samples

Sample	Spiked Concentration, mg %	Peak Height[a], cm	Response Factor[b]
1	0	1.16	—
2	0.05	3.04	37.60
3	0.10	5.12	39.60
4	0.20	9.10	39.70
5	0.30	12.70	38.47
6	0.50	19.60	36.88
Average ± *SD*			38.45 ± 1.232

[a] The detector sensitivity was set at 0.005 *A* full scale, and a 25.4-cm recorder chart paper was used. [b] Response factor = (peak height from spiked sample—peak height from unspiked sample)/spiked creatinine concentration.

(Fig. 1). The creatinine peak was not as well resolved as that observed in plasma or serum samples using simple deproteinization (5).

Methylene chloride in the sample preparation served two purposes. It removed interfering substances from saliva through extraction. It also concentrated the aqueous supernate as compared to the previous deproteinization procedure (5), since essentially all acetonitrile remained with the methylene chloride layer in the last step. Our preliminary study indicated that most creatinine remains in the upper aqueous layer. In other words, about a threefold increase in sensitivity can be achieved by the present extraction method.

In our previous study (5), a variable wavelength detector set at 215 nm was used for creatinine quantitation. Although creatinine absorption at 254 nm in the mobile phase used here was only ~28% of that at 215 nm, the higher signal-to-noise ratio using the 254-nm fixed wavelength detector as compared to the variable wavelength detector (7) would still make the former detector more sensitive. Based on a criterion of a signal-to-noise ratio of 3, one could estimate the lower limit for quantitation with the present method as 0.0065 mg %.

The satisfactory creatinine peak height linearity with increasing concentrations was demonstrated by the response factor studies (Table I). The coefficient of variation in the range studied was 3.2%. The coefficients of variation for the intraassay and interassay studies (n = 6) using a saliva sample with 0.048 mg % creatinine were 4.2 and 6.7%, respectively. The coefficients of variation were reduced to 2 and 5.5%, respectively, with a 0.248-mg % saliva creatinine sample. Over several months, many hundred saliva samples have been satisfactorily analyzed by the present method.

In most of our saliva creatinine studies, the recorder chart speed was 10 cm/hr. The advantages of such a slow chart speed were discussed previously (8). In the present study, a micrometer[5] with its dial graduated in 0.1-mm increments was used for the measurement of peak heights.

(1) W. L. Chiou and F. H. Hsu, *J. Clin. Pharmacol.*, **15**, 427 (1975).
(2) W. L. Chiou and F. H. Hsu, *Res. Commun. Chem. Pathol. Pharmacol.*, **10**, 315 (1975).
(3) W. L. Chiou, F. H. Hsu, C. Westenfelder, and N. A. Kurtzman, *ibid.*, **16**, 549 (1977).
(4) R. S. Lott and W. L. Hayton, *Drug Intell. Clin. Pharm.*, **12**, 140 (1978).
(5) W. L. Chiou, M. A. F. Gadalla, and G. W. Peng, *J. Pharm. Sci.*, **67**, 182 (1978).
(6) W. L. Chiou, G. W. Peng, M. A. F. Gadalla, and S. T. Nerenberg, *ibid.*, **67**, 292 (1978).
(7) N. K. Athanikar, G. W. Peng, R. L. Nation, S. M. Huang, and W. L. Chiou, *J. Chromatogr. Biomed. Appl.*, in press.
(8) W. L. Chiou, *Clin. Chem.*, **25**, 197 (1979).

[5] Vernier Caliper, Fisher Scientific Co., Chicago, Ill.

Frances S. Pu
Win L. Chiou ˣ
Clinical Pharmacokinetics Laboratory and Department of Pharmacy
College of Pharmacy
University of Illinois at the Medical Center
Chicago, IL 60612

Received November 9, 1978.
Accepted for publication January 9, 1979.
Abstracted from a thesis submitted by F. S. Pu to the Graduate College, University of Illinois at the Medical Center, in partial fulfillment of the Master of Science degree requirements.

Potential Antiarthritic Agents I: Benzoylacetonitriles

Keyphrases □ Antiarthritic agents—benzoylacetonitriles, synthesis, screened in rats, structure–activity relationships □ Benzoylacetonitriles—antiarthritis activity, synthesis, screened in rats, structure–activity relationships

To the Editor:

Rheumatoid arthritis, a chronic inflammatory disorder of unknown etiology, is treated largely with agents useful only in ameliorating the acute inflammatory symptoms, *i.e.*, pain and swelling. Clearly, nontoxic drugs effective in the remission of joint and cartilage destruction are critically needed. We screened compounds in the chronic Freund's adjuvant-induced arthritis model (1) and discovered that benzoylacetonitrile (I) and its monofluorophenyl analogs (II–IV) were highly effective in this assay.

Concurrently, we found this series to be inactive against carrageenan-induced edema in rats and urate synovitis in dogs and only weakly active in suppressing UV-induced erythema in guinea pigs. When tested for the suppression of prostaglandin synthesis *in vitro*, benzoylacetonitrile had only one-third of the potency of aspirin. Additionally, I and IV displayed little or no ulcerogenic potential in rats at total daily doses as high as 800 mg/kg. These facts suggest that prostaglandin synthesis inhibition is unlikely to ac-

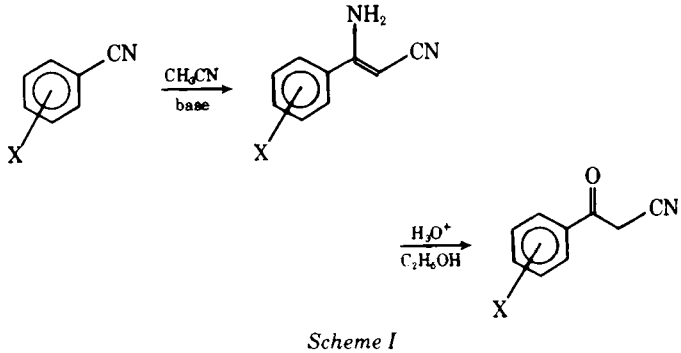

Scheme I

© 1979, American Pharmaceutical Association

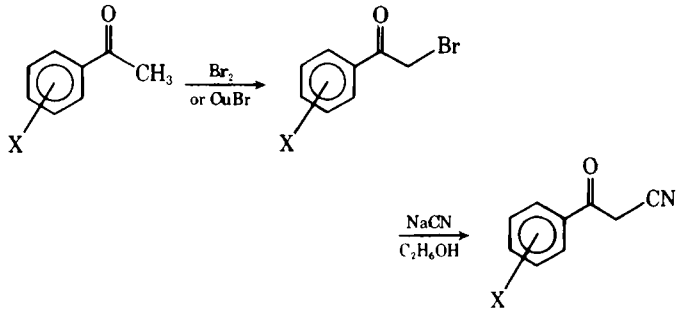

Scheme II

count for this striking suppression of developing adjuvant arthritis.

A series of phenyl-substituted benzoylacetonitriles was prepared and screened for activity in the above-mentioned assays. These analogs were easily obtained, as in Scheme I, *via* the β-aminocinnamonitriles (2) followed by acid hydrolysis.

The most useful conditions for enamine intermediate preparation employed 1 equivalent of sodium hydride in refluxing ether with 0.1 equivalent of *tert*-butyl alcohol. Alternatively, benzoylacetonitriles were prepared by cyanide displacement on a phenacyl bromide (3) as in Scheme II. Table I lists some representative benzoylacetonitriles from the many prepared in this investigation.

The compounds listed in Table I were screened in the rat adjuvant arthritis assay as described previously (1). Measurements of swelling and weight gain were made 14 days following challenge with Freund's adjuvant. Compounds that produced a statistically significant percent inhibition of the control swelling were accepted as active. Only benzoylacetonitrile (I) and its fluoro analogs (II–IV) displayed activity in this model.

Table II presents dose–response data for I and IV on adjuvant arthritis in rats. These compounds showed marked suppression of both primary and secondary lesions. Additionally, they suppressed both lesions for at least 7 days after cessation of treatment.

Table I—Benzoylacetonitrile Analogs

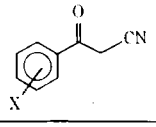

Compound	X	Method	Yield, %	Melting Point	Reference
I[a]	H	—	—	79–80°	4 (mp 80–81°)
II	2-F	I	87	53–54°	5 (mp 53°)
III	3-F	II	37	69–70°	6
IV	4-F	I	80	78–80°	6
V	2-Cl	I	77	50–54°	7 (mp 56–57°)
VI	4-Cl	I	53	126–130°	3 (mp 128°)
VII	3-Br	I	88	93–95°	7 (mp 88–89°)
VIII	4-Br	II	42	164–165°	3 (mp 158°), 7 (mp 160–161°)
IX	4-CH_3	II	40	106–106.5°	3 (mp 102°)
X	4-OH[b]	II	38	168–172° dec.	5, 7 (mp 182–183°)
XI[a]	4-NH_2	—	—	157–160°	7 (mp 157–158°)

[a] Obtained from Aldrich Chemical Co. [b] Elemental analysis acceptable to within 0.4% for $C_9H_7NO_2 \cdot 1/4\ H_2O$.

Table II—Effect of Benzoylacetonitrile (I) and *p*-Fluorobenzoylacetonitrile (IV) on Developing Adjuvant Arthritis in Rats (Pooled Data)[a]

Compound	Oral Dose, mg/kg	Number of Animals	Mean Weight Gain, g	Inhibition of Swelling, % Primary Lesion	Inhibition of Swelling, % Secondary Lesion
Normal rats	—	186	77	—	—
Adjuvant controls		630	36	0	0
Indomethacin	4		Toxic		
	2	57	68	51	38
	1	54	63	46	34
	0.5	54	53	40	25
I	400	18	31*	81	84
	200	18	56	73	70
	100	36	49	63	70
	50	54	53	51	52
	25	36	54	54	40
	12.5	18	49	37	43
IV	400	18	42*	75	72
	200	18	67	52	63
	100	18	63	46	44
	50	36	61	56	13
	25	18	55*	33	25
	12.5	18	62	34	22

[a] All values in the treated groups, other than those marked with an asterisk, were significantly different from the adjuvant arthritic controls; $p < 0.05$ by t test.

Analogs II and III also were effective in the rat adjuvant arthritis assay and were inactive when tested in the prostaglandin-mediated assays (*i.e.*, rat carrageenan edema and guinea pig UV erythema).

We concluded that these agents (I–IV) act by a pharmacological mechanism different from that of the classical aspirin-like anti-inflammatory drugs and have a unique potential as structurally novel agents for antiarthritic therapy. Initial animal studies suggest that reticuloendothelial stimulation may be one possible mechanism of action. A detailed discussion of the chemical and pharmacological aspects of this work will be published.

(1) A. E. Sloboda and A. C. Osterberg, *Inflammation*, **1** (4), 415 (1976).

(2) S. A. Lang and E. Cohen, *J. Med. Chem.*, **18**, 441 (1975).

(3) H. K. Gakhar, G. S. Gill, and J. S. Multani, *J. Indian Chem. Soc.*, **48**, 953 (1971).

(4) J. B. Dorsch and S. McElvain, *J. Am. Chem. Soc.*, **54**, 2960 (1932).

(5) O. Hromatka and D. Binder, Ger. Offen. 2, 221, 623 (Nov. 30, 1972); through *Chem. Abstr.*, **78**, 72241n (1973).

(6) V. Pihl, H. Siilbek, T. Tenno, A. Ranne, and A. Talvik, *Reakts. Sposobn. Org. Soedin.*, **5**, 27 (1968); through *Chem. Abstr.*, **69**, 100208s (1968).

(7) N. S. Vul'fson, *Sb. Statei, Nauchno-Issled. Inst. Org. Poluprovod. Krasetelei*, **2**, 128 (1961); through *Chem. Abstr.*, **56**, 10031 (1961).

J. W. Hanifin
B. D. Johnson
J. Menschik
D. N. Ridge [x]
A. E. Sloboda

Metabolic Disease Research Section
Medical Research Division
American Cyanamid Company
Lederle Laboratories
Pearl River, NY 10965

Received November 27, 1978.

Accepted for publication January 26, 1979.

The authors thank Dr. V. Grosso and his group, particularly Ms. L. Harten, and the staffs of L. Brancone and W. Fulmor.

A publication of the
American Pharmaceutical Association—
the National Professional Society
of Pharmacists

JOURNAL OF PHARMACEUTICAL SCIENCES

INDEX TO AUTHORS
INDEX TO SUBJECTS

VOLUME 68
JANUARY TO DECEMBER, 1979

Published monthly under the supervision of the Board of Trustees

MARY H. FERGUSON
Editor

SHELLY ELLIOTT
Production Editor

MARCIA GARTRELL
Copy Editor

NICOLETTE TRIANTAFELLU
Copy Editor

EDWARD G. FELDMANN
Contributing Editor

SAMUEL W. GOLDSTEIN
Contributing Editor

BELLE R. BECK
Editorial Secretary

DAVID BOHARDT
Director of Publications

L. LUAN CORRIGAN
Assistant Director of Publications

EDITORIAL ADVISORY BOARD

John Autian
Norman R. Farnsworth
William O. Foye
William J. Jusko
Herbert A. Lieberman
David E. Mann, Jr.
Gerald J. Papariello
Edward G. Rippie

MAY 1979
VOLUME 68 NUMBER 5

JOURNAL OF PHARMACEUTICAL SCIENCES

MARY H. FERGUSON
Editor

SHELLY ELLIOTT
Production Editor

JANIS KELLY
Copy Editor

EDWARD G. FELDMANN
Contributing Editor

SAMUEL W. GOLDSTEIN
Contributing Editor

BELLE R. BECK
Editorial Secretary

DAVID BOHARDT
Director of Publications

L. LUAN CORRIGAN
Assistant Director of Publications

EDITORIAL ADVISORY BOARD

JOHN AUTIAN
HERBERT A. LIEBERMAN
NORMAN R. FARNSWORTH
DAVID E. MANN, JR.
WILLIAM O. FOYE
GERALD J. PAPARIELLO
WILLIAM J. JUSKO
EDWARD G. RIPPIE

The *Journal of Pharmaceutical Sciences* (ISSN 0022-3549) is published monthly by the American Pharmaceutical Association (APhA) at 2215 Constitution Ave., N.W., Washington, DC 20037. Second-class postage paid at Washington, D.C., and at additional mailing office.

All expressions of opinion and statements of supposed fact appearing in articles or editorials carried in this journal are published on the authority of the writer over whose name they appear and are not to be regarded as necessarily expressing the policies or views of APhA.

Offices—Editorial, Advertising, and Subscription: 2215 Constitution Ave., N.W., Washington, DC 20037. Printing: 20th & Northampton Streets, Easton, PA 18042.

Annual Subscriptions—United States and foreign, industrial and government institutions $50, educational institutions $50, individuals *for personal use only* $30; single copies $5. All foreign subscriptions add $5 for postage. Subscription rates are subject to change without notice. Members of APhA may elect to receive the *Journal of Pharmaceutical Sciences* as a part of their annual $70 (foreign $75) APhA membership dues.

Claims—Missing numbers will not be supplied if dues or subscriptions are in arrears for more than 60 days or if claims are received more than 60 days after the date of the issue, or if loss was due to failure to give notice of change of address. APhA cannot accept responsibility for foreign delivery when its records indicate shipment has been made.

Change of Address—Members and subscribers should notify at once both the Post Office and APhA of any change of address.

Photocopying—The code at the foot of the first page of an article indicates that APhA has granted permission for copying of the article beyond the limits permitted by Sections 107 and 108 of the U.S. Copyright Law provided that the copier sends the per copy fee stated in the code to the Copyright Clearance Center, Inc., P.O. Box 8891, Boston, MA 02114. Copies may be made for personal or internal use only and not for general distribution.

Microfilm—Available from University Microfilms International, 300 N. Zeeb Road, Ann Arbor, MI 48106.

© Copyright 1979, American Pharmaceutical Association, 2215 Constitution Ave., N.W., Washington, DC 20037; all rights reserved.

BUREAUCRATIC OVERKILL

Those who have had the good fortune of being able to read newspapers or periodicals in which columnist James J. Kilpatrick's writings appear are familiar with his uncanny ability to discuss rules and regulations that smack of "overkill." He is able to write about such measures in a manner that—while entertaining and amusing—leads the reader persuasively along a pathway to the conclusion that the regulation is absurd, ridiculous, and even beyond belief.

Recently, we read his column concerning a particular regulation that previously had our casual support. However, by the time we finished reviewing Mr. Kilpatrick's analysis and commentary, we were squirming in embarrassment for the poor agency official who had innocently promulgated the requirement.

Mr. Kilpatrick's remarkable ability to blow away all the extraneous aspects and to expose the utter absurdity of the underlying requirement came to mind recently in connection with one of the ancillary provisions of the Food and Drug Administration's revised and expanded Good Manufacturing Practices regulations.

This massive tome, which was released last fall, constitutes FDA's effort to codify who may manufacture drugs and how such manufacturing facilities shall be outfitted, organized, staffed, and operated. While opinions may vary, we happen to feel that this basic objective is a good thing. Hence, our immediate, general inclination is to support these reorganized and expanded GMP regulations. We suspect that this attitude is shared by most people in the pharmaceutical field including the majority of our readers.

But tucked away in this huge document is a provision that, in our opinion at least, constitutes the regulatory "overkill" that would cause Mr. Kilpatrick's ire to rise and his typewriter to hum.

Specifically, John W. West, a pharmacist at a Holland, Michigan, community hospital, has called attention to FDA's declaration that hospitals that do packaging for unit dose dispensing must now comply with the full GMP regulations. He notes with astonishment and disbelief that, "*These regulations are the same as those required of the pharmaceutical manufacturing industry. They mandate extensive stability testing, in-process inspections, a separate quality control unit,* etc. *Unlike industry, the community hospital pharmacy simply does not have these extensive control facilities.*"

Now, if the hospital pharmacy were engaged in drug manufacturing in the usual and conventional sense, then there would be no quarrel about FDA's sweeping application of these requirements. But a unit dose dispensing system simply enables the pharmacist to dispense the medication in a convenient and ready-to-administer form. For example, individual tablets or capsules are dispensed in a single packet bearing the name of the drug, its strength, its control number, and any other pertinent information.

Unit dose drug distribution systems have been encouraged by APhA, and other professional pharmacy organizations, because their adoption and use have been shown to reduce the incidence of medication errors, decrease the cost of delivering medication to the patient, and facilitate in drug identification, control, and storage. The system has other obvious advantages from the standpoint of minimizing contamination and maintaining drug purity and potency.

A goodly number of drugs can be obtained directly from the manufacturer in unit dose package form. But many other drugs are not so available. To fill this gap, hospital pharmacists use a simple packaging machine to produce unit dose packets in the hospital pharmacy.

It is regarding this operation that the long arm of the FDA has reached in and grabbed on grounds that it is "manufacturing" and that it eliminates the pharmacy's exemption from having to comply with the complete GMP requirements which apply to full scale drug manufacturing plants.

The regulations in the *Federal Register* discussed strip-packaging and related types of repackaging by "pharmacies and hospitals in particular," and in this context concluded by saying:

> "*When a hospital or pharmacy is engaged in drug repackaging or relabeling operations that are beyond the usual conduct of dispensing or selling drugs at retail, however, the exemptions of the act cease to apply; the establishment is required to register and is subject to regular inspections under section 704 of the act. Furthermore, appropriate current good manufacturing practice must be complied with.*"

High quality pharmaceutical service is something that should be encouraged. Regrettably, this ill-conceived regulation will discourage such quality service by forcing institutional pharmacies to abandon the unit dose concept.

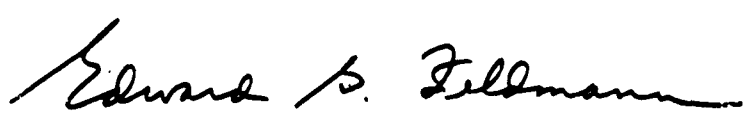

Capsule Dissolution

I take exception to Dr. Moore's implicit criticism and conclusions in his letter "Nondisintegration of a Capsule's Contents" in the February 1979 Open Forum[1].

First, it does not strike me as unexpected to find *in vitro* differences, using discriminating methods, in dosage forms as fundamentally different as tablets, capsules, and timed-release tablets. It seems grossly unjustified to impute "top manufacturers" on such a finding because it fails to take into account special patient needs, the clinical effects resulting from such differences, and the label claims of the manufacturer.

Second, I do not believe that the slower dissolution observed with the capsule was failure to disintegrate but more likely a failure of the capsule contents to wet readily. Incidentally, wetting problems are easily identified by sprinkling the contents onto water and noting whether they float. Under any conditions, I would not presume that a disintegration failure could be extrapolated to a general industry need and opportunity to make a fortune based only on dissolution test values.

Finally, for a more detailed discussion on capsule wetting problems and how to overcome them, readers are invited to read my paper[2] "Dissolution of Lithium and Magnesium from Lithium Carbonate Capsules Containing Magnesium Stearate."

Henry C. Caldwell
Research and Development
Smith Kline & French Laboratories
Philadelphia, PA 19101

Received March 15, 1979.

[1] W. E. Moore, *J. Pharm. Sci.*, 68 (2), IV (1979).
[2] H. C. Caldwell, *ibid.*, 63, 770 (1974).

Antibiotic Certification

I would like to comment on the editorial, "Antibiotic Certification—Obsolete and Archaic," in the February issue[1] of *J. Pharm. Sci.* I read it the day after retiring from FDA after 31 years plus of service in the subject field.

I agree with Dr. Feldmann and Dr. George Schneller that, when antibiotics were first marketed, they were extremely crude and that conventional methods were not applicable to assure their potency. I also agree that advances in manufacture have allowed the making of these pharmaceuticals with a degree of purity comparable to other chemicals.

I also agree that antibiotics should not be treated differently from other potent medicinal agents on the market.

I do, however, feel that to assure compliance through regular enforcement activities is not sufficient nor optimal.

Test results from postdistribution testing in the National Center of Drug Analysis have shown that some drug categories have 10–25% defective lots. None of these products was tested for sterility or absence of pyrogenicity, which could make the rate even higher.

I also know that the experience gained in the certification program has been beneficial in overall drug evaluations. Let me cite a few of many examples:

1. Expiration dates, required for antibiotics since the program began, were deemed necessary for *all* drug products in the most recent GMP regulations.
2. Metal particles were first observed in antibiotic ointments (ophthalmic), and limits for their presence are now prescribed for all drug products.
3. Full knowledge of manufacturers and their products was essential for the certification program, and Drug Registration lagged far behind in other areas.

Finally, having shown that such thorough hands-on experience does contribute to public safety and health, let me put the claim of increased cost of medicines in a proper perspective.

The certification service, which covers more positions than those used for the testing only (new antibiotic drug evaluation, inspection, *etc.*), has a budget near $6 million. This amount is about 0.3% in an industry where the total sales are estimated to be about $2 billion.

Peter J. Weiss
(Former Director, National
Center for Antibiotic Analysis, FDA)
1309 Caddington Avenue
Silver Spring, MD 20901

Received March 6, 1979.

[1] E. G. Feldmann, *J. Pharm. Sci.*, 68 (2), I (1979).

Capsule Dissolution

I take exception to Dr. Moore's implicit criticism and conclusions in his letter "Nondisintegration of a Capsule's Contents" in the February 1979 Open Forum[1].

First, it does not strike me as unexpected to find *in vitro* differences, using discriminating methods, in dosage forms as fundamentally different as tablets, capsules, and timed-release tablets. It seems grossly unjustified to impute "top manufacturers" on such a finding because it fails to take into account special patient needs, the clinical effects resulting from such differences, and the label claims of the manufacturer.

Second, I do not believe that the slower dissolution observed with the capsule was failure to disintegrate but more likely a failure of the capsule contents to wet readily. Incidentally, wetting problems are easily identified by sprinkling the contents onto water and noting whether they float. Under any conditions, I would not presume that a disintegration failure could be extrapolated to a general industry need and opportunity to make a fortune based only on dissolution test values.

Finally, for a more detailed discussion on capsule wetting problems and how to overcome them, readers are invited to read my paper[2] "Dissolution of Lithium and Magnesium from Lithium Carbonate Capsules Containing Magnesium Stearate."

Henry C. Caldwell
Research and Development
Smith Kline & French Laboratories
Philadelphia, PA 19101

Received March 15, 1979.

[1] W. E. Moore, *J. Pharm. Sci.*, 68 (2), IV (1979).
[2] H. C. Caldwell, *ibid.*, 63, 770 (1974).

Antibiotic Certification

I would like to comment on the editorial, "Antibiotic Certification—Obsolete and Archaic," in the February issue[1] of *J. Pharm. Sci.* I read it the day after retiring from FDA after 31 years plus of service in the subject field.

I agree with Dr. Feldmann and Dr. George Schneller that, when antibiotics were first marketed, they were extremely crude and that conventional methods were not applicable to assure their potency. I also agree that advances in manufacture have allowed the making of these pharmaceuticals with a degree of purity comparable to other chemicals.

I also agree that antibiotics should not be treated differently from other potent medicinal agents on the market.

I do, however, feel that to assure compliance through regular enforcement activities is not sufficient nor optimal.

Test results from postdistribution testing in the National Center of Drug Analysis have shown that some drug categories have 10–25% defective lots. None of these products was tested for sterility or absence of pyrogenicity, which could make the rate even higher.

I also know that the experience gained in the certification program has been beneficial in overall drug evaluations. Let me cite a few of many examples:

1. Expiration dates, required for antibiotics since the program began, were deemed necessary for *all* drug products in the most recent GMP regulations.
2. Metal particles were first observed in antibiotic ointments (ophthalmic), and limits for their presence are now prescribed for all drug products.
3. Full knowledge of manufacturers and their products was essential for the certification program, and Drug Registration lagged far behind in other areas.

Finally, having shown that such thorough hands-on experience does contribute to public safety and health, let me put the claim of increased cost of medicines in a proper perspective.

The certification service, which covers more positions than those used for the testing only (new antibiotic drug evaluation, inspection, *etc.*), has a budget near $6 million. This amount is about 0.3% in an industry where the total sales are estimated to be about $2 billion.

Peter J. Weiss
(Former Director, National
Center for Antibiotic Analysis, FDA)
1309 Caddington Avenue
Silver Spring, MD 20901

Received March 6, 1979.

[1] E. G. Feldmann, *J. Pharm. Sci.*, 68 (2), I (1979).

JOURNAL OF PHARMACEUTICAL SCIENCES

MAY 1979
VOLUME 68 NUMBER 5

RESEARCH ARTICLES

Anti-Inflammatory Activity of Sesquiterpene Lactones and Related Compounds

I. H. HALL *x, K. H. LEE *, C. O. STARNES *, Y. SUMIDA *, R. Y. WU *, T. G. WADDELL ‡, J. W. COCHRAN ‡, and K. G. GERHART ‡

Received August 11, 1978, from the *Division of Medicinal Chemistry, School of Pharmacy, University of North Carolina, Chapel Hill, NC 27514, and the ‡Department of Chemistry, University of Tennessee at Chattanooga, Chattanooga, TN 37401. Accepted for publication October 23, 1978.

Abstract □ Some sesquiterpene lactones and related compounds were tested for anti-inflammatory activity in rodents. In the edema-induced carrageenan inflammation screen, the α-methylene-γ-lactone moiety of the sesquiterpene lactones was required for inhibitory activity. The 6-hydroxy group of helenalin also was required for potency. In the tenulin series, the 2,3-epoxy derivatives were marginally active. The same structure was required for inhibition of the writhing reflex. In the chronic adjuvant arthritic screen, compounds containing the α-methylene-γ-lactone moiety, the β-unsubstituted cyclopentenone ring, and the α-epoxy cyclopentenone system afforded significant inhibition at 2.5 mg/kg/day. The sesquiterpene lactones were marginally effective against induced pleurisy. The delayed hypersensitivity was suppressed by these agents whereas immunoglobulin synthesis was slightly stimulated. No deleterious side effects were observed with these agents from the limited tests performed.

Keyphrases □ Lactones, sesquiterpene—anti-inflammatory activity, structure-activity relationships, edema, arthritis, pleurisy, immunoglobulin synthesis, rats □ Anti-inflammatory agents—sesquiterpene lactones, structure-activity relationships, edema, arthritis, pleurisy, immunoglobulin synthesis, rats □ Structure-activity relationships—sesquiterpene lactones, anti-inflammatory activity

The anti-inflammatory drugs ethacrynic acid and *N*-ethylmaleimide have been shown to bind sulfhydryl groups (1). Cysteine, a sulfhydryl-donating compound, reversed the anti-inflammatory activity of these agents, indicating that sulfhydryl groups participate in the inflammatory process. In addition, the sulfhydryl-binding properties of drugs, *e.g.*, salicylates and indomethacin, were related to their anti-inflammatory activity (1). Other researchers (2–5) showed that sulfhydryl and disulfide interactions are altered in rat adjuvant arthritis, human connective tissue disease, and anti-inflammatory drug therapy.

Mechanism of action studies with sesquiterpene lactones showed that the α-methylene-γ-lactone and cyclopentenone moieties undergo Michael-type addition with L-cysteine, glutathionine, and a number of sulfhydryl-bearing cell enzymes (6–10). Metabolic studies with sesquiterpene lactones in mammalian cancer cells demonstrated that these agents are potent inhibitors of the lysosomal enzymes, oxidative phosphorylation, and protein synthesis and that they significantly elevate cellular cyclic AMP levels (7, 11, 12). A number of clinically useful anti-inflammatory agents have similar effects on cell metabolism. Moreover, certain sesquiterpene lactone-producing plants, such as *Eupatorium formosanum*, have been used as anti-inflammatory herbal remedies as well as antipyretic drugs (13). Thus, it was decided to test these agents for anti-inflammatory activity.

EXPERIMENTAL

Test Compounds—Twenty-nine sesquiterpene lactones and related compounds were studied. Some were natural products isolated from plant species by literature techniques (14): helenalin (I) from *Balduina angustifolia* (15), tenulin (XI) (6) and aromaticin (XVII) (6, 16) from *Helenium amarum*, eupatolide (XVIII) from *Eupatorium formosanum* (17), deoxyelephantopin (XIX) from *Elephantopus carolinianus* (18), eupahyssopin (XX) from *Eupatorium hyssopifolium* (19), eupaformosanin (XXI) from *Eupatorium formosanum* (20), and molephantin (XXII) (21), molephantinin (XXIII) (22), and phantomolin (XXIV) (23) from *Elephantopus mollis*.

Plenolin (II) was obtained by hydrogenation of helenalin to give a compound identical to the naturally occurring product (24). 2,3-Dihydrohelenalin (III), 2,3,11,13-tetrahydrohelenalin (IV), 2,3-epoxyhelenalin (IX), and 2,3-epoxyplenolin (X) were chemically modified from helenalin (24), as was dimeric helenalin (V) (12), helenalin dimethylamine adduct (VI) (25), 2,3-epoxyhelenalin dimethylamine adduct (VII) (26), and helenalin pyrrolidine adduct (VIII) (25). 2,3-Dihydrotenulin (XII), 2,3-epoxytenulin (XIII), isotenulin (XIV), 2,3-epoxyisotenulin (XV), and dihydroisotenulin (XVI) were prepared by a literature method (27). Thymine α-methylene-γ-lactone (XXV) and its corresponding trimethoxybenzoyl ester (XXVI) were prepared by literature techniques (28), as was α-methylene-β,β-dicarbethoxy-γ-butyrolactone (XXVIII) (29). α-Methylene-γ-lactone (XXVII) was prepared by the published method (30).

0022-3549/79/0500-0537$01.00/0
© 1979, American Pharmaceutical Association

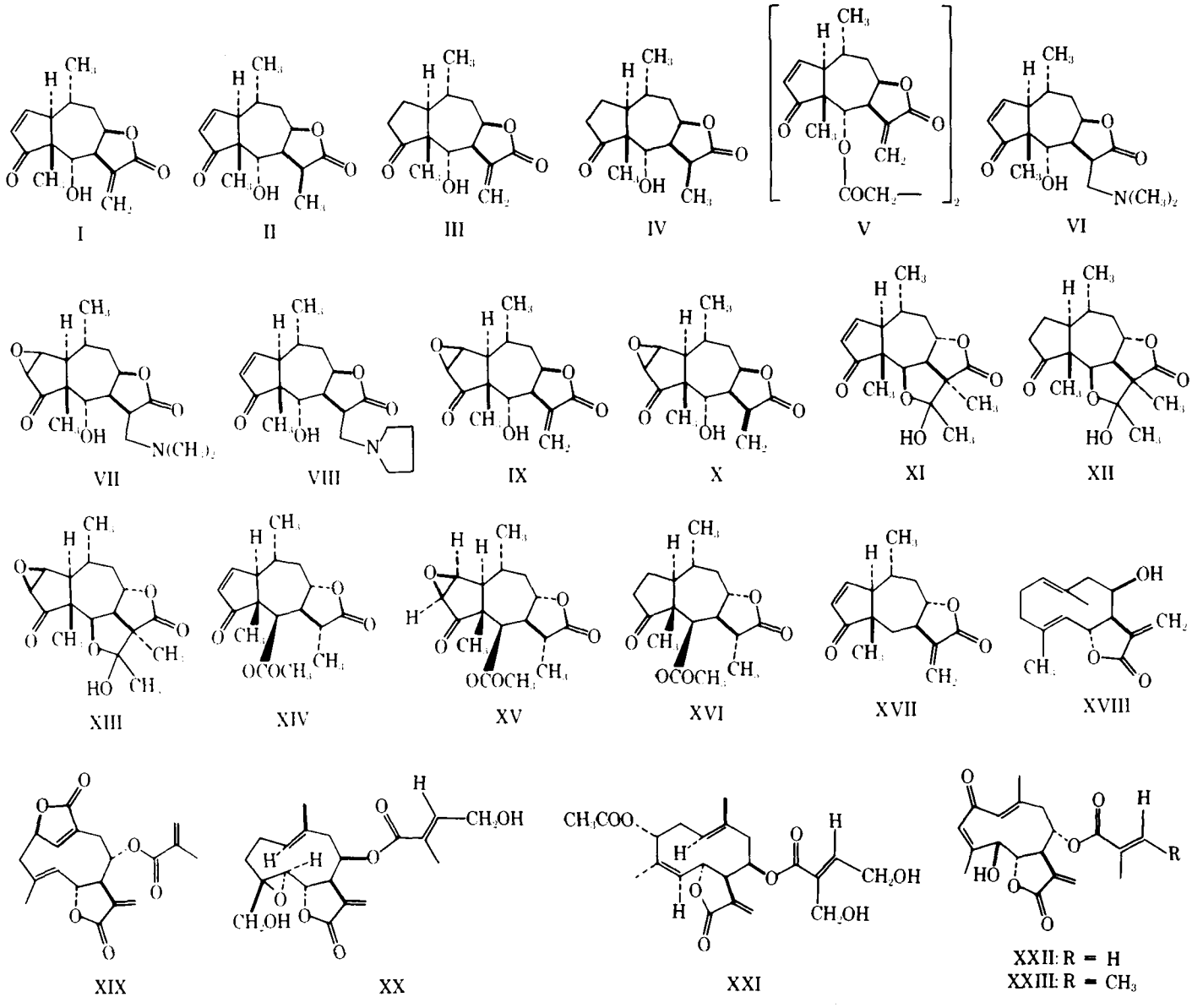

The following were purchased from commercial sources: 2-cyclopentenone[1] (XXIX), indomethacin[2] (XXX), phenylbutazone[3] (XXI), diethylstilbestrol[4], and ethynyl estradiol[4].

Anti-Inflammatory Screen—Sprague-Dawley male rats, ~160 g, were administered test drugs at 2.5 mg/kg ip in 0.05% polysorbate 80, 3 hr and 30 min prior to the injection of 0.2 ml of 1% carrageenan in 0.9% saline into the plantar surface of the right hindfoot. Isotonic saline was injected into the left hindfoot, which served as a baseline. After 3 hr, both feet were excised at the tibiotarsal (ankle) joint according to a modified method (31, 32), resulting in an average 0.655-g foot weight increase for controls.

Antipyretic Screen—Sprague-Dawley rats, ~200 g, were administered 2 ml of 44% baker's yeast solution subcutaneously (31) 18 hr prior to the injection of drugs at 2.5 or 5 mg/kg ip, resulting in an average body temperature elevation of 3.46 °F. Rats were also administered 0.25 mg of *Mycobacterium butyricum*[5] (33) subcutaneously prior to drug administration. Rectal temperatures were taken at 0, 2, 4, and 6 hr.

Analgesic Screen—The hot-plate-tail flick method (34) was employed with CF_1 male mice, ~30 g, who were administered test drugs at 20 mg/kg ip 5 min prior to the analgesic test. Normal reaction time was 9.3 sec. Morphine, 10 mg/kg, increased the reaction time to over 1 min.

The writhing reflex was also utilized. Mice were administered test drugs at 20 mg/kg ip 20 min (35) prior to the administration of 0.5 ml of 0.6% acetic acid (36). After 5 min, the number of stretches, characterized by repeated contractures of the abdominal musculature accompanied by extension of the hindlimbs, was counted for the next 10 min. The control mice averaged 78 stretch reflexes/10 min.

Chronic Adjuvant Arthritic Screen—Male Sprague-Dawley rats, ~160 g, were injected at the base of the tail with 0.2 ml of 100 mg of dried *M. butyricum* solution and 40 mg of digitonin in 20 ml of light mineral oil (37). Test drugs were administered on Day 3 through Day 30 at 2.5 mg/kg/day ip. Animals were sacrificed on Day 21, and the feet were excised and weighed. Control animals achieved a 0.830-g average net weight gain.

Pleurisy Anti-Inflammatory Screen—Sprague-Dawley rats were administered test drugs at 2.5 mg/kg ip 1 hr before and 3 hr after injection into the pleural cavity of 0.05 ml of 0.316% Evan's Blue and carrageenan (38). Six hours later, the rats were sacrificed, and the fluid was collected from the pleural cavity. Control rats produced an average 2.5 ml of fluid.

Passive Cutaneous Anaphylaxis Screen (Antiallergy)—Egg albumin (10 mg/kg) with 1.5 ml of *Bordetella pertussis* vaccine (8 protective units/ml) was used to induce homocytotropic antibody production in Sprague-Dawley male rats (39). Blood was collected by tail vein bleeding, and the serum was separated and frozen. New rats were shaved,

[1] Aldrich.
[2] Merck Sharp and Dohme
[3] Geigy.
[4] Sigma.
[5] Difco.

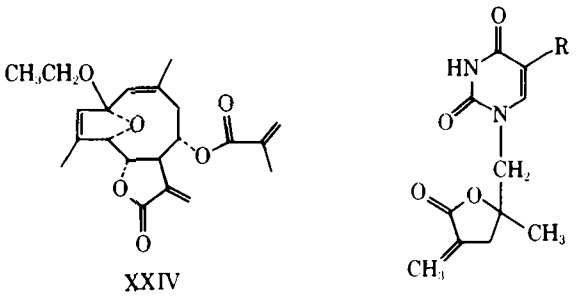

XXIV

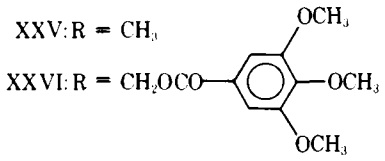

XXV: R = CH_3

XXVI: R = CH_2OCO

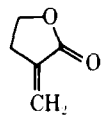

XXVII

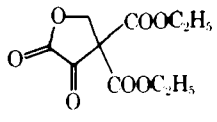

XXVIII

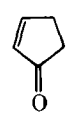

XXIX

and 0.1 ml of serum antibodies (diluted 1:2 with isotonic phosphate saline buffer) was injected intradermally at three sites. Forty-eight hours later, the rats were given test drugs at 2.5 mg/kg ip. The rats were challenged 45 min later intravenously with 0.3 ml of 1% egg albumin in pH 7.2 isotonic saline and 0.25% solution of Evan's Blue. The animals were sacrificed 30 min later, and the blue wheals were measured at the serum antibody injection sites (40, 41). Control animals gave an average response of 22.4 mm (diameter).

Histamine-Induced Anaphylaxis or Hypersensitivity—Female HLA-SW mice, ~35 g, received 0.15 ml of reconstituted *B. pertussis* vaccine in 0.9% saline intravenously 4 days prior to the administration of test drugs at 20 mg/kg. Histamine base (1 mg) was injected intraperitoneally 30 min later (42). Histamine anaphylaxis resulted in 88% mortality for the control animals.

Antibody Production—CF_1 male mice, ~30 g, were administered sheep red blood cells as an antigen intraperitoneally. On Days 2–4, test compounds were administered at 5 and 10 mg/kg/day. On Day 5, the spleens were removed and the lymphocytes were harvested. Lymphocytes were incubated with sheep red blood cells and guinea pig complement on 1% agarose slides according to the Jerne plaque microassay technique (43), and the plaques were counted. The control animals produced 275 plaques/10^6 lymphocytes. Animals were treated similarly with chicken red blood cells, blood was collected by tail vein bleeding on Day 5, and the serum was separated. Chromium 51 was incubated with, and taken up by, chicken nucleated red blood cells (44). Labeled cells were then incubated with serum antibodies from the mice. Normal mouse serum resulted in an average 22% release of chromium 51 from the chicken red blood cells and a maximum 95% release with 3% acetic acid.

Mitogenic Test—CF_1 male mice were given helenalin (I) at 5 mg/kg 2 hr prior to sacrifice or on Days 1–3 and 10 μCi of [^{14}C-*methyl*]thymidine (49.2 mCi/mmole) was injected intraperitoneally on Day 4 (6). After 1 hr, the mice were sacrificed, the spleen was excised, and lymphocytes were prepared. The ^{14}C-thymidine incorporation into lymphocyte deoxyribonucleic acid was determined. In an analogous manner, spleen lymphocytes from 2 hr-treated mice were analyzed by radioimmunoassay for cyclic AMP.

Delayed Hypersensitivity Screen—Sprague–Dawley rats, ~160 g, were administered methylated bovine serum albumin as antigen subcutaneously on Days 0 and 7 (45–47). Test drugs were administered daily at 2.5 mg/kg ip. On Day 21, the rats were challenged with antigen injected into the right plantar footpad. The left hindfoot acted as the control. Animals were sacrificed 24 hr later, and the paw weight was obtained.

In the second experiment, rats were administered chicken egg albumin as antigen on Days 0 and 7. However, dosing with test compounds at 2.5 mg/kg only occurred on Days 18–20. The methylated bovine serum albumin resulted in a net increase of 119 mg whereas the egg albumin resulted in a net increase of only 46 mg upon challenge with the respective antigens.

Antifertility and Teratogenic Effects of Drugs—CF_1 female mice, ~30 g, were administered test compounds at 6 mg/kg/day for 28 days. On Day 10, they were exposed to males (two females per male) for the remainder of the experiment. On Days 27–30, pregnant females were sacrificed and the number of viable fetuses and intrauterine deaths were tabulated (48, 49). Fetuses were examined for teratogenic effects by literature methods (50). Uterotropic effects were determined in female rats, ~50 g, by published methods (51).

Adverse Side Effects—Central nervous system (CNS) effects such as drowsiness, convulsions, hyperexcitability, and reflex activity loss were determined by observation of all animal species used in the screens at various doses. Ulcerogenic (estrogenic side effects) tests were carried out in Sprague–Dawley rats, ~160 g, who were administered test drugs at 2.5 mg/kg/day for 3 weeks. After food had been removed for 18 hr, the last dose was administered on Day 21. Four hours later, the rats were sacrificed and the gastric and duodenal linings were examined for bleeding and/or ulcers (52).

In an analogous experiment, animals were bled on Day 21 by tail vein and the red and white blood cells were counted in a hemocytometer and expressed as numbers of cells × $10^6/cm^3$. Hematocrits were also obtained (53). *In vitro* effects of test drugs on aerobic respiration of rat liver homogenates were also determined at 0.75 μmole as previously outlined (12).

RESULTS

In the edema-induced inflammation test, at 2.5 mg/kg twice, III, IX, X, XIII, XIX, XX, XXIV, and XXV caused at least 40% inhibition, while I caused 72% inhibition (Table I). At 2.5 or 5 mg/kg, the sesquiterpene

Table I—Anti-Inflammatory Activity of Sesquiterpene Lactones and Germacranolides

Compound (n = 8)	Percent Control: Anti-Inflammatory Screen, Sprague–Dawley Rats, 2.5 mg/kg twice, $\bar{x} \pm SD$	Percent Control: Writhing Reflex, CF_1 Mice, 20 mg/kg, $\bar{x} \pm SD$
I Helenalin	28 ± 15[a]	7 ± 3[a]
II Plenolin	89 ± 16	83 ± 8[b]
III 2,3-Dihydrohelenalin	51 ± 19[a]	50 ± 11[a]
IV 2,3,11,13-Tetrahydrohelenalin	96 ± 15	93 ± 13
V Dimeric helenalin	68 ± 11[a]	64 ± 5[a]
VI Helenalin dimethylamine adduct	74 ± 16[b]	79 ± 8[a]
VII 2,3-Epoxyhelenalin dimethylamine adduct	75 ± 13[b]	86 ± 7[c]
VIII Helenalin pyrrolidine adduct	72 ± 16[b]	73 ± 6[a]
IX 2,3-Epoxyhelenalin	54 ± 3[a]	47 ± 5[a]
X 2,3-Epoxyplenolin	49 ± 7	77 ± 12
XI Tenulin	84 ± 18	95 ± 7
XII 2,3-Dihydrotenulin	93 ± 8	81 ± 8[a]
XIII 2,3-Epoxytenulin	57 ± 19[a]	28 ± 6[a]
XIV Isotenulin	84 ± 17	87 ± 12
XV 2,3-Epoxyisotenulin	69 ± 9[a]	64 ± 9[a]
XVI 2,3-Dihydroisotenulin	92 ± 15	101 ± 16
XVII Aromaticin	65 ± 6[a]	77 ± 11[a]
XVIII Eupatolide	70 ± 12[a]	64 ± 9[a]
XIX Deoxyelephantopin	49 ± 11[a]	47 ± 7[a]
XX Eupahyssopin	43 ± 6[a]	32 ± 5[a]
XXI Eupaformosanin	69 ± 8[a]	62 ± 5[a]
XXII Molephantin	67 ± 8[a]	46 ± 8[a]
XXIII Molephantinin	68 ± 17[b]	53 ± 6[a]
XXIV Phantomolin	54 ± 19[a]	53 ± 9[a]
XXV Thymine α-methylene-γ-lactone	57 ± 7[a]	59 ± 7[a]
XXVI Trimethoxybenzoyl ester of thymine lactone	83 ± 9[c]	69 ± 7[a]
XXVII α-Methylene-γ-lactone	64 ± 13[a]	78 ± 5[a]
XXVIII α-Methylene-β,β-dicarbethoxy-γ-butyrolactone	75 ± 11[b]	—
XXIX 2-Cyclopentenone	77 ± 13[b]	79 ± 8[a]
XXX Indomethacin (10 mg twice)	22 ± 8[a]	43 ± 7[a]
XXXI Phenylbutazone (50 mg twice)	53 ± 13[a]	—
XXXII 0.05% Polysorbate 80	100 ± 12 (0.655 g)	100 ± 9

[a] $p = 0.001$. [b] $p = 0.005$. [c] $p = 0.010$.

Table II—Antiarthritis Screen Test Drugs in Sprague-Dawley Rats

Compound (2.5 mg/kg for 3 weeks) (n = 6)	Percent Control
0.05% Polysorbate 80	100 (0.830 g)
I	23
VI	59
IX	54
XI	47
XII	92
XIII	33
XIV	47
XV	37
XVIII	70
XIX	31
XX	34
XXII	40
XXVII	17
XXX (10 mg/kg/day)	55

Table III—Antipleurisy Activity of Sesquiterpene Lactones in Rats

Compound (2.5 mg/kg/day) (n = 6)	Fluid Increase, ml	Percent Control
0.05% Polysorbate 80	2.50	—
I	2.02	81
XI	1.58	63
XIX	1.50	60
XX	1.60	64

Table IV—Passive Cutaneous Anaphylaxis Test of Antiallergy Effects in Rats

Compound (2.5 mg/kg/day) (n = 8)	Antigen Challenge, Average Diameter, cm	Percent Control
0.05% Polysorbate 80	2.24	—
I	1.67	74
XI	1.65	73
XIX	2.04	91
XX	1.78	79

lactones afforded no activity against induced hyperpyrexia in rats. In the hot-plate test, which more closely relates to narcotic analgesic activity, these analogs were inactive at 20 mg/kg. The writhing reflex text (Table I), which is more closely related to inflammation pain, showed that III, IX, XIII, XIX, XX, and XXII–XXV caused greater than 40% inhibition; I caused 93% reflex inhibition; XIII caused 72% inhibition; and XX caused 68% inhibition. Compounds I, XII, XV, XIX, XX, and XXVII at 2.5 mg/kg/day caused greater than 60% inhibition of induced adjuvant arthritis in rats (Table II). Compounds VI, IX, XI, XIV, and XXII showed greater than 40% inhibition.

In the antipleurisy screen, I, XI, XIX, and XX caused 20–40% inhibition of pleural edema at 2.5 mg/kg twice (Table III). These same compounds offered only minimal protection in the passive cutaneous anaphylaxis text (antiallergy) in rats (Table IV) and offered no protection against histamine-induced anaphylaxis in mice.

The sesquiterpene lactones (I, XI, and XXIX) caused a slight, but significant, increase in serum immunoglobulin production in mice (Table V). Chromium 51 release from nucleated chicken red blood cells also demonstrated the increase in antibody synthesis after I and XI administration. Sesquiterpene lactones suppressed T cell delayed hypersensitivity with both methylated bovine albumin and chicken egg albumin (Table VI). Short-term dosing prior to antigen challenge caused the most suppression of T cell function compared to continued dosing, although different antigens were used. Compound I caused 81% inhibition, XI caused 32% inhibition, XIX caused 68% inhibition, and XX caused 47% inhibition. Compound I demonstrated 46% inhibition of delayed hypersensitivity to methylated bovine serum albumin. Helenalin (I) was judged to have mitogenic effects on spleen lymphocytes since 5 mg/kg/day resulted in a 342% increase in ^{14}C-thymine incorporation into DNA after 2 hr and a 445% increase after 3 days. Cyclic AMP levels were reduced 51% after 2 hr.

The sesquiterpene lactones had no effects on fertility in mice at 6 mg/kg/day (Table VII). The viable fetuses and intrauterine deaths were

Table V—Jerne Plaque: Immunosuppressant/Stimulation Activity of Sesquiterpene Lactones in CF_1 Male Mice Administered 0.2 ml of Sheep Erythrocytes

Compound[a]	Jerne Plaque, % control	Chromium 51, % released
0.05% Polysorbate 80	100 ± 11[b]	22.2[c]
I (0.125 mg/day)	138 ± 11	65.9
XI (0.25 mg/day)	123 ± 11	76.3
XIX (0.25 mg/day)	104 ± 9	—
XXIX (0.25 mg/day)	140 ± 12	—
Melphalan (0.1 mg/day)	51 ± 8	—

[a] Intraperitoneal administration on Days 2–4. [b] 275 plaques/10^6 spleen cells. [c] Maximum release 95%.

Table VI—Effects of Sesquiterpene Lactones on Delayed Hypersensitivity in Rats

Compound (2.5 mg/kg/day) (n = 6)	Egg Albumin		Methylated Bovine Serum Albumin	
	mg Increase	% Control	mg Increase	% Control
0.05% Polysorbate 80	46.1	—	119	—
I	8.6	18.6	64	54
XI	31.2	68.0	112	94
XIX	14.9	32.0	86	72
XX	24.5	53.1	93	78

Table VII—Effects of Sesquiterpene Lactones on Reproduction

Compound (n = 8)	Fertility in CF_1 Female Mice	
	% Pregnant	Viable Fetuses per Litter
I (6 mg/kg/day)	100	11 ± 2
XI (6 mg/kg/day)	100	9 ± 3
Diethylstilbesterol	0[a]	0[a]
1% Carboxymethylcellulose	100	12 ± 3

Compound (n = 6)	Uterotropic Effects in Rats, mg increase
I (20 mg/kg/day)	63 ± 5
XI (20 mg/kg/day)	73 ± 7
XX (20 mg/kg/day)	87 ± 10
Ethynyl estradiol (10 μg/kg/day)	184 ± 9[a]
1% Carboxymethylcellulose	84 ± 8

[a] p = 0.001.

within normal control limits. No teratogenic or congenital abnormalities were noted in the viable fetuses. The sesquiterpene lactones had no estrogenic effects on immature female rats. After 3 weeks of drug administration in rats, no gastric or duodenal bleeding or ulcerogenic effects were noted. White and red blood cell counts were within normal control limits, and hematocrit values were also normal. No abnormal CNS effects were observed in any of the animals while being administered drugs. Sesquiterpene lactones at equivalent doses had no effect on liver aerobic respiration. In Tables I–VII, the number of animals per group is expressed as n; the mean of the percent of control and standard deviation is expressed as $\bar{x} \pm SD$. The significance level p was determined by the Student t test (54).

DISCUSSION

The general anti-inflammatory screen of induced edema by carrageenan demonstrated that the α-methylene-γ-lactone sesquiterpene lactone moiety and related compounds (compare I–XXIX) was required for activity. When the 11,13-methylene group was saturated (II) or otherwise masked (XI), significant activity was lost. Among the compounds studied, helenalin (I), which contains a cyclopentenone ring in addition to this essential α-methylene-γ-lactone moiety, was the most active. The β-unsubstituted cyclopentenone ring (XXIX) demonstrated minimal inhibitory activity and probably is responsible for the slight anti-inflammatory activity of II, XI, and XIV. Saturation of the 2,3-double bond resulted in the loss of this slight activity, as seen with IV, XII, and XVI, and the reduced activity of III.

The 6-hydroxy group of helenalin may play a significant role in receptor binding since esterification (as in V) or elimination of this group (as in XVII, which has a transfused lactone ring) drastically reduced anti-inflammatory activity. The 2,3-epoxy derivatives in the tenulin and isotenulin series (XIII and XV) afforded increased anti-inflammatory ac-

tivity; however, the 2,3-epoxy of helenalin (IX) did not improve the anti-inflammatory activity of helenalin. If the α-methylene-γ-lactone was converted to the dimethylamine adduct (VI) or the pyrrolidine adduct (VIII), activity was reduced. The adducts may be hydrolyzed slowly *in vivo* to give back the α-methylene-γ-lactone, which would account for the observed activity. Here again, the 2,3-epoxy derivative (VII) of the dimethylamine adduct caused no increase in activity.

The structural types of sesquiterpene lactones might affect their anti-inflammatory potency; thus, the pseudoguaianolide 2,3-dihydrohelenalin (III, 49% inhibition) is more active than the germacranolide, eupatolide (XVIII, 30% inhibition). The difference in the degree of potency (57–30%) among the germacranolides tested (XVIII–XXIV) might be due to their dissimilar conformations as well as to functional groups, *e.g.*, eupahyssopin (XX) which, in addition to the essential α-methylene-γ-lactone moiety, contains an allylic ester, an epoxy ring, and a primary hydroxyl group, any one of which may be responsible for the additional activity. The simple α-methylene-γ-lactones (XXVII and XXVIII) caused minimal anti-inflammatory activity, indicating again that there are other steric requirements for potent pharmacological activity.

The writhing reflex test demonstrated the same structural requirements as did the general anti-inflammatory screen; *i.e.*, the α-methylene-γ-lactone in the *cis*-position with relation to the central cycloheptane ring resulted in the best activity. Here again the 6-hydroxy group of the cycloheptane ring appeared to play a functional role and the β-unsubstituted cyclopentenone ring resulted in only minimal activity. Of the germacranolides tested, eupahyssopin and deoxyelephantopin again showed the best inhibitory effects. The simple α-methylene-γ-lactones possessed only minimal activity. In the chronic adjuvant arthritic screen, at a relatively low dose, the simple α-methylene-γ-lactone (XXVII) possessed the best inhibitory activity against arthritis.

Helenalin (I), which contains both the α-methylene-γ-lactone moiety and β-unsubstituted cyclopentenone ring, was very potent. The dimethylamine adduct (VI) of helenalin showed less activity, as did the 2,3-epoxy derivative (IX). In the tenulin series (XI and XIV), the β-unsubstituted cyclopentenone appeared to play a major role in inhibitory activity against arthritis. Saturation of the ring led to loss of activity (XII). The tenulin epoxy derivatives (XIII and XV) had improved activity. Of the germacranolides tested, the allylic ester-bearing deoxyelephantopin (XIV), eupahyssopin (XX), and molephantin (XXII) all were more active than the simple germacranolide, eupatolide (XVIII). Thus, the structural requirements for chronic arthritic inhibition were not as rigid as those for general anti-inflammatory activity.

The sesquiterpene lactones at 2.5 mg/kg had only marginal inhibitory effects in the pleurisy screen, with helenalin (I) having less effect than the germacranolides. As antiallergy agents, the sesquiterpene lactones were essentially inactive. The effects of these agents on the immunological system were twofold. First, the serum antibody production seemed to be elevated with agents containing the β-substituted cyclopentenone ring. Second, T lymphocyte production seemed to be depressed, with helenalin (I) having the best effects. The mitogenic effects of helenalin would explain the immunostimulant effects on B cells.

Chronic arthritis in humans has been treated with BCG vaccine, levamisole, tilorone, and various immunological fractions like transfer factor, which are immunostimulants (55, 56). Complement, T cells, and IgM of rheumatoid factor have been found in the joint synovium or pannus (57–59). The exact etiology of rheumatoid arthritis is unknown. It is believed to be related to persistent viral (60, 61), mycoplasma, or bacterial infection or to an autoimmune disease due to uncoiled IgG autoantibody formation and a deficiency of suppressor T cell function (62). Substances of T cells, *e.g.*, lymphotoxin, migration inhibition factor (MIF), and blastogenic factor, were found in the synovial fluid of patients with rheumatoid arthritis (63, 64). For these reasons, immunosuppressors, *e.g.*, azathioprine, cyclophosphamide, D-penicillamine (56), and gold (55), are used. Whether elevated T cell responses are due to the primary pathogenesis of chronic arthritis or to secondary changes in the disease state, *e.g.*, response against phagocytic products or vasoamine release, is not known. Thus, the sesquiterpene lactones offer an alternative to the current anti-inflammatory therapy. The dose required for antiarthritic activity is relatively low compared to marketed drugs. No deleterious side effects were noted in rodents with the sesquiterpene lactones at the doses employed. The exact mode of action as antiarthritic agents is being studied.

REFERENCES

(1) A. L. Oronsky, L. Triner, O. S. Steinsland, and G. G. Nahas, *Nature*, **223**, 619 (1969).

(2) A. Lorber, *Clin. Res.*, **14**, 334 (1966).

(3) M. Butler, T. Giannina, D. Cargill, D. I. Popick, and B. G. Steinitz, *Proc. Soc. Exp. Biol. Med.*, **132**, 484 (1969).

(4) D. A. Gerber, R. Guistra, and N. Cohen, *Arthritis Rheum.*, **9**, 507 (1966).

(5) D. A. Gerber, N. Cohen, and R. Guistra, *Biochem. Pharmacol.*, **16**, 115 (1967).

(6) I. H. Hall, K. H. Lee, E. C. Mar, C. O. Starnes, and T. G. Waddell, *J. Med. Chem.*, **20**, 333 (1977).

(7) K. H. Lee, I. H. Hall, E. C. Mar, C. O. Starnes, S. A. ElGebaly, T. G. Waddell, R. I. Hadgraft, C. G. Ruffner, and I. Weidner, *Science*, **196**, 533 (1977).

(8) C. H. Smith, J. Larner, A. M. Thomas, and S. M. Kupchan, *Biochim. Biophys. Acta*, **276**, 94 (1972).

(9) S. M. Kupchan, D. C. Fessler, M. A. Eakin, and T. J. Giacobbe, *Science*, **168**, 376 (1970).

(10) R. L. Hanson, H. A. Lardy, and S. M. Kupchan, *ibid.*, **168**, 378 (1970).

(11) I. H. Hall, K. H. Lee, and S. A. ElGebaly, *J. Pharm. Sci.*, **67**, 552 (1978).

(12) I. H. Hall, K. H. Lee, C. O. Starnes, S. A. ElGebaly, T. Ibuka, Y. S. Wu, T. Kimura, and K. Haruna, *ibid.*, **67**, 1235 (1978).

(13) W. S. Kan, "Pharmaceutical Botany," National Research Institute of Chinese Medicine, Taiwan, Republic of China, 1969, p. 561.

(14) K. H. Lee and T. A. Geissman, *Phytochemistry*, **9**, 403 (1970).

(15) K. H. Lee, D. C. Anuforo, E. S. Huang, and C. Piantadosi, *J. Pharm. Sci.*, **61**, 626 (1972).

(16) R. A. Lucas, S. Rovinski, R. J. Kiesel, L. Dortman, and H. B. MacPhillamy, *J. Org. Chem.*, **29**, 1549 (1964).

(17) K. H. Lee, H. C. Huang, E. S. Huang, and H. Furukawa, *J. Pharm. Sci.*, **61**, 629 (1972).

(18) K. H. Lee, C. M. Cowherd, and M. T. Walo, *ibid.*, **64**, 1572 (1975).

(19) K. H. Lee, T. Kimura, M. Okamoto, C. M. Cowherd, A. T. McPhail, and K. D. Onan, *Tetrahedron Lett.*, **14**, 1051 (1976).

(20) K. H. Lee, T. Kimura, M. Haruna, A. T. McPhail, K. D. Onan, and H. C. Huang, *Phytochemistry*, **16**, 1068 (1977).

(21) K. H. Lee, H. Furukawa, M. Kozuka, H. C. Huang, P. A. Luchan, and A. T. McPhail, *J. Chem. Soc., Chem. Commun.*, **1973**, 476.

(22) K. H. Lee, T. Ibuka, H. C. Huang, and D. L. Harris, *J. Pharm. Sci.*, **64**, 1077 (1975).

(23) A. T. McPhail, K. D. Onan, K. H. Lee, T. Ibuka, M. Kozuka, T. Shingu, and H. C. Huang, *Tetrahedron Lett.*, **1974**, 2739.

(24) K. H. Lee, T. Ibuka, A. T. McPhail, K. D. Onan, T. A. Geissman, and T. G. Waddell, *ibid.*, **1974**, 1149.

(25) K. H. Lee, H. Furukawa, and E. S. Huang, *J. Med. Chem.*, **15**, 609 (1972).

(26) K. H. Lee, S. H. Kim, H. Furukawa, and C. Piantadosi, *ibid.*, **18**, 59 (1975).

(27) T. G. Waddell, A. M. Austin, J. W. Cochran, K. G. Gerhart, I. H. Hall, and K. H. Lee, *J. Pharm. Sci.*, in press.

(28) K. H. Lee, Y. S. Wu, and I. H. Hall, *J. Med. Chem.*, **20**, 911 (1977).

(29) K. H. Lee, T. Ibuka, S. H. Kim, B. R. Vestal, and I. H. Hall, *ibid.*, **18**, 812 (1975).

(30) G. M. Ksander, J. E. McMurry, and M. Johnson, *J. Org. Chem.*, **42**, 1180 (1977).

(31) A. P. Roszkowski, W. H. Rooks, A. Tomolonis, and L. M. Miller, *J. Pharmacol. Exp. Ther.*, **179**, 114 (1971).

(32) C. A. Winter, E. A. Risley, and G. W. Nuss, *Proc. Soc. Exp. Biol. Med.*, **111**, 544 (1962).

(33) L. O. Randall and H. Baruth, *Arch. Int. Pharmacodyn Ther.*, **220**, 94 (1976).

(34) W. L. Dewey, L. S. Harris, J. E. Howes, and J. A. Nuit, *J. Pharmacol. Exp. Ther.*, **175**, 435 (1970). *Ibid.*, **179**, 652 (1971).

(35) L. C. Hendershot and J. Forsaith, *ibid.*, **125**, 237 (1959).

(36) R. Vingar, J. F. Traux, and J. L. Selph, *Eur. J. Pharmacol.*, **37**, 23 (1976).

(37) B. H. Waksman, C. M. Pearson, and J. T. Sharp, *J. Immunol.*, **85**, 403 (1960).

(38) L. F. Sancilio, *Proc. Soc. Exp. Biol. Med.*, **127**, 597 (1968).

(39) I. Mota, *Immunology*, **7**, 681 (1964).

(40) J. Goose and A. M. J. Blair, *ibid.*, **16**, 749 (1969).

(41) D. R. Buckle, N. J. Morgan, J. W. Ross, H. Smith, and B. A. Spicer, *J. Med. Chem.*, **16**, 1334 (1973).

(42) Y. Matsumura, E. M. Tan, and J. H. Vaughan, *J. Allergy Clin. Immunol.*, **58**, 387, 395 (1976).

(43) N. K. Jerne and D. A. Nordin, *Science*, **140**, 405 (1963).
(44) T. Igarashi, M. Okada, S. Kishimoto, and Y. Yamamura, *Immunology*, **28**, 37 (1975).
(45) E. M. Uyeki, R. S. Klassen, and V. Llacer, *Proc. Exp. Biol. Med.*, **132**, 1140 (1969).
(46) A. J. Crowle and C. C. Hu, *Proc. Soc. Exp. Biol.*, **127**, 190 (1968).
(47) A. J. Crowle, C. C. Hu, and A. Patruce, *J. Allergy*, **42**, 140 (1968).
(48) B. Baggett, I. H. Hall, R. G. Boelgi, K. H. Palmer, and M. Wall, *Fertil. Steril.*, **21**, 68 (1970).
(49) I. Hall, G. L. Carlson, G. S. Abernethy, and C. Piantadosi, *J. Med. Chem.*, **17**, 1253 (1974).
(50) J. G. Wilson, in "First Fertility Conference on Congenital Malformations," General Principles in Experimental Teratology, Lippincott, Philadelphia, Pa., 1961, pp. 187–194.
(51) C. W. Emmens, *Methods Horm. Res.*, **2**, 61 (1970).
(52) D. A. Brodie and B. J. Chase, *J. Gastroenterol.*, **53**, 604 (1967).
(53) S. A. Lang, B. D. Johnson, E. Cohen, A. E. Sloboda, and E. Greenblatt, *J. Med. Chem.*, **19**, 1404 (1976).
(54) G. W. Snedecor, "Statistical Methods," Iowa State College Press, Ames, Iowa, 1956.
(55) E. Arrigoni-Mantelli, "Inflammation and Anti-inflammatories," Spectrum, New York, N.Y., 1977.
(56) Y. H. Chang, *Annu. Rep. Med. Chem.*, **11**, 138 (1976).
(57) O. J. Mellbye, J. B. Natvig, T. E. Michaelson, and H. M. Hoyeraal, in "The Immunological Basis of Connective Tissue Disorders," L. G. Silvestri, Ed., North-Holland Publishing, Amsterdam, The Netherlands, 1975.
(58) P. Davies and R. J. Bonney, *Annu. Rep. Med. Chem.*, **12**, 152 (1977).
(59) E. Munthe and J. B. Natvig, *Scand. J. Immunol.*, **1**, 217 (1972).
(60) D. Hamerman, in "The Immunological Basis of Connective Tissue Disorders," L. G. Silvestri, Ed., North-Holland Publishing, Amsterdam, The Netherlands, 1975, p. 17.
(61) D. Hurwitz, N. E. Cremer, F. Quismorio, E. H. Lennette, and G. J. Friou, *J. Rheum. (Suppl.)*, **1**, 120 (1974).
(62) A. C. Allison, *Ann. Rheum. Dis.*, **32**, 283 (1973).
(63) P. Stastny, *Arthritis Rheum.*, **16**, 572 (1972).
(64) J. B. Peter, T. Konen, K. Stenepel, and C. Cardin, *ibid.*, **14**, 179 (1971).

ACKNOWLEDGMENTS

The authors acknowledge financial support from the following sources: University of North Carolina Research Council Grant VF475 awarded to I. H. Hall, NIH Grant CA-17625 and American Cancer Society Grants CH-19A and CH-19B awarded to K. H. Lee, and the Research Corporation of America grant and the American Chemical Society grant awarded to T. G. Waddell.

Simultaneous Solubilization of Steroid Hormones II: Androgens and Estrogens

B. LUNDBERG ˣ, T. LÖVGREN, and B. HEIKIUS

Received March 1, 1978, from the *Department of Biochemistry and Pharmacy, Åbo Akedemi, Porthansgatan 3, 20500 Åbo 50, Finland.* Accepted for publication October 18, 1978.

Abstract □ The simultaneous solubilization of some androgens and estrogens in aqueous polysorbate 40, tetradecyltrimethylammonium bromide, and sodium lauryl sulfate was studied. The solubilizations of estradiol and testosterone were independent of each other in all three association colloids. However, if the estrogen component was ethinyl estradiol, the solubilization was dependent on the addition order. The estrogen precipitates more readily than testosterone in polysorbate 40 and tetradecyltrimethylammonium bromide, but the opposite is true in sodium lauryl sulfate. The simultaneous solubilizations of methyltestosterone or ethisterone with the estrogens tested were different from those of testosterone. The solubilization behavior of the steroids is discussed, starting with the pseudophase model and different solubilization loci. Results indicated that the free energy change of micellar binding, ΔG_b, decreases with increased steroid polarity. The simultaneous solubilization cannot be predicted by ΔG_b but may be explained by differences in the solubilization mechanism.

Keyphrases □ Solubilization—androgens and estrogens in various association colloids □ Androgens—solubilization in various association colloids □ Estrogens—solubilization in various association colloids

The solubilization of poorly soluble drugs is of great pharmaceutical interest. The surfactants used may be important in drug bioavailability (1).

The solubilization of steroid hormones by aqueous solutions of surfactants was reviewed previously (2). More recent reports (3–7) indicated that solubilization continues to be of interest.

A recent report from this laboratory (8) dealt with the simultaneous solubilization of estrogens and C_{21}-steroids in aqueous solutions of association colloids. The poorly soluble estrogen, estradiol, solubilized independently of the C_{21}-steroids, whereas the solubilization of ethinyl estradiol was independent of corticosterone and hydrocortisone but dependent on the presence of progesterone and desoxycorticosterone (21-hydroxyprogesterone).

This report deals with the dissolution behavior of estrogens and androgens simultaneously solubilized in aqueous solutions of three association colloids chosen as representatives of nonionic, cationic, and anionic types.

EXPERIMENTAL

Materials—Purification methods and the tests of purity of the steroid hormones and the association colloids were described previously (8). The association colloids used were sodium lauryl sulfate[1], tetradecyltrimethylammonium bromide[2], and polysorbate 40[3].

Solubilization Experiments—The solubility studies were carried out as previously described (8). The procedures were: saturation of the solution of association colloid with the first steroid and quantitation of solubilized steroid, saturation with the second steroid, and, finally, UV spectroscopic quantitation of both solubilized steroids. Special notice was paid to complete equilibration of the solutions. The solubilization temperatures were 20° for tetradecyltrimethylammonium bromide and polysorbate 40 and 40° for sodium lauryl sulfate.

The UV absorbance of the steroid solutions was recorded at around

[1] Koch-Light Laboratories.
[2] K & K Laboratories.
[3] Tween 40, Atlas Chemical Industries.

0022-3549/79/0500-0542$01.00/0
© 1979, American Pharmaceutical Association

(43) N. K. Jerne and D. A. Nordin, *Science*, **140**, 405 (1963).
(44) T. Igarashi, M. Okada, S. Kishimoto, and Y. Yamamura, *Immunology*, **28**, 37 (1975).
(45) E. M. Uyeki, R. S. Klassen, and V. Llacer, *Proc. Exp. Biol. Med.*, **132**, 1140 (1969).
(46) A. J. Crowle and C. C. Hu, *Proc. Soc. Exp. Biol.*, **127**, 190 (1968).
(47) A. J. Crowle, C. C. Hu, and A. Patruce, *J. Allergy*, **42**, 140 (1968).
(48) B. Baggett, I. H. Hall, R. G. Boelgi, K. H. Palmer, and M. Wall, *Fertil. Steril.*, **21**, 68 (1970).
(49) I. Hall, G. L. Carlson, G. S. Abernethy, and C. Piantadosi, *J. Med. Chem.*, **17**, 1253 (1974).
(50) J. G. Wilson, in "First Fertility Conference on Congenital Malformations," General Principles in Experimental Teratology, Lippincott, Philadelphia, Pa., 1961, pp. 187–194.
(51) C. W. Emmens, *Methods Horm. Res.*, **2**, 61 (1970).
(52) D. A. Brodie and B. J. Chase, *J. Gastroenterol.*, **53**, 604 (1967).
(53) S. A. Lang, B. D. Johnson, E. Cohen, A. E. Sloboda, and E. Greenblatt, *J. Med. Chem.*, **19**, 1404 (1976).
(54) G. W. Snedecor, "Statistical Methods," Iowa State College Press, Ames, Iowa, 1956.
(55) E. Arrigoni-Mantelli, "Inflammation and Anti-inflammatories," Spectrum, New York, N.Y., 1977.
(56) Y. H. Chang, *Annu. Rep. Med. Chem.*, **11**, 138 (1976).
(57) O. J. Mellbye, J. B. Natvig, T. E. Michaelson, and H. M. Hoyeraal, in "The Immunological Basis of Connective Tissue Disorders," L. G. Silvestri, Ed., North-Holland Publishing, Amsterdam, The Netherlands, 1975.
(58) P. Davies and R. J. Bonney, *Annu. Rep. Med. Chem.*, **12**, 152 (1977).
(59) E. Munthe and J. B. Natvig, *Scand. J. Immunol.*, **1**, 217 (1972).
(60) D. Hamerman, in "The Immunological Basis of Connective Tissue Disorders," L. G. Silvestri, Ed., North-Holland Publishing, Amsterdam, The Netherlands, 1975, p. 17.
(61) D. Hurwitz, N. E. Cremer, F. Quismorio, E. H. Lennette, and G. J. Friou, *J. Rheum. (Suppl.)*, **1**, 120 (1974).
(62) A. C. Allison, *Ann. Rheum. Dis.*, **32**, 283 (1973).
(63) P. Stastny, *Arthritis Rheum.*, **16**, 572 (1972).
(64) J. B. Peter, T. Konen, K. Stenepel, and C. Cardin, *ibid.*, **14**, 179 (1971).

ACKNOWLEDGMENTS

The authors acknowledge financial support from the following sources: University of North Carolina Research Council Grant VF475 awarded to I. H. Hall, NIH Grant CA-17625 and American Cancer Society Grants CH-19A and CH-19B awarded to K. H. Lee, and the Research Corporation of America grant and the American Chemical Society grant awarded to T. G. Waddell.

Simultaneous Solubilization of Steroid Hormones II: Androgens and Estrogens

B. LUNDBERG ˣ, T. LÖVGREN, and B. HEIKIUS

Received March 1, 1978, from the *Department of Biochemistry and Pharmacy, Åbo Akedemi, Porthansgatan 3, 20500 Åbo 50, Finland.* Accepted for publication October 18, 1978.

Abstract □ The simultaneous solubilization of some androgens and estrogens in aqueous polysorbate 40, tetradecyltrimethylammonium bromide, and sodium lauryl sulfate was studied. The solubilizations of estradiol and testosterone were independent of each other in all three association colloids. However, if the estrogen component was ethinyl estradiol, the solubilization was dependent on the addition order. The estrogen precipitates more readily than testosterone in polysorbate 40 and tetradecyltrimethylammonium bromide, but the opposite is true in sodium lauryl sulfate. The simultaneous solubilizations of methyltestosterone or ethisterone with the estrogens tested were different from those of testosterone. The solubilization behavior of the steroids is discussed, starting with the pseudophase model and different solubilization loci. Results indicated that the free energy change of micellar binding, ΔG_b, decreases with increased steroid polarity. The simultaneous solubilization cannot be predicted by ΔG_b but may be explained by differences in the solubilization mechanism.

Keyphrases □ Solubilization—androgens and estrogens in various association colloids □ Androgens—solubilization in various association colloids □ Estrogens—solubilization in various association colloids

The solubilization of poorly soluble drugs is of great pharmaceutical interest. The surfactants used may be important in drug bioavailability (1).

The solubilization of steroid hormones by aqueous solutions of surfactants was reviewed previously (2). More recent reports (3–7) indicated that solubilization continues to be of interest.

A recent report from this laboratory (8) dealt with the simultaneous solubilization of estrogens and C_{21}-steroids in aqueous solutions of association colloids. The poorly soluble estrogen, estradiol, solubilized independently of the C_{21}-steroids, whereas the solubilization of ethinyl estradiol was independent of corticosterone and hydrocortisone but dependent on the presence of progesterone and desoxycorticosterone (21-hydroxyprogesterone).

This report deals with the dissolution behavior of estrogens and androgens simultaneously solubilized in aqueous solutions of three association colloids chosen as representatives of nonionic, cationic, and anionic types.

EXPERIMENTAL

Materials—Purification methods and the tests of purity of the steroid hormones and the association colloids were described previously (8). The association colloids used were sodium lauryl sulfate[1], tetradecyltrimethylammonium bromide[2], and polysorbate 40[3].

Solubilization Experiments—The solubility studies were carried out as previously described (8). The procedures were: saturation of the solution of association colloid with the first steroid and quantitation of solubilized steroid, saturation with the second steroid, and, finally, UV spectroscopic quantitation of both solubilized steroids. Special notice was paid to complete equilibration of the solutions. The solubilization temperatures were 20° for tetradecyltrimethylammonium bromide and polysorbate 40 and 40° for sodium lauryl sulfate.

The UV absorbance of the steroid solutions was recorded at around

[1] Koch-Light Laboratories.
[2] K & K Laboratories.
[3] Tween 40, Atlas Chemical Industries.

0022-3549/79/0500-0542$01.00/0
© 1979, American Pharmaceutical Association

Table I—Influence of the Addition Order on Solubilization Capacities of Surfactants for Hormonal Steroids

Order of Addition of Steroid		Moles of Steroid per Mole of Surfactant[a]					
		I		II		III	
First	Second	First	Second	First	Second	First	Second
Testosterone	Estradiol	0.027	0.013	0.13	0.068	0.20	0.025
Estradiol	Testosterone	0.013	0.027	0.068	0.13	0.025	0.20
Testosterone	Ethinyl estradiol	0.027	0.18	0.12	0.25	0.04	0.13
Ethinyl estradiol	Testosterone	0.063	0.027	0.078	0.024	0.065	0.18
Methyltestosterone	Ethinyl estradiol	0.046	0.18	0.13	0.25	—	—
Ethinyl estradiol	Methyltestosterone	0.18	0.046	0.27	0.12	—	—
Ethisterone	Estradiol	—	—	0.005	0.068	—	—
Estradiol	Ethisterone	—	—	0.068	0.005	—	—

[a] I = polysorbate 40, II = tetradecyltrimethylammonium bromide, and III = sodium lauryl sulfate.

280 nm for the estrogens and around 240 nm for the androgens. The molar absorptivity of the steroids in different colloid solutions was investigated. The steroids did not affect the molar absorptivity of each other.

RESULTS

The simultaneous solubilization of the estrogens estradiol and ethinyl estradiol and the androgens testosterone, methyltestosterone, and ethisterone in the three association colloids tetradecyltrimethylammonium bromide, polysorbate 40, and sodium lauryl sulfate was investigated. If excess estradiol was added to a solution saturated with testosterone, or *vice versa*, the steroids were solubilized in all three association colloids as if they had been added independently. The amount of steroids solubilized increased linearly with the concentration of association colloid.

When ethinyl estradiol was used as the estrogen component together with testosterone, the solubilization was dependent on the order of addition. If excess ethinyl estradiol was added to a saturated solution of testosterone in polysorbate 40, the two steroids solubilized independently (Fig. 1*a*). However, if the addition was done in the opposite order, the micellar solubilization of ethinyl estradiol dropped to 35% of its maximal value while testosterone was solubilized almost maximally (Fig. 1*b*). If excesses of both steroids were added at the same time, testosterone was solubilized maximally while the micellar solubility of ethinyl estradiol dropped to the same order of magnitude (~30%) as if it were added first.

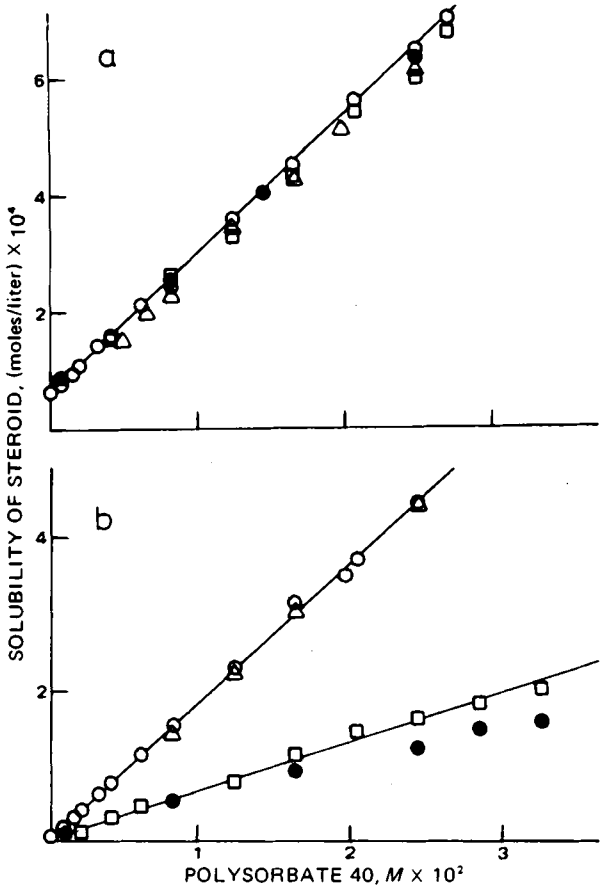

Figure 1—(a) *Solubility of testosterone in aqueous solutions of polysorbate 40. Key:* ○, *testosterone only;* △, *testosterone first and ethinyl estradiol second;* □, *ethinyl estradiol first and testosterone second; and* ●, *testosterone and ethinyl estradiol at the same time.* (b) *Solubility of ethinyl estradiol in aqueous solutions of polysorbate 40. Key:* ○, *ethinyl estradiol only;* △, *testosterone first and ethinyl estradiol second;* □, *ethinyl estradiol first and testosterone second; and* ●, *testosterone and ethinyl estradiol at the same time.*

In tetradecyltrimethylammonium bromide, 8% of the solubilized testosterone precipitated on addition of excess ethinyl estradiol which, in turn, reached 93% of its maximal saturation (Fig. 2*a*). If the saturations were done in the opposite order, 71% of the solubilized ethinyl estradiol precipitated while testosterone reached only 72% of its maximal saturation (Fig. 2*b*).

In a solution of sodium lauryl sulfate, the simultaneous solubilization of testosterone and ethinyl estradiol was strikingly different from that in polysorbate 40 and tetradecyltrimethylammonium bromide. Eighty percent of the solubilized testosterone precipitated on addition of excess ethinyl estradiol while the estrogen component solubilized maximally (Fig. 3*a*). If the saturation were carried out in the opposite direction, 50% of the ethinyl estradiol precipitated and testosterone was solubilized almost maximally (Fig. 3*b*).

Methyltestosterone showed a different solubility behavior from testosterone. In polysorbate 40, the solubilities of methyltestosterone and ethinyl estradiol were independent of each other (Fig. 4). In the opposite direction, 17% of methyltestosterone precipitated and the estrogen component reached 93% of its maximal value (Fig. 4).

Ethisterone was also studied. This androgen hormone has the lowest micellar solubility of all steroids tested. It was solubilized independently of estradiol in tetradecyltrimethylammonium bromide.

The solubilization capacities of the three surfactants for the different steroids were calculated (Table I).

DISCUSSION

Solubilization was defined as the transfer of cosolute (X) from the pure state, either crystalline (c) or liquid (l), to micelles (9). The process must be distinguished from micellar binding, which involves the transfer of cosolute from an aqueous (aq) solution into the micelle (m). The equilibrium between X_{aq} and X_m may be governed by the distribution law, or nonlinear isotherms (plot of $[X_m]$ against $[X_{aq}]$) are obtained for micellar binding (9). To determine the micellar constants from solubility measurements alone, the micellar binding has to be governed by the distribution law. If the law is obeyed, saturation solubilities may be used for determination of the partition constant K_p (9).

The linear relationship between surfactant concentration and quantity of solubilized steroid in unsaturated systems is indicative of solubility governed by the distribution law. The linearity was confirmed for a

Table II—Free Energy Change, ΔG_b, of Micellar Binding of Hormonal Steroids in Aqueous Solutions of Surfactants

Steroid	ΔG_b, J mole^{-1}		
	I[a]	II	III
Testosterone	14,322	18,217	19,285
Ethisterone	14,583	19,254	20,594
Estradiol	16,256	20,353	17,874
Ethinyl estradiol	21,258	22,263	20,452

[a] See footnote *a*, Table I.

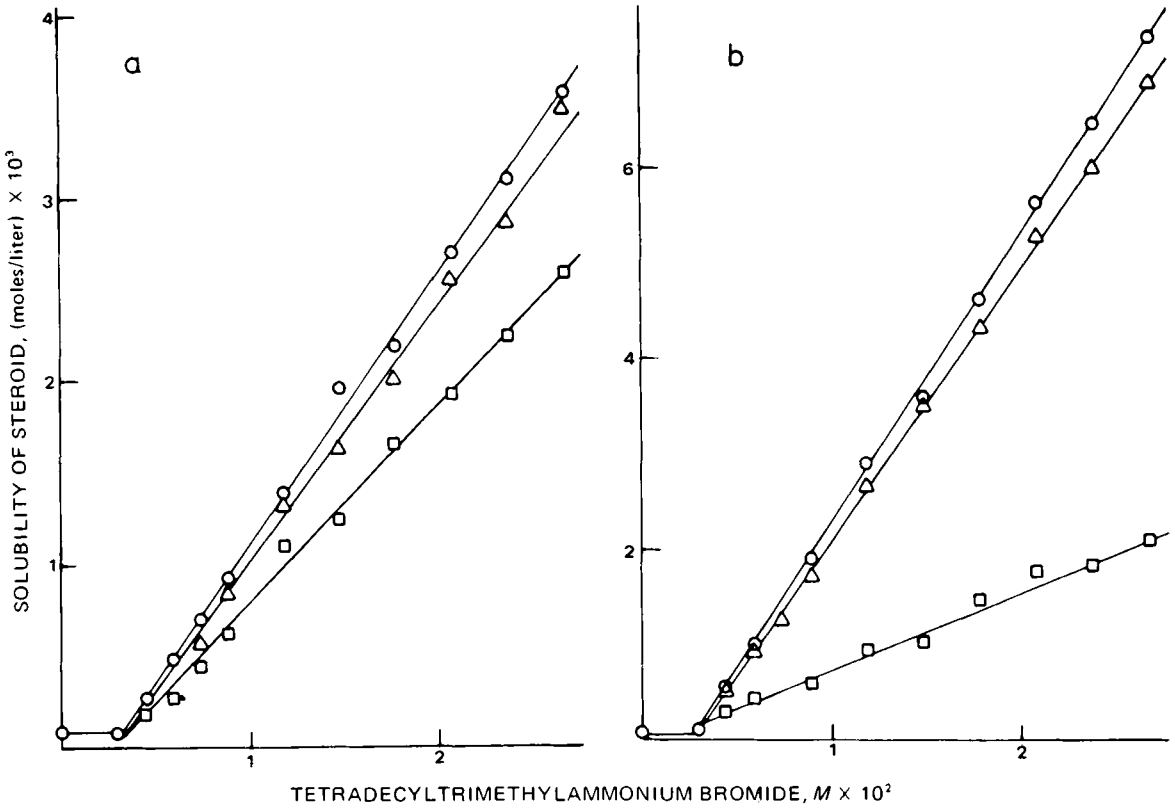

Figure 2—(a) *Solubility of testosterone in aqueous solutions of tetradecyltrimethylammonium bromide. Key:* ○, *testosterone only;* △, *testosterone first and ethinyl estradiol second; and* □ *ethinyl estradiol first and testosterone second.* (b) *Solubility of ethinyl estradiol in aqueous solutions of tetradecyltrimethylammonium bromide. Key:* ○, *ethinyl estradiol only;* △, *testosterone first and ethinyl estradiol second; and* □, *ethinyl estradiol first and testosterone second.*

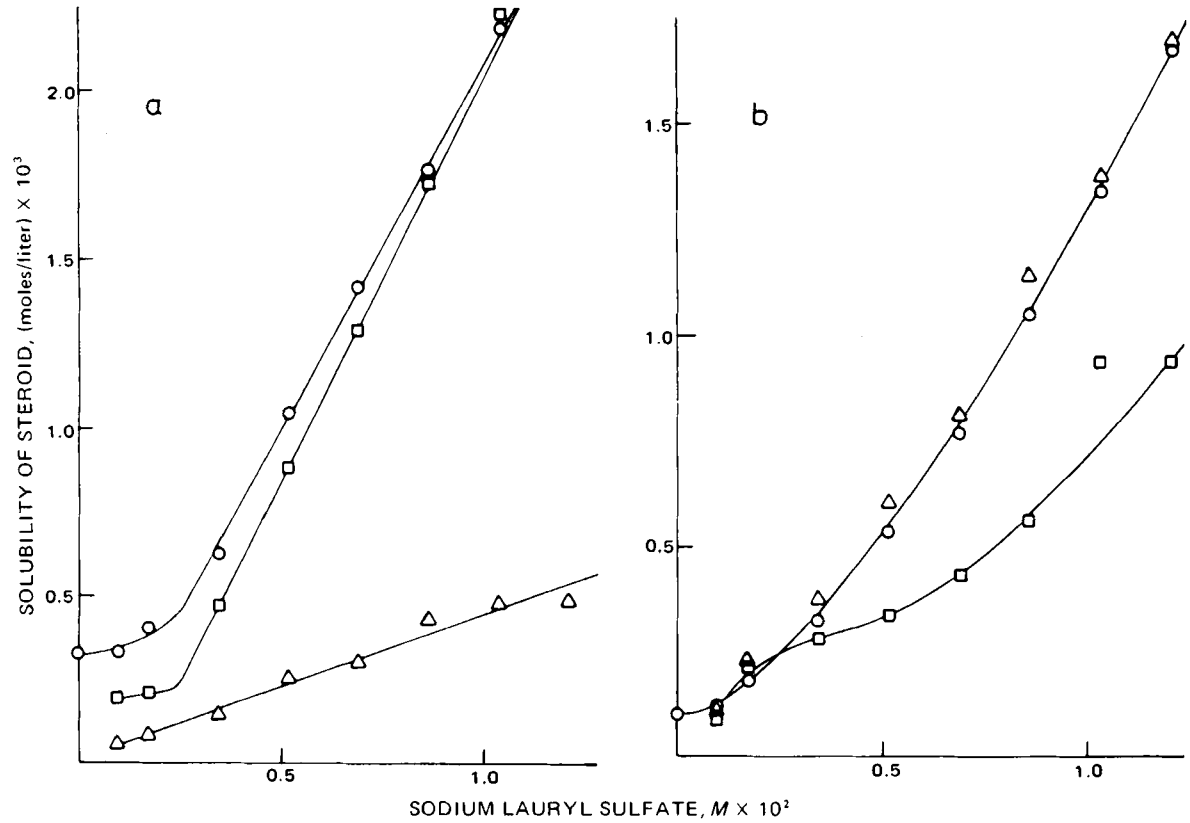

Figure 3—(a) *Solubility of testosterone in aqueous solutions of sodium lauryl sulphate. Key:* ○, *testosterone only;* △, *testosterone first and ethinyl estradiol second; and* □, *ethinyl estradiol first and testosterone second.* (b) *Solubility of ethinyl estradiol in aqueous solutions of sodium lauryl sulfate. Key:* ○, *ethinyl estradiol only;* △, *testosterone first and ethinyl estradiol second; and* □, *ethinyl estradiol first and testosterone second.*

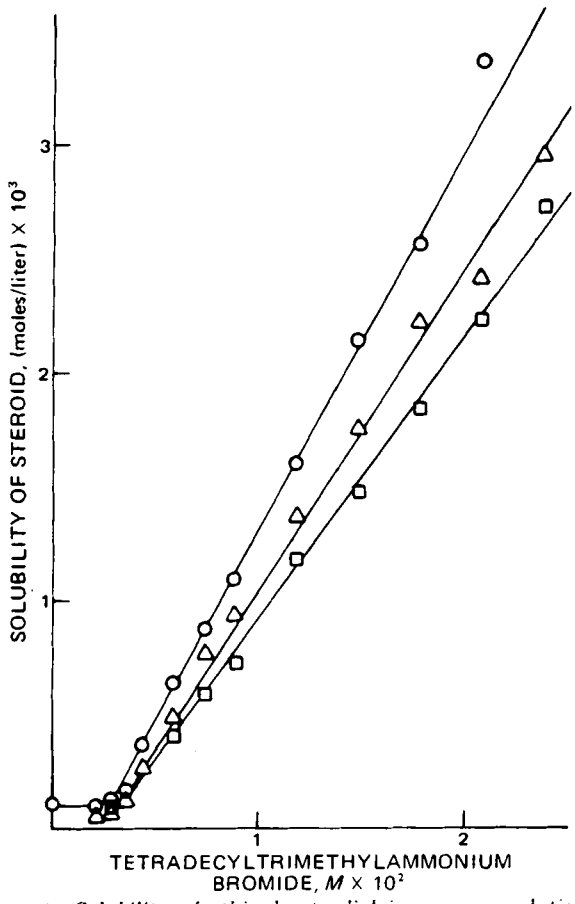

Figure 4—*Solubility of ethinyl estradiol in aqueous solutions of tetradecyltrimethylammonium bromide. Key:* ○, *methyltestosterone only;* △, *methyltestosterone first and ethinyl estradiol second; and* □, *ethinyl estradiol first and methyltestosterone second.*

number of steroids by dialysis experiments (10). Thus, the partition constant between micellar and nonmicellar steroids can be defined by (9, 11):

$$K_p = \frac{[X^s_m]}{[X^s_{aq}]} \qquad \text{(Eq. 1)}$$

where K_p is the partition constant, $[X^s_m]$ is the saturation solubility of steroid in the "micellar phase," and $[X^s_{aq}]$ is the saturation solubility of steroid in water.

Although the two-phase model is inappropriate for describing monomer–micelle equilibria, it is useful for solubilizing systems. Accordingly, Eq. 2 (9, 11) can be used to calculate the free energy change of micellar binding ΔG_b (J mole^{-1}):

$$\Delta G_b = -RT \ln K_p \qquad \text{(Eq. 2)}$$

By starting with the values of the water solubility of steroids (12) and solubilization capacities, ΔG_b values of steroids solubilized separately and simultaneously were calculated (Table II). The ΔG_b values differed considerably.

The introduction of an ethinyl group into the 17 α-position of estradiol decreased the ΔG_b value greatly while the effect on testosterone was minor. This apparent contradiction can be explained by the effect of the ethinyl group on the polarity of the steroid molecule, increasing the net dipole moment of estradiol but reducing that of testosterone (13). Thus, ΔG_b depends on the balance of hydrophilicity between the ends of the molecule, which determine the orientation of the molecules in the micelle.

These results clearly indicate that ΔG_b decreases with increased steroid polarity in contradiction to an earlier study (10). This result can be explained by different solubilization mechanisms; nonpolar species are solubilized by the hydrocarbon core while the polar ones penetrate the palisade layer of the micelle. Furthermore, the location of the cosolute in the palisade layer can be characterized as deep or short penetration (14). Presumably, the polar steroids decrease the interfacial energy by orientating themselves in the palisade layer with the polar groups at the micelle–water interface. The solubilization of nonpolar species is determined by the volume of the hydrocarbon core of the micelle (15).

The fact that testosterone and estradiol can be simultaneously solubilized independently of each other is consistent with the idea that steroids can be solubilized in different loci. Testosterone has a larger net dipole moment (13) and is likely to penetrate the palisade layer while estradiol is solubilized in the hydrocarbon core. This assumption is supported by observations indicating that testosterone is associated with the polar part of the micelle (16).

The simultaneous solubilization of steroids cannot be predicted by the free energy of micellar binding (Table II). Other factors obviously influence the behavior of the steroids in the micellar solution.

Ethinyl estradiol has a more negative ΔG_b than testosterone but is solubilized only to ~30% of its maximal value, while testosterone is solubilized maximally. This contradiction may be explained by differences in the solubilization mechanism. Both ethinyl estradiol and testosterone are rather polar and are supposed to be solubilized in the palisade layer. However, the less polar testosterone is most likely to be solubilized by deep penetration while ethinyl estradiol could be solubilized by short penetration. Thus, the solubilization loci of the two steroids partly overlap. During simultaneous solubilization, a new state of equilibrium for the micelle has to be considered. Testosterone does not precipitate in polysorbate 40 and tetradecyltrimethylammonium bromide solutions when excess ethinyl estradiol is added because testosterone is more deeply embedded in the micelle. On the other hand, ethinyl estradiol precipitates on addition of testosterone because the microenvironment of the micelle is changed in an unfavorable direction for solubilization of ethinyl estradiol.

From the present data, the enthalpy and entropy contributions to the free energy of solubilization cannot be deduced, but some hypothetical conclusions can be drawn. If the micelle is assumed to be in liquid state (17), the partial molar entropy of solubilization is given by:

$$\Delta S^\circ_s = (S_s - S_l)_{p,t} + (S_l - S_c)_{p,t} \qquad \text{(Eq. 3)}$$

where S_s, S_l, and S_c are the entropies in the solubilized, liquid, and crystalline states, respectively. The transfer from the crystalline to liquid state implies an increase in entropy, which is assumed to be almost the same for all steroids. Hence, the entropy change of the transfer from pure liquid to micelle is most important and is dependent on the type of micelle and the interaction between the surfactant and cosolute.

A similar change in enthalpy can be expected for the steroids dissolving in the micellar core. A different enthalpy change is observed for molecules solubilized at the micelle surface. This factor, in addition to the entropy change, may be important in the simultaneous solubilization of steroids.

REFERENCES

(1) S. Feldman and M. Gibaldi, *J. Pharm. Sci.*, **58**, 425 (1969).

(2) L. Sjöblom, in "Solvent Properties of Surfactant Solutions," K. Shinoda, Ed., Dekker, New York, N.Y., 1967, p. 189.

(3) K. J. Simons and C. T. Rhodes, *Pharmazie*, **26**, 623 (1971).

(4) N. H. Choulis, *ibid.*, **28**, 376 (1973).

(5) L. H. Loh, N. H. Choulis, and C. T. Rhodes, *Can. J. Pharm. Sci.*, **8**, 93 (1973).

(6) L. S. C. Wan and P. F. S. Lee, *ibid.*, **10**, 69 (1975).

(7) Y. W. Chien and H. J. Lambert, *Chem. Pharm. Bull.*, **23**, 1085 (1975).

(8) T. Lövgren, B. Heikius, B. Lundberg, and L. Sjöblom, *J. Pharm. Sci.*, **67**, 1419 (1978).

(9) P. Molyneux and C. T. Rhodes, *Kolloid-Z. Z. Polym.*, **250**, 886 (1972).

(10) B. W. Barry and D. J. D. El Eini, *J. Pharm. Pharmacol.*, **26**, 87 P (1974).

(11) K. J. Humphreys and C. T. Rhodes, *J. Pharm. Sci.*, **57**, 79 (1968).

(12) P. Kabasakalian, E. Britt, and M. D. Yudis, *ibid.*, **55**, 642 (1966).

(13) M. M. Gale and L. Saunders, *Biochim. Biophys. Acta*, **248**, 466 (1971).

(14) S. Riegelman, N. A. Allawala, M. K. Hrenoff, and L. A. Strait, *J. Colloid Sci.*, **13**, 208 (1958).

(15) B. A. Mulley, in "Advances in Pharmaceutical Sciences," H. S. Bean, A. H. Beckett, and J. E. Carless, Eds., Academic, New York, N.Y., 1964.

(16) A. L. Thakkar and N. A. Hall, *J. Pharm. Sci.*, **57**, 1394 (1968).

(17) K. Shinoda and T. Soda, *J. Phys. Chem.*, **67**, 2072 (1963).

Dynamic Dialysis in Drug–Erythrocyte Interactions

D. L. PARSONS and J. J. VALLNER ˣ

Received June 2, 1978, from the *Department of Pharmaceutics, School of Pharmacy, University of Georgia, Athens, GA 30602.* Accepted for publication October 4, 1978.

Abstract □ Application of dynamic dialysis to drug binding to erythrocytes was found to be more complex than previously described. Drug molecules located intracellularly in erythrocytes must diffuse through erythrocyte membranes before diffusing through the dialysis membrane to the external sink in dynamic dialysis. One must consider drug within the dialysis sack and within the erythrocyte and their corresponding volumes. When binding occurs in these internal compartments, different equations result for computing D_t, the total drug within the dialysis bag. With these equations and theoretically generated data, the results of "double dialysis" on the data produced in dynamic dialysis studies of drug–erythrocyte interactions were examined. The intracellular binding of drug by the erythrocyte to a single class of preexisting noninteracting sites could be misinterpreted as cooperative binding, or binding to at least two classes of sites, when the data of dynamic dialysis are treated in the Scatchard format.

Keyphrases □ Dialysis, dynamic—drug–erythrocyte interactions □ Erythrocytes—drug interactions, dynamic dialysis analysis

Dynamic dialysis (1) has been used to quantitate drug binding in whole blood and to suspended erythrocytes (2). However, due to the structure of the red blood cell, the technique of dynamic dialysis may not be quantitatively applicable to many drug–erythrocyte interactions.

BACKGROUND

The red blood cell's lipid-like membrane is perforated with positively charged aqueous channels of various diameters (3). Molecules may enter red blood cells by dissolving in the lipid phase or by passively diffusing through aqueous channels. The drug entry rate is governed primarily by the drug's lipid solubility, which is affected by drug ionization.

Drug may be bound (or adsorbed) by the erythrocyte membrane, but most drug taken up by the erythrocytes usually interacts with intracellular components, especially hemoglobin. Thus, to be bound, the drug must pass through the erythrocyte membrane and travel to the intracellular binding site(s). Drug transport is time dependent and is affected by the drug's physical properties (3). For example, a steady-state cell–medium ratio is obtained in less than 5 min for antipyrine and procainamide, 3 hr for serotonin, 7 hr for epinephrine, and >8 hr for norepinephrine. Drug may also exist in the intracellular fluid of the erythrocyte in a free form. Therefore, drug binding is more complicated in erythrocytes than in serum proteins such as albumin.

Cruze and Meyer (2), utilizing dynamic dialysis, reported that salicylate is bound by suspended erythrocytes and that the results obtained may be due to either cooperative binding or the presence of hemolysate. McArthur *et al.* (4), utilizing equilibrium dialysis, also reported salicylate to be bound by red blood cells. However, other studies (5–8) found that salicylate is not bound by red blood cells but is freely permeable to the erythrocyte membrane. Erythrocytes act as a salicylate reservoir, but the salicylate concentration inside the cell is equal to the free salicylate concentration in the plasma. These studies (5–8) suggested that salicylate within the red blood cell is in a free, diffusible form.

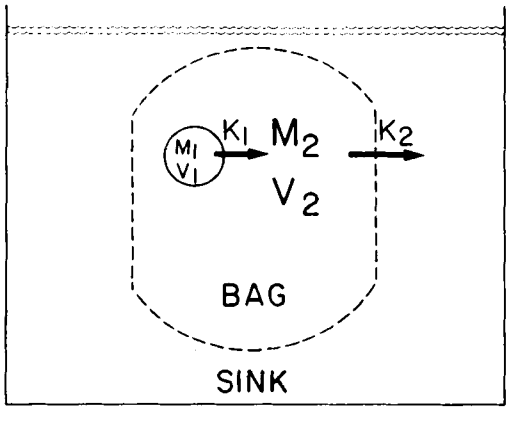

Figure 1—*Schematic representation of the double dialysis theory. For meaning of designations, see text.*

Dynamic dialysis (1) is based on the fact that ligand reversibly bound to protein within a dialysis bag is nondiffusible. The rate of loss of ligand from this compartment to an external sink of buffer is directly proportional to the concentration of unbound ligand. In the absence of protein, the movement of drug from the dialysis bag to the sink is first order and obeys:

$$-\frac{d[D_t]}{dt} = K[D_f] \qquad \text{(Eq. 1)}$$

where:

$[D_t]$ = total molar drug concentration within the dialysis bag at any time, t

K = first-order rate constant for the diffusion of drug out of the dialysis bag (hour^{-1})

$[D_f]$ = molar concentration of unbound drug within the dialysis bag at $[D_t]$

The rate constant, K, is found by dynamic dialysis in the absence of protein. In the presence of protein, the rate of loss of drug is no longer first order, and a plot of log $[D_t]$ *versus* t exhibits marked curvature. The instantaneous rate $-d[D_t]/dt$ at any particular value of $[D_t]$ may then be used, along with K, to determine $[D_f]$ using Eq. 1. In this way, a series of values of $[D_t]$ and their corresponding $[D_f]$ values may be obtained from a single dynamic dialysis experiment.

Since the drug movement across the erythrocyte membrane to its binding site(s) is not instantaneous, the incubation time of a drug–erythrocyte solution before addition of this solution to the dialysis sack may be critical in dynamic dialysis. This factor is not critical in dynamic dialysis studies of drug–albumin interactions since the actual chemical equilibrium of the binding reaction is normally reached within a fraction of a second (9, 10) and drug does not have to pass through a membrane to reach its binding sites.

A more serious potential problem is the effect of drug movement out of the erythrocyte and into the surrounding medium within the dialysis bag on the drug transport rate out of the dialysis bag into the external sink. In such a case, the drug movement out of the dialysis bag may be thought of as involving a double dialysis, *i.e.*, movement of drug out of the red blood cell to the surrounding medium followed by movement of drug through the dialysis membrane to the external sink.

Table I—Constants Used in the Double Dialysis Theory in the Presence of Intracellular Drug Binding

Figure	Curve	K_1, ml/hr	k, M^{-1}	$\frac{K_1}{K_2}$
5	K	0.375	1×10^4	0.25
	L	0.750	1×10^4	0.50
6	M	6	1×10^4	4.00
	N	150	1×10^4	100.00
	P	1,500	1×10^4	1,000.00
	Q	15,000	1×10^4	10,000.00
7	R	0.375	1×10^6	0.25
	S	0.750	1×10^6	0.50
	T	6	1×10^6	4.00
	U	150	1×10^6	100.00
	V	1,500	1×10^6	1,000.00
	W	15,000	1×10^6	10,000.00

0022-3549/79/0500-0546$01.00/0
© 1979, American Pharmaceutical Association

THEORETICAL

The double dialysis theory is represented schematically in Fig. 1. In this figure, the circle represents the erythrocytes of total volume V_1 that contain a mass of drug, M_1. Before dynamic dialysis, the drug within the red blood cells is in equilibrium with the mass of drug, M_2, outside the erythrocytes but within the dialysis bag. Drug mass M_2 is contained within volume V_2, which is equal to the total volume within the dialysis bag, V_t, minus V_1. The dotted line represents the dialysis membrane. K_2 (milliliter per hour) is the rate constant for movement of drug from V_2 to the sink, and K_1 (milliliters per hour) is the rate constant for the net movement of drug out of the erythrocyte during dynamic dialysis.

The simplest case of dynamic dialysis represented by Fig. 1 is when the drug is not bound by the erythrocyte and when, at $t = 0$, $(M_1/V_1) = (M_2/V_2)$. With the assumption that drug transport out of the red blood cell obeys Fick's law of diffusion (11), the equilibria are described by:

$$\frac{dM_1}{dt} = -K_1\left[\frac{M_1}{V_1} - \frac{M_2}{V_2}\right] \qquad \text{(Eq. 2)}$$

$$\frac{dM_2}{dt} = -\frac{K_2M_2}{V_2} + K_1\left[\frac{M_1}{V_1} - \frac{M_2}{V_2}\right] \qquad \text{(Eq. 3)}$$

where:

$$K_2 = \frac{D_eA_e}{h_e}$$

$$K_1 = \frac{D_mA_m}{h_m}$$

D_e = diffusion coefficient of the erythrocyte membrane
A_e = surface area of the erythrocyte membrane
h_e = effective thickness of the erythrocyte membrane
D_m = diffusion coefficient of the dialysis membrane
A_m = surface area of the dialysis membrane
h_m = effective thickness of the dialysis membrane

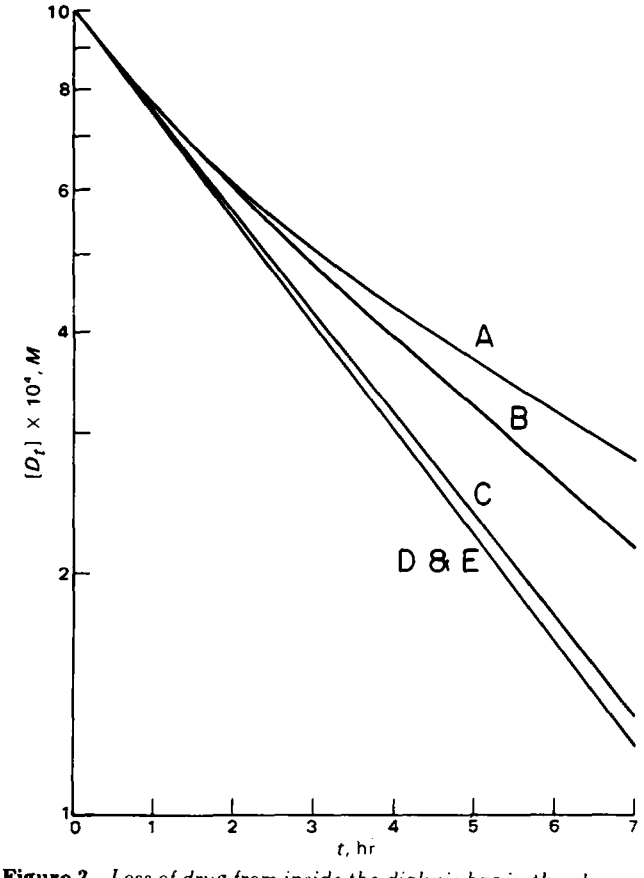

Figure 2—*Loss of drug from inside the dialysis bag in the absence of drug binding by erythrocyte. The value of* K_2 *(milliliters per hour) for each curve is: A, 0.375; B, 0.750; C, 6; and D, 150. Curve E represents drug loss in the absence of protein.*

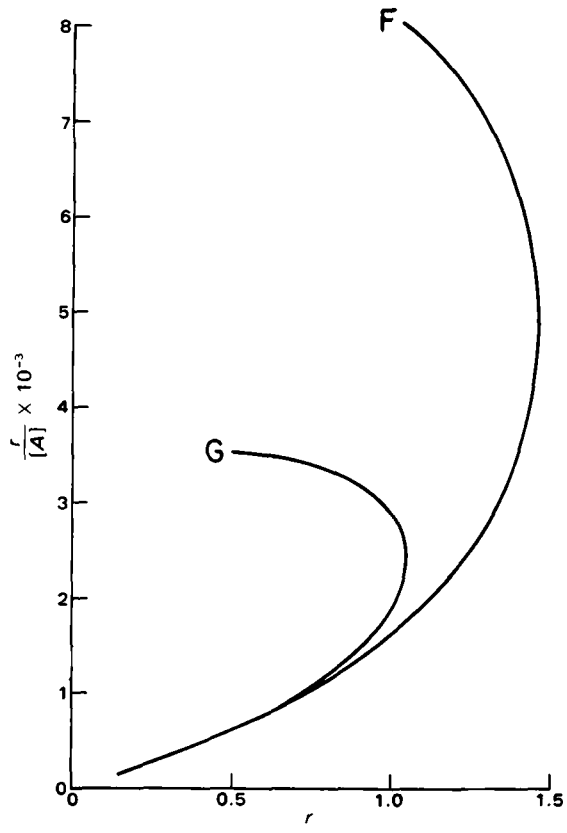

Figure 3—*Scatchard plots resulting from curves A and B of Fig. 2 using* $K = 0.3\ hr^{-1}$.

At $t = 0$, let $M_2 = (M_2)_0$ and $M_1 = (M_1)_0$. Equations 2 and 3 may be integrated to yield:

$$M_1 = \frac{(B - Aa)e^{-at} - (B - Ab)e^{-bt}}{b - a} \qquad \text{(Eq. 4)}$$

$$M_2 = \frac{(B' - A'a)e^{-at} - (B' - A'b)e^{-bt}}{b - a} \qquad \text{(Eq. 5)}$$

where:

$$a = \tfrac{1}{2}\left[\frac{K_1 + K_2}{V_2} + \frac{K_1}{V_1} + \sqrt{\left(\frac{K_1 + K_2}{V_2} + \frac{K_1}{V_1}\right)^2 - \frac{4K_1K_2}{V_1V_2}}\right]$$

$$b = \tfrac{1}{2}\left[\frac{K_1 + K_2}{V_2} + \frac{K_1}{V_1} - \sqrt{\left(\frac{K_1 + K_2}{V_2} + \frac{K_1}{V_1}\right)^2 - \frac{4K_1K_2}{V_1V_2}}\right]$$

$$A = (M_1)_0$$

$$B = (M_1)_0\left(\frac{K_1 + K_2}{V_2}\right) + \frac{(M_2)_0K_1}{V_2}$$

$$A' = (M_2)_0$$

$$B' = \frac{K_1}{V_1}[(M_1)_0 + (M_2)_0]$$

The total mass of drug within the dialysis bag, M_t, at any time t is equal to $M_1 + M_2$. Therefore, upon addition of Eqs. 4 and 5, Eq. 6 is obtained:

$$M_t = \frac{e^{-at}[B + B' - a(A + A')] - e^{-bt}[B + B' - b(A + A')]}{b - a} \qquad \text{(Eq. 6)}$$

or, in terms of concentration:

$$[D_t] = \frac{e^{-at}[B + B' - a(A + A')] - e^{-bt}[B + B' - b(A + A')]}{V_t(b - a)} \qquad \text{(Eq. 7)}$$

where $[D_t]$ is the total drug concentration within the dialysis bag. Equation 7 may be used to generate theoretical data that would result

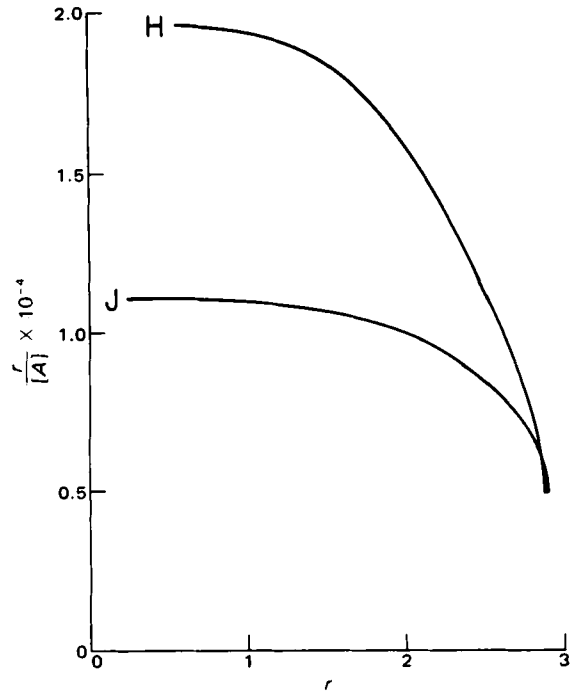

Figure 4—*Scatchard plots resulting from curves A and B of Fig. 2 using corrected* K *of 0.516 hr*$^{-1}$.

from the situation represented by Fig. 1 in the absence of drug binding by erythrocytes.

The drug may be bound by the intracellular components of the erythrocyte. Reversible binding of a ligand by a macromolecule is described by (12):

$$r = \sum_{i=1}^{m} \frac{n_i k_i [A]}{1 + k_i [A]} \qquad \text{(Eq. 8)}$$

where:

- r = mole of ligand bound per total mole of macromolecule in the system
- n_i = number of binding sites in the ith class of sites
- k_i = intrinsic association constant for the binding of drug to the ith class of sites
- $[A]$ = molar concentration of unbound ligand

This equation holds for a macromolecule that only contains noninteracting classes of preexisting binding sites. In the present case of drug binding to intracellular components of erythrocytes, Eq. 8 may be restated as:

$$\frac{M_b}{P} = \sum_{i=1}^{m} \frac{n_i k_i \frac{M_1}{V_1}}{1 + k_i \frac{M_1}{V_1}} \qquad \text{(Eq. 9)}$$

where:

- M_b = moles of drug bound by intracellular components of erythrocytes
- P = moles of macromolecule in the system
- M_1 = moles of drug within the erythrocyte in the free, diffusible form

Equation 9 may be rearranged to obtain:

$$M_b = \sum_{i=1}^{m} \frac{n_i k_i M_1 P}{V_1 + k_i M_1} \qquad \text{(Eq. 10)}$$

When drug is bound by the intracellular components of the red blood cells, the total mass of drug within the dialysis bag, M_t, at any time t is equal to $M_1 + M_2 + M_b$. Therefore, using Eq. 6:

$$M_t = \frac{e^{-at}[B + B' - a(A + A')] - e^{-bt}[B + B' - b(A + A')]}{b - a} + M_b \qquad \text{(Eq. 11)}$$

which may be stated as the following by use of Eqs. 4 and 10:

$$M_t = \frac{e^{-at}[B + B' - a(A + A')] - e^{-bt}[B + B' - b(A + A')]}{b - a} + \sum_{i=1}^{m} \frac{n_i k_i P[(B - Aa)e^{-at} - (B - bA)e^{-bt}]}{V_1(b - a) + k_i[(B - Aa)e^{-at} - (B - bA)e^{-bt}]} \qquad \text{(Eq. 12)}$$

or, in terms of concentration:

$$[D_t] = \frac{e^{-at}[B + B' - a(A + A')] - e^{-bt}[B + B' - b(A + A')]}{V_t(b - a)} + \sum_{i=1}^{m} \frac{n_i k_i P[(B - Aa)e^{-at} - (B - bA)e^{-bt}]}{V_1 V_t(b - a) + V_t k_i[(B - Aa)e^{-at} - (B - bA)e^{-bt}]} \qquad \text{(Eq. 13)}$$

Equation 13 may be used to generate theoretical data that would result from the situation represented by Fig. 1 in the presence of intracellular drug binding by erythrocytes.

To utilize Eq. 1 to find $[D_f]$ (or $[A]$ as defined herein) at the corresponding value of $[D_t]$, the instantaneous slope $d[D_t]/dt$ must be found. In the theoretical work, this instantaneous slope is found by differentiation of the applicable equation used to generate the data. Thus, for the data of Eq. 7:

$$\frac{d[D_t]}{dt} = \frac{-a[B + B' - a(A + A')]e^{-at} + b[B + B' - b(A + A')]e^{-bt}}{V_t(b - a)} \qquad \text{(Eq. 14)}$$

and for the data of Eq. 13:

$$\frac{d[D_t]}{dt} = \frac{-a[B + B' - a(A + A')]e^{-at} + b[B + B' - b(A + A')]e^{-bt}}{V_t(b - a)} + \sum_{i=1}^{m} \frac{n_i k_i P V_1 V_t (b - a)[b(B - Ab)e^{-bt} - a(B - Aa)e^{-at}]}{[V_1 V_t(b - a) + V_t k_i[(B - Aa)e^{-at} - (B - Ab)e^{-bt}]]^2} \qquad \text{(Eq. 15)}$$

THE MODEL

By using Eq. 7 and by choosing values for its constants, the effect of K_1 on the drug diffusion rate out of the bag could be examined theoretically. In this simple model, the total volume within the dialysis bag was 5 ml. The erythrocyte concentration used was the same concentration normally found in blood (2). Assumption of a 46% hematocrit with 9% extracellular fluid in the packed red blood cell mass (3) gives:

$$V_1 = 5 \text{ ml}[46\% - (9\%)(46\%)] = 2.093 \text{ ml} \qquad \text{(Eq. 16)}$$

$$V_2 = V_t - V_1 = 2.907 \text{ ml} \qquad \text{(Eq. 17)}$$

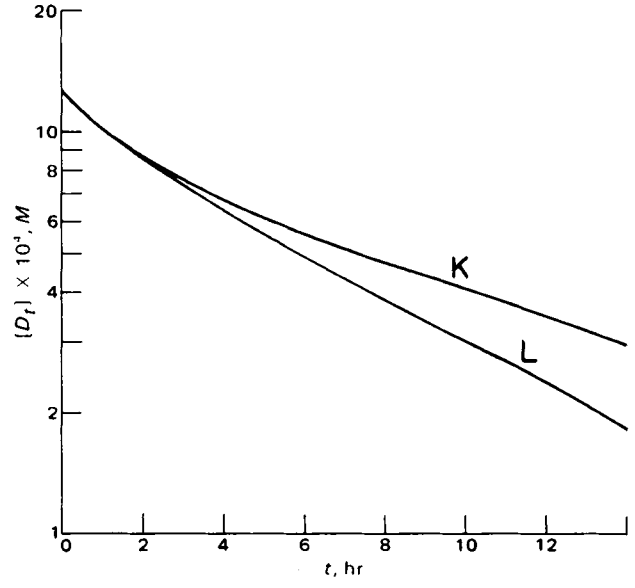

Figure 5—*Loss of drug from inside the dialysis bag in the presence of drug binding by intracellular components of the erythrocyte. See Table I for constants used in generation of individual curves.*

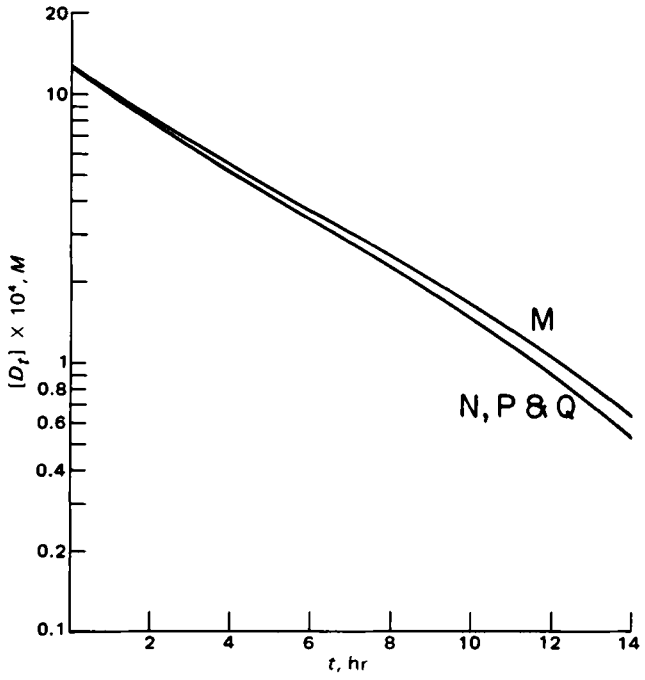

Figure 6—*Loss of drug from inside the dialysis bag in the presence of drug binding by intracellular components of the erythrocyte. See Table I for constants used in generation of individual curves.*

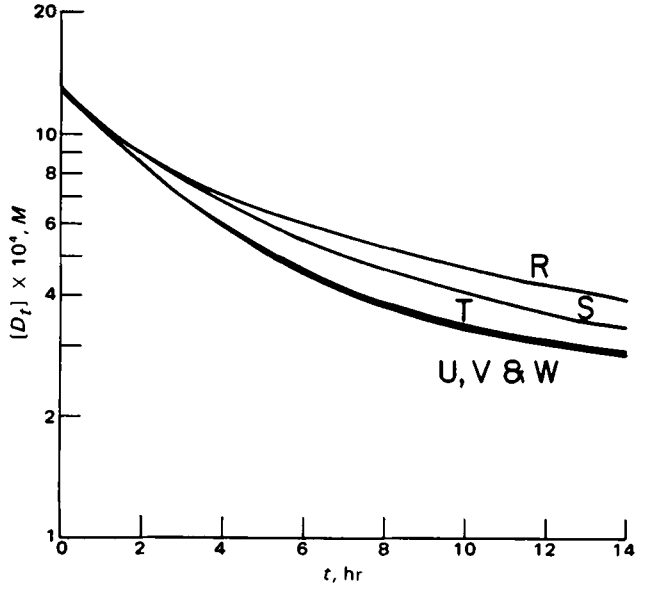

Figure 7—*Loss of drug from inside the dialysis bag in the presence of drug binding by intracellular components of the erythrocyte. See Table I for constants used in generation of individual curves.*

Also, $K = 0.3\ hr^{-1}$ and $[D_t]_0 = 1 \times 10^{-3}\ M$. Therefore, the following values resulted: $K_2 = 1.5$ ml/hr, $(M_1)_0 = 2.093 \times 10^{-6}$ mole, and $(M_2)_0 = 2.907 \times 10^{-6}$ mole.

By using these constants and Eq. 7, the value of $[D_t]$ at any value of t could be found at various values of K_1 in the absence of drug binding by erythrocytes.

By using Eq. 13 and the constants already given, the value of $[D_t]$ at any value of t could be found at various values of k_i and K_1 in the presence of drug binding by intracellular components of erythrocytes. For the construction of Scatchard plots, a 1% concentration of protein of 69,000 molecular weight was assumed, as was done by Cruze and Meyer[1] (2). A different method of constructing Scatchard plots of drug–erythrocyte interactions was proposed recently (13). A single class of sites of $n = 2$ was assumed also.

RESULTS AND DISCUSSION

Figure 2 was obtained using Eq. 7 for the double dialysis in the absence of drug binding by erythrocytes. This figure shows that as drug is "held" in a free state by the erythrocyte, the lower values of K_1 result in slower drug loss from the dialysis bag. This presentation gives the false appearance of drug–erythrocyte binding. This false appearance of binding decreases as K_1 increases and is not visible at $K_1 = 150$ ml/hr where curve D cannot be distinguished from the line obtained for drug loss from the dialysis bag in the absence of protein (curve E). As the ratio of K_1 to K_2 increases, the false appearance of binding decreases.

Scatchard plots of the data obtained using $K_1 = 0.375$ ml/hr and $K_1 = 0.750$ ml/hr indicative of this false binding situation (using Eqs. 1 and 14) are presented as curves F and G, respectively, of Fig. 3. Such unusual Scatchard plots probably result since no binding is occurring. In addition, the value of K of $0.3\ hr^{-1}$ found in the absence of protein in the bag may be adding to the unusual appearance. This value of K, if corrected for the decrease in V_2 that occurs as a result of the presence of erythrocytes, is:

$$\text{corrected } K = \frac{K_2}{V_2} = 0.51600\ hr^{-1} \qquad \text{(Eq. 18)}$$

and, when substituted for the uncorrected K in Eq. 1, results in the Scatchard plots of Fig. 4. Curves H and J are obtained for $K_1 = 0.375$ and 0.750 ml/hr, respectively. These Scatchard plots also have an unusual appearance and could be misinterpreted as resulting from a drug–erythrocyte interaction even though no direct interaction is occurring.

Figures 5–7 show drug loss from inside the dialysis bag in the presence of drug binding by intracellular erythrocyte components. The data were obtained using Eq. 13 for drug binding by erythrocytes. The constants listed in Table I were used to generate the figures.

Curve K of Fig. 5 and the curves of Fig. 7 all have the decreasing slope characteristic of drug–protein interactions. However, curve L of Fig. 5 and the curves of Fig. 6 exhibit first a decreasing and then an increasing slope, similar to those obtained from the dynamic dialysis of both salicylate and sulfathiazole in the presence of either bovine whole blood or suspended erythrocytes (2). These theoretical curves were obtained at a moderate binding strength ($k = 1 \times 10^4\ M^{-1}$) and at all but the lowest K_1 to K_2 ratio. There is only a small change in the curves obtained using a K_1 to K_2 ratio of 4 or 10,000 (Fig. 6). In the case of drug binding by in-

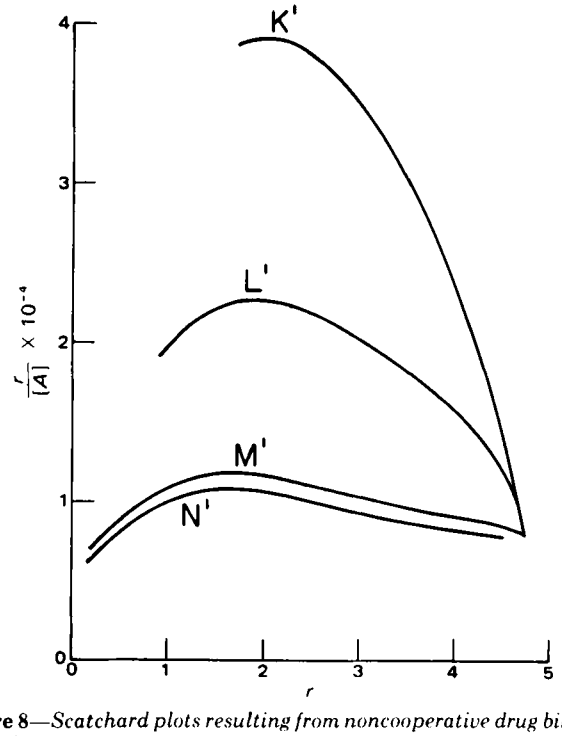

Figure 8—*Scatchard plots resulting from noncooperative drug binding by erythrocyte.*

[1] M. C. Meyer, College of Pharmacy, University of Tennessee Center for the Health Sciences, Memphis, Tenn., personal communication, Oct. 28, 1977.

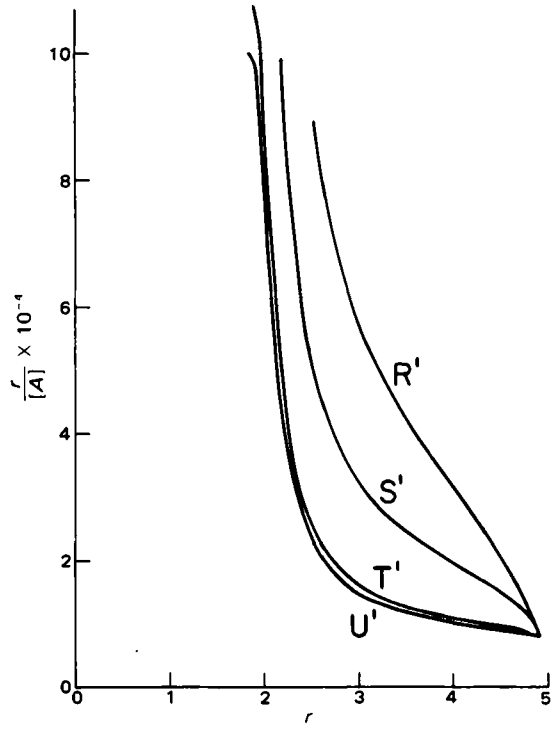

Figure 9—*Scatchard plots resulting from drug binding by a single class of sites on the erythrocyte.*

tracellular erythrocyte components, even at a K_1 to K_2 ratio of 10,000, the double dialysis theory is important, and ignoring it may result in a misinterpretation of dynamic dialysis results. Although the value of K_2 used to obtain these figures may be somewhat low, the results would be similar at higher values of K_2 with the same K_1 to K_2 ratios. In the presence of binding, identical drug escape curves (Figs. 6 and 7) were obtained for all values of the K_1 to K_2 ratio greater than 150.

The Scatchard plots shown in Figs. 8 and 9 were obtained for the data shown in Figs. 5–7. Each Scatchard plot is denoted by the prime of the letter used to identify the curve for drug loss from the dialysis bag. The

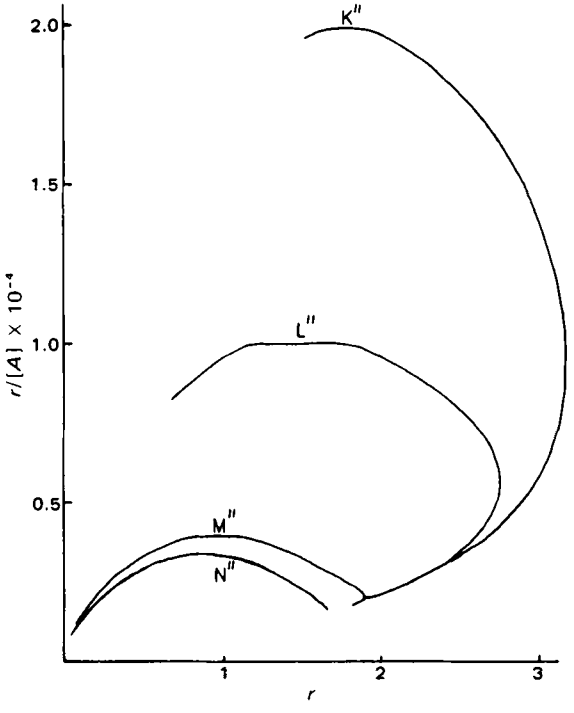

Figure 10—*Scatchard plots resulting from Figs. 5 and 6 using* K = *0.3* hr^{-1}.

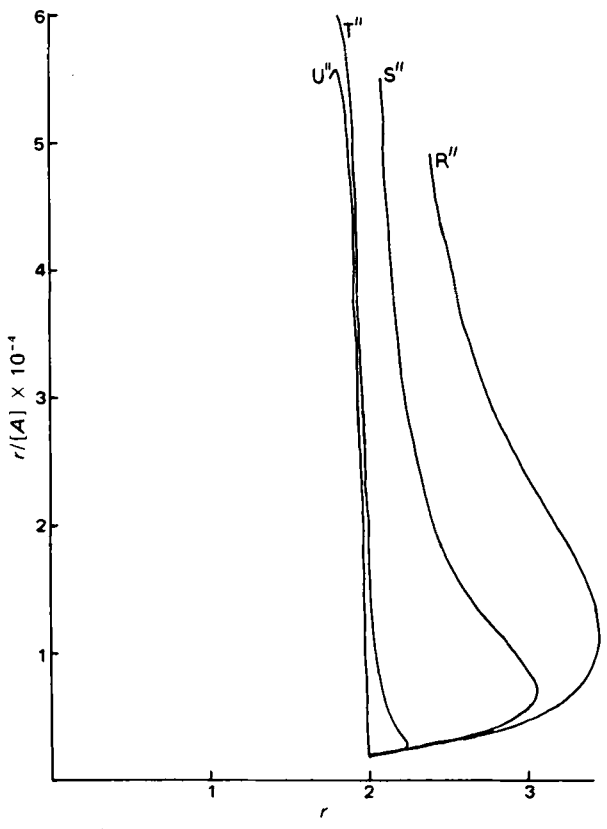

Figure 11—*Scatchard plot resulting from Fig. 7 using* K = *0.3* hr^{-1}.

Scatchard plots were obtained using Eqs. 13 and 1 with the corrected value of K.

The Scatchard plots of Fig. 8 show how the noncooperative drug binding by intracellular erythrocyte components could be misinterpreted as a cooperative drug–erythrocyte interaction. Again, this occurs even at a K_1 to K_2 ratio of 100.

The Scatchard plots of Fig. 9 could also be misinterpreted as a result of ignoring the double dialysis. These curves, especially T′ and U′ obtained at the higher ratios of K_1 to K_2, could be misinterpreted as the interaction of drug with two classes of erythrocyte binding sites. This misinterpretation would be even more likely since the corresponding curves for drug loss from the dialysis bag (Fig. 7) have the constantly decreasing slope that normally results from a drug–protein interaction.

Scatchard plots obtained for the data shown in Figs. 5–7 using the uncorrected K value of 0.3 hr^{-1} in Eq. 1 are shown in Figs. 10 and 11. Each Scatchard plot is denoted by the double prime of the letter used to identify the curve for drug loss from the dialysis bag. The curves may be misinterpreted as being cooperative at $k = 1 \times 10^4$ or as linear but with a slope unequal to $-k$ at $k = 1 \times 10^6$.

Dynamic dialysis studies of drug–erythrocyte interactions could be misinterpreted if double dialysis is ignored. Therefore, such quantitative analysis of drug–erythrocyte interactions should be conducted carefully and compared to results from another experimental method. Equation 15 could be used to interpret correctly the interaction of drug and erythrocytes by dynamic dialysis. However, with the availability of less complex experimental methods such as equilibrium dialysis, the use of dynamic dialysis may prove less than satisfactory. One problem that immediately surfaces with dynamic dialysis is deciding whether a plot of drug loss from the dialysis bag that has a constantly decreasing slope is due to the double dialysis effect alone (Fig. 2) or to drug binding in addition to the double dialysis effect (Fig. 7). Again, equilibrium dialysis should be able to distinguish between these two effects, although this method is not totally free of technical difficulties.

Erythrocytes may be important reservoirs for some drugs without the drug being bound. The drug may exist within the erythrocyte in a free, diffusible form. Thus, no true drug–protein interaction occurs. At equilibrium, the drug concentration within the erythrocyte would be equal to the free drug concentration in the extracellular fluid. Such an entrapment of drug may have the same effect as drug binding by plasma

proteins. These results show that entrapment of drug could resemble a drug–protein interaction at a sufficiently low ratio of K_1 to K_2. This results from the decrease in drug available for diffusion from V_2 to the external sink. At low values of the K_1 to K_2 ratio, as drug is removed from V_2, it is not immediately replaced by drug from within the erythrocytes; the end result is the same as if the drug had actually been bound by the erythrocyte.

Dynamic dialysis may be a useful method for the study of drug entrapment since equilibrium methods cannot be used to determine transport rate constants of drug out of erythrocytes. However, it is important not to confuse drug entrapment by erythrocytes with true drug–erythrocyte complexation.

REFERENCES

(1) M. C. Meyer and D. E. Guttman, *J. Pharm. Sci.*, **57**, 1627 (1968).

(2) C. A. Cruze and M. C. Meyer, *ibid.*, **65**, 33 (1976).

(3) L. S. Schanker, P. A. Nafpliotis, and J. M. Johnson, *J. Pharmacol. Exp. Ther.*, **133**, 325 (1961).

(4) J. N. McArthur, P. D. Dawkins, and M. J. H. Smith, *J. Pharm. Pharmacol.*, **23**, 32 (1971).

(5) D. Lester, G. Lolli, and L. A. Greenberg, *J. Pharmacol. Exp. Ther.*, **87**, 329 (1946).

(6) P. K. Smith, H. L. Gleason, C. G. Stoll, and S. Ogorzalek, *ibid.*, **87**, 237 (1946).

(7) M. H. Bickel, *J. Pharm. Pharmacol.*, **27**, 733 (1975).

(8) R. C. Baselt and C. B. Stewart, *Res. Commun. Chem. Pathol. Pharmacol.*, **15**, 351 (1976).

(9) S. P. Colowick and F. W. Womack, *J. Biol. Chem.*, **244**, 774 (1969).

(10) H. Sund, in "New Techniques in Amino Acid, Peptide, and Protein Analysis," A. Niederwieser and G. Pataki, Eds., Ann Arbor Science Publishers, Ann Arbor, Mich., 1971, pp. 405–411.

(11) J. G. Wagner, "Biopharmaceutics and Relevant Pharmacokinetics," Drug Intelligence, Hamilton, Ill., 1971, p. 268.

(12) M. C. Meyer and D. E. Guttman, *J. Pharm. Sci.*, **57**, 895 (1968).

(13) D. L. Parsons and J. J. Vallner, *ibid.*, **67**, 1344 (1978).

ACKNOWLEDGMENTS

Presented at the APhA Academy of Pharmaceutical Sciences, Montreal meeting, May 1978.

D. L. Parsons thanks the American Foundation for Pharmaceutical Education for support. The authors express sincere thanks to Ms. J. Cole for her help in manuscript preparation.

High-Performance Liquid Chromatographic Separation and Identification of Epimeric 17-Ketone Impurities in Commercial Sample of Dexamethasone Sodium Phosphate

ERIC C. JUENGE ˣ **and JAMES F. BROWER**

Received July 12, 1978, from the *National Center for Drug Analysis, Food and Drug Administration, St. Louis, MO 63101.* Accepted for publication October 3, 1978.

Abstract □ A commercial sample of dexamethasone sodium phosphate solution for injection was found to contain 56% of the label concentration and to be extensively contaminated (~50%) with a white insoluble solid, which was identified as a mixture of the 16α- and 16β-methyl epimers of 9-fluoro-11β-hydroxy-16-methylandrosta-1,4-diene-3,17-dione. High-performance liquid chromatography (HPLC) was used to separate, identify, and quantitate these epimers and to determine their presence in commercial samples. One epimer was identified by HPLC comparison with a synthesized specimen of 9-fluoro-11β-hydroxy-16α-methylandrosta-1,4-diene-3,17-dione. The second peak was identified as the 16β-epimer by epimerization of the synthesized α-component with alkali to obtain a product whose chromatogram matched that of the impurity. These conclusions are supported by data obtained by IR and UV spectrophotometry, TLC, and the blue tetrazolium test.

Keyphrases □ Dexamethasone sodium phosphate—analysis, high-performance liquid chromatography, identification of impurities in a commercial sample, epimerization □ High-performance liquid chromatography—analysis of dexamethasone sodium phosphate and impurities in a commercial sample □ Epimerization—dexamethasone sodium phosphate in a commercial solution

Drug samples contain various impurities: drug intermediates, by-products, and degradation products introduced during manufacture, packaging, or storage, as well as products of the interaction of such substances with excipients in the sample or with the drug itself. These impurities constitute physiological and mechanical hazards. For example, during degradation, the structure of the compound may retain active or modified active centers that, through structural relationship to the intact drug, may bestow undesirable physiological activity or toxic properties on the decomposition product. An example of a physical or mechanical hazard is the presence or formation of insoluble substances during intravenous injection.

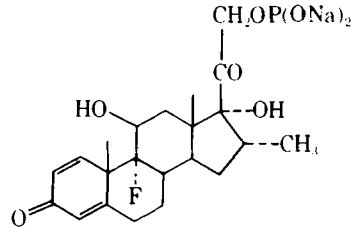

I

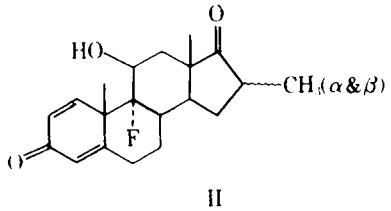

II

0022-3549/79/0500-0551$01.00/0

© 1979, American Pharmaceutical Association

proteins. These results show that entrapment of drug could resemble a drug–protein interaction at a sufficiently low ratio of K_1 to K_2. This results from the decrease in drug available for diffusion from V_2 to the external sink. At low values of the K_1 to K_2 ratio, as drug is removed from V_2, it is not immediately replaced by drug from within the erythrocytes; the end result is the same as if the drug had actually been bound by the erythrocyte.

Dynamic dialysis may be a useful method for the study of drug entrapment since equilibrium methods cannot be used to determine transport rate constants of drug out of erythrocytes. However, it is important not to confuse drug entrapment by erythrocytes with true drug–erythrocyte complexation.

REFERENCES

(1) M. C. Meyer and D. E. Guttman, *J. Pharm. Sci.*, **57**, 1627 (1968).

(2) C. A. Cruze and M. C. Meyer, *ibid.*, **65**, 33 (1976).

(3) L. S. Schanker, P. A. Nafpliotis, and J. M. Johnson, *J. Pharmacol. Exp. Ther.*, **133**, 325 (1961).

(4) J. N. McArthur, P. D. Dawkins, and M. J. H. Smith, *J. Pharm. Pharmacol.*, **23**, 32 (1971).

(5) D. Lester, G. Lolli, and L. A. Greenberg, *J. Pharmacol. Exp. Ther.*, **87**, 329 (1946).

(6) P. K. Smith, H. L. Gleason, C. G. Stoll, and S. Ogorzalek, *ibid.*, **87**, 237 (1946).

(7) M. H. Bickel, *J. Pharm. Pharmacol.*, **27**, 733 (1975).

(8) R. C. Baselt and C. B. Stewart, *Res. Commun. Chem. Pathol. Pharmacol.*, **15**, 351 (1976).

(9) S. P. Colowick and F. W. Womack, *J. Biol. Chem.*, **244**, 774 (1969).

(10) H. Sund, in "New Techniques in Amino Acid, Peptide, and Protein Analysis," A. Niederwieser and G. Pataki, Eds., Ann Arbor Science Publishers, Ann Arbor, Mich., 1971, pp. 405–411.

(11) J. G. Wagner, "Biopharmaceutics and Relevant Pharmacokinetics," Drug Intelligence, Hamilton, Ill., 1971, p. 268.

(12) M. C. Meyer and D. E. Guttman, *J. Pharm. Sci.*, **57**, 895 (1968).

(13) D. L. Parsons and J. J. Vallner, *ibid.*, **67**, 1344 (1978).

ACKNOWLEDGMENTS

Presented at the APhA Academy of Pharmaceutical Sciences, Montreal meeting, May 1978.

D. L. Parsons thanks the American Foundation for Pharmaceutical Education for support. The authors express sincere thanks to Ms. J. Cole for her help in manuscript preparation.

High-Performance Liquid Chromatographic Separation and Identification of Epimeric 17-Ketone Impurities in Commercial Sample of Dexamethasone Sodium Phosphate

ERIC C. JUENGE ˣ **and JAMES F. BROWER**

Received July 12, 1978, from the *National Center for Drug Analysis, Food and Drug Administration, St. Louis, MO 63101.* Accepted for publication October 3, 1978.

Abstract □ A commercial sample of dexamethasone sodium phosphate solution for injection was found to contain 56% of the label concentration and to be extensively contaminated (~50%) with a white insoluble solid, which was identified as a mixture of the 16α- and 16β-methyl epimers of 9-fluoro-11β-hydroxy-16-methylandrosta-1,4-diene-3,17-dione. High-performance liquid chromatography (HPLC) was used to separate, identify, and quantitate these epimers and to determine their presence in commercial samples. One epimer was identified by HPLC comparison with a synthesized specimen of 9-fluoro-11β-hydroxy-16α-methylandrosta-1,4-diene-3,17-dione. The second peak was identified as the 16β-epimer by epimerization of the synthesized α-component with alkali to obtain a product whose chromatogram matched that of the impurity. These conclusions are supported by data obtained by IR and UV spectrophotometry, TLC, and the blue tetrazolium test.

Keyphrases □ Dexamethasone sodium phosphate—analysis, high-performance liquid chromatography, identification of impurities in a commercial sample, epimerization □ High-performance liquid chromatography—analysis of dexamethasone sodium phosphate and impurities in a commercial sample □ Epimerization—dexamethasone sodium phosphate in a commercial solution

Drug samples contain various impurities: drug intermediates, by-products, and degradation products introduced during manufacture, packaging, or storage, as well as products of the interaction of such substances with excipients in the sample or with the drug itself. These impurities constitute physiological and mechanical hazards. For example, during degradation, the structure of the compound may retain active or modified active centers that, through structural relationship to the intact drug, may bestow undesirable physiological activity or toxic properties on the decomposition product. An example of a physical or mechanical hazard is the presence or formation of insoluble substances during intravenous injection.

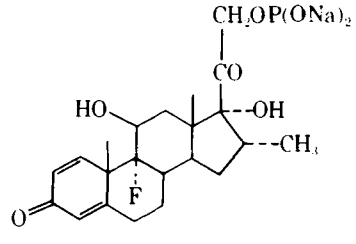

I

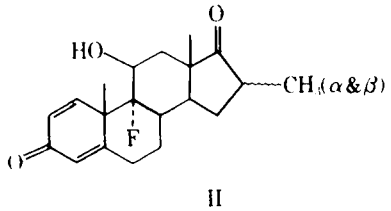

II

0022-3549/79/0500-0551$01.00/0

© 1979, American Pharmaceutical Association

A sample of dexamethasone sodium phosphate [9-fluoro-11β,17,21-trihydroxy-16α-methylpregna-1,4-diene-3,20-dione 21-(dihydrogen phosphate) disodium] (I) solution for injection was found to contain a suspended white solid. After examination by high-performance liquid chromatography (HPLC), TLC, UV and IR spectrophotometry, thermal microscopy, and reaction with blue tetrazolium, the solid was identified as a mixture of the 16α- and 16β-methyl epimers of 9-fluoro-11β-hydroxy-16-methylandrosta-1,4-diene-3,17-dione (II).

EXPERIMENTAL

Materials—Dexamethasone and dexamethasone sodium phosphate NF reference standards were used. Reagent grade chloroform, methylene chloride, methanol, acetone, hexane, squalane, sodium bicarbonate, sodium sulfite, tetrabutylammonium hydroxide, anhydrous magnesium sulfate, acetic acid, and concentrated hydrochloric acid were used as received.

Dexamethasone acetate[1] was checked by melting point and comparison of its IR spectrum with a published spectrum (1). Sodium bismuthate analytical reagent[2] (assay for $NaBiO_3$, 80.0–85.0%) was used as obtained. A reagent grade solution of sodium hydroxide[3] (50% by weight) was used for the epimerization work.

Instruments—A grating IR spectrophotometer[4] (mineral oil mulls on sodium chloride plates), a UV/near-IR spectrophotometer[5] (UV spectra obtained from solutions in methanol), and a high-performance liquid chromatograph[6] were used. All melting points were taken by thermal microscopy with a microscope[7] and a Kofler melting-point stage.

HPLC—Instrument parameters included a microparticulate, reversed-phase column[8], 3.9 mm × 30 cm; a 50% methanol–water mobile phase; and a flow rate of 2.0 ml/min. Retention times, in terms of the distance from injection to peak appearance on the chart paper in concomitant runs, were converted to capacity factors (2).

Sublimation—Sublimation was effected by placing crude material in a 0.5-ml sublimation beaker, covered with a watch glass, directly on a hot stage maintained within 230–240°.

TLC—A limited study was made with TLC strips or plates, 6–7 cm long, by upward development in an equilibrated chamber. Chromatographic sheets[9], high-performance plates[10], and reversed-phase plates[10] were used. All thin-layer materials contained a fluorescent indicator. Spots were visually located by placing the plates or strips under shortwave UV light.

Preparation of 9-Fluoro-11β-hydroxy-16α-methylandrosta-1,4-diene-3,17-dione (IIa)—Following the procedure of Rausser and Oliveto (3), 240 mg of dexamethasone was oxidized by sodium bismuthate; 140 mg of product should have been obtained (3). However, yields of only 22–30 mg were consistently obtained. The reduced yield was attributed to the insolubility of the product in the highly dilute acetic acid solution and could be improved by modifications described under *Results and Discussion*.

The synthetic 17-ketone (IIa) was dissolved in methanol and examined by HPLC. A capacity factor (2) of 8.01 was observed, and the areas of extraneous peaks in the chromatogram were estimated as being less than 1% of the area of the major component.

Epimerization of IIa to 16-Methyl Epimeric Mixture (II) Favoring β-Isomer—To 15 mg of the 17-ketone (IIa) was added 1 ml of anhydrous methanol and 0.5 ml of 50% aqueous sodium hydroxide, resulting in a pale-orange solution. The mixture was stirred at room temperature for 10 min, followed by addition of 5 ml of distilled water, which caused precipitation of a white solid. The solid (10 mg) was collected, washed three times with distilled water, and allowed to dry overnight.

The solid was subjected to thermal microscopy (2°/min), which gave sintering at 136°, initial needle formation at 222° with the entire mass laced with needles at 239°, and melting at 250–254° to an orange liquid. The material was dissolved in methanol and examined by HPLC. Capacity factors (2) of 7.96 and 8.97, which correspond to a relative retention α (2) of 1.13, were observed. The areas of extraneous peaks in the chromatogram were estimated as being less than 1% of those of the major components.

Description and Preparation of Sample—The vials contained a white precipitate in a pale-yellow solution of pH 7.2–7.3. The contents of each drug vial, 5 ml, labeled to indicate 4 mg of dexamethasone phosphate (equivalent to 4.4 mg of dexamethasone sodium phosphate)/ml, were extracted three times with a total of 20 ml of chloroform. The separated chloroform layers were combined and then washed with 10 ml of deionized water containing 1 drop of 50% NaOH, followed by a wash with 15 ml of deionized water. The chloroform was removed by evaporation under a nitrogen flush while the mixture was warmed gently on a steam bath.

The residue was dissolved in methanol for UV examination (λ_{max} 240 nm) and HPLC study (capacity factors 7.93 and 8.92, relative retention 1.12). If treatment with the dilute alkali wash was omitted, the same HPLC peaks with the same relative peak heights were obtained, but paraben (preservative) peaks also appeared. The paraben-free residue was dried over phosphorus pentoxide overnight, leaving a crude white solid, mp 249–252° dec. Observed with a melting-point stage (1°/min), rapid sublimation began at 223° and colorless needles developed from the residual solid; as these needles melted, the mass laced with needles became an orange melt. Some sintering with formation of orange spots occurred during melting.

The residue isolated from the sample was soluble in chloroform, methanol, and acetone and was insoluble in ether, hexane, water, and dilute aqueous sodium hydroxide. It was recrystallized from acetone–hexane by dissolving the material in acetone and adding hexane in small portions while boiling until turbidity developed. On cooling in an ice bath, crystals separated immediately and were collected and washed with cold hexane–acetone (3:1) to give a white solid, mp 246–250°.

A solution of the crude impurity in methanol did not reduce blue tetrazolium[11]. Therefore, the impurity contained neither free dexamethasone nor other steroidal α-ketols.

UV spectra of all materials were examined just before analysis by HPLC to assure that a maximum absorbance appeared at 240 nm. This precaution was necessary because these materials decomposed under certain conditions; a methanolic solution of the drug impurity exhibited maximum absorbance at 253 nm after storage in a clear glass container for about 1 month.

RESULTS AND DISCUSSION

The synthesized α-epimer (IIa), the synthesized epimeric mixture (II), and the impurity from the sample gave spectra that, in the IR carbonyl region (1600–1800 cm^{-1}) and UV region (λ_{max} 240 nm), were identical. The IR spectrum of II closely matched that of the impurity; both spectra showed peaks at 1744, 1770, 1630, 1615, 1238, 1010, and 920 cm^{-1}. The IR spectrum of the α-epimer closely matched the major peaks reported for that compound by Gut (4).

Two modifications were devised to recover additional adsorbed product (α-epimer) from the spent sodium bismuthate oxidant. First, in a method similar to one used by Gut (4), the solids collected by filtration were treated with aqueous sodium sulfite and concentrated hydrochloric acid until they dissolved, and the chloroform extraction procedure was repeated on the solution. This procedure yielded an additional 160–175 mg of product. Alternatively, it was found that the solids could be dried in air and then extracted with acetone in a soxhlet apparatus. After the extract was dried with anhydrous magnesium sulfate and the acetone was removed on a steam bath, this modification yielded an additional 170–190 mg of product. The latter procedure is preferred, because it avoids any possibility of halogenation.

The batches of IIa obtained by these procedures were examined by thermal microscopy (1°/min) and gave a melting point of 244–247° [lit. (4) mp 245–249°]; practically all material passed quickly into the melt; a few crystals lingered to the higher temperature range, suggesting the occurrence of thermal epimerization. Hardly any sublimation was observed.

The 17-keto impurity was determined quantitatively by extracting a new vial of the sample injection with chloroform, evaporating the chloroform, dissolving the residue in methanol, and injecting the methanolic

[1] Schering Corp., Kenilworth, NJ 07033.
[2] Mallinckrodt Chemical Works, St. Louis, MO 63160.
[3] Taylor Chemical Co., St. Louis, MO 63144.
[4] Model 337, Perkin-Elmer Corp., Norwalk, CT 06856.
[5] Model ACTA MIV, Beckman Instruments, Fullerton, CA 92634.
[6] Model 3500B, Spectra-Physics, Santa Clara, CA 95051.
[7] Carl Zeiss, New York, NY 10018.
[8] μBondapak C_{18}, Waters Associates, Milford, MA 01757.
[9] Chromagram, silica gel 6060 and alumina 6063, Eastman Organic Chemicals Division, Eastman Kodak Co., Rochester, NY 14650.
[10] QHPF and RPF Nano/gram, Quantum Industries, Fairfield, NJ 07006.
[11] Sigma Chemical Co., St. Louis, MO 63178.

Table I—TLC of Drug Impurity, 16α-Methyl-17-ketone (IIa), Epimeric Product from 16α-Methyl-17-ketone, and Dexamethasone Acetate

Adsorbent	Solvent System[a]	R_f[b]
Silica gel	Methanol–water	0.80
	Butyl acetate	0.62
Alumina	Methanol–water	0.81
Alumina with 2% squalane[c]	Methanol–water	0.62
Reversed phase	Methanol–water	0.00
	Butyl acetate	0.92
	Acetonitrile–water	0.45
High-performance silica gel	Methanol–water	0.80

[a] Mixed solvents were used in 1:1 proportions. [b] Single values given because all compounds gave identical R_f values in each system. [c] Each plate was dipped twice in 2% squalane in *n*-pentane just before use.

solution into the chromatograph. The reference standard used was a portion of the dried residue previously isolated from a chloroform extract of three other vials and examined by IR and TLC. The amount of 17-keto impurity found was 1.4 mg/ml (corresponding to 2.2 mg of dexamethasone sodium phosphate/ml) and was calculated by use of the larger of the two peaks in the epimeric mixture. Analysis for dexamethasone sodium phosphate by the USP XIX procedure (5) gave 2.45 mg of dexamethasone sodium phosphate/ml, 56% of the stated value (4.4 mg/ml). The amount of impurity thus calculated accounts for the shortage and suggests oxidation of a dexamethasone derivative as the source of the impurity.

Primary TLC screening consistently suggested that the white, water-insoluble precipitate in the dexamethasone sodium phosphate sample was comprised of a single component and that it was dexamethasone acetate. This latter compound generated R_f values identical with those of the impurity from the sample in various systems (Table I). In most cases, aqueous methanol was used as the developing solvent since this solvent was used in HPLC. Two adsorbents, reversed-phase precoated plates[10] and squalane on alumina, were used to approximate the reversed-phase conditions provided by the high-resolution HPLC column[8]. In reference to thermal microscopy of dexamethasone acetate, Ref. 6 notes that rods develop from the residual crystals during the melting-point determination; this phenomenon also was observed in this laboratory when the melting point of the impurity was determined with a melting-point stage.

Despite these data, the IR spectrum of dexamethasone acetate was distinctly different from that of the impurity. Dexamethasone acetate displayed two sharp carbonyl peaks at 1730 and 1750 cm^{-1}, whereas the impurity showed only the peak at 1744 cm^{-1}. In addition, when a mixture of dexamethasone acetate and the impurity was examined, a depressed melting point was observed. HPLC on the reversed-phase column demonstrated that the impurity consisted of two components, which eluted as a single peak when 40% acetonitrile was used as the mobile phase but separated into two peaks when 50% methanol was employed. This result confirmed that the impurity was not dexamethasone acetate, which had a much larger capacity factor (13.80).

An attempt was made to separate the epimers by sublimation. Long, fine, single needles grew from the material up toward the watch glass. These long needles were easily separated from the remaining material and melted at 257–259°; no signs of sintering (orange coloration) before melting were noted. A smaller amount of material, including some fine short needles, mp 237–257°, collected on the watch glass.

TLC of the crude, recrystallized, and sublimed (mp 257–259°) materials on silica gel gave spots with the same R_f when the chromatogram was developed with methanol–water (1:1). HPLC demonstrated that the sublimate was still a mixture, now containing a majority of the epimer that eluted last. Recrystallization gave a product that contained approximately equal amounts of the epimers.

The integrity of the steroidal A ring in the impurity was indicated by absorption in the UV region. Both Δ^4- and $\Delta^{1,4}$-3-ketone moieties in the A ring show absorption at 240 nm (7). The observed shift of the UV wavelength of maximum absorbance in aged methanolic solutions of the impurity, stored in closed, clear glass containers, probably resulted from a photochemical transformation at the A ring of the steroid. Prednisolone acetate, for example, can undergo such photocatalyzed transformations at the $\Delta^{1,4}$-3-keto group, leading to other compounds that absorb in the UV region (8). The IR spectrum of the impurity was also similar to that obtained for steroids with A rings that contain an α,β-unsaturated carbonyl function and showed absence of bands characteristic of the $-CH_2OPO_2O-$ group found in dexamethasone phosphate or its sodium salt.

The negative blue tetrazolium reaction for steroidal α-ketols suggested that cleavage had occurred at the C_{17} position. Cleavage may result from oxidation at the C_{17} side chain, and the possible products from such a reaction—aldehydes, acids (such as etianic acids), and the 17-ketone—were discussed by Cohen in his review on dexamethasone (7). Of these candidates, the IR examination appeared to eliminate aldehydes. Furthermore, it seemed likely that the acidic compounds could be eliminated from consideration, since they would be expected to elute rapidly from the lipophilic HPLC column or to be removed in the sample preparation steps when the chloroform extracts were washed with dilute aqueous alkali. Thus, the 17-ketone was the most likely candidate.

To confirm this deduction, an independent synthesis of the 17-ketone analog of dexamethasone by the method of Rausser and Oliveto (3) was undertaken. Because only minute quantities of impurity were available, it was decided to use direct syntheses of the 16α- and 16β-methyl components of the impurity as reference standards instead of fractional crystallization, sublimation, or isolation and identification by HPLC; since the compounds were not completely resolved, the latter technique would have required careful timing during the collection of the eluted fractions.

HPLC (Fig. 1, curve 2) of the synthesized 17-ketone (IIa) gave a single peak and showed a retention time identical with that of the first peak (Fig. 1, curve 1) in the chromatogram of the impurity. This match established the first, larger peak in the chromatogram of the impurity as the one representing the α-epimer of II, since there is no reason to expect inversion or even racemization at the C_{16} position of dexamethasone after oxidation with sodium bismuthate.

An epimerization of the 16α-methyl-17-ketone (IIa) was devised to generate the epimeric 16-methyl mixture of the 17-ketone (II), and these epimers showed retention times in HPLC (Fig. 1, curve 3) that were identical with those of the two components in the impurity of the drug sample. The IR spectrum of the impurity closely matched that of the epimeric mixture of the 17-ketone obtained by alkali treatment of the 16α-methyl optical isomer. TLC consistently gave spots with the same R_f values (Table I) for the synthesized 16α-methyl isomer of the 17-ketone (IIa), the epimerized ketone (II), and the impurity, and the epimers did not separate with the chromatographic systems used.

The synthesized α-epimer showed less tendency to sublime in the mass during melting-point determination than did the impurity containing the β-epimer. The sublimed long needles growing from the impurity were higher melting and were shown by HPLC to be predominantly the β-epimer. Some sublimate, which collected on the watch glass cover of the sublimation apparatus, melted at a lower temperature but showed no change in the ratio of the HPLC peaks when compared to the original impurity and may have suffered slight decomposition during sublimation. The long needles appeared to collect at a higher temperature near the

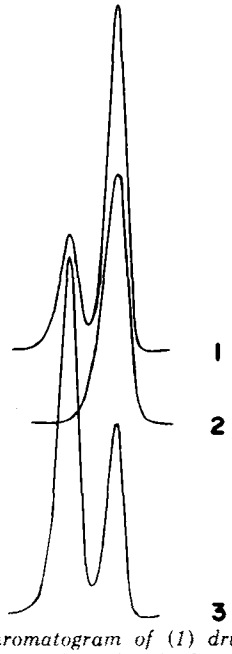

Figure 1—*Liquid chromatogram of (1) drug impurity, (2) 16α-methyl-17-ketone (IIa), and (3) epimerized 16α-methyl-17-ketone (II). Only that portion of the chromatogram showing 17-ketones is reproduced.*

hot stage by seeding directly on the material so as to favor the β-epimer.

The presence of the solid impurity was somewhat obscured by the dark glass container used to protect the injection solution from decomposition. The mechanical hazards from the presence of large amounts of an insoluble 17-ketone (II) in an injection solution are obvious. Possible adverse physiological activities, especially in larger doses, are obscure, because pharmacological studies on such impurities are limited. The situation is further complicated by the fact that the 16α- and 16β-methyl compounds (II) may show distinctly different activities.

Lodge *et al.* (9) reported that, of six manufacturers of dexamethasone for the Canadian market, five produced products containing up to 2% of the 17-ketone (II). These investigators found the same extent of contamination with the corresponding 17-oxo oxidation product in prednisone and prednisolone tablets on the Canadian market. Massive contamination (50%), as described in this report, and even lower levels could result in pronounced physiological activity caused by the presence of the 17-oxo contaminant, since patients on corticosteroid therapy may already be exposed to 0.4 mg of oxidation products daily. Some androgenic side effects of corticosteroids may be due to impurities (10).

Concerned that known unfavorable anabolic–androgenic ratios, which can occur from 17-keto or 17-hydroxy substitution, might be observed with dexamethasone, Lodge *et al.* (9) studied the anabolic and androgenic activities. They found that II had no demonstrable organ-stimulating effect; it caused a significant decrease in weight in the levator ani muscle but showed no inhibition of androgenic and anabolic activities. Their results (9) did indicate possible catabolic activity for this impurity; dexamethasone, particularly, is known to have catabolic effects (11). Drugs related to betamethasone may be expected to be subject to the same type of contamination from a 17-oxo product, consisting of, in this case, the 16β-methyl epimer (II*b*) (peak to the left in Fig. 1, curve 1). Alternatively, the same epimeric mixture obtained from the dexamethasone sodium phosphate sample would be expected when oxidation is accompanied by epimerization at the ketonic α-position.

The analysis method described here would apply in either case and possibly also in cases where cleavage occurred at a steroidal C_{17} position to generate a 17-ketone. The presence of an epimeric 17-oxo product as an impurity in dexamethasone sodium phosphate suggests that the oxidation occurred under acidic or basic conditions favorable to epimerization at the α-position of ketones. Dexamethasone itself is known to be highly sensitive to air oxidation; under basic conditions, 50% oxidation of the α-ketol side chain occurs within 6–8 min (12). This reaction and its mechanism have been studied extensively in the case of the kinetics of the base-catalyzed degradation of prednisolone (13).

In this study, the ease with which the dexamethasone degradation products could be determined by HPLC and the possible resolution provided by the reversed-phase column (14) simplified laboratory analysis. These advantages also gave a fast solution to problems encountered in the initial work by TLC, which did not separate the epimers and gave coincidental matching of R_f values with the R_f value of dexamethasone acetate during the first attempts to identify the impurity.

Significant interest has developed in the use of HPLC for analysis of epimers, *e.g.*, the determination of the 15-epimer of dinoprost in bulk drugs (15) and the assay for foreign epimeric steroidal impurities in methandrostenolone (16). In the latter case, one epimeric impurity exhibits an unfavorable anabolic–androgenic ratio; because of this serious problem, the presence of the impurity in any significant amount is undesirable and its detection is important. The use of HPLC for detection of epimers or various diastereoisomers responsible for specific undesirable physiological properties may become increasingly important in quality assurance programs.

A TLC method that distinguishes between the oxidation products was reported recently (17) (R_f values reported for the 16-methyl 17-ketones of dexamethasone and betamethasone were 0.60 and 0.59, respectively). A new quantitative TLC method, which is sensitive enough to allow determination of α to β ratios and which is useful for the analysis of large numbers of these 16-methyl-17-ketones in quality assurance programs, will shortly be reported by this laboratory.

REFERENCES

(1) "Infrared and Ultraviolet Spectra of Some Compounds of Pharmaceutical Interest," rev. ed., Association of Official Analytical Chemists, Washington, D.C., 1975, p. 128.

(2) J. J. Kirkland, "Modern Practice of Liquid Chromatography," Wiley, New York, N.Y., 1971, pp. 10, 14.

(3) R. Rausser and E. P. Oliveto, U.S. pat. 3,010,958 (1961); through *Chem. Abstr.*, **57,** 3524 (1962).

(4) M. Gut, U.S. pat. 3,529,598 (1970); through *Chem. Abstr.*, **74,** 54113 (1971).

(5) "The United States Pharmacopeia," 19th rev., Mack Publishing Co., Easton, Pa., 1975, p. 125.

(6) "Handbook of Analytical Toxicology," I. Sunshine, Ed., Chemical Rubber Co., Cleveland, Ohio, 1969, p. 428.

(7) E. M. Cohen, in "Analytical Profiles of Drug Substances," vol. 2, K. Florey, Ed., Academic, New York, N.Y., 1973, pp. 163–197.

(8) D. H. R. Barton and W. C. Taylor, *J. Chem. Soc.*, **1968,** 2500.

(9) B. A. Lodge, H. Watanabe, and L. Watts, *Can. J. Pharm. Sci.*, **10,** 107 (1975); through *Chem. Abstr.*, **84,** 26327 (1976).

(10) J. A. Vida, "Androgens and Anabolic Agents," Academic, New York, N.Y., 1969, pp. 77–91.

(11) H. E. B. Astwood and C. E. Cassidy, "Clinical Endocrinology," Greene & Stratton, New York, N.Y., 1968, p. 499.

(12) M. Pesez and J. Bartos, *Bull. Soc. Chim. Fr.*, **56,** 1928 (1962).

(13) D. E. Guttman and P. D. Meister, *J. Am. Pharm. Assoc., Sci. Ed.*, **47,** 773 (1958).

(14) "Manual No. CU 27386, Rev. B," Waters Associates, Milford, Mass., Sept. 1976.

(15) T. J. Roseman, S. S. Butler, and S. L. Douglas, *J. Pharm. Sci.*, **65,** 673 (1976).

(16) A. G. Butterfield, B. A. Lodge, N. J. Pound, and R. W. Sears, *ibid.*, **64,** 441 (1975).

(17) M. Lanquette and B. A. Lodge, *J. Chromatogr.*, **129,** 475 (1976).

ACKNOWLEDGMENTS

The authors thank Matthew L. Dow and William B. Furman for helpful suggestions, Paul Flinn for technical assistance, and John C. Black for assistance in the preparation of the figures.

High-Performance Liquid Chromatographic Analysis of Penicillin V Benzathine Oral Suspensions

MICHAEL LeBELLE, KEITH GRAHAM, and WILLIAM L. WILSON ˣ

Received June 20, 1978, from the *Drug Research Laboratories, Health Protection Branch, Health and Welfare Canada, Tunney's Pasture, Ottawa, Ontario, Canada K1A 0L2.* Accepted for publication October 6, 1978.

Abstract □ A rapid high-performance liquid chromatographic assay for penicillin V content of penicillin V benzathine bulk drug and oral suspensions is described. Dilution of the oral suspension with methanol containing 1,3,5-trimethoxybenzene as the internal standard allowed for direct analysis on a reversed-phase column with a mobile phase of 53% methanol in 0.05 *M* aqueous pH 3.5 phosphate buffer. A relative standard deviation of less than 1% was obtained on commercial formulations, and the system was linear over a range of 10–40 μg injected.

Keyphrases □ Penicillin V—analysis in penicillin V benzathine bulk drug and oral suspensions, high-performance liquid chromatography □ Penicillin V benzathine—high-performance liquid chromatographic analysis of penicillin V content in bulk drug and oral suspensions □ High-performance liquid chromatography—penicillin V analysis in penicillin V benzathine bulk drug and oral suspensions

The iodometric assay (1–3) is the official designated potency method for penicillin V benzathine drug substance and formulations (4). Normally in this method, a sample and reference standard of the same chemical species are analyzed under identical conditions. With the benzathine salt of penicillin V, however, the drug is assayed against a penicillin V acid standard. Moreover, the inactivated and blank solutions are titrated at a different pH. Under these conditions, benzathine was reported to react with iodine in the sample blank solution (5), resulting in reduced thiosulfate titers and values for the penicillin V content that are 5–10% low.

An absorptivity test is also specified in the "Code of Federal Regulations" (4) for the penicillin V benzathine bulk drug. This method is nonspecific since a known impurity, *p*-hydroxyphenoxymethylpenicillin, interferes (6).

Because of these problems, a new analytical approach was needed. High-performance liquid chromatography (HPLC) has been used for the analysis of other penicillins (7–11), and its application as a specific, rapid, and accurate assay for penicillin V benzathine products was examined.

EXPERIMENTAL

Apparatus—The liquid chromatograph was equipped with two constant-flow pumps[1], a solvent programer[2], a septumless injector[3], and a commercial 4.6-mm × 25-cm prepacked reversed-phase column[4]. A variable-wavelength spectrophotometer[5] operating at 274 nm and 0.20 aufs was used for detection. Peak areas and calculations were computed using a chromatographic data system[6].

Reagents—A low UV cutoff, distilled-in-glass grade of methanol[7] was employed. All other chemicals were reagent grade.

Chromatographic Parameters—The mobile phase, 53% methanol in phosphate buffer (v/v), was prepared by adding 53% solution of methanol in 0.05 *M* aqueous phosphoric acid to 53% methanol in 0.05 *M* sodium dihydrogen phosphate until pH 3.5 was obtained. A flow rate of 1.0 ml/min (600 psi) was employed, and injection volumes were 5 μl.

Internal Standard Solution—A stock solution of 1,3,5-trimethoxybenzene[8] (45 mg/ml) was prepared in methanol.

Standard Preparation—European Pharmacopoeia[9] (EP) reference standard phenoxymethylpenicillin CRS (labeled 100% potency) and USP phenoxymethylpenicillin reference standard[10] (labeled 98.06% potency) were dried as required before use. Penicillin V USP bulk drug powder[11] was employed as a working standard and used as received. Solutions were

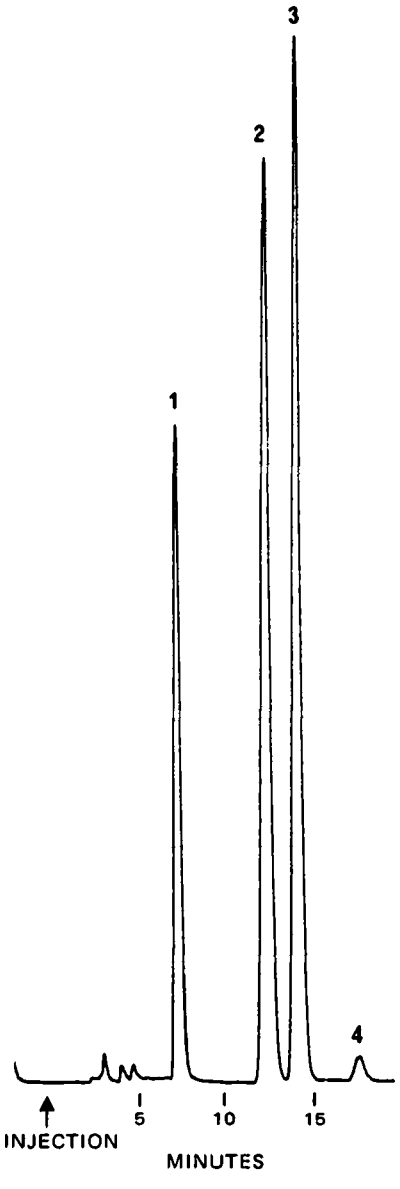

Figure 1—*HPLC analysis of a commercial penicillin V benzathine oral suspension. Key: 1, methylparaben and sodium benzoate; 2, penicillin V; 3, the internal standard; and 4, propylparaben.*

[1] Model 6000A, Waters Associates, Milford, Mass.
[2] Model 660, Waters Associates, Milford, Mass.
[3] Model U6K, Waters Associates, Milford, Mass.
[4] RP-8, 10 μm, Brownlee Laboratories, Santa Clara, Calif.
[5] Model 155-40, Altex Scientific Inc., Berkeley, Calif.
[6] SP4000, Spectra-Physics, Santa Clara, Calif.
[7] Burdick & Jackson Laboratories, Muskegon, Mich.
[8] Aldrich Chemical Co., Milwaukee, Wis.
[9] European Pharmacopoeia Commission, Strasbourg, France.
[10] Lot H2.
[11] Wyeth Ltd., Windsor, Canada.

0022-3549/79/0500-0555$01.00/0
© 1979, American Pharmaceutical Association

Table I—Retention Times of Various Common Excipients and Penicillin V Impurities

Compound	Retention Time, min
FD&C Red No. 2	2.7
FD&C Yellow No. 6	3.0
p-Hydroxyphenoxymethylpenicillin	4.9
Phenoxyacetic acid	5.6
Benzathine	6.0
Penicillin V penicilloic acid	6.4
Penicillin V penilloic acid	7.2
Sodium benzoate	7.7
Methylparaben	8.1
Penicillin G	8.3
Penicillin V	12.3
Propylparaben	16.0
Penicillin V penicillenic acid	18.2

prepared in methanol to contain 9 mg/ml of the internal standard and either 3 or 6 mg/ml of penicillin V.

Sample Preparation—*Penicillin V Benzathine Bulk Drug*—Solutions (6 mg/ml) were prepared in the same way as for the standards.

Penicillin V Benzathine Oral Suspension—Approximately 2.5 ml of suspension was weighed accurately into a 25-ml volumetric flask. Internal standard solution, 5.0 ml, and about 15 ml of methanol were added. The flasks were swirled to disperse the suspension, methanol was added to volume, and insoluble materials were allowed to settle.

RESULTS AND DISCUSSION

The EP phenoxymethylpenicillin standard, with a labeled potency of 100%, chromatographed as a single peak in this HPLC system and was used as a reference standard. Penicillin V benzathine chromatographed as two separate entities. A typical chromatogram of a commercial formulation is shown in Fig. 1. The concentration of methanol in the mobile phase was critical to achieve baseline separation between penicillin V (peak 2) and the internal standard (peak 3). The benzathine portion of the molecule was eluted prior to peak 1 but was not detected at the wavelength used. With a conventional fixed-wavelength detector (254 nm), the benzathine was visible as a broad peak eluting with a retention time of about 6 min. This type of detector may also be used.

Figure 1 shows that common formulation excipients such as methylparaben and propylparaben, sodium benzoate, and coloring agents did not interfere. Methylparaben and sodium benzoate had nearly identical retention times (peak 1). Common degradation products such as the penicillenic, penicilloic, and penilloic acids, the congener penicillin G, and the precursor phenoxyacetic acid were resolved from the penicillin V peak. Table I lists the retention times obtained for these compounds in the system described.

Both the USP and working standard penicillin V contained a small amount of an impurity with a retention time of 4.9 min. Relative to the penicillin V peak and based on relative peak areas, 1 and 3% of this product were found in the USP and working standard, respectively. This impurity was collected from HPLC using 50% methanol–water as the mobile phase, and rechromatography indicated its integrity. This material had an absorbance maximum at 287 nm, which underwent a phenolic shift in base to 303 nm, suggesting that the product was *p*-hydroxyphenoxymethylpenicillin, an impurity known to be occasionally present in penicillin V (6, 12, 13). PMR spectrometry[12] confirmed this structure.

With six solutions (2–8 mg/ml), a linear calibration curve ($r = 0.9995$) was obtained over the range tested (10–40 μg injected) with a linear regression of $y = 0.0303x + 0.005$.

The precision of the method was determined by analysis of 10 aliquots of a commercial sample of a 150-mg/5 ml penicillin V benzathine suspension. A mean assay of 24.89 mg/g of suspension and a relative standard deviation of 0.94% was obtained (Table II).

There was good agreement between the HPLC and iodometric values for both the USP and working standard penicillin V (Table III). Similarly, excellent agreement between the HPLC and official (4) absorptivity assays for penicillin V content of the penicillin V benzathine bulk drug was obtained. The iodometric assay of this product exhibited the interference previously mentioned (5).

[12] WP-80, Bruker Spectrospin Ltd., Mississauga, Canada.

Table II—Precision of HPLC Determination of Penicillin V in a Penicillin V Benzathine Oral Suspension (150 mg/5 ml)

Determination	Amount of Penicillin V[a]
1	24.93
2	24.46
3	24.76
4	24.72
5	25.13
6	25.00
7	25.01
8	25.25
9	24.80
10	24.91
Mean	24.89
RSD, %	0.94

[a] Results are expressed as milligrams of penicillin V per gram of suspension.

Table III—Analysis of Penicillin V and Penicillin V Benzathine Bulk Drug and Oral Suspension

Product	Penicillin V, %	
	HPLC	Official[a]
USP penicillin V reference standard (98.06% label claim)	98.7	97.6
Penicillin V working standard	95.9	97.8
Penicillin V benzathine bulk drug	66.0	65.9
Oral Suspension A (300 mg/5 ml)	54.7, 54.0[b]	49.0, 49.2[b]
Oral Suspension B (300 mg/5 ml)	54.2, 54.7[b]	49.8, 50.3[b]

[a] Iodometric assay except for penicillin V benzathine bulk drug which is the UV absorptivity method. [b] Results are expressed as milligrams of penicillin V per gram of suspension.

Table III also shows a comparison of the assay results using the two methods for two commercial formulations of penicillin V benzathine (300 mg/5 ml) from different manufacturers. The values listed are expressed as milligrams of penicillin V per gram of suspension. For potency determination, conversion to milligrams per dose is required and is effected by determination of the specific gravity of the suspension, because problems are encountered when pipetting such viscous preparations. The difference between the HPLC and iodometric assay values for these oral suspensions is due to the interference by the benzathine in the iodometric method (5).

The HPLC procedure can be used for the analysis of other penicillin V products and as a combined identity and purity test to control the quality of these antibiotics.

REFERENCES

(1) J. F. Alicino, *Ind. Eng. Chem. Anal. Ed.*, **18**, 619 (1946).

(2) B. Ortenblad, *Acta Chem. Scand.*, **4**, 518 (1950).

(3) P. J. Weiss, *Antibiot. Chemother.*, **9**, 660 (1959).

(4) "Code of Federal Regulations," Part 440, Title 21, 1976.

(5) M. J. LeBelle and W. L. Wilson, *J. Pharm. Sci.*, **67**, 1495 (1978).

(6) A. S. Hughes and C. R. Popplestone, *Proc. Anal. Div. Chem. Soc.*, **14**, 288 (1977).

(7) K. Tsuji and J. H. Robertson, *J. Pharm. Sci.*, **64**, 1542 (1975).

(8) J. M. Blaha, A. M. Knevel, and S. L. Hem, *ibid.*, **64**, 1384 (1975).

(9) J. M. Blaha, A. M. Knevel, D. P. Kessler, J. W. Mincy, and S. L. Hem, *ibid.*, **65**, 1165 (1976).

(10) V. Hartmann and M. Rödiger, *Chromatographia*, **9**, 266 (1976).

(11) E. R. White, M. A. Carrol, and J. E. Zarembo, *J. Antibiot.*, **30**, 811 (1977).

(12) "European Pharmacopoeia, 1971," Maisonneuve S. A., France, 1971, p. 339.

(13) "British Pharmacopoeia, 1973," Her Majesty's Stationery Office, London, England, 1973, p. 362.

ACKNOWLEDGMENTS

Presented at the APhA Academy of Pharmaceutical Sciences, Hollywood, Fla., meeting, November 1978.

Simple and Specific Electron-Capture GLC Assay for Plasma and Urine Ephedrine Concentrations following Single Doses

K. K. MIDHA ˣ, J. K. COOPER, and I. J. McGILVERAY

Received June 13, 1978, from the *Drug Research Laboratories, Health Protection Branch, Health & Welfare Canada, Ottawa, Ontario, Canada.* Accepted for publication October 18, 1978.

Abstract □ An electron-capture GLC procedure for determination of plasma ephedrine concentrations is described. The procedure is capable of determining 2 ng/ml of ephedrine and is adequate for following profiles after 25-mg single doses. Pentane extraction of the drug and the internal standard and formation of the *N*-pentafluorobenzoyl derivatives were followed by GLC. Plasma ephedrine concentrations following a 24-mg dose of ephedrine hydrochloride to a human volunteer are presented. Formation of *N*-trifluoroacetyl, *N*-pentafluoropropionyl, *N*-heptafluorobutryl, and *N*-pentafluorobenzoyl derivatives and their GLC–mass spectrometric identification are discussed together with comparative electron-capture sensitivities of these derivatives toward a nickel-63 detector. The detection of the *N*-pentafluorobenzoyl derivative of ephedrine is at least 100-fold greater in sensitivity than detection of the *N*-trifluoroacetyl derivative.

Keyphrases □ Ephedrine—electron-capture GLC analysis in human plasma and urine □ Electron-capture GLC—comparison of various fluoroacyl derivatives of ephedrine □ GLC, electron capture—analysis, ephedrine in plasma and urine

Ephedrine (I) is widely used in the treatment of asthma, either alone or in combination with theophylline and a barbiturate. Several GLC methods (1–4) are adequate for determining plasma and urine ephedrine concentrations following therapeutic doses but are not sensitive enough for single-dose pharmacokinetic and bioavailability studies.

GLC with flame ionization has been used to estimate ephedrine and its congeners in urine (1). Heptafluorobutyryl ephedrine derivatives following benzene extraction of basified serum were used for electron-capture analysis of blood levels at therapeutic dosages (2). Previously reported procedures have been insufficiently sensitive for clinical use (3, 4).

No details are available on a modification of an electron-capture GLC assay for pseudoephedrine and norpseudoephedrine, which may have the sensitivity required for single-dose bioavailability studies (5).

A simple and specific electron-capture GLC assay of ephedrine and norephedrine is described. This procedure has a 2-ng/ml sensitivity and is used routinely for assay of ephedrine bioavailability following a single dose of the drug either alone or in combination with theophylline and a barbiturate.

EXPERIMENTAL

Reagents—Glass-distilled *n*-pentane[1] and analytical grade amyl acetate[2] were employed. Pentafluorobenzoyl chloride[3], trifluoroacetic anhydride[3], heptafluorobutyric anhydride[3], pentafluoropropionic anhydride[3], and pyridine[3] were all GLC grade. *d,l*-Ephedrine hydrochloride[4], *d,l*-norephedrine hydrochloride[4], and 3,4-dimethoxyamphetamine hydrochloride[4] were donated. *d,l*-Ephedrine[5] free base, *p*-hydroxyephedrine[5], and *p*-hydroxynorephedrine[5] were purchased. All other chemicals were analytical reagent grade.

Stock solutions of I (100 μg/ml) and the internal standard 3,4-dimethoxyamphetamine (II) (100 μg/ml) were prepared weekly by dissolving their hydrochloride salts in water. Appropriate dilutions were made daily as required.

Plasma Level Study—Ephedrine hydrochloride (24 mg) was administered in a combination tablet[6], which also contained theophylline (130 mg) and phenobarbital (8 mg), to a healthy 67.6-kg male volunteer. Blood samples, 10 ml, were withdrawn from the cubital vein into heparinized tubes[7] at 10 appropriate time intervals. The blood samples were centrifuged, and the plasma was transferred to another tube before storage at −10°.

Extraction of Ephedrine—To 1 ml of plasma or 0.1 ml of urine diluted to 1 ml with distilled water, in a 15-ml glass round-bottom tube[8], were added 1 ml of aqueous solution of II (100 ng/ml) and 0.5 ml of 10 *N* NaOH. The sample was mixed[9] for 30 sec, and 7.0 ml of glass-distilled pentane[1] was added before mixing[10] for 10 min followed by centrifugation[11] (5 min at 0° at 6000 rpm). The clear organic extract was transferred by Pasteur pipet to an 8-ml polytef[12]-lined, screw-capped, round-bottom tube[13].

Pentafluorobenzoyl chloride[3], 0.1% in pentane (200 μl), was added to the extract. The tube was tightly stoppered and incubated[14] at 65° for 90 min. Then the tube was allowed to reach room temperature, and a small antibumping granule[2] was added. The sample was evaporated[14] at 65° without nitrogen until just dry.

To the dried reaction mixture, 0.5 ml of 0.1 *N* NH_4OH was added and the sample was mixed[9] for 30 sec. Amyl acetate[2] (50 μl) was added, and the sample was mixed[9] for 30 sec and centrifuged[15] for 2 min at 2500 rpm. Approximately 25 μl of the amyl acetate solution was transferred to a 1-ml disposable screw-capped vial[13]. About 2–3 μl of the sample was injected into the gas chromatograph.

GLC—The gas chromatograph[16] was equipped with a ^{63}Ni electron-capture detector. The column was a spiral glass tube[17], 0.9 m long × 2.0 mm i.d., packed with 3% phenyl cyanopropyl methyl silicone[18] coated by fluidization on acid-washed, dimethylchlorosilane-treated, 100–120-mesh, high-performance, flux-calcined diatomite support[19].

The column was conditioned at 245° for 48 hr with low nitrogen flow. For plasma analysis, the injection port, outlet, and oven temperatures were 250, 260, and 235°, respectively. Argon–methane (95:5) as a carrier gas was maintained at 93 ml/min. The ^{63}Ni detector was operated at 325° with a standing current of 3.0 namp.

For determination of the response of various ephedrine derivatives, the column was operated from 170 to 230°. The detector was operated at a standing current of 2.0 namp.

Calculations—Peak height ratios were calculated by dividing the peak height from the *N*-pentafluorobenzoyl derivative of I (1.40 min) by that of the *N*-pentafluorobenzoyl derivative of II (3.82 min). Calibration

[1] Caledon Laboratories Ltd., Georgetown, Ontario, Canada.
[2] British Drug House, Toronto, Ontario, Canada.
[3] Pierce Chemical Co., Rockford Ill.
[4] Dr. Keith Bailey, Drug Identification Division, Drug Research Laboratories, Health Protection Branch, Ottawa, Ontario, Canada.
[5] Aldrich Chemical Co., Milwaukee, Wis.
[6] Tedral, Warner-Chilcott Laboratories Co., Toronto, Ontario, Canada.
[7] Vacutainers, Becton Dickinson and Co., Mississauga, Ontario, Canada.
[8] Corex, Sorvall Inc., Newtown, Conn.
[9] Vortex Genie, Fisher Scientific Co., Montreal, Quebec, Canada.
[10] Evapo-Mix, Fisher Scientific Co., Montreal, Quebec, Canada.
[11] RC2-B centrifuge, Sorvall Inc., Newtown, Conn.
[12] Teflon, du Pont.
[13] Fisher Scientific Co., Montreal, Quebec, Canada.
[14] Thermolyne Dri-Bath, Fisher Scientific Co., Montreal, Quebec, Canada.
[15] HNS, Fisher Scientific Co., Montreal, Quebec, Canada.
[16] Model 3920, Perkin-Elmer, Montreal, Quebec, Canada.
[17] Chromatographic Specialties, Brockville, Ontario, Canada.
[18] OV-225, Chromatographic Specialties, Brockville, Ontario, Canada.
[19] Chromosorb W, Chromatographic Specialties, Brockville, Ontario, Canada.

0022-3549/79/0500-0557$01.00/0
© 1979, American Pharmaceutical Association

Table I—Electron-Capture Sensitivity and Retention Times of Ephedrine Derivatives

Derivative	Response, coulombs × 10^3/mole	Retention Time, min	Column[a] Temperature
Pentafluorobenzoyl	14.303	1.42	230°
Heptafluorobutyryl	0.971	1.04	170°
Pentafluoropropionyl	0.812	1.28	170°
Trifluoroacetyl	0.013	1.46	170°

[a] Chromatographed on OV-225.

curves were constructed by plotting the spiked control plasma peak height ratios against the concentrations of I (nanograms per milliliter of plasma).

Electron-Capture Response of Various Ephedrine Derivatives—*Stock Solution of* d,l-*Ephedrine*—A solution of *d,l*-ephedrine free base (1000 μg/ml) in glass-distilled pentane was prepared.

N-*Trifluoroacetyl,* N-*Heptafluorobutyryl, and* N-*Pentafluoropropionyl Derivatives*—To 1 ml of I stock solution (1000 μg) in an 8-ml polytef-lined, screw-capped, round-bottom tube[13] were added either 0.5 ml of trifluoroacetic anhydride[3] or 200 μl of heptafluorobutyric[3] or pentafluoropropionic anhydride[3] and 20 μl of pyridine[3]. The tubes were tightly stoppered and incubated for 60 min at 45° for trifluoroacylation or for 90 min at 65° for other derivatives. The tubes were cooled to room temperature, a small antibumping granule was added to each, and excess anhydride was removed by evaporation without nitrogen until just dry at 45° for trifluoroacetic anhydride and at 65° for other anhydrides. Then 1 ml of 1 *N* NaOH and 0.5 ml of amyl acetate[2] were added, and the contents of the tube were mixed for 5 min and centrifuged for 2 min at 2500 rpm. Appropriate dilutions of each derivative were made with amyl acetate to yield final concentrations of 13.33 ng/μl for the *N*-trifluoroacetyl derivative and 6.66 ng/μl for the other two derivatives.

N-*Pentafluorobenzoyl Derivative*—The reaction was the same as described for the other *N*-acyl derivatives. In this case, dilution of 10 μl of pentyl acetate to 15 ml yielded a final concentration of 0.67 ng/μl. Flame-ionization GLC analysis of the three undiluted reaction mixtures described previously showed that at least 95% of I was present as the corresponding *N*-monoacyl derivative.

Di-Derivatives of Ephedrine with Trifluoroacetic Anhydride, Heptafluorobutyric Anhydride, and Pentafluoropropionic Anhydride—The reactions for the di-derivatives of I were the same as described for each reagent, except that the derivative was back-extracted following the addition of 1 ml of 0.1 *N* NH_4OH instead of 1 ml of 1 *N* NaOH.

Measurement of Electron-Capture Response—The electron-capture response of the ephedrine amide derivatives was determined by mixing the pentafluorobenzoyl derivative with each derivative separately at a ratio of exactly 1:1 (v/v). This step was necessary because the former three derivatives did not separate completely under the chromatographic conditions employed. No change in the response of the *N*-pentafluorobenzoyl derivative was observed when it was chromatographed separately or as a mixture with any of the three derivatives. The response of the other three derivatives was calculated using the *N*-pentafluorobenzoyl derivative as a reference.

Each fluoroacyl derivative gave a sharp symmetrical peak when chromatographed under the conditions described. The response of each derivative was expressed in 10^3 coulombs/mole and was calculated for each derivative from its peak area (width of the peak at half height × peak height) by converting the area to coulombs from the chart speed and the current for full-scale deflection.

RESULTS AND DISCUSSION

N-Pentafluorobenzoyl derivatives of I, norephedrine, and the internal standard (II) gave sharp peaks (a, b, and c, Fig. 1B) with retention times of 1.40, 2.38, and 3.82 min, respectively. The presence of these *N*-pentafluorobenzoyl derivatives was established by GLC–mass spectrometry[20].

The GLC–mass spectra of the *N*-pentafluorobenzoyl derivative of I and norephedrine did not give molecular ions, but diagnostic ions for the derivative of I were at *m/e* 252, 253, 234, 195, 167, 107, 105, 79, and 77. For the derivative of norephedrine, they were at *m/e* 238, 239, 195, 167, 107, 105, 79, and 77. The GLC–mass spectrum of the *N*-pentafluorobenzoyl derivative of II gave a molecular ion at *m/e* 389 and other characteristic ions at *m/e* 238, 178, 151, 121, 195, 167, 91, and 77. These mass spectra indicate that peaks a, b, and c (Fig. 1) were due to *N*-monoacyl derivatives.

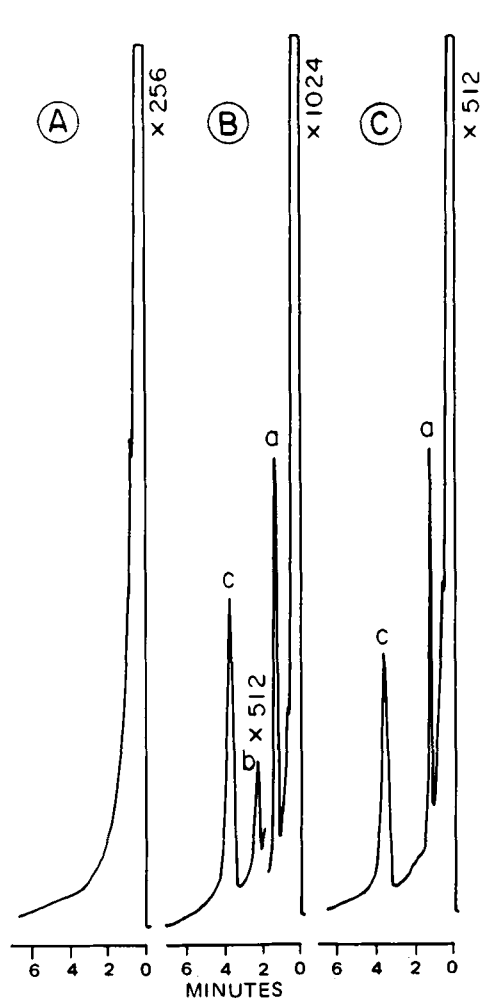

Figure 1—*Typical chromatograms of human plasma. Key: A, blank control plasma; B, spiked plasma containing 100 ng of ephedrine, 100 ng of norephedrine, and 100 ng of 3,4-dimethoxyamphetamine; C, plasma (0.5-hr sample) from a dosed volunteer who received a combination tablet (containing 24 mg of ephedrine hydrochloride) containing 57.14 ng of ephedrine and 100 ng of 3,4-dimethoxyamphetamine; peak a,* N-*pentafluorobenzamide of ephedrine; peak b,* N-*pentafluorobenzamide of norephedrine; and peak c,* N-*pentafluorobenzamide of 3,4-dimethoxyamphetamine.*

Derivatization of I and norephedrine with pentafluorobenzoyl chloride followed by GLC did not give any peaks other than for *N*-monoacyl derivatives, which suggested that the β-hydroxy group did not undergo acylation. However, on increasing the reaction time to 7 hr with subsequent GLC examination, a small peak (5% by peak area) eluted (retention time of 0.5 min) just before peak a. The GLC–mass spectrum of this peak gave a base peak at *m/e* 195 and other diagnostic ions at *m/e* 342, 341, 252, 238, 208, 168, 167, 105, and 77. The absence of ions at *m/e* 253 and 107 is diagnostic for the formation of the *O*-pentafluorobenzoyl derivative[21].

Similarly, reactions of I and norephedrine with heptafluorobutyric anhydride, pentafluoropropionic anhydride, and trifluoroacetic anhydride as checked by GLC–mass spectrometry yielded *N,O*-diacyl derivatives as the main products equal to 95% peak area compared to *N*-monoacyl derivatives. *N,O*-Diacyl derivatives of I were not hydrolyzed with 0.1 *N* NH_4OH. Shaking of diacyl derivatives with 1 *N* NaOH gave *N*-monoacyl derivatives, showing that the *O*-acyl, and not the *N*-acyl, functions of these derivatives are hydrolyzed with 1 *N* NaOH.

N-Pentafluorobenzoyl derivatives of phenylalkylamines have great

[20] GC–MS-data system model HP5985, Hewlett-Packard Corp., Ottawa, Ontario, Canada.

[21] K. K. Midha, J. W. Hubbard, J. K. Cooper, and D. Gagné, to be published.

electron-capturing affinity (1, 6). In the present study, the electron-capturing affinity of the *N*-pentafluorobenzoyl derivative of I was nearly 15 times that of the *N*-heptafluorobutyryl derivative, 18 times that of the *N*-pentafluoropropionyl derivative, and 1100 that of the *N*-trifluoroacetyl derivative of I (Table I).

Figure 1 shows a typical chromatogram obtained by processing control blank plasma without the internal standard. No extraneous peaks are observed. Similar chromatograms of urine extracts were as clean as those from plasma. A chromatogram obtained when the method was applied to spiked human plasma containing 100 ng each of I, norephedrine, and II is also shown in Fig. 1.

Figure 1 also shows a chromatogram of the plasma sample (1 ml) from blood withdrawn from a male volunteer (67.6 kg) at 0.5 hr after administration of 24 mg of I in a combination tablet[6] containing theophylline and phenobarbital. Analysis time was 6 min, and a 57.14-ng/ml level of I was found in this 0.5-hr sample.

Ether was the solvent of choice for the extraction of ephedrines from biological fluids in several studies (3, 4, 7, 8). Recently, degradation of I during extraction with ether was observed (9, 10). In the present study, ether was tried as a solvent for the extraction of I and II from plasma at different pH values. The extraction from plasma with ether at pH 12 and subsequent derivatization of I and II with pentafluorobenzoyl chloride yielded chromatograms with many endogenous interfering peaks and irreproducible peak height ratios (I to II). Back-extracting the ethereal extract of plasma containing I and II into aqueous acid, basifying the aqueous layer to pH 12, extracting with ether, and derivatizing with pentafluorobenzoyl chloride did not eliminate all interfering peaks. Raising the pH to 14 and extracting with pentane eliminated all interfering peaks, which may have been from phenolic substances that would not be extracted into a nonpolar solvent such as pentane at pH 14.

When two known phenolic metabolites of I, *p*-hydroxyephedrine and *p*-hydroxynorephedrine, were carried through the extraction and derivatization procedures, neither was observed by GLC. However, peaks for the *N*-pentafluorobenzoyl derivatives of these metabolites were observed when they were not carried through the extraction but were derivatized directly[22].

After extraction and derivatization of I and II with pentafluorobenzoyl chloride, the excess reagent was hydrolyzed with 0.1 *N* NH_4OH, and the derivatives of I and II were extracted with amyl acetate. The pentyl acetate extract had to be removed from contact with the ammonium hydroxide within 20 min or slow hydrolysis of the derivatives occurred, as shown by a decrease in peak heights. Once the amyl acetate was removed from contact with the ammonia layer, these derivatives were stable for several months.

Nitrogen evaporation of pentane extracts of derivatized or underivatized drug caused perceptible loss of derivative and even greater loss of free drug. Even after reaction and evaporation to dryness without nitrogen, the derivative was lost if the samples were left too long in the bath. Thus, the samples were evaporated without the use of nitrogen and removed immediately when dry.

Different GLC stationary phases such as phenyl methyl dimethyl silicone[23] and phenyl methyl (50:50) silicone[24] were tried but were not suitable for quantitation. The drug and internal standard were poorly resolved with the former, and broad peaks were obtained with the latter. A column of methyl phenyl silicone containing about 75% phenyl silicone[25] gave sharp peaks for I and the internal standard. However, norephedrine, the major metabolite of I (which was extracted in the procedure) could not be separated from I. A liquid phase of phenyl cyanopropyl and methyl silicone[17], however, separated the *N*-pentafluorobenzamide derivatives of I and norephedrine.

After repeated injections into the gas chromatograph, a noisy baseline was occasionally observed, and the ratios of I to II became irreproducible. This result was initially considered to be due to detector contamination. However, baking the detector at 350° over 24 hr did not remedy the problem. When the glass liner in the injection port of the gas chromatograph was examined, a white coating of small particles was observed on the inside. After cleaning the glass liner by soaking it in a chromic acid solution in an ultrasonic bath overnight, reproducible ratios of I to II were obtained. The irreproducible ratios may have been caused by buildup of endogenous materials contained in derivatized plasma extracts and/or by septum particles. By changing the glass liner in the injection port either weekly or after approximately 500 injections, the problem of irreproducible ratios was overcome.

Table II—Calibration Curve of Ephedrine Extracted from Plasma [a]

Nanograms per Milliliter	*n*	Mean	±*SD*	±*CV*, %
5	8	0.113	0.0046	4.09
10	7	0.216	0.0089	4.13
20	8	0.445	0.0169	3.77
30	9	0.659	0.0190	2.89
50	11	1.092	0.0436	3.98
100	9	2.128	0.0755	3.55

[a] Mean *CV* = 3.74%, slope = 0.0215 ± 0.0002, and correlation = 0.9986.

Table III—Recovery of Ephedrine and 3,4-Dimethoxyamphetamine from Plasma

Nanograms Added to 1 ml of Plasma	*n*	Mean Nanograms Recovered	Percent Recovery, mean ± *SD*
	Recovery of Ephedrine		
20	4	19.51	97.56 ± 1.16
100	4	96.94	96.94 ± 1.18
Mean			97.25 ± 1.13
	Recovery of 3,4-Dimethoxyamphetamine		
100	4	51.74	51.74 ± 0.85

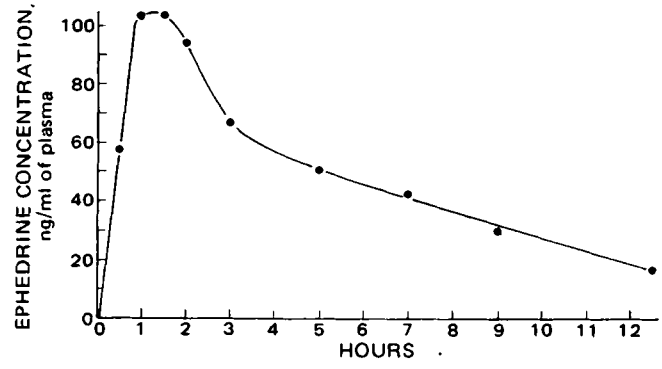

Figure 2—*Ephedrine concentrations in the plasma of a human volunteer (67.6 kg) following a single 24-mg dose of ephedrine hydrochloride in a combination tablet.*

The accuracy and precision of the GLC assay are demonstrated in Table II. Results are based on at least seven determinations of each concentration of I, ranging from 5.0 to 100.0 ng/ml. The overall coefficient of variation was 3.98%. The calibration curve obtained by plotting the peak height ratio of the *N*-pentafluorobenzoyl derivatives of I:II *versus* the I concentration was linear ($y = mx$) over the 5.0–100.0-ng of I/ml of plasma range. A mean slope value of 0.0215 ± 0.0002 ($r^2 = 0.999$) was obtained.

The overall recoveries of I and II from plasma were 97.25 ± 1.13 and 51.74 ± 0.85%, respectively (Table III). The procedure described has been applied to numerous plasma sample analyses. However, since II is a restricted drug in Canada, an alternative internal standard may be desirable. 3,4-Dimethoxyphenethylamine[5], a commercially available chemical, was suitable, and its *N*-pentafluorobenzoyl derivative gave a sharp symmetrical peak at 4.3 min, well separated from the peak due to the derivative of I. Recovery under the extraction conditions and the sensitivity of the procedure using this alternative internal standard were approximately equivalent to those with II.

The application of the present method to the determination of plasma I concentrations is shown in Fig. 2. A combination tablet[6] containing ephedrine hydrochloride (24 mg), theophylline, and phenobarbital was given as outlined in the *Experimental* section, and aliquots of the sampled plasma were assayed for I by GLC. Plasma concentrations over 24 hr in the subject fit a one-compartment model from which the elimination half-life was calculated (4.8 hr).

[22] Bonded Carbowax; C. R. Hastings, J. M. Augl, S. Kapila, and W. A. Aue, *J. Chromatogr.*, 87, 49 (1973).
[23] OV-7, Chromatographic Specialties, Brockville, Ontario, Canada.
[24] OV-17, Chromatographic Specialties, Brockville, Ontario, Canada.
[25] OV-25, Chromatographic Specialties, Brockville, Ontario, Canada.

REFERENCES

(1) G. R. Wilkinson and A. H. Beckett, *J. Pharmacol. Exp. Ther.*, **162**, 139 (1968).

(2) L. M. Cummins and M. J. Fourier, *Anal. Lett.*, **2**, 403 (1969).

(3) M. E. Pickup and J. W. Paterson, *J. Pharm. Pharmacol.*, **26**, 561 (1974).

(4) C. Bye, H. M. Hill, D. T. D. Hughes, and A. W. Peck, *Eur. J. Clin. Pharmacol.*, **8**, 47 (1975).

(5) E. T. Lin and L. Z. Benet, "Abstracts, APhA Academy of Pharmaceutical Sciences," 19th National Meeting, Atlanta, Ga., 1975, p. 155.

(6) S. B. Matin and M. Rowland, *J. Pharm. Sci.*, **61**, 1235 (1972).

(7) A. H. Beckett and B. Testa, *J. Pharm. Pharmacol.*, **25**, 382 (1973).

(8) P. S. Sever, L. G. Dring, and R. T. Williams, *Eur. J. Clin. Pharmacol.*, **9**, 193 (1975).

(9) A. H. Beckett and G. R. Jones, *Tetrahedron*, **33**, 3313 (1977).

(10) A. H. Beckett, G. R. Jones, and D. A. Hollingsbee, *J. Pharm. Pharmacol.*, **30**, 15 (1978).

ACKNOWLEDGMENTS

Presented at the APhA Academy of Pharmaceutical Sciences, Montreal meeting, May 1978.

Effects of Amorphous Silicon Dioxides on Drug Dissolution

K. Y. YANG *, R. GLEMZA ‡, and C. I. JAROWSKI ˣ

Received February 13, 1978, from the *Department of Allied Health and Industrial Sciences, College of Pharmacy and Allied Health Professions, St. John's University, Jamaica, NY 11439.* Accepted for publication October 6, 1978.

*Present address: Natcon Chemical Co., Plainview, N.Y. ‡Present address: Davison Chemical Division, W. R. Grace & Co., Baltimore, Md.

Abstract □ The dissolution profiles of prednisone, digoxin, and griseofulvin in simulated GI fluids were determined after solvent deposition or ball milling with three commercially available grades of amorphous silicon dioxide. The former procedure resulted in adsorbates showing evidence of drug entrapment by the two grades with larger average pore diameters. Ball milling the drugs with the grade possessing the largest average particle diameter produced triturations with the slowest dissolution rates. A relationship between drug dissolution and extent of dilution with the amorphous silicon dioxides was shown. Particle-size measurements revealed that the ball milling procedure was more apt to broaden the size distribution as compared with the solvent-deposition method of drug incorporation.

Keyphrases □ Dissolution rate—effects of amorphous silicon dioxides on prednisone, digoxin, griseofulvin, simulated GI fluids, solvent deposition compared to ball milling □ Silicon dioxide, amorphous—effect on dissolution rates of prednisone, digoxin, griseofulvin in simulated GI fluids, solvent deposition compared to ball milling □ Dispersions, solid—effect of amorphous silicon dioxides on prednisone, digoxin, griseofulvin, simulated GI fluids, solvent deposition compared to ball milling

Various water-insoluble drugs, solvent deposited on fumed silicon dioxide, have been reported to have more rapid dissolution rates than the pure micronized drugs. Surface area of the acidified and basified silica gel adsorbents was a controlling factor for the increased dissolution rate of these adsorbate samples (1).

This study evaluated the effects of three commercial grades of amorphous silicon dioxide on the dissolution rates of digoxin, griseofulvin, and prednisone. The micrometer-sized, synthetic, amorphous silicon dioxides possess a unique combination of properties. Purity, nontoxicity, uniformity, chemical inertness, large surface area and porosity, controlled particle size, and a high adsorptive capacity for both oil and water characterize these versatile products. The three grades selected differ from one another in surface pH, particle size, surface area, and pore volume and diameter (Table I).

In addition to the customary procedure of solvent deposition, ball milling was used to spread each drug on the amorphous silicon dioxide surfaces. Earlier studies had shown that ball milling was superior to solvent deposition for preparing drug–lactose triturations (2, 3). Besides comparison of these two methods, the effect of pore diameter on the dissolution rate of entrapped drug molecules was studied.

EXPERIMENTAL

Materials—The following were obtained from commercial sources: amorphous silicon dioxides[1], digoxin[2] USP, griseofulvin[3] USP, prednisone[4] USP, sodium hydroxide[5] USP, monobasic sodium phosphate[6] USP, sodium chloride[7] USP, reagent grade hydrochloric acid[5], and absolute ethanol[8].

Equipment—The following were used: the USP XIX dissolution test basket assembly[9]; a constant-temperature shaker bath[10]; a grating spectrophotometer with digital display[11]; a jar mill, 10.16-cm (4-in.) diameter with 1.27-cm (0.5-in.) diameter porcelain balls[12]; a pH meter[11]; a particle-size counter[13]; a U.S. standard sieve, 60 mesh[14]; a Swinny adapter[15], 13 mm; and filter paper, 0.45-μm porosity[15].

Preparation of Drug–Amorphous Silicon Dioxide Triturations—The drug–amorphous silicon dioxide triturations were prepared in a weight ratio of 1:20. Simple blends were prepared by manual bottle tumbling for 15 min. Ball milled triturations were prepared from homogeneous simple blends. Ball milling was carried out for 48 hr in a jar mill half-filled with porcelain balls.

Solvent deposition consisted of dissolving prednisone or griseofulvin in sufficient absolute ethanol (80% ethanol was used for digoxin) and uniformly wetting the various silicas contained in a beaker. The mixture was stirred with a magnetic stirrer while the solvent was evaporated in an air stream. The residues were dried at 37° for 24 hr and passed through a 60-mesh screen to break up any agglomerates. The sieved material was bottle blended to ensure homogeneity.

[1] Syloid 63, 72, and 266, Davison Chemical Division, W. R. Grace & Co., Baltimore, Md.
[2] Roussel Corp., New York, N.Y.
[3] Ayerst Laboratories, New York, N.Y.
[4] The Upjohn Co., Kalamazoo, Mich.
[5] J. T. Baker Chemical Co., Phillipsburg, N.J.
[6] Fisher Scientific Co., Fair Lawn, N.J.
[7] Apache Chemicals, Seward, Ill.
[8] U.S. Industrial Chemicals Co., New York, N.Y.
[9] Hanson Research Corp., Northridge, Calif.
[10] Model WBR, New Brunswick Scientific Co., New Brunswick, N.J.
[11] Model DB-GT, Beckman Instruments, Fullerton, Calif.
[12] Paul O. Abbe Inc., Little Falls, N.J.
[13] Model T, Coulter Electronics Inc., Hialeah, Fla.
[14] Dual Manufacturing Co., Chicago, Ill.
[15] Millipore Corp., Bedford, Mass.

0022-3549/79/0500-0560$01.00/0

© 1979, American Pharmaceutical Association

REFERENCES

(1) G. R. Wilkinson and A. H. Beckett, *J. Pharmacol. Exp. Ther.*, **162**, 139 (1968).

(2) L. M. Cummins and M. J. Fourier, *Anal. Lett.*, **2**, 403 (1969).

(3) M. E. Pickup and J. W. Paterson, *J. Pharm. Pharmacol.*, **26**, 561 (1974).

(4) C. Bye, H. M. Hill, D. T. D. Hughes, and A. W. Peck, *Eur. J. Clin. Pharmacol.*, **8**, 47 (1975).

(5) E. T. Lin and L. Z. Benet, "Abstracts, APhA Academy of Pharmaceutical Sciences," 19th National Meeting, Atlanta, Ga., 1975, p. 155.

(6) S. B. Matin and M. Rowland, *J. Pharm. Sci.*, **61**, 1235 (1972).

(7) A. H. Beckett and B. Testa, *J. Pharm. Pharmacol.*, **25**, 382 (1973).

(8) P. S. Sever, L. G. Dring, and R. T. Williams, *Eur. J. Clin. Pharmacol.*, **9**, 193 (1975).

(9) A. H. Beckett and G. R. Jones, *Tetrahedron*, **33**, 3313 (1977).

(10) A. H. Beckett, G. R. Jones, and D. A. Hollingsbee, *J. Pharm. Pharmacol.*, **30**, 15 (1978).

ACKNOWLEDGMENTS

Presented at the APhA Academy of Pharmaceutical Sciences, Montreal meeting, May 1978.

Effects of Amorphous Silicon Dioxides on Drug Dissolution

K. Y. YANG *, R. GLEMZA ‡, and C. I. JAROWSKI ˣ

Received February 13, 1978, from the *Department of Allied Health and Industrial Sciences, College of Pharmacy and Allied Health Professions, St. John's University, Jamaica, NY 11439.* Accepted for publication October 6, 1978.

*Present address: Natcon Chemical Co., Plainview, N.Y. ‡Present address: Davison Chemical Division, W. R. Grace & Co., Baltimore, Md.

Abstract □ The dissolution profiles of prednisone, digoxin, and griseofulvin in simulated GI fluids were determined after solvent deposition or ball milling with three commercially available grades of amorphous silicon dioxide. The former procedure resulted in adsorbates showing evidence of drug entrapment by the two grades with larger average pore diameters. Ball milling the drugs with the grade possessing the largest average particle diameter produced triturations with the slowest dissolution rates. A relationship between drug dissolution and extent of dilution with the amorphous silicon dioxides was shown. Particle-size measurements revealed that the ball milling procedure was more apt to broaden the size distribution as compared with the solvent-deposition method of drug incorporation.

Keyphrases □ Dissolution rate—effects of amorphous silicon dioxides on prednisone, digoxin, griseofulvin, simulated GI fluids, solvent deposition compared to ball milling □ Silicon dioxide, amorphous—effect on dissolution rates of prednisone, digoxin, griseofulvin in simulated GI fluids, solvent deposition compared to ball milling □ Dispersions, solid—effect of amorphous silicon dioxides on prednisone, digoxin, griseofulvin, simulated GI fluids, solvent deposition compared to ball milling

Various water-insoluble drugs, solvent deposited on fumed silicon dioxide, have been reported to have more rapid dissolution rates than the pure micronized drugs. Surface area of the acidified and basified silica gel adsorbents was a controlling factor for the increased dissolution rate of these adsorbate samples (1).

This study evaluated the effects of three commercial grades of amorphous silicon dioxide on the dissolution rates of digoxin, griseofulvin, and prednisone. The micrometer-sized, synthetic, amorphous silicon dioxides possess a unique combination of properties. Purity, nontoxicity, uniformity, chemical inertness, large surface area and porosity, controlled particle size, and a high adsorptive capacity for both oil and water characterize these versatile products. The three grades selected differ from one another in surface pH, particle size, surface area, and pore volume and diameter (Table I).

In addition to the customary procedure of solvent deposition, ball milling was used to spread each drug on the amorphous silicon dioxide surfaces. Earlier studies had shown that ball milling was superior to solvent deposition for preparing drug–lactose triturations (2, 3). Besides comparison of these two methods, the effect of pore diameter on the dissolution rate of entrapped drug molecules was studied.

EXPERIMENTAL

Materials—The following were obtained from commercial sources: amorphous silicon dioxides[1], digoxin[2] USP, griseofulvin[3] USP, prednisone[4] USP, sodium hydroxide[5] USP, monobasic sodium phosphate[6] USP, sodium chloride[7] USP, reagent grade hydrochloric acid[5], and absolute ethanol[8].

Equipment—The following were used: the USP XIX dissolution test basket assembly[9]; a constant-temperature shaker bath[10]; a grating spectrophotometer with digital display[11]; a jar mill, 10.16-cm (4-in.) diameter with 1.27-cm (0.5-in.) diameter porcelain balls[12]; a pH meter[11]; a particle-size counter[13]; a U.S. standard sieve, 60 mesh[14]; a Swinny adapter[15], 13 mm; and filter paper, 0.45-μm porosity[15].

Preparation of Drug–Amorphous Silicon Dioxide Triturations—The drug–amorphous silicon dioxide triturations were prepared in a weight ratio of 1:20. Simple blends were prepared by manual bottle tumbling for 15 min. Ball milled triturations were prepared from homogeneous simple blends. Ball milling was carried out for 48 hr in a jar mill half-filled with porcelain balls.

Solvent deposition consisted of dissolving prednisone or griseofulvin in sufficient absolute ethanol (80% ethanol was used for digoxin) and uniformly wetting the various silicas contained in a beaker. The mixture was stirred with a magnetic stirrer while the solvent was evaporated in an air stream. The residues were dried at 37° for 24 hr and passed through a 60-mesh screen to break up any agglomerates. The sieved material was bottle blended to ensure homogeneity.

[1] Syloid 63, 72, and 266, Davison Chemical Division, W. R. Grace & Co., Baltimore, Md.
[2] Roussel Corp., New York, N.Y.
[3] Ayerst Laboratories, New York, N.Y.
[4] The Upjohn Co., Kalamazoo, Mich.
[5] J. T. Baker Chemical Co., Phillipsburg, N.J.
[6] Fisher Scientific Co., Fair Lawn, N.J.
[7] Apache Chemicals, Seward, Ill.
[8] U.S. Industrial Chemicals Co., New York, N.Y.
[9] Hanson Research Corp., Northridge, Calif.
[10] Model WBR, New Brunswick Scientific Co., New Brunswick, N.J.
[11] Model DB-GT, Beckman Instruments, Fullerton, Calif.
[12] Paul O. Abbe Inc., Little Falls, N.J.
[13] Model T, Coulter Electronics Inc., Hialeah, Fla.
[14] Dual Manufacturing Co., Chicago, Ill.
[15] Millipore Corp., Bedford, Mass.

0022-3549/79/0500-0560$01.00/0

© 1979, American Pharmaceutical Association

Table I—Physicochemical Analyses of Amorphous Silicon Dioxides

Property	Silica 63[a]	Silica 72[b]	Silica 266[c]
Total volatiles (1750° F), %	5.9	5.5	7.7
pH (5% slurry)	3.8	6.8	8.0
Na_2O, %	0.035	0.062	0.09
Sulfate, %	0.07	0.065	0.05
Al_2O_3, %	0.03	0.074	0.05
CaO, %	0.034	0.13	0.09
Fe, ppm	50	70	70
NH_3, %	—	0.02	0.02
Oil adsorption, lb/100 lb	75	195	315
Through 325 mesh, %	99.95	100	100
Bulk density, g/c^3	0.34	0.145	0.08
Centrifuge density, g/cm^3	0.57	0.28	0.15
Surface area, m^2/g	760	290	295
Pore volume, ml/g	0.43	1.08	—
Average pore diameter, Å	20	150	210
Average particle size, μm	11.1	4.85	2

[a] Lot 334. [b] Lot 4072. [c] Lot 189; typical analysis.

Table II—Wavelengths of UV Light Used in Development of Calibration Curves for the Three Drugs in Various Solvents

Solvent	Wavelength of Light, nm		
	Digoxin	Griseofulvin	Prednisone
Simulated gastric fluid (without pepsin)	222	296	242
Simulated intestinal fluid (without pancreatin)	222	296	245
Absolute ethanol	—	290	240
80% Ethanol	220	—	—

Triturations were assayed spectrophotometrically for content uniformity. Only samples containing 100 ± 5% of the required amount of drug were used in the dissolution studies.

Spectrophotometric Absorption and Calibration Curves—Stock solutions were prepared by dissolving 100 mg of each drug in 50 ml of absolute ethanol or 80% ethanol (digoxin). Aliquots were diluted with appropriate solvents to develop absorption spectral and calibration curves. The following solution concentrations were employed: prednisone, 20 μg/ml; griseofulvin, 10 μg/ml; and digoxin, 40 μg/ml.

To blank out interference of colloidal silica particles on the UV measurements, stock suspensions of the silicas were prepared. Aliquots were added 20:1 (w/w) to the drug solutions. The suspensions were filtered through a 0.45-μm membrane filter before determination of the absorption spectral and calibration curves. Only in the case of digoxin was an interference found. An absorption spectral curve of one amorphous silicon dioxide (silica 63) in 80% ethanol showed a maximum absorbance at 228 nm. The maximum absorbance values for digoxin ranged from 220 to 222 nm. Thus, the blanks used for the spectrophotometric measurements of digoxin solutions were the corresponding solvents plus the appropriate silica. For the measurements of prednisone and griseofulvin, the appropriate solvent without silica addition was adequate.

All calibration curves determined at the wavelength of maximum absorbance obeyed Beer's law. The wavelengths employed for calibration curves are summarized in Table II.

Assay of the Drug–Silica Triturations—The various drug-silica triturations were extracted with absolute or 80% ethanol. The extracts were passed through a 0.45-μm membrane filter. After dilution with solvent, the absorbance was determined spectrophotometrically and the concentration was ascertained from the calibration curves.

Dissolution Studies—The dissolution studies were conducted in simulated gastric fluid (without pepsin) and simulated intestinal fluid (without pancreatin) (4). The stability of the three drugs was satisfactory in these dissolution media after 2 hr of exposure at 37°. An insignificant change in absorbance occurred after addition of 20-fold excesses of either silica 63 or 266. On the basis of these observations, the possibility of drug adsorption by the silicas during the dissolution rate determinations was discounted (Fig. 1).

A modification of the procedure of Monkhouse and Lach (1) was used to determine the dissolution rates of the three drugs and the various triturations. Simulated gastric fluid, 200 ml, was brought to 37° in a constant-temperature bath. The dissolution medium was stirred with the basket used in the USP dissolution test. The stirrer was vertically centered at a depth 2 cm from the beaker bottom and was maintained at 60 rpm.

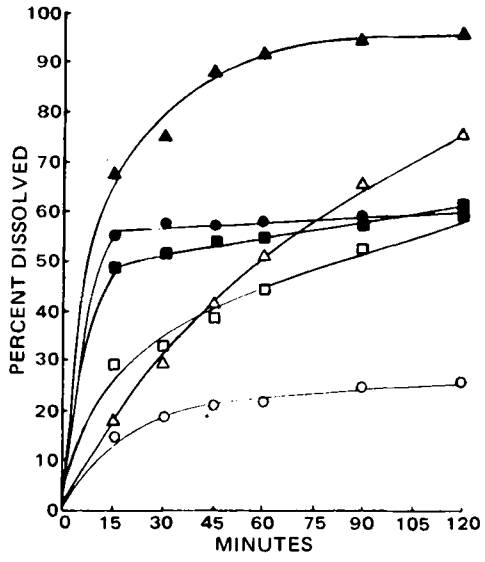

Figure 1—*Dissolution rate in simulated gastric fluids of selected samples of griseofulvin, digoxin, and prednisone solvent deposited on amorphous silicon dioxide (drug–silica 63 ratio, 1:20) compared with the pure drugs. Key: ○, griseofulvin (simulated intestinal fluid); ●, griseofulvin–silica 63 (simulated intestinal fluid); □, digoxin (simulated gastric fluid); ■, digoxin–silica 63 (simulated gastric fluid); △, prednisone (simulated gastric fluid); and ▲, prednisone–silica 63 (simulated gastric fluid).*

Accurately weighed samples, equivalent to a quantity of drug to ensure sink conditions, were spread over the medium surface (digoxin, 9.44 mg; grisofulvin, 1.45 mg; and prednisone, 8 mg). Any large aggregates that formed at this stage were lightly broken up within 10 sec after sample addition. Aliquots of the dissolution medium were withdrawn periodically and passed through a 0.45-μm membrane filter. After appropriate dilution, the absorbance was determined spectrophotometrically.

Immediately after withdrawing an aliquot, an equal quantity of dissolution medium was added to the beaker to maintain a constant volume. Cumulative corrections were made for the previously withdrawn aliquots in calculating the total amount of drug dissolved. Each point on the dissolution curves represents at least two determinations.

In another series of experiments, 500 ml of dissolution medium was used. The quantity of sample added was 2.5-fold greater than that used in the experiments with 200 ml. The dissolution rate data are summarized in Tables III and IV.

Initial screening experiments showed that the dissolution rates were not significantly altered when 0.02% polysorbate 80 was present in the media, so it was not used.

Particle-Size Measurement—Pure drug, each of the three silica grades, and the drug–silica triturations were ultrasonically dispersed in an aqueous medium buffered at pH 2. The concentrations of the resulting aqueous dispersions were less than 0.01%. Aperture diameters ranged from 30 to 280 μm, and two apertures were routinely used. Each particle-size determination was completed in less than 10 min. The particle-size data are summarized in Table V.

RESULTS AND DISCUSSION

A significant drop in digoxin potency resulted from 48-hr ball milling, making dissolution rate determination impossible. This potency drop was unexpected, since such ball milling operations were conducted at room temperature with ingredients previously dried at 37°[16].

Digoxin (4.8%), solvent deposited on the three grades of silica, did not show a significant improvement in dissolution rate in simulated gastric fluids (Samples 4–6 and 10–12) compared with the pure drug. However, the best of the three proved to be silica 63 (Samples 4 and 10) due to its larger surface area (Table I). Indications of digoxin instability were encountered with the digoxin–silica 63 trituration but not with either of the other two[17].

The data in Table IV clearly show that the dissolution rate of digoxin in simulated gastric fluid increased as the quantity of silica 63 increased

[16] Details of these observations will be presented in a future publication.
[17] The stability studies will be described in a future publication.

Table III—Dissolution of Digoxin, Griseofulvin, Prednisone, and Their 1:20 Drug–Silica Triturations in Simulated Gastric Fluids at 37° (Volume of Solvent, 200 ml)

Sample	Solvent		Method of Preparation			Grade of Silica			Percentage Dissolved					
	Simulated Gastric	Simulated Intestinal	Solvent Deposition	Simple Blend	Ball Milling	63	72	266	15 min	30 min	45 min	60 min	90 min	120 min
1. Digoxin	+								28.9	32.8	37.7	43.8	52.4	59.2
2. Digoxin[a]	+		+						37.0	43.2	46.9	51.6	59.7	67.8
3. Digoxin	+			+		+			20.4	22.2	24.8	27.1	30.5	34.9
4. Digoxin	+		+			+			48.8	51.7	54.6	55.4	58.5	61.2
5. Digoxin	+		+				+		33.3	37.3	39.0	42.7	46.0	49.2
6. Digoxin	+		+					+	32.6	33.3	35.1	36.7	39.8	44.3
7. Digoxin		+							17.6	19.1	21.2	22.9	26.9	29.0
8. Digoxin		+	+						30.3	34.3	38.3	40.3	41.5	42.2
9. Digoxin		+		+		+			12.5	14.0	16.5	17.8	20.1	22.0
10. Digoxin		+	+			+			55.3	57.1	59.2	61.1	62.8	63.7
11. Digoxin		+	+				+		48.9	46.9	47.4	47.9	48.5	50.8
12. Digoxin		+	+					+	43.0	44.4	46.2	46.4	47.2	50.5
13. Griseofulvin	+								19.1	29.7	35.3	41.6	47.7	53.4
14. Griseofulvin[a]	+		+						8.7	10.5	13.2	16.6	19.9	22.9
15. Griseofulvin	+			+		+			51.6	55.6	56.6	61.8	65.8	69.2
16. Griseofulvin	+		+			+			32.0	34.2	35.3	36.9	36.8	37.7
17. Griseofulvin	+		+				+		31.0	35.3	37.7	39.4	42.6	45.3
18. Griseofulvin	+		+					+	31.0	34.8	37.5	39.6	42.6	45.3
19. Griseofulvin	+				+	+			19.7	22.6	24.0	25.5	26.6	28.3
20. Griseofulvin	+				+		+		23.2	45.0	48.1	50.8	54.0	56.8
21. Griseofulvin	+				+			+	46.6	50.8	54.7	57.1	60.5	63.6
22. Griseofulvin		+							14.0	18.2	20.5	21.4	24.4	25.7
23. Griseofulvin[a]		+	+						10.0	11.9	13.0	16.1	20.4	23.5
24. Griseofulvin		+		+		+			33.8	36.9	42.6	46.0	49.2	52.6
25. Griseofulvin		+	+			+			54.5	57.0	56.5	57.7	59.0	58.7
26. Griseofulvin		+	+				+		30.5	33.1	36.1	37.9	38.8	40.5
27. Griseofulvin		+	+					+	33.1	36.8	38.2	40.4	42.2	44.3
28. Griseofulvin		+			+	+			30.9	38.4	43.5	47.4	51.7	55.2
29. Griseofulvin		+			+		+		49.9	53.1	55.2	56.8	59.6	62.2
30. Griseofulvin		+			+			+	50.0	53.2	56.8	59.0	63.4	65.2
31. Prednisone	+								16.9	29.9	40.9	50.8	65.8	75.4
32. Prednisone[a]	+		+						16.0	29.0	40.0	51.6	66.2	73.6
33. Prednisone	+			+		+			32.2	40.6	46.2	51.4	59.1	65.1
34. Prednisone	+		+			+			67.6	75.1	87.7	91.7	94.7	96.4
35. Prednisone	+		+				+		29.4	43.0	50.1	55.0	60.2	65.0
36. Prednisone	+		+					+	44.5	52.6	55.8	56.8	58.8	59.5
37. Prednisone	+				+	+			15.6	17.4	19.5	20.8	21.4	21.8
38. Prednisone	+				+		+		40.0	49.0	53.9	55.7	57.3	57.4
39. Prednisone	+				+			+	43.9	54.3	58.9	61.2	63.6	64.7
40. Prednisone		+							23.0	35.1	45.7	59.3	69.4	82.0
41. Prednisone[a]		+	+						22.8	34.9	45.0	58.9	68.2	80.4
42. Prednisone		+		+		+			22.3	29.1	37.2	43.1	52.3	58.5
43. Prednisone		+	+			+			38.8	46.3	51.0	54.4	59.4	64.6
44. Prednisone		+	+				+		65.5	75.7	76.4	76.6	76.9	78.1
45. Prednisone		+	+					+	58.6	63.9	66.4	67.5	68.3	69.1
46. Prednisone		+			+	+			16.1	22.1	26.9	29.1	34.4	37.1
47. Prednisone		+			+		+		42.6	49.6	50.4	50.5	51.2	51.6
48. Prednisone		+			+			+	55.0	59.0	60.4	61.2	62.1	63.6

[a] Each drug was dissolved in absolute or 80% ethanol (digoxin). The solvent was evaporated in the absence of silica in an air stream and then dried at 37° for 24 hr. The crystalline residue was passed through a 60-mesh screen.

(Samples 49–56). Minimal improvement in the dissolution rates of drugs with the addition of fumed silicon dioxide above 10% was reported (1). The dissolution profiles in Table IV reveal that increased dilutions of the amorphous silicon dioxides favor a more rapid digoxin dissolution rate. The increased dissolution rate became apparent only in the 120-min study, which is why it was missed by previous researchers using a 14-min experimental design (1). The 120-min dissolution study clearly shows the advantage of adding additional adsorbent.

Significant portions of the total drug went into solution within the first 15 min (Table III). Thus, while 55.5% (Sample 55) of the digoxin had dissolved within the first 15 min, only 12.4% more dissolved after an additional 105 min. The dissolution profiles reported previously (1) also are indicative of a reduction in rate after 14 min. Increased dissolution of solvent-deposited phenylbutazone with increased silicon dioxide concentration has been reported (5). In agreement with our findings, these authors also showed that incomplete recovery of the solvent-deposited phenylbutazone occurred with the more concentrated triturations.

Whereas the simple blend was not of value for digoxin (Sample 3), it enhanced the griseofulvin dissolution rate in simulated gastric fluid (Sample 15). Solvent deposition of 4.8% griseofulvin on each of the three silicas produced equally inefficient triturations as measured in simulated gastric fluid (Samples 16–18). In simulated intestinal fluid, the dissolution rate of pure griseofulvin was much slower (Samples 22 and 23). In this dissolution medium, the simple blend (Sample 24) and the three silica triturations prepared by solvent deposition (Samples 25–27) all showed significant improvement over micronized griseofulvin (Sample 22).

Solvent deposition of 4.8% griseofulvin on silica 63 showed the expected rapid dissolution rate in simulated intestinal fluid (Sample 25).

Griseofulvin, 4.8%, with silica 266 unexpectedly yielded the best dissolution rate after 48 hr of ball milling (Sample 30), followed by silica 72 (Sample 29). This order is exactly the rank order in average particle size (Tables I and V). Thus, silica 266, with the finest particle size (2.05 μm) significantly increased in particle size when ball milled (15.3 μm) or when treated with solvent (22.4 μm). Such increases probably result from an aggregation of particles with little further reduction in size of individual silica 266 particles.

Silica 63 has the largest particle size (9.2 μm), and one would expect the generation of more fines from its ball milling. Ball milling silica 63[18] with griseofulvin yielded a trituration with smaller particle size and a very broad cumulative particle-size distribution (7.8 μm; $V = 2.6$). Thus, an increase in the production of fines and a decrease in particle size might possibly favor the trapping of drug particles beneath and between the fine particles of silica 63. With silica 266, the large increase in average particle size may be due primarily to the buildup of large, softer agglomerates from which the drug particles can be expected to dissolve more readily. Silica 72[19] had an intermediate average particle size (3.4 μm). It yielded an intermediate particle-size increase on ball milling with griseofulvin (10.3 μm). Solvent treatment of silica 63[20] led to an insig-

[18] Lot 22288.
[19] Lot 3580.
[20] Lot 334.

Table IV—Dissolution of Digoxin, Griseofulvin, Prednisone, and Various Drug–Silica 63 Triturations Prepared by Solvent Deposition (Volume of Simulated Gastric Fluid, 500 ml)

Sample	Concentration of Drug in Sample, %	Percentage Dissolved					
		15 min	30 min	45 min	60 min	90 min	120 min
49. Digoxin	100	19.5	22.0	24.3	30.4	35.9	42.3
50. Digoxin[a]	100	26.5	33.3	37.8	41.2	47.3	51.0
51. Digoxin	90	19.1	18.8	20.2	21.1	22.6	24.2
52. Digoxin	80	23.8	24.4	26.5	29.4	31.1	34.6
53. Digoxin	50	36.5	43.1	47.1	48.6	49.3	52.8
54. Digoxin	25	47.5	52.9	57.1	57.7	59.5	62.4
55. Digoxin	10	55.5	57.7	61.4	63.8	65.2	67.9
56. Digoxin	4.8	56.8	59.9	61.0	62.7	66.7	68.6
57. Griseofulvin	100	18.2	25.5	33.4	43.5	51.4	53.8
58. Griseofulvin[a]	100	7.3	9.7	12.7	15.2	17.9	21.7
59. Griseofulvin	90	9.2	12.1	15.3	16.8	20.6	23.4
60. Griseofulvin	80	6.9	11.6	13.8	13.9	17.0	19.9
61. Griseofulvin	50	22.1	26.5	32.1	38.7	38.2	41.0
62. Griseofulvin	25	20.5	24.5	27.0	29.5	33.1	37.7
63. Griseofulvin	10	33.4	36.8	39.2	41.9	46.4	50.5
64. Griseofulvin	4.8	28.4	32.2	34.5	36.1	37.7	39.4
65. Prednisone	100	15.2	27.1	41.1	49.6	62.3	74.9
66. Prednisone[a]	100	17.0	26.0	39.5	50.6	68.7	75.8
67. Prednisone	90	22.2	39.6	51.4	58.7	72.1	83.4
68. Prednisone	80	41.8	50.9	60.2	68.3	76.2	84.2
69. Prednisone	50	64.5	68.8	75.2	78.8	85.0	86.5
70. Prednisone	25	57.7	63.6	65.6	68.7	73.4	74.4
71. Prednisone	10	34.0	40.2	46.4	50.6	57.2	61.6
72. Prednisone	4.8	46.5	52.3	59.8	62.0	67.4	69.3

[a] Each drug was dissolved in absolute or 80% ethanol (digoxin). The solvent was evaporated in the absence of silica 63 in an air steam and then dried at 37° for 24 hr. The crystalline residue was passed through a 60-mesh screen.

Table V—Particle-Size Data of Griseofulvin, Prednisone, and Selected Drug–Silica Triturations

Sample	Method of Preparation		Dual Aperture Diameters, μm	Average Particle Size, μm	Width[a], V
	Solvent Deposition	Ball Milling			
Silica 63, lot 22288					
Silica 63			50 + 140	9.2	1.15
Silica 63		+	50 + 140	12.0	2.4
Silica 63 + griseofulvin 4.8%		+	50 + 140	7.8	2.6
Silica 63 + prednisone 4.8%		+	50 + 140	8.6	2.5
Silica 63[b]	+		50 + 140	9.9	1.15
Silica 63 + griseofulvin 4.8%	+		50 + 140	9.5	1.15
Silica 63 + prednisone 4.8%	+		50 + 140	9.6	1.15
Silica 63, lot 334					
Silica 63			50 + 140	11.1	1.15
Silica 63 + prednisone 4.8%	+		50 + 140	12.2	1.15
Silica 63 + prednisone 9%	+		50 + 140	13.4	1.15
Silica 63 + prednisone 25%	+		140 + 280	13.5	1.15
Silica 63 + prednisone 50%	+		140 + 280	15.3	1.3
Silica 63 + prednisone 80%	+		140 + 280	23	1.3
Silica 63 + prednisone 90%	+		140 + 280	21	1.15
Silica 72, lot 4072					
Silica 72			30 + 100	4.85	1.15
Silica 72, lot 3580					
Silica 72			30 + 100	3.4	1.15
Silica 72		+		9.7	2.15
Silica 72 + griseofulvin 4.8%		+		10.3	2.1
Silica 72 + prednisone 4.8%		+	50 + 100	9.4	2.05
Silica 72[b]	+			6–8	—[c]
Silica 72 + griseofulvin 4.8%	+			4.0	0.9
Silica 72 + prednisone 4.8%	+			4.3	1.4
Silica 266, lot 158					
Silica 266			30 + 70	2.05	1.15
Silica 266		+	100 + 200	15.3	2.15
Silica 266 + griseofulvin 4.8%		+		13.7	2.2
Silica 266 + prednisone 4.8%		+		11.0	1.7
Silica 266[b]	+			22.4	3.4
Silica 266 + griseofulvin 4.8%	+			19.9	3.2
Silica 266 + prednisone 4.8%	+			15.8	2.4
Pure drugs					
Prednisone				59	0.85
Prednisone	+			28	0.95
Griseofulvin	+			31	0.85
Griseofulvin				7.7	0.95

[a] The parameter V is a measure of the width of a particle-size distribution. Mathematically such width corresponds to dispersion around a central measure such as the average, mean, median, or mode. V is dimensionless and is calculated from the 84% (D_1) and 16% (D_2) points of the cumulative curve: $V = \sqrt{D_2/D_1} - 1$. For a true log normal distribution, $V = \sigma_g - 1$, where σ_g is the geometric standard deviation. In practice, most distributions are skewed, and $V + 1$ is then only an approximation to σ_g. Since relative, rather than absolute, measures of width of nonsymmetrical distributions were of interest, the tedious calculations associated with σ_g were avoided by using V as a basis for comparison. For disperse systems, the range of V is as follows: $V = 0$, monosize particles; $V = 0.5$, narrow distribution; $V = 1.5$, broad distribution; and $V \geq 2.0$, very broad distribution. The Coulter reproducibility of V is ±0.05% at $V = 1$ and ±10% at V above 1.5. [b] The pure silica was wet with ethanol. The solvent was evaporated in the absence of drug in an air stream and then dried at 37° for 24 hr. The residue was passed through a 60-mesh screen. Alternatively, the drug was dissolved in ethanol and the solution was evaporated to dryness in an air stream and then dried at 37° for 24 hr. The crystalline residue was passed through a 60-mesh screen. [c] Full distribution could not be determined because of the failure of agglomerates to pass through the 50-μm aperture.

Table VI—Dissolution Rates of Selected Samples in Simulated Gastric Fluids at 37° Plotted in First-Order Fashion (Ratio of Drug to Amorphous Silicon Dioxide, 1:20)

Number and Description of Sample	Simulated Gastric Fluid			Simulated Intestinal Fluid		
	K_1, min^{-1} (×0.0001)	K_2, min^{-1} (×0.0001)	t_{50}[a], min	K_1, min^{-1} (×0.0001)	K_2, min^{-1} (×0.0001)	t_{50}, min
1 and 7. Digoxin	—	54.4	127	—	14.9	465
4 and 10. Digoxin (solvent deposited on silica 63)	—	25.3	274	—	2.0	3500
13 and 22. Griseofulvin	—	50.5	137	—	12.9	537
16 and 25. Griseofulvin (solvent deposited on silica 63)	—	7.7	902	—	12.2	568
19 and 28. Griseofulvin (ball milled with silica 63)	—	9.8	704	—	39.7	175
31 and 40. Prednisone	118	115	60	140	134	52
34 and 43. Prednisone (solvent deposited on silica 63)	139	138	50	66	42	165
37 and 46. Prednisone (ball milled with silica 63)	14.1	2.3	3000	38	20	347
39 and 48. Prednisone (ball milled with silica 266)	80.8	15.7	441	31.8	10.7	648

[a] Some first-order plots exhibited steeper slopes from 15 to 60 min (Figs. 4 and 5). The t_{50} values were calculated from the less steep slopes generated from the dissolution data beyond 60 min.

nificant increase in particle size, whereas silica 72[19] and 266 increased particle size significantly.

The dissolution profiles (Table IV) demonstrated that griseofulvin solvent deposited on silica 63 in concentrations greater than 50% inefficiently dissolved in simulated gastric fluid (Samples 59 and 60). Micronized griseofulvin attained the highest percentage in solution after 120 min (Sample 57). Solvent deposition of griseofulvin in the absence of silica 63 exhibited a poor dissolution rate (Sample 58). This difference can be explained on the basis of particle size. Thus, the average particle size of the solvent-deposited griseofulvin was fourfold greater than the micronized material (Table V).

Solvent deposition of 4.8% prednisone on silica 63 showed the fastest dissolution rate in simulated gastric fluid (Table III, Sample 34). Solvent deposition of a similar quantity on silica 72 produced a trituration with the fastest dissolution rate in simulated intestinal fluid (Sample 45). On the other hand, ball milled triturations containing 4.8% drug showed silica 266 to give the best dissolution in both simulated gastric media (Fig. 2, Samples 39 and 48).

Solvent deposition of prednisone on silica 63 at various drug concentrations produced triturations exhibiting unusual dissolution profiles in simulated gastric fluid (Table IV, Samples 65–72). Triturations with drug concentrations of 50% exhibit dissolution rates faster than 80 or 90% triturations. After 120 min, the three triturations achieved virtually the same extent of dissolution. However, further dilution with silica 63 resulted in less efficiently dissolving triturations (Samples 70–72).

During the dissolution experiments, the three grades of amorphous silicon dioxides did not tend to adsorb dissolved drug under the sink conditions employed. However, there was an indication of drug entrapment within the pores of silicas 72 and 266 in samples prepared by solvent deposition. Thus, silica 63, which has the smallest average pore diameter (20 Å), usually showed the most rapid drug release when compared with silicas 72 (150 Å) and 266 (210 Å). Digoxin (Table III, Sample 4) dissolved most rapidly in simulated gastric fluid after solvent deposition on silica 63. Griseofulvin (Sample 25) dissolved most rapidly in simulated intestinal fluid after solvent deposition on silica 63, whereas prednisone, after solvent deposition on silica 63, showed the most rapid dissolution in simulated gastric fluid (Sample 34).

The selected samples exhibited in Figs. 1 and 2 highlight some key points. The significance of the data presented in Table V may be more quickly grasped by inspection of Fig. 3. Ball milling silica 63, which had the largest average particle size of the three amorphous silicon dioxides used, significantly broadened the particle-size distribution. Solvent

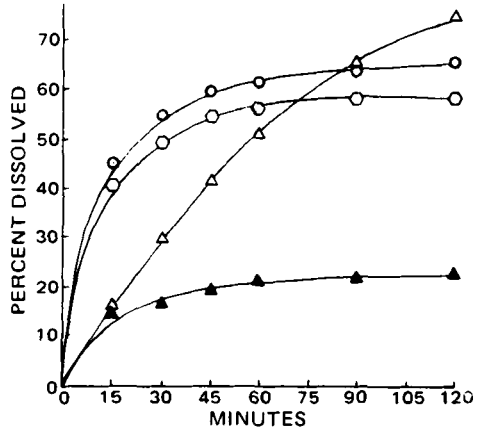

Figure 2—*Dissolution rate in simulated gastric fluid at 37° of selected samples of prednisone ball milled with various amorphous silicon dioxides (ratio of drug–silica, 1:20). Key: △, prednisone; ▲, prednisone–silica 63; ○, prednisone–silica 72; and ○, prednisone–silica 266.*

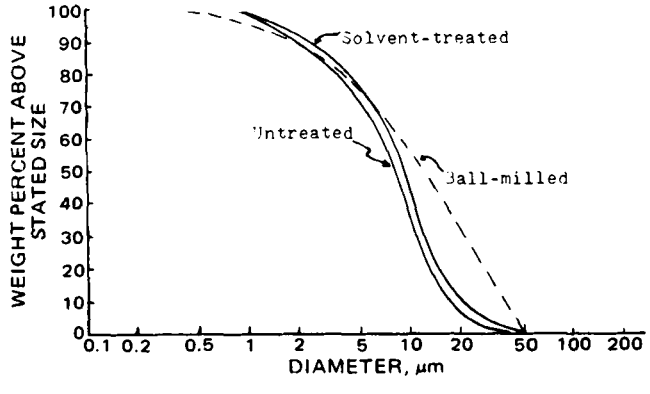

Figure 3—*Particle-size analysis (dual aperture, 50 and 140 μm) of amorphous silicon dioxide (silica 63, lot 22288) in pH 2 buffer before and after treatment with solvent or ball milled for 48 hr.*

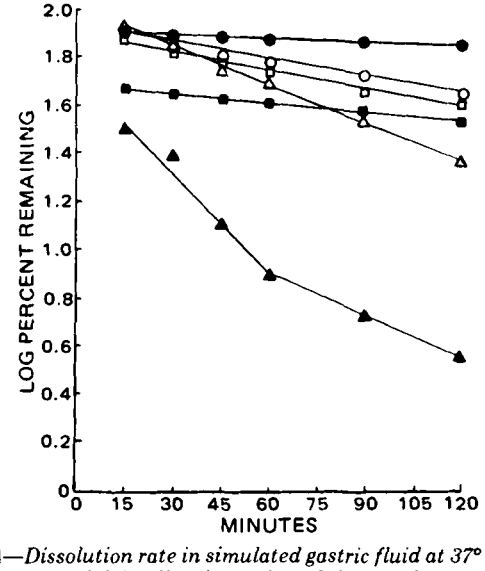

Figure 4—*Dissolution rate in simulated gastric fluid at 37° of selected samples of griseofulvin, digoxin, and prednisone solvent deposited or ball milled with amorphous silicon dioxide (drug–silica 63 ratio, 1:20). Key: △, prednisone; ▲, prednisone–silica 63 (solvent deposited); ○, griseofulvin; ●, griseofulvin–silica 63 (ball milled); □, digoxin; and ■, digoxin–silica 63 (solvent deposited).*

treatment of silica 63, however, resulted in an insignificant change in the particle-size distribution.

In Table VI and Fig. 4, the data gathered on selected samples are plotted in first-order fashion. The values for K_1 and K_2 were determined from the slopes of the lines, and the dissolution half-lives were calculated from the K_2 values. Where two first-order processes were evident, K_2 represented the slower process that occurred 60 min after dissolution had commenced (Fig. 4, prednisone–silica 63, solvent deposited). The data in Table VI clearly show that a significant change in dissolution half-life can be affected by solvent deposition on, or ball milling with, the amorphous silicon dioxides.

REFERENCES

(1) D. C. Monkhouse and J. L. Lach, *J. Pharm. Sci.*, **61**, 1430 (1972).

(2) C. Ampolsuk, J. V. Mauro, A. A. Nyhuis, N. Shah, and C. I. Jarowski, *ibid.*, **63**, 117 (1974).

(3) N. Shah, R. Pytelewski, H. Eisen, and C. I. Jarowski, *ibid.*, **63**, 339 (1974).

(4) "The United States Pharmacopeia," 19th rev., Mack Publishing Co., Easton, Pa., 1975, p. 765.

(5) H. Johansen and N. Møller, *J. Pharm. Sci.*, **67**, 134 (1978).

Fusion of Disubstituted Benzenes

ERIC MARTIN, SAMUEL H. YALKOWSKY ˣ, and JOHN E. WELLS

Received June 9, 1978, from the *Pharmacy Research Unit, The Upjohn Company, Kalamazoo, MI 49001.* Accepted for publication October 3, 1978.

Abstract □ The entropy of fusion of 84 disubstituted benzenes was essentially constant and independent of the participation of the compounds in intramolecular or intermolecular hydrogen bonding. It was also independent of the shapes, sizes, and dipole moments of the rigid molecules studied. While the entropy of fusion was independent of these parameters, the melting point and the heat of fusion showed a direct dependence on molecular properties.

Keyphrases □ Entropy of fusion—disubstituted benzenes, independent of hydrogen bonding, shape, size, dipole moment of rigid molecules, structure-activity relationships □ Melting point—analysis, disubstituted benzenes, structure-activity relationships □ Benzenes, disubstituted—entropy of fusion, melting point, heat of fusion, structure-activity relationships

The ability to predict the melting point, entropy of fusion, and heat of fusion from chemical structure would make possible the design of compounds having a specified physical state or even a specified melting range. The aqueous solubility of many organic compounds can be predicted from their melting points, entropies of fusion, and octanol–water partition coefficients (1). Since partition coefficients can be predicted by several group contribution methods (2, 3), the estimation of fusion properties makes possible the estimation of aqueous solubility. This possibility has direct implications for drug delivery.

BACKGROUND

In 1908, Walden (4) proposed that entropy of fusion is constant for many classes of compounds. Most elements have entropies of fusion of 2–3 entropy units (eu = cal/deg/mole); salts and small organic molecules usually have entropies of fusion of 5–7 eu; most organic molecules have entropies around 13 eu.

The entropy of fusion rule for organic compounds was later refined to account for molecular geometry (5). If heat of fusion is plotted *versus* melting point, molecules fall into groups according to molecular shape. The data for the chain-like, disk-like, and spherical molecules fall into regions (6) characterized by:

$$\frac{\Delta H_f}{T_m - a} = K \qquad \text{(Eq. 1)}$$

where ΔH_f is the heat of fusion, T_m is the melting point, and the constants K and a are characteristic of the spatial form of the molecules. Since at the melting point:

$$\Delta S_f = \frac{\Delta H_f}{T_m} \qquad \text{(Eq. 2)}$$

the entropy of fusion is dependent on the melting point for each class of compounds:

$$\Delta S_f = K - \frac{Ka}{T_m} \qquad \text{(Eq. 3)}$$

The entropy of fusion of flexible chain-like molecules increases as R ln 3 for the addition of each CH_2 group to a chain because there are three potential minima for rotation about a carbon–carbon bond (7). This theory explains the apparent dependencies of ΔS_f on area and volume (8, 9).

The entropy of fusion of rigid molecules does not vary directly with surface area (10, 11) or with molecular volume. The entropy of fusion of rigid hydrocarbons varies according to their moments of inertia and symmetry. Strong dipoles and hydrogen bonding have also been assumed to lower the entropy of fusion by hindering rotation in the liquid.

The purposes of this report are to determine the effect of molecular shape, hydrogen bonding, and dipole moment on ΔS_f for rigid nonspherical organic molecules and to consider the effects of these parameters on heat of fusion and melting point.

EXPERIMENTAL

Data Set—The compounds studied were all disubstituted benzene molecules. They included all 84 combinations of the substituents CH_3, Cl, Br, NO_2, OH, NH_2, and COOH in the *ortho*, *meta*, and *para* positions. The entropy of fusion was either determined experimentally or found in the literature for all compounds solid at room temperature as well as for many that are liquid. These compounds were chosen because of their similar size, shape and symmetry, but the substituents cover a wide range of dipole strengths and hydrogen bonding sites. Entropy of fusion differences due to symmetry and shape should have been minimal, while those due to dipole interactions and hydrogen bonding should have been readily apparent.

Determination of Entropy of Fusion—All entropies of fusion were calculated from the heats of fusion and melting points. These quantities were either obtained from the literature (12) or determined experimentally on a differential thermal analyzer[1] with a high-pressure differential scanning calorimeter cell. The literature values were obtained at atmospheric pressure. The experimental values were obtained at 500 psi to inhibit sublimation of the more volatile compounds. This pressure had little or no effect on the entropy of fusion of nonvolatile compounds and was assumed to have no effect on the entropy of fusion of the volatile crystals.

Reliable values for the entropy of fusion of three solids could not be determined experimentally. *p*-Aminophenol decomposed before melting, even under 1000 psi of nitrogen. Phthalic acid dehydrated to phthalic anhydride upon melting. Terephthalic acid sublimed, even under 1000 psi of nitrogen, as shown by a coating of compound around the inside of the calorimeter cell. This coating was insoluble in dilute sodium hydroxide and had the texture of a polymer, suggesting that some chemical

[1] Dupont model 900.

0022-3549/79/0500-0565$01.00/0

© 1979, American Pharmaceutical Association

treatment of silica 63, however, resulted in an insignificant change in the particle-size distribution.

In Table VI and Fig. 4, the data gathered on selected samples are plotted in first-order fashion. The values for K_1 and K_2 were determined from the slopes of the lines, and the dissolution half-lives were calculated from the K_2 values. Where two first-order processes were evident, K_2 represented the slower process that occurred 60 min after dissolution had commenced (Fig. 4, prednisone–silica 63, solvent deposited). The data in Table VI clearly show that a significant change in dissolution half-life can be affected by solvent deposition on, or ball milling with, the amorphous silicon dioxides.

REFERENCES

(1) D. C. Monkhouse and J. L. Lach, *J. Pharm. Sci.*, **61**, 1430 (1972).

(2) C. Ampolsuk, J. V. Mauro, A. A. Nyhuis, N. Shah, and C. I. Jarowski, *ibid.*, **63**, 117 (1974).

(3) N. Shah, R. Pytelewski, H. Eisen, and C. I. Jarowski, *ibid.*, **63**, 339 (1974).

(4) "The United States Pharmacopeia," 19th rev., Mack Publishing Co., Easton, Pa., 1975, p. 765.

(5) H. Johansen and N. Møller, *J. Pharm. Sci.*, **67**, 134 (1978).

Fusion of Disubstituted Benzenes

ERIC MARTIN, SAMUEL H. YALKOWSKY ˣ, and JOHN E. WELLS

Received June 9, 1978, from the *Pharmacy Research Unit, The Upjohn Company, Kalamazoo, MI 49001.* Accepted for publication October 3, 1978.

Abstract □ The entropy of fusion of 84 disubstituted benzenes was essentially constant and independent of the participation of the compounds in intramolecular or intermolecular hydrogen bonding. It was also independent of the shapes, sizes, and dipole moments of the rigid molecules studied. While the entropy of fusion was independent of these parameters, the melting point and the heat of fusion showed a direct dependence on molecular properties.

Keyphrases □ Entropy of fusion—disubstituted benzenes, independent of hydrogen bonding, shape, size, dipole moment of rigid molecules, structure-activity relationships □ Melting point—analysis, disubstituted benzenes, structure-activity relationships □ Benzenes, disubstituted—entropy of fusion, melting point, heat of fusion, structure-activity relationships

The ability to predict the melting point, entropy of fusion, and heat of fusion from chemical structure would make possible the design of compounds having a specified physical state or even a specified melting range. The aqueous solubility of many organic compounds can be predicted from their melting points, entropies of fusion, and octanol–water partition coefficients (1). Since partition coefficients can be predicted by several group contribution methods (2, 3), the estimation of fusion properties makes possible the estimation of aqueous solubility. This possibility has direct implications for drug delivery.

BACKGROUND

In 1908, Walden (4) proposed that entropy of fusion is constant for many classes of compounds. Most elements have entropies of fusion of 2–3 entropy units (eu = cal/deg/mole); salts and small organic molecules usually have entropies of fusion of 5–7 eu; most organic molecules have entropies around 13 eu.

The entropy of fusion rule for organic compounds was later refined to account for molecular geometry (5). If heat of fusion is plotted *versus* melting point, molecules fall into groups according to molecular shape. The data for the chain-like, disk-like, and spherical molecules fall into regions (6) characterized by:

$$\frac{\Delta H_f}{T_m - a} = K \qquad \text{(Eq. 1)}$$

where ΔH_f is the heat of fusion, T_m is the melting point, and the constants K and a are characteristic of the spatial form of the molecules. Since at the melting point:

$$\Delta S_f = \frac{\Delta H_f}{T_m} \qquad \text{(Eq. 2)}$$

the entropy of fusion is dependent on the melting point for each class of compounds:

$$\Delta S_f = K - \frac{Ka}{T_m} \qquad \text{(Eq. 3)}$$

The entropy of fusion of flexible chain-like molecules increases as R ln 3 for the addition of each CH_2 group to a chain because there are three potential minima for rotation about a carbon–carbon bond (7). This theory explains the apparent dependencies of ΔS_f on area and volume (8, 9).

The entropy of fusion of rigid molecules does not vary directly with surface area (10, 11) or with molecular volume. The entropy of fusion of rigid hydrocarbons varies according to their moments of inertia and symmetry. Strong dipoles and hydrogen bonding have also been assumed to lower the entropy of fusion by hindering rotation in the liquid.

The purposes of this report are to determine the effect of molecular shape, hydrogen bonding, and dipole moment on ΔS_f for rigid nonspherical organic molecules and to consider the effects of these parameters on heat of fusion and melting point.

EXPERIMENTAL

Data Set—The compounds studied were all disubstituted benzene molecules. They included all 84 combinations of the substituents CH_3, Cl, Br, NO_2, OH, NH_2, and COOH in the *ortho*, *meta*, and *para* positions. The entropy of fusion was either determined experimentally or found in the literature for all compounds solid at room temperature as well as for many that are liquid. These compounds were chosen because of their similar size, shape and symmetry, but the substituents cover a wide range of dipole strengths and hydrogen bonding sites. Entropy of fusion differences due to symmetry and shape should have been minimal, while those due to dipole interactions and hydrogen bonding should have been readily apparent.

Determination of Entropy of Fusion—All entropies of fusion were calculated from the heats of fusion and melting points. These quantities were either obtained from the literature (12) or determined experimentally on a differential thermal analyzer[1] with a high-pressure differential scanning calorimeter cell. The literature values were obtained at atmospheric pressure. The experimental values were obtained at 500 psi to inhibit sublimation of the more volatile compounds. This pressure had little or no effect on the entropy of fusion of nonvolatile compounds and was assumed to have no effect on the entropy of fusion of the volatile crystals.

Reliable values for the entropy of fusion of three solids could not be determined experimentally. *p*-Aminophenol decomposed before melting, even under 1000 psi of nitrogen. Phthalic acid dehydrated to phthalic anhydride upon melting. Terephthalic acid sublimed, even under 1000 psi of nitrogen, as shown by a coating of compound around the inside of the calorimeter cell. This coating was insoluble in dilute sodium hydroxide and had the texture of a polymer, suggesting that some chemical

[1] Dupont model 900.

0022-3549/79/0500-0565$01.00/0

© 1979, American Pharmaceutical Association

Table I—Input Data for Disubstituted Benzenes

Name	ΔS_f	MP	σ	α	DM	QM	HNO	IHB
o-CH3-CH3	13.20	−25.00	2.00	14.40	0.62	0.27	0.00	0.00
m-CH3-CH3	12.40	−47.40	2.00	14.40	0.40	0.27	0.00	0.00
p-CH3-CH3	14.30	13.50	4.00	14.40	0.00	0.27	0.00	0.00
o-CH3-CL	—	−35.10	1.00	14.50	1.38	2.24	0.00	0.00
m-CH3-CL	—	−47.80	1.00	14.50	1.79	2.24	0.00	0.00
p-CH3-CL	12.90	7.50	2.00	14.50	1.96	2.24	0.00	0.00
o-CH3-BR	—	−28.00	1.00	15.50	1.45	2.33	0.00	0.00
m-CH3-BR	—	−40.00	1.00	15.50	1.77	2.33	0.00	0.00
p-CH3-BR	12.00	28.50	2.00	15.50	1.99	2.33	0.00	0.00
o-CH3-NO2	—	−9.60	1.00	14.80	3.72	9.75	0.00	0.00
m-CH3-NO2	11.40	16.00	1.00	14.80	4.20	9.75	0.00	0.00
p-CH3-NO2	12.60	54.50	2.00	14.80	4.47	9.75	0.00	0.00
o-CH3-OH	12.40	30.90	1.00	13.20	1.45	2.24	2.00	0.00
m-CH3-OH	9.00	11.50	1.00	13.20	1.61	2.24	2.00	0.00
p-CH3-OH	9.60	34.80	2.00	13.20	1.58	2.24	2.00	0.00
o-CH3-NH2	—	−23.70	1.00	13.90	1.59	2.33	2.00	0.00
m-CH3-NH2	—	−30.40	1.00	13.90	1.45	2.33	2.00	0.00
p-CH3-NH2	13.50	43.70	2.00	13.90	1.36	2.33	2.00	0.00
o-CH3-COOH	12.80	107.00	1.00	15.00	1.70	9.75	2.00	0.00
m-CH3-COOH	9.90	112.00	1.00	15.00	2.05	9.75	2.00	0.00
p-CH3-COOH	12.40	182.00	2.00	15.00	2.05	9.75	2.00	0.00
o-COOH-COOH	—	231.00	2.00	15.60	2.45	19.22	4.00	2.00
m-COOH-COOH	18.90	348.00	2.00	15.60	2.27	19.22	4.00	0.00
p-COOH-COOH	—	440.00	4.00	15.60	0.00	19.22	4.00	0.00
o-BR-BR	11.00	7.10	2.00	16.60	2.05	5.99	0.00	0.00
m-BR-BR	12.10	−7.00	2.00	16.60	1.47	5.99	0.00	0.00
p-BR-BR	13.50	87.30	4.00	16.60	0.00	5.99	0.00	0.00
o-BR-NO2	16.30	43.00	1.00	15.90	4.19	20.72	0.00	0.00
m-BR-NO2	13.70	56.00	1.00	15.90	3.44	20.72	0.00	0.00
p-BR-NO2	10.00	127.00	2.00	15.90	2.66	20.72	0.00	0.00
o-BR-OH	9.70	5.60	1.00	14.30	1.37	5.10	2.00	0.00
m-BR-OH	—	33.00	1.00	14.30	2.15	5.10	2.00	0.00
p-BR-OH	10.50	66.40	2.00	14.30	2.27	5.10	2.00	0.00
o-BR-NH2	13.00	32.00	1.00	15.00	1.71	5.18	2.00	0.00
mBR-NH2	—	18.50	1.00	15.00	2.66	5.18	2.00	0.00
p-BR-NH2	14.40	66.40	2.00	15.00	2.95	5.18	2.00	0.00
o-BR-COOH	13.20	150.00	1.00	16.10	2.73	12.60	2.00	0.00
m-BR-COOH	11.90	155.00	1.00	16.10	2.17	12.60	2.00	0.00
p-BR-COOH	15.50	254.00	2.00	16.10	2.10	12.60	2.00	0.00
o-OH-OH	14.40	105.00	2.00	12.00	2.62	4.20	4.00	0.00
m-OH-OH	13.30	111.00	2.00	12.00	2.09	4.20	4.00	0.00
p-OH-OH	14.60	174.00	4.00	12.00	1.40	4.20	4.00	0.00
o-OH-NH2	12.80	174.00	1.00	12.70	1.85	4.29	6.00	0.00
m-OH-NH2	11.20	123.00	1.00	12.70	1.90	4.29	6.00	0.00
p-OH-NH2	—	187.00	2.00	12.70	1.45	4.29	6.00	0.00
o-OH-COOH	10.80	159.00	1.00	13.80	2.65	11.71	4.00	1.00
m-OH-COOH	14.70	202.00	1.00	13.80	2.39	11.71	4.00	0.00
p-OH-COOH	12.20	215.00	2.00	13.80	2.76	11.71	4.00	0.00
o-CL-CL	12.10	−17.00	2.00	14.60	2.20	5.78	0.00	0.00
m-CL-CL	12.30	−24.70	2.00	14.60	1.35	5.78	0.00	0.00
p-CL-CL	13.40	53.10	4.00	14.60	0.00	5.78	0.00	0.00
o-CL-BR	—	−12.30	1.00	15.60	2.20	5.88	0.00	0.00
m-CL-BR	12.20	−21.50	1.00	15.60	1.52	5.88	0.00	0.00
p-CL-BR	13.30	68.00	2.00	15.60	0.00	5.88	0.00	0.00
o-CL-NO2	13.70	34.00	1.00	14.90	4.30	20.61	0.00	0.00
m-CL-NO2	16.10	46.00	1.00	14.90	3.30	20.61	0.00	0.00
p-CL-NO2	11.70	83.60	2.00	14.90	2.59	20.61	0.00	0.00
o-CL-OH	9.10	9.00	1.00	13.30	1.31	4.99	2.00	0.00
m-CL-OH	9.20	33.00	1.00	13.30	2.15	4.99	2.00	0.00
p-CL-OH	11.10	43.50	2.00	13.30	2.25	4.99	2.00	0.00
o-CL-NH2	—	−14.00	1.00	14.00	1.79	5.18	2.00	0.00
m-CL-NH2	—	−10.30	1.00	14.00	2.70	5.18	2.00	0.00
p-CL-NH2	13.80	72.50	2.00	14.00	2.99	5.18	2.00	0.00
o-CL-COOH	14.90	142.00	1.00	15.10	2.50	12.60	2.00	0.00
m-CL-COOH	13.30	158.00	1.00	15.10	2.22	12.60	2.00	0.00
p-CL-COOH	15.00	243.00	2.00	15.10	2.02	12.60	2.00	0.00
o-NH2-NH2	12.00	102.00	2.00	13.40	1.45	4.38	4.00	0.00
m-NH2-NH2	11.50	101.00	2.00	13.40	1.79	4.38	4.00	0.00
p-NH2-NH2	10.40	140.00	4.00	13.40	1.52	4.38	4.00	0.00
o-NH2-COOH	11.70	147.00	1.00	14.50	1.52	11.80	6.00	1.00
m-NH2-COOH	11.60	174.00	1.00	14.50	2.73	11.80	6.00	0.00
p-NH2-COOH	10.90	189.00	2.00	14.50	3.39	11.80	6.00	0.00
o-NO2-NO2	14.00	118.50	2.00	15.20	6.04	35.45	0.00	0.00
m-NO2-NO2	12.50	90.20	2.00	15.20	3.83	35.45	0.00	0.00
p-NO2-NO2	15.00	174.00	4.00	15.20	0.58	35.45	0.00	0.00
o-NO2-OH	12.50	45.50	1.00	13.60	3.15	19.83	2.00	1.00
m-NO2-OH	13.80	97.00	1.00	13.60	3.91	19.83	2.00	0.00
p-NO2-OH	13.00	115.00	2.00	13.60	5.05	19.83	2.00	0.00
o-NO2-NH2	11.20	71.50	1.00	14.30	4.28	19.91	4.00	1.00
m-NO2-NH2	14.70	114.00	1.00	14.30	4.85	19.91	4.00	0.00
p-NO2-NH2	12.00	149.00	2.00	14.30	6.32	19.91	4.00	0.00
o-NO2-COOH	15.90	147.00	1.00	15.40	3.82	27.33	2.00	2.00
m-NO2-COOH	11.30	141.00	1.00	15.40	3.50	27.33	2.00	0.00
p-NO2-COOH	17.20	242.00	2.00	15.40	3.50	27.33	2.00	0.00

Table II—Results of Regression Analyses

Dependent Variable		Independent Variable Estimated Coefficient (T Value)							
s	r^2	σ	α	QM	HNO	IHB	MP	DM	Intercept
ΔS_f: 1.83	0.179	0.49	0.31	0.08	0.09	−0.09		−0.01	6.31
		(1.64)	(1.17)	(2.03)	(0.58)	(−0.12)		(−0.04)	(1.51)
MP: 43.2	0.796	29.7	28.7	5.40	41.8	−28.5		−10.2	−492
		(4.60)	(4.80)	(6.44)	(12.90)	(−2.02)		(−1.87)	(−5.30)
MP: 44.6	0.778	36.9	30.2	4.07	40.4				−535
		(6.44)	(5.06)	(6.58)	(12.54)				(−6.01)
ΔH_f: 1169	0.476	540	491	75	526				−5231
		(3.13)	(2.94)	(4.36)	(5.50)				(−266)
ΔH_f: 672	0.829	−27.6	−79.7	−2.01	−268		21.4		4474
		(−0.25)	(−0.74)	(−0.17)	(−3.02)		11.4		(2.65)
ΔH_f: 735	0.783						17.7		3065
							(15.5)		(21.9)

change (possibly to a linear anhydride) occurred as well. These data were excluded from the analysis.

Variables—One purpose of this study was to determine whether the thermodynamic properties of melting point, MP, heat of fusion, ΔH_f, and entropy of fusion, ΔS_f, are dependent on other, easily predicted properties. Molecular properties rather than bulk properties were chosen as parameters for two reasons. First, they can be estimated from the molecular structure so they can be used for predictions about little-studied compounds and about compounds that have not yet been synthesized. Second, the effects of molecular properties are more easily interpreted and are more valuable in explaining and understanding any discovered relationship.

Because these three thermodynamic properties are directly related [$\Delta H_f = (\Delta S_f) \times T_m$, where T_m is the Kelvin melting point], only two of them need be determined to obtain all three. Melting point is among the most difficult properties to predict. Fortunately, it is easily determined and frequently reported, so it is usually known. The entropy of fusion is largely predictable from previous work. The effects of certain electronic factors have not yet been determined and were the focus of this study.

The maximum possible number of hydrogen bonds (HNO) and the dipole moment (DM) were selected because they are known to affect the degree of disorder in the liquid state. They also affect the entropy of fusion. The simulated quadrapole moment (QM) accounted for electronic effects that are strong in the closely packed crystal but weak at the greater intermolecular distances in the liquid. The parameters (HNO, DM, and QM) can be predicted accurately from molecular structure alone (3), although experimental literature values were used in most cases.

The orientational symmetry number, σ, accounted for the statistical likelihood of finding a molecule properly oriented for incorporation into the crystal. Sigma is defined as the orientational degeneracy of a molecule, *i.e.*, the number of orientations of the molecule that will appear identical when viewed from a given point. The *ortho*-, *meta*-, and *para*-dichlorobenzenes have sigma values of 2, 2, and 4, respectively; *ortho*-, *meta*-, and *para*-bromochlorobenzenes have values of 1, 1, and 2, respectively. In this report, polyatomic groups such as CH_3, NH_2, NO_2, OH, and COOH are treated as monoatomic substituents which are coplanar with the benzene ring.

The polarizability, α, reflected the ability of the compound to interact with dipoles or induced dipoles. Polarizabilities were calculated from the following group incremental values: C_6H_4, 10.0; CH_3, 2.2; Cl, 2.3; Br, 3.3; NO_2, 2.6; NH_2, 1.7; OH, 1.0; and COOH, 2.8.

The dipole moments (DM) for all compounds were found in Ref. 13 except for *m*-bromophenol, terephthalic acid, and *p*-hydroxyaniline. The bromo compound was assigned the same value as the corresponding chloro compound because their group contributions were similar. *p*-Hydroxyaniline was estimated as being in the same ratio to *p*-dihydroxybenzene and *p*-diaminobenzene as the corresponding *ortho* and *meta* values. Terephthalic acid was assumed to be zero by its planarity and symmetry.

The simulated quadrapole moment is an artificial variable. It is the sum of the squares of the group dipole contributions from the two substituents:

$$QM = \mu_1^2 + \mu_2^2 \qquad \text{(Eq. 4)}$$

The squares were used because quadrapole moment is defined by $q = \Sigma er^2$, where e is the charge and r is the distance between the charges, whereas dipole moment is simply proportional to the distance:

$$\mu = \Sigma er \qquad \text{(Eq. 5)}$$

The maximum number of possible hydrogen bonds touching each molecule was the smaller of:

$$HNO = 2 \times H_a \qquad \text{(Eq. 6}a\text{)}$$

or:

$$HNO = 2 \times H_d \qquad \text{(Eq. 6}b\text{)}$$

where H_a is the number of hydrogen bond acceptor sites (electron pairs on oxygen or nitrogen) and H_d is the number of hydrogen bond donor sites (hydrogen attached to oxygen or nitrogen). The smaller of the two values was used instead of the number of protons because repeating networks of association in the liquid must have an acceptor for each donor.

The IHB variable indicated the ability of a molecule to form intramolecular hydrogen bonds. Internal hydrogen bonding competes with external (intermolecular) hydrogen bonding and thus would be expected to decrease melting point. The IHB is unity if the compound is capable of forming a hydrogen bond in a six- or seven-membered ring and zero if it is not. Thus, for resorcinol and related compounds, IHB = 0.0.

The data were analyzed by multiple linear regression using the Statistical Analysis System. The r^2 value was used as a measure of correlation for each set tested. Values above 0.9 were considered quantitatively useful; values above 0.7 were considered a qualitative correlation, indicative of a trend but not good enough for accurate predictions; values below 0.7 were considered random. The T values were used to determine the significance of each independent variable's contribution to the whole equation in multiple regressions. Values above 3 were considered to be borderline correlations, and values above 4 were considered to be significant contributions. The results of these tests are given in Tables I and II.

RESULTS AND DISCUSSION

The data consisted of ΔS_f, MP, σ, α, DM, QM, HNO, and IHB values for all 84 compounds (Table I). The ΔH_f and ΔS_f have been determined for only 69 compounds. If any of the variables were missing for a compound in a given analysis, that compound was not included in that run. The number of common values determined the size of the data set for each regression.

The results of the more interesting regression analyses for ΔS_f, ΔH_f, and MP are given in Table II.

Inspection of Table II shows that ΔS_f does not depend on any of the parameters against which it was measured ($r^2 < 0.40$). It is independent of the number of hydrogen bonds, of dipole moment, and of other measures of attractive electronic factors. It is approximately constant, with a value of 12.7 ± 2 eu (mean ± SD) for all 69 data points. Constancy is also shown by the low estimated coefficients,which indicate an approximately horizontal slope. The low T value for σ (Table II) indicates that the effect of molecular geometry is also insignificant. Symmetry, moment of inertia, and other structurally related properties do not affect the entropy of fusion for these compounds. However, because this set of compounds was chosen to minimize these geometrical effects, this result cannot be generalized.

The fact that the entropy of fusion is independent of the electronic attractive factors (Table III) contradicts previous reports (10). For the 24 compounds in the upper left quadrant (Table III), neither substituent has a hydrogen bond-forming hydrogen. The average value of ΔS_f for this group is 13.0 ± 1.48 eu. The upper right quadrant is occupied by the 30 compounds with one hydrogen bond-forming substituent. The mean ΔS_f for these compounds is 12.7 ± 2.20 eu. (Two compounds with questionable values were excluded.) The average for all three groups is between 12.5 and 13 eu, with no systematic decrease apparent.

Bondi (10) stated that any factors that interfere with free rotation in the liquid would decrease the entropy. Hydrogen bonds and strong di-

Table III—Fusion Entropies (eu) of Disubstituted Benzene Compounds

Substituents	CH_3	Cl	Br	NO_2	OH	NH_2	CO_2H
CH_3: *o*	13.2	*L*[a]	*L*	*L*	12.4	*L*	12.8
m	12.4	*L*	*L*	11.4	9.0	*L*	9.9
p	14.2	12.9	12.0	12.6	9.6	13.5	12.4
Cl: *o*		12.1	*L*	13.7	9.1	*L*	14.9
m		12.3	12.2	16.1	9.2	*L*	13.3
p		13.4	13.3	11.7	11.1	13.8	15.0
Br: *o*			11.0	16.3	9.7	[13.0][b]	[13.15]
m			12.1	13.7	*L*	*L*	[11.9]
p			13.5	[10.0]	10.5	[14.4]	[15.5]
NO_2: *o*				14.0	12.5	11.2	15.9
m				12.5	13.8	14.7	11.3
p				15.0	13.0	12.0	17.2
OH: *o*					14.4	[12.8]	[10.8]
m					13.3	[11.2]	[14.7]
p					14.6	—[c]	[12.2]
NH_2: *o*						[12.0]	11.7
m						[11.5]	11.6
p						[10.4]	10.9
CO_2H: *o*							[23.3][d]
m							[18.9]
p							[31.3][e]

[a] *L* = liquid at room temperature. [b] Values in brackets were determined experimentally by differential scanning calorimetry. All others are literature values. [c] Decomposed before melting. [d] Evidence of reaction during melting. *Not used.* [e] Evidence of reaction and sublimation during melting. *Not used.*

Table IV—Entropy of Fusion Differences between Substituted Phenols and Their Hydrocarbon Homomorphs

Hydroxy Derivative	Hydrocarbon Homomorph	$\Delta\Delta S_f$
o-Hydroxytoluene	*o*-Toluene	0.8
m-Hydroxytoluene	*m*-Toluene	3.4
p-Hydroxytoluene	*p*-Toluene	4.6
o-Chlorophenol	*o*-Chlorotoluene	—
m-Chlorophenol	*m*-Chlorotoluene	—
p-Chlorophenol	*p*-Chlorotoluene	1.8
o-Bromophenol	*o*-Bromotoluene	—
m-Bromophenol	*m*-Bromotoluene	—
p-Bromophenol	*p*-Bromotoluene	−2.4
o-Nitrophenol	*o*-Nitrotoluene	—
m-Nitrophenol	*m*-Nitrotoluene	2.4
p-Nitrophenol	*p*-Nitrotoluene	0.4
o-Aminophenol	*o*-Aminotoluene	—
m-Aminophenol	*m*-Aminotoluene	—
p-Aminophenol	*p*-Aminotoluene	—
o-Dihydroxybenzene	*o*-Hydroxytoluene	−2.0
m-Dihydroxybenzene	*m*-Hydroxytoluene	−3.3
p-Dihydroxybenzene	*p*-Hydroxytoluene	−5.0
o-Hydroxybenzoic acid	*o*-Toluic acid	2.0
m-Hydroxybenzoic acid	*m*-Toluic acid	−4.8
p-Hydroxybenzoic acid	*p*-Toluic acid	−0.2
R-C_6H_4OH	R-$C_6H_4CH_3$	−0.18[a]

[a] Average.

poles restrict free rotation and decrease the disorder in the liquid state. The lack of effect of these phenomena on the entropy of fusion can be explained on the basis of the effect of hydrogen bonding in the crystal.

Entropy is related to disorder by a logarithmic function:

$$\Delta S_{or} = R \ln \frac{\Omega_r}{\Omega_{tor}} \qquad \text{(Eq. 7)}$$

The orientational contribution to the entropy is determined by the ratio of the number of complexions available in the liquid to the number of complexions available in the crystal. If the magnitude of the torsional oscillations were restricted in the crystal by the same percentage as the rotations are restricted in the liquid, there would be no change in entropy. The effect of hydrogen bonding on bulk crystalline properties such as packing density and melting point shows that factors that lead to association in the liquid also hold the molecules more tightly in the solid. The smaller A-B intermolecular distances and the appearance of A-H···B vibrational modes in the IR regions provide evidence that hydrogen bonds might restrict these torsional oscillations in the crystal (14).

The lack of a consistent effect of hydrogen bonding can be demonstrated by comparing the entropy of fusion of hydroxyl compounds with that of their methyl homomorphs (Table IV).

The heat of fusion equals the product of the entropy and the melting point. If the entropy is a constant, ΔH_f should depend only on MP. Therefore, the value of the correlation coefficient of the regression ΔH_f *versus* MP indicates how well 12.7 approximates the entropy of the set of compounds tested. Table II shows that ΔH_f does indeed depend only on MP. The r^2 value of 0.78 shows that a strong correlation exists but accurate values must be determined experimentally.

The regression analysis of melting point is also given in Table II. Four parameters were necessary to obtain a definite trend. These results were difficult to interpret because of the low r^2 value for the number of parameters and the large contribution of the sigma parameter, which probably includes a large variety of unspecified factors. The most interesting results is the much larger contribution of QM than DM as a result of the proximity of the molecules in the crystal. In the tightly packed, highly ordered crystal lattice, the molecules arrange themselves so that the negative parts of one molecule are closest to the positive portions of neighboring molecules. At these distances, a negative group is strongly attracted to the positive charge adjacent to it, but it is largely unaffected by the repulsive forces at the other end of the molecule since quadrapole fields fall off so rapidly with distance (much more rapidly than dipoles). Although no definite conclusions can be drawn from the melting-point correlations, they provide some encouragement for the eventual ability to understand and predict melting point.

REFERENCES

(1) S. Yalkowsky, in "Design of Biopharmaceutical Properties through Prodrugs and Analogs," E. B. Roche, Ed., APhA, Washington, D.C., 1977, chap. 13, p. 392.

(2) C. Hansch, A. Leo, and D. Nikaitani, *J. Org. Chem.*, **37**, 3090 (1972).

(3) G. G. Nys and R. F. Rekker, *Eur. J. Med. Chem.*, **9**, 361 (1974).

(4) P. Walden, *Z. Electrochem.*, **14**, 713 (1908).

(5) J. Pirsch, *Ber.*, **70**, 12 (1937).

(6) J. Pirsch, *Mikrochim. Acta.*, **1-6**, 992 (1956).

(7) R. H. Aranow, L. Witten, and D. H. Andrews, *J. Phys. Chem.*, **62**, 812 (1958).

(8) A. Luttinghaus and G. Vierk, *Ber.*, **82**, 376 (1949).

(9) H. Shinke and F. Sauerwald, *Z. Phys. Chem.*, **216**, 26 (1961).

(10) A. Bondi, "Physical Properties of Molecular Crystals, Liquids, and Glasses," Wiley, New York, N.Y., 1968.

(11) A. Bondi, *Chem. Rev.*, **67**, 565 (1967).

(12) R. C. Weast, "Handbook of Chemistry and Physics," CRC, Cleveland, Ohio, 1975.

(13) A. L. McClellan, "Tables of Dipole Moments," Freeman, San Francisco, Calif., 1963.

(14) G. C. Pimentel and A. L. McClellan, "The Hydrogen Bond," Freeman, San Francisco, Calif., 1960.

Use of a Nitrogen-Specific Detector for GLC Determination of Plasma Bucainide

HERSCHEL H. C. LI ˣ, WILLIAM P. FEENEY, and MARTHA M. JOHNSTON

Received April 12, 1978, from the *Department of Biochemistry and Drug Disposition, USV Pharmaceutical Corp., Tuckahoe, NY 10707.* Accepted for publication October 18, 1978.

Abstract □ A sensitive and specific GLC determination of plasma bucainide was developed using a nitrogen-specific detector. The method permits the determination of bucainide as low as 5.0 ng/ml of plasma and provides sufficient sensitivity and reproducibility for clinical use.

Keyphrases □ GLC—bucainide, analysis in plasma □ Bucainide—GLC analysis in plasma □ Antiarrhythmic—bucainide, GLC analysis in plasma

Bucainide maleate[1] (I), 1-(*N*-isobutyl)benzimidoyl-4-(*N*-hexyl)piperazine dimaleate, is a novel, potent antiarrhythmic agent. The antiarrhythmic effect was demonstrated in the following animal models: mouse chloroform-induced ventricular arrhythmias, refractory period prolongation in guinea pig isolated atria, aconitine-induced atrial arrhythmias in the dog, ventricular arrhythmias following coronary artery ligation in the dog, and ouabain-induced ventricular tachyarrhythmias in the dog (1). The drug also possesses local anesthetic effects and is a weak central nervous system depressant[2].

The development of a reliable, specific, and sensitive determination of bucainide in plasma was initiated to support clinical and related studies. Recent advances in GLC detector technology indicated that a nitrogen-specific detector would be feasible. The use of a nitrogen-specific detector for the determination of imipramine and desipramine (2), cocaine (3), and theophylline (4) in biological fluids was reported. Bucainide, due to the three nitrogen atoms on the molecule, appeared to be a promising candidate for this mode of detection.

EXPERIMENTAL

GLC—The gas chromatograph[3] was equipped with a nitrogen-phosphorus detector (NPD). A 1.8-m × 0.2-cm i.d. glass column was packed with 3% phenyl methyl silicone fluid coated on acid-washed, dimethylchlorosilane-treated (80–100-mesh) diatomite support[4]. Retention times and peak areas were measured by a single-channel computing integrator[5].

The gas chromatograph was run in the isothermal mode at a column temperature of 240°. The flow rate of the carrier gas (helium) was 40 ml/min, while the detector gases were set at 100 ml/min for air and 3 ml/min for hydrogen.

The standing current of the detector was calibrated daily by adjustment of the potentiometer so that a 50% full-scale response was obtained on the recorder at an attenuation setting of 64 on the integrator.

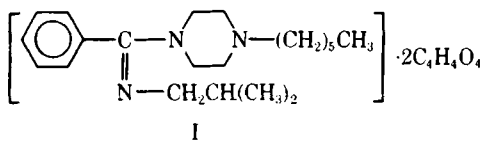

I

Reagents and Materials—Hexane, acetone, *n*-butyl chloride, and 2-propanol were "distilled-in-glass" grade[6]. The aqueous solution of saturated sodium bicarbonate was filtered[7] before use.

N^1-Hexyl-N^4-benzoylpiperazine maleate[1] (II) was selected as the internal standard. Oxalated dog plasma[8], which was kept frozen in polypropylene containers, was employed for standard curves.

All glassware was kept in chromic acid overnight. After cleaning, the glassware was rinsed with acetone prior to use.

Procedure—Aliquots of 7.5, 15, 30, 60, 90, 120, and 150 μl of bucainide maleate aqueous stock solution (equivalent to 14.8 ng/10 μl as base) were added to 2.0 ml of control dog plasma samples in 15-ml polytef-lined screw-capped tubes. In addition, an aliquot of 50 μl of the internal standard aqueous stock solution (equivalent to 14.1 ng/10 μl as base) was added to each tube. These samples were used to generate a standard curve. An equal aliquot of the internal standard solution was added to all unknown samples.

After an addition of 2.0 ml of saturated sodium bicarbonate solution to each plasma sample, bucainide was extracted with 5.0 ml of *n*-butyl chloride–2-propanol (90:10 v/v) by shaking at 120 oscillations/min for 15 min on a reciprocating shaker[9]. The organic phase was transferred to a second extraction tube containing 5.0 ml of hexane. Bucainide was then extracted with 1 ml of 0.1 *M* H_2SO_4. The addition of hexane to lower the solvent polarity of the organic phase enhanced the extraction of bucainide into acid.

After the solution was alkalinized with 3.0 ml of saturated sodium bicarbonate solution, the drug was back-extracted into 5.0 ml of *n*-butyl chloride–2-propanol (90:10 v/v). The organic extract was evaporated[10] to dryness under nitrogen at 30°, and the residue was redissolved with 25 μl of acetone by vigorous vortexing. To avoid evaporation, the sample was kept on ice prior to GLC analysis, which used an aliquot of 5.0 μl.

RESULTS AND DISCUSSION

Solvent Extraction—The extractibility of bucainide and II as a function of pH was studied in separate experiments with *n*-butyl chloride–2-propanol (90:10 v/v) as the solvent. Bucainide, together with *n*-dososane[11] as an internal standard, was spiked into pH 6, 7, 8, 9, 10, 11, and 12 buffers. The organic extracts were evaporated to dryness and redissolved in acetone before detection by flame ionization. The results showed that after an initial increase from pH 6 to 7, no significant increase in bucainide extraction was observed between pH 7 and 12. Similarly, II was found equally extractible over the pH 6–12 range.

The extraction efficiency of bucainide with II as the internal standard was studied by comparing the relative areas of the extracted spiked plasma samples with those of the unextracted reference standards. An average of 98.5% recovery was observed for the range of 7.5–111.8 ng/ml of plasma.

Plasma Standard Curves—Figure 1 is a typical chromatogram of a spiked plasma sample used for the standard curve. The peak at 150 sec represents 66.6 ng/ml of bucainide, whereas the peak at 210 sec represents 35.3 ng/ml of the internal standard.

Four plasma standard curves for the range of 5.6–111.0 ng/ml were analyzed over 3 weeks (Table I). The standard error was 9.1% for 5.6 ng/ml and 1.8% for 111.0 ng/ml. The composite standard curve was determined by regression analysis, the equation of which was: $y = 0.01445x + 0.05788$, where y represents the relative areas of bucainide to II and x is the bucainide concentration in nanograms per milliliter.

[1] Synthesized by the Medicinal Chemistry Department, USV Pharmaceutical Corp., Tuckahoe, NY 10707; purity was certified by the Analytical Research and Development Department.

[2] J. S. Shroff and P. Cervoni, paper presented at the Second Joint Conference of the Chemical Institute of Canada/American Chemical Society, Montreal, Canada, May 1977.

[3] Perkin-Elmer Corp., Norwalk, CT 06582.

[4] OV-17 on Supelcoport, Supelco, Inc., Bellefonte, PA 16823.

[5] Minigrator, Spectra-Physics, Piscataway, NJ 08854.

[6] Burdick & Jackson Laboratories, Muskegon, MI 49442.

[7] Type HA filter of 0.45 μm, Millipore Corp., Bedford, MA 01730.

[8] Pel Freez Biologicals, Rogers, AR 72756.

[9] Arthur H. Thomas Co., Philadelphia, PA 19105.

[10] Organomation Associates, Shrewsbury, MA 01545.

[11] Applied Science Laboratories, State College, PA 16801.

0022-3549/79/0500-0569$01.00/0
© 1979, American Pharmaceutical Association

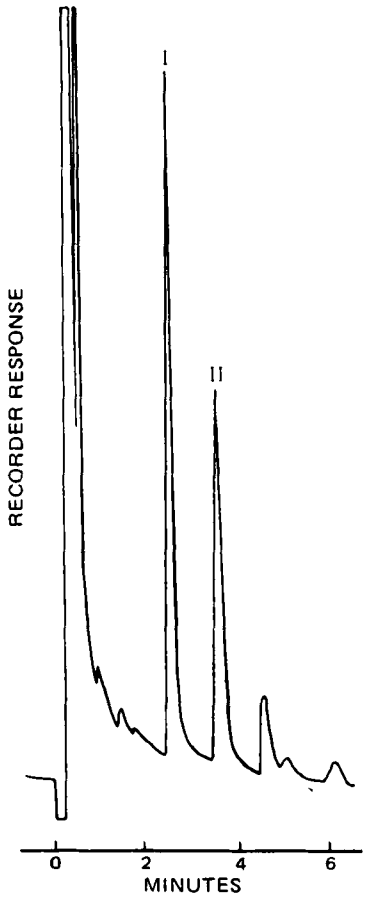

Figure 1—*Chromatogram of a control dog plasma sample, which was spiked with the bucainide reference standard and the internal standard. The peaks at 150 and 210 sec represent 66.6 ng of bucainide and 35.3 ng of II/ml of plasma, respectively.*

The standard curve was linear for the range studied (r = 0.986).

Specificity—To study the possible interference due to endogenous materials in the plasma, plasma samples of four different subjects from a clinical study were extracted as already described and analyzed without addition of the internal standard under the established GLC conditions. The samples represent either predose plasma blanks or samples at various time intervals from subjects receiving a placebo. No interference peaks at the retention times of bucainide or II were observed.

Similarly, another set of plasma samples from a multiple-dose clinical study was analyzed by the same procedure without the internal standard. These samples were obtained after the fourth intravenous dose of 50 mg at 10 min and 1, 3, and 6 hr. None of these samples showed any interference peaks at the II retention time.

Subsequently, GLC–mass spectrometry[12] was employed to substantiate further the absence of interference due to either unidentified metabolites or plasma endogenous materials coextracted and cochromatographed with bucainide or II. A set of plasma samples from the same subject at 0 and 15 min and 1, 2, and 3 hr after the fourth intravenous dose was spiked with the internal standard and extracted as described. The pooled extract was analyzed using chemical ionization with isobutane as the reactant gas.

For each fraction, the chemical-ionization mass spectra showed a base peak at m/e 330 and 275, corresponding to the expected protonated molecular ions, MH^+, of bucainide and the internal standard. Minor peaks at m/e 202 for bucainide and m/e 140 for the internal standard also were observed. These minor peaks were the breakdown products of the corresponding MH^+ ions. These assignments were supported by the identical spectra of the respective unextracted reference standards. Based on these studies, the present method was specific for the determination of bucainide in plasma samples from controlled clinical studies when the subjects were free from other medication.

Clinical Samples—A complete profile of the plasma bucainide levels of one subject from a multiple-dose clinical study is shown in Table II. The subject received four intravenous doses of 50 mg at a dose interval of 4 hr. The predose levels of bucainide at Doses 2 and 3 were approximately 5 ng/ml. The levels of the samples taken immediately after Doses 1, 2, 3, and 4 were about 500–1000 ng/ml.

[12] Chemical-ionization mass spectra were obtained using a Varian MAT 112 GLC-mass spectrometer interfaced to a Varian MAT SS-100C data processing system, Varian MAT, Florham Park, NJ 07832.

Table I—Composite Plasma Standard Curve [a]

Plasma Concentration, ng/ml	Mean Relative Area ± *SE*	*SE*, %
5.6	0.11 ± 0.01	9.1
11.1	0.23 ± 0.02	8.7
22.2	0.42 ± 0.03	7.1
44.4	0.65 ± 0.01	1.5
66.6	1.03 ± 0.04	3.9
88.8	1.28 ± 0.07	5.5
111.0	1.70 ± 0.03	1.8

[a] Composite of four standard curves, and each concentration point was determined in duplicate; $y = 0.01445x + 0.05788$ (r = 0.986).

Table II—Plasma Bucainide Levels for One Subject [a]

Sample Time	Dose 1	Dose 2	Dose 3	Dose 4
Predose[b]	0.0	5.2	5.6	—
"Zero"[c]	940.2	497.0	533.9	482.8
10 min	49.5	—	—	52.1
20 min	34.8	—	—	30.7
1 hr	9.3	—	—	27.6
2 hr	10.2	—	—	12.3

[a] Subject received four intravenous doses of 50 mg of bucainide at a dose interval of 4 hr. [b] Predose samples were taken 10 min prior to dosing. [c] Samples were taken immediately after a 2-min intravenous infusion of the drug.

REFERENCES

(1) J. R. Shroff and P. Cervoni, "Proceedings of the Third International Congress Iranian Chemical Society, Shiraz, Iran," Mar. 1975, p. 130.

(2) D. N. Bailey and P. I. Jatlow, *Clin. Chem.*, **22**, 1697 (1976).

(3) P. I. Jatlow and D. N. Bailey, *ibid.*, **21**, 1918 (1975).

(4) J. D. Lowry, L. J. Williamson, and V. A. Raisys, *J. Chromatogr.*, **143**, 83 (1977).

ACKNOWLEDGMENTS

Presented in part at the Eighth Northeast Regional Meeting, American Chemical Society, June 1978.

The authors gratefully acknowledge the technical assistance of Dr. R. Biniakewitz and Mr. N. Ruzza, the Analytical Research and Development Department, USV Pharmaceutical Corp., for the GLC–mass spectrometry analysis.

Rotating-Disk Method for Determining Cutaneous Metabolism

L. C. LEUNG and H. Y. ANDO ˣ

Received September 13, 1978, from the *Department of Pharmacy, Philadelphia College of Pharmacy and Science, Philadelphia, PA 19104.* Accepted for publication October 19, 1978.

Abstract □ Since design and evaluation of topical dosage forms should account for both skin permeation and cutaneous metabolism, an *in vitro* system was formulated to determine the metabolic component of viable guinea pig skin utilizing the diffusion layer property of the rotating disk. The drug investigated was vidarabine, an antiviral agent, which was rapidly metabolized to 9-β-D-arabinofuranosylhypoxanthine. The aqueous diffusion coefficient of the drug was determined by the capillary cell method. The rotating-disk system was standardized using benzoic acid. The dorsal skin of a guinea pig was removed after shaving, and the epidermal section was excised by a keratome. After the section was mounted on the stainless steel disk with a tissue adhesive, the preparation was immersed in a 10-ml beaker containing 5 ml of drug solution at 37°. At suitable intervals, samples were withdrawn, separated by TLC, and assayed by liquid scintillation. The enzyme rate constant was 1.54×10^{-1} sec^{-1}.

Keyphrases □ Rotating disk—analysis, cutaneous metabolism of vidarabine, guinea pig, *in vitro* study □ Skin—metabolism of vidarabine, rotating-disk method, guinea pig, *in vitro* study □ Antiviral agents—vidarabine, cutaneous metabolism, rotating-disk method, guinea pig, *in vitro* study □ Vidarabine—cutaneous metabolism, analysis by rotating-disk method, guinea pig, *in vitro* study

Recently (1, 2), an *in vitro* model was proposed for determining the simultaneous transport and metabolism of vidarabine (I) into 9-β-D-arabinofuranosylhypoxanthine (II) in hairless mouse skin. However, some experimental parameters required for the metabolic rate constant calculation were not determined, namely, the aqueous diffusion coefficient of I, D_{aqA}, and the diffusion layer thickness, h.

The objectives of the present investigation were to assess these parameters and to determine the enzyme metabolic rate constant. A capillary cell method (3) was used for the determination of D_{aqA}. By using the rotating-disk theory (4) and benzoic acid standardization (5), h was calculated. These parameters were then used for the calculation of the cutaneous metabolic enzyme rate constant.

EXPERIMENTAL

Apparatus—A constant-speed synchronized motor[1], a 50-μl syringe[2], a liquid scintillation counter[3], a laboratory press[4], two variable-speed synchronized motors[5], a light tachometer[6], 10-ml micropipets[7], a membrane filter[8], an electric shaver[9], a keratome[10], and silica GF plates[11] were used.

Reagents and Materials—The following were used: vidarabine[12], ^{3}H-vidarabine[13], 9-β-D-arabinofuranosylhypoxanthine[12], benzoic acid (primary standard)[14], ^{14}C-benzoic acid, a commercially prepared liquid scintillation cocktail[15], 0.01 *N* HCl[14], female albino guinea pigs (500–600 g), and pentobarbital sodium.

Aqueous Diffusion Coefficient, D_{aqA}, Determination—The upper reservoir of the diffusion cell (3) was nylon, and the capillary portion was a 50-μl gas-tight syringe[2] ground flat to the zero calibration mark. The value of D_{aqA} was determined by Saraf's method (3) using ^{3}H-vidarabine and liquid scintillation.

Estimation of Aqueous Diffusion Layer, h—The stainless steel rotating disk consisted of an outer cone-shaped manifold and an inner cylindrical disk (Fig. 1). Experimental deviations from the Levich (4) theory due to geometry and hydrodynamics were assessed using a benzoic acid standardization (5, 6).

By recrystallizing 0.1 mCi (0.9 mg) of ^{14}C-labeled and 9 g of primary standard benzoic acid from alcohol, radioactive benzoic acid crystals were obtained. Pellets of this material were prepared on a laboratory press by directly compressing about 500 mg of the crystals in a flat surface die (1.27 cm i.d.) with an average force of 4086 kg (9000 lb).

For each dissolution run, 5 ml of 0.01 *N* HCl, preequilibrated at 37°, was pipetted into a 10-ml beaker in a 37° controlled bath. The benzoic acid pellet was firmly seated in the outer cone-shaped manifold, which was connected to a synchronized motor. The rotation speed was determined with a light tachometer and adjusted to 300 rpm. After the disk was immersed in the hydrochloric acid solution, 10-μl samples were withdrawn with a micropipet at 5-min intervals and were assayed by liquid scintillation counting.

Metabolism Study of Vidarabine (I)—*Preparation of Radioactive Solution*—A 600 μ*M* I solution was prepared by dissolving 16.0 mg of I in 100 ml of Delbecco buffer (7) and filtering the solution through a 0.22-μm filter. By successive serial dilutions, stock solutions of 0.25, 0.5, 0.75, 1.0, and 6.0 μ*M* were obtained. Five-milliliter samples of these solutions were spiked with 10 μCi of ^{3}H-vidarabine (I) prior to each experiment.

Preparation of Skin—A female albino guinea pig, 500–600 g, was anesthetized with pentobarbital sodium (100 mg/kg ip). The dorsal skin was shaved first with an animal shaver and then with a manual razor. The area was washed with distilled water and dried with a stream of warm air. After removal from the animal, the dorsal skin was stapled onto a wooden board. The animal was then sacrificed with pentobarbital sodium.

A keratome set at 0.2 mm removed a thin layer of the epidermis plus some underlying dermis from the skin. The inner disk was removed from the outer manifold and placed over the shaved surface; tissue adhesive[16] was used to secure the skin to the side of the disk. To expose a constant surface area of the skin, polytef tape was wrapped around the skin on the cylindrical surface and secured with tissue adhesive. The outer cone-shaped manifold was then replaced on the inner disk (Fig. 1). This preparation was connected to a synchronized motor and immediately immersed in the 5 ml of radioactive I solution prepared prior to each experiment and maintained at 37°.

Five microliters of this solution was spotted with 1.5 μg of nonradioactive I and II onto prescored silica GF plates under a nitrogen stream. The plates were immediately developed in the solvent system described previously (8). After separation, I and II were scraped into vials and assayed by liquid scintillation. As a control, the experiment was duplicated twice without the skin.

RESULTS AND DISCUSSION

Aqueous Diffusion Coefficient Determination—The aqueous diffusion coefficient for Compound *A*, D_{aqA}, can be determined from (9):

$$D_{aqA} = \frac{4L^2}{\pi^2 T} \ln\left(\frac{8C_0}{\pi^2 C_a}\right) \qquad \text{(Eq. 1)}$$

[1] Hurst Manufacturing Co., Princeton, Ind.
[2] Hamilton Co., Whittier, Calif.
[3] Packard Tri-Carb model 3385, Packard Instrument Co., Downers Grove, Ill.
[4] Fred Carver Inc., Summit, N.J.
[5] GT210 laboratory stirrer, Gerald K. Hiller Co.
[6] Power Instruments Inc., Skokie, Ill.
[7] Bio-Rad Laboratories, Richmond, Calif.
[8] Millipore Corp., Boston, Mass.
[9] Oster Co., Milwaukee, Wis.
[10] Storz Surgical Instruments, St. Louis, Mo.
[11] Altech, Inc., Newark, Del.
[12] PL-Biochemicals, Milwaukee, Wis.
[13] New England Nuclear, Boston, Mass.
[14] Fisher Co., Pittsburgh, Pa.
[15] Aquasol, New England Nuclear, Boston, Mass.
[16] Eastman-910, Kodak, Rochester, N.Y.

0022-3549/79/0500-0571$01.00/0
© 1979, American Pharmaceutical Association

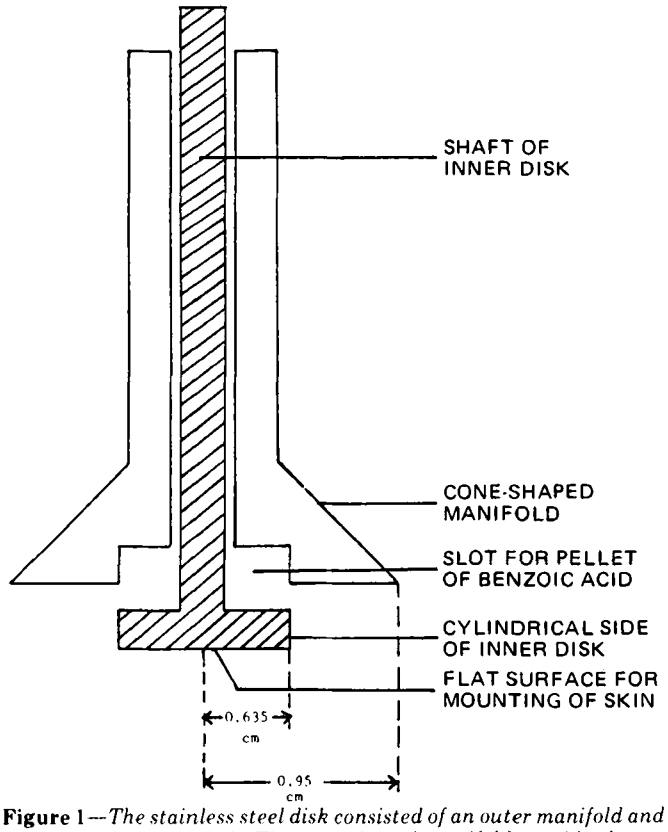

Figure 1—*The stainless steel disk consisted of an outer manifold and an inner cylindrical disk. The cone-shaped manifold provides better hydrodynamic conditions and serves as a slot for the benzoic acid pellet. The inner cylindrical disk is for the anchorage of skin in the metabolism experiments.*

where C_a and C_0 are the solute concentrations of A at time T and time zero, respectively, and L is the capillary length in centimeters. Compound I was found to have an average D_{aqA} of $(1.05 \pm 0.01) \times 10^{-5}$ cm^2/sec at 37° (Table I).

This value appears to be a little high compared with that of cyclic adenosine monophosphate (III), which was reported as 4.44×10^{-6} cm^2/sec at 20° (10). This difference may be due to the difficulty in the measurement and in the accurate reproduction of the capillary length. However, this higher value may be justified partly by the Stoke-Einstein equation (10). First, I was at a higher temperature, so the viscosity of the solvent was lower. Second, I has a smaller molecular weight and a lesser degree of solvation than III due to the absence of the phosphate group.

Estimation of Aqueous Diffusion Layer Thickness—When Compound A diffuses out of a rotating disk into an aqueous liquid, a theoretical diffusion layer thickness, h_{th}, which retards the loss of A, is described by the Levich (4) relationship:

$$h_{th} = (1.612)(D_{aqA}^{1/3})(\nu^{1/6})(\omega^{-1/2}) \qquad \text{(Eq. 2)}$$

where D_{aqA} is the aqueous diffusion coefficient (square centimeters per second), ν is the kinematic viscosity (centimeters per second), and ω is the angular velocity (radians per second). This equation requires that the disk have an infinite diameter and that it rotate with a constant velocity in a liquid of infinite volume. Therefore, the finite size and shape

Table I—Parameters in Determination of Aqueous Diffusion Coefficient of I by Capillary Cell Method [a]

Time[b], sec	L, cm	C_0, cpm	C_a, cpm	D_{aqA}, (cm^2/sec) $\times 10^5$
87,900	2.300	24,731.1	13,037.4	1.051
86,400	2.415	20,779.7	11,528.0	1.307
86,460	2.415	20,900.2	11,459.1	1.069
86,400	2.725	6,314.7	3,665.2	1.043
86,580	2.350	4,608.2	2,474.6	1.064

[a] The average value of the coefficient is $(1.05 \pm 0.01) \times 10^{-5}$ cm^2/sec. [b] About 24 hr.

Table II—Dissolution Profile of Benzoic Acid Pellets (A = 1.27 cm^2) in 0.01 N HCl at 300 rpm

Minutes	Concentration, mg/ml	ΔC[a], mg/ml
5	1.21	0.87
10	2.08	0.62
15	2.70	0.46
20	3.16	0.34
25	3.50	0.25
30	3.75	

[a] Concentration differential between successive time periods.

of the disk and the hydrodynamic condition within a real system may cause h to be considerably different from h_{th}. If h is the effective diffusion layer thickness in the experimental system, then let:

$$R = \frac{h}{h_{th}} \qquad \text{(Eq. 3)}$$

To determine R, consider the Levich relationship for the flux from the disk (4), assuming sink conditions:

$$J_{th} = (0.62)(D_{aqA}^{2/3})(\nu^{-1/6})(\omega^{1/2})(C_s) \qquad \text{(Eq. 4)}$$

where C_s is the saturation concentration of A.

Combining Eqs. 2 and 4 gives:

$$J_{th} = \left(\frac{D_{aqA}}{h_{th}}\right)(C_s) \qquad \text{(Eq. 5)}$$

which is Fick's first law. Since this law must hold for the experimental system as well:

$$J = \left(\frac{D_{aqA}}{h}\right)(C_s) \qquad \text{(Eq. 6)}$$

Then R can be determined by combining Eqs. 5 and 6 to give:

$$R = \frac{J_{th}}{J} \qquad \text{(Eq. 7)}$$

The dissolution of benzoic acid was used to standardize the disk for the determination of J_{th} since its aqueous diffusion coefficient is well known.

Data Treatment—Three dissolution experiments of benzoic acid pellets rotating at 300 rpm in 0.01 N HCl (Table II) showed the relation between the concentration and the successive concentration differential and time. The dissolution rate constant, K, was determined from these data (11) (Fig. 2) assuming a first-order equation. This constant was 6.17 $\pm$ 1.19 min^{-1}. The experimental flux was determined from:

$$J_{exp} = (K)(C_s)\left(\frac{V}{A}\right) \qquad \text{(Eq. 8)}$$

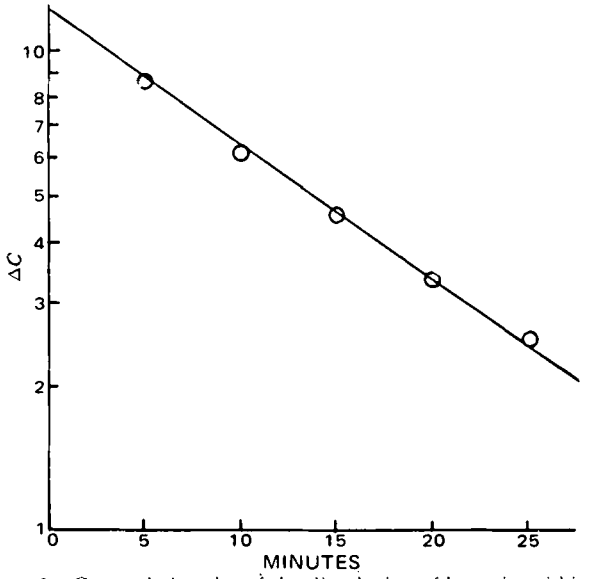

Figure 2—*Guggenheim plot of the dissolution of benzoic acid in 0.01 N HCl;* $C_t = C_{(t+i)} - C_t$, *where* i *is the sampling interval (5 min).*

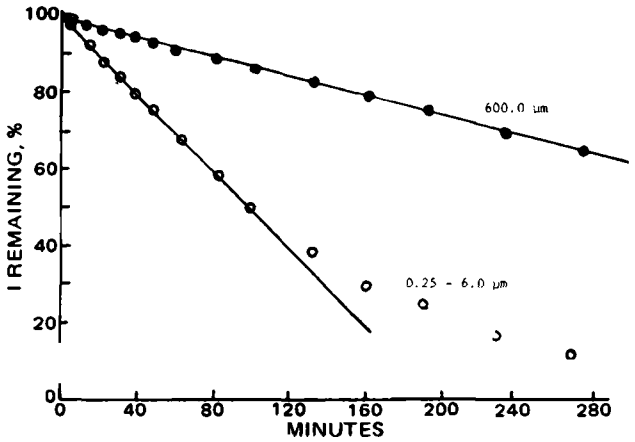

Figure 3—*Metabolism of I by guinea pig skin rotating at 300 rpm and 37°. Plots for concentrations of 0.25–6.0 μM were similar.*

where (V/A) is the volume to surface area ratio (3.95 cm in this system). The flux J_{exp} was 0.244 ± 0.047 C_s.

By using reported values of the aqueous diffusion coefficient of benzoic acid (1.40×10^{-5} cm²/sec) (12) and the aqueous kinematic viscosity (0.00699 cm²/sec) (13), the theoretical flux and the diffusion layer thickness, under the same experimental conditions, were computed to be 0.277 C_s and 27.57 μm, respectively. From Eq. 3, R was estimated to be 1.135. This value of R predicts an experimental aqueous diffusion layer thickness, h, of 31.3 μm, which differs from h_{th} by 13.5%.

This high discrepancy came as a surprise since the cone-shaped design is accepted as the best configuration for a rotating-disk system (14). However, this deviation can be explained by the fact that within the rotating system, the solvent does not have an infinite volume, nor does the disk have an infinite diameter, as required by the Levich (4) equation. Also, as benzoic acid dissolution continued, surface erosion occurred, disturbing the flow pattern. All of these nonideal hydrodynamic conditions, as well as the continual solvent evaporation, contributed to the 13.5% deviation, which is similar to that previously reported (5).

Metabolism Study of Vidarabine—Vidarabine (I) was metabolized to 9-β-D-arabinofuranosylhypoxanthine by the cutaneous enzyme system (Fig. 3). The initial slope was derived from the regression analysis, which included all data points up to 100 min. These regression coefficients were all greater than 0.995.

The flux of I, F_A, was then calculated from:

$$F_A = \left(\frac{V}{A}\right)\left(\frac{dC}{dt}\right) \qquad \text{(Eq. 9)}$$

where V is the solution volume in milliliters, A is the area of the exposed skin (square centimeters), and (dC/dt) is the initial slope of metabolism (percent per minute) (Table III). Statistical analysis of the fluxes showed a significant difference between 600.0 μM and the other concentrations. The mean flux was 1.75 ± 0.09%/min.

Determination of Cutaneous Metabolic Rate Constant—As shown in Eq. 10, the enzyme metabolic rate constant, k_m, can be expressed in terms of the initial substrate concentration, $C_A(h)$; the flux of the substrate in the system, F_A; the aqueous diffusion coefficient, D_{aqA}; the epidermal layer thickness, M; and the diffusion layer thickness, h:

$$k_m = \left(1 \Big/ \left[\frac{C_A(h)}{-F_A} - \frac{h}{D_{aqA}}\right]\right)(M) \qquad \text{(Eq. 10)}$$

This equation is derived by using Eq. 25 of previous work (2) and taking the limit of $\theta \to 0$, such that $\tanh \theta \to 0$. By substituting into Eq. 10 the reported epidermal thickness of 20.85 μm (15) and the other experimentally determined parameters, the enzyme metabolic rate constant was found to be 1.56×10^{-1} sec^{-1}.

In the controlled metabolism study, I remained unchanged at the initial concentration of 98.1% over 6 hr in the presence of the stainless steel rotating disk. The stability of I during the storage period was also investigated. The stock solution had been sterilized by being passed through a 0.22-μm filter and was then stored in an enclosed sterile vial and refrigerated. There was no apparent adsorption of I onto the filter. At the end of the 40th day, when all of the stock solutions were used up, the I purity was determined to be 97.9%. These findings show that the degradation of I into II was the sole result of the enzyme system existing in the viable guinea pig epidermal slice.

Table III—Fluxes of I at Different Concentrations

Concentration, μM	Flux, %/cm²/min	Mean Flux, %/cm²/min
0.25	1.630	1.826
	1.956	
	1.892	
0.50	1.888	1.283
	0.797	
	1.164	
0.75	1.662	1.679
	1.713	
	1.717	
1.0	1.691	1.616
	1.921	
	1.230	
6.0	1.568	1.839
	1.787	
	2.144	
600.0	0.388	0.378
	0.399	
	0.346	

The enzyme that converts I into II is adenosine deaminase, which metabolizes adenosine and various adenine nucleoside drug analogs, rendering them pharmacologically inactive. Calf intestinal mucosa adenosine deaminase has a metabolic rate constant of 0.8×10^{-1} sec^{-1} mg^{-1} (16). Although no direct comparison can be drawn, it can be concluded that adenosine deaminase is present in abundance in guinea pig skin.

In the final calculation of the enzyme rate constant from Eq. 10, the I flux and the epidermal thickness were the two most important parameters.

Since the flux depends on the concentration data of I and II, the assumption of mass balance used in their determination was evaluated. The criterion for mass balance is that the sum of the activities of I and II on the TLC plate is equal to the total activities of the sample. This assumption holds if II is the only major metabolite of I and if I and II bind identically to the tissue.

Several 6th-hr samples of the metabolism experiments were examined. The entire plate was scraped into scintillation vials in strips of 2 cm. It was found that I and II accounted for over 98% of the total activities.

Possible binding of I and II to the tissue was investigated statistically. From the raw data from five experiments at 0.5 μM, the corresponding activities of I and II were plotted *versus* time. The slope for the disappearance of I was 31.44 cpm/min, while the appearance rate of II was 31.48 cpm/min. Since the appearance rate of II was accompanied by an equivalent amount of disappearance of I, and since I and II accounted for over 98% of all activities, the assumption of mass balance was valid.

The average flux was obtained from the results of all concentrations except those of 600.0 and 0.5 μM. The former was rejected because it was significantly different from the others. The latter was excluded on the ground that two of the values were obtained from animals that did not meet the protocol.

The epidermal thickness is another important parameter in the determination of the rate constant. The model calls for the use of only the epidermal thickness on the assumption that the dermis is less active enzymatically than the epidermis. However, the dermis does contribute to the overall metabolism (17). Variation of hand pressure and speed of dermatoming caused variation in skin thickness, which was usually about 0.3 mm microscopically. Future studies may investigate the possibility of preparing epidermal slices of reproducible thickness using a motor-driven constant-pressure dermatome device. A method for accurate measurement of skin thickness must be developed also.

Future studies may determine the epidermal diffusion coefficient of the drug. With this parameter and the present data, one can estimate how metabolism and, possibly, formulation adjuvants can modify the bioavailability of the drug as it is administered in a topical dosage form.

REFERENCES

(1) H. Y. Ando, N. F. H. Ho, and W. I. Higuchi, *J. Pharm. Sci.*, **66**, 755 (1977).

(2) *Ibid.*, **66**, 1525 (1977).

(3) D. N. Saraf, A. A. Witherspoon, and L. H. Cohen, *Science*, **142**, 955 (1963).

(4) V. G. Levich, "Physiochemical Hydrodynamics," Prentice Hall,

Englewood Cliffs, N.J., 1962.
(5) S. Prakongpan, W. I. Higuchi, K. H. Kwan, and A. M. Molokhia, *J. Pharm. Sci.*, **65**, 685 (1976).
(6) C. V. King and S. S. Brodie, *J. Chem. Soc.*, **59**, 1375 (1937).
(7) D. J. Merchant, R. H. Kant, and W. H. Murphy, Jr., "Handbook of Cell and Organ Culture," Burgess, Minneapolis, Minn., 1969.
(8) J. C. Drack and J. M. Novack, *Anal. Biochem.*, **52**, 633 (1973).
(9) J. H. Wang, *J. Chem. Soc.*, **74**, 1182 (1952).
(10) D. Dworkin and K. Keller, *J. Biol. Chem.*, **252**, 864 (1977).
(11) P. J. Niebergall and E. T. Sugita, *J. Pharm. Sci.*, **57**, 1805 (1968).
(12) S. Prakongpan, Ph.D. thesis, University of Michigan, Ann Arbor, Mich., 1974, p. 89.
(13) H. Nogami, T. Nagai, and A. Suzuki, *Chem. Pharm. Bull.*, **14**, 329 (1966).
(14) A. Riddiford, in "Advances in Electrochemistry and Electrochemical Engineering," vol. 4, P. Delahay, Ed., Interscience, New York, N.Y., 1966.
(15) I. Sarkany and P. M. Gaylarde, *Trans. St. John's Hosp. Dermatol. Soc.*, **59**, 241 (1973).
(16) J. Cory and R. Suhadolnik, *Biochemistry*, **4**, 1733 (1965).
(17) O. D. Laerum, *J. Invest. Dermatol.*, **52**, 204 (1969).

GLC Assay of Verapamil in Plasma: Identification of Fluorescent Metabolites after Oral Drug Administration

R. G. McALLISTER, Jr. *, T. G. TAN *, and D. W. A. BOURNE ‡x

Received August 21, 1978, from the **Department of Medicine, Veterans Administration Hospital, and the School of Medicine and the* ‡*College of Pharmacy, University of Kentucky, Lexington, KY 40506.* Accepted for publication October 20, 1978.

Abstract □ The fluorometric assay for verapamil in plasma is not useful after oral drug administration because of interference by inactive, but fluorescent, metabolites extracted along with the parent drug. A GLC method using a flame-ionization detector after silylation allows the separation of unchanged active verapamil from the metabolites and quantitation to a sensitivity of 0.025 μg/ml. After a single oral dose of drug in dogs, up to 80% of "fluorescent verapamil" represented inactive metabolites.

Keyphrases □ Verapamil—GLC analysis, plasma fluorometric analysis, metabolite interference □ GLC—analysis, verapamil in plasma □ Vasodilators—verapamil, GLC analysis in plasma

Verapamil, 5-[(3,4-dimethoxyphenethyl)methylamino]-2-(3,4-dimethoxyphenyl)-2-isopropylvaleronitrile (I), is an experimental antiarrhythmic and antianginal agent (1–5) and is currently undergoing clinical evaluation in the United States. Its pharmacological activity is related to suppression of transmembrane calcium fluxes in cardiac and other tissues (6, 7). These "slow" calcium currents may be involved in the genesis of fatal arrhythmias during myocardial ischemia and associated with sudden cardiac death (8).

BACKGROUND

A fluorometric assay for verapamil in plasma (9) has been used to determine its elimination kinetics in dogs after intravenous injection (10) and to demonstrate a linear correlation between plasma drug concentrations and both electrophysiologic and hemodynamic effects in dogs following systemic dosing (11). However, after oral administration of verapamil to dogs, no relationship between plasma level and effect was found (12), raising the possibility that metabolites generated during the first passage through the liver interfere with the fluorometric assay.

Verapamil is known to be metabolized extensively in rats and dogs, primarily to *O*- and *N*-dealkylated derivatives through loss of the 3,4-dimethoxyphenylethyl moiety (13). Schomerus *et al.* (14) used mass fragmentography to confirm the extensive metabolism of the drug in three normal human subjects after a single oral dose but did not identify the specific metabolites produced.

Since verapamil may become an important addition to the drugs available for treatment of cardiovascular disorders, the assay validity must be defined before further kinetic and pharmacological studies can be carried out. Two major metabolites of verapamil, 5-amino-2-(3,4-dimethoxyphenyl)-2-isopropylvaleronitrile (D620) (II) and 5-methylamino-2-(3,4-dimethoxyphenyl)-2-isopropylvaleronitrile (D617) (III)[1], were studied to determine possible interference with the fluorometric assay for parent verapamil. Furthermore, a GLC procedure specific for unchanged verapamil in the presence of II or III was developed and is described.

EXPERIMENTAL

Fluorometric Assay—The fluorometric assay for verapamil in plasma (9) involves extraction of drug from alkaline plasma with heptane and back-extraction into acid. Fresh plasma from normal drug-free human subjects was pooled. To one group of aliquots, verapamil was added to achieve concentrations of 0.1, 0.5, and 1.0 μg/ml; to two other aliquots, II or III were added similarly. All samples were prepared in triplicate.

The fluorometric assay was performed on each sample by an experienced technician under blind conditions, and the resulting fluorescence at an excitation/emission spectra of 275/310 nm was recorded[2]. The calculated recovery from these standards ranged from 85 to 94%.

To additional aliquots of plasma from the same pool, combinations of verapamil and II and III were added, each in a concentration of 0.5 μg/ml. The assay was carried out as previously described, and total fluorescence was determined[2].

GLC Assay—All reagents and solvents were of analytical grade, and glassware was cleaned by superheating after a distilled water rinse (15). Fresh plasma was collected from normal human volunteers as well as from drug-free mongrel dogs; no differences were found between the two for the work described here, and the term "plasma" used here may apply equally to either species.

Known amounts of verapamil and/or II and III were added to 2-ml plasma samples. After addition of 1.0 ml of 1 *N* NaOH and 5.0 ml of heptane, the mixture was shaken for 15 min and centrifuged at 1800 rpm for 10 min. Four milliliters of the heptane layer was transferred to a 15-ml centrifuge tube containing 2.0 ml of 0.1 *N* HCl; each tube was shaken and centrifuged as before. The heptane layer was aspirated and discarded, and the aqueous phase was washed twice with 2.0 ml of heptane. One milliliter of 1.0 *N* NaOH was added, and the acid layer was extracted with 4.0 ml of heptane, with agitation and centrifugation as before.

Three milliliters of the heptane layer was then transferred to another tube and evaporated under a nitrogen stream during heating to 60° on

[1] Kindly supplied by Prof. K. Hahn, Knoll AG, Ludwigshafen, West Germany.

[2] Aminco-Bowman spectrophotofluorometer with ratio photometer unit, American Instrument Co.

0022-3549/79/0500-0574$01.00/0
© 1979, American Pharmaceutical Association

Englewood Cliffs, N.J., 1962.
(5) S. Prakongpan, W. I. Higuchi, K. H. Kwan, and A. M. Molokhia, *J. Pharm. Sci.*, **65**, 685 (1976).
(6) C. V. King and S. S. Brodie, *J. Chem. Soc.*, **59**, 1375 (1937).
(7) D. J. Merchant, R. H. Kant, and W. H. Murphy, Jr., "Handbook of Cell and Organ Culture," Burgess, Minneapolis, Minn., 1969.
(8) J. C. Drack and J. M. Novack, *Anal. Biochem.*, **52**, 633 (1973).
(9) J. H. Wang, *J. Chem. Soc.*, **74**, 1182 (1952).
(10) D. Dworkin and K. Keller, *J. Biol. Chem.*, **252**, 864 (1977).
(11) P. J. Niebergall and E. T. Sugita, *J. Pharm. Sci.*, **57**, 1805 (1968).
(12) S. Prakongpan, Ph.D. thesis, University of Michigan, Ann Arbor, Mich., 1974, p. 89.
(13) H. Nogami, T. Nagai, and A. Suzuki, *Chem. Pharm. Bull.*, **14**, 329 (1966).
(14) A. Riddiford, in "Advances in Electrochemistry and Electrochemical Engineering," vol. 4, P. Delahay, Ed., Interscience, New York, N.Y., 1966.
(15) I. Sarkany and P. M. Gaylarde, *Trans. St. John's Hosp. Dermatol. Soc.*, **59**, 241 (1973).
(16) J. Cory and R. Suhadolnik, *Biochemistry*, **4**, 1733 (1965).
(17) O. D. Laerum, *J. Invest. Dermatol.*, **52**, 204 (1969).

GLC Assay of Verapamil in Plasma: Identification of Fluorescent Metabolites after Oral Drug Administration

R. G. McALLISTER, Jr. *, T. G. TAN *, and D. W. A. BOURNE ‡x

Received August 21, 1978, from the **Department of Medicine, Veterans Administration Hospital, and the School of Medicine and the* ‡*College of Pharmacy, University of Kentucky, Lexington, KY 40506.* Accepted for publication October 20, 1978.

Abstract □ The fluorometric assay for verapamil in plasma is not useful after oral drug administration because of interference by inactive, but fluorescent, metabolites extracted along with the parent drug. A GLC method using a flame-ionization detector after silylation allows the separation of unchanged active verapamil from the metabolites and quantitation to a sensitivity of 0.025 μg/ml. After a single oral dose of drug in dogs, up to 80% of "fluorescent verapamil" represented inactive metabolites.

Keyphrases □ Verapamil—GLC analysis, plasma fluorometric analysis, metabolite interference □ GLC—analysis, verapamil in plasma □ Vasodilators—verapamil, GLC analysis in plasma

Verapamil, 5-[(3,4-dimethoxyphenethyl)methylamino]-2-(3,4-dimethoxyphenyl)-2-isopropylvaleronitrile (I), is an experimental antiarrhythmic and antianginal agent (1–5) and is currently undergoing clinical evaluation in the United States. Its pharmacological activity is related to suppression of transmembrane calcium fluxes in cardiac and other tissues (6, 7). These "slow" calcium currents may be involved in the genesis of fatal arrhythmias during myocardial ischemia and associated with sudden cardiac death (8).

BACKGROUND

A fluorometric assay for verapamil in plasma (9) has been used to determine its elimination kinetics in dogs after intravenous injection (10) and to demonstrate a linear correlation between plasma drug concentrations and both electrophysiologic and hemodynamic effects in dogs following systemic dosing (11). However, after oral administration of verapamil to dogs, no relationship between plasma level and effect was found (12), raising the possibility that metabolites generated during the first passage through the liver interfere with the fluorometric assay.

Verapamil is known to be metabolized extensively in rats and dogs, primarily to *O*- and *N*-dealkylated derivatives through loss of the 3,4-dimethoxyphenylethyl moiety (13). Schomerus *et al.* (14) used mass fragmentography to confirm the extensive metabolism of the drug in three normal human subjects after a single oral dose but did not identify the specific metabolites produced.

Since verapamil may become an important addition to the drugs available for treatment of cardiovascular disorders, the assay validity must be defined before further kinetic and pharmacological studies can be carried out. Two major metabolites of verapamil, 5-amino-2-(3,4-dimethoxyphenyl)-2-isopropylvaleronitrile (D620) (II) and 5-methylamino-2-(3,4-dimethoxyphenyl)-2-isopropylvaleronitrile (D617) (III)[1], were studied to determine possible interference with the fluorometric assay for parent verapamil. Furthermore, a GLC procedure specific for unchanged verapamil in the presence of II or III was developed and is described.

EXPERIMENTAL

Fluorometric Assay—The fluorometric assay for verapamil in plasma (9) involves extraction of drug from alkaline plasma with heptane and back-extraction into acid. Fresh plasma from normal drug-free human subjects was pooled. To one group of aliquots, verapamil was added to achieve concentrations of 0.1, 0.5, and 1.0 μg/ml; to two other aliquots, II or III were added similarly. All samples were prepared in triplicate.

The fluorometric assay was performed on each sample by an experienced technician under blind conditions, and the resulting fluorescence at an excitation/emission spectra of 275/310 nm was recorded[2]. The calculated recovery from these standards ranged from 85 to 94%.

To additional aliquots of plasma from the same pool, combinations of verapamil and II and III were added, each in a concentration of 0.5 μg/ml. The assay was carried out as previously described, and total fluorescence was determined[2].

GLC Assay—All reagents and solvents were of analytical grade, and glassware was cleaned by superheating after a distilled water rinse (15). Fresh plasma was collected from normal human volunteers as well as from drug-free mongrel dogs; no differences were found between the two for the work described here, and the term "plasma" used here may apply equally to either species.

Known amounts of verapamil and/or II and III were added to 2-ml plasma samples. After addition of 1.0 ml of 1 *N* NaOH and 5.0 ml of heptane, the mixture was shaken for 15 min and centrifuged at 1800 rpm for 10 min. Four milliliters of the heptane layer was transferred to a 15-ml centrifuge tube containing 2.0 ml of 0.1 *N* HCl; each tube was shaken and centrifuged as before. The heptane layer was aspirated and discarded, and the aqueous phase was washed twice with 2.0 ml of heptane. One milliliter of 1.0 *N* NaOH was added, and the acid layer was extracted with 4.0 ml of heptane, with agitation and centrifugation as before.

Three milliliters of the heptane layer was then transferred to another tube and evaporated under a nitrogen stream during heating to 60° on

[1] Kindly supplied by Prof. K. Hahn, Knoll AG, Ludwigshafen, West Germany.

[2] Aminco-Bowman spectrophotofluorometer with ratio photometer unit, American Instrument Co.

0022-3549/79/0500-0574$01.00/0
© 1979, American Pharmaceutical Association

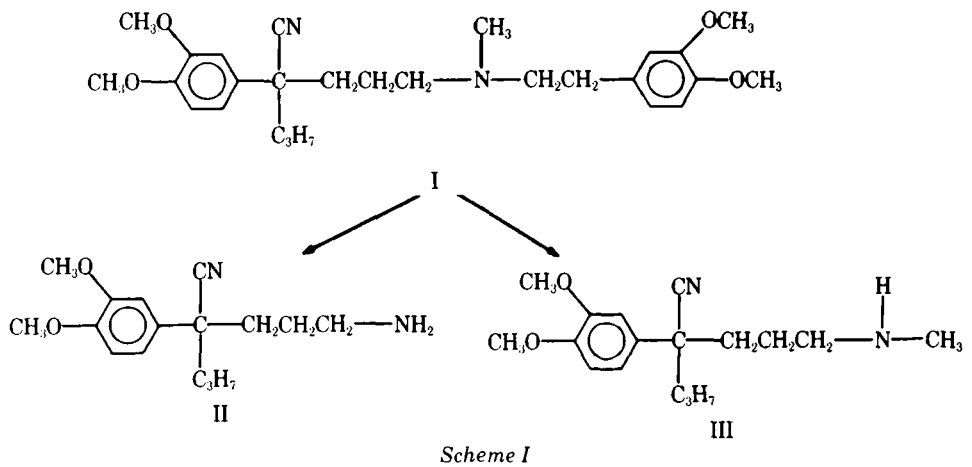

Scheme I

a waterbath. To the residue was added 100 μl of *N*-methyl-*N*-trimethylsilyltrifluoroacetamide (IV)[3], with heating for 1 hr at 65–70°. After cooling, evaporation was again effected under a nitrogen stream; the sample was then reconstituted with 25 μl of methanol, and 5-μl amounts were injected into the gas chromatograph.

The gas chromatograph[4] was equipped with a glass column (1.8 m × 2 mm i.d.) packed with 3% Dexsil-300[3] on 100–200-mesh WHP[3]. The column was silanized and conditioned at 325° for 72 hr prior to use. The conditions were as follows: carrier gas (nitrogen) flow rate, 30 ml/min; inlet temperature, 310°; column temperature, 270°; and detector temperature, 350°. The flame-ionization unit was supplied with hydrogen at 30 ml/min and with air at 300 ml/min. Detector responses were recorded[5], and peak areas were integrated electronically[6].

Animal Study—Verapamil (3 mg/kg in 30 ml of water) was administered by nasogastric tube to a healthy 20-kg mongrel dog which had been fasted overnight. Serial blood samples were collected over the following 4 hr. Plasma was analyzed for verapamil by the fluorometric method (9) and the GLC technique described here.

RESULTS AND DISCUSSION

Fluorometric Assay—The fluorescence of verapamil, II, and III is shown in Fig. 1. Both metabolites fluoresced maximally at the same excitation/emission wavelength combination as the parent drug, and both were extracted with high recoveries (80–90%) in the plasma–heptane–acid procedure used for verapamil. The potential for interference by these metabolites with the fluorometric verapamil assay is illustrated in Fig. 2; various combinations of the compounds were extracted from plasma, and total fluorescence was determined. Both II and III showed a concentration–fluorescence intensity relationship similar to that for unchanged verapamil; addition of one or both metabolites to plasma containing the parent drug resulted in a proportionate increase in total fluorescence.

The pharmacological activity of these fluorescent metabolites has not

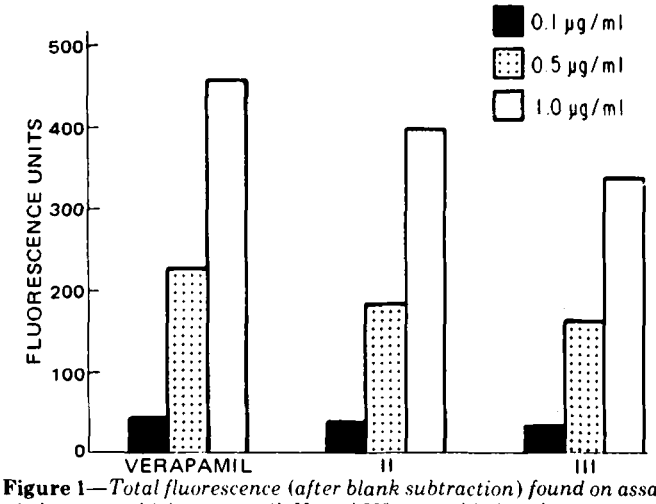

Figure 1—*Total fluorescence (after blank subtraction) found on assay of plasma to which verapamil, II, and III were added in the concentrations shown.*

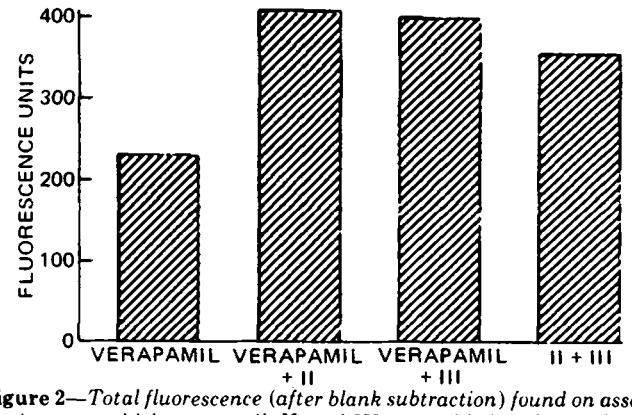

Figure 2—*Total fluorescence (after blank subtraction) found on assay of plasma to which verapamil, II, and III were added in the combinations indicated; 0.500 μg of each compound/ml was present.*

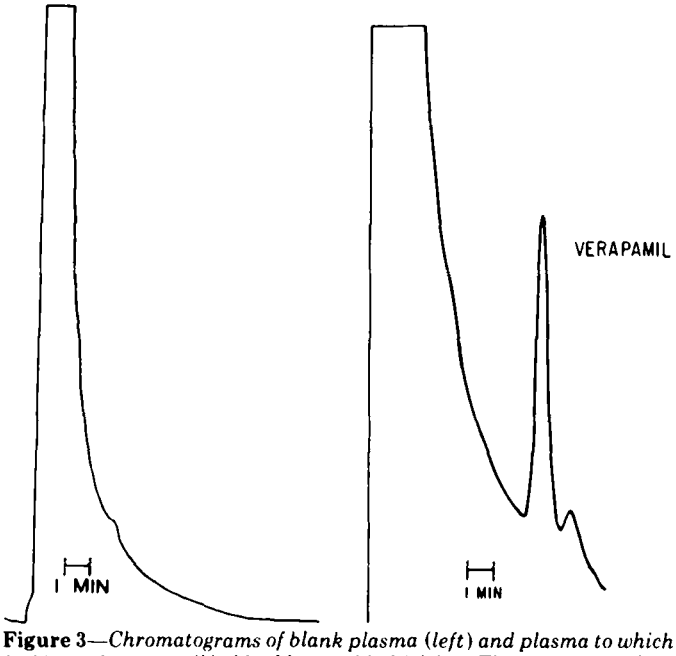

Figure 3—*Chromatograms of blank plasma (left) and plasma to which 0.100 μg of verapamil/ml had been added (right). The assay procedure is described in the text.*

[3] Pierce Chemical Co., Rockford, Ill.
[4] Model 3700 dual-column gas chromatograph, Varian Co., Walnut Creek, Calif.
[5] Model 9176 recorder, Varian Co., Walnut Creek, Calif.
[6] CDS 111 integrator, Varian Co., Walnut Creek, Calif.

Table I—Linearity and Precision of Plasma Verapamil Concentrations Measured by GLC

Plasma Concentration, μg/ml	Peak Area[a], mean ± *SD* × 10^4	*CV*, %
0.025	0.514 ± 0.056	10.8
0.050	1.013 ± 0.106	10.4
0.100	2.030 ± 0.168	8.3
0.250	6.531 ± 0.521	7.9
0.500	12.123 ± 0.885	7.3
1.000	24.674 ± 1.517	6.1

[a] $n = 6$ at each plasma concentration.

Figure 4—*Chromatograms of plasma to which II or III was added, using a column temperature of 220°. Both compounds were added in a concentration of 0.100 μg/ml.*

been specifically determined. However, since the concentration of plasma verapamil determined fluorometrically is linearly related to the drug's effects after intravenous administration (10, 11) but not after oral administration (12), these (and possibly other) fluorescent metabolites probably are generated during the first passage through the liver and are either inactive or have little pharmacological effect. In any event, the fluorometric assay for verapamil in plasma is not a valid reflection of the concentration of active drug in the presence of drug metabolites after oral dosing.

GLC Assay—Under the conditions described, verapamil could be extracted from plasma with good recoveries (range of 89–96%) in a concentration range of 0.025–1.000 μg/ml. Figure 3 shows chromatograms of blank plasma and of plasma containing 0.100 μg of added verapamil/ml. The retention time for verapamil was 7.3 min. Table I gives data on the reproducibility and sensitivity of the GLC procedure. The assay was linear over the concentration range studied ($r = 0.9995$; $p < 0.001$), which reflects the plasma drug concentrations likely to be of clinical interest (10, 11).

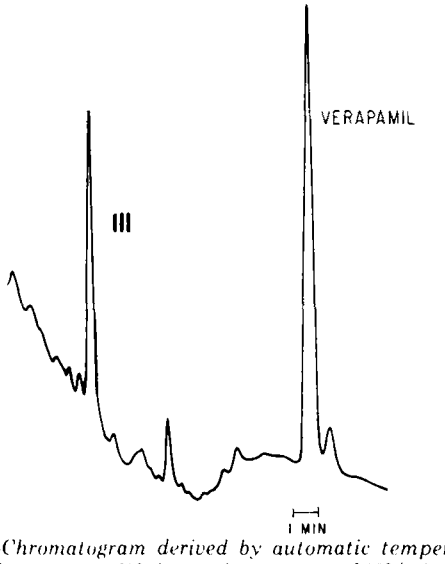

Figure 5—*Chromatogram derived by automatic temperature programming, from 190 to 270°, increasing at a rate of 10°/min. Compound III eluted at a column temperature of approximately 220°, while verapamil emerged at 270°.*

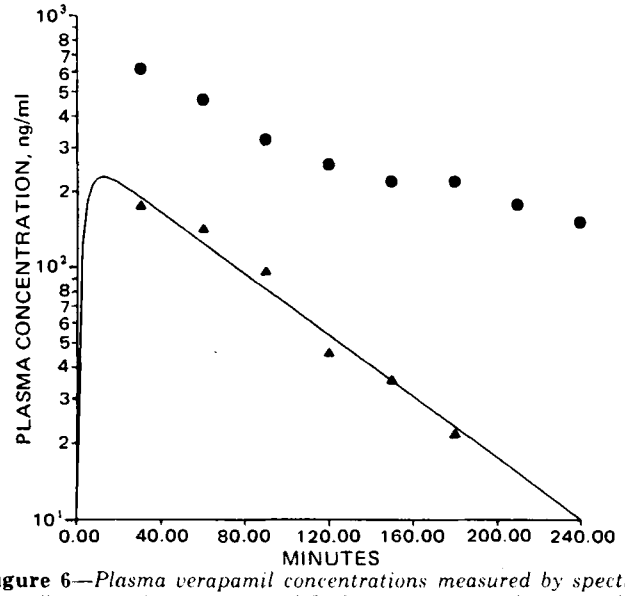

Figure 6—*Plasma verapamil concentrations measured by spectrophotofluorometric assay (●) and GLC (▲); serial samples were taken from a 20-kg mongrel dog given 3 mg of verapamil/kg at time zero.*

Of the two metabolites studied, II did not appear to form a silyl derivative and could not be detected under the GLC conditions used. Compound III, however, was easily and quantitatively detected at a column temperature of 220° (Fig. 4). Automatic temperature programming, beginning at a column temperature of 190° and increasing at 10°/min, could be used to detect both III and parent verapamil in the same plasma sample (Fig. 5). At the column temperature of 270° used to measure parent verapamil concentrations, III emerged with the solvent front.

Since this assay is specific for unchanged verapamil, it will be particularly useful in pharmacokinetic and pharmacodynamic studies of the drug after oral dosing. For example, when both spectrophotofluorometric and GLC techniques were used to measure serial drug plasma levels in a dog given a single oral dose of verapamil, fluorometric analysis gave results four- to fivefold higher than those measured by GLC, indicating the presence of metabolites interfering with the fluorometric procedure (Fig. 6).

On the basis of these and prior studies (10–12), it appears that the fluorometric assay for plasma verapamil is a valid reflection of the concentration of unchanged, active drug only after intravenous verapamil administration. After oral doses, a more specific assay, such as the described GLC procedure, must be used to quantitate the parent compound.

REFERENCES

(1) B. N. Singh and E. M. Vaughan Williams, *Cardiovasc. Res.*, **6**, 109 (1972).

(2) F. Hagemeijer, *Circulation*, **57**, 751 (1978).

(3) L. Schamroth, D. M. Krikler, and C. Garrett, *Br. Med. J.*, **1**, 660 (1972).

(4) W. G. Nayler, A. Grau, and A. Slade, *Cardiovasc. Res.*, **10**, 650 (1976).

(5) O. Parodi, I. Simonetti, and A. Maseri, *Circulation (Suppl. III)*, **55–56**, 224 (1977).

(6) M. R. Rosen, J. P. Ilvento, H. Gelband, and C. Merker, *J. Pharmacol. Exp. Ther.*, **189**, 414 (1974).

(7) A. L. Wit and P. R. Cranefield, *Circulation (Suppl. III)*, **49–50**, 146 (1974).

(8) B. Surawicz, *Am. J. Cardiol.*, **33**, 689 (1974).

(9) R. G. McAllister and S. M. Howell, *J. Pharm. Sci.*, **65**, 431 (1976).

(10) R. G. McAllister, D. W. A. Bourne, and L. W. Dittert, *J. Pharmacol. Exp. Ther.*, **202**, 38 (1977).
(11) L. M. Mangiardi, R. Hariman, R. G. McAllister, V. Bhargava, B. Surawicz, and R. Shabetai, *Circulation*, **57**, 366 (1978).
(12) A. L. Cornish, H. G. Hanley, T. G. Tan, T. A. Patrick, and R. G. McAllister, *Clin. Res.*, **26**, 288 (1978).
(13) H. M. McIlhenny, *J. Med. Chem.*, **14**, 1178 (1971).
(14) M. Schomerus, B. Spiegelhalder, B. Stieren, and M. Eichelbaum, *Cardiovasc. Res.*, **10**, 605 (1976).
(15) S. M. Howell and R. G. McAllister, *Lab. Med.*, **7**, 34 (1976).

ACKNOWLEDGMENTS

R. G. McAllister, Jr., is a clinical investigator in the Veterans Administration Career Development Program.

The authors are grateful for the encouragement and support of Dr. Michael Grozier.

Stability-Indicating High-Performance Liquid Chromatographic Determination of Chlorpropamide, Tolbutamide, and Their Respective Sulfonamide Degradates

D. L. ROBERTSON, A. G. BUTTERFIELD, H. KOLASINSKI, E. G. LOVERING, and F. F. MATSUI ˣ

Received October 19, 1977, from the *Drug Research Laboratories, Health Protection Branch, Health and Welfare Canada, Ottawa, Canada K1A 0L2.* Accepted for publication October 19, 1978.

Abstract □ A quantitative high-performance liquid chromatographic method for the determination of chlorpropamide, tolbutamide, and their respective hydrolysis products, *p*-chlorobenzenesulfonamide and *p*-toluenesulfonamide, in solid dosage forms was developed. The method is stability indicating and can be used to determine the sulfonamide hydrolysis product and the intact drug in the presence of minor degradates. Method reproducibility, demonstrated by repeated injections of a calibration standard, was 1.21%. The lower limit of quantitation of the hydrolysis products, *p*-chlorobenzenesulfonamide and *p*-toluenesulfonamide, was 0.2 μg/5-μl injection. The accuracy of the method for intact drugs was determined by comparison of the HPLC results to those obtained by the appropriate USP or BP assays. The mean of the results obtained by the two methods differed by 0.7% for chlorpropamide and 0.3% for tolbutamide. Pure drug samples were spiked with amounts of the hydrolysis products ranging from 20 to 120% of the intact drug content. The mean percent recovery for *p*-chlorobenzenesulfonamide was 98.6%; for *p*-toluenesulfonamide, it was 100.6%. A qualitative TLC procedure for the detection of chlorpropamide, *p*-chlorobenzenesulfonamide, dipropylurea, propylurea, *n*-propylamine, tolbutamide, *p*-toluenesulfonamide, dibutylurea, butylurea, and *n*-butylamine is also described.

Keyphrases □ High-performance liquid chromatography—analysis of chlorpropamide, tolbutamide, *p*-chlorobenzenesulfonamide, *p*-toluenesulfonamide, stability in solid pharmaceutical dosage forms □ Chlorpropamide—high-performance liquid chromatographic analysis of stability in solid pharmaceutical dosage forms, sulfonamide degradates □ Tolbutamide—high-performance liquid chromatographic analysis of stability in solid pharmaceutical dosage forms, sulfonamide degradates □ Sulfonamides—degradation products of chlorpropamide and tolbutamide, high-performance liquid chromatographic analysis □ Antidiabetic agents—chlorpropamide, tolbutamide, high-performance liquid chromatographic analysis of stability and sulfonamide degradation products

The antidiabetic agents chlorpropamide and tolbutamide decompose under various experimental conditions. The major degradation route is hydrolysis (1, 2), mainly to *p*-chlorobenzenesulfonamide or *p*-toluenesulfonamide, but thermal dissociation in various solvents has been reported also (3, 4).

The USP XIX (5) spectrophotometric assay for tablets containing these drugs lacks specificity since the sulfonamide degradates retain the UV chromophore of the intact drug. The BP 1973 (6) titrimetric procedures are selective because the sulfonamide degradates are weak acids that are not neutralized by the aqueous solution of sodium hydroxide. However, the method cannot be used to assay highly discolored samples due to interference in the visual detection of the end-point.

Colorimetric procedures have been reported (2, 7, 8), but these methods require prior separation of the degradates before the intact drug can be quantitated. A high-performance liquid chromatographic (HPLC) method for the quantitation of sulfonylureas in pharmaceuticals has been reported (9), but separation and quantitation of the hydrolysis products were not demonstrated. An HPLC procedure for the determination of chlorpropamide in tablet formulations was described (10) but was not suitable for resolution of the sulfonamide from the main drug.

This paper describes a TLC technique for the detection of the major degradates of chlorpropamide and tolbutamide and an HPLC assay of intact chlorpropamide, tolbutamide, and their sulfonamide impurities, *p*-chlorobenzenesulfonamide and *p*-toluenesulfonamide, in solid dosage formulations.

EXPERIMENTAL

Materials—Chlorpropamide[1] and tolbutamide[2] were recrystallized from acetone and found to meet USP XIX (5) specifications. *p*-Chlorobenzenesulfonamide[3], *p*-toluenesulfonamide[4], *n*-propylurea[3], *n*-butylurea[4], *n*-dipropylurea[5], *n*-dibutylurea[6], *n*-propylamine[7], *n*-butylamine[3], micronized prednisone[8], acetic acid[9], hydrochloric acid[9], chlo-

[1] F. W. Horner Ltd., Montreal, Quebec, Canada.
[2] Paul Maney Laboratories, Toronto, Ontario, Canada.
[3] Aldrich Chemical Co., Milwaukee, Wis.
[4] Eastman Organic Chemicals, Rochester, N.Y.
[5] Authentic samples, B.P. Commission.
[6] K & K Laboratories, Plainsview, N.Y.
[7] J. T. Baker Chemical Co., Phillipsburg, N.J.
[8] Roussel (Canada) Ltd., Montreal, Quebec, Canada.
[9] Analytical reagent grade.

0022-3549/79/0500-0577$01.00/0
© 1979, American Pharmaceutical Association

(10) R. G. McAllister, D. W. A. Bourne, and L. W. Dittert, *J. Pharmacol. Exp. Ther.*, **202**, 38 (1977).
(11) L. M. Mangiardi, R. Hariman, R. G. McAllister, V. Bhargava, B. Surawicz, and R. Shabetai, *Circulation*, **57**, 366 (1978).
(12) A. L. Cornish, H. G. Hanley, T. G. Tan, T. A. Patrick, and R. G. McAllister, *Clin. Res.*, **26**, 288 (1978).
(13) H. M. McIlhenny, *J. Med. Chem.*, **14**, 1178 (1971).
(14) M. Schomerus, B. Spiegelhalder, B. Stieren, and M. Eichelbaum, *Cardiovasc. Res.*, **10**, 605 (1976).
(15) S. M. Howell and R. G. McAllister, *Lab. Med.*, **7**, 34 (1976).

ACKNOWLEDGMENTS

R. G. McAllister, Jr., is a clinical investigator in the Veterans Administration Career Development Program.

The authors are grateful for the encouragement and support of Dr. Michael Grozier.

Stability-Indicating High-Performance Liquid Chromatographic Determination of Chlorpropamide, Tolbutamide, and Their Respective Sulfonamide Degradates

D. L. ROBERTSON, A. G. BUTTERFIELD, H. KOLASINSKI, E. G. LOVERING, and F. F. MATSUI ˣ

Received October 19, 1977, from the *Drug Research Laboratories, Health Protection Branch, Health and Welfare Canada, Ottawa, Canada K1A 0L2.* Accepted for publication October 19, 1978.

Abstract □ A quantitative high-performance liquid chromatographic method for the determination of chlorpropamide, tolbutamide, and their respective hydrolysis products, *p*-chlorobenzenesulfonamide and *p*-toluenesulfonamide, in solid dosage forms was developed. The method is stability indicating and can be used to determine the sulfonamide hydrolysis product and the intact drug in the presence of minor degradates. Method reproducibility, demonstrated by repeated injections of a calibration standard, was 1.21%. The lower limit of quantitation of the hydrolysis products, *p*-chlorobenzenesulfonamide and *p*-toluenesulfonamide, was 0.2 μg/5-μl injection. The accuracy of the method for intact drugs was determined by comparison of the HPLC results to those obtained by the appropriate USP or BP assays. The mean of the results obtained by the two methods differed by 0.7% for chlorpropamide and 0.3% for tolbutamide. Pure drug samples were spiked with amounts of the hydrolysis products ranging from 20 to 120% of the intact drug content. The mean percent recovery for *p*-chlorobenzenesulfonamide was 98.6%; for *p*-toluenesulfonamide, it was 100.6%. A qualitative TLC procedure for the detection of chlorpropamide, *p*-chlorobenzenesulfonamide, dipropylurea, propylurea, *n*-propylamine, tolbutamide, *p*-toluenesulfonamide, dibutylurea, butylurea, and *n*-butylamine is also described.

Keyphrases □ High-performance liquid chromatography—analysis of chlorpropamide, tolbutamide, *p*-chlorobenzenesulfonamide, *p*-toluenesulfonamide, stability in solid pharmaceutical dosage forms □ Chlorpropamide—high-performance liquid chromatographic analysis of stability in solid pharmaceutical dosage forms, sulfonamide degradates □ Tolbutamide—high-performance liquid chromatographic analysis of stability in solid pharmaceutical dosage forms, sulfonamide degradates □ Sulfonamides—degradation products of chlorpropamide and tolbutamide, high-performance liquid chromatographic analysis □ Antidiabetic agents—chlorpropamide, tolbutamide, high-performance liquid chromatographic analysis of stability and sulfonamide degradation products

The antidiabetic agents chlorpropamide and tolbutamide decompose under various experimental conditions. The major degradation route is hydrolysis (1, 2), mainly to *p*-chlorobenzenesulfonamide or *p*-toluenesulfonamide, but thermal dissociation in various solvents has been reported also (3, 4).

The USP XIX (5) spectrophotometric assay for tablets containing these drugs lacks specificity since the sulfonamide degradates retain the UV chromophore of the intact drug. The BP 1973 (6) titrimetric procedures are selective because the sulfonamide degradates are weak acids that are not neutralized by the aqueous solution of sodium hydroxide. However, the method cannot be used to assay highly discolored samples due to interference in the visual detection of the end-point.

Colorimetric procedures have been reported (2, 7, 8), but these methods require prior separation of the degradates before the intact drug can be quantitated. A high-performance liquid chromatographic (HPLC) method for the quantitation of sulfonylureas in pharmaceuticals has been reported (9), but separation and quantitation of the hydrolysis products were not demonstrated. An HPLC procedure for the determination of chlorpropamide in tablet formulations was described (10) but was not suitable for resolution of the sulfonamide from the main drug.

This paper describes a TLC technique for the detection of the major degradates of chlorpropamide and tolbutamide and an HPLC assay of intact chlorpropamide, tolbutamide, and their sulfonamide impurities, *p*-chlorobenzenesulfonamide and *p*-toluenesulfonamide, in solid dosage formulations.

EXPERIMENTAL

Materials—Chlorpropamide[1] and tolbutamide[2] were recrystallized from acetone and found to meet USP XIX (5) specifications. *p*-Chlorobenzenesulfonamide[3], *p*-toluenesulfonamide[4], *n*-propylurea[3], *n*-butylurea[4], *n*-dipropylurea[5], *n*-dibutylurea[6], *n*-propylamine[7], *n*-butylamine[3], micronized prednisone[8], acetic acid[9], hydrochloric acid[9], chlo-

[1] F. W. Horner Ltd., Montreal, Quebec, Canada.
[2] Paul Maney Laboratories, Toronto, Ontario, Canada.
[3] Aldrich Chemical Co., Milwaukee, Wis.
[4] Eastman Organic Chemicals, Rochester, N.Y.
[5] Authentic samples, B.P. Commission.
[6] K & K Laboratories, Plainsview, N.Y.
[7] J. T. Baker Chemical Co., Phillipsburg, N.J.
[8] Roussel (Canada) Ltd., Montreal, Quebec, Canada.
[9] Analytical reagent grade.

0022-3549/79/0500-0577$01.00/0
© 1979, American Pharmaceutical Association

Table I—TLC Data [a]

Compound	R_f Values: Absolute (× 100)	Relative[b]	Absolute (× 100)	Relative[b]
	Sil G-25 UV 254		Silica Gel G/MH	
Chlorpropamide	42	1.0	50	1.0
p-Chlorobenzenesulfonamide	30	0.71	36	0.72
Dipropylurea	20	0.48	25	0.52
Propylurea	12	0.29	14	0.28
n-Propylamine	0	0	0	0
	Silica Gel 60 F-254		Silica Gel G/HL	
Tolbutamide	44	1.0	35	1.0
p-Toluenesulfonamide	29	0.66	24	0.69
Dibutylurea	35	0.80	30	0.86
Butylurea	16	0.36	16	0.46
n-Butylamine	0	0	0	0

[a] Development and visualization details given in the text. [b] Relative to chlorpropamide or tolbutamide.

roform[9], absolute ethanol[9], ethyl acetate[10], *n*-hexane[10], tetrahydrofuran[10], toluene[9], sodium hypochlorite solution[11], and phenothiazine[12] were used as received.

TLC Procedures—For chlorpropamide, 0.25-mm Sil G-25 UV 254[13] or silica gel G/MH[14] plates were used. For tolbutamide, 0.25-mm silica gel 60 F-254[15] or silica gel G/HL[14] plates were used.

The solvent system was toluene–ethyl acetate–chloroform–acetic acid (80:15:5:10). The detection agents were: A, 0.2% ninhydrin aerosol[7]; B, 0.6% (v/v) aqueous sodium hypochlorite; C, 1% (w/v) phenothiazine in chloroform (prepared fresh each week); and D, 20% (v/v) acetic acid in ethanol.

Sample Preparation—An accurately weighed amount of powdered tablet was tumbled[16] for 30 min in a screw-capped test tube with sufficient acetone to yield a 25-mg/ml final solution. The sample was centrifuged, 10 μl of the supernate was applied to the appropriate TLC plate, and the plate was developed 15 cm in a filter paper-lined chromatographic chamber, which had been equilibrated with the solvent system for 1 hr prior to use.

Visualization—The plate was air dried, and the origin was sprayed with Detection Agent A to disclose *n*-propylamine in chlorpropamide or *n*-butylamine in tolbutamide. Detection Agent B was then applied. The plate was dried with a warm air stream until free of chlorine odor and then sprayed consecutively with Detection Agents C and D. The main component and the potential degradates appeared as green spots on a white background. The R_f values are given in Table I.

HPLC Procedure—*Apparatus*—A liquid chromatograph[17] equipped with a fixed wavelength UV detector (254 nm)[17], a septumless injector port[17], and a computing integrator[18] were used. The detector was operated at an attenuation of 0.02 absorbance unit full scale (aufs), and the integrator output to the recorder was attenuated ×16 throughout. Integrator malfunction would necessitate peak height quantitation of the degradates. If peak height is to be utilized for the degradate determination, the signal from the chromatograph electrometer to the recorder would be 0.02 aufs. At this signal level, 2% impurity levels were seen and measured easily.

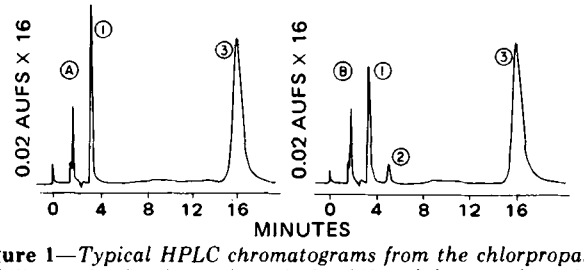

Figure 1—*Typical HPLC chromatograms from the chlorpropamide stability study of an intact formulation (A) and the same formulation exposed to 60° and 70% RH for 6 weeks (B). Key: 1, chlorpropamide; 2, p-chlorobenzenesulfonamide; and 3, prednisone.*

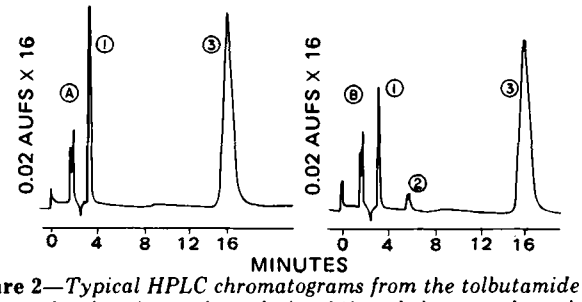

Figure 2—*Typical HPLC chromatograms from the tolbutamide stability study of an intact formulation (A) and the same formulation exposed to 60° and 70% RH for 6 weeks (B). Key: 1, tolbutamide; 2, p-toluenesulfonamide; and 3, prednisone.*

Column—A 250 × 3.2-mm i.d. column was packed with 10-μm diameter silica gel[19], using a balanced density slurry technique (11). All chromatographic operations were performed at ambient temperature and at a flow rate of 60 ml/hr (35 bar).

Mobile Phase—A mixture of 4% absolute ethanol, 8% tetrahydrofuran, and 0.06% acetic acid in *n*-hexane was prepared as required, degassed (reflux, 5 min), and stored in the solvent reservoir of the instrument.

Internal Standard Solution—A solution of micronized prednisone in ethyl acetate (0.70 mg/ml) was used.

Linearity—Solutions containing 0.3–3.0 mg/ml of chlorpropamide and tolbutamide (15–150% of label claim) were assayed; 2 mg/ml of drug substance was chosen as the 100% level. Solutions containing 0.04–1.2 mg/ml of *p*-chlorobenzenesulfonamide and *p*-toluenesulfonamide (2–60% of label claim) were prepared and analyzed.

Calibration Standards—A calibration standard was prepared in a 50-ml glass tube to contain accurately weighed amounts (about 50 mg) of chlorpropamide or tolbutamide and about 10 mg of the respective impurity.

System Check Sample—Powdered, well-mixed composites were prepared from a minimum of 20 tablets of chlorpropamide or tolbutamide previously shown by TLC to contain a sulfonamide impurity. The tablet composites were analyzed repeatedly for intact drug and impurity content. An aliquot of this powdered tablet substance, equivalent to ~50 mg of intact drug, was accurately weighed into a 50-ml glass tube.

Chromatography—To the calibration standard tube and the system check sample tube were added 4.0 ml of 10% (v/v) aqueous hydrochloric acid and 25.0 ml of the internal standard solution. Both tubes were agitated for 30 min on a shaker[20] and centrifuged[21] for 5 min. Duplicate 5-μl aliquots of the organic phases of both tubes were chromatographed.

If the check sample assay fell within the limits of experimental error (Table II), the system was established as functioning satisfactorily and tablet formulations were sampled. The system check sample was injected periodically to detect any changes within the chromatographic system.

Tablet Analysis—Powdered tablet substance aliquots, equivalent to ~50 mg of drug, were accurately weighed into separate 50-ml glass tubes and treated as previously described.

Calculations—Peak area ratio was determined by electronic integration of the sample and the internal standard.

RESULTS AND DISCUSSION

The ideal stability assay would measure the undegraded drug and all possible degradates without prior separation. A chromatographic technique such as HPLC generally comes closest to meeting this criterion. Preliminary TLC stability studies showed that the main degradation products of chlorpropamide and tolbutamide are the respective sulfonamides and alkylamines. The alkylamines, propyl and dipropylurea, and butyl and dibutylurea did not interfere with the HPLC assay because these compounds give no absorbance at 254 nm. Prior separation of these

[10] Glass distilled, low UV cutoff, Burdick & Jackson Laboratories, Muskegon, Mich.
[11] Javex 1-10 dilution, Bristol-Myers Canada Ltd., Toronto, Canada.
[12] Fisher Scientific Co., Fair Lawn, N.J.
[13] Macherey-Nagel precoat, Brinkmann Instruments, Rexdale, Ontario, Canada.
[14] Analtech precoat, Analtech Inc., Newark, Del.
[15] Merck precoat, E. Merck, Darmstadt, Germany.
[16] Multi-purpose rotator, Scientific Industries, Springfield, Mass.
[17] Model 4100, Varian Aerograph, Palo Alto, Calif.
[18] Autolab System 1, Spectra-Physics, Santa Clara, Calif.
[19] LiChrosorb Si-60, Brinkmann Instruments, Rexdale, Ontario, Canada.
[20] Eberbach Corp., Ann Arbor, Mich.
[21] Model K, International Equipment Co., Needham Heights, Mass.

Table II—HPLC Linearity Data

Compound	Range, mg/ml	Correlation Coefficient[a], r^2	Slope[b]	y-Intercept[c]
Chlorpropamide	0.3–3.0	0.9997	0.0825	−0.00164
p-Chlorobenzenesulfonamide	0.04–1.2	0.9986	0.0522	−0.00059
Tolbutamide	0.3–3.0	0.9996	0.0576	−0.00130
p-Toluenesulfonamide	0.04–1.2	0.9998	0.0576	−0.00347

[a] Five points were subjected to regression analysis with each compound. [b] The slope was obtained by dividing the count ratio of the compound to the internal standard by the weight ratio of the compound to the internal standard. [c] The y-coordinate for a value of $x = 0$.

compounds from the intact drug and the sulfonamide impurity was not necessary.

An important prerequisite for an HPLC stability study is separation reproducibility over time. The forward-phase technique on microparticulate silica gel fulfills this need. The chromatograms in Figs. 1 and 2 are typical of the separation achieved.

Chlorpropamide and tolbutamide exhibited linear responses between 0.3 and 3.0 mg/ml (1.5 and 15 μg/injection). The respective sulfonamide impurities exhibited linear responses between 0.04 and 1.2 mg/ml (0.2 and 6.0 μg/injection) (Table II).

The precision of the quantitation of the main drugs and the respective sulfonamide impurities was determined by analyzing a degraded formulation on different days (Table III). The reproducibility of the chromatographic system over a single day was shown by injecting 12, 5-μl aliquots of the ethyl acetate layer of a calibration standard (2.90 mg/ml of

Table III—HPLC Assay of Degraded[a] Chlorpropamide (A) and Tolbutamide (B) Composites on Different Days

	Composite A				Composite B		
Day	Chlorpropamide by HPLC, %	p-Chlorobenzenesulfonamide by HPLC, %	Total by HPLC, %	Assay by USP XIX, %	Tolbutamide by HPLC, %	p-Toluenesulfonamide by HPLC, %	Tolbutamide by BP 1973, %
1	79.0	18.3			87.6	10.9	
2	79.8	18.2			86.2	11.2	
3	78.4	18.2			85.9	10.9	
4	79.1	19.1					
Mean assay (% label claim)	79.1 (±0.6[b])	18.5 (±0.4[b])	97.6	96.0	86.6 (±0.9[b])	11.0 (±0.2[b])	83.9

[a] Stored at 60° and 70% RH for 3 months. [b] Standard deviation.

Table IV—HPLC Analysis of Impurity-Free Chlorpropamide and Tolbutamide Tablet Grinds Spiked with Known Amounts of the Respective Sulfonamide

	Chlorpropamide				Tolbutamide			
		p-Chlorobenzenesulfonamide Spike				p-Toluenesulfonamide Spike		
Aliquot	Intact Drug, % label claim	Calc., %	Found by HPLC, %	Recovery, %	Intact Drug, % label claim	Calc., %	Found by HPCL, %	Recovery, %
1	99.3	11.3	10.4	92.0	98.8	11.7	11.4	97.4
2	101.2	21.2	20.5	96.7	99.9	28.5	28.5	100.0
3	101.1	46.1	47.9	103.8	99.4	32.4	32.7	100.9
4	99.6	57.2	58.3	101.8	100.1	66.2	68.9	104.1
Mean recovery, %	100.3			98.6	99.6			100.6
CV, %	±1.0			±5.4	±0.6			±2.8
Mean assay, %	101.0[a,b]				99.3[a,c]			

[a] Assay value obtained on tablet triturate before spiking with impurity. [b] USP XIX. [c] BP 1973.

Table V—Assay of Chlorpropamide Formulations by USP XIX and HPLC Procedures

Formulation	Storage Condition	USP XIX, Chlorpropamide, % label claim	HPLC		
			Chlorpropamide, % label claim	p-Chlorobenzenesulfonamide[a]	Total, % label claim
1	Ambient	98.1	97.8	Nil	97.8
1	60°, 70% RH for 3 months	96.0[b], 80.1[c]	79.1	18.7	97.8
2	Ambient	103.4	106.1	Nil	106.1
2	60°, 70% RH for 3 months	101.1[b], 70.8[c]	66.7	39.6	106.3
3	Ambient	101.0	98.8	Nil	98.8
3	60°, 70% RH for 3 months	99.5[b], 71.6[c]	70.7	32.1	102.8

[a] Expressed as equivalent weight of intact drug. [b] Uncorrected for p-chlorobenzenesulfonamide. [c] Corrected assay value determined by calculating the contribution of p-chlorobenzenesulfonamide to USP XIX assay from the known absorptivity of this compound and its actual level in the formulation as determined by HPLC.

Table VI—Assay of Tolbutamide Formulations by BP 1973 and HPLC Procedures

Formulation	Storage Condition	BP 1973, Tolbutamide, % label claim	HPLC		
			Tolbutamide, % label claim	p-Toluenesulfonamide[a]	Total, % label claim
1	Ambient	97.7	99.1	Nil	99.1
1	60°, 70% RH for 3 months	83.9	86.9	11.0	97.9
2	Ambient	99.3	101.4	Nil	101.4
2	60°, 70% RH for 3 months	95.7	97.2	3.9	101.1
3	Ambient	98.6	99.7	Nil	99.7
3	60°, 70% RH for 3 months	72.9	73.4	25.7	99.1

[a] Expressed as equivalent weight of intact drug.

chlorpropamide and 0.697 mg/ml of the internal standard). The relative standard deviation of the peak area ratios was 1.21%. The lower limit of quantitation[22] of *p*-chlorobenzenesulfonamide or *p*-toluenesulfonamide was 0.2 μg/5-μl injection. This impurity level is ~2% of the label claim of chlorpropamide or tolbutamide.

Several injections at the low impurity level were made to analyze the error involved in quantitating the sulfonamide impurity. For *p*-toluenesulfonamide at the 1.95% level, the relative standard deviation of the count ratio of the substance to the internal standard was 3.77%, an estimate of the error expected at the lower limit of quantitation.

The accuracy of the intact drug quantitation was established by analysis of individual tablet composites of chlorpropamide and tolbutamide, shown to be free of impurities by TLC. The samples were analyzed by the official method and also by HPLC. Additional weighings of these samples were spiked with known amounts of the respective sulfonamide impurity and reanalyzed by the HPLC method (Table IV).

To establish that quantitative partitioning of the intact drug and the related sulfonamide impurity was obtained, accurately weighed tablet composite samples, equivalent to 50 mg of the intact drug, were partitioned between 10, 20, and 30 ml of ethyl acetate and 4 ml of 10% (v/v) aqueous hydrochloric acid. Duplicate 5-μl aliquots of the organic layer were chromatographed. The assay values obtained after partition with 20 and 30 ml of ethyl acetate were not significantly different. The partitioning experiment was repeated with tablets that had been partially degraded by exposure to 60° and 70% relative humidity (RH). The total amount of intact drug and impurity obtained after partition with 20 and 30 ml of ethyl acetate was not significantly different. These data indicated that 25 ml of ethyl acetate was sufficient to extract completely the intact drug and impurities from degraded formulations.

The time required for complete extraction was determined by shaking replicate samples for 15, 30, and 45 min with 4.0 ml of 10% aqueous hydrochloric acid solution and 25.0 ml of the internal standard solution. There was no difference in assay value after 30 min of shaking. The aqueous layers of a calibration standard and of a decomposed formulation extracted with ethyl acetate for 30 min were chromatographed. No peaks were detected in these layers, indicating that complete extraction had taken place.

The system check sample in combination with the calibration standard indicated the status of the total system. Reproducible check sample values showed that the calibration standard factors were correct and that the sampling procedure had been carried out properly. For chlorpropamide and *p*-chlorobenzenesulfonamide, the relative standard deviations of these calibration factors were 1.42 and 3.11%, respectively, over ~8 weeks. For tolbutamide and *p*-toluenesulfonamide, the relative standard deviations of the calibration factors were 1.39 and 2.37%, respectively. These values indicate that the method is reproducible over an extended time.

[22] Defined as the level of impurity that, on repeated analysis, gives a relative standard deviation of ~4%.

Tablet formulations of chlorpropamide and tolbutamide stored for 3 months at ambient temperature (range of 21–23°) and ambient relative humidity and replicate samples stored at 60° and 70% RH (12) were analyzed by HPLC for the intact drug and the sulfonamide degradates. The samples were also analyzed by the appropriate compendial method.

Chlorpropamide samples were analyzed by the USP XIX (5) spectrophotometric technique. From the known absorptivity of *p*-chlorobenzenesulfonamide and its HPLC-determined level in the formulation, the contribution to the measured total absorbance was estimated, and the absorbance due to the intact drug was calculated. The percent recoveries of the undegraded drug determined by the two methods are given in Table V.

Similarly, the BP 1973 (6) titrimetric procedure was utilized for the tolbutamide formulations (Table VI). Because the degradate, *p*-toluenesulfonamide, is not titratable, this method allowed for a direct determination of the intact drug. The method was not applicable to some decomposed samples because discoloration in the tablets interfered with the end-point.

Comparison of the data in Tables V and VI indicates that the HPLC method is equivalent or superior to existing techniques with respect to accuracy. The HPLC method could be used to determine levels of the sulfonamide impurities in amounts less than 2% by increasing the amount of sample injected onto the column; however, the levels of chlorpropamide and tolbutamide might exceed the linear range of the system. The TLC method can be used to follow the stability profile of formulations in a stability study and to estimate semiquantitatively the concentration of impurities.

REFERENCES

(1) K. K. Kaistha and W. N. French, *J. Pharm. Sci.*, **57**, 459 (1968).

(2) K. K. Kaistha, *ibid.*, **58**, 235 (1969).

(3) F. Bottari, M. Mannelli, and M. F. Saettone, *ibid.*, **59**, 1663 (1970).

(4) F. Bottari, B. Giannaccini, E. Nannipieri, and M. F. Seattone, *ibid.*, **61**, 602 (1972).

(5) "The United States Pharmacopeia," 19th rev., Mack Publishing Co., Easton, Pa., 1975.

(6) "The British Pharmacopoeia 1973," University Printing House, Cambridge, England, 1973.

(7) T. Kuriki, T. Tsujiyama, and N. Suzuki, *Jpn. Anal.*, **22**, 91 (1973).

(8) T. Kuriki, T. Tsujiyama, T. Akaogi, and N. Suzuki, *ibid.*, **23**, 181 (1974).

(9) W. F. Beyer, *Anal. Chem.*, **44**, 1312 (1972).

(10) D. Molins, C. K. Wong, D. M. Cohen, and K. P. Munnelly, *J. Pharm. Sci.*, **64**, 123 (1975).

(11) R. E. Majors, *Anal. Chem.*, **44**, 1722 (1972).

(12) "Annual Book of ASTM Standards" part 35, American Society for Testing and Materials, Philadelphia, Pa., 1975, p. 852.

Enthalpy of Bile Salt–Lecithin Mixed Micelle Formation

RUPERT O. ZIMMERER, Jr. *, and SIEGFRIED LINDENBAUM ˣ

Received July 17, 1978, from the *Department of Pharmaceutical Chemistry, McCollum Laboratories, University of Kansas, Lawrence, KS 66044.* Accepted for publication October 20, 1978. *Present address: Analytical Research Department, Endo Laboratories Inc., Garden City, NY 11530.

Abstract □ The enthalpies for the dissolution of lecithin by sodium salts of cholic, deoxycholic, and chenodeoxycholic acids and their glycine and taurine conjugates are reported. Exothermic enthalpies were found in each case. It is suggested that heat evolution is due to a bile salt–lecithin interaction other than hydrophobic interactions. These results provide strong support for the "mixed disk" model for the complex lecithin–bile salt micelle, which requires that a substantial fraction of the bile salt molecules be incorporated within a lecithin bilayer where hydrogen-bonded pair formation can occur. Calorimetric studies of the interaction between sodium cholate and nonionic, cationic, and anionic detergents yielded exothermic heats. These results suggest that these bile salt molecules partition into the detergent micelle interior as hydrogen-bonded pairs.

Keyphrases □ Enthalpy—dissolution of lecithin in aqueous bile salt solutions, micelle formation, hydrogen bonding □ Lecithin—dissolution in aqueous bile salt solutions, micelle formation, enthalpy, hydrogen bonding □ Bile salts, solutions—dissolution of lecithin, micelle formation, enthalpy, hydrogen bonding

Recent clinical success in dissolving cholesterol gallstones by chenodeoxycholic acid administration has renewed interest in the role of bile salts in the dissolution of cholesterol and other lipids (1, 2).

Whereas bile salts are essential for cholesterol solubilization, bile salts alone in aqueous solution increase cholesterol solubility only slightly: 30–100 bile salt molecules are required to solubilize one cholesterol molecule (3). Therefore, bile salts by themselves cannot account for lipid solubilization and transport in digestion or for maintenance of cholesterol in solution in the gallbladder. Lecithin (phosphatidylcholine) is an essential component of bile; in fact, the bile salt–lecithin combination is required for the solubilization of cholesterol and other lipids (5). Bile

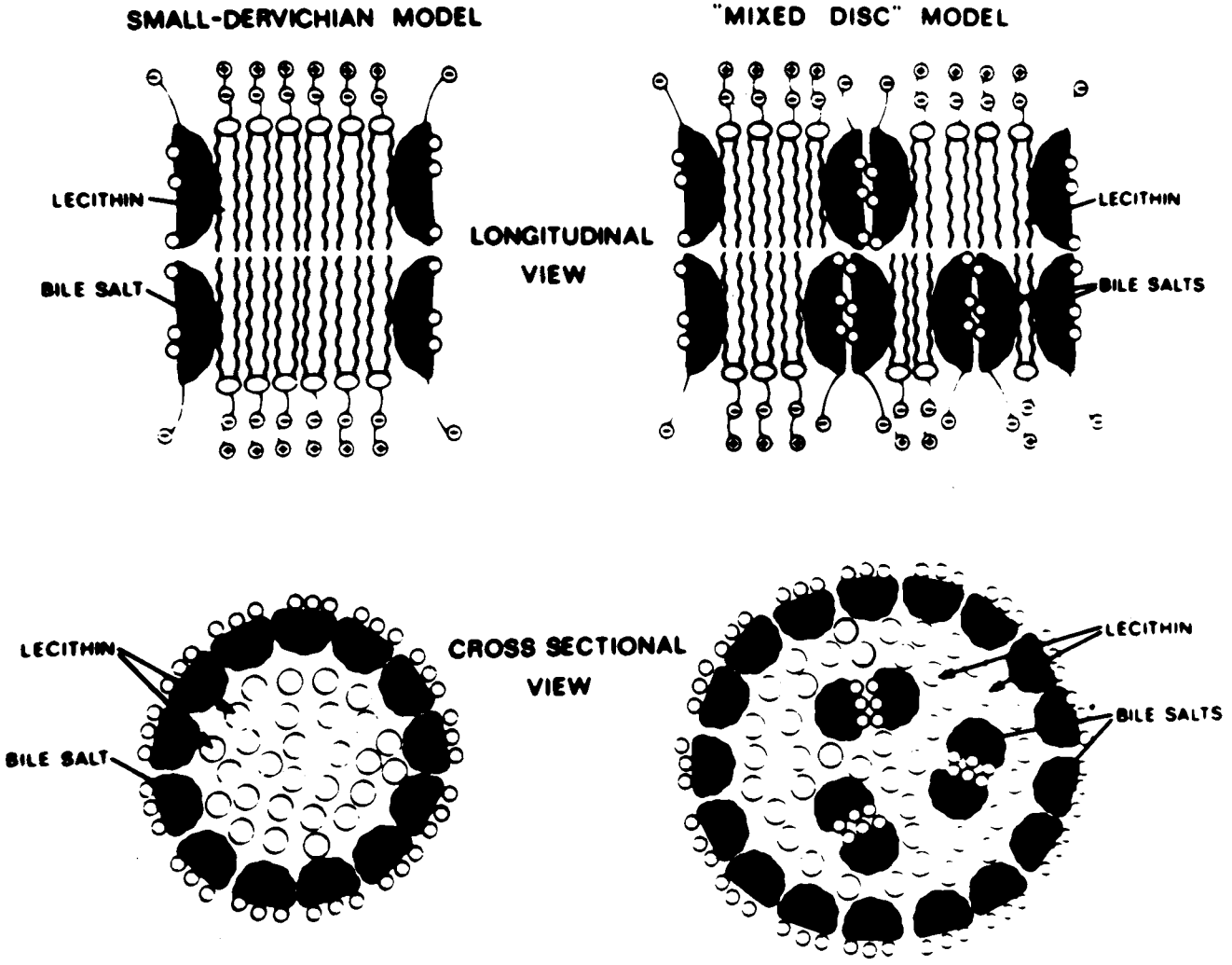

Figure 1—*Schematic models for the structure of the bile salt–lecithin mixed micelle. (Reprinted from Ref. 8 with permission of Plenum Press.)*

0022-3549/79/0500-0581$01.00/0
© 1979, American Pharmaceutical Association

Table I—Structures and Common Names of Bile Salts Used in This Study

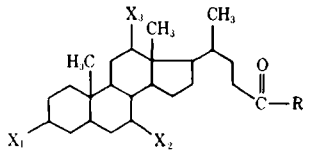

Common Name	X_1	X_2	X_3	R
Cholic acid	OH	OH	OH	OH
Glycocholic acid	OH	OH	OH	$NHCH_2CO_2H$
Taurocholic acid	OH	OH	OH	$NHCH_2CH_2SO_3H$
Chenodeoxycholic acid	OH	OH	H	OH
Glycochenodeoxycholic acid	OH	OH	H	$NHCH_2CO_2H$
Taurochenodeoxycholic acid	OH	OH	H	$NHCH_2CH_2SO_3H$
Deoxycholic acid	OH	H	OH	OH
Glycodeoxycholic acid	OH	H	OH	$NHCH_2CO_2H$
Taurodeoxycholic acid	OH	H	OH	$NHCH_2CH_2SO_3H$

salts have been shown to solubilize lecithin efficiently, forming a micellar solution (3, 5).

On the basis of phase equilibrium and X-ray diffraction studies, a model for the bile salt–lecithin mixed micelle was proposed (6, 7). According to this model (Fig. 1), a disk-shaped micelle is formed on the association of lecithin with bile salt. The disk core consists of the hydrocarbon alkyl chains of the lecithin molecules surrounded by a ring of bile salt molecules. Thus, the disk-shaped micelle exterior presents to the aqueous solvent only the hydrophilic end groups of the phosphatidylcholine and the hydrophilic sides of the bile salt.

Recently, a modified model was proposed on the basis of quasielastic light-scattering data (8). The revised model allowed for the presence of both lecithin and bile salt molecules within the micelle interior (Fig. 1). The bile salt molecules within the micelle interior are presumed to exist as hydrogen-bonded dimers. Recently, other researchers suggested that hydrogen-bonded dimer formation also occurs in dilute aqueous bile salt solutions (9).

The purposes of this study were to measure the enthalpy accompanying the formation of the lecithin–bile salt mixed micellar solution and to correlate the results with the proposed models for these complex micelles.

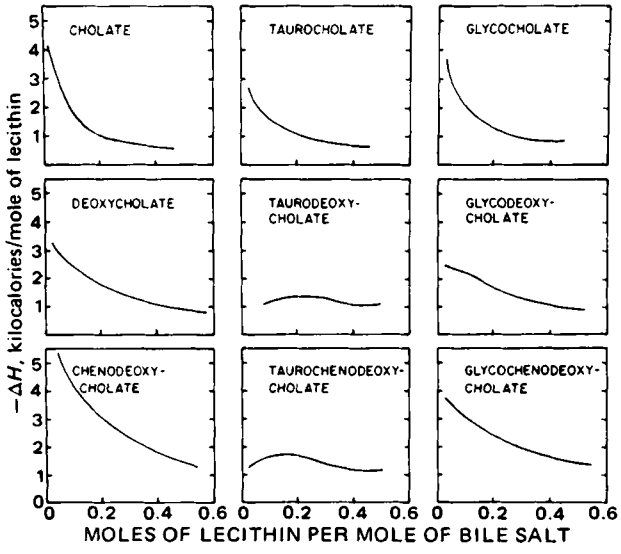

Figure 2—*Enthalpy per mole of lecithin, −ΔH, as a function of the molar ratio of lecithin to sodium salt of bile acid at 25°.*

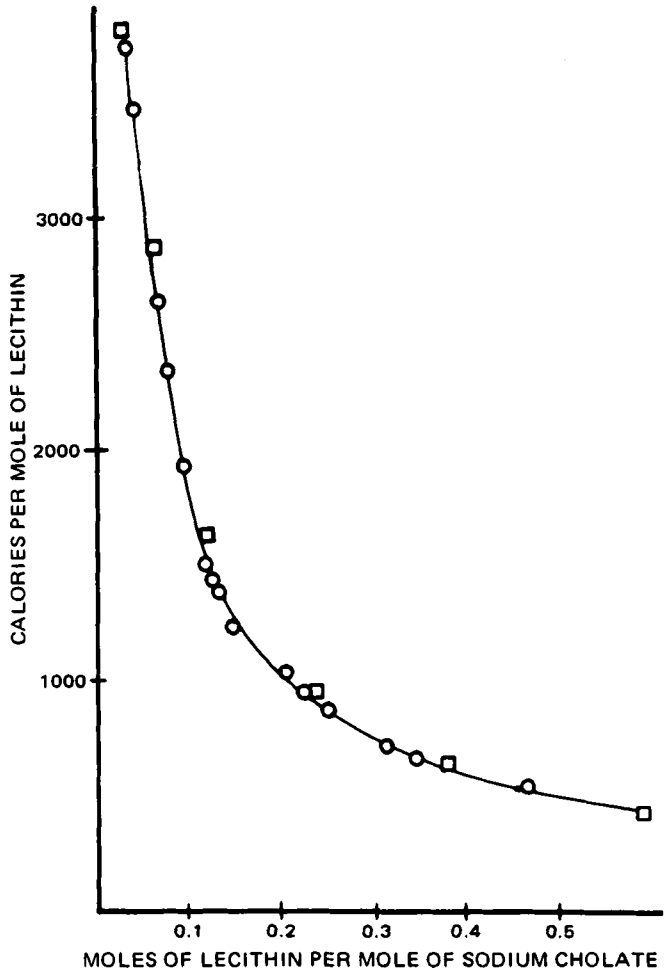

Figure 3—*Enthalpy for the dissolution of lecithin by sodium cholate in water (○) and deuterium oxide (□) solutions at 25°.*

EXPERIMENTAL

Materials—L-α-Lecithin (egg phosphatidylcholine), obtained commercially[1], had been purified by chromatography over alumina and silica gel. The lecithin yielded a milky white suspension when mixed with water on a vortex mixer[2]. TLC showed one spot after visualization with iodine vapor. The bile salts used (Table I) were the highest purity available commercially[3]. They were purchased as the sodium salts, with the exception of glycocholic acid, which was obtained as the free acid. The free acid in 25% ethanol was titrated to pH 9 with sodium hydroxide and lyophilized.

Each bile salt was tested by TLC to estimate the number and approximate concentration of the impurities present. Quantitative TLC was performed using a densitometer[4] in the diffuse reflectance mode. The only major impurities were other bile acids, and in no case did the impurity represent greater than 1% of the total bile salt. Some salts were titrated with percholic acid in acetic acid as a further check on purity. Sodium taurocholate was recrystallized from ethanol–ether before use.

Deuterium oxide, 99.8 atom %D, was used as received[5].

Sodium lauryl sulfate[6] was recrystallized from ethanol. Cetrimonium bromide[3] was recrystallized from water–ethanol. "Scintillation grade" polyoxyethylated *tert*-octylphenol[7] was used without further purification. All other chemicals were reagent grade and were used as received. Aqueous solutions were prepared with deionized water.

Apparatus—Heats of dissolution of lecithin in aqueous bile salt sus-

[1] Avanti Biochemicals Inc., Birmingham, AL 35226.
[2] Vortex Genie, Scientific Products, McGaw Park, IL 60085.
[3] Sigma Chemical Co., St. Louis, MO 63178. Calbiochem, Dallas, TX 75247.
[4] Chromaflex K49500, Kontes, Vineland, NJ 08360.
[5] Aldrich Chemical Co., Milwaukee, WI 53233.
[6] Eastman Organic Chemicals, Rochester, NY 14650.
[7] Triton X-100, Yorktown Research, South Hackensack, NJ 07606.

Table II—Enthalpies of Dissolution of Lecithin in Aqueous Solutions of Sodium Salts of Bile Acids at 25°

Cholate		Deoxycholate		Chenodeoxycholate		Taurocholate		Taurodeoxycholate		Taurochenodeoxycholate		Glycocholate		Glycodeoxycholate		Glycochenodeoxycholate	
R^a	$-\Delta H^b$	R	$-\Delta H$	R	$-\Delta H$	R	$-\Delta H$	R	$-\Delta H$	R	$-\Delta H$	R	$-\Delta H$	R	$-\Delta H$	R	$-\Delta H$
0.4671	550	0.5777	776	0.5411	1285	0.4569	663	0.6135	1036	0.5036	1118	0.4563	834	0.5226	882	0.5464	1329
0.3492	665	0.4626	924	0.4414	1595	0.3514	751	0.5000	1055	0.4012	1254	0.4278	846	0.3222	1275	0.4489	1563
0.3139	714	0.3920	1082	0.3830	1992	0.2565	932	0.4510	1078	0.3195	1335	0.3943	893	0.2559	1489	0.3640	1750
0.2520	870	0.3414	1224	0.3455	2156	0.1409	1329	0.3926	994	0.2842	1467	0.3688	907	0.2065	1635	0.3087	1897
0.2249	954	0.2865	1433	0.2860	2232	0.1170	1459	0.3531	1233	0.2053	1616	0.3438	950	0.2047	1622	0.2718	1929
0.2048	1040	0.2026	1813	0.1929	2948	0.0957	1600	0.2949	1354	0.1376	1794	0.3039	1074	0.1539	1859	0.2105	2392
0.1495	1257	0.1886	1875	0.1221	4035	0.0706	1935	0.2877	1240	0.1376	1634	0.2681	1003	0.1506	1925	0.1904	2510
0.1332	1391	0.1581	2051	0.0884	4652	0.0458	2291	0.2588	1242	0.0918	1586	0.2302	1135	0.1187	2144	0.1567	2723
0.1262	1446	0.1391	2040	0.0427	5381	0.0229	2709	0.2256	1213	0.0773	1671	0.2049	1274	0.1035	2276	0.0957	3103
0.1210	1511	0.1011	2880	0.0369	5613			0.2124	1083	0.0610	1457	0.1684	1362	0.0862	2291	0.0943	3161
0.0955	1940	0.0734	2913	0.0178	5704			0.1887	1263	0.0545	1430	0.1522	1470	0.0704	2252	0.0746	3388
0.0784	2352	0.0702	2942					0.1885	1333	0.0426	1522	0.1296	1595	0.0543	2333	0.0478	3352
0.0684	2644	0.0690	3347					0.1457	1544	0.0268	1257	0.0970	2017	0.0485	2422	0.0264	3627
0.0424	3485	0.0365	3230					0.1317	1270	0.0240	1028	0.0787	2340	0.0455	2443		
0.0350	3751	0.0287	3197					0.1298	1173	0.0229	1069	0.0518	2821	0.0440	2237		
0.0266	4084	0.0282	3195					0.1099	1277			0.0462	2813	0.0288	2374		
0.0235	4233							0.1013	1096			0.0252	3682	0.0224	2425		
								0.0960	1180			0.0129	3700				
								0.0756	1014								
								0.0718	921								
								0.0688	1087								
								0.0670	1099								
								0.0508	782								
								0.0508	782								
								0.0345	767								
								0.0203	683								

[a] Moles of lecithin per mole of bile salt. [b] Calories per mole of lecithin; 1 calorie = 4.184 joules.

Table III—Heat of Mixing of Lecithin Suspended in Deuterium Oxide with Sodium Cholate in Deuterium Oxide Solution at 25°

R^a	$-\Delta H^b$
0.5955	461
0.3817	642
0.2399	954
0.1213	1635
0.0629	2878
0.0306	3819

[a] Moles of lecithin per mole of sodium cholate. [b] Calories per mole of lecithin.

pensions were measured in a batch microcalorimeter[8] described previously (10). The normal calorimeter strip-chart recorder with an integrator was replaced with a digital output device. The potential from the calorimeter thermopile was amplified[9], and the output was fed sequentially to a voltage-to-frequency converter[10] and to a counter[11].

Heats of mixing of aqueous sodium cholate solutions with aqueous solutions of nonionic, cationic, and anionic detergents were measured with a titration calorimeter[12] interfaced with a minicomputer[13]. The computer counted and recorded the number of pulses representing the calorimeter heat output. It also controlled the on–off timing of the buret and calibration heater[14].

Methods—The techniques and methods of calibration of the batch microcalorimeter were described previously (11). Heats of dissolving aqueous suspensions of egg lecithin with bile salt solutions were obtained by mixing 1–4 ml of 0.1 molal solutions of sodium bile salt with 0.25–2 ml of 0.01–0.05 molal suspensions of lecithin in the batch microcalorimeter. Solutions and suspensions were prepared by weight and injected into the calorimeter cell with syringes, which were weighed before and after delivery of solution.

Enthalpies for the dissolution of lecithin by sodium cholate in the presence of sodium chloride were measured in the same way, except that aqueous sodium chloride solutions were substituted for distilled water in the preparation of lecithin suspensions and sodium cholate solutions.

[8] Model 10700-2, LKB Instruments, Rockville, MD 20852.
[9] Model 150 B microvolt ammeter, Keithley Instrument Co., Cleveland, OH 44139.
[10] Designed by Dr. Wesley White, Chemistry Department, University of Kansas.
[11] Model 5330 B preset counter, Hewlett-Packard, Santa Clara, CA 95050.
[12] Model 550 isothermal titration calorimeter, Tronac Inc., Orem, UT 84057.
[13] Model 2100A, Hewlett-Packard, Cupertino, CA 95014.
[14] The computer interface and programs for the operation of the calorimeter were provided by Dr. Wesley White.

Table IV—Heat of Dissolution of Lecithin by Sodium Cholate in Aqueous Sodium Chloride Solutions at 25°

0.1 M NaCl		0.2 M NaCl	
R^a	$-\Delta H^b$	R	$-\Delta H$
0.4904	589	0.5021	596
0.4061	676	0.3894	703
0.3082	824	0.2787	923
0.2661	931	0.2483	1036
0.1988	1219	0.2009	1270
0.1511	1569	0.1437	1703
0.1192	1953	0.1184	2055
0.0890	2466	0.0894	2557
0.0827	2617	0.0753	2786
0.0515	3348	0.0426	3501
		0.0240	3945

[a] Moles of lecithin per mole of sodium cholate. [b] Calories per mole of lecithin.

Likewise, the enthalpy measurements in deuterium oxide were performed with deuterium oxide substituted for distilled water in the solutions and suspensions.

Heats of mixing aqueous solutions of sodium cholate with aqueous surfactant solutions were measured by placing 20 ml of 0.03 molal sodium cholate in the isothermal reaction vessel and titrating with 0.05 molal surfactant with the motor-driven syringe buret. Detailed procedures for the operation and calibration of the titration calorimeter were published (12, 13). The batch and titration calorimeter gave results in good agreement with literature values for the heat of dilution and heats of mixing for standard reactions.

RESULTS

Heats of dissolution of suspended lecithin by aqueous bile salt solutions are given in Table II and Fig. 2 as calories per mole of lecithin as a function of the final system composition expressed as moles of lecithin per mole of bile salt. For the dissolution of lecithin by sodium cholate solutions, these experiments were repeated in deuterium oxide (Table III and Fig. 3) and in 0.1 and 0.2 M NaCl (Table IV and Fig. 4). In all cases, the initially cloudy lecithin suspension formed a clear solution after mixing in the calorimeter with the bile salt solution. Over the concentration range studied, the measured heats were a function only of the lecithin to bile salt ratio and not of the total lipid concentration.

Enthalpy values for the mixing of surfactant solutions with aqueous sodium cholate solutions are given in Table V and Fig. 5 as calories per mole of surfactant as a function of moles of surfactant per mole of sodium cholate.

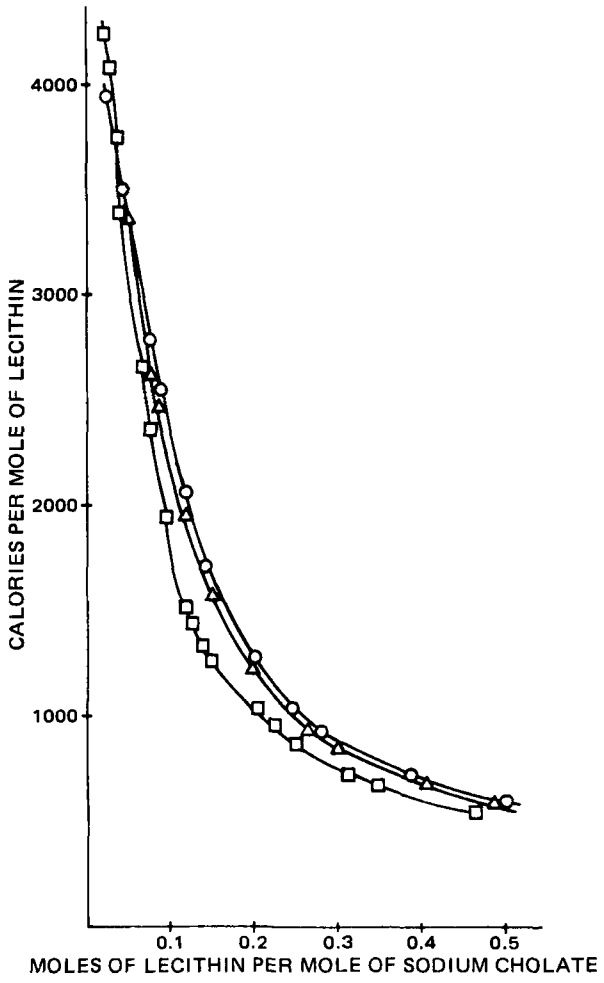

Figure 4—*Enthalpy of dissolution of lecithin by sodium cholate in the presence of added sodium chloride at 25°. Key: □, water; △, 0.1 M NaCl; and ○, 0.2 M NaCl.*

DISCUSSION

The dissolution of suspended hydrated lecithin by bile salt solutions was accompanied in every case by the evolution (negative ΔH) of large amounts of heat (Fig. 2). Previous observations of heats of micelle formation generally yielded small and positive values for the enthalpy (14–18). It has generally been assumed, therefore, that the driving force for micelle formation is the positive entropy change associated with a hydrophobic species leaving the aqueous environment to form a micelle (17). Micelle formation of surfactants is attributed to the hydrophobic effect phenomenon, similar to the stabilization of proteins in their native configuration in an aqueous environment (17, 19).

The large exothermic heats obtained in these studies suggest that the process is not simply "hydrophobic" micelle formation. The process investigated here is shown in Scheme I:

$$x\mathrm{L}(\mathrm{H_2O}) + y(\mathrm{BS})_{\mathrm{sol}} \rightarrow \mathrm{L}_x(\mathrm{BS})_y$$

Scheme I

in which x moles of hydrated lecithin (L) interact with y moles of bile salts (BS) in aqueous solution to form a complex micellar solution. In an aqueous dispersion, lecithin is presumably in the form of liposomes (20–22) consisting of concentric envelopes of lipid bilayers. The milky-white lipid bilayer dispersions are solubilized in the presence of bile salt solutions to form optically clear micellar solutions. Under the experimental conditions, the heat measured may be seen as the sum of the heat of simple bile salt micelle dissociation and the heat of mixed micelle formation with lecithin.

Dilution heat studies on sodium cholate solutions showed that the enthalpy of simple micelle dissociation is negligible compared to the total heat observed for the dissolution of lecithin by bile salt solution. The observed heat is, therefore, virtually entirely the heat of mixed micelle formation. Heat evolution during this process is difficult to understand

Table V—Heat of Mixing Aqueous Surfactant Solutions with Aqueous Sodium Cholate at 25°

Anionic[a] Detergent		Nonionic[b] Detergent		Cationic[c] Detergent	
R[d]	$-\Delta H$[e]	R	$-\Delta H$	R	$-\Delta H$
0.0352	4784	0.0247	6474	0.0244	3779
0.0704	4186	0.0495	6200	0.0489	3323
0.1056	3870	0.0743	5398	0.0733	2936
0.1408	3637	0.0990	4794	0.1222	2601
0.2112	3203	0.1485	3974	0.1711	2344
0.2816	2899	0.1980	3473	0.2200	2082
0.3520	2697	0.2476	3152	0.2689	1883
0.4224	2553	0.2971	2922	0.3178	1754
0.4928	2408	0.3961	2578		
0.5632	2289	0.4950	2315		

[a] Sodium lauryl sulfate. [b] Polyoxyethylated *tert*-octylphenol. [c] Cetrimonium bromide. [d] Moles of surfactant per mole of sodium cholate. [e] Calories per mole of surfactant.

in terms of the Small–Dervichian model (Fig. 1) since no new chemical bonds are formed in the mixed micelle. In the mixed disk model, however, a substantial fraction of the bile salt molecules are partitioned into the bilayer interior as hydrogen-bonded pairs. It may be assumed that in the low dielectric micelle interior, the bile salt molecules are hydrogen bonded to each other to a much greater extent than in the aqueous phase. The partition of bile salt molecules from the aqueous phase to the micelle interior would be accompanied by increased hydrogen bonding and heat evolution.

Recently, Oakenfull and Fisher (9) suggested that bile salts are associated by hydrogen bonding in aqueous solution. This finding, based on conductance and volume studies, is in conflict with earlier models for bile salt association. It has generally been assumed that premicellar association of bile salts occurs by hydrophobic interaction between the nonpolar flat surfaces of the bile salt molecules. This hydrophobic association model was suggested on the basis of NMR studies of aqueous bile salt solutions (23). This conflict remains to be resolved. It seems reasonable to assume that any hydrogen-bonded association in the aqueous phase will be enhanced in a less polar medium. Hydrogen bonding between bile salt molecules in a lecithin bilayer also would be consistent with spectroscopic evidence for hydrogen-bonded association of di- and trihydroxy methylcholanoates in carbon tetrachloride (24).

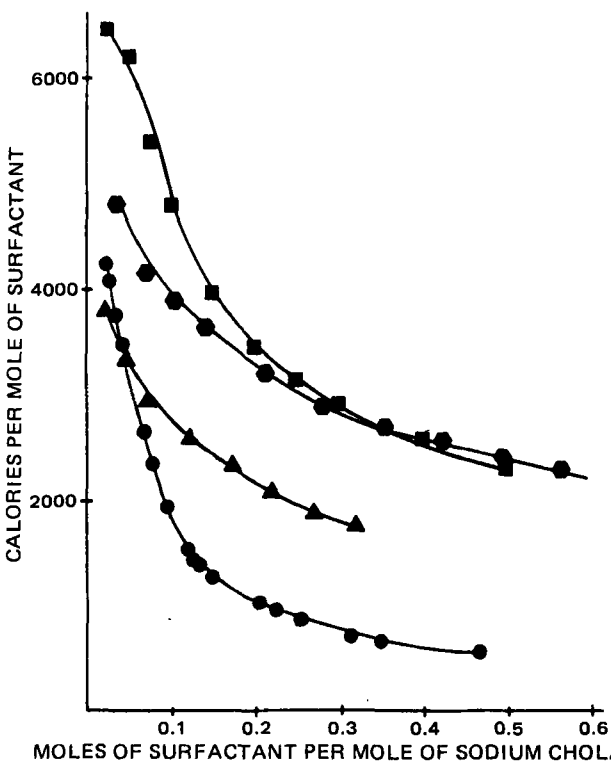

Figure 5—*Enthalpy of mixing surfactant solutions with sodium cholate solution at 25°. Key: ●, lecithin; ■, polyoxyethylated* tert*-octylphenol; ▲, cetrimonium bromide; and ●, sodium lauryl sulfate.*

According to the mixed disk model (8), the ratio of lecithin to cholate within the micelle interior is 2:1, not including the cholate molecules that make up the circumference of the disk.

This 2:1 ratio is also the proportion observed at the phase limit (7, 25, 26). Therefore, for each mole of lecithin solubilized, there is 0.5 mole of bile salt within the micelle. If each pair of bile salt molecules is attached by two hydrogen bonds, then one-half of a hydrogen bond is formed for each lecithin molecule solubilized. The enthalpy for hydrogen bond formation in alcohols varies from −3 to −10 kcal/mole (27, 28). If a value of −6 kcal/mole is assumed, then the heat accompanying the dissolution of 1 mole of lecithin would be −3 kcal/mole. This crude estimate of the enthalpy change expected assumes that hydrogen bonding is the most important contribution. Since other processes such as hydrophobic effects and changes in hydration also contribute, the expected enthalpy value cannot be estimated more accurately.

Comparison of the dissolution heat of lecithin by sodium cholate in water and deuterium oxide (Fig. 3) shows that the results are indistinguishable. These results also suggest that the extent of interaction of the bile salt in the micellar interior determines the enthalpy observed and that hydrophobic forces in the aqueous phase play only a minor role.

In several cases (Fig. 2), the enthalpy per mole of lecithin dissolved increased sharply as the lecithin to bile salt ratio decreased. This result suggests that as this ratio decreases, more bile salt partitions into the micelle phase, with a concomitant increase in hydrogen bonding. An increase in bile salt partition into the micellar phase as the aqueous bile salt concentration increases would be expected to occur if the distribution of bile salt between the micelle interior and the aqueous phase is seen as a mass action phenomenon. For taurocholate and taurochenodeoxycholate, equilibrium dialysis studies have shown that the micellar concentration of bile salt increases with the aqueous bile salt concentration (29).

The effect of added electrolyte on the enthalpy of dissolution of lecithin by sodium cholate is shown in Fig. 4. The enthalpy values become more negative as the concentration of added sodium chloride increases. This enhancement may be caused by increased partition of bile salt into the micelle due to "salting out" of the bile salt from the aqueous phase. The increased penetration of bile salt into the micellar phase is expected to lead to increased hydrogen-bonded association and, therefore, to more heat evolution.

Bile salts form complex micellar solutions with ampiphilic substances other than lecithin (3). It was hoped that an examination of the thermodynamic properties of the interaction between bile salts and other ampiphiles would shed further light on the bile salt–lecithin association.

Enthalpies of mixing sodium cholate solutions with solutions of a nonionic detergent (polyoxyethylated *tert*-octylphenol), a cationic detergent (cetrimonium bromide), and an anionic detergent (sodium lauryl sulfate) were measured. The results (Fig. 5) were compared with the lecithin data. In each case, even larger, more exothermic values for the complex micelle formation heat were obtained.

A detailed discussion of the differences in enthalpies between the different detergents would be highly speculative on the basis of the limited information available. However, these results are consistent with the suggestion that, in each case, the heat evolution is due to enhanced hydrogen-bonded association of the bile salt molecules in the micellar interior.

REFERENCES

(1) J. L. Thistle and L. J. Schoenfield, *J. Lab. Clin. Med.*, **74**, 1020 (1969).

(2) D. M. Small, *Postgrad. Med.*, **51**, 187 (1972).

(3) D. M. Small, in "The Bile Acids," vol. 1, P. P. Nair and D. Kritchevsky, Eds., Plenum, New York, N.Y., 1971, chap. 8.

(4) B. Isaksson, *Acta Soc. Med. Ups.*, **59**, 296 (1954).

(5) D. M. Small, *Adv. Chem. Ser.*, **84**, 31 (1968).

(6) D. M. Small, *Gastroenterology*, **51**, 607 (1967).

(7) D. G. Dervichian, *Adv. Chem. Ser.*, **84**, 78 (1968).

(8) N. A. Mazer, R. F. Kwasnick, M. C. Carey, and G. B. Benedek, in "Micellization, Solubilization, and Microemulsions," vol. 1, K. L. Mittal, Ed., Plenum, New York, N.Y., 1977, p. 383.

(9) D. G. Oakenfull and L. R. Fisher, *J. Phys. Chem.*, **81**, 1838 (1977).

(10) I. Wadsö, *Acta Chem. Scand.*, **22**, 927 (1968).

(11) A. S. Levine and S. Lindenbaum, *J. Solution Chem.*, **2**, 445 (1973).

(12) D. J. Eatough, J. J. Christensen, and R. M. Izatt, "Experiments in Thermometric Titration Calorimetry," Brigham Young University Press, Provo, Utah, 1973.

(13) B. D. Anderson, J. H. Rytting, S. Lindenbaum, and T. Higuchi, *J. Phys. Chem.*, **79**, 2340 (1975).

(14) J. M. Corkill, J. F. Goodman, P. B. Robison, and J. R. Tate, *Trans. Faraday Soc.*, **62**, 987 (1966).

(15) J. M. Corkill, J. F. Goodman, and J. R. Tate, *ibid.*, **60**, 996 (1964).

(16) J. M. Corkill, J. F. Goodman, and S. P. Harrold, *ibid.*, **60**, 202 (1964).

(17) C. Tanford, "The Hydrophobic Effect," Wiley, New York, N.Y., 1973.

(18) N. Muller and F. E. Platko, *J. Phys. Chem.*, **75**, 547 (1971).

(19) W. Kauzmann, *Adv. Protein Chem.*, **14**, 1 (1959).

(20) A. D. Bangham, *Prog. Biophys. Mol. Biol.*, **18**, 29 (1968).

(21) A. Darke, E. G. Finer, A. G. Flook, and M. C. Phillips, *J. Mol. Biol.*, **63**, 265 (1972).

(22) E. Forslind and R. Kjellander, *J. Theoret. Biol.*, **51**, 97 (1975).

(23) D. M. Small, S. A. Penkett, and D. Chapman, *Biochim. Biophys. Acta*, **176**, 178 (1969).

(24) W. S. Bennet, G. Eglinton, and S. Kovac, *Nature*, **214**, 776 (1969).

(25) W. Shankland, *Chem. Phys. Lipids*, **4**, 109 (1970); **19**, 20 (1977).

(26) D. M. Small, M. C. Bourges, and D. G. Dervichian, *Biochim. Biophys. Acta*, **125**, 563 (1966).

(27) S. N. Vinogradov and R. H. Linnell, "Hydrogen-Bonding," Van Nostrand Reinhold, New York, N.Y., 1971, p. 143.

(28) M. D. Joesten and L. J. Schaad, "Hydrogen-Bonding," Dekker, New York, N.Y., 1974, p. 284.

(29) W. C. Duane, *Biochem. Biophys. Res. Commun.*, **74**, 223 (1977).

ACKNOWLEDGMENTS

Abstracted in part from a dissertation submitted by R. O. Zimmerer, Jr., to the University of Kansas in partial fulfillment of the Doctor of Philosophy degree requirements.

Supported by grants from the National Institutes of Health (AM-18084) and the General Research Fund of the University of Kansas.

The authors thank Dr. N. A. Mazer for reading the manuscript and offering constructive criticism.

R. O. Zimmerer, Jr., is the recipient of an American Foundation for Pharmaceutical Education–Mead Johnson Fellowship.

Decreased Tetracycline Bioavailability Caused by a Bismuth Subsalicylate Antidiarrheal Mixture

K. S. ALBERT ˣ, R. D. WELCH, K. A. DeSANTE, and A. R. DiSANTO

Received April 3, 1978, from *The Upjohn Company, Kalamazoo, MI 49001.* Accepted for publication August 3, 1978.

Abstract □ Oral coadministration of a single 250-mg tetracycline capsule and 60 ml of a bismuth subsalicylate antidiarrheal mixture reduced tetracycline absorption by 34% without appearing to perturb its absorption or disposition rate. A pronounced increase in intersubject tetracycline absorption variability also was noted. Apparently, the reduction in tetracycline bioavailability previously reported with a kaolin–pectin suspension is not peculiar to kaolin–pectin but can be expected with almost any antidiarrheal whose mechanism of action is adsorptive in nature.

Keyphrases □ Tetracycline—bioavailability, decreased by coadministered bismuth subsalicylate antidiarrheal □ Bismuth subsalicylate—antidiarrheal mixture, interference with bioavailability of coadministered tetracycline □ Antibiotics—tetracycline, bioavailability decreased by coadministered bismuth subsalicylate □ Antidiarrheals—bismuth subsalicylate, interference with bioavailability of coadministered tetracycline □ Drug-antibiotic interactions—bismuth subsalicylate interference with tetracycline bioavailability

Several studies (1–8) demonstrated that kaolin–pectin-containing antidiarrheal mixtures[1] interfere with the absorption of some concomitantly administered oral drugs. Retrospective *in vitro* experiments[2] suggested that drugs that can exist as cations in solution (*e.g.*, clindamycin, lincomycin, and tetracycline) are most susceptible to irreversible adsorption by negatively charged components of the antidiarrheal, but neutral molecules that can hydrogen bond (*e.g.*, digoxin, which contains a large sugar molecule) also may interact in an untoward way.

This paper describes the effect of a bismuth subsalicylate antidiarrheal mixture[3] on the bioavailability of the cationic drug tetracycline. Concomitant administration of both products markedly decreased the antibiotic bioavailability, suggesting that, in general, any antidiarrheal whose mechanism of action is adsorptive may interfere with the absorption of coadministered cationic and hydrogen-bonded drugs.

EXPERIMENTAL

The 16 normal, nonobese adult volunteers, whose average age was 26 years (range of 20–37 years) and whose average weight was 79 kg (range of 69–90 kg), exhibited normal vital signs and selected laboratory parameters and were without evidence of cardiac, renal, or GI abnormalities. These subjects did not receive any antibacterial medication for 30 days before initiation of the protocol. During the study, volunteers received only the medication prescribed, with 7 days separating each administered treatment.

Subjects were fasted (food and beverage) from 10:00 pm the night before their allocated treatment until 4 hr after drug administration. To ensure adequate urine output, subjects were required to drink at least 360 ml of water with their noon meal. Smoking was permitted if it was the usual custom of a subject. Volunteers did not engage in strenuous or athletic activities during the days the drug was given.

Each subject received a 250-mg tetracycline capsule[4] with and without bismuth subsalicylate suspension in crossover fashion (Table I). Serum samples were obtained at 0, 0.5, 1.0, 2.0, 2.5, 3.0, 4.0, 5.0, 6.0, 8.0, 10.0, 12.0, 16.0, and 24.0 hr. Urine specimens were collected at the following time intervals during each treatment period: predose (to serve as a urine blank), 0–12, 12–24, 24–48, and 48–72 hr. All samples were kept frozen until assayed microbiologically for tetracycline-like activity (9).

RESULTS

The bismuth subsalicylate antidiarrheal preparation effect on average tetracycline serum levels and urinary excretion for the 15 subjects who completed the study is summarized in Tables II and III, respectively; Fig. 1 shows the serum tetracycline time course through 24 hr. It is evident from Table II and the figure that, at every sampling, significantly lower serum antibiotic levels were found following coadministration with the antidiarrheal mixture. With the exception of the 24–48-hr interval, Table III shows that the urinary tetracycline excretion was reduced as well.

The average times of individual peak serum levels were comparable for the two treatments, which suggests that absorption rates were similar (Table II). In contrast, Table II shows that, following the bismuth subsalicylate treatment, the individual peak average concentration was decreased by 27% and the average 24-hr area under the antibiotic curve

Table I—Dosage Schedule and Treatments

Group	Subjects in Group	Treatment for Phase Number[a] I	II
I	1, 3, 6, 9, 10, 12, 14, 16	A	B
II	2, 4, 5, 7, 8, 11, 13, 15	B	A

[a] Treatment A was 60 ml of Pepto-Bismol (lot 830547, Norwich Products) followed immediately by one Panmycin H.F.C., 250 mg (lot 532EK, Upjohn), administered orally with 90 ml of water. Treatment B was one Panmycin H.F.C., 250 mg (lot 532EK, Upjohn), administered orally with 90 ml of water.

Table II—Effect of Bismuth Subsalicylate Antidiarrheal Mixture on Mean Serum Tetracycline Levels

Parameter	Treatment Average[a] A	B	Level of Significance between Treatments, *p*
Serum tetracycline level, μg/ml, at:			
0.5 hr	0.08	0.53	<0.0001
1.0 hr	0.84	1.30	<0.001
1.5 hr	1.25	1.69	<0.01
2.0 hr	1.45	1.92	<0.0025
2.5 hr	1.50	1.98	<0.001
3.0 hr	1.54	2.04	<0.001
4.0 hr	1.44	1.97	<0.001
5.0 hr	1.22	1.85	<0.0001
6.0 hr	1.07	1.64	<0.0001
7.0 hr	1.02	1.55	<0.001
8.0 hr	0.91	1.40	<0.0001
10.0 hr	0.80	1.23	<0.0001
12.0 hr	0.68	1.02	<0.0001
16.0 hr	0.47	0.73	<0.0001
24.0 hr	0.30	0.47	<0.001
Average of individual peak serum levels, μg/ml	1.60	2.18	<0.001
Time of individual peak serum levels, hr	2.80	3.03	NS[b]
AUC through 24 hr, μg/ml × hr	17.5	26.1	<0.0001
Half-life, hr	8.38	9.13	<0.05
Renal clearance, ml/min	79.6	80.7	NS

[a] See Table I. [b] NS = not significant.

[1] Kaopectate or Kaopectate Concentrate, The Upjohn Co., Kalamazoo, MI 49001.
[2] Unpublished data.
[3] Pepto-Bismol, Norwich Products, Norwich, NY 13815.
[4] Panmycin H.F.C., 250 mg, The Upjohn Co., Kalamazoo, MI 49001.

0022-3549/79/0500-0586$01.00/0
© 1979, American Pharmaceutical Association

Table III—Effect of Bismuth Subsalicylate Antidiarrheal Mixture on Mean Urinary Tetracycline Excretion

Time Interval, hr	Amount Excreted[a], mg A	Amount Excreted[a], mg B	Level of Significance between Treatments, p
0–12	56.7	86.7	<0.001
12–24	26.2	45.5	<0.001
24–48	18.3	21.0	NS[b]
48–72	3.72	5.38	<0.005
0–72	105	159	<0.001

[a] See Table I. [b] NS = not significant.

(*AUC*) was reduced 33%, while Table III shows that the 72-hr urinary tetracycline recovery was reduced by 33%. These results indicated that the antidiarrheal disturbed either the absorption or the disposition of the antibiotic. All 15 subjects showed lower 24-hr serum antibiotic *AUC* values in the presence of the antidiarrheal, while 14 of 15 subjects showed the same trend in 72-hr urinary recoveries (Table III).

Two parameters free from absorption influences, renal clearance and half-life, also were evaluated to ascertain whether the bismuth subsalicylate product altered tetracycline disposition. Mean renal clearances were virtually identical while treatment half-lives differed by only 8% (Table II). Apparently, the interaction between the antidiarrheal and the antibiotic affected only absorption, not disposition.

An estimate of the antidiarrheal influence on absorption can be made utilizing a model-independent method described previously (10). This technique bases bioavailability assessment on total urinary recovery (U_∞) and renal clearance ($\dot{V}_{cl,r}$) and assumes that changes in serum clearance ($\dot{V}_{cl,s}$) would be manifested as observed differences in renal clearance among treatments.

Individual relative bioavailability estimates utilizing this approach are summarized in Table IV. Even though average treatment renal clearances were virtually equal, individual subject values did vary between study days. To compensate for these observed differences, adjustments in serum clearance were made on the assumption that individual nonrenal elimination components did not change. With the exception of Subject 8, bioavailability ratios were less than unity, indicating that the antidiarrheal had an adverse effect on absorption. On the average, tetracycline bioavailability when coadministered with bismuth subsalicylate was only 66% ($F^A/F^B = 0.66$, $p < 0.001$).

The effect of the bismuth subsalicylate antidiarrheal mixture on intersubject tetracycline variability is summarized in Table V. Except for time to peak, the data show that the variabilities exhibited by the parameters peak maximum, area under the curve, and urinary recovery were greater for the bismuth subsalicylate treatment. Since the two disposition parameters (renal clearance and half-life) exhibited similar ranges and percent standard deviations between treatments, the greater variation

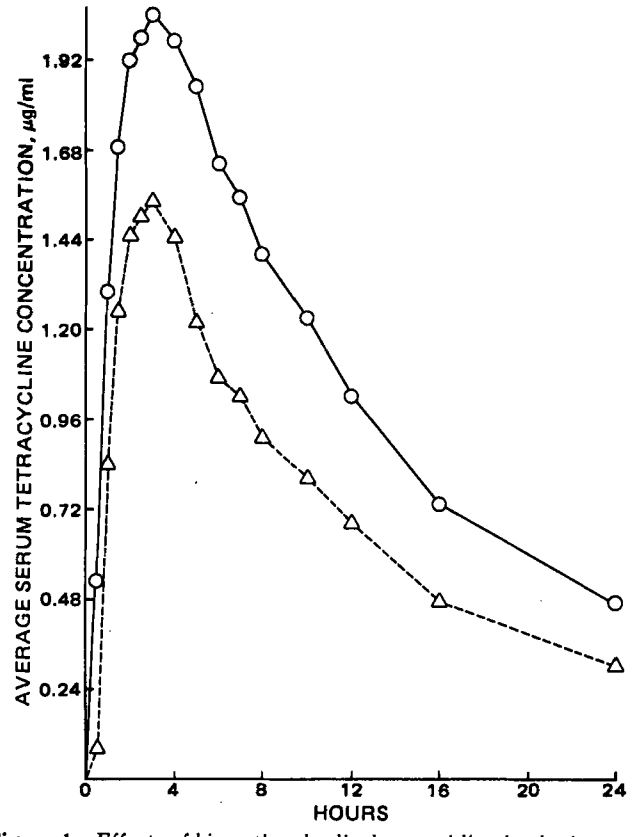

Figure 1—*Effects of bismuth subsalicylate antidiarrheal mixture on serum tetracycline levels following concomitant administration of both drugs. Key: ○, tetracycline alone; and △, tetracycline plus bismuth subsalicylate.*

associated with antidiarrheal coadministration can be attributed predominantly to a perturbation in tetracycline absorption. These results parallel the findings on absorption efficiency already described.

DISCUSSION

The only previous studies of antidiarrheal effect on coadministered oral drug absorption involved kaolin–pectin products (1–8). These studies

Table IV—Model-Independent Relative Bioavailability Estimate[a]

Subject[b]	Clearances, ml/min A $\dot{V}_{cl,r}$	Clearances, ml/min A $(\dot{V}_{cl,s})'_{ex}$	Clearances, ml/min B $\dot{V}_{cl,r}$	Clearances, ml/min B $(\dot{V}_{cl,s})_{ex}$	Urinary Recovery, mg A	Urinary Recovery, mg B	Relative Amount Absorbed, F^A/F^B
1	89.3	124.0	85.2	119.9	97.7	175.8	0.560
2	93.0	111.4	125.7	144.1	84.2	216.0	0.330
4	53.3	111.8	81.2	139.7	88.5	143.7	0.629
5	72.2	133.2	77.8	138.8	108.6	137.4	0.796
6	70.3	111.3	82.3	123.3	122.1	164.6	0.730
7	82.4	129.8	95.5	142.9	94.8	166.9	0.556
8	89.9	165.6	95.0	170.7	173.4	121.4	1.44
9	56.8	126.5	64.1	133.8	80.8	156.7	0.513
10	84.8	123.7	100.7	139.6	103.0	178.3	0.557
11	64.1	129.5	64.9	130.3	42.2	122.9	0.344
12	80.9	113.2	25.8	58.1	96.3	108.4	0.720
13	54.2	74.2	74.1	94.4	148.3	193.4	0.685
14	81.5	126.4	93.5	138.4	140.3	168.0	0.820
15	70.6	124.2	67.4	121.0	58.8	137.7	0.426
16	151.1	175.9	77.3	102.1	135.0	187.2	0.809
Mean	79.6	125.4	80.7	126.5	104.9	158.6	0.661[c]
CV, %	37.3	18.6	33.8	20.7	32.8	18.8	40.5

[a] Calculated according to the method of Kwan and Till (10) where:

$$(\dot{V}^B_{cl,s})_{ex} = \frac{(\dot{V}^B_{cl,r})(D^B)}{U^B_\infty}$$

$$(\dot{V}^A_{cl,s})'_{ex} = \dot{V}^A_{cl,r} + (\dot{V}^B_{cl,s})_{ex} - \dot{V}^B_{cl,r}$$

$$F^A/F^B = \frac{U^A_\infty (\dot{V}^A_{cl,s})'_{ex}}{(D^A)(\dot{V}^A_{cl,r})}$$

[b] Subject 3 did not complete the study. [c] Statistically significantly different from unity using t test ($p < 0.001$).

Table V—Bismuth Subsalicylate Antidiarrheal Mixture Effect on Tetracycline Product Variability

Parameter	Range A	Range B	SD, % A	SD, % B
Peak serum level, μg/ml	0.69–2.29	1.79–2.52	24.4	9.34
Peak time, hr	2.50–4.0	2.50–5.0	18.9	37.6
AUC through 24 hr, μg/ml × hr	7.13–27.9	21.1–30.5	28.9	11.0
Urinary recovery through 72 hr, mg	42.2–173	108–216	32.8	18.8
Half-life, hr	7.09–10.8	7.58–11.8	11.4	15.1
Renal clearance, ml/min	53.3–151	25.8–126	29.7	27.3

suggested that the antidiarrheal influence on antibiotic absorption is dose dependent.

In the present study, 60 ml of a bismuth subsalicylate antidiarrheal product was administered concomitantly with a 250-mg tetracycline hydrochloride capsule. Since the "active" bismuth subsalicylate concentration was not given on the package, molar comparisons of "active" bismuth subsalicylate antidiarrheal to "active" kaolin–pectin products were impossible. Nonetheless, the 34% decrease in relative tetracycline bioavailability was consistent with the kaolin–pectin with tetracycline data and indicated that similar drug interactions are likely with any antidiarrheal whose mechanism of action is adsorptive.

REFERENCES

(1) J. G. Wagner, *Can. J. Pharm. Sci.*, **1**, 55 (1966).

(2) J. G. Wagner, *Drug Intell.*, **2**, 38 (1968).

(3) P. F. Binnion, in "Symposium on Digitalis," O. Storstein, Ed., Glydenal Norsk Forlag, Oslo, Norway, 1973, p. 216.

(4) D. D. Brown and R. P. Juhl, *N. Engl. J. Med.*, **295**, 1034 (1976).

(5) W. M. Gouda, *Abstr., Acad. Pharm. Sci.*, **6**, 117 (1976).

(6) K. A. DeSante, A. R. DiSanto, R. G. Stoll, R. D. Welch, T. J. Vecchio, and K. S. Albert, *ibid.*, **7**, 116 (1977).

(7) K. S. Albert, J. W. Ayres, D. J. Weidler, E. Sakmar, M. R. Hallmark, R. G. Stoll, K. A. DeSante, A. R. DiSanto, and J. G. Wagner, *ibid.*, **7**, 116 (1977).

(8) K. S. Albert, K. A. DeSante, R. D. Welch, and A. R. DiSanto, *ibid.*, **7**, 115 (1977).

(9) D. C. Grove and W. A. Randall, in "Medical Encyclopedia," H. Welch and F. Marti-Ibasey, Eds., Medical Encyclopedia Inc., New York, N.Y., 1955, p. 238.

(10) K. C. Kwan and A. E. Till, *J. Pharm. Sci.*, **62**, 1494 (1973).

ACKNOWLEDGMENTS

The authors thank Ms. Mariann Holthouse for secretarial assistance and W. L. Lummis for performing the microbiological assays.

Molecular Weight Determination of Commercial Heparin Sodium USP and Its Sterile Solutions

H. J. RODRIGUEZ * and A. J. VANDERWIELEN ˣ

Received June 19, 1978, from *Control Analytical Research and Development, The Upjohn Company, Kalamazoo, MI 49001.* Accepted for publication September 8, 1978. *Present address: Waters Associates, Milford, MA 01757.

Abstract □ A liquid chromatographic assay for the characterization of heparin sodium USP and heparin sterile solutions was developed. The method employs size exclusion chromatography and computer-based data collection and manipulation. An examination of commercially available heparin showed only minor differences between the heparins extracted from beef lung and porcine intestinal mucosa. The molecular weight averages of the material and its sterile solutions were 9000–12,000 daltons. A correlation was observed between average molecular weight and anticoagulant activity for the heparin sodium samples examined.

Keyphrases □ Heparin sodium—molecular weight determination of commercial products and sterile solutions using liquid chromatography □ Molecular weight determination—commercial heparin sodium USP and its sterile solutions, liquid chromatography □ Liquid chromatography—molecular weight determination of commercial heparin sodium USP and its sterile solutions □ Anticoagulants—heparin sodium, molecular weight determination, liquid chromatography

Several methods for the molecular weight fractionation of heparin sodium have been reported (1–3), gel filtration being most commonly used (4). In most cases, analysis requires several hours per sample and complicated detection procedures. Recently, a fast and reliable method was developed (5, 6) using high-performance liquid chromatography (HPLC) with refractive index detection for the determination of molecular weight averages of heparin sodium USP and injectable heparin sodium solutions (6).

The literature contains conflicting reports regarding the relationship of molecular weight and anticoagulant activity (7–9). There are also significant differences in the reported molecular weights of commercially available heparin (5, 6, 10). This paper presents the results of an examination of sterile injectable heparin sodium from commercial sources. The liquid chromatographic method recently developed (5) was modified and used to determine if any relationship exists between molecular weight and anticoagulant activity.

EXPERIMENTAL

A liquid chromatograph[1] was equipped with a refractive index detector and a syringe loop injector. A minicomputer[2] was used to monitor the refractive index detector signals and to run the molecular weight calculation programs. The detector–computer interface is shown in Fig. 1.

Chromatographic Conditions—Two sets of columns were used. The hand-packed set was used initially to compare molecular weight fractions for their relationship to anticoagulant activity. Commercially available columns were used for the comparative study on heparin sterile solutions.

A set of three columns was tap packed with various pore sizes of 5–10-μm glycophase-controlled porous glass. These columns were packed

[1] Waters Associates model ALC/GPC 244 equipped with a RI (R-404) and a U6K injector.

[2] PDP-11/40, Digital Equipment Co.; the interfacing was developed in-house.

0022-3549/79/0500-0588$01.00/0

© 1979, American Pharmaceutical Association

Table V—Bismuth Subsalicylate Antidiarrheal Mixture Effect on Tetracycline Product Variability

Parameter	Range A	Range B	SD, % A	SD, % B
Peak serum level, μg/ml	0.69–2.29	1.79–2.52	24.4	9.34
Peak time, hr	2.50–4.0	2.50–5.0	18.9	37.6
AUC through 24 hr, μg/ml × hr	7.13–27.9	21.1–30.5	28.9	11.0
Urinary recovery through 72 hr, mg	42.2–173	108–216	32.8	18.8
Half-life, hr	7.09–10.8	7.58–11.8	11.4	15.1
Renal clearance, ml/min	53.3–151	25.8–126	29.7	27.3

suggested that the antidiarrheal influence on antibiotic absorption is dose dependent.

In the present study, 60 ml of a bismuth subsalicylate antidiarrheal product was administered concomitantly with a 250-mg tetracycline hydrochloride capsule. Since the "active" bismuth subsalicylate concentration was not given on the package, molar comparisons of "active" bismuth subsalicylate antidiarrheal to "active" kaolin–pectin products were impossible. Nonetheless, the 34% decrease in relative tetracycline bioavailability was consistent with the kaolin–pectin with tetracycline data and indicated that similar drug interactions are likely with any antidiarrheal whose mechanism of action is adsorptive.

REFERENCES

(1) J. G. Wagner, *Can. J. Pharm. Sci.*, **1**, 55 (1966).

(2) J. G. Wagner, *Drug Intell.*, **2**, 38 (1968).

(3) P. F. Binnion, in "Symposium on Digitalis," O. Storstein, Ed., Glydenal Norsk Forlag, Oslo, Norway, 1973, p. 216.

(4) D. D. Brown and R. P. Juhl, *N. Engl. J. Med.*, **295**, 1034 (1976).

(5) W. M. Gouda, *Abstr., Acad. Pharm. Sci.*, **6**, 117 (1976).

(6) K. A. DeSante, A. R. DiSanto, R. G. Stoll, R. D. Welch, T. J. Vecchio, and K. S. Albert, *ibid.*, **7**, 116 (1977).

(7) K. S. Albert, J. W. Ayres, D. J. Weidler, E. Sakmar, M. R. Hallmark, R. G. Stoll, K. A. DeSante, A. R. DiSanto, and J. G. Wagner, *ibid.*, **7**, 116 (1977).

(8) K. S. Albert, K. A. DeSante, R. D. Welch, and A. R. DiSanto, *ibid.*, **7**, 115 (1977).

(9) D. C. Grove and W. A. Randall, in "Medical Encyclopedia," H. Welch and F. Marti-Ibasey, Eds., Medical Encyclopedia Inc., New York, N.Y., 1955, p. 238.

(10) K. C. Kwan and A. E. Till, *J. Pharm. Sci.*, **62**, 1494 (1973).

ACKNOWLEDGMENTS

The authors thank Ms. Mariann Holthouse for secretarial assistance and W. L. Lummis for performing the microbiological assays.

Molecular Weight Determination of Commercial Heparin Sodium USP and Its Sterile Solutions

H. J. RODRIGUEZ * and A. J. VANDERWIELEN ˣ

Received June 19, 1978, from *Control Analytical Research and Development, The Upjohn Company, Kalamazoo, MI 49001.* Accepted for publication September 8, 1978. *Present address: Waters Associates, Milford, MA 01757.

Abstract □ A liquid chromatographic assay for the characterization of heparin sodium USP and heparin sterile solutions was developed. The method employs size exclusion chromatography and computer-based data collection and manipulation. An examination of commercially available heparin showed only minor differences between the heparins extracted from beef lung and porcine intestinal mucosa. The molecular weight averages of the material and its sterile solutions were 9000–12,000 daltons. A correlation was observed between average molecular weight and anticoagulant activity for the heparin sodium samples examined.

Keyphrases □ Heparin sodium—molecular weight determination of commercial products and sterile solutions using liquid chromatography □ Molecular weight determination—commercial heparin sodium USP and its sterile solutions, liquid chromatography □ Liquid chromatography—molecular weight determination of commercial heparin sodium USP and its sterile solutions □ Anticoagulants—heparin sodium, molecular weight determination, liquid chromatography

Several methods for the molecular weight fractionation of heparin sodium have been reported (1–3), gel filtration being most commonly used (4). In most cases, analysis requires several hours per sample and complicated detection procedures. Recently, a fast and reliable method was developed (5, 6) using high-performance liquid chromatography (HPLC) with refractive index detection for the determination of molecular weight averages of heparin sodium USP and injectable heparin sodium solutions (6).

The literature contains conflicting reports regarding the relationship of molecular weight and anticoagulant activity (7–9). There are also significant differences in the reported molecular weights of commercially available heparin (5, 6, 10). This paper presents the results of an examination of sterile injectable heparin sodium from commercial sources. The liquid chromatographic method recently developed (5) was modified and used to determine if any relationship exists between molecular weight and anticoagulant activity.

EXPERIMENTAL

A liquid chromatograph[1] was equipped with a refractive index detector and a syringe loop injector. A minicomputer[2] was used to monitor the refractive index detector signals and to run the molecular weight calculation programs. The detector–computer interface is shown in Fig. 1.

Chromatographic Conditions—Two sets of columns were used. The hand-packed set was used initially to compare molecular weight fractions for their relationship to anticoagulant activity. Commercially available columns were used for the comparative study on heparin sterile solutions.

A set of three columns was tap packed with various pore sizes of 5–10-μm glycophase-controlled porous glass. These columns were packed

[1] Waters Associates model ALC/GPC 244 equipped with a RI (R-404) and a U6K injector.

[2] PDP-11/40, Digital Equipment Co.; the interfacing was developed in-house.

0022-3549/79/0500-0588$01.00/0

© 1979, American Pharmaceutical Association

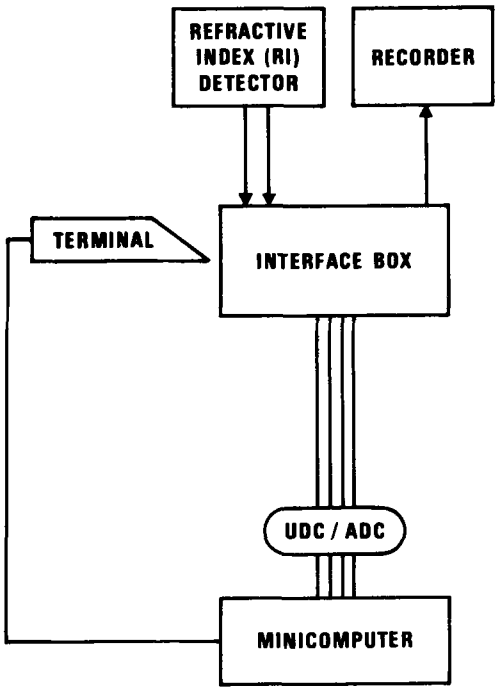

Figure 1—*Interface of refractive index detector to the minicomputer system. UDC = universal digital controller. ADC = analog to digital converter.*

by adding very small quantities (25–30 mg) of material and tapping the column 50–100 times. This procedure was repeated until the column appeared full. The column was then pressurized at 3500 psi, and any void observed was repacked. This procedure was repeated until no void was observed after pressurizing.

This column set consisted of three different lengths of 2.3-mm i.d. tubing packed as follows: 10 cm of 40-Å pore size, 25 cm of 100-Å pore size, and 60 cm of 250-Å pore size. The mobile phase used was 0.1 *M* sodium acetate (0.01% in sodium azide to inhibit bacterial growth) in double-distilled water at a flow of 0.1 ml/min (2500 psi).

All columns were calibrated using heparin sodium samples[3] of varied molecular weights. Retention times of these standards were plotted against molecular weight(s).

Efficient molecular sizing columns that can be used for molecular weight determinations are commercially available. These columns[4] consisted of 30-cm × 3.9-mm i.d. stainless steel tubing packed with microparticles (10 μm) of a fully porous silica–ether [$Si(RO)_xCH_3$].

After examination of various combinations of the available columns,

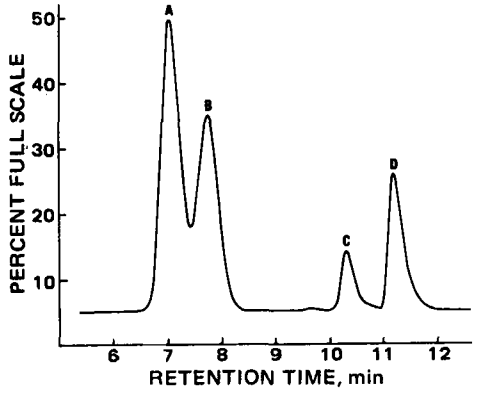

Figure 2—*Chromatogram of standard samples. Key: A, heparin of 5500 daltons (weight average); B, heparin of 12,100 daltons (weight average); C, injection artifact; and D, methanol. Full scale was 1.92 × 10^{-4} refractive index unit.*

[3] These standards (14K, 12K, 8K, and 5.5K) were obtained from J. A. Cifonelli.

[4] μBondagel, Waters Associates, Milford, MA 01757.

Table I—Calibration Results for Commercial Columns

Relative Retention Time[a] (Heparin–Methanol)	Molecular Weight, daltons × 1000
0.627	14.0
0.636	12.9
0.645	12.1
0.652	11.1
0.662	9.8
0.682	8.0
0.709	5.5

[a] Slope = −104.1, intercept = 79.8, correlation coefficient = 0.997, and estimated standard deviation of the line = 0.231.

a set consisting of one column of 125-Å pore size packing and two columns that were a blend of 125-, 300-, 500-, and 1000-Å pore size packing gave adequate resolution, reproducible measurements, and fast analyses (about 12 min/sample). A chromatogram showing the typical resolution obtained is shown in Fig. 2. This figure also shows the peaks due to methanol and an injection artifact resulting from changes in the refractive index due to inorganic salts (5, 6). Methanol (eluting at the total permeation volume) was used as an internal standard.

The columns were calibrated using seven samples of heparin sodium of known molecular weight. Three of these samples (14K, 8.0K, and 5.5K) were characterized previously using ultracentrifugation. The remaining samples were fractions collected on the original hand-packed columns, and their average molecular weights were determined on these columns (calibrated using four standards). The calibration was performed by a linear least-squares analysis on the relative retention time of heparin (relative to methanol) *versus* the weight average molecular weight. A well-characterized sample of sodium heparin was run with each set of analyses to monitor the performance of the columns and to correct the data for the comparative study (eliminate column and preparation variations).

Samples and Analysis—The samples consisted of commercially available material[5]. The powdered heparin sodium was dissolved (~12 mg/ml) in mobile phase containing 4% by volume methanol. Approximately 9 μl of this solution was injected. All sterile solutions were diluted accurately to a final concentration of 1000 USP units/ml by adding an appropriate amount of the mobile phase–methanol solution.

Molecular Weight Calculations—Molecular weight averages were calculated by literature methods (5, 11) using a FORTRAN program. The data were collected on-line by the system depicted in Fig. 1. The programs to collect the data and to perform the calculations were developed for this project to save time and calculation errors.

Anticoagulant Activity Determination—The samples were tested for potency (anticoagulant activity) using the USP assay (12).

RESULTS AND DISCUSSION

The results of a typical calibration are shown in Table I. Statistical treatment showed that molecular weight averages could be determined accurately to about ±500 daltons (*SD*) when the columns were calibrated properly. Figure 3 shows chromatograms of beef lung and intestinal porcine mucosal heparin. The chromatograms also indicate a difference that was noted previously (5): beef lung heparin sodium gave a fairly

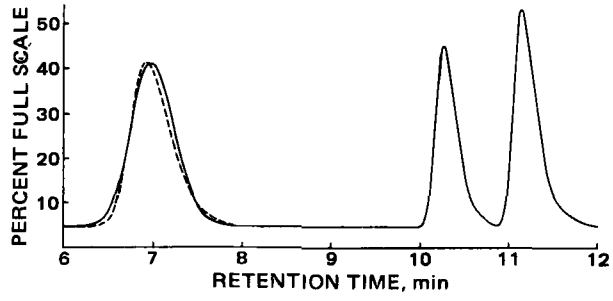

Figure 3—*Chromatograms of beef lung (—) and porcine intestinal mucosal (---) sodium heparin. Full scale was 0.48 × 10^{-4} refractive index unit.*

[5] The Upjohn Co., Riker Laboratories, Abbott Laboratories, Organon, Inolex, ASRY-Medical, and Pasadena Research Laboratories.

Table II—Comparison between Molecular Weight and Potency of Heparin Sodium Fractions

Fraction	Molecular Weight, weight average in daltons	Anticoagulant Activity, USP units/mg
1	13,800	167
2	12,900	157
3	12,100	155
4	11,100	145
5	9,800	124
6	9,100	100
7	8,000	76
8	7,500	50

Table III—Data on Heparin Sodium USP Grade Relation of Molecular Weight to Potency

Molecular Weight, daltons	Origin[a]	Anticoagulant Activity[b], USP units/mg
11,900	B	169
11,600	B	174
11,000	M	155–157
10,800	B, M	157–159
10,600	B, M	149–150
10,400	B	135–145
10,200	B	141–143
9,900	B	133–140
9,600	B	123–128

[a] B = beef lung, and M = porcine intestinal mucosa. [b] The ranges were obtained from two to four samples for each range.

symmetrical peak about the maxima whereas most porcine intestinal mucosal heparin gave a peak that was skewed toward low molecular weights.

Eight heparin fractions were collected using the hand-packed columns. When enough of each fraction had been collected, the heparin sodium was precipitated out of the mobile phase by adding methanol. In all cases, the heparin sodium precipitated at approximately a 1:2 ratio of methanol to mobile phase. After centrifuging and drying, the fractions were characterized accurately. The molecular weight was determined by the HPLC method, and the anticoagulant activities were determined by the USP method (Table II and Fig. 4).

These results show that there was a relationship between molecular weight and anticoagulant activity; however, this relationship was linear only over a narrow range of molecular weights (8000–12,000 daltons). Johnson and Mulloy (10), using intrinsic viscosity to measure molecular weight, observed this same relationship. In addition, they noted that the

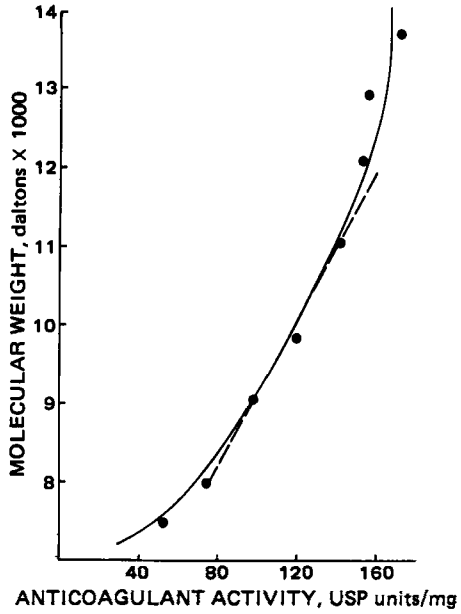

Figure 4—*Plot of anticoagulant activity of fractions* versus *molecular weight.*

Table IV—Molecular Weight of Commercial Heparin Sterile Solutions (1000 USP units/ml)

Sample[a]	Type	Molecular Weight, daltons: Weight Average	High	Low
A-1	Mucosal	10,400	15,400	2000
A-2	Mucosal	10,500	16,200	2500
A-3	Mucosal	10,100	16,800	2500
A-4	Mucosal	10,400	15,900	2400
X-1	Mucosal	10,900	16,100	2400
X-2	Mucosal	11,200	16,600	3500
Y	Mucosal	10,600	16,600	2400
D-1	Mucosal	10,900	17,300	4400
D-2	Beef lung	10,800	17,600	1700
W	Beef lung	10,600	16,900	1500
U-1	Beef lung	10,500	16,300	3700
U-2	Beef lung	10,200	16,200	2900

[a] Samples with the same letter designation are from the same commercial source.

Table V—Molecular Weight Comparison to Potency by Liquid Chromatography and Spectroscopy

Sample	Molecular Weight, daltons: HPLC	Spectroscopic[a]	Anticoagulant Activity, USP units/mg
CX-1	9,600	6,300	123
DF	10,000	7,600	136
CX-2	11,600	16,900	174
Average	10,400	10,300	

[a] Results obtained by Chromatrix, Sunnyvale, Calif., using a low-angle laser light-scattering technique.

anticoagulant activity decreased for molecular weights above 20,000 daltons.

The molecular weight and anticoagulant activity were determined on 32 different lots[6] of heparin sodium USP (24 of beef lung origin and eight of porcine intestinal mucosal origin). The results (Table III) show that the relationship observed for the heparin fractions also held true for the samples of commercial grade heparin. A linear regression analysis showed good correlation (0.93) and an estimated error of about 9 USP units (2 *SD*) for the anticoagulant activity. Although there was considerable overlap, these results indicate that one can expect differences in anticoagulants when the molecular weights differ by 1000 daltons or more.

In contrast to previously reported results (6), these results (Table III) show that beef lung heparin cannot be distinguished from porcine mucosal heparin on the basis of molecular weight analyses.

Twelve lots of sterile solution from the different manufacturers were analyzed by the HPLC method on the commercial columns. The results (Table IV) show a molecular weight range from 11,200 to 10,100 daltons. As noted previously (5), some lots of beef lung heparin had a distribution that was wider than porcine intestinal mucosal heparin (*e.g.*, compare Sample D-1 to D-2).

Sugisaka and Petracek recently (6) stated that porcine mucosal heparin has an average molecular weight somewhere between 21,000 and 24,000 daltons and that beef lung heparin has an average molecular weight between 16,000 and 19,000 daltons. This study shows that there is very little difference between commercial heparin extracted from beef lung and porcine intestinal mucosa and that the average molecular weight is 9000–12,000 daltons. The major difference between the results on the average molecular weight of sterile solutions is the calibration method. In this study, standardized heparin sodium was used to calibrate the liquid chromatographic column whereas Sugisaka and Petracek (6) used dextrans of various molecular weights.

The difference observed is not unexpected since molecular size is the property responsible for the separation observed by HPLC. Differences in molecular shape can appear as differences in molecular weight in size exclusion chromatography. The higher results obtained when the columns are calibrated with dextrans (6) are to be expected if the dextran molecules are smaller than molecules of heparin of equivalent weight. Accurate calibration, therefore, requires that the standards have the same molecular shape as the samples.

To check the accuracy of these results, the molecular weights of three samples were determined using a low-angle laser light-scattering tech-

[6] Manufactured by Upjohn, Abbott, and Inolex.

nique. This technique requires no reference to external standards since the molecular weight is obtained from a simple linear extrapolation to zero concentration of the light-scattering data obtained at a single angle from two or more solutions of different solute concentrations (13–16). The results (Table V) show that the HPLC molecular weight determinations were in fair agreement with those of the light-scattering technique. The average of the three samples agreed within 100 daltons, although there was considerable sample-to-sample variation. Both the HPLC and spectroscopic results showed a good correlation between molecular weight and anticoagulant activity.

REFERENCES

(1) G. Totolani and E. Romagnoli, *Anal. Biochem.*, **66**, 29 (1975).

(2) H. B. Nader, N. M. McDuffie, and C. P. Dietrich, *Biochem. Biophys. Res. Commun.*, **57**, 488 (1974).

(3) J. A. Cifonelli and J. King, *Biochim. Biophys. Acta*, **320**, 331 (1973).

(4) J. Ehrlich and S. S. Stavila, *J. Pharm. Sci.*, **62**, 617 (1973).

(5) H. J. Rodriguez, *Anal. Lett.*, **9**, 497 (1976).

(6) N. Sugisaka and F. J. Petracek, *Fed. Proc.*, **36**, 89 (1977).

(7) S. S. Stivala, L. Yuan, J. Echlich, and P. A. Liberti, *Biochem. Biophys.*, **122**, 32 (1967).

(8) G. H. Barlow, N. D. Sanderson, and P. G. McNeill, *Arch. Biochem. Biophys.*, **115**, 360 (1961).

(9) T. C. Laurent, *ibid.*, **92**, 224 (1961).

(10) E. A. Johnson and B. Mulloy, *Carbohydr. Res.*, **51**, 119 (1976).

(11) R. Guliana and L. Wild, *J. Polym. Sci., A2*, **5**, 1087 (1967).

(12) "The United States Pharmacopeia," 19th rev., Mack Publishing Co., Easton, Pa., 1975, p. 229.

(13) W. Kaye and A. J. Havlik, *Appl. Opt.*, **12**, 541 (1973).

(14) H. J. Cantow, E. Siefert, and R. Kuhn, *Chem. Eng. Technol.*, **38**, 1032 (1966).

(15) A. C. Ouano and W. Kaye, *J. Polym. Sci.*, **12**, 1151 (1974).

(16) A. C. Ouano, *J. Chromatogr.*, **118**, 303 (1976).

ACKNOWLEDGMENTS

The authors thank Dr. Lloyd Fox and Mr. Norman Young for providing the interface for the refractive index detector and Mr. Bill Frailing for providing the FORTRAN programs for on-line data collection and manipulation. They also appreciate the assistance of P. A. Hartman, E. C. Berro, and M. C. Walker.

Heterocyclic Analogs of Amphetamine: Thioureas, Dithiocarbamates, and Negatively Substituted Amides

WILLIAM O. FOYE ˣ and SUCHINTA TOVIVICH

Received September 1, 1978, from the *Samuel M. Best Research Laboratory, Massachusetts College of Pharmacy, Boston, MA 02115.* Accepted for publication October 20, 1978.

Abstract □ A series of heterocyclic analogs of amphetamine was synthesized. The heterocycles employed included the 2-furyl, 2-thienyl, 3-methyl-2-thienyl, 3-pyridyl, and 6-methyl-2-pyridyl rings. The aliphatic amine group was converted to the *N*-methylthiourea, dithiocarbamate, methanesulfonyl, trifluoromethanesulfonyl, and trifluoroacetyl functions since similar conversions of the β-phenethylamine structure had shown blood pressure-lowering effects and some loss of behavioral effects. *p*-Chlorophenyl and 1-naphthyl analogs were also converted to these derivatives. Behavioral and other biological effects, including antiarthritic, passive cutaneous anaphylactic, and antimicrobial, were observed. The 3-methyl-2-thienyl analog of amphetamine significantly increased papillary muscle contractile force without producing arrhythmias.

Keyphrases □ Amphetamine analogs—thioureas, dithiocarbamates, negatively substituted amides, synthesis, behavioral effects, antiarthritis effects, cutaneous anaphylaxis, antimicrobial effects, blood pressure, rats □ Structure–activity relationships—amphetamine analogs, thioureas, dithiocarbamates, negatively substituted amides, synthesis, behavioral and biological effects, rats □ Motor activity—effects of amphetamine analogs, rats □ Antiarthritis agents—amphetamine analogs, rats □ Blood pressure—effects of amphetamine analogs, rats

Formation of negatively substituted amides on the aliphatic nitrogen of amphetamine and related structures has produced compounds with blood pressure-lowering effects (1). This result occurred also with negatively substituted amides of the β-phenethylamine structure as well as dithiocarbamate and thiourea derivatives (2, 3). Conversion of the aliphatic nitrogen to a neutral or acidic function thus led to a depressor response from a basic structure having motor stimulant activity. Previously, inclusion of the alkanesulfonamide group in the aromatic ring of phenethanolamines conferred either adrenergic stimulant or blocking activity (the latter generally appearing with an isopropyl or larger group on the aliphatic nitrogen) (4, 5).

DISCUSSION

A number of dithiocarbamates of the β-phenethylamine structure showed varying degrees of amphetamine-like behavioral effects (6). The presence of heterocyclic rings, in place of the phenyl, generally resulted in a loss of amphetamine behavioral effects. Diethyldithiocarbamate had previously been shown to deplete brain norepinephrine and to maintain the conditioned avoidance response of the rat (7). The dithiocarbamates of the heterocyclic ethylamines failed to alter this response (6). Antiobesity manifestations were observed in rats with some negatively substituted amides, dithiocarbamates, and thioureas of the β-phenethylamines and amphetamine derivatives. The possibility existed, therefore, of removing many or all of the behavioral attributes of the basic amphetamine structure while retaining depressor and antiobesity effects by appropriate substitutions on the nitrogen and inclusion of heterocyclic rings.

A series of heterocyclic analogs of amphetamine, including neutral or negatively substituted functions on the aliphatic nitrogen, was synthesized to determine if behavioral activity could be diminished and other useful effects retained. Corresponding derivatives of *p*-chloroamphetamine and the 1-naphthyl analog were prepared for similar observations. Negatively substituted amides prepared included the methanesulfonamide, trifluoromethanesulfonamide, and trifluoroacetyl as well as dithiocarbamates and methylthioureas. Both thioureas and dithiocarbamates have shown inhibitory activity against dopamine-β-hydroxylase (8, 9), so these derivatives were expected to produce depressor effects.

Previously, the furyl and thienyl analogs of amphetamine were obtained, and their motor effects were compared to those of amphetamine (10). Amphetamine and its thienyl analog were more active motor stimulants than the furyl analog, but both the heterocyclic analogs were less toxic than amphetamine.

0022-3549/79/0500-0591$01.00/0

© 1979, American Pharmaceutical Association

nique. This technique requires no reference to external standards since the molecular weight is obtained from a simple linear extrapolation to zero concentration of the light-scattering data obtained at a single angle from two or more solutions of different solute concentrations (13–16). The results (Table V) show that the HPLC molecular weight determinations were in fair agreement with those of the light-scattering technique. The average of the three samples agreed within 100 daltons, although there was considerable sample-to-sample variation. Both the HPLC and spectroscopic results showed a good correlation between molecular weight and anticoagulant activity.

REFERENCES

(1) G. Totolani and E. Romagnoli, *Anal. Biochem.*, **66**, 29 (1975).

(2) H. B. Nader, N. M. McDuffie, and C. P. Dietrich, *Biochem. Biophys. Res. Commun.*, **57**, 488 (1974).

(3) J. A. Cifonelli and J. King, *Biochim. Biophys. Acta*, **320**, 331 (1973).

(4) J. Ehrlich and S. S. Stavila, *J. Pharm. Sci.*, **62**, 617 (1973).

(5) H. J. Rodriguez, *Anal. Lett.*, **9**, 497 (1976).

(6) N. Sugisaka and F. J. Petracek, *Fed. Proc.*, **36**, 89 (1977).

(7) S. S. Stivala, L. Yuan, J. Echlich, and P. A. Liberti, *Biochem. Biophys.*, **122**, 32 (1967).

(8) G. H. Barlow, N. D. Sanderson, and P. G. McNeill, *Arch. Biochem. Biophys.*, **115**, 360 (1961).

(9) T. C. Laurent, *ibid.*, **92**, 224 (1961).

(10) E. A. Johnson and B. Mulloy, *Carbohydr. Res.*, **51**, 119 (1976).

(11) R. Guliana and L. Wild, *J. Polym. Sci., A2*, **5**, 1087 (1967).

(12) "The United States Pharmacopeia," 19th rev., Mack Publishing Co., Easton, Pa., 1975, p. 229.

(13) W. Kaye and A. J. Havlik, *Appl. Opt.*, **12**, 541 (1973).

(14) H. J. Cantow, E. Siefert, and R. Kuhn, *Chem. Eng. Technol.*, **38**, 1032 (1966).

(15) A. C. Ouano and W. Kaye, *J. Polym. Sci.*, **12**, 1151 (1974).

(16) A. C. Ouano, *J. Chromatogr.*, **118**, 303 (1976).

ACKNOWLEDGMENTS

The authors thank Dr. Lloyd Fox and Mr. Norman Young for providing the interface for the refractive index detector and Mr. Bill Frailing for providing the FORTRAN programs for on-line data collection and manipulation. They also appreciate the assistance of P. A. Hartman, E. C. Berro, and M. C. Walker.

Heterocyclic Analogs of Amphetamine: Thioureas, Dithiocarbamates, and Negatively Substituted Amides

WILLIAM O. FOYE ˣ and SUCHINTA TOVIVICH

Received September 1, 1978, from the *Samuel M. Best Research Laboratory, Massachusetts College of Pharmacy, Boston, MA 02115.* Accepted for publication October 20, 1978.

Abstract □ A series of heterocyclic analogs of amphetamine was synthesized. The heterocycles employed included the 2-furyl, 2-thienyl, 3-methyl-2-thienyl, 3-pyridyl, and 6-methyl-2-pyridyl rings. The aliphatic amine group was converted to the *N*-methylthiourea, dithiocarbamate, methanesulfonyl, trifluoromethanesulfonyl, and trifluoroacetyl functions since similar conversions of the β-phenethylamine structure had shown blood pressure-lowering effects and some loss of behavioral effects. *p*-Chlorophenyl and 1-naphthyl analogs were also converted to these derivatives. Behavioral and other biological effects, including antiarthritic, passive cutaneous anaphylactic, and antimicrobial, were observed. The 3-methyl-2-thienyl analog of amphetamine significantly increased papillary muscle contractile force without producing arrhythmias.

Keyphrases □ Amphetamine analogs—thioureas, dithiocarbamates, negatively substituted amides, synthesis, behavioral effects, antiarthritis effects, cutaneous anaphylaxis, antimicrobial effects, blood pressure, rats □ Structure–activity relationships—amphetamine analogs, thioureas, dithiocarbamates, negatively substituted amides, synthesis, behavioral and biological effects, rats □ Motor activity—effects of amphetamine analogs, rats □ Antiarthritis agents—amphetamine analogs, rats □ Blood pressure—effects of amphetamine analogs, rats

Formation of negatively substituted amides on the aliphatic nitrogen of amphetamine and related structures has produced compounds with blood pressure-lowering effects (1). This result occurred also with negatively substituted amides of the β-phenethylamine structure as well as dithiocarbamate and thiourea derivatives (2, 3). Conversion of the aliphatic nitrogen to a neutral or acidic function thus led to a depressor response from a basic structure having motor stimulant activity. Previously, inclusion of the alkanesulfonamide group in the aromatic ring of phenethanolamines conferred either adrenergic stimulant or blocking activity (the latter generally appearing with an isopropyl or larger group on the aliphatic nitrogen) (4, 5).

DISCUSSION

A number of dithiocarbamates of the β-phenethylamine structure showed varying degrees of amphetamine-like behavioral effects (6). The presence of heterocyclic rings, in place of the phenyl, generally resulted in a loss of amphetamine behavioral effects. Diethyldithiocarbamate had previously been shown to deplete brain norepinephrine and to maintain the conditioned avoidance response of the rat (7). The dithiocarbamates of the heterocyclic ethylamines failed to alter this response (6). Antiobesity manifestations were observed in rats with some negatively substituted amides, dithiocarbamates, and thioureas of the β-phenethylamines and amphetamine derivatives. The possibility existed, therefore, of removing many or all of the behavioral attributes of the basic amphetamine structure while retaining depressor and antiobesity effects by appropriate substitutions on the nitrogen and inclusion of heterocyclic rings.

A series of heterocyclic analogs of amphetamine, including neutral or negatively substituted functions on the aliphatic nitrogen, was synthesized to determine if behavioral activity could be diminished and other useful effects retained. Corresponding derivatives of *p*-chloroamphetamine and the 1-naphthyl analog were prepared for similar observations. Negatively substituted amides prepared included the methanesulfonamide, trifluoromethanesulfonamide, and trifluoroacetyl as well as dithiocarbamates and methylthioureas. Both thioureas and dithiocarbamates have shown inhibitory activity against dopamine-β-hydroxylase (8, 9), so these derivatives were expected to produce depressor effects.

Previously, the furyl and thienyl analogs of amphetamine were obtained, and their motor effects were compared to those of amphetamine (10). Amphetamine and its thienyl analog were more active motor stimulants than the furyl analog, but both the heterocyclic analogs were less toxic than amphetamine.

0022-3549/79/0500-0591$01.00/0

© 1979, American Pharmaceutical Association

Table I—1-Aryl-2-nitropropenes

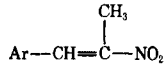

Ar	Formula	Yield, %	Melting Point	Analysis, %	Calc.	Found
2-Furyl	$C_7H_7NO_3$	65	47–48°[a]		—	—
2-Thienyl	$C_7H_7NO_2S$	44	67–68°	C	49.69	49.55
				H	4.17	4.42
				N	8.27	8.02
				S	18.95	18.68
3-Methyl-2-thienyl	$C_8H_9NO_2S$	65.5	67–69°	C	52.46	52.52
				H	4.92	5.34
				N	7.65	7.51
				S	17.47	17.33
3-Pyridyl	$C_8H_8N_2O_2$	18	61–63°	C	58.53	58.33
				H	4.91	5.04
				N	17.06	17.15
6-Methyl-2-pyridyl	$C_9H_{10}N_2O_2$	39	68–69°	C	60.67	60.54
				H	5.61	5.71
				N	15.73	15.72
4-Chlorophenyl	$C_9H_8ClNO_2$	64	86–87°[b]		—	—
1-Naphthyl	$C_{13}H_{11}NO_2$	81	64–65°	C	73.23	73.02
				H	5.11	5.49
				N	6.57	6.60

[a] Lit. (12) mp 50–51°. [b] Lit. (13) mp 88–89°.

Table II—1-Aryl-2-aminopropanes

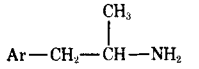

Compound	Ar	Formula	Yield, %	Boiling Point or Melting Point	Analysis, %	Calc.	Found
I	2-Furyl	$C_7H_{11}NO$	65	66–70° (20 mm)[a]		—	—
II	2-Thienyl	$C_7H_{11}NS$	39	146–150° (20 mm)		—	—
	2-Thienyl hydrochloride	$C_7H_{12}ClNS$	—	149–152°	C	47.32	47.50
					H	6.81	6.85
					N	7.88	7.62
					S	18.04	17.76
III	3-Methyl-2-thienyl	$C_8H_{13}NS$	90	125–130° (20 mm)		—	—
	3-Methyl-2-thienyl hydrochloride	$C_8H_{14}ClNS$	—	148–150°	C	50.13	49.69
					H	7.31	7.28
					N	7.31	7.12
					S	16.71	16.60
IV	3-Pyridyl	$C_8H_{12}N_2$	37	125–130° (20 mm)		—	—
V	6-Methyl-2-pyridyl	$C_9H_{14}N_2$	68	100–105° (20 mm)		—	—
	6-Methyl-2-pyridyl hydrochloride	$C_9H_{15}ClN_2$	—	160–161°	C	57.90	57.73
					H	8.04	8.45
					N	15.01	14.89
VI	4-Chlorophenyl hydrochloride	$C_9H_{12}ClN$	—	166–168°[b]		—	—
VII	1-Naphthyl	$C_{13}H_{15}N$	81	160–165° (20 mm)		—	—
	1-Naphthyl hydrochloride	$C_{13}H_{16}ClN$	—	212–215°	C	70.43	70.27
					H	7.22	7.21
					N	6.32	6.29

[a] Lit. (12) bp 68–75° (20 mm). [b] Lit. (14) mp 163–169°.

Table III—Amide, Thiourea, and Dithiocarbamate Derivatives

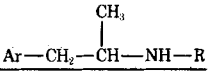

Compound	Ar	R	Formula	Yield, %	Melting Point	Analysis, %	Calc.	Found
VIII	2-Furyl	$CS_2^-(C_2H_5)_3NH^+$	$C_{14}H_{25}N_2OS_2 \cdot 1\frac{1}{2}H_2O$	94	Oil	C	51.06	50.74
						H	7.60	7.73
						N	8.51	8.22
						S	19.45	18.96
IX	2-Thienyl	SO_2CH_3	$C_8H_{13}NO_2S_2$	70.5	63–64°	C	43.83	43.80
						H	5.93	5.78
						N	6.39	6.33
						S	29.20	28.88
X	2-Thienyl	$COCF_3$	$C_9H_{10}F_3NOS$	16	59–61°	C	45.56	45.76
						H	4.24	4.16
						N	5.90	5.73
						S	13.50	14.00
XI	2-Thienyl	SO_2CF_3	$C_8H_{10}F_3NO_2S_2$	22	35–37°	C	35.16	35.11
						H	3.66	3.95
						N	5.12	5.06
						S	23.44	23.70
XII	2-Thienyl	$CNHCH_3$ (S above C)	$C_9H_{14}N_2S_2$	75.5	Oil	C	50.46	50.18
						H	6.54	6.76
						N	13.08	12.92
						S	29.90	29.51

Table III—*Continued*

Ar—CH(CH₃)—CH—NH—R

Compound	Ar	R	Formula	Yield, %	Melting Point	Analysis, %	Calc.	Found
XIII	2-Thienyl	$CS_2^-(C_2H_5)_3NH^+$	$C_{14}H_{26}N_2S_3 \cdot 1/2H_2O$	64.5	Oil	C	51.38	51.62
						H	8.17	7.75
						N	8.56	8.34
						S	29.35	29.11
XIV	3-Methyl-2-thienyl	SO_2CH_3	$C_9H_{15}NO_2S_2$	51.5	41–43°	C	46.35	46.80
						H	6.43	6.34
						N	6.00	5.85
						S	27.46	27.40
XV	3-Methyl-2-thienyl	$COCF_3$	$C_{10}H_{12}F_3NOS$	82	57–58°	C	47.81	47.44
						H	4.78	5.12
		S ‖				N	5.58	5.69
						S	12.75	13.19
XVI	3-Methyl-2-thienyl	$CNHCH_3$	$C_{10}H_{16}N_2S_2$	74.5	Oil	C	52.63	53.02
						H	7.02	7.13
						S	24.56	24.69
XVII	3-Methyl-2-thienyl	$CS_2^-(C_2H_5)_3NH^+$	$C_{15}H_{28}N_2S_3 \cdot 1\frac{1}{2}H_2O$	34.5	Oil	C	50.14	49.80
						H	7.80	7.55
						N	7.80	7.50
						S	26.74	27.01
XVIII	3-Pyridyl	SO_2CH_3	$C_9H_{14}N_2O_2S$	30.5	114–115°	C	50.46	50.72
						H	6.54	6.56
						N	13.08	12.93
						S	14.95	15.20
XIX	3-Pyridyl	$COCF_3$	$C_{10}H_{11}F_3N_2O \cdot CF_3CO_2H$	55	112–113°	C	41.76	41.83
						H	2.89	3.32
		S ‖				N	8.09	8.10
XX	3-Pyridyl	$CNHCH_3$	$C_{10}H_{15}N_3S$	72	Oil	C	57.41	57.01
						H	7.18	7.40
						N	20.09	19.64
						S	15.30	14.92
XXI	3-Pyridyl	$CS_2^-(C_2H_5)_3NH^+$	$C_{15}H_{26}N_3S_2 \cdot 1\frac{1}{2}H_2O$	75	Oil	C	53.09	53.54
						H	7.66	7.72
						N	12.39	12.70
						S	18.87	18.66
XXII	6-Methyl-2-pyridyl	SO_2CH_3	$C_{10}H_{16}N_2O_2S$	59	Oil	C	52.63	53.03
						H	7.02	7.17
						N	12.28	12.41
						S	14.03	13.86
XXIII	6-Methyl-2-pyridyl	$COCF_3$	$C_{11}H_{13}F_3N_2O$	71	43–44°	C	53.66	53.73
						H	5.28	5.35
						N	11.38	11.15
XXIV	6-Methyl-2-pyridyl	$CS_2^-(C_2H_5)_3NH^+$	$C_{16}H_{29}N_3S_2 \cdot H_2O$	35	Oil	C	55.65	55.48
						H	8.98	8.91
						N	12.17	12.34
XXV	4-Chlorophenyl	SO_2CH_3	$C_{10}H_{15}ClNO_2S$	36	55–57°	C	48.48	48.57
						H	5.66	5.70
						N	5.66	5.77
						S	12.93	13.21
XXVI	4-Chlorophenyl	$COCF_3$	$C_{11}H_{11}ClF_3NO$	90	127–128°	C	49.71	49.92
						H	4.14	4.02
		S ‖				N	5.27	5.40
XXVII	4-Chlorophenyl	$CNHCH_3$	$C_{11}H_{15}ClN_2S$	70	Oil	C	54.42	54.73
						H	6.23	6.56
						N	11.54	11.13
XXVIII	4-Chlorophenyl	$CS_2^-(C_2H_5)_3NH^+$	$C_{16}H_{27}ClN_2S \cdot 2H_2O$	53	66–68°	C	50.20	50.47
						H	7.06	6.80
						N	7.32	7.39
						S	16.73	17.20
XXIX	1-Naphthyl	SO_2CH_3	$C_{14}H_{17}NO_2S$	97	63–65°	C	63.88	63.65
						H	6.46	6.56
						N	5.32	5.19
						S	12.16	12.03
XXX	1-Naphthyl	$COCF_3$	$C_{15}H_{14}F_3NO$	73	106–107°	C	64.06	63.84
						H	4.98	5.10
						N	4.98	5.01

The heterocyclic analogs of amphetamine were synthesized by reduction of the intermediate nitropropenes. The nitropropenes were obtained by a base-catalyzed condensation of aromatic aldehyde and nitroethane (11). Physical constants of the nitropropenes are listed in Table I. The nitropropenes were reduced to amphetamines with lithium aluminum hydride (12) (Scheme I). The amines were generally isolated as the hydrochlorides. Physical constants of the amines are listed in Table II.

The methanesulfonamides were prepared from reaction of the respective amines with methanesulfonyl chloride and triethylamine, giving up to 97% yields. The trifluoroacetamides were obtained from reaction with trifluoroacetic anhydride, with yields up to 90%. The trifluoromethanesulfonamides were obtained from reaction with trifluoromethanesulfonyl chloride and triethylamine. Dark, sticky liquids were usually obtained, and they could not be purified by distillation; prolonged refrigeration generally produced semisolids that could be recrystallized.

The methylthioureas were prepared by reaction of the amine with

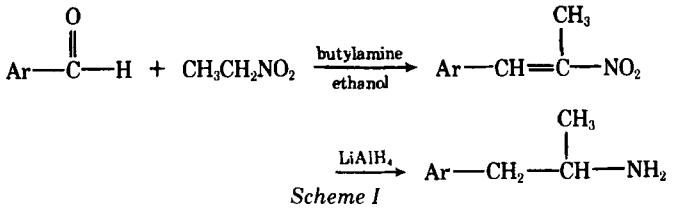

Scheme I

methyl isothiocyanate. The resulting liquids could not be distilled without decomposition. Therefore, the crude products were washed with petroleum ether and thoroughly dried, giving yields of analytically acceptable products of about 70%.

The dithiocarbamates were prepared as the triethylammonium salts on reaction of the amines with carbon disulfide and triethylamine. Generally, yellow liquids were obtained, and they gave hygroscopic solids on washing with anhydrous ether. The compounds were isolated as hydrates, as verified by the IR spectra (Table III).

EXPERIMENTAL[1]

Melting points were determined in capillaries with a melting-point block[2] and are uncorrected. IR absorption spectra were obtained with a grating spectrophotometer[3]. Silica gel TLC was carried out, and products were detected by exposure to iodine vapor.

The aldehydes and nitroethane were commercially prepared[4]. Methanesulfonyl chloride[5], trifluoromethanesulfonyl chloride[5], trifluoroacetic anhydride[5], methyl isothiocyanate[5], carbon disulfide[5], and lithium aluminum hydride in ether[6] (1 *M*) were used as received.

The following procedures are representative.

1-(2-Thienyl)-2-nitropropene—A mixture of 56.0 g (0.5 mole) of 2-thiophenecarboxaldehyde, 37.5 g (0.5 mole) of nitroethane, 90 ml of absolute ethanol, and 10 ml of *n*-butylamine was stirred in the dark at room temperature for 5 days. The resulting yellow crystalline mass was filtered and recrystallized from absolute ethanol, giving 37.5 g (44.4% yield) of yellow needles, mp 67–68°; IR (KBr): 1640 (C=C), 1510 (NO_2), and 1300 (NO_2) cm^{-1}.

1-(2-Thienyl)-2-aminopropane Hydrochloride—To 300 ml of anhydrous ether was added 7.6 g (0.2 mole) of lithium aluminum hydride, and the mixture was stirred until the hydride dissolved. A solution of 16.8 g (0.1 mole) of 1-(2-thienyl)-2-nitropropene in 100 ml of anhydrous ether was added dropwise at such a rate that the capacity of the condenser was not exceeded, requiring 30–60 min. The mixture was stirred for 3 hr after the addition, the reaction flask was placed in an ice bath, and water was added dropwise until hydrogen evolution ceased.

The ether layer was separated, the solvent was removed by flash evaporation, and the product was distilled at 146–150° (20 mm), giving 5.5 g (39% yield) of amber liquid. Addition of dry hydrogen chloride to an ethereal solution of the amine produced the hydrochloride, mp 149–152°; IR (KBr): 2900–3000 (NH_3^+) and 720 (ring CH) cm^{-1}.

***N*-Methanesulfonyl-1-(2-thienyl)-2-aminopropane**—To a cooled solution of 2.8 g (0.02 mole) of 1-(2-thienyl)-2-aminopropane in 25 ml of benzene were added dropwise, with stirring, 1.67 ml (0.022 mole) of methanesulfonyl chloride in 20 ml of methylene chloride and 3 ml (0.022 mole) of triethylamine in 20 ml of methylene chloride. The mixture was stirred at 25° for 15 hr, and the resulting solution was washed with dilute hydrochloric acid and water and distilled *in vacuo*. The residue was recrystallized from ethanol, giving 3.1 g (70.5% yield) of colorless needles, mp 63–64°; IR (KBr): 3320 (NH), 1310 (SO_2), and 1125 (SO_2) cm^{-1}.

***N*-Trifluoroacetyl-1-(2-thienyl)-2-aminopropane**—To a cooled solution of 4.2 g (0.03 mole) of 1-(2-thienyl)-2-aminopropane in 50 ml of benzene was added dropwise, with stirring, 6.7 g (0.03 mole) of trifluoroacetic anhydride. The mixture was stirred for 3 hr and refrigerated overnight. The solvent was removed under reduced pressure, and the resulting semisolid was refrigerated. The solid obtained was washed with dilute hydrochloric acid and water and recrystallized from dilute ethanol, giving 1.1 g (16.4% yield) of colorless needles, mp 59–61°; IR (KBr): 3310 (NH), 1690 (C=O), and 1160–1180 (CF_3) cm^{-1}.

***N*-Trifluoromethanesulfonyl-1-(2-thienyl)-2-aminopropane**—To a cooled solution of 2.2 g (0.02 mole) of 1-(2-thienyl)-2-aminopropane in 25 ml of methylene chloride were added, with stirring, 3.36 g (0.02 mole) of trifluoromethanesulfonyl chloride in 20 ml of methylene chloride and 3 ml (0.022 mole) of triethylamine in 20 ml of methylene chloride. The mixture was stirred at room temperature for 12 hr, and the resulting solution was washed with dilute hydrochloric acid and water.

The solvent was removed under reduced pressure, and the residue was dissolved in anhydrous ether and decolorized with charcoal. The solvent was removed in a rotary evaporator, and the residue was refrigerated for 1 week. The resulting semisolid was recrystallized from petroleum ether, giving 1.2 g (22% yield) of colorless crystals, mp 35–37°; IR (KBr): 3300 (NH), 1375 (SO_2), 1190 (CF_3), and 1145 (SO_2) cm^{-1}.

Table IV—Behavioral Effects in Rats

Compound	Dose, mg/kg po	Observations
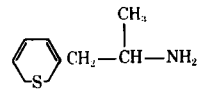 II	100	Ataxia
	200	Bizarre behavior
	25	High body posture
	25	Curiosity increase
	200	Cyanosis
	25	Exophthalmos
	50	Hypersensitivity
	50	Hyperthermia
	100	Motor activity decrease
	50	Motor activity increase
	25	Mydriasis
	25	Piloerection
	200	Placing reflex inhibition
	100	Prostration
	200	Respiratory distress
	200	Salivation, tremors
	200	Stereotyped behavior
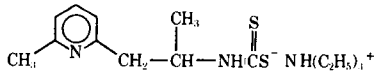 XXIV	200	Bizarre behavior
	200	Curiosity increase
	200	Hyperthermia
	200	Motor activity increase
	200	Mastication
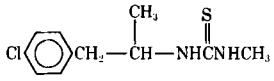 XXVII	200	High body posture
	50	Low body posture
	200	Curiosity increase
	50	Hypersensitivity
	200	Hyperthermia
	200	Lacrimation
	100	Motor activity decrease
	50	Motor activity increase
	200	Mydriasis
	200	Piloerection
	200	Placing reflex inhibition
	200	Prostration
	50	Salivation
	200	Semiprostration
	200	Stereotyped behavior
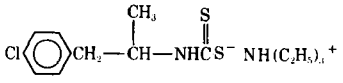 XXVIII	200	Bizarre behavior
	200	Curiosity increase
	200	Hyperthermia
	200	Mastication
	200	Motor activity increase
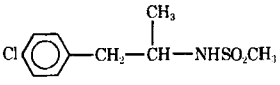 XXV	200	Ataxia
	200	Low body posture
	200	Grasp reflex inhibition
	200	Hypotonia
	200	Motor activity decrease
	200	Myotactic reflex inhibition
	200	Myotatic reflex inhibition
	200	Ptosis

[1] Elemental analyses were performed by Strauss Microanalytical Laboratory, Oxford, England.
[2] Mel-Temp.
[3] Model 457A, Perkin-Elmer.
[4] Aldrich Chemical Co.
[5] Fisher Scientific Co.
[6] Ventron Corp.

Table V—Antimicrobial Activity

Compound	Minimum Inhibitory Concentration, 1/*M*: *Staphylococcus aureus*[a] (ATCC 6538)	*Escherichia coli*[a] (ATCC 1129)	*Aspergillus niger*[b] (ATCC 16404)	*Candida albicans*[b] (ATCC 10231)
IX	<10,000	<10,000	<10,000	<100,000
XI	<10,000	<10,000	<10,000	<100,000
XIII	<1,000	<10,000	<100,000	<100,000
XIV	<10,000	<10,000	<10,000	<10,000
XVII	<1,000	—	<100,000	<100,000
XVIII	<10,000	<10,000	<10,000	<100,000
XXI	<1,000	<100	<10,000	<100,000
XXV	<10,000	<10,000	<10,000	<10,000
XXVIII	<10,000	<1,000	<100,000	<100,000
Sulfathiazole	<2,000[c]			

[a] Determined in brain heart infusion broth after 24–48 hr at 37°. [b] Determined in Sabouraud broth after 48–78 hr at 25°. [c] Reference 15.

1-Methyl-3-[1-methyl-2-(2-thienyl)-ethyl]thiourea—A solution of 1.125 g (0.025 mole) of methyl isothiocyanate in 10 ml of absolute ethanol was added dropwise, with stirring, to a cooled solution of 2.8 g (0.02 mole) of 1-(2-thienyl)-2-aminopropane in 25 ml of absolute ethanol. The mixture was refluxed for 12 hr and allowed to cool. The solvent was removed in a rotary evaporator under reduced pressure, and the residue was washed several times with petroleum ether and dried *in vacuo*. A yield of 3.23 g (75.5%) of viscous oil was obtained; IR (film): 3260 (NH) and 1340 (C=S) cm^{-1}.

Triethylammonium 1-Methyl-2-(2-thienyl)-ethyldithiocarbamate—Triethylamine (3.03 g, 0.03 mole) was added, with stirring, to a cooled solution of 2.2 g (0.02 mole) of 1-(2-thienyl)-2-aminopropane in 25 ml of absolute ethanol. To this mixture was added dropwise 2.28 g (0.03 mole) of carbon disulfide, and stirring was continued for 24 hr. The solvent was removed in a rotary evaporator, and the yellow residue was washed with anhydrous ether and dried *in vacuo*, giving 4.1 g (64.5% yield); IR (film): 2960–2990 (NH^+), 1290 (C=S), and 965 (C=S) cm^{-1}.

RESULTS[7]

Rats were observed continuously for 6 hr and daily for 7 days after dosing (Table IV). The 2-thienyl analog of amphetamine (II) produced a behavior pattern similar to that of amphetamine. The dithiocarbamate of the 6-methyl-2-pyridyl analog (XXIV) showed few behavioral effects. The methylthiourea of the *p*-chloro analog (XXVII) also showed many behavioral effects of amphetamine, whereas the methanesulfonamide (XXV) and the dithiocarbamate (XXVIII) showed fewer of these effects.

Passive cutaneous anaphylaxis tests were conducted for XIV, XVII, XXII, and XXV. No inhibition was seen except for XVII, which gave 31% inhibition at a 5.0-mg/kg dose. Antiarthritic activity of X, XV, XVIII, and XXVI was observed *via* the adjuvant-induced arthritis test. A significant decrease in the inflamed hindleg volume of the treated rat was found for XXVI at a 50-mg/kg dose.

Blood pressure effects have not been determined yet for these compounds, but III gave a significant increase (42%) in papillary muscle contractile force *in vitro* at a 1.10-μg/ml dose. No arrhythmia was produced.

Tests for antimicrobial activity were also carried out by both the agar plate method and *in vitro* serial dilution (Table V). Results are expressed in terms of the minimum inhibitory concentration (1/*M*) of compound for inhibition of 24-hr broth cultures of Gram-positive and Gram-negative bacteria, a mold, and a yeast. Appreciable activity was observed against *Candida albicans* for most of the compounds tested and against *Aspergillus niger* for the dithiocarbamates. Previously, thiourea and dithiocarbamate derivatives of β-phenethylamine and 4-substituted β-phenethylamines showed significant antimicrobial activity against these organisms (2).

[7] Behavioral observations, antiarthritic tests, passive cutaneous anaphylaxis tests, and papillary muscle contractile force measurements were carried out at Smith Kline and French Laboratories through the courtesy of Dr. Blaine Sutton.

REFERENCES

(1) W. O. Foye and J. N. Sane, *J. Pharm. Sci.*, **66**, 923 (1977).

(2) W. O. Foye and J. C. Anderson, *ibid.*, **58**, 1558 (1969).

(3) W. O. Foye, J. C. Anderson, and J. N. Sane, *ibid.*, **60**, 1095 (1971).

(4) R. H. Uloth, J. R. Kirk, W. A. Gould, and A. A. Larsen, *J. Med. Chem.*, **9**, 88 (1966).

(5) A. A. Larsen, W. A. Gould, H. R. Roth, W. J. Comer, R. H. Uloth, K. W. Dungan, and P. M. Lish, *ibid.*, **10**, 462 (1967).

(6) W. O. Foye and J. P. Speranza, *Eur. J. Med. Chem.*, **9**, 177 (1974).

(7) K. D. Krantz and L. S. Seiden, *J. Pharm. Pharmacol.*, **20**, 166 (1968).

(8) G. A. Johnson, S. J. Boukma, and E. G. Kim, *J. Pharmacol. Exp. Ther.*, **171**, 80 (1970).

(9) J. Jonsson, H. Grobecker, and L.-M. Gunne, *J. Pharm. Pharmacol.*, **19**, 201 (1967).

(10) G. A. Alles and G. A. Feigen, *J. Pharmacol. Exp. Ther.*, **72**, 265 (1941).

(11) E. Knoevenagel and L. Walter, *Chem. Ber.*, **37**, 4502 (1904).

(12) W. C. McCarthy and R. J. Kahl, *J. Org. Chem.*, **21**, 1118 (1956).

(13) M. Piank, *J. Sci. Food Agr.*, **14**, 48 (1963).

(14) F. Benington, R. D. Morin, and L. C. Clark, Jr., *J. Med. Chem.*, **8**, 100 (1965).

(15) G. J. Harper and W. C. Cawston, *J. Pathol. Bacteriol.*, **57**, 59 (1945).

ACKNOWLEDGMENTS

Presented at the VIth International Symposium on Medicinal Chemistry, Brighton, United Kingdom, September 1978.

Abstracted from a thesis submitted by S. Tovivich to the Massachusetts College of Pharmacy in partial fulfillment of the Doctor of Philosophy degree requirements.

Supported by funds from the John R. and Marie K. Sawyer Memorial Fund, Massachusetts College of Pharmacy.

The authors are indebted to the Pharmacology Department of Smith Kline and French Laboratories, Philadelphia, Pa., for the behavioral observations, passive cutaneous anaphylaxis tests, antiarthritic tests, and papillary muscle contractile force measurements.

Percutaneous Absorption of Butylparaben through Guinea Pig Skin *In Vitro*

HIDEO KOMATSU ˣ **and MASAMI SUZUKI**

Received July 10, 1978, from *Pola Laboratories, 27-1, Takashimadai, Kanagawa-ku, Yokohama, Japan.* Accepted for publication October 20, 1978.

Abstract □ Percutaneous absorption of aqueous butylparaben through guinea pig dorsal skin was studied using a diffusion chamber. Polysorbate 80 increased the solubilized concentration but decreased penetration of the preservative. Polyethylene glycol 400 also reduced the amount of penetration. Propylene glycol was less effective than polyethylene glycol 400. Preservative activities of these systems on several microorganisms were evaluated on agar plates. The relationship between the butylparaben penetration and preservative activity is discussed.

Keyphrases □ Percutaneous absorption—butylparaben, guinea pig, *in vitro*, effect of surfactants, relation to preservative activities □ Butylparaben—percutaneous absorption, effect of surfactants, guinea pig, *in vitro*, relation of absorption and preservative activities □ Surfactants—effect on percutaneous absorption of butylparaben, guinea pig, *in vitro* □ Preservatives—butylparaben, percutaneous absorption, effect of surfactants, relation of absorption and preservative activities, guinea pig, *in vitro*

The preservative activity of a system is dependent on the aqueous concentration of the preservative (1–3). This fact suggests that organic compounds employed as preservatives will be somewhat solubilized in the aqueous phase in systems such as foods, ointments, and cosmetics. Such organic preservatives have affinities to both water and oil and are expected to penetrate into the skin easily (4, 5).

Many studies have concerned the percutaneous absorption of preservatives, especially hexachlorophene (6–9), and their preservative activities in various systems (3, 10). However, few reports concerning butylparaben (I) have been published, despite its wide use as a preservative, and there are few reports on the relationship between preservative activity and percutaneous preservative absorption.

Although recent reports stated that esters of *p*-hydroxybenzoic acid did not pass through a natural membrane 15 hr after application (11), these substances must penetrate into the skin since they induce allergic reactions (12, 13). A whole body autoradiography study of hairless mice (14) showed that I was percutaneously absorbed from several ointments.

In this paper, percutaneous absorption *in vitro* and preservative activity of I in an aqueous system were measured; the relationship between the preservative activity and the percutaneous preservative absorption is discussed.

EXPERIMENTAL

^{14}C-Butylparaben[1] was obtained with a specific activity of 1.65 mCi/mmole. Propylene glycol, polyethylene glycol 400, and polysorbate 80 were reagent grade[2].

Vehicle compositions are listed in Table I. A 2-ml aliquot of each system was used for the diffusion study.

Male guinea pigs (Hartley strain), ~320 g, were used. The dorsal hair was removed with a hair clipper immediately prior to the experiment. The residual hair was 0.5 mm long. The adipose tissue was removed after the dorsal skin was excised from the sacrificed animal. The skin sample was then punched into a 3-cm diameter disk.

The disk was placed in a modified diffusion chamber (15). The area of the donor side was 3.14 cm^2, and the volume of the receptor space was 4.4 ml. The dermal side receptor fluid was saline and flowed through the chamber continuously at ~8 ml/hr. The eluted solution was fractionally collected in test tubes. The chamber was placed in a controlled 37° water bath throughout the experiment.

Aliquots (1 ml) of eluted I were pipetted from each test tube into a vial containing 10 ml of Bray's scintillation fluid (16). The radioactivity was measured by a liquid scintillation counter[3].

Preservative activities were studied according to a modified method of Ishizeki (17). The test sample was mixed with each solution of *Escherichia coli* (IFO[4] 3043) plus *Staphylococcus aureus* (IFO 3061), *Bacillus subtilis* (IFO 3024), *Pseudomonas aeruginosa* (IFO 3445), *Aerobacter aerogenes* (IFO 3320), *Aspergillus niger* (IAM[5] 3001) plus *Penicillium citrinum* (IAM 7316), and *Candida albicans* (IFO 0583). After several intervals of up to 7 days at 32°, each mixture was transferred onto an agar plate[6]. For *P. aeruginosa* and *A. aerogenes*, glucose was added to the agar; for *A. niger* plus *P. citrinum* and *C. albicans*, Sabouraud medium[6] was employed.

Colonies were counted after 24 hr of incubation at 37° for bacteria and after 48 hr of incubation at 30° for fungi and yeasts. Preservative activities were evaluated by counting the days before all colonies disappeared. The score was 8 when no colonies were found on the plate zero day after addition of the test sample. The score decreased with time; when colonies were still observed after 7 days, the score was 0.

RESULTS AND DISCUSSION

The penetration flux, J, of a solute through the skin is expressed as:

$$J = \frac{Q}{At} = \frac{(D)(PC)(C_v)}{l} \qquad \text{(Eq. 1)}$$

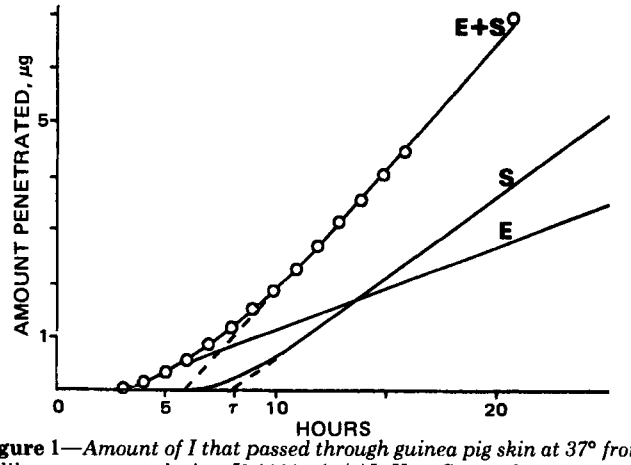

Figure 1—*Amount of I that passed through guinea pig skin at 37° from a dilute aqueous solution [0.002% (w/v)]. Key:* S, *steady-state penetration through epidermis;* E, *early penetration through appendages;* S + E, *observed amount of penetration; and* τ, *lag time.*

[1] Daiichi Pure Chemicals Co., Tokyo, Japan.
[2] Wako Pure Chemical Industries, Tokyo, Japan.
[3] Model LSC-601, Aloka Co., Mitaka, Tokyo, Japan.
[4] Institute for Fermentation, Osaka, Japan.
[5] Institute of Applied Microbiology, Tokyo, Japan.
[6] Eiken Chemical Co., Tokyo, Japan.

0022-3549/79/0500-0596$01.00/0
© 1979, American Pharmaceutical Association

Table I—Vehicle Composition

System	Compound I, % (w/v)	Polysorbate 80, % (w/v)	Propylene Glycol, % (v/v)	Polyethylene Glycol 400, % (v/v)
A	0.015	—	—	—
B	0.02	—	10	—
C	0.02	—	—	10
D	0.02	—	20	—
E	0.02	—	—	20
F	0.1	1.0	—	—
G	0.1	1.0	10	—
H	0.1	1.0	—	10
I	0.1	2.0	—	—
J	0.1	2.0	10	—
K	0.1	2.0	—	10

where Q is the amount of solute that diffuses across the area, A, in time, t; PC is the skin–vehicle partition coefficient of the solute; D is the solute diffusion constant in the skin of thickness l; and C_v is the solute concentration in the vehicle (18, 19). The permeability constant, k_p, which represents a penetration rate, is given by J/C_v.

Figure 1 shows the total amount of I absorbed from an aqueous vehicle through the skin as a function of time. Transient penetration through appendages becomes less important than the steady-state penetration through an unbroken membrane over time (18). In Fig. 1, however, the amount of early penetration, E, was comparable to the steady-state penetration, S. In the present study, therefore, the observed penetration was explained as the sum of two diffusion processes ($E + S$) (20).

A lag time, τ, was given by the intercept of the line S on the t-axis. The lag time is the time required for the solute to pass transepidermally through skin of thickness l with the diffusion constant D (20):

$$\tau = \frac{l^2}{6 \times D} \qquad \text{(Eq. 2)}$$

The penetration of I increased with time from Systems A–K (Tables I and II and Figs. 2 and 3). The average thickness of the skin samples from 22 animals without subcutaneous fat was 0.134 cm (SD 0.017 cm). This value was used for the diffusion constant calculations.

Percutaneous solute absorption is reportedly enhanced by solvents such as dimethyl sulfoxide and chloroform–methanol (21–24) because, perhaps, of stratum corneum changes (23, 24). Although there was a small D value deviation in the 11 systems in the present study ($D = 3.63 \pm 0.47 \times 10^{-4}$ cm^2/hr), no correlation was found between the system compositions and D values. The I partition coefficient varied markedly with the systems. Propylene glycol reduced the value significantly, but the effect was much less than that of polyethylene glycol 400. The effect of polysorbate 80 on the decrease of the partition coefficient was much more drastic. When polyethylene glycol 400 was coexistent with the surfactant, further reduction of the partition coefficient occurred. Propylene glycol addition had no effect.

The percentage of the solute passing through the skin from the system correlated well with the partition coefficient, indicating that the system–skin partition coefficient determined the penetration flux.

Preservative activities were evaluated qualitatively. Since the solubility of I in water is 0.015% (w/v), the I concentration in System A was slightly less than that in Systems B–E. The System E score was relatively high, but the preservative levels of these five systems were comparable (Table III). This finding suggested that there were no interactions between the solubilizers and I that would deactivate the preservative.

Table II—Values of Diffusion Constant (D), Permeability Constant (k_p), and Partition Coefficient (PC) of the Steady-State Penetration, and Percentage Penetration of the Total Amount Applied

System	D, $\times 10^{-4}$ cm^2/hr	k_p, $\times 10^{-4}$ cm/hr	PC	Penetration of Total Amount Applied, %
A	3.43	70.82	2.77	23.70
B	4.53	53.70	1.59	20.22
C	4.26	16.76	0.53	5.70
D	3.38	26.88	1.07	9.54
E	3.04	7.52	0.33	1.95
F	3.28	9.36	0.38	3.64
G	3.34	12.04	0.48	3.54
H	3.46	7.08	0.27	2.17
I	3.39	4.28	0.17	1.40
J	3.51	4.60	0.18	1.47
K	4.31	1.98	0.04	1.10

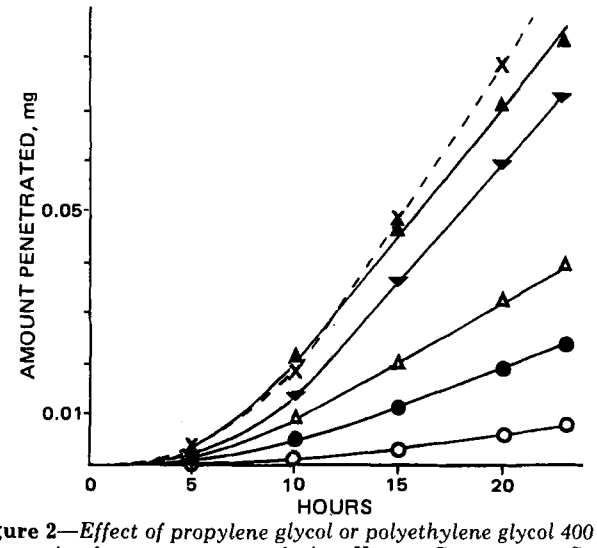

Figure 2—*Effect of propylene glycol or polyethylene glycol 400 on I penetration from an aqueous solution. Key: ▼, System A; ▲, System B; ●, System C; △, System D; ○, System E; and ×, supposed amount of penetration from 0.02% aqueous I solution.*

The increase in I concentration with polysorbate 80 did not improve preservative activity. On the contrary, the activity was reduced (Table III). Since the preservative activity is dependent on the effective aqueous I concentration (1), these results indicate that the surfactant increased the amount of I trapped in micelles and reduced the I concentration in the outer phase (3, 25).

Since the partition coefficient is also regarded as an index of mutual affinity between the preservative and vehicle (26), a low partition coefficient reflects the tendency of the preservative to remain in the vehicle. Therefore, the addition of propylene glycol or polyethylene glycol 400 to water, which increased the I solubility, decreased the partition coefficient. If the aqueous solubility were 0.02% (w/v) and the concentration were not increased by the solubilizers, the penetrated amount would be reduced in Systems B–E (Fig. 2). System A contained only 0.015% I, so the addition of solubilizers decreased the partition coefficient and increased I concentration. The latter was larger than the former in System B (Fig. 2), whereas the decrease in the partition coefficient was much more effective in Systems C–E. Polyethylene glycol 400 induced a greater decrease in the penetrated amount (or partition coefficient) than propylene glycol, as shown by a preliminary experiment. The saturated I concentration in 10% aqueous polyethylene glycol 400 was 0.050% (w/v) while that in 10% aqueous propylene glycol was 0.032% (w/v). These values were obtained by spectrophotometry[7] at 256 nm. An increase in

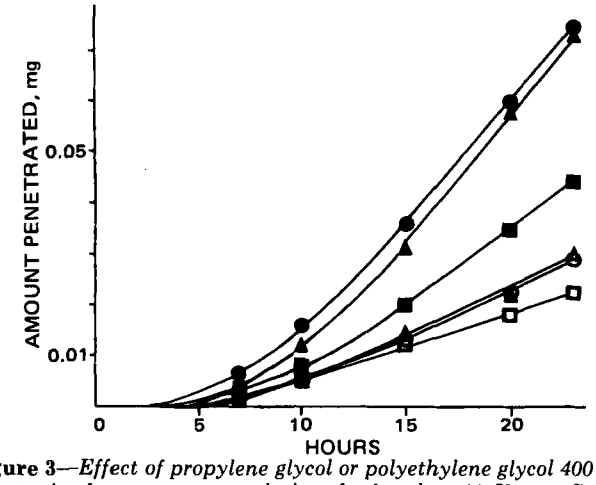

Figure 3—*Effect of propylene glycol or polyethylene glycol 400 on I penetration from an aqueous solution of polysorbate 80. Key: ●, System F; ▲, System G; ■, System H; ○, System I; △, System J; and □, System K.*

[7] Model 139 UV-VIS spectrophotometer, Hitachi Co., Tokyo, Japan.

Table III—Preservative Score

System	*A. niger* plus *P. citrinum*	*C. albicans*	*B. subtilis*	*E. coli* plus *S. aureus*	*A. aerogenes*	*P. aeruginosa*	Total Score
A	0	7	7	7	6	0	27
B	0	3	7	7	7	0	24
C	0	3	7	7	3	3	23
D	0	3	7	6	7	3	26
E	0	6	8	7	7	7	35
F	0	3	7	0	0	0	10
G	0	3	6	0	0	0	12
H	0	6	6	7	7	7	33
I	0	0	6	0	0	0	6
J	0	0	7	0	0	0	7
K	0	0	7	6	0	0	13

solubility means an increase in affinity to the system, which results in a decrease in the partition coefficient.

The preservative activity increased following addition of polyethylene glycol 400 to the surfactant solution (Table III), indicating that the I concentration in the outer phase increased due to alteration of the aqueous phase–micelle partition coefficient. The increase in I concentration in the outer phase (Table III) and the decrease in the amount passing through the skin (Fig. 2) caused by polyethylene glycol 400 help explain the percutaneous absorption results for Systems F–K.

The effect of the polyethylene glycol 400 addition in Fig. 3 was not so great as that in Fig. 2, where the surfactant was not present. Although the value of the skin–vehicle partition coefficient was reduced by the addition of polyethylene glycol 400, the effective concentration in the outer phase, which can contribute to penetration (19), was increased. Thus, the product of the effective outer phase concentration and the partition coefficient showed only a slight decrease in the penetrated amount.

The effect of propylene glycol was not so great as that of polyethylene glycol 400 on either permeability or preservative activity. Propylene glycol induced only a small increase in I concentration in the outer phase, which was counteracted by a small decrease in the partition coefficient, resulting in a smaller permeability change.

Some other factors also affected penetration from a surfactant solution since the amount of penetration from System F was similar to that from System A, although the preservative activities of these two were significantly different. Malik *et al.* (27) suggested that a surfactant increased the drug–skin affinity but that the excess addition of a surfactant decreased drug absorption, an effect also seen in Systems F and I in this study. Ostrenga *et al.* (28) suggested that the whole vehicle was absorbed or that the vehicle was separated on the skin after application. These reports reflect the difficulty of comparing the amount of penetration from systems with and without surfactant on the basis of the concentration and partition coefficient only. It was possible, however, to evaluate the effect of propylene glycol and polyethylene glycol 400 in each system on the basis of these two factors.

Although the addition of excess surfactant is an effective way to prevent a preservative from penetrating into the skin, such a system was inactive on microorganisms. Moreover, it is very dangerous to apply a large amount of a preservative on living skin since the compositions of the system change with time due to water evaporation and the secretion of sebum and sweat. The results in this study suggest that both the increase in preservative activity and the reduction of percutaneous preservative absorption can occur following the addition of a solubilizer, *i.e.*, polyethylene glycol 400, to the system.

REFERENCES

(1) H. S. Bean, S. M. Heman-Ackah, and J. Thomas, *J. Soc. Cosmet. Chem.*, **16**, 15 (1965).

(2) E. R. Garrett, *J. Pharm. Pharmacol.*, **18**, 589 (1966).

(3) H. S. Bean, G. H. Konning, and S. A. Malcolm, *ibid.*, **21**, suppl. 173 (1969).

(4) F. N. Marzulli, J. F. Callahan, and D. W. C. Brown, *J. Invest. Dermatol.*, **44**, 339 (1965).

(5) R. E. Dempski, J. B. Portnoff, and A. W. Wase, *J. Pharm. Sci.*, **58**, 579 (1969).

(6) J. B. Black and D. Howes, *J. Soc. Cosmet. Chem.*, **26**, 205 (1975).

(7) B. Calensnick, C. H. Costello, J. P. Ryan, and G. J. DiGregorio, *Toxicol. Appl. Pharmacol.*, **32**, 204 (1975).

(8) D. W. C. Brown and A. G. Ulsamer, *Food Cosmet. Toxicol.*, **13**, 81 (1975).

(9) P. G. T. Bye, W. Morison, and E. L. Rhodes, *Br. J. Dermatol.*, **93**, 209 (1975).

(10) B. Croshaw, *J. Soc. Cosmet. Chem.*, **28**, 3 (1977).

(11) G. M. Smith and G. E. Peck, *J. Pharm. Sci.*, **65**, 727 (1976).

(12) W. D. Schorr and A. H. Mohajerin, *Arch. Dermatol.*, **93**, 721 (1966).

(13) F. N. Marzulli and H. I. Maibach, *J. Soc. Cosmet. Chem.*, **24**, 399 (1973).

(14) M. Suzuki, H. Komatsu, K. Asaba, and S. Kato, *J. Jpn. Cosmet. Chem. Assoc.*, **9**, 16 (1974).

(15) I. H. Blank, *J. Invest. Dermatol.*, **43**, 415 (1964).

(16) G. A. Bray, *Anal. Biochem.*, **1**, 279 (1960).

(17) C. Ishizeki, *Iyakuhin Kenkyu*, **4**, 175 (1973).

(18) R. J. Scheuplein, in "Pharmacology and the Skin," W. Montagna, R. B. Stoughton, and E. J. van Scott, Eds., Meredith, New York, N.Y., 1972, p. 125.

(19) B. Idson, *J. Pharm. Sci.*, **64**, 901 (1975).

(20) R. J. Scheuplein, *J. Invest. Dermatol.*, **48**, 79 (1967).

(21) H. Baker, *ibid.*, **50**, 283 (1968).

(22) T. M. Sweeney and D. T. Downing, *ibid.*, **55**, 135 (1970).

(23) R. J. Scheuplein and L. Ross, *J. Soc. Cosmet. Chem.*, **21**, 853 (1970).

(24) L. J. Vinson, E. J. Singer, W. R. Koehler, M. D. Lehman, and T. Masurat, *Toxicol. Appl. Pharmacol.*, **7**, 7 (1965).

(25) F. D. Pisano and H. B. Kostenbauder, *J. Am. Pharm. Assoc., Sci. Ed.*, **48**, 310 (1959).

(26) B. J. Poulsen, in "Pharmacology and the Skin," W. Montagna, R. B. Stoughton, and E. J. van Scott, Eds., Meredith, New York, N.Y., 1972, p. 495.

(27) S. N. Malik, D. H. Canahan, and M. W. Gouda, *J. Pharm. Sci.*, **64**, 987 (1975).

(28) J. Ostrenga, J. Haleblian, B. Poulsen, B. Ferrell, N. Mueller, and S. Shastri, *J. Invest. Dermatol.*, **56**, 392 (1971).

ACKNOWLEDGMENTS

The authors thank Miss Toshiko Suzuki, Miss Tamiko Nakamura, and Mr. Masaaki Takahashi for carrying out the preservative test.

High-Performance Liquid Chromatographic Assay for the Antiprotozoal Agent, Tinidazole, in Human Plasma

K. B. ALTON ˣ and J. E. PATRICK

Received August 7, 1978, from *Ortho Pharmaceutical Corporation, Raritan, NJ 08869.* Accepted for publication October 20, 1978.

Abstract □ A rapid and specific high-performance liquid chromatographic (HPLC) assay for the quantitative determination of tinidazole in human plasma is described. After a simple extraction procedure, the compound is analyzed by HPLC using a reversed-phase column and a UV detector. Quantitation is accomplished using an external standard, and peak areas are determined with an integrating computer. The average recovery of tinidazole over a concentration range of 0.20–20.0 μg/ml was 86.9 ± 2.8% *SD*. The maximum sensitivity of the assay is approximately 0.10 μg/ml; it is suitable for use in pharmacokinetic studies following administration of therapeutic levels of tinidazole to humans.

Keyphrases □ Tinidazole—high-performance liquid chromatographic assay, human plasma □ High-performance liquid chromatography—analysis, tinidazole in human plasma □ Antiprotozoal agents—high-performance liquid chromatographic analysis in human plasma □ High-performance liquid chromatography—analysis, tinidazole in human plasma

The antitrichomonal agent tinidazole, ethyl-2-(2-methyl-5-nitro-1-imidazolyl ethyl) sulfone (I), is one of the most active compounds in a series of nitroimidazole derivatives (1) active against *Trichomonas vaginalis* (2–5). Attempts to measure tinidazole or other *N*-1-substituted nitroimidazoles in plasma samples have included polarography (6–8), absorptiometry (9, 10), GLC (10), TLC (10, 11), *in vitro* agar diffusion (12), and high-performance liquid chromatography (HPLC) (13).

Quantitation of both tinidazole and metronidazole (7, 8) based on the polarographic assay described by Kane (6) lacks specificity since all drug-related species possessing the nitroimidazole nucleus are similarly detected. The *in vitro* agar diffusion assay (12), the absorptiometry method (9, 10), and the HPLC procedure (13) have maximum sensitivities of 0.5–1.0 μg/ml for the *N*-1-substituted 5-nitroimidazoles. This sensitivity limitation may diminish their usefulness in describing the initial phase of drug absorption or the terminal portion of the elimination phase in humans.

The absorptiometric method and the pulsed polarographic and electron-capture GLC procedures (10) require time-consuming isolation of the intact, parent *N*-substituted nitroimidazole by TLC before quantitation. In a modified TLC–densitometry method (11), direct quantitation of tinidazole and metronidazole was achieved, but this method is not as rapid as conventional HPLC or GLC, which can be automated to handle a large number of clinical samples.

This report describes a simple and specific HPLC method for the rapid estimation of tinidazole in human plasma at concentrations suitable for pharmacokinetic studies. No interference from two known urinary metabolites (II and III) (14, 15) of tinidazole was encountered.

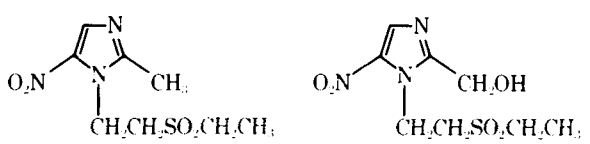

I

II

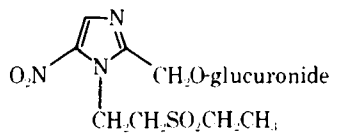

III

EXPERIMENTAL

Apparatus—Analyses were performed on a liquid chromatograph[1] operated at ambient temperature and equipped with a differential UV (313 nm) detector[2]. Separations were accomplished on a 30-cm × 3.9-mm i.d. reversed-phase column[3]. Samples were introduced onto the column through a septumless injector[4] with a 25-μl syringe[5]. Chromatograms were traced on a strip-chart recorder[6], and peak area integrations were performed by an integrating computer[7] interfaced with the detector by an analog–digital converter[8].

Reagents and Solvents—Tinidazole (I) and two known metabolites of tinidazole, ethyl[2-(2-hydroxymethyl-5-nitro-1-imidazolyl)-ethyl] sulfone (II) and the *O*-glucuronide conjugate of II (III), were used as received[9]. All chemicals and reagents except methanol[10] were reagent grade. Both 2-butanone and water were distilled before use.

Chromatographic Conditions—The mobile phase was 0.05 *M* pH 7.0 KH_2PO_4–NaOH buffer–methanol (86:14 v/v) with the flow rate adjusted to 2.0 ml/min (~2000 psi). The solvent mixture was prepared daily and degassed under reduced pressure before use.

Extraction Procedure—An aliquot (1.0 ml) of plasma was transferred to a 15-ml vial (16 × 125 mm) fitted with a polytef-lined screw cap and diluted with 2.0 ml of 0.05 *M* pH 7.0 KH_2PO_4–NaOH buffer. This aqueous portion was extracted by vigorous shaking with 7.0 ml of petroleum ether (bp 30–60°). The mixture was centrifuged (2 min at 1500×*g*) to obtain a clear supernate, and the organic (upper) layer was discarded. The aqueous layer was extracted twice with ethyl acetate (7.0 ml) by manual shaking for 1 min, and the phases were separated by centrifugation at 1500×*g* for 3 min.

The organic layers were removed with a Pasteur pipet, pooled, taken to dryness under a nitrogen stream in a water bath (55°), and then transferred to a 2.5-ml conical centrifuge tube using ethyl acetate. The ethyl acetate was concentrated as described, the residue was dissolved in 2-butanone (0.1–0.5 ml), and aliquots (5–20 μl) were injected onto the HPLC column.

Extraction Efficiency—Blood from several untreated volunteers was drawn into heparinized containers[11] and centrifuged to generate a plasma pool from which an extraction efficiency was established. Known amounts of tinidazole dissolved in methanol were added to each of six 11.0-ml drug-free plasma pool samples to obtain concentrations of 0.20, 0.39, 1.93, 4.82, 9.82, and 20.0 μg/ml. The plasma pools were thoroughly mixed on a tube rotator for 30 min. Aliquots (1.0 ml) of plasma from each pool were transferred to 15-ml screw-capped vials and stored frozen (−20°) until extracted as described.

[1] Model ALC 204, Waters Associates, Milford, Mass.
[2] Model 440, Waters Associates, Milford, Mass.
[3] μBondapak/phenyl, Waters Associates, Milford, Mass.
[4] Model U6K, Waters Associates, Milford, Mass.
[5] Pressure-Lok B-110, Precision Sampling Corp., Baton Rouge, La.
[6] Servo/riter II, Texas Instruments, Houston, Tex.
[7] Model 3352B, Hewlett-Packard, Avondale, Pa.
[8] Model 18652A, Hewlett-Packard, Avondale, Pa.
[9] Tinidazole and the metabolite standards were synthesized and supplied by Pfizer Ltd., Sandwich, Kent, England.
[10] Distilled in glass, Burdick & Jackson Laboratories, Muskegon, Mich.
[11] Vacutainers, Becton-Dickenson, Rutherford, N.J.

0022-3549/79/0500-0599$01.00/0
© 1979, American Pharmaceutical Association

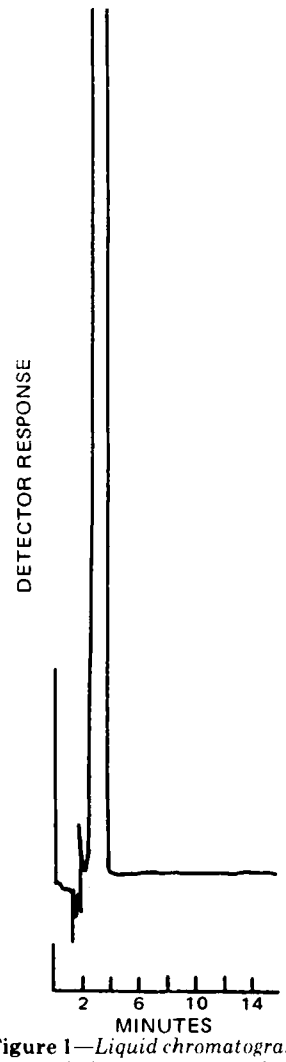

Figure 1—*Liquid chromatogram of an ethyl acetate extract from drug-free plasma. The mobile phase consisted of 0.05* M *KH_2PO_4–NaOH buffer–methanol (86:14 v/v) with the flow rate adjusted to 2.0 ml/min.*

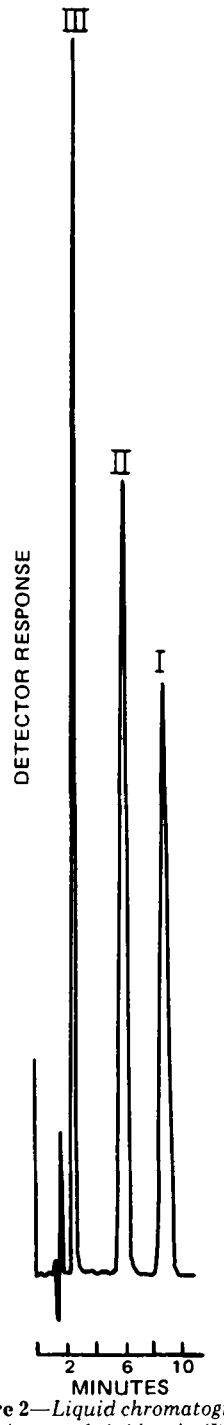

Figure 2—*Liquid chromatogram of a mixture of tinidazole (I), II, and III. Approximately 0.2 μg of each standard was injected for analysis.*

Since the prepared drug concentrations ranged over two orders of magnitude (0.20–20.0 μg/ml), varying volumes of the final 2-butanone dilutions were injected for analysis by HPLC. Typically, when the drug concentration approached 0.2 μg/ml, one-fifth (20 μl/100 μl) of the final dissolved residue volume was analyzed; at a concentration of 20 μg/ml, only one-one hundreth (5 μl/500 μl) of the final dissolved residue was injected. All samples were analyzed in duplicate. After chromatography, quantitation of tinidazole was accomplished by use of the external standard method.

Calibration and Standard Preparation—Tinidazole (10.0 mg) was dissolved in 2-butanone and diluted in a 10.0-ml volumetric flask to 1.0 μg/μl. Two additional stock solutions were prepared containing 0.10 and 0.01 μg/μl of tinidazole by serial dilution of the 1.0-μg/μl stock solution with 2-butanone. Since the external standard method prepared from the software section of the computer assumes a linear relationship between micrograms injected and peak area (microvolt-seconds as reported by the integrating computer), this relationship was initially evaluated by repeated ($n \geq 5$) injections of 0.25, 0.20, 0.15, 0.10, 0.05, and 0.025 μg of tinidazole from the 2-butanone stock solutions. Thereafter, an average calibration response factor was established by the computer following triplicate injections equivalent to 0.15 μg of tinidazole.

Specificity—Assay specificity was determined by analyzing a methanolic solution containing a mixture (0.2 μg) of tinidazole and two of its known urinary metabolites (II and III). A portion of an extract (20 μg/100 μl) from a drug-free plasma sample was evaluated chromato-

Table I—Recovery of Tinidazole (n = 11) from Human Plasma at Various Concentrations

Theoretical Plasma Concentration, μg/ml	Average Observed Plasma Concentration, μg/ml	Average Recovery[a], %
0.20	0.18	89.8 ± 3.7
0.39	0.34	88.2 ± 3.3
1.93	1.64	85.2 ± 2.3
4.82	4.16	86.2 ± 2.6
9.82	8.20	83.5 ± 2.5
20.0	17.7	88.6 ± 2.5
		$\bar{x}$ = 86.9 ± 2.8[b]

[a] $\bar{x} \pm SD$. [b] CV = 3.2%.

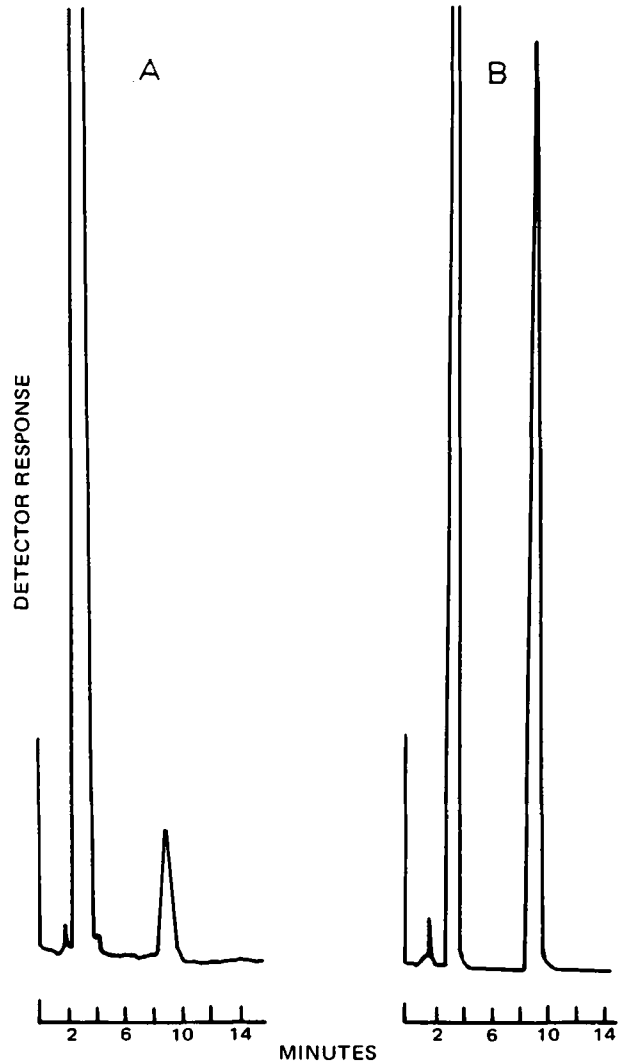

Figure 3—*Representative chromatograms of ethyl acetate extracts from human plasma spiked with 0.2 (A) and 20.0 (B) μg/ml of tinidazole. Detector response was at 0.005 aufs.*

graphically for the presence of any extractable ethyl acetate UV-absorbing (313 nm) material that might interfere with tinidazole measurement.

RESULTS AND DISCUSSION

A successful chromatographic assay for drug levels in the large number of plasma samples generated from a clinical study would provide highly reproducible drug recovery, specificity, sensitivity, precise measurement, and rapid throughput of samples.

The average recovery of drug from plasma samples to which tinidazole had been added was 86.9 ± 2.8% *SD* (Table I). Linear regression analysis of percent recovery *versus* plasma concentration revealed no statistically significant slope (β) ($p = 0.7431$). These data, therefore, suggest that there is no concentration dependence on extraction efficiencies over the range of expected plasma drug levels (10–12).

Tinidazole was monitored at 313 nm since its λ_{max} was observed in methanol at 310 nm ($\epsilon = 9070$). Ethyl acetate extracts from drug-free plasma were free of interfering UV- (313 nm) absorbing peaks (Fig. 1). Preextraction with petroleum ether eliminated nonpolar material that would otherwise be highly retained on this reversed-phase system. Little or no loss of tinidazole was encountered in this step.

Baseline resolution among tinidazole, II, and III was achieved under the chromatographic conditions described (Fig. 2). The observed retention times (t_r) for III, II, and I were 2.73, 6.12, and 8.96 min, respectively. Representative chromatograms of plasma extracts containing 0.20 and 20.0 μg/ml of tinidazole are shown in Fig. 3.

Linear regression analysis of the curve described by plotting microvolt-seconds (area) *versus* micrograms injected indicated a linear fit of the data ($r^2 = 0.9994$) from 0.025 to 0.25 μg. The slope was 474.75 μv-sec/ng; the intercept, which was not significantly different from zero ($p < 0.05$), was 1512 μv-sec. Over 2 months, the slope of this line demonstrated little change, with a coefficient of variation equal to 3.83% ($n = 16$).

REFERENCES

(1) M. W. Miller, H. L. Howes, and A. R. English, *Antimicrob. Agents Chemother.*, **1969**, 257.

(2) J. Daels, D. Janssens, and W. Stroobants, *Tijdschr. Geneesk*, **15** 747 (1970).

(3) P. Dubois, R. Lambotte, and G. Plomteux, *Rev. Med. Liège*, **18**, 586 (1970).

(4) J. Frick and A. Decristofero, *Therapiewoche*, **21**, 472 (1971).

(5) B. Flotho and H. Koelbl, *Wien. Med. Wochenschr.*, **121**, 707 (1971).

(6) P. O. Kane, *J. Polarogr. Sci.*, **8**, 73 (1961).

(7) J. A. Taylor, J. R. Migiliardi, and M. Schack von Wittenau, *Antimicrob. Agents Chemother.*, **1970**, 267.

(8) P. O. Kane, J. A. McFadzean, and S. Squires, *Br. J. Venerol. Dis.*, **37**, 276 (1961b).

(9) E. Lau, C. Yao, M. Lewis, and B. Senkowski, *J. Pharm. Sci.*, **58**, 55 (1969).

(10) J. A. F. de Silva, N. Munno, and N. Strojny, *ibid.*, **59**, 201 (1970).

(11) P. G. Welling and A. M. Monro, *Arzneim.-Forsch.*, **22**, 2128 (1972).

(12) T. Ripa, L. Weström, P.-A. Mardh, and K.-E. Andersson, *Chemotherapy*, **23**, 227 (1977).

(13) J. Nachbaur and H. Joly, *J. Chromatogr.*, **145**, 325 (1978).

(14) B. A. Wood, D. Rycroft, and A. M. Monro, *Xenobiotica*, **3**, 801 (1973).

(15) Y. Kimura, K. Ohki, K. Hiroshi, and Y. Noguchi, *Oyo Yakuri*, **8**, 573 (1974).

ACKNOWLEDGMENTS

The authors thank Dr. B. A. Wood of Pfizer Ltd., Sandwich, Kent, England, for providing samples of tinidazole metabolites.

Thermal Characterization of Citric Acid Solid Dispersions with Benzoic Acid and Phenobarbital

ROBERT J. TIMKO and NICHOLAS G. LORDI ×

Received April 24, 1978, from the *College of Pharmacy, Rutgers—The State University, Busch Campus, Piscataway, NJ 08854.* Accepted for publication October 25, 1978.

Abstract □ The glass transition temperatures of citric acid glass were determined by differential scanning calorimetry to be 10.2 and 13.5° for *in situ* and bulk-prepared samples, respectively. Mechanical stress on citric acid glass induced foci for crystallization. Benzoic acid addition to citric acid glass decreased its glass transition temperature while phenobarbital addition increased its glass transition temperature, the latter forming a glass solution.

Keyphrases □ Glass transition temperature—citric acid glass, benzoic acid, mechanical stress, phenobarbital □ Citric acid—glass formation, glass transition temperature, benzoic acid, phenobarbital □ Glass formation—citric acid, benzoic acid, phenobarbital □ Phenobarbital—glass formation with citric acid

A glass is generally defined as a noncrystalline solid formed by continuous hardening or solidification of a liquid (1, 2). The use of organic compounds capable of glass formation to reduce the particle size of a drug and to increase its dissolution and absorption rates was first suggested by Chiou and Riegelman (3). They proposed the formation of a glass dispersion of a poorly water-soluble drug and a physiologically inert carrier such as citric acid. The concepts involved in glass solution and glass suspension formation were discussed previously (4).

Glass dispersions are metastable and, as a result, exhibit rapid dissolution. In a study with griseofulvin (3), the citric acid–griseofulvin glass solution had the fastest dissolution rate of the solid dispersion systems examined. However, griseofulvin decomposition occurred in the presence of citric acid during manufacturing. Citric acid was also an unacceptable sulfabenzamide carrier (5). As with griseofulvin, thermal drug degradation occurred during sample preparation.

Summers and Enever (6–8) studied citric acid–primidone glass dispersions and found the glass solutions formed to be unstable and rapidly devitrified. The devitrified dispersion systems, however, still exhibited more rapid dissolution than the pure drug or drug and carrier mixtures. The citric acid glass transition temperature increased with increasing primidone concentration (8). The

0022-3549/79/0500-0601$01.00/0

© 1979, American Pharmaceutical Association

graphically for the presence of any extractable ethyl acetate UV-absorbing (313 nm) material that might interfere with tinidazole measurement.

RESULTS AND DISCUSSION

A successful chromatographic assay for drug levels in the large number of plasma samples generated from a clinical study would provide highly reproducible drug recovery, specificity, sensitivity, precise measurement, and rapid throughput of samples.

The average recovery of drug from plasma samples to which tinidazole had been added was 86.9 ± 2.8% *SD* (Table I). Linear regression analysis of percent recovery *versus* plasma concentration revealed no statistically significant slope (β) ($p = 0.7431$). These data, therefore, suggest that there is no concentration dependence on extraction efficiencies over the range of expected plasma drug levels (10–12).

Tinidazole was monitored at 313 nm since its λ_{max} was observed in methanol at 310 nm ($\epsilon = 9070$). Ethyl acetate extracts from drug-free plasma were free of interfering UV- (313 nm) absorbing peaks (Fig. 1). Preextraction with petroleum ether eliminated nonpolar material that would otherwise be highly retained on this reversed-phase system. Little or no loss of tinidazole was encountered in this step.

Baseline resolution among tinidazole, II, and III was achieved under the chromatographic conditions described (Fig. 2). The observed retention times (t_r) for III, II, and I were 2.73, 6.12, and 8.96 min, respectively. Representative chromatograms of plasma extracts containing 0.20 and 20.0 μg/ml of tinidazole are shown in Fig. 3.

Linear regression analysis of the curve described by plotting microvolt-seconds (area) *versus* micrograms injected indicated a linear fit of the data ($r^2 = 0.9994$) from 0.025 to 0.25 μg. The slope was 474.75 μv-sec/ng; the intercept, which was not significantly different from zero ($p < 0.05$), was 1512 μv-sec. Over 2 months, the slope of this line demonstrated little change, with a coefficient of variation equal to 3.83% ($n = 16$).

REFERENCES

(1) M. W. Miller, H. L. Howes, and A. R. English, *Antimicrob. Agents Chemother.*, **1969**, 257.

(2) J. Daels, D. Janssens, and W. Stroobants, *Tijdschr. Geneesk*, **15** 747 (1970).

(3) P. Dubois, R. Lambotte, and G. Plomteux, *Rev. Med. Liège*, **18**, 586 (1970).

(4) J. Frick and A. Decristofero, *Therapiewoche*, **21**, 472 (1971).

(5) B. Flotho and H. Koelbl, *Wien. Med. Wochenschr.*, **121**, 707 (1971).

(6) P. O. Kane, *J. Polarogr. Sci.*, **8**, 73 (1961).

(7) J. A. Taylor, J. R. Migiliardi, and M. Schack von Wittenau, *Antimicrob. Agents Chemother.*, **1970**, 267.

(8) P. O. Kane, J. A. McFadzean, and S. Squires, *Br. J. Venerol. Dis.*, **37**, 276 (1961b).

(9) E. Lau, C. Yao, M. Lewis, and B. Senkowski, *J. Pharm. Sci.*, **58**, 55 (1969).

(10) J. A. F. de Silva, N. Munno, and N. Strojny, *ibid.*, **59**, 201 (1970).

(11) P. G. Welling and A. M. Monro, *Arzneim.-Forsch.*, **22**, 2128 (1972).

(12) T. Ripa, L. Weström, P.-A. Mardh, and K.-E. Andersson, *Chemotherapy*, **23**, 227 (1977).

(13) J. Nachbaur and H. Joly, *J. Chromatogr.*, **145**, 325 (1978).

(14) B. A. Wood, D. Rycroft, and A. M. Monro, *Xenobiotica*, **3**, 801 (1973).

(15) Y. Kimura, K. Ohki, K. Hiroshi, and Y. Noguchi, *Oyo Yakuri*, **8**, 573 (1974).

ACKNOWLEDGMENTS

The authors thank Dr. B. A. Wood of Pfizer Ltd., Sandwich, Kent, England, for providing samples of tinidazole metabolites.

Thermal Characterization of Citric Acid Solid Dispersions with Benzoic Acid and Phenobarbital

ROBERT J. TIMKO and NICHOLAS G. LORDI ×

Received April 24, 1978, from the *College of Pharmacy, Rutgers—The State University, Busch Campus, Piscataway, NJ 08854.* Accepted for publication October 25, 1978.

Abstract □ The glass transition temperatures of citric acid glass were determined by differential scanning calorimetry to be 10.2 and 13.5° for *in situ* and bulk-prepared samples, respectively. Mechanical stress on citric acid glass induced foci for crystallization. Benzoic acid addition to citric acid glass decreased its glass transition temperature while phenobarbital addition increased its glass transition temperature, the latter forming a glass solution.

Keyphrases □ Glass transition temperature—citric acid glass, benzoic acid, mechanical stress, phenobarbital □ Citric acid—glass formation, glass transition temperature, benzoic acid, phenobarbital □ Glass formation—citric acid, benzoic acid, phenobarbital □ Phenobarbital—glass formation with citric acid

A glass is generally defined as a noncrystalline solid formed by continuous hardening or solidification of a liquid (1, 2). The use of organic compounds capable of glass formation to reduce the particle size of a drug and to increase its dissolution and absorption rates was first suggested by Chiou and Riegelman (3). They proposed the formation of a glass dispersion of a poorly water-soluble drug and a physiologically inert carrier such as citric acid. The concepts involved in glass solution and glass suspension formation were discussed previously (4).

Glass dispersions are metastable and, as a result, exhibit rapid dissolution. In a study with griseofulvin (3), the citric acid–griseofulvin glass solution had the fastest dissolution rate of the solid dispersion systems examined. However, griseofulvin decomposition occurred in the presence of citric acid during manufacturing. Citric acid was also an unacceptable sulfabenzamide carrier (5). As with griseofulvin, thermal drug degradation occurred during sample preparation.

Summers and Enever (6–8) studied citric acid–primidone glass dispersions and found the glass solutions formed to be unstable and rapidly devitrified. The devitrified dispersion systems, however, still exhibited more rapid dissolution than the pure drug or drug and carrier mixtures. The citric acid glass transition temperature increased with increasing primidone concentration (8). The

0022-3549/79/0500-0601$01.00/0

© 1979, American Pharmaceutical Association

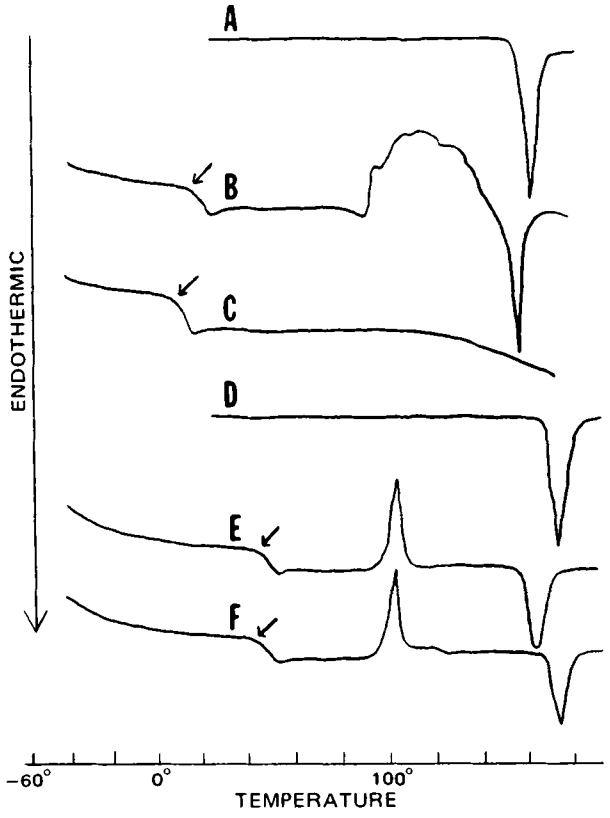

Figure 1—*Thermograms of anhydrous citric acid (A), bulk-prepared citric acid solidified melt (B),* in situ *prepared citric acid glass (C), phenobarbital (D),* in situ *prepared phenobarbital glass crystallizing as polymorphic Form IV (E), and* in situ *prepared phenobarbital glass crystallizing as polymorphic Form I (F). The glass transition temperatures are indicated by arrows.*

increased primidone dissolution rate was a result of its reduced particle size and increased wettability in the systems.

Most glass dispersion studies concentrate on the drug. Little information is available on carrier stability or the effect of additives on stability. This article reports some observations on citric acid glass stability; the effect of two additives, benzoic acid and phenobarbital, on its glass transition temperature; and the nature of the dispersion systems these materials form. Benzoic acid, a crystalline material, has not been reported capable of glass formation. Phenobarbital has been suggested to be capable of glass formation by rapid melt cooling (9) and has been reported to form a glass solution with citric acid (3).

EXPERIMENTAL

Materials—Citric acid[1] (mp 152–156°), benzoic acid[2] (mp 121–124°), and phenobarbital[3] (mp 174–178°) were used as received.

Thermal Analysis—A differential scanning calorimeter[4] was used to determine the glass transition temperatures and stabilities. Observed temperature values were corrected for chromel alumel thermocouples from −60 to 200° using indium metal as the standard. All determinations were made at least in duplicate.

A 10–15-mg sample size was necessary to obtain reproducible and distinct transition temperatures. Samples were scanned at 10°/min in a static air atmosphere using an empty aluminum pan as the reference.

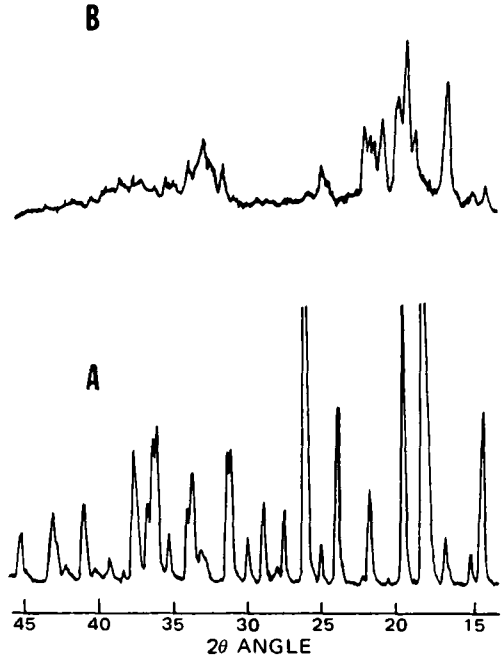

Figure 2—*X-ray diffraction pattern of anhydrous citric acid (A) and bulk-prepared citric acid solidified melt (B).*

The sensitivities were 1.0°/in. for pure materials and physical mixtures and 0.2°/in. for solidified melts and glass systems. A 20°/in. temperature scale was used.

Two procedures were used for sample preparation, an *in situ* method and a bulk procedure. In the *in situ* procedure, citric acid or mixtures of citric acid and benzoic acid or phenobarbital in the desired ratio were weighed accurately directly into an aluminum sample pan. An aluminum cover was placed on the sample, and the pan was transferred to the sample holder of the differential scanning calorimeter. After the sample was heated to melting, the melt was rapidly cooled to −60° by purging the sample holder of the instrument with liquid nitrogen. The solidified melt was reheated, and the thermogram was recorded.

Bulk glass system preparation involved melting 50 g of citric acid or mixtures of citric acid and benzoic acid or phenobarbital in the desired ratio in an electric frying pan[5] heated to 170°. Samples were stirred continually until melting was complete. The melt was rapidly solidified by transferring it to an aluminum foil boat located on a dry ice block hollowed out to fit the boat dimensions. After solidification, the melt was removed from the dry ice and placed in a desiccator over silica gel at 23° for 24 hr. The solidified melt was pulverized in a rotary granulator[6].

Samples of the solidified melts, prepared by both the *in situ* method (removed from the sample holder after cooling to −60°) and the bulk procedure, were placed in desiccators at 4, 23, and 37°. Thermograms were run periodically to examine the effects of aging on physical stability.

The melting temperatures of the physical mixtures were determined by differential scanning calorimetry and a conventional capillary tube melting-point apparatus[7]. Both the onset of melting temperature and the complete fusion temperature are reported. When using the differential scanning calorimetry, melting onset was defined as the temperature at which there was an initial endothermic deviation in the thermogram baseline. Its value was the curve extrapolation crossing point on each side of the baseline deviation. The complete fusion temperature was the endothermic peak temperature. If a sharp peak was not obtained, the sides of the peak were extrapolated and the crossing point was used as the value of the endothermic peak. With the capillary tube method, the melting onset and the complete fusion temperatures were visually estimated with a magnifying glass. The heating rate was ~10°/min.

The area under the exothermic peak in the bulk-prepared citric acid melts was determined by a cut and weigh method. Areas were calculated according to the standard area weight. Results are reported as area under the peak in square centimeters per milligram of sample weight.

[1] Anhydrous, J. T. Baker Chemical Co., Phillipsburg, N.J.
[2] Reagent grade, Fisher Scientific Co., Fair Lawn, N.J.
[3] USP, Mallinckrodt Chemical Works, St. Louis, Mo.
[4] DuPont 900 thermal analyzer with a No. 900600 differential scanning calorimeter cell, E. I. DuPont DeNemours and Co., Wilmington, Del.
[5] Sunbeam Corp., Chicago, Ill.
[6] Type TG-2, Erweka-G.m.b.H., Frankfurt, West Germany.
[7] Model JM-110, Scientific Glass Inc., Bloomfield, N.J.

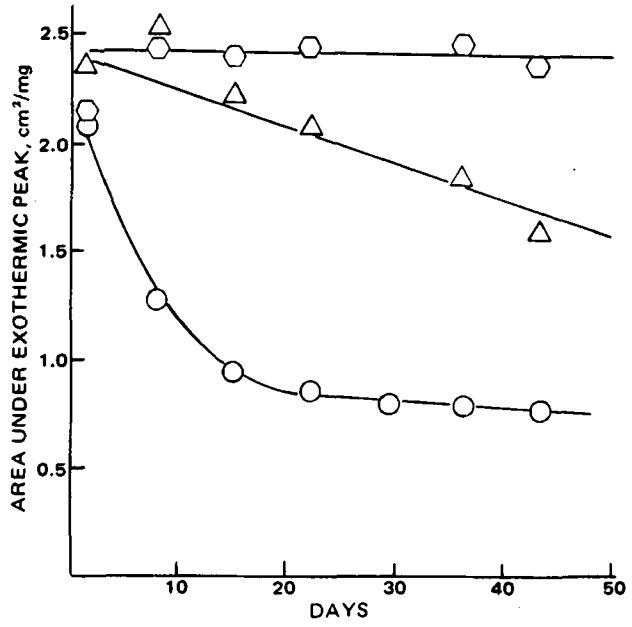

Figure 3—*Storage temperature effect on the area under the exothermic peak of bulk-prepared citric acid solidified melt. Key:* ○, *4°;* △, *23°; and* ○, *37°.*

X-Ray Diffraction—An X-ray diffractiometer[8] was used to determine the bulk-prepared solidified citric acid melt. Powdered mixed particle-size samples were mounted on a screen sample holder, and the X-ray diffraction pattern was determined using Cu K_α radiation. A powdered citric acid sample was run for comparison.

NMR Studies—Citric acid stability during sample preparation was examined by NMR[9]. The fused sample citric acid spectra, prepared by both the *in situ* and bulk methods, were compared with those of unfused citric acid and aconitic acid[10], a possible dehydration decomposition product of citric acid. The solvent was deuterium oxide, and tetramethylsilane was the internal standard.

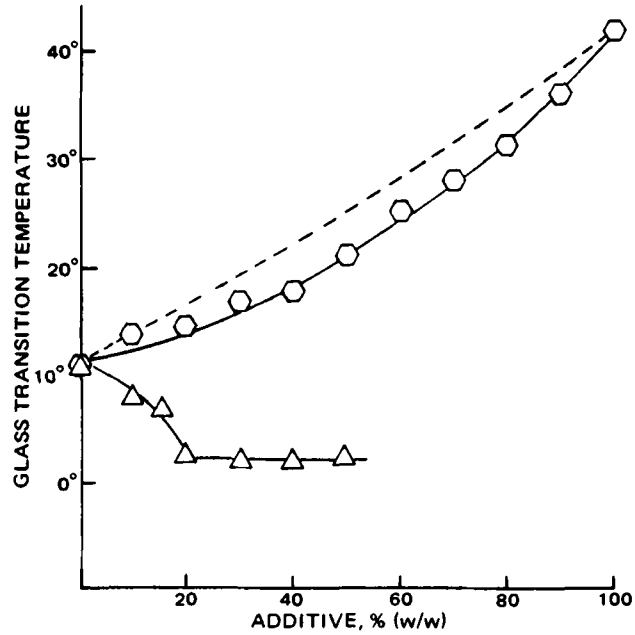

Figure 4—*Effect of benzoic acid (*△*) and phenobarbital (*○*) on the citric acid glass transition temperature. The dashed line represents the values of the glass transition temperatures of the phenobarbital–citric acid glass system predicted by Eq. 1.*

[8] Model GE XRD-6, General Electric Co.
[9] Varian T-60 NMR spectrometer, Varian Instrument Division, Palo Alto, Calif.
[10] Aldrich Chemical Co., Milwaukee, Wis.

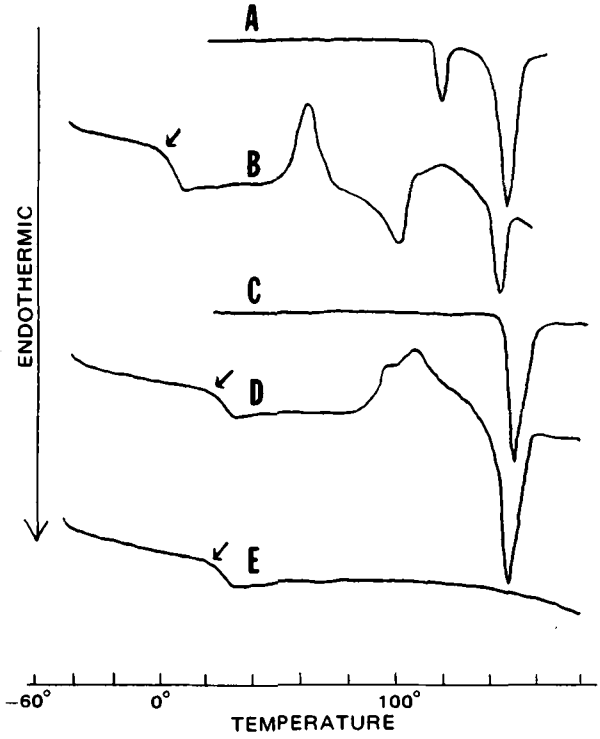

Figure 5—*Thermograms of 1:4 benzoic acid–citric acid physical mixture (A), 1:4 benzoic acid–citric acid* in situ *prepared glass (B), 1:1 phenobarbital–citric acid physical mixture (C), 1:1 phenobarbital–citric acid bulk-prepared solidified melt (D), and 1:1 phenobarbital–citric acid* in situ *prepared glass (E). Glass transition temperatures are indicated by arrows.*

RESULTS AND DISCUSSION

Glass is a fourth state of matter, distinct from both the crystalline and liquid states, yet exhibiting characteristics of both. Like a crystal, a glass exhibits ridigity; like a liquid, it has random molecular arrangement (1, 10, 11).

The crystalline and liquid states are delineated from each other by a definite temperature: the melting point of the crystalline material. The transition between a glass and a liquid is more ambiguous (12). In differential scanning calorimetry, it is indicated by a marked shift in the thermogram baseline due to an increase in the material's specific heat. The glass transition temperature (T_g) is the upper boundary of this transitional temperature range (10), and it is this temperature that is reported as the T_g of the glass system studied. Experimentally, it was determined by extrapolating the curve on each side of the onset of the baseline shift; the crossing point of the extrapolated lines was used as the T_g value.

Crystalline citric acid is highly hydrogen bonded (13). Citric acid glass formation has been attributed to this hydrogen bonding capacity, which may prevent its crystallization (14). Citric acid glass formation may be due also to its partial decomposition by dehydration into aconitic acid during melting (4).

Citric acid stability during sample preparation was examined by NMR. No changes were observed in the fused citric acid spectra when compared to the spectrum of unfused citric acid. A molten citric acid sample held isothermally at 175° for 5 min and then cooled rapidly also showed no spectral changes. The thermogram of this material was identical to that of citric acid melt prepared in the normal manner.

Thermal citric acid studies indicate possible anhydride formation on continuous heating at ~185° (15). Decomposition does not occur until about 200° (15, 16), where citric acid begins to decompose to a mixture of itaconic and citraconic acid anhydrides.

The thermograms of bulk-prepared citric acid melt and *in situ* prepared citric acid glass are shown in Fig. 1. The bulk and *in situ* glass transitions were 13.5 and 10.2°, respectively. These results are in conflict with a previously reported T_g of −23° for bulk-prepared citric acid glass (8). In preliminary studies with bulk-prepared citric acid melts, a small baseline shift was observed at −23°, in addition to the transition at 13.5°, when the heating rate was 2°/min. Since this shift was not observed at

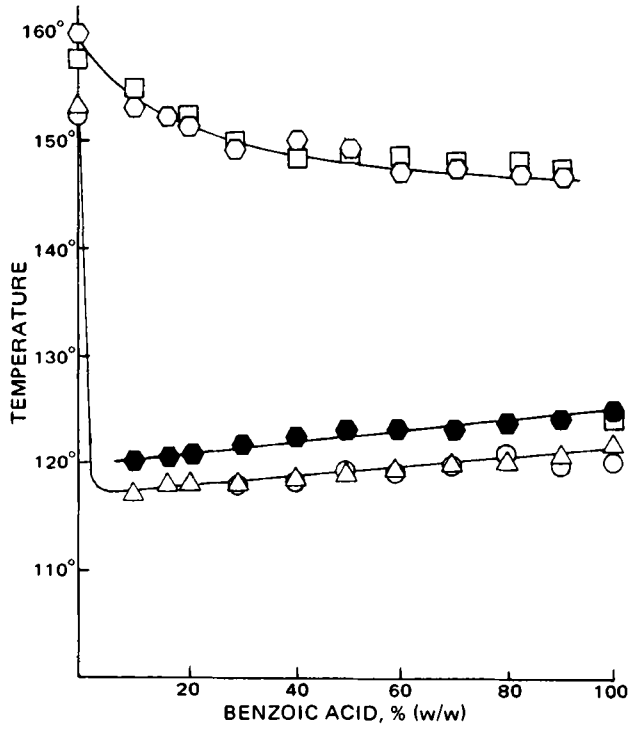

Figure 6—*Melting temperatures of the benzoic acid–citric acid binary system determined from physical mixtures. Key (differential scanning calorimetry): △, initial endothermic temperature deviation in the thermogram baseline; ○, citric acid endothermic peak temperature; and ●, endothermic benzoic acid peak temperature. Key (capillary tube method): ○, melting onset temperature; and □, complete physical mixture fusion temperature.*

heating rates of 5, 10, and 20°/min, it was not considered to be the true citric acid glass T_g but rather an artifact or a secondary transition in the sample as a result of molecular relaxation within the solidified melt (17).

The thermogram of the bulk-prepared melt exhibited a broad exothermic transition, onset at ~80°, followed by an endotherm. The exotherm was present in all samples but varied in size and shape. The *in situ* samples did not exhibit an exotherm. No changes were observed in their thermograms after 4 weeks of storage under the test conditions. When the *in situ* sample surface was scratched with a metal probe and the scan was recorded, an exotherm similar to the one observed in the bulk samples was noted. X-ray diffraction data (Fig. 2) indicated that the bulk-prepared citric acid melt consisted of an amorphous and crystalline citric acid mixture. Mechanical manipulation of the citric acid melt during processing induced crystallization foci, and the exotherm in the bulk-prepared citric acid melt thermograms was due to crystallization. The endotherm was crystallized solid melting.

The bulk-prepared citric acid melt crystallization rate can be studied by monitoring the rate of change in area under the exothermic peak. The smaller the area, the more crystalline is the material. Although the areas under the peak differed among batches of bulk citric acid melt because of stress variability, similar trends were observed (Fig. 3). Little area change was observed in melt samples stored at 4°. At 23°, the area gradually decreased with time. At 37°, there was a rapid initial decrease followed by a slower rate of change. The abrupt change in slope corresponded to the disappearance of the glass transition. An initial rapid crystallization was followed by a slower secondary crystallization. Possibly, crystallites formed in the primary process were regrouped and a more perfect crystalline state was formed.

The benzoic acid effect on the citric acid glass T_g is shown in Fig. 4. Benzoic acid up to 20% (w/w) decreased the T_g. Above this concentration, the limit of benzoic acid incorporation into citric acid glass was reached, and no further T_g reduction was observed. Excess benzoic acid crystallized upon cooling of the melt, forming a macrocrystal dispersion in the citric acid–benzoic acid glass matrix and disrupting the glass system. Figure 5 shows thermograms of a benzoic acid–citric acid (1:4) mixture and its rapidly cooled melt. The glass system was thermally unstable; the components crystallized and then melted as the temperature was increased.

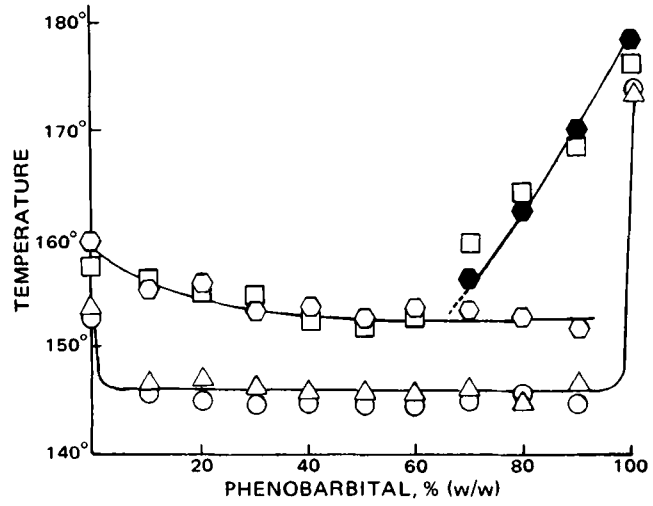

Figure 7—*Phenobarbital–citric acid binary system melting temperatures determined from physical mixtures. Key (differential scanning calorimetry): △, initial endothermic temperature deviation in the thermogram baseline; ○, citric acid endothermic peak temperature; and ●, phenobarbital endothermic peak temperature. Key (capillary tube method): ○, melting onset temperature; and □, complete physical mixture fusion temperature.*

The use of the melting characteristics of pharmaceutical mixtures to detect possible interactions between materials has been demonstrated (18, 19). Figure 6 shows the melting data for the benzoic acid–citric acid system. The results obtained by the capillary tube method were in good agreement with the melting onset and the complete fusion temperatures determined with the differential scanning calorimeter. Little interaction between benzoic acid and citric acid was indicated since the physical mixture melting temperatures showed little change when compared to the melting temperatures of the pure materials. The slight depression of the citric acid melting temperature in the mixtures was probably due to the presence of molten benzoic acid.

Phenobarbital also formed a glass on rapid cooling of its melt with a T_g of 41.9°. The thermograms (Fig. 1) showed an exotherm, onset at 90°, on continued heating above the T_g followed by an endotherm. The exotherm was attributed to crystallization, and the endotherm was attributed to crystallized phenobarbital melting. The phenobarbital crystallized into either of two polymorphic forms. A previous study of phenobarbital polymorphism showed similar results (9).

In polymeric systems, the mixture T_g of two miscible glasses can be estimated by (20):

$$\frac{1}{T_g} = \frac{W_a}{T_{ga}} + \frac{W_b}{T_{gb}} \qquad \text{(Eq. 1)}$$

where T_{ga} and T_{gb} are the glass transition temperatures of the two components of the mixture in degrees Kelvin, and W_a and W_b are their respective weight fractions. For the phenobarbital–citric acid glass system, the observed T_g values were lower than those predicted (Fig. 4), probably because the bonding between citric acid and phenobarbital molecules is less than that between either citric acid or phenobarbital molecules alone.

A thermogram of 1:1 bulk-prepared phenobarbital–citric acid melt (Fig. 5) resembled that for bulk-prepared citric acid melt (Fig. 1). As in that case, the exotherm was attributed to crystallization, and the endotherm was attributed to melting of the crystallized solid. No difference from the *in situ* T_g was observed.

The phenobarbital–citric acid mixture melting temperatures are shown in Fig. 7. As with the benzoic acid–citric acid system, the results obtained by the capillary tube method were in good agreement with those obtained using the differential scanning calorimeter. At compositions below 70% (w/w) phenobarbital, a single sharp endotherm was observed by differential scanning calorimetry. At 70% (w/w) phenobarbital and above, two endothermic peaks were observed in the thermogram. This finding indicates that the phenobarbital was dissolving in the molten citric acid. A second endothermic peak became visible in the thermogram only when the phenobarbital reached its solubility limit in the molten citric acid. The appearance of the second endothermic peak corresponded with the instability of the ≥70% (w/w) phenobarbital glass systems to tempera-

tures above the T_g. Thermograms of these systems showed an exotherm followed by an endotherm, indicating crystallization followed by melting.

Citric acid and phenobarbital seem to form glass solutions rather than dispersions as in the case of citric acid and benzoic acid. Visual examination of the melts of citric acid and phenobarbital mixtures in a capillary tube, under a hot-stage microscope[11], and during bulk preparation showed them to be a single homogeneous phase.

The *in situ* procedure is useful for screening potential glass-forming materials and glass-forming drug–carrier combinations. Physical mixture and solidified melt thermograms and the T_g data indicate whether a drug–carrier mixture will form a glass solution or suspension and what optimum drug–carrier combination can be obtained. In systems that exhibit mechanical and/or thermal instability or that have a T_g below or only slightly above room temperature, the material would not be rigid enough to withstand normal handling operations and could be eliminated from further investigation.

Of particular interest would be the preparation of glass systems containing large quantities of drugs. For example, it might be possible to stabilize the glassy state of a glass-forming drug by mixing it with a small amount of a compatible inert glassy carrier. This procedure would permit the use of less carrier, thereby reducing bulk volume, and aid in the formulation of glass dispersion systems into solid dosage forms.

REFERENCES

(1) J. H. Gibbs and E. A. DiMarzio, *J. Chem. Phys.*, **28**, 373 (1958).

(2) P. Chaudhari and D. Trunbull, *Science*, **199**, 11 (1978).

(3) W. L. Chiou and S. Riegelman, *J. Pharm. Sci.*, **58**, 1505 (1969).

(4) *Ibid.*, **60**, 1281 (1971).

(5) J. W. McGinty, D. D. Maness, and G. J. Yakatan, *Drug Dev. Commun.*, **1**, 369 (1974–1975).

(6) M. P. Summers and R. P. Enever, *J. Pharm. Pharmacol.*, **26**, 83P (1974).

(7) M. P. Summers and R. P. Enever, *J. Pharm. Sci.*, **65**, 1613 (1976).

(8) *Ibid.*, **66**, 825 (1977).

(9) R. J. Mesley, R. L. Clements, B. Flaherty, and K. Goodhead, *J. Pharm. Pharmacol.*, **20**, 329 (1968).

(10) G. S. Parks and H. M. Huffman, *J. Phys. Chem.*, **31**, 1842 (1927).

(11) G. S. Parks, H. M. Huffman, and F. R. Cattoir, *ibid.*, **32**, 1366 (1928).

(12) G. O. Jones, "Glass," Wiley, New York, N.Y., 1958, p. 46.

(13) C. E. Nordman, A. S. Weldon, and A. L. Patterson, *Acta Crystallogr.*, **13**, 418 (1960).

(14) D. Fox, M. M. Labes, and A. Weissberger, "Physics and Chemistry of the Organic Solid State," Interscience, New York, N.Y., 1963, p. 572.

(15) W. W. Wendlandt and J. A. Hoiberg, *Anal. Chim. Acta*, **28**, 506 (1963).

(16) M. T. Saibova, V. K. Bukins, and E. L. Abramova, *Usb. Khim. Zh.*, **9**, 54 (1965); through *Chem. Abstr.*, **63**, 16197c (1965).

(17) L. E. Nielson, "Mechanical Properties of Polymers and Composites," vol. 1, Dekker, New York, N.Y., 1974, p. 215.

(18) J. K. Guillory, S. C. Hwang, and J. L. Lach, *J. Pharm. Sci.*, **58**, 301 (1969).

(19) W. L. Chiou and S. Niazi, *ibid.*, **60**, 1333 (1971).

(20) L. E. Nielson, "Mechanical Properties of Polymers and Composites," vol. 1, Dekker, New York, N.Y., 1974, p. 25.

[11] Leitz Orthblux microscope equipped with a model 350 heating stage, E. Leitz, Inc., New York, N.Y.

ACKNOWLEDGMENTS

Appreciation is expressed to the Gillette Co. of Boston, Mass., for a fellowship to R. J. Timko.

Paired-Ion Reversed-Phase High-Pressure Liquid Chromatographic Assay of Pentobarbital–Pyrilamine Suppositories

JOHN H. BLOCK ˣ, HOWARD L. LEVINE, and JAMES W. AYRES

Received July 17, 1978, from the *School of Pharmacy, Oregon State University, Corvallis, OR 97331.* Accepted for publication October 23, 1978.

Abstract □ The assay of suppositories containing pentobarbital and/or pyrilamine in a water-soluble polyethylene glycol base by high-pressure liquid chromatography is described. No extraction is required. The suppository is dissolved in the mobile phase. This solution is diluted with an internal standard stock solution containing phenobarbital. Chromatographic conditions include a C_{18} bonded microporous silica column and a mobile phase of 65% 4×10^{-3} *M* *n*-butyl sodium sulfonate in 1% acetic acid and 35% acetonitrile. The procedure using commercial products gave results comparable to those obtained by GLC.

Keyphrases □ Pentobarbital–pyrilamine suppositories—analysis, paired-ion reversed-phase high-pressure liquid chromatography, compared to GLC □ Suppositories, pentobarbital–pyrilamine—analysis, paired-ion reversed-phase high-pressure liquid chromatography, compared to GLC □ High-pressure liquid chromatography—analysis, pentobarbital–pyrilamine suppositories, compared to GLC

A pharmacokinetic study involving suppositories containing pentobarbital and/or pyrilamine maleate required in-house manufacturing. This need led to the development of an assay for accurately determining the drug content and uniformity in each lot of suppositories. The rapid high-pressure liquid chromatographic (HPLC) procedure was verified by GLC using commercial products.

Several GLC assays for barbiturates (1–3) and antihistamines (4–7) have been published. In each, appropriate extraction procedures must be carried out to separate the acidic barbiturate from the basic antihistamine. Because the suppositories were made using a water-soluble polyethylene glycol base, reversed-phase HPLC seemed to be the logical approach.

EXPERIMENTAL

Reagents and Chemicals—Authentic samples of pentobarbital sodium[1], pyrilamine maleate[1], phenobarbital[2], propylparaben[1], and

[1] City Chemical.
[2] Mallinckrodt.

0022-3549/79/0500-0605$01.00/0

© 1979, American Pharmaceutical Association

tures above the T_g. Thermograms of these systems showed an exotherm followed by an endotherm, indicating crystallization followed by melting.

Citric acid and phenobarbital seem to form glass solutions rather than dispersions as in the case of citric acid and benzoic acid. Visual examination of the melts of citric acid and phenobarbital mixtures in a capillary tube, under a hot-stage microscope[11], and during bulk preparation showed them to be a single homogeneous phase.

The *in situ* procedure is useful for screening potential glass-forming materials and glass-forming drug–carrier combinations. Physical mixture and solidified melt thermograms and the T_g data indicate whether a drug–carrier mixture will form a glass solution or suspension and what optimum drug–carrier combination can be obtained. In systems that exhibit mechanical and/or thermal instability or that have a T_g below or only slightly above room temperature, the material would not be rigid enough to withstand normal handling operations and could be eliminated from further investigation.

Of particular interest would be the preparation of glass systems containing large quantities of drugs. For example, it might be possible to stabilize the glassy state of a glass-forming drug by mixing it with a small amount of a compatible inert glassy carrier. This procedure would permit the use of less carrier, thereby reducing bulk volume, and aid in the formulation of glass dispersion systems into solid dosage forms.

REFERENCES

(1) J. H. Gibbs and E. A. DiMarzio, *J. Chem. Phys.*, **28**, 373 (1958).

(2) P. Chaudhari and D. Trunbull, *Science*, **199**, 11 (1978).

(3) W. L. Chiou and S. Riegelman, *J. Pharm. Sci.*, **58**, 1505 (1969).

(4) *Ibid.*, **60**, 1281 (1971).

(5) J. W. McGinty, D. D. Maness, and G. J. Yakatan, *Drug Dev. Commun.*, **1**, 369 (1974–1975).

(6) M. P. Summers and R. P. Enever, *J. Pharm. Pharmacol.*, **26**, 83P (1974).

(7) M. P. Summers and R. P. Enever, *J. Pharm. Sci.*, **65**, 1613 (1976).

(8) *Ibid.*, **66**, 825 (1977).

(9) R. J. Mesley, R. L. Clements, B. Flaherty, and K. Goodhead, *J. Pharm. Pharmacol.*, **20**, 329 (1968).

(10) G. S. Parks and H. M. Huffman, *J. Phys. Chem.*, **31**, 1842 (1927).

(11) G. S. Parks, H. M. Huffman, and F. R. Cattoir, *ibid.*, **32**, 1366 (1928).

(12) G. O. Jones, "Glass," Wiley, New York, N.Y., 1958, p. 46.

(13) C. E. Nordman, A. S. Weldon, and A. L. Patterson, *Acta Crystallogr.*, **13**, 418 (1960).

(14) D. Fox, M. M. Labes, and A. Weissberger, "Physics and Chemistry of the Organic Solid State," Interscience, New York, N.Y., 1963, p. 572.

(15) W. W. Wendlandt and J. A. Hoiberg, *Anal. Chim. Acta*, **28**, 506 (1963).

(16) M. T. Saibova, V. K. Bukins, and E. L. Abramova, *Usb. Khim. Zh.*, **9**, 54 (1965); through *Chem. Abstr.*, **63**, 16197c (1965).

(17) L. E. Nielson, "Mechanical Properties of Polymers and Composites," vol. 1, Dekker, New York, N.Y., 1974, p. 215.

(18) J. K. Guillory, S. C. Hwang, and J. L. Lach, *J. Pharm. Sci.*, **58**, 301 (1969).

(19) W. L. Chiou and S. Niazi, *ibid.*, **60**, 1333 (1971).

(20) L. E. Nielson, "Mechanical Properties of Polymers and Composites," vol. 1, Dekker, New York, N.Y., 1974, p. 25.

[11] Leitz Orthblux microscope equipped with a model 350 heating stage, E. Leitz, Inc., New York, N.Y.

ACKNOWLEDGMENTS

Appreciation is expressed to the Gillette Co. of Boston, Mass., for a fellowship to R. J. Timko.

Paired-Ion Reversed-Phase High-Pressure Liquid Chromatographic Assay of Pentobarbital–Pyrilamine Suppositories

JOHN H. BLOCK ˣ, HOWARD L. LEVINE, and JAMES W. AYRES

Received July 17, 1978, from the *School of Pharmacy, Oregon State University, Corvallis, OR 97331.* Accepted for publication October 23, 1978.

Abstract □ The assay of suppositories containing pentobarbital and/or pyrilamine in a water-soluble polyethylene glycol base by high-pressure liquid chromatography is described. No extraction is required. The suppository is dissolved in the mobile phase. This solution is diluted with an internal standard stock solution containing phenobarbital. Chromatographic conditions include a C_{18} bonded microporous silica column and a mobile phase of 65% 4×10^{-3} *M* *n*-butyl sodium sulfonate in 1% acetic acid and 35% acetonitrile. The procedure using commercial products gave results comparable to those obtained by GLC.

Keyphrases □ Pentobarbital–pyrilamine suppositories—analysis, paired-ion reversed-phase high-pressure liquid chromatography, compared to GLC □ Suppositories, pentobarbital–pyrilamine—analysis, paired-ion reversed-phase high-pressure liquid chromatography, compared to GLC □ High-pressure liquid chromatography—analysis, pentobarbital–pyrilamine suppositories, compared to GLC

A pharmacokinetic study involving suppositories containing pentobarbital and/or pyrilamine maleate required in-house manufacturing. This need led to the development of an assay for accurately determining the drug content and uniformity in each lot of suppositories. The rapid high-pressure liquid chromatographic (HPLC) procedure was verified by GLC using commercial products.

Several GLC assays for barbiturates (1–3) and antihistamines (4–7) have been published. In each, appropriate extraction procedures must be carried out to separate the acidic barbiturate from the basic antihistamine. Because the suppositories were made using a water-soluble polyethylene glycol base, reversed-phase HPLC seemed to be the logical approach.

EXPERIMENTAL

Reagents and Chemicals—Authentic samples of pentobarbital sodium[1], pyrilamine maleate[1], phenobarbital[2], propylparaben[1], and

[1] City Chemical.
[2] Mallinckrodt.

0022-3549/79/0500-0605$01.00/0

© 1979, American Pharmaceutical Association

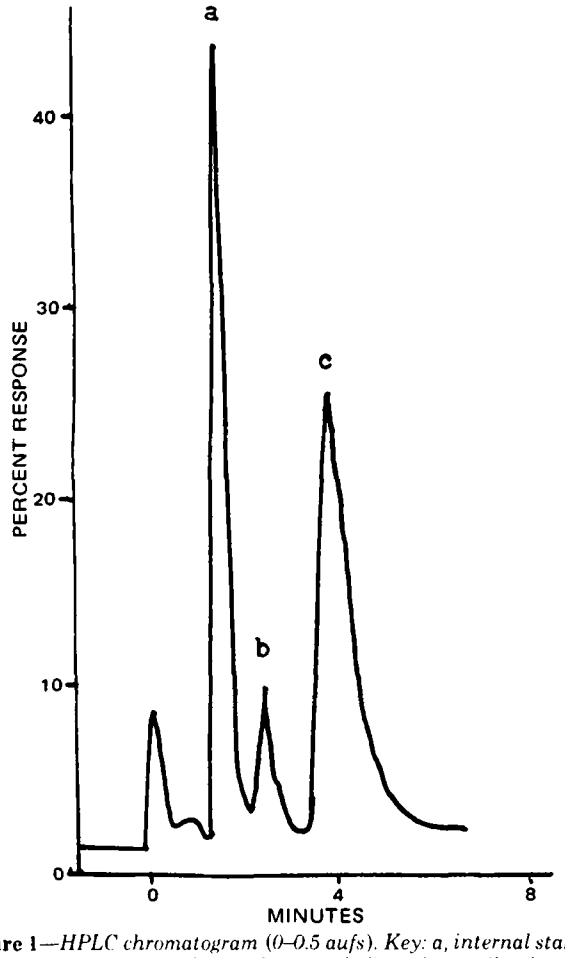

Figure 1—*HPLC chromatogram (0–0.5 aufs). Key: a, internal standard (phenobarbital); b, pentobarbital (3.5 mg/ml); and c, pyrilamine (0.972 mg/ml).*

chlorpheniramine maleate[3] were used. Reagent grade solvents were used as received. *n*-Butyl sodium sulfonate[4] was used as the anion that paired with pyrilamine. Commercial suppositories containing pentobarbital and pyrilamine maleate were purchased from local pharmacies.

HPLC Conditions—The mobile phase consisted of two parts. Solution A consisted of 1% (v/v) acetic acid and 4×10^{-3} *M* *n*-butyl sodium sulfonate (640 mg/liter). Solution B was acetonitrile. Each solution was degassed by stirring under a vacuum. They were then mixed in the ratio of 65A:35B by a solvent-flow programmer[5].

A liquid chromatograph was equipped with two constant-flow pumps[6], an on-stream injector[7], a variable-wavelength spectrophotometer[8], a 254-nm dual-pen recorder[9], and a 25-cm column packed with 10-μm porous silica chemically bonded with octadecylsilane[10]. The flow rate was 2.0 ml/min. Phenobarbital was the internal standard. An injection volume of 10 μl was used for all assays.

Each product was analyzed three times, and each analysis was done in triplicate. The spectrophotometer was set at 254 nm.

GLC Conditions—A gas chromatograph was equipped with a flame-ionization detector[11] and a 180-cm, 2-mm i.d., 6-mm o.d. U-shaped column packed with 3% phenylmethyl silicone on a silane-treated 100–120-mesh support[12]. The oven temperatures were 175 and 220° for pentobarbital and pyrilamine, respectively. For both drugs, the settings were: flash heater, 280°; detector, 310°; nitrogen carrier gas, 35 ml/min; hydrogen, 60 ml/min; and air, 400 ml/min.

[3] Amend Drug and Chemical Co.
[4] Eastman Kodak Co.
[5] Waters Associates model 660.
[6] Waters Associates model ALC 201/202 with M-6000 pumps.
[7] Waters Associates model U-6K.
[8] Varian Technicon model 635 LC.
[9] Soltec.
[10] Waters Associates μBondapak C_{18}.
[11] Hewlett-Packard model 402B.
[12] Commercially coated OV-17 on Gas Chrom Q, Applied Science Laboratories.

A 5-μl injection volume was used for all assays. All injections were made in triplicate. Each product was analyzed three times.

HPLC Stock Solutions—*Phenobarbital Internal Standard Solution*—Phenobarbital (2.200 g) was dissolved in 500 ml of warmed mobile phase. The solute remained in solution at room temperature.

Pyrilamine Stock Solution—Pyrilamine maleate, 205 mg, was dissolved in 100 ml of the mobile phase.

Pentobarbital Stock Solution—Pentobarbital sodium was dissolved in distilled water, acidified with 10% (v/v) HCl, extracted two or three times with chloroform, evaporated to dryness, and recrystallized from hot water. Then 0.700 g was dissolved in 100 ml of mobile phase.

GLC Stock Solution—Propylparaben, 400 mg, and chlorpheniramine maleate, 160 mg, were dissolved in 40 ml of ethanol and brought to 100 ml with distilled water. This stock solution was diluted 1:10 with distilled water.

GLC Standard Solutions—A separate standard solution was prepared for each suppository strength by dissolving the appropriate amount of each drug in ~10 ml of ethanol and bringing to 50 ml with distilled water. Each standard solution contained both pentobarbital and pyrilamine maleate in amounts equivalent to labeled amounts.

HPLC Procedure—*Standard Curve*—The stock solutions for each drug were diluted in the following manner. Solution 1 was prepared by diluting each stock solution 1:1 with the internal standard solution to yield a 1:2 dilution. For Solution 2, each stock solution was diluted 1:1 with mobile phase and then this new solution was diluted 1:1 with the internal standard to yield a 1:4 dilution. Solution 3 was made by diluting each stock solution 1:4 with mobile phase and then diluting this solution 1:1 with the internal standard, yielding a 1:8 dilution.

Each of the three standard solutions was prepared in triplicate, and 10 μl of each solution was injected on the column.

Suppositories—Commercially available suppositories containing 50 mg of pyrilamine maleate and 100 mg of pentobarbital were dissolved by shaking a suppository and about 30 ml of mobile phase in a 50-ml volumetric flask for 30 min. The suppositories containing lesser amounts of pentobarbital were dissolved by shaking a suppository and about 15 ml of mobile phase in a 25-ml volumetric flask for 30 min. Both solutions were brought to volume with additional mobile phase. Each resulting

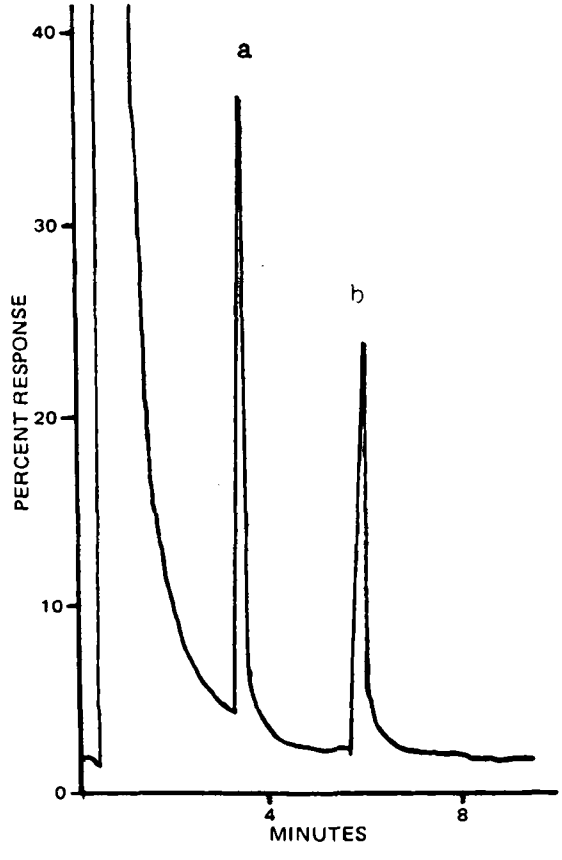

Figure 2—*GLC chromatogram (2.5×10^{-10} amps full scale). Key: a, internal standard (propylparaben); and b, pentobarbital sodium.*

Table I—GLC and HPLC Analyses of Commercial Samples

Suppository	Label, mg	Found by GLC[a], mg	Found by HPLC[a], mg	CV[b], %
Pentobarbital	30	29.21 (28.28–30.28)	28.96 (27.66–30.75)	3.04
Pyrilamine	25	24.05 (23.01–25.04)	24.10 (23.12–24.96)	2.25
Pentobarbital	45	43.79 (42.56–43.35)	44.21 (42.99–45.24)	1.81
Pyrilamine	50	48.32 (47.44–49.44)	48.38 (47.24–49.69)	1.65
Pentobarbital	100	99.47 (97.80–101.26)	96.22 (94.43–98.35)	1.64
Pyrilamine	50	47.20 (46.09–48.06)	47.48 (46.41–48.70)	1.73

[a] Average of nine injections (range). [b] Percent coefficient of variation = (*SD*/mean) × 100.

suppository stock solution was diluted 1:1 with internal standard stock solution and injected.

GLC Procedure—A suppository was placed in a 50-ml volumetric flask and dissolved in distilled water by shaking. The assay preparation for pentobarbital consisted of 2.0 ml of the suppository solution and 2.0 ml of the internal standard solution, both of which were placed in a 10-ml screw-capped vial. The pentobarbital and its propylparaben internal standard were extracted by adding 2 drops of concentrated hydrochloric acid and 2 ml of ether and shaking for 5 min. After the layers separated, 5 μl of the ether layer was injected.

The assay preparation for pyrilamine was prepared by placing a fresh 2.0-ml aliquot of the solution containing the suppository and 2.0 ml of the internal standard solution into a 10-ml screw-capped vial. A drop of phenolphthalein test solution was added, and the solution was made basic by the dropwise addition of 10 *N* NaOH. Ether, 2 ml, was added, and the mixture was shaken for 5 min. After the layers separated, 5 μl of the ether layer was injected.

These extraction procedures were repeated using 2.0-ml quantities of the stock solution corresponding to the labeled content of the suppository to be analyzed.

HPLC Calculations—A standard curve was constructed for each drug.

GLC Calculations—The following formula was used:

$$\text{mg of drug/suppository} = (0.05C)\left(\frac{b}{a}\right)\left(\frac{A}{B}\right) \qquad \text{(Eq. 1)}$$

where C = concentration (micrograms per milliliter) of drug in the standard preparation, A = peak height of the internal standard in the standard preparation, B = peak height of the drug in the standard preparation, a = peak height of the internal standard in the assay preparation, and b = peak height of the drug in the assay preparation.

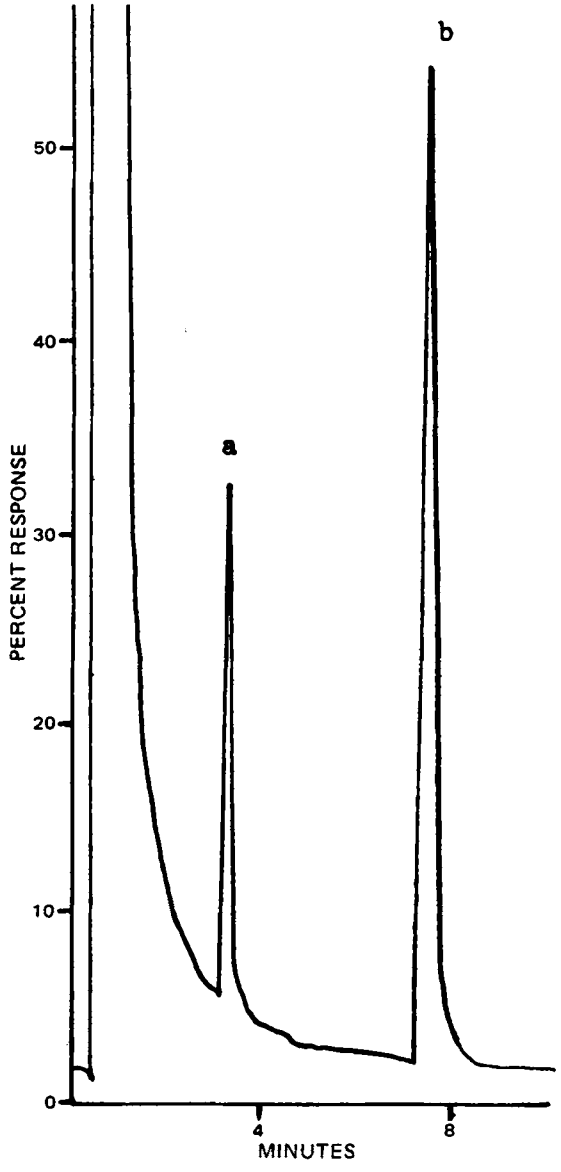

Figure 3—*GLC chromatogram (2.5 × 10⁻¹⁰ amps full scale). Key: a, internal standard (chlorpheniramine maleate); and b, pyrilamine maleate.*

RESULTS AND DISCUSSION

The objective of this study was to develop a rapid procedure for the quantitative analysis of suppositories containing pentobarbital and/or pyrilamine maleate. The described HPLC procedure eliminates the extraction steps required for GLC. The water-soluble suppository base and dyes are eluted from the reversed-phase column with the solvent front and, therefore, do not interfere with the assay. In the concentration range studied, the standard curves are straight lines: r = 1.000 for both drugs; coefficient of variation = 2.76% for pyrilamine maleate and 3.64% for pentobarbital.

Figure 1 shows a typical HPLC tracing, and Figs. 2 and 3 show GLC tracings. Table I contains a comparison of GLC and HPLC results. The only significant difference is ease of sample handling. With this particular type of suppository base, HPLC is superior since no extractions are required.

The use of the paired-ion technique produced the best separation. Initially, an acid-buffered mobile phase was tried. Good retention times were obtained for phenobarbital, but the protonated pyrilamine was eluted with the solvent front. The results were worse with a basic mobile phase. The charged barbiturate was eluted with the solvent front and pyrilamine, while having an acceptable retention time, showed considerable tailing. This procedure does not appear to affect the column since this same column was used for several months after completion of this project.

It is obvious from the chromatogram shown in Fig. 1 that pentobarbital has low sensitivity relative to the antihistamine. At the same time, pyrilamine has a very good UV-sensitive chromophore. Although a variable-wavelength detector was utilized, the 254-nm wavelength common to most fixed-wavelength detectors was selected to see if the procedure could be adapted to most instruments. Nevertheless, a wavelength closer to the end absorption of unionized pentobarbital (230 nm and lower) or perhaps a refractive index detector would produce a more esthetically satisfying chromatogram (8). An alternative procedure for obtaining a more sensitive response from pentobarbital would be to utilize the recently described postionization technique whereby pH 10 borate buffer is added to the column effluent before it enters the detector (9).

REFERENCES

(1) E. Brochmann-Hanssen, "Theory and Application of Gas Chromatography in Industry and Medicine," H. Kroman and S. R. Bender, Eds., Grune & Stratton, New York, N.Y., 1968, p. 132.

(2) J. L. Sibert and F. L. Fricke, *J. Assoc. Offic. Anal. Chem.*, **51**, 1326 (1968).

(3) H. W. Schultz and C. Paveenbampen, *J. Pharm. Sci.*, **62**, 1995 (1973).
(4) A. MacDonald, Jr., and R. T. Pflaum, *ibid.*, **52**, 816 (1963).
(5) *Ibid.*, **53**, 887 (1964).
(6) B. R. Rader, *ibid.*, **58**, 1535 (1969).
(7) T. J. Reiss, *J. Assoc. Offic. Anal. Chem.*, **53**, 609 (1970).
(8) "Pharmaceuticals: Ultraviolet Spectra R480-U," Sadtler Research Laboratories, Philadelphia, Pa., 1963.
(9) G. R. Clark and J. L. Chan, *Anal. Chem.*, **50**, 635 (1978).

ACKNOWLEDGMENTS

Presented at the Pharmaceutical Analysis and Control Section, APhA Academy of Pharmaceutical Sciences, Phoenix meeting, November 1977.

Supported by the General Research Fund administered by Oregon State University's Research Council.

The authors are grateful to Susan Strahl, Arnar-Stone Laboratories, Mount Prospect, Ill., for providing the GLC procedure.

Percutaneous Nitroglycerin Absorption in Rats

S. T. HORHOTA * and HO-LEUNG FUNG ×

Received June 16, 1978, from the *Department of Pharmaceutics, State University of New York at Buffalo, Amherst, NY 14260.* Accepted for publication October 24, 1978. *Present address: Pharmacy Research and Development Department, Ayerst Laboratories, Rouses Point, NY 12979.

Abstract □ Percutaneous nitroglycerin absorption was studied in shaved rats by monitoring unchanged plasma drug concentrations for up to 4 hr. Drug absorption from the neat liquid state or from an alcoholic solution was considerably poorer than that from a commercial ointment. This observation was unanticipated since the driving force for percutaneous drug absorption was assumed to be drug thermodynamics. Potential artifacts such as drug volatilization from the skin, reduction of surface area through droplet formation, and vehicle occlusion were investigated, but they did not appear to be responsible for the observed results. Two experimental aqueous nitroglycerin gels were prepared with polyethylene glycol 400. One gel contained just sufficient polyethylene glycol to solubilize the nitroglycerin; the other had excess polyethylene glycol to solubilize nitroglycerin far below saturation. Both gels gave extremely low plasma nitroglycerin levels. The composite data suggested that percutaneous nitroglycerin absorption is highly vehicle dependent and that this dependency cannot be explained by simple consideration of drug thermodynamic activity.

Keyphrases □ Absorption, percutaneous—nitroglycerin, various topical dosage forms, rats □ Nitroglycerin—percutaneous absorption, various topical dosage forms, rats □ Dosage forms, topical—nitroglycerin, percutaneous absorption, rats

Topical nitroglycerin ointments produce sustained and clinically beneficial hemodynamic responses in patients with various cardiovascular ailments. Application of a 2% nitroglycerin preparation on 150–230 cm^2 of skin surface reduced the frequency and severity of exercise-induced angina attacks (1, 2) and decreased heart workload and myocardial oxygen consumption (3).

Systemic availability is the primary goal of topical nitroglycerin application. However, there is little information about the physical and physiological factors influencing its percutaneous absorption. The relatively large clinical nitroglycerin ointment doses and the extensive surface area needed for therapeutic effect suggest that transdermal delivery of nitroglycerin, at present, is inefficient and that attempts to increase percutaneous nitroglycerin absorption may be worthwhile.

The purpose of this investigation was to examine various factors that may affect the rate and extent of topical nitroglycerin absorption. *In vivo* and *in vitro* models were used to gather data to form a rational basis for improving transdermal drug delivery. The relationship between thermodynamic activity and *in vivo* nitroglycerin absorption was examined.

BACKGROUND

The skin is one of the most impermeable tissues of the body. It functions as a barrier against attack by microorganisms, viruses, and many toxic chemicals. At the same time, it limits the loss of physiologically essential components, such as water. The extensive skin barrier properties have caused it to be regarded as a poor route for systemic drug administration. Recently, serious attempts have been made to fabricate devices for controlled, sustained delivery through the dermal route. A tape capable of delivering a constant rate of transdermal scopolamine for up to 3 days was described (4).

Several factors influence percutaneous drug absorption (5, 6) including drug permeability through the stratum corneum, the drug's physical–chemical properties, the vehicle in which the drug is incorporated, the drug's ionization state, the skin's hydration state, the skin's lipid content, and regional variations in skin properties. The quantitative relationship between drug transfer and several of these factors is (7):

$$dQ/dt = KC_vDA/T \qquad \text{(Eq. 1)}$$

where dQ/dt is the steady-state drug transfer rate across a skin barrier, K is the effective skin–vehicle drug partition coefficient, C_v is the drug concentration dissolved in the vehicle, D is the drug diffusivity through the barrier, A is the surface area of application of the vehicle, and T is the effective barrier thickness.

The model assumes that the skin represents a simple diffusional barrier to drug transfer. When the surface area of application, drug diffusivity through the skin, and barrier thickness are constant, the equation addresses the role of thermodynamics in determining percutaneous absorption rates. Specifically, absorption will be enhanced from vehicles with a low affinity for the drug and in which the drug concentration approaches saturated solubility. Therefore, approaches toward optimizing drug delivery should maximize the drug's thermodynamic activity in the vehicle, as represented by the product term KC_v in Eq. 1. The validity of the thermodynamic relationship has been confirmed qualitatively (8, 9), and Eq. 1 has provided valuable guidance in the development of improved vehicles for topical application of new drug entities.

While the thermodynamic approach does include skin characteristics—*viz.*, D and T, in determining absorption rate, these parameters are usually difficult to measure as functions of vehicle changes. Therefore, they are often assumed to be independent of vehicle effects. This assumption is not always valid since topical formulations are known to affect these parameters (5, 6, 10). Vehicle-induced changes in these variables may be of sufficient magnitude to override the contribution of the thermodynamic term, KC_v. In such cases, thermodynamic considerations alone, although predictive for *in vitro* drug release, may not explain absorption differences in animals or humans.

0022-3549/79/0500-0608$01.00/0
© 1979, American Pharmaceutical Association

(3) H. W. Schultz and C. Paveenbampen, *J. Pharm. Sci.*, **62**, 1995 (1973).
(4) A. MacDonald, Jr., and R. T. Pflaum, *ibid.*, **52**, 816 (1963).
(5) *Ibid.*, **53**, 887 (1964).
(6) B. R. Rader, *ibid.*, **58**, 1535 (1969).
(7) T. J. Reiss, *J. Assoc. Offic. Anal. Chem.*, **53**, 609 (1970).
(8) "Pharmaceuticals: Ultraviolet Spectra R480-U," Sadtler Research Laboratories, Philadelphia, Pa., 1963.
(9) G. R. Clark and J. L. Chan, *Anal. Chem.*, **50**, 635 (1978).

ACKNOWLEDGMENTS

Presented at the Pharmaceutical Analysis and Control Section, APhA Academy of Pharmaceutical Sciences, Phoenix meeting, November 1977.

Supported by the General Research Fund administered by Oregon State University's Research Council.

The authors are grateful to Susan Strahl, Arnar-Stone Laboratories, Mount Prospect, Ill., for providing the GLC procedure.

Percutaneous Nitroglycerin Absorption in Rats

S. T. HORHOTA * and HO-LEUNG FUNG ×

Received June 16, 1978, from the *Department of Pharmaceutics, State University of New York at Buffalo, Amherst, NY 14260.* Accepted for publication October 24, 1978. *Present address: Pharmacy Research and Development Department, Ayerst Laboratories, Rouses Point, NY 12979.

Abstract □ Percutaneous nitroglycerin absorption was studied in shaved rats by monitoring unchanged plasma drug concentrations for up to 4 hr. Drug absorption from the neat liquid state or from an alcoholic solution was considerably poorer than that from a commercial ointment. This observation was unanticipated since the driving force for percutaneous drug absorption was assumed to be drug thermodynamics. Potential artifacts such as drug volatilization from the skin, reduction of surface area through droplet formation, and vehicle occlusion were investigated, but they did not appear to be responsible for the observed results. Two experimental aqueous nitroglycerin gels were prepared with polyethylene glycol 400. One gel contained just sufficient polyethylene glycol to solubilize the nitroglycerin; the other had excess polyethylene glycol to solubilize nitroglycerin far below saturation. Both gels gave extremely low plasma nitroglycerin levels. The composite data suggested that percutaneous nitroglycerin absorption is highly vehicle dependent and that this dependency cannot be explained by simple consideration of drug thermodynamic activity.

Keyphrases □ Absorption, percutaneous—nitroglycerin, various topical dosage forms, rats □ Nitroglycerin—percutaneous absorption, various topical dosage forms, rats □ Dosage forms, topical—nitroglycerin, percutaneous absorption, rats

Topical nitroglycerin ointments produce sustained and clinically beneficial hemodynamic responses in patients with various cardiovascular ailments. Application of a 2% nitroglycerin preparation on 150–230 cm^2 of skin surface reduced the frequency and severity of exercise-induced angina attacks (1, 2) and decreased heart workload and myocardial oxygen consumption (3).

Systemic availability is the primary goal of topical nitroglycerin application. However, there is little information about the physical and physiological factors influencing its percutaneous absorption. The relatively large clinical nitroglycerin ointment doses and the extensive surface area needed for therapeutic effect suggest that transdermal delivery of nitroglycerin, at present, is inefficient and that attempts to increase percutaneous nitroglycerin absorption may be worthwhile.

The purpose of this investigation was to examine various factors that may affect the rate and extent of topical nitroglycerin absorption. *In vivo* and *in vitro* models were used to gather data to form a rational basis for improving transdermal drug delivery. The relationship between thermodynamic activity and *in vivo* nitroglycerin absorption was examined.

BACKGROUND

The skin is one of the most impermeable tissues of the body. It functions as a barrier against attack by microorganisms, viruses, and many toxic chemicals. At the same time, it limits the loss of physiologically essential components, such as water. The extensive skin barrier properties have caused it to be regarded as a poor route for systemic drug administration. Recently, serious attempts have been made to fabricate devices for controlled, sustained delivery through the dermal route. A tape capable of delivering a constant rate of transdermal scopolamine for up to 3 days was described (4).

Several factors influence percutaneous drug absorption (5, 6) including drug permeability through the stratum corneum, the drug's physical–chemical properties, the vehicle in which the drug is incorporated, the drug's ionization state, the skin's hydration state, the skin's lipid content, and regional variations in skin properties. The quantitative relationship between drug transfer and several of these factors is (7):

$$dQ/dt = KC_vDA/T \qquad \text{(Eq. 1)}$$

where dQ/dt is the steady-state drug transfer rate across a skin barrier, K is the effective skin–vehicle drug partition coefficient, C_v is the drug concentration dissolved in the vehicle, D is the drug diffusivity through the barrier, A is the surface area of application of the vehicle, and T is the effective barrier thickness.

The model assumes that the skin represents a simple diffusional barrier to drug transfer. When the surface area of application, drug diffusivity through the skin, and barrier thickness are constant, the equation addresses the role of thermodynamics in determining percutaneous absorption rates. Specifically, absorption will be enhanced from vehicles with a low affinity for the drug and in which the drug concentration approaches saturated solubility. Therefore, approaches toward optimizing drug delivery should maximize the drug's thermodynamic activity in the vehicle, as represented by the product term KC_v in Eq. 1. The validity of the thermodynamic relationship has been confirmed qualitatively (8, 9), and Eq. 1 has provided valuable guidance in the development of improved vehicles for topical application of new drug entities.

While the thermodynamic approach does include skin characteristics—*viz.*, D and T, in determining absorption rate, these parameters are usually difficult to measure as functions of vehicle changes. Therefore, they are often assumed to be independent of vehicle effects. This assumption is not always valid since topical formulations are known to affect these parameters (5, 6, 10). Vehicle-induced changes in these variables may be of sufficient magnitude to override the contribution of the thermodynamic term, KC_v. In such cases, thermodynamic considerations alone, although predictive for *in vitro* drug release, may not explain absorption differences in animals or humans.

0022-3549/79/0500-0608$01.00/0
© 1979, American Pharmaceutical Association

Nitroglycerin is a liquid at room temperature. Absorption of pure drug applied to the skin would be uncomplicated by vehicle and/or particle dissolution effects. Unless a positive deviation from Raoult's law results when nitroglycerin is formulated in topical vehicles, the neat liquid state should give the maximal thermodynamic activity for drug penetration. This mode of application could serve as a convenient thermodynamic reference point for trials of experimental formulations.

In this study, *in vivo* nitroglycerin absorption from the neat liquid was compared to that from a clinical ointment[1]. The latter contains 2% nitroglycerin formulated in an oleaginous vehicle. Because of the favorable solubility of nitroglycerin in nonpolar solvents, a strict interpretation of Eq. 1 would suggest reduced nitroglycerin absorption from the ointment when compared to the neat state. This hypothesis was tested.

Followup experiments explored other factors, *e.g.*, evaporative loss and occlusion, that may influence nitroglycerin absorption. Aqueous polymer gels reflecting widely divergent thermodynamic activities of nitroglycerin, as estimated from partitioning and solubility data, were also prepared. The *in vitro* release and *in vivo* absorption of nitroglycerin from these formulations were compared to those of the ointment. The importance of thermodynamic considerations in optimizing transdermal nitroglycerin delivery was evaluated.

EXPERIMENTAL

Materials—All reagents were analytical grade unless otherwise noted.

Isolation and Assay of Nitroglycerin Raw Material—Nitroglycerin lactose triturate[2] (10% w/w) was packed as a column and eluted with anhydrous ether[3]. The solvent was evaporated from the eluate under a stream of dry compressed air for 6–8 hr. Nitroglycerin was recovered as a liquid, and its purity was determined by the USP XIX (11) procedure or by GLC (12).

Partitioning of Nitroglycerin between Isooctane and Polyethylene Glycol 400–Water—Solutions containing varying concentrations of polyethylene glycol 400 in distilled water were equilibrated with an equal volume of isooctane[4] containing 2.60 μg of nitroglycerin/ml. The mixtures were rotated end-over-end for 24 hr in a 20 ± 0.5° water bath. Duplicate samples were prepared for each composition. After centrifugation, aliquots of the two phases were diluted with absolute methanol and assayed by the kinetic procedure (13, 14).

In the concentrations used, polyethylene glycol did not affect the calibration curve in this kinetic assay. With 100% polyethylene glycol 400, nitroglycerin was overwhelmingly distributed into the polyethylene glycol phase. Therefore, assay of the organic nitrate in the isooctane phase was conducted by GLC.

***In Vitro* Nitroglycerin Release from Topical Preparations**—Aqueous polymer gels containing 2% nitroglycerin were prepared by dissolving raw nitroglycerin (96% purity) into polyethylene glycol–water solutions with stirring. Microcrystalline cellulose[5] (~29% w/w) was added to gel these solutions. All blends were assayed and used within 24 hr of preparation.

A modification of the *in vitro* release model described by Poulsen *et al.* (8) was used. The formulation was introduced into a tared 60-mm diameter × 15-mm petri dish cover[6], leveled to the top edge with a microscope slide, and weighed accurately. The cover was lowered into a 250-ml beaker, which was then placed in a 20 ± 0.5° water bath. A three-blade propeller-stirrer, 27 mm in radius, was positioned 1.5 cm above the test material surface. A variable-speed motor drive[7] was set for 10 rpm. Isopropyl myristate[8] (100.0 ml) previously equilibrated at 20° was added with care over the formulation. Samples of isopropyl myristate (1.0 ml) were taken at specified intervals, and the volume was replaced by fresh solvent equilibrated at the same temperature.

The nitroglycerin concentration in the isopropyl myristate receptor phase was determined by GLC after appropriate dilution with hexane. The total amount of drug released into the medium at each point was corrected for sampling. The area under the percent nitroglycerin released *versus* time curve (0–60 min) was calculated by the trapezoidal rule.

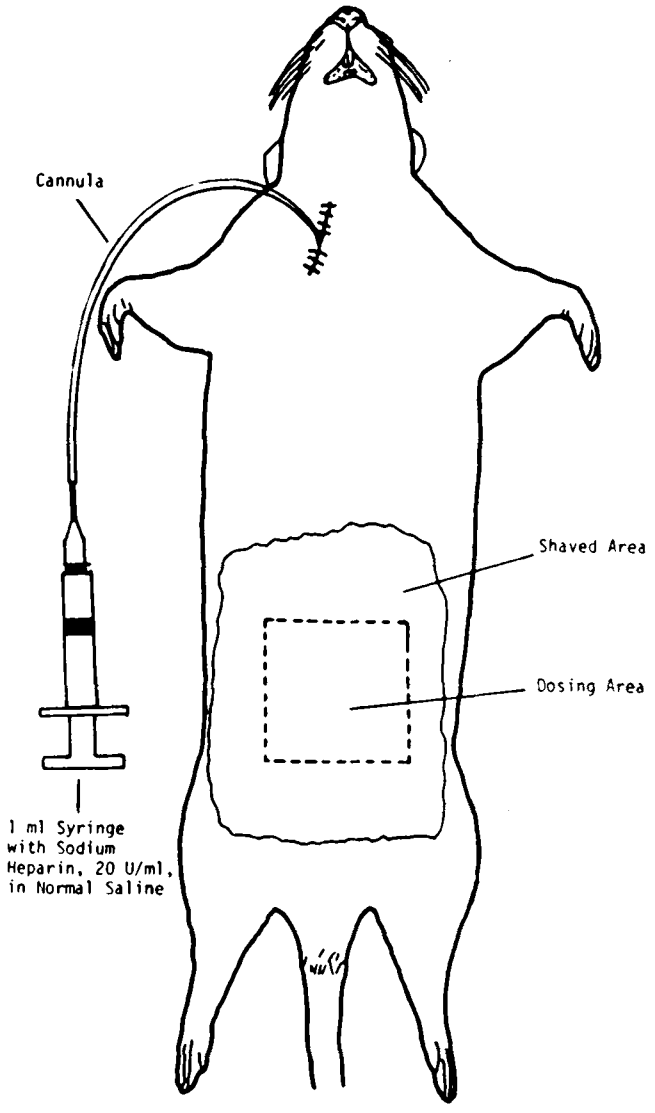

Figure 1—*Schematic representation of animal preparation and abdominal dosing area used in topical absorption studies.*

***In Vivo* Absorption Studies**—An abdominal dosing site (Fig. 1) on male Sprague–Dawley rats[9], 280–390 g, was prepared as described previously (15). The following dosage forms were investigated at 20 mg/kg: A, 2% nitroglycerin ointment[1]; B, 6.9% nitroglycerin solution in alcohol; C, neat nitroglycerin, isolated by evaporating a known volume of the alcoholic solution on a microscope slide and uniformly transferring the material to the dosing area; D, occlusion of the dosing site with polytef tape[10] 1 hr after application of the alcoholic solution; and E, 2% nitroglycerin experimental formulations, described previously. The area under the plasma concentration–time curve was evaluated from 0 to 4 hr after dosing (AUC_{0-4}) using the trapezoidal rule.

Nitroglycerin Recovery from Tissue Sections—Rat abdominal tissue sections from Treatments B and C were excised at the end of the experiments and minced. These tissue preparations were shaken with 25.0 ml of isomeric hexanes for 1 hr and allowed to sit overnight at room temperature. Appropriate dilutions with hexanes produced concentrations of 50–150 ng of nitroglycerin/ml. The internal standard was added to a final concentration of 250 ng/ml, and nitroglycerin was assayed by GLC. The extraction efficiency for this procedure was determined by excising and treating skin sections immediately after nitroglycerin application. In two experiments, a mean recovery of 75.8% was obtained.

RESULTS AND DISCUSSION

Results from trials involving abdominal dosing of 18 animals, allocated

[1] Nitro-Bid Ointment, lot T4808, Marion Laboratories, Kansas City, MO 64137.
[2] SDM 17, lot D-17-H2, ICI Americas, Atlas Explosives Division, Tamaqua, PA 18252.
[3] Mallinckrodt, St. Louis, MO 63147.
[4] J. T. Baker Chemical Co., Phillipsburg, NJ 08865.
[5] Avicel PH-105, FMC Corp., Marcus Hook, PA 19061.
[6] Corning Glass 3160, supplied through VWR Scientific, Buffalo, N.Y.
[7] Model 4440, Cole Parmer, Chicago, IL 60648.
[8] Technical grade, Pfaltz & Bauer, Flushing, NY 11368.
[9] Blue Spruce Farms, Altamont, N.Y.
[10] Chemfluor Lab-Tape, Chemplast, Inc., Wayne, NJ 07470.

Table I—Comparison of Areas under the Plasma Nitroglycerin *versus* Time Curve (0–4 hr) after Different Treatments

	Treatment		
	Ointment	Solution	Neat
	252.1[a]	2.2	36.9
	200.1	49.3	43.2
	72.3	49.3	29.3
	121.6	31.0	24.6
	71.1	15.3	20.1
	88.6	17.0	55.7
Mean	134.3	27.3	35.0
SD	75.2	19.3	13.1
	$p < 0.01$	$p > 0.05$	
	$p < 0.02$		

[a] In ng-hr/ml.

randomly to three treatment groups, are shown in Fig. 2. The clinically used nitroglycerin ointment yielded average 30–40-ng/ml plasma levels within 1 hr, while neat and alcohol applications gave mean concentrations below 10 ng/ml. The wide standard error ranges (Fig. 2) indicate that there was a large degree of individual variability in percutaneous nitroglycerin absorption. Comparison of AUC_{0-4} is presented in Table I. Despite the observed variability, analyses of variance [Kruskall–Wallis rank method (16)] with multiple comparisons indicated the ointment treatment to be significantly different from both the neat ($p < 0.02$) and the alcohol ($p < 0.01$) administrations. The latter cases were statistically indistinguishable, suggesting that they represent equivalent topical dosing modes.

Both neat and alcohol solution treatments were studied because neat nitroglycerin represented a small volume of drug, which may have been subjected to significant transfer errors, while the alcohol solution represented a more manageable volume for uniform dosing, but the effect of the solvent on the skin could not be predetermined. The results show that the application appeared adequate in both cases and that the alcohol solvent did not significantly alter skin characteristics *vis-à-vis* nitroglycerin absorption.

The finding of reduced absorption from neat nitroglycerin was unanticipated from thermodynamic considerations of Eq. 1. Possible explanations include: (*a*) evaporative loss of neat drug from the absorption site, (*b*) alteration in skin permeability by an occlusion effect caused by the ointment, (*c*) artifactual reductions in total surface contact in the case of neat nitroglycerin, (*d*) positive deviations from Raoult's law (*i.e.*, increases in thermodynamic activity) due to a specific interaction between the drug and some vehicle component, and (*e*) nonspecific effects produced by certain components of the ointment vehicle that increase nitroglycerin penetration.

Experiments were carried out to assess each of these possible factors.

Nitroglycerin Loss from Absorption Site—The volatility of nitroglycerin sublingual tablets has been documented extensively (17–19). While the thermodynamic activity of nitroglycerin and, hence, its potential for absorption were expected to be maximized in the neat state,

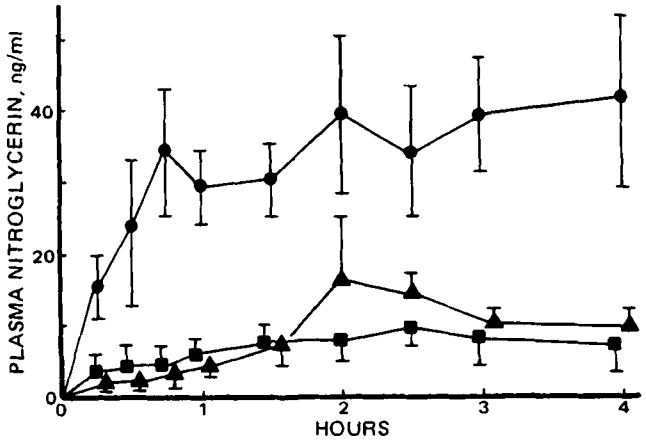

Figure 2—In vivo *absorption of nitroglycerin after topical application (20 mg/kg) to the abdominal skin surface of rats. Key:* ●, *2% nitroglycerin commercial ointment;* ■, *6.9% nitroglycerin alcoholic solution; and* ▲, *neat nitroglycerin. Each point represents the mean* (±SEM) *of six animals.*

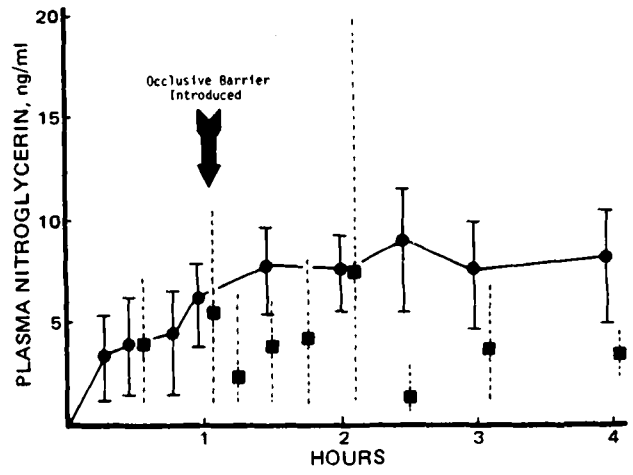

Figure 3—*Effect of polytef tape occlusion on topical absorption of nitroglycerin from alcoholic solution. Key:* ●, *no occlusion, bars indicate standard errors; and* ■, *occlusion with polytef tape after 1 hr. Each point represents the mean of three animals. Broken lines indicate experimental range.*

the energy balance would simultaneously favor nitroglycerin escape to the atmosphere. This phenomenon might lead to reduced absorption because of volatilization of drug from the dosing site.

To investigate this possibility, tissue sections representing the entire dosing area were excised after the 4-hr absorption experiments and the amount of nitroglycerin remaining was determined. An average of nearly 60% of the applied drug could be recovered from the surface skin sections (Table II). The unrecovered 40% of the dose might have been in the systemic circulation or still moving through the epidermal layers. Nevertheless, the evidence suggests that there was no extensive evaporative loss of drug at the absorption site after application of neat nitroglycerin or the alcoholic solution. Significant quantities of drug were still available for absorption at the dosing site, even at the end of the experimental period. This conclusion is supported by results from the occlusion experiment.

Effect of Skin Occlusion—Skin hydration is often considered to be the most crucial parameter affecting percutaneous absorption of chemical compounds (5). Increasing the water content of the stratum corneum has been shown to alter the rate and extent of transdermal drug passage (20). Oleaginous vehicles and occlusive dressings offer certain advantages by inhibiting transepidermal water loss. Thus, the petrolatum–lanolin ointment base possibly increased percutaneous nitroglycerin absorption primarily through an occlusive effect.

To test this hypothesis, an alcoholic solution of nitroglycerin was applied to the shaved abdominal surfaces of three rats. The dosing site remained exposed for the 1st hr during which blood samples were collected to establish control values for plasma nitroglycerin concentrations. At 1 hr, the area was covered with polytef tape and sampling was continued. Enhanced nitroglycerin absorption after this time point would suggest a positive influence of an occlusive effect. The results showed, however, that the plasma concentrations were unaffected by occlusion (Fig. 3). Thus, it is unlikely that occlusion was responsible for the greater absorption of nitroglycerin from the ointment preparation.

Polytef tape presents a barrier to water mass transfer (21), and preliminary studies demonstrated a resistance to nitroglycerin transfer. The polytef tape not only prevented water loss from the skin but should have retarded significant volatilization of nitroglycerin from the dosing site.

Table II—Percent Recovery [a] of Nitroglycerin from Rat Tissue Sections 4 hr after Abdominal Application of a 20-mg/kg Dose

Application[b]	Recovery, %
Neat	50.8
Neat	64.1
Neat	55.2
Neat	49.7
Alcohol solution	60.9
Alcohol solution	74.1
Mean	59.1

[a] Corrected for extraction. [b] Each listing represents an individual tissue section from separate animals.

Because there was no increase in plasma nitroglycerin levels after enclosure of the dosing site with polytef tape, evaporative drug loss after application of neat nitroglycerin and its alcoholic solution could not have been extensive.

Surface Area Considerations—As clearly stated in Eq. 1, the conditions required for testing the thermodynamic concept must include a constant surface area for drug application. The total abdominal dosing area was controlled at 9 cm^2 for all experiments. This region could, however, represent only an apparent dosing area if the interfacial tension between nitroglycerin and the skin was of sufficient magnitude to cause poor "wetting," reducing the actual contact area through droplet formation.

Gross examination of the skin after dosing showed nothing to suggest that uniform film formation had not taken place. Microscopic examination and photographic documentation proved difficult because of the low level of contrast between the deposited drug, a clear to slightly yellowish liquid, and the skin background. Attempts to visualize the drug on the skin using oil-soluble dyes or fluorescent markers were also inconclusive. Thus, within the visualization capability of the experiment, surface area artifacts arising from droplet formation from neat nitroglycerin appeared to be absent. This conclusion will be substantiated further by comparison of *in vivo* absorption of nitroglycerin from ointment and experimental gels.

Comparison of *In Vitro* Nitroglycerin Release between Experimental Gels and Ointment—Aqueous nitroglycerin solubility at 20° was determined to be 1.77 mg/ml, in close agreement with literature reports (22). Nitroglycerin partitioning between isooctane and polyethylene glycol 400–water combinations is shown in Fig. 4. Because of extensive nitroglycerin solubility in alcohols, the partition coefficients (oil-water) were reduced drastically in the presence of significant concentrations of polyethylene glycol 400. The observed partition coefficients and measured water solubility value were used to estimate nitroglycerin solubility in the different water-polyethylene glycol 400 mixtures (Fig. 4). This method of solubility estimation was used instead of the classical excess compound technique to avoid handling large quantities of pure nitroglycerin.

Gels were prepared using polyethylene glycol 400–water mixtures and microcrystalline cellulose. Simple mixing of components yielded pharmaceutically suitable preparations of uniform texture and acceptable viscosity. Preliminary experiments involving gels prepared with different concentrations of microcrystalline cellulose showed that this material did not inhibit nitroglycerin diffusion out of the gels. This finding suggests that drug binding or adsorption to microcrystalline cellulose is insignificant in the presence of polyethylene glycol 400.

From the calculated solubility profile, it was determined that a 2% nitroglycerin gel could be prepared near saturated solubility using 70% polyethylene glycol 400 in water (Gel A). This formulation presented nitroglycerin at a near maximal thermodynamic state when compared to similar formulations in which 2% nitroglycerin did not represent saturated solubility. In 100% polyethylene glycol 400, the estimated nitroglycerin solubility was approximately 150-fold greater than in 70% polyethylene glycol 400. Thus, a 2% nitroglycerin gel prepared with 100% polyethylene glycol 400 (with microcrystalline cellulose added for viscosity) (Gel B) presented nitroglycerin at a 150-fold reduction in thermodynamic activity compared to that produced by Gel A.

Estimation of nitroglycerin thermodynamic activity in the ointment could not be made because of solubility problems. Information on the composition of this ointment was not available, and the saturated solubility of nitroglycerin in the ointment could not be determined easily. The relative thermodynamic activity of nitroglycerin in the gels and the ointment could be determined by the relative *in vitro* release rates.

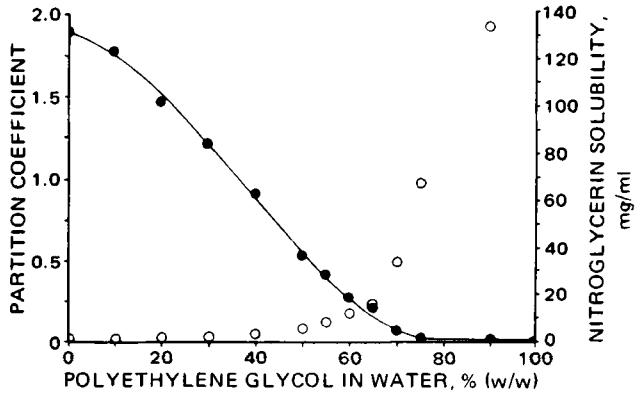

Figure 4—*Partitioning and estimated solubility of nitroglycerin at 20°. Key: ●, observed partition coefficient (isooctane–aqueous–polymer) for nitroglycerin; and ○, calculated solubility of nitroglycerin in water–polymer mixtures.*

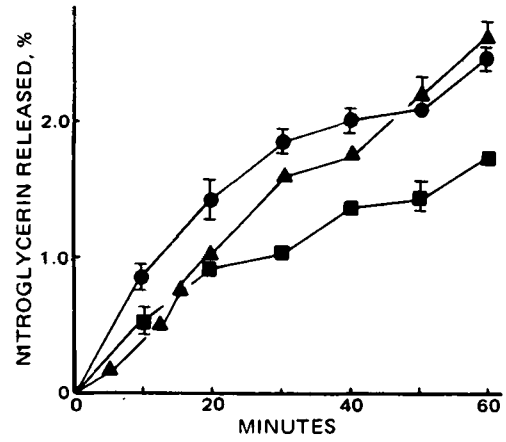

Figure 5—*In vitro release of nitroglycerin from 2% topical preparations into isopropyl myristate. Key: ●, Gel A; ■, Gel B; and ▲, commercial ointment. Each point represents the mean of two trials. Bars indicate the range of observed values. Where bars are not shown, the observed range was within the area covered by the symbols used.*

Comparative *in vitro* release rates from Gels A and B and the ointment into isopropyl myristate were evaluated. A hydrocarbon solvent such as isooctane could not be used because it caused rapid dissolution of the oleaginous vehicle. On the other hand, higher molecular weight alcohols such as octanol brought about disintegration of the polyethylene glycol-based gels. Isopropyl myristate was chosen as a compromise because both polyethylene glycol and water were immiscible with it while ointment dissolution, although present, was considerably less rapid. To avoid further artifactual results from ointment dissolution, a very slow stirring rate for the receptor phase was used. Sampling was conducted for 1 hr to compare the initial release characteristics from the three preparations (Fig. 5).

The areas under the percent release–time curves (in percent release-min) were 94.2 and 85.3 for Gel A, 55.6 and 55.1 for Gel B, and 80.2 and 75.9 for the ointment. The data suggested that Gel A released nitroglycerin about two times faster than Gel B. This result is in qualitative agreement with a prediction based on solubility arguments, but Gel A did not release nitroglycerin 150 times faster than Gel B, as would be expected if the drug solubility in the vehicle is inversely related to release. Isopropyl myristate, however, is a much better solvent for nitroglycerin than is isooctane. Thus, differences in partitioning with the latter solvent may be greatly reduced because of the solvent "leveling" effect of isopropyl myristate. At any rate, nitroglycerin release from the ointment was not statistically different from that produced by Gel A. This finding suggests that nitroglycerin is not present in the ointment at an abnormally high thermodynamic activity. Thus, a positive deviation from Raoult's law cannot be invoked for the increased nitroglycerin absorption from the ointment over the neat liquid. The absence of an enhanced "escaping tendency" of nitroglycerin in the ointment was further indicated by the following observation: when several ointment samples were placed unmixed and allowed to equilibrate with water at 20°, the resultant aqueous concentrations measured at 1 and 2 weeks did not exceed the aqueous solubility of nitroglycerin.

The lack of quantitative correlation between the *in vitro* release rate and solubility in Gels A and B might have been due to the slow stirring rate used. Release rates from topical steroid preparations using a similar *in vitro* test system were reported to be sensitive to stirring rates of less than 30 rpm (8). This degree of agitation could not be accommodated in the present study without erosion of the ointment base by the solvent. An alternative approach using a dialysis membrane[11] to separate the vehicle and isopropyl myristate was unsuccessful because polyethylene glycol 400 rapidly diffused through the artificial membrane.

***In Vivo* Nitroglycerin Absorption from Polymer Gels**—The *in vivo* study of percutaneous absorption of Gels A and B produced unan-

[11] Spectrapor membrane tubing, mol. wt. cutoff 6000–8000, Spectrum Medical Industries, Los Angeles, CA 90054.

ticipated results. In contrast to the ointment, where a plateau drug level of 30–40 ng/ml was achieved, both gels (three animals in each trial) gave negligible (<1 ng/ml) plasma nitroglycerin concentrations over 4 hr. The *in vivo* absorption data did not correlate with the *in vitro* release results.

The composite data suggest a specific skin–vehicle interaction with the ointment, which has the net effect of increasing nitroglycerin permeability or decreasing the effective skin barrier thickness. Alternatively, poor nitroglycerin absorption from the neat material, alcoholic solution, and polyethylene glycol gels may have arisen from unfavorable interactions with the skin. A recent study showed that benzocaine diffusion through human stratum corneum decreased in the presence of relatively high amounts of low molecular weight polyethylene glycol (23). These researchers also showed that polyethylene glycol significantly affected the surface structure of the stratum corneum. These effects may be tested by comparing the absorption of a marker chemical following application of neat nitroglycerin or polyethylene glycol gels on the skin to absorption through untreated skin.

The ointment may increase transdermal nitroglycerin delivery by inhibiting skin metabolism. Enzymatic process in the skin and considerations of the skin as an active metabolizing barrier were discussed recently (24, 25). Previous studies also showed a total body nitroglycerin clearance from the rat in excess of reasonable hepatic clearance (26), suggesting extensive tissue degradation of this drug. The skin may represent a first-pass metabolic site for topically applied nitroglycerin. Interference with this process can affect the amount of intact nitroglycerin reaching the systemic circulation. This aspect of nitroglycerin transdermal delivery will be investigated.

REFERENCES

(1) J. O. Parker, R. J. Augustine, J. P. Burton, R. O. West, and P. W. Armstrong, *Am. J. Cardiol.*, **38**, 162 (1976).

(2) M. E. Davidov and W. J. Mroczek, *Angiology*, **27**, 205 (1976).

(3) P. W. Armstrong, M. T. Matthew, K. Boroomand, and J. O. Parker, *Am. J. Cardiol.*, **38**, 474 (1976).

(4) J. E. Shaw, S. K. Chandrasekaran, A. S. Michaels, and L. Taskovich, in "Animal Models in Dermatology," H. Maibach, Ed., Churchill Livingstone, New York, N.Y., 1975, p. 138.

(5) B. Idson, *J. Pharm. Sci.*, **64**, 901 (1975).

(6) R. J. Scheuplein and I. H. Blank, *Physiol. Rev.*, **51**, 702 (1971).

(7) T. Higuchi, *J. Soc. Cosmet. Chem.*, **11**, 85 (1960).

(8) B. J. Poulsen, E. Young, V. Coquilla, and M. Katz, *J. Pharm. Sci.*, **57**, 928 (1968).

(9) J. Ostrenga, C. Steinmetz, and B. Poulsen, *ibid.*, **60**, 1175 (1971).

(10) P. Grasso and A. B. G. Lansdown, *J. Soc. Cosmet. Chem.*, **23**, 481 (1972).

(11) "The United States Pharmacopeia," 19th rev., Mack Publishing Co., Easton, Pa., 1975.

(12) P. S. K. Yap, E. F. McNiff, and H.-L. Fung, *J. Pharm. Sci.*, **67**, 582 (1978).

(13) H.-L. Fung, P. Dalecki, E. Tse, and C. T. Rhodes, *ibid.*, **62**, 696 (1973).

(14) S. K. Yap, C. T. Rhodes, and H.-L. Fung, *Anal. Chem.*, **47**, 1183 (1975).

(15) S. T. Horhota and H.-L. Fung, *J. Pharm. Sci.*, **67**, 1345 (1978).

(16) D. Colquhoun, "Lectures on Biostatistics," Clarendon Press, Oxford, England, 1971.

(17) B. A. Edelman, A. M. Contractor, and R. F. Shangraw, *J. Am. Pharm. Assoc.*, **NS11**, 30 (1971).

(18) M. J. Pikal, A. L. Lukes, and L. F. Ellis, *J. Pharm. Sci.*, **65**, 1278 (1976).

(19) R. F. Shangraw and A. M. Contractor, *J. Am. Pharm. Assoc.*, **NS12**, 633 (1972).

(20) A. W. McKenzie and R. B. Stoughton, *Arch. Dermatol.*, **86**, 608 (1962).

(21) E. W. Rosenberg, H. Blank, and S. Resnik, *J. Am. Med. Assoc.*, **179**, 809 (1962).

(22) "Encyclopedia of Chemical Technology," vol. 8, 2nd ed., Interscience, New York, N.Y., 1968, p. 602.

(23) A. A. Belmonte and W. Tsai, *J. Pharm. Sci.*, **67**, 517 (1978).

(24) H. Y. Ando, N. F. Hitto, and W. I. Higuchi, *ibid.*, **66**, 755 (1977).

(25) *Ibid.*, **66**, 1525 (1977).

(26) P. S. K. Yap and H.-L. Fung, *J. Pharm. Sci.*, **67**, 584 (1978).

ACKNOWLEDGMENTS

Abstracted in part from a thesis submitted by S. T. Horhota to the Graduate School, State University of New York at Buffalo, in partial fulfillment of the Doctor of Philosophy degree requirements.

Supported in part by National Institutes of Health General Research Support Grant RR05454-15.

S. T. Horhota was a Fellow of the American Foundation for Pharmaceutical Education.

The authors thank Dr. E. Shefter and Dr. B. Poulsen for helpful discussions.

Kinetics of Dopamine Oxidation by Dialkylaminoalkylphenothiazine Cation Radicals

MARIA ROSA GASCO ˣ and MARIA EUGENIA CARLOTTI

Received March 28, 1978, from the *Istituto di Chimica Farmaceutica e Tossicologica dell'Universita' di Torino, Corso Raffaello 31, Torino, Italy.* Accepted for publication October 26, 1978.

Abstract □ The kinetics of dopamine oxidation by dialkylaminoalkylphenothiazine cation radicals (with two- or three-carbon side chains) were investigated. The two-carbon side-chain derivatives have reaction rates higher than the three-carbon ones. For chlorpromazine and promazine, extrapolation of pH 1–6 data shows that reaction rates become very fast at physiological pH.

Keyphrases □ Dopamine—oxidation by phenothiazine cation radicals, kinetics, structure–activity relationships □ Phenothiazine derivatives—oxidation of dopamine, kinetics, structure–activity relationships □ Structure–activity relationships—phenothiazine cation radicals, oxidation of dopamine, kinetics

Several reports (1–4) pointed out that transformation of chlorpromazine [2-chloro-*N*,*N*-dimethyl-10H-phenothiazine-10-propamine] (I) is necessary for some *in vitro* enzyme inhibitions. A I intermediate, the cation radical [obtained also *in vivo* (5)], was shown to inhibit (Na^+, K^+) adenosine triphosphatase (6). The cation radical also inhibited microsomal brain enzyme (7) and uridine diphosphate glucose dehydrogenase (8).

0022-3549/79/0500-0612$01.00/0

© 1979, American Pharmaceutical Association

ticipated results. In contrast to the ointment, where a plateau drug level of 30–40 ng/ml was achieved, both gels (three animals in each trial) gave negligible (<1 ng/ml) plasma nitroglycerin concentrations over 4 hr. The *in vivo* absorption data did not correlate with the *in vitro* release results.

The composite data suggest a specific skin–vehicle interaction with the ointment, which has the net effect of increasing nitroglycerin permeability or decreasing the effective skin barrier thickness. Alternatively, poor nitroglycerin absorption from the neat material, alcoholic solution, and polyethylene glycol gels may have arisen from unfavorable interactions with the skin. A recent study showed that benzocaine diffusion through human stratum corneum decreased in the presence of relatively high amounts of low molecular weight polyethylene glycol (23). These researchers also showed that polyethylene glycol significantly affected the surface structure of the stratum corneum. These effects may be tested by comparing the absorption of a marker chemical following application of neat nitroglycerin or polyethylene glycol gels on the skin to absorption through untreated skin.

The ointment may increase transdermal nitroglycerin delivery by inhibiting skin metabolism. Enzymatic process in the skin and considerations of the skin as an active metabolizing barrier were discussed recently (24, 25). Previous studies also showed a total body nitroglycerin clearance from the rat in excess of reasonable hepatic clearance (26), suggesting extensive tissue degradation of this drug. The skin may represent a first-pass metabolic site for topically applied nitroglycerin. Interference with this process can affect the amount of intact nitroglycerin reaching the systemic circulation. This aspect of nitroglycerin transdermal delivery will be investigated.

REFERENCES

(1) J. O. Parker, R. J. Augustine, J. P. Burton, R. O. West, and P. W. Armstrong, *Am. J. Cardiol.*, **38**, 162 (1976).

(2) M. E. Davidov and W. J. Mroczek, *Angiology*, **27**, 205 (1976).

(3) P. W. Armstrong, M. T. Matthew, K. Boroomand, and J. O. Parker, *Am. J. Cardiol.*, **38**, 474 (1976).

(4) J. E. Shaw, S. K. Chandrasekaran, A. S. Michaels, and L. Taskovich, in "Animal Models in Dermatology," H. Maibach, Ed., Churchill Livingstone, New York, N.Y., 1975, p. 138.

(5) B. Idson, *J. Pharm. Sci.*, **64**, 901 (1975).

(6) R. J. Scheuplein and I. H. Blank, *Physiol. Rev.*, **51**, 702 (1971).

(7) T. Higuchi, *J. Soc. Cosmet. Chem.*, **11**, 85 (1960).

(8) B. J. Poulsen, E. Young, V. Coquilla, and M. Katz, *J. Pharm. Sci.*, **57**, 928 (1968).

(9) J. Ostrenga, C. Steinmetz, and B. Poulsen, *ibid.*, **60**, 1175 (1971).

(10) P. Grasso and A. B. G. Lansdown, *J. Soc. Cosmet. Chem.*, **23**, 481 (1972).

(11) "The United States Pharmacopeia," 19th rev., Mack Publishing Co., Easton, Pa., 1975.

(12) P. S. K. Yap, E. F. McNiff, and H.-L. Fung, *J. Pharm. Sci.*, **67**, 582 (1978).

(13) H.-L. Fung, P. Dalecki, E. Tse, and C. T. Rhodes, *ibid.*, **62**, 696 (1973).

(14) S. K. Yap, C. T. Rhodes, and H.-L. Fung, *Anal. Chem.*, **47**, 1183 (1975).

(15) S. T. Horhota and H.-L. Fung, *J. Pharm. Sci.*, **67**, 1345 (1978).

(16) D. Colquhoun, "Lectures on Biostatistics," Clarendon Press, Oxford, England, 1971.

(17) B. A. Edelman, A. M. Contractor, and R. F. Shangraw, *J. Am. Pharm. Assoc.*, **NS11**, 30 (1971).

(18) M. J. Pikal, A. L. Lukes, and L. F. Ellis, *J. Pharm. Sci.*, **65**, 1278 (1976).

(19) R. F. Shangraw and A. M. Contractor, *J. Am. Pharm. Assoc.*, **NS12**, 633 (1972).

(20) A. W. McKenzie and R. B. Stoughton, *Arch. Dermatol.*, **86**, 608 (1962).

(21) E. W. Rosenberg, H. Blank, and S. Resnik, *J. Am. Med. Assoc.*, **179**, 809 (1962).

(22) "Encyclopedia of Chemical Technology," vol. 8, 2nd ed., Interscience, New York, N.Y., 1968, p. 602.

(23) A. A. Belmonte and W. Tsai, *J. Pharm. Sci.*, **67**, 517 (1978).

(24) H. Y. Ando, N. F. Hitto, and W. I. Higuchi, *ibid.*, **66**, 755 (1977).

(25) *Ibid.*, **66**, 1525 (1977).

(26) P. S. K. Yap and H.-L. Fung, *J. Pharm. Sci.*, **67**, 584 (1978).

ACKNOWLEDGMENTS

Abstracted in part from a thesis submitted by S. T. Horhota to the Graduate School, State University of New York at Buffalo, in partial fulfillment of the Doctor of Philosophy degree requirements.

Supported in part by National Institutes of Health General Research Support Grant RR05454-15.

S. T. Horhota was a Fellow of the American Foundation for Pharmaceutical Education.

The authors thank Dr. E. Shefter and Dr. B. Poulsen for helpful discussions.

Kinetics of Dopamine Oxidation by Dialkylaminoalkylphenothiazine Cation Radicals

MARIA ROSA GASCO ˣ and MARIA EUGENIA CARLOTTI

Received March 28, 1978, from the *Istituto di Chimica Farmaceutica e Tossicologica dell'Universita' di Torino, Corso Raffaello 31, Torino, Italy.* Accepted for publication October 26, 1978.

Abstract □ The kinetics of dopamine oxidation by dialkylaminoalkylphenothiazine cation radicals (with two- or three-carbon side chains) were investigated. The two-carbon side-chain derivatives have reaction rates higher than the three-carbon ones. For chlorpromazine and promazine, extrapolation of pH 1–6 data shows that reaction rates become very fast at physiological pH.

Keyphrases □ Dopamine—oxidation by phenothiazine cation radicals, kinetics, structure–activity relationships □ Phenothiazine derivatives—oxidation of dopamine, kinetics, structure–activity relationships □ Structure–activity relationships—phenothiazine cation radicals, oxidation of dopamine, kinetics

Several reports (1–4) pointed out that transformation of chlorpromazine [2-chloro-*N*,*N*-dimethyl-10H-phenothiazine-10-propamine] (I) is necessary for some *in vitro* enzyme inhibitions. A I intermediate, the cation radical [obtained also *in vivo* (5)], was shown to inhibit (Na^+, K^+) adenosine triphosphatase (6). The cation radical also inhibited microsomal brain enzyme (7) and uridine diphosphate glucose dehydrogenase (8).

0022-3549/79/0500-0612$01.00/0

© 1979, American Pharmaceutical Association

Table I—Structures of Investigated Compounds and Spectral Characteristics of the Corresponding Radicals

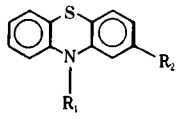

Compound	R_1	R_2	ϵ, $10^{-3}\ M^{-1}\ cm^{-1}$	λ_{max}
I Chlorpromazine[a] (2-chloro-*N,N*-dimethyl-10H-phenothiazine-10-propanamine)	$-CH_2CH_2CH_2N(CH_3)_2$	Cl	11.2 ± 0.5	523
II Promazine[a] (*N,N*-dimethyl-10H-phenothiazine-10-propanamine)	$-CH_2CH_2CH_2N(CH_3)_2$	H	9.2 ± 0.3	513
III Dietazine[a] (*N,N*-diethyl-10H-phenothiazine-10-ethanamine)	$-CH_2CH_2N(C_2H_5)_2$	H	10.5 ± 0.4	511
IV Parsidol[a] (*N,N*-diethyl-α-methyl-10H-phenothiazine-10-ethanamine)	$-CH_2CH(CH_3)N(C_2H_5)_2$	H	9.5 ± 0.3	515
V Promethazine[a] (*N,N,α*-trimethyl-10H-phenothiazine-10-ethanamine)	$-CH_2CH(CH_3)N(CH_3)_2$	H	9.3 ± 0.4	515
VI Isopromethazine[a] (*N,N,β*-trimethyl-10H-phenothiazine-10-ethanamine)	$-CH(CH_3)CH_2N(CH_3)_2$	H	8.8 ± 0.4	524

[a] Rhône-Poulenc, France.

Barras and Coult (9) observed that phenothiazine tranquillizers accelerated enzymatic biogenic amine oxidation while phenothiazines lacking clinical tranquillizing activity had no effect. Løvstad (10, 11), investigating ceruloplasmine-catalyzed phenothiazine oxidation, found that a three-carbon side chain was essential for a rapid enzymatic oxidation to the cation radical and for further oxidation by the same cation radicals of biogenic amines.

A previous paper reported the oxidation kinetics of tricyclic amines to the corresponding radicals with Ce(IV) (12); cation radical formation rates decreased while the reduction potentials increased, passing from the drugs with antidepressant action [imipramine (5H-dibenz[*b,f*]azepine-5-propanamine, 10,11-dihydro-*N,N*-dimethyl) and 10(9H)-acridinepropanamine, *N,N*,9,9-tetramethyl (dimetacrine)] to dialkylaminoalkylphenothiazines with a two-carbon side chain and then to dialkylaminoalkylphenothiazines with a three-carbon side chain.

In the present study, the reduction kinetics of phenothiazine cation radicals with different pharmacodynamic activities (Table I) by dopamine [1,2-benzenediol-4-(2-aminoethyl)] (VII) are investigated.

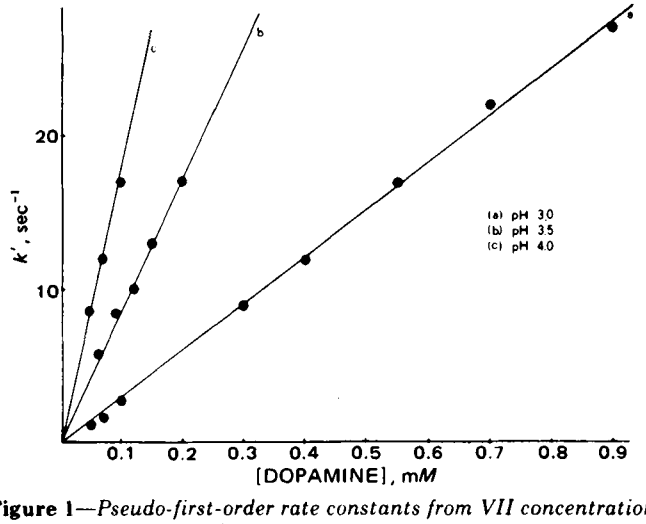

Figure 1—*Pseudo-first-order rate constants from VII concentration at different pH values (for II).*

EXPERIMENTAL

Reagents—The phenothiazine compounds (I–VI, Table I) were employed as chlorhydrates. Compound VII[1] and potassium exachloriridate were reagent grade.

Procedure—Cation radical solutions were obtained immediately before use either by adding potassium exachloriridate in slight deficiency to a solution of phenothiazine derivatives or by platinum electrode electrooxidation. Unoxidized phenothiazine had no effect on kinetics. The kinetic runs were carried out with a stopped-flow spectrophotometer[2] at the wavelength of maximum cation radical absorption (Table I). The cell path length was 2.00 cm.

Measurements were performed at different acidities: the pH ≤ 3 was obtained with perchloric acid, while the pH 3–6 range was obtained with potassium phthalate buffers. The pH measured by the potentiometer[3] was constant within 0.05 unit.

Pseudo-first-order conditions were chosen when possible; second-order conditions were adopted for the faster reactions. The cation radical concentration ranged between 5.0×10^{-6} and $5.0 \times 10^{-5}\ M$; the VII concentration ranged between 5.0×10^{-6} and $5.0 \times 10^{-4}\ M$.

The rate constants were evaluated by the least-squares method. Cation radical instability allowed a wide pH range investigation of I and II only; for other derivatives, only high acidity 0.1 *M* $HClO_4$ runs were performed. Since many radicals are unstable at high pH, the cation radical solutions were obtained at pH 3–6 with $1.0 \times 10^{-3}\ M$ $HClO_4$ and mixed with the solution of VII buffered at the desired pH. (The final pH variation was within 0.1 unit.) The cation radical decomposition rates, reported previously (13), were negligible compared to the ones in this study.

The initial cation radical concentration was estimated, when second-order conditions were used, by initial transmittance. Kinetic runs were carried out at 25° and, for I and II, at 35°.

[1] Dopamine, Merck, Schuchardt.
[2] Durrum-Gibson, Palo Alto, California.
[3] Polymetron 42/B.

Table II—Pseudo-First-Order Constants for Reaction between II Cation Radical and VII at 25° at Different Acidities[a]

VII, m*M*	pH 1.00[b]	2.00[b]	2.52[c]	3.00[d]	3.50[d]	4.00[d]	4.60[d]
0.050	—	—	—	1.2_5	—	8.6	—
0.060	—	—	—	—	5.8	—	33
0.070	—	—	—	1.8_5	—	12	—
0.090	—	—	—	—	8.4	—	58
0.100	—	—	—	2.8	—	17	—
0.120	—	—	—	—	10	—	74
0.15	—	—	—	—	13	—	—
0.20	—	—	—	—	17	—	—
0.30	—	4.7	6.2	9.0	—	—	—
0.40	2.18	—	—	12	—	—	—
0.50	3.40	7.8	8.8	—	—	—	—
0.55	—	—	—	17	—	—	—
0.70	4.30	10.5	12	22	—	—	—
0.90	—	13	—	27	—	—	—
1.00	—	—	17	—	—	—	—
1.50	—	—	25	—	—	—	—
5.00	27.0	—	—	—	—	—	—

[a] For pH 1.0–4.6, other kinetic runs were performed also in second-order conditions. For pH >4.60, the runs were performed in second-order conditions. [b] 5.0×10^{-6} *M* II cation radical. [c] 2.5×10^{-5} *M* II cation radical. [d] 5.0×10^{-5} *M* II cation radical.

RESULTS AND DISCUSSION

Stoichiometry—By adding successive VII aliquots to a cation radical solution in 0.1 *M* $HClO_4$, the decrease in absorbance at the proper wavelength was measured and the stoichiometric ratio was determined. The overall reaction can be depicted as:

$$2P^{+\cdot} + H_3D^+ \rightarrow 2P + DQ^+ + 2H^+$$

Scheme I

where P represents the phenothiazine derivative, $P^{+\cdot}$ is the corresponding cation radical, H_3D^+ is the fully protonated VII, and DQ^+ is the protonated dopamine quinone VIII.

Since the H_3D^+/DQ^+ reduction potential is ~0.78–0.79 v (14, 15), the reaction is shifted toward the right side with phenothiazine derivatives that exhibit higher reduction potentials or a higher pH. In the kinetic runs with less oxidizing cation radicals and excess VII, T_∞ transmittance at equilibrium came very close to 1.00. At pH 5, VIII can produce the corresponding aminochrome (16); however, the aminochrome formation rate is negligible compared to the reaction rates in this study (17).

Reaction Kinetics—In pseudo-first-order conditions, plots of $\ln(A_t - A_\infty)$ (where A_∞ and A_t represent the absorbance at equilibrium and at time t, respectively) as a function of time were linear for at least 80% of the reaction process (Table II).

The observed rate constants also exhibited a linear dependence on the VII concentration (Fig. 1). With second-order conditions, the related second-order plots were also satisfactorily linear. When the reaction rate

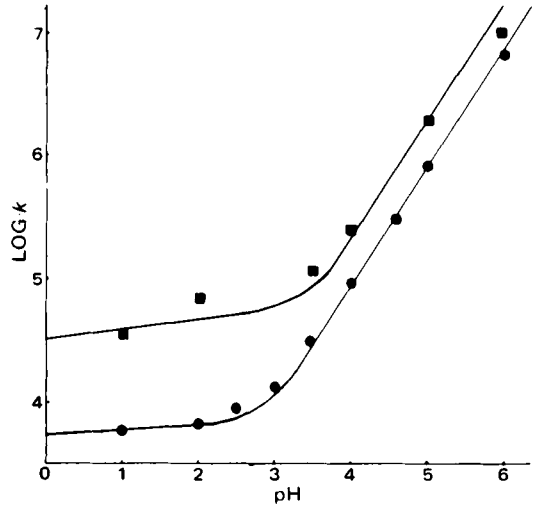

Figure 2—*The pH dependence of second-order rate constants, k, for VII oxidation with cation radicals (I and II) at 25°. The points (● for II and ■ for I) are experimental data. The curves were computed according to Eq. 2 with the values reported in Table III.*

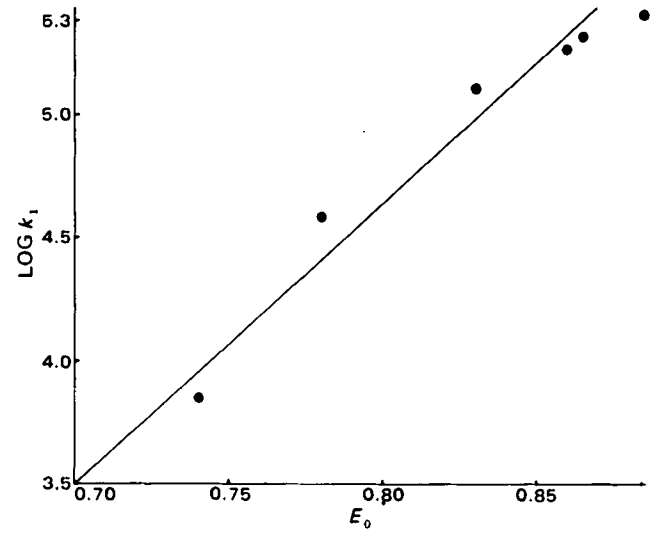

Figure 3—*Log* k_1 versus E_0 *plot of different phenothiazine cation radicals.*

was first order and dependent on each reagent concentration, the following rate law pertained:

$$-\frac{1d[P^{+\cdot}]}{2dt} = k[P^{+\cdot}][\text{dopamine}] \qquad \text{(Eq. 1)}$$

where [dopamine] represents the stoichiometric VII concentration. The observed rate constant values are reported in Table III.

pH Dependence—The data reported in Table III show that the rate constants were affected by the solution pH. This pH dependence can be explained by the different VII protonation states represented by:

$$H_3D^+ \underset{H^+}{\overset{K_1}{\rightleftharpoons}} H_2D \underset{H^+}{\overset{K_2}{\rightleftharpoons}} HD^-$$

Scheme II

where $pK_1 \cong 9$ and $pK_2 \cong 10$ (18).

Recent research (18) suggested that these dissociation constants represent competitive deprotonation and cannot be assigned to the ammonium or phenolic groups.

The acidity dependence can be ascribed to competitive paths such as:

$$P^{+\cdot} + H_3D^+ \xrightarrow{k_1} P + H_2D^{+\cdot} + H^+$$

Scheme III

Table III—Second-Order Constants for Reaction between VII and Different Phenothiazine Cation Radicals at 25°

pH	I	II	III	IV	V	VI
0.5	—	—	1.2×10^5	1.6×10^5	—	2.1×10^5
1.0	3.75×10^4	5.9×10^3	—	—	1.75×10^5	1.9×10^5
2.0	7.1×10^4	6.7×10^3	—	—	—	—
2.5	—	8.9×10^3	—	—	—	—
3.0	—	1.32×10^4	—	—	—	—
3.5	1.2×10^5	3.13×10^4	—	—	—	—
4.0	2.5×10^5	9.36×10^4	—	—	—	—
4.6	—	3.06×10^5	—	—	—	—
5.0	2×10^6	8.5×10^5	—	—	—	—
6.0	1×10^7	6.7×10^6	—	—	—	—

Table IV—VII Oxidation Rate Constants with Different Cation Radicals at 25°

Compound	E_0	k_1, M^{-1} sec^{-1}	k_2K_1, sec^{-1}
I	0.78	$(3.7 \pm 0.4) \times 10^4$	(20 ± 8)
II	0.72	$(6.0 \pm 0.8) \times 10^3$	(7.9 ± 0.9)
III	0.83	$(1.2 \pm 0.1) \times 10^5$	—
IV	0.86	$(1.6 \pm 0.2) \times 10^5$	—
V	0.86_5	$(1.75 \pm 0.2) \times 10^5$	—
VI	0.88_5	$(2.1 \pm 0.2) \times 10^5$	—

$$P^{+\cdot} + H_2D \xrightarrow{k_2} P + H_2D^{+\cdot}$$

Scheme IV

and then follows the fast reaction:

$$P^{+\cdot} + H_2D \rightarrow P + DQ^+ + H^+$$

Scheme V

This leads to the rate law:

$$-\frac{1d[P^{+\cdot}]}{2dt} = \frac{(k_1 + k_2K_1[H^+]^{-1})[\text{dopamine}][P^{+\cdot}]}{1 + k_1[H^+]^{-1}} \qquad \text{(Eq. 2)}$$

which with $K_1[H^+]^{-1} \ll 1$ in the pH range investigated reduced to:

$$-\frac{1d[P^{+\cdot}]}{2dt} = (k_1 + k_2K_1[H^+]^{-1})[\text{dopamine}][P^{+\cdot}] \qquad \text{(Eq. 3)}$$

Figure 2 compares the experimental points and a curve calculated with Eq. 3. The parameters k_1 and, when available, k_2K_1, were collected and were $\Delta H^{\neq} = 7.3 \pm 1.1$ kcal/mol and $\Delta S^{\neq} = -17 \pm 4$ cal deg^{-1} mole^{-1} for path I and $\Delta H^{\neq} = 4.8 \pm 1.3$ kcal/mole and $\Delta S^{\neq} = -38 \pm 4$ cal deg^{-1} mole^{-1} for path II. These values are overall data, including the contribution of dissociation constant K_1 and of the diffusion-controlled term.

CONCLUSIONS

For the observed reaction between a cation radical and an organic substrate, an electron-transfer mechanism can be proposed (19–21). When this mechanism is operating, a relationship between the reaction rates and the oxidizing agent reduction potentials is expected (22, 23). This provision is fulfilled for the acid-independent path. In fact, where the phenothiazine derivative reduction potentials are reported (12), the compounds with higher reduction potential exhibit the higher reaction rates (Table IV). This can be seen in Fig. 3, where a linear relationship between log k_1 and E_0 is shown. The acid-independent path, however, although investigated for only two compounds, shows a close rate, k_2K_1. [In fact, while the ratio of k_1(II)/k_1(I) is 6.2, the ratio of k_2(II)/k_2(I) is only 2.5.]

The values of the specific rate constant k_2 could be estimated by knowing K_1, for which the value around 10^{-9} mole/liter can be suggested (19–21). This procedure leads to k_2 values of 7.9×10^9 and 2.0×10^{10} liters mole/sec for I and II, respectively, which are very close to the diffusion-controlled limit (24).

When such conditions are reached, the contribution of the activation-controlled reaction can be expressed by (25):

$$\frac{1}{k_{obs}} = \frac{1}{k_{diff}} + \frac{1}{k_{act}} \qquad \text{(Eq. 4)}$$

Consequently, it should be possible, knowing k_{diff}, to derive k_{act}, the activation-controlled electron-transfer rate. If $k_{diff} = 3.0 \times 10^{10}$ liters/mole sec (24), it follows that $k_{act} = 1.0 \times 10^{10}$ and 6.0×10^{10} liters/mole sec for I and II, respectively. The ratio $k_{2act(II)}/k_{2act(I)}$ should be approximately equal to that observed for the ratio of an independent path. This suggests that the rate of path electron transfer is also related to the oxidizing species reduction potentials. Obviously, this agreement could be fortuitous, owing to the uncertainty on k_1 and k_{diff}. The observed rate constants become very fast at physiological pH. With these conditions, VII oxidation could be a way of disappearance of I and II cation radicals.

Since dialkylaminoalkylphenothiazines with two-carbon side chains have a higher reduction potential, their cation radicals show a quicker oxidation reaction than the ones with three-carbon side chains. There is, therefore, a correlation between VII oxidation rates and the side-chain structure. The higher cation radical oxidation potential of derivatives with two-carbon side chains could explain their different behavior (11) in enzymatic oxidation of VII. This parameter might also explain the difference in their pharmacodynamic activities.

REFERENCES

(1) H. Low, *Biochim. Biophys. Acta*, **32**, 11 (1959).

(2) H. J. Carver, *Biochem. Pharmacol.*, **12**, 19 (1963).

(3) M. Wollemann and P. Elodi, *ibid.*, **6**, 228 (1961).

(4) M. Wollemann and T. Keleti, *Arzneim.-Forsch.*, **12**, 360 (1962).

(5) I. S. Forrest, A. G. Bolt, and R. C. Aber, *Aggressologie*, **9**, 259 (1968).

(6) T. Akera and T. M. Brody, *Mol. Pharm.*, **4**, 600 (1968).

(7) T. Akera and T. M. Brody, *Biochem. Pharmacol.*, **21**, 1403 (1972).

(8) L. Levy and T. M. Burbridge, *ibid.*, **16**, 1249 (1967).

(9) B. C. Barras and D. E. Coult, *ibid.*, **21**, 677 (1972).

(10) R. A. Løvstad, *ibid.*, **23**, 1045 (1974).

(11) *Ibid.*, **24**, 475 (1975).

(12) M. R. Gasco and M. E. Carlotti, *Pharm. Acta Helv.*, **52**, 296 (1977).

(13) T. M. Tozer and L. D. Tuck, *J. Pharm. Sci.*, **54**, 1169 (1965).

(14) W. M. Clark, "Oxidation Reduction Potentials of Organic Systems," Williams & Wilkins, Baltimore, Md., 1960, p. 373.

(15) A. Brun and R. Rossett, *Electroanal. Chem. Interfacial Chem.*, **49**, 287 (1974).

(16) R. A. Heacock, *Adv. Heterocycl. Chem.*, **5**, 205 (1965).

(17) E. Pelizzetti, E. Mentasti, and E. Pramauro, *J. Chem. Soc. Perkin II*, **1976**, 1651.

(18) R. K. Boggess and R. B. Martin, *J. Am. Chem. Soc.*, **97**, 3076 (1975).

(19) N. Winograd and T. Kurvanz, *ibid.*, **93**, 18 (1971).

(20) B. A. Kowert, L. Marcoux, and A. J. Bard, *ibid.*, **94**, 18 (1971).

(21) A. Yamagishi, *Bull. Chem. Soc. Jpn.*, **48**, 3475 (1975).

(22) N. Sutin, in "Inorganic Biochemistry," vol. 2, G. L. Eichorn, Ed., Elsevier, Amsterdam, The Netherlands, 1973, p. 611.

(23) W. L. Reynolds and R. W. Lunery "Mechanism of Electron Transfer," Ronald, New York, N.Y., 1966, p. 117.

(24) S. Petrucci, in "Ionic Interactions," vol. 2, S. Petrucci, Ed., Academic, New York, N.Y., 1971, p. 39.

(25) R. A. Marcus, *J. Phys. Chem.*, **72**, 891 (1968).

Chemical Reactions in Cephalosporin Allergy: High-Pressure Liquid Chromatographic Analysis of Cephalosporin Aminolysis Kinetics

AKIRA TSUJI, ETSUKO MIYAMOTO, and TSUKINAKA YAMANA ˣ

Received May 2, 1978, from the *Faculty of Pharmaceutical Sciences, Kanazawa University, Takara-machi, Kanazawa 920, Japan.* Accepted for publication October 30, 1978.

Abstract □ Cephalosporin reaction with protein amino groups is fundamental to cephalosporin allergy. Cephalothin and cefazolin reaction kinetics with ε-aminocaproic acid, β-alanine, and glycine in aqueous solution were investigated. All reactions were conducted at 35° and 0.5 ionic strength and were followed by ion-exchange high-pressure liquid chromatography. The aminolysis rate constants can be expressed as terms representing uncatalyzed or water-catalyzed amine reaction, self-assisted nucleophilic reaction, and hydroxide-ion-catalyzed nucleophilic amine attack on the β-lactam moiety. Cephalothin and cefazolin react with amines as readily as penicillin G. The UV spectra of several cephalothin–glycine reaction products were recorded, and their possible structures are discussed.

Keyphrases □ Cephalosporins—aminolysis kinetics, allergy, high-pressure liquid chromatography □ Aminolysis—cephalosporins, allergy, kinetic analysis, high-pressure liquid chromatography □ Kinetics—cephalosporin aminolysis, high-pressure liquid chromatography □ High-pressure liquid chromatography—analysis, cephalosporins, aminolysis kinetics, aminolysis products □ Antibacterials—cephalothin, deacetylcephalothin, and cefazolin, aminolysis kinetics, cephalosporin allergy, high-pressure liquid chromatography

Since cephalosporin reaction with free amino groups on tissue proteins to yield cephalosporoyl conjugates *in vivo* may be largely responsible for cephalosporin immunogenicity (1), a knowledge of cephalosporin aminolysis and reaction products is important. Such protein conjugates prepared *in vitro* have been strongly immunogenic in animals (2–6).

Although kinetic studies on penicillin aminolysis have been reported (7–17), little work has been performed using cephalosporins, probably due to analysis difficulties, reaction complexity, and the dearth of information on these compounds. Cephalosporin aminolysis kinetic analysis by differential UV spectrophotometry was reported recently (18, 19). Spectrophotometric analysis has been useful for following cephalosporin hydrolysis (18–23).

This paper reports the high-pressure liquid chromatographic (HPLC) analysis of cephalosporin aminolysis kinetics. This method seems to be a powerful tool for quantifying reactions, separating the hydrolysis and aminolysis products, and investigating degradation products. HPLC analysis of the kinetics and mechanism of aqueous cephalosporin hydrolysis as a function of pH was reported previously (23, 24).

EXPERIMENTAL

Materials—Cephalothin sodium[1] (944 μg/mg), deacetylcephalothin sodium[1], and cefazolin sodium[2] (966 μg/mg) were used as received.

All other chemicals were the highest grade and were used without further purification.

Kinetic Procedure—Three amino acid types, glycine, β-alanine, and ε-aminocaproic acid, were used both as buffers to maintain a constant pH and as nucleophiles. The amine buffers were prepared just before use with calculated amounts of amino acid and standard sodium hydroxide solution. The ionic strength was adjusted to 0.5 with potassium chloride. The kinetic technique was almost the same as one used previously for penicillin aminolysis (12–14).

To avoid the possible change in the kinetic solution pH[3] during the reaction, a constant pH was maintained with a pH-stat[4]. All reactions were conducted at 35.0 ± 0.1° with the total amine concentration in large excess over the reacting substrate concentration to maintain pseudo-first-order kinetics. In most cases, the initial cephalosporin concentration was 5×10^{-3} *M* and the total amine concentration was 0.04–0.60 *M*. Reaction solution aliquots (1 ml) were withdrawn at intervals, neutralized to quench the reaction by addition of 1 ml of 0.2 *M* phosphate buffer (pH 6.0) in a cooled water bath to give the final pH of 7–8, and analyzed by HPLC as described later.

Table I—Apparent First-Order Rate Constants, k_{obs}, for Cephalothin Aminolysis in Various Amine Buffers at 0.5 Ionic Strength and 35°

Buffer			pH[a]	k_{obs}, hr^{-1}
$[NH_3^+CH_2COO^-]$	[NaOH]	[KCl]		
0.060	0.033	0.467	9.50	0.274
0.120	0.066	0.434	9.50	0.499
0.060	0.043	0.457	9.80	0.533
0.120	0.088	0.412	9.84	1.11
0.180	0.131	0.369	9.84	1.86
0.060	0.044	0.456	9.85	0.638
0.120	0.096	0.404	10.00	1.28
0.180	0.143	0.357	10.00	2.24
0.300	0.239	0.261	10.00	4.94
$[NH_3^+(CH_2)_2COO^-]$	[NaOH]	[KCl]		
0.060	0.020	0.480	9.70	0.460
0.380	0.131	0.369	9.70	2.85
0.600	0.207	0.293	9.70	6.11
0.038	0.019	0.481	10.00	0.830
0.075	0.038	0.462	10.00	1.10
0.150	0.077	0.423	10.00	1.95
0.300	0.150	0.347	10.00	4.50
0.050	0.033	0.467	10.30	1.90
0.080	0.054	0.446	10.30	2.37
0.100	0.068	0.432	10.30	2.89
0.200	0.135	0.365	10.30	5.61
0.300	0.203	0.297	10.30	9.25
0.050	0.038	0.462	10.50	3.00
0.060	0.046	0.454	10.50	3.26
0.150	0.115	0.385	10.50	6.25
0.200	0.153	0.347	10.50	8.20
$[NH_3^+(CH_2)_5COO^-]$	[NaOH]	[KCl]		
0.050	0.011	0.489	10.00	1.09
0.100	0.022	0.478	10.00	1.85
0.150	0.033	0.467	10.00	2.80
0.200	0.044	0.456	10.00	3.90
0.040	0.014	0.486	10.30	2.17
0.100	0.035	0.465	10.30	4.15
0.120	0.042	0.458	10.30	4.91
0.150	0.053	0.447	10.30	6.74
0.020	0.013	0.487	10.80	6.12
0.047	0.030	0.470	10.80	9.76
0.094	0.060	0.440	10.80	17.7

[a] The pH was maintained by a pH-stat.

[1] Shionogi & Co., Osaka, Japan.
[2] Fujisawa Pharmaceutical Co., Osaka Japan.
[3] PHM26 pH-meter, Radiometer, Copenhagen, Denmark.
[4] A pH-stat titrimeter assembly consisting of a TTT11 titrator, a PHM26 pH-meter, and an ABU12b autoburet, Radiometer, Copenhagen, Denmark.

0022-3549/79/0500-0616$01.00/0
© 1979, American Pharmaceutical Association

Table II—Apparent First-Order Rate Constants, k_{obs}, for Deacetylcephalothin Aminolysis in Glycine Buffer at 0.5 Ionic Strength and 35°

Buffer			pH[a]	k_{obs}, hr^{-1}
$[NH_3^+CH_2COO^-]$	[NaOH]	[KCl]		
0.120	0.066	0.434	9.50	0.185
0.180	0.099	0.401	9.50	0.359
0.060	0.048	0.452	10.00	0.258

[a] The pH was maintained by a pH-stat.

Table III—Apparent First-Order Rate Constants, k_{obs}, for Cefazolin Aminolysis in Various Amine Buffers at 0.5 Ionic Strength and 35°

Buffer			pH[a]	k_{obs}, hr^{-1}
$[NH_3^+CH_2COO^-]$	[NaOH]	[KCl]		
0.080	0.049	0.451	9.60	0.340
0.200	0.122	0.378	9.60	1.40
0.300	0.182	0.318	9.60	2.82
0.120	0.094	0.406	10.00	1.06
0.190	0.153	0.347	10.00	2.28
0.250	0.198	0.302	10.00	3.51
0.300	0.236	0.264	10.00	5.19
$[NH_3^+(CH_2)_2COO^-]$	[NaOH]	[KCl]		
0.060	0.020	0.480	9.70	0.277
0.150	0.052	0.448	9.70	0.790
0.300	0.103	0.397	9.70	1.96
0.380	0.131	0.369	9.70	2.96
0.585	0.201	0.299	9.70	6.29
0.080	0.054	0.446	10.30	1.52
0.150	0.102	0.398	10.30	2.90
0.200	0.135	0.365	10.30	4.40
0.210	0.142	0.358	10.30	4.55
0.300	0.203	0.297	10.30	7.96
0.050	0.040	0.460	10.60	1.96
0.100	0.081	0.419	10.60	3.42
0.168	0.136	0.364	10.60	6.11
$[NH_3^+(CH_2)_5COO^-]$	[NaOH]	[KCl]		
0.050	0.011	0.489	10.00	0.741
0.100	0.022	0.478	10.00	1.46
0.150	0.033	0.467	10.00	2.38
0.217	0.048	0.452	10.00	3.99
0.040	0.014	0.486	10.30	1.53
0.070	0.025	0.475	10.30	2.60
0.120	0.043	0.457	10.30	4.77
0.146	0.052	0.448	10.30	6.00
0.160	0.058	0.442	10.30	7.07
0.200	0.072	0.428	10.30	9.66

[a] The pH was maintained by a pH-stat.

The pseudo-first-order rate constants, k_{obs}, were usually calculated from the slope of the semilogarithmic plots of the residual concentration starting materials *versus* time by the least-squares treatment. Tables I–III summarize the amine buffer compositions and the k_{obs} values.

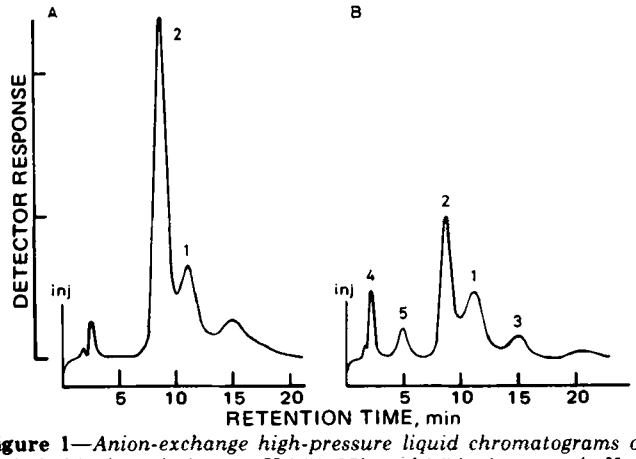

Figure 1—*Anion-exchange high-pressure liquid chromatograms of cephalothin degradation at pH 9.50, 35°, and 0.5 ionic strength. Key: A, sample after 10 hr of hydrolysis; and B, sample after 5 hr of reaction with 0.12 M glycine.*

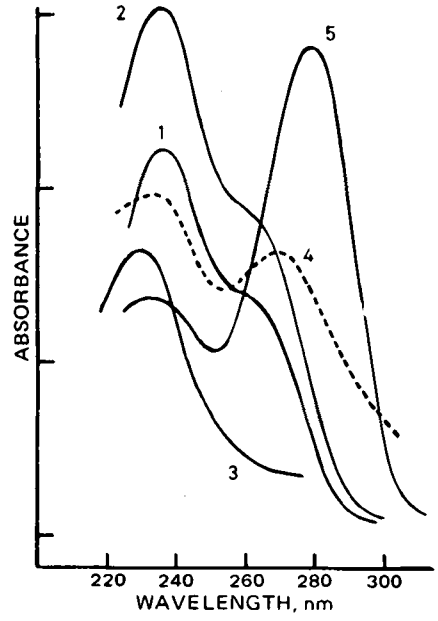

Figure 2—*UV spectra of peaks 1–5 in Fig. 1B.*

HPLC Study—The liquid chromatograph[5] was equipped with a double-beam, variable-wavelength UV detector[6] set at 254 nm. The stationary phase was strong anion-exchange resin prepacked into a stainless steel column, 2.1 mm i.d.[7]. The mobile phases were aqueous 0.02 *M* NaH_2PO_4 adjusted to pH 8.5 with sodium hydroxide for cephalothin and aqueous 0.2 *M* CH_3COONa adjusted to pH 5.0 for cefazolin. The operating parameters for the instrument were: pressure, 40–100 kg/cm^2 (changed to obtain suitable retention time for analysis); temperature, ambient; and UV attenuation, 0.16–0.32 aufs.

A 5-μl sample was injected using a 10-μl syringe and a stopped-flow mode. The cephalothin and deacetylcephalothin or cefazolin content was determined by comparing the peak heights with those of similarly chromatographed standards. Calibration curves for the substances were prepared daily.

TLC Study—TLC was employed to identify the degradation products and to verify HPLC results. Aliquots (10 μl) of the 0.01 *M* cephalothin–glycine reaction solution were applied to glass plates (5 × 20 cm) precoated with 250-μm silica gel[8]. Chromatograms were run for 15 cm in acetic acid–ethanol–chloroform (1:7:12). Spots corresponding to cephalosporins were visualized with iodine vapor. Authentic cephalothin and deacetylcephalothin samples showed R_f values of 0.39 and 0.18, respectively. The standard *N*-acetylglycine solution showed a spot at R_f 0.36, which was visualized with bromcresol green (18).

RESULTS AND DISCUSSION

Monitoring Hydrolysis and Aminolysis of Cephalothin by HPLC—Figure 1A represents the typical chromatogram of the 10-hr aged hydrolysis solution of cephalothin at 35°, μ = 0.5, and pH 9.5 maintained with a pH-stat. Several peaks appeared; two could be assigned, as demonstrated previously (23), to cephalothin itself (peak 1) and deacetylcephalothin (peak 2) resulting from 3-acetoxy moiety hydrolysis. Others were regarded as β-lactam cleavage products.

The cephalothin hydrolytic pathway in alkaline solution has been established kinetically (18, 23) as represented in Scheme I, where k_1 and k_3 represent the rate constants for cleavage of cephalothin and deacetylcephalothin β-lactam rings, and k_2 is the rate constant for cephalothin deacetylation. Simultaneous and quantitative cephalothin and deacetylcephalothin determination at pH 9.5, 35°, and μ = 0.5 was made by HPLC. Kinetic parameters (Scheme I) were computed by the nonlinear least-squares[9] method to be (in hr^{-1}): k_1 = 0.070, k_2 = 0.137, and k_3 = 0.069. Detailed kinetics (18, 23) and the mechanism (23) of cepha-

[5] Shimadzu-DuPont model 830, Kyoto, Japan.
[6] UV 202 recording spectrophotometer, Shimadzu, Kyoto, Japan.
[7] Zipax SAX, 0.5 or 1 m, DuPont Instruments, Wilmington, Del.
[8] E. Merck, Darmstadt, West Germany.
[9] FORTRAN IV computer program written by the authors. A digital computer, FACOM 230-35, was used at the Data Processing Center, Kanazawa University.

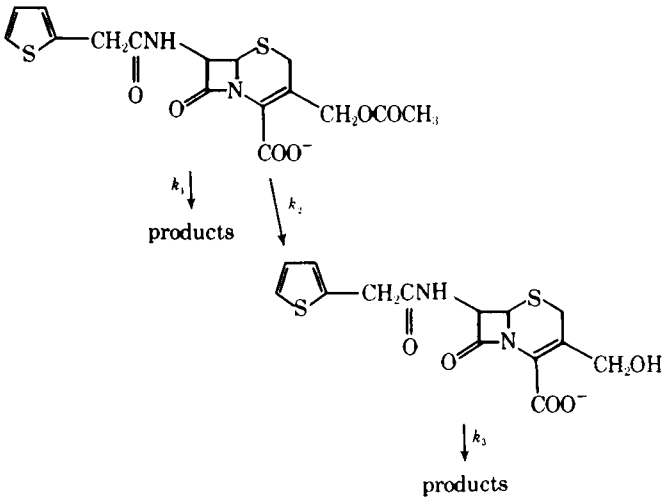

Scheme I

lothin hydrolysis were reported previously. The hydrolysis rate constants for k_1, k_2, and k_3 can be defined, in nonbuffer solutions, as $(k_1)_{pH}$, $(k_2)_{pH}$, and $(k_3)_{pH}$ and obey Eqs. 1*a*–1*c* above pH 9:

$$(k_1)_{pH} = (k_1)_{OH}a_{OH^-} \quad \text{(Eq. 1}a\text{)}$$

$$(k_2)_{pH} = (k_2)_{OH}a_{OH^-} \quad \text{(Eq. 1}b\text{)}$$

$$(k_3)_{pH} = (k_3)_{OH}a_{OH^-} \quad \text{(Eq. 1}c\text{)}$$

where $(k_i)_{OH}$ is the specific hydroxide ion-catalyzed rate constant for the respective hydrolytic reactions and a_{OH^-} is the hydroxide-ion activity and can be calculated at 35° from (25):

$$a_{H^+}a_{OH^-} = 10^{-13.68} \quad \text{(Eq. 2)}$$

The $(k_i)_{OH}$ average values (35°, μ = 0.5) for $(k_i)_{pH}$ from the data determined by HPLC and previously (23), according to Eqs. 1*a*–1*c*, were 1.06 × 10^3, 1.82 × 10^3, and 1.01 × 10^3 M^{-1} hr^{-1}, respectively.

A typical 5-hr chromatogram of cephalothin with 0.12 *M* glycine (pH 9.5, 35°, μ = 0.5) is shown in Fig. 1B. There were some differences in the product peaks between hydrolysis (Fig. 1A) and aminolysis at the same pH. UV spectra of these peaks are shown in Fig. 2. Peaks 1 and 2 had two characteristic absorption maxima at 235 and 260 nm, consistent with those of cephalothin and deacetylcephalothin (26). Peaks 3–5 were assigned to the glycinolysis products of cephalothin and/or deacetylcephalothin. These findings indicate that the cephalothin aminolysis is also represented as Scheme I.

The time course (mole percent) for cephalothin and deacetylcephalothin during cephalothin glycinolysis at pH 9.5 (Fig. 3) showed good agreement with values calculated from the nonlinear least-squares analysis[9]. The rate constants computed were (in hr^{-1}): k_1 = 0.345 ± 0.008, k_2 = 0.161 ± 0.007, and k_3 = 0.184 ± 0.018 (*SD*). No detectable *N*-

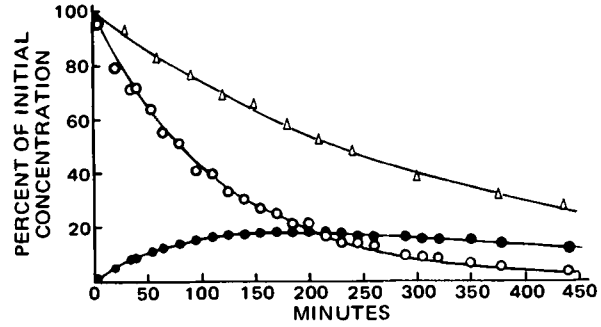

Figure 3—*Time course for cephalothin* (○) *and deacetylcephalothin* (●) *during cephalothin aminolysis and that for deacetylcephalothin aminolysis* (△), *both with 0.12* M *glycine at pH 9.50, 35°, and 0.5 ionic strength. Points for cephalothin aminolysis were from several experiments by HPLC under the same conditions. The curves were calculated according to Scheme I by the use of the following rate constants (in hours*$^{-1}$*):* k_1 = *0.345,* k_2 = *0.164, and* k_3 = *0.184.*

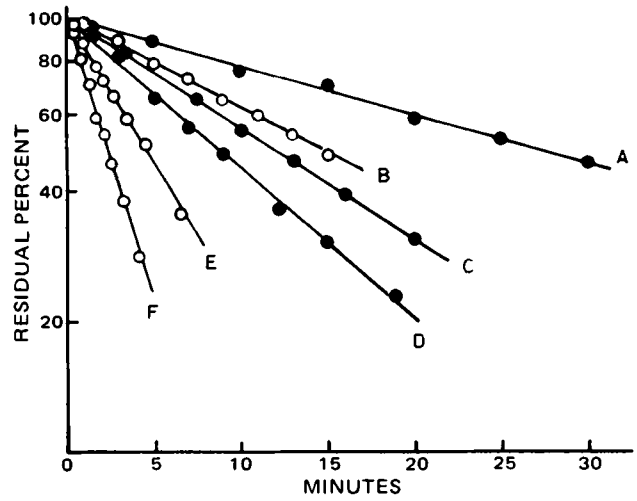

Figure 4—*Apparent first-order plots determined by HPLC for the aminolysis of cephalothin* (○) *and cefazolin* (●) *at 35° and 0.5 ionic strength. Key: A, 0.08* M *β-alanine at pH 10.30; B, 0.38* M *β-alanine at pH 9.70; C, 0.25* M *glycine at pH 10.00; D, 0.12* M *ε-aminocaproic acid at pH 10.30; E, 0.30* M *β-alanine at pH 10.30; and F, 0.094* M *ε-aminocaproic acid at pH 10.80.*

acetylglycine formation was found on TLC, as previously observed (18). These kinetic and TLC results indicate no significant ester moiety aminolysis at the cephalothin 3-position. The deacetylcephalothin reaction in 0.12 *M* glycine buffer (pH 9.5, 35°, μ = 0.5) is shown in Fig. 3. The first-order degradation rate constant was k_3 = 0.183 $hr,^{-1}$ which is in fair agreement with that computed from the cephalothin glycinolysis under the same conditions.

For other aminolysis reactions followed by HPLC, cephalothin disappearance followed first-order kinetics (Fig. 4). The pseudo-first-order rate constant, k_{obs}, can be commonly expressed for the reactions in all amine solutions as:

$$k_{obs} = k_{pH} + k_{amine} \quad \text{(Eq. 3)}$$

where k_{pH} is the cephalothin first-order hydrolysis rate constant and is equal to $(k_1)_{pH}$ + $(k_2)_{pH}$ and k_{amine} is the first-order rate constant depending on the concentration of amines.

Monitoring Cefazolin Aminolysis—Typical chromatograms of cefazolin aminolysis with ε-aminocaproic acid are shown in Fig. 5 as a function of time. Cefazolin aminolysis occurs only at the β-lactam moiety. The semilogarithmic plots of the remaining cefazolin percentage were reasonably linear (Fig. 4), indicating that the cefazolin degradation followed first-order kinetics. The pseudo-first-order rate constant, k_{obs}, obtained from the slopes is the sum of the competing rate constants, k_{pH} for hydrolysis and k_{amine} for aminolysis, and is given by Eq. 3. Cefazolin hydrolysis k_{pH} obeys Eq. 4 above pH 9, as verified previously (18, 23):

$$k_{pH} = k_{OH}a_{OH^-} \quad \text{(Eq. 4)}$$

The value of k_{OH} used for the calculation was 1.14 × 10^3 M^{-1} hr^{-1} (23).

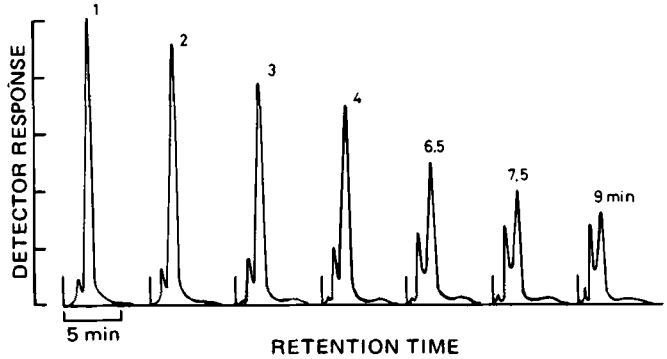

Figure 5—*HPLC changes for the cefazolin reaction with 0.10* M *ε-aminocaproic acid at pH 10.60, 35°, and 0.5 ionic strength with time in minutes (listed in graph).*

Table IV—Aminolysis Rate Constants of Cephalosporins and Penicillin G at 0.5 or 1.0 Ionic Strength (μ) and 35°

Amine	pKa[a]	Rate Constant[b]	β-Lactam Antibiotics: Cephalothin μ = 0.5	Cephalothin μ = 1.0[c]	Deacetylcephalothin μ = 0.5	Deacetylcephalothin μ = 1.0[c]	Cefazolin μ = 0.5	Cefazolin μ = 1.0[c]	Penicillin G μ = 0.5[a]	Penicillin G μ = 1.0[c]
ε-Aminocaproic acid	10.55	k_n	9.6	9.0	—	—[d]	9.1	9.6	5.3	24
		k_{gb}	873	1280	—	420	874	1380	1770	1100
		$k_{gOH} \times 10^{-4}$	12	12[e]	—	10	13	10[e]	10	16[e]
β-Alanine	9.98	k_n	2.0	3.0	—	1.2	3.4	3.0	1.0	6.0
		k_{gb}	109	258	—	114	122	270	213	240
		$k_{gOH} \times 10^{-4}$	3.5	3.2[e]	—	—[d]	2.1	3.2[e]	4.2	5.5
Glycine[f]	9.41	k_n	0.78	1.2	—[d]	—[d]	0.83	—[d]	0.40	3.6
		k_{gb}	73.6	150	27.7	48	81.5	162	90.6	96.0

[a] Determined previously (13). [b] Defined in Eq. 5; k_n in M^{-1} hr^{-1} and k_{gb} and k_{gOH} in M^{-2} hr^{-1}. [c] Values reported by Bundgaard (18). [d] Undetectable. [e] Recalculated from the reported values (18) according to the definition in Eq. 5 by use of the relationship (18) $\log[OH^-] = \log a_{OH^-} + 0.12$. [f] The k_{gOH} constant could not be determined.

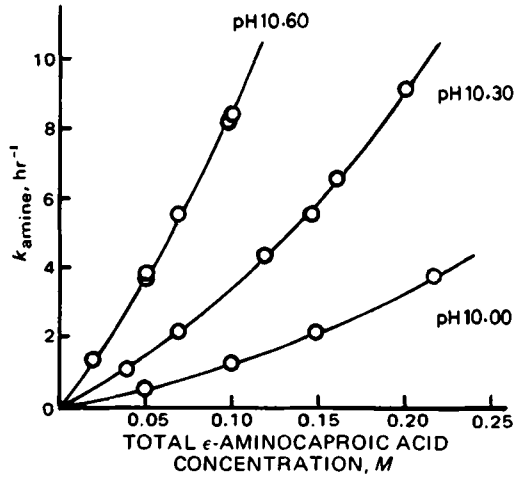

Figure 6—*Pseudo-first-order rate constants* versus *total amine concentration for cefazolin reaction with ε-aminocaproic acid at 35° and 0.5 ionic strength. Curves were calculated from Eq. 5 and rate constants in Table I.*

Aminolysis Kinetics—Typical plots of the aminolysis rate constant, k_{amine}, *versus* total amine concentration, $[amine]_T$ (Fig. 6) showed upward curvature at any pH. These pseudo-first-order rate constants apparently obey the general relationship reported previously for penicillins (7, 10, 13, 18) and cephalosporins (18):

$$k_{amine} = k_n[amine] + k_{gb}[amine]^2 + k_{gOH}[amine]a_{OH^-} \quad \text{(Eq. 5)}$$

where k_n represents the unassisted or water-catalyzed reaction of free amine on the β-lactam moiety, k_{gb} represents the general base-catalyzed and nucleophilic reaction with assistance by the amine second molecule, and k_{gOH} is the hydroxide ion-catalyzed third-order rate constant of nucleophilic displacement by the amine. The concentration of free amine can be calculated from:

$$[amine] = \frac{K_a}{K_a + a_{H^+}}[amine]_T \quad \text{(Eq. 6)}$$

where K_a is the conjugated amine acid dissociation constant. The pKa values determined previously under the same conditions (13) were used for the calculation.

Rearrangement of Eq. 5 leads to:

$$\frac{k_{amine}}{[amine]} = k_n + k_{gOH}a_{OH^-} + k_{gb}[amine] \quad \text{(Eq. 7)}$$

Equation 7 predicts that plots of $k_{amine}/[amine]$ *versus* [amine] provide k_{gb} as a slope of $k_n + k_{gb}a_{OH^-}$ as an intercept. One such plot is given in Fig. 7 for cephalothin, deacetylcephalothin, and cefazolin glycinolysis,

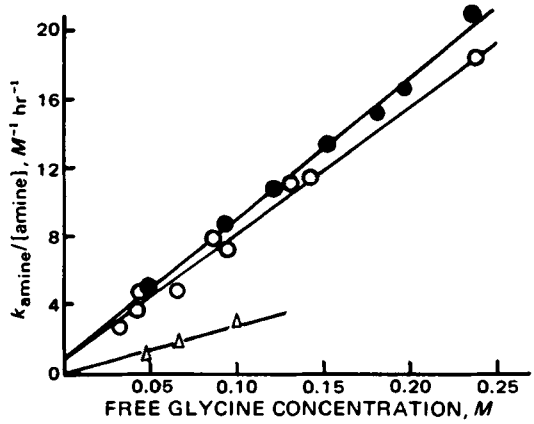

Figure 7—*Apparent second-order rate constants* versus *free amine concentration for the reactions of cephalothin (○), cefazolin (●), and deacetylcephalothin (△) with glycine at 35° and 0.5 ionic strength.*

Table V—Effect of Ionic Strength on the Reaction Rate Constants of Cephalothin with 0.12 *M* Glycine at pH 9.50 and 35°

Ionic Strength[a]	Rate Constant, hr^{-1}: k_{obs}[b]	k_{pH}[b,c]	k_{amine}[d]
0.5	0.506	0.207	0.299
1.0	0.649	0.213	0.436
2.0	0.772	0.217	0.555

[a] Adjusted with potassium chloride. [b] Determined by HPLC analysis. [c] $k_{pH} = (k_1)pH + (k_2)_{pH}$. [d] $k_{amine} = k_{obs} - k_{pH}$.

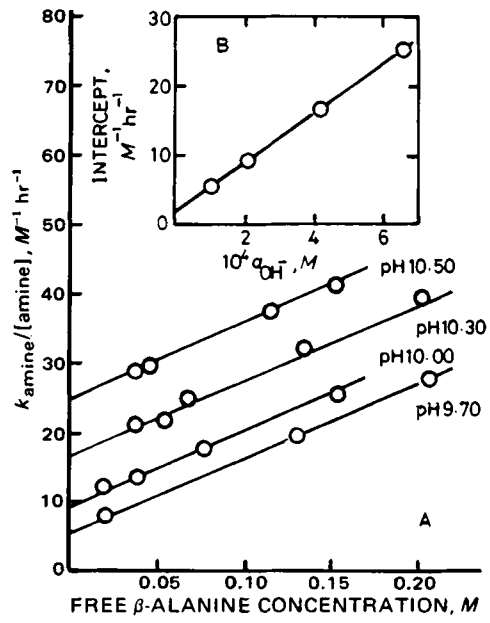

Figure 8—*Apparent second-order rate constants* versus *free amine concentration (A) and the intercepts of Fig. 8A* versus *hydroxide-ion activity (B) for cephalothin reaction with β-alanine at 35° and 0.5 ionic strength.*

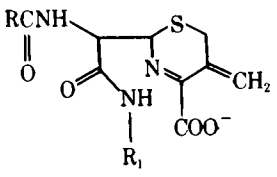

I

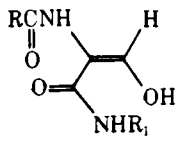

II

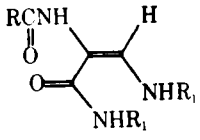

III

showing a single line in each case with different slopes. Another typical plot with different intercepts and the same slope is illustrated in Fig. 8, predicting significant contribution of the kinetic term of k_{gOH}.

The weighed multiple linear regression analysis according to Eq. 7 provides (with $R > 0.98$) the rate constants for the uncatalyzed (or water-assisted), general base-catalyzed, and hydroxide ion-catalyzed reactions of cephalosporins with a number of amines (Table IV). The solid lines in Figs. 6–8 were calculated from the rate law (Eq. 5) and the parameters in Table IV and show satisfactory agreement with the data.

In cephalosporin aminolysis, the rate constants of k_{gb} were 50% lower at $\mu = 0.5$ than those determined spectrophotometrically (18) for similar aminolysis at 35° and $\mu = 1.0$ (Table IV). The UV spectrophotometric analysis (18) of the present reaction solutions gave rate constants almost identical to those determined by HPLC. This significant difference may be attributed to the different ionic strength rather than to the analytical method.

This speculation was substantiated in cephalothin glycinolysis at ionic strengths of 0.5–2.0 (Table V). The aminolysis rate constants, k_{amine}, compared to the hydrolysis rate constants, k_{pH}, increased significantly with the ionic strength increase. The ionic strength effect was similar to that for phenyl acetate aminolysis in which a high concentration of potassium chloride increased the reaction rates (27, 28).

General base-catalyzed cephalosporin aminolysis was favored by ionic strength increases and presumably proceeded through activated complexes of more ionic character than the starting materials. For the cephalosporin aminolysis (Table IV), the influence of ionic strength on the uncatalyzed (or water-assisted) and hydroxide-ion-catalyzed rate constants (k_n and k_{gOH}) was small compared to that on the amine-catalyzed rate constants (k_{gb}). In contrast to cephalosporin reactivity, the marked increase of k_n compared to k_{gb} and k_{gOH} by an increase of ionic strength was noted for penicillin aminolysis.

The rate constants for penicillin G aminolysis determined at $\mu = 0.5$ in this laboratory (13) and those determined previously at $\mu = 1.0$ (18) under the same temperature condition (35°) are also listed in Table IV. The rate constants k_n of penicillin G at $\mu = 0.5$ increased significantly five to nine times at $\mu = 1.0$, while the catalyzed rate constants were almost unchanged. These different reaction rate sensitivities to the ionic strength between pencillin and cephalosporin may result from the difference in the mechanism and/or ionic nature of the transition state.

There was no significant difference in cephalosporin aminolysis rate constants as obtained by HPLC and differential UV spectrometry. The HPLC method requires no assumption on the UV absorbability of the reaction products and permits simultaneous determination of the starting materials and degradation products. The UV data for the first three to five half-lives, when treated by literature methods (29), also provide reliable rate constants (18, 19).

Mechanism of Cephalosporin Aminolysis—The amine and hydroxide-ion-catalyzed reactions of cephalosporins are likely to be catalyzed nucleophilic amine displacements on the β-lactam moiety, yielding the corresponding cephalosporoylamide, as demonstrated for penicillin aminolysis (13, 16). The uncatalyzed or water-assisted kinetic term of Eq. 5 may represent a nucleophilic displacement reaction to yield the cephalosporoylamides or a kinetically equivalent general base-catalyzed hydrolysis to yield cephalosporoic acids. For penicillin aminolysis, this reaction was nucleophilic (13, 16). Cephalosporin reaction with one amine molecule represents nucleophilic displacement (18). Since the experimental evidence strongly suggested the dominance of the nucleophilic reaction, no further experiments were performed.

Relative Reactivity, Aminolysis Products, and Chemical Aspects of Cephalosporin Allergy—There are two striking differences between the chemistry of cephalosporins and penicillins. One is the relative rate of aminolysis. Change in the acylamide side chain in penicillin molecules produces no significant change in the aminolysis rate (7, 16, 30, 31), whereas the cephalosporin aminolysis rate is markedly influenced by the nature of the cephalosporin molecules.

In comparison with the reactivity of cephalosporins containing 7-position thienyl side chains, deacetylcephalothin is less reactive than cephalothin, as seen by the glycinolysis rates (Table IV). This difference can be attributed either to the inductive effect on the 3-methylene substituent (18) or to the leavability of the 3-methylene moiety in activating the β-lactam ring toward nucleophilic attack (32). As a result, cephalosporins containing a strong electron-withdrawing or good leaving group in the 3-position, such as cephaloridine, are readily destroyed in the presence of amines (18). Cefazolin and cephalothin reaction with amino acid primary amino groups resembled that of penicillin G (Table IV). These clinically used cephalosporins may conjugate with free protein amino groups in the body as readily as does penicillin G.

Furthermore, the penicillin β-lactam ring can be opened to give a relatively stable D-α-penicilloate without further molecular degradation. The presence of a Δ^3-double bond in cephalosporins leads to more extensive cleavage on hydrolysis and aminolysis (33, 34). The initial aminolysis product (I) with λ_{max} 230 nm was followed by chromophores with λ_{max} 270 and 278 nm (attributed to molecular fragmentation) and penaldates (II) and penamaldates (III) (33, 34). These actual structures are not completely understood. UV spectra of HPLC peaks, which appeared during cephalothin glycinolysis (Fig. 1B), revealed characteristic λ_{max} absorptions at 230 and 270 nm (Fig. 2). The UV spectrum of peak 5, which increased in peak height with time at the last aminolysis stage, exhibited λ_{max} at 278 nm. On the basis of reported chemical and spectroscopic evidence (33, 34) on the cephalosporin aminolysis product, peaks 3, 4, and 5 from the cephalothin glycinolysis may correspond to I, II, and III, respectively.

REFERENCES

(1) M. A. Schwartz, *J. Pharm. Sci.*, **58**, 643 (1969).

(2) M. W. Brandriss, J. W. Smith, and H. G. Steinmann, *J. Immunol.*, **94**, 696 (1965).

(3) F. R. Batchelor, J. M. Dewdney, R. D. Weston, and A. W. Wheeler, *Immunology*, **10**, 21 (1966).

(4) K. Shibata, T. Atsumi, Y. Horiuchi, and K. Mashimo, *Nature (London)*, **212**, 419 (1966).

(5) Y. Mine, M. Nishida, S. Goto, and S. Kuwahara, *J. Antibiot.*, **23**, 195 (1970).

(6) J. M. T. Hamilton-Miller and E. P. Abraham, *Biochem. J.*, **123**, 183 (1971).

(7) M. A. Schwartz and G.-M. Wu, *J. Pharm. Sci.*, **55**, 550 (1966).

(8) M. A. Schwartz, *ibid.*, **57**, 1209 (1968).

(9) C. H. Schneider and A. L. de Weck, *Biochim. Biophys. Acta*, **168**, 27 (1968).

(10) H. Bundgaard, *Dan. Tidsskr. Farm.*, **46**, 29 (1972).

(11) H. Bundgaard, *J. Pharm. Pharmacol.*, **24**, 985 (1972).

(12) T. Yamana, A. Tsuji, E. Miyamoto, and E. Kiya, *ibid.*, **27**, 283 (1975).

(13) A. Tsuji, T. Yamana, E. Miyamoto, and E. Kiya, *ibid.*, **27**, 580 (1975).

(14) T. Yamana, A. Tsuji, E. Miyamoto, and E. Kiya, *ibid.*, **27**, 771 (1975).

(15) H. Bundgaard, *ibid.*, **28**, 725 (1976).

(16) H. Bundgaard, *Arch. Pharm. Chemi, Sci. Ed.*, **4**, 91 (1976).

(17) H. Bundgaard, *Acta Pharm. Suec.*, **14**, 391 (1977).

(18) H. Bundgaard, *Arch. Pharm. Chemi, Sci. Ed.*, **3**, 94 (1975).

(19) H. Bundgaard, *Acta Pharm. Suec.*, **13**, 299 (1976).

(20) P. P. K. Ho, R. D. Towner, J. M. Indelicato, W. J. Wilham, W. A. Spitzer, and G. A. Koppel, *J. Antibiot.*, **26**, 313 (1973).

(21) J. M. Indelicato, T. T. Norvilas, R. R. Pfeiffer, W. J. Wheeler, and W. L. Wilham, *J. Med. Chem.*, **17**, 523 (1974).

(22) R. D. Kinget and M. A. Schwartz, *J. Pharm. Sci.*, **58**, 1102 (1969).

(23) T. Yamana and A. Tsuji, *ibid.*, **65**, 1563 (1976).

(24) J. Konecny, E. Felber, and J. Gruner, *J. Antibiot.*, **26**, 135 (1973).

(25) H. S. Harned and W. J. Hamer, *J. Am. Chem. Soc.*, **55**, 2194 (1933).

(26) E. Van Heyningen, *J. Med. Chem.*, **8**, 22 (1965).

(27) W. P. Jencks and J. Carriuolo, *J. Am. Chem. Soc.*, **82**, 675 (1960).

(28) W. P. Jencks and M. Gilchrist, *ibid.*, **88**, 104 (1966).

(29) E. A. Guggenheim, *Phil. Mag.*, **2**, 538 (1926).
(30) H. Bundgaard, *Dan. Tidsskr. Farm.*, **46**, 85 (1972).
(31) T. Yamana, A. Tsuji, E. Kiya, and E. Miyamoto, *J. Pharm. Sci.*, **66**, 861 (1977).
(32) D. B. Boyd, R. B. Hermann, D. E. Presti, and M. M. Marsh, *J. Med. Chem.*, **18**, 408 (1975).
(33) J. M. T. Hamilton-Miller, G. G. F. Newton, and E. P. Abraham, *Biochem. J.*, **116**, 371 (1970).
(34) J. M. T. Hamilton-Miller, E. Richards, and E. P. Abraham, *ibid.*, **116**, 385 (1970).

ACKNOWLEDGMENTS

The authors acknowledge the gifts of cephalosporins from Shionogi & Co. and Fujisawa Pharmaceutical Co., Japan. They also thank Ms. A. Ito, Ms. T. Takamura, and Ms. K. Matsui for assistance.

Localization of Low Molecular Weight ^{99m}Tc-Labeled Dimercaptodicarboxylic Acids in Kidney Tissue

DAVID O. KUBIATOWICZ, THEODORE F. BOLLES, JAMES C. NORA, and DIONYSSIS S. ITHAKISSIOS ˣ

Received March 18, 1977, from the *Medical Products Division, 3M Co., 3M Center, St. Paul, MN 55101.* Accepted for publication October 27, 1978.

Abstract □ Kidney localization of low molecular weight ^{99m}Tc-dimercaptodicarboxylic acid complexes was examined in mice. The complexes ^{99m}Tc-dimercaptosuccinic acid, ^{99m}Tc-dimercaptoglutaric acid, and ^{99m}Tc-dimercaptoadipic acid were formed by reducing sodium ^{99m}Tc-pertechnetate with stannous chloride in the presence of 2–10-fold excess ligand at pH 2.5 or 7.5. Kidney specificity decreased as chain length between the mercapto groups increased. Optimum kidney retention occurred with complexes formed at pH 2.5. Complexes prepared at pH 7.5 were rapidly excreted through the urine and feces. Kidney localization of complexes prepared at one pH was not altered if the pH was later changed.

Keyphrases □ Technetium mercaptan complexes—localization in kidney tissue, synthesis, low molecular weight, structure–activity relationships □ Radionuclide imaging, renal—technetium mercaptan complexes, low molecular weight, localization in kidney tissue, synthesis, structure–activity relationships □ Kidney—radionuclide imaging, technetium mercaptan complexes, structure–activity relationships □ Structure–activity relationships—technetium mercaptan complexes, localization in kidney tissue

Radionuclide diagnosis of renal disease saves time in routine renal function tests and allows external kidney monitoring for clearance and morphological studies. The ^{203}Hg- and ^{197}Hg-labeled agents previously used have been replaced by ^{99m}Tc-labeled agents to decrease the high absorbed radiation dose *in vivo* (1).

Initial work on technetium mercaptan complexes as organ imaging agents led to the introduction of ^{99m}Tc-dihydrothioctic acid as a replacement for rose bengal in liver, gallbladder, and biliary tract studies (2). Other unpublished studies indicated that technetium complexes with short chain mono- and dimercaptodicarboxylic acids accumulated in kidney tissue. ^{99m}Tc-Dimercaptodicarboxylic acids were found to have better localization characteristics than their monomercapto analogs, especially ^{99m}Tc-dimercaptosuccinic acid, which has become well known as a renal imaging agent (1).

This *in vivo* study concerned organ localization of low molecular weight ^{99m}Tc-dimercaptodicarboxylic acids as affected by the number of carbon atoms between the mercapto groups and by the pH of complex formation.

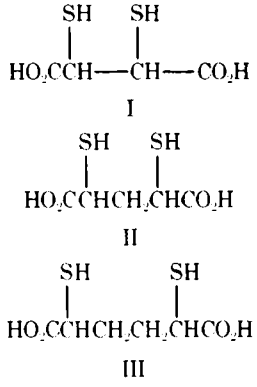

I

II

III

EXPERIMENTAL

Dimercaptosuccinic acid[1] (I) was used without further purification.

Dimercaptoglutaric acid (II) was synthesized according to a literature procedure (3). Glutaric acid was brominated and esterified to form dimethyl 2,4-dibromoglutarate. The dibromide was reacted with potassium thioacetate to form the acetyl dithio ester. This derivative was subjected to alkaline hydrolysis in the presence of iodine and recrystallized from ethyl acetate to yield 1,2-dithiolane-3,5-dicarboxylic acid (the disulfide of II), mp 190–192° [lit. (3) mp 193–194°]. The structure for the disulfide was confirmed by elemental analysis, NMR, and mass spectrometry. Dimercaptoglutaric acid was generated from its disulfide, just prior to technetium complex formation, by reduction with aqueous sodium borohydride at pH 8, a technique that has been demonstrated in related compounds (4).

Dimercaptoadipic acid (III) was synthesized by incubating 2,2′-dibromoadipic acid[2] with aqueous potassium xanthogenate, followed by alkaline hydrolysis of the xanthate derivative in methanol and acidification. The solid was further purified by recrystallization from boiling water to yield pure crystalline III, mp 186–189° [lit. (5) mp 187–189°]. The structure for III was confirmed by elemental analysis and NMR.

^{99m}Tc-Dimercaptodicarboxylic Acid Complexes—These complexes were prepared in a nitrogen atmosphere by adding 0.1–2 ml of sodium pertechnetate ($Na^{99m}TcO_4$) (IV) eluate from ^{99}Mo-^{99m}Tc-generator[3] to 1–3 ml of stock tin–dimercaptodicarboxylic acid solution (pH 2.5 or 7.5), followed by 5–15 min of incubation at room temperature. The

[1] J. T. Baker, Phillipsburg, N.J.
[2] ICN Laboratories, Cleveland, Ohio.
[3] Mallinckrodt, St. Louis, Mo.

0022-3549/79/0500-0621$01.00/0
© 1979, American Pharmaceutical Association

(29) E. A. Guggenheim, *Phil. Mag.*, **2**, 538 (1926).
(30) H. Bundgaard, *Dan. Tidsskr. Farm.*, **46**, 85 (1972).
(31) T. Yamana, A. Tsuji, E. Kiya, and E. Miyamoto, *J. Pharm. Sci.*, **66**, 861 (1977).
(32) D. B. Boyd, R. B. Hermann, D. E. Presti, and M. M. Marsh, *J. Med. Chem.*, **18**, 408 (1975).
(33) J. M. T. Hamilton-Miller, G. G. F. Newton, and E. P. Abraham, *Biochem. J.*, **116**, 371 (1970).
(34) J. M. T. Hamilton-Miller, E. Richards, and E. P. Abraham, *ibid.*, **116**, 385 (1970).

ACKNOWLEDGMENTS

The authors acknowledge the gifts of cephalosporins from Shionogi & Co. and Fujisawa Pharmaceutical Co., Japan. They also thank Ms. A. Ito, Ms. T. Takamura, and Ms. K. Matsui for assistance.

Localization of Low Molecular Weight ^{99m}Tc-Labeled Dimercaptodicarboxylic Acids in Kidney Tissue

DAVID O. KUBIATOWICZ, THEODORE F. BOLLES, JAMES C. NORA, and DIONYSSIS S. ITHAKISSIOS ˣ

Received March 18, 1977, from the *Medical Products Division, 3M Co., 3M Center, St. Paul, MN 55101.* Accepted for publication October 27, 1978.

Abstract □ Kidney localization of low molecular weight ^{99m}Tc-dimercaptodicarboxylic acid complexes was examined in mice. The complexes ^{99m}Tc-dimercaptosuccinic acid, ^{99m}Tc-dimercaptoglutaric acid, and ^{99m}Tc-dimercaptoadipic acid were formed by reducing sodium ^{99m}Tc-pertechnetate with stannous chloride in the presence of 2–10-fold excess ligand at pH 2.5 or 7.5. Kidney specificity decreased as chain length between the mercapto groups increased. Optimum kidney retention occurred with complexes formed at pH 2.5. Complexes prepared at pH 7.5 were rapidly excreted through the urine and feces. Kidney localization of complexes prepared at one pH was not altered if the pH was later changed.

Keyphrases □ Technetium mercaptan complexes—localization in kidney tissue, synthesis, low molecular weight, structure–activity relationships □ Radionuclide imaging, renal—technetium mercaptan complexes, low molecular weight, localization in kidney tissue, synthesis, structure–activity relationships □ Kidney—radionuclide imaging, technetium mercaptan complexes, structure–activity relationships □ Structure–activity relationships—technetium mercaptan complexes, localization in kidney tissue

Radionuclide diagnosis of renal disease saves time in routine renal function tests and allows external kidney monitoring for clearance and morphological studies. The ^{203}Hg- and ^{197}Hg-labeled agents previously used have been replaced by ^{99m}Tc-labeled agents to decrease the high absorbed radiation dose *in vivo* (1).

Initial work on technetium mercaptan complexes as organ imaging agents led to the introduction of ^{99m}Tc-dihydrothioctic acid as a replacement for rose bengal in liver, gallbladder, and biliary tract studies (2). Other unpublished studies indicated that technetium complexes with short chain mono- and dimercaptodicarboxylic acids accumulated in kidney tissue. ^{99m}Tc-Dimercaptodicarboxylic acids were found to have better localization characteristics than their monomercapto analogs, especially ^{99m}Tc-dimercaptosuccinic acid, which has become well known as a renal imaging agent (1).

This *in vivo* study concerned organ localization of low molecular weight ^{99m}Tc-dimercaptodicarboxylic acids as affected by the number of carbon atoms between the mercapto groups and by the pH of complex formation.

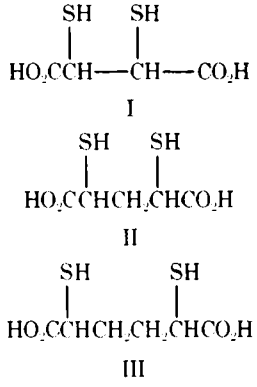

I

II

III

EXPERIMENTAL

Dimercaptosuccinic acid[1] (I) was used without further purification.

Dimercaptoglutaric acid (II) was synthesized according to a literature procedure (3). Glutaric acid was brominated and esterified to form dimethyl 2,4-dibromoglutarate. The dibromide was reacted with potassium thioacetate to form the acetyl dithio ester. This derivative was subjected to alkaline hydrolysis in the presence of iodine and recrystallized from ethyl acetate to yield 1,2-dithiolane-3,5-dicarboxylic acid (the disulfide of II), mp 190–192° [lit. (3) mp 193–194°]. The structure for the disulfide was confirmed by elemental analysis, NMR, and mass spectrometry. Dimercaptoglutaric acid was generated from its disulfide, just prior to technetium complex formation, by reduction with aqueous sodium borohydride at pH 8, a technique that has been demonstrated in related compounds (4).

Dimercaptoadipic acid (III) was synthesized by incubating 2,2′-dibromoadipic acid[2] with aqueous potassium xanthogenate, followed by alkaline hydrolysis of the xanthate derivative in methanol and acidification. The solid was further purified by recrystallization from boiling water to yield pure crystalline III, mp 186–189° [lit. (5) mp 187–189°]. The structure for III was confirmed by elemental analysis and NMR.

^{99m}Tc-Dimercaptodicarboxylic Acid Complexes—These complexes were prepared in a nitrogen atmosphere by adding 0.1–2 ml of sodium pertechnetate ($Na^{99m}TcO_4$) (IV) eluate from ^{99}Mo-^{99m}Tc-generator[3] to 1–3 ml of stock tin–dimercaptodicarboxylic acid solution (pH 2.5 or 7.5), followed by 5–15 min of incubation at room temperature. The

[1] J. T. Baker, Phillipsburg, N.J.
[2] ICN Laboratories, Cleveland, Ohio.
[3] Mallinckrodt, St. Louis, Mo.

0022-3549/79/0500-0621$01.00/0
© 1979, American Pharmaceutical Association

Table I—Distribution of ^{99m}Tc-Dimercaptodicarboxylic Acid Complexes in Mice [a]

Organ	^{99m}Tc-Dimercaptosuccinic Acid		^{99m}Tc-Dimercaptoglutaric Acid		^{99m}Tc-Dimercaptoadipic Acid	
	pH 2.5[b]	pH 7.5	pH 2.5	pH 7.5	pH 2.5	pH 7.5
Kidneys	31.5 ± 2.9[c]	3.2 ± 0.8	15.3 ± 3.2	2.6 ± 0.9	8.7 ± 1.4	6.6 ± 0.6
Liver	6.1 ± 1.1	1.1 ± 0.3	2.6 ± 1.0	1.4 ± 0.2	10.3 ± 1.7	6.7 ± 1.1
Intestine	3.4 ± 0.8	1.3 ± 0.1	3.2 ± 0.2	3.8 ± 0.4	3.4 ± 0.5	6.2 ± 0.9
Blood	28.2 ± 3.2	13.9 ± 2.1	15.8 ± 4.6	5.1 ± 0.6	33.1 ± 5.1	24.8 ± 3.2
Urine and feces	28.4 ± 4.3	83.4 ± 9.6	65.4 ± 15.1	89.8 ± 10.8	30.5 ± 4.2	53.1 ± 9.3

[a] Four hours after injection of complexes (percent total). Complexes were prepared *via* reduction of sodium pertechnetate with stannous chloride. [b] The pH at which complexes were formed. [c] Percent total ± *SD*. Average results from four replications.

Table II—Distribution of ^{99m}Tc-Dimercaptosuccinic Acid in Mice [a]

Organ	Hours[b]					
	0.02	0.5	1.0	2.0	4.0	24.0
Kidneys	9.4 ± 1.3[c]	29.3 ± 3.8	39.5 ± 4.1	45.6 ± 6.7	54.8 ± 6.7	75.5 ± 12.2
Liver	28.6 ± 2.4	12.8 ± 1.7	9.4 ± 2.1	6.8 ± 1.8	3.8 ± 0.8	2.7 ± 0.7
Intestine	11.9 ± 2.1	7.2 ± 2.1	8.2 ± 1.9	4.8 ± 1.3	3.4 ± 1.0	2.1 ± 0.9
Blood	40.9 ± 5.8	30.4 ± 4.1	26.9 ± 4.0	20.4 ± 3.1	21.3 ± 4.5	8.4 ± 1.2
Urine and feces	9.2 ± 1.6	20.3 ± 3.8	16.0 ± 3.8	22.4 ± 2.6	16.7 ± 3.4	11.7 ± 3.1

[a] The complex was prepared *via* sodium hexabromotechnetate (action of hydrogen bromide on sodium pertechnetate). [b] Following injection. [c] Percent total ± *SD*. Average results from three replications.

stock solutions were made by mixing stannous chloride dissolved in oxygen-free 1 *M* HCl with 3 m*M* I, II, or III such that the ligand to tin ratio was 3:1. The stock solution pH was adjusted with 1 *M* $NaHCO_3$.

Following incubation, the complexes were analyzed for unreacted IV by TLC on silica gel 6060 paper[4] with acetone as the developing solvent; IV moved with the solvent front while reduced technetium remained at the origin. Unreacted IV was always less than 2%. If a mixture of acetone (100 parts) and 12 *M* HCl (0.5 part) was used as a developing solvent, the complexes migrated (R_f ~0.8) while IV moved with the solvent front.

To avoid accidental contamination of the complex with undesirable metal ions, all preparation steps were carried out in glass vessels and with highly pure reagents.

***In Vivo* Distribution Study**—The 84 female Swiss Webster mice[5] were from the same shipment and weighed 20–24 g. Prior to experimentation, the animals were housed in groups of six for 3 days. They were allowed free access to food and tap water.

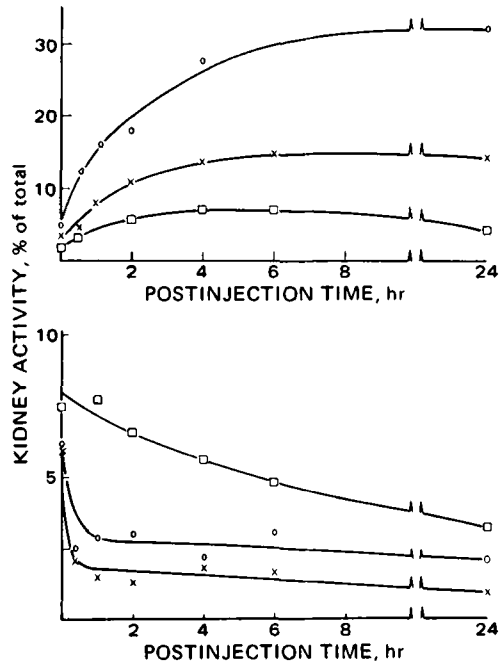

Figure 1—*Kidney localization of ^{99m}Tc-dimercaptosuccinic acid (○) compared with that of homologs ^{99m}Tc-dimercaptoglutaric acid (×) and ^{99m}Tc-dimercaptoadipic acid (□). Complexes were formed at pH 2.5 (top) and pH 7.5 (bottom).*

[4] Eastman.
[5] Bio-Lab, Centerville, Minn.

The *in vivo* distribution of ^{99m}Tc-dimercaptodicarboxylic acids in mice *versus* time was studied by intravenous injection of 1.5 mg/kg into the tail vein. The animals were injected at random and were killed at 0.02, 0.5, 1, 2, 4, 6, and 24 hr after injection by exposure to a carbon dioxide atmosphere. Blood samples were obtained by cardiac puncture immediately after death. The organs were assayed for radioactivity, and the results were reported as percent of total injected radioactivity. The experiment was replicated four times.

RESULTS AND DISCUSSION

Preparation of ^{99m}Tc-Dimercaptodicarboxylic Acid Complexes—This paper describes the reduction of radioactive pertechnetate IV and its reaction with excess dimercaptodicarboxylic acid complexes. Dimercaptodicarboxylic acids are by themselves reducing agents. Therefore, the technetium complexes could be formed simply by heating a solution of the acid with IV at 100° for 15–30 min. The addition of trace quantities (1 μg) of cupric sulfate or ferric chloride reduced the reaction time to 5 min.

A drawback of this method was that oxidation of mercaptan groups sometimes occurred, producing incomplete labeling and formation of labeled dimercaptodicarboxylic acid fragments. This problem was eliminated by room temperature labeling in the presence of an oxidizable, lower valence metal salt such as ferrous chloride or stannous chloride under a nitrogen atmosphere and use of double-distilled water diluent. The ligand to tin ratio could vary from 2:1 to 10:1, and the labeling could be done at any pH between 2 and 9. ^{99m}Tc-Dimercaptosuccinic acid (V), ^{99m}Tc-dimercaptoglutaric acid (VI), and ^{99m}Tc-dimercaptoadipic acid (VII) prepared under these conditions were stable for at least 6 hr at room temperature.

The stannous chloride reduction was adequate for the formation of the low molecular weight ^{99m}Tc-dimercaptodicarboxylic acid complexes described in this study; however, a modified method was required for several other mercaptan derivatives that precipitated in the presence of tin. ^{99m}Tc-Mercaptan complexes were made by first reacting the sodium pertechnetate eluate with 9 *M* HBr at 100° under nitrogen to form sodium hexabromotechnetate, $Na_2{}^{99m}TcBr_6$ (VIII) (6, 7). Then the mixture was evaporated to dryness over a nitrogen stream, and a slightly red solid (VIII) residue was obtained (8). This residue was dissolved in ethanol and mixed with an equal volume of an ethanolic solution of mercaptan ligand. Afterward, the organic solvent was evaporated and the resulting ^{99m}Tc-mercaptan complex was dissolved in saline.

In all studies, the extent of reduction and the complex stability were followed by TLC and radiation monitoring since IV had a distinctly different R_f value than its complexed forms.

Kidney Localization of ^{99m}Tc-Dimercaptodicarboxylic Acids—^{99m}Tc-Dimercaptodicarboxylic acids, prepared at pH 2.4 and 7.5 and having a 3:1 ligand–tin ratio, were injected. The complexes circulated in the blood and either accumulated in kidneys and, to a lesser extent, in the liver (<10%) or were excreted.

Table I shows the distribution and excretion of the complexes formed in acidic or basic solutions in mice killed 4 hr after injection. The average

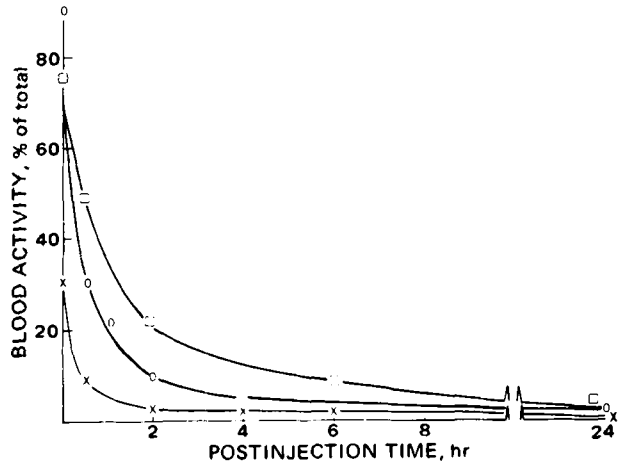

Figure 2—*Comparison of blood clearance rates of* ^{99m}*Tc-dimercaptosuccinic acid* (○), ^{99m}*Tc-dimercaptoglutaric acid* (×), *and* ^{99m}*Tc-dimercaptoadipic acid* (□) *formed at pH 2.5.*

kidney accumulation of V–VII *versus* postinjection time is shown in Fig. 1. Within a few hours after injection of the acidic complexes, V concentrated most highly in kidney tissue, plateauing at slightly above 30% of the total injected radioactivity. Five-carbon VI reached a maximum of 15%, and six-carbon VII concentrated least of all, plateauing at 8%. Paired *t* test analysis showed the curves to be significantly different ($p < 0.05$) for periods greater than 2 hr.

In contrast, the basic complexes showed an initial low kidney accumulation that radically dropped a short time after administration. Least sensitive of all to pH changes was VII, which showed very low kidney uptake of both acidic and basic preparations. In all cases, as the radioactivity in kidney tissue decreased, a marked increase in activity was found in the animal's excreta.

Figure 2 shows the average blood clearance of the three complexes formulated at pH 2.5. Slowest to clear was VII. The relative blood clearance rates were the same for complexes prepared at pH 7.5, but the individual clearance rates were faster. These complexes were excreted within 0.5 hr of injection.

Further studies indicated that low pH preparations were necessary for high kidney localization of the complexes. Complexes prepared at pH 2.5 and then raised to pH 7.5 by sodium bicarbonate addition prior to *in vivo* injection localized strongly in the kidney. However, complexes prepared at pH 7.5 and then lowered to pH 2.5 by hydrochloric acid addition still showed low kidney localization and were excreted rapidly. These observations are in agreement with those previously reported (9).

The ligand to tin ratio during complex formation and the injection time after complex preparation did not significantly affect the degree of complex localization in kidney tissue. During these studies, the ligand to tin ratio varied from 2:1 to 10:1, and the complexes were injected from 30 min to 6 hr after their preparation. If the complexes were not prepared using pure ligand and reagents and in an inert atmosphere, they rapidly decomposed into fragments that concentrated in the liver.

The nature of the technetium complexes formed is uncertain. The presence of two mercapto groups in the dicarboxylic acid molecules was necessary for good kidney uptake of the complexes. Comparative studies in this laboratory[6] using various monomercapto homologs such as ^{99m}Tc-mercaptoacetic acid and ^{99m}Tc-thiolactic acid showed that these complexes were more rapidly excreted and that their renal uptake was lower.

Reduction of pertechnetate with stannous chloride was used in this study because it was easy, rapid, and convenient. The complexes prepared by this method accumulated sufficiently in the kidney. However, reduction with hydrogen bromide, which can be used for a variety of mercaptan compounds, gave a higher deposition in the kidney with a considerable reduction in the excretion rate. Table II shows the distribution of V prepared by this method. The reason for the higher uptake is unknown. It may be due to the formation of a purer complex than that formed by tin reduction or to formation of an entirely different complex with higher specificity for kidney tissue.

Further studies are in progress to investigate the nature of complex formation as well as the chemical structure–kidney localization relationship.

REFERENCES

(1) M. D. Blaufox, L. R. Chervu, and I. M. Freeman, in "Radiopharmaceuticals," G. Subramanian, B. S. Rhodes, J. F. Cooper, and V. J. Sodd, Eds., Society of Nuclear Medicine, New York, N.Y., 1975, p. 385.

(2) R. A. Jackson, T. F. Bolles, D. O. Kubiatowicz, and G. E. Krejcarek, *J. Nucl. Med.*, **14**, 411 (1973).

(3) M. O. Hedblom, *Swedish J. Agric. Res.*, **1**, 43 (1971).

(4) I. C. Gunsalus, L. S. Barton, and W. Gruber, *J. Am. Chem. Soc.*, **78**, 1765 (1956).

(5) A. Fredga, *Chem. Ber.*, **71**, 289 (1928).

(6) L. Ossicini, F. Saracino, and M. Lederer, *J. Chromatogr.*, **16**, 524 (1964).

(7) J. Dalziel, N. S. Gill, R. S. Nyholm, and R. D. Peacock, *J. Chem. Soc.* **1958**, 4012.

(8) K. V. Kotegov, O. N. Pavlov, and V. P. Shvedov, in "Advances in Inorganic Chemistry and Radiochemistry," vol. 11, H. J. Emeleus and A. G. Sharre, Eds., Academic, New York, N.Y., 1968, pp 30–32.

(9) G. E. Krejcarek, J. H. Wicks, P. E. Heerwald, K. L. Tucker, V. M. Kubik, R. A. Newmark, and R. C. Williams, *J. Nucl. Med.*, **17**, 565 (1976).

[6] Unpublished data.

Hydrocortisone Stability in Human Feces

JANIS J. MacKICHAN ˣ and WILLIAM J. JUSKO

Received July 31, 1978, from the *Clinical Pharmacokinetics Laboratory, Department of Pharmaceutics, School of Pharmacy, State University of New York at Buffalo,* and *Millard Fillmore Hospital, Buffalo, NY 14209.* Accepted for publication November 1, 1978.

Abstract □ Hydrocortisone stability in human feces was studied under various conditions to determine whether stability accounts for the variable effects of hydrocortisone enemas. Recovery from feces and assay specificity were assured using dual isotopes, TLC separation, and liquid scintillation counting. Hydrocortisone degraded slightly from 7 to 26% in 24 hr when incubated in fresh human feces at 37°. Less than 7% degradation occurred in feces stored at 10°, and negligible degradation occurred with hydrocortisone in water at 37°. Fecal bacteria may account for the observed degradation. Hydrocortisone stability in feces may contribute to local persistence and may account partly for its efficacy in ulcerative colitis treatment.

Keyphrases □ Hydrocortisone—degradation, human feces, various rectal dosage forms □ Dosage forms—hydrocortisone, various rectal dosage forms, degradation in human feces □ Stability—hydrocortisone in human feces, various rectal dosage forms

Rectally administered hydrocortisone (cortisol) is an established mode of long-term ulcerative colitis therapy. It has the proposed advantage of direct drug delivery without excessive systemic absorption and the attendant

0022-3549/79/0500-0623$01.00/0
© 1979, American Pharmaceutical Association

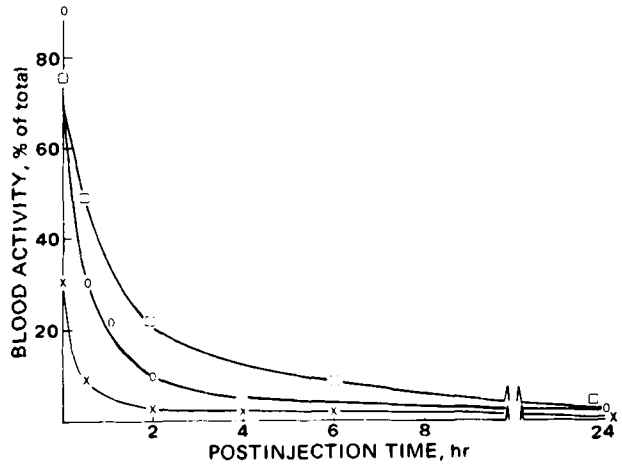

Figure 2—*Comparison of blood clearance rates of* ^{99m}*Tc-dimercaptosuccinic acid* (○), ^{99m}*Tc-dimercaptoglutaric acid* (×), *and* ^{99m}*Tc-dimercaptoadipic acid* (□) *formed at pH 2.5.*

kidney accumulation of V–VII *versus* postinjection time is shown in Fig. 1. Within a few hours after injection of the acidic complexes, V concentrated most highly in kidney tissue, plateauing at slightly above 30% of the total injected radioactivity. Five-carbon VI reached a maximum of 15%, and six-carbon VII concentrated least of all, plateauing at 8%. Paired *t* test analysis showed the curves to be significantly different ($p < 0.05$) for periods greater than 2 hr.

In contrast, the basic complexes showed an initial low kidney accumulation that radically dropped a short time after administration. Least sensitive of all to pH changes was VII, which showed very low kidney uptake of both acidic and basic preparations. In all cases, as the radioactivity in kidney tissue decreased, a marked increase in activity was found in the animal's excreta.

Figure 2 shows the average blood clearance of the three complexes formulated at pH 2.5. Slowest to clear was VII. The relative blood clearance rates were the same for complexes prepared at pH 7.5, but the individual clearance rates were faster. These complexes were excreted within 0.5 hr of injection.

Further studies indicated that low pH preparations were necessary for high kidney localization of the complexes. Complexes prepared at pH 2.5 and then raised to pH 7.5 by sodium bicarbonate addition prior to *in vivo* injection localized strongly in the kidney. However, complexes prepared at pH 7.5 and then lowered to pH 2.5 by hydrochloric acid addition still showed low kidney localization and were excreted rapidly. These observations are in agreement with those previously reported (9).

The ligand to tin ratio during complex formation and the injection time after complex preparation did not significantly affect the degree of complex localization in kidney tissue. During these studies, the ligand to tin ratio varied from 2:1 to 10:1, and the complexes were injected from 30 min to 6 hr after their preparation. If the complexes were not prepared using pure ligand and reagents and in an inert atmosphere, they rapidly decomposed into fragments that concentrated in the liver.

The nature of the technetium complexes formed is uncertain. The presence of two mercapto groups in the dicarboxylic acid molecules was necessary for good kidney uptake of the complexes. Comparative studies in this laboratory[6] using various monomercapto homologs such as ^{99m}Tc-mercaptoacetic acid and ^{99m}Tc-thiolactic acid showed that these complexes were more rapidly excreted and that their renal uptake was lower.

Reduction of pertechnetate with stannous chloride was used in this study because it was easy, rapid, and convenient. The complexes prepared by this method accumulated sufficiently in the kidney. However, reduction with hydrogen bromide, which can be used for a variety of mercaptan compounds, gave a higher deposition in the kidney with a considerable reduction in the excretion rate. Table II shows the distribution of V prepared by this method. The reason for the higher uptake is unknown. It may be due to the formation of a purer complex than that formed by tin reduction or to formation of an entirely different complex with higher specificity for kidney tissue.

Further studies are in progress to investigate the nature of complex formation as well as the chemical structure–kidney localization relationship.

REFERENCES

(1) M. D. Blaufox, L. R. Chervu, and I. M. Freeman, in "Radiopharmaceuticals," G. Subramanian, B. S. Rhodes, J. F. Cooper, and V. J. Sodd, Eds., Society of Nuclear Medicine, New York, N.Y., 1975, p. 385.

(2) R. A. Jackson, T. F. Bolles, D. O. Kubiatowicz, and G. E. Krejcarek, *J. Nucl. Med.*, **14**, 411 (1973).

(3) M. O. Hedblom, *Swedish J. Agric. Res.*, **1**, 43 (1971).

(4) I. C. Gunsalus, L. S. Barton, and W. Gruber, *J. Am. Chem. Soc.*, **78**, 1765 (1956).

(5) A. Fredga, *Chem. Ber.*, **71**, 289 (1928).

(6) L. Ossicini, F. Saracino, and M. Lederer, *J. Chromatogr.*, **16**, 524 (1964).

(7) J. Dalziel, N. S. Gill, R. S. Nyholm, and R. D. Peacock, *J. Chem. Soc.* **1958**, 4012.

(8) K. V. Kotegov, O. N. Pavlov, and V. P. Shvedov, in "Advances in Inorganic Chemistry and Radiochemistry," vol. 11, H. J. Emeleus and A. G. Sharre, Eds., Academic, New York, N.Y., 1968, pp 30–32.

(9) G. E. Krejcarek, J. H. Wicks, P. E. Heerwald, K. L. Tucker, V. M. Kubik, R. A. Newmark, and R. C. Williams, *J. Nucl. Med.*, **17**, 565 (1976).

[6] Unpublished data.

Hydrocortisone Stability in Human Feces

JANIS J. MacKICHAN ˣ and WILLIAM J. JUSKO

Received July 31, 1978, from the *Clinical Pharmacokinetics Laboratory, Department of Pharmaceutics, School of Pharmacy, State University of New York at Buffalo,* and *Millard Fillmore Hospital, Buffalo, NY 14209.* Accepted for publication November 1, 1978.

Abstract □ Hydrocortisone stability in human feces was studied under various conditions to determine whether stability accounts for the variable effects of hydrocortisone enemas. Recovery from feces and assay specificity were assured using dual isotopes, TLC separation, and liquid scintillation counting. Hydrocortisone degraded slightly from 7 to 26% in 24 hr when incubated in fresh human feces at 37°. Less than 7% degradation occurred in feces stored at 10°, and negligible degradation occurred with hydrocortisone in water at 37°. Fecal bacteria may account for the observed degradation. Hydrocortisone stability in feces may contribute to local persistence and may account partly for its efficacy in ulcerative colitis treatment.

Keyphrases □ Hydrocortisone—degradation, human feces, various rectal dosage forms □ Dosage forms—hydrocortisone, various rectal dosage forms, degradation in human feces □ Stability—hydrocortisone in human feces, various rectal dosage forms

Rectally administered hydrocortisone (cortisol) is an established mode of long-term ulcerative colitis therapy. It has the proposed advantage of direct drug delivery without excessive systemic absorption and the attendant

0022-3549/79/0500-0623$01.00/0
© 1979, American Pharmaceutical Association

Table I—Extraction of Hydrocortisone from Feces: Percent Recovery of Added Radiochemical

Sample	4-^{14}C-Hydrocortisone	1,2-^{3}H-Hydrocortisone
1	69.2	70.7
2	74.7	74.7
3	76.8	72.6
4	74.2	78.7
5	70.2	72.9
6	66.8	67.5
Mean	72.0	72.9
CV, %	5.3	5.2

risk of side effects (1–3).

Reported systemic hydrocortisone absorption following rectal administration is 0–50% of that seen after oral administration (1, 3). The reason for incomplete rectal absorption is uncertain. In particular, hydrocortisone stability in the colo-rectal environment has never been demonstrated. Fecal bacteria are capable of 21-dehydroxylating certain corticoids (4, 5) and may degrade hydrocortisone in feces.

This paper describes the analysis and *in vitro* stability of hydrocortisone in human feces incubated at 37°.

EXPERIMENTAL

Materials—1,2-^{3}H-Hydrocortisone [250 μCi/0.002 mg in 0.25 ml of benzene–ethanol (9:1)] and 4-^{14}C-hydrocortisone [50 μCi/0.33 mg in 2.5 ml of benzene–ethanol (9:1)] were received[1] in sealed ampuls. The ^{3}H-hydrocortisone was diluted to 15 ml with benzene–ethanol (9:1).

Hydrocortisone as the free alcohol[2] and two commercial hydrocortisone rectal enema suspensions[3] were used as received. Acetone, ethanol, trichloroacetic acid, benzene, methylene chloride, sodium chloride, and sodium hydroxide were reagent grade. Reagents and standards were prepared with distilled and deionized water.

Fecal samples were collected in 1-liter polytef-lined[4] metal paint cans[5]. Hydrocortisone was extracted from fecal homogenate using 50-ml conical polyethylene tubes[6], and extracts were separated on silica gel 60 F-254 precoated TLC plates[7]. Radioactive samples and quenched standards were prepared with a universal liquid scintillation cocktail[8].

Apparatus—Hydrocortisone on TLC plates was visualized using a short wavelength (254 nm) UV visualizing cabinet[9]. Dual-labeled samples were counted with a liquid scintillation spectrometer[10].

Radiochemical Standards—Dilute stock solutions of ^{3}H- and ^{14}C-hydrocortisone were prepared. Aliquots (0.3 ml) of ^{3}H-hydrocortisone (16.7 μCi/ml) and ^{14}C-hydrocortisone (20 μCi/ml) were transferred to separate 50-ml volumetric flasks and diluted to volume with benzene–ethanol (9:1). These solutions were stored in amber, glass-stoppered bottles at 10°.

Ethanolic radioactive hydrocortisone standard solutions were prepared as needed by evaporating small volumes (3–5 ml) of the stock solutions under nitrogen and reconstituting immediately with equal volumes of pure ethanol. These solutions were used for no longer than 72 hr and were stored in darkness at 10°.

Quenched Standards—A set of quenched standards was prepared for ^{3}H- and ^{14}C-hydrocortisone to facilitate counting efficiency determination of each isotope.

To each of six scintillation vials were added 10 ml of scintillation cocktail, 3 ml of water, and 100 μl of either ^{3}H- or ^{14}C-hydrocortisone stock solution. Acetone was added as a quenching agent so that one vial in each set contained 0, 0.1, 0.3, 0.5, 0.7, or 0.9 ml.

Standard curves were prepared by plotting the external standards ratio (an index of quench) *versus* the counting efficiency of each label in two preset energy channels.

[1] New England Nuclear, Boston, Mass.
[2] Sigma Chemical Co., St. Louis, Mo.
[3] I-Rectoid, Pharmacia; II-Cortenema, Rowell Laboratories.
[4] Teflon, du Pont.
[5] Glidden Paint Co., Buffalo, N.Y.
[6] Becton, Dickinson and Co., Cockeysville, Md.
[7] E. Merck, Darmstadt, West Germany.
[8] Scinti-Verse, Fisher Scientific Co., Springfield, N.J.
[9] Ultra-Violet Products, San Gabriel, Calif.
[10] Packard Instrument Co., Downers Grove, Ill.

Stability Protocol—Hydrocortisone stability was tested as three different formulations in biological specimens and under various conditions:

1. Incubation in feces at 37°—hydrocortisone enema I, three subjects; hydrocortisone enema II, one subject; and hydrocortisone free alcohol, one subject.
2. Incubation in feces at 10°—hydrocortisone enema I, one subject.
3. Incubation in water at 37°—hydrocortisone enema II, one subject.

Fecal Collection—Fresh fecal samples were collected from three healthy volunteers in clean dry-weighed metal cans. The cans were weighed again, an equal weight of water was added, and the contents were shaken vigorously for 1 hr.

Incubation—Each test series consisted of 1-g aliquots of fecal homogenate or water in six 50-ml plastic tubes. To each set of tubes was added hydrocortisone enema I, II, or aqueous hydrocortisone free alcohol so that the resulting hydrocortisone concentration in each sample was 0.25 mg/g.

Freshly prepared ethanolic ^{14}C-hydrocortisone solution (150 μl, ~39,960 dpm) was added to each tube, and the contents were vortexed for 30 sec. The tubes were sealed, covered with foil, and placed in either a constant-temperature water bath at 37° or a refrigerator at 10°.

Samples from each test series were removed from incubation at 0, 3, 6, 11, 14, and 24 hr. Freshly prepared ^{3}H-hydrocortisone in ethanol (150 μl, ~33,300 dpm) was added immediately to each tube to serve as an internal recovery standard and to account for losses during extraction. Six milliliters of trichloroacetic acid (6%) was added, and the contents were vortexed for 1 min. Following centrifugation at 3000 rpm for 10 min, the supernate was transferred to a clean plastic tube and stored at 10°.

Analytical Procedure—*Extraction*—To the supernate were added 4 ml of saturated sodium chloride solution and 35 ml of methylene chloride. After shaking vigorously for 30 min, the mixture was centrifuged at 3000 rpm for 5 min. The aqueous layer was aspirated and discarded. Then 10 ml of 0.1 *N* NaOH was added, and the mixture was vortexed for 15 sec. Following centrifugation at 3000 rpm for 5 min, the aqueous layer was again aspirated and discarded. The resultant methylene chloride phase was evaporated to dryness in the same tube under nitrogen with gentle heat (55°) provided by a water bath.

TLC—The residue was reconstituted with 100 μl of methylene chloride. Approximately 20 μl of this solution was spotted on the TLC plate with a 5-μl capillary tube. A known hydrocortisone standard in methylene chloride (0.5 mg/ml) was also spotted on the plate. Plates were developed in benzene–acetone (50:50) for the entire length of the plate (18 cm). The steroid R_f was 0.4. The hydrocortisone in each sample was visualized under UV light at 254 nm and compared to the hydrocortisone standard. Degradation products were observed but were not identified.

Liquid Scintillation Spectrometry—The silica was scraped from sections of the plate corresponding to unchanged hydrocortisone and placed in a scintillation vial containing 10 ml of scintillation cocktail and 3 ml of water. Cocktails were prepared to quantitate the actual disintegrations per minute in the ethanol solutions of ^{3}H- and ^{14}C-hydrocortisone that were added to these samples.

All samples were run with the two quenched standards sets and counted for approximately 10 min or 10,000 cpm under preset dual-label counting conditions.

Calculations—Unchanged ^{14}C-hydrocortisone radioactivity (disintegrations per minute) was analyzed as a function of time in all test groups. The amount of unchanged ^{14}C-hydrocortisone in each sample before extraction was determined as follows.

The disintegrations per minute of carbon 14 in a sample was determined by:

$$^{14}\text{C dpm} = {}^{14}\text{C cpm/efficiency of } {}^{14}\text{C in } {}^{14}\text{C channel} \quad \text{(Eq. 1)}$$

The counts per minute of hydrogen 3 in each sample was corrected for its efficiency in the hydrogen 3 window as well as the efficiency of carbon 14 in the hydrogen 3 window:

$$^{3}\text{H dpm} = \frac{{}^{3}\text{H cpm} - ({}^{14}\text{C dpm} \times \text{efficiency of } {}^{14}\text{C in } {}^{3}\text{H window})}{\text{efficiency of } {}^{3}\text{H in } {}^{3}\text{H window}} \quad \text{(Eq. 2)}$$

The internal standard (^{3}H-hydrocortisone) recovery efficiency was determined by:

$$\text{recovery efficiency} = \frac{{}^{3}\text{H dpm}}{\text{known } {}^{3}\text{H dpm added to sample}} \quad \text{(Eq. 3)}$$

The unchanged ^{14}C-hydrocortisone present in the sample before extraction was then calculated:

$$\text{actual } ^{14}\text{C dpm} = \frac{^{14}\text{C dpm calculated}}{\text{recovery efficiency}} \qquad \text{(Eq. 4)}$$

Extraction Efficiency and Reproducibility—^{14}C-Hydrocortisone and ^{3}H-hydrocortisone were added to six 1-g fecal homogenate samples, and the extraction procedure was performed. Following extraction, the methylene chloride phase was transferred to an empty scintillation vial and dried under nitrogen with gentle heat. Scintillation cocktail and water were added to the vials, and they were counted using the dual-label setting. The mean recovery of each labeled compound from feces was determined as well as the variability in recovery.

Added Radioactivity Recovery—The appearance of ^{14}C-hydrocortisone degradation products with time was quantitated for one incubated fecal sample set. After the regions corresponding to unchanged hydrocortisone had been scraped from the TLC plates, the remaining silica gel for the 0-, 11-, and 24-hr samples was scraped into separate vials and counted. Added ^{14}C-hydrocortisone recovery (unchanged and degraded) was calculated for each sample.

RESULTS

Extraction Technique—The efficiency and reproducibility of the technique are shown in Table I. The similarity in recoveries of the two labeled compounds in each sample indicates that either compound may be used as an internal recovery standard for the other. The extraction procedure reproducibility was good with a variation coefficient of about 5%.

Stability Studies—Hydrocortisone degradation over time under various conditions is presented in Fig. 1. Hydrocortisone enema I degradation in the feces of three different subjects ranged from 4.4 to 12.3% in 6 hr and from 7 to 26% in 24 hr (Fig. 1A). This same formulation showed negligible degradation when incubated at 37° in water (Fig. 1B). A study comparing hydrocortisone degradation in the feces of one subject under different temperature conditions (Fig. 1C) showed only 6.5% degradation at 10° as compared to 26% at 37° in 24 hr.

The degradation of three hydrocortisone formulations in the incubated feces of one subject (Fig. 1D) ranged from 13.6 to 26%, with the least degradation occurring with hydrocortisone free alcohol.

Added Radioactivity Recovery—At 0, 11, and 24 hr, the total carbon 14 percent present on the TLC plate as degradation product was 3.5, 9.6, and 15.6%, respectively. The added carbon 14 percent recovery, as both unchanged and degraded hydrocortisone, was 102, 89.3, and 83.1 for the 0-, 11-, and 24-hr samples, respectively. Inability to extract degradation products from feces as efficiently as unchanged hydrocortisone may account for the observed decrease in total radioactivity recovery with time. These results might also be explained by increased binding of unchanged hydrocortisone to incubated feces over time.

DISCUSSION

Hydrocortisone incubation in human feces resulted in as much as 26% degradation over 24 hr. Hydrocortisone given as an enema, however, is rarely retained in the rectum and colon longer than 6 hr, and the maximum observed degradation was 12% at this time.

Fecal material itself causes hydrocortisone degradation rather than temperature and hydrolysis (Fig. 1B). Relative hydrocortisone stability in water at 65° was previously reported (6) as a degradation $t_{1/2}$ of 25 days. A lower temperature apparently confers protection against degradation in feces (Fig. 1C). This phenomenon may be consistent with bacterial hydrocortisone degradation. Other investigators (4, 5) recently isolated and characterized in human feces bacterial organisms capable of metabolizing corticosteroids.

The small amount of hydrocortisone added to feces in the study (0.25 mg/g of fecal homogenate) was chosen to provide realistic exposure of hydrocortisone to fecal material, thus maximizing any possible degradation. The usual rectal hydrocortisone dose is 100 mg. Because the fecal samples were diluted twofold, the hydrocortisone concentration was actually 0.5 mg/g of feces. This concentration was selected assuming an average of 200 g of feces in the rectum at the time of hydrocortisone administration.

Because the greatest hydrocortisone loss was 26% in 24 hr at 0.5 mg/g of feces, only 6.5% of the drug should degrade in 6 hr if the process is first order. Extrapolation of these results to the clinical situation shows that even with a large fecal content in the rectum and thorough mixing of the

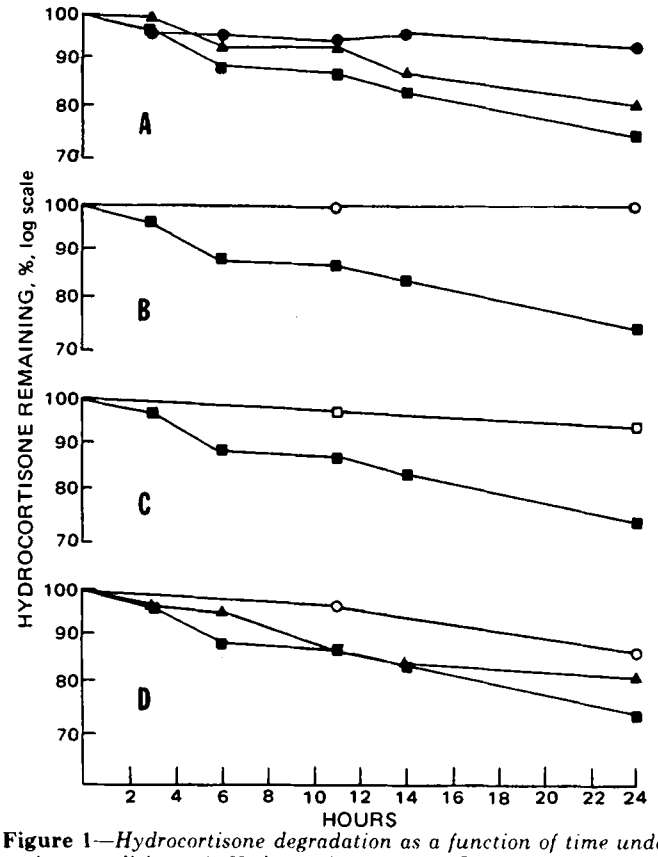

Figure 1—*Hydrocortisone degradation as a function of time under various conditions. A. Hydrocortisone enema I degradation in fecal samples from three human volunteers. Samples were incubated at 37°. B. Hydrocortisone enema I degradation in water (○) and human feces (■) at 37°. C. Hydrocortisone enema I degradation in fecal samples incubated at 37° (■) and refrigerated at 10° (□). D. Comparison of three hydrocortisone product degradations in human feces at 37°. Key: ○, hydrocortisone free alcohol in aqueous solution; ■, hydrocortisone enema I; and ▲, hydrocortisone enema II.*

administered hydrocortisone with rectal contents, little of the drug should actually be degraded during retention. For a 100-mg dose, only 6.5 mg should degrade in 6 hr.

It is widely assumed that the therapeutic benefit of hydrocortisone enemas is due in part to local action on the intestinal mucosa of ulcerative colitis patients. Previous studies (1, 3) suggested that hydrocortisone is incompletely absorbed through the intestinal mucosa and, therefore, persists in and acts upon the large intestine and rectum. A local effect could also result from lower GI tract exposure to the steroid during absorption. This demonstration of minimal hydrocortisone degradation in fecal material excludes one potential factor responsible for incomplete systemic availability of rectally administered hydrocortisone. Other factors that may account for incomplete systemic hydrocortisone availability include first-pass intestinal mucosa and/or liver metabolism and slow absorption and inadequate retention in the lower bowel.

REFERENCES

(1) M. Patterson, *Tex. Rep. Biol. Med.*, **16**, 508 (1958).

(2) J. C. Truelove, *Postgrad. Med. J.*, **37**, 76 (1961).

(3) R. G. Farmer and O. P. Schumacher, *Am. J. Gastroenterol.*, **54**, 229 (1970).

(4) V. D. Bokkenheuser, J. B. Suzuki, S. B. Polovsky, J. Winter, and W. G. Kelly, *Appl. Microbiol.*, **30**, 82 (1975).

(5) V. D. Bokkenheuser, J. Winter, P. Dehazya, and W. G. Kelly, *Appl. Environ. Microbiol.*, **34**, 571 (1977).

(6) V. D. Gupta, *J. Pharm. Sci.*, **67**, 299 (1978).

ACKNOWLEDGMENTS

Supported in part by a grant-in-aid from Pharmacia Laboratories and by Grant 24211 from the National Institute of General Medical Sciences.

Plasma Pentazocine Radioimmunoassay

J. E. PETERSON ˣ, M. GRAHAM, W. F. BANKS, D. BENZIGER, E. A. ROWE, S. CLEMANS, and J. EDELSON

Received September 19, 1978, from the *Department of Drug Metabolism and Disposition, Sterling-Winthrop Research Institute, Rensselaer, NY 12144.* Accepted for publication October 31, 1978.

Abstract □ A sensitive and specific radioimmunoassay of dog and human plasma pentazocine is described. Rabbit antiserum and the second antibody method separated bound from free pentazocine. The radioimmunoassay employed an ^{125}I-labeled radioligand and required extraction from the sample prior to quantitation. The method had a detection limit of approximately 200 pg/assay tube (1 ng/ml). The assay was used successfully to measure pentazocine in the plasma of beagle hounds given 0.3 mg of pentazocine/kg iv. The decline in plasma levels fitted a two-compartment body model with a 100-min mean overall half-life and a 3.2-liters/hr mean plasma clearance rate.

Keyphrases □ Pentazocine—radioimmunoassay, dog and human plasma, pharmacokinetics □ Radioimmunoassay—pentazocine, dog and human plasma □ Pharmacokinetics—pentazocine, dog and human plasma, radioimmunoassay □ Analgesics—pentazocine, radioimmunoassay, dog and human plasma, pharmacokinetics

Pentazocine, (2α,6α,11R*)-(±)-1,2,3,4,5,6-hexahydro-6,11- dimethyl-3- (3-methyl-2- butenyl) -2,6- methano-3-benzazocin-8-ol[1] (Ia), is a member of the benzomorphan series of compounds (1). Pentazocine is a potent analgesic and a weak narcotic antagonist, possessing little dependence potential (2). Both oral and parenteral formulations have found widespread clinical use. To estimate the plasma pentazocine concentration accurately and conveniently, a rapid and sensitive method was needed. Previous methods include a fluorometric technique with a sensitivity of 30–50 ng/ml of plasma (3) and a GLC method with greater specificity and sensitivity (3 ng/ml) but which was more difficult to perform (4). A radioimmunoassay using ^{3}H-pentazocine (5) had no advantage in sensitivity over the GLC method.

This study reports a new radioimmunoassay, using a ^{125}I-labeled pentazocine derivative, with sensitivity in the subnanogram range. This assay has been used to measure pentazocine in both human and dog plasma. The technique permitted determination of pentazocine pharmacokinetic parameters in dogs that received a 0.3-mg/kg iv dose.

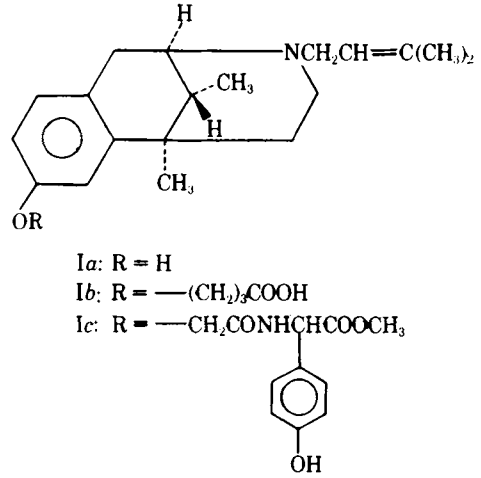

Ia: R = H
Ib: R = —$(CH_2)_3$COOH
Ic: R = —$CH_2CONHCHCOOCH_3$

EXPERIMENTAL

Solutions—Iodination buffer contained 0.5 *M* Na_2HPO_4–0.5 *M* NaH_2PO_4 (4:1), adjusted to a final pH of 7.5. Dilute iodination buffer was the same buffer diluted 1:10 with water. Phosphate-buffered saline was prepared by dissolving 24.51 g of NaCl, 1.77 g of $NaH_2PO_4 \cdot H_2O$, 3.21 g of Na_2HPO_4, and 0.285 g of thimerosal[2] in 3 liters of distilled water and adjusting the pH to 7.0. The assay buffer contained 0.1% (w/v) gelatin dissolved in phosphate-buffered saline. Nonimmune normal rabbit serum was diluted 1:400 in phosphate-buffered saline containing 0.05 *M* edetate sodium[3].

Antipentazocine Serum Preparation—A carbodiimide condensation (6) conjugated a pentazocine hapten[4] (Ib) with bovine serum albumin basic amino acid residues. Approximately 17 hapten molecules were conjugated to each albumin molecule, as shown by a trinitrobenzenesulfonic acid free amino group determination (7). The hapten-protein conjugate (2.0–3.0 mg/rabbit) was emulsified in complete Freund's adjuvant[5] and injected intradermally at several sites on the backs of seven Dutch belted rabbits (8). Conjugate (1.0 mg/rabbit) in incomplete Freund's adjuvant was administered as a booster immunization at approximately 3-week intervals for 3 months. Serum was obtained from blood collected from rabbit marginal ear veins.

Second Antibody Preparation—Rabbit γ-globulin[6] (100 μg), emulsified in complete Freund's adjuvant, was injected subcutaneously at monthly intervals into an adult female goat to obtain anti-rabbit γ-globulin. The goat was bled 2 weeks after each immunization, and serum was obtained. The appropriate second antibody dilution was determined by a progesterone assay[7]; a 1:16 dilution was used.

Radioiodination—At room temperature, a methyl tyrosinate pentazocine derivative[8] (Ic) was radiolabeled by a modified method (9). Sodium ^{125}I-iodide[9] (1.0 mCi) was added to a vial containing 50 μl of iodination buffer and 10 μl of the methyl tyrosinate derivative (1 mg/ml of methanol). The vial was stoppered, and the contents were gently agitated. Thirty micrograms of chloramine-T[10] in 15 μl of dilute iodination buffer was added, and the mixture was allowed to react for 2 min. Then 60 μg of sodium metabisulfite in 30 μl of dilute iodination buffer was added to the vial to stop the reaction.

A solution (100 μl) containing 16% (w/v) of sucrose dissolved in assay buffer was added, and the sample was transferred to a 0.5 × 20-cm gel filtration[11] column, which had been equilibrated with assay buffer. Then 70 μl of 8% (w/v) sucrose dissolved in assay buffer was used to rinse the vial, and the wash solution was added to the column. The column was eluted with assay buffer, and 1.0-ml fractions were collected and counted to determine the radioactivity.

Extraction Procedure—Duplicate samples (0.1 or 0.2 ml) of pentazocine-containing plasma were added to extraction tubes (15 × 85 mm). Pentazocine standards (1–100 ng/ml) were included. Water (0.8 or 0.9 ml) and saturated sodium bicarbonate–sodium carbonate extraction buffer (0.1 ml) were added to the plasma in each extraction tube. Ben-

[1] Talwin, Winthrop Laboratories, New York, N.Y.

[2] Sigma Chemical Co., St. Louis, Mo.

[3] Ethylenediaminetetraacetic acid, sodium salt, Sigma Chemical Co., St. Louis, Mo.

[4] 4-[1,2,3,4,5,6- Hexahydro-*cis*-6,11-dimethyl-3- (3-methyl-2- butenyl)-2,6-methano-3-benzazocin-8-yloxy]butanoic acid.

[5] Difco Laboratories, Detroit, Mich.

[6] Fraction II, Miles Laboratories, Kankakee, Ill.

[7] J. E. Peterson and G. D. Niswender, unpublished data.

[8] Methyl *N*-(2-[1,2,3,4,5,6-hexahydro-*cis*-6,11-dimethyl-3-(3-methyl-2-butenyl)-2,6- methano-3-benzazocin-8- yl]oxy]-1-oxoethyl)tyrosinate hydrochloride.

[9] New England Nuclear, Boston, Mass.

[10] Eastman Kodak, Rochester, N.Y.

[11] Sephadex G-25-150, Sigma Chemical Co., St. Louis, Mo.

0022-3549/79/0500-0626$01.00/0
© 1979, American Pharmaceutical Association

Table I—Relative Affinities of Pentazocine and Related Compounds to the Antiserum

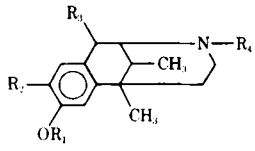

Number	R_1	R_2	R_3	R_4	Relative Affinity
I	H	H	H	$-CH_2CH=C(CH_3)_2$	1.000
II	H	H	H	$-CH_2C(-CH_3)=CH(CH_3)_2$	0.045
III	$-CH_2COOH$	H	H	$-CH_2CH=C(CH_3)_2$	0.032
IV	H	H	H	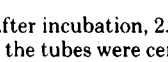	0.008
V	H	H	H	$-CH_2CH=CH_2$	0.007
VI	H	H	H	$-CH_2CH_2CH_3$	0.007
VII	H	H	H	$-CH_2-CH=C(-CH_3)-CH_2OH$	0.006
VIII	H	H	=O	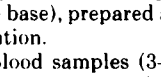	0.003
IX	H	H	H	H	0.002
X	H	H	H	$-CH_2CH=C(-CH_3)-COOH$	0.001

zene[12] (8 ml) was added, and the tubes were shaken mechanically for 15 min. Then tubes were centrifuged for 5 min at 2200×*g*, and duplicate benzene aliquots were removed and placed in appropriately labeled tubes (12 × 75 mm) for the assay. The benzene was evaporated under a nitrogen stream, and the residue was dissolved in 0.5 ml of assay buffer. The tubes were mixed, stoppered, and left overnight at 4°.

Radioimmunoassay—The pentazocine radioimmunoassay was similar to procedures reported for steroids (10). The antipentazocine serum (200 μl), at a dilution of 1:15,000 in normal rabbit serum, was added to the assay tubes containing the plasma extracts. Radioiodinated tyrosinate pentazocine derivative (25,000–30,000 cpm/100 μl) was added. The tubes were incubated for 4–6 hr at 4°. Appropriately diluted second antibody (200 μl) was added, and the incubation was continued overnight.

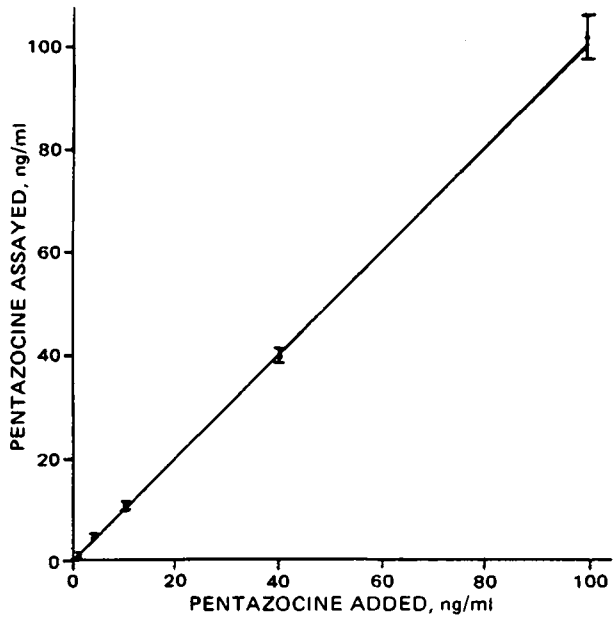

Figure 1—*Correlation of pentazocine added to human plasma with the mean values obtained by radioimmunoassay. Slope = 1.020, intercept = 0.034, and r (correlation coefficient) = 0.9705. The short vertical lines represent 2* SE (n = *8).*

[12] Analytical reagent, Mallinckrodt, St. Louis, Mo.

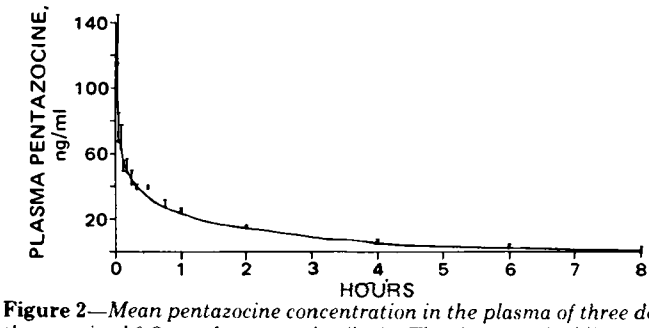

Figure 2—*Mean pentazocine concentration in the plasma of three dogs that received 0.3 mg of pentazocine/kg iv. The short vertical lines represent 1* SE.

After incubation, 2.5 ml of cold phosphate-buffered saline was added, and the tubes were centrifuged at 2500 rpm for 30 min. The supernatant solutions were discarded, and the precipitates were counted. Duplicate standards (1–100 ng/ml) were included in each assay run.

Dog Study—One male (12.6 kg) and two female (9.6 and 17.2 kg) beagle hounds were given 0.3 mg of pentazocine/kg iv (calculated as the free base), prepared as a 3-mg of pentazocine/ml of physiological saline solution.

Blood samples (3–5 ml) were collected from an indwelling venous catheter from 1.0 min to 8 hr after administration. Potassium oxalate was the anticoagulant. The samples were centrifuged, and the plasma was frozen until analyzed.

RESULTS AND DISCUSSION

All seven rabbits produced antiserum within 6 months; the antiserum titers ranged from 1:1000 to 1:20,000. The 1:15,000 antiserum dilution (~1:75,000 final dilution in the assay tube) resulted in 50–55% radioligand binding.

The antiserum specificity was assessed by three related methods. First, the ability of several related compounds, including known pentazocine metabolites, to compete with the radioiodinated pentazocine tyrosinate derivative for antibody binding was determined by comparing the amount of each compound required for 50% radioactivity binding inhibition with the pentazocine standard curves (11). Second, the percent displacement of the related compounds was evaluated (12). Third, the percent cross-reactivity of the related compounds was determined in extracted plasma.

The antiserum exhibiting the least cross-reactivity was selected for all subsequent work. The relative affinities of the related compounds for this antiserum are shown in Table I. The two compounds (II and III) that demonstrated a slight cross-reactivity with pentazocine (I) are not metabolites and posed no problem. The known metabolites (13) of pentazocine (*trans*-acid, *trans*-alcohol, and norpentazocine; X, VII, and IX, respectively) showed little affinity for this pentazocine antiserum.

The assay sensitivity or detection limit (14) is the smallest compound amount that is significantly different from zero at the 95% confidence limit. The human plasma blank gave a detection limit of 0.21 ng/assay tube. The dog plasma blanks gave a limit of 0.19 ng/tube. These values correspond to about 1 ng of compound/ml of plasma.

Precision was tested by calculating the within-assay and between-assay variances. The within-assay variance was evaluated by duplicate measurements of the same sample, and the between-assay variance was evaluated by duplicate measurements in different assays using samples with a wide range of concentrations. The variation coefficient from the mean duplicate determinations was estimated (15). The within-assay variation coefficient ranged from 7.4 to 10.1% (mean 8.2%, $n = 18$). The between-assay variation coefficient ranged from 10.5 to 13.2% (mean 11.6%, $n = 3$). These values are within the range reported for steroid radioimmunoassays (11).

Exogenous pentazocine was accurately quantitated in human plasma by the pentazocine radioimmunoassay system (Fig. 1). A similar correlation was found for canine plasma. No statistical difference was found between canine and human plasma standards.

The mean plasma pentazocine concentrations in the three dogs are shown in Fig. 2. Plasma levels declined biexponentially with time, suggesting that a two-compartment model could be applied. Pharmacokinetic parameters were computer fitted by a modified program (16) (Table II). Previous work indicated that the two-compartment model was applicable to pentazocine pharmacokinetics in dogs (17). The re-

Table II—Pharmacokinetic Parameters for the Disappearance of Dog Plasma Pentazocine following an Intravenous Dose of 0.3 mg/kg

Animal Weight, kg, and Sex	Rate Constants, hr^{-1}			Plasma Clearance Rate, liters/hr	Apparent Distribution, Volume, Steady State, liters	$t_{1/2}^{a}$, min	Area under the Curve, ng hr/ml
	K_{12}	K_{21}	K_{10}				
17.2 F	2.27	1.89	1.05	2.88	6.04	100.2	99.6
9.6 F	2.02	3.41	0.65	3.99	9.80	106.8	80.7
12.6 M	14.6	5.26	1.67	2.68	6.07	99.6	107
Mean	6.29	3.52	1.12	3.18	7.30	102.2	95.9
±*SEM*	±4.15	±0.97	±0.29	±0.41	±1.25	±2.3	±7.95

[a] Calculated from $\frac{0.693}{1/2[(K_{12}+K_{21}+K_{10})-\{(K_{12}+K_{21}+K_{10})^2-4K_{12}K_{21}\}^{1/2}]}$.

ported pentazocine terminal elimination half-life of 150 min in dogs is in good agreement with the present estimate (102 min, Table II). The two-compartment model was used recently to describe pentazocine pharmacokinetics in healthy humans (18) where the average terminal disposition half-life was 203 min.

REFERENCES

(1) S. Archer, N. F. Albertson, L. S. Harris, A. K. Pierson, J. G. Bird, A. S. Keats, J. Telford, and C. N. Papadopoulous, *Science*, **137**, 541 (1962).

(2) S. Archer and W. F. Michne, *Prog. Res.*, **20**, 45 (1976).

(3) B. A. Berkowitz, J. H. Asling, S. M. Shnider, and E. L. Way, *Clin. Pharmacol. Ther.*, **10**, 320 (1969).

(4) K. A. Pittman and C. Davison, *J. Pharm. Sci.*, **62**, 765 (1973).

(5) T. A. Williams and K. A. Pittman, *Res. Commun. Chem. Pathol. Pharmacol.*, **7**, 119 (1974).

(6) B. F. Erlanger, *Pharmacol. Rev.*, **25**, 271 (1973).

(7) A. F. S. A. Habeeb, *Anal. Biochem.*, **14**, 328 (1966).

(8) J. Vaitukaitus, J. B. Robbins, E. Neischlag, and G. T. Ross, *J. Clin. Endocrinol. Metab.*, **33**, 988 (1971).

(9) F. C. Greenwood and W. M. Hunter, *Biochem. J.*, **89**, 114 (1963).

(10) G. D. Niswender and A. R. Midgley, in "Immunologic Methods in Steroid Determination," F. G. Peron and B. V. Caldwell, Eds., Plenum, New York, N.Y., 1970, pp. 149–173.

(11) G. E. Abraham, *Acta Endocrinol. (Kobenhaven)* [*Suppl. 183*], **75**, 1 (1974).

(12) S. deLauzon, N. Cittanova, B. Desfosses, and M. F. Jayle, *Steroids*, **22**, 747 (1973).

(13) K. A. Pittman, D. Rosi, R. Cherniak, A. J. Merola, and W. D. Conway, *Biochem. Pharmacol.*, **18**, 1673 (1969).

(14) G. E. Abraham, F. S. Manlimds, and R. Garza, in "Handbook of Radioimmunoassay," G. E. Abraham, Ed., Dekker, New York, N.Y., 1977, p. 638.

(15) G. E. Abraham, R. Swerdloff, D. Tulchinsky, and W. D. Odell, *J. Clin. Endocrinol. Metab.*, **32**, 619 (1971).

(16) M. Pfeffer, *J. Pharmacokinet. Biopharm.*, **1**, 137 (1973).

(17) L. E. Davis and B. L. Sturm, *Am. J. Vet. Res.*, **31**, 1631 (1970).

(18) M. Ehrnebo, L. O. Boreus, and U. Lönroth, *Clin. Pharmacol. Ther.*, **22**, 888 (1977).

ACKNOWLEDGMENTS

The authors thank K. O. Gelotte and A. G. Hlavac of the Sterling-Winthrop Research Institute for assistance in the synthesis of the compounds required to develop the radioimmunoassay.

Drug Entrapment for Controlled Release in Radiation-Polymerized Beads

MASARU YOSHIDA, MINORU KUMAKURA, and ISAO KAETSU ×

Received June 20, 1978, from the *Takasaki Radiation Chemistry Research Establishment, Japan Atomic Energy Research Institute, Takasaki, Gunma, Japan.* Accepted for publication October 31, 1978.

Abstract □ The preparation of beads including polymer, vinyl monomer, and drug was carried out by low temperature, radiation-induced polymerization. Complete spherical particles were obtained when ethanol was the precipitation medium. Polymers such as polymethyl methacrylate and polystyrene were dissolved in various glass-forming monomers, and the drug was dispersed in the mixture. The mixture was dropped into cold precipitation media. The formed monomeric particle was irradiated at low temperatures to produce polymerization. The drug release profiles from polymerized particles were changed by varying the glass-forming monomer and the precipitation medium.

Keyphrases □ Dosage forms—controlled-release delivery devices, radiation-polymerized beads, potassium chloride □ Potassium chloride—controlled-release delivery devices, radiation-polymerized beads □ Polymers—controlled-release delivery devices, beads, potassium chloride

Controlled drug release may improve effectiveness and safety in drug use (1–3). Drug entrapment in polymerized matrixes may be an effective way to control release. Various bioactive materials, such as enzymes or microbial cells, could first be attached effectively to a carrier surface and then incorporated into a polymer by means of radiation-induced polymerization at low temperatures (4, 5). This method can be performed using monomers that form stable glass-like states when supercooled and that can be readily polymerized at low temperatures (6).

This method can be applied to entrapping low molecular weight drugs for controlled release as well as high molecular weight bioactive substances. Entrapping drugs in fine polymer particles, such as microspheres, could have practical advantages. Trapping enzymes or microbial cells on a carrier surface is desirable for the contact with the substrate (7). Immobilized enzyme or microbial cell microspheres were obtained by suspension polymerization of a hydrophobic glass-forming monomer and a buffered enzyme solution at low temperatures or by polymerization

0022-3549/79/0500-0628$01.00/0

© 1979, American Pharmaceutical Association

Table II—Pharmacokinetic Parameters for the Disappearance of Dog Plasma Pentazocine following an Intravenous Dose of 0.3 mg/kg

Animal Weight, kg, and Sex	Rate Constants, hr^{-1}			Plasma Clearance Rate, liters/hr	Apparent Distribution, Volume, Steady State, liters	$t_{1/2}^{a}$, min	Area under the Curve, ng hr/ml
	K_{12}	K_{21}	K_{10}				
17.2 F	2.27	1.89	1.05	2.88	6.04	100.2	99.6
9.6 F	2.02	3.41	0.65	3.99	9.80	106.8	80.7
12.6 M	14.6	5.26	1.67	2.68	6.07	99.6	107
Mean	6.29	3.52	1.12	3.18	7.30	102.2	95.9
±*SEM*	±4.15	±0.97	±0.29	±0.41	±1.25	±2.3	±7.95

[a] Calculated from $\frac{0.693}{1/2[(K_{12}+K_{21}+K_{10})-\{(K_{12}+K_{21}+K_{10})^2-4K_{12}K_{21}\}^{1/2}]}$.

ported pentazocine terminal elimination half-life of 150 min in dogs is in good agreement with the present estimate (102 min, Table II). The two-compartment model was used recently to describe pentazocine pharmacokinetics in healthy humans (18) where the average terminal disposition half-life was 203 min.

REFERENCES

(1) S. Archer, N. F. Albertson, L. S. Harris, A. K. Pierson, J. G. Bird, A. S. Keats, J. Telford, and C. N. Papadopoulous, *Science*, **137**, 541 (1962).

(2) S. Archer and W. F. Michne, *Prog. Res.*, **20**, 45 (1976).

(3) B. A. Berkowitz, J. H. Asling, S. M. Shnider, and E. L. Way, *Clin. Pharmacol. Ther.*, **10**, 320 (1969).

(4) K. A. Pittman and C. Davison, *J. Pharm. Sci.*, **62**, 765 (1973).

(5) T. A. Williams and K. A. Pittman, *Res. Commun. Chem. Pathol. Pharmacol.*, **7**, 119 (1974).

(6) B. F. Erlanger, *Pharmacol. Rev.*, **25**, 271 (1973).

(7) A. F. S. A. Habeeb, *Anal. Biochem.*, **14**, 328 (1966).

(8) J. Vaitukaitus, J. B. Robbins, E. Neischlag, and G. T. Ross, *J. Clin. Endocrinol. Metab.*, **33**, 988 (1971).

(9) F. C. Greenwood and W. M. Hunter, *Biochem. J.*, **89**, 114 (1963).

(10) G. D. Niswender and A. R. Midgley, in "Immunologic Methods in Steroid Determination," F. G. Peron and B. V. Caldwell, Eds., Plenum, New York, N.Y., 1970, pp. 149–173.

(11) G. E. Abraham, *Acta Endocrinol. (Kobenhaven)* [*Suppl. 183*], **75**, 1 (1974).

(12) S. deLauzon, N. Cittanova, B. Desfosses, and M. F. Jayle, *Steroids*, **22**, 747 (1973).

(13) K. A. Pittman, D. Rosi, R. Cherniak, A. J. Merola, and W. D. Conway, *Biochem. Pharmacol.*, **18**, 1673 (1969).

(14) G. E. Abraham, F. S. Manlimds, and R. Garza, in "Handbook of Radioimmunoassay," G. E. Abraham, Ed., Dekker, New York, N.Y., 1977, p. 638.

(15) G. E. Abraham, R. Swerdloff, D. Tulchinsky, and W. D. Odell, *J. Clin. Endocrinol. Metab.*, **32**, 619 (1971).

(16) M. Pfeffer, *J. Pharmacokinet. Biopharm.*, **1**, 137 (1973).

(17) L. E. Davis and B. L. Sturm, *Am. J. Vet. Res.*, **31**, 1631 (1970).

(18) M. Ehrnebo, L. O. Boreus, and U. Lönroth, *Clin. Pharmacol. Ther.*, **22**, 888 (1977).

ACKNOWLEDGMENTS

The authors thank K. O. Gelotte and A. G. Hlavac of the Sterling-Winthrop Research Institute for assistance in the synthesis of the compounds required to develop the radioimmunoassay.

Drug Entrapment for Controlled Release in Radiation-Polymerized Beads

MASARU YOSHIDA, MINORU KUMAKURA, and ISAO KAETSU ×

Received June 20, 1978, from the *Takasaki Radiation Chemistry Research Establishment, Japan Atomic Energy Research Institute, Takasaki, Gunma, Japan.* Accepted for publication October 31, 1978.

Abstract □ The preparation of beads including polymer, vinyl monomer, and drug was carried out by low temperature, radiation-induced polymerization. Complete spherical particles were obtained when ethanol was the precipitation medium. Polymers such as polymethyl methacrylate and polystyrene were dissolved in various glass-forming monomers, and the drug was dispersed in the mixture. The mixture was dropped into cold precipitation media. The formed monomeric particle was irradiated at low temperatures to produce polymerization. The drug release profiles from polymerized particles were changed by varying the glass-forming monomer and the precipitation medium.

Keyphrases □ Dosage forms—controlled-release delivery devices, radiation-polymerized beads, potassium chloride □ Potassium chloride—controlled-release delivery devices, radiation-polymerized beads □ Polymers—controlled-release delivery devices, beads, potassium chloride

Controlled drug release may improve effectiveness and safety in drug use (1–3). Drug entrapment in polymerized matrixes may be an effective way to control release. Various bioactive materials, such as enzymes or microbial cells, could first be attached effectively to a carrier surface and then incorporated into a polymer by means of radiation-induced polymerization at low temperatures (4, 5). This method can be performed using monomers that form stable glass-like states when supercooled and that can be readily polymerized at low temperatures (6).

This method can be applied to entrapping low molecular weight drugs for controlled release as well as high molecular weight bioactive substances. Entrapping drugs in fine polymer particles, such as microspheres, could have practical advantages. Trapping enzymes or microbial cells on a carrier surface is desirable for the contact with the substrate (7). Immobilized enzyme or microbial cell microspheres were obtained by suspension polymerization of a hydrophobic glass-forming monomer and a buffered enzyme solution at low temperatures or by polymerization

0022-3549/79/0500-0628$01.00/0

© 1979, American Pharmaceutical Association

Table I—Properties and Preparation of Polymer, Glass-Forming Monomer, and Potassium Chloride Beads in Low Temperature Polymerization

Sample	Polymer-Monomer Composition, wt. %	Precipitation Condition			Property of Beads		
		Medium	Temperature	W, %	Shape	D_{av}, mm	C_{KCl}, mg/particle
1	100% Diethylene glycol dimethacrylate	Methanol	−78°	3.8	Nonparticle (block composite)	—	—
2	5% Polymethyl methacrylate–95% diethylene glycol dimethacrylate	Methanol	−78°	3.3	Ellipsoid	—	19
3	10% Polymethyl methacrylate–90% diethylene glycol dimethacrylate	Methanol	−78°	3.6	Ellipsoid	—	21
4	20% Polymethyl methacrylate–80% diethylene glycol dimethacrylate	Methanol	−78°	3.1	Ellipsoid	—	23
5	10% Polymethyl methacrylate–90% diethylene glycol dimethacrylate	Ethanol	−78°	2.7	Sphere	2.2 ± 0.1	18
6	10% Polymethyl methacrylate–90% diethylene glycol dimethacrylate	n-Butanol	−78°	3.6	Ellipsoid	—	20
7	10% Polymethyl methacrylate–90% diethylene glycol dimethacrylate	n-Hexane	−78°	3.4	Ellipsoid	—	19
8	10% Polymethyl methacrylate–90% diethylene glycol dimethacrylate	Ethanol	−24°	—	Nonparticle (block composite)	—	—
9	10% Polymethyl methacrylate–90% hydroxyethyl acrylate	Ethanol	−78°	64.5	Sphere	2.1 ± 0.1	16
10	10% Polymethyl methacrylate–90% glycidyl methacrylate	Ethanol	−78°	4.2	Sphere	1.9 ± 0.1	17
11	10% Polymethyl methacrylate–90% hydroxyethyl methacrylate	Ethanol	−78°	32.0	Sphere	2.0 ± 0.1	17
12	10% Polymethyl methacrylate–90% trimethylolpropane trimethacrylate	Ethanol	−78°	2.6	Sphere	2.1 ± 0.1	20
13	100% Glycidyl methacrylate	Ethanol	−78°	4.0	Nonparticle (block composite)	—	—
14	10% Polystyrene–90% glycidyl methacrylate	Ethanol	−78°	3.8	Sphere	2.0 ± 0.1	23
15	20% Polystyrene–80% glycidyl methacrylate	Ethanol	−78°	3.5	Sphere	2.2 ± 0.1	21

of the salted-out hydrophilic glass-forming monomer and a buffered enzyme solution.

Drugs also can be entrapped inside the microsphere polymer matrix, because low molecular weight substances leach too rapidly from the surface-sorbed state. In this report, a new method for small solid particle preparation incorporating drugs inside the matrix by means of radiation-induced polymerization at low temperatures was investigated.

EXPERIMENTAL

Materials—Potassium chloride[1] was the drug used.

2-Hydroxyethyl methacrylate[2], diethylene glycol dimethacrylate[3], trimethylolpropane trimethacrylate[3], glycidyl methacrylate[2], and hydroxyethyl acrylate[2] were the glass-forming monomers. Methyl methacrylate[2] was the nonglass-forming monomer.

Reagent grade methanol[2], ethanol[2], n-buthanol[2], n-hexane[2], and 1,4-butanediol[2] were the precipitation media. Polymethyl methacrylate[4], polyethylene glycol 600[2], and polystyrene[5] were the polymers used.

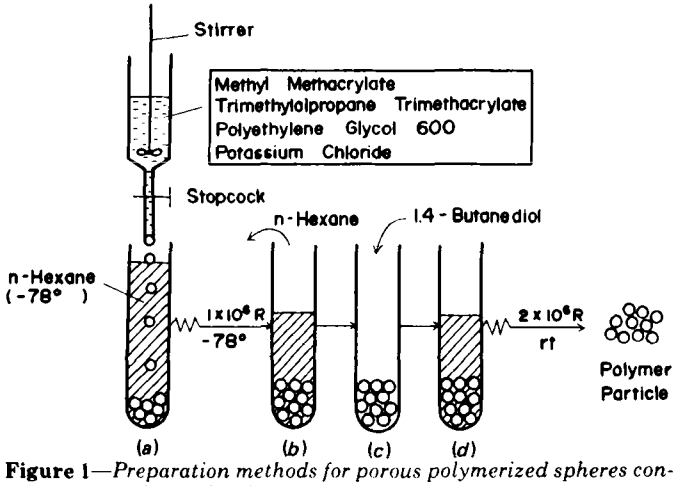

Figure 1—*Preparation methods for porous polymerized spheres containing potassium chloride.*

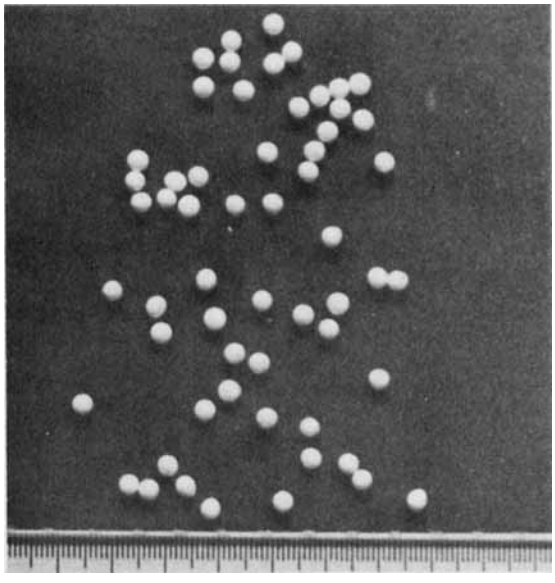

Figure 2—*Photograph of spherical particles.*

Preparation of Radiation-Polymerized Beads—Drops of polymer, monomer, and drug (potassium chloride) mixtures were allowed to fall into a cold (−78°) precipitation medium with the equipment shown in Fig. 1*a*. The solid globules were irradiated at −78° (dry ice–methanol) or −24° for 2 hr at 1×10^6 rads/hr with ^{60}Co γ-rays. After irradiation, the polymerized spheres were removed and dried. When polyethylene glycol 600 replaced the polymers polymethyl methacrylate or polystyrene, the solidified globules were irradiated for 1 hr at 1×10^6 rads/hr. Then the original n-hexane precipitation medium was replaced by cooled 1,4-butanediol, and polymerization was continued for 2 hr at room temperature at the same rate.

Properties of Spheres—The mean particle diameter, D_{av}, was measured by optical microscopic observation[6], and the mean potassium chloride amount, C_{KCl}, was estimated from the potassium chloride released from the beads. To estimate the polymer hydrophilicity, water content, W, was determined according to:

[1] About 48-mesh powder, Otsuka Pharmaceuticals Co.

[2] Tokyo Kasei Kogyo Co. Monomers were purified by distillation according to conventional methods.

[3] Shin-Nakamura Chemical Co. Monomers were purified by washing with 1% NaOH, passing over Amberlite A-27 (Rohm & Haas), and drying over molecular sieves 4A.

[4] Mitsubishi Rayon Co.

[5] Denki Kagaku Co.

[6] Model SMZ-6, Nippon Kogaku Co.

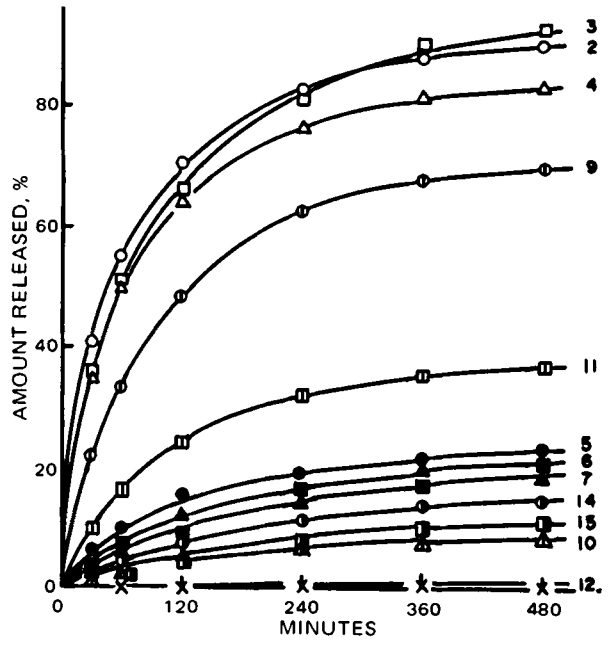

Figure 3—*Potassium chloride release profile from polymerized particles. Numbers refer to compositions (Table I).*

$$W\,(\%) = \frac{W_w}{W_p + W_w} \times 100 \qquad \text{(Eq. 1)}$$

where W_w and W_p are the weights of the water required to saturate the polymer and of the dried polymer, respectively.

Dissolution of Potassium Chloride from Polymerized Spheres—The dissolution test was carried out at 37°, 100 rpm, with the dissolution apparatus[7] based on USP XIX. The basket was immersed in the vessel containing 1000 ml of dissolution medium, usually water at pH 6.0. At selected intervals over 480 min, 5 ml of the dissolution medium was sampled and the released potassium chloride was assayed spectrophotometrically[8] (8).

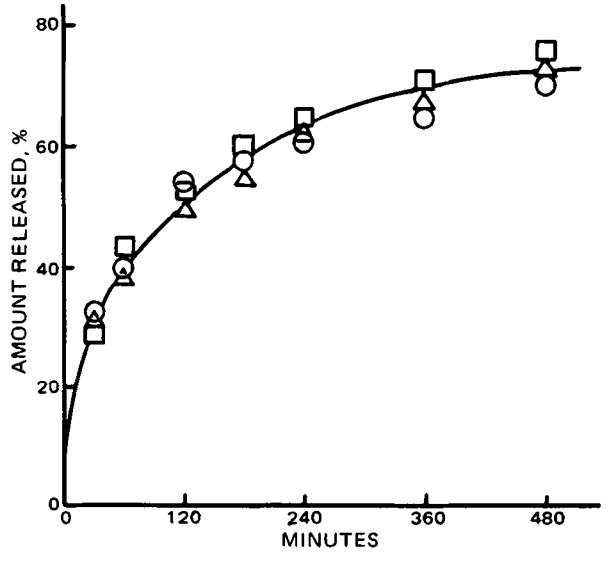

Figure 4—*Potassium chloride release from spheres as a binary monomer composition function in 30% monomers–70% polyethylene glycol 600. Key (monomer composition): ○, 70% methyl methacrylate–30% trimethylolpropane trimethacrylate; □, 50% methyl methacrylate–50% trimethylolpropane trimethacrylate; and △, 30% methyl methacrylate–70% trimethylolpropane trimethacrylate.*

[7] Model TR-5S, Toyama Sangyo Co.
[8] Model UV-200 Shimazu double-beam spectrophotometer.

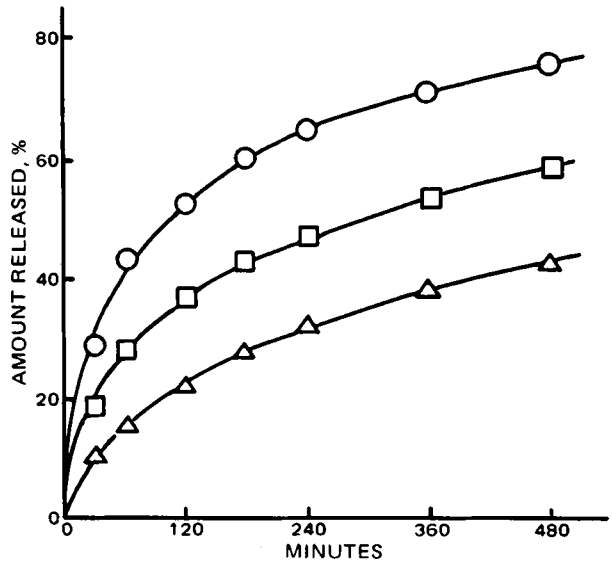

Figure 5—*Potassium chloride release from spheres as a function of polyethylene glycol 600 concentration in 50% methyl methacrylate–50% trimethylolpropane trimethacrylate monomer system. Key (polyethylene glycol 600 concentration): ○, 70%; □, 50%; and △, 30%.*

RESULTS AND DISCUSSION

Nonglass-Forming Monomers—Methyl methacrylate required at least 6% polymethyl methacrylate to form stabilized globules when dropped into cold methanol. Otherwise, the monomer-polymer-drug mixture formed threads or simply coalesced into an immiscible layer. Other precipitation media produced similar results. Methyl methacrylate polymerization did not yield solid spheres at cold temperatures and merely coalesced above 0°.

Glass-Forming Monomers—These monomers gave well-formed solid globules when mixed with polymer and potassium chloride and supercooled. They were easily polymerized by irradiation at the low temperatures used.

Globule Formation—Ethanol as the supercooled precipitation me-

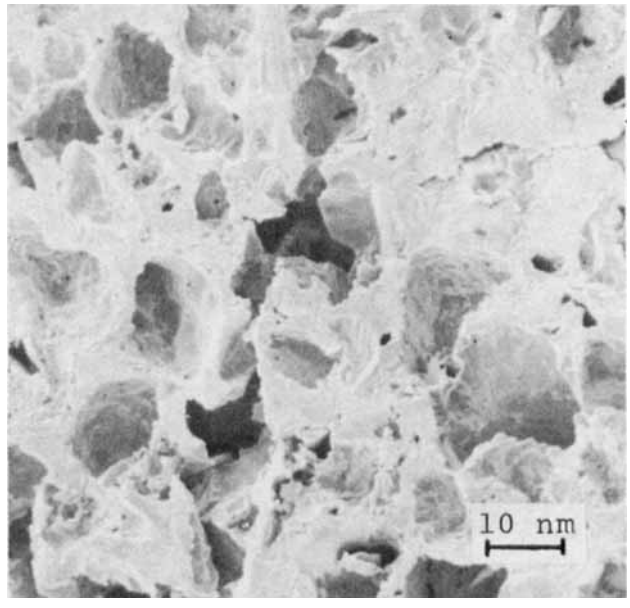

Figure 6—*Scanning electron micrograph of sphere structure. The spheres (2.4 ± 0.2 mm in diameter) were prepared with 30% (methyl methacrylate–trimethylolpropane trimethacrylate)–70% polyethylene glycol 600, a monomer composition of 50% methyl methacrylate–50% trimethylolpropane trimethacrylate, ethanol as the precipitation medium, and a precipitation temperature of −78°. Irradiation was carried out under the conditions shown in Fig. 1.*

dium yielded spherical globules (Fig. 2[9]). Methanol, *n*-butanol, and *n*-hexane formed ellipsoidal globules. Globule formation seemed dependent on the polymer present in the mixture and on a precipitation medium temperature not above −24°. When these conditions were not met, coalescence but not stabilization occurred.

Release of Potassium Chloride—In the spheres containing polymethyl methacrylate as the polymer and diethylene glycol dimethacrylate as the monomer (Samples 2–7), the methanol precipitation medium increased potassium chloride release (Fig. 3). In nonmethanol precipitation media, release from relatively strongly hydrophilic beads (Samples 9 and 11) was faster than that from less hydrophilic matrixes.

The binary monomer spheres containing polyethylene glycol 600 in place of polymer showed a release rate independent of the methyl methacrylate–trimethylolpropane trimethacrylate proportions (Fig. 4). The polyethylene glycol 600 concentration strongly affected potassium chloride release (Fig. 5). Larger polyethylene glycol 600 proportions together with 1,4-butanediol in the final polymerization step yielded spheres with a markedly porous internal structure (Fig. 6[10]).

[9] Nikon F, Nippon Kogaku Co.
[10] Model JSM-U3, Japan Electron Optics Laboratory Co.

REFERENCES

(1) Y. W. Chien, H. J. Lambert, and D. E. Grant, *J. Pharm. Sci.*, **63**, 365 (1974).

(2) V. W. Winkler, S. Borodkin, S. K. Webel, and J. T. Mannebach, *ibid.*, **66**, 816 (1977).

(3) R. W. Croswell and C. H. Becker, *ibid.*, **63**, 440 (1974).

(4) I. Kaetsu, M. Kumakura, M. Yoshida, and M. Asano, "26th IUPAC Congress," Tokyo, Japan, 1977, p. 262.

(5) M. Yoshida, M. Kumakura, and I. Kaetsu, *Polym. Prepr., Jpn.*, **26**, 698 (1977).

(6) I. Kaetsu, H. Okubo, A. Ito, and K. Hayashi, *J. Polym. Sci.*, **A1**, 2203 (1972).

(7) M. Yoshida, M. Kumakura, and I. Kaetsu, *Polym. Prepr., Jpn.*, **27**, 252 (1978).

(8) W. Uchiumi, *Nippon Kagaku Zasshi*, **73**, 835 (1952).

ACKNOWLEDGMENTS

The authors thank Dr. N. O. Nuessle for useful suggestions.

UV Studies of Nucleic Acid Base Complexation with Isoproterenol in Different Solvents

HASSAN M. TAHA, FAHAD A. AL-OBEIDI *, and HANNA N. BORAZAN ˣ

Received August 3, 1977, from the *Department of Pharmaceutical Chemistry, College of Pharmacy, University of Baghdad, Baghdad, Republic of Iraq.* Accepted for publication October 31, 1978. *Present address: Department of Chemistry, University of Arizona, Tucson, AZ 85721.

Abstract □ Charge transfer complex formation between nucleic acid bases and isoproterenol was demonstrated from UV absorption measurements. The solvent polarity effects on equilibrium constants were investigated. The solvent systems containing 0.1 *N* HCl were 20% aqueous ethanol, water, and water containing sodium chloride. The equilibrium constants, calculated from UV absorption data by the application of the Benesi–Hildebrand equation, were small and increased with increasing ionic strength. Equilibrium constant wavelength dependence was demonstrated in some cases.

Keyphrases □ Complexes, charge transfer—nucleic acid bases with isoproterenol, various solvents, UV absorption study □ Nucleic acid bases—charge transfer complex formation with isoproterenol, various solvents, UV absorption study □ Solvents, various—charge transfer complex formation, nucleic acid bases with isoproterenol, UV absorption study

Catechol forms the catecholamine aromatic nucleus and anchors these molecules to their receptors (1). The adrenergic sites and the biogenic amine storage granules are known to contain adenosine triphosphate, phosphate, and magnesium ions (2, 3). Complex formation between these ions and catecholamines has been demonstrated (4, 5). Evidence for charge transfer complex formation between catechol, epinephrine, and nucleic acid bases has been presented (6–8).

The present study was undertaken to trace the catecholamine action mechanism, to obtain more information about adrenergic receptors, and to investigate adenosine triphosphate-like action of some other storage granule nucleoside triphosphates. UV absorption was used to study the interactions between the nucleic acid bases and isoproterenol in the following solvents containing 0.1 *N* HCl: 20% aqueous ethanol, water, and water containing sodium chloride.

EXPERIMENTAL

Isoproterenol sulfate dihydrate[1], thymine[2], cytosine[2], standard hydrochloric acid solution[2], adenine[3], uracil[3], and sodium chloride[4] (BP) were the highest commercially available purity (>99%) and were used without further purification.

Solutions containing a fixed nucleic acid base concentration (0.02 *M*, except cytosine-containing solutions in 20% alcohol, fixed at 0.01 *M*) and different isoproterenol sulfate concentrations (0.3–0.8 *M*) were prepared by dilution from concentrated standard solutions.

The solvents used were 20% aqueous ethanol containing 0.1 *N* HCl, 0.1 *N* aqueous HCl, and water solutions containing 0.1 *N* HCl and different amounts of sodium chloride.

All solutions were freshly prepared, and their spectra were recorded within 6 hr in 1-cm path length rectangular cells with stoppers. Most experimental work was carried out in subdued light to avoid isoproterenol light oxidation and at room temperature (20–25°).

The spectrophotometers[5] were checked and calibrated with an oxide film[6]. Cell holders were thermostated to maintain the temperature at 25°. The baseline was recorded before the experiments with the same solvent in the reference and in the sample compartments.

[1] Aldrich Chemical Co., Milwaukee, Wis.
[2] BDH Chemical Co., Poole, England.
[3] Hopkin and Williams Chemical Co., Chadwell Heath, Essex, England.
[4] Evans Medical Ltd., Liverpool, England.
[5] Perkin-Elmer model 402 and Pye Unicam model SP 800 UV-visible.
[6] Holmium.

0022-3549/79/0500-0631$01.00/0

© 1979, American Pharmaceutical Association

dium yielded spherical globules (Fig. 2[9]). Methanol, *n*-butanol, and *n*-hexane formed ellipsoidal globules. Globule formation seemed dependent on the polymer present in the mixture and on a precipitation medium temperature not above −24°. When these conditions were not met, coalescence but not stabilization occurred.

Release of Potassium Chloride—In the spheres containing polymethyl methacrylate as the polymer and diethylene glycol dimethacrylate as the monomer (Samples 2–7), the methanol precipitation medium increased potassium chloride release (Fig. 3). In nonmethanol precipitation media, release from relatively strongly hydrophilic beads (Samples 9 and 11) was faster than that from less hydrophilic matrixes.

The binary monomer spheres containing polyethylene glycol 600 in place of polymer showed a release rate independent of the methyl methacrylate–trimethylolpropane trimethacrylate proportions (Fig. 4). The polyethylene glycol 600 concentration strongly affected potassium chloride release (Fig. 5). Larger polyethylene glycol 600 proportions together with 1,4-butanediol in the final polymerization step yielded spheres with a markedly porous internal structure (Fig. 6[10]).

[9] Nikon F, Nippon Kogaku Co.
[10] Model JSM-U3, Japan Electron Optics Laboratory Co.

REFERENCES

(1) Y. W. Chien, H. J. Lambert, and D. E. Grant, *J. Pharm. Sci.*, **63**, 365 (1974).

(2) V. W. Winkler, S. Borodkin, S. K. Webel, and J. T. Mannebach, *ibid.*, **66**, 816 (1977).

(3) R. W. Croswell and C. H. Becker, *ibid.*, **63**, 440 (1974).

(4) I. Kaetsu, M. Kumakura, M. Yoshida, and M. Asano, "26th IUPAC Congress," Tokyo, Japan, 1977, p. 262.

(5) M. Yoshida, M. Kumakura, and I. Kaetsu, *Polym. Prepr., Jpn.*, **26**, 698 (1977).

(6) I. Kaetsu, H. Okubo, A. Ito, and K. Hayashi, *J. Polym. Sci.*, **A1**, 2203 (1972).

(7) M. Yoshida, M. Kumakura, and I. Kaetsu, *Polym. Prepr., Jpn.*, **27**, 252 (1978).

(8) W. Uchiumi, *Nippon Kagaku Zasshi*, **73**, 835 (1952).

ACKNOWLEDGMENTS

The authors thank Dr. N. O. Nuessle for useful suggestions.

UV Studies of Nucleic Acid Base Complexation with Isoproterenol in Different Solvents

HASSAN M. TAHA, FAHAD A. AL-OBEIDI *, and HANNA N. BORAZAN ˣ

Received August 3, 1977, from the *Department of Pharmaceutical Chemistry, College of Pharmacy, University of Baghdad, Baghdad, Republic of Iraq.* Accepted for publication October 31, 1978. *Present address: Department of Chemistry, University of Arizona, Tucson, AZ 85721.

Abstract □ Charge transfer complex formation between nucleic acid bases and isoproterenol was demonstrated from UV absorption measurements. The solvent polarity effects on equilibrium constants were investigated. The solvent systems containing 0.1 *N* HCl were 20% aqueous ethanol, water, and water containing sodium chloride. The equilibrium constants, calculated from UV absorption data by the application of the Benesi–Hildebrand equation, were small and increased with increasing ionic strength. Equilibrium constant wavelength dependence was demonstrated in some cases.

Keyphrases □ Complexes, charge transfer—nucleic acid bases with isoproterenol, various solvents, UV absorption study □ Nucleic acid bases—charge transfer complex formation with isoproterenol, various solvents, UV absorption study □ Solvents, various—charge transfer complex formation, nucleic acid bases with isoproterenol, UV absorption study

Catechol forms the catecholamine aromatic nucleus and anchors these molecules to their receptors (1). The adrenergic sites and the biogenic amine storage granules are known to contain adenosine triphosphate, phosphate, and magnesium ions (2, 3). Complex formation between these ions and catecholamines has been demonstrated (4, 5). Evidence for charge transfer complex formation between catechol, epinephrine, and nucleic acid bases has been presented (6–8).

The present study was undertaken to trace the catecholamine action mechanism, to obtain more information about adrenergic receptors, and to investigate adenosine triphosphate-like action of some other storage granule nucleoside triphosphates. UV absorption was used to study the interactions between the nucleic acid bases and isoproterenol in the following solvents containing 0.1 *N* HCl: 20% aqueous ethanol, water, and water containing sodium chloride.

EXPERIMENTAL

Isoproterenol sulfate dihydrate[1], thymine[2], cytosine[2], standard hydrochloric acid solution[2], adenine[3], uracil[3], and sodium chloride[4] (BP) were the highest commercially available purity (>99%) and were used without further purification.

Solutions containing a fixed nucleic acid base concentration (0.02 *M*, except cytosine-containing solutions in 20% alcohol, fixed at 0.01 *M*) and different isoproterenol sulfate concentrations (0.3–0.8 *M*) were prepared by dilution from concentrated standard solutions.

The solvents used were 20% aqueous ethanol containing 0.1 *N* HCl, 0.1 *N* aqueous HCl, and water solutions containing 0.1 *N* HCl and different amounts of sodium chloride.

All solutions were freshly prepared, and their spectra were recorded within 6 hr in 1-cm path length rectangular cells with stoppers. Most experimental work was carried out in subdued light to avoid isoproterenol light oxidation and at room temperature (20–25°).

The spectrophotometers[5] were checked and calibrated with an oxide film[6]. Cell holders were thermostated to maintain the temperature at 25°. The baseline was recorded before the experiments with the same solvent in the reference and in the sample compartments.

[1] Aldrich Chemical Co., Milwaukee, Wis.
[2] BDH Chemical Co., Poole, England.
[3] Hopkin and Williams Chemical Co., Chadwell Heath, Essex, England.
[4] Evans Medical Ltd., Liverpool, England.
[5] Perkin-Elmer model 402 and Pye Unicam model SP 800 UV-visible.
[6] Holmium.

0022-3549/79/0500-0631$01.00/0

© 1979, American Pharmaceutical Association

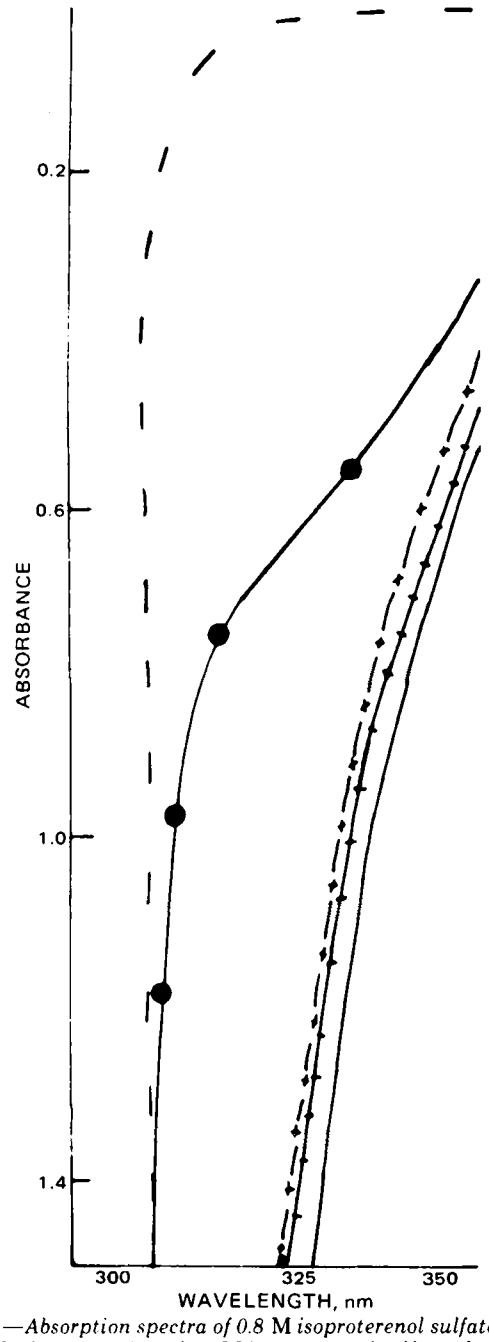

Figure 1—*Absorption spectra of 0.8 M isoproterenol sulfate (-●-), 2 × 10^{-2} M adenine (– –), and 0.8 M isoproterenol sulfate plus 2 × 10^{-2} M adenine (—) in aqueous solutions containing 0.1 N HCl at an ionic strength of 3.0; —+—+— and -×-×- represent the absorption spectra of the mixture at ionic strengths of 3.5 and 4.0, respectively. Measurements were at 25 ± 0.5°.*

RESULTS AND DISCUSSION

A representative nucleic acid base–isoproterenol UV absorption spectrum (Fig. 1) showed a shift toward longer wavelengths. The increase in absorption at longer wavelengths (Table I) was attributed to weakly bonded complex formation.

Isoproterenol and the nucleic acid base absorption at the specified wavelengths depended only on concentration. This result was to be expected if no self-association had taken place. The pH deviation (~0.8) from the initial working acidity, as well as changes in temperature and ionic strength, did not affect the pure component absorption spectra, further supporting the suggestion that the increased absorbance observed in the mixtures was due to complex formation.

Absorbances at different isoproterenol concentrations were estimated from the difference between the mixture absorbance and a sum of the absorbances of the individual substances having concentrations identical to those in the mixture. The absorbances at different wavelengths were calculated from molar absorptivities.

All UV binding interaction measurements were made at fixed wavelengths; for each mixture examined, measurements were made at several wavelengths. The complex absorbance was measured in regions where the free component absorptions were small and the complex absorption was appreciable. The accuracy of these measurements was ±0.01 unit of absorbance.

The complex equilibrium constants were calculated by assuming simple complex formation:

$$A + D = AD \qquad \text{(Eq. 1)}$$

and by application of the Benesi–Hildebrand equation:

$$\frac{[A_0]}{A_\lambda^{AD}} = \frac{1}{\epsilon_\lambda^{AD}} + \frac{1}{(K_c^{AD})(\epsilon_\lambda^{AD})[D_0]} \qquad \text{(Eq. 2)}$$

where K_c^{AD} is the equilibrium constant; $[A_0]$ and $[D_0]$ are the initial concentrations of the reactant species; and A_λ^{AD} and ϵ_λ^{AD} represent the absorbance and molar absorptivity of the complex, respectively, at the wavelength λ.

Equation 2 is based upon the assumption that $[D] \simeq [D_0]$ when designing an experiment such that $[D_0] \gg [A_0]$.

A plot of $[A_0]/A_\lambda^{AD}$ *versus* $1/[D_0]$ leads to an intercept of $1/\epsilon_\lambda^{AD}$ and a slope of $1/K_c^{AD}\epsilon_\lambda^{AD}$, whereby the molar absorptivity and the equilibrium constant can be calculated graphically.

The standard free energy changes associated with various interactions, $\Delta G°$, are calculated from the following well-known equation:

$$\Delta G° = -RT \ln K_c^{AD} \qquad \text{(Eq. 3)}$$

where R is the gas constant and T is the absolute temperature. Representative Benesi–Hildebrand plots are presented in Fig. 2; the thermo-

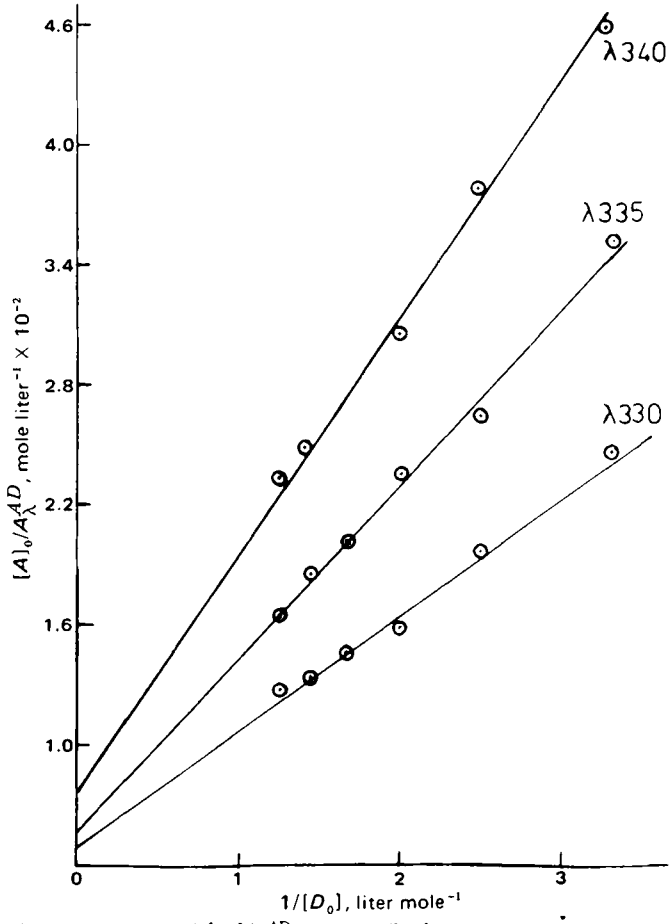

Figure 2—*Plots of* $[A_0]/A_\lambda^{AD}$ versus $1/[D_0]$ *of isoproterenol sulfate containing cytosine in 20% alcoholic solutions with 0.1 N HCl. The cytosine total concentration,* $[A_0]$, = 10^{-2} M, *and the isoproterenol total concentration,* $[D_0]$, = 0.3–0.8 M. *The* A_λ^{AD} *represents the absorbance of the complex at the wavelength. Measurements were at 25 ± 0.5°.*

Table I—Equilibrium Constants (K) and Standard Free Energy Changes ($\Delta G°$) Associated with Interactions of Nucleic Acid Bases with Isoproterenol Sulfate in Different Solvents Together with Molar Absorptivities (ϵ) at Different Wavelengths (λ) [a]

Nucleic Acid Base	λ, nm	ε	K, M^{-1} ± 0.01	$\Delta G°$, kcal/mole
	20% Alcoholic Solutions Containing 0.1 *N* HCl			
Adenine	325	71.4	2.12	−0.44
	330	42.3	1.77	−0.34
Cytosine	330	200	0.88	0.07
	335	178	0.65	0.25
	340	131	0.60	0.30
Thymine	310	50	1.31	−0.16
	315	31	1.15	−0.08
Uracil	310	27.2	5.10	−0.96
	Aqueous Solutions Containing 0.1 *N* HCl			
Adenine	323	89	1.70	−0.31
	325	78	1.44	−0.22
Cytosine	340	76	1.13	−0.07
	345	71	0.60	0.30
Thymine	312	100	0.59	0.31
	315	93	0.58	0.32
	Aqueous Solutions Containing 0.1 *N* HCl at Different Ionic Strengths (I)			
Adenine[b]	330	91	1.00	0.00
	335	78	1.60	−0.28
Cytosine[b]	340	100	0.71	0.20
	345	68	0.87	0.08
Adenine[c]	330	41	4.00	−0.82
	335	23	4.70	−0.92
Cytosine[c]	340	58	2.10	−0.44
	345	45	2.08	−0.43
Adenine[d]	330	36	5.90	−1.05

[a] Measurements were at 25 ± 0.5°. [b] At I = 3.0. [c] At I = 3.5. [d] At I = 4.0.

dynamic constants and molar absorptivities are summarized in Table I.

The molar absorptivities of adenine–isoproterenol and thymine–isoproterenol complexes were higher in water than in water–ethanol; the reverse was obtained with cytosine–isoproterenol. Furthermore, the adenine–isoproterenol and cytosine–isoproterenol complex molar absorptivities were ionic strength dependent.

In general, the equilibrium constants were sensitive to changes in the wavelengths at which the measurements were taken, except for thymine–isoproterenol in water. Almost all equilibrium constants were less than two, except for uracil–isoproterenol in 20% alcohol. Therefore, $\Delta G°$ values were small. The equilibrium constants of adenine–isoproterenol and thymine–isoproterenol (Table I) decreased as the solvent was changed from alcoholic to aqueous, while the cytosine–isoproterenol complex equilibrium constants increased.

Three- and fourfold increases in adenine–isoproterenol equilibrium constants at λ335 and λ330 nm, respectively, were produced by increasing the ionic strength of aqueous solutions from 3.0 to 3.5. A sixfold increase could be obtained at λ330 nm by increasing the ionic strength from 3.0 to 4.0. The same trend was observed for cytosine–isoproterenol equilibrium constants; 2.4- and threefold increases were produced by changing the ionic strength from 3.0 to 3.5 at λ345 and λ340 nm, respectively.

The increase in absorbance at longer wavelength was attributed to charge transfer complex formation where the nucleic acid bases were assumed to act as electron acceptors with catechol or epinephrine as electron donors (6–8). Similar donor and acceptor species may be hypothesized for isoproterenol–nucleic acid base complexes.

Exact complex geometry cannot be determined from UV absorption measurements, but parallel stacking interactions between nucleic acid bases and isoproterenol can be proposed. This mechanism was suggested previously for a similar system (9–12). The geometry is likely to be affected by the stoichiometry (13–17), but the present results are best interpreted by a 1:1 stoichiometry.

To account for the decrease in adenine–isoproterenol and thymine–isoproterenol equilibrium constants as the solvent polarity increases (Table I), the complex dipole moment was assumed to be larger in the excited state than in the ground state, resulting in the formation of a highly polar complex that was more solvated than the sum of the uncombined components. The reverse situation can be assumed for the cytosine–isoproterenol complex (18–20).

Little work has been done on the salt effect on the equilibrium constants. The large increase in equilibrium constants as salt concentrations were increased (Table I) can be explained by assuming ion-pair formation between the chloride ions and the protonated centers around the interacting molecules, resulting in an electrostatic repulsion decrease. Other weaker forces seem to dominate the repulsive forces. The same explanation accounted for the decrease in the equilibrium constants (21–25). Borazan (13, 17) showed that the equilibrium constants of nucleoside self-association and aqueous complex formation are similar to those obtained at higher salt concentrations.

The equilibrium constant wavelength dependence (Table I) could indicate the formation of more than one complex type; the wavelength independence was explained as due to the formation of one complex type in solution (26).

REFERENCES

(1) P. Pratesi, E. Grana, and L. Villa, "Physico-Chemical Aspects of Drug Actions," 1st ed., E. J. Ariens, Ed., Pergamon, Oxford, England, 1968, p. 283.

(2) A. Korolkovas, "Essentials of Molecular Pharmacology," Wiley, New York, N.Y., 1970, p. 234.

(3) "Second Symposium on Catecholamines," G. H. Acheson, Ed., Williams & Wilkins, Baltimore, Md., 1966, pp. 401–456.

(4) J. Seifter, E. Seifter, and G. Guideri, *Am. J. Med. Sci.*, **263**, 261 (1972).

(5) H. G. Weder and U. W. Wiegand, *FEBS Lett.*, **38**, 64 (1973).

(6) F. A. Al-Obeidi, M.S. thesis, University of Baghdad, Baghdad, Iraq, 1975.

(7) F. A. Al-Obeidi and H. N. Borazan, *J. Pharm. Sci.*, **65**, 892 (1976).

(8) *Ibid.*, **65**, 982 (1976).

(9) P. O. P. Ts'o, I. S. Melvin, and A. C. Olson, *J. Am. Chem. Soc.*, **85**, 1289 (1963).

(10) A. D. Broom, M. P. Schweizer, and P. O. P. Ts'o, *ibid.*, **89**, 3612 (1967).

(11) J. L. Dimicoli and C. Helene, *ibid.*, **95**, 1036 (1973).

(12) M. P. Schweizer, A. D. Broom, P. O. P. Ts'o, and D. P. Hollis, *ibid.*, **90**, 1042 (1968).

(13) H. N. Borazan, *J. Pharm. Sci.*, **64**, 770 (1975).

(14) F. M. Goyan and H. N. Borazan, *ibid.*, **57**, 861 (1968).

(15) H. N. Borazan, Ph.D. thesis, University of California, San Francisco, Calif., 1969.

(16) H. N. Borazan and F. M. Goyan, *J. Pharm. Sci.*, **62**, 923 (1973).

(17) H. N. Borazan, *ibid.*, **62**, 1982 (1973).

(18) J. Grundnes and S. D. Christian, *J. Am. Chem. Soc.*, **90**, 2239 (1968).

(19) S. D. Christian and J. Grundnes, *Nature*, **214**, 1111 (1967).

(20) H. W. Offen and M. S. F. A. Abidi, *J. Chem. Phys.*, **44**, 4642 (1966).

(21) E. M. Kosower and J. C. Burbach, *J. Am. Chem. Soc.*, **78**, 5838 (1956).

(22) D. Brooke and D. E. Guttman, *J. Pharm. Sci.*, **57**, 1206 (1968).

(23) C. Helene, H. Borazan, J. L. Dimicoli, J. C. Maurizot, M. Durand, and J. J. Toulme, "Proceedings of the 23rd Annual Meeting of the Societe de Chimie Physique over the Dynamic Aspects of Conformation Changes in Biological Macromolecules," Orleans, France, 1973, p. 349.

(24) M. Durand, H. N. Borazan, J. C. Maurizot, J. L. Dimicoli, and C. Helene, *Biochimie*, **58**, 395 (1976).

(25) M. Durand, J. C. Maurizot, H. N. Borazan, and C. Helene, *Biochemistry*, **14**, 563 (1975).

(26) G. D. Johnson and R. E. Bowen, *J. Am. Chem. Soc.*, **87**, 1655 (1965).

ACKNOWLEDGMENTS

Presented at the 35th International Congress of Pharmaceutical Sciences, Dublin, Ireland, September 1975.

Abstracted in part from a dissertation submitted by H. M. Taha to the University of Baghdad in partial fulfillment of the Master of Science degree requirements.

The authors thank Professor Hatif H. Al-Jalil for encouragement. They also thank the University of Baghdad for financial support.

In Vitro and *In Vivo* Availability of Hydrophilized Phenytoin from Capsules

C. F. LERK ˣ, M. LAGAS, L. LIE-A-HUEN, P. BROERSMA, and K. ZUURMAN

Received July 31, 1978, from the *Laboratory for Pharmaceutical Technology, University of Groningen, Antonius Deusinglaan 2, 9713 AW Groningen, The Netherlands.* Accepted for publication November 9, 1978.

Abstract □ The effect of phenytoin hydrophilization on the liquid penetration rate into prepared plugs, on the disintegration time, on the *in vitro* release rate, and on *in vivo* absorption in humans was studied. Hydrophilization was performed by intensive mixing of the hydrophobic drug with a small amount of methylcellulose solution. Liquid penetration into the treated plugs was independent of the liquid wetting potency and extremely high compared to the pure drug plugs. Analogous results were obtained for the disintegration time and *in vitro* release rates from capsules loaded with pure and treated drug. A bioavailability study in seven healthy volunteers showed immediate absorption of the treated drug but a 1-hr absorption lag time for the pure drug.

Keyphrases □ Phenytoin, hydrophilized—*in vitro* and *in vivo* availability from capsules □ Bioavailability—hydrophilized phenytoin, capsule formulation, *in vitro* release rates □ Anticonvulsants—phenytoin, effect of hydrophilization, *in vitro* and *in vivo* availability

When a disintegratable tablet or capsule is administered orally to humans, gastric fluid must penetrate the porous mass before disintegration and absorption can occur. Any factor influencing the penetration rate may influence the absorption rate.

The liquid penetration rate into a porous mass is given by the Washburn (1) equation:

$$\frac{dl}{dt} = \frac{m\gamma \cos\theta}{2l\eta} \qquad \text{(Eq. 1)}$$

where l is the penetrated length at time t, m is the hydraulic pore radius, γ is the penetrating liquid surface tension, θ is the contact angle between solid and liquid, and η is the liquid viscosity. The penetration rate is strongly dependent on the solid contact angle.

In earlier studies on pharmaceutical powder wettability (2, 3), reported contact angles varied from 0° for dicalcium phosphate dihydrate up to 125° for chloramphenicol palmitate. Recently (4), the effect on the capsule release rate of surface hydrophilic binder distribution over a hydrophobic drug was studied. The increased hydrophilized hexobarbital release rate was independent of the dissolution medium wetting potency, in contrast to the untreated drug.

The purpose of this investigation was to examine the penetration rate effect on the *in vitro* and *in vivo* availability of poorly soluble, hydrophobic drugs from capsules. Phenytoin was selected as a prototype drug, exhibiting a contact angle of 102°. Phenytoin bioavailability is important because of the closeness of the therapeutic and toxic levels. Marked bioavailability differences between different products have been reported (5–9).

EXPERIMENTAL

Materials—Phenytoin[1] was NF grade. The mean particle size, based on air permeability measurement[2], was 5 μm. Methylcellulose[3], polysorbate[4], β-glucuronidase[5] (purified lyophilized powder, 5×10^6 units/g), 5-(*p*-methylphenyl)-5-phenylhydantoin[6], and 5-(*p*-hydroxyphenyl)-5-phenylhydantoin[6] were used as received. Trimethylanilinium hydroxide[7] was used as a 0.1 *M* solution in methanol, and tetramethylammonium hydroxide[8] was used as a 25% solution in water.

All solvents and other chemicals were analytical grade, except *n*-heptane which was spectrophotometric grade[9]. The methylene chloride used as a mobile phase component in the high-pressure liquid chromatographic (HPLC) procedure was freshly distilled and 50% saturated with water before use.

Methods—*Treatment of Drug*—Methylcellulose dispersion over the phenytoin surface was carried out in a small high-speed mixer[10]. The drug (20 g) was placed in the mixer, 6 ml of a 3% aqueous binder solution was added, and the mixer was run for 6 min at ~9000 rpm. The mixing was interrupted every 0.5 min to mix, with a spatula, material from dead spots in the mixer. The material was dried in a tray drier at 40° for 1 hr and

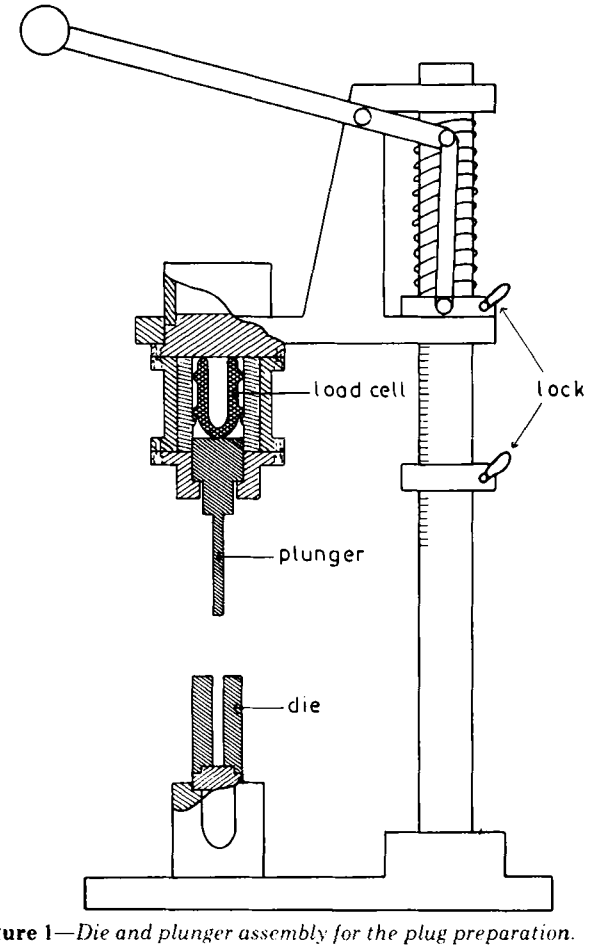

Figure 1—*Die and plunger assembly for the plug preparation.*

[1] Parke-Davis, Mijdrecht, The Netherlands.
[2] Model 95, Fisher Scientific Co., Pittsburgh, Pa.
[3] Celacol M20, British Celanese Ltd., Derby, England.
[4] Tween 80, Atlas Chemie, Essen, West Germany.
[5] Sigma, St. Louis, Mo.
[6] Aldrich Europe, Beerse, Belgium.
[7] B.D.H., Poakstoone, England.
[8] Serva, Heidelberg, West Germany.
[9] Merck AG, Darmstadt, West Germany.
[10] MX 32, Braun AG, Frankfurt/M., West Germany.

0022-3549/79/0500-0634$01.00/0
© 1979, American Pharmaceutical Association

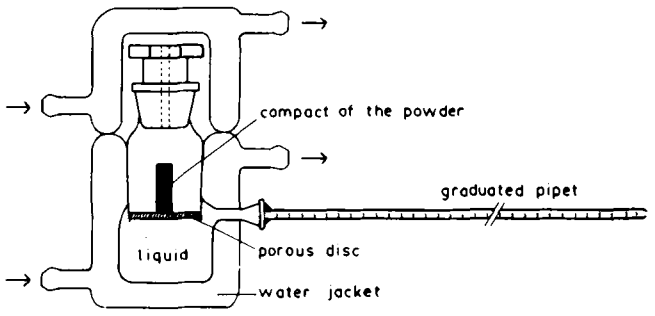

Figure 2—*Thermostated apparatus for measuring unidimensional liquid penetration into the plugs.*

screened through an 80-μm sieve. Treated drug particle-size determination (measured value of 6 μm) and electron micrographs of the untreated and treated powder showed that no milling and hardly any granulation had occurred during preparation.

Wettability—Pure and hydrophilized phenytoin wettability was characterized by contact angle determination as described previously (4).

Plug Preparation—Most commercial capsules are filled by compressing the powder and loading it into the capsule body. To reproduce this process, the pure and treated drugs were compressed with a 120 ± 5 N force to 300-mg plugs (1.8-cm length × 0.6-cm diameter) using a special die and plunger assembly (Fig. 1). The plunger was connected to a load cell for compression force registration.

Capsule Filling—Prepared plugs were manually loaded into No. 1 hard gelatin capsules[11] for the disintegration measurements, the *in vitro* release studies, and the *in vivo* availability studies.

Liquid Penetration—The unidimensional liquid penetration rate into the phenytoin plugs was measured by placing the plug on a modified thermostated apparatus glass filter plate (Fig. 2) (10). The liquid uptake rate was read from the graduated pipet. The penetrations were carried out at 37 ± 0.2° with distilled water or water to which different amounts of polysorbate had been added.

The all-side liquid penetration was measured at room temperature by registration of the phenytoin plug weight increase during penetration. The powder plug was placed in a small glass cylinder with a porous bottom and a gauze cover to prevent floating (Fig. 3). The whole was immersed in the penetrating liquid and connected to an electronic balance[12] with automatic recording. Unidimensional penetration measurements were made four times and averaged. All-side penetrations were so reproducible that they were performed in duplicate only. No significant difference in experimental results was found when the penetrating liquid was presaturated with phenytoin.

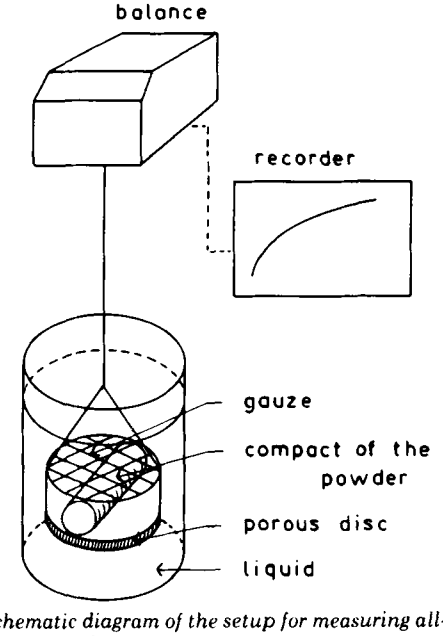

Figure 3—*Schematic diagram of the setup for measuring all-side liquid penetration into the plugs.*

[11] Snap-fit, Capsugel AG, Basel, Switzerland.

[12] PR 1200, Mettler, Greifensee-Zürich, Switzerland.

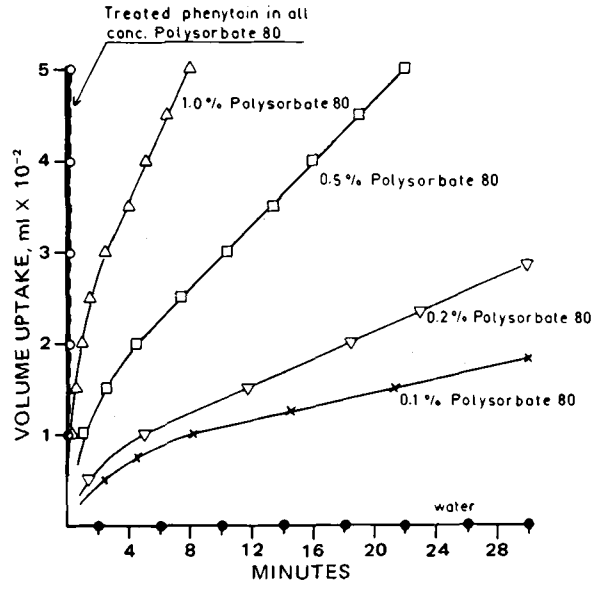

Figure 4—*Unidimensional liquid penetration profiles as a function of the polysorbate concentration. Key: ●, ×, ▽, □, and △, penetration of water and 0.1, 0.2, 0.5, and 1.0% polysorbate into plugs of untreated phenytoin, respectively; and ○, penetration of all concentrations of polysorbate into plugs of treated phenytoin.*

Disintegration—The capsule disintegration time was determined according to the BP 1973. Measurements were carried out without disks at 37 ± 0.5° in water with different polysorbate concentrations. Disintegration measurements were made eight times and averaged.

Dissolution and Solubility—A water-jacketed 1-liter beaker containing the dissolution medium (900 ml) was maintained at 37 ± 0.5°. The dissolution medium consisted of water with different polysorbate concentrations (pH < 5.5). The capsule was held in a stainless steel wire spiral located centrally 2 cm above the beaker bottom. Stirring was with a 5-cm diameter straight four-bladed impeller, rotated at 60 ± 1 rpm 3.5 cm above the capsule (11).

Samples were taken at convenient time intervals through membrane filters (0.8-μm pore diameter) and analyzed by a modified UV spectrophotometric method (12). To a 4.0-ml sample (first diluted, if necessary, with water or the test medium) in a glass-stoppered 25-ml test tube were added 0.5 g of potassium permanganate and 8 ml of 8 *N* NaOH. After

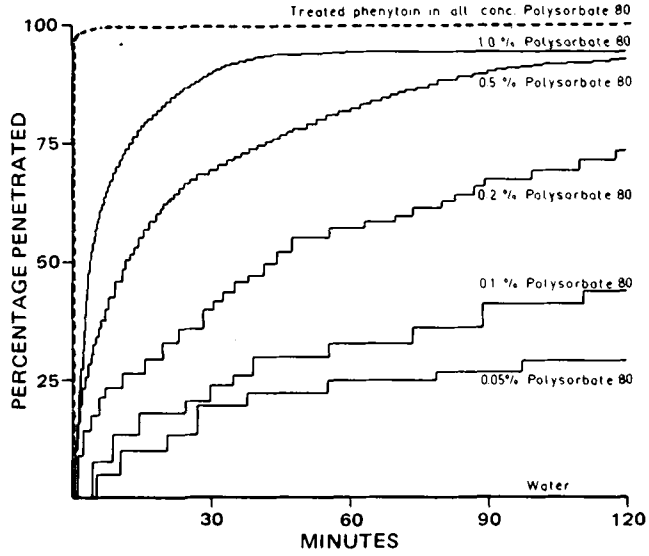

Figure 5—*All-side liquid penetration profiles into plugs of treated and untreated phenytoin as function of the polysorbate concentration. Key: —, untreated phenytoin; and - - -, treated phenytoin.*

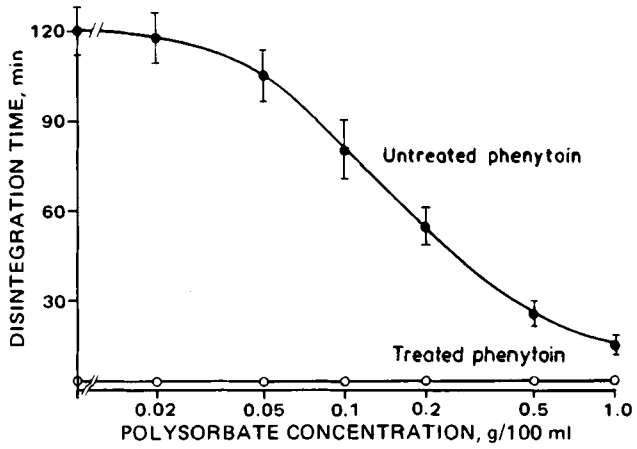

Figure 6—*Untreated and treated phenytoin capsule disintegration time as a function of the polysorbate concentration. Key:* ● *and* ○, *untreated and treated phenytoin, respectively; and* I, *standard deviation.*

being shaken for several minutes, the tubes were immersed in an 80° water bath for 30 min. The samples were allowed to cool to room temperature, and 5.0 ml of *n*-heptane was added. The mixture was shaken for an additional 15 min; after separation of the two layers, the heptane layer absorbance was measured[13] at 247 nm against a suitable blank.

Calibration curves showed that Beer's law was obeyed with slopes of 0.017, 0.026, and 0.057 for water and 0.1 and 0.25% polysorbate, respectively. The correlation coefficients were at least 0.999. Each dissolution profile is the average of three to six determinations. The ranges are indicated in the graphs.

The saturated phenytoin solubility in the different solutions was determined by placing excess solute (about 300 mg) in glass vials filled with each test medium. The vials were closed and rotated at 25 ± 1 rpm in a water bath at 37 ± 0.5° until no increase in the amount dissolved could be measured. Samples were taken at convenient time intervals through membrane filters and analyzed as described for the dissolution study.

For the dissolution and solubility studies, all glass syringes, pipets, and the filter apparatus were prewarmed to prevent drug precipitation.

Absorption—Absorption studies were carried out with nine healthy

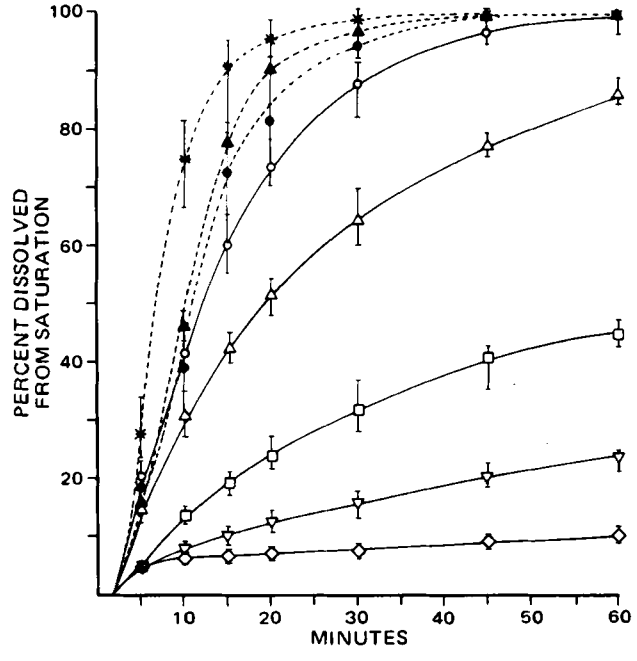

Figure 7—*Treated and untreated phenytoin capsule release profiles as a function of the polysorbate concentration. Open symbols are for untreated phenytoin, and solid symbols are for treated drug. Key:* ◊, *0% polysorbate 80 (γ_{LV}° = 70.1 dynes/cm);* ▽, *0.1% polysorbate 80 (39.9 dynes/cm);* □, *0.2% polysorbate 80 (38.9 dynes/cm);* △, *0.5% polysorbate 80 (37.8 dynes/cm);* ○, *1.0% polysorbate 80 (37.7 dynes/cm);* ✱, *polysorbate solutions with 0–0.2% polysorbate 80;* ▲, *polysorbate solution with 0.5% polysorbate 80;* ●, *polysorbate solutions with 1.0% polysorbate 80; and* I, *intercapsule variation.*

[13] Model 25 UV spectrophotometer, Beckman Instruments Co., Fullerton, Calif.

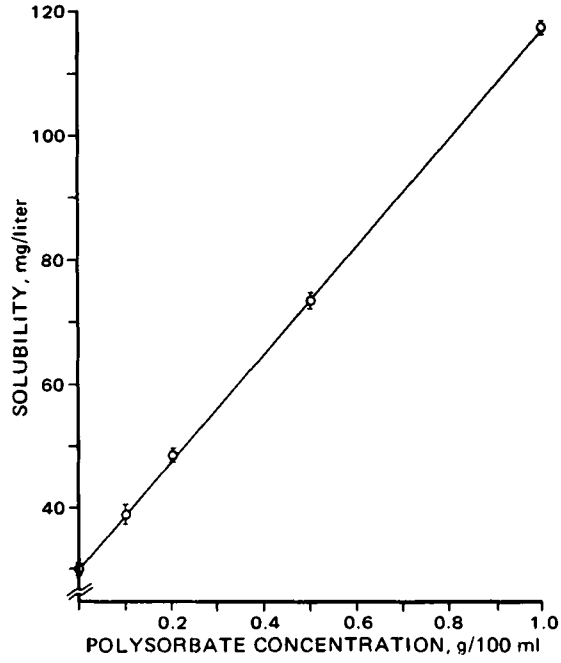

Figure 8—*Phenytoin solubility as a function of the polysorbate concentration (*I = *standard deviation).*

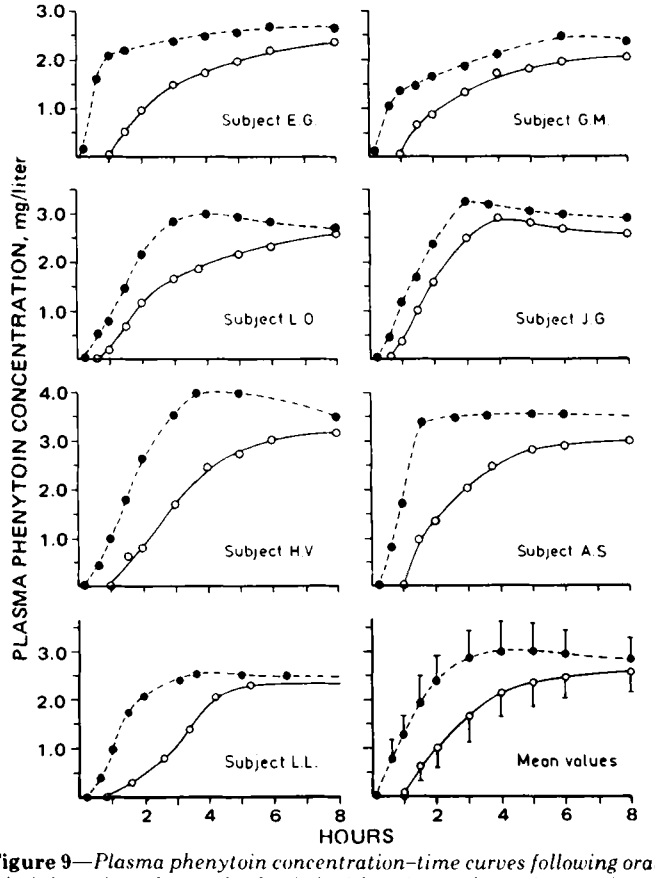

Figure 9—*Plasma phenytoin concentration–time curves following oral administration of capsules loaded with 300-mg plugs of treated and untreated drug. Key:* ● *and* ○, *treated and untreated phenytoin, respectively; and* T, *standard deviation.*

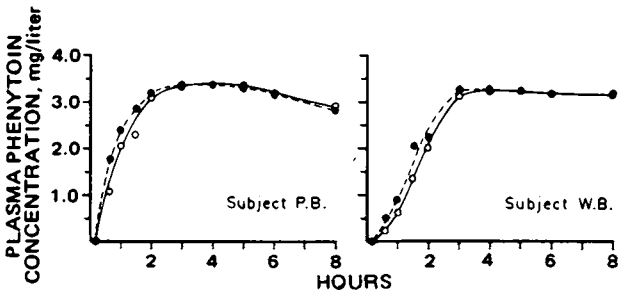

Figure 10—*Plasma phenytoin concentration–time curves following oral administration of a capsule loaded with a plug of 300 mg of treated drug and of a suspension of 300 mg of phenytoin in water. Key: ●, capsule; and ○, suspension.*

volunteers (66–87 kg, 21–28 years of age). Seven subjects received one capsule (300 mg) of pure phenytoin or one capsule of hydrophilized phenytoin. The two administrations were at least 2 weeks apart. The capsules were taken with 200 ml of water after an overnight fast, and no food was allowed for 4 hr after administration. Two subjects received one capsule with 300 mg of hydrophilized phenytoin; 2 weeks later, they received 300 mg of phenytoin dispersed in water.

Blood samples (8 ml) were taken from a forearm vein at 10, 40, 60, and 90 min and 2, 3, 4, 5, 6, 8, 12, 24, 30, and 48 hr. The heparinized blood samples were centrifuged, and the plasma was stored in a refrigerator until analyzed. Urine was collected at (convenient) time intervals over 48 hr. Volumes were recorded, and samples were refrigerated until assayed.

The plasma phenytoin levels were measured by HPLC[14] according to a method developed for carbamazepine (13). The column was 15 cm × 3 mm (i.d.) stainless steel, packed by a balanced-density slurry technique (14) with 5-μm porous particle silicic acid[15]. The solvent system was 5% tetrahydrofuran in methylene chloride. The flow rate was 1.2 ml/min, and the pressure required was ~10 MPa (1500 psi). Nitrazepam was the internal standard. The absorbance[16] was measured at 254 nm. The mean recovery from plasma was 95% with a relative standard deviation of ±2.5% (n = 32). The relative standard deviation of the calibration graph data down to 0.4-μg of phenytoin/ml of plasma did not exceed ±3% (n = 7).

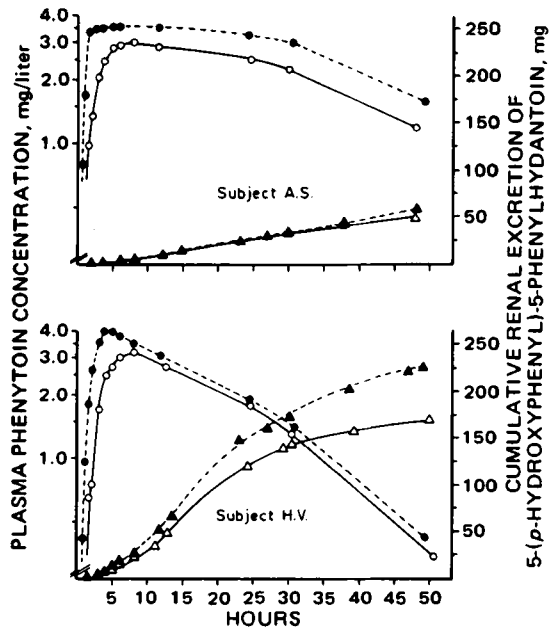

Figure 11—*Plasma phenytoin concentration–time curves and cumulative renal excretion of the total amount of 5-(p-hydroxyphenyl)-5-phenylhydantoin following oral administration of 300-mg treated and untreated phenytoin capsules. Key: ● and ▲, plasma and urine after the treated drug, respectively; and ○ and △, plasma and urine after the untreated drug, respectively.*

5-(*p*-Hydroxyphenyl)-5-phenylhydantoin and its conjugate, the main phenytoin metabolite in humans (15, 16), were assayed in the urine by a modified GLC method (17). To 1.0 ml of urine were added 0.5 ml of 0.066 *M* phosphate buffer (pH 6.9) and 250 units of β-glucuronidase. The samples were incubated for 15 hr at 37°. To the hydrolyzed samples were added 100 μl of an internal standard solution [50 μg/ml of 5-(*p*-methylphenyl)-5-phenylhydantoin in 0.01 *N* NaOH] and 1 ml of 3 *M* phosphate buffer (pH 4.5). After extraction with 8 ml of ether for 15 min and centrifugation, 7 ml of the organic phase was transferred to another test tube. Then 40 μl of 0.1 *M* trimethylanilinium hydroxide dissolved in methanol and 40 μl of 0.54 *M* tetramethylammonium hydroxide dissolved in water were added, and the tube was shaken for 10 min.

After centrifugation, 1 μl of the lower phase was injected into a gas chromatograph[17] equipped with a flame-ionization detector. The coiled glass tubing column, 1.5 m long × 2.2 mm i.d., was packed with 3% OV-17 on 80–100-mesh Chromosorb G.H.P. Operating conditions were: injection port, 300°; column oven, 240°; and detector, 275°. The nitrogen flow rate was 20 ml/min. Hydrogen and compressed air flow rates were adjusted to give maximum response. The relative standard deviation of the calibration graph data down to 15 μg of 5-(*p*-hydroxyphenyl)-5-phenylhydantoin/ml of urine did not exceed ±4% (n = 9).

All plasma and urine samples were analyzed in duplicate.

Liquid Properties—Liquid surface tensions and viscosities were determined with a tensiometer[18] and a capillary tube viscometer[19].

RESULTS AND DISCUSSION

In Fig. 4, the distilled water and polysorbate 80 solution uptakes into pure and hydrophilized phenytoin plugs are graphed against penetration time. As expected, no distilled water penetration into plugs of nontreated drug could be detected because of the strongly hydrophobic nature of the solid and the distilled water surface tension (70.1 dynes/cm at 37°). Addition of 0.1% polysorbate 80 to the penetrating liquid produced a measurable volume uptake. The penetration rate increased with increasing surfactant, decreasing the penetrating liquid surface tension to 37.7 dynes/cm at a 1% concentration.

The wetting of a powder mass by a liquid containing a surfactant is a dynamic process during which surfactant monomers are adsorbed on the substrate. The surfactant micelles are broken down to monomers, which diffuse to the liquid–solid interfaces. During the dynamic penetration process, the micelle breakdown in the capillaries may result in a micelle diffusion from the bulk of the solution into the pores of the mass. In this case, the wetting potency is not limited by the critical micelle concentration [polysorbate 80 = 0.04% (w/v) at 37°]. This is consistent with the theory (18) that micelle diffusion and breakdown will be the rate-limiting steps.

Since the penetration rate into a porous mass is, according to the Washburn equation, strongly dependent on the contact angle of the solid, the extremely hydrophobic phenytoin, exhibiting a contact angle of 102°, was hydrophilized by hydrophilic binder distribution over the solid surface. Methylcellulose treatment decreased the contact angle to 51°. The penetration rate into the hydrophilized phenytoin plugs was strongly increased (Fig. 4). The extremely fast penetration rate was independent of the penetrating liquid wetting potency.

The all-side penetration profiles are represented in Fig. 5. Again no penetration of distilled water into pure phenytoin plugs could be detected. Addition of polysorbate 80 to distilled water resulted in penetrations that increased with increasing surfactant concentrations. The steps in the recorded curves were caused by air bubbles escaping from the porous mass. The hydrophilized phenytoin plugs exhibited instant uptake, which was again independent of the penetrating liquid wetting potency.

The effect of drug hydrophilization on the disintegration of capsules loaded with 300-mg plugs of phenytoin is shown in Fig. 6. The untreated drug capsule disintegration time was 2 hr in distilled water. The disintegration time decreased with increasing surfactant concentration down to 15 min at 1% polysorbate 80. The hydrophilized phenytoin capsules all exhibited, independent of the polysorbate 80 concentration, disintegration times of 3 min, corresponding with the time in which enough of the gelatin had dissolved to open the capsule shell completely.

Analogous results were obtained for the hydrophilization effect on the *in vitro* phenytoin release rate from the different capsules (Fig. 7). The results are expressed as the percentage dissolved from saturation against time. A strong increase in the percentage dissolved for the nontreated

[14] Model M-6000 B, Waters Associates, Milford, Mass.
[15] Partisil, Chrompack, Middelburg, The Netherlands.
[16] Model 440, Waters Associates, Milford, Mass.
[17] Model 5750, Hewlett-Packard, Avondale, Pa.
[18] Du Noüy, 8600 EE, Krüss, Hamburg, West Germany.
[19] Type Ubbelohde, Tamson, Zoetermeer, The Netherlands.

Table I—Area under the Curves for Seven Volunteers after Administration of Capsules Loaded with 300-mg Plugs of Pure or Hydrophilized Phenytoin

Subject	*AUC*, mg min/liter, 0–8 hr		*AUC*, mg min/liter, 0–48 hr	
	Untreated Drug	Treated Drug	Untreated Drug	Treated Drug
A.S.	995	1337	6336	8452
G.M.	673	905	4760	6075
J.G.	991	1192	4184	5324
L.O.	781	1109	4833	5103
E.G.	713	1098	4187	4783
H.V.	943	1447	4821	5661
L.L.	693	1096	—	5194
Mean	827	1169	4853	5900
SD	145	178	787	1328
p^a	<0.001		<0.01	

[a] Evaluated with the Student test for paired observations.

drug was found, along with a slight decrease for the treated drug with increasing surfactant concentrations. The slight decrease in the percentage dissolved from saturation corresponds with an absolute increase in the amount dissolved because of the increased phenytoin solubility with an increasing polysorbate 80 concentration. The latter was due to the strongly solubilizing surfactant (Fig. 8).

Comparative absorption studies were performed in humans. In Fig. 9, all of the individual and the mean plasma curves are given for two capsule preparations loaded with 300 mg of either pure or hydrophilized phenytoin. The plasma levels for all individuals were significantly higher for the treated phenytoin than for the pure drug. Moreover, phenytoin absorption from capsules with untreated drug showed an ~1-hr lag time whereas the hydrophilized drug was absorbed immediately. The area under the plasma level–time curve, evaluated by the trapezoidal rule from 0 to 8 and 0 to 48 hr, showed higher values for the hydrophilized powder than for the pure drug (Table I) ($p < 0.01$).

In two subjects, absorption profiles were compared following oral administration of a 300-mg hydrophilized drug capsule and of a 300-mg phenytoin/200 ml of water suspension (Fig. 10). Nearly identical plasma curves were obtained. The areas under the plasma concentration–time curves from 0 to 8 hr for the capsule and the suspension were 1394 and 1357 mg min/liter for one subject and 1251 and 1244 mg min/liter for the other, respectively. Differences between the areas from 0 to 48 hr after administration were similar.

The total amount of the hydroxylated phenytoin metabolite in the urine over 48 hr is shown in Fig. 11 together with the plasma drug levels in two subjects after pure and hydrophilized drug administration. The results showed remarkable intersubject variation in excretion rates and could not be used to predict relative drug absorption rates from different preparations.

These availability studies are based only on a comparison of hydrophilized drug with pure strongly hydrophobic drug without any adjuvants (*i.e.*, disintegrating agents).

REFERENCES

(1) E. L. Washburn, *Phys. Rev.*, **17**, 273 (1921).

(2) C. F. Lerk, A. J. M. Schoonen, and J. T. Fell, *J. Pharm. Sci.*, **65**, 843 (1976).

(3) C. F. Lerk, M. Lagas, J. P. Boelstra, and P. Broersma, *ibid.*, **66**, 1480 (1977).

(4) C. F. Lerk, M. Lagas, J. T. Fell, and P. Nauta, *ibid.*, **67**, 935 (1978).

(5) K. Arnold, N. Gerber, and G. Levy, *Can. J. Pharm. Sci.*, **5**, 89 (1970).

(6) L. Lund, *Eur. J. Clin. Pharmacol.*, **7**, 119 (1974).

(7) M. J. Steward, B. R. Ballinger, E. J. Declin, A. Y. Miller, and A. C. Ramsey, *ibid.*, **9**, 209 (1975).

(8) P. J. Pentikäinen, P. J. Neuvonen, and S. M. Elfving, *ibid.*, **9**, 213 1975.

(9) B. Rambeck, H. E. Boenigk, and E. Stenzel, *ibid.*, **12**, 285 (1977).

(10) O. Enslin, *Dis. Chem. Falrik*, **6**, 147 (1933).

(11) M. Lagas and C. F. Lerk, *Pharm. Weekbl.*, **112**, 845 (1977).

(12) J. E. Wallace and H. E. Hamilton, *J. Pharm. Sci.*, **63**, 1795 (1974).

(13) H. G. M. Westenberg and R. A. de Zeeuw, *J. Chromatogr.*, **118**, 217 (1976).

(14) R. E. Majors, *Anal. Chem.*, **44**, 1722 (1972).

(15) T. C. Butler, *J. Pharmacol. Exp. Ther.*, **119**, 1 (1957).

(16) A. J. Glazko, T. Chang, J. Baukema, W. A. Dill, J. R. Gaulet, and R. A. Buchanan, *Clin. Pharmacol. Ther.*, **10**, 498 (1969).

(17) B. Karlen, M. Carle, A. Rane, M. Gutova, and B. Lindborg, *Eur. J. Clin. Pharmacol.*, **8**, 359 (1975).

(18) N. Schönfeld, "Grenzflächenaktive Äthylenoxid-Addukte," 1st ed., Wissenschaftliche Verlagsgesellschaft mbH, Stuttgart, West Germany, 1976, p. 185.

ACKNOWLEDGMENTS

The authors thank Parke-Davis for phenytoin. They thank Mr. P. Bouma, Laboratory of Hospital Pharmacy, Mr. J. Visser, Laboratory of Pharmacotherapy and Dispensing, and Mr. D. Smith, Laboratory of Pharmacognosy, for their technical advice. These laboratories of the University of Groningen are acknowledged for providing their facilities. The medical supervision in the *in vivo* experiments of Dr. Wesseling, Department of Clinical Pharmacology, State University, Groningen, The Netherlands, is also gratefully acknowledged.

Alkaline Hydrolysis of 1,3-Dimethylphenobarbital

JAMES LESLIE

Received August 31, 1978, from the *School of Pharmacy, University of Maryland, Baltimore, MD 21201.* Accepted for publication November 6, 1978.

Abstract □ The reaction of 1,3-dimethylphenobarbital (I) with 0.02–0.32 *M* KOH in aqueous methanol was studied. The barbiturate ring cleaved reversibly at the 1,6-position, forming a malonuric acid which was stable to further hydrolysis but which could readily recyclize to I. *N,N*-Dimethylethylphenylmalondiamide arose from decarboxylation of the carbamic acid formed by a 1,2-ring opening; this irreversible decarboxylation determined the diamide as the only final reaction product. The malonuric acid, which could be isolated in solid form, appeared as *N*-methyl-2-phenylbutyramide (GLC) following thermal decarboxylation and degradation of the acid. The I disappearance rate was biphasic, and the kinetics were consistent with the described reaction. The individual rate constants and the equilibrium constant for the reaction between I, the malonuric acid, and hydroxide were determined.

Keyphrases □ Dimethylphenobarbital—alkaline hydrolysis, kinetics, reaction products □ Hydrolysis, alkaline—dimethylphenobarbital, kinetics, reaction products □ Kinetics—dimethylphenobarbital alkaline hydrolysis

The 5,5-disubstituted barbituric acid alkaline hydrolysis has recently received attention (1–5). The pyrimidine ring may cleave at the 1,6-position, yielding a malonuric acid, or at the 1,2-position, forming a carbamic acid. Further hydrolysis leads to the acetic acid derivative and urea. The predominant pathway depends on the barbituric acid ionization state (2) and on the C-5 substituent size (1).

1,3-Dimethyl-5,5-disubstituted barbituric acid hydrolysis yielded only the *N,N'*-dimethylmalondiamides (6). Neither a malonuric acid nor a carbamic acid was isolated from the hydrolysis of phenobarbital, its *N*-methyl derivative (7), and 1,3-dimethylphenobarbital (6). A diamide was the main product in 1,3-dimethylbarbital alkaline hydrolysis, which also produced an acid intermediate. Acid intermediates that can recyclize to the parent barbituric acids have been reported (2, 3).

As a result of a related study (8), interest arose in the base-catalyzed degradation of 1,3-dimethylphenobarbital (I) and the alkaline hydrolysis of I in aqueous methanol was examined. Initial results were sufficiently different from those found with other barbituric acids to warrant detailed study. This paper presents a kinetic and product analysis investigation of the I reaction with potassium hydroxide.

EXPERIMENTAL

Materials—Compound I and *N*-methyl-2-phenylbutyramide (VI) were obtained as described previously (8). Compound IV was prepared by I hydrolysis in 0.7 *M* KOH in methanol–water for 24 hr. After acidification, the reaction mixture was extracted with chloroform and IV was purified by treatment with charcoal[1] in ethanol. The product, mp 106–110° [lit. (6) mp 108–109°], was characterized by mass spectrometry and yielded a single peak by GLC. Ethylphenylmalonate ethyl ester[2] was purified by distillation under reduced pressure.

The malonuric acid (II) was prepared by treating I with 0.1 *M* KOH in methanol–water for a few minutes, acidifying, and extracting with chloroform. The organic layer was shaken with pH 7 phosphate buffer, and the chloroform phase was discarded. Compound II was then obtained by chloroform extraction of the acidified aqueous phase.

All salts and solvents were reagent grade.

GLC—GLC[3] was performed on a 1.82-m × 2-mm i.d. silanized glass column packed with OV-17 on Chromosorb WHP[4]. The carrier gas was nitrogen (30 ml/min). The injection port temperature was maintained at 280°, as was the flame-ionization detector. For detailed reaction product examination, the oven temperature was programmed from 160 to 260° at 10°/min. In the kinetic studies, it was programmed from 220 to 260° at 10°/min.

TLC—TLC[5] was performed using silica gel sheets with a fluorescent indicator[6]. Petroleum ether (bp 60–110°)–ether (65:35) was used to separate reaction products. The R_f values were: I, 0.65; VI, 0.15; and IV, 0.06. In some experiments, ethanol–chloroform was used to isolate II (R_f 0.75). In this latter system, I, IV, and VI moved with the solvent front. The compounds were visualized under UV light, and the spots were scraped off the sheet and eluted with chloroform or methanol.

Kinetic Studies—Kinetic measurements were made at 25° in various potassium hydroxide concentrations with potassium chloride added to

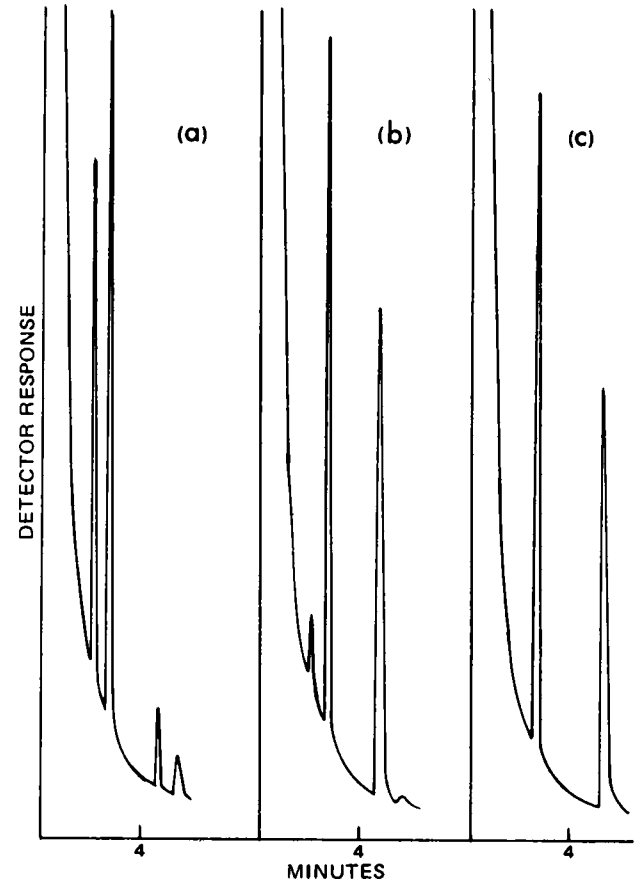

Figure 1—*Gas chromatograms of the reaction mixture of 1,3-dimethylphenobarbital with potassium hydroxide. Key:* a, *0.319* M *KOH after 1 min;* b, *0.0199* M *KOH after 2 min; and* c, *0.319* M *KOH after 50 min. Peaks in order of increasing retention time are* N*-methyl-2-phenylbutyramide, internal standard, 1,3-dimethylphenobarbital, and* N,N'*-dimethylethylphenylmalondiamide.*

[1] Norit-A, Fisher Scientific Co.
[2] Eastman.
[3] Hewlett-Packard 7620A.
[4] Applied Science Laboratories.
[5] Eastman chromatogram chamber set.
[6] Eastman 6060.

0022-3549/79/0500-0639$01.00/0
© 1979, American Pharmaceutical Association

Table I—Rate and Equilibrium Constants [a] for the Reaction of 1,3-Dimethylphenobarbital with Potassium Hydroxide in 50% Aqueous Methanol at 25°

[KOH], M	λ_1	λ_2	k_1	k_2	k_3	k_3[b]	K[c]	K[d]
0.319	0.101	—	16.9[e]	3.14[f]	0.658[g]	0.660	16.9	20.6
0.239	0.0867	—	9.47[e]	2.35[f]	0.449[g]	0.474	16.9	18.6
0.160	0.0713	—	4.25[e]	1.56[f]	0.275[g]	0.277	17.0	20.4
0.0798	0.0486	1.85	1.04	0.738	0.122	0.119	17.6	18.4
0.0606	0.0373	1.33	0.678	0.607	0.0817	0.0894	18.4	18.8
0.0399	0.0223	0.600	0.253	0.329	0.0407	0.0430	19.3	16.2
0.0303	0.0155	0.451	0.164	0.277	0.0252	0.0267	19.5	17.6
0.0199	0.00761	0.229	0.0685	0.157	0.0111	0.0114	21.9	17.1

[a] Rate constants are in minutes^{-1}. [b] Determined from $(\Delta IV/\Delta t)/[I]$. [c] Calculated from $(k_1/k_2)/[KOH]$. [d] Calculated from $([II]/[I])_{max}/[KOH]$. [e] Extrapolated from plot of k_1 and $[KOH]^2$. [f] Extrapolated from plot of k_2 and [KOH]. [g] Calculated using k_1, k_2, and λ_1.

maintain a 0.32 ionic strength. Stock I solutions were prepared by dissolving 10 mg of I in 5 ml of methanol and diluting to 10 ml with water. After thermal equilibration, 0.200 ml of the hydroxide solution in methanol–water was added rapidly to 0.200 ml of the stock I solution. The solution was mixed[7] rapidly and allowed to stand in a constant-temperature bath for the required time.

The solution was then acidified rapidly with hydrochloric acid, 0.400 ml of the internal standard solution (ethylphenylmalonate ethyl ester, 44 mg/100 ml of chloroform) was added, and the mixture was agitated vigorously for 1 min. This volume of solvent and duration of mixing were sufficient to extract the reaction products completely from the aqueous phase. Immediately after the layers had settled, 4 μl of the chloroform solution was injected into the gas chromatograph.

The I and IV peak height ratios to the internal standard were assumed to be proportional to the concentration of these compounds studied (0–0.5 μg/μl). The relative response of I to IV was determined by comparing the peak heights of I aliquots before and after completion of the reaction with potassium hydroxide. Since VI was a decomposition product in GLC and tailed on the packing used, peak height ratios were only an approximate measure of the II concentration.

IR, NMR, and Mass Spectra—IR[8] spectra were obtained in potassium bromide pellets. The NMR[9] spectrum was determined in deuterated chloroform[10] containing 1% tetramethylsilane. Mass spectra were obtained as described previously (8).

RESULTS

Compound I reacted slowly with potassium hydroxide in methanol but readily in the presence of water. The hydrolysis was studied in 50% (v/v) methanol–water.

Hydrolysis Products—When the chloroform extracts of the acidified reaction mixtures were injected into the gas chromatograph, three peaks in addition to that of the internal standard generally were observed (Fig. 1). On the basis of retention times and mass spectrometry (8), the peaks were identified as the butyramide VI, I, and the diamide IV, in order of increasing retention times. The relative peak heights depended on the reaction time and hydroxide concentration. Details are presented under *Kinetic Studies*.

TLC of the extracts using the petroleum ether–ether system showed three spots. Upon elution and GLC, two spots corresponded to I and IV, as did the R_f values. The third spot, at the origin, did not have the VI R_f value, although it yielded the butyramide by GLC. Similar behavior was observed with TLC using ethanol–acetone except that the reference I, IV, and VI moved with the solvent front, as did all of the reaction mixture components except the one that yielded VI by GLC. Since VI initially increased and then decreased to zero as hydrolysis proceeded, it must be derived from an intermediate.

Compound VI did not appear on the gas chromatograms when the reaction chloroform extract was shaken with pH 7 phosphate buffer prior to injection. This finding suggested that the VI precursor was acidic. This extraction procedure was used as the basis for VI isolation.

The IR spectrum of the intermediate was consistent with II, a malonuric acid formed by 1,6-cleavage of the pyrimidine ring (broad regions centered around 3000 cm^{-1}, 1730 cm^{-1}, —COOH; 3280, 1680, 1635, and 1530 cm^{-1}, amide functions). Solubility difficulties precluded obtaining an NMR spectrum. The intermediate melted at ~115° with effervescence. After melting, the product did not correspond on TLC to any of the previously mentioned compounds, although it yielded VI upon GLC. Its R_f value was 0.4 in petroleum ether–ether. An IR spectrum was consistent with the acetylureide V; the carboxyl group bands were no longer present, but bands at 3300, 1700, 1655, and 1530 cm^{-1} showed that the amide functions were intact. The V structure was confirmed by NMR of material purified by TLC: δ 7.29 (s, 5H, C_6H_5), 6.69 (broad peak, 1H, NH), 3.77 (t, 1H, CH), 3.22 (s, 3H, NCH_3), 2.87 [d, 3H, N-(H)CH_3], 1.87 (broad, diffuse, probably —CH_2—), and 0.88 (t, 3H, CH_3).

The possibility that the intermediate was the carbamic acid derivative was ruled out since it would have formed the diamide IV upon decarboxylation.

Samples of II gradually produced increasing I quantities on standing in methanol or chloroform or on a TLC sheet, indicating the capability of the malonuric acid to recyclize back to I. This recyclization was shown to be base catalyzed by treating the isolated intermediate with hydroxide for a short time and acidifying. Substantial I quantities were demon-

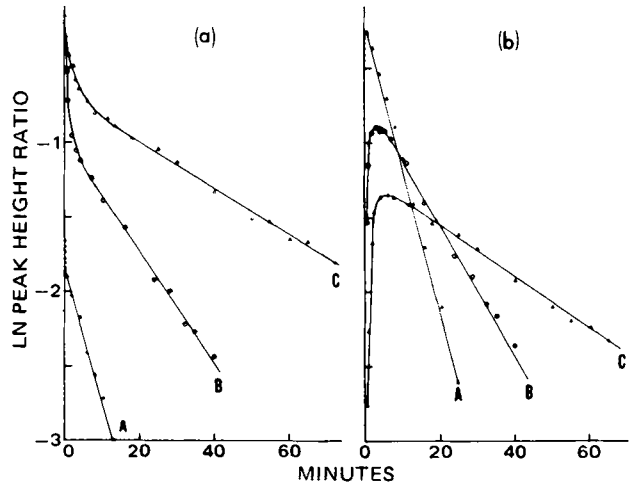

Figure 2—*Rate of change of 1,3-dimethyphenobarbital* (a) *and the intermediate (as N-methyl-2-phenylbutyramide)* (b). *Key: A* (▲), *0.239* M *KOH; B* (○), *0.0606* M *KOH; and C* (△), *0.0303* M *KOH.*

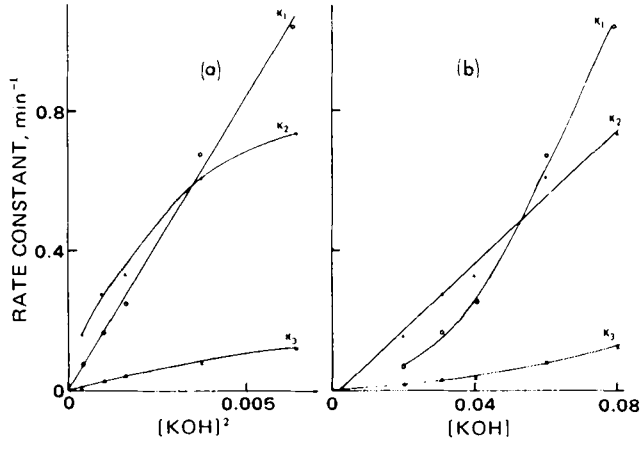

Figure 3—*Plots of* k_1, k_2, *and* k_3 *against* $[KOH]^2$ (a) *and* [KOH] (b).

[7] Vari-Whirl, VWR Scientific Inc.
[8] Perkin-Elmer 257 grating spectrophotometer.
[9] Varian T60.
[10] Norell Chemical Co.

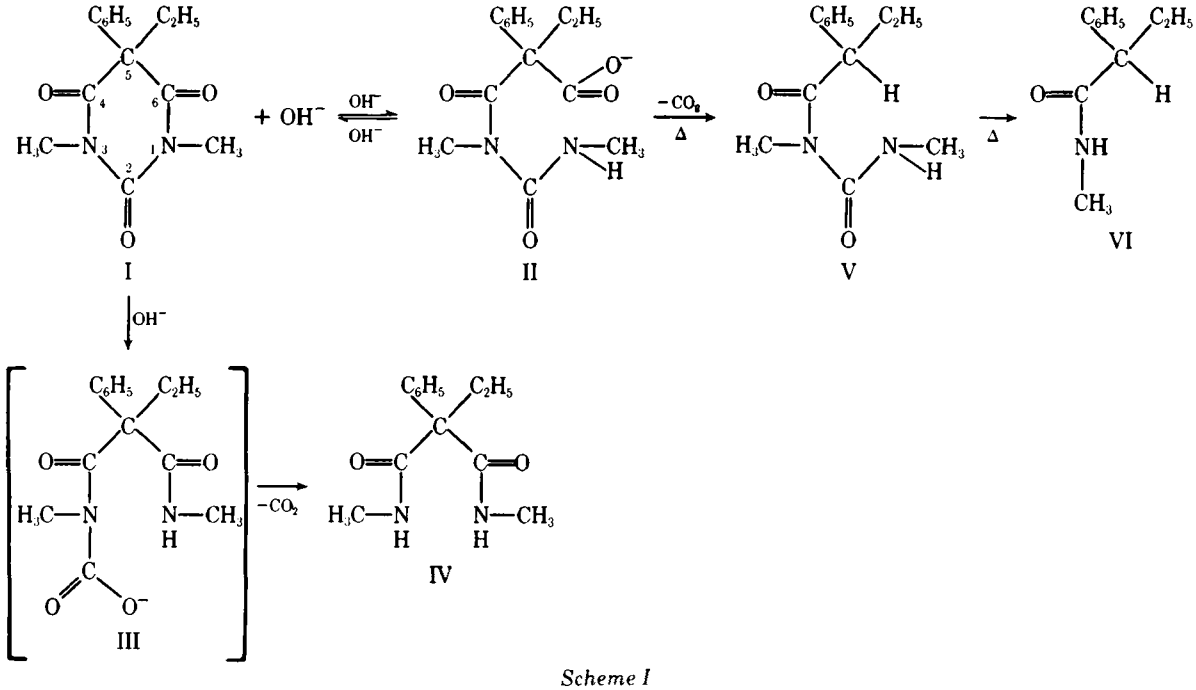

Scheme I

strated by GLC and TLC. Chloroform extraction of an alkaline (no acidification before extraction) II solution resulted in all of it being converted to I (except for a small amount converted to IV). This finding showed that malonurate anion recyclization occurs rapidly and that as I is formed it is removed continuously into the organic layer. When II was allowed to react to completion with potassium hydroxide, only IV could be isolated. Scheme I summarizes the previous reactions.

Kinetic Studies—At all hydroxide concentrations used, the I disappearance rate and the II change rate were biphasic; *i.e.*, a rapid change was followed by a more gradual one, the final phase being linear on a semilogarithmic plot (Fig. 2). The extent of the initial change and the terminal phase slope were strongly dependent on the hydroxide concentration. The initial phase was so fast in hydroxide concentrations greater than 0.1 *M* that it could not be followed kinetically.

The biphasic I disappearance could be fitted to:

$$[I] = Ae^{-\lambda_1 t} + Be^{-\lambda_2 t} \qquad \text{(Eq. 1)}$$

using standard curve-fitting techniques (9); A and B are constants, and λ_1 and λ_2 are rate constants (arbitrarily $\lambda_2 > \lambda_1$). This equation is consistent with the reaction sequence shown in Scheme II.

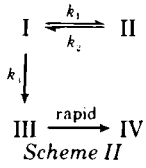

Scheme II

The constant A is the terminal line intercept at $t = 0$. From the observed A, λ_1, and λ_2 values, the rate constants k_1, k_2, and k_3 were calculated (Table I) using:

$$k_2 = \lambda_1 + A(\lambda_2 - \lambda_1)/[I]_0 \qquad \text{(Eq. 2)}$$

$$k_3 = \lambda_1\lambda_2/k_2 \qquad \text{(Eq. 3)}$$

$$k_1 = \lambda_1 + \lambda_2 - k_2 - k_3 \qquad \text{(Eq. 4)}$$

The rate constants k_1, k_2, and k_3 were plotted against various hydroxide concentration functions. The best correlations (Fig. 3) for k_1 and k_2 were:

$$k_1 = 166[OH^-]^2 + 0.0118 \qquad r = 0.996 \qquad \text{(Eq. 5)}$$

$$k_2 = 9.97[OH^-] - 0.0382 \qquad r = 0.993 \qquad \text{(Eq. 6)}$$

No hydroxide function was found that yielded a satisfactory correlation with k_3: the plots of k_3 *versus* [KOH] and [KOH]^2 (Fig. 3) show a definite curvature.

In principle, the rate constants could also be obtained from the II rate of change with time. However, at all potassium hydroxide concentrations, the terminal slope, *i.e.*, λ_1 for the II disappearance rate, measured by GLC as VI, was slightly higher than the rate for I. This finding was attributed to the nonlinearity of the peak height ratios with II concentration because of column tailing. The error is amplified in obtaining λ_2. Since II is an unstable compound, no standard response on the GLC can be obtained and the II concentration at the intercept that is needed for the rate constant calculation can only be approximated. The response factor was approximated by calculating the II concentration from the difference between the amount of I added and the amount of I unreacted and IV formed.

With the following appropriate relationships:

$$k_1 = (\text{intercept of terminal line}) \times (\lambda_2 - \lambda_1)/[I]_0 \qquad \text{(Eq. 7)}$$

$$k_2 + k_3 = \lambda_1 + \lambda_2 - k_1 \qquad \text{(Eq. 8)}$$

$$k_2k_3 = \lambda_1\lambda_2 \qquad \text{(Eq. 9)}$$

k_1, k_2, and k_3 can be estimated from the corrected peak height ratios. For example, for the reaction in 0.0606 *M* KOH, λ_1, λ_2, k_1, k_2, and k_3 were estimated to be 0.0421, 1.05, 0.558, 0.436, and 0.102 min^{-1}, respectively, compared to 0.0373, 1.33, 0.678, 0.607, and 0.0817 min^{-1}, respectively, obtained for the I rate of change. The agreement is reasonable considering the approximations made; the data are consistent with the reactions in Scheme II.

Since the III to IV conversion is rapid, the IV formation rate is proportional to the I concentration. Therefore, approximate values for k_3 can be derived using:

$$(\Delta IV/\Delta t)/[I] \simeq k_3 \qquad \text{(Eq. 10)}$$

By using increments of IV and time from [IV] *versus* t plots, approximate k_3 values were calculated (Table I). The agreement with the k_3 values obtained by the previous method is remarkable but to some extent fortuitous.

Since $d[II]/dt = k_1[I] - k_2[II] = 0$ at the maximum of the plot of [II] *versus* time, and since k_1 is proportional to [KOH]^2 and k_2 is proportional to [KOH], Eq. 11 can be derived:

$$([II]/[I])_{max}/[KOH] = (k_1/k_2)/[KOH] = K \qquad \text{(Eq. 11)}$$

where K is the equilibrium constant for the reaction between I and II and $([II]/[I])_{max}$ is the ratio of the I and II concentrations at the maximum in II. Values of K obtained in this way using the maximum obtained graphically are listed in Table I, as are values of $(k_1/k_2)/[KOH]$. Although there is a 12-fold change in hydroxide concentration, the values of K are reasonably constant.

Although λ_2 could not be obtained directly from the experimental data for the higher hydroxide concentrations, the rate and equilibrium constants were estimated as indicated in the footnotes of Table I.

DISCUSSION

Unlike 1-methylphenobarbital and phenobarbital itself (7), I alkaline hydrolysis yielded only the substituted diamide IV. Although this compound could be the result of decarboxylation of a carbamic acid intermediate formed by a 1,2-ring opening, the acid intermediate actually isolated was identified as a malonuric acid formed by a 1,6-ring opening. The formation of the diamide as the sole final reaction product is in agreement with a previous report (6), although no acid intermediates were isolated in that work, probably due to the relatively low hydroxide concentrations used and to the reaction mixture manipulation.

The malonurate (II) did not decarboxylate but recyclized to the parent barbituric acid. The overall irreversibility of IV hydrolysis was due to the decarboxylation of a carbamic acid, which was too unstable to isolate. Phenobarbital and its *N*-methyl derivative yielded acetylureides and diamides, but no malonuric acids (7), upon hydrolysis. The simplicity of I hydrolysis is due to dimethylated diamide and malonuric acid stability. A diamide is the only product of 1,3-dimethylbarbital hydrolysis (3). An acid intermediate proposed to be a carbamic acid could be a malonuric acid in rapid equilibrium with the barbituric acid.

A malonurate anion would not be expected to recyclize readily, but similar compounds form cyclic products. Diethylacetylurea cyclizes to barbital (2), 2-ureidobenzoate forms 2,4-dihydroxyquinazoline at a rate proportional to the hydroxide-ion activity (10), and 2-iodo-3-ureidopropionic acid yields 2-amino-2-oxazoline-3-carboxylic acid (11).

The observed reaction kinetics of I with hydroxide are consistent with the reaction sequence in Scheme I and agree with the qualitative observations that ring opening occurs predominantly at the 1,6-position. This is the first report of a biphasic decrease in barbiturate concentration upon alkaline hydrolysis, and its observation is due in part to the reaction mixtures being analyzed by a technique that permits separation of products. The simplicity of the reactions enabled the rate constants and equilibrium constant to be determined. The terminal disappearance of the barbituric acid is not a simple function but depends on all of the rate constants in Scheme II.

The rate of II formation is dependent on the second power of the hydroxide concentration. This result can be explained by tetrahedral complex formation between I and hydroxide ion, followed by a base-catalyzed ring opening to the malonurate. Such a sequence was proposed (12) for barbituric acid hydrolysis. The reverse reaction cyclization would have to be first order in hydroxide concentration, as was observed in this study.

The lack of a simple k_3 dependence on hydroxide concentration probably reflects the fact that the irreversible step is complex, involving ring opening and decarboxylation. Although a carbamic acid was not isolated in this work, it may be present in the reaction mixture and undergo decarboxylation during the workup. In view of carbamic acid instability, the quantity would be insignificant.

Although the reaction rate of I is biphasic, this behavior becomes modified at the lower and higher hydroxide concentrations and approaches first-order kinetics. Therefore, the complex behavior observed in the hydrolysis of barbituric acids possibly could be explained by closer examination of the experimental data.

The pyrimidine ring in 1,3-dimethylphenobarbital is preferably cleaved at the 1,6-position, as established by detailed kinetic studies, whereas final product analysis could lead to the conclusion that ring opening occurs at the 1,2-position. This system may serve as a useful model for a study of the effects of substituents at the 5 carbon without the complications of ionization or degradation to a large number of products.

REFERENCES

(1) H. V. Maudling, J. Nazareno, J. Polesuk, and A. Michaelis, *J. Pharm. Sci.*, **61**, 1389 (1972).

(2) E. R. Garrett, J. T. Bojarski, and G. J. Yakatan, *ibid.*, **60**, 1145 (1971).

(3) J. Bojarski, *Rocz. Chem.*, **47**, 1417 (1973).

(4) T. Hermann, *Pharmazie* **31**, 618 (1976).

(5) L. A. Gardner and J. E. Goyan, *J. Pharm. Sci.*, **62**, 1026 (1973).

(6) H. Aspelund, *Acta Acad. Abo., Ser. B*, **29**, 1 (1969).

(7) F. Fretwurst, *Arzneim.-Forsch.*, **8**, 44 (1948).

(8) P. S. Callery and J. Leslie, *J. Pharm. Sci.*, **66**, 578 (1977).

(9) D. S. Riggs, "The Mathematical Approach to Physiological Problems," M.I.T. Press, Cambridge, Mass., 1970, p. 146.

(10) A. F. Hegarty and T. C. Bruice, *J. Am. Chem. Soc.*, **92**, 6584 (1970).

(11) M. Buehler and E. G. Sander, *Biochem. Biophys. Res. Commun.*, **82**, 196 (1978).

(12) S. O. Eriksson and C.-G. Regardh, *Acta Pharm. Suec.*, **5**, 457 (1968).

ACKNOWLEDGMENTS

The author thanks Dr. S. E. Krikorian for assistance in the IR and NMR determinations, Dr. P. S. Callery for the mass spectrometric analyses, and Mr. Frank C. Fiery for assistance in some of the early kinetic measurements.

Oxybutynin Influence on Autonomic Measures in Dogs

BERNARD KOROL *x **and LOWELL D. MILLER** ‡§

Received March 4, 1977, from the *Veterans Administration Medical Center, St. Louis, MO 63125, and the ‡Department of Psychiatry, St. Louis University School of Medicine, St. Louis, MO 63104. Accepted for publication November 1, 1978. §Present address: Marion Laboratories, Kansas City, MO 64137.

Abstract □ In the conscious dog, the most apparent oxybutynin effect was a dose-related tachycardia. Associated with this heart rate increase were a very slight, sometimes significant, elevation in diastolic pressure and an insignificant increase in systolic pressure. Under pentobarbital anesthesia, the systolic/diastolic arterial pressure oxybutynin responses were reversed and showed a dose-related systolic and diastolic hypotension. However, the tachycardic response to oxybutynin still appeared. The arterial pressure and heart rate responses produced by the autonomic agents were altered by the oxybutynin treatment in a pattern indicative of an anticholinergic mechanism of action. Differences in many response profiles were observed with either conscious or anesthetized dogs, but the statistically significant inhibition of the acetylcholine-induced systolic and diastolic arterial pressure and bradycardic responses were constant in both conditions. Oxybutynin is an anticholinergic agent with mild to moderate cardiovascular activity.

Keyphrases □ Oxybutynin—effect on autonomic functions in conscious and phenobarbital-anesthetized dogs □ Autonomic functions—effect of oxybutynin, conscious and phenobarbital-anesthetized dogs □ Phenobarbital—effect on oxybutynin response, autonomic functions, dogs

Previous studies indicated that the tertiary amine oxybutynin chloride (4-diethylamino-2-butynyl α-phenylcyclohexaneglycolate hydrochloride) had a weakly anticholinergic mechanism of action. In an anesthetized dog, a cumulative intravenous dose of 750 μg/kg (last dose of 400 μg/kg) completely blocked the hypotensive acetylcholine-induced response and partially (60%) inhibited the hypotensive response to vagal stimulation. Atropine, 10 μg/kg, produced a 66% reduction of the vagal blood pressure response and a 30% inhibition of the acetylcholine depressor response.

Table I—Effects of Graded Intravenous Oxybutynin Doses on Mean Basal Level and Mean Response Amplitude in Six Conscious Beagle Dogs

Treatment	Systolic, mm Hg	Diastolic, mm Hg	Heart Rate, beats/min	Respiration Rate, breaths/min
Basal level	133 (8.9)[a]	87 (6.2)	107 (5.3)	42 (5.5)
Oxybutynin				
0.1 mg/kg	+5 (3.4)	+1 (0.8)	+1 (2.6)	+8 (4.3)
0.3 mg/kg	+3 (4.3)	+2[b] (0.7)	+21[b] (5.5)	+6 (5.9)
1.0 mg/kg	+9 (5.9)	+6[b] (2.4)	+35[b] (11.8)	+2 (0.9)
3.0 mg/kg	−7 (8.8)	+3 (6.7)	+52[b] (12.5)	+7 (3.5)

[a] Standard errors are given in parentheses. [b] $p \leq 0.05$.

Table III—Effects of Graded Intravenous Oxybutynin Doses on Mean Basal Level and Mean Response Amplitude in Six Anesthetized Beagle Dogs

Treatment	Systolic, mm Hg	Diastolic, mm Hg	Heart Rate, beats/min	Respiration Rate, breaths/min
Basal level	125 (9.5)[a]	89 (9.3)	140 (8.2)	22 (5.1)
Oxybutynin				
0.1 mg/kg	0	+2 (1.1)	+4 (2.4)	+1 (0.7)
0.3 mg/kg	0	0	+1 (2.2)	+1 (0.3)
1.0 mg/kg	−8 (4.6)	−5 (3.2)	+12[b] (2.0)	+1 (0.6)
3.0 mg/kg	−30[b] (6.2)	−26[b] (5.8)	+25[b] (5.7)	+6 (2.9)
10.0 mg/kg	−31[b] (2.4)	−37[b] (3.7)	+1 (3.5)	+17[b] (6.3)

[a] Standard errors are given in parentheses. [b] $p \leq 0.05$.

The physiological state of the experimental preparation can influence the quality and amplitude of a response profoundly. In the anesthetized dog, the alkaloid ibogaine produced a marked hypotension, which was not evident in the conscious dog (1). In anesthetized dogs, the alkaloid yohimbine lowered arterial pressure due to a peripheral α-adrenergic blocking effect (2). In these same animals, while conscious, an equivalent intravenous yohimbine dose produced a hypertension and tachycardia; both responses endured for 30 min or longer. The response from the conscious dog was an expression of the yohimbine central sympathetic nervous system stimulating effect, which was not evoked in the anesthetized (barbiturate) animal.

A recent study in chronically prepared dogs investigated anesthesia influence on cardiovascular responses to cryptenamine, an alkaloid from *Veratrum veride* (3). In

Table II—Effects of a Cumulative Oxybutynin Dose of 4.4 mg/kg iv on Autonomic Response in Six Conscious Beagle Dogs

Treatment	Systolic, mm Hg	Diastolic, mm Hg	Heart Rate, beats/min	Respiration Rate, breaths/min
		Control Response		
Bilateral carotid occlusion	+92 (73)[a]	+45 (54.2)	+20 (12)	+2 (1)
Tyramine	+58 (18.8)	+22 (4.6)	+18 (3.6)	+1 (0.8)
Acetyl choline	−21 (6.1)	−17 (5.3)	+20 (11.3)	+4 (1.2)
Epinephrine	+33 (4.9)	+21 (3.5)	+11 (5.7)	+4 (5.4)
Histamine	−26 (2.4)	−23 (3.1)	+48 (10.7)	+1 (1)
Norepinephrine	+34 (4.7)	+18 (7)	−2 (1.9)	+5 (2.3)
Isoproterenol	−29 (8.6)	−30 (8.8)	+78 (13.8)	+23 (7.4)
5-Hydroxytryptamine	+29 (9.2)	+13 (5.1)	+12 (10.5)	−2 (4.3)
		After Oxybutynin		
Bilateral carotid occlusion	+48 (17.4)	+33 (8.3)	−4 (4.9)	+1 (1.8)
Tyramine	+75 (21.3)[b]	+42 (9.8)[b]	+3 (1.3)[b]	+11 (6.7)
Acetylcholine	−11 (4.3)[b]	−3 (4.9)[b]	+4 (7.6)[b]	−10 (9.1)
Epinephrine	+42 (11.8)	+27 (5.2)[b]	−1 (4)[b]	+13 (10.2)
Histamine	−30 (3.5)	−35 (6.8)	+83 (19.4)[b]	−3 (4.4)
Norepinephrine	+32 (6.3)	+14 (5.4)	−28 (1)[b]	+4 (2.4)
Isoproterenol	−36 (8.9)	−55 (8.4)[b]	+54 (11.1)	+12 (9.2)
5-Hydroxytryptamine	+17 (5.9)	+9 (4.3)	−4 (4.3)	+8 (10)

[a] Standard errors are given in parentheses. [b] $p \leq 0.05$.

0022-3549/79/0500-0643$01.00/0
© 1979, American Pharmaceutical Association

Table IV—Effects of a Cumulative Oxybutynin Dose of 14.4 mg/kg iv on Autonomic Response in Six Anesthetized Beagle Dogs

Treatment	Systolic, mm Hg	Diastolic, mm Hg	Heart Rate, beats/min	Respiration Rate, breaths/min
		Control Response		
Bilateral carotid occlusion	+11 (6.7)[a]	+17 (1.7)	+35 (35)	+3 (4.1)
Tyramine	+122 (30.5)	+49 (20.5)	+18 (17)	−3 (1.8)
Acetylcholine	−26 (2.4)	−27 (3.1)	+21 (5.3)	+2 (1.5)
Epinephrine	+33 (7)	+22 (8)	−1 (3.9)	+4 (1.6)
Histamine	−24 (3.3)	−28 (6.7)	+12 (4.8)	+2 (1.3)
Norepinephrine	+39 (5.2)	+27 (5.7)	−22 (4.5)	0
Isoproterenol	−32 (9.2)	−45 (5.2)	+101 (11.1)	+11 (3.8)
5-Hydroxytryptamine	+5 (4.5)	+1 (2.7)	+6 (5.8)	+7 (4.1)
		After Oxybutynin		
Bilateral carotid occlusion	+15 (3)	+27 (12.5)	+48 (17)	+2 (0.5)
Tyramine	+106 (30.3)	+61 (23.3)	+53 (15.6)	+7 (7.1)
Acetylcholine	+1 (0.8)[b]	+1 (1.5)[b]	−3 (2.9)[b]	+2 (0.9)
Epinephrine	+76 (13.8)[b]	+39 (14.4)[b]	+22 (12.9)[b]	+24 (21.7)
Histamine	−30 (3.9)	−27 (7.9)	+10 (1.4)	+6 (2.8)
Norepinephrine	+92 (11.8)[b]	+47 (7.2)[b]	+21 (10.5)[b]	+2 (0.6)[b]
Isoproterenol	−34 (6.9)	−59 (3.3)[b]	+82 (8.3)	+8 (4)
5-Hydroxytryptamine	0	−5 (5.4)	+1 (1.8)	+10 (3.2)

[a] Standard errors are given in parentheses. [b] $p \leq 0.05$.

32 paired conscious and anesthetized dogs, pentobarbital anesthesia significantly lowered basal systolic/diastolic arterial pressures, raised basal heart rate, and altered responses to autonomic treatments. Pentobarbital anesthesia also significantly increased the cryptenamine dose required for inhibition of the hypotensive and/or bilateral carotid occlusion pressor response. The conscious dog systolic depressor response to cryptenamine is the most sensitive and accurate bioassay for cryptenamine potency evaluation.

Earlier studies on oxybutynin were performed only in anesthetized animals. This paper reports its effects on autonomic functions and responses to autonomimetic treatments in conscious and anesthetized matched paired dogs.

EXPERIMENTAL

Six male and female beagle dogs were surgically prepared with externalized bilateral carotid artery loops (4). Each animal was its own control and was utilized both conscious and anesthetized (~35 mg of pentobarbital sodium/kg iv). This preparation permits direct systolic and diastolic arterial pressure measurement, induction of a reflex pressure response to bilateral carotid occlusion, and measurement of other autonomic functions such as ECG, heart rate, and respiration on conscious, slightly restrained animals (5).

Direct systolic and diastolic arterial pressure (lateral) was measured from an externalized carotid artery cannula[1]. The cannula was connected to a pressure transducer[2], which supplied input into a recorder coupler[3]. Cannula patency was maintained by slow retrograde saline infusion through the pressure transducer. The infusion rate did not alter the arterial pressure measurements.

Heart rate was measured by the conversion of the R-R wave interval by a cardiotachometer coupler[4] from a bipolar electrocardiograph input obtained through biopotential electrodes positioned and affixed to the skin over the sternum. A homemade sodium chloride electrode paste (0.154 mole/kg)[5] was used to facilitate conduction.

Respiration rate and amplitude were measured indirectly through a pneumograph belt positioned around the thoracico-abdominal junction and connected to a pressure transducer[2], which was connected to a coupler[3].

Recording was on a multichannel recorder[6] at a paper speed of 5 mm/sec.

[1] Medicon AR-3218.
[2] Statham model P-23AA.
[3] Beckman strain-gauge coupler 9872.
[4] Beckman cardiotachometer coupler 9857.
[5] In Unibase.
[6] Beckman type R dynograph.

Table V—Difference in Mean Basal Level and Mean Amplitude of Cardiovascular Response to Graded Oxybutynin Doses in Six Beagle Dogs Examined in the Conscious and Anesthetized States

Treatment	Systolic, mm Hg	Diastolic, mm Hg	Heart Rate, beats/min	Respiration Rate, breaths/min
Basal level	+8	−2	−33[a]	+20[a]
Oxybutynin				
0.1 mg/kg	+5	−1	−4	+7
0.3 mg/kg	+3	+2	+20[a]	+6
1.0 mg/kg	+16[a]	+11[a]	+23[a]	+1
3.0 mg/kg	+23[a]	+29[a]	+27[a]	+1

[a] $p \leq 0.05$.

To control for order effect, the six animals were treated in a random order in both the conscious and anesthetized states.

All dogs had an indwelling venocatheter (PE-50) in the branchial-cephalic or saphenous vein for drug solution administration. They were anesthetized with pentobarbital sodium, 30–35 mg/kg. Care was taken to position the pressure transducer at the appropriate level (heart horizontal) for each dog, particularly when anesthesia was employed.

Fresh aqueous oxybutynin solutions were prepared prior to use, and the concentrations were adjusted so that equivolumes were administered at each dose level. The oxybutynin doses were 0.1, 0.3, 1.0, 3.0, and 10.0[7] mg/kg iv in equivolumes of 0.1 ml/kg. Systolic and diastolic arterial pressures, heart rate, ECG, and respiration rate were measured.

After a 10–15-min equilibration, the animal received an autonomic treatment series. The autonomic agonists and their dose levels (salt weight) were: bilateral carotid occlusion, 30 sec; tyramine hydrochloride, 0.20 mg/kg; acetylcholine chloride, 0.6 μg/kg; epinephrine hydrochloride, 2 μg/kg; histamine phosphate, 2 μg/kg; norepinephrine bitartrate, 2 μg/kg; isoproterenol hydrochloride, 2 μg/kg; and serotonin diphosphate, 10 μg/kg. The autonomic treatments were repeated after the highest oxybutynin dose. The direction and amplitude of the autonomic responses were described previously (6).

The data were analyzed for statistical significance by the matched-pair t test (7).

RESULTS AND DISCUSSION

The data are summarized in Tables I–IV.

Oxybutynin effects in the conscious dog are reviewed in Tables I and II. At a mean basal systolic arterial pressure level of 133 mm Hg, oxybutynin doses of 0.1, 0.3, 1.0, and 3.0 mg/kg iv produced statistically insignificant changes in systolic pressure (Table I). The mean basal diastolic pressure of 87 mm Hg was significantly elevated following treatment with 0.3 and 1.0 mg of oxybutynin/kg. Diastolic pressure increased insignificantly (3 mm Hg) after the 3.0-mg/kg dose. These changes in diastolic

[7] Given only if an absent or a weak response resulted from lower dose.

pressure were statistically significant but physiologically inconsequential.

Oxybutynin produced apparently dose-related tachycardia. A significant peak tachycardic response (21 beats/min) appeared after the 0.3-mg/kg dose, and a significant peak (52 beats/min) occurred after the 3.0-mg/kg iv dose. Although there was a consistent tachypnea after each oxybutynin dose, none of the respiratory changes was significant.

The effects of the cumulative 4.4-mg/kg iv oxybutynin dose on the autonomic responses in conscious dogs are summarized in Table II. Oxybutynin produced several significant autonomic responses. The tyramine-induced pressor response was significantly enhanced. The tyramine-evoked tachycardic response was significantly depressed to +3.2 beats/min. The acetylcholine-induced depressor and associated tachycardic responses were significantly inhibited. The epinephrine pressor response amplitude was significantly enhanced by oxybutynin treatment, although the associated heart rate response was inhibited by from +11 to −1 beats/min. Other significant changes included enhanced histamine tachycardia, increased norepinephrine brachycardia, and increased diastolic depressor response to isoproterenol.

When oxybutynin was administered to anesthetized dogs, the systolic and diastolic pressure responses were opposite to those observed in the conscious state (Table III). Oxybutynin (1.0, 3.0, and 10.0 mg/kg iv) produced systolic/diastolic depressor responses of −8/−5, −30/−26, and −31/−37 mm Hg, respectively. The associated significant tachycardic responses occurred only after the 1.0- and 3.0-mg/kg doses. The 10.0-mg/kg oxybutynin dose produced profound and significant depressor responses but insignificantly increased heart rate. Perhaps at this dose in the anesthetized dog the heart rate response, which appears to be compensatory to the systolic/diastolic depression, is pharmacologically antagonized by oxybutynin. The possibility of a toxicologic response to the 10.0-mg/kg dose is supported by the appearance of a marked and statistically significant tachypnea (+17 breaths/min).

Table IV describes the effects of a total cumulative 14-mg/kg iv oxybutynin dose of the autonomic treatment responses of anesthetized dogs. The acetylcholine-induced arterial pressure depressor response was inhibited. Similarly, the acetylcholine-induced tachycardia was markedly inhibited following oxybutynin. The epinephrine pressor response was enhanced, as was the heart rate response. The systolic/diastolic pressures and heart rate response to norepinephrine were also significantly altered. The respiratory rate response to norepinephrine was slightly, but significantly, increased. Only the diastolic pressure response to isoproterenol was significantly increased following oxybutynin.

Divergent responses due to the "state-of-the-animal" were reported previously (1–3). The influence of differential state on response must be considered when interpreting the experimental data, particularly from the anesthetized preparation.

The differences in systolic/diastolic arterial pressures, heart rates, and respiration rates are summarized in Table V. Basal heart rate was considerably lower in the conscious state, while basal respiratory rate was significantly greater. The amplitude of the changes indicated that the conscious animal exhibits greater oxybutynin sensitivity and response intensity. Greater oxybutynin tachycardic response in conscious animals can be explained on the basis of the Law of Initial Values (8).

In the conscious dog, the oxybutynin response was pressor; following pentobarbital anesthesia, the same oxybutynin doses evoked a systolic/diastolic arterial depressor response. These findings are inexplicable.

The consistent and significant tachycardia produced by oxybutynin in conscious and anesthetized dogs and the selective oxybutynin inhibition of the acetylcholine-induced cardiovascular responses in both conditions support the earlier pharmacological report. Oxybutynin has mild to moderate cardiovascular effects, probably through an anticholinergic mechanism of action.

REFERENCES

(1) J. A. Schneider and R. K. Rinehart, *Arch. Int. Pharmacodyn. Ther.*, **110**, 92 (1957).

(2) S. Gershon and W. J. Lang, *ibid.*, **135**, 31 (1962).

(3) B. Korol, *J. Pharm. Sci.*, **60**, 488 (1971).

(4) M. L. Brown and B. Korol, *Physiol. Behav.*, **3**, 207 (1968).

(5) B. Korol, W. J. Lang, M. L. Brown, and S. Gershon, *Nature*, **209**, 1249 (1966).

(6) B. Korol and M. L. Brown, *Arch. Int. Pharmacodyn. Ther.*, **170**, 371 (1967).

(7) A. L. Edwards, "Experimental Design in Psychological Research," 3rd ed., Holt, Rinehart & Winston, New York, N.Y., 1968, pp. 164, 165.

(8) J. Wilder, *Ann. N.Y. Acad. Sci.*, **98**, 1211 (1962).

Amino Acid Effect on Aspirin Stability in Propylene Glycol

PREM K. NARANG * and JAMES K. LIM *

Received July 6, 1978, from the *School of Pharmacy, West Virginia University, Morgantown, WV 26506.* Accepted for publication November 6, 1978. *Present address: School of Pharmacy, University of Maryland, Baltimore, MD 21201.

Abstract □ Temperature stability studies were conducted on 0.36 *M* (6.5% w/v) aspirin solutions including either 0.02 *M* L-methionine or 0.02 *M* histidine in propylene glycol. Aspirin was determined spectrophotofluorometrically as salicylic acid content at 412 nm. A 0.36 *M* aspirin in polyethylene glycol 400 solution was studied concurrently. Aspirin degradation rate constants, *k*, obtained from semilogarithmic plots of percent drug remaining *versus* time at 30–70 ± 0.5° were used for preparing Arrhenius plots. Good correlation was seen between predicted aspirin stability and experimental $k_{25°}$ values. L-Methionine and histidine markedly reduced aspirin stability.

Keyphrases □ Aspirin—stability in propylene glycol, effect of L-methionine and histidine, temperature □ Stability—aspirin in propylene glycol, effect of L-methionine and histidine, temperature □ Propylene glycol—stability of aspirin solutions, effect of L-methionine and histidine, temperature

Aspirin remains the most sought-after, nonprescription analgesic. It possesses a combination of anti-inflammatory, antipyretic, and analgesic properties unparalleled by other "aspirin-like" compounds. Aspirin is, however, a notoriously unstable drug and degrades to the less potent salicylic acid in the presence of moisture (1). Liquid aspirin dosage forms present a challenging pharmaceutical problem because of this instability in water and in vehicles containing traces of water.

Numerous attempts to stabilize aspirin solutions, especially in nonaqueous solvents such as polyethylene glycol 400 (2), glycerol and propylene glycol (3, 4), ethanol, (5), and esterified polyethylene glycols (6) have been reported. The objective of the present study was to measure

0022-3549/79/0500-0645$01.00/0

© 1979, American Pharmaceutical Association

pressure were statistically significant but physiologically inconsequential.

Oxybutynin produced apparently dose-related tachycardia. A significant peak tachycardic response (21 beats/min) appeared after the 0.3-mg/kg dose, and a significant peak (52 beats/min) occurred after the 3.0-mg/kg iv dose. Although there was a consistent tachypnea after each oxybutynin dose, none of the respiratory changes was significant.

The effects of the cumulative 4.4-mg/kg iv oxybutynin dose on the autonomic responses in conscious dogs are summarized in Table II. Oxybutynin produced several significant autonomic responses. The tyramine-induced pressor response was significantly enhanced. The tyramine-evoked tachycardic response was significantly depressed to +3.2 beats/min. The acetylcholine-induced depressor and associated tachycardic responses were significantly inhibited. The epinephrine pressor response amplitude was significantly enhanced by oxybutynin treatment, although the associated heart rate response was inhibited by from +11 to −1 beats/min. Other significant changes included enhanced histamine tachycardia, increased norepinephrine brachycardia, and increased diastolic depressor response to isoproterenol.

When oxybutynin was administered to anesthetized dogs, the systolic and diastolic pressure responses were opposite to those observed in the conscious state (Table III). Oxybutynin (1.0, 3.0, and 10.0 mg/kg iv) produced systolic/diastolic depressor responses of −8/−5, −30/−26, and −31/−37 mm Hg, respectively. The associated significant tachycardic responses occurred only after the 1.0- and 3.0-mg/kg doses. The 10.0-mg/kg oxybutynin dose produced profound and significant depressor responses but insignificantly increased heart rate. Perhaps at this dose in the anesthetized dog the heart rate response, which appears to be compensatory to the systolic/diastolic depression, is pharmacologically antagonized by oxybutynin. The possibility of a toxicologic response to the 10.0-mg/kg dose is supported by the appearance of a marked and statistically significant tachypnea (+17 breaths/min).

Table IV describes the effects of a total cumulative 14-mg/kg iv oxybutynin dose of the autonomic treatment responses of anesthetized dogs. The acetylcholine-induced arterial pressure depressor response was inhibited. Similarly, the acetylcholine-induced tachycardia was markedly inhibited following oxybutynin. The epinephrine pressor response was enhanced, as was the heart rate response. The systolic/diastolic pressures and heart rate response to norepinephrine were also significantly altered. The respiratory rate response to norepinephrine was slightly, but significantly, increased. Only the diastolic pressure response to isoproterenol was significantly increased following oxybutynin.

Divergent responses due to the "state-of-the-animal" were reported previously (1–3). The influence of differential state on response must be considered when interpreting the experimental data, particularly from the anesthetized preparation.

The differences in systolic/diastolic arterial pressures, heart rates, and respiration rates are summarized in Table V. Basal heart rate was considerably lower in the conscious state, while basal respiratory rate was significantly greater. The amplitude of the changes indicated that the conscious animal exhibits greater oxybutynin sensitivity and response intensity. Greater oxybutynin tachycardic response in conscious animals can be explained on the basis of the Law of Initial Values (8).

In the conscious dog, the oxybutynin response was pressor; following pentobarbital anesthesia, the same oxybutynin doses evoked a systolic/diastolic arterial depressor response. These findings are inexplicable.

The consistent and significant tachycardia produced by oxybutynin in conscious and anesthetized dogs and the selective oxybutynin inhibition of the acetylcholine-induced cardiovascular responses in both conditions support the earlier pharmacological report. Oxybutynin has mild to moderate cardiovascular effects, probably through an anticholinergic mechanism of action.

REFERENCES

(1) J. A. Schneider and R. K. Rinehart, *Arch. Int. Pharmacodyn. Ther.*, **110**, 92 (1957).

(2) S. Gershon and W. J. Lang, *ibid.*, **135**, 31 (1962).

(3) B. Korol, *J. Pharm. Sci.*, **60**, 488 (1971).

(4) M. L. Brown and B. Korol, *Physiol. Behav.*, **3**, 207 (1968).

(5) B. Korol, W. J. Lang, M. L. Brown, and S. Gershon, *Nature*, **209**, 1249 (1966).

(6) B. Korol and M. L. Brown, *Arch. Int. Pharmacodyn. Ther.*, **170**, 371 (1967).

(7) A. L. Edwards, "Experimental Design in Psychological Research," 3rd ed., Holt, Rinehart & Winston, New York, N.Y., 1968, pp. 164, 165.

(8) J. Wilder, *Ann. N.Y. Acad. Sci.*, **98**, 1211 (1962).

Amino Acid Effect on Aspirin Stability in Propylene Glycol

PREM K. NARANG * and JAMES K. LIM *

Received July 6, 1978, from the *School of Pharmacy, West Virginia University, Morgantown, WV 26506.* Accepted for publication November 6, 1978. *Present address: School of Pharmacy, University of Maryland, Baltimore, MD 21201.

Abstract □ Temperature stability studies were conducted on 0.36 *M* (6.5% w/v) aspirin solutions including either 0.02 *M* L-methionine or 0.02 *M* histidine in propylene glycol. Aspirin was determined spectrophotofluorometrically as salicylic acid content at 412 nm. A 0.36 *M* aspirin in polyethylene glycol 400 solution was studied concurrently. Aspirin degradation rate constants, *k*, obtained from semilogarithmic plots of percent drug remaining *versus* time at 30–70 ± 0.5° were used for preparing Arrhenius plots. Good correlation was seen between predicted aspirin stability and experimental $k_{25°}$ values. L-Methionine and histidine markedly reduced aspirin stability.

Keyphrases □ Aspirin—stability in propylene glycol, effect of L-methionine and histidine, temperature □ Stability—aspirin in propylene glycol, effect of L-methionine and histidine, temperature □ Propylene glycol—stability of aspirin solutions, effect of L-methionine and histidine, temperature

Aspirin remains the most sought-after, nonprescription analgesic. It possesses a combination of anti-inflammatory, antipyretic, and analgesic properties unparalleled by other "aspirin-like" compounds. Aspirin is, however, a notoriously unstable drug and degrades to the less potent salicylic acid in the presence of moisture (1). Liquid aspirin dosage forms present a challenging pharmaceutical problem because of this instability in water and in vehicles containing traces of water.

Numerous attempts to stabilize aspirin solutions, especially in nonaqueous solvents such as polyethylene glycol 400 (2), glycerol and propylene glycol (3, 4), ethanol, (5), and esterified polyethylene glycols (6) have been reported. The objective of the present study was to measure

0022-3549/79/0500-0645$01.00/0

© 1979, American Pharmaceutical Association

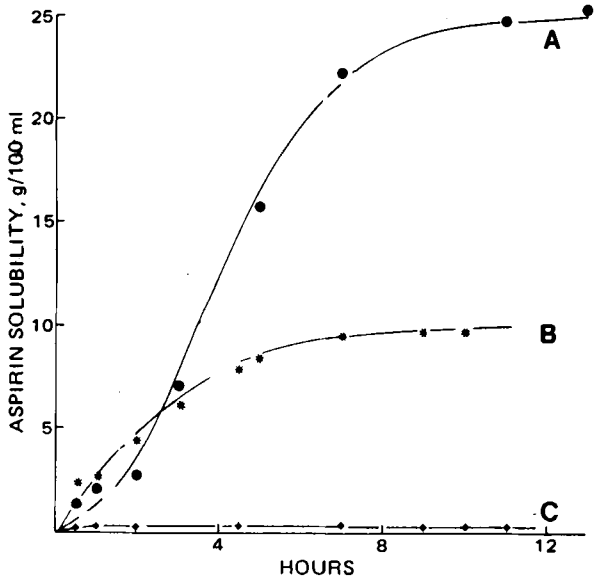

Figure 1—*Aspirin dissolution rates in polyethylene glycol 400 (A), propylene glycol (B), and water (C) by mechanical rotary agitation at 25 ± 0.1°.*

Table I—Aspirin Formulations I–IV

Formulation	Aspirin, 6.5% w/v (0.36 *M*)	Histidine, 0.32% w/v (0.02 *M*)	L-Methionine, 0.30% w/v (0.02 *M*)	Propylene Glycol	Polyethylene Glycol 400
I	+			+	
II	+		+	+	
III	+	+		+	
IV	+				+

aspirin stability in propylene glycol and in the presence of several amino acids. L-Methionine and histidine were chosen since they were slightly soluble in this solvent; furthermore, past reports indicated that histidine pro-

Table II—Predicted Stability of Aspirin Formulations I–IV for $t_{10\%}$ at 25 and 5°

Formulation[a]	$t_{10\%}$ 25°	$t_{10\%}$ 5°
I	151.2 days	55.8 months
II	75.6 days	20.4 months
III	55 days	13.3 months
IV	18.8 days	2.88 months

[a] See Table I for formulation contents.

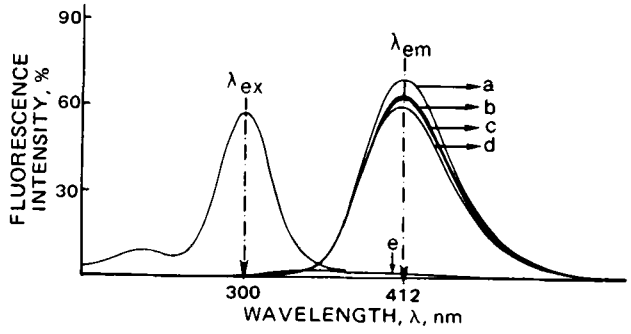

Figure 2—*Effect of 3.6 × 10^{-4} M aspirin solution and 3.6 × 10^{-4} M salicylic acid solution in pH 7 phosphate buffer on fluorescence intensity. Key: a, 11 μl of salicylic acid solution plus 40 μl of aspirin solution; b, 10 μl of salicylic acid solution; c, 10 μl of salicylic acid solution plus 10 μl of aspirin solution; d, 10 μl of salicylic acid solution plus 20 μl of aspirin solution; and e, 20 μl of aspirin solution.*

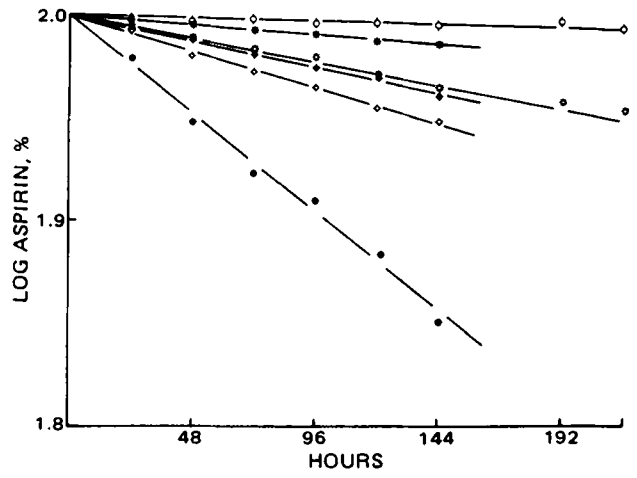

Figure 3—*Percent aspirin remaining as a function of time and temperature for I. Key: ◇, 30°; ✱, 40°; ☼, 50°; ◆, 55°; ◈, 60°; and ●, 70°.*

duced remedial effects in the treatment of peptic ulcers (7) and that methionine effected favorable histological changes in parenchymal cells of the liver (8).

EXPERIMENTAL

Materials—Aspirin[1], histidine[2], L-methionine[3], propylene glycol[2], polyethylene glycol 400[4], and salicylic acid[2] were used as received. Methanol[2] was spectroscopic grade.

Aspirin Formulations—Aspirin and the amino acids were dissolved in the glycol solvents by mechanical agitation for 4–6 hr on a rotary shaker[5] at ambient room temperatures. All aspirin formulations con-

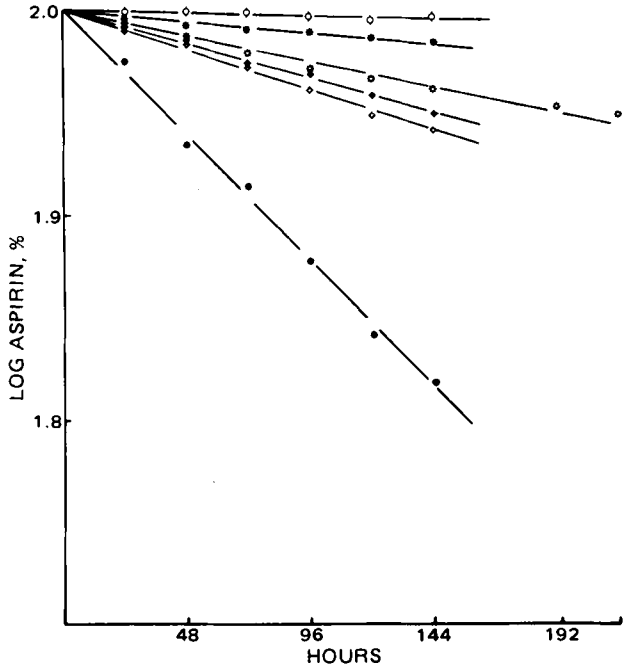

Figure 4—*Percent aspirin remaining as a function of time and temperature for II. Key: ◇, 30°; ✱, 40°; ☼, 50°; ◆, 55°; ◈, 60°; and ●, 70°.*

[1] Amend Drugs and Chemicals, Irvington, N.J.
[2] Fisher Scientific Co., Fair Lawn, N.J.
[3] Mann Research Laboratories, New York, N.Y.
[4] Ruger Chemical Co., Irvington, N.J.
[5] Gyrotory shaker, model S3, New Brunswick Scientific Co., New Brunswick, N.J.

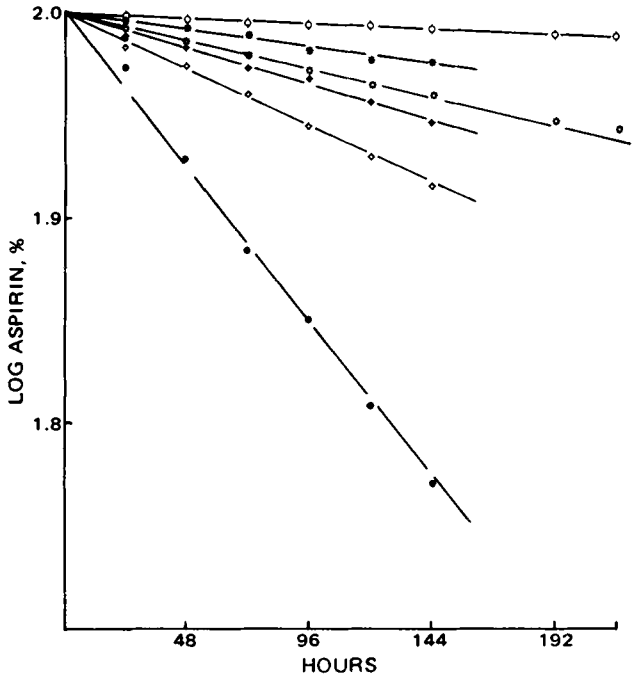

Figure 5—*Percent aspirin remaining as a function of time and temperature for III. Key: ○, 30°; ✱, 40°; ☼, 50°; ◆, 55°; ⊖, 60°; and ●, 70°.*

tained 0.36 *M* (6.5% w/v) aspirin and 0.02 *M* of either amino acid (II or III). A 0.36 *M* aspirin in polyethylene glycol 400 (IV) solution was included for comparison (Table I).

Aspirin Content Analysis—Aspirin was assayed as salicylic acid in pH 7 phosphate buffer at 25 ± 0.1°, using a spectrophotofluorometer[6] equipped with a 150-w xenon lamp/LP 21 photomultiplier tube, at the excitation and emission wavelengths of 300 and 412 nm, respectively. A 1.3 conversion factor, representing the aspirin to salicylic acid molecular weight ratio, was used to compute aspirin concentrations from salicylic acid concentrations. Salicylic acid concentrations were determined from

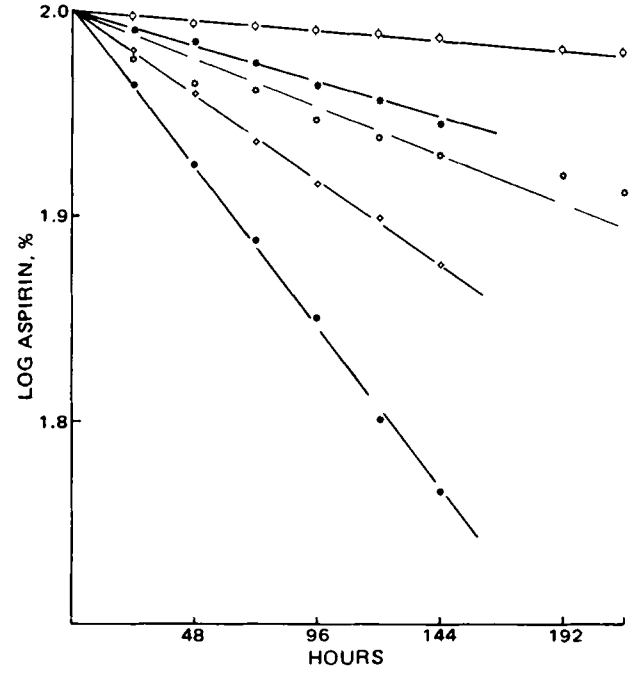

Figure 6—*Percent aspirin remaining as a function of time and temperature for IV. Key: ○, 30°; ✱, 40°; ☼, 50°; ⊖, 60°; and ●, 70°.*

[6] Aminco-Bowman, American Instrument Co., Silver Spring, Md.

Table III—Effect of Water Dilution on pH of Formulations I–III

Formulation	Percent Water (v/v) 0	10	25	50	70
I	3.1	3.1	3.1	3.0	3.0
II	3.8	3.8	3.7	3.3	3.0
III	3.9	3.9	3.8	3.5	3.1

a standard plot of salicylic acid, prepared from a fresh 0.36 *M* salicylic acid stock solution in glycol or methanol and appropriately diluted with pH 7 phosphate buffer for the fluorescence measurements.

Stability Studies—The aspirin formulations were placed in screw-capped, 30-ml, amber-colored prescription bottles and were immersed in controlled temperature water baths at 30–70 ± 0.5°. At 24-hr intervals, analytical samples were pipetted into ice-cold tubes, sealed, and stored at refrigeration temperatures until analysis. Semilogarithmic plots of percent aspirin remaining as a function of time and temperature were used to obtain the degradation rate constants, *k*. Arrhenius plots based on these rate constants were derived to predict aspirin stability at 25 and 5°. These predictions were compared with the experimental values from samples left at ambient room temperatures (25 ± 2°).

RESULTS AND DISCUSSION

Complete solubility of 6.5% (w/v) aspirin in propylene glycol or polyethylene glycol 400 was attainable within 6–8 hr of continuous agitation at 40 oscillations/min on a shaker bath maintained at 25 ± 0.1° (Fig. 1). This concentration represents the average adult dose (~325 mg/teaspoonful). Figure 2 shows the relative salicylic acid fluorescence intensity as a function of wavelength. Aspirin exerted negligible fluorescence at 412 nm.

Figures 3–6 show the semilogarithmic plots of percent aspirin remaining as a function of time and temperature for I–IV. The degradation rate constants, *k*, derived from these plots show that IV was the least stable (Fig. 7). This result may be attributed to transesterification (6) between aspirin and the polyethylene glycols. Formulation II ($k = 0.54 \times 10^{-4}$ hr^{-1}) exhibited almost twice the I degradation rate, indicating that amino acids decrease aspirin stability in propylene glycol. Table II summarizes the predicted shelflife stability at 25 and 5° for I–IV in terms of a 10% aspirin breakdown. As anticipated, the shortened shelflife of aspirin in propylene glycol due to the presence of the amino acids cor-

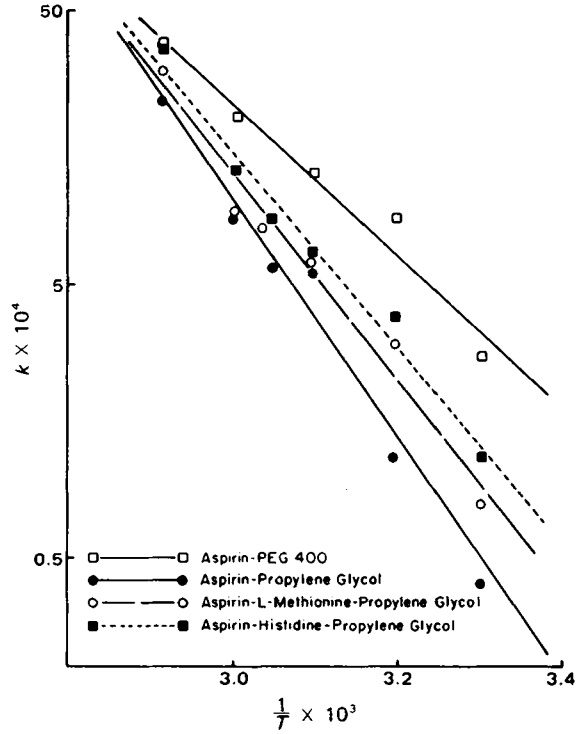

Figure 7—*Arrhenius plot showing aspirin degradation rate constants, k, in I–IV exposed to 30–70 ± 0.5°.*

Table IV—Predicted (Extrapolated) and Experimental (Actual) Degradation Rate Constants at 25° for Formulations I–IV

Formulation	Degradation Rate Constants, $k \times 10^{-4}$	
	Experimental[a]	Predicted
I	0.28	0.29
II	0.54	0.58
III	0.72	0.79
IV	3.49	2.33

[a] Ambient room temperature, 25 ± 2°.

responded with the slight increases in pH on dilution with water (Table III).

A fair correlation was evident between the predicted and experimental degradation rate constants, $k_{25°}$ (Table IV), thus supporting the predicted stability values (Table II). Preliminary IR studies showed a carbonyl band shift from 1595 cm^{-1} of L-methionine[7], where no bonding takes place, to 1640 cm^{-1} when the amino acid was dissolved in propylene glycol, indicating weak hydrogen bonding. Similarly, weak hydrogen bonding was indicated between aspirin and propylene glycol because of a slight carbonyl band shift to a higher frequency.

[7] Kaydol, Ruger Chemical Co., Irvington, N.J.

REFERENCES

(1) L. Lasagna, *Am. J. Med. Sci.*, **242**, 620 (1961).

(2) T. W. Schwarz, N. G. Shvemar, and R. G. Renaldi, *J. Am. Pharm. Assoc., Pract. Ed.*, **19**, 40 (1958).

(3) M. Faeges, U.S. pat. 3,316,150 (Feb. 26, 1964); through *Chem. Abstr.*, **67**, 67578w (1967).

(4) H. R. Mehta and F. G. Drommond, *J. Am. Pharm. Assoc., Pract. Ed.*, **15**, 103 (1954).

(5) H. W. Tomski and L. J. Waller, *Pharm. J.*, **144**, 53 (1940).

(6) H. W. Jun, C. W. Whitworth, and L. A. Luzzi, *J. Pharm. Sci.*, **61**, 1160 (1972).

(7) A. Frohlich, *Med. Klin.*, **33**, 933 (1937); through "United States Dispensatory," 25th ed., Lippincott, Philadelphia, Pa., 1960, p. 650.

(8) A. J. Beams and E. T. Endicott, *Gastroenterology*, **9**, 718 (1947).

ACKNOWLEDGMENTS

Abstracted in part from a thesis submitted by P. K. Narang to the Graduate School, West Virginia University, in partial fulfillment of the Master of Science degree requirements.

The authors thank Dr. Joseph K. H. Ma for assistance in the aspirin fluorescence determination and Dr. John P. O'Donnell for valuable advice on the IR analysis.

Radiochemical Plasma Salicylamide Assay Using Ring-Labeled Tritiated Salicylamide

V. J. STELLA ˣ, S. A. VARIA, and M. RIEDY

Received May 4, 1978, from the *Department of Pharmaceutical Chemistry, University of Kansas, Lawrence, KS 66045.* Accepted for publication November 6, 1978.

Abstract □ A rat plasma salicylamide assay was developed using ring-labeled tritiated salicylamide, synthesized by reacting salicylamide with tritium oxide in the presence of heptafluorobutyric acid. The reaction yielded ^3H-salicylamide of specific activity up to 8.41 mCi/mmole, 60% yield. Plasma containing ^3H-salicylamide and its metabolites was extracted with a toluene-based scintillation fluid, which was subsequently counted. Specificity for free salicylamide was demonstrated by radiochemical and standard fluorescence plasma salicylamide level–time curves. Specificity resulted from nonextraction of the salicylamide sulfate and glucuronide metabolites. Sulfatase and β-glucuronidase treatment allowed the analysis of plasma sulfate and glucuronide conjugates as free salicylamide. This procedure should be effective for the analysis of salicylamide and its metabolites in the presence of similar phenolic compounds.

Keyphrases □ Salicylamide—radiochemical analysis, from plasma, compared to fluorescence assay, rats □ Radiochemistry—analysis, salicylamide in plasma, compared to fluorescence assay, rats □ Fluorometry—analysis, salicylamide in plasma, compared to radiochemical assay, rats

In a study of the effects of alternate substrates on their ability to block temporarily the first-pass metabolism (1, 2) of phenolic drugs, the oral administration of salicylamide to rats was chosen as a suitable animal model because of the similarity of salicylamide's metabolic behavior in rats (3–7) and humans (8, 9). Numerous assays for salicylamide have been proposed (9–11). The fluorometric assay of Barr and Riegelman (9) is the most extensively used procedure for the analysis of salicylamide and its metabolites in biological fluids. This sensitive and specific fluorometric assay, along with a few modifications, has been the assay of choice in numerous studies (3, 9, 12).

Since the long-term objective of this project was to screen the effects of various alternate substrates on their ability to block temporarily the sulfation–glucuronidation first-pass effect of a model phenolic compound, salicylamide, many of the alternate substrates would most likely be other phenolic compounds. Some of these phenolic alternate substrates have physical, chemical, and fluorescense properties so similar to salicylamide that they interfere with the fluorometric procedure (9). For this reason, an assay for salicylamide and its metabolites was developed using ring-labeled tritiated salicylamide. The assay selectivity was due to the separation of salicylamide from its sulfate and glucuronide metabolites by a relatively nonpolar organic solvent.

EXPERIMENTAL

Reagents and Materials—All reagents were analytical grade, and all aqueous solutions were prepared using glass-distilled, deionized water. The scintillation fluid was prepared by stirring overnight 1000 ml of toluene[1] with 0.5 g of 1,4-bis[2-(4-methyl-5-phenyloxazolyl)]benzene[2] and 4 g of 2,5-diphenyloxazole[2].

[1] Scintillation grade, Research Products International Corp., Grove Village, Ill.

[2] Amersham/Searle Corp., Arlington Heights, Ill.

0022-3549/79/0500-0648$01.00/0

© 1979, American Pharmaceutical Association

Table IV—Predicted (Extrapolated) and Experimental (Actual) Degradation Rate Constants at 25° for Formulations I–IV

Formulation	Degradation Rate Constants, $k \times 10^{-4}$	
	Experimental[a]	Predicted
I	0.28	0.29
II	0.54	0.58
III	0.72	0.79
IV	3.49	2.33

[a] Ambient room temperature, 25 ± 2°.

responded with the slight increases in pH on dilution with water (Table III).

A fair correlation was evident between the predicted and experimental degradation rate constants, $k_{25°}$ (Table IV), thus supporting the predicted stability values (Table II). Preliminary IR studies showed a carbonyl band shift from 1595 cm^{-1} of L-methionine[7], where no bonding takes place, to 1640 cm^{-1} when the amino acid was dissolved in propylene glycol, indicating weak hydrogen bonding. Similarly, weak hydrogen bonding was indicated between aspirin and propylene glycol because of a slight carbonyl band shift to a higher frequency.

[7] Kaydol, Ruger Chemical Co., Irvington, N.J.

REFERENCES

(1) L. Lasagna, *Am. J. Med. Sci.*, **242**, 620 (1961).

(2) T. W. Schwarz, N. G. Shvemar, and R. G. Renaldi, *J. Am. Pharm. Assoc., Pract. Ed.*, **19**, 40 (1958).

(3) M. Faeges, U.S. pat. 3,316,150 (Feb. 26, 1964); through *Chem. Abstr.*, **67**, 67578w (1967).

(4) H. R. Mehta and F. G. Drommond, *J. Am. Pharm. Assoc., Pract. Ed.*, **15**, 103 (1954).

(5) H. W. Tomski and L. J. Waller, *Pharm. J.*, **144**, 53 (1940).

(6) H. W. Jun, C. W. Whitworth, and L. A. Luzzi, *J. Pharm. Sci.*, **61**, 1160 (1972).

(7) A. Frohlich, *Med. Klin.*, **33**, 933 (1937); through "United States Dispensatory," 25th ed., Lippincott, Philadelphia, Pa., 1960, p. 650.

(8) A. J. Beams and E. T. Endicott, *Gastroenterology*, **9**, 718 (1947).

ACKNOWLEDGMENTS

Abstracted in part from a thesis submitted by P. K. Narang to the Graduate School, West Virginia University, in partial fulfillment of the Master of Science degree requirements.

The authors thank Dr. Joseph K. H. Ma for assistance in the aspirin fluorescence determination and Dr. John P. O'Donnell for valuable advice on the IR analysis.

Radiochemical Plasma Salicylamide Assay Using Ring-Labeled Tritiated Salicylamide

V. J. STELLA ˣ, S. A. VARIA, and M. RIEDY

Received May 4, 1978, from the *Department of Pharmaceutical Chemistry, University of Kansas, Lawrence, KS 66045.* Accepted for publication November 6, 1978.

Abstract □ A rat plasma salicylamide assay was developed using ring-labeled tritiated salicylamide, synthesized by reacting salicylamide with tritium oxide in the presence of heptafluorobutyric acid. The reaction yielded ^3H-salicylamide of specific activity up to 8.41 mCi/mmole, 60% yield. Plasma containing ^3H-salicylamide and its metabolites was extracted with a toluene-based scintillation fluid, which was subsequently counted. Specificity for free salicylamide was demonstrated by radiochemical and standard fluorescence plasma salicylamide level–time curves. Specificity resulted from nonextraction of the salicylamide sulfate and glucuronide metabolites. Sulfatase and β-glucuronidase treatment allowed the analysis of plasma sulfate and glucuronide conjugates as free salicylamide. This procedure should be effective for the analysis of salicylamide and its metabolites in the presence of similar phenolic compounds.

Keyphrases □ Salicylamide—radiochemical analysis, from plasma, compared to fluorescence assay, rats □ Radiochemistry—analysis, salicylamide in plasma, compared to fluorescence assay, rats □ Fluorometry—analysis, salicylamide in plasma, compared to radiochemical assay, rats

In a study of the effects of alternate substrates on their ability to block temporarily the first-pass metabolism (1, 2) of phenolic drugs, the oral administration of salicylamide to rats was chosen as a suitable animal model because of the similarity of salicylamide's metabolic behavior in rats (3–7) and humans (8, 9). Numerous assays for salicylamide have been proposed (9–11). The fluorometric assay of Barr and Riegelman (9) is the most extensively used procedure for the analysis of salicylamide and its metabolites in biological fluids. This sensitive and specific fluorometric assay, along with a few modifications, has been the assay of choice in numerous studies (3, 9, 12).

Since the long-term objective of this project was to screen the effects of various alternate substrates on their ability to block temporarily the sulfation–glucuronidation first-pass effect of a model phenolic compound, salicylamide, many of the alternate substrates would most likely be other phenolic compounds. Some of these phenolic alternate substrates have physical, chemical, and fluorescense properties so similar to salicylamide that they interfere with the fluorometric procedure (9). For this reason, an assay for salicylamide and its metabolites was developed using ring-labeled tritiated salicylamide. The assay selectivity was due to the separation of salicylamide from its sulfate and glucuronide metabolites by a relatively nonpolar organic solvent.

EXPERIMENTAL

Reagents and Materials—All reagents were analytical grade, and all aqueous solutions were prepared using glass-distilled, deionized water. The scintillation fluid was prepared by stirring overnight 1000 ml of toluene[1] with 0.5 g of 1,4-bis[2-(4-methyl-5-phenyloxazolyl)]benzene[2] and 4 g of 2,5-diphenyloxazole[2].

[1] Scintillation grade, Research Products International Corp., Grove Village, Ill.

[2] Amersham/Searle Corp., Arlington Heights, Ill.

0022-3549/79/0500-0648$01.00/0

© 1979, American Pharmaceutical Association

Tritiated Salicylamide Synthesis—A screw-capped Pyrex glass tube containing 300 mg of salicylamide[3], 20 μl of tritium oxide[4], and 200 μl of heptafluorobutyric acid[5] was maintained in a sealed metal container at 200–210° for 4 days. After being cooled to room temperature, the solidified contents were dissolved in a minimal amount of 0.25 *N* NaOH (~15 ml).

The solution pH was adjusted to 6 with 1 *N* HCl, and this solution was then extracted with 30 ml of ethyl acetate. The ethyl acetate layer was separated, washed twice with 30 ml of saturated sodium bicarbonate solution, and dried over anhydrous magnesium sulfate. The ethyl acetate was evaporated on a rotary evaporator[6].

The solid white material obtained was purified by vacuum sublimation at 10 mm Hg and 118–122°. The isolated salicylamide specific activity varied from 5.24 to 8.41 mCi/mmole. Labile tritium was assayed by standard methods and was negligible[7]. The radiochemical purity was determined by TLC[8]. Chemical purity, checked qualitatively by melting points and quantitatively by fluorescence spectrophotometry, was 99–99.5%. The ^{3}H-salicylamide final yield was 180–200 mg.

Animal Studies—Sixteen male Sprague–Dawley rats[9] (250–275 g) were used. The rats were fed standard rat chow and water *ad libitum*. Prior to oral salicylamide administration, the rats were fasted overnight.

The oral salicylamide dose, 500 mg/kg, was prepared by dissolving the appropriate salicylamide and ^{3}H-salicylamide amounts in 1 *N* NaOH[10] and adjusting the pH to 10 with dropwise addition of 1 *N* HCl. For example, a 250-g rat received 4.2 mg of ^{3}H-salicylamide (8.4 mCi/mmole) and 120.8 mg of salicylamide. This aqueous salicylamide solution (1.5–2 ml depending on the weight of the animal) was administered orally by intubation. After drug administration, the animals were placed in metabolism cages.

Five minutes prior to predetermined times (15, 30, 60, or 90 min postdosing), each rat was anesthetized with ether, and 5-ml blood samples were removed from the inferior vena cava (after an abdominal incision) into an edetate sodium pretreated syringe. After centrifugation, duplicate 50-μl plasma samples were assayed for free salicylamide, salicylamide sulfate, and salicylamide glucuronide by the fluorescence and radiochemical assays.

Radiochemical Assay—Free plasma salicylamide was determined by adding 100 μl of a pH 7.0 phosphate buffer (0.2 *M*) to 50 μl of plasma in a 50-ml screw-capped centrifuge tube[11] and extracting with 16 ml of the toluene-based scintillation fluid. After agitation for 2 min and centrifugation, 15 ml of the upper toluene layer was transferred by disposable pipet to a 20-ml scintillation vial[12]. The vial was stored in a dark place for 12–24 hr prior to counting.

Radioactivity was determined by liquid scintillation counting[13] using the ^{3}H optimized window. A blank was prepared from predosed tail vein plasma. Free salicylamide was determined from a previously prepared plasma standard curve. Correction for counting efficiency was not necessary because the external standard channel ratio remained essentially constant and equal for the standard curve and the measured plasma samples.

Plasma salicylamide glucuronide was determined as free salicylamide obtained after salicylamide glucuronide hydrolysis with β-glucuronidase[14]. β-Glucuronidase (25 μl, 125 units) and 0.5 ml of 0.1 *M* pH 5.0 acetate buffer were added to the 50-μl plasma sample and incubated in a constant-temperature shaking water bath[15] at 37° for 16 hr. The incubation mixture was assayed for free salicylamide as described.

Salicylamide sulfate was determined as free salicylamide after hydrolysis of a 50-μl plasma sample with sulfatase (175 units), β-glucuronidase (875 units)[16], and 100 μl of 0.1 *M* pH 5.2 acetate buffer. Salicylamide glucuronide and salicylamide sulfate concentrations were calculated as described previously (5).

Fluorometric Assay—The salicylamide fluorometric assay was described previously (5, 9, 12). The plasma salicylamide conjugates were determined as free salicylamide after sulfatase and β-glucuronidase treatment.

RESULTS AND DISCUSSION

The fluorometric salicylamide assay is selective for salicylamide in the presence of its metabolites and can detect salicylamide levels as low as 2 μg/ml from 50-μl plasma samples. However, this assay is prone to interferences from other fluorescent or fluorescence quenching phenolic compounds.

The two major metabolites of salicylamide are the highly polar and charged sulfate and glucuronide conjugates (5). Polarity differences between salicylamide and these metabolites make possible a specific radiochemical salicylamide assay. Similar assays were reported for other radiolabeled phenolic compounds (13, 14).

As stated under *Experimental*, ring-labeled tritiated salicylamide was prepared by the reaction of salicylamide with tritium oxide in the presence of heptafluorobutyric acid. The salicylamide hydroxy group is electron donating and tends to promote electrophilic substitution reactions such as the acid-catalyzed tritium–hydrogen exchange. The carboxamide group tends to be deactivating (electron withdrawing). For this reason, the conditions necessary for the acid-catalyzed tritium incorporation were severe and had to be optimized for this particular system. Heptafluorobutyric acid was more useful than trifluoroacetic acid because of its lower volatility (15). The conditions required for equilibrium tritium incorporation into salicylamide (ring substitution[17]) were worked out using deuterium incorporation, substituting deuterium oxide for tritium oxide. Deuterium incorporation was followed by mass spectral analysis of the P, P + 1, and P + 2 peaks. The high temperature and extended heating period finally used were necessary for maximum tritium incorporation with minimal product decomposition.

The white crystalline material obtained from the final sublimation showed only one spot, corresponding to salicylamide, by TLC. Spectrofluorometric analysis showed the product to be >99–99.5% pure. It was necessary, for maximum purification, to collect small fractions (~50 mg) of the sublimed material from the sublimation apparatus cold finger to prevent excess accumulation, which produced material that was only ~90% pure. This enclosed sublimation system was found to be the most efficient both in terms of the purification and recovery of ^{3}H-salicylamide. Once the synthesis procedure was standardized, ^{3}H-salicylamide of >99% purity and 5.24–8.4 mCi/mmole specific activity was consistently obtained.

The radiochemical assay for free salicylamide involved a one-step extraction. The detection limit (100 cpm above background) was 0.002 μg (0.04 μg/ml from 50-μl plasma samples)[18]. No chemiluminescence problems occurred, although routinely the samples were stored in the dark for 12–24 hr prior to counting. The overall mean ± *SD* (3.1–25 μg/ml, n = 17) toluene-based scintillation fluid ^{3}H-salicylamide extraction efficiency was 89.7 ± 0.8% (3.1 μg/ml, n = 6, 89.9 ± 0.7%; 6.25 μg/ml, n = 3, 89.5 ± 1.1%; 12.5 μg/ml, n = 4, 89.1 ± 0.5%; 25 μg/ml, n = 4, 90.1 ± 0.7%).

Salicylamide (^{3}H-salicylamide to salicylamide ratio of 1:29) was administered at 500 mg/kg to rats as an oral solution (pH ~10) to minimize problems associated with administering different crystalline forms and particle sizes. In initial studies, salicylamide in suspension in methylcellulose gave spurious results because the larger ^{3}H-salicylamide crystals dissolved more slowly than the salicylamide powder in the rat GI tract.

The fluorescent and radiochemical plasma level–time curves for salicylamide and its major metabolites are shown in Fig. 1. Each point is the mean of four animals. The areas under the curve for the fluorometric *versus* radiochemical assay (in microgram minutes per milliliter) calculated *via* the trapezoidal method for 0–90 min were 4363 and 4512 for free salicylamide, 1548 and 1570 for salicylamide sulfate, and 1405 and 1425 for salicylamide glucuronide, respectively. Plots of plasma salicylamide,

[3] Eastman Kodak Co., Rochester, N.Y.
[4] Specific activity of 5 Ci/ml, Amersham/Searle Corp., Arlington Heights, Ill.
[5] Aldrich Chemical Co., Milwaukee, Wis.
[6] Buchi Rotavapor, Brinkmann Instruments, Westbury, N.Y.
[7] Approximately 5 mg of ^{3}H-salicylamide was dissolved in 10 ml of methanol and allowed to stand for 2 hr. The methanol was evaporated on a rotary evaporator, and the total number of counts in the collected methanol was determined. Labile tritium represented <0.01% of total counts per minute. Repetition of this procedure showed no further labile tritium.
[8] Run on Polygram Sil G precoated plates for TLC, Brinkmann Instruments, Westbury, N.Y. Solvents were ethyl acetate–ammonium hydroxide (9:1, R_f 0.47) and isopropanol–chloroform–ammonium hydroxide (3:1.5:0.5, R_f 0.58).
[9] ARA/Sprague–Dawley, Madison, Wis.
[10] Fisher Scientific Co., Fair Lawn, N.J.
[11] Pyrex tubes 8062.
[12] Scientific Products, Kansas City, Mo.
[13] Beckman LS-3133T, Fullerton, Calif.
[14] Glucurase, β-glucuronidase solution from bovine liver, Sigma Chemical Co., St. Louis, Mo.
[15] American Optical Corp., Buffalo, N.Y.
[16] Glusulase, Endo Laboratories, Garden City, N.Y.
[17] Ring substitution is assumed because tritium incorporated in the hydroxyl group and carboxamide group readily exchanged. The only position for stable tritium to be incorporated into the molecule is on the phenyl ring.
[18] This limit is dependent on the specific activity of the ^{3}H-salicylamide batch.

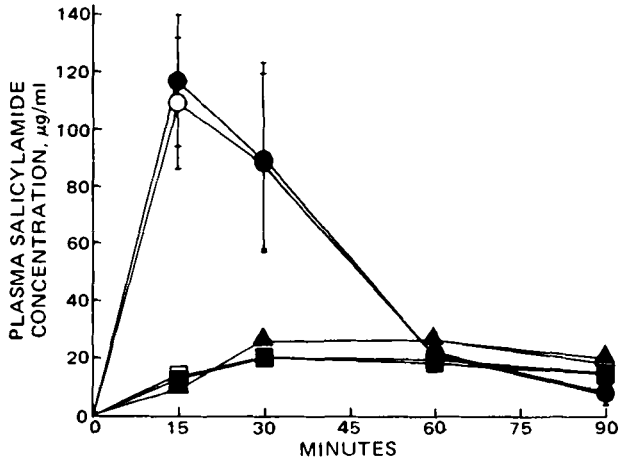

Figure 1—*Plasma concentration* ± SEM versus *time profiles for salicylamide (○, fluorescence assay; ●, radiochemical assay), salicylamide sulfate (□, fluorescence assay; ■, radiochemical assay), and salicylamide glucuronide (△, fluorescence assay; ▲, radiochemical assay) after oral administration of 500 mg of salicylamide/kg to rats. Each point is the mean of four animals. If no error bars are noted, the standard error of the mean was within the size of the symbol.*

salicylamide sulfate, and salicylamide glucuronide assayed radiochemically *versus* levels determined fluorometrically had slopes (±*SEM*) of 1.06 ± 0.02 (r = 0.99), 1.11 ± 0.14 (r = 0.81), and 0.96 ± 0.07 (r = 0.98), respectively. An overall plot combining all 48 data points gave a 1.06 ± 0.01 slope (r = 0.99). The new assay gives ~6% higher plasma salicylamide analysis than does the fluorescence assay, probably due to a slight total plasma radioactivity carryover into the extraction medium. The poorer correlation coefficients for plasma sulfate and glucuronide analyses were probably due to concentration calculation by differences (5) rather than to errors in the assay.

The radiochemical assay gave levels of salicylamide and its conjugates that were statistically equivalent ($p < 0.05$) to those determined by the fluorescence assay (Fig. 1). The large standard errors for the salicylamide levels at 15 and 30 min (Fig. 1) were due to animal differences and not to assay variations. The plasma free salicylamide levels generated in this study were considerably higher than the free salicylamide levels reported previously (3) for rats administered 500 mg of salicylamide suspension/kg. Reported glucuronide levels were larger than those generated in this study. These differences are probably attributable to the more efficient metabolism of salicylamide from the suspension compared to the solution. Similar effects were seen in a human study (12), which showed that a sodium salicylamide solution produced significantly higher free salicylamide bioavailability than salicylamide tablets. These differences were due to more efficient first-pass salicylamide metabolism from the slowly dissolving tablets. Sodium salicylamide partially saturated the enzymes responsible for the first-pass effect, which allowed more unmetabolized drug to enter the general circulation (12).

In conclusion, the advantages of the radiochemical assay just described are: (*a*) its ability to determine specifically salicylamide and its conjugates in the presence of other phenolic substances capable of exhibiting fluorescence or of quenching the fluorescence of salicylamide and (*b*) the low level of detection it can afford. This last point, of course, will be dependent on the specific activity of ^{3}H-salicylamide that can be synthesized. Another important advantage is that once the salicylamide has been extracted into the scintillant fluid, the vials can be counted at the investigator's convenience. In the fluorometric assay, the fluoresence intensity of extracted salicylamide (in 0.25 *N* NaOH) did deteriorate with time. The single-step extraction directly into the scintillant fluid used in the radiochemical assay increased its ruggedness by minimizing technical errors while speeding up the analysis. Balanced against these advantages were the problems of synthesis and handling of the ^{3}H-salicylamide.

REFERENCES

(1) M. Gibaldi, R. N. Boyes, and S. Feldman, *J. Pharm. Sci.*, **60,** 1338 (1971).

(2) M. Rowland, S. Riegelman, P. A. Harris, S. D. Sholkoff, and E. J. Eyring, *Nature*, **215** (1967).

(3) J. B. Houston and G. Levy, *J. Pharmacol. Exp. Ther.*, **198,** 284 (1976).

(4) J. B. Houston and G. Levy, *Nature*, **255,** 78 (1975).

(5) G. Levy and T. Matsuzawa, *J. Pharmacol. Exp. Ther.*, **156,** 285 (1976).

(6) G. Levy and J. Procknal, *J. Pharm. Sci.*, **57,** 1330 (1968).

(7) G. Levy and H. Yamada, *ibid.*, **60,** 215 (1971).

(8) W. H. Barr, *Drug Intell. Bull.*, **3,** 27 (1969).

(9) W. H. Barr and S. Riegelman, *J. Pharm. Sci.*, **59,** 154 (1970).

(10) W. E. Lange, D. G. Floriddia, and F. J. Pruyn, *ibid.*, **58,** 771 (1969).

(11) M. Kakemi, T. Kobayashi, C. Manuro, M. Ueda, and T. Koizumi, *Chem. Pharm. Bull.*, **24,** 2254 (1976).

(12) L. Fleckenstein, G. R. Mundy, R. Horovitz, and J. M. Mazzullo, *Clin. Pharmacol. Ther.*, **19,** 451 (1976).

(13) G. M. Cohen, O. M. Bakke, and D. S. Davies, *J. Pharm. Pharmacol.*, **26,** 348 (1974).

(14) R. A. Franklin and A. Aldridge, *Xenobiotica*, **6,** 499 (1976).

(15) R. A. W. Hanzlik and T. J. Gillesse, *J. Lab. Comp. Radiopharm.*, in press.

ACKNOWLEDGMENTS

Supported by Grant GM22357 from the National Institutes of Health.

The authors acknowledge the help of Dr. R. Hanzlik and Mr. T. Gillesse who provided guidance and equipment for the preparation of ^{3}H-salicylamide.

High Steady-State Levels of Uric Acid Produced in Rats by Dietary Training and Potassium Oxonate

JEROLD NEWBURGER, TING-FENG HSU, and ALAN B. COMBS ˣ

Received August 17, 1978, from the *College of Pharmacy, University of Texas, Austin, TX 78712.* Accepted for publication October 18, 1978.

Abstract □ To reduce the inherent variability in serum uric acid levels of animals allowed *ad libitum* exposure to food containing potassium oxonate and uric acid, male Sprague–Dawley rats were trained to eat their daily food allotment in a 1.25-hr period each morning. After training, the rats were fed a food mixture containing 5% potassium oxonate and 2% uric acid (w/w each). Serum blood levels of uric acid reached a steady state within 2 hr; these levels were maintained for an additional 4 hr. It is believed that the stomach emptying rate is a zero-order process under these experimental conditions.

Keyphrases □ Uric acid—steady-state serum levels, rats, dietary training, potassium oxonate □ Hyperuricemia—animal models, rats □ Potassium oxonate—used to produce hyperuricemia in rats

Hyperuricemia can result in clinical gout (1) and can complicate the treatment of certain neoplastic diseases (2). The drugs presently used in the treatment of hyperuricemia all have distinct disadvantages and can cause adverse effects (3, 4).

A potential alternative therapy may be indicated by recent reports characterizing the *in vitro* decomposition of uric acid in the presence of light and riboflavin (5, 6). The selection of an animal model for *in vivo* testing of phototherapy is difficult, because most naturally hyperuricemic animals are typically exotic, protected, expensive, or nonmammalian (7–10). However, a murine model for hyperuricemia was reported recently. Rats given the uricase inhibitor oxonic acid can become hyperuricemic (11, 12). Moreover, these animals will develop gouty renal pathology after chronic oral feeding of oxonate and uric acid (13, 14).

We recently demonstrated that serum uric acid levels of rats fed *ad libitum* a ground laboratory ration containing potassium oxonate and uric acid are subject to a diurnal variation with higher morning levels (15). The variability produced by this method complicated the evaluation of phototherapy effects on serum uric acid. This paper reports the effects on serum uric acid levels of feeding potassium oxonate and uric acid to rats trained to eat their total daily food allotment within a short period.

EXPERIMENTAL

Male Sprague–Dawley rats[1], 150–200-g initial weights, were housed individually in hanging cages and were maintained on 12-hr light–dark cycles. They were allowed water *ad libitum* throughout the study. The animals were fed a standard pelleted laboratory ration[2] *ad libitum* for 1 week before dietary training. Following a previously reported procedure for dietary training and synchronization (16, 17), the rats were fed their laboratory ration as a ground powder given for only 1.25 hr each morning. By the end of 1 week, most animals had learned to eat their total daily ration during this brief feeding period. Animal body weights stabilized and generally began to increase again after 2 weeks. The animals were maintained on this feeding schedule for 4 weeks prior to use in the study.

On the morning of the study, animals were fed the ground laboratory ration mixed with 5% potassium oxonate[3] and 2% uric acid[4] (w/w each). The duration of feeding was the usual 1.25 hr. Animals were sacrificed for serum uric acid determinations immediately prior to drug administration and at 2, 4, 6, and 24 hr afterward. The animals were anesthetized with ether, and 3–5 ml of blood was drawn from each into heparinized syringes *via* the inferior vena cava. Analysis of serum uric acid was performed by high-pressure liquid chromatography as previously described (6). Statistical comparisons were made using analysis of variance followed by Scheffé's method of multiple contrasts (18).

RESULTS

The animal weights and the amounts of food, potassium oxonate, and uric acid ingested are listed in Table I. Serum uric acid levels as a function of time after the mixture was presented to the animals are shown in Fig. 1. The rats became hyperuricemic within 2 hr. The blood levels remained high and essentially constant for a minimum of another 4 hr. Levels returned to control values by 24 hr.

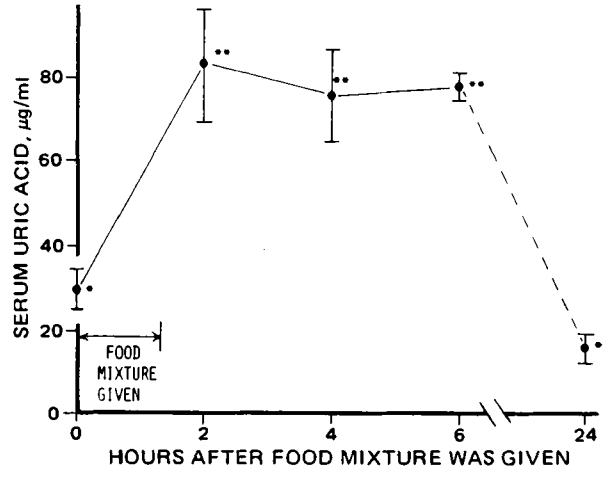

Figure 1—*Serum uric acid levels as a function of time after exposure of rats to a food mixture containing 5% potassium oxonate and 2% uric acid (w/w each). The animals were trained to eat their full daily food rations during a 1.25-hr period each morning. Each data point represents the mean ± SEM for three animals; for * versus **, $p < 0.05$ by analysis of variance followed by Scheffé's method of multiple contrasts.*

[1] Tempco Breeding Laboratories, Houston, Tex.
[2] Wayne Lab Blox, Allied Mills.
[3] Calbiochem, San Diego, Calif.
[4] Fisher Scientific Co., Fair Lawn, N.J.

0022-3549/79/0500-0651$01.00/0
© 1979, American Pharmaceutical Association

Table I—Values Observed on Day of Experiment [a]

Parameter	Value
Animal weight, g	225 ± 38
Amount of mixture eaten, g/kg[b]	57.1 ± 7.2
Potassium oxonate ingested, g/kg	2.86 ± 0.36
Uric acid ingested, g/kg	1.14 ± 0.14

[a] Values are reported as mean ± *SD*. [b] Mixture consisted of ground laboratory ration containing 5% potassium oxonate and 2% uric acid (w/w each).

Accumulation to a plateau would be expected to occur with a zero-order administration process (19). The absorption of uric acid from the rat intestine, however, has been reported to be first order (20). Therefore, gastric emptying rather than intestinal absorption may be rate limiting. Reported data (16, 17) for untreated control animals trained by this technique are consistent with a zero-order stomach emptying rate for the first 10–12 hr following the daily feeding. This animal model will be used to test the efficacy of light and riboflavin in the reduction of serum uric acid.

REFERENCES

(1) J. R. Klinenberg, R. Bluestone, L. Schlosstein, J. Waisman, and M. W. Whitehouse, *Ann. Intern. Med.*, **78**, 99 (1973).

(2) I. H. Krakoff and R. L. Meyer, *J. Am. Med. Assoc.*, **193**, 1 (1965).

(3) W. N. Kelley and J. B. Wyngaarden, *Semin. Drug Treat.*, **1**, 119 (1971).

(4) "The Pharmacological Basis of Therapeutics," 5th ed., L. S. Goodman and A. Gilman, Eds. Macmillan, New York, N.Y., 1975, pp. 340, 342, 351, 863, 864, 1496.

(5) J. Newburger and A. B. Combs, *Life Sci.*, **17**, 443 (1975).

(6) J. Newburger, A. B. Combs, and T. F. Hsu, *J. Pharm. Sci.*, **66**, 1561 (1977).

(7) W. E. C. Wacker, *N. Engl. J. Med.*, **283**, 151 (1970).

(8) P. Christen, W. C. Peacock, A. E. Christen, and W. E. C. Wacker, *Eur. J. Biochem.*, **12**, 3 (1970).

(9) M. D. Skeith and L. A. Healey, *Am. J. Physiol.*, **214**, 582 (1968).

(10) T. K. Shnitka and M. M. Youngman, *J. Ultrastructure Res.*, **16**, 598 (1966).

(11) B. Stavric, W. J. Johnson, and H. C. Grice, *Proc. Soc. Exp. Biol. Med.*, **131**, 512 (1969).

(12) W. J. Johnson, B. Stavric, and A. Chartrand, *ibid.*, **131**, 8 (1969).

(13) B. Stavric, E. A. Neva, W. J. Johnson, and F. A. Salem, *Invest. Urol.*, **11**, 3 (1973).

(14) R. Bluestone, J. Waisman, and J. R. Klinenberg, *Lab. Invest.*, **33**, 273 (1975).

(15) J. Newburger, A. B. Combs, and T. F. Hsu, *Drug Chem. Toxicol.*, in press.

(16) S. H. Dieke, *Proc. Soc. Exp. Biol. Med.*, **76**, 788 (1951).

(17) S. N. Giri and S. Rice, *Life Sci.*, **9**, 1109 (1970).

(18) W. L. Hays, "Statistics," Holt, Rinehart and Winston, New York, N.Y., 1963, pp. 485–487.

(19) "Principles of Drug Action," 2nd ed., A. Goldstein, L. Aronow, and S. M. Kalman, Eds., Wiley, New York, N.Y., 1974, p. 311.

(20) J. H. Oh, J. B. Dossetor, and I. T. Beck, *Can. J. Physiol. Pharmacol.*, **45**, 121 (1967).

ACKNOWLEDGMENTS

Supported in part by Biomedical Sciences Support Grant 26-16994-0650 from the University of Texas at Austin.

The authors thank Mr. Paul Godley and Mr. Joseph Lew for their assistance.

High-Performance Liquid Chromatographic Determination of Cephacetrile

ALBERTO MANGIA ˣ, SILVESTRO SILINGARDI, FULVIO BORTESI, GIAMPIERO GRISANTI, and MAURO DI BITETTO

Received June 6, 1978, from the *Research Laboratories, Pierrel SpA, Via Degli Artigianelli 10, 20159 Milan, Italy* Accepted for publication October 19, 1978.

Abstract □ A rapid and accurate quantitative determination of cephacetrile in finished bulk and dosage forms is reported. The high-performance liquid chromatographic method is free of interference by acetyl hydrolysis products and synthesis by-products. The assay can be performed in about 15 min, affording <0.7% coefficients of variation within and between days. The chromatographic results are in good agreement with the microbiological assay requested by the "Code of Federal Regulations" for certification of cephacetrile sodium.

Keyphrases □ High-performance liquid chromatography—analysis, cephacetrile in various dosage forms □ Cephacetrile—high-performance liquid chromatographic analysis in various dosage forms □ Antibacterials—cephacetrile, high-performance liquid chromatographic analysis in various dosage forms

Cephacetrile (I) sodium [7-cyanoacetamido-3-acetoxymethyl-3-cephem-4-carboxylic acid, sodium salt] is a new cephalosporin antibacterial for parenteral use (1). The approved methods of analysis for certification are the microbiological agar diffusion assay and the hydroxylamine colorimetric assay (2).

This report outlines a more selective, rapid, and accurate method for the quantitative determination of cephacetrile in bulk drugs and pharmaceutical formulations using high-performance liquid chromatography (HPLC). The method is free of interference by acetyl hydrolysis products and synthesis by-products. Furthermore, the desacetyl derivative (II) of cephacetrile and lactone (III) can be detected accurately up to 0.1%.

EXPERIMENTAL

Materials—Cephacetrile FDA reference standard (microbiological potency of 885 μg/mg, lot 9/72) was used as received. Desacetyl derivative (II) of cephacetrile was prepared by enzymatic hydrolysis with acetyl esterase (3), while lactone (III) was synthesized by reacting trifluoroacetic acid with cephacetrile. Cephalosporins (IV*a* and IV*b*) were obtained by reaction of V with the proper acid chloride in acetone in the presence of urea (4), while IV*c* was prepared by reaction of methanesulfonyl chloride with the silyl derivative of V in dichloroethane (Scheme I). Cefazolin was Pierrel working standard. Methanol[1], acetic acid[2], and 1 *N* NaOH[2] were analytical reagent grade.

Apparatus—A liquid chromatograph[3], equipped with a 20-μl valve

[1] E. Merck, Darmstadt, West Germany.
[2] C. Erba, Milan, Italy.
[3] Model 1084 A, Hewlett-Packard, Böblingen, West Germany.

0022-3549/79/0500-0652$01.00/0

© 1979, American Pharmaceutical Association

Table I—Values Observed on Day of Experiment [a]

Parameter	Value
Animal weight, g	225 ± 38
Amount of mixture eaten, g/kg[b]	57.1 ± 7.2
Potassium oxonate ingested, g/kg	2.86 ± 0.36
Uric acid ingested, g/kg	1.14 ± 0.14

[a] Values are reported as mean ± *SD*. [b] Mixture consisted of ground laboratory ration containing 5% potassium oxonate and 2% uric acid (w/w each).

Accumulation to a plateau would be expected to occur with a zero-order administration process (19). The absorption of uric acid from the rat intestine, however, has been reported to be first order (20). Therefore, gastric emptying rather than intestinal absorption may be rate limiting. Reported data (16, 17) for untreated control animals trained by this technique are consistent with a zero-order stomach emptying rate for the first 10–12 hr following the daily feeding. This animal model will be used to test the efficacy of light and riboflavin in the reduction of serum uric acid.

REFERENCES

(1) J. R. Klinenberg, R. Bluestone, L. Schlosstein, J. Waisman, and M. W. Whitehouse, *Ann. Intern. Med.*, **78**, 99 (1973).

(2) I. H. Krakoff and R. L. Meyer, *J. Am. Med. Assoc.*, **193**, 1 (1965).

(3) W. N. Kelley and J. B. Wyngaarden, *Semin. Drug Treat.*, **1**, 119 (1971).

(4) "The Pharmacological Basis of Therapeutics," 5th ed., L. S. Goodman and A. Gilman, Eds. Macmillan, New York, N.Y., 1975, pp. 340, 342, 351, 863, 864, 1496.

(5) J. Newburger and A. B. Combs, *Life Sci.*, **17**, 443 (1975).

(6) J. Newburger, A. B. Combs, and T. F. Hsu, *J. Pharm. Sci.*, **66**, 1561 (1977).

(7) W. E. C. Wacker, *N. Engl. J. Med.*, **283**, 151 (1970).

(8) P. Christen, W. C. Peacock, A. E. Christen, and W. E. C. Wacker, *Eur. J. Biochem.*, **12**, 3 (1970).

(9) M. D. Skeith and L. A. Healey, *Am. J. Physiol.*, **214**, 582 (1968).

(10) T. K. Shnitka and M. M. Youngman, *J. Ultrastructure Res.*, **16**, 598 (1966).

(11) B. Stavric, W. J. Johnson, and H. C. Grice, *Proc. Soc. Exp. Biol. Med.*, **131**, 512 (1969).

(12) W. J. Johnson, B. Stavric, and A. Chartrand, *ibid.*, **131**, 8 (1969).

(13) B. Stavric, E. A. Neva, W. J. Johnson, and F. A. Salem, *Invest. Urol.*, **11**, 3 (1973).

(14) R. Bluestone, J. Waisman, and J. R. Klinenberg, *Lab. Invest.*, **33**, 273 (1975).

(15) J. Newburger, A. B. Combs, and T. F. Hsu, *Drug Chem. Toxicol.*, in press.

(16) S. H. Dieke, *Proc. Soc. Exp. Biol. Med.*, **76**, 788 (1951).

(17) S. N. Giri and S. Rice, *Life Sci.*, **9**, 1109 (1970).

(18) W. L. Hays, "Statistics," Holt, Rinehart and Winston, New York, N.Y., 1963, pp. 485–487.

(19) "Principles of Drug Action," 2nd ed., A. Goldstein, L. Aronow, and S. M. Kalman, Eds., Wiley, New York, N.Y., 1974, p. 311.

(20) J. H. Oh, J. B. Dossetor, and I. T. Beck, *Can. J. Physiol. Pharmacol.*, **45**, 121 (1967).

ACKNOWLEDGMENTS

Supported in part by Biomedical Sciences Support Grant 26-16994-0650 from the University of Texas at Austin.

The authors thank Mr. Paul Godley and Mr. Joseph Lew for their assistance.

High-Performance Liquid Chromatographic Determination of Cephacetrile

ALBERTO MANGIA ˣ, SILVESTRO SILINGARDI, FULVIO BORTESI, GIAMPIERO GRISANTI, and MAURO DI BITETTO

Received June 6, 1978, from the *Research Laboratories, Pierrel SpA, Via Degli Artigianelli 10, 20159 Milan, Italy* Accepted for publication October 19, 1978.

Abstract □ A rapid and accurate quantitative determination of cephacetrile in finished bulk and dosage forms is reported. The high-performance liquid chromatographic method is free of interference by acetyl hydrolysis products and synthesis by-products. The assay can be performed in about 15 min, affording <0.7% coefficients of variation within and between days. The chromatographic results are in good agreement with the microbiological assay requested by the "Code of Federal Regulations" for certification of cephacetrile sodium.

Keyphrases □ High-performance liquid chromatography—analysis, cephacetrile in various dosage forms □ Cephacetrile—high-performance liquid chromatographic analysis in various dosage forms □ Antibacterials—cephacetrile, high-performance liquid chromatographic analysis in various dosage forms

Cephacetrile (I) sodium [7-cyanoacetamido-3-acetoxymethyl-3-cephem-4-carboxylic acid, sodium salt] is a new cephalosporin antibacterial for parenteral use (1). The approved methods of analysis for certification are the microbiological agar diffusion assay and the hydroxylamine colorimetric assay (2).

This report outlines a more selective, rapid, and accurate method for the quantitative determination of cephacetrile in bulk drugs and pharmaceutical formulations using high-performance liquid chromatography (HPLC). The method is free of interference by acetyl hydrolysis products and synthesis by-products. Furthermore, the desacetyl derivative (II) of cephacetrile and lactone (III) can be detected accurately up to 0.1%.

EXPERIMENTAL

Materials—Cephacetrile FDA reference standard (microbiological potency of 885 μg/mg, lot 9/72) was used as received. Desacetyl derivative (II) of cephacetrile was prepared by enzymatic hydrolysis with acetyl esterase (3), while lactone (III) was synthesized by reacting trifluoroacetic acid with cephacetrile. Cephalosporins (IV*a* and IV*b*) were obtained by reaction of V with the proper acid chloride in acetone in the presence of urea (4), while IV*c* was prepared by reaction of methanesulfonyl chloride with the silyl derivative of V in dichloroethane (Scheme I). Cefazolin was Pierrel working standard. Methanol[1], acetic acid[2], and 1 *N* NaOH[2] were analytical reagent grade.

Apparatus—A liquid chromatograph[3], equipped with a 20-μl valve

[1] E. Merck, Darmstadt, West Germany.
[2] C. Erba, Milan, Italy.
[3] Model 1084 A, Hewlett-Packard, Böblingen, West Germany.

0022-3549/79/0500-0652$01.00/0

© 1979, American Pharmaceutical Association

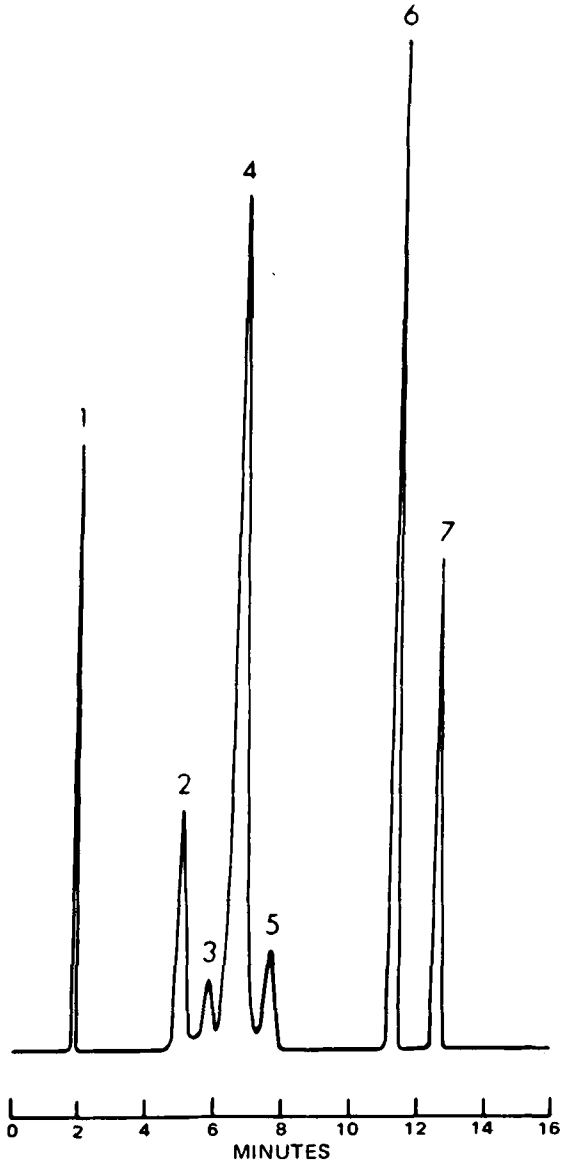

Figure 1—*High-performance liquid chromatogram of an artificial mixture of cephalosporins (I–IV). Key: 1, II; 2, III; 3, IVc; 4, I; 5, IVa; 6, cefazolin; and 7, IVb.*

and loop injector[4] and a fixed-wavelength UV detector (254 nm), was used. The prepacked[5] stainless steel column (25 × 0.45 cm i.d.) was operated at 40° at a flow rate of 2 ml/min.

Mobile Phase—An acetic acid–sodium acetate pH 4.2 buffer (0.01 ionic strength) and methanol were used as the mobile phase. The elution (5% of methanol) was isocratic for 5 min; then a linear gradient was programmed, reaching 30% of methanol in 7 min.

Standard Solutions—*Internal Standard Solution*—Approximately 25 mg of cefazolin was weighed accurately in a 50-ml volumetric flask and dissolved and diluted to volume with the pH 4.2 buffer.

Cephacetrile Standard Solution—Approximately 15 mg of the reference standard was weighed accurately in a 25-ml volumetric flask and dissolved and diluted to volume with the pH 4.2 buffer. Fresh standard solutions were prepared daily.

Standard Calibration Solution—Five standard calibration solutions were prepared daily by adding 1, 2, 3, 4, and 5 ml of cephacetrile standard solution and 3 ml of internal standard solution to five 10-ml volumetric flasks and then diluting to volume with the pH 4.2 buffer.

Sample Analyses—Approximately 15 mg of cephacetrile samples was accurately weighed in a 25-ml volumetric flask, dissolved with the pH 4.2 buffer, and diluted to volume. A 5.0-ml aliquot was pipetted into a 10-ml volumetric flask together with 3.0 ml of the internal standard solution and diluted to volume. Aliquots (20 μl) of the solution were injected onto the chromatograph.

[4] Model 7120, Rheodyne, Berkeley, Calif.

[5] Lichrosorb RP8, 10 μm, Brownlee Laboratories, Berkeley, Calif.

Table I—Same-Day Reproducibility of HPLC Cephacetrile Sodium Assay

Sample	Cephacetrile, % purity[a] Run 1	Run 2	Run 3	Mean	*CV*, %
		Day 1			
1	85.8	85.7	85.8	85.77	0.13
2	85.2	84.6	85.1	84.97	0.38
3	76.1	77.0	76.4	76.5	0.6
4	77.2	77.7	77.5	77.47	0.32
5	78.5	78.6	78.1	78.4	0.33
Pooled standard error = 0.3%					
		Day 2			
1	85.4	86.0		85.7	0.5
2	87.1	86.9		87.0	0.16
3	77.7	77.4		77.55	0.27
4	79.8	79.3		79.55	0.44
5	79.7	79.9		79.8	0.18
Pooled standard error = 0.34%					
		Day 3			
1	85.5	85.2		85.35	0.25
2	87.5	87.6		87.55	0.08
3	75.7	76.1		75.9	0.37
4	80.1	79.8		79.95	0.27
5	80.3	80.3		80.3	0
Pooled standard error = 0.23%					

[a] Calculated as free acid (molecular weight 339.3).

RESULTS AND DISCUSSION

Synthesis—Cephacetrile is synthesized (Scheme I) by reaction of 7-amino-3-acetoxymethyl-3-cephem-4-carboxylic acid (V) with mixed anhydrides (VIa–VIc) of cyanoacetic acid, both carboxylic (3) and sulfonic[6]. Crude cephacetrile is accompanied by variable amounts of by-products (IV), as shown by TLC. Moreover, II and III, arising from I through the acid hydrolysis removal of the acetyl group, can be formed during the workup of the reaction mixture and, therefore, be present in the finished product after a long storage. The described HPLC method is a rapid and accurate tool for isolating and measuring cephacetrile.

Evaluation of Chromatographic Systems—Reversed-phase chromatography was chosen because of the stability of the resins over time and a wide pH range, easy preparation, and low cost of mobile phases. The retention times of products (I–IV) can be changed by varying the amount and type of the organic modifier and the buffer pH. With cephacetrile as the reference peak, at a constant concentration of the organic

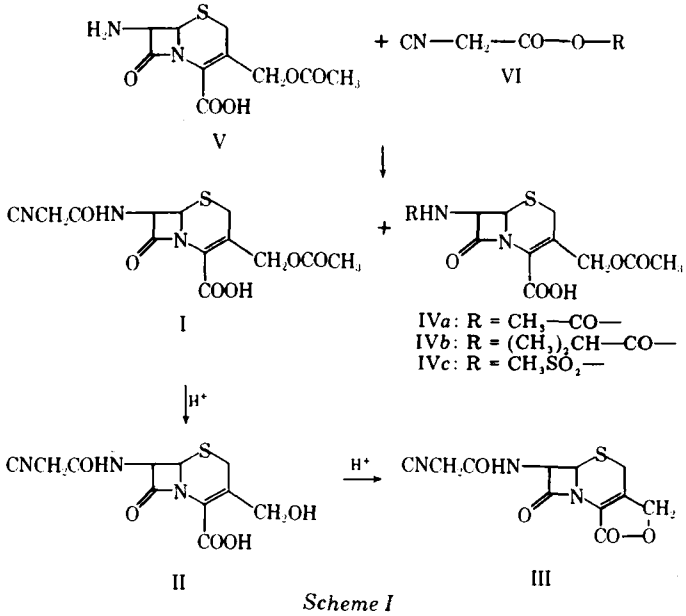

Scheme I

[6] Unpublished data.

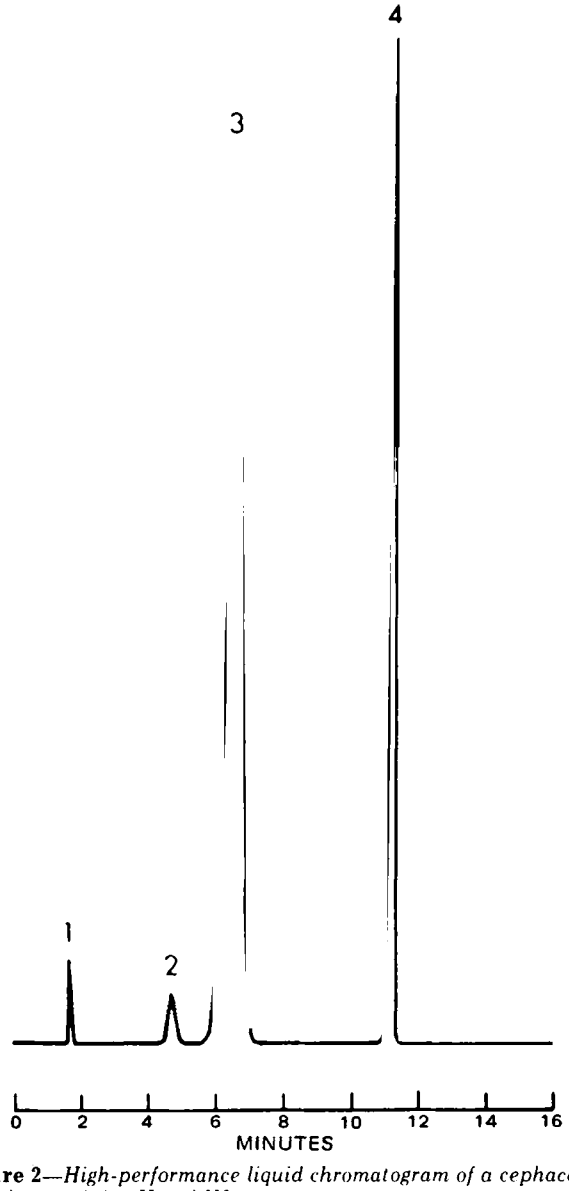

Figure 2—*High-performance liquid chromatogram of a cephacetrile sample containing II and III.*

solvent, III was rapidly eluted while the retention time of IV*a* was increased by lowering the pH from 7.2 phosphate buffer to 4.2 acetate buffer. The elution of IV*c* was not affected by changing the pH and type of the organic modifier, while IV*b* was eluted only by using a proper gradient. Methanol allowed a better partition between the components than acetonitrile. Cefazolin was selected as the internal standard because of its efficient separation from I–IV.

Figure 1 shows a chromatogram of an artificial mixture of cephalosporins I–IV and cefazolin. The peaks of the compounds were well resolved in less than 15 min. Figure 2 shows a typical chromatogram of a cephacetrile sample containing desacetyl (II) and lactone (III) impurities.

Table II—Comparison of Analysis by HPLC and Official Methods for Certification [a] of Cephacetrile Sodium

	Percent Purity (Acid)			
Sample	HPLC[b]	Microbiological[c] Method	Hydroxylamine[c] Method	Perchloric Acid[c] Method
A	85.6	82.5	91.9	89.6
B	85.3	87.3	94.7	89.6
C	87.0	85.7	92.2	91.6
D	86.3	86.1	90.8	89.1
E	78.8	77.8	88.9	90.9
F	82.7	85.3	92.7	91.3
G	79.3	81.6	88.5	90.9
H	82.3	81.6	87.4	90.3
I[d]	70.5	73	71.2	80.8
L[d]	70.9	72.5	78.2	83.5
M[d]	76.6	80.4	87.7	94.3
Average	80.48	81.3	87.6	89.3

[a] Reference 2. [b] Mean of three determinations. [c] Mean of two determinations. [d] Lyophilized salts containing 10% mannitol (w/w).

Reproducibility and Accuracy—The calibration curve was linear in the range of cephacetrile content examined [correlation coefficient (5) of 0.99993]. The within-day standard error was less than 0.4% (Table I). The pooled standard error from different days was less than 0.5%.

Specificity—As shown in Fig. 1, the hydrolysis products (II and III) and the potential impurities (IV*a*–IV*c*) cannot interfere with the quantitative HPLC determination of cephacetrile. While the desacetyl derivatives and lactones do not interfere with the *Bacillus subtilis* assay of cephalosporins, if present in a quantity lower than 15% (6), they do interfere with the colorimetric hydroxylamine assay mandated by the "Code of Federal Regulations." A comparison of the analyses of I by HPLC, the microbiological determination, the hydroxylamine colorimetric method, and the perchloric acid titration is given in Table II. Samples were selected from freshly crystallized salts (Samples A–D), aged salts (E–H), and sterile lyophilized forms (I–M) to show the dependability of the HPLC analysis. The deviation between the HPLC method and the microbiological determination was less than 1%. The other two official assays were less accurate.

REFERENCES

(1) C. H. Nightingale, D. S. Greene, and R. Quintiliani, *J. Pharm. Sci.*, **64**, 1899 (1975).

(2) "Code of Federal Regulations," Title 21, Paragraph 442.19 (1977).

(3) Ciba, British pat. 1,109,525 (1966).

(4) H. M. Higgins (to Eli Lilly and Co.), U.S. pat. 3,351,597 (1967).

(5) G. W. Snedecor and W. G. Cochran, "Statistical Methods," Iowa State University Press, Ames, Iowa, 1967.

(6) F. Kavanagh, "Analytical Microbiology," vol. II, Academic, New York, N.Y., 1972, p. 200.

ACKNOWLEDGMENTS

The authors thank Dr. Chiarani and his staff for microbiological determinations and Prof. G. Pagani, University of Milan, for reviewing this manuscript.

Preparation of Semisynthetic (+)-Tubocurarine Chloride

JANETTE NAGHAWAY [x] **and T. O. SOINE** [†]

Received September 5, 1978, from the *Department of Medicinal Chemistry, College of Pharmacy, University of Minnesota, Minneapolis, MN 55455.* Accepted for publication October 25, 1978. [†]Deceased.

Abstract □ Semisynthetic (+)-tubocurarine chloride (II) was prepared by monoquaternization of (+)-tubocurine. The method involved treating (+)-tubocurine with a 0.5 *M* equivalent of hydrochloric acid prior to quaternization with methyl iodide, followed by neutralization and iodide–chloride ion-exchange. Column chromatography and crystallization procedures were utilized for pure semisynthetic II preparation. The neuromuscular junction blocking activities of the semisynthetic and commercial II were determined by the *in vivo* cat hypoglossal nerve–tongue muscle preparation. No detectable differences among physical constants, spectral data, and neuromuscular junction blocking activities were noted between the commercial product and the semisynthetic II. This result substantiates the chemical and biological data for the well-accepted new formula for II. The unexplained M + *n*14 mass spectral peaks shown by the curare-type bases are characteristic of the molecular species rather than a result of contaminants.

Keyphrases □ Tubocurarine chloride—chemical synthesis, comparison to naturally derived material, NMR analysis □ Neuromuscular blocking effect—tubocurarine chloride, comparison of synthesized and naturally derived materials □ NMR spectroscopy—analysis, tubocurarine chloride

The isolation and original structural characterization of crystalline (+)-tubocurarine chloride (I) were achieved by King (1, 2), who identified I as a bisbenzyltetrahydroisoquinoline alkaloid in which both nitrogen atoms were quaternary. Subsequent structural revision (3) revealed that the bisquaternary structural assignment was erroneous and that (+)-tubocurarine chloride was actually a monoquaternary–monotertiary species (II) with the quaternary function in the tetrahydroisoquinoline ring bearing the free phenolic hydroxyl group. The new structure was soon confirmed (4) by X-ray crystallography, as was the assignment of the quaternary function to the phenolic tetrahydroisoquinoline ring system.

Although the new structure is well accepted, direct chemical synthesis or semisynthesis should be provided as confirmatory evidence. The successful synthesis of II from unequivocal sources would confirm the structure and permit comparative tests of biological activity. Pure II was also needed for determining whether the anomalous M + *n*14 mass spectral peaks observed (5, 6) in natural curare bases and similar type alkaloids were characteristic of such compounds or due to *O*-methylated contaminants.

DISCUSSION

The successful preparation of (+)-isotubocurarine chloride (III) from (+)-tubocurine (IV) (7) suggested the possiblity of preparing II by similar means. NMR spectra and TLC data obtained during the preparation of III by interaction of IV with a 0.5 *M* equivalent of methyl iodide showed that II was being formed in small yields. The small yields of II mandated a modified route for quaternization such as that employed (8) on the calabash curare alkaloids. This method involved the use of a 0.5 *M* equivalent of hydrochloric acid added prior to quaternization with methyl iodide, followed by neutralization. Treating IV sequentially with hydrochloric acid and methyl iodide, followed by neutralization, produced a multicomponent product.

TLC examination of this product on silica gel revealed four spots with R_f values corresponding to those of IV, neutralized II, neutralized III, and (+)-chondocurarine iodide (V). The presence of a higher proportion

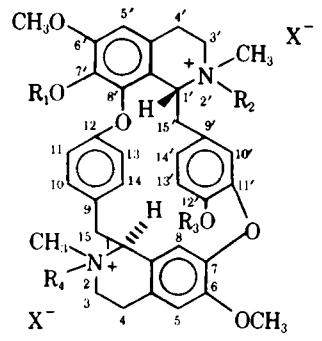

I: $R_1 = R_3 = H$, $R_2 = R_4 = CH_3$, X = Cl
II: $R_1 = R_3 = R_4 = H$, $R_2 = CH_3$, X = Cl
III: $R_1 = R_2 = R_3 = H$, $R_4 = CH_3$, X = Cl
IV: $R_1 = R_3 = H$ (R_2, R_4, and X absent)
V: $R_1 = R_3 = H$, $R_2 = R_4 = CH_3$, X = I

of neutralized II than III was evident from the TLC plate and the NMR spectrum, which showed two NCH_3 signals: the neutralized III 2′-NCH_3 resonance (at δ 2.10) and the neutralized II 2-NCH_3 resonance (at δ 2.42) in a ratio of 1:2. The reaction mixture iodide content was ion exchanged for chloride ions, and neutralized II was isolated through column chromatography over alumina. Following treatment with hydrochloric acid to convert the product to its hydrochloride, II was crystallized from 0.1 *N* HCl by seeding with a few crystals of commercial (+)-tubocurarine chloride, followed by recrystallization from 0.1 *N* HCl to provide the pure compound.

The lesser basicity and nucleophilicity of the amine function of IV at the 2′-nitrogen center, evident by the lower magnitudes of protonation and alkylation at this position, are probably reflections of a steric factor, although solvation effects could contribute to the observed differences. A Dreiding model of IV shows that the trisubstituted aromatic ring, because of some free movement at position C-15′, could easily exert steric hindrance at the 2′-nitrogen center. On the other hand, such steric interaction cannot be invoked at the 2-nitrogen heterocyclic ring since the disubstituted aromatic ring at C-15 cannot be brought near the 2-nitrogen reaction site.

Semisynthetic II was identified by TLC, melting-point, and spectral (IR, UV, and NMR) data, which were in good agreement with those of the commercial samples. The mass spectral data indicated the base peak at *m/e* 298 and a molecular ion at *m/e* 594 with relative intensities in accord with literature values (9). The spectra[1] showed the expected *m/e* 594 major peak, resulting from the conversion of II to a ditertiary molecular ion (M), and definite M + 14 and M + 28 peaks with relative intensities of 3.7 and 0.5% of the base peak, respectively.

Previous reports (9) suggested that the formation of the ditertiary species is through loss of methyl chloride, presumably before ionization, probably in a purely thermal process similar to that observed in GLC (10) and mass spectra (11) of quaternary methiodide salts of amines. The only peaks for (+)-tubocurarine chloride cited (9) were those having an abundance greater than 5% of the base peak, although a greater significance was attached by other investigators (5) to a very low relative intensity peak (0.2%), which was assigned as the M^+ for a similar (but ditertiary) type of alkaloid.

Peaks at 14 mass units above the molecular ion in the mass spectra of bisbenzyltetrahydroisoquinoline alkaloids (5, 6) have been attributed to either contamination by a more highly methylated impurity (5) or to a thermally induced intermolecular methyl transfer (6). Thermal methyl transfer was an inadequate explanation for the II mass spectral data, since II lacks the necessary methylating group (12). Furthermore, the inten-

[1] The mass spectra of commercial II samples were determined on a Hitachi Perkin-Elmer RMU-6D spectrometer and/or an AEI-MS 30 high-resolution mass spectrometer at a 70-ev ionizing voltage and a 200° chamber temperature.

0022-3549/79/0500-0655$01.00/0
© 1979, American Pharmaceutical Association

sities of the higher peaks relative to the M^+ peak were expected to vary with changes in the vaporization temperature (12), but this was not the case with II. Since all commercial II is crystallized from natural sources, contamination by *O*-methylated congeners is possible. Small amounts of these contaminants could be detected in the mass spectrum and would not unduly distort the physical criteria of the compound but could affect the biological activity through the greater blocking potencies of the more highly *O*- and *N*-methylated congeners (13).

The M + *n*14 peaks shown by pure II indicate that this mass spectral behavior may be characteristic of the quaternary curare bases. The higher peaks may be due to preliminary thermal dequaternization, followed by generation of these peaks from the tertiary base, since pure (−)-curine and (+)-tubocurine give spectra with peaks at *m/e* 608 and 622. A thermally induced Hofmann elimination could account for the M + 14 peak from the quaternary base and coupled with radical formation from the tertiary base which could combine with generated methyl radicals to account for the higher peak(s).

EXPERIMENTAL[2]

Semisynthetic (+)-Tubocurarine Chloride (II)—A stirred solution of (+)-tubocurine[3] (1.0 g, 1.68 mmoles) in 80 ml of acetone–water (3:1) was slowly treated with 16.76 ml of 0.1 *N* HCl (1.68 mmoles). Immediate evaporation of the solvent to dryness under reduced pressure was followed by dissolution of the residue in methanol (35 ml) and the subsequent addition of methyl iodide (10 ml). The mixture was stirred for 17 min and then evaporated to dryness under reduced pressure. TLC examination of the residue on silica gel showed four spots with R_f values of 0.83, 0.43, 0.26, and 0.06. These R_f values were similar to those for (+)-tubocurine (IV), (+)-tubocurarine chloride (II) neutralized with sodium bicarbonate, neutralized (+)-isotubocurarine chloride (III), and (+)-chondocurarine iodide (V), respectively. The intensity of the R_f 0.43 spot was greater than that of R_f 0.26.

Crystallization of the residue from a methanol–chloroform mixture (15) provided V (0.38 g), which was dissolved in methanol and converted to I by passage through a column[4] (15 × 1.5 cm, chloride cycle). Methanolic solvent evaporation gave an amorphous I residue (0.28 g). Crystallization of I from absolute ethanol gave a product with a melting point of 246–247° (frothing). The methanol–chloroform mother liquor iodide content was also exchanged for chloride, and the effluent solution was evaporated to dryness. The residue (0.92 g) was suspended in water (30 ml) and extracted with chloroform (3 × 100 ml).

The aqueous layer was evaporated to dryness under reduced pressure, leaving a yellowish-white residue (0.56 g). The residue (0.37 g) was dissolved in methanol, adsorbed on a small amount of neutral alumina (grade V), and air dried. This dry powder was packed on top of a neutral alumina column (grade V, 60 g) and eluted with ethyl acetate to provide unchanged IV (0.056 g) in the early fractions. The eluting solvent was enriched with methanol, followed by enrichment with 2.5% aqueous ammonia, so that elution took place over 10–12 hr with a mixture of ethyl acetate–methanol–2.5% aqueous ammonia (8:1.5:0.5) and separated the remaining components into two yellow bands with an intermediate diffuse yellow zone.

Extrusion of the column contents enabled mechanical separation of the bands. The faster moving band was repeatedly extracted with hot methanol (300 ml). The residue left after solvent evaporation was treated with excess 1 *N* HCl, followed by evaporation of the solution to dryness under reduced pressure. The residue (0.20 g) showed trace amounts of the other components when examined by TLC. Crystallization from 0.1 *N* HCl by seeding with a few crystals of commercial II[5] provided a crop of crystals, which was used for seeding other quantities of column-separated semisynthetic II. TLC on silica gel of the crystalline product showed one spot with a higher R_f (~0.83) in addition to that at 0.43, which represents II.

Further purification was carried out by treating an aqueous solution of the foregoing crystals (0.02 g in 5 ml) with a few drops of 10% ammonium hydroxide and extracting with chloroform (6 × 30 ml). The aqueous layer was acidified with 1 *N* HCl and evaporated to dryness, affording a white solid (0.014 g), which now showed only one spot (R_f 0.43). Recrystallization from 0.1 *N* HCl provided white crystals, mp 255–257° (frothing at 263°) [lit. (16) mp 270°]; $[\alpha]_D^{25}$ +204.3° (c 0.60, methanol) [lit. (16) $[\alpha]_D$ +219° (c 0.785, methanol)]. IR and NMR spectra were similar to those of the commercial sample used for seeding; UV: λ_{max} (log ϵ) 225 (4.56) and 282 (3.90) nm; mass spectrum[6]: *m/e* (relative intensity) 622 (0.5), 609 (1.4), 608 (3.7), 595 (6.0), 594 (17.0), 593 (15.0), and 298 (100.0) [lit. (9) *m/e* (relative intensity) 595 (6.0), 594 (17.0), 593 (12.0), and 298 (100.0)].

Neuromuscular Junction Blocking Bioassay—The neuromuscular junction blocking potencies of semisynthetic and authentic II were determined by employing the *in vivo* cat hypoglossal nerve-tongue muscle preparation, which was described earlier (17). The results indicated identical blocking potencies for the two compounds.

REFERENCES

(1) H. King, *J. Chem. Soc.*, **1935**, 1381.

(2) H. King, *Chem. Ind.*, **45**, 739 (1935).

(3) A. J. Everett, L. A. Lowe, and S. Wilkinson, *Chem. Commun.*, **1970**, 1020.

(4) P. W. Codding and M. N. G. James, *J. Chem. Soc. Chem. Commun.*, **1972**, 1174.

(5) D. C. Dejongh, S. R. Shrader, and M. P. Cava, *J. Am. Chem. Soc.*, **88**, 1052 (1966).

(6) D. H. R. Barton, G. W. Kirby, and A. Wiechers, *J. Chem. Soc.*, **1966**, 2313.

(7) T. O. Soine and J. Naghaway, *J. Pharm. Sci.*, **63**, 1643 (1974).

(8) W. V. Philipsborn, H. Schmid, and P. Karrer, *Helv. Chim. Acta*, **29**, 913 (1956).

(9) G. W. A. Milne and J. R. Plimmer, *J. Chem. Soc.*, **1966**, 1966.

(10) L. D. Metcalfe, *J. Am. Oil Chem. Soc.*, **40**, 25 (1963).

(11) M. Hesse, W. Vetter, and H. Schmid, *Helv. Chim. Acta*, **48**, 674 (1965).

(12) D. W. Thomas and K. Biemann, *J. Am. Chem. Soc.*, **87**, 5447 (1965).

(13) H. O. J. Collier, S. K. Paris, and L. I. Woolfe, *Nature*, **161**, 817 (1948).

(14) M. Shamma, N. C. Deno, and J. F. Remar, *Tetrahedron Lett.*, **1966**, 1375.

(15) J. D. Dutcher, *J. Am. Chem. Soc.*, **74**, 2221 (1952).

(16) "The Merck Index," 8th ed., Merck & Co., Rahway, N.J., 1968.

(17) P. W. Erhardt and T. O. Soine, *J. Pharm. Sci.*, **64**, 53 (1975).

[2] Melting points were determined on a Mel-Temp apparatus and are uncorrected. Optical rotations were measured on a Perkin-Elmer 141 polarimeter. UV spectra were taken in methanol solutions with a Cary 14 recording spectrophotometer. IR spectra were obtained in KBr pellets with a Perkin-Elmer 237 grating IR spectrophotometer. NMR spectra were measured with a Varian Associates model A-60D or XL-100 NMR spectrometer with sodium 2,2-dimethyl-2-silapentane-5-sulfonate as an internal standard. Mass spectral determinations were performed by the Mass Spectroscopy Laboratory Service, Department of Chemistry, University of Minnesota, Minneapolis, Minn., with a Hitachi Perkin-Elmer RMU-6D mass spectrometer or an AEI-MS 30 high-resolution mass spectrometer.

TLC was conducted on 0.25-mm Brinkmann silica gel HF-254 plates using 10% aqueous ammonia–methanol–ethyl acetate–isopropyl alcohol (2:2:1:1) as the developing solvent. Visualization was done with both UV lamp and iodine vapor. Activity grade V Woelm neutral alumina was employed in column chromatography. (+)-Tubocurarine chloride was obtained from Sigma Chemical Co., St. Louis, MO 63118, Abbott Laboratories, North Chicago, IL 60064, and Organon Inc., West Orange, NJ 07052.

[3] Prepared by the dequaternization of II with sodium thiophenoxide (14). It showed only one spot (R_f 0.83) when examined by TLC.

[4] Amberlite IRA-410, medium porosity, Mallinckrodt.

[5] Obtained from Abbott Laboratories, North Chicago, IL 60064. Its melting-point behavior showed collapse of the sample at 255°, followed by vigorous frothing with decomposition at 263°. It also showed $[\alpha]_D^{25}$ +214° (c 0.79, methanol). When examined by TLC, it showed only one spot (R_f 0.43).

[6] The mass spectrum of semisynthetic II was obtained using an RMU-6D Hitachi Perkin-Elmer mass spectrometer with a 70-ev ionization voltage and a 200° chamber temperature.

Differential Pulse Polarographic Determination of 2,3-Dimercaptosuccinic Acid and Tin(II) in Radiopharmaceuticals

A. J. ROSS*, H. A. MOORE‡§x, C. O. RITTER‡, and S. A. MOROS*

Received May 18, 1978, from the *Quality Control Department, Hoffmann-La Roche Inc., Nutley, NJ 07110, and the ‡Medi+Physics Inc., Emeryville, CA 94608. Accepted for publication October 30, 1978. §Present address: New England Nuclear, Billerica, Mass.

Abstract □ A differential pulse polarographic procedure was developed for the assay of dimercaptosuccinic acid and tin(II), components of a commercially available pharmaceutical kit for kidney scintigraphy. The method is quantitative and qualitative for both the chelated and unchelated forms of dimercaptosuccinic acid and tin(II) in a mixture of the two.

Keyphrases □ Dimercaptosuccinic acid—analysis, differential pulse polarography, in radiopharmaceuticals, and tin □ Tin—analysis, differential pulse polarography, in radiopharmaceuticals, and dimercaptosuccinic acid □ Polarography, differential pulse—analysis, dimercaptosuccinic acid and tin in radiopharmaceuticals □ Scintigraphy, kidney—analysis of dimercaptosuccinic acid and tin(II) in commercial preparations, differential pulse polarography

Dimercaptosuccinic acid (I) possesses clinical importance as a detoxification agent for mercury, arsenic, and other heavy metals (1) and, more recently, in conjunction with tin(II) and ^{99m}technetium as a radiopharmaceutical for kidney scintigraphy (2–4). Although the chemistry of several I chelates has been studied (5) with application to biological systems (6, 7), little work has been done to develop a specific analytical procedure.

UV procedures (8, 9) depend on the I thiol reducing properties and are inappropriate in the presence of another reducing agent. Since tin(II) is present in the kidney reagent final product (3 m*M* I + 1 m*M* $SnCl_2$), an alternative means of analysis is necessary. Krejcarek *et al.* (10) employed differential pulse polarography to analyze both tin(II) and I but gave few details of their unpublished procedure. McBride *et al.* (11) employed the same technique to quantitate tin(II) in pyrophosphate and polyphosphate radiopharmaceutical kits.

This paper expands on this recent work and presents a quantitative and qualitative technique to analyze both the chelated and unchelated forms of I and tin(II) in a mixture of the two. The method was successfully applied to ampuls of final product reagent.

EXPERIMENTAL

Reagents and Chemicals—The reagents and chemicals used were *meso*-dimercaptosuccinic acid, anhydrous stannous chloride[1], and analytical grade lithium perchlorate[2], sodium phosphate·$7H_2O$[3], and citric acid[3]. The mercury[4] used was triple distilled.

Instrumentation—A polarographic analyzer[5], equipped with a drop-time assembly[6], was used in conjunction with a three-electrode system consisting of a dropping mercury electrode, a silver–silver chloride reference electrode, and a platinum counter electrode. The mercury column height was 60 cm; the automatic drop time was 0.5 sec. At this column height, the dropping mercury electrode had an open circuit drop time of 7.36 sec and a mercury flow rate of 0.93 mg/sec in the buffer.

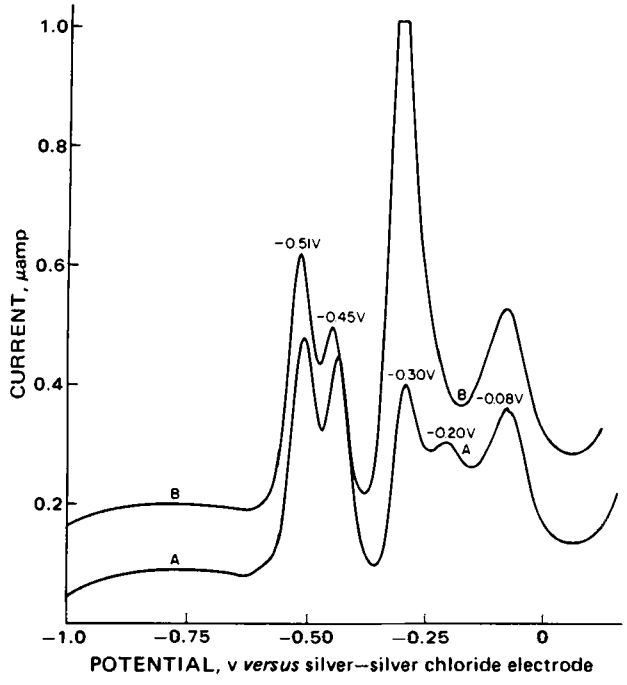

Figure 1—*Sample polarograms of ampul in supporting electrolyte (polarogram A) and with addition of excess I (polarogram B).*

A scan rate of 2 mv/sec and a pulse amplitude of 25 mv were employed. The current range was set at 1 μamp, and the scan range was 0.75 v. The samples were scanned positively from −0.70 to +0.05 v against silver–silver chloride, and the differential pulse polarograms were obtained on an *x*–*y* recorder[7].

Dissolved air was removed from solutions by bubbling prepurified nitrogen through the cell for 5 min and passing it over the solution during polarography.

Determination of I and Tin(II) in Kidney Reagent—Dilute tin(II) solutions such as those used in this procedure are susceptible to oxidation, especially when exposed to light. Consequently, it is essential to establish a technique that minimizes exposure to air and light. Dimercaptosuccinic acid slowly hydrolyzes in solution; standards and reagents containing this material should be prepared just before use.

A 150-μl aliquot of the freshly opened ampul of kidney reagent final product was diluted to 10 ml with deaerated pH 3.0, 0.1 *N* $LiClO_4$–0.1 *M* citrate–phosphate buffer supporting electrolyte, and the polarogram was recorded. The peak current at −0.30 v (due to the unchelated I) was measured and compared to a standard calibration curve for unchelated I. A second peak current at about −0.51 v (due to the reduction of chelated stannous ion) was measured also and compared to a standard curve for chelated tin(II). This second value was then normalized with respect to stoichiometry [at this pH, the chelate formula is $Sn(I)_2$] and added to the unchelated I value to arrive at the total I concentration (Fig. 1A).

Another 150-μl aliquot of the ampul contents was transferred to a

[1] Purity >99%, Medi+Physics Inc., Emeryville, CA 94608.
[2] ROC/RIC.
[3] Mallinckrodt.
[4] Bethlehem Instruments.
[5] Princeton Applied Research model 174 A.
[6] Princeton Applied Research model 174/70.
[7] Hewlett-Packard model 7001 AM.

0022-3549/79/0500-0657$01.00/0
© 1979, American Pharmaceutical Association

Table I—Peak Currents of I and Tin(II) Solutions

I Concentration, m*M*	Tin(II) Concentration, m*M*	i_p (microamperes) at E = −0.51 v	E = −0.30 v	E = −0.20 v	E = −0.08 v
0.0580	—	—	1.13	—	—
0.0580	0.0108	0.28	0.68	—	0.16
0.0580	0.0161	0.40	0.49	—	0.21
0.0580	0.0215	0.52	0.20	0.05	0.26
0.0580	0.0269	0.61	Shoulder	0.12	0.28
0.0580	0.0323	0.71	—	0.25	0.31

second 10-ml volumetric flask, flooded with excess deaerated I solution (1.5 ml of 1 m*M* solution) to ensure complete chelation of the tin, and diluted to volume with deaerated supporting electrolyte. The solution was analyzed polarographically and the peak current was measured at −0.51 v. Comparison to the standard curve of chelated tin gave the total stannous content (Fig. 1B).

Standard free I and chelated tin(II) curves were prepared. Five solutions, ranging in concentration from 0.012 to 0.018 m*M* of both I in the absence of tin and tin(II) flooded by an excess of I, were diluted in supporting electrolyte. The I solutions were analyzed polarographically, and the peak currents measured at −0.30 v were plotted against the respective concentrations to obtain the free I calibration curve. Similarly, for tin(II) solutions in an excess of I, the peak currents at −0.51 v were measured and plotted against concentration to obtain the chelated tin(II) calibration curve.

RESULTS AND DISCUSSION

Tin(II) in the absence of I had two distinct polarographic peaks in pH 3.0, 0.1 *N* $LiClO_4$–0.1 *M* citrate–phosphate buffer. One, at −0.20 v, was due to the tin(II) to tin(IV) oxidation. The second, at −0.45 v, was due to the reduction to tin metal. When tin(II) was chelated by I, these peaks shifted to −0.45 and −0.51 v, respectively. The standard curve was linear with concentration, demonstrating that the method can be used to determine chelated tin(II). Tin(IV) will produce a reduction peak only in the presence of high hydrogen-ion and chloride-ion concentrations (12) and does not interfere in this electrolyte.

The I wave at −0.30 v is due to the oxidation of mercury to form the mercury mercaptide salt and not to oxidation of the sulfhydryl group itself (13–16). At 0.15–0.6 m*M* levels, the peak current appeared to be independent of concentration, remaining virtually the same as the concentration was increased fourfold. A second standard curve at much lower concentrations (0.012–0.018 m*M*), however, was linear. The mercury mercaptide product apparently coats the mercury drop, preventing further oxidation. This phenomenon could also have produced the erratic baselines encountered when the scan was initiated at 0.0 v and scanned negatively. To avoid this result, all polarograms were begun at −0.70 v and scanned positively.

Adding tin(II) to I decreased the peak at −0.30 v, while a new peak at −0.08 (chelated I) grew. Further addition of tin(II) resulted in the complete elimination of the free I peak and the emergence of a second new peak at −0.20 v [unchelated tin(II)] (Table I). Since the total I concentration was known and the remaining free I and the chelated tin(II) concentrations could be evaluated, the stoichiometry of the chelate could be determined. At this pH, tin(II) was complexed to two I molecules, confirming the previous work (10) where the same ratio was determined by difference UV spectroscopy. Electrolytically reducing an aliquot of the final product at −0.75 v *versus* silver–silver chloride produced only the free I peak at −0.30 v when analyzed polarographically. These additional data provide convincing evidence of complexation.

Table II—Final Product Kidney Results

Ampul	I, m*M*	Tin(II), m*M*
First of filling operation	3.05	1.02
Middle of filling operation	3.05	1.01
Last of filling operation	3.17	1.03
Middle of filling operation	3.13, 3.10, 3.09	1.00, 0.99, 0.97
	3.11 ± σ of 0.02	0.987 ± σ of 0.015

Three ampuls taken at various stages of a production filling operation were analyzed for I and tin(II) content. A fourth ampul was analyzed in triplicate for both components. The results (Table II) are precise and show good correlation with the quantities added.

REFERENCES

(1) I. E. Okonishnikova, *Prom. Toksikol. Klin. Prof. Zabolevanii Khim. Etiol.*, **1962**, 205 (1962).

(2) T. H. Lin, A. Khentigan, and H. S. Winchell, *J. Nucl. Med.*, **15**, 34 (1974).

(3) R. W. Arnold and F. D. Thomas, *ibid.*, **16**, 357 (1975).

(4) A. Ando, T. Aburano, K. Hisada, T. Hiraki, and I. Ando, *Radioisotopes*, **24**, 36 (1975).

(5) G. R. Lenz and A. E. Martell, *Inorg. Chem.*, **4**, 378 (1965).

(6) L. G. Egorova, I. E. Okonishnikova, Y. L. Niremburg, and I. Postovskii, *Khim.-Farm. Zh.*, **5**, 26 (1972).

(7) *Ibid.*, **6**, 14 (1972).

(8) T. J. Bydalek, J. E. Poldoski, and J. D. Bagenda, *Anal. Chem.*, **42**, 929 (1970).

(9) D. R. Grassetti and J. F. Murray, *Arch. Biochem. Biophys.*, **119**, 41 (1967).

(10) G. E. Krejcarek, P. E. Heerwald, K. L. Tucker, and J. H. Wicks, "First International Symposium on Radiopharmaceutical Chemistry," Brookhaven, Long Island, N.Y., 1976.

(11) M. H. McBride, R. E. George, W. V. Kessler, and S. M. Shaw, *J. Pharm. Sci.*, **66**, 870 (1977).

(12) I. M. Kolthoff and J. J. Lingane, "Polarography," vol. II, 2nd ed., Interscience, New York, N.Y., 1952, p. 526.

(13) L. Meites, "Polarographic Techniques," Interscience, New York, N.Y., 1965, p. 675.

(14) W. Stricks and I. M. Kolthoff, *J. Am. Chem. Soc.*, **74**, 4646 (1952).

(15) I. M. Kolthoff and C. Barnum, *ibid.*, **62**, 3061 (1940).

(16) D. L. Rabenstein and R. Saetre, *Anal. Chem.*, **49**, 1036 (1977).

ACKNOWLEDGMENTS

The authors thank Dr. T. H. Lin for assistance in providing the dimercaptosuccinic acid and Dr. V. Toome and Dr. C. G. Scott for determining the purity of this material.

Simultaneous Determination of Isosorbide Dinitrate and Its Mononitrates in Human Plasma by Capillary Column GLC

M. T. ROSSEEL ˣ **and M. G. BOGAERT**

Received August 21, 1978, from the *J. F. & C. Heymans Institute of Pharmacology, University of Ghent, De Pintelaan 135, B-9000 Ghent, Belgium.* Accepted for publication October 25, 1978.

Abstract □ A previously described electron-capture GLC method for determination of isosorbide dinitrate in human plasma was adapted for the simultaneous determination of isosorbide dinitrate, isosorbide 2-mononitrate, and isosorbide 5-mononitrate using a capillary column. Quantitation was done with two internal standards. The lower limits of detection were approximately 0.5 ng/ml of plasma for isosorbide dinitrate, 2 ng/ml for isosorbide 2-mononitrate, and 20 ng/ml for isosorbide 5-mononitrate.

Keyphrases □ Isosorbide dinitrate—and mononitrates, simultaneous electron-capture GLC analysis, human plasma □ GLC, electron capture—analysis, isosorbide dinitrate and mononitrates, human plasma □ Isosorbide mononitrates—and dinitrate, simultaneous electron-capture GLC analysis, human plasma

The mononitrated metabolites of isosorbide dinitrate, isosorbide 2-mononitrate and isosorbide 5-mononitrate, are pharmacologically active and may contribute to the drug's therapeutic effect (1–4). Therefore, it is of interest to measure the levels of these metabolites together with the parent compound in plasma.

A method was described previously for the quantitative determination of isosorbide dinitrate in human plasma with electron-capture GLC (5), but quantitative mononitrate determination is sometimes difficult because of interfering peaks. This paper presents a modified method for simultaneous determination of isosorbide dinitrate and its two metabolites using a capillary column.

EXPERIMENTAL

Reagents and Materials—Ethyl acetate was pesticide grade[1]. Isosorbide 2-mononitrate, isosorbide 5-mononitrate, isoidide mononitrate, and isomannide dinitrate were prepared as previously described (6). Isosorbide dinitrate was available as a powder[2]. Charcoal, activated and neutralized, was washed three times with ethyl acetate[3].

Instrumental Conditions—The analysis was performed on a gas chromatograph[4] equipped with a linear ^{63}Ni-electron-capture detector[5]. The detector was operated with methane (5% v/v) in argon at a flow rate of 22.5 ml/min. The 25-m × 0.5-mm i.d. glass capillary column was deactivated and wall coated with OV-17[6]. The carrier gas was helium, prefiltered through a gas purifier[7] at a flow rate of 7.5 ml/min. Temperatures were: injector, 200°; column, 165°; and detector, 250°. Direct on-column injection without stream splitting was used. The peak areas were recorded on a recording integrator[8].

Procedure—All glassware was silanized as described previously (5).

The extraction procedure reported earlier (5) was slightly modified. To 2-ml of plasma in a glass-stoppered 10-ml centrifuge tube were added the internal standards isoidide mononitrate (25 ng) and isomannide dinitrate (200 ng). The plasma was extracted twice with 4 ml of ethyl acetate by shaking for 10 min. After separation from the aqueous phase by centrifugation (10 min, 6000 rpm), the organic phase was removed, avoiding the lipoprotein interface.

To the combined organic phase in another 10-ml tube, 55 mg of charcoal was added. The solution was shaken a few times by hand and centrifuged for 20 min at 7000 rpm. The organic phase was transferred into a 6-ml glass-stoppered conical tube and evaporated to dryness under a nitrogen flow at room temperature. The residue was immediately dissolved in 20 μl of ethyl acetate and stored at −18° until analysis. After evaporation of the ethyl acetate to approximately 5 μl under nitrogen, 0.3 μl was injected into the wide-bore glass capillary column.

Quantitation and Reproducibility—As the internal standard for the mononitrates, isoidide mononitrate was used; for isosorbide dinitrate, isomannide dinitrate was used. Human plasma samples spiked with increasing concentrations of isosorbide dinitrate (5–40 ng/2 ml), isosorbide 2-mononitrate (5–100 ng/2 ml), and isosorbide 5-mononitrate (50–1000 ng/2 ml) were carried through the whole procedure. The ratios of the test product peak areas to the internal standard peak areas were plotted *versus* the test product concentrations, and a least-squares linear regression analysis was performed. Values of unknown plasma drug concentrations were determined from this calibration graph.

RESULTS AND DISCUSSION

Typical chromatograms of a blank plasma sample and of a spiked plasma sample are shown in Fig. 1. When the ratios of the peak area of isosorbide dinitrate to that of its internal standard were calculated and plotted *versus* the isosorbide dinitrate concentrations in spiked plasma

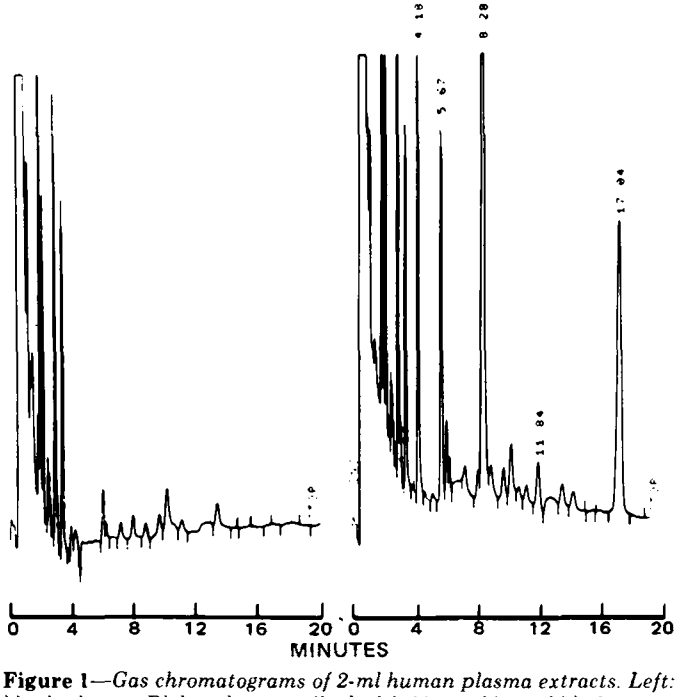

Figure 1—*Gas chromatograms of 2-ml human plasma extracts. Left: blank plasma. Right: plasma spiked with 20 ng of isosorbide 2-mononitrate (retention time of 4.18 min), 25 ng of isoidide mononitrate (5.67 min), 200 ng of isosorbide 5-mononitrate (8.28 min), 5 ng of isosorbide dinitrate (11.84 min), and 200 ng of isomannide dinitrate (17.04 min).*

[1] Carlo Erba, Italy.
[2] Cedona, The Netherlands.
[3] Sigma, St. Louis, Mo.
[4] Hewlett-Packard 5730 A series.
[5] Hewlett-Packard model 18713 A.
[6] RSL, Belgium.
[7] Alltech Associates.
[8] Hewlett-Packard 3380 A.

0022-3549/79/0500-0659$01.00/0
© 1979, American Pharmaceutical Association

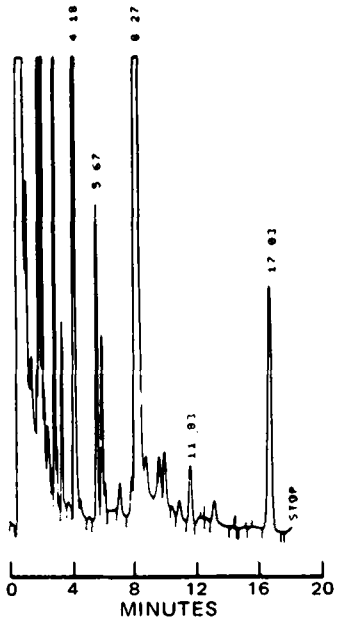

Figure 2—*Gas chromatogram of a 2-ml plasma sample extract obtained from a subject 6 hr after intake of 120 mg of isosorbide dinitrate slow-release preparation; 25 ng of isoidide mononitrate (retention time of 5.67 min) and 200 ng of isomannide dinitrate (17.03 min) were added as internal standards. Key (retention time): 4.18 min, isosorbide 2-mononitrate; 8.27 min, isosorbide 5-mononitrate; and 11.83 min, isosorbide dinitrate.*

samples, a linear relationship was found for the concentration range studied, and the intercept of the standard curve was negligible. The same was true for isosorbide 2-mononitrate and isosorbide 5-mononitrate.

As for isosorbide dinitrate (5), the recoveries of the mononitrates from plasma were quantitative. The relative standard deviations for analyses performed on different days were 7.01 for isosorbide dinitrate (11 samples, 5–20 ng), 9.13 for isosorbide 2-mononitrate (11 samples, 10–30 ng), and 10.96 for isosorbide 5-mononitrate (11 samples, 100–300 ng). The lower limits of detection were approximately 0.5 ng/ml of plasma for isosorbide dinitrate, 2 ng/ml for isosorbide 2-mononitrate, and 20 ng/ml for isosorbide 5-mononitrate.

After daily injections on the column, the glass injector adaptor was replaced weekly.

Figure 2 shows a typical plasma chromatogram 6 hr after intake of 120 mg of an isosorbide dinitrate slow-release preparation.

Several investigators reported difficulties with the quantitative mononitrate determination by conventional packed column GLC due to peak interference mainly with isosorbide 5-mononitrate (7–9). The wall-coated capillary column used here provides a suitable means of analyzing the isosorbide mononitrates with the required efficiency and specificity.

REFERENCES

(1) M. G. Bogaert and M. T. Rosseel, *Arch. Pharmacol.*, **275**, 339 (1972).

(2) R. L. Wendt, *J. Pharmacol. Exp. Ther.*, **180**, 732 (1972).

(3) M. Stauch, N. Grewe, and H. Nissen, *Verh. Dtsch. Ges. Kreislaufforschg.*, **41**, 182 (1975).

(4) M. Stauch, N. Grewe, and H. Nissen, *Herz.*, **3**, 223 (1978).

(5) M. T. Rosseel and M. G. Bogaert, *J. Pharm. Sci.*, **62**, 754 (1973).

(6) M. T. Rosseel and M. G. Bogaert, *Biochem. Pharmacol.*, **22**, 67 (1973).

(7) D. A. Chin, D. G. Prue, J. Michelucci, B. T. Kho, and C. R. Warner, *J. Pharm. Sci.*, **66**, 1143 (1977).

(8) L. Richard, G. Klein, and J. M. Orr, *Clin. Chem.*, **22**, 2060 (1976).

(9) J. O. Malbica, K. Monson, K. Neilson, and R. Sprissler, *J. Pharm. Sci.*, **66**, 384 (1977).

ACKNOWLEDGMENTS

Supported by Grant 3900171 from the National Fund for Medical Research, Belgium.

Improved Method for Morphine Extraction from Biological Samples

G. L. SPRAGUE and A. E. TAKEMORI ˣ

Received June 19, 1978, from the *Department of Pharmacology, University of Minnesota, Minneapolis, MN 55455.* Accepted for publication October 31, 1978.

Abstract □ Methadone, morphine, or naloxone extraction from brain homogenates, plasma, and urine is described. An aqueous sample was loaded on a surgical gauze support, which was washed with extracting solvents. Aqueous samples remained on the support, and nonpolar drugs partitioned into the lipophilic extracting solvent. The procedure recovered 80–100% of nanogram levels of methadone, morphine, or naloxone from biological samples. In addition, an approximate 10-fold timesaving capacity was demonstrated compared to standard liquid–liquid extraction techniques.

Keyphrases □ Methadone—analysis, liquid–liquid extraction, brain, blood, plasma, urine □ Morphine—analysis, liquid–liquid extraction, brain, blood, plasma, urine □ Naloxone—analysis, liquid–liquid extraction, brain, blood, plasma, urine □ Liquid–liquid extraction—analysis, methadone, morphine, naloxone, brain, blood, plasma, urine □ Narcotic analgesics—methadone, morphine, naloxone, liquid–liquid extraction, brain, blood, plasma, urine

Determination of tissue narcotic drug levels frequently involves radiolabeled drug administration. Following alkalinization, the lipophilic drugs are extracted from tissue preparations using standard liquid–liquid extraction techniques (1–5). These techniques typically involve partitioning the drug between two immiscible liquids by shaking, phase separation by centrifugation, and drug analysis in the nonpolar solvent phase or in the aqueous phase after back-extraction. Improved methods for morphine and related drug extraction have not altered the basic liquid–liquid extraction technique (4, 6).

A rapid, efficient extraction technique for tissue morphine and related drug determination is presented here. Extraction of tritiated methadone, morphine, and naloxone from brain, plasma, and urine samples is described. A polar support (gauze sponges) held an aqueous tissue ho-

0022-3549/79/0500-0660$01.00/0
© 1979, American Pharmaceutical Association

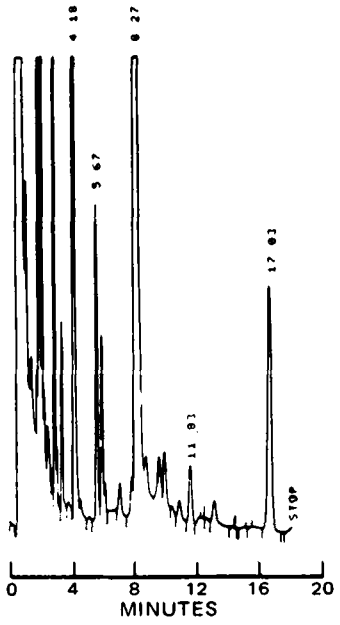

Figure 2—*Gas chromatogram of a 2-ml plasma sample extract obtained from a subject 6 hr after intake of 120 mg of isosorbide dinitrate slow-release preparation; 25 ng of isoidide mononitrate (retention time of 5.67 min) and 200 ng of isomannide dinitrate (17.03 min) were added as internal standards. Key (retention time): 4.18 min, isosorbide 2-mononitrate; 8.27 min, isosorbide 5-mononitrate; and 11.83 min, isosorbide dinitrate.*

samples, a linear relationship was found for the concentration range studied, and the intercept of the standard curve was negligible. The same was true for isosorbide 2-mononitrate and isosorbide 5-mononitrate.

As for isosorbide dinitrate (5), the recoveries of the mononitrates from plasma were quantitative. The relative standard deviations for analyses performed on different days were 7.01 for isosorbide dinitrate (11 samples, 5–20 ng), 9.13 for isosorbide 2-mononitrate (11 samples, 10–30 ng), and 10.96 for isosorbide 5-mononitrate (11 samples, 100–300 ng). The lower limits of detection were approximately 0.5 ng/ml of plasma for isosorbide dinitrate, 2 ng/ml for isosorbide 2-mononitrate, and 20 ng/ml for isosorbide 5-mononitrate.

After daily injections on the column, the glass injector adaptor was replaced weekly.

Figure 2 shows a typical plasma chromatogram 6 hr after intake of 120 mg of an isosorbide dinitrate slow-release preparation.

Several investigators reported difficulties with the quantitative mononitrate determination by conventional packed column GLC due to peak interference mainly with isosorbide 5-mononitrate (7–9). The wall-coated capillary column used here provides a suitable means of analyzing the isosorbide mononitrates with the required efficiency and specificity.

REFERENCES

(1) M. G. Bogaert and M. T. Rosseel, *Arch. Pharmacol.*, **275**, 339 (1972).

(2) R. L. Wendt, *J. Pharmacol. Exp. Ther.*, **180**, 732 (1972).

(3) M. Stauch, N. Grewe, and H. Nissen, *Verh. Dtsch. Ges. Kreislaufforschg.*, **41**, 182 (1975).

(4) M. Stauch, N. Grewe, and H. Nissen, *Herz.*, **3**, 223 (1978).

(5) M. T. Rosseel and M. G. Bogaert, *J. Pharm. Sci.*, **62**, 754 (1973).

(6) M. T. Rosseel and M. G. Bogaert, *Biochem. Pharmacol.*, **22**, 67 (1973).

(7) D. A. Chin, D. G. Prue, J. Michelucci, B. T. Kho, and C. R. Warner, *J. Pharm. Sci.*, **66**, 1143 (1977).

(8) L. Richard, G. Klein, and J. M. Orr, *Clin. Chem.*, **22**, 2060 (1976).

(9) J. O. Malbica, K. Monson, K. Neilson, and R. Sprissler, *J. Pharm. Sci.*, **66**, 384 (1977).

ACKNOWLEDGMENTS

Supported by Grant 3900171 from the National Fund for Medical Research, Belgium.

Improved Method for Morphine Extraction from Biological Samples

G. L. SPRAGUE and A. E. TAKEMORI ˣ

Received June 19, 1978, from the *Department of Pharmacology, University of Minnesota, Minneapolis, MN 55455.* Accepted for publication October 31, 1978.

Abstract □ Methadone, morphine, or naloxone extraction from brain homogenates, plasma, and urine is described. An aqueous sample was loaded on a surgical gauze support, which was washed with extracting solvents. Aqueous samples remained on the support, and nonpolar drugs partitioned into the lipophilic extracting solvent. The procedure recovered 80–100% of nanogram levels of methadone, morphine, or naloxone from biological samples. In addition, an approximate 10-fold timesaving capacity was demonstrated compared to standard liquid–liquid extraction techniques.

Keyphrases □ Methadone—analysis, liquid–liquid extraction, brain, blood, plasma, urine □ Morphine—analysis, liquid–liquid extraction, brain, blood, plasma, urine □ Naloxone—analysis, liquid–liquid extraction, brain, blood, plasma, urine □ Liquid–liquid extraction—analysis, methadone, morphine, naloxone, brain, blood, plasma, urine □ Narcotic analgesics—methadone, morphine, naloxone, liquid–liquid extraction, brain, blood, plasma, urine

Determination of tissue narcotic drug levels frequently involves radiolabeled drug administration. Following alkalinization, the lipophilic drugs are extracted from tissue preparations using standard liquid–liquid extraction techniques (1–5). These techniques typically involve partitioning the drug between two immiscible liquids by shaking, phase separation by centrifugation, and drug analysis in the nonpolar solvent phase or in the aqueous phase after back-extraction. Improved methods for morphine and related drug extraction have not altered the basic liquid–liquid extraction technique (4, 6).

A rapid, efficient extraction technique for tissue morphine and related drug determination is presented here. Extraction of tritiated methadone, morphine, and naloxone from brain, plasma, and urine samples is described. A polar support (gauze sponges) held an aqueous tissue ho-

0022-3549/79/0500-0660$01.00/0
© 1979, American Pharmaceutical Association

Table I—Methadone, Morphine, and Naloxone Recovery from Brain, Plasma, and Urine Samples

Drug	Tissue	Drug Added, ng	Percent Recovered	Solvent
Methadone	Brain	15–85	91.0 ± 2.3[a]	Ether
	Plasma	2–19	91.4 ± 4.9	Ether
	Urine	185	98.0 ± 0.8	Ether
Morphine	Brain	2–15	98.0 ± 3.3	Ethanol–chloroform (10:90)
	Plasma	1–18	94.3 ± 3.1	Ethanol–chloroform (10:90)
	Urine	0.5–1	80.3 ± 0.8	Ethanol–chloroform (10:90)
Naloxone	Brain	4–55	104.4 ± 1.8	Chloroform
	Plasma	2–230	95.6 ± 3.4	Chloroform
	Urine	2.5–70	83.2 ± 1.8	Chloroform

[a] Mean ± *SEM*, n = 6–9.

mogenate or a sample containing radioactive drug. A nonpolar, water-immiscible solvent was passed through the column, collected, and evaporated, and the drug concentration was determined.

EXPERIMENTAL

Drugs and Reagents—All solvents were reagent grade. The drugs used included morphine sulfate, methadone hydrochloride, naloxone hydrochloride, ^{3}H-methadone hydrobromide (161.0 mCi/mmole), ^{3}H-morphine (23 Ci/mmole), and ^{3}H-naloxone (4.54 mCi/mmole). All drug concentrations were expressed in terms of the base.

Extraction Columns—These columns were similar to commercially available[1] ones but were made from inexpensive, common laboratory materials. The columns consisted of 12-ml disposable syringe barrels into which one folded and tightly rolled piece of surgical gauze (10.2 × 10.2-cm, 8-ply gauze sponge) was placed. A 21-gauge needle fitted with a piece of polyethylene tubing (PE90) was attached to a three-way stopcock, which, in turn, was attached to the extraction column (syringe tip) and was used to regulate the effluent flow.

TLC—Radioactivity extracted from brain homogenates, plasma, or urine was identified as unchanged drug (*e.g.*, methadone, morphine, or naloxone) using TLC. Tritiated drug radioactive purity was verified by TLC. After extraction, excess solvent from selected samples was evaporated using nitrogen; the resulting concentrated samples were applied to individual plastic TLC plates coated with silica gel along with appropriate standards.

The solvent systems for methadone, morphine, and naloxone were ethyl acetate–butanol–ethanol–ammonium hydroxide (70:10:15:1), ethanol–acetic acid–water (60:30:10), and ethyl acetate–hexane–ethanol–ammonium hydroxide (60:25:14:1), respectively. The radioactivity in each area was determined by cutting the chromatogram into 1-cm sections and placing them in scintillation vials containing scintillation cocktail.

Biological Tissues and Fluids—Brains and blood samples were obtained from male Swiss-Webster mice killed with carbon dioxide. Blood was removed by cardiac puncture using a heparinized syringe, and plasma was obtained following centrifugation of blood samples. Brains were removed, weighed, and homogenized in four volumes of cold, distilled water using a motor-driven polytef pestle in a Potter homogenizer. Human urine was used in all cases.

Method of Extraction—The following procedure was used to extract morphine or naloxone from mouse brain homogenates. A brain homogenate aliquot (0.2 ml) was diluted with an equal volume of glycine buffer (0.5 *M*, pH 9.0) and added to the extraction column. The column capacity was 2 ml. Two minutes after the buffered homogenate was added to the column, 10 ml of solvent was added. The effluent was collected in a scintillation vial after a 2-min equilibration period. The column was washed twice with 5 ml of solvent and allowed a 2-min equilibration with each wash.

The combined effluent (20 ml) was evaporated to dryness in a water bath, and 15 ml of scintillation cocktail was added. Radioactivity was measured by liquid scintillation spectrometry, and an internal standard (^{3}H-toluene) was used to determine counting efficiency. The procedure for methadone extraction from brain homogenates was identical except that sufficient 0.1 *N* NaOH was added to the brain homogenate to adjust the pH to 10.5 prior to extraction.

[1] Jetubes, Manhattan Instruments, Santa Monica, Calif.

A similar procedure was used to extract drugs from plasma and urine samples. Aliquots (0.05 ml) of plasma or urine containing morphine or naloxone were diluted with nine volumes of glycine buffer, and the total volume added to the extraction column was 0.5 ml in each case. The upper limit of plasma or urine that was applied to the column was 1.0 ml; extraction efficiency was not reduced by applying smaller volumes. The pH of plasma or urine samples containing methadone was adjusted to 10.5 after nine volumes of glycine buffer were added. The extraction solvents were ether for methadone, ethanol–chloroform (10:90) for morphine, and chloroform for naloxone.

Determination of Percent Recovery—The specific activity of tritiated methadone, morphine, and naloxone was known. The purity was determined using TLC and appropriate standards. A measured radiolabeled drug amount was added to a sample (brain homogenate, plasma, or urine), the sample pH was adjusted, and drug was extracted. The radioactivity was measured after solvent evaporation in certain samples, and the identity of radioactivity was confirmed by TLC in others. The percent recovery was calculated, and corrections were made for the purity of added radioactivity as well as the amount of radioactivity lost in the transfer of 0.4-ml aliquots to the extraction columns.

Drug Extraction from Tissues after Subcutaneous Administration—Tritiated methadone, morphine, or naloxone was administered subcutaneously to mice to measure the extraction of metabolites and unchanged drug(s) from brain and blood. Mice were killed with carbon dioxide 20 min after drug administration, and whole brains and blood samples were obtained. Brains were homogenized, plasma was obtained, and radioactivity was extracted as already described. The percent of total radioactivity corresponding to unchanged methadone, morphine, or naloxone was determined using TLC.

RESULTS AND DISCUSSION

Table I shows the percent tritiated methadone, morphine, and naloxone recovery from brain homogenate, plasma, or urine. In each case, the extracted radioactivity was chromatographically identical to authentic methadone, morphine, or naloxone. These results demonstrate highly efficient extraction of the three drugs from mouse brain homogenates even at very low drug concentrations. The concentrations used represented values typical of pharmacological studies.

The recovery of methadone, morphine, or naloxone from brain samples in other studies using standard liquid–liquid extraction techniques was between 66.0 and 96.2% (1, 4, 6, 7). The highest recoveries required three consecutive liquid–liquid extractions. A recent study (4) reported 90% morphine recovery (0.125–0.5 μg added) from biological tissues using standard liquid–liquid extraction methods and siliconized glassware. The present extraction procedure provided efficient recovery of morphine (98.0%) from brain homogenates at low morphine concentrations (1–20 ng added) without special precautions such as siliconized glassware.

The present procedure also provided efficient methadone recovery from plasma and urine samples (91.4 and 98.0%, respectively). Extraction of morphine and naloxone from plasma samples was also efficient (94.3 and 95.6%, respectively). Morphine and naloxone recovery from urine samples (80.3 and 83.2%, respectively) was significantly lower than morphine and naloxone recovery from plasma but was acceptable. The buffered urine sample pH was not significantly lower than the buffered plasma pH, so reduced urine morphine and naloxone extraction efficiency may have been related to the procedure. Urine alkalinization (7) and extraction with a polar solvent might improve the efficiency.

Subcutaneous methadone, morphine, or naloxone was administered to mice to measure selective extraction of parent drugs and metabolites from brain and plasma. The total radioactivity extracted from brain was

chromatographically identical to methadone (80.5%), morphine (95.5%), and naloxone (100%). Total extracted plasma radioactivity represented methadone (76.9%), morphine (75.5%), or naloxone (91.8%). Parent drug extraction selectivity in each case was acceptable.

Timesaving is the greatest advantage of this method. Extraction of 20 tissue samples required 10–15 min; 1.5–2 hr was required with standard liquid–liquid extraction. Since brain and plasma drug concentrations are routinely required in pharmacological studies, the utility of the present method is obvious. Theoretically, the present procedure could be substituted for any organic base or acid solvent extraction from biological fluids and tissues.

REFERENCES

(1) F. C. Tulunay, I. Yano, and A. E. Takemori, *Eur. J. Pharmacol.*, **35**, 285 (1976).

(2) L. Manara, *Res. Commun. Chem. Pathol. Pharmacol.*, **17**, 183 (1977).

(3) G. L. Sprague and A. E. Takemori, *Fed. Proc.*, **37**, 567 (1978).

(4) H. N. Bhargava, *J. Pharm. Sci.*, **66**, 1044 (1977).

(5) E. L. Way and T. K. Adler, *Bull. WHO*, **25**, 227 (1961).

(6) J. Ramsey and D. B. Campbell, *J. Chromatogr.*, **63**, 303 (1971).

(7) J. M. Fujimoto, E. L. Way, and C. H. Hine, *J. Lab. Clin. Med.*, **44**, 627 (1954).

ACKNOWLEDGMENTS

Supported by U.S. Public Health Service Grants DA 00289 and DA 05076.

The authors thank Miss Joan Naeseth for technical assistance.

Effect of Water-Soluble Carriers on Morphine Sulfate Release from a Silicone Polymer

JAMES W. McGINITY ˣ, LOUIS A. HUNKE, and ALAN B. COMBS

Received August 14, 1978, from the *Drug Dynamics Institute, College of Pharmacy, University of Texas, Austin, TX 78712.* Accepted for publication November 2, 1978.

Abstract □ The influence of gelatin, sodium lauryl sulfate, lactose, and sodium alginate on morphine sulfate diffusion from cylindrical silicone polymer pellets was examined in isotonic pH 7.4 phosphate buffer. These water-soluble carriers caused the pellets to swell in aqueous media. Sodium alginate exerted the greatest influence on drug release. The morphine sulfate diffusion rate from the cylindrical pellets increased as the matrix alginate content increased up to 20%. Water-soluble carrier incorporation into silicone polymeric matrixes permits controlled release of water-soluble drugs that otherwise would be released extremely slowly from the polymer. Drug diffusion from the silicone matrix containing sodium alginate followed second-order kinetics. The release mechanism probably involves the creation of pores or pathways through the matrix secondary to the swelling.

Keyphrases □ Morphine sulfate—release from silicone polymer, effect of water-soluble carriers □ Drug delivery systems—morphine sulfate, release from silicone polymer, effect of water-soluble carriers □ Silicone polymers—release of morphine sulfate, effect of water-soluble carriers □ Dosage forms, controlled release—morphine sulfate, release from silicone polymer, effect of water-soluble carriers

The drug release rate from an inert matrix is dependent on solute solubility in the matrix and diffusivity as well as on parameters independent of the particular drug (1). Previous silicone polymer work has been concerned largely with developing long acting steroidal delivery systems and investigating factors controlling drug release from silicone devices (2–9).

The divergent *in vitro* silicone polymer release patterns of four progesterone-type steroids with similar diffusion coefficients were attributed to differences in the polymer steroid solubilities (5). The release of salts and water-soluble drugs from silicone polymers has received little attention. Since polymer drug solubility is an important drug release determinant, water-soluble drug diffusion from a silicone polymer would be expected to be extremely slow.

The present study examined the influence of water-soluble carriers on the *in vitro* morphine sulfate release from a polysiloxane polymer. Recent studies (10, 11) demonstrated that polysiloxane rubber implants containing morphine sulfate and a water-soluble carrier are excellent drug delivery systems for inducing morphine dependence in rats.

EXPERIMENTAL

The following items were used: simethicone liquid[1], polydimethylsiloxane polymer and silica filler[2], stannous octoate[3], morphine sulfate, polysorbate 80[4], sodium alginate[5], sodium chloride, 0.1 *N* HCl, lactose, sodium lauryl sulfate, monobasic sodium phosphate, dibasic sodium phosphate, and microcrystalline cellulose[6].

Pellets were prepared by the addition of simethicone fluid to polydimethylsiloxane elastomer (1:1), followed by homogeneous mixing with the powders to be added. The pellets contained 25% (w/w) morphine sulfate. The drug and water-soluble carrier (lactose, sodium lauryl sulfate, gelatin, or sodium alginate) were passed through a 100-mesh screen prior to mixing with the silicone polymer. To polymerize the mixture, stannous octoate catalyst, 25 mg/g of mixture, was added and dispersed uniformly. Next, the mixture was added rapidly to a plastic tablet mold, and the pellets were allowed to cure for 24 hr.

The cylindrical pellets were 5.5 mm in diameter and 3.5 mm in thickness. The mean weights varied from 78 to 88 mg, depending on the amount of powder embedded in the pellet. Surface area measurements were made with a micrometer. Homogeneity studies were carried out by cutting individual pellets into small pieces and extracting them in 100 ml of purified water for 48 hr. Recoveries of 99 ± 2% were obtained (n = 6).

Drug release from the pellets was studied in screw-capped vials, 1.5 cm diameter × 10.5 cm length, containing 15 ml of phosphate buffer (0.13 *N*, pH 7.4). These vials were maintained at 37° and rotated end-over-end at 15 rpm. Aliquots of 5 ml were withdrawn from the vials at various times and assayed by UV spectrophotometry for morphine. To maintain sink conditions, 5-ml volumes of fresh medium were added to each vial after

[1] Medical fluid 360, 200 cps, Dow Corning Corp., Midland, Mich.
[2] Silastic 382 medical grade elastomer, Dow Corning Corp., Midland, Mich.
[3] Catalyst M, Dow Corning Corp., Midland, Mich.
[4] Tween 80, City Chemical Corp., New York, N.Y.
[5] Kelco Gell LV, Kelco Co., Clark, N.J.
[6] Avicel, FMC Corp., Marcus Hook, Pa.

0022-3549/79/0500-0662$01.00/0

© 1979, American Pharmaceutical Association

chromatographically identical to methadone (80.5%), morphine (95.5%), and naloxone (100%). Total extracted plasma radioactivity represented methadone (76.9%), morphine (75.5%), or naloxone (91.8%). Parent drug extraction selectivity in each case was acceptable.

Timesaving is the greatest advantage of this method. Extraction of 20 tissue samples required 10–15 min; 1.5–2 hr was required with standard liquid–liquid extraction. Since brain and plasma drug concentrations are routinely required in pharmacological studies, the utility of the present method is obvious. Theoretically, the present procedure could be substituted for any organic base or acid solvent extraction from biological fluids and tissues.

REFERENCES

(1) F. C. Tulunay, I. Yano, and A. E. Takemori, *Eur. J. Pharmacol.*, **35**, 285 (1976).

(2) L. Manara, *Res. Commun. Chem. Pathol. Pharmacol.*, **17**, 183 (1977).

(3) G. L. Sprague and A. E. Takemori, *Fed. Proc.*, **37**, 567 (1978).

(4) H. N. Bhargava, *J. Pharm. Sci.*, **66**, 1044 (1977).

(5) E. L. Way and T. K. Adler, *Bull. WHO*, **25**, 227 (1961).

(6) J. Ramsey and D. B. Campbell, *J. Chromatogr.*, **63**, 303 (1971).

(7) J. M. Fujimoto, E. L. Way, and C. H. Hine, *J. Lab. Clin. Med.*, **44**, 627 (1954).

ACKNOWLEDGMENTS

Supported by U.S. Public Health Service Grants DA 00289 and DA 05076.

The authors thank Miss Joan Naeseth for technical assistance.

Effect of Water-Soluble Carriers on Morphine Sulfate Release from a Silicone Polymer

JAMES W. McGINITY ˣ, LOUIS A. HUNKE, and ALAN B. COMBS

Received August 14, 1978, from the *Drug Dynamics Institute, College of Pharmacy, University of Texas, Austin, TX 78712.* Accepted for publication November 2, 1978.

Abstract □ The influence of gelatin, sodium lauryl sulfate, lactose, and sodium alginate on morphine sulfate diffusion from cylindrical silicone polymer pellets was examined in isotonic pH 7.4 phosphate buffer. These water-soluble carriers caused the pellets to swell in aqueous media. Sodium alginate exerted the greatest influence on drug release. The morphine sulfate diffusion rate from the cylindrical pellets increased as the matrix alginate content increased up to 20%. Water-soluble carrier incorporation into silicone polymeric matrixes permits controlled release of water-soluble drugs that otherwise would be released extremely slowly from the polymer. Drug diffusion from the silicone matrix containing sodium alginate followed second-order kinetics. The release mechanism probably involves the creation of pores or pathways through the matrix secondary to the swelling.

Keyphrases □ Morphine sulfate—release from silicone polymer, effect of water-soluble carriers □ Drug delivery systems—morphine sulfate, release from silicone polymer, effect of water-soluble carriers □ Silicone polymers—release of morphine sulfate, effect of water-soluble carriers □ Dosage forms, controlled release—morphine sulfate, release from silicone polymer, effect of water-soluble carriers

The drug release rate from an inert matrix is dependent on solute solubility in the matrix and diffusivity as well as on parameters independent of the particular drug (1). Previous silicone polymer work has been concerned largely with developing long acting steroidal delivery systems and investigating factors controlling drug release from silicone devices (2–9).

The divergent *in vitro* silicone polymer release patterns of four progesterone-type steroids with similar diffusion coefficients were attributed to differences in the polymer steroid solubilities (5). The release of salts and water-soluble drugs from silicone polymers has received little attention. Since polymer drug solubility is an important drug release determinant, water-soluble drug diffusion from a silicone polymer would be expected to be extremely slow.

The present study examined the influence of water-soluble carriers on the *in vitro* morphine sulfate release from a polysiloxane polymer. Recent studies (10, 11) demonstrated that polysiloxane rubber implants containing morphine sulfate and a water-soluble carrier are excellent drug delivery systems for inducing morphine dependence in rats.

EXPERIMENTAL

The following items were used: simethicone liquid[1], polydimethylsiloxane polymer and silica filler[2], stannous octoate[3], morphine sulfate, polysorbate 80[4], sodium alginate[5], sodium chloride, 0.1 *N* HCl, lactose, sodium lauryl sulfate, monobasic sodium phosphate, dibasic sodium phosphate, and microcrystalline cellulose[6].

Pellets were prepared by the addition of simethicone fluid to polydimethylsiloxane elastomer (1:1), followed by homogeneous mixing with the powders to be added. The pellets contained 25% (w/w) morphine sulfate. The drug and water-soluble carrier (lactose, sodium lauryl sulfate, gelatin, or sodium alginate) were passed through a 100-mesh screen prior to mixing with the silicone polymer. To polymerize the mixture, stannous octoate catalyst, 25 mg/g of mixture, was added and dispersed uniformly. Next, the mixture was added rapidly to a plastic tablet mold, and the pellets were allowed to cure for 24 hr.

The cylindrical pellets were 5.5 mm in diameter and 3.5 mm in thickness. The mean weights varied from 78 to 88 mg, depending on the amount of powder embedded in the pellet. Surface area measurements were made with a micrometer. Homogeneity studies were carried out by cutting individual pellets into small pieces and extracting them in 100 ml of purified water for 48 hr. Recoveries of 99 ± 2% were obtained (n = 6).

Drug release from the pellets was studied in screw-capped vials, 1.5 cm diameter × 10.5 cm length, containing 15 ml of phosphate buffer (0.13 *N*, pH 7.4). These vials were maintained at 37° and rotated end-over-end at 15 rpm. Aliquots of 5 ml were withdrawn from the vials at various times and assayed by UV spectrophotometry for morphine. To maintain sink conditions, 5-ml volumes of fresh medium were added to each vial after

[1] Medical fluid 360, 200 cps, Dow Corning Corp., Midland, Mich.
[2] Silastic 382 medical grade elastomer, Dow Corning Corp., Midland, Mich.
[3] Catalyst M, Dow Corning Corp., Midland, Mich.
[4] Tween 80, City Chemical Corp., New York, N.Y.
[5] Kelco Gell LV, Kelco Co., Clark, N.J.
[6] Avicel, FMC Corp., Marcus Hook, Pa.

0022-3549/79/0500-0662$01.00/0

© 1979, American Pharmaceutical Association

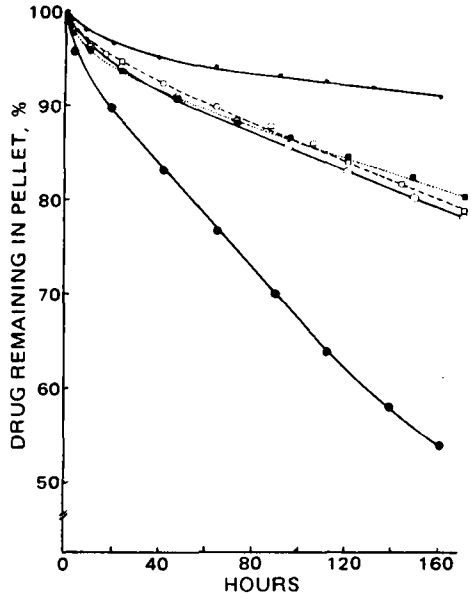

Figure 1—*Influence of various carriers (10% each) on 25% morphine sulfate release from silicone pellets. Key: •, drug alone; ■, gelatin; □, sodium lauryl sulfate; ○, lactose; and ●, sodium alginate.*

sample withdrawal. The reported data represent the means of three or more runs.

RESULTS AND DISCUSSION

The influence of water-soluble carriers on morphine sulfate release from silicone pellets is shown in Fig. 1. As expected, the release of the water-soluble salt from the polymer in the absence of any carrier was very slow; after 1 week, only 9% of the drug was removed from the pellet. This result confirmed the expectation that water-soluble drugs are released slowly from lipophilic silicone matrixes.

The presence of 10% gelatin, sodium lauryl sulfate, or lactose in the silicone matrix all produced similar effects on drug release: approximately 20% of the morphine had diffused from the pellet after 1 week. This value increased to 50% when sodium alginate was incorporated into the matrix.

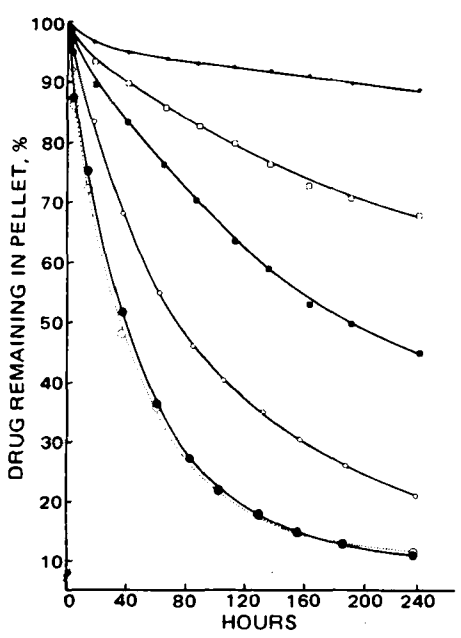

Figure 2—*Influence of sodium alginate concentration formulated within the silicone matrix on 25% morphine sulfate release. Key: •, 0%; □, 5%; ■, 10%; ○, 15%; ●, 20%; and ○, 25%.*

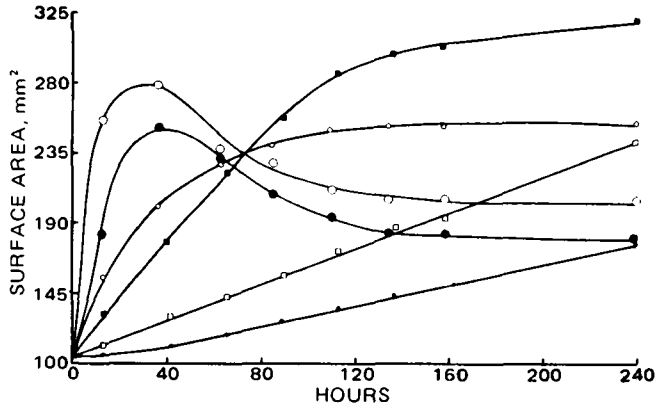

Figure 3—*Plots of Surface area as a function of time for the pellet formulations in Fig. 2.*

With all systems, an initial burst of drug from the pellet lasted for 10–15 hr.

As the sodium alginate content in the matrix was increased, so did the morphine diffusion rate from the polymer (Fig. 2). This influence appeared to be maximal at 20% alginate. One prominent action of each carrier was to swell the pellet. The influence of alginate content on silicone matrix swelling is shown in Fig. 3. Morphine sulfate dissolution from the matrix is probably facilitated by this swelling, which creates microscopic pores or channels from carrier hydration. In the absence of the swelling agent, pellets containing morphine sulfate alone increased in surface area at a uniform rate over the 10-day period studied. This increase was the smallest of the pellets studied, however.

Swelling rates increased during the first 30 hr as the level of sodium alginate in the pellet increased. Pellets containing 20 and 25% alginate achieved maximal surface area at approximately 40 and 30 hr, respectively. The matrix then began to shrink as both the drug and carrier were removed from it (Fig. 3). This phenomenon can be monitored by taking transverse sections of the pellet and measuring the core and the translucent depletion zone.

Morphine diffusion from the silicone matrix (Fig. 4) appeared to follow second-order kinetics with respect to morphine sulfate concentration. The second-order profile correlation coefficients (Fig. 4) for morphine sulfate release from silicone matrixes containing 10, 15, and 20% sodium

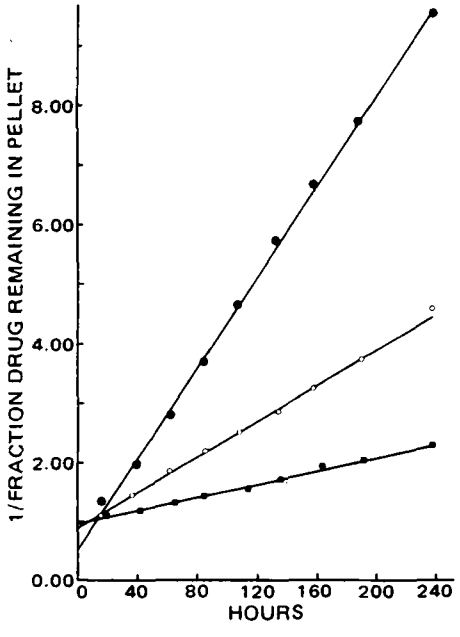

Figure 4—*Second-order profiles for silicone matrixes containing 25% morphine sulfate and three sodium alginate concentrations. Key: ■, 10% sodium alginate; ○, 15% sodium alginate; and ●, 20% sodium alginate.*

alginate were 0.9982, 0.9987, and 0.9983, respectively. The processes giving rise to the second-order elimination from the matrix are not apparent immediately since a shrinking core phenomenon with decreasing core surface area is occurring.

This technique of controlling the diffusion rate from silicone polymers was recently applied by the authors to salts of amphetamine and the barbiturates, and preliminary *in vitro* and *in vivo* results are encouraging. This simple method of drug delivery may find use also in chronic toxicity studies in small animals.

REFERENCES

(1) T. J. Roseman and S. H. Yalkowsky, *J. Pharm. Sci.*, **63**, 1639 (1974).

(2) P. J. Dzuik and B. Cook, *Endocrinology*, **78**, 208 (1966).

(3) C. C. Chang and F. A. Kincl, *Fertil. Steril.*, **21**, 134 (1970).

(4) T. J. Roseman and W. I. Higuchi, *J. Pharm. Sci.*, **59**, 353 (1970).

(5) T. J. Roseman, *ibid.*, **61**, 46 (1972).

(6) J. Haleblian, R. Runkel, N. Mueller, J. Christopherson, and K. Ng, *ibid.*, **60**, 541 (1971).

(7) P. Kratochvil, G. Benagiano, and F. A. Kincl, *Steroids*, **13**, 505 (1970).

(8) Y. W. Chien and H. J. Lambert, *J. Pharm. Sci.*, **63**, 515 (1974).

(9) Y. W. Chien, H. J. Lambert, and D. E. Grant, *ibid.*, **63**, 365 (1974).

(10) J. W. McGinity, C. S. Mehta, and A. B. Combs, "Proceedings of First International Conference on Pharmaceutical Technology," Paris, France, 1976, p. 235.

(11) J. W. McGinity and C. S. Mehta, *Pharmacol. Biochem. Behav.*, **9**, 705 (1978).

ACKNOWLEDGMENTS

Supported in part by a grant from the University Research Institute, University of Texas at Austin.

Wikstromol, Antitumor Lignan from *Wikstroemia foetida* var. *oahuensis* Gray and *Wikstroemia uva-ursi* Gray (Thymelaeaceae)

STERLING J. TORRANCE, JOSEPH J. HOFFMANN, and JACK R. COLE ×

Received September 11, 1978, from the *Department of Pharmaceutical Sciences, College of Pharmacy, University of Arizona, Tucson, AZ 85721.* Accepted for publication November 1, 1978.

Abstract □ The ethanol extracts of *Wikstroemia foetida* var. *oahuensis* and *Wikstroemia uva-ursi* showed antitumor activity against the P-388 lymphocytic leukemia (3PS) test system. One PS-active constituent of both plants was the lignan wikstromol. Several inactive compounds were identified as daphnoretin, pinoresinol, and syringaresinol.

Keyphrases □ Wikstromol—isolation from plant material, antineoplastic activity □ Antineoplastic agents—wikstromol, isolated from plant material

In the continuing search for plants having antitumor constituents, it was found that the chloroform fractions of *Wikstroemia foetida* var. *oahuensis* Gray and *Wikstroemia uva-ursi* Gray[1] (Thymelaeaceae) ethanol extracts were active against the P-388 lymphocytic leukemia (3PS) test system[2].

DISCUSSION

The lignan wikstromol (I) was isolated from both *Wikstroemia* species. This compound was isolated recently from *Wikstroemia viridiflora* (1) and *Daphne odora* (Thymelaeaceae) (2). Wikstromol is the enantiomer of nortrachelogenin (II, also called pinopalustrin), isolated from *Trachelospermum asiaticum* var. *intermedium* (Apocynaceae) (3) and *Pinus palustris* (Pinaceae) (4).

Comparison of the sample spectra (IR, PMR, and mass) with literature values (1, 3) for wikstromol and nortrachelogenin and comparison of the sample's physical constants with those of these two lignans (Table I) suggested that it was wikstromol. Confirmation was by direct comparison of authentic spectra[3] (IR and PMR) and of the sample[3] of the nortrachelogenin dimethyl ether with the study sample dimethyl ether. The spectra were identical, and TLC behaviors were indistinguishable. Unfortunately, the study sample could not be made to crystallize, and an authentic sample of wikstromol, or its dimethyl ether, was unobtainable.

In addition to the PS-active wikstromol, three inactive compounds were isolated from both *W. foetida* var. *oahuensis* and *W. uva-ursi*. These compounds were daphnoretin (III), pinoresinol (IV), and syringaresinol (V). In each case, identity was confirmed by comparison with authentic specimens[4].

Wikstromol (I) demonstrated activities of 154, 146, 137, 141, and 130% test/control (T/C) at does of 16, 10, 4, 2, and 1 mg/kg, respectively. Activity in the PS test system is defined as an increase in the survival of treated animals over that of control animals resulting in a T/C ≥ 130%[5].

EXPERIMENTAL[6]

Wikstromol was isolated similarly from *W. foetida* var. *oahuensis* and *W. uva-ursi*. The procedure for isolation from the former follows.

Whole *W. foetida* var. *oahuensis* plants were ground in a Wiley mill and stored at −10° prior to extraction. The ground material (9 kg) was exhaustively extracted in a Lloyd-type extractor with petroleum ether

[1] *W. foetida* var. *oahuensis* and *W. uva-ursi* were collected in Hawaii in September 1975 and March 1973, respectively. Identification was confirmed by Dr. Robert E. Perdue, Jr., Medicinal Plant Resources Laboratory, U.S. Department of Agriculture, Bethesda, Md. Reference specimens are maintained by the Department of Agriculture.

[2] Of the Drug Evaluation Branch, Drug Research and Development, Division of Cancer Treatment, National Cancer Institute, National Institutes of Health, Bethesda, Md.

[3] The authors are indebted to Prof. Dr. Sansei Nishibe, Department of Pharmacognosy, Higashi Nippon Gakuen University, Ishikari-Tobetsu, Hokkaido, Japan, for spectra and sample of nortrachelogenin dimethyl ether.

[4] The authors thank Prof. Dr. G. Legler, Institute für Biochemie der Universität Köln, Germany, for sample of daphnoretin. They are grateful also to Dr. Cornelius Steelink, Department of Chemistry, University of Arizona, Tucson, Ariz., for specimens of pinoresinol and syringaresinol.

[5] John D. Douros, Natural Products Branch, National Cancer Institute, Bethesda, Md., personal communication, Sept. 1977.

[6] Melting points were determined on a Kofler hot-stage apparatus and are uncorrected. IR and mass spectra were recorded on a Beckman IR-33 and Hewlett-Packard quadrupole spectrometer (model 4930), respectively. PMR spectra were recorded on Varian T-60 and EM-360L spectrometers, and optical rotations were taken on a Perkin-Elmer model 241 MC polarimeter.

0022-3549/79/0500-0664$01.00/0

© 1979, American Pharmaceutical Association

alginate were 0.9982, 0.9987, and 0.9983, respectively. The processes giving rise to the second-order elimination from the matrix are not apparent immediately since a shrinking core phenomenon with decreasing core surface area is occurring.

This technique of controlling the diffusion rate from silicone polymers was recently applied by the authors to salts of amphetamine and the barbiturates, and preliminary *in vitro* and *in vivo* results are encouraging. This simple method of drug delivery may find use also in chronic toxicity studies in small animals.

REFERENCES

(1) T. J. Roseman and S. H. Yalkowsky, *J. Pharm. Sci.*, **63**, 1639 (1974).

(2) P. J. Dzuik and B. Cook, *Endocrinology*, **78**, 208 (1966).

(3) C. C. Chang and F. A. Kincl, *Fertil. Steril.*, **21**, 134 (1970).

(4) T. J. Roseman and W. I. Higuchi, *J. Pharm. Sci.*, **59**, 353 (1970).

(5) T. J. Roseman, *ibid.*, **61**, 46 (1972).

(6) J. Haleblian, R. Runkel, N. Mueller, J. Christopherson, and K. Ng, *ibid.*, **60**, 541 (1971).

(7) P. Kratochvil, G. Benagiano, and F. A. Kincl, *Steroids*, **13**, 505 (1970).

(8) Y. W. Chien and H. J. Lambert, *J. Pharm. Sci.*, **63**, 515 (1974).

(9) Y. W. Chien, H. J. Lambert, and D. E. Grant, *ibid.*, **63**, 365 (1974).

(10) J. W. McGinity, C. S. Mehta, and A. B. Combs, "Proceedings of First International Conference on Pharmaceutical Technology," Paris, France, 1976, p. 235.

(11) J. W. McGinity and C. S. Mehta, *Pharmacol. Biochem. Behav.*, **9**, 705 (1978).

ACKNOWLEDGMENTS

Supported in part by a grant from the University Research Institute, University of Texas at Austin.

Wikstromol, Antitumor Lignan from *Wikstroemia foetida* var. *oahuensis* Gray and *Wikstroemia uva-ursi* Gray (Thymelaeaceae)

STERLING J. TORRANCE, JOSEPH J. HOFFMANN, and JACK R. COLE ×

Received September 11, 1978, from the *Department of Pharmaceutical Sciences, College of Pharmacy, University of Arizona, Tucson, AZ 85721.* Accepted for publication November 1, 1978.

Abstract □ The ethanol extracts of *Wikstroemia foetida* var. *oahuensis* and *Wikstroemia uva-ursi* showed antitumor activity against the P-388 lymphocytic leukemia (3PS) test system. One PS-active constituent of both plants was the lignan wikstromol. Several inactive compounds were identified as daphnoretin, pinoresinol, and syringaresinol.

Keyphrases □ Wikstromol—isolation from plant material, antineoplastic activity □ Antineoplastic agents—wikstromol, isolated from plant material

In the continuing search for plants having antitumor constituents, it was found that the chloroform fractions of *Wikstroemia foetida* var. *oahuensis* Gray and *Wikstroemia uva-ursi* Gray[1] (Thymelaeaceae) ethanol extracts were active against the P-388 lymphocytic leukemia (3PS) test system[2].

DISCUSSION

The lignan wikstromol (I) was isolated from both *Wikstroemia* species. This compound was isolated recently from *Wikstroemia viridiflora* (1) and *Daphne odora* (Thymelaeaceae) (2). Wikstromol is the enantiomer of nortrachelogenin (II, also called pinopalustrin), isolated from *Trachelospermum asiaticum* var. *intermedium* (Apocynaceae) (3) and *Pinus palustris* (Pinaceae) (4).

Comparison of the sample spectra (IR, PMR, and mass) with literature values (1, 3) for wikstromol and nortrachelogenin and comparison of the sample's physical constants with those of these two lignans (Table I) suggested that it was wikstromol. Confirmation was by direct comparison of authentic spectra[3] (IR and PMR) and of the sample[3] of the nortrachelogenin dimethyl ether with the study sample dimethyl ether. The spectra were identical, and TLC behaviors were indistinguishable. Unfortunately, the study sample could not be made to crystallize, and an authentic sample of wikstromol, or its dimethyl ether, was unobtainable.

In addition to the PS-active wikstromol, three inactive compounds were isolated from both *W. foetida* var. *oahuensis* and *W. uva-ursi*. These compounds were daphnoretin (III), pinoresinol (IV), and syringaresinol (V). In each case, identity was confirmed by comparison with authentic specimens[4].

Wikstromol (I) demonstrated activities of 154, 146, 137, 141, and 130% test/control (T/C) at does of 16, 10, 4, 2, and 1 mg/kg, respectively. Activity in the PS test system is defined as an increase in the survival of treated animals over that of control animals resulting in a T/C ≥ 130%[5].

EXPERIMENTAL[6]

Wikstromol was isolated similarly from *W. foetida* var. *oahuensis* and *W. uva-ursi*. The procedure for isolation from the former follows.

Whole *W. foetida* var. *oahuensis* plants were ground in a Wiley mill and stored at −10° prior to extraction. The ground material (9 kg) was exhaustively extracted in a Lloyd-type extractor with petroleum ether

[1] *W. foetida* var. *oahuensis* and *W. uva-ursi* were collected in Hawaii in September 1975 and March 1973, respectively. Identification was confirmed by Dr. Robert E. Perdue, Jr., Medicinal Plant Resources Laboratory, U.S. Department of Agriculture, Bethesda, Md. Reference specimens are maintained by the Department of Agriculture.

[2] Of the Drug Evaluation Branch, Drug Research and Development, Division of Cancer Treatment, National Cancer Institute, National Institutes of Health, Bethesda, Md.

[3] The authors are indebted to Prof. Dr. Sansei Nishibe, Department of Pharmacognosy, Higashi Nippon Gakuen University, Ishikari-Tobetsu, Hokkaido, Japan, for spectra and sample of nortrachelogenin dimethyl ether.

[4] The authors thank Prof. Dr. G. Legler, Institute für Biochemie der Universität Köln, Germany, for sample of daphnoretin. They are grateful also to Dr. Cornelius Steelink, Department of Chemistry, University of Arizona, Tucson, Ariz., for specimens of pinoresinol and syringaresinol.

[5] John D. Douros, Natural Products Branch, National Cancer Institute, Bethesda, Md., personal communication, Sept. 1977.

[6] Melting points were determined on a Kofler hot-stage apparatus and are uncorrected. IR and mass spectra were recorded on a Beckman IR-33 and Hewlett-Packard quadrupole spectrometer (model 4930), respectively. PMR spectra were recorded on Varian T-60 and EM-360L spectrometers, and optical rotations were taken on a Perkin-Elmer model 241 MC polarimeter.

0022-3549/79/0500-0664$01.00/0

© 1979, American Pharmaceutical Association

Table I—Comparison of Physical Constants

Constant	Wikstromol	Study Sample	Nortrachelogenin	Daphne Lignan	Pinopalustrin
Melting point	Amorphous	Amorphous	Amorphous	Amorphous	Amorphous
$[\alpha]_D$	+72° (chloroform)	+41° (chloroform)	−17° (ethanol)	+48°	—
		Dimethyl Ethers			
Melting point	96–97°	Amorphous	97–98.5°	—	96–97°, 127–128°
$[\alpha]_D$	+35° (chloroform)	+26° (chloroform)	−46° (ethanol)	—	−39° (chloroform)

(bp 30–60°) followed by 95% ethanol. The air-dried ethanol extract was partitioned between chloroform and water (1:1). Removal of the solvent from the chloroform phase provided a sticky, green residue (227 g). The latter was extracted with hexane (5 × 0.5 liter) and ether (4 × 0.5 liter), and the hexane-insoluble, ether-soluble material (84 g after solvent removal) was chromatographed over silica gel 60[7] (2 kg, 9.5 × 80 cm). Elution was begun with chloroform–methanol (98:2 v/v), and wikstromol (I) was eluted with chloroform–methanol (97:3 v/v). Final purification of wikstromol was by preparative TLC [chloroform–methanol–water (188:12:1 v/v/v)].

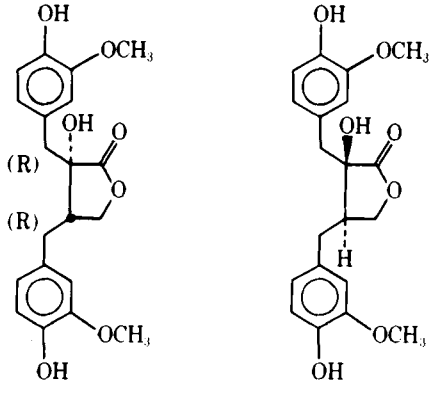

I

II

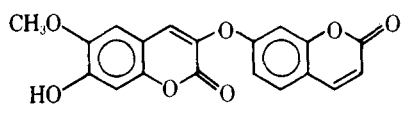

III

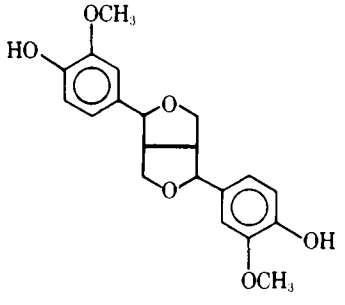

IV

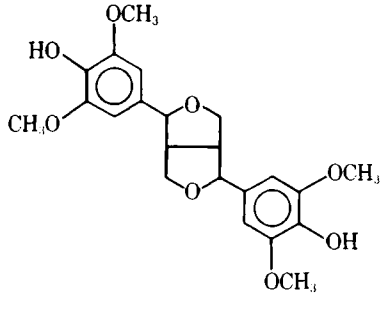

V

Wikstromol was obtained as an amorphous powder, $[\alpha]_D^{25}$ +41° (c 0.93, $CHCl_3$) whose IR, PMR, and mass spectra were identical to those reported for wikstromol (1) and nortrachelogenin (3).

Wikstromol dimethyl ether, prepared in the usual way with diazomethane, was obtained as an amorphous semisolid, $[\alpha]_D^{25}$ +26.3° (c 1.09, $CHCl_3$). Its spectra (IR, PMR, and mass) were in accord with those in the literature (1, 3), and its IR and PMR spectra were identical in all respects with authentic nortrachelogenin dimethyl ether spectra[3]. In several solvent systems, TLC behaviors of our material and authentic nortrachelogenin dimethyl ether[3] were indistinguishable.

Daphnoretin (III) and syringaresinol (V) were isolated from other fractions of the preparative TLC used to obtain wikstromol. Daphnoretin was obtained as yellow needles, mp 246–248°. Recrystallization from methanol–chloroform provided colorless needles, mp 261–262°. Comparison with an authentic sample (identical IR spectra and undepressed mixed melting point) confirmed its identity. The PMR and mass spectra were in accord with Structure III. Syringaresinol was obtained as colorless cubelets from methanol, mp 178–180°. Comparison with an authentic specimen[4] (identical IR and undepressed mixed melting point) confirmed its identity.

Pinoresinol (IV) was obtained from the wikstromol-containing column fraction by preparative TLC using benzene–ethyl acetate–methanol (30:10:2 v/v/v). Recrystallization from ether gave colorless cubelets, mp 120–121°, identical (superimposable IR spectra and undepressed mixed melting point) with an authentic sample[4].

REFERENCES

(1) S. Tandon, and R. P. Rastogi, *Phytochemistry*, **1976**, 1789.

(2) S. Kogiso, K. Wada, and K. Munakata, "Report of the 26th International Congress of Pure and Applied Chemistry," Tokyo, Japan, 1977, p. 291.

(3) S. Nishibe, S. Hisada, and I. Inagaki, *Phytochemistry*, **1971**, 2231. S. Nishibe, S. Hisada, and I. Inagaki, *Chem. Pharm. Bull.*, **19** (4), 866 (1971). *Ibid.*, **20** (9), 2075 (1972). *Ibid.*, **20** (12), 2710 (1972). *Ibid.*, **21** (5), 1108 (1973).

(4) B. Carnmalm, H. G. H. Erdtman, G. C. Harris, and T. F. Sanderson, *Acta Chem. Scand.*, **B31**, 433 (1977).

ACKNOWLEDGMENTS

Supported in part by Contract NOI-CM-33750 from the Division of Cancer Treatment, National Cancer Institute, National Institutes of Health, Bethesda, MD 20014; The Elsa U. Pardee Foundation, Midland, MI 48640; and Grant 1-R01-CA22336-01A1 from the National Cancer Institute.

[7] Merck.

Effect of UV Irradiation and Tritiation on Hydroxyzine

Keyphrases □ Hydroxyzine—decomposition by UV irradiation, tritiation, degradation products □ Tranquilizers, minor—hydroxyzine, UV photodecomposition, tritiation, degradation products □ Chlorobenzophenone—degradation product of hydroxyzine following UV irradiation

To the Editor:

Hydroxyzine, a diphenylmethane minor tranquilizer, is commercially available as a tablet, syrup, suspension, and solution. It is an effective antianxiety agent (1) and is particularly useful in its ability to render disturbed patients more approachable and amenable to psychotherapy. Recently, it was shown to be more effective than cyproheptadine in pruritus treatment (2).

An aqueous hydroxyzine solution turned dark brown in the air (3), and hydroxyzine was photodegraded by UV light to give three spots on TLC (4). During the purification of tritiated hydroxyzine for the metabolic study (5), the tritiated hydroxyzine solution gradually turned dark brown in the air under room light. Therefore, hydroxyzine susceptibility to oxidative deterioration in the presence of light is apparent. Since the nature of the degradative products of hydroxyzine is still unknown, the effect of UV irradiation on hydroxyzine was studied. In a preliminary experiment, the aqueous hydroxyzine solution turned slightly brown in the dark and >90% of the hydroxyzine remained unchanged.

Three grams of hydroxyzine hydrochloride was dissolved in 20 ml of distilled water and irradiated under a UV lamp (3660 Å, 100 w) at a distance of 20 cm for 3 days. The reaction mixture, which was white material in the brown solution, was extracted three times with two volumes of cyclohexane. The combined extracts were dehydrated over anhydrous sodium sulfate and filtered through 10 g of activated magnesium silicate in a Büchner funnel. The solvent was evaporated *in vacuo*, and the colorless residue was sublimed at 70° at 5 mm Hg pressure to give white crystals.

The product was soluble in organic solvent and insoluble in water. It was negative to Dragendorff and iodoplatinate reagents, indicating the absence of a piperazine ring. It was positive to the 2,4-dinitrophenylhydrazine test, and its IR spectrum showed a strong peak at 6.1 μm attributable to a ketone group. It gave a positive Beilstein test, indicating the presence of a chloride atom. It fluoresced strongly under UV light, implicating a highly conjugated system in the structure. The information suggested that the product was *p*-chlorobenzophenone.

Anal.—Calc. for $C_{13}H_9ClO$: C, 72.07; H, 4.7. Found: C, 71.96; H, 4.24.

Moreover, the product had TLC behavior, UV (UV_{max} 211 and 261 in ethanol) and IR spectra, and a melting point (77–78° uncorrected) identical to those of authentic *p*-chlorobenzophenone. Therefore, the product was identified as *p*-chlorobenzophenone. The yield was ~13%. The mother liquor of the reaction mixture was yellowish brown and became darker on standing in the air at room temperature. The mixture contained at least four yellowish Dragendorff-positive compounds separable by silica gel TLC in chloroform containing 2% methanol. Characterization of the products was not attempted further.

This finding prompted us to identify the tritiation degradation products of hydroxyzine. Hydroxyzine (1 g) was tritiated[1] according to Wilzbach's method (6) by exposing it to 3 Ci of tritium gas at 250 mm Hg pressure at 26° for 2 weeks. The unpurified product gave five distinct dark spots on the fluorogram (7) of the silica gel sheet[2], developed in cyclohexane–benzene–diethylamine (75:15:10), with R_f values and percentages of radioactivity as follows: 0, 16%; 0.24, 12%; 0.46, 19%; 0.70, 8%; and 0.88, 45%.

The silica gel zones with R_f 0.46 and 0.88 were scraped off, purified, chromatographed in other solvent systems, and identified as hydroxyzine and *p*-chlorobenzophenone, respectively. The tritiated product was purified according to Wilzbach (8). The specific activities of the tritiated hydroxyzine before and after purification were 154 and 16.3 μCi/mg, respectively. The decrease in specific activity after purification indicated that contaminants with high specific activities formed during the tritiation procedure were removed.

This study indicates that hydroxyzine in aqueous solution is very unstable on UV irradiation and that hydroxyzine is also vulnerable to tritiation. In either case, *p*-chlorobenzophenone was a main decomposition product.

(1) S. F. Barranco and W. Bridger, *Curr. Ther. Res.*, **22**, 217 (1977).
(2) C. S. Barof, *ibid.*, **19**, 32 (1976).
(3) E. R. Hammarlund and G. L. Van Pevenage, *J. Pharm. Sci.*, **55**, 1448 (1966).
(4) J. Pawlaczyk, *Poznan. Tow. Przyjl. Nauk Wydz. Lek. Pr. Kom. Farm.*, **5**, 117 (1966).
(5) S. F. Pong and C. L. Huang, *J. Pharm. Sci.*, **63**, 1527 (1974).
(6) K. E. Wilzbach, *J. Am. Chem. Soc.*, **79**, 1913 (1957).
(7) U. Luthi and P. G. Waser, *Nature*, **205**, 1190 (1965).
(8) K. E. Wilzbach, *Adv. Tracer Methodol.*, **1**, 4 (1963).

S. F. Pong [*x]
C. L. Huang [‡]
Department of Pharmacology
School of Pharmacy
University of Mississippi
University, MS 38677

Received December 8, 1978.
Accepted for publication March 14, 1979.
Abstracted in part from a dissertation submitted by S. F. Pong to the University of Mississippi in partial fulfillment of the Doctor of Philosophy degree requirements.
Supported by Public Health Service Grant MH-11927 from the National Institute of Mental Health, Bethesda, MD 20014.
Hydroxyzine was generously supplied by Chas. Pfizer & Co., New York, N.Y.

*Present address: Norwich-Eaton Pharmaceuticals, Norwich, NY 13815.
‡Present address: Medicinal Research Laboratories, Takeda Chemical Industries, Ltd., Osaka, Japan.

[1] New England Nuclear Corp., Boston, Mass.
[2] Eastman Chromagram 6060.

0022-3549/79/0500-0666$01.00/0
© 1979, American Pharmaceutical Association

Synthesis of 9-Allyladenine N^1-Oxide

Keyphrases □ Allyl adenine N^1-oxide—chemical synthesis □ Hypolipidemic agents—allyl adenine N^1-oxide, chemical synthesis

To the Editor:

During our investigations of novel hypolipidemic agents (1), we desired to synthesize 9-(2,3-epoxypropyl)adenine (III) by the reaction of *m*-chloroperoxybenzoic acid with 9-allyladenine (I) as described previously (2). Compound III was not obtained, although the decomposition point and NMR data in trifluoroacetic acid were consistent with the literature (2). For comparison, the spectrum of I in trifluoroacetic acid was taken. No difference in the chemical shifts of the protons in the side chain between I and the oxidized material was observed (Scheme I). However, there was a difference in the ring protons.

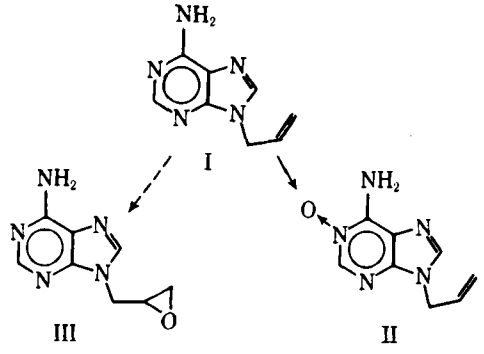

Scheme I

A spectrum of the oxidized material in dimethyl sulfoxide-d_6 was obtained by using a Fourier transform NMR (650 scans, saturated 1.5-ml sample). This spectrum was consistent with the N^1-oxide (II). A shift downfield of the C_2 ring proton and a splitting of the nitrogen protons occurred[1]. The fact that no change in the chemical shift of the olefinic protons in dimethyl sulfoxide-d_6 was observed establishes this material as the N^1-oxide. This product also is more consistent with the literature, since peroxidation of 9-substituted adenines using hydrogen peroxide or *m*-chloroperoxybenzoic acid gives the N^1-oxide (3).

(1) W. S. DiMenna, C. Piantadosi, and R. Lamb, *J. Med. Chem.*, **21**, 1073 (1978).

(2) K. Kondo, K. Kuwata, and K. Takemoto, *Makromol. Chem.*, **160**, 341 (1972).

(3) J. P. Miller and R. K. Robins, *Ann. Rep. Med. Chem.*, **11**, 291 (1976).

William S. DiMenna ˣ
Claude Piantadosi
Department of Medicinal Chemistry
School of Pharmacy
University of North Carolina
Chapel Hill, NC 27514

Received December 12, 1978.
Accepted for publication March 14, 1979.

[1] Fourier transform NMR (dimethyl sulfoxide-d_6): δ 8.58 and 8.23 (2s, 2, adenine CH), 7.89 and 7.59 (m, 2, NH_2), 6.05 (m, 1, olefinic CH), 5.23 (m, 2, olefinic), and 4.82 (m, 2, CH_2). Analyzed ($C_8H_9N_5O$) for carbon, hydrogen, and nitrogen.

Temperature-Dependent Aqueous Solubilities of Lidocaine, Mepivacaine, and Bupivacaine

Keyphrases □ Lidocaine—aqueous solubility, effect of temperature □ Mepivacaine—aqueous solubility, effect of temperature □ Bupivacaine—aqueous solubility, effect of temperature □ Local anesthetics—aqueous solubility, effect of temperature

To the Editor:

We previously prepared 3-hydroxy-2-naphthoates of lidocaine, mepivacaine, and bupivacaine to prolong the duration of action of these local anesthetics through their sparingly soluble salt forms and studied their dissolution characteristics at 37° in 0.7 *M* phosphate buffer, pH 7.46 (1). Only the bupivacaine salt exhibited unusual dissolution characteristics. At equilibrium, the solution was saturated incongruously with respect to the base and the acid component. Further studies with the bupivacaine salt at 25° showed no such unusual behavior. The unusual behavior at 37° resulted from the fact that the concentration of the base component dissolved out of the solid salt exceeded the solubility of the base at 37° (2).

These observations prompted us to examine the temperature dependency of aqueous solubilities of bupivacaine and its structural analogs, lidocaine and mepivacaine. The only available data on the solubility of these local anesthetics at different temperatures were those of Setnikar (3), who reported lidocaine solubility in an alkaline medium to be 16 m*M* at 20° and 15 m*M* at 37°.

Lidocaine base[1] and mepivacaine base[2] were used as received. Bupivacaine hydrochloride[2] was converted to the base for solubility determination. Excess base was placed in a 20-ml glass-stoppered test tube together with a small magnetic stirring bar. Two milliliters of either 0.5 *M* phosphate buffer[3], pH 7.4[4], or 1–4 m*M* NaOH was added to it. The test tube was placed in a jacketed beaker and mounted on the platform of a magnetic stirrer, together with a magnet bar and water. The water temperature inside the jacketed beaker was maintained constant with water circulated through the jacket by a constant-temperature circulator[5].

After equilibration for 16–48 hr at different temperatures, the solid phase was separated by vacuum filtration through a glass filter. All glassware used in the filtration process and subsequent sampling was preincubated to the study temperature. The filtrate was suitably diluted for spectrophotometric assay for lidocaine and mepivacaine at 262 nm. The bupivacaine equilibrium concentration was determined, after extraction with methylene chloride, by GLC[6], using a 3% OV-17 column (4) and mepivacaine as an internal standard.

As with bupivacaine (2), lidocaine and mepivacaine showed decreases in solubility with increasing temperature

[1] Fujisawa Pharmaceutical Co., Osaka, Japan.
[2] Yoshitomi Pharmaceutical Industries, Osaka, Japan.
[3] Composition at the time of preparation was 0.427 *M* Na_2HPO_4 and 0.0710 *M* NaH_2PO_4.
[4] Digital 112 research pH meter, Corning Scientific Instruments, Medfield, Mass.
[5] Haake model FK 10.
[6] Shimadzu model GC-4BM gas chromatograph.

0022-3549/79/0500-0667$01.00/0
© 1979, American Pharmaceutical Association

Synthesis of 9-Allyladenine N^1-Oxide

Keyphrases □ Allyl adenine N^1-oxide—chemical synthesis □ Hypolipidemic agents—allyl adenine N^1-oxide, chemical synthesis

To the Editor:

During our investigations of novel hypolipidemic agents (1), we desired to synthesize 9-(2,3-epoxypropyl)adenine (III) by the reaction of *m*-chloroperoxybenzoic acid with 9-allyladenine (I) as described previously (2). Compound III was not obtained, although the decomposition point and NMR data in trifluoroacetic acid were consistent with the literature (2). For comparison, the spectrum of I in trifluoroacetic acid was taken. No difference in the chemical shifts of the protons in the side chain between I and the oxidized material was observed (Scheme I). However, there was a difference in the ring protons.

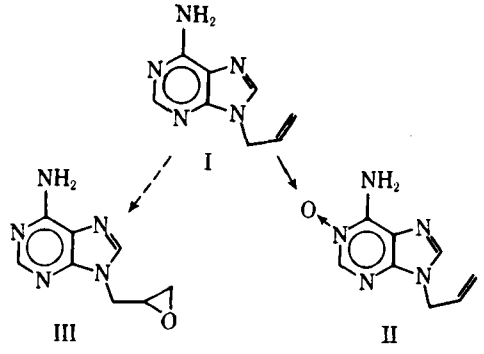

Scheme I

A spectrum of the oxidized material in dimethyl sulfoxide-d_6 was obtained by using a Fourier transform NMR (650 scans, saturated 1.5-ml sample). This spectrum was consistent with the N^1-oxide (II). A shift downfield of the C_2 ring proton and a splitting of the nitrogen protons occurred[1]. The fact that no change in the chemical shift of the olefinic protons in dimethyl sulfoxide-d_6 was observed establishes this material as the N^1-oxide. This product also is more consistent with the literature, since peroxidation of 9-substituted adenines using hydrogen peroxide or *m*-chloroperoxybenzoic acid gives the N^1-oxide (3).

(1) W. S. DiMenna, C. Piantadosi, and R. Lamb, *J. Med. Chem.*, **21**, 1073 (1978).

(2) K. Kondo, K. Kuwata, and K. Takemoto, *Makromol. Chem.*, **160**, 341 (1972).

(3) J. P. Miller and R. K. Robins, *Ann. Rep. Med. Chem.*, **11**, 291 (1976).

William S. DiMenna ˣ
Claude Piantadosi
Department of Medicinal Chemistry
School of Pharmacy
University of North Carolina
Chapel Hill, NC 27514

Received December 12, 1978.
Accepted for publication March 14, 1979.

[1] Fourier transform NMR (dimethyl sulfoxide-d_6): δ 8.58 and 8.23 (2s, 2, adenine CH), 7.89 and 7.59 (m, 2, NH_2), 6.05 (m, 1, olefinic CH), 5.23 (m, 2, olefinic), and 4.82 (m, 2, CH_2). Analyzed ($C_8H_9N_5O$) for carbon, hydrogen, and nitrogen.

Temperature-Dependent Aqueous Solubilities of Lidocaine, Mepivacaine, and Bupivacaine

Keyphrases □ Lidocaine—aqueous solubility, effect of temperature □ Mepivacaine—aqueous solubility, effect of temperature □ Bupivacaine—aqueous solubility, effect of temperature □ Local anesthetics—aqueous solubility, effect of temperature

To the Editor:

We previously prepared 3-hydroxy-2-naphthoates of lidocaine, mepivacaine, and bupivacaine to prolong the duration of action of these local anesthetics through their sparingly soluble salt forms and studied their dissolution characteristics at 37° in 0.7 *M* phosphate buffer, pH 7.46 (1). Only the bupivacaine salt exhibited unusual dissolution characteristics. At equilibrium, the solution was saturated incongruously with respect to the base and the acid component. Further studies with the bupivacaine salt at 25° showed no such unusual behavior. The unusual behavior at 37° resulted from the fact that the concentration of the base component dissolved out of the solid salt exceeded the solubility of the base at 37° (2).

These observations prompted us to examine the temperature dependency of aqueous solubilities of bupivacaine and its structural analogs, lidocaine and mepivacaine. The only available data on the solubility of these local anesthetics at different temperatures were those of Setnikar (3), who reported lidocaine solubility in an alkaline medium to be 16 m*M* at 20° and 15 m*M* at 37°.

Lidocaine base[1] and mepivacaine base[2] were used as received. Bupivacaine hydrochloride[2] was converted to the base for solubility determination. Excess base was placed in a 20-ml glass-stoppered test tube together with a small magnetic stirring bar. Two milliliters of either 0.5 *M* phosphate buffer[3], pH 7.4[4], or 1–4 m*M* NaOH was added to it. The test tube was placed in a jacketed beaker and mounted on the platform of a magnetic stirrer, together with a magnet bar and water. The water temperature inside the jacketed beaker was maintained constant with water circulated through the jacket by a constant-temperature circulator[5].

After equilibration for 16–48 hr at different temperatures, the solid phase was separated by vacuum filtration through a glass filter. All glassware used in the filtration process and subsequent sampling was preincubated to the study temperature. The filtrate was suitably diluted for spectrophotometric assay for lidocaine and mepivacaine at 262 nm. The bupivacaine equilibrium concentration was determined, after extraction with methylene chloride, by GLC[6], using a 3% OV-17 column (4) and mepivacaine as an internal standard.

As with bupivacaine (2), lidocaine and mepivacaine showed decreases in solubility with increasing temperature

[1] Fujisawa Pharmaceutical Co., Osaka, Japan.
[2] Yoshitomi Pharmaceutical Industries, Osaka, Japan.
[3] Composition at the time of preparation was 0.427 *M* Na_2HPO_4 and 0.0710 *M* NaH_2PO_4.
[4] Digital 112 research pH meter, Corning Scientific Instruments, Medfield, Mass.
[5] Haake model FK 10.
[6] Shimadzu model GC-4BM gas chromatograph.

0022-3549/79/0500-0667$01.00/0
© 1979, American Pharmaceutical Association

Table I—Temperature-Dependent Solubilities [a] (Millimolar) of Lidocaine, Mepivacaine, and Bupivacaine in 0.5 *M* Phosphate Buffer, pH 7.4 [b], and 1–4 m*M* NaOH [c]

Temperature [d]	Lidocaine		Mepivacaine		Bupivacaine	
	0.5 *M* Phosphate Buffer	1–4 m*M* NaOH	0.5 *M* Phosphate Buffer	1–4 m*M* NaOH	0.5 *M* Phosphate Buffer	1–4 m*M* NaOH
14.5°	30.3 ± 1.4	—	17.1	—	1.35	—
14.9°	—	18.5 ± 0.5	—	13.6 ± 0.3	—	0.375 ± 0.003
25.0°	22.9 ± 0.1	16.3 ± 0.1	13.5	10.2 ± 0.4	0.850 ± 0.020	0.318 ± 0.002
34.5°	—	14.6 ± 0.1	—	9.91 ± 0.20	—	0.313 ± 0.004
37.0°	16.5	—	9.90	—	0.575 ± 0.008	—

[a] Either the result of a single determination or average (two or three determinations) ± *SE*. [b] Composition at the time of preparation was 0.427 *M* Na_2HPO_4 and 0.0710 *M* NaH_2PO_4, pH 7.40 ± 0.01 at 25° and 7.38 ± 0.01 at 37°. [c] The pH varied from 10.43 (1 m*M* at 34.5°) to 11.86 (4 m*M* at 14.9°). [d] Temperature control was ±0.1°.

in the phosphate buffer (Table I). Since the pKa of these bases varied at 23° from 7.78 for mepivacaine to 8.09 for bupivacaine (5), at pH 7.4 these local anesthetics existed as a mixture of protonated and unprotonated forms. Thus, the solubilities of the unprotonated base species were determined in 1–4 m*M* NaOH. The solubilities in these high pH media were independent of hydroxyl-ion concentration and increased with decreasing temperature (Table I), although this trend was not as great as in the phosphate buffer.

The difference in temperature dependency is now being studied in our laboratories and is probably due to a measurable decrease in the pKa values of the bases with increasing temperature whereas the phosphate buffer pH remains relatively constant (Table I, footnote *b*). Our preliminary determination of lidocaine pKa values at different temperatures by the solubility method indicated that they vary from 8.2 at 15° to 7.7 at 35°. With increasing temperature, therefore, the gap between the medium pH and the pKa diminishes. Thus, the proportion of the soluble protonated base, BH^+, decreases with increasing temperature, which is reflected greatly in the total solubility, S_t, of the base at pH around 7.4; *i.e.*, S_t is given by (6):

$$S_t = [B] + [BH^+] = S_0\left(1 + \frac{[H^+]}{K_a}\right) \qquad \text{(Eq. 1)}$$

where $[B] = S_0$ is the solubility of the unprotonated species and K_a is the acid dissociation constant of BH^+. Since S_0 decreases and K_a increases as the temperature is increased (Eq. 1) at pH 7.4, both of these effects contribute to lower solubility at higher temperatures.

Since the unusual temperature-dependent solubility is likely to extend over a fairly wide pH range, including physiological pH, the following clinical problem could arise. In parenteral dosage forms of these drugs as local anesthetics, solution is effected by means of their hydrochloride salts. Therefore, the pH of these preparations can be as low as 3.0–4.5 (7). The results of the present study suggest possible precipitation of the base at the injection site from the following two points: (*a*) an increase in pH to the tissue pH after injection, as was suggested earlier for lidocaine (8); and (*b*) a lowering of free base solubility at body temperature relative to ambient temperature.

For most organic compounds, solubilities are usually assumed to increase with temperature. These local anesthetics, however, behave differently. Even if the decrease in solubility with increasing temperature at pH values of around 7.4 is mainly attributable to a decrease in the fraction of protonated species because of a shift in pKa with increasing temperature, the unprotonated species also show atypical temperature-dependent solubilities. Only a few organic medicinal compounds are known to exhibit such behavior. These include anhydrous ampicillin (9), dactinomycin (10), aminopyrine and propyphenazone (11), and colchicine (12).

(1) N. I. Nakano, N. Kawahara, T. Amiya, Y. Gotoh, and K. Furukawa, *Chem. Pharm. Bull.*, **26**, 936 (1978).

(2) N. I. Nakano and A. Setoya, *J. Pharm. Pharmacol.*, in press.

(3) I. Setnika, *J. Pharm. Sci.*, **55**, 1190 (1966).

(4) A. Berlin, E. A. Persson, and P. Belfrage, *J. Pharm. Pharmacol.*, **25**, 466 (1973).

(5) P. Friberger and G. Åberg, *Acta Pharm. Suec.*, **8**, 361 (1971).

(6) S. F. Kramer and G. L. Flynn, *J. Pharm. Sci.*, **61**, 1896 (1972).

(7) "British Pharmacopoeia 1973," Her Majesty's Stationery Office, London, England, 1973, pp. 70, 265.

(8) B. E. Ballard, *J. Pharm. Sci.*, **64**, 781 (1975).

(9) L. W. Poole and C. K. Bahal, *ibid.*, **59**, 1265 (1970).

(10) S. N. Giri and L. R. Kartt, *Experientia*, **31**, 482 (1974).

(11) Y. Morimoto, R. Hori, and T. Arita, *Chem. Pharm. Bull.*, **22**, 2217 (1974).

(12) M. Nakano, Y. Uematsu, and T. Arita, *ibid.*, **25**, 1109 (1977).

Naomi I. Nakano

Hokkaido Institute of Pharmaceutical Sciences
Otaru 047-02, Japan

Received March 27, 1978.

Accepted for publication March 6, 1979.

I thank Mr. T. Oshio, Miss A. Setoya, and Miss A. Kotsutsumi for technical assistance.

Carbocyclic Analog of Cytarabine

Keyphrases □ Cytarabine, analogs—synthesis, carbocyclic analog, antileukemic activity □ Antineoplastic agents—cytarabine, carbocyclic analog, synthesis □ Antineoplastic activity—cytarabine, carbocyclic analog

To the Editor:

Cytarabine (1-β-D-arabinofuranosylcytosine, Ara-C) inhibits a variety of experimental neoplasma (1, 2), produces remissions in some patients with acute myelocytic or acute lymphocytic leukemia (3–5), and is considered the most effective single-drug treatment for acute myelogenous leukemia (6). It is also effective in suppressing the replication of certain DNA viruses (2) and is a useful agent for the clinical treatment of herpes virus infections (7). Recently, we reported (8) the synthesis and activity of the carbocyclic analog (carbodine, I) of cytidine against a murine leukemia (L-1210). Brockman *et al.* (9) showed that carbodine inhibits both DNA and RNA synthesis in

0022-3549/79/0500-0668$01.00/0

© 1979, American Pharmaceutical Association

Table I—Temperature-Dependent Solubilities [a] (Millimolar) of Lidocaine, Mepivacaine, and Bupivacaine in 0.5 *M* Phosphate Buffer, pH 7.4 [b], and 1–4 m*M* NaOH [c]

Temperature [d]	Lidocaine		Mepivacaine		Bupivacaine	
	0.5 *M* Phosphate Buffer	1–4 m*M* NaOH	0.5 *M* Phosphate Buffer	1–4 m*M* NaOH	0.5 *M* Phosphate Buffer	1–4 m*M* NaOH
14.5°	30.3 ± 1.4	—	17.1	—	1.35	—
14.9°	—	18.5 ± 0.5	—	13.6 ± 0.3	—	0.375 ± 0.003
25.0°	22.9 ± 0.1	16.3 ± 0.1	13.5	10.2 ± 0.4	0.850 ± 0.020	0.318 ± 0.002
34.5°	—	14.6 ± 0.1	—	9.91 ± 0.20	—	0.313 ± 0.004
37.0°	16.5	—	9.90	—	0.575 ± 0.008	—

[a] Either the result of a single determination or average (two or three determinations) ± *SE*. [b] Composition at the time of preparation was 0.427 *M* Na_2HPO_4 and 0.0710 *M* NaH_2PO_4, pH 7.40 ± 0.01 at 25° and 7.38 ± 0.01 at 37°. [c] The pH varied from 10.43 (1 m*M* at 34.5°) to 11.86 (4 m*M* at 14.9°). [d] Temperature control was ±0.1°.

in the phosphate buffer (Table I). Since the pKa of these bases varied at 23° from 7.78 for mepivacaine to 8.09 for bupivacaine (5), at pH 7.4 these local anesthetics existed as a mixture of protonated and unprotonated forms. Thus, the solubilities of the unprotonated base species were determined in 1–4 m*M* NaOH. The solubilities in these high pH media were independent of hydroxyl-ion concentration and increased with decreasing temperature (Table I), although this trend was not as great as in the phosphate buffer.

The difference in temperature dependency is now being studied in our laboratories and is probably due to a measurable decrease in the pKa values of the bases with increasing temperature whereas the phosphate buffer pH remains relatively constant (Table I, footnote *b*). Our preliminary determination of lidocaine pKa values at different temperatures by the solubility method indicated that they vary from 8.2 at 15° to 7.7 at 35°. With increasing temperature, therefore, the gap between the medium pH and the pKa diminishes. Thus, the proportion of the soluble protonated base, BH^+, decreases with increasing temperature, which is reflected greatly in the total solubility, S_t, of the base at pH around 7.4; *i.e.*, S_t is given by (6):

$$S_t = [B] + [BH^+] = S_0\left(1 + \frac{[H^+]}{K_a}\right) \qquad \text{(Eq. 1)}$$

where $[B] = S_0$ is the solubility of the unprotonated species and K_a is the acid dissociation constant of BH^+. Since S_0 decreases and K_a increases as the temperature is increased (Eq. 1) at pH 7.4, both of these effects contribute to lower solubility at higher temperatures.

Since the unusual temperature-dependent solubility is likely to extend over a fairly wide pH range, including physiological pH, the following clinical problem could arise. In parenteral dosage forms of these drugs as local anesthetics, solution is effected by means of their hydrochloride salts. Therefore, the pH of these preparations can be as low as 3.0–4.5 (7). The results of the present study suggest possible precipitation of the base at the injection site from the following two points: (*a*) an increase in pH to the tissue pH after injection, as was suggested earlier for lidocaine (8); and (*b*) a lowering of free base solubility at body temperature relative to ambient temperature.

For most organic compounds, solubilities are usually assumed to increase with temperature. These local anesthetics, however, behave differently. Even if the decrease in solubility with increasing temperature at pH values of around 7.4 is mainly attributable to a decrease in the fraction of protonated species because of a shift in pKa with increasing temperature, the unprotonated species also show atypical temperature-dependent solubilities. Only a few organic medicinal compounds are known to exhibit such behavior. These include anhydrous ampicillin (9), dactinomycin (10), aminopyrine and propyphenazone (11), and colchicine (12).

(1) N. I. Nakano, N. Kawahara, T. Amiya, Y. Gotoh, and K. Furukawa, *Chem. Pharm. Bull.*, **26**, 936 (1978).

(2) N. I. Nakano and A. Setoya, *J. Pharm. Pharmacol.*, in press.

(3) I. Setnika, *J. Pharm. Sci.*, **55**, 1190 (1966).

(4) A. Berlin, E. A. Persson, and P. Belfrage, *J. Pharm. Pharmacol.*, **25**, 466 (1973).

(5) P. Friberger and G. Åberg, *Acta Pharm. Suec.*, **8**, 361 (1971).

(6) S. F. Kramer and G. L. Flynn, *J. Pharm. Sci.*, **61**, 1896 (1972).

(7) "British Pharmacopoeia 1973," Her Majesty's Stationery Office, London, England, 1973, pp. 70, 265.

(8) B. E. Ballard, *J. Pharm. Sci.*, **64**, 781 (1975).

(9) L. W. Poole and C. K. Bahal, *ibid.*, **59**, 1265 (1970).

(10) S. N. Giri and L. R. Kartt, *Experientia*, **31**, 482 (1974).

(11) Y. Morimoto, R. Hori, and T. Arita, *Chem. Pharm. Bull.*, **22**, 2217 (1974).

(12) M. Nakano, Y. Uematsu, and T. Arita, *ibid.*, **25**, 1109 (1977).

Naomi I. Nakano

Hokkaido Institute of Pharmaceutical Sciences
Otaru 047-02, Japan

Received March 27, 1978.

Accepted for publication March 6, 1979.

I thank Mr. T. Oshio, Miss A. Setoya, and Miss A. Kotsutsumi for technical assistance.

Carbocyclic Analog of Cytarabine

Keyphrases □ Cytarabine, analogs—synthesis, carbocyclic analog, antileukemic activity □ Antineoplastic agents—cytarabine, carbocyclic analog, synthesis □ Antineoplastic activity—cytarabine, carbocyclic analog

To the Editor:

Cytarabine (1-β-D-arabinofuranosylcytosine, Ara-C) inhibits a variety of experimental neoplasma (1, 2), produces remissions in some patients with acute myelocytic or acute lymphocytic leukemia (3–5), and is considered the most effective single-drug treatment for acute myelogenous leukemia (6). It is also effective in suppressing the replication of certain DNA viruses (2) and is a useful agent for the clinical treatment of herpes virus infections (7). Recently, we reported (8) the synthesis and activity of the carbocyclic analog (carbodine, I) of cytidine against a murine leukemia (L-1210). Brockman *et al.* (9) showed that carbodine inhibits both DNA and RNA synthesis in

0022-3549/79/0500-0668$01.00/0

© 1979, American Pharmaceutical Association

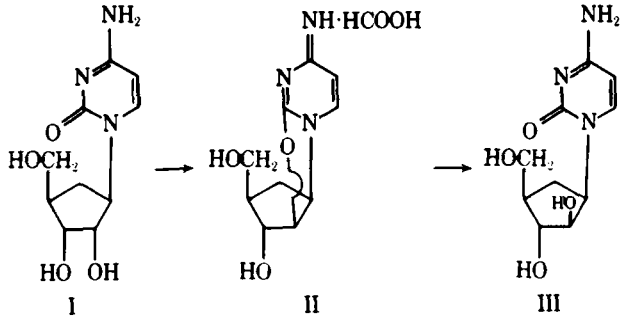

Scheme I

L-1210 cells and that it is phosphorylated to the mono-, di-, and triphosphate stages. Collectively, these facts provided the rationale for the synthesis of the carbocyclic analog (III) of cytarabine.

Carbodine served as the precursor of III (Scheme I). Treatment of I with dimethylformamide–thionyl chloride reagent in excess dimethylformamide, a method reported (10) for the conversion of cytidine to cytarabine, produced the carbocyclic analog (II) of 2,2′-anhydrocytidine (cyclocytidine). A solution of I (500 mg) in the reagent solution (0.75 ml of thionyl chloride in 5 ml of dimethylformamide stirred for 0.5 hr at room temperature prior to the addition of I) was stirred for 3 hr at room temperature, diluted with water (2.5:1), sparged with nitrogen to remove sulfur dioxide, and applied to a column of a cation-exchange resin[1] in the pyridinium salt form. Elution of the column with 0.1 *M* pyridinium formate, combination of fractions containing II[2], and concentration of the solution *in vacuo* furnished a viscous syrupy residue that contained II, as well as pyridinium formate.

A solution of this residue in 1 *N* aqueous ammonia was heated at 80° for 15 min to hydrolyze II to III. The reaction solution was concentrated *in vacuo*, and an aqueous solution of the residue was chromatographed on a strong cation-exchange resin[1] in the pyridinium salt form, as already described. Fractions containing III[2] were concentrated *in vacuo*, and an aqueous solution of the residue was applied to a column of a strongly acidic cation-exchange resin[3]. The column was washed thoroughly with water and then eluted with 2 *N* aqueous ammonia.

The portion of the eluate containing III[2] was concentrated to dryness *in vacuo*, and the white, solid residue was recrystallized from ethanol–water; 60% yield from I; mp 227–230° dec.; mass spectrum (1 m*A*, direct-inlet probe, 240°): *m/e* 242 (M + 1), 241 (M), 224 (M − OH), 223 (M − H_2O), 210 (M − CH_2OH), and 138 (cytosinyl group + C_2H_4); UV: λ_{max} 283 (ϵ 14,500) and 214 (10,100) at pH 1, 274 (10,000) and 225 (sh) at pH 7 or pH 13; PMR (dimethylsulfoxide-d_6, δ in parts per million downfield from tetramethylsilane): 1.5–2.05 (m, CH_2 and CH at positions 5 and 4 of the cyclopentane ring), 3.25–3.7 (m, CH_2OH and CH at position 3 of the cyclopentane ring), 3.7–3.9 (m, CH at position 2 of the cyclopentane ring), 4.46–4.85 (m, OH of CH_2OH), 4.85–5.14 (m, CH at position 1 and OH at positions 2 and 3 of the cyclopentane ring), 5.65 (center of doublet, CH at position 5 of the pyrimidine ring), 6.94 (broad singlet, NH_2), and 7.57 (center of doublet, CH at position 6 of the pyrimidine ring).

Compound III moved slightly faster than I on a thin-layer plate of silica gel with 2-propanol–1 *M* ammonium acetate (7:3) as developing solvent.

Anal.—Calc. for $C_{10}H_{15}N_3O_4$: C, 49.79; H, 6.27; N, 17.42. Found (after drying at 100° for 4 hr): C, 49.57; H, 6.30; N, 17.45.

The carbocyclic analog (II) of cyclocytidine was isolated from another reaction of I with dimethylformamide–thionyl chloride. The mixture of II and pyridinium formate, obtained by chromatographing the reaction product on the pyridinium cation-exchange resin[1], as already described, was stored in a high vacuum for an extended period to volatilize pyridine and formic acid. The residue was triturated several times with ether and then with cold ethanol. Ethanol evaporation, addition of a second portion of cold ethanol, and drying of the crystalline precipitate at 56° afforded II formate as a hydrate; TLC, one spot [40 or 80 μg on silica gel, 2-propanol–1 *N* ammonium acetate (7:3)[4], UV detection]; mass spectrum: *m/e* 223 (M), 192 (M − CH_2OH), and 46 (HCOOH); UV: λ_{max} 269 (ϵ 9500) and 232 (9000) at pH 1.

Anal.—Calc. for $C_{10}H_{13}N_3O_3 \cdot HCOOH \cdot \frac{3}{4}H_2O$: C, 46.39; H, 5.84; N, 14.76. Found: C, 46.29; H, 5.54; N, 15.28.

Kikugawa and Ichino (10) reported the preparation of cytarabine from cytidine through the intermediate formation of cyclocytidine with dimethylformamide–thionyl chloride reagent. The overall yield of cytarabine was about 27%. When the first procedure outlined for the preparation of III was applied to the preparation of cytarabine from cytidine, the yield of product obtained from the second ion-exchange column[1] was 41%.

Analysis of the product by high-pressure liquid chromatography showed it to be a mixture of cytarabine and cytidine (55:45) and indicated an overall yield of about 23% of cytarabine. In comparison, the yield of III free of I was 68% at the same stage.

In tests performed by standard protocols (11), the carbocyclic analog of cytarabine was active against L-1210 leukemia in mice (Table I).

Table I—Tests of Compound III against L-1210 Leukemia [a]

Dose, mg/kg/day	Weight Change[b], T − C	Average Lifespan, T/C	Increase in Lifespan, %
150	−2.2	16.6/8.1	104
100	−0.8	13.8/8.7	58
67	−1.5	11.4/8.1	40

[a] Mice were implanted intraperitoneally with 10^5 L-1210 cells on Day 0. Treatment was begun on Day 1 and continued through Day 9 (*q.d.* 1–9). T = treated mice; C = control mice. [b] The weight change is the difference on Day 5 between the average change in weight of treated mice and the average change in weight of control mice.

[1] Styrene-sulfonic acid-type resin, analytical grade (AG-50W-X4, Bio-Rad Laboratories, Richmond, Calif.).

[2] Fractions of the eluate containing II or III were located by monitoring the effluent with a UV spectrophotometric monitor.

[3] Amberlite CG-120, H^+ form.

[4] In this TLC system, II moved more slowly than I and III.

(1) J. S. Evans, E. A. Musser, L. Bostwick, and G. D. Mengel, *Cancer Res.*, **24**, 1285 (1964).

(2) W. A. Creasey, in "Antineoplastic and Immunosuppressive Agents," Part II, A. C. Sartorelli and D. G. Johns. Eds., Springer-Verlag, New York, N.Y., 1975, chap. 42.

(3) G. P. Bodey, E. J. Freireich, R. W. Monto, and J. S. Hewlett, *Cancer Chemother. Rep.*, **53**, 59 (1969).

(4) R. R. Ellison, J. F. Holland, M. Weil, C. Jacquillat, M. Boiron, J. Bernard, A. Sawitsky, F. Rosner, B. Gussoff, R. T. Silver, A. Karanas, J. Cuttner, C. L. Spurr, D. M. Hayes, J. Blom, L. A. Leone, F. Haurani, R. Kyle, J. L. Hutchison, R. J. Forcier, and J. H. Moon, *Blood*, **32**, 507 (1968).

(5) B. D. Clarkson, M. D. Dowling, T. S. Gee, I. B. Cunningham, and J. H. Burchenal, *Cancer*, **36**, 775 (1975).

(6) F. Maley, in "Cancer, A Comprehensive Treatise," vol. 5, F. F. Becker, Ed., Plenum, New York, N.Y., 1977, chap. 12.

(7) A. W. Chow, J. Foerster, and W. Hryniuk, in "Antimicrobial Agents and Chemotherapy–1970," G. L. Hobby, Ed., American Society for Microbiology, Bethesda, Md., 1971, pp. 214–217.

(8) Y. F. Shealy and C. A. O'Dell, *J. Heterocycl. Chem.*, **13**, 1353 (1976).

(9) R. W. Brockman, J. W. Carpenter, C. A. O'Dell, Y. F. Shealy, and L. L. Bennett, Jr., *Fed. Proc.*, **37**, 234 (1978).

(10) K. Kikugawa and M. Ichino, *Tetrahedron Lett.*, **1970**, 867.

(11) R. I. Geran, N. H. Greenberg, M. M. Macdonald, A. M. Schumacher, and B. J. Abbott, *Cancer Chemother. Rep., Part 3*, **3**, 1 (1972).

Y. Fulmer Shealy ˣ
C. Allen O'Dell
Kettering-Meyer Laboratory
Southern Research Institute
Birmingham, AL 35205

Received December 21, 1978.
Accepted for publication February 14, 1979.
Supported by the Division of Cancer Treatment, National Cancer Institute, National Institutes of Health, Contract NO1-CM-43762, and by Southern Research Institute.
Testing against L-1210 leukemia was performed in this Institute under the supervision of Dr. F. M. Schabel, Jr., and Dr. W. R. Laster, Jr., and was supported by Contract NO1-CM-43756 with the Division of Cancer Treatment, National Cancer Institute, National Institutes of Health.
Mass spectra were determined by M. C. Kirk; NMR spectra were determined by Martha C. Thorpe.

Absorption of Insulin Delivered to Rabbit Trachea Using Aerosol Dosage Form

Keyphrases □ Insulin—aerosol dosage forms, tracheal administration, absorption, rabbits □ Dosage forms, aerosol—insulin, tracheal administration, absorption, rabbits □ Proteins—aerosol dosage forms, insulin, tracheal administration, absorption, rabbits

To the Editor:

Insulin, an endogenous hormone used in treatment of diabetes mellitus, has been administered parenterally rather than orally because it readily decomposes in the GI tract. However, some effective approaches have been developed for oral (1–3), nasal (4), and rectal and aerosol (5, 6) dosage forms. The aerosol dosage form has been receiving much attention because it can be used by diabetic patients with little difficulty.

Wigley *et al.* (5) reported that insulin delivered to patients and volunteers by aerosol inhalation using a nebulizer was absorbed through the respiratory tract epithelium and was an effective therapeutic form for diabetes mellitus (5). However, little has been mentioned about the pharmaceutical factor that governs insulin absorption from aerosol dosage forms.

The present study was undertaken to investigate the bioavailability of powdered aerosol insulin when administered intratracheally to rabbits.

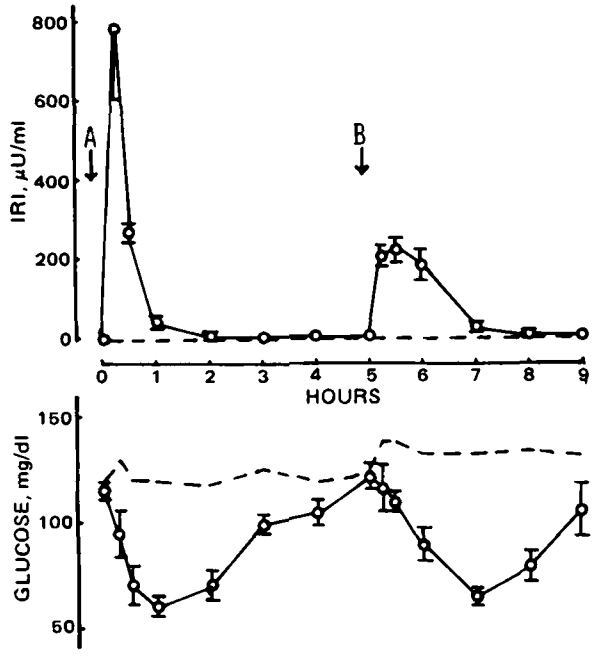

Figure 1—*Plasma concentration profiles of immunoreactive insulin (IRI) and glucose after intravenous (A, 1 U/kg) or intratracheal (B, 2.5 U/kg) insulin administration. Each point represents the mean ± SEM of three experiments. Broken lines denote immunoreactive insulin and glucose levels in sham-operated rabbits.*

White male rabbits, 2.8–3.1 kg, were anesthetized with pentobarbital sodium and maintained under anesthesia for the entire experiment. After the animal was secured in a supine position, insulin solution (1.0 U/kg) or physiological saline (as the control) was injected into the ear vein.

Blood samples were collected from the femoral vein at timed intervals to monitor immunoreactive insulin and glucose levels in plasma. Four hours after intravenous insulin injection, the rabbit trachea was exposed and polyethylene tubing was inserted through a tracheal incision. Insulin aerosol was sprayed into the trachea 1 hr after surgical treatment, and the appearance of immunoreactive insulin and the blood glucose level then were determined at timed intervals.

The insulin aerosol formulation was composed of: monocomponent porcine insulin[1], 5 mg; lactose, 75 mg; acetylglycerin monostearate, 50 mg; dichlorodifluoromethane, 3.6 g; and dichlorotetrafluoroethane, 2.4 g. A metered aerosol valve was designed to release 0.058 mg (1.5 U) of insulin/delivery. The plasma glucose level was measured by the method of Hyvärinen and Nikkilä (7), and immunoreactive insulin in plasma was determined by the method of Desbuquois and Aurbach (8).

Figure 1 shows the time courses of immunoreactive insulin and glucose concentrations in plasma after intravenous injection and after intratracheal aerosol insulin administration. After intravenous administration, there was a sharp increase in plasma immunoreactive insulin and a decrease in plasma glucose. The decline in plasma glucose continued for about 3 hr, although the plasma immuno-

[1] Crystals, lot S 837301 (biological potency 26.6 I.U./mg), Novo Industry Co., Copenhagen, Denmark.

0022-3549/79/0500-0670$01.00/0
© 1979, American Pharmaceutical Association

(4) R. R. Ellison, J. F. Holland, M. Weil, C. Jacquillat, M. Boiron, J. Bernard, A. Sawitsky, F. Rosner, B. Gussoff, R. T. Silver, A. Karanas, J. Cuttner, C. L. Spurr, D. M. Hayes, J. Blom, L. A. Leone, F. Haurani, R. Kyle, J. L. Hutchison, R. J. Forcier, and J. H. Moon, *Blood*, **32**, 507 (1968).

(5) B. D. Clarkson, M. D. Dowling, T. S. Gee, I. B. Cunningham, and J. H. Burchenal, *Cancer*, **36**, 775 (1975).

(6) F. Maley, in "Cancer, A Comprehensive Treatise," vol. 5, F. F. Becker, Ed., Plenum, New York, N.Y., 1977, chap. 12.

(7) A. W. Chow, J. Foerster, and W. Hryniuk, in "Antimicrobial Agents and Chemotherapy–1970," G. L. Hobby, Ed., American Society for Microbiology, Bethesda, Md., 1971, pp. 214–217.

(8) Y. F. Shealy and C. A. O'Dell, *J. Heterocycl. Chem.*, **13**, 1353 (1976).

(9) R. W. Brockman, J. W. Carpenter, C. A. O'Dell, Y. F. Shealy, and L. L. Bennett, Jr., *Fed. Proc.*, **37**, 234 (1978).

(10) K. Kikugawa and M. Ichino, *Tetrahedron Lett.*, **1970**, 867.

(11) R. I. Geran, N. H. Greenberg, M. M. Macdonald, A. M. Schumacher, and B. J. Abbott, *Cancer Chemother. Rep., Part 3*, **3**, 1 (1972).

Y. Fulmer Shealy ˣ
C. Allen O'Dell
Kettering-Meyer Laboratory
Southern Research Institute
Birmingham, AL 35205

Received December 21, 1978.
Accepted for publication February 14, 1979.
Supported by the Division of Cancer Treatment, National Cancer Institute, National Institutes of Health, Contract NO1-CM-43762, and by Southern Research Institute.
Testing against L-1210 leukemia was performed in this Institute under the supervision of Dr. F. M. Schabel, Jr., and Dr. W. R. Laster, Jr., and was supported by Contract NO1-CM-43756 with the Division of Cancer Treatment, National Cancer Institute, National Institutes of Health.
Mass spectra were determined by M. C. Kirk; NMR spectra were determined by Martha C. Thorpe.

Absorption of Insulin Delivered to Rabbit Trachea Using Aerosol Dosage Form

Keyphrases □ Insulin—aerosol dosage forms, tracheal administration, absorption, rabbits □ Dosage forms, aerosol—insulin, tracheal administration, absorption, rabbits □ Proteins—aerosol dosage forms, insulin, tracheal administration, absorption, rabbits

To the Editor:

Insulin, an endogenous hormone used in treatment of diabetes mellitus, has been administered parenterally rather than orally because it readily decomposes in the GI tract. However, some effective approaches have been developed for oral (1–3), nasal (4), and rectal and aerosol (5, 6) dosage forms. The aerosol dosage form has been receiving much attention because it can be used by diabetic patients with little difficulty.

Wigley *et al.* (5) reported that insulin delivered to patients and volunteers by aerosol inhalation using a nebulizer was absorbed through the respiratory tract epithelium and was an effective therapeutic form for diabetes mellitus (5). However, little has been mentioned about the pharmaceutical factor that governs insulin absorption from aerosol dosage forms.

The present study was undertaken to investigate the bioavailability of powdered aerosol insulin when administered intratracheally to rabbits.

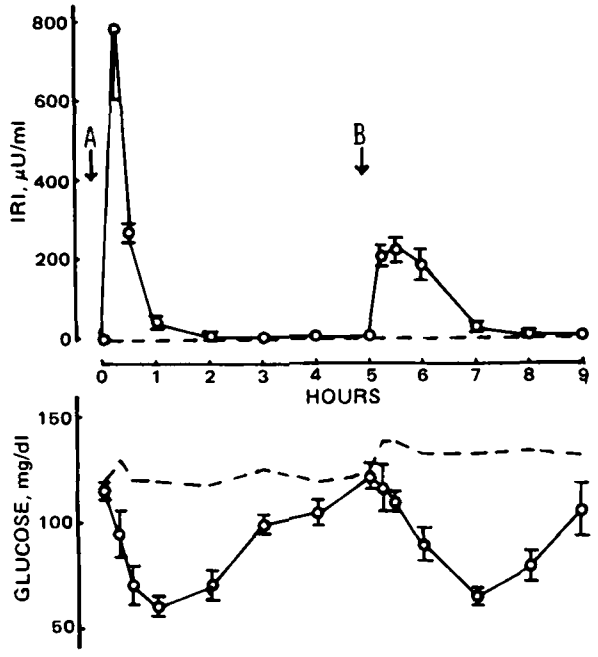

Figure 1—*Plasma concentration profiles of immunoreactive insulin (IRI) and glucose after intravenous (A, 1 U/kg) or intratracheal (B, 2.5 U/kg) insulin administration. Each point represents the mean ± SEM of three experiments. Broken lines denote immunoreactive insulin and glucose levels in sham-operated rabbits.*

White male rabbits, 2.8–3.1 kg, were anesthetized with pentobarbital sodium and maintained under anesthesia for the entire experiment. After the animal was secured in a supine position, insulin solution (1.0 U/kg) or physiological saline (as the control) was injected into the ear vein.

Blood samples were collected from the femoral vein at timed intervals to monitor immunoreactive insulin and glucose levels in plasma. Four hours after intravenous insulin injection, the rabbit trachea was exposed and polyethylene tubing was inserted through a tracheal incision. Insulin aerosol was sprayed into the trachea 1 hr after surgical treatment, and the appearance of immunoreactive insulin and the blood glucose level then were determined at timed intervals.

The insulin aerosol formulation was composed of: monocomponent porcine insulin[1], 5 mg; lactose, 75 mg; acetylglycerin monostearate, 50 mg; dichlorodifluoromethane, 3.6 g; and dichlorotetrafluoroethane, 2.4 g. A metered aerosol valve was designed to release 0.058 mg (1.5 U) of insulin/delivery. The plasma glucose level was measured by the method of Hyvärinen and Nikkilä (7), and immunoreactive insulin in plasma was determined by the method of Desbuquois and Aurbach (8).

Figure 1 shows the time courses of immunoreactive insulin and glucose concentrations in plasma after intravenous injection and after intratracheal aerosol insulin administration. After intravenous administration, there was a sharp increase in plasma immunoreactive insulin and a decrease in plasma glucose. The decline in plasma glucose continued for about 3 hr, although the plasma immuno-

[1] Crystals, lot S 837301 (biological potency 26.6 I.U./mg), Novo Industry Co., Copenhagen, Denmark.

0022-3549/79/0500-0670$01.00/0
© 1979, American Pharmaceutical Association

reactive insulin was almost completely cleared within 1 hr. After intratracheal insulin administered by aerosol, the circulating plasma immunoreactive insulin showed a significant rise and there was a sustained decline in the plasma glucose level.

The bioavailability calculated from the area under the plasma immunoreactive insulin curves after intratracheal aerosol administration of about 2.5 U of insulin/kg was almost the same as that after intravenous injection of 1 U/kg. Wigley *et al.* (5) reported that the plasma immunoreactive insulin area with aerosol delivery of about 3 U/kg was 7–16% of that after intravenous injection of 0.2 U/kg. This low bioavailability might depend on many factors such as adherence to the glass nebulizer, the mouth, and the throat. Our results indicated that most of the insulin (~40%) delivered directly into the trachea in an aerosol formulation is absorbed into the bloodstream through the epithelial layer of the respiratory tract. Accordingly, if an aerosol formulation could be administered directly into the trachea, it could be an effective tool for clinical applications of proteins and peptides.

(1) R. H. Engel, S. J. Riggi, and M. J. Fahrenbach, *Nature*, **219**, 8561 (1968).

(2) C. W. Crane, M. C. Path, and G. R. W. N. Luntz, *Diabetes*, **17**, 625 (1968).

(3) H. M. Patel and B. E. Ryman, *FEBS Lett.*, **62**, 60 (1976).

(4) S. Hirai, T. Ikenaga, and T. Matsuzawa, *Diabetes*, **27**, 296 (1978).

(5) F. M. Wigley, J. H. Londono, S. H. Wood, J. C. Shipp, and R. H. Waldman, *ibid.*, **20**, 552 (1971).

(6) S. Lee and J. J. Sciarra, *J. Pharm. Sci.*, **65**, 567 (1976).

(7) A. Hyvärinen and E. A. Nikkilä, *Clin. Chim. Acta*, **7**, 140 (1962).

(8) B. Desbuquois and G. D. Aurbach, *J. Clin. Endocrinol. Metab.*, **33**, 732 (1971).

Hisahiro Yoshida
Katsuhiko Okumura ˣ
Ryohei Hori
Institute of Pharmaceutical Sciences
Hiroshima University School of Medicine
Kasumi, Hiroshima, Japan

Toshio Anmo
Hiroshi Yamaguchi
Research Laboratory
Taisho Pharmaceutical Co., Ltd.
Yoshino-cho, Omiya, Japan

Received January 22, 1979.
Accepted for publication February 14, 1979.

BOOKS

REVIEWS

Analysis of Drugs and Metabolites by Gas Chromatography–Mass Spectrometry. Vol. 1: Respiratory Gases, Volatile Anesthetics, Ethyl Alcohol, and Related Toxicological Materials; Vol. 2: Hypnotics, Anticonvulsants, and Sedatives; Vol. 3: Antipsychotic, Antiemetic, and Antidepressant Drugs; Vol. 4: Central Nervous System Stimulants; Vol. 5: Analgesics, Local Anesthetics, and Antibiotics. By BENJAMIN J. GUDZINOWICZ and MICHAEL J. GUDZINOWICZ. Dekker, 270 Madison Avenue, New York, NY 10016, Vol. 1: 1977, 223 pp., 15 × 23 cm, Price $23.75; Vol. 2: 1977, 493 pp., 15 × 23 cm, Price $45.00; Vol. 3: 1977, 268 pp., 15 × 23 cm, Price $29.75; Vol. 4: 1978, 458 pp., 15 × 23 cm, Price $45.00; Vol. 5: 1978, 541 pp., 15 × 23 cm, Price $55.00.

The above titles are the first five volumes in what the publisher promises to be a continuing series. Indeed, the flyleaf of Volume 5 states that Volume 6 will cover cardiovascular, antihypertensive, hypoglycemic, and thyroid-related agents. The stated purposes of this series are: to provide a chronological literature compilation of the GLC and GLC–mass spectrometry procedures for the analysis of specific drugs and their metabolites; to provide qualitative and quantitative procedures in such detail that they might be reproduced "faithfully" in the reader's laboratory; to present the results, precision, accuracy, and limits of detection achieved by a given procedure; and to indicate, wherever possible, the procedure's applicability to pharmacokinetic studies.

Each volume has a separate author and subject index. These indexes are not cumulative, but that is not necessary since each volume is self-contained. The authors assume that the reader is familiar with GLC and GLC–mass spectrometry. No pages are wasted on cursory introductory chapters, although the authors do include a few sketches of special instrument modifications such as sampling traps and injection ports. Where appropriate, the chemistry of a chemical class is described in an expanded discussion, which usually contains the structures and sometimes the biotransformations. Each chapter contains representative GLC tracings and tabulated retention data. Some mass spectra or printouts of mass fragment values are presented.

A logical question is: Does this series duplicate or overlap *Analytical Profiles*? To a limited extent, the answer is yes, only because GLC and mass spectra analyses are found in *Analytical Profiles*. Whereas the latter deals more with the pure drug, *Analysis of Drugs and Metabolites by Gas Chromatography–Mass Spectrometry* emphasizes the analysis of mixtures that include the specific drugs under discussion. The two series complement each other, and the volumes covered in this review discuss a much larger group of compounds.

Volume 1 consists of two chapters of about equal length. The first chapter discusses respiratory gases, volatile anesthetics, and related toxicological materials. The second includes sterilizing agents, common organic solvents found in blood, and riot-control aerosol irritants. The second chapter also features ethanol and volatile trace components in breath, body fluids, and body tissues. The term "volatile" may be a little misleading, because the discussion on urine includes screening of urinary steroids and acids plus other chemicals.

The topics become more pharmaceutically oriented in the remaining volumes. About half of Volume 2 is devoted to barbiturates. One-third of the volume is a chapter that includes chloral derivatives, tertiary acetylenic alcohols, cyclic ethers, carbamates and ureides, piperdinediones, quinazalones, benzodiazepines, and carbamazepine. The third and final chapter makes up about 20 percent of the book and covers the traditional anticonvulsants including hydantoins, succinimides, primidone, paramethadione and trimethadione, and some miscellaneous anticonvulsants.

Volume 3 has two chapters of about equal length. Chapter 1 covers phenothazines, butyrophenones, and thioxanthines; Chapter 2 includes a moderate discussion on monoamine oxidase inhibitors and a rather complete coverage of the tricyclic antidepressants.

Volume 4 also contains two chapters of about equal length. Most of Chapter 1 is devoted to the amphetamines and related compounds, with the remainder including the xanthines and pentylenetetrazol. Chapter 2 mainly covers the phenylethylamine-related compounds, with the balance devoted to tryptamine- and propranolol-related compounds.

reactive insulin was almost completely cleared within 1 hr. After intratracheal insulin administered by aerosol, the circulating plasma immunoreactive insulin showed a significant rise and there was a sustained decline in the plasma glucose level.

The bioavailability calculated from the area under the plasma immunoreactive insulin curves after intratracheal aerosol administration of about 2.5 U of insulin/kg was almost the same as that after intravenous injection of 1 U/kg. Wigley *et al.* (5) reported that the plasma immunoreactive insulin area with aerosol delivery of about 3 U/kg was 7–16% of that after intravenous injection of 0.2 U/kg. This low bioavailability might depend on many factors such as adherence to the glass nebulizer, the mouth, and the throat. Our results indicated that most of the insulin (~40%) delivered directly into the trachea in an aerosol formulation is absorbed into the bloodstream through the epithelial layer of the respiratory tract. Accordingly, if an aerosol formulation could be administered directly into the trachea, it could be an effective tool for clinical applications of proteins and peptides.

(1) R. H. Engel, S. J. Riggi, and M. J. Fahrenbach, *Nature*, **219**, 8561 (1968).

(2) C. W. Crane, M. C. Path, and G. R. W. N. Luntz, *Diabetes*, **17**, 625 (1968).

(3) H. M. Patel and B. E. Ryman, *FEBS Lett.*, **62**, 60 (1976).

(4) S. Hirai, T. Ikenaga, and T. Matsuzawa, *Diabetes*, **27**, 296 (1978).

(5) F. M. Wigley, J. H. Londono, S. H. Wood, J. C. Shipp, and R. H. Waldman, *ibid.*, **20**, 552 (1971).

(6) S. Lee and J. J. Sciarra, *J. Pharm. Sci.*, **65**, 567 (1976).

(7) A. Hyvärinen and E. A. Nikkilä, *Clin. Chim. Acta*, **7**, 140 (1962).

(8) B. Desbuquois and G. D. Aurbach, *J. Clin. Endocrinol. Metab.*, **33**, 732 (1971).

Hisahiro Yoshida
Katsuhiko Okumura ˣ
Ryohei Hori
Institute of Pharmaceutical Sciences
Hiroshima University School of Medicine
Kasumi, Hiroshima, Japan

Toshio Anmo
Hiroshi Yamaguchi
Research Laboratory
Taisho Pharmaceutical Co., Ltd.
Yoshino-cho, Omiya, Japan

Received January 22, 1979.
Accepted for publication February 14, 1979.

BOOKS

REVIEWS

Analysis of Drugs and Metabolites by Gas Chromatography–Mass Spectrometry. Vol. 1: Respiratory Gases, Volatile Anesthetics, Ethyl Alcohol, and Related Toxicological Materials; Vol. 2: Hypnotics, Anticonvulsants, and Sedatives; Vol. 3: Antipsychotic, Antiemetic, and Antidepressant Drugs; Vol. 4: Central Nervous System Stimulants; Vol. 5: Analgesics, Local Anesthetics, and Antibiotics. By BENJAMIN J. GUDZINOWICZ and MICHAEL J. GUDZINOWICZ. Dekker, 270 Madison Avenue, New York, NY 10016, Vol. 1: 1977, 223 pp., 15 × 23 cm, Price $23.75; Vol. 2: 1977, 493 pp., 15 × 23 cm, Price $45.00; Vol. 3: 1977, 268 pp., 15 × 23 cm, Price $29.75; Vol. 4: 1978, 458 pp., 15 × 23 cm, Price $45.00; Vol. 5: 1978, 541 pp., 15 × 23 cm, Price $55.00.

The above titles are the first five volumes in what the publisher promises to be a continuing series. Indeed, the flyleaf of Volume 5 states that Volume 6 will cover cardiovascular, antihypertensive, hypoglycemic, and thyroid-related agents. The stated purposes of this series are: to provide a chronological literature compilation of the GLC and GLC–mass spectrometry procedures for the analysis of specific drugs and their metabolites; to provide qualitative and quantitative procedures in such detail that they might be reproduced "faithfully" in the reader's laboratory; to present the results, precision, accuracy, and limits of detection achieved by a given procedure; and to indicate, wherever possible, the procedure's applicability to pharmacokinetic studies.

Each volume has a separate author and subject index. These indexes are not cumulative, but that is not necessary since each volume is self-contained. The authors assume that the reader is familiar with GLC and GLC–mass spectrometry. No pages are wasted on cursory introductory chapters, although the authors do include a few sketches of special instrument modifications such as sampling traps and injection ports. Where appropriate, the chemistry of a chemical class is described in an expanded discussion, which usually contains the structures and sometimes the biotransformations. Each chapter contains representative GLC tracings and tabulated retention data. Some mass spectra or printouts of mass fragment values are presented.

A logical question is: Does this series duplicate or overlap *Analytical Profiles*? To a limited extent, the answer is yes, only because GLC and mass spectra analyses are found in *Analytical Profiles*. Whereas the latter deals more with the pure drug, *Analysis of Drugs and Metabolites by Gas Chromatography–Mass Spectrometry* emphasizes the analysis of mixtures that include the specific drugs under discussion. The two series complement each other, and the volumes covered in this review discuss a much larger group of compounds.

Volume 1 consists of two chapters of about equal length. The first chapter discusses respiratory gases, volatile anesthetics, and related toxicological materials. The second includes sterilizing agents, common organic solvents found in blood, and riot-control aerosol irritants. The second chapter also features ethanol and volatile trace components in breath, body fluids, and body tissues. The term "volatile" may be a little misleading, because the discussion on urine includes screening of urinary steroids and acids plus other chemicals.

The topics become more pharmaceutically oriented in the remaining volumes. About half of Volume 2 is devoted to barbiturates. One-third of the volume is a chapter that includes chloral derivatives, tertiary acetylenic alcohols, cyclic ethers, carbamates and ureides, piperdinediones, quinazalones, benzodiazepines, and carbamazepine. The third and final chapter makes up about 20 percent of the book and covers the traditional anticonvulsants including hydantoins, succinimides, primidone, paramethadione and trimethadione, and some miscellaneous anticonvulsants.

Volume 3 has two chapters of about equal length. Chapter 1 covers phenothazines, butyrophenones, and thioxanthines; Chapter 2 includes a moderate discussion on monoamine oxidase inhibitors and a rather complete coverage of the tricyclic antidepressants.

Volume 4 also contains two chapters of about equal length. Most of Chapter 1 is devoted to the amphetamines and related compounds, with the remainder including the xanthines and pentylenetetrazol. Chapter 2 mainly covers the phenylethylamine-related compounds, with the balance devoted to tryptamine- and propranolol-related compounds.

Volume 5 covers a mixed group of drugs. Chapter 1 is about 40 percent of the book and includes natural and synthetic narcotics and narcotic antagonists. The balance of Volume 5, Chapter 2, discusses antipyretics, antiinflammatory and antihyperuricemic agents, local anesthetics, and antibiotics. Since these volumes are part of a continuing series, it would have seemed more appropriate to include antibiotics in a volume covering antiinfective and chemotherapeutic agents.

At first glance, from the authors' goals, the reader might expect a combination of an exhaustive treatise and laboratory manual for each subject. An examination of any volume will show that this was not necessary. The general format of each section is: (*a*) a general literature review including the chemistry and biochemical transformation of the drug class under discussion; (*b*) a discussion of derivatization, sensitivity, and quantitation; and (*c*) several specific examples. A limited number of actual procedures is found in the latter part of each chapter. All information is well referenced. Perhaps the best way to describe this series is to say that each chapter is a very extensive review article.

Unless an individual is an analytical laboratory director, there is little reason to purchase the entire set. On the other hand, individual volumes are highly recommended to scientists needing to be knowledgeable in the analysis of a specific drug group. The entire set should be purchased by libraries whose collections include books dealing with instrumental analysis.

Reviewed by John H. Block
School of Pharmacy
Oregon State University
Corvallis, OR 97331

Aromatic and Heteroaromatic Chemistry, Volume 6. A Review of the Literature Abstracted between 7/76 and 6/77. By H. SUSCHITZKY and O. METH-COHN. Chemical Society, Burlington House, London, W1V OBN, England. 1978. 326 pp. 14 × 22 cm. Price $47.50.

This latest volume in the series of Specialist Periodical Reports reviews the literature on aromatic and heteroaromatic chemistry abstracted between July 1976 and June 1977 and covered by Volumes 85 and 86 of *Chemical Abstracts*.

The two new senior reporters, Professors Suschitzky and Meth-Cohn, have partially reorganized the chapters of this volume in an attempt to reduce the cost and to aid the reader in locating particular topics quickly, in the absence of a subject index. The high cost and lack of a subject index were the only previous criticisms of this series. The reorganization was successful in both endeavors, although the cost of the book is still relatively high.

The senior reporters have retained all other aspects developed by their predecessors, Professors Bird and Cheeseman, and have maintained the high quality presentation of a large amount of factual information so valuable to the scientist interested in this area.

The liberal use of structures and reaction schemes and the practice of placing references as footnotes on the page cited have been retained and maintain the excellent readability and continuity of the previous volumes.

The new chapter titles include: Three and Four-Membered Ring Systems; Five-Membered Ring Systems; Six-Membered Ring Systems; Six-Membered Heterocycles; Seven-Membered Ring Systems; Medium-Sized Rings and Macrocycles; and Electrophilic Substitution Reactions. Chapter titles retained include: Nucleophilic Substitution Reactions; Aromatic Substitution by Free Radicals, Carbenes, and Nitrenes; Porphyrins and Related Compounds; Naturally Occurring Aromatic Oxygen-Ring Compounds; and Other Naturally Occurring Aromatic Compounds. Not included, due to the illness of its reporter, was the new chapter entitled Six-Membered Homocycles. The volume has a complete author index containing over 4300 names, and the 11 chapters include over 2200 literature citations.

Like the previous volumes, this one provides a systematic, critical, in-depth account of the progress in aromatic and heteroaromatic chemistry.

Reviewed by Edward F. LaSala
Massachusetts College of Pharmacy
Boston, MA 02115

Analysis of Steroid Hormone Drugs. By S. GÖRÖG and GY. SZÁSZ. Akadémie Kiadó, Budapest, Hungary, and Elsevier Scientific Publishing Co., Amsterdam, The Netherlands. 1978. 426 pp. Price $59.

Every scientist interested in the analysis of steroid pharmaceuticals should acquire this book. The literature on steroid analysis has become so extensive that many review articles have degenerated into mere taxonomy, like the bienniel *Analytical Chemistry* reviews on drug analysis. In contrast, this book provides an informed and intelligent review of the subject. It is a volume one can read through as a text, browse in for intellectual stimulation, or use as a reference for a specific question.

Organization of the book could well serve as a paradigm for other monographs. The chapters are titled, "Fundamental Steroid Hormone Chemistry," "Brief Outline of the Therapeutic Use of Steroid Hormones," "Development of, and Current Trends in, Methods of Steroid Hormone Analysis," "Chromatography of Steroid Hormones," "Gas Chromatography of Steroid Hormones," "Functional Group Analysis," "Assay of Dosage Forms," and "Analysis of Raw Materials for the Semi-syntheses of Steroid Hormones." The author of each chapter or section is identified, and each chapter has references. There are author and subject indexes.

HPLC methods now are probably the most useful for assay of steroids and their pharmaceutical dosage forms. Discussion of this technique in the book is much shorter than for GC, which it has largely supplanted. Nevertheless, the text is oriented to chemical principles, so it is unlikely to be dated rapidly by the appearance of new technology.

Reviewed by Lester Chafetz
Analytical Research
Warner-Lambert Company
Morris Plains, NJ 07950

Volume 5 covers a mixed group of drugs. Chapter 1 is about 40 percent of the book and includes natural and synthetic narcotics and narcotic antagonists. The balance of Volume 5, Chapter 2, discusses antipyretics, antiinflammatory and antihyperuricemic agents, local anesthetics, and antibiotics. Since these volumes are part of a continuing series, it would have seemed more appropriate to include antibiotics in a volume covering antiinfective and chemotherapeutic agents.

At first glance, from the authors' goals, the reader might expect a combination of an exhaustive treatise and laboratory manual for each subject. An examination of any volume will show that this was not necessary. The general format of each section is: (*a*) a general literature review including the chemistry and biochemical transformation of the drug class under discussion; (*b*) a discussion of derivatization, sensitivity, and quantitation; and (*c*) several specific examples. A limited number of actual procedures is found in the latter part of each chapter. All information is well referenced. Perhaps the best way to describe this series is to say that each chapter is a very extensive review article.

Unless an individual is an analytical laboratory director, there is little reason to purchase the entire set. On the other hand, individual volumes are highly recommended to scientists needing to be knowledgeable in the analysis of a specific drug group. The entire set should be purchased by libraries whose collections include books dealing with instrumental analysis.

Reviewed by John H. Block
School of Pharmacy
Oregon State University
Corvallis, OR 97331

Aromatic and Heteroaromatic Chemistry, Volume 6. A Review of the Literature Abstracted between 7/76 and 6/77. By H. SUSCHITZKY and O. METH-COHN. Chemical Society, Burlington House, London, W1V OBN, England. 1978. 326 pp. 14 × 22 cm. Price $47.50.

This latest volume in the series of Specialist Periodical Reports reviews the literature on aromatic and heteroaromatic chemistry abstracted between July 1976 and June 1977 and covered by Volumes 85 and 86 of *Chemical Abstracts*.

The two new senior reporters, Professors Suschitzky and Meth-Cohn, have partially reorganized the chapters of this volume in an attempt to reduce the cost and to aid the reader in locating particular topics quickly, in the absence of a subject index. The high cost and lack of a subject index were the only previous criticisms of this series. The reorganization was successful in both endeavors, although the cost of the book is still relatively high.

The senior reporters have retained all other aspects developed by their predecessors, Professors Bird and Cheeseman, and have maintained the high quality presentation of a large amount of factual information so valuable to the scientist interested in this area.

The liberal use of structures and reaction schemes and the practice of placing references as footnotes on the page cited have been retained and maintain the excellent readability and continuity of the previous volumes.

The new chapter titles include: Three and Four-Membered Ring Systems; Five-Membered Ring Systems; Six-Membered Ring Systems; Six-Membered Heterocycles; Seven-Membered Ring Systems; Medium-Sized Rings and Macrocycles; and Electrophilic Substitution Reactions. Chapter titles retained include: Nucleophilic Substitution Reactions; Aromatic Substitution by Free Radicals, Carbenes, and Nitrenes; Porphyrins and Related Compounds; Naturally Occurring Aromatic Oxygen-Ring Compounds; and Other Naturally Occurring Aromatic Compounds. Not included, due to the illness of its reporter, was the new chapter entitled Six-Membered Homocycles. The volume has a complete author index containing over 4300 names, and the 11 chapters include over 2200 literature citations.

Like the previous volumes, this one provides a systematic, critical, in-depth account of the progress in aromatic and heteroaromatic chemistry.

Reviewed by Edward F. LaSala
Massachusetts College of Pharmacy
Boston, MA 02115

Analysis of Steroid Hormone Drugs. By S. GÖRÖG and GY. SZÁSZ. Akadémie Kiadó, Budapest, Hungary, and Elsevier Scientific Publishing Co., Amsterdam, The Netherlands. 1978. 426 pp. Price $59.

Every scientist interested in the analysis of steroid pharmaceuticals should acquire this book. The literature on steroid analysis has become so extensive that many review articles have degenerated into mere taxonomy, like the bienniel *Analytical Chemistry* reviews on drug analysis. In contrast, this book provides an informed and intelligent review of the subject. It is a volume one can read through as a text, browse in for intellectual stimulation, or use as a reference for a specific question.

Organization of the book could well serve as a paradigm for other monographs. The chapters are titled, "Fundamental Steroid Hormone Chemistry," "Brief Outline of the Therapeutic Use of Steroid Hormones," "Development of, and Current Trends in, Methods of Steroid Hormone Analysis," "Chromatography of Steroid Hormones," "Gas Chromatography of Steroid Hormones," "Functional Group Analysis," "Assay of Dosage Forms," and "Analysis of Raw Materials for the Semi-syntheses of Steroid Hormones." The author of each chapter or section is identified, and each chapter has references. There are author and subject indexes.

HPLC methods now are probably the most useful for assay of steroids and their pharmaceutical dosage forms. Discussion of this technique in the book is much shorter than for GC, which it has largely supplanted. Nevertheless, the text is oriented to chemical principles, so it is unlikely to be dated rapidly by the appearance of new technology.

Reviewed by Lester Chafetz
Analytical Research
Warner-Lambert Company
Morris Plains, NJ 07950

Volume 5 covers a mixed group of drugs. Chapter 1 is about 40 percent of the book and includes natural and synthetic narcotics and narcotic antagonists. The balance of Volume 5, Chapter 2, discusses antipyretics, antiinflammatory and antihyperuricemic agents, local anesthetics, and antibiotics. Since these volumes are part of a continuing series, it would have seemed more appropriate to include antibiotics in a volume covering antiinfective and chemotherapeutic agents.

At first glance, from the authors' goals, the reader might expect a combination of an exhaustive treatise and laboratory manual for each subject. An examination of any volume will show that this was not necessary. The general format of each section is: (*a*) a general literature review including the chemistry and biochemical transformation of the drug class under discussion; (*b*) a discussion of derivatization, sensitivity, and quantitation; and (*c*) several specific examples. A limited number of actual procedures is found in the latter part of each chapter. All information is well referenced. Perhaps the best way to describe this series is to say that each chapter is a very extensive review article.

Unless an individual is an analytical laboratory director, there is little reason to purchase the entire set. On the other hand, individual volumes are highly recommended to scientists needing to be knowledgeable in the analysis of a specific drug group. The entire set should be purchased by libraries whose collections include books dealing with instrumental analysis.

Reviewed by John H. Block
School of Pharmacy
Oregon State University
Corvallis, OR 97331

Aromatic and Heteroaromatic Chemistry, Volume 6. A Review of the Literature Abstracted between 7/76 and 6/77. By H. SUSCHITZKY and O. METH-COHN. Chemical Society, Burlington House, London, W1V OBN, England. 1978. 326 pp. 14 × 22 cm. Price $47.50.

This latest volume in the series of Specialist Periodical Reports reviews the literature on aromatic and heteroaromatic chemistry abstracted between July 1976 and June 1977 and covered by Volumes 85 and 86 of *Chemical Abstracts*.

The two new senior reporters, Professors Suschitzky and Meth-Cohn, have partially reorganized the chapters of this volume in an attempt to reduce the cost and to aid the reader in locating particular topics quickly, in the absence of a subject index. The high cost and lack of a subject index were the only previous criticisms of this series. The reorganization was successful in both endeavors, although the cost of the book is still relatively high.

The senior reporters have retained all other aspects developed by their predecessors, Professors Bird and Cheeseman, and have maintained the high quality presentation of a large amount of factual information so valuable to the scientist interested in this area.

The liberal use of structures and reaction schemes and the practice of placing references as footnotes on the page cited have been retained and maintain the excellent readability and continuity of the previous volumes.

The new chapter titles include: Three and Four-Membered Ring Systems; Five-Membered Ring Systems; Six-Membered Ring Systems; Six-Membered Heterocycles; Seven-Membered Ring Systems; Medium-Sized Rings and Macrocycles; and Electrophilic Substitution Reactions. Chapter titles retained include: Nucleophilic Substitution Reactions; Aromatic Substitution by Free Radicals, Carbenes, and Nitrenes; Porphyrins and Related Compounds; Naturally Occurring Aromatic Oxygen-Ring Compounds; and Other Naturally Occurring Aromatic Compounds. Not included, due to the illness of its reporter, was the new chapter entitled Six-Membered Homocycles. The volume has a complete author index containing over 4300 names, and the 11 chapters include over 2200 literature citations.

Like the previous volumes, this one provides a systematic, critical, in-depth account of the progress in aromatic and heteroaromatic chemistry.

Reviewed by Edward F. LaSala
Massachusetts College of Pharmacy
Boston, MA 02115

Analysis of Steroid Hormone Drugs. By S. GÖRÖG and GY. SZÁSZ. Akadémie Kiadó, Budapest, Hungary, and Elsevier Scientific Publishing Co., Amsterdam, The Netherlands. 1978. 426 pp. Price $59.

Every scientist interested in the analysis of steroid pharmaceuticals should acquire this book. The literature on steroid analysis has become so extensive that many review articles have degenerated into mere taxonomy, like the bienniel *Analytical Chemistry* reviews on drug analysis. In contrast, this book provides an informed and intelligent review of the subject. It is a volume one can read through as a text, browse in for intellectual stimulation, or use as a reference for a specific question.

Organization of the book could well serve as a paradigm for other monographs. The chapters are titled, "Fundamental Steroid Hormone Chemistry," "Brief Outline of the Therapeutic Use of Steroid Hormones," "Development of, and Current Trends in, Methods of Steroid Hormone Analysis," "Chromatography of Steroid Hormones," "Gas Chromatography of Steroid Hormones," "Functional Group Analysis," "Assay of Dosage Forms," and "Analysis of Raw Materials for the Semi-syntheses of Steroid Hormones." The author of each chapter or section is identified, and each chapter has references. There are author and subject indexes.

HPLC methods now are probably the most useful for assay of steroids and their pharmaceutical dosage forms. Discussion of this technique in the book is much shorter than for GC, which it has largely supplanted. Nevertheless, the text is oriented to chemical principles, so it is unlikely to be dated rapidly by the appearance of new technology.

Reviewed by Lester Chafetz
Analytical Research
Warner-Lambert Company
Morris Plains, NJ 07950

A publication of the
American Pharmaceutical Association—
the National Professional Society
of Pharmacists

JOURNAL OF PHARMACEUTICAL SCIENCES

INDEX TO AUTHORS
INDEX TO SUBJECTS

VOLUME 68
JANUARY TO DECEMBER, 1979

Published monthly under the supervision of the Board of Trustees

MARY H. FERGUSON
Editor

SHELLY ELLIOTT
Production Editor

MARCIA GARTRELL
Copy Editor

NICOLETTE TRIANTAFELLU
Copy Editor

EDWARD G. FELDMANN
Contributing Editor

SAMUEL W. GOLDSTEIN
Contributing Editor

BELLE R. BECK
Editorial Secretary

DAVID BOHARDT
Director of Publications

L. LUAN CORRIGAN
Assistant Director of Publications

EDITORIAL ADVISORY BOARD

John Autian
Norman R. Farnsworth
William O. Foye
William J. Jusko
Herbert A. Lieberman
David E. Mann, Jr.
Gerald J. Papariello
Edward G. Rippie

JUNE 1979
VOLUME 68 NUMBER 6

JOURNAL OF PHARMACEUTICAL SCIENCES

MARY H. FERGUSON
Editor

SHELLY ELLIOTT
Production Editor

JANIS KELLY
Copy Editor

EDWARD G. FELDMANN
Contributing Editor

SAMUEL W. GOLDSTEIN
Contributing Editor

BELLE R. BECK
Editorial Secretary

DAVID BOHARDT
Director of Publications

L. LUAN CORRIGAN
Assistant Director of Publications

EDITORIAL ADVISORY BOARD

JOHN AUTIAN
HERBERT A. LIEBERMAN
NORMAN R. FARNSWORTH
DAVID E. MANN, JR.
WILLIAM O. FOYE
GERALD J. PAPARIELLO
WILLIAM J. JUSKO
EDWARD G. RIPPIE

The *Journal of Pharmaceutical Sciences* (ISSN 0022-3549) is published monthly by the American Pharmaceutical Association (APhA) at 2215 Constitution Ave., N.W., Washington, DC 20037. Second-class postage paid at Washington, D.C., and at additional mailing office.

All expressions of opinion and statements of supposed fact appearing in articles or editorials carried in this journal are published on the authority of the writer over whose name they appear and are not to be regarded as necessarily expressing the policies or views of APhA.

Offices—Editorial, Advertising, and Subscription: 2215 Constitution Ave., N.W., Washington, DC 20037. Printing: 20th & Northampton Streets, Easton, PA 18042.

Annual Subscriptions—United States and foreign, industrial and government institutions $50, educational institutions $50, individuals *for personal use only* $30; single copies $5. All foreign subscriptions add $5 for postage. Subscription rates are subject to change without notice. Members of APhA may elect to receive the *Journal of Pharmaceutical Sciences* as a part of their annual $70 (foreign $75) APhA membership dues.

Claims—Missing numbers will not be supplied if dues or subscriptions are in arrears for more than 60 days or if claims are received more than 60 days after the date of the issue, or if loss was due to failure to give notice of change of address. APhA cannot accept responsibility for foreign delivery when its records indicate shipment has been made.

Change of Address—Members and subscribers should notify at once both the Post Office and APhA of any change of address.

Photocopying—The code at the foot of the first page of an article indicates that APhA has granted permission for copying of the article beyond the limits permitted by Sections 107 and 108 of the U.S. Copyright Law provided that the copier sends the per copy fee stated in the code to the Copyright Clearance Center, Inc., P.O. Box 8891, Boston, MA 02114. Copies may be made for personal or internal use only and not for general distribution.

Microfilm—Available from University Microfilms International, 300 N. Zeeb Road, Ann Arbor, MI 48106.

© Copyright 1979, American Pharmaceutical Association, 2215 Constitution Ave., N.W., Washington, DC 20037; all rights reserved.

TOO MANY REGULATIONS?

Out in Fairfax County, Virginia, where this writer resides, we enjoy—or are afflicted with, depending upon one's viewpoint—an apparent surfeit of dogs. Moreover, the owners of many of these pets exercise exceedingly little restraint or control over the canine population.

This situation has led to the county adopting a so-called "leash law," which requires every dog to be maintained on a leash whenever the animal is off its owner's property. After being in effect for a full year, however, we see no discernible change in behavior, simply because the police do not enforce the law and the malefactors who own the dogs are well aware of that fact. Consequently, what seemed to be a good solution in theory turned out to be an exercise in futility.

We also have certain main roads designated as "snow emergency routes," and any car getting stuck there due to ice and snow is subject to being ticketed. Well, this past February, the Washington, D.C., area was hit with its worst blizzard in 50 years. Although efforts were made to keep the main arteries open, this quickly proved hopeless due to stalled cars that were abandoned on the roadways, preventing the snow removal equipment from doing its job.

In one newspaper account, a reporter asked the traffic department why the offending cars were not being ticketed. The response offered by the police was that to do so would be "unfair because the cars were snowed in." But since no one gets stuck in snow purposely, why maintain such a law on the books if it is not to be enforced?

We are reminded of these examples because we recently heard an APhA member offer the same time-worn and simplistic solution that pharmacy often employs in an effort to solve some problem situation or behavior; namely, the "there-ought-to-be-a-law" syndrome.

A pharmaceutical company house organ publication crossed our desk a few weeks ago that carried an article, the heading of which was a direct quote from a book entitled "Spirit of the Law," written in 1748 by the French state philosopher Charles de Montesquieu. The quote read: "*Superfluous laws detract from the effectiveness of those that are necessary.*"

Increasingly, there are signs and evidence that the United States in general, and the health field in particular, are becoming the victims of over-regulation. Productivity and effectiveness are gradually being strangled by excessive regulatory requirements.

This problem has gotten to the point that the federal government itself, in the form of the Carter Administration, is initiating various reviews to assess whether this trend might be reversed. Although we may be pessimistic or even cynical about such pronouncements, it is encouraging that there is some recognition of the danger posed by unbridled policy to solve problems through imposing new regulations.

Moreover, Mary Munson Runge, quoted several months ago before assuming the APhA Presidency, expressed chagrin at the "overlegislated" state of the profession of pharmacy. Who is to blame for the mountain of mandates that is slowly taking shape throughout the country? She believes that pharmacists themselves are at fault: "*Pharmacists have brought some of these things on themselves by not doing them voluntarily. I understand fully the reasons for all the mandates that are being legislated, and I think it's the fault of the profession.*"

From our perspective, she is right on target. Most new statutes and regulations come about because something wasn't working as it should have been, and a need was perceived by someone to legislate a solution.

Requirements affecting the drug industry—and especially the Good Manufacturing Practices and Good Laboratory Practices regulations—can generally be traced to some sloppy or shoddy performance by at least a part of the industry.

Similarly, in this month's issue of APhA's professional periodical, *American Pharmacy*, there is an article titled "Kelsey's Commandos: FDA Investigates the Investigators." This article deals with all the rules that have sprung up in the past decade to regulate scientists who conduct clinical investigations on new drugs. Again, as the article reveals, these people brought it on themselves through the scandalous performance of some of their own.

But if it's any consolation, the investigators-of-the-investigators are increasingly getting rapped on their back-sides also! There have been several cases lately where FDA is being dragged into court to account for its alleged failure to perform and is being slapped with requirements to speed up certain processes, to release certain information, or to complete certain projects. A big headline in the March 9 issue of *The Washington Post* serves as a cryptic example: "Judge is Asked to Force FDA to Move on Ineffective Drugs." As the story notes, "More than 16 years and one court order" after Congress passed the provision that the government halt sales of any drug lacking substantial evidence of its efficacy, some 482 prescription products lacking such evidence remain on the market.

FDA's usual excuse is that Congress is quick to pass laws but slow to appropriate funds for their implementation.

We are not sure what the answer is to the over-regulation problem. But we suspect that much of the problem is preventable if people, organizations, and agencies all performed up to the reasonable standard expected of them by society. —EGF

Benzoyl Peroxide Analysis

In a recent paper[1] in this Journal, "High-Pressure Liquid Chromatographic Assay of Benzoyl Peroxide in Dermatological Gels and Lotions," the authors questioned the validity of a TLC system described by our laboratories in a paper[2] entitled "The Stability of a Benzoyl Peroxide Acne Cream Product." The reliance on removing and measuring spectrophotometrically an extract from the solvent front of a chromatogram was recognized, and a subsequent paper[3], "An Improved TLC Procedure for the Quantitative Determination of Benzoyl Peroxide in Acne Creams," was published. This procedure utilized acetonitrile–water (1:1) in a reversed-phase system on an acetylated support, and complete resolution was achieved with benzoyl peroxide (R_f 0.42), benzoic acid (R_f 0.9–1.0), and other isolable impurities. Excellent assay agreement was obtained between this method and an iodometric titration procedure in deliberately degraded cream formulations. The fact that the iodometric titration procedure was proven to be stability indicating suggests its use as an assay method in terms of economics and simplicity over chromatographic methods.

D. L. Simmons
Research and Development
Frank W. Horner Ltd.
Montreal, Canada H3C 2W6

Received March 26, 1979.

[1] F. W. Burton, R. R. Gadde, and W. L. McKenzie, *J. Pharm. Sci.*, **68**, 280 (1979).
[2] D. L. Simmons, H. S. L. Wood, J. J. Liston, and R. J. Ranz, *Can. J. Pharm. Sci.*, **2**, 101 (1967).
[3] D. L. Simmons *et al.*, *ibid.*, **4**, 46 (1969).

Drug Stability in Veterinary Dosage Forms

The January 1979 issue of this Journal contained an editorial on "Consistency in Stability Testing"[1]. This timely editorial was of great interest to the Review Chemists in the Bureau of Veterinary Medicine of the Food and Drug Administration because they are deeply involved in the review and evaluation of stability testing of drug products.

The Bureau of Veterinary Medicine is a counterpart to the Bureau of Drugs, though with a smaller contingent of Review Chemists. The public only hears about veterinary medicine on such issues as DES, nitrites, nitrofurazones, and low-level antibiotics. The Bureau, however, has a much larger responsibility in approving drugs for animal use. Such critical areas as animal safety and human safety must be considered in addition to the effectiveness of the drug. The process of approval is just as intense as that for human products. In many cases, the approval is more critical since food products are involved.

Veterinary drug products are sold as pharmaceutical dosage forms (identical in many cases to the human dosage forms except for labeling), as medicated feed preparations (premixes, supplements, and complete feeds), and as other forms such as medicated blocks.

Bureau Review Chemists are responsible for evaluating the manufacturing operations related to the production of the final products to ensure that they meet the standards they purport to possess.

Stability is an important issue for veterinary products just as it is for human products. In fact, the issue is much more complex because of the variety of products and use patterns. Because of these complexities and often questionable areas of stability testing for veterinary products, the Bureau of Veterinary Medicine developed a set of guidelines for industry and reviewer use. The Bureau issued the Guidelines in July 1976 with a *Federal Register*[2] notice of availability in November of the same year. The Guidelines were updated in February 1978.

For veterinary products, stability is probably more critical and harder to focus on. Because of obvious reasons, human drug products enjoy a much higher plateau in the various fields of research and methods development. Human products are often used under controlled situations or conditions—stored in pharmacies and used in clinics, hospitals, and households. Probably the only controlled conditions for veterinary product usage, however, are in veterinary clinics, hospitals, or offices. Use by farmers of drugs purchased by them or dispensed to them leaves much to be desired as far as stability and shelflife are concerned. Many animal drugs are subjected to higher temperatures and abuse than human drug counterparts. However, as provided under our laws, a veterinary drug is a "drug" and must meet the requirements and individual standards of strength, quality, purity, and identity as proclaimed by the Act. The drug must also be manufactured under the cGMPs as published by the FDA.

We, in the Bureau of Veterinary Medicine, feel the Guidelines we have issued are meaningful and provide the guidance needed by industry. Many companies concerned with human pharmaceuticals are currently using our Guidelines. The Guidelines represent our best scientific judgment on the topic and should be used as just that—"guidelines." Our general position is that every product is unique and must "stand on its own" as far as stability is concerned.

Copies of the drug Guidelines can be obtained by writing to the: Food and Drug Administration, Bureau of Veterinary Medicine, Industry Relations Branch, HFV-226, 5600 Fishers Lane, Rockville, MD 20857.

John R. Markus
Scientific Evaluation
Bureau of Veterinary Medicine
Food and Drug Administration
Rockville, MD 20852

Received April 19, 1979.

[1] E. G. Feldmann, *J. Pharm. Sci.*, **68** (1), I (1979).
[2] *Fed. Regist.*, **44**, 48150 (Nov. 2, 1976).

Unified Theory of Anesthesia

The current diversity of theories of narcosis indicates a lack of understanding of the mechanism of anesthesia at the molecular level. Ecanow and coworkers[1,2] have proposed a hypothesis that integrates the descriptive, clinical, and laboratory data concerning individuals in a state of anesthesia.

This hypothesis is based on the concept that neuronal cells, like all cells, have membranes in the coacervate state; that is, the membrane exists as an aqueous phase that is in a different thermodynamic state than that of the surrounding aqueous plasma and interstitial fluids[3]. The addition of a small increment of drug to a coacervate phase produces a change in structuring, which results in a free energy change which is chiefly entropic. Accompanying the free energy change are pharmacological changes[1–3].

The colloid theory initially proposed by Claude Bernard in 1875 and subsequently elaborated by others suggested that a reversible aggregation of cell colloids causes or accompanies anesthesia. This reversible aggregation is precisely what occurs upon the introduction of an anesthetic agent to the colloidal system known as the coacervate phase. The change in aggregation relationships is measured by changes in physicochemical properties[3]. These changes, in turn, correlate with the ranking of clinical potencies in a series of depressant drugs[2].

The lipid theory advanced by Meyer and Overton proposes a direct parallelism between the affinity for a lipid phase and its resultant central nervous system (CNS) depressant action. The affinity is

Benzoyl Peroxide Analysis

In a recent paper[1] in this Journal, "High-Pressure Liquid Chromatographic Assay of Benzoyl Peroxide in Dermatological Gels and Lotions," the authors questioned the validity of a TLC system described by our laboratories in a paper[2] entitled "The Stability of a Benzoyl Peroxide Acne Cream Product." The reliance on removing and measuring spectrophotometrically an extract from the solvent front of a chromatogram was recognized, and a subsequent paper[3], "An Improved TLC Procedure for the Quantitative Determination of Benzoyl Peroxide in Acne Creams," was published. This procedure utilized acetonitrile–water (1:1) in a reversed-phase system on an acetylated support, and complete resolution was achieved with benzoyl peroxide (R_f 0.42), benzoic acid (R_f 0.9–1.0), and other isolable impurities. Excellent assay agreement was obtained between this method and an iodometric titration procedure in deliberately degraded cream formulations. The fact that the iodometric titration procedure was proven to be stability indicating suggests its use as an assay method in terms of economics and simplicity over chromatographic methods.

D. L. Simmons
Research and Development
Frank W. Horner Ltd.
Montreal, Canada H3C 2W6

Received March 26, 1979.

[1] F. W. Burton, R. R. Gadde, and W. L. McKenzie, *J. Pharm. Sci.*, **68**, 280 (1979).
[2] D. L. Simmons, H. S. L. Wood, J. J. Liston, and R. J. Ranz, *Can. J. Pharm. Sci.*, **2**, 101 (1967).
[3] D. L. Simmons *et al.*, *ibid.*, **4**, 46 (1969).

Drug Stability in Veterinary Dosage Forms

The January 1979 issue of this Journal contained an editorial on "Consistency in Stability Testing"[1]. This timely editorial was of great interest to the Review Chemists in the Bureau of Veterinary Medicine of the Food and Drug Administration because they are deeply involved in the review and evaluation of stability testing of drug products.

The Bureau of Veterinary Medicine is a counterpart to the Bureau of Drugs, though with a smaller contingent of Review Chemists. The public only hears about veterinary medicine on such issues as DES, nitrites, nitrofurazones, and low-level antibiotics. The Bureau, however, has a much larger responsibility in approving drugs for animal use. Such critical areas as animal safety and human safety must be considered in addition to the effectiveness of the drug. The process of approval is just as intense as that for human products. In many cases, the approval is more critical since food products are involved.

Veterinary drug products are sold as pharmaceutical dosage forms (identical in many cases to the human dosage forms except for labeling), as medicated feed preparations (premixes, supplements, and complete feeds), and as other forms such as medicated blocks.

Bureau Review Chemists are responsible for evaluating the manufacturing operations related to the production of the final products to ensure that they meet the standards they purport to possess.

Stability is an important issue for veterinary products just as it is for human products. In fact, the issue is much more complex because of the variety of products and use patterns. Because of these complexities and often questionable areas of stability testing for veterinary products, the Bureau of Veterinary Medicine developed a set of guidelines for industry and reviewer use. The Bureau issued the Guidelines in July 1976 with a *Federal Register*[2] notice of availability in November of the same year. The Guidelines were updated in February 1978.

For veterinary products, stability is probably more critical and harder to focus on. Because of obvious reasons, human drug products enjoy a much higher plateau in the various fields of research and methods development. Human products are often used under controlled situations or conditions—stored in pharmacies and used in clinics, hospitals, and households. Probably the only controlled conditions for veterinary product usage, however, are in veterinary clinics, hospitals, or offices. Use by farmers of drugs purchased by them or dispensed to them leaves much to be desired as far as stability and shelflife are concerned. Many animal drugs are subjected to higher temperatures and abuse than human drug counterparts. However, as provided under our laws, a veterinary drug is a "drug" and must meet the requirements and individual standards of strength, quality, purity, and identity as proclaimed by the Act. The drug must also be manufactured under the cGMPs as published by the FDA.

We, in the Bureau of Veterinary Medicine, feel the Guidelines we have issued are meaningful and provide the guidance needed by industry. Many companies concerned with human pharmaceuticals are currently using our Guidelines. The Guidelines represent our best scientific judgment on the topic and should be used as just that—"guidelines." Our general position is that every product is unique and must "stand on its own" as far as stability is concerned.

Copies of the drug Guidelines can be obtained by writing to the: Food and Drug Administration, Bureau of Veterinary Medicine, Industry Relations Branch, HFV-226, 5600 Fishers Lane, Rockville, MD 20857.

John R. Markus
Scientific Evaluation
Bureau of Veterinary Medicine
Food and Drug Administration
Rockville, MD 20852

Received April 19, 1979.

[1] E. G. Feldmann, *J. Pharm. Sci.*, **68** (1), I (1979).
[2] *Fed. Regist.*, **44**, 48150 (Nov. 2, 1976).

Unified Theory of Anesthesia

The current diversity of theories of narcosis indicates a lack of understanding of the mechanism of anesthesia at the molecular level. Ecanow and coworkers[1,2] have proposed a hypothesis that integrates the descriptive, clinical, and laboratory data concerning individuals in a state of anesthesia.

This hypothesis is based on the concept that neuronal cells, like all cells, have membranes in the coacervate state; that is, the membrane exists as an aqueous phase that is in a different thermodynamic state than that of the surrounding aqueous plasma and interstitial fluids[3]. The addition of a small increment of drug to a coacervate phase produces a change in structuring, which results in a free energy change which is chiefly entropic. Accompanying the free energy change are pharmacological changes[1–3].

The colloid theory initially proposed by Claude Bernard in 1875 and subsequently elaborated by others suggested that a reversible aggregation of cell colloids causes or accompanies anesthesia. This reversible aggregation is precisely what occurs upon the introduction of an anesthetic agent to the colloidal system known as the coacervate phase. The change in aggregation relationships is measured by changes in physicochemical properties[3]. These changes, in turn, correlate with the ranking of clinical potencies in a series of depressant drugs[2].

The lipid theory advanced by Meyer and Overton proposes a direct parallelism between the affinity for a lipid phase and its resultant central nervous system (CNS) depressant action. The affinity is

Benzoyl Peroxide Analysis

In a recent paper[1] in this Journal, "High-Pressure Liquid Chromatographic Assay of Benzoyl Peroxide in Dermatological Gels and Lotions," the authors questioned the validity of a TLC system described by our laboratories in a paper[2] entitled "The Stability of a Benzoyl Peroxide Acne Cream Product." The reliance on removing and measuring spectrophotometrically an extract from the solvent front of a chromatogram was recognized, and a subsequent paper[3], "An Improved TLC Procedure for the Quantitative Determination of Benzoyl Peroxide in Acne Creams," was published. This procedure utilized acetonitrile–water (1:1) in a reversed-phase system on an acetylated support, and complete resolution was achieved with benzoyl peroxide (R_f 0.42), benzoic acid (R_f 0.9–1.0), and other isolable impurities. Excellent assay agreement was obtained between this method and an iodometric titration procedure in deliberately degraded cream formulations. The fact that the iodometric titration procedure was proven to be stability indicating suggests its use as an assay method in terms of economics and simplicity over chromatographic methods.

D. L. Simmons
Research and Development
Frank W. Horner Ltd.
Montreal, Canada H3C 2W6

Received March 26, 1979.

[1] F. W. Burton, R. R. Gadde, and W. L. McKenzie, *J. Pharm. Sci.*, **68**, 280 (1979).
[2] D. L. Simmons, H. S. L. Wood, J. J. Liston, and R. J. Ranz, *Can. J. Pharm. Sci.*, **2**, 101 (1967).
[3] D. L. Simmons *et al.*, *ibid.*, **4**, 46 (1969).

Drug Stability in Veterinary Dosage Forms

The January 1979 issue of this Journal contained an editorial on "Consistency in Stability Testing"[1]. This timely editorial was of great interest to the Review Chemists in the Bureau of Veterinary Medicine of the Food and Drug Administration because they are deeply involved in the review and evaluation of stability testing of drug products.

The Bureau of Veterinary Medicine is a counterpart to the Bureau of Drugs, though with a smaller contingent of Review Chemists. The public only hears about veterinary medicine on such issues as DES, nitrites, nitrofurazones, and low-level antibiotics. The Bureau, however, has a much larger responsibility in approving drugs for animal use. Such critical areas as animal safety and human safety must be considered in addition to the effectiveness of the drug. The process of approval is just as intense as that for human products. In many cases, the approval is more critical since food products are involved.

Veterinary drug products are sold as pharmaceutical dosage forms (identical in many cases to the human dosage forms except for labeling), as medicated feed preparations (premixes, supplements, and complete feeds), and as other forms such as medicated blocks.

Bureau Review Chemists are responsible for evaluating the manufacturing operations related to the production of the final products to ensure that they meet the standards they purport to possess.

Stability is an important issue for veterinary products just as it is for human products. In fact, the issue is much more complex because of the variety of products and use patterns. Because of these complexities and often questionable areas of stability testing for veterinary products, the Bureau of Veterinary Medicine developed a set of guidelines for industry and reviewer use. The Bureau issued the Guidelines in July 1976 with a *Federal Register*[2] notice of availability in November of the same year. The Guidelines were updated in February 1978.

For veterinary products, stability is probably more critical and harder to focus on. Because of obvious reasons, human drug products enjoy a much higher plateau in the various fields of research and methods development. Human products are often used under controlled situations or conditions—stored in pharmacies and used in clinics, hospitals, and households. Probably the only controlled conditions for veterinary product usage, however, are in veterinary clinics, hospitals, or offices. Use by farmers of drugs purchased by them or dispensed to them leaves much to be desired as far as stability and shelflife are concerned. Many animal drugs are subjected to higher temperatures and abuse than human drug counterparts. However, as provided under our laws, a veterinary drug is a "drug" and must meet the requirements and individual standards of strength, quality, purity, and identity as proclaimed by the Act. The drug must also be manufactured under the cGMPs as published by the FDA.

We, in the Bureau of Veterinary Medicine, feel the Guidelines we have issued are meaningful and provide the guidance needed by industry. Many companies concerned with human pharmaceuticals are currently using our Guidelines. The Guidelines represent our best scientific judgment on the topic and should be used as just that—"guidelines." Our general position is that every product is unique and must "stand on its own" as far as stability is concerned.

Copies of the drug Guidelines can be obtained by writing to the: Food and Drug Administration, Bureau of Veterinary Medicine, Industry Relations Branch, HFV-226, 5600 Fishers Lane, Rockville, MD 20857.

John R. Markus
Scientific Evaluation
Bureau of Veterinary Medicine
Food and Drug Administration
Rockville, MD 20852

Received April 19, 1979.

[1] E. G. Feldmann, *J. Pharm. Sci.*, **68** (1), I (1979).
[2] *Fed. Regist.*, **44**, 48150 (Nov. 2, 1976).

Unified Theory of Anesthesia

The current diversity of theories of narcosis indicates a lack of understanding of the mechanism of anesthesia at the molecular level. Ecanow and coworkers[1,2] have proposed a hypothesis that integrates the descriptive, clinical, and laboratory data concerning individuals in a state of anesthesia.

This hypothesis is based on the concept that neuronal cells, like all cells, have membranes in the coacervate state; that is, the membrane exists as an aqueous phase that is in a different thermodynamic state than that of the surrounding aqueous plasma and interstitial fluids[3]. The addition of a small increment of drug to a coacervate phase produces a change in structuring, which results in a free energy change which is chiefly entropic. Accompanying the free energy change are pharmacological changes[1–3].

The colloid theory initially proposed by Claude Bernard in 1875 and subsequently elaborated by others suggested that a reversible aggregation of cell colloids causes or accompanies anesthesia. This reversible aggregation is precisely what occurs upon the introduction of an anesthetic agent to the colloidal system known as the coacervate phase. The change in aggregation relationships is measured by changes in physicochemical properties[3]. These changes, in turn, correlate with the ranking of clinical potencies in a series of depressant drugs[2].

The lipid theory advanced by Meyer and Overton proposes a direct parallelism between the affinity for a lipid phase and its resultant central nervous system (CNS) depressant action. The affinity is

measured in a lipid phase, which is usually a vegetable or organic liquid. By contrast, coacervates can be prepared from true lipids as well as other surfactants. Use of a coacervate as the lipid phase is more realistic to test for affinity and confirms the above parallelism[3]. Further, coacervates with their ability to show a continuum of subtle responses to the addition of anesthetics parallel the subtle responses characteristic of biophase reactions. The coacervate with its composition of lipids, colloids, water, and electrolytes is of the same composition as the biophase. On the other hand, the oils used in oil–water partition studies are at best single-point approximations of the physical–chemical properties of the biophase[3].

The cell permeability theory advanced by Hoher and others states that anesthetics stabilize the cell membrane and thus decrease the ion exchanges that normally accompany depolarization. This stabilizing of the cell membrane has been shown to accompany the increasing matrix structuring that occurs on the addition of anesthetics to a coacervate phase. This result is reflected by the increased resistance to electrical conductivity of a coacervate phase when the depressant drugs are added to the coacervate. The conductivity, in turn, parallels the clinical potency of the anesthetics added to the coacervate phase[2,5].

The increased red cell permeability to glucose normally produced by carbon dioxide can be seen by bubbling carbon dioxide through a coacervate phase and following the increasing glucose solubility (permeability). This increased permeability is inhibited upon the addition of an anesthetic agent to the coacervate phase.

In current neurophysiologocal theory, there is no satisfactory explanation for the observation that decreased synaptic transmission can be caused by anesthetic agents while, at the same time, axonal conduction remains unimpaired. We explain this observation as follows. The aqueous matrix in a synaptic cleft is a structured aqueous medium, thermodynamically different from neuronal cytoplasm and adjacent aqueous plasma. In effect, it constitutes three different states of aqueous media. The addition of an anesthetic agent concentrates in and further increases the synaptic aqueous matrix structuring, thus impairing synaptic transmission while axonal transmission remains unimpaired[2].

The Pauling and Miller concept of the structuring of water molecules around the anesthetic agent within the CNS focuses attention on the role of water. However, by focusing on water structuring as opposed to total matrix structuring, the theory suffers from the fact that the suggested stability is not likely to occur under conditions of normal body temperatures. The water–lipid equilibrium phase known as protoplasm is a coacervate and has no such limitation. The coacervate matrix at body temperature can readily become increasingly stable. The point to be emphasized is that the coacervate phase is both an aqueous phase and a lipoidal phase. As such, it integrates the attractive features of both the water structuring theory and the lipid theory of anesthetic mechanism.

The concept that general anesthetics expand the lipid phase of a membrane[4] correlates directly with the expansion of a coacervate phase as it becomes increasingly structured by the addition of clinical amounts of the anesthetic agent. High pressures that reverse anesthetic-induced expansion of the biomembrane also reduce expanded structures of coacervates. Many artificial phospholipid membranes used to confirm the expansion concept by means of electron-spin resonance are really phospholipid aqueous matrixes that are coacervate phases.

The concept of the membrane as a coacervate phase capable of undergoing subtle changes in structuring that correspond to different degrees of anesthesia supplies a fundamental predictive and experimentally verifiable basis for a unified theory to account for cellular changes produced by anesthetics as well as other drugs and metabolites. Finally, the membrane can undergo a continuum of free energy changes from polar to nonpolar properties. The anesthetic state occupies one range on this continuum.

Bernard Ecanow
Bernard H. Gold
University of Illinois
at the Medical Center
Chicago, IL 60612

Charles S. Ecanow
Ecanow and Associates, Inc.
Wilmette, IL 60091

Received April 9, 1979.

[1] B. Ecanow, B. Gold, and P. Tunkunas, in "Application of Physical Chemistry Principles to the Study of Anxiety and Depression; Psychotherapy and Psychosomatic," J. Ruesch, Ed., S. Karger, Basel, Switzerland, 1972.

[2] B. Ecanow and H. Klawans, in "Models of Human Neurological Disease," H. Klawans, Ed., Excerpta Medica, Amsterdam. The Netherlands, 1974.

[3] H. Takruri, B. Ecanow, and R. Balagot, *J. Pharm. Sci.*, **66**, 283 (1977).

[4] "The Pharmacological Basis of Therapeutics," 5th ed., L. Goodman and A. Gilman, Eds., Macmillan, New York, N.Y., 1976, pp. 56–58.

[5] B. Ecanow, J. Wosnicki, and J. Webster, unpublished data.

JOURNAL OF PHARMACEUTICAL SCIENCES

JUNE 1979
VOLUME 68 NUMBER 6

RESEARCH ARTICLES

Mechanistic and Quantitative Evaluation of Precorneal Pilocarpine Disposition in Albino Rabbits

VINCENT HON-LEUNG LEE and JOSEPH R. ROBINSON ˣ

Received July 6, 1978, from the *School of Pharmacy, University of Wisconsin, Madison, WI 53706.* Accepted for publication December 13, 1978.

Abstract □ The low ocular bioavailability of topically applied pilocarpine is attributed to extensive precorneal drug loss in conjunction with the resistance to corneal penetration. Several elements of precorneal loss were reported earlier, but a complete mechanistic understanding has not been available. The present study was designed to gain a better understanding of the mechanisms governing pilocarpine disposition in the precorneal areas as well as the relative influence of these parameters on ocular drug bioavailability. Radioactive pilocarpine and glycerin solutions were instilled into the precorneal area of the albino rabbit eye under various experimental conditions, and the drug concentration in the lacrimal lake was monitored as a function of time. The results demonstrated that nonconjunctival loss of pilocarpine, vasodilation due to the drug, and lacrimation due to vehicle formulation are additional aspects of precorneal drug disposition. The individual influence of all precorneal loss parameters on drug bioavailability was then assessed using a mathematical model formulated from experimental findings on both precorneal and intraocular drug disposition. Drainage and vasodilation, as well as nonconjunctival pilocarpine loss, exerted major influences on drug loss at the absorption site.

Keyphrases □ Pilocarpine—precorneal disposition, mechanistic and quantitative evaluation □ Precorneal area—pilocarpine disposition, mechanistic and quantitative evaluation □ Distribution, ocular—pilocarpine, mechanistic and quantitative evaluation □ Dosage forms, topical—pilocarpine, precorneal disposition, mechanistic and quantitative evaluation □ Cholinergics, ophthalmic—pilocarpine, precorneal disposition, mechanistic and quantitative evaluation

The mechanisms by which a topically applied dose of drug disappears from the precorneal area of the eye are important from the standpoint of improving ocular drug delivery systems. Pilocarpine, an important agent in glaucoma management, was selected as the probe drug for investigating this aspect of drug action.

Previous studies with pilocarpine established that solution drainage (1, 2), drug protein binding (3–5), tear turnover (1, 6), and conjunctival absorption (7) compete with corneal absorption for the drug from the precorneal area. Only 1–2% or less of an instilled pilocarpine dose gains access to the internal eye structures (8, 9). While drainage removes a substantial portion of a dose within minutes of instillation, this parameter alone cannot explain the low pilocarpine bioavailability, nor can a combination of the other parameters.

In a similar manner, the large first-order rate constant, $\sim 0.6\ min^{-1}$, associated with the decline of the pilocarpine concentration in the tear film[1] for the critical first 5 min postinstillation is inconsistent with the values reported for the rate constants governing corneal absorption, tear turnover, and conjunctival absorption. Even though drainage has an associated rate constant whose value is $\sim 0.5\ min^{-1}$, it cannot be responsible for the large rate constant associated with precorneal drug loss because drainage is not expected to influence directly tear film drug concentration. In essence, this description for precorneal pilocarpine disposition implies that some as yet unidentified factors, with sizable rate constants, are present.

The purpose of the present study was to gain a better understanding of the mechanisms governing pilocarpine disposition in the precorneal area as well as of the relative influence of these parameters on ocular drug bioavailability.

MODEL

The evolution of mathematical models to describe pilocarpine disposition in the eye reflects the state of knowledge concerning the mechanisms governing its precorneal and intraocular disposition. Scheme I is an example of a commonly used model to describe the fate of pilocarpine

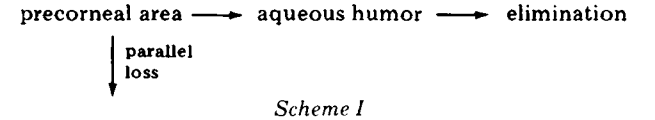

Scheme I

[1] The term tear film or pool is used interchangeably with lacrimal lake. It is assumed that instilled drugs are uniformly mixed with tear fluid.

0022-3549/79/0600-0673$01.00/0
© 1979, American Pharmaceutical Association

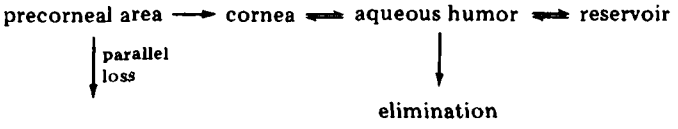

Scheme II

following topical instillation. Two deficiencies of such a model are that it considers the cornea as a single membrane with no apparent role in the disposition process and that it lumps all precorneal drug disposition constants into one large rate constant.

A more recent model (10) (Scheme II) corrects for the first deficiency by including the cornea as a component. However, it does not distinguish the specific roles exercised by the corneal epithelium and corneal stroma in the movement of pilocarpine through the cornea (11).

Both models suffer from the additional drawback of not considering the effects of instilled drop size explicitly. This important precorneal factor forms a component of a recently proposed model (12) which, for simplicity, treats the cornea as a single membrane, as in Scheme I. In summary, all of these models are incomplete descriptions of the fate of pilocarpine in the precorneal area and in the various ocular tissues.

The present study began with construction of a model that was cognizant of the deficiencies mentioned (Scheme III). The model partitions the precorneal loss rate constant into its component parts for a mechanistic understanding of the processes involved. In addition, it incorporates the findings of Sieg and Robinson (11) on pilocarpine disposition: (*a*) the corneal epithelium serves as both a barrier and a depot, and (*b*) the corneal stroma and endothelium are kinetically indistinguishable from the aqueous humor. Table I details the model parameters. The major assumptions introduced while constructing the model were:

1. Instantaneous and complete mixing of instilled drug solution and tears occurs.
2. Pilocarpine metabolism in the tear fluid is negligible.
3. The tissues comprising the compartments are homogeneous.
4. The iris, ciliary body, lens, and vitreous humor constitute the reservoir.

Moreover, the present model will not explicitly consider either pilocarpine protein binding in tear fluid or ocular tissues or the resistance offered by diffusional boundary layers to membrane drug transport.

Proceeding from these assumptions, appropriate differential equations can be written to account for the rate of change in the *mass* of drug in the compartments shown in Scheme III. The volume element of disposition kinetics in the precorneal area is treated in a manner akin to that described previously (12), which is based on the concept of mass balance in open systems advanced earlier (13). Drug transfer, on the other hand, is considered to be a series of simple diffusion steps taking place simultaneously and in succession, with each step governed by Fick's first law of diffusion, in much the same manner as Teorell (14) derived formulas to describe the amount of drug in the body as a function of time. Accordingly, the amount of drug transferred per unit time, M, can be written (15):

$$M = k_p S\,\Delta C \qquad \text{(Eq. 1)}$$

where k_p is the permeability coefficient in centimeters per second, S is the effective surface area in square centimeters, and ΔC is the concentration difference in grams per cubic centimeters. Since k_p and S have not been determined, they are treated in the present model as a single coefficient denoted as p and given by $p = k_p S$ with units of cubic centimeters per second.

Equation 2 describes the rate of change in amount of pilocarpine in the precorneal area:

$$\frac{dV_A(t)[A]}{dt} = -p_p([A] - [B]) - k_d[V_A(t) - V_0][A] - Q_T(t)[A] - p_n[A] \qquad \text{(Eq. 2)}$$

Table I—Parameters of the Model Described in Scheme III

Parameter	Coefficient Associated With[a]
p_p	Transfer of pilocarpine between precorneal area and corneal epithelium
p_n	Nonproductive loss
k_d	Drainage
$Q_T(t)$	Tear flow
p_a	Transfer of pilocarpine between epithelium and corneal stroma–endothelium–aqueous chamber
p_m	Drug loss *via* metabolism in or lateral diffusion from epithelium
p_{ao}	Drug elimination from aqueous humor
p_r	Transfer of pilocarpine between corneal stroma–endothelium–aqueous chamber and reservoir
p_{ro}	Pilocarpine elimination from reservoir

[a] With the exception of k_d, the coefficients have dimensions of microliters per minute. See text for details.

where $[A]$ denotes the drug concentration in the precorneal area (or tear chamber), $[B]$ is the drug concentration in the corneal epithelium, $V_A(t)$ is the volume of fluid in the tear chamber at a given time, V_0 is the normal resident tear volume, and all other symbols are as previously described. Sink conditions are assumed to be maintained in the blood supplying the conjunctiva and related structures.

Thus, from Eq. 2, the change in amount of pilocarpine in the precorneal area is due to corneal absorption, solution drainage, tear flow, and nonproductive loss. As will be evident in the *Discussion* section, nonproductive loss is composed of conjunctival absorption, nonconjunctival loss, and the influence of pilocarpine vasodilation on several of these processes. Likewise, tear flow is composed of normal tear turnover and induced lacrimation.

Induced lacrimation is interpreted here as increased tear flow rate; consequently, it will not change the resident precorneal volume appreciably since a corresponding volume will leave the area. This appears to be the case, as there was no visually apparent fluid accumulation in the precorneal area following dosing. In essence, this treatment views induced lacrimation and instilled volume-dependent drainage as noninteracting entities. This simplification is justifiable based on an earlier study (1) in which the influence of pH on lacrimation could be estimated. The technetium sulfur colloid preparation pH was not reported in that study but was ~6.5, which was close to the pH of most pilocarpine solutions employed in the present study. Therefore, in terms of a change in precorneal fluid volume, the k_d values thus determined account not only for the contribution of instilled volume but also for that of induced lacrimation. Interestingly, the k_d value determined (1) for an instilled volume of 25 μl is consistent with that determined recently (16) by microscintigraphy for a pH 6.24 sodium pertechnetate solution. Combining this observation with the vehicle-induced lacrimation demonstrated in the present study suggests that Eq. 3 is appropriate for describing the rate of change in precorneal fluid volume:

$$\frac{dV_A(t)}{dt} = -k_d[V_A(t) - V_0] \qquad \text{(Eq. 3)}$$

Upon integration, Eq. 3 yields:

$$V_A(t) = V_0 + V_i \exp(-k_d t) \qquad \text{(Eq. 4)}$$

where V_i is the instilled volume. Equation 3 can be combined with Eq. 2:

$$\frac{d[A]}{dt} = -\left(\frac{p_p + p_n}{V_A(t)} + \frac{Q_T(t)}{V_A(t)}\right)[A] + \frac{p_p}{V_A(t)}[B] \qquad \text{(Eq. 5)}$$

In Eq. 5, $Q_T(t)$, like $V_A(t)$, is a time-dependent quantity, as shown in the empirical expression:

$$\frac{dQ_T(t)}{dt} = -k_l[Q_T(t) - Q_0] \qquad \text{(Eq. 6)}$$

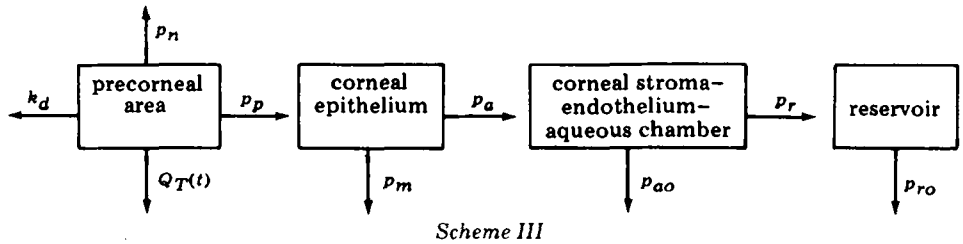

Scheme III

Table II—Apparent Rate Constants for Routes of Precorneal Loss Established for Pilocarpine prior to the Present Study

Loss Route	Associated Rate Constant	Reference
Corneal absorption	0.004 min^{-1}	10, 11
Drainage, 25 μl	0.54 min^{-1}	1
Tear flow	0.66 μl/min	1
Nonproductive loss[a]	0.0217 min^{-1}	7

[a] This reported value was attributed to conjunctival absorption.

which is analogous in form to Eq. 3. Upon integration, Eq. 6 yields:

$$Q_T(t) = Q_0 + Q_i \exp(-k_l t) \qquad \text{(Eq. 7)}$$

According to this equation, the tear flow rate immediately following dosing (*i.e.*, $t = 0$) is the sum of the normal tear flow rate, Q_0, and that due to the instillation of a dose, Q_i. Eventually, the contribution of induced lacrimation to tear flow disappears, and the rate at which this occurs is governed by the rate constant k_l.

The essential feature of Eq. 5 concerns the dimension of the quantity:

$$\left[\frac{p_p + p_n}{V_A(t)} + \frac{Q_T(t)}{V_A(t)}\right]$$

which is that of a first-order rate constant. Nevertheless, it should not be considered as a constant since $V_A(t)$ and $Q_T(t)$ are functions of time. Thus, the quantity derived from the slope of a semilogarithmic plot of tear film drug concentration *versus* time is time averaged. The implication is that to convert the experimental first-order rate constant to the parameters p_p and p_n, knowledge of a time-averaged volume is needed. Of course, if a nonsampling technique that continuously monitors tear film drug concentration is available, $d[A]/dt$ will be known accurately as a function of time and a time-averaged volume is not needed. In this report, the first approach will be adopted, but $V_A(t)$ cannot be construed as a constant in subsequent computer simulations. The procedure for finding the time-averaged volume will be presented under *Discussion*.

For the case in which:

$$\frac{p_p}{V_A(t)}[B] \ll \left(\frac{p_p + p_n + Q_T(t)}{V_A(t)}\right)[A]$$

and $k_l = k_d$, Eq. 5 can be combined with Eqs. 4 and 7 to give an expression which, upon integration, yields a final expression describing the time dependence of drug concentration in the precorneal area following topical instillation:

$$[A] = [A]_i \left(\frac{V_i}{V_A(0)}\right)\left(\frac{V_A(0)}{V_A(t)}\right)^b \exp(-k''t) \qquad \text{(Eq. 8)}$$

where $[A]_i$ is the instilled drug concentration, V_i is the instilled volume, and:

$$b = \left(\frac{p_p + p_n + Q_0}{V_0} - \frac{Q_i}{V_i}\right)\frac{1}{k_d}$$

$$k'' = \frac{p_p + p_n + Q_0}{V_0}$$

$$V_A(0) = V_i + V_0$$

Several features of Eq. 8 are of interest. First, the parameters governing nonproductive loss, p_n, and pilocarpine transfer between the precorneal area and the corneal epithelium, p_p, contribute, along with the parameter governing normal tear flow, Q_0, to the exponent b. This result will not be obtained when one neglects the effect of volume on apparent first-order rate constants (17), in which case only Q_0 contributes. Second, the initial dilution of an instilled dose is accounted for by the term $V_i/V_A(0)$. Third, the equation accounts for the peculiar influence of drainage on drug concentration decline, which is one of deceleration. The key to the preceding statement lies in the terms $[V_A(0)/V_A(t)]^b$ and $\exp(-k''t)$ in Eq. 8. Whereas the term $\exp(-k''t)$ decreases continuously with time, the term $[V_A(0)/V_A(t)]^b$ increases with time [until $V_A(t)$ = normal resident tear volume], thereby counteracting the diminishing effect of the former. Fourth, the term $[V_A(0)/V_A(t)]^b$ yields the expected curvature observed in a semilogarithmic plot of tear film drug concentration *versus* time.

Equation 8 will be employed, as shown in the *Appendix*, to establish an expression relating the coefficient p and the apparent first-order rate constant k_a for a given parameter associated with the decline of the pilocarpine concentration in the precorneal area. Whether it is a good approximate equation to use depends largely on the relative magnitude of b and k''; the approximation improves as b exceeds k'' by a factor of at least 5. For the range of parameter values encountered in this study, the error due to the approximation does not exceed 7%, a tolerable error for these purposes[2].

Finally, mass balance equations similar to Eq. 5 can be written for the other compartments in Scheme III. They are:

$$V_B \frac{d[B]}{dt} = p_p([A] - [B]) - p_m[B] - p_a([B] - [C]) \qquad \text{(Eq. 9)}$$

$$V_C \frac{d[C]}{dt} = p_a([B] - [C]) - p_r([C] - [D]) - p_{ao}[C] \qquad \text{(Eq. 10)}$$

$$V_D \frac{d[D]}{dt} = p_r([C] - [D]) - p_{ro}[D] \qquad \text{(Eq. 11)}$$

In Eqs. 9–11, A represents the precorneal area, B represents the corneal epithelium, C is the corneal stroma–endothelium–aqueous chamber, and D is the reservoir; the V's refer to the volumes of the compartments indicated by the subscripts. Analytical expressions that might be obtained from these equations are too complicated to have practical value. Fortunately, much can be learned about the behavior of pilocarpine in the eye by solving the system of first-order linear differential equations, *i.e.*, Eqs. 3, 5, 6, and 9–11, using numerical methods. This approach was used in the simulation studies.

Simulation studies with the precorneal drug loss parameter values listed in Table II failed to duplicate tear film drug loss, suggesting the need for additional loss routes to complete the profile. Establishing these loss routes and quantifying the influence of all precorneal factors on ocular drug bioavailability are the purposes of this report.

EXPERIMENTAL

Materials—Tritiated pilocarpine alkaloid (specific activity of 4.2 Ci/mmole) in ethanol was obtained commercially[3] and purified by vacuum evaporation immediately prior to each run, as previously described (8). [^{14}C]-Glycerol[3] sterile aqueous solution (specific activity of 96.0 μCi/mg) was used as received. All other chemicals were either reagent or analytical grade and were used as received.

Male albino rabbits[4], 1.8–2.4 kg, were used throughout the studies. They were fed a regular diet with no restrictions on food or water consumed. Lighting and auditory stimuli were maintained on a 24-hr basis in the caging facility.

Solution Preparation—*0.01* M *Pilocarpine Alkaloid Solution*—A 0.01 *M* pilocarpine alkaloid solution, prepared in Sorensen phosphate buffer at the appropriate pH (6.24 or 7.38), was added to the labeled material prior to each experiment. Solutions were made isoosmotic with tears using sodium chloride. Each microliter of the resulting solution had an activity of ~75,000 cpm.

0.14 M *Glycerin Solution*—An aqueous aliquot of the isotopic species was added, prior to each experiment, to a 0.14 *M* glycerin solution prepared in pH 6.24 Sorensen phosphate buffer. The resulting solution was isoosmotic with tear fluid, and each microliter of solution had an activity of ~10,000 cpm.

0.14 M *Glycerin Solution Containing 0.01* M *Pilocarpine Alkaloid*—Equal portions of a 0.28 *M* glycerin solution and a 0.02 *M* pilocarpine alkaloid solution, both in pH 6.24 Sorensen phosphate buffer, were mixed immediately prior to each experiment. An aqueous aliquot of [^{14}C]-glycerin was added to the mixture, and the resulting solution was made isoosmotic with tears using sodium chloride. Each microliter of the final solution had an activity of ~10,000 cpm.

The small amount of labeled substances added to these three solutions did not appreciably alter the molarity of the final solutions. The final counts per minute for each solution was selected to achieve optimal counting efficiency.

0.1% Epinephrine Bitartrate and 0.25% Histamine Dihydrochloride Solutions—A 0.1% epinephrine bitartrate solution was prepared by diluting a commercial solution[5] with isoosmotic pH 7.38 Sorensen phosphate buffer. A 0.25% histamine dihydrochloride solution was prepared by dissolving the salt[6] with the same buffer. To minimize any direct irritating effect from these solutions on precorneal pilocarpine disposition, pilocarpine solutions were not instilled onto the eyes of experimental

[2] Unpublished calculations.
[3] New England Nuclear, Boston, Mass.
[4] Klubertanz, Edgerton, Wis.
[5] Epitrate (2%), Ayerst Laboratories, New York, N.Y.
[6] Sigma Chemical Co., St. Louis, Mo.

animals until 15 min had elapsed following application of the histamine or epinephrine solutions.

Epinephrine bitartrate was employed for its vasoconstrictive effect on blood vessels perfusing the nictitating membrane and the conjunctiva, whereas histamine dihydrochloride was employed for its vasodilating effect. The concentration of each agent was selected based on conventional usage and appeared, by visual inspection, to exert the desired effect over the experiments.

Anesthesia—When necessary, anesthesia was induced and maintained by phenobarbital sodium (50 mg/ml iv) administered *via* the marginal ear vein. The rabbits were anesthetized ~15 min prior to instillation of the pilocarpine solution.

Tear Film Pilocarpine Concentration–Time Profile—Disappearance of pilocarpine from the tear film was monitored under the following experimental conditions: (*a*) normal unanesthetized rabbits, (*b*) normal anesthetized rabbits, (*c*) unanesthetized rabbits whose ocular surfaces were treated with 25 μl of a 0.1% epinephrine bitartrate solution 15 min prior to instillation of the pilocarpine solution, (*d*) anesthetized rabbits whose ocular surfaces were treated as in (*c*), (*e*) unanesthetized rabbits whose ocular surfaces were dosed with 25 μl of a 0.01 *M* nonradioactive pilocarpine solution 15 min prior to instillation of the dosing solution, (*f*) unanesthetized rabbits whose ocular surfaces were dosed with 25 μl of a 0.25% histamine dihydrochloride solution 15 min prior to instillation of the pilocarpine solution, and (*h*) unanesthetized rabbits receiving 25-μl doses of a 0.01 *M* pilocarpine solution at pH 7.38.

During the experiments, all test animals were kept in restraining boxes in a normal upright posture. Both eyes of the rabbit were employed. Pilocarpine solution, 25 μl, was instilled directly onto the cornea of the test animal, collecting in the cul-de-sac. During instillation, the upper lid was slightly raised and the lower lid was pulled slightly away from the globe. The lids were immediately returned to their normal position after instillation.

One-microliter tear samples were removed at 0.25, 1, 2, 3, 4, and 5 min postinstillation using 1-μl disposable glass capillary pipets[7]. The earliest sample was taken 15 sec after instillation to allow for mixing of the instilled solution with the tear fluid. During the early time period following drug instillation, sample removal has a small influence on the overall rate constant governing the decline in pilocarpine concentration since the precorneal tear volume is substantial and the number of samples taken is small. Moreover, removal of a small volume of fluid from the tear film–drug pool has only an indirect influence on drug concentration in subsequent samples.

During sampling, extreme care was exercised to avoid eye irritation. Thus, the capillary pipet tip was placed into the tear pool in contact with the cornea along the lower lid margin without touching any eye tissue. For consistency, all samples were withdrawn from the center of the marginal tear strip. On those rare occasions when the entire pipet was not filled with tear fluid, the volume of sample withdrawn was estimated from the depth to which the capillary pipet was filled. Pipets containing tear samples were transferred to vials[8] containing 5 ml of prerefrigerated scintillation cocktail[9] and counted in a liquid scintillation spectrometer[10] after 24 hr of storage in the dark. The presence of glass capillaries in the scintillation cocktail did not alter the counting efficiency or affect the results in any way, in agreement with earlier findings (18).

After suitable corrections, the data in number of counts per minute per microliter of tear fluid were plotted semilogarithmically as a function of time and subjected to linear regression analysis. First-order rate constants were obtained for the decline of the pilocarpine concentration in the precorneal area of each rabbit.

Tear Film Glycerin Concentration–Time Profile—Only anesthetized rabbits were employed in this portion of the study. The dosing solutions were: (*a*) glycerin solution containing no pilocarpine and (*b*) glycerin solution with 0.01 *M* pilocarpine. Positioning of the test animals, dosing and sampling procedures, and data analysis were as described in the preceding sections.

Influence of Instilled Dose Volume on Pilocarpine Disappearance from Tear Film—Ten microliters of a 0.01 *M* pilocarpine alkaloid solution was instilled onto the cornea of anesthetized rabbits as described. Sampling procedure and data analysis were as described.

Computer Simulation Studies—The computer program to simulate pilocarpine disposition in the albino rabbit eye consists of two major subroutines, DERIVS and INTGRT. The system of differential equations is presented in the subroutine DERIVS, which is introduced into the main program *via* the differential equation routine DEPC[11]. DEPC employs the predictor–corrector method outlined previously (19) to solve numerically initial value problems of ordinary first-order differential equations.

The subroutine INTGRT performs integration by Simpson's rule on the results produced by the differential equation routine. In addition to simulating single-dose situations, the program is capable of treating: (*a*) multiple-dose problems with variable dose size and volume given at intervals that need not be equal and (*b*) situations where the dose is removed before absorption is complete.

All computer calculations were performed on a digital computer[12], and the specific simulations carried out are indicated under *Results* and *Discussion*.

Table III—Compilation of First-Order Rate Constants Governing Initial Decline in Drug (Pilocarpine and Glycerin) Concentration under Various Experimental Conditions

Experimental Condition	k_a, min^{-1}
Pilocarpine (pH 6.24, 25-μl dose)	
Unanesthetized	0.63 (0.06)[a] [10][b]
Pretreated with epinephrine	0.40 (0.050) [7]
Pretreated with pilocarpine	0.68 (0.11) [4]
Pretreated with histamine	1.03 (0.14) [6]
Anesthetized	0.30 (0.05) [5]
Pretreated with epinephrine	0.072 (0.012) [6]
Pilocarpine (pH 6.24, 10-μl dose)	
Anesthetized	0.46 (0.009) [7]
Pilocarpine (pH 7.38, 25-μl dose)	
Unanesthetized	0.43 (0.042) [6]
Glycerin (pH 6.24, 25-μl dose)	
Anesthetized	0.13 (0.014) [8]
Dosing solution incorporated with pilocarpine	0.39 (0.043) [5]

[a] Number in parentheses represents standard error of the mean. [b] Number in brackets represents number of determinations.

RESULTS

Disposition of Pilocarpine and Glycerin in Precorneal Area—With the possible exception of histamine dihydrochloride, the compounds instilled into the cul-de-sac of the rabbits at the concentrations employed do not damage the corneal epithelium (20, 21). Consequently, alteration in apparent rate constants could not be due to enhanced absorption of pilocarpine as a result of corneal damage from these compounds.

In fitting the data to first-order decline by linear regression analysis, no attempt was made to force the best fit line through the theoretical counts per minute per microliter of tear fluid at time zero, due mainly to uncertainties in the mixing efficiency of instilled dose with the resident tear fluid. On the average, the deviations of the time zero values given by these best fit lines from the corresponding values calculated by assuming instantaneous mixing were less than 5%. In most cases, the coefficient of determination for the regression exceeded 0.95.

Following topical instillation of a given volume of pilocarpine solution in the eye, the tear film drug concentration declined rapidly. Figure 1 is an example of a semilogarithmic plot of counts per minute per microliter of tear fluid against time. Table III summarizes the apparent first-order rate constants governing tear film drug concentration decline under various experimental conditions. In normal unanesthetized rabbits, the decline in pilocarpine concentration had an associated rate constant of 0.63 min^{-1}. Changing the instilled solution pH from 6.24 to 7.38 produced a 1.5-fold reduction in the associated rate constant. In contrast, in the presence of anesthesia, the rate constant was reduced by ~50%. Predosing the eye with vasoactive agents also modified the first-order rate constant. Specifically, histamine dihydrochloride, a vasodilator, increased the rate constant by a factor of 1.5; epinephrine bitartrate, a vasoconstrictor, reduced it by the same factor. The reduction in the rate constant due to epinephrine was more prominent when anesthesia was present (Table III).

Table III also shows that, in the presence of anesthesia, glycerin disappeared from the precorneal area with an associated rate constant ~50% less than that for pilocarpine. However, when administered in combination with pilocarpine, the associated rate constant increased and was

[7] Curtis Matheson Scientific, Houston, Tex.
[8] Mini Vial, Research Products International Corp., Elk Grove Village, Ill.
[9] Aquasol, New England Nuclear, Boston, Mass.
[10] Model 2002, Packard Instrument Corp., Downers Grove, Ill.
[11] Differential Equations Reference Manual for the 1108, Madison Academic Computing Center, Madison, Wis.
[12] UNIVAC 1110, Madison Academic Computing Center, Madison, Wis.

Table IV—Significance Testing [a] for Selected Cases Listed in Table III

Experimental Condition	p
Unanesthetized[b] *versus* (unanesthetized + pilocarpine)	<0.3366
Unanesthetized *versus* (unanesthetized + epinephrine)	<0.0036
Unanesthetized *versus* (unanesthetized + histamine)	<0.0106
Anesthetized[b] *versus* (anesthetized + epinephrine)	<0.0009
Anesthetized (25 μl) *versus* anesthetized (10 μl)	<0.0056
Anesthetized (glycerin) *versus* anesthetized (pilocarpine)	<0.0041
[Anesthetized (glycerin) + pilocarpine] *versus* anesthetized (pilocarpine)	<0.1004
Unanesthetized *versus* anesthetized (10 μl)	<0.0047
Unanesthetized (pH 6.24) *versus* unanesthetized (pH 7.38)	<0.0065
Anesthetized (pH 6.24) *versus* unanesthetized (pH 7.38)	<0.0366

[a] Student t-test. [b] Unless otherwise indicated, these cases referred to those in which pilocarpine was the drug employed.

statistically indistinguishable from that obtained for pilocarpine at the 95% confidence level (Table IV).

Finally, the first-order rate constant of decline increased by a factor of 1.5 when the instilled volume was reduced from 25 to 10 μl. At the 95% confidence level, this difference was statistically significant (Table IV).

Computer Simulation of Precorneal and Intraocular Pilocarpine Disposition—Table V lists the literature-adapted parameter values used in the initial simulation (1, 7, 11, 17, 22). Each parameter, p, associated with drug transfer between compartments, *e.g.*, aqueous humor → reservoir, was obtained by multiplying the corresponding first-order rate constant by the donor compartment volume. Since the corneal epithelium and stroma volumes were not determined, only their estimates are included. In regard to precorneal factors, the associated first-order rate constants (Table II) were employed. The exception was nonproductive loss, for which a value of 0.258 min^{-1} was shown (17) to yield better agreement with the tear film pilocarpine concentration–time profile established in the present study. For estimating p_p and p_n, a time-averaged precorneal fluid volume was employed; its rationale was discussed earlier. The final version of the precorneal parameter values is presented in Table VI. The initial estimates shown in Table V were modified only slightly.

Table V—Initial Estimates of the Parameter Values Associated with Ocular Distribution of Pilocarpine in the Albino Rabbit

Parameter	Value
Precorneal factors	
p_p	0.13 μl/min
k_d	0.54 min^{-1}
p_n	8.38 μl/min
Q_0	0.66 μl/min
Q_i	2.48 μl/min
k_l	0.54 min^{-1}
Intraocular factors	
p_a	0.6 μl/min
p_{ao}	4.04 μl/min
p_r	2.02 μl/min
p_{ro}	0 μl/min
Volumes	
V_0	7.5 μl
V_B	6 μl
V_C	250 μl[a,b]
V_D	325 μl[b]

[a] Volume of stroma is assumed to be 32 μl. [b] V_C and V_D add up to the volume of distribution value of 575 μl reported by Conrad and Robinson (22).

Figure 2 displays the simulated tear film drug concentration profile in unanesthetized rabbits for the first 5 min postinstillation. The slight curvature evident was due to drainage. Unless the experimental data are extremely precise, this curvature usually will not be detected. Consequently, the initial decline in drug concentration can often be approximated by a first-order process. The slope of the best-fit line yielded a first-order rate constant of 0.68 min^{-1}, which resided within the 95% confidence interval of the experimental value. This observation, in conjunction with the values reported for previously identified precorneal disposition factors, supported the notion that additional factors are critical to precorneal loss of pilocarpine.

The corresponding plot for the amount of drug in the tear film is depicted in Fig. 3. Here, the slope was approximately 1.5 times larger than that governing the decline in drug concentration. The important point is that the apparent first-order rate constant controlling the decline in drug concentration is not necessarily that controlling the decline in the amount of drug.

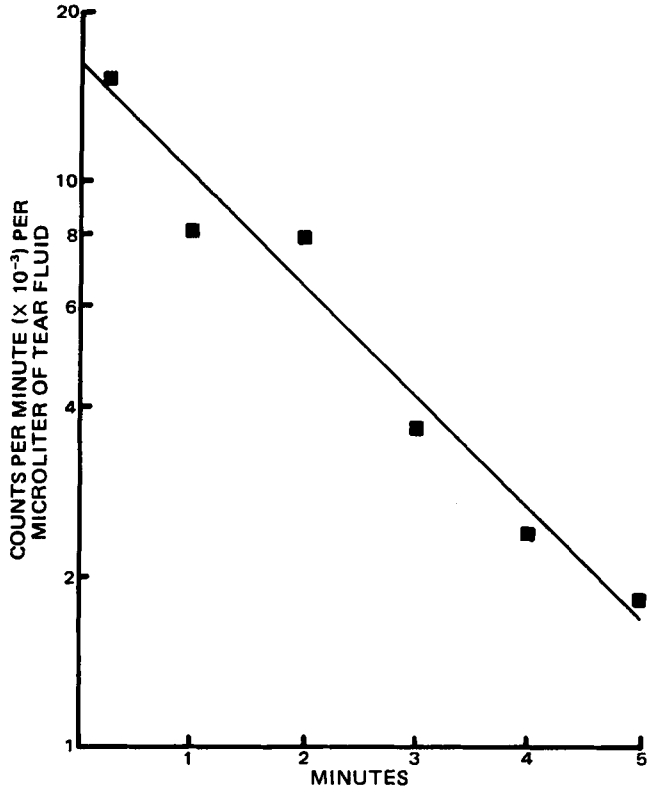

Figure 1—*Decline in the pilocarpine concentration (expressed as counts per minute per microliter of tear fluid) in the tear film following instillation of 10 μl of a 0.01* M *pilocarpine solution in an anesthetized rabbit.*

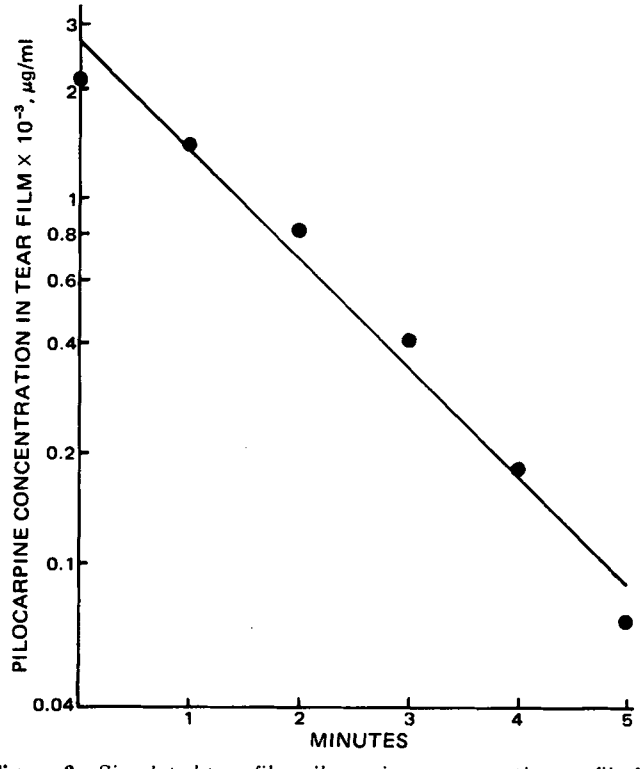

Figure 2—*Simulated tear film pilocarpine concentration profile for the first 5 min postinstillation. The solid circles represent the concentration of drug in the tear film calculated for a given time from the parameter values listed in Table V. The solid line represents the best-fit line, with* $R^2 = 0.98$ *and slope* $= -0.68\ min^{-1}$.

Table VI—Relationship between the Volume-Independent Value and First-Order Rate Constant of Precorneal Drug Loss Parameters

Parameter Associated with	p^a, μl/min	k^b, min^{-1} Unanesthetized	Anesthetized
Corneal absorption	0.13	0.006	0.005
Conjunctival absorption	0.71	0.033	0.025
Nonconjunctival loss	2.80	0.13	0.10
Vasodilation due to pilocarpine	4.76	0.22	0.17
Normal tear flow	0.66	0.031	0
Induced lacrimation	4.75	0.22	0
Decline in induced lacrimation	—	2	0
Drainage	—	0.54	0.18
Equation relating p and k		$k = 0.047p$	$k = 0.036p$

[a] Volume-independent value. [b] Apparent first-order rate constant.

Figure 4 is a simulated aqueous humor drug concentration profile, and the fit to experimental data is good. Based on the profiles displayed in Figs. 2 and 4, the proposed model is excellent in describing precorneal disposition of pilocarpine. A deficiency of the model concerns accounting for pilocarpine disposition within the cornea beyond 20-min postinstillation. In particular, the amount of pilocarpine in the cornea for this time interval, calculated according to the model, is approximately twice that obtained experimentally. As a result of systematically varying the magnitude of relevant parameter values, it becomes clear that a model that satisfactorily describes both precorneal and corneal disposition of pilocarpine must await additional studies on drug movement within the cornea.

DISCUSSION

Mechanisms Governing Precorneal Pilocarpine Disposition—The existence of efficient parallel loss processes acting in concert to remove drug from the precorneal area of the eye is unequivocal. This is attested to by the early peak time established in the corneal epithelium and aqueous humor following instillation of a pilocarpine solution (10, 11) and by the small fraction of an instilled dose that successfully gains access to the internal eye structures (8, 9). The large rate constant, 0.63 min^{-1}, associated with the decline in pilocarpine concentration in the tear film of unanesthetized rabbits provides a quantitative measure of the overall parallel loss effect. Obviously, from the standpoint of improving ocular drug bioavailability by formulating maximally efficacious ocular drug delivery systems, it would be helpful to identify all components of precorneal drug loss as well as the associated rate constants.

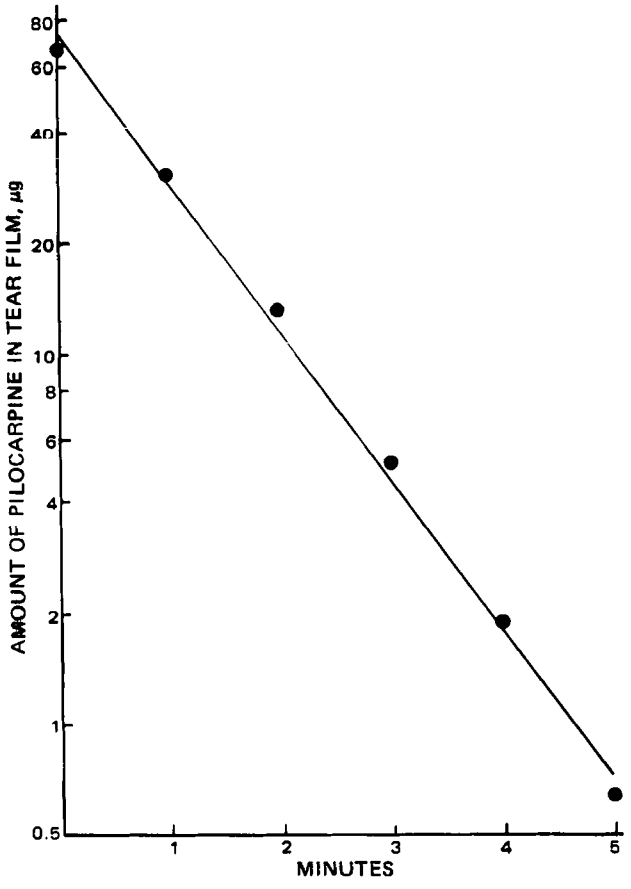

Figure 3—*Simulated profile for amount of pilocarpine in tear film for the first 5 min postinstillation. The solid circles represent the amount of drug in the tear film calculated for a given time from the parameter values listed in Table V. The solid line represents the best-fit line, with* $R^2 = 0.99$ *and slope* $= -0.93\ min^{-1}$.

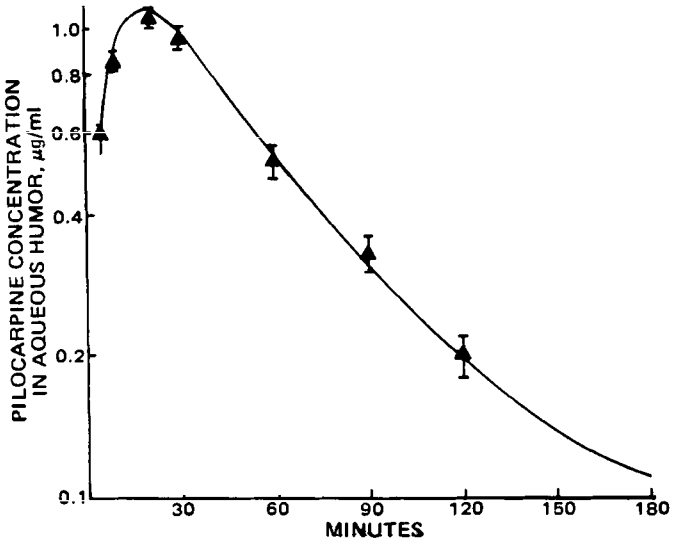

Figure 4—*Concentration of pilocarpine in aqueous humor of albino rabbits following topical instillation of a 0.01* M *solution. Key:* ▲, *data from Ref. 11; and —, simulated profile generated with parameter values listed in Table V.*

As mentioned earlier, the reported loss parameters of solution drainage (1, 2), drug protein binding (3–5), tear turnover (1, 6), and conjunctival absorption (7), by themselves, cannot account for the large first-order rate constant governing precorneal pilocarpine loss. To reconcile this discrepancy, several possibilities can be proposed, and each will be examined here in turn.

Incorrect Reported Rate Constants

1. Underestimation of Reported Rate Constants—The two reported loss routes of interest are corneal and conjunctival absorption. Although the rate constant for corneal pilocarpine absorption has not been determined, good estimates place it at least one or two orders of magnitude less than the rate constant governing conjunctival absorption and overall tear film drug loss. As a result, it is of minor consequence to the overall tear film drug loss rate constant.

The 0.0217 min^{-1} rate constant reported for nonproductive loss due to conjunctival pilocarpine absorption is in line with reported values for other substances, including the rate constant (23) for passive diffusion of sodium and chloride ions across the conjunctiva. Additional support comes from a consideration of the difference in surface area of the cornea and conjunctiva available for drug absorption (24) and of the data of a recent study (25) on conjunctival absorption. Therefore, it can be concluded that the reported conjunctival absorption rate constant for pilocarpine (7) is probably accurate.

2. Volume Effect on Apparent First-Order Rate Constants—It is of interest to evaluate the extent to which the discrepancy between 0.30 min^{-1}, observed in the anesthesia experiment[13], and 0.0217 min^{-1}, reported for nonproductive loss, can be attributed to a volume effect on apparent rate constants. In the study by Patton and Robinson (7), the experiment that yielded the nonproductive loss rate constant of 0.0217 min^{-1} was conducted in rabbits whose drainage apparatus were mechanically blocked. Under such circumstances, the precorneal fluid volume at all times would be approximately 32.5 μl, essentially the sum of instilled volume (25 μl) and resident tear fluid volume (7.5 μl). In contrast, the present study was performed with rabbits possessing functional drainage apparatus, meaning that the fluid volume in the precorneal area

[13] Ignoring the additional routes of precorneal drug loss for the moment leaves nonproductive loss as the only loss route available in the presence of anesthesia.

underwent an approximate fourfold change, from 32.5 μl at the moment of drop instillation to 7.5 μl shortly thereafter.

Teorell (14) showed that the first-order rate constant associated with drug movement from one compartment to the next is inversely related to the fluid volume in the donor compartment. In the present study, the effect of instilled volume on k_a was established in the experiment in which a 10-μl rather than a 25-μl dose was instilled into the cul-de-sacs of anesthetized rabbits. Table III shows that k_a underwent a 1.5-fold increase for a 2.5-fold reduction in instilled volume. On this basis, this volume effect by itself can *at most* contribute a factor of approximately 4.5, in which case a rate constant of 0.094 min^{-1} is obtained for nonproductive loss. Clearly, while volume influences the magnitude of the rate constant, it is not the principal explanation for the large rate constant associated with precorneal pilocarpine loss.

Different Mechanism for Corneal Pilocarpine Uptake—Some years ago, Kakemi *et al.* (26–29) reported that the amount of drug absorbed in the GI tract correlated well with its extent of binding to mucin lining the mucosa; they suggested that drug binding to mucin constituted the first step in absorption. Conceivably, the same phenomenon can occur in the mucin layer that coats the corneal surface (30). The anesthesia experiment in the present study, however, minimized the possibility of rapid uptake of pilocarpine by some component(s), including mucin, on the corneal surface as being primarily responsible for the large rate constant, k_a, associated with a decline in precorneal pilocarpine concentration. For this mechanism to be operative, k_a should register no appreciable change in its value under anesthesia.

Additional Loss Routes

1. Induced Lacrimation—If an increase in tear flow rate due to instilling a pilocarpine solution is a parallel loss route, the apparent rate constant, k_a, governing drug loss from the precorneal area must show a reduction in its value in the presence of anesthesia since lacrimation as well as normal tear flow is inhibited under this condition (1). The experimental value of 0.30 min^{-1} obtained in anesthetized rabbits, an appreciable reduction when compared with the value of 0.63 min^{-1}, indicates that induced lacrimation is indeed a pathway of drug loss. It is not the only route, however, because k_a does not converge to the value of 0.0217 min^{-1} determined (7) for nonproductive loss of pilocarpine to tissues surrounding the tear chamber.

The results of the experiment using a pH 7.38 instead of a pH 6.24 solution demonstrate that much of the lacrimation effect is due to vehicle formulation. Although this observation is consistent with other findings (16) on vehicle influence on drug bioavailability, it is inconsistent with those of Patton and Robinson (7). In particular, Patton and Robinson (7) can account fully for the difference in k_a between anesthetized and unanesthetized rabbits, both with blocked drainage apparatus, by merely including normal tear turnover. This apparent inhibition of lacrimation upon blocking the drainage apparatus has also been observed in humans (31). Aside from invoking a compensatory mechanism that resists an increase in tear volume beyond the large volume already present, no explanation is forthcoming at the present time. There is little doubt, however, that in normal unanesthetized rabbits, induced lacrimation is a component of the precorneal pilocarpine loss mechanism.

2. Nonconjunctival Loss of Pilocarpine (Uptake of Drug by Nictitating Membrane)—Examination of the anatomy of the rabbit's tear chamber reveals the nictitating membrane to be a structure that potentially can act in conjunction with the conjunctiva and the cornea to remove drug from the precorneal area. This discussion of nonconjunctival pilocarpine loss will focus on uptake by the nicitating membrane, even though additional components of nonconjunctival loss are possible.

Like the conjunctiva, the nictitating membrane is a vascularized tissue (32). It is not clear what gives it an apparent advantage over the conjunctiva in removing drug from the precorneal area. A direct determination of drug levels in the nictitating membrane as a function of time may not establish if it is the dominant factor in causing drug loss. So long as it is in contact with the fluid bathing the precorneal area, its concentration–time profile will probably show an early peak time of 5 min just like that for the corneal epithelium. On the other hand, surgical removal of the nictitating membrane may change the tear chamber volume and possibly the drainage process, just to name a few. Therefore, a simple approach of manipulating the vascularization of this tissue was adopted.

The role of blood flow on drug absorption was studied in the GI tract (33, 34) and was recently reviewed (35). In the eye, if the nictitating membrane contributes substantially more to precorneal drug loss than does the conjunctiva, in the presence of a vasoconstrictor the apparent rate constant of decline should register a corresponding reduction in value. Indeed, in the anesthetized rabbit, it is reduced by a factor of 4 upon the application of a 0.1% epinephrine bitartrate solution. The change is less dramatic in the unanesthetized rabbit because induced lacrimation due to vehicle formulation, which is not expected to be affected by this procedure, is still present. The difference in the magnitude of the rate constant obtained in unanesthetized and anesthetized rabbits was the same regardless of epinephrine pretreatment (Table III). This difference amounted to 0.33 min^{-1} and may be ascribed to tear flow, of which induced lacrimation is a part.

Just as vasoconstriction is accompanied by a substantial reduction in the apparent rate constant of parallel loss, it is reasonable to expect opposite changes in the aforementioned rate constant when vasodilation or inflammation is present. Indeed, histamine dihydrochloride, a potent vasodilator (36), at an instilled concentration of 0.25% caused an upward shift of the rate constant from 0.63 to 1.03 min^{-1}. This result may not be a pure vasodilation effect, however, because histamine at a concentration as low as 5×10^{-6} *M* loosened the superficial epithelial cells of excised beef corneas after several hours of incubation (37), an effect that could enhance corneal pilocarpine absorption. However, the contact time in the present experiment was short enough to preclude a surface effect.

3. Vasodilation due to Pilocarpine—Since pilocarpine itself is a vasodilator (36), this pharmacological effect is expected to manifest itself in the rate constant governing disappearance of the drug from the precorneal area. The vasodilation effect appears to be immediate since predosing the eye with an equivalent amount of pilocarpine yielded a rate constant that was statistically indistinguishable from that obtained under normal circumstances (Table IV). In contrast, when glycerin, which is devoid of vasodilation properties, was administered in combination with pilocarpine, the rate constant associated with the glycerin concentration decline increased by a factor of 3. Moreover, glycerin then disappeared from the precorneal area with a rate constant similar to that governing pilocarpine decline. Induced lacrimation was not a concern here since anesthetized rabbits were employed.

By taking the difference in rate constants obtained for pilocarpine and glycerin, both in anesthetized rabbits, a value of 0.17 min^{-1} was obtained. This value may be denoted as the rate constant due to vasodilation induced by pilocarpine in *anesthetized* rabbits. Suitable corrections for the influence of anesthesia on the drainage rate constant (1) must be applied in calculating the corresponding value for unanesthetized animals.

An implication associated with vasodilation induced by pilocarpine is its expected variation with instilled concentration. This, if operative, will be reflected in the pilocarpine levels obtained in a given tissue, *e.g.*, aqueous humor, and, obviously, the magnitude of the rate constant governing precorneal drug loss. The linearity of the dose–aqueous humor concentration (at 20 min postinstillation) profile over six orders of magnitude in dose (10^{-6}–10^{-1} *M*) (8) suggests that either the rate constant due to pilocarpine-induced vasodilation is a weak function of instilled concentration or, less likely, maximum vasodilation is attained at the lowest instilled concentration of 10^{-6} *M*. The dose–aqueous humor concentration plot is a log–log plot so that small differences will not be discerned.

Not only does induced lacrimation appear to be suppressed when the drainage apparatus is blocked, but the same is true for pilocarpine-induced vasodilation. This effect can be seen by comparing the magnitude of the rate constants involved: 0.17 min^{-1} for the vasodilation determined in this study *versus* 0.0217 min^{-1} for nonproductive loss reported elsewhere (7). Undoubtedly, a volume effect is making a contribution. Thus, in anesthetized rabbits with blocked drainage apparatus, the rate constant ascribed to vasodilation assumes a theoretical value of 0.11 min^{-1}, which is five times larger than the reported 0.0217-min^{-1} value. The difference can be reconciled, in part, by attributing the preponderance of vasodilator effect to the nictitating membrane, a consideration consistent with the view that the nictitating membrane, in some unknown fashion, does not participate in precorneal drug disposition as soon as the drainage apparatus is blocked. Whether this phenomenon is peculiar to pilocarpine can possibly be disclosed in an experiment involving other drugs such as glycerin.

Thus far, the volume effect on apparent first-order rate constants has been identified, the notion of rapid pilocarpine uptake by some components on the corneal surface has been mentioned, and induced lacrimation due to vehicle formulation, nonconjunctival pilocarpine loss, and vasodilation due to the drug have been established as additional aspects of precorneal pilocarpine disposition. It is still unclear why these additional, and yet critical, parameters controlling precorneal disposition are absent when the drainage apparatus is blocked. Similarly, there is the observation by DeSantis and Schoenwald (38) that disputes the importance of the nictitating membrane as a pathway contributing to pilocarpine loss

Table VII—Influence of Individual Parallel Loss Factors on Bioavailability

Parallel Loss Factor Present	Ratio A[a]	Ratio B[b]
Drainage	0.24	30.4
Normal tear flow	0.18	22.1
Induced lacrimation	0.13	16.4
Conjunctival absorption	0.16	20.9
Vasodilation due to pilocarpine	0.03	3.5
Nonconjunctival loss	0.05	5.9
All factors present	0.007	1.0

[a] Ratio A is referenced to the case when no parallel loss factors are present (*AUC* in aqueous humor is 9716 μg/ml min). [b] Ratio B is referenced to the case when all parallel loss factors are present (*AUC* in aqueous humor is 77.0 μg/ml min).

from the precorneal area. They monitored changes in pupil diameters as a result of surgical removal of the nictitating membrane. However, pupillary diameter measurements, as compared with aqueous humor drug level determinations (8), are not a sensitive indicator for pilocarpine bioavailability.

What remains to be done is to integrate these additional pathways responsible for precorneal pilocarpine loss with the previously identified pathways by assessing the relative importance of each to ocular drug bioavailability. But first it is necessary to derive from the experimental data the coefficients, p, associated with each pathway of loss shown in Scheme III because the experimental results, presented as first-order rate constants, were obtained in both anesthetized and unanesthetized rabbits and the rate of change in precorneal fluid volume differs under these conditions. In other words, the presence of drainage conceals the actual contribution of each pathway to total drug loss. With this background, one can proceed, as outlined in the *Appendix*, to calculate the volume-independent coefficients, p, associated with various routes of precorneal drug loss.

Table VI summarizes the values computed for various parameters associated with precorneal pilocarpine disposition. The corresponding k values for anesthetized and unanesthetized rabbits are obtained by applying Eqs. A1 and A3, respectively (see *Appendix*). From the volume-independent values, one can see that, in terms of effectiveness of removing drug from the precorneal area, the rank order of various precorneal disposition factors appears to be: vasodilation due to pilocarpine > nonconjunctival loss > conjunctival absorption > normal tear turnover > corneal absorption. How induced lacrimation fits into this sequence is not as straightforward because of its time dependence. The same is true of drainage, due to lack of knowledge of an effective volume to properly weight this parameter. Computer simulations will be employed to examine the relative importance of these precorneal factors in effecting drug loss.

Relative Importance of Precorneal Drug Disposition Factors on Extent of Drug Absorption—Tables VII and VIII list the various cases to be considered in an effort to understand the relative importance of precorneal drug disposition factors, alone or in combination, in influencing the extent to which pilocarpine is absorbed across the corneal epithelium. The area under the curve (*AUC*) from 0 to 120 min in the aqueous humor will serve as an indicator for the amount of drug absorbed. Ideally, the entire, rather than the truncated, *AUC* should be used. However, since only relative values are of interest, the *AUC* from 0 to 120 min is used.

Each case listed in Tables VII and VIII is referenced to two special cases. Ratio A is referenced to the ideal case in which no parallel loss factors are present and is, therefore, roughly equivalent to the fraction of dose absorbed in the presence of certain loss factors. Ratio B is referenced to the case corresponding to normal physiological conditions when all parallel loss factors are present and, therefore, reflects the improvement in bioavailability when one or more parallel loss factors are suppressed. As an illustration, Table VII shows that when all parallel loss factors except normal tear flow are suppressed: (*a*) the apparent fraction of dose absorbed (Ratio A) is 0.18, and (*b*) relative to normal physiological conditions, there should be a 22-fold increase in the amount of pilocarpine recovered in aqueous humor (Ratio B).

Consider Ratio A in greater detail. According to Table VII, when only a single parallel loss factor is present, the amount of dose absorbed is reduced by at least 75%. Under the usual circumstances of more than one parallel loss factor being operative, it is reduced by an additional 80% (Table VIII). From these two tables, one can establish, in principle, a single sequence ranking the various parallel loss factors in terms of their effectiveness in removing pilocarpine from the precorneal area. To this end, the most efficient parallel loss factor can be identified as the one possessing a Ratio A that has the smallest value in Table VII but the largest in Table VIII. Quite unexpectedly, two sequences differing only in the ranking of drainage are obtained. Whereas Table VII indicates that drainage is the *least* efficient parallel loss factor, Table VIII indicates that it is the *most* efficient one.

Table VIII—Influence of Combinations of Parallel Loss Factors on Bioavailability

Parallel Loss Factor Absent	Ratio A[a]	Ratio B[b]
Drainage	0.014	1.78
Induced lacrimation	0.0085	1.07
Conjunctival absorption	0.0084	1.06
Vasodilation due to pilocarpine	0.013	1.67
Nonconjunctival loss	0.010	1.29
All factors present	0.007	1.0

[a,b] See footnotes to Table VII for details.

These conflicting results can be explained by noting that the proposed model allows drug diffusion from the epithelium into the tear film, a realistic situation. Within this framework, the portion of drug that has diffused into the tear film is completely available for reabsorption as soon as normal resident tear volume is attained, so long as drainage is the only loss factor present. When factors in addition to drainage are present, the same portion of drug is subjected to continuous removal by routes in addition to corneal absorption. Of relevance here is the first case listed in Table VIII. It can be seen that eliminating drainage brings about the most improvement in bioavailability, equivalent to saying that drainage is the most efficient parallel loss factor.

Simply stated, when parallel loss factors are evaluated in the manner prescribed by Table VII, the conclusion of drainage being the least efficient parallel loss factor is an artifact of the system. Thus, the relative effectiveness of precorneal disposition factors in removing drug should be: drainage ≃ vasodilation > nonconjunctival loss > induced lacrimation ≃ conjunctival absorption > normal tear turnover.

Implications of Precorneal Drug Loss in Ocular Drug Delivery System Design—Having established the contributions of various precorneal drug disposition factors to precorneal loss of pilocarpine, their implications in designing ocular drug delivery systems that optimize ocular pilocarpine bioavailability can be examined. The aforementioned precorneal disposition factors can first be grouped into vehicle- and drug-related categories. Drainage and induced lacrimation belong to the category of vehicle-related factors, whereas conjunctival absorption, nonconjunctival loss, vasodilation, and corneal absorption are drug-related factors. Based on the magnitude associated with each parameter, impairing a single route of loss will not bring about more than a twofold improvement, on the average, in the fraction of dose absorbed (Ratio B, Table VIII).

By far, the route that has received the most attention is drainage. Previous studies (39–41) showed that delaying drainage by a factor of 10 through use of polymer solutions as vehicles results in only a factor of 2 improvement in bioavailability. As an alternative to polymer solutions, one can employ solid or semisolid dosage forms such as ointment (42), soft contact lenses (43–46), and controlled-release devices including the Ocusert (47, 48). With the possible exception of the Ocusert, this approach has thus far not met with satisfactory results.

Induced lacrimation, another vehicle-related loss factor, can be suppressed by formulating the solution at physiological pH and tonicity so long as they are compatible with drug stability. According to the proposed model, this approach alone causes no dramatic improvement in the amount of drug absorbed either. There is a 1.6-fold improvement in aqueous humor pilocarpine levels as the pH is varied (42).

The remaining factors, vasodilation, nonconjunctival loss (of which drug uptake by the nictitating membrane is a component), and conjunctival absorption, are more drug than vehicle related. Unfortunately, they include those factors that play dominant roles in causing drug loss. This finding suggests prodrug derivative formation to minimize vasodilation, thereby improving bioavailability for pilocarpine. Alternatively, administration of vasoconstrictors prior to instillation of pilocarpine solution shows promise for improving its bioavailability. The proposed model, in conjunction with the experimental data obtained in the present study, predicts a 2.5-fold improvement when a 0.1% epinephrine bitartrate solution is administered 15 min prior to instilling the dose. Chrai *et al.* (2) reported only a 1.16-fold increase, but these investigators administered both drugs in combination.

Since the nictitating membrane is absent in humans, drug uptake by this structure is not a concern in designing ocular drug delivery systems for humans.

From this discussion, it is clear that a combination of physical and

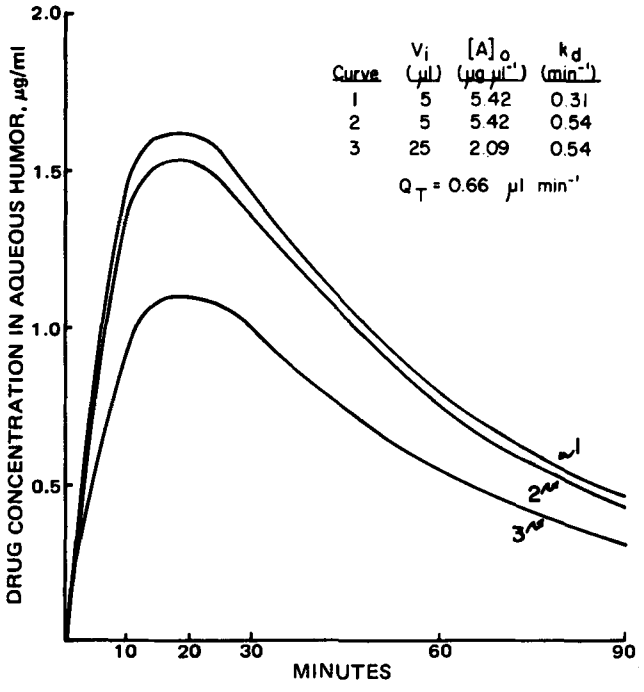

Figure 5—*Effect on aqueous humor drug levels upon varying instilled concentration and volume while holding amount of drug administered constant. Tear flow is present. Key:* V_i, *instilled volume;* $[A]_0$, *initial concentration of drug in tear film; and* k_d, *drainage rate constant. These profiles were generated for an instilled concentration of 13.56 μg/μl contained in a volume of 5 μl and for 2.71 μg/μl in 25 μl.*

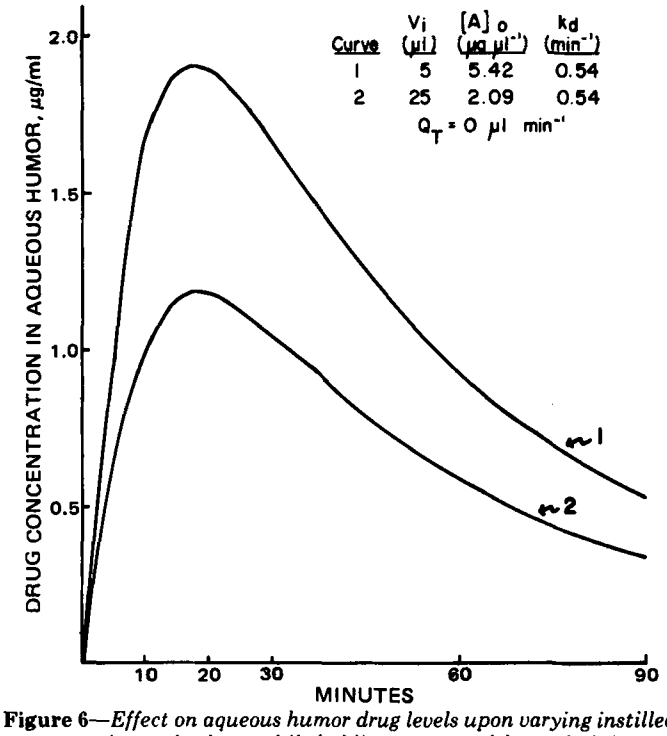

Figure 6—*Effect on aqueous humor drug levels upon varying instilled concentration and volume while holding amount of drug administered constant. Tear flow is absent. Key:* V_i, *instilled volume;* $[A]_0$, *initial concentration of drug in tear film; and* k_d, *drainage rate constant. These profiles were generated for an instilled concentration of 13.56 μg/μl contained in a volume of 5 μl and for 2.71 μg/μl in 25 μl.*

chemical approaches is needed to achieve maximum improvement in bioavailability of topically applied pilocarpine. Assuming that the enzymes necessary for bioconversion are available, one can design a prodrug derivative possessing the desirable attributes of favorable uptake by the corneal epithelium (a highly lipophilic structure), minimal vasodilating properties, and, ideally, minimal uptake by the conjunctiva. Such a derivative can then be placed into a suitable controlled-release device, which must satisfy the anatomical and physiological constraints imposed by the precorneal area of the eye. One may argue that administering larger amounts of drug would give the desired drug levels in ocular tissues, but there exists the concern of systemic toxicity since most of the applied drug is then available for systemic absorption (49).

Important Aspects Relating to Drainage—With the spectrum of of precorneal pilocarpine disposition factors placed in some perspective, the remaining sections of this report are devoted to some important aspects relating to drainage, the factor deemed to be crucial in precorneal drug loss.

Role of Instilled Dose Parameters in Ocular Drug Bioavailability—Given the strategic role of drainage in the parallel loss process and its sensitivity to the volume of dose instilled, it is instructive to compare the concentration–time profiles in a given intraocular tissue when a fixed amount of drug is delivered in various combinations of volume and concentration. Compartment pharmacokinetics will predict identical profiles under these conditions; this result can be seen in Eq. 12, which expresses the concentration, C, of drug in the central compartment as a function of time for a drug that obeys one-compartment model kinetics:

$$C = \frac{FD}{V_d}\left(\frac{k_a}{k_a - k_e}\right)(e^{-k_e t} - e^{-k_a t}) \qquad \text{(Eq. 12)}$$

where k_a is the absorption rate constant, k_e is the elimination rate constant, D is the amount of drug administered, F is the fraction of dose absorbed, and V_d is the apparent volume of distribution. In contrast, our model, like a previous one (12), predicts characteristic intraocular tissue concentration–time profiles for each combination of instilled concentration and volume. Figure 5 illustrates this point. In this figure, two curves (1 and 2) are included for the 5-μl case. Curve 1 represents the case where the drainage rate constant, k_d, possesses a value characteristic of this volume, *i.e.*, $k_d = 0.31$ min^{-1}; curve 2 represents the case where k_d is the same as that for a 25-μl dose, *i.e.*, $k_d = 0.54$ min^{-1}. In both cases, the concentration at any time is higher than that for a 25-μl dose (curve 3). This finding indicates that the differences that arise from the dose volume instilled are not due to a volume-dependent drainage effect alone; the initial concentration established in the tear film also plays a role. Moreover, since the volume instilled indirectly influences the contribution of tear flow, $Q_T(t)$, to parallel loss, it is necessary to see if the profiles would continue to be different even when $Q_T(t)$ is set equal to zero.

The answer is provided by the profiles displayed in Fig. 6. Again, the 5-μl dose gives a higher concentration than the 25-μl dose, indicating that the increase in extent of drug absorption from a smaller dose volume cannot be due largely to the indirect influence exerted by drainage on tear flow. Drainage is present in all these instances. Hence, when it ceases to be a parallel loss factor, the results given by the present model should coincide with those given by the pharmacokinetic treatment described earlier. In essence, the dose volume administered influences the tissue concentration–time profiles only if the fluid volume at the absorption site undergoes a time-dependent change in response to the volume administered. Therefore, this volume effect should be observed in regions of the body, *e.g.*, precorneal area, rectum, and skeletal muscles (50–53), which have a limited capacity to accommodate volume and/or to possess a small resident volume of fluid to begin with. The influence that fluid volumes may exert on the absorption of orally dosed drugs begins to be recognized. This influence is complex, as illustrated by studies on aspirin (54), amoxicillin and ampicillin (55), and erythromycin stearate (56).

For completeness, the role of the initial concentration as it relates to drug bioavailability from topical instillation should be explored. According to Table IX, the *AUC* in aqueous humor, and hence the amount of drug absorbed, is greater for a 25-μl dose than for a 5-μl dose, despite the negative influence of drainage experienced by the larger volume of dose. The increase is due to a larger amount of drug administered with the larger volume of dose. Also of interest in the same table is the higher instilled concentration associated with the 5-μl dose, yet the extent of drug absorbed still favors the 25-μl dose.

Thus, the relationship between instilled concentration and amount relative to drug bioavailability is an intricate one. On an absolute basis, for a given amount of drug, a small volume allows more drug to be absorbed. For a given initial or instilled concentration, the opposite is the case. However, in terms of the fraction of dose absorbed, as reflected by the value obtained on dividing the *AUC* by the instilled amount, a small volume of dose is still more efficient than a large one (Table IX). Such a volume effect was implied by previous studies in this laboratory (1, 2) and, more recently, was confirmed experimentally in rabbits (49, 57) and humans (58).

Table IX—Effect of Initial Concentration in Tear Film on Area under the Curve (*AUC*) in Aqueous Humor

Volume Instilled, μl	Instilled Concentration, μg/μl	Instilled Amount, μg	Initial Concentration, μg/μl	*AUC* in Aqueous Humor[a], μg/ml min	*AUC* ÷ Instilled Amount, μg/ml min/μg
5	5.22	26.08	2.09	43.6	1.67
25	2.71	67.82	2.09	77.0	1.14

[a] From 0 to 120 min.

Role of Drainage in Determining Early Peak Time in Corneal Epithelial Drug Concentration–Time Profile—Not only does drainage exercise a definite role in controlling the fraction of instilled dose available for absorption, it also complicates the interpretation of the early peak time observed in the corneal epithelium. Despite the magnitude of the drainage rate constant, the peak time obtained when it is the only parallel loss factor is about three times *longer* than that obtained when it is the only one absent (Table X). This observation says that, by itself, drainage is less effective than the other parallel loss factors combined in causing an early peak time in the epithelium concentration–time profile.

The picture changes when drainage is allowed to act in conjunction with at least one other parallel loss factor. As an example, in the presence of tear flow, drainage gives a peak time of 10 min, as compared with the 20 min obtained otherwise. This example illustrates an additional important point; so long as drainage is an integral component of the precorneal drug loss mechanism, the peak time derived from a corneal epithelial drug concentration–time profile is an insensitive indicator for the existence of such equally efficient parallel loss pathways as vasodilation and uptake of drug into the nictitating membrane. The present study demonstrates that only by directly monitoring tear film drug levels, under a variety of experimental conditions, can a complete picture of precorneal drug disposition emerge.

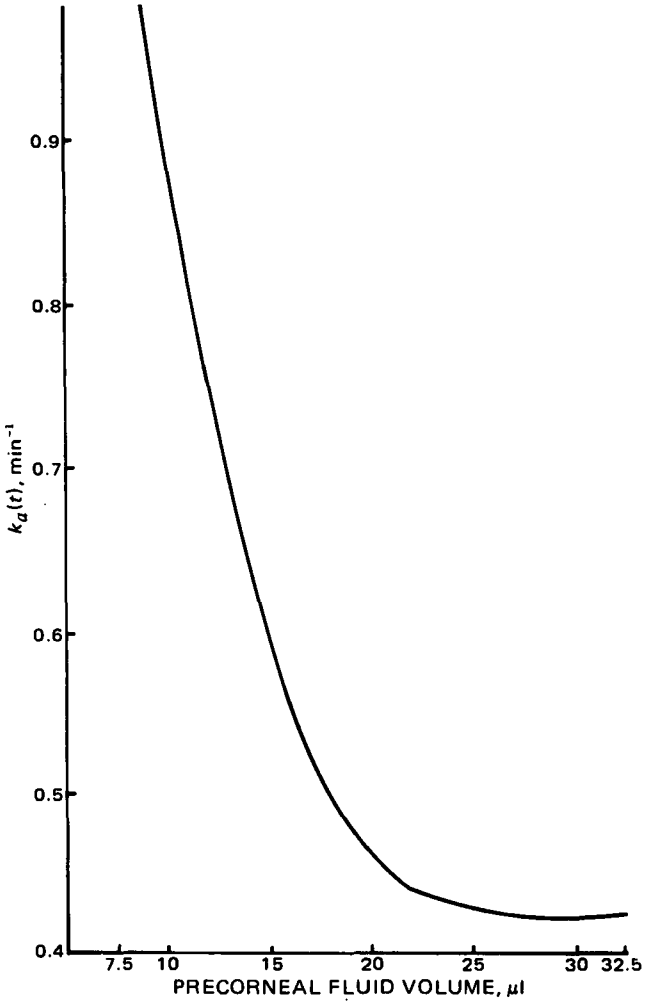

Figure 7—*Plot of* $k_a(t)$ *versus volume,* $V_A(t)$, *of precorneal fluid at a given time. See text for meaning of* $k_a(t)$.

Role of Precorneal Fluid Volume in Influencing Magnitude of Apparent First-Order Rate Constants Associated with Decline in Tear Film Drug Levels—Treatment of data according to compartment pharmacokinetics carries with it the implicit assumption of a single rate constant being adequate to describe the change in both amount and concentration of drug with time. Table XI indicates that this assumption does not hold in the precorneal area of the eye since the volume of fluid there continuously changes with time in an effort to attain resident tear volume. As expected, the apparent rate constant is larger for amount than for concentration, the difference being due to drainage, which exerts a direct influence on amount as opposed to an indirect one on concentration.

Furthermore, this apparent rate constant is time dependent. This is evident in Eq. 13, which describes the change in tear film drug concentration for the first 5 min postinstillation when the drug contribution from the epithelium to tear film drug levels is negligible:

$$\frac{d[A]}{dt} = -\left(\frac{p_p + p_n + Q_T(t)}{V_A(t)}\right)[A] \qquad \text{(Eq. 13)}$$

where the term within parentheses can be identified with the apparent first-order rate constant, $k_a(t)$, governing the decline in drug concentration. Notice that $Q_T(t)$ and $V_A(t)$ are functions of time. Thus:

$$k_a(t) = \frac{p_p + p_n + Q_T(t)}{V_A(t)} \qquad \text{(Eq. 13}a\text{)}$$

The first-order rate constant derived from the slope of a semilogarithmic plot of drug concentration *versus* time is, therefore, a time-averaged quantity, as indicated earlier. It is denoted as $\bar{k}_a$ and, conforming to experimental conditions in the present study, is given by:

$$\bar{k}_a = \frac{1}{V_A(5) - V_A(0)} \int_{V_A(0)}^{V_A(5)} k_a(t)\, dV_A(t) \qquad \text{(Eq. 14)}$$

where $V_A(0)$ is the fluid volume in the precorneal area at time zero and $V_A(5)$ is that at 5 min. Evaluation of the integral in Eq. 14 is simplified if $Q_T(t)$ is constant or zero. The result of the integration by assuming $Q_T(t) = 0$ is:

$$\bar{k}_a = \frac{p_p + p_n}{V_A(5) - V_A(0)} \ln\left(\frac{V_A(5)}{V_A(0)}\right) \qquad \text{(Eq. 15)}$$

For a 25-μl dose:

$$\bar{k}_a = \frac{p_p + p_n}{29.0} \qquad \text{(Eq. 16)}$$

whereas for a 10-μl dose:

$$\bar{k}_a = \frac{p_p + p_n}{18.9} \qquad \text{(Eq. 17)}$$

The conditions leading to Eqs. 16 and 17 are resident tear volume V_0 = 12 μl and drainage rate constant k_d = 0.177 min^{-1}. Equation 16 is very similar to Eq. A1 obtained by the procedure detailed in the *Appendix*. The essence of Eqs. 16 and 17 is twofold. First, contrary to what one might anticipate, the effective volume contributing to $\bar{k}_a$ is neither the instilled volume nor the total volume at time zero. Second, $\bar{k}_a$ is larger for a smaller instilled volume. Dividing Eq. 17 by Eq. 16 gives a ratio of 1.5, in excellent agreement with experimental findings on anesthetized rabbits, thus lending credence to the interpretation of apparent first-order rate constants offered by Eq. 14.

When $Q_T(t)$ is not equal to zero, the integral in Eq. 14 can be evaluated graphically. With the parameter values listed in Table VI, a plot of $k_a(t)$ *versus* $V_A(t)$ can be generated (Fig. 7). From this plot, a $\bar{k}_a$ of 0.41 min^{-1} is derived, which is less than the value of 0.63 min^{-1} obtained from the slope of a semilogarithmic plot of tear film drug concentration *versus* time. The discrepancy can be partly ascribed to rounding-off errors incurred in graphical integration.

An expression analogous to Eq. 15 for the time-averaged rate constant, $\bar{k}'$, governing the decline in amount of drug in the tear film can now be obtained. Equation 2 is cast into its equivalent form:

$$\frac{dA_t}{dt} = -\left(\frac{p_p + p_n + Q_T(t) - k_d V_0}{V_A(t)}\right) A_t - k_d A_t \qquad \text{(Eq. 18)}$$

Table X—Influence of Selected Parallel Loss Factors on Peak Time in Corneal Epithelial Drug Concentration–Time Profile

Parameter	Peak Time, min
Tear flow	9
Drainage	20
Drainage and tear flow	10
All but drainage	6

where A_t is the amount of drug in the tear film. Equation 18 assumes that the contribution from the term $p_p[B]$ is negligible. It follows that the apparent first-order rate constant, $k'(t)$, is given by:

$$k'(t) = \frac{p_p + p_n + Q_T(t)}{V_A(t)} + k_d\left(1 - \frac{V_0}{V_A(t)}\right) \qquad \text{(Eq. 19)}$$

Then:

$$\bar{k}' = \frac{1}{V_A(5) - V_A(0)} \int_{V_A(0)}^{V_A(5)} k'(t)\, dV_A(t) \qquad \text{(Eq. 20)}$$

where the symbols are as previously defined. Again, for $Q_T(t) = 0$, Eq. 20 becomes:

$$\bar{k}' = \frac{p_p + p_n}{V_A(5) - V_A(0)} \ln\left(\frac{V_A(5)}{V_A(0)}\right) + k_d\left[1 - \frac{V_0}{V_A(5) - V_A(0)} \ln\left(\frac{V_A(5)}{V_A(0)}\right)\right] \qquad \text{(Eq. 21)}$$

Equation 21 differs from Eq. 15 by the additional term containing k_d. For a 25-μl dose, $\bar{k}' = 0.036p + 0.10$ where $p = p_p + p_n$.

CONCLUSIONS

A picture concerning the mechanisms that control precorneal pilocarpine disposition following topical instillation (Scheme IV) has been presented. Through experimentation and computer simulation, it was found that competing with corneal pilocarpine absorption from the precorneal area are the processes of solution drainage, vasodilation due to the drug, nonconjunctival loss (of which uptake of drug by the nictitating membrane is a component), conjunctival absorption, induced lacrimation, and normal tear turnover, with some of these processes being more efficient than others. The enormous influence of drainage on ocular drug bioavailability was recognized.

Equally as important, the analysis showed that the burden of removing drug from the precorneal area was shared almost equally by drainage, vasodilation due to pilocarpine, and nonconjunctival loss. Consequently, suppressing a single factor only results in a modest improvement in pilocarpine bioavailability. The experience with manipulating drainage is an illuminating example. It follows that the strategy for optimizing absorption efficiency through controlled drug delivery should involve both physical and chemical approaches. This process should be enhanced since estimates on the magnitude of precorneal disposition parameters are now available.

An additional aspect of this study centers on defining the effect of instilled volume on the magnitude of the apparent first-order rate constant governing the decline in concentration and amount of drug in the precorneal area. According to the proposed model, the rate constant controlling drug loss is a time-dependent quantity. Strictly speaking, it should be denoted as a coefficient rather than as a rate constant. The time-average first-order rate constant is shown to be a function of, among other parameters, the initial volume of fluid in the precorneal area. In contrast to the situation where the volume of fluid at the absorption site remains essentially constant with time, the first-order drug loss rate constant viewed in the context of the proposed model varies depending on whether concentration or amount is being considered.

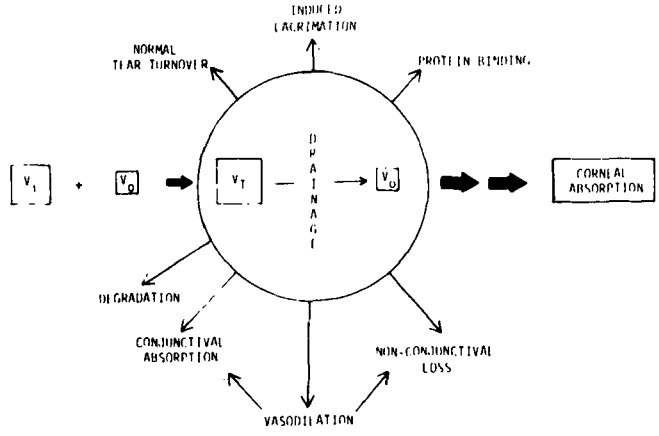

Scheme IV—Precorneal disposition of pilocarpine in the albino rabbit

Table XI—Apparent First-Order Rate Constants Governing Decline in Amount and Concentration of Pilocarpine in Tear Film following Instillation of 25 μl of 0.01 M Solution

Condition	k_a, min^{-1} [a]	
	Amount[b]	Concentration[c]
Unanesthetized	0.90	0.63
Anesthetized	0.40	0.30

[a] For the first 5 min postinstillation. [b] Calculated value. See text for details. [c] Experimental value.

Additionally, as a result of analyzing instilled dose parameters such as volume and concentration in terms of influence on the rate and extent of absorption, the contention that the volume of dose instilled affects ocular drug bioavailability through a combined influence on initial concentration established in the tear film and on the magnitude of drainage that results was put on a relatively definitive basis.

The proposed model is satisfactory from the standpoints of physical meaning as well as a quantitative description concerning precorneal disposition, of accounting for the role of instilled volume in ocular drug bioavailability, and of exposing the hidden aspects of time dependence as it pertains to first-order rate "constants" commonly employed to describe drug distribution.

APPENDIX

This section outlines the procedure for computing the values for various precorneal disposition parameters from experimental results listed in Table III. Of central importance in these calculations is Eq. 8. According to this equation, $[A]$ can be estimated if p_n (the coefficient associated with nonproductive loss) and Q_i (the coefficient associated with induced lacrimation) are known since values for the other parameters are available. Only one unknown remains if the condition of anesthesia is selected, in which case $Q_0 = Q_i = 0$. Thus, one can calculate $[A]$ for a given value of p_n for $t = 0, 1, 2, 3, 4$, and 5 min. These numbers are then plotted semilogarithmically against t. From the slope of this plot, an apparent first-order rate constant is derived. The same procedure is then repeated for other p_n values. On correlating the resulting slopes with the corresponding p_n values, an equation relating the volume-independent value (p, in microliters per minute) and the apparent first-order rate constant (k, in minute^{-1}) for a given parameter is obtained.

Consider now the experiment in which a 25-μl dose of pilocarpine solution was instilled onto the cornea of anesthetized rabbits. Under this condition, the apparent first-order rate constant has a value of 0.30 min^{-1} (Table III). Chrai *et al.* (1) reported that in the presence of anesthesia, the normal resident volume of tear fluid is 12 μl, the drainage rate constant has a value of 0.177 min^{-1}, and tear turnover is inhibited, *i.e.*, $Q_i = Q_0 = 0$ μl min^{-1}. With this information, the equation relating p and k takes the form:

$$k = \frac{p}{28.0} = 0.036p \qquad \text{(Eq. A1)}$$

Equation A1 holds for anesthetized rabbits only. For $k = 0.30$ min^{-1}, $p = 8.40$ μl/min. This, when applied to an instilled dose of 10 μl in anesthetized rabbits, yields $k = 0.46$ min^{-1}, in excellent agreement with the observed value (Table III).

The key elements involved in partitioning $p = 8.40$ μl/min just obtained into its components are as follows. Since $p = p_p + p_n$ and p_p has been estimated to be 0.13 μl/min (Table V), $p_n = 8.27$ μl/min. The parameter p_n is the sum of p_{nc}, p_{nm}, and p_{nd}, where p_{nc} refers to conjunctival absorption, p_{nm} refers to nonconjunctival loss, and p_{nd} refers to vasodilation induced by pilocarpine. Among these values, an estimate for p_{nc} is available. It is 0.71 μl/min, calculated from 0.0217 min^{-1}, the first-order rate constant associated with conjunctival absorption, and 32.5 μl, the volume of fluid under the prevailing experimental conditions (7). The first-order rate constant governing vasodilation is 0.17 min^{-1}. According to Eq. A1, this value corresponds to a p_{nd} of 4.76 μl/min. Now p_{nc} can be shown to take on a value of (8.27 − 0.71 − 4.76) or 2.80 μl/min. The only parameters remaining to be calculated are Q_i and k_l, which will

be discussed after the companion form of Eq. A1 for unanesthetized rabbits is obtained.

In this instance, the procedure is essentially that outlined for anesthetized rabbits, the exception being that the resident tear volume is 7.5 μl. Since Q_i is weighted with V_i instead of V_0 (Eq. 8), it is set equal to zero to simplify calculations. Accordingly, Eq. A2 is the appropriate form relating p and k in unanesthetized rabbits, provided that induced lacrimation is not a loss factor:

$$k = \frac{p}{14.1} = 0.071p \qquad \text{(Eq. A2)}$$

Applying Eq. A2 to the sum of p_p, p_n, and Q_0, *i.e.*, 9.06 μl/min, produces a value of 0.64 min^{-1}, implying that induced lacrimation is not needed to explain the apparent first-order rate constant obtained in normal unanesthetized rabbits. On the one hand, this finding is consistent with the assumption made on induced lacrimation in deriving Eq. A2. On the other hand, it appears to contradict the data on the influence of instilled solution pH on the apparent first-order rate constant. In essence, Eq. A2 is not obeyed by unanesthetized rabbits for whom pH-induced lacrimation constitutes a pathway of drug loss.

To take this factor into account, two assumptions are appropriate: (*a*) no induced lacrimation occurs with an instilled solution at pH 7.38 and (*b*) alterations in solution pH cause no significant changes in the remaining precorneal disposition parameters. By noting that the apparent first-order rate constant for the condition under which these assumptions hold is 0.43 min^{-1} (Table III), Eq. A3 can be obtained:

$$k = \frac{p}{21.1} = 0.047p \qquad \text{(Eq. A3)}$$

With this background, the parameters associated with induced lacrimation can be estimated. In the proposed model, they include the induced lacrimation rate constant, Q_i, and the rate constant, k_l, governing its decline. In the absence of additional information, the situation consists of solving one equation with two unknowns. Consequently, one has less confidence in these computed values as compared with others. In any event, from Eq. A3, one can obtain p = 13.29 μl/min for k = 0.63 min^{-1} (Table III). Subtracting p_p, p_{nm}, p_{nc}, and p_{nd} from p yields a value of 4.89 μl/min, which presumably can be attributed to induced lacrimation. Computer-simulation results suggest a value of 4.75 μl/min for the induced lacrimation rate constant, whose decline appears to be controlled by a rate constant with a value in the order of 2 min^{-1}. Applying these estimates to the case in which the ocular surfaces were pretreated with epinephrine (Table III) generates an apparent first-order rate constant of 0.2 min^{-1}, which is in only fair agreement with the observed value of 0.4 min^{-1}.

Table VI summarizes the values computed for the various parameters associated with precorneal disposition of pilocarpine.

REFERENCES

(1) S. S. Chrai, T. F. Patton, A. Mehta, and J. R. Robinson, *J. Pharm. Sci.*, **62**, 1112 (1973).

(2) S. S. Chrai, M. C. Makoid, S. P. Eriksen, and J. R. Robinson, *ibid.*, **63**, 333 (1974).

(3) T. J. Mikkelson, S. S. Chrai, and J. R. Robinson, *ibid.*, **62**, 1648 (1973).

(4) *Ibid.*, **62**, 1942 (1973).

(5) S. S. Chrai and J. R. Robinson, *J. Pharm. Sci.*, **65**, 437 (1976).

(6) T. F. Patton and J. R. Robinson, *ibid.*, **64**, 267 (1975).

(7) *Ibid.*, **65**, 1295 (1976).

(8) S. S. Chrai and J. R. Robinson, *Am. J. Ophthalmol.*, **77**, 735 (1974).

(9) R. Lazare and M. Horlington, *Exp. Eye Res.*, **21**, 281 (1975).

(10) M. C. Makoid and J. R. Robinson, *J. Pharm. Sci.*, **68**, 435 (1979).

(11) J. W. Sieg and J. R. Robinson, *ibid.*, **65**, 1816 (1976).

(12) K. J. Himmelstein, I. Guvenir, and T. F. Patton, *ibid.*, **67**, 603 (1978).

(13) K. B. Bischoff and R. L. Dedrick, *ibid.*, **57**, 1346 (1968).

(14) T. Teorell, *Arch Int. Pharmacodyn. Ther.*, **57**, 205 (1937).

(15) D. S. Riggs, "The Mathematical Approach to Physiological Problems," Williams & Wilkins, Baltimore, Md., 1963, p. 185.

(16) J. M. Conrad, W. A. Reay, R. E. Polcyn, and J. R. Robinson, *J. Parent. Drug Assoc.*, **32**, 149 (1978).

(17) V. H. L. Lee, M.S. thesis, University of Wisconsin, Madison, Wis., 1978.

(18) T. F. Patton, Ph.D. thesis, University of Wisconsin, Madison, Wis., 1975.

(19) R. W. Hamming, "Numerical Methods for Scientists and Engineers," 2nd ed., McGraw-Hill, New York, N.Y., 1973, pp. 393–411.

(20) H. Herrmann and F. H. Hickman, *Bull. Johns Hopkins Hosp.*, **82**, 182 (1948).

(21) R. R. Pfister and N. Burstein, *Invest. Ophthalmol.*, **15**, 246 (1976).

(22) J. M. Conrad and J. R. Robinson, *J. Pharm. Sci.*, **66**, 219 (1977).

(23) D. M. Maurice, *Exp. Eye Res.*, **15**, 527 (1973).

(24) N. Ehlers, *Acta Ophthalmol.*, **43**, 205 (1965).

(25) M. G. Doane, A. D. Jensen, and C. H. Dohlman, *Am. J. Ophthalmol.*, **85**, 383 (1978).

(26) K. Kakemi, T. Arita, R. Hori, R. Konishi, and K. Nishimura, *Chem. Pharm. Bull.*, **15**, 1883 (1967).

(27) *Ibid.*, **17**, 248 (1969).

(28) *Ibid.*, **17**, 255 (1969).

(29) K. Kakemi, H. Tezaki, S. Muranishi, and Y. Tsujimura, *Chem. Pharm. Bull.*, **17**, 1650 (1969).

(30) S. Mishima, *Arch. Ophthalmol.*, **73**, 233 (1965).

(31) M. S. Norn, *Acta Ophthalmol.*, **55**, 674 (1977).

(32) I. Eglitis, in "The Rabbit in Eye Research," J. H. Prince, Ed., Charles C Thomas, Springfield, Ill., 1964, p. 55.

(33) D. Winne and H. Ochsenfahrt, *J. Theor. Biol.*, **14**, 293 (1967).

(34) W. G. Crouthamel, L. Diamond, L. W. Dittert, and J. T. Doluisio, *J. Pharm. Sci.*, **64**, 664 (1975).

(35) D. Winne, *J. Pharmacokinet. Biopharm.*, **6**, 55 (1978).

(36) S. Gartner, *Arch. Ophthalmol.*, **32**, 464 (1944).

(37) H. Herrmann, *Bull. Johns Hopkins Hosp.*, **82**, 208 (1948).

(38) L. M. DeSantis and R. D. Schoenwald, *J. Pharm. Sci.*, **67**, 1189 (1978).

(39) S. S. Chrai and J. R. Robinson, *ibid.*, **63**, 1218 (1974).

(40) T. F. Patton and J. R. Robinson, *ibid.*, **64**, 1312 (1975).

(41) C. A. Adler, D. M. Maurice, and M. E. Paterson, *Exp. Eye Res.*, **11**, 34 (1971).

(42) J. W. Sieg and J. R. Robinson, *J. Pharm. Sci.*, **66**, 1222 (1977).

(43) S. M. Podos, B. Becker, C. Asseff, and J. Hartstein, *Am. J. Ophthalmol.*, **73**, 336 (1972).

(44) R. M. Ramer and A. R. Gasset, *Ann. Ophthalmol.*, **6**, 1325 (1974).

(45) M. Ruben and R. Watkins, *Br. J. Ophthalmol.*, **59**, 455 (1975).

(46) J. S. Hillman, J. B. Marsters, and A. Broad, *Trans. Ophthalmol. Soc., U.K.*, **95**, 79 (1975).

(47) M. F. Armaly and K. R. Rao, *Invest. Ophthalmol.*, **12**, 491 (1973).

(48) H. A. Quigley, I. P. Pollack, and T. S. Harbin, *Arch. Ophthalmol.*, **93**, 771 (1975).

(49) T. F. Patton and M. Francoeur, *Am. J. Ophthalmol.*, **85**, 225 (1978).

(50) H. Schriftman and A. A. Kondritzer, *Am. J. Physiol.*, **191**, 591 (1957).

(51) R. B. Sund and J. Schou, *Acta Pharmacol. Toxicol.*, **21**, 313 (1964).

(52) T. Nishimura, H. Kobayashi, K. Okumura, S. Muranishi, and H. Sezaki, *Chem. Pharm. Bull.*, **22**, 1275 (1974).

(53) M. Hashida, Y. Takahashi, S. Muranishi, and H. Sezaki, *J. Pharmacokin. Biopharm.*, **5**, 241 (1977).

(54) B. K. Martin, *Adv. Pharm. Sci.*, **3**, 107 (1971).

(55) P. G. Welling, H. Huang, P. A. Koch, W. A. Craig, and P. O. Madsen, *J. Pharm. Sci.*, **66**, 549 (1977).

(56) P. G. Welling, H. Huang, P. F. Hewitt, and L. L. Lyons, *ibid.*, **67**, 764 (1978).

(57) T. F. Patton, *ibid.*, **66**, 1058 (1977).

(58) M. Sugaya and S. Nagataki, *Jpn. J. Ophthalmol.*, **22**, 127 (1978).

ACKNOWLEDGMENTS

Supported by Allergan Pharmaceuticals, Irvine, CA 92664, and Grant EY-01681 from the National Institutes of Health.

The authors thank Mr. Ho-Wah Hui for technical assistance.

Boron Betaine Analogs: Antitumor Activity and Effects on Ehrlich Ascites Tumor Cell Metabolism

I. H. HALL *x, C. O. STARNES *, B. F. SPIELVOGEL ‡x, P. WISIAN-NEILSON ‡, M. K. DAS ‡, and L. WOJNOWICH ‡

Received March 6, 1978, from the *Division of Medicinal Chemistry, School of Pharmacy, University of North Carolina at Chapel Hill, Chapel Hill, NC 27514, and the ‡Paul M. Gross Chemical Laboratory, Duke University, Durham, NC 27706. Accepted for publication November 15, 1978.

Abstract □ Several newly synthesized boron betaine analogs had antitumor activity in Ehrlich ascites, Walker 256 ascites carcinosarcoma, and Lewis lung screens and marginal activity in the B-16 melanotic melanoma screen. *In vivo* testing demonstrated that trimethylamine-cyanoborane inhibited Ehrlich ascites cell DNA and protein syntheses as well as gene modulation by chromatin protein phosphorylation and methylation. Trimethylamine-cyanoborane increased cyclic-AMP levels. *In vitro* testing showed that nuclear DNA polymerase, thymidylate synthetase, *S*-adenosylmethyltransferase, nonhistone chromatin methylation, deoxyribonuclease, ribonuclease, and cathepsin were inhibited by the boron analogs. These compounds did not demonstrate high antitumor activity at the doses employed, but blockage of methyl transfer from *S*-adenosylmethionine was established as a feasible method for controlling cell proliferation.

Keyphrases □ Antineoplastic agents—betaine, boron analogs, metabolic effects, protein synthesis, nucleic acid synthesis, methyl transfer □ Betaine analogs—boron, antineoplastic activity, metabolic effects, protein synthesis, nucleic acid synthesis, methyl transfer □ Protein synthesis—effect of boron betaine analogs □ Methylation—effect of boron betaine analogs □ Nucleic acid synthesis—effect of boron betaine analogs

Blockage of methyl group transfer from choline *via* betaine to L-homocysteine would ultimately inhibit L-methionine and protein syntheses. Since *S*-adenosyl-L-methionine requires L-methionine as a precursor, its synthesis would be reduced, as would be the availability of the methyl transfer from *S*-adenosyl-L-methionine to transfer or ribosomal RNAs and to ribosomal, regulating enzyme, and chromatin protein amino acid residues (1–4). *S*-Adenosyl-L-methionine may play a minor role as the methyl donor cofactor to the enzyme thymidylate synthetase (1, 2). Cancer cells have more methylated chromatin protein and nucleotide bases, particularly transfer RNA, and higher methyl transferase activity than normal tissue.

Numerous reports cite the utilization of folate cofactor antimetabolites to block the methyl transfer to uracil for thymine synthesis. Few studies have investigated the blockage of methyl transfer from *S*-adenosyl-L-methionine since an initial attempt produced ethionine, the ethyl analog of L-methionine, which is a liver carcinogen. A boron analog series of possible betaine or choline antimetabolites was selected to test this premise.

A previous note reported the synthesis of isoelectronic and isostructural boron α-amino acid analogs (5). Trimethylamine-carboxyborane, the protonated boron analog of betaine [$(CH_3)_3N^+CH_2CO_2^-$], its *N*-ethylamide, and a series of related compounds were prepared from trimethylamine-cyanoborane. Because of their structural similarity to betaine, these compounds will be referred to as boron betaine analogs. These boron analogs were evaluated for their antineoplastic activity in a number of tumor models.

EXPERIMENTAL[1]

Chemistry—*Reagents*—The following compounds were purchased: *tert*-butylamine borane[2] [$(CH_3)_3CNH_2{:}BH_3$] (I), morpholine borane[2] [$O(CH_2CH_2)_2NHBH_3$] (II), trimethylamine borane[3] [$(CH_3)_3N{:}BH_3$] (III), and dimethylamine borane[3] [$(CH_3)_2NH{:}BH_3$] (IV).

Trimethylamine-cyanoborane [$(CH_3)_3NBH_2CN$] (*V*)—Compound V was synthesized in high yields (83%) by reacting sodium cyanoborohydride with trimethylamine hydrochloride in dry tetrahydrofuran (7). The product was purified by sublimation, mp 62° [lit. (8) mp 63°]; ^{1}H-NMR (C_6H_6): δ 2.25 (s, CH_3) ppm; BH_2 not observed.

Dimethylamine-cyanoborane [$(CH_3)_2NHBH_2CN$] (*VI*)—Compound VI was synthesized similarly, except that dimethylamine hydrochloride was used and produced a 53% yield, mp 55–57° [lit. (9) mp 56–57°]; ^{1}H-NMR (CD_3CN): δ 2.0 (q, J_{BH} = 100 Hz, BH_2), 2.35 (t, J_{HNCH} = 6 Hz, CH_3), and 4.48 (s, NH_2) ppm.

Anal.—Calc. for $C_3H_9BN_2$: C, 42.93; H, 10.81; B, 12.88; N, 33.38. Found: C, 43.11; H, 10.57; B, 12.66; N, 33.17.

Trimethylamine-N-ethylamidoborane [$(CH_3)_3NBH_2C(O)N(CH_2CH_3)H$] (*VII*)—A solution of V (11.9 g, 0.12 mole) and $(CH_3CH_2)_3OBF_4$ (250 ml, 0.1 *N* in methylene chloride) was refluxed under nitrogen for 24 hr (Scheme I). The reaction mixture was cooled to 0°, and 1.0 *N* NaOH was added slowly with vigorous stirring until the solution was basic. After stirring for 1 hr at room temperature, the organic layer was separated and the aqueous layer was extracted three times with methylene chloride. The organic portions were combined and dried over magnesium sulfate, and the solvent was removed *in vacuo*.

The remaining viscous liquid was distilled *in vacuo* with minimum heating to give VII (13.1 g, 75% yield, bp 80°/0.15 torr); IR[4]: 3430 (m), 3350 (vs), 3010 (m), 2990 (s), 2950 (s), 2890 (m), 2420 (sh), 2370 (s, br), 2320 (m), 2290 (m), 2240 (w), 2200 (w), 1600 (s), 1480 (s), 1460 (s), 1435 (s), 1400 (m), 1375 (w), 1345 (w), 1295 (w), 1255 (s), 1140 (s), 1100 (s), 1050 (s), 1010 (w), 990 (s), 970 (m), 895 (w), 860 (s), 720 (w), and 670 (w) cm^{-1}; ^{1}H-NMR ($CDCl_3$): δ 1.07 (t, *J* = 8 Hz, CH_2CH_3), 2.75 (s, CH_3N), 3.57 (m, CH_2CH_3), and 5.43 (broad s, NH) ppm; ^{13}C-NMR ($CDCl_3$): δ 15.3 (CH_3CH_2), 31.5 (CH_2CH_3), 51.8 (CH_3N), and 182.8 (CO) ppm; ^{11}B ($CDCl_3$, 50°): δ 7.4 (1:2:1 t, *J* = 90 Hz) ppm.

Trimethylamine-carboxyborane [$(CH_3)_3NBH_2COOH$] (*VIII*)—Compound V (20.8 g, 0.214 mole) and triethyloxonium tetrafluoroborate (450 ml, 0.1 *N* in methylene chloride) were refluxed for 24 hr. The solvent and the reaction by-product, boron trifluoride etherate, were removed *in vacuo*, and water was added to the solid residue. After stirring at room temperature for 2–3 days, the solution was extracted with five 75-ml portions of methylene chloride. The organic extractions were combined and dried over magnesium sulfate, and the solvent was removed *in vacuo*.

The solid residue was recrystallized from hot water and dried under vacuum to give VIII (13.8 g, 55.5% yield, mp 131° dec.); IR[3]: 3050 (vs, br), 2950 (s), 2860 (s, sh), 2720 (m), 2620 (m), 2580 (m), 2380 (s), 2290 (w), 2210

$$V \xrightarrow{(CH_3CH_2)_3OBF_4} (CH_3)_3NBH_2CNCH_2CH_3^+BF_4^- \xrightarrow[NaOH]{1\ N} VII$$

Scheme I

[1] IR spectra were measured on a Perkin-Elmer model 297 spectrometer. Liquid samples were run neat between sodium chloride disks, and solid samples were run as potassium bromide pellets. Elemental analysis was performed by Galbraith Laboratories, Knoxville, Tenn. Triethyloxonium tetrafluoroborate was obtained commercially as 0.1 *N* solutions in methylene chloride or was prepared as described in the literature (6).

[2] Alfa Products.

[3] Aldrich Chemical.

[4] Legend: s = strong, m = medium, w = weak, sh = shoulder, br = broad, and v = very.

0022-3549/79/0600-0685$01.00/0
© 1979, American Pharmaceutical Association

Table I—Boron Analog Toxicity and Antitumor Activity in Rodents

Compound	Ehrlich Ascites, 20 mg/kg/day, CF_1 Male Mice, % inhibition	Walker 256, 2.5 mg/kg/day, Sprague–Dawley Rats, T/C	P-388 Leukemia, 20 mg/kg/day, DBA/2 Mice, T/C	B-16 Melanoma, 20 mg/kg/day, C_{57} BL/6 Mice, T/C	Lewis Lung, 20 mg/kg/day, C_{57} BL/6 Mice, T/C	LD_{50}, CF_1 Male Mice, mg/kg
I	Toxic	137	Toxic	Toxic	Toxic	16
II	37	162	117	108	139	475
III	83	145	113	141	87	740
IV	96	156	111	90	178	200
V	98	202	109	143	144	70
VI	81	103	86	113	91	39
VII	69	178	132	145	174	320
VIII	82	174	98	134	144	1800
IX	53	125	116	117	154	250
X	32	105	113	92	Toxic	100
Phenylalanine mustard	99	317	—	—	—	—
Fluorouracil	—	—	186	164	—	—
Cyclophosphamide	—	—	—	—	140	—
Control[a]	100	100	100	100	100	—
Activity required for significant activity	80	125	125	140	140	—

[a] 0.05% Tween 80–water.

(w), 2165 (w), 2100 (w), 1650 (s, br), 1480 (sh), 1465 (s), 1405 (w), 1360 (w), 1245 (s), 1125 (s), 1065 (s), 1020 (m), 980 (m), 975 (m), 915 (m), 865 (s), 810 (m), 725 (w), and 665 (m) cm^{-1}; ^{1}H-NMR (D_2O): δ 2.72 (s, CH_3N) and 4.65 (s, HDO) ppm.

Anal.—Calc. for $C_4H_{12}BNO_2$: C, 41.08; H, 10.34; B, 9.24; N, 11.98. Found: C, 41.14; H, 10.45; B, 9.23; N, 11.85.

Trimethylamine-iodoborane [$(CH_3)_3NBH_2I$] (*IX*)—This compound was prepared using the literature method (10) and was sublimed before use, mp 73° [lit. (11, 12) mp 73°]; ^{1}H-NMR (CD_2Cl_2): δ 2.82 (s, CH_3) ppm.

Hexakis(ammonia-cyanoborane)sodium Iodide {[$Na(NH_3BH_2CN)_6$]I} (*X*)—Compound X was synthesized from ammonia, sodium cyanide, and IX and was recrystallized from ether (13).

Anal.—Calc. for $C_6H_{30}B_6IN_{12}Na$: C, 14.86; H, 6.24; B, 13.38; N, 34.66. Found: C, 15.05; H, 6.37; B, 12.71; N, 34.91.

Pharmacological Screens—Toxicity studies were carried out in CF_1 male mice (~30 g) using a literature method (14).

Antitumor screening was carried out at doses that preliminary screening for V demonstrated to be nontoxic. In the Ehrlich ascites screen, 10^6 tumor cells were implanted intraperitoneally into CF_1 male mice (~30 g). Test compounds were suspended in 0.05% polysorbate 80–water and homogenized. Each compound was injected at 20 mg/kg/day ip. On the 8th day, the mice were sacrificed. The total ascites tumor volume and packed tumor cells (ascrit) volume were determined to calculate the percent inhibition (15). Mercaptopurine and melphalan were used as positive controls for the screen.

In the Walker 256 carcinosarcoma screen, 10^6 tumor cells were implanted intraperitoneally into Sprague–Dawley male rats (~80 g). Test compounds were administered at 2.5 mg/kg/day ip, and the day of death was recorded. The T/C values were calculated according to the NIH protocol (16). Melphalan was used as a positive standard.

Screening was carried out in DBA/2 male mice (~25 g) for the P-388 lymphocytic leukemia model. On Day 0, 10^6 cells were implanted intraperitoneally and test compounds were administered at 20 mg/kg/day. The T/C values were calculated from the group survival times (16). Fluorouracil was used as a positive standard.

In the melanotic melanoma B-16 screens, 1 g of tumor was homogenized in 10 ml of Hanke's balanced salt medium, and 0.5 ml of homogenate was implanted subcutaneously in the inguinal region of C_{57}BL/6 male mice. Test compounds were administered at 20 mg/kg/day ip. The T/C values were calculated (16). Cyclophosphamide was used as a positive control.

In the Lewis lung screen, 2×10^6 tumor cells were implanted intramuscularly in the hindlegs of C_{57}BL/6 male mice. Test compounds were administered at 20 mg/kg/day ip, and T/C values were calculated. Cyclophosphamide was used as an internal standard.

The glioma 26 and 261 and ependymoblastoma brain tumor screens were carried out in a manner analogous to the B-16 screen. Cyclophosphamide and melphalan were the positive controls.

Biochemical Assays—Male CF_1 mice (~30 g) were implanted intraperitoneally on Day 0 with 10^6 Ehrlich ascites tumor cells. For the *in vivo* studies, animals were treated intraperitoneally with 0.25 mg of test compounds on Days 7, 8, and 9. Animals were sacrificed on Day 10, and the ascites fluid was collected from the peritoneal cavity. The number of tumor cells per milliliter and the 0.4% trypan blue uptake were determined with a hemocytometer (17).

In vitro enzymatic and oxidative phosphorylation studies were performed on untreated 10-day Ehrlich ascites cells. Thymidine incorporation into DNA was determined (18). One hour prior to sacrifice, 10 μCi of [methyl-^{14}C]-thymidine (54 mCi/mmole) was injected intraperitoneally. The DNA was isolated, and the ^{14}C content was determined in 0.4% 2,5-diphenyloxazole and 0.01% 1,4-bis[2-(5-phenyloxazolyl)]benzene in a solvent of two parts of toluene and one part of octoxynol, corrected for quenching. DNA concentration was determined by UV spectrophotometry at 260 nm using a calf thymus DNA standard.

Uridine incorporation into RNA was determined in an analogous manner utilizing 10 μCi of 5-^{3}H-uridine (24.2 Ci/mmole). RNA was extracted (19). Leucine incorporation into protein was determined (20) using 1 μCi of 1-^{14}C-leucine (56.9 mCi/mmole). The boron analog effect on 1-^{14}C-acetic acid (57.8 mCi/mmole) incorporation into Ehrlich ascites cell cholesterol was measured also (21, 22). Histone phosphorylation and methylation were determined by injecting intraperitoneally 10 μCi of (γ-^{32}P)-ATP (7.97 Ci/mmole) or [methyl-^{14}C]-choline chloride (49 mCi/mmole) 1 hr prior to sacrifice. The nuclei were isolated (23), and the histone chromatin protein was extracted (24).

Nonhistone chromatin phosphorylation and methylation were determined on isolated nuclei (25) utilizing 2 mmoles of γ-^{32}P-ATP or [methyl-^{14}C]-choline chloride. Chromatin protein was collected on nitrocellulose membrane filters (25). Cyclic-AMP levels were determined by a radioimmunoassay (26) using ^{3}H(G)-cyclic-AMP (39.8 Ci/mmole).

Table II—Trimethylamine-cyanoborane (V) Effects on *In Vivo* Ehrlich Ascites Tumor Metabolism

In Vivo (n = 6)	Percent Control: Control[a]	Percent Control: Treated, 0.25 mg on Days 7, 8, and 9
^{14}C-Thymidine incorporation into DNA	100 ± 10	48 ± 4[b]
^{3}H-Uridine incorporation into RNA	100 ± 24	100 ± 29
^{14}C-Leucine incorporation into protein	100 ± 27	10 ± 2[b]
^{14}C-Acetic acid incorporation into cholesterol	100 ± 4	75 ± 6[b]
[methyl-^{14}C]-Choline incorporation into RNA	100 ± 11	51 ± 13[b]
[methyl-^{14}C]-Choline incorporation into protein	100 ± 15	42 ± 10[b]
[methyl-^{14}C]-Choline incorporation into nonhistones	100 ± 2	44 ± 5[b]
[methyl-^{14}C]-Choline incorporation into histones	100 ± 16	132 ± 9[c]
^{32}P-γ-ATP incorporation into nonhistones	100 ± 3	41 ± 7[b]
^{32}P-γ-ATP incorporation into histones	100 ± 8	53 ± 4[b]
Cyclic-AMP level	100 ± 5	269 ± 8[b]
Number of tumor cells per milliliter	100 ± 19	33 ± 14[b]

[a] 0.05% Tween 80. [b] $p = 0.001$. [c] $p = 0.005$.

Table III—*In Vitro* Boron Analog Effects on 10-Day Ehrlich Ascites Tumor Enzymatic Activities

Compound (6 μg)	Percent Control (n = 6)						
	DNA Polymerase Activity[a]	Thymidylate Synthetase Activity[b]	S-Adenosyl-L-methionine Methyl-transferase Activity[c]	Methylation of Nonhistone Protein[d]	DNase Activity[e]	RNase Activity[f]	Cathepsin Activity[g]
I	75 ± 6[h]	44 ± 7[h]	81 ± 4[i]	76 ± 4[h]	7 ± 3[h]	72 ± 14[i]	80 ± 12
II	65 ± 9[h]	85 ± 2[h]	75 ± 12[i]	53 ± 6[h]	28 ± 8[h]	51 ± 16[h]	53 ± 18[j]
III	51 ± 8[h]	62 ± 2[h]	68 ± 10[h]	77 ± 8[h]	10 ± 4[h]	68 ± 12[i]	44 ± 19[h]
IV	71 ± 6[h]	68 ± 5[h]	66 ± 7[h]	78 ± 10[j]	19 ± 6[h]	70 ± 17[i]	33 ± 15[h]
V	46 ± 3[h]	48 ± 15[h]	49 ± 5[h]	44 ± 5[h]	14 ± 5[h]	47 ± 12[h]	68 ± 13[j]
VII	40 ± 8[h]	66 ± 2[h]	75 ± 9[i]	95 ± 10	47 ± 11[h]	98 ± 17	19 ± 8[h]
VIII	37 ± 6[h]	79 ± 2[h]	39 ± 19[h]	47 ± 5[h]	25 ± 9[h]	60 ± 9[h]	64 ± 20[i]
IX	53 ± 7[h]	—	—	—	—	—	—
X	54 ± 4[h]	—	—	—	—	—	—
Iodoacetate	41 ± 4	—	—	—	—	—	—
Fluorouracil	—	39 ± 7[h]	99 ± 13	—	—	—	—
Control[k]	100 ± 15	100 ± 3	100 ± 15	100 ± 5	100 ± 8	100 ± 19	100 ± 17

Control values for 10-day Ehrlich ascites tumor cells were as follows: [a] 7561 dpm/mg of protein. [b] 103,328 dpm/mg of protein. [c] 3268 dpm/mg of protein. [d] 8000 dpm/mg of chromatin protein. [e] 35 μg of DNA hydrolyzed/mg of protein/30 min. [f] 24 μg of RNA hydrolyzed/mg of protein/30 min. [g] 0.90 mg of protein hydrolyzed/mg of protein/30 min. [h] $p = 0.001$. [i] $p = 0.025$. [j] $p = 0.005$. [k] 0.05% Tween 80–water.

In vitro DNA polymerase activity was determined on washed (three times) isolated nuclei (23). The incubation system was that of Sawada *et al.* (27), except that 2-^{14}C-deoxythymidylate triphosphate (45 mCi/mmole) was used. The insoluble nucleic acids were collected on glass fiber GF/F by vacuum suction. Deoxythymidylate kinase and deoxythymidylate diphosphate kinase activities were determined by a method (28) based on the disappearance of reduced nicotinamide adenosine dinucleotide at 340 nm for 20 min. *In vitro* thymidylate synthetase activity was assayed by a method (29) utilizing a postmitochondrial supernate (9000×*g* for 10 min) and 5 μCi of 5′-^{3}H-deoxyuridine monophosphate (11 Ci/mmole). S-Adenosyl-L-methionine methyltransferase activity was determined (30) using S-[methyl-^{14}C]-adenosyl-L-methionine (53 mCi/mmole).

The effects of the boron analogs on the tumor cell hydrolytic enzymes were also determined. Deoxyribonuclease activity, at pH 5.0, was measured by a modification of the deDuve method (31). Ribonuclease and cathepsin activities, at pH 5.0, were determined by the method of Cho-Chung and Gullino (32). *In vitro* effects of boron analogs on Ehrlich ascites tumor cell oxidative phosphorylation processes were measured (33) in the presence and absence of adenosine diphosphate, utilizing succinate or α-ketoglutarate as the substrate. Protein was determined by the Lowry method (34).

All *in vitro* tests were carried out at 6 μmoles of test compounds/ml of assay mixture. *In vitro* UV binding studies were conducted with test compounds (0.2 μg/ml) and DNA (38 μg/ml) or deoxyguanosine monophosphate (38 μg/ml) in 0.1 *M* phosphate buffer, pH 7.2, over a range of 200–340 nm for 24 hr (22). Data in Tables II and III are the means of control and standard deviation percentages ($\bar{x} \pm SD$). The probable significance level (p) was determined by the Student t test (35).

RESULTS

Compounds III–V and VIII significantly inhibited Ehrlich ascites tumor growth at 1 mg/kg/day. Compounds I–V, VII, and VIII were significantly active (T/C ≧ 125) in the Walker 256 carcinosarcoma survival screen at a relatively low dose, 2.5 mg/kg/day. In the P-388 lymphocytic leukemia screen at 20 mg/kg/day, only VII had significant activity. In the B-16 melanoma screen, III, V, and VII demonstrated significant activity (T/C ≧ 140). In the Lewis lung survival system, IV, V, VII, IX, and X demonstrated activity at 20 mg/kg/day. Compound V was inactive in the brain tumor screens, glioma 26 and 261 and ependymoblastoma (Table I).

Boron analog effects on several biochemical events necessary for rapid cell proliferation were examined. ^{14}C-Thymidine incorporation into DNA for 10-day Ehrlich ascites cells was 280,629 dpm/mg of DNA. DNA synthesis was inhibited 52% by V, 45% by VII, and 60% by VIII (Table II). ^{3}H-Uridine incorporation into Ehrlich ascites cell RNA was unaffected by boron analogs. The UV spectral studies with V, VII, and VIII and DNA or deoxyguanosine monophosphate demonstrated no binding between drugs and nucleotides, indicating that the DNA template was intact for transcription.

^{14}C-Leucine incorporation into protein for the 10-day control Ehrlich ascites cells was 6238 dpm/mg of protein and was inhibited 90% after V administration. Cholesterol synthesis for newly synthesized cell membranes for the control 10-day tumor was 132,809 dpm/mg of protein. Cholesterol synthesis was inhibited 25% by V, 48% by VII, and 62% by VIII. The methyl transfer from choline to transfer and ribosomal RNA for the control animals was 1086 dpm/mg of RNA, which was inhibited 49% by treatment with V.

Protein methylation by the choline donor for the 10-day Ehrlich ascites cells was 1225 dpm/mg of protein. Compound V inhibited protein methylation 58%. Nonhistone chromatin protein methylation for the control was 8118 dpm/mg of chromatin protein; treatment with V resulted in 56% inhibition. Histone methylation was 40,976 dpm/mg of chromatin protein for the control, whereas administration of V caused a 32% elevation. Phosphorylation of the regulatory proteins controlling gene activity was 9803 dpm/mg of nonhistone chromatin protein and 2954 dpm/mg of histone chromatin protein. Treatment with V resulted in a 59 and a 65% reduction, respectively, of chromatin protein phosphorylation.

The cyclic-AMP level for 10-day Ehrlich ascites cells was 3.65 pmoles/10^6 cells, which was elevated 169% by V administration. The number of tumor cells per milliliter on Day 10 was 223 × 10^6, which was suppressed 67% by treatment with V. The boron analogs were also tested for their *in vitro* effects on specific enzymes of 10-day Ehrlich ascites cells (Table III). Nuclei DNA polymerase activities were suppressed by all compounds tested. Compounds V, VII, and VIII possessed the best inhibitory activity: 54, 60, and 63% inhibition, respectively. Thymidylate mono- and diphosphate kinase activities were not affected by the boron analogs. Thymidylate synthetase activity was inhibited significantly by I and V and marginally by III, IV, and VIII. S-Adenosyl-L-methionine transferase activity was inhibited 51% by V and 61% by VIII with marginal inhibition by II–IV and VII. Nonhistone methylation dependent on S-adenosyl-L-methionine-methyltransferase activity was inhibited significantly by V (56%) and VIII (53%), with marginal inhibition by I–IV.

Treatment with the boron analogs reduced the activity of deoxyribonuclease, ribonuclease and cathepsin. Deoxyribonuclease activity was affected the most drastically. Compound I reduced activity 93%, II 72%, III 90%, IV 81%, V 86%, and VIII 75%. Ribonuclease activity was inhibited significantly by V (53%) and II (49%) with marginal inhibition by I, III, IV, and VIII. Cathepsin activity was reduced 47% by II, 56% by III, 67% by IV, 32% by V and VIII, and 81% by VII. Basal and adenosine diphosphate-stimulated respiration of 10-day Ehrlich ascites cells was unaffected by V, VII, and VIII at 6 μmoles.

DISCUSSION

The major boron analog effects were on Ehrlich ascites tumor cell protein and DNA syntheses. Protein synthesis inhibition may be the direct result of the α-amino boron analog on the translocation process or by blocking L-methionine synthesis. Enzymes required for DNA synthesis are synthesized in the early stages of cell proliferation (32). DNA polymerase activity was inhibited significantly whereas thymidylate kinases were unaffected by the boron analogs. Elevated cyclic-AMP levels resulting from boron analog administration are associated with cessation of cholesterol synthesis (36), reduced cellular proliferation, and reduction of H-1 histone phosphorylation, an event necessary for template activity (37).

Other protein kinases that are modulated by cyclic nucleotide levels

are those that phosphorylate nonhistone chromatin proteins which regulate transcription and differentiation. Compound V effectively blocks nonhistone and histone phosphorylation. The necessary phosphorus is derived from the γ-P of ATP, but Ehrlich ascites cell oxidative phosphorylation was not inhibited by the boron analogs. Lysosomal enzymatic activity is high prior to the mitotic apparatus formation, and membrane surface proteolytic activity is increased in cells undergoing rapid proliferation and metastasis (38). Elevated cyclic-AMP levels are associated with lysosomal membrane stabilization and blockage of the hydrolytic enzyme release (39).

Deoxyribonuclease activity was inhibited significantly by the boron analogs. Cathepsin proteolytic activity was inhibited moderately. *S*-Adenosyl-L-methionine transferase activity as well as the *S*-adenosyl-L-methionine-dependent methyl group transfer from choline was inhibited by the boron analogs. Protein and RNA methylation was suppressed significantly by boron analog treatment (1–4). Chromatin methylation is elevated in Novikoff hepatoma (40) and Hela cells (41). Cultured pancreatic anlase cells require *S*-adenosyl-L-methionine for proliferation and differentiation. Conversely, histone methylation by protein methylase III is highest late in the S and G_2 phases, indicating a cessation of replication (42). Boron analogs slightly increased histone methylation. Thymidylate synthetase activity also was inhibited by these agents, apparently producing cell death through thymine deprivation.

Generally, the degree of methyltransferase inhibition followed the antineoplastic activity demonstrated by these boron analogs in the Ehrlich ascites screen, with V having the highest activity in both areas. Boron betaine analogs are potent inhibitors of the protein synthesis and methyl transfer necessary for rapidly proliferating cells.

REFERENCES

(1) G. L. Cantoni, *Annu. Rev. Biochem.*, **44**, 435 (1975).

(2) G. R. Shepherd, J. M. Hardin, and B. J. Norland, *Arch. Biochem. Biophys.*, **143**, 1 (1971).

(3) M. Friedkin, *Adv. Enzymol.*, **28**, 235 (1973).

(4) W. K. Paik and S. Kim, *ibid.*, **42**, 227 (1975).

(5) B. F. Spielvogel, L. Wojnowich, M. K. Das, A. T. McPhail, and K. D. Hargrave, *J. Am. Chem. Soc.*, **98**, 5702 (1976).

(6) H. Meerwein, *Org. Synth.*, **46**, 113 (1966).

(7) B. F. Spielvogel, M. K. Das, and P. Wisian-Neilson, *Inorg. Chem.*, **17**, 2327 (1978).

(8) S. S. Uppal and H. C. Kelly, *J. Chem. Soc., Chem. Commun.*, **1970**, 1619.

(9) O. T. Beachley, Jr., and B. Washburn, *Inorg. Chem.*, **14**, 120 (1975).

(10) A. T. McPhail, K. D. Onan, B. F. Spielvogel, and P. Wisian-Neilson, *J. Chem. Res.*, **5**, 205 (1978).

(11) W. H. Myers, G. E. Ryschkewitsch, M. A. Mathur, and R. W. King, *Inorg. Chem.*, **14**, 2874 (1975).

(12) M. P. Brown, R. W. Heseltine, P. A. Smith, and P. J. Walker, *J. Chem. Soc. A*, **1970**, 410.

(13) B. F. Spielvogel, P. Wisian-Neilson, A. T. McPhail, and K. D. Hargrave, *J. Chem. Soc. Dalton*, **1976**, 353.

(14) J. T. Litchfield and F. Wilcoxon, *J. Pharmacol. Exp. Ther.*, **96**, 99 (1949).

(15) C. Piantadosi, C. S. Kim, and J. L. Irvin, *J. Pharm. Sci.*, **58**, 821 (1969).

(16) R. I. Geran, N. H. Greenberg, M. M. MacDonald, A. M. Schmasdon, and B. J. Abbott, *Cancer Chem. Rep., Part 3*, **3**(2) (1972).

(17) I. H. Hall, K. H. Lee, E. C. Mar, C. O. Starnes, and T. G. Waddell, *J. Med. Chem.*, **20**, 333 (1977).

(18) C. B. Chae, J. L. Irvine, and C. Piantadosi, *Proc. Am. Assoc. Cancer Res.*, **9**, 44 (1968).

(19) R. G. Wilson, R. H. Bodner, and G. E. MacHorter, *Biochim. Biophys. Acta*, **378**, 260 (1975).

(20) A. C. Sartorelli, *Biochem. Biophys. Res. Commun.*, **27**, 26 (1967).

(21) G. T. Haven, J. R. Frzemien, and T. T. Nquyea, *Res. Commun. Chem. Pathol. Pharmacol.*, **6**, 253 (1973).

(22) F. Wada, K. Hirata, and Y. Sakamoto, *J. Biol. Chem.*, **65**, 171 (1969).

(23) W. C. Hymer and E. L. Kuff, *J. Histochem. Cytochem.*, **12**, 359 (1964).

(24) A. Raineri, R. C. Simsimau, and R. K. Boutwell, *Cancer Res.*, **33**, 134 (1973).

(25) Y. M. Kish and L. J. Kleinsmith, *Methods Enzymol.*, **40**, 201 (1975).

(26) A. C. Gilman, *Proc. Natl. Acad. Sci., USA*, **67**, 305 (1970). Calbiochem. cAmp assay kit.

(27) H. Sawada, K. Tatsumi, M. Sasada, S. Shirakawa, T. Nakumura, and G. Wakisaka, *Cancer Res.*, **33**, 41 (1974).

(28) F. Maley and S. Ochoa, *J. Biol. Chem.*, **233**, 1538 (1958).

(29) A. Kampf, R. L. Barfknecht, P. J. Shaffer, O. Osaki, and M. P. Mertes, *J. Med. Chem.*, **19**, 903 (1976).

(30) R. T. Borchardt, J. A. Huber, and Y. S. Wu, *ibid.*, **19**, 1094 (1976).

(31) I. H. Hall, K. S. Ishaq, and C. Piantadosi, *J. Pharm. Sci.*, **63**, 625 (1974).

(32) Y. S. Cho-Chung and P. M. Gullino, *J. Biol. Chem.*, **248**, 4743 (1973).

(33) I. H. Hall, K. H. Lee, and S. A. ElGebaly, *J. Pharm. Sci.*, **67**, 552 (1978).

(34) O. H. Lowry, N. J. Rosebrough, A. L. Farr, and R. J. Randell, *J. Biol. Chem.*, **193**, 265 (1975).

(35) G. W. Snedecor, in "Statistical Methods," Iowa State College Press, Ames, Iowa, 1956, section 2.

(36) L. A. Bricker and G. S. Levy, *J. Biol. Chem.*, **247**, 4914 (1972).

(37) C. S. Rubin and O. M. Roseu, *Annu. Rev. Biochem.*, **44**, 831 (1975).

(38) H. P. Schnebli, in "Proteases and Proteases Inhibitors in Neoplasia in Proteinase Inhibition," H. Fritz, H. Tschnesche, L. J. Green, and E. Truscheit, Eds., Springer-Verlag, New York, N.Y., 1974, p. 615.

(39) H. Bourne, L. Lichenstein, K. Melmom, C. Henney, E. Weinstein, and C. Shearer, *Science*, **184**, 19 (1974).

(40) W. K. Paik, H. W. Lee, and H. P. Morris, *Cancer Res.*, **32**, 37 (1972).

(41) H. W. Lee, W. K. Paik, and T. W. Borum, *J. Biol. Chem.*, **248**, 4194 (1973).

(42) I. Parsa, N. H. Marsh, and P. J. Fitzgerald, *J. Exp. Res.*, **73**, 49 (1972).

ACKNOWLEDGMENTS

Supported by grants from the University of North Carolina, the American Cancer Society (IN-15R), and the U.S. Army (DAAG29-77-G-0099).

Controlled Drug Release from Polymeric Delivery Devices V: Hydroxy Group Effects on Drug Release Kinetics and Thermodynamics

Y. W. CHIEN *x, D. M. JEFFERSON, J. G. COONEY, and H. J. LAMBERT

Received August 7, 1978, from the *New Product Development Department, Searle Laboratories, Division of G. D. Searle & Co., Skokie, IL 60077.* Accepted for publication November 15, 1978. *Present address: Pharmaceutical R&D Department, Endo Laboratories, Garden City, NY 11530.

Abstract □ The effects of progesterone hydroxylation on silicone matrix drug release kinetics and thermodynamics were investigated. Hydroxylation at positions 11, 17, and/or 21 substantially reduced progesterone release. The magnitude of this reduction depended on the number and position of the hydroxy groups and could be attributed to decreased polymer matrix diffusivity (D_m) and polymer solubility (C_p). Thermodynamically, hydroxy group addition to positions 11 and/or 21 reduced the activation energy for matrix diffusion ($E_{d,m}$) but increased the solvation energy for dissolution in silicone polymer ($\Delta H_{T,m}$). Adding an hydroxy group to position 17 increased the $E_{d,m}$ but decreased the $\Delta H_{T,m}$. The overall ($E_{d,m} + \Delta H_{T,m}$) values were relatively constant and independent of hydroxylation.

Keyphrases □ Dosage forms—controlled release, progesterone from silicone matrix, effect of hydroxylation, kinetics, thermodynamics □ Progesterone—controlled-release dosage forms, effect of hydroxylation on release from silicone matrix □ Hydroxylation—progesterone, effect on release from silicone matrix □ Steroids—controlled-release dosage forms, progesterone, effect of hydroxylation on release from silicone matrix

The idea of replacing daily drug administration with a polymeric controlled-release device has recently generated much interest (1). The high silicone polymer steroid permeability has led to development of drug-filled and drug-dispersed silicone devices for long-term intrauterine, intravaginal, subcutaneous, and transdermal drug administration (2–15).

An *in vitro* system for direct, rapid drug release characterization was recently developed (16). Two types of drug release mechanisms, matrix controlled and partition controlled, were observed when the drug release profiles from silicone devices were followed daily using this system (17–19). Controlled drug release kinetics and thermodynamics under these two processes were analyzed (18–20).

Normalized steroid permeability coefficients appear to depend on the steroidal structure (21). For drugs with a high permeability coefficient (across the vaginal membrane) (P_m), like progesterone, intravaginal absorption is mainly controlled by the permeability of the vaginal surface aqueous hydrodynamic diffusion layer. For drugs with a low P_m value, such as hydrocortisone, intravaginal uptake is determined mainly by molecular transport across the vaginal membrane. This difference in absorption may be due to the hydroxy groups in the steroid. The transdermal permeability constants were also reported to be influenced by the presence of hydroxy groups on the progesterone molecules (22).

Effects of hydroxy groups on the controlled-release kinetics and thermodynamics of progesterone and its derivatives were studied in this investigation as a step in the design of controlled-release drug delivery systems.

EXPERIMENTAL

Silicone devices were prepared by thoroughly mixing 0.5–2.0 parts of progesterone derivative crystals, 7.5 parts of dimethyl polysiloxane elastomer[1], and one part of silicone fluid[2] with a rotator[3] at 1000 rpm for 7 min. One drop (0.02 ml) of stannous octoate[1], as catalyst, was then incorporated and thoroughly mixed for another minute. The mixture was deaerated under vacuum for 4 min and delivered by an extrusion pump[4] into Tygon tubing[5] (0.63-cm i.d.). The silicone polymer was allowed to cure at 60° for 1 hr. After proper cross-linking, the resulting medicated silicone device was removed from the tubing mold and cut into the desired lengths for *in vitro* drug elution studies.

The *in vitro* drug elution studies were conducted by immersing one medicated silicone device in each test tube containing 10 ml of 50% (v/v) polyethylene glycol 400–water. The test tubes were sealed with screw caps and shaken at a constant 40 oscillations/min in a water bath thermostated at 37, 45, 50, or 55°. The medicated silicone devices were transferred to new elution solution every 24 hr for 7 days. The drug concentration in each test tube was analyzed spectrophotometrically[6] after appropriate dilution with spectral grade methanol. The drug released every 24 hr from each device and the drug released from a unit surface area of the device (Q) were calculated.

The techniques for determining drug solubility in silicone polymer and in 50% (v/v) polyethylene glycol 400–water were reported previously (16).

RESULTS AND DISCUSSION

***In Vitro* Progesterone Derivative Release**—The chemical structures and hydroxy group locations of progesterone derivatives are illustrated in Table I. Their *in vitro* release profiles are shown in Fig. 1. Controlled release of progesterone and its hydroxy derivative from silicone devices at steady state followed the matrix-controlled process previously seen for other progesterone derivatives (6, 19). As expected from Eq. 1, the cumulative amount of progesterone derivative released (Q) is linearly proportional to the square root of time ($t^{1/2}$) (18):

$$Q = [D_m(2A - C_p)C_p t]^{1/2} \quad \text{(Eq. 1)}$$

where D_m is the effective drug diffusivity in the polymer matrix, A is the drug content in a unit volume of silicone device, and C_p is the drug solubility in the silicone polymer. The drug release flux is defined as:

$$Q/t^{1/2} = [D_m(2A - C_p)C_p]^{1/2} \quad \text{(Eq. 2)}$$

and can be estimated from the slope of the Q *versus* $t^{1/2}$ plots (Fig. 1). Hydroxylation of progesterone reduced $Q/t^{1/2}$. This reduction depended on the hydroxy group number and location (Table II). An hydroxy group at either the 11- or 17-position had the most drastic effect on progesterone release from a silicone device, producing a more than fivefold decrease in $Q/t^{1/2}$ compared to a 1.5-fold reduction when the hydroxy group was at the 21-position.

The presence of two hydroxy groups further reduced $Q/t^{1/2}$. Hydroxy groups at the 11- and 21-positions yielded a 13.5-fold reduction in $Q/t^{1/2}$ and hydroxy groups at 17 and 21 resulted in a 28-fold decrease. The addition of a second hydroxy group at the 17-position had a more significant

[1] Silastic 382 medical grade, Dow Corning Corp., Midland, MI 48640.
[2] Silicone medical fluid 360, Dow Corning Corp., Midland, MI 48640.
[3] Cole-Parmer Instrument, Chicago, IL 60680.
[4] Searle Laboratories, Chicago, IL 60680.
[5] R5340-3, Norton, Inc., Akron, OH 44309.
[6] Coleman 124D spectrophotometer (double beam), Perkin-Elmer.

0022-3549/79/0600-0689$01.00/0
© 1979, American Pharmaceutical Association

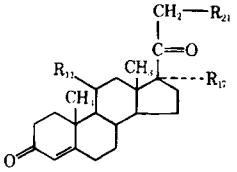

Table I—Melting Points of Progesterone Derivatives

	Compound	R_{21}	R_{11}	R_{17}	Melting Point[a]
I	Progesterone	H	H	H	129.0°
II	Desoxycorticosterone	OH	H	H	141.5°
III	11α-Hydroxyprogesterone	H	OH	H	165.5°
IV	17α-Hydroxyprogesterone	H	H	OH	215.0°
V	Corticosterone	OH	OH	H	181.0°
VI	17α-Hydroxydesoxycorticosterone	OH	H	OH	216.8°
VII	Hydrocortisone	OH	OH	OH	220.0°

[a] Median value of the literature melting-point range.

influence on $Q/t^{1/2}$ than did a second hydroxy group at the 11-position (compare VI with V). With three hydroxy groups (VII), $Q/t^{1/2}$ was reduced by 35 times, from 3.368 mg/cm²/day$^{1/2}$ for progesterone to 0.096 mg/cm²/day$^{1/2}$ for hydrocortisone (Table II).

Mechanistic Analysis of Hydroxy Group Effects—Equation 2 suggests that the reductions in $Q/t^{1/2}$ in response to the addition of hydroxy groups could reflect changes in the progesterone matrix diffusivity (D_m) and/or the polymer solubility (C_p). Theoretically, hydroxy groups should add hydrophilicity and change the progesterone stereochemical configuration.

Equation 2 indicates that $Q/t^{1/2}$ should be linearly dependent on $(2A - C_p)^{1/2}$ (Fig. 2). The slope of $Q/t^{1/2}$ *versus* $(2A - C_p)^{1/2}$ should be defined by $(D_m C_p)^{1/2}$. If the value of C_p, the progesterone derivative solubility in silicone polymer, is known or experimentally determined, the magnitude of D_m, the matrix diffusivity in a silicone device, can be calculated (Table III).

The addition of hydroxy groups to progesterone decreased D_m and C_p but increased C_s, the solubility of progesterone derivatives in 50% (v/v) polyethylene glycol 400–water (Table III). The decrease in matrix diffusivity (D_m) could be due to the alterations in the stereochemical configuration of the progesterone molecule. On the other hand, the increase in C_s and the decrease in C_p could be related to increased progesterone hydrophilicity due to the addition of hydrophilic hydroxy groups.

If hydroxy groups change progesterone hydrophilicity, they also should change the progesterone partitioning behavior from the silicone device toward the elution solution. As expected, the K_{obs} calculated from C_s/C_p varied with the number and position of hydroxy groups added (Table III). The partition coefficient, K_{obs}, is theoretically related to the standard Gibbs free energy (ΔF_d) of desorption, *i.e.*, the energy gained by a molecule on desorption from the polymer phase into the elution solution (23):

$$\Delta F_d = -RT \ln K_{obs} \qquad \text{(Eq. 3)}$$

If it is assumed (24) that ΔF_d can be expressed additively in terms of the individual contributions of the nonpolar progesterone skeleton (ΔF_p) and the polar hydroxy group (ΔF_{OH}), then:

$$\Delta F_d = \Delta F_p + n(\Delta F_{OH}) \qquad \text{(Eq. 4)}$$

It is also known that:

$$\Delta F_p = -RT \ln K_p \qquad \text{(Eq. 5)}$$

where K_p is the solution–polymer partition coefficients for progesterone itself. Combining Eqs. 3–5 yields:

$$\ln K_{obs} = \ln K_p - \frac{n(\Delta F_{OH})}{RT} \qquad \text{(Eq. 6a)}$$

or:

$$\log K_{obs} = \log K_p - \frac{n(\Delta F_{OH})}{2.303RT} \qquad \text{(Eq. 6b)}$$

As expected from Eq. 6*b*, the K_{obs} values were first order dependent on the number (n) of hydroxy groups on the progesterone molecule (Fig. 3). From the slope ($-\Delta F_{OH}/2.303RT$) of the linear log K_{obs} *versus* n plots, the ΔF_{OH} values were computed (Table IV). Depending on the system temperature, the addition of hydroxy groups onto the progesterone molecule yielded a contribution of ΔF_{OH} from −1.419 to −1.684 kcal/mole to the Gibbs free energy of desorption (ΔF_d). Without the hydroxy groups, the progesterone molecule partitioning from a silicone device toward an elution solution required a Gibbs free energy of desorption (ΔF_p) of 0.321–0.108 kcal/mole; with the hydroxy groups, the overall ΔF_d was improved to −1.098–−1.550 kcal/mole (Table IV). In other words, the addition of hydroxy groups enhanced the interfacial partitioning of the progesterone molecule from a silicone device to an elution medium.

As reported previously (24), K_{obs} for monosubstituted hydroxy progesterone was also dependent on the substituent hydroxy group position (Table III). From the following relationship:

$$\Delta F_{OH} = -2.303RT(\log K_{obs} - \log K_p) \qquad \text{(Eq. 7)}$$

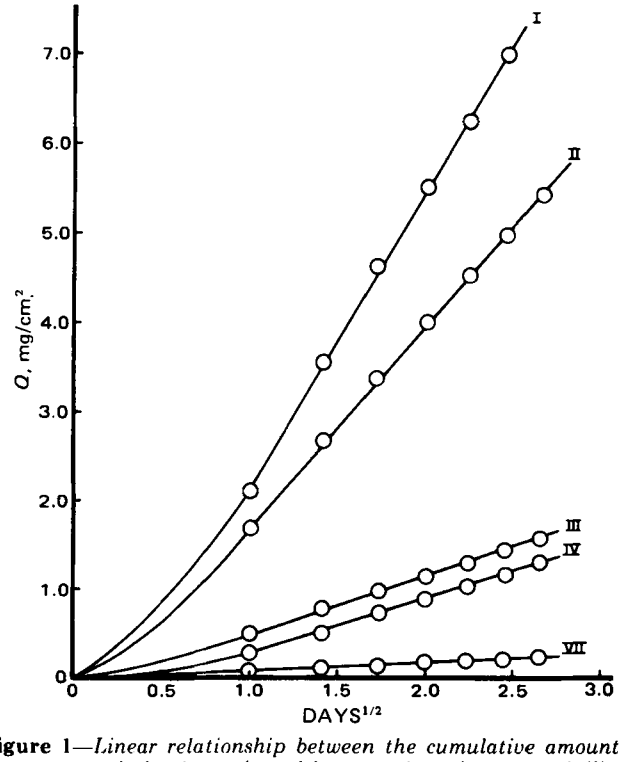

Figure 1—*Linear relationship between the cumulative amount of progesterone derivatives released from a unit surface area of silicone device* (Q) *and time* (t) *in days at 45°.*

Table II—Hydroxy Group Effect on $Q/t^{1/2}$ of Progesterone Derivatives through Silicone Device[a]

Compound	$Q/t^{1/2}$, mg/cm²/day$^{1/2}$
I	3.368
II	2.280
III	0.663
IV	0.623
V	0.249
VI	0.120
VII	0.096

[a] Determined from a silicone device (A = 117.4 mg/cm³) in 50% (v/v) polyethylene glycol 400–water at 45°.

Table III—Hydroxy Group Effect on the Polymer Matrix Diffusivity (D_m)[a], the Solubilities, and the Solution-Polymer Partition Coefficients (K_{obs}) of Progesterone Derivatives

Compound	$D_m \times 10^2$, cm²/day	Solubility, μg/ml ± SD		K_{obs}[d]
		C_s[b]	C_p[c]	
I	6.34	353.3 ± 16.2	594.7 ± 32.3	0.59
II	4.51	1402.1 ± 75.4	205.9 ± 5.4	6.81
III	2.96	575.0 ± 31.8	9.1 ± 0.3	63.2
IV	1.82	442.0 ± 37.4	26.5 ± 1.1	16.7
V	5.82	839.0 ± 9.2	1.23 ± 0.06	682.1
VI	4.16	994.1 ± 57.5	1.48 ± 0.18	671.7
VII	0.76	3987.6 ± 48.2	3.78 ± 0.29	1054.9

[a] Determined at 45°. [b] Aqueous solubility in 50% (v/v) polyethylene glycol 400 solution at 37°. [c] Polymer solubility in silicone medical fluid (20 cv) at 37°. [d] Ratio of C_s over C_p.

the ΔF_{OH} values for 21-OH, 17α-OH, and 11α-OH groups were estimated to be −1.51, −2.06, and −2.88 kcal/mole, respectively, at 37°.

Controlled Drug Release Thermodynamics—The temperature dependency of $Q/t^{1/2}$ is defined by the following relationship (19):

$$\log (Q/t^{1/2}) = \text{constant} - \left(\frac{(E_{d,m} + \Delta H_{T,m})}{4.606R}\right)\left(\frac{1}{T}\right) \quad \text{(Eq. 8)}$$

where $E_{d,m}$ is the activation energy a drug molecule requires to diffuse in a polymer matrix, $\Delta H_{T,m}$ is the energy required for the solvation of drug molecules in the polymer structure, R is the gas constant (1.9872 cal/mole/deg), and T is the absolute temperature. As expected from Eq. 8, the linear log $(Q/t^{1/2})$ *versus* T^{-1} was followed very well (Fig. 4). The values of $(E_{d,m} + \Delta H_{T,m})$ for progesterone and its hydroxy derivatives were similar, ranging from 13.52 (±1.02) to 16.70 (±0.87) kcal/mole (Table V). Compound VI had a slightly higher value (23.62 ± 2.44 kcal/mole). Except for VI, additional hydroxy groups did not significantly affect the total energy requirements for the controlled progesterone derivative release.

Diffusion of drug molecules in the polymer structure is energy dependent (25); the matrix diffusion of progesterone and its hydroxy derivatives requires the activation energy ($E_{d,m}$) defined in the following expression:

$$\log D_m = \log D_m^0 - \left(\frac{E_{d,m}}{2.303R}\right)\left(\frac{1}{T}\right) \quad \text{(Eq. 9)}$$

The linear relationship between log D_m and T^{-1} was followed very well for all compounds tested (Fig. 5). A significant difference in $E_{d,m}$ values was noticed among the progesterone derivatives (Table VI).

The $\Delta H_{T,m}$ values, which were computed from the difference between $(E_{d,m} + \Delta H_{T,m})$ (Table V) and $E_{d,m}$ (Table VI), are also given in Table VI. Again, a significant variation in $\Delta H_{T,m}$ values was observed from one progesterone derivative to another. The results in Table VI suggested that hydroxy group addition to position 11 or 21 reduced the matrix

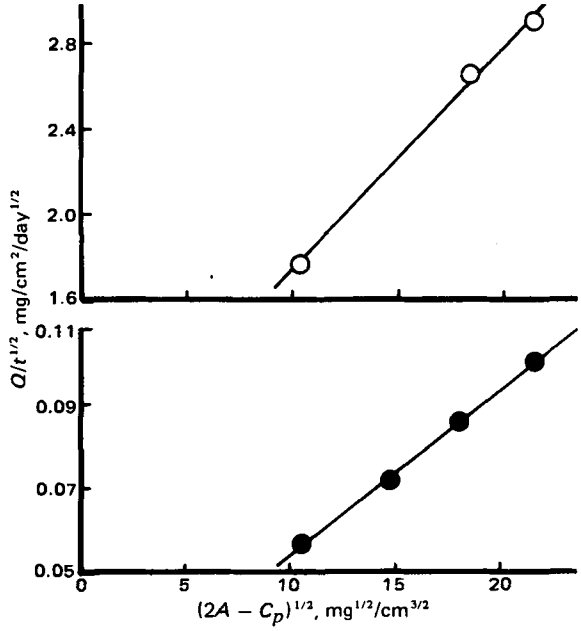

Figure 2—*Dependency of* $Q/t^{1/2}$ *values on* $(2A - C_p)^{1/2}$. *The slope is defined by* $(D_m C_p)^{1/2}$. *Key:* ○, *progesterone; and* ●, *hydrocortisone.*

Table IV—Gibbs Free Energies of Desorption of Hydroxyprogesterones at Various Tmperatures

Temperature	ΔF_{OH}, kcal/mole	ΔF_p, kcal/mole	ΔF_d, kcal/mole
37°	−1.419	0.321	−1.098
45°	−1.515	0.256	−1.259
50°	−1.638	0.108	−1.530
55°	−1.684	0.134	−1.550

Table V—Energy Required for the Controlled Release of Progesterone and Its Hydroxy-Substituted Derivatives from Silicone Devices

Compound	$(E_{d,m} + \Delta H_{T,m})$[a], kcal/mole ± SD
I	15.25 ± 2.26
II	13.52 ± 1.02
III	14.95 ± 0.75
IV	14.30 ± 1.42
V	16.30 ± 0.32
VI	23.62 ± 2.44
VII	16.70 ± 0.87

[a] Mean ±SD of the measurements from four drug concentrations (54.25–228.81 mg/cm³) at four temperatures (37–55°).

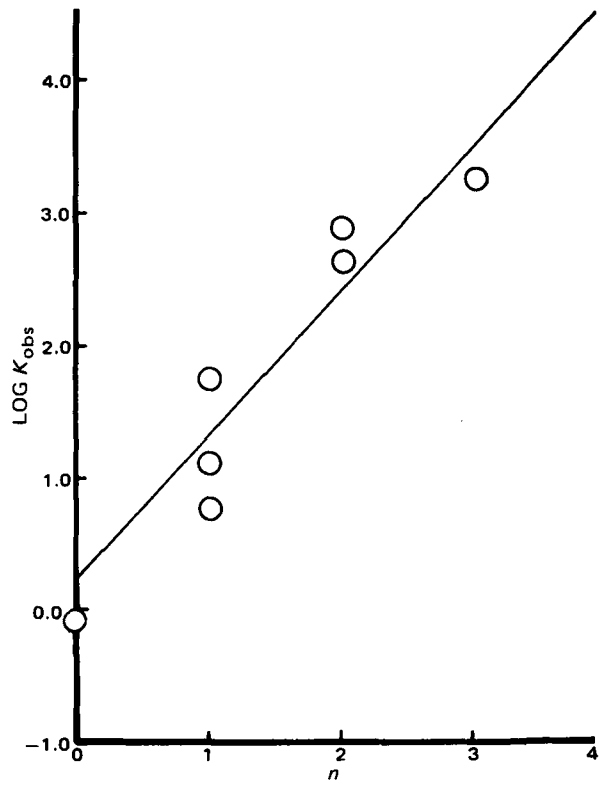

Figure 3—*Dependence of log* K_{obs}, *solution-polymer partition coefficient, on the number of hydroxy groups* (n) *on the progesterone molecule (Eq. 6). From the slope, a* ΔF_{OH} *value of 1.515 kcal/mole was computed (45°).*

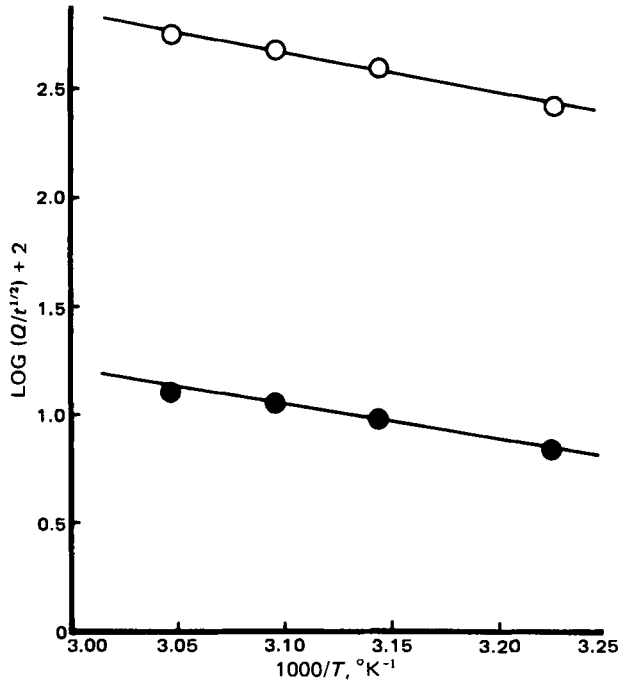

Figure 4—*Temperature dependence of* $Q/t^{1/2}$ *of progesterone* (○) *and hydrocortisone* (●). *The values of* $(E_{d,m} + \Delta H_{T,m})$ *were calculated from the slopes as 16.61 and 17.07 kcal/mole for progesterone and hydrocortisone, respectively.*

diffusion activation energy ($E_{d,m}$) but increased the solvation energy ($\Delta H_{T,m}$). Hydroxy group addition to position 17 increased $E_{d,m}$ but decreased $\Delta H_{T,m}$ (Table VI). The addition of more than one hydroxy group to the progesterone molecule gave a composite effect.

The $\Delta H_{T,m}$ values can also be determined from the temperature dependency of drug solubility (C_p) in a liquid silicone polymer (19), as expected from:

$$\log C_p = \text{constant} - \left(\frac{\Delta H_{T,m}}{2.303R}\right)\left(\frac{1}{T}\right) \qquad \text{(Eq. 10)}$$

A good $\log C_p$ *versus* T^{-1} linearity was achieved experimentally (Fig. 6). The $\Delta H_{T,m}$ values determined in the liquid silicone polymer (Table VII) agreed with the data generated in the polymerized, solid silicone matrix (Table VI), except for progesterone derivatives with one hydroxy group

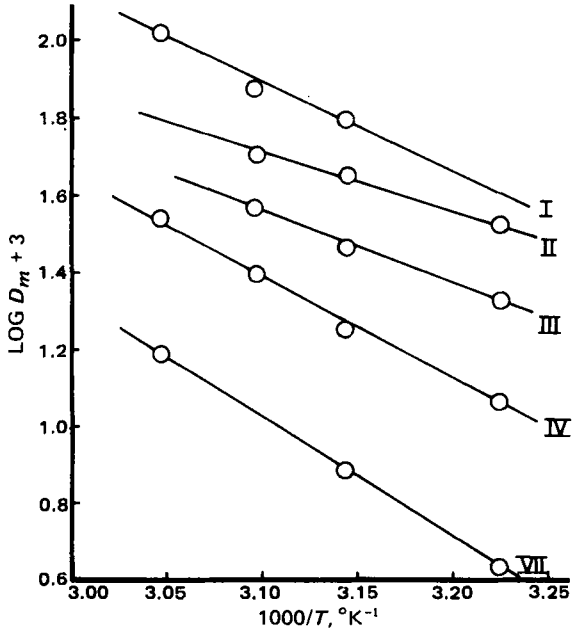

Figure 5—*Temperature dependency of* D_m *(effective diffusivity in silicone matrix) of progesterone derivatives.*

Table VI—Hydroxy Group Effect on the Activation Energy for Matrix Diffusion ($E_{d,m}$) and the Solvation Energy ($\Delta H_{T,m}$) of Progesterone Derivatives in Silicone Polymer

Compound	$E_{d,m}$, kcal/mole	$\Delta H_{T,m}$, kcal/mole ± *SD*
I	10.39	4.86 ± 2.26
II	6.34	7.18 ± 1.02
III	6.88	8.07 ± 0.75
IV	12.19	2.11 ± 1.42
V	3.12	13.18 ± 0.32
VI	11.04	12.58 ± 2.44
VII	14.43	3.01 ± 0.50

Table VII—$\Delta H_{T,s}$ and $\Delta H_{T,m}$ Values for Progesterone and Its Hydroxyl Derivatives

Compound	Solvation Energies, kcal/mole[a]	
	$\Delta H_{T,s}$[b]	$\Delta H_{T,m}$[c]
I	10.22	5.49
II	7.17	8.80
III	6.55	7.88
IV	6.11	8.27
V	7.42	12.99
VI	6.74	8.72
VII	6.48	12.71

[a] Determined at four temperatures (37–55°). [b] Solvation energy in 50% (v/v) polyethylene glycol 400 solution. [c] Solvation energy in silicone medical fluid (20 cv).

at position 17. Apparently, the addition of an hydroxy group at position 17 produces stereochemical configuration and/or physicochemical changes, which become apparent only in a solid polymer matrix and not in a polymer fluid.

The aqueous solubility (C_s) of progesterone and its hydroxy derivatives was also temperature dependent (19), as defined by:

$$\log C_s = \text{constant} - \left(\frac{\Delta H_{T,S}}{2.303R}\right)\left(\frac{1}{T}\right) \qquad \text{(Eq. 11)}$$

As expected from Eq. 11, $\log C_s$ is linearly dependent on T^{-1} (Fig. 6). The hydroxy group addition reduced $H_{T,s}$, the solvation energy (by 3.48 ± 0.48 kcal/mole) (Table VII), leading to an improvement of aqueous solubility (C_s in Table III). However, the number of hydroxy groups did not

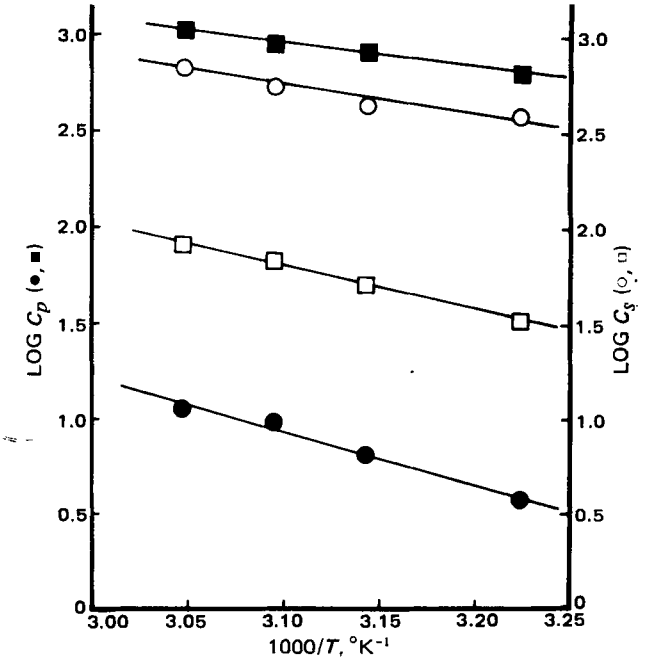

Figure 6—*Temperature dependency of polymer solubility* (C_p) *and aqueous solubility* (C_s) *of progesterone* (■ *or* □) *and hydrocortisone* (● *or* ○). *The* $\Delta H_{T,m}$ *and* $\Delta H_{T,s}$ *values were 5.49 and 10.22 kcal/mole for progesterone and 12.71 and 6.48 kcal/mole for hydrocortisone, respectively.*

change $\Delta H_{T,s}$ [mean value ($\pm SD$) of 6.75 ($\pm$0.48) kcal/mole], although the more hydroxy groups added, the higher the aqueous solubility. The C_s value increased 1.25–11.29-fold.

The data in Table III indicated that the addition of an hydroxy group at position 21 remarkably affected the solution solubility (C_s). With the addition of a 21-OH group, the C_s increased almost fourfold, from 353.3 ($\pm$16.2) (I) to 1402.1 ($\pm$75.4) (II) μg/ml. The significance of the 21-OH group in progesterone derivative solubility enhancement can be demonstrated by removing the 21-OH group by acetylation. Desoxycorticosterone acetate formation reduced C_s substantially to 249.9 ($\pm$2.1) μg/ml. The reduction of C_s was accompanied by an increase in $\Delta H_{T,s}$, the solvation energy, from 7.17 to 10.99 kcal/mole. For desoxycorticosterone acetate, C_s and $\Delta H_{T,s}$ were very close to the value for progesterone (353.3 ± 16.2 μg/ml and 10.22 kcal/mole, respectively). A similar result was achieved when the 21-OH group of hydrocortisone (VII) was acetylated to form hydrocortisone acetate.

REFERENCES

(1) Y. W. Chien, in "Sustained and Controlled Release Drug Delivery Systems," J. Robinson, Ed., Dekker, New York, N.Y., 1978, chap. 4.

(2) Y. W. Chien, S. E. Mares, J. Berg, S. Huber, H. J. Lambert, and K. F. King, *J. Pharm. Sci.*, **64**, 1776 (1975).

(3) L. L. Doyle and T. H. Clewe, *Am. J. Obstet. Gynecol.*, **101**, 564 (1968).

(4) A. Scommegna, G. N. Pandya, M. Christ, A. W. Lee, and M. R. Cohen, *Fertil. Steril.*, **21**, 201 (1970).

(5) A. Scommegna, T. Avila, M. Luna, and W. P. Dmowski, *Obstet. Gynecol.*, **43**, 769 (1974).

(6) Y. W. Chien, L. F. Rozek, and H. J. Lambert, in "Controlled Release Polymeric Formulations," D. R. Paul and F. W. Harris, Eds., ACS Symposium Series No. 33, American Chemical Society, Washington, D.C., 1976, chap. 6.

(7) Y. W. Chien, *Chem. Pharm. Bull.*, **24**, 1471 (1976).

(8) D. R. Mishell, Jr., M. Talas, A. F. Parlow, and D. L. Moyer, *Am. J. Obstet. Gynecol.*, **107**, 100 (1970).

(9) M. Thiery, D. Vandekerckhove, M. Dhont, A. Vermeulen, and J. M. Decoster, *Contraception*, **13**, 605 (1976).

(10) A. Vermeulen, M. Dhont, M. Thiery, and D. Vandekerckhove, *Fertil. Steril.*, **27**, 773 (1976).

(11) F. Z. Stanczyk, M. Hiroi, U. Goebelsmann, P. F. Brenner, M. E. Lumkin, and D. R. Mishell, Jr., *Contraception*, **12**, 279 (1975).

(12) D. R. Mishell, Jr., D. E. Moore, S. Roy, P. F. Brenner, and M. A. Page, *Am. J. Obstet. Gynecol.*, **130**, 55 (1978).

(13) L. Viinikka, A. Victor, O. Janne, and J. P. Raynaud, *Contraception*, **12**, 309 (1975).

(14) N. H. Lauerson and K. H. Wilson, *Prostaglandins (Suppl.)*, **12**, 63 (1976).

(15) J. H. Duenhoelter, R. S. Ramos, L. Milewich, and P. C. MacDonald, *Contraception*, **17**, 51 (1978).

(16) Y. W. Chien, H. J. Lambert, and D. E. Grant, *J. Pharm. Sci.*, **63**, 365 (1974).

(17) Y. W. Chien and H. J. Lambert, *ibid.*, **63**, 515 (1974).

(18) Y. W. Chien, H. J. Lambert, and T. K. Lin, *ibid.*, **64**, 1643 (1975).

(19) Y. W. Chien, in "Controlled Release Polymeric Formulations," D. R. Paul and F. W. Harris, Eds., ACS Symposium Series No. 33, American Chemical Society, Washington, D.C., 1976, chap. 5.

(20) Y. W. Chien and E. P. K. Lau, *J. Pharm. Sci.*, **65**, 488 (1976).

(21) N. F. H. Ho, L. Suhardja, S. Hwang, E. Owada, A. Molokhia, G. L. Flynn, W. I. Higuchi, and J. Y. Park, *ibid.*, **65**, 1578 (1976).

(22) R. J. Scheuplein and I. H. Blank, *Physiol. Rev.*, **51**, 702 (1971).

(23) J. T. Davies and E. K. Rideal, "Interfacial Phenomena," Academic, New York, N.Y., 1963.

(24) G. L. Biagi, A. M. Barbaro, O. Grandolfi, M. C. Guerra, and G. Cantelli-Forti, *J. Med. Chem.*, **18**, 873 (1975).

(25) J. Crank and G. S. Park, "Diffusion in Polymers," Academic, New York, N.Y., 1968, chaps. 2 and 3.

ACKNOWLEDGMENTS

The authors thank Ms. Geri Vargason for editorial comments and Ms. Freddi Haas and Ms. Lynelle Sachen for assistance in manuscript preparation.

Cobaltous Chloride-Induced Hypothermia II: Pretreatment with Sympathoplegics, Antihistamines, and Narcotic Antagonists

DAVID H. BURKE ˣ **and JACK C. BROOKS**

Received August 25, 1978, from the *Divisions of Pharmacology and Physiology, School of Dentistry, Marquette University, Milwaukee, WI 53233.* Accepted for publication November 13, 1978.

Abstract □ Body temperature depression was noted in rats, mice, and hamsters following intraperitoneal cobaltous chloride administration (25 mg/kg). Intracerebral cobalt injection elicited hypothermia in rats and mice but not in hamsters. Body temperature depression appeared to be centrally mediated in rats and mice and peripherally mediated in hamsters. The effect of intraperitoneal and intracerebral pretreatment with phentolamine, diphenhydramine, propranolol, cimetidine, and naloxone on the mouse rectal temperature response to cobalt (25 mg/kg ip) was noted. Systemic phentolamine injection (intraperitoneal) did not alter the cobalt response, whereas intracerebral administration partially antagonized cobalt-induced hypothermia, indicating that antagonism was mediated centrally. Pretreatment with propranolol and cimetidine failed to modify the temperature response. Intracerebral diphenhydramine did not influence cobalt hypothermia. However, this agent reduced the cobalt response when given intraperitoneally, presumably through a peripheral inhibitory mechanism. The intracerebral injection of naloxone 30 min prior to cobalt slightly enhanced hypothermia, apparently through a central action. Intracerebral 6-hydroxydopamine injection depleted brain norepinephrine and dopamine but exhibited no apparent influence on cobalt-induced hypothermia.

Keyphrases □ Hypothermia—cobaltous chloride induced, effect of phentolamine, diphenhydramine, propranolol, cimetidine, naloxone, rats, mice, hamsters, species specificity, central *versus* peripheral effects □ Cobaltous chloride—hypothermia, rats, mice, hamsters, effect of phentolamine, diphenhydramine, propranolol, cimetidine, naloxone, species specificity □ Sympathoplegics—effect on cobaltous chloride-induced hypothermia □ Antihistamines—effect on cobaltous chloride-induced hypothermia □ Narcotic antagonists—effect on cobaltous chloride-induced hypothermia

Many agents interfere with thermoregulatory control as a result of their influence on the central nervous system (CNS). Intracerebral dopamine and norepinephrine injections into conscious mice caused hypothermia (1). Similarly, histamine and oxotremorine injection into the lateral ventricles produced a dose-related fall in body temperature (2–4). Hypothermia, due solely to a decrease in heat production, was reported following a single central morphine injection in rats (5, 6).

Recent studies in this laboratory showed that cobaltous

0022-3549/79/0600-0693$01.00/0

© 1979, American Pharmaceutical Association

change $\Delta H_{T,s}$ [mean value ($\pm SD$) of 6.75 ($\pm$0.48) kcal/mole], although the more hydroxy groups added, the higher the aqueous solubility. The C_s value increased 1.25–11.29-fold.

The data in Table III indicated that the addition of an hydroxy group at position 21 remarkably affected the solution solubility (C_s). With the addition of a 21-OH group, the C_s increased almost fourfold, from 353.3 ($\pm$16.2) (I) to 1402.1 ($\pm$75.4) (II) μg/ml. The significance of the 21-OH group in progesterone derivative solubility enhancement can be demonstrated by removing the 21-OH group by acetylation. Desoxycorticosterone acetate formation reduced C_s substantially to 249.9 ($\pm$2.1) μg/ml. The reduction of C_s was accompanied by an increase in $\Delta H_{T,s}$, the solvation energy, from 7.17 to 10.99 kcal/mole. For desoxycorticosterone acetate, C_s and $\Delta H_{T,s}$ were very close to the value for progesterone (353.3 ± 16.2 μg/ml and 10.22 kcal/mole, respectively). A similar result was achieved when the 21-OH group of hydrocortisone (VII) was acetylated to form hydrocortisone acetate.

REFERENCES

(1) Y. W. Chien, in "Sustained and Controlled Release Drug Delivery Systems," J. Robinson, Ed., Dekker, New York, N.Y., 1978, chap. 4.

(2) Y. W. Chien, S. E. Mares, J. Berg, S. Huber, H. J. Lambert, and K. F. King, *J. Pharm. Sci.*, **64**, 1776 (1975).

(3) L. L. Doyle and T. H. Clewe, *Am. J. Obstet. Gynecol.*, **101**, 564 (1968).

(4) A. Scommegna, G. N. Pandya, M. Christ, A. W. Lee, and M. R. Cohen, *Fertil. Steril.*, **21**, 201 (1970).

(5) A. Scommegna, T. Avila, M. Luna, and W. P. Dmowski, *Obstet. Gynecol.*, **43**, 769 (1974).

(6) Y. W. Chien, L. F. Rozek, and H. J. Lambert, in "Controlled Release Polymeric Formulations," D. R. Paul and F. W. Harris, Eds., ACS Symposium Series No. 33, American Chemical Society, Washington, D.C., 1976, chap. 6.

(7) Y. W. Chien, *Chem. Pharm. Bull.*, **24**, 1471 (1976).

(8) D. R. Mishell, Jr., M. Talas, A. F. Parlow, and D. L. Moyer, *Am. J. Obstet. Gynecol.*, **107**, 100 (1970).

(9) M. Thiery, D. Vandekerckhove, M. Dhont, A. Vermeulen, and J. M. Decoster, *Contraception*, **13**, 605 (1976).

(10) A. Vermeulen, M. Dhont, M. Thiery, and D. Vandekerckhove, *Fertil. Steril.*, **27**, 773 (1976).

(11) F. Z. Stanczyk, M. Hiroi, U. Goebelsmann, P. F. Brenner, M. E. Lumkin, and D. R. Mishell, Jr., *Contraception*, **12**, 279 (1975).

(12) D. R. Mishell, Jr., D. E. Moore, S. Roy, P. F. Brenner, and M. A. Page, *Am. J. Obstet. Gynecol.*, **130**, 55 (1978).

(13) L. Viinikka, A. Victor, O. Janne, and J. P. Raynaud, *Contraception*, **12**, 309 (1975).

(14) N. H. Lauerson and K. H. Wilson, *Prostaglandins (Suppl.)*, **12**, 63 (1976).

(15) J. H. Duenhoelter, R. S. Ramos, L. Milewich, and P. C. MacDonald, *Contraception*, **17**, 51 (1978).

(16) Y. W. Chien, H. J. Lambert, and D. E. Grant, *J. Pharm. Sci.*, **63**, 365 (1974).

(17) Y. W. Chien and H. J. Lambert, *ibid.*, **63**, 515 (1974).

(18) Y. W. Chien, H. J. Lambert, and T. K. Lin, *ibid.*, **64**, 1643 (1975).

(19) Y. W. Chien, in "Controlled Release Polymeric Formulations," D. R. Paul and F. W. Harris, Eds., ACS Symposium Series No. 33, American Chemical Society, Washington, D.C., 1976, chap. 5.

(20) Y. W. Chien and E. P. K. Lau, *J. Pharm. Sci.*, **65**, 488 (1976).

(21) N. F. H. Ho, L. Suhardja, S. Hwang, E. Owada, A. Molokhia, G. L. Flynn, W. I. Higuchi, and J. Y. Park, *ibid.*, **65**, 1578 (1976).

(22) R. J. Scheuplein and I. H. Blank, *Physiol. Rev.*, **51**, 702 (1971).

(23) J. T. Davies and E. K. Rideal, "Interfacial Phenomena," Academic, New York, N.Y., 1963.

(24) G. L. Biagi, A. M. Barbaro, O. Grandolfi, M. C. Guerra, and G. Cantelli-Forti, *J. Med. Chem.*, **18**, 873 (1975).

(25) J. Crank and G. S. Park, "Diffusion in Polymers," Academic, New York, N.Y., 1968, chaps. 2 and 3.

ACKNOWLEDGMENTS

The authors thank Ms. Geri Vargason for editorial comments and Ms. Freddi Haas and Ms. Lynelle Sachen for assistance in manuscript preparation.

Cobaltous Chloride-Induced Hypothermia II: Pretreatment with Sympathoplegics, Antihistamines, and Narcotic Antagonists

DAVID H. BURKE ˣ **and JACK C. BROOKS**

Received August 25, 1978, from the *Divisions of Pharmacology and Physiology, School of Dentistry, Marquette University, Milwaukee, WI 53233.* Accepted for publication November 13, 1978.

Abstract □ Body temperature depression was noted in rats, mice, and hamsters following intraperitoneal cobaltous chloride administration (25 mg/kg). Intracerebral cobalt injection elicited hypothermia in rats and mice but not in hamsters. Body temperature depression appeared to be centrally mediated in rats and mice and peripherally mediated in hamsters. The effect of intraperitoneal and intracerebral pretreatment with phentolamine, diphenhydramine, propranolol, cimetidine, and naloxone on the mouse rectal temperature response to cobalt (25 mg/kg ip) was noted. Systemic phentolamine injection (intraperitoneal) did not alter the cobalt response, whereas intracerebral administration partially antagonized cobalt-induced hypothermia, indicating that antagonism was mediated centrally. Pretreatment with propranolol and cimetidine failed to modify the temperature response. Intracerebral diphenhydramine did not influence cobalt hypothermia. However, this agent reduced the cobalt response when given intraperitoneally, presumably through a peripheral inhibitory mechanism. The intracerebral injection of naloxone 30 min prior to cobalt slightly enhanced hypothermia, apparently through a central action. Intracerebral 6-hydroxydopamine injection depleted brain norepinephrine and dopamine but exhibited no apparent influence on cobalt-induced hypothermia.

Keyphrases □ Hypothermia—cobaltous chloride induced, effect of phentolamine, diphenhydramine, propranolol, cimetidine, naloxone, rats, mice, hamsters, species specificity, central *versus* peripheral effects □ Cobaltous chloride—hypothermia, rats, mice, hamsters, effect of phentolamine, diphenhydramine, propranolol, cimetidine, naloxone, species specificity □ Sympathoplegics—effect on cobaltous chloride-induced hypothermia □ Antihistamines—effect on cobaltous chloride-induced hypothermia □ Narcotic antagonists—effect on cobaltous chloride-induced hypothermia

Many agents interfere with thermoregulatory control as a result of their influence on the central nervous system (CNS). Intracerebral dopamine and norepinephrine injections into conscious mice caused hypothermia (1). Similarly, histamine and oxotremorine injection into the lateral ventricles produced a dose-related fall in body temperature (2–4). Hypothermia, due solely to a decrease in heat production, was reported following a single central morphine injection in rats (5, 6).

Recent studies in this laboratory showed that cobaltous

0022-3549/79/0600-0693$01.00/0

© 1979, American Pharmaceutical Association

Table I—Body Temperature Changes 30 min after Itracerebral Cobaltous Chloride Injection in Various Species

Species	Water[a] Initial Temperature	Water[a] Temperature Change (Mean ± SE)[b]	Cobaltous Chloride[a] Initial Temperature	Cobaltous Chloride[a] Temperature Change (Mean ± SE)[b]
Mice	37.19°	−0.12 ± 0.04°	37.24°	−4.08 ± 0.19°[c]
Rats	37.67°	+0.03 ± 0.09°	37.69°	−3.56 ± 0.18°[c]
Hamsters	37.24°	−0.26 ± 0.13°	37.46°	−0.18 ± 0.16°

[a] Each animal received 0.01 ml of water or a 0.25% cobaltous chloride solution. [b] Temperature changes represent the difference between body temperature recorded initially and that obtained 30 min following water or cobalt treatment in groups of 12 animals. [c] Compared to water in the corresponding species, $p < 0.05$.

chloride causes pronounced hypothermia in mice, apparently through a centrally mediated decrease in heat production (7). Although pretreatment with atropine, hexamethonium, and nicotine failed to modify the cobalt response, a partial antagonism was noted after pretreatment with chlorpromazine.

This paper describes cobalt-induced hypothermia and modification of this response by pretreatment with histaminergic, noradrenergic, or "opioid" receptor blocking agents.

EXPERIMENTAL

Animals—The experiments were performed on male Swiss albino mice, 18–25 g, on male Wistar rats, 140–160 g, and on male Syrian hamsters, 50–70 g. The animals were housed in groups of six to 20 with *ad libitum* access to laboratory food[1] and water for at least 3 days prior to use. For 24 hr before and including the time of the experiment, the animals were kept in a room free from drafts at a constant environmental temperature (23 ± 1°).

Drugs—Fresh drug and chemical solutions were prepared with distilled water in concentrations (calculated as the salt) 0.01 ml/g of body weight. Intracerebral injections were administered in a fixed volume of 0.01 ml/animal. Cobaltous chloride[2], phentolamine mesylate[3], propranolol hydrochloride[4], diphenhydramine hydrochloride[5], cimetidine hydrochloride[6], naloxone hydrochloride[7], and 6-hydroxydopamine[8] were used.

Body Temperature Recording—A thermistor thermometer[9] was used for obtaining body temperature. Rectal temperatures were recorded with a thermistor probe inserted ~2.5 cm (5 cm for rats) and held in position until constant readings were attained.

At the start of daily testing, the animals were placed singly in circular wire-mesh cages and individual weights were recorded with a triple-beam balance[10]. Immediately following weight determination, initial temperatures were recorded and treatments were administered. Temperatures were recorded again at various intervals. Unless otherwise stated, treatments were intraperitoneal. Control animals received distilled water (0.01 ml/g). To study the influence of various drugs on cobalt-induced hypothermia, pretreatment injections (water, phentolamine, propranolol, diphenhydramine, cimetidine, naloxone, and 6-hydroxydopamine) were given at specified intervals prior to recording initial temperatures.

Intracerebral Injections—Intracerebral injections were carried out according to a literature method (8). Agents were injected 2 mm lateral to the midline on a line joining the anterior bases of the ears. A 27-gauge needle attached to a microliter syringe[11] was inserted perpendicularly through the skull to a depth of 3 mm. Similar prior injection of several animals with methylene blue (0.5%) resulted in dye localization in the third and fourth ventricles.

[1] Wayne Lab-Blox.
[2] J. T. Baker Chemical Co.
[3] Ciba Pharmaceutical Co.
[4] Ayerst Laboratories.
[5] Parke-Davis & Co.
[6] SK&F Lab Co.
[7] Endo Laboratories.
[8] Sigma Chemical Co.
[9] Model 46 Tele-Thermometer, Yellow Springs Instrument Co., Yellow Springs, Ohio.
[10] Ohaus.
[11] Hamilton.

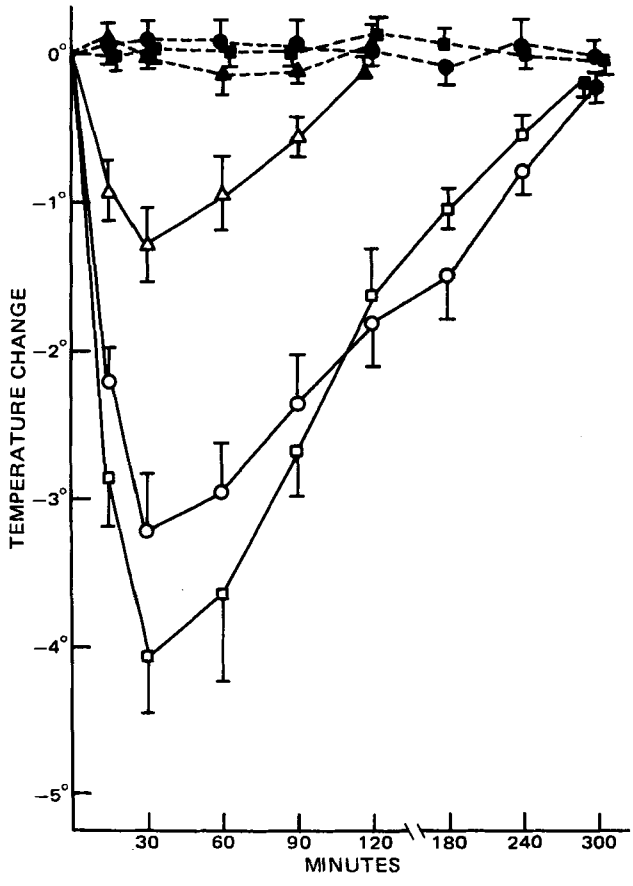

Figure 1—*Time course of the effect of 0.01 ml/g ip distilled water (- - -) and cobaltous chloride (25 mg/kg ip) (—) on rectal temperature in hamsters (▲), rats (●), and mice (■). Water or cobaltous chloride were administered at zero time. Open symbols denote significant difference ($p < 0.05$) from water treatment at the corresponding time interval. Each point represents the average of 12 determinations. Vertical bars represent standard errors.*

Catecholamine Assay—Dopamine and norepinephrine were extracted from the brain and quantitated as the trihydroxyindoles (9). Amines were isolated from deproteinized brain homogenates by chromatography on a cation-exchange resin[12]. The individual amines were quantitated fluorometrically[13] with standard curves relating relative fluorescence to concentration.

Statistics—Results are expressed as mean ± standard error. Significance was calculated using the Student *t* test. Differences were considered significant at the probability level of 5% or less.

RESULTS

Core temperature changes were recorded at various intervals for 5 hr following cobaltous chloride administration (25 mg/kg ip) to unrestrained mice, rats, and hamsters (Fig. 1). Maximum body temperature depression (~1.2°) was evident 30 min after cobalt injection in hamsters. Hypothermia duration in this species was ~90 min. Cobaltous chloride caused more body temperature depression in rats (3.2°) and mice (4.1°). In each case, maximum hypothermia occurred within 30 min. A 4-hr hypothermia duration was noted in rats and mice.

Body temperature changes were noted 30 min after intracerebral cobaltous chloride injection (25 μg) in mice, rats, and hamsters (Table I). Mice and rats exhibited respective drops of 4.08 and 3.56°. Visible shivering and increased muscle tone were absent throughout the body temperature response. In both species, hypothermia was accompanied by depression of locomotor activity. Cobaltous chloride failed to elicit a significant body temperature depression when injected intracerebrally in hamsters.

[12] Dowex 50-X8.
[13] Aminco-Bowman SPF spectrophotofluorometer.

Table II—Effect of Intraperitoneal (ip) and Intracerebral (ic) Pretreatment with Various Agents on the Hypothermic Response to Cobaltous Chloride in Mice

Pretreatment[a]	Route	Dose	Water		Cobaltous Chloride (25 mg/kg)	
			Initial Temperature	Temperature Change (Mean ± SE)[b]	Initial Temperature	Temperature Change (Mean ± SE)[b]
Water	ip	—	37.36°	+0.01 ± 0.07°	37.45°	−4.28 ± 0.22°[c]
Water	ic	—	37.11°	−0.10 ± 0.07°	37.08°	−3.93 ± 0.11°[d]
Phentolamine mesylate	ip	10 mg/kg	37.20°	−0.12 ± 0.10°	37.21°	−4.14 ± 0.25°
Phentolamine mesylate	ic	10 μg	36.72°	−0.24 ± 0.07°	36.85°	−3.05 ± 0.15°[e]
Propranolol hydrochloride	ip	10 mg/kg	37.13°	+0.10 ± 0.08°	37.54°	−4.68 ± 0.23°
Propranolol hydrochloride	ic	10 μg	36.59°	−0.21 ± 0.15°	36.78°	−4.06 ± 0.14°
Diphenhydramine hydrochloride	ip	5 mg/kg	37.24°	+0.09 ± 0.08°	37.38°	−3.48 ± 0.14°[f]
Diphenhydramine hydrochloride	ic	5 μg	37.10°	+0.03 ± 0.08°	37.07°	−3.85 ± 0.14°
Cimetidine hydrochloride	ip	30 mg/kg	37.36°	−0.05 ± 0.07°	37.46°	−4.13 ± 0.13°
Cimetidine hydrochloride	ic	30 μg	37.42°	−0.17 ± 0.09°	37.12°	−4.03 ± 0.16°
Naloxone hydrochloride	ip	1 mg/kg	37.60°	−0.06 ± 0.05°	37.96°	−4.18 ± 0.12°
Naloxone hydrochloride	ic	1 μg	37.44°	−0.02 ± 0.09°	37.30°	−4.45 ± 0.11°[e]

[a] Pretreatments were administered 30 min before intraperitoneal water and cobalt to groups of 30 animals. [b] Temperature changes represent the difference between body temperature recorded initially and that obtained 30 min after treatment. [c] Compared to intraperitoneal water–intraperitoneal water (pretreatment–treatment), $p < 0.05$. [d] Compared to intracerebral water–intraperitoneal water (pretreatment–treatment), $p < 0.05$. [e] Compared to intracerebral water–intraperitoneal cobalt (pretreatment–treatment), $p < 0.05$. [f] Compared to intraperitoneal water–intraperitoneal cobalt (pretreatment–treatment), $p < 0.05$.

Table III—Effect of Intracerebral Pretreatment with 6-Hydroxydopamine on the Hypothermic Response to Cobaltous Chloride in Mice

Pretreatment[a]	Pretreatment–Treatment Interval, days	Water (0.01 ml/g ip)		Cobaltous Chloride (25 mg/kg ip)	
		Initial Temperature	Temperature Change (Mean ± SE)[b]	Initial Temperature	Temperature Change (Mean ± SE)[b]
Vehicle[c]	14	38.63°	−0.31 ± 0.11°	38.56°	−5.31 ± 0.25°[d]
6-Hydroxydopamine	14	38.84°	−0.36 ± 0.10°	38.31°	−5.42 ± 0.30°
Vehicle	42	38.62°	−0.39 ± 0.11°	38.79°	−5.41 ± 0.30°[e]
6-Hydroxydopamine	42	38.78°	−0.30 ± 0.07°	38.81°	−5.34 ± 0.32°

[a] Pretreatments (intracerebral) were administered 14 and 42 days before intraperitoneal water and cobaltous chloride to groups of 18 mice. [b] Temperature changes represent the difference between body temperature recorded initially and that obtained 30 min after treatment. [c] Aqueous ascorbic acid solution (0.5%) with pH adjusted to 5.5. [d] Compared to vehicle–water (pretreatment–treatment) at the 14-day pretreatment–treatment interval, $p < 0.05$. [e] Compared to vehicle–water (pretreatment–treatment) at the 42-day pretreatment–treatment interval, $p < 0.05$.

The effect of intraperitoneal and intracerebral pretreatment with phentolamine mesylate, propranolol hydrochloride, diphenhydramine hydrochloride, cimetidine hydrochloride, and naloxone hydrochloride on the body temperature response to cobaltous chloride (25 mg/kg) in mice is shown in Table II. Pretreatment doses were incapable of causing significant body temperature alteration. Intracerebral phentolamine administration partially attenuated the hypothermic response to cobalt. Phentolamine produced no significant effect upon cobalt hypothermia when given intraperitoneally. Propranolol did not modify cobalt-induced hypothermia by either the intraperitoneal or intracerebral route. Systemic diphenhydramine administration partially inhibited cobalt hypothermia. No antagonism occurred following intracerebral administration. Cobaltous chloride-induced body temperature depression was not significantly altered by intraperitoneal naloxone, but a hypothermia potentiation was observed after intracerebral naloxone.

Table III describes the effect of intracerebral 6-hydroxydopamine pretreatment (100 μg) on the hypothermic response to cobaltous chloride (25 mg/kg ip) in mice. Pretreatment 14 and 42 days prior to cobalt treatment did not affect the body temperature response.

At 14 days following intracerebral 6-hydroxydopamine injection, mouse brain norepinephrine and dopamine concentrations were reduced by 59.09 and 71.43%, respectively (Table IV). A similar reduction in catecholamine concentrations was noted 42 days after the central administration of 6-hydroxydopamine.

DISCUSSION

The body temperature response to cobaltous chloride was species dependent. Hypothermia intensity and duration were greater in rats and mice than in hamsters.

Intracerebral cobalt injection did not produce hypothermia in hamsters but did produce body temperature depression in mice and rats, apparently through a central mechanism. The small drop in hamster body temperature produced by intraperitoneal injection was probably due to peripheral activity.

Since catecholamine, histamine, and opioid receptor stimulation within the CNS is associated with hypothermia in mice (1, 10–12), it seemed logical that cobalt might accomplish body temperature depression through its influence on one or more of these receptive sites. Intracerebral, but not systemic, phentolamine partially antagonized cobalt-induced hypothermia. It is possible, therefore, that cobalt hypothermia is mediated, in part, either through a direct influence on α-adrenergic receptors or through norepinephrine release within the CNS.

The absence of an intracerebral or intraperitoneal propranolol effect on cobalt hypothermia indicates that cobalt does not act through central or peripheral β-receptors.

The H_1 and H_2 receptor blocking agents diphenhydramine and cimetidine did not modify cobalt hypothermia when injected intracerebrally and intraventricularly, respectively. Cobalt hypothermia apparently is not mediated through activity upon central H_1 or H_2 receptors.

On the other hand, intraperitoneal diphenhydramine partially antagonized the temperature response to cobalt. Cobalt-induced hypothermia may be mediated, in part, peripherally either through histamine release or through a direct influence on H_1 receptors.

Intracerebral naloxone slightly enhanced cobalt-induced hypothermia, apparently through a central action.

The catecholamine-depleting agent 6-hydroxydopamine markedly reduced brain norepinephrine and dopamine levels (~59 and 72%, respectively) at 2 and 6 weeks following pretreatment (Table IV). However, 6-hydroxydopamine had no effect on cobalt hypothermia. It is possible, therefore, that cobalt produces hypothermia through mechanisms other than norepinephrine or dopamine release. Over a period of time, however, receptors for these amines may have become "supersensitive." Thus, less released norepinephrine or dopamine could have caused a more intense response.

Little information is available concerning brain dopamine depletion in mice following central 6-hydroxydopamine administration. Tabakoff and Ritzmann (13) reported that intracerebrally administered 6-hydroxydopamine (50 μg) depleted norepinephrine but had little effect on dopamine and serotonin levels. The present results show that intracerebral 6-hydroxydopamine (100 μg) depleted mouse brain dopamine.

Previous experiments in this laboratory showed that cobalt-induced hypothermia is partially attenuated by chlorpromazine pretreatment (7). Antagonism in the case of this phenothiazine was not mediated through a central anticholinergic action, since atropine, as well as nicotine, failed to achieve a similar blockade. In addition to anticholinergic activity,

Table IV—Intracerebral 6-Hydroxydopamine Effect on Norepinephrine and Dopamine Concentration in Mice Brains

Days after Injection[a]	Norepinephrine			Dopamine		
	Vehicle[b], μg/g ± SE	6-Hydroxydopamine, μg/g ± SE	Change, %	Vehicle, μg/g ± SE	6-Hydroxydopamine, μg/g ± SE	Change, %
14	0.308 ± 0.02	0.126 ± 0.03[c]	−59.09	0.287 ± 0.03	0.082 ± 0.03[c]	−71.43
42	0.336 ± 0.01	0.135 ± 0.03[c]	−59.82	0.298 ± 0.02	0.082 ± 0.02[c]	−72.48

[a] The mice brains (groups of six) were removed and assayed for catecholamine content 14 and 42 days following the intracerebral water or 6-hydroxydopamine injection (100 μg). [b] Aqueous ascorbic acid solution (0.5%) with pH adjusted to 5.5. [c] Compared to the appropriate vehicle, $p < 0.05$.

chlorpromazine possesses adrenolytic and antihistaminic qualities (14). Chlorpromazine may partially reverse the cobalt response through a central α-receptor blockade and/or peripheral antihistaminic activity.

REFERENCES

(1) R. T. Brittain and S. L. Handley, *J. Physiol.*, **192**, 805 (1967).
(2) G. G. Shaw, *Br. J. Pharmacol.*, **42**, 205 (1971).
(3) P. Spencer, *Life Sci.*, **5**, 1015 (1966).
(4) W. E. Kirkpatrick, *Proc. West. Pharmacol. Soc.*, **10**, 51 (1967).
(5) R. M. Paolino and B. K. Bernard, *Life Sci.*, **7**, 857 (1968).
(6) V. J. Lotti, P. Lomax, and R. George, *J. Pharmacol.*, **150**, 135 (1965).
(7) D. H. Burke, *J. Pharm. Sci.*, **67**, 799 (1978).
(8) T. Haley and W. McCormick, *Br. J. Pharmacol.*, **12**, 12 (1957).
(9) S. Snyder and K. Taylor, in "Research Methods in Neurochemistry," vol. 1, N. Marks and R. Rodnight, Eds., Plenum, New York, N.Y., 1972, p. 287.
(10) G. G. Shaw, *Br. J. Pharmacol.*, **42**, 205 (1971).
(11) C. J. Estler, *Proc. Int. Pharmacol. Meet., 1st*, **8**, 153 (1962).
(12) A. A. Menon and B. J. Pleuvry, *J. Pharm. Pharmacol.*, **28**, 827 (1976).
(13) B. Tabakoff and R. F. Ritzmann, *J. Pharmacol. Exp. Ther.*, **203**, 319 (1977).
(14) S. Courvoisier, J. Fournel, R. Ducrat, M. Kolsky, and P. Koetschet, *Arch. Int. Pharmacodyn. Ther.*, **92**, 305 (1953).

ACKNOWLEDGMENTS

Presented at the Pharmacology Section, APhA Academy of Pharmaceutical Sciences, Hollywood, Fla., meeting, November 1978.

Supported in part by a grant from the Marquette University Committee on Research and National Institutes of Health Grant RR-09016.

The authors are indebted to Julie Baron, Carol Marshall, Robert Ryan, Susan Treml, and Donald Zuech for their assistance.

Antifertility and Antiproteolytic Activity of Activated *N*-Carbobenzoxy Amino Acid Esters

I. H. HALL ˣ, J. H. DREW, Z. SAJADI, and L. J. LOEFFLER

Received July 31, 1978, from the *Division of Medicinal Chemistry, School of Pharmacy, University of North Carolina, Chapel Hill, NC 27514.* Accepted for publication November 16, 1978.

Abstract □ *N*-Carbobenzoxy L-phenylalanine, glycine, L-leucine, and L-proline derivatives, their vinyl esters, and their 1,2-dibromoethyl esters were tested for antifertility activity in mice. Intraperitoneal administration reduced the pregnancy percentage and the number of fetuses per litter. Intravaginal administration reduced the pregnancy percentage significantly, with *N*-carbobenzoxyglycine vinyl ester, *N*-carbobenzoxyglycine-1,2-dibromoethyl ester, *N*-carbobenzoxy-L-leucine-1,2-dibromoethyl ester, and *N*-carbobenzoxy-L-proline-1,2-dibromoethyl ester producing 100% inhibition at 10 mg/kg/day. Sperm enzyme hydrolysis of the nonspecific substrate azocasein was inhibited significantly by certain *N*-carbobenzoxy amino acid esters *in vitro*. Specific substrate *N*-benzoyl-L-arginine ethyl ester hydrolysis was also inhibited. Compounds that inhibited *N*-benzoyl-L-arginine ethyl ester hydrolysis also demonstrated *in vivo* intravaginal antifertility activity.

Keyphrases □ Carbobenzoxy amino acid esters—contraceptive activity, antiproteolytic activity, mice □ Contraceptives, potential—activated *N*-carbobenzoxy amino acid esters, mice □ Enzyme activity—effect of activated *N*-carbobenzoxy amino acid esters on sperm proteolysis, mice □ Sperm—enzymes, effect of *N*-carbobenzoxy amino acid esters, mice

Recently, numerous activated *N*-protected amino acid esters were synthesized as possible latent proteolytic inhibitors (1, 2). These agents resemble known trypsin and chymotrypsin inhibitors. Certain members of the series effectively inhibited *in vivo* cathepsin activity and *in vitro* chymotrypsin activity (3). Since proteolytic enzyme inhibitors block sperm acrosin activity, capacitation, and fertility, the effects of this series on reproduction were investigated.

EXPERIMENTAL

Chemistry—*N*-Carbobenzoxy-L-phenylalanine (I), *N*-carbobenzoxyglycine (II), *N*-carbobenzoxy-L-leucine (III), and *N*-carbobenzoxy-L-proline (IV) were prepared by the standard procedure (4) (Table I). The *N*-carbobenzoxy amino acids were converted to the corresponding vinyl esters V, VI, VII, and VIII by refluxing with vinyl acetate in the presence of palladium chloride and were purified by column chromatography. The vinyl esters were treated with bromine in chloroform to give the 1,2-dibromo esters IX, X, XI, and XII, which were purified by fractional crystallization or column chromatography (1, 2). *N*-α-Tosyl-L-lysylchloromethyl ketone (XIII), tosyl-L-phenylalanylchloromethyl ketone (XIV), carbobenzoxy-L-phenylalanine chloromethyl ketone (XV), 17-ethinyl estradiol (XVI), and diethylstilbestrol (XVII) were purchased[1].

Antifertility Screens—For 28 days, virgin CF_1 female mice (~28 g), which had been isolated for 4 weeks, were administered test compounds suspended in 1% carboxymethylcellulose at 10 mg/kg/day (0.2 ml) ip. On Day 10, female mice were exposed to male mice (two females per male) for the remainder of the experiment. Male mice were rotated once a week to assure fertility. On gestation Days 17–21, the females were sacrificed;

[1] Sigma Chemical Co. or Cyclo Chemicals.

0022-3549/79/0600-0696$01.00/0

© 1979, American Pharmaceutical Association

Table IV—Intracerebral 6-Hydroxydopamine Effect on Norepinephrine and Dopamine Concentration in Mice Brains

Days after Injection[a]	Norepinephrine			Dopamine		
	Vehicle[b], μg/g ± SE	6-Hydroxydopamine, μg/g ± SE	Change, %	Vehicle, μg/g ± SE	6-Hydroxydopamine, μg/g ± SE	Change, %
14	0.308 ± 0.02	0.126 ± 0.03[c]	−59.09	0.287 ± 0.03	0.082 ± 0.03[c]	−71.43
42	0.336 ± 0.01	0.135 ± 0.03[c]	−59.82	0.298 ± 0.02	0.082 ± 0.02[c]	−72.48

[a] The mice brains (groups of six) were removed and assayed for catecholamine content 14 and 42 days following the intracerebral water or 6-hydroxydopamine injection (100 μg). [b] Aqueous ascorbic acid solution (0.5%) with pH adjusted to 5.5. [c] Compared to the appropriate vehicle, $p < 0.05$.

chlorpromazine possesses adrenolytic and antihistaminic qualities (14). Chlorpromazine may partially reverse the cobalt response through a central α-receptor blockade and/or peripheral antihistaminic activity.

REFERENCES

(1) R. T. Brittain and S. L. Handley, *J. Physiol.*, **192**, 805 (1967).
(2) G. G. Shaw, *Br. J. Pharmacol.*, **42**, 205 (1971).
(3) P. Spencer, *Life Sci.*, **5**, 1015 (1966).
(4) W. E. Kirkpatrick, *Proc. West. Pharmacol. Soc.*, **10**, 51 (1967).
(5) R. M. Paolino and B. K. Bernard, *Life Sci.*, **7**, 857 (1968).
(6) V. J. Lotti, P. Lomax, and R. George, *J. Pharmacol.*, **150**, 135 (1965).
(7) D. H. Burke, *J. Pharm. Sci.*, **67**, 799 (1978).
(8) T. Haley and W. McCormick, *Br. J. Pharmacol.*, **12**, 12 (1957).
(9) S. Snyder and K. Taylor, in "Research Methods in Neurochemistry," vol. 1, N. Marks and R. Rodnight, Eds., Plenum, New York, N.Y., 1972, p. 287.
(10) G. G. Shaw, *Br. J. Pharmacol.*, **42**, 205 (1971).
(11) C. J. Estler, *Proc. Int. Pharmacol. Meet., 1st*, **8**, 153 (1962).
(12) A. A. Menon and B. J. Pleuvry, *J. Pharm. Pharmacol.*, **28**, 827 (1976).
(13) B. Tabakoff and R. F. Ritzmann, *J. Pharmacol. Exp. Ther.*, **203**, 319 (1977).
(14) S. Courvoisier, J. Fournel, R. Ducrat, M. Kolsky, and P. Koetschet, *Arch. Int. Pharmacodyn. Ther.*, **92**, 305 (1953).

ACKNOWLEDGMENTS

Presented at the Pharmacology Section, APhA Academy of Pharmaceutical Sciences, Hollywood, Fla., meeting, November 1978.

Supported in part by a grant from the Marquette University Committee on Research and National Institutes of Health Grant RR-09016.

The authors are indebted to Julie Baron, Carol Marshall, Robert Ryan, Susan Treml, and Donald Zuech for their assistance.

Antifertility and Antiproteolytic Activity of Activated *N*-Carbobenzoxy Amino Acid Esters

I. H. HALL ˣ, J. H. DREW, Z. SAJADI, and L. J. LOEFFLER

Received July 31, 1978, from the *Division of Medicinal Chemistry, School of Pharmacy, University of North Carolina, Chapel Hill, NC 27514.* Accepted for publication November 16, 1978.

Abstract □ *N*-Carbobenzoxy L-phenylalanine, glycine, L-leucine, and L-proline derivatives, their vinyl esters, and their 1,2-dibromoethyl esters were tested for antifertility activity in mice. Intraperitoneal administration reduced the pregnancy percentage and the number of fetuses per litter. Intravaginal administration reduced the pregnancy percentage significantly, with *N*-carbobenzoxyglycine vinyl ester, *N*-carbobenzoxyglycine-1,2-dibromoethyl ester, *N*-carbobenzoxy-L-leucine-1,2-dibromoethyl ester, and *N*-carbobenzoxy-L-proline-1,2-dibromoethyl ester producing 100% inhibition at 10 mg/kg/day. Sperm enzyme hydrolysis of the nonspecific substrate azocasein was inhibited significantly by certain *N*-carbobenzoxy amino acid esters *in vitro*. Specific substrate *N*-benzoyl-L-arginine ethyl ester hydrolysis was also inhibited. Compounds that inhibited *N*-benzoyl-L-arginine ethyl ester hydrolysis also demonstrated *in vivo* intravaginal antifertility activity.

Keyphrases □ Carbobenzoxy amino acid esters—contraceptive activity, antiproteolytic activity, mice □ Contraceptives, potential—activated *N*-carbobenzoxy amino acid esters, mice □ Enzyme activity—effect of activated *N*-carbobenzoxy amino acid esters on sperm proteolysis, mice □ Sperm—enzymes, effect of *N*-carbobenzoxy amino acid esters, mice

Recently, numerous activated *N*-protected amino acid esters were synthesized as possible latent proteolytic inhibitors (1, 2). These agents resemble known trypsin and chymotrypsin inhibitors. Certain members of the series effectively inhibited *in vivo* cathepsin activity and *in vitro* chymotrypsin activity (3). Since proteolytic enzyme inhibitors block sperm acrosin activity, capacitation, and fertility, the effects of this series on reproduction were investigated.

EXPERIMENTAL

Chemistry—*N*-Carbobenzoxy-L-phenylalanine (I), *N*-carbobenzoxyglycine (II), *N*-carbobenzoxy-L-leucine (III), and *N*-carbobenzoxy-L-proline (IV) were prepared by the standard procedure (4) (Table I). The *N*-carbobenzoxy amino acids were converted to the corresponding vinyl esters V, VI, VII, and VIII by refluxing with vinyl acetate in the presence of palladium chloride and were purified by column chromatography. The vinyl esters were treated with bromine in chloroform to give the 1,2-dibromo esters IX, X, XI, and XII, which were purified by fractional crystallization or column chromatography (1, 2). *N*-α-Tosyl-L-lysylchloromethyl ketone (XIII), tosyl-L-phenylalanylchloromethyl ketone (XIV), carbobenzoxy-L-phenylalanine chloromethyl ketone (XV), 17-ethinyl estradiol (XVI), and diethylstilbestrol (XVII) were purchased[1].

Antifertility Screens—For 28 days, virgin CF_1 female mice (~28 g), which had been isolated for 4 weeks, were administered test compounds suspended in 1% carboxymethylcellulose at 10 mg/kg/day (0.2 ml) ip. On Day 10, female mice were exposed to male mice (two females per male) for the remainder of the experiment. Male mice were rotated once a week to assure fertility. On gestation Days 17–21, the females were sacrificed;

[1] Sigma Chemical Co. or Cyclo Chemicals.

0022-3549/79/0600-0696$01.00/0

© 1979, American Pharmaceutical Association

Table I—Structures of the *N*-Carbobenzoxy-Activated Amino Acids

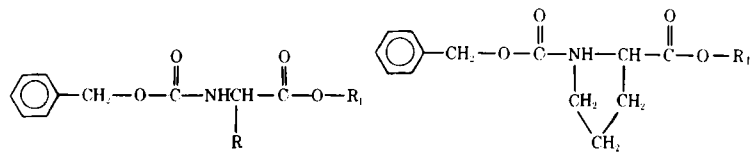

I-III, V-VII, IX-XI

IV, VIII, XII

Compound	R	R_1	Melting Point	Preparation Method (Reference)
I *N*-Carbobenzoxy-L-phenylalanine	$-CH_2-C_6H_5$	—H	86–89°	4
II *N*-Carbobenzoxyglycine	—H	—H	117–119.5°	4
III *N*-Carbobenzoxy-L-leucine	$-CH_2CH(CH_3)_2$	—	Oil	4
V *N*-Carbobenzoxy-L-phenylalanine vinyl ester	$-CH_2-C_6H_5$	$-CH=CH_2$	Oil	1
VI *N*-Carbobenzoxyglycine vinyl ester	—H	$-CH=CH_2$	Oil	2
VII *N*-Carbobenzoxy-L-leucine vinyl ester	$-CH_2CH(CH_3)_2$	$-CH=CH_2$	Oil	2
IX *N*-Carbobenzoxy-L-phenylalanine-1,2-dibromoethyl ester	$-CH_2-C_6H_5$	$-CHBr-CH_2Br$	Oil	1
X *N*-Carbobenzoxyglycine-1,2-dibromoethyl ester	—H	$-CHBr-CH_2Br$	Oil	2
XI *N*-Carbobenzoxy-L-leucine-1,2-dibromoethyl ester	$-CH_2CH(CH_3)_2$	$-CHBr-CH_2Br$	60–61°	2
IV *N*-Carbobenzoxy-L-proline		—H	Oil	4
VIII *N*-Carbobenzoxy-L-proline vinyl ester		$-CH=CH_2$	Oil	2
XII *N*-Carbobenzoxy-L-proline-1,2-dibromoethyl ester		$-CHBr-CH_2Br$	Oil	2

Table II—Antifertility Screen of Activated Esters of *N*-Carbobenzoxy Amino Acids in CF_1 Females at 10 mg/kg/day

	Intraperitoneal Administration				Intravaginal Administration			
Compound	*n*	Percent Pregnant	Number of Viable Fetuses per Litter	Number of Intrauterine Deaths per Litter	*n*	Percent Pregnant	Number of Viable Fetuses per Litter	Number of Intrauterine Deaths per Litter
I	7	28	7.5	0.00	8	25	6.5	0.0
II	7	57	8.5	0.00	8	25	9.5	0.0
III	7	71	7.5	0.40	8	12	7.0	3.0
IV	8	38	9.6	0.33	8	25	8.0	0.0
V	10	100	10.7	0.10	8	25	7.0	0.0
VI	8	12	11.0	0.00	8	0	0.0	0.0
VII	8	62	11.8	0.00	8	25	7.0	0.0
VIII	6	43	7.3	0.00	8	25	10.5	0.0
IX	6	67	8.0	0.16	8	25	8.5	0.5
X	8	38	10.3	0.25	8	0	0.0	0.0
XI	8	38	12.4	0.13	8	0	0.0	0.0
XII	8	31	12.4	0.13	8	0	0.0	0.0
XIII	7	71	8.6	0.20	7	0	0.0	0.0
XIV	—	—	—	—	8	0	0.0	0.0
XV	8	88	11.6	0.14	8	38	9.0	0.0
XVI	8	0	0.0	0.0	—	—	—	—
XVII	8	0	0.0	0.0	—	—	—	—
1% Carboxymethylcellulose	8	12.0 ± 3	0.48	—	—	—	—	—
40% Lactose	—	—	—	—	8	100	11.0	0.70
6% Carboxymethylcellulose	—	—	—	—	8	75	8.8	0.66

the viable fetuses, intrauterine deaths, and implantation sites were tabulated (5, 6). Viable fetuses were examined for teratogenic effects as outlined previously (7).

For intravaginal testing, the compounds were homogenized in 40% lactose or 6% carboxymethylcellulose and administered at 10 mg/kg/day (0.03–0.05 ml) for 28 days using a tuberculin syringe without the needle or a low dose (0.5-ml) insulin syringe with a 1–100-μl eppendorf pipet tip modified to fit the syringe. On Day 10 and all subsequent days, females were exposed to males for 1 hr and the previously described protocol was followed. Dose–response curves for intravaginal administration were obtained over the 0.5–10-mg/kg/day range. Activated *N*-protected amino acid ester toxicity (LD_{50}) in CF_1 male mice (~30 g) was determined (8).

Enzymatic Studies—The acrosin enzyme was isolated from the epididymides of four Sprague–Dawley rats (~250 g) or 10 CF_1 mice (~30 g). The epididymides were sliced in 0.25 *M* sucrose–0.001 *M* disodium (ethylenedinitrilo)tetraacetate, pH 6.5. The sperm suspension was filtered through two sterile cheesecloth layers to remove debris, centrifuged at 600×*g* for 15 min using a swinging bucket-type rotor head, and washed twice. The spermatozoa were resuspended in 20 ml of 0.25 *M* sucrose and frozen at −20° (9, 10). After freeze thawing, the tubes were vortexed for 30 sec and centrifuged at 1000×*g* for 15 min at 0°. The spermatozoa were resuspended, vortexed, and centrifuged again. The denuded spermatozoa were taken up in 5 ml of sucrose, and the pH was adjusted to 2.5 with hydrochloric acid. Acrosin was recovered in the supernate after centrifugation at 36,000×*g* for 15 min at 0° (9, 10).

Acrosin proteolytic enzymatic activity was determined (11). The incubation medium contained 0.7 ml of 0.1 *M* phosphate buffer, pH 7.6, and 0.3 ml of extracted crude rat acrosin, which were preincubated for 5 min at 30°. One milliliter of 2% azocasein and 1.5 μmoles of test compound in 0.2 ml of 40% lactose were added, and the mixture was incubated for 10 min at 30°. Tests were run in triplicate. The reaction was stopped with 5% trichloroacetic acid, and the mixture was centrifuged at 3500×*g* for 10 min. Absorbance of the trichloroacetic acid-soluble peptides produced by azocasein hydrolysis was measured at 366 nm. Enzymatic activity was calculated as the increase in absorbance of 0.730 unit/hr/mg of protein (11, 12).

N-Benzoyl-L-arginine ethyl ester hydrolysis was followed as described previously (12). Two milliliters of buffer, 0.3 ml of substrate, 0.1 ml of crude mouse acrosin, and 1.5 μmoles of test sample in 0.2 ml of 40% lactose

Table III—Effects of *N*-Carbobenzoxy-Activated Esters at 1.5 μmoles on *In Vitro* Sperm Proteolytic Activity[a]

Compound	Percent Inhibition: Rat Azocasein Proteolytic Activity[b]	Percent Inhibition: Mouse *N*-Benzoyl-L-arginine Ethyl Ester Proteolytic Activity[c]	LD_{50}, mg/kg
I	93 ± 15	69 ± 5	250
II	63 ± 5	60 ± 1	380
III	68 ± 7	83 ± 7	>1000
IV	38 ± 4	77 ± 4	>1000
V	100 ± 1	57 ± 14	>2000
VI	96 ± 3	91 ± 2	500
VII	90 ± 14	68 ± 4	500
VIII	92 ± 2	79 ± 3	500
IX	85 ± 7	58 ± 3	74
X	100 ± 0	82 ± 1	148
XI	94 ± 2	85 ± 2	81
XII	94 ± 12	91 ± 1	225
XIII	100 ± 0	91 ± 1	—
XIV	100 ± 0	17 ± 2	75
XV	100 ± 0	35 ± 4	—

[a] All data in table have a $p = 0.001$ as calculated by the Student t test. [b] A 0.730-unit absorbance increase/hr/mg of protein. [c] A 0.328-unit absorbance increase/30 min/mg of protein.

were mixed, and the rise in absorbance at 253 nm was determined at 0 and 30 min. The control resulted in an absorbance increase of 0.328 unit/mg of protein (11, 12).

RESULTS

In the intraperitoneal antifertility screen, I, IV, VI, VIII, and X–XII produced greater than 50% pregnancy inhibition at 10 mg/kg/day compared to diethylstilbestrol and 17-ethinyl estradiol, which produced 100% pregnancy inhibition (Table II).

In the intravaginal antifertility screen, all tested compounds produced 75% or greater fertility inhibition. Compounds VI and X–XII caused 100% inhibition, as did the standard proteolytic inhibitors XIII and XIV. Dose-response curves were determined for VI, X, XI, and XIV at 0.5, 1, 5, and 10 mg/kg/day. Compounds VI, X, and XI caused 100% pregnancy inhibition at 1 mg/kg/day, whereas XIV required 10 mg/kg/day. No teratogenic effects were observed in the viable fetuses. Reabsorptions and intrauterine deaths were within normal limits (Table II).

Compounds I, V–VIII, and X–XV produced 90% rat acrosome proteolytic activity inhibition *in vitro*. Compounds III, VI, and X–XIII produced greater than 80% inhibition of *N*-benzoyl-L-arginine ethyl ester hydrolysis by mouse sperm acrosin *in vitro;* the remaining compounds produced greater than 50% inhibition (Table III).

DISCUSSION

Prior to fertilization, the sperm must undergo capacitation. This process involves sperm hydrolytic enzyme activation to permit penetration of the cervical mucus and external oval membranes as well as labilization of the external sperm membrane. Spermal acrosin (EC 3.4.21.10) has been isolated from various mammalian sperm (13) and apparently is responsible for zona pellucida penetration.

Acrosin, an endopeptidase that cleaves the carboxyl bond of arginyl and lysyl derivatives (13–15), can be inhibited by trypsin inhibitors (16–20). Endogenous acrosin inhibitors have been isolated from seminal plasma (21, 22), cervix uteri secretions (12), and pancreatic tissue (11). Normally, these inhibitors are removed as the sperm moves through the female reproductive tract, allowing the proteolytic enzyme to become active.

Screening demonstrated that the activated *N*-carbobenzoxy amino acid esters possessed antifertility activity in mice. Since the acrosome contains a number of proteolytic enzymes, any of which may hydrolyze azocasein, azocasein hydrolysis inhibition by the test compounds, chymotrypsin inhibitors (XIV and XV), and the trypsin inhibitor (XIII) was not surprising. Compounds VI and X–XII, which caused 100% pregnancy inhibition, also inhibited 80% of the hydrolysis of *N*-benzoyl-L-arginine ethyl ester, a substrate specific for acrosin and trypsin. Carbobenzoxy-activated esters also inhibit cathepsin (3). Thus, in addition to inhibiting sperm acrosin or trypsin, they may be reducing other proteolytic acrosomal enzymes. Since these *N*-carbobenzoxy-activated esters of L-proline, L-leucine, and glycine have no apparent teratogenic or toxic effects, they may have contraceptive potential.

REFERENCES

(1) L. J. Loeffler, Z. Sajadi, and I. H. Hall, *J. Med. Chem.*, **20,** 1578 (1977).

(2) *Ibid.*, **20,** 1581 (1977).

(3) I. H. Hall, Z. Sajadi, and L. J. Loeffler, *J. Pharm. Sci.*, **67,** 1726 (1978).

(4) M. Bergmann and L. Zervas, *Chem. Ber.*, **65,** 1192 (1932).

(5) B. Baggett, I. H. Hall, R. G. Boegli, K. H. Palmer, and M. Wall, *Fertil. Steril.*, **21,** 68 (1970).

(6) I. H. Hall, G. L. Carlson, G. S. Abernethy, and C. Piantadosi, *J. Med. Chem.*, **17,** 1253 (1974).

(7) J. G. Wilson, in "First International Conference on Congenital Malformations, General Principles in Experimental Teratology," Lippincott, Philadelphia, Pa., 1961, pp. 187–194.

(8) J. T. Litchfield and F. A. Wilcoxon, *J. Pharmacol. Exp. Ther.*, **96,** 99 (1949).

(9) C. R. Brown and E. F. Hartree, *J. Reprod. Fertil.*, **46,** 249 (1976).

(10) C. R. Brown, Z. Audani, and E. F. Hartree, *Biochem. J.*, **149,** 133 (1975).

(11) W. D. Schleuning and H. Fritz, *Methods Enzymol.*, **45,** 330 (1976).

(12) G. W. Schwert and Y. Takenaka, *Biochim. Biophys. Acta*, **16,** 570 (1955).

(13) R. A. McRorie and W. L. Williams, *Annu. Rev. Biochem.*, **43,** 777 (1974).

(14) R. B. L. Gwatkin, *Ann. Rep. Med. Chem.*, **10,** 240 (1975).

(15) L. J. D. Zaneveld, B. M. Dragoje, and G. F. B. Shumacher, *Science*, **177,** 702 (1972).

(16) R. Stambaugh, B. G. Brackett, and L. Mastroianni, *Biol. Reprod.*, **1,** 223 (1969).

(17) L. J. D. Zaneveld, R. T. Robertson, and W. L. Williams, *FEBS Lett.*, **11,** 345 (1970).

(18) A. K. Bhattacharyya, L. J. D. Zaneveld, B. M. Dargoje, G. F. B. Schumacher, and J. Travis, *J. Reprod. Fertil.*, **47,** 97 (1976).

(19) K. L. Polakoski, W. L. Williams, and R. A. McRorie, *Fed. Proc.*, **31,** 278 (1972).

(20) P. Stambaugh and J. Buckley, *J. Reprod. Fertil.*, **19,** 423 (1969).

(21) C. R. Brown and E. F. Hartree, *Hoppe-Seyler's Z. Physiol. Chem.*, **356,** 1909 (1975).

(22) L. J. D. Zaneveld, R. T. Robertson, M. Kessler, and W. L. Williams, *J. Reprod. Fertil.*, **25,** 387 (1971).

Bioavailability and Dissolution Behavior of Trisulfapyrimidine Suspensions

L. K. MATHUR *§, J. M. JAFFE *¶×, R. I. POUST *, H. BARRY, III *, T. J. GOEHL *‖, V. P. SHAH ‡, and J. L. COLAIZZI *•

Received June 6, 1978, from the **Department of Pharmaceutics, School of Pharmacy, University of Pittsburgh, Pittsburgh, PA 15261*, and the ‡*Division of Biopharmaceutics, Food and Drug Administration, Washington, DC 20204.* Accepted for publication November 20, 1978. §Present address: Wyeth Laboratories, Philadelphia, PA 19101. ¶Present address: Sandoz Pharmaceuticals, East Hanover, NJ 07936. ‖Present address: Division of Biopharmaceutics, Food and Drug Administration, Washington, DC 20204. •Present address: College of Pharmacy, Rutgers—The State University, Piscataway, NJ 08854.

Abstract □ The bioavailability of seven commercial trisulfapyrimidine suspensions was studied in 14 adult male volunteers. Fifteen blood samples were collected over a 48-hr period following administration of a 1-g dose of each suspension. Serum was assayed for each component (sulfadiazine, sulfamerazine, and sulfamethazine) by high-pressure liquid chromatography. Analysis of variance indicated several significant differences among the seven commercial preparations with respect to C_{max}, T_{max}, and *AUC* for sulfadiazine, sulfamerazine, and sulfamethazine. The *in vitro* behavior of each suspension was then studied by the paddle method of the Food and Drug Administration. A 0.5-ml sample was introduced into 900 ml of hydrochloric acid (2.2×10^{-4} *M*) at 37° and dissolved using a paddle speed of 25 rpm. Samples withdrawn at 15 and 30 min were analyzed by high-pressure liquid chromatography, and the percent of sulfadiazine, sulfamerazine, and sulfamethazine was calculated. Significant correlation was obtained between an *in vivo* parameter (C_{max} for sulfadiazine) and an *in vitro* parameter (percent sulfadiazine dissolved in 30 min). Results indicate that this method is suitable for the *in vitro* screening of trisulfapyrimidine suspensions.

Keyphrases □ Bioavailability—trisulfapyrimidine suspensions, compared to *in vitro* dissolution behavior, various commercial preparations, screening methods □ Trisulfapyrimidine suspensions—bioavailability, compared to *in vitro* dissolution behavior, various commercial preparations, screening methods □ Dissolution, *in vitro*—trisulfapyrimidine suspensions, compared to bioavailability, various commercial preparations, screening methods □ Screening methods—trisulfapyrimidine suspensions, bioavailability compared to *in vitro* dissolution behavior, various commercial preparations

In vitro dissolution testing offers a convenient and inexpensive means of predicting bioavailability differences among different tablet and capsule formulations of the same drug. However, *in vitro* studies for suspension dosage forms have not been reported. Because suspensions exposed to aqueous fluids are similar to the disintegrated form of tablets and capsules, these dosage forms also may show dissolution rate-limited absorption. Thus, *in vitro* dissolution rate studies are needed on drugs commonly available on a multisource basis as suspensions. Drugs of this type include various sulfonamide derivatives.

Such studies also require *in vivo* testing of various brands of the same drug to establish comparative bioavailability. The results of *in vitro* testing can then be correlated with *in vivo* results and also can be used as a test of lot-to-lot variability of suspensions produced by the same manufacturer. With this type of information, *in vivo* testing can be eliminated, lot-to-lot specifications can be developed, and rapid screening procedures for new sulfa drug suspensions could become available.

Several reports (1–3) dealt with the dissolution behavior of drugs in suspensions. The bioavailability and dissolution rates of sulfa drugs also were investigated (4–11). Although bioavailability differences among various sulfonamide dosage forms were reported, attempts to correlate *in vitro* dissolution data with *in vivo* bioavailability data were unsuccessful (7–11).

The objective of this research was to establish a suitable dissolution test method for correlating *in vivo* comparative bioavailability data of different commercially available oral trisulfapyrimidine suspensions. This objective required investigation of both the *in vitro* and *in vivo* parameters. By using a specific high-pressure liquid chromatographic (HPLC) method, the behavior of each trisulfapyrimidine component was studied separately.

EXPERIMENTAL

Bioavailability Study—Prior to admission to the study, 14 healthy adult males were given a complete medical examination; a medical history was taken, and laboratory tests were performed, including complete blood and urine tests. Subjects were accepted for the study only if all laboratory test results were within the normal range accepted by the examining physician. The average age of the subjects was 23.4 years (range of 21.2–29.3 years), the mean weight was 77.6 kg (range of 61.2–86.2 kg), and the mean height was 182.5 cm (range of 175.3–193.0 cm). They could not take chronic medications of any kind for a week prior to the study and any drugs during the entire test period.

Subjects were informed of all study details, the potential hazards of participation, and the benefits. They were also informed that they could withdraw from the study at any time for any reason. Toward the latter stages of the study, one subject developed a rash. It probably appeared gradually and was noticed only after administration of the fifth dose of the drug. This subject was not allowed to receive the remaining two scheduled treatments (Weeks 6 and 7), and the missing values were estimated statistically by the method of Li (12).

The seven (A–G) commercial trisulfapyrimidine suspensions[1] were supplied by the Food and Drug Administration (FDA). To eliminate any possible residual effects, each subject received the seven different brands (A–G) in a complete crossover design. A 10-ml dose of each suspension (providing a total of 1.0 g of sulfa drug) was administered in the morning to the subjects after an overnight fast. The suspensions were shaken well, and 10-ml doses were withdrawn into glass syringes. The doses were then administered by emptying the contents of the syringe into the mouth. The syringe was rinsed once with 10 ml of water, which was also emptied into the subject's mouth. Drug dose delivery was accurate to within 0.1% of the stated volume.

Each subject was then instructed to drink an additional 110 ml of water. Subjects were allowed to eat lunch after abstaining from all food for 3 hr after drug administration. Doses were administered every alternate week, the time interval of 2 weeks being considered adequate for virtually complete drug elimination.

Preliminary pharmacokinetic data indicated that 15 blood samples were adequate to obtain a complete blood level profile. Samples were collected at 0, 0.167, 0.332, 0.50, 0.75, 1.0, 2.0, 3.0, 4.0, 6.0, 8.0, 12.0, 24.0, 30.0, and 48.0 hr. All blood samples were obtained by venipuncture with

[1] A, Trisem, lot C53747, Beecham-Massengill Pharmaceutics, Bristol, Tenn; B, Terfonyl, lot 60080, E. R. Squibb and Sons, Princeton, N.J.; C, Sulfaloid, lot 17612, Westerfield Laboratories, Cincinnati, Ohio; D, Trisureid, lot 5M249, Reid Provident Laboratories, Atlanta, Ga.; E, Quad-Ramoid, lot 28431, Paul B. Elder Co., Bryan, Ohio; F, Sulfose, lot 1951619, Wyeth Laboratories, Philadelphia, Pa.; and G, Neotrizine, lot 9ND79A, Eli Lilly and Co., Indianapolis, Ind.

0022-3549/79/0600-0699$01.00/0
© 1979, American Pharmaceutical Association

Table I—Mean (±*SD*) Values of *In Vivo* Parameters of Sulfadiazine (I), Sulfamerazine (II), and Sulfamethazine (III) Obtained for Seven Commercial Trisulfapyrimidine Suspensions (A–G) after Administration to 14 Subjects

In Vivo Parameter	Product						
	A	B	C	D	E	F	G
C_{max}, μg/ml							
I	12.1 ± 2.0	11.9 ± 1.7	11.2 ± 1.6	10.4 ± 2.4	9.3 ± 2.1	9.1 ± 2.5	6.0 ± 1.6
II	27.3 ± 3.5	27.4 ± 4.1	25.3 ± 3.7	24.1 ± 4.5	23.0 ± 3.4	24.3 ± 4.4	18.0 ± 4.9
III	19.6 ± 4.3	19.6 ± 5.3	18.5 ± 5.0	15.8 ± 4.1	16.3 ± 5.0	16.3 ± 5.2	18.0 ± 5.7
T_{max}, hr							
I	3.9 ± 1.3	3.3 ± 1.1	4.4 ± 1.6	4.3 ± 1.4	4.9 ± 1.3	5.1 ± 1.5	4.6 ± 1.4
II	2.6 ± 1.4	2.8 ± 1.3	3.9 ± 1.8	4.1 ± 2.0	4.8 ± 1.7	4.7 ± 1.8	5.6 ± 2.6
III	1.1 ± 0.9	1.2 ± 0.7	1.3 ± 0.7	2.1 ± 1.1	2.7 ± 1.0	2.1 ± 0.9	1.5 ± 0.8
$AUC_0^\infty \times K_e$, μg/ml							
I	13.9 ± 2.3	12.6 ± 2.2	12.1 ± 3.0	11.0 ± 2.7	10.8 ± 2.5	11.1 ± 3.4	7.8 ± 2.6
II	29.0 ± 2.8	28.6 ± 4.1	28.7 ± 6.0	27.6 ± 4.4	27.6 ± 3.2	28.5 ± 3.9	25.6 ± 6.6
III	19.4 ± 3.9	20.4 ± 4.5	20.4 ± 4.6	18.5 ± 5.2	20.0 ± 4.7	29.6 ± 4.2	20.6 ± 5.4

Table II—Mean (±*SD*) Percent of Sulfadiazine, Sulfamerazine, and Sulfamethazine Dissolved in 15 and 30 min by the Paddle Method

Product	Sulfadiazine		Sulfamerazine		Sulfamethazine	
	15 min	30 min	15 min	30 min	15 min	30 min
A	64.9 ± 3.4	84.2 ± 3.7	71.4 ± 2.4	91.1 ± 2.3	63.3 ± 2.4	84.5 ± 2.3
B	79.5 ± 1.8	92.5 ± 2.3	84.8 ± 2.6	98.3 ± 2.2	84.2 ± 2.7	97.8 ± 2.7
C	44.3 ± 3.9	67.3 ± 4.4	39.0 ± 3.5	58.9 ± 4.1	44.6 ± 4.0	65.0 ± 4.2
D	84.5 ± 2.4	99.1 ± 1.2	83.8 ± 2.6	98.7 ± 1.4	83.9 ± 2.6	98.9 ± 1.4
E	46.4 ± 4.7	53.5 ± 4.9	28.3 ± 3.0	32.7 ± 3.3	19.5 ± 1.8	25.7 ± 1.5
F	21.6 ± 2.9	41.7 ± 4.4	41.7 ± 2.9	42.5 ± 5.1	23.0 ± 3.5	42.1 ± 6.6
G	8.3 ± 1.7	23.5 ± 3.0	10.2 ± 2.4	26.6 ± 3.5	11.9 ± 2.5	28.9 ± 3.5

6-ml silicone-coated vacuum tubes[2]. Samples were refrigerated and allowed to clot before being centrifuged at 3500 rpm. Serum was separated from the clot with the aid of a Pasteur pipet, transferred to a 4-ml glass vial, and frozen until assayed. Samples were assayed for sulfadiazine, sulfamerazine, and sulfamethazine by the HPLC procedure described here.

Dissolution Methodology—The dissolution of seven trisulfapyrimidine suspensions (A–G) was determined at 37° in 900 ml of a dissolution medium (Medium M) consisting of 899 ml of distilled water to which 1.0 ml of 0.2 *M* HCl was added. The medium pH was checked at the start and at the end of each experiment and was fairly constant at 3.4. A low stirring rate of 25 rpm was chosen since other work had demonstrated very rapid dissolution of some trisulfapyrimidine suspensions with higher stirring rates.

The apparatus consisted of a cylindrical 1000-ml round-bottom flask[3], which was secured in a multiple-spindle dissolution drive apparatus[4] and immersed in a controlled-temperature bath[5] maintained at 37°. Each spindle was provided with an independent clutch so that any spindle could be stopped without disturbing the others. The apparatus was capable of achieving speeds from 25 to 250 rpm ± 5% of the preset speed. The flask was equipped with a Plexiglas cover with a center port for entry of the paddle shaft and three side ports for sample introduction and removal. The paddle[6], consisting of a 7.6-cm polytef[7] blade attached to a polytef-coated, 0.95-cm stainless steel shaft, was positioned exactly 2.5 cm above the flask bottom.

The suspension (0.5 ml) was introduced carefully into the bottom of the flask using a 1-ml syringe with an attached 17.8-cm stainless steel needle[8]. Paddle rotation was engaged and controlled at a constant 25 rpm. Previous dissolution trials indicated that Products A–D dissolved at a much greater rate than did Products E and F, and that the dissolution of Product G was very slow. On the basis of the preliminary data, 15- and 30-min sampling times were selected.

Samples were withdrawn with 5-ml glass syringes through an attached 7.6-cm, 20-gauge stainless steel needle[9] secured to the flask cover and positioned to extend 6.8 cm into the dissolution medium. Thirty seconds prior to sample removal, the needle was cleared of any remaining fluid by withdrawing 3 ml of the medium and replacing it into the flask immediately. A 3-ml sample was then removed, filtered through a 13-mm, 0.2-μm membrane filter[10] using a Swinny adaptor, and analyzed by HPLC for sulfadiazine, sulfamerazine, and sulfamethazine. An equal volume of drug-free Medium M was replaced in the flask immediately after sample withdrawal.

After removal of the 30-min sample, the stirring rate was increased 10-fold to ensure complete dissolution of the suspension; a final 90-min sample was removed for analysis. Several additional samples were withdrawn after the 90-min sample in a few cases and were found to contain amounts of drug identical to the 90-min sample. The amount of drug dissolved at 15 and 30 min was expressed as a percentage of this last sample.

Analytical—All samples were analyzed for sulfadiazine, sulfamerazine, and sulfamethazine by an HPLC method developed in this laboratory (13). Samples of sulfadiazine[11], sulfamerazine[12], sulfamethazine[13], and sulfamethizole[14] were used as received. All other materials were reagent grade.

For the *in vivo* study, a stock solution of trisulfapyrimidines was prepared by dissolving 100 mg each of sulfadiazine, sulfamerazine, and sulfamethazine in 0.1 *M* NaOH and adjusting the volume to 50 ml in a volumetric flask. The internal standard stock solution was prepared by dissolving 50 mg of sulfamethizole in 1 *M* NaOH and adjusting to volume in a 100-ml volumetric flask. Serum standards were prepared by taking appropriate small volumes of the stock triple-sulfa solutions and adding these to control serum[15]. Ten microliters of internal standard solution was added to 0.2 ml of sample (standard or unknown) in a 1-ml vial[16] followed by 0.1 ml of a 14% trichloroacetic acid solution. The samples were mixed and centrifuged[17] at 2500 rpm for 15 min.

Five microliters of the clear supernate was injected onto the column[18]. Peak height ratios were calculated by dividing the peak height of the drug by the peak height of the internal standard. Calibration curves were constructed daily from results obtained from spiked control serum samples containing equal amounts of each trisulfapyrimidine in the 1–30-μg/ml range by plotting peak height ratios *versus* concentration of the individual sulfa drug.

For the *in vitro* study, a stock trisulfapyrimidine solution was prepared by dissolving 100 mg each of sulfadiazine, sulfamerazine, and sulfamethazine in 0.1 *N* NaOH and adjusting the volume to 100 ml in a volu-

[2] Vacutainers, silicone-coated interior, 7-ml capacity, 13 × 100 mm, Becton Dickinson and Co., Rutherford, N.J.
[3] No. 333710-51, Kimble Products, Owens, Ill.
[4] Spec. 72B, Hanson Research Corp., Northridge, Calif.
[5] Blue M Electric Co., Blue Island, Ill.
[6] Paddle shaft (⅜ in.) 65-700-001 with 3-in. Teflon blade 65-700-300, Hansen Research Corp., Northridge, Calif.
[7] Teflon, du Pont.
[8] Transfer set needle, Travenol Laboratories, Morton Grove, Ill.
[9] Pitkin spinal needle 1162, Becton Dickinson and Co., Rutherford, N.J.
[10] Gelman Instrument Co., Ann Arbor, Ill.
[11] Lot R02114, Eli Lilly and Co., Indianapolis, Ind.
[12] Lot M07059, Eli Lilly and Co., Indianapolis, Ind.
[13] Lot R02011, Eli Lilly and Co., Indianapolis, Ind.
[14] Lot R159178, Ayerst Laboratories, New York, N.Y.
[15] Obtained from the Central Blood Bank, Pittsburgh, Pa.
[16] Reacti-Vials 13261, Pierce, Inc., Rockford, Ill.
[17] IEC EXD centrifuge 460G, Damon/IEC Division, Needham Heights, Mass.
[18] Waters Associates prepacked μBondapak C-18 column.

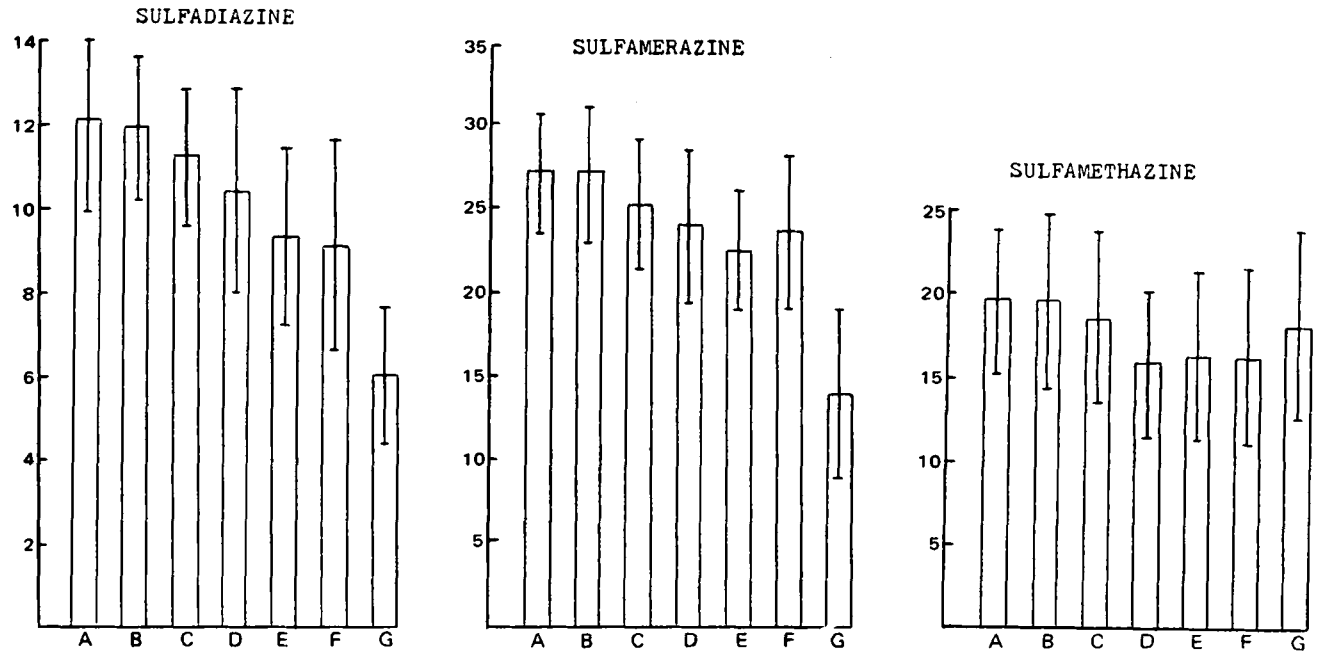

Figure 1—*Mean* (±SD) *maximum serum concentrations (micrograms per milliliter) of sulfadiazine, sulfamerazine, and sulfamethazine observed in 14 subjects after oral administration of seven commercial trisulfapyrimidine suspensions.*

metric flask. Standards (2, 4, 10, 20, and 30 μg/ml) were prepared by diluting appropriate small volumes of the stock solution with 0.1 *M* NaOH. The internal standard solution was prepared by dissolving 100 mg of acetaminophen[19] in hot water and adjusting the volume to 100 ml in a volumetric flask when cold. The solution prepared in this manner corresponded to a concentration of 1 mg/ml. Ten microliters of internal standard solution was added to 0.2 ml of filtered dissolution medium sample in a 5-ml culture tube. The sample was mixed, and 5 μl was injected onto the column[18]. Standards were treated similarly, calibration plots being constructed daily by plotting individual sulfa drug peak height ratios *versus* concentration.

Data Analysis—The peak serum concentration (C_{max}) and the time of the peak concentration (T_{max}) were obtained from the individual serum level *versus* time curves. The areas under the curve from 0 to 48 hr (AUC_0^{48}) were calculated by the trapezoidal rule and then corrected for the area beyond the last data point to obtain the total area (AUC_0^∞). The individual AUC_0^∞ values were then "normalized" (14) by multiplying the calculated AUC_0^∞ by the elimination rate constant (K_E) obtained from the terminal linear portion of the serum level *versus* time curves. These normalized areas were obtained for each of the three sulfa drugs in the suspensions: sulfadiazine (I), sulfamerazine (II), and sulfamethazine (III).

For each parameter, one-way analysis of variance was carried out by the computerized statistical program BMD 08V (15). A repeated-measures design permitted tests in the same subject of treatment interactions that would not be seen if each treatment were given to a different subject. The *F* ratios were compared with tabulated *F* ratios to determine the level of statistical significance (with seven treatments and 14 subjects, df = 6/76, taking into account two missing values, the minimum *F* value is 2.13 for $p < 0.05$ and 2.89 for $p < 0.01$). Any statistical differences found among treatments were compared further to determine differences between treatment pairs by Tukey's HSD tests (16).

Dissolution data were based on the amount of drug added to the dissolution medium. Thus, the concentration of the last sample (after complete dissolution of the suspension) represented 100%. Concentrations at all other sampling periods were expressed as a percentage of this last sample to obtain the percentage of drug dissolved in 15 and 30 min. For each sulfa drug, the means of 12 determinations for each trisulfapyrimidine suspension were used for calculation of the linear correlation coefficients (r) between these *in vitro* measurements and the *in vivo* data obtained from the subjects. Tables of r values were used for determining the statistical significance of the correlations (with df = 5 for the preparations, the minimum r values are 0.75 for $p < 0.05$ and 0.83 for $p < 0.02$).

[19] Lot X1667, Ruger Chemical Co., Irvington, N.J.

RESULTS

For the 14 subjects, mean values of the *in vivo* parameters are summarized in Table I for sulfadiazine (I), sulfamerazine (II), and sulfamethazine (III), respectively, for each of five parameters.

Observed Maximum Serum Concentration (C_{max})—The analysis of variance indicated statistically significant ($p < 0.01$) differences among the seven treatments administered with respect to I–III. The *F* ratios were 21.68 for I, 17.62 for II, and 5.85 for III. Tukey's HSD tests indicated that Product G was significantly ($p < 0.01$) different from all the other products and produced a much lower C_{max} value for I and II but not for III (Fig. 1). With respect to III, significantly low C_{max} values were observed with Product D.

Time for Maximum Serum Concentration (T_{max})—The analysis of variance indicated statistically significant ($p < 0.01$) differences among the seven treatments administered with respect to I–III. The *F* ratios were 3.85 for I, 6.80 for II, and 8.06 for III. Tukey's HSD tests indicated that the T_{max} values were significantly higher with Products E and F for I, with Product G for II, and with Product E for III.

Areas under the Curve—The analysis of variance of normalized areas indicated a significant ($p < 0.01$) difference among the seven treatments only with respect to I (F = 12.53). Tukey's HSD tests applied to I indicated significantly low values for Products G, D, E, and F.

***In Vitro* Study**—The mean (±*SD*) percentage of I–III dissolved in 15 and 30 min is shown in Table II for the seven trisulfapyrimidine suspensions. Analysis of variance of the data indicated large differences among the seven products with respect to I–III. Tukey's HSD tests indicated statistically significant ($p < 0.01$) differences between most pairs of suspensions.

***In Vivo–In Vitro* Correlation**—For the three drugs, each *in vivo* parameter was correlated with the percent of drug dissolved in 15 and 30 min for the seven suspensions. Significant values of the linear correlation coefficient were observed between: (*a*) percent of I dissolved in 30 min and C_{max} ($r = 0.86, p < 0.02$), (*b*) percent of I dissolved in 15 min and C_{max} ($r = 0.80, p < 0.05$), (*c*) percent of II dissolved in 30 min and C_{max} ($r = 0.76, p < 0.05$), (*d*) percent of II dissolved in 30 min and T_{max} ($r = -0.85, p < 0.02$), and (*e*) percent of II dissolved in 15 min and T_{max} ($r = -0.83, p < 0.05$).

DISCUSSION

Significant bioavailability differences among commercial trisulfapyrimidine suspensions were revealed by differences in the rate and extent of absorption of the individual suspension components. A number of differences were observed for C_{max} and T_{max}, but only a few were found for *AUC*. Thus, while the relative trisulfapyrimidine suspension bio-

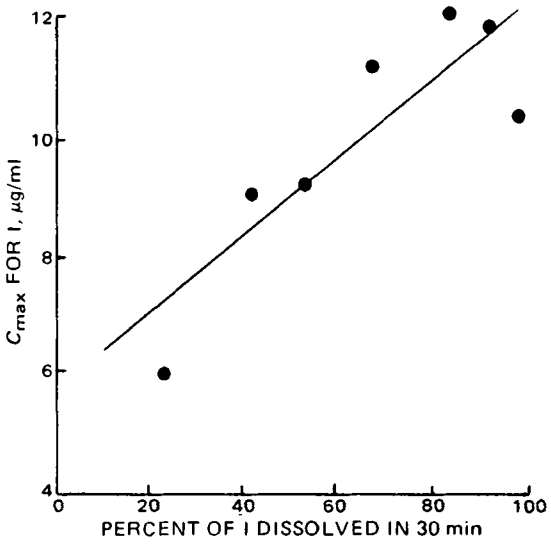

Figure 2—*Relationship between the* in vivo *measure of* C_{max} *and the* in vitro *measure of percentage of sulfadiazine (I) for the seven commercial trisulfapyrimidine suspensions, showing the regression line for the correlation coefficient of* +0.86 ($p < 0.02$).

availability was fairly uniform in terms of the extent of absorption, the absorption rate as shown by C_{max} and T_{max} was more variable.

Of all the statistically significant differences observed for the comparative bioavailability (bioequivalency) of the trisulfapyrimidine suspensions, the largest F ratio was in the C_{max} parameter for I. Product G showed the lowest mean C_{max} value for I. Since significant differences in the AUC values also were observed only for I, the dissolution characteristics of I were the most closely monitored and the variables in the dissolution study were controlled in such a way as to correspond to these *in vivo* study results.

With the FDA paddle method, the dissolution medium (pH 3.4) that was most suitable for the trisulfapyrimidine suspensions contained 2.2×10^{-4} M HCl with no added salts at a 37° temperature and a 25-rpm stirring rate. The dissolution data indicated large significant variations among the products. However, the absence of statistically significant ($p < 0.05$) differences among the 12 determinations on any one product indicated that the dissolution method was very reproducible.

Of all the significant correlations for C_{max} or T_{max} with *in vitro* parameters, the greatest r value was between C_{max} for I and the percent of I dissolved in 30 min (Fig. 2). The greatest bioavailability differences among the products also were observed for the C_{max} parameter for I. The paddle dissolution method thus appeared to be a very strong indicator of the *in vivo* situation and suitable to set standards for the I and II components of trisulfapyrimidine suspensions in terms of the percent of drug dissolved in 30 min.

A suitable guideline for determination of a minimal dissolution standard might be the mean percentage of drug (I or II) dissolved in 30 min for Products A–D. These values were 85% for I and 87% for II. While dissolution standards could be set for I and II, it was not possible to set a dissolution standard for III since a suitable *in vivo–in vitro* correlation was not obtained for this component. However, the establishment of actual standards that require minimal performance of only one or two components of a multicomponent product would be a matter to be decided upon by the appropriate regulatory agency.

Additional work carried out in these laboratories suggests that simple UV measurements for total trisulfapyrimidines could be used by determining dissolution rate profiles of the suspensions. The possibility of correlating *in vitro* data with *in vivo* parameters is being explored.

REFERENCES

(1) A. J. Aguiar, J. E. Zelmar, and A. W. Kinkel, *J. Pharm. Sci.*, **56**, 1243 (1967).

(2) T. R. Bates, J. M. Young, C. M. Wu, and H. A. Rosenberg, *ibid.*, **63**, 643 (1974).

(3) R. K. Reddy, S. A. Khalil, and M. W. Gouda, *ibid.*, **65**, 115 (1976).

(4) Y. Langlois, A. Gagnon, and L. Tetraeult, *J. Clin. Pharmacol.*, **12**, 196 (1972).

(5) V. Bernareggi, G. Bugada, A. Cassola, G. Levy, and F. Moncalvo, *Boll. Chim. Farm.*, **112**, 196 (1972).

(6) S. Khalil, M. Moustafa, A. Ebian, and M. Motaivi, *J. Pharm. Sci.*, **61**, 1615 (1972).

(7) M. J. Taraszka and R. A. Delor, *ibid.*, **58**, 207 (1969).

(8) G. R. van Petten, G. C. Becking, R. J. Withey, and H. F. Lettau, *J. Clin. Pharmacol.*, **11**, 27 (1971).

(9) *Ibid.*, **12**, 35 (1972).

(10) R. J. Withey, G. R. van Petten, and H. F. Lettau, *J. Clin. Pharmacol.*, **12**, 190 (1972).

(11) G. Mattock and I. McGilveray, *J. Pharm. Sci.*, **61**, 746 (1972).

(12) C. C. Li, "Introduction to Experimental Statistics," McGraw-Hill, New York, N.Y., 1964, pp. 237–239.

(13) T. J. Goehl, L. K. Mathur, J. D. Strum, J. M. Jaffe, W. H. Pitlick, V. P. Shah, R. I. Poust, and J. L. Colaizzi, *J. Pharm. Sci.*, **67**, 404 (1978).

(14) J. G. Wagner, "Fundamentals of Clinical Pharmacokinetics," 1st ed., Drug Intelligence Publications, Hamilton, Ill., 1975, p. 348.

(15) P. Sampson, in "BMD, Biomedical Computer Programs," 3rd ed., W. J. Dixon, Ed., University of California Press, Berkeley, Calif., 1973, pp. 693–704.

(16) R. E. Kirk, "Experimental Design Procedures for the Behavioral Sciences," Brooks and Cole, Monterey, Calif., 1968, p. 112.

ACKNOWLEDGMENTS

Abstracted from a thesis submitted by L. K. Mathur to the University of Pittsburgh in partial fulfillment of the Doctor of Philosophy degree requirements.

Supported by Food and Drug Administration Contract 223-76-3010.

The authors thank Mr. Chan-Loi Yong for technical assistance.

High-Performance Liquid Chromatographic Assay for Imipramine, Desipramine, and Their 2-Hydroxylated Metabolites

TAMARA A. SUTFIN and WILLIAM J. JUSKO ×

Received August 28, 1978, from the *Clinical Pharmacokinetics Laboratory, Department of Pharmaceutics, School of Pharmacy, State University of New York at Buffalo, and the Millard Fillmore Hospital, Buffalo, NY 14209.* Accepted for publication November 20, 1978.

Abstract □ A high-performance liquid chromatographic method is presented for the simultaneous determination of imipramine, desipramine, and their 2-hydroxylated metabolites in plasma. The method involves a simple plasma extraction at basic pH with organic solvent, chromatography on a silica gel column, and fluorescence detection. Correlation with a GLC–mass spectrometric method for imipramine and desipramine is illustrated. The method can detect 1 ng of each component/ml of plasma, sufficient sensitivity for pharmacokinetic studies.

Keyphrases □ High-performance liquid chromatography—analysis, imipramine, desipramine, 2-hydroxylated metabolites in plasma □ Desipramine—analysis in plasma, high-performance liquid chromatography □ Imipramine—analysis in plasma, high-performance liquid chromatography, metabolites □ Antidepressants, tricyclic—imipramine, desipramine, high-performance liquid chromatographic analysis in plasma

Clinical monitoring of plasma imipramine is complicated by biotransformation of the tricyclic antidepressant into another therapeutic entity, desipramine, and by their low plasma concentrations (1). Recent studies also identified hydroxylated metabolites in the brain following acute intoxication (2) and demonstrated biological activity of the 2-hydroxy metabolites of both compounds (3–7). An appropriate assay is needed to assess the potential importance of these metabolites in psychopharmacological and pharmacokinetic studies.

Several methods for tricyclic antidepressant analysis by TLC (8–10), GLC (11, 12), and high-pressure liquid chromatography (HPLC) (13–16) have been published. However, few were applied to imipramine and desipramine determination in biological specimens, and none dealt with the 2-hydroxy metabolites. The imipramine and desipramine assays required either sophisticated instrumentation not readily available or multistep extraction and/or derivatization. The sensitivity achieved generally was not adequate for pharmacokinetic studies, even when large samples were used.

An HPLC method for the simultaneous determination of plasma imipramine, 2-hydroxyimipramine, desipramine, and 2-hydroxydesipramine was developed. The procedure involves a simple extraction followed by separation of all four components and an internal standard in a single injection. High fluorescence sensitivity permits detection of 1 ng of each drug and metabolite in 1 ml of plasma.

EXPERIMENTAL

Reagents—Acetonitrile[1], ammonium hydroxide[2], *n*-butyl alcohol[1], hexane[1], and methanol[1] were spectroanalytical grade.

Equipment—A high-performance liquid chromatograph[3] with a syringe-loading sample injector[4], a 10-mv recorder[5], and a fluorescence detector[6] were used. An excitation wavelength of 240 nm and a 370-nm emission filter gave optimum fluorescence under the assay conditions. Detector range settings of 0.05–0.2 μamp were sufficient for most analyses; limits of the range settings were 0.01–1.0 μamp. Chromatography was done on a 0.46 × 25-cm, stainless steel column packed with 5-μm (particle diameter) silica B/5[7].

Assay Standards—Stock methanol solutions of desipramine hydrochloride[8] (113 mg/100 ml), imipramine hydrochloride[9] (113 mg/100 ml), 2-hydroxydesipramine free base[10] (10 mg/10 ml), and 2-hydroxyimipramine free base[10] (10 mg/10 ml) were prepared.

Plasma standards were prepared by spiking drug-free plasma with the methanol solutions to give final concentrations of 5–500 ng of imipramine and desipramine/ml and 5–150 ng of the 2-hydroxy metabolites/ml. The internal standard was 200 μg of *N*-desmethylclomipramine hydrochloride[9]/10 ml of methanol.

Extraction—To 1 ml of plasma standard or unknown, 50 μl of internal standard solution and 300 μl of ammonium hydroxide were added in polypropylene test tubes. The mixtures were extracted with 1 ml of 20% *n*-butyl alcohol in hexane for 15 min on a reciprocating shaker. After centrifugation, the upper organic layers were transferred to clean polypropylene tubes and evaporated to dryness at ambient temperature under nitrogen. Each extract was reconstituted just prior to chromatography with 100 μl of methanol, and 50 μl was injected.

Chromatography—All chromatography was done at ambient temperature. The mobile phase was methanol–acetonitrile (1:5) plus am-

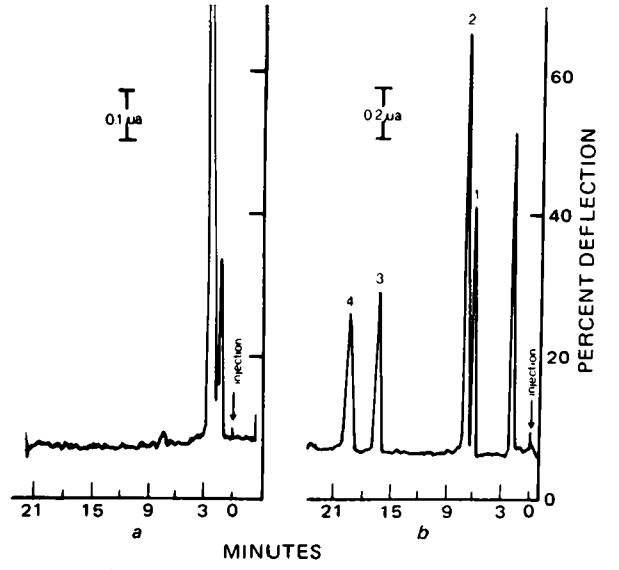

Figure 1—(a) *Chromatogram of an extract of 1 ml of blank plasma. The extract was reconstituted with 100 μl of methanol and the entire extract was injected.* (b) *Chromatogram of 100 μl of a methanol solution containing 50 ng/100 μl each of imipramine (1), 2-hydroxyimipramine (2), desipramine (3), and 2-hydroxydesipramine (4).*

[1] Burdick & Jackson Laboratories, Muskegon, Mich.
[2] "Baker Analyzed" reagent, VWR, Rochester, N.Y.
[3] DuPont model 848, Wilmington, Del.
[4] Rheodyne model 7105 injection valve, Perkin-Elmer, Norwalk, Conn.
[5] Linear Instruments Corp., Scientific Products, Rochester, N.Y.
[6] F. S. 970 L. C. fluorometer, Schoeffel Instrument Corp., Westwood, N.J.
[7] Perkin-Elmer Instrument Division, Norwalk, Conn.
[8] USV Pharmaceutical Corp., Tuckahoe, N.Y.
[9] Ciba Pharmaceutical Co., Summit, N.J.
[10] Gift of Dr. Albert A. Manian, National Institute of Mental Health (NIMH), Rockville, Md.

0022-3549/79/0600-0703$01.00/0
© 1979, American Pharmaceutical Association

Table I—Reproducibility of HPLC Standards

Concentration, ng/ml	n	Imipramine Mean Peak Height Ratio	Imipramine Slope[a]	Imipramine CV, %	2-Hydroxyimipramine Mean Peak Height Ratio	2-Hydroxyimipramine Slope[a]	2-Hydroxyimipramine CV, %	Desipramine Mean Peak Height Ratio	Desipramine Slope[a]	Desipramine SD, %	2-Hydroxydesipramine Mean Peak Height Ratio	2-Hydroxydesipramine Slope[a]	2-Hydroxydesipramine CV, %
5	6	0.17	0.034	5.8	0.32	0.064	9.4	0.18	0.036	11.1	0.11	0.022	13.6
50	6	1.57	0.031	10.8	3.12	0.062	10.6	1.09	0.022	8.3	0.91	0.018	8.8
150	6	5.07	0.034	5.5	9.61	0.064	7.4	3.15	0.021	6.0	2.84	0.019	2.5
300	3	10.01	0.033	7.2	—	—	—	6.34	0.021	7.3	—	—	—

[a] Slope = mean peak height ratio/concentration.

Table II—Recovery and Within-Run Precision

Concentration, ng/ml	n	Imipramine %	Imipramine SD	Imipramine CV, %	Desipramine %	Desipramine SD	Desipramine CV, %
10	5	68.6	1.8	2.6	64.0	1.4	2.2
50	10	69.5	2.3	3.3	64.8	2.5	3.9
150	10	68.3	2.6	3.8	66.1	2.6	3.9
300	6	67.6	1.5	2.2	67.2	1.7	2.5
Mean		68.5	2.0	3.0	65.5	2.0	3.1
		2-Hydroxyimipramine			2-Hydroxydesipramine		
10	5	84.6	2.5	2.9	94.3	2.8	2.9
50	4	79.2	1.3	1.6	76.9	3.2	4.2
100	5	81.4	2.1	2.6	84.6	3.1	3.7
Mean		81.7	2.0	2.4	85.3	3.0	3.6

monium hydroxide (4 ml/liter). The flow rate was 1.8 ml/min (~1100 psig).

Quantitation—Peak height ratios of the drug or metabolite to the internal standard were plotted against concentration to obtain standard calibration curves for each compound. Plasma standards were included with each assay.

RESULTS AND DISCUSSION

Imipramine, desipramine, and their 2-hydroxy metabolites were separated and eluted in ~21 min (Fig. 1*b*). Blank plasma extracts yielded no interference from endogenous plasma components (Fig. 1*a*).

Detector response was linear to plasma imipramine and desipramine concentrations of 5–500 ng/ml and to plasma 2-hydroxyimipramine and 2-hydroxydesipramine concentrations of at least 5–150 ng/ml. All four lines passed through the origin. At least 1 ng of each component/ml could be detected by injecting the entire 1-ml plasma extract.

Standard curve reproducibility for 1 month is indicated by Table I. The mean peak height ratio variation coefficients were approximately 5–10% for each compound. Plasma with added imipramine and desipramine stored in polypropylene tubes at −4° was stable for at least 3 months. Similarly stored clinical serum specimens also were stable for at least 3 months.

Drug and metabolite recoveries from plasma were estimated by comparing the peak heights from spiked plasma extracts directly with those of methanol solutions. The entire plasma extract was injected, and the methanol solution concentrations were calculated to permit injections of the same volumes. Table II shows reproducible recoveries of each compound over the concentration ranges studied and within-run variability of <5%. Studies of different concentrations were performed on separate days.

Several drugs were tested chromatographically in methanol solutions for use as internal standards and for interference (Table III). Drugs with relative retention times within 10% of the relative retention time of the experimental components could interfere with the assay. Therefore, complete medication histories are recommended before clinical or pharmacokinetic studies.

Two other imipramine and desipramine metabolites, 2-hydroxyiminodibenzyl and didesmethylimipramine, were chromatographed; only the former metabolite was incompletely separated. Previous evidence suggests that this metabolite is present only in small amounts (17) and that its potential interference is insignificant.

Other drugs that did not give fluorescent peaks within the analysis time were nortriptyline, protriptyline, diazepam, flurazepam, clorazepate, chlordiazepoxide, and scopolamine.

N-Desmethylclomipramine was chosen as the internal standard because it eluted near, but was completely separated from, the experimental components and did not add to total analysis time. It is reproducibly extracted from plasma by the method presented but is unlikely to be present in specimens from patients receiving other tricyclics. Figure 2*a* illustrates a chromatogram of a patient specimen with added internal standard. The patient was receiving a daily (150 mg) imipramine main-

Table III—Relative Chromatographed Drug Retention Times

Drug	Relative Retention Time
Fluphenazine	0.05
Perphenazine	0.65
Amitriptyline	0.68
Chlorpromazine	0.68
Mepazine	0.70
Doxepin	0.70
Promazine	0.93
Imipramine	1.00
Prochlorperazine	1.10
2-Hydroxyiminodibenzyl	1.14
2-Hydroxyimipramine	1.15
Didesmethylimipramine	1.32
Trifluopromazine	1.35
Trifluoperazine	1.80
Mesoridazine	1.90
Thioridazine	2.10
N-Desmethylclomipramine	2.15
Desipramine	2.40
2-Hydroxydesipramine	2.90

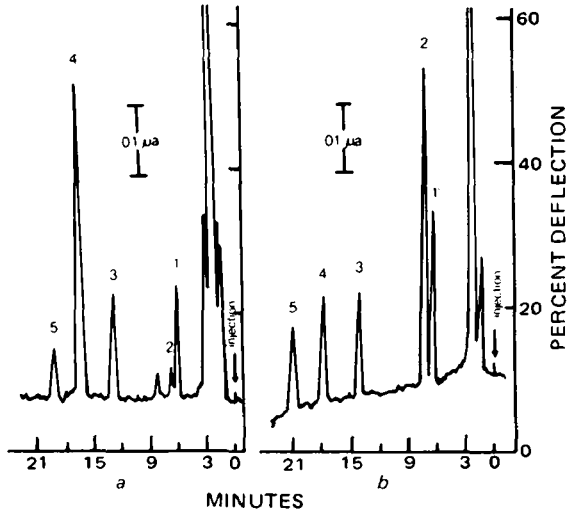

Figure 2—(a) *Chromatogram of the extract of 1 ml of serum from a patient receiving imipramine. The extract was reconstituted with 100 μl of methanol; 50 μl was injected. Concentrations measured were: imipramine (1), 32 ng/ml; 2-hydroxyimipramine (2), 5 ng/ml; internal standard (3); desipramine (4), 134 ng/ml; and 2-hydroxydesipramine (5), 29 ng/ml.* (b) *Chromatogram of a 1-ml blank plasma extract spiked with 50 ng/ml each of the drugs and metabolites. The extract was reconstituted with 100 μl of methanol; 50 μl was injected. Peak identification is the same as in Fig.* 2a.

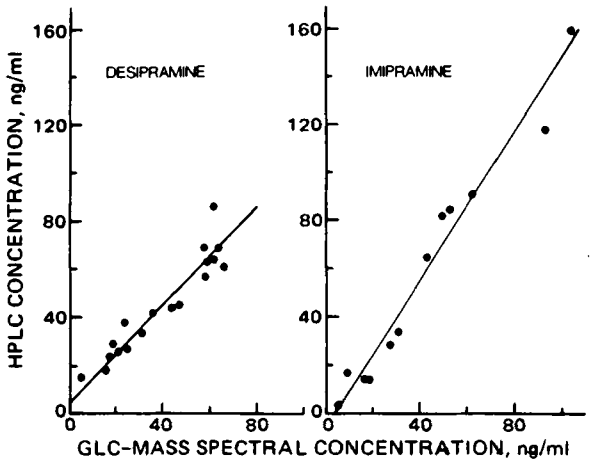

Figure 3—*Correlation between HPLC and GLC–mass spectral methods for plasma imipramine and desipramine analysis. For desipramine, the slope = 1.01, the intercept = 4.7, and the correlation coefficient = 0.943. For imipramine, the slope = 1.55, the intercept = −7.2, and the correlation coefficient = 0.960.*

tenance dose. Figure 2*b* shows a chromatogram of a plasma standard containing 50 ng/ml of each drug and metabolite and added internal standard. One milliliter each of the plasma standard and patient sample were extracted, and one-half of the extract was injected according to the procedure.

Eighteen plasma specimens from seven patients participating in an NIMH study (5) and receiving imipramine or desipramine were assayed by the HPLC method and a GLC–mass spectrometric method (18) (Fig. 3). The two assays showed excellent correlation, with a slope of nearly unity (1.01) for desipramine. The HPLC assay yielded higher results than the GLC–mass spectral method for imipramine. Imipramine and desipramine are stable at least 3 months in plasma stored at −4°. The NIMH samples were 6–15 months old at the time of HPLC analysis; therefore, interference in the fluorescence assay due to some unidentified degradation component(s) may explain the discrepancy between the methods for imipramine. Further comparison studies with fresh patient samples and spiked plasma are in progress. Data for the 2-hydroxy metabolites quantitated by GLC–mass spectra were not available for comparison.

REFERENCES

(1) L. F. Gram, *Clin. Pharmacokinet.*, **2**, 237 (1977).

(2) J. Christiansen and L. F. Gram, *J. Pharm. Pharmacol.*, **25**, 604 (1973).

(3) A. H. Glassman, J. M. Perel, M. Shostak, S. J. Kantor, and J. L. Fleiss, *Arch. Gen. Psychiat.*, **34**, 197 (1977).

(4) S. B. Jandhyala, M. L. Steenberg, J. M. Perel, A. A. Manian, and J. P. Buckley, *Eur. J. Pharmacol.*, **42**, 403 (1977).

(5) W. Z. Potter, A. P. Zavadil, and F. K. Goodwin, *Psychopharmacol. Bull.*, **14**, 29 (1978).

(6) W. Z. Potter, H. M. Calil, A. A. Manian, A. P. Zavadil, and F. K. Goodwin, in press.

(7) R. E. Heikkila, S. S. Goldfinger, and H. Orlansky, *Res. Commun. Chem. Pathol. Pharmacol.*, **13**, 237 (1976).

(8) D. C. Fenimore, C. J. Meyer, and C. M. Davis, *J. Chromatogr.*, **142**, 399 (1977).

(9) P. N. Kaul, L. R. Whitfield, and M. L. Clark, *J. Pharm. Sci.*, **67**, 60 (1978).

(10) A. Nagy and L. Treiber, *J. Pharm. Pharmacol.*, **25**, 599 (1973).

(11) D. N. Bailey and P. I. Jatlow, *Clin. Chem.*, **22**, 1697 (1976).

(12) R. G. Jenkins and R. O. Friedel, *J. Pharm. Sci.*, **67**, 17 (1978).

(13) J. C. Kraak and P. Bijster, *J. Chromatogr.*, **143**, 499 (1977).

(14) F. L. Vandemark, R. F. Adams, and G. J. Schmidt, *Clin. Chem.*, **24**, 87 (1978).

(15) J. H. M. Van Den Berg, H. J. J. M. DeRuwe, and R. S. Deelder, *J. Chromatogr.*, **138**, 431 (1977).

(16) I. D. Watson and M. J. Stewart, *ibid.*, **132**, 155 (1977).

(17) L. F. Gram, *Dan. Med. Bull.*, **21**, 218 (1974).

(18) M. Claeys, G. Muscettola, and S. P. Markey, *Biomed. Mass Spectrom.*, **3**, 110 (1976).

ACKNOWLEDGMENTS

Supported by Grant 20852 from the National Institutes of General Medical Sciences, National Institutes of Health.

The provision of GLC–mass spectral assay samples and GLC–mass spectral results by Dr. William Z. Potter of the National Institute of Mental Health and Dr. Anthony P. Zavadil, III, of the National Institutes of General Medical Sciences, the gifts of drug metabolites by Dr. Albert A. Manian of the National Institute of Mental Health, and the clinical assistance of Dr. Richard E. Wolin are appreciated.

Chemistry of 8-Chloroberberine

JEROME L. MONIOT, TINA M. KRAVETZ, ABD EL RAHMAN H. ABD EL RAHMAN, and MAURICE SHAMMA ˣ

Received June 1, 1978, from the *Department of Chemistry, Pennsylvania State University, University Park, PA 16802.* Accepted for publication November 21, 1978.

Abstract □ 8-Chloroberberine (V), obtained by treatment of oxyberberine (I) with phosphorus oxychloride, is a reactive intermediate. Treatment with ammonia, methylamine, *n*-propylamine, aniline, and *p*-toluidine furnished the 8-berberinylidene derivatives IV and VII–X. Reaction of V with malononitrile, ethyl acetoacetate, and ethyl malonate anions yielded the 8-berberinylidene derivatives XII–XIV. Acid hydrolysis of XIV gave 8-berberinylacetic acid (XV) whose reduction provided 8-canadinylacetic acid (XVI). Grignard reagents react readily with V. Methylmagnesium iodide, ethylmagnesium iodide, and benzylmagnesium iodide led to 8,8-dimethyldihydroberberine (XVII), 8,8-diethyldihydroberberine (XIX), and the benzyl derivative XX, respectively. Sodium borohydride reduction of XX gave rise to 8-benzylcanadine (XXI).

Keyphrases □ Chloroberberine—synthesis, derivatives □ Protoberberine salts—chloroberberine, synthesis, derivatives □ Antibacterials—chloroberberine, synthesis, derivatives □ Antiarrhythmics—chloroberberine, synthesis, derivatives □ Tranquilizers—chloroberberine, synthesis, derivatives

Protoberberine salts and tetrahydroprotoberberine bases have wide pharmacological potency including tranquilizing, antimicrobial, antifungal, hypotensive, antiulcer, uterine, antiarrhythmic, neuroleptic, and antipsychotic effects. Protoberberine salt pharmacology was reviewed recently (1, 2).

The present report describes the structure of 8-chloroberberine (V), a compound characterized partially by

© 1979, American Pharmaceutical Association

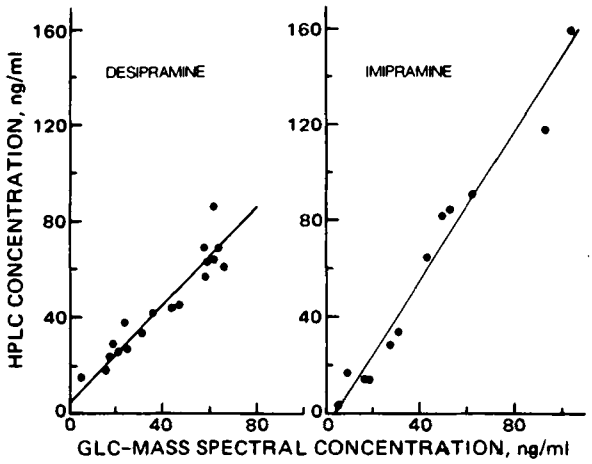

Figure 3—*Correlation between HPLC and GLC–mass spectral methods for plasma imipramine and desipramine analysis. For desipramine, the slope = 1.01, the intercept = 4.7, and the correlation coefficient = 0.943. For imipramine, the slope = 1.55, the intercept = −7.2, and the correlation coefficient = 0.960.*

tenance dose. Figure 2*b* shows a chromatogram of a plasma standard containing 50 ng/ml of each drug and metabolite and added internal standard. One milliliter each of the plasma standard and patient sample were extracted, and one-half of the extract was injected according to the procedure.

Eighteen plasma specimens from seven patients participating in an NIMH study (5) and receiving imipramine or desipramine were assayed by the HPLC method and a GLC–mass spectrometric method (18) (Fig. 3). The two assays showed excellent correlation, with a slope of nearly unity (1.01) for desipramine. The HPLC assay yielded higher results than the GLC–mass spectral method for imipramine. Imipramine and desipramine are stable at least 3 months in plasma stored at −4°. The NIMH samples were 6–15 months old at the time of HPLC analysis; therefore, interference in the fluorescence assay due to some unidentified degradation component(s) may explain the discrepancy between the methods for imipramine. Further comparison studies with fresh patient samples and spiked plasma are in progress. Data for the 2-hydroxy metabolites quantitated by GLC–mass spectra were not available for comparison.

REFERENCES

(1) L. F. Gram, *Clin. Pharmacokinet.*, **2**, 237 (1977).

(2) J. Christiansen and L. F. Gram, *J. Pharm. Pharmacol.*, **25**, 604 (1973).

(3) A. H. Glassman, J. M. Perel, M. Shostak, S. J. Kantor, and J. L. Fleiss, *Arch. Gen. Psychiat.*, **34**, 197 (1977).

(4) S. B. Jandhyala, M. L. Steenberg, J. M. Perel, A. A. Manian, and J. P. Buckley, *Eur. J. Pharmacol.*, **42**, 403 (1977).

(5) W. Z. Potter, A. P. Zavadil, and F. K. Goodwin, *Psychopharmacol. Bull.*, **14**, 29 (1978).

(6) W. Z. Potter, H. M. Calil, A. A. Manian, A. P. Zavadil, and F. K. Goodwin, in press.

(7) R. E. Heikkila, S. S. Goldfinger, and H. Orlansky, *Res. Commun. Chem. Pathol. Pharmacol.*, **13**, 237 (1976).

(8) D. C. Fenimore, C. J. Meyer, and C. M. Davis, *J. Chromatogr.*, **142**, 399 (1977).

(9) P. N. Kaul, L. R. Whitfield, and M. L. Clark, *J. Pharm. Sci.*, **67**, 60 (1978).

(10) A. Nagy and L. Treiber, *J. Pharm. Pharmacol.*, **25**, 599 (1973).

(11) D. N. Bailey and P. I. Jatlow, *Clin. Chem.*, **22**, 1697 (1976).

(12) R. G. Jenkins and R. O. Friedel, *J. Pharm. Sci.*, **67**, 17 (1978).

(13) J. C. Kraak and P. Bijster, *J. Chromatogr.*, **143**, 499 (1977).

(14) F. L. Vandemark, R. F. Adams, and G. J. Schmidt, *Clin. Chem.*, **24**, 87 (1978).

(15) J. H. M. Van Den Berg, H. J. J. M. DeRuwe, and R. S. Deelder, *J. Chromatogr.*, **138**, 431 (1977).

(16) I. D. Watson and M. J. Stewart, *ibid.*, **132**, 155 (1977).

(17) L. F. Gram, *Dan. Med. Bull.*, **21**, 218 (1974).

(18) M. Claeys, G. Muscettola, and S. P. Markey, *Biomed. Mass Spectrom.*, **3**, 110 (1976).

ACKNOWLEDGMENTS

Supported by Grant 20852 from the National Institutes of General Medical Sciences, National Institutes of Health.

The provision of GLC–mass spectral assay samples and GLC–mass spectral results by Dr. William Z. Potter of the National Institute of Mental Health and Dr. Anthony P. Zavadil, III, of the National Institutes of General Medical Sciences, the gifts of drug metabolites by Dr. Albert A. Manian of the National Institute of Mental Health, and the clinical assistance of Dr. Richard E. Wolin are appreciated.

Chemistry of 8-Chloroberberine

JEROME L. MONIOT, TINA M. KRAVETZ, ABD EL RAHMAN H. ABD EL RAHMAN, and MAURICE SHAMMA ˣ

Received June 1, 1978, from the *Department of Chemistry, Pennsylvania State University, University Park, PA 16802.* Accepted for publication November 21, 1978.

Abstract □ 8-Chloroberberine (V), obtained by treatment of oxyberberine (I) with phosphorus oxychloride, is a reactive intermediate. Treatment with ammonia, methylamine, *n*-propylamine, aniline, and *p*-toluidine furnished the 8-berberinylidene derivatives IV and VII–X. Reaction of V with malononitrile, ethyl acetoacetate, and ethyl malonate anions yielded the 8-berberinylidene derivatives XII–XIV. Acid hydrolysis of XIV gave 8-berberinylacetic acid (XV) whose reduction provided 8-canadinylacetic acid (XVI). Grignard reagents react readily with V. Methylmagnesium iodide, ethylmagnesium iodide, and benzylmagnesium iodide led to 8,8-dimethyldihydroberberine (XVII), 8,8-diethyldihydroberberine (XIX), and the benzyl derivative XX, respectively. Sodium borohydride reduction of XX gave rise to 8-benzylcanadine (XXI).

Keyphrases □ Chloroberberine—synthesis, derivatives □ Protoberberine salts—chloroberberine, synthesis, derivatives □ Antibacterials—chloroberberine, synthesis, derivatives □ Antiarrhythmics—chloroberberine, synthesis, derivatives □ Tranquilizers—chloroberberine, synthesis, derivatives

Protoberberine salts and tetrahydroprotoberberine bases have wide pharmacological potency including tranquilizing, antimicrobial, antifungal, hypotensive, antiulcer, uterine, antiarrhythmic, neuroleptic, and antipsychotic effects. Protoberberine salt pharmacology was reviewed recently (1, 2).

The present report describes the structure of 8-chloroberberine (V), a compound characterized partially by

© 1979, American Pharmaceutical Association

previous researchers (3). 8-Chloroberberine was then used as an intermediate in the preparation of new berberine derivatives.

DISCUSSION

Initial investigations of phosphorus oxychloride–oxyberberine (I) reaction products identified oxyberberrubine (II) and a reactive chlorinated derivative, tentatively assigned Structure III (3). Treatment of the chlorinated derivative with ammonia yielded iminoberberine (IV), characterized as its hydrochloride salt. When iminoberberine was subjected to aqueous alkali, hydrolysis to I took place (3).

Refluxing I with phosphorus oxychloride produced the stable but moisture-sensitive orange crystalline salt 8-chloroberberine (V), which readily hydrolyzed to I in water, ethanol, or aqueous alkali. The V high-resolution mass spectrum contained the molecular ion *m/e* 370 for $C_{20}H_{17}NO_4Cl$. The berberine and V trifluoroacetic acid PMR spectra were nearly identical, the major difference being the absence in V of the proton singlet at δ10.1 assigned to H-8 in the spectrum of berberine chloride. Thus, the phosphorus oxychloride product from I is the C-8 monochloro berberine analog V rather than the dichloro compound III. The high V reactivity toward oxygen nucleophiles was extended to other entering groups including primary amines, carbanions, and Grignard reagents.

Reaction of V with anhydrous ammonia produced Perkin's yellow "iminoberberine" (IV), here designated 8-berberinylideneimine. Acetylation of this material produced the yellow *N*-acetyl amide VI. Mild VI hydrolysis with sodium bicarbonate regenerated IV.

Similarly, V reacted with methylamine, *n*-propylamine, aniline, and *p*-toluidine to give the 8-berberinylidene derivatives VII–X. As partial verification of these results, IV methylation with methyl iodide produced 8-berberinylidenemethylimine (VII), identical to that obtained by direct treatment of V with methylamine.

Imine bases VII–X hydrolysis with sodium hydroxide regenerated I while reduction of the bases with sodium borohydride in ethanol supplied canadine (XI) (4).

Since V reacts readily with basic nitrogen nucleophiles, V reaction with carbanions was also investigated. Treatment of V with the malononitrile anion furnished the dark-orange 8-berberinylidenemalononitrile (XII). Reaction of V with ethyl acetoacetate and ethyl malonate anions yielded the 8-berberinylidene derivatives XIII and XIV, respectively. Acid hydrolysis of XIV was accompanied by decarboxylation and produced the orange 8-berberinylacetic acid (XV). Reduction of this quaternary salt with sodium borohydride in ethanol generated 8-canadinylacetic acid (XVI).

Another aspect of V chemistry is its reactivity toward Grignard reagents. With methylmagnesium iodide, a good yield of 8,8-dimethyldihydroberberine (XVII) was obtained; with ethylmagnesium iodide, 8,8-diethyldihydroberberine (XVIII) was produced. The latter compound was reduced with sodium borohydride to 8,8-diethylcanadine (XIX). Monoalkylation of V with the bulkier benzylmagnesium bromide gave the benzyl derivative XX whose borohydride reduction product was identical with 8-benzylcanadine (XXI) (5).

Clearly, the readily available V is a useful synthetic intermediate for the generation of 8-substituted berberine and canadine derivatives.

EXPERIMENTAL[1]

8-Chloroberberine (V)—An oxyberberine (I) slurry (5 g, 14.2 mmoles) in phosphorus oxychloride (10 ml) was refluxed for 2 hr. After cooling, the orange-red crystalline residue was collected, washed with chloroform and then ether, and dried *in vacuo* to yield 4.5 g (85%) of V as orange-red crystals, mp >300°; PMR (trifluoroacetic acid): δ 3.30 (t, 2H, J = 7 Hz, H-5), 4.23 (s, 6H, 2 OCH_3), 5.20 (t, 2H, J = 7 Hz, H-6), 6.13 (s, 2H, OCH_2O), 6.97 (s, 1H, H-4), 7.47 (s, 1H, H-1), 8.10 (s, 2H, H-11,12), and 8.47 (s, 1H, H-13); mass spectrum: *m/e* M^+ 370 (10), 355 (10), and 335 (100); high-resolution mass spectrum: calc. for $C_{20}H_{17}ClNO_4$, 370.0845; found *m/e* 370.0876.

Compound V Hydrolysis—Compound V was decolorized rapidly with water, ethanol, or aqueous alkali and gave I exclusively.

8-Berberinylideneimine (IV)—Anhydrous ammonia gas was bubbled through a V slurry (1 g, 2.7 mmoles) in benzene (20 ml) for 1 hr. Following solvent removal, the residue was washed with water and partitioned between chloroform and aqueous sodium bicarbonate. The organic layer was dried, and the solvent was evaporated to afford yellow needles (0.9 g, 95%), which were recrystallized from chloroform, mp >300° [lit. (2) mp >280°]; IR: $\nu_{max}^{CHCl_3}$ 1640 and 3300 cm^{-1}; UV: $\lambda_{max}^{ethanol}$ 282 (log ε 3.48), 358 (3.76), 377 sh (3.61), and 400 (3.41) nm; UV: $\lambda_{max}^{ethanol,H^+}$ 233 (log ε 4.05), 253 sh (3.77), 343 (3.83), 386 (3.48), and 403 sh (3.40) nm; PMR ($CDCl_3$): δ 2.87 (t, 2H, J = 7 Hz, H-5), 3.88 (s, 3H, OCH_3), 3.92 (s, 3H, OCH_3), 4.23 (t, 2H, H-6), 5.93 (s, 2H, OCH_2O), 6.12 (s, 1H, H-13), 6.63 (s, 1H, H-4), 7.05 (s, 2H, H-11,12), and 7.13 (s, 1H, H-1); PMR (trifluoroacetic acid): δ 3.17 (t, 2H, J = 7 Hz, H-5), 4.14 (s, 3H, OCH_3), 4.27 (s, 3H, OCH_3), 4.35 (t, 2H, H-6), 6.10 (s, 2H, OCH_2O), 5.85 (br s, 3H, NH), 6.91 (s, 1H, H-4), 7.32 (s, 1H, H-1), 7.50 (s, 1H, H-13), and 7.80 (s, 2H, H-11, 12); mass spectrum: *m/e* M^+ 350 (100), 335 (80), 321 (20), and 293 (50).

Sodium borohydride in ethanol reduction of IV provided (±)-canadine (XI), mp 172–173° [lit. (4) mp 170–171°], quantitatively.

The IV·HCl had a melting point of 165–166° (methanol).

Anal.—Calc. for $C_{20}H_{18}N_2O_4$·HCl: C, 62.24; H, 4.93. Found: C, 61.98; H, 5.05.

***N*-Acetyl-8-berberinylideneimine (VI)**—A slurry of IV (1 g, 2.8 mmoles) in pyridine (10 ml) and acetic anhydride (5 ml) was stirred overnight. After solvent removal, the residue crystallized from methanol as tan needles (0.84 g, 2.1 mmoles, 75%), mp 226–228°; IR: ν_{max}^{KBr} 1655 cm^{-1}; UV: $\lambda_{max}^{ethanol}$ 263 (log ε 4.22), 348 (4.23), 408 (3.68), and 420 (3.69) nm; PMR (trifluoroacetic acid): δ 2.70 (s, 3H, CH_3CO), 3.18 (t, 2H, J = 7 Hz, H-5),

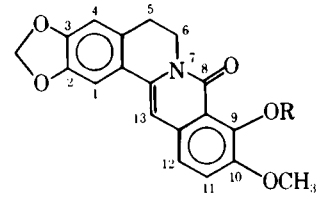

I: R = CH_3
II: R = H

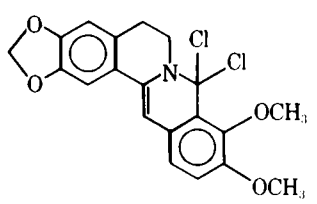

III

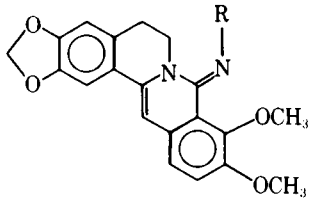

IV: R = H
VI: R = $COCH_3$
VII: R = CH_3
VIII: R = $CH_3CH_2CH_2$
IX: R = Ph
X: R = p-$CH_3C_6H_5$

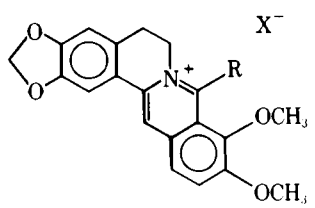

V: R = Cl
XV: R = CH_2COOH
XX: R = $CH_2C_6H_5$

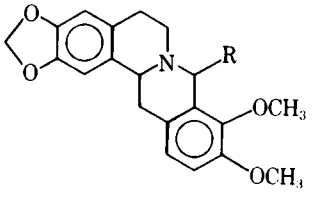

XI: R = H
XVI: R = CH_2COOH
XXI: R = $CH_2C_6H_5$

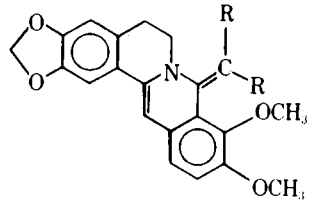

XII: R = CN
XIII: R = $COOC_2H_5$, $COCH_3$
XIV: R = $COOC_2H_5$

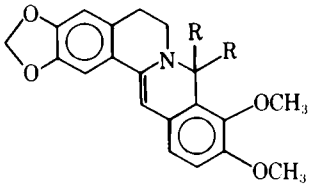

XVII: R = CH_3
XVIII: R = C_2H_5

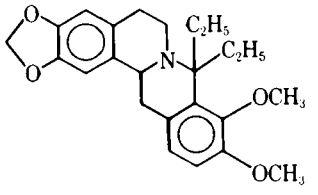

XIX

[1] PMR spectra were obtained at 60 MHz in deuterochloroform, unless specified otherwise, with tetramethylsilane as the internal standard. Mass spectra were run at 70 ev. TLC utilized Merck 254 silica gel plates. Microanalyses were done at Midwest Microlab, Indianapolis, Ind.

4.24 (s, 3H, OCH_3), 4.37 (s, 3H, OCH_3), 4.72 (t, 2H, J = 7 Hz, H-6), 6.18 (s, 2H, OCH_2O), 6.94 (s, 1H, ring A aromatic H), 7.49 (s, 1H, ring A aromatic H), 8.40 (s, 1H, H-13), and 8.08 (s, 2H, ring D aromatic H); mass spectrum: m/e M^+ 392 (5), 377 (5), 361 (100), 352 (15), 335 (17), 320 (10), 305 (5), and 291 (25); high-resolution mass spectrum: calc. for $C_{22}H_{20}N_2O_5$, 392.1373; found m/e 392.1387.

Compound VI hydrolysis with aqueous sodium bicarbonate and chloroform extraction produced IV in near-quantitative yield.

Preparations of 8-Berberinylidenemethylamine (VII), 8-Berberinylidene-*n*-propylamine (VIII), 8-Berberinylideneaniline (IX), and 8-Berberinylidene-*p*-toluidine (X)—The anhydrous amine, in excess, was added to a stirred V benzene slurry, and the mixture was stirred for 1 hr. After dilution with ether, dry hydrogen chloride gas was added until precipitation was complete. The collected solid was washed with water and dissolved in chloroform, and the solution was dried. Solvent evaporation was followed by crystallization. The yields were around 80%.

Compound VII, $C_{21}H_{20}N_2O_4$, was obtained as light-yellow needles, mp 122° (methanol); IR: $\nu_{max}^{CHCl_3}$ 1570 and 1640 cm^{-1}; UV: $\lambda_{max}^{ethanol}$ 283 (log ϵ 3.83) and 360 (4.16) nm; UV: $\lambda_{max}^{ethanol,\ H^+}$ 253 (log ϵ 4.18), 340 (4.25), and 395 (3.78) nm; PMR (trifluoroacetic acid): δ 3.15 (t, 2H, J = 7, H-5), 3.51 (s, 3H, NCH_3), 4.18 (s, 3H, OCH_3), 4.30 (s, 3H, OCH_3), 4.54 (t, 2H, J = 7 Hz, H-6), 61.0 (s, 2H, OCH_2O), 6.91 (s, 1H, aromatic H), 7.32 (s, 1H, aromatic H), 7.50 (s, 1H, aromatic H), and 7.80 (s, 2H, H-11,12); mass spectrum: m/e M^+ 364 (30), 350 (90), 335 (100), and 291 (10); high-resolution mass spectrum: calc. for $C_{21}H_{20}N_2O_4$, 364.1419; found m/e 364.1446.

The VII·HCl salt had a melting point of 187–189° (methanol).

Compound VIII, $C_{23}H_{24}N_2O_4$, was obtained as light-yellow needles, mp 170–172° (ether); UV: $\lambda_{max}^{ethanol}$ 283 (log ϵ 4.09) and 363 (4.22) nm; UV: $\lambda_{max}^{ethanol,\ H^+}$ 254 (log ϵ 4.36), 340 (4.42), and 397 (3.90) nm; NMR (trifluoroacetic acid): δ 1.13 (t, 3H, J = 7 Hz, $CH_3CH_2CH_2$), 1.90 (m, 2H, $CH_3CH_2CH_2$), 3.10 (t, 2H, J = 7 Hz, H-5), 3.72 (m, 2H, $CH_3CH_2CH_2$), 4.17 (s, 3H, OCH_3), 4.28 (s, 3H, OCH_3), 4.34 (t, 2H, J = 7 Hz, H-6), 6.17 (s, 2H, OCH_2O), 6.97 (s, 1H, H-4), 7.32 (s, 1H, H-13), 7.50 (s, 1H, H-1), and 7.80 (s, 2H, H-11,12); mass spectrum: m/e M^+ 392 (100), 378 (70), 363 (80), 361 (50), 347 (60), 335 (30), 334 (30), 333 (30), 320 (25), 306 (20), 281 (25), and 207 (50).

The VIII·HCl had a melting point of 219–220° (methanol).

Anal.—Calc. for $C_{23}H_{24}N_2O_4$·HCl: C, 64.37; H, 5.88. Found: C, 63.98; H, 6.07.

Compound IX, $C_{26}H_{22}N_2O_4$, was obtained as yellow needles, mp 167–169° (methanol–ether); UV: $\lambda_{max}^{ethanol}$ 285 (log ϵ 3.95), 328 (3.75), and 370 (3.90) nm; UV: $\lambda_{max}^{ethanol,\ H^+}$ 258 (log ϵ 4.06), 343 (4.06), 395 sh (3.48), and 422 (3.54) nm; mass spectrum: m/e M^+ 426 (100), 411 (40), 395 (30), 335 (30), and 321 (25).

The IX·HCl had a melting point of 186–187° (methanol).

Anal.—Calc. for $C_{26}H_{22}N_2O_4$·HCl: C, 67.42; H, 5.01. Found: C, 67.17; H, 5.29.

Compound X, $C_{27}H_{24}N_2O_4$, hydrochloride salt was obtained as gold prisms, mp 160–162° (methanol–water–ether); UV: $\lambda_{max}^{ethanol,\ H^+}$ 236 (log ϵ 4.50), 257 (4.40), 342 (4.38), and 420 (3.90) nm; mass spectrum (free base): m/e M^+ 440 (40), 425 (10), 335 (5), 107 (100), and 106 (98); high-resolution mass spectrum (free base): calc. for $C_{27}H_{24}N_2O_4$, 440.1731; found m/e 440.1749.

Anal.—Calc. for $C_{27}H_{24}N_2O_4$·HCl·H_2O: C, 65.49; H, 5.50. Found: C, 65.27; H, 5.66.

Conversion of IV to VII—A solution of IV (1 g, 2.85 mmoles) in methyl iodide (3 ml) and acetonitrile (10 ml) was refluxed for 0.5 hr and cooled, and the solvent was evaporated. The residue, after basification with aqueous sodium bicarbonate and chloroform extraction, provided VII in high yield.

8-Berberinylidenemalononitrile (XII)—Malononitrile (0.6 g, 9.1 mmoles) was added to dry tetrahydrofuran (20 ml), followed by sodium hydride (0.2 g, 8.3 mmoles). Following gas evolution, V (1.5 g, 4.08 mmoles) was added, and the mixture was stirred for 30 min. The red mixture was diluted with an equal volume of ether and filtered. The solid was slurried in chloroform and filtered, and the filtrate crystallized upon addition of ether. Recrystallization from methanol afforded 1.1 g (2.75 mmoles, 68%) of XII as reddish-orange crystals, mp 276–277°; IR: $\nu_{max}^{CHCl_3}$ 2102 cm^{-1}; UV: $\lambda_{max}^{ethanol}$ 255 sh (log ϵ 3.97), 278 (3.85), 345 (3.84), 368 sh (3.73), and 466 (3.51) nm; PMR (trifluoroacetic acid): δ 3.25 (t, 2H, J = 7 Hz, H-5), 4.90 (t, 2H, J = 7 Hz, H-6), 4.17 (s, 3H, OCH_3), 4.28 (s, 3H, OCH_3), 6.23 (s, 2H, OCH_2O), 6.30 [s, 1H, $HC(CN)_2$], 7.06 (s, 1H, aromatic H), 7.47 (s, 1H, aromatic H), 7.87 (s, 1H, aromatic H), and 8.06 (s, 2H, H-11,12); mass spectrum: m/e M^+ 399 (100), 384 (20), 359 (60), 334 (40), and 322 (40); high-resolution mass spectrum: calc. for $C_{23}H_{17}N_3O_4$, 399.1218; found m/e 399.1225.

Ethyl 8-Berberinylideneacetoacetate (XIII)—Ethyl acetoacetate (1.2 ml, 8.3 mmoles) was added to a stirred slurry of sodium hydride (0.2 g, 8.3 mmoles) in dry tetrahydrofuran (50 ml). After gas evolution, V (1 g, 2.7 mmoles) was added, and the mixture was stirred for 30 min. The product was partitioned between chloroform and water, the organic layer was dried, and the solvent was evaporated. Trituration with ether gave a product, which was recrystallized from methanol to give 1.04 g (2.15 mmoles, 80%) of XIII as dark-red plates, mp 263–264°; IR: ν_{max}^{KBr} 1620 and 1670 cm^{-1}; UV: $\lambda_{max}^{ethanol}$ 232 (log ϵ 4.53), 267 (4.62), 337 (4.33), and 432 (3.73) nm; UV: $\lambda_{max}^{ethanol,H^+}$ 232 (log ϵ 4.60), 267 (4.48), 352 (4.38), and 440 (3.72) nm; mass spectrum: m/e M^+ 463 (5), 432 (100), 403 (50), and 358 (80).

Anal.—Calc. for $C_{26}H_{25}NO_7$·CH_3OH: C, 65.45; H, 5.85. Found: C, 65.37; H, 5.58.

Diethyl 8-Berberinylidenemalonate (XIV)—Salt V (1.5 g, 4 mmoles) was treated with the anion of ethyl malonate as described to yield, after similar workup and treatment with dry methanolic hydrochloric acid, 1.54 g (3.14 mmoles, 79%) of XIV as the hydrochloride salt as light-orange needles, mp >300° (methanol–ether), and red needles of free base, mp 238° (methanol); UV: $\lambda_{max}^{ethanol}$ 260 (log ϵ 4.31), 332 (4.15), 402 (3.78), and 428 sh (3.72) nm; mass spectrum: m/e M^+ 493 (2), 448 (2), 421 (10), 390 (30), 376 (40), 361 (45), 346 (40), 334 (100), and 318 (30).

Anal.—Calc. for $C_{27}H_{27}NO_8$·HCl: C, 61.30; H, 5.11. Found: C, 61.18; H, 4.90.

8-Berberinylacetic Acid (XV) Chloride Salt—A solution of XIV (1.36 g, 2.76 mmoles) in methanol (20 ml) containing concentrated hydrochloric acid (5 ml) was heated at 60° for 1 hr, diluted with water, and extracted with chloroform. The organic layer was dried, filtered, and evaporated. The residue was recrystallized from ethanol–ether to afford 0.85 g (2.16 mmoles, 78%) of XV, mp >300°; IR: ν_{max}^{KBr} 1600, 1720, and 3350 cm^{-1}; UV: $\lambda_{max}^{ethanol}$ 272 (log ϵ 4.26), 353 (4.22), 411 sh (3.70), and 430 sh (3.68) nm; PMR (trifluoroacetic acid): δ 3.32 (t, 2H, J = 7 Hz, H-5), 4.28 (s, 6H, 2 OCH_3), 4.96 (t, 2H, J = 7 Hz, H-6), 5.25 (s, 2H, CH_2COOH), 6.20 (s, 2H, OCH_2O), 7.01 (s, 1H, aromatic H), 7.59 (s, 1H, aromatic H), 8.56 (s, 1H, aromatic H), and 8.14 (s, 2H, H-11,12).

Anal.—Calc. for $C_{22}H_{20}ClNO_6$·C_2H_5OH: C, 60.58; H, 5.46. Found: C, 60.95; H, 5.38.

8-Canadinylacetic Acid (XVI)—A solution of XV (0.9 g, 2.3 mmoles) in ethanol (50 ml) was treated with excess sodium borohydride, giving an oil that crystallized from methanolic hydrogen chloride solution. Recrystallization from methanol afforded 0.8 g (2.0 mmoles, 87%) of XVI as very light-yellow needles of the hydrochloride salt, mp 212–214°; IR: $\nu_{max}^{CHCl_3}$ 1480, 1720, 2400, and 3400 cm^{-1}; UV: $\lambda_{max}^{ethanol,\ H^+}$ 267 sh (log ϵ 3.44) and 287 (3.86) nm; mass spectrum: m/e M^+ 397 (30), 382 (10), 338 (100), 322 (10), 306 (7), 278 (10), 236 (15), 206 (25), 126 (25), and 169 (20).

Anal.—Calc. for $C_{22}H_{23}NO_6$·HCl: C, 60.89; H, 5.57. Found: C, 61.00; H, 5.88.

8,8-Dimethyldihydroberberine (XVII) Hydroiodide—To a rapidly stirred suspension of magnesium turnings (1 g) in ether (20 ml) was added portionwise a solution of methyl iodide (1 ml) in ether (20 ml) at a rate to maintain vigorous reflux. The mixture was cooled, a suspension of V (1 g, 2.67 mmoles) in ether (20 ml) was added, and the mixture was refluxed for 30 min. The product was poured over ice, mixed with concentrated sulfuric acid (5 ml), and extracted with chloroform. The organic layer was worked up and treated with methanolic hydrogen iodide to furnish 0.78 g (60%) of the hydroiodide salt, mp 222° dec.; PMR (trifluoroacetic acid): δ 2.21 (s, 6H, 2 CH_3), 3.26 (t, 2H, J = 7 Hz, H-5), 4.04 (s, 3H, OCH_3), 4.16 (s, 3H, OCH_3), 4.31 (t, 2H, J = 7 Hz, H-6), 4.70 (s, 2H, H-13), 6.19 (s, 2H, OCH_2O), 6.93 (s, 1H, H-4), 7.19 (s, 2H, H-11,12), and 7.50 (s, 1H, H-1).

Anal.—Calc. for $C_{22}H_{23}NO_4$·HI: C, 53.52; H, 4.90. Found: C, 53.12; H, 4.90.

8,8-Diethyldihydroberberine (XVIII) Hydroiodide—By a procedure similar to that described but using ethylmagnesium bromide, XVIII was obtained in 66% yield as orange needles of the hydroiodide salt, mp 290° dec. (methanol).

Anal.—Calc. for $C_{24}H_{27}NO_4$·HI·CH_3OH: C, 54.25; H, 5.68. Found: C, 54.35; H, 5.39.

8-Benzylberberinium Bromide (XX)—An ethereal V suspension (1 g, 2.7 mmoles) was treated with excess ethereal benzylmagnesium bromide. Workup provided 0.99 g (2.32 mmoles, 86%) of XX as light-red needles, mp 232–233° (methanol); UV: $\lambda_{max}^{ethanol}$ 285 (log ϵ 4.04), 365 (3.87), 400 (3.44), and 450 (3.28) nm; PMR (trifluoroacetic acid): δ 3.08 (t, 2H, J = 7 Hz, C-5), 3.85 (s, 3H, OCH_3), 4.20 (s, 3H, OCH_3), 4.87 (t, 2H, J = 7 Hz, H-6), 5.53 (s, 2H, $PhCH_2$), 6.15 (s, 2H, OCH_2O), 6.90 (s, 1H, H-4), 7.08–7.43 (m, 5H, ArH), 7.55 (s, 1H, H-1), 8.10 (s, 2H, H-11,12), and 8.55 (s, 1H, H-13); mass spectrum: m/e M^+ 425 (100), 410 (53), 394 (24), and

334 (80); high-resolution mass spectrum: calc. for $C_{27}H_{23}NO_4$, 425.1627; found *m/e* 425.1615.

8,8-Diethylcanadine (XIX)—A XVIII solution (0.1 g, 0.25 mmole) in ethanol (20 ml) was treated with excess sodium borohydride (0.4 g). Workup and recrystallization from methanol furnished 0.096 g (96%) of XIX as tan plates, mp 168–169°; UV: $\lambda_{max}^{ethanol}$ 233 (log ϵ 4.31) and 288 (3.81) nm; mass spectrum: *m/e* M^+ 395 (5), 367 (100), 335 (10), 220 (35), and 175 (40); high-resolution mass spectrum: calc. for $C_{24}H_{29}NO_4$, 395.2096; found *m/e* 395.2125.

8-Benzylcanadine (XXI)—Sodium borohydride reduction of XX (1 g, 2.3 mmoles) in ethanol yielded 0.98 g (99%) of the known XXI, mp 165–166° (methanol) [lit. (5) mp 163–165°].

REFERENCES

(1) M. Shamma, "The Isoquinoline Alkaloids," Academic, New York, N.Y., 1972, pp. 268–314.

(2) M. Shamma and J. L. Moniot, "Isoquinoline Alkaloids Research, 1972–1977," Plenum, New York, N.Y., 1978, pp. 209–259.

(3) R. D. Haworth, W. H. Perkin, Jr., and H. S. Pink, *J. Chem. Soc.*, **1925**, 1709.

(4) A. C. Santosy and P. Adkilen, *J. Am. Chem. Soc.*, **54**, 2923 (1932).

(5) J. R. Gear and I. D. Spenser, *Can. J. Chem.*, **41**, 783 (1963).

ACKNOWLEDGMENTS

Supported by Grant HL-12971 from the National Heart, Lung and Blood Institute, U.S. Public Health Service, National Institutes of Health.

A. H. Abd el Rahman, of the Department of Chemistry, Mansura University, Mansura, Egypt, was the recipient of a postdoctoral fellowship from the Egyptian government.

Comparative Studies on Eight Dissolution Methods Using 21 Commercial Chloramphenicol Tablets and a Nondisintegrating Benzoic Acid Tablet

HIROYASU OGATA ˣ, TOSHIO SHIBAZAKI, TETSUO INOUE, and AKIRA EJIMA

Received April 25, 1978, from the *Division of Drug, National Institute of Hygienic Sciences, 1-18-1, Kamiyoga Setagaya-ku, Tokyo, Japan.* Accepted for publication November 17, 1978.

Abstract □ Eight dissolution methods (beaker, rotating basket, oscillating basket, solubility simulator, rotating flask, and column) were evaluated using 21 commercial film-coated chloramphenicol (I) tablets and a nondisintegrating benzoic acid (II) tablet. The relative agitating intensities obtained from different dissolution methods were compared through the relative zero-order nondisintegrating tablet dissolution rate constants. Correlation coefficients between I dissolution rate parameters (lag time, T_{20}, T_{50}, and T_{80}) were determined. Significant correlation was observed for the lag time among seven methods, and all pairwise regression lines passed through zero except one. The regression line slopes reflected the relative destructive force intensities produced by each dissolution method on the coated I tablet films. The seven dissolution methods could be classified into two main groups according to correlations of four dissolution rate parameters. This classification criterion agreed well with that based on the agitation method. However, dissolution methods may not be interchangeable even though they belong to the same dissolution method group.

Keyphrases □ Dissolution testing systems—eight systems compared, chloramphenicol tablets and powder, benzoic acid tablet □ Dissolution rates—chloramphenicol tablets and powder, benzoic acid tablet □ Chloramphenicol—dissolution rates, tablets and powder, eight testing systems compared □ Benzoic acid—dissolution rate, tablet, eight testing systems compared

Since the dissolution rate was first recognized as a significant factor in determining *in vivo* drug bioavailability, many methods for testing solid dosage form dissolution have been reported (1, 2). These methods differ in hydrodynamic properties, agitating intensities, and mechanical destructive forces to the intact drug. There are three basic dissolution testing devices (2, 3): the stirred-tank reactor with a mechanical agitator such as Levy's beaker method (4) or the rotating-basket method (5), the rotating vessel reactor such as the rotating flask (6) or the solubility simulator[1], and the stream reactor such as the column method (7–9).

Several investigators compared the relative agitating intensities or hydrodynamic properties of selected dissolution devices by using a nondisintegrating model tablet (10–12). Bathe *et al.* (3) studied dissolution rates by beaker, rotating-basket, and flow column methods under eight different conditions. However, detailed comparisons of disintegrating tablet dissolution methods have not been made.

In the present study, eight representative dissolution testing methods were compared and evaluated. They can be divided into three categories: (*a*) stirrer-tank reactor type (beaker, rotating basket, and oscillating basket), (*b*) rotating-vessel reactor type (rotating flask and solubility simulator[1]), and (*c*) stream reactor type (column). Disintegrating tablets—21 chloramphenicol (I) brands available in Japan—and nondisintegrating tablets—benzoic acid (II)—were used as markers. The two drugs were selected because of their moderate solubilities in acidic solutions (2–4 mg/ml).

EXPERIMENTAL

Materials—Twenty-one different sugar-coated I tablets were obtained from 16 manufacturers in Japan. Tablets A–E each contained 50 mg of I while Tablets F–U each contained 250 mg of I. A powder of I[2] was included for comparison. Nondisintegrating and uncoated tablets containing 100 mg of II[3] were used.

[1] Sartorius-Membranfilter GmbH, Göttingen, West Germany.
[2] Yamanouchi Pharmaceutical Co., Tokyo, Japan.
[3] Supplied by Dr. Ikeda and Dr. Nishimura, Sankyo Co., Tokyo, Japan.

0022-3549/79/0600-0708$01.00/0

© 1979, American Pharmaceutical Association

334 (80); high-resolution mass spectrum: calc. for $C_{27}H_{23}NO_4$, 425.1627; found *m/e* 425.1615.

8,8-Diethylcanadine (XIX)—A XVIII solution (0.1 g, 0.25 mmole) in ethanol (20 ml) was treated with excess sodium borohydride (0.4 g). Workup and recrystallization from methanol furnished 0.096 g (96%) of XIX as tan plates, mp 168–169°; UV: $\lambda_{max}^{ethanol}$ 233 (log ϵ 4.31) and 288 (3.81) nm; mass spectrum: *m/e* M^+ 395 (5), 367 (100), 335 (10), 220 (35), and 175 (40); high-resolution mass spectrum: calc. for $C_{24}H_{29}NO_4$, 395.2096; found *m/e* 395.2125.

8-Benzylcanadine (XXI)—Sodium borohydride reduction of XX (1 g, 2.3 mmoles) in ethanol yielded 0.98 g (99%) of the known XXI, mp 165–166° (methanol) [lit. (5) mp 163–165°].

REFERENCES

(1) M. Shamma, "The Isoquinoline Alkaloids," Academic, New York, N.Y., 1972, pp. 268–314.

(2) M. Shamma and J. L. Moniot, "Isoquinoline Alkaloids Research, 1972–1977," Plenum, New York, N.Y., 1978, pp. 209–259.

(3) R. D. Haworth, W. H. Perkin, Jr., and H. S. Pink, *J. Chem. Soc.*, **1925**, 1709.

(4) A. C. Santosy and P. Adkilen, *J. Am. Chem. Soc.*, **54**, 2923 (1932).

(5) J. R. Gear and I. D. Spenser, *Can. J. Chem.*, **41**, 783 (1963).

ACKNOWLEDGMENTS

Supported by Grant HL-12971 from the National Heart, Lung and Blood Institute, U.S. Public Health Service, National Institutes of Health.

A. H. Abd el Rahman, of the Department of Chemistry, Mansura University, Mansura, Egypt, was the recipient of a postdoctoral fellowship from the Egyptian government.

Comparative Studies on Eight Dissolution Methods Using 21 Commercial Chloramphenicol Tablets and a Nondisintegrating Benzoic Acid Tablet

HIROYASU OGATA ˣ, TOSHIO SHIBAZAKI, TETSUO INOUE, and AKIRA EJIMA

Received April 25, 1978, from the *Division of Drug, National Institute of Hygienic Sciences, 1-18-1, Kamiyoga Setagaya-ku, Tokyo, Japan.* Accepted for publication November 17, 1978.

Abstract □ Eight dissolution methods (beaker, rotating basket, oscillating basket, solubility simulator, rotating flask, and column) were evaluated using 21 commercial film-coated chloramphenicol (I) tablets and a nondisintegrating benzoic acid (II) tablet. The relative agitating intensities obtained from different dissolution methods were compared through the relative zero-order nondisintegrating tablet dissolution rate constants. Correlation coefficients between I dissolution rate parameters (lag time, T_{20}, T_{50}, and T_{80}) were determined. Significant correlation was observed for the lag time among seven methods, and all pairwise regression lines passed through zero except one. The regression line slopes reflected the relative destructive force intensities produced by each dissolution method on the coated I tablet films. The seven dissolution methods could be classified into two main groups according to correlations of four dissolution rate parameters. This classification criterion agreed well with that based on the agitation method. However, dissolution methods may not be interchangeable even though they belong to the same dissolution method group.

Keyphrases □ Dissolution testing systems—eight systems compared, chloramphenicol tablets and powder, benzoic acid tablet □ Dissolution rates—chloramphenicol tablets and powder, benzoic acid tablet □ Chloramphenicol—dissolution rates, tablets and powder, eight testing systems compared □ Benzoic acid—dissolution rate, tablet, eight testing systems compared

Since the dissolution rate was first recognized as a significant factor in determining *in vivo* drug bioavailability, many methods for testing solid dosage form dissolution have been reported (1, 2). These methods differ in hydrodynamic properties, agitating intensities, and mechanical destructive forces to the intact drug. There are three basic dissolution testing devices (2, 3): the stirred-tank reactor with a mechanical agitator such as Levy's beaker method (4) or the rotating-basket method (5), the rotating vessel reactor such as the rotating flask (6) or the solubility simulator[1], and the stream reactor such as the column method (7–9).

Several investigators compared the relative agitating intensities or hydrodynamic properties of selected dissolution devices by using a nondisintegrating model tablet (10–12). Bathe *et al.* (3) studied dissolution rates by beaker, rotating-basket, and flow column methods under eight different conditions. However, detailed comparisons of disintegrating tablet dissolution methods have not been made.

In the present study, eight representative dissolution testing methods were compared and evaluated. They can be divided into three categories: (*a*) stirrer-tank reactor type (beaker, rotating basket, and oscillating basket), (*b*) rotating-vessel reactor type (rotating flask and solubility simulator[1]), and (*c*) stream reactor type (column). Disintegrating tablets—21 chloramphenicol (I) brands available in Japan—and nondisintegrating tablets—benzoic acid (II)—were used as markers. The two drugs were selected because of their moderate solubilities in acidic solutions (2–4 mg/ml).

EXPERIMENTAL

Materials—Twenty-one different sugar-coated I tablets were obtained from 16 manufacturers in Japan. Tablets A–E each contained 50 mg of I while Tablets F–U each contained 250 mg of I. A powder of I[2] was included for comparison. Nondisintegrating and uncoated tablets containing 100 mg of II[3] were used.

[1] Sartorius-Membranfilter GmbH, Göttingen, West Germany.
[2] Yamanouchi Pharmaceutical Co., Tokyo, Japan.
[3] Supplied by Dr. Ikeda and Dr. Nishimura, Sankyo Co., Tokyo, Japan.

0022-3549/79/0600-0708$01.00/0

© 1979, American Pharmaceutical Association

Table I—Benzoic Acid Dissolution Rate Constants from Nondisintegrating Tablet under Sink Condition

Method	K_d, mg/min	Relative K_d
a	0.896	1.00
b (in)[a]	0.221	0.25
b (out)[b]	0.288	0.32
c-I (in)	1.012	1.13
c-I (out)	0.294	0.33
c-III (in)	1.132	1.26
c-III (out)	0.500	0.56
d	0.974	1.09
e	0.123	0.14
f	0.339	0.38

[a] Tablet was placed in the basket. [b] Tablet was placed out of the basket.

Dissolution Methods—*Beaker: Method a*—A cylindrical flat-bottom vessel for the disintegration test (JP IX) was used. One liter of the dissolution medium kept at 37° was stirred at 120 rpm with a three-bladed impeller (4.5 × 1.5 cm), which was held 4.5 cm from the vessel bottom. The tablets were placed at the vessel bottom during dissolution.

Rotating Basket: Method b—The test was carried out according to USP XIX specifications at 120 rpm.

Oscillating Basket: Method c—The disintegration test (JP IX) device was used, with the basket-rack assembly attached under three different conditions: (*a*) without the disk (c-I), (*b*) with the disk as specified in JP IX (c-II), and (*c*) with the disk located so that it touched the vessel bottom at the lowest point on the downward stroke (c-III). Tablets were placed into one of six open-ended glass tubes. The medium volume was 1 liter.

Rotating Flask: Method d—A 2-liter round-bottom flask was used as the vessel into which 150 g of glass beads (8-mm diameter) and 75 g of butyl rubber pieces (15 × 15 × 5 mm) were added with 900 ml of the medium. The flask was attached to a device for rotation[4] and immersed into the water bath maintained at 37° at 165° angle against the horizontal axis. The flask rotation speed was 18 rpm. The medium was sampled continuously through steel tubing attached to the flask.

Solubility Simulator: Method e—The thermostated (37°) solubility chamber (100 ml), which contained 170 g of glass beads (8-mm diameter) and 100 ml of the medium, was rotated horizontally at 1.2 rpm. A fixed sample volume was automatically removed from the chamber through a membrane filter at definite intervals. As the sample was taken, an identical fresh dissolution medium volume flowed into the chamber. The sampling volume and interval were set at 2.5 ml and 2.5 min, respectively.

Column: Method f—An ultrafiltration[5] cell with support screens[6] on both ends was used. The membrane filter was not used because the high-speed upward flow of the medium caused the dispersed particles to clog the upper filter. Dissolution medium was circulated through the column at 35 ml/min. The effluent was returned to a sink, which was stirred by the same procedure as in Method a. The total dissolution medium volume was 1 liter.

Rate Determination—Dissolution was determined for a single tablet in each procedure. Except in Method e, the dissolution medium was circulated through a flowcell (5-mm cell length) by a microtube pump[7] at 3.0 ml/min, and the medium absorbance was determined spectrophotometrically at two wavelengths[8]. In Methods a and b, the sampling tubing, with a glass filter at its end, was placed on the side and midheight

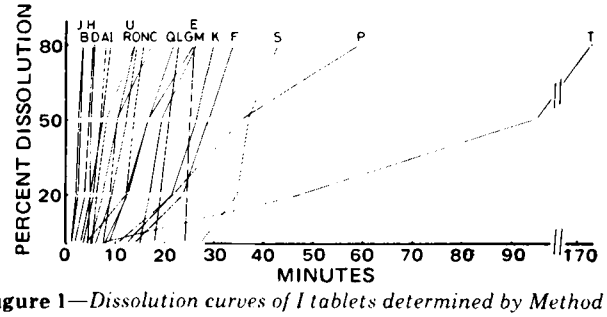

Figure 1—*Dissolution curves of I tablets determined by Method a.*

[4] Japan Servo Co., Tokyo, Japan.
[5] Millipore xx 42 025 00.
[6] Millipore xx 30 025 10.
[7] Tokyo Rikakikai Co., Tokyo, Japan.
[8] Hitachi 156.

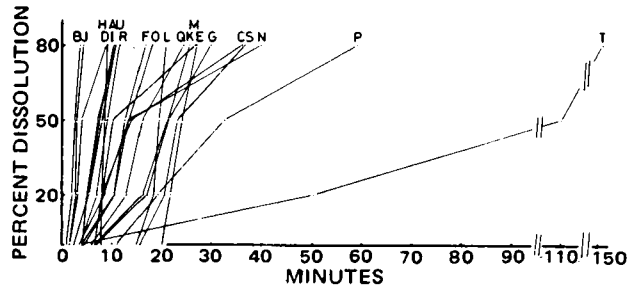

Figure 2—*Dissolution curves of I tablets determined by Method b.*

in the dissolution vessel. In Methods c and d, the filter was attached to the oscillating basket-rack bottom or to the round-bottom flask bottom and immersed into the medium.

In all methods except Method e for I tablets, the asymptotic absorbance was used as the value of 100% dissolution. In Method e, the drug absorbance in the medium removed from the chamber was determined and the cumulative amount dissolved was calculated. The asymptotic value was then substituted as the amount of 100% dissolution.

The I tablet dissolution rates were represented by four parameters: lag time (T_0), T_{20}, T_{50}, and T_{80}, where T_{20}, T_{50}, and T_{80} represent 20, 50, and 80% dissolution times, respectively. In II tablets, the absolute dissolved II amount was determined; the dissolution rate constant (milligrams per minute) was obtained from the slope of the earlier straight line of the dissolution curve. In all experiments, the dissolution medium was simulated gastric fluid without enzymes (JP VIII).

Disintegration and Hardness Measurements—Disintegration measurements were carried out according to JP IX. Hardness was measured by a hardness tester[9]. The disintegration time and hardness values reported are the average values of six tablets.

RESULTS

Dissolution Rate Constant of Nondisintegrating II Tablets—The drug dissolution rate can be represented by the Noyes–Nernst equation (13):

$$J = SK(C_s - C) \qquad \text{(Eq. 1)}$$

where J, S, K, C_s, and C represent the dissolution rate, surface area available to dissolution, dissolution rate constant, solubility, and drug concentration in the medium, respectively. According to the diffusion layer theory (14), the dissolution rate constant is a function of two parameters:

$$K = \frac{D}{h} \qquad \text{(Eq. 2)}$$

where D and h represent the diffusion coefficient and diffusion layer thickness, respectively. When $C_s \gg C$, Eq. 3 is obtained from Eqs. 1 and 2:

$$J = \frac{DS}{h} C_s = K_d \qquad \text{(Eq. 3)}$$

Thus, if the dissolution rate is measured under sink condition, the dissolution process follows apparent zero-order kinetics. When the same nondisintegrating tablet is tested using different dissolution methods, the differences in K_d should reflect only variations in h as a function of the dissolution method because D, S, and C_s are held constant. From

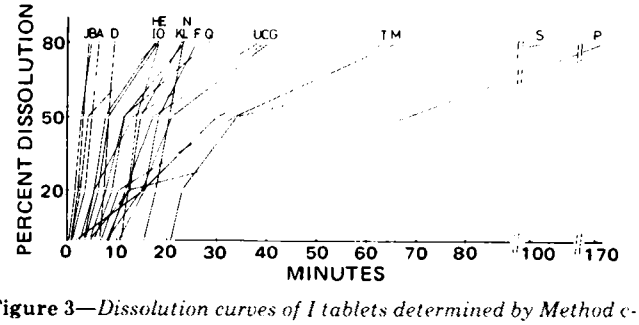

Figure 3—*Dissolution curves of I tablets determined by Method c-I.*

[9] Kiya Seisakusho, Tokyo, Japan.

Table II—Correlation Coefficients between the Dissolution Parameters

Parameter		Disintegration Time	a	b	c-I	c-II	c-III	d	e
Hardness	Lag	0.453	0.367	0.169	0.341	0.407	0.584	0.281	0.330
	T_{20}		0.573[a]	0.461	0.429	0.156	0.426	0.345	0.425
	T_{50}		0.372	0.198	0.197	0.217	0.457	0.274	0.436
	T_{80}		0.242	0.095	0.040	0.100	0.436	0.229	0.456
Disintegration Time	Lag		0.415	0.265	0.507	0.628[a]	0.563[a]	0.514	0.578[a]
	T_{20}		0.367	0.255	0.639[a]	0.738[a]	0.850[a]	0.711[a]	0.678[a]
	T_{50}		0.215	0.100	0.171	0.617[a]	0.900[a]	0.652[a]	0.680[a]
	T_{80}		0.096	0.050	0.006	0.326	0.835[a]	0.594[a]	0.607[a]
a	Lag			0.870[a]	0.796[a]	0.722[a]	0.863[a]	0.872[a]	0.686[a]
	T_{20}			0.911[a]	0.800[a]	0.564[a]	0.583[a]	0.702[a]	0.582[a]
	T_{50}			0.959[a]	0.558[a]	0.783[a]	0.341	0.325	0.421
	T_{80}			0.972[a]	0.405	0.709[a]	0.375	0.203	0.310
b	Lag				0.826[a]	0.693[a]	0.756[a]	0.905[a]	0.606[a]
	T_{20}				0.652[a]	0.416	0.375	0.539[a]	0.542[a]
	T_{50}				0.439	0.705[a]	0.177	0.148	0.382
	T_{80}				0.409	0.694[a]	0.323	0.084	0.315
c-I	Lag					0.823[a]	0.850[a]	0.878[a]	0.685[a]
	T_{20}					0.841[a]	0.861[a]	0.840[a]	0.749[a]
	T_{50}					0.598[a]	0.381	0.089	0.312
	T_{80}					0.681[a]	0.325	0.002	0.119
c-II	Lag						0.880[a]	0.864[a]	0.776[a]
	T_{20}						0.914[a]	0.730[a]	0.663[a]
	T_{50}						0.739[a]	0.565[a]	0.562[a]
	T_{80}						0.629[a]	0.448	0.332
c-III	Lag							0.832[a]	0.652[a]
	T_{20}							0.780[a]	0.730[a]
	T_{50}							0.674[a]	0.660[a]
	T_{80}							0.637[a]	0.595[a]
d	Lag								0.831[a]
	T_{20}								0.679[a]
	T_{50}								0.336
	T_{80}								0.208

[a] Significant ($p < 0.05$).

these considerations, the zero-order dissolution rate constant emerges as the parameter reflecting the relative dissolution method agitation intensity. Table I shows the II dissolution rate constants. The relative values were normalized against the value obtained by Method a.

I Tablet Dissolution—Figures 1–7 show the dissolution curves measured by Methods a–e. The curves were constructed by linking the four points used for further treatment: lag time, T_{20}, T_{50}, and T_{80}.

The I dissolution rates were compared pairwise. Correlation coefficients are reported in Table II. Significant correlations ($p < 0.05$) for all four parameters were found for Method a *versus* b and c-II, b *versus* a, c-I *versus* c-II, c-III *versus* c-II, d and e, and disintegration time *versus* c-III and e. The I tablet disintegration and hardness values are listed in Table III.

Table III—Disintegration Times and Hardness of Chloramphenicol Tablets

Tablet	Disintegration Time, min	Hardness, kg
A	9.2	9.9
B	4.4	13.1
C	10.2	5.9
D	4.2	14.8
E	5.5	10.6
F	16.9	14.0
G	14.5	>20[a]
H	5.9	11.1
I	7.9	>20
J	2.5	5.8
K	18.6	16.4
L	19.2	16.6
M	5.5	16.4
N	9.7	16.0
O	12.7	>20
P	7.8	11.7
Q	12.2	>20
R	7.9	13.9
S	13.4	>20
T	7.8	>20
U	3.4	10.7

[a] More than 20 kg.

Interpretation of Lag Time—The dissolution lag time was the time required for the mechanical destruction of the coated tablet film. Thus, a shorter lag time represents a stronger destructive force. Significant correlations among the seven dissolution methods were observed regarding lag time (Table II). Except for the pairwise comparisons involving Method e, the least-squares regression lines passed through the origin. In these cases, the regression line slope obtained with lag time apparently reflected the relative destructive force intensity to the coated tablet film. Table IV shows the regression line slopes calculated for all combinations except those involving Method e. Thus, a slope of 1.64 for Method a *versus* b indicated that Method b gave 1.64 times the destructive force of a.

DISCUSSION

Agitating Intensity—The K_d values from nondisintegrating tablets (Table I) reasonably reflected the relative agitation intensities produced by the different dissolution methods. Method d had the lowest agitating intensity, and Method c-III (in) had the highest among the methods tested. Methods c-III, d, and e gave relatively sharp sigmoidal dissolution curves for all tablets, while Methods a, b, c-I, and c-II gave sigmoidal curves with smaller slopes, especially after 50% dissolution. Although Method e produced the mildest intensity, it gave comparatively sharp dissolution curves (Fig. 6). This finding suggests that the agitating intensity, as represented by the II dissolution rate from a nondisintegrating tablet, was not the rate-determining factor for disintegrating tablets.

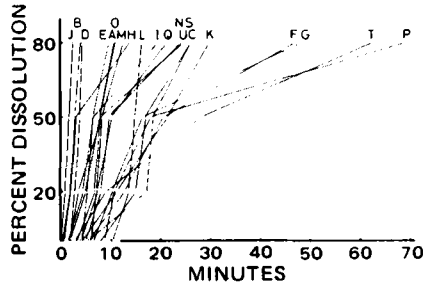

Figure 4—*Dissolution curves of I tablets determined by Method c-II.*

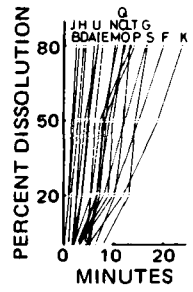

Figure 5—*Dissolution curves of I tablets determined by Method c-III.*

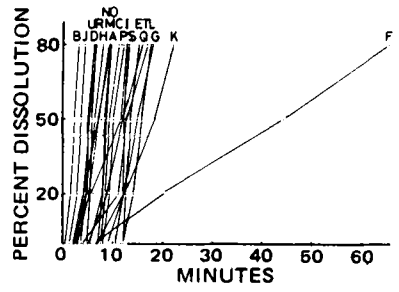

Figure 6—*Dissolution curves of I tablets determined by Method d.*

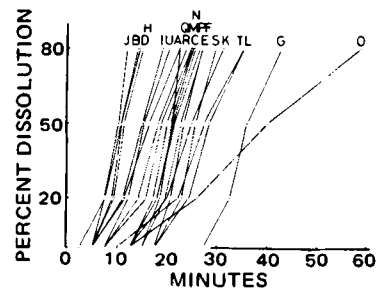

Figure 7—*Dissolution curves of I tablets determined by Method e.*

Because Method e used a rotating-vessel type reactor, "mound" formation of particles was prevented in spite of mild agitating intensity.

Tablets T and P showed very slow dissolution rates as determined by Methods a, b, c-I, and c-II but faster rates with Methods c-III, d, and e. The dispersing intensity was highly dependent on the stirring mode. Methods a, b, and c (the stirred-tank reaction type) could not prevent mound formation. On the other hand, the rotating-vessel devices, such as Methods d and e, generated high dispersing intensity in spite of low rotation speed, perhaps because of the unique stirring method.

Destructive Intensity to Coated I Tablet Films—The destructive intensity followed the descending order Method c-III ≥ c-II > d ≥ c-I > b > a (Table IV). Method e was not included in the comparison because of the inaccuracy in the lag time determination due to discontinuous sampling.

Correlation of I Tablet Dissolution Rates—Correlations between hardness and dissolution rates with all four rate parameters (lag time, T_{20}, T_{50}, and T_{80}) were insignificant statistically (Table II). Dissolution rate prediction from hardness is, therefore, impossible in this case. These results differ from those reported for other drugs (15, 16).

The relation among the methods is schematically represented in Scheme I. In this scheme, any two methods having a significant correlation for all four rate parameters were connected with a solid line. The results suggested two conclusions:

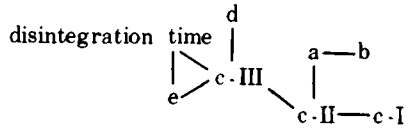

Scheme I—Relation among the methods of dissolution

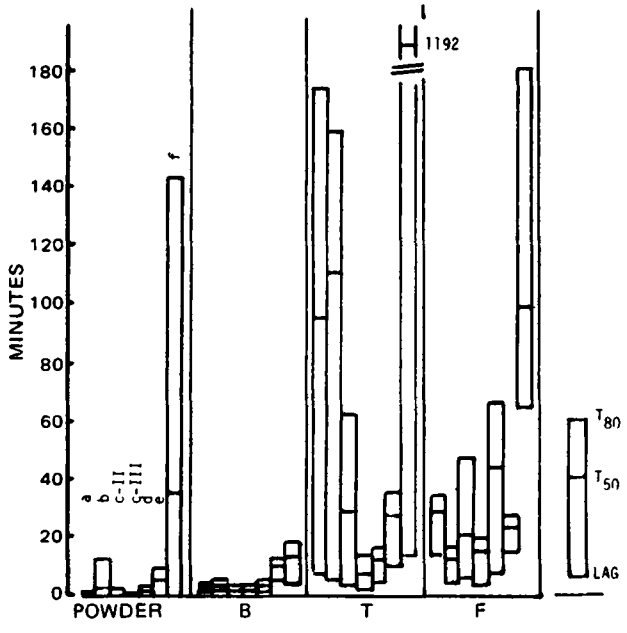

Figure 8—*Schematic representation of the dissolution rates of four samples determined by Method f and other methods.*

Table IV—Regression Line Slope Resulting from Pairwise Comparison of Lag Time Obtained with Different Dissolution Methods

	x-Axis					
y-Axis	a	b	c-I	c-II	c-III	d
a	1.0	1.64	2.50	4.55	3.70	2.00
b	—	1.0	1.61	3.23	2.56	1.20
c-I	—	—	1.0	1.49	2.13	1.32
c-II	—	—	—	1.0	1.20	0.71
c-III	—	—	—	—	1.0	0.50
d	—	—	—	—	—	1.0
Average relative intensity	1.0	1.56	2.33	4.01	4.40	2.40

1. Two different device types were distinguishable: stirred-tank reactors and rotating-vessel reactors. Only Method c-III correlated with both groups.

2. Among similar devices, a significant correlation was not observed among all methods. Thus, dissolution methods are not interchangeable, even if they belong to the same group.

Dissolution Rates Using Method f—Method f was inadequate for disintegrating tablet evaluation due to filter clogging. To avoid this problem, experiments were carried out without the filter. The modified device was similar in nature to that used in Method a for well-dispersed tablets since most disintegrated particles were returned to the impeller-stirred vessel. For poorly dispersed tablets, however, the dissolution rate may be evaluated more accurately with Method f because the drug remained longer in the column. Thus, despite the clogging defect, Method f was used for selected dissolution tests.

Figure 8 shows the dissolution rates of four I samples, *i.e.*, the powder and three commercial tablets, as determined by different methods. Surprisingly, the powder took much longer to dissolve using Method f than with the other methods. This result might have occurred because of the small agitating intensity produced by Method f (Table I) or because the laminar flow produced much less dispersing ability than that achieved with turbulent flow in the other methods. The dissolution lag times observed with Method f were generally longer than those obtained with other methods. This finding suggests that the Method f destructive force to coated film was far less than that of other methods. These data indicate that Method f is suitable for testing the intrinsic dissolution rate of a nondisintegrating drug matrix because of its controlled hydrodynamic flow but is unsuitable for evaluating the drug dissolution rate from disintegrating tablets and capsules.

REFERENCES

(1) J. Swarbrick, "Current Concepts in the Pharmaceutical Sciences: Biopharmaceutics," Lea & Febiger, Philadelphia, Pa., 1970, p. 265.

(2) W. H. Barr, *Pharmacology*, **8**, 55 (1972).

(3) R. V. Bathe, O. Hafliger, F. Langenbucher, and D. Schonleber, *Pharm. Acta Helv.*, **50**, 3 (1975).

(4) G. Levy and B. A. Hayes, *N. Engl. J. Med.*, **262**, 1053 (1960).

(5) "The United States Pharmacopeia," 19th rev., Mack Publishing Co., Easton, Pa., 1975.

(6) M. Gibaldi and H. Weintraub, *J. Pharm. Sci.*, **59**, 725 (1970).

(7) D. G. Baun and G. C. Walker, *ibid.*, **58**, 611 (1969).

(8) J. E. Tingstad and S. Riegelman, *ibid.*, **59**, 692 (1970).

(9) O. Umezawa and S. Yamamoto, *J. Nippon Hosp. Pharm. Assoc.*, **2**, 73 (1976).

(10) J. Tingstad, E. Gropper, L. Lachman, and E. Shami, *J. Pharm. Sci.*, **63**, 925 (1974).
(11) F. L. Underwood and D. E. Cadwallader, *ibid.*, **65**, 697 (1976).
(12) M. Ikeda and K. Nishimura, "Abstract 91st Annual Meeting of the Pharmaceutical Society of Japan," Fukuoka, Japan, Apr. 1971, p. 323.
(13) A. Noyes and J. Whitney, *J. Am. Chem. Soc.*, **19**, 930 (1897).
(14) W. Nernst, *Z. Phys. Chem.*, **47**, 52 (1904).
(15) S. Kitazawa, I. Johno, Y. Ito, S. Teramura, and J. Okada, *J. Pharm. Pharmacol.*, **27**, 765 (1975).
(16) T. Higuchi, R. A. Narsimha, L. W. Busse, and J. V. Swintosky, *J. Am. Pharm. Assoc., Sci. Ed.*, **42**, 194 (1953).

ACKNOWLEDGMENTS

The authors thank Dr. H.-L. Fung, State University of New York at Buffalo, for discussions.

Dissolution Systems for Chloramphenicol Tablet Bioavailability

HIROYASU OGATA ˣ, TOSHIO SHIBAZAKI, TETSUO INOUE, and AKIRA EJIMA

Received April 25, 1978, from the *Division of Drug, National Institute of Hygienic Sciences, 1-18-1, Kamiyoga Setagaya-ku, Tokyo, Japan.* Accepted for publication November 17, 1978.

Abstract □ The relationship between chloramphenicol (I) tablet bioavailability and *in vitro* dissolution rates was examined. The effect of solid food on the I tablet and powder bioavailability was also studied. Five tablets of I were selected for bioavailability testing on the basis of the dissolution rates of 18 I tablets (250 mg) determined by several methods. Compound I, 500 mg, was administered orally to five subjects, following overnight fasting, according to a crossover design. The bioavailability parameters were obtained from urinary I excretion. Among the five formulations studied, only one tablet (F) showed significantly poorer bioavailability. The dissolution rates at pH 1.2 did not give the same rank order as the bioavailability. The dissolution rate of Tablet F showed remarkable pH dependency. The dissolution rates at pH 4 showed good correlation with *in vivo* bioavailability data. The bioavailability of I powder was not affected by solid food. Tablet F, which had poor bioavailability in the fasting state, showed good bioavailability when administered just after the standard breakfast.

Keyphrases □ Chloramphenicol—various dosage forms, bioavailability correlated with dissolution rates □ Bioavailability—chloramphenicol, various dosage forms, correlated with dissolution rates □ Dissolution rates—chloramphenicol, various dosage forms, correlated with bioavailability □ Antibacterials—chloramphenicol, various dosage forms, bioavailability correlated with dissolution rates

The dissolution rates of 21 chloramphenicol (I) tablets manufactured in Japan were reported previously (1). In this paper, the *in vivo* bioavailability of selected I tablets was correlated with *in vitro* dissolution tests. The bioavailability of nine different I tablets available in Japan was determined previously by Watanabe *et al.* (2, 3), who showed significant correlation of *in vivo* bioavailability with disintegration time and dissolution rate as measured by a disintegration apparatus[1] using water as the medium.

The dissolution devices used in that study (beaker, rotating basket, oscillating basket, and disintegration[1] methods) all belonged to the stirred-tank reactor type (1). *In vivo–in vitro* correlation with rotating-flask type dissolution devices was not attempted. These investigators (2, 3) also reported better correlation of *in vitro* dissolution rate and *AUC* (area under plasma level–time curve) following oral administration of I tablets with water as the dissolution medium instead of the pH 1.2 solution recommended in JP IX. Chloramphenicol dissolution in an unbuffered medium could have complicated the system since the pH value changed as the tablet dissolved.

Comparative bioavailability studies of five I tablets are described in this report. These tablets were selected based on dissolution rates of 18 I tablets (250 mg) and I powder determined by seven methods (1). The relationship between *in vivo* bioavailability and *in vitro* dissolution was examined. The effect of food on the I bioavailability was also studied.

EXPERIMENTAL

Materials—The I tablets and powder were the same as those described previously (1), except for Tablets V and V′ which were of the same brand but different lot numbers.

***In Vitro* Studies**—The methods and procedures for determining the dissolution rate were the same as those reported previously (1): beaker (a), rotating basket (b), oscillating basket (c-II and c-III), rotating flask (d), solubility simulator (e)[2], and column (f). The dissolution medium pH was controlled by a pH stat. No corrections were made for acidic dissolution media adjusted at pH 1.2.

Bioavailability Studies—Six healthy adult male volunteers, 55–72 kg and 29–49 years old, participated after being informed about the study and the drug. All subjects received no barbiturates or other enzyme-inducing agents for 30 days before and for the duration of the studies. They also received no other medication or alcoholic beverages for 7 days before and for the duration of the studies.

Study I—The bioavailability of five I tablets was studied using a Latin square. Treatments were separated by 1 week. Subjects fasted for 10 hr prior to dosing and took two I tablets (total of 500 mg) with 300 ml of water. They took 200 ml of water at 2 hr and had lunch at 4 hr after administration. Urine samples were collected at 0, 0.5, 1, 1.5, 2, 3, 4, 5, 6, 8, 12, 16, 24, and 28 hr after dosing. The exact sampling times and the volume were recorded.

Study II—The effect of solid food on Tablet F and I powder bioavailability was studied with four subjects using a Latin square. Tablet F or I powder (500 mg) was taken either with 300 ml of water in the fasting state or immediately after a standard breakfast of 100 g of toast, 20 g of butter, 35 g of cucumber, 65 g of boiled egg, 200 ml of milk, and 100 ml of water. The urine collection procedure was the same as that for Study I.

Study III—One subject participated in a study of the relationship

[1] Erweka.

[2] Sartorius-Membranfilter GmbH, Göttingen, West Germany.

0022-3549/79/0600-0712$01.00/0
© 1979, American Pharmaceutical Association

(10) J. Tingstad, E. Gropper, L. Lachman, and E. Shami, *J. Pharm. Sci.*, **63**, 925 (1974).
(11) F. L. Underwood and D. E. Cadwallader, *ibid.*, **65**, 697 (1976).
(12) M. Ikeda and K. Nishimura, "Abstract 91st Annual Meeting of the Pharmaceutical Society of Japan," Fukuoka, Japan, Apr. 1971, p. 323.
(13) A. Noyes and J. Whitney, *J. Am. Chem. Soc.*, **19**, 930 (1897).
(14) W. Nernst, *Z. Phys. Chem.*, **47**, 52 (1904).
(15) S. Kitazawa, I. Johno, Y. Ito, S. Teramura, and J. Okada, *J. Pharm. Pharmacol.*, **27**, 765 (1975).
(16) T. Higuchi, R. A. Narsimha, L. W. Busse, and J. V. Swintosky, *J. Am. Pharm. Assoc., Sci. Ed.*, **42**, 194 (1953).

ACKNOWLEDGMENTS

The authors thank Dr. H.-L. Fung, State University of New York at Buffalo, for discussions.

Dissolution Systems for Chloramphenicol Tablet Bioavailability

HIROYASU OGATA ˣ, TOSHIO SHIBAZAKI, TETSUO INOUE, and AKIRA EJIMA

Received April 25, 1978, from the *Division of Drug, National Institute of Hygienic Sciences, 1-18-1, Kamiyoga Setagaya-ku, Tokyo, Japan.* Accepted for publication November 17, 1978.

Abstract □ The relationship between chloramphenicol (I) tablet bioavailability and *in vitro* dissolution rates was examined. The effect of solid food on the I tablet and powder bioavailability was also studied. Five tablets of I were selected for bioavailability testing on the basis of the dissolution rates of 18 I tablets (250 mg) determined by several methods. Compound I, 500 mg, was administered orally to five subjects, following overnight fasting, according to a crossover design. The bioavailability parameters were obtained from urinary I excretion. Among the five formulations studied, only one tablet (F) showed significantly poorer bioavailability. The dissolution rates at pH 1.2 did not give the same rank order as the bioavailability. The dissolution rate of Tablet F showed remarkable pH dependency. The dissolution rates at pH 4 showed good correlation with *in vivo* bioavailability data. The bioavailability of I powder was not affected by solid food. Tablet F, which had poor bioavailability in the fasting state, showed good bioavailability when administered just after the standard breakfast.

Keyphrases □ Chloramphenicol—various dosage forms, bioavailability correlated with dissolution rates □ Bioavailability—chloramphenicol, various dosage forms, correlated with dissolution rates □ Dissolution rates—chloramphenicol, various dosage forms, correlated with bioavailability □ Antibacterials—chloramphenicol, various dosage forms, bioavailability correlated with dissolution rates

The dissolution rates of 21 chloramphenicol (I) tablets manufactured in Japan were reported previously (1). In this paper, the *in vivo* bioavailability of selected I tablets was correlated with *in vitro* dissolution tests. The bioavailability of nine different I tablets available in Japan was determined previously by Watanabe *et al.* (2, 3), who showed significant correlation of *in vivo* bioavailability with disintegration time and dissolution rate as measured by a disintegration apparatus[1] using water as the medium.

The dissolution devices used in that study (beaker, rotating basket, oscillating basket, and disintegration[1] methods) all belonged to the stirred-tank reactor type (1). *In vivo–in vitro* correlation with rotating-flask type dissolution devices was not attempted. These investigators (2, 3) also reported better correlation of *in vitro* dissolution rate and *AUC* (area under plasma level–time curve) following oral administration of I tablets with water as the dissolution medium instead of the pH 1.2 solution recommended in JP IX. Chloramphenicol dissolution in an unbuffered medium could have complicated the system since the pH value changed as the tablet dissolved.

Comparative bioavailability studies of five I tablets are described in this report. These tablets were selected based on dissolution rates of 18 I tablets (250 mg) and I powder determined by seven methods (1). The relationship between *in vivo* bioavailability and *in vitro* dissolution was examined. The effect of food on the I bioavailability was also studied.

EXPERIMENTAL

Materials—The I tablets and powder were the same as those described previously (1), except for Tablets V and V′ which were of the same brand but different lot numbers.

***In Vitro* Studies**—The methods and procedures for determining the dissolution rate were the same as those reported previously (1): beaker (a), rotating basket (b), oscillating basket (c-II and c-III), rotating flask (d), solubility simulator (e)[2], and column (f). The dissolution medium pH was controlled by a pH stat. No corrections were made for acidic dissolution media adjusted at pH 1.2.

Bioavailability Studies—Six healthy adult male volunteers, 55–72 kg and 29–49 years old, participated after being informed about the study and the drug. All subjects received no barbiturates or other enzyme-inducing agents for 30 days before and for the duration of the studies. They also received no other medication or alcoholic beverages for 7 days before and for the duration of the studies.

Study I—The bioavailability of five I tablets was studied using a Latin square. Treatments were separated by 1 week. Subjects fasted for 10 hr prior to dosing and took two I tablets (total of 500 mg) with 300 ml of water. They took 200 ml of water at 2 hr and had lunch at 4 hr after administration. Urine samples were collected at 0, 0.5, 1, 1.5, 2, 3, 4, 5, 6, 8, 12, 16, 24, and 28 hr after dosing. The exact sampling times and the volume were recorded.

Study II—The effect of solid food on Tablet F and I powder bioavailability was studied with four subjects using a Latin square. Tablet F or I powder (500 mg) was taken either with 300 ml of water in the fasting state or immediately after a standard breakfast of 100 g of toast, 20 g of butter, 35 g of cucumber, 65 g of boiled egg, 200 ml of milk, and 100 ml of water. The urine collection procedure was the same as that for Study I.

Study III—One subject participated in a study of the relationship

[1] Erweka.

[2] Sartorius-Membranfilter GmbH, Göttingen, West Germany.

0022-3549/79/0600-0712$01.00/0
© 1979, American Pharmaceutical Association

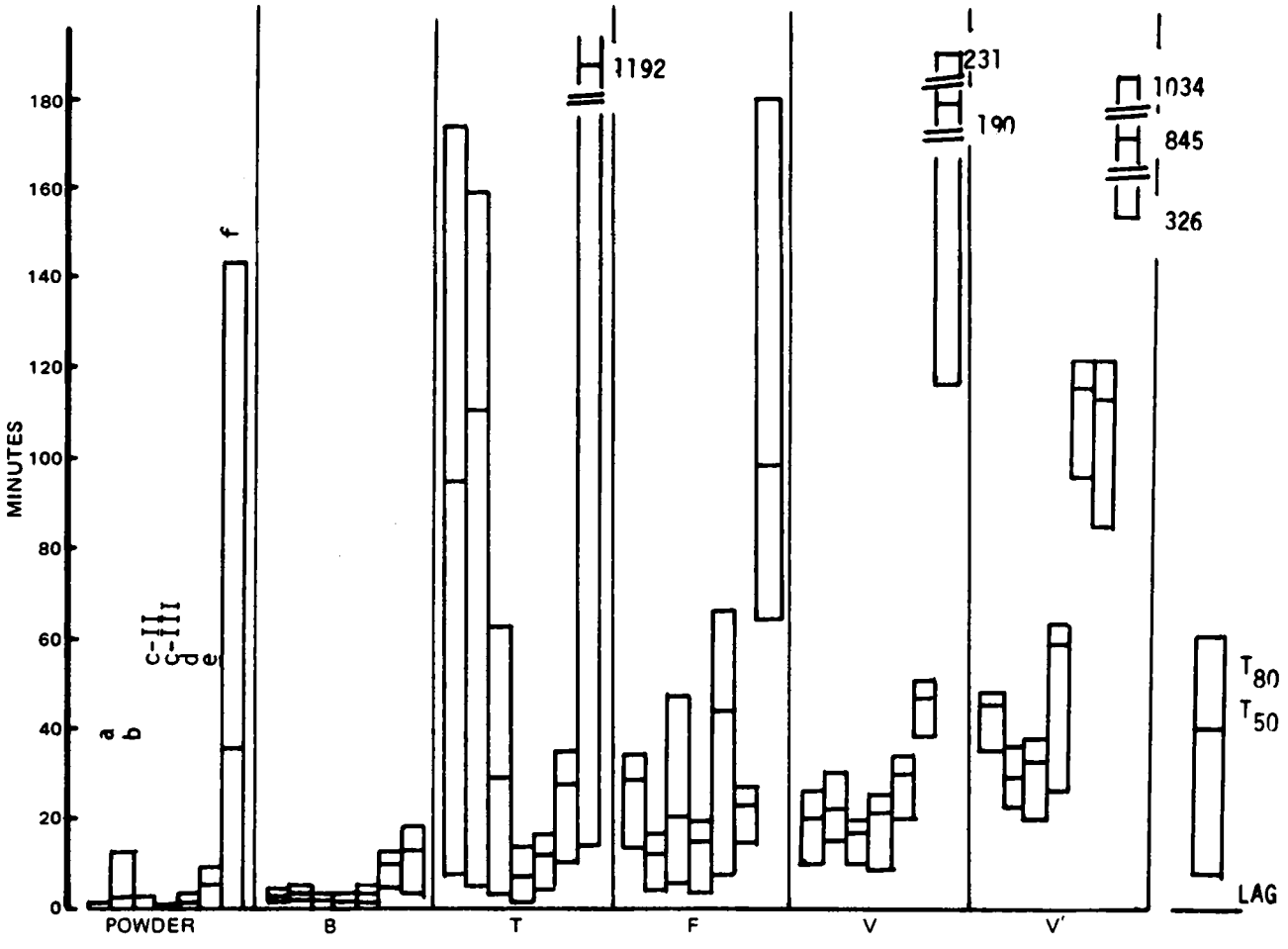

Figure 1—*Dissolution rates of six I formulations.*

between urinary recovery and dose. Oral I doses of 155, 250, and 500 mg of powder were given according to the protocol described for Study I.

Assay—Unchanged and total urine nitro I compounds were determined by colorimetry as described by Maruyama and Suzuki (4) with slight modifications.

Total Nitro I Compounds—Urine, 1 ml, was diluted to 100 ml with water, and 4 ml of 0.25 *N* NaOH and 0.3 ml of 2% $Na_2S_2O_4$ were added to 1 ml of the solution and mixed well. After the solution stood for 15 min at room temperature, 0.5 ml of 2.5% $NaNO_2$ and 1.0 ml of 4 *N* HCl were added and mixed well. After 5 min, 0.5 ml of 5% sulfamic acid was added; the solution was shaken and allowed to stand for 5 min. Then 0.5 ml of 0.5% Tsuda's reagent solution was added, and the mixture was allowed to stand for 90 min at 37°. The solution absorbance was determined spectrophotometrically[3] at 650 and 560 nm.

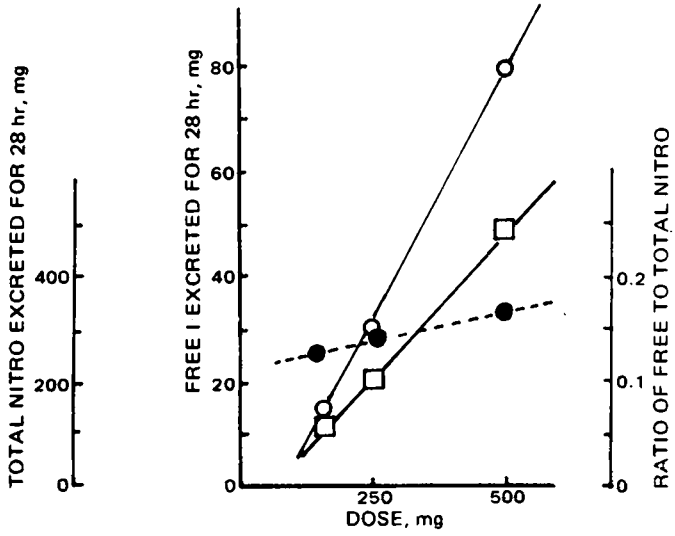

Figure 2—*Dose dependency of urinary excretion of free and total nitro following oral I powder administration. Key:* ○, *free I;* □, *total nitro compounds; and* ●, *ratio of free to total nitro.*

Unchanged I—An aliquot of urine was diluted 20 times with water, 4 ml of pH 6.0 phosphate buffer (0.2 *M*) and 12 ml of ethyl acetate were added to 2 ml of the solution, and the solution was shaken for 10 min mechanically. After centrifugation, the aqueous layer was removed and 10 ml of fresh phosphate buffer (pH 6.0) was added. The mixture was shaken for 10 min and centrifuged. Ten milliliters of the organic layer was evaporated to dryness under reduced pressure in a boiling water bath. Water (4.5 ml) was added, and the solution was heated for 5 min to dissolve I completely. After the solution cooled, 0.5 ml of 1.0 *N* NaOH and 0.3 ml of 2% $Na_2S_2O_4$ were added. The assay then followed the procedure described for total nitro compounds.

Aqueous solutions of 2% $Na_2S_2O_4$ and 2.5% $NaNO_2$ were prepared just prior to addition. The absorbance due to the urine composition was almost constant and very small in comparison with other colorimetric methods (5, 6). The urine sample collected just prior to dosing could be used as the urine blank with very slight error.

RESULTS AND DISCUSSION

***In Vitro* Studies**—Figure 1 shows the relative dissolution rates of the five I tablets and powder as reflected by lag time, time for 50% dissolution (T_{50}), and time for 80% dissolution (T_{80}). Each formulation showed a distinguishing dissolution rate profile. Tablet B had very fast dissolution rates by all seven methods. The powder dissolution behavior was similar to that of Tablet B in all dissolution methods except Method f. Tablet T showed especially slow dissolution rates in Methods a, b, and f, which have poor dispersing intensity (1).

The Tablet T dissolution lag time was small. Tablet V' appeared to

[3] Hitachi 156.

Table I—Mean Chloramphenicol Bioavailability Parameters from the Five Formulations

Parameter[a]	Formulation B	T	F	V	V′	Results of ANOVA	Tukey's Allowable Difference
Excretion lag time, hr	0.2[b]	0.4	5.2	1.2	1.4	$p < 0.05$	B < T < V < V′ < F[c]
Maximum urinary excretion rate, mg/hr	15.42	14.34	3.44	14.24	13.64	$p < 0.05$	B > T > V > V′ > F
Time of maximum urinary excretion rate, hr	1.46	2.30	15.45	2.15	2.50	$p < 0.05$	B < V < T < V′ < F
Cumulative amount excreted in urine for 28 hr, mg	77.12	73.36	41.76	78.12	71.34	$p < 0.05$	V > B > T > V′ > F
Ratio of free to total nitro excreted for 28 hr	0.159	0.164	0.156	0.159	0.152	NS[d]	

[a] Obtained from the urinary excretion of unchanged compound. [b] Mean of five subjects. [c] Formulations not underscored by the same line differ significantly in their mean values for the parameter ($p < 0.05$). [d] Not significant ($p > 0.05$).

Table II—Chloramphenicol Dissolution Rates in Two Different Media

Formulation	Time of 50% Dissolution, min Method d SJ[a]	Method d DW[b]	Method c-III SJ	Method c-III DW
Powder	1.1	1.5	0.3	1.0
Tablet B	3.6	4.2	1.6	3.2
Tablet T	12.6	10.9	7.3	12.6
Tablet F	44.4	>1140	15.0	114.0
Tablet V	29.0	170.0	21.1	34.5
Tablet V′	116.0	1022.0	59.5	49.4

[a] Simulated gastric juice without enzyme, pH 1.2. [b] Distilled water.

have a strongly coated film; its lag time was very long, but dissolution after the lag time was comparatively fast. The rotating vessel reactor dissolution methods (d and e) showed especially poor destructive intensity against Tablet V′. Tablet V showed fast dissolution after the lag time by all methods except Method f. Tablet F showed especially poor dissolution by Method d but comparatively good dissolution by other methods.

Dose Dependency of I Urinary Excretion—Figure 2 shows the relationship between dose and the cumulative amount excreted in 28 hr following oral administration of I powder in one subject (Study III). The excreted free and total nitro I compounds were proportional to the dose administered, but the ratio of free to total nitro compounds increased slightly with dose from 0.128 to 0.162. This result suggested that urinary I excretion in humans can be treated by linear pharmacokinetics within the dose range studied.

Bioavailability—The bioavailability parameters following five different treatments are summarized in Table I. Based on ANOVA (analysis of variance), statistically significant differences were found among the treatments in all parameters except the ratio of free to total nitro I compounds. Tablet F showed significant differences from the other tablets in all parameters except the ratio of free to total nitro compounds excreted. Tablet F showed an excretion lag time of about 5 hr. This tablet took the longest time to reach the maximum excretion rate, which was also the smallest value among the treatments. The total amount excreted in 28 hr after dosing with Tablet F was about one-half of the amount excreted after the other tablets. The poor Tablet F bioavailability, however, appeared not to be due to *in vitro* dissolution rates (Fig. 1).

All dissolution tests in Fig. 1 were carried out at pH 1.2. The *in vitro* dissolution was reexamined using water as the dissolution medium as suggested by Watanabe *et al.* (3).

Table II showed that, with Method d, the Tablet F dissolution rate in water was remarkably slower than that determined at pH 1.2, as were the dissolution rates of Tablets V and V′. With Method c-III, only Tablet F showed a slower dissolution. With water as the dissolution medium, the pH changed as dissolution progressed; the change was dependent on the formulation.

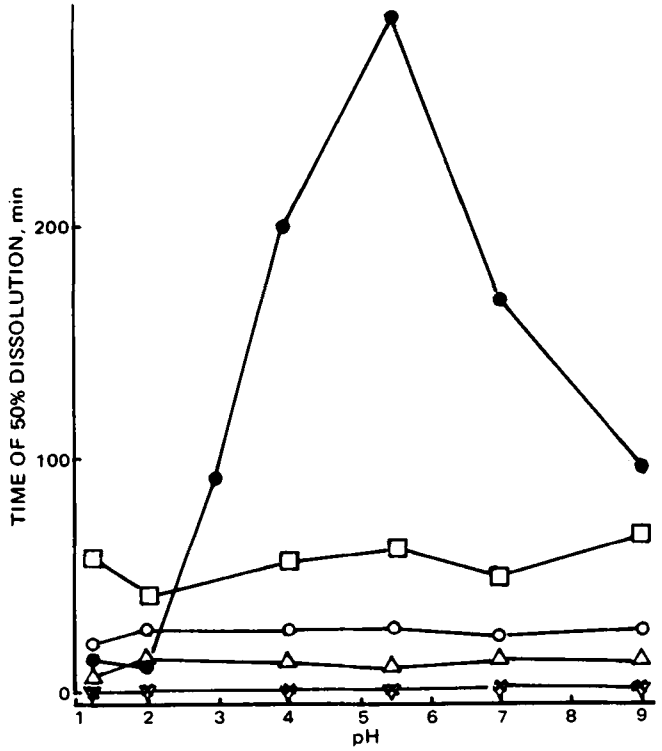

Figure 3—*Effect of pH on time of 50% I formulation dissolution. Key:* ▽, *powder;* ×, *Tablet B;* △, *Tablet T;* ●, *Tablet F;* ○, *Tablet V; and* □, *Tablet V′.*

Figure 3 represents the dissolution rates determined by Method c-III when the medium pH was controlled *via* pH stat. Tablet F was the only tablet whose dissolution showed a remarkable pH dependency. Since the powder dissolution rate was not a function of pH, the pH dependency shown by Tablet F might have been caused by the white shellac tablet coating.

Figure 4 shows the relationship between *in vivo* bioavailability and *in vitro* dissolution of the five tablets tested. The *in vitro* dissolution rates were determined by Method c-III at pH 4.0. From Fig. 4, there appeared to be a critical dissolution rate point distinguishing the equivalent from

Table III—Effect of Food on Chloramphenicol Powder and Tablet F Bioavailabilities

Parameter[a]	Powder Fasting	Powder Nonfasting	Powder Paired *t* Test	Tablet F Fasting	Tablet F Nonfasting	Tablet F Paired *t* Test
Excretion lag time, hr	0.13[b]	0.50	NS[c]	5.20	2.60	NS
Maximum urinary excretion rate, mg/hr	15.00	15.15	NS	3.44	14.95	$p < 0.025$
Time of maximum urinary excretion rate, hr	1.63	2.53	NS	15.45	4.06	$p < 0.025$
Cumulative amount excreted for 28 hr, mg	76.73	89.55	NS	41.76	82.85	$p < 0.05$

[a] Obtained from the urinary excretion of unchanged compound. [b] Mean of four subjects. [c] Not significant ($p > 0.05$).

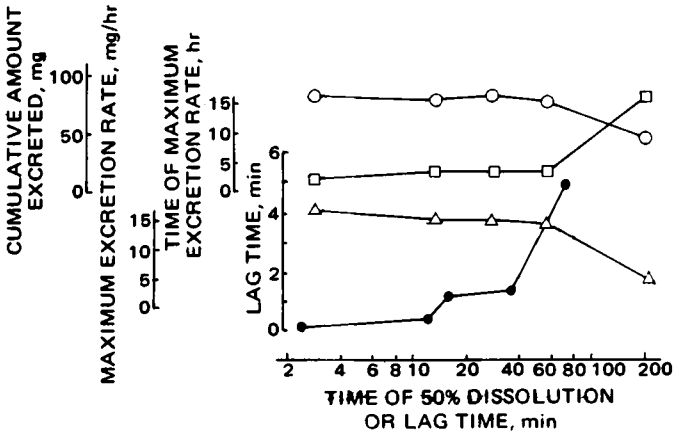

Figure 4—*Correlation of* in vitro *parameters (time of 50% dissolution and lag time) with urinary excretion* in vivo. *Key:* ●, *urinary excretion lag time;* △, *maximum urinary excretion rate;* □, *time of maximum urinary excretion rate; and* ○, *cumulative amount excreted in urine for 28 hr. These values were estimated by means of the urinary excretion of unchanged compound.*

the nonequivalent tablets. Since only one tablet was detected as nonequivalent in this study, the critical point could not be determined clearly. However, an approximate critical T_{50} point appeared to be more than 50 min. The critical value occurred surprisingly late, even though the *in vitro* rates were determined by the dissolution method that had the most vigorous agitating, dispersing, and destructive intensities among the seven methods studied.

Effect of Food on Bioavailability—The relative bioavailability of the powder and Tablet F was studied under fasting and nonfasting conditions. Table III shows the bioavailability parameters compared by the paired t test. The powder showed equivalent bioavailability with the tablets, except for Tablet F under fasting condition, and did not show any bioavailability difference between fasting and nonfasting states. Tablet F, which had poor bioavailability after fasting, became equivalent in bioavailability with the other formulations when it was administered just after the standard breakfast. Possibly, the more violent movement of the tablet in the GI tract after food might have increased drug absorption.

CONCLUSIONS

Film-coated I tablet absorption in humans is related to dissolution. The dissolution device that correlated well with bioavailability was one with a comparatively violent destructive force for the coated tablet film and high test medium agitation. The test medium pH must also be considered because dissolution of certain tablet coatings was pH dependent.

REFERENCES

(1) H. Ogata, T. Shibazaki, T. Inoue, and A. Ejima, *J. Pharm. Sci.*, **68**, 708 (1979).

(2) Y. Watanabe, T. Nagai, Y. Tanaka, and K. Motohashi, *Yakugaku Zasshi*, **95**, 599 (1975).

(3) Y. Watanabe, K. Motohashi, Y. Mitsui, R. Yoneda, and Y. Tanaka, *ibid.*, **96**, 1468 (1976).

(4) M. Maruyama and Y. Suzuki, *Takamine Kenkyusho Nempo*, **10**, 158 (1958).

(5) M. Yamazaki, S. Shigeo, and A. Kamada, *Yakuzaigaku*, **34**, 97 (1974).

(6) K. Kakemi and S. Ohashi, *Yakugaku Zasshi*, **82**, 338 (1962).

ACKNOWLEDGMENTS

The authors thank Dr. Y. Watanabe, Tokyo National Chest Hospital, and Dr. H.-L. Fung, State University of New York at Buffalo, for suggestions and discussions.

Antitumor Agents: Structure–Activity Relationships in Tenulin Series

THOMAS G. WADDELL *x, ANNE-MARIE AUSTIN *, JANICE W. COCHRAN *, KARL G. GERHART *, IRIS H. HALL ‡, and K. H. LEE ‡

Received May 25, 1978, from the **Department of Chemistry, University of Tennessee at Chattanooga, Chattanooga, TN 37401*, and the ‡*Department of Medicinal Chemistry, School of Pharmacy, University of North Carolina, Chapel Hill, NC 27514.* Accepted for publication November 21, 1978.

Abstract □ Systematic structural modifications were performed on the natural sesquiterpene lactone tenulin to define those groupings essential to, or significant in, its *in vivo* antitumor activity. Accordingly, the following tenulin analogs were prepared: dihydrotenulin, 2,3-epoxytenulin, isotenulin, dihydroisotenulin, 2,3-epoxyisotenulin, and tetrahydrodeacetylisotenulin. Both the cyclopentenone and the hemiketal units in tenulin were necessary for high *in vivo* activity.

Keyphrases □ Tenulin—antineoplastic activity, structure-activity relationships, *in vivo* study □ Antineoplastic activity—tenulin, structure-activity relationships, *in vivo study*

The sesquiterpene lactone tenulin (I) is a major bitter principle in several species of the plant genus *Helenium* (Family Compositae) (1–6). High *in vivo* tenulin antitumor activity toward the Ehrlich ascites and Walker 256 carcinosarcoma screens and, to a lesser extent, toward P-388 leukemia has been demonstrated (7, 8). The tenulin cyclopentenone unit may act as a Michael acceptor in cellular enzyme essential sulfhydryl group alkylation.

Tenulin forms a Michael addition product with L-cysteine to give the zwitterionic compound II (7, 8). The adduct II, containing the cyclopentanone group, showed 84% activity loss toward the Ehrlich ascites screen, suggesting that a cyclopentenone unit is important for high activity. Low II activity also might be the result of lower solubility in lipid membranes.

In the present study, the tenulin structure was modified in ways not significantly affecting drug transport. This structure–*in vivo* antitumor activity work reveals those tenulin features necessary for high activity.

RESULTS AND DISCUSSION

Chemistry—Tenulin (I), isolated after extraction of *Helenium amarum* (6, 7), was subjected to catalytic hydrogenation conditions to give dihydrotenulin (III) (1). A new compound, 2,3-epoxytenulin (IV), was prepared in quantitative yield from tenulin upon brief treatment with cold, basic hydrogen peroxide solution. 2,3-Epoxytenulin, $C_{17}H_{22}O_6$ (by exact mass measurement), had a 194–197° melting point and IR ab-

0022-3549/79/0600-0715$01.00/0
© 1979, American Pharmaceutical Association

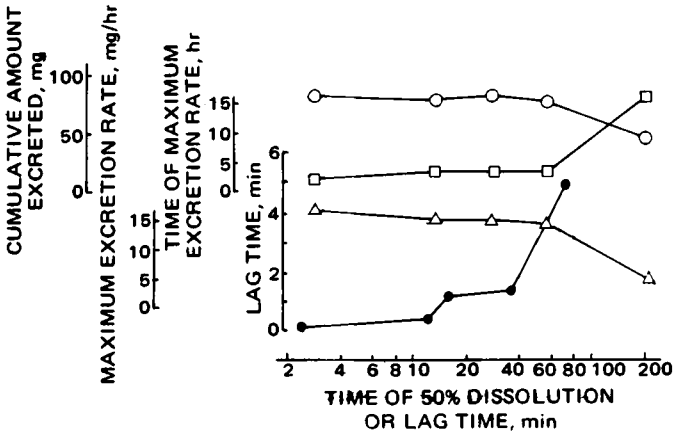

Figure 4—*Correlation of* in vitro *parameters (time of 50% dissolution and lag time) with urinary excretion* in vivo. *Key:* ●, *urinary excretion lag time;* △, *maximum urinary excretion rate;* □, *time of maximum urinary excretion rate; and* ○, *cumulative amount excreted in urine for 28 hr. These values were estimated by means of the urinary excretion of unchanged compound.*

the nonequivalent tablets. Since only one tablet was detected as nonequivalent in this study, the critical point could not be determined clearly. However, an approximate critical T_{50} point appeared to be more than 50 min. The critical value occurred surprisingly late, even though the *in vitro* rates were determined by the dissolution method that had the most vigorous agitating, dispersing, and destructive intensities among the seven methods studied.

Effect of Food on Bioavailability—The relative bioavailability of the powder and Tablet F was studied under fasting and nonfasting conditions. Table III shows the bioavailability parameters compared by the paired t test. The powder showed equivalent bioavailability with the tablets, except for Tablet F under fasting condition, and did not show any bioavailability difference between fasting and nonfasting states. Tablet F, which had poor bioavailability after fasting, became equivalent in bioavailability with the other formulations when it was administered just after the standard breakfast. Possibly, the more violent movement of the tablet in the GI tract after food might have increased drug absorption.

CONCLUSIONS

Film-coated I tablet absorption in humans is related to dissolution. The dissolution device that correlated well with bioavailability was one with a comparatively violent destructive force for the coated tablet film and high test medium agitation. The test medium pH must also be considered because dissolution of certain tablet coatings was pH dependent.

REFERENCES

(1) H. Ogata, T. Shibazaki, T. Inoue, and A. Ejima, *J. Pharm. Sci.*, **68**, 708 (1979).

(2) Y. Watanabe, T. Nagai, Y. Tanaka, and K. Motohashi, *Yakugaku Zasshi*, **95**, 599 (1975).

(3) Y. Watanabe, K. Motohashi, Y. Mitsui, R. Yoneda, and Y. Tanaka, *ibid.*, **96**, 1468 (1976).

(4) M. Maruyama and Y. Suzuki, *Takamine Kenkyusho Nempo*, **10**, 158 (1958).

(5) M. Yamazaki, S. Shigeo, and A. Kamada, *Yakuzaigaku*, **34**, 97 (1974).

(6) K. Kakemi and S. Ohashi, *Yakugaku Zasshi*, **82**, 338 (1962).

ACKNOWLEDGMENTS

The authors thank Dr. Y. Watanabe, Tokyo National Chest Hospital, and Dr. H.-L. Fung, State University of New York at Buffalo, for suggestions and discussions.

Antitumor Agents: Structure–Activity Relationships in Tenulin Series

THOMAS G. WADDELL *x, ANNE-MARIE AUSTIN *, JANICE W. COCHRAN *, KARL G. GERHART *, IRIS H. HALL ‡, and K. H. LEE ‡

Received May 25, 1978, from the **Department of Chemistry, University of Tennessee at Chattanooga, Chattanooga, TN 37401*, and the ‡*Department of Medicinal Chemistry, School of Pharmacy, University of North Carolina, Chapel Hill, NC 27514.* Accepted for publication November 21, 1978.

Abstract □ Systematic structural modifications were performed on the natural sesquiterpene lactone tenulin to define those groupings essential to, or significant in, its *in vivo* antitumor activity. Accordingly, the following tenulin analogs were prepared: dihydrotenulin, 2,3-epoxytenulin, isotenulin, dihydroisotenulin, 2,3-epoxyisotenulin, and tetrahydrodeacetylisotenulin. Both the cyclopentenone and the hemiketal units in tenulin were necessary for high *in vivo* activity.

Keyphrases □ Tenulin—antineoplastic activity, structure-activity relationships, *in vivo* study □ Antineoplastic activity—tenulin, structure-activity relationships, *in vivo study*

The sesquiterpene lactone tenulin (I) is a major bitter principle in several species of the plant genus *Helenium* (Family Compositae) (1–6). High *in vivo* tenulin antitumor activity toward the Ehrlich ascites and Walker 256 carcinosarcoma screens and, to a lesser extent, toward P-388 leukemia has been demonstrated (7, 8). The tenulin cyclopentenone unit may act as a Michael acceptor in cellular enzyme essential sulfhydryl group alkylation.

Tenulin forms a Michael addition product with L-cysteine to give the zwitterionic compound II (7, 8). The adduct II, containing the cyclopentanone group, showed 84% activity loss toward the Ehrlich ascites screen, suggesting that a cyclopentenone unit is important for high activity. Low II activity also might be the result of lower solubility in lipid membranes.

In the present study, the tenulin structure was modified in ways not significantly affecting drug transport. This structure–*in vivo* antitumor activity work reveals those tenulin features necessary for high activity.

RESULTS AND DISCUSSION

Chemistry—Tenulin (I), isolated after extraction of *Helenium amarum* (6, 7), was subjected to catalytic hydrogenation conditions to give dihydrotenulin (III) (1). A new compound, 2,3-epoxytenulin (IV), was prepared in quantitative yield from tenulin upon brief treatment with cold, basic hydrogen peroxide solution. 2,3-Epoxytenulin, $C_{17}H_{22}O_6$ (by exact mass measurement), had a 194–197° melting point and IR ab-

0022-3549/79/0600-0715$01.00/0
© 1979, American Pharmaceutical Association

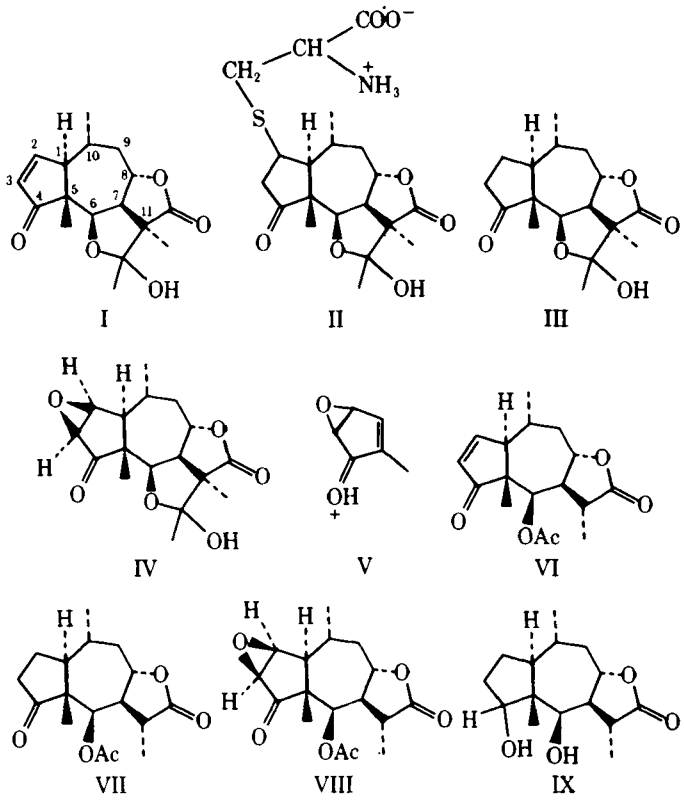

I II III IV V VI VII VIII IX

sorption at 3575 (OH), 1770 (γ-lactone), and 1750 (cyclopentanone) cm^{-1}. The UV spectrum revealed no enone absorption band at 225 nm.

The IV structure was confirmed by a high-resolution mass spectrum. Most significant of several fragment ions (see *Experimental*) were the molecular ion at *m/e* 322, an $M^+ - H_2O$ ion at *m/e* 304 indicating the presence of a hydroxyl group in IV, and the base peak at *m/e* 111 corresponding to the ion V. These and other peaks in the 2,3-epoxytenulin mass spectrum were easily interpretable in terms of Structure IV and principles recently put forth (9) regarding pseudoguaianolide mass spectra (9).

The stereochemistry of the IV 2,3-epoxide was determined by circular dichroism (Table I). The negative Cotton effect at 311 nm ($[\theta] = -6628$) corresponded to the $n \rightarrow \pi^*$ saturated ketone absorption and indicated a β-epoxide according to an inverse octant rule for epoxyketones described in the literature (10–12). This assignment for IV stereochemistry was supported by an analogous epoxidation reaction in the steroid series where 5α-androst-15-en-17-one yielded the corresponding 15β,16β-epoxy-17-ketone as the only product (13, 14).

Tenulin and 5α-androst-15-en-17-one molecular models revealed no definitive difference in steric hindrance between the molecular α- and β-faces. Therefore, an orbital explanation for the exclusive β-epoxide production from tenulin was sought. Both molecular models and circular dichroism measurements (Table I and Ref. 10) indicated that the tenulin and 5α-androst-15-en-17-one enone system was not planar but was skewed with the convex surface on the β-face (15, 16). An application of the orbital distortion technique (17) to this situation indicated that the lobes of the lowest unoccupied enone molecular orbital were distorted toward the β-face. Therefore, the attacking hydroperoxide anion should prefer to approach from this direction, as was observed experimentally.

Isotenulin (VI), prepared from tenulin by a literature method (3), yielded dihydroisotenulin (VII) (6) upon catalytic hydrogenation and 2,3-epoxyisotenulin (VIII) (6) when briefly exposed to cold, basic hydrogen peroxide solution. 2,3-Epoxyisotenulin, $C_{17}H_{22}O_6$, showed a negative Cotton effect at 312 nm (Table I) for the $n \rightarrow \pi^*$ ketone absorption, indicating that the newly introduced oxygen atom was beta. TLC showed that VIII had a higher R_f value than IV.

To prepare a derivative with a reduced ketone or lactone grouping, tenulin was reacted with sodium borohydride and with lithium aluminum hydride. In both experiments, low complex mixture yields were obtained. A sodium borohydride reduction of III produced more satisfactory results, giving, in low yield, a new compound, tetrahydrodeacetylisotenulin (IX). Compound IX, $C_{15}H_{24}O_4$, mp 161–163°, showed IR absorption at 3400 (OH) and 1755 (γ-lactone) cm^{-1}. The IX mass spectrum indicated the molecular ion at *m/e* 268 (M^+) and fragment ions at *m/e* 250 ($M^+ - H_2O$) and 232 ($M^+ - 2H_2O$), supporting the hypothesis of two hydroxyl groups. The NMR spectrum of IX (detailed under *Experimental*) was completely in accord with the assigned structure. Presumably, IX was formed in this reaction by sequential ketone reduction, retro-aldol cleavage of the hemiketal, and reductive cleavage of the resulting acetate ester.

Table I—Ketone $n \rightarrow \pi^*$ Cotton Effects for Tenulin and Derivatives

Compound	λ_{max}, nm	$[\theta]$
I	329	−3169
VI	330	−4850
IV	311	−6628
VIII	312	−9383

Biological Evaluation—Tenulin and the prepared derivatives were assayed for *in vivo* antitumor activity in Sprague–Dawley rats implanted with Walker 256 ascites carcinosarcoma cells and in DBA/2 mice implanted with P-388 lymphocytic leukemia according to published procedures (7) (Table II). Only tenulin showed significant activity in the P-388 screen. Since changes in activity are more pronounced in the sensitive Walker 256 screen, the following structure–activity relationship discussion focuses on those data.

Within the tenulin series (I, III, and IV), modification of the cyclopentenone ring by hydrogenation to III or epoxidation to IV was accompanied by decreased antitumor activity. Although less dramatic, this trend was evident also in the isotenulin series (VI–VIII) where both VII and VIII are less active than VI. These results confirmed that the tenulin and isotenulin cyclopentenone unit is needed for high *in vivo* antitumor activity. These conclusions are in accordance with those of Hall *et al.* (7) and Lee *et al.* (8), who demonstrated the tenulin cyclopentenone unit *S*-alkylating ability and related this reactivity to the action mechanism of antitumor agents bearing this enone system.

Compounds III and IV have nearly identical activities, as do VII and VIII. Furthermore, the epoxides IV and VIII, themselves potential alkylating agents, nevertheless showed decreased antitumor activity when compared to their progenitors I and VI, respectively. These observations suggest that in the tenulin–isotenulin series, the marginally active cyclopentenone epoxides are not acting significantly as *S*-alkylating agents *in vivo*.

Other systematic comparisons revealed the importance of the hemiketal unit to high antitumor activity. Within the hemiketal present–hemiketal absent pairs of I and VI, III and VII, and IV and VIII, the compound with the hemiketal intact was more active than its acetate ester counterpart. The hemiketal hydroxyl grouping may hydrogen bond the sesquiterpene antitumor agent to the cellular receptor site.

Tetrahydrodeacetylisotenulin (IX) inactivity supported the postulates regarding cyclopentenone and hemiketal importance to antitumor activity in the tenulin series.

EXPERIMENTAL[1]

***In Vivo* Tumor Screens**—*In vivo* tumor screens (Walker 256 ascites carcinosarcoma and P-388 lymphocytic leukemia) were performed according to published procedures (7). In the Walker 256 ascites carcinosarcoma screen, 10^6 tumor cells were implanted into 80 ± 10-g Sprague–Dawley male rats. In the P-388 lymphocytic leukemia screen, 10^6 cells were implanted into DBA/2 male mice (~18 g) on Day 0.

Test compounds were homogenized in 0.05% polysorbate 80–water and injected at 2.5 mg/kg/day ip for the rats and at 25 mg/kg/day ip for the mice. The day of death was recorded, and the treated/control (T/C) values for the average days survived were calculated according to the National Institutes of Health protocol 1.500 (18). Melphalan and fluorouracil were used as positive standards in these screens. Controls with 0.05% polysorbate 80–water give T/C = 100.

Isolation of Tenulin (I) from *H. amarum*[2]—A 476-g sample of *H.*

[1] Melting points were determined on a Thomas-Hoover apparatus and are corrected. IR spectra were determined with a Perkin-Elmer model 700 recording spectrophotometer. The circular dichroism curves were taken with methanol as the solvent, $c = 10^{-3}$ g/ml, using a Cary 60 instrument. Elemental analyses were performed by Galbraith Laboratories, Knoxville, Tenn.

[2] The plant material was identified as *Helenium amarum* (Raf.) H. Rock (Compositae) by Dr. Gene S. Van Horn, Department of Biology, University of Tennessee at Chattanooga. A voucher specimen (HAM-81074-FAR) is available for inspection at the Department of Chemistry, University of Tennessee at Chattanooga.

Table II—Antitumor Activity of Test Compounds [a]

Compound	Walker 256 Ascites		P-388 Lymphocytic Leukemia	
	Average Days Survived	T/C[b]	Average Days Survived	T/C[b]
I	22.16/8.33	266	13.8/10.2	135
III	24.0/16.3	147	9.5/10.2	93
IV	13.4/9.6	140	12.4/10.2	122
VI	14.6/9.6	152	11.5/10.2	113
VII	21.0/16.3	129	11.5/10.2	113
VIII	16.5/13.0	127	11.8/10.2	116
IX	15.9/15.6	102	—	—
Melphalan[c]	23.0/7.25	317	—	—
Fluorouracil[d]	—	—	19.7/10.6	186

[a] Six animals were used per group. [b] T/C ≥ 125% for minimum significant activity. [c] Wellcome Research Laboratories, Research Triangle Park, N.C. [d] Calbiochem, La Jolla, Calif.

amarum (Raf.) H. Rock leaves and stems[3] was cut into 1.27-cm pieces and extracted with chloroform by maceration for 4 days at room temperature. After decanting, the plant material was extracted twice in the same manner. The combined extracts were evaporated to dryness, leaving a dark-green tar (48.6 g). The crude extract was stirred for 30 min with 400 ml of water–ethanol (3:1) and filtered through diatomaceous earth.

The aqueous filtrate was extracted with five 100-ml portions of chloroform, and the combined organic phase was dried over anhydrous magnesium sulfate. Filtration and evaporation *in vacuo* left 19.4 g of the final extract as an amber oil. Trituration of this oil with benzene gave 6.27 g of crude I (mp 181–183°), which was recrystallized from ethanol–water, mp 186–188° [lit. (4) mp 184–186°]; IR ($CHCl_3$): 3600–3200 (OH), 1770 (γ-lactone), 1705 (cyclopentenone), and 1590 (C=C) cm^{-1}; UV (ethanol): 225 (ε 8215) nm; circular dichroism (methanol): $[\theta]_{329}$ −3169.

Anal.[4]—Calc. for $C_{17}H_{22}O_5 \cdot 0.20C_6H_6$: C, 67.91; H, 7.21. Found: C, 67.94; H, 6.90.

A direct comparison of this material with authentic I[5] established its identity. The mixed melting point of this sample was not depressed compared to authentic tenulin, the IR spectra were superimposable, and the two samples (mixed or separated) cochromatographed on TLC in numerous solvent systems. The NMR spectrum was identical to published I spectra.

Tenulin used in the experiments described in this paper showed one spot on TLC (R_f 0.50, 20% acetone in chloroform, silica gel).

Dihydrotenulin (III)—Tenulin (0.500 g) was hydrogenated in 25 ml of ethanol containing 0.20 g of 5% palladium-on-charcoal to give III (0.415 g), mp 170–171° [lit. (1) mp 172°]; IR ($CHCl_3$): 1760 (γ-lactone) and 1740 (cyclopentanone) cm^{-1}.

2,3-Epoxytenulin (IV)—To 0.203 g of I in 5 ml of methanol at 0° was added dropwise, with constant stirring, a solution containing 0.25 ml of 30% hydrogen peroxide, 0.60 ml of water, and 0.041 g of sodium carbonate. The cooled reaction mixture was stirred for 10 min, and 10 ml of distilled water was added. This aqueous solution was extracted with two 20-ml portions of chloroform, and the combined organic phase was dried (magnesium sulfate), filtered, and evaporated to dryness under reduced pressure. 2,3-Epoxytenulin was isolated as a clear glass in quantitative yield and showed a single circular spot on TLC in various solvent systems.

Efforts to crystallize this material were initially unsuccessful due to extensive decomposition. However, a crystalline sample of IV, mp 194–197°, was eventually obtained in low yield; IR ($CHCl_3$): 3575 (OH), 1770 (γ-lactone), and 1750 (cyclopentanone) cm^{-1}; circular dichroism (methanol): $[\theta]_{311}$ −6628; mass spectrum (9): *m/e* 322.1412 (M^+), calc. for $C_{17}H_{22}O_6$, 322.1416; 307 ($M^+ - CH_3$), 304 ($M^+ - H_2O$), 280, 279, 262, 261, 251, 235, 234, 233, 207, 191, 189, 163, 137, 135, 124, 123, 122, and 111 (base peak).

Isotenulin (VI)—Isotenulin was prepared in 82% yield from tenulin (3). The product VI was recrystallized from benzene–ether mixtures to give material with a melting point of 154–156° [lit. (2) mp 152–153°]; IR ($CHCl_3$): 1760 (γ-lactone), 1750 (OAc), 1705 (cyclopentenone), and 1580 (C=C) cm^{-1}; circular dichroism (methanol): $[\theta]_{330}$ −4850.

Dihydroisotenulin (VII)—Isotenulin (0.500 g) was hydrogenated in 25 ml of ethanol containing 0.231 g of 5% palladium-on-charcoal to give VII (0.441 g), mp 148–149° [lit. (6) mp 147–149°]; IR ($CHCl_3$): 1740–1760 cm^{-1}, unresolved.

2,3-Epoxyisotenulin (VIII)—2,3-Epoxyisotenulin was prepared in 74% yield from VI by the method of Lucas *et al.* (6), who obtained the product as an amorphous glass. The solid reaction product in the present case was crystallized from ethyl acetate–ether to give material with a 148–149° melting point; IR ($CHCl_3$): 1785–1755 and 1720 (shoulder) cm^{-1}; circular dichroism (methanol): $[\theta]_{312}$ −9383.

Anal.—Calc. for $C_{17}H_{22}O_6$: C, 63.35; H, 6.83. Found: C, 63.53; H, 7.01.

Tetrahydrodeacetylisotenulin (IX)—To 0.415 g of III in 10 ml of methanol was added 0.316 g of sodium borohydride in portions with constant stirring. After 45 min at room temperature, the reaction mixture was diluted to 50 ml with distilled water and extracted with three 25-ml portions of chloroform. The combined organic phase was washed once with 25 ml of water, dried (magnesium sulfate), filtered,and evaporated to dryness under reduced pressure. The crude, oily product (0.321 g) showed four components on TLC and was chromatographed on a column of silica gel (1.5 × 36 cm), eluting with chloroform followed by 20% acetone in chloroform.

From the later fractions, IX (20 mg) crystallized, mp 162–163°; IR ($CHCl_3$): 3400 (OH) and 1755 (γ-lactone) cm^{-1}; NMR ($CDCl_3$): δ 1.14 (3H, s, 5-CH_3), 1.16 (3H, d, J = 7 Hz, 10-CH_3), 1.46 (3H, d, J = 7 Hz, 11-CH_3), 3.24 (1H, m, H-11), 4.10 (1H, br, H-4), 4.18 (1H, d, J = 6 Hz, H-6), and 4.84 (1H, triplet of doublets, J = 3, 11 Hz, H-8); mass spectrum; *m/e* 268.1675 (M^+), calc. for $C_{15}H_{24}O_4$, 268.1673; 250 ($M^+ - H_2O$), 235 ($M^+ - H_2O - CH_3$), 232 ($M^+ - 2H_2O$), 224 ($M^+ - CO_2$), 208, 191, 178, 150, 136, 120, 117, 104, 103, and 102.

Anal.—Calc. for $C_{15}H_{24}O_4$: C, 67.16; H, 8.96. Found: C, 67.24; H, 9.03.

Earlier fractions from the crude reaction product chromatography yielded 3 mg of a second crystalline compound whose IR spectrum (3450, 1760, and 1720 cm^{-1}) was consistent with that expected for tetrahydroisotenulin, a possible intermediate in the production of IX.

REFERENCES

(1) E. P. Clark, *J. Am. Chem. Soc.*, **61**, 1836 (1939).

(2) H. E. Ungnade and E. C. Hendley, *ibid.*, **70**, 3921 (1948).

(3) D. H. R. Barton and P. De Mayo, *J. Chem. Soc.*, **1956**, 142.

(4) B. A. Parker and T. A. Geissman, *J. Org. Chem.*, **27**, 4127 (1962).

(5) W. Herz, W. A. Rohde, K. Rabindran, P. Jayaraman, and N. Viswanathan, *J. Am. Chem. Soc.*, **84**, 3857 (1962).

(6) R. A. Lucas, S. Rovinski, R. J. Kiesel, L. Dorfman, and H. B. MacPhillamy, *J. Org. Chem.*, **29**, 1549 (1964).

(7) I. H. Hall, K. H. Lee, E. C. Mar, C. O. Starnes, and T. G. Waddell, *J. Med. Chem.*, **20**, 333 (1977).

(8) K. H. Lee, I. H. Hall, E. C. Mar, C. O. Starnes, S. A. Elgebaly, T. G. Waddell, R. I. Hadgraft, C. G. Ruffner, and I. Weidner, *Science*, **196**, 533 (1977).

(9) L. Tsai, R. J. Highet, and W. Herz, *J. Org. Chem.*, **34**, 945 (1969).

(10) R. Bonnett and J. G. Davin, "Some Newer Physical Methods in Structural Chemistry," United Trade Press, London, England, 1967, pp. 159–161.

(11) C. Djerassi, W. Klyne, T. Norin, G. Ohloff, and E. Klein, *Tetrahedron*, **21**, 163 (1965).

(12) K. Schaffner and G. Snatzke, *Helv. Chim. Acta*, **48**, 347 (1965).

(13) C. Djerassi and G. Von Mutzenbecher, *Proc. Chem. Soc.*, **1963**, 377.

[3] Collected in Bledsoe County, Tenn.

[4] The ability of tenulin to form strong associations with benzene is in accord with results of Ungnade and Hendley (2).

[5] Supplied by Dr. W. Herz, Florida State University.

(14) C. Djerassi, G. Von Mutzenbecher, J. Fajkos, D. H. Williams, and H. Budzikiewicz, *J. Am. Chem. Soc.*, **87**, 817 (1965).
(15) W. Stocklin, T. G. Waddell, and T. A. Geissman, *Tetrahedron*, **26**, 2397 (1970).
(16) W. Herz, M. V. Lakshmikantham, and J. J. Schmid, *ibid.*, **22**, 1709 (1966).
(17) C. L. Liotta, *Tetrahedron Lett.*, **1975**, 519.
(18) R. I. Geran, N. H. Greenberg, M. M. MacDonald, A. M. Schumacher, and B. J. Abbott, *Cancer Chemother. Rep. Part 3*, **3**, 9, 15 (1972).

ACKNOWLEDGMENTS

Supported in part by a grant to T. G. Waddell from the Research Corporation of America and by Grant CA 17625 to K. H. Lee from the National Cancer Institute. Acknowledgment is also made to the Donors of the Petroleum Research Fund, administered by the American Chemical Society, for partial support of this research.

The authors thank Dr. Howard E. Smith, Vanderbilt University, for the use of the Cary 60 instrument for circular dichroism measurements and Colleen McCarty for technical assistance.

GLC Determination of Whole Blood Antimalarial Concentrations

T. NAKAGAWA *§, T. HIGUCHI *, J. L. HASLAM ‡x, R. D. SHAFFER ‡, and D. W. MENDENHALL *

Received April 18, 1977, from the **Department of Pharmaceutical Chemistry, University of Kansas, Lawrence, KS 66045, and ‡INTERx Research Corporation, Lawrence, KS 66044.* Accepted for publication November 21, 1978. §Present address: Faculty of Pharmaceutical Sciences, Kyoto University, Kyoto 606, Japan..

Abstract □ An assay was developed for determining mefloquine (quinolinemethanol) and pyridinemethanol derivative concentrations in whole blood. The method involved ion-pair extraction or usual solvent extraction for drug recovery from whole blood followed by trimethylsilylation. The silylated compounds were then submitted to GLC with electron-capture or flame-ionization detection. Mass spectrometry combined with GLC of the trimethylsilyl derivatives indicated that substitution of one trimethylsilyl group had occurred on the hydroxyl group. A phenyl methyl silicone column with temperature programming separated the drugs from normal blood extracts. The determination limit was 10 ng/ml of whole blood when an electron-capture detector was used with ion-pair extraction. Quantitation was achieved by using one antimalarial as an internal standard for the assay of the other. The utility of the present method was demonstrated by following the whole blood level time course after a single oral 250-mg tablet in beagle dogs.

Keyphrases □ Mefloquine—analysis, GLC, blood □ Pyridinemethanol derivatives—analysis, GLC, blood □ Antimalarials—analysis, GLC, blood □ GLC, electron capture—analysis, mefloquine, pyridinemethanol derivatives, blood □ GLC, flame ionization—analysis, mefloquine, pyridinemethanol derivatives, blood

Mefloquine (I), DL-*erythro*-α-(2-piperidyl)-2,8-bis-(trifluoromethyl)-4-quinolinemethanol, is curative for drug-resistant falciparum malaria (1–3). This compound has an extremely long biological half-life and is distributed rapidly into the body tissue (4), suggesting that the amount of the drug circulating in blood is low and persistent.

DL-*threo*-α-2′-Piperidyl-2-(4-trifluoromethylphenyl)-6-trifluoromethyl-4-pyridinemethanol (II) is a new antimalarial with activity against *Plasmodium berghei* (5). Sensitive and specific assays for whole blood concentrations of both compounds were needed.

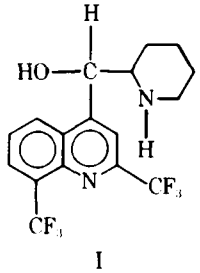

I

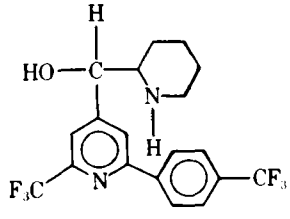

II

Several methods have been used for antimalarial analysis, including high-pressure liquid chromatography (HPLC) (6, 7), GLC (8), fluorometry (8), and liquid scintillation counting (9), but no reports have dealt with GLC determination of I and II in blood. Of these methods, HPLC combines better reproducibility and specificity than the fluorometry or radioactivity methods with a simple pretreatment procedure; it was used for I determination. However, HPLC sensitivity was limited by the relatively low I extinction coefficient at the readily accessible wavelengths, 280 and 254 nm; GLC combined with an electron-capture detector was expected to give more sensitive and specific measurements. This paper describes whole blood I and II determinations by electron-capture GLC.

EXPERIMENTAL

Reagents and Materials—Free bases of I and II were prepared by alkalizing the corresponding hydrochloride salts using equimolar sodium hydroxide in ethanol. The elemental analysis data (I—calc.: C, 53.97; H, 4.26; N, 7.41. Found: C, 54.29; H, 4.09; N, 7.59. II—calc.: C, 56.43; H, 4.49; N, 6.93. Found: C, 56.45; H, 4.47; N, 6.79), TLC, and GLC supported the purity of both free bases. The trimethylsilylating reagent[1] was a mixture of hexamethyldisilazane and trimethylchlorosilane dissolved in pyridine. Fresh human blood was obtained from volunteers. All other chemicals were commercially available analytical grades and were used without further purification.

GLC—The gas chromatograph[2] was equipped with an electron-capture detector and a flame-ionization detector. A U-shaped glass column (183

[1] TriSil, Pierce Chemical Co., Rockford, Ill.
[2] Varian Aerograph model 2100, Walnut Creek, Calif.

0022-3549/79/0600-0718$01.00/0
© 1979, American Pharmaceutical Association

(14) C. Djerassi, G. Von Mutzenbecher, J. Fajkos, D. H. Williams, and H. Budzikiewicz, *J. Am. Chem. Soc.*, **87**, 817 (1965).
(15) W. Stocklin, T. G. Waddell, and T. A. Geissman, *Tetrahedron*, **26**, 2397 (1970).
(16) W. Herz, M. V. Lakshmikantham, and J. J. Schmid, *ibid.*, **22**, 1709 (1966).
(17) C. L. Liotta, *Tetrahedron Lett.*, **1975**, 519.
(18) R. I. Geran, N. H. Greenberg, M. M. MacDonald, A. M. Schumacher, and B. J. Abbott, *Cancer Chemother. Rep. Part 3*, **3**, 9, 15 (1972).

ACKNOWLEDGMENTS

Supported in part by a grant to T. G. Waddell from the Research Corporation of America and by Grant CA 17625 to K. H. Lee from the National Cancer Institute. Acknowledgment is also made to the Donors of the Petroleum Research Fund, administered by the American Chemical Society, for partial support of this research.

The authors thank Dr. Howard E. Smith, Vanderbilt University, for the use of the Cary 60 instrument for circular dichroism measurements and Colleen McCarty for technical assistance.

GLC Determination of Whole Blood Antimalarial Concentrations

T. NAKAGAWA *§, T. HIGUCHI *, J. L. HASLAM ‡x, R. D. SHAFFER ‡, and D. W. MENDENHALL *

Received April 18, 1977, from the **Department of Pharmaceutical Chemistry, University of Kansas, Lawrence, KS 66045, and ‡INTERx Research Corporation, Lawrence, KS 66044.* Accepted for publication November 21, 1978. §Present address: Faculty of Pharmaceutical Sciences, Kyoto University, Kyoto 606, Japan..

Abstract □ An assay was developed for determining mefloquine (quinolinemethanol) and pyridinemethanol derivative concentrations in whole blood. The method involved ion-pair extraction or usual solvent extraction for drug recovery from whole blood followed by trimethylsilylation. The silylated compounds were then submitted to GLC with electron-capture or flame-ionization detection. Mass spectrometry combined with GLC of the trimethylsilyl derivatives indicated that substitution of one trimethylsilyl group had occurred on the hydroxyl group. A phenyl methyl silicone column with temperature programming separated the drugs from normal blood extracts. The determination limit was 10 ng/ml of whole blood when an electron-capture detector was used with ion-pair extraction. Quantitation was achieved by using one antimalarial as an internal standard for the assay of the other. The utility of the present method was demonstrated by following the whole blood level time course after a single oral 250-mg tablet in beagle dogs.

Keyphrases □ Mefloquine—analysis, GLC, blood □ Pyridinemethanol derivatives—analysis, GLC, blood □ Antimalarials—analysis, GLC, blood □ GLC, electron capture—analysis, mefloquine, pyridinemethanol derivatives, blood □ GLC, flame ionization—analysis, mefloquine, pyridinemethanol derivatives, blood

Mefloquine (I), DL-*erythro*-α-(2-piperidyl)-2,8-bis-(trifluoromethyl)-4-quinolinemethanol, is curative for drug-resistant falciparum malaria (1–3). This compound has an extremely long biological half-life and is distributed rapidly into the body tissue (4), suggesting that the amount of the drug circulating in blood is low and persistent.

DL-*threo*-α-2′-Piperidyl-2-(4-trifluoromethylphenyl)-6-trifluoromethyl-4-pyridinemethanol (II) is a new antimalarial with activity against *Plasmodium berghei* (5). Sensitive and specific assays for whole blood concentrations of both compounds were needed.

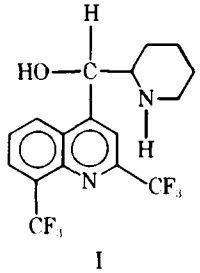

I

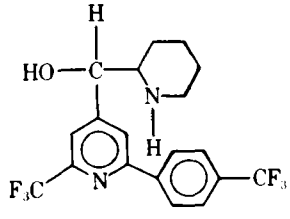

II

Several methods have been used for antimalarial analysis, including high-pressure liquid chromatography (HPLC) (6, 7), GLC (8), fluorometry (8), and liquid scintillation counting (9), but no reports have dealt with GLC determination of I and II in blood. Of these methods, HPLC combines better reproducibility and specificity than the fluorometry or radioactivity methods with a simple pretreatment procedure; it was used for I determination. However, HPLC sensitivity was limited by the relatively low I extinction coefficient at the readily accessible wavelengths, 280 and 254 nm; GLC combined with an electron-capture detector was expected to give more sensitive and specific measurements. This paper describes whole blood I and II determinations by electron-capture GLC.

EXPERIMENTAL

Reagents and Materials—Free bases of I and II were prepared by alkalizing the corresponding hydrochloride salts using equimolar sodium hydroxide in ethanol. The elemental analysis data (I—calc.: C, 53.97; H, 4.26; N, 7.41. Found: C, 54.29; H, 4.09; N, 7.59. II—calc.: C, 56.43; H, 4.49; N, 6.93. Found: C, 56.45; H, 4.47; N, 6.79), TLC, and GLC supported the purity of both free bases. The trimethylsilylating reagent[1] was a mixture of hexamethyldisilazane and trimethylchlorosilane dissolved in pyridine. Fresh human blood was obtained from volunteers. All other chemicals were commercially available analytical grades and were used without further purification.

GLC—The gas chromatograph[2] was equipped with an electron-capture detector and a flame-ionization detector. A U-shaped glass column (183

[1] TriSil, Pierce Chemical Co., Rockford, Ill.
[2] Varian Aerograph model 2100, Walnut Creek, Calif.

0022-3549/79/0600-0718$01.00/0
© 1979, American Pharmaceutical Association

Table I—Compound I Recovery from Spiked Blood Samples by Ion-Pair Extraction followed by Electron-Capture and Flame-Ionization GLC Determinations

Blood Level, ng/ml	Recovery (Mean ± *SD*), %[a]
1070[b]	87.7 ± 4.6
535[b]	88.3 ± 4.6
107[b]	94.0 ± 5.2
10.4[c]	92.9 ± 9.4
5.3[c]	94.4 ± 15.3
1.04[c]	100.5 ± 19.1
Average	93.0 ± 9.7

[a] From three replicate samples. [b] Flame-ionization detection. [c] Electron-capture detection.

cm × 4 mm i.d.) was packed with 3% phenyl methyl silicone gum[3] coated on a flux-calcined diatomite support[4] (100–200 mesh, acid washed, dimethylchlorosilane treated). The electron-capture detection used an 8 mCi ^{63}Ni-radiation source, a 90-v dc cell voltage, and $1.0–1.2 \times 10^{-9}$ amp standing current. For flame-ionization detection, 30 ml of hydrogen gas/min, 300 ml of dry air/min, and a 300-v dc cell voltage were employed. The temperature was maintained at 250° for both the detector and the injector.

The column temperature was programmed to increase 1°/min from 160 to 250°, followed by flash heating to 280° to elute the high boiling materials from the column. The nitrogen carrier gas was adjusted to a 30-ml/min flow rate with a mass flow controller.

Sample Preparation Procedure—For statistical analysis, human blood was spiked with known amounts of the standard free bases to make 1–1000-ng/ml blood levels and equilibrated by shaking for 30 min. In the dog experiments, a 2- or 5-ml whole blood portion was withdrawn from a beagle dog, transferred immediately to a heavy-duty centrifuge tube, and weighed accurately. Two drops of 15% ethylenediaminetetracarboxylic acid disodium salt solution were added as an anticoagulant. The blood samples thus prepared were then extracted.

Ion-Pair Extraction—To the 5-ml blood sample, 4 ml of 0.2 *N* H_2SO_4 and 10 ml of ether were added. After the mixture had been shaken at room temperature for 10 min, it was centrifuged at 2000 rpm for 15 min. The ether layer was removed and discarded. Four milliliters of aqueous 3% trichloroacetic acid solution was added to the remaining blood layer, which was extracted three times using 10 ml of ether. An additional 1 ml of trichloroacetic acid was added with the ether on the second and third extractions.

For each extraction, the mixture was shaken for 30 min and centrifuged at 2000 rpm for 15 min, after which the ether layer was transferred to a separator. The combined ether extracts were washed with 10 ml of 10% NaOH and 10 ml of 10% aqueous ammonium hydroxide. After the aqueous layer had been drained, the ether layer was transferred to a conical flask and evaporated almost to dryness. The flask was further dried in a desiccator.

Ethyl Acetate Extraction—To a 5-ml blood sample in a centrifuge tube were added 1.8 ml of 0.1 *N* NaOH and 10 ml of ethyl acetate. The

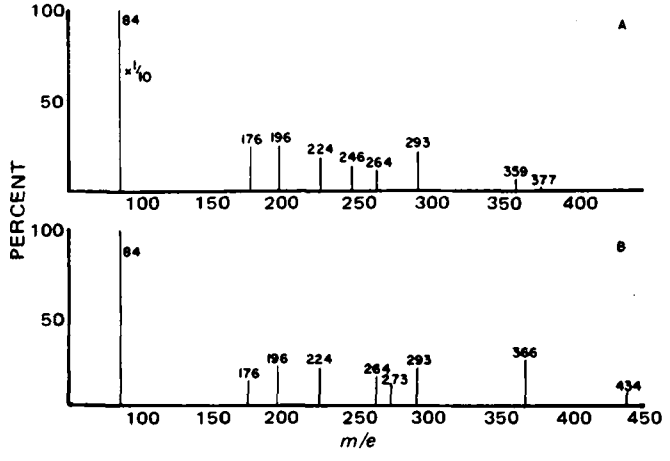

Figure 1—*Gas chromatogram–mass spectra of the free base (A) and trimethylsilane derivative (B) of mefloquine.*

[3] OV-17, Applied Science Laboratories, State College, Pa.
[4] Chromosorb W, Anspec Co., Ann Arbor, Mich.

Table II—Compound I Recovery from Spiked Blood by Ethyl Acetate Extraction followed by Electron-Capture GLC Determination

Blood Level, ng/ml	Recovery (Mean ± *SD*), %[a]
1044	68.7 ± 5.17
104.3	76.3 ± 2.77
10.5	90.1 ± 42.2
Average	78.4 ± 16.7

[a] From three replicate samples.

tube was shaken for 30 min and centrifuged at 3200 rpm for 15 min. The extraction was repeated twice. The ethyl acetate layers were transferred to a conical flask and evaporated almost to dryness. The extracts were completely dried in a desiccator.

Ether Extraction—To a 2-ml blood sample were added 0.5 ml of 0.1 *N* NaOH and 5 ml of ether. After the mixture had been shaken for 15 min at room temperature, the ether layer was separated by centrifugation at 2000 rpm for 10 min and transferred to a conical flask. The remaining layer was extracted two more times with 5 ml of ether. The combined extracts were evaporated to near dryness, and the residue was dried in a desiccator.

Trimethylsilylation—The dried residue was dissolved in ~1 ml of ether and transferred to a small conical test tube. The internal standard solution in ethyl acetate was added to the tube based on an estimated sample compound concentration. After the solvent had been evaporated carefully under a nitrogen stream, 100 μl of the trimethylsilylating reagent (200 μl if the concentration was expected to be about 500 ng/ml) was added, and the solution was left to stand for 10 min at room temperature. An appropriate volume (0.2–2.0 μl) of this solution was injected onto the GLC column.

Quantitation—A peak height ratio method was employed. The weight ratio for the calibration plot was varied by changing the mixing ratio of the standard free bases I and II in ethyl acetate solution. The mixed solution was evaporated to complete dryness and trimethylsilylated according to the described procedure. The calibration plots thus obtained showed good linearity for the flame-ionization detection over 1:5 and 5:1 weight ratios. The electron-capture detection gave a slightly concave curve in the same region; however, a 1:2–2:1 weight ratio range produced a linear electron-capture detection response. The determination limit was 10 ng/ml for I when the electron-capture detection was used in combination with ion-pair extraction, but the flame-ionization detection could detect concentrations of 100 ng/ml for both I and II.

Dog Experiment—An *in vivo* experiment was conducted using three female beagle dogs. Each dog was fasted 24 hr prior to dosing. One dog (7.75 kg) was orally dosed with one 250-mg I tablet; two dogs (13.7 and 9.0 kg) were dosed with one 250-mg II tablet (both drugs as hydrochloride salt). From the dog dosed with I, blood was withdrawn through the jugular vein at 0, 1, 2, 2.5, 3, 3.5, 4, 4.5, 5, 6, 8, 12, 24, 72, and 144 hr, and at 2, 3, 4, 5, 6, 7, and 9 weeks after administration. The blood volume taken was 2 ml for the first 6 days and 5 ml thereafter. From the dogs dosed with II, 2 ml of blood was taken at 0, 1, 2, 3, 4, 5, 6, 8, 12, 48, and 72 hr after dosing.

RESULTS AND DISCUSSION

Since the average blood I level was expected to be lower than the II level from the same dosage, ion-pair extraction was used to obtain a better I recovery. An ethyl acetate extraction was examined as a possible procedural simplification. Tables I and II list the results for the statistical analysis of I recovery from spiked blood by ion-pair extraction and by ethyl acetate extraction, respectively. The ion-pair extraction gave higher I recovery and better reproducibility than ethyl acetate extraction; however, the standard deviation increased gradually at the lower levels. The ethyl acetate extraction was applicable to levels above 100 ng/ml. The recovery of II from the spiked blood was studied by ethyl ether extraction; a very high recovery with good reproducibility was observed for all levels examined (Table III).

In Tables I–III, the electron-capture detection and the flame-ionization detection were used for recovery determination. Electron-capture detection is highly sensitive to antimalarials that contain two trifluoromethyl groups per molecule but has a lower sensitivity to cholesterols, the major extracted blood component. The solvent peak tailing which sometimes interferes with drug peak separation in flame-ionization detection can be reduced by using low electron affinity solvents. Electron-capture detection has a relatively narrow dynamic range compared with flame-ionization detection, and detector stability and sensitivity depend

Table III—Compound II Recovery from Spiked Blood by Ether Extraction followed by Electron-Capture GLC Determination

Spiked Level, ng/ml	Recovery, %
1000	99.6
500	96.2
100	99.6
50	103.8
10	106.0
Mean ± *SD*	101.0 ± 2.8

more subtly on the detector condition than does flame-ionization detection. The detection limits for each drug were 1 ng/ml with the electron-capture detection (the limit of accurate determination is 10 ng/ml, Table I) and 100 ng/ml with the flame-ionization detection under the best condition. Thus, the electron-capture detection was used for blood levels of 10–1000 ng/ml and the flame-ionization detection was limited to levels higher than 100 ng/ml.

The I and II free bases without trimethylsilyl derivative formation gave tailing peaks on the chromatogram, which subsequently overlapped normal blood component background peaks. The trimethylsilyl derivatization produced sharper and higher peaks with shorter retention times, which helped separate the derivatives from the background peaks.

The reaction conditions used to prepare the trimethylsilyl derivatives were studied. The I and II free bases recovered from 2 or 5 ml of whole blood were completely derivatized with 100 μl of the silylating reagent at room temperature. An additional 100 μl of the reagent was used when a higher level of drug was found; the sample was further diluted so as to fall in the electron-capture detection sensitivity range. Silylation reaction time dependence was examined by injecting samples at 1, 5, 10, and 30 min after silylating reagent addition. The 1-min sample indicated about a 50% silyl derivative yield; just a trace amount of the unreacted species was found in the 5-min sample. For reaction times between 10 min and 1 day, neither a peak due to unreacted species nor measurable changes in the peak intensity were observed.

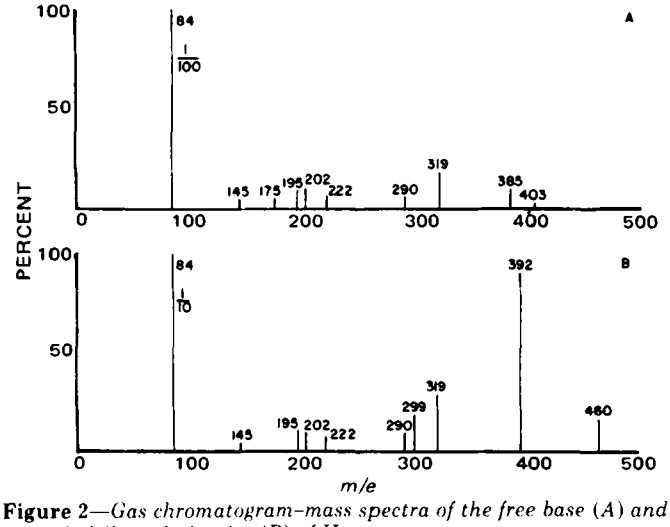

Figure 2—*Gas chromatogram–mass spectra of the free base (A) and trimethylsilane derivative (B) of II.*

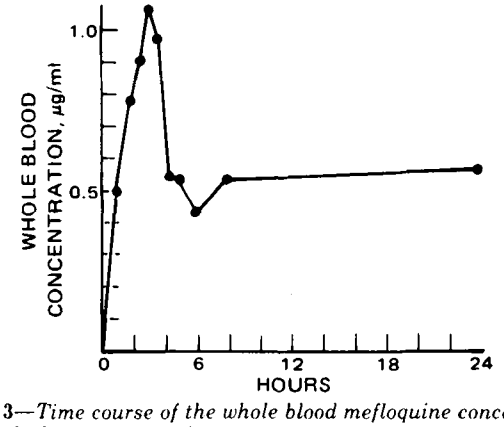

Figure 3—*Time course of the whole blood mefloquine concentration in a beagle dog given a single 250-mg tablet.*

To confirm the structure of the trimethylsilyl derivative, GLC–mass spectra of the derivatized and underivatized free bases were obtained. The spectrum for trimethylsilyl-I (Fig. 1B) indicates the formation of the $(M - 1 - CH_3)^+$ ion at *m/e* 434; the I free base had an $(M - 1)^+$ ion at *m/e* 377 (Fig. 1A). The assignments of some possible fragment ions are summarized as:

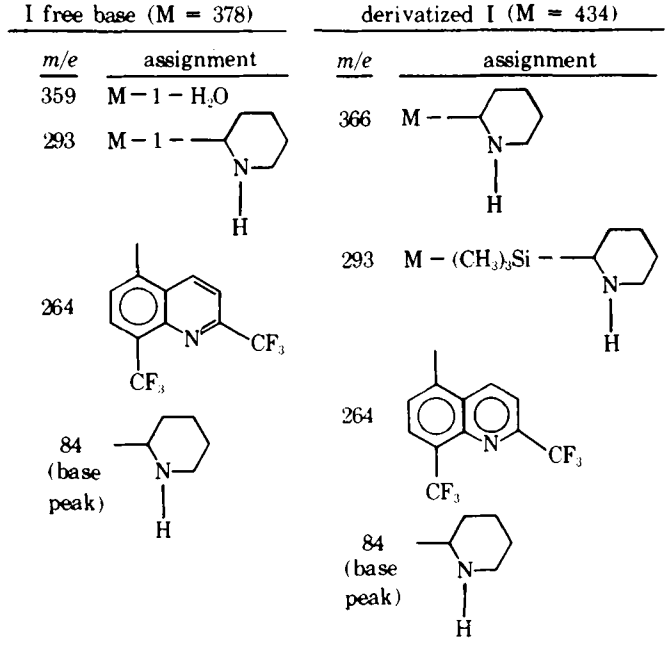

The trimethylsilyl-II spectrum (Fig. 2B) similarly indicated $(M - 1 - CH_3)^+$ ion formation at *m/e* 460, and II free base (Fig. 2A) gave the $(M - 1)^+$ ion at *m/e* 403. Some other fragment ions are shown below:

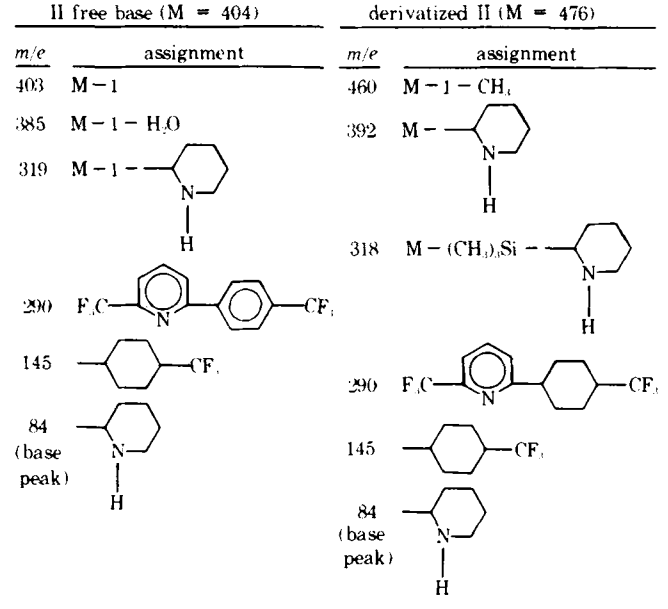

Spectra for free bases and trimethylsilyl derivatives confirmed that one trimethylsilyl group had been substituted at the hydroxy group.

In vivo experiments were carried out to examine the utility of the present method (Figs. 3–5). The flame-ionization detection was used for the samples taken in the 1st week; the electron-capture detection was used for the samples taken thereafter. Figures 3 and 4 indicate the time course of whole blood I levels for the first 24 hr and for the following 42 days, respectively. A rapid increase in the blood I level was observed up to the maximum point at 3 hr, followed by a very slow decrease to a level of 18 ng/ml at 7 weeks. No measurable level was observed in the 9th-week blood sample. A semilogarithmic plot of the data in Figs. 3 and 4 led to a I elimination half-life of 10.2 days with a 0.068 day^{-1} rate constant.

Figure 5 shows the II time course plots given as the mean of two experiments. The blood II level increased during the first 3 hr after administration, reached a maximum level which was maintained for about

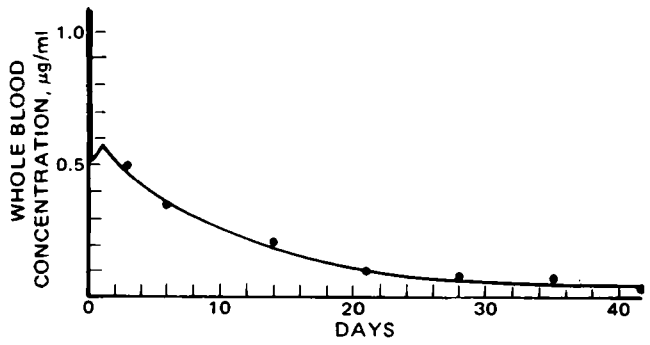

Figure 4—*Time course of the whole blood mefloquine concentration in a beagle dog given a single 250-mg tablet.*

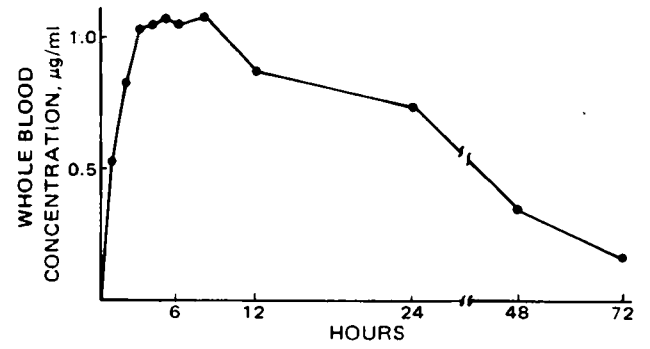

Figure 5—*Time course of the average whole blood II concentration in two beagle dogs given 250-mg tablets.*

5 hr, and then decreased slowly. From the semilogarithmic time course data plot, an elimination half-life and an elimination rate constant for II were estimated to be 24.8 hr and 0.028 hr^{-1}, respectively. The results for I and II suggested that I is about 10 times more persistent than II in its elimination from dogs.

REFERENCES

(1) C. J. Canfield and R. S. Rozman, *Bull. WHO*, **50**, 203 (1974).

(2) G. M. Trenholme, R. L. Williams, R. E. Desjardins, H. Fischer, P. E. Carson, K. H. Rieckmann, and C. J. Canfield, *Science*, **190**, 792 (1975).

(3) K. H. Rieckmann, G. M. Trenholme, R. L. Williams, P. E. Carson, H. Fischer, and R. E. Desjardins, *Bull. WHO*, **51**, 375 (1974).

(4) J. Y. Mu, Z. H. Israili, and P. G. Dayton, *Drug Metab. Dispos.*, **3**, 198 (1975).

(5) M. P. Lamontagne, A. Markovac, and A. Blumbergs, *J. Med. Chem.*, **17**, 519 (1974).

(6) J. M. Grindel, P. F. Tilton, and R. D. Shaffer, *J. Pharm. Sci.*, **66**, 834 (1977).

(7) H. Okada, V. Stella, J. Haslam, and N. Yata, *ibid.*, **64**, 1665 (1975).

(8) A. W. Burg, Final Report to U.S. Army Medical Research and Development Command, Report No. 9, "Development of Analytical Methods for the Determination of Experimental Antimalarials in Biological Fluids," Contract DADA17-72-C-2182 with Arthur D. Little, Inc., Cambridge, Mass, Dec. 8, 1974.

(9) J. M. Grindel, R. S. Rozman, D. M. Leahy, N. A. Molek, and H. H. Grillum, *Drug Metab. Dispos.*, **4**, 133 (1976).

ACKNOWLEDGMENTS

Supported by a grant from the Department of the Army, U.S. Army Medical Research Development Command.

This paper is Contribution 1447 to the Army Research Program on Malaria, Contract DADA17-73-C-3125.

Powder Homogenization Using a Hammer Mill

CHARLES C. YEUNG * **and JOHN A. HERSEY** ‡×

Received September 12, 1978, from the *Victorian College of Pharmacy Ltd. and the ‡Institute of Drug Technology Ltd., Parkville, Victoria, 3052, Australia. Accepted for publication November 30, 1978.

Abstract □ Hammer mill applicability in the comixing milling operation is discussed with reference to a 1:1000 microfine salicylic acid–sucrose binary system. The hammer mill would not serve as a mixing machine under most circumstances because of the low holdup capacity. Grinding of pure materials was preferable to mixture grinding since active ingredients could be lost during the milling operation. Remixing was always necessary following comminution of the mixture in the hammer mill. Grinding followed by remixing considerably enhanced mixture homogeneity. A large size range was produced by comminution, which resulted in the segregation of ordered units such that the final mixture could be described as a randomized ordered mixture.

Keyphrases □ Powders—homogenization using a hammer mill, sucrose–salicylic acid □ Pharmaceutical formulations—powders, homogenization using a hammer mill, sucrose–salicylic acid □ Hammer mill—powder homogenization, sucrose–salicylic acid

Many raw materials are supplied in a form requiring no further processing. However, grinding or cutting may be indicated with waxes and vegetable drugs or when agglomeration of starting materials occurs on storage. If grinding is a necessary stage in manufacturing or is required to attain a desired homogeneity, the hammer mill is frequently used for comminution.

Mixing is impossible when σ_R, the theoretical standard deviation of the fully randomized system, is equal to or greater than σ_A, the specification index (1). The σ_R value can be calculated from the sample size and the known proportions of the powders to be mixed using Lacey's equation (2):

$$\sigma_R^2 = \frac{XY}{N} \qquad \text{(Eq. 1)}$$

where X and Y are the proportions of the two ingredients and N is the number of particles in the samples. The σ_A value is calculated from the desired homogeneity of the powder mixture (3). The value of σ_R can be reduced by increasing the particle number per sample, which implies that size reduction is necessary.

Even though the hammer mill has been extensively used in the pharmaceutical industry for size reduction, limited evaluation has been carried out on the mixing performance of industrial comminution equipment. Most equipment used in comminution was ineffective for powder mixing operations because of the low holdup capacity (4). With nonflowing materials, passing a preblend through a ham-

0022-3549/79/0600-0721$01.00/0
© 1979, American Pharmaceutical Association

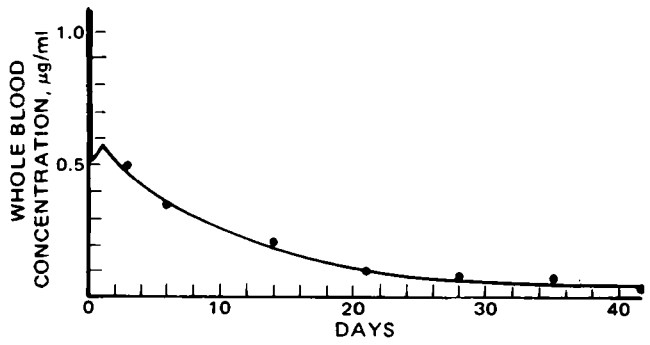

Figure 4—*Time course of the whole blood mefloquine concentration in a beagle dog given a single 250-mg tablet.*

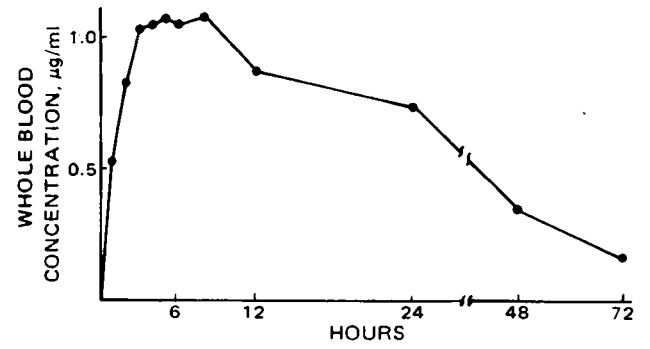

Figure 5—*Time course of the average whole blood II concentration in two beagle dogs given 250-mg tablets.*

5 hr, and then decreased slowly. From the semilogarithmic time course data plot, an elimination half-life and an elimination rate constant for II were estimated to be 24.8 hr and 0.028 hr^{-1}, respectively. The results for I and II suggested that I is about 10 times more persistent than II in its elimination from dogs.

REFERENCES

(1) C. J. Canfield and R. S. Rozman, *Bull. WHO*, **50**, 203 (1974).

(2) G. M. Trenholme, R. L. Williams, R. E. Desjardins, H. Fischer, P. E. Carson, K. H. Rieckmann, and C. J. Canfield, *Science*, **190**, 792 (1975).

(3) K. H. Rieckmann, G. M. Trenholme, R. L. Williams, P. E. Carson, H. Fischer, and R. E. Desjardins, *Bull. WHO*, **51**, 375 (1974).

(4) J. Y. Mu, Z. H. Israili, and P. G. Dayton, *Drug Metab. Dispos.*, **3**, 198 (1975).

(5) M. P. Lamontagne, A. Markovac, and A. Blumbergs, *J. Med. Chem.*, **17**, 519 (1974).

(6) J. M. Grindel, P. F. Tilton, and R. D. Shaffer, *J. Pharm. Sci.*, **66**, 834 (1977).

(7) H. Okada, V. Stella, J. Haslam, and N. Yata, *ibid.*, **64**, 1665 (1975).

(8) A. W. Burg, Final Report to U.S. Army Medical Research and Development Command, Report No. 9, "Development of Analytical Methods for the Determination of Experimental Antimalarials in Biological Fluids," Contract DADA17-72-C-2182 with Arthur D. Little, Inc., Cambridge, Mass, Dec. 8, 1974.

(9) J. M. Grindel, R. S. Rozman, D. M. Leahy, N. A. Molek, and H. H. Grillum, *Drug Metab. Dispos.*, **4**, 133 (1976).

ACKNOWLEDGMENTS

Supported by a grant from the Department of the Army, U.S. Army Medical Research Development Command.

This paper is Contribution 1447 to the Army Research Program on Malaria, Contract DADA17-73-C-3125.

Powder Homogenization Using a Hammer Mill

CHARLES C. YEUNG * **and JOHN A. HERSEY** ‡×

Received September 12, 1978, from the *Victorian College of Pharmacy Ltd. and the ‡Institute of Drug Technology Ltd., Parkville, Victoria, 3052, Australia. Accepted for publication November 30, 1978.

Abstract □ Hammer mill applicability in the comixing milling operation is discussed with reference to a 1:1000 microfine salicylic acid–sucrose binary system. The hammer mill would not serve as a mixing machine under most circumstances because of the low holdup capacity. Grinding of pure materials was preferable to mixture grinding since active ingredients could be lost during the milling operation. Remixing was always necessary following comminution of the mixture in the hammer mill. Grinding followed by remixing considerably enhanced mixture homogeneity. A large size range was produced by comminution, which resulted in the segregation of ordered units such that the final mixture could be described as a randomized ordered mixture.

Keyphrases □ Powders—homogenization using a hammer mill, sucrose–salicylic acid □ Pharmaceutical formulations—powders, homogenization using a hammer mill, sucrose–salicylic acid □ Hammer mill—powder homogenization, sucrose–salicylic acid

Many raw materials are supplied in a form requiring no further processing. However, grinding or cutting may be indicated with waxes and vegetable drugs or when agglomeration of starting materials occurs on storage. If grinding is a necessary stage in manufacturing or is required to attain a desired homogeneity, the hammer mill is frequently used for comminution.

Mixing is impossible when σ_R, the theoretical standard deviation of the fully randomized system, is equal to or greater than σ_A, the specification index (1). The σ_R value can be calculated from the sample size and the known proportions of the powders to be mixed using Lacey's equation (2):

$$\sigma_R^2 = \frac{XY}{N} \qquad \text{(Eq. 1)}$$

where X and Y are the proportions of the two ingredients and N is the number of particles in the samples. The σ_A value is calculated from the desired homogeneity of the powder mixture (3). The value of σ_R can be reduced by increasing the particle number per sample, which implies that size reduction is necessary.

Even though the hammer mill has been extensively used in the pharmaceutical industry for size reduction, limited evaluation has been carried out on the mixing performance of industrial comminution equipment. Most equipment used in comminution was ineffective for powder mixing operations because of the low holdup capacity (4). With nonflowing materials, passing a preblend through a ham-

0022-3549/79/0600-0721$01.00/0
© 1979, American Pharmaceutical Association

Table I—Actual Mixing Time (Minutes) for Each Preblend

Preblend	Initial Mixing in Cube Mixer	Remixing after Passing through Hammer Mill Once	Remixing after Passing through Hammer Mill Twice	Final Remixing after Passing through Hammer Mill Three Times
1	1	1 (2)	2 (4)	6 (10)
2	2	2 (4)	6 (10)	10 (20)
3	4	6 (10)	10 (20)	20 (40)
4	160	160 (320)	—	—

mer mill increased the mixture homogeneity (5). The main problems associated with grinding were cost, contamination, and segregation (6).

Random mixing theory has been established for 25 years, but, in practice, mixtures rarely attain full randomization due to particulate size, shape, and density differences. Ordered mixtures exist in which one constituent adheres onto the surface of the other in a fixed proportion (7). The purpose of the present work was to investigate the application of the hammer mill to powder mixing operations with particular reference to ordered mixing. The binary system used had previously been shown to give an ordered mixture under some circumstances.

EXPERIMENTAL

Sucrose was the oversized fraction remaining when granulated sugar[1] was sieved through a 630-μm mesh screen[2]. Salicylic acid was previously sized using an air permeability technique (at 3.4-μm average diameter).

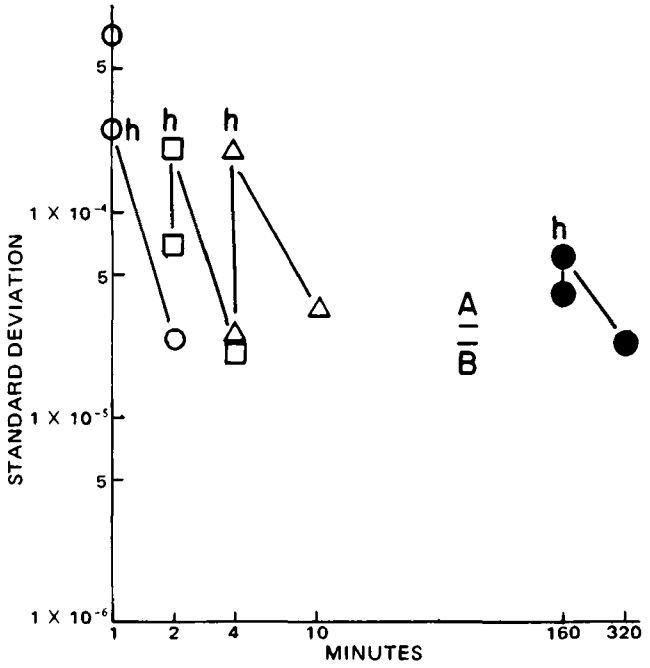

Figure 1—*Effect of passing the salicylic acid–sucrose mixture (1:1000) through the hammer mill once. Key: A and B, standard deviations of a fully randomized equivalent system before and after passing through the hammer mill, respectively;* h, *mixture that has been passed through the hammer mill;* ○, *Preblend 1;* □, *Preblend 2;* △, *Preblend 3; and* ●, *Preblend 4.*

[1] C. S. R. brand 1A.
[2] No. 29 mesh.

Table II—Sucrose Size Distribution [a] (Weight Fraction Undersize) before and after Passing through the Hammer Mill

Particle Size, μm	Number of Passes through Hammer Mill			
	Zero	One	Two	Three
1003	1	1	1	1
853	0.930			
710	0.492	0.902	0.985	0.999
600	0.065	0.710	0.923	0.988
500	0.016	0.565	0.834	0.956
425		0.516	0.788	0.932
355		0.468	0.731	0.895
250		0.380	0.605	0.794
180		0.291	0.459	0.645
150		0.264	0.415	0.593
75		0.163	0.248	0.364
<75		0	0	0
Σfw	335.63 μg	131.80 μg	47.64 μg	16.12 μg

[a] Determined by a nest of sieves and a sieve shaker.

The sucrose size distribution was determined using a nest of sieves and a test sieve-shaker[3]. The sucrose and salicylic acid densities were determined by air comparison pycnometry to be 1.44 and 1.59 g/cm, respectively (8).

Preblends were prepared by mixing 3.6 kg of powders (salicylic acid–sucrose, 1:1000) in a 7.5-kg stainless steel revolvo-cube mixer[4] for 1, 2, 4, or 160 min. Each preblend was subsequently passed through the hammer mill[5]. The revolvo-cube mixer was fitted with an internal agitator rotating at 37 rpm while the cube mixer rotated at 17 rpm.

After grinding, the mixture was reloaded into the revolvo-cube mixer and remixed according to the procedure given in Table I. The whole comminution and remixing process was repeated three times. Twenty random samples (250 mg) were taken immediately before grinding and before remixing in the revolvo-cube mixer at each cycle for each preblend. To investigate the sample size effect on the standard deviation, different sample weights were collected using a set of concentric cylindrical sampling thieves. The samples were individually assayed by dissolving the contents in 50% ethanol. The absorbance was measured at 300 nm using a spectrophotometer[6] connected to an autosampling unit. The blank consisted of 50% ethanol with an equivalent amount of sucrose. For

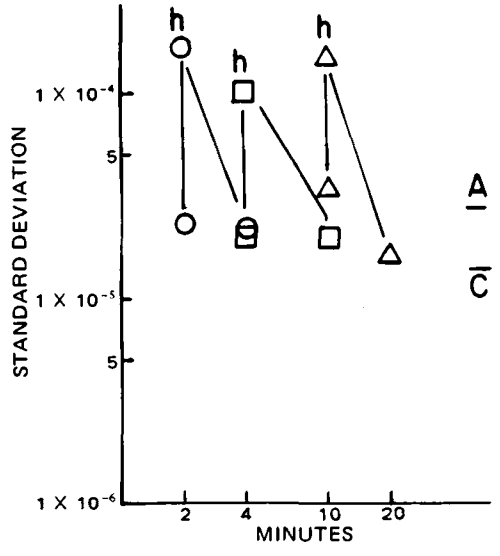

Figure 2—*Effect of passing the salicylic acid–sucrose mixture (1:1000) through the hammer mill twice. Key: A and C, standard deviations of a fully randomized equivalent system before and after passing through the hammer mill twice, respectively;* h, *mixture that has been passed through the hammer mill;* ○, *Preblend 1;* □, *Preblend 2; and* △, *Preblend 3.*

[3] A. C. Cheers Pty. Ltd.
[4] Garwood and Goodyear Pty. Ltd.
[5] Bauhnecht (Glen Creston Ltd.).
[6] Techtron model 634, Varian.

Table III—Salicylic Acid Content (Percent) for Each Group of 20 Samples Taken at Various Stages of the Experiment

Stage[a]	Preblend 1	2	3	4
m	112.7	89.9	98.7	96.8
m/h	100.8	109.1	97.4	100.0
m/h/m	99.5	101.2	98.5	103.9
m/h/m/h	98.0	95.6	89.4	
m/h/m/h/m	99.4	96.9	96.4	
m/h/m/h/m/h	94.8	95.4	90.1	
m/h/m/h/m/h/m	95.3	96.3	93.6	

[a] *m* = a single stage of mixing in the cube mixer, and *h* = a single passage through the hammer mill.

comparison, data previously obtained using salicylic acid and sucrose mixtures in a revolvo-cube mixer were used (8).

RESULTS

The sucrose size distribution is shown in Table II; the median diameter was 710 μm. The hammer mill comminution effect resulted in size reduction as the mix was passed through the hammer mill each time (Table II). Mixing was examined by the analysis of the samples removed at various stages, *i.e.*, after mixing and/or milling. The standard sample concentration deviation was calculated from:

$$S = \sqrt{\frac{\Sigma(x_i - \bar{x})^2}{n - 1}} \qquad \text{(Eq. 2)}$$

where x_i was the sample concentration and $\bar{x}$ was the mean sample concentration estimated from n number of samples.

Preblends were investigated after 1, 2, 4, and 160 min (Preblends 1–4, respectively). Figures 1–3 show the effect of passing the four preblends through the hammer mill once, twice, and three times. Preblend 4 was only passed through the hammer mill once. The graphs are plots of standard deviation against time. The *x*-axis is the cumulative time that the mixture was mixed in the revolvo-cube mixer.

Figure 4 shows the mixing of salicylic acid and sucrose or icing sugar in the revolvo-cube mixer. The effect of sample size on the standard deviation for Preblend 3 is shown in Fig. 5. Table III shows the mean salicylic acid content for the four preblends at different stages.

DISCUSSION

Figures 1–3 indicate that grinding should never be the last stage in any mixing operation. The comminution effect of the hammer mill induces segregation due to size differences; since the holdup capacity of the mill

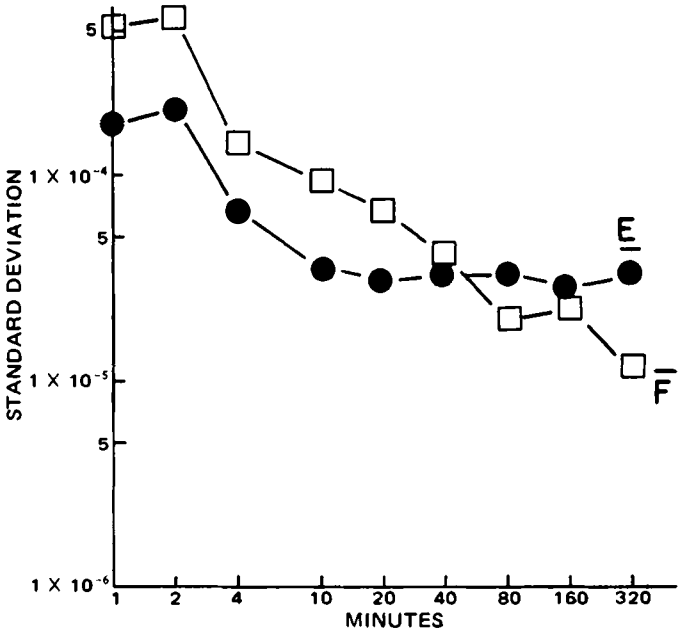

Figure 4—*Mixing of salicylic acid and sucrose/icing sugar (1:1000) in a cube mixer. Key:* E *and* F, *theoretical deviations of fully randomized mixtures of salicylic acid and sucrose and salicylic acid and icing sugar, respectively;* ●, *coarse sucrose system; and* □, *fine icing sugar system.*

is so low, no general mixing is possible. Therefore, before the materials are processed further, they must be mixed to improve homogeneity. Of the four different preblends, homogeneity increased during milling only when the preblend has been mixed in the cube mixer for the very limited period of 1 min.

The value of σ_R, the theoretical standard deviation of a fully randomized system, was calculated (9). There was a slight increase in mixture homogeneity through each cycle. This effect probably was due to the particle-size reduction and particles number increase.

If grinding is a necessary stage in the manufacturing process, it may be desirable to reduce the size of pure materials instead of the whole mixture. Table III shows the slight salicylic acid content decrease at each stage. Because of the highly cohesive microfine salicylic acid, the vigorous hammer grinding action possibly produces electrically charged fine particles and consequent particle attraction onto the mill and collecting bag walls. Thus, the salicylic acid content could vary from batch to batch.

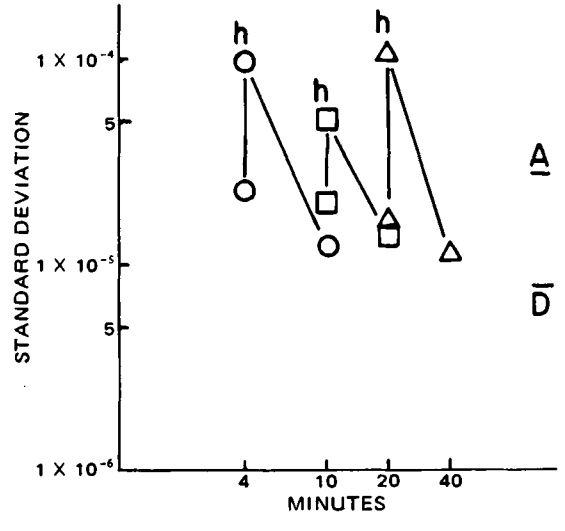

Figure 3—*Effect of passing the salicylic acid–sucrose mixture (1:1000) through the hammer mill three times. Key: A and D, standard deviations of a fully randomized equivalent system before and after passing through the hammer mill three times, respectively;* h, *mixture that has been passed through the hammer mill;* ○, *Preblend 1;* □, *Preblend 2; and* △, *Preblend 3.*

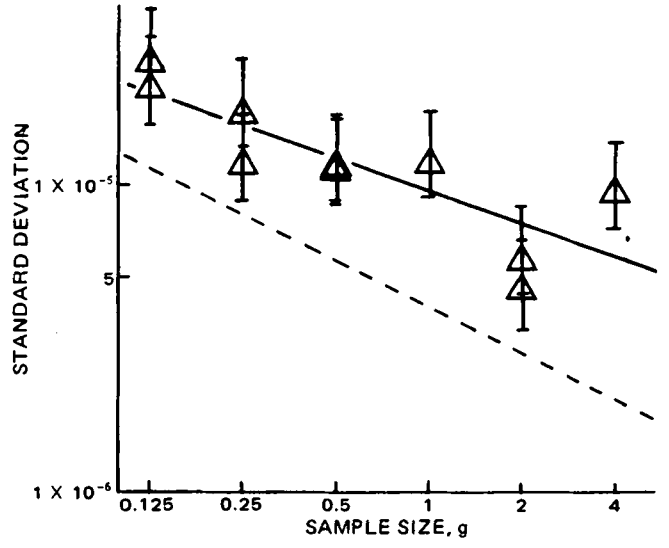

Figure 5—*Effect of sample size on standard deviation for Preblend 3 that was remixed after passing through the hammer mill three times. The dotted line represents the standard deviation for a fully equivalent randomized system. Error bars are 95% confidence limits for individual results.*

The active ingredient loss was only significant after three passes through the hammer mill.

Comparison of Fig. 1 with Fig. 4 shows that if the materials could be purchased in a fine form, it would probably be more economical to mix the preground fine material instead of grinding and mixing the coarser powders. The ordered mixture formation rate is slow when fine–fine components are mixed in a revolvo-cube mixer. With hammer mill mixture grinding, new surfaces are created by fracture of the coarse crystals. This procedure provides more area for drug particle adhesion. Furthermore, aggregates are broken down more rapidly in the hammer mill to facilitate mixing. Nevertheless, the cost of longer mixing time in the revolvo-cube mixer for fine–fine mixtures will be compensated by less handling of the mix than when the hammer mill is used.

Figure 4 also shows the mixing of a fine–coarse system in a revolvo-cube mixer where the desired degree of homogeneity is achieved after 10 min and the ordered mixture is stable and not prone to segregation (8). Even though homogeneity increases for fine particles, other problems such as fine powder flow (10) and storage effects (11) cannot be overlooked.

The sample size effect on the standard deviation for Preblend 3 is shown in Fig. 5. For a randomized mixture, the slope of the line will be −0.5. For an ordered mixture, it will approach zero. The 95% confidence limits for the slope were −0.554–−0.166. The mixture could not be classified as either completely randomized or completely ordered. In fact, it may have been a mixture of both systems, a description that may satisfy most powder mixtures used in pharmaceutical practice. A system with a large particle-size range is unlikely to be fully randomized due to size segregation. In practice, some degree of adhesional-type ordered mixture (12) may be formed. Due to the size differences of carrier particles, they will undergo ordered unit segregation (13, 14). Further mixing of this system will produce the randomized ordered unit powder mixture.

REFERENCES

(1) J. A. Hersey, *Aust. J. Pharm. Sci.*, **NS1**, 76 (1972).

(2) P. M. C. Lacey, *Trans. Inst. Chem. Eng.*, **21**, 53 (1943).

(3) J. A. Hersey, *J. Pharm. Pharmacol.*, **19**, 168S (1967).

(4) D. Train, *Pharm. J.*, **185**, 129 (1960).

(5) J. B. Gary, *Chem. Eng. Prog.*, **53**, 25 (1957).

(6) J. A. Hersey and J. Cooper, *Process Chem. Eng.*, No. 2, 11 (1978).

(7) C. W. Yip and J. A. Hersey, *Powder Technol.*, **16**, 189 (1977).

(8) C. C. Yeung and J. A. Hersey, *ibid.*, **22**, 127 (1979).

(9) K. R. Poole, F. R. Taylor, and G. P. Wall, *Trans. Inst. Chem. Eng.*, **41**, T305 (1964).

(10) R. J. Winters, *Chem. Eng. Prog.*, **73**, 82 (1977).

(11) R. C. Oppenheim and J. A. Hersey, *J. Powder Bulk Solids Technol.*, **1**, 3 (1977).

(12) J. A. Hersey, *Aust. J. Pharm. Sci.*, **6**, 29 (1977).

(13) M. J. Crooks and R. Ho, *Powder Technol.*, **14**, 161 (1976).

(14) C. W. Yip and J. A. Hersey, *ibid.*, **16**, 149 (1977).

ACKNOWLEDGMENTS

Supported by the Pharmaceutical Society of Victoria and the Australian Research Grants Committee.

The authors thank the Pharmacy Department, Western Australian Institute of Technology, for providing the microfine salicylic acid and the Chemical Engineering Department, Monash University, for use of laboratory test sieves. They also thank Dr. W. J. Thiel and Mr. P. Stephenson for valuable discussions.

Vehicle Effects on Ocular Drug Bioavailability III: Shear-Facilitated Pilocarpine Release from Ointments

JAMES W. SIEG * and JOSEPH R. ROBINSON ˣ

Received June 5, 1978, from the *School of Pharmacy, University of Wisconsin, Madison, WI 53706.* Accepted for publication November 29, 1978. *Present address: College of Pharmacy, University of Kentucky, Lexington, KY 40506.

Abstract □ Pilocarpine release from water-in-oil emulsion ointments was studied *in vitro* and *in vivo*, using albino rabbits. Pilocarpine release from the vehicle to the ocular fluids was dependent on shear, *i.e.*, blinking, and the dosing system emulsifying efficiency. A mechanical shearing component was vital for correlating corneal drug penetration and the *in vitro* pilocarpine release pattern. Simple diffusion studies with the vehicles did not predict drug *in vivo* release, but the ointment systems were all superior to an aqueous pilocarpine solution. Incorporation of a mechanical shearing component to mimic blinking gave good correlation of *in vitro* and *in vivo* results. Also, increasing the vehicle emulsifying efficiency by surfactant addition decreased shear-facilitated drug release and *in vivo* performance. Finally, increasing the internal aqueous phase volume fraction decreased *in vivo* performance and was linked to the influence of effective drug concentration in the vehicle.

Keyphrases □ Dosage forms, ocular—pilocarpine, shear-facilitated release, ointments □ Pilocarpine—release, shear facilitated, ocular ointments □ Shear—facilitation of pilocarpine release from ocular ointments □ Ointments—pilocarpine, shear-facilitated release, ocular

Important considerations in vehicle design are the anatomical and physiological aspects of the drug delivery site. To improve drug bioavailability, ocular drug delivery system designs are based on comfort, contact time, and dose volume, each of which recognizes an important anatomical/physiological constraint. An additional ocular limitation is blinking, which can both increase and decrease drug bioavailability. On the positive side, blinking spreads instilled solution or ointment across the cornea, thus promoting corneal contact and drug absorption. On the negative side, it forces drug away from the precorneal area and into the drainage apparatus.

An important blinking feature is the shear that occurs when a vehicle is placed in the eye and blinking occurs. The proximity of the eyelids to the eyeball exposes an instilled vehicle to a considerable shearing stress during blinking. Non-Newtonian fluid vehicles should undergo rheological changes during blinking, and ointments should have an altered drug release profile. This report describes an ointment drug release that is dependent on blinking and on the shear created by blinking.

Drug solubility, prolonged contact time, and modest sustained release are some positive features of ointments. Unfortunately, ointments sometimes create blurred vision and are apparently less accepted by the patient than simple aqueous solutions. Nevertheless, one generally has greater control over drug release from an ointment than from a corresponding aqueous based product in terms of drug solubility, emulsion *versus* nonemulsion form, and contact time. Generally, drug release from an ointment is attributed to partitioning and/or diffusion, depending on the drug properties and the specific vehicle selected. A third possibility for drug release, specifically from water-

0022-3549/79/0600-0724$01.00/0

© 1979, American Pharmaceutical Association

The active ingredient loss was only significant after three passes through the hammer mill.

Comparison of Fig. 1 with Fig. 4 shows that if the materials could be purchased in a fine form, it would probably be more economical to mix the preground fine material instead of grinding and mixing the coarser powders. The ordered mixture formation rate is slow when fine–fine components are mixed in a revolvo-cube mixer. With hammer mill mixture grinding, new surfaces are created by fracture of the coarse crystals. This procedure provides more area for drug particle adhesion. Furthermore, aggregates are broken down more rapidly in the hammer mill to facilitate mixing. Nevertheless, the cost of longer mixing time in the revolvo-cube mixer for fine–fine mixtures will be compensated by less handling of the mix than when the hammer mill is used.

Figure 4 also shows the mixing of a fine–coarse system in a revolvo-cube mixer where the desired degree of homogeneity is achieved after 10 min and the ordered mixture is stable and not prone to segregation (8). Even though homogeneity increases for fine particles, other problems such as fine powder flow (10) and storage effects (11) cannot be overlooked.

The sample size effect on the standard deviation for Preblend 3 is shown in Fig. 5. For a randomized mixture, the slope of the line will be −0.5. For an ordered mixture, it will approach zero. The 95% confidence limits for the slope were −0.554–−0.166. The mixture could not be classified as either completely randomized or completely ordered. In fact, it may have been a mixture of both systems, a description that may satisfy most powder mixtures used in pharmaceutical practice. A system with a large particle-size range is unlikely to be fully randomized due to size segregation. In practice, some degree of adhesional-type ordered mixture (12) may be formed. Due to the size differences of carrier particles, they will undergo ordered unit segregation (13, 14). Further mixing of this system will produce the randomized ordered unit powder mixture.

REFERENCES

(1) J. A. Hersey, *Aust. J. Pharm. Sci.*, **NS1**, 76 (1972).

(2) P. M. C. Lacey, *Trans. Inst. Chem. Eng.*, **21**, 53 (1943).

(3) J. A. Hersey, *J. Pharm. Pharmacol.*, **19**, 168S (1967).

(4) D. Train, *Pharm. J.*, **185**, 129 (1960).

(5) J. B. Gary, *Chem. Eng. Prog.*, **53**, 25 (1957).

(6) J. A. Hersey and J. Cooper, *Process Chem. Eng.*, No. 2, 11 (1978).

(7) C. W. Yip and J. A. Hersey, *Powder Technol.*, **16**, 189 (1977).

(8) C. C. Yeung and J. A. Hersey, *ibid.*, **22**, 127 (1979).

(9) K. R. Poole, F. R. Taylor, and G. P. Wall, *Trans. Inst. Chem. Eng.*, **41**, T305 (1964).

(10) R. J. Winters, *Chem. Eng. Prog.*, **73**, 82 (1977).

(11) R. C. Oppenheim and J. A. Hersey, *J. Powder Bulk Solids Technol.*, **1**, 3 (1977).

(12) J. A. Hersey, *Aust. J. Pharm. Sci.*, **6**, 29 (1977).

(13) M. J. Crooks and R. Ho, *Powder Technol.*, **14**, 161 (1976).

(14) C. W. Yip and J. A. Hersey, *ibid.*, **16**, 149 (1977).

ACKNOWLEDGMENTS

Supported by the Pharmaceutical Society of Victoria and the Australian Research Grants Committee.

The authors thank the Pharmacy Department, Western Australian Institute of Technology, for providing the microfine salicylic acid and the Chemical Engineering Department, Monash University, for use of laboratory test sieves. They also thank Dr. W. J. Thiel and Mr. P. Stephenson for valuable discussions.

Vehicle Effects on Ocular Drug Bioavailability III: Shear-Facilitated Pilocarpine Release from Ointments

JAMES W. SIEG * and JOSEPH R. ROBINSON ˣ

Received June 5, 1978, from the *School of Pharmacy, University of Wisconsin, Madison, WI 53706.* Accepted for publication November 29, 1978. *Present address: College of Pharmacy, University of Kentucky, Lexington, KY 40506.

Abstract □ Pilocarpine release from water-in-oil emulsion ointments was studied *in vitro* and *in vivo*, using albino rabbits. Pilocarpine release from the vehicle to the ocular fluids was dependent on shear, *i.e.*, blinking, and the dosing system emulsifying efficiency. A mechanical shearing component was vital for correlating corneal drug penetration and the *in vitro* pilocarpine release pattern. Simple diffusion studies with the vehicles did not predict drug *in vivo* release, but the ointment systems were all superior to an aqueous pilocarpine solution. Incorporation of a mechanical shearing component to mimic blinking gave good correlation of *in vitro* and *in vivo* results. Also, increasing the vehicle emulsifying efficiency by surfactant addition decreased shear-facilitated drug release and *in vivo* performance. Finally, increasing the internal aqueous phase volume fraction decreased *in vivo* performance and was linked to the influence of effective drug concentration in the vehicle.

Keyphrases □ Dosage forms, ocular—pilocarpine, shear-facilitated release, ointments □ Pilocarpine—release, shear facilitated, ocular ointments □ Shear—facilitation of pilocarpine release from ocular ointments □ Ointments—pilocarpine, shear-facilitated release, ocular

Important considerations in vehicle design are the anatomical and physiological aspects of the drug delivery site. To improve drug bioavailability, ocular drug delivery system designs are based on comfort, contact time, and dose volume, each of which recognizes an important anatomical/physiological constraint. An additional ocular limitation is blinking, which can both increase and decrease drug bioavailability. On the positive side, blinking spreads instilled solution or ointment across the cornea, thus promoting corneal contact and drug absorption. On the negative side, it forces drug away from the precorneal area and into the drainage apparatus.

An important blinking feature is the shear that occurs when a vehicle is placed in the eye and blinking occurs. The proximity of the eyelids to the eyeball exposes an instilled vehicle to a considerable shearing stress during blinking. Non-Newtonian fluid vehicles should undergo rheological changes during blinking, and ointments should have an altered drug release profile. This report describes an ointment drug release that is dependent on blinking and on the shear created by blinking.

Drug solubility, prolonged contact time, and modest sustained release are some positive features of ointments. Unfortunately, ointments sometimes create blurred vision and are apparently less accepted by the patient than simple aqueous solutions. Nevertheless, one generally has greater control over drug release from an ointment than from a corresponding aqueous based product in terms of drug solubility, emulsion *versus* nonemulsion form, and contact time. Generally, drug release from an ointment is attributed to partitioning and/or diffusion, depending on the drug properties and the specific vehicle selected. A third possibility for drug release, specifically from water-

0022-3549/79/0600-0724$01.00/0

© 1979, American Pharmaceutical Association

in-oil emulsions, is physical exchange of the internal emulsion phase with the neighboring tears. This report describes the properties of, and bioavailability from, such systems.

EXPERIMENTAL

Materials—Tritiated pilocarpine alkaloid (4.1 Ci/mmole) was obtained commercially[1] and purified by vacuum distillation immediately before each experiment to prevent problems with tritium exchange in the solvent. The ophthalmic ointment vehicles were commercially available, petrolatum-based products[2,3].

Male albino rabbits[4], 1.8–2.4 kg, were fed a regular diet with no restrictions on food and water consumption.

Pilocarpine Ointment Preparation—The 5% water-in-oil emulsion ointments were prepared by mixing a 0.05-ml aliquot of distilled water containing 2.08 mg of tritiated pilocarpine with sufficient ointment base to make 1 g of product. This procedure provided a 10^{-2} *M* pilocarpine ointment containing 5% water with a specific activity of 0.25 mCi/g, or approximately 160,000 cpm/mg.

For procedures in which the percent water in the ointment was increased, the ointments were prepared by adding more water in the initial step. The anhydrous ointment was prepared by geometrically mixing the tritiated pilocarpine alkaloid directly with the ointment vehicle. Surfactants were added directly to the ointment vehicles as required.

Drug distribution homogeneity was verified by the reproducibility of measured radioactivity among weighed ointment samples. Ointments were always prepared fresh prior to the experiment.

***In Vivo* Ointment Dosing Technique**—Individual ointment doses were weighed on an analytical balance. A standard 25-mg dose was used throughout the *in vivo* procedures. The weighed dose was carefully transferred to a microspatula and placed inside the center of the lower lid (cul-de-sac), with care being exercised not to irritate the eye or touch the corneal surface. The lower lid was gently moved once across the cornea to spread the dose uniformly and then released. No further manual action was performed, and normal precorneal ointment disposition was allowed to progress.

Aqueous Humor Drug Concentration–Time Profiles—The basic techniques used for monitoring aqueous humor drug levels after topical ocular dosing were described previously (1). Aqueous humor samples, 100 μl, were removed from the anterior chamber at specified times after dosing and analyzed for pilocarpine by liquid scintillation. Prior to sample removal, the precorneal area was rinsed thoroughly and the corneal surface was wiped gently with tissue to avoid contamination by any remaining ointment dose.

***In Vitro* Ointment Drug Release Study**—A 200-mg tritiated pilocarpine ointment sample was placed in the center of a 10-cm petri dish, covering a circular area 15 mm in diameter. The total pilocarpine was 416 μg, and the surface area figure was chosen to correspond to the average rabbit cornea. At the start of each release study, 35 ml of distilled water was added and the system was stirred using a magnetic stirrer and stirring bar positioned away from the ointment mass. One hundred-microliter samples were removed from the system at specified times and transferred to scintillation vials for liquid scintillation counting.

In studies where the ointment was sheared, the shearing action was accomplished manually. The ointment was positioned in the petri dish, as previously described; a microspatula, whose flat end was bent perpendicular to the rest of the handle, was used to shear the ointment against the bottom of the dish. The microspatula was rotated against the ointment, and an attempt was made to keep constant the ointment area exposed to the bathing fluid. Shear rates were predetermined and controlled by the operator. Despite the simplicity and crudeness of the system, very good reproducibility was obtained.

RESULTS

Effect of Ointment Vehicle Emulsifying Efficiency on Ocular Pilocarpine Penetration—In preliminary work (2), it was noted that the Absorption Base A[2] emulsifying efficiency was quite low compared with other hydrophilic absorption bases. Although this ointment vehicle can emulsify water to produce a relatively stable water-in-oil emulsion, 10% water is the limit. Since this vehicle was highly effective for intraocular pilocarpine penetration with a 5% water-in-oil emulsion system, this noteworthy *in vivo* success might be attributable to its low water emulsifying ability.

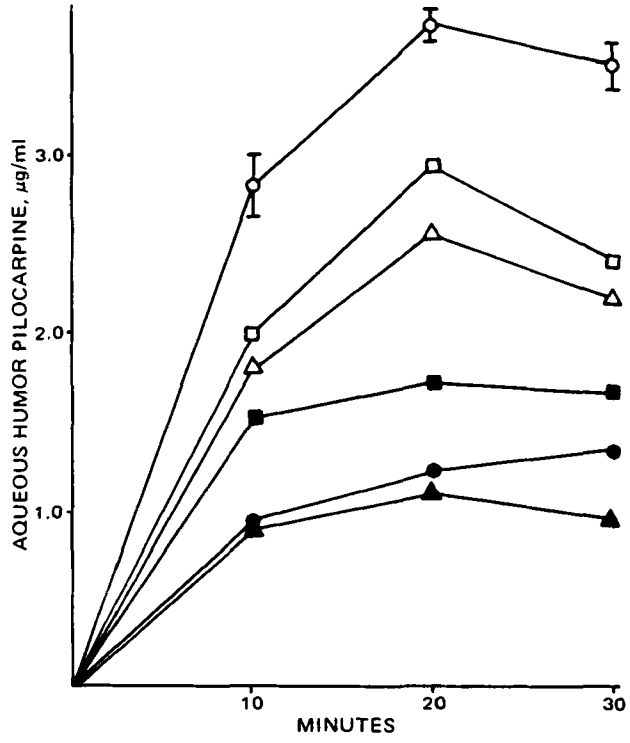

Figure 1—*Pilocarpine concentration in aqueous humor after dosing with various ointment vehicles and aqueous solution. Key:* ○, *Absorption Base A–5% water;* □, *Absorption Base A–2% sorbitan monooleate–5% water;* △, *Absorption Base A anhydrous;* ■, *Absorption Base B–5% water;* ●, *Absorption Base B–25% water; and* ▲, 10^{-2} M *aqueous solution, pH 6.24. Ointment doses were 25 mg, and the solution dose was 25 μl. At least 10 eyes were used for each data point, and representative variation in data is shown for only one system for clarity.*

Figure 1 presents current *in vivo* experiments performed to investigate this parameter. The superiority of the Absorption Base A–5% water system is readily apparent from the figure, especially when it is compared to the profile obtained from a 25-μl dose of 10^{-2} *M* pilocarpine aqueous solution (which contains the same total drug amount as the ointment). Peak aqueous humor pilocarpine levels occurred at 20-min postinstillation for both systems, but these levels are about four times higher for the ointment. The mechanism of transcorneal pilocarpine permeation and vehicle effects were extensively discussed in previous publications (3).

The next step was to incorporate 2% sorbitan monoleate[5] into the Absorption Base A vehicle to improve its emulsifying capability. A qualitative assessment of this parameter was made microscopically, and the base emulsifying efficiency was vastly improved[6] by surfactant addition. The *in vivo* experiments with this vehicle (Fig. 1) showed that aqueous humor pilocarpine levels decreased by about 25%.

At this point, the vehicle was changed to Absorption Base B[3] since its excellent emulsifying ability is well known. This base was mixed 50:50 with liquid petrolatum because the pure base did not melt at the rabbit body temperature. The mixture still possessed extremely good emulsifying efficiency, as indicated by microscopic inspection, while at the same time exhibiting melting and spreading characteristics in the eye similar to Absorption Base A. The data presented in Fig. 1 clearly indicated a further ocular drug penetration reduction when this vehicle was used.

The effect of increasing the vehicle percent water content was also investigated. Absorption Base B was used for these procedures since Absorption Base A would not accept more than about 10% water without serious "bleeding" problems. The 25% water addition decreased aqueous

[1] New England Nuclear, Boston, Mass.
[2] Lacri-Lube, Allergan Pharmaceuticals, Irvine, Calif.
[3] Aquaphor, Duke Laboratories, South Norwalk, Conn.
[4] Klubertanz, Edgerton, Wis.
[5] Span 80, Atlas Powder Co., Wilmington, Del.
[6] Homogeneity, size of internal phase, and ease of incorporation of water into the base were subjective guides in ranking bases as to their emulsifying efficiency.

Table I—*In Vitro* Shear-Facilitated Pilocarpine Release from Various Ointment Vehicles

Vehicle	Emulsifying Efficiency Ranking[a]	Maximum Amount[b] Released by Diffusion/ Partition	Maximum Amount Released by Shearing[c]
Absorption Base A–5% water	4 (poorest)	8	416
Absorption Base A–2% sorbitan monooleate–5% water	3	7	391
Absorption Base B–5% water	1 (best)	6	175
Absorption Base B–25% water	2	8	182
Absorption Base A anhydrous	NA[d]	4	216

[a] Emulsifying efficiency ranking was made by microscopic analysis. [b] All values represent micrograms of pilocarpine released. [c] Total amount of pilocarpine in each system was 416 μg. [d] Not applicable.

humor drug levels relative to the Absorption Base B–5% water system (Fig. 1).

To provide a clearer baseline for assessing relative water-in-oil emulsion vehicle effectiveness, an anhydrous pilocarpine ointment was prepared using Absorption Base A. This system was intermediate in its effectiveness for intraocular pilocarpine penetration. The pilocarpine alkaloid was not soluble in this vehicle, as discussed previously (2).

***In Vitro* Pilocarpine Release from Ointment Vehicles under Nonshear and Shear Conditions**—Shearing is an appropriate consideration for the present study with ophthalmic ointments owing to the natural shear forces that arise during blinking. These experiments were designed to determine if shear-facilitated drug release is a characteristic of such systems.

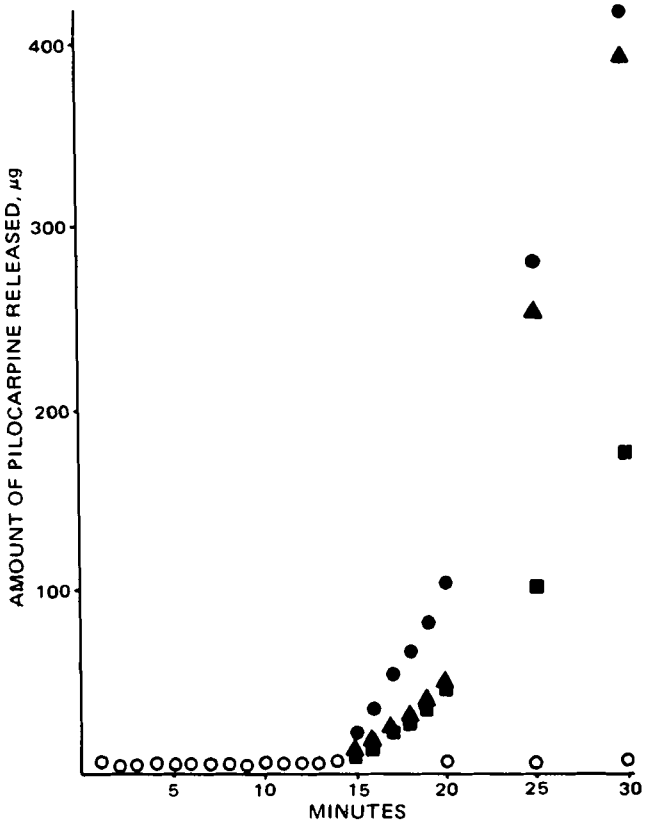

Figure 2—In vitro *pilocarpine release from various ointment vehicles under shear and nonshear conditions. Key:* ○, *Absorption Base A–5% water, no shearing;* ●, *Absorption Base A–5% water, shearing;* ■, *Absorption Base B–5% water, shearing; and* ▲, *Absorption Base A–2% sorbitan monooleate–5% water, shearing. The time interval from 0 to 15 min represents no shearing (simple diffusion), the time interval from 15 to 20 min represents a shear rate of 2/min, and the intervals from 20 to 25 min and from 25 to 30 min represent continuous shear conditions. Total pilocarpine in each system was 416 μg.*

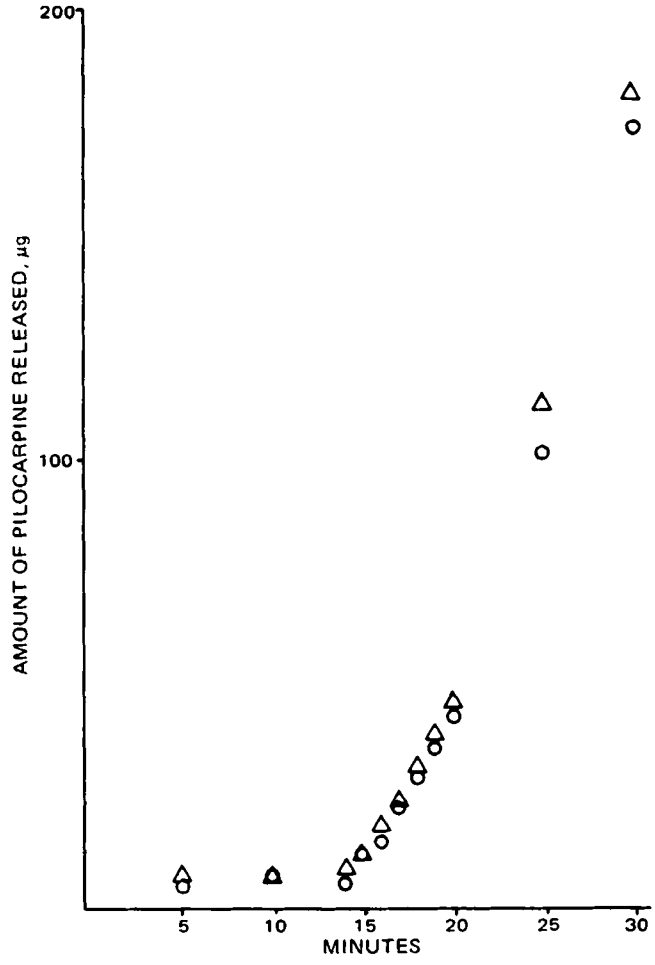

Figure 3—*Shear-facilitated pilocarpine release from absorption base B–5% water (○) and Absorption Base B–25% water (△). The time intervals representing specified shear conditions are the same as those indicated in Fig. 2. Total pilocarpine in each system was 416 μg.*

Figure 2 depicts the *in vitro* pilocarpine release patterns for three ointment vehicles. The data in each case represent an average of at least two determinations. The results of the nonshearing study using the Absorption Base A–5% water vehicle show that pilocarpine was not readily released by simple diffusion. In fact, the initial drug release, which was about 6–8 μg out of 416 μg, remained unchanged for the full 30 min of the studies.

A similar situation was observed with the other ointment vehicles. The interval from 0 to 15 min (Fig. 2) in the shearing experiments was actually a period of nonshear, or simple diffusion, drug release. The 15-min values for all systems are similar; values prior to this time point were omitted from the graph for clarity. The nonshear drug release for each system is presented in Table I.

At times beyond 15 min, addition of a mechanical shearing component to the *in vitro* release study dramatically changed the observed pilocarpine release pattern for each vehicle. The shear rate was 2/min in the interval from 15 to 20 min. The interval from 20 to 30 min represented continuous shear application during which time the operator attempted to liberate the maximum pilocarpine from the systems. The total drug released from each vehicle by the shearing procedures is listed in Table I.

Shearing caused immediate increased pilocarpine release from all vehicles (Fig. 2). The observed shear-facilitated release was consistent with microscopic assessment of the vehicle emulsifying ability. In each case, the shear-facilitated release rate was dependent on the shear rate, as indicated by the changes in slope at the 15- and 20-min points. In addition, within a given time interval with a specific shear rate, the release rate for each vehicle was a function of its emulsifying efficiency. The steepest slopes were observed for vehicles with the poorest emulsifying efficiency.

Figure 3 compares the shear-facilitated *in vitro* release patterns of the Absorption Base B–5% water and Absorption Base B–25% water vehicles.

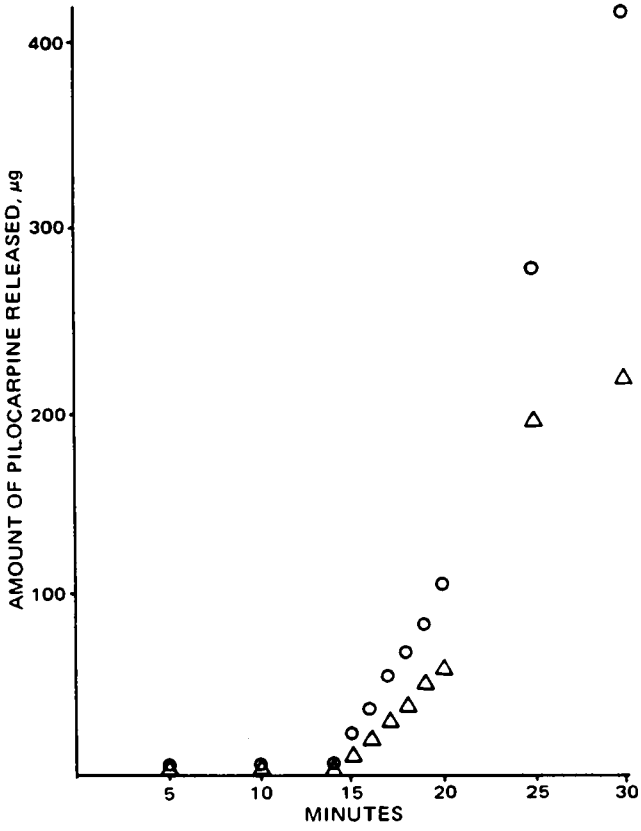

Figure 4—*Shear-facilitated pilocarpine release from Absorption Base A–5% water (○) and Absorption Base A anhydrous (△). The time intervals representing specified shear conditions are the same as those indicated in Fig. 2. Total pilocarpine in each system was 416 μg.*

These two systems showed nearly identical *in vitro* pilocarpine release. Figure 4 compares Absorption Base A–5% water and Absorption Base A anhydrous systems. The water-in-oil emulsion vehicle was clearly superior. This finding is in accord with the results of the *in vivo* experiments. A comparison of the data presented in Fig. 1 and in Table I shows that a good correlation between *in vitro* shear-facilitated drug release and *in vivo* corneal pilocarpine penetration was obtained for all of the vehicles studied. The Absorption Base A anhydrous vehicle also suffered a falloff of pilocarpine release during the terminal period of continuous shear application, a situation that is not apparent in the emulsion system for the time interval studied.

DISCUSSION

The results from *in vitro* and *in vivo* ointment studies show that pilocarpine release from the vehicles to the ocular fluids was dependent on shear and on the dosing system emulsifying efficiency. In particular, the mechanical shearing component was vitally important in correlating *in vitro* release patterns and *in vivo* performance. A literature search did not indicate that this approach had been used with *in vivo–in vitro* correlations for ophthalmic vehicles.

If the pilocarpine ointment studies are considered strictly in terms of simple partition–diffusion considerations, a number of apparent inconsistencies arise:

1. The simple *in vitro* diffusion study (without shearing) using the water-in-oil emulsion ointment vehicles did not indicate that drug release would occur *in vivo;* studies with albino rabbits, however, showed that these were excellent *in vivo* dosing systems and were as much as four times better than an aqueous solution containing the same pilocarpine amount.

2. Additional surfactant incorporation into the absorption vehicle improved the water-in-oil emulsion and increased the internal phase surface area. However, this result decreased the *in vivo* system performance.

3. Increasing the internal phase volume fraction, which decreased the oily diffusion barrier (external phase) thickness, also decreased *in vivo* performance.

A concise review of the parameters governing *in vitro* release of water-soluble drugs from water-in-oil emulsions using a simplified model was presented (4). In developing a qualitative interpretation, the following assumptions are commonly made: (*a*) the emulsion must be stable during the study time, (*b*) drug release occurs by simple diffusion or partition rather than by degradation or breaking of the emulsion, (*c*) the receptor medium acts as a perfect sink for the drug as it is released from the vehicle, and (*d*) the drug is dissolved in the aqueous phase.

Water-in-oil emulsion ointment vehicle stability was verified by checking the final product homogeneity during several storage days. Individually weighed ointment samples were analyzed for radioactivity distribution, and visual assessments of emulsion integrity were made using a microscope. No indications of instability were evident at any time for any of the vehicles studied.

The receptor medium for the *in vitro* release studies was also assumed to approximate a perfect drug sink. The relative amount of ointment and the medium volumes prevented pilocarpine concentration buildup during an individual experiment.

Pilocarpine solubility in the internal (aqueous) phase of the water-in-oil vehicles was verified previously (2). Pilocarpine resided almost totally within the aqueous component, and dissolution in the oleaginous portion of the base was highly unfavorable.

Drug release from ointment vehicles such as those under consideration is dependent upon several processes: (*a*) partitioning, (*b*) diffusion, and (*c*) "facilitated release," which refers to mechanical rupture of dispersed droplets in a water-in-oil emulsion system.

The mechanical shearing action affects each of these processes. The shearing force continually exposes new surface areas to the partitioning process between the vehicle and the receptor phase. Thus, the partitioning interface is altered by each successive shear input. The diffusion process may also be altered by a shearing component, since the diffusion layer thickness is changing. Finally, the mechanical shearing force greatly influences systems in which drug release is facilitated by coalescence and rupture of the dispersed droplets in a water-in-oil emulsion.

These considerations may be included in a discussion of the apparent inconsistencies regarding the *in vitro* and *in vivo* performance of the vehicles used in the present study. The first inconsistency can be eliminated by simply adding a mechanical shearing component to the *in vitro* drug release study. Good correlations between *in vitro* drug release and *in vivo* corneal drug penetration are thus achieved, whereas lack of such a component makes these correlations impossible. Such a shear component is intimately linked to the major drug release mechanism for the systems studied.

A qualitative measure of this shear release mechanism can be inferred from the slopes of the *in vitro* release rate profiles. The slopes are all very steep under shear conditions, suggesting that partitioning and diffusion are probably less important than shear-facilitated release. Undoubtedly, all three mechanisms operate simultaneously, but the shear-dependent mechanism is the more important and releases drug at a faster rate.

The second problem involves the addition of greater amounts of surfactant and the resulting increased internal phase surface area. While an increase in the internal surface area would be expected to increase drug release, this parameter is also a direct consequence of the emulsifying efficiency of the system and the "goodness" of the emulsion. The *in vivo* data correlate with this parameter in a unique manner. The best *in vivo* system (Absorption Base A–5% water) possessed the lowest emulsifying efficiency. Thus, surfactant addition decreased the *in vivo* performance. This observation must reflect the dependence of these systems on the shear component. Shear-facilitated drug release by emulsion rupture seems reasonable.

Finally, the decreased *in vivo* performance resulting from increasing the internal phase volume fraction may be explained on the basis of the effective pilocarpine concentration in the vehicle. A preliminary discussion of this parameter was reported (2). Since the pilocarpine is only soluble in the aqueous component of the water-in-oil emulsion vehicles, the drug will be present almost exclusively in the internal phase. However, since this phase comprises only a fraction of the total volume, the effective pilocarpine concentration in the ointments will be higher than an aqueous solution of the same volume. In other words, a 25-mg dose of 10^{-2} *M* pilocarpine in an Absorption Base A–5% water vehicle will possess an effective aqueous pilocarpine concentration 20 times higher than a 25-μl dose of 10^{-2} *M* aqueous pilocarpine solution. Similarly, the concentrations in the Absorption Base B–5% water and Absorption Base B–25% water vehicles differ by a factor of five due to different internal phase volumes.

The data in Fig. 3 show similar *in vitro* release patterns from these two vehicles, although the *in vivo* data presented in Fig. 1 show that the 5% water vehicle is superior. This finding has important implications re-

garding effective concentration influences. The *in vitro* system for measuring drug release could not distinguish between these two systems due to the large receptor medium volume. The effective concentration parameter was swamped by the excess receptor fluid. However, this result did not occur *in vivo* due to the limited volume (about 7 μl) of precorneal fluid present. This finding also points out problems that can arise when such *in vitro* tests are used to predict *in vivo* performance for systems containing high effective drug concentrations.

The *in vivo* data for these two vehicles (Fig. 1) may not reflect the fivefold difference in effective concentration since the aqueous humor levels produced by the Absorption Base B–25% water vehicle were decreased by less than one-half those values achieved by the Absorption Base B–5% water vehicle. However, these results were quite reasonable if the dilution factor arising from the normal resident tear pool volume (7.5 μl) was considered. The water volume in a 25-mg dose of the Absorption Base B–25% water vehicle was 6.25 μl, with one-fifth this amount (1.25 μl) being present in an equivalent dose of the Absorption Base B–5% water vehicle. If each volume were to be mixed with the tear pool, the calculated decrease in precorneal drug concentration would be no more than 40%. Of course, such mixing would not be instantaneous in either case, but these considerations do explain the observed results.

The data in Fig. 4 show that the Absorption Base A–5% water vehicle was able to release more pilocarpine *in vivo via* shearing than was the Absorption Base A anhydrous vehicle. Inspection of the *in vivo* data presented in Fig. 1 also shows the emulsion system to be superior. The reason for this result may be that as the percent water in the vehicle is reduced to zero, the rate-controlling process is switched from mechanical rupture of the emulsion to dissolution or diffusion control. Further work to determine this mechanism is indicated.

A shearing component is a necessary feature for *in vitro–in vivo* data correlations with ophthalmic ointments. Since some form of shearing action, such as inunction, is common to nearly every semisolid topical dosing system and to many parenteral products, this parameter should have almost universal importance.

These studies show that significant drug bioavailability increases can be achieved by careful design of a system that incorporates shear-facilitated drug release. More importantly, the results also demonstrate that such systems can be used to reduce the total drug amount required for topical ophthalmic dosing. This implies a reduced systemic drug load and decreased side effects, particularly important points for pediatric dosing.

REFERENCES

(1) J. W. Sieg and J. R. Robinson, *J. Pharm. Sci.*, **64**, 931 (1975).

(2) *Ibid.*, **66**, 1222 (1977).

(3) *Ibid.*, **65**, 1816 (1976).

(4) J. J. Windheuser, M. Best, and J. H. Perrin, *Bull. Parenter. Drug Assoc.*, **24**, 286 (1970).

ACKNOWLEDGMENTS

Supported by Allergan Pharmaceuticals, Irvine, CA 92664, and Grant EY-01332 from the National Institutes of Health.

Enhanced Chartreusin Solubility by Hydroxybenzoate Hydrotropy

G. K. POOCHIKIAN ˣ and J. C. CRADOCK

Received October 6, 1978, from the *Analytical and Product Development Section, Pharmaceutical Resources Branch, National Cancer Institute, National Institutes of Health, Bethesda, MD 20014.* Accepted for publication November 30, 1978.

Abstract □ The apparent aqueous solubility of the water-insoluble cytotoxic agent, chartreusin, was increased at neutral pH in the presence of hydroxybenzoates. Water molecules play an important role in the chartreusin conformation. Studies included solubility and spectral examinations. The weakest and strongest interactants with chartreusin were sodium benzoate and sodium trihydroxybenzoate, respectively, while the effect of mono- and dihydroxybenzoates was intermediate. A plane-to-plane orientation of chartreusin and the ligand molecules brought together by electrostatic and hydrophobic interactions is postulated. The dramatic chartreusin aqueous solubility increase relative to its aglycone, chartarin, under similar conditions was best rationalized by micellization.

Keyphrases □ Chartreusin—aqueous solubility enhanced by hydroxybenzoates, conformation □ Hydroxybenzoates—electrostatic and hydrophobic interactions, stability constants □ Cytotoxic agents—chartreusin, aqueous solubility enhanced by hydroxybenzoates □ Antineoplastic agents, potential—chartreusin, aqueous solubility enhanced by hydroxybenzoates

Chartreusin[1] (I) produced by *Streptomyces chartreusis* was originally reported in 1953 (1), but its chemical structure was not fully elucidated until 1964 (2, 3). The chartreusin aglycone, chartarin (II), possesses essentially a planar ring system. The phenolic group at C-10 is glycosidically (β) bound to a D-fucose, which, in turn, is linked

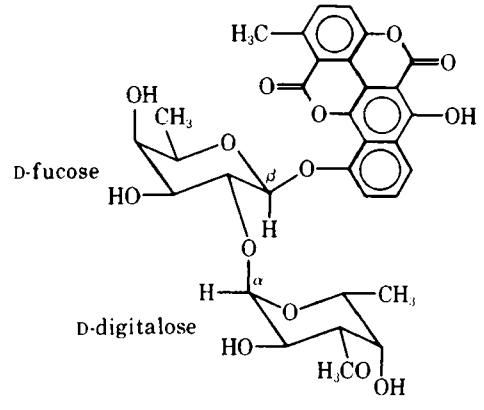

I

by an α-glycosidic linkage to D-digitalose. Chartreusin has exhibited substantial chemotherapeutic activity in mice against the P-388 and L-1210 leukemias and, to some extent, against B16 melanoma (4). Biochemical studies demonstrated that I binds to DNA and inhibits RNA and DNA syntheses (5).

Low chartreusin solubility (15 μg/ml) inhibits preparation of reasonably concentrated aqueous solutions. Although the solubility may be increased to 2 mg/ml at a high pH (>9), these solutions may be irritating and incompatible with physiological fluids. More importantly, significant irreversible decomposition of these solutions is evi-

[1] Benzo[*h*][*l*]benzopyrano[5,4,3-*cde*][*l*]benzopyran-5,12-dione, 10-[[6-deoxy-2-*O*-(6-deoxy-3-*O*-methyl-α-D-galactopyranosyl)-β-D-galactopyranosyl]oxy]-6-hydroxy-1-methyl.

0022-3549/79/0600-0728$01.00/0

© 1979, American Pharmaceutical Association

garding effective concentration influences. The *in vitro* system for measuring drug release could not distinguish between these two systems due to the large receptor medium volume. The effective concentration parameter was swamped by the excess receptor fluid. However, this result did not occur *in vivo* due to the limited volume (about 7 μl) of precorneal fluid present. This finding also points out problems that can arise when such *in vitro* tests are used to predict *in vivo* performance for systems containing high effective drug concentrations.

The *in vivo* data for these two vehicles (Fig. 1) may not reflect the fivefold difference in effective concentration since the aqueous humor levels produced by the Absorption Base B–25% water vehicle were decreased by less than one-half those values achieved by the Absorption Base B–5% water vehicle. However, these results were quite reasonable if the dilution factor arising from the normal resident tear pool volume (7.5 μl) was considered. The water volume in a 25-mg dose of the Absorption Base B–25% water vehicle was 6.25 μl, with one-fifth this amount (1.25 μl) being present in an equivalent dose of the Absorption Base B–5% water vehicle. If each volume were to be mixed with the tear pool, the calculated decrease in precorneal drug concentration would be no more than 40%. Of course, such mixing would not be instantaneous in either case, but these considerations do explain the observed results.

The data in Fig. 4 show that the Absorption Base A–5% water vehicle was able to release more pilocarpine *in vivo via* shearing than was the Absorption Base A anhydrous vehicle. Inspection of the *in vivo* data presented in Fig. 1 also shows the emulsion system to be superior. The reason for this result may be that as the percent water in the vehicle is reduced to zero, the rate-controlling process is switched from mechanical rupture of the emulsion to dissolution or diffusion control. Further work to determine this mechanism is indicated.

A shearing component is a necessary feature for *in vitro–in vivo* data correlations with ophthalmic ointments. Since some form of shearing action, such as inunction, is common to nearly every semisolid topical dosing system and to many parenteral products, this parameter should have almost universal importance.

These studies show that significant drug bioavailability increases can be achieved by careful design of a system that incorporates shear-facilitated drug release. More importantly, the results also demonstrate that such systems can be used to reduce the total drug amount required for topical ophthalmic dosing. This implies a reduced systemic drug load and decreased side effects, particularly important points for pediatric dosing.

REFERENCES

(1) J. W. Sieg and J. R. Robinson, *J. Pharm. Sci.*, **64**, 931 (1975).

(2) *Ibid.*, **66**, 1222 (1977).

(3) *Ibid.*, **65**, 1816 (1976).

(4) J. J. Windheuser, M. Best, and J. H. Perrin, *Bull. Parenter. Drug Assoc.*, **24**, 286 (1970).

ACKNOWLEDGMENTS

Supported by Allergan Pharmaceuticals, Irvine, CA 92664, and Grant EY-01332 from the National Institutes of Health.

Enhanced Chartreusin Solubility by Hydroxybenzoate Hydrotropy

G. K. POOCHIKIAN ˣ and J. C. CRADOCK

Received October 6, 1978, from the *Analytical and Product Development Section, Pharmaceutical Resources Branch, National Cancer Institute, National Institutes of Health, Bethesda, MD 20014.* Accepted for publication November 30, 1978.

Abstract □ The apparent aqueous solubility of the water-insoluble cytotoxic agent, chartreusin, was increased at neutral pH in the presence of hydroxybenzoates. Water molecules play an important role in the chartreusin conformation. Studies included solubility and spectral examinations. The weakest and strongest interactants with chartreusin were sodium benzoate and sodium trihydroxybenzoate, respectively, while the effect of mono- and dihydroxybenzoates was intermediate. A plane-to-plane orientation of chartreusin and the ligand molecules brought together by electrostatic and hydrophobic interactions is postulated. The dramatic chartreusin aqueous solubility increase relative to its aglycone, chartarin, under similar conditions was best rationalized by micellization.

Keyphrases □ Chartreusin—aqueous solubility enhanced by hydroxybenzoates, conformation □ Hydroxybenzoates—electrostatic and hydrophobic interactions, stability constants □ Cytotoxic agents—chartreusin, aqueous solubility enhanced by hydroxybenzoates □ Antineoplastic agents, potential—chartreusin, aqueous solubility enhanced by hydroxybenzoates

Chartreusin[1] (I) produced by *Streptomyces chartreusis* was originally reported in 1953 (1), but its chemical structure was not fully elucidated until 1964 (2, 3). The chartreusin aglycone, chartarin (II), possesses essentially a planar ring system. The phenolic group at C-10 is glycosidically (β) bound to a D-fucose, which, in turn, is linked

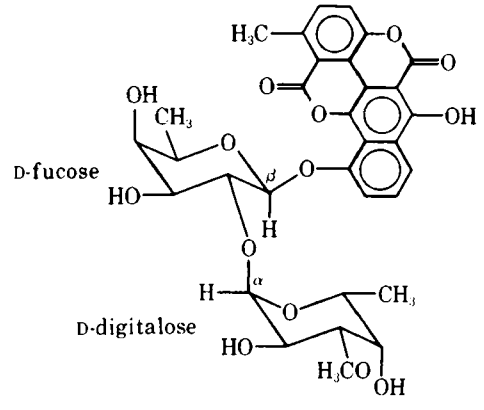

I

by an α-glycosidic linkage to D-digitalose. Chartreusin has exhibited substantial chemotherapeutic activity in mice against the P-388 and L-1210 leukemias and, to some extent, against B16 melanoma (4). Biochemical studies demonstrated that I binds to DNA and inhibits RNA and DNA syntheses (5).

Low chartreusin solubility (15 μg/ml) inhibits preparation of reasonably concentrated aqueous solutions. Although the solubility may be increased to 2 mg/ml at a high pH (>9), these solutions may be irritating and incompatible with physiological fluids. More importantly, significant irreversible decomposition of these solutions is evi-

[1] Benzo[*h*][*l*]benzopyrano[5,4,3-*cde*][*l*]benzopyran-5,12-dione, 10-[[6-deoxy-2-*O*-(6-deoxy-3-*O*-methyl-α-D-galactopyranosyl)-β-D-galactopyranosyl]oxy]-6-hydroxy-1-methyl.

0022-3549/79/0600-0728$01.00/0

© 1979, American Pharmaceutical Association

dent within a few hours at room temperature. However, at neutral pH, various hydroxybenzoic acids increase chartreusin solubility.

This report describes the preparation of relatively concentrated aqueous chartreusin solutions and the qualitative and quantitative nature of the interactions with various mono-, di-, and trihydroxybenzoic acid sodium salts.

EXPERIMENTAL

Materials—Benzoic acid, salicylic acid, *m*-hydroxybenzoic acid, *p*-hydroxybenzoic acid, 2,4-dihydroxybenzoic acid, 2,5-dihydroxybenzoic acid, 2,6-dihydroxybenzoic acid, and 2,4,6-trihydroxybenzoic acid from the same commercial source[2] were used directly[3]. Chartreusin[4] (NSC-5159), mp 246–249° (benzene–methylene chloride), and chartarin[5], mp 311–314° [lit. (2) mp 315–316°], were used as received. All other chemicals were analytical reagent grade and were used without further purification.

Solubility Studies—Ligand stock solutions of known concentrations were prepared by dissolving the necessary ligand quantities in equimolar amounts of aqueous sodium bicarbonate solution. Excess chartreusin or chartarin was added to 15-ml screw-capped vials containing different aliquots of the proper stock ligand solution, and sufficient water was added to yield 10 ml of aqueous media. The vials were stirred mechanically in a constant-temperature water bath[6] (25 ± 0.1°). To prevent excessive hydroxybenzoate oxidation and to avoid chartreusin or chartarin hydrolysis, no samples remained in solution for more than 48 hr. Chartreusin and chartarin were stable in these solutions (pH ~ 6.0[7]) during the study period, which was sufficient to ensure equilibrium with all ligands tested.

The mixtures were centrifuged for 5 min at 25° and then filtered[8]. An aliquot of the filtrate was diluted quickly with a small amount of water, and the resulting solution was extracted with fixed volumes of chloroform. The combined organic extracts were dried over anhydrous sodium sulfate, filtered, and diluted to the desired volume with additional dry chloroform. The solubilized chartreusin concentration was then measured spectrophotometrically[9]. The extraction procedure was necessary due to the limited chartarin solubility in water.

Following extraction with chloroform, the ligand concentration in the aqueous phase accounted for most (>98%) of the original ligand present as measured spectrophotometrically in the UV region. These same aqueous solutions had no absorption in the visible region, thus indicating that chartreusin and chartarin had partitioned essentially completely into chloroform and that the measured chloroform solution absorbances were due only to the free forms. The I and II concentrations were calculated from appropriate Beer–Lambert plots; I, λ_{max} (chloroform): 424 (log ϵ 4.31) nm; and II, λ_{max} (chloroform): 427 (log ϵ 4.26) nm.

The chartreusin and chartarin solubility diagrams were obtained at 25 ± 0.1° by plotting the observed solubilities against the added benzoate concentrations. The apparent stability constants for both compounds were calculated by the solubility method (7).

Precise solution surface tension[10] measurements were obtained using the Ring method by direct reading (dynes per centimeter).

RESULTS AND DISCUSSION

The solvent effects on the UV–visible spectra of chartreusin (0.025–0.027 × 10^{-3} *M*) in chloroform, ethanol, and water are shown in Fig. 1. The noticeable spectral perturbations in the strong protic solvent, water, may indicate intramolecular associations. These observations, based on the fact that water molecules can influence macromolecular conformation (8, 9) if they change any of the noncovalent bonds that stabilize macromolecular conformation, may explain the observed low chartreusin aqueous solubility. Such information, along with inspection of models, indicated a conformational change in the chartreusin molecule involving an intramolecular association or the folding up of the sugar portion over the aromatic moiety. Furthermore, the D-fucose 3-hydroxyl hydrogen is conformationally capable of hydrogen bonding to the digitalose pyranoside oxygen (10, 11). Such a possibility would create a cage-type chartreusin molecular conformation and diminish its hydration, resulting in the observed low water solubility.

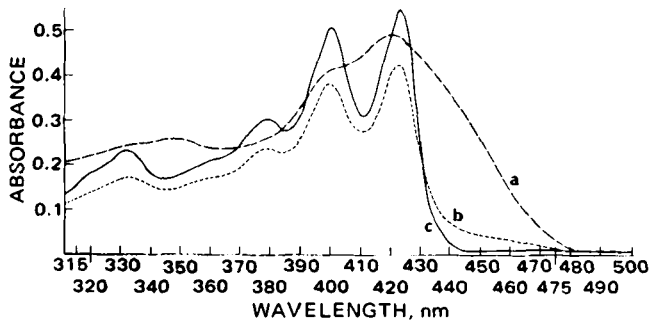

Figure 1—*Chartreusin UV–visible absorption spectra in water (a,– –), 95% ethanol (b,- - -), and chloroform (c,—).*

Hydroxybenzoates have a definite solubilizing action on chartreusin. As shown in Fig. 2, the amount of chartreusin in equilibrium with its solid phase increased progressively with the hydroxybenzoate concentration. The chartreusin solubility increase may be attributed partially to complex formation; however, due to the high reaction product solubilities and instabilities, the exact stoichiometry could not be determined. Nevertheless, the plots indicate that the dependency was nonlinear. The observations strongly support the suggestion that more than one ligand molecule interacts with an individual chartreusin molecule.

The I solubility diagram indicates that, among the ligands studied, the weakest interactant with chartreusin was the unsubstituted benzoate while the strongest was the 2,4,6-trihydroxybenzoate. Between these two were sodium benzoates with different hydroxyl substituents, all increasing I solubility.

The introduction of a hydroxyl group into the ring markedly enhanced the carboxylate "binding" tendencies. With the assumption of 1:1 and 1:2 interactions, the $K_{1:1}$ and $K_{1:2}$ association constants were calculated by the least-squares method (Table I) (7). The *ortho*-substituent had the strongest solubilizing effect on chartreusin. The enhancement effect of *meta*- and *para*-isomers on chartreusin solubility was somewhat less but still appreciable (Fig. 2 and Table I).

The sequential addition of a second or third hydroxyl group at different positions on the aromatic ring intensified chartreusin solubility on a mole to mole basis (Fig. 2). However, due to the limited solubility (0.15 *M*) of sodium 2,4,6-trihydroxybenzoate in water at 25 ± 0.1°, the apparent chartreusin solubility could not be increased more than 120-fold relative to that of water. The additional hydroxyl substitutions may lead to formation of other complexes independent of the original complex or may increase the initial complex strength while maintaining the same structure and, consequently, increase chartreusin solubility. Various ligands may have differently oriented interaction sites with chartreusin, or two complexes of different structures may coexist.

The chartreusin solubility equilibrium in the presence of dihydroxy-

Table I—Apparent 1:1 and 1:2 Stability Constants (M^{-1}) for Chartreusin and Chartarin Interactions with Various Benzoates in Water at 25 ± 0.1° Determined by the Solubility Method

Compound	Chartreusin		Chartarin	
	$K_{1:1}$	$K_{1:2}$	$K_{1:1}$	$K_{1:2}$
Benzoate	3.5	2.1	—[a]	—[a]
p-Hydroxybenzoate	5.9	9.0	—[a]	—[a]
m-Hydroxybenzoate	26.4	2.8	—[a]	—[a]
o-Hydroxybenzoate	5.7	29.1	0.25	10.5
2,4-Dihydroxybenzoate	17.2	48.3	—[a]	—[a]
2,5-Dihydroxybenzoate	30.5	27.5	1.6	28.1
2,6-Dihydroxybenzoate	32.5	38.6	—[a]	—[a]
2,4,6-Trihydroxybenzoate	263.7	17.4	7.9	29.1

[a] Interactions of these benzoates were not studied due to limited chartarin availability.

[2] Aldrich Chemical Co., Milwaukee, WI 53233.

[3] When used at the proper concentrations, the materials received were found to contain no significant impurities that interfered with chartreusin absorption in the region studied.

[4] Chartreusin occurs in several crystalline forms, and its melting point varies according to the degree of hydration and the recrystallization solvent, *i.e.*, mp 180° [acetone (1)], mp 184–186° [methylene chloride–ethanol (6)], and mp 244–246° [benzene–methylene chloride (5)].

[5] Cancer Research Unit, The Upjohn Co., Kalamazoo, MI 49001.

[6] Haake model E52, Haake, Saddle Brook, NJ 07662.

[7] Beckman Zeromatic pH meter, Beckman Instruments, Irvine, CA 92664.

[8] Millex, 0.45-μm Millipore filter, Bedford, MA 01730.

[9] UV–visible Cary 15 recording spectrophotometer, Varian Subsidiary, Monrovia, CA 91016.

[10] Du Nouy tensiometer.

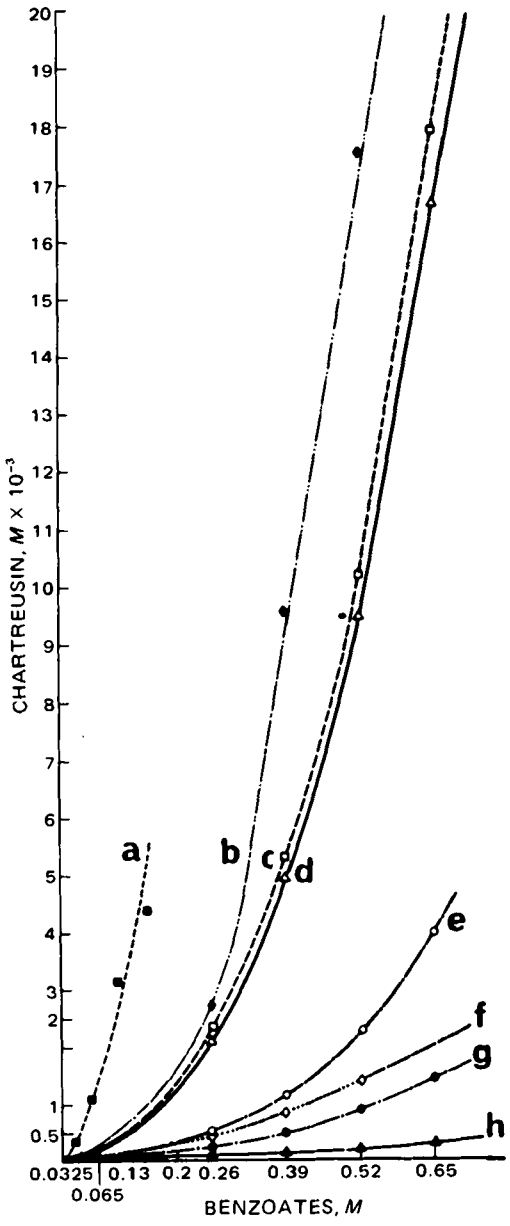

Figure 2—*Chartreusin solubility diagrams in the presence of sodium 2,4,6-trihydroxybenzoate (a, ■), sodium 2,6-dihydroxybenzoate (b, ♦), sodium 2,5-dihydroxybenzoate (c, □), sodium 2,4-dihydroxybenzoate (d, △), sodium salicylate (e, ○), sodium* m*-hydroxybenzoate (f, ◊), sodium* p*-hydroxybenzoate (g, ●), and sodium benzoate (h, ▲) in water at 25 ± 0.1°.*

benzoates, contrary to that with benzoate and monohydroxybenzoates, was achieved quickly (5 min) at concentrations up to 0.5 *M*. Higher ligand concentrations required 30 hr for equilibrium (Fig. 3). Moreover, a difference in the chartreusin solubility equilibration time with benzoate and various monohydroxybenzoates existed, the former being the slowest. Hence, the benzoate hydroxyl group(s) must play a key role in solubility equilibrium and in improving chartreusin solubility.

The increased chartreusin solubility in the presence of monohydroxybenzoates may be rationalized as follows. A hydroxyl group would stabilize the carboxylate anion by delocalization of the negative charge in the following order: *o*-hydroxybenzoate > *m*-hydroxybenzoate > *p*-hydroxybenzoate (12). Such a process would create a π-excessive aromatic system. Furthermore, in *o*-hydroxybenzoate, "ion-dipole interaction" between the phenolic hydrogen and the carboxylate anion (13) tends to keep the carbonyl group in a position coplanar with the benzene ring. Consequently, the carboxylate function π-electrons resonate with the aromatic ring π-electrons and thus increase the area of the π-cloud above and below the plane of the aromatic molecule.

Similarly, the two hydroxyl moieties in 2,6-dihydroxybenzoate are

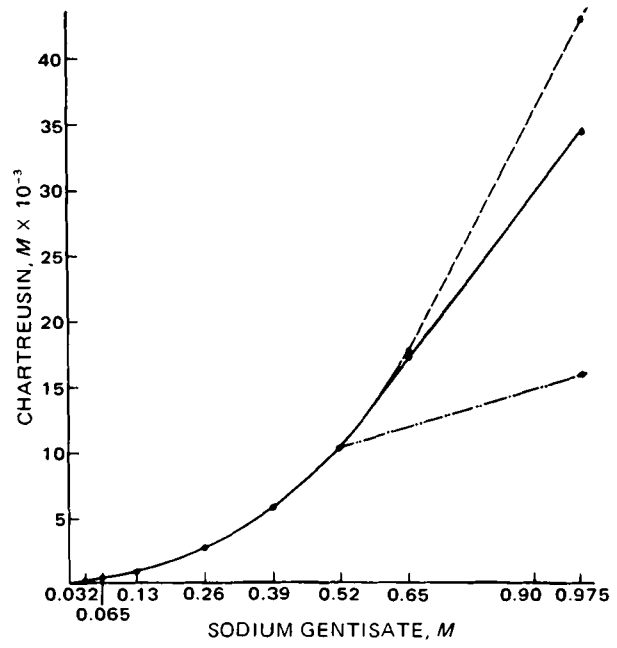

Figure 3—*Chartreusin solubility at 5 min (····), 24 hr (—), and 30 and 48 hr (- -) in the presence of increasing concentrations of sodium gentisate in water at 25 ± 0.1°.*

capable of forming two simultaneous intramolecular hydrogen bonds with the carboxylate anion, resulting in a greater planar π-cloud area relative to the 2,5- and 2,4-dihydroxybenzoates. Such an increase in the benzoate planar surface area may intensify the π–π interaction with the chartreusin aglycone portion, which possesses essentially a planar ring system, and, consequently, explain the observed solubility data: 2,4,6- > 2,6- > 2,5- > 2,4- > *o*- > *m*- > *p*- > sodium benzoate. Thus, charge delocalization on the carboxylate ion coupled with the increase in the ligand molecule π-cloud area would account partially for the difference in apparent chartreusin solubility in the presence of various benzoates. In addition, this relationship parallels the increasing pKa order of their respective acids (14), which reflects the inductive and resonance effects (12, 15).

The area correlation is good evidence for the gross structure of these interactions in solution, which may be described as a plane-to-plane orientation of the substrate and ligand molecules. Such molecular ar-

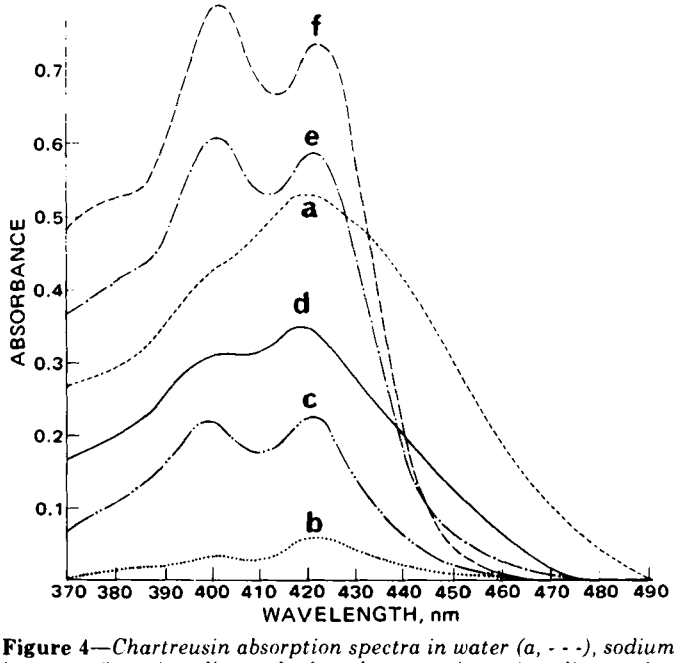

Figure 4—*Chartreusin absorption spectra in water (a, - - -), sodium benzoate (b, . . .), sodium* p*-hydroxybenzoate (c, ·—·), sodium* m*-hydroxybenzoate (d, —), sodium salicylate (e, —·), and sodium dihydroxybenzoate (f, - -) in water at 25 ± 0.1°.*

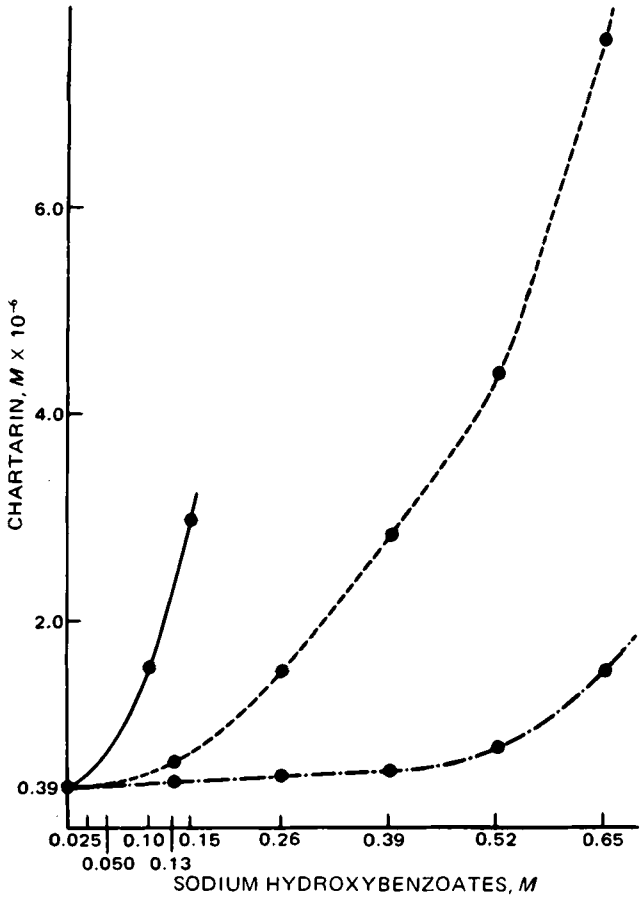

Figure 5—*Chartarin solubility diagrams in the presence of sodium salicylate (·–·), sodium 2,4-dihydroxybenzoate (- - -), and sodium 2,4,6-trihydroxybenzoate (—) in water at 25 ± 0.1°.*

rangements in solution may also indicate electrostatic interactions. Charge transfer forces have orientational properties (16), and their complexes are formed in simple molecular ratios (17). Figure 4 shows the I spectra in the presence of water and various benzoates. The chartreusin spectrum in the presence of benzoate(s) was modified to the extent that it resembled the chartreusin spectrum in chloroform (Fig. 1). This change was most prominent with di- and trihydroxybenzoates. This may be visualized as the chartreusin molecule unfolding due to its interaction with the benzoate, enabling the sugar portion to interact with water as well as with excess benzoate molecules and resulting in enhanced water solubility. Furthermore, a bathochromic shift (2 nm) of the 399- and 421-nm peaks, as well as a marked hyperchromic shift at 399 nm (Fig. 4), was observed.

These ligand-induced spectral changes suggested orientations favoring intermolecular interaction such as local dipole–dipole or dipole-induced–dipole interactions with perhaps some contact-type charge transfer contribution. Interestingly, the hydroxybenzoate sequence 2,4,6 > 2,6 > 2,5 > 2,4 > *o*-hydroxybenzoate > *m*-hydroxybenzoate > *p*-hydroxybenzoate that increased the chartreusin solubility is in the same order as their electron donor strengths, as would be expected from their

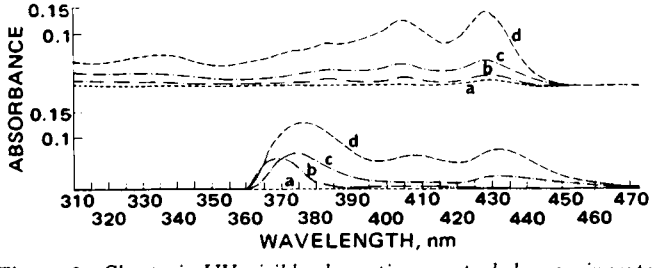

Figure 6—*Chartarin UV-visible absorption spectral changes in water (a, - - -) and in the presence of 0.13* M *(b, ·–·–·), 0.26* M *(c, ·–·), and 0.52* M *(d, – –) sodium gentisate (bottom) and following extraction of these solutions into chloroform (top).*

Table II—Chartarin Spectral Changes in the Presence of Different Benzoate Concentrations

Benzoate Concentration, *M*	Sodium Salicylate λ_{max}, nm	Sodium Gentisate λ_{max}, nm	Sodium 2,4,6-Trihydroxybenzoate λ_{max}, nm
0.025	—	—	328
0.050	—	—	335
0.10	—	—	342
0.13	—	369	—
0.15	—	—	345
0.26	342	373	—
0.39	343	—	—
0.52	344	377	—
0.65	345	—	—

ionization energies (18–20). Conjugation (21, 22) and electron donor groups decrease the π-electron ionization potential (23). Moreover, the polarization model for substituent effects gives qualitatively correct predictions. The addition of two substituent groups having opposite dipole moment directions with respect to the aromatic ring resulted in an ionization potential increasing in the order *o*-hydroxybenzoate > *m*-hydroxybenzoate > *p*-hydroxybenzoate (23). The effects of such substituents are additive but not necessarily linear. However, when studying electron donor–acceptor interactions in aromatic compounds containing heteroatom(s) capable of ρ–π-conjugation, one should recognize that *n*-donor or π-donor properties depend on certain factors (24).

To shed additional light on the interactions that increased chartreusin solubility, the chartreusin aglycone was studied. Chartarin is virtually water insoluble. The effect of various ligands on chartarin solubility is shown in Fig. 5. The shape of the curves corresponds to that of chartreusin. The order of the ligands that increased chartarin solubility was identical to that of chartreusin: trihydroxybenzoate > dihydroxybenzoate > monohydroxybenzoate. With the assumption of 1:1 and 1:2 interactions between chartarin and the ligand, the $K_{1:1}$ and $K_{1:2}$ stability constants were calculated (7) (Table I).

The characteristic chartarin UV-visible maxima were obtained in chloroform[11]. However, due to the low chartarin solubility, the corresponding UV-visible spectrum in water was unobtainable. Significant chartarin spectral changes were induced in the presence of various aqueous benzoates. These changes were observed as the difference spectra of ligand *versus* chartarin plus ligand. A typical difference spectrum is shown in Fig. 6. The $\lambda_{max}^{H_2O}$ at 404 and 427 nm had a 5-nm bathochromic shift, while all other bands[11] present in chloroform disappeared. However, a new absorption band appeared between λ_{325} and λ_{380} nm, depending on the ligand used (Table II). The new peak became the predominant one in the spectrum.

The magnitude of the bathochromic shift was dependent on the ligand concentration (Table II), and the extent of the red shift was more noticeable in the presence of the ligand with greater binding tendencies. On extraction with chloroform, the spectrum of each organic solution was identical to the original spectrum in chloroform (Fig. 6), while the remaining aqueous phase quantitatively accounted (>98%) for the ligand. The increase in chartarin solubility and the significant spectral changes in the presence of sodium hydroxybenzoate(s) support the charge transfer (24) interaction hypothesis.

There also appears to be hydrophobic contribution to the complex stabilization, since there is a direct relationship between the ligand surface area and the stability constants. Such interactions may be important for the association of solute molecules in water, although they may not be the dominant ones. Water, in addition to its role in hydrophobic bonding, may influence the stability of these complexes. Various investigators (25, 26) observed a qualitative correlation between complex stability and solvent surface tension. The solvent surface tension is the "master variable" in determining the complex stability (27). Chartreusin alone and chartreusin plus gentisic acid in chloroform afforded superimposable spectra in the visible region. In water, however, in addition to a significant reduction in the broadness of the shoulder between λ_{435} and λ_{475} nm, red shifts (5 nm) at λ_{421} and λ_{399} nm were observed.

These interactions, although operable in both chartreusin and chartarin, do not account for the remarkable preferential increase in chartreusin solubility. For example, chartarin solubility in the presence of 0.52 *M* sodium gentisate at 25 ± 0.1° was enhanced 10-fold relative to that in water, while chartreusin solubility was intensified more than 300-fold

[11] Chartarin: λ_{max} ($CHCl_3$) 266 (log ϵ 4.53), 274 (4.48), 338 (3.78), 383 (3.95), 404 (4.20), and 427 (4.26) nm.

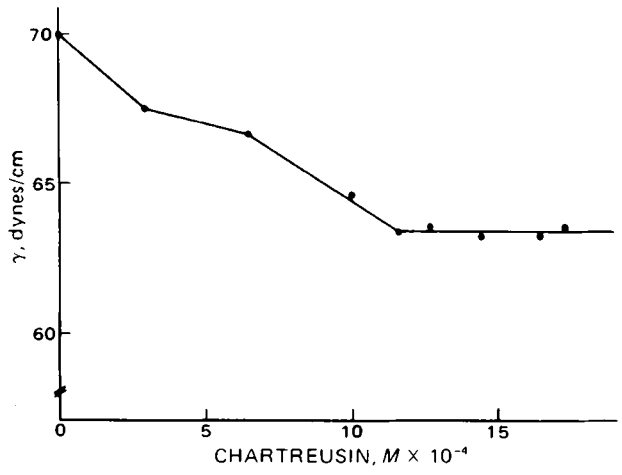

Figure 7—*Surface tension* versus *the chartreusin concentration in 0.26* M *aqueous sodium gentisate solution at 25 ± 0.1°.*

under identical conditions. Such a significant increase may be due to micellization. The commonly accepted picture of micelle structure comes from studies on compounds having a hydrophobic tail joined to a hydrophilic head. The micelles formed by these compounds above the critical micelle concentration (CMC) are nearly spherical aggregates with the heads on the surface and the tails forming a core. Such aggregates are stabilized by hydrophobic interaction between the hydrocarbon tails.

Chartreusin, once unfolded on interaction with the ligand, may be visualized as having a hydrophobic polyaromatic moiety joined to a hydrophilic disaccharide portion. Thus, one can assume that chartreusin molecule aggregates, similar to those of conventional detergent molecules, are built up by hydrophobic interactions between the aromatic surfaces, with the hydrophilic "heads" pointing outward and available to hydrogen bond with the excess ligand as well as with solvent molecules. Where conditions favor the formation of larger secondary micelles, two or more primary micelles could be linked by hydrogen bond donor and acceptor groups. Preliminary surface tension studies of chartreusin and sodium gentisate mixtures indicated possible micelle formation. When the chartreusin concentration was increased ($0–1.72 \times 10^{-5}$ *M*) in the presence of a fixed sodium gentisate concentration (0.26 *M*), a drop in surface tension to a constant minimum value was observed (Fig. 7) (28–30).

Thus, no single mechanism explains hydrotropy, but all of the above-mentioned factors play contributing roles in increasing chartreusin solubility.

REFERENCES

(1) B. E. Leach, K. M. Calhoun, L. E. Johnson, C. M. Teeters, and W. G. Jackson, *J. Am. Chem. Soc.*, **75**, 4011 (1953).

(2) E. Simonitsh, W. Eisenhuth, D. A. Stamm, and H. Schmid, *Helv. Chim. Acta*, **47**, 1459 (1964).

(3) W. Eisenhuth, D. A. Stamm, and H. Schmid, *ibid.*, **47**, 1475 (1964).

(4) J. P. McGovren, G. L. Neil, S. L. Crampton, M. I. Robinson, and J. D. Douros, *Cancer Res.*, **37**, 1666 (1977).

(5) L. H. Li and T. A. Clark, *Proc. Am. Assoc. Cancer Res.*, **17**, 96 (1976).

(6) J. Berger, L. H. Sternbach, R. G. Pollock, E. R. La Sala, S. Kaiser, and M. W. Goldberg, *J. Am. Chem. Soc.*, **80**, 1636 (1958).

(7) T. Higuchi and H. Kristiansen, *J. Pharm. Sci.*, **59**, 1601 (1970).

(8) O. Sinanoglu and S. Abdulnur, *Fed. Proc. Fed. Am. Soc. Exp. Biol.*, **24**, Suppl. 15, S-12 (1965).

(9) I. M. Klotz, *ibid.*, **24**, Suppl. 15, S-24 (1965).

(10) R. K. McMullan, W. Saeger, I. Fayos, and D. Mootz, *Carbohydr. Res.*, **31**, 211 (1973).

(11) B. Casu, M. Reggiani, G. G. Gallo, and A. Vigevani, *Tetrahedron*, **22**, 3061 (1966).

(12) D. Lloyd and D. R. Marshall, *Chem. Ind. (London)*, **1972**, 335.

(13) J. C. Darden and W. F. Forkes, *Can. J. Chem.*, **38**, 1837 (1960).

(14) G. Kortum, W. Vogel, and K. Andrusson, "Dissociation Constants of Organic Acids in Aqueous Solution," Butterworths, London, England, 1961, p. 236.

(15) L. Pauling, "Nature of the Chemical Bond," 3rd ed., Cornell University Press, Ithaca, N.Y., 1960, p. 278.

(16) R. Mulliken, *J. Am. Chem. Soc.*, **64**, 811 (1952).

(17) S. D. Ross and I. Kuntz, *J. Am. Chem. Soc.*, **76**, 74 (1954).

(18) G. Briegleb, "Molekulverbindungen und Koordination-Verbindungen in Eizebdarstellungen Elektronen-Donator-Acceptor Komplex," Springer-Verlag, Berlin, Germany, 1961.

(19) A. Streitwieser, Jr., "Molecular Orbital Theory," Wiley, New York, N.Y., 1962, p. 188.

(20) J. Rose, "Molecular Complexes," Pergamon, New York, N.Y., 1967, pp. 8, 94, and references cited therein.

(21) W. C. Price, *Chem. Rev.*, **41**, 257 (1947).

(22) G. Briegleb, *Angew Chem. Int. Ed. Engl.*, **3**, 617 (1964).

(23) G. F. Crable and G. L. Kearns, *J. Phys. Chem.*, **66**, 436 (1962).

(24) E. N. Gufyanova, I. P. Goldstein, and I. P. Romm, "Donor-Acceptor Bond," Wiley, New York, N.Y., 1975, p. 311.

(25) R. E. Moser and H. G. Cassidy, *J. Am. Chem. Soc.*, **87**, 3463 (1965).

(26) H. Kristiansen, M. Nakano, N. I. Nakano, and T. Higuchi, *J. Pharm. Sci.*, **59**, 1103 (1970).

(27) K. A. Connors and S. Sun, *J. Am. Chem. Soc.*, **93**, 7239 (1971).

(28) J. J. Bikerman, "Physical Surfaces," Academic, New York, N.Y., 1970, p. 73.

(29) A. W. Adamson, "The Physical Chemistry of Surfaces," Interscience, New York, N.Y., 1967, pp. 73, 92.

(30) P. H. Elworthy, A. T. Florence, and C. B. Macfarlane, "Solubilization by Surface-Active Agents," Chapman and Hall, London, England, 1968, p. 13.

ACKNOWLEDGMENTS

Presented in part at the Basic Pharmaceutics Section, APhA Academy of Pharmaceutical Sciences, Montreal meeting, May 1978.

The authors thank Dr. John A. Beisler, Laboratory of Medicinal Chemistry and Biology, National Cancer Institute, for helpful discussions and Dr. J. P. McGovren, The Upjohn Co., for providing the chartarin sample.

Stability-Indicating Analysis of Injectable Estrogen–Androgen Combinations in Formulations Containing Corn Oil

R. ROMAN *x, C. H. YATES, J. F. MILLAR, J. O'NEILL, and J. S. ZWEIG ‡

Received August 25, 1978, from the *Pharmacy Research and Development Department, Merck Frosst Research Laboratories, Point Claire-Dorval, Quebec, Canada.* Accepted for publication November 27, 1978. *Present address: Merck Sharp and Dohme Research Laboratories, West Point, PA 19486. ‡Merck Sharp and Dohme Research Laboratories, Rahway, NJ 07065.

Abstract □ A method was developed for the analysis of testosterone 17-enanthate 3-benzilic acid hydrazone, 17-β-estradiol 3,17-dienanthate, and estradiol benzoate combinations dissolved in an oily vehicle. Testosterone 17-enanthate 3-benzilic acid hydrazone was separated from the other drugs and vehicle components by chromatography on an acetonitrile–infusorial earth column followed by quantitation using UV spectroscopy. The estradiol esters were separated from the oil by an additional chromatographic step using a heptane–silanized infusorial earth column prior to quantitation by GLC. Subjecting formulations to elevated temperatures resulted in detectable losses for testosterone 17-enanthate 3-benzilic acid hydrazone and 17-β-estradiol 3,17-dienanthate. For both drugs, degradation was due to hydrolysis; the degradation products, testosterone 17-enanthate and 17-β-estradiol 17-enanthate, did not interfere with the intact drug determination. Methods also were developed to estimate degradation product levels in the formulation.

Keyphrases □ Estrogens—analysis, stability in formulations containing corn oil, chromatography, separation from degradation products □ Androgens—analysis, stability in formulations containing corn oil, chromatography, separation from degradation products □ Stability—estrogens and androgens in formulations containing corn oil, chromatography, separation from degradation products □ Corn oil—analysis, formulations with estrogens and androgens, stability

Testosterone 17-enanthate 3-benzilic acid hydrazone (I), a novel androgen, produces prolonged hormonal effects following subcutaneous injection (1). This drug is an ingredient in two injectable steroid formulations[1,2] that also contain 17-β-estradiol 3,17-dienanthate (II) and estradiol benzoate (III). One product[1] contains 150 mg of I, 7.5 mg of II, and 1 mg of III/ml; the other[2] contains the same amount of I and II but 3 mg of III/ml. The vehicle for both products is a corn oil–benzyl benzoate–benzyl alcohol mixture.

Drug determination in formulations containing vegetable oil usually requires separation of the drug substances from the oil components prior to quantitation (2–6). The added requirement that the method be stability indicating can add to the procedural complexity. In the present study, drug degradation products were characterized to demonstrate method selectivity.

Additional methodology was developed to estimate the degradation product level so as to establish a mass balance between intact ingredient loss and degradate formation.

EXPERIMENTAL

Reagents—All solvents and chemicals were reagent grade unless otherwise specified.

Assay—*Sample Preparation*—Approximately 500 mg of the formulation[1,2] was weighed accurately into a 5-ml volumetric flask. The sample

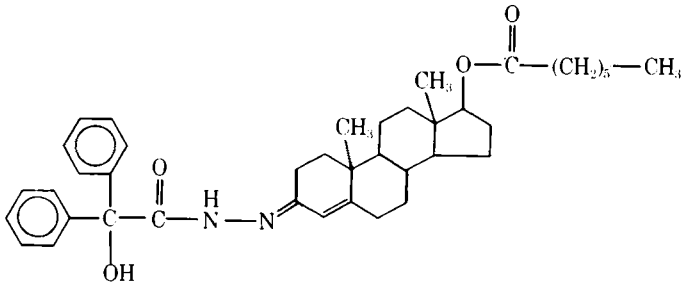

I

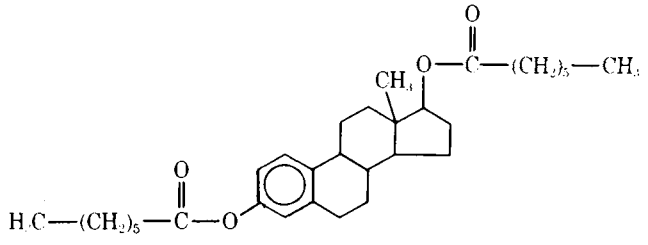

II

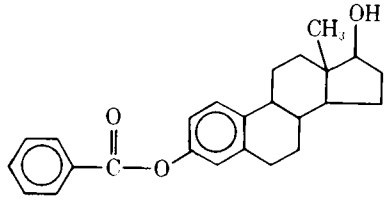

III

was dissolved in *n*-heptane (saturated with 90% ethanol) and diluted to volume with the same solvent.

Standard Solutions—For I[3], 0.75 mg/ml in denatured alcohol (ethanol 90%, methanol 10%) was prepared.

For II[3] and III[4], either 0.75 mg of II/ml and 0.1 mg of III/ml in chloroform (formulations containing 1 mg of III/ml) or 0.75 mg of II/ml and 0.3 mg of III/ml in chloroform (formulations containing 3 mg of III/ml) were prepared.

For the internal standard (for II and III determination), 0.75 mg of 17-β-estradiol 3,17-dicaproate (IV[5])/ml of chloroform was prepared.

I Determination—A 1.0-ml aliquot of the sample solution was transferred to the top of a chromatography column[6] containing 9 ml of acetonitrile (saturated with heptane) supported on 8 g of infusorial earth[7]. The column was eluted using 300 ml of heptane (saturated with acetonitrile) at a flow rate of ~8 ml/min. The eluate was retained for II and III determination (Eluate A).

When the solvent level reached the support surface, the elution was continued using 100 ml of chloroform. The eluate (Eluate B) was collected, the solvent was evaporated, the residue was transferred quanti-

[1] Climacteron Injection, Charles E. Frosst, Montreal, Quebec, Canada.
[2] Lactostat Injection, Charles E. Frosst, Montreal, Quebec, Canada.
[3] Merck Frosst Production Laboratories, Valleyfield, Quebec, Canada.
[4] Roussel Ltd., Montreal, Quebec, Canada.
[5] Prepared by the esterification of 17-β-estradiol.
[6] A 2.4-cm × 16-cm glass column equipped with a stopcock.
[7] Celite 545, Johns-Manville Product Corp., New York, NY 10016.

0022-3549/79/0600-0733$01.00/0
© 1979, American Pharmaceutical Association

tatively to a 100-ml volumetric flask using denatured alcohol, and the solution was diluted to volume with the same solvent. A 5.0-ml aliquot of this solution was transferred into a 50-ml volumetric flask, and the volume was brought to ~40 ml with denatured alcohol. A 1.0-ml aliquot of the standard I solution (0.75 mg/ml) was diluted in a parallel manner. Both flasks were heated to 70° for 0.5 hr, cooled, and diluted to volume with denatured alcohol. The UV spectra[8] for sample and standard were recorded, and the absorbance maximum at 282 nm was used for quantitation.

II and III Determination—A 1.0-ml aliquot of the internal standard solution (0.75 mg of IV/ml) was transferred to the 300 ml of heptane eluate (Eluate A). The solvent was evaporated, the oily residue was dissolved in about 2 ml of heptane (saturated with 90% ethanol), and the bulk of the solution was then transferred to a liquid chromatography column[6] containing 4 ml of heptane (saturated with 90% ethanol) supported on 6 g of silanized infusorial earth (2).

The column was eluted with 90 ml of 90% ethanol (saturated with heptane), the eluate was collected (Eluate C), the solvent was evaporated, and the residue was dissolved in ~1 ml of silylation reagent[9].

One-milliliter aliquots of the standard II–III solution and the IV solution were combined, the solvent was removed, and the residue was dissolved in ~1 ml of silylation reagent.

Approximately 2 μl of the sample was injected into a gas chromatograph[10] equipped with a 1.8-m × 2-mm i.d. glass column packed with 5% OV-101 on Gas Chrom Q[11] (80–100 mesh).

Following the injection, the oven temperature was programmed from 290 to 300° at 2°/min and was maintained at the higher temperature until the diglycerides from the vehicle eluted. The injection and temperature programming were repeated for the silylated standard. Areas[12] of the peaks for II–IV from sample and standard chromatograms were used for quantitation.

Degradation Product Identification and Estimation—*Testosterone Enanthate*—Replicate heat-stressed formulation[1] samples were passed through the normal and reversed-phase partitioning steps of the assay procedure. A series of experiments was performed on the ethanol fractions (Eluate C) to demonstrate the presence of testosterone-17-enanthate (V):

1. The solvent was removed from one sample, the residue was silylated, and 2 μl was injected onto a 5% OV-101[11] column with a column temperature at 290°[10].

2. Two microliters of the silylated residue from 1 was also injected onto a 1% Silar 10C[13] column maintained at 250°[10].

3. The residue from a replicate sample was saponified by heating at reflux in alcoholic sodium hydroxide (1 *N*) for 2 hr. After solvent removal, the organic residue was dissolved in chloroform and injected into a 5% OV-101 column[11] with the oven at 260°[10].

4. Another sample was concentrated to ~1 ml, and a portion was spotted on a TLC plate[14]. The plate was developed with benzene–ether (1:1) and visualized using iodine vapor and UV.

Benzilic Acid Hydrazide—An aged formulation[1] sample was applied to the acetonitrile–infusorial earth column, and the chloroform eluate containing I was taken to dryness. The residue was dissolved in 1 ml of *p*-nitrobenzaldehyde in methanol (2.18 mg/ml), a drop of acetic acid was added, and the solution was refluxed for 15 min. The reaction mixture was transferred to a 100-ml volumetric flask and diluted to volume with methanol–water (1:1). A similar reaction and dilution were performed on pure benzilic acid hydrazide[3] (VI).

The sample was filtered through a 0.4-μm membrane[15] to remove undissolved I, and 50 μl was injected into a high-pressure liquid chromatograph[16]. With a 25-cm × 4.6-mm stainless steel column packed with octadecylsilane permanently bonded to 10-μm silica[17], a mobile phase of methanol–water (1:1), a flow rate of 1.5 ml/min [~1500 psi (105 kg/cm^2)], and a column temperature of 40°, derivatized VI was separated from other formulation components. Quantitation was achieved by comparing the peak area[11] from the sample chromatogram to that for pure VI.

Table I—Formulation[a] Ingredient Elution on an Infusorial Earth–Acetonitrile Column

Component	Elution Volume, ml
Corn oil	<50
Benzyl benzoate	<50
II	<50
III	175
Benzyl alcohol	250
I	450

[a] Climacteron Injection, Charles E. Frosst, Montreal, Quebec, Canada.

Estradiol Monoenanthate—A formulation[2] sample stored at 40° for 1 year was subjected to the usual analytical procedure, except that the silanized residue was split into two portions. One portion, analyzed by the routine method using an OV-101 column[11], showed a 12% II loss. Examination of the other portion by GLC–mass spectrometry[18] (Silar 10C[13], 240°) indicated a component with the same retention time and mass spectrum as 17-β-estradiol 17-enanthate (VII). TLC also indicated a component with the R_f and visualization characteristics of VII.

17-β-Estradiol 17-Enanthate Preparation—A II sample dissolved in benzyl benzoate (7.5 mg/ml) was heated at 160° for 4 days. Examination by GLC indicated a 50% II loss with the formation of a more volatile product having 45% of the original II area.

The mixture was chromatographed over alumina, and the degradation product present in the methanol eluate was isolated as an oil in approximately 98% purity (GLC). Maceration of the oil with petroleum ether yielded a solid, mp 96–98°. The solid IR spectrum (chloroform) showed absorption at 3595 cm^{-1} [within the band expected for phenolic —OH stretch, a somewhat longer wavelength than would be expected for a secondary alcohol (7)] and at 1720 cm^{-1} (ester C=O). On TLC[14] with benzene–ether (9:1) as a developing solvent, the substance migrated as a single UV-absorbing spot (R_f 0.5), which gave a positive test when the plate was treated with *p*-nitrobenzenediazonium fluoroborate spray reagent. These data indicate that the product was 17-β-estradiol 17-enanthate.

A GLC–mass spectrometric[18] study gave evidence consistent with this finding. Approximately 500 μg of the solid was dissolved in 200 μl of

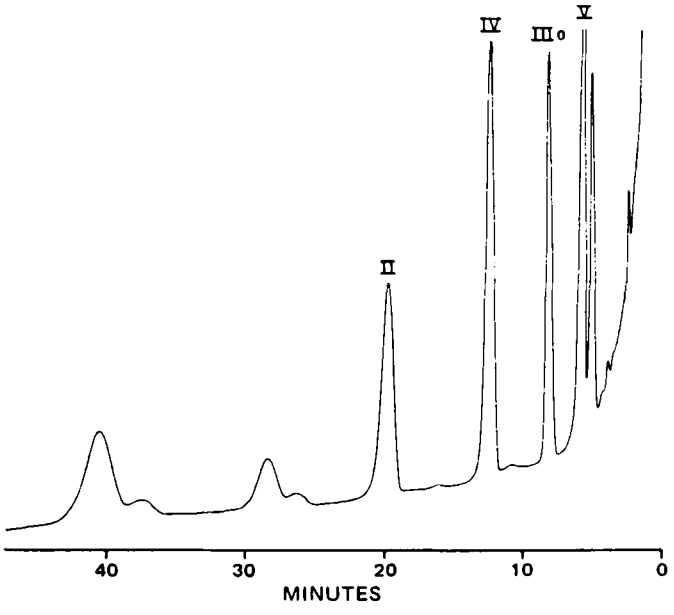

Figure 1—*Chromatogram of the fraction containing II and III obtained from a formulation. Chromatographic conditions were: column, 5% OV-101 on Gas Chrom Q; column temperature, 290–300° at 2°/min and then isothermal at 300°; injector, 310°; manifold, 330°; and nitrogen flow, 25 ml/min.*

[8] Beckman model DB-G.
[9] TRISIL, Pierce Chemical Co., Rockford, Ill.
[10] Perkin-Elmer model 900. The chromatographic conditions were: nitrogen flow, 25 ml/min; hydrogen flow, 40 ml/min; air flow, 500 ml/min; injector temperature, 310°; and manifold temperature, 330°.
[11] Prepared by the solution coating technique using a 5% (w/v) solution of OV-101 in chloroform, followed by fluidized drying. The column was conditioned at 300° for 18 hr prior to use.
[12] Hewlett-Packard model 3380 A digital integrator.
[13] Prepared by the solution coating technique using a 1% (w/v) solution of Silar 10C in chloroform coated on Chromosorb W, which was sieved, acid washed, and silanized in these laboratories.
[14] Silica gel G 60 F254, 250 μm on aluminum, E. Merck.
[15] Nuclepore Corp., Pleasanton, Calif.
[16] DuPont model 830 equipped with a sampling valve, a variable-wavelength detector, and a thermostated oven.
[17] Partisil-1025 ODS, Whatman Inc., Clifton, N.J.
[18] LKB model 9000, ionizing voltage 70 ev.

Table II—Replicate Sample[a] Assays

	I, mg/ml	II[b], mg/ml	III, mg/ml
	149.0	7.99	0.996
	147.8	8.14	0.964
	145.4	8.18	0.986
	152.6	7.93	1.010
	150.4	7.97	0.988
	144.8	7.78	0.954
Mean	148.3	8.00	0.983
SD	±2.7	±0.13	±0.019
CV, %	±1.8	±1.7	±1.9

[a] Climacteron Injection, Charles E. Frosst, Montreal, Quebec, Canada. [b] There is a 5% overage for II (theoretical input of 7.875 mg/ml).

Sylon-HTP[19]. This solution gave one GLC peak (Silar 10C, 1.4%, 0.91 m × 2 mm, 240°, retention time of 3 min). The mass spectrum showed a very strong molecular ion and the fragmentation pattern expected for the 3-trimethylsilyl ether of estradiol 17-enanthate (8–10) [*m/e* 458 (relative intensity 12%), 457 (37), 456 (M^+, 100), 441 (3), 343 (1), 328 (2), 327 (6), 298 (2), 297 (4), 257 (1), 245 (3), 244 (8), 232 (4), 231 (8), 229 (2), 219 (2), 218 (7), 217 (2), 205 (5), 113 (5), 85 (2), 75 (2), 73 (10), 57 (2), 55 (2), and 43 (11)]. A different fragmentation pattern would be expected if the carboxylate moiety were attached to the steroid aromatic A ring.

RESULTS AND DISCUSSION

Assay—Quantitation of I–III required separation of the three drugs from the other vehicle components.

I Determination—The acetonitrile–infusorial earth column retained I while allowing II, III, corn oil, benzyl alcohol, and benzyl benzoate to be eluted with heptane (Table I). Initial experiments using a nitromethane–infusorial earth column resulted in less effective I and III separation.

Compound I was eluted from the column with chloroform, a solvent of sufficiently high polarity to strip the acetonitrile liquid phase and any retained compounds from the column. The large I quantity in the formulation coupled with its high absorptivity ($A^{1\%}_{1cm}$ 492 at 282 nm) made any interference from other compounds negligible. Prior to UV determination, the eluted I was heated at 70° for 30 min to ensure that the *syn–anti* isomerization had reached equilibrium (11).

Quantitation was achieved by comparing the I sample absorbance to that for a standard I solution that had been similarly equilibrated. The Beer–Lambert law was valid for the equilibrium mixture of the two I isomers in the concentration range used for UV measurements.

II and III Determination—Following elution from the reversed-phase column, the ethanol solution containing II and III was evaporated and treated with silylation reagent. Compound III reacted to form the 17-trimethylsilyl ether (III*a*); the major corn oil components present in this fraction, the diglycerides of oleic and linoleic acid, also reacted to form trimethylsilyl derivatives.

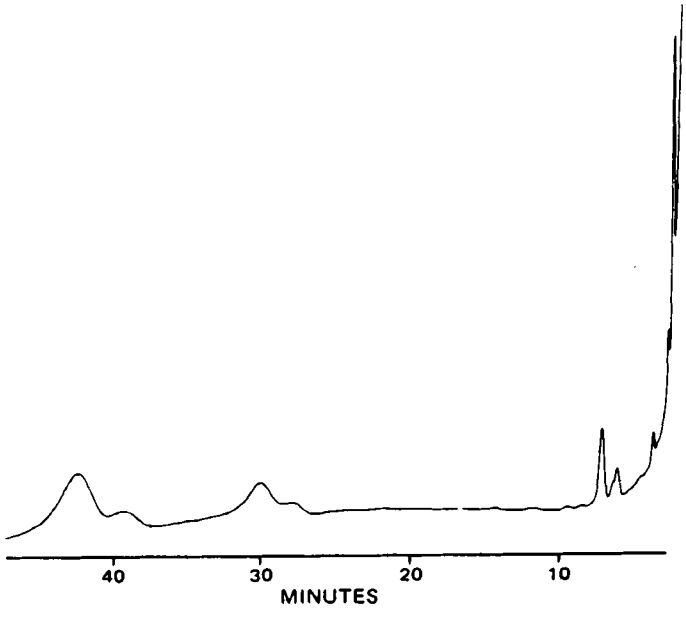

Figure 2—*Chromatogram of pharmaceutical vehicle without drugs. Conditions were the same as for Fig. 1.*

[19] Supelco, Bellefonte, Pa.

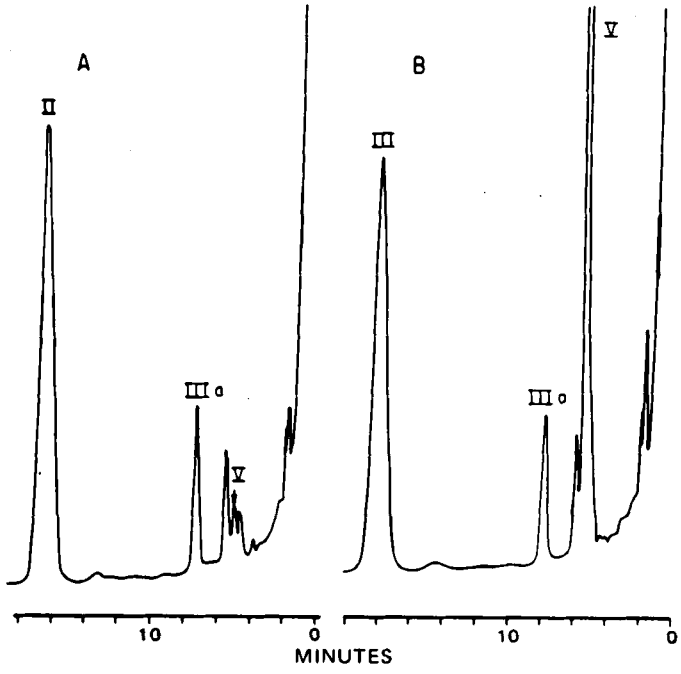

Figure 3—*(A) Chromatogram of the fraction containing II and III from a freshly prepared formulation. (B) Chromatogram of the fraction containing II and III from the same sample after storage for 12 weeks at 50°. Conditions were the same as for Fig. 1.*

A typical gas chromatogram obtained during formulation[1] analysis (Fig. 1) illustrates that II, III*a*, and the internal standard (IV) were well separated from each other as well as from V and the silylated diglycerides. Benzyl benzoate and benzyl alcohol were obscured in the solvent front. A chromatogram for the vehicle alone, after it has passed through the whole analytical procedure, is shown in Fig. 2.

The general method employed for II and III quantitation involved comparing the sample internal standard (IV) peak ratios with the corresponding ratios for a standard solution. GLC response *versus* concentration plots for II and III*a* were linear, demonstrating that a single standard with concentrations approximating those present in the sample is adequate for the quantitative analysis of the two estrogens.

Assay Precision—Results of six replicate assays carried out on a single formulation[1] over several weeks are shown in Table II. Between assays, the sample was stored at −20° to eliminate degradation. The method had adequate precision, and the drug recovery posed no problem.

Degradation Product Identification and Estimation—*I Degradation*—Benzilic acid hydrazones undergo acid hydrolysis (12). For I, this reaction would produce V and VI. Compound V could be readily detected in the formulation during the GLC analysis of II and III. Like II and III, V was eluted from both normal and reversed-phase liquid chromatographic columns. A V peak can be seen in Fig. 1.

Compound I degradation could be monitored by the size of the V peak in the chromatogram, although interfering components from the corn oil prevented accurate V quantitation. Figure 3A shows a chromatogram obtained from freshly prepared formulation[1]. A small V peak, representing less than 0.2% of the I content, was barely discernible. A chromatogram obtained after storing the sample for 12 weeks at 50° is shown in Fig. 3B. Comparison of the V peak area to that of authentic material indicated about 6.2 mg/ml (equivalent to a loss of 9.2 mg/ml for I) while the UV I assay indicated a 10.8-mg/ml loss from the initial value.

The component shown in Fig. 3 was V and not a product formed from corn oil degradation. The retention time of the component was compared to that for an authentic V sample on a 5% OV-101 column and on a 1% Silar 10C column. The latter column was prepared with a very polar cyanosilicone liquid phase and had markedly different selectivity than the nonpolar OV-101 column. On both columns, there was good agreement between the retention times for V and the component from the heat-stressed formulation[1]. Additionally, a sample of this heat-stressed for-

mulation was saponified and analyzed by GLC. The reaction mixture showed a component with the same retention time as testosterone. A spot characteristic of V was observed also when the heat-stressed sample was examined by TLC.

The other fragment (VI) from the hydrolytic I degradation was not routinely detected during the assay. A very polar compound, VI is retained on the acetonitrile–infusorial earth column and is eluted with I by chloroform. Since VI had a weak absorbance at the I maximum, $A^{1\%}_{1cm} < 1$ at 282 nm, its presence did not interfere significantly with the I determination.

The VI in a heat-stressed formulation[1] sample was detected by allowing the hydrazide to react with excess *p*-nitrobenzaldehyde and subjecting the mixture to HPLC analysis. This analysis indicated the presence of 2.6 mg of VI/ml (equivalent to hydrolysis of 6.8 mg of I/ml). UV assay showed 141.2 mg of I/ml (a loss of 8.8 mg/ml).

II and III Degradation—Hydrolysis would be expected to be the major mode of degradation for II and III, as it is for I. Compound II would be expected to give 17-β-estradiol 17-enanthate (VII) and/or 17-β-estradiol 3-enanthate (VIII). Compound III would be expected to give 17-β-estradiol. Since III was stable under extremely stressful conditions (120° for 48 hr), its decomposition was not considered further. On the other hand, II decomposed demonstrably with time.

A VII sample was prepared by heating II in benzyl benzoate. The isolated material's structure was verified by IR, GLC–mass spectrometry, and TLC. Examination of a severely stressed formulation[2] by GLC–mass spectrometry indicated a component with the same retention time and mass spectrum as VII. Evidence confirming the presence of VII in the stressed formulation was obtained by TLC.

The VII retention time on the OV-101 column was similar to that for V; when mixed, the two components eluted as a single peak. Thus, if present in the formulations, VII would not be detected in a normal analysis. The two steroids were separated on a Silar 10C column. Analysis of a heat-stressed formulation[2] using this column showed the presence of 0.85 mg of VII/ml (equivalent to a loss of 0.95 mg of II/ml) while the analysis for II using the OV-101 column resulted in a value of 6.94 mg/ml (a loss of 0.96 mg/ml from the initial value).

REFERENCES

(1) C. H. Gleason and J. M. Parker, *Endocrinology*, **65**, 508 (1959).

(2) E. Smith, *J. Pharm. Sci.*, **56**, 630 (1967).

(3) T. James, *J.A.O.A.C.*, **54**, 1192 (1971).

(4) E. Smith, *J. Am. Oil Chem. Soc.*, **49**, 409 (1972).

(5) R. H. King, L. T. Grady, and J. T. Reamer, *J. Pharm. Sci.*, **63**, 1591 (1974).

(6) R. E. Graham, E. R. Biehl, and C. T. Kenner, *ibid.*, **67**, 360 (1978).

(7) L. J. Bellamy, "The Infrared Spectra of Complex Molecules," Chapman and Hall, London, England, 1975, p. 108.

(8) C. Djerassi, J. M. Wilson, H. Budzikiewicz, and J. W. Chamberlain, *J. Am. Chem. Soc.*, **84**, 4544 (1962).

(9) H. Budzikiewicz, C. Djerassi, and D. H. Williams, "Structure Elucidation of Natural Products by Mass Spectrometry," vol. 2, Holden Day, San Francisco, Calif., 1964, p. 50.

(10) R. A. Okerholm, S. J. Clark, and H. H. Wotiz, *Anal. Biochem.*, **44**, 1 (1971).

(11) R. Roman, C. H. Yates, and J. F. Millar, *J. Pharm. Sci.*, **68**, 736 (1979).

(12) British pat. 738,230 (1955).

syn–anti Isomerization in Testosterone 17-Enanthate 3-Benzilic Acid Hydrazone

R. ROMAN *x, C. H. YATES, and J. F. MILLAR

Received August 25, 1978, from the *Pharmacy Research and Development Department, Merck Frosst Research Laboratories, Point Claire-Dorval, Quebec, Canada.* Accepted for publication November 28, 1978. *Present address: Merck Sharp and Dohme Research Laboratories, West Point, PA 19486.

Abstract □ UV spectrophotometry, high-pressure liquid chromatography, and NMR were used to investigate *syn–anti* isomerization in testosterone 17-enanthate 3-benzilic acid hydrazone. In the crystalline state, the isomeric ratio is dependent on the crystallization solvent. In solutions, including injectable pharmaceutical formulations, an equilibrium isomer mixture (2:1) is formed.

Keyphrases □ Testosterone hydrazones—isomerization, UV spectrophotometry, high-pressure liquid chromatography, NMR, effect of crystallization solvent □ Isomerization—testosterone hydrazones, effect of crystallization solvent

Compounds containing an azo function can exist in *syn*- or *anti*-configuration. Most phenylhydrazones, semicarbazones, and thiosemicarbazones form equilibrium isomer mixtures in solution (1). *syn–anti* Isomerization was detected by NMR in the 3-oximes of a series of testosterone derivatives (2). Separation of 17α-ethynyl-17β-acetoxy-19-norandrost-4-en-3-one oxime isomers using high-pressure liquid chromatography (HPLC) was also reported (3).

The object of the present study was to determine whether testosterone 17-enanthate 3-benzilic acid hydrazone (I), a long-acting androgen, exists as a single isomer or as a *syn–anti* mixture.

EXPERIMENTAL

Stock solutions of I[1] in methanol or ethanol, ~0.75 mg/ml, were used for equilibration studies. These solutions were diluted 1 to 50 prior to UV measurement[2].

High-pressure liquid chromatograms were obtained using an instrument[3] with a 254-nm fixed-wavelength detector and a column[4] (25 cm × 2 mm i.d.) packed with 6-μm silica particles. The mobile phase was

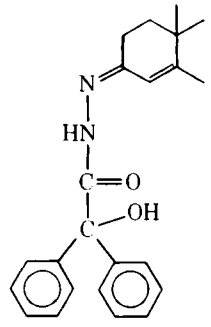

Ia

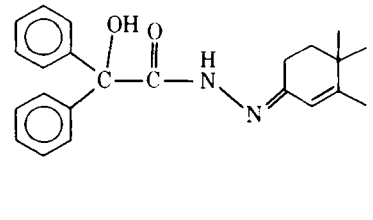

Ib

[1] Merck Frosst Production Laboratories, Valleyfield, Quebec, Canada.
[2] Beckman model DB-G and Cary model 15.
[3] DuPont model 830.
[4] Zorbax-SIL, DuPont.

0022-3549/79/0600-0736$01.00/0

© 1979, American Pharmaceutical Association

mulation was saponified and analyzed by GLC. The reaction mixture showed a component with the same retention time as testosterone. A spot characteristic of V was observed also when the heat-stressed sample was examined by TLC.

The other fragment (VI) from the hydrolytic I degradation was not routinely detected during the assay. A very polar compound, VI is retained on the acetonitrile–infusorial earth column and is eluted with I by chloroform. Since VI had a weak absorbance at the I maximum, $A^{1\%}_{1cm} < 1$ at 282 nm, its presence did not interfere significantly with the I determination.

The VI in a heat-stressed formulation[1] sample was detected by allowing the hydrazide to react with excess *p*-nitrobenzaldehyde and subjecting the mixture to HPLC analysis. This analysis indicated the presence of 2.6 mg of VI/ml (equivalent to hydrolysis of 6.8 mg of I/ml). UV assay showed 141.2 mg of I/ml (a loss of 8.8 mg/ml).

II and III Degradation—Hydrolysis would be expected to be the major mode of degradation for II and III, as it is for I. Compound II would be expected to give 17-β-estradiol 17-enanthate (VII) and/or 17-β-estradiol 3-enanthate (VIII). Compound III would be expected to give 17-β-estradiol. Since III was stable under extremely stressful conditions (120° for 48 hr), its decomposition was not considered further. On the other hand, II decomposed demonstrably with time.

A VII sample was prepared by heating II in benzyl benzoate. The isolated material's structure was verified by IR, GLC–mass spectrometry, and TLC. Examination of a severely stressed formulation[2] by GLC–mass spectrometry indicated a component with the same retention time and mass spectrum as VII. Evidence confirming the presence of VII in the stressed formulation was obtained by TLC.

The VII retention time on the OV-101 column was similar to that for V; when mixed, the two components eluted as a single peak. Thus, if present in the formulations, VII would not be detected in a normal analysis. The two steroids were separated on a Silar 10C column. Analysis of a heat-stressed formulation[2] using this column showed the presence of 0.85 mg of VII/ml (equivalent to a loss of 0.95 mg of II/ml) while the analysis for II using the OV-101 column resulted in a value of 6.94 mg/ml (a loss of 0.96 mg/ml from the initial value).

REFERENCES

(1) C. H. Gleason and J. M. Parker, *Endocrinology*, **65**, 508 (1959).

(2) E. Smith, *J. Pharm. Sci.*, **56**, 630 (1967).

(3) T. James, *J.A.O.A.C.*, **54**, 1192 (1971).

(4) E. Smith, *J. Am. Oil Chem. Soc.*, **49**, 409 (1972).

(5) R. H. King, L. T. Grady, and J. T. Reamer, *J. Pharm. Sci.*, **63**, 1591 (1974).

(6) R. E. Graham, E. R. Biehl, and C. T. Kenner, *ibid.*, **67**, 360 (1978).

(7) L. J. Bellamy, "The Infrared Spectra of Complex Molecules," Chapman and Hall, London, England, 1975, p. 108.

(8) C. Djerassi, J. M. Wilson, H. Budzikiewicz, and J. W. Chamberlain, *J. Am. Chem. Soc.*, **84**, 4544 (1962).

(9) H. Budzikiewicz, C. Djerassi, and D. H. Williams, "Structure Elucidation of Natural Products by Mass Spectrometry," vol. 2, Holden Day, San Francisco, Calif., 1964, p. 50.

(10) R. A. Okerholm, S. J. Clark, and H. H. Wotiz, *Anal. Biochem.*, **44**, 1 (1971).

(11) R. Roman, C. H. Yates, and J. F. Millar, *J. Pharm. Sci.*, **68**, 736 (1979).

(12) British pat. 738,230 (1955).

syn–anti Isomerization in Testosterone 17-Enanthate 3-Benzilic Acid Hydrazone

R. ROMAN *x, C. H. YATES, and J. F. MILLAR

Received August 25, 1978, from the *Pharmacy Research and Development Department, Merck Frosst Research Laboratories, Point Claire-Dorval, Quebec, Canada.* Accepted for publication November 28, 1978. *Present address: Merck Sharp and Dohme Research Laboratories, West Point, PA 19486.

Abstract □ UV spectrophotometry, high-pressure liquid chromatography, and NMR were used to investigate *syn–anti* isomerization in testosterone 17-enanthate 3-benzilic acid hydrazone. In the crystalline state, the isomeric ratio is dependent on the crystallization solvent. In solutions, including injectable pharmaceutical formulations, an equilibrium isomer mixture (2:1) is formed.

Keyphrases □ Testosterone hydrazones—isomerization, UV spectrophotometry, high-pressure liquid chromatography, NMR, effect of crystallization solvent □ Isomerization—testosterone hydrazones, effect of crystallization solvent

Compounds containing an azo function can exist in *syn*- or *anti*-configuration. Most phenylhydrazones, semicarbazones, and thiosemicarbazones form equilibrium isomer mixtures in solution (1). *syn–anti* Isomerization was detected by NMR in the 3-oximes of a series of testosterone derivatives (2). Separation of 17α-ethynyl-17β-acetoxy-19-norandrost-4-en-3-one oxime isomers using high-pressure liquid chromatography (HPLC) was also reported (3).

The object of the present study was to determine whether testosterone 17-enanthate 3-benzilic acid hydrazone (I), a long-acting androgen, exists as a single isomer or as a *syn–anti* mixture.

EXPERIMENTAL

Stock solutions of I[1] in methanol or ethanol, ~0.75 mg/ml, were used for equilibration studies. These solutions were diluted 1 to 50 prior to UV measurement[2].

High-pressure liquid chromatograms were obtained using an instrument[3] with a 254-nm fixed-wavelength detector and a column[4] (25 cm × 2 mm i.d.) packed with 6-μm silica particles. The mobile phase was

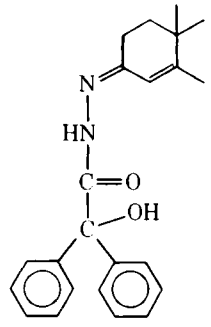

Ia

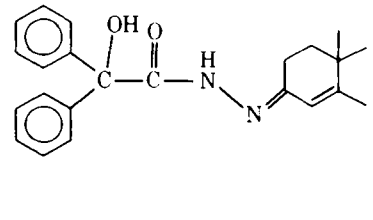

Ib

[1] Merck Frosst Production Laboratories, Valleyfield, Quebec, Canada.
[2] Beckman model DB-G and Cary model 15.
[3] DuPont model 830.
[4] Zorbax-SIL, DuPont.

0022-3549/79/0600-0736$01.00/0

© 1979, American Pharmaceutical Association

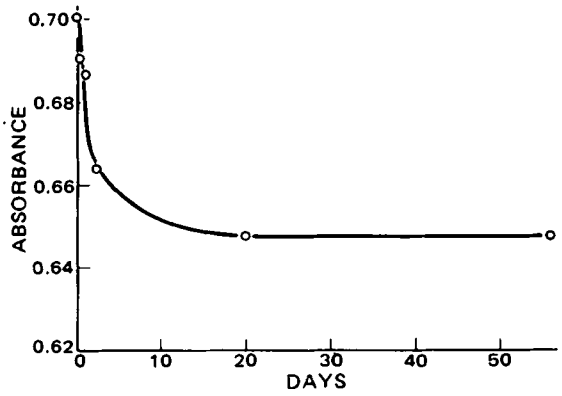

Figure 1—*Absorbance at 282 nm* versus *time for a I solution in methanol (0.0125 mg/ml).*

pentane–ether–concentrated ammonia (50:50:1). The flow rate was 0.5 ml/min. Continual column use led to resolution loss and changing retention times due to mobile phase water absorption by the silica. The column could be regenerated with anhydrous ether as the mobile phase.

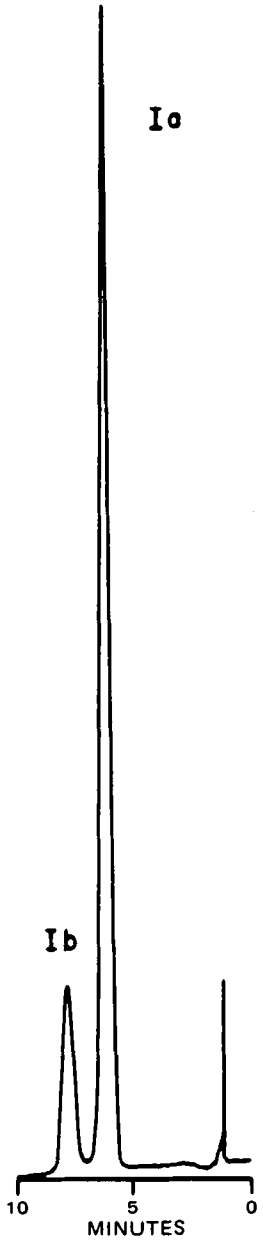

Figure 2—*Chromatograms of I stored for 2 months in methanol (0.75 mg/ml). The chromatographic conditions were: column, Zorbax-SIL; mobile phase, pentane–ether–concentrated ammonia (50:50:1); flow, 0.5 ml/min; pressure, 1000 psi; injection volume, 3 μl; wavelength, 254 nm; and attenuation, 0.08 aufs.*

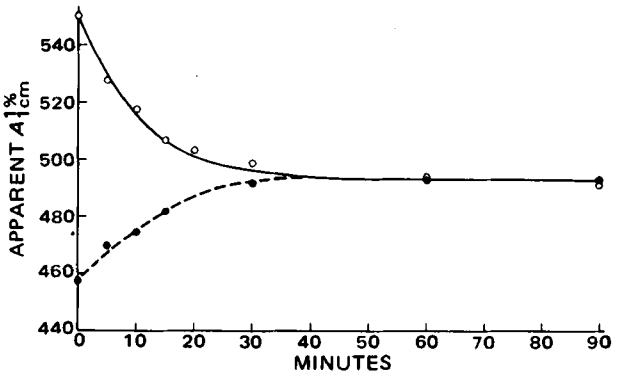

Figure 3—*Apparent* $A^{1\%}_{1cm}$ *at 282 nm* versus *time for I crystallized from aqueous acetone (○) and for I crystallized from aqueous ethanol (●) dissolved in ethanol at 70°.*

A 60-MHz NMR spectrometer[5] was used to record NMR spectra. Solutions were prepared by dissolving ~60 mg of the samples in 0.6 ml of deuterated chloroform. Tetramethylsilane was used as an internal reference standard.

RESULTS AND DISCUSSION

Since the azo group of I is conjugated to the 4,5-double bond, *syn*-(I*a*) and *anti*-(I*b*) isomers might be expected to have different UV spectra,

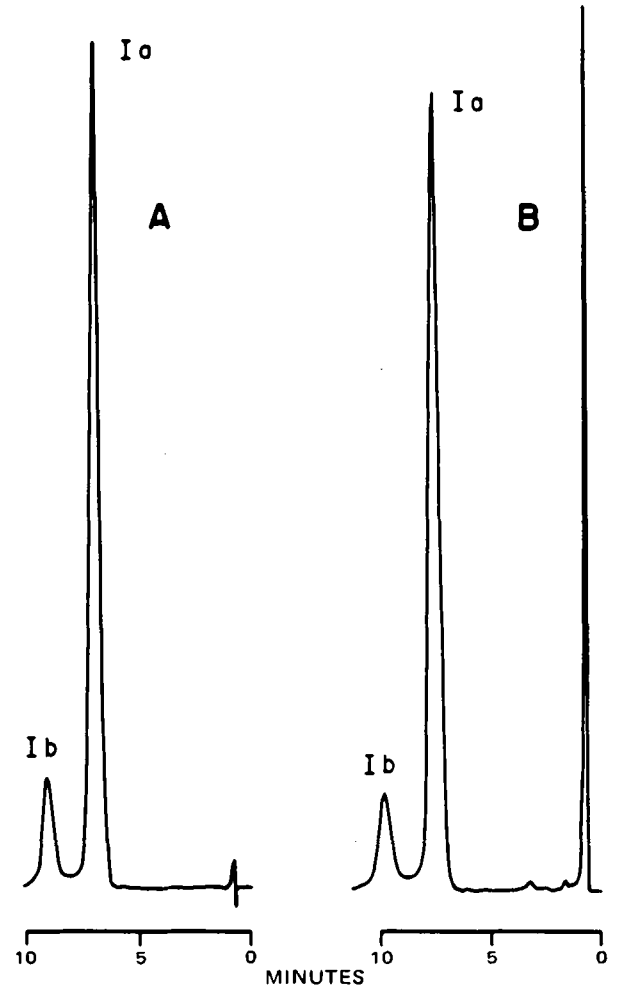

Figure 4—*(A) Chromatogram of I equilibrated in methanol (0.75 mg/ml). (B) Chromatogram of dilute formulation (1:200 in chloroform). Conditions were as in Fig. 2.*

[5] Varian model A-60-D.

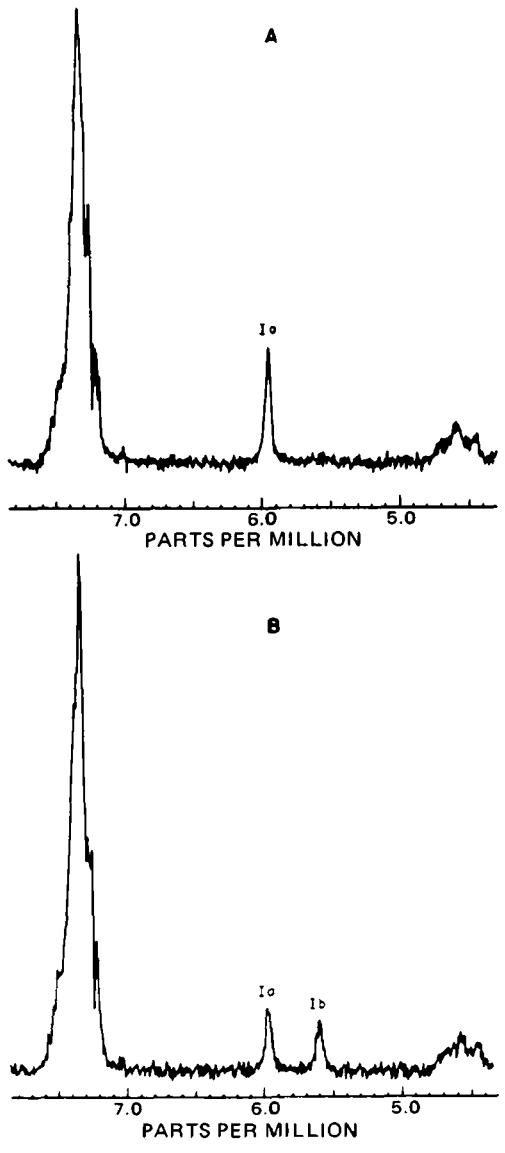

Figure 5—*(A) NMR spectrum of I crystallized from aqueous acetone (~100 mg/ml in deuterated chloroform). (B) NMR spectrum of I crystallized from aqueous ethanol (~100 mg/ml in deuterated chloroform).*

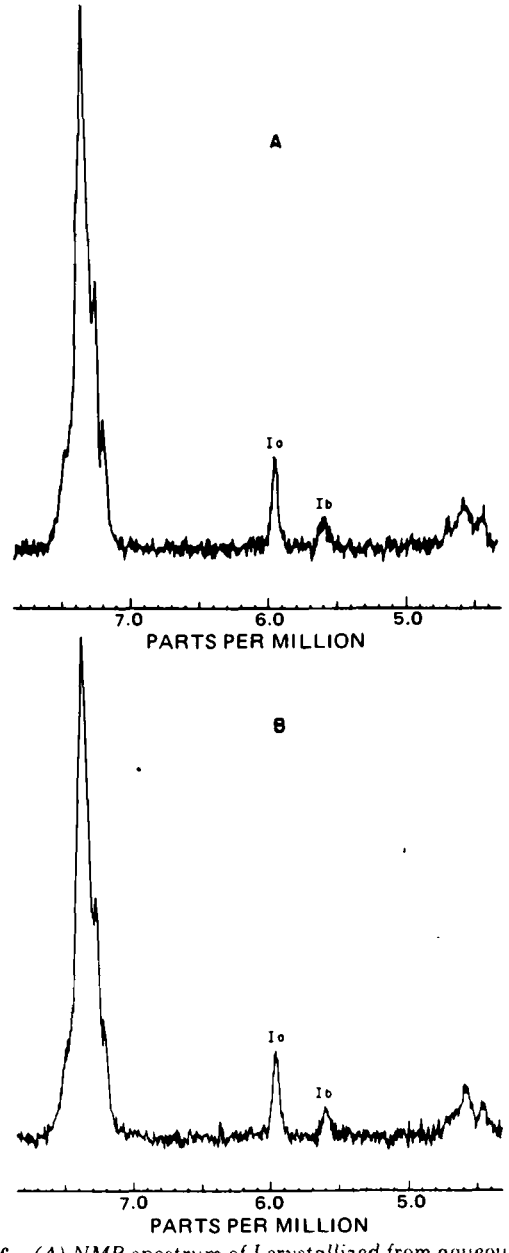

Figure 6—*(A) NMR spectrum of I crystallized from aqueous acetone after storage for 6 days in deuterated chloroform. (B) NMR spectrum of I crystallized from aqueous ethanol after storage for 6 days in deuterated chloroform.*

as was observed for 2,4-dinitrophenyl hydrazones (4). In fact, the first indication for the presence of two I isomers was the observation that the absorbance (at the UV maximum near 282 nm) of a methanolic I solution decreased with time. After a loss of 7.5%, the absorbance remained constant (Fig. 1). That this decrease in absorbance was due to a reversible equilibrium was shown by the following experiment. The methanol was evaporated from a I solution in which the absorbance had decreased ~7.5%, and the residue was crystallized from isopropyl ether. This solvent was then evaporated, and the entire residue was redissolved in methanol. The absorbance of this solution was the same as that observed for the freshly prepared solution. On storage, the solution absorbance again decreased.

Figure 2 illustrates the HPLC separation of the two isomers present in an aged I solution in methanol. Examination of a number of I solutions indicated a correlation between the UV properties and the amount of I*b* determined by HPLC. On standing, the apparent $A^{1\%}_{1cm}$ of the solutions decreased as the amount of I*b* increased.

Freshly prepared I solutions also indicated a small amount of I*b*. The extent of this isomerization depended on the method used to crystallize I. For pharmaceutical formulations, I is crystallized from isopropyl ether. A freshly prepared solution of this material had an apparent $A^{1\%}_{1cm}$ of 523 at 282 nm with ~5% isomer I*b* by area on HPLC; I crystallized from acetone–water (10:2) had an apparent $A^{1\%}_{1cm}$ of 550 at 282 nm with ~1% I*b*. The apparent $A^{1\%}_{1cm}$ of I crystallized from aqueous ethanol varied from 465 to 430. These values are lower than those measured for the equilibrium mixture dissolved in ethanol ($A^{1\%}_{1cm}$ 492 at 282 nm).

The solution equilibration rate was increased by exposure to UV radiation and heat. The elevated temperature effect is shown in Fig. 3 where I crystallized from aqueous acetone ($A^{1\%}_{1cm}$ 550) and I crystallized from aqueous ethanol ($A^{1\%}_{1cm}$ 457) equilibrated to the same isomer ratio in 30 min at 70°. This heating period was incorporated into the analysis of I in pharmaceutical formulations to assure complete equilibration prior to UV measurement (5).

The extent of isomerization in a marketed pharmaceutical formulation was determined. A chromatogram obtained from the HPLC analysis of a formulation[6] freshly dissolved in chloroform was compared to a chromatogram from an equilibrated I solution in methanol (Fig. 4). The similarity of the two chromatograms indicates that the equilibrium isomer ratio is the same in the formulation and in methanol.

Although crystallization from acetone yielded isomer I in reasonable purity, a pure sample of the thermodynamically less stable isomer was unobtainable. Without knowledge of the I*b* UV spectrum, the amounts

[6] Climacteron Injection, Charles E. Frosst, Montreal, Quebec, Canada.

of the two isomers could not be determined by UV measurement. This determination was possible using NMR. As observed for the testosterone oxime (2), the vinyl proton had a different chemical shift for the two isomers. The spectra (over the 4–8-ppm range) for I crystallized from acetone and from aqueous ethanol are shown in Fig. 5. Crystallized I from acetone had a single resonance attributable to the vinyl proton at 5.95 ppm; I crystallized from aqueous ethanol ($A^{1\%}_{1cm}$ 457 at 282 nm) had resonances at 5.95 and 5.60 ppm. That the resonance at 5.60 ppm was due to *Ib* was confirmed by monitoring changes in the two resonances with time. After storage for 144 hr with exposure to daily diffuse sunlight, the acetone-crystallized I had developed a resonance at 5.60 ppm (Fig. 6A). In the sample crystallized from aqueous ethanol, the resonance at 5.60 ppm had become smaller and the one at 5.95 ppm had become larger than in the initial spectrum (Fig. 6B).

The vinyl resonance integration values for the aqueous ethanol-crystallized sample showed the mixture to be 50% *Ia* and 50% *Ib*. After 144 hr in solution, both crystal types showed 67% *Ia* and 33% *Ib*. Using these ratios along with an apparent $A^{1\%}_{1cm}$ of 457 for I crystallized from ethanol and an apparent $A^{1\%}_{1cm}$ of 492 for the equilibrium mixture, the $A^{1\%}_{1cm}$ of *Ia* was calculated as 554 and that for *Ib* was 365 at 282 nm.

For the oximes of testosterone derivatives, Mazur (2) observed that the vinyl proton in the *anti*-isomer always resonated about 40 Hz upfield from the *syn*-isomer. For I, the 22-Hz upfield shift of *Ib* relative to *Ia* suggests that *Ia* is the *syn*-isomer and *Ib* is *anti*. This assignment is consistent with an ~20-Hz shift to lower field predicted when the vinyl proton is *cis* to the azo group(*syn*) compared to *trans* (*anti*) (1).

REFERENCES

(1) G. J. Karabatsos, F. M. Vane, R. A. Taller, and N. His, *J. Am. Chem. Soc.*, **86**, 3351 (1964).

(2) R. J. Mazur, *J. Org. Chem.*, **28**, 248 (1963).

(3) R. E. Huettemann, and A. P. Shroff, *J. Chromatogr. Sci.*, **13**, 357 (1975).

(4) F. Ramirez and A. F. Kirby, *J. Am. Chem. Soc.*, **76**, 1037 (1954).

(5) R. Roman, C. H. Yates, J. F. Millar, J. O'Neill, and J. S. Zweig, *J. Pharm. Sci.*, **68**, 733 (1979).

ACKNOWLEDGMENTS

The authors thank Mr. James Ryan for performing the NMR experiments.

Spectrophotometric Determination of Tolbutamide, Thiamine Hydrochloride, and Pyridoxine Hydrochloride in Combination Products

M. ABDEL-HADY ELSAYED *x, SAIED F. BELAL, ABDEL-FATTAH M. ELWALILY, and HASSAN ABDINE

Received April 26, 1978, from the *Faculty of Pharmacy, University of Alexandria, Alexandria, Egypt.* Accepted for publication December 4, 1978.

*Present address: Department of Pharmacy, University of Nigeria, Nsukka, Nigeria.

Abstract □ The first derivative curve is used for tolbutamide determination in unit-dose tablets and in combination products. The absorbance contribution from tablet excipient and coexisting components, thiamine and pyridoxine, is thereby nullified. The interference from tolbutamide during thiamine and pyridoxine determination is eliminated by solvent extraction and pH-induced differential spectrophotometry. Thiamine is measured at the isosbestic point of pyridoxine. The latter is determined by the differential absorbance measurement at two wavelengths with the consequent computation of the delta absorbance value.

Keyphrases □ Tolbutamide—analysis, combination tablets with thiamine and pyroxidine, spectrophotometry, first derivative curve □ Thiamine—analysis, combination tablets with tolbutamide and pyridoxine, spectrophotometry, first derivative curve □ Pyridoxine—analysis, combination tablets with thiamine and tolbutamide, spectrophotometry, first derivative curve □ Spectrophotometry—analysis, tolbutamide in combination tablets □ Antidiabetic agents—tolbutamide, spectrophotometric analysis, in combination tablets

Spectrophotometric determination of a weakly absorbing compound like tolbutamide in tablets without any interference from the tablet excipients is challenging. The problem is made more difficult when such a compound is combined with thiamine hydrochloride and pyridoxine hydrochloride.

Quantitation methods for multicomponent mixtures often employ multiple separation steps using chromatography or solvent extraction (1, 2). UV spectrophotometric methods that demand solution of simultaneous equations have also been used (3). Mixtures of two known absorbing substances have been determined spectrophotometrically (4). This method was modified (5) in terms of the extinction ratio. The application of the absorbance ratio to binary mixture analysis was recommended (6, 7).

The orthogonal function method was proposed in two-component spectrophotometric analysis (8). Recently, dual wavelength spectrophotometry (9) was applied to the simultaneous determination of mixtures (10) and to masking of unwanted components (11). The first derivative curve was useful in distinguishing substances with overlapping spectra (12) and in the quantitative analysis of two-component mixtures (13).

The present investigation was concerned with tolbutamide determination in unit-dose tablets and combination products by use of the first derivative curve. pH-Induced difference spectrophotometry (14–16) was utilized for thiamine and pyridoxine determination by independent absorbance measurements.

EXPERIMENTAL

Materials—Tolbutamide[1], thiamine hydrochloride[2], and pyridoxine hydrochloride[1] unit-dose tablets[3] contained 500 mg of tolbutamide/tablet. The combination product[4] contained 500 mg of tolbutamide, 5 mg of thiamine hydrochloride, and 3 mg of pyridoxine hydrochloride.

Reagents—All reagents were analytical grade, and solvents were spectroscopic grade.

[1] El-Nile Co. for Pharmaceutical and Chemical Industries, Cairo, Egypt.
[2] Alexandria Co. for Pharmaceutical and Chemical Industries, Egypt.
[3] Batch 039, Hoechst Orient Saa, Cairo, Egypt.
[4] Batch 14364, El-Nile Co. for Pharmaceutical and Chemical Industries, Cairo, Egypt.

0022-3549/79/0600-0739$01.00/0

© 1979, American Pharmaceutical Association

of the two isomers could not be determined by UV measurement. This determination was possible using NMR. As observed for the testosterone oxime (2), the vinyl proton had a different chemical shift for the two isomers. The spectra (over the 4–8-ppm range) for I crystallized from acetone and from aqueous ethanol are shown in Fig. 5. Crystallized I from acetone had a single resonance attributable to the vinyl proton at 5.95 ppm; I crystallized from aqueous ethanol ($A^{1\%}_{1cm}$ 457 at 282 nm) had resonances at 5.95 and 5.60 ppm. That the resonance at 5.60 ppm was due to *Ib* was confirmed by monitoring changes in the two resonances with time. After storage for 144 hr with exposure to daily diffuse sunlight, the acetone-crystallized I had developed a resonance at 5.60 ppm (Fig. 6A). In the sample crystallized from aqueous ethanol, the resonance at 5.60 ppm had become smaller and the one at 5.95 ppm had become larger than in the initial spectrum (Fig. 6B).

The vinyl resonance integration values for the aqueous ethanol-crystallized sample showed the mixture to be 50% *Ia* and 50% *Ib*. After 144 hr in solution, both crystal types showed 67% *Ia* and 33% *Ib*. Using these ratios along with an apparent $A^{1\%}_{1cm}$ of 457 for I crystallized from ethanol and an apparent $A^{1\%}_{1cm}$ of 492 for the equilibrium mixture, the $A^{1\%}_{1cm}$ of *Ia* was calculated as 554 and that for *Ib* was 365 at 282 nm.

For the oximes of testosterone derivatives, Mazur (2) observed that the vinyl proton in the *anti*-isomer always resonated about 40 Hz upfield from the *syn*-isomer. For I, the 22-Hz upfield shift of *Ib* relative to *Ia* suggests that *Ia* is the *syn*-isomer and *Ib* is *anti*. This assignment is consistent with an ~20-Hz shift to lower field predicted when the vinyl proton is *cis* to the azo group(*syn*) compared to *trans* (*anti*) (1).

REFERENCES

(1) G. J. Karabatsos, F. M. Vane, R. A. Taller, and N. His, *J. Am. Chem. Soc.*, **86**, 3351 (1964).

(2) R. J. Mazur, *J. Org. Chem.*, **28**, 248 (1963).

(3) R. E. Huettemann, and A. P. Shroff, *J. Chromatogr. Sci.*, **13**, 357 (1975).

(4) F. Ramirez and A. F. Kirby, *J. Am. Chem. Soc.*, **76**, 1037 (1954).

(5) R. Roman, C. H. Yates, J. F. Millar, J. O'Neill, and J. S. Zweig, *J. Pharm. Sci.*, **68**, 733 (1979).

ACKNOWLEDGMENTS

The authors thank Mr. James Ryan for performing the NMR experiments.

Spectrophotometric Determination of Tolbutamide, Thiamine Hydrochloride, and Pyridoxine Hydrochloride in Combination Products

M. ABDEL-HADY ELSAYED *x, SAIED F. BELAL, ABDEL-FATTAH M. ELWALILY, and HASSAN ABDINE

Received April 26, 1978, from the *Faculty of Pharmacy, University of Alexandria, Alexandria, Egypt.* Accepted for publication December 4, 1978.

*Present address: Department of Pharmacy, University of Nigeria, Nsukka, Nigeria.

Abstract □ The first derivative curve is used for tolbutamide determination in unit-dose tablets and in combination products. The absorbance contribution from tablet excipient and coexisting components, thiamine and pyridoxine, is thereby nullified. The interference from tolbutamide during thiamine and pyridoxine determination is eliminated by solvent extraction and pH-induced differential spectrophotometry. Thiamine is measured at the isosbestic point of pyridoxine. The latter is determined by the differential absorbance measurement at two wavelengths with the consequent computation of the delta absorbance value.

Keyphrases □ Tolbutamide—analysis, combination tablets with thiamine and pyroxidine, spectrophotometry, first derivative curve □ Thiamine—analysis, combination tablets with tolbutamide and pyridoxine, spectrophotometry, first derivative curve □ Pyridoxine—analysis, combination tablets with thiamine and tolbutamide, spectrophotometry, first derivative curve □ Spectrophotometry—analysis, tolbutamide in combination tablets □ Antidiabetic agents—tolbutamide, spectrophotometric analysis, in combination tablets

Spectrophotometric determination of a weakly absorbing compound like tolbutamide in tablets without any interference from the tablet excipients is challenging. The problem is made more difficult when such a compound is combined with thiamine hydrochloride and pyridoxine hydrochloride.

Quantitation methods for multicomponent mixtures often employ multiple separation steps using chromatography or solvent extraction (1, 2). UV spectrophotometric methods that demand solution of simultaneous equations have also been used (3). Mixtures of two known absorbing substances have been determined spectrophotometrically (4). This method was modified (5) in terms of the extinction ratio. The application of the absorbance ratio to binary mixture analysis was recommended (6, 7).

The orthogonal function method was proposed in two-component spectrophotometric analysis (8). Recently, dual wavelength spectrophotometry (9) was applied to the simultaneous determination of mixtures (10) and to masking of unwanted components (11). The first derivative curve was useful in distinguishing substances with overlapping spectra (12) and in the quantitative analysis of two-component mixtures (13).

The present investigation was concerned with tolbutamide determination in unit-dose tablets and combination products by use of the first derivative curve. pH-Induced difference spectrophotometry (14–16) was utilized for thiamine and pyridoxine determination by independent absorbance measurements.

EXPERIMENTAL

Materials—Tolbutamide[1], thiamine hydrochloride[2], and pyridoxine hydrochloride[1] unit-dose tablets[3] contained 500 mg of tolbutamide/tablet. The combination product[4] contained 500 mg of tolbutamide, 5 mg of thiamine hydrochloride, and 3 mg of pyridoxine hydrochloride.

Reagents—All reagents were analytical grade, and solvents were spectroscopic grade.

[1] El-Nile Co. for Pharmaceutical and Chemical Industries, Cairo, Egypt.
[2] Alexandria Co. for Pharmaceutical and Chemical Industries, Egypt.
[3] Batch 039, Hoechst Orient Saa, Cairo, Egypt.
[4] Batch 14364, El-Nile Co. for Pharmaceutical and Chemical Industries, Cairo, Egypt.

0022-3549/79/0600-0739$01.00/0

© 1979, American Pharmaceutical Association

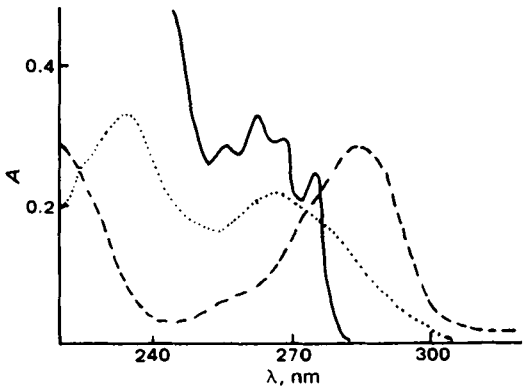

Figure 1—*UV absorption spectra of 0.15 mg of tolbutamide/ml (—), 0.01 mg of thiamine hydrochloride/ml (···), and 0.01 mg of pyridoxine hydrochloride/ml (- -). The solvent was 95% ethanol.*

Instruments—A photoelectric spectrophotometer[5] with 1-cm silica cells was used for all measurements.

Assay of Tolbutamide in Unit-Dose Tablets—Twenty tablets were powdered and mixed, and an accurately weighed quantity (~0.6 g) was extracted with 95% ethanol. The solution was diluted with ethanol to give ~0.25 mg of tolbutamide/ml. The absorbance was measured at 274 and 276 nm using 95% ethanol in the reference cell. The absorbance difference between 274 and 276 nm, $\Delta A(274 - 276)$, was computed.

Assay for Combination Product—For the tolbutamide component, the above-mentioned method was used. For the thiamine and pyridoxine components, another ~0.6-g powdered tablet portion was weighed accurately, extracted, and diluted with water. Two equal volumes were suitably diluted, with 0.1 *N* H_2SO_4 or 0.01 *N* NaOH, to give ~0.016 mg of thiamine/ml and 0.01 mg of pyridoxine/ml. The acid solution absorbance was measured at 265 nm using an alkaline solution in the reference cell (thiamine component). The alkaline solution absorbance was measured at 300 and 310 nm using an acid solution in the reference cell (pyridoxine component).

RESULTS AND DISCUSSION

The tolbutamide absorption spectrum (Fig. 1) showed three absorption maxima at 256, 262, and 274 nm and a shoulder at 268 nm. The first derivative curve, obtained by plotting $\Delta A(\lambda_1 - \lambda_2)$ *versus* λ_m [where $\lambda_m = (\lambda_1 + \lambda_2)/2$], is presented in Fig. 2. The working wavelengths chosen for the tolbutamide assay were 274 and 276 nm rather than the peaks located at shorter wavelengths.

The choice of these wavelengths was based on the high $\Delta A(274 - 276)$ with a consequent increase in sensitivity. The absorbance contribution from tablet excipients (mostly nonbenzenoid) at longer wavelengths was expected to be nil since the diverse components were characterized by constant absorption spectra (*i.e.*, with zero slope). More important, the absorption spectrum slopes of the coexisting components (thiamine and pyridoxine) in the compound tablets were opposite to each other and distinctly lower (Fig. 1) than the tolbutamide spectrum slope. Consequently, the first derivative curves of thiamine and pyridoxine contribute equally but with opposite signs (Fig. 2). Therefore, they canceled each other with the net result of no interference from these compounds. The first derivative curve in the tolbutamide determination in unit-dose tablets and in combination products gave highly accurate results (Tables I and II).

The tolbutamide concentration was calculated from the following regression equation[6], derived by using the least-squares method (17):

$$\Delta A(274 - 276) = 0.0053 + 0.915C \qquad \text{(Eq. 1)}$$

with[7] $r = 0.9998$, which was obtained by application of the procedure described for tolbutamide assay in tablets to known tolbutamide concentrations. Within a 0.1–0.7-mg/ml range, $\Delta A(274 - 276)$ *versus* C was linear.

Thiamine and pyridoxine in combination products could be determined using their pH-induced spectral changes. The interference from the major component, tolbutamide, was thereby eliminated since it is barely soluble in water, the solvent used for the tablet powder extraction. More important, tolbutamide exhibits virtually identical spectra in acid and alkaline media. Consequently, the pH-induced tolbutamide solution differential spectrum (prepared by extracting 500 mg of tolbutamide with water and subsequent acidification or alkalinization) displayed a negligible contribution (Fig. 3).

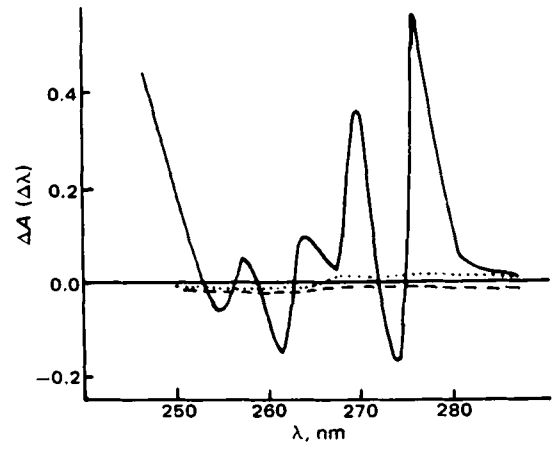

Figure 2—*First derivative curves from absorption spectra of tolbutamide (—), thiamine hydrochloride (···), and pyridoxine hydrochloride (- -).*

When the acid solution absorbance was measured against that of alkaline solution at 265 nm, thiamine could be determined without interference from pyridoxine since the latter showed an isosbestic point (Fig. 3). The delta absorbance measurement [A(acid) − A(alkaline)] at 265 nm was linearly related to the thiamine concentration over the 0.008–0.056-mg/ml range. The following regression equation, derived from ΔA_{265} measurements of known thiamine concentrations, describes the calibration curve:

$$\Delta A_{265} = -0.0108 + 3.03C \qquad \text{(Eq. 2)}$$

where $r = 0.9998$. For pyridoxine estimation, the delta absorbance at two wavelengths (300 and 310 nm) was measured with subsequent subtraction to obtain a value of $\Delta(\Delta A)(310 - 300)$. Such a choice for the two wavelengths satisfied the following fundamental conditions. The coexisting

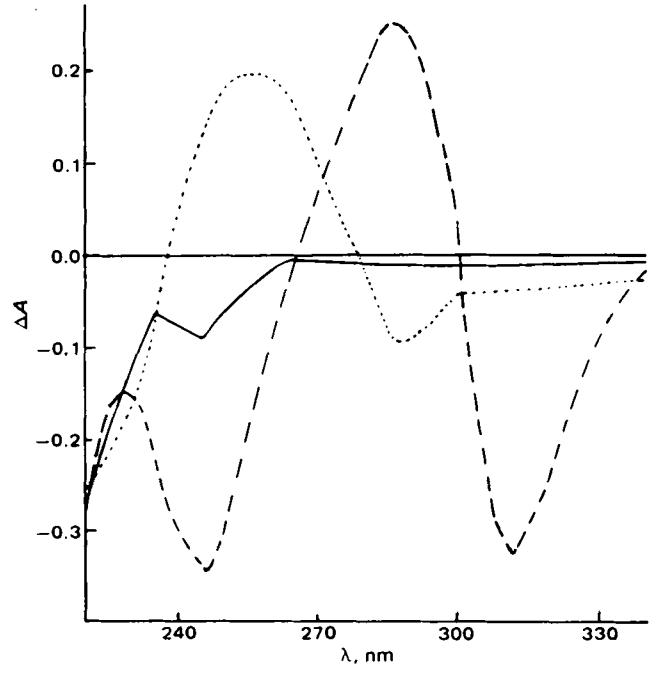

Figure 3—*Differential curves of 0.15 mg of tolbutamide/ml (—), 0.01 mg of thiamine hydrochloride/ml (···), and 0.01 mg of pyridoxine hydrochloride/ml (- -).*

[5] Prolabo, Paris.

[6] Concentrations in this equation and in subsequent equations are in milligrams per milliliter.

[7] r = correlation coefficient.

Table I—Tolbutamide in Unit-Dose Tablets

Tablet	Mean[a] Percentage[b] ± *SD*	
	A_{max} Method	$\Delta A(274 - 276)$ Method
Laboratory made	101.78 ± 0.42	100.58 ± 0.59
	9.476[c]	2.198[c]
Commercial product[d]	101.38 ± 0.47	100.07 ± 0.36
	6.565[c]	4.16[c]

[a] Mean of five determinations. [b] Percentage recovery in laboratory made and percentage found in commercial. [c] Calculated t-value for which theoretical t at 99% confidence level ($\alpha = 0.01$) = 4.604. [d] Rastinon.

components (thiamine and the soluble portion of tolbutamide) exhibited the same absorbance at these wavelengths [*i.e.*, $\Delta(\Delta A)(310 - 300)$ = zero], so variations in their concentrations had no influence on absorbance measurements. Furthermore, $\Delta(\Delta A)(310 - 300)$ was linearly related to concentration in the 0.004–0.028-mg/ml range of pyridoxine, thus permitting its determination. The regression equation derived from the data obtained is as follows:

$$\Delta(\Delta A)(310 - 300) = 0.0058 + 26.89C \qquad \text{(Eq. 3)}$$

where $r = 0.9999$.

The applicability of Eq. 1 in the tolbutamide assay and of Eqs. 2 and 3 in thiamine and pyridoxine determination was tested by analysis of laboratory-made mixtures. The results obtained are of good accuracy and reproducibility (Table II).

The first derivative curve method [$\Delta A(274 - 276)$] for tolbutamide determination in unit-dose tablets was compared with the traditional spectrophotometric method (A_{max} method). The latter was carried out by direct absorbance measurement at λ_{max} 262 nm, and the following equation was used for the concentration calculation:

$$A_{262} = 0.019 + 2.170C \qquad \text{(Eq. 4)}$$

where $r = 0.9999$.

The unit-dose tablets were analyzed using $\Delta A(274 - 276)$ and A_{max} methods (Table I). By applying the t test (17), the results were subjected to statistical analysis. At the 99% confidence level ($p = 0.01$), the ΔA method gave a value not significantly different from the true value whereas the A_{max} method gave a value significantly different from the true value. Therefore, the former method was more accurate than the latter method.

In combination tablets, tolbutamide–thiamine–pyridoxine were present in the ratio 166:1.66:1. Although tolbutamide represented the major component, the interference from strongly absorbing coexisting components was significant because of the weak absorptivity of tolbutamide (Fig. 1). In term of absorbance, the interference from thiamine and pyridoxine was about 20%. The first derivative curve method diminished such interference since the slope of the tolbutamide absorption curve was distinctly higher than the slopes of the coexisting component spectra (Figs. 1 and 2). The interference from the coexisting components was eliminated completely because of the opposite slopes of the thiamine and pyridoxine curves.

Table II—Three Components in Tolbutamide Combination Tablets

Preparation	Mean Percentage[a] ± *SD*		
	Tolbutamide[b]	Thiamine[c]	Pyridoxine[c]
Laboratory made	100.82 ± 0.56	100.04 ± 0.39	100.16 ± 0.49
Commercial[d]	101.63 ± 0.45	106.61 ± 0.59	106.99 ± 0.66

[a] Percentage recovery in laboratory-made mixture and percentage found in commercial tablets. [b] Mean of 15 determinations. [c] Mean of 10 determinations. [d] Tolvit.

REFERENCES

(1) "Pharmaceutical Analysis," T. Higuchi and E. Brochmann-Hanssen, Eds., Interscience, New York, N.Y., 1961, pp. 313–543.

(2) "Official Methods of Analysis of the Association of Official Analytical Chemists," Association of Official Analytical Chemists, Washington, D.C., 1970, pp. 620–649.

(3) A. W. Clayton and R. E. Theirs, *J. Pharm. Sci.*, **55**, 5 (1966).

(4) "Spectrophotometry in Medicine," Heilmeyer, Adam Hilger Ltd., London, England, 1943, p. 7.

(5) A. L. Glenn, *J. Pharm. Pharmacol.*, **12**, 595 (1960).

(6) M. Pernarowski, A. M. Knevel, and J. E. Christian, *J. Pharm. Sci.*, **50**, 943, 946 (1961).

(7) M. Pernarowski and F. Yokoyama, *ibid.*, **50**, 953 (1961).

(8) A. L. Glenn, *J. Pharm. Pharmacol., Suppl.*, **15**, 123T (1963).

(9) S. Shibata, M. Furukawa, and K. Goto, *Anal. Chim. Acta*, **46**, 271 (1969).

(10) *Ibid.*, **53**, 369 (1971).

(11) S. Shibata, K. Goto, and Y. Ishiguro, *Anal. Chim. Acta*, **62**, 305 (1972).

(12) A. M. Wahbi and S. Ebel, *ibid.*, **70**, 57 (1974).

(13) M. A. Elsayed, H. Abdine, and Y. M. Elsayed, *Acta Pharm. Jugoslav.*, **27**, 161 (1977).

(14) G. Aulin-Erdtman, *Chem. Ind.*, **74**, 581 (1955).

(15) G. M. Junejo and A. L. Glenn, *ibid.*, **75**, 813 (1956).

(16) K. Capek and R. Holch, *Pharm. Acta Helv.*, **33**, 163 (1958).

(17) M. R. Spiegel, "Theory and Problems of Probability and Statistics," McGraw-Hill, New York, N.Y., 1975, pp. 229, 270.

Effect of Serum Protein Binding on Sulfisoxazole Distribution, Metabolism, and Excretion in Rats

AVRAHAM YACOBI and GERHARD LEVY ×

Received July 17, 1978, from the *Department of Pharmaceutics, School of Pharmacy, State University of New York at Buffalo, Amherst, NY 14260.* Accepted for publication December 13, 1978.

Abstract □ This investigation determined the effect of serum protein binding on the kinetics of sulfisoxazole distribution, metabolism, and excretion. Adult rats, whose serum free fraction of sulfisoxazole (at a total concentration of 81 ± 6 μg/ml) was 0.05–0.24, received a rapid intravenous injection of 20 mg/kg. Sulfisoxazole concentrations in plasma declined biexponentially with time. There were pronounced and reproducible interindividual differences in the total, metabolic, and renal sulfisoxazole clearances, each positively correlated with the serum free fraction of sulfisoxazole. The renal sulfisoxazole clearance had a component unaffected by serum protein binding. The apparent central compartment volume increased with an increasing serum free sulfisoxazole fraction, but the latter had no apparent effect on the first exponential term of the biexponential equation describing sulfisoxazole elimination kinetics in rats. Serum protein binding was a major determinant of intersubject differences in sulfisoxazole excretion and biotransformation kinetics.

Keyphrases □ Protein binding, serum—sulfisoxazole, distribution, metabolism, excretion, rats □ Serum proteins—binding, sulfisoxazole, distribution, metabolism, excretion, rats □ Sulfisoxazole—distribution, metabolism, excretion, effect of serum protein binding, rats □ Antibacterials—sulfisoxazole, distribution, metabolism, excretion, effect of serum protein binding

The pharmacokinetic characteristics of drugs can be markedly influenced by serum protein binding (1–3). For drugs with linear, not blood flow rate-limited, elimination kinetics, total clearance is proportional to the serum or plasma free fraction (4–8). Since there are pronounced interindividual differences in the serum protein binding of some drugs even among healthy animals and humans (9–12), serum protein binding can be a major determinant of interindividual differences in drug elimination kinetics.

Previous studies focused on the relationship between the serum free fraction and the pharmacokinetic constants that describe the multiexponential decline of plasma dicumarol (12) and warfarin (4) concentrations in rats after rapid intravenous injection. These studies have now been extended to sulfisoxazole.

The selection of sulfisoxazole was based primarily on the following considerations:

1. The average serum free sulfisoxazole fraction value in rats is one to two orders of magnitude larger than that of warfarin, which, in turn, is one to two orders of magnitude larger than that of dicumarol.
2. Significant interindividual differences in the serum free sulfisoxazole fraction have been demonstrated in rats (13) and humans (9).
3. Sulfisoxazole serum protein binding in humans is affected by their pathophysiologic status (14).
4. Unlike dicumarol and warfarin, which are eliminated almost entirely by biotransformation, sulfisoxazole is eliminated largely by renal excretion.

The investigation was designed to permit assessment not only of total clearance but also of metabolic and renal clearance values individually.

EXPERIMENTAL

Adult male Sprague–Dawley rats[1], 360–475 g, were used. A two-piece silicone rubber–polyethylene cannula was implanted in the right jugular vein under light ether anesthesia (15, 16). One or 2 days later, the rats were placed in individual metabolism cages with food and water freely available. They received a single sulfisoxazole injection, 20 mg/kg iv, through the cannula; blood samples (0.25 ml) were then obtained at 0.1, 0.25, 0.5, 1.0, 1.5, 2.0, 3.0, 4.0, 6.0, 8.0, and 10.0 hr, using a technique described previously (16).

Plasma was separated and assayed for sulfisoxazole by the Bratton–Marshall method (17). At the end of the experiment, 3 ml of blood was obtained for the determination of the serum free sulfisoxazole fraction by equilibrium dialysis (14) at 37° against pH 7.4 phosphate buffer containing sulfisoxazole, 100 μg/ml. Urine was collected for 24 hr and assayed for sulfisoxazole and its acetylated and conjugated metabolites following selective extraction with and without prior hydrolysis (18). However, rather than performing the Bratton–Marshall reaction in the ethyl acetate phase with solutions of reagents in acetone (18), the ethyl acetate solution was evaporated under nitrogen, the residue was redissolved in 0.5 ml of 3 *N* HCl and 0.2 ml of 30% trichloroacetic acid, and the Bratton–Marshall reaction was carried out in the usual manner. This modification obviated the stability problems encountered previously (18) and resulted in excellent reproducibility.

The sulfisoxazole concentration data for individual animals were fitted to the equation $C_t = Ae^{-\alpha t} + Be^{-\beta t}$ for plasma concentration C_t at time t by nonlinear least-squares regression (19). Convergence was defined as a relative change in the residual sum of squares $<10^{-4}$. Data in all functions were weighted numerically equal. Apparent distribution volumes and total clearance values were determined from the biexponential equation constants (20). Renal and metabolic clearance values were determined from the product of the total clearance and the dose fraction excreted in the urine as sulfisoxazole and as sulfisoxazole metabolite(s), respectively. The product of the total clearance and the dose fraction not recovered in the urine was designated as the clearance of an unknown.

RESULTS

The free sulfisoxazole fraction in the serum of the 13 rats used ranged from 0.052 to 0.235 at an average ± *SD* total concentration of 81 ± 6 μg/ml. Plasma sulfisoxazole concentrations declined biexponentially with time after rapid intravenous injection (Fig. 1). Excellent replication of plasma concentrations was obtained in six rats that received intravenous sulfisoxazole on two occasions, 1 week apart (Fig. 2). The correlations between total clearance values obtained in the two experiments on each of the six rats and between the serum free fraction values were very strong; there was little quantitative difference between values in any one animal (Figs. 3 and 4). An average of ~88% of the dose was recovered in the urine within 24 hr after injection; the 24–48-hr urine (collected from some animals) contained less than 3% of the dose. About 10% of the amount excreted was in the form of metabolite(s) [*i.e.*, substance(s) assayable by the Bratton–Marshall procedure following organic solvent extraction only after acid hydrolysis].

Table I summarizes the pharmacokinetic data obtained from 13 rats in the first experiment. The renal and metabolic clearance values were determined on the basis of the fraction of the dose excreted in the urine as sulfisoxazole and sulfisoxazole metabolites, respectively, during 24 hr after drug injection. The unknown clearance, based on the fraction of the dose not recovered in the urine, is a reflection of possible extrarenal elimination, conversion of the drug to metabolites that are not determinable by the Bratton–Marshall procedure even upon hydrolysis, and (probably largely) technical imperfections such as incomplete urine re-

[1] Blue Spruce Farms, Altamont, N.Y.

0022-3549/79/0600-0742$01.00/0
© 1979, American Pharmaceutical Association

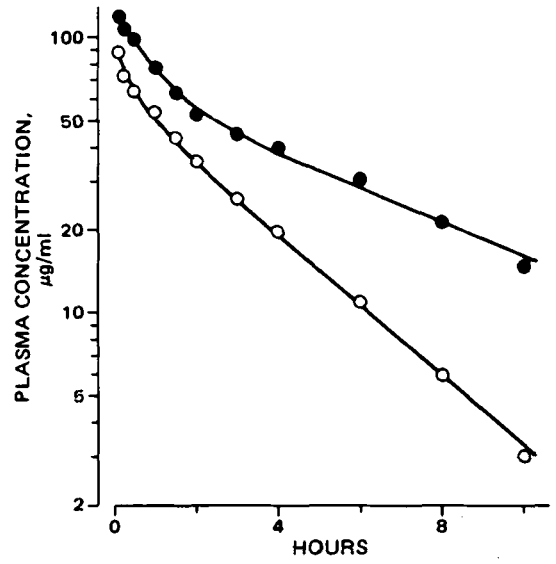

Figure 1—*Time course of plasma sulfisoxazole concentrations of the rat with the lowest serum free fraction (f) value (●, f = 0.052) and the rat with the highest f value (○, f = 0.235) after 20 mg/kg iv. Curves were fitted by nonlinear least-squares regression.*

covery. Consequently, the range of unknown clearance values is wide. More important, there were substantial interindividual differences in the total, renal, and metabolic sulfisoxazole clearances. Therefore, the relationship between these clearance values and the serum free sulfisoxazole fraction in individual animals can be examined.

Figure 5 is a plot of the total sulfisoxazole clearance against the serum free drug fraction. A highly significant correlation was obtained when only data from the first experiment on 13 animals were used for the statistical analysis (a procedure followed also in all subsequent analyses). The total clearance *versus* the free fraction relationship appeared linear but exhibited a substantial positive intercept on the clearance axis. A similarly high correlation and apparently linear relationship were observed between the renal clearance and serum free sulfisoxazole fraction, again with a pronounced positive intercept on the clearance axis (Fig. 6). A highly statistically significant correlation existed between metabolic clearance and serum free fraction, but a plot of these parameters had an intercept close to zero if the animal with the highest metabolic clearance, an apparent outlier, was excluded (Fig. 7). There was no statistically

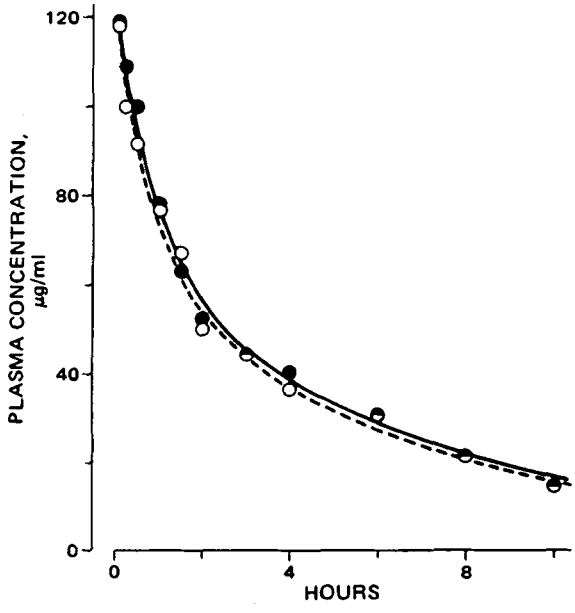

Figure 2—*Time course of plasma sulfisoxazole concentrations of Rat 1 after 20 mg/kg iv in two experiments, 1 week apart. Curves were fitted by nonlinear least-squares regression.*

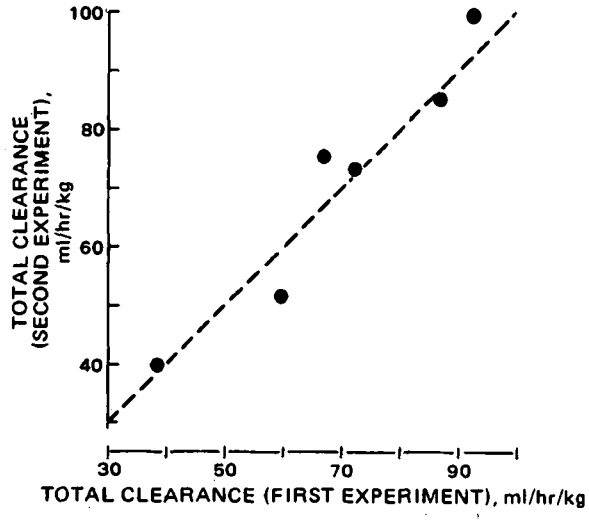

Figure 3—*Relationship between total clearance values for sulfisoxazole determined in two experiments, 1 week apart, in the same six rats. Correlation coefficient equals 0.967, p < 0.005. The broken line in this figure and in several subsequent figures has a slope of unity, indicative of perfect correlation.*

significant correlation between unknown clearance and the serum free sulfisoxazole fraction.

The volume of the apparent central compartment for sulfisoxazole increased significantly with an increasing serum free fraction (Fig. 8, lower panel). A similar trend was evident for the apparent distribution volume (V_{area}), but the relationship was not statistically significant (Fig. 8, upper panel). An examination of the relationships between each biexponential equation constant describing the time course of plasma sulfisoxazole concentrations and the serum free fraction value in individual animals indicated that there was a statistically significant negative correlation between A and the free fraction ($r = -0.666$, $p < 0.02$) but no apparent correlation between B and the free fraction and that there was a statistically very significant positive correlation between β and the free fraction but no apparent correlation between α and the free fraction (Fig. 9).

DISCUSSION

Theoretically, the metabolic clearance of drugs with linear pharmacokinetics should be proportional to their serum free fraction provided that the clearance is much lower than the blood flow rate to the metabolizing organ or tissue (1–3). A linear relationship between *in vivo* total clearance and serum free fraction in rats was demonstrated previously with respect to dicumarol (5), warfarin (1, 4), and bilirubin (6), all of which are eliminated almost entirely by biotransformation.

The hepatic and renal blood flow rates in rats are about 1.7 ml/min/g of liver and 4 ml/min/g of kidneys (21). Based on a liver weight of 30 g/kg

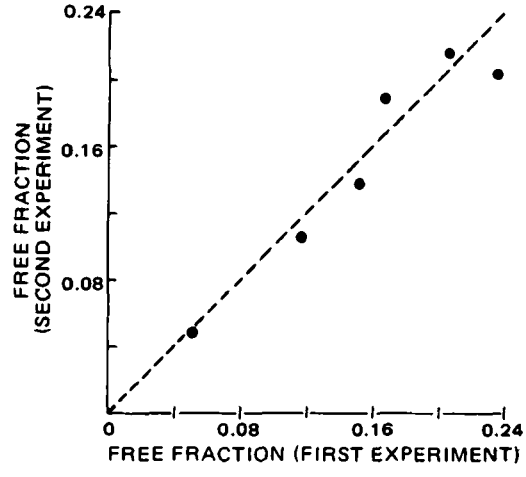

Figure 4—*Relationship between serum free sulfisoxazole fraction determined at the end of two experiments, 1 week apart, in the same six rats. Correlation coefficient equals 0.957, p < 0.005.*

Table I—Sulfisoxazole Pharmacokinetics in Rats

Constant	Mean Value[a]	Range
A, μg/ml[b]	47.4	27.6–61.1
B, μg/ml[b]	65.1	42.8–89.8
α, hr^{-1}	1.08	0.314–1.44
β, hr^{-1}	0.245	0.144–0.313
$t_{1/2}$, hr	2.91	2.21–4.81
V_c, ml/kg	180	149–206
V_{area}, ml/kg	272	215–324
Free fraction in serum	0.144	0.052–0.235
Total clearance, ml/hr/kg	66.5	38.4–92.7
Renal clearance, ml/hr/kg	51.9	27.7–77.9
Metabolic clearance, ml/hr/kg	6.15	2.37–14.1
Unknown clearance[c], ml/hr/kg	8.35	0.742–12.2

[a] $n = 13$. [b] For a 20-mg/kg dose. [c] Total clearance times the fraction of dose not recovered in urine.

of body weight and a kidney weight of 5.7 g/kg of body weight (22), about 3000 ml of blood/hr/kg of body weight flows through the liver, and about 1400 ml of blood/hr/kg of body weight flows through the kidneys. These flow rates are much higher than the total sulfisoxazole clearance observed in this investigation. Consistent with theoretical predictions, the metabolic sulfisoxazole clearance increased proportionately with the serum free drug fraction. Considering the results of this study and of previous investigations on other drugs (4, 5), the proportionality between metabolic clearance and serum free fraction has now been demonstrated at serum free fraction values ranging over three orders of magnitude.

An important discovery in this investigation was the pronounced positive intercept on the clearance axis when renal clearance (and, therefore, also total clearance) was plotted against the serum free fraction. Pending the outcome of studies now in progress, these observations suggest that renal clearance has at least one component that is independent of the serum free sulfisoxazole fraction and at least one other component that is proportional to the serum free fraction. To confirm this preliminary conclusion, it will be necessary to determine the intrinsic and "conventional" renal sulfisoxazole clearances as functions of urine flow rate, urine pH, and drug concentration in plasma so that possible artifacts can be ruled out.

Renal sulfonamide excretion is the net result of glomerular filtration, renal tubular secretion, and partial nonionic back-diffusion from the renal tubular lumen. There is some indirect evidence that the first two of these processes are functions of the plasma free drug concentration and that tubular secretion is describable by Michaelis-Menten kinetics in rabbits (23). Further studies are needed, but this investigation did show that the

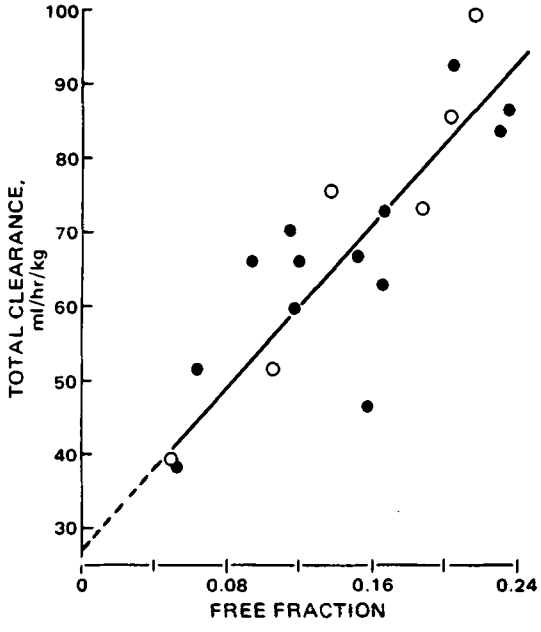

Figure 5—*Relationship between total clearance and serum free sulfisoxazole fraction in 13 rats (●) and in six of these rats retested 1 week later (○). Regression line and correlation coefficient (r) are based on data from first experiment only: r = 0.792, p < 0.005.*

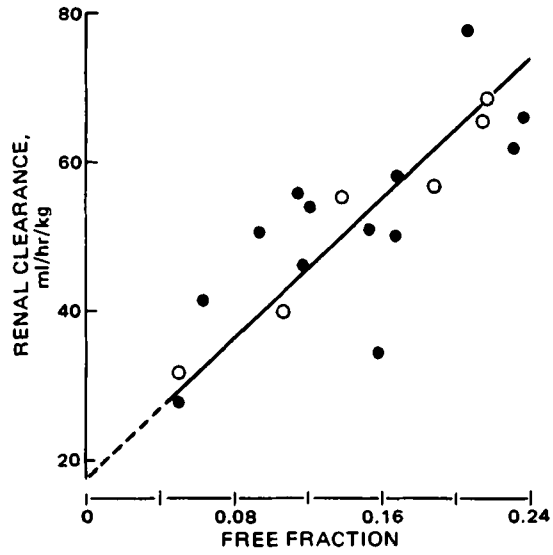

Figure 6—*Relationship between renal clearance and serum free sulfisoxazole fraction. See legend of Fig. 5 for other information; r = 0.732, p < 0.005.*

renal sulfisoxazole clearance increases with increasing serum free fraction.

As previously found with warfarin (4) but not with dicumarol (12), the volume of the apparent central compartment (V_c) for sulfisoxazole increases with an increasing serum free fraction. Therefore, this apparent volume is not the volume of a distinct homogeneous, instantaneously accessible (by intravenous injection) physiologic space such as plasma water. Consistent with this view, the V_c for sulfisoxazole is much larger than the plasma water space, even when extrapolated to a serum free fraction value of zero (Fig. 8).

There is no correlation between α, the exponent of the biexponential equation that characterizes the slope of what is conventionally considered to be the distribution phase of sulfisoxazole elimination, and the serum free sulfisoxazole fraction. A similar lack of correlation was found for dicumarol and warfarin (4, 12). On the other hand, and consistent with previous observations on dicumarol and warfarin (4, 12), there is a strong positive relationship between β and the serum free sulfisoxazole fraction.

Theoretical considerations indicate that β is primarily a function of the free drug fraction in tissues rather than in plasma (24). The weighted

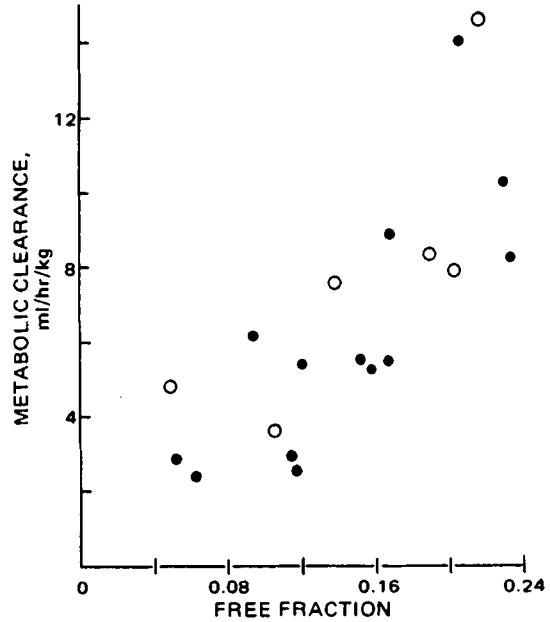

Figure 7—*Relationship between metabolic clearance and serum free sulfisoxazole fraction. See legend of Fig. 5 for other information; r = 0.784, p < 0.005.*

Table II—Serum Protein Binding and Estimated Tissue Binding of Dicumarol, Warfarin, and Sulfisoxazole in Rats[a]

Parameter	Dicumarol	Warfarin	Sulfisoxazole
f_p	0.000497	0.0123	0.144
f_T	0.00258	0.0610	0.399
f_T/f_p	5.19	4.96	2.77

[a] See text for method of tissue binding estimation and sources of data; f_p is the free fraction of drug in plasma or serum, and f_T is the free fraction of drug in tissues.

average apparent free drug fraction in tissues (f_T) can be estimated from the apparent distribution volume (V_{ss}), the free fraction in plasma or serum (f_p), and the real volumes of the body water space (V_w) and the plasma water space (V_p) according to the following relationship (25, 26):

$$V_{ss} = V_p + \frac{f_p}{f_T}(V_w - V_p) \qquad \text{(Eq. 1)}$$

Values of f_T for dicumarol, warfarin, and sulfisoxazole in adult rats were estimated on the basis of average data obtained in this and previous (4, 12) studies, assuming V_w = 700 ml/kg and V_p = 30 ml/kg. These estimates (Table II) indicate substantial binding of all three drugs in tissues. Previously, it was also established that interindividual differences in dicumarol and warfarin f_p are associated with corresponding differences in f_T such that the ratio of f_T to f_p for any one drug is relatively constant over a wide f_p range (27). The β of dicumarol and warfarin increases with increasing f_p, presumably because of the relatively constant relationship between f_p and f_T. The strong positive correlation between sulfisoxazole β and f_p and the inferential indication of significant ($\simeq$ 60%) tissue drug binding suggest that interindividual differences in sulfisoxazole f_p may be associated with corresponding differences in f_T.

The estimated f_T/f_p ratios of dicumarol, warfarin, and sulfisoxazole are quite similar despite large differences in their average f_p values (Table II). The drug f_T/f_p ratio can remain relatively unaffected by compounds that displace the drug from plasma protein binding sites since similar

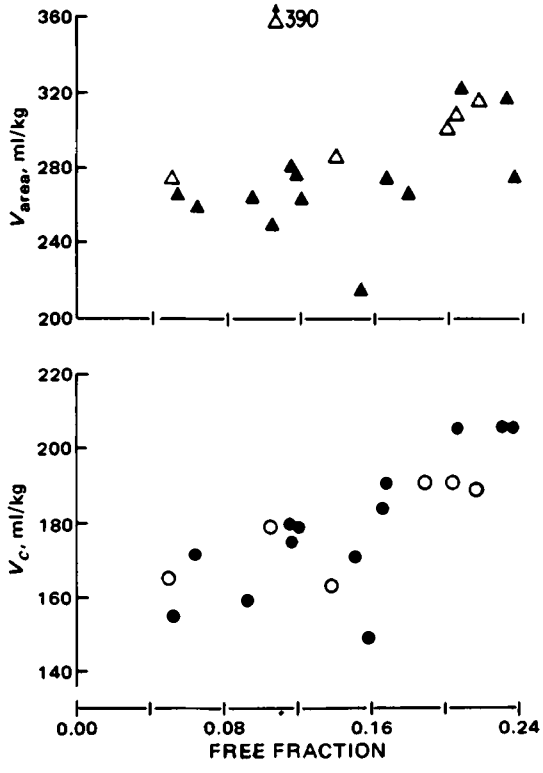

Figure 8—*Relationship between serum free fraction and apparent volume of distribution (V_{area}, upper panel) or apparent volume of the hypothetical central compartment (V_c, lower panel) of sulfisoxazole in rats. Solid symbols are for the first experiment, and open symbols are for the second experiment. Correlation between free fraction and V_c is statistically significant: r = 0.766, p < 0.005. (Correlation between free fraction and V_{area} is not significant: r = 0.454).*

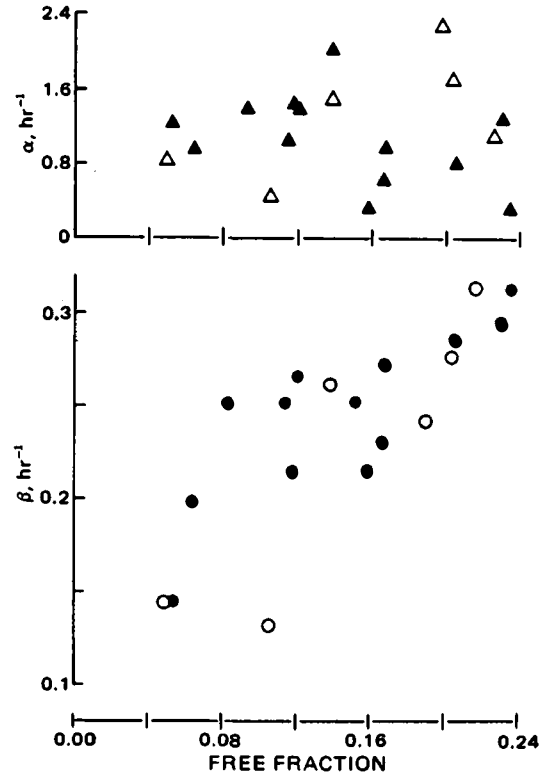

Figure 9—*Relationship between serum free fraction and α (upper panel) or β (lower panel), the exponential constants of the biexponential equation describing the elimination kinetics of sulfisoxazole in rats. Solid symbols are for the first experiment, and open symbols are for the second experiment. Correlation between free fraction and β is statistically significant: r = 0.821, p < 0.001.*

displacement from tissue binding sites may occur (28). This would increase β with little or no change in the apparent distribution volume. The situation is more complicated when drug binding is nonlinear (29).

The serum free sulfisoxazole fraction in 22 healthy adult humans varied from 0.082 to 0.125 at a total concentration of ~9 mg/100 ml (9); it was substantially larger in patients with impaired renal function (14). Serum protein binding may, therefore, be an important determinant of interindividual differences in human sulfisoxazole clearance. The same consideration probably applies to certain other sulfonamides. Consequently, *in vitro–in vivo* correlations, pharmacogenetic characterizations, and similar pharmacokinetic interpretations of the biotransformation of extensively protein-bound sulfonamides should be based on their intrinsic rather than on their total clearance values.

REFERENCES

(1) G. Levy and A. Yacobi, *J. Pharm. Sci.*, **63**, 805 (1974).

(2) G. Levy, in "The Effect of Disease States on Drug Pharmacokinetics," L. Z. Benet, Ed., American Pharmaceutical Association, Washington, D.C., 1976, chap. 9.

(3) G. Wilkinson and D. G. Shand, *Clin. Pharmacol. Ther.*, **18**, 377 (1975).

(4) A. Yacobi and G. Levy, *J. Pharm. Sci.*, **66**, 567 (1977).

(5) C.-M. Lai and G. Levy, *ibid.*, **66**, 1739 (1977).

(6) S. Øie and G. Levy, *ibid.*, **64**, 1433 (1975).

(7) A. Yacobi, J. A. Udall, and G. Levy, *Clin. Pharmacol. Ther.*, **19**, 552 (1976).

(8) R. Gugler and D. L. Azarnoff, *Clin. Pharmacokinet.*, **1**, 25 (1976).

(9) A. Yacobi and G. Levy, *J. Pharm. Sci.*, **66**, 1285 (1977).

(10) J. T. Slattery, A. Yacobi, and G. Levy, *Life Sci.*, **19**, 447 (1976).

(11) A. Yacobi, T. Lampman, and G. Levy, *Clin. Pharmacol. Ther.*, **21**, 283 (1977).

(12) A. Yacobi, C.-M. Lai, and G. Levy, *J. Pharm. Sci.*, **66**, 1741 (1977).

(13) A. Yacobi, S. Øie, and G. Levy, *ibid.*, **66**, 1025 (1977).

(14) G. Levy, T. Baliah, and J. A. Procknal, *Clin. Pharmacol. Ther.*, **20**, 512 (1976).

(15) J. R. Weeks and J. D. Davis, *J. Appl. Physiol.*, **19**, 540 (1964).
(16) J. J. Ashley and G. Levy, *Res. Commun. Chem. Pathol. Pharmacol.*, **4**, 297 (1972).
(17) A. C. Bratton and E. K. Marshall, *J. Biol. Chem.*, **128**, 537 (1939).
(18) J. Rieder, *Chemotherapy*, **17**, 1 (1972).
(19) C. M. Metzler, "NONLIN, a Computer Program for Parameter Estimation in Nonlinear Situations," The Upjohn Co., Kalamazoo, Mich., 1969.
(20) M. Gibaldi and D. Perrier, "Pharmacokinetics," Dekker, New York, N.Y., 1975.
(21) R. A. Roth, Jr., and R. J. Rubin, *Drug Metab. Disp.*, **4**, 460 (1976).
(22) C.-M. Lai, A. Yacobi, and G. Levy, *J. Pharmacol. Exp. Ther.*, **199**, 74 (1976).
(23) R. Hori, K. Sunayashiki, and A. Kamiya, *J. Pharm. Sci.*, **65**, 463 (1976).
(24) M. Gibaldi, G. Levy, and P. J. McNamara, *Clin. Pharmacol. Ther.*, **24**, 1 (1978).
(25) J. R. Gillette, *Ann. N.Y. Acad. Sci.*, **179**, 43 (1971).
(26) M. Gibaldi and P. J. McNamara, *J. Pharm. Sci.*, **66**, 1211 (1977).
(27) G. Levy, C.-M. Lai, and A. Yacobi, *ibid.*, **67**, 229 (1978).
(28) C.-M. Lai and G. Levy, *ibid.*, **67**, 1492 (1978).
(29) P. J. McNamara, G. Levy, and M. Gibaldi, *J. Pharmacokinet. Biopharm.*, in press.

ACKNOWLEDGMENTS

Supported in part by Grant GM-20852 from the National Institute of General Medical Sciences, National Institutes of Health.

Analysis of Hydrophobic Amine Antimalarials in Biological Fluids with the Plastic Ion-Selective Electrode

DOUGLAS W. MENDENHALL, TAKERU HIGUCHI, and LARRY A. STERNSON ˣ

Received September 11, 1978, from the *Department of Pharmaceutical Chemistry, University of Kansas, Lawrence, KS 66045.* Accepted for publication December 5, 1978.

Abstract □ Plastic ion-selective electrode analysis of the hydrophobic amine antimalarial mefloquine in blood samples was investigated. The direct electrode response in plasma samples provided poor drug sensitivity due to high mefloquine protein binding. The drug was analyzed in whole blood by initial extraction into ether as its trichloroacetate ion-pair. Mefloquine was monitored in whole blood extracts with the electrode to moderately low levels (to 0.4 μg/ml). Rapid blood mefloquine level monitoring by this electrode was demonstrated in a bioavailability study. Mefloquine alkylation with various alkyl halides produced derivatives detectable by the electrode at much lower levels (up to two orders of magnitude) than the parent. A kinetic study of this alkylation reaction revealed that an alkyl amine base was necessary to scavenge the acid produced during reaction and to allow the reaction to go to completion. At room temperature, with benzyl bromide as the reagent, reaction was 99% complete in 30 min and mefloquine could be detected to $\sim 10^{-8}$ *M*, a 100-fold improvement in sensitivity over electrode monitoring of underivatized mefloquine.

Keyphrases □ Electrodes, plastic ion selective—analysis, mefloquine and derivatives in blood, dogs, hydrophobic amines □ Mefloquine—analysis, in blood, plastic ion-selective electrodes, derivatives □ Hydrophobic amines—mefloquine, analysis in blood, plastic ion-selective electrodes □ Antimalarials—mefloquine, analysis in blood, plastic ion-selective electrodes

Recent interest in routine drug level monitoring in biological samples (*e.g.*, blood, plasma, and urine) for determining pharmacokinetic parameters and individualizing dosage regimens had produced a need for analytical methods that can be practically applied in the clinical laboratory. These methods should be rapid, simple, and sensitive, should require minimal sample preparation, and should employ inexpensive instrumentation.

One such method recently was reported (1) from these laboratories for urine methadone analysis. A plastic ion-selective electrode was used that detects hydrophobic cations in aqueous solutions (2, 3). This report describes further studies quantitating hydrophobic amines to low levels in whole blood samples. Amines could be derivatized for detection by the plastic ion-selective electrode, increasing sensitivity up to two orders of magnitude.

The model compounds selected for these studies were the quinolinemethanol antimalarial series mefloquine (I), II, and III, presently under investigation for the treatment of persistent disease caused by *Plasmodia* strains. Problems associated with the blood concentration determination of such hydrophobic amines include glass adsorption, protein binding, and poor sensitivity by conventional detection methods [*e.g.*, high-performance liquid chromatography (HPLC) using UV detection].

EXPERIMENTAL

Materials—Mefloquine, II, and III were used as obtained[1]. The free mefloquine base was precipitated from an alkaline salt solution and recrystallized from water–ethanol to a constant melting point (174–175°). Dodecyl, octyl, and hexyl iodides and tetrabutylammonium bromide were used as obtained from commercial sources. Benzyl bromide was freshly distilled (55–56°/0.03 mm Hg) under nitrogen and stored protected from light under nitrogen until used; at the first sign of a yellow color, fresh reagent was distilled. Methanol and acetonitrile were reagent grade and were distilled in glass prior to use. Electrodes were fabricated as described previously (1).

Fresh whole blood was obtained from beagle dogs and maintained under refrigeration until used, usually within 48 hr. Anticoagulants (usually sodium citrate) were added at collection. Plasma was prepared from whole blood by centrifugation at 5000 rpm for 40 min and collection of the clear supernatant fraction.

Electrodes—Coated wire electrodes were prepared as previously described (1). All electrodes were checked for response to tetrabutylammonium ion before use, and a minimum −56-mv/decade slope (*versus* theoretical −59 mv) was required for electrode acceptability.

Apparatus—All potentiometric measurements were made with a

[1] Through INTERx Research Corp., Lawrence, Kans., from Walter Reed Army Research Institute.

0022-3549/79/0600-0746$01.00/0
© 1979, American Pharmaceutical Association

(15) J. R. Weeks and J. D. Davis, *J. Appl. Physiol.*, **19**, 540 (1964).
(16) J. J. Ashley and G. Levy, *Res. Commun. Chem. Pathol. Pharmacol.*, **4**, 297 (1972).
(17) A. C. Bratton and E. K. Marshall, *J. Biol. Chem.*, **128**, 537 (1939).
(18) J. Rieder, *Chemotherapy*, **17**, 1 (1972).
(19) C. M. Metzler, "NONLIN, a Computer Program for Parameter Estimation in Nonlinear Situations," The Upjohn Co., Kalamazoo, Mich., 1969.
(20) M. Gibaldi and D. Perrier, "Pharmacokinetics," Dekker, New York, N.Y., 1975.
(21) R. A. Roth, Jr., and R. J. Rubin, *Drug Metab. Disp.*, **4**, 460 (1976).
(22) C.-M. Lai, A. Yacobi, and G. Levy, *J. Pharmacol. Exp. Ther.*, **199**, 74 (1976).
(23) R. Hori, K. Sunayashiki, and A. Kamiya, *J. Pharm. Sci.*, **65**, 463 (1976).
(24) M. Gibaldi, G. Levy, and P. J. McNamara, *Clin. Pharmacol. Ther.*, **24**, 1 (1978).
(25) J. R. Gillette, *Ann. N.Y. Acad. Sci.*, **179**, 43 (1971).
(26) M. Gibaldi and P. J. McNamara, *J. Pharm. Sci.*, **66**, 1211 (1977).
(27) G. Levy, C.-M. Lai, and A. Yacobi, *ibid.*, **67**, 229 (1978).
(28) C.-M. Lai and G. Levy, *ibid.*, **67**, 1492 (1978).
(29) P. J. McNamara, G. Levy, and M. Gibaldi, *J. Pharmacokinet. Biopharm.*, in press.

ACKNOWLEDGMENTS

Supported in part by Grant GM-20852 from the National Institute of General Medical Sciences, National Institutes of Health.

Analysis of Hydrophobic Amine Antimalarials in Biological Fluids with the Plastic Ion-Selective Electrode

DOUGLAS W. MENDENHALL, TAKERU HIGUCHI, and LARRY A. STERNSON ˣ

Received September 11, 1978, from the *Department of Pharmaceutical Chemistry, University of Kansas, Lawrence, KS 66045.* Accepted for publication December 5, 1978.

Abstract □ Plastic ion-selective electrode analysis of the hydrophobic amine antimalarial mefloquine in blood samples was investigated. The direct electrode response in plasma samples provided poor drug sensitivity due to high mefloquine protein binding. The drug was analyzed in whole blood by initial extraction into ether as its trichloroacetate ion-pair. Mefloquine was monitored in whole blood extracts with the electrode to moderately low levels (to 0.4 μg/ml). Rapid blood mefloquine level monitoring by this electrode was demonstrated in a bioavailability study. Mefloquine alkylation with various alkyl halides produced derivatives detectable by the electrode at much lower levels (up to two orders of magnitude) than the parent. A kinetic study of this alkylation reaction revealed that an alkyl amine base was necessary to scavenge the acid produced during reaction and to allow the reaction to go to completion. At room temperature, with benzyl bromide as the reagent, reaction was 99% complete in 30 min and mefloquine could be detected to $\sim 10^{-8}$ *M*, a 100-fold improvement in sensitivity over electrode monitoring of underivatized mefloquine.

Keyphrases □ Electrodes, plastic ion selective—analysis, mefloquine and derivatives in blood, dogs, hydrophobic amines □ Mefloquine—analysis, in blood, plastic ion-selective electrodes, derivatives □ Hydrophobic amines—mefloquine, analysis in blood, plastic ion-selective electrodes □ Antimalarials—mefloquine, analysis in blood, plastic ion-selective electrodes

Recent interest in routine drug level monitoring in biological samples (*e.g.*, blood, plasma, and urine) for determining pharmacokinetic parameters and individualizing dosage regimens had produced a need for analytical methods that can be practically applied in the clinical laboratory. These methods should be rapid, simple, and sensitive, should require minimal sample preparation, and should employ inexpensive instrumentation.

One such method recently was reported (1) from these laboratories for urine methadone analysis. A plastic ion-selective electrode was used that detects hydrophobic cations in aqueous solutions (2, 3). This report describes further studies quantitating hydrophobic amines to low levels in whole blood samples. Amines could be derivatized for detection by the plastic ion-selective electrode, increasing sensitivity up to two orders of magnitude.

The model compounds selected for these studies were the quinolinemethanol antimalarial series mefloquine (I), II, and III, presently under investigation for the treatment of persistent disease caused by *Plasmodia* strains. Problems associated with the blood concentration determination of such hydrophobic amines include glass adsorption, protein binding, and poor sensitivity by conventional detection methods [*e.g.*, high-performance liquid chromatography (HPLC) using UV detection].

EXPERIMENTAL

Materials—Mefloquine, II, and III were used as obtained[1]. The free mefloquine base was precipitated from an alkaline salt solution and recrystallized from water–ethanol to a constant melting point (174–175°). Dodecyl, octyl, and hexyl iodides and tetrabutylammonium bromide were used as obtained from commercial sources. Benzyl bromide was freshly distilled (55–56°/0.03 mm Hg) under nitrogen and stored protected from light under nitrogen until used; at the first sign of a yellow color, fresh reagent was distilled. Methanol and acetonitrile were reagent grade and were distilled in glass prior to use. Electrodes were fabricated as described previously (1).

Fresh whole blood was obtained from beagle dogs and maintained under refrigeration until used, usually within 48 hr. Anticoagulants (usually sodium citrate) were added at collection. Plasma was prepared from whole blood by centrifugation at 5000 rpm for 40 min and collection of the clear supernatant fraction.

Electrodes—Coated wire electrodes were prepared as previously described (1). All electrodes were checked for response to tetrabutylammonium ion before use, and a minimum −56-mv/decade slope (*versus* theoretical −59 mv) was required for electrode acceptability.

Apparatus—All potentiometric measurements were made with a

[1] Through INTERx Research Corp., Lawrence, Kans., from Walter Reed Army Research Institute.

0022-3549/79/0600-0746$01.00/0
© 1979, American Pharmaceutical Association

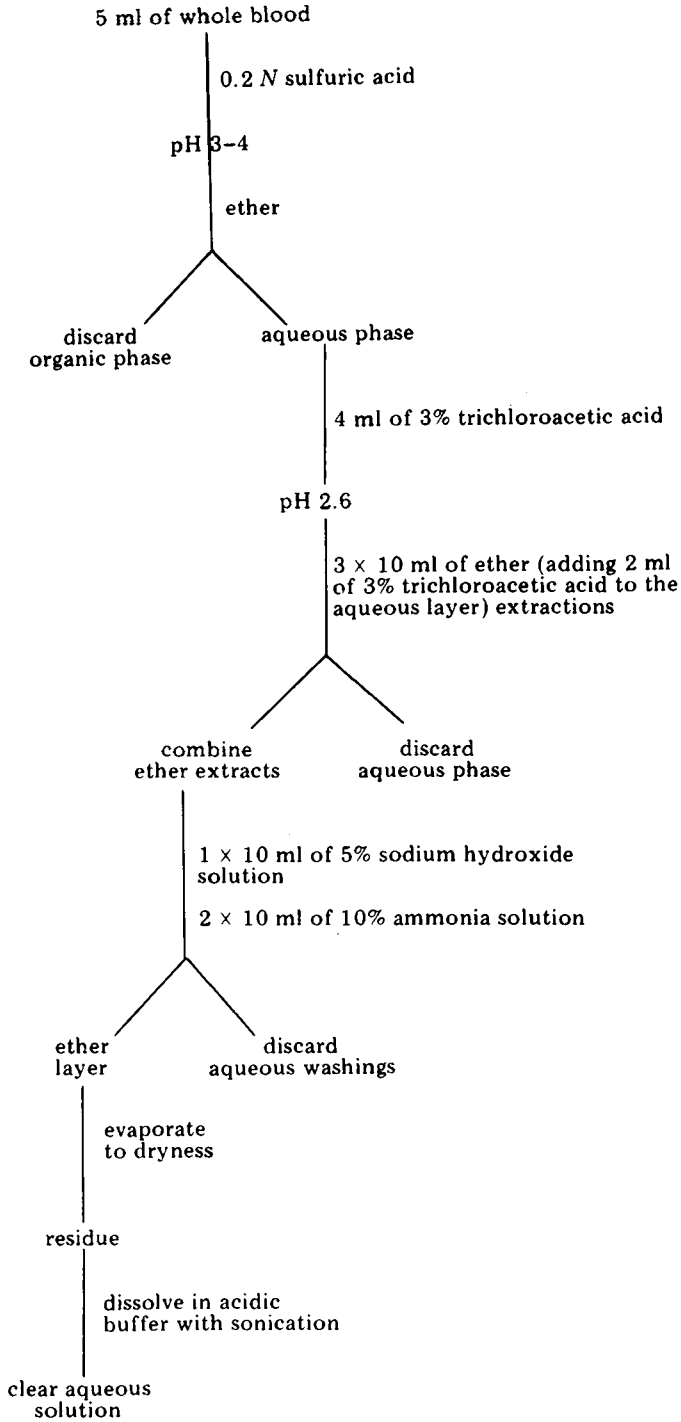

Scheme I—Ion-pair extraction scheme for mefloquine from whole blood.

digital ionanalyzer equipped with a miniature saturated calomel electrode (fiber junction[2]).

HPLC analysis was carried out with a component system[3] fitted with a column containing 10-μm silica with bonded octadecylsilane and an absorbance detector (280-nm phosphor). Detector output was monitored on a 10-mv strip-chart recorder, and peak areas were determined with a polar planimeter.

Plastic Ion-Selective Electrode Determination—The plastic electrode–calomel electrode pair was immersed in a stirred aqueous sample solution, and the potential was measured after the electrode equilibrated for 3 min. Electrodes were removed from the sample solution and washed thoroughly with deionized water before reuse. Analytes were

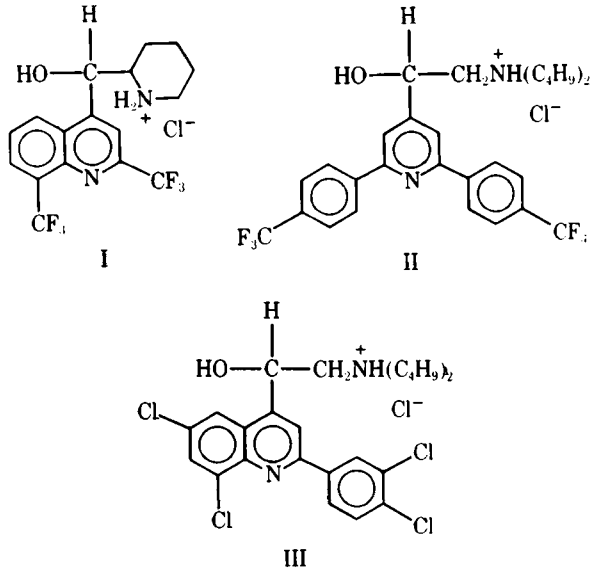

I II III

quantitated by comparison of the unknown solution potential with a standard curve constructed after plastic electrode analysis of a series of samples containing known analyte amounts prepared in the matrix (*e.g.*, plasma, whole blood, or water) in which the unknown was present.

Direct Plastic Ion-Selective Electrode Determination in Plasma—Plasma samples (1.0 ml) spiked with mefloquine (0.414–414 μg/ml) were adjusted to pH 4–5 with 0.3 ml of 0.1 *N* HCl, and the solution was diluted to 10 ml with water. Potentials were determined with the plastic electrode. Samples containing II were treated similarly; however, the pH was adjusted to 3 prior to electrode monitoring.

Blood Mefloquine Analysis—Fresh whole blood samples containing mefloquine were transferred to 35-ml heavy duty screw-capped culture tubes and extracted by the ion-pair technique (4) (Scheme I). The extracts were evaporated to dryness, and the residue was redissolved in 250 μl of acetone and 4.75 ml of 0.001 *M* phosphate buffer (pH 6.0). Extracted blanks, used as standards, were spiked with known mefloquine amounts before dilution with buffer. The plastic electrode response was determined and transformed to concentration units by comparison of the response with a standard curve constructed by analysis of whole blood samples spiked with known mefloquine amounts (0.414–41.4 μg/ml).

Mefloquine Derivation with Benzyl Bromide—Alkylation kinetics were determined with 2-ml samples containing mefloquine (7×10^{-4} *M*) dissolved in acetonitrile to which was added 200 μl of benzyl bromide. The mixture was analyzed by HPLC. Samples (50 μl) were withdrawn at timed intervals and diluted with methanol (to 1.0 ml), and a 50-μl aliquot was chromatographed. Components were eluted isocratically with methanol–0.012 *M* ammonium dihydrogen phosphate (69:31) pumped through the system at 2 ml/min. Standard methanolic mefloquine (V_r = 9.1 ml) and *N*-benzylmefloquine (V_r = 11.5 ml) solutions were injected periodically to determine if instrument performance was deteriorating.

For characterization purposes, *N*-alkylmefloquines were synthesized by refluxing equimolar alkyl halide and I in acetone (acetonitrile for benzyl bromide) for 48 hr. The mixture was cooled and diluted threefold with ether, and the product was precipitated as the hydrochloride salt by the addition of one volume of 5% hydrochloric acid. The solid was collected and recrystallized from ether–acetone or methanol–water, and its structure was confirmed by elemental analysis.

Animal Studies—Beagle dogs were given mefloquine orally as a 250-mg tablet[4] followed by 100 ml of water by gastric lavage or as an intravenous bolus of 50 mg of mefloquine in 5 ml of 20% propylene glycol–6% dextrose solution into one jugular vein over 2 min. Blood samples (5 ml) taken from the other jugular vein just prior to drug administration and at various times postadministration were processed by ion-pair extraction and were analyzed with the plastic ion-selective electrode.

RESULTS AND DISCUSSION

Solutions containing mefloquine, II, or III prepared in dilute aqueous acid (10^{-4} *N* H_2SO_4) could be quantified by direct measurement with

[2] Corning 476017.
[3] μBondapak C18, Waters Associates, Milford, Mass.
[4] Lot B-512, INTERx Research Corp., Lawrence, Kans.

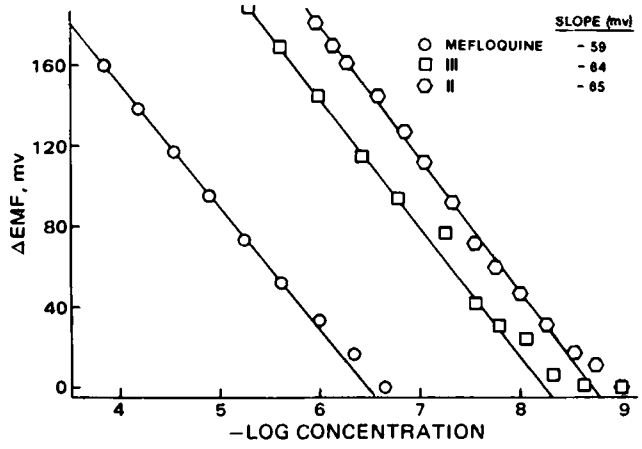

Figure 1—*Plastic ion selective response to hydrophobic antimalarials. Key:* ○, *mefloquine in* 10^{-4} N H_2SO_4; ○, *II in* 10^{-3} N *HCl containing 0.1% methanol; and* □, *III in* 10^{-3} N *HCl containing 1% methanol.*

the plastic ion-selective electrode. The potential response was linearly related to analyte concentration over three orders of magnitude (Fig. 1). In this simple aqueous matrix, measurements could be made with ±4% accuracy and ±2% precision over the linear concentration range.

Electrodes were thoroughly washed with deionized water (*e.g.*, 5 min) after removal from sample solutions to achieve this accuracy and precision. After determinations in more concentrated solutions, electrodes were immersed in stirred deionized water for 3 hr and air dried before reuse on a dilute sample. Failure to take such precautions reduced accuracy and precision and produced meaningless results.

The electrode response increased with the analyte hydrophobicity. For the more hydrophobic drugs (II and III), sensitivity approaching 10^{-9} *M* could be achieved; mefloquine could be quantified to 10^{-7} *M*. The Nernst equation predicts a change of 59 mv/decade in the activity of a species to which the electrode responds (5). A near-Nernstian linear response was observed in aqueous acid. The slightly super-Nernstian slopes (>59 mv) seen with the more hydrophobic compounds may arise from alterations in the membrane caused by adsorbed analyte, producing a more favorable environment for subsequent analyte partitioning into the membrane phase, an explanation consistent with the proposed mechanism for the plastic ion-selective electrode (3).

Direct Determination of Plasma Antimalarials—Compared with aqueous solutions, a loss of two orders of magnitude in sensitivity was observed for plastic ion-selective electrode response to mefloquine and II in buffered plasma. In both cases, linear responses were observed, although slopes were sub-Nernstian (I, −49 mv; and II, −53 mv). This loss in sensitivity is accounted for by the extensive protein binding observed with hydrophobic molecules (6), which reduces the free drug activity in solution. Mefloquine is 98% protein bound in plasma (7).

Attempts to dislodge mefloquine from protein binding sites and thereby to allow detection at lower levels by pH manipulation or heat denaturation were unsuccessful. Sample matrix effects severely hampered

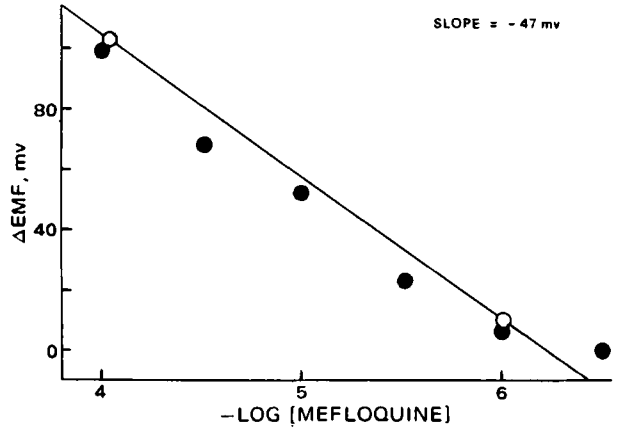

Figure 2—*Plastic ion-selective electrode determination of mefloquine in ion-pair extracts of whole blood dissolved in 5% acetone-pH 6 buffer spiked before (●) and after (○) extraction. Potential was measured versus a saturated calomel electrode.*

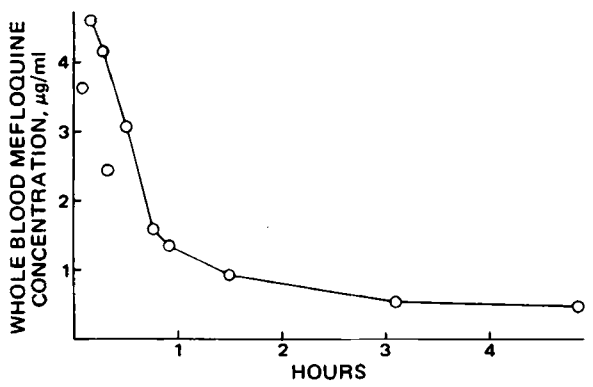

Figure 3—*Blood mefloquine level versus time profile after intravenous administration of 50 mg of the drug (as the hydrochloride) to a beagle dog.*

the assay accuracy (±25%) and precision when carried out directly in biological fluid. Therefore, methods were necessary to remove the drug from the biological matrix prior to plastic ion-selective electrode monitoring.

Blood Mefloquine Analysis—The drug was separated from blood components by extraction. Direct extraction from neutral or basic solution was ineffective because of drug loss due to adsorption to glass surfaces; interference from endogenous amines coextracted from blood, especially when derivatization with alkyl halides was indicated; and incomplete dissolution into aqueous acid after evaporation of the extracts to dryness, apparently due to lipid material coextracted with the drug. Therefore, a more selective, ion-pair extraction was used for mefloquine isolation (Scheme I).

Nakagawa *et al.* (4) showed that mefloquine was extracted into ether from blood acidified to pH 3 as a 1:1 ion-pair with trichloroacetate, giving excellent recoveries (88–100%) over a broad concentration range (1–1000 ng/ml). Initial extraction of acidified blood with ether in the absence of an ion-pairing agent removed acidic compounds, lipids, and other neutral materials that may otherwise have interfered with subsequent drug detection. The extraction scheme (Scheme I) utilized ether, an electron-donating species, as the extractant instead of the proton-donating solvent (*e.g.*, chloroform) normally indicated for solvation (extraction) of a large cation–small anion ion-pair (8). This procedure minimized extraction of potentially interfering, less hydrophobic amines while maintaining efficient analyte recovery (9).

The extracted drug was reconstituted in aqueous buffer (pH 6.0), and the concentration was determined using the plastic electrode. The plastic electrode potential *versus* the log of the spiked blood sample-concentration curve (Fig. 2) indicated a linear response to 10^{-6} *M* drug (0.4 μg/ml free base), the same limit found in aqueous systems. Extractive mefloquine removal from biological fluid returned the analyte to a more uniform matrix. Measurements could be made with ±8% accuracy and ±6% precision. These statistics also reflect the sample to sample variation (±5%) in mefloquine extraction efficiency from a biological sample.

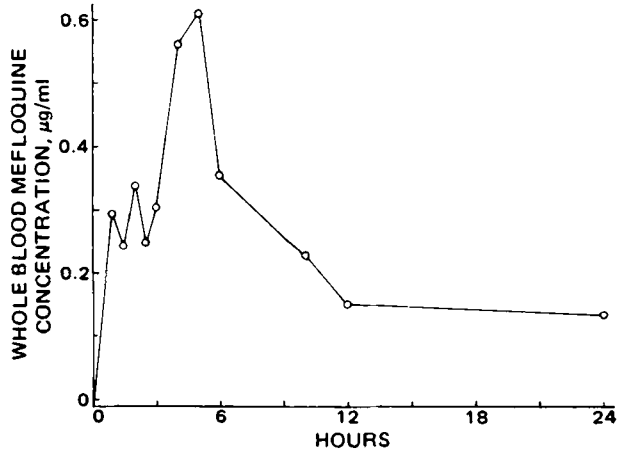

Figure 4—*Blood mefloquine level versus time profile after oral administration of 250-mg mefloquine hydrochloride tablet to a beagle dog.*

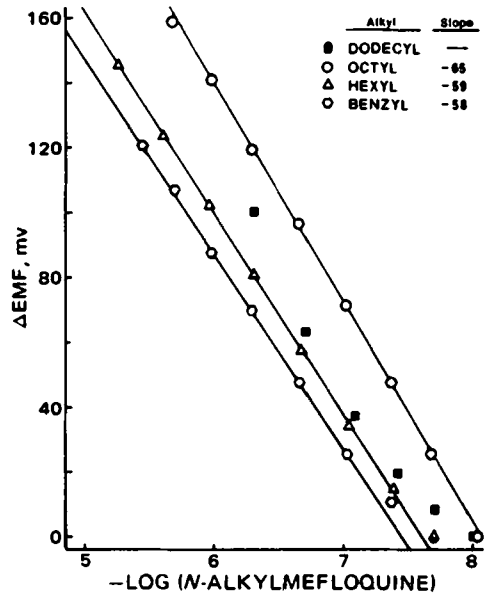

Figure 5—*Plastic ion-selective electrode response to* N-*alkylmefloquines in* 10^{-4} N H_2SO_4 *(dodecyl solutions contained 1% methanol). Potential was measured* versus *a saturated calomel electrode.*

The depressed slope (−47 mv *versus* a theoretical slope of −59 mv) was consistently seen with blood extracts and may have been due to some undefined effect of coextracted blood components on electrode response. Nonetheless, a linear response over the range of interest is adequate as a useful analytical detector. Blank blood samples were alternatively spiked after ion-pair extraction and used to generate a standard response curve (open circles in Fig. 2). An apparent consistent ~85% recovery (as determined by deviations from the theoretical 100% response line in Fig. 2) was indicated by this method, in good agreement with literature results over this concentration range (4).

The use of this method for bioavailability studies evaluating various mefloquine formulations in dogs was demonstrated by analyzing blood samples drawn from two beagles after administration of two experimental formulations. The results (Figs. 3 and 4) indicate adequate sensitivity for formulations having good availability but limited accuracy beyond peak levels for poorly absorbed formulations.

Amine Derivatization for Plastic Ion-Selective Electrode Detection—After hydrophobic amine isolation by a relatively selective procedure such as ion-pair extraction, simple alkylation with a relatively lipophilic alkyl halide prior to plastic ion-selective electrode detection provided a rapid method for dramatically increasing detector sensitivity. Figure 5 illustrates the increased sensitivity limits to various *N*-alkylated mefloquine derivatives, showing up to two orders of magnitude improvement in sensitivity over the parent compound. *N*-Dodecylmefloquine required an organic cosolvent (1% methanol) to achieve dissolution and showed an erratic response to the plastic electrode. The octyl derivative showed the same super-Nernstian slope (−65 mv) previously observed for II and III and may be similarly explained.

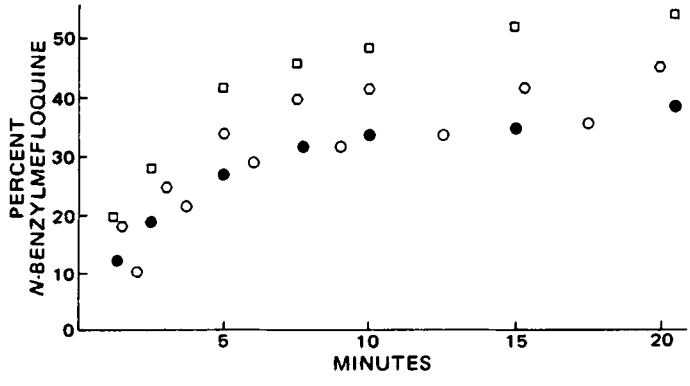

Figure 6—*Effect of added hydrobromic acid and 2,6-di-*tert*-butylpyridine on the percent of mefloquine ([mefloquine]*$_0$ *=* 7×10^{-4} *M) converted to* N*-benzylmefloquine as a function of time. Key ([hydrobromic acid]): □, 0.0; ○,* 3.5×10^{-5} M; ○, 7×10^{-5} M; *and* ●, 7×10^{-5} M *plus* 2.8×10^{-3} M *2,6-di-*tert*-butylpyridine.*

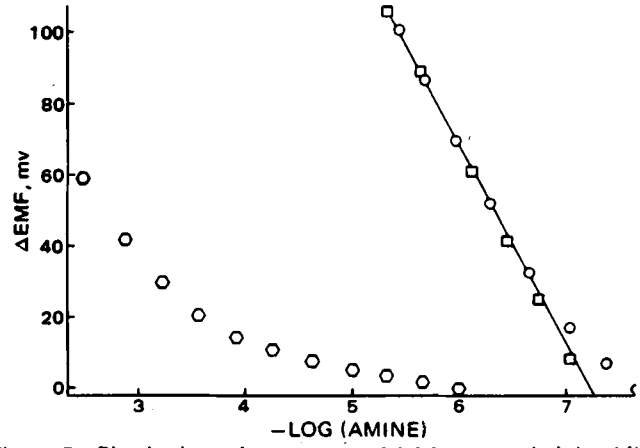

Figure 7—*Plastic electrode response to 2,2,6,6-tetramethylpiperidine (○) and to* N*-benzylmefloquine in the presence (□) and absence (○) of excess benzyl bromide in* 10^{-4} N H_2SO_4. *Potential was measured* versus *a saturated calomel electrode.*

To optimize reaction conditions for alkylation of nanogram quantities of mefloquine from blood extracts, a brief study of alkylation reaction kinetics was undertaken. Of the alkylated mefloquines, the octyl and benzyl derivatives were the most likely derivatives for plastic electrode detection, the former because of its greater sensitivity and the latter because of its anticipated faster formation rate from I. Only the benzyl bromide–mefloquine reaction kinetics were studied in detail since preliminary experiments indicated that the reaction rate between octyl iodide and the drug was too slow to be useful as a derivatization procedure.

Amine alkylation rates involving bulky reactants are slow (10). Therefore, a large (10,000-fold) alkyl halide excess was used to accelerate the reaction rate since the amine concentration available for the presumed second-order reaction was small. Benzyl bromide (neat) was added to stirred mefloquine free base solutions in acetonitrile; aliquots were periodically removed, the reaction was quenched in methanol, and the mefloquine and *N*-benzylmefloquine concentrations were determined by HPLC. Essentially 100% of the initial mefloquine concentration could be accounted for by the parent and *N*-benzylmefloquine peaks in all experiments, indicating that no unexpected side reactions were occurring; no detectable benzyl bromide loss was observed under the reaction conditions, indicating that the reagent was stable over the reaction period.

Initial mefloquine benzylation studies gave unexpected results. The reaction proceeded rapidly initially, but the rate declined substantially after less than half the mefloquine had been consumed. Furthermore, the data could not be plotted in the expected pseudo-first-order manner. The reaction could be of a higher order than the assumed first-order dependency, which would produce an exaggerated drop in rate as amine was consumed. Variation in initial mefloquine concentration, however, failed to show the concentration dependence that would be expected for such a mechanism.

If the reaction proceeded by an S_N1 mechanism and bromide ion effectively competed with the amine for the reactive benzyl carbonium ion, a depression in rate would be expected as the bromide-ion concentration increased over the reaction course. Addition of relatively high bromide-ion concentrations (two times the initial mefloquine concentration) failed to depress the reaction rate, eliminating this possibility. Addition of hydrogen bromide to the reaction mixture, however, depressed the reaction rate (Fig. 6), indicating that hydrogen bromide produced during the reaction was protonating the secondary amine, effectively reducing the mefloquine concentration available for alkylation and, therefore, the rate. Addition of a sterically hindered (to prevent alkylation) pyridine base (2,6-di-*tert*-butylpyridine) failed to reverse the hydrogen bromide effect (Fig. 6). However, when 2,2,6,6-tetramethylpiperidine was added to the reaction mixture, the expected first-order plot was obtained, indicating that piperidine is a significantly stronger base in acetonitrile than pyridine and, therefore, capable of more effectively trapping the liberated hydrogen bromide.

Under the reaction conditions employed (5 μl of benzyl bromide/50 μl of acetonitrile solution of the amine to be determined, containing 0.001 *M* piperidine base), the pseudo-first-order rate constant (0.146 min^{-1})

predicts that the reaction is essentially (~99%) complete after 30 min at room temperature.

As shown in Fig. 7, 100:1 dilution of this reaction mixture with 10^{-4} N H_2SO_4 allowed direct plastic electrode determination of the alkylated amine without separation from the excess reactants since no interference from benzyl bromide or the piperidine base was seen.

CONCLUSION

Previous reports reviewed the many difficulties in handling and analyzing hydrophobic amines in biological samples, including glass adsorption, protein binding, and poor detector sensitivity (11–15). Coupled with ion-pair extraction, the plastic ion-selective electrode detection method described here offers potential advantages for efficient isolation and quantitation of hydrophobic drugs in whole blood at low levels. Furthermore, the derivatization procedure affords a means of enhancing plastic electrode detector sensitivity up to two orders of magnitude and may, therefore, extend the applicability of the method to other, less hydrophobic primary and secondary amines.

REFERENCES

(1) S. Srianujata, W. R. White, T. Higuchi, and L. A. Sternson, *Anal. Chem.*, **50**, 232 (1978).

(2) T. Higuchi, C. R. Illian, and J. L. Tossounian, *ibid.*, **42**, 1674 (1970).

(3) J. R. Luch, Ph.D. thesis, University of Kansas, Lawrence, Kans., 1976.

(4) T. Nakagawa, T. Higuchi, J. L. Haslam, R. D. Shaffer, and D. W. Mendenhall, *J. Pharm. Sci.*, in press.

(5) G. Eisenman, in "Advances in Analytical Chemistry and Instrumentation," vol. 4, C. N. Reilly, Ed., Wiley, New York, N.Y., 1965, pp. 213–369.

(6) B. B. Brodie, in "Transport Function of Plasma Proteins," P. Desgrez and P. M. DeTraverse, Eds., Elsevier, Amsterdam, The Netherlands, 1966, pp. 137–145.

(7) J. Y. Mu, Z. H. Israili, and P. G. Dayton, *Drug Metab. Disp.*, **3**, 198 (1976).

(8) T. Higuchi, A. F. Michaelis, T. Tan, and A. Hurwitz, *Anal. Chem.*, **39**, 974 (1967).

(9) D. W. Mendenhall, Ph.D. thesis, University of Kansas, Lawrence, Kans., 1977, pp. 3–34.

(10) J. March, "Advanced Organic Chemistry," McGraw-Hill, New York, N.Y., 1968, pp. 251–375.

(11) B. B. Brodie, in "Handbook of Experimental Pharmacology," vol. 28, part 2, O. Eichler, Series Ed., Springer-Verlag, Berlin, Germany, 1971.

(12) C. R. Jones, in "Methodological Developments in Biochemistry," vol. 5, E. Reid, Ed., North-Holland, Amsterdam, The Netherlands, 1976, pp. 107–113.

(13) E. O. Titus, in "Fundamentals of Drug Metabolism and Drug Disposition," B. N. LaDu, H. G. Mandel, and E. L. Way, Eds., Williams & Wilkins, Baltimore, Md., 1971, pp. 419–436.

(14) G. Schill, in "Methodological Developments in Biochemistry," vol. 5, E. Reid, Ed., North-Holland, Amsterdam, The Netherlands, 1976, pp. 87–102.

(15) K. Thakker, T. Higuchi, and L. A. Sternson, *J. Pharm. Sci.*, **68**, 93 (1979).

ACKNOWLEDGMENTS

Supported in part by NIH Grant CA-09242 from the National Cancer Institute and by grants from the U.S. Army Research and Development Command and INTERx Research Corp.

Colorimetric Acetaminophen Determination in Pharmaceutical Formulations

S. BELAL ˣ, M. ABDEL-HADY ELSAYED *, A. EL-WALIELY, and H. ABDINE

Received April 14, 1978, from the *Pharmaceutical Analytical Chemistry Department, Faculty of Pharmacy, University of Alexandria, Alexandria, Egypt.* Accepted for publication December 6, 1978.

*Present address: Department of Pharmacy, University of Nigeria, Nsukka, Nigeria.

Abstract □ Different approaches for the colorimetric determination of acetaminophen, based on its coupling with diazotized *o*-nitroaniline, are described. Copper(II) chelation with the coupled compound makes the method highly selective. Sensitivity is increased when the acetaminophen assay is carried out indirectly through the determination of the chelate's copper content. Optimum conditions for performing the different approaches are described. The stoichiometric balance for the reactants in the coupled compound and chelate is determined. The degree of dissociation and the instability constant are computed. The rectilinear relationship between the absorbance of the different products and the concentration of acetaminophen allows for its determination in different pharmaceutical formulations. Compared with the official method, the proposed methods give more accurate results.

Keyphrases □ Acetaminophen—analysis, colorimetry, various pharmaceutical formulations □ Colorimetry—analysis, acetaminophen in various pharmaceutical formulations □ Analgesics—acetaminophen, analysis, colorimetry, various pharmaceutical formulations □ Antipyretics—acetaminophen, analysis, colorimetry, various pharmaceutical formulations

Acetaminophen hydrolysis with subsequent condensation with anisaldehyde (1), *p*-dimethylaminobenzaldehyde (2), *p*-dimethylaminocinnamaldehyde (3), or vanillin (4) or reaction with alkaline 2-naphthol (5) has been used for colorimetric acetaminophen determination in unit-dose formulations. Other methods were based on the reaction with phenol together with hypobromite (6), hypochlorite in the presence of metaarsenite (7), or ferricyanide (8). Nitrosatin (9) and nitration (10, 11) were utilized also for colorimetric determination. Most of these methods are not selective.

The fluorometric method, based on acetaminophen oxidation with alkali ferricyanide (12, 13) or on its hydrolysis followed by reaction with benzylamine (14), is sensitive to many interfering substances present in pharmaceutical formulations.

Acetaminophen was also determined by cerimetric titration (15, 16), gravimetry (17), titration of the hydrolytic product with nitrite (18), and polarography (19). These methods are not sufficiently sensitive.

Acetaminophen, containing the acetamido group $NHCOCH_3$, was determined by hydrolysis, diazotization

0022-3549/79/0600-0750$01.00/0

© 1979, American Pharmaceutical Association

predicts that the reaction is essentially (~99%) complete after 30 min at room temperature.

As shown in Fig. 7, 100:1 dilution of this reaction mixture with 10^{-4} N H_2SO_4 allowed direct plastic electrode determination of the alkylated amine without separation from the excess reactants since no interference from benzyl bromide or the piperidine base was seen.

CONCLUSION

Previous reports reviewed the many difficulties in handling and analyzing hydrophobic amines in biological samples, including glass adsorption, protein binding, and poor detector sensitivity (11–15). Coupled with ion-pair extraction, the plastic ion-selective electrode detection method described here offers potential advantages for efficient isolation and quantitation of hydrophobic drugs in whole blood at low levels. Furthermore, the derivatization procedure affords a means of enhancing plastic electrode detector sensitivity up to two orders of magnitude and may, therefore, extend the applicability of the method to other, less hydrophobic primary and secondary amines.

REFERENCES

(1) S. Srianujata, W. R. White, T. Higuchi, and L. A. Sternson, *Anal. Chem.*, **50**, 232 (1978).

(2) T. Higuchi, C. R. Illian, and J. L. Tossounian, *ibid.*, **42**, 1674 (1970).

(3) J. R. Luch, Ph.D. thesis, University of Kansas, Lawrence, Kans., 1976.

(4) T. Nakagawa, T. Higuchi, J. L. Haslam, R. D. Shaffer, and D. W. Mendenhall, *J. Pharm. Sci.*, in press.

(5) G. Eisenman, in "Advances in Analytical Chemistry and Instrumentation," vol. 4, C. N. Reilly, Ed., Wiley, New York, N.Y., 1965, pp. 213–369.

(6) B. B. Brodie, in "Transport Function of Plasma Proteins," P. Desgrez and P. M. DeTraverse, Eds., Elsevier, Amsterdam, The Netherlands, 1966, pp. 137–145.

(7) J. Y. Mu, Z. H. Israili, and P. G. Dayton, *Drug Metab. Disp.*, **3**, 198 (1976).

(8) T. Higuchi, A. F. Michaelis, T. Tan, and A. Hurwitz, *Anal. Chem.*, **39**, 974 (1967).

(9) D. W. Mendenhall, Ph.D. thesis, University of Kansas, Lawrence, Kans., 1977, pp. 3–34.

(10) J. March, "Advanced Organic Chemistry," McGraw-Hill, New York, N.Y., 1968, pp. 251–375.

(11) B. B. Brodie, in "Handbook of Experimental Pharmacology," vol. 28, part 2, O. Eichler, Series Ed., Springer-Verlag, Berlin, Germany, 1971.

(12) C. R. Jones, in "Methodological Developments in Biochemistry," vol. 5, E. Reid, Ed., North-Holland, Amsterdam, The Netherlands, 1976, pp. 107–113.

(13) E. O. Titus, in "Fundamentals of Drug Metabolism and Drug Disposition," B. N. LaDu, H. G. Mandel, and E. L. Way, Eds., Williams & Wilkins, Baltimore, Md., 1971, pp. 419–436.

(14) G. Schill, in "Methodological Developments in Biochemistry," vol. 5, E. Reid, Ed., North-Holland, Amsterdam, The Netherlands, 1976, pp. 87–102.

(15) K. Thakker, T. Higuchi, and L. A. Sternson, *J. Pharm. Sci.*, **68**, 93 (1979).

ACKNOWLEDGMENTS

Supported in part by NIH Grant CA-09242 from the National Cancer Institute and by grants from the U.S. Army Research and Development Command and INTERx Research Corp.

Colorimetric Acetaminophen Determination in Pharmaceutical Formulations

S. BELAL ˣ, M. ABDEL-HADY ELSAYED *, A. EL-WALIELY, and H. ABDINE

Received April 14, 1978, from the *Pharmaceutical Analytical Chemistry Department, Faculty of Pharmacy, University of Alexandria, Alexandria, Egypt.* Accepted for publication December 6, 1978.

*Present address: Department of Pharmacy, University of Nigeria, Nsukka, Nigeria.

Abstract □ Different approaches for the colorimetric determination of acetaminophen, based on its coupling with diazotized *o*-nitroaniline, are described. Copper(II) chelation with the coupled compound makes the method highly selective. Sensitivity is increased when the acetaminophen assay is carried out indirectly through the determination of the chelate's copper content. Optimum conditions for performing the different approaches are described. The stoichiometric balance for the reactants in the coupled compound and chelate is determined. The degree of dissociation and the instability constant are computed. The rectilinear relationship between the absorbance of the different products and the concentration of acetaminophen allows for its determination in different pharmaceutical formulations. Compared with the official method, the proposed methods give more accurate results.

Keyphrases □ Acetaminophen—analysis, colorimetry, various pharmaceutical formulations □ Colorimetry—analysis, acetaminophen in various pharmaceutical formulations □ Analgesics—acetaminophen, analysis, colorimetry, various pharmaceutical formulations □ Antipyretics—acetaminophen, analysis, colorimetry, various pharmaceutical formulations

Acetaminophen hydrolysis with subsequent condensation with anisaldehyde (1), *p*-dimethylaminobenzaldehyde (2), *p*-dimethylaminocinnamaldehyde (3), or vanillin (4) or reaction with alkaline 2-naphthol (5) has been used for colorimetric acetaminophen determination in unit-dose formulations. Other methods were based on the reaction with phenol together with hypobromite (6), hypochlorite in the presence of metaarsenite (7), or ferricyanide (8). Nitrosatin (9) and nitration (10, 11) were utilized also for colorimetric determination. Most of these methods are not selective.

The fluorometric method, based on acetaminophen oxidation with alkali ferricyanide (12, 13) or on its hydrolysis followed by reaction with benzylamine (14), is sensitive to many interfering substances present in pharmaceutical formulations.

Acetaminophen was also determined by cerimetric titration (15, 16), gravimetry (17), titration of the hydrolytic product with nitrite (18), and polarography (19). These methods are not sufficiently sensitive.

Acetaminophen, containing the acetamido group $NHCOCH_3$, was determined by hydrolysis, diazotization

0022-3549/79/0600-0750$01.00/0

© 1979, American Pharmaceutical Association

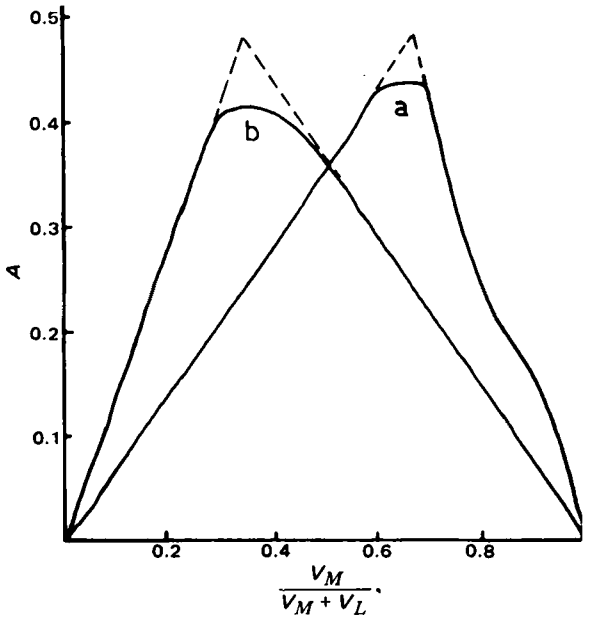

Figure 1—*Continuous variation plot for:* (a) *diazotized* o-*nitroaniline* (V_M)-*acetaminophen* (V_L) *coupled compound, and* (b) *2,6-di-(o-nitrophenylazo)-4-acetamidophenol* (V_L)-*copper(II) ion* (V_M).

of the resulting amine, and subsequent coupling with *N*-1-naphthylethylenediamine (20).

Acetaminophen as a phenolic compound can couple with a chromogenic reagent, diazotized *o*-nitroaniline. The coupled compound can be used as a chelating agent to copper(II) ion. These approaches constitute the bases for the acetaminophen assay described in this article.

EXPERIMENTAL

Apparatus, Reagents, and Materials—All reagents were analytical grade.

A photoelectric spectrophotometer[1] with 1-cm cells was used.

Acetaminophen[2] (BP 1973), acetaminophen tablets[3], acetaminophen syrup[4], and acetaminophen drops[5] were used.

Preparation of Assay Solution—*Tablets*—Twenty tablets were powdered and mixed; an accurately weighed amount, equivalent to one tablet, was transferred to a 100-ml graduated flask. The sample was dissolved as completely as possible in water, diluted to volume, and filtered. An aliquot of filtrate was removed, after the first portion was discarded, measured, suitably diluted, and treated as described for Procedure A, B, or C.

Syrups or Drops—An aliquot was diluted with water to attain a concentration suitable for Procedure A, B, or C.

Procedure A—*Coupling with Diazotized Nitroaniline*—One milliliter of *o*-nitroaniline solution (1 mg/ml of 1.5 *N* HCl) was transferred to a 25-ml graduated flask to which 2 ml of sodium nitrite solution (3% aqueous) had been added. The contents were mixed and left for 10 min. An aliquot of acetaminophen solution (0.4 mg in water) was added, followed by 3 ml of 1 *N* NaOH. The contents were mixed, left for 5 min, and diluted to volume with water. The absorbance was measured at 426 nm against a blank.

Stoichiometric Reactant Balance—Using Procedure A, 0.5–4.5 ml of 2×10^{-3} *M* (V_M) samples of *o*-nitroaniline were diazotized and coupled with the corresponding complementary volume of 2×10^{-3} *M* acetaminophen (V_L) to make a total 5-ml volume for $V_M + V_L$.

Procedure B—*Subsequent Chelation with Copper(II) Ion*—*o*-Nitroaniline (1 ml) and sodium nitrite solution (2 ml) were transferred to a 100-ml separator. The contents were mixed and left to stand for 10 min.

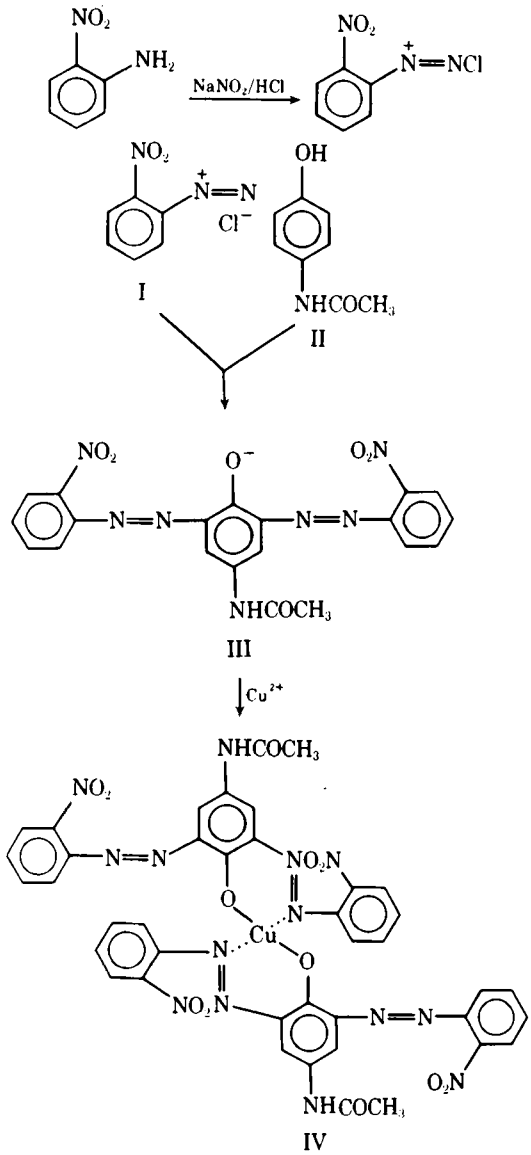

Scheme I

Acetaminophen solution (0.3 mg/5.0 ml of water) was added followed by 3 ml of 1 *N* NaOH. The contents were mixed and left to stand for 5 min. A copper(II) sulfate solution (5 ml, 0.125 *M*) was added followed by 6 ml of 1 *N* H_2SO_4. The mixture was extracted three times with a total of 25 ml of chloroform. The absorbance was measured at 400 nm against a blank.

Stoichiometric Balance—Procedure B was used on 0.5–4.5 ml of 2×10^{-3} *M* acetaminophen (V_L) previously coupled with diazotized *o*-nitroaniline and treated with the corresponding complementary volume of copper(II) sulfate (V_M) to give a total volume of 5 ml for V_M and V_L in each case.

Procedure C: Indirect Determination—The copper(II) chelate chloroform extract (5.0 ml) obtained by applying Procedure B was transferred to a 10-ml graduated flask. The volume was completed with 5.0 ml of sodium diethyldithiocarbamate solution (0.5 g % in ethanol). The contents were mixed, and the absorbance was measured at 442 nm against a blank.

RESULTS

Coupling with Diazotized *o*-Nitroaniline—The phenolic hydroxyl group *para* to the acetamido group ($NHCOCH_3$) in acetaminophen causes coupling with diazotized *o*-nitroaniline to occur *ortho* to the hydroxyl group. To investigate the molecular reactant ratio, Job's method of continuous variation (21) was employed (Fig. 1*a*). The maximum absorbance was attained when $V_M/(V_L + V_M)$ equaled 0.66. This finding indicated that the diazonium salt-acetaminophen molecular ratio was

[1] Aprolabo.
[2] Alexandria Co. for Pharmaceutical and Chemical Industries, Egypt.
[3] Paracetamol, Misr Co. for Pharmaceutical Industries, Cairo, Egypt.
[4] Paracetamol, Misr Co. for Pharmaceutical Industries; and pyral, Elkahira Pharmaceutical and Chemical Industries Co., Cairo, Egypt.
[5] Pyral, Elkahira Pharmaceutical and Chemical Industries Co., Cairo, Egypt.

Table I—Acetaminophen in Different Pharmaceutical Formulations

Pharmaceutical Formulation	Mean Percentage ± *SD*			
	Official Method (n = 12)[a]	Procedure A (n = 14)	Procedure B (n = 16)	Procedure C (n = 14)
Laboratory-made tablet	—	100.24 ± 0.28	100.35 ± 0.51	100.37 ± 0.67
Acetaminophen tablets	101.02 ± 0.8	99.56 ± 0.41 (5.99)[b]	99.60 ± 0.60 (5.38)	99.54 ± 0.45 (5.93)
Acetaminophen syrup	101.75 ± 1.09	103.71 ± 0.29 (3.44)	103.77 ± 51.0 (3.18)	103.46 ± 0.39 (4.14)
Acetaminophen syrup	107.53 ± 0.73	105.38 ± 0.24 (10.41)	105.25 ± 0.44 (10.28)	105.57 ± 0.38 (8.77)
Acetaminophen drops	102.32 ± 0.20	101.36 ± 0.32 (8.98)	101.72 ± 0.37 (5.07)	101.57 ± 0.31 (7.19)

[a] n = number of experiments. [b] Figures in parentheses are the calculated values for which theoretical value $t_{0.975}$ equals 2.06.

2:1, as was anticipated due to the two free positions *ortho* to the acetaminophen hydroxyl when the diazonium salt coupling was assumed to occur (Compound III, Scheme I).

The coupled product stability was attained by: (*a*) keeping the *o*-nitroaniline with nitrous acid under the conditions previously mentioned for 10 min; (*b*) making the medium alkaline after addition of acetaminophen since the alkaline medium was essential for the coupling reaction, and (*c*) leaving the coupled product for 5 min before dilution with water. For alkalinization, 3 ml of 1 *N* NaOH was the optimum; a lower concentration was not sufficient for the full color development, and a higher concentration caused azo dye precipitation.

The colored azo dye (λ_{max} 426 nm) was stable for 6 hr. The dissociation degree, α, and the instability constant, K_i (22), equaled 0.0952 and 6.1105 × 10^{-6}, respectively.

Coupling and Subsequent Chelation—The investigation was extended to utilize the coupled compound as a chelating agent for copper(II) ion since the former has a free hydroxyl group with an easily replaceable proton and a diazo group (—N=N—) that offers a lone electron pair. The copper (II) chelate was hardly soluble in water but was easily extracted with chloroform to give a yellow solution (λ_{max} 400 nm).

The stoichiometric balance (Fig. 1*b*) determined by Job's method of continuous variation equaled 2:1 [2,6-di-(*o*-nitrophenylazo)-4-acetamidophenol–copper(II) ion]. The copper(II) ion satisfied its four coordination valency by combination with two free acetaminophen hydroxyl groups and with two diazo groups (Compound IV, Scheme I). The chelate was stable in chloroform for at least 4 hr after extraction. The dissociation degree, α, and the instability constant, K_i, for the chelate equaled 0.1375 and 19.2899 × 10^{-6}, respectively.

An acidic medium favored copper(II) chelate formation. Addition of 6 ml of 1 *N* H_2SO_4 ensured maximum quantitative chelate extraction. More important, the order of reagent addition (copper sulfate followed by sulfuric acid) was essential since addition of acid before copper(II) sulfate destroyed the azo dye.

Linearity of Beer's Plots—Standard curves for the azo dye and its copper(II) chelate were constructed by plotting observed absorbance readings *versus* the acetaminophen concentration treated similarly as described for Procedures A and B. Such a relationship followed Beer's law within a concentration range of 0.4–2.8 mg % (Procedure A) or 0.4–4 mg (Procedure B) of acetaminophen calculated in the final dilution. The regression equations, derived by the least-squares method (23), for the calibration curves were:

$$A_{426} = -0.0020 + 0.2503C \quad \text{(Procedure A)} \qquad \text{(Eq. 1)}$$

$$A_{400} = -0.0025 + 0.1216C \quad \text{(Procedure B)} \qquad \text{(Eq. 2)}$$

for which the percentage fits (24) were 99.97 and 99.91, respectively.

The validity of these equations was tested by analyzing known acetaminophen amounts mixed with common tablet excipients or additives in a ratio approximating sample commercial tablet weights. The results (Table I) were highly accurate, indicating no interference from tablet base ingredients.

Indirect Method—In spite of the high copper(II) chelate stability in chloroform, addition of 5 ml of diethyldithiocarbamate (0.5 g % ethanolic solution) displaced 2,6-di-(*o*-nitrophenylazo)-4-acetamidophenol to give copper(II) diethyldithiocarbamate, a complex of λ_{max} 442 nm. The absorbance was proportional to the acetaminophen concentration in the 0.2–2 mg % range. The calibration curve was described by the following regression equation:

$$A_{442} = -0.0047 + 0.3081C \quad \text{(Procedure C)} \qquad \text{(Eq. 3)}$$

for which the percentage fits equaled 99.59.

DISCUSSION

Acetaminophen coupling with diazotized *o*-nitroaniline had an advantage over the method involving acetaminophen hydrolysis with subsequent diazotization and coupling (20, 21). In the latter technique, any hydrolytic product present in pharmaceutical formulations during unsuitable storage interfered during the analysis. Any phenolic compound could interfere with Procedure A. To increase the method selectivity, coupling with subsequent chelation was proposed. The common analgesic–antipyretics likely to be present with acetaminophen exhibited no interference. Aspirin, codeine, caffeine, and salicylamide did not interfere[6].

The slope of the calibration curve for Procedure C was 1.23- or 2.53-fold higher than that for Procedure A or B, respectively. This finding indicated the high indirect method sensitivity.

BP 1973 (25) described a UV assay for acetaminophen in which diluents and binders in tablets or sweetening agents, preservatives, and coloring matter in syrups interfere during analysis. Therefore, it is not surprising that the proposed procedures give more accurate results than the official method since t-calculated exceeds t-theoretical (Table I).

REFERENCES

(1) A. A. D'Sanza and K. G. Shenoy, *Can. J. Pharm. Sci.*, **3**, 90 (1968).

(2) D. R. Vishwasrao, *Indian J. Pharm.*, **35**, 172 (1973).

(3) I. Tetsuo, T. Masayoshi, L. Shu-Chi, and I. Toyozo, *J. Hyg. Chem.*, **21**, 313 (1975); through *Anal. Abstr.*, **31**, 1E 29 (1976).

(4) J. B. Vaughan, *J. Pharm. Sci.*, **58**, 469 (1969).

(5) J. Kos, *Farm. Glas.*, **22**, 51 (1966); through *Anal. Abstr.*, **14**, 3529 (1967).

(6) R. M. Welch and A. H. Conney, *Clin. Chem.*, **11**, 1004 (1965).

(7) D. R. Davies, A. G. Fogg, D. T. Burns, and J. S. Wragg, *Analyst*, **99**, 12 (1974).

(8) R. O. Deodhar, M. R. Shastri, and R. C. Mehta, *Indian J. Pharm.*, **35**, 120 (1973).

(9) M. C. Inamdar and N. N. Kaji, *ibid.*, **31**, 79 (1969).

(10) C. Hanegroaff and N. Chastaigner, *Ann. Pharm. Fr.*, **27**, 663 (1969).

(11) F. Le Perdriel, C. Hanegroaff, N. Chastaigner, and E. De Monrety, *ibid.*, **26**, 227 (1968).

(12) K. Tsunetoshi, S. Kazuhiko, and Y. Ito-Yagu *J. Pharm. Soc. Jpn.*, **94**, 633 (1974); through *Anal. Abstr.*, **30**, 2E 34 (1976).

(13) K. Tsunetoshi, K. Kagi, and I. Toshili, *Jpn. Anal.*, **20**, 801 (1971); through *Anal. Abstr.*, **23**, 2776 (1972).

(14) K. Tsunetoshi and S. Kazuhiko, *J. Pharm. Soc. Jpn.*, **94**, 639 (1974); through *Anal. Abstr.*, **30**, 2E 33 (1976).

(15) Z. E. Kalinowska and H. Hasztar, *Pharm. Pol.*, **21**, 570 (1965); through *Anal. Abstr.*, **14**, 370 (1967).

(16) *Ibid.*, **23**, 447 (1967); through *Anal. Abstr.*, **15**, 4978 (1968).

(17) W. Poethke and H. Kahne, *Pharm. Zentralh.*, **104**, 630 (1965); through *Anal. Abstr.*, **14**, 370 (1967).

(18) M. C. Inamdar, J. C. Saboo, C. N. Kamdar, and N. M. Sanghavi, *Indian J. Pharm.*, **35**, 187 (1973).

(19) G. Brockelt, *Pharmazie*, **20**, 136 (1965).

(20) M. C. Inamdar, M. A. Gore, and R. V. Bhide, *Indian J. Pharm.*,

[6] Unpublished data.

36, 7 (1974).
(21) J. Rose, "Advanced Physico-Chemical Experiments," Pitman, London, England, 1964, p. 54.
(22) A. E. Harvey and D. L. Manning, *J. Am. Chem. Soc.*, **72**, 4488 (1950).
(23) M. R. Siegel, "Theory and Problems of Probability and Statistics," McGraw-Hill, New York, N.Y., 1975, pp. 215, 259.
(24) O. L. Davies and P. Goldsmith, "Statistical Methods in Research and Production," 4th ed., Oliver and Boyd, Edinburgh, Scotland, 1972, p. 178.
(25) "British Pharmacopoeia 1973," Her Majesty's Stationery Office, London, England, 1973, p. 340.

Pharmacokinetics of Morphine and Its Surrogates III: Morphine and Morphine 3-Monoglucuronide Pharmacokinetics in the Dog as a Function of Dose

EDWARD R. GARRETT ˣ **and ANDRÉ J. JACKSON** *

Received September 12, 1978, from *The Beehive, College of Pharmacy, J. Hillis Miller Health Center, University of Florida, Gainesville, FL 32610.* Accepted for publication November 21, 1978. *Present address: College of Pharmacy, Howard University, Washington, DC 20059.

Abstract □ The pharmacokinetics of morphine and its derived metabolite, morphine 3-monoglucuronide, were studied in normal and bile-cannulated dogs. High doses (7.2–7.7 mg/kg iv) caused renal and biliary shutdowns and time lags in urinary drug and metabolite excretion and in biliary secretion of the hepatically formed conjugate. Intermediate doses (0.41–0.47 mg/kg iv) inhibited urine flow but not renal clearance. Low doses (0.019–0.07 mg/kg iv) had no apparent effect. Dose-related effects on the total, metabolic, and biliary clearances imply saturable enzymes and/or dose-inhibited hepatic flows, accounting for the major elimination half-lives of 83 ± 8 and 37 ± 13 min at the high and low doses, respectively. The slow terminal phase in plasma morphine and metabolite elimination and urinary accumulation is due apparently to the enterohepatic metabolite recirculation after biliary excretion, gastrointestinal hydrolysis, and hepatic first-pass reconjugation. Bile-cannulated dogs showed no fecal drug and no slow terminal plasma and urine elimination phases. Intravenous morphine 3-monoglucuronide was eliminated only renally and showed neither biliary excretion nor prolonged hepatically formed glucuronide elimination. Hepatic morphine clearances at normal therapeutic doses parallel hepatic blood flow and explain the lack of oral morphine bioavailability by anticipating complete first-pass liver metabolism. Renal morphine and morphine conjugate clearances were 85 (± 9 *SEM*) and 41 (± 4 *SEM*) ml/min, respectively, indicating glomerular filtration for the latter and glomerular filtration plus tubular secretion for the former. Urinary morphine and morphine conjugate excretion accounted for ~83% of the dose. Biliary secretion accounted for 11–14% of the dose. Morphine showed dose-independent plasma protein binding of 36 (± 1 *SEM*) % and a red cell–plasma water partition coefficient of 1.11 ± 0.04 *SD*. New equations were developed to model the discontinuous morphine and morphine metabolite pharmacokinetics.

Keyphrases □ Morphine—pharmacokinetics, dose related, dogs □ Morphine monoglucuronide—pharmacokinetics, dose related, dogs □ Pharmacokinetics—morphine, morphine monoglucuronide, dose related, dogs

Early studies on the distribution and disposition of morphine were largely descriptive (1–6). Rigorous pharmacokinetic studies were limited and usually only related to the parent compound at high doses. Early time course studies (7–10) in the dog were conducted at large time intervals and at high 30-mg/kg levels (human therapeutic dose is 0.14 mg/kg) due to color complex assay sensitivity limitations (10). Early morphine studies (9) estimated that 78–97% of the administered morphine was recoverable in urinary and fecal excretions, 14% as free morphine and 55% as presumed glucuronide conjugate in the urine, and 6–26% in the feces with less than 2% of the total drug as the conjugate. The plasma [*N*-^{14}C-*methyl*]morphine half-life was estimated at ~1 hr (11).

BACKGROUND

A fluorometric method with a sensitivity of 1 μg/ml of plasma was used by Kupferberg *et al.* (12) in a single rabbit study of six time samples at 15 mg/kg to demonstrate apparent biphasic morphine decay in plasma with a terminal half-life that could be roughly estimated as 1 hr.

Only in the last decade has the morphine time course been monitored with sufficient attention to warrant any pharmacokinetic data analysis.

A highly sensitive GLC method was used to monitor the time course of morphine at 2.5 mg/kg iv in the rat (13). At least three exponentials were needed to fit the plasma level–time curve.

Radioimmunoassay was used to monitor morphine, 0.14 mg/kg iv, in human plasma (14, 15), and the results indicated an apparent triphasic loss that included a rapid initial decline during the first 5–10 min, a subsequent slower but precipitous decline with a half-life of 1.0–3.1 hr, and a terminal slow disappearance of 10–44 hr at plasma levels of <10 ng/ml. A separate study (16) at 1 mg/kg infused over 12 min could only demonstrate a two-compartment body model when conducted for 2 hr after the completion of the infusion. Total clearance was 378 ± 63 ml/min. The apparent half-lives were similar to those of the previous studies; mean values were 1 ± 1 and 137 ± 14 min, with the latter phase ranging from 1.3 to 3.5 hr. These half-lives were similar to those for the lower 0.14-mg/kg dose and suggested that the assumption of a saturable or capacity-limited process for morphine was not warranted. Since different subjects were used for the different doses, this concept cannot be rigorously concluded. Mean apparent volumes of distribution of the central compartment and the total apparent distribution space were 9 and 102% of body weight, respectively.

Radiolabeled morphine at 0.14 mg/kg in humans (17, 18) showed an initially fast distribution phase and an apparent terminal half-life of 2.1–2.6 hr. The sensitivity of 20–30 ng/ml of plasma may not have permitted the observation of a slow terminal phase. Conjugate quickly appeared in the plasma close to its maximum value at ~40 min. Cumulative urinary excretion of free morphine and of the conjugate was 8.5–9.3 and 66–70% of the dose, respectively. The renal drug and metabolite clearances were given as 109–171 and 50–115 ml/min, respectively. The qualitative formation of *N*-demethylated morphine was observed by following the time course of expired $^{14}CO_2$.

Catlin (19) investigated morphine pharmacokinetics in the rabbit by morphine radioimmunoassay methods with the intent of confirming the presence of multiphasic pharmacokinetics as indicated by previous studies that apparently demonstrated a terminal half-life of many hours or days. He clearly demonstrated that a two- or three-compartment body model in the rabbit could be observed, dependent on antiserum specificity and on possible interaction with metabolites. He stated that he would reject the third compartment for the rabbit and retain only two half-lives of 13 and 72 min. No pharmacokinetic dose dependency was observed between the 1- and 10-mg/kg doses. Catlin (19) issued the caveat for the previously cited radioimmunoassay studies in humans (14, 15), where an apparently long terminal half-life was observed, that "providing the antiserum used . . . did not seriously cross-react with morphine metabolites, it appears that in man the two compartment model is not sufficient

0022-3549/79/0600-0753$01.00/0
© 1979, American Pharmaceutical Association

36, 7 (1974).
(21) J. Rose, "Advanced Physico-Chemical Experiments," Pitman, London, England, 1964, p. 54.
(22) A. E. Harvey and D. L. Manning, *J. Am. Chem. Soc.*, **72**, 4488 (1950).
(23) M. R. Siegel, "Theory and Problems of Probability and Statistics," McGraw-Hill, New York, N.Y., 1975, pp. 215, 259.
(24) O. L. Davies and P. Goldsmith, "Statistical Methods in Research and Production," 4th ed., Oliver and Boyd, Edinburgh, Scotland, 1972, p. 178.
(25) "British Pharmacopoeia 1973," Her Majesty's Stationery Office, London, England, 1973, p. 340.

Pharmacokinetics of Morphine and Its Surrogates III: Morphine and Morphine 3-Monoglucuronide Pharmacokinetics in the Dog as a Function of Dose

EDWARD R. GARRETT ˣ **and ANDRÉ J. JACKSON** *

Received September 12, 1978, from *The Beehive, College of Pharmacy, J. Hillis Miller Health Center, University of Florida, Gainesville, FL 32610.* Accepted for publication November 21, 1978. *Present address: College of Pharmacy, Howard University, Washington, DC 20059.

Abstract □ The pharmacokinetics of morphine and its derived metabolite, morphine 3-monoglucuronide, were studied in normal and bile-cannulated dogs. High doses (7.2–7.7 mg/kg iv) caused renal and biliary shutdowns and time lags in urinary drug and metabolite excretion and in biliary secretion of the hepatically formed conjugate. Intermediate doses (0.41–0.47 mg/kg iv) inhibited urine flow but not renal clearance. Low doses (0.019–0.07 mg/kg iv) had no apparent effect. Dose-related effects on the total, metabolic, and biliary clearances imply saturable enzymes and/or dose-inhibited hepatic flows, accounting for the major elimination half-lives of 83 ± 8 and 37 ± 13 min at the high and low doses, respectively. The slow terminal phase in plasma morphine and metabolite elimination and urinary accumulation is due apparently to the enterohepatic metabolite recirculation after biliary excretion, gastrointestinal hydrolysis, and hepatic first-pass reconjugation. Bile-cannulated dogs showed no fecal drug and no slow terminal plasma and urine elimination phases. Intravenous morphine 3-monoglucuronide was eliminated only renally and showed neither biliary excretion nor prolonged hepatically formed glucuronide elimination. Hepatic morphine clearances at normal therapeutic doses parallel hepatic blood flow and explain the lack of oral morphine bioavailability by anticipating complete first-pass liver metabolism. Renal morphine and morphine conjugate clearances were 85 (± 9 *SEM*) and 41 (± 4 *SEM*) ml/min, respectively, indicating glomerular filtration for the latter and glomerular filtration plus tubular secretion for the former. Urinary morphine and morphine conjugate excretion accounted for ~83% of the dose. Biliary secretion accounted for 11–14% of the dose. Morphine showed dose-independent plasma protein binding of 36 (± 1 *SEM*) % and a red cell–plasma water partition coefficient of 1.11 ± 0.04 *SD*. New equations were developed to model the discontinuous morphine and morphine metabolite pharmacokinetics.

Keyphrases □ Morphine—pharmacokinetics, dose related, dogs □ Morphine monoglucuronide—pharmacokinetics, dose related, dogs □ Pharmacokinetics—morphine, morphine monoglucuronide, dose related, dogs

Early studies on the distribution and disposition of morphine were largely descriptive (1–6). Rigorous pharmacokinetic studies were limited and usually only related to the parent compound at high doses. Early time course studies (7–10) in the dog were conducted at large time intervals and at high 30-mg/kg levels (human therapeutic dose is 0.14 mg/kg) due to color complex assay sensitivity limitations (10). Early morphine studies (9) estimated that 78–97% of the administered morphine was recoverable in urinary and fecal excretions, 14% as free morphine and 55% as presumed glucuronide conjugate in the urine, and 6–26% in the feces with less than 2% of the total drug as the conjugate. The plasma [*N*-^{14}C-*methyl*]morphine half-life was estimated at ~1 hr (11).

BACKGROUND

A fluorometric method with a sensitivity of 1 μg/ml of plasma was used by Kupferberg *et al.* (12) in a single rabbit study of six time samples at 15 mg/kg to demonstrate apparent biphasic morphine decay in plasma with a terminal half-life that could be roughly estimated as 1 hr.

Only in the last decade has the morphine time course been monitored with sufficient attention to warrant any pharmacokinetic data analysis.

A highly sensitive GLC method was used to monitor the time course of morphine at 2.5 mg/kg iv in the rat (13). At least three exponentials were needed to fit the plasma level–time curve.

Radioimmunoassay was used to monitor morphine, 0.14 mg/kg iv, in human plasma (14, 15), and the results indicated an apparent triphasic loss that included a rapid initial decline during the first 5–10 min, a subsequent slower but precipitous decline with a half-life of 1.0–3.1 hr, and a terminal slow disappearance of 10–44 hr at plasma levels of <10 ng/ml. A separate study (16) at 1 mg/kg infused over 12 min could only demonstrate a two-compartment body model when conducted for 2 hr after the completion of the infusion. Total clearance was 378 ± 63 ml/min. The apparent half-lives were similar to those of the previous studies; mean values were 1 ± 1 and 137 ± 14 min, with the latter phase ranging from 1.3 to 3.5 hr. These half-lives were similar to those for the lower 0.14-mg/kg dose and suggested that the assumption of a saturable or capacity-limited process for morphine was not warranted. Since different subjects were used for the different doses, this concept cannot be rigorously concluded. Mean apparent volumes of distribution of the central compartment and the total apparent distribution space were 9 and 102% of body weight, respectively.

Radiolabeled morphine at 0.14 mg/kg in humans (17, 18) showed an initially fast distribution phase and an apparent terminal half-life of 2.1–2.6 hr. The sensitivity of 20–30 ng/ml of plasma may not have permitted the observation of a slow terminal phase. Conjugate quickly appeared in the plasma close to its maximum value at ~40 min. Cumulative urinary excretion of free morphine and of the conjugate was 8.5–9.3 and 66–70% of the dose, respectively. The renal drug and metabolite clearances were given as 109–171 and 50–115 ml/min, respectively. The qualitative formation of *N*-demethylated morphine was observed by following the time course of expired $^{14}CO_2$.

Catlin (19) investigated morphine pharmacokinetics in the rabbit by morphine radioimmunoassay methods with the intent of confirming the presence of multiphasic pharmacokinetics as indicated by previous studies that apparently demonstrated a terminal half-life of many hours or days. He clearly demonstrated that a two- or three-compartment body model in the rabbit could be observed, dependent on antiserum specificity and on possible interaction with metabolites. He stated that he would reject the third compartment for the rabbit and retain only two half-lives of 13 and 72 min. No pharmacokinetic dose dependency was observed between the 1- and 10-mg/kg doses. Catlin (19) issued the caveat for the previously cited radioimmunoassay studies in humans (14, 15), where an apparently long terminal half-life was observed, that "providing the antiserum used . . . did not seriously cross-react with morphine metabolites, it appears that in man the two compartment model is not sufficient

0022-3549/79/0600-0753$01.00/0
© 1979, American Pharmaceutical Association

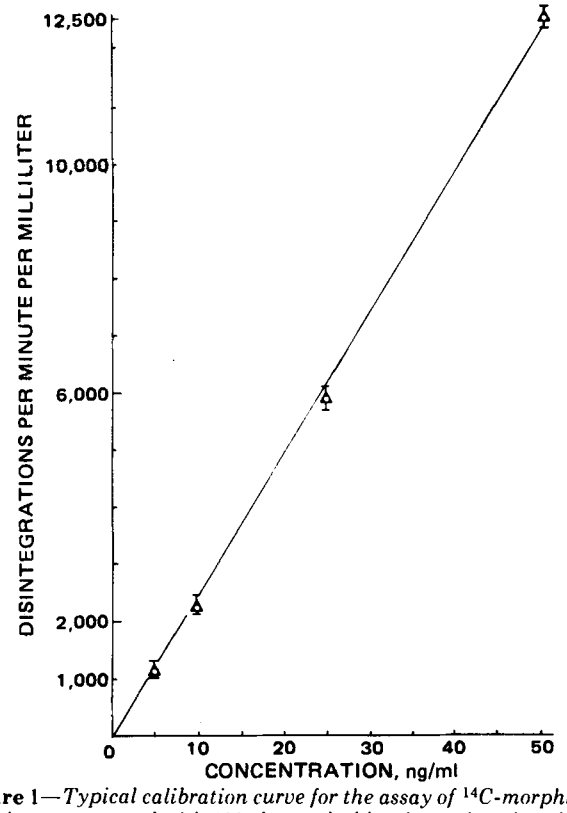

Figure 1—*Typical calibration curve for the assay of ^{14}C-morphine in dog plasma extracted with 10% butanol–chloroform after the addition of 0.5 g of $NaHCO_3$ to 2 ml of plasma by liquid scintillation spectrometry in the absence (△) and presence (○) of 100 ng/ml of ^{14}C-morphine-3-glucuronide. The vertical bars give the ± SD of four replicate determinations.*

to describe the data." Stripped of its niceties, the statement implies that radioimmunoassay assays for low morphine levels in the presence of metabolites are suspect and that the assumption of a deep compartment in humans is not assured.

Definitive pharmacokinetic studies in other animal species and humans still are needed to prove the presence of a deep compartment characterized by a slow terminal release of administered morphine from the body. The reported studies were designed to challenge the hypothesis of a deep morphine compartment with slow terminal release.

The only attempt to challenge systematically dose-dependent morphine pharmacokinetics was made by Catlin (19) in the rabbit. His conclusion of nondose dependence is surprising in the light of known morphine pharmacology. Although morphine is used primarily as an analgesic agent, it elicits many other pharmacodynamic responses (20) including cardiovascular and respiratory effects such as peripheral vasodilation, blood pressure decrease, blood compartment volume changes, and respiratory depression. Morphine increased biliary pressure and caused biliary tract spasms which could impede biliary excretion.

Handley and Moyer (21) showed that intravenous doses of 1 mg/kg or more to the dog produced not only a pronounced fall in mean blood pressure but also an abrupt and sustained depression of the glomerular filtration rate and renal plasma flow and a maximal rate of dextrose reabsorption by the renal tubules. Such pharmacological effects should have a decided "feedback" effect on morphine pharmacokinetics as a function of dose. This paper reports on the apparent perturbations of morphine pharmacokinetics by its dose-dependent pharmacological effects.

These potential problems offer a challenge in proper pharmacokinetic modeling. Not only must nonlinearities that may not conform to simple saturation models be taken into account, but discontinuities in pharmacokinetic processes must be considered. Such discontinuities can be caused by shutdowns in renal and biliary processes and the holdup of significant drug and metabolite quantities in the kidneys and bile.

Pharmacokinetic studies have not monitored the constancies of renal and metabolic clearances of morphine and its metabolites as a function of dose. These canine studies were designed to permit a pharmacokinetically unified appraisal of the time courses of intravenous morphine and its principal metabolite (2, 3), morphine-3-monoglucuronide, in plasma, urine, bile, and feces over a wide spectrum of doses. It is believed (2, 3, 6) that the formation of other metabolites in the dog is negligible.

The separation techniques used here permit the specific monitoring of radiolabeled morphine and its conjugates in the various biological fluid studied (22). The analytical methods used were equivalent to several independent nonradioactive assays.

EXPERIMENTAL

Materials—The following were used: nanograde chloroform[1], analytical grade butanol[1], *N*-^{14}C-*methyl*-morphine hydrochloride[2], morphine sulfate USP[3], silicone solution[4], thin-layer plates[5], chromatogram sheets[6], a scintillant (Handifluor[1]), sodium bicarbonate[1], *tert*-butylhydroperoxide[7], heparin sodium[8] (10,000 units/ml), and pentobarbital sodium[9].

Purity of *N*-^{14}C-*methyl*-Morphine—Vendor analysis of the *N*-^{14}C-*methyl*-morphine hydrochloride (143 μCi/mg) (1 μCi = 2.2 × 10^6 dpm) stated a 98% radiolabeled purity in carbon tetrachloride–*n*-butanol–methanol–5 *N* ammonia (40:30:30:4). TLC[6] in the system of *n*-propanol–acetone–acetic acid–5% ammonium hydroxide–water (9:3:2:2:4) (23) separated morphine (R_f 0.67) from the other alkaloids. One-centimeter sections of the developed chromatogram were scraped into vials, dissolved in 1.0 ml of water, and counted in a scintillation counter[10].

^{14}C-Morphine and ^{14}C-Morphine Glucuronide Assay in Biological Fluids—All glassware was silylated because of morphine adsorption by glass at low concentrations (24). Sodium bicarbonate (0.5 g) was added to 2 ml of plasma, urine, or bile containing morphine. This solution was shaken with 9 ml of 10% butanol–chloroform for 10 min and separated by centrifugation[11] at 1000 rpm. The upper aqueous phase was removed by aspiration, and an appropriate organic phase aliquot was evaporated in a scintillation vial under nitrogen in a water bath at 50°. Scintillant (10 ml)[12] was added, and the resultant ^{14}C-morphine solution was counted.

The original plasma, urine, or bile ^{14}C-morphine concentration was calculated by dividing by the extraction efficiency and the specific activity. A typical linear calibration curve for ^{14}C-morphine in dog plasma in the absence and presence of ^{14}C-morphine-3-glucuronide is given in Fig. 1.

The morphine extraction efficiency from a buffered 2.0-ml plasma sample with 9 ml of 10% butanol–chloroform was 0.84 ± 0.03 (*SD*). The solvent–plasma partition coefficient was 1.17, calculated from:

$$K = \frac{A_o V_w}{V_o(A - A_o)} = \frac{C_o}{C_w} \qquad \text{(Eq. 1)}$$

where $A_o/(A - A_o)$ is the ratio of the organic phase concentration (0.84 *A*) to the aqueous plasma concentration (0.16 *A*); V_w (2 ml) and V_o (9 ml) are the plasma and organic solution volumes, respectively; and *A* is the total plasma concentration before extraction. Where the organic solvent volume (V_o) and/or the extracted plasma volume (V_w) were varied, the total extracted plasma morphine fraction (f_{ex}) was calculated from:

$$f_{ex} = A_o/A = 1/(1 + V_w/V_oK) \qquad \text{(Eq. 2)}$$

where K = 1.167.

The extraction efficiency of morphine from buffered urine (2 ml with 9 ml of organic solvent) was 0.87 ± 0.02 to give a partition coefficient from urine of K = 1.49 (Eq. 1). The fraction extracted from a different volume of urine was calculated from Eq. 2.

The plasma, urine, or bile concentration (disintegrations per minute per milliliter) of the unextractable morphine metabolite was determined from the difference between the experimentally determined total disintegrations per minute per milliliter of unextracted plasma, urine, or bile and the calculated disintegrations per minute per milliliter assigned to the morphine concentration in these biological fluids. Unextracted

[1] Mallinckrodt Chemical Works, St. Louis, MO 63160.
[2] Amersham/Searle, Arlington Heights, IL 60005.
[3] Merck Sharp and Dohme, West Point, PA 19486.
[4] Siliclad, Clay Adams, Parsippany, NJ 07054.
[5] Uniplate, Analtech Inc., Newark, DE 19711.
[6] Eastman Kodak Co., Rochester, NY 14650.
[7] Matheson Coleman and Bell, Norwood, OH 45212.
[8] The Upjohn Co., Kalamazoo, Mich.
[9] Nembutal Sodium, Abbott Laboratories, North Chicago, Ill.
[10] Beckman Instrument Co., Fullerton, CA 92634.
[11] International centrifuge, model K, International Equipment Co., Needham Heights, Mass.
[12] Handifluor, Mallinckrodt Chemical Works, St. Louis, MO 63160.

plasma, urine, or bile (0.2 ml) was counted by adding 1.0 ml of water plus 10 ml of scintillant.

All counts per minute were converted to disintegrations per minute by dividing by the counting efficiencies. Nanogram morphine base equivalents were determined by dividing the disintegration per minute values by the specific activity of the morphine free base. The counting efficiencies of plasma, urine, bile, fecal slurries (10% w/v homogenate in water), and their extracts were determined by adding a known standard ^{14}C-toluene amount to previously counted samples and recounting. The counting efficiency was the ratio of the difference in counts per minute values to the disintegrations per minute added. Blood and bile samples were digested with 0.5 ml of 1 *N* NaOH and bleached with 0.5 ml of *tert*-butylhydroperoxide prior to extraction and counting.

^{14}C-Morphine-3-monoglucuronide Isolation—The metabolite was isolated from the urine of dogs administered ^{14}C-morphine. A literature procedure (24) was used, except that TLC was substituted for anionic-exchange separation. Urine (30 ml) was shaken with 2 g of charcoal in a 50-ml centrifuge tube for 1 hr and centrifuged for 3 min. The aqueous layer was decanted, and the residual charcoal was washed twice with 30 ml of water. The adsorbed morphine and metabolites were extracted from the charcoal by shaking it with 10 ml of acetic acid for 30 min and centrifuging for 10 min. This procedure was repeated three times.

The resulting extracts were collected and filtered through filter paper to remove the finer charcoal particles. The clear liquid was evaporated under reduced pressure[13], and the residue was dissolved in 10 ml of water. This solution was chromatographed[5] in *n*-propanol–acetone–acetic acid–5% ammonium hydroxide–water (9:3:2:2:4) to separate morphine from its metabolite. The chromatogram was developed for 15 cm, and the metabolite spot (R_f 0.48) was scraped from the plate and eluted with hot water. The silica gel slurry was filtered to give a metabolite solution.

Metabolite Purity—The purity of the radiolabeled morphine-3-monoglucuronide metabolite was based on the R_f values of the isolated compound *versus* an authentic nonradioactive standard[14]. The following systems were used to verify the purity: System I (R_f 0.48), *n*-propanol–acetone–acetic acid–5% ammonium hydroxide–water (9:3:2:4:4) (3); and System II (R_f 0.0), chloroform–ethanol–water–acetic acid (20:10:15:1) (4). The morphine-3-monoglucuronide was visualized under UV light, and 1-cm sections were scraped into scintillation vials and counted. The chromatographic purity was 96%.

Metabolite Purity by Extraction—One hundred nanograms (10 μl) of the radiolabeled metabolite was added to each of three test tubes containing 2 ml of water to give a final concentration of the metabolite of 50 ng/ml. Each tube was extracted three times after the addition of 0.5 g of $NaHCO_3$ with 9 ml of 10% butanol–chloroform. Then 8 ml of each total extract was collected, dried, and counted. Less than 1.4% (1.1, 1.4, and 1.2) was extracted by this procedure.

Attempted Identification of Additional Major Metabolites—Plasma ultrafiltrates and urine samples from several dogs administered morphine were analyzed by TLC (System I). Two compounds were visualized, and their R_f values were determined by radioactive analysis of scrapings. They were morphine glucuronide (R_f 0.48) and morphine (R_f 0.67). These plasma and urine samples were also extracted with tetrahydrofuran at pH 1, 8, and 10, and the extracts were chromatographed in System I. Each chromatogram was developed to 15 cm, and 1-cm sections were scraped into scintillation vials and counted after the addition of 1 ml of water. Additional compounds were not observed at other R_f values.

Protein Binding—The binding of ^{14}C-morphine and ^{14}C-morphine 3-monoglucuronide was studied by an ultrafiltration method (25). When these drugs were dissolved in buffer and ultrafiltered through the cone membrane[15], no significant cone binding of drugs was observed. Standard morphine solutions were prepared in plasma at 10 and 100 ng/ml and at 2.48 μg/ml. The ultrafiltration cones were soaked in water and spun dry prior to use. The dried cones were placed in ultrafiltration cone supports in centrifuge tubes.

One milliliter of 0.05 *M* phosphate buffer, at ionic strength 0.154 and pH values of 7.4, 7.5, and 7.8, was placed in each cone. The appropriate standard plasma solution concentration was added, with agitation to effect mixing, until a volume of 5.0 ml was obtained. An aliquot (0.2 ml) was analyzed for total radioactivity. The samples were allowed to stand at room temperature for 3 min, 12 min, or 1 hr and then were centrifuged at 2000 rpm for 10 min to half-filtration. The ultrafiltrates were assayed by liquid scintillation spectrophotometry.

Similar studies were conducted with dog plasma at 100 ng of morphine-3-glucuronide/ml at pH values of 7.1 and 7.4.

Red Blood Cell Partition—The partition of ^{14}C-morphine and ^{14}C-morphine-3-monoglucuronide into the red blood cells was studied as a function of drug concentration and time. Fresh heparinized dog blood was added with gentle shaking to 10-ml volumetric flasks containing enough ^{14}C-morphine to achieve concentrations of 1, 10, 100, and 1000 ng/ml. Dog blood also was added to another set of volumetric flasks containing sufficient ^{14}C-metabolite to achieve concentrations of 50 and 500 ng/ml. Hematocrits were determined, and aliquots (3 ml) were taken after 30 sec and 30 min at room temperature and assayed for total radioactivity. The remaining blood was centrifuged at 1000 rpm for 10 min, and the plasma was analyzed for total radioactivity.

Pharmacokinetics of Morphine and Its Derived Metabolite—The dogs were fasted for 24 hr before each experiment and then weighed. Chronic jugular vein catheterization was done with medical grade tubing[16] at least 48 hr before the scheduled experiment. All blood sampling was done through this catheter.

On the day of the experiment, the dog was placed on a table in a standing position and restrained by separate straps around the fore- and hindlegs, which were fixed to a horizontal bar above. A water load of 15 ml/kg was administered through stomach tubing. A continuous 0.9% NaCl drip (1 ml/min) was maintained for 500 min. A transurethral catheter[17] was used to collect bladder urine for the first 12 hr. After 12 hr, urine was collected from the metabolic cages, with completeness achieved by acute catheterization. After anaerobic collection, the blood pH and P_{CO_2} were routinely determined on the gas analyzer[18]. Hematocrits were determined utilizing a microhematocrit centrifuge and reader[19].

Sterile procedures were used for blood handling when red blood cells were to be readministered. After separation from plasma, the packed cells were stored at 5°. At the end of the experiment, they were resuspended in normal saline and reinfused into the animal; 200,000 units of procaine penicillin G in dihydrostreptomycin sulfate[20] solution were administered intramuscularly.

Hematology showed negative results for microfilaria. Body weights and the intravenous morphine doses are listed in Table I. A minimum period of 2 weeks was allowed between any two experiments on the same dog.

^{14}C-Morphine hydrochloride was diluted with morphine sulfate USP, and the specific activity of the final mixture determined. The morphine was administered intravenously, as freshly prepared solutions in plasma, into the jugular catheter over 10 sec for the 0.02- and 0.07-mg/kg doses; it was injected into the cephalic vein for the 0.4–0.5- and 7.2–7.7-mg/kg doses. Drug administration was followed by a 5-ml flush of normal saline to free the catheter of residual drug. At the highest dose, the dogs exhibited a phenomenon known as sham rage and had to be physically restrained so that blood could be sampled.

Blood samples were taken from the jugular catheter after the dead space volume was removed and the catheter was filled with fresh undiluted blood. Sterile disposable syringes containing approximately 50 μl of heparin (10,000 units/ml) were used to collect blood samples. The blood was transferred to a 15-ml centrifuge tube and centrifuged at 1500 rpm for 10 min, with 2 ml of the supernatant plasma being transferred to tubes containing 0.5 g of sodium bicarbonate for extraction. Blood samples (5 ml) were taken at 0.5, 1, 2, 5, 10, and 20 min after the morphine injection; 8-ml samples were taken at 30, 45, 75, 110, and 180 min; 1-ml samples were taken hourly thereafter to 12 hr and finally every 12 hr up to 50 hr. When pH and hematocrit values were to be evaluated, a small portion of the sample was left in the syringe.

Urine was collected every 10 min up to 1 hr, then hourly up to 12 hr, and then every 12 hr up to 100 hr. The volume was noted, and the urine was stored in bottles and refrigerated at 5°.

Feces were collected at 24-hr intervals.

Pharmacokinetics of ^{14}C-Morphine-3-monoglucuronide—The purified metabolite morphine-3-monoglucuronide was administered intravenously to Dog A, which had not been used in a previous phar-

[13] Büchi Rotavapor, Brinkmann Instruments, Westbury, NY 11590.

[14] National Institute of Mental Health, Center for Studies of Narcotic and Drug Abuse, Bethesda, Md.

[15] Centriflo CF 50 membrane filter cone with CSTL support, Amicon Co., Lexington, Mass.

[16] Silastic tubing, Dow Corning Corp. Medical Products, Midland, MI 48640.

[17] French size 6, Bard Inc., Murray Hill, N.J.

[18] Model 113-S-1 pH-blood gas analyzer, Instrumentation Laboratories, Boston, Mass.

[19] Damon/I.E.C. Division, Needham Heights, MA 02194.

[20] Distrycillin, 200,000 units, 0.25 g/ml, E. R. Squibb and Sons, New Brunswick, NJ 08903.

Table I—Pharmacokinetics of Intravenous Morphine in Dogs

Parameter	High Doses			Intermediate Doses			Low Doses	
Dose (D_0), mg	109.2	109.0	107.0	6.43	5.70	0.792	0.225	0.208
Dose (D_0), mg/kg	7.68	7.22	7.60	0.406	0.471	0.070	0.0191	0.0189
Specific activity, dpm/ng	1.17	0.624	0.792	5.99	14.92	128	416	438
Dog	C	C	E	C	D	B	B	A
Weight, kg	14.2	15.1	14.0	16.0	11.5	11.4	11.8	11.0
Bile cannulated	Yes	No	No	Yes	No	No	No	No
Parameters[a] from plasma data								
A, ng/ml	1200	5600	3700	82.8	111	40	12.5	17.5
B	2200	2200	2800	47	51	21.3	4.0	5.4
α, min^{-1} ($t_{1/2}$, min)	0.0974 (7.1)	0.175 (4.0)	0.0534 (13)	0.0344 (20)	0.0613 (11)	0.159 (4.4)	0.201 (3.4)	0.234 (3.0)
β	7.78×10^{-3} (89)	8.45×10^{-3} (82)	8.96×10^{-3} (77)	9.50×10^{-3} (73)	1.40×10^{-2} (50)	2.06×10^{-2} (34)	1.53×10^{-2} (45)	1.86×10^{-2} (37)
Parameters[a] from urine data								
β, min^{-1} ($t_{1/2}$, min)	7.73×10^{-3} (90)	9.4×10^{-3} (74)	8.6×10^{-3} (81)	1.03×10^{-2} (67)	9.14×10^{-3} (76)	2.84×10^{-2} (24)	1.41×10^{-2} (49)	1.80×10^{-2} (39)
γ	0.0	8.6×10^{-4} (808)	4.6×10^{-4} (1509)	0.0	5.04×10^{-4} (1375)	1.45×10^{-3} (477)	1.31×10^{-3} (531)	5.5×10^{-4} (1264)
Clearances, ml/min								
Cl^M_{tot} [b]	370	359	290	784	886	586	694	554
Cl^M_{ren} [c]	98	67	56	115	115	69	98	62
Cl^M_{met} [d]	272 (322)	292 (232)	234 (215)	669 (454)	771	517	596	492
$Cl^M_{met} - Cl_B$ [e]	—	205	182	—	256	341	417	207
Cl_B [f]	—	87 (150)[g]	52	—	515	176	179	285
Cl^{MG}_{ren} [h]	57	45	38	50	34	48	33	24
Disposition, fractions of dose								
$\Sigma U^\infty_M/D_0$	0.148	0.099	0.070	0.139	0.151	0.124	0.145	0.123
$\Sigma U^\infty_{MG}/D_0$	0.785	0.674	0.794	0.508	0.620	0.813	0.736	0.720
$\Sigma B^\infty_{exp}/D_0$	0.143	—	—	0.109	—	—	—	—
Theoretical fraction of drug not in urine[i]	0.063	0.227	0.136	0.353	0.229	0.063	0.119	0.147
Theoretical fraction of drug excreted in bile[i], $\frac{\Sigma B^{tot}_{calc}}{D_0}$	—	0.295	0.186	—	0.582	0.286	0.258	0.514
$\Sigma MG^\infty_{ent}/D_0$ [k]	—	0.156	0.145	—	0.333	0.258	0.129	0.367
$\Sigma MG^{theo}_{feces}/D_0 = B'_\infty$ [l]	0.0	0.139	0.041	0.0	0.249	0.028	0.129	0.147
$\Sigma MG^{exp}_{feces}/D_0$	0.0	0.087	0.053	0.0	0.135	—	—	—
Apparent volumes of distribution, liters								
V^M_c [m]	32	14	16	19	5.2	13	14	9
V^M_d [n]	48	42	66	23	63	30	46	31
V^M_{extrap} [o]	50	50	38	50	35	37	56	39
V_{MG} [p]	-(4.2)	5.05 (4.2)	4.23 (3.96)	-(2.85)	2.03	1.52	0.51	1.68
Time of commencement, min								
Renal function	60	65	105	0	0	0	0	0
Bile function	16	35	0–10	0	0	0	0	0
$[MG]_{max}$, ng/ml as morphine	8800	6400	10,300	360	330	92	50	26
$10^5 [MG]_{max}/D_0$	8.1	5.9	9.6	5.6	5.8	120	22	9.6

[a] Parameters estimated from best fit of $[M]_{exp}$ as morphine base in plasma against time to $[M] = Ae^{-\alpha t} + Be^{-\beta t} + Ce^{-\gamma t}$ or from urine data where the γ parameter was determinable solely from slopes of plots of ln $|\Sigma U_\infty - \Sigma U|$ *versus* time t and ln $\Delta U_M/\Delta t$ *versus* time t_{mid}, where ΣU_M is the cumulative morphine base excreted into urine at time t and $\Delta U_M/\Delta t$ is the amount of morphine base excreted in a time interval of midtime, t_{mid}. A C and γ of 20 ng/ml and 8.7×10^{-4} min^{-1} ($t_{1/2}$ = 798 min), respectively, could be estimated from plasma for Dog C, not bile cannulated, at the 109-mg dose in column 2. With the two intermediate doses, a quickly vanishing exponential $A'e^{-\alpha' t}$ should also be added to best fit the plasma–time data where the values of A' and α' ($t_{1/2})_{\alpha'}$ were 212 ng/ml and 0.242 min^{-1} (2.9 min), respectively, for the 6.43-mg dose in the bile-cannulated Dog C and 930 ng/ml and 0.921 min^{-1} (0.75 min), respectively, for the 5.70-mg dose in the non-bile-cannulated Dog D. [b] Total morphine base clearance estimated from ratio of dose to total area under plasma $[M]$ *versus* t curve, D_0/AUC_M^∞. [c] Renal morphine base clearance estimated from the slope of $\Delta U/\Delta t$ *versus* $[M]$ plots and the best fit of ΣU *versus* t data generated from $Cl_{ren}^M (AUC_M^t - AUC_M^{t_0})$, where AUC_M is the area under the plasma $[M]$ *versus* t curve up to time t and $AUC_M^{t_0}$ is the area up to a time, t_0, where renal processes start at the high doses. [d] Estimated metabolic clearance of morphine base to morphine conjugate, MG, normally calculated from $Cl_{tot}^M - Cl_{ren}^M$. The parenthetical values were determined from appropriate plots of:

$$\frac{\Sigma U_{MG}^{exp} + \Sigma B_{MG}^{exp}}{[MG]_{exp}} = Cl_{met}^M \frac{AUC_M}{[MG]} - V_{MG} \quad \text{or} \quad \frac{\Sigma U_{MG}^{exp} + \Sigma B_{MG}^{exp}}{AUC_M} = -V_{MG} \frac{[MG]_{exp}}{AUC_M} + Cl_{met}^M$$

where the ΣB_{MG}^{exp} data were the cumulative excretions of the conjugate in the bile experimentally determined for the study in the bile-cannulated dog at the same dose. [e] Obtained from appropriate data plots in accordance with $\Sigma U_{MG}^{exp}/AUC_M = V_{MG}[MG]_{exp}/AUC_M + (Cl_{met}^M - Cl_B)$ or $\Sigma U_{MG}^{exp}/[MG]_{exp} = (Cl_{met}^M - Cl_B) AUC_M/[MG]_{exp} - V_{MG}$ on the assumption of a constant immediate biliary clearance, Cl_B, of the formed conjugate. [f] Calculated constant biliary conjugate clearance, immediately after formation, obtained from the difference between $Cl_{met}^M = Cl_{tot}^M - Cl_{ren}^M$ and the $Cl_{met}^M - Cl_B$ value defined in footnote *e*. [g] This parenthetical biliary clearance value is from the best fit of the ΣB_{exp} *versus* t data from the bile-cannulated study from $Cl_B(AUC_M^t - AUC_M^{t_0})$, where $AUC_M^{t_0}$ is the area up to a time, t_0, where biliary clearance is presumed to start at this high dose. [h] Renal conjugate clearance (as morphine base equivalents) from the slope of $\Delta U_{MG}/\Delta t$ *versus* $[MG]$ plots and the best fit of ΣU_{MG} *versus* t data generated from $Cl_{ren}^{MG} (AUC_M^t - AUC_M^{t_0})$, where renal processes start at t_0. [i] $1 - (\Sigma U_{MG}^\infty + \Sigma U_M^\infty)/D_0$. [j] $\Sigma B_{calc}^{tot} = Cl_B AUC_M^\infty$ on the assumption of constant biliary clearance, Cl_B, and no enterohepatic recirculation. [k] Fraction of drug enterohepatically recirculated is calculated from $\Sigma MG_{ent}^\infty = \Sigma B^{tot} - \Sigma B'_\infty$ where $\Sigma B'_\infty = Cl_{met}^M AUC_M^\infty - \Sigma U_{MG}^\infty$. [l] Theoretical fraction excreted elsewhere, most probably in feces, from $\Sigma MG_{feces}^{theo} = \Sigma B'_\infty = Cl_{met}^M AUC_M^\infty - \Sigma U_{MG}^\infty$. [m] Apparent central compartment volume referenced to morphine base concentration in plasma, $V_c^m = [(D_0)/(A' + A + B)]$. [n] Apparent overall distribution volume, referenced to morphine base concentration in plasma, $V_d^m = [(D_0)/(AUC_M^\infty)(\beta)]$. [o] Apparent volume of distribution on assumption of rapid equilibration so that α or α' is extremely fast, *i.e.*, $V_{extrap} = D_0/B$, or for the intermediate doses where an α' existed, $V_{extrap} = (D_0)/(A + B)$. [p] Apparent overall distribution volume for the formed conjugate, MG, as determined from appropriate plots as specified in footnote *e*. The parenthetical estimates of this volume were determined from the appropriate plots as specified in footnote *d*.

Table II—Morphine Fraction Bound to Plasma Protein[a]

pH	Concentration, ng/ml									Average ± *SD*
	10			100			2,480			
7.4	0.37	0.26	0.33	0.33	0.36	0.40	0.36	0.35	0.34	0.344 ± 0.038
7.6	0.45	0.31	0.36	0.42	0.41	0.39	0.28	0.28	0.29	0.354 ± 0.066
7.8	0.40	0.36	0.37	0.37	0.40	0.38	0.35	0.37	0.33	0.370 ± 0.022
Average ± *SD*	0.357 ± 0.054			0.384 ± 0.028			0.328 ± 0.037			0.356 ± 0.046

[a] As determined at 3 min, 12 min, and 1 hr after addition to dog plasma.

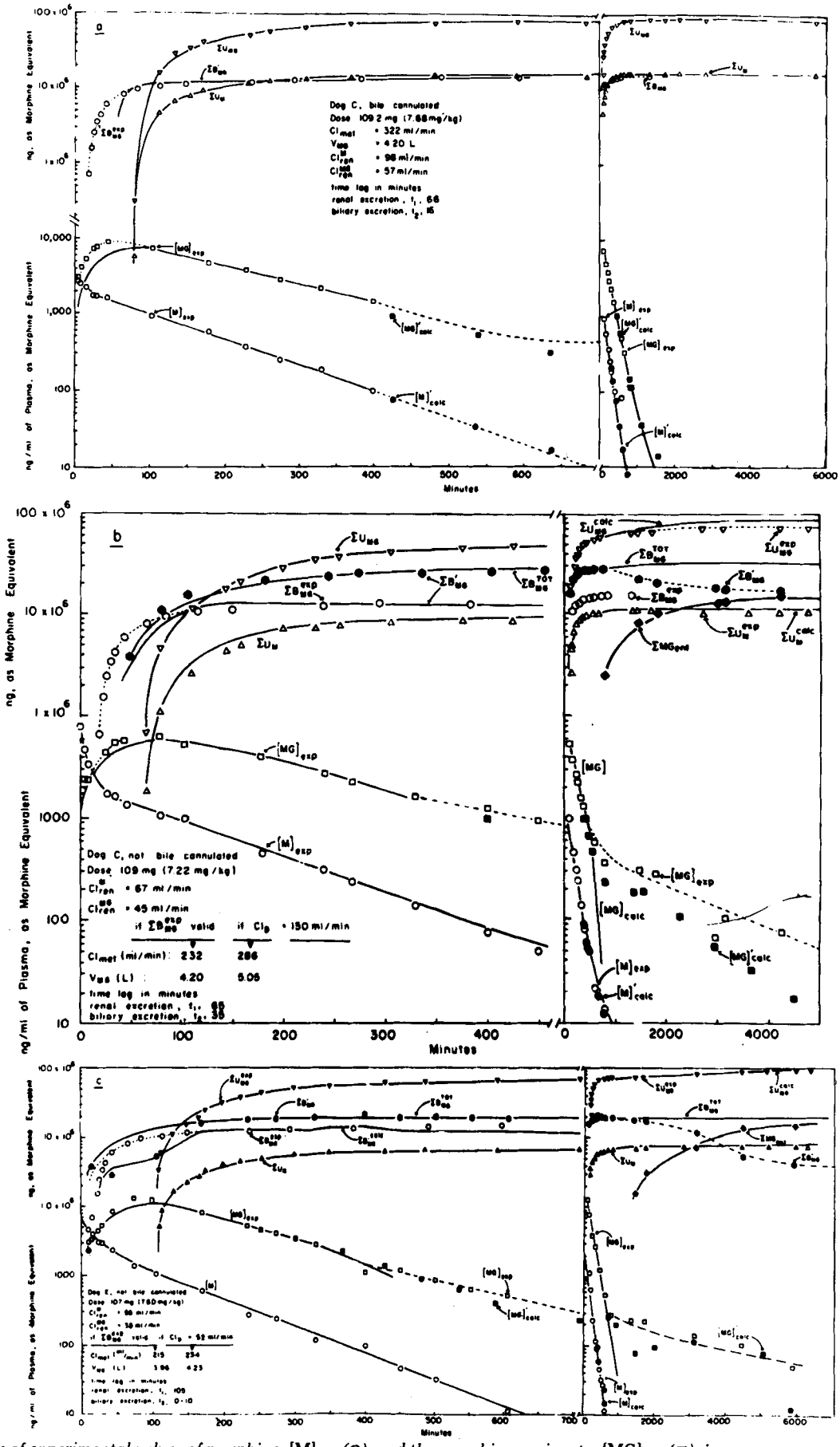

Figure 2—*Plots of experimental values of morphine,* $[M]_{exp}$ (⊙), *and the morphine conjugate,* $[MG]_{exp}$ (⊡), *in nanograms per milliliter of plasma as morphine equivalents against time at high morphine base doses, ~7.5 mg/kg iv. The solid line through the experimental* [M] *values was calculated*

from the polyexponential fit, $[M] = Ae^{-\alpha t} + Be^{-\beta t} + Ce^{-\gamma t}$. *(See Table I for parameters.) The solid line through the experimental* $[MG]_{exp}$ *values was calculated on the assumption of a constant metabolic morphine clearanee,* Cl^{M}_{met}, *so that* $[MG] = (Cl_{met}AUC_M - \Sigma B_{MG} - \Sigma U^{exp}_{MG})/V_{MG}$ *as in Eq. A13. The* Cl_{met} *and* V_{MG} *values for each dog could be obtained from appropriate plots of the data in accordance with Eqs. A11 and A12 (Fig. 7) based on the assumed validity of the* ΣB^{exp}_{MG} *data (○) from the bile-cannulated dog for the normal dog. The* [MG] *values were also calculated for the normal dog from estimates of* $Cl_{met} = Cl_{tot} - Cl^{ren}_{M}$, *where* $Cl_{tot} = dose/AUC_M$, *and* $\Sigma B_{MG} = Cl_B AUC_M$, *where* $Cl_{met} - Cl_B$ *and* V_{MG} *values were estimated from plots in accordance with Eqs. A16 and A17 (Figs. 8 and 9).*

The experimental values of cumulative morphine, ΣU^{exp}_{M} *(△), and its conjugate,* ΣU^{exp}_{MG} *(▽), in urine are also plotted against time. The solid lines through the data points are the theoretical values calculated from* $\Sigma U_M = Cl^{M}_{ren}(AUC_M - AUC^{u}_{M})$ *and* $\Sigma U_{MG} = Cl^{MG}_{ren}(AUC_{MG} - AUC^{u}_{MG})$, *where* AUC^{u}_{M} *and* AUC^{u}_{MG} *are the respective areas under the* [M] *and* [MG] versus *time curves up to the time,* t_1, *of onset of renal excretion. The renal clearances,* Cl^{M}_{ren} *and* Cl^{MG}_{ren}, *were consistent with the values obtained from the slopes of the renal clearance plots of* $\Delta U/\Delta t$ versus *plasma level (Fig. 5).*

The calculated values of $\Sigma B'_{MG} = Cl^{M}_{met} AUC_M - \Sigma U^{exp}_{MG} - V_{MG}[MG]_{exp}$ *of Eq. A22 are represented by the solid line through the experimental values of* ΣB^{exp}_{MG} *(○), which were obtained from studies with the bile-cannulated dog at the same dose (Fig. 2a). The* Cl_{met} *and* V_{MG} *values were obtained from appropriate plots of the data in accordance with Eqs. A11 and A12 (Fig. 7).*

Alternative estimates of cumulative conjugate in the bile, $\Sigma B'_{MG}$ *(●), of the normal (not bile cannulated) dog (Figs. 2b and 2c) were based on the* Cl_{met} *and* V_{MG} *values obtained from appropriate data plots in accordance with Eqs. A16 and A17 (Figs. 8 and 9). The solid line through these data (●) was based on the assumed constant biliary clearance obtained from these plots and was calculated from* $\Sigma B^{tot}_{MG} = Cl_B(AUC_M - AUC^{t_2}_{M})$, *where* $AUC^{t_2}_{M}$ *is the area under the* [M] versus *time curve up to the time,* t_2, *of onset of biliary excretion. The difference between this total amount of conjugate excreted in the bile,* ΣB^{tot}_{MG}, *and the amount presumed to remain there,* $\Sigma B'_{MG}$, *estimates the amount of conjugate enterohepatically recirculated to the systemic circulation,* $\Sigma MG_{ent} = \Sigma B^{tot}_{MG} - \Sigma B'_{MG}$.

Terminal values of $[M]_{exp}$ *(○) and* $[MG]_{exp}$ *(□) tend to have larger errors since the liquid scintillation counts approach background. The respective solid symbols are the plasma level of* $[M]'_{calc}$ *(●) and* $[MG]'_{calc}$ *(■) calculated from the estimated renal clearances and the observed* ΣU^{exp}_{M} *and* ΣU^{exp}_{MG} *values, respectively (Eq. A27).*

macokinetic study. A freshly prepared solution of the material containing 50% plasma was injected into the jugular catheter over 10 sec.

The same sampling schedule as for morphine was used. Urine was collected for 800 min. The dog was kept in the sling support for 8 hr and then placed in the metabolic cage.

Biliary Excretion—Dog C was anesthetized with 30 mg/kg of pentobarbital sodium, a laparotomy was performed, the cystic duct was tied and cut, and the common bile duct was cannulated with tubing[21] (0.2 cm i.d. and 0.3 cm o.d.). The other end was used to cannulate the caudal end of the common bile duct to provide for normal bile flow into the duodenum. The tubing loop resulting from the cannulation was pulled cephalically subcutaneously and brought to the surface through an incision in the skin at the back of the neck. This loop was cut, and a connecting piece of tubing was inserted which, when removed, allowed for continuous bile sampling.

The animal was allowed to recover from the surgical procedure and was administered a 7.7-mg/kg dose. After 3 weeks, this bile-cannulated animal was given a 0.41-mg/kg dose. Blood and urine were collected as in other experiments. Bile was collected under heptane at 4.7, 7.8, 10, 13, 16, 20, 25, 31, 43, 57, 86, 176, 290, 382, 520, 600, 730, and 800 min. The volume was measured, and the bile was stored at 0° until analyzed by liquid scintillation counting in the manner described previously.

Infusion Study—The procedure for this study was the same as for the other pharmacokinetic studies with the following changes. The infusion line was connected to the jugular vein catheter, using a 19-gauge needle introduced through the flash ball injection site of the Plexitron administration set[22] for the chloride drip. This apparatus was attached to the catheter by a 14-gauge needle[23] and a three-way stopcock. The drug (3750 μg of ^{14}C-morphine) was prepared in 286.6 ml of sterile 75% isotonic saline plasma solution. The infusion rate (10 μg/min) was attained using an infusion pump[24].

Blood (5 ml) was sampled at 30, 60, 90, 180, 280, 300, 310, 320, and 340 min during the infusion. Postinfusion samples were collected at 3 and 9 min, then at 30-min intervals up to 150-min postinfusion, and then at 90-min intervals up to 1200-min postinfusion. Urine was collected every 20 min during the infusion. Following the infusion, urine was collected every 40 min for the 1st hr, then at 2-hr intervals up to 700-min postinfusion, and subsequently every 8 hr up to 4000-min postinfusion.

RESULTS AND DISCUSSION

Protein Binding—The results of these studies in dog plasma are given in Table II. There was no significant concentration or pH effect on the 36 ± 1% (*SEM*) morphine binding to plasma protein. No significant differences were observed among the samples centrifuged at different times after the spiking of dog plasma, so equilibration at least within 3 min, the earliest time studied, must be concluded. No significant protein binding (<2%) in dog plasma of morphine-3-monoglucuronide (100 ng/ml) was observed at pH 7.1 and 7.4.

The protein binding of 32.8% at 2.5 μg/ml (Table I) is consistent with the estimates of 30% (26) for dog plasma studied in the ranges of 2.5–15 μg of morphine/ml and is not too different from the 35.7 ± 0.9% given for normal human plasma (27).

Red Blood Cell–Plasma Water Partition Coefficient—This coefficient, *D*, the ratio of the drug concentration in the red blood cells, $[A_{RBC}]$, to that in the plasma water, $[A^u_p]$, can be calculated (28) from the experimentally determined concentration, $[A_p]$, of drug in the plasma when the concentration in whole blood, $[A_B]$, the fraction bound to plasma protein, *f*, and the hematocrit, *H*, are known:

$$D = \frac{[A_{RBC}]}{[A^u_p]} = \left\{\frac{[A_B]}{[A_p](1-f)(1-H)} - \frac{f}{(1-f)} - 1\right\}\frac{1-H}{H} \quad \text{(Eq. 3)}$$

There was no apparent time or concentration dependence for the red blood cell–plasma water partition coefficient of morphine (1.11 ± 0.04 *SD*) or its glucuronide metabolite (0.66 ± 0.05) (Table III).

The following cited equations, labeled with the prefix A, are derived and given in *Appendix I.* The symbols used are defined in *Appendix II.* The experimental disposition of various morphine doses, the clearances, and the best fit pharmacokinetic parameters are given in Table I, and the fitting is demonstrated in Figs. 2–4.

Morphine Pharmacokinetics at High Doses—Plasma morphine levels, [*M*], with time in the bile-cannulated dog, C, where the bile was completely collected, were best fitted by the two-compartment body model (Fig. 2a and Table I). There was no significant terminal plateau in $[MG]_{exp}$ or $[MG]'_{calc}$ values that could be assigned to the return of the conjugate or its precursor, *M*, from a deep compartment. Significant urine flow was not observed until after 53 min of drug administration at this 7.7-mg/kg dose when 1.5 ml was obtained.

Significant morphine, ΣU_M, and conjugate, ΣU_{MG}, in the urine were first observed in the interval of 53–80 min. The calculated amounts (Eqs. A6 and A8) of ΣU_M and ΣU_{MG} renally excreted (solid lines in Fig. 2a) were consistent only with the experimental data, the obtained renal clearances (Fig. 5) and areas, AUC_M, under the morphine and conjugate

Table III—Dog Red Blood Cell–Plasma Water Partition Coefficients (*D*)[a] of Morphine and Its Glucuronide Metabolite

Time of Measurement	Morphine, ng/ml				Morphine-3-monoglucuronide, ng/ml	
	1	10	100	1000	50	500
30 sec	1.03	1.13	1.13	1.14	0.71	0.63
30 min	1.10	1.10	1.12	1.11	0.60	0.70
Average ± *SD*	1.11 ± 0.35				0.66 ± 0.53	

[a] The values used in Eq. 3 for these calculations were $H = 0.35$ and $f = 0.32$ for morphine and $f = 0$ for the glucuronide.

[21] Tygon, Scientific Products, Chamblee, GA 30341.
[22] Travenol Laboratories, Deerfield, IL 60015.
[23] Becton Dickinson and Co., Rutherford, N.J.
[24] Model 600-950, Harvard Apparatus, Dover, Mass.

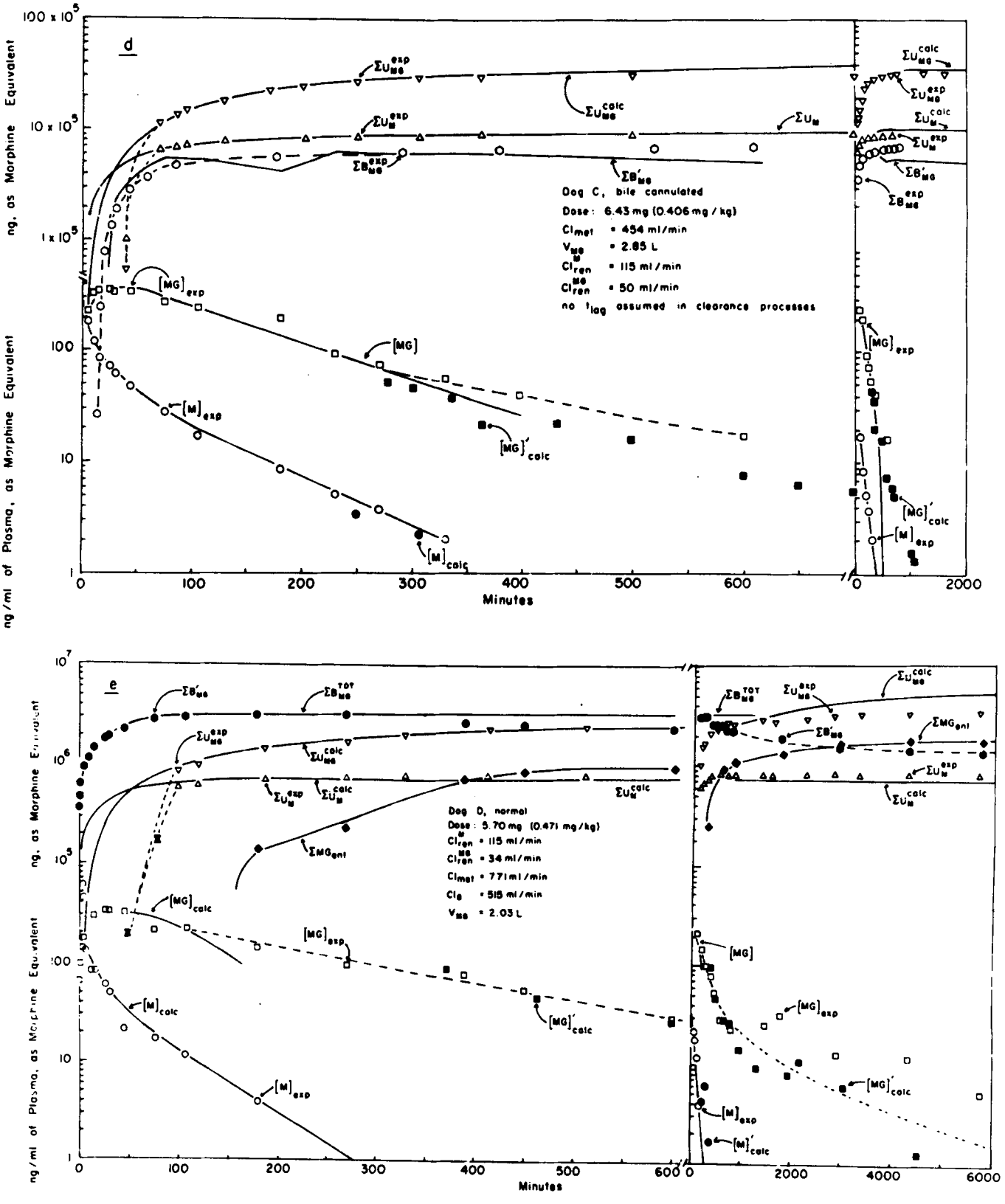

Figure 3—*Plots of experimental values of morphine,* $[M]_{exp}$ (⊙), *and the morphine conjugate,* $[MG]_{exp}$ (⊡), *in nanograms per milliliter of plasma as morphine equivalents against time at intermediate morphine base doses, 0.41 and 0.47 mg/kg iv. The solid line through the experimental* [M] *values was calculated from the polyexponential fit,* $[M] = A'e^{-\alpha' t} + Ae^{-\alpha t} + Be^{-\beta t}$. *(See Table I for parameters.) The solid line through the experimental* $[MG]_{exp}$ *values was calculated on the assumption of a constant metabolic morphine clearance,* Cl^{M}_{met}, *so that* $[MG] = (Cl_{met} AUC_M - \Sigma B_{MG} - \Sigma U^{exp}_{MG})/V_{MG}$. *The* Cl_{met} *and* V_{MG} *values for the bile-cannulated Dog C in Fig. 3d were obtained from an appropriate data plot in accordance with Eqs. A11 and A12 (Fig. 7) based on the assumed validity of the* ΣB^{exp}_{MG} *data (○). The MG values were calculated for the normal Dog D in Fig. 3e from estimates of* $Cl_{met} = Cl_{tot} - Cl^{ren}_{M}$, *where* $Cl_{tot} = dose/AUC_M$, *and* $\Sigma B_{MG} = Cl_B AUC_M$, *where* $Cl_{met} - Cl_B$ *and* V_{MG} *values were estimated from plots in accordance with Eqs. A16 and A17 (Figs. 8 and 9).*

The experimental values of cumulative morphine, ΣU^{exp}_{M} (△), *and its conjugate,* ΣU^{exp}_{MG} (▽), *in urine are also plotted against time. The solid*

lines through the data points are the theoretical values calculated from $\Sigma U_M = Cl^M_{ren}\,AUC_M$ *and* $\Sigma U_{MG} = Cl^{MG}_{ren}AUC_{MG}$. *The renal clearances,* Cl^M_{ren} *and* Cl^{MG}_{ren}, *were consistent with the values obtained from the slopes of the renal clearance plots of* $\Delta U/\Delta t$ versus *plasma level (Fig. 5).*

The calculated values of $\Sigma B'_{MG} = Cl^M_{met}\,AUC_M - \Sigma U^{exp}_{MG} - V_{MG}\,[MG]_{exp}$ *for the bile-cannulated dog (Fig. 3d) are represented by the solid line through the experimental values of* ΣB^{exp}_{MG} (○). *The* Cl_{met} *and* V_{MG} *values were obtained from appropriate data plots in accordance with Eqs. A11 and A12 (Fig. 7).*

Estimates of cumulative conjugate in the bile, $\Sigma B'_{MG}$ (●), *of the normal (not bile cannulated) dog (Fig. 3e) were based on the* Cl_{met} *and* V_{MG} *values obtained from appropriate data plots in accordance with Eqs. A16 and A17 (Figs. 8 and 9). The solid line through these data (●) was based on the assumed constant biliary clearance obtained from these plots and was calculated from* $\Sigma B^{tot}_{MG} = Cl_B AUC_M$. *The difference between this total amount of conjugate excreted in the bile,* ΣB^{tot}_{MG}, *and the amount presumed to remain there,* $\Sigma B'_{MG}$, *estimates the amount of conjugate enterohepatically recirculated to the systemic circulation (◆),* $\Sigma MG_{ent} = \Sigma B^{tot}_{MG} - \Sigma B'_{MG}$.

Terminal values of $[M]_{exp}$ (○) *and* $[MG]_{exp}$ (□) *tend to have larger errors since the liquid scintillation counts approach background. The respective solid symbols are the plasma levels of* $[M]'_{calc}$ (●) *and* $[MG]'_{calc}$ (■) *calculated from the estimated renal clearances and the observed* ΣU^{exp}_M *and* ΣU^{exp}_{MG} *values, respectively (Eq. A27).*

plasma level–time curves when renal processes were not considered operative until a time, t_0, of 65 min after drug administration.

The only major discrepancy in the fitting of the data for the bile-cannulated dog in Fig. 2*a* was that the calculated $\Sigma B'^{calc}_{MG}$ (Eq. A14) and $[MG]_{calc}$ (Eq. A13) values based on the 4200-ml value of V_{MG} underestimated the experimental values of ΣB^{exp}_{MG} and $[MG]_{exp}$, respectively, for the first 45 min, even when ΣU_{MG} was taken as zero for this time. The assumption of an average V_{MG} of 2500 ml for this interval improved the fit (dashed lines before 45 min in Fig. 2*a*) with the experimental data. This finding strongly indicates that the apparent conjugate distribution volume may have increased during this interval, which is not consistent with the assumption of a one-compartment body model for $[MG]$ immediately after its production. A period of time may be necessary for the conjugate to equilibrate in its apparent overall distribution volume.

Biliary conjugate secretion also was inhibited at the high morphine doses. The use of a time lag of 16 min and the determined variable biliary clearance, Cl_B (Fig. 6), which depended on the bile flow, gave the fit to the ΣB^{exp}_{MG} data demonstrated by the dashed line before 45 min in accordance with $\Sigma B^{calc}_{MG} = \Sigma Cl_B(AUC'_M - AUC'^{t_0=16\,min}_M)$ as described in Eq. A3.

The fact that no radioactivity was observed in the collected feces of this bile-collected dog shows that the fecal source of drug must be assigned to the biliary excretion.

Studies (Fig. 2*b*) of both the same Dog C at a similar dose, 7.2 mg/kg, and Dog E at 7.6 mg/kg (Fig. 2*c*) without biliary cannulation showed similar pharmacokinetic patterns, except for terminal elevations of plasma metabolite levels and pronounced drug and metabolite in the feces (Table I). Direct plasma conjugate measurements were consistent, $[MG]_{exp}$, with $[MG]'_{calc}$ values calculated by Eq. A27 from the presumed renal clearance, Cl'_{ren}, of the conjugate and the cumulative amount, ΣU^{exp}_{MG}, excreted in the urine.

This elevation in plasma and concomitant urine conjugate in the non-bile-cannulated dog can be assigned to material returned to the system by enterohepatic recirculation of the bile contents.

The cumulative amounts of enterohepatically recirculated drug in normal Dogs C and E, ΣMG_{ent}, are plotted in Figs. 2*b* and 2*c* as based on Eqs. A21–A23. The premise for the calculation is that the intravenously administered morphine was almost completely cleared by 100 min, as indicated by the data for bile-cannulated Dog C (Fig. 2*a*).

The data for the normal dogs in Figs. 2*b* and 2*c* were fitted in two manners. In one, the same biliary excretion, ΣB^{exp}_{MG}, was postulated as when the dog was biliary cannulated and the total bile was collected (Fig. 2*a*). The estimated V_{MG} and Cl_{met} values for the normal dogs at this dose (Eqs. A11 and A12) were 4.2 liters and 232 ml/min, respectively, for Dog C and 3.96 liters and 215 ml/min, respectively, for Dog E (Fig. 7). The solid lines ($\Sigma B'_{MG}$) in Figs. 2*b* and 2*c* through the ΣB^{exp}_{MG} data obtained from the bile-cannulated Dog C at the same dose were calculated from Eq. A22 with these parameters and fit well except at the early times. The solid lines for $[MG]_{calc}$ through the $[MG]_{exp}$ data were calculated from Eq. A13 with these parameters and were reasonable for all times up to when enterohepatic return from the bile was postulated, as indicated by the plotting of terminal dashed lines. A better fit of the initial $[MG]_{exp}$ data up to 45 min in Fig. 2*b* is given by the dashed lines when it was postulated that no drug was eliminated in the bile until ~50 min.

The alternative manner of fitting was to postulate a constant biliary clearance which only commenced a specified time after drug administration. This premise does not demand a specific knowledge of the amount of conjugate in the bile (Eqs. A16 and A17). The obtained respective values of V_{MG} and Cl_{met} were 5.05 liters and 292 ml/min for Dog C (Figs. 8 and 9) and 4.23 liters and 234 ml/min for Dog E. The calculated $\Sigma B'^{calc}_{MG}$ values (Eq. A22) based on these parameters are given in Figs. 2*b* and 2*c*. The solid lines through these data (ΣB^{tot}_{MG}) assumed a constant biliary clearance, Cl_B (Eq. A3), and no enterohepatic conjugate recirculation in the bile. Obviously, when these values diverged from the $\Sigma B'^{calc}_{MG}$ values, the difference could be attributed to those amounts returned from the bile to the systemic circulation, *i.e.*, ΣMG_{ent}.

Morphine Pharmacokinetics at Intermediate Doses—The plasma morphine levels, $[M]$, with time in the bile-cannulated Dog C at the 0.406-mg/kg dose were consistent with those observed with the high dose and were best fitted by the two-compartment body model (Fig. 3*d* and Table I). Again, no significant drug appeared in the feces, and there was no significant terminal plateau in $[MG]_{exp}$ or $[MG]'_{calc}$ values that could be assigned to the return of the conjugate or its precursor, M, from a deep compartment in the bile-cannulated dog. The non-bile-cannulated dog at the same dose (Fig. 3*e*) showed terminal plasma metabolite elevations and pronounced drug and metabolite in the feces (Table I).

Although the urine flow was negligible up to 75 min after morphine administration in both the bile-cannulated and normal dogs at this dose, the calculated amounts (Eqs. A6 and A8) of ΣU_M and ΣU_{MG} renally excreted after that time were consistent with the experimental data, the obtained renal clearances (Fig. 5) and the *total* areas (*i.e.*, uncorrected for a time lag in commencement of renal processes) under the morphine and conjugate plasma level–time curves. Thus, in contrast with the higher dose, complete renal shutdown by the drug does not have to be postulated. The delay in renal morphine and conjugate excretion can be attributed solely to the lack of urine flow necessary to eliminate the morphine and metabolite trapped in the tubules.

The solid line, $\Sigma B'^{calc}_{MG}$, in Fig. 3*d* through the experimentally obtained cumulative conjugate excreted in the bile, ΣB^{exp}_{MG} (dashed line), obtained from the bile-cannulated dog was calculated from Eq. A22 where the pertinent Cl_{met} and V_{MG} values were obtained by application of Eqs. A11 and A12 (Figs. 8 and 9). The solid line, ΣB^{tot}_{MG}, in Fig. 3*e* through the calculated (Eq. A22) cumulative conjugate in the biliary system of the noncannulated dog, $\Sigma B'^{calc}_{MG}$, was estimated on the premises of a constant biliary clearance, Cl_B, of immediately formed metabolite and nonenterohepatic return to the system. The pertinent Cl_{met}, Cl_B, and V_{MG} values were obtained by application of Eqs. A16–A20; the values of the pharmacokinetic parameters are given in Table I. The difference between ΣB^{tot}_{MG} and $\Sigma B'^{calc}_{MG}$ (Eq. A23) estimates the cumulative amounts of drug returned to the systemic circulation, ΣMG_{ent}.

Morphine Pharmacokinetics at Low Doses—The pharmacokinetics at these doses in normal animals (Figs. 4*f*–4*h*) were similar to those for the normal animal at the intermediate dose, except that urine flow was not highly inhibited and no tubular entrapment of morphine and/or its metabolite had to be postulated. There was only one minor anomaly in the fitting of these data. Although the calculated (Eq. A8) and experimentally determined amounts of conjugate in the urine, ΣU_{MG}, were reasonably consistent until 500–700 min, less was excreted than anticipated with the presumption of the constant renal clearance, which conformed to the greatest extent of the clearance plots (Fig. 5). This finding could indicate a lessened renal clearance of ΣU_{MG} when the values of $[MG]$ were less than 1.0–2.0 ng/ml of plasma. Alternatively, this result could be an artifact of studies at high morphine specific activities. The terminal values of unextracted radioactivity considered as $[MG]_{exp}$ after ~600 min could contain a higher quantity of radiolabeled impurities or other long-lived undefinable, unextractable morphine metabolites in plasma and could give an anomalous terminal radioactivity elevation that would overestimate the urine metabolite accumulation for a presumed constant clearance.

Renal Clearances and Eliminations of Morphine and Its Metabolite—The morphine and metabolite clearances showed remarkable constancies as long as the renal function was operative and there was adequate urine flow (Fig. 5). There were no significant dose effects on these clearances (Table I), which averaged to significantly different values

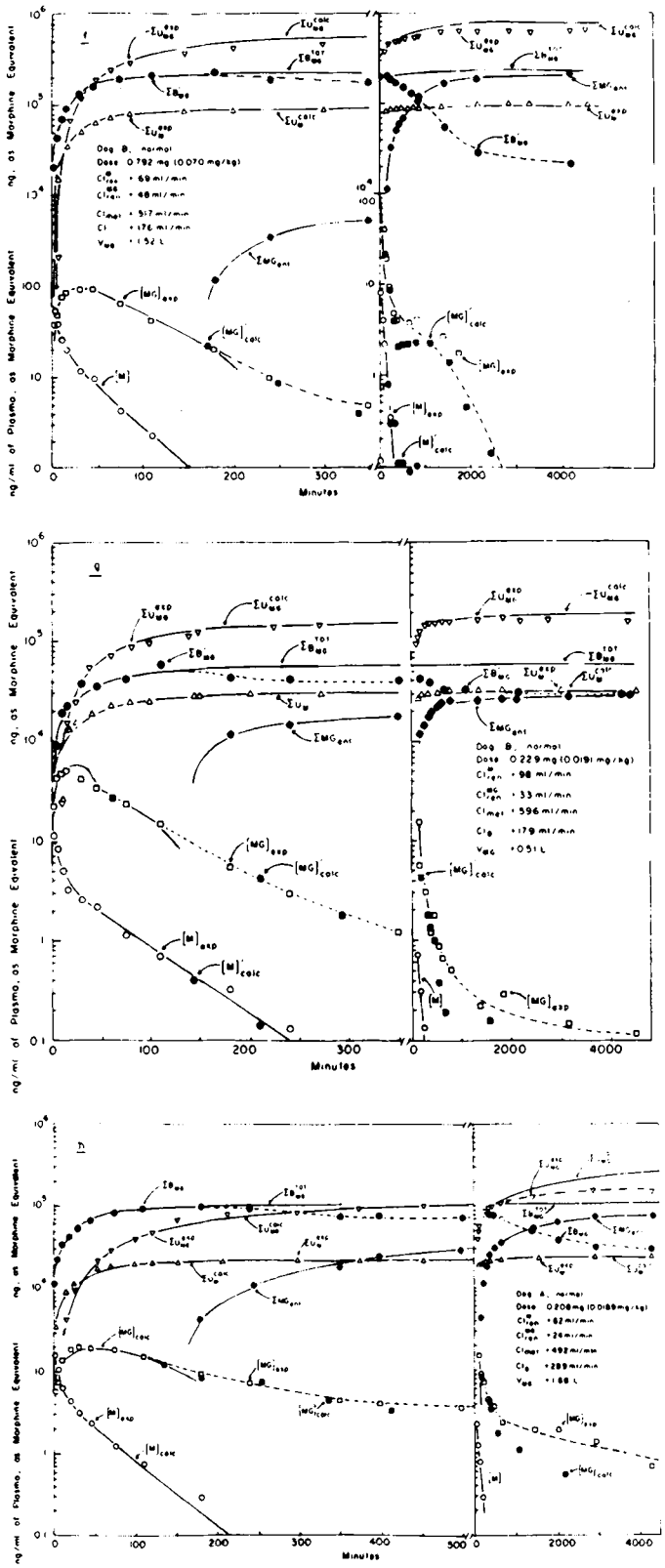

Figure 4—*Plots of experimental values of morphine, $[M]_{exp}$ (⊙), and the morphine conjugate, $[MG]_{exp}$ (⊡), in nanograms per milliliter of plasma as morphine equivalents against time at low morphine base doses, 0.07 and ~0.019 mg/kg iv. The solid line through the experimental [M] values was calculated from the polyexponential fit, $[M] = Ae^{-\alpha t} + Be^{-\beta t}$. (See Table I for parameters.) The solid line through the experimental $[MG]_{exp}$ values was calculated on the assumption of a constant metabolic morphine clearance, Cl^{M}_{met}, so that $[MG] = (Cl_{met}AUC_M - \Sigma B_{MG} - \Sigma U^{exp}_{MG})/V_{MG}$. The [MG] values were calculated for the normal dog from estimates of $Cl_{met} = Cl_{tot} - Cl^{ren}_{M}$, where $Cl_{tot} = dose/AUC_M$, and $\Sigma B_{MG} = Cl_B AUC_M$, where $Cl_{met} - Cl_B$ and V_{MG} values were estimated from plots in accordance with Eqs. A16 and A17 (Figs. 8 and 9).*

The experimental values of cumulative morphine, ΣU^{exp}_{M} (△), and its conjugate, ΣU^{exp}_{MG} (▽), in urine are also plotted against time. The solid lines through the data points are the theoretical values calculated from $\Sigma U_M = Cl^{M}_{ren}AUC_M$ and $\Sigma U_{MG} = Cl^{MG}_{ren}AUC_{MG}$. The renal clearances, Cl^{M}_{ren} and Cl^{MG}_{ren}, were consistent with the values obtained from the slopes of the renal clearance plots of $\Delta U/\Delta t$ versus plasma level (Fig. 5).

Estimates of cumulative conjugate in the bile, $\Sigma B'_{MG} = Cl^{M}_{met}AUC_M - \Sigma U^{exp}_{MG} - V_{MG}[MG]_{exp}$, were based on the Cl_{met} and V_{MG} values obtained from appropriate data plots in accordance with Eqs. A16 and A17 (Figs. 8 and 9). The solid line through these data (●) was based on the assumed biliary clearance obtained from these plots and was calculated from $\Sigma B^{tot}_{MG} = Cl_B AUC_M$. The difference between this total amount of conjugate excreted in the bile, ΣB^{tot}_{MG}, and the amount presumed to remain there, $\Sigma B'_{MG}$, estimates the amount of conjugate enterohepatically recirculated to the systemic circulation (◆), $\Sigma MG_{ent} = \Sigma B^{tot}_{MG} - \Sigma B'_{MG}$.

Terminal values of $[M]_{exp}$ (○) and $[MG]_{exp}$ (□) tend to have larger errors since the liquid scintillation counts approach background. The respective solid symbols are the plasma levels of $[M]_{calc}$ (●) and $[MG]_{calc}$ (■) calculated from the estimated renal clearances and the observed ΣU^{exp}_{M} and ΣU^{exp}_{MG} values, respectively (Eq. A27).

for Cl^{M}_{ren} of 85 ± 9 and 41 ± 4 (*SEM*) ml/min, respectively, in contrast to the respective values of 66 and 80 ml/min cited previously for the dog (3). The morphine clearance with respect to drug unbound to plasma proteins (67%) was 127 ± 13 (*SEM*) ml/min; the morphine glucuronide showed negligible protein binding.

These differences in renal clearances imply different processes for the drug and its conjugate. Since the calculated renal clearance for inulin (glomerular filtration) for a 12-kg dog is 51 ± 12 ml/min (29), the glucuronide probably was eliminated solely by glomerular filtration and the intravenously administered morphine probably was eliminated by both filtration and tubular secretion.

No pronounced differences in fractions of the intravenous dose excreted in the urine were observed among doses (Table I): 12 ± 3 (*SD*) % as unchanged morphine and 71 ± 10 (*SD*) % as morphine conjugate.

In the three noncannulated dogs (C, 109 mg; E, 107 mg; and D, 0.471 mg) where feces were collected, 9, 5, and 14% of the total radioactivity were found in the feces, respectively, with 47, 43, and 5% of the excreted amounts extractable as morphine, respectively. These values contrast with those previously reported (9), where negligible conjugate was observed in the feces of dogs. Unfortunately, the possibility of fecal conjugate hydrolysis or fecal morphine degradation does not provide incontrovertible proof of high degrees of GI hydrolysis of biliary secreted conjugate, the major drug form in bile. Less than 0.5% of the total drug excreted into bile was as free morphine in the two studies with the bile-cannulated dog.

The fraction of the administered radioactivity that appeared in the saliva drippings collected from Dog D at the 5.7-mg dose was an extremely low 0.087%.

"Deep" Compartment for Morphine—The plasma morphine levels with time generally could be fit to a sum of two exponentials. However, the data in the normal dog showed a terminal positive deviation in $[M]_{exp}$ from this fitting in some instances (Figs. 2*b*, 4*g*, and 4*h*), indicating the presence of a slower elimination process. The radioactive counts of extracted morphine were too close to background levels to make a definite conclusion. Conclusive demonstration of such a slower elimination process was clearly manifested in urinary morphine elimination, ΣU^{exp}_{M}. The semilogarithmic plots of amounts yet to be excreted against time (Figs. 10 and 11) showed a terminal phase, γ (Table I), whose half-lives averaged 994 ± 16 (*SEM*) min for all studies in the normal dog, with no apparent dose dependency. The fact that no such terminal phase was observable with the urinary data (Fig. 10) from the cannulated dog where total bile was collected is strong evidence that this slow morphine elimination is due to the recycling of amounts secreted into the bile. Since negligible free morphine is bile secreted, the conjugate must be gastrointestinally hydrolyzed, either in the lumen or gut wall, before reabsorption into the systemic circulation.

When 3.7 mg of morphine was infused at a constant rate of 10.7 μg/min into a dog, reasonable steady-state values of plasma morphine were achieved by 60 min and maintained during the 350 min of infusion at an average of 57 ± 4 (*SEM*) ng/ml. At cessation of infusion, there was a

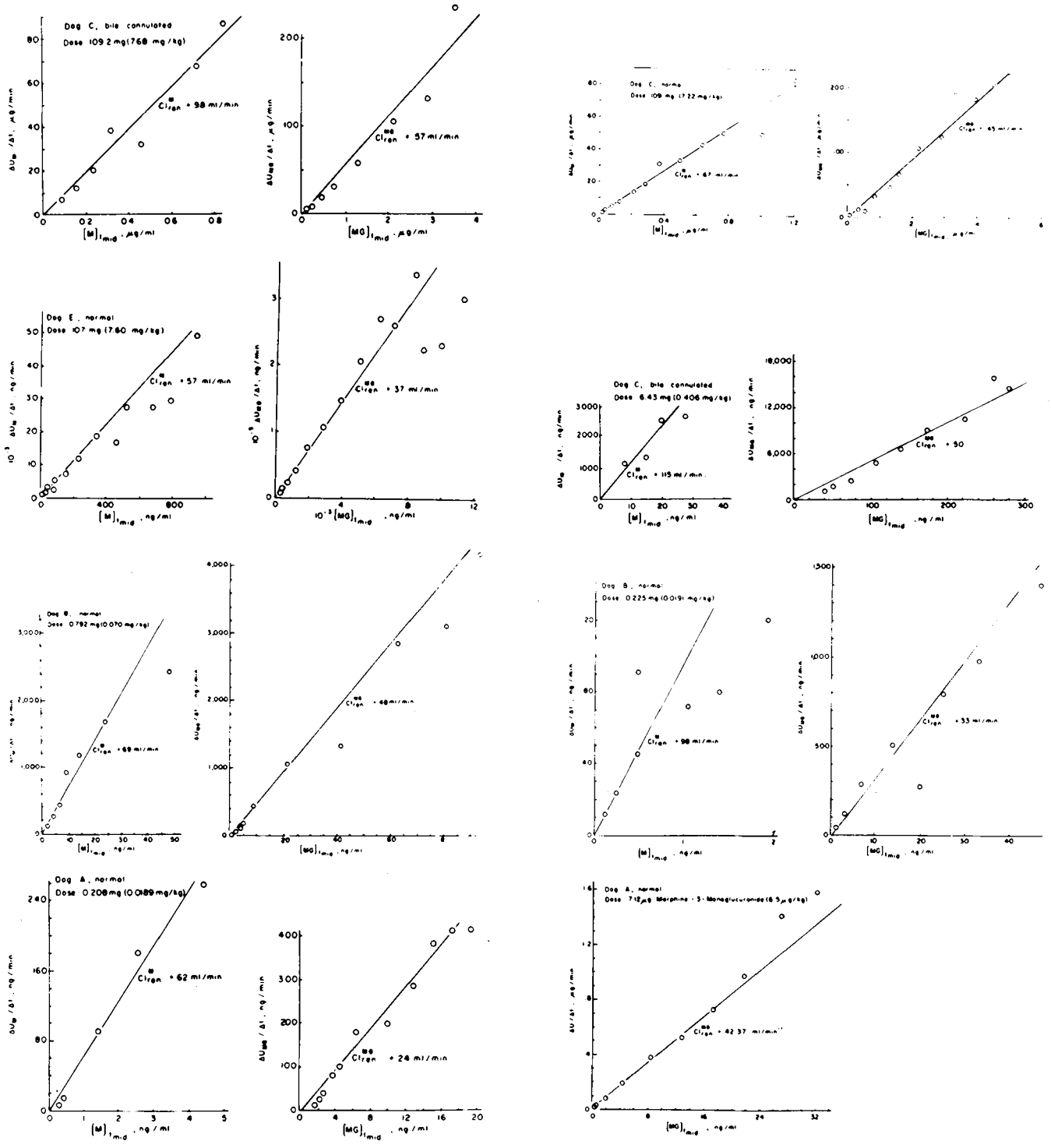

Figure 5—*Renal clearance plots for morphine,* M *(left), and its conjugate,* MG *(right), when morphine was administered. Rates of drug amounts excreted* versus *plasma levels were obtained at the midtimes of the urine-collection intervals. The lower right clearance plot is for morphine-3-glucuronide administration.*

precipitous drop until plasma levels of both morphine [0.45 ± 0.03 (*SEM*) ng/ml of plasma, $n = 7$] and glucuronide [34.1 ± 0.9 (*SEM*) ng/ml of plasma] remained invariant over the studied period from 250 to 850 min after the cessation of the infusion. The plasma morphine levels monitored by liquid scintillation counting were four times the background radiation level. This evidence is considered valid for the slow enterohepatic return of both morphine and its conjugate from bile to show an apparent deep compartment in the dog. The total percent of the dose excreted in the urine was 85.8%, 68.5% as the conjugate and 17.3% as unchanged morphine.

The terminal elevation in plasma and urine morphine glucuronide levels in normal dogs (Figs. 2–4) was in decided contrast to the studies in the bile-cannulated dog and is proper evidence for enterohepatic recirculation. The lack of morphine and the conjugate in the feces of the cannulated dog, but not in the normal, confirms this hypothesis and agrees with the observations of Woods (8). The conjugate, even when significantly hydrolyzed in the lumen or gut wall, must be largely reconjugated in the liver prior to its return to the systemic circulation for this hypothesis to be true. The return of small amounts of morphine could be responsible for the frequent observation of a slow terminal morphine loss in the plasma. It is estimated (Table I) that 27 ± 0.05 (*SEM*) % of the dose is enterohepatically recirculated at doses less than 0.5 mg/kg. It is possible that the 15% observed in the two studies at 7–8 mg/kg may signify a dose dependency.

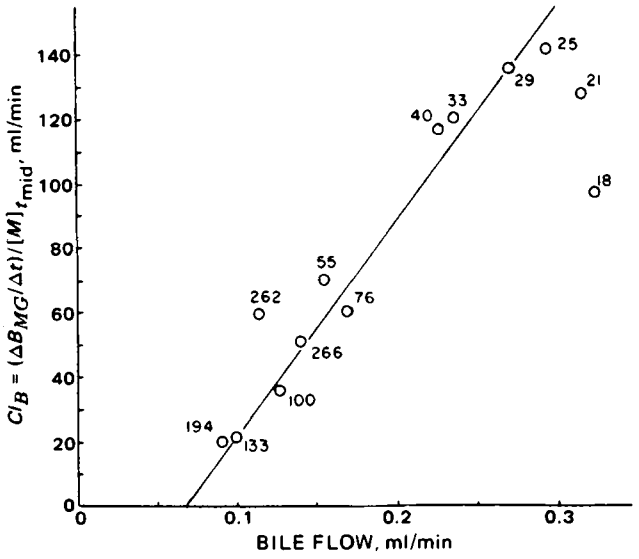

Figure 6—*Demonstration of the linear dependence of the apparent biliary clearance,* Cl_B, *of immediately formed metabolite,* MG, *on the rate of bile flow for the bile-cannulated Dog C at the 109.2-mg dose (7.68 mg/kg):* Cl_B *(ml/min) = 671 × bile flow (ml/min) − 45.6. The values are labeled with the measured times in minutes.*

Dose Effects in Morphine Pharmacokinetics—The anticipated "feedback" effects of morphine's pharmacology (20, 21) on its pharmacokinetics in the dog were observed. The 7.2–7.7-mg/kg doses of morphine caused an instantaneous cessation of renal processes (Figs. 2*a*–2*c*) that did not resume until 60–105 min after intravenous administration when the plasma morphine level reached 1000 ng/ml. At these doses, the dogs were completely unconscious for at least 3 hr after administration and lay supine upon the table.

The same doses inhibited biliary secretion for 10–35 min after intravenous administration and demonstrated uneven bile flows and concomitant uneven biliary clearances thereafter (Fig. 6), which readily confirmed the statements (20) that the drug causes biliary tract spasms and constrictions that can impede biliary excretion. The estimated average biliary clearances, Cl_B (Eqs. A16–A20), of formed metabolite were 52 and 87 ml/min at these high doses in the normal dog and 213 ± 36 (*SEM*) ml/min (range of 176–285) at the lowest doses of 0.019–0.07 mg/kg.

Morphine at the intermediate doses of 0.4–0.5 mg/kg (Figs. 3*d* and 3*e*) did not shut down the renal processes but did have a pronounced effect on urine flow. The time courses of the drug and its metabolite could best be fit on the premise of maintained viable renal processes with delayed elimination into the urine. The time courses at the lowest doses studied could be fit (Figs. 4*f* and 4*g*) without the postulations of such drug-induced discontinuities in pharmacokinetic processes.

Total morphine clearance is clearly dose related (Table I). At the highest doses of 7.2–7.7 mg/kg, Cl_{tot} averaged 340 ± 43 (*SD*) for the range of 290–370 ml/min in contrast to the average of 701 ± 138 (*SD*) for the range of 554–886 ml/min at doses below 0.5 mg/kg. Since renal clearances are relatively invariant with dose, this finding implies that the hepatic metabolism of morphine is dose dependent. The estimated average ± *SD* (*SEM*) (range) values for Cl_{met} were 261 ± 41 (17) (215–322) ml/min at the high dose and 609 ± 114 (51) (492–771) at the other doses. The fraction of formed metabolite partitioned into the bile, Cl_B/Cl_{met}, cannot be concluded to be dose dependent, however. About 25% was partitioned into the bile in two high-dose and two low-dose cases.

The hepatic blood flow in the 14-kg dog is in the range of 420–630 ml/min (30) and is the same as the range of metabolic clearances at the low doses. This finding could imply that the high dose of 7 mg/kg decreases blood flow to the liver and/or that the metabolizing enzymes are saturable. However, the fact that negligible plasma morphine levels occur in the dog orally administered 30 mg/kg (9) is indicative of the complete metabolism of orally administered drug by its first pass in the liver even at these enormous doses.

The dose dependencies of total and metabolic clearances are clearly reflected in the apparent rate constants and half-lives for the elimination of the major morphine fraction in the β-phase of the two-compartment body model (Table I). Excellent agreement was obtained with the urinary data for this phase when semilogarithmic plots of amounts yet to be excreted (after correction for the slow terminal phase) and rates of urinary elimination were made against time (Figs. 10 and 11). The half-lives for the high dose (7–8 mg/kg) were 83 ± 6 (*SD*) min from plasma and 82 ± 8 (*SD*) min from urine. They were 39 ± 6 (*SD*) min from plasma and 37 ± 13 (*SD*) min from urine for the lowest doses.

There were no significant differences among the apparent morphine distribution volumes. The estimated central compartment volume is 15.3 ± 2.8 (*SEM*) liters, and the overall volume is 44 ± 6 (*SEM*) liters.

Pharmacokinetics of Morphine-3-monoglucuronide and Its Significance in Morphine Pharmacokinetics—The intravenous administration of ^{14}C-morphine-3-monoglucuronide to the 11-kg Dog A (71.2 μg, 6.5 μg/kg, specific activity of 273 dpm/ng) clearly demonstrated a two-compartment body model (Fig. 12), where the plasma level could be defined for time, *t*, in minutes as:

$$[MG],\ \text{ng/ml} = 33.3e^{-0.245t} + 26.4e^{-1.46\times10^{-2}t} \qquad \text{(Eq. 4)}$$

and the respective half-lives of the α- and β-phases were 2.8 and 47.6 min, respectively. The semilogarithmic plots of amounts yet to be excreted and amounts per unit of time against time showed respective rate constants of 56 and 51 min, in agreement with the terminal phase. The recovery of the total radioactivity in the urine was complete; the actual calculation was 116%. No free morphine was extractable either from the plasma or urine. The total clearance from the ratio of dose and the area under the curve was 37.1 ml/min, and the renal clearance from the classical plot (Fig. 5) was consistent at 42 ml/min. The conclusion is that renal excretion is the sole route of systemic glucuronide elimination. The apparent overall glucuronide distribution volume from the ratio of the total clearance and the terminal rate constant was 2541 ml, whereas the value from the quotient of the dose and the intercept of the extrapolated β-phase was 2696 ml.

The fact that there was not the prolonged terminal phase in the plasma or urine for the administered glucuronide that appeared when morphine was injected (Figs. 2–4) demonstrates that its appearance is a consequence of a process unique to morphine metabolism. The hepatically conjugated morphine is partitioned into bile in the liver, whereas the systemic conjugate is not. This hepatically formed conjugate is gut hydrolyzed to be slowly reabsorbed as morphine, whereas the systemic conjugate is not. The time lag in the enterohepatic recirculation with concomitant gallbladder storage (3) postpones the return of biliary secreted drug and metabolite to maintain persistent levels in plasma and urine.

The calculated 2500 ml of apparent overall distribution volume in intravenous glucuronide administration, V_{MG}, is consistent with the volumes calculated for morphine doses below 0.5 mg/kg from Eqs. A11, A12, A16, and A17 and validate the premises upon which they were based. The significantly greater calculated volumes of 4200–5050 ml for glucuronide at 7.2–7.7 mg of morphine/kg must be related to the demonstrated extreme pharmacological effects at this dose.

APPENDIX I: METHODS AND PROCEDURES FOR PHARMACOKINETIC ANALYSES

Renal Clearances and Time Durations of Drug Inhibitions of Such Processes—When the drug concentration time course in the plasma, such as morphine [*M*], can be monitored, the cumulative drug excreted unchanged into the urine (ΣU_M) and bile (ΣB_M) and metabolized into a metabolite such as morphine glucuronide (ΣMG) at a time *t* can be estimated from the respective clearances Cl^M_{ren}, Cl^M_B, and Cl^M_{met}, provided that these clearances are not plasma level dependent. Thus, the cumulative amounts excreted at time *t* would be:

$$\Sigma U_M = Cl^M_{ren}\int_{t_0}^{t}[M]dt = Cl^M_{ren}\,AUC^{t-t_0}_M \qquad \text{(Eq. A1)}$$

$$\Sigma MG = Cl^M_{met}\int_{t_0}^{t}[M]dt = Cl^M_{met}\,AUC^{t-t_0}_M \qquad \text{(Eq. A2)}$$

$$\Sigma B_M = Cl^M_B\int_{t_0}^{t}[M]dt = Cl^M_B AUC^{t-t_0}_M \qquad \text{(Eq. A3)}$$

where AUC_M is the needed area under the morphine plasma level–time curve from t_0 to *t*, where t_0 is the time of onset of the specific clearance process. These equations are a consequence of first-order differential equations such as:

$$d(MG)/dt = k_{M,MG}V[M] = Cl_{met}[M] \qquad \text{(Eq. A4)}$$

which, on integration, gives:

$$\Sigma MG = \int_0^{MG} d(MG) = Cl^M_{met}\int_{t_0}^{t}[M]dt$$

$$= Cl^M_{met}\,AUC^{t-t_0}_M \qquad \text{(Eq. A5)}$$

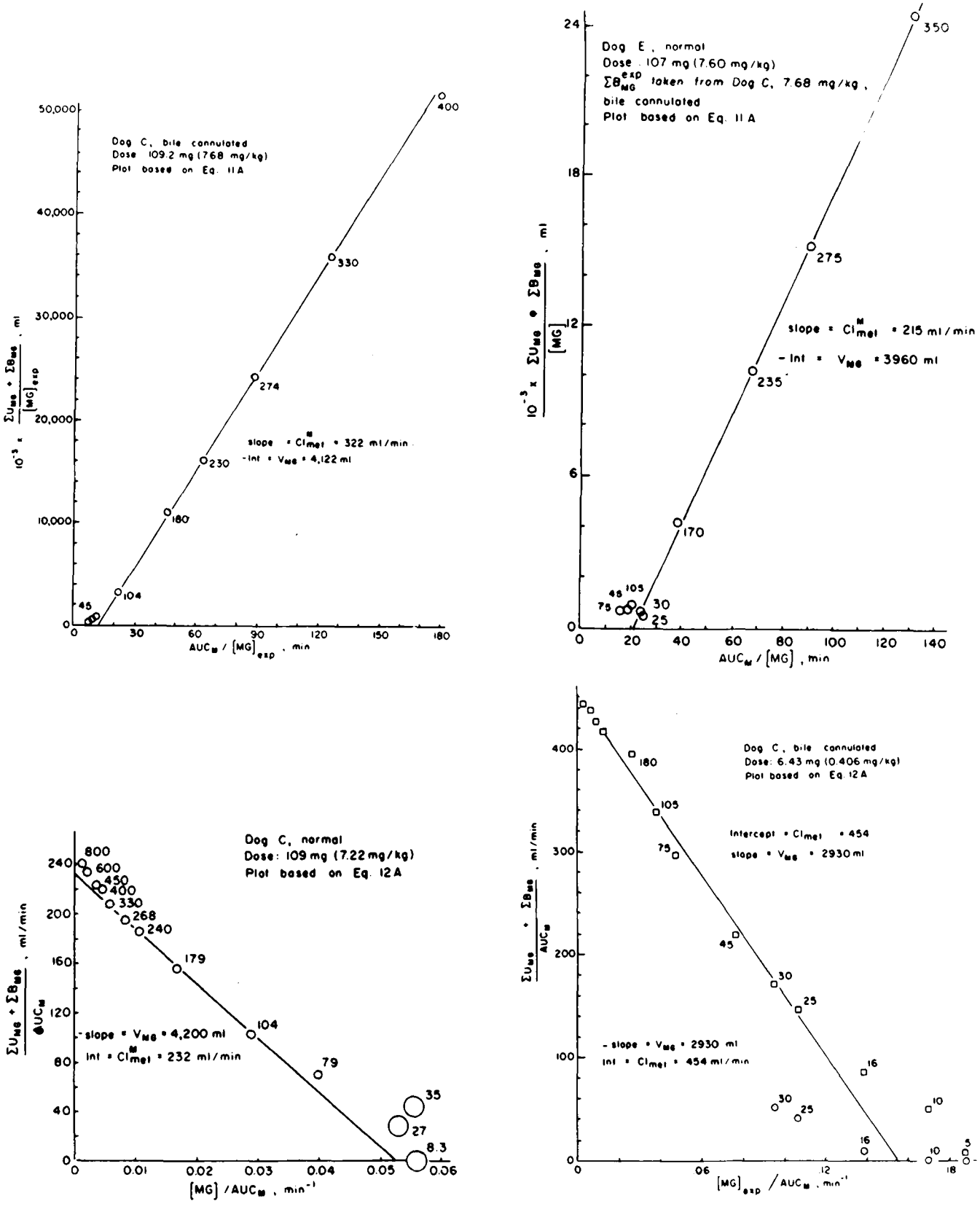

Figure 7—*Data for dogs administered morphine in accordance with the premise that the amounts of cumulative conjugate excreted in the bile, ΣB_{MG}^{exp}, were monitored (Eqs. A11 and A12). The ΣB_{MG} values used in the normal dogs were taken from the studies on the bile-cannulated Dog C at the high dose. The values are labeled with the times at which the AUC_M and $[MG]_{exp}$ values were taken. The ΣU_{MG}^{exp} and ΣB_{MG}^{exp} values were estimated for these same times from interpolations in the respective plots of their values against time. The experimental values at the earlier times in these plots are expected to be aberrant because inadequate urine flow at the high systemic drug levels did not permit proper estimates of ΣU_{MG} values. Deviations of experimental values at the later times in the non-bile-cannulated dogs were due to the perturbations effected by enterohepatic recirculation that gave estimates of ΣU_{MG}^{exp} and $[MG]_{exp}$ in excess of those anticipated by the premises underlying the equation used, which did not take such delayed return to the system into account.*

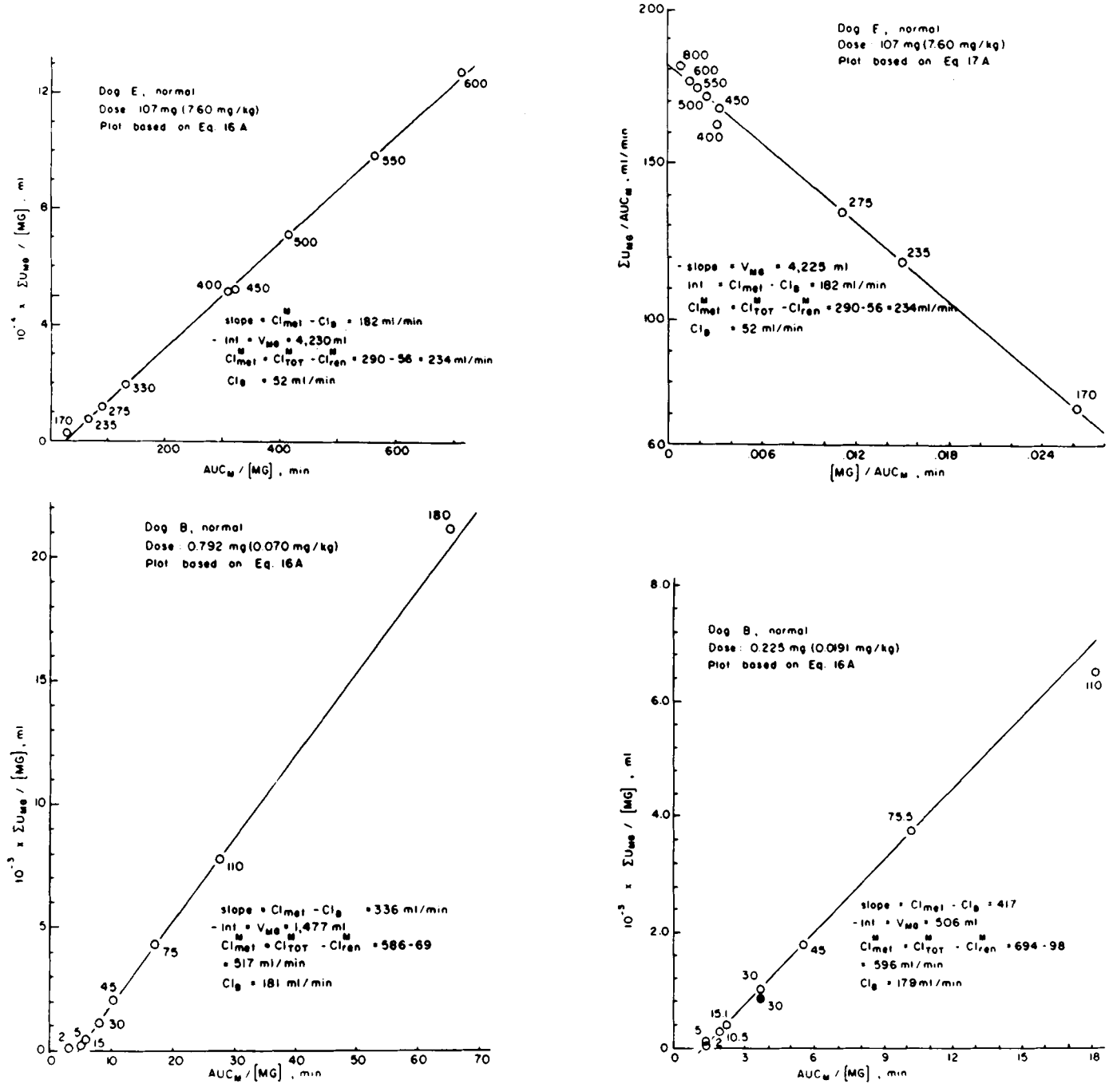

Figure 8—*Data for normal, non-bile-cannulated dogs in accordance with* $\Sigma U^{exp}_{MG}/[MG]_{exp} = (Cl_{met} - Cl_B)(AUC_M/[MG]_{exp}) - V_{MG}$ *(Eq. A16) or Eq. A17 on the premises that biliary clearance,* Cl_B*, of the metabolite is a constant fraction of the metabolic clearance,* Cl_{met}*, of morphine and that there is a negligible time lag in biliary process initiations. The values are labeled with the times at which the* AUC_M *and* $[MG]_{exp}$ *values were taken. The* ΣU^{exp}_{MG} *values were estimated for these same times from interpolations in plots of these values against time. Deviations of experimental values at the later times are due to the perturbations effected by enterohepatic recirculation that gave estimates of* ΣU^{exp}_{MG} *and* $[MG]_{exp}$ *in excess of those anticipated by the premises underlying Eq. A16, which did not take such delayed return to the system into account.*

The metabolism of morphine to the conjugate is apparently initiated at a time, t_0, of zero since there appears to be no lag in conjugate appearance, $[MG]$, in plasma at any studied dose (Figs. 2–4).

However, the renal excretion of the drug and conjugate at high morphine doses (Figs. 2 and 10) may be inhibited by the action of the drug so that:

$$\Sigma U_M = Cl^M_{ren}\left(\int_0^t [M]dt - \int_0^{t_0} [M]dt\right) = Cl^M_{ren}(AUC^t_M - AUC^{t_0}_M) \quad \text{(Eq. A6)}$$

where the parenthetical expression represents the difference between the total area under the plasma morphine concentration–time curve up to time t and the area up to time t_0 when the renal process commenced.

As a consequence of:

$$dU_{MG}/dt = Cl^{MG}_{ren}[MG] \quad \text{(Eq. A7)}$$

the cumulative renal excretion of the metabolite (ΣU_{MG}) would be related to a similar difference in the areas under the plasma metabolite concentration–time curve:

$$\Sigma U_{MG} = Cl^{MG}_{ren}\left(\int_0^t [MG]dt - \int_0^{t_0} [MG]dt\right) = Cl^{MG}_{ren}(AUC^t_{MG} - AUC^{t_0}_{MG}) = Cl^{MG}_{ren}(AUC^{t-t_0}_{MG}) \quad \text{(Eq. A8)}$$

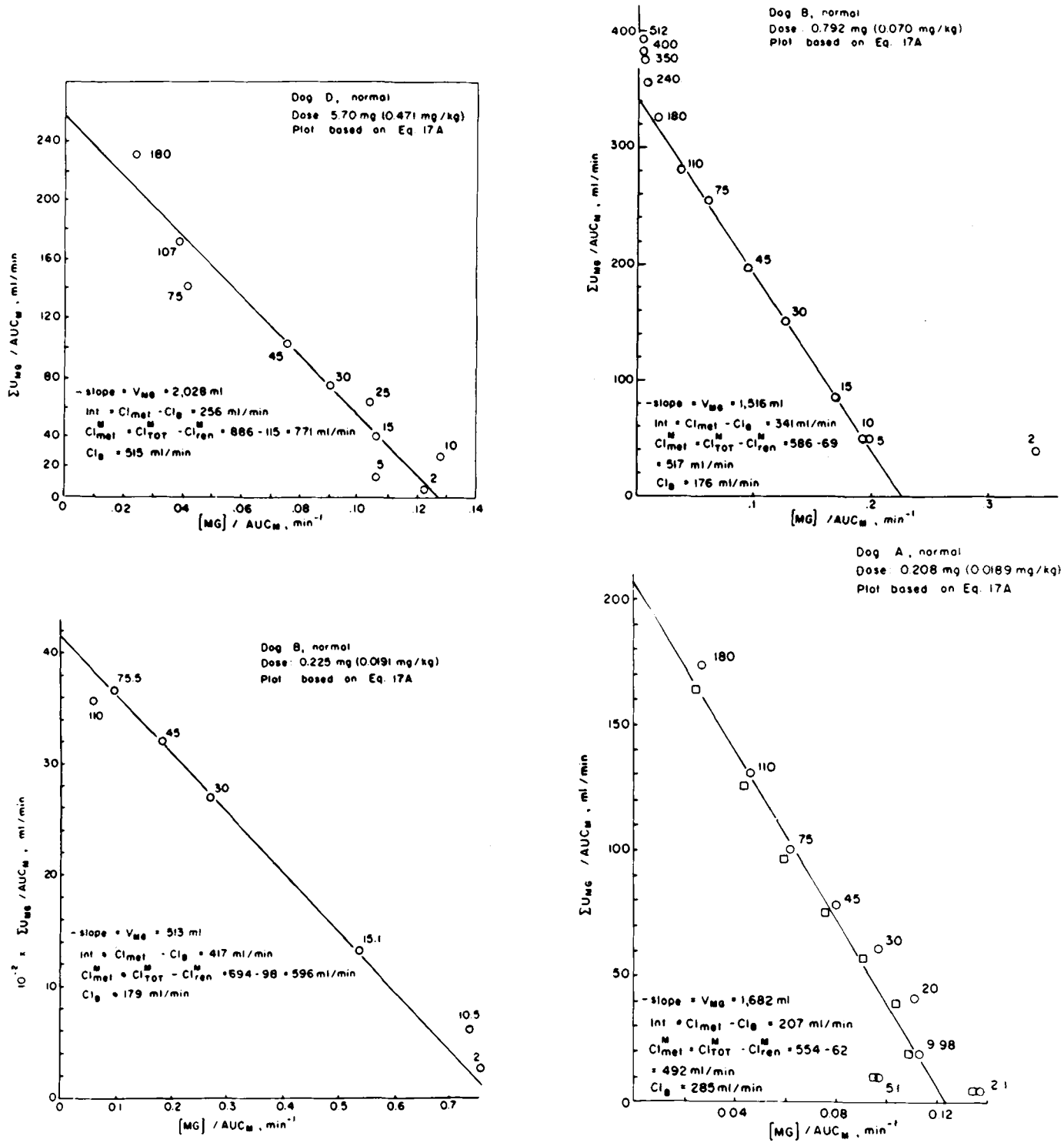

Figure 9—*Data for normal, non-bile-cannulated dogs in accordance with* $\Sigma U^{exp}_{MG}/AUC_M = V_{MG}([MG]_{exp}/AUC_M) + Cl_{met} - Cl_B$ *(Eq. A17) on the premises that biliary clearance,* Cl_B*, of the metabolite is a constant fraction of the metabolic clearance,* Cl_{met}*, of morphine and that there is a negligible time lag in biliary process initiation. The values are labeled with the times at which the* AUC_M *and* $[MG]_{exp}$ *values were taken. The* ΣU^{exp}_{MG} *values were estimated for those same times from interpolations in plots of these values against time. Deviations of experimental values at the later times are due to the perturbations effected by enterohepatic recirculation that gave estimates of* ΣU^{exp}_{MG} *and* $[MG]_{exp}$ *in excess of those anticipated by the premises underlying Eq. A17, which did not take such delayed return to the system into account. The values plotted for Dog A (0.208-mg dose) are based on two estimates of* AUC_M*: that calculated from the best-fit sum of exponentials (○) and that estimated by the trapezoidal rule (□) for* $[M]_{exp}$ *values with time.*

The clearances can be estimated from the slopes of $\Delta U_M/\Delta t$ ($\sim dU_M/dt$) *versus* $[M]_{t_{mid}}$ and $\Delta U_{MG}/\Delta t$ ($\sim dU_{MG}/dt$) *versus* $[MG]_{t_{mid}}$ in accordance with relations such as Eq. A7 where the plasma concentrations are taken at the midtime of the monitored excretory interval, Δt. Such anticipated linear plots were obtained (Fig. 5) and permitted the estimation of plasma level-independent renal clearances (Table I).

Thus, the values of ΣU_M and ΣU_{MG} could be generated from Eqs. A6 and A8. The appropriate choice of a time, t_0, for the renal process commencement should permit the generated values to agree with the experimental (Figs. 2–4).

It is possible that an amount of morphine in bile, ΣB_M, could be generated by a similar equation with a time of commencement of such a

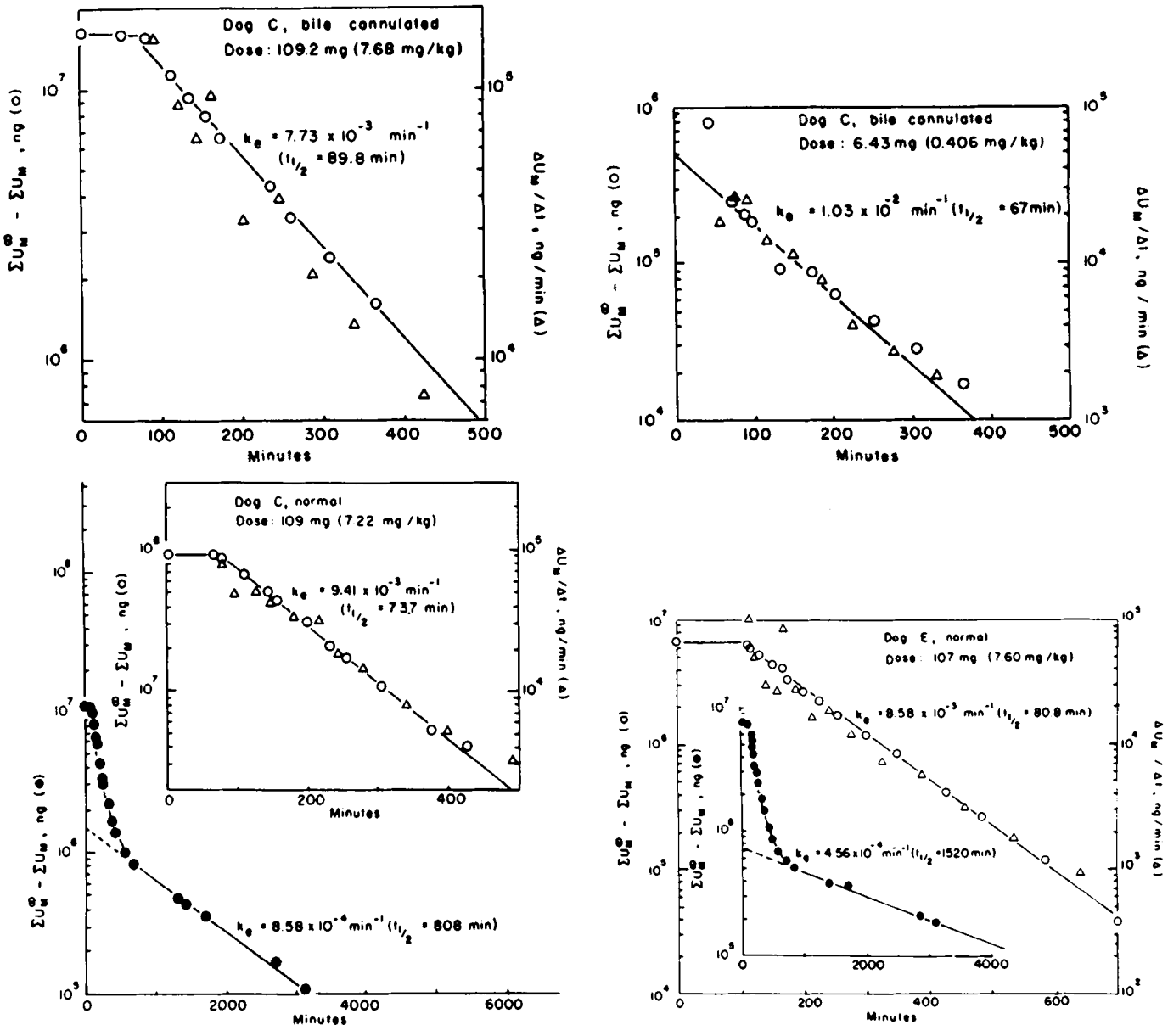

Figure 10—*Estimation of first-order rate constants, k_e, of urinary elimination from semilogarithmic plots of unchanged morphine not yet excreted, $\Sigma U_M^\infty - \Sigma U^M$ (○, ●), and rates of elimination, $\Delta U_M/\Delta t$ (Δ), against time in the bile-cannulated dog and at high doses in the normal dog. The former were plotted over the entire time interval (●) and then plotted according to the method of residuals (○). The time delay in elimination can be clearly noted.*

process at time t_0 (Eq. A3). However, the total amount of unchanged morphine that was experimentally determined in the bile was less than 0.005 of the dose in the two bile cannulation studies and was considered negligible.

Evaluation of Metabolic Clearances of Morphine in Bile-Cannulated Animal—The challenging of the validity of Eq. A2 for metabolite formation is not as simple. The metabolic clearance, Cl^M_{met}, is not readily obtained since the total metabolite produced, ΣMG, at a given time has to be constructed from the sums of amounts of the metabolite in the body, bile, and urine, respectively:

$$\Sigma MG = V_{MG}[MG]_{exp} + \Sigma B^{exp}_{MG} + \Sigma U^{exp}_{MG} \qquad \text{(Eq. A9)}$$

where V_{MG} is the apparent metabolite distribution volume on the postulation of instantaneous equilibration in the body fluids on its formation.

In the intact animal, ΣB_{MG} at a given time and V_{MG} are not readily obtainable. The ΣB^{exp}_{MG} value can be estimated from studies on a bile-cannulated dog. Substitution of Eq. A9 into Eq. A2 on the presumption of a constant metabolic clearance starting at time $t_0 = 0$ gives:

$$V_{MG}[MG]_{exp} + \Sigma B^{exp}_{MG} + \Sigma U^{exp}_{MG} = Cl^M_{met} AUC_M \qquad \text{(Eq. A10)}$$

which can be rearranged to:

$$\frac{\Sigma U_{MG} + \Sigma B_{MG}}{[MG]} = Cl^M_{met}\frac{AUC_M}{[MG]} - V_{MG} \qquad \text{(Eq. A11)}$$

or:

$$\frac{\Sigma U_{MG} + \Sigma B_{MG}}{AUC_M} = -V_{MG}\frac{[MG]}{AUC_M} + Cl^M_{met} \qquad \text{(Eq. A12)}$$

Thus, plots of the experimentally available $(\Sigma U_{MG} + \Sigma B_{MG})/[MG]$ or $(\Sigma U_{MG} + \Sigma B_{MG})/AUC_M$ against $AUC_M/[MG]$ or $[MG]/AUC_M$, respectively, can permit the estimation of V_{MG} and Cl^M_{met} values (Table I) from the slope and intercept of such plots (Fig. 7). The validity of these values can be ascertained by generating $[MG]_{calc}$ from a modification of Eq. A11 or A12:

$$[MG]_{calc} = \frac{\Sigma MG - \Sigma B^{exp}_{MG} - \Sigma U^{exp}_{MG}}{V_{MG}} = \frac{Cl^M_{met}AUC_M - \Sigma B^{exp}_{MG} - \Sigma U^{exp}_{MG}}{V_{MG}} \qquad \text{(Eq. A13)}$$

and the resultant calculated values of plasma metabolite concentration can be compared to those obtained experimentally, $[MG]_{exp}$ (Figs. 2–4).

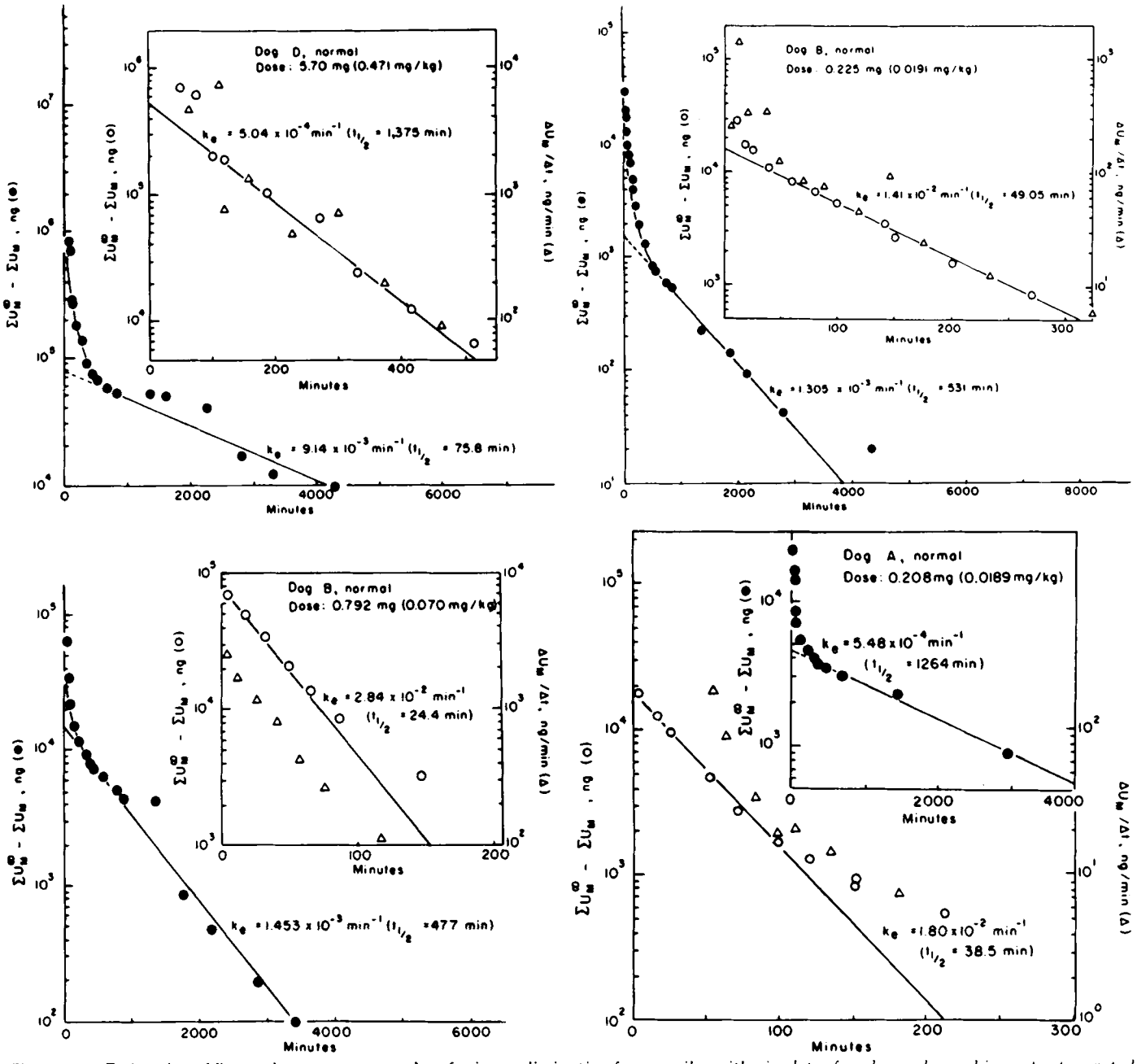

Figure 11—*Estimation of first-order rate constants, k_e, of urinary elimination from semilogarithmic plots of unchanged morphine not yet excreted, $\Sigma U_M - \Sigma U^M$ (○, ●), and rates of elimination, $\Delta U_M/\Delta t$ (Δ), against time at intermediate and low doses in the normal dog. The former were plotted over the entire time interval (●) and then plotted according to the method of residuals (○).*

Alternatively, the experimental values of metabolite concentration can be used to estimate the amounts of the metabolite, $\Sigma' B^{calc}_{MG}$, bile excreted from these estimates of Cl^M_{met} and V_{MG} (Eqs. A11 and A12) since:

$$\sum B^{calc}_{MG} = \sum MG - \sum U^{exp}_{MG} - V_{MG}[MG]_{exp}$$
$$= Cl^M_{met} AUC_M - \sum U^{exp}_{MG} - V_{MG}[MG]_{exp} \quad \text{(Eq. A14)}$$

Thus, the coincidences of $\Sigma' B^{calc}_{MG}$ with ΣB^{exp}_{MG} values and $[MG]_{calc}$ with $[MG]_{exp}$ can confirm or deny the validity of these postulates.

Evaluation of Metabolic Morphine Clearances in the Non-Bile-Cannulated Animal—If the amount of conjugate excreted in the bile is not specifically known, a constant biliary clearance, Cl_B, of hepatically formed conjugate can be postulated and Eq. A10 can be modified to:

$$V_{MG}[MG]_{exp} + Cl_B AUC_M + \sum U^{exp}_{MG} = Cl_{met} AUC_M \quad \text{(Eq. A15)}$$

where $Cl_B AUC_M/\Sigma MG = Cl_B/Cl_{met}$ is the fraction of conjugate formed in the liver that is partitioned immediately into the bile. If the biliary process is drug affected, a more accurate definition of the second term would be $Cl_B(AUC^t_M - AUC^{t_0}_M)$, where $AUC^{t_0}_M$ is the area under the plasma morphine level curve up to the time, t_0, of initiation of the biliary processes.

Thus, Eq. 15A can be rearranged to:

$$\frac{\sum U^{exp}_{MG}}{[MG]_{exp}} = (Cl_{met} - Cl_B)\frac{AUC_M}{[MG]_{exp}} - V_{MG} + \frac{Cl_B AUC^{t_0}_M}{[MG]_{exp}} \quad \text{(Eq. A16)}$$

or:

$$\frac{\sum U^{exp}_{MG}}{AUC_M} = -V_{MG}\frac{[MG]_{exp}}{AUC_M} + (Cl_{met} - Cl_B) + \frac{Cl_B AUC^{t_0}_M}{AUC_M} \quad \text{(Eq. A17)}$$

where the last term of both Eqs. A16 and A17 vanishes if there is no time lag in the initiation of the biliary process.

In the absence of such a time lag and the maintenance of a constant biliary partitioning of formed metabolite, V_{MG} and $I = Cl_{met} - Cl_B$ can

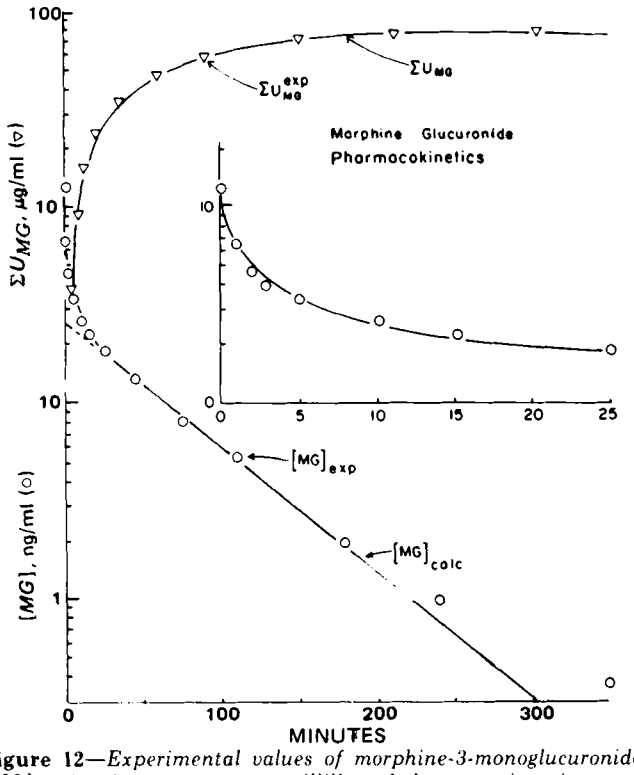

Figure 12—*Experimental values of morphine-3-monoglucuronide,* $[MG]_{exp}$ *(○), in nanograms per milliliter of plasma against time at an intravenous dose of 71.2 μg (6.5 μg/kg) to Dog A. The solid line through the experimental values was calculated from the polyexponential fit of Eq. 4. The solid line through the experimental values of cumulative conjugate in the urine,* ΣU_{MG}^{exp}*, are the theoretical values calculated from* $\Sigma U_{MG}^{calc} = Cl_{ren}^{MG} AUC_{MG}$ *for a renal clearance of 40 ml/min.*

be obtained from the slopes and intercepts of appropriate data plots in accordance with Eqs. A16 (Fig. 8) and A17 (Fig. 9), where $AUC_M^{\infty} = 0$. If the total clearance of morphine can be estimated from:

$$Cl_{tot} = \text{dose}/AUC_M \qquad \text{(Eq. A18)}$$

then:

$$Cl_{met} = Cl_{tot} - Cl_{ren}^{M} \qquad \text{(Eq. A19)}$$

and:

$$Cl_B = Cl_{met} - I = Cl_{met} - (Cl_{met} - Cl_B) \qquad \text{(Eq. A20)}$$

The premises for the absolute validity of these relations of Eqs. A18–A20 demand constant metabolic, biliary, and renal clearances of the drug and metabolite and no time lags in their initiation.

The levels of the conjugate $[MG]_{calc}$ in the normal dog also can be estimated from Eq. A13. However, the cumulative amount of formed metabolite totally secreted in the bile must be calculated from:

$$\Sigma B_{MG}^{tot} = Cl_B AUC_M \qquad \text{(Eq. A21)}$$

The $[MG]_{calc}$ and $[MG]_{exp}$ values will diverge if and when there is significant enterohepatic recirculation of the conjugate secreted into the bile.

Evaluation of Extent of Enterohepatic Recirculation of Morphine Metabolite (*MG*)—The biliary partition of the hepatically formed conjugate can be calculated in the normal animal from the determined Cl_B value by Eq. A21, which gives the amount secreted into the bile.

On the postulation of stoichiometry being preserved, the *actual* amount of conjugate in the biliary system would be:

$$\Sigma B_{MG}^{'calc} = \Sigma MG_{formed}^{tot} - \Sigma U_{MG}^{exp} - MG_{body}$$
$$= Cl_{met} AUC_M - \Sigma U_{MG}^{exp} - V_{MG}[MG]_{exp} \qquad \text{(Eq. A22)}$$

The difference between the calculated values of Eqs. A21 and A22 estimates the amount of conjugate at any given time that has been enterohepatically recirculated into the systemic circulation:

$$\Sigma MG_{ent} = \Sigma B_{MG}^{calc} - \Sigma B_{MG}^{'calc} \qquad \text{(Eq. A23)}$$

Estimation of Low Values of Morphine and Its Metabolite in Plasma—The estimates of the experimentally determined terminal plasma values of morphine, $[M]_{exp}$, and its conjugate, $[MG]_{exp}$, tend to have large errors since their estimates by liquid scintillation counting approach background. Alternative estimates are $[M]'_{calc}$ and $[MG]'_{calc}$, which can be determined from the estimated renal clearances, Cl_{ren}^{M} and Cl_{ren}^{MG}, and the experimentally determined values of cumulative urinary excretions, ΣU_M^{exp} and ΣU_{MG}^{exp}.

The area under the plasma level–time curve at time $t_{(i+1)}$ can be estimated from the quotient of the cumulative drug in the urine at that time and the renal clearance:

$$AUC_{t_{(i+1)}} = (\Sigma U)_{t_{(i+1)}}/Cl_{ren} = AUC_{t_i} + \Delta AUC \qquad \text{(Eq. A24)}$$

This area is the sum of a known area, AUC_{t_i}, where the plasma concentration is C_{t_i} at time t_i and an increase in area, ΔAUC, which can be defined as:

$$\Delta AUC = AUC_{t_{(i+1)}} - AUC_{t_i} = \left(\frac{C_{t_i} + C_{t_{(i+1)}}}{2}\right)\Delta t$$
$$= \frac{C_{t_i} + C_{t_{(i+1)}}}{2}(t_{(i+1)} - t_i) \qquad \text{(Eq. A25)}$$

Thus, the plasma drug concentration at time $t_{(i+1)}$ can be estimated from:

$$C_{t_{i+1}} = \frac{2(\Delta AUC)}{t_{(i+1)} - t_i} - C_{t_i} \qquad \text{(Eq. A26)}$$

so that, on consideration of Eq. A24:

$$C_{t_{i+1}} = \frac{2[(\Sigma U)t_{(i+1)}/Cl_{ren} - AUC_{t_i}]}{(t_{(i+1)} - t_i)} - C_{t_i} \qquad \text{(Eq. A27)}$$

where $C_{t_{i+1}}$ can be $[M]'_{calc}$ or $[MG]'_{calc}$ plasma values at t_{i+1}. It is necessary to have one initial experimental set of values of C_{t_1} and AUC_{t_1} at time t_1 to substitute into Eq. A27 for the first calculation of a plasma concentration of C_{t_2} at t_2 from $(\Sigma U)_{t_2}$ and t_2. Subsequent calculations of $C_{t_3}, C_{t_4}, \ldots, C_{t_{(i+1)}}$ can then be made in accordance with Eq. A27 since prior $C_{t_2}, C_{t_3}, \ldots, C_{t_i}$ and AUC_{t_i} values were available. The new AUC_{t_i} can be estimated by adding the calculated ΔAUC obtained from Eq. A25 to the prior estimated AUC at a previous time, $AUC_{(t_{i-1})}$. Plasma values obtained in this manner tended to oscillate unless averaged. Thus:

$$\overline{C}_{t_i} = \frac{C_{t_{(i+1)}} + C_{t_i}}{2} \qquad \text{for } t'_i = \frac{t_{(i+1)} + t_i}{2} \qquad \text{(Eq. A28)}$$

$$\overline{C}_{t'_{(i+1)}} = \frac{C_{t_{(i+2)}} + C_{t_{(i+1)}}}{2} \qquad \text{for } t'_{(i+1)} = \frac{t_{(i+2)} + t_{(i+1)}}{2} \qquad \text{(Eq. A29)}$$

etc., can provide monotonically decreasing values of $[M]'_{calc}$ and $[MG]'_{calc}$ with time with minimum scatter about a smooth curve drawn through the points.

APPENDIX II: GLOSSARY OF SYMBOLS

Concentrations of morphine, *M*, and morphine conjugate, *MG*, are given as nanograms of equivalent morphine base in plasma, whereas amounts in urine or bile are given as nanograms of equivalent morphine base.

$[M]_{exp}$—experimental morphine concentration per milliliter of plasma.

$[M]'_{calc}$—morphine concentration per milliliter of plasma calculated from experimental values of $\Sigma U_{M_{t_{(i+1)}}}$ at a time, $t_{(i+1)}$, from a known renal clearance, Cl_{ren}^{M}, and the known AUC_M and $[M]$ values of previous time, t_i (Eq. A27).

$[M]$—morphine concentration per milliliter of plasma calculated at a time, t, from a best-fitted linear sum of exponentials, $[M] = Ae^{-\alpha t} + Be^{-\beta t} + Ce^{-\gamma t}$.

$[MG]_{exp}$—experimental morphine conjugate concentration per milliliter of plasma.

$[MG]'_{calc}$—morphine conjugate concentration per milliliter of plasma as calculated from experimental values of $\Sigma U_{MG_{t_{(i+1)}}}$ at a time, $t_{(i+1)}$, from a known renal clearance, Cl_{ren}^{MG}, and the known AUC_{MG} and $[MG]$ values at a previous time, t_i (Eq. A27).

$[MG]$ or $[MG]_{calc}$—morphine conjugate concentration per milliliter of plasma as calculated from the difference between the cumulative amount of conjugate generated, ΣU_{MG}, and the experimental cumulative amounts of conjugate in bile and urine and divided by a volume of distribution, V_{MG} (Eq. A13). In the non-bile-cannulated dog, the

cumulative amount of conjugate in the bile must be calculated on the assumption of a constant biliary clearance of metabolized morphine (Eq. A21).

ΣMG or ΣMG^{tot}—cumulative morphine conjugate produced by metabolic morphine clearance, Cl^{M}_{met} (Eqs. A2, A5, and A9).

ΣU^{exp}_{M}—cumulative experimental morphine excreted in urine.

ΣU^{calc}_{M}—calculated cumulative morphine excreted in urine, based on renal clearance, Cl^{M}_{ren}, of plasma morphine (Eqs. A1 and A6).

ΣU^{exp}_{MG}—cumulative experimental morphine conjugate excreted in urine.

ΣU^{calc}_{MG}—calculated cumulative morphine conjugate excreted in urine, based on renal clearance, Cl^{MG}_{ren}, of plasma conjugate (Eq. A8).

ΣB^{exp}_{MG}—experimental cumulative morphine conjugate excreted in bile in the bile-cannulated dog.

ΣB^{calc}_{MG} or ΣB^{tot}_{MG}—calculated total cumulative morphine conjugate excreted in bile, based on biliary clearance, Cl_B, of metabolized morphine (Eqs. A3 and A21).

$\Sigma B'^{calc}_{MG}$—actual morphine conjugate in the biliary system calculated from the difference in the total formed, ΣMG, and the amounts of conjugate experimentally determined in the urine and in the body (Eq. A22).

ΣMG_{ent}—conjugate presumably enterohepatically recirculated from the bile to the systemic circulation as estimated from the difference between ΣB^{calc}_{MG} and $\Sigma B'^{calc}_{MG}$ (Eq. A23).

ΣMG^{exp}_{feces}—experimental conjugate excreted in feces.

ΣMG^{theo}_{feces}—conjugate calculated to be in feces based on the difference in calculated total conjugate formation and total amount excreted in urine.

ΣU^{∞} or ΣB^{∞}—total drug or metabolite in urine or bile at infinite time.

Cl^{M}_{tot}—total morphine clearance, in milliliters per minute (Eq. A18).

Cl^{M}_{ren}—renal morphine clearance, in milliliters per minute, basically estimated from $\Delta\Sigma U_M/\Delta t/[M]_{t_{mid}}$.

Cl^{MG}_{ren}—renal morphine conjugate clearance, in milliliters per minute, basically estimated from $\Delta\Sigma U_{MG}/\Delta t/[MG]_{t_{mid}}$.

Cl_{met} or Cl^{M}_{met}—metabolic morphine clearance, in milliliters per minute, which can be estimated directly in the bile-cannulated dog (Eqs. A11 and A12) and indirectly in the non-bile-cannulated dog (Eq. A19).

Cl_B or Cl^{M}_{B}—biliary clearance of a morphine conjugate fraction formed by morphine metabolism, in milliliters per minute, which can be estimated from $\Delta\Sigma B^{exp}_{MG}/\Delta t/[M]_{exp}$ in the bile-cannulated dog and indirectly estimated on the assumption of dose independence in the non-bile-cannulated dog (Eqs. A16, A17, and A20). The biliary clearance of systemic morphine conjugate is not presumed.

V^{M}_{C}—apparent distribution volume, in liters, of central compartment referenced to morphine base concentration in plasma.

V^{M}_{d}—apparent overall distribution volume, in liters, referenced to morphine base concentration in plasma.

V^{M}_{extrap}—apparent distribution volume, in liters, referenced to morphine based concentration in plasma on assumption of instantaneous equilibration in body fluids.

V_{MG}—apparent overall distribution volume, in liters, for the formed conjugate, MG, of morphine (Eqs. A11, A12, A16, and A17).

REFERENCES

(1) H. Krueger, N. B. Eddy, and M. Sumualt, "The Pharmacology of the Opium Alkaloids," parts I and II, U.S. Public Health Reports, Supplement 165, 1941 and 1943.

(2) E. L. Way and T. K. Adler, *Pharmacol. Rev.*, **12**, 383 (1960).

(3) E. L. Way and T. K. Adler, *Bull. WHO*, **25**, 227 (1961).

(4) *Ibid.*, **26**, 51 (1962).

(5) *Ibid.*, **26**, 261 (1962).

(6) *Ibid.*, **27**, 359 (1962).

(7) L. A. Woods and H. E. Muehlenbeck, *J. Pharmacol. Exp. Ther.*, **110**, 54 (1954).

(8) L. A. Woods, *ibid.*, **112**, 158 (1954).

(9) J. Cochin, J. Haggart, L. A. Woods, and M. H. Seevers, *ibid.*, **111**, 74 (1954).

(10) L. A. Woods, J. Cochin, E. G. Fornefeld, and M. H. Seevers, *ibid.*, **111**, 64 (1954).

(11) S. Y. Mulé and L. A. Woods, *ibid.*, **136**, 232 (1962).

(12) H. Kupferberg, A. Burkhalter, and E. L. Way, *ibid.*, **145**, 247 (1964).

(13) B. E. Dahlstrom and L. K. Paalzow, *J. Pharmacokinet. Biopharm.*, **3**, 293 (1975).

(14) S. Spector and E. S. Vesell, *Science*, **174**, 421 (1971).

(15) B. A. Berkowitz, S. H. Ngai, J. C. Yang, J. Hempstead, and S. Spector, *Clin. Pharmacol. Ther.*, **17**, 629 (1975).

(16) D. R. Stanski, D. J. Greenblatt, D. G. Lappas, J. Koch-Weser, and E. Lowenstein, *ibid.*, **19**, 752 (1976).

(17) S. F. Brunk and M. Delle, *ibid.*, **16**, 51 (1974).

(18) S. F. Brunk, M. Delle, and W. R. Wilson, *ibid.*, **15**, 283 (1974).

(19) D. H. Catlin, *J. Pharmacol. Exp. Ther.*, **200**, 224 (1977).

(20) "The Pharmacological Basis of Therapeutics," 5th ed., L. S. Goodman and A. Gilman, Eds., Macmillan, New York, N.Y., 1975, pp. 245–283.

(21) C. A. Handley and J. H. Moyer, *Arch. Int. Pharmacodyn. Ther.* **90**, 185 (1952).

(22) E. R. Garrett and T. Gürkan, *J. Pharm. Sci.*, **67**, 1512 (1978).

(23) H. Yoshimura, K. Oguri, and H. Tsukamato, *Biochem. Pharmacol.*, **18**, 279 (1968).

(24) A. E. Takemori, *ibid.*, **17**, 1627 (1968).

(25) P. H. Hinderling, J. Brès, and E. R. Garrett, *J. Pharm. Sci.*, **61**, 138 (1972).

(26) D. J. Blaney and L. A. Woods, *J. Pharmacol. Exp. Ther.*, **116**, 7 (1956).

(27) G. D. Olsen, *Clin. Pharmacol. Ther.*, **17**, 31 (1975).

(28) E. R. Garrett and H. J. Lambert, *J. Pharm. Sci.*, **62**, 550 (1973).

(29) H. M. Smith, "Principles of Renal Physiology," Oxford University Press, New York, N.Y., 1956, p. 32.

(30) P. L. Altman and D. S. Dittmer, "Respiration and Circulation," Biological Handbooks, American Societies for Experimental Biology, Bethesda, Md., 1971, p. 429.

ACKNOWLEDGMENTS

Supported in part by Grant 2-R01-DA-00743 from the National Institute of Drug Abuse, Rockville, MD 20852.

The technical assistance of Kathy Eberst and the contribution in surgical techniques of Dr. Lester L. Rolf, Jr., are gratefully acknowledged.

Monoamine Oxidase Inhibition by β-Carbolines: A Quantum Chemical Approach

FRANCISCO TOMÁS [x] **and JOSÉ M. AULLÓ**

Received July 8, 1977, from the *Departamento de Química Física, Facultad de Ciencias, Universidad de Valencia, Burjasot, Valencia, Spain.* Accepted for publication December 5, 1978.

Abstract □ Monoamine oxidase inhibition by β-carboline derivatives is related to the energy change, ΔE, arising from complex formation between the inhibitor and the enzyme. The energy change was expressed in terms of electronic indexes, which were estimated for a set of aromatic β-carbolines. The electronic indexes were correlated to the experimental activity indexes by a simplified quantum chemical perturbational treatment with a multiple regression procedure. A characteristic structure for the inhibitor–enzyme complex was derived from the correlation. The molecules are linked by two kinds of bond. One involves the lone pyridine nitrogen pair of β-carbolines; the other is due to a π-electronic interaction between the inhibitor indole fragment and a suitable area of the enzyme. Such a model explains the competitive inhibition by β-carbolines compared to tryptamine and other aromatic amines that are monoamine oxidase substrates.

Keyphrases □ β-Carbolines—monoamine oxidase inhibition, quantum chemistry □ Monoamine oxidase—inhibition by β-carbolines, quantum chemistry □ Monoamine oxidase inhibitors—β-carbolines, quantum chemistry

Some β-carboline (9*H*-pyrido[3,4-*b*]indole) derivatives are inhibitors of monoamine oxidase in oxidative cerebral amine deamination. *In vitro* studies using tryptamine as the substrate in deamination found that some derivatives were potent competitive inhibitors (1–8). The common β-carboline structure is the tricyclic aromatic system. Substituents enhance or diminish activity.

The present work was designed to relate the inhibitory activity to the aromatic β-carboline derivative electronic structure. An inhibition mechanism was derived from the correlation between experimental data and estimated electronic properties.

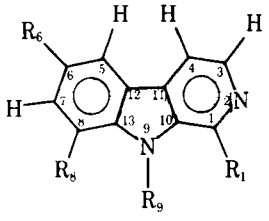

	R_1	R_6	R_8	R_9
β-carboline (I)	H	H	H	H
1-methyl-β-carboline (II)	$-CH_3$	H	H	H
9-methyl-β-carboline (III)	H	H	H	$-CH_3$
6-methyl-β-carboline (IV)	H	$-CH_3$	H	H
8-methyl-β-carboline (V)	H	H	$-CH_3$	H
6,9-dimethyl-β-carboline (VI)	H	$-CH_3$	H	$-CH_3$
8,9-dimethyl-β-carboline (VII)	H	H	$-CH_3$	$-CH_3$
1-amino-β-carboline (VIII)	$-NH_2$	H	H	H
6-amino-β-carboline (IX)	H	$-NH_2$	H	H
8-amino-β-carboline (X)	H	H	$-NH_2$	H
6-methoxy-β-carboline (XI)	H	$-OCH_3$	H	H
8-methoxy-β-carboline (XII)	H	H	$-OCH_3$	H
6-methoxy-9-methyl-β-carboline (XIII)	H	$-OCH_3$	H	$-CH_3$

EXPERIMENTAL

Molecular Orbital Calculations—The "valence shell" molecular orbital theory and the INDO (intermediate neglect of differential overlap) semiempirical method (9) were used. Calculations were performed with the CNINDO program (10) using the parameters implicit in the program.

The molecular conformation was built according to the following criteria:

1. Molecular tricyclic structure was considered to be planar, as inferred from electronic delocalization.
2. Substituents did not alter the tricyclic system conformation significantly.
3. The tricyclic system geometry derived from that of the glycyl-L-tryptophan (11) and pyridine (12) cyclic fragments.

The substituent bond lengths are given in Table I. The geometric parameters used in the calculations are given in Table I and Fig. 1.

Theoretical Considerations on Inhibitory Activity—The inhibitory activity is expressed by I_{50}, the inhibitor concentration that diminishes the enzyme activity by 50%. To compare all β-carbolines, the I_{50} must be measured using the same experimental conditions. With the assumption that the β-carboline derivatives inhibit the catalytic action of monoamine oxidase on tryptamine oxidation by a competitive mechanism, such a mechanism was analyzed considering the formation of the inhibitor–enzyme complex. The equilibrium constant for complex formation can be derived from experimental I_{50} data (1–8) and also can be estimated from theoretical electronic structure calculations. The aim is to find a correlation between the complex equilibrium constant and the inhibitor electronic properties.

The equilibrium constant can be derived from reported I_{50} values. Literature studies (1–8) suggested that the inhibitor and the substrate (tryptamine) are competitive toward the same enzyme centers. The competitive mechanism can be expressed by:

$$S + E \underset{k_2}{\overset{k_1}{\rightleftarrows}} SE \xrightarrow{k_3} P + E$$

Scheme I

$$B + E \overset{K_i}{\rightleftarrows} BE$$

Scheme II

where *S*, *E*, *B*, *SE*, and *BE* are the substrate, the enzyme, the inhibitor, the substrate–enzyme complex, and the inhibitor–enzyme complex, re-

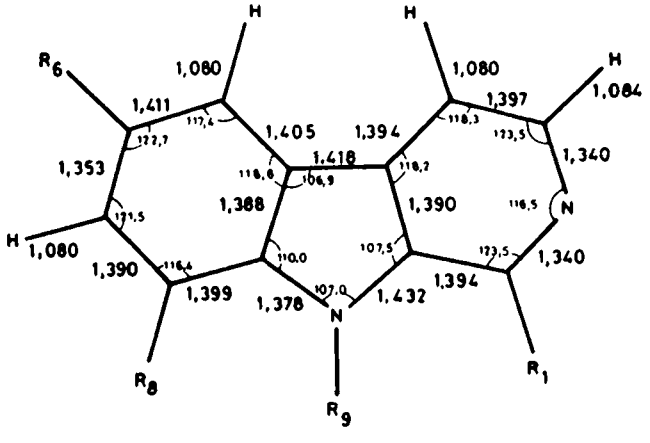

Figure 1—*Geometrical β-carboline tricyclic conformation.*

0022-3549/79/0600-0772$01.00/0
© 1979, American Pharmaceutical Association

Table I—Substituent Bond Lengths

Bond	Length, Å	Reference.
C_1-H	1.084	13
C_6-H	1.080	14
C_8-H	1.080	14
N_9-H	1.090	15
C_1-CH_3	1.500	16
C_6-CH_3	1.500	16
C_8-CH_3	1.500	16
N_9-CH_3	1.460	17
C-H	1.110	16
C_1-NH_2	1.360	18
C_6-NH_2	1.360	18
C_8-NH_2	1.360	18
N-H	1.040	18
C_6-OCH_3	1.360	19
C_8-OCH_3	1.360	19
O-CH_3	1.350	19
C-H	1.110	16

spectively; k_1, k_2, and k_3 are the rate constants; and K_i is the equilibrium constant:

$$K_i = \frac{[BE]}{[B][E]} \qquad \text{(Eq. 1)}$$

By applying the steady-state hypothesis, the degree of inhibition, i, is (20):

$$i = \frac{K_A K_i [B]}{K_A(1 + K_i[B]) + [S]} \qquad \text{(Eq. 2)}$$

where $K_A = k_2 + k_3/k_1$, the Michaelis constant, referred to the substrate; and S and B are the concentrations of the substrate and inhibitor, respectively, in the experiment.

From the I_{50} definition, Eq. 2 can be written:

$$K_i = \frac{K_A + [S]}{K_A I_{50}} \qquad \text{(Eq. 3)}$$

This expression can be simplified by suitable planning of the experiment. The value $K_A = 8.1 \times 10^{-5}$ was reported when the same initial tryptamine concentration, $[S] = 6 \times 10^{-2}$ mole/liter, was used for every experiment (1). Under these experimental conditions when $[S] > 100 \times K_A$, the oxidation kinetics can be considered to be zero order (with less than 1% deviation). Consequently, Eq. 3 reduces to:

$$K_i = \frac{K_{AS}}{I_{50}} \qquad \text{(Eq. 4)}$$

where:

$$K_{AS} = \frac{K_A + [S]}{K_A} \qquad \text{(Eq. 5)}$$

Obviously, K_{AS} depends on the experimental conditions, but it will be constant if $[S]$ is constant. In the experiments quoted, the conditions were constant for all β-carbolines. Thus, Eq. 4 or its logarithmic form:

$$\log K_i = \log K_{AS} + pI_{50} \qquad \text{(Eq. 6)}$$

where:

$$pI_{50} = -\log I_{50} \qquad \text{(Eq. 7)}$$

can be used to estimate the equilibrium constants for inhibitor–enzyme complex formation. From the experimental data (1), $\log K_{AS} = 2.870$. The values of pI_{50} and K_i derived by applying Eq. 6 to the experimental data are given in Table II.

Quantum Chemical Treatment of Inhibition—After an experimental estimate of the equilibrium constant K_i was obtained, the next step was to relate K_i to electronic and/or structural properties. No correlation was found between atomic electronic properties and β-carboline inhibitory activity in any previous work (21).

According to statistical thermodynamics, K_i is expressed by:

$$K_i = \frac{f_{BE}}{f_B f_E} \exp(-\Delta E_i/kT) \qquad \text{(Eq. 8)}$$

where ΔE_i is the difference between the complex energy and the separate enzyme and inhibitor energies, all at ground state; f is the partition function, and k is the Boltzmann constant. Structural similarities permit the simplification of Eq. 8 for the entire β-carboline set. The partition quotient can be considered nearly constant for all β-carbolines (22).

Table II—Inhibitory Activity Parameter (pI_{50}) and Equilibrium Constant for the β-Carbolines–Monoamine Oxidase Complexes

Compound	pI_{50} Experimental[a]	pI_{50} Calculated[b]	$K_i \times 10^{-6}$ liter/mole Calculated[b]
I	4.538	4.537	25.54
II	3.854	3.890	5.30
III	5.000	5.012	74.13
IV	3.921	3.844	6.18
V	4.143	4.153	10.30
VI	4.155	4.173	10.59
VII	4.699	4.696	37.07
VIII	3.824	3.796	4.94
IX	3.201	3.237	1.19
X	3.237	3.215	1.28
XI	4.367	4.366	17.22
XII	3.921	3.967	6.18
XIII	4.553	4.527	26.49
Tryptamine	—	—	3.15

[a] Reference 6. [b] This work.

The energy variation in complex formation can be developed into several components:

$$\Delta E_i = \Delta E_n^i + \Delta E_e^i + \Delta E_{st}^i + \Delta E_{sv}^i \qquad \text{(Eq. 9)}$$

where ΔE_n^i represents the difference due to nuclear rotation and vibration, ΔE_{st}^i expresses the variation from steric rearrangements, ΔE_{sv}^i concerns the solvation phenomenon, and ΔE_e^i expresses the change of electronic energy. The most important contribution to ΔE_i is ΔE_e^i (23). It is also the differential factor of each molecule in the ΔE_i estimation because the formation mechanism must be equal for all compounds. Equation 9 can be simplified to:

$$\Delta E_i = \Delta E_e^i + C \qquad \text{(Eq. 10)}$$

where C includes all contributions except the electronic ones and is constant for the β-carbolines.

From these considerations, the equilibrium constant is:

$$K_i = D(T) \exp(-\Delta E_e^i/kT) \qquad \text{(Eq. 11)}$$

where:

$$D(T) = \frac{f_{BE}}{f_B f_E} \exp(-C/kT) \qquad \text{(Eq. 12)}$$

$D(T)$ depends on temperature but is the same for all β-carbolines. In a logarithmic form, Eq. 11 can be written:

$$\log K_i = A(T) - \frac{\Delta E_e^i}{kT} \qquad \text{(Eq. 13)}$$

where $A(T) = \log D(T)$. Finally, from Eqs. 6 and 13, the inhibitory activity expressed by pI_{50} can be related to the complex formation electronic energy by:

$$pI_{50}^i = a + b\,\Delta E_e^i \qquad \text{(Eq. 14)}$$

where $a = A(T) - \log K_{AS}$ and $b = -1/kT$; a and b are constants for a temperature and for the entire β-carboline set.

Unfortunately, the direct ΔE_e^i calculation is not feasible. The monoamine oxidase molecular structure is unknown, and the electronic energy cannot be calculated. A greater difficulty appears in the electronic energy calculation of the inhibitor–enzyme complex, because the nature of the complex is unknown. The only energy that can be calculated is the inhibitor electronic energy in the geometrical conformations proposed.

Nevertheless, perturbational treatment (24, 25) was performed on the complex, considering its nature and stability. The important features observed in the β-carbolines were:

1. All compounds inhibited monoamine oxidase catalysis on aromatic amines and, more precisely, on tryptamine.
2. The inhibitory mechanism seemed to be common.
3. The inhibition was produced because the β-carbolines blocked the enzyme active centers on which the substrate was to be fixed.
4. The inhibitory mechanism reversibility implied molecular attraction rather than covalent bonding between molecules.
5. The pyridine nitrogen as well as the delocalized electronic system was essential for the inhibitory behavior. Carbazole, having a similar electronic structure to β-carboline but lacking the pyridine nitrogen, does not present inhibitory properties (26).
6. Substituents only altered the activity located at the delocalized tricyclic system.

Table III—Net Charges (e) of the Most Significant Atoms in Eq. 22

Compound	Q_5	Q_6	Q_9	Q_{13}
I	0.0297	−0.0054	−0.1656	0.1462
II	0.0299	−0.0054	−0.1647	0.1462
III	0.0294	−0.0047	−0.1283	0.1684
IV	0.0172	0.0056	−0.1653	0.1416
V	0.0241	−0.0016	−0.1655	0.1367
VI	0.0167	0.0060	−0.1279	0.1342
VII	0.0236	−0.0011	−0.1271	0.1286
VIII	0.0312	−0.0064	−0.1589	0.1457
IX	−0.0553	0.1619	−0.1663	0.1080
X	−0.0222	0.0297	−0.1600	0.0721
XI	−0.0523	0.2048	−0.1650	0.1208
XII	−0.0034	0.0234	−0.1564	0.0859
XIII	−0.0524	0.2046	−0.1275	0.1138
Tryptamine	0.0216	−0.0125	−0.1109	0.1359

Table IV—Superdelocalizability Indexes of the Most Significant Atoms in Eq. 22

Compound	$S_5^{(e)}$	$S_6^{(e)}$	$S_8^{(e)}$	$S_9^{(e)}$	$S_{13}^{(e)}$
I	−0.1941	−0.1950	−0.2009	−0.2682	−0.1852
II	−0.1940	−0.1951	−0.2024	−0.2676	−0.1788
III	−0.1939	−0.1928	−0.2001	−0.2683	−0.1800
IV	−0.2004	−0.1931	−0.2005	−0.2681	−0.1805
V	−0.1955	−0.1996	−0.1960	−0.2671	−0.1811
VI	−0.2028	−0.1928	−0.2003	−0.2688	−0.1813
VII	−0.2154	−0.1943	−0.1965	−0.2679	−0.1788
VIII	−0.1950	−0.1963	−0.2010	−0.2703	−0.1797
IX	−0.2164	−0.1759	−0.1988	−0.2729	−0.1881
X	−0.2079	−0.1943	−0.1801	−0.2714	−0.1918
XI	−0.2037	−0.1714	−0.1959	−0.2673	−0.1821
XII	−0.1999	−0.1921	−0.1789	−0.2675	−0.1845
XIII	−0.2035	−0.1739	−0.1957	−0.2688	−0.1834
Tryptamine	−0.2005	−0.2019	−0.2281	−0.2614	−0.1837

The electronic interaction energy between a pair of atoms, b from the inhibitor B and e from the enzyme E, can be expressed (27) by:

$$\Delta E_{be} = Q_b Q_e (bb|ee) + \sum_m \sum_{n'} \frac{d_{mb} d_{n'e}}{\epsilon_m - \epsilon_{n'}} \beta_{be}^2 + \sum_{m'} \sum_n \frac{d_{m'b} d_{ne}}{\epsilon_{m'} - \epsilon_n} \beta_{be}^2 \quad \text{(Eq. 15)}$$

where Q_b and Q_e are the net charges over the atoms and β_{be} is the resonance integral; $d_{ks} = \Sigma_j 2c_{kj}$ is the orbital charge of atom s in molecular orbital ϕ_k, where c_{kj} are the coefficients of the atomic orbitals from the atom s in ϕ_k. The indexes m' and n' denote the virtual orbitals of inhibitor and enzyme, respectively, and m and n stand for the doubly occupied orbitals of the corresponding molecules. The ϵ values are the molecular orbital energies; $(bb|ee)$ is the repulsion energy between the electrons occupying orbitals centered on b and e atoms. The hypothesis of INDO formalism gives a constant value for the repulsion integral $(bb|ee)$ among the atoms b and e valence orbitals despite the kind of such orbitals. The value of β_{be} is independent of the kind of atomic orbitals because the molecular nature of the complex does not involve covalent bonds.

By extending Eq. 15 to all pairs of interacting atoms, p, it can be written:

$$\Delta E_e^i = \sum_p \left\{ Q_b^p Q_e^p (bb|ee) + \beta_{be}^2 \sum_m \frac{d_{mb}^p}{\epsilon_m - \bar{\epsilon}_{n'}} \sum_{n'} d_{n'e}^p + \beta_{be}^2 \sum_{m'} \frac{d_{m'b}^p}{\epsilon_{m'} - \bar{\epsilon}_n} \sum_n d_{ne}^p \right\} \quad \text{(Eq. 16)}$$

This expression has been written with the consideration that the occupied molecular orbitals of one molecule and the virtual orbitals of the other have very different energies, as in a charge controlled process. The following approach may be used:

$$\epsilon_m - \epsilon_{n'} = \epsilon_m - \bar{\epsilon}_{n'} \quad \text{(Eq. 17)}$$

$$\epsilon_{m'} - \epsilon_n = \epsilon_{m'} - \bar{\epsilon}_n \quad \text{(Eq. 18)}$$

where $\bar{\epsilon}$ is the average of the corresponding energies.

Since the atoms from the tricyclic system, which are the same for all β-carbolines, are the only ones involved in complex formation and since the complexes are formed with the same atoms of the enzyme, some of the magnitudes appearing in Eq. 16 probably are constant for all β-carbolines. The integrals $(bb|ee)$, the resonance integrals β_{be}, the summations referring the enzyme coefficients, and the average enzyme orbital energies may be considered constant.

Otherwise, the summations concerning the β-carboline orbitals are closely related to the generalized superdelocalizability indexes (28, 29) and are expressed by:

$$S_b^{(e)} = \sum_m \frac{d_{mb}}{\epsilon_m} \quad \text{(Eq. 19}a\text{)}$$

$$S_b^{(n)} = \sum_{m'} \frac{d_{m'b}}{\epsilon_{m'}} \quad \text{(Eq. 19}b\text{)}$$

where $S^{(e)}$ is the electrophilic index and $S^{(n)}$ is the nucleophilic index.

Since the enzymatic terms in Eqs. 16 and 19 are constant, the following expression for the electronic energy variation can be written:

$$\Delta E_e^i = \sum_p \{A_p Q_p^2 + B_p S_b^{(e)p} + C_p S_b^{(n)p}\} \quad \text{(Eq. 20)}$$

The coefficients A_p, B_p, and C_p are constants for all β-carbolines, and the indexes Q and S are variables for each complex.

Finally, by introducing Eq. 20 in Eq. 14 and rearranging, the following expression can be found:

$$pI_{50} = a + \sum_p (c_{1p} Q_p + c_{2p} S_p^{(e)} + c_{3p} S_p^{(n)}) \quad \text{(Eq. 21)}$$

In this equation, the summation is extended over all of the atoms of the aromatic β-carboline tricyclic system, and the coefficients c_{ip} are constant. Equation 21 relates the experimentally found inhibitory activity to the theoretically estimated electronic indexes. This equation holds if the enzyme–β-carboline complex is well approximated by the proposed molecular model, *i.e.*, if it is a molecular charge-controlled complex without covalent bonds. A statistical study of the applicability of Eq. 21 to the molecules considered was performed to identify the coefficients that gave the best statistical correlation.

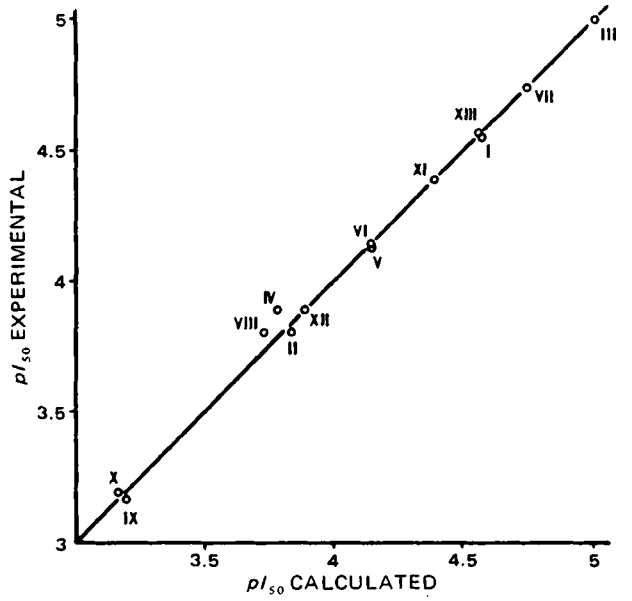

Figure 2—*Experimental* pI_{50} *values* versus *calculated values from Eq. 22.*

RESULTS AND DISCUSSION

The calculated values for the electronic indexes appearing in Eq. 21 are summarized in Tables III and IV. The statistical fitting of Eq. 21 was performed by means of stepwise linear regression techniques with pI_{50} as the dependent variable and the electronic indexes as independent variables. More than 400 combinations of electronic indexes were performed; the best correlated expression found is Eq. 2 , where the numerical values for the coefficients of Eq. 21 are shown:

$$pI_{50} = 31.806 + 11.782\, Q_9 + 140.546\, S_9^{(e)} + 14.405\, Q_6 + 18.199\, S_6^{(e)} + 42.378\, Q_5 - 28.496\, S_5^{(e)} + 22.284\, Q_{13} - 101.543\, S_{13}^{(e)} + 63.959\, S_8^{(e)} \quad \text{(Eq. 22)}$$

Table V—t-Test for Significance of Coefficients in Eq. 22

Variable	t Value	p
Q_9	13.003	<0.0005
$S_9^{(e)}$	10.307	<0.0025
Q_6	10.165	<0.0025
$S_2^{(e)}$	2.32	= 0.05
$S_8^{(e)}$	10.684	<0.0025
Q_5	10.491	<0.0025
$S_5^{(e)}$	9.291	<0.0025
Q_{13}	10.608	<0.0025
$S_{13}^{(e)}$	13.067	<0.005

Equation 22 has a multiple correlation coefficient (R) of 0.999 that represents a significance better than 99.9%, a mean standard deviation (MSD) of 0.011_7, and a residual standard deviation (RSD) of 0.042_4. A detailed statistical analysis is given in the *Appendix*.

The next best correlation is given by:

$$pI_{50} = 34.157 + 16.215\,Q_9 + 139.164\,S_9^{(e)} + 10.245\,Q_6 + 24.402\,Q_5 + 14.753\,Q_{13} - 75.452\,S_{13}^{(e)} + 32.385\,S_8^{(e)} \quad \text{(Eq. 23)}$$

with the following statistical parameters: $R = 0.972$, $MSD = 0.053_2$, and $RSD = 0.192$.

The pI_{50} values taken from the literature (1–8) and the ones estimated by Eq. 22 are summarized in Table II, which also shows the estimated equilibrium constants. The experimental pI_{50} values are fitted *versus* the calculated ones in Fig. 2.

As can be derived from Eq. 22, the inhibitory activity was not closely related to any individual atomic property but to a definite set of electronic indexes located on some tricyclic system atoms. The electrophilic index $S_9^{(e)}$ was the most important term influencing the activity. The inhibitory activity of any aromatic β-carboline could be predicted from the corresponding electronic indexes of its ring atoms using Eq. 22. The significant features from the statistical analysis were:

1. The electronic indexes corresponding to pyridine nitrogen, N_2, did not appear in any tested regression giving an acceptable statistical analysis.
2. The same circumstance was observed for C_1, C_3, and C_4 belonging to the pyridine β-carboline fragment.
3. The benzene fragment electronic indexes, as well as the pyrrole fragment indexes, showed the best correlation found for the entire β-carboline indolic part.
4. In all significant regressions studied, the Q_9 and $S_9^{(e)}$ indexes gave important contributions to the regression.

Only the indole fragment is involved in β-carboline–enzyme complex formation. The pyridine nitrogen, N_2, is essential to the inhibitory activity of β-carbolines but does not contribute to the complex formation.

From an electronic point of view, the indole group exhibited a delocalized charge with some accumulations and depletions over its atoms (Table III); it was a good system to form molecular or π-electronic complexes. The pyridine nitrogen is an electron donor system, responsible for the basicity of β-carbolines. The electronic characteristics of both molecular regions are responsible for the interaction with monoamine oxidase. β-Carbolines and monoamine oxidase form a molecular complex on which the molecules are linked by two interactions. The first one arises from the molecular electronic complex between the β-carboline indole fragment and a suitable fixing region of monoamine oxidase (Fig. 3). This

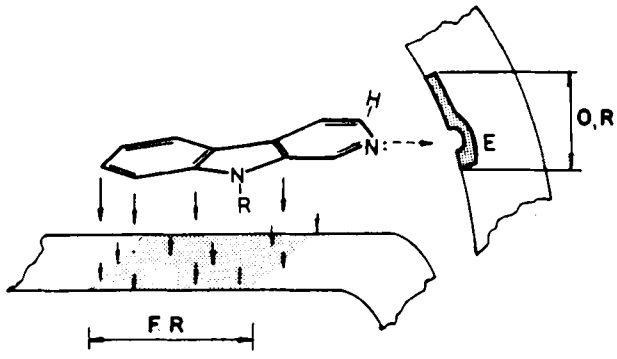

Figure 3—*Interaction model between inhibitor and enzyme. FR = fixing region, and OR = oxidizing region.*

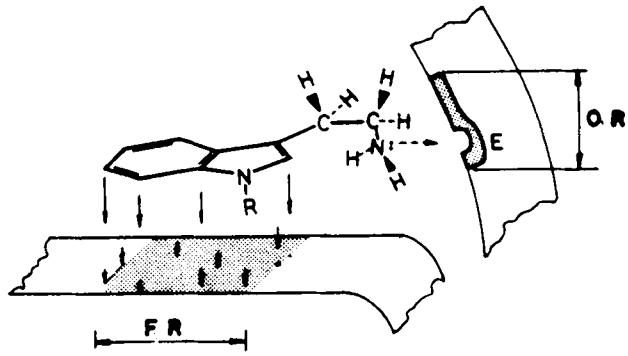

Figure 4—*Interaction model between tryptamine and the enzyme.*

complex has π-complex characteristics, like Mulliken's external complex ($b\pi$–$a\pi$) (30). The indole system acts as an electron donor by means of N_9, C_6, and C_8.

The second interaction is due to pyridine nitrogen, N_2, which acts as an electron donor over an electrophilic monoamine oxidase center located in a region identified as OR (oxidizing region) (Fig. 3). This interaction must be stronger than the former because of its electronic nature. Such a model involves specific structures at the enzyme interaction regions, the so-called FR and OR. The OR interacts with N_2 by means of a strong bond (dative covalent, hydrogen bonding, *etc.*). The FR must have a delocalized structure to match the electronic singularities of the inhibitor indole fragment. Some kind of conformational change is involved in the enzyme itself in order to bind adequately to the inhibitor.

Such a model adequately explains the competitive inhibition of tryptamine and probably of other aromatic cerebral amines. Tryptamine has an indole structure that can form a complex with the enzyme FR in a similar mode to β-carboline. Also, the tryptamine side chain can take a suitable conformation facing the nitrogen of the amino group to the enzyme OR (Fig. 4). In such a conformation, the nitrogen atom reacts, breaking the C–N bond and initiating the oxidative degradation that inactivates the amine. After the oxidation, the complex between the indole fragment and the FR region opens again, releasing the inactivated product.

The inhibitory β-carboline behavior can be explained as the result of a mimetic mechanism forming the same bonds with the same enzymatic regions; the difference is that β-carboline cannot be oxidized because of the stability of its delocalized electronic structure. If such a model works, the competition for the formation of the complex with the enzyme and, consequently, the inhibitory activity are due to the more stable complexes formed by β-carbolines with the enzyme FR than by tryptamine. Thus, the tryptamine–FR complex stability is estimated using Eq. 22, with the electronic indexes corresponding to the indole group of tryptamine (Tables III and IV). A value of 3.15×10^6 liters/mole was found for the equilibrium constant in the reaction tryptamine + FR(enzyme) ⇌ complex.

This value is similar to those found for β-carbolines (Table II). From Table II, it can be seen that the greatest inhibitory activity belongs to the greatest difference between the estimated equilibrium constants of β-carboline and tryptamine. Such a result sustains the model proposed.

APPENDIX

The analysis of variance of Eq. 22 gives $F_{9,3} = 208.53$, giving a very high significance for this equation ($p < 0.0005$). The t-test values of the coefficients of Eq. 22 are shown in Table V. All of them are significant (significance limits of 95–99.9%); consequently, the corresponding indexes influence the values of pI_{50} and K_i.

The introduction or elimination of any other index decreases substantially the regression equation significance level.

Finally, the regression equation referring to the β-carboline benzene ring atoms, together with their most important statistical parameters, are:

$$pI_{50} = 33.991 + 31.452\,S_6^{(e)} + 8.732\,Q_6 + 16.228\,S_7^{(e)} + 97.778\,Q_7 - 28.030\,S_{13}^{(e)} + 14.143\,Q_{13} - 30.809\,S_5^{(e)} + 172.652\,S_8^{(e)} + 133.849\,Q_{12} \quad \text{(Eq. A1)}$$

with $RSD = 0.100$, $R = 0.995$, $MSD = 0.028$, $F_{9,3} = 37.12$, and $p < 0.01$. The equation of regression and the statistical parameters for the atoms

of the pyrrole fragment are:

$$pI_{50} = 105.773 + 503.033\,S_9^{(e)} + 27.992\,Q_9 - 183.106\,S_{13}^{(e)} + 8.801\,Q_{13} - 62.903\,S_{11}^{(e)} - 176.198\,Q_{11} - 46.928\,Q_{12} - 63.207\,Q_{10} \quad \text{(Eq. A2)}$$

with $RSD = 0.10$, $R = 0.994$, $MSD = 0.028$, $F_{8,4} = 41.67$, and $p < 0.005$. These correlations are poorer than the one found for the indole group.

REFERENCES

(1) B. T. Ho, W. M. McIsaac, K. E. Walker, and V. Estevez, *J. Pharm. Sci.*, **57**, 269 (1968).

(2) B. T. Ho, W. M. McIsaac, and K. E. Walker, *ibid.*, **57**, 1364 (1968).

(3) B. T. Ho, W. M. McIsaac, L. W. Tansey, and K. E. Walker, *ibid.*, **58**, 219 (1969).

(4) B. T. Ho, W. M. McIsaac, and L. W. Tansey, *ibid.*, **58**, 998 (1969).

(5) B. T. Ho, G. E. Fritchie, P. M. Kralik, L. W. Tansey, K. E. Walker, and W. M. McIsaac, *ibid.*, **58**, 1423 (1969).

(6) B. T. Ho, K. Li, K. E. Walker, L. W. Tansey, P. M. Kralik, and W. M. McIsaac, *ibid.*, **59**, 1445 (1970).

(7) B. T. Ho, P. M. Gardner, and K. E. Walker, *ibid.*, **62**, 36 (1973).

(8) B. T. Ho, P. M. Gardner, S. F. Pong, and K. E. Walker, *Experientia*, **29**, 527 (1973).

(9) J. A. Pople, D. L. Beveridge, and P. A. Dobosh, *J. Chem. Phys.*, **47**, 2026 (1966).

(10) Quantum Chemistry Program Exchange, QCPE 141, Indiana University, Bloomington, Ind. "Approximate Molecular Orbital Theory," J. A. Pople and D. L. Beveridge, Eds., McGraw-Hill, New York, N.Y., 1970, p. 163.

(11) R. A. Pasternak, *Acta Crystallogr.*, **9**, 341 (1956).

(12) B. Bak, L. Hansen-Nygaard, and J. Rastrup-Andersen, *J. Mol. Spectrosc.*, **2**, 361 (1958).

(13) A. Lanseth and B. P. Stoicheff, *Can. J. Phys.*, **34**, 350 (1956).

(14) W. S. Wilcox and J. H. Goldstein, *J. Chem. Phys.*, **20**, 1656 (1952).

(15) F. A. Keidel and S. H. Bauer, *ibid.*, **25**, 1218 (1956).

(16) D. J. Sutor, *Acta Crystallogr.*, **11**, 83 (1958).

(17) F. P. Billingsley and J. E. Bloor, *Theor. Chim. Acta*, **11**, 325 (1968).

(18) G. Erlandsson, *Ark. Fys.*, **8**, 341 (1954).

(19) T. H. Goodwin, M. Przykylaska, and J. M. Robertson, *Acta Crystallogr.*, **3**, 279 (1950).

(20) K. J. Laidler and P. S. Bunting, "The Chemical Kinetics of Enzyme Action," Oxford University Press, Oxford, England, 1973, chap. 3.

(21) J. M. Aulló, Ph.D. thesis, University of Valencia, Valencia, Spain, 1976.

(22) M. J. S. Dewar and C. C. Thompson, *J. Am. Chem. Soc.*, **87**, 4414 (1965).

(23) R. Daudel, R. Lefebvre, and C. M. Moser, "Quantum Chemistry," Interscience, New York, N.Y., 1959.

(24) G. Klopman and R. F. Hudson, *Theor. Chim. Acta*, **8**, 165 (1967).

(25) G. Klopman, *J. Am. Chem. Soc.*, **90**, 223 (1968).

(26) W. M. McIsaac and V. Estevez, *Biochem. Pharmacol.*, **15**, 1625 (1969).

(27) F. Peradejordi, A. N. Martin, and A. Cammarata, *J. Pharm. Sci.*, **60**, 576 (1971).

(28) K. Fukui, T. Yonezawa, and C. Nagata, *Bull. Chem. Soc. Jpn.*, **27**, 423 (1954).

(29) K. Fukui, T. Yonezawa, and C. Nagata, *J. Chem. Phys.*, **27**, 1247 (1957).

(30) R. S. Mulliken and W. B. Person, "Molecular Complexes," Wiley, New York, N.Y., 1969.

ACKNOWLEDGMENTS

The authors are indebted to Prof. J. I. Fernán dez Alonso, Department of Physical and Quantum Chemistry, Universidad Autónoma de Madrid, Spain, and to the Instituto de Agroquímica y Tecnología de Alimentos from Valencia, Spain, for the computer facilities. The authors are also grateful to V. Sanz for reviewing the manuscript.

New Biphenyl Derivatives II: 1-(4-Biphenylyl)-1-hydroxy-2-aminoethanes and 1-(4-Biphenylyl)-1-chloro-2-aminoethanes as Potential β-Adrenoceptor Blocking Agents

RAGAB M. SHAFIK ˣ and ABDEL-FATTAH A. A. ASKAR

Received September 6, 1978, from the *Department of Pharmaceutical Chemistry, Faculty of Pharmacy, University of Alexandria, Alexandria, Egypt.* Accepted for publication December 5, 1978.

Abstract □ Series of 1-(4-biphenylyl)-1-hydroxy-2-aminoethanes and 1-(4-biphenylyl)-1-chloro-2-aminoethanes were synthesized. Newly developed reaction conditions for aryl aminomethyl ketone reduction and reductive alkylation, using sodium borohydride, are described. The prepared compounds were examined for adrenergic blocking activity on an anesthetized dog blood pressure preparation and on isolated toad hearts. β-Adrenergic blockade was investigated using isoproterenol as the agonist. The benzylamino and cyclohexylamino analogs exhibited marked β-adrenoceptor blocking activity, for which the latter derivatives were more potent.

Keyphrases □ β-Adrenergic blocking activity—biphenyl derivatives, synthesis, structure–activity relationships □ Biphenyl derivatives, various—synthesized, evaluated for β-adrenergic blocking activity, structure–activity relationships □ Structure–activity relationships—biphenyl derivatives, β-adrenergic blocking activity

Optimum β-adrenoceptor blockade occurs when 1-phenyl-1-hydroxy-2-aminoethane structures (I) bear certain substituents at the phenyl 4- or 3,4-position and an isopropyl grouping on the amine head (1). 1-(3,4-Dichlorophenyl)-1-hydroxy-2-isopropylaminoethane (2) (II), 1-(2-naphthyl)-1-hydroxy-2-isopropylaminoethane (pronethalol) (3, 4) (III), and 1-(4-nitrophenyl)-1-hydroxy-2-isopropylaminoethane (5) (IV) are well-known examples.

In vitro hydrolysis of 1-aryl-1-chloro-2-aminoethanes to 1-aryl-1-hydroxy-2-aminoethanes was used to prepare a series of 1-chloro-2-aminoethanes related to III (6, 7).

0022-3549/79/0600-0776$01.00/0

© 1979, American Pharmaceutical Association

of the pyrrole fragment are:

$$pI_{50} = 105.773 + 503.033\,S_9^{(e)} + 27.992\,Q_9 - 183.106\,S_{13}^{(e)} + 8.801\,Q_{13} - 62.903\,S_{11}^{(e)} - 176.198\,Q_{11} - 46.928\,Q_{12} - 63.207\,Q_{10} \quad \text{(Eq. A2)}$$

with $RSD = 0.10$, $R = 0.994$, $MSD = 0.028$, $F_{8,4} = 41.67$, and $p < 0.005$. These correlations are poorer than the one found for the indole group.

REFERENCES

(1) B. T. Ho, W. M. McIsaac, K. E. Walker, and V. Estevez, *J. Pharm. Sci.*, **57**, 269 (1968).

(2) B. T. Ho, W. M. McIsaac, and K. E. Walker, *ibid.*, **57**, 1364 (1968).

(3) B. T. Ho, W. M. McIsaac, L. W. Tansey, and K. E. Walker, *ibid.*, **58**, 219 (1969).

(4) B. T. Ho, W. M. McIsaac, and L. W. Tansey, *ibid.*, **58**, 998 (1969).

(5) B. T. Ho, G. E. Fritchie, P. M. Kralik, L. W. Tansey, K. E. Walker, and W. M. McIsaac, *ibid.*, **58**, 1423 (1969).

(6) B. T. Ho, K. Li, K. E. Walker, L. W. Tansey, P. M. Kralik, and W. M. McIsaac, *ibid.*, **59**, 1445 (1970).

(7) B. T. Ho, P. M. Gardner, and K. E. Walker, *ibid.*, **62**, 36 (1973).

(8) B. T. Ho, P. M. Gardner, S. F. Pong, and K. E. Walker, *Experientia*, **29**, 527 (1973).

(9) J. A. Pople, D. L. Beveridge, and P. A. Dobosh, *J. Chem. Phys.*, **47**, 2026 (1966).

(10) Quantum Chemistry Program Exchange, QCPE 141, Indiana University, Bloomington, Ind. "Approximate Molecular Orbital Theory," J. A. Pople and D. L. Beveridge, Eds., McGraw-Hill, New York, N.Y., 1970, p. 163.

(11) R. A. Pasternak, *Acta Crystallogr.*, **9**, 341 (1956).

(12) B. Bak, L. Hansen-Nygaard, and J. Rastrup-Andersen, *J. Mol. Spectrosc.*, **2**, 361 (1958).

(13) A. Lanseth and B. P. Stoicheff, *Can. J. Phys.*, **34**, 350 (1956).

(14) W. S. Wilcox and J. H. Goldstein, *J. Chem. Phys.*, **20**, 1656 (1952).

(15) F. A. Keidel and S. H. Bauer, *ibid.*, **25**, 1218 (1956).

(16) D. J. Sutor, *Acta Crystallogr.*, **11**, 83 (1958).

(17) F. P. Billingsley and J. E. Bloor, *Theor. Chim. Acta*, **11**, 325 (1968).

(18) G. Erlandsson, *Ark. Fys.*, **8**, 341 (1954).

(19) T. H. Goodwin, M. Przykylaska, and J. M. Robertson, *Acta Crystallogr.*, **3**, 279 (1950).

(20) K. J. Laidler and P. S. Bunting, "The Chemical Kinetics of Enzyme Action," Oxford University Press, Oxford, England, 1973, chap. 3.

(21) J. M. Aulló, Ph.D. thesis, University of Valencia, Valencia, Spain, 1976.

(22) M. J. S. Dewar and C. C. Thompson, *J. Am. Chem. Soc.*, **87**, 4414 (1965).

(23) R. Daudel, R. Lefebvre, and C. M. Moser, "Quantum Chemistry," Interscience, New York, N.Y., 1959.

(24) G. Klopman and R. F. Hudson, *Theor. Chim. Acta*, **8**, 165 (1967).

(25) G. Klopman, *J. Am. Chem. Soc.*, **90**, 223 (1968).

(26) W. M. McIsaac and V. Estevez, *Biochem. Pharmacol.*, **15**, 1625 (1969).

(27) F. Peradejordi, A. N. Martin, and A. Cammarata, *J. Pharm. Sci.*, **60**, 576 (1971).

(28) K. Fukui, T. Yonezawa, and C. Nagata, *Bull. Chem. Soc. Jpn.*, **27**, 423 (1954).

(29) K. Fukui, T. Yonezawa, and C. Nagata, *J. Chem. Phys.*, **27**, 1247 (1957).

(30) R. S. Mulliken and W. B. Person, "Molecular Complexes," Wiley, New York, N.Y., 1969.

ACKNOWLEDGMENTS

The authors are indebted to Prof. J. I. Fernán dez Alonso, Department of Physical and Quantum Chemistry, Universidad Autónoma de Madrid, Spain, and to the Instituto de Agroquímica y Tecnología de Alimentos from Valencia, Spain, for the computer facilities. The authors are also grateful to V. Sanz for reviewing the manuscript.

New Biphenyl Derivatives II: 1-(4-Biphenylyl)-1-hydroxy-2-aminoethanes and 1-(4-Biphenylyl)-1-chloro-2-aminoethanes as Potential β-Adrenoceptor Blocking Agents

RAGAB M. SHAFIK ˣ and ABDEL-FATTAH A. A. ASKAR

Received September 6, 1978, from the *Department of Pharmaceutical Chemistry, Faculty of Pharmacy, University of Alexandria, Alexandria, Egypt.* Accepted for publication December 5, 1978.

Abstract □ Series of 1-(4-biphenylyl)-1-hydroxy-2-aminoethanes and 1-(4-biphenylyl)-1-chloro-2-aminoethanes were synthesized. Newly developed reaction conditions for aryl aminomethyl ketone reduction and reductive alkylation, using sodium borohydride, are described. The prepared compounds were examined for adrenergic blocking activity on an anesthetized dog blood pressure preparation and on isolated toad hearts. β-Adrenergic blockade was investigated using isoproterenol as the agonist. The benzylamino and cyclohexylamino analogs exhibited marked β-adrenoceptor blocking activity, for which the latter derivatives were more potent.

Keyphrases □ β-Adrenergic blocking activity—biphenyl derivatives, synthesis, structure–activity relationships □ Biphenyl derivatives, various—synthesized, evaluated for β-adrenergic blocking activity, structure–activity relationships □ Structure–activity relationships—biphenyl derivatives, β-adrenergic blocking activity

Optimum β-adrenoceptor blockade occurs when 1-phenyl-1-hydroxy-2-aminoethane structures (I) bear certain substituents at the phenyl 4- or 3,4-position and an isopropyl grouping on the amine head (1). 1-(3,4-Dichlorophenyl)-1-hydroxy-2-isopropylaminoethane (2) (II), 1-(2-naphthyl)-1-hydroxy-2-isopropylaminoethane (pronethalol) (3, 4) (III), and 1-(4-nitrophenyl)-1-hydroxy-2-isopropylaminoethane (5) (IV) are well-known examples.

In vitro hydrolysis of 1-aryl-1-chloro-2-aminoethanes to 1-aryl-1-hydroxy-2-aminoethanes was used to prepare a series of 1-chloro-2-aminoethanes related to III (6, 7).

0022-3549/79/0600-0776$01.00/0

© 1979, American Pharmaceutical Association

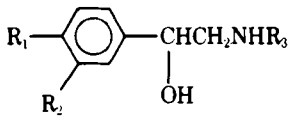

I: $R_1 = R_2 = R_3 = H$
II: $R_1 = R_2 = Cl$, $R_3 = CH(CH_3)_2$
III: R_1 and R_2 = parts in naphthalene ring, $R_3 = CH(CH_3)_2$
IV: $R_1 = NO_2$, $R_2 = H$, $R_3 = CH(CH_3)_2$

Their β-adrenergic blockade was concordant with that given by their corresponding 1-hydroxy-2-aminoethanes, thus proving the presumed *in vivo* hydrolysis. β-Adrenergic blockade studies on compounds possessing other phenyl or substituted phenyl groupings on the I aromatic function were unreported. Interest in new biphenyl derivatives (8) prompted the synthesis and subsequent pharmacological testing of some 1-biphenylyl-2-aminoethane (V) derivatives. The present investigation describes the preparation and preliminary biological evaluation of 1-(4-biphenylyl)-1-hydroxy-2-aminoethanes (VI) and their corresponding 1-chloro analogs (VII).

RESULTS AND DISCUSSION

Chemistry—Halohydrin amination and aminomethyl ketone reduction and/or reductive alkylation using any previously reported conditions (9), were unreliable for production of VI. The present work is confined to the reduction and reductive alkylation approaches using sodium borohydride. In this respect, the observed differences in reactivities for the various aryl aminomethyl ketones is believed to result from a shift in the keto–enol equilibrium that should exist at pH 8 (Scheme I) and which might be due to the aromatic function resonance contribution.

The most pronounced effect was given by the biphenylyl radical; its aminomethyl ketone could exist almost entirely as the enol (X). The latter would be converted completely to the enolate anion (XI) at pH > 8, leading to decomposition demonstrated by a darkening in the solution color. The predominance of X at pH 8 was substantiated by primary aminomethyl ketone stability at such a pH and by the failure of 4-biphenylyl aminomethyl ketone hydrochloride (XIII) acetylation at pH > 8.

These observations also were supported by the similarity in chemical behavior between derivatives of 2-aminophenol and X. The most important properties were the ability of both groups to undergo diazotization (10) and to give the characteristic phenol ferric chloride test. The enol form of the secondary aminomethyl ketone derivative, 4-biphenylyl isopropylaminomethyl ketone (XVI*a*), solubilized in caustic alkali solutions without appreciable decomposition. Moreover, a stable enol form for the secondary amino derivative 4-biphenylyl anilinomethyl ketone (XVI*b*), namely 1-(4-biphenylyl)-1-hydroxy-2-anilinoethene (XVII), could be isolated.

Sodium borohydride ketonic group reduction *via* hydride-ion transfer followed by exchange with the hydroxylic solvent requires reactive borohydride anion production through sodium borohydride alkalinity (11). Such alkalinity ordinarily would not interfere with the reduction if the equilibrium (Scheme I) were shifted toward the keto form (IX); otherwise, an increase in the enol form (X) equilibrium shift would effect the conversion to the enolate anion (XI), resulting in decomposition rather than reduction of the aminomethyl ketone. The latter effect was prominent with XIII due to its relatively strong acidic enol form.

To maintain the medium pH at ≃ 8, polyhydroxy compounds, *e.g.*, glycerol and mannitol, were incorporated into the reaction mixture. Their ability to react with the liberated boric acid from sodium borohydride produced stronger acids. The best reduction medium was methanol–glycerol–water. For reductive alkylation, the produced glyceroboric acid could also catalyze the initial Schiff-base formation step with aldehydes or ketones. Water provided H^+ and OH^- ions necessary for the reaction. The described reductive alkylation procedure was applied successfully with aliphatic and aromatic aldehydes as well as with aliphatic and alicyclic ketones.

The synthesis of VI and VII (Table I) is outlined in Scheme II. The required 4-biphenylylaminomethyl ketones (XVI) were obtained by 4-biphenylylbromomethyl ketone amination (XII) (12). The primary aminomethyl ketone (XIII) key intermediate was prepared by reacting XII with hexamine in carbon tetrachloride followed by hydrolysis of the separated adduct. Treatment of a cooled aqueous XIII suspension with acetic anhydride and sodium acetate afforded the 4-biphenylylacetamidomethyl ketone (XIV).

The unexpected strong liability for dehydration of XIV to 5-(4-biphenylyl)-2-methyloxazole (XV) was seen upon treatment with aluminum isopropoxide in isopropanol under the usual Meerwein–Ponndorf–Verley reduction conditions. Unequivocal synthesis of XV was achieved by refluxing a XIV solution in acetic anhydride. The described reduction and reductive alkylation processes were applied for the preparation of the different 1-(4-biphenylyl)-1-hydroxy-2-aminoethanes (VI)

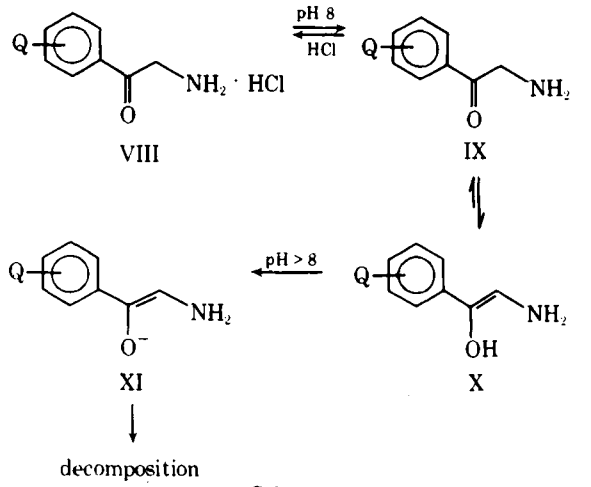

Scheme I

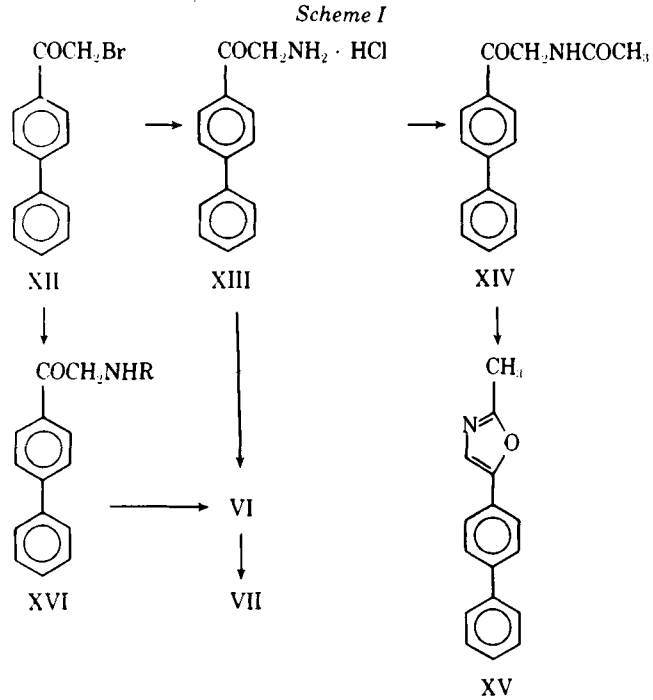

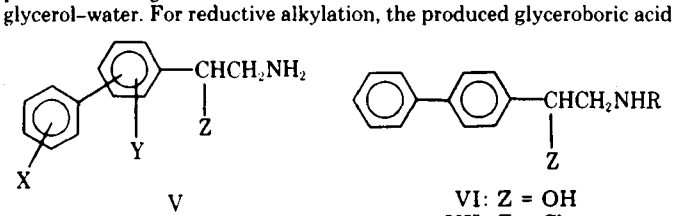

V

VI: Z = OH
VII: Z = Cl

Scheme II

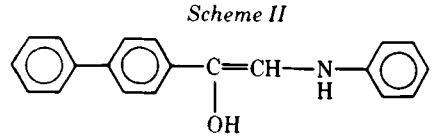

XVII

Table I—1-(4-Biphenylyl)-1-hydroxy-2-aminoethanes (VI) and 1-(4-Biphenylyl)-1-chloro-2-aminoethanes (VII)

Compound	Z	R	Method	Yield, %	Melting Point[a]	Formula	Analysis, %	Calc.	Found
VI*a*	OH	H	C	90	234–236° dec.	$C_{14}H_{16}ClNO$[b,c]	C	67.3	67.2
							H	6.5	6.6
							Cl	14.2	14.2
							N	5.6	5.6
VI*b*	OH	$CH(CH_3)_2$	C, D[d]	89, 84	200–202°[e]	$C_{17}H_{22}ClNO$[b,f]	C	70.0	69.9
							H	7.6	7.2
							Cl	12.2	12.4
							N	4.8	4.6
VI*c*	OH	$CH_2CH(CH_3)_2$	D[g]	81	223–225°	$C_{18}H_{24}ClNO$[b]	C	70.7	70.4
							H	7.9	7.7
							Cl	11.6	11.2
							N	4.6	5.0
VI*d*	OH	$CH(CH_3)CH_2CH_3$	D[h]	72	212–214°	$C_{18}H_{24}BrNO$[i]	C	61.7	61.7
							H	6.9	6.6
							Br	22.8	23.2
							N	4.0	3.8
VI*e*	OH	$CH_2C_6H_5$	D[j]	68	245–247°	$C_{21}H_{22}ClNO$[b]	C	74.2	74.4
							H	6.5	6.4
							Cl	10.4	10.6
							N	4.1	4.5
VI*f*	OH	C_6H_{11}[k]	D[l]	74	245–247° dec.	$C_{20}H_{26}ClNO$[b]	C	72.4	72.0
							H	7.9	7.8
							Cl	10.7	10.5
							N	4.2	4.5
VII*a*	Cl	H	E	68	195–196° dec.	$C_{14}H_{15}Cl_2N$[b]	C	62.7	62.3
							H	5.6	5.2
							Cl	26.4	26.4
							N	5.2	5.0
VII*b*	Cl	$CH(CH_3)_2$	E	73	209–211°	$C_{17}H_{21}Cl_2N$[b]	C	65.8	65.9
							H	6.8	6.5
							Cl	22.9	23.1
							N	4.5	4.5
VII*c*	Cl	$CH_2CH(CH_3)_2$	E	70	173–175° dec.	$C_{18}H_{23}Cl_2N$[b]	C	66.7	67.0
							H	7.1	7.1
							Cl	21.9	22.2
							N	4.3	4.6
VII*d*	Cl	$CH(CH_3)CH_2CH_3$	E	65	170–172° dec.	$C_{18}H_{23}Cl_2N$[b]	C	66.7	66.6
							H	7.1	7.1
							Cl	21.9	22.2
							N	4.3	4.0
VII*e*	Cl	$CH_2C_6H_5$	E	54	174–176° dec.	$C_{21}H_{21}Cl_2N$[b]	C	70.4	70.2
							H	5.9	6.0
							Cl	19.8	20.2
							N	3.9	3.5
VII*f*	Cl	C_6H_{11}[k]	E	78	199–201° dec.	$C_{20}H_{25}Cl_2N$[b]	C	68.6	68.4
							H	7.2	7.5
							Cl	20.2	19.9
							N	4.0	3.8

[a] Recrystallization was done from methanol–ethyl acetate. [b] Hydrochloride. [c] Lit. (16) mp 209–211° dec. [d] Acetone was used. [e] Admixture of the products obtained by Methods C and D showed no melting-point depression. [f] Lit. (16) mp 175–177°. [g] Isobutyraldehyde was used. [h] Methyl ethyl ketone was used. [i] Hydrobromide. [j] Benzaldehyde was used. [k] Cyclohexyl. [l] Cyclohexanone was used.

from XIII and XVI*a*. The 1-(4-biphenylyl)-1-chloro-2-aminoethanes (VII) were produced by reacting the appropriate VI with thionyl chloride, either in chloroform or benzene (6). Structures were confirmed by IR and PMR studies.

Pharmacology—Compounds VI*a*–VI*f* and VII*a*–VII*f* were tested for cardiovascular activity on an anesthetized dog blood pressure preparation and isolated toad hearts. β-Adrenoceptor blocking was investigated using isoproterenol as the agonist.

For the anesthetized dog blood pressure method (13), anesthesia was induced by ether inhalation and was maintained by intravenous chloralose–urethan. The compounds were dissolved in water and injected into the femoral vein, and blood pressure was recorded from the carotid artery. The dose levels were 3×10^{-5} and 15×10^{-4} mole/kg. Each biphenylylhydroxyaminoethane and its chloro analog (VI*b* and VII*b*) gave the same type and magnitude of biological activity. No hypotensive effect was observed for the primary amine derivatives (VI*a* and VII*a*).

Table II compares the hypotensive effects obtained for VI*b*–VI*f* and VII*b*–VII*f*. With the exception of the cyclohexylamino derivatives (VI*f* and VII*f*), the hypotensive effects for all other *N*-substituted analogs (VI*b*–VI*e* and VII*b*–VII*e*) were not antagonized by pronethalol. On the other hand, they antagonized the epinephrine agonist effect in the order isopropylamino (VI*b* and VII*b*) > benzylamino (VI*e* and VII*e*) > *sec*-butylamino (VI*c* and VII*c*) > isobutylamino (VI*d* and VII*d*) derivatives.

Compounds VI*b* and VII*b* did not display any isoproterenol antagonism. The other *N*-substituted analogs (VI*c*–VI*f* and VII*c*–VII*f*) exhibited isoproterenol antagonism of the order cyclohexylamino (VI*f* and VII*f*) > benzylamino (VI*e* and VII*e*) ≫ *sec*-butylamino (VI*c* and VII*c*) > isobutylamino (VI*d* and VII*d*) derivatives. In all cases, gradual β-blockade onset was observed. Table II indicates that VI*b* and VII*b* might possess α-adrenoceptor blocking activity whereas VI*e*, VI*f*, VII*e*, and VII*f* revealed significant β-adrenoceptor blockades.

For the isolated toad heart method (14), the doses were 3×10^{-5} and 3×10^{-4} mole/ml. The experiments showed hypotensive effects for all tested compounds. This effect could not be blocked by atropine (3×10^{-5} mole/ml) and thus indicated direct myocardial depression. Isoproterenol antagonism, *i.e.*, β-blockade, was only exhibited by VI*e* and VII*e* and VI*f* and VII*f* analogs. The most pronounced effect was produced by VI*f* and VII*f*.

EXPERIMENTAL[1]

4-Biphenylylaminomethyl Ketone Hydrochloride (XIII)—A hot suspension of hexamine (9.8 g, 0.07 mole) in carbon tetrachloride (100 ml) was gradually added to a hot stirred XII solution (13.8 g, 0.05 mole) in carbon tetrachloride (50 ml). The reaction mixture was stirred for 1.5

[1] IR spectra were determined on a Unicam SP 200 spectrophotometer with Nujol mulls. PMR spectra were determined on a Perkin-Elmer R 12 spectrometer with tetramethylsilane as the internal standard. Melting points were determined in open glass capillaries and are uncorrected. Microanalyses were performed by the Microanalytical Unit, Faculty of Science, University of Cairo, Cairo, Egypt.

Table II—Comparison of the Hypotensive Effects[a] of VIb–VIf and VIIb–VIIf Using the Anesthetized Dog Blood Pressure Method

Compound[b,c]	Mean Percent Reduction[d] of Agonist Response ± SE: Epinephrine[b] Antagonism	Isoproterenol[e] Antagonism
VIb	23.33 ± 0.83	—
VIc	11.70 ± 1.18	10.83 ± 0.94
VId	10.00 ± 1.44	6.66 ± 0.83
VIe	13.33 ± 0.83	49.33 ± 2.24
VIf[f]	—	67.50 ± 1.44
VIIb	21.70 ± 1.67	—
VIIc	10.83 ± 0.83	10.00 ± 1.03
VIId	9.16 ± 1.66	6.00 ± 0.76
VIIe	12.50 ± 1.44	47.50 ± 1.44
VIIf[f]	—	64.17 ± 0.83

[a] Not antagonized by pronethalol (3×10^{-5} mole/kg). [b] The dose used was 15×10^{-4} mole/kg. [c] Aqueous solutions were used. [d] Average of three experiments. [e] The dose was 3×10^{-5} mole/kg. [f] The hypotensive effect was antagonized by pronethalol (3×10^{-5} mole/kg).

hr. It was then refluxed for 1 hr, cooled, diluted with acetone (50 ml), and filtered. The crude adduct, 4-biphenylylhexamethylene tetraammonium methyl ketone bromide, was triturated with cold ethanol, filtered, and dried in air. The yield was 17.5 g (84%), mp 162°.

Hydrolysis of the adduct (12.5 g, 0.03 mole) was affected by brief heating on a water bath with ethanol (50 ml) and concentrated hydrochloric acid (9 ml). The reaction mixture was treated with 10% HCl dropwise until turbidity appeared. It was then decolorized by boiling with charcoal, filtered, concentrated *in vacuo*, and left to crystallize. The product was recrystallized from 10% HCl to yield 5.6 g (74%) of product, mp > 300°; IR: 3000 (b, NH_3^+) and 1680 (C=O) cm^{-1}.

Anal.—Calc. for $C_{14}H_{14}ClNO$: C, 67.8; H, 5.7; Cl, 14.4; N, 5.6. Found: C, 67.4; H, 5.8; Cl, 14.0; N, 5.3.

4-Biphenylylacetamidomethyl Ketone (XIV)—Acetic anhydride (3.1 g, 0.03 mole) was added, in one portion, to a XIII suspension (3.7 g, 0.015 mole) in water (25 ml) and crushed ice (50 g). The mixture was treated dropwise, while being stirred, with a sodium acetate solution (5 g, 0.06 mole) in water (20 ml) at a rate such that the temperature was not allowed to rise above 5°. The reaction mixture was allowed to reach room temperature and was treated with 10% HCl (20 ml).

The product was filtered, washed with water several times, dried, and recrystallized from benzene–petroleum ether (bp 40–60°). The yield was 2.6 g (71%), mp 164–166° [lit. (15) mp 151°]; IR: 3400 (NH), 1685 (C=O), and 1645, 1550, and 1295 (amide I, II, and III, respectively) cm^{-1}.

Anal.—Calc. for $C_{16}H_{15}NO_2$: C, 75.9; H, 6.0; N, 5.4. Found: C, 75.7; H, 5.9; N, 5.3.

5-(4-Biphenylyl)-2-methyloxazole (XV)—*Method A*—Under strictly anhydrous conditions, a stirred mixture of XIV (1.2 g, 0.005 mole) and an aluminum isopropoxide solution (1.5 g, 0.0075 mole) in dry isopropanol (50 ml) was heated at 90° in a 100-ml flat-bottom flask. The flask was fitted with a reflux air condenser and an upper distillation head, which was attached to a downside condenser connected to a water pump *via* a buchner receiver. The reaction mixture was distilled slowly, at a rate not exceeding 7–10 drops/min at 40 mm Hg. No acetone was detected in the distillate collected during 1.5 hr.

The residue was cooled, and the remaining complex was treated with crushed ice. The mixture was extracted with benzene, washed with water, dried over anhydrous sodium sulfate, and filtered; then the solvent was removed *in vacuo*. The product was recrystallized from benzene–petroleum ether (bp 40–60°) to yield 0.9 g (76%), mp 167°.

Method B—A mixture of XIV (1.2 g, 0.005 mole) and acetic anhydride (20 g, 0.2 mole) was refluxed for 30 min. The reaction mixture was concentrated *in vacuo* to a small volume and then treated with crushed ice. The medium was made alkaline with sodium carbonate, and the product was filtered, washed with water, dried, and recrystallized from benzene–petroleum ether (bp 40–60°). The yield was 0.95 g (80%), mp 167°.

Admixture of the products obtained by Methods A and B showed no melting-point depression; IR: 1670 (C=N) and 1240 (aromatic C–O–C) cm^{-1}.

Anal.—Calc. for $C_{16}H_{13}NO$: C, 81.7; H, 5.6; N, 6.0. Found: C, 82.0; H, 5.2; N, 6.0.

4-Biphenylylisopropylaminomethyl Ketone (XVIa) Hydrochloride—A solution of isopropylamine (0.59 g, 0.01 mole) in carbon tetrachloride (20 ml) was gradually added, with stirring, to a solution of XII (2.8 g, 0.01 mole) in carbon tetrachloride (20 ml) at 0°. The stirring was maintained for an additional 2 hr. The reaction mixture was refluxed for 30 min, cooled, and extracted with 5 *N* NaOH. The alkaline extract was washed twice with benzene and made strongly acidic with concentrated hydrochloric acid. The product was filtered, washed with acetone, and recrystallized from methanol–ethyl acetate. The yield was 0.5 g (17%); IR: 2750 (NH_2^+) and 1680 (C=O) cm^{-1}.

Anal.—Calc. for $C_{17}H_{20}ClNO$: C, 70.4; H, 6.9; Cl, 12.2; N, 4.9. Found: C, 70.2; H, 6.6; Cl, 12.5; N, 4.5.

4-Biphenylylanilinomethyl Ketone (XVIb) and 1-(4-Biphenylyl)-1-hydroxy-2-anilinoethene (XVII)—A solution of aniline (0.93 g, 0.01 mole) in carbon tetrachloride (20 ml) was gradually added, with stirring, to a solution of XII (2.8 g, 0.01 mole) in carbon tetrachloride (20 ml) at 0°. The stirring was maintained for an additional 2 hr. The reaction mixture was refluxed for 30 min, cooled, and shaken with 5 *N* NaOH (20 ml). The carbon tetrachloride layer was washed twice with water and dried over anhydrous sodium sulfate, and the solvent was removed *in vacuo*.

The residue was boiled with methanol and filtered. From the methanolic extract, XVIb was crystallized out as colorless needles to yield 0.3 g (10%), mp 125–128°. The methanol-insoluble fraction was recrystallized from acetone as bright-yellow flakes (XVII) to yield 2.1 g (70%), mp 185–186°. The colorless XVIb changed to the yellow XVII within 84 hr at room temperature; IR (XVIb): 3390 (C=O) cm^{-1}; IR (XVII): 3410 (NH) and 3100 (b, OH) cm^{-1}; PMR (XVII, $CDCl_3$): δ 4.60 (s, 1H, OH), 4.90 (b, 1H, NH), 7.20 (m, 1H, CH), and 8.10 (m, 14H, aromatic) ppm.

Anal.—Calc. for $C_{20}H_{17}NO$: C, 83.6; H, 6.0; N, 4.9. Found: C, 83.3; H, 6.1; N, 4.8.

1-(4-Biphenylyl)-1-hydroxy-2-aminoethanes—*Method C (VIa and VIb)*—Sodium borohydride (0.95 g, 0.025 mole) was added in portions during 1.5 hr to a 0° cooled and stirred mixture of the appropriate 4-biphenylylaminomethyl ketone (XIII and XVIa, 0.01 mole), glycerol (23 g, 0.25 mole), water (2 ml), and methanol (100 ml). Cooling and stirring were maintained for 3 hr, and the reaction mixture was stirred at room temperature for a further 15 hr. It was then treated with concentrated hydrochloric acid dropwise until just acidic to litmus, concentrated *in vacuo*, and made strongly alkaline with 5 *N* NaOH. The product was extracted with benzene, washed twice with water, dried over anhydrous sodium sulfate, and filtered. Dry hydrogen chloride gas was bubbled into the filtrate, and the separated salt was collected and recrystallized.

Method D (VIb–VIf)—Sodium borohydride (1.4 g, 0.036 mole) was added in portions during 1.5 hr to a 0° cooled and stirred mixture of XIII (2.75 g, 0.01 mole), the proper aldehyde or ketone (0.1 mole), glycerol (33.2 g, 0.36 mole), water (2 ml), and methanol (100 ml). The reaction mixture was worked up as detailed under *Method C*, and the appropriate salt was prepared in the usual manner and recrystallized; IR (VIa–VIf): 3350–3300 (OH) and 2500–2400 (with several splits, NH_2^+) cm^{-1}; PMR (VIb, CD_3OD–$CDCl_3$): δ 1.35 (d, 6H, $2CH_3$ of isopropyl), 3.10 (m, 2H, methylene), 3.40 (m, 1H, CH of isopropyl), 5.15 (m, 1H, CH), 6.85 (b, 1H, OH), 7.45 (m, 9H, aromatic), and 8.15 (b, 1H, NH) ppm.

1-(4-Biphenylyl)-1-chloro-2-aminoethanes (VII)—*Method E*—Thionyl chloride (2.4 g, 0.02 mole) was added dropwise to a stirred suspension of the proper VI (0.01 mole) in either chloroform or benzene (75 ml). The reaction mixture was refluxed for 1.5 hr, and the solvent was removed *in vacuo*. The residue was recrystallized.

REFERENCES

(1) P. Somani, R. T. Bachand, Jr., W. Murmann, and L. Almirante, *J. Med. Chem.*, **9**, 823 (1966).

(2) C. E. Powell and I. H. Slater, *J. Pharmacol. Exp. Ther.*, **122**, 480 (1958).

(3) J. W. Black and J. S. Stephenson, *Lancet*, **2**, 311 (1962).

(4) P. Somani, H. F. Hardman, and B. K. B. Lum, *Pharmacologist*, **5**, 260 (1963).

(5) P. Somani and B. K. B. Lum, *J. Pharmacol. Exp. Ther.*, **147**, 194 (1965).

(6) R. Howe, *J. Med. Chem.*, **13**, 398 (1970).

(7) F. Wolfheim, *Chem. Ber.*, **47**, 1440 (1914).

(8) R. M. Shafik, R. Soliman, and A. M. M. Hassan, *J. Pharm. Sci.*, **67**, 991 (1978).

(9) R. Howe, A. F. Crowther, J. S. Stephenson, B. S. Rao, and L. H. Smith, *J. Med. Chem.*, **11**, 1000 (1968).

(10) W. A. Skinner, H. F. Gram, C. W. Mosher, and B. R. Baker, *J. Am. Chem. Soc.*, **81**, 4639 (1959).

(11) H. O. House, "Modern Synthetic Reactions," Benjamin, New York, N.Y., 1965, p. 24.

(12) N. L. Drake and J. Bronitsky, *J. Am. Chem. Soc.*, **52**, 3715 (1930).
(13) J. W. Black, W. A. M. Dungan, and R. G. Shanks, *Br. J. Pharmacol.*, **25**, 577 (1965).
(14) J. H. Gaddum, "Pharmacology," 5th ed., Oxford University Press, London, England, 1959, p. 296.
(15) E. D. Sych, *Ukr. Khim. Zh.*, **22**, 217 (1956); through *Chem. Abstr.*, **51**, 372h (1957).
(16) J. Sam, K. Aparajithan, and R. Shafik, *J. Pharm. Sci.*, **57**, 567 (1968).

ACKNOWLEDGMENTS

The authors are grateful to Mr. Shaker A. Mousa, Department of Pharmacology, Faculty of Pharmacy, University of Alexandria, Alexandria, A. R. Egypt, for the pharmacological examinations.

Modified USP Assay for Simultaneous Determination of Aspirin and Nonaspirin Salicylates in Aspirin and Buffered Aspirin Tablets

JOSEPH R. LUBER ˣ, ANTHONY J. VISALLI, and DAHYABHAI M. PATEL

Received October 6, 1978, from the *Analytical and Physical Chemistry Department, Research and Development Division, William H. Rorer, Inc., Fort Washington, PA 19034.* Accepted for publication December 14, 1978.

Abstract □ Modified USP procedures are described for the simultaneous determination of nonaspirin salicylates and aspirin in aspirin and buffered aspirin tablets. The existing USP procedures are not stability indicating for intact aspirin when significant levels of nonaspirin salicylates are present, as is often the case in short-term, high temperature stability programs. The modified procedures yield considerably shorter analysis times and stability-indicating assays for intact aspirin without the need for sophisticated equipment other than that presently required by USP XIX.

Keyphrases □ Aspirin—analysis, modified USP method, liquid chromatography, spectrophotometry, stability, buffered and unbuffered tablets □ Liquid chromatography—analysis, aspirin in buffered and unbuffered tablets, modified USP method, stability □ Analgesics—aspirin, analysis, buffered and unbuffered tablets, modified USP method, liquid chromatography, spectrophotometry, stability

The USP methods (1) for the quantitative determination of aspirin and nonaspirin salicylates in aspirin and buffered aspirin tablets are time consuming and nonspecific for evaluation of intact aspirin stability. The aspirin assay is based mainly on the work of Levine (2). A sample preparation in chloroform is passed through a sodium bicarbonate-treated, infusorial earth-packed column, which separates aspirin from tablet excipients. Following its elution, the aspirin is quantitated spectrophotometrically.

Although the method is reliable for production control, its accuracy as a stability-indicating assay is questionable because it does not isolate aspirin from its degradation product salicylic acid. Since the bicarbonate column concurrently traps both aspirin and salicylic acid, the result of their simultaneous elution is a positive interference in the aspirin UV absorption at 280 nm.

Another weakness in the USP method is that separate procedures are required for the aspirin and nonaspirin salicylates assays; hence, the complete analysis of aspirin tablets is quite lengthy. The USP nonaspirin salicylates assay is based on several studies (3–7). A sample is triturated in chloroform in the presence of citric acid monohydrate. Insoluble salts of aspirin or salicylic acid, if present, are converted to chloroform-extractable free acids by hydrochloric acid. Finally, the salicylic acid is separated from aspirin using an infusorial earth column treated with ferric chloride and urea, which complexes salicylic acid. The salicylic acid is eluted and quantitated spectrophotometrically.

This paper reports a modified USP method that simultaneously determined aspirin and nonaspirin salicylates in aspirin and buffered aspirin dosage forms. Complexing the nonaspirin salicylates on a ferric chloride–urea infusorial earth column and collecting the intact aspirin eluate achieved effective separation. Aspirin in the eluate was determined spectrophotometrically. The complexed nonaspirin salicylates were eluted and likewise determined spectrophotometrically. The results of this modification were a considerably shorter analysis time, a stability-indicating assay for aspirin, and a method that could be performed without sophisticated equipment other than that already required by the USP.

EXPERIMENTAL

Reagents and Chemicals—All chemicals and reagents were USP or ACS grade and were used without further purification.

Aspirin Tablet Assay—*Chromatographic Column*—A column was packed as described under the nonaspirin salicylates procedure in the USP. It was washed with a 25-ml portion of chloroform.

Aspirin Standard Preparation—About 50 mg of USP aspirin reference standard, accurately weighed, was dissolved in glacial acetic acid–chloroform (1:99) and diluted to 50 ml in a volumetric flask. A 5.0-ml portion was transferred to a 100-ml volumetric flask containing 2.0 ml of methanol, diluted to volume with glacial acetic acid–chloroform, and mixed.

Salicylic Acid Standard Preparation—A suitable, accurately weighed, quantity of salicylic acid was dissolved in chloroform to obtain a solution containing 30 μg of salicylic acid/ml. A 5.0-ml portion was transferred

Table I—Recovery of Added Aspirin (50.00 mg) by USP Procedure

Salicylic Acid Added, mg	Aspirin Recovered, mg	Recovery, %
0.00	50.00	100.0
0.75	50.35	100.7
1.50	50.95	101.9
2.25	51.50	103.0
3.00	52.10	104.2

0022-3549/79/0600-0780$01.00/0
© 1979, American Pharmaceutical Association

(12) N. L. Drake and J. Bronitsky, *J. Am. Chem. Soc.*, **52**, 3715 (1930).
(13) J. W. Black, W. A. M. Dungan, and R. G. Shanks, *Br. J. Pharmacol.*, **25**, 577 (1965).
(14) J. H. Gaddum, "Pharmacology," 5th ed., Oxford University Press, London, England, 1959, p. 296.
(15) E. D. Sych, *Ukr. Khim. Zh.*, **22**, 217 (1956); through *Chem. Abstr.*, **51**, 372h (1957).
(16) J. Sam, K. Aparajithan, and R. Shafik, *J. Pharm. Sci.*, **57**, 567 (1968).

ACKNOWLEDGMENTS

The authors are grateful to Mr. Shaker A. Mousa, Department of Pharmacology, Faculty of Pharmacy, University of Alexandria, Alexandria, A. R. Egypt, for the pharmacological examinations.

Modified USP Assay for Simultaneous Determination of Aspirin and Nonaspirin Salicylates in Aspirin and Buffered Aspirin Tablets

JOSEPH R. LUBER ˣ, ANTHONY J. VISALLI, and DAHYABHAI M. PATEL

Received October 6, 1978, from the *Analytical and Physical Chemistry Department, Research and Development Division, William H. Rorer, Inc., Fort Washington, PA 19034.* Accepted for publication December 14, 1978.

Abstract □ Modified USP procedures are described for the simultaneous determination of nonaspirin salicylates and aspirin in aspirin and buffered aspirin tablets. The existing USP procedures are not stability indicating for intact aspirin when significant levels of nonaspirin salicylates are present, as is often the case in short-term, high temperature stability programs. The modified procedures yield considerably shorter analysis times and stability-indicating assays for intact aspirin without the need for sophisticated equipment other than that presently required by USP XIX.

Keyphrases □ Aspirin—analysis, modified USP method, liquid chromatography, spectrophotometry, stability, buffered and unbuffered tablets □ Liquid chromatography—analysis, aspirin in buffered and unbuffered tablets, modified USP method, stability □ Analgesics—aspirin, analysis, buffered and unbuffered tablets, modified USP method, liquid chromatography, spectrophotometry, stability

The USP methods (1) for the quantitative determination of aspirin and nonaspirin salicylates in aspirin and buffered aspirin tablets are time consuming and nonspecific for evaluation of intact aspirin stability. The aspirin assay is based mainly on the work of Levine (2). A sample preparation in chloroform is passed through a sodium bicarbonate-treated, infusorial earth-packed column, which separates aspirin from tablet excipients. Following its elution, the aspirin is quantitated spectrophotometrically.

Although the method is reliable for production control, its accuracy as a stability-indicating assay is questionable because it does not isolate aspirin from its degradation product salicylic acid. Since the bicarbonate column concurrently traps both aspirin and salicylic acid, the result of their simultaneous elution is a positive interference in the aspirin UV absorption at 280 nm.

Another weakness in the USP method is that separate procedures are required for the aspirin and nonaspirin salicylates assays; hence, the complete analysis of aspirin tablets is quite lengthy. The USP nonaspirin salicylates assay is based on several studies (3–7). A sample is triturated in chloroform in the presence of citric acid monohydrate. Insoluble salts of aspirin or salicylic acid, if present, are converted to chloroform-extractable free acids by hydrochloric acid. Finally, the salicylic acid is separated from aspirin using an infusorial earth column treated with ferric chloride and urea, which complexes salicylic acid. The salicylic acid is eluted and quantitated spectrophotometrically.

This paper reports a modified USP method that simultaneously determined aspirin and nonaspirin salicylates in aspirin and buffered aspirin dosage forms. Complexing the nonaspirin salicylates on a ferric chloride–urea infusorial earth column and collecting the intact aspirin eluate achieved effective separation. Aspirin in the eluate was determined spectrophotometrically. The complexed nonaspirin salicylates were eluted and likewise determined spectrophotometrically. The results of this modification were a considerably shorter analysis time, a stability-indicating assay for aspirin, and a method that could be performed without sophisticated equipment other than that already required by the USP.

EXPERIMENTAL

Reagents and Chemicals—All chemicals and reagents were USP or ACS grade and were used without further purification.

Aspirin Tablet Assay—*Chromatographic Column*—A column was packed as described under the nonaspirin salicylates procedure in the USP. It was washed with a 25-ml portion of chloroform.

Aspirin Standard Preparation—About 50 mg of USP aspirin reference standard, accurately weighed, was dissolved in glacial acetic acid–chloroform (1:99) and diluted to 50 ml in a volumetric flask. A 5.0-ml portion was transferred to a 100-ml volumetric flask containing 2.0 ml of methanol, diluted to volume with glacial acetic acid–chloroform, and mixed.

Salicylic Acid Standard Preparation—A suitable, accurately weighed, quantity of salicylic acid was dissolved in chloroform to obtain a solution containing 30 μg of salicylic acid/ml. A 5.0-ml portion was transferred

Table I—Recovery of Added Aspirin (50.00 mg) by USP Procedure

Salicylic Acid Added, mg	Aspirin Recovered, mg	Recovery, %
0.00	50.00	100.0
0.75	50.35	100.7
1.50	50.95	101.9
2.25	51.50	103.0
3.00	52.10	104.2

0022-3549/79/0600-0780$01.00/0
© 1979, American Pharmaceutical Association

Table II—Statistical Evaluation

Determination	Aspirin Tablet Procedure: Recovered Aspirin, %	Aspirin Tablet Procedure: Recovered Nonaspirin Salicylates, %	Buffered Aspirin Tablet Procedure: Recovered Aspirin, %	Buffered Aspirin Tablet Procedure: Recovered Nonaspirin Salicylates, %
1	100.2	100.9	99.97	99.30
2	100.8	100.5	99.80	99.07
3	99.44	100.5	99.75	100.2
4	100.2	100.5	100.2	98.14
5	100.3	100.5	99.98	97.44
6	99.97	100.0	99.50	99.54
Mean	100.2	100.5	99.87	98.95
SD	±0.537	±0.356	±0.276	±1.090
Precision, %	±0.54	±0.35	±0.28	±1.10

to a 100-ml volumetric flask containing 20.0 ml of methanol, 5 drops of concentrated hydrochloric acid, and 20.0 ml of a 1:9 solution of glacial acetic acid in water-saturated ether. Chloroform was added to volume and mixed.

Assay Preparation—A quantity of finely ground tablets equivalent to 50 mg of aspirin was weighed accurately in a 50-ml beaker. Then 10 ml of chloroform was added, and the beaker was swirled for 3 min. The entire sample was transferred onto the chromatographic column.

Procedure—Without delay, the beaker and column were washed, in portions, with 90 ml of chloroform. The washings were collected in a 100-ml volumetric flask containing 1.0 ml of glacial acetic acid, diluted to volume with chloroform, and mixed. A 10.0-ml portion was transferred to a 100-ml volumetric flask containing 1.0 ml of glacial acetic acid and 2.0 ml of methanol. Chloroform was added to volume and mixed. The absorbances of the assay preparation and the aspirin standard preparation were determined at 278 nm in 1-cm cells *versus* chloroform as the blank.

To the column containing the ferric–salicylate complex was added 20.0 ml of a 1:9 solution of glacial acetic acid in water-saturated ether, followed by 60 ml of chloroform. The eluate was collected in a 100-ml volumetric flask containing 20.0 ml of methanol and 5 drops of concentrated hydrochloric acid. Chloroform was added to volume and mixed. The absorbances of the assay preparation and the salicylic acid standard preparation were determined at 306 nm in 5-cm cells *versus* a blank of the same solvent composition as that of the salicylic acid standard preparation.

Calculations—The quantity, in milligrams, of aspirin per tablet was calculated as follows:

$$\text{mg of aspirin/tablet} = \frac{C(A_u/A_s)(A.W.)}{W} \qquad \text{(Eq. 1)}$$

where C is the concentration, in micrograms of aspirin per milliliter, in the standard preparation; A_u and A_s are the absorbances of the assay preparation and the standard preparation at 278 nm, respectively; $A.W.$ is the average tablet weight; and W is the weight of sample in the assay preparation.

The quantity, in milligrams, of salicylic acid per tablet was calculated as follows:

$$\text{mg of salicylic acid/tablet} = \frac{C(A_u/A_s)(A.W.)}{W} \qquad \text{(Eq. 2)}$$

where C is the concentration, in milligrams of salicylic acid per 100 ml, in the standard preparation; A_u and A_s are the absorbances of the assay preparation and the standard preparation at 306 nm, respectively; $A.W.$ is the average tablet weight; and W is the weight of sample in the assay preparation.

Buffered Aspirin Tablet Assay—*Chromatographic Column*—The column was prepared as directed under *Aspirin Tablet Assay*.

Aspirin Standard Preparation and Salicylic Acid Standard Preparation—These standards were prepared as directed under *Aspirin Tablet Assay* except that the concentrations were doubled.

Table III—Effect of Methanol on Aspirin Assay

Methanol Added, ml	Wavelength Maximum, nm	Absorbance
0.0	279	0.802
2.0	278	0.740
6.0	277	0.702
10.0	276	0.690

Table IV—Assay Results on Commercial Aspirin Tablets

Product	Aspirin, %: Modified Method	Aspirin, %: USP Method	Nonaspirin Salicylates, %: Modified Method	Nonaspirin Salicylates, %: USP Method
A	99.2	99.4	0.09	0.05
B	99.9	99.5	0.10	0.09
C	100.2	99.6	0.07	0.07
D	98.1	98.6	0.04	0.06
E	100.1	100.7	0.04	0.04

Assay Preparation—A quantity of finely ground tablets equivalent to 100 mg of aspirin was weighed accurately in a 50-ml beaker. About 700 mg of citric acid monohydrate and 40 ml of chloroform were added, and the beaker was swirled for 1 min. The mixture was filtered through coarse filter paper into a 200-ml volumetric flask. The beaker and filter paper were rinsed with two 25-ml portions of chloroform, and the rinsings were collected in the volumetric flask.

The filter paper was allowed to dry, and the residue was transferred to a 125-ml separator containing 10 ml of 1 *N* HCl. It was then extracted with two 25-ml portions of chloroform and passed through nonabsorbent cotton into the 200-ml volumetric flask. Chloroform was added to volume and mixed.

Procedure—A 20.0-ml portion of the assay preparation was transferred onto the chromatographic column, and, without delay, the column was washed in portions with 90 ml of chloroform. The washings were collected in a 100-ml volumetric flask containing 1.0 ml of glacial acetic acid and 2.0 ml of methanol, diluted to volume with chloroform, and mixed. The absorbances of the assay preparation and the aspirin standard preparation were determined at 278 nm in 1-cm cells *versus* chloroform as the blank.

The ferric–salicylate complex was eluted from the column, and the absorbance was determined as described under *Aspirin Tablet Assay*.

Calculations—The quantity, in milligrams, of aspirin per tablet was calculated as follows:

$$\text{mg of aspirin/tablet} = \frac{C(A_u/A_s)(10)(A.W.)}{W} \qquad \text{(Eq. 3)}$$

where C is the concentration, in micrograms of aspirin per milliliter, in the standard preparation; A_u and A_s are the absorbances of the assay preparation and the standard preparation at 278 nm, respectively; $A.W.$ is the average tablet weight; and W is the weight of sample in the assay preparation.

The quantity, in milligrams, of salicylic acid per tablet was calculated as follows:

$$\text{mg of salicylic acid/tablet} = \frac{C(A_u/A_s)(10)(A.W.)}{W} \qquad \text{(Eq. 4)}$$

where C is the concentration, in milligrams of salicylic acid per 100 ml, in the standard preparation; A_u and A_s are the absorbances of the assay preparation and the standard preparation at 306 nm, respectively; $A.W.$ is the average tablet weight; and W is the weight of sample in the assay preparation.

RESULTS AND DISCUSSION

Aspirin Recovery by USP Procedure—The interference of salicylic acid with aspirin recovery was studied. Mixtures were prepared in chloroform containing 50.00 mg of aspirin and various amounts of salicylic acid. One milliliter of hydrochloric acid–methanol (1:49) was added to each mixture. The solution was diluted to 50.0 ml with chloroform.

The mixtures were assayed for aspirin content by the USP procedure. As shown in Table I, a positive interference was introduced in the USP aspirin assay, making it nonspecific for stability evaluation of aspirin products.

Table V—Assay Results on Commercial Buffered Aspirin Tablets

Product	Aspirin, %: Modified Method	Aspirin, %: USP Method	Nonaspirin Salicylates, %: Modified Method	Nonaspirin Salicylates, %: USP Method
A	99.4	100.9	0.65	0.64
B	97.1	97.6	0.32	0.37
C	96.6	97.4	0.84	0.82
D	99.2	100.4	0.73	0.73
E	97.3	96.5	0.82	0.82

Linearity of Modified USP Procedure—The linearity for the aspirin tablet and buffered aspirin tablet assays was examined. For the aspirin assay, mixtures of varying amounts of aspirin with 0.15 mg of salicylic acid for the aspirin tablet assay and 3.0 mg of salicylic acid for the buffered aspirin tablet assay were determined. The amounts of salicylic acid added were equivalent to the maximum amount allowed by the USP, assuming sample weights equivalent to 50 and 100 mg of aspirin, respectively. For the nonaspirin salicylates assay, mixtures of varying amounts of salicylic acid with 50 mg of aspirin for the aspirin tablet assay and 100 mg of aspirin for the buffered aspirin assay were determined. The amounts of aspirin added represented the quantity specified in the modified USP procedures.

The aspirin assay was linear in the 0–75- and 0–130-mg ranges for the aspirin tablet assay and the buffered aspirin tablet assay, respectively. The nonaspirin salicylates assay was linear in the 0–0.3- and 0–5.0-mg ranges for the aspirin tablet assay and the buffered aspirin tablet assay, respectively.

Precision of Modified USP Procedures—A statistical evaluation of the precision of the modified methods was performed on the assay results of two sets of six accurately weighed preparations. The sets used contained either ~0.15 mg of salicylic acid and 50 mg of aspirin or 0.30 mg of salicylic acid and 100 mg of aspirin (Table II).

Effects of Methanol on Aspirin Assay—Methanol was used in the modified USP aspirin assay to clarify the column eluate, which was often turbid due to the physical removal of water by chloroform from the chromatographic column. Methanol had to be added accurately to both the assay preparation and the standard preparation since the presence of methanol affected the magnitude of the absorbance and the wavelength maximum of the aspirin peak (Table III). Aspirin was stable in this solvent mixture for at least 6 hr. The absorbance of an aspirin solution at 278 nm after this time was 99.5% of the initial value. After 24 hr, however, the absorbance dropped to 75% of the initial value.

Comparison of Modified USP Assay and USP Assay—The results of studies on several commercially available aspirin and buffered aspirin tablets are summarized in Tables IV and V. The results indicate a good correlation between methods.

REFERENCES

(1) "The United States Pharmacopeia," 19th rev., Mack Publishing Co., Easton, Pa., 1975, p. 39.

(2) J. Levine, *J. Pharm. Sci.*, **50**, 506 (1961).

(3) J. Levine and J. D. Weber, *ibid.*, **57**, 631 (1968).

(4) J. D. Weber and J. Levine, *ibid.*, **55**, 78 (1966).

(5) J. D. Weber, *J. Assoc. Off. Anal. Chem.*, **48**, 1151 (1965).

(6) D. E. Guttman, *J. Pharm. Sci.*, **57**, 1685 (1968).

(7) D. E. Guttman and G. W. Salomon, *ibid.*, **58**, 120 (1969).

Evaluation of Lanolin Alcohol Films and Kinetics of Triamcinolone Acetonide Release

BALASUBRAMANIAN V. IYER and RAVINDRA C. VASAVADA ×

Received June 26, 1978, from the *School of Pharmacy, University of the Pacific, Stockton, CA 95211.* Accepted for publication December 15, 1978.

Abstract □ The film-forming potential of lanolin alcohol was evaluated. Inclusion of ethylcellulose in lanolin alcohol improved film integrity. The hardness and modulus of elasticity of these lanolin alcohol–ethylcellulose films were improved by incorporating propylene glycol or cetyl alcohol. *Triamcinolone acetonide release from selected film compositions was* investigated. The data were analyzed from the viewpoint of the first-order kinetic theory and the release from a planar system having a homogeneous or granular matrix. The results suggest that the drug release follows a diffusion-controlled matrix model and a square root of time release profile. The release rate constants were proportional to drug concentration. Drug release was maximal from a system containing the drug in a near-saturated solution.

Keyphrases □ Lanolin alcohol—films, kinetics of triamcinolone acetonide release, topical dosage forms □ Triamcinolone acetonide—release from lanolin alcohol films, kinetics, topical dosage forms, □ Dosage forms, topical—lanolin alcohol films, kinetics of triamcinolone acetonide release □ Glucocorticoids—triamcinolone acetonide, release from lanolin alcohol films, kinetics

Protective films containing therapeutically active agents have been used for dermatological and surgical applications (1–3). An inert polymeric matrix impregnated with pilocarpine has been utilized to achieve prolonged and steady release of the drug for ocular administration (4). In certain dermatological applications, polymeric films containing a drug could offer advantages over conventional dosage forms. These potential advantages include enhanced therapeutic effect, predictable control over rate and extent of absorption, occlusion of the skin surface, and improved patient acceptance.

Although several polymeric substances have been studied for their film-forming characteristics (5–7) and potential application in topical drug delivery systems, the nonpolymeric, high molecular weight substances apparently have not been investigated. Furthermore, the applicability of this concept to topical drug delivery system design has not been explored fully.

THEORETICAL

Drug release from a planar system having a drug dispersed in a homogeneous insoluble matrix was shown (8) to follow:

$$Q = \sqrt{Dt(2A - C_s)C_s} \qquad \text{(Eq. 1)}$$

where Q is the amount of drug released per unit area at time t, D is the drug diffusion coefficient in the matrix, A is the total amount of drug present in the matrix per unit volume, and C_s is the drug solubility in the matrix. The relationship for release from a planar system having a granular matrix was shown to be (9) diffusion controlled and is given by:

$$Q = \sqrt{\frac{D\epsilon}{\tau}(2A - \epsilon C_s)C_s t} \qquad \text{(Eq. 2)}$$

where D and C_s refer to the diffusion coefficient and drug solubility in the permeating fluid, τ is the tortuosity of the matrix, and ϵ is the porosity of the matrix.

Both these equations describe drug release as being linear with the square root of time:

$$Q = kt^{1/2} \qquad \text{(Eq. 3)}$$

where k is the release rate constant. For a homogeneous matrix system:

$$k = \sqrt{D(2A - C_s)C_s} \qquad \text{(Eq. 4)}$$

and for a granular matrix system:

$$k = \sqrt{\frac{D\epsilon}{\tau}(2A - C_s)C_s} \qquad \text{(Eq. 5)}$$

These relationships were confirmed experimentally using plastic and wax matrixes (10–15).

0022-3549/79/0600-0782$01.00/0

© 1979, American Pharmaceutical Association

Linearity of Modified USP Procedure—The linearity for the aspirin tablet and buffered aspirin tablet assays was examined. For the aspirin assay, mixtures of varying amounts of aspirin with 0.15 mg of salicylic acid for the aspirin tablet assay and 3.0 mg of salicylic acid for the buffered aspirin tablet assay were determined. The amounts of salicylic acid added were equivalent to the maximum amount allowed by the USP, assuming sample weights equivalent to 50 and 100 mg of aspirin, respectively. For the nonaspirin salicylates assay, mixtures of varying amounts of salicylic acid with 50 mg of aspirin for the aspirin tablet assay and 100 mg of aspirin for the buffered aspirin assay were determined. The amounts of aspirin added represented the quantity specified in the modified USP procedures.

The aspirin assay was linear in the 0–75- and 0–130-mg ranges for the aspirin tablet assay and the buffered aspirin tablet assay, respectively. The nonaspirin salicylates assay was linear in the 0–0.3- and 0–5.0-mg ranges for the aspirin tablet assay and the buffered aspirin tablet assay, respectively.

Precision of Modified USP Procedures—A statistical evaluation of the precision of the modified methods was performed on the assay results of two sets of six accurately weighed preparations. The sets used contained either ~0.15 mg of salicylic acid and 50 mg of aspirin or 0.30 mg of salicylic acid and 100 mg of aspirin (Table II).

Effects of Methanol on Aspirin Assay—Methanol was used in the modified USP aspirin assay to clarify the column eluate, which was often turbid due to the physical removal of water by chloroform from the chromatographic column. Methanol had to be added accurately to both the assay preparation and the standard preparation since the presence of methanol affected the magnitude of the absorbance and the wavelength maximum of the aspirin peak (Table III). Aspirin was stable in this solvent mixture for at least 6 hr. The absorbance of an aspirin solution at 278 nm after this time was 99.5% of the initial value. After 24 hr, however, the absorbance dropped to 75% of the initial value.

Comparison of Modified USP Assay and USP Assay—The results of studies on several commercially available aspirin and buffered aspirin tablets are summarized in Tables IV and V. The results indicate a good correlation between methods.

REFERENCES

(1) "The United States Pharmacopeia," 19th rev., Mack Publishing Co., Easton, Pa., 1975, p. 39.

(2) J. Levine, *J. Pharm. Sci.*, **50**, 506 (1961).

(3) J. Levine and J. D. Weber, *ibid.*, **57**, 631 (1968).

(4) J. D. Weber and J. Levine, *ibid.*, **55**, 78 (1966).

(5) J. D. Weber, *J. Assoc. Off. Anal. Chem.*, **48**, 1151 (1965).

(6) D. E. Guttman, *J. Pharm. Sci.*, **57**, 1685 (1968).

(7) D. E. Guttman and G. W. Salomon, *ibid.*, **58**, 120 (1969).

Evaluation of Lanolin Alcohol Films and Kinetics of Triamcinolone Acetonide Release

BALASUBRAMANIAN V. IYER and RAVINDRA C. VASAVADA ×

Received June 26, 1978, from the *School of Pharmacy, University of the Pacific, Stockton, CA 95211.* Accepted for publication December 15, 1978.

Abstract □ The film-forming potential of lanolin alcohol was evaluated. Inclusion of ethylcellulose in lanolin alcohol improved film integrity. The hardness and modulus of elasticity of these lanolin alcohol–ethylcellulose films were improved by incorporating propylene glycol or cetyl alcohol. *Triamcinolone acetonide release from selected film compositions was* investigated. The data were analyzed from the viewpoint of the first-order kinetic theory and the release from a planar system having a homogeneous or granular matrix. The results suggest that the drug release follows a diffusion-controlled matrix model and a square root of time release profile. The release rate constants were proportional to drug concentration. Drug release was maximal from a system containing the drug in a near-saturated solution.

Keyphrases □ Lanolin alcohol—films, kinetics of triamcinolone acetonide release, topical dosage forms □ Triamcinolone acetonide—release from lanolin alcohol films, kinetics, topical dosage forms, □ Dosage forms, topical—lanolin alcohol films, kinetics of triamcinolone acetonide release □ Glucocorticoids—triamcinolone acetonide, release from lanolin alcohol films, kinetics

Protective films containing therapeutically active agents have been used for dermatological and surgical applications (1–3). An inert polymeric matrix impregnated with pilocarpine has been utilized to achieve prolonged and steady release of the drug for ocular administration (4). In certain dermatological applications, polymeric films containing a drug could offer advantages over conventional dosage forms. These potential advantages include enhanced therapeutic effect, predictable control over rate and extent of absorption, occlusion of the skin surface, and improved patient acceptance.

Although several polymeric substances have been studied for their film-forming characteristics (5–7) and potential application in topical drug delivery systems, the nonpolymeric, high molecular weight substances apparently have not been investigated. Furthermore, the applicability of this concept to topical drug delivery system design has not been explored fully.

THEORETICAL

Drug release from a planar system having a drug dispersed in a homogeneous insoluble matrix was shown (8) to follow:

$$Q = \sqrt{Dt(2A - C_s)C_s} \qquad \text{(Eq. 1)}$$

where Q is the amount of drug released per unit area at time t, D is the drug diffusion coefficient in the matrix, A is the total amount of drug present in the matrix per unit volume, and C_s is the drug solubility in the matrix. The relationship for release from a planar system having a granular matrix was shown to be (9) diffusion controlled and is given by:

$$Q = \sqrt{\frac{D\epsilon}{\tau}(2A - \epsilon C_s)C_s t} \qquad \text{(Eq. 2)}$$

where D and C_s refer to the diffusion coefficient and drug solubility in the permeating fluid, τ is the tortuosity of the matrix, and ϵ is the porosity of the matrix.

Both these equations describe drug release as being linear with the square root of time:

$$Q = kt^{1/2} \qquad \text{(Eq. 3)}$$

where k is the release rate constant. For a homogeneous matrix system:

$$k = \sqrt{D(2A - C_s)C_s} \qquad \text{(Eq. 4)}$$

and for a granular matrix system:

$$k = \sqrt{\frac{D\epsilon}{\tau}(2A - C_s)C_s} \qquad \text{(Eq. 5)}$$

These relationships were confirmed experimentally using plastic and wax matrixes (10–15).

0022-3549/79/0600-0782$01.00/0

© 1979, American Pharmaceutical Association

Table I—Effect of Change in Lanolin Alcohol–Ethylcellulose Ratio on Sward Hardness and Modulus of Elasticity of Films Containing Propylene Glycol at Room Temperature (22 ± 0.5°)

Lanolin Alcohol–Ethylcellulose–Propylene Glycol Ratio[a]	Mean Dry Film Thickness (× 10^3)[b], inches	Constant for Varying Thickness, $K_t \times 10^{10}$	Sward Hardness (R)[c], rocks	Modulus of Elasticity (E), psi (kg/cm^2)
9.50:0.00:0.50	0.189	0.030	2	3.55 (0.25)
9.00:0.50:0.50	0.252	0.068	3	11.47 (0.81)
8.50:1.00:0.50	0.402	0.450	4	44.19 (3.11)
8.00:1.50:0.50	0.724	3.200	4	53.87 (3.79)
7.50:2.00:0.50	1.047	9.000	4	50.16 (3.53)
7.00:2.50:0.50	1.063	9.200	4	51.27 (3.60)
6.50:3.00:0.50	1.425	45.000	3	41.97 (2.95)

[a] All films were cast from a 10% (w/v) solution of film formers in isopropyl alcohol. [b] Thicknesses are expressed as mean values of five measurements. [c] Sward hardnesses are expressed as mean values of three measurements rounded to the nearest whole number.

Table II—Effect of Change in Lanolin Alcohol–Ethylcellulose Ratio on Sward Hardness and Modulus of Elasticity of Films Containing Cetyl Alcohol at Room Temperature (22 ± 0.5°)

Lanolin Alcohol–Ethylcellulose–Cetyl Alcohol Ratio[a]	Mean Dry Film Thickness (× 10^3)[b], inches	Constant for Varying Thickness, $K_t \times 10^{10}$	Sward Hardness (R)[c], rocks	Modulus of Elasticity (E), psi (kg/cm^2)
9.50:0.00:0.50	0.189	0.030	2	3.55 (0.25)
9.00:0.50:0.50	0.193	0.031	3	11.66 (0.85)
8.50:1.00:0.50	0.504	0.850	4	42.52 (2.99)
8.00:1.50:0.50	0.650	2.200	4	51.36 (3.61)
7.50:2.00:0.50	0.480	0.700	4	40.43 (2.84)
7.00:2.50:0.50	0.441	0.600	4	44.80 (3.15)
6.50:3.00:0.50	1.284	30.000	3	38.31 (2.69)

[a] All films were cast from a 10% (w/v) solution of film formers in isopropyl alcohol. [b] Thicknesses are expressed as mean values of five measurements. [c] Sward hardnesses are expressed as mean values of three measurements rounded to the nearest whole number.

This paper reports a preliminary evaluation of films formed by lanolin alcohol. Propylene glycol or cetyl alcohol was used as the plasticizer and primary solvent for the test drug. The films formed by lanolin alcohol in combination with a known film former, ethylcellulose (16), also were tested in the presence of the mentioned plasticizers. The prepared films were evaluated by measuring the hardness and modulus of elasticity.

This paper also describes studies of drug release from the films of selected compositions, showing the effect of change in proportion of film formers and the plasticizer and the nature of the plasticizer. Triamcinolone acetonide was chosen as the model drug.

EXPERIMENTAL

Materials—The materials used for the preparation of the films were lanolin alcohol[1] (mp 61–64°), ethylcellulose[2], propylene glycol USP[3], and cetyl (hexadecyl) alcohol (cosmetic grade, d 0.84)[4]. Triamcinolone acetonide USP (solubility in distilled water at 37° is 0.03 mg/ml)[5] and 1,2,3(n)-^{3}H-triamcinolone acetonide[6] were used as the drugs. The solvents were isopropyl alcohol NF[7] and anhydrous methanol[7] (spectral grade). A premade dioxane cocktail[8] was the scintillation fluid.

Film Preparations—For the initial screening, all films were cast from a 10% (w/v) solution of film former(s) and plasticizer in isopropyl alcohol. The films were cast on the mercury substrate. Sufficient solution was poured within a stainless steel ring (9.2-cm i.d., 3-mm height, which had been placed on a mercury surface contained in a 140 × 10-mm glass petri dish, and the solution was spread evenly across the mercury surface within the area bound by the ring. The petri dish was partially covered with its lid, and the solvent was allowed to evaporate overnight.

The entire operation was carried out in a humidity-controlled room at 30° and 40% relative humidity (RH). Partially covering the petri dish helped to control the solvent evaporation rate and the blistering of the deposited film surface. Film formation was easily noted by observing the mercury substrate after complete solvent evaporation. The film could be retrieved intact by slowly lifting the ring from the mercury substrate. The isolated films were stored between sheets of wax paper in a desiccator.

Determination of Film Hardness and Modulus of Elasticity—Film hardness was determined on film cast on aluminum plates. For each composition tested, a 10% (w/v) solution of film former(s) and plasticizer was prepared in isopropyl alcohol and was cast on an aluminum plate using an applicator[9] with a wet film thickness of ~1 mm. These plates were then dried in a humidity-controlled room at 30° and 40% RH. The exact thickness of the dried film was determined using a thickness measuring gauge[10]. Film hardness was determined using a hardness tester[11]. The rocker was calibrated before each measurement by checking for 100 oscillations on a standard glass plate. From the Sward hardness R (number of oscillations of rocker on the test film), the modulus of elasticity (E) was calculated with:

$$E = \frac{KR^3}{T^3} \qquad \text{(Eq. 6)}$$

The values of the constant K for thickness (T) were obtained from the literature (17).

Solubility Studies—The solubilities of triamcinolone acetonide in propylene glycol and cetyl alcohol were determined at room temperature (22°) and at 37°.

Solubility was determined by adding excess steroid to 25 ml of propylene glycol or cetyl alcohol in 50-ml glass bottles with screw caps. A polytef-coated magnetic bar was placed in each bottle prior to capping it tightly. The bottles were kept in water baths on magnetic stirrers for 6 days. All studies were conducted in triplicate.

Prior to sampling, the stirring was stopped and the excess steroid was allowed to settle. An aliquot was filtered using a filter[12] with 0.22-μm filter paper. The filtration and sampling apparatus was allowed to equilibrate for 48 hr prior to use. The first 5 ml of the filtrate was rejected in each case to avoid any reduction in solubility values due to steroid adsorption in the filter paper (18). All operations were conducted in a constant-temperature room.

The steroid concentration in the solvent was determined using a scanning spectrophotometer[13] after appropriate dilutions of the solvent

[1] Super Hartolan, Croda Inc., New York, N.Y.
[2] Ethyl Cellulose N-50, Hercules Inc., Wilmington, Del.
[3] Ruger Chemical Co., Irvington, N.J.
[4] Branched-chain hexadecyl alcohol, M. Michel and Co., New York, N.Y.
[5] Dermatological Division, Johnson and Johnson, New Brunswick, N.J.
[6] Amersham/Searle Corp., Arlington Heights, Ill.
[7] Mallinckrodt Chemical Works, St. Louis, Mo.
[8] Hydroscint, ICN Chemical and Radioisotope Division, Irvine, Calif.
[9] Multiple-clearance applicator, Gardner Laboratory, Bethesda, Md.
[10] Minitector (model N), Gardner Laboratory, Bethesda, Md.
[11] I.C.I. automatic Sward hardness rocker, Gardner Laboratory, Bethesda, Md.
[12] Swinnex-25, Millipore Filter Corp., Bedford, Mass.
[13] Perkin-Elmer model-202, Coleman Instruments Division, Oak Brook, Ill.

Table III—Effect of Change in Lanolin Alcohol–Propylene Glycol Ratio on Sward Hardness and Modulus of Elasticity of Films at Room Temperature (22 ± 0.5°)

Lanolin Alcohol–Ethylcellulose–Propylene Glycol Ratio[a]	Mean Dry Film Thickness ($\times 10^3$)[b], inches	Constant for Varying Thickness, $K_t \times 10^{10}$	Sward Hardness (R)[c], rocks	Modulus of Elasticity (E), psi (kg/cm^2)
8.50:1.50:0.00	0.669	2.80	3	25.22 (1.77)
8.25:1.50:0.25	0.606	1.12	4	31.58 (2.22)
8.00:1.50:0.50	0.724	3.20	4	53.87 (3.79)
7.75:1.50:0.75	0.755	4.54	4	66.68 (4.69)
7.50:1.50:1.00	0.809	5.52	4	66.58 (4.68)
7.25:1.50:1.25	0.693	3.13	4	59.64 (4.19)
7.00:1.50:1.50	0.874	6.54	4	62.31 (4.38)
6.50:1.50:2.00	0.740	4.05	4	63.12 (4.44)
6.00:1.50:2.50	0.724	3.91	4	65.66 (4.62)
5.50:1.50:3.00	0.622	1.52	4	39.89 (2.80)
5.00:1.50:3.50	0.622	1.52	4	39.89 (2.80)

[a] All films were cast from a 10% (w/v) solution of film formers in isopropyl alcohol. [b] Thicknesses are expressed as mean values of five measurements. [c] Sward hardnesses are expressed as mean values of three measurements rounded to the nearest whole number.

with anhydrous methanol. The steroid solubility was determined at 239 nm in propylene glycol and at 265 nm in cetyl alcohol.

Apparent Solubility in Lanolin Alcohol—The apparent solubility was estimated by determining the effective partition coefficient of the steroid in a lanolin alcohol–water system at 22 and 37°.

About 100–200 mg of the melted lanolin alcohol was coated as a thin film in the bottom of a preweighed, 50-ml, flat-bottom polypropylene beaker and allowed to cool to room temperature. The beaker was weighed again to determine the exact film weight. Then 20 ml of a 0.002% (w/v) mixture of cold and radiolabeled triamcinolone acetonide was added. The beaker was covered with Parafilm and kept in a temperature-controlled water bath until equilibrium was reached. One-milliliter samples were withdrawn from the aqueous phase at suitable intervals into a scintillation vial, and 10 ml of scintillation fluid was added to each. They were then analyzed radiochemically using a liquid scintillation counter[14].

The apparent partition coefficient, K_e, was then determined using the equation proposed previously (19):

$$K_e = \frac{A_1/W_1}{A_a/W_a} = \frac{(A_a' - A_a)W_a}{A_a W_1} \qquad \text{(Eq. 7)}$$

where A_1 and A_a are the amounts of the drug in the lanolin alcohol and in the aqueous phase, respectively; A_a' is the initial amount of drug in water; and W_1 and W_a are the weights of lanolin alcohol and water, respectively.

The apparent solubility was calculated from:

$$K_e = \frac{C_s^1}{C_s^w} \qquad \text{(Eq. 8)}$$

where C_s^1 is the apparent solubility in lanolin alcohol and C_s^w is the solubility in water.

Determination of Release Rate—Lanolin alcohol, ethylcellulose, and propylene glycol or cetyl alcohol were added in required quantities to 5 ml of isopropyl alcohol and allowed to go into solution by gentle heating. The solution was cooled to room temperature, and the required concentration of cold triamcinolone acetonide was added and allowed to go into solution. The radiolabeled steroid (10 μCi) in isopropyl alcohol was added to this solution, and the total volume was made up to 10 ml in a volumetric flask. Two milliliters of this solution was pipetted into a preweighed aluminum petri dish and allowed to spread evenly on the flat bottom (7.5 cm in diameter; area of 44.2 cm^2).

The petri dish was kept on a level surface for 24 hr, and the solvent was allowed to evaporate to form a uniform film of 5–8-μm thickness. Complete solvent evaporation was confirmed by weighing the petri dish to a constant weight. The film-coated petri dish was stored in a desiccator containing anhydrous calcium chloride for at least 24 hr prior to the release studies. The good adherence of the film to the petri dish ensured that only the exposed surface area (44.2 cm^2) was available for release. The film was examined visually at the end of each experiment. No visible pores or "peeling" of the film from the petri dish was observed.

The release studies were conducted in a dissolution assembly[15] with the following modifications. The dissolution flasks were replaced by 1000-ml flat-bottom polypropylene beakers, and the dissolution basket assemblies were replaced by stainless steel stirrers with a propeller diameter of 4.5 cm. The film-coated petri dishes were placed in the bottom of the beakers. The beakers were held in position by Plexiglas disks with central circular ports for the stirrers and a small sampling port. The stirring assembly was set in position, 300 ml of preheated (37°) distilled water was added carefully to each, and the stirring was maintained at 40 rpm. The water bath was maintained at 37°.

One-milliliter samples were drawn frequently over 24 hr and were replaced by 1 ml of distilled water. Each sample was pipetted into a scintillation vial to which 10 ml of scintillation fluid was added. The samples were then analyzed using a liquid scintillation counter. The external standard ratio method was employed for calculation of counting efficiency using a standard quench curve.

The release data were computed and analyzed by a computer[16] using a FORTRAN program. Appropriate corrections were applied for the sample withdrawn, and medium was added. All release studies were conducted in triplicate.

RESULTS AND DISCUSSION

Film Characteristics—Lanolin alcohol was found to form thin, isolatable films. The lanolin alcohol films with a minimum thickness of 65 μm could be easily recovered intact from the mercury substrate. The lanolin alcohol films with less than 65-μm thickness were fragile, and their uniformity and integrity during isolation could not be assured due, in part, to associated tackiness. The inclusion of appropriate amounts of solvent-plasticizer, *e.g.*, propylene glycol or cetyl alcohol, reduced film tackiness. The lanolin alcohol film integrity was enhanced by ethylcellulose. When the solvent-plasticizer concentration was kept constant at 5% (w/w), the modulus of elasticity increased with the increasing proportion of ethylcellulose and a corresponding decrease in the proportion of lanolin alcohol. The modulus of elasticity reached a maximum value at an ethylcellulose concentration of 15% (w/w) with a corresponding lanolin alcohol concentration of 80% (w/w) (Tables I and II).

The effect of variation in the lanolin alcohol–propylene glycol ratio on film properties also was studied while the ethylcellulose content was held constant at 15% (w/w) (Table III). Compositions with 75–77.5% (w/w) lanolin alcohol and 7.5–10% (w/w) propylene glycol produced films with a high modulus of elasticity (Table III). These compositions also gave perceptibly good films. A further increase in the proportion of propylene glycol up to 25% (w/w) with a corresponding decrease in the proportion of lanolin alcohol did not substantially alter the film characteristics. However, an increase in the propylene glycol concentration beyond 25% (w/w) resulted in films that were definitely tacky and had a low modulus of elasticity.

Solubility Studies—Triamcinolone acetonide solubility in propylene glycol at 22 and 37° was 8.04 ± 0.19 and 12.09 ± 0.18 mg/ml, respectively. The solubility in cetyl alcohol at 22 and 37° was 0.92 ± 0.3 and 1.25 ± 0.05 mg/ml, respectively. The solubility values are expressed as the mean ± *SD* of three determinations. The attainment of equilibrium solubility in 3 days was noted by the fact that there was no difference in absorbance between the samples analyzed at the end of 3 and 6 days. Since the cetyl alcohol had a strong absorption at 239 nm, the side of the absorption band was used. Actual measurements of steroid concentration were made at 265 nm after verifying compliance with Beer's law.

[14] Beckman CPM-100 counter.
[15] Hanson Research Corp., Northridge, Calif.
[16] Burroughs B6700.

Table IV—Comparison of *Q versus* $t^{1/2}$ and First-Order Treatments of Triamcinolone Acetonide Release Data from Films Containing Propylene Glycol as Plasticizer at 37 ± 0.5°

Lanolin Alcohol–Ethylcellulose–Propylene Glycol Ratio	Drug Concentration[a], %	*Q versus* $t^{1/2}$ [b]			First Order		
		t_{lag}, min	Correlation Coefficient	$k \times 10^3$, mg cm^2 min$^{-1/2}$	t_{lag}, min	Correlation Coefficient	$K \times 10^3$, min^1
8.0:1.5:0.5	0.50	24.05	0.992	0.405	−54.51	0.990	0.639
8.0:1.5:0.5	0.99	4.70	0.995	1.056	−56.62	0.983	1.169
8.0:1.5:0.5	1.96	0.35	0.994	1.650	−195.74	0.978	0.696
8.0:1.5:0.5	2.91	6.26	0.994	2.849	−113.20	0.986	0.858
8.5:1.0:0.5	0.50	17.14	0.997	0.448	−65.47	0.996	0.764
8.5:1.0:0.5	0.99	−0.53	0.980	1.131	−41.54	0.919	1.833
8.5:1.0:0.5	1.96	7.18	0.996	1.969	−92.23	0.995	0.929
8.5:1.0:0.5	2.91	−0.07	0.979	2.384	−258.55	0.957	0.636

[a] Weight of drug per weight of dry film. Drug concentration exceeded solubility in all cases. [b] All correlation coefficients and k and K values were computed from the regression line drawn from the data obtained by triplicate runs at each level by using the TEKTRONIX (model 4005-1) graphics terminal.

The apparent solubility of triamcinolone acetonide in lanolin alcohol at 22 and 37° was 0.13 ± 0.01 and 0.41 ± 0.01 mg/g, respectively. The attainment of equilibrium in 5 days was noted by running the partitioning experiment for 8 days with daily sampling of the aqueous phase. No further reduction in aqueous phase radioactivity was observed after 5 days.

Release Kinetics—Higuchi (9) showed that the *Q versus* $t^{1/2}$ relationship is common to homogeneous as well as to granular matrix systems during unidirectional leaching or extraction from a simple planar surface (Eqs. 1–5). It is necessary that A be greater than C_s (for homogeneous) or ϵC_s (for granular matrix) by a factor of three or four. A first-order release mechanism in which the release rate is proportional to the amount of drug left in the matrix also might be considered possible for drug release from polymeric systems of this type (11, 15, 16). This can be shown as:

$$\log (Q_\infty - Q) = \frac{-Kt}{2.303} + \log Q_\infty \qquad \text{(Eq. 9)}$$

where Q_∞ is the initial amount of drug present per unit area of the film, Q is the amount of drug present per unit area at time t, and K is the first-order rate constant.

In this study, the release data were analyzed to determine which release mechanism might be operative. The data comparing both of these treatments for triamcinolone acetonide release from matrixes containing propylene glycol as plasticizer are shown in Table IV and Figs. 1 and 2. The linear square root of time plots had high correlation coefficients. The observed lag times were relatively small, and the release rate constant, k, increased with the increase in drug concentration, as predicted by Eqs. 1 and 2. On the other hand, relatively high correlation coefficients also were obtained for the first-order treatment of the release data. However, highly negative lag times and a lack of constancy in the first-order constants (Table IV) strongly point against this mechanism. An initial curvature effect also was noticed in all first-order treatments of the data. A representative plot of the first-order data is shown in Fig. 5. Similar results were seen with systems containing cetyl alcohol as the plasticizer.

Figures 1–4 show the *Q versus* $t^{1/2}$ treatment of the data for different concentrations of triamcinolone acetonide in matrixes containing propylene glycol or cetyl alcohol. All plots show the mean of three observations because of small standard deviations involved in most cases. The maximum amount of drug released varied from 7.6 to 46.0% of its solubility in distilled water at 37°. A good linear fit was observed in all cases, with slight negative deviation at longer time intervals and for higher drug concentrations. This deviation might be due to the exhaustion of the drug in the suspension phase and to the increase in diffusion distance for the

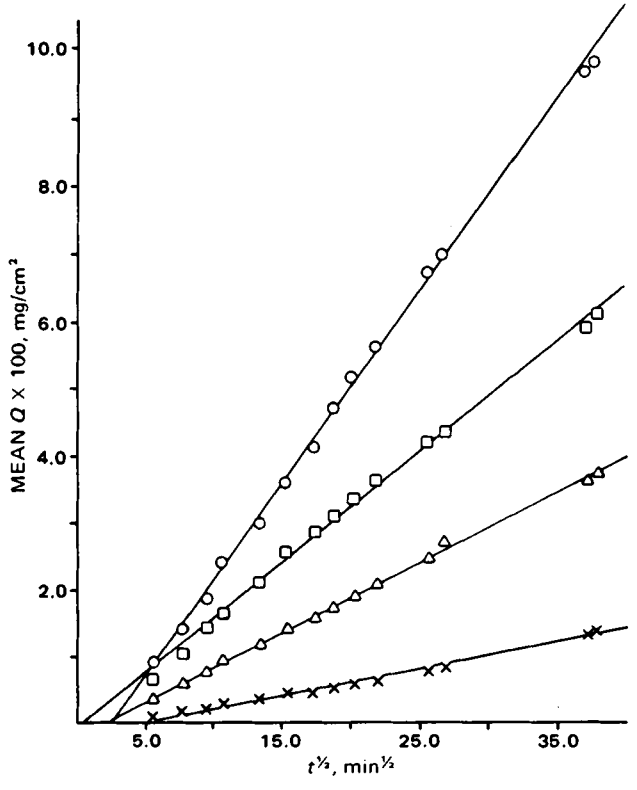

Figure 1—*Drug release from films containing lanolin alcohol–ethylcellulose–propylene glycol (8.0:1.5:0.5) at different concentrations of triamcinolone acetonide. Key: ×, 0.50%; △, 0.99%; □, 1.96%; and ○, 2.91%.*

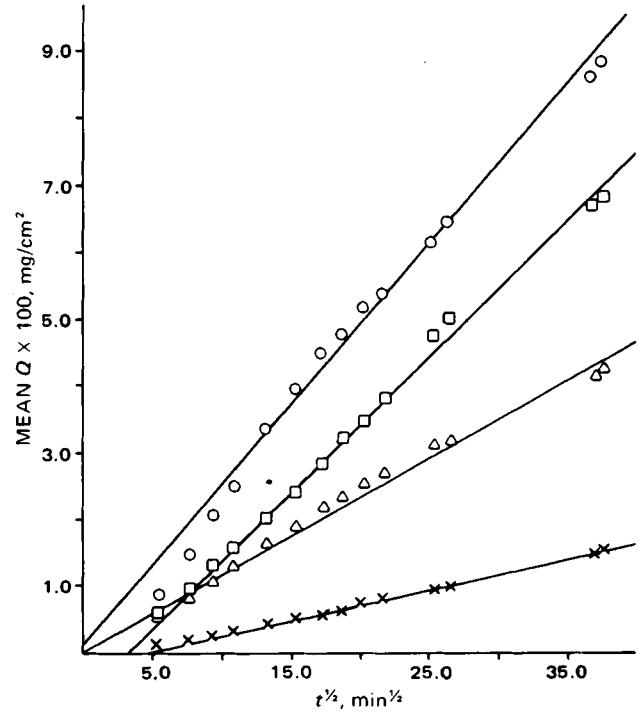

Figure 2—*Drug release from films containing lanolin alcohol–ethylcellulose–propylene glycol (8.5:1.0:0.5) at different concentrations of triamcinolone acetonide. Key: ×, 0.50%; △, 0.99%; □, 1.96%; and ○, 2.91%.*

Table V—*Q versus* $t^{1/2}$ Treatments of Triamcinolone Acetonide Release Data from Films Containing Cetyl Alcohol as Plasticizer at 37 ± 0.5°

Lanolin Alcohol–Ethylcellulose–Cetyl Alcohol Ratio	Drug Concentration[a], %	$k \times 10^3$ [b], mg cm^2 min$^{-1/2}$	t_{lag}, min	Correlation Coefficient
8.0:1.5:0.5	0.50	0.454	5.94	0.990
8.0:1.5:0.5	0.99	1.270	0.52	0.965
8.0:1.5:0.5	1.96	2.116	0.14	0.967
8.0:1.5:0.5	2.91	2.926	−0.07	0.932
8.5:1.0:0.5	0.50	0.540	−3.72	0.957
8.5:1.0:0.5	0.99	0.940	5.26	0.996
8.5:1.0:0.5	1.96	1.940	0.06	0.974
8.5:1.0:0.5	2.91	2.756	1.98	0.982

[a] Weight of drug per weight of dry film. Drug concentration exceeded solubility in all cases. [b] All k values and correlation coefficients were computed from the regression line drawn from the data obtained by triplicate runs at each level by using the TEKTRONIX (model 4005-1) graphics terminal.

drug in the film. The observed lag times never exceeded 1.7% of the total release period (24 hr).

Effect of Drug Concentration—The densities of lanolin alcohol and ethylcellulose were determined to be 0.98 and 1.38 g/ml using the pycnometric method. The weight per weight drug concentrations (Tables IV and V) were converted to weight per volume (A values) concentrations. The effect of the changing the drug concentration on the release rate constant, k, was tested using these concentrations of triamcinolone acetonide for each composition of the film tested. In all cases, the k *versus* A plots were slightly more linear (r = 0.992) than the k *versus* $A^{1/2}$ plots (r = 0.960). While Eqs. 4 and 5 predict a linear relationship between k and $A^{1/2}$, the observed results also could be explained in terms of a granular matrix system alone if the initial porosity were assumed to be very small. Such as assumption appears to be reasonable since these matrixes contain a plasticizer. Higuchi (9) showed that in those instances where initial porosity is very small or where the fraction of the matrix volume occupied by the drug is relatively large, $\epsilon \cong KA$ and Eq. 5 reduces to:

$$k = A\sqrt{\frac{DK}{\tau}(2 - KC_s)C_s} \qquad \text{(Eq. 10)}$$

where K is equal to the specific volume of the drug if A is expressed in terms of grams of drug per milliliter.

Effect of Change in Plasticizer—According to Eq. 4, one would expect k to decrease substantially when the solvent-plasticizer is changed from propylene glycol to cetyl alcohol in view of the nearly eightfold difference in drug solubility in that vehicle. This expectation would be valid if D, the diffusion coefficient of the drug in the matrix, were not altered significantly by the change of the solvent-plasticizer. Alternatively, in the same release medium, Eq. 5 would predict comparable k values for the two systems differing only in the nature of solvent-plasticizer, provided that volume, porosity, and tortuosity of the matrix are not significantly altered. This might well be the case for the systems studied since the k values for the cetyl alcohol systems (Table V) were comparable to those for the propylene glycol systems (Table IV).

Effect of Vehicle Composition—Table VI describes the effect of drug solubilization on drug release by varying the propylene glycol–lanolin alcohol concentration. The steroid concentration (0.10%, w/w) was chosen, in part, to permit this study in films of sufficient integrity. The

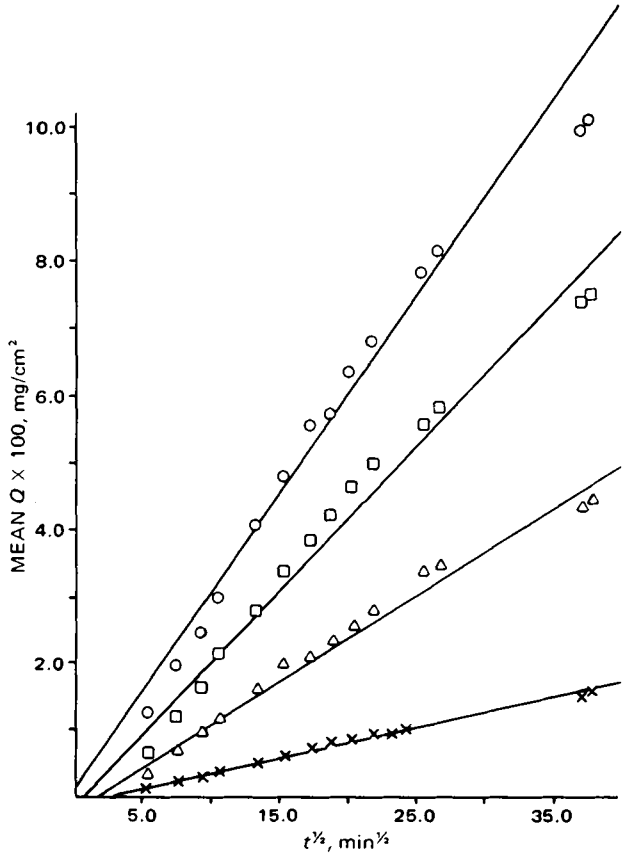

Figure 3—*Drug release from films containing lanolin alcohol–ethylcellulose–cetyl alcohol (8.0:1.5:0.5) at different concentrations of triamcinolone acetonide. Key:* ×, *0.50%;* △, *0.99%;* □, *1.96%; and* ○, *2.91%.*

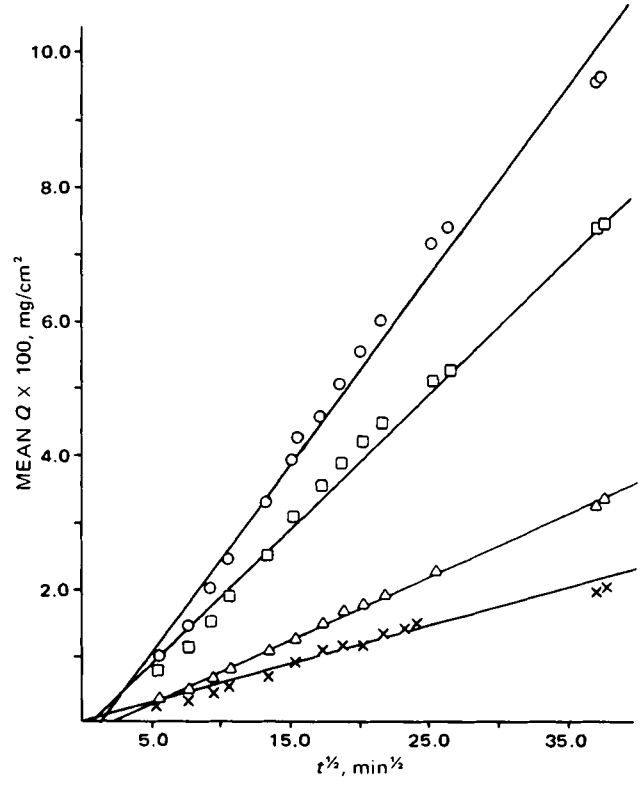

Figure 4—*Drug release from films containing lanolin alcohol–ethylcellulose–cetyl alcohol (8.5:1.0:0.5) at different concentrations of triamcinolone acetonide. Key:* ×, *0.50%;* △, *0.99%;* □, *1.96%; and* ○, *2.91%.*

Table VI—Release of 0.10% (w/w) Triamcinolone Acetonide from Matrixes Containing Different Percentages of Propylene Glycol after 6 hr at 37°

Lanolin Alcohol–Ethylcellulose–Propylene Glycol Ratio	Amount[a] Released, %
8.5:1.5:0.0	37.11 ± 0.62
8.0:1.5:0.5	40.46 ± 1.12
7.7:1.5:0.8	32.38 ± 0.71
7.0:1.5:1.5	30.48 ± 0.29

[a] All values are expressed as the means ± *SD* of three runs.

maximum release of drug was obtained with systems containing the drug in a near-saturated solution (5% propylene glycol). The release rate decreased with systems containing no propylene glycol (major solubilizer) as well as with systems containing the solubilizer in excess of that required to dissolve the steroid completely (8 and 15% propylene glycol). These vehicle effects are consistent with those reported for fluocinolone acetonide from propylene glycol–water gels (20).

Conclusion—This film-forming capability of lanolin alcohol is potentially significant and appears to have remained unrecognized in spite of the use of this material in cosmetic and dermatologic preparations. Additional work is planned to explain its film-forming ability.

The release of suspended triamcinolone acetonide from films of lanolin alcohol in combination with ethylcellulose and propylene glycol or cetyl alcohol followed the diffusion-controlled granular matrix model (9). The *in vitro* skin penetration work in progress may help to determine the rate-limiting step during topical drug absorption.

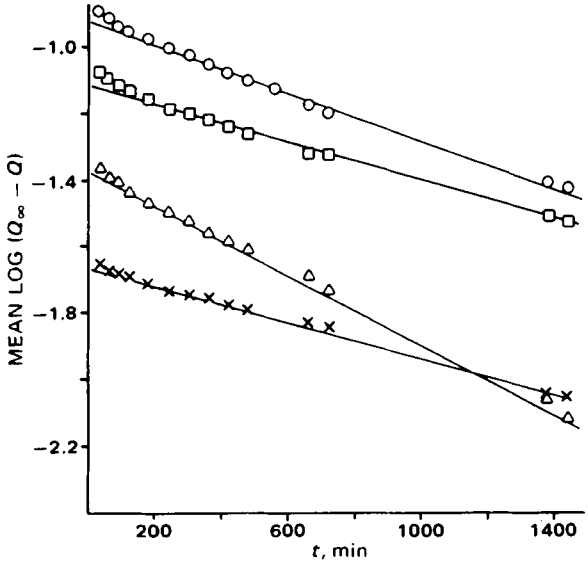

Figure 5—*First-order plots of drug release from films containing lanolin alcohol–ethylcellulose–propylene glycol (8.0:1.5:0.5) at different concentrations of triamcinolone acetonide. Key: ×, 0.50%; △, 0.99%; □, 1.96%; and ○, 2.91%.*

REFERENCES

(1) M. Luongo, J. J. Sciarra, and C. O. Ward, *J. Pharm. Sci.*, **63**, 1376 (1974).

(2) M. J. Groves and J. N. Hague, British pat. 1213295 (1970).

(3) F. E. Gould, U.S. pat. 3,577,516 (1971).

(4) N. Applezweig, U.S. pat. 3,536,809 (1970).

(5) J. J. Sciarra and R. N. Gidwani, *J. Pharm. Sci.*, **61**, 754 (1972).

(6) S. Borodkin and F. E. Tucker, *ibid.*, **64**, 1289 (1975).

(7) J. A. Conrady, Amherst, and C. H. Stockman, U.S. pat. 3,590,118 (1971).

(8) T. Higuchi, *J. Pharm. Sci.*, **50**, 874 (1961).

(9) *Ibid.*, **52**, 1145 (1963).

(10) S. J. Desai, A. P. Simonelli, and W. I. Higuchi, *J. Pharm. Sci.*, **54**, 1459 (1965).

(11) J. B. Schwartz, A. P. Simonelli, and W. I. Higuchi, *ibid.*, **57**, 274 (1968).

(12) *Ibid.*, **57**, 278 (1968).

(13) P. Singh, S. J. Desai, A. P. Simonelli, and W. I. Higuchi, *J. Pharm. Sci.*, **56**, 1542 (1967).

(14) *Ibid.*, **56**, 1548 (1967).

(15) S. Borodkin and F. E. Tucker, *J. Pharm. Sci.*, **63**, 1359 (1974).

(16) J. J. Sciarra and R. N. Gidwani, *J. Soc. Cosmet. Chem.*, **21**, 667 (1970).

(17) R. A. Cass, *J. Paint Technol.*, **38**, 281 (1966).

(18) W. L. Chiou, *Can. J. Pharm. Sci.*, **10**, 112 (1975).

(19) Z. T. Chowhan and R. Pritchard, *J. Pharm. Sci.*, **64**, 754 (1975).

(20) B. J. Poulsen, E. Young, V. Coquilla, and M. Katz, *ibid.*, **57**, 928 (1968).

ACKNOWLEDGMENTS

Presented at the Basic Pharmaceutics Section, APhA Academy of Pharmaceutical Sciences, Hollywood, Fla., meeting, November 1978.

Abstracted in part from a dissertation submitted by B. V. Iyer to the School of Pharmacy, University of the Pacific, in partial fulfillment of the Doctor of Philosophy degree requirements.

The authors thank Dr. Boyd J. Poulsen, Institute of Pharmaceutical Sciences, Syntex Research, Palo Alto, Calif., for helpful discussions and Dr. John R. Marvel, Dermatological Division, Johnson and Johnson, New Brunswick, N.J., for providing triamcinolone acetonide. They also thank Dr. John Kent and Mr. Mark Yost of Syntex Laboratories, Palo Alto, Calif., for density determinations on the Quantasorb Sorption System (Quantachrome Corp., Greenvale, N.Y.).

Nortropacocaine Hydrochloride Conformation in Aqueous and Hydrophobic Media

ALEXANDROS MAKRIYANNIS ˣ **and GILBERT HITE**

Received August 14, 1978, from the *Department of Medicinal Chemistry, School of Pharmacy, and the Institute of Materials Science, University of Connecticut, Storrs, CT 06268.* Accepted for publication December 7, 1978.

Abstract □ The nortropacocaine hydrochloride PMR spectra in deuterium oxide and in deuterochloroform differed markedly. A detailed conformational analysis using vicinal ^1H-^1H coupling constants revealed the molecular conformation to be identical in both solvents. The preferred conformation was one in which the piperidine component existed as a deformed chair. The spectral differences were due to a decreased deshielding of the protonated nitrogen on the neighboring bicyclic ring protons, resulting in chemical shift changes.

Keyphrases □ Nortropacocaine—conformation, effect of solvents, PMR spectra, structure-activity relationships □ Cocaine analogs—nortropacocaine, conformation, structure-activity relationships, effect of solvents, PMR spectra □ Anesthetics, local—nortropacocaine, conformation, structure-activity relationships □ Stimulants, central—nortropacocaine, conformation, structure-activity relationships

Cocaine, the most prominent tropane alkaloid obtained from *Erythroxylon coca* leaves, possesses dual pharmacological activity (1). Systemic administration interferes with the uptake of catecholamines by adrenergic nerve terminals, and local application blocks nerve conduction. Therefore, the drug has central nervous system stimulant as well as local anesthetic properties.

One explanation for this dual activity is that cocaine interacts in two different conformations (2, 3). The catecholamine uptake inhibition is associated with a noncontiguous transoid phenethylamine cocaine conformation (2) while the local anesthetic activity is associated with a piperidine boat conformation (3). This hypothesis is similar to that of Schueler (4), according to which acetylcholine in a "cisoid" conformation stimulates the nicotinic receptors while acetylcholine in a "transoid" conformation stimulates the muscarinic receptors.

BACKGROUND

Although examples of 4-piperidinols in boat conformations have been reported (5, 6), no tropane analogs have been shown to possess such a conformation. X-ray diffraction studies on salts of cocaine (7) and its analogs (8) provided no evidence for a piperidine boat. Similarly, cocaine free base was found in a conformation having the piperidine ring in a chair form. However, a boat conformation was reported (9) to be a necessary intermediate during the reversible acid-catalyzed N → O acyl migration in *N*-benzoylnortropine and several of its analogs.

This study investigated the conformation of *O*-benzoylnortropine (nortropacocaine) (Structure I) hydrochloride, a monosubstituted tropane analog resembling cocaine only in those structural features believed to favor a piperidine boat conformation (Structure II). Such a boat conformation would be stabilized through an interaction—electrostatic or hydrogen bonding—between the ^+NH group and the *O*-benzoyloxy oxygen.

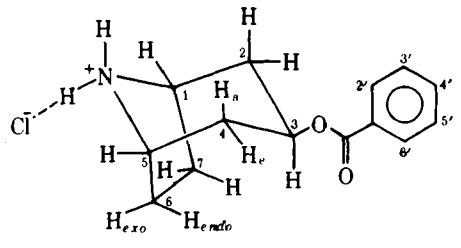

I

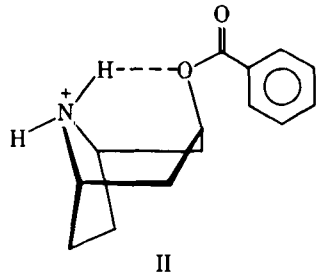

II

Conformational analyses of several tropane alkaloid free bases in deuterochloroform (8) and of tropane salts in deuterium oxide (10–12) have been carried out from their PMR spectra. However, the conformations of tropane salts in hydrophobic media have not been investigated. The present study represents a detailed conformational analysis of a cocaine analog salt in aqueous and in hydrophobic media, with special emphasis on the possible role of the solvent. This study is also the first conformational analysis of a tropane salt in hydrophobic media.

Solvent changes have been reported to produce pronounced effects on some molecular conformations (6, 13). To observe any such solvent effects, the nortropacocaine hydrochloride conformation was determined in deuterium oxide and in deuterochloroform using high-resolution PMR. Nonpolar solvents, in addition to representing more accurately the nerve membrane hydrophobic environment, should favor the boat conformation by enhancing the H_2N^+–O interaction. This study is further justified by the great interest in tropane analogs as models of various drug pharmacophoric conformations (14).

EXPERIMENTAL

The ^1H resonance spectra were measured at 270 MHz (Figs. 1*a* and 1*b*) using 0.10 *M* solutions in deuterochloroform and in deuterium oxide at an ambient temperature of 20°. Chemical shifts were measured from tetramethylsilane and sodium 2,2-dimethyl-2-silatane-5-sulfonate, which were used as internal standards. Nortropacocaine hydrochloride (9) was obtained by *N*-demethylating tropacocaine using 2,2,2-trichloroethylchloroformate (15). Tropacocaine hydrochloride was obtained commercially.

All of the ^1H chemical shifts and ^1H-^1H coupling constants for the protons in the piperidine component of the tropane nucleus could be

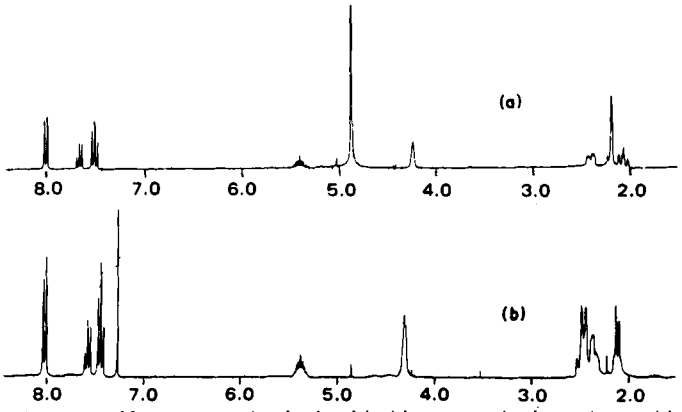

Figure 1—*Nortropacocaine hydrochloride spectra in deuterium oxide* (a) *and in deuterochloroform* (b).

0022-3549/79/0600-0788$01.00/0
© 1979, American Pharmaceutical Association

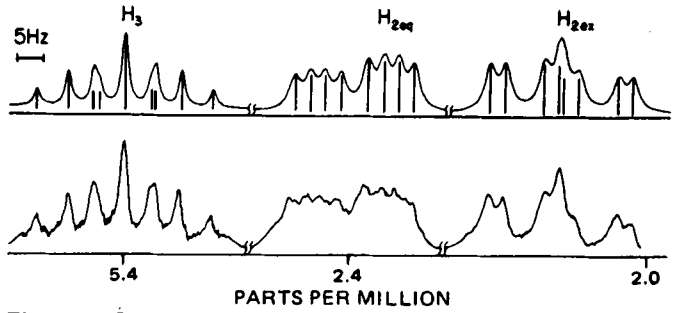

Figure 2—*Real (bottom) and simulated (top) spectral regions from the ^1H-nortropacocaine hydrochloride spectrum in deuterium oxide.*

extracted by analyzing the spectral portions due to the methine proton on C_3 and the methylene protons on C_2. The absorption signals due to the H_3 methine proton were analyzed as the *C* portion of an *AA'BB'C* system. Signals due to each geminal proton on C_2 were sufficiently separated to allow their analysis as the *AB* portion of an *ABCD* system. In the preliminary analysis, the *AA'BB'C* and *ABCD* spectra were correspondingly approximated as $(AB)_2X$ and *ABKY* systems. Initial spectral parameter estimates were obtained by standard methods (16) with the aid of ^1H-^1H spin decoupling, when necessary, and were then refined by spectral simulation and iteration using the ITRCAL program. This program is an implementation of the LAOCN 3 algorithm (17) on a minicomputer. It requires a 12K computer system and a disk memory. Experimental and "best-fit" simulated spectra are shown in Figs. 2 and 3.

Due to overlap, the spectral portions corresponding to the protons on C_6 and C_7 of the ethylene bridge were not amenable to detailed analysis. Only approximate individual chemical shifts could be extracted directly from the spectra with the help of ^1H-^1H spin decoupling.

RESULTS AND DISCUSSION

The nortropacocaine hydrochloride spectra in deuterium oxide (Figs. 1*a* and 2) and in deuterochloroform (Figs. 1*b* and 3) had similar H_3 proton resonances but varied markedly in other regions. Spectral assignments in the crucial $H_{2,4}$ region (Figs. 2 and 3) could be made only after ^1H-^1H spin decoupling. The variations between the two spectra could be attributed to differences in coupling constants, chemical shifts, or both.

Coupling Constants—The preferred molecular conformation could be determined unambiguously from the piperidine ring proton coupling constants. In both solvents, the coupling constants showed no appreciable differences, indicating that no significant conformational changes occurred when an aqueous medium was substituted for a hydrophobic solvent. The most direct information on this tropane analog conformation came from the C_3 proton signal. The coupling constants ($J_{2ax,3}$ and $J_{2eq,3}$) between this proton and its neighboring methylene protons are consistent with H_{ax}-H_{ax} and H_{ax}-H_{eq} coupling, indicating that the piperidine ring exists as a slightly distorted chair (Structure III). In this chair, the H_3 proton occupies an axial position. Consequently, the benzoyloxy group is equatorial. The $J_{2eq,3}$ and $J_{2ax,3}$ were assumed to have like signs and to be positive since vicinal couplings in substituted ethanes have the same sign and are regarded as positive (18). The $J_{2ax,2eq}$ was assumed to be negative since the geminal proton coupling is negative for most CH_2 groups (18). Additional evidence for a distorted piperidine chair conformation was provided by the coupling constants ($J_{1,2ax}$ and $J_{1,2eq}$) of the C_2 protons with the C_1 bridge carbon proton.

If nortropacocaine hydrochloride is assumed to exist as a single conformer in solution, the piperidine ring distortion can be evaluated by comparing the vicinal ^1H-^1H coupling constants with the coupling constants calculated for a "perfect" chair. This procedure, which makes use of substituent electronegativities (19), was developed (20) for perfectly staggered 1,2-disubstituted ethanes and has given good results in the past

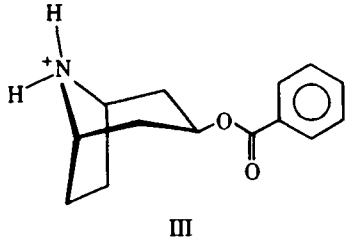

III

Table I—^1H Vicinal Coupling Constants for Nortropacocaine Hydrochloride

Constant	Deuterochloroform	Deuterium Oxide	Calculated
$J_{1,2eq}$	2.9	3.25	2.37
$J_{1,2ax}$	2.35	2.85	3.63
$J_{2eq,3}$	5.8	5.75	5.19
$J_{2ax,3}$	10.8	10.75	12.70
$J_{2ax,2eq}$	−13.95	−13.85	—

(21). First, coupling constants for a perfectly staggered piperidine ring were calculated (20). The values thus obtained were compared to the experimentally determined coupling constants of the piperidine ring in nortropacocaine hydrochloride (Table I), and the following dihedral angles were calculated for nortropacocaine hydrochloride in deuterochloroform and in deuterium oxide, respectively: $\phi(H_1C_1C_1$-$H_{2ax}) = 66$ and 64°, $\phi(H_1C_1C_2H_{2eq}) = 56$ and 54°, $\phi(H_{2ax}C_2C_3H_{3ax}) = 158$ and 157°, and $\phi(H_{2eq}C_2C_3H_3) = 58$ and 58°.

Because of the dangers involved in using quantitative correlations to obtain precise dihedral angles, such values are only approximate. The dihedral angles deviations from ideality were compatible with a piperidine ring slightly flattened at the C_3 position and more puckered at the $^+NH_2$ group (Structure III).

Similar conclusions about the piperidine ring distortion were reached using a method (22, 23) for the qualitative determination of six-membered ring distortions from the ratios of J_{trans}-J_{cis} vicinal coupling constants.

Chemical Shifts—The pronounced changes that the nortropacocaine hydrochloride proton spectrum underwent when the solvent was changed from deuterochloroform to deuterium oxide were due almost exclusively to different individual proton chemical shift changes. The variation in these chemical shift changes could be attributed to a reduction in the protonated nitrogen deshielding influence on the neighboring protons in the bicyclic ring when deuterochloroform was replaced with deuterium oxide. Such solvent modification of the charged nitrogen deshielding influence was demonstrated elsewhere (24). The highly polar deuterium oxide presumably (24) decreases the effect of the positive charge through direct solvation of the positive ion. The result is that in deuterium oxide the protons in close proximity to the protonated nitrogen are shifted upfield relative to the corresponding protons in the less polar deuterochloroform.

An attempt was made to relate the chemical shift differences in the

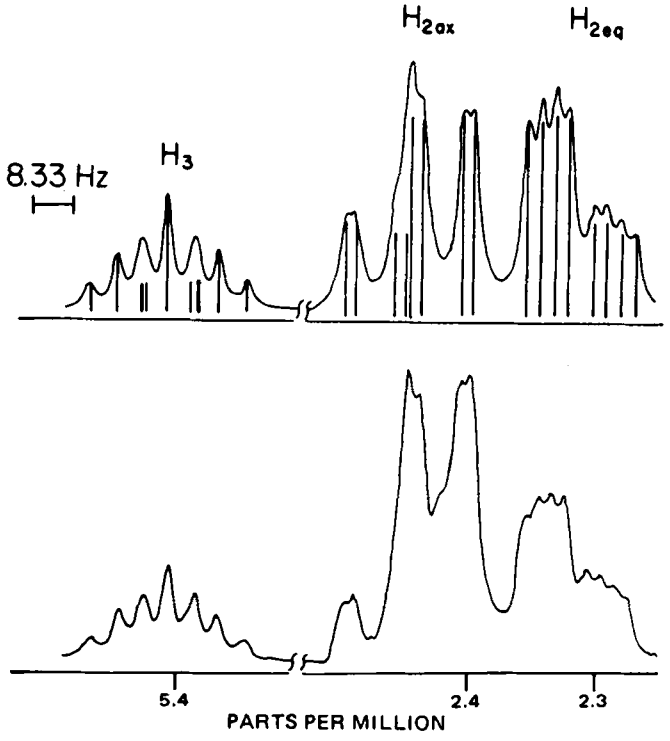

Figure 3—*Real (bottom) and simulated (top) spectral regions from the ^1H-nortropacocaine hydrochloride spectrum in deuterochloroform. In the real spectrum, H_{2ax} and H_7 protons are overlapping.*

Table II—^{1}H Chemical Shifts for Nortropacocaine Hydrochloride (270 MHz)

Proton	Chemical Shift, ppm		Difference, Hz
	Deuterochloroform	Deuterium Oxide	
$H_{1,5}$	4.29	4.24	14
$H_{2eq,4eq}$	2.31	2.39	−22
$H_{2ax,4ax}$	2.44	2.06	103
H_3	5.37	5.40	−8
$H_{6endo,7endo}$	2.07	2.18	−30
$H_{6exo,7exo}$	2.42	2.18	65
$H_{2',6'}$	8.08	8.04	11
$H_{3',5'}$	7.45	7.54	−24
$H_{4'}$	7.59	7.70	−30

two solvents to the relative distances between the protonated nitrogen and the neighboring protons based on the described conformation. Examination of the chemical shift differences (Table II) revealed that the $H_{2ax,4ax}$ as well as the $H_{6exo,7exo}$ protons that showed large downfield shifts lay in close proximity to the positively charged nitrogen. On the other hand, the $H_{2eq,4eq}$, $H_{6endo,7endo}$, and H_3 protons that were farthest removed from the nitrogen showed the small upfield shifts generally observed when the solvent was changed from deuterium oxide to deuterochloroform. On the whole, the correlation between chemical shift differences and nitrogen–proton distances was very good and supported the conformational assignments.

The chemical shift changes on the phenyl ring protons could be explained by using a similar argument. The carbonyl group contributes to the deshielding of the ring protons, which lie in the same plane with it (25). The diminished deshielding resulting from carbonyl group solvation when deuterium oxide was used as a solvent was more pronounced on the nearest *ortho*-protons and decreased progressively with the *meta*- and *para*-protons.

Reports of changes in the proton chemical shifts following a solvent change were interpreted as a conformational change in the molecule. The results reported here point out that conformational interpretations based solely on changes in chemical shifts should be made cautiously. Preferably, such results should be supplemented with coupling constant measurements, still the most reliable information source on the conformations of small molecules in solution.

Failure to demonstrate significant quantities of a piperidine boat conformation in this cocaine-like molecule in solution indicated that such a species is unstable and suggested that it does not participate in events leading to local anesthesia. The occurrence of a chair to boat conformational change when the molecule comes in contact with the nerve membrane could not, however, be excluded. The conformation of cocaine and its analogs in the presence of membrane preparations is currently under investigation.

REFERENCES

(1) "The Pharmacological Basis of Therapeutics," 5th ed., L. S. Goodman and A. Gilman, Eds., Macmillan, New York, N.Y., 1975, p. 386.

(2) R. A. Maxwell, E. Chaplin, S. B. Eckardt, J. R. Soares, and G. Hite, *J. Pharmacol. Exp. Ther.*, **173,** 158 (1970).

(3) M. Shen, J. R. Ruble, and G. Hite, *Acta Crystallogr. Sect. B,* **31,** 2706 (1975).

(4) F. W. Schueler, *J. Am. Pharm. Assoc., Sci. Ed.*, **45,** 197 (1956).

(5) R. E. Lyle, *J. Org. Chem.*, **22,** 1280 (1957).

(6) A. F. Casy, *J. Med. Chem.*, **11,** 188 (1968).

(7) E. J. Gabe and W. H. Barnes, *Acta Crystallogr.*, **16,** 796 (1963).

(8) A. Sinnema, L. Maat, A. J. Van der Guzten, and H. C. Beyerman, *Recl. Trav. Chim. Pays-Bas*, **87,** 1027 (1968).

(9) G. Fodor and K. Nador, *Nature (London)*, **169,** 462 (1952).

(10) A. F. Casy, "PMR Spectroscopy in Medicinal and Biological Chemistry," Academic, New York, N.Y., 1971, pp. 249–251.

(11) G. Chappell, B. F. Grabowski, R. A. Sandmann, and D. M. Yourtee, *J. Pharm. Sci.*, **62,** 414 (1973).

(12) J. Feeney, R. Forster, and E. P. Piper, *J. Chem. Soc., Perkin Trans.* **II,** 1202 (1977).

(13) T. Jen and C. Kaiser, *J. Med. Chem.*, **20,** 693 (1977).

(14) S. J. Daum, C. M. Martini, R. K. Kullnig, and R. L. Clarke, *J. Med. Chem.*, **18,** 436 (1975).

(15) T. A. Montzka, J. D. Matiskella, and R. A. Partyka, *Tetrahedron Lett.*, **1974,** 1325.

(16) J. W. Emsley, J. Feeney, and L. H. Sutcliffe, in "High Resolution Nuclear Magnetic Resonance Spectroscopy," vol. 2, Pergamon, Oxford, England, 1965, pp. 419–428.

(17) S. Castellano and A. A. Bothner-By, *J. Chem. Phys.*, **41,** 3863 (1964).

(18) J. W. Emsley, J. Feeney, and L. H. Sutcliffe, in "High Resolution Nuclear Magnetic Resonance Spectroscopy," vol. 2, Pergamon, Oxford, England, 1965, p. 681.

(19) M. L. Higgins, *J. Am. Chem. Soc.*, **75,** 4123 (1961).

(20) R. J. Abraham and G. Gatti, *J. Chem. Soc. B,* **1966,** 961.

(21) A. Makriyannis, R. F. Sullivan, and H. G. Mautner, *Proc. Natl. Acad. Sci. USA*, **69,** 3416 (1972).

(22) J. B. Lambert, *J. Am. Chem. Soc.*, **89,** 1836 (1967).

(23) J. B. Lambert, R. G. Keske, and D. K. Weary, *J. Am. Chem. Soc.*, **89,** 5921 (1967).

(24) W. F. Reynolds and U. R. Priller, *Can. J. Chem.*, **46,** 2787 (1968).

(25) J. A. Pople, *Proc. R. Soc. London, Ser. A,* **239,** 550 (1957).

ACKNOWLEDGMENTS

Presented at the APhA Academy of Pharmaceutical Sciences, Montreal meeting, May 1978.

Supported by grants from the University of Connecticut Research Foundation (UCRF 257,298) and the U.S. Public Health Service (RR05743).

The authors thank the Yale NMR regional facility where the 270-MHz spectra were obtained.

Dissolution Rate of *p*-Aminobenzoates from Solid Xylitol Dispersions

ILARI SIRENIUS, VELI E. KROGERUS ˣ, and TUULA LEPPÄNEN

Received July 25, 1978, from the *Division of Pharmaceutical Technology, School of Pharmacy, University of Helsinki, Fabianinkatu 35, SF-00170 Helsinki 17, Finland.* Accepted for publication November 15, 1978.

Abstract □ Xylitol was studied as a carrier in solid dispersions because of its low melting point and stability up to 180°. It is more stable than sucrose and does not enter into Maillard reactions. Solid dispersions were prepared from esters of *p*-aminobenzoic acid and xylitol by the melting method and were compressed into tablets. The *p*-aminobenzoate dissolution rates were determined by a modified beaker method. The increase in the dissolution rates was greatest at the lowest drug levels. When the dispersion drug content exceeded 20–30%, the dissolution rate per unit area remained nearly constant. In the latter case, the increase in the dissolution rate was primarily due to an increase in area. When the carbon chain length was increased in the homologous series, the dissolution rate from the xylitol dispersions showed a nearly linear decrease.

Keyphrases □ *p*-Aminobenzoic acid—rate of dissolution from solid xylitol dispersions □ Xylitol—carrier, solid dispersions of *p*-aminobenzoic acid esters □ Dissolution rate—*p*-aminobenzoic acid esters from solid xylitol dispersions □ Dosage forms, solid—dispersions, *p*-aminobenzoic acid esters in xylitol, dissolution rate

Solid dispersions have been used to increase the dissolution rate and bioavailability of drugs that are only slightly water soluble. The carriers used have been physiologically inert compounds that are readily water soluble. To reduce sulfathiazole particle size, eutectic mixtures, for example, have been prepared from urea and slightly water-soluble sulfathiazole by the melting method (1). However, the high temperatures required by the melting method may cause either the drug or the carrier to decompose.

p-Aminobenzoic acid esters, particularly the higher homologous ones, are only slightly soluble in water (2). Xylitol was studied as a carrier for solid dispersions of *p*-aminobenzoates because of its low melting point and stability up to 180°. Xylitol is almost equal to sucrose in water solubility and is more stable chemically; when xylitol is heated in the presence of amino groups, it does not undergo the Maillard ("browning") reaction (3, 4).

The melting range of xylitol is 93–94.5°, and it begins to decompose at 179–186° (3). When xylitol is used as the dispersing medium, the dissolution process is endothermic. The relatively high negative heat of xylitol solution is 145.7 J/g (3).

EXPERIMENTAL

Materials—The *p*-aminobenzoic acid esters studied were methyl *p*-aminobenzoate[1], ethyl *p*-aminobenzoate[1] (benzocaine), propyl *p*-aminobenzoate[2] (risocaine), and butyl *p*-aminobenzoate[1] (butamben). Xylitol[3] was used as a carrier.

Solid Dispersion Preparation—Solid dispersions were prepared using the direct melting method (1). A physical mixture of the drug and xylitol was made, and this mixture was heated in an IR bath[4]. The mixture of xylitol and methyl *p*-aminobenzoate was heated to 114°, and the other mixtures were heated to 96–98°. The molten mixture was cooled quickly by pouring it onto a stainless steel plate in an ice bath. The mixture was left to stabilize for 24 hr at room temperature.

Sample Preparation—The dispersion used in the tablets was pulverized to 0.71-mm particles. For dissolution rate determination, the solid dispersions were compressed into cylindrical tablets (18 mm in diameter; 750 mg) using a hydraulic press[5] in the same way as potassium bromide disks are prepared for IR spectroscopy. Pure drug tablets were prepared using the same pressure, 400 MPa.

Dissolution Rate Determination—The dissolution rates were determined using a modified beaker method (5). Each determination was run in 600 ml of distilled water in a 800-ml beaker at 37°. The tablet was placed on a sieve net (mesh 2.0 mm) positioned 2 cm from the bottom of the beaker. A sieve net basket (4 × 4 × 1 cm) was placed over the tablet (6). A three-blade stirrer[6] was placed 5 cm from the bottom of the beaker. The stirring speed was 60 rpm.

The tablet was placed on the sieve net, and the solvent was poured into the beaker. The dissolution test time was 3 min. Samples were taken at the stirring blade level through a filter[7] using a peristaltic pump which let the sample solution into the spectrophotometer flow-through cells[8]. The sample solution absorbance was registered automatically at 284 nm. Xylitol did not interfere. The dissolution rate was determined per tablet unit area (milligrams per square centimeter per hour).

RESULTS AND DISCUSSION

At a low drug content (<10%), the molten mixture solidification was slow. When the drug content was increased, however, the dispersion solidified quickly. A solid dispersion of xylitol–*p*-aminobenzoates increased

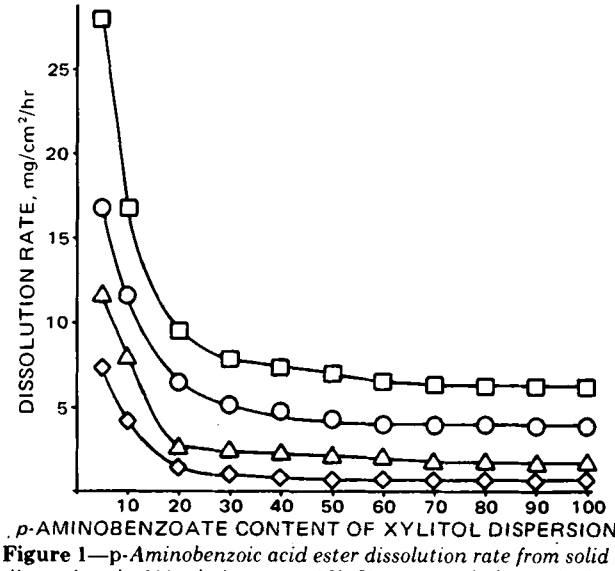

Figure 1—p-*Aminobenzoic acid ester dissolution rate from solid xylitol dispersions in 600 ml of water at 37°. Key:* □, *methyl* p-*aminobenzoate;* ○, *ethyl* p-*aminobenzoate;* △, *propyl* p-*aminobenzoate; and* ◇, *butyl* p-*aminobenzoate.*

[1] Purum, Fluka AG.
[2] ICN Pharmaceuticals.
[3] Pharmaceutical grade, Sokerikemia Oy, Xyrofin Ltd.
[4] Ströhlein, Düsseldorf-Stuttgart, West Germany.
[5] Matra-Werke G.M.B.H., type M 177.2, Frankfurt, West Germany.
[6] Nalgene 6160.
[7] Millipore, 0.22 μm.
[8] Unicam SP. 800A, Unicam Instruments Ltd.

0022-3549/79/0600-0791$01.00/0
© 1979, American Pharmaceutical Association

the *p*-aminobenzoate dissolution rate. The difference between several dissolution rate tests was less than ±5% during the first 3 min of dissolution when the surface areas of the tablets were still nearly identical. The dissolution rate was calculated over the portion of the dissolution profile that followed zero-order kinetics.

The increase in the dissolution rate as compared with that of pure drug tablets was greatest when the drug content was lowest. The dissolution rate of a xylitol dispersion containing 5% butyl *p*-aminobenzoate was about 10 times, per unit area, the pure drug dissolution rate. When the increase in area caused by dispersion of the drug with xylitol (1:20) was considered, the dissolution rate of a 5% dispersion was about 200-fold that of the pure drug. The dissolution rate of the methyl *p*-aminobenzoate dispersion was fivefold per unit area, which corresponds to a 100-fold increase in the dissolution rate of the pure drug when the increase in area is considered. When the dispersion drug content was 20–30%, the changes in the dissolution rate per unit area decreased. In this case, the increase in the dissolution rate was primarily due to an increase in area.

A curve depicting the dissolution rates as a function of the drug content of the dispersion was of nearly the same shape for each compound (Fig. 1). When the *p*-aminobenzoic acid ester alkyl group carbon chain was increased, the xylitol dispersion dissolution rate showed a nearly linear decrease.

REFERENCES

(1) K. Sekiguchi and N. Obi, *Chem. Pharm. Bull.*, **9**, 866 (1961).

(2) J. Büchi, X. Perlia, and A. Strässle, *Arzneim.-Forsch.*, **16**, 1657 (1966).

(3) F.-K. Grütte and H. Rödel, *Ernährungsforschung*, **20**, 74 (1975).

(4) F. Kracher, *Kak. Zucker*, **27**, 68 (1975).

(5) G. Levy and B. A. Hayes, *N. Engl. J. Med.*, **262**, 1053 (1960).

(6) E. Kristoffersson and S. Halme, *Acta Pharm. Fenn.*, **87**, 61 (1978).

ACKNOWLEDGMENTS

Supported by a grant from Suomen farmaseuttinen yhdistys (Society of Pharmaceutical Sciences in Finland).

Pharmacokinetics of Drugs Subject to Enterohepatic Circulation

HSIAO-SHENG GEORGE CHEN and JOSEPH F. GROSS ×

Received October 16, 1978, from the *Department of Internal Medicine and the Department of Chemical Engineering, University of Arizona, Tucson, AZ 85721.* Accepted for publication November 15, 1978.

Abstract □ The influence of the changes in biliary excretion and reabsorption rates on the pharmacokinetics of drugs subject to enterohepatic circulation was examined analytically. A recently proposed two-compartment model with drug elimination occurring in each compartment was adapted to represent the body and the GI tract. Enhanced reabsorption was equivalent to biliary excretion rate reduction, except that the latter always decreased α and prolonged the α-phase half-life while the former always increased α and shortened the half-life. However, depending on the relative values of the two elimination rate constants, biliary excretion reduction (or reabsorption enhancement) could either increase or decrease the terminal drug half-life (β-phase). Whether the terminal drug half-life was prolonged or shortened, a biliary excretion reduction always increased the area under the plasma decay curve for intravenous and oral doses and also raised the steady-state drug level in the body for constant-rate intravenous infusion. As a consequence, the lethality, toxicity, or effectiveness of the drug will be increased for patients with impaired bile flow or enhanced drug reabsorption; therefore, the clinical dosage may have to be reduced.

Keyphrases □ Enterohepatic circulation—effect of biliary excretion and reabsorption rates on drug pharmacokinetics, two-compartment model □ Distribution—enterohepatic circulation, effect of biliary excretion and reabsorption rates, pharmacokinetics, two-compartment model □ Pharmacokinetics—enterohepatic circulation, effect of biliary excretion and reabsorption rates, two-compartment model

When a substance is excreted into the bile, passes through the lumen of the intestine, is reabsorbed, and then is carried to the liver *via* blood flow, it undergoes enterohepatic circulation or cycling. Many endogenous and exogenous substances (bile salts, morphine, methadone, methotrexate, digitoxin, *etc.*) can undergo enterohepatic circulation (1). Pharmacokinetic study of drugs subject to enterohepatic circulation has gained importance in recent years.

A two-compartment model representing the body and the GI tract was recently proposed by Harrison and Gibaldi (2) to describe the influence of cholestasis (bile flow reduction or discontinuance) on the elimination of drugs undergoing enterohepatic circulation. Scheme I shows the

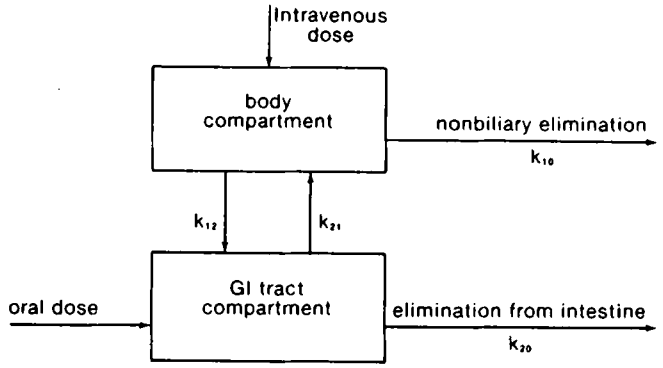

Scheme I—Pharmacokinetic model for a drug subject to enterohepatic circulation.

pharmacokinetic model of the biliary excretion (k_{12}) and reabsorption process (k_{21}) of a drug eliminated by both compartments. Cholestasis was simulated numerically by reducing the transfer rate constant k_{12}. Results (2) suggested that cholestasis can either increase or decrease the terminal drug half-life ($T^{\beta}_{1/2}$), depending on the ratio of the two elimination rate constants k_{10}/k_{20}. If the ratio is greater than unity, cholestasis will increase β and reduce the drug half-life. The reverse is true if the ratio is less than unity. In contrast, a biliary excretion reduction will always decrease α and prolong the α-phase half-life.

Although the terminal drug half-life may be decreased, many experiments showed that drug lethality and toxicity are greater in animals with a ligated bile duct than in normal animals (1). Furthermore, since enterohepatic circulation is characterized by biliary excretion and reabsorption, the reabsorption influence on drug disposition should also be studied. In the present work, the effects of both processes on the pharmacokinetics of drugs undergoing enterohepatic circulation were examined analytically. The dependence of the drug half-lives, the area

0022-3549/79/0600-0792$01.00/0

© 1979, American Pharmaceutical Association

the *p*-aminobenzoate dissolution rate. The difference between several dissolution rate tests was less than ±5% during the first 3 min of dissolution when the surface areas of the tablets were still nearly identical. The dissolution rate was calculated over the portion of the dissolution profile that followed zero-order kinetics.

The increase in the dissolution rate as compared with that of pure drug tablets was greatest when the drug content was lowest. The dissolution rate of a xylitol dispersion containing 5% butyl *p*-aminobenzoate was about 10 times, per unit area, the pure drug dissolution rate. When the increase in area caused by dispersion of the drug with xylitol (1:20) was considered, the dissolution rate of a 5% dispersion was about 200-fold that of the pure drug. The dissolution rate of the methyl *p*-aminobenzoate dispersion was fivefold per unit area, which corresponds to a 100-fold increase in the dissolution rate of the pure drug when the increase in area is considered. When the dispersion drug content was 20–30%, the changes in the dissolution rate per unit area decreased. In this case, the increase in the dissolution rate was primarily due to an increase in area.

A curve depicting the dissolution rates as a function of the drug content of the dispersion was of nearly the same shape for each compound (Fig. 1). When the *p*-aminobenzoic acid ester alkyl group carbon chain was increased, the xylitol dispersion dissolution rate showed a nearly linear decrease.

REFERENCES

(1) K. Sekiguchi and N. Obi, *Chem. Pharm. Bull.*, **9**, 866 (1961).

(2) J. Büchi, X. Perlia, and A. Strässle, *Arzneim.-Forsch.*, **16**, 1657 (1966).

(3) F.-K. Grütte and H. Rödel, *Ernährungsforschung*, **20**, 74 (1975).

(4) F. Kracher, *Kak. Zucker*, **27**, 68 (1975).

(5) G. Levy and B. A. Hayes, *N. Engl. J. Med.*, **262**, 1053 (1960).

(6) E. Kristoffersson and S. Halme, *Acta Pharm. Fenn.*, **87**, 61 (1978).

ACKNOWLEDGMENTS

Supported by a grant from Suomen farmaseuttinen yhdistys (Society of Pharmaceutical Sciences in Finland).

Pharmacokinetics of Drugs Subject to Enterohepatic Circulation

HSIAO-SHENG GEORGE CHEN and JOSEPH F. GROSS ×

Received October 16, 1978, from the *Department of Internal Medicine and the Department of Chemical Engineering, University of Arizona, Tucson, AZ 85721.* Accepted for publication November 15, 1978.

Abstract □ The influence of the changes in biliary excretion and reabsorption rates on the pharmacokinetics of drugs subject to enterohepatic circulation was examined analytically. A recently proposed two-compartment model with drug elimination occurring in each compartment was adapted to represent the body and the GI tract. Enhanced reabsorption was equivalent to biliary excretion rate reduction, except that the latter always decreased α and prolonged the α-phase half-life while the former always increased α and shortened the half-life. However, depending on the relative values of the two elimination rate constants, biliary excretion reduction (or reabsorption enhancement) could either increase or decrease the terminal drug half-life (β-phase). Whether the terminal drug half-life was prolonged or shortened, a biliary excretion reduction always increased the area under the plasma decay curve for intravenous and oral doses and also raised the steady-state drug level in the body for constant-rate intravenous infusion. As a consequence, the lethality, toxicity, or effectiveness of the drug will be increased for patients with impaired bile flow or enhanced drug reabsorption; therefore, the clinical dosage may have to be reduced.

Keyphrases □ Enterohepatic circulation—effect of biliary excretion and reabsorption rates on drug pharmacokinetics, two-compartment model □ Distribution—enterohepatic circulation, effect of biliary excretion and reabsorption rates, pharmacokinetics, two-compartment model □ Pharmacokinetics—enterohepatic circulation, effect of biliary excretion and reabsorption rates, two-compartment model

When a substance is excreted into the bile, passes through the lumen of the intestine, is reabsorbed, and then is carried to the liver *via* blood flow, it undergoes enterohepatic circulation or cycling. Many endogenous and exogenous substances (bile salts, morphine, methadone, methotrexate, digitoxin, *etc.*) can undergo enterohepatic circulation (1). Pharmacokinetic study of drugs subject to enterohepatic circulation has gained importance in recent years.

A two-compartment model representing the body and the GI tract was recently proposed by Harrison and Gibaldi (2) to describe the influence of cholestasis (bile flow reduction or discontinuance) on the elimination of drugs undergoing enterohepatic circulation. Scheme I shows the

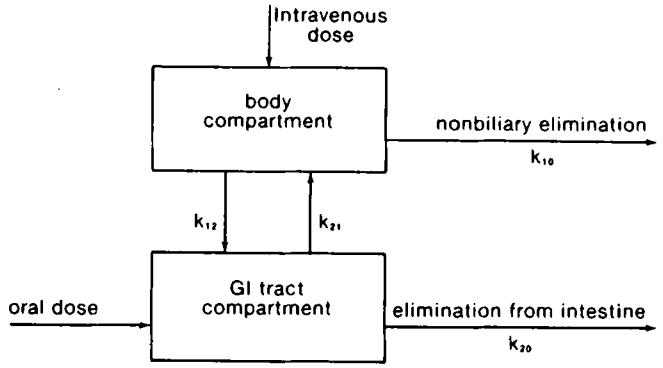

Scheme I—Pharmacokinetic model for a drug subject to enterohepatic circulation.

pharmacokinetic model of the biliary excretion (k_{12}) and reabsorption process (k_{21}) of a drug eliminated by both compartments. Cholestasis was simulated numerically by reducing the transfer rate constant k_{12}. Results (2) suggested that cholestasis can either increase or decrease the terminal drug half-life ($T^{\beta}_{1/2}$), depending on the ratio of the two elimination rate constants k_{10}/k_{20}. If the ratio is greater than unity, cholestasis will increase β and reduce the drug half-life. The reverse is true if the ratio is less than unity. In contrast, a biliary excretion reduction will always decrease α and prolong the α-phase half-life.

Although the terminal drug half-life may be decreased, many experiments showed that drug lethality and toxicity are greater in animals with a ligated bile duct than in normal animals (1). Furthermore, since enterohepatic circulation is characterized by biliary excretion and reabsorption, the reabsorption influence on drug disposition should also be studied. In the present work, the effects of both processes on the pharmacokinetics of drugs undergoing enterohepatic circulation were examined analytically. The dependence of the drug half-lives, the area

0022-3549/79/0600-0792$01.00/0

© 1979, American Pharmaceutical Association

under the plasma decay curve, and the steady-state drug level after intravenous infusion on changes in biliary drug excretion and reabsorption rates were studied.

THEORETICAL

The model used by Harrison and Gibaldi (2) was adopted, although it involved the assumption that the bile flow is a continuous process. The drug can be administered either as an intravenous bolus injection into the body compartment or as an oral bolus dose into the GI tract. Drug elimination occurs linearly in both compartments. The rate constant k_{10} represents the sum of all first-order rate constants associated with nonbiliary elimination; the constant k_{20} is the drug disappearance rate from the reabsorption sites (intestine) by biotransformation in the intestine or by fecal elimination.

The biliary excretion and reabsorption rates are represented by the constants k_{12} and k_{21} separately. Disease states like cholestasis that reduce biliary excretion or mechanisms (1) that enhance bile flow can all be simulated by corresponding changes in k_{12}. Similarly, changes in the conjugate hydrolysis rate due to intestinal microorganisms and subsequent deconjugated product reabsorption can be simulated by changing the value of k_{21}.

The amount of drug in the body, A, as a function of time after different administration routes can be solved easily to yield the following analytic expressions.

After intravenous bolus injection of dose D, the drug level in the body is:

$$A_{iv} = \frac{(\alpha - k_{21} - k_{20})D}{\alpha - \beta}\exp(-\alpha t) + \frac{(k_{21} + k_{20} - \beta)D}{\alpha - \beta}\exp(-\beta t) \quad \text{(Eq. 1)}$$

where:

$$\alpha = \tfrac{1}{2}(k_{21} + k_{20} + k_{12} + k_{10} + \nabla) \quad \text{(Eq. 2)}$$

$$\beta = \tfrac{1}{2}(k_{21} + k_{20} + k_{12} + k_{10} - \nabla) \quad \text{(Eq. 3)}$$

and:

$$\nabla^2 = (k_{21} + k_{20} + k_{12} + k_{10})^2 - 4(k_{12}k_{20} + k_{10}k_{21} + k_{10}k_{20}) \quad \text{(Eq. 4)}$$

The area under the intravenous injection plasma decay curve is then obtained by integrating Eq. 1:

$$CXT_{iv} = \left(\frac{D}{V}\right)\left(\frac{k_{21} + k_{20}}{k_{12}k_{20} + k_{21}k_{10} + k_{10}k_{20}}\right) \quad \text{(Eq. 5)}$$

where V is the distribution volume.

After oral administration of dose D, the drug level in the body is:

$$A_{oral} = \frac{Dk_{21}}{\alpha - \beta}[\exp(-\beta t) - \exp(-\alpha t)] \quad \text{(Eq. 6)}$$

Since the area under the plasma decay curve for oral dosing is:

$$CXT_{oral} = \left(\frac{D}{V}\right)\left(\frac{k_{21}}{k_{12}k_{20} + k_{21}k_{10} + k_{10}k_{20}}\right) \quad \text{(Eq. 7)}$$

the oral dose availability (or the fraction absorbed into the body) is:

$$F = \frac{k_{21}}{k_{21} + k_{20}} \quad \text{(Eq. 8)}$$

Following the oral dose, the peak drug level and the time required to reach it are:

$$A_{max} = \frac{Dk_{21}}{\alpha}\left(\frac{\alpha}{\beta}\right)^{-\beta/\alpha-\beta} \quad \text{(Eq. 9)}$$

$$t_{peak} = \frac{1}{\alpha - \beta}\ln\frac{\alpha}{\beta} \quad \text{(Eq. 10)}$$

Following intravenous drug infusion at constant rate k_0, the drug level in the body as a function of time is:

$$A_{infusion} = \frac{k_0(k_{21} + k_{20})}{\alpha\beta} - \frac{k_0(\alpha - k_{21} - k_{20})}{\alpha(\alpha - \beta)}\exp(-\alpha t) - \frac{k_0(k_{21} + k_{20} - \beta)}{\beta(\alpha - \beta)}\exp(-\beta t) \quad \text{(Eq. 11)}$$

As time proceeds, the drug level reaches a steady state:

$$A_{ss} = \frac{k_0(k_{21} + k_{20})}{k_{21}k_{10} + k_{12}k_{20} + k_{10}k_{20}} \quad \text{(Eq. 12)}$$

The drug half-lives are then given by:

$$T^{\alpha}_{1/2} = \frac{\ln 2}{\alpha} \quad \text{(Eq. 13)}$$

and:

$$T^{\beta}_{1/2} = \frac{\ln 2}{\beta} \quad \text{(Eq. 14)}$$

where $T^{\beta}_{1/2}$ is the terminal drug half-life.

The influences of biliary excretion and reabsorption processes on drug disposition can be simulated by changing the rate constants k_{12} and k_{21}. It can be shown (*Appendix*) that:

$$\frac{\partial\beta}{\partial k_{12}} > 0 \quad \text{if } k_{20} > k_{10} \quad \text{(Eq. 15)}$$

$$\frac{\partial\beta}{\partial k_{12}} = 0 \quad \text{if } k_{20} = k_{10} \quad \text{(Eq. 16)}$$

$$\frac{\partial\beta}{\partial k_{12}} < 0 \quad \text{if } k_{20} < k_{10} \quad \text{(Eq. 17)}$$

The physical meaning of a multivariable function partial differentiation with respect to one of its variables is the rate of change of that function with respect to the variable while the other variables are held constant. Therefore, β will increase as k_{12} increases and will decrease as k_{12} decreases if $k_{20} > k_{10}$. If $k_{20} < k_{10}$, β will decrease while k_{12} is increased. If $k_{20} = k_{10}$, the value of β will be independent of the changes in k_{12}.

Similarly, no matter what the relative values of k_{20} and k_{10}, the partial derivative of α with respect to k_{12} is always greater than zero. Thus, a biliary excretion reduction will decrease α and produce a longer α-phase half-life. However, by observing Eqs. 5, 7, and 12, it is obvious that a reduction of k_{12} will increase CXT_{iv}, CXT_{oral}, and A_{ss}.

The influence of changing the reabsorption rate k_{21} on the drug elimination can be studied similarly. It can be proved that:

$$\frac{\partial\beta}{\partial k_{21}} < 0 \quad \text{if } k_{20} > k_{10} \quad \text{(Eq. 18)}$$

$$\frac{\partial\beta}{\partial k_{21}} = 0 \quad \text{if } k_{20} = k_{10} \quad \text{(Eq. 19)}$$

$$\frac{\partial\beta}{\partial k_{21}} > 0 \quad \text{if } k_{20} < k_{10} \quad \text{(Eq. 20)}$$

Thus, an increase in the drug reabsorption rate will have the same effect on β and $T^{\beta}_{1/2}$ as a biliary excretion reduction. However, $\partial\alpha/\partial k_{21}$ is always positive for any combination of variables. An enhancement in the reabsorption rate will thus increase α and shorten the α-phase half-life.

The effect of k_{21} on the values of CXT_{iv}, CXT_{oral}, and A_{ss} cannot be as easily observed as with k_{12}. However, Eqs. 5, 7, and 12 can be rewritten in the form:

$$CXT_{iv} = \left(\frac{D}{V}\right)\left[\frac{1}{k_{10}} - \frac{k_{12}k_{20}}{k_{10}(k_{12}k_{20} + k_{21}k_{10} + k_{10}k_{20})}\right] \quad \text{(Eq. 21)}$$

An increase in k_{21} will decrease the second term in the parenthesis and increase CXT_{iv}. Hence, an increase in the drug reabsorption rate will increase CXT_{iv}, CXT_{oral}, and A_{ss} while a reduction of k_{21} will decrease these quantities.

DISCUSSION

The influence of the biliary excretion and reabsorption rates on the disposition of drugs subject to enterohepatic circulation was studied analytically using the model of Harrison and Gibaldi (2). The results are:

1. If $k_{20} > k_{10}$, a biliary excretion reduction or reabsorption rate increase will decrease β and produce a longer half-life $T^{\beta}_{1/2}$. If $k_{20} < k_{10}$, a decrease in biliary excretion or reabsorption enhancement will increase β and shorten the drug half-life. If $k_{20} = k_{10}$, the terminal half-life will be independent of the changes in either rate.
2. A reduction of biliary drug excretion will always decrease the value of α and increase the α-phase half-life, while an increase in the reabsorption rate will have the reverse effects, regardless of the combination of variables.
3. A biliary excretion reduction or an increase in the reabsorption rate will always increase the area under the plasma decay curve for intravenous and oral doses and will also raise the steady-state drug level in the body following a constant-rate intravenous infusion.

Biliary excretion enhancement or drug reabsorption decrease will produce the opposite effects on drug disposition.

Although the terminal half-life may be reduced by biliary dysfunction or reabsorption enhancement (when $k_{20} < k_{10}$), CXT_{iv}, CXT_{oral}, and A_{ss} will always be increased by these changes. Since drug effectiveness and toxicity are closely related to CXT values after intravenous or oral dosing and to A_{ss}, the steady-state drug level, after infusion, they will increase for patients with biliary dysfunction or enhanced reabsorption. To avoid toxicity, the drug dosage may have to be reduced accordingly.

APPENDIX

From Eq. 3, partial differentiation of β with respect to k_{12} yields:

$$\frac{\partial\beta}{\partial k_{12}} = \frac{1}{2\nabla}[\nabla - (k_{21} + k_{12} + k_{10} - k_{20})] \quad \text{(Eq. A1)}$$

Since ∇ is always positive, if $k_{20} \geq k_{21} + k_{12} + k_{10}$, then $\partial\beta/\partial k_{12}$ will be positive. If $k_{21} + k_{12} + k_{10} > k_{20}$, $\partial\beta/\partial k_{12}$ has the same sign as $\nabla^2 - (k_{21} + k_{12} + k_{10} - k_{20})^2$. Thus:

$$\nabla^2 - (k_{21} + k_{12} + k_{10} - k_{20})^2 = 4k_{21}(k_{20} - k_{10}) \quad \text{(Eq. A2)}$$

and, therefore:

$$\frac{\partial\beta}{\partial k_{12}} > 0 \quad \text{if } k_{20} > k_{10} \quad \text{(Eq. A3)}$$

$$\frac{\partial\beta}{\partial k_{12}} = 0 \quad \text{if } k_{20} = k_{10} \quad \text{(Eq. A4)}$$

$$\frac{\partial\beta}{\partial k_{12}} < 0 \quad \text{if } k_{20} < k_{10} \quad \text{(Eq. A5)}$$

Similarly, partial differentiation of β with respect to k_{21} gives:

$$\frac{\partial\beta}{\partial k_{21}} = \frac{1}{2\nabla}[\nabla - (k_{21} + k_{12} + k_{20} - k_{10})] \quad \text{(Eq. A6)}$$

which is similar to Eq. A1 except that the order of k_{20} and k_{10} is reversed. Therefore:

$$\frac{\partial\beta}{\partial k_{21}} < 0 \quad \text{if } k_{20} > k_{10} \quad \text{(Eq. A7)}$$

$$\frac{\partial\beta}{\partial k_{21}} = 0 \quad \text{if } k_{20} = k_{10} \quad \text{(Eq. A8)}$$

$$\frac{\partial\beta}{\partial k_{21}} > 0 \quad \text{if } k_{20} < k_{10} \quad \text{(Eq. A9)}$$

REFERENCES

(1) G. L. Plaa, in "Handbook of Experimental Pharmacology," vol. 28, part 3, J. R. Gillette, T. R. Mitchell, and P. S. Randall, Eds., Springer-Verlag, New York, N.Y., 1975, pp 130–149.

(2) L. I. Harrison and M. Gibaldi, *J. Pharm. Sci.*, **65**, 1346 (1976).

ACKNOWLEDGMENTS

Supported in part by Grant CA-17094 from the National Cancer Institute.

Progestin Permeation through Polymer Membranes III: Polymerization Solvent Effect on Progesterone Permeation through Hydrogel Membranes

G. M. ZENTNER, J. R. CARDINAL ˣ, and D. E. GREGONIS

Received August 4, 1978, from the *Department of Pharmaceutics, College of Pharmacy, University of Utah, Salt Lake City, UT 84112.* Accepted for publication November 13, 1978.

Abstract □ Hydrogels prepared from poly(hydroxyethyl methacrylate) are biocompatible and highly permeable to low molecular weight solutes. Permeation rates can be varied by altering the cross-linker concentration or using copolymers; the latter are chosen to alter the hydrogel equilibrium hydration. These factors suggest that hydrogels are good candidates for controlled-release drug delivery devices. Hydrogels may be synthesized using various temperatures, initiators (nature and concentration), and solvents (nature and concentration). This study demonstrated that progesterone permeation through poly(hydroxyethyl methacrylate) films is independent of polymerization solvent (nature and concentration) for the solvents, water, ethanol, and *tert*-butyl alcohol. The importance of hydrogel equilibrium hydration in progesterone permeation is emphasized.

Keyphrases □ Hydrogels, poly(hydroxyethyl methacrylate)—progesterone permeation, effect of various nonaqueous polymerization solvents □ Hydroxyethyl methacrylate—hydrogel films, progesterone permeation, effect of various nonaqueous polymerization solvents □ Progesterone—permeation through hydrogel membranes, effect of various nonaqueous polymerization solvents □ Delivery devices, controlled—hydrogel membranes, progesterone permeation, effect of various nonaqueous polymerization solvents

Hydrogels are biocompatible (1) and potentially useful for controlled-release drug delivery systems (2–9). Monomer composition and cross-linker type and composition determine hydrogel drug release rates.

The physical–chemical properties of hydrogels depend on polymerization conditions (10). In poly(hydroxyalkyl methacrylate) synthesis, polymerization at the gel equilibrium water content is convenient. However, varying the initial solvent composition is often advantageous in fabricating controlled-release drug delivery devices. Certain fabrication problems may be overcome through nonaqueous polymerization (4, 7). However, polymer chain organization, degree of cross-linking, and other properties may be altered, resulting in a different polymer when water is omitted. These changes could affect the permeability of these films relative to those polymerized in the presence of water.

For these reasons, a systematic study of polymerization solvent effects on progesterone permeability through films polymerized from hydroxyethyl methacrylate was undertaken. Films prepared without cross-linker were chosen because the permeabilities of these films are highly sensitive to small changes in cross-link density (9, 11, 12).

Also included in the present study are the effects of the solvents ethanol and *tert*-butyl alcohol. Based on thermodynamic (13) and swelling arguments (14), ethanol and, to a greater extent, *tert*-butyl alcohol are better solvents for poly(hydroxyethyl methacrylate) than is water. These solvents are expected to offer certain advantages in the polymerization of films containing high concentrations of cross-linking agents and aid in dissolving drugs that nor-

0022-3549/79/0600-0794$01.00/0
© 1979, American Pharmaceutical Association

Although the terminal half-life may be reduced by biliary dysfunction or reabsorption enhancement (when $k_{20} < k_{10}$), CXT_{iv}, CXT_{oral}, and A_{ss} will always be increased by these changes. Since drug effectiveness and toxicity are closely related to CXT values after intravenous or oral dosing and to A_{ss}, the steady-state drug level, after infusion, they will increase for patients with biliary dysfunction or enhanced reabsorption. To avoid toxicity, the drug dosage may have to be reduced accordingly.

APPENDIX

From Eq. 3, partial differentiation of β with respect to k_{12} yields:

$$\frac{\partial\beta}{\partial k_{12}} = \frac{1}{2\nabla}[\nabla - (k_{21} + k_{12} + k_{10} - k_{20})] \quad \text{(Eq. A1)}$$

Since ∇ is always positive, if $k_{20} \geq k_{21} + k_{12} + k_{10}$, then $\partial\beta/\partial k_{12}$ will be positive. If $k_{21} + k_{12} + k_{10} > k_{20}$, $\partial\beta/\partial k_{12}$ has the same sign as $\nabla^2 - (k_{21} + k_{12} + k_{10} - k_{20})^2$. Thus:

$$\nabla^2 - (k_{21} + k_{12} + k_{10} - k_{20})^2 = 4k_{21}(k_{20} - k_{10}) \quad \text{(Eq. A2)}$$

and, therefore:

$$\frac{\partial\beta}{\partial k_{12}} > 0 \quad \text{if } k_{20} > k_{10} \quad \text{(Eq. A3)}$$

$$\frac{\partial\beta}{\partial k_{12}} = 0 \quad \text{if } k_{20} = k_{10} \quad \text{(Eq. A4)}$$

$$\frac{\partial\beta}{\partial k_{12}} < 0 \quad \text{if } k_{20} < k_{10} \quad \text{(Eq. A5)}$$

Similarly, partial differentiation of β with respect to k_{21} gives:

$$\frac{\partial\beta}{\partial k_{21}} = \frac{1}{2\nabla}[\nabla - (k_{21} + k_{12} + k_{20} - k_{10})] \quad \text{(Eq. A6)}$$

which is similar to Eq. A1 except that the order of k_{20} and k_{10} is reversed. Therefore:

$$\frac{\partial\beta}{\partial k_{21}} < 0 \quad \text{if } k_{20} > k_{10} \quad \text{(Eq. A7)}$$

$$\frac{\partial\beta}{\partial k_{21}} = 0 \quad \text{if } k_{20} = k_{10} \quad \text{(Eq. A8)}$$

$$\frac{\partial\beta}{\partial k_{21}} > 0 \quad \text{if } k_{20} < k_{10} \quad \text{(Eq. A9)}$$

REFERENCES

(1) G. L. Plaa, in "Handbook of Experimental Pharmacology," vol. 28, part 3, J. R. Gillette, T. R. Mitchell, and P. S. Randall, Eds., Springer-Verlag, New York, N.Y., 1975, pp 130–149.

(2) L. I. Harrison and M. Gibaldi, *J. Pharm. Sci.*, **65**, 1346 (1976).

ACKNOWLEDGMENTS

Supported in part by Grant CA-17094 from the National Cancer Institute.

Progestin Permeation through Polymer Membranes III: Polymerization Solvent Effect on Progesterone Permeation through Hydrogel Membranes

G. M. ZENTNER, J. R. CARDINAL ˣ, and D. E. GREGONIS

Received August 4, 1978, from the *Department of Pharmaceutics, College of Pharmacy, University of Utah, Salt Lake City, UT 84112.* Accepted for publication November 13, 1978.

Abstract □ Hydrogels prepared from poly(hydroxyethyl methacrylate) are biocompatible and highly permeable to low molecular weight solutes. Permeation rates can be varied by altering the cross-linker concentration or using copolymers; the latter are chosen to alter the hydrogel equilibrium hydration. These factors suggest that hydrogels are good candidates for controlled-release drug delivery devices. Hydrogels may be synthesized using various temperatures, initiators (nature and concentration), and solvents (nature and concentration). This study demonstrated that progesterone permeation through poly(hydroxyethyl methacrylate) films is independent of polymerization solvent (nature and concentration) for the solvents, water, ethanol, and *tert*-butyl alcohol. The importance of hydrogel equilibrium hydration in progesterone permeation is emphasized.

Keyphrases □ Hydrogels, poly(hydroxyethyl methacrylate)—progesterone permeation, effect of various nonaqueous polymerization solvents □ Hydroxyethyl methacrylate—hydrogel films, progesterone permeation, effect of various nonaqueous polymerization solvents □ Progesterone—permeation through hydrogel membranes, effect of various nonaqueous polymerization solvents □ Delivery devices, controlled—hydrogel membranes, progesterone permeation, effect of various nonaqueous polymerization solvents

Hydrogels are biocompatible (1) and potentially useful for controlled-release drug delivery systems (2–9). Monomer composition and cross-linker type and composition determine hydrogel drug release rates.

The physical–chemical properties of hydrogels depend on polymerization conditions (10). In poly(hydroxyalkyl methacrylate) synthesis, polymerization at the gel equilibrium water content is convenient. However, varying the initial solvent composition is often advantageous in fabricating controlled-release drug delivery devices. Certain fabrication problems may be overcome through nonaqueous polymerization (4, 7). However, polymer chain organization, degree of cross-linking, and other properties may be altered, resulting in a different polymer when water is omitted. These changes could affect the permeability of these films relative to those polymerized in the presence of water.

For these reasons, a systematic study of polymerization solvent effects on progesterone permeability through films polymerized from hydroxyethyl methacrylate was undertaken. Films prepared without cross-linker were chosen because the permeabilities of these films are highly sensitive to small changes in cross-link density (9, 11, 12).

Also included in the present study are the effects of the solvents ethanol and *tert*-butyl alcohol. Based on thermodynamic (13) and swelling arguments (14), ethanol and, to a greater extent, *tert*-butyl alcohol are better solvents for poly(hydroxyethyl methacrylate) than is water. These solvents are expected to offer certain advantages in the polymerization of films containing high concentrations of cross-linking agents and aid in dissolving drugs that nor-

0022-3549/79/0600-0794$01.00/0
© 1979, American Pharmaceutical Association

Table I—Progesterone Permeation Parameters in Poly(hydroxyethyl methacrylate) Films as a Function of Polymerization Solvent Type and Concentration

Concentration, % v/v	$D \times 10^9$, cm²/sec	K_d	$U \times 10^7$, cm²/sec	H
		Water		
0	5.54	102	5.65	0.47
	4.96	109	5.41	0.46
	5.89	100	5.89	0.47
5	5.05	85	4.29	0.45
	4.99	99	4.94	0.46
10	5.08	104	5.28	0.46
	4.79	107	5.13	0.45
20	6.02	92	5.54	0.46
	5.29	107	5.66	0.51
40	6.85	103	7.06	0.47
	4.66	120	5.59	0.52
	3.81	133	5.07	0.52
	4.77	124	5.91	0.53
	4.23	134	5.67	0.50
	4.48	131	5.87	0.48
		Ethanol		
20	4.34	101	4.38	0.45
	4.77	111	5.30	0.46
	4.55	114	5.19	0.51
40	5.50	107	5.89	0.48
	4.81	96	4.62	0.50
		tert-Butyl Alcohol		
20	5.46	110	6.01	0.48
40	4.64	107	4.96	0.53
	6.84	103	7.04	0.45
Average ± *SD*	5.10 ± 0.76	109 ± 13	5.49 ± 0.69	0.48 ± 0.03

mally are not soluble in hydroxyethyl methacrylate–water solutions during polymerization. When water is used as the polymerization solvent, phase separation tends to occur during polymerization, a problem that is overcome through the use of ethanol or *tert*-butyl alcohol.

EXPERIMENTAL

Hydrogel films were prepared by free radical polymerization using azobis(methyl isobutyrate) (15) (7.84 mmoles/liter of monomer) as the initiator. Hydroxyethyl methacrylate[1] was used as received and contained the major impurities methacrylic acid (0.06%), ethylene glycol dimethacrylate (0.024%), and diethylene glycol methacrylate (0.29%).

Hydroxyethyl methacrylate mixtures with 0, 5, 10, 20, and 40% (v/v) deionized water, 20 and 40% (v/v) ethanol[2], and 20 and 40% (v/v) *tert*-butyl alcohol[3] were polymerized between sealed polyethylene plates at 60° for 24 hr. All films were transparent and homogeneous after polymerization. Subsequent to polymerization, all films were equilibrated in water (changed repeatedly) for 3–4 weeks prior to the permeation studies.

Unlabeled progesterone[4] and 1,2-^{3}H-progesterone[5] were used as received to prepare aqueous 11.2-μg of progesterone/ml solutions for the permeation and partition experiments.

Diffusion and partition experiments were conducted as described previously (8, 9). Film thicknesses, ~0.07 cm, were measured on the water-swollen hydrogels using a lightwave micrometer[6].

Hydration values were obtained as described previously (11).

RESULTS AND DISCUSSION

Progesterone diffusion coefficients in the hydrogel films were calculated using (16):

$$\ln\left(1 - \frac{2C_t}{C_0}\right) = -\left(\frac{1}{V_1} + \frac{1}{V_2}\right)\frac{AUt}{l} \qquad \text{(Eq. 1)}$$

where C_t is the progesterone concentration at time t, C_0 is the initial progesterone concentration, A is the polymer film area (14.9 cm²), l is the film thickness, V_1 and V_2 are the compartment volumes (176 ml), and U is the permeation coefficient defined as:

$$U = DK_d \qquad \text{(Eq. 2)}$$

where D is the diffusion coefficient and K_d is the partition coefficient.

Values for U, D, K_d, and H [the membrane hydration, defined as (film water concentration/bulk water concentration)] are given in Table I, as are the average values and standard deviations for each parameter. The values in each row represent results from a single polymer film.

Progesterone permeability, diffusivity, and partitioning in poly(hydroxyethyl methacrylate) films did not change when: (*a*) the initial polymerization mixture water content was varied from 0 to 40% (v/v), (*b*) the polymerization solvent was changed from water to ethanol or *tert*-butyl alcohol, and (*c*) the alcohol concentration was changed from 20 to 40% (Table I). The equilibrium hydration of the poly(hydroxyethyl methacrylate) films in water was independent of the polymerization conditions.

It was demonstrated previously (14) that the equilibrium water swelling of hydrogels polymerized in different solvents was independent of the solvent type and was dependent only on the monomer volume fraction present in the polymerization medium. This conclusion is consistent with the present study, which demonstrates that polymer hydration is independent of both solvent type and concentration, regardless of the dimensional changes that occur with water equilibration.

Hydration and permeability of hydrogel films have been theoretically related (17) and experimentally verified (9). Mechanistic interpretations of poly(hydroxyethyl methacrylate) film permeation suggest a "pore-flow" mechanism for progesterone (9). This information and the present data indicate that equally hydrated gels display an "effective porosity" independent of the polymerization solvent. Hydration is an inherent property of the gel network formed under conditions of fixed monomer type, temperature, and initiator type and concentration. Furthermore, it appears that any differences in the gel network organization that arise from polymerization solvent changes are secondary to hydration in determining progesterone permeability in hydrogel films.

[1] Courtesy of Hydron Laboratories, New Brunswick, N.J. Impurities in the sample were determined by Hydron Laboratories.
[2] IMC Chemical Group, Agnew, Calif.
[3] J. T. Baker Chemical Co., Phillipsburg, N.J.
[4] Steraloids Inc., Pauling, N.Y.
[5] New England Nuclear, Boston, Mass.
[6] Van Kueren Co., Watertown, Mass.

REFERENCES

(1) J. D. Andrade, *Med. Instrum.*, **1**, 110 (1973).

(2) M. Tollar, M. Stol, and K. Kliment, *J. Biomed. Mater. Res.*, **3**, 305 (1969).

(3) V. Majkus, F. Horakova, F. Vymola, and M. Stol, *ibid.*, **3**, 443 (1969).

(4) J. M. Anderson, T. Koinis, T. Nelson, M. Horst, and D. S. Love, in "Hydrogels for Medical and Related Applications," J. D. Andrade, Ed., American Chemical Society Symposium Series 31, 1976, p. 167.

(5) D. R. Cowsar, O. R. Tarwater, and A. C. Tanguary, in *ibid.*, p. 180.

(6) J. Drobnik, P. Spacek, and O. Wichterle, *J. Biomed. Mater. Res.*, **8**, 45 (1974).

(7) R. A. Abrahams and S. H. Ronel, *ibid.*, **9**, 355 (1975).

(8) G. M. Zentner, J. R. Cardinal, and S. W. Kim, *J. Pharm. Sci.*, **67**, 1347 (1978).

(9) *Ibid.*, **67**, 1352 (1978).

(10) B. D. Ratner and A. S. Hoffman, in "Hydrogels for Medical and Related Applications," J. D. Andrade, Ed., American Chemical Society Symposium Series 31, 1976, p. 1.

(11) S. J. Wisniewski, D. E. Gregonis, S. W. Kim, and J. D. Andrade, in *ibid.*, p. 80.

(12) R. Y. S. Chen, *Polym. Preprints*, **15** (2), 387 (1974).

(13) P. J. Flory, "Principles of Polymer Chemistry," Cornell University Press, Ithaca, N.Y., 1953.

(14) O. Wichterle and R. Chromecek, *J. Polym. Sci., Part C*, **16**, 4677 (1969).

(15) G. A. Mortimer, *J. Org. Chem.*, **30**, 1632 (1964).

(16) G. L. Flynn, S. H. Yalkowsky, and T. J. Roseman, *J. Pharm. Sci.*, **63**, 479 (1974).

(17) H. Yasuda, C. E. Lamaze, and A. Peterlin, *J. Polym. Sci., A-2*, **9**, 1117 (1971).

ACKNOWLEDGMENTS

Supported by NIH Grant HD-09791.

The authors thank Dr. Sung-Wan Kim for helpful comments.

High-Pressure Liquid Chromatographic Analysis of Veterinary Anthelmintics I: Quantitative Determination of Tetramisole

D. MOUROT ˣ, B. DELÉPINE, J. BOISSEAU, and G. GAYOT

Received May 3, 1978, from the *Laboratoire National des Médicaments Vétérinaires, Direction de la Qualité, Ministère de l'Agriculture, Javené 35300 Fougeres, France.* Accepted for publication November 15, 1978.

Abstract □ High-pressure liquid chromatography was used with a 10-μm C_8-type bonded silica gel column to quantitate the tetramisole in veterinary anthelmintic preparations. The chromatographic elution time was less than 10 min, and other compounds present in the products analyzed did not interefere.

Keyphrases □ Tetramisole—high-pressure liquid chromatographic analysis, veterinary preparations □ High-pressure liquid chromatography—analysis, tetramisole in veterinary preparations □ Anthelmintics—tetramisole, high-pressure liquid chromatographic analysis in veterinary preparations

Tetramisole (*dl*-2,3,5,6-tetrahydro-6-phenylimidazo[2,1-*b*]thiazole) hydrochloride (1) is a potent, broad-spectrum anthelmintic; it exhibits high activity against several GI and pulmonary nematode species. Tetramisole is often used in veterinary therapeutics, either alone or with other anthelmintics such as bithionol, bithionol sulfoxide, and oxyclozanide.

UV spectrophotometry cannot be used directly for identifying tetramisole because the tetramisole absorption maximum (214 nm) is shared by other organic substances. TLC separation of tetramisole from its thermal degradation products was reported (2) but was not quantitative. A partition column chromatographic method (3) resolved tetramisole from other interfering substances prior to UV measurement but was time consuming and unsuitable for routine analysis.

High-pressure liquid chromatography (HPLC) offers a viable alternative for the quantitative analysis of tetramisole in commercial products and is applicable to various formulations.

EXPERIMENTAL

Equipment—The liquid chromatograph[1] was operated at ambient temperature and was equipped with a UV detector for monitoring the column effluent at 254 nm. The stainless steel column, 15 cm × 4.7 mm (i.d.), was packed with a C_8-type permanently bonded silica gel[2]. The liquid chromatographic detector was connected to a computing integrator[3] for obtaining the chromatogram peak areas.

Reagents—Tetramisole hydrochloride[4] and phenol[5] were the reference and internal standards, respectively.

Analytical reagent grade acetonitrile[5] and sulfuric acid[5] were used for the mobile phase preparation.

Mobile Phase—A mixture of 1% concentrated sulfuric acid in water–acetonitrile (80:20 v/v) was used.

Internal Standard Solution—Accurately weighed phenol (~500 mg) in a 100-ml volumetric flask was dissolved in, and diluted to volume with, the mobile phase.

Standard Solution—Accurately weighed tetramisole standard (~100 mg) in a 100-ml volumetric flask was dissolved in, and diluted to volume with, water. A tetramisole standard–phenol solution mixture (1:1) in a suitable vessel was mixed well.

Sample Solution—An anthelmintic sample equivalent to 100 mg of tetramisole was pipetted accurately into a 100-ml volumetric flask and diluted to volume with water. A 1:1 sample solution–phenol solution mixture in a suitable vessel was mixed well.

Formulations Containing Bithionol and Oxyclozanide—Veterinary formulations containing tetramisole–bithionol or tetramisole–oxyclozanide are suspensions. The formulation was mixed thoroughly, and an aliquot equivalent to 100 mg of tetramisole was pipetted quickly into a 50-ml glass-stoppered centrifuge tube. Water (25 ml) was added, and the solution was mixed thoroughly and centrifuged at 2000 rpm for 5 min. The supernate was transferred into a 100-ml volumetric flask, and the residue was extracted with 4 × 10 ml of water. The combined extracts in the 100-ml flask were diluted to volume with water.

Chromatography—The column was conditioned 0.5 hr with mobile phase (flow rate of 1.6 ml/min). Four-microliter standard solution aliquots were injected onto the column, and the tetramisole (2.4 min) and phenol (6.0 min) peaks were identified. The relative area response ratio was determined by replicate standard solution injections. When the response ratio deviation was less than 2%, the sample dilution was injected.

Linearity—The method was evaluated for tetramisole response linearity at concentrations ranging from 0.02 to 2% of tetramisole. Four microliters of each solution was injected into the chromatograph, and the tetramisole–internal standard area ratio was calculated and plotted *versus* the tetramisole concentration. The chromatographic response was linear up to the highest tetramisole concentration tested (2%).

RESULTS AND DISCUSSION

The results (Table I) show that tetramisole can be assayed in veterinary anthelmintic formulations using a simple HPLC method. However, these results could not be tested against an alternative (tested or official) method because no such method exists. The HPLC analyses gave a linear response with tetramisole concentrations between 0.02 and 2%. An aqueous 0.1% tetramisole standard was assayed with each batch of samples, and the sample concentration calculations were based upon this standard.

The commercial anthelmintic preparations generally contained bithionol, bithionol sulfoxide, or oxyclozanide in addition to tetramisole, but these agents did not interfere with the tetramisole assay since they were not eluted under the conditions described. Bithionol, bithionol sulfoxide, and oxyclozanide remaining on the column were subsequently eluted by changing the mobile phase to acetonitrile (1 ml/min) and eluting for 20 min after every series of 20 samples had been run.

Although 254 nm is the most commonly used wavelength, tetramisole elution was monitored at its absorption maximum (214 nm); detection

Table I—Percent Tetramisole Concentration in Anthelmintic Veterinary Formulations

Sample	Labeled Tetramisole	Found Tetramisole[a]
1[b]	7.5	7.9 ± 0.1
2[c]	3.4	3.4 ± 0.05
3[d]	3.4	3.51 ± 0.05
4	3.4	3.48 ± 0.05
5[e]	3.4	3.46 ± 0.05

[a] Mean of three sample preparations and standard error. [b] Containing tetramisole free base. [c] Containing oxyclozanide (3.4%). [d] Containing bithionol (8%). [e] Containing bithionol sulfoxide (10%).

[1] Varian 8500.
[2] Lichrosorb RP8, 10 μ, Merck & Co.
[3] System I, Spectra-Physics.
[4] Lot CA 76.007.00, Specia, Paris, France
[5] Merck & Co.

0022-3549/79/0600-0796$01.00/0
© 1979, American Pharmaceutical Association

at 214 nm was eightfold more sensitive and would be useful in residue analysis.

REFERENCES

(1) D. Thienpont, O. F. J. Vanparijs, A. H. M. Raeymaekers, J. Vandenberk, P. J. A. Demoen, F. T. N. Allewijn, R. P. H. Marsboom, C. J. E. Niemegaers, K. H. L. Schellekens and P. A. J. Janssen, *Nature*, **209**, 1084 (1966).

(2) N. A. Dickinson, H. E. Hudson, and P. J. Taylor, *Analyst*, **96**, 235 (1971).

(3) *Ibid.*, **96**, 244 (1971).

Possibility for Error in FDA Diffusion Assays

M. A. FOGLESONG ˣ, F. KAVANAGH, and J. V. DIETZ

Received September 26, 1978, from *Eli Lilly and Company, Indianapolis, IN 46206.* Accepted for publication November 20, 1978.

Abstract □ Computational procedures specified for the FDA single-dose diffusion assay for antibiotics may cause substantial error in estimated sample potency. An unrecognized mistake in reference solution concentration is the source of error. It is caused by correcting responses from standard and sample plates differently. The error can be avoided by correcting both standard and sample responses to the observed reference response.

Keyphrases □ FDA—assay, antibiotics, correction □ Antibiotics—analysis, FDA diffusion assay, corrections

The single-dose diffusion assay of the Food and Drug Administration (FDA) has been a satisfactory antibiotic assay for more than 30 years. The method is about as accurate as any other diffusion method.

Since samples and standards are on different petri plates, sample responses must be corrected for variations in zone sizes attributable to plates. To this end, one-half of the responses on sample plates are from a reference solution, which is also the middle concentration of the standard line.

The correction procedures specified in the FDA regulations (1) are different for standards and samples and can cause substantial error under certain circumstances. Causes of errors, their sizes, and procedures for avoiding them will be discussed.

DISCUSSION

The standard line used in this assay was relatively short to avoid complication caused by excessive curvature. Standard concentrations did not follow a 1.35 multiplier exactly but were adjusted to concentrations that could be prepared accurately using volumetric pipets and flasks. The standard lines were computed by linear regression analysis and not by the modified least-squares formula of the "Code of Federal Regulations" (CFR) 436.105 (1).

The data for this investigation were obtained from a *Bacillus subtilis* (ATCC 6633) pen-cylinder agar diffusion assay for cephalexin. For the assay, plastic petri plates (100 × 15 mm) contained a single 10-ml layer of Medium 1 (2) seeded with *B. subtilis* spores. Standard and sample solutions were made from a freshly prepared stock solution in pH 6.0 buffer. Standards containing 2.00, 2.75, 3.75, 5.00, or 6.50 μg of cephalexin activity/ml and samples containing 2.75, 3.00, 4.00, or 6.00 μg of activity/ml were applied at a dosage of 0.2 ml/cylinder. The solution used for the 2.75-μg/ml sample was the same solution used for the 2.75-μg/ml standard. Plates were incubated at 30° for 16–18 hr, and inhibition zones were measured to the nearest 0.01 mm with an antibiotic zone reader[1] as described elsewhere (3).

Zone diameters are given in Table I. A standard line graph is given in

Table I—Standard and Sample Responses

Standard, μg/ml	Response, mm	
	Standard	Reference
2.00	14.25	16.14
2.75	15.71	16.08
(3.75)	(16.12)	—
5.00	18.12	16.07
6.50	19.31	16.18
	Response, mm	
Sample	Sample	Reference
1	16.12	16.19
2	19.14	16.31
3	17.21	16.01
4[a]	15.20	15.61

[a] The plates for this sample were purposely incubated at a temperature slightly different from the standard plates.

Fig. 1. Estimated potencies computed as required by the CFR 436.105 (1) and by two modifications are given in Table II. All potencies were interpolated from the best straight line through the standard responses. The reference standard was purposely made at 3.0 μg/ml and not of the 3.75 μg/ml its label indicated. This fact placed a small bias in all potencies, as could be inferred from Fig. 1.

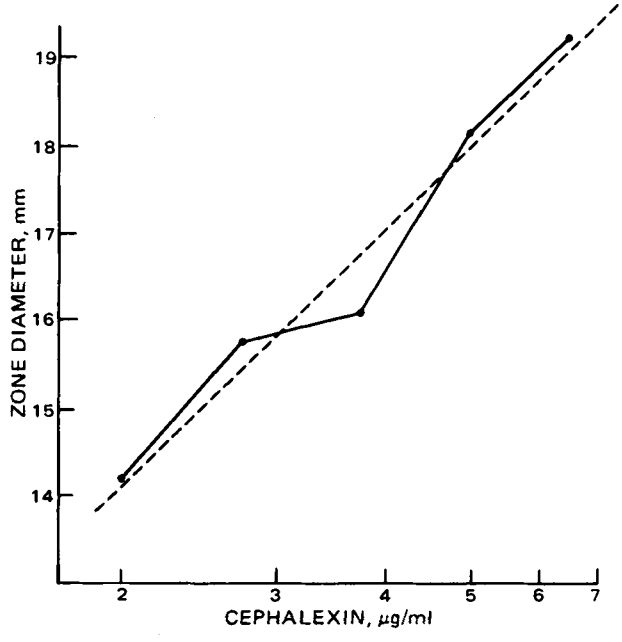

Figure 1—*Calibration line for an assay of cephalexin by* B. subtilis *(ATCC 6633). The true concentration of the reference solution (3.75 μg/ml) point is 3.00 μg/ml. The dashed line is the least-squares best line through the five points.*

[1] Fisher-Lilly.

0022-3549/79/0600-0797$01.00/0

© 1979, American Pharmaceutical Association

at 214 nm was eightfold more sensitive and would be useful in residue analysis.

REFERENCES

(1) D. Thienpont, O. F. J. Vanparijs, A. H. M. Raeymaekers, J. Vandenberk, P. J. A. Demoen, F. T. N. Allewijn, R. P. H. Marsboom, C. J. E. Niemegaers, K. H. L. Schellekens and P. A. J. Janssen, *Nature*, **209**, 1084 (1966).

(2) N. A. Dickinson, H. E. Hudson, and P. J. Taylor, *Analyst*, **96**, 235 (1971).

(3) *Ibid.*, **96**, 244 (1971).

Possibility for Error in FDA Diffusion Assays

M. A. FOGLESONG ˣ, F. KAVANAGH, and J. V. DIETZ

Received September 26, 1978, from *Eli Lilly and Company, Indianapolis, IN 46206.* Accepted for publication November 20, 1978.

Abstract □ Computational procedures specified for the FDA single-dose diffusion assay for antibiotics may cause substantial error in estimated sample potency. An unrecognized mistake in reference solution concentration is the source of error. It is caused by correcting responses from standard and sample plates differently. The error can be avoided by correcting both standard and sample responses to the observed reference response.

Keyphrases □ FDA—assay, antibiotics, correction □ Antibiotics—analysis, FDA diffusion assay, corrections

The single-dose diffusion assay of the Food and Drug Administration (FDA) has been a satisfactory antibiotic assay for more than 30 years. The method is about as accurate as any other diffusion method.

Since samples and standards are on different petri plates, sample responses must be corrected for variations in zone sizes attributable to plates. To this end, one-half of the responses on sample plates are from a reference solution, which is also the middle concentration of the standard line.

The correction procedures specified in the FDA regulations (1) are different for standards and samples and can cause substantial error under certain circumstances. Causes of errors, their sizes, and procedures for avoiding them will be discussed.

DISCUSSION

The standard line used in this assay was relatively short to avoid complication caused by excessive curvature. Standard concentrations did not follow a 1.35 multiplier exactly but were adjusted to concentrations that could be prepared accurately using volumetric pipets and flasks. The standard lines were computed by linear regression analysis and not by the modified least-squares formula of the "Code of Federal Regulations" (CFR) 436.105 (1).

The data for this investigation were obtained from a *Bacillus subtilis* (ATCC 6633) pen-cylinder agar diffusion assay for cephalexin. For the assay, plastic petri plates (100 × 15 mm) contained a single 10-ml layer of Medium 1 (2) seeded with *B. subtilis* spores. Standard and sample solutions were made from a freshly prepared stock solution in pH 6.0 buffer. Standards containing 2.00, 2.75, 3.75, 5.00, or 6.50 μg of cephalexin activity/ml and samples containing 2.75, 3.00, 4.00, or 6.00 μg of activity/ml were applied at a dosage of 0.2 ml/cylinder. The solution used for the 2.75-μg/ml sample was the same solution used for the 2.75-μg/ml standard. Plates were incubated at 30° for 16–18 hr, and inhibition zones were measured to the nearest 0.01 mm with an antibiotic zone reader[1] as described elsewhere (3).

Zone diameters are given in Table I. A standard line graph is given in

Table I—Standard and Sample Responses

Standard, μg/ml	Response, mm	
	Standard	Reference
2.00	14.25	16.14
2.75	15.71	16.08
(3.75)	(16.12)	—
5.00	18.12	16.07
6.50	19.31	16.18
	Response, mm	
Sample	Sample	Reference
1	16.12	16.19
2	19.14	16.31
3	17.21	16.01
4[a]	15.20	15.61

[a] The plates for this sample were purposely incubated at a temperature slightly different from the standard plates.

Fig. 1. Estimated potencies computed as required by the CFR 436.105 (1) and by two modifications are given in Table II. All potencies were interpolated from the best straight line through the standard responses. The reference standard was purposely made at 3.0 μg/ml and not of the 3.75 μg/ml its label indicated. This fact placed a small bias in all potencies, as could be inferred from Fig. 1.

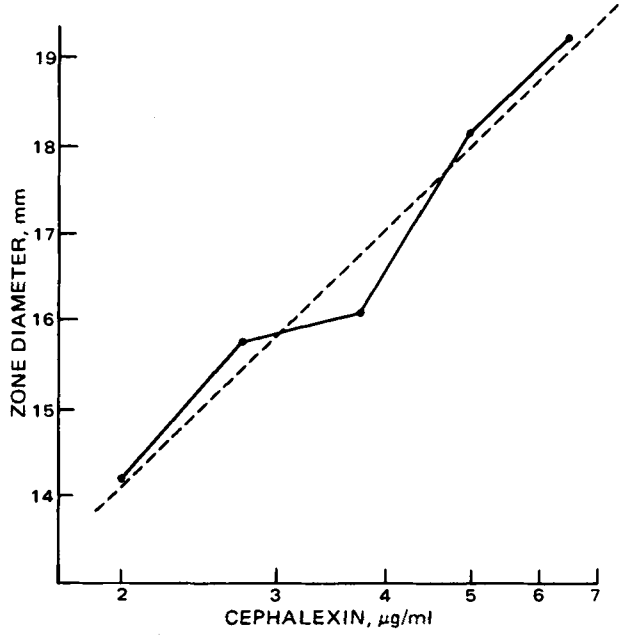

Figure 1—*Calibration line for an assay of cephalexin by* B. subtilis *(ATCC 6633). The true concentration of the reference solution (3.75 μg/ml) point is 3.00 μg/ml. The dashed line is the least-squares best line through the five points.*

[1] Fisher-Lilly.

0022-3549/79/0600-0797$01.00/0

© 1979, American Pharmaceutical Association

Table II—Potencies Computed by FDA and Lilly Procedures from the Best Straight Lines

Sample	True Concentration, μg/ml	Five-Point Line, Including Reference Point		Four-Point Line Excluding Reference Point, Lilly
		FDA	Lilly	
1	3.00	3.69	3.15	3.02
2	6.00	7.36	6.27	6.02
3	4.00	4.99	4.26	4.09
4	2.75	3.40	2.90	2.79
Reference, mm		16.79	16.12	16.12
Mean computational error, %		+24	+5	0

Standard responses were corrected to the observed mean reference concentration response ("3.75" μg/ml) on all standard plates. Sample plate responses were corrected to the theoretical reference response, the 3.75-μg/ml point on the best straight line through the five standards as required by regulations (1). These results are given in the "FDA" column of Table II.

A second set of potencies was obtained from the same data by correcting sample zones to the observed reference as was done for standards and interpolating from the same straight line. These results are given in the "Lilly" column of Table II. A third set of potencies was obtained by correcting to the observed reference and by rejecting the obviously erroneous reference response when computing the best straight line. These results were taken as the true sample assay.

The computational error of +24% in the FDA procedure was caused by the computed reference diameter required by the CFR (1). The error caused by including the erroneous reference point in the calculation of the best straight line was about 5%.

The plates for Sample 4 were incubated at a temperature slightly different from that of the standard plates. Since each response was corrected to the reference concentration, this difference in temperature and the resultant reduction in zone diameters had no effect on the calculated sample potency.

The correction procedure of Ref. 1 is without error only when the observed mean reference diameter is identical with that interpolated from the best straight line. Since this is an unlikely occurrence, a different correction scheme should be used. Correcting both standard and sample responses to the response observed for the reference and then calculating estimated potencies from the regression equation will avoid the errors of the CFR (1).

Proper plate correction is of more than academic interest because computational errors as great as 40% have been reported from other laboratories[2]. Such an error was caused by using a reference about three-fourths as concentrated as it was thought to be. Large errors seem to be rare, but smaller ones are not. In one series of 40 response lines from 16 laboratories, seven of the reference zones, including the one just mentioned, were obviously in error and nine other standard zones had errors. Except for the reference, errors were evenly distributed among the other four standards. Three calibration lines had two obvious errors in them. All of these lines were used in the laboratories reporting the work.

REFERENCES

(1) "Code of Federal Regulations," Title 21, Part 436.105, 1977.

(2) "Code of Federal Regulations," Title 21, Part 436.102, 1977.

(3) F. Kavanagh, *J. Pharm. Sci.*, **64**, 1224 (1975).

ACKNOWLEDGMENTS

The authors thank Dr. H. S. Ragheb for furnishing the information about the errors in standard lines from the 17 laboratories.

[2] Dr. H. S. Ragheb, Department of Biochemistry, Purdue University Agricultural Experiment Section, West Lafayette, IN 47907, personal communication.

High-Pressure Liquid Chromatographic Feprazone Determination in Pharmaceutical Formulations

ANGELO BONORA ˣ and PIER ANDREA BOREA

Received September 12, 1978, from the *Istituto di Farmacologia, Università di Ferrara, 44100 Ferrara, Italy.* Accepted for publication November 30, 1978.

Abstract □ A high-pressure liquid chromatographic method was developed for the quantitative determination of feprazone, a nonsteroidal anti-inflammatory agent, in different pharmaceutical formulations. The results agree with those obtained with GLC and UV spectrophotometric assays.

Keyphrases □ High-pressure liquid chromatography—analysis, feprazone in various pharmaceutical formulations □ Feprazone—analysis, high-pressure liquid chromatography, various pharmaceutical formulations □ Analgesics—feprazone, analysis in various pharmaceutical formulations, high-pressure liquid chromatography

Feprazone (4-prenyl-1,2-diphenyl-3,5-pyrazolidinedione) is a nonsteroidal analgesic, antipyretic, and anti-inflammatory agent with a low ulcerogenic potential. Feprazone has been determined in pharmaceutical formulations and in body fluids by potentiometric titration (1), UV spectrophotometry (2), TLC (3), GLC (4–6), and radioisotopic techniques (7).

This paper describes the quantitative determination of feprazone in capsule, suppository, and cream formulations by a simple and rapid high-pressure liquid chromatographic (HPLC) procedure.

The proposed HPLC method was compared to GLC (5) and UV spectrophotometric (2) assays.

EXPERIMENTAL[1]

HPLC—*Equipment and Operating Conditions*—A liquid chromatograph[2], equipped with a UV–visible detector[3] and with a septum injector[2], was used. The column[4] was 50 cm × 2.2 mm i.d., and the microcell[5] volume was 8 μl. The flow rate was 0.49 ml/min under a constant pressure

[1] All solvents were BDH AnalaR grade and were used without further purification.

[2] Series 4000, Varian Aerograph, Palo Alto, Calif.

[3] Beckman DU, Beckman Instruments, Fullerton, Calif.

[4] Micropak SI 10, Varian Aerograph, Palo Alto, Calif.

[5] Circus, Milan, Italy.

0022-3549/79/0600-0798$01.00/0

© 1979, American Pharmaceutical Association

Table II—Potencies Computed by FDA and Lilly Procedures from the Best Straight Lines

Sample	True Concentration, μg/ml	Five-Point Line, Including Reference Point		Four-Point Line Excluding Reference Point, Lilly
		FDA	Lilly	
1	3.00	3.69	3.15	3.02
2	6.00	7.36	6.27	6.02
3	4.00	4.99	4.26	4.09
4	2.75	3.40	2.90	2.79
Reference, mm		16.79	16.12	16.12
Mean computational error, %		+24	+5	0

Standard responses were corrected to the observed mean reference concentration response ("3.75" μg/ml) on all standard plates. Sample plate responses were corrected to the theoretical reference response, the 3.75-μg/ml point on the best straight line through the five standards as required by regulations (1). These results are given in the "FDA" column of Table II.

A second set of potencies was obtained from the same data by correcting sample zones to the observed reference as was done for standards and interpolating from the same straight line. These results are given in the "Lilly" column of Table II. A third set of potencies was obtained by correcting to the observed reference and by rejecting the obviously erroneous reference response when computing the best straight line. These results were taken as the true sample assay.

The computational error of +24% in the FDA procedure was caused by the computed reference diameter required by the CFR (1). The error caused by including the erroneous reference point in the calculation of the best straight line was about 5%.

The plates for Sample 4 were incubated at a temperature slightly different from that of the standard plates. Since each response was corrected to the reference concentration, this difference in temperature and the resultant reduction in zone diameters had no effect on the calculated sample potency.

The correction procedure of Ref. 1 is without error only when the observed mean reference diameter is identical with that interpolated from the best straight line. Since this is an unlikely occurrence, a different correction scheme should be used. Correcting both standard and sample responses to the response observed for the reference and then calculating estimated potencies from the regression equation will avoid the errors of the CFR (1).

Proper plate correction is of more than academic interest because computational errors as great as 40% have been reported from other laboratories[2]. Such an error was caused by using a reference about three-fourths as concentrated as it was thought to be. Large errors seem to be rare, but smaller ones are not. In one series of 40 response lines from 16 laboratories, seven of the reference zones, including the one just mentioned, were obviously in error and nine other standard zones had errors. Except for the reference, errors were evenly distributed among the other four standards. Three calibration lines had two obvious errors in them. All of these lines were used in the laboratories reporting the work.

REFERENCES

(1) "Code of Federal Regulations," Title 21, Part 436.105, 1977.

(2) "Code of Federal Regulations," Title 21, Part 436.102, 1977.

(3) F. Kavanagh, *J. Pharm. Sci.*, **64**, 1224 (1975).

ACKNOWLEDGMENTS

The authors thank Dr. H. S. Ragheb for furnishing the information about the errors in standard lines from the 17 laboratories.

[2] Dr. H. S. Ragheb, Department of Biochemistry, Purdue University Agricultural Experiment Section, West Lafayette, IN 47907, personal communication.

High-Pressure Liquid Chromatographic Feprazone Determination in Pharmaceutical Formulations

ANGELO BONORA ˣ and PIER ANDREA BOREA

Received September 12, 1978, from the *Istituto di Farmacologia, Università di Ferrara, 44100 Ferrara, Italy.* Accepted for publication November 30, 1978.

Abstract □ A high-pressure liquid chromatographic method was developed for the quantitative determination of feprazone, a nonsteroidal anti-inflammatory agent, in different pharmaceutical formulations. The results agree with those obtained with GLC and UV spectrophotometric assays.

Keyphrases □ High-pressure liquid chromatography—analysis, feprazone in various pharmaceutical formulations □ Feprazone—analysis, high-pressure liquid chromatography, various pharmaceutical formulations □ Analgesics—feprazone, analysis in various pharmaceutical formulations, high-pressure liquid chromatography

Feprazone (4-prenyl-1,2-diphenyl-3,5-pyrazolidinedione) is a nonsteroidal analgesic, antipyretic, and anti-inflammatory agent with a low ulcerogenic potential. Feprazone has been determined in pharmaceutical formulations and in body fluids by potentiometric titration (1), UV spectrophotometry (2), TLC (3), GLC (4–6), and radioisotopic techniques (7).

This paper describes the quantitative determination of feprazone in capsule, suppository, and cream formulations by a simple and rapid high-pressure liquid chromatographic (HPLC) procedure.

The proposed HPLC method was compared to GLC (5) and UV spectrophotometric (2) assays.

EXPERIMENTAL[1]

HPLC—*Equipment and Operating Conditions*—A liquid chromatograph[2], equipped with a UV–visible detector[3] and with a septum injector[2], was used. The column[4] was 50 cm × 2.2 mm i.d., and the microcell[5] volume was 8 μl. The flow rate was 0.49 ml/min under a constant pressure

[1] All solvents were BDH AnalaR grade and were used without further purification.

[2] Series 4000, Varian Aerograph, Palo Alto, Calif.

[3] Beckman DU, Beckman Instruments, Fullerton, Calif.

[4] Micropak SI 10, Varian Aerograph, Palo Alto, Calif.

[5] Circus, Milan, Italy.

0022-3549/79/0600-0798$01.00/0

© 1979, American Pharmaceutical Association

Table I—Comparison of HPLC, GLC, and UV Methods for Feprazone Determination in Capsule Formulations [a]

Sample	HPLC	GLC	UV
1	201.4	203.6	203.5
2	203.7	199.7	201.5
3	198.3	201.2	197.7
4	201.1	203.8	204.6
5	198.5	201.4	198.0
6	196.7	198.3	200.3
7	200.1	204.2	201.4
8	198.5	201.5	199.1
Average	199.8	201.7	200.8
SD	2.2	2.1	2.5

[a] All results are reported as milligrams per capsule based on a pool of five capsules.

Table II—Comparison of HPLC, GLC, and UV Methods for Feprazone Determination in Suppository Formulations [a]

Sample	HPLC	GLC	UV
1	302.1	302.8	301.7
2	296.8	296.1	298.0
3	296.4	297.2	298.1
4	301.5	302.3	304.3
5	300.5	298.3	295.6
6	301.2	301.4	301.8
7	296.9	296.2	298.7
8	296.2	297.6	299.5
Average	298.9	299.0	298.1
SD	2.6	2.8	2.8

[a] All results are reported as milligrams per suppository based on a pool of five suppositories.

Table III—Comparison of HPLC, GLC, and UV Methods for Feprazone Determination in Cream Formulations [a]

Sample	HPLC	GLC	UV
1	4.92	5.01	5.00
2	5.00	5.02	4.90
3	4.94	5.02	4.92
4	5.10	4.83	5.03
5	4.82	4.82	4.82
6	5.10	4.92	5.11
7	5.00	4.81	4.86
8	4.87	4.98	5.00
Average	4.97	4.93	4.96
SD	0.10	0.09	0.10

[a] All results are reported as milligrams percent based on a pool of five cream samples.

of 1000 psi (70.3 kg/cm^2). Detection was by UV absorbance at 265 nm.

The optimum wavelength was determined from the UV spectrum of feprazone obtained by a stop-flow technique (8). The flow was interrupted by means of a two-stem valve[6] placed between the constant pressure pump and the septum injector when an absorbance, previously determined by comparison with the solvent absorbance (and, therefore, belonging to the substance under examination), was detected. The complete sample spectrum was then recorded in the 320–220-nm range.

Reagents—As a reference standard, pure feprazone[7] was used. Promethazine chlorhydrate[8] was the internal standard. The mobile phase was methanol–32% ammonia (150:2 v/v).

Standard Solutions—Standard feprazone solutions were prepared by dissolving accurately weighed aliquots of the pure substance in the mobile phase to produce final concentrations of 0.1–3.2 mg/ml. All standard solutions contained 2.5 mg of promethazine/ml.

Capsules—Pools of five capsules[7] were crushed in a porcelain mortar to a fine powder. Then aliquots of 25 mg of powder plus 50 mg of the internal standard were dissolved in 25 ml of chloroform. After filtration, the solution was evaporated at 40° and the residue was dissolved in 25 ml of mobile phase.

Suppositories—An aliquot of a suppository[7] mixture, one-third of the weight of a suppository, and 200 mg of the internal standard were dissolved in 50 ml of carbon disulfide. After filtration and evaporation, the residue was dissolved in the mobile phase.

Cream—Cream (0.50 g) and 50 mg of the internal standard were dissolved in a water bath in 25 ml of ethanol. Then 1 ml of this solution was filtered, evaporated, and redissolved in 1 ml of mobile phase.

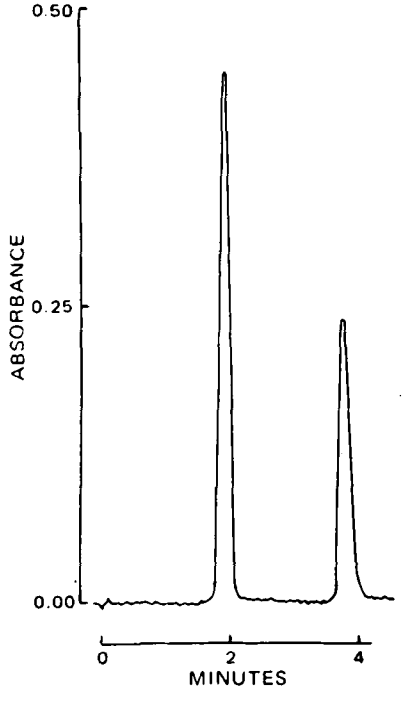

Figure 1—*Typical liquid chromatogram of feprazone (left) and internal standard (right) from capsules.*

GLC—A gas chromatograph[9], fitted with a dual-flame ionization detector and coiled glass columns[9] (1500 × 40 mm) packed with 2.5% SE-30 on 100–120-mesh Gas Chrom Q[9], was used. All working conditions were as described previously (5).

UV Spectrophotometry—A UV-visible spectrophotometer[3] was used, and the absorbance of feprazone was determined at 263 nm in 0.1 *N* NaOH. All working conditions were as described previously (2).

RESULTS AND DISCUSSION

Standard Curve—Linearity was shown by injecting into the column various amounts of feprazone over the concentration range 0.1–3.2 mg/ml with a constant amount of the internal standard (2.5 mg/ml). The mobile phase was methanol–32% ammonia (150:2 v/v). The standard curve was calculated by regression analysis as $y = 0.02 + 0.43x$ ($r = 1.0$), where y is the ratio of the feprazone peak area to the internal standard peak area, calculated at a sensitivity of 0.5 aufs deflection, and x is milligrams of feprazone per milliliter. To estimate the peak area standard deviations, five determinations were carried out for each concentration. Standard deviations were 3.1%.

HPLC—Eight samples of each pharmaceutical formulation were injected into the column using the stop-flow technique. Figure 1 shows a typical chromatogram of feprazone and the internal standard obtained from the capsule extraction. The retention times were 1.52 min for feprazone and 3.46 min for the internal standard. All measurements were carried out at room temperature (25°).

Recovery—Feprazone recovery from the pharmaceutical formulations was estimated. Formulations to which known feprazone amounts were added prior to extraction had an average percent recovery of 99.9, 99.9, and 99.8 with 95% confidence limits of 99.5–100.3, 99.4–100.4, and 99.2–100.4, respectively, for capsules, suppositories, and cream.

Peak Identification—Feprazone identification was accomplished by comparison with the pure standard retention times.

Suitable quantities of the liquid chromatograph cell effluent were collected corresponding to the drug chromatographic peak and were tested for homogeneity by qualitative monodimensional TLC using silica gel precoated glass plates (20 × 20 cm, 0.25 mm thick). Three solvents

[6] Whitey Co., Oakland, Calif.
[7] De Angeli Institute, Milan, Italy.
[8] Farmitalia Pharmaceuticals, Milan, Italy.
[9] Carlo Erba, Milan, Italy.

were used: (*a*) chloroform–acetone–ethanol (70:30:3 v/v); (*b*) cyclohexane–ethyl acetate–methanol–water (100:100:60:8 v/v); and (*c*) benzene–acetic acid (95:5 v/v). After each development, the plates were dried at 110° and spots were visualized in iodine vapors. The chromatograms corresponded perfectly in color (brown) and R_f values to those obtained with the reference compounds.

Comparison of HPLC, GLC, and UV Methods—The proposed HPLC method was compared to GLC (5) and UV spectrophotometric (2) assays. The results (Tables I–III) show that the proposed method is in good agreement with the GLC and UV assays.

The HPLC procedure described here provides a rapid, sensitive (the lower sensitivity limit is about 10 ng on the column), and precise assay of feprazone in pharmaceutical formulations.

REFERENCES

(1) R. Perego, A. Gallazzi, P. C. Vanoni, and I. Lucarella, *Arzneim.-Forsch.*, **22**, 177 (1972).

(2) G. Coppi, G. Bonardi, and R. Perego, *ibid.*, **22**, 234 (1972).

(3) C. Schutz and H. Schutz, *ibid.*, **23**, 428 (1973).

(4) G. Coppi, A. Vidi, A. Gallazzi, and R. Perego, *ibid.*, **24**, 801 (1974).

(5) A. Gallazzi and P. C. Vanoni, *Il Farmaco, Ed. Pratica*, **30**, 147 (1975).

(6) D. J. Berry, *J. Chromatogr.*, **144**, 159 (1975).

(7) H. G. Dean, B. Donovan, and P. Rylett, *Arzneim.-Forsch.*, **26**, 1574 (1976).

(8) A. Bonora and P. A. Borea, *Experientia*, **34**, 1486 (1978).

GLC–Mass Spectrometry of *Teucrium polium* Oil

M. M. A. HASSAN ˣ, F. J. MUHTADI, and A. A. AL-BADR

Received June 6, 1978, from the *Faculty of Pharmacy, University of Riyad, Riyad, Saudi Arabia.* Accepted for publication December 14, 1978.

Abstract □ The essential oil of *Teucrium polium*, growing in Saudi Arabia, was thoroughly investigated for its constituents by GLC–mass spectrometry, TLC, and spectrophotometric methods. This investigation revealed the presence of 10 terpenoidal compounds including the hydrocarbons β-pinene, limonene, α-phellandrene, and γ- and δ-cadinenes and the alcohols linalool, terpine-4-ol, cedrol, cedrenol, and guaiol. The oil was rich in alcohols and devoid of esters. Preliminary pharmacological screening showed that the oil possesses powerful antispasmodic activity.

Keyphrases □ GLC–mass spectrometry—analysis, *Teucrium polium* oil, antispasmodics, folk medicine □ *Teucrium polium*—oil, GLC–mass spectrometry □ Antispasmodics—analysis, *Teucrium polium* oil, GLC–mass spectrometry, folk medicine □ Folk medicine—antispasmodics, *Teucrium polium* oil, GLC–mass spectrometry

Teucrium polium (Family Labiatae) is one of the most fragrant plants in Saudi Arabia and is fairly distributed throughout the country (1). In folk medicine, it is used as an antispasmodic, antirheumatic, carminative, and flavoring agent. In an admixture with other powdered herbs, it is claimed to be therapeutic for peptic ulcer.

The aroma of this plant is due to its essential oil content (2). A literature review revealed that the oil constituents had not been investigated thoroughly (4). The present work was carried out to investigate the composition of this potentially therapeutic plant oil.

EXPERIMENTAL

Material—The plant was collected in the spring at the flowering stage from Sudair (Central Zone), 180 km from Riyad. Its identity as *T. polium* was confirmed[1]. It was dried and powdered.

Successive quantities (1 kg each) were subjected to steam distillation, which produced a volatile oil (average yield, 1.55 g).

The physical properties of the oil are presented in Table I.

TLC—TLC was done on precoated silica gel thin-layer plates[2] developed in chloroform–benzene (1:1) and chloroform–benzene (4:1) solvent systems (3). After development, the spots were visualized by spraying with anisaldehyde reagent (3).

Table I—Comparative Physicochemical Data

Property	Isolated Oil	Sardinian Oil
Color	Light yellow, darkens upon standing	Blue
Odor	Fragrant, characteristic	Agreeable, pungent
Refractive index[a]	n_D^{24}, 1.4850	n_D^{20}, 1.475 and 1.488
Optical rotation[b]	$[\alpha]_D^{24}$ +4.7° (10% in ethanol)	$[\alpha]_D^{20}$ +12.75°
Acetyl value[c]	117	47.45–47.59
IR[d]	1633, 1655, 1700, 2900, and 3400 cm^{-1}	—
NMR[e]	Broad singlets at 332, 306, 280, and 268 Hz; broad singlet at 217 Hz; singlet at 98 Hz; doublet at 73 Hz; two overlapping doublets centered at 58 Hz	—

[a] Zeiss Abbe refractometer. [b] Bellingham and Stanley polarimeter. [c] According to the BP method (5). [d] As film on Perkin-Elmer 567 grating IR spectrophotometer. [e] In deuterochloroform on Varian T 60A with tetramethylsilane as the internal standard.

GLC–Mass Spectrometry—Mass spectra of the volatile oil constituents were obtained using a gas chromatograph–mass spectrometer[3]. The chromatographic column (1.8 m long) was packed with 3% OV-17. The column was conditioned isothermally at 100° for 10 min, and then the temperature was programmed at 5 min until 260°. The injection port temperature was 185°, the separation temperature was 252°, and the ion source temperature was 290°. Mass spectra were obtained by operating at 60 MHz and with an ionization energy of 70 ev.

RESULTS AND DISCUSSION

The isolated oil was compared with Saridinian *T. polium* oil (4) (Table I). The IR and NMR data revealed free alcohols (3400 cm^{-1}; broad singlet at 217 Hz, disappeared on deuteration), alkene and highly conjugated

[1] The plant material was identified as *Teucrium polium* Linneus (Labiatae) by Dr. A. M. Migahid, Department of Botany, Faculty of Science, University of Riyad, Riyad, Saudi Arabia. A voucher specimen is available in the herbarium of Riyad University.

[2] GF plants, Anachem.

[3] Model 9000, LKB-Produkter, Brommo, Sweden.

0022-3549/79/0600-0800$01.00/0

© 1979, American Pharmaceutical Association

were used: (*a*) chloroform–acetone–ethanol (70:30:3 v/v); (*b*) cyclohexane–ethyl acetate–methanol–water (100:100:60:8 v/v); and (*c*) benzene–acetic acid (95:5 v/v). After each development, the plates were dried at 110° and spots were visualized in iodine vapors. The chromatograms corresponded perfectly in color (brown) and R_f values to those obtained with the reference compounds.

Comparison of HPLC, GLC, and UV Methods—The proposed HPLC method was compared to GLC (5) and UV spectrophotometric (2) assays. The results (Tables I–III) show that the proposed method is in good agreement with the GLC and UV assays.

The HPLC procedure described here provides a rapid, sensitive (the lower sensitivity limit is about 10 ng on the column), and precise assay of feprazone in pharmaceutical formulations.

REFERENCES

(1) R. Perego, A. Gallazzi, P. C. Vanoni, and I. Lucarella, *Arzneim.-Forsch.*, **22**, 177 (1972).

(2) G. Coppi, G. Bonardi, and R. Perego, *ibid.*, **22**, 234 (1972).

(3) C. Schutz and H. Schutz, *ibid.*, **23**, 428 (1973).

(4) G. Coppi, A. Vidi, A. Gallazzi, and R. Perego, *ibid.*, **24**, 801 (1974).

(5) A. Gallazzi and P. C. Vanoni, *Il Farmaco, Ed. Pratica*, **30**, 147 (1975).

(6) D. J. Berry, *J. Chromatogr.*, **144**, 159 (1975).

(7) H. G. Dean, B. Donovan, and P. Rylett, *Arzneim.-Forsch.*, **26**, 1574 (1976).

(8) A. Bonora and P. A. Borea, *Experientia*, **34**, 1486 (1978).

GLC–Mass Spectrometry of *Teucrium polium* Oil

M. M. A. HASSAN ˣ, F. J. MUHTADI, and A. A. AL-BADR

Received June 6, 1978, from the *Faculty of Pharmacy, University of Riyad, Riyad, Saudi Arabia.* Accepted for publication December 14, 1978.

Abstract □ The essential oil of *Teucrium polium*, growing in Saudi Arabia, was thoroughly investigated for its constituents by GLC–mass spectrometry, TLC, and spectrophotometric methods. This investigation revealed the presence of 10 terpenoidal compounds including the hydrocarbons β-pinene, limonene, α-phellandrene, and γ- and δ-cadinenes and the alcohols linalool, terpine-4-ol, cedrol, cedrenol, and guaiol. The oil was rich in alcohols and devoid of esters. Preliminary pharmacological screening showed that the oil possesses powerful antispasmodic activity.

Keyphrases □ GLC–mass spectrometry—analysis, *Teucrium polium* oil, antispasmodics, folk medicine □ *Teucrium polium*—oil, GLC–mass spectrometry □ Antispasmodics—analysis, *Teucrium polium* oil, GLC–mass spectrometry, folk medicine □ Folk medicine—antispasmodics, *Teucrium polium* oil, GLC–mass spectrometry

Teucrium polium (Family Labiatae) is one of the most fragrant plants in Saudi Arabia and is fairly distributed throughout the country (1). In folk medicine, it is used as an antispasmodic, antirheumatic, carminative, and flavoring agent. In an admixture with other powdered herbs, it is claimed to be therapeutic for peptic ulcer.

The aroma of this plant is due to its essential oil content (2). A literature review revealed that the oil constituents had not been investigated thoroughly (4). The present work was carried out to investigate the composition of this potentially therapeutic plant oil.

EXPERIMENTAL

Material—The plant was collected in the spring at the flowering stage from Sudair (Central Zone), 180 km from Riyad. Its identity as *T. polium* was confirmed[1]. It was dried and powdered.

Successive quantities (1 kg each) were subjected to steam distillation, which produced a volatile oil (average yield, 1.55 g).

The physical properties of the oil are presented in Table I.

TLC—TLC was done on precoated silica gel thin-layer plates[2] developed in chloroform–benzene (1:1) and chloroform–benzene (4:1) solvent systems (3). After development, the spots were visualized by spraying with anisaldehyde reagent (3).

Table I—Comparative Physicochemical Data

Property	Isolated Oil	Sardinian Oil
Color	Light yellow, darkens upon standing	Blue
Odor	Fragrant, characteristic	Agreeable, pungent
Refractive index[a]	n_D^{24}, 1.4850	n_D^{20}, 1.475 and 1.488
Optical rotation[b]	$[\alpha]_D^{24}$ +4.7° (10% in ethanol)	$[\alpha]_D^{20}$ +12.75°
Acetyl value[c]	117	47.45–47.59
IR[d]	1633, 1655, 1700, 2900, and 3400 cm^{-1}	—
NMR[e]	Broad singlets at 332, 306, 280, and 268 Hz; broad singlet at 217 Hz; singlet at 98 Hz; doublet at 73 Hz; two overlapping doublets centered at 58 Hz	—

[a] Zeiss Abbe refractometer. [b] Bellingham and Stanley polarimeter. [c] According to the BP method (5). [d] As film on Perkin-Elmer 567 grating IR spectrophotometer. [e] In deuterochloroform on Varian T 60A with tetramethylsilane as the internal standard.

GLC–Mass Spectrometry—Mass spectra of the volatile oil constituents were obtained using a gas chromatograph–mass spectrometer[3]. The chromatographic column (1.8 m long) was packed with 3% OV-17. The column was conditioned isothermally at 100° for 10 min, and then the temperature was programmed at 5 min until 260°. The injection port temperature was 185°, the separation temperature was 252°, and the ion source temperature was 290°. Mass spectra were obtained by operating at 60 MHz and with an ionization energy of 70 ev.

RESULTS AND DISCUSSION

The isolated oil was compared with Saridinian *T. polium* oil (4) (Table I). The IR and NMR data revealed free alcohols (3400 cm^{-1}; broad singlet at 217 Hz, disappeared on deuteration), alkene and highly conjugated

[1] The plant material was identified as *Teucrium polium* Linneus (Labiatae) by Dr. A. M. Migahid, Department of Botany, Faculty of Science, University of Riyad, Riyad, Saudi Arabia. A voucher specimen is available in the herbarium of Riyad University.

[2] GF plants, Anachem.

[3] Model 9000, LKB-Produkter, Brommo, Sweden.

0022-3549/79/0600-0800$01.00/0

© 1979, American Pharmaceutical Association

Table II—Constituents of the Oil by GLC-Mass Spectrometry

Compound	Retention Time, min	Molecular Weight	M^+
1 β-Pinene	1.0	136.23	136
2 Limonene	1.3	136.23	136
3 α-Phellandrene	1.6	136.23	136
4 Linalool	2.3	154.24	136
5 Terpine-4-ol	3.9	154.24	154
6 γ-Cadinene	17.2	204.34	204
7 Cedrenol	20.7	222.36	220
8 δ-Cadinene	22.5	204.34	204
9 Guaiol	22.9	222.36	222
10 Cedrol	23.4	222.36	222

alkenes [1633 (m)[4] and 1655 (m) cm^{-1}; broad peaks at 332, 306, 280, 268 Hz], alicyclic structures (singlet at 98 Hz, doublet at 73 Hz, and triplet formed of two overlapping doublets at 58 Hz), and the absence of esters, other carbonyl compounds, and aromatic functions. TLC screening of the oil showed both hydrocarbons and alcohols.

GLC–mass spectrometry studies indicated the presence of several compounds (Table II and Fig. 1). The major components on the GLC trace (Fig. 1) are identified by sequence numbers that correspond to the mass spectral sequence numbers.

The mass spectra so obtained were compared with the authentic compounds and demonstrated almost identical fragmentation characteristics (6). The mass fragmentation pattern of most components showed molecular ion peaks at atomic mass units equivalent to their molecular weights. The linalool mass fragmentation pattern exhibited an M^+ at 136 amu instead of at 154 amu. The M − 18 fragment was attributed to the formation of a triene compound from the parent ion by the loss of water (7).

The cedrenol mass spectrum did not show an M^+ at 222 amu; the M − 2 fragment at 220 amu represented the loss of two hydrogen atoms (7).

From the data obtained, the volatile oil was considered to be one of the alcoholic volatile oils since 50% of the components were alcohols. The absence of esters may indicate that the plant is unable to esterify these alcohols.

Preliminary pharmacological screening of the isolated oil showed that it possessed potent antispasmodic activity and that it markedly antagonized the effects of the agonists nicotine, acetylcholine, histamine, and serotonin.

[4] Medium.

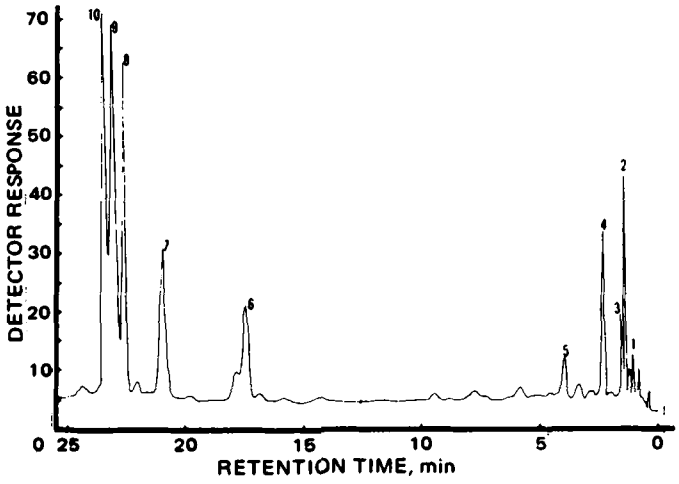

Figure 1—*Gas chromatogram of the isolated oil.*

The aqueous extract of the herb had low antispasmodic activity compared to the oil. The results of this study partially justified the use of this plant in folk medicine.

REFERENCES

(1) A. M. Migahid and M. A. Hammouda, "Flora of Saudi Arabia," Riyad University Publications, Riyad, Saudi Arabia, 1974.

(2) G. M. Wassel and S. S. Ahmed, *Pharmazie*, **29**, 8 (1974).

(3) E. Stahl, "Thin Layer Chromatography," 2nd ed., Allen & Unwin, London, England, 1967, p. 857.

(4) I. E. Puxeddu, *Ann. Chim. Appl.*, **15**, 159 (1925).

(5) "British Pharmacopoeia, 1973," Her Majesty's Stationery Office, London, England, 1973.

(6) E. Stenhagen, S. Abrahamasson, and F. W. McLafferty, "Registry of Mass Spectra Data," vols. I and II, Wiley, New York, N.Y., 1974.

(7) H. Budzikiewicz, C. Djerassi, and D. H. William, "Interpretation of Mass Spectra of Organic Compounds," Holden-Day, San Francisco, Calif., 1965, pp. 32, 33.

ACKNOWLEDGMENTS

The authors thank The Upjohn Co., Kalamazoo, Mich., for the GLC–mass spectrometric data and A. M. S. Ahmed for assistance.

Comparison of High-Pressure Liquid Chromatographic and Ion-Exchange Membrane Methods for Creatinine

Keyphrases □ High-pressure liquid chromatography—analysis of creatinine, membrane method □ Creatinine—high-pressure liquid chromatography analysis, membrane method

To the Editor:

Chiou *et al.* (1) described a high-pressure liquid chromatographic (HPLC) method for creatinine and stated that previously published methods "lack specificity" or are "subject to interferences." In particular, they stated that in the cation-exchange membrane method of Vedsø *et al.* (2), the membrane is used "to remove proteins and interfering substances from serum samples . . . . Acetoacetate and possibly some other interfering substances are not removed. Therefore, interferences occur at least in samples from ketotic patients."

In fact, the cation-exchange membrane is used to *remove creatininium ions* from diluted serum at pH 3.1. Acetoacetate, acetone, glucose, and pyruvate are not removed (3); therefore, interference by these substances does *not* occur. (This is clearly stated in the original article.)

Chiou *et al.* (1) also stated that the membrane method "would probably take about 30 min for each assay," while their own method requires "only about 5 min for completion." In fact, an assay with the membrane method takes about 1.5 hr (the original article clearly stated that ion exchange takes 1 hr and desorption requires 20 min). Since the membrane method is a batch technique, a routine workload of 250 determinations (representing 100 sample duplicates) can be accomplished by one technician in 2.5 hr. This quantity is in contrast to the method of Chiou *et al.* (1) in which the throughput appears to be about 12 determinations/chromatograph hr, which is hardly suitable for routine workloads.

The membrane method has been improved since publication in 1974. The picrate reagent now contains 9.8 mmoles of picric acid/liter and 82 mmoles of sodium hydroxide/liter. The reagent blank is now about 0.030*A*, and the slope of the standard curve is about 2.0*A* mole^{-1} liter $\times 10^3$. With the improved method, the coefficient of variation at 50 μmoles/liter (0.57 mg %) is about 5%; in the normal range, it is about 4%. These values are in sharp contrast to those of Moss *et al.* (4), who found a coefficient of variation of 14% for creatinine values of 67 μmoles/liter (0.76 mg %).

Chiou *et al.* (1) erroneously stated that Moss *et al.* (4) did not report on the reproducibility of measurements of concentrations below 1 mg %. In fact, the article of Moss *et al.* is one of the few that *does* give this information. However, Chiou *et al.* do not report the reproducibility of their method below 1 mg %.

(1) W. L. Chiou, M. A. F. Gadalla, and G. W. Peng, *J. Pharm. Sci.*, **67**, 182 (1978).

(2) S. Vedsø, C. Rud, and J. F. Place, *Scand. J. Clin. Lab. Invest.*, **34**, 275 (1974).

(3) A. C. Teger-Nilsson, *ibid.*, **13**, 326 (1961).

(4) G. A. Moss, R. J. L. Bondar, and D. M. Buzzelli, *Clin. Chem.*, **21**, 1422 (1975).

John F. Place
Department of Clinical Chemistry
Vejle Hospital
7100 Vejle, Denmark

Received September 26, 1978.
Accepted for publication November 22, 1978.

Creatinine IX: Specificity and Sensitivity of High-Performance Liquid Chromatographic and Ion-Exchange Membrane Methods for Determination of Endogenous Creatinine

Keyphrases □ Creatinine—analysis, high-performance liquid chromatography, ion-exchange membrane assay □ High-performance liquid chromatography—analysis, creatinine

To the Editor:

In commenting on our extensive studies (1) on the development of a simple, rapid, and micro high-pressure liquid chromatographic (HPLC) method for the determination of endogenous "true" creatinine, it appears that Place (2) has misunderstood the content of our paper. Our paper clearly stated that in the ion-exchange membrane method by Vedsø *et al.* (3), "the subsequent reaction of creatinine desorbed from the membrane with the alkaline picrate." Although the ion-exchange membrane method was claimed to be specific (3), it can only be considered more specific than some other published methods using the alkaline picrate reagent. This is obvious since there is no guarantee that other endogenous substance(s) not tested by them or other workers cannot react with the alkaline picrate in their method. In commenting on the kinetic method of Larsen (4), Vedsø *et al.* (3) erroneously implied that they achieved a *total specificity* in their membrane method.

The accuracy and specificity of the original membrane method (1) also can be questioned due to the unusually high absorbance for their blank sample. The blank absorbance, calculated by this author, is equivalent to 1.70 mg % of creatinine. Plasma or serum creatinine levels ranging from 0.4 to 0.8 mg % are quite commonly found in patients.

There should be no doubt that the HPLC methods (1, 5, 6) for the assay of creatinine in serum or plasma should be more specific than the other assays published to date. The automated analyzer method, generally considered to be quite specific, overestimated creatinine by as much as 45% in our studies and ~200% in others (5) in certain samples when compared with the HPLC methods. In our laboratory, a range of ~20–70% of overestimation also was recently found in many serum samples with low creatinine

0022-3549/79/0600-0802$01.00/0
© 1979, American Pharmaceutical Association

Comparison of High-Pressure Liquid Chromatographic and Ion-Exchange Membrane Methods for Creatinine

Keyphrases □ High-pressure liquid chromatography—analysis of creatinine, membrane method □ Creatinine—high-pressure liquid chromatography analysis, membrane method

To the Editor:

Chiou *et al.* (1) described a high-pressure liquid chromatographic (HPLC) method for creatinine and stated that previously published methods "lack specificity" or are "subject to interferences." In particular, they stated that in the cation-exchange membrane method of Vedsø *et al.* (2), the membrane is used "to remove proteins and interfering substances from serum samples . . . . Acetoacetate and possibly some other interfering substances are not removed. Therefore, interferences occur at least in samples from ketotic patients."

In fact, the cation-exchange membrane is used to *remove creatininium ions* from diluted serum at pH 3.1. Acetoacetate, acetone, glucose, and pyruvate are not removed (3); therefore, interference by these substances does *not* occur. (This is clearly stated in the original article.)

Chiou *et al.* (1) also stated that the membrane method "would probably take about 30 min for each assay," while their own method requires "only about 5 min for completion." In fact, an assay with the membrane method takes about 1.5 hr (the original article clearly stated that ion exchange takes 1 hr and desorption requires 20 min). Since the membrane method is a batch technique, a routine workload of 250 determinations (representing 100 sample duplicates) can be accomplished by one technician in 2.5 hr. This quantity is in contrast to the method of Chiou *et al.* (1) in which the throughput appears to be about 12 determinations/chromatograph hr, which is hardly suitable for routine workloads.

The membrane method has been improved since publication in 1974. The picrate reagent now contains 9.8 mmoles of picric acid/liter and 82 mmoles of sodium hydroxide/liter. The reagent blank is now about 0.030*A*, and the slope of the standard curve is about 2.0*A* mole^{-1} liter $\times 10^3$. With the improved method, the coefficient of variation at 50 μmoles/liter (0.57 mg %) is about 5%; in the normal range, it is about 4%. These values are in sharp contrast to those of Moss *et al.* (4), who found a coefficient of variation of 14% for creatinine values of 67 μmoles/liter (0.76 mg %).

Chiou *et al.* (1) erroneously stated that Moss *et al.* (4) did not report on the reproducibility of measurements of concentrations below 1 mg %. In fact, the article of Moss *et al.* is one of the few that *does* give this information. However, Chiou *et al.* do not report the reproducibility of their method below 1 mg %.

(1) W. L. Chiou, M. A. F. Gadalla, and G. W. Peng, *J. Pharm. Sci.*, **67**, 182 (1978).

(2) S. Vedsø, C. Rud, and J. F. Place, *Scand. J. Clin. Lab. Invest.*, **34**, 275 (1974).

(3) A. C. Teger-Nilsson, *ibid.*, **13**, 326 (1961).

(4) G. A. Moss, R. J. L. Bondar, and D. M. Buzzelli, *Clin. Chem.*, **21**, 1422 (1975).

John F. Place
Department of Clinical Chemistry
Vejle Hospital
7100 Vejle, Denmark

Received September 26, 1978.
Accepted for publication November 22, 1978.

Creatinine IX: Specificity and Sensitivity of High-Performance Liquid Chromatographic and Ion-Exchange Membrane Methods for Determination of Endogenous Creatinine

Keyphrases □ Creatinine—analysis, high-performance liquid chromatography, ion-exchange membrane assay □ High-performance liquid chromatography—analysis, creatinine

To the Editor:

In commenting on our extensive studies (1) on the development of a simple, rapid, and micro high-pressure liquid chromatographic (HPLC) method for the determination of endogenous "true" creatinine, it appears that Place (2) has misunderstood the content of our paper. Our paper clearly stated that in the ion-exchange membrane method by Vedsø *et al.* (3), "the subsequent reaction of creatinine desorbed from the membrane with the alkaline picrate." Although the ion-exchange membrane method was claimed to be specific (3), it can only be considered more specific than some other published methods using the alkaline picrate reagent. This is obvious since there is no guarantee that other endogenous substance(s) not tested by them or other workers cannot react with the alkaline picrate in their method. In commenting on the kinetic method of Larsen (4), Vedsø *et al.* (3) erroneously implied that they achieved a *total specificity* in their membrane method.

The accuracy and specificity of the original membrane method (1) also can be questioned due to the unusually high absorbance for their blank sample. The blank absorbance, calculated by this author, is equivalent to 1.70 mg % of creatinine. Plasma or serum creatinine levels ranging from 0.4 to 0.8 mg % are quite commonly found in patients.

There should be no doubt that the HPLC methods (1, 5, 6) for the assay of creatinine in serum or plasma should be more specific than the other assays published to date. The automated analyzer method, generally considered to be quite specific, overestimated creatinine by as much as 45% in our studies and ~200% in others (5) in certain samples when compared with the HPLC methods. In our laboratory, a range of ~20–70% of overestimation also was recently found in many serum samples with low creatinine

0022-3549/79/0600-0802$01.00/0
© 1979, American Pharmaceutical Association

levels[1]. A boiling alkaline picrate method claimed for the determination of "true" creatinine has also been shown to give an average 32.4 ± 27.2% (*SD*) overestimation, with the highest overestimation being 102% (7).

We did not advocate that our method be used routinely for all creatinine determinations in patients. Since plasma or serum samples as small as 10 μl are sufficient in our method, we suggested that the method would be "particularly valuable to the monitoring of the renal function in premature and mature infants, children, and adults with collapsed vascular veins. In these patients, the sample required can be obtained easily from the fingertip or the heel in the case of tiny, premature infants."

Place misunderstood our paper regarding the analysis time for each sample. We stated in the Abstract that: "Each assay required only about 5 min for completion." This statement was mistaken by Place to mean 5 min per chromatographic time. In fact, we meant that the time from the receipt of a plasma or serum sample to the reporting of the creatinine level of the sample is ~5 min. Less time is required for multiple-sample analyses. This time compares favorably with the membrane method, which requires ~90 min for emergency cases. The proposed HPLC method can certainly be modified and automated. The potential clinical application of the HPLC method for creatinine assay was examined in two recent papers (5, 6).

Regarding Place's (2) comment on the work of Moss *et al.* (8), it should be pointed out that the lowest creatinine concentration shown in their standard curve is 2 mg %, although the use of a 1 mg % solution was mentioned in the text. Certainly, it is not most desirable to perform the reproducibility study using the creatinine level below the range used for the standard curve.

Although the data on reproducibility of measurements of concentrations <1 mg % were not presented explicitly in our papers (1, 7), they were clearly implied. Excellent reproducible results were always obtained for low creatinine levels in our many standard curve and plasma level studies (1, 7). Using a modified mobile phase and a 254-nm fixed wavelength detector, the coefficient of variation for 0.5 mg % serum sample is only about 2% (9). Our comment (1) on the interferences in samples from ketotic patients should have been directed to the colorimetric method of Heinegård and Tiderström (10) and not to the ion-exchange membrane method.

It is important to point out that in using our HPLC method (1) for creatinine, the filter device[2] to separate plasma or serum from blood cells should not be used; chemicals leached out from the device will interfere with the assay. The possibility of such interference in other HPLC methods should be studied prior to their use.

(1) W. L. Chiou, M. A. F. Gadalla, and G. W. Peng, *J. Pharm. Sci.*, **67**, 182 (1978).

(2) J. F. Place, *ibid.*, **68**, 802 (1979).

(3) S. Vedsø, C. Rud, and J. F. Place, *Scand. J. Clin. Lab. Invest.*, **34**, 275 (1974).

(4) K. Larsen, *Clin. Chim. Acta*, **41**, 209 (1972).

(5) S. J. Soldin and J. G. Hill, *Clin. Chem.*, **24**, 747 (1978).

(6) N. D. Brown, H. C. Sing, W. E. Neeley, and S. E. Koetitz, *Clin. Chem.*, **23**, 1281 (1977).

(7) W. L. Chiou, G. W. Peng, M. A. F. Gadalla, and S. T. Nerenberg, *J. Pharm. Sci.*, **67**, 292 (1978).

(8) G. A. Moss, R. J. L. Bondar, and D. M. Buzzelli, *Clin. Chem.*, **21**, 1422 (1975).

(9) F. S. Pu, Master's thesis, University of Illinois at the Medical Center, Chicago, Ill., 1978.

(10) D. Hengård and G. Tiderström, *Clin. Chim. Acta*, **43**, 305 (1973).

Win L. Chiou
Clinical Pharmacokinetics Laboratory
and Department of Pharmacy
College of Pharmacy
University of Illinois at the Medical Center
Chicago, IL 60612

Received December 5, 1978.
Accepted for publication January 23, 1979.

[1] Unpublished data.
[2] Filter sampler blood serum filter, Glassrock Products, Fairburn, GA 30212.

Effect of Sodium Sulfate on Acetaminophen Elimination by Rats

Keyphrases □ Sodium sulfate—effect on acetaminophen elimination, protection against acetaminophen toxicity, rats □ Acetaminophen—toxicity, prevention by sodium sulfate, effect on elimination □ Analgesics—acetaminophen, toxicity, prevention by sodium sulfate

To the Editor:

Accidental or intentional ingestion of large acetaminophen overdoses can cause hepatotoxicity and damage to other vital organs, sometimes with lethal outcome (1, 2). This toxic effect is produced by a reactive metabolite, which is formed in parallel with acetaminophen glucuronide and acetaminophen sulfate, the two major drug metabolites (3). Pharmacokinetic analysis of acetaminophen disposition in acutely intoxicated patients and certain other evidence from studies in humans indicate that the reactive acetaminophen metabolite is formed by apparent first-order kinetics while the two major conjugated metabolites are formed by capacity-limited kinetics (4, 5). Results of acetaminophen conjugation interaction studies in humans suggest that the availability of sulfate is rate limiting in the formation of acetaminophen sulfate (6, 7). If the formation of acetaminophen sulfate can be accelerated by administration of sodium sulfate or another suitable sulfate source, then the amount of reactive metabolite formed and, therefore, the acetaminophen toxicity should be decreased.

Preliminary studies in mice showed that intraperitoneal administration of sodium sulfate significantly increased the median lethal dose (*i.e.*, decreased the toxicity) of acetaminophen (8), but the effect of sodium sulfate on acetaminophen disposition was not determined. There is some indication that acetaminophen sulfate formation by rats is capacity limited and that treatment with sodium sulfate increases the urinary excretion of the conjugate (9, 10). However, the reported data do not establish definitively the effect of sodium sulfate on acetaminophen elimination kinetics since acetaminophen concentrations in plasma were not determined and urine collections were terminated before the excretion of drug and metabolites was completed.

In view of the potential clinical utility of sodium sulfate

© 1979, American Pharmaceutical Association

levels[1]. A boiling alkaline picrate method claimed for the determination of "true" creatinine has also been shown to give an average 32.4 ± 27.2% (*SD*) overestimation, with the highest overestimation being 102% (7).

We did not advocate that our method be used routinely for all creatinine determinations in patients. Since plasma or serum samples as small as 10 μl are sufficient in our method, we suggested that the method would be "particularly valuable to the monitoring of the renal function in premature and mature infants, children, and adults with collapsed vascular veins. In these patients, the sample required can be obtained easily from the fingertip or the heel in the case of tiny, premature infants."

Place misunderstood our paper regarding the analysis time for each sample. We stated in the Abstract that: "Each assay required only about 5 min for completion." This statement was mistaken by Place to mean 5 min per chromatographic time. In fact, we meant that the time from the receipt of a plasma or serum sample to the reporting of the creatinine level of the sample is ~5 min. Less time is required for multiple-sample analyses. This time compares favorably with the membrane method, which requires ~90 min for emergency cases. The proposed HPLC method can certainly be modified and automated. The potential clinical application of the HPLC method for creatinine assay was examined in two recent papers (5, 6).

Regarding Place's (2) comment on the work of Moss *et al.* (8), it should be pointed out that the lowest creatinine concentration shown in their standard curve is 2 mg %, although the use of a 1 mg % solution was mentioned in the text. Certainly, it is not most desirable to perform the reproducibility study using the creatinine level below the range used for the standard curve.

Although the data on reproducibility of measurements of concentrations <1 mg % were not presented explicitly in our papers (1, 7), they were clearly implied. Excellent reproducible results were always obtained for low creatinine levels in our many standard curve and plasma level studies (1, 7). Using a modified mobile phase and a 254-nm fixed wavelength detector, the coefficient of variation for 0.5 mg % serum sample is only about 2% (9). Our comment (1) on the interferences in samples from ketotic patients should have been directed to the colorimetric method of Heinegård and Tiderström (10) and not to the ion-exchange membrane method.

It is important to point out that in using our HPLC method (1) for creatinine, the filter device[2] to separate plasma or serum from blood cells should not be used; chemicals leached out from the device will interfere with the assay. The possibility of such interference in other HPLC methods should be studied prior to their use.

(1) W. L. Chiou, M. A. F. Gadalla, and G. W. Peng, *J. Pharm. Sci.*, **67**, 182 (1978).

(2) J. F. Place, *ibid.*, **68**, 802 (1979).

(3) S. Vedsø, C. Rud, and J. F. Place, *Scand. J. Clin. Lab. Invest.*, **34**, 275 (1974).

(4) K. Larsen, *Clin. Chim. Acta*, **41**, 209 (1972).

(5) S. J. Soldin and J. G. Hill, *Clin. Chem.*, **24**, 747 (1978).

(6) N. D. Brown, H. C. Sing, W. E. Neeley, and S. E. Koetitz, *Clin. Chem.*, **23**, 1281 (1977).

(7) W. L. Chiou, G. W. Peng, M. A. F. Gadalla, and S. T. Nerenberg, *J. Pharm. Sci.*, **67**, 292 (1978).

(8) G. A. Moss, R. J. L. Bondar, and D. M. Buzzelli, *Clin. Chem.*, **21**, 1422 (1975).

(9) F. S. Pu, Master's thesis, University of Illinois at the Medical Center, Chicago, Ill., 1978.

(10) D. Hengård and G. Tiderström, *Clin. Chim. Acta*, **43**, 305 (1973).

Win L. Chiou
Clinical Pharmacokinetics Laboratory
and Department of Pharmacy
College of Pharmacy
University of Illinois at the Medical Center
Chicago, IL 60612

Received December 5, 1978.
Accepted for publication January 23, 1979.

[1] Unpublished data.
[2] Filter sampler blood serum filter, Glassrock Products, Fairburn, GA 30212.

Effect of Sodium Sulfate on Acetaminophen Elimination by Rats

Keyphrases □ Sodium sulfate—effect on acetaminophen elimination, protection against acetaminophen toxicity, rats □ Acetaminophen—toxicity, prevention by sodium sulfate, effect on elimination □ Analgesics—acetaminophen, toxicity, prevention by sodium sulfate

To the Editor:

Accidental or intentional ingestion of large acetaminophen overdoses can cause hepatotoxicity and damage to other vital organs, sometimes with lethal outcome (1, 2). This toxic effect is produced by a reactive metabolite, which is formed in parallel with acetaminophen glucuronide and acetaminophen sulfate, the two major drug metabolites (3). Pharmacokinetic analysis of acetaminophen disposition in acutely intoxicated patients and certain other evidence from studies in humans indicate that the reactive acetaminophen metabolite is formed by apparent first-order kinetics while the two major conjugated metabolites are formed by capacity-limited kinetics (4, 5). Results of acetaminophen conjugation interaction studies in humans suggest that the availability of sulfate is rate limiting in the formation of acetaminophen sulfate (6, 7). If the formation of acetaminophen sulfate can be accelerated by administration of sodium sulfate or another suitable sulfate source, then the amount of reactive metabolite formed and, therefore, the acetaminophen toxicity should be decreased.

Preliminary studies in mice showed that intraperitoneal administration of sodium sulfate significantly increased the median lethal dose (*i.e.*, decreased the toxicity) of acetaminophen (8), but the effect of sodium sulfate on acetaminophen disposition was not determined. There is some indication that acetaminophen sulfate formation by rats is capacity limited and that treatment with sodium sulfate increases the urinary excretion of the conjugate (9, 10). However, the reported data do not establish definitively the effect of sodium sulfate on acetaminophen elimination kinetics since acetaminophen concentrations in plasma were not determined and urine collections were terminated before the excretion of drug and metabolites was completed.

In view of the potential clinical utility of sodium sulfate

© 1979, American Pharmaceutical Association

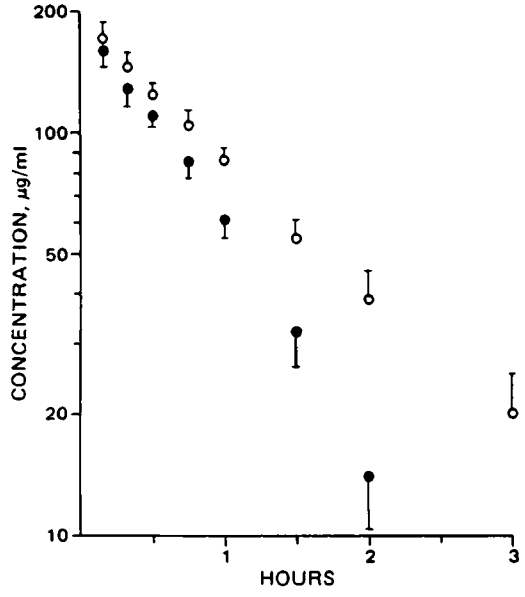

Figure 1—*Effect of sodium sulfate on elimination of acetaminophen, 150 mg/kg iv, by male Sprague–Dawley rats. Sodium sulfate was administered intraperitoneally (142 mg/kg 15 min before acetaminophen) and by intravenous infusion (about 21 mg/kg/hr for 2 hr, starting at the time of acetaminophen injection). Shown are the acetaminophen concentrations in plasma (mean + or − SD, n = 7) as a function of time in control (○) and sulfate-treated (●) animals. Concentrations differed significantly (p < 0.02) from 20 min on.*

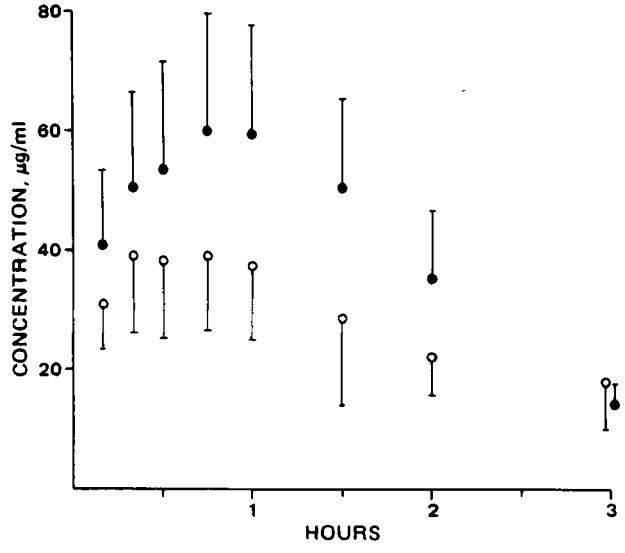

Figure 2—*Acetaminophen sulfate concentrations (expressed in terms of acetaminophen) as a function of time in plasma of control (○) and sodium sulfate-treated (●) rats (mean + or − SD, n = 7). The areas under the two curves from zero time to 3 hr differed significantly (p < 0.05).*

for preventing or reducing acetaminophen toxicity (5), a comprehensive study of the effect of sodium sulfate on acetaminophen elimination kinetics has been instituted. Reported here are results of a preliminary study which showed that sodium sulfate does substantially accelerate acetaminophen elimination in rats.

Fourteen adult male Sprague–Dawley rats, 280–320 g, had a cannula implanted in the right jugular vein (11, 12) 1 day before the study. Food and water were withdrawn in the morning at the beginning of the experiment. Acetaminophen, 150 mg/kg (25 mg dissolved in 1 ml of 40% propylene glycol in water at 40°), was injected intravenously. Seven animals received a bolus dose of sodium sulfate, 142 mg in 3 ml of water/kg ip 15 min before acetaminophen and an intravenous sodium sulfate infusion, 142 mg in 10 ml of water, over 2 hr beginning at the time of acetaminophen injection. Seven control rats received an intraperitoneal injection and an intravenous infusion of sodium chloride solution containing the same sodium concentrations as the sodium sulfate solutions.

Blood samples (0.45 ml) were obtained periodically over 4 hr. Plasma was separated and assayed for acetaminophen and acetaminophen sulfate by high-performance liquid chromatography. The assay was a modification of a published procedure (13) with the following changes: μBondapak C-18 column[1], 4-fluorophenol as the internal standard, 2-ml/min flow rate, isopropanol in the mobile phase reduced to 1.0 part, and 50% trichloroacetic acid (1 part/2 parts of plasma) for plasma protein precipitation.

Sodium sulfate caused plasma acetaminophen concentrations to decline much more rapidly in the experimental animals than in control rats (Fig. 1). Other data, to be reported later, show that acetaminophen elimination is dose dependent even though the plasma drug concentration decline is apparently exponential. The time required for acetaminophen concentrations to decrease by 50% was 55 ± 7 min in control rats and 32 ± 5 min in sodium sulfate-treated rats (mean ± *SD*, $p < 0.001$) under the experimental conditions. Conversely, plasma acetaminophen sulfate concentrations were significantly higher in sodium sulfate-treated than in control animals (Fig. 2).

This study demonstrated that sodium sulfate increases acetaminophen sulfate formation and thereby accelerates acetaminophen elimination in rats. Inferentially, such treatment should reduce the formation of other metabolites by competing pathways, particularly those, like the reactive acetaminophen metabolite, that are formed by apparently linear kinetics. These conclusions are consistent with the observation that sodium sulfate reduces acetaminophen toxicity in mice (8). If clinical studies, now in progress, yield similar results, then incorporating sodium sulfate or another sulfate source in pharmaceutical products containing acetaminophen (14) will deserve serious consideration.

[1] Waters Associates, Milford, MA 01757.

(1) J. Koch-Weser, *N. Engl. J. Med.*, **295**, 1297 (1976).
(2) B. H. Rumack and H. Matthew, *Pediatrics*, **55**, 871 (1975).
(3) J. R. Mitchell, S. Thorgeirsson, W. Z. Potter, D. J. Jollow, and H. Keiser, *Clin. Pharmacol. Ther.*, **16**, 676 (1974).
(4) M. Davis, C. J. Simmons, N. G. Harrison, and R. Williams, *Q. J. Med.*, **45**, 181 (1976).
(5) J. T. Slattery and G. Levy, *Clin. Pharmacol. Ther.*, **25**, 184 (1979).
(6) J. B. Houston and G. Levy, *J. Pharm. Sci.*, **65**, 1218 (1976).
(7) G. Levy and H. Yamada, *ibid.*, **60**, 215 (1971).
(8) J. T. Slattery and G. Levy, *Res. Commun. Chem. Pathol. Pharmacol.*, **18**, 167 (1977).
(9) H. Büch, K. Pfleger, and W. Rüdiger, *Z. Klin. Chem. Klin. Biochem.*, **5**, 110 (1967).
(10) H. Büch, C. H. Eschrich, and K. Pfleger, *Arch. Exp. Pathol. Pharmakol.*, **255**, 6 (1966).
(11) J. R. Weeks and J. D. Davis, *J. Appl. Physiol.*, **19**, 540 (1964).
(12) J. J. Ashley and G. Levy, *Res. Commun. Chem. Pathol. Pharmacol.*, **4**, 297 (1972).
(13) P. I. Adriaenssens and L. F. Prescott, *Br. J. Clin. Pharmacol.*, **6**,

87 (1978).
(14) G. Levy, in "Conjugation Reactions in Drug Biotransformation," A. Aitio, Ed., Elsevier/North-Holland Biomedical Press, Amsterdam, The Netherlands, 1978, pp. 469–476.

Raymond E. Galinsky
John T. Slattery
Gerhard Levy ˣ

Department of Pharmaceutics
School of Pharmacy
State University of New York at Buffalo
Amherst, NY 14260

Received February 22, 1979.
Accepted for publication March 22, 1979.
Supported in part by Grant GM 19568 from the National Institutes of Health.

BOOKS

REVIEWS

Essentials of Toxicology, 3rd Ed. By TED A. LOOMIS. Lea & Febiger, 600 Washington Square, Philadelphia, PA 19106. 1978. 245 pp. 15 × 24 cm. Price $12.50.

The newest edition of this basic toxicology text differs little from the previous edition in both form and content. The type is slightly larger and thus easier to read. Many chapters have few, if any, alterations. Some of the additional or revised material to be found includes: updated statistics on poisoning and mortality from chemical exposure; an amplified section on the influence of the microsomal P-450 enzyme system on chemical toxicity; a table of genetically based alterations which account for individual variations in response to drugs and chemicals; a section differentiating the concepts of biological half-life of a compound *versus* "half-life for toxicity," using as an example fatty deposition in liver after exposure to ethanol; and a brief description of behavioral toxicity studies in animals.

A table on page 60 lists formaldehyde as the toxic metabolite of methanol, although recently published data indicated that formate, and not formaldehyde, is responsible for ocular toxicity in monkeys and presumably in humans.

Each chapter is adequately referenced to provide the interested student with sources of more detailed information. This book cannot be compared to other texts such as Casarett and Doull's "Toxicology, The Basic Science of Poisons" (Macmillan) or portions of Goldstein, Aronow, and Kalman's "Principles of Drug Action" (Wiley), both of which deal more extensively with toxicologic subject matter. However, "Essentials of Toxicology" provides a well-organized introductory approach to toxicology and can serve a useful purpose in an orientation course to this highly diversified science.

Reviewed by Ray Orzechowski
Philadelphia College of Pharmacy and Science
Philadelphia, PA 19104

Blood Drugs and Other Analytical Challenges (in Methodological Surveys in Biochemistry), Vol. 7. Edited by E. REID. Ellis Horwood Ltd., Market Cross House, 1 Cooper Street, Chichester, Sussex, England (U.S. distributor: Halstead Press, a division of John Wiley & Sons, 605 Third Avenue, New York, NY 10016). 1978. 355 pp. 14.8 × 22.6 cm. Price $47.50.

This volume (Volume 7) compliments its predecessor (Volume 5) and is based on the papers presented at Bioanalytical Forum held at the University of Surrey in 1977. The book provides practical information of value to the bioanalytical researcher and attempts to present methodological rationale rather than mere recipes. The first four chapters are subdivided into sections, and the fifth chapter represents the notes, comments, and discussion in the form of questions and answers on the preceding four chapters.

The first chapter, "The Framework," sets out the general philosophy for development of analytical methods, discusses quality control and sources of errors in assays, and presents an overview on analytical method evaluation. The second chapter describes aspects of gas chromatography (GLC) with problems associated with capillary and packed columns and detectors (AFID and ECD). Their applications in drug analysis as well as derivatization procedures are discussed also.

In the third chapter, mass spectrometric methods for drug and endogenous compound analyses in biological fluids are presented, with suitable examples, together with considerations concerning accuracy and precision. Discussions of more recent approaches in this field such as negative-ion mass spectrometry and HPLC—mass spectrometry are particularly valuable.

The fourth chapter discusses the applications of HPLC to drug analysis. Interesting and useful discussions with relevant examples are provided on ion-pair HPLC of acid and basic drugs, metabolites, and endogenous compounds. Various aspects of HPLC such as electrochemical detection, sample handling, chemical derivatization including fluorescence labeling, and prechromatographic methods in biomedical trace analysis are presented with useful comments and suitable examples.

The analytical case histories on the assays of bendrofluzide, biperidin, and labetalol and its metabolites are interesting and informative. The notes and comments in the fifth chapter along with analytical case histories of drugs including metoclopramide, procetofenic acid, tienlilic acid, practolol, amitriptyline, nortriptyline and benzodiazepines make particularly enjoyable reading for the analyst.

In summary, the reviewer found this book to be a well-balanced blend of the theoretical and practical aspects of present techniques and their potential applications of trace drug analysis in biological fluids.

The book is effective in its scope, variety of experiments, and presentation style. It is well planned, emphasizes the rationale of developing successful analytical methods for drug analysis by chromatographic techniques, and should be useful to analytical chemists working with biological fluids.

Reviewed by K. K. Midha
Drug Research Laboratories
Health Protection Branch
Health & Welfare Canada
Ottawa, Ontario
K1A 0L2 Canada

Lange's Handbook of Chemistry, Twelfth Edition. Edited by JOHN A. DEAN. McGraw-Hill, New York, NY 10020. 1978. 1470 pp. 15 × 23 cm. Price $28.50.

This new edition of *Lange's Handbook of Chemistry* is a valuable updating of a classic one-volume reference.

A major improvement on the previous edition is the revised section on thermodynamics. The new section reflects currently recommended values for heats of formation and Gibbs energies of formation, entropies, heat capacities at five different temperatures, and heats of melting, vaporization, and sublimation for 2400 inorganic and 1500 organic compounds.

87 (1978).
(14) G. Levy, in "Conjugation Reactions in Drug Biotransformation," A. Aitio, Ed., Elsevier/North-Holland Biomedical Press, Amsterdam, The Netherlands, 1978, pp. 469–476.

Raymond E. Galinsky
John T. Slattery
Gerhard Levy ˣ

Department of Pharmaceutics
School of Pharmacy
State University of New York at Buffalo
Amherst, NY 14260

Received February 22, 1979.
Accepted for publication March 22, 1979.
Supported in part by Grant GM 19568 from the National Institutes of Health.

BOOKS

REVIEWS

Essentials of Toxicology, 3rd Ed. By TED A. LOOMIS. Lea & Febiger, 600 Washington Square, Philadelphia, PA 19106. 1978. 245 pp. 15 × 24 cm. Price $12.50.

The newest edition of this basic toxicology text differs little from the previous edition in both form and content. The type is slightly larger and thus easier to read. Many chapters have few, if any, alterations. Some of the additional or revised material to be found includes: updated statistics on poisoning and mortality from chemical exposure; an amplified section on the influence of the microsomal P-450 enzyme system on chemical toxicity; a table of genetically based alterations which account for individual variations in response to drugs and chemicals; a section differentiating the concepts of biological half-life of a compound *versus* "half-life for toxicity," using as an example fatty deposition in liver after exposure to ethanol; and a brief description of behavioral toxicity studies in animals.

A table on page 60 lists formaldehyde as the toxic metabolite of methanol, although recently published data indicated that formate, and not formaldehyde, is responsible for ocular toxicity in monkeys and presumably in humans.

Each chapter is adequately referenced to provide the interested student with sources of more detailed information. This book cannot be compared to other texts such as Casarett and Doull's "Toxicology, The Basic Science of Poisons" (Macmillan) or portions of Goldstein, Aronow, and Kalman's "Principles of Drug Action" (Wiley), both of which deal more extensively with toxicologic subject matter. However, "Essentials of Toxicology" provides a well-organized introductory approach to toxicology and can serve a useful purpose in an orientation course to this highly diversified science.

Reviewed by Ray Orzechowski
Philadelphia College of Pharmacy and Science
Philadelphia, PA 19104

Blood Drugs and Other Analytical Challenges (in Methodological Surveys in Biochemistry), Vol. 7. Edited by E. REID. Ellis Horwood Ltd., Market Cross House, 1 Cooper Street, Chichester, Sussex, England (U.S. distributor: Halstead Press, a division of John Wiley & Sons, 605 Third Avenue, New York, NY 10016). 1978. 355 pp. 14.8 × 22.6 cm. Price $47.50.

This volume (Volume 7) compliments its predecessor (Volume 5) and is based on the papers presented at Bioanalytical Forum held at the University of Surrey in 1977. The book provides practical information of value to the bioanalytical researcher and attempts to present methodological rationale rather than mere recipes. The first four chapters are subdivided into sections, and the fifth chapter represents the notes, comments, and discussion in the form of questions and answers on the preceding four chapters.

The first chapter, "The Framework," sets out the general philosophy for development of analytical methods, discusses quality control and sources of errors in assays, and presents an overview on analytical method evaluation. The second chapter describes aspects of gas chromatography (GLC) with problems associated with capillary and packed columns and detectors (AFID and ECD). Their applications in drug analysis as well as derivatization procedures are discussed also.

In the third chapter, mass spectrometric methods for drug and endogenous compound analyses in biological fluids are presented, with suitable examples, together with considerations concerning accuracy and precision. Discussions of more recent approaches in this field such as negative-ion mass spectrometry and HPLC—mass spectrometry are particularly valuable.

The fourth chapter discusses the applications of HPLC to drug analysis. Interesting and useful discussions with relevant examples are provided on ion-pair HPLC of acid and basic drugs, metabolites, and endogenous compounds. Various aspects of HPLC such as electrochemical detection, sample handling, chemical derivatization including fluorescence labeling, and prechromatographic methods in biomedical trace analysis are presented with useful comments and suitable examples.

The analytical case histories on the assays of bendrofluzide, biperidin, and labetalol and its metabolites are interesting and informative. The notes and comments in the fifth chapter along with analytical case histories of drugs including metoclopramide, procetofenic acid, tienlilic acid, practolol, amitriptyline, nortriptyline and benzodiazepines make particularly enjoyable reading for the analyst.

In summary, the reviewer found this book to be a well-balanced blend of the theoretical and practical aspects of present techniques and their potential applications of trace drug analysis in biological fluids.

The book is effective in its scope, variety of experiments, and presentation style. It is well planned, emphasizes the rationale of developing successful analytical methods for drug analysis by chromatographic techniques, and should be useful to analytical chemists working with biological fluids.

Reviewed by K. K. Midha
Drug Research Laboratories
Health Protection Branch
Health & Welfare Canada
Ottawa, Ontario
K1A 0L2 Canada

Lange's Handbook of Chemistry, Twelfth Edition. Edited by JOHN A. DEAN. McGraw-Hill, New York, NY 10020. 1978. 1470 pp. 15 × 23 cm. Price $28.50.

This new edition of *Lange's Handbook of Chemistry* is a valuable updating of a classic one-volume reference.

A major improvement on the previous edition is the revised section on thermodynamics. The new section reflects currently recommended values for heats of formation and Gibbs energies of formation, entropies, heat capacities at five different temperatures, and heats of melting, vaporization, and sublimation for 2400 inorganic and 1500 organic compounds.

87 (1978).
(14) G. Levy, in "Conjugation Reactions in Drug Biotransformation," A. Aitio, Ed., Elsevier/North-Holland Biomedical Press, Amsterdam, The Netherlands, 1978, pp. 469–476.

Raymond E. Galinsky
John T. Slattery
Gerhard Levy ˣ

Department of Pharmaceutics
School of Pharmacy
State University of New York at Buffalo
Amherst, NY 14260

Received February 22, 1979.
Accepted for publication March 22, 1979.
Supported in part by Grant GM 19568 from the National Institutes of Health.

BOOKS

REVIEWS

Essentials of Toxicology, 3rd Ed. By TED A. LOOMIS. Lea & Febiger, 600 Washington Square, Philadelphia, PA 19106. 1978. 245 pp. 15 × 24 cm. Price $12.50.

The newest edition of this basic toxicology text differs little from the previous edition in both form and content. The type is slightly larger and thus easier to read. Many chapters have few, if any, alterations. Some of the additional or revised material to be found includes: updated statistics on poisoning and mortality from chemical exposure; an amplified section on the influence of the microsomal P-450 enzyme system on chemical toxicity; a table of genetically based alterations which account for individual variations in response to drugs and chemicals; a section differentiating the concepts of biological half-life of a compound *versus* "half-life for toxicity," using as an example fatty deposition in liver after exposure to ethanol; and a brief description of behavioral toxicity studies in animals.

A table on page 60 lists formaldehyde as the toxic metabolite of methanol, although recently published data indicated that formate, and not formaldehyde, is responsible for ocular toxicity in monkeys and presumably in humans.

Each chapter is adequately referenced to provide the interested student with sources of more detailed information. This book cannot be compared to other texts such as Casarett and Doull's "Toxicology, The Basic Science of Poisons" (Macmillan) or portions of Goldstein, Aronow, and Kalman's "Principles of Drug Action" (Wiley), both of which deal more extensively with toxicologic subject matter. However, "Essentials of Toxicology" provides a well-organized introductory approach to toxicology and can serve a useful purpose in an orientation course to this highly diversified science.

Reviewed by Ray Orzechowski
Philadelphia College of Pharmacy and Science
Philadelphia, PA 19104

Blood Drugs and Other Analytical Challenges (in Methodological Surveys in Biochemistry), Vol. 7. Edited by E. REID. Ellis Horwood Ltd., Market Cross House, 1 Cooper Street, Chichester, Sussex, England (U.S. distributor: Halstead Press, a division of John Wiley & Sons, 605 Third Avenue, New York, NY 10016). 1978. 355 pp. 14.8 × 22.6 cm. Price $47.50.

This volume (Volume 7) compliments its predecessor (Volume 5) and is based on the papers presented at Bioanalytical Forum held at the University of Surrey in 1977. The book provides practical information of value to the bioanalytical researcher and attempts to present methodological rationale rather than mere recipes. The first four chapters are subdivided into sections, and the fifth chapter represents the notes, comments, and discussion in the form of questions and answers on the preceding four chapters.

The first chapter, "The Framework," sets out the general philosophy for development of analytical methods, discusses quality control and sources of errors in assays, and presents an overview on analytical method evaluation. The second chapter describes aspects of gas chromatography (GLC) with problems associated with capillary and packed columns and detectors (AFID and ECD). Their applications in drug analysis as well as derivatization procedures are discussed also.

In the third chapter, mass spectrometric methods for drug and endogenous compound analyses in biological fluids are presented, with suitable examples, together with considerations concerning accuracy and precision. Discussions of more recent approaches in this field such as negative-ion mass spectrometry and HPLC—mass spectrometry are particularly valuable.

The fourth chapter discusses the applications of HPLC to drug analysis. Interesting and useful discussions with relevant examples are provided on ion-pair HPLC of acid and basic drugs, metabolites, and endogenous compounds. Various aspects of HPLC such as electrochemical detection, sample handling, chemical derivatization including fluorescence labeling, and prechromatographic methods in biomedical trace analysis are presented with useful comments and suitable examples.

The analytical case histories on the assays of bendrofluzide, biperidin, and labetalol and its metabolites are interesting and informative. The notes and comments in the fifth chapter along with analytical case histories of drugs including metoclopramide, procetofenic acid, tienlilic acid, practolol, amitriptyline, nortriptyline and benzodiazepines make particularly enjoyable reading for the analyst.

In summary, the reviewer found this book to be a well-balanced blend of the theoretical and practical aspects of present techniques and their potential applications of trace drug analysis in biological fluids.

The book is effective in its scope, variety of experiments, and presentation style. It is well planned, emphasizes the rationale of developing successful analytical methods for drug analysis by chromatographic techniques, and should be useful to analytical chemists working with biological fluids.

Reviewed by K. K. Midha
Drug Research Laboratories
Health Protection Branch
Health & Welfare Canada
Ottawa, Ontario
K1A 0L2 Canada

Lange's Handbook of Chemistry, Twelfth Edition. Edited by JOHN A. DEAN. McGraw-Hill, New York, NY 10020. 1978. 1470 pp. 15 × 23 cm. Price $28.50.

This new edition of *Lange's Handbook of Chemistry* is a valuable updating of a classic one-volume reference.

A major improvement on the previous edition is the revised section on thermodynamics. The new section reflects currently recommended values for heats of formation and Gibbs energies of formation, entropies, heat capacities at five different temperatures, and heats of melting, vaporization, and sublimation for 2400 inorganic and 1500 organic compounds.

87 (1978).
(14) G. Levy, in "Conjugation Reactions in Drug Biotransformation," A. Aitio, Ed., Elsevier/North-Holland Biomedical Press, Amsterdam, The Netherlands, 1978, pp. 469–476.

Raymond E. Galinsky
John T. Slattery
Gerhard Levy ˣ

Department of Pharmaceutics
School of Pharmacy
State University of New York at Buffalo
Amherst, NY 14260

Received February 22, 1979.
Accepted for publication March 22, 1979.
Supported in part by Grant GM 19568 from the National Institutes of Health.

BOOKS

REVIEWS

Essentials of Toxicology, 3rd Ed. By TED A. LOOMIS. Lea & Febiger, 600 Washington Square, Philadelphia, PA 19106. 1978. 245 pp. 15 × 24 cm. Price $12.50.

The newest edition of this basic toxicology text differs little from the previous edition in both form and content. The type is slightly larger and thus easier to read. Many chapters have few, if any, alterations. Some of the additional or revised material to be found includes: updated statistics on poisoning and mortality from chemical exposure; an amplified section on the influence of the microsomal P-450 enzyme system on chemical toxicity; a table of genetically based alterations which account for individual variations in response to drugs and chemicals; a section differentiating the concepts of biological half-life of a compound *versus* "half-life for toxicity," using as an example fatty deposition in liver after exposure to ethanol; and a brief description of behavioral toxicity studies in animals.

A table on page 60 lists formaldehyde as the toxic metabolite of methanol, although recently published data indicated that formate, and not formaldehyde, is responsible for ocular toxicity in monkeys and presumably in humans.

Each chapter is adequately referenced to provide the interested student with sources of more detailed information. This book cannot be compared to other texts such as Casarett and Doull's "Toxicology, The Basic Science of Poisons" (Macmillan) or portions of Goldstein, Aronow, and Kalman's "Principles of Drug Action" (Wiley), both of which deal more extensively with toxicologic subject matter. However, "Essentials of Toxicology" provides a well-organized introductory approach to toxicology and can serve a useful purpose in an orientation course to this highly diversified science.

Reviewed by Ray Orzechowski
Philadelphia College of Pharmacy and Science
Philadelphia, PA 19104

Blood Drugs and Other Analytical Challenges (in Methodological Surveys in Biochemistry), Vol. 7. Edited by E. REID. Ellis Horwood Ltd., Market Cross House, 1 Cooper Street, Chichester, Sussex, England (U.S. distributor: Halstead Press, a division of John Wiley & Sons, 605 Third Avenue, New York, NY 10016). 1978. 355 pp. 14.8 × 22.6 cm. Price $47.50.

This volume (Volume 7) compliments its predecessor (Volume 5) and is based on the papers presented at Bioanalytical Forum held at the University of Surrey in 1977. The book provides practical information of value to the bioanalytical researcher and attempts to present methodological rationale rather than mere recipes. The first four chapters are subdivided into sections, and the fifth chapter represents the notes, comments, and discussion in the form of questions and answers on the preceding four chapters.

The first chapter, "The Framework," sets out the general philosophy for development of analytical methods, discusses quality control and sources of errors in assays, and presents an overview on analytical method evaluation. The second chapter describes aspects of gas chromatography (GLC) with problems associated with capillary and packed columns and detectors (AFID and ECD). Their applications in drug analysis as well as derivatization procedures are discussed also.

In the third chapter, mass spectrometric methods for drug and endogenous compound analyses in biological fluids are presented, with suitable examples, together with considerations concerning accuracy and precision. Discussions of more recent approaches in this field such as negative-ion mass spectrometry and HPLC—mass spectrometry are particularly valuable.

The fourth chapter discusses the applications of HPLC to drug analysis. Interesting and useful discussions with relevant examples are provided on ion-pair HPLC of acid and basic drugs, metabolites, and endogenous compounds. Various aspects of HPLC such as electrochemical detection, sample handling, chemical derivatization including fluorescence labeling, and prechromatographic methods in biomedical trace analysis are presented with useful comments and suitable examples.

The analytical case histories on the assays of bendrofluzide, biperidin, and labetalol and its metabolites are interesting and informative. The notes and comments in the fifth chapter along with analytical case histories of drugs including metoclopramide, procetofenic acid, tienlilic acid, practolol, amitriptyline, nortriptyline and benzodiazepines make particularly enjoyable reading for the analyst.

In summary, the reviewer found this book to be a well-balanced blend of the theoretical and practical aspects of present techniques and their potential applications of trace drug analysis in biological fluids.

The book is effective in its scope, variety of experiments, and presentation style. It is well planned, emphasizes the rationale of developing successful analytical methods for drug analysis by chromatographic techniques, and should be useful to analytical chemists working with biological fluids.

Reviewed by K. K. Midha
Drug Research Laboratories
Health Protection Branch
Health & Welfare Canada
Ottawa, Ontario
K1A 0L2 Canada

Lange's Handbook of Chemistry, Twelfth Edition. Edited by JOHN A. DEAN. McGraw-Hill, New York, NY 10020. 1978. 1470 pp. 15 × 23 cm. Price $28.50.

This new edition of *Lange's Handbook of Chemistry* is a valuable updating of a classic one-volume reference.

A major improvement on the previous edition is the revised section on thermodynamics. The new section reflects currently recommended values for heats of formation and Gibbs energies of formation, entropies, heat capacities at five different temperatures, and heats of melting, vaporization, and sublimation for 2400 inorganic and 1500 organic compounds.

New to this edition are structure-correlation tables for PMR and IR spectroscopy, ionization potentials of molecular and radical species, potentials of reference electrodes for water–organic solvent mixtures, and a wavenumber/wavelength conversion table.

In the original edition of this handbook, Dr. N. A. Lange described his effort "to select material to meet the needs of chemists who cannot command the unlimited time available to the research specialist, or who lack the facilities of a large technical library . . . (or who) may find this volume of value as a time-saver because of the many tables of numerical data which have been especially computed for this purpose." The present edition contains clear, comprehensive tables entirely consistent with the original editor's purpose. The compilations of commonly used information in mathematics, atomic and molecular structure, inorganic chemistry, analytical chemistry, electrochemistry, organic chemistry, and spectroscopy are complemented by succinct, well-written summaries of basic theory in each area.

This excellent, relatively inexpensive volume would be a useful addition to the library of anyone involved in pharmaceutical research.

Staff Review

Progress in Drug Research, Vol. 22. Edited by ERNST JUCKER. Birkhauser Verlag, P.O. Box 34, CH-4010, Basel, Switzerland. 1978. 412 pp. 16 × 24 cm. Price Fr. 168.

This volume of "Progress in Drug Research" contains eight chapters of diverse character and subject matter. However, all are expert accounts of recent progress or current activity in a particular area of drug research.

The first contribution, "Aspects of Social Pharmacology," discusses this emerging discipline. Social pharmacology is described as drawing on disciplines (*e.g.*, sociology and economics) outside pharmacology in order to better evaluate the effects of drugs as they are usually employed, *i.e.*, after controlled clinical studies. The second contribution, "Fundamental Structures in Drug Research II," is a companion piece to Part I, which appeared in Vol. 19 of "Progress in Drug Research." The basic approach is one of showing how the structures of members of a therapeutic group evolve from a lead or prototypical compound. Included in Part II are antimicrobials, antiprotozoals, anthelmintics, antibiotics, antivirals, antineoplastics, steroidal and peptidal hormones, prostaglandins, and vitamins. This work can be useful in several ways, one of which is as an efficient summary or outline of structural types associated with particular pharmacological activity.

Chapter three, "Antifungal Agents," is a good treatment of the clinically useful antifungal agents. For each agent, there is a summary of pertinent chemistry and thorough reviews of mechanism(s) of action, mechanism(s) of resistance, and assessments of current clinical utility. Chapter four, "Analgesics and Their Antagonists: Recent Developments," covers the literature since 1970 in a thorough and well-written review of synthesis and structure-activity relationships among opium alkaloids and synthetic analgesics. A good account of the opioid peptides is included also.

The fifth contribution, "The Benzodiazepine Story," recounts interesting personal research experiences of Leo H. Sternbach in the development of this field of medicinal agents. Additionally, this chapter is a good overview of the development of, and the present directions of research in, benzodiazepines and related compounds. Chapter six, "Antiviral Agents," carefully reviews recent advances. The agents are grouped by chemical type where feasible. Chemical modifications and antiviral activities for each group are given.

The seventh contribution, "Klinisch-Pharmakologische Kriterien in der Bewertung Eines Neuen Antibiotikums. Grundlagen and Methodische Gesichtspunkte," describes problems encountered and procedures involved in the clinical evaluation of new drug entities. A good general treatment of the factors involved in antibiotics evaluation is presented. The concluding chapter, "Drug Research and Human Sleep," is a concise account of the state of the art in the study of the drug effects on sleep in human subjects. Included are discussions of factors to be considered in accurately measuring drug effects on sleep and the problem of determining the significance of these effects.

The present volume offers a high quality and varied bill of fare. Each contribution is current and is authoritatively written. Volume 22 upholds the series' reputation as one of the classic and indispensable reference works for any college of pharmacy library.

Reviewed by Eugene I. Isaacson
College of Pharmacy
Idaho State University
Pocatello, ID 83209

Animal Health Products: Design and Evaluation. DONALD C. MONKHOUSE. American Pharmaceutical Association, 2215 Constitution Ave., N.W., Washington, DC 20037. 152 pp. 15 × 23 cm, soft cover, $14.00 ($9.00 APhA Member Rate).

The increasing likelihood of a global food shortage is drawing more attention to the area of animal health products, particularly those designed to improve agricultural productivity. *Animal Health Products: Design and Evaluation* is the first booklength compilation of concepts and ideas related to research in this field and will doubtless serve as a reference text for teaching and for defining future research. As such, it is an important and readable contribution to an area largely neglected in pharmaceutical journals and texts and rarely addressed by the curricula of schools of pharmacy.

The APhA Annual Meeting symposium from which this volume evolved was designed to acquaint scientists working primarily in human therapeutics with the rapidly expanding area of veterinary research. The growing importance of pharmaceutical support for animal husbandry is one reason this volume should be of interest to scientists in this and in related fields. Another reason is that the growth of government regulatory requirements for animal products—which are generally stiffer than those for human products—is increasing the need for cooperative work between scientists in various areas, particularly in toxicology and metabolic studies.

A final attraction is the pure intellectual challenge of this area of pharmacy. As Dr. Lloyd H. Conover wrote in the "overview" Chapter:

> *"The dip-bath constitutes the greatest challenge I know to the art and science of pharmacy. Dip-baths are water-filled vats in which cattle or sheep take periodic involuntary 'dips.' The active ectoparasiticidal agent, usually in the form of an emulsifiable concentrate, is maintained at an effective concentration by periodic additions to the bath. Thousands of animals may pass through a dip-bath in the course of a week, and as they do, excreta, soil, microorganisms and other miscellaneous debris accumulate. The emulsion must retain its chemical and physical integrity in the murky bath for months, while the ectoparasiticidal film left on the skin and hair of dipped animals must withstand tropical rains and sun for at least a week. Think on this, if you are accustomed to working with elegant human dosage forms!"*

Animal Health Products covers several of the major problems in veterinary pharmacy, with particularly good information on the pharmacokinetics of oral dosage forms in multigastric animals, the analyses and metabolism of tissue residues, the problems of incorporating drugs into feed, and the special stability problems of veterinary formulations.

Staff Review

New to this edition are structure-correlation tables for PMR and IR spectroscopy, ionization potentials of molecular and radical species, potentials of reference electrodes for water–organic solvent mixtures, and a wavenumber/wavelength conversion table.

In the original edition of this handbook, Dr. N. A. Lange described his effort "to select material to meet the needs of chemists who cannot command the unlimited time available to the research specialist, or who lack the facilities of a large technical library . . . (or who) may find this volume of value as a time-saver because of the many tables of numerical data which have been especially computed for this purpose." The present edition contains clear, comprehensive tables entirely consistent with the original editor's purpose. The compilations of commonly used information in mathematics, atomic and molecular structure, inorganic chemistry, analytical chemistry, electrochemistry, organic chemistry, and spectroscopy are complemented by succinct, well-written summaries of basic theory in each area.

This excellent, relatively inexpensive volume would be a useful addition to the library of anyone involved in pharmaceutical research.

Staff Review

Progress in Drug Research, Vol. 22. Edited by ERNST JUCKER. Birkhauser Verlag, P.O. Box 34, CH-4010, Basel, Switzerland. 1978. 412 pp. 16 × 24 cm. Price Fr. 168.

This volume of "Progress in Drug Research" contains eight chapters of diverse character and subject matter. However, all are expert accounts of recent progress or current activity in a particular area of drug research.

The first contribution, "Aspects of Social Pharmacology," discusses this emerging discipline. Social pharmacology is described as drawing on disciplines (*e.g.*, sociology and economics) outside pharmacology in order to better evaluate the effects of drugs as they are usually employed, *i.e.*, after controlled clinical studies. The second contribution, "Fundamental Structures in Drug Research II," is a companion piece to Part I, which appeared in Vol. 19 of "Progress in Drug Research." The basic approach is one of showing how the structures of members of a therapeutic group evolve from a lead or prototypical compound. Included in Part II are antimicrobials, antiprotozoals, anthelmintics, antibiotics, antivirals, antineoplastics, steroidal and peptidal hormones, prostaglandins, and vitamins. This work can be useful in several ways, one of which is as an efficient summary or outline of structural types associated with particular pharmacological activity.

Chapter three, "Antifungal Agents," is a good treatment of the clinically useful antifungal agents. For each agent, there is a summary of pertinent chemistry and thorough reviews of mechanism(s) of action, mechanism(s) of resistance, and assessments of current clinical utility. Chapter four, "Analgesics and Their Antagonists: Recent Developments," covers the literature since 1970 in a thorough and well-written review of synthesis and structure-activity relationships among opium alkaloids and synthetic analgesics. A good account of the opioid peptides is included also.

The fifth contribution, "The Benzodiazepine Story," recounts interesting personal research experiences of Leo H. Sternbach in the development of this field of medicinal agents. Additionally, this chapter is a good overview of the development of, and the present directions of research in, benzodiazepines and related compounds. Chapter six, "Antiviral Agents," carefully reviews recent advances. The agents are grouped by chemical type where feasible. Chemical modifications and antiviral activities for each group are given.

The seventh contribution, "Klinisch-Pharmakologische Kriterien in der Bewertung Eines Neuen Antibiotikums. Grundlagen and Methodische Gesichtspunkte," describes problems encountered and procedures involved in the clinical evaluation of new drug entities. A good general treatment of the factors involved in antibiotics evaluation is presented. The concluding chapter, "Drug Research and Human Sleep," is a concise account of the state of the art in the study of the drug effects on sleep in human subjects. Included are discussions of factors to be considered in accurately measuring drug effects on sleep and the problem of determining the significance of these effects.

The present volume offers a high quality and varied bill of fare. Each contribution is current and is authoritatively written. Volume 22 upholds the series' reputation as one of the classic and indispensable reference works for any college of pharmacy library.

Reviewed by Eugene I. Isaacson
College of Pharmacy
Idaho State University
Pocatello, ID 83209

Animal Health Products: Design and Evaluation. DONALD C. MONKHOUSE. American Pharmaceutical Association, 2215 Constitution Ave., N.W., Washington, DC 20037. 152 pp. 15 × 23 cm, soft cover, $14.00 ($9.00 APhA Member Rate).

The increasing likelihood of a global food shortage is drawing more attention to the area of animal health products, particularly those designed to improve agricultural productivity. *Animal Health Products: Design and Evaluation* is the first booklength compilation of concepts and ideas related to research in this field and will doubtless serve as a reference text for teaching and for defining future research. As such, it is an important and readable contribution to an area largely neglected in pharmaceutical journals and texts and rarely addressed by the curricula of schools of pharmacy.

The APhA Annual Meeting symposium from which this volume evolved was designed to acquaint scientists working primarily in human therapeutics with the rapidly expanding area of veterinary research. The growing importance of pharmaceutical support for animal husbandry is one reason this volume should be of interest to scientists in this and in related fields. Another reason is that the growth of government regulatory requirements for animal products—which are generally stiffer than those for human products—is increasing the need for cooperative work between scientists in various areas, particularly in toxicology and metabolic studies.

A final attraction is the pure intellectual challenge of this area of pharmacy. As Dr. Lloyd H. Conover wrote in the "overview" Chapter:

> *"The dip-bath constitutes the greatest challenge I know to the art and science of pharmacy. Dip-baths are water-filled vats in which cattle or sheep take periodic involuntary 'dips.' The active ectoparasiticidal agent, usually in the form of an emulsifiable concentrate, is maintained at an effective concentration by periodic additions to the bath. Thousands of animals may pass through a dip-bath in the course of a week, and as they do, excreta, soil, microorganisms and other miscellaneous debris accumulate. The emulsion must retain its chemical and physical integrity in the murky bath for months, while the ectoparasiticidal film left on the skin and hair of dipped animals must withstand tropical rains and sun for at least a week. Think on this, if you are accustomed to working with elegant human dosage forms!"*

Animal Health Products covers several of the major problems in veterinary pharmacy, with particularly good information on the pharmacokinetics of oral dosage forms in multigastric animals, the analyses and metabolism of tissue residues, the problems of incorporating drugs into feed, and the special stability problems of veterinary formulations.

Staff Review

New to this edition are structure-correlation tables for PMR and IR spectroscopy, ionization potentials of molecular and radical species, potentials of reference electrodes for water–organic solvent mixtures, and a wavenumber/wavelength conversion table.

In the original edition of this handbook, Dr. N. A. Lange described his effort "to select material to meet the needs of chemists who cannot command the unlimited time available to the research specialist, or who lack the facilities of a large technical library . . . (or who) may find this volume of value as a time-saver because of the many tables of numerical data which have been especially computed for this purpose." The present edition contains clear, comprehensive tables entirely consistent with the original editor's purpose. The compilations of commonly used information in mathematics, atomic and molecular structure, inorganic chemistry, analytical chemistry, electrochemistry, organic chemistry, and spectroscopy are complemented by succinct, well-written summaries of basic theory in each area.

This excellent, relatively inexpensive volume would be a useful addition to the library of anyone involved in pharmaceutical research.

Staff Review

Progress in Drug Research, Vol. 22. Edited by ERNST JUCKER. Birkhauser Verlag, P.O. Box 34, CH-4010, Basel, Switzerland. 1978. 412 pp. 16 × 24 cm. Price Fr. 168.

This volume of "Progress in Drug Research" contains eight chapters of diverse character and subject matter. However, all are expert accounts of recent progress or current activity in a particular area of drug research.

The first contribution, "Aspects of Social Pharmacology," discusses this emerging discipline. Social pharmacology is described as drawing on disciplines (*e.g.*, sociology and economics) outside pharmacology in order to better evaluate the effects of drugs as they are usually employed, *i.e.*, after controlled clinical studies. The second contribution, "Fundamental Structures in Drug Research II," is a companion piece to Part I, which appeared in Vol. 19 of "Progress in Drug Research." The basic approach is one of showing how the structures of members of a therapeutic group evolve from a lead or prototypical compound. Included in Part II are antimicrobials, antiprotozoals, anthelmintics, antibiotics, antivirals, antineoplastics, steroidal and peptidal hormones, prostaglandins, and vitamins. This work can be useful in several ways, one of which is as an efficient summary or outline of structural types associated with particular pharmacological activity.

Chapter three, "Antifungal Agents," is a good treatment of the clinically useful antifungal agents. For each agent, there is a summary of pertinent chemistry and thorough reviews of mechanism(s) of action, mechanism(s) of resistance, and assessments of current clinical utility. Chapter four, "Analgesics and Their Antagonists: Recent Developments," covers the literature since 1970 in a thorough and well-written review of synthesis and structure-activity relationships among opium alkaloids and synthetic analgesics. A good account of the opioid peptides is included also.

The fifth contribution, "The Benzodiazepine Story," recounts interesting personal research experiences of Leo H. Sternbach in the development of this field of medicinal agents. Additionally, this chapter is a good overview of the development of, and the present directions of research in, benzodiazepines and related compounds. Chapter six, "Antiviral Agents," carefully reviews recent advances. The agents are grouped by chemical type where feasible. Chemical modifications and antiviral activities for each group are given.

The seventh contribution, "Klinisch-Pharmakologische Kriterien in der Bewertung Eines Neuen Antibiotikums. Grundlagen and Methodische Gesichtspunkte," describes problems encountered and procedures involved in the clinical evaluation of new drug entities. A good general treatment of the factors involved in antibiotics evaluation is presented. The concluding chapter, "Drug Research and Human Sleep," is a concise account of the state of the art in the study of the drug effects on sleep in human subjects. Included are discussions of factors to be considered in accurately measuring drug effects on sleep and the problem of determining the significance of these effects.

The present volume offers a high quality and varied bill of fare. Each contribution is current and is authoritatively written. Volume 22 upholds the series' reputation as one of the classic and indispensable reference works for any college of pharmacy library.

Reviewed by Eugene I. Isaacson
College of Pharmacy
Idaho State University
Pocatello, ID 83209

Animal Health Products: Design and Evaluation. DONALD C. MONKHOUSE. American Pharmaceutical Association, 2215 Constitution Ave., N.W., Washington, DC 20037. 152 pp. 15 × 23 cm, soft cover, $14.00 ($9.00 APhA Member Rate).

The increasing likelihood of a global food shortage is drawing more attention to the area of animal health products, particularly those designed to improve agricultural productivity. *Animal Health Products: Design and Evaluation* is the first booklength compilation of concepts and ideas related to research in this field and will doubtless serve as a reference text for teaching and for defining future research. As such, it is an important and readable contribution to an area largely neglected in pharmaceutical journals and texts and rarely addressed by the curricula of schools of pharmacy.

The APhA Annual Meeting symposium from which this volume evolved was designed to acquaint scientists working primarily in human therapeutics with the rapidly expanding area of veterinary research. The growing importance of pharmaceutical support for animal husbandry is one reason this volume should be of interest to scientists in this and in related fields. Another reason is that the growth of government regulatory requirements for animal products—which are generally stiffer than those for human products—is increasing the need for cooperative work between scientists in various areas, particularly in toxicology and metabolic studies.

A final attraction is the pure intellectual challenge of this area of pharmacy. As Dr. Lloyd H. Conover wrote in the "overview" Chapter:

> *"The dip-bath constitutes the greatest challenge I know to the art and science of pharmacy. Dip-baths are water-filled vats in which cattle or sheep take periodic involuntary 'dips.' The active ectoparasiticidal agent, usually in the form of an emulsifiable concentrate, is maintained at an effective concentration by periodic additions to the bath. Thousands of animals may pass through a dip-bath in the course of a week, and as they do, excreta, soil, microorganisms and other miscellaneous debris accumulate. The emulsion must retain its chemical and physical integrity in the murky bath for months, while the ectoparasiticidal film left on the skin and hair of dipped animals must withstand tropical rains and sun for at least a week. Think on this, if you are accustomed to working with elegant human dosage forms!"*

Animal Health Products covers several of the major problems in veterinary pharmacy, with particularly good information on the pharmacokinetics of oral dosage forms in multigastric animals, the analyses and metabolism of tissue residues, the problems of incorporating drugs into feed, and the special stability problems of veterinary formulations.

Staff Review

A publication of the
American Pharmaceutical Association—
the National Professional Society
of Pharmacists

JOURNAL OF PHARMACEUTICAL SCIENCES

INDEX TO AUTHORS
INDEX TO SUBJECTS

VOLUME 68
JANUARY TO DECEMBER, 1979

Published monthly under the supervision of the Board of Trustees

MARY H. FERGUSON
Editor

SHELLY ELLIOTT
Production Editor

MARCIA GARTRELL
Copy Editor

NICOLETTE TRIANTAFELLU
Copy Editor

EDWARD G. FELDMANN
Contributing Editor

SAMUEL W. GOLDSTEIN
Contributing Editor

BELLE R. BECK
Editorial Secretary

DAVID BOHARDT
Director of Publications

L. LUAN CORRIGAN
Assistant Director of Publications

EDITORIAL ADVISORY BOARD

John Autian
Norman R. Farnsworth
William O. Foye
William J. Jusko
Herbert A. Lieberman
David E. Mann, Jr.
Gerald J. Papariello
Edward G. Rippie

JULY 1979
VOLUME 68 NUMBER 7

JOURNAL OF PHARMACEUTICAL SCIENCES

MARY H. FERGUSON
Editor

SHELLY ELLIOTT
Production Editor

MARCIA GARTRELL
Copy Editor

JANIS KELLY
Copy Editor

EDWARD G. FELDMANN
Contributing Editor

SAMUEL W. GOLDSTEIN
Contributing Editor

BELLE R. BECK
Editorial Secretary

DAVID BOHARDT
Director of Publications

L. LUAN CORRIGAN
Assistant Director of Publications

EDITORIAL ADVISORY BOARD

JOHN AUTIAN
HERBERT A. LIEBERMAN
NORMAN R. FARNSWORTH
DAVID E. MANN, JR.
WILLIAM O. FOYE
GERALD J. PAPARIELLO
WILLIAM J. JUSKO
EDWARD G. RIPPIE

The *Journal of Pharmaceutical Sciences* (ISSN 0022-3549) is published monthly by the American Pharmaceutical Association (APhA) at 2215 Constitution Ave., N.W., Washington, DC 20037. Second-class postage paid at Washington, D.C., and at additional mailing office.

All expressions of opinion and statements of supposed fact appearing in articles or editorials carried in this journal are published on the authority of the writer over whose name they appear and are not to be regarded as necessarily expressing the policies or views of APhA.

Offices—Editorial, Advertising, and Subscription: 2215 Constitution Ave., N.W., Washington, DC 20037. Printing: 20th & Northampton Streets, Easton, PA 18042.

Annual Subscriptions—United States and foreign, industrial and government institutions $50, educational institutions $50, individuals *for personal use only* $30; single copies $5. All foreign subscriptions add $5 for postage. Subscription rates are subject to change without notice. Members of APhA may elect to receive the *Journal of Pharmaceutical Sciences* as a part of their annual $70 (foreign $75) APhA membership dues.

Claims—Missing numbers will not be supplied if dues or subscriptions are in arrears for more than 60 days or if claims are received more than 60 days after the date of the issue, or if loss was due to failure to give notice of change of address. APhA cannot accept responsibility for foreign delivery when its records indicate shipment was made.

Change of Address—Members and subscribers should notify at once both the Post Office and APhA of any change of address.

Photocopying—The code at the foot of the first page of an article indicates that APhA has granted permission for copying of the article beyond the limits permitted by Sections 107 and 108 of the U.S. Copyright Law provided that the copier sends the per copy fee stated in the code to the Copyright Clearance Center, Inc., P.O. Box 8891, Boston, MA 02114. Copies may be made for personal or internal use only and not for general distribution.

Microfilm—Available from University Microfilms International, 300 N. Zeeb Road, Ann Arbor, MI 48106.

© Copyright 1979, American Pharmaceutical Association, 2215 Constitution Ave., N.W., Washington, DC 20037; all rights reserved.

A PLEA FOR FDA STABILITY

Kings, popes, and presidents come and go with the passing of time. It should not be strange, therefore, that the same is true of Food and Drug Administration Commissioners.

Nevertheless, the departure of the last several FDA Commissioners has seemed to us to have come too soon, too abruptly, and all too unexpectedly. Indeed, each of them seems to have little more than arrived, got settled in office, established an operating style, developed a rapport with the health professions and the regulated industry, when "poof!"—they were gone from office!

Our editorial comments in the November 1976 issue were written on the occasion of the previous Commissioner's (Alexander M. Schmidt) departure. Under the column heading "Passing the Baton at FDA," we recounted the strengths, weaknesses, and operating styles of the succession of modern era FDA Commissioners beginning with the celebrated James L. Goddard, the first noncareer official to ascend to the office in the agency's history. We concluded on a plaintive note that what the agency most needed at that point was "someone at the helm 'who can get it all together!' "

Well, whoever the Almighty has in charge of answering such prayers evidently heard our plea, with the rather unexpected and unlikely selection of an academic research biologist in the person of Ph.D., Donald Kennedy.

The initial Washington reaction to this choice was that the primary qualification possessed by Dr. Kennedy was that he was virtually unknown to the respective Washington political, scientific, and health communities, and therefore no one had a significant basis for mounting opposition to his appointment. Given the operating process in this politically sensitive city, there was much logic to this line of reasoning.

But it was no time at all until Dr. Kennedy had demonstrated himself to be a very energetic, articulate, and personable individual, as well as one with a quick mind and the intellectual ability to grasp the peculiar facets of FDA's regulatory responsibilities and the difficult policy issues with which it was grappling. After his two years in office, there is almost a universal consensus that he proved to be a very able Commissioner.

Moreover, if we were to single out one special achievement that he made, we would cite his "humanization" of FDA. He met with countless groups, engaging them in the most lively and informal discussion and inspiring such a feeling of openness and credibility that he came to be nicknamed "The Visible Commissioner."

So, his announcement that he would be resigning in late June to return to Stanford University as Provost and Vice-President for Academic Affairs was met with widespread disappointment. In discussing his resignation with the press, it is reported that the timing of his decision was at least in part due to the Ethics in Government Act. This is a new federal statute that becomes effective July 1, 1979. The Act is designed to restrict former federal employees in their postemployment contacts with their former agencies. The objective is to prevent even the appearance of conflict-of-interest or other undue influence. It is this Ethics in Government Act that has led to a whole rash of other recent resignations from federal office, particularly within the Department of HEW.

In discussing the impact of this new law on personnel recruiting efforts, an HEW representative recently stated that it has become much more difficult to find people on the outside who are willing to fill these high level vacancies. The pay scale for such positions is generally below that of comparable levels in the private sector; the security is tenuously tied to the fortunes of the elected Administration; and now the Ethics Act will prevent such people from easily returning to employment where their knowledge, skills, and experience would be most suited. Both Dr. Schmidt and Dr. Kennedy had simply taken leaves of absence to serve in FDA, which made it readily convenient for them to return to their respective academic institutions at such time as they felt the situation might dictate. The HEW representative went on to state that this effect of much greater difficulty in recruiting qualified outside persons would probably necessitate substantially more appointments from within the present career staff of the respective agencies.

Our first reaction is that such an outcome would be unfortunate because it deprives the agency of new thinking, fresh ideas, and the broadest choice of qualified people from which to select. However, there is another likely result that would generally be beneficial. In short, people will be far less inclined to bounce in and out of high level federal positions, for the simple reason that there will be little place for them to bounce to—at least for one year.

If this result contributes to greater stability in the FDA Commissionership, it will at least constitute one very significant compensating feature—one that our experience over the past decade has taught us to value.

Edward G. Feldmann

Drug Repackaging

I would like to comment on the editorial[1] "Bureaucratic Overkill," which appeared in the May issue of this Journal. I feel strongly that some agency must regulate drug repackaging in hospital pharmacies.

I am actively engaged with a local hospital in determining the stability of drugs after repackaging in unit dose forms. We have found that serious stability problems are possible unless proper quality control procedures are followed. For example, a number of tablets had rusty spots because the repackaging machine was not cleaned properly. Furthermore, repacked neomycin sulfate tablets had absorbed about 4.5% of moisture in less than 1 month and had become discolored. Tablets in the original container (same lot) did not change color and absorbed very little moisture. The expiration date was still a couple of years away. Moreover, aminophylline tablets had problems similar to neomycin sulfate tablets. Needless to say, all of these dosage forms had to be removed from the shelves.

V. Das Gupta
Department of Pharmaceutics
College of Pharmacy
University of Houston
Houston, TX 77004

Received May 29, 1979.

[1] E. G. Feldmann, *J. Pharm. Sci.*, 68(5), I (1979).

Thiazide Bioavailability Studies

There is a paucity of reports on the absorption and mode of elimination of the thiazide diuretics. However, there is general agreement[1,2] that when a thiazide is dissolved in water (in which it is slightly soluble), hydrolysis occurs and an equilibrium is established. The extent of this hydrolysis *in vivo* varies with the thiazide. Our studies reveal that for cyclothiazide and methyclothiazide, it varies from one individual to another and even in the same individual at different times.

The hydrolysis product common to the thiazides is 4-amino-6-chloro-*m*-benzenedisulfonamide (I). This compound, which is more soluble in water than the thiazides, is absorbed and displays diuretic activity[3]. According to Tust[4], "in saline-loaded rats the diuretic activity is equivalent to chlorothiazide." We found that I is excreted slowly in humans and can be measured in urine 96 hr after a 250-mg dose of chlorothiazide.

The more potent thiazides normally hydrolyze more extensively *in vivo* to furnish I in the urine. Examination of the urine of 28 male subjects who had been dosed with cyclothiazide, using the Bratton–Marshall colorimetric method, revealed that the 24-hr urinary excretions of I plus cyclothiazide, calculated as thiazide, ranged from 10.3 to 57.8% (average 25.4) of the ingested dose. Most of the urines were also assayed by a high-performance liquid chromatographic (HPLC) method to measure cyclothiazide and I. The urines examined contained 5–35% of the cyclothiazide as I.

When urines are extracted with ethyl acetate to recover thiazide, I, even as its hydrochloride salt from urines acidified with hydrochloric acid, is also essentially quantitatively recovered. The Bratton–Marshall method measures the I formed by hydrolysis of the thiazide both *in vivo* and *in vitro* and, therefore, usually furnishes higher urinary levels than the HPLC method when only thiazide is assayed.

Interferences by urinary constituents when the Bratton–Marshall method was used for the determination of sulfonamides in the urine were recognized early by Marshall *et al.*[5]. As more potent thiazide diuretics than chlorothiazide were subsequently introduced, less dilution of the urine was possible and these interferences became more troublesome[6]. The purple color, which develops more slowly (and is more stable) than the red color from the Bratton–Marshall, is produced by certain urinary constituents[1]. The purple color from human urine displays a broad absorption band with a maximum at 545 nm. However, by a special extraction procedure and measurement of the red color at 500 nm, the interference from urinary constituents in humans can be substantially eliminated.

Urine samples are made alkaline with sodium hydroxide solution and heated on a steam bath for about 3 hr to destroy emulsifying components, which frequently produce very stable emulsions with urine and ethyl acetate. The urine samples are then made acidic with an excess of hydrochloric acid, which increases the salt concentration and favors more complete extraction of the thiazide and I hydrochloride by ethyl acetate. The ethyl acetate is separated, washed with a small volume of distilled water, and then extracted quickly (10–15 sec) with two portions of 0.1 *N* NaOH.

The sodium hydroxide extracts are combined and allowed to stand for about 30 min, which permits hydrolysis of dissolved ethyl acetate and a drop in pH to about 8.0. This slightly alkaline solution is then extracted with fresh ethyl acetate. The ethyl acetate layer is separated and evaporated to dryness with a stream of air or nitrogen. The residue is completely hydrolyzed to I by treatment with 5 *N* NaOH and evaporation to dryness on a steam bath. The residue from this treatment is dissolved in strong hydrochloric acid[1] to a predetermined volume, and the I is diazotized in the usual manner and coupled with *N*-1-naphthylethylenediamine. The absorbance at 500 nm is determined 15–30 min after the diamine solution has been added.

This reaction is more complex than a simple diazotization[2]. Examination of the red color produced by TLC on silica gel revealed the presence of at least four components. The absorption maximum of the red color is 510 nm; by measuring absorbance at 500 nm instead of at 518 nm, as is frequently used, less than a 4% loss in intensity is encountered. However, measurement at 500 nm decreases any small interference from human urinary constituents by about 40%.

Although the HPLC method will measure a thiazide in the urine with good precision[7], I believe a more meaningful measure of bioavailability of the thiazide diuretics, especially those given in smaller doses where more of the drug is hydrolyzed, requires an HPLC method that measures both I and the thiazide. My recommendation is that all thiazide obtained from urine be converted to I and that I be measured by an HPLC method to give maximum precision and sensitivity.

Hubert W. Murphy
Analytical Development Division
Eli Lilly and Company
Indianapolis, IN 46206

Received May 24, 1979.

[1] J. E. Baer, H. L. Leidy, A. V. Brooks, and K. H. Beyer, *J. Pharmacol. Exp. Ther.*, **125**, 295 (1959).
[2] C. R. Rehm and J. B. Smith, *J. Am. Pharm. Assoc., Sci. Ed.*, **49**, 386 (1960).
[3] G. DeStevens, "Diuretics Chemistry and Pharmacology," Academic, New York, N.Y., 1963, p. 81.
[4] R. H. Tust, Cardiovascular Research Group, Eli Lilly & Co., Indianapolis, Ind., personal communication.
[5] E. K. Marshall, Jr., K. Emerson, and W. C. Cutting, *J. Am. Med. Assoc.*, **108**, 953 (1937).
[6] H. Sheppard, T. F. Mowles, and A. J. Plummer, *J. Am. Pharm. Assoc., Sci. Ed.*, **49**, 722 (1960).
[7] D. E. Resetarits and T. R. Bates, *J. Pharm. Sci.*, **68**, 126 (1979).

Drug Repackaging

I would like to comment on the editorial[1] "Bureaucratic Overkill," which appeared in the May issue of this Journal. I feel strongly that some agency must regulate drug repackaging in hospital pharmacies.

I am actively engaged with a local hospital in determining the stability of drugs after repackaging in unit dose forms. We have found that serious stability problems are possible unless proper quality control procedures are followed. For example, a number of tablets had rusty spots because the repackaging machine was not cleaned properly. Furthermore, repacked neomycin sulfate tablets had absorbed about 4.5% of moisture in less than 1 month and had become discolored. Tablets in the original container (same lot) did not change color and absorbed very little moisture. The expiration date was still a couple of years away. Moreover, aminophylline tablets had problems similar to neomycin sulfate tablets. Needless to say, all of these dosage forms had to be removed from the shelves.

V. Das Gupta
Department of Pharmaceutics
College of Pharmacy
University of Houston
Houston, TX 77004

Received May 29, 1979.

[1] E. G. Feldmann, *J. Pharm. Sci.*, 68(5), I (1979).

Thiazide Bioavailability Studies

There is a paucity of reports on the absorption and mode of elimination of the thiazide diuretics. However, there is general agreement[1,2] that when a thiazide is dissolved in water (in which it is slightly soluble), hydrolysis occurs and an equilibrium is established. The extent of this hydrolysis *in vivo* varies with the thiazide. Our studies reveal that for cyclothiazide and methyclothiazide, it varies from one individual to another and even in the same individual at different times.

The hydrolysis product common to the thiazides is 4-amino-6-chloro-*m*-benzenedisulfonamide (I). This compound, which is more soluble in water than the thiazides, is absorbed and displays diuretic activity[3]. According to Tust[4], "in saline-loaded rats the diuretic activity is equivalent to chlorothiazide." We found that I is excreted slowly in humans and can be measured in urine 96 hr after a 250-mg dose of chlorothiazide.

The more potent thiazides normally hydrolyze more extensively *in vivo* to furnish I in the urine. Examination of the urine of 28 male subjects who had been dosed with cyclothiazide, using the Bratton–Marshall colorimetric method, revealed that the 24-hr urinary excretions of I plus cyclothiazide, calculated as thiazide, ranged from 10.3 to 57.8% (average 25.4) of the ingested dose. Most of the urines were also assayed by a high-performance liquid chromatographic (HPLC) method to measure cyclothiazide and I. The urines examined contained 5–35% of the cyclothiazide as I.

When urines are extracted with ethyl acetate to recover thiazide, I, even as its hydrochloride salt from urines acidified with hydrochloric acid, is also essentially quantitatively recovered. The Bratton–Marshall method measures the I formed by hydrolysis of the thiazide both *in vivo* and *in vitro* and, therefore, usually furnishes higher urinary levels than the HPLC method when only thiazide is assayed.

Interferences by urinary constituents when the Bratton–Marshall method was used for the determination of sulfonamides in the urine were recognized early by Marshall *et al.*[5]. As more potent thiazide diuretics than chlorothiazide were subsequently introduced, less dilution of the urine was possible and these interferences became more troublesome[6]. The purple color, which develops more slowly (and is more stable) than the red color from the Bratton–Marshall, is produced by certain urinary constituents[1]. The purple color from human urine displays a broad absorption band with a maximum at 545 nm. However, by a special extraction procedure and measurement of the red color at 500 nm, the interference from urinary constituents in humans can be substantially eliminated.

Urine samples are made alkaline with sodium hydroxide solution and heated on a steam bath for about 3 hr to destroy emulsifying components, which frequently produce very stable emulsions with urine and ethyl acetate. The urine samples are then made acidic with an excess of hydrochloric acid, which increases the salt concentration and favors more complete extraction of the thiazide and I hydrochloride by ethyl acetate. The ethyl acetate is separated, washed with a small volume of distilled water, and then extracted quickly (10–15 sec) with two portions of 0.1 *N* NaOH.

The sodium hydroxide extracts are combined and allowed to stand for about 30 min, which permits hydrolysis of dissolved ethyl acetate and a drop in pH to about 8.0. This slightly alkaline solution is then extracted with fresh ethyl acetate. The ethyl acetate layer is separated and evaporated to dryness with a stream of air or nitrogen. The residue is completely hydrolyzed to I by treatment with 5 *N* NaOH and evaporation to dryness on a steam bath. The residue from this treatment is dissolved in strong hydrochloric acid[1] to a predetermined volume, and the I is diazotized in the usual manner and coupled with *N*-1-naphthylethylenediamine. The absorbance at 500 nm is determined 15–30 min after the diamine solution has been added.

This reaction is more complex than a simple diazotization[2]. Examination of the red color produced by TLC on silica gel revealed the presence of at least four components. The absorption maximum of the red color is 510 nm; by measuring absorbance at 500 nm instead of at 518 nm, as is frequently used, less than a 4% loss in intensity is encountered. However, measurement at 500 nm decreases any small interference from human urinary constituents by about 40%.

Although the HPLC method will measure a thiazide in the urine with good precision[7], I believe a more meaningful measure of bioavailability of the thiazide diuretics, especially those given in smaller doses where more of the drug is hydrolyzed, requires an HPLC method that measures both I and the thiazide. My recommendation is that all thiazide obtained from urine be converted to I and that I be measured by an HPLC method to give maximum precision and sensitivity.

Hubert W. Murphy
Analytical Development Division
Eli Lilly and Company
Indianapolis, IN 46206

Received May 24, 1979.

[1] J. E. Baer, H. L. Leidy, A. V. Brooks, and K. H. Beyer, *J. Pharmacol. Exp. Ther.*, **125**, 295 (1959).
[2] C. R. Rehm and J. B. Smith, *J. Am. Pharm. Assoc., Sci. Ed.*, **49**, 386 (1960).
[3] G. DeStevens, "Diuretics Chemistry and Pharmacology," Academic, New York, N.Y., 1963, p. 81.
[4] R. H. Tust, Cardiovascular Research Group, Eli Lilly & Co., Indianapolis, Ind., personal communication.
[5] E. K. Marshall, Jr., K. Emerson, and W. C. Cutting, *J. Am. Med. Assoc.*, **108**, 953 (1937).
[6] H. Sheppard, T. F. Mowles, and A. J. Plummer, *J. Am. Pharm. Assoc., Sci. Ed.*, **49**, 722 (1960).
[7] D. E. Resetarits and T. R. Bates, *J. Pharm. Sci.*, **68**, 126 (1979).

JOURNAL OF PHARMACEUTICAL SCIENCES

JULY 1979
VOLUME 68 NUMBER 7

RESEARCH ARTICLES

5-Azacytidine Hydrolysis Kinetics Measured by High-Pressure Liquid Chromatography and ^{13}C-NMR Spectroscopy

KENNETH K. CHAN [x], DONALD D. GIANNINI *, JAMES A. STAROSCIK, and WOLFGANG SADEE [‡]

Received August 18, 1978, from the *School of Pharmacy, Stauffer Pharmaceutical Sciences Center, University of Southern California, Los Angeles, CA 90033.* Accepted for publication January 22, 1979. *Postdoctoral fellow, Chemistry Department, California Institute of Technology. Present address: Eastman Kodak Research Laboratory, Rochester, NY 14650. [‡]School of Pharmacy, University of California, San Francisco, CA 94143.

Abstract □ Hydrolysis of 5-azacytidine, an experimental anticancer drug, in aqueous buffers was measured using a high-pressure liquid chromatographic (HPLC) procedure and a ^{13}C-NMR method. The former utilized a 17.5-μm Aminex A-6 strong cation-exchanger column eluted with 0.4 *M*, pH 4.6 ammonium formate buffer at a flow rate of 0.4 ml/min. The hydrolysis sequence as well as the existence of a labile intermediate, *N*-formylguanylribosylurea, was unequivocally established using 6-^{13}C-5-azacytidine and NMR spectral techniques. A reversible ring opening step to the *N*-formylguanylribosylurea with an equilibrium constant of 0.58 ± 0.03 between pH 5.6 and 8.5, followed by an irreversible formation of guanylribosylurea, was found by HPLC. The data confirm previous assumptions on the hydrolytic kinetics. The pH dependency of hydrolysis was examined, and the hydrolysis profile gave a normal V shape with the most stable pH at 7.0. Rather stable intravenous dosage forms can be formulated.

Keyphrases □ 5-Azacytidine—hydrolysis kinetics, aqueous solutions, high-pressure liquid chromatography, ^{13}C-NMR □ Hydrolysis kinetics—5-azacytidine, aqueous solutions □ Antineoplastic agents—5-azacytidine, hydrolysis kinetics, aqueous solutions

A cytidine analog, 5-azacytidine[1] (I), first synthesized in 1964 (1) and subsequently isolated from *Streptoverticillium ladakanus* (2, 3), has shown antitumor activity against several animal neoplasms including L-1210 leukemia (4) and T-4 lymphoma (5). Clinically, it has also demonstrated activity against various solid tumors (6) as well as leukemias (7) and is currently undergoing phase II trials (8).

This compound has long been known to be unstable in aqueous solution. Its lability has been attributed to the facile hydrolytic cleavage across the 5,6-bond (9–11). Consequently, proper formulation has been a problem in its clinical use. In addition, not only has the metabolic evidence indicated that ring cleavage is a major process of its disposition (12–14), the facile process may have a possible relationship to its still unclear overall biological activity. Therefore, the nature and sequence of its hydrolysis must be understood. While hydrolysis of I has been investigated (9–11, 15), the lack of a suitable analytical method has hampered a complete and unequivocal kinetic analysis, although certain information concerning hydrolysis has been obtained through spectroscopic resolution in a complex hydrolytic mixture (10).

Recently, specific information was obtained through TLC, NMR (11), and high-pressure liquid chromatography (HPLC) (15), including the isolation and identification of the labile intermediate; however, a systematic kinetic analysis is still lacking. This paper describes an HPLC method for the simultaneous analysis of I and its labile intermediate, *N*-formylribosylguanylurea (II), which occurs during formation of the hydrolytic product 1-β-D-ribofuranosyl-3-guanylurea (III). Corroborated with Fourier transform ^{13}C-NMR, using a 6-^{13}C-5-azacytidine previously synthesized in this laboratory (14), a detailed kinetic analysis of the hydrolysis of I in aqueous solution is presented.

EXPERIMENTAL

Chemicals and Reagents—All solvents were either analytical or liquid chromatographic grade. 5-Azacytidine was greater than 99% pure by HPLC and was used without further purification. Ninety percent labeled 6-^{13}C-5-azacytidine was synthesized as described previously (14). 1-β-D-Ribofuranosyl-3-guanylurea (III) was synthesized according to

[1] 4-Amino-1-β-D-ribofuranosyl-1,3,5-triazin-2-one, NSC-102816, CAS Reg. No. 320-67-2. Supplied by the Drug Synthesis and Chemistry Branch, Developmental Therapeutics Program, Division of Cancer Treatment, National Cancer Institute, Bethesda, MD 20014.

0022-3549/79/0700-0807$01.00/0
© 1979, American Pharmaceutical Association

the procedure of Pithova *et al.* (9). Sodium formate[2] and 90% enriched 1-^{13}C-sodium acetate[3], used as internal standards, were also pure by ^{13}C-NMR.

Analytical Procedure—Methanolic or aqueous solutions of 5-azacytidine were injected into a liquid chromatograph[4,5] *via* a 20-μl high-pressure sample injection valve[5]. The solution was eluted into a 500 × 2-mm i.d. stainless steel column[5] packed with 17.5-μm Aminex A-6[6] strong cation-exchanger with 0.40 *M*, pH 4.6 ammonium formate buffer at a flow rate of 0.4 ml/min. The components emerging from the column were detected *via* a UV detector[5] set at 254 nm. The UV-absorbing components were quantitated using either peak height or peak area as estimated *via* a mechanical disk integrator on a strip-chart recorder[7]. No significant difference was observed between these two quantitative methods.

^{13}C-NMR—NMR studies of 5-azacytidine, 6-^{13}C-5-azacytidine, and guanylribosylurea were recorded in dimethyl sulfoxide or in aqueous buffers at pH 8.0 *via* a 25.2-MHz Fourier transform NMR spectrometer[8]. Typical parameters for the measurements were: acquisition time, 0.8 sec; pulse delay, 1.2 sec; sweep width, 5000 Hz, 8 K data points; and tip angle, 30°.

For kinetic measurements, an aqueous solution of 90% enriched 6-^{13}C-5-azacytidine, 0.1 *M* in pH 8.0, 0.067 *M* phosphate buffer, was placed in the sample tube, which was inserted into the spectrometer probe. The probe temperature was maintained at 38 ± 0.1°. Rapid pulses at a pulse width of 8 were generated, and the appropriate number of transients was accumulated to acquire an adequate signal-to-noise ratio. A timer was started when the 5-azacytidine solution was mixed and placed inside the spectrometer. At the end of each accumulation, the time was noted.

Kinetic Measurements—The hydrolytic degradation of 5-azacytidine was studied quantitatively by HPLC at 25 and 37° in 0.067 *M* sodium phosphate buffer and acetate buffer at pH 4.5–9.1.

All experiments were duplicated. A gas-tight syringe was filled with a solution of 5-azacytidine at either 4.10×10^{-4} or 8.20×10^{-4} *M* in a phosphate buffer of the desired pH. For the 25° runs, the filled syringe was allowed to remain at room temperature in the high-pressure injector valve module. At approximately 10-min intervals, aliquots were pushed into the sample loop and injected immediately. For the 37° runs, the syringe was filled, capped, and placed in a constant-temperature bath. It was then removed at specific intervals to fill the injector loop and quickly replaced in the bath.

The 5-azacytidine concentrations were followed by either the peak height or the peak area method. Stability evaluations were made in Ringer's lactate and in normal saline at room temperature as well as at refrigerated temperature (5°).

RESULTS

Drug Assay—With either methanolic or aqueous solutions of 5-azacytidine kept at ice temperature before injection, a straight line was observed in the $0.041–8.20 \times 10^{-4}$ *M* range when either peak heights or peak areas were plotted against concentrations. The variance of 10 separate injections at 0.20×10^{-4} *M* was less than 1%.

When 5-azacytidine was dissolved in a phosphate buffer, 0.067 *M* at pH 8.0, and chromatographed, in addition to a peak emerging at 3.4 min (peak 1) corresponding to 5-azacytidine, a small, slower running peak emerged at 7.3 min (peak 2) and the intensity of peak 2 appeared to increase with time (Fig. 1). Their peak height ratio (peak 1 to peak 2) appeared to be constant at approximately 3:2 after 150 min. The intensities of these two peaks then diminished with time while maintaining an essentially constant ratio.

Each component was collected into a separate tube at room temperature. Reinjection of peak 1 immediately following collection yielded a single peak corresponding to 5-azacytidine. However, similar treatment of peak 2 gave two components corresponding to peaks 1 and 2, the latter at a higher intensity. After a longer period, repetition of the injection of either peak 1 or 2 revealed two peaks, this time with a peak 1 to peak 2 ratio of approximately 3:2 but with both at much diminished intensities. Collection of peak 2 at ice temperature did not appear to change the reversal of peak 2 to peak 1.

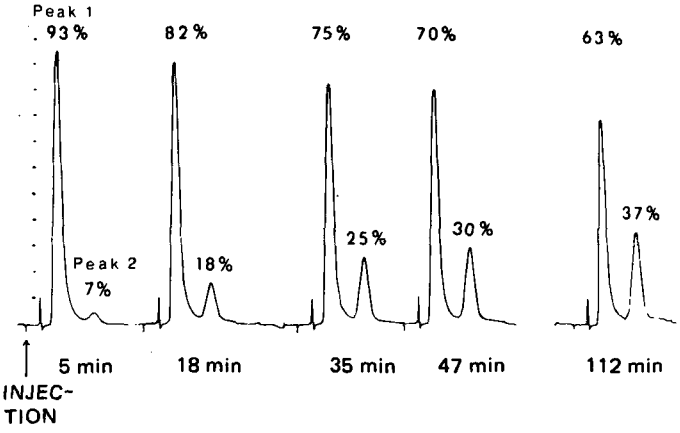

Figure 1—*High-pressure liquid chromatograms of 5-azacytidine, 8.2 × 10^{-4} M in pH 8.0, 0.067 M potassium phosphate at 25°, using 0.4 M, pH 4.6 ammonium formate at 0.4 ml/min.*

Attempts to isolate peak 2 by collecting it into a tube in a dry ice–acetone bath followed by lyophilization failed[9]. Dissolving the residue in water and injecting it into the liquid chromatograph did not give significant amounts of a UV-absorbing peak (254 nm). TLC analysis of the residue using the literature procedure (14) indicated that guanylribosylurea (III) was a major component.

^{13}C-NMR Analysis—The naturally abundant proton-decoupled NMR spectra of 5-azacytidine and guanylribosylurea spiked with formate in aqueous buffer are shown in Figs. 2 and 3, respectively. The chemical shift assignments of 5-azacytidine under the present conditions were referenced from reported values (16), and those for guanylribosylurea were assigned by direct comparison with those of I (Table I). Differences of the chemical shifts of guanylribosylurea from 5-azacytidine were seen in C-2, C-4, and C-1, as expected from the structure.

When a 5-azacytidine solution in pH 8 phosphate buffer was subjected to Fourier transform NMR analysis, new sets of signals not accounted for on the basis of the 5-azacytidine and ribosylguanylurea spectra appeared with time. A new signal appeared at 171.7 ppm, subsequently identified as formate by signal enhancement with the addition of sodium formate. Furthermore, the signal at 157.5 ppm was particularly broadened (Fig. 4).

The kinetic detections of 6-^{13}C-5-azacytidine hydrolysis in a buffered solution are shown in Fig. 5. A known concentration of ^{13}C-sodium acetate was added to the buffered solution in an attempt to quantitate the decomposition kinetics. The signals ratio between the C-6 of 5-azacytidine and the C-1 of sodium acetate was essentially constant until after 17 min. A small signal appeared at 167.8 ppm and increased with time. After 90 min, a second signal at 171.7 ppm appeared. Both new signals increased at the expense of the C-6 of 5-azacytidine, as indicated by slowly decreasing ratios of the signal intensity of the C-6 of 5-azacytidine to the C-1 of acetate. After 270 min, the intensity of the lower field signal exceeded that of the higher field one. The time course of the ratios between the C-6 signal of 5-azacytidine and the C-1 of acetate, an added internal standard, is shown in Fig. 6.

The identity of these new signals was confirmed by off-resonance decoupled NMR measurements, which assess the ^{13}C–H coupling. In this experiment, all signals exhibited a doublet except the signal of acetate (Fig. 5*h*), which indicated the attachment of one proton to each carbon. The chemical shift of the signal at 171.7 ppm coincided with that of the formate. On the basis of the chemical rationale of hydrolysis, UV absorption property *via* HPLC, and C–H coupling *via* the NMR off-resonance decoupling experiments, the signal at 167.8 ppm was assigned as derived from the formyl carbon of the labile intermediate, *N*-formylguanylribosylurea.

Kinetic Analysis—5-Azacytidine hydrolysis was carried out in 0.067 *M* phosphate buffers at pH 4.5–9.1 and at 25 and 37°. Selected hydrolysis profiles as measured by concentrations of 5-azacytidine *versus* times are shown in Fig. 7. Either monophasic or biphasic profiles were observed in all of the pH and temperature studies on semilog plots. At low pH as well as in the vicinity of neutral pH, biphasic profiles were observed, with

[2] Mallinckrodt.
[3] Merck & Co., St. Louis, Mo.
[4] Chromatronix model 3510.
[5] Spectra-Physics, Santa Clara, Calif.
[6] Packed in this laboratory with the resin supplied by Bio-Rad Laboratories, Richmond, Calif.
[7] Varian Aerograph, model 20, Varian Associates, Palo Alto, Calif.
[8] Varian XL-100, Varian Associates, Palo Alto, Calif.

[9] Recently, Beisler (11) was able to isolate and characterize *N*-formylribosylguanylurea by HPLC using a C-18 reversed-phase column and water as the eluant. In the present case, the low pH and high salt content during the lyophilization procedure may have caused the decomposition of this labile intermediate.

Table I—Chemical Shifts [a] of 5-Azacytidine and Guanylribosylurea

Carbon	I	III
C-4	166.4	162.2
C-6	157.5	—
C-2	156.1	165.4
C-1′	91.8	85.5
C-4′	84.6	83.9
C-3′	74.9	74.3
C-2′	69.6	71.2
C-5′	61.1	62.7

[a] Measured in dimethyl sulfoxide and expressed in parts per million with tetramethylsilane as the internal standard.

the most pronounced being at pH 7 and 8. At high pH, *i.e.*, 9.1, the first phase was too rapid to be discernible so that an apparently monophasic profile was observed. Similar biphasic profiles of 5-azacytidine were observed in Ringer's lactate as well as in normal saline, although the terminal phases declined very slowly.

From this evidence for the existence of an initial equilibrium phase between *N*-formylguanylribosylurea and 5-azacytidine, the biphasic behavior of these hydrolysis profiles were attributed to the kinetic scheme of Pithova *et al.* (9) (Path A, Scheme I).

The appropriate rate constants can be solved by making several assumptions: (*a*) the initial process is a rapid equilibrium, (*b*) *N*-formylguanylribosylurea exists at an approximate steady state throughout the hydrolysis, and (*c*) $k_{-1} \gg k_2$. These assumptions were supported by subsequent estimated data, generating a self-consistency. Then k_1 and k_{-1} are solvable by:

$$K_{eq} = \frac{k_1}{k_{-1}} \qquad \text{(Eq. 1)}$$

and (17, 18):

$$\log\left(\frac{A_0 - A_{eq}}{A - A_{eq}}\right) = \frac{k_1 + k_{-1}}{2.303} t \qquad \text{(Eq. 2)}$$

k_2 is solvable by the first-order degradation of the second phase:

$$A = A_0 e^{-Kt} \qquad \text{(Eq. 3)}$$

$$K = K_{eq} k_2 \qquad \text{(Eq. 4)}$$

The estimated rate constants for 5-azacytidine hydrolysis in aqueous buffer solutions at different pH values and at two temperatures are shown in Table II. The stability profile at 25 and 37° as expressed by plotting log k_1 *versus* pH is shown in Fig. 8. The profile at both temperatures followed a typical V shape, with the most stable pH at 7.0.

DISCUSSION

As was first proposed by Pithova *et al.* (9), 5-azacytidine in aqueous solution undergoes hydrolysis according to Scheme I in strong aqueous acid. Glycosidic linkage cleavage to yield 5-azacytosine, 5-azauracil, and D-ribose (Path B) was the major degradative pathway. In neutral and basic media, a facile ring cleavage to yield an instable *N*-formylguanylribosylurea intermediate followed by a loss of formate to form ribosylguanylurea was proposed as the major degradative pathway (Path A). Notari and DeYoung (10) proposed a refined scheme to include the hydration step across the 5,6-double bond as the first step.

In those studies, UV spectral techniques were used to quantify the hydrolysis kinetics of I. Using a TLC and PMR method, Israili *et al.* (15) studied the hydrolysis of 5-azacytidine and found that its degradation in aqueous buffers as well as in human plasma under various conditions followed first-order kinetics, but only monoexponential declines were reported.

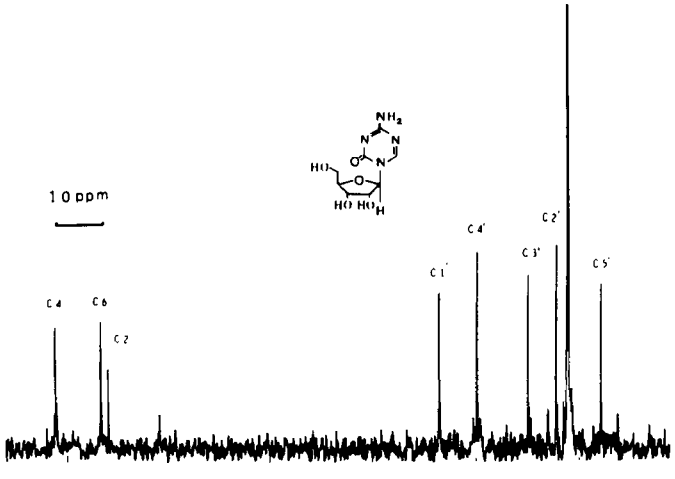

Figure 2—^{13}C-*NMR spectrum of 0.15* M *5-azacytidine at 30°. The solvent was deuterium oxide–water.*

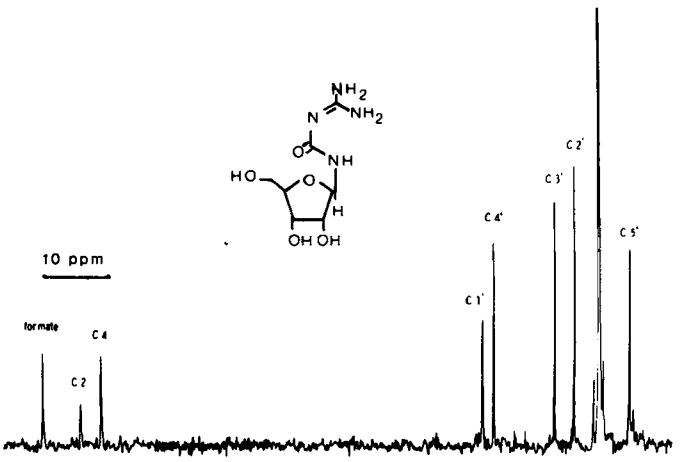

Figure 3—^{13}C-*NMR spectrum of guanylribosylurea (0.15* M*) and sodium formate (0.32* M*) in deuterium oxide–water at pH 10.2 and 30°.*

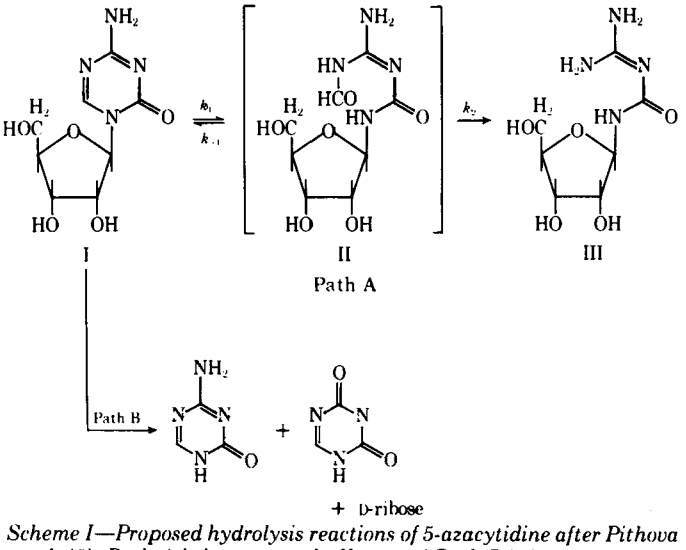

Scheme I—Proposed hydrolysis reactions of 5-azacytidine after Pithova et al. *(9). Path A is in aqueous buffers, and Path B is in strong acids.*

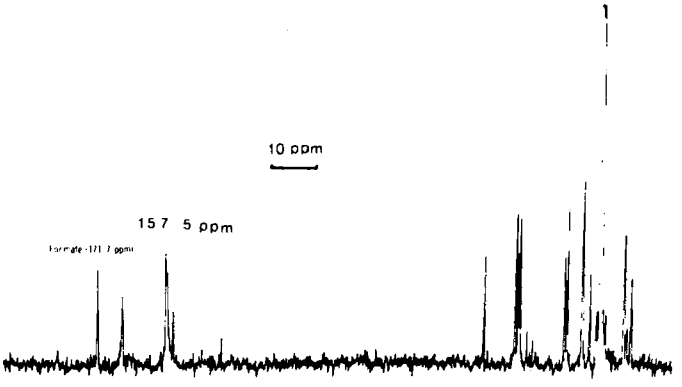

Figure 4—^{13}C-*NMR spectrum of 5-azacytidine in pH 8.0 phosphate buffer (0.15* M*) after 4 hr at 30°.*

Table II—Estimated Rate Constants[a] for 5-Azacytidine Hydrolysis in Aqueous Buffer Solutions

	25°				30°		
pH	$k_1 \times 10^{-3}$ M, min^{-1}	$k_{-1} \times 10^{-3}$ M, min^{-1}	K_{eq}	$k_2 \times 10^{-3}$ M, min^{-1}	$k_1 \times 10^{-3}$ M, min^{-1}	$k_{-1} \times 10^{-3}$ M, min^{-1}	K_{eq}
4.5	7.67 ± 0.37	17.50 ± 0.40	0.44	4.10	15.60 ± 0.40	32.30 ± 1.40	0.48
5.6	6.27 ± 0.37	11.20 ± 1.20	0.57	1.30	11.20 ± 0.60	19.60 ± 1.50	0.58
7.0	3.22 ± 0.02	5.73 ± 0.04	0.56	0.77	7.33 ± 0.00	13.05 ± 0.00	0.56
7.4	4.36 ± 0.04	7.95 ± 0.24	0.55	0.93	12.8 ± 0.50	22.20 ± 0.50	0.58
8.0	9.92 ± 0.03	17.20 ± 0.50	0.58	1.70	35.00 ± 1.80	60.80 ± 1.70	0.58
8.5	24.00 ± 1.10	39.20 ± 1.8	0.61	—	—	—	—
9.1	62.20 ± 3.80	101.0 ± 6.0	0.61	10.80	—	—	—

[a] Calculations were based on the molar concentrations of remaining 5-azacytidine since the *N*-formyl intermediate possesses different extinction coefficients (10, 11). At those times where initial equilibrium was observed and used for calculation, insignificant amounts of irreversible degradation occurred, consistent with the assumptions made, *i.e.*, $k_{-1} \gg k_2$, and with the experimental observations (^{13}C-NMR). This finding is also consistent with the observations in Ref. 11.

None of the previous studies isolated and characterized the *N*-formylguanylribosylurea intermediate. In a preliminary study (19) in this laboratory, the *N*-formyl intermediate was isolated and characterized by ^{13}C-NMR. Recently, using HPLC and PMR, Beisler (11) also isolated and characterized the *N*-formyl intermediate and reported its biological activity. However, no detailed kinetic analysis of the hydrolysis of I was presented.

The aims of this study were to use ^{13}C-NMR coupled with specific stable isotopic labeling to demonstrate unequivocally the existence of the unstable intermediates and the sequence of the degradation and to use an assay method to quantitate the kinetics and hydrolysis of 5-azacytidine as a function of pH and temperature.

^{13}C-NMR—Because of the high sensitivity and speed in data acquisition, Fourier transform ^{13}C-NMR has been used in studying reaction mechanisms (20, 21). In the present studies, the large differences in chemical shifts among the imino carbon of I, the *N*-formyl carbon of II, and the formic acid carbon were utilized for analysis. The C–H coupling (*i.e.*, doublet) should provide a positive identification of their location. Initially, it was anticipated that NMR studies on the basis of naturally abundant C-13 would provide the necessary evidence for the hydrolysis; however, no additional signals at the low field region except the formate carbon have been revealed in the hydrolysate. Subsequently, it was found that, due to the overlapping signal between the C-6 of *N*-formyl carbon and the C-4 and 5-azacytidine, it was not possible to follow the kinetics of the generation of II using naturally abundant ^{13}C-compounds. This problem was circumvented by the use of ^{13}C-5-azacytidine labeled at the C-6 position synthesized previously (14).

Use of 90% labeled 6-^{13}C-5-azacytidine revealed the generation of *N*-formylribosylguanylurea and subsequently formic acid from a solution of 5-azacytidine in pH 8.0 phosphate buffer. The chemical shifts and multiplicity in off-resonance decoupled ^{13}C-NMR and UV absorption characteristics detected from the HPLC studies are all consistent with the assigned *N*-formylguanylribosylurea structure. In addition to the off-resonance decoupled experiment, the formate carbon identity comes from enhancement of signal intensity with addition of sodium formate. On the basis of the timed ^{13}C-NMR studies, the generation sequence of *N*-formylguanylribosylurea and formate was proven unequivocally. Although carbinolamine formation as the first step of hydration across the 5,6-double bond (10) appeared to be reasonable, its detection by ^{13}C-NMR has not yet been accomplished, possibly because of its short life or very low concentration. Thus, this study also demonstrates the use of stable isotope labeling and ^{13}C-NMR in the study of reaction mechanisms.

Since the relaxation mechanism and T_1 of 5-azacytidine and *N*-formylguanylribosylurea are likely to be similar, it was thought that by selecting a reference atom with a similar chemical shift, the degradation kinetics could be followed. Thus, 90% 1-^{13}C-sodium acetate equimolar to 6-^{13}C-5-azacytidine was added to the solution for the kinetic measurement. Decomposition kinetics were followed by a change in the signal ratios between the C-6 of 5-azacytidine and the C-1 of acetate (Fig. 6). However, as shown, the ratio remained relatively constant for the initial several minutes and declined afterwards. The kinetic profile was not consistent with the HPLC data and remained difficult to interpret. The difference was perhaps due to in part to errors in Fourier transform NMR arising from limitations because of the number of data points available in the computer system and from the nonuniformity in numbers of pulses for each time spent. Therefore, steady state may not have been achieved in the experiments with few pulses.

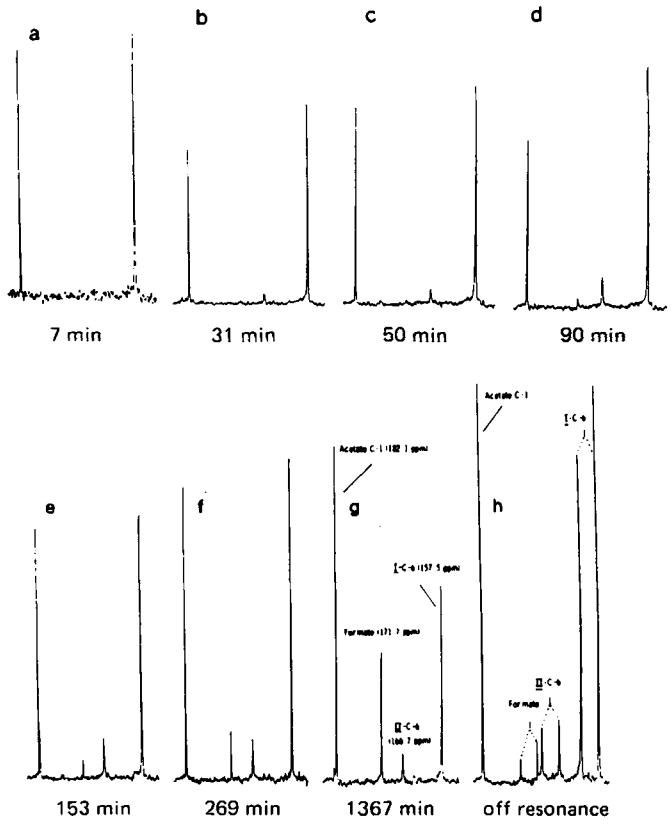

Figure 5—*^{13}C-NMR spectrum of 90% enriched 6-^{13}C-5-azacytidine (0.148 M) in pH 8.0, 0.067 M potassium phosphate buffer containing 30% deuterium oxide and ^{13}C-sodium acetate (0.20 M) at 27°. Figures 5a–5h are spectra at selected times. For complete number of time points, see Fig. 6.*

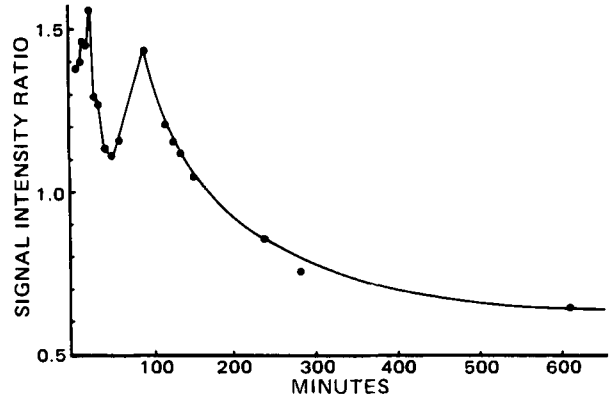

Figure 6—*Kinetic profiles of 90% enriched 6-^{13}C-5-azacytidine (0.158 M) hydrolysis in pH 8.0, 0.067 M potassium phosphate buffer containing 30% deuterium oxide and ^{13}C-sodium acetate (0.20 M) at 27° using ^{13}C-NMR measurements. Vertical axis is signal intensity ratios between 5-azacytidine and sodium acetate.*

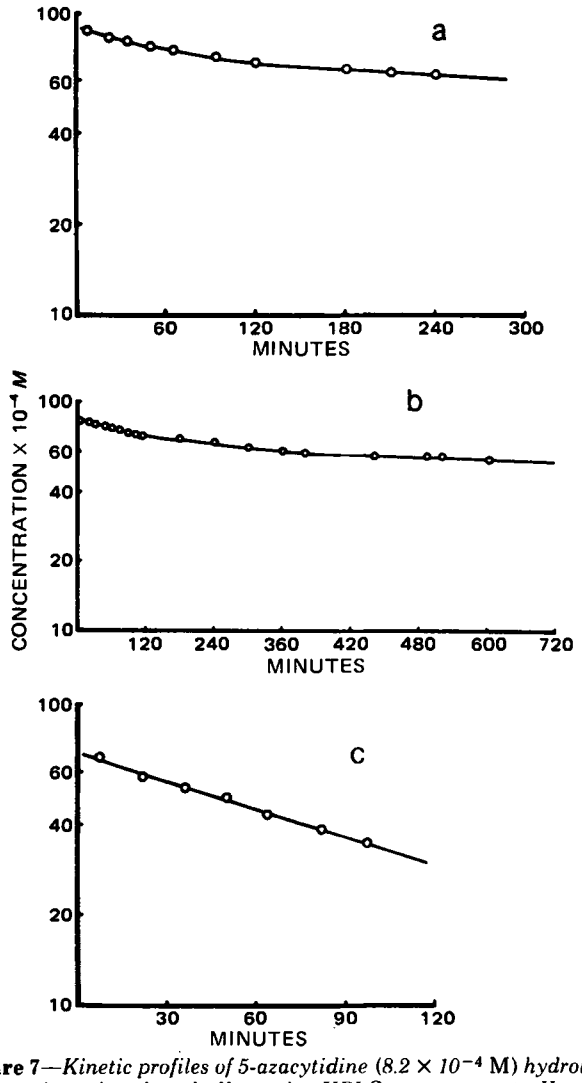

Figure 7—*Kinetic profiles of 5-azacytidine (8.2 × 10^{-4} M) hydrolysis in potassium phosphate buffers using HPLC measurements. Key:* (a), *pH 5.6 and 2.5°;* (b), *pH 7.0 and 25°; and* (c), *pH 9.1 and 25°.*

Kinetics Studies—Using UV measurement at 242 nm, Pithova *et al.* (9) first observed an initial increase followed by a subsequent decline when the extinction coefficient of 5-azacytidine in pH 6.6–7.8 borate buffers was plotted against time. Using similar UV measurements at two different wavelengths, Notari and De Young (10) observed biphasic profiles when 5-azacytidine absorbances in buffer solutions were plotted against time; the decrease or increase with time of the initial phase depended on whether the sample was acidified initially or not. The initial phase decreased with time using initially acidified sample and increased using nonacidified 5-azacytidine.

In the present study (Fig. 7), in buffers from pH 4.5 to 8.5, biphasic declines were observed when 5-azacytidine concentrations were plotted against time. At pH 9.1, the profile appeared to be monophasic and probably resulted from a very rapid equilibrium so that the first phase was not readily discernible. On the basis of the kinetic scheme (Scheme I), the individual rate constants were estimated (Table II). The direct kinetic measurements showed a rapid equilibrium between 5-azacytidine and *N*-formylribosylguanylurea, followed by a slower degradation of the latter to ribosylguanylurea.

As was evident at room temperature and various pH values, the rate constants, k_{-1}, for the ring closure were several times larger than those of the guanylribosylurea formation, k_2, consistent with the assumption made. This observation is reasonable in view of the chemical nature of the cleavages since the latter step requires the breakage of an amide bond. The k_{-1} values were also slightly greater than the k_2 values, the rate constant for the ring opening, yielding an equilibrium constant of 0.58 ± 0.03 between pH 5.6 and 8.5. This value is close to the constant ratio of 0.41 between II and I reported in water (pH unknown) (11). At 37° the equilibrium constants (0.58 ± 0.01) remained essentially unchanged (pH 5.6–8.0). The equilibrium constant decreased slightly at a lower pH (4.5). These observations are qualitatively consistent with the HPLC and PMR observations as well as with reported data (10, 11).

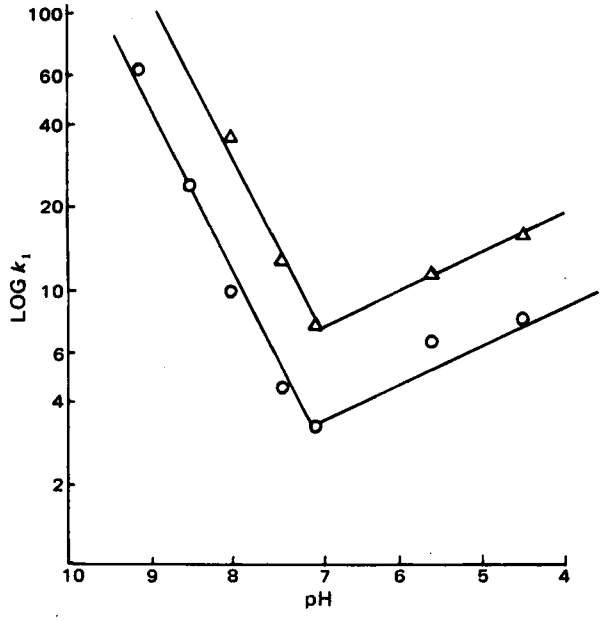

Figure 8—*The pH stability profile of 5-azacytidine (8.2 × 10^{-4} M) in aqueous buffers (potassium phosphate buffer, 0.067 M) at 25° (○) and 37° (△).*

pH-Dependent Hydrolysis—As shown in Table II, the rate constants of the hydrolysis varied with pH. When log k values were plotted against pH at 25 and 37°, a V-shaped curve resulted with both minima at pH 7.0 (Fig. 8), a value slightly different than the pH 6.5 reported (10). The slopes on the basic and acidic portions of the curve were +0.630 and −0.152, respectively. A similar trend was also observed if log k_2 values were plotted against pH. The hydrolysis, therefore, appears to be acid and base catalyzed, similar to the other known examples (22, 23). The deviation of the slopes from +1 and −1 on the basic and acidic pH portions of the curve, respectively, suggests that the hydrolysis may be susceptible to general acid and base catalyses (17). These pH profiles of the hydrolyses were markedly different from those reported by Notari and De Young (10) who described a more complex profile not readily interpretable on the basis of acid and base catalyses.

The hydrolysis kinetics observed were qualitatively similar to those reported using HPLC, PMR, and UV; however, quantitation differences were observed with those reported and may be attributed to differences in experimental conditions as well as methodologies. Under comparable experimental conditions such as those in Ringer's lactate, comparable results were obtained.

Stability Evaluation of 5-Azacytidine in Aqueous Buffers and Other Solutions—Although 5-azacytidine hydrolysis is subject to acid and base catalyses, the rate constants for the reversible formation of *N*-formlyribosylguanylurea as well as for the irreversible formation of ribosylguanylurea are smaller in magnitude than at the basic pH. Since ribosylguanylurea itself does not seem to possess significant cytotoxicity, rapid degradation of 5-azacytidine to this compound will result in a loss of efficacy. Recent biological data suggest that *N*-formylribosylguanylurea also has little cytotoxicity (11), although the evidence was not clearcut. However, other researchers found that aqueous solutions of 5-azacytidine, after long standing at room temperature, resulted in higher cytotoxicity (24, 25). Although formation of *N*-formylribosylguanylurea is reversible, in the absence of more definitive data it is desirable to formulate 5-azacytidine in media where the ring opening reaction is retarded. The pH profile of hydrolysis and kinetic data in Table II show that the rate constants for the hydrolysis in acidic pH are smaller in magnitude than those in basic pH. Therefore, a pH lower than 7.0 will result in slower ring hydrolysis.

In patients, slow infusion of 5-azacytidine in Ringer's lactate has lowered GI toxicity. The present study demonstrated that 5-azacytidine is very stable in this medium (pH 6.4), yielding a terminal $t_{1/2}$ of 4.8 days at room temperature, a value close to the reported one of 4.2 days (15). The $t_{1/2}$ in this medium at refrigerated temperature (0–5°) was considerably longer (31.3 days).

REFERENCES

(1) A. Piskala and F. Sorm, *Collect. Czech. Chem. Commun.*, **29**, 2060 (1964).

(2) L. J. Hanka, J. S. Evans, D. S. Mason, and A. Dietz, *Actimicrob. Agents Chemother.*, **1966**, 619.

(3) M. E. Bergy and R. R. Herr, *ibid.*, **1966**, 625.

(4) J. S. Evans and L. J. Hanka, *Experientia*, **24**, 922 (1968).

(5) L. J. Hanka and J. F. Clark, *Proc. Am. Cancer Res.*, **16**, 113 (1975).

(6) A. J. Weiss, J. E. Stambaugh, M. J. Mastrangelo, J. F. Laucius, and R. E. Bellet, *Cancer Chemother. Rep.*, **56**, 413 (1972).

(7) K. B. McCredie, G. P. Bodey, M. A. Burgess, J. U. Gutterman, V. Rodriguez, M. P. Sullivan, and E. J. Freireich, *ibid.*, **57**, 319 (1973).

(8) A. J. Weiss, G. E. Metter, T. F. Nealon, J. P. Keanan, G. Ramirez, A. Swiminathan, W. S. Fletcher, S. E. Moss, and R. W. Manthei, *Cancer Treatment Rep.*, **61**, 55 (1977).

(9) P. Pithova, A. Piskala, J. Pitha, and F. Sorm, *Collect. Czech. Chem. Commun.*, **30**, 2801 (1965).

(10) R. E. Notari and J. L. De Young, *J. Pharm. Sci.*, **64**, 1148 (1975).

(11) J. A. Beisler, *J. Med. Chem.*, **21**, 205 (1978).

(12) M. Surovcik, K. Raska, Jr., Z. Sormova, and F. Sorm., *Collect. Czech. Chem. Commun.*, **30**, 3370 (1965).

(13) G. L. Neil, T. E. Moxley, S. L. Kuentzel, R. C. Manak, and L. J. Hanka, *Cancer Chemother. Rep.*, **59**, 459 (1975).

(14) K. K. Chan, J. A. Staroscik, and W. Sadee, *J. Med. Chem.*, **20**, 598 (1977).

(15) Z. H. Israili, W. R. Vogler, E. S. Mingioli, J. L. Pirkle, R. W. Smithwick, and J. H. Goldstein, *Cancer Res.*, **36**, 1453 (1976).

(16) A. J. Jones, D. M. Grant, M. W. Winkley, and R. K. Robins, *J. Phys. Chem.*, **74**, 2684 (1970).

(17) A. N. Martin, J. Swarbrick, and A. Cammarata, "Physical Pharmacy," 2nd ed., Lea & Febiger, Philadelphia, Pa., 1969, pp. 383–387.

(18) A. A. Frost and R. G. Pearson, "Kinetics and Mechanism," 2nd ed., Wiley, New York, N.Y., 1961, pp. 143–196.

(19) K. K. Chan, J. Staroscik, D. D. Giannini, and W. Sadee, "Abstracts," APhA Academy of Pharmaceutical Sciences, Atlanta meeting, Nov. 1975.

(20) E. Hadaya and M. E. Kent, *J. Am. Chem. Soc.*, **93**, 3283 (1971).

(21) J. B. Stothers, I. S. Y. Wang, D. Ouchi, and E. W. Warnhoff, *ibid.*, **93**, 6702 (1971).

(22) S. Siegel, L. Lachman, and L. Malspeis, *J. Am. Pharm. Assoc., Sci. Ed.*, **48**, 431 (1959).

(23) K. T. Koshy and J. L. Lach, *J. Pharm. Sci.*, **50**, 113 (1961).

(24) P. L. Lomen, L. H. Baker, G. L. Neil, and M. K. Samson, *Cancer Chemother. Rep.*, **59**, 1123 (1975).

(25) H. H. Lloyd, E. A. Dulmadge, and L. J. Wilkoff, *ibid.*, **56**, 585 (1972).

ACKNOWLEDGMENTS

Presented in part at the Pharmaceutical Analysis and Control Section, APhA Academy of Pharmaceutical Sciences, Atlanta meeting, November 1975.

Supported in part by LAC/USC Cancer Center Grant Unit 5, P01-CA14089-2, and by Western Cancer Study Group Grant SR05 CA05186-13, Pharmacokinetic Section, both of the National Cancer Institute. The ^{13}C-NMR measurements were performed at the California Institute of Technology.

The authors thank Mr. Alfonso Barrientos for technical assistance and the National Cancer Institute for support.

GI Absorption of β-Lactam Antibiotics III: Kinetic Evidence for *In Situ* Absorption of Ionized Species of Monobasic Penicillins and Cefazolin from the Rat Small Intestine and Structure–Absorption Rate Relationships

AKIRA TSUJI, ETSUKO MIYAMOTO, OSAMU KUBO, and TSUKINAKA YAMANA ˣ

Received July 6, 1978, from the *Faculty of Pharmaceutical Sciences, Kanazawa University, Takara-machi, Kanazawa 920, Japan.* Accepted for publication December 20, 1978.

Abstract □ Absorption rates of monobasic β-lactam antibiotics were measured as a function of lumen solution pH between 4 and 9 by utilizing the rat intestinal recirculating method *in situ*. Between pH 6.5 and 9, the absorption rate constants of ionized antibiotics were almost identical; but, at pH 4, the unionized species were highly absorbed, depending on their lipophilicity through the GI membrane lipoidal barrier. The structure-absorption rate relationship was established with the unstirred layer model.

Keyphrases □ Absorption, GI—various monobasic penicillins and cefazolin, effect of ionization, pH, structure–activity relationships □ Penicillins, various—GI absorption, effect of ionization, structure–activity relationships □ Cefazolin—GI absorption, effect of ionization, structure–activity relationships □ Antibiotics—penicillins and cefazolin, GI absorption, effect of ionization, structure–activity relationships

The GI absorption rate of a monobasic penicillin in rats deviated significantly from the pH-partition hypothesis (1). This shift was interpreted successfully by the absorption mechanism of penicillins through the aqueous diffusion layer of the lumen side of the GI membrane, which is restricted by the lipophilicity of the undissociated species (1).

In *in vitro* experiments utilizing an isolated gut technique, the transport of phenoxypenicillin derivatives exhibited a saturable process, but additional study did not produce evidence of active transport (2). A similar *in vitro* study (3) provided evidence for the passive transport of β-lactam antibiotics at pH 7.4. Perrier and Gibaldi (4) attributed the larger absorption of dicloxacillin than of penicillin G and ampicillin from the *in situ* rat intestinal loop to the larger lipophilicity of dicloxacillin. A good correlation was found (5) between the rate of *in situ* intestinal cephalexin and cefazolin absorption in rats and their *in vitro* release rate from liposomes.

Recent studies in this laboratory on the *in situ* absorption kinetics of low lipophilic and completely ionized amphoteric β-lactam antibiotics, such as amoxicillin (6), cyclacillin (7), and cephradine (7), indicated that their intestinal absorption is governed by simple diffusion fol-

0022-3549/79/0700-0812$01.00/0

© 1979, American Pharmaceutical Association

REFERENCES

(1) A. Piskala and F. Sorm, *Collect. Czech. Chem. Commun.*, **29**, 2060 (1964).

(2) L. J. Hanka, J. S. Evans, D. S. Mason, and A. Dietz, *Actimicrob. Agents Chemother.*, **1966**, 619.

(3) M. E. Bergy and R. R. Herr, *ibid.*, **1966**, 625.

(4) J. S. Evans and L. J. Hanka, *Experientia*, **24**, 922 (1968).

(5) L. J. Hanka and J. F. Clark, *Proc. Am. Cancer Res.*, **16**, 113 (1975).

(6) A. J. Weiss, J. E. Stambaugh, M. J. Mastrangelo, J. F. Laucius, and R. E. Bellet, *Cancer Chemother. Rep.*, **56**, 413 (1972).

(7) K. B. McCredie, G. P. Bodey, M. A. Burgess, J. U. Gutterman, V. Rodriguez, M. P. Sullivan, and E. J. Freireich, *ibid.*, **57**, 319 (1973).

(8) A. J. Weiss, G. E. Metter, T. F. Nealon, J. P. Keanan, G. Ramirez, A. Swiminathan, W. S. Fletcher, S. E. Moss, and R. W. Manthei, *Cancer Treatment Rep.*, **61**, 55 (1977).

(9) P. Pithova, A. Piskala, J. Pitha, and F. Sorm, *Collect. Czech. Chem. Commun.*, **30**, 2801 (1965).

(10) R. E. Notari and J. L. De Young, *J. Pharm. Sci.*, **64**, 1148 (1975).

(11) J. A. Beisler, *J. Med. Chem.*, **21**, 205 (1978).

(12) M. Surovcik, K. Raska, Jr., Z. Sormova, and F. Sorm., *Collect. Czech. Chem. Commun.*, **30**, 3370 (1965).

(13) G. L. Neil, T. E. Moxley, S. L. Kuentzel, R. C. Manak, and L. J. Hanka, *Cancer Chemother. Rep.*, **59**, 459 (1975).

(14) K. K. Chan, J. A. Staroscik, and W. Sadee, *J. Med. Chem.*, **20**, 598 (1977).

(15) Z. H. Israili, W. R. Vogler, E. S. Mingioli, J. L. Pirkle, R. W. Smithwick, and J. H. Goldstein, *Cancer Res.*, **36**, 1453 (1976).

(16) A. J. Jones, D. M. Grant, M. W. Winkley, and R. K. Robins, *J. Phys. Chem.*, **74**, 2684 (1970).

(17) A. N. Martin, J. Swarbrick, and A. Cammarata, "Physical Pharmacy," 2nd ed., Lea & Febiger, Philadelphia, Pa., 1969, pp. 383–387.

(18) A. A. Frost and R. G. Pearson, "Kinetics and Mechanism," 2nd ed., Wiley, New York, N.Y., 1961, pp. 143–196.

(19) K. K. Chan, J. Staroscik, D. D. Giannini, and W. Sadee, "Abstracts," APhA Academy of Pharmaceutical Sciences, Atlanta meeting, Nov. 1975.

(20) E. Hadaya and M. E. Kent, *J. Am. Chem. Soc.*, **93**, 3283 (1971).

(21) J. B. Stothers, I. S. Y. Wang, D. Ouchi, and E. W. Warnhoff, *ibid.*, **93**, 6702 (1971).

(22) S. Siegel, L. Lachman, and L. Malspeis, *J. Am. Pharm. Assoc., Sci. Ed.*, **48**, 431 (1959).

(23) K. T. Koshy and J. L. Lach, *J. Pharm. Sci.*, **50**, 113 (1961).

(24) P. L. Lomen, L. H. Baker, G. L. Neil, and M. K. Samson, *Cancer Chemother. Rep.*, **59**, 1123 (1975).

(25) H. H. Lloyd, E. A. Dulmadge, and L. J. Wilkoff, *ibid.*, **56**, 585 (1972).

ACKNOWLEDGMENTS

Presented in part at the Pharmaceutical Analysis and Control Section, APhA Academy of Pharmaceutical Sciences, Atlanta meeting, November 1975.

Supported in part by LAC/USC Cancer Center Grant Unit 5, P01-CA14089-2, and by Western Cancer Study Group Grant SR05 CA05186-13, Pharmacokinetic Section, both of the National Cancer Institute. The ^{13}C-NMR measurements were performed at the California Institute of Technology.

The authors thank Mr. Alfonso Barrientos for technical assistance and the National Cancer Institute for support.

GI Absorption of β-Lactam Antibiotics III: Kinetic Evidence for *In Situ* Absorption of Ionized Species of Monobasic Penicillins and Cefazolin from the Rat Small Intestine and Structure–Absorption Rate Relationships

AKIRA TSUJI, ETSUKO MIYAMOTO, OSAMU KUBO, and TSUKINAKA YAMANA ˣ

Received July 6, 1978, from the *Faculty of Pharmaceutical Sciences, Kanazawa University, Takara-machi, Kanazawa 920, Japan.* Accepted for publication December 20, 1978.

Abstract □ Absorption rates of monobasic β-lactam antibiotics were measured as a function of lumen solution pH between 4 and 9 by utilizing the rat intestinal recirculating method *in situ*. Between pH 6.5 and 9, the absorption rate constants of ionized antibiotics were almost identical; but, at pH 4, the unionized species were highly absorbed, depending on their lipophilicity through the GI membrane lipoidal barrier. The structure-absorption rate relationship was established with the unstirred layer model.

Keyphrases □ Absorption, GI—various monobasic penicillins and cefazolin, effect of ionization, pH, structure–activity relationships □ Penicillins, various—GI absorption, effect of ionization, structure–activity relationships □ Cefazolin—GI absorption, effect of ionization, structure–activity relationships □ Antibiotics—penicillins and cefazolin, GI absorption, effect of ionization, structure–activity relationships

The GI absorption rate of a monobasic penicillin in rats deviated significantly from the pH-partition hypothesis (1). This shift was interpreted successfully by the absorption mechanism of penicillins through the aqueous diffusion layer of the lumen side of the GI membrane, which is restricted by the lipophilicity of the undissociated species (1).

In *in vitro* experiments utilizing an isolated gut technique, the transport of phenoxypenicillin derivatives exhibited a saturable process, but additional study did not produce evidence of active transport (2). A similar *in vitro* study (3) provided evidence for the passive transport of β-lactam antibiotics at pH 7.4. Perrier and Gibaldi (4) attributed the larger absorption of dicloxacillin than of penicillin G and ampicillin from the *in situ* rat intestinal loop to the larger lipophilicity of dicloxacillin. A good correlation was found (5) between the rate of *in situ* intestinal cephalexin and cefazolin absorption in rats and their *in vitro* release rate from liposomes.

Recent studies in this laboratory on the *in situ* absorption kinetics of low lipophilic and completely ionized amphoteric β-lactam antibiotics, such as amoxicillin (6), cyclacillin (7), and cephradine (7), indicated that their intestinal absorption is governed by simple diffusion fol-

0022-3549/79/0700-0812$01.00/0

© 1979, American Pharmaceutical Association

lowing first-order kinetics at a high dose and is favored by some forms of a carrier-mediated transport process following Michaelis–Menten kinetics at low doses. However, the kinetics and mechanism for the transport of ionized species of monobasic β-lactam antibiotics across the intestinal mucosa are not clearly understood.

In the present absorption study, attention was paid to lumen solution pH, and simultaneous absorption and degradation were assessed. Discussion by others (4) on the absorption of ionized penicillin species seems to harbor some questions because of the pH change and β-lactam ring degradation, both of which may occur during absorption experiments, especially with the *in situ* method. In this report, kinetic evidence is presented for the *in situ* intestinal absorption of ionized forms of monobasic penicillins and cefazolin. Furthermore, based on the unstirred layer theory, which is applicable to the absorption of undissociated β-lactam antibiotic molecules (1), the relationship between the absorption rate of antibiotics and their oil–water partition coefficients has been established.

EXPERIMENTAL

Materials—The following β-lactam antibiotics were used as supplied: penicillin V potassium[1] (1490 units/mg), phenethicillin potassium[1] (1444 units/mg), propicillin potassium[2] (993 μg/mg), oxacillin sodium[3] (840 μg/mg), cloxacillin sodium[1] (907 μg/mg), dicloxacillin sodium[1] (900 μg/mg), floxacillin sodium[4] (893 μg/mg), and cefazolin sodium[4] (966 μg/mg). Solutions of penicilloic acids of propicillin and dicloxacillin were prepared according to the method of Schwartz and Delduce (8).

All other chemicals were reagent grade and were used without further purification, except for imidazole which was purified by double recrystallization from benzene followed by thorough washing with ether.

***In Situ* Intestinal Absorption Procedure**—Male albino Wistar rats, 225 ± 25 g, were fasted over 20 hr prior to the experiments, but water was given freely. The rats were anesthetized with urethan, 1.3 g/kg ip.

The recirculating perfusion procedure for studying *in situ* intestinal absorption was essentially the same as that described previously (1, 9), except for the use of the upper 30-cm portion of the small intestine. The bile duct was ligated in all experiments. The small intestine was washed with 50 ml of perfusion solution, and a 5-ml solution of a penicillin or of a penicilloic acid (5 mg/ml, unless otherwise stated) was recirculatingly perfused at 2 ml/min. The drug solution was prepared with isotonic buffer (10), and the lumen solution pH was maintained at the desired pH with a pH-stat[5] (1, 9) during the absorption experiments.

The perfusion periods were 1 hr at pH 4.0 and 2 hr at other pH values. At the end of the absorption experiment, the recirculating drug solution of about 9 ml and a fresh isotonic buffer perfused to wash the intestine were collected into a 50-ml volumetric flask; the required amount of the same buffer was added to obtain 50 ml. To obtain a final sample, the solution was passed through a 0.45-μm filter[6] to remove any solid materials. The initial sample was prepared by diluting 5 ml of the initial drug solution (5 mg/ml) with the isotonic buffer to obtain 50 ml.

Analytical Procedures—The antibiotic concentration was determined by three methods: UV spectrophotometry (11), high-pressure liquid chromatography (HPLC), and spectrofluorometry (12). Due to the interference by unknown materials with UV absorbance in the sample solution of penicillins having an isoxazole group (oxacillin, cloxacillin, dicloxacillin, and floxacillin) (4), these samples were analyzed only by HPLC.

HPLC—The chromatograph[7] was equipped with a variable-wavelength UV detector[8] set at 210 or 254 nm. A reversed-phase column[9], prepacked with octadecylsilane chemically bonded on totally porous silica gel, was used for the determination of unchanged β-lactam antibiotics. The eluent was 10–30% (v/v) aqueous acetonitrile containing 0.01 *M* ammonium acetate. For the determination of penicilloic acids, an anion-exchange column[10] was utilized with 0.02 *M* KH_2PO_4 adjusted to pH 5 as the eluent; a 100-μl sample was injected through a loop injector on flow. Peak heights were used for quantification. A standard solution of the corresponding penicilloic acids was prepared according to the procedure described by Schwartz and Delduce (8).

Spectrofluorometry—Spectrofluorometry was used in the analysis of relatively lower propicillin concentrations and of the sample from the absorption experiment with penicilloic acid. This analytical method was based on the formation of a fluorescent Schiff base resulting from the reaction between 5-dimethylaminonaphthalene-1-sulfonylhydrazine and penilloaldehyde (12), which can be produced from the reaction of penicilloic acid and mercuric chloride at pH 2.5. This method has the advantage of simultaneous determination of the intact penicillin and its product, penicilloic acid (12). The detailed procedure was described elsewhere (12)[11].

RESULTS AND DISCUSSION

Simultaneous Absorption and Degradation—Table I shows the percentage of remaining penicillins and the percentage of penicilloic acids that appeared after 2 hr in the *in situ* intestinal recirculating absorption experiments for propicillin, dicloxacillin, penicillin V, and cefazolin. Samples were analyzed by HPLC for all penicillins and cefazolin and by spectrofluorometry for propicillin and penicilloic acids. There were significant degradations in the β-lactam moiety of penicillin derivatives. Cefazolin degradation was negligible during the experiments since the corresponding product peak, which was observed in *in vitro* degradation for a sufficiently long period under the same condition, was not detected.

Possible absorption of penicilloic acids was examined under similar conditions. Both penicilloic acids of propicillin and dicloxacillin were absorbed to the same extent (16.1 ± 6.8%) at the end of 2 hr at pH 7.4. From these results, the overall pathway of β-lactam antibiotics in the intestinal lumen solution can be represented as in Scheme I.

As seen in Table I, the widespread change of the initial propicillin concentration between 100 and 5000 μg/ml produced an almost constant disappearance of 23% and an appearance of 10% of the penicilloic acid at pH 7.4. A similar result was reported (2) for penicillin V disappearance in the 0.6–160-μg/ml range from rat intestinal lumen solution at pH 7.4. These findings indicate that all rate processes in Scheme I follow apparent first-order kinetics, at least for propicillin and penicillin V. If one assumes that a similar kinetic process applies to other β-lactam antibiotics according to Scheme I, the ratios of a remaining antibiotic (α_1) and an apparent penicilloic acid (α_2) at time t to the initial antibiotic dose would be expressed by:

$$\alpha_1 = e^{-(k_a + k_d)t} \qquad \text{(Eq. 1)}$$

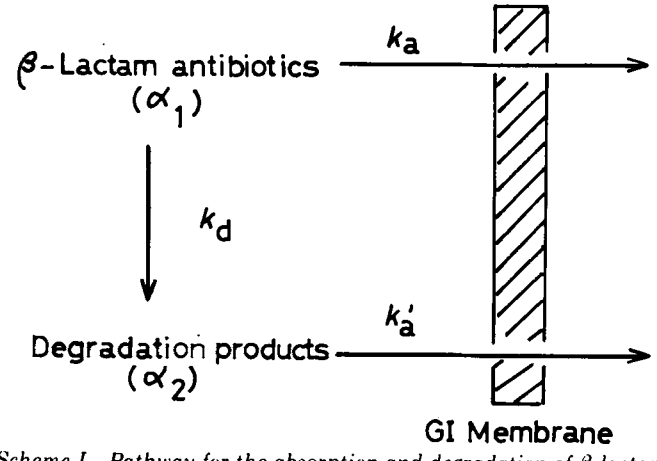

Scheme I—Pathway for the absorption and degradation of β-lactam antibiotics. (For the meaning of α_i, see text.)

[1] Meiji Seika Kaisha, Tokyo, Japan.
[2] Takeda Chemical Industries, Osaka, Japan.
[3] Banyu Pharmaceutical Co., Tokyo, Japan.
[4] Fujisawa Pharmaceutical Co., Osaka, Japan.
[5] pH-Stat titrator assembly consisting of TTT2 titrator and ABU12b autoburette, Radiometer, Copenhagen, Denmark.
[6] Sartorius-Membranfilter GmbH, Göttingen, Germany.
[7] Model FLC-A700, Japan Spectroscopic Co., Tokyo, Japan.
[8] Model UVIDEC-100, Japan Spectroscopic Co., Tokyo, Japan.
[9] μBondapak-C_{18}, 30 cm × 4 mm i.d., Waters Associate, Milford, Mass.
[10] Zipax-SAX, 50 cm × 2.1 mm i.d., DuPont Instrument, Wilmington, Del.
[11] In the previous paper (12), the concentration of 5-dimethylaminonaphthalene-1-sulfonylhydrazine reagent was erroneously referred to as 10%. The correct concentration is 0.1%.

Table I—Summary of the Data Determined for Penicillin, Penicilloic Acid, and Cefazolin in the *In Situ* Absorption Experiments through the Small Intestine of the Rat

β-Lactam Antibiotic	pH	Dose, μg/ml	Remaining Antibiotic[a], % (100 × α_1)	Appearance of Penicilloic Acid[a], % (100 × α_2)	Rate Constant[b], 10^3 min^{-1}	
					k_a or k'_a	k_d
Propicillin	6.5	5,000	69.1	7.1	2.30	0.78
	7.4	100	69.1	15.6	1.38	1.70
	7.4	100	70.0	8.8	2.02	0.96
	7.4	100	84.9	7.6	0.61	0.75
	7.4	500	80.2	5.7	1.26	0.58
	7.4	500	84.8	2.8	1.10	0.28
	7.4	500	84.9	9.5	0.43	0.94
	7.4	1,000	67.4	15.2	1.61	1.68
	7.4	1,000	87.2	4.8	0.67	0.47
	7.4	5,000	74.0	8.6	1.60	0.91
	7.4	5,000	73.9	15.0	0.93	1.59
	7.4	5,000	66.9	18.0	1.35	2.00
	7.4	10,000	87.0	0.8	1.08	0.08
	7.4	10,000	84.9	7.5	0.62	0.74
	7.4	10,000	98.6	0.3	0.09	0.03
	7.4	10,000	86.5	5.8	0.64	0.57
	8.0	5,000	79.1	3.6	1.59	0.37
	8.5	5,000	82.8	3.8	1.19	0.38
	8.5	5,000	80.9	5.4	1.22	0.55
	9.0	5,000	69.6	19.4	0.91	2.11
	9.0	5,000	79.0	7.0	1.25	0.72
Dicloxacillin	6.5	5,000	74.5	15.1	0.86	1.59
	7.4	5,000	79.8	7.9	1.08	0.80
	7.4	5,000	69.6	4.9	2.49	0.53
	8.0	5,000	73.3	7.5	1.79	0.80
	8.5	5,000	75.2	7.1	1.63	0.74
	8.5	5,000	84.0	7.0	0.76	0.69
	8.5	5,000	76.9	9.0	1.26	0.93
	9.0	5,000	79.2	12.8	0.63	1.31
Penicillin V	6.5	5,000	77.7	7.0	1.38	0.72
	7.4	5,000	82.8	10.4	0.53	1.04
	8.5	5,000	78.5	8.2	1.18	0.84
	8.5	5,000	81.2	8.2	0.91	0.83
	9.0	5,000	69.6	18.1	1.05	1.97
Penicilloic acid of propicillin	7.4	5,000	88.1	—	1.06	—
	7.4	5,000	89.9	—	0.90	—
	7.4	5,000	84.0	—	1.45	—
Penicilloic acid of dicloxacillin	7.4	5,000	83.7	—	1.48	—
	7.4	5,000	74.7	—	2.43	—
Cefazolin	7.4	5,000	89.4	—	0.93	—
	7.4	5,000	89.2	—	0.95	—
	7.4	5,000	92.4	—	0.66	—

[a] Determined at the end of 2-hr experiments. [b] Calculated from Eqs. 4 and 5 by use of $\alpha_0 = 0.839$, which is the average of values determined for penicilloic acids of propicillin and dicloxacillin.

$$\alpha_2 = \frac{k_d}{(k_a + k_d) - k'_a}\left[e^{-k'_a t} - e^{-(k_a + k_d)t}\right] \qquad \text{(Eq. 2)}$$

where k_a and k'_a represent the apparent first-order absorption rate constants of a penicillin and its penicilloic acid, respectively, and k_d is the apparent first-order penicillin degradation rate constant. The absorption rate constant, k'_a, can be calculated from:

$$\alpha_0 = e^{-k'_a t} \qquad \text{(Eq. 3)}$$

where α_0 is the ratio of the remaining penicilloic acid to the initial dose, which is determined under the same conditions in a separate absorption experiment for penicilloic acid. In the present kinetic treatment, the value of k'_a or α_0 was regarded as independent of lumen solution pH and of the kind of penicilloic acids, being equal to 1.46×10^{-3} min^{-1} or 0.839 of the mean value of k'_a or α_0 as determined for the penicilloic acids of dicloxacillin and propicillin. By using the data of α_1, α_2, and α_0, the penicillin absorption rate constant, k_a, and degradation rate constant, k_d, could be calculated from Eqs. 1–3 using:

$$k_a = -\frac{1}{t}\left(\ln \alpha_1 + \frac{\alpha_2}{\alpha_0 - \alpha_1} \ln \alpha_0/\alpha_1\right) \qquad \text{(Eq. 4)}$$

$$k_d = \frac{\alpha_2}{t(\alpha_0 - \alpha_1)} \ln \alpha_0/\alpha_1 \qquad \text{(Eq. 5)}$$

The raw data of α_1, α_2, and α_0 and k_a and k_d of penicillins and cefazolin determined under various conditions are summarized in Table I, and their mean values are listed in Table II.

The rate constants of chemical degradation under similar conditions were known to be almost independent of the kinds of penicillins but dependent on lumen solution pH. They were evaluated, based on previous kinetic data (13), as 1.0×10^{-4}, 1.3×10^{-4}, and 6.0×10^{-4} min^{-1} in isotonic buffer of pH 6.5, 7.4, and 9.0, respectively. When comparing the degradation rate constants of penicillins under *in situ* and *in vitro* conditions, it must be emphasized that, at pH 9.0, both were in a similar range. At a neutral pH of 6.5–7.4, however, the degradation rate constants *in situ* were ~6–10 times greater than those *in vitro*. These results suggest that in the intestinal lumen and/or at the intestinal mucosa, β-lactam cleavage other than chemical reaction takes place in an apparently first-order kinetic fashion under physiological pH conditions.

The present kinetic study provided evidence for the significant absorption of ionized penicillins and cefazolin and also for the absorption of penicilloic acids. If the intestinal absorption of ionized β-lactam antibiotics is the result of transport through the lipoidal barrier, as was verified (1) for the undissociated forms, significant differences in the extent of absorption may be expected among penicillins. In spite of the 10-fold difference at maximum in the oil–water partition coefficient (14) of the ionized forms of penicillin V, propicillin, and dicloxacillin, the ionized species of these penicillins and cefazolin were absorbed to an almost identical extent (Table II).

This result suggests that intestinal absorption of ionized β-lactam antibiotics below the concentration of 5 mg/ml follows apparent first-order kinetics such as, for example, simple diffusion through water channels in the membrane and that it is almost insensitive to the lipophilicity of transport molecules. However, due to the slight decrease of propicillin absorption at 10 mg/ml (Table II), the possibility cannot be

Table II—Mean Values Describing the Kinetic Behavior of β-Lactam Antibiotics and Penicilloic Acid in Rat Lumen Solution and Dose Effect on the Absorption of Propicillin

Antibiotic	Dose, μg/ml	Total Disappearance[a], % ± SD	Appearance of Penicilloic Acid[a] % ± SD	Rate Constant[b], 10^3 min^{-1} ± SD: Absorption, k_a or k'_a	Rate Constant[b], 10^3 min^{-1} ± SD: Degradation, k_d	Number of Experiments
Propicillin	100[c]	25.3 ± 8.9	10.7 ± 4.3	1.34 ± 0.71	1.14 ± 0.50	3
	500[c]	16.7 ± 2.7	6.0 ± 3.4	0.93 ± 0.44	0.60 ± 0.33	3
	1,000[c]	22.7	10.0	1.14	1.08	2
	5,000[c]	28.4 ± 4.1	13.9 ± 4.8	1.29 ± 0.34	1.50 ± 0.55	3
	5,000[d]	25.0 ± 5.7	9.8 ± 6.1	1.37 ± 0.42	1.05 ± 0.68	9
	10,000[c]	10.8 ± 6.3	3.6 ± 3.6	0.61 ± 0.41	0.36 ± 0.35	4
Dicloxacillin	5,000[d]	23.4 ± 4.4	8.9 ± 3.4	1.31 ± 0.63	0.92 ± 0.35	8
Penicillin V	5,000[d]	22.0 ± 5.1	10.4 ± 4.5	1.01 ± 0.32	1.08 ± 0.51	5
Penicilloic[e] acid	5,000[c]	16.1 ± 6.8	—	1.46 ± 0.59	—	5
Cefazolin	5,000[c]	9.7 ± 1.8	—	0.85 ± 0.16	—	3

[a] Observed values at the end of 2-hr experiments. [b] Calculated value by Eqs. 4 and 5. [c] Averaged value at pH 7.4. [d] Averaged value between pH 6.5 and 9. [e] Penicilloic acids of propicillin and dicloxacillin prepared by Schwartz and Delduce (8).

excluded that a specialized mechanism of intestinal carrier-mediated transport of the ionized species exists, as was proposed for the intestinal absorption of completely ionized and highly hydrophilic aminopenicillins and aminocephalosporins (6, 7).

Effect of pH on Intestinal Absorption and Structure–Absorption Rate Relationships—Figure 1 shows the plots of *in situ* absorption rate constants, k_a, of penicillins *versus* perfusion solution pH, which was maintained with a pH-stat (1, 9). Absorption rate constants at pH 4.0 were calculated, assuming the degradation to be negligible in comparison to absorption, while those at other pH values were derived from Eq. 4.

Between pH 6.5 and 9, the penicillin absorption was independent of the lumen solution pH, with average rate constants, k_a, of 1.27×10^{-3} min^{-1}; it was almost identical among penicillin molecules (Table II). Below pH 6, the rate constants increased significantly with a decrease of the lumen solution pH depending on the lipophilicity of the undissociated species. Therefore, k_a can be expressed as:

$$k_a = k_u + k_i \qquad \text{(Eq. 6)}$$

where k_u and k_i are the apparent first-order absorption rate constants for unionized and ionized species of penicillins, respectively. A previous study (1) verified that k_u can be expressed by Eq. 7, which is derived from the kinetic model of membrane permeation across the lipoidal barrier of undissociated penicillin species transported through the aqueous diffusion layer with thickness L_I adjacent to the surface of the lipoidal membrane with thickness L_{II}:

$$k_u = \frac{SD_{aq}}{VL_I}\left(\frac{f_u}{T + f_u}\right) \qquad \text{(Eq. 7)}$$

where:

$$T = \frac{L_{II}D_{aq}}{L_I D_{lip} Pl_u R} \qquad \text{(Eq. 8)}$$

$$f_u = \frac{a_{H^+}}{K_a + a_{H^+}} \qquad \text{(Eq. 9)}$$

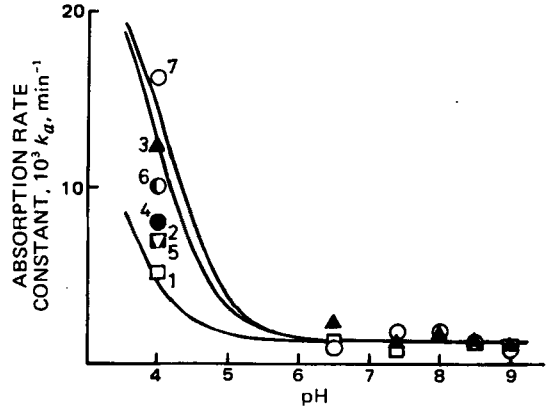

Figure 1—*Plots of* in situ *rat intestinal absorption rate constants,* k_a, *for penicillins* versus *pH of the perfusion solution at 37°. The compounds are numbered as in Table III. The points are experimental values, and the solid lines were generated from Eqs. 6, 12, and 14;* k_i = 1.27×10^{-3} min^{-1} *for Compounds 1, 3, and 7.*

where V is the volume of the recirculating drug solution; D_{aq} and D_{lip} are the diffusion coefficients of the drug in water and lipid, respectively; Pl_u is the partition coefficient of the undissociated drug between the lipid membrane and aqueous solution; f_u is the fraction of undissociated species; a_{H^+} is the hydrogen-ion activity of the lumen solution; K_a is the penicillin dissociation constant; and R is the ratio of the true interfacial area to the geometrical area, S, of the membrane.

Parameters V, L_I, L_{II}, S, and R can be regarded as constant since V and L_I depend only on experimental conditions and the others depend on the membrane. By using the relationship of Eq. 10 (10, 15) for a diffusion coefficient, D, and of Eq. 11 (10) for a partition coefficient, Pl_u, Eq. 7 can be simplified to Eq. 12:

$$D = \beta_1(\sqrt{MW})^{-1} \qquad \text{(Eq. 10)}$$

$$Pl_u = \beta_2 P_u \qquad \text{(Eq. 11)}$$

$$k_u = k_a - k_i = \frac{1}{a\sqrt{MW}}\left(\frac{f_u P_u}{b + f_u P_u}\right) \qquad \text{(Eq. 12)}$$

where MW and P_u represent the molecular weight and the partition coefficient between two immiscible liquids of the undissociated species of the transport antibiotics, respectively, and β_1 and β_2 are proportionality constants.

The rearrangement of Eq. 12 leads to:

$$(k_u\sqrt{MW})^{-1} = ab(f_u P_u)^{-1} + a \qquad \text{(Eq. 13)}$$

To verify Eq. 13, the intestinal absorption of several penicillins at pH 4.0 was examined (Table III and Fig. 2). The P_u values in the octanol–water system and the K_a values used for the calculation were determined previously (14). The plots of $1/(k_u\sqrt{MW})$ *versus* $1/(f_u P_u)$ according to Eq. 13 gave a good linear relationship (Fig. 2), and the following equation was obtained:

$$(k_u\sqrt{MW})^{-1} = 70.0(f_u P_u)^{-1} + 1.95 \qquad \text{(Eq. 14)}$$

The solid line in Fig. 1 was calculated for dicloxacillin, propicillin, and penicillin V from Eqs. 6, 12, and 14 and was in fair agreement with ex-

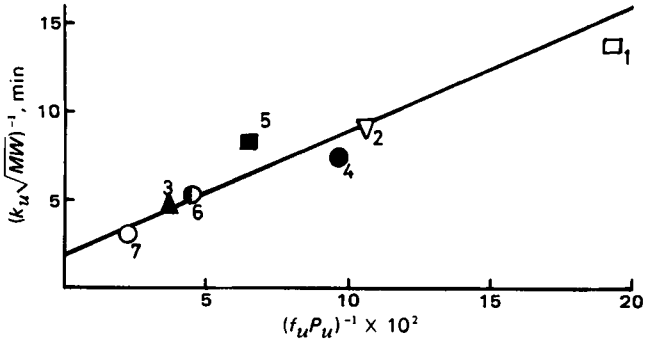

Figure 2—*Plots of* $(k_u\sqrt{MW})^{-1}$ *against* $(f_u P_u)^{-1}$ *for penicillins in* in situ *perfusion experiments at pH 4. The compounds are numbered as in Table III.*

Table III—Absorption Rate Constants at pH 4.0 and Related Parameters for Penicillins

Number	Penicillin	Molecular Weight (MW)[a]	pKa[b]	log P_u^b	k_a, 10^3 min^{-1}
1	Penicillin V	350.4	2.79	1.95	5.22
2	Phenethicillin	364.4	2.80	2.20	7.08
3	Propicillin	378.4	2.76	2.70	12.48
4	Oxacillin	401.4	2.73	2.31	8.05
5	Cloxacillin	435.9	2.78	2.43	7.05
6	Floxacillin	453.9	2.76	2.61	10.15
7	Dicloxacillin	470.3	2.76	2.91	16.25

[a] As free acid. [b] P_u is the partition coefficient of the undissociated penicillins in the octanol–water system. All data were at 37° and taken from Ref. 14.

perimental values. This finding indicates that the absorption of monobasic penicillins, excluding amphoteric ones such as amoxicillin and cyclacillin (6, 7), follows the common mechanisms of: (*a*) the lipoidal membrane transport of the undissociated species permeating the aqueous diffusion layer barrier and (*b*) the apparent first-order transport of the ionized species permeating some forms of the barrier almost insensitive to antibiotic lipophilicity.

A previous study (1) revealed that, below pH 6, the intestinal absorption rate of propicillin is about 100 times faster than the gastric absorption rate. This significant difference is undoubtedly due to the relative surface area in the alimentary tract. Naturally, other monobasic β-lactam antibiotics can be expected to exhibit absorption behavior similar to propicillin. The present and previous results (1, 9) indicate that a small amount of these orally ingested antibiotics may be absorbed in the stomach while almost all absorption takes place in the duodenum, where the fluid pH is relatively lower, and that absorption occurs *via* passive diffusion of the undissociated species, largely dependent on their lipophilicity. A small amount may be also absorbed by ionic transport during the slow transit through the intestine. Poor absorbability (16) of orally ingested cephalosporins such as cefazolin, the P_u of which is about one-thirtieth lower than that of penicillin V (17), may be due to the considerable reduction of k_u values effective both in the stomach and upper duodenum.

REFERENCES

(1) A. Tsuji, E. Miyamoto, N. Hashimoto, and T. Yamana, *J. Pharm. Sci.*, **67**, 1705 (1978).

(2) I. M. Rollo, *Can. J. Physiol. Pharmacol.*, **50**, 986 (1972).

(3) S. C. Penzotti, Jr., and J. W. Poole, *J. Pharm. Sci.*, **63**, 1803 (1974).

(4) D. Perrier and M. Gibaldi, *ibid.*, **62**, 1486 (1973).

(5) M. Yasuhara, Y. Miyoshi, A. Yuasa, T. Kimura, S. Muranishi, and H. Sezaki, *Chem. Pharm. Bull.*, **25**, 675 (1977).

(6) A. Tsuji, E. Nakashima, I. Kagami, N. Honjo, and T. Yamana, *J. Pharm. Pharmacol.*, **29**, 707 (1977).

(7) A. Tsuji, E. Nakashima, I. Kagami, T. Asano, R. Nakashima, and T. Yamana, *ibid.*, **30**, 508 (1978).

(8) M. A. Schwartz and A. J. Delduce, *J. Pharm. Sci.*, **58**, 1137 (1969).

(9) A. Tsuji, E. Miyamoto, I. Kagami, H. Sakaguchi, and T. Yamana, *ibid.*, **67**, 1701 (1978).

(10) T. Koizumi, T. Arita, and K. Kakemi, *Chem. Pharm. Bull.*, **12**, 413 (1964).

(11) H. Bundgaard and K. Ilver, *J. Pharm. Pharmacol.*, **24**, 790 (1972).

(12) A. Tsuji, E. Miyamoto, and T. Yamana, *ibid.*, **30**, 811 (1978).

(13) T. Yamana, A. Tsuji, and Y. Mizukami, *Chem. Pharm. Bull.*, **22**, 1186 (1974).

(14) A. Tsuji, O. Kubo, E. Miyamoto, and T. Yamana, *J. Pharm. Sci.*, **66**, 1675 (1977).

(15) B. E. Ballard and E. Nelson, *J. Pharmacol. Exp. Ther.*, **135**, 120 (1962).

(16) C. H. Nightingale, D. S. Greene, and R. Quintiliani, *J. Pharm. Sci.*, **64**, 1899 (1975).

(17) T. Yamana, A. Tsuji, E. Miyamoto, and O. Kubo, *ibid.*, **66**, 747 (1977).

ACKNOWLEDGMENTS

The authors acknowledge the gifts of penicillins and cefazolin from Meiji Seika Kaisha, Banyu Pharmaceutical Co., Takeda Chemical Industries, and Fujisawa Pharmaceutical Co.

Pyridones as Potential Antitumor Agents

DENG RUEY HWANG * and JOHN S. DRISCOLL ˣ

Received September 28, 1978, from the *Drug Design and Chemistry Section, Laboratory of Medicinal Chemistry and Biology, Developmental Therapeutics Program, Division of Cancer Treatment, National Cancer Institute, National Institutes of Health, Bethesda, MD 20014.* Accepted for publication December 20, 1978. *Present address: Technicon Inc., Tarrytown, NY 10591.

Abstract □ Based on the finding that 3-acetoxy-2-pyridone had reproducible activity against murine P-388 lymphocytic leukemia, derivatives in this series were synthesized and evaluated to determine structural parameters important for activity. Of the 32 compounds tested, 10 were active. At least two oxygen-containing functional groups are required for P-388 activity, and the 2,3-isomeric arrangement provides the greatest activity. Carbamate or acyloxy groups in the 3-position produced the most active 2-pyridones.

Keyphrases □ Pyridone derivatives—antineoplastic activity, structure–activity relationships, mice □ Antineoplastic agents, potential—pyridone derivatives, structure–activity relationships, mice □ Structure–activity relationships—pyridone derivatives, antineoplastic activity, mice

During an investigation of hydroxypyridine derivatives, it was discovered that 3-acetoxy-2-pyridone (I) possessed reproducible activity against P-388 leukemia in mice. There are other scattered reports of pyridone antitumor activity. A nucleoside presently undergoing clinical evaluation, which can be classed as a pyridone, is 3-deazauridine (1, 2). Mimosine, a naturally occurring 4-pyridone, was reported as active against Walker 256 carcinosarcoma (3) and B16 melanotic melanoma (4). Other pyridones studied possess less antitumor activity (5–8). Based on the antitumor properties of I, a study was undertaken to determine the structural parameters important for activity.

RESULTS AND DISCUSSION

Compounds I–XXXII were evaluated. 3-Hydroxy-2-pyridone (II) was reacted with various acid chlorides, anhydrides, and isocyanates to produce 3-substituted and 1,3-disubstituted 2-pyridones. 2-Pyridone (VII) was oxidized to 5-hydroxy-2-pyridone (IV) by the Elbs persulfate reaction. UV and other spectral data were consistent with those expected for 2-pyridones (9, 10). The properties of these compounds are shown in Table I.

Antitumor activity was evaluated in the P-388 lymphocytic leukemia system using standard protocols (11) of the National Cancer Institute. Multiple biological tests were carried out with each compound using a dose response on the QD 1–9 treatment schedule. Physiological saline was the vehicle. Drugs were administered intraperitoneally to mice with

0022-3549/79/0700-0816$01.00/0

© 1979, American Pharmaceutical Association

Table III—Absorption Rate Constants at pH 4.0 and Related Parameters for Penicillins

Number	Penicillin	Molecular Weight (MW)[a]	pKa[b]	log P_u^b	k_a, 10^3 min^{-1}
1	Penicillin V	350.4	2.79	1.95	5.22
2	Phenethicillin	364.4	2.80	2.20	7.08
3	Propicillin	378.4	2.76	2.70	12.48
4	Oxacillin	401.4	2.73	2.31	8.05
5	Cloxacillin	435.9	2.78	2.43	7.05
6	Floxacillin	453.9	2.76	2.61	10.15
7	Dicloxacillin	470.3	2.76	2.91	16.25

[a] As free acid. [b] P_u is the partition coefficient of the undissociated penicillins in the octanol–water system. All data were at 37° and taken from Ref. 14.

perimental values. This finding indicates that the absorption of monobasic penicillins, excluding amphoteric ones such as amoxicillin and cyclacillin (6, 7), follows the common mechanisms of: (*a*) the lipoidal membrane transport of the undissociated species permeating the aqueous diffusion layer barrier and (*b*) the apparent first-order transport of the ionized species permeating some forms of the barrier almost insensitive to antibiotic lipophilicity.

A previous study (1) revealed that, below pH 6, the intestinal absorption rate of propicillin is about 100 times faster than the gastric absorption rate. This significant difference is undoubtedly due to the relative surface area in the alimentary tract. Naturally, other monobasic β-lactam antibiotics can be expected to exhibit absorption behavior similar to propicillin. The present and previous results (1, 9) indicate that a small amount of these orally ingested antibiotics may be absorbed in the stomach while almost all absorption takes place in the duodenum, where the fluid pH is relatively lower, and that absorption occurs *via* passive diffusion of the undissociated species, largely dependent on their lipophilicity. A small amount may be also absorbed by ionic transport during the slow transit through the intestine. Poor absorbability (16) of orally ingested cephalosporins such as cefazolin, the P_u of which is about one-thirtieth lower than that of penicillin V (17), may be due to the considerable reduction of k_u values effective both in the stomach and upper duodenum.

REFERENCES

(1) A. Tsuji, E. Miyamoto, N. Hashimoto, and T. Yamana, *J. Pharm. Sci.*, **67**, 1705 (1978).

(2) I. M. Rollo, *Can. J. Physiol. Pharmacol.*, **50**, 986 (1972).

(3) S. C. Penzotti, Jr., and J. W. Poole, *J. Pharm. Sci.*, **63**, 1803 (1974).

(4) D. Perrier and M. Gibaldi, *ibid.*, **62**, 1486 (1973).

(5) M. Yasuhara, Y. Miyoshi, A. Yuasa, T. Kimura, S. Muranishi, and H. Sezaki, *Chem. Pharm. Bull.*, **25**, 675 (1977).

(6) A. Tsuji, E. Nakashima, I. Kagami, N. Honjo, and T. Yamana, *J. Pharm. Pharmacol.*, **29**, 707 (1977).

(7) A. Tsuji, E. Nakashima, I. Kagami, T. Asano, R. Nakashima, and T. Yamana, *ibid.*, **30**, 508 (1978).

(8) M. A. Schwartz and A. J. Delduce, *J. Pharm. Sci.*, **58**, 1137 (1969).

(9) A. Tsuji, E. Miyamoto, I. Kagami, H. Sakaguchi, and T. Yamana, *ibid.*, **67**, 1701 (1978).

(10) T. Koizumi, T. Arita, and K. Kakemi, *Chem. Pharm. Bull.*, **12**, 413 (1964).

(11) H. Bundgaard and K. Ilver, *J. Pharm. Pharmacol.*, **24**, 790 (1972).

(12) A. Tsuji, E. Miyamoto, and T. Yamana, *ibid.*, **30**, 811 (1978).

(13) T. Yamana, A. Tsuji, and Y. Mizukami, *Chem. Pharm. Bull.*, **22**, 1186 (1974).

(14) A. Tsuji, O. Kubo, E. Miyamoto, and T. Yamana, *J. Pharm. Sci.*, **66**, 1675 (1977).

(15) B. E. Ballard and E. Nelson, *J. Pharmacol. Exp. Ther.*, **135**, 120 (1962).

(16) C. H. Nightingale, D. S. Greene, and R. Quintiliani, *J. Pharm. Sci.*, **64**, 1899 (1975).

(17) T. Yamana, A. Tsuji, E. Miyamoto, and O. Kubo, *ibid.*, **66**, 747 (1977).

ACKNOWLEDGMENTS

The authors acknowledge the gifts of penicillins and cefazolin from Meiji Seika Kaisha, Banyu Pharmaceutical Co., Takeda Chemical Industries, and Fujisawa Pharmaceutical Co.

Pyridones as Potential Antitumor Agents

DENG RUEY HWANG * and JOHN S. DRISCOLL ˣ

Received September 28, 1978, from the *Drug Design and Chemistry Section, Laboratory of Medicinal Chemistry and Biology, Developmental Therapeutics Program, Division of Cancer Treatment, National Cancer Institute, National Institutes of Health, Bethesda, MD 20014.* Accepted for publication December 20, 1978. *Present address: Technicon Inc., Tarrytown, NY 10591.

Abstract □ Based on the finding that 3-acetoxy-2-pyridone had reproducible activity against murine P-388 lymphocytic leukemia, derivatives in this series were synthesized and evaluated to determine structural parameters important for activity. Of the 32 compounds tested, 10 were active. At least two oxygen-containing functional groups are required for P-388 activity, and the 2,3-isomeric arrangement provides the greatest activity. Carbamate or acyloxy groups in the 3-position produced the most active 2-pyridones.

Keyphrases □ Pyridone derivatives—antineoplastic activity, structure–activity relationships, mice □ Antineoplastic agents, potential—pyridone derivatives, structure–activity relationships, mice □ Structure–activity relationships—pyridone derivatives, antineoplastic activity, mice

During an investigation of hydroxypyridine derivatives, it was discovered that 3-acetoxy-2-pyridone (I) possessed reproducible activity against P-388 leukemia in mice. There are other scattered reports of pyridone antitumor activity. A nucleoside presently undergoing clinical evaluation, which can be classed as a pyridone, is 3-deazauridine (1, 2). Mimosine, a naturally occurring 4-pyridone, was reported as active against Walker 256 carcinosarcoma (3) and B16 melanotic melanoma (4). Other pyridones studied possess less antitumor activity (5–8). Based on the antitumor properties of I, a study was undertaken to determine the structural parameters important for activity.

RESULTS AND DISCUSSION

Compounds I–XXXII were evaluated. 3-Hydroxy-2-pyridone (II) was reacted with various acid chlorides, anhydrides, and isocyanates to produce 3-substituted and 1,3-disubstituted 2-pyridones. 2-Pyridone (VII) was oxidized to 5-hydroxy-2-pyridone (IV) by the Elbs persulfate reaction. UV and other spectral data were consistent with those expected for 2-pyridones (9, 10). The properties of these compounds are shown in Table I.

Antitumor activity was evaluated in the P-388 lymphocytic leukemia system using standard protocols (11) of the National Cancer Institute. Multiple biological tests were carried out with each compound using a dose response on the QD 1–9 treatment schedule. Physiological saline was the vehicle. Drugs were administered intraperitoneally to mice with

0022-3549/79/0700-0816$01.00/0

© 1979, American Pharmaceutical Association

Table I—Physical and Chemical Data

Compound	Melting Point	Yield, %	Formula	Analysis, %	
				Calc.	Found
V	166–168°	39	$C_7H_7NO_3$	C 54.88	54.85
				H 4.61	4.86
				N 9.18	9.21
XI	150–151°	74	$C_8H_9NO_3$	C 57.46	57.20
				H 5.42	5.11
				N 8.41	8.31
XII	84–88°	10	$C_8H_9NO_3$	C 57.46	57.19
				H 5.42	5.32
				N 8.41	8.20
XIII	196–198°	72	$C_9H_9NO_3$	C 60.31	60.36
				H 5.06	5.29
				N 7.85	8.05
XIV	128–129°	24	$C_{10}H_{13}NO_3$	C 61.51	61.40
				H 6.71	6.88
				N 7.20	7.05
XV	176–178°	62	$C_{16}H_{19}NO_3$	C 70.29	70.08
				H 7.01	6.95
				N 5.15	5.21
XVI	139–141°	37	$C_8H_9NO_4$	C 52.44	52.18
				H 4.95	5.17
				N 7.68	7.96
XVII	174–176°	59	$C_{12}H_9NO_3$	C 66.95	66.83
				H 4.21	4.41
				N 6.53	6.73
XVIII	200–202°	69	$C_{12}H_8FNO_3$	C 61.79	61.85
				H 3.46	3.66
				N 6.03	5.76
XIX	208°	35	$C_{12}H_8N_2O_5$	C 55.37	55.66
				H 3.09	3.42
				N 10.81	11.00
XX	269°	84	$C_{12}H_{17}N_3O_7$	C 47.20	46.90
				H 2.31	2.29
				N 13.82	13.81
XXI	190–192°	76	$C_{13}H_{11}NO_4$	C 63.66	63.52
				H 4.52	4.75
				N 5.73	5.74
XXII	164–165°	51	$C_7H_8N_2O_3$	C 49.97	49.87
				H 4.79	5.09
				N 16.72	16.49
XXIII	159–160°	50	$C_9H_{11}N_3O_4$	C 47.96	47.71
				H 4.92	5.17
				N 18.72	18.85
XXIV	138–139°	76	$C_8H_{10}N_2O_3$	C 52.71	52.74
				H 5.52	5.80
				N 15.43	15.18
XXV	178–179°	86	$C_{12}H_{16}N_2O_3$	C 60.97	61.14
				H 6.82	6.81
				N 11.90	11.71
XXVI	111–113°	18	$C_{11}H_{13}Cl_2N_3O_4$	C 40.81	40.94
				H 4.49	4.21
				N 13.03	12.84
XXVII	190–192°	33	$C_8H_{10}N_2O_3$	C 52.71	52.25
				H 5.53	5.44
				N 15.43	15.16
XXVIII	176–178°	81	$C_{12}H_{10}N_2O_3$	C 62.57	62.66
				H 4.38	4.40
				N 12.21	12.15
XXIX	197–199°	60	$C_{12}H_9FN_2O_3$	C 58.04	57.71
				H 3.65	3.84
				N 11.33	11.18
XXX	138–139°	53	$C_8H_9NO_4$	C 52.44	52.57
				H 4.95	4.89
				N 7.67	7.87
XXXI	182–184°	17	$C_6H_7NO_4S$	C 38.08	37.94
				H 3.73	3.70
				N 7.43	7.63
XXXII	172–173°	2	$C_7H_9NO_2S_2$	C 31.45	31.47
				H 3.39	3.44
				N 5.26	5.24

intraperitoneally implanted tumors. Active compounds are defined (11) as those that produce a T/C value[1] equal to or greater than 125%.

Antitumor data for the 10 reproducibly active compounds (*i.e.*, two or more T/C values ≥ 125%) are given in Table II. The compounds shown in Table I but not Table II were inactive in duplicate or two of three tests.

The initial part of this study involved a determination of whether both oxygen functions were necessary for activity and the importance of the isomeric relationship of these two groups.

That none of the monooxygenated pyridine analogs (VII–X) related to I possessed P-388 antitumor activity was readily established.

Evaluation of the isomeric hydroxy-2-pyridones (III–VI) related to I showed that the 5-hydroxy (IV) but not the 4- or 6-hydroxy (III or VI) analogs were active. This finding is consistent with the chemical similarity of the 3- and 5-positions of the pyridine ring. The activity of the 5-acetoxy derivative (V) was variable (T/C 132, 121, and 119%). Neither 5-hydroxy analog was as active as the corresponding 3-substituted isomer. 4-Hy-

[1] T/C = (survival time of treated mice/survival time of control mice) × 100%.

I: X = 3-OCOCH$_3$
II: X = 3-OH
III: X = 4-OH
IV: X = 5-OH
V: X = 5-OCOCH$_3$
VI: X = 6-OH

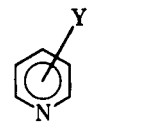

VII: Y = 2-OH
VIII: Y = 3-OH
IX: Y = 3-OCOCH$_3$
X: Y = 4-OH

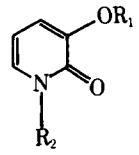

XI: R_1 = COC_2H_5, R_2 = H
XII: R_1 = $COCH_3$, R_2 = CH_3
XIII: R_1 = CO(cyclopropyl), R_2 = H
XIV: R_1 = CO(*tert*-butyl), R_2 = H
XV: R_1 = CO(1-adamantyl), R_2 = H
XVI: R_1 = $COCH_2OCH_3$, R_2 = H
XVII: R_1 = COC_6H_5, R_2 = H
XVIII: R_1 = COC_6H_4F(4-substituted); R_2 = H
XIX: R_1 = $COC_6H_4NO_2$(4-substituted), R_2 = H
XX: R_1 = $COC_6H_3(NO_2)_2$(2,4-disubstituted), R_2 = H
XXI: R_1 = $COC_6H_4OCH_3$(4-substituted), R_2 = H
XXII: R_1 = $CONHCH_3$, R_2 = H
XXIII: R_1 = R_2 = $CONHCH_3$
XXIV: R_1 = $CONHC_2H_5$, R_2 = H
XXV: R_1 = CONH(cyclohexyl), R_2 = H
XXVI: R_1 = R_2 = $CONHCH_2CH_2Cl$
XXVII: R_1 = $CON(CH_3)_2$, R_2 = H
XXVIII: R_1 = $CONHC_6H_5$, R_2 = H
XXIX: R_1 = $CONHC_6H_4F$(4-substituted), R_2 = H
XXX: R_1 = $COOC_2H_5$, R_2 = H
XXXI: R_1 = SO_2CH_3, R_2 = H
XXXII: R_1 = R_2 = SO_2CH_3

droxy-2-pyridone (III), the parent base for 3-deazauridine, had no P-388 activity, in contrast to the activity shown by both that nucleoside and II in this tumor system.

With the knowledge that at least two oxygen functions were required for antitumor activity and that 2,3-substitution was optimum, several derivatives of II were planned, prepared, and evaluated. Based on the observation that I was more active than II, several different types of derivatives were prepared at the 3-hydroxy position. Most of the derivatives were capable of hydrolysis since it was established early in the series that the ethers prepared in the 3-position were not active.

3-Acetoxy-2-pyridone (I) had good activity at high doses (Table II). The parent compound, 3-hydroxy-2-pyridone (II), also was active but somewhat less so than I. *N*-Methylation of I to give XII provided an active but toxic compound.

Variations in the alkyl portion of the acyl group in the 3-position produced both active and inactive materials. An ethyl group (XI) provided reproducible activity, while the cyclopropyl (VIII), methoxymethyl (XVI), *tert*-butyl (XIV), and adamantyl (XV) compounds were inactive. The aryl substitution (XVII–XXI), which was chosen to affect the ester hydrolysis rate, produced no activity differences and uniformly abolished activity.

The reaction of II with isocyanates to provide alkyl- or arylaminocarbonyl analogs (carbamates) produced several active compounds (XXII–XXIV, XXVIII, and XXIX). In some instances (XXIII and XXVI), *N*- as well as *O*-substitution occurred. The methylamino and ethylamino compounds (XXII and XXIV) were active, but the cyclohexylamino (XXV) and dimethylamino (XXVII) analogs were not. Although 2-chloroethylisocyanate formed a diadduct (XXVI), which was inactive, the methylisocyanate diadduct (XXIII) was one of the most active derivatives prepared. Neither the monoadduct (XXXI) nor the diadduct (XXXII) from methanesulfonyl chloride was active. While the ethylcarbamate (XXIV) was active, the corresponding carbonate (XXX) was not.

This investigation indicates that derivatives of 3-hydroxy-2-pyridone can provide moderate activity against P-388 leukemia. At least two oxygen functions are required, with the 2,3-isomer being the most active.

Table II—2-Pyridones Reproducibly Active against P-388 Lymphocytic Leukemia [a]

Compound	Optimum Dose[b], mg/kg/day	T/C[c]	T − C[d]
I	600	163	−2.8
II	400	138	−2.4
IV	200	128	+0.8
XI	400	143	−0.8
XII	600	144	−5.0
XXII	400	153	−4.6
XXIII	150	161	−3.3
XXIV	200	129	−1.7
XXVIII	100	132	−4.6
XXIX	25	134	−2.0

[a] With 10^6 cells implanted intraperitoneally in CDF_1 mice. [b] Dose giving the maximum T/C value on the intraperitoneal QD 1–9 treatment schedule. [c] At least one other active test (T/C ≥ 125%) was obtained in a separate, duplicate experiment. [d] Weight difference between treated and control animals 5 days after tumor implant.

Bioisosteres, 4-pyridones, and pyridone nucleosides are being studied currently. Also under investigation is the possibility that biological oxidation of the hydroxypyridones to quinoid forms may be involved in antitumor activity.

EXPERIMENTAL[2]

5-Hydroxy-2(1*H*)-pyridone (IV)—This compound was prepared in a 20% yield from 0.4 mole of VII using the Elbs peroxydisulfate oxidation procedure of Behrman and Pitt (12), mp 245–250° dec. [lit. (12) mp 250–260° dec.].

5-Acetoxy-2(1*H*)-pyridone (V)—To a stirred dry mixture of IV (1.67 g, 0.015 mole) and pyridine (1.30 ml, 0.016 mole) in dry benzene (10 ml) was added acetic anhydride (1.5 ml, 0.016 mole) by syringe through a septum. The mixture was refluxed for 26 hr. After the solvent was removed *in vacuo*, ethyl acetate was added to the dark-brown semisolid. Cooling at 3° gave a gray precipitate, which was decolorized with charcoal in a small volume of ethyl acetate–ethanol to give 0.91 g (39%) of a white solid, mp 166–168°; NMR: δ 2.27 (s, 3H, CH_3), 6.33 (m, 1H, CH), 6.97 (m, 2H, CH), and 11.48 (broad, 1H, NH) ppm; UV: 306 (log ε 3.83) and 231 (4.05) nm; IR: 1740, 1665, and 1625 cm^{-1}.

3-Propionyloxy-2(1*H*)-pyridone (XI)—A mixture of II (27.75 g, 0.25 mole), propionic anhydride (80 ml), and dry pyridine (50 ml) was refluxed for 89 hr, and the solvent was evaporated *in vacuo* to yield a crude solid product, which was washed with ethyl acetate. Recrystallization from anhydrous ethanol gave white crystals (30.90 g, 74%), mp 150–151°; NMR: δ 1.08 (t, 3H, CH_3), 2.48 (m, 2H, CH_2), 6.15 (t, 1H, CH), 7.28 (d, 2H, CH), and 11.98 (broad, 1H, NH) ppm; UV: 226 (log ε 3.79) and 297 (3.81) nm; IR: 1760 and 1655 cm^{-1}.

1-Methyl-3-acetyloxy-2(1*H*)-pyridone (XII)—To a cold, stirred solution of I (12.25 g, 0.08 mole) in dry dimethylformamide (50 ml) was slowly added (35 min) sodium hydride (50% mineral oil suspension, 3.86 g, 0.16 mole) under nitrogen. As the mixture became harder to stir, additional dry dimethylformamide (30 ml) was added. The mixture was stirred in an ice water bath for 3 hr, at which time methyl iodide (5.05 ml, 11.51 g, 0.081 mole) was added by syringe over 15 min. Sodium iodide separated during the addition. The mixture was stirred for 2.5 hr at room temperature. Acetic acid (7 ml), followed by portions of methylene chloride, was added.

The combined methylene chloride extracts were quickly washed with water and dried (sodium sulfate). After solvent evaporation *in vacuo*, the resulting red oil was distilled (ambient to 150° at 0.1 torr) to give a yellow oil, which was triturated with petroleum ether to remove mineral oil. Upon cooling, a solid precipitated. This solid was dissolved in methylene chloride and reprecipitated by addition to petroleum ether. The resulting solid was a light-sensitive, white, crystalline material (1.48 g, 10%), mp

[2] All melting points were recorded on a Thomas-Hoover capillary apparatus and are uncorrected. Elemental analyses were performed by the National Institute of Arthritis, Metabolism, and Digestive Diseases, National Institutes of Health, Bethesda, Md. Compounds I–III, VI, and VII–X were obtained commercially. When several compounds were prepared by comparable procedures, only one representative example is included in this section. Reference should be made to Table I for supplementary information.

New compounds were identified by NMR, UV, and IR spectra. These spectra were determined in dimethyl sulfoxide-d_6, 95% ethanol, and Nujol, respectively, unless otherwise indicated. NMR data are relative to tetramethylsilane.

84–88° [lit. (13) mp 99–101°]; NMR (deuterochloroform): δ 2.30 (s, 3H, NCH_3), 3.53 (s, 3H, CH_3), 6.05, and 7.11 (m, 3H, aromatic) ppm; UV: 236.5 (log ε 3.65) and 298 (3.94) nm; IR (chloroform): 1775 and 1665 cm^{-1}.

1,2-Dihydro-2-oxo-cyclopropanecarboxylic Acid-3-pyridinyl Ester (XIII) (General Procedure for XV, XVI, XVIII–XXI, XXVII, XXX, and XXXI)—A mixture of II (5.56 g, 0.05 mole), cyclopropanecarboxylic acid chloride (4.63 ml, 0.05 mole), dry pyridine (4.04 ml, 0.05 mole), and dry tetrahydrofuran (50 ml) was refluxed for 24 hr under nitrogen. Addition of methylene chloride to the ambient solution produced a solid, which was a mixture of XIII and pyridine hydrochloride. Recrystallization from absolute ethanol with charcoal gave 6.42 g (72%) of XIII as white crystals, mp 196–198°; NMR: 0.97 (m, 4H, CH_2), 1.80 (m, 1H, CH), 6.12 (t, 1H, CH), 7.25 (d, 2H, CH), and 11.88 (broad, 1H, NH) ppm; UV: 226.5 (log ε 3.79) and 297.5 (3.81) nm; IR: 1750 and 1650 cm^{-1}.

3-Benzoyloxy-2(1*H*)-pyridone (XVII) (General Procedure for XIV and XXXII)—A mixture of II (2.22 g, 0.02 mole), benzoyl chloride (2.44 ml, 0.021 mole), anhydrous potassium carbonate (2.90 g, 0.021 mole), and dry acetone (15 ml) was refluxed for 28 hr. Methylene chloride (20 ml) was added, followed by water (5 ml). Additional methylene chloride was added, and the mixture was thoroughly stirred. The layers were separated, the suspended solid was discarded, and the aqueous phase was extracted with two 20-ml portions of methylene chloride.

The combined organic extracts were washed with water (3 × 20 ml), dried over sodium sulfate, and evaporated *in vacuo*. Trituration of the resulting solid with toluene gave a white solid, which was recrystallized from ethyl acetate to give white crystals (2.51 g, 59%), mp 174–176°; NMR (deuterochloroform): 6.18 (t, 1H, CH), 7.40 (m, 5H, CH), 8.17 (m, 2H, CH), and 13.32 (broad, 1H, NH) ppm; UV: 228 (log ε 4.26) and 297 (3.92) nm; IR (chloroform): 1735, 1655, and 1615 cm^{-1}.

3-[[(Methylamino)carbonyl]oxy]-2(1*H*)-pyridone (XXII) (General Procedure for XXIV, XXV, XXVIII, and XXIX)—A mixture of II (5.51 g, 0.05 mole), methyl isocyanate (3.1 ml, 0.052 mole), dry triethylamine (8 drops), and dry dimethylformamide (35 ml) was stirred at room temperature for 44 hr. Solvent evaporation gave a red-brown material, which was stirred with hot ethyl acetate to remove 0.39 g of the disubstituted product, XXIII, mp 159–160°. The material insoluble in ethyl acetate was dissolved in warm ethanol. Scratching the cold filtrate produced XXII (4.28 g, 51%), mp 164–165°; NMR: 2.63 (d, 3H, CH_3), 6.08 (t, 1H, CH), 7.17 (d, 2H, CH), 7.45 (broad, 1H, NH), and 11.67 (broad, 1H, NH) ppm; UV: 227 (log ε 3.77) and 297 (3.81) nm; IR: 1725 and 1665 cm^{-1}.

***N*-Methyl-3-[[(methylamino)carbonyl]oxy]-2-oxo-1(2*H*)-pyridinecarboxamide (XXIII)**—Compound XXIII, mp 161–162°, was prepared in a 49% yield using a 1:2 molar ratio of II to methylisocyanate and the procedure described for XXII; NMR (deuterochloroform): 2.75 (d, 3H, CH_3), 2.87 (d, 3H, CH_3), 5.15 (broad, 1H, NH), 6.17 (t, 1H, CH), 7.15 (m, 1H, CH), 8.18 (m, 1H, CH), and 10.08 (broad, 1H, NH) ppm; UV: 220 (shoulder) and 306 (log ε 3.70) nm; IR (chloroform): 3430, 3160, 1745, and 1655 cm^{-1}.

***N*-(2-Chloroethyl)-3-[[(2-chloroethylamino)carbonyl]oxy]-1(2*H*)-pyridinecarboxamide (XXVI)**—A mixture of II (5.56 g, 0.05 mole), 2-chloroethylisocyanate (5.38 g, 0.051 mole), dry triethylamine (8 drops), and dry dimethylformamide (30 ml) was stirred at room temperature for 19 hr with occasional warming to 40° to dissolve suspended solids. The solvents were removed *in vacuo*, ethyl acetate (50 ml) was added to the residue, and the mixture was cooled to 0° overnight. The resulting solid (II, 2.4 g) was removed, the ethyl acetate was evaporated, and chloroform was added. This solution was extracted with three 30-ml portions of water, dried with sodium sulfate, and evaporated *in vacuo* to give a gray solid. Dissolution in ethyl acetate, followed by the addition of petroleum ether, yielded a gray-white solid (4.97 g, 55%), mp 111–113°; NMR (deuterochloroform): 3.52 (m, 8H, CH_2), 5.83 (broad, 1H, NH), 7.28 (m, 1H, CH), 8.25 (m, 1H, CH), and 10.72 (broad, 1H, NH) ppm; UV: 226 (shoulder) and 305 (log ε 3.83) nm; IR: 3410, 3120, 1730, and 1655 cm^{-1}.

REFERENCES

(1) A. Bloch, G. Dutschman, B. L. Currie, R. K. Robins, and M. J. Robins, *J. Med. Chem.*, **16**, 294 (1973).

(2) R. W. Brockman, S. C. Shaddix, M. Williams, J. A. Nelson, L. M. Rose, and F. M. Schabel, *Ann. N.Y. Acad. Sci.*, **255**, 501 (1975).

(3) W. D. De Wys and T. C. Hall, *Eur. J. Cancer*, **19**, 281 (1973).

(4) T. A. Khwaja, T. C. Hall, and K. M. Sheikh, in "Cancer Chemotherapy II," K. Hellmann and T. A. Connors, Eds., Plenum, New York, N.Y., 1975, p. 77.

(5) S. Danishefsky and S. J. Etheredge, *J. Org. Chem.*, **39**, 3430 (1974).

(6) T. Fujii, S. Yoshifuji, Y. Hatanaka, K. Yoshida, M. Ohba, K. Yamada, M. Ohkuma, H. Shinoda, and D. Mizuno, *J. Pharm. Soc. Jpn.*, **97**, 685 (1977).

(7) T. Kato, H. Kimura, A. Wagai, T. Sasaki, M. Ohkuma, H. Shinoda, M. Kohno, and D. Mizuno, *ibid.*, **97**, 676 (1977).

(8) S. Nesnow, T. Miyazaki, T. Khwaja, R. B. Meyer, and C. Heidelberger, *J. Med. Chem.*, **16**, 524 (1973).

(9) H. Meislich, in "Pyridine and Its Derivatives, Part Three," E. Klingsberg, Ed., Interscience, New York, N.Y., 1962, p. 509.

(10) H. Tieckelmann, in "Pyridine and Its Derivatives, Vol. 14 Supplement, Part Three," R. A. Abramovitch, Ed., Interscience, New York, N.Y., 1974, p. 597.

(11) R. I. Geran, N. H. Greenberg, M. M. Macdonald, A. M. Schumacher, and B. J. Abbott, *Cancer Chemother. Rep., Part 3*, **3** (2), 1 (1972).

(12) E. J. Behrman and B. M. Pitt, *J. Am. Chem. Soc.*, **80**, 3717 (1958).

(13) H. W. Chambers and J. E. Casida, *Toxicol. Appl. Pharmacol.*, 14, 249 (1969).

ACKNOWLEDGMENTS

The authors thank Dr. George Proctor, University of Strathclyde, Glasgow, Scotland, for helpful technical discussions and the synthesis of XII.

D. R. Hwang was a National Institutes of Health Visiting Postdoctoral Fellow, 1976–1977.

Metabolic Conversion of Fluorenone Oxime to Phenanthridinone by Hepatic Enzymes

YECHIEL GOLANDER and LARRY A. STERNSON ˣ

Received September 5, 1978, from the *Department of Pharmaceutical Chemistry, University of Kansas, Lawrence, KS 66045.* Accepted for publication December 18, 1978.

Abstract □ Fluorenone oxime is converted to phenanthridinone by enzymes present in rat liver homogenates. The reaction is analogous to the chemical Beckman rearrangement. The oxime–amide rearrangement enzyme is localized primarily in the microsomes, with some activity in the cytosol. The reaction requires reduced nicotinamide adenine dinucleotide phosphate and observes Michaelis–Menten kinetics. The reaction is relatively slow (V_{max} = 7.75 ± 2.01 nmoles of phenanthridinone formed/100 mg of liver/15 min), but the enzyme reaches maximum velocity at relatively low substrate concentrations (K_m = 3.90 ± 1.85 × 10^{-5} M). The reaction is strongly competitively inhibited by 1-decylimidazole (K_I = 3.75 ± 1.77 × 10^{-7} M) and inhibited to a lesser extent by the chelating agents bipyridyl (K_I = 1.33 ± 0.21 × 10^{-3} M) and ethylenediamine tetraacetate (K_I = 1.00 ± 0.28 × 10^{-3} M) and the sulfhydryl binding agent *p*-chloromercuribenzoate (K_I = 2.71 ± 0.07 × 10^{-4} M). Studies also suggest that the reaction mechanism does not involve initial enzymatic substrate esterification through acetylation, glucuronidation, phosphorylation, or sulfation.

Keyphrases □ Fluorenone oxime—metabolic conversion to phenanthridinone by hepatic enzymes, *in vitro*, kinetics □ Phenanthridinone—produced from fluorenone oxime by hepatic enzymes, *in vitro*, kinetics □ Enzymes, hepatic—conversion of fluorenone oxime to phenanthridinone, *in vitro*, kinetics

Oximes are metabolic products formed by liver microsomal oxidation of primary aliphatic amines (1, 2). Although these products were considered to be metabolically unreactive, they were susceptible to enzymatic reduction to the corresponding hydroxylamine and amine in several animal species (3, 4). Fluorenone oxime (I), when administered intravenously to rats, is converted (Scheme I) to phenanthridinone (II), which is subsequently excreted in the urine (5). The enzymes responsible for this transformation are localized primarily in the liver microsomes (6), with minor activity in the nuclear and mitochondrial fractions.

This report describes the enzymatic transformation kinetics and provides information to help characterize the oxime–amide rearrangement enzyme.

EXPERIMENTAL

Apparatus—High-performance liquid chromatography (HPLC) was performed on a component system[1], and analytes were detected with an absorbance detector operated at 254 nm.

Materials—Fluorenone oxime and phenanthridinone were synthesized by literature methods (7). Liver enzymes were prepared from male Sprague–Dawley rats, 200–250 g, as described previously (8).

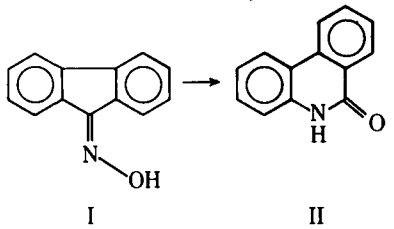

I II

Scheme I

Enzymatic Assay—Incubation mixtures contained enzyme equivalent to 100 mg of liver, a reduced nicotinamide adenine dinucleotide phosphate (III)-generating system [nicotinamide adenine dinucleotide phosphate (1 μmole), glucose-6-phosphate (20 μmoles), glucose-6-phosphate dehydrogenase (1 unit), and magnesium chloride (100 μmoles)], fluorenone oxime, and phosphate buffer (0.05 M, pH 7.4) adjusted to a final volume of 5 ml.

Incubations were carried out for 15 min with agitation in a Dubnoff metabolic incubator at 37°. All reagents in the system used to generate III were in excess with respect to requirements for III during the entire incubation.

Analytical Methodology—Incubations were terminated by the addition of 10 ml of chloroform to the reaction mixture. The mixture was shaken for 20 min and centrifuged at 2500×*g*. The organic layer was recovered [extraction efficiency of II ≥98% (6)] and evaporated to dryness under nitrogen. The mixture was dissolved in 200 μl of dimethylformamide containing 20.8 nmoles of phenanthrene, present as an internal standard.

Aliquots (10 μl) of this mixture were analyzed by HPLC on a 4-mm o.d. × 30-cm column[2]. Components were separated using methanol–methylene chloride–water (60:5:35) as the mobile phase (flow rate of 2 ml/min). Under these conditions, the retention volumes (V_R) were: phenanthridinone, 7.1 ml; fluorenone oxime, 10.4 ml; and phenanthrene (added as internal standard), 26.7 ml. Quantitation of II was based on comparison of the peak height ratio (analyte–internal standard) with a standard curve prepared after analysis of liver homogenate samples containing known amounts of I and II in the 8.6 × 10^{-6}–1.4 × 10^{-4} M range. This response was related linearly to concentration, yielding the line $y = 0.05x - 0.005$ (zero-order correlation 0.99) after least-squares analysis.

Kinetic Measurement—The Michaelis constants (K_m) and the maximum velocity (V_{max}) for the conversion of I to II were determined from double-reciprocal (Lineweaver–Burk) plots of initial velocity against substrate concentration (9), which varied over the range of 62–1000 μM. The line of best fit was determined by least-squares regression analysis. In experiments to determine the effect of various chemicals on enzyme activity, the test compounds were added to the incubation mixture concurrently with the substrate (I). Microsomes isolated by centrifugation of the 9000×*g* supernate of liver homogenates at 105,000×*g* were not subjected to additional purification.

RESULTS AND DISCUSSION

A previous report (6) showed that the conversion of I to II in liver homogenates is an enzymatic process. Now it is shown that the major oxime–amide rearrangement enzyme responsible for the rearrangement of fluorenone oxime (present at concentrations of 10^{-4} M) is present in liver microsomes (6.04 ± 1.25 nmoles of phenanthridinone formed/100 mg of liver/15 min), with the cytosol exhibiting ~38% of this activity (2.32 ± 0.02 nmoles of phenanthridinone formed/100 mg of liver/15 min).

Minor activity was observed in nuclear and mitochondrial subcellular liver fractions. Repeated washings (six times) of the microsomal pellet (resuspending the pellet in the buffer and then centrifugating at 105,000×*g* for 45 min) caused no loss in enzyme activity, suggesting that the enzyme is bound relatively tightly to the membrane surface. Essentially no oxime–amide rearrangement was observed in the buffer used to wash the microsomal pellet.

Compound III was required as a cofactor for activity in both microsomes and cytosol (6). Neither oxidized nor reduced nicotinamide adenine dinucleotide nor oxidized nicotinamide adenine dinucleotide phosphate (NADP) was an effective cofactor for these enzymes. The role of III in

[1] Waters Associates, Milford, Mass.

[2] μBondapak C-18, Waters Associates, Milford, Mass.

0022-3549/79/0700-0820$01.00/0
© 1979, American Pharmaceutical Association

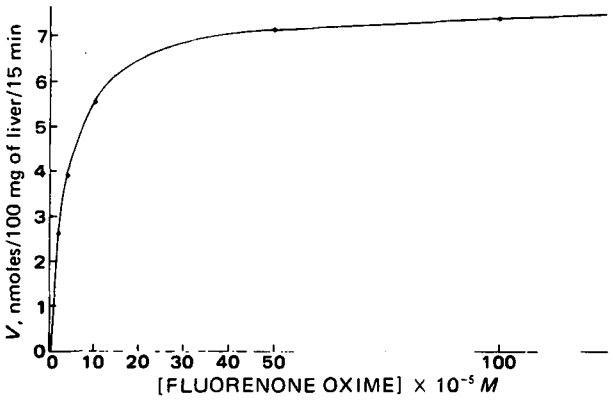

Figure 1—*Rate of fluorenone oxime rearrangement to phenanthridinone determined as a function of the substrate concentration.*

the transformation of I to II has not been elucidated. Conversion of I to II results in no net change in the oxidation state, so the involvement of III in a redox role is questionable.

Incubation of I with tritiated III resulted in the formation of II with no incorporation of tritium in the product. Compound III was consumed during both the microsomal- and cytosol-catalyzed rearrangement of I, as determined by monitoring the reaction spectrophotometrically at 340 nm. Although this result could suggest that the cofactor plays an electron-transfer role in the oxime–amide rearrangement enzyme-catalyzed reaction, the experiment was inconclusive because HPLC analysis of incubation mixtures showed that I was converted to products other than II (particularly in microsomes), and these transformations probably required III. This supposition is supported by the fact that III was consumed more rapidly than can be attributed solely to the enzymatic formation of II. Biotransformation of I occurred with III consumption, but its role in the reaction under study could not be segregated from the total substrate biodegradation.

Microsomal oxime–amide rearrangement enzyme-catalyzed reaction kinetics were determined by measuring the initial I–II conversion rate at substrate concentrations of 10^{-3}, 5×10^{-4}, 10^{-4}, 4×10^{-5}, and 2×10^{-5} *M*. Since microsomes were used without further purification, the observed K_m and K_i values may have been influenced by nonspecific substrate binding to proteins other than the oxime–amide rearrangement enzyme(s). Double-reciprocal plots of initial velocity data *versus* substrate concentration yielded the straight line $v^{-1} = 5.03 \times 10^{-6} S^{-1} + 0.13$ ($r = 0.99$). The plot linearity indicates Michaelis–Menten kinetics (10).

Values of K_m and V_{max} extracted from these plots were $3.90 \pm 1.85 \times 10^{-5}$ *M* and 7.75 ± 2.01 nmoles of II formed/100 mg of liver/15 min (for eight determinations), respectively. Therefore, the reaction was quite slow, but the enzyme reached maximum velocity at relatively low substrate concentrations. Figure 1 shows reaction rate as a function of substrate concentration.

The microsomal oxime–amide rearrangement enzyme system was further investigated by assessing the ability of certain compounds to inhibit the conversion of I to II. Three compounds that are structurally similar to I, carbazole, 2-nitrofluorene, and 9-aminofluorene, had no effect on the reaction in question when I was incubated with the microsomal system at a 10^{-4} *M* concentration and the potential inhibitors were present in a concentration of 10^{-7}, 10^{-6}, 10^{-5}, or 10^{-4} *M*. At substrate (I) concentrations of 10^{-4} *M*, ethyl 2,2-diphenylvalerate failed to inhibit the reaction when present at concentrations below 10^{-5} *M*; however, when this potential inhibitor was added at concentrations of 10^{-3} *M*, reaction was inhibited 62% during a 15-min incubation period.

N-Decylimidazole, a known inhibitor of microsomal mixed-function oxidases (11), was a potent competitive inhibitor of the microsomal oxime–amide rearrangement system (Table I), inhibiting the conversion of I to II by 77% when the substrate and inhibitor were present at concentrations of 10^{-4} and 10^{-3} *M*, respectively. However, cytochrome P-450 was not involved in the reaction since conversion of I to II was not effected by either carbon monoxide (6) or microsome preexposure to UV light. The imidazole inhibitory role in this reaction is, therefore, probably not that normally associated with this class of inhibitors.

Chelating agents bipyridyl and edetate sodium also inhibited the biotransformation of I to II (Table I), suggesting that metal ions may play a role in the enzymatic reaction. However, when the substrate was incubated with microsomes and III (*not* a reduced nicotinamide adenine dinucleotide phosphate-*generating* system but III itself), the rearrangement was not inhibited when magnesium ion was totally excluded from the incubation mixture. Thus, the observed inhibitory effects of chelating agents on the enzymatic I → II conversion apparently do not result from an inhibition of III formation (when an NADPH-generating system is used) due to complexation of the magnesium ion required for III formation.

Table I—Inhibition Constants for Various Compounds toward Microsomal Oxime–Amide Rearrangement Activity [a,b]

Inhibitor	Inhibitor Concentration, *M*	$K_I \pm SEM$[c], *M*
N-Decylimidazole	10^{-3}, 10^{-6}, 5×10^{-7}	$3.75 \pm 1.77 \times 10^{-7}$
Bipyridyl	10^{-3}	$1.33 \pm 0.21 \times 10^{-3}$
Edetate sodium	10^{-3}	$1.00 \pm 0.28 \times 10^{-3}$
p-Chloromercuribenzoate	10^{-3}	$2.71 \pm 0.07 \times 10^{-4}$

[a] Oxime–amide rearrangement activity assayed as described previously (6) using fluorenone oxime as the substrate. [b] Fluorenone oxime incubated at concentrations of 20, 40, 100, and 500 μ*M*. [c] Each inhibitor showed linear competitive kinetics, and inhibition constants were calculated from Lineweaver–Burke plots (9, 15).

Microsomal oxime–amide rearrangement enzymes also were sensitive to the sulfhydryl binding reagent *p*-chloromercuribenzoate; this reagent also competitively inhibited the rearrangement (Table I), suggesting the possible involvement of a thiol linkage in the transformation. Chelating agents and sulfhydryl binding agents rarely exhibit competitive kinetics with regard to reactions such as the one under investigation. No explanation is offered at this time for this observation.

Microsomal oxime–amide rearrangement activity also was studied as a function of pH. With a substrate concentration of 5×10^{-4} *M* ($13 K_m$), maximum activity was observed at pH 7.1 with diminished activity on either side of this maximum (Fig. 2) over the pH 6.0–8.2 range. All of the experiments in the study were carried out at pH 7.4 to compare oxime–amide rearrangement activity with other microsomal enzyme (mixed-function oxidase) processes acting on fluorenone oxime and to provide an environment for the microsomal suspension that was most similar to that encountered *in vivo*.

It was postulated (5, 6) that the role of the oxime–amide rearrangement enzyme may be to esterify the oxime, producing an intermediate with a high propensity for formation of a transitory nitrenium ion (IV), which undergoes facile rearrangement to yield the amide (II, Scheme II). This mechanism is identical with one that occurs during the Beckman rearrangement (12) of I to II. Four enzymatic esterifying systems were investigated as potential catalysts for the reaction: acetylation, glucuronidation, phosphorylation, and sulfation. Incubation of either microsomal or cytosol fractions with acetyl CoA (an acetylating substrate), uridinediphosphoglucuronic acid (a glucuronidation precursor), or adenosine triphosphate (a phosphorylating reagent) failed to facilitate the conversion of I to II.

The sulfation reaction was studied in greater detail because of its participation in the analogous enzymatic conversion of arylhydroxylamines to electrophilic intermediates (13). However, reaction of I (at levels of 10^{-4} *M*) with cytosol and/or microsomal homogenates to produce

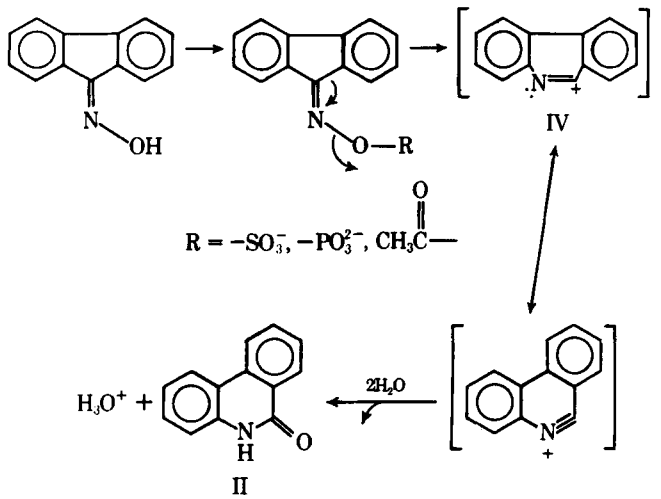

Scheme II—Postulated mechanism for enzymatic transformation of fluorenone oxime to phenanthridinone.

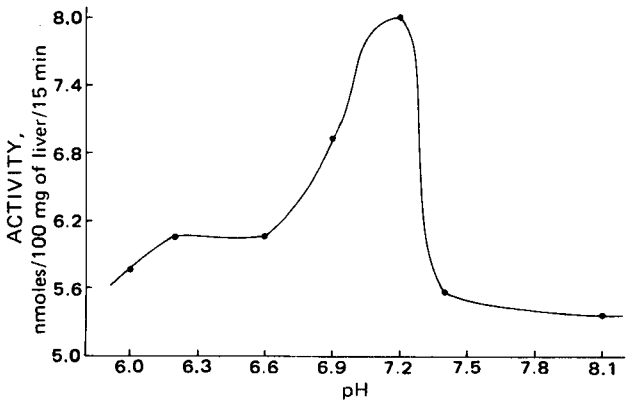

Figure 2—*Hepatic microsomal oxime-amide rearrangement enzyme activity toward fluorenone oxime determined as a function of pH. Each point is the average of six determinations.*

II was not stimulated by the addition of either inorganic sulfate (6.5×10^{-4} *M*) or adenosine triphosphate plus sulfate. Furthermore, the reaction was not inhibited by *p*-nitrophenol (1×10^{-4} *M*), a known consumer of sulfate (14) (and, therefore, a potential competitive inhibitor of the oxime-amide rearrangement system), or 3′,5′-adenosine diphosphate, another known sulfation inhibitor (14). These results suggest that enzymatic conversion of I to II does not involve oxime substrate esterification prior to rearrangement. The reaction mechanism remains a mystery but is being studied.

REFERENCES

(1) H. B. Hucker, B. M. Michniewicz, and R. E. Rhodes, *Biochem. Pharmacol.*, **20**, 2123 (1971).
(2) R. W. Fuller, C. J. Parli, and B. B. Molloy, *ibid.*, **22**, 2059 (1973).
(3) J. Hes and L. A. Sternson, *Drug Metab. Disp.*, **2**, 245 (1974).
(4) L. A. Sternson and J. Hes, *Pharmacology*, **13**, 234 (1975).
(5) L. A. Sternson and F. Hincal, *Experientia*, **33**, 1079 (1977).
(6) L. A. Sternson and F. Hincal, *Biochem. Pharmacol.*, **27**, 1919 (1978).
(7) H. L. Pan and T. L. Fletcher, *J. Med. Chem.*, **12**, 822 (1969).
(8) R. A. Wiley, L. A. Sternson, H. A. Sasame, and J. R. Gillette, *Biochem. Pharmacol.*, **21**, 3235 (1972).
(9) H. Lineweaver and D. Burke, *J. Am. Chem. Soc.*, **56**, 658 (1934).
(10) L. Michaelis and M. L. Menten, *Biochem. Z.*, **49**, 333 (1913).
(11) K. C. Liebman, *Chem. Biol. Interact.*, **3**, 289 (1971).
(12) B. J. Gregory, R. B. Moodie, and K. Schofield, *J. Chem. Soc. B*, **1970**, 338.
(13) E. C. Miller and J. A. Miller, *Pharmacol. Rev.*, **18**, 805 (1966).
(14) R. K. Banerjee and A. B. Roy, *Biochim. Biophys. Acta*, **151**, 573 (1968).
(15) W. W. Cleland, *ibid.*, **67**, 173 (1963).

ACKNOWLEDGMENTS

Supported in part by Grant CA-18615 awarded by the National Institutes of Health.

Stabilization of 5-Azacytidine by Nucleophilic Addition of Bisulfite Ion

DULAL C. CHATTERJI ˣ **and JOSEPH F. GALLELLI**

Received June 30, 1978, from the *Pharmaceutical Development Service, Pharmacy Department, The Clinical Center, National Institutes of Health, Bethesda, MD 20014.* Accepted for publication December 18, 1978.

Abstract □ 5-Azacytidine (I) stability was increased approximately 10-fold over its stability in water or lactated Ringer injection by the addition of excess sodium bisulfite and the maintenance of pH ~2.5. The increased stability in the presence of bisulfite at pH 2.5 was attributed to the addition of bisulfite across the 5–6 protonated imine bond of I, which prevented the hydrolytic attack on this labile double bond. However, above pH 4, bisulfite increased I degradation. At higher pH, the compound was no longer protonated and bisulfite did not form the stable addition product. The addition compound quickly decomposed above pH 6 to give back the parent compound and, thus, acted as a I prodrug. The intact drug remaining was assayed by high-pressure liquid chromatography (HPLC), and the reversibility of the bisulfite–I addition product above pH 6 was demonstrated by UV spectrophotometry and HPLC. The potential utility of the bisulfite–I addition product as a I prodrug in parenteral and possible oral dosage forms is discussed.

Keyphrases □ Azacytidine—prodrugs, sodium bisulfite, stabilization in aqueous solutions, effect of pH □ Sodium bisulfite—stabilization of azacytidine in aqueous solutions, effect of pH, prodrugs □ Prodrugs—azacytidine, stabilization by sodium bisulfite □ Antineoplastic agents—azacytidine, prodrugs, sodium bisulfite complex

The use of 5-azacytidine (I) in acute myelogenous leukemia (1–3) is often limited by severe and sometimes dose-limiting nausea and vomiting (4, 5). Although the GI toxicity can be controlled effectively by administering the drug as a slow infusion (6, 7), extreme drug instability (8–10) poses a serious problem. Even when I is infused in lactated Ringer injection, which provides optimum stability conditions for the drug at pH 6.4, ~10% of I is lost in 2 hr at room temperature (8).

BACKGROUND

Systematic kinetic studies on the I hydrolysis (8–10) revealed that hydrolysis proceeds by the classical acid-catalyzed hydration of the 5–6 imine double bond (Scheme I), followed by deamination to yield the formyl derivative, *N*-(formylamidino)-*N*-β-D-ribofuranosylurea (II).

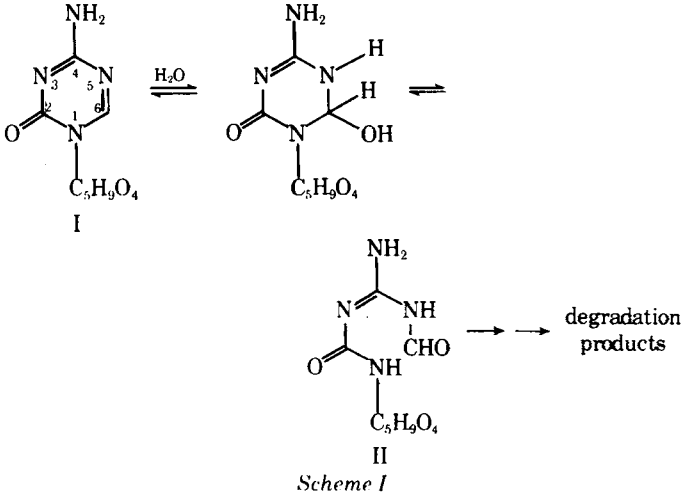

Scheme I

0022-3549/79/0700-0822$01.00/0
© 1979, American Pharmaceutical Association

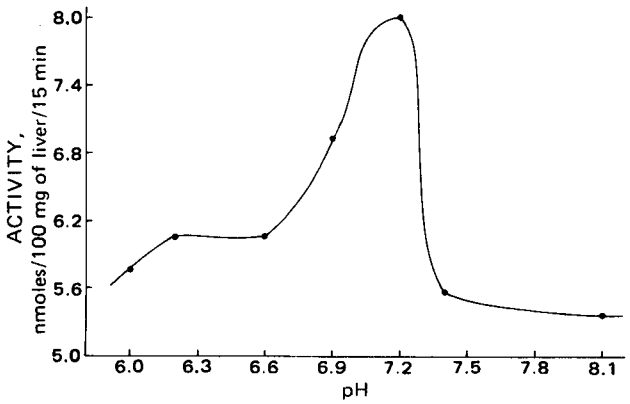

Figure 2—*Hepatic microsomal oxime-amide rearrangement enzyme activity toward fluorenone oxime determined as a function of pH. Each point is the average of six determinations.*

II was not stimulated by the addition of either inorganic sulfate (6.5×10^{-4} *M*) or adenosine triphosphate plus sulfate. Furthermore, the reaction was not inhibited by *p*-nitrophenol (1×10^{-4} *M*), a known consumer of sulfate (14) (and, therefore, a potential competitive inhibitor of the oxime-amide rearrangement system), or 3′,5′-adenosine diphosphate, another known sulfation inhibitor (14). These results suggest that enzymatic conversion of I to II does not involve oxime substrate esterification prior to rearrangement. The reaction mechanism remains a mystery but is being studied.

REFERENCES

(1) H. B. Hucker, B. M. Michniewicz, and R. E. Rhodes, *Biochem. Pharmacol.*, **20**, 2123 (1971).
(2) R. W. Fuller, C. J. Parli, and B. B. Molloy, *ibid.*, **22**, 2059 (1973).
(3) J. Hes and L. A. Sternson, *Drug Metab. Disp.*, **2**, 245 (1974).
(4) L. A. Sternson and J. Hes, *Pharmacology*, **13**, 234 (1975).
(5) L. A. Sternson and F. Hincal, *Experientia*, **33**, 1079 (1977).
(6) L. A. Sternson and F. Hincal, *Biochem. Pharmacol.*, **27**, 1919 (1978).
(7) H. L. Pan and T. L. Fletcher, *J. Med. Chem.*, **12**, 822 (1969).
(8) R. A. Wiley, L. A. Sternson, H. A. Sasame, and J. R. Gillette, *Biochem. Pharmacol.*, **21**, 3235 (1972).
(9) H. Lineweaver and D. Burke, *J. Am. Chem. Soc.*, **56**, 658 (1934).
(10) L. Michaelis and M. L. Menten, *Biochem. Z.*, **49**, 333 (1913).
(11) K. C. Liebman, *Chem. Biol. Interact.*, **3**, 289 (1971).
(12) B. J. Gregory, R. B. Moodie, and K. Schofield, *J. Chem. Soc. B*, **1970**, 338.
(13) E. C. Miller and J. A. Miller, *Pharmacol. Rev.*, **18**, 805 (1966).
(14) R. K. Banerjee and A. B. Roy, *Biochim. Biophys. Acta*, **151**, 573 (1968).
(15) W. W. Cleland, *ibid.*, **67**, 173 (1963).

ACKNOWLEDGMENTS

Supported in part by Grant CA-18615 awarded by the National Institutes of Health.

Stabilization of 5-Azacytidine by Nucleophilic Addition of Bisulfite Ion

DULAL C. CHATTERJI ˣ **and JOSEPH F. GALLELLI**

Received June 30, 1978, from the *Pharmaceutical Development Service, Pharmacy Department, The Clinical Center, National Institutes of Health, Bethesda, MD 20014.* Accepted for publication December 18, 1978.

Abstract □ 5-Azacytidine (I) stability was increased approximately 10-fold over its stability in water or lactated Ringer injection by the addition of excess sodium bisulfite and the maintenance of pH ~2.5. The increased stability in the presence of bisulfite at pH 2.5 was attributed to the addition of bisulfite across the 5–6 protonated imine bond of I, which prevented the hydrolytic attack on this labile double bond. However, above pH 4, bisulfite increased I degradation. At higher pH, the compound was no longer protonated and bisulfite did not form the stable addition product. The addition compound quickly decomposed above pH 6 to give back the parent compound and, thus, acted as a I prodrug. The intact drug remaining was assayed by high-pressure liquid chromatography (HPLC), and the reversibility of the bisulfite–I addition product above pH 6 was demonstrated by UV spectrophotometry and HPLC. The potential utility of the bisulfite–I addition product as a I prodrug in parenteral and possible oral dosage forms is discussed.

Keyphrases □ Azacytidine—prodrugs, sodium bisulfite, stabilization in aqueous solutions, effect of pH □ Sodium bisulfite—stabilization of azacytidine in aqueous solutions, effect of pH, prodrugs □ Prodrugs—azacytidine, stabilization by sodium bisulfite □ Antineoplastic agents—azacytidine, prodrugs, sodium bisulfite complex

The use of 5-azacytidine (I) in acute myelogenous leukemia (1–3) is often limited by severe and sometimes dose-limiting nausea and vomiting (4, 5). Although the GI toxicity can be controlled effectively by administering the drug as a slow infusion (6, 7), extreme drug instability (8–10) poses a serious problem. Even when I is infused in lactated Ringer injection, which provides optimum stability conditions for the drug at pH 6.4, ~10% of I is lost in 2 hr at room temperature (8).

BACKGROUND

Systematic kinetic studies on the I hydrolysis (8–10) revealed that hydrolysis proceeds by the classical acid-catalyzed hydration of the 5–6 imine double bond (Scheme I), followed by deamination to yield the formyl derivative, *N*-(formylamidino)-*N*-β-D-ribofuranosylurea (II).

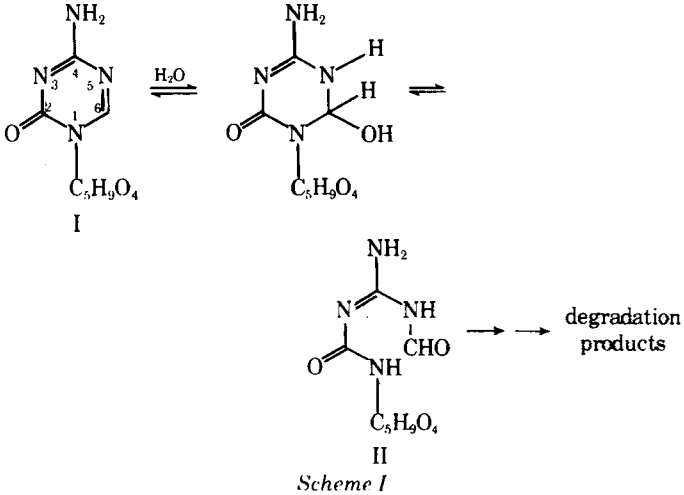

Scheme I

0022-3549/79/0700-0822$01.00/0
© 1979, American Pharmaceutical Association

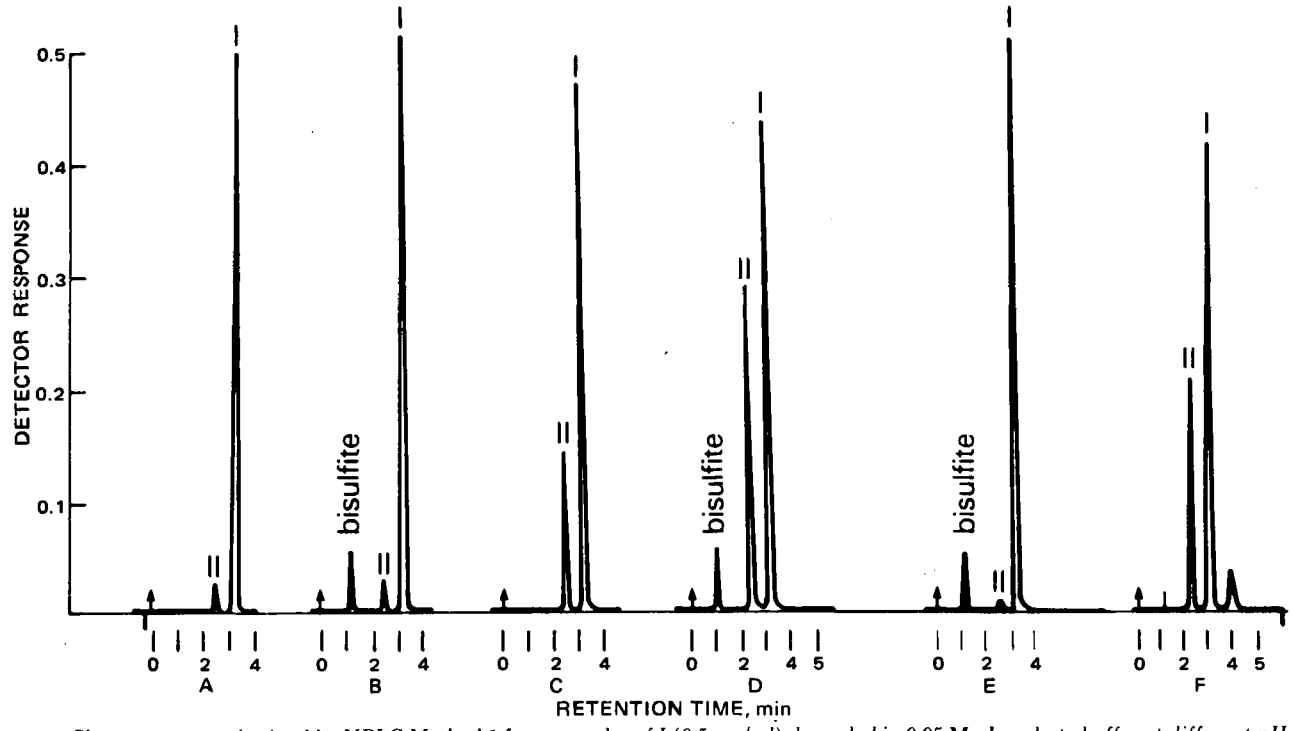

Figure 1—*Chromatograms obtained by HPLC Method 1 from samples of I (0.5 mg/ml) degraded in 0.05 M phosphate buffer at different pH values and room temperatures. Key: A, freshly prepared solutions of I in pH 7.0 phosphate; B, freshly prepared solution of I in pH 7.0 or 2.5 buffer containing 5 mg of sodium bisulfite/ml; C, sample in 1A after 70 min; D, sample in 1B with pH 7.0 buffer after 70 min; E, sample in 1B with pH 2.5 buffer after 70 min; and F, solution of I in pH 2.5 buffer in the absence of bisulfite after 70 min.*

The formyl derivative, II, can either reverse back to I or degrade subsequently (8–10).

The I hydrolysis rate, which is dictated by the pH dependence of hydration and deamination steps, is slowest around pH 6.5–7.0. However, even at this pH of maximum stability, drug degradation is too fast. Therefore, a different approach to improve I stability was needed.

The key to the instability of I is its 5–6 double bond, and saturating this double bond could improve drug stability. Synthesis of one such stable compound, 5,6-dihydro-5-azacytidine, was reported (11). Although the stability of this dihydro compound is excellent, approximately 20 times the dose of I is needed to yield an equivalent antitumor activity in experimental animals (11, 12).

Another approach to render the 5–6 double bond of I stable to water attack would be to add a stronger nucleophile capable of attacking the 5–6 double bond preferentially over water. Such a nucleophile should assure that the addition product does not undergo subsequent deamination; it should be stable in the infusion solution and, most important, it should quickly convert back to I under physiological conditions. The nucleophile should also be physiologically compatible.

Sodium bisulfite is a strong nucleophile and a common antioxidant additive in various pharmaceutical preparations. The nucleophilic addition of the bisulfite ion across the 5–6 double bond of I was demonstrated (9), but no attempt was made to study the results of this reaction or the stabilizing effect of sodium bisulfite on I. This paper reports the effect of sodium bisulfite on I stability in aqueous solutions.

EXPERIMENTAL

Materials—5-Azacytidine for injection (100 mg) was used as received[1]. Water was double distilled in an all-glass apparatus. All other chemicals were reagent grade.

Equipment—A high-pressure liquid chromatograph[2] equipped with a fixed-volume loop-type injection valve[3] and a variable-wavelength detector with a wavelength drive[4] attached to a computing integrator[5] were used. The columns used were a 250-mm × 4.6-mm i.d. reversed-phase column[6] and a 250-mm × 3.2-mm i.d. strong cation-exchange column[7]. Spectrophotometric analyses were carried out on a recording spectrophotometer[8]. All pH measurements[9] were taken at room temperature.

Degradation Studies—Solutions of I (0.5 mg/ml unless otherwise specified) were made by accurately weighing ~10 mg of I in a 20-ml screw-capped vial and adding 20.0 ml of the required buffer. Sodium bisulfite, when required, was incorporated into the buffer before adjustment of its final pH. The solutions were stored at room temperature (22–26°) and at refrigeration temperature (2–6°). The amount of intact I remaining at various time intervals was assayed by high-pressure liquid chromatography (HPLC) as described under *HPLC Method 1*. The time for 10% I degradation was obtained by extrapolation from the amount of intact I remaining at various time intervals.

UV Spectrum—The bisulfite–I mixture[10] was diluted 25-fold with pH 2.5 and 6.5 buffers (0.05 *M* phosphate), and their respective UV spectra using appropriate blanks were recorded[8]. UV spectra of I alone in pH 2.5 and 6.5 buffers were also recorded after appropriate dilution.

Assay and Identification Methods—*HPLC Method 1*—A reversed-phase column[6] with the mobile phase (0.02 *M* phosphate buffer, pH 6.5) at a flow rate of 2.0 ml/min was used to assay I. A 10-μl full loop sample volume was injected quantitatively, and the recorder was set at 0.64 full scale (254-nm detector). The area of the peak due to I was used to calculate the amount of intact I remaining in the sample. Typical run times were less than 6 min. The UV spectrum of the peaks were recorded when needed for identification by stopping the flow at the maximum of the peak and scanning them from 300 to 220 nm using the wavelength drive of the detector[4].

HPLC Method 2—A strong cation-exchange column[7] was used for separation of I from the I–sodium bisulfite addition product. The mobile phase consisted of 0.01 *M* NaCl with 0.01 *M* HCl in water (pH 2), and it was pumped at 1.25 ml/min. A 10-μl full loop sample volume was injected, and the recorder was set at 0.32 full scale (254-nm detector).

[1] Lot BV-77-270, Ben Venue Laboratories, Bedford, Ohio.
[2] Model 3500B, Spectra-Physics, Santa Clara, Calif.
[3] Velco type valve, Spectra-Physics, Santa Clara, Calif.
[4] Model SF770 spectroflow monitor with SFA339 wavelength drive, Schoeffel Instrument Corp., Westwood, N.J.
[5] Autolab System I, Spectra-Physics, Santa Clara, Calif.
[6] Zorbax C-8 column, 6-μm average particle size, DuPont Instruments, Wilmington, Del.
[7] Partisil 10 SCX, 10-μm average particle size, Altex Scientific, Berkeley, Calif.
[8] Cary 17, Varian Instrument Division, Palo Alto, Calif.
[9] Expandomatic SS-2 pH meter, Beckman Instruments, Fullerton, Calif.
[10] Unless otherwise specified, the bisulfite–I mixture was 0.5 mg of I and 5 mg of sodium bisulfite/ml of 0.05 *M* phosphate with the pH adjusted to 2.5.

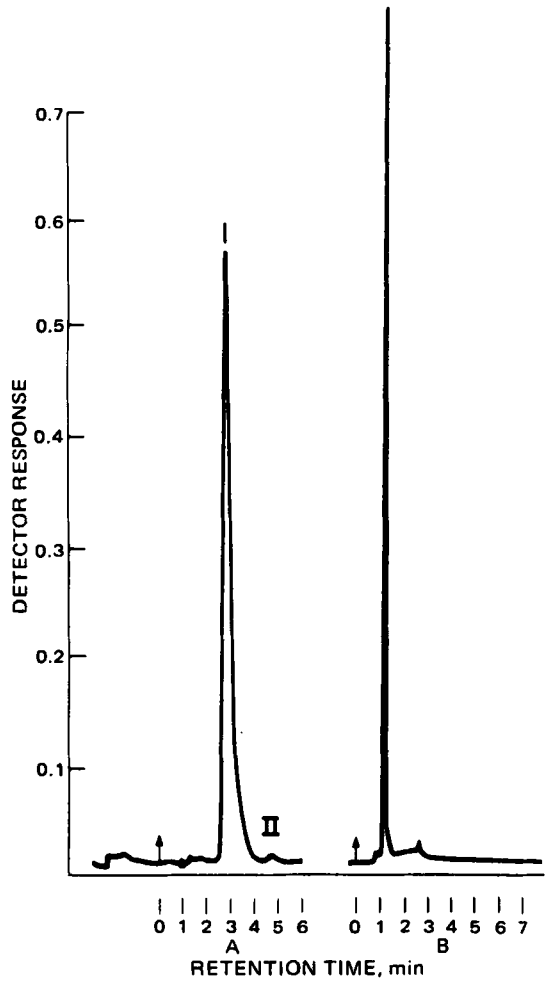

Figure 2—*Chromatograms obtained by HPLC Method 2 from samples of I (0.5 mg/ml) in 0.05 M phosphate buffers at different pH values and room temperature. Key: A, freshly prepared solution of I in pH 7.0 buffer; and B, freshly prepared solution of I in pH 2.5 buffer containing 5 mg of sodium bisulfite/ml.*

RESULTS AND DISCUSSION

HPLC Method 1 was similar in principle to the reversed-phase HPLC method used previously (8) to separate I and II. However, a different reversed-phase column[6] and mobile phase were used. A pH 6.5 buffer (0.02 *M* phosphate) was chosen as the mobile phase to prevent the retention time of I from changing when samples in concentrated buffers at low pH (2.5) were analyzed. Also, as discussed later, the maintenance of a high pH (>6) of the mobile phase was essential for the instant decomposition of the bisulfite–I addition product to yield I during the HPLC analysis.

As seen in Fig. 1F, the column[6] clearly separated the major degradation product, II (retention time of 150 sec), and an unidentified reaction product (retention time of 245 sec) from the peak due to I (retention time of 190 sec). Peak areas of I increased linearly with concentration from 0.3 to 0.5 mg/ml and were used for the calculation of intact I present in the samples.

Figure 1A shows the chromatogram of a freshly prepared solution of I in pH 7.0 buffer using HPLC Method 1. In addition to the major peak (I), a small peak (II) was present. Figure 1C is a chromatogram of the sample in Fig. 1A after 70 min at room temperature. Loss of I (~7%) was accompanied by an increase in peak II. Figure 1F shows the chromatogram of a I solution at pH 2.5 after standing for 70 min at room temperature. As is evident, I was less stable at pH 2.5 than at pH 7.0.

The chromatograms of freshly prepared solutions of I with bisulfite in either pH 2.5 or 7.0 buffer were identical (Fig. 1B). Peak I had the same retention time in all samples shown in Fig. 1. However, after 70 min at room temperature, the sample kept at pH 7.0 degraded almost 15% (Fig. 1D) whereas the same sample (Fig. 1B) kept at pH 2.5 showed little degradation (Fig. 1E). This finding indicates that bisulfite has a strong stabilizing effect on I hydrolysis at pH 2.5 (compare Figs. 1C–1E). This effect is more evident when the chromatogram of the I sample at pH 2.5 in the absence of bisulfite (Fig. 1F) is compared with that in Fig. 1E.

Table I—Time for I to Reach 90% of Its Original Concentration (0.5 mg/ml) in Buffer Solutions at Room Temperature (23–26°)

pH	Buffer	Time to Reach 90%, hr With Bisulfite[a]	Time to Reach 90%, hr Without Bisulfite
6.3	Lactated Ringer injection	—	2.3
7.0	0.05 *M* phosphate	0.8	2.6
6.5	0.05 *M* phosphate	1.2	2.3
6.0	0.05 *M* phosphate	1.0	1.5
4.0	0.05 *M* acetate	1.3	1.4
3.2	0.05 *M* phosphate	8.7	1.2
2.5	0.05 *M* phosphate	20	1.1
2.5	0.05 *M* phosphate	18[b]	—
2.5	0.05 *M* phosphate	6[c]	—
2.5	0.05 *M* phosphate	96[d]	—

[a] Sodium bisulfite, 5 mg/ml, unless specified otherwise. [b] Sodium bisulfite, 3 mg/ml. [c] Sodium bisulfite, 1 mg/ml. [d] Refrigeration temperature (2–6°).

Table I summarizes the effect of bisulfite on I stability at various pH values. Bisulfite increased the I degradation rate when the solution pH was maintained above 4.0. However, below pH 4.0, bisulfite slowed I degradation; the stabilization was more pronounced as the solution pH approached 2.5. Furthermore, at pH 2.5, increasing the amount of bisulfite increased the stabilization. At pH 2.5 in the presence of a 10-fold excess of bisulfite (5 mg of sodium bisulfite/ml with 0.5 mg of I/ml), ~20 hr was required for 10% I degradation at room temperature. This represents almost one order of magnitude improvement over the stability of I in the presently used clinical formulation of drug in lactated Ringer injection.

The large increase in I stability by bisulfite at acidic pH cannot be attributed to the effects of ionic strength but must be attributed to the protection of I by some direct interaction. To confirm that the peaks at 190 sec (Figs. 1B and 1E) (pH 2.5 sample) were due to I and not to the bisulfite–I product (III), the UV spectra of all peaks at 190 sec (Figs. 1A–1E) were recorded and found to be identical to those obtained from pure I. This finding demonstrates that whatever the stabilization mechanism, the addition product (III) eluted as I during HPLC Method 1. However, when the mobile phase had a pH of 2 (HPLC Method 2), the peak corresponding to I was missing in the chromatogram of the bisulfite–I mixture (Figs. 2A and 2B). The chromatogram in Fig. 2A was obtained from the sample represented in Fig. 1A; the chromatogram in Fig. 2B, which shows the absence of peak I, was obtained from the pH 2.5 sample represented in Fig. 1B. Therefore, in spite of high dilution during the HPLC procedure, when the mobile phase of low pH (pH 2) was used, III remained intact and did not elute as a peak corresponding to I. However, at pH 6.5, III rapidly reverted back to I; therefore, the peak resulting from III corresponds to I alone.

Another indication of the reversibility of III to I at pH 6.5 was obtained when equimolar (based on molar concentration of I) concentrations of I and the bisulfite–I mixture gave similar UV spectra (Fig. 3) at pH 6.5 (both I and the bisulfite–I mixture had λ_{max} of 239 nm, ϵ = 6800). However, at pH 2.5, the spectrum (Fig. 3) obtained from the bisulfite–I mixture was much less intense and different from that obtained with I (at pH 2.5, I had λ_{max} at 241, ϵ = 3700, and the bisulfite–I mixture had λ_{max} at 243, ϵ = 1900). Since the loss of absorption at 240 nm reflects the loss of the 5–6 double bond (8, 9), it is reasonable to suggest that the lower ϵ value at pH 2.5 of the bisulfite–I mixture was due to addition of bisulfite across this bond.

Stabilization Mechanism—The results of the present study indicate that bisulfite forms an addition product with I across the 5–6 double bond that is stable at low pH (*i.e.*, 2.5) and thus prevents the hydrolytic attack on the 5-azacytosine ring. The addition reaction at pH 2.5 is reversible and requires excess bisulfite to maintain the equilibrium in favor of the addition product. As seen in Table I, at pH 2.5, when the bisulfite concentration decreased, I stability also decreased. Based on these observations and in accordance with the hydrolysis mechanism proposed for I (9), it appears that the major reaction responsible for stabilization of I is as shown in Scheme II.

The formation of III proceeds through the protonation of N-5, similar to the protonation that usually precedes the nucleophilic attack on imine bonds (13) and as suggested for I hydrolysis (9). Therefore, formation of III (and, hence, stabilization of I against hydrolysis) is expected to increase as the pH is lowered and more I is protonated. If the pKa of I is assumed to be of the order of 2–3 from the reported pKa of the related

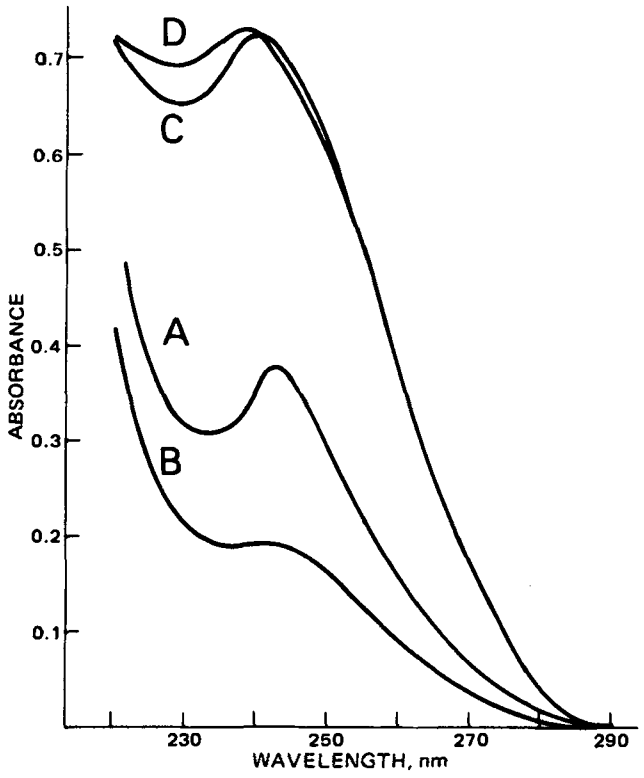

Figure 3—*UV spectrum of I and the bisulfite–I mixture in 0.05* M *phosphate buffer at different pH values. Concentration of I (or its equivalent) in the spectrophotometer cell was 30 μg/ml. Key: A, I in pH 2.5 buffer; B, bisulfite–I mixture in pH 2.5 buffer; C, I in pH 6.5 buffer; and D, bisulfite–I mixture in pH 6.5 buffer.*

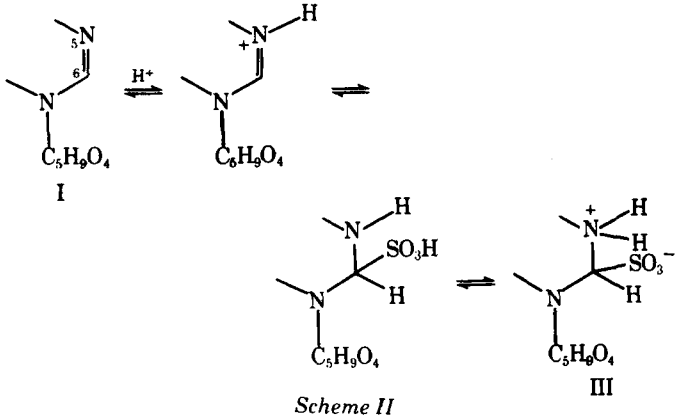

Scheme II

compound 5-azacytosine (9), the stabilization would be expected to increase as the pH is lowered below 4, provided the concentration of reactive nucleophile, bisulfite anion (HSO_3^-), is constant.

A substantial portion of sulfurous acid species would exist as the bisulfite anion up to pH 1.5 (pK_1 of sulfurous acid is 1.7), and increased I stability was observed up to pH 1.5. However, in strongly acidic solutions (*i.e.*, 1 *N* HCl), although I is expected to be completely protonated, the fraction of reactive nucleophile, bisulfite anion, is extremely small. Therefore, at very low pH, the addition reaction is expected to be slower. This was the case when a mixture of I and sodium bisulfite in 1 *N* HCl showed almost 90% free I after 1 min and 40% free I after 8 min (HPLC Method 2) whereas a mixture of the same concentrations of I and sodium bisulfite adjusted to pH 2 showed no free I (HPLC Method 2) even after 30 sec. This finding shows that the III formation rate is very fast at pH 2 but relatively slower in 1 *N* HCl.

To demonstrate that this slower rate is not due to an increase in the rate of reverse (desulfonation) reaction at this low pH, the bisulfite–I mixture[10] (where almost all I existed as III, Fig. 2B) was diluted with an equal volume of 2 *N* HCl and the resulting solution was analyzed by HPLC Method 2. The peak height due to I was 3, 20, and 40% of the theoretical amount of I after 0.5, 8, and 20 min, respectively. This finding

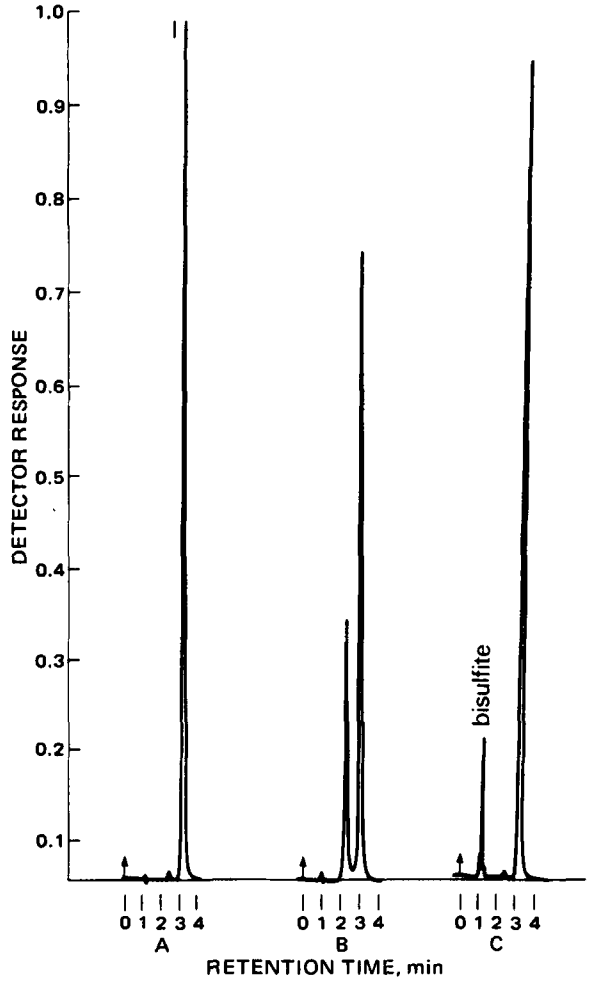

Figure 4—*Chromatograms obtained by HPLC Method 1 from samples of I (0.5 mg/ml). Key: A, freshly prepared solution of I in water; B, freshly prepared solution of I in 0.01* N *HCl; and C, sample in 4B after addition of sodium bisulfite (5.0 mg/ml).*

demonstrates that III does not decompose to I instantly in acidic solutions.

The degree of stabilization would also be influenced by the reverse reaction rate. The data presented in this paper indicate that the desulfonation rate of III to I is relatively slow at acidic pH whereas desulfonation is instantaneous at pH 6.5. It is unlikely that this fast reaction above pH 6 would be due to a direct replacement of bisulfite by hydroxyl ion followed by dehydration to yield I because (*a*) the hydroxyl-ion concentration is too small at pH 6.5 to compete effectively with bisulfite ion and (*b*) the product formed by the attack of hydroxyl ion would be expected to deaminate very fast at pH 6.5 (13). A more likely explanation is that, above pH 6, the cationic nitrogen of III would lose the proton and the resulting lone pair of electrons in N-5 would help in the desulfonation of III to I. At low pH (*i.e.*, pH ~2), the N-5 still would be protonated and desulfonation would be relatively slow. No further studies of this reaction were performed.

Catalysis of I Hydrolysis by Bisulfite at Neutral pH—The described stabilization mechanism of I by bisulfite does not explain why the I degradation rate above pH 4 is increased in the presence of bisulfite compared to buffer alone (Table I). As seen in Figs. 1C and 1D, the degradation product in the presence or absence of bisulfite at pH 7.0 is the same, *i.e.*, II. Therefore, the sulfurous acid species present at these pH values (pH 4–7) apparently does not form any other reaction product but catalyses I hydrolysis. Furthermore, the sulfite dianion appears to be a stronger catalyst than the bisulfite anion because bisulfite decreased I stability by a factor of 3 at pH 7 whereas the stability decrease was only 15% at pH 6, even though the total sulfurous acid concentration was the same (Table I). Since the pK_2 of sulfurous acid is ~6.7, it is reasonable to assume that faster degradation of I at pH 7.0 in bisulfite compared to that at pH 6.0 is due to the presence of a higher fraction of sulfurous acid species in the sulfite dianion form. No attempts were made to elucidate

further the mechanism of bisulfite-ion catalysis of I degradation.

Pharmaceutical Significance—*Parenteral Route*—The results of this study indicate that if the solution in I is maintained at pH 2.5 and if a five- to 10-fold excess of sodium bisulfite (relative to the concentration of I) is provided, I is stable (<10% degradation) for 20 hr at room temperature and for ~4 days at refrigeration temperature. This conclusion represents a substantial improvement in the stability of I in solutions. Further, the ready reversibility of the bisulfite–I addition product (III) to yield I at neutral pH values indicates that III will quickly convert to I in the body and thus act as a I prodrug. Such increased stability will assure better control over the preparation of the I infusion solutions and over the dose being administered.

The results of this study also indicate that 1–2 g of sodium bisulfite would be necessary to provide a stable solution of 200 mg of I[11] to be infused over 24 hr. Infusions of similar amounts of sodium bisulfite in commercial amino acid solution are used routinely, so it appears unlikely that addition of bisulfite would add significantly to the drug toxicity.

Oral Route—The mixture of I with bisulfite also holds promise as an oral dosage form. The administration of I alone is not practicable because of its relatively short stability at 37° over the pH range of the stomach and intestine. Furthermore, at the highly acidic stomach pH, a substantial portion of I would be in the hydrated form (IV) and, as suggested (9), the bioreversibility of IV to I at physiological pH may not be complete. Above pH 6.0, a significant portion of IV probably would deaminate to II and subsequent degradation products, and conversion of IV to I may not be quantitative.

This argument is supported by comparing the chromatogram of a solution of I in 0.01 *N* HCl (Fig. 4B) with that of the same concentrations of I in water (Fig. 4A) using HPLC Method 1. There was a 25% decrease in peak I and an increase in peak II immediately after dissolving I in 0.01 *N* HCl. After further storage, there was a more gradual decrease in peak I in Fig. 4B (an additional 10% decrease in peak I after 20 min at room temperature). Based on the stability studies of I at acidic pH (9), it is unlikely that a 25% loss of I would occur instantly at pH 2 (0.01 *N* HCl); therefore, it must be attributed to the decomposition of IV during HPLC with pH 6.5 buffer as the mobile phase. This conclusion is substantiated by the fact that when bisulfite was added to the solution of I in 0.01 *N* HCl (Fig. 4B), the chromatogram showed complete loss of peak II and an increase in peak I to approximately the original height of peak I in Fig. 4A (Fig. 4C). If II were already present in the sample of Fig. 4B in 0.01 *N* HCl, it is unlikely that it would cyclize immediately and yield I upon addition of the bisulfite. Therefore, in the presence of bisulfite in acidic pH, IV apparently is converted to III, which then elutes as I in HPLC Method 1 as discussed earlier.

This discussion indicates that a significant portion of IV resulting from dissolving I in acidic pH in the absence of bisulfite does not reverse back to I on reaching physiological pH. However, a mixture of I and sodium bisulfite would quickly form a relatively stable compound (III) in the acidic pH of the stomach and then rapidly revert back to I above pH 6. Thus, drug absorbed in the stomach probably would quickly release I on reaching the higher pH (7.4) of blood. Although the stability of the bisulfite–I mixture at the higher pH of the ileum is uncertain, a mixture of I with bisulfite as an oral preparation holds promise as a stabilized dosage form during its passage through the stomach and warrants further investigation by the oral route. The toxicity and efficacy of III and its application in developing suitable dosage forms of I are presently being investigated.

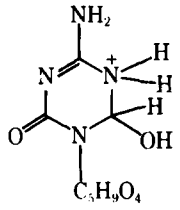

IV

[11] Usual daily dose of I is 100–200 mg/ml.

REFERENCES

(1) D. D. Von Hoff, M. Slavik, and F. M. Muggia, *Ann. Intern. Med.*, **85**, 237 (1976).

(2) M. Karon, S. Sieger, S. Leimbrock, J. E. Finkelstein, M. Nesbit, and J. J. Swaney, *Blood*, **42**, 259 (1973).

(3) K. B. McCredie, G. P. Bodey, M. A. Burgess, J. U. Gutterman, V. Rodriguez, M. P. Sullivan, and E. T. Freireich, *Cancer Chemother. Rep.*, **57**, 319 (1973).

(4) W. R. Vogler, S. Arkun, and E. Velez-Garcia, *ibid.*, **58**, 895 (1974).

(5) C. G. Moertel, A. J. Schutt, R. J. Reitemeier, and R. G. Hahn, *ibid.*, **56**, 649 (1972).

(6) W. R. Vogler, D. S. Miller, and J. W. Keller, *Blood*, **48**, 331 (1976).

(7) P. L. Lomen, L. H. Baker, G. L. Neil, and M. K. Samson, *Cancer Chemother. Rep.*, **59**, 1123 (1975).

(8) J. A. Beisler, *J. Med. Chem.*, **21**, 204 (1978).

(9) R. E. Notari and J. L. DeYoung, *J. Pharm. Sci.*, **64**, 1148 (1975).

(10) P. Pithova, A. Piskala, J. Pittia, and F. Sorm, *Collect. Czech. Chem. Commun.*, **30**, 2801 (1965).

(11) J. A. Beisler, M. M. Abbasi, and J. S. Driscoll, *Cancer Treatment Rep.*, **60**, 1671 (1976).

(12) J. A. Beisler, M. M. Abbasi, J. A. Kelley, and J. S. Driscoll, *J. Med. Chem.*, **20**, 806 (1977).

(13) W. P. Jencks, "Catalysis in Chemistry and Enzymology," McGraw-Hill, New York, N.Y., 1969, pp. 490–496.

In Vitro Nitrosation of Methapyrilene

WILLIAM J. MERGENS *x, FLOIE M. VANE *, STEVEN R. TANNENBAUM ‡, LAURA GREEN ‡, and PAUL L. SKIPPER ‡

Received October 5, 1978, from **Hoffmann-La Roche Inc., Nutley, NJ 07110*, and the ‡*Massachusetts Institute of Technology, Cambridge, MA 02139.* Accepted for publication December 18, 1978.

Abstract □ The reactions of sodium nitrite and methapyrilene were studied in aqueous solution at neutral pH and under simulated gastric fluid conditions. Reaction product formation was much more complex than nitrosation of the parent molecule dimethylamino moiety to form nitrosodimethylamine. Several new nitroso compounds were formed under the reaction conditions studied. The simultaneous incorporation of 2 moles of ascorbic acid/mole of nitrite ion prevented any destruction of methapyrilene under all conditions studied. The implications of these observations with respect to nitrosation theory, the general carcinogenicity of nitroso compounds, and methapyrilene dosage formulation are discussed.

Keyphrases □ Methapyrilene—nitrosation, *in vitro*, with sodium nitrite, nitrosodimethylamine formation, effect of pH, prevented by ascorbic acid □ Ascorbic acid—methapyrilene nitrosation, prevention of nitrosodimethylamine formation, *in vitro* □ Nitrosodimethylamine—formation from methapyrilene, prevention by ascorbic acid, *in vitro* □ Carcinogens—nitrosodimethylamine, formation from methapyrilene, prevention by ascorbic acid, *in vitro*

The formation of *N*-nitroso compounds by interaction of nitrite or other nitrosating agents such as gaseous nitrogen dioxide or dinitrogen trioxide with susceptible amines has received much attention over the past few years (1). A recent survey showed that of 100 nitrosamines studied, 80% were carcinogenic in animal studies (2).

BACKGROUND

No animal species has proved immune so far to the carcinogenicity of *N*-nitroso compounds (3, 4). Dimethylnitrosamine, the simplest dialkyl nitrosamine, is carcinogenic in a wide variety of species including the mouse, hamster, mink, rat, guinea pig, rabbit, and rainbow trout. Dimethylnitrosamine is carcinogenic in the mink at the lowest dose tested in rodents, 50 μg/kg, given twice per week in the diet (5). In addition, the carcinogenicity of *N*-nitrosamines is organospecific. In the rat, for example, dimethylnitrosamine is a liver carcinogen regardless of the administration route (6).

These results are of particular concern to humans, because many of these suceptible amines are commonly ingested as pharmaceuticals, pesticide residues, and normal components of food. Additionally, nitrite is produced by microbiological nitrate reduction in the mouth and is ingested from exogenous sources such as cured meat products and many vegetables.

Ascorbic acid inhibits this reaction, as was first demonstrated in an *in vitro* study (7) in 1972. This protective effect of ascorbic acid was extended to *in vivo* studies (8), which demonstrated that aminopyrine–nitrite-induced hepatotoxicity in rats could be completely abolished by the concomitant feeding of sodium ascorbate.

The mechanism of this protective effect by ascorbic acid is currently believed to be due to the ability of ascorbic acid to compete successfully with susceptible amines for the available nitrite (nitrosating species) ion. This premise is based on detailed studies (9) of the anaerobic oxidation of ascorbic acid by nitrous acid. The initial attack by the nitrosating species on the 3-hydroxy group of ascorbic acid forms the nitrite ester, which subsequently decomposes to yield the semiquinone. Further reaction of the semiquinone with an additional mole of nitrosating species completes ascorbate oxidation to dehydroascorbic acid. This work was extended (10) to aerobic systems, and a kinetic model was developed that predicted the amount of ascorbate required to inhibit completely nitrosation of an amine in the presence of ascorbic acid.

Since that time, the conditions required for ascorbic acid to prevent nitrite-induced reactions involving many different amine substrates have needed evaluation. The subject of the present study is methapyrilene, a tertiary pharmaceutical amine found in many over-the-counter antihistamine and sleep aid products. A significant incidence of liver tumors and other liver lesions was reported in rats fed an aqueous solution of methapyrilene plus sodium nitrite (11). The authors presumed that this hepatotoxicity was due to dimethylnitrosamine formation in the stomach of the test animals. The present study was undertaken to investigate the methapyrilene reaction with nitrite and the potential utility of ascorbic acid in protection of methapyrilene from such reactions.

EXPERIMENTAL

Materials and Methods—Methapyrilene hydrochloride[1] was commercial grade. Sodium nitrite[2] and isopentyl nitrite[3] were used as sources of nitrosating intermediates. Redistilled methylene chloride was used for all sample extractions and workups.

Nitrosated Standards—*Nitrosation of* N-(*2-Pyridyl*)-N′-*dimethylethylenediamine* (*VIII*)—The amine was purified by dissolving it in hydrochloric acid, extracting with methylene chloride, basifying the aqueous phase, and extracting the amine with ether.

The amine (165 mg, 1 mmole) was dissolved in 4 ml of ether and treated with 1 ml of isopentyl nitrite. After standing overnight, a gummy residue precipitated. The ether solution was decanted and heated to evaporate the solvent. Alcohol (7 ml) was added, and the resultant solution was evaporated by boiling and then under a nitrogen stream. The product (IX) was obtained as a reddish oil, pure by TLC.

Nitrosation of 2-(2-Thienylmethylamino)pyridine (*V*)—The recrystallized amine had a sharp melting point and dissolved cleanly in ether. One millimole (190 mg) was treated with 1.5 ml of isopentyl nitrite in 4 ml of ether for 2 days. The product (VI) was worked as for IX and yielded a reddish oil, pure by TLC. Both products were confirmed as nitrosamines by the use of UV photolysis and Griess reagent on their chromatograms.

Analyses—Methapyrilene determinations were performed by GLC[4] on an instrument equipped with a flame-ionization detector. The column, a 1.83-m × 0.635-cm o.d. 8% methyl silicone gum rubber[5] glass U-tube, was operated isothermally at 240° with a helium flow rate of 50 ml/min. Samples were injected as the free base after the reaction mixture had been rendered alkaline with sodium hydroxide and the compound had been extracted into distilled methylene chloride.

The reaction products of methapyrilene with sodium nitrite were extracted as outlined and analyzed by a combined GLC–mass spectrometer[6] system interfaced with a data dystem[7]. Methane was used as the GLC carrier gas and as the chemical-ionization reagent gas. A 1.02-m × 0.32-cm o.d. 3% methyl silicone gum rubber[5] column was used at an initial temperature of 140° and a programmed rate increase of 10°/min. The mass range of *m/e* 60–460 was scanned in 2 sec.

Electron-ionization mass spectrometry of the nitrosated standards of *N*-(2-pyridyl)-*N*′-dimethylethylenediamine and 2-(2-thienylmethylamino)pyridine were obtained by mass spectrometry[8] using a chamber voltage of 70 (standard ionizing voltage). Several columns were tried for GLC–electron-ionization mass spectrometry, with terephthalic acid-treated polyethylene glycol[9] proving the most useful. Injector temperatures of 150–200° and lower were compared.

TLC studies were performed using precoated 15-cm silica plates with and without the fluorescent additive for visualizing UV-absorbing compounds, as required. The solvent system was hexane–ether–meth-

[1] Lot 072/02470, J. B. Williams Co., Jersey City, N.J.
[2] J. T. Baker Chemical Co., Phillipsburg, N.J.
[3] Aldrich Chemical Co., Milwaukee, Wis.
[4] Model 220, Tracor Instruments, Austin, Tex.
[5] Se-30.
[6] Model 1015D, Finnigan Corp., Sunnyvale, Calif.
[7] Model 6000, Finnigan Corp., Sunnyvale, Calif.
[8] Hitachi-Perkin-Elmer RMU 6E mass spectrometer, Perkin-Elmer Corp., Norwalk, Conn.
[9] Carbowax 20M/TPA.

0022-3549/79/0700-0827$01.00/0
© 1979, American Pharmaceutical Association

Table I—TLC R_f Values for Methapyrilene and Some Reaction Products on Silica Gel G

Compound	R_f Value	Reaction to Spray Reagent		
		Iodoplatinate	Griess	Isatin
I	0.5	+	−	+
III	0.4	+	−	+
VIII	0.25	+	−	−
IX	0.55	+	+	−

ylene chloride–methanol–concentrated ammonium hydroxide (40:15:20:10:0.25).

All compounds were visualized by UV on fluorescent plates. Nitrosamines were further identified by spraying the plate with Griess reagent followed by exposure to longwave UV light, which caused them to appear as pink spots. Basic nitrogen compounds were differentiated by spraying with iodoplatinate reagent, and thienyl compounds were detected by isatin reagent (12). The R_f values were not highly reproducible (probably because some components of the solvent system are very volatile). The compounds, in order of increasing R_f values, were VIII, I, IX, V, and VI (Scheme I and Table I).

Nitrosamine analyses are most conveniently and quite specifically performed using a thermal energy analyzer (13). This detector can be coupled with either a gas or liquid chromatograph. The nitrogen–nitrogen bond of the nitrosamine (nitrosamide) is thermally split in a pyrolysis chamber. The resulting reaction products, parent amine (or amide) plus the liberated nitric oxide radical, and any other components that emerge from the pyrolysis oven are then swept through a cold trap. The nitric oxide radical, one of the few substances that will not be trapped, passes into the reaction chamber where it is oxidized with ozone to yield an excited nitrogen dioxide molecule. As this molecule relaxes to the ground

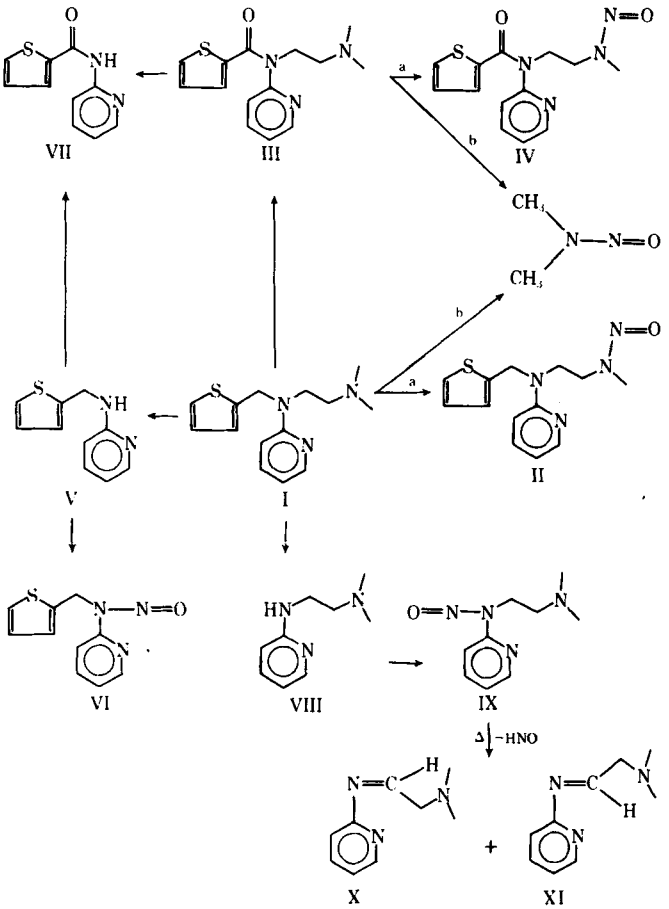

Scheme I—Proposed reaction products of methapyrilene with sodium nitrite. The reaction products of I and III arise through nitrosative attack on the dimethylamino group. When the leaving group is $-CH_3$, the resulting product is the unsymmetrical dialkylnitrosamine (path a). When the leaving group is the substituted ethyl, both I and III yield nitrosodimethylamine (path b).

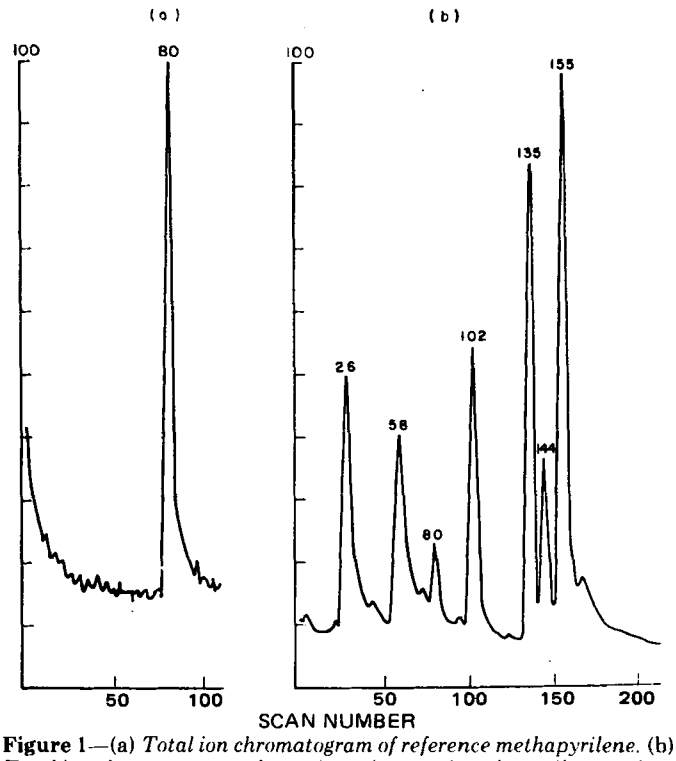

Figure 1—(a) *Total ion chromatogram of reference methapyrilene.* (b) *Total ion chromatogram of reaction mixture of methapyrilene and nitrite.*

state, it emits a characteristic energy (in the near IR), which is detected using a photomultiplier tube.

Nitrosodimethylamine analyses were performed by a GLC–thermal energy analyzer using a column of polyethylene glycol[10] on a potassium hydroxide-treated support. Methylene chloride solutions were generally analyzed isothermally at 145° and an attenuation of 0.1. Some analyses were performed using a temperature program between 100 and 180° at an attenuation of 0.1, when solvent tailing under isothermal conditions presented an analytical problem.

Compounds VI, IX, nitrosodimethylamine, and the reaction products of methapyrilene and nitrite at 37° were examined using a high-pressure liquid chromatography (HPLC)–thermal energy analyzer. These studies employed a prepacked column[11] and a mobile phase of 95% isooctane/5% acetone at a flow rate of 2 ml/min. The thermal energy analyzer detector was operated with an oven temperature of 450° and a reaction chamber pressure of 2 torr. The cold trap was held in a dry ice–isopropyl alcohol bath.

Reactivity of Methapyrilene with Nitrite as a Function of Temperature—Methapyrilene solutions (1 mg/ml) were prepared in pH 3.7 acetate buffer. Mole ratios of sodium nitrite to methapyrilene were adjusted by adding solid sodium nitrite to the solution to yield 8.6, 4.3, 1.0, and 0.5 mole ratios. Reactions were carried out by sealing 10-ml aliquots of the reaction mixtures in 20-ml amber all-glass ampuls. Reaction temperatures of 90, 70, 50, and 37° were maintained by immersion of the samples in constant-temperature water baths. Reaction time was 4 hr. Samples were stored under refrigeration pending analyses. In this particular study, nitrosodimethylamine determinations were performed by GLC using an electrolytic conductivity detector[12] operated in the reductive mode without a catalyst (14).

Mild Reaction Conditions—Studies were performed under simulated gastric fluid conditions at 37° and pH 3.7 for 4 hr in glass-stoppered vessels. The methapyrilene concentration was 1 mg/ml, and the sodium nitrite concentration was 2 mg/ml.

For a similar experiment involving the production of nitrosodimethylamine over 1–5 days under room temperature conditions at pH 6.2, the following sample workup was used. During storage, the samples were shielded from light. Afterwards, each sample was extracted with 3 × 100 ml of methylene chloride, dried over sodium sulfate, and con-

[10] Carbowax 20M.

[11] μPorisil, Waters Associates, Milford, Mass.

[12] Model 310, Hall electrolytic conductivity detector, Tracor Instruments, Austin, Tex.

Table II—Reaction of Methapyrilene with Nitrite as a Function of Temperature and Mole Ratio [a]

Nitrite–Methapyrilene Mole Ratio	Methapyrilene Analysis, % retention				Nitrosodimethylamine at 90°, % of theory
	90°	70°	50°	37°	
8.6:1	2	50	97	99	12
4.3:1	7	59	96	99	8
1:1	47	67	98	99	0.1
0.5:1	75	82	98	100	<0.04

[a] Reaction time was 4 hr using pH 3.7 acetate buffer. Methapyrilene = 1 mg/ml.

centrated to 10 ml in an apparatus[13]. Heptane, 1 ml, was added, and the sample was further concentrated to 1 ml with nitrogen. Samples were then quantitatively vacuum transferred to remove nonvolatile material and analyzed by the GLC–thermal energy analyzer on a polyethylene glycol[10]–potassium hydroxide-treated column at 100°.

Ascorbic Acid Influence—The influence of ascorbic acid on the nitrite–methapyrilene reaction was evaluated by incorporating 0–2 moles of ascorbic acid/mole of sodium nitrite present. In all cases, the reaction mixture pH was adjusted to compensate for the acid addition.

RESULTS AND DISCUSSION

Methapyrilene Reaction Products—The methapyrilene molecule contains a dimethylamine moiety, which could be a potential source of nitrosodimethylamine. Tertiary amines have been reported to undergo nitrosative dealkylation to form a nitrosamine in the presence of a nitrosating intermediate (15, 16). The optimum condition for many aqueous nitrosations is usually about pH 3.4, the pKa for nitrous acid. This pH generally reflects the mutual optimization of the two reactive species: (*a*) the formation of the nitrosating intermediate, which increases with increasing acid concentration, and (*b*) the concentration of the unprotonated, more electrophilic form of the amine, which is, of course, dependent on the pKa of the specific base.

Reaction Products of Methapyrilene and Nitrite—Methapyrilene nitrosation at pH 3.7 was investigated as a function of temperature and mole ratio of nitrite (Table II). At 90° with an 8.6 mole excess of nitrite, the parent amine almost completely disappeared. As the temperature and mole ratios decreased, the stability of methapyrilene substantially increased.

GLC-Chemical-Ionization Mass Spectrometric Analysis—These analyses were performed to identify the reaction products at 90° and the highest mole ratio of nitrite. The total ion chromatograms for the reference standard (methapyrilene base) and a sample containing a mixture of the methylene chloride-extractable reaction products obtained under different reaction conditions are reproduced in Fig. 1. Proposed structures for the individual reaction products can be found in Scheme I and Table III. No definite structure could be made for scan 144. The presence of a carbonyl function in III, IV, and VII was confirmed by GLC coupled to an IR detection system[14].

At 90°, the major reaction product appeared to be III, in which the methylene bridge between the ethylenediamine and thienyl moieties had been oxidized to a keto group. One possible mechanism for the formation of such an amide structure would involve attack of the nitrosyl ion on this group to form a C-nitroso compound, which could rearrange to the corresponding oxime. Hydrolysis of the oxime would subsequently yield the amide plus hydroxylamine.

One interesting aspect of this experiment can be seen in Table II. At 90°, a definite break in both methapyrilene retention and nitrosodimethylamine formation occurred at nitrite–methapyrilene mole ratios at and below 1:1 compared to the higher ratios. Not only was the retention of the parent compound improved, but the conversion of methapyrilene to nitrosodimethylamine was almost negligible. One interpretation of this observation would indicate that the parent amine consumes 1 mole of nitrite prior to attack of the dimethylamino function. This idea is supported by the fact that III was the principal oxidation product under these conditions. Moreover, the dealkylation products observed at 90° involved cleavage of the parent molecule in the ethylenediamine portion of the molecule and not in the thienyl moiety (*viz.*, V and VII).

Table III—Molecular Weights of the Products of the Reaction of Methapyrilene (I) and Sodium Nitrite

Peak, scan number	Molecular Weight	Possible Structure
26	190	V
58	204	VII
80	261	I
102	275	III
135	276	II
155	290	IV

[13] Kuderna-Danish, SGA Scientific Inc., Bloomfield, N.J.
[14] RS1, Norcon Inc., Norwalk, Conn.

Room Temperature Storage—Based on these findings, the system was reexamined using considerably less stringent reaction conditions to identify the initial reaction products. Solutions of 1 mg of methapyrilene/ml of distilled water were stored at room temperature in the presence of 2 mg of sodium nitrite/ml. The pH of this mixture was 6.6. Under these conditions, substantial conversion (~1%/day) of the parent compound into *N*-(2-pyridyl)-*N'*-dimethylethylenediamine (VIII) was observed (Table IV). In the absence of nitrite, on the other hand, no deterioration of the parent compound was observed under identical storage periods. The appearance of this particular secondary amine is not unusual because its synthesis involves a cleavage of the activated methapyrilene methylene bond. One can only speculate as to why it was not observed at 90°.

Compound VIII was isolated by TLC at R_f 0.25 (Table I), and its identity was confirmed by GLC–mass spectrometric analysis of both the free amine and its trimethylsilyl derivative. Furthermore, it behaved identically to a known standard in all tests performed. The nitrosation of VIII was studied in simulated gastric fluid (pH 1.3) and acetate buffer (pH 3.7) using the same amine and nitrite-ion concentrations described for methapyrilene. After 4 hr of reaction, both samples were more than 90% converted to the corresponding nitrosamine. After 24 hr, the reaction was essentially complete in both cases as estimated by TLC.

The nitrosamine was separated from the reaction mix with methylene chloride and isolated by solvent evaporation. IR spectrophotometry confirmed the presence of a nitroso group and indicated a structure compatible with IX. The fact that VIII reacted more readily with nitrite than methapyrilene is understandable since it is a secondary amine. Secondary amines classically are the most readily nitrosated amines, with the exception of the tertiary amine aminopyrine (17).

Further confirmation of the structure of the nitroso derivative of VIII by direct mass spectrometry was attempted. The compound yielded a fairly clean spectrum in which the highest *m/e* was 163, corresponding to M − 31 for the *N*-nitroso derivative of VIII (inlet temperature of 160°). When the inlet temperature was lowered to 65°, a similar spectrum was obtained, but with additional peaks at *m/e* 164 and 179, presumably M − 30 and M − 15, respectively. In neither case was the molecular ion observed, so the resulting spectra, while consistent with the structure of IX, cannot be considered firm evidence that the desired product was obtained. GLC–mass spectrometry on terephthalic acid-treated polyethylene glycol[9] yielded complex chromatograms with injector temperatures at 150–200°. Lower injector temperatures gave simpler chromatograms, but this result may have been due either to less decomposition or simply to fewer components being flash evaporated.

Useful mass spectra were obtained for only two of these components. Both gave an apparent molecular ion at *m/e* 163 and probably correspond to the isomeric imines formed by HNO elimination of the parent nitrosamine during GLC (X and XI, Scheme I).

Similarly prepared samples were also analyzed for nitrosodimethyl-

Table IV—Oxidation of Methapyrilene (1 mg/ml) in Water at pH 6.6 in the Presence of Nitrite (2 mg/ml)

Hours at Room Temperature	Percent VIII[a]
24	0.5
48	1.8
72	2.5
98	4
168	7.5

[a] Estimations by TLC compared to an authentic standard.

Table V—Effect of Ascorbic Acid on the Methapyrilene–Nitrite Reactions

Ascorbic Acid–Nitrite Mole Ratio	Concentrations[a]	Reaction Conditions[b]	pH	Percent Present			
				Methapyrilene[c]	III[d]	VII[d]	Nitrosamine[d]
0:1	A	1	3.7	91	+	+	—
0.5:1	A	1	3.7	94	+	+	—
1:1	A	1	3.7	98	+	+	—
2:1	A	1	3.7	100	ND	ND	—
0:1	B	1	3.7	89	+	+	—
0.5:1	B	1	3.7	99	+	+	—
1:1	B	1	3.7	100	+	+	—
2:1	B	1	3.7	100	ND	ND	—
0:1	A	2	3.7	—	—	10	+
0.5:1	A	2	3.7	—	—	5	+
1:1	A	2	3.7	—	—	1–2	+
2:1	A	2	3.7	—	—	ND	ND
0:1	B	2	3.7	—	—	10	+
0.5:1	B	2	3.7	—	—	4	+
1:1	B	2	3.7	—	—	2	+
2:1	B	2	3.7	—	—	ND	—
0:1	A	3	6.6	—	ND	1	—
2:1	A	3	6.6	—	ND	ND	—
0:1	A	4	6.6	—	ND	4	—
2:1	A	4	6.6	—	ND	ND	—
0:1	A	5	1.0	—	ND	2	—
2:1	A	5	1.0	—	ND	ND	—
0:1	A	5	2.0	—	ND	<0.2	—
2:1	A	5	2.0	—	ND	ND	—
0:1	A	5	3.0	—	ND	<0.2	—
2:1	A	5	3.0	—	ND	ND	—
0:1	A	5	4.0	—	ND	<0.2	—
2:1	A	5	4.0	—	ND	ND	—
0:1	A	5	5.0	—	ND	0.2	—
2:1	A	5	5.0	—	ND	ND	—

[a] A, sodium nitrite = 2 mg/ml and methapyrilene = 1 mg/ml; and B, sodium nitrite = 10 mg/ml and methapyrilene = 5 mg/ml. [b] 1 = acetate buffer, 37°, 36 hr; 2 = acetate buffer, room temperature, 10 days; 3 = distilled water, room temperature, 21 hr; 4 = distilled water, room temperature, 4 days; and 5 = simulated gastric fluid, 37°, 4 hr. [c] Analysis by GLC. [d] Estimation by TLC. The + indicates that the compound was present but not estimated, and ND indicates that none was detected. Estimation of VII was based on a methapyrilene standard.

amine with the GLC–thermal energy analyzer after 1- and 5-day periods. The 1-day sample contained 0.33 ppm and the 5-day contained 0.104 ppm of nitrosodimethylamine. These values correspond to 16.5 and 5.2 μg of nitrosodimethylamine/50 mg of methapyrilene. The nitrosodimethylamine loss between Days 1 and 5 was due to chemical–physical factors that caused aqueous solutions of this nitrosamine to be unstable over long periods. The fact remains, however, that some production of nitrosodimethylamine can take place even under such mild conditions.

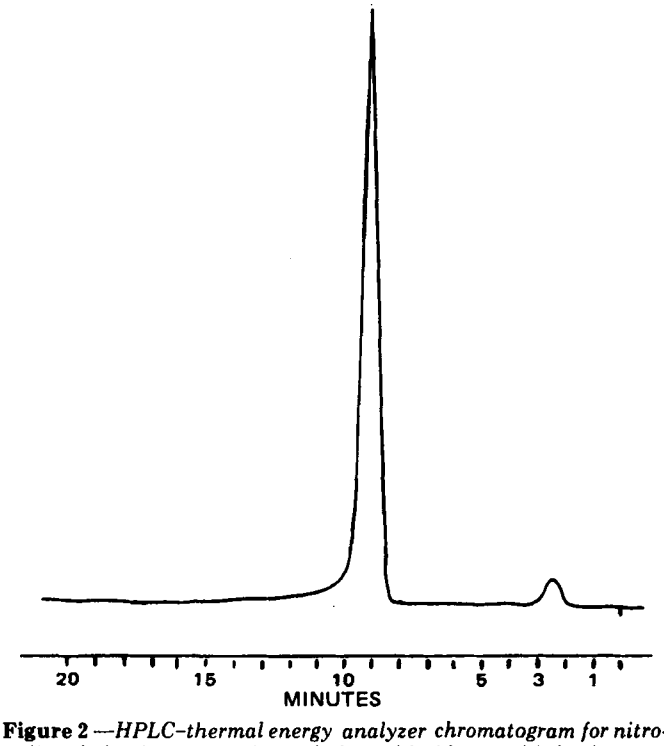

Figure 2—*HPLC–thermal energy analyzer chromatogram for nitrosodimethylamine, 5 ppm in methylene chloride, 10-μl injection, and attenuation 128×.*

Gastric Fluid Conditions—The potential for nitrosamine formation between an amine and nitrite is greatly enhanced under gastric fluid conditions as compared to the neutral solution. This situation directly relates to the hydrogen-ion influence on the nitrosating intermediate formation through the nitrite–nitrous acid equilibria (Schemes II and III):

$$NO_2^- + H^+ \rightleftharpoons HONO$$

Scheme II

$$2HONO \rightleftharpoons N_2O_3 + H_2O$$

Scheme III

The studies performed here for the methapyrilene system after 4 hr under simulated conditions yielded the following results. Conversion of methapyrilene to nitrosodimethylamine was 150 ng/ml from a maximum theoretical yield of 250 μg/ml, which represents a 0.06% conversion by GLC–thermal energy analyzer analysis. In addition to nitrosodimethylamine, several other peaks appeared in the HPLC–thermal energy analyzer chromatogram. The first peak in all HPLC–thermal energy analyzer chromatograms, appearing at 3 min after injection, was a solvent front response; it did not correspond to an *N*-nitroso compound, and its magnitude was unimportant. The remaining peaks corresponded to the same peaks derived from the nitroso derivative of V and the nitroso derivative of VIII standards, although not all peaks could be accounted for in this manner. Nitroso V represented yet another nitrosamine derivative, which could be formed from methapyrilene (Figs. 2–4).

These observations have important implications with respect to the experimental handling of methapyrilene–nitrite solutions, especially in animal feeding experiments such as those described previously (11). The present results indicate that the experimental protocol of mixing methapyrilene and sodium nitrite in drinking water prior to ingestion by test animals could lead to preformed nitrosodimethylamine in quantities (0.1–0.3 ppm in drinking water) comparable to those formed by incubation under simulated gastric fluid conditions for 4 hr. In addition, the substantial conversion of the parent amine to VIII complicates the scheme by introducing a secondary amine that has been shown to nitrosate much more rapidly than the parent amine under simulated gastric fluid conditions at 37°. For this and other reasons, caution should

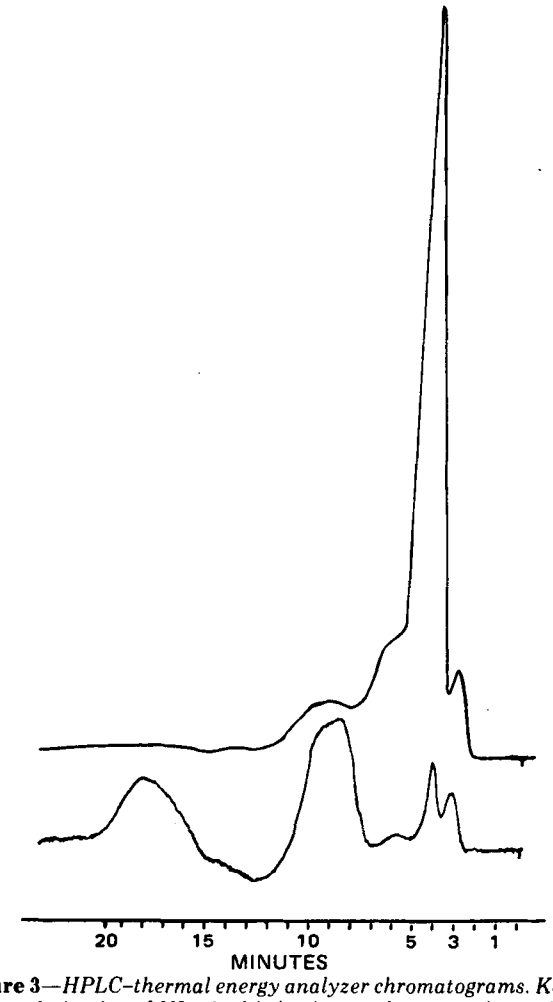

Figure 3—*HPLC–thermal energy analyzer chromatograms. Key: top, nitroso derivative of VI, 10-μl injection, and attenuation 128×; and bottom, nitroso derivative of IX, 10-μl injection, and attenuation 32×.*

be used in the interpretation of carcinogenicity experiments as solely the result of *in vivo* nitrosation of the parent amine.

Ascorbic Acid Effect—Ascorbic acid was applied successfully as a nitrosamine inhibitor in a number of *in vivo* (8, 18) and *in vitro* (7) systems involving drug nitrosation. Table V summarizes the results for the application of various mole ratios of ascorbic acid to nitrite ion for two different concentrations of nitrite and methapyrilene under different reaction conditions. As predicted (10), the presence of 2 moles of ascorbic acid/mole of nitrite was effective in preventing oxidative and nitrosative damage to the methapyrilene molecule. This result was true for all reaction conditions (Table V). Results not reported in Table V indicate that ascorbic acid is just as effective a protective agent at 90°. Although TLC results can be considered encouraging, this procedure lacks the sensitivity and specificity afforded by the thermal energy analyzer.

Analyses of methapyrilene–nitrite mixtures containing 2 moles of ascorbic acid/mole of nitrite were performed with the thermal energy analyzer. The reaction conditions were the same as those described under *Experimental* for 5 days at room temperature and 4 hr in simulated gastric fluid at 37°. No thermal energy analyzer responsive peaks were detected in either sample (Fig. 5). Based on the lowest detectable limit for nitrosodimethylamine under the conditions of analysis, a maximum of 0.0001% of nitrosodimethylamine could be present in the ascorbic acid-containing samples in contrast to 0.06 and 0.03% of this nitrosamine found in the gastric fluid and 1-day room temperature samples, respectively. These results indicate that ascorbic acid is an extremely effective agent in protecting against methapyrilene nitrosation. Hence, it follows that susceptible pharmaceutical amines could be safeguarded against *in vivo* nitrosation if they were compounded with ascorbic acid.

This suggestion has already been made (7). Technologically, however, other considerations come into play. If the nitrosation rate of the amine is sufficiently slower than the ascorbate and nitrite reaction, one can safely conclude that *in vivo* nitrosation of the amine will be halted successfully. Aside from kinetic considerations, this would presume that the ascorbic acid solution rate is comparable to or better than that for the susceptible amine. One formulation approach to assure this could be a T-T tablet with ascorbic acid comprising the outer tablet.

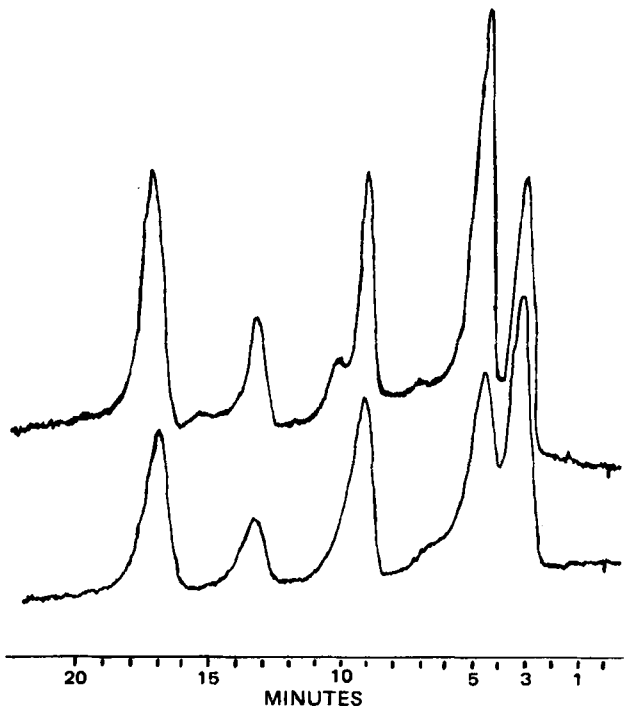

Figure 4—*HPLC–thermal energy analyzer chromatograms. Key: top, methapyrilene dissolved in sterile distilled water and immediately reacted with nitrite for 4 hr at 37°, 10-μl injection of methylene chloride extract, and attenuation 16×; and bottom, methapyrilene incubated at room temperature in sterile distilled water for 7 days and then reacted with nitrite for 4 hr at 37°, 10-μl injection of methylene chloride extract, and attenuation 32×.*

Recent experimental work has shown that yet another precaution must be taken. Aminopyrine is a popular headache remedy on the European market. It is also a tertiary amine, which nitrosates extremely rapidly in

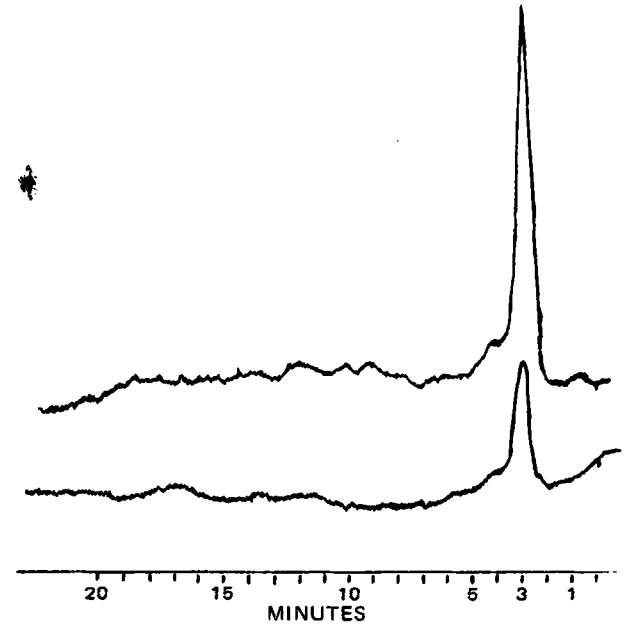

Figure 5—*HPLC–thermal energy analyzer chromatograms. Key: top, same as Fig. 4 (top) with twice molar ascorbic acid added with nitrite, 10-μl injection of methylene chloride extract, and attenuation 16×; and bottom, same as Fig. 4 (bottom) with twice molar ascorbic acid, 10-μl injection of methylene chloride extract, and attenuation 16×.*

the presence of nitrite to yield nitrosodimethylamine (20). Eisenbrand *et al.* (21) showed that tablets containing 300 mg of aminopyrine and protected with 160 mg of ascorbic acid contained 88, 89, and 57 μg/kg of nitrosodimethylamine as purchased. These same tablets, when exposed for about 12 hr to a continuous air flow containing 1 ppm of nitrogen dioxide, comparable to many urban atmospheres (chamber volume of 50 m^3, air flow of 50 m^3/hr), were found to contain 5090 μg/kg of nitrosodimethylamine. Obviously, the heterogeneous admixture of aminopyrine and ascorbic acid in a tablet of this nature is less than effective in protecting the aminopyrine crystals from attack by nitrogen dioxide molecules.

Aminopyrine is unusual in being a tertiary amine that is more rapidly nitrosated than most secondary amines. This fact is at least justified under aqueous nitrosation conditions if one considers that its pKa is 5.04. Whether or not the same aberrant behavior extends to its ability to be directly nitrosated by gaseous nitrogen dioxide as compared to other amines is not known.

Successful tablet formulations containing ascorbic acid to protect against the nitrosation of a susceptible amine should preclude the possibility of direct gas phase exposure of the amine to nitrogen dioxide or contain suitable experimental assurances that this nitrosation route is not possible. Protection of this type of susceptible amine would probably involve encapsulation of the amine crystals or possibly the entire tablet with a suitable barrier.

SUMMARY AND CONCLUSIONS

Methapyrilene contains a dimethylamine moiety, which, on the basis of previous studies (8, 15), was suspected of reacting with a nitrosating intermediate to form nitrosodimethylamine, a potent animal carcinogen. The present studies demonstrated that very small yields of nitrosodimethylamine are obtained in neutral solutions at room temperature after 1 day and also under conditions simulating gastric digestion (*i.e.*, 4 hr at 37° at pH 3.7). Severe reaction conditions (4 hr at 90° at pH 3.7) are required to obtain high yields (over 20%) in the reaction of methapyrilene with nitrite.

In near neutral solution at room temperature and under conditions simulating the environment of the stomach, the major pathway for the reaction of methapyrilene and nitrite is completely different than that leading to nitrosodimethylamine formation. One observed reaction is the formation of the secondary amine *N*-(2-pyridyl)-*N'*-dimethylethylenediamine (VIII) through nitrite oxidation of the thiophene-activated methylene bridge of the parent amine. A recent report (22) indicating that methapyrilene is metabolized *in vivo* to nonsulfur-containing metabolites tends to support this finding. Another secondary amine can be formed by removal of the side chain on the central nitrogen in the molecule leading to 2-(2-thienylmethylamino)pyridine. Evidence suggests that the formation of these secondary amines could lead to the generation of the corresponding nitrosamines under the acid conditions of the stomach.

Ascorbic acid, when present in a 2:1 molar ratio to nitrite ion, was completely effective in preventing the oxidative and nitrosative damage of the methapyrilene molecule in all systems studied.

The production of small, but toxicologically significant, amounts of nitrosodimethylamine and ~1%/day of VIII from methapyrilene under neutral aqueous conditions in the presence of nitrite indicates that caution should be exercised in any experimental protocol involving solution storage for the following reasons. Animal feeding studies cannot preclude the presence of preformed nitrosamines (*e.g.*, nitrosodimethylamine). In addition, ~1%/day of VIII, a secondary amine that has been shown to nitrosate much more rapidly than methapyrilene under simulated gastric fluid conditions, is formed.

The concept of protecting susceptible pharmaceutical amines from nitrosation by using ascorbic acid, either as its acid or salt form, is probably a viable goal. However, consideration must be given not only to aqueous sources of nitrosating intermediates but also to gaseous ones.

REFERENCES

(1) S. S. Mirvish, *J. Toxicol. Environ. Health*, **2**, 1267 (1977).

(2) M. C. Archer, *ACS Abstr. Paper*, **172** (Sept. 3), 18 (1976).

(3) P. N. Magee and J. M. Barnes, *Adv. Cancer Res.*, **10**, 163 (1967).

(4) H. Druckrey, A. Schildbach, D. Schmall, R. Preussmann, and S. Ivankovic, *Arzneim.-Forsch.*, **13**, 841 (1963).

(5) N. Koppang and H. Rimslatten, in "Environmental *N*-Nitroso Compounds. Analysis and Formation," E. A. Walker, P. Bogovski, and L. Gricuite, Eds., Publication 14, International Agency for Research on Cancer, Lyon, France, 1976, pp. 443–452.

(6) H. Druckrey, R. Preussmann, S. Ivankovic, and D. Schmall, *Z. Krebsforsch.*, **69**, 103 (1967).

(7) S. S. Mirvish, L. Wallcave, M. Egan, and P. Shubik, *Science*, **177**, 65 (1972).

(8) J. J. Kamm, T. Dashman, A. H. Conney, and J. J. Burns, *Proc. Natl. Acad. Sci. USA*, **70**, 747 (1973).

(9) H. Dahn, L. Loewe, and C. A. Bunton, *Helv. Chim. Acta*, **43**, 320 (1960).

(10) M. Archer, S. R. Tannenbaum, T.-Y. Fan, and M. Weisman, *J. Natl. Cancer Inst.*, **54**, 1203 (1975).

(11) W. Lijinsky and H. N. Taylor, *Food Cosmet. Toxicol.*, **15**, 269 (1977).

(12) "Thin Layer Chromatography: A Laboratory Handbook," E. Stahl, Ed., Springer-Verlag, New York, N.Y., 1969, pp. 854–905 (reagents 148 and 147).

(13) D. H. Fine, F. Rufeh, and B. Gunther, *Anal. Lett.*, **6** (8), 731 (1973).

(14) J. W. Rhoades and D. F. Johnson, *J. Natl. Cancer Inst.*, **48**, 1841 (1972).

(15) W. Lijinsky and G. M. Singer, in "*N*-Nitroso Compounds in the Environment," P. Bogovoski and E. A. Walker, Eds., Publication 9, International Agency for Research on Cancer, Lyon, France, 1974, pp. 111–114.

(16) P. A. S. Smith and R. N. Loeppky, *J. Am. Chem. Soc.*, **89**, 1147 (1967).

(17) S. S. Mirvish, *Toxicol. Appl. Pharmacol.*, **31**, 325 (1975).

(18) M. Greenblatt, *J. Natl. Cancer Inst.*, **50**, 1055 (1973).

(19) W. Fiddler, J. W. Pensabene, E. G. Piotrowski, R. C. Doerr, and A. E. Wasserman, *J. Food Sci.*, **38**, 1084 (1973).

(20) W. Lijinsky, E. Conrad, and R. Van De Bogart, *Nature*, **239**, 167 (1972).

(21) G. Eisenbrand, B. Spiegelhalder, C. Janzowski, J. Kann, and R. Preussman, paper presented at 5th Meeting on Analysis and Formation of *N*-Nitroso Compounds, World Health Organization, International Agency for Research on Cancer, Durham, N.H., Aug. 1977.

(22) R. E. Schirmer and R. J. Pierson, *J. Pharm. Sci.*, **62**, 2052 (1973).

ACKNOWLEDGMENTS

The technical assistance of Mr. J. P. Keating and Mr. M. P. Lanyi of Hoffmann-La Roche Inc. and Dr. J. S. Wishnok and Mr. W. Bishop of the Massachusetts Institute of Technology is gratefully acknowledged. The *N*-(2-pyridyl)-*N'*-dimethylethylenediamine standard was graciously supplied by Dr. W. Schroeder of Burdick and Jackson Laboratories.

Prostaglandin Prodrugs I: Stabilization of Dinoprostone (Prostaglandin E_2) in Solid State through Formation of Crystalline C_1-Phenyl Esters

W. MOROZOWICH ˣ, T. O. OESTERLING, W. L. MILLER, C. F. LAWSON, J. R. WEEKS, R. G. STEHLE, and S. L. DOUGLAS

Received September 15, 1975, from the *Research Laboratories, The Upjohn Company, Kalamazoo, MI 49001.* Accepted for publication December 28, 1978.

Abstract □ Dinoprostone *para*-substituted phenyl esters were synthesized in attempt to improve the solid-state stability of the parent prostaglandin. A phenol series covering a wide melting-point range was employed, and a linear relationship was observed between the phenol melting points and the resulting prostaglandin C_1-ester melting points. The crystalline esters showed improved solid-state stability over the parent compound, and many esters were biologically active.

Keyphrases □ Prostaglandins—dinoprostone, prodrugs, stabilization in solid state of crystalline C_1-phenyl esters, biological activity □ Prodrugs—dinoprostone, stabilization in solid state of crystalline C_1-phenyl esters, biological activity

Prostaglandins are naturally occurring long chain substituted carboxylic acids with various biological effects *in vivo* (1–3). These compounds are undergoing extensive molecular modification in attempts to increase potency and specificity and to improve pharmaceutical and biological properties. Chemical programs aimed at increasing potency or specificity involve the creation of analogs through substituent synthesis or skeletal modification, whereas biopharmaceutical properties are modified *via* prodrugs.

BACKGROUND

Following the identification of several highly active prostaglandin analogs (4–7), attention has been directed toward improving pharmaceutical or biological properties through the *in vivo* reversible modification known as the prodrug (8). Many highly active prostaglandin analogs do not have optimal pharmaceutical properties such as solubility, stability, and crystallinity nor optimal biological properties such as absorption and duration of action (9). These problems may be solved through prodrug synthesis.

Two pressing problems with prostaglandins are E-series prostaglandin instability and difficulty in handling many prostaglandins that occur as liquids (9). This report focuses on the utility of crystalline C_1-esters in improving the solid-state stability of dinoprostone (I).

Dinoprostone (I) instability is due to the 9,11β-ketol system in which the activated C_{11}-hydroxyl undergoes facile elimination to give prostaglandin A_2 (10). Attempts to stabilize this prostaglandin have included solvent stabilization (11), complex formation (12, 13), and bisulfite formation at C_9 (14).

Crystalline high-melting C_1-esters were synthesized to improve the solid-state stability of I based on the following reasoning. Compound I is a crystalline solid (mp 63°) stable at room temperature for short periods but liquefies and decomposes rapidly after a few months. High melting I C_1-esters might maintain crystal integrity and improve the solid-state stability. Prediction of the ester melting points was not possible *a priori* from structural formula inspection, but, intuitively, phenols capable of strong intermolecular interaction were expected to provide high melting esters. The melting point of the parent phenol used in ester formation reflects the intermolecular interaction strength; therefore, higher melting phenols would be expected to give higher melting esters.

This work describes the synthesis of various I C_1-esters using a phenol series covering a wide melting-point range in an attempt to explore the: (*a*) relationship between the phenol and corresponding prostaglandin ester melting points, (*b*) utility of crystalline dinoprostone esters in improving the parent prostaglandin solid-state stability, and (*c*) influence of esterification on bioactivity.

RESULTS AND DISCUSSION

Synthesis—Prostaglandin C_1-esters have been synthesized by numerous routes including the *N,N*-dicyclohexylcarbodiimide procedure (15), carboxyl activation with pivaloyl chloride (16), and carboxyl activation with sulfonyl halides (17). In this work the isobutyl chlorocarbonate carboxyl activation route widely used in peptide synthesis (18) was chosen.

Reaction of I with isobutyl chlorocarbonate (II) gave the acylisobutylcarbonate mixed anhydride (III); upon reaction with 1.5–4 mole equivalents of the appropriate phenol in pyridine at room temperature, III gave the desired C_1-esters (V) (Scheme I). The use of a small excess (0.1–0.5 mole equivalents) of II generally gave quantitative I esterification in less than 15 min; for convenience, the reactions were allowed to stand at room temperature for up to 3 hr before workup.

The esters were purified by silica gel column chromatography and, upon recrystallization, they were shown to be pure by silica gel TLC. The structures were verified by combustion analyses (Table I) and, in some cases, by mass spectral analyses.

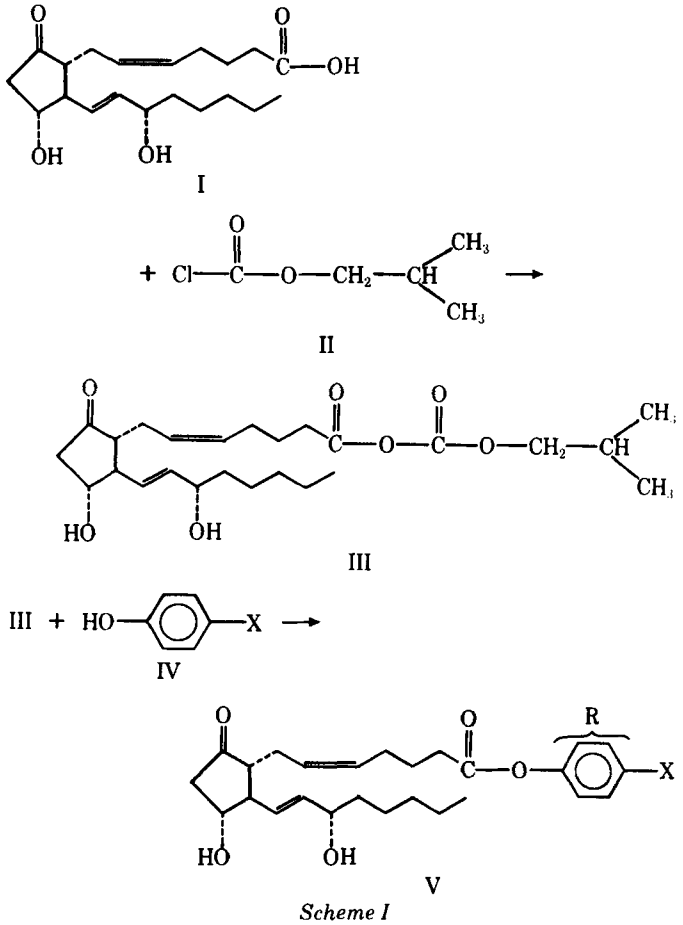

Scheme I

0022-3549/79/0700-0833$01.00/0
© 1979, American Pharmaceutical Association

Table I—Physical Constants of Dinoprostone C_1-Esters

Compound	C_1-Ester (R in V)	Recrystallization Solvent	Melting Point: C_1-Ester	Melting Point: Parent Phenol	Empirical Formula	Combustion Analyses, %: Calc.	Combustion Analyses, %: Found
Va		—	Liquid	43°	$C_{26}H_{36}O_5$	—[a]	—
Vb	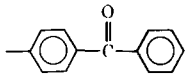	—	Liquid	130–133°	$C_{33}H_{40}O_6$	—[b]	—
Vc	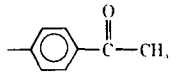	Ethyl acetate diluted with hexane	76.8–77.8°	108–110°	$C_{28}H_{38}O_6$	C 71.46 H 8.14	71.46 8.13
Vd	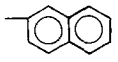	Ethyl acetate diluted with hexane	79.3–80.3°	122–124°	$C_{30}H_{38}O_5$	C 75.38 H 8.00	75.44 7.73
Ve	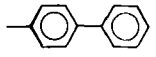	Ethyl acetate diluted with hexane	91.8–92.8°	165°	$C_{32}H_{40}O_5$	C 76.16 H 7.99	76.26 7.86
Vf	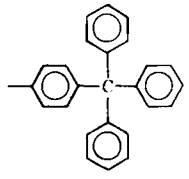	Ethyl acetate diluted with hexane	96.3–97.8°	283°	$C_{45}H_{50}O_5$	C 80.56 H 7.51	79.52 7.81
Vg	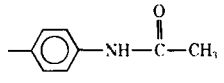	Ethyl acetate diluted with hexane	102.3–103.3°	167–169°	$C_{28}H_{29}NO_6$	C 69.25 H 8.09 N 2.88	69.36 8.27 2.87
Vh	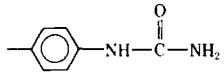	Ethyl acetate diluted with hexane	105.3–108.3°	170–172°	$C_{27}H_{38}N_2O_6$	C 66.64 H 7.87 N 5.76	66.73 8.13 5.83
Vi	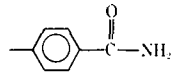	Acetonitrile diluted with water	106.3–108.3°	196–197°	$C_{27}H_{37}NO_6$	C 68.76 H 7.91 N 2.97	68.36 7.71 2.95
Vj	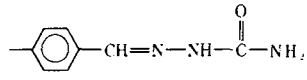	Hot acetonitrile	125.3–126.5°	224°	$C_{28}H_{39}N_3O_6$	C 65.48 H 7.65 N 8.18	65.62 7.76 8.27
Vk	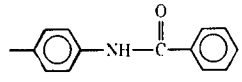	Tetrahydrofuran diluted with hexane	132.8–135.0°	218°	$C_{33}H_{41}NO_6$	C 72.37 H 7.55 N 2.56	71.95 7.34 2.55
Vl	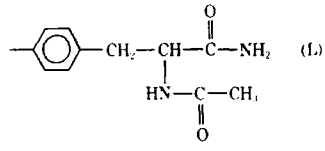 (L)	Warm acetone diluted with hexane	137.3–140.8°	223–225°	$C_{31}H_{44}N_2O_7$	C 66.88 H 7.97 N 5.03	66.46 8.03 5.27
Vm	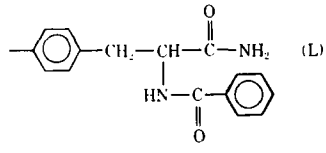 (L)	Hot acetone	160.8–164.8°	205–208°	$C_{36}H_{46}N_2O_7$	C 69.88 H 7.49 N 4.53	69.80 7.80 4.89
Vn	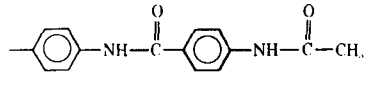	Hot acetone	173.2–176.2°	275–277°	$C_{35}H_{44}N_2O_7$	C 69.51 H 7.33 N 4.63	69.30 7.25 4.69
Vo	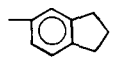	—	44.5–48.0°[c]	51–53°	$C_{29}H_{39}O_5$	—	—

[a] Characterized by mass spectral analysis of the bis(trimethylsilyl) derivative showing a molecular ion at *m/e* 572 and a fragmentation pattern consistent with the structure. [b] Characterized by mass spectral analysis of the bis(trimethylsilyl) derivative. A partial list of fragment ions includes *m/e* 605 ($M^+ - 71$), 586 ($M^+ - 90$), 571 ($M^+ - 90 - 15$), and 515 ($M^+ - 90 - 71$). [c] Reference 19.

Table II—Biological Activity of Dinoprostone C_1-Esters

Compound	Hamster Antifertility Assay: Percent Nonpregnant	Hamster Antifertility Assay: Dose, μg/animal	Gerbil Colon[a]	Rat Blood Pressure (Depressor)[a]
I[b]	100	200[c]	2 (1.4–2.6)[d]	0.6 (0.4–1.1)[d]
V*a*	50	234[e]	1–3	0.1–0.3
V*b*	17	302[e]	1–3	0.1–0.3
V*c*	100	267	1–3	0.1–0.3
	17	134		
V*d*	0	272[e]	0.3–1	0.1–0.3
V*e*	17	286[e]	0.1–0.3	0.01–0.03
V*f*	17	381[e]	0.01–0.03	Inactive
	100	1000		
V*g*	0	100	0.01–0.03	0.1–0.3
V*h*	50	276[e]	1–3	0.1–0.3
V*i*	33	268[e]	0.3–1	0.1–0.3
V*j*	17	291[e]	0.3–1	0.1–0.3
V*k*	33	1000	0.1–0.3	0.1–0.3
V*l*	17	316[e]	1–3	0.3–1
V*m*	0	351[e]	0.3–1	0.1–0.3
V*n*	0	100	0.1–0.3	0.1–0.3

[a] Prostaglandin E = 1. [b] Reference compound. [c] Minimal effective dose (MED_{100}) for 100% inhibition of pregnancy. [d] Relative potency and 95% confidence interval in parenthesis. [e] Amount equivalent to 200 μg of I.

Melting Points—Plotting the I C_1-ester melting points *versus* the starting phenol[1] melting points (Fig. 1) showed that higher melting phenols generally gave higher melting esters. The lowest melting ester on the plot was that of 5-indanol (19).

The least-squares line is shown without the most deviant point (V*f*, the *p*-tritylphenyl ester). The correlation coefficient was 0.937 (slope, 0.57; intercept, 10.1°). Inclusion of V*f* decreased the correlation coefficient to 0.780 (slope, 0.43; intercept, 31.1°). The reason for the large deviation of V*f* is not clear but could be the isolation of an unusually low melting polymorph or a different crystal packing arrangement caused by exceptional ester bulkiness.

Structurally, the amido-substituted phenyl esters provided higher melting points than the acyl- or aromatic-substituted phenyl esters, presumably due to strong amido moiety hydrogen bonding (20). The melting points increased progressively from the *p*-acetamidophenyl ester (V*g*) to the *p,p'*-acetamidobenzamidophenyl ester (V*n*). The latter ester is remarkably effective in raising the melting point of I and is the highest melting ester (173.2–176.2°) recorded to date.

Stability—Storage of crystalline esters V*c*–V*e*, V*g*–V*l*, and V*n* at room temperature for 23–30 months resulted in no detectable degradation as shown by silica gel TLC; the esters remained as white solids. The free acid I, on the other hand, underwent 44–59% degradation in 12 months at room temperature with partial liquefaction. Since the liquid esters V*a* and V*b* underwent decomposition as well as discoloration upon storage at room temperature, the improved solid-state stability of the crystalline esters apparently is due to the stabilization by the crystal lattice.

Biological Activity—The ester biological activities in three test screening systems are summarized in Table II. Significant activity was observed in the antifertility assay for all compounds except V*d*, V*m*, and V*n*. Full activity was attained with V*c*. Some esters were nearly as active as I in the gerbil colon assay, but all compounds were less active than I in the rat blood pressure assay.

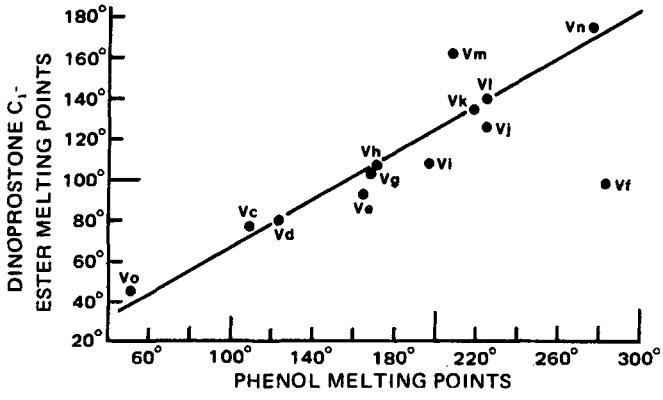

Figure 1—*Plot of the melting points of starting phenols* versus *the melting points of resulting dinoprostone C_1-esters. The least-squares line is shown omitting ester V*f.

[1] The melting-point range midpoint was used.

EXPERIMENTAL

Materials and Methods—Compound I[2] (mp 63°) purity was verified by silica gel TLC using ethyl acetate–acetic acid (97:3). The phenols, except those synthesized below, were obtained commercially[3]. Pyridine (analytical reagent) was dried over molecular sieves[4] for 1 week before use. All other solvents were glass-distilled quality[5]. Acetone and tetrahydrofuran were dried by stirring 100 ml of the solvent with 50 g of alumina[6] for 15 min followed by filtration under nitrogen.

Column chromatography was conducted on 0.063–0.2-mm silica gel[7]. In most cases, the support was deactivated by stirring 1 kg of silica gel with 4 liters of ethyl acetate containing 30 ml of water. After the slurry settled for about 2 min, the supernate was decanted and the remaining thick slurry was poured into glass columns. Silica gel TLC was conducted on 250-μm layer plates[8]. The compounds were visualized by spraying the developed plates with aqueous 15% ammonium sulfate followed by charring on a hot plate.

Synthesis—p-*Benzamidophenol*—A solution of 20 g of *p*-aminophenol in 200 ml of dry pyridine was treated with 20 g of benzoic anhydride. After 4 hr at room temperature, the solvent was removed under vacuum at 45°, and the residue was dissolved in 200 ml of hot methanol. Dilution with 300 ml of water gave 22 g of tan crystals. An 11.2-g portion of the product was recrystallized from 350 ml of hot acetonitrile, affording 8.5 g of white crystals, mp 218.0–218.5°. The product was soluble in alkali, indicative of a phenol, and the mass spectrum revealed a molecular ion at *m/e* 213.

Anal.—Calc. for $C_{13}H_{11}NO_2$: C, 73.22; H, 5.20; N, 6.56. Found: C, 73.49; H, 5.30; N, 6.47.

p,p'-*Acetamidobenzamidophenol*—A solution of 12.5 g of *p*-acetamidobenzoic acid in 250 ml of dry tetrahydrofuran was treated with 11.1 ml of triethylamine, and partial crystallization of the triethylammonium salt occurred. Isobutyl chlorocarbonate (10.4 ml) was added to the suspension with stirring, and a voluminous precipitate occurred. After 5 min of stirring at room temperature, a solution of 13.3 g of *p*-aminophenol in 80 ml of dry pyridine was added. The suspension was stirred for 40 min and then diluted with 2 liters of water, affording 14.3 g of a brown solid. Then the product was dissolved in 500 ml of hot methanol. After partial decolorization with 1 g of charcoal, the solution was diluted with 300 ml of water, giving 5.9 g of white crystals, mp 275.0–277.0°.

Anal.—Calc. for $C_{15}H_{14}N_2O_3$: C, 66.69; H, 5.18; N, 10.36. Found (corrected for 3.87% H_2O): C, 66.08; H, 5.36; N, 10.33.

The compound was rendered anhydrous by drying under vacuum at 110° overnight.

[2] Supplied by the Research Division, The Upjohn Co.
[3] Aldrich Chemical Co., Milwaukee, Wis., and Eastman Kodak Co., Rochester, N.Y.
[4] Beads, 10–16 mesh, 4 Å, Davison Chemical Co., Baltimore, Md.
[5] Burdick & Jackson, Muskegon, Mich.
[6] Woelm alumina, ICN Pharmaceuticals, Cleveland, Ohio.
[7] Silica gel 60, EM Laboratories, Elmsford, N.Y.
[8] Uniplate, Analtech Inc., Newark, Del.

p-*Benzamidophenyl Ester of Dinoprostone* (*Vk*)—A solution of 260 mg (0.74 mmole) of I in 20 ml of dry acetone was treated with 0.206 ml (1.48 mmoles) of triethylamine. While under a positive nitrogen atmosphere, the solution was cooled to −5°, and 0.194 ml (1.47 mmoles) of isobutyl chlorocarbonate was added. Rapid crystallization of triethylamine hydrochloride occurred. After 3 min at −5°, a solution of 0.8 g (3.76 mmoles) of *p*-benzamidophenol in 8 ml of dry pyridine was added.

After 3 hr at room temperature, the solvent was removed under vacuum at 45°, and the resulting oily residue was purified by column chromatography on 80 g of silica gel. Elution was achieved with 150 ml of ethyl acetate followed by acetonitrile. TLC showed the product was in tubes 25–30 (15 ml each); upon solvent removal under vacuum at 45°, a white solid was obtained. The product was dissolved in 20 ml of tetrahydrofuran and diluted with 20 ml of hexane, affording 269 mg of white crystals, mp 132.8–135.0°, after drying under vacuum at 50°. The product was pure by silica gel TLC with ethyl acetate as the developing solvent.

Anal.—Calc. for $C_{33}H_{41}NO_6$: C, 72.37; H, 7.55; N, 2.56. Found: C, 71.95; H, 7.34; N, 2.55.

Mass spectral analysis showed a peak at *m/e* 529 corresponding to $M^+ - H_2O$, and the fragmentation pattern supported the structure.

The other I C_1-esters were synthesized by similar methods.

Biological Assays—*Hamster Antifertility*—The esters were evaluated for their ability to inhibit pregnancy in adult female hamsters, as reported previously (21). The compounds were administered subcutaneously in 0.5 ml of a vehicle containing 30% ethanol and 70% physiological saline. (In some cases, the ethanol concentration was increased slightly to achieve dissolution.) The solutions were stored at −30° until used. The ester doses were equivalent to 200 μg of I/animal unless otherwise indicated. The minimum I dose giving 100% pregnancy inhibition was 200 μg. The percentage inhibition of pregnancy was determined from the number of animals pregnant in a six to 12 animal group.

Isolated Gerbil Colon—The male gerbil ascending colon was used to evaluate smooth muscle stimulating activity, as previously described (21). Generally, two colons were used for each test. The response to 3.2 and 10 ng/ml of prostaglandin E_1 was obtained, and increasing ester concentrations were tested until a response was obtained between the two standard concentrations. The standard concentration to test concentration ratio was calculated, and the activity was expressed as the range of these two ratios.

Rat Blood Pressure—Direct blood pressure measurement was made from a common carotid artery of anesthetized, mature female rats as described previously (21). Generally, only one rat was used for each test. The depressor response of 1 and 3.2 μg/kg of prostaglandin E_1 was determined following intravenous administration, and increasing test compound doses were administered intravenously until a response was obtained between the two standard doses. Activity was expressed as indicated for the gerbil colon.

REFERENCES

(1) T. O. Oesterling, W. Morozowich, and T. J. Roseman, *J. Pharm. Sci.*, **61**, 1861 (1972).

(2) J. R. Weeks, *Annu. Rev. Pharmacol.*, **12**, 317 (1972).

(3) J. W. Hinman, *Annu. Rev. Biochem.*, **41**, 161 (1972).

(4) W. P. Schneider, in "The Prostaglandins, Progress in Research," S. M. M. Karim, Ed., Medical and Technical Publishing, Oxford, England, 1972, p. 293.

(5) U. F. Axen, J. E. Pike, and A. W. Schneider, in "Progress in the Total Synthesis of Natural Products," vol. I, J. ApSimon, Ed., Wiley, New York, N.Y., 1973, p. 81.

(6) G. L. Bundy, *Annu. Rep. Med. Chem.*, **7**, 157 (1972).

(7) M. P. L. Caton, in "The Prostaglandins, Pharmacological and Therapeutic Advances," M. F. Cuthbert, Ed., William Heineman Medical Books, London, England, 1973, p. 1.

(8) A. A. Sinkula and S. H. Yalkowsky, *J. Pharm. Sci.*, **64**, 181 (1975).

(9) W. Morozowich, "Abstracts, 121st Annual Meeting of the American Pharmaceutical Association," 1974, p. 45.

(10) D. C. Monkhouse, L. V. VanCampen, and A. J. Aguiar, *J. Pharm. Sci.*, **62**, 576 (1973).

(11) R. G. Stehle and T. O. Oesterling (to The Upjohn Co.), U.S. pat. 3,749,800 (1974).

(12) Ono Pharmaceutical Co., South African pat. 3398 (1971).

(13) A. C. O'Rouke and J. S. Kent (to Syntex Inc.), U.S. pat. 3,826,823 (1974).

(14) D. C. Monkhouse (to Pfizer Inc.), U.S. pat. 3,851,052 (1974).

(15) J. E. Pike, F. H. Lincoln, and W. P. Schneider, *J. Org. Chem.*, **34**, 3552 (1969).

(16) Ono Pharmaceutical Co., Belgian pat. 775,106 (1972).

(17) Ono Pharmaceutical Co., Belgian pat. 776,294 (1972).

(18) A. Kapoor, *J. Pharm. Sci.*, **59**, 1 (1970).

(19) Pfizer Inc., German pat. 2,365,205 (1974).

(20) T. Gramstad and W. I. Fluglevik, *Acta Chem. Scand.*, **16**, 1369 (1962).

(21) J. R. Weeks, D. W. DuCharme, W. E. Magee, and W. L. Miller, *J. Pharmacol. Exp. Ther.*, **186**, 67 (1973).

Prostaglandin Prodrugs II: New Method for Synthesizing Prostaglandin C_1-Aliphatic Esters

W. MOROZOWICH ˣ, T. O. OESTERLING, W. L. MILLER, and S. L. DOUGLAS

Received September 15, 1975, from the *Research Laboratories, The Upjohn Company, Kalamazoo, MI 49001.* Accepted for publication December 28, 1978.

Abstract □ A new method for synthesizing C_1-aliphatic esters of dinoprost and dinoprostone without using hydroxyl protective groups is described. Reaction of the prostaglandin with an alkyl halide in the presence of the sterically hindered amine *N,N*-diisopropylethylamine proceeds smoothly to give C_1-esters in various solvents at ambient or slightly elevated temperatures. Polar solvents were strongly catalytic, and even the hindered *tert*-butyl esters were synthesized by employing solvents such as dimethylformamide or dimethyl sulfoxide. Biological evaluation in the hamster antifertility assay showed that some esters maintained high bioactivity.

Keyphrases □ Prostaglandins—prodrugs, dinoprost, dinoprostone, C_1-aliphatic esters, synthesis, biological activity □ Prodrugs–dinoprost and dinoprostone, C_1-aliphatic esters, synthesis, biological activity □ Dinoprost—prodrugs, C_1-aliphatic esters, synthesis □ Dinoprostone—prodrugs, C_1-aliphatic esters, synthesis

The conversion of prostaglandins to C_1-methyl esters has resulted in increased or more rapid intestinal absorption (1, 2), as well as in greater potency following intravenous administration (3). Since few prostaglandin C_1-aliphatic esters have been reported, various aliphatic esters of dinoprost (I) and dinoprostone (II) were synthesized for evaluation of their utility as prodrugs in continuation of our effort on prostaglandin prodrugs (4).

The S_N2 reaction of inorganic metal salts of carboxylic acids and alkyl halides produces C_1-alkyl esters (5), but the

0022-3549/79/0700-0836$01.00/0

© 1979, American Pharmaceutical Association

p-*Benzamidophenyl Ester of Dinoprostone* (*Vk*)—A solution of 260 mg (0.74 mmole) of I in 20 ml of dry acetone was treated with 0.206 ml (1.48 mmoles) of triethylamine. While under a positive nitrogen atmosphere, the solution was cooled to −5°, and 0.194 ml (1.47 mmoles) of isobutyl chlorocarbonate was added. Rapid crystallization of triethylamine hydrochloride occurred. After 3 min at −5°, a solution of 0.8 g (3.76 mmoles) of *p*-benzamidophenol in 8 ml of dry pyridine was added.

After 3 hr at room temperature, the solvent was removed under vacuum at 45°, and the resulting oily residue was purified by column chromatography on 80 g of silica gel. Elution was achieved with 150 ml of ethyl acetate followed by acetonitrile. TLC showed the product was in tubes 25–30 (15 ml each); upon solvent removal under vacuum at 45°, a white solid was obtained. The product was dissolved in 20 ml of tetrahydrofuran and diluted with 20 ml of hexane, affording 269 mg of white crystals, mp 132.8–135.0°, after drying under vacuum at 50°. The product was pure by silica gel TLC with ethyl acetate as the developing solvent.

Anal.—Calc. for $C_{33}H_{41}NO_6$: C, 72.37; H, 7.55; N, 2.56. Found: C, 71.95; H, 7.34; N, 2.55.

Mass spectral analysis showed a peak at *m/e* 529 corresponding to $M^+ - H_2O$, and the fragmentation pattern supported the structure.

The other I C_1-esters were synthesized by similar methods.

Biological Assays—*Hamster Antifertility*—The esters were evaluated for their ability to inhibit pregnancy in adult female hamsters, as reported previously (21). The compounds were administered subcutaneously in 0.5 ml of a vehicle containing 30% ethanol and 70% physiological saline. (In some cases, the ethanol concentration was increased slightly to achieve dissolution.) The solutions were stored at −30° until used. The ester doses were equivalent to 200 μg of I/animal unless otherwise indicated. The minimum I dose giving 100% pregnancy inhibition was 200 μg. The percentage inhibition of pregnancy was determined from the number of animals pregnant in a six to 12 animal group.

Isolated Gerbil Colon—The male gerbil ascending colon was used to evaluate smooth muscle stimulating activity, as previously described (21). Generally, two colons were used for each test. The response to 3.2 and 10 ng/ml of prostaglandin E_1 was obtained, and increasing ester concentrations were tested until a response was obtained between the two standard concentrations. The standard concentration to test concentration ratio was calculated, and the activity was expressed as the range of these two ratios.

Rat Blood Pressure—Direct blood pressure measurement was made from a common carotid artery of anesthetized, mature female rats as described previously (21). Generally, only one rat was used for each test. The depressor response of 1 and 3.2 μg/kg of prostaglandin E_1 was determined following intravenous administration, and increasing test compound doses were administered intravenously until a response was obtained between the two standard doses. Activity was expressed as indicated for the gerbil colon.

REFERENCES

(1) T. O. Oesterling, W. Morozowich, and T. J. Roseman, *J. Pharm. Sci.*, **61**, 1861 (1972).

(2) J. R. Weeks, *Annu. Rev. Pharmacol.*, **12**, 317 (1972).

(3) J. W. Hinman, *Annu. Rev. Biochem.*, **41**, 161 (1972).

(4) W. P. Schneider, in "The Prostaglandins, Progress in Research," S. M. M. Karim, Ed., Medical and Technical Publishing, Oxford, England, 1972, p. 293.

(5) U. F. Axen, J. E. Pike, and A. W. Schneider, in "Progress in the Total Synthesis of Natural Products," vol. I, J. ApSimon, Ed., Wiley, New York, N.Y., 1973, p. 81.

(6) G. L. Bundy, *Annu. Rep. Med. Chem.*, **7**, 157 (1972).

(7) M. P. L. Caton, in "The Prostaglandins, Pharmacological and Therapeutic Advances," M. F. Cuthbert, Ed., William Heineman Medical Books, London, England, 1973, p. 1.

(8) A. A. Sinkula and S. H. Yalkowsky, *J. Pharm. Sci.*, **64**, 181 (1975).

(9) W. Morozowich, "Abstracts, 121st Annual Meeting of the American Pharmaceutical Association," 1974, p. 45.

(10) D. C. Monkhouse, L. V. VanCampen, and A. J. Aguiar, *J. Pharm. Sci.*, **62**, 576 (1973).

(11) R. G. Stehle and T. O. Oesterling (to The Upjohn Co.), U.S. pat. 3,749,800 (1974).

(12) Ono Pharmaceutical Co., South African pat. 3398 (1971).

(13) A. C. O'Rouke and J. S. Kent (to Syntex Inc.), U.S. pat. 3,826,823 (1974).

(14) D. C. Monkhouse (to Pfizer Inc.), U.S. pat. 3,851,052 (1974).

(15) J. E. Pike, F. H. Lincoln, and W. P. Schneider, *J. Org. Chem.*, **34**, 3552 (1969).

(16) Ono Pharmaceutical Co., Belgian pat. 775,106 (1972).

(17) Ono Pharmaceutical Co., Belgian pat. 776,294 (1972).

(18) A. Kapoor, *J. Pharm. Sci.*, **59**, 1 (1970).

(19) Pfizer Inc., German pat. 2,365,205 (1974).

(20) T. Gramstad and W. I. Fluglevik, *Acta Chem. Scand.*, **16**, 1369 (1962).

(21) J. R. Weeks, D. W. DuCharme, W. E. Magee, and W. L. Miller, *J. Pharmacol. Exp. Ther.*, **186**, 67 (1973).

Prostaglandin Prodrugs II: New Method for Synthesizing Prostaglandin C_1-Aliphatic Esters

W. MOROZOWICH ˣ, T. O. OESTERLING, W. L. MILLER, and S. L. DOUGLAS

Received September 15, 1975, from the *Research Laboratories, The Upjohn Company, Kalamazoo, MI 49001.* Accepted for publication December 28, 1978.

Abstract □ A new method for synthesizing C_1-aliphatic esters of dinoprost and dinoprostone without using hydroxyl protective groups is described. Reaction of the prostaglandin with an alkyl halide in the presence of the sterically hindered amine *N,N*-diisopropylethylamine proceeds smoothly to give C_1-esters in various solvents at ambient or slightly elevated temperatures. Polar solvents were strongly catalytic, and even the hindered *tert*-butyl esters were synthesized by employing solvents such as dimethylformamide or dimethyl sulfoxide. Biological evaluation in the hamster antifertility assay showed that some esters maintained high bioactivity.

Keyphrases □ Prostaglandins—prodrugs, dinoprost, dinoprostone, C_1-aliphatic esters, synthesis, biological activity □ Prodrugs–dinoprost and dinoprostone, C_1-aliphatic esters, synthesis, biological activity □ Dinoprost—prodrugs, C_1-aliphatic esters, synthesis □ Dinoprostone—prodrugs, C_1-aliphatic esters, synthesis

The conversion of prostaglandins to C_1-methyl esters has resulted in increased or more rapid intestinal absorption (1, 2), as well as in greater potency following intravenous administration (3). Since few prostaglandin C_1-aliphatic esters have been reported, various aliphatic esters of dinoprost (I) and dinoprostone (II) were synthesized for evaluation of their utility as prodrugs in continuation of our effort on prostaglandin prodrugs (4).

The S_N2 reaction of inorganic metal salts of carboxylic acids and alkyl halides produces C_1-alkyl esters (5), but the

0022-3549/79/0700-0836$01.00/0

© 1979, American Pharmaceutical Association

Table I—Physical Constants and Biological Activity of Prostaglandin C_1-Esters

Compound	C_1-Ester	Halide Used	Conditions	Formula	Melting Point	Characteristic Mass Spectra Ions (m/e)[a]					Hamster Antifertility Assay[b]	
						M^+	$M^+ - 15$	$M^+ - 31$	$M^+ - 71$	$M^+ - 90$	Percent Non-pregnant	Dose, μg/animal, sc
IIIa	$-CH_3$	Iodide	Acetonitrile, room temperature, 1 hr	$C_{21}H_{36}O_5$	Liquid	—[c]	—	—	—	—	100	100
IIIb	$-C_2H_5$	Iodide	Dimethyl sulfoxide, room temperature, overnight	$C_{22}H_{38}O_5$	Liquid	598	583	—	508	493	100	50
IIIc	$-n-C_3H_7$	Iodide	Acetonitrile, room temperature, overnight	$C_{23}H_{40}O_5$	Liquid	612	597	—	541	522	83	50
IIId	$-iso-C_3H_7$	Bromide	Dimethyl sulfoxide, 50°, 4 hr	$C_{23}H_{40}O_5$	Liquid	612	597	—	541	522	83	50
IIIe	$-n-C_4H_9$	Iodide	Dimethyl sulfoxide, room temperature, overnight	$C_{24}H_{42}O_5$	Liquid	626	611	—	555	536	100	1000
IIIf	$-iso-C_4H_9$	Iodide	Dimethyl sulfoxide, room temperature, overnight	$C_{24}H_{42}O_5$	Liquid	626	611	—	555	536	40	100
IIIg	$-sec-C_4H_9$	Iodide	Dimethyl sulfoxide, room temperature, overnight	$C_{24}H_{42}O_5$	Liquid	626	611	—	555	536	67	100
IIIh	$-CH(C_2H_5)_2$	Iodide	Dimethyl sulfoxide, room temperature, overnight	$C_{25}H_{44}O_5$	Liquid	640	—	—	569	550	33	100
IIIi	$-n-C_6H_{13}$	Bromide	Dimethyl sulfoxide, room temperature, overnight	$C_{26}H_{46}O_5$	Liquid	654	639	—	583	564	33	100
IIIj	$-n-C_{10}H_{21}$	Iodide	Acetonitrile, room temperature, 32 hr	$C_{30}H_{54}O_5$	43.5–44.0°[d]	—[e]	—	—	—	—	83	200
IIIk	$-CH_2-C_6H_5$	Bromide	Acetonitrile, room temperature, overnight	$C_{27}H_{40}O_5$	Liquid	660	545	—	589	570	100	1000
IIIl	$-CH_2-C_6H_4-p-NO_2$	Bromide	Acetonitrile–dimethyl sulfoxide, room temperature, 3 hr	$C_{27}H_{39}NO_7$	Liquid	705	690	—	634	615	—	—
IVa	$-C_2H_5$[f]	Iodide	Dimethyl sulfoxide, room temperature, 3 hr	$C_{22}H_{36}O_5$	Liquid	553	538	522	482	463	83	1000
IVb	$-n-C_3H_7$	Iodide	Acetonitrile, room temperature, 24 hr	$C_{23}H_{38}O_5$	Liquid	567	552	536	496	477	66	1000
IVc	$-iso-C_3H_7$	Bromide	Dimethyl sulfoxide, room temperature, 24 hr	$C_{23}H_{38}O_5$	Liquid	567	552	536	496	477	100	200
IVd	$-n-C_4H_9$[f]	Iodide	Acetonitrile, room temperature, 24 hr	$C_{24}H_{40}O_5$	Liquid	581	566	550	510	491	100	1000
IVe	$-sec-C_4H_9$	Iodide	Acetonitrile–dimethyl sulfoxide (1:1), room temperature, 24 hr	$C_{24}H_{40}O_5$	Liquid	581	566	550	510	491	100	1000
IVf	$-tert-C_4H_9$	Iodide	Dimethyl sulfoxide, 40°, 3 hr	$C_{24}H_{40}O_5$	Liquid	581	566	550	510	491	17	100
IVg	$-n-C_{10}H_{21}$[f]	Iodide	Acetonitrile, room temperature, 24 hr	$C_{30}H_{52}O_5$	44.9–47.3°[d]	636	621	—	565	546	17	200[g]
IVh	$-CH_2-C_6F_5$	Bromide	Acetonitrile–dimethyl sulfoxide (1:1), room temperature, 1 hr	$C_{27}H_{33}F_5O_5$	50.8–51.8°[d]	676	661	—	605	586	17	100
IVi	$-CH_2-C_6H_4-p-NO_2$	Bromide	Acetonitrile–dimethyl sulfoxide (2:1), room temperature, 3 hr	$C_{27}H_{37}NO_7$	40.0–45.0°[d]	660	645	629	589	—	20	100

[a] Conducted on the trimethylsilyl derivatives of the II esters and on the trimethylsilyl–methoxime derivatives of the IV esters unless otherwise indicated. [b] The minimum effective doses for 100% pregnancy inhibition are 100 μg of I/animal and 200 μg of II/animal. The dose is stated as the equivalent amount of the parent prostaglandin. [c] Characterized by silica gel TLC and GLC as identical to authentic I methyl ester prepared by diazomethane (13). [d] Compound crystallized upon storage in a freezer. [e] Mass spectral analysis was conducted on nonderivatized ester. Key fragmentation pattern: m/e 476 ($M^+ - 18$), 458 ($M^+ - 36$), and 405 ($M^+ - 18 - 71$). [f] Prepared previously by the diazoalkane route (8). [g] Administered in 95% ethanol. Compound was inactive in the standard vehicle.

reaction generally is slow due to the use of a heterogeneous medium. A recent communication reported that prostaglandins could be converted rapidly to C_1-*p*-nitrophenacyl esters by reaction of the prostaglandin with *p*-nitrophenacyl bromide in the presence of a small excess of the sterically hindered amine *N,N*-diisopropylethylamine (6). The competing quaternary ammonium side reaction between this sterically hindered amine and the phenacyl halide was slower than the esterification reaction, thereby allowing successful phenacyl ester formation.

This report shows that prostaglandin C_1-aliphatic esters can be synthesized rapidly at ambient or slightly elevated temperatures using the prostaglandin, *N,N*-diisopropylethylamine, and an alkyl halide in a suitable solvent.

RESULTS AND DISCUSSION

Synthesis—The general method for synthesizing the aliphatic I and II C_1-esters involved reaction of the parent prostaglandin in a suitable solvent with a 3–10-mole alkyl halide excess in the presence of a 2–4-mole *N,N*-diisopropylethylamine excess (Scheme I).

The reaction was monitored by silica gel TLC, and greater than 90% esterification generally occurred with the linear alkyl halides in 1–24 hr at room temperature; in some cases, mildly elevated temperatures (40–50°) were employed. Polar solvents showed a remarkable catalytic effect as illustrated by the facile synthesis of the *tert*-butyl II ester. Reaction of II in dimethyl sulfoxide with *tert*-butyl iodide and *N,N*-diisopropylethylamine gave about 70% of the *tert*-butyl ester in 3 hr at 40°, as evidenced by silica gel TLC; in acetonitrile, about a 10% reaction occurred in the same time period.

Esterification of II in polar solvents generally gave a small amount (<10%) of a side product slightly less polar than the desired C_1-ester (IV). The by-product subsequently was removed by column chromatography and was identified tentatively as the II 8-iso C_1-ester since the II 8-isomer is slightly less polar than II by silica gel TLC. Previously, it was shown that prostaglandin E_1 undergoes isomerization at C_8 under mildly basic conditions (7). Presumably, the excess amine in the esterification medium was responsible for isomerization of either II or the resulting C_1-ester. Indeed, in the absence of an alkyl halide, treatment of II with a 3–20-mole excess of *N,N*-diisopropylethylamine in dimethyl sulfoxide or dimethylformamide gave about 5% of the II 8-isomer in 24 hr at room tempera-

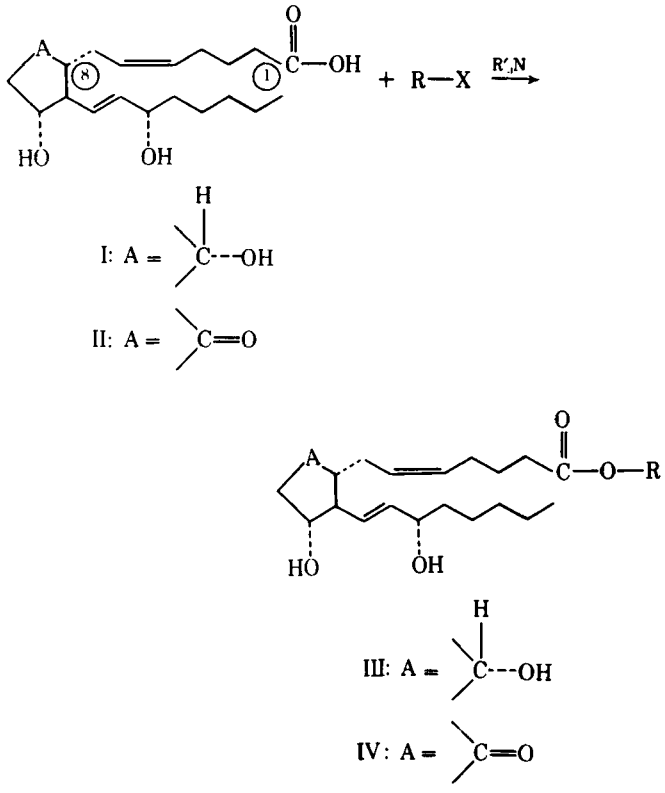

Scheme I

ture. The II 8-isomer was identified by TLC in comparison with the authentic compound.

No II isomerization occurred in acetonitrile under the same conditions, in accord with similar observations reported previously (6).

Excepting the branched esters, the crude ester yield as shown by TLC generally was quantitative with I and about 90% with II due to formation of by-products. The esters were purified by conventional column chromatography using silica gel, and purity was verified by TLC. Table I lists the esters synthesized along with some of the mass spectral fragment ions observed. The only esters isolated as crystalline solids were the *n*-decyl esters (IV*g* and III*j*), the pentafluorobenzyl ester (IV*h*), and the *p*-nitrobenzyl ester (IV*i*).

The simplicity of the alkyl halide esterification method makes it an attractive alternative to previous methods that employed diazoalkanes (8), *N,N*-dicyclohexylcarbodiimide (9), dimethylsulfate (10), and acid chloride–carboxyl activation (11).

Biological—Preliminary prostaglandin C_1-ester screening in the subcutaneous hamster antifertility assay showed that all compounds were active in the range of 50–1000 μg (weight basis)/animal (Table I). Some of the esters, such as the isopropyl ester (III*d*), appeared to be more active than I, for which the minimal effective dose for 100% inhibition of pregnancy was 100 μg/animal.

Initial evaluation of orally administered ethyl ester (III*b*) and propyl ester (III*c*) in hamsters showed that both esters gave 33% inhibition of pregnancy at 500 μg/animal, but I was ineffective in inhibiting pregnancy at this dose. The results indicate improved oral absorption.

EXPERIMENTAL

Materials and Methods—The purity of I[1] and II[1] was verified by silica gel TLC using ethyl acetate–acetic acid (97:3). The alkyl halides were obtained commercially[2]. All solvents were glass-distilled quality[3].

Column chromatography was conducted on 0.063–0.2-mm silica gel[4]. Silica gel TLC was conducted on 250-μm layer plates[5], and visualization was achieved by spraying the developed plates with aqueous 15% ammonium sulfate followed by charring on a hot plate. The mass spectra[6] of the I esters were obtained after conversion to the trimethylsilyl derivatives using a mixture of bis(trimethylsilyl)acetamide–trimethylchlorosilane–hexamethyldisilazane–pyridine (1:1:1:3). The II esters were converted initially to the C_9-methoxime derivatives by reaction of ~1 mg of the ester with 0.2 ml of a saturated solution of hydroxylamine hydrochloride in pyridine for 6 hr at 50°. The methoxination reaction mixture was treated with 0.5–1 ml of the silylating mixture followed by mass spectral analysis.

Ester Synthesis—Representative examples of the methods for synthesizing C_1-esters are given here. All other esters were synthesized by similar procedures.

Dinoprostone Ethyl Ester (IV*a*)—A solution of 181 mg of II in a mixture of 2 ml of dimethyl sulfoxide, 0.2 ml of *N,N*-diisopropylethylamine, and 1 ml of ethyl iodide was allowed to stand at room temperature for 3 hr. Silica gel TLC (ethyl acetate–acetic acid, 97:3) showed greater than 95% conversion of II to the less polar ester. The solution was diluted with 100 ml of ethyl acetate and extracted with 100 ml of aqueous 3% citric acid, and the organic phase was dried with sodium sulfate. After solvent removal at 40° under vacuum, the brown oily residue was chromatographed over 50 g of silica gel with ethyl acetate–methanol (99:1) as the eluant. The product fractions were identified by silica gel TLC. After solvent removal, 75 mg of a colorless oil was isolated.

Dinoprost Benzyl Ester (III*k*)—A solution of 116 mg of I in a mixture of 0.2 ml of *N,N*-diisopropylethylamine, 0.3 ml of benzyl bromide, and 3 ml of acetonitrile was stored at room temperature overnight. Silica gel TLC (ethyl acetate–acetic acid, 97:3) showed quantitative esterification. After extraction and column chromatography as for IV*a*, 85 mg of a colorless oil was isolated.

Biological: Hamster Antifertility Assay—The esters were evaluated for their ability to inhibit pregnancy following subcutaneous injection in adult female hamsters in estrus as reported previously (4, 12) using an ethanol–physiological saline (3:7) vehicle.

REFERENCES

(1) W. E. Magee, S. B. Armour, and O. V. Miller, *Biochim. Biophys. Acta*, **306**, 270 (1973).

(2) A. Robert, W. E. Magee, O. V. Miller, and J. E. Nezamis, *ibid.*, **348**, 269 (1974).

(3) N. Wiqvist, J. N. Martin, M. Bygdeman, and K. Green, *Prostaglandins*, **9**, 255 (1975).

(4) W. Morozowich, T. O. Oesterling, W. L. Miller, C. F. Lawson, J. R. Weeks, R. G. Stehle and S. L. Douglas, *J. Pharm. Sci.*, **68**, 833 (1979).

(5) H. Henecka, in "Methoden Der Organischen Chemie, Houben-Weyl," vol. 8, E. Müller, Ed., G. Thieme Verlag, Stuttgart, West Germany, 1952, p. 503.

(6) W. Morozowich and S. L. Douglas, *Prostaglandins*, **10**, 19 (1975).

(7) E. G. Daniels, W. C. Krueger, F. P. Kupiecki, J. E. Pike, and W. P. Schneider, *J. Am. Chem. Soc.*, **90**, 5894 (1968).

(8) Ono Pharmaceutical Co., Ltd., German pat. 2,118,242, 1973.

(9) J. E. Pike, F. H. Lincoln, and W. P. Schneider, *J. Org. Chem.*, **34**, 3552 (1969).

(10) M. F. Jones, *J. Pharm. Pharmacol.*, **25**, 900 (1973).

(11) M. Kurono, F. Lomoto, T. Chiba, and M. Hayashi (to Ono Pharmaceutical Co.), U.S. pat. 3,821,279 (1974).

(12) J. R. Weeks, D. W. DuCharme, W. E. Magee, and W. L. Miller, *J. Pharmacol. Exp. Ther.*, **186**, 67 (1973).

(13) E. J. Corey, N. M. Weinshenker, T. K. Schaaf, and W. Huber, *J. Am. Chem. Soc.*, **91**, 5675 (1969).

ACKNOWLEDGMENTS

The authors thank Mr. F. H. Lincoln and Mr. J. R. Kinner for providing samples of I and II, Mr. L. H. Humphrey for obtaining the mass spectral analyses, and Miss M. J. Sutton for technical assistance.

[1] Supplied by the Research Division, The Upjohn Co.

[2] Aldrich Chemical Co., Milwaukee, Wis., and Eastman Kodak Co., Rochester, N.Y.

[3] Burdick & Jackson, Muskegon, Mich.

[4] Silica gel 60, EM Laboratories, Inc., Elmsford, N.Y.

[5] Uniplate, Analtech Inc., Newark, Del.

[6] LBK 9000 spectrometer.

Molecular Topology and Aqueous Solubility of Aliphatic Alcohols

ARTHUR CAMMARATA

Received August 31, 1978, from the *School of Pharmacy, Temple University, Philadelphia, PA 19140.* Accepted for publication December 28, 1978.

Abstract □ A physically based method for arriving at topological indexes is described. The derived indexes correlate with molecular surface areas and with the molecular connectivity index. The newly derived index seems to account better for the expected distinctions among primary, secondary, and tertiary alcohol aqueous solubilities. This study suggests that the Del Re method for calculating molecular charges and dipole moments also may be used, without appreciable change, to provide estimates of molecular refraction.

Keyphrases □ Alcohols, aliphatic—molecular topology, aqueous solubility, structure–activity relationships □ Topological indexes—aliphatic alcohols, molecular surface area, molecular connectivity, aqueous solubility, structure–activity relationships □ Solubility, aqueous—aliphatic alcohols, molecular topology, structure–activity relationships □ Structure–activity relationships—aliphatic alcohols, molecular topology, aqueous solubility

About 3 years ago, an approach was presented (1) for assigning a numerical index to acyclic hydrocarbons and for ranking them according to their degree of branching. To each atom (vertex) of a molecular structure (graph) was assigned a value $1/\nu^{1/2}$, where ν is the vertex valency. The valency may be taken as the number of valence electrons less the number of hydrogens associated with an atom. Each molecular bond (edge) was characterized by the product of associated atom values: $1/(\nu_i\nu_j)^{1/2}$. The branching index was obtained by summing all bond values appropriate to a molecule. Reciprocal values were used to distinguish bond types since the branching indexes thus derived parallel the ordering for branched structures arrived at from a binary representation of their connectivity (bonding or topological) matrixes.

BACKGROUND

This approach has been extended considerably (2). In particular, the treatment of cyclic aliphatics, alkenes, aromatics, and heteroatomic substances was left unspecified previously (1). The definition for ν [also termed δ (2)] was extended to include first row atoms of the periodic table (C, N, and O) irrespective of the nature of the bonding; valency values for the halogens and for sulfur were established empirically; and an adjustment to the branching index (termed χ), which is appropriate to cyclic aliphatics, was provided (2).

No physical definition for the branching index exists, although it appears to be related to molecular refraction or to molecular volume by the nature of its construction. The physical properties of branched aliphatic substances frequently differ from those of corresponding n-aliphatic substances. Hence, a graph of a physical property (or its logarithm) against an integer (1, 2, . . .) representing the number of carbon atoms in a side chain generally will be linear for the n-aliphatic substances, but considerable departures from this line most often will be noted for branched aliphatic substances. An index such as that described, which allows both n-aliphatic and branched aliphatic substances to lie on a line when graphed against a physical property, reflects a change due to branching in molecular refraction or to molecular volume, because these are the principal physical attributes of n-aliphatic substances.

In a sense, the derivation of branching indexes by the described approach corresponds to the determination of a molecular refraction value using bond refractions adjusted according to the nature of the immediate molecular environment. That is, molecular refractions, which are usually considered to be additive–constitutive properties, are in reality only approximately additive–constitutive; more accurate estimates require consideration of the perturbations induced by differing atomic environments. Such a perturbational approach has been taken (3, 4) for molecular dipole calculation. Bond dipoles are vectorially additive, but the effect of differing atomic environments has to be taken into account for more accurate molecular dipole estimates.

In this study, the perturbational approach described previously (3–5) was applied topologically to arrive at numerical indexes appropriate to a given molecule. The indexes obtained for a hydrocarbon series have the same general attributes as the molecular connectivity index. The indexes obtained for a series of 51 aliphatic alcohols correlate with their aqueous solubilities similarly to the correlations reported when their molecular surface areas (6) or connectivity indexes (7) were used. These results suggest that the perturbational approach may provide a means of arriving at topographically consistent molecular refraction and charge estimates.

EXPERIMENTAL

Isolated atoms, when bonded, have their properties changed. The electron affinity toward an isolated atom differs from the electron affinity for a bonded atom. Hence, depending on the bonding about an atom, the electronegativity and, consequently, the charge and polarizability characteristics of the atom will vary. For a molecule such as isobutane (I) (hydrogen atoms suppressed for simplicity), a given atomic property for a bonded atom, δ_i, may be said to be perturbed from the isolated atom value, δ_i^0, in a linear manner with respect to each similar atomic property for its immediate neighbors. Thus, a set of equations may be written (one equation for each atom of the molecule) that represents the existing perturbations within a molecule (Eqs. 1*a*–1*d*):

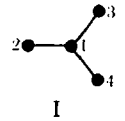

I

$$\delta_1 = \delta_1^0 + \gamma_{12}\delta_2 + \gamma_{13}\delta_3 + \gamma_{14}\delta_4 \quad \text{(Eq. 1}a\text{)}$$

$$\delta_2 = \delta_2^0 + \gamma_{21}\delta_1 \quad \text{(Eq. 1}b\text{)}$$

$$\delta_3 = \delta_3^0 + \gamma_{31}\delta_1 \quad \text{(Eq. 1}c\text{)}$$

$$\delta_4 = \delta_4^0 + \gamma_{41}\delta_1 \quad \text{(Eq. 1}d\text{)}$$

The coefficients γ_{ij} provide a measure of the influence of bonded atom i on bonded atom j. With numerical values for γ_{ij} and δ_i^0, one can solve the simultaneous equations represented by Eq. 2 so as to estimate the atomic properties, δ_i, appropriate to the atoms in a given molecule:

$$\begin{vmatrix} 1 & -\gamma_{12} & -\gamma_{13} & -\gamma_{14} \\ -\gamma_{21} & 1 & 0 & 0 \\ -\gamma_{31} & 0 & 1 & 0 \\ -\gamma_{41} & 0 & 0 & 1 \end{vmatrix} \begin{vmatrix} \delta_1 \\ \delta_2 \\ \delta_3 \\ \delta_4 \end{vmatrix} = \begin{vmatrix} \delta_1^0 \\ \delta_2^0 \\ \delta_3^0 \\ \delta_4^0 \end{vmatrix} \quad \text{(Eq. 2)}$$

Inspection of Eq. 2 shows that the matrix of the γ_{ij} coefficients has the form of a bonding or topological matrix. Therefore, a consistently applied set of arbitrary values for δ_i^0 and γ_{ij} may be used to arrive at topographically meaningful indexes for the atoms of a molecule. The sum of the atom indexes would then provide a branching index. In this work, the following conditions were applied: (*a*) molecular structures were represented with the hydrogen atoms suppressed; (*b*) δ_i^0 values were chosen to correspond to the number of valence electrons on an atom ($\delta_C^0 = 4$; $\delta_O^0 = 6$); and (*c*) the value of γ_{ij} ($\gamma_{ij} = \gamma_{ji}$) was taken as 0.1 for C–C and C–O bonds because such a value provides computed atom indexes, δ_i, that are all positive.

0022-3549/79/0700-0839$01.00/0
© 1979, American Pharmaceutical Association

Table I—Aqueous Solubilities of Aliphatic Alcohols and Topological Indexes

Compound	Mole Fraction Solubility, $-\log X_2$[a]	M'	A'	A'_R	TSA[a]	χ[b]
1-Butanol	1.7500	26.11	0.972	0.624	272.1	2.414
2-Methylpropanol	1.7428	26.20	0.971	0.625	263.8	2.269
2-Butanol	1.7244	26.24	0.972	0.641	264.1	2.269
1-Pentanol	2.3318	31.09	1.173	0.825	303.9	2.914
3-Methylbutanol	2.2544	31.20	1.171	0.823	291.4	2.807
2-Methylbutanol	2.2071	31.19	1.172	0.826	289.4	2.769
2-Pentanol	2.0246	31.22	1.172	0.841	295.9	2.769
3-Pentanol	1.9609	31.23	1.173	0.844	293.5	2.807
3-Methyl-2-butanol	1.9259	31.33	1.172	0.843	284.3	2.641
2-Methyl-2-butanol	1.6085	31.43	1.171	0.855	282.5	2.561
2,2-Dimethyl-1-propanol	2.0295	31.43	1.167	0.823	283.5	2.561
1-Hexanol	2.9574	36.09	1.373	1.025	335.7	3.414
2-Hexanol	2.6122	36.22	1.373	1.042	327.7	3.269
3-Hexanol	2.5419	36.23	1.373	1.044	325.3	3.307
3-Methyl-3-pentanol	2.1086	36.47	1.371	1.056	305.8	3.122
2-Methyl-2-pentanol	2.2327	36.44	1.371	1.055	314.3	3.061
2-Methyl-3-pentanol	2.4452	36.35	1.372	1.044	314.3	3.179
3-Methyl-2-pentanol	2.4585	36.35	1.371	1.042	311.3	3.179
2,3-Dimethyl-2-butanol	2.1176	36.58	1.369	1.055	301.2	2.943
3,3-Dimethylbutanol	2.8703	36.39	1.368	1.021	307.5	3.061
3,3-Dimethyl-2-butanol	2.3593	36.55	1.368	1.040	296.7	2.943
4-Methylpentanol	2.7370	36.20	1.371	1.023	323.0	3.269
4-Methyl-2-pentanol	2.5338	36.33	1.371	1.041	314.9	3.124
2-Ethylbutanol	2.9558	36.44	1.371	1.055	308.6	3.345
Cyclohexanol	2.1645	37.35	1.324	0.995	290.5	3.393
1-Heptanol	3.5545	41.08	1.573	1.225	367.5	3.914
2-Methyl-2-hexanol	2.8195	41.43	1.571	1.255	346.1	3.561
3-Methyl-3-hexanol	2.7286	41.48	1.571	1.257	337.7	3.622
3-Ethyl-3-pentanol	2.5785	41.47	1.572	1.259	324.4	3.683
2,3-Dimethyl-2-pentanol	2.6154	41.59	1.569	1.255	323.8	3.481
2,3-Dimethyl-3-pentanol	2.5875	41.58	1.570	1.257	321.8	3.504
2,4-Dimethyl-2-pentanol	2.6775	41.54	1.569	1.253	328.6	3.416
2,4-Dimethyl-3-pentanol	2.9621	41.44	1.572	1.246	331.7	3.552
2,2-Dimethyl-3-pentanol	2.8934	41.56	1.569	1.243	326.1	3.481
3-Heptanol	3.1322	41.22	1.574	1.240	357.1	3.807
4-Heptanol	3.1333	41.22	1.574	1.245	357.1	3.807
1-Octanol	4.0906	46.08	1.773	1.226	399.4	4.414
2,2,3-Trimethyl-3-pentanol	3.0184	46.84	1.766	1.461	335.2	3.811
2-Octanol	3.8105	46.21	1.773	1.435	391.0	4.269
2-Ethylhexanol	3.9150	46.22	1.722	1.427	371.3	4.345
1-Nonanol	4.7449	51.07	1.974	1.374	431.2	4.914
2-Nonanol	4.4895	51.20	1.973	1.643	423.2	4.769
3-Nonanol	4.4024	51.21	1.974	1.644	420.8	4.807
4-Nonanol	4.3298	51.20	1.974	1.644	420.8	4.807
5-Nonanol	4.2396	51.21	1.974	1.645	420.8	4.807
2,6-Dimethyl-3-heptanol	4.2534	51.41	1.972	1.643	394.0	5.517
3,5-Dimethyl-4-heptanol	4.0458	51.49	1.971	1.645	379.3	4.628
1,1-Diethylpentanol	4.1650	51.46	1.973	1.660	372.5	4.683
7-Methyloctanol	4.2396	51.20	1.971	1.623	418.7	4.769
3,5,5-Trimethylhexanol	4.2506	51.49	1.968	1.620	376.6	4.454
1-Decanol	5.4438	56.07	2.174	1.826	463.0	5.414

[a] From Ref. 6. [b] From Ref. 7.

RESULTS AND DISCUSSION

The 51 aliphatic alcohols listed in Table I were the subject of a study correlating molecular surface area with aqueous solubility (6). The same alcohols were included in an investigation correlating aqueous solubility with the molecular connectivity index, χ (7). These compounds represent a variety of *n*-aliphatic and branched aliphatic alcohols and constitute a good series for testing the relation between the newly derived branching index, M', and the molecular connectivity index. Linear regression performed on the indexes leads to the correlation equation:

$$\chi = 0.0990(\pm 0.0031)M' - 0.3981(\pm 0.1292) \qquad \text{(Eq. 3)}$$
$$n = 51 \quad s = 0.175 \quad r = 0.976 \quad F(1,49) = 982.7$$

where n is the total number of compounds, s is the standard error of the estimate, r is the correlation coefficient, and F is the computed F ratio for the correlation. The values in parentheses beside each regression coefficient are the standard errors for the regression coefficient estimates. The correlation between the two indexes is highly significant ($p < 0.01$).

A comparison of atom indexes for select molecules is instructive. In the surface area approach (6) and the molecular connectivity approach (2), hydrogen atoms bonded to carbon are taken into account either explicitly in terms of their contribution to a van der Waals radius or implicitly as the difference between the valence electron number and the number of hydrogens bonded to an atom. In the present approach, hydrogen atoms are not considered either explicitly or implicitly; a molecule is viewed as a linked chain of C and O atoms and with no other distinction.

Table II compares indexes for the methyl and methylene groups in 1-nonanol. The surface area approach shows that the terminal methyl group differs from the methylene groups and that the methylene groups nearest the terminal points of the chain differ from those more central in the chain. A similar pattern is noted for the atom indexes obtained in this work but not for the bond indexes obtained from the molecular connectivity approach. The molecular connectivity approach distinguishes a terminal methyl group from internal methyl groups since the product $(1/v_i^{1/2}v_j^{1/2})$ differs in each instance; but the methylene groups in the chain necessarily are identical as in this instance the product $(1/v_i^{1/2}v_j^{1/2})$ is the same. Since the results of this work are purely topographical in origin, methyl and methylene group distinctions apparently are a necessary consequence of both molecular topography (geometry) and atomic valency. The perturbational approach described in this work can be extended to include hydrogens. In principle, both topographical and valency effects can be taken into account.

Molecular branching or cyclization can affect the molecular physical properties by reducing the surface exposed to an external environmental influence. For example, neopentane as opposed to pentane has the central carbon atom effectively shielded from external influences by the methyl groups bonded to it. Cyclohexane as opposed to *n*-hexane has the inner

Table II—Methyl and Methylene Group Distinctions in 1-Nonanol

CH_3–CH_2–CH_2–CH_2–CH_2–CH_2–CH_2–CH_2–CH_2–OH
9 8 7 6 5 4 3 2 1

Group	Atom Index: Exposed Surface Area[a]	δ_i	$1/\nu_i^{1/2}$[b]
OH	59.15	6.51	1.000
CH_2(1)	45.43	5.15	0.707
CH_2(2)	39.80	5.01	0.707
CH_2(3)	31.82	5.00	0.707
CH_2(4)	31.82	5.00	0.707
CH_2(5)	31.82	4.99	0.707
CH_2(6)	31.82	4.99	0.707
CH_2(7)	31.82	4.99	0.707
CH_2(8)	42.75	4.94	0.707
CH_3(9)	84.92	4.49	1.000

[a] From Ref. 6. [b] These atom indexes are used to derive a bond index, which is the basis of the approach in Ref. 1.

surfaces of the ring atoms shielded from external influences to a greater extent than the outer surfaces of the ring atoms. Branched or cyclic substances will be expected to have lower surface areas, molecular refractions, and molecular volumes when compared with isomeric straight-chain substances. A branching index, irrespective of its origin, seeks to mirror this expectation.

Table III compares the total surface area, the perturbationally derived index M', and the connectivity index χ for these illustrative compounds. The connectivity index for the acyclic hydrocarbons mirrors the order of their computed total surface areas, but a comparison of cyclic and straight-chain isomers shows that the order is reversed. Since the molecular connectivity approach is bond centered and cyclic hydrocarbons contain one more bond than their acyclic counterparts, an amount corresponding to the additional bond contribution should be subtracted from the computed χ value for cyclic hydrocarbons when making such comparisons (2). This adjustment properly orders χ with respect to total surface area in a comparison of cyclic with noncyclic hydrocarbons.

Since the perturbationally derived index is atom centered rather than bond centered, no adjustment for cyclic hydrocarbon indexes seems necessary. However, a comparison of M' with the total surface areas for the molecules in Table III shows that in each case the order is the reverse of that expected. This result can be traced to the fact that in the perturbational approach the more highly substituted atoms have higher derived atom indexes. Hence, atoms that are more shielded from external environmental influences are weighted more heavily in M' ($\equiv \Sigma\, \delta_i$).

An index that would weight shielded atoms less than those that are more external would be more physically realistic. For simplicity, one may make the definition $A' = \Sigma\, (1/\delta_i)$, although such a definition still will tend to overweight heavily shielded atoms. This index provides the expected surface area ordering for the compounds of Table III. When compared to the χ index, the A' index is slightly less satisfactory than M', as a statistical comparison for Eqs. 3 and 4 shows:

$$\chi = 2.573(\pm 0.088)A' - 0.317(\pm 0.138) \qquad \text{(Eq. 4)}$$
$$n = 51 \quad s = 0.197 \quad r = 0.972 \quad F(1,49) = 841.2$$

The correlation coefficients and calculated F ratios for Eqs. 5 and 6 show that the χ index has a slight statistical edge over A' in correlating the total surface areas (TSA) for the alcohols in Table I:

$$A' = 0.0060(\pm 0.0003)\text{TSA} - 0.515(\pm 0.103) \qquad \text{(Eq. 5)}$$
$$n = 51 \quad s = 0.105 \quad r = 0.943 \quad F(1,49) = 394.4$$

$$\chi = 0.0162(\pm 0.0006)\text{TSA} - 1.883(\pm 0.230) \qquad \text{(Eq. 6)}$$
$$n = 51 \quad s = 0.234 \quad r = 0.960 \quad F(1,49) = 579.7$$

The alcohol aqueous solubilities (Table I) have been correlated with total surface area (6) and with the χ index (7). There are four fewer alcohols in Table I than in the total surface area study (6); the four alcohols not considered are all long chain n-aliphatic alcohols and are equivalent to those in the study involving χ. The solubilities can be correlated by the respective indexes (Eqs. 7–9):

$$-\log X_2 = 0.0185(\pm 0.0006)\text{TSA} - 3.309(\pm 0.220) \qquad \text{(Eq. 7)}$$
$$n = 51 \quad s = 0.224 \quad r = 0.972 \quad F(1,49) = 832.8$$

$$-\log X_2 = 2.833(\pm 0.140)A' - 1.337(\pm 0.218) \qquad \text{(Eq. 8)}$$
$$n = 51 \quad s = 0.311 \quad r = 0.945 \quad F(1,49) = 408.2$$

Table III—Accessible Area Distinctions between Select Molecules

Compound	Structure	Molecular Index: Total Surface Area[a]	M'	χ	A'
n-Pentane		287.0	23.84	2.414	1.048
Neopentane		270.1	24.15	2.000	1.043
n-Hexane	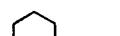	319	28.84	2.914	1.248
Cyclohexane		279.1	29.94	3.000	1.200

[a] Reference 6.

$$-\log X_2 = 1.093(\pm 0.042)\chi - 0.961(\pm 0.155) \qquad \text{(Eq. 9)}$$
$$n = 51 \quad s = 0.248 \quad r = 0.965 \quad F(1,49) = 673.5$$

The computed correlation coefficients and F ratios for these correlations indicate that total surface area provides a better fit and A' a poorer fit of the data than does χ. All fits, however, are highly significant.

For any isomeric aliphatic alcohol series, the aqueous solubility increases in the order: primary < secondary < tertiary. The increase in solubility tends to parallel the carbonium-ion stability and suggests a distinction in the C–O bond character among primary, secondary, and tertiary alcohols. Such isomeric alcohols can be distinguished using the indexes described in the following way: (*a*) surface areas—separate the hydroxyl surface area (OHSA) from the total surface area to provide a hydrocarbon residue surface area (HYSA); (*b*) molecular connectivity—separate the C–O bond contribution (C_{CO}) from χ to provide the residual hydrocarbon index χ_R; and (*c*) perturbational—sum the atom indexes for a C–O bond (A'_{CO}) and separate the result from A' to provide the residual hydrocarbon index A'_R. A regression analysis of the alcohol solubilities using the respective hydroxyl and hydrocarbon residue indexes leads to:

$$-\log X_2 = 0.0265(\pm 0.0028)\text{OHSA} + 0.0184(\pm 0.0006)\text{HYSA} - 3.6227(\pm 0.2332) \qquad \text{(Eq. 10)}$$
$$n = 51 \quad s = 0.209 \quad r = 0.976 \quad F(2,48) = 480.7$$

$$-\log X_2 = 25.62(\pm 2.59)A'_{CO} + 2.91(\pm 0.11)A'_R - 8.94(\pm 0.88) \qquad \text{(Eq. 11)}$$
$$n = 51 \quad s = 0.230 \quad r = 0.971 \quad F(2,48) = 394.5$$

$$-\log X_2 = 3.060(\pm 0.444)C_{CO} + 1.064(\pm 0.043)\chi_R - 2.074(\pm 0.304) \qquad \text{(Eq. 12)}$$
$$n = 51 \quad s = 0.253 \quad r = 0.965 \quad F(2,48) = 323.4$$

For this analysis, the surface area values provide only slightly better correlation than do the corresponding perturbational indexes. These correlations are somewhat more significant than the correlation using molecular connectivity indexes.

A comparison of the correlation coefficients for the single-parameter and two-parameter relations (Eqs. 7–9 *versus* Eqs. 10–12) is instructive. No appreciable increase in the correlation coefficient is noted for the relations involving either the surface area index or the molecular connectivity index. However, for the correlations involving the perturbational index, the correlation coefficient is improved. Apparently, the expected hydroxyl group influence in primary, secondary, and tertiary alcohols on aqueous solubility is reflected better by the perturbational approach than by either the surface area or molecular connectivity approach.

CONCLUSIONS

The perturbational approach described previously (3–5) for the calculation of molecular charges and dipole moments contains the essential features for arriving at a topographical index[1]. The original parameterization given for the calculation of molecular charges probably can be maintained unchanged and the calculations can provide a topographical index related to molecular refraction and volume as well as charges. A

[1] Molecular connectivity indexes were derived for atoms, and these indexes were shown to correlate with CNDO/2 calculated electronic charges in alkanes. See L. H. Hall and L. B. Kier, *Tetrahedron*, 33, 1953 (1977).

combination of charge and molecular refraction indexes could extend greatly the applicability range of solubility-related correlation analyses such as have been reported for aromatic substances (8, 9). Since this approach is atom centered rather than bond centered, it appears highly suitable for arriving at molecular descriptors for pattern recognition studies (10, 11).

REFERENCES

(1) M. Randic, *J. Am. Chem. Soc.*, **97**, 6609 (1975).

(2) L. B. Kier and L. H. Hall, "Molecular Connectivity in Chemistry and Drug Research," Academic, New York, N.Y., 1978.

(3) G. Del Re, *J. Chem. Soc.*, **1958**, 4031.

(4) G. Del Re, B. Pullman, and T. Yonezawa, *Biochim. Biophys. Acta*, **75**, 153 (1963).

(5) A. N. Martin, J. Swarbrick, and A. Cammarata, "Physical Pharmacy," 2nd ed., Lea & Febiger, Philadelphia, Pa., 1969, p. 590.

(6) G. L. Amidon, S. H. Yalkowsky, and S. Leung, *J. Pharm. Sci.*, **63**, 1858 (1974).

(7) L. H. Hall, L. B. Kier, and W. J. Murray, *ibid.*, **64**, 1974 (1975).

(8) K. S. Rogers and A. Cammarata, *J. Med. Chem.*, **12**, 692 (1969).

(9) A. Cammarata and K. S. Rogers, *ibid.*, **14**, 269 (1971).

(10) A. Cammarata and G. K. Menon, *ibid.*, **19**, 739 (1976).

(11) G. K. Menon and A. Cammarata, *J. Pharm. Sci.*, **66**, 304 (1977).

Rheological and Drug Release Properties of Oil Gels Containing Colloidal Silicon Dioxide

M. SHERRIFF * **and R. P. ENEVER** ˣ

Received July 25, 1978, from the *Department of Pharmaceutics, School of Pharmacy, University of London, London WC1N 1AX, England.* Accepted for publication December 27, 1978. *Present address: Department of Pharmaceutical Chemistry, School of Pharmacy, University of London, London WC1N 1AX, England.

Abstract □ The rheological properties of oil gels prepared by dispersing colloidal silica in *n*-dodecane and 1-dodecanol were examined. The differences in gel strength using these two media were accounted for by the difference in the extent of hydrogen bond formation between the silanol groups on the silica surface. The incorporation of methyl salicylate further modified the rheological properties of the gels. The drug was capable of hydrogen bonding with silanol groups in the *n*-dodecane gels, which increase gel strength at low concentrations; at high concentrations, the drug acted as a plasticizer. In 1-dodecanol systems, the drug acted solely as a plasticizer. Adsorption studies showed that methyl salicylate was adsorbed only on the silica particles in the *n*-dodecane medium. Interaction of the drug with the silanol groups in the *n*-dodecane systems did not appear to effect methyl salicylate release from the gels.

Keyphrases □ Gels—colloidal silica in *n*-dodecane and 1-dodecanol, rheological analysis, hydrogen bonding, methyl salicylate incorporation and release □ Colloidal silica—in *n*-dodecane and 1-dodecanol gels, rheological analysis, hydrogen bonding, methyl salicylate incorporation and release □ *n*-Dodecane—gels, colloidal silica, rheological analysis, methyl salicylate incorporation and release □ 1-Dodecanol—gels, colloidal silica, rheological analysis, methyl salicylate incorporation and release □ Methyl salicylate—gels, colloidal silica, *n*-dodecane, 1-dodecanol, rheological analysis

Colloidal silicon dioxide (fumed silica), produced by the vapor-phase hydrolysis of silicon tetrachloride, is used widely in the pharmaceutical industry as a binder and glidant in tablets and as a suspending agent and viscosity modifier in suspensions, ointments, and suppositories. Its use as a viscosity modifier is largely attributable to the ability of the very small silica particles to form a network structure throughout the medium by interparticle hydrogen bonding *via* the silanol groups on the silica surface. In addition to these particle interactions, there is possible bonding between the silanol groups and other components that are also capable of hydrogen bond formation. A detailed investigation of this type of interaction was published (1).

Modification of the magnitude of the interparticle interactions and production of ointment bases of different consistencies are possible by selecting, as dispersion media, oils that differ from each other in hydrogen bonding ability. Incorporation of a drug capable of hydrogen bonding into such bases might be expected to influence not only their rheological characteristics but also their drug release properties.

The object of this work was to quantify some of these phenomena by incorporating methyl salicylate into model gel systems prepared by dispersing fumed silica in the nonhydrogen bonding *n*-dodecane and the hydrogen bonding analog 1-dodecanol. The influences of silica and drug concentration on rheological and release properties are reported.

EXPERIMENTAL

Materials—Specially pure (99%) 1-dodecanol[1], laboratory reagent grade *n*-dodecane[1] and BP quality methyl salicylate[2] were used as received. Colloidal silicon dioxide[3] was dried for 1 hr at 150° and stored in a desiccator prior to use.

Gel Preparation—The requisite amount of continuous phase, containing drug where appropriate, was added to the silica, and the system was sonicated[4] for 30 sec to obtain a uniform dispersion. The gel was transferred to a glass container, sealed, and stored at 40°.

Rheological Properties—Dynamic rheological properties were measured using a modified Weissenberg rheogoniometer[5] in conjunction with a digital transfer function analyzer[6]. This rheogoniometer is one of the few commercially available instruments with facilities for both oscillatory (dynamic) and continuous shear measurements. The viscoelastic properties of materials may be evaluated using the oscillatory technique, and its application to pharmaceutical semisolid systems was described previously (2, 3).

Parallel plate geometry (platen radius of 3.75 cm) was used, and all gels were tested over the frequency range of 0.01–25.0 Hz using two torsion strips (Nos. 6 and 7) to minimize problems associated with natural resonance (4). The measurement temperature, as monitored by a thermocouple system[7] embedded in the top platen, was 37 ± 0.5°. Samples were

[1] British Drug Houses Ltd., Poole, Dorset, England.
[2] McCarthys Ltd., Romford, Essex, England.
[3] Aerosil 300, Bush, Beach and Segner Bayley Ltd., London, England.
[4] Kerry PUL 55 ultrasonic bath, Kerry Ultrasonics Ltd., Hitchin, Herts, England.
[5] R16, Sangamo Ltd., Bogner Regis, England.
[6] JM1600/JX1606, Solartron Ltd., Farnborough, Hampshire, England.
[7] Type 1604 electronic thermometer, Comark Electronics Ltd., Littlehampton, Sussex, England.

0022-3549/79/0700-0842$01.00/0
© 1979, American Pharmaceutical Association

combination of charge and molecular refraction indexes could extend greatly the applicability range of solubility-related correlation analyses such as have been reported for aromatic substances (8, 9). Since this approach is atom centered rather than bond centered, it appears highly suitable for arriving at molecular descriptors for pattern recognition studies (10, 11).

REFERENCES

(1) M. Randic, *J. Am. Chem. Soc.*, **97**, 6609 (1975).

(2) L. B. Kier and L. H. Hall, "Molecular Connectivity in Chemistry and Drug Research," Academic, New York, N.Y., 1978.

(3) G. Del Re, *J. Chem. Soc.*, **1958**, 4031.

(4) G. Del Re, B. Pullman, and T. Yonezawa, *Biochim. Biophys. Acta*, **75**, 153 (1963).

(5) A. N. Martin, J. Swarbrick, and A. Cammarata, "Physical Pharmacy," 2nd ed., Lea & Febiger, Philadelphia, Pa., 1969, p. 590.

(6) G. L. Amidon, S. H. Yalkowsky, and S. Leung, *J. Pharm. Sci.*, **63**, 1858 (1974).

(7) L. H. Hall, L. B. Kier, and W. J. Murray, *ibid.*, **64**, 1974 (1975).

(8) K. S. Rogers and A. Cammarata, *J. Med. Chem.*, **12**, 692 (1969).

(9) A. Cammarata and K. S. Rogers, *ibid.*, **14**, 269 (1971).

(10) A. Cammarata and G. K. Menon, *ibid.*, **19**, 739 (1976).

(11) G. K. Menon and A. Cammarata, *J. Pharm. Sci.*, **66**, 304 (1977).

Rheological and Drug Release Properties of Oil Gels Containing Colloidal Silicon Dioxide

M. SHERRIFF * **and R. P. ENEVER** ˣ

Received July 25, 1978, from the *Department of Pharmaceutics, School of Pharmacy, University of London, London WC1N 1AX, England.* Accepted for publication December 27, 1978. *Present address: Department of Pharmaceutical Chemistry, School of Pharmacy, University of London, London WC1N 1AX, England.

Abstract □ The rheological properties of oil gels prepared by dispersing colloidal silica in *n*-dodecane and 1-dodecanol were examined. The differences in gel strength using these two media were accounted for by the difference in the extent of hydrogen bond formation between the silanol groups on the silica surface. The incorporation of methyl salicylate further modified the rheological properties of the gels. The drug was capable of hydrogen bonding with silanol groups in the *n*-dodecane gels, which increase gel strength at low concentrations; at high concentrations, the drug acted as a plasticizer. In 1-dodecanol systems, the drug acted solely as a plasticizer. Adsorption studies showed that methyl salicylate was adsorbed only on the silica particles in the *n*-dodecane medium. Interaction of the drug with the silanol groups in the *n*-dodecane systems did not appear to effect methyl salicylate release from the gels.

Keyphrases □ Gels—colloidal silica in *n*-dodecane and 1-dodecanol, rheological analysis, hydrogen bonding, methyl salicylate incorporation and release □ Colloidal silica—in *n*-dodecane and 1-dodecanol gels, rheological analysis, hydrogen bonding, methyl salicylate incorporation and release □ *n*-Dodecane—gels, colloidal silica, rheological analysis, methyl salicylate incorporation and release □ 1-Dodecanol—gels, colloidal silica, rheological analysis, methyl salicylate incorporation and release □ Methyl salicylate—gels, colloidal silica, *n*-dodecane, 1-dodecanol, rheological analysis

Colloidal silicon dioxide (fumed silica), produced by the vapor-phase hydrolysis of silicon tetrachloride, is used widely in the pharmaceutical industry as a binder and glidant in tablets and as a suspending agent and viscosity modifier in suspensions, ointments, and suppositories. Its use as a viscosity modifier is largely attributable to the ability of the very small silica particles to form a network structure throughout the medium by interparticle hydrogen bonding *via* the silanol groups on the silica surface. In addition to these particle interactions, there is possible bonding between the silanol groups and other components that are also capable of hydrogen bond formation. A detailed investigation of this type of interaction was published (1).

Modification of the magnitude of the interparticle interactions and production of ointment bases of different consistencies are possible by selecting, as dispersion media, oils that differ from each other in hydrogen bonding ability. Incorporation of a drug capable of hydrogen bonding into such bases might be expected to influence not only their rheological characteristics but also their drug release properties.

The object of this work was to quantify some of these phenomena by incorporating methyl salicylate into model gel systems prepared by dispersing fumed silica in the nonhydrogen bonding *n*-dodecane and the hydrogen bonding analog 1-dodecanol. The influences of silica and drug concentration on rheological and release properties are reported.

EXPERIMENTAL

Materials—Specially pure (99%) 1-dodecanol[1], laboratory reagent grade *n*-dodecane[1] and BP quality methyl salicylate[2] were used as received. Colloidal silicon dioxide[3] was dried for 1 hr at 150° and stored in a desiccator prior to use.

Gel Preparation—The requisite amount of continuous phase, containing drug where appropriate, was added to the silica, and the system was sonicated[4] for 30 sec to obtain a uniform dispersion. The gel was transferred to a glass container, sealed, and stored at 40°.

Rheological Properties—Dynamic rheological properties were measured using a modified Weissenberg rheogoniometer[5] in conjunction with a digital transfer function analyzer[6]. This rheogoniometer is one of the few commercially available instruments with facilities for both oscillatory (dynamic) and continuous shear measurements. The viscoelastic properties of materials may be evaluated using the oscillatory technique, and its application to pharmaceutical semisolid systems was described previously (2, 3).

Parallel plate geometry (platen radius of 3.75 cm) was used, and all gels were tested over the frequency range of 0.01–25.0 Hz using two torsion strips (Nos. 6 and 7) to minimize problems associated with natural resonance (4). The measurement temperature, as monitored by a thermocouple system[7] embedded in the top platen, was 37 ± 0.5°. Samples were

[1] British Drug Houses Ltd., Poole, Dorset, England.
[2] McCarthys Ltd., Romford, Essex, England.
[3] Aerosil 300, Bush, Beach and Segner Bayley Ltd., London, England.
[4] Kerry PUL 55 ultrasonic bath, Kerry Ultrasonics Ltd., Hitchin, Herts, England.
[5] R16, Sangamo Ltd., Bogner Regis, England.
[6] JM1600/JX1606, Solartron Ltd., Farnborough, Hampshire, England.
[7] Type 1604 electronic thermometer, Comark Electronics Ltd., Littlehampton, Sussex, England.

0022-3549/79/0700-0842$01.00/0
© 1979, American Pharmaceutical Association

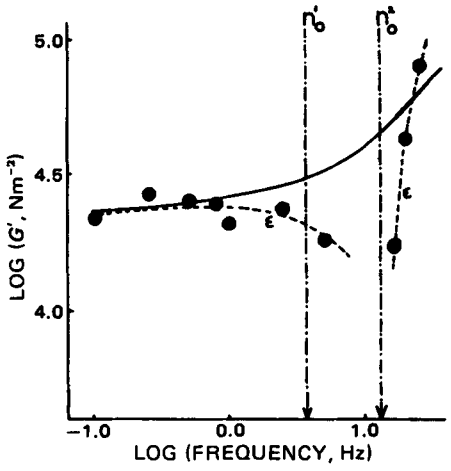

Figure 1—*Frequency dependence of log G′ for n-dodecane gel containing 8% (w/w) silica at 37°. The lines labeled ϵ represent the lower bounds of error due to the discontinuity in the data produced as the test frequency passed through the natural frequency of the rheogoniometer; n_0^1 is the resonance frequency for torsion strip No. 6, and n_0^2 is that for torsion strip No. 7.*

equilibrated for 30 min between the platens prior to measurement. For the 1-dodecanol gels, the gap width between platens was maintained at 0.05 ± 0.002 cm.

The analysis of Walters and Kemp (5) was used to evaluate the inertia parameter, α^2. The inertia parameter of the system is related to the complex dynamic viscosity of the test material, η^*, in the following manner:

$$\alpha^2 = \frac{-i\omega\rho}{\eta^*} \qquad \text{(Eq. 1)}$$

where i is the square root of -1, ω is the frequency of sinusoidal oscillation, and ρ is the density of the test sample.

For a linear viscoelastic system undergoing small amplitude oscillations, η^* is expressed as a combination of real and imaginary parts:

$$\eta^* = \eta^1 - \frac{iG'}{\omega} \qquad \text{(Eq. 2)}$$

where η^1 is the dynamic viscosity and G' is termed the real component of the complex shear modulus, G^*.

Once the inertia parameter has been determined, all test material parameters can be evaluated. Equation 2 can be transformed to give:

$$G^* = G' + iG'' \qquad \text{(Eq. 3)}$$

since the imaginary component, G'', of the complex shear modulus is given by:

$$G'' = \eta^1\omega \qquad \text{(Eq. 4)}$$

and G', the real component, describes the elastic properties of the system, and G'', the imaginary component, describes the viscous properties.

With parallel plate geometry, the upper platen is constrained by the torsion strip and the lower platen is oscillated with a frequency of ω Hz

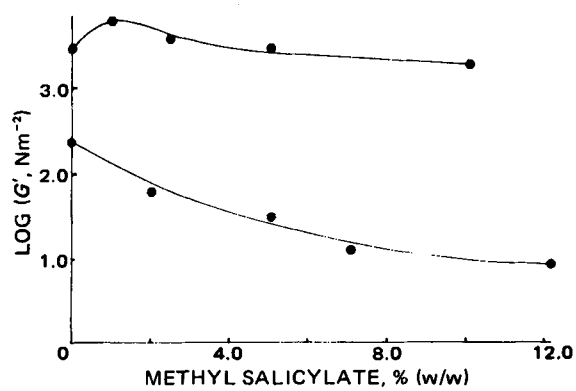

Figure 2—*Variation of G′ with methyl salicylate concentration for gels containing 8% (w/w) silica at 37°. Oscillation frequency was 0.25 Hz. Key: ●, n-dodecane; and ●, 1-dodecanol.*

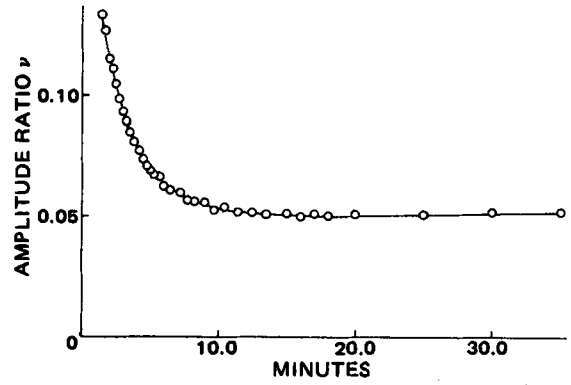

Figure 3—*Variation of amplitude ratio, ν, with time for 8% (w/w) silica in 1-dodecanol containing 12% (w/w) methyl salicylate at 37°. Oscillation frequency was 0.25 Hz.*

and amplitude θ_2. The platens are coupled through the sample under test; its rheological properties result in a phase lag, C, between the constrained and driven platens. In addition, the constrained platen oscillates with an amplitude of θ_1. The experimentally measured parameters for the sample were thus the amplitude ratio, ν, (θ_1/θ_2), and the phase lag, C, which were used to calculate α^2 using an iterative procedure, since:

$$\frac{\exp(iC)}{\nu} = \cos\alpha h + S\alpha h \sin\alpha h \qquad \text{(Eq. 5)}$$

where h was the gap between the platens and S was defined by the test geometry.

Subsequently, α was used to calculate G' and G'' using Eqs. 1–3.

Methyl Salicylate Adsorption—Methyl salicylate solutions ranging in concentration from 0.008 to 0.04 mg/ml were prepared in *n*-dodecane and 1-dodecanol. Ten milliliters of each solution was equilibrated with 0.1 g of silica in glass-stoppered vessels for 24 hr at 37°. The supernatant solutions were subsequently centrifuged[8] to remove the residual silica and assayed for equilibrium methyl salicylate content by UV spectrophotometry[9] using the 308-nm absorption maximum.

Drug Release from Gels—Approximately 10 ml of each gel was placed in a Perspex holder and covered with a cellophane membrane[10] so that there was complete contact between the gel and the 20.43 cm² of membrane area. The holder was placed at the bottom of a 1-liter, flat-bottom, glass reaction vessel containing 500 ml of pH 2.0 Clark and Lub buffer (6) at 37°. A stainless steel paddle stirrer was placed in the surface of the medium and rotated at 75 rpm. Aliquots were removed at 5-min intervals and assayed spectrophotometrically[9] for methyl salicylate with the absorption maximum at 238 nm.

Methyl Salicylate Partition Coefficients—Five-milliliter volumes of 1-mg/ml solutions of methyl salicylate in *n*-dodecane and 1-dodecanol were equilibrated with 5-ml volumes of pH 2.0 buffer at 37° for 1 week. Drug concentrations in organic and aqueous phases were determined spectrophotometrically[9] with the absorption maximum at 308 nm. The mean values of four determinations were used to calculate the partition coefficient (organic phase–pH 2.0 buffer).

RESULTS AND DISCUSSION

Preliminary experiments established that the gel properties were critically dependent on the preparation method; for this reason, the dispersion technique using an ultrasonic bath was used.

The *n*-dodecane gels exhibited a linear viscoelastic response under the test conditions. At any given silica concentration, G' increased slightly with frequency. Specimen data for a gel containing 8% (w/w) silica are shown in Fig. 1. The discontinuity was due to the test frequency passing through the natural frequency range of the rheogoniometer, n_0 (7). At any given frequency, G' increased as the silica concentration increased from 6 to 11% (w/w); G'' was lower than G' under all experimental conditions. These results are characteristic of the plateau region of viscoelastic response where there is reversible elastic deformation of the gel structure. Figure 2 shows the influence of methyl salicylate concentration on G' for *n*-dodecane gels containing 8% (w/w) silica. There was an initial

[8] Junior centrifuge, Gallenkamp Ltd., London, England.
[9] Unicam SP1800 UV spectrophotometer, Pye-Unicam Ltd., Cambridge, England.
[10] Visking tubing, Scientific Instrument Centre, London, England.

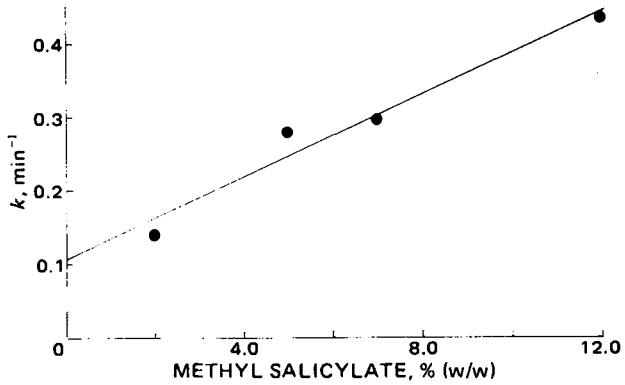

Figure 4—*Variation of first-order rate constant for gel breakdown, k, with methyl salicylate concentration for 1-dodecanol gels containing 8% (w/w) silica at 37°. Oscillation frequency was 0.25 Hz.*

increase in G' with drug concentration to a maximum of ~2% (w/w) methyl salicylate, followed by a progressive decline thereafter.

In contrast, the 1-dodecanol gels exhibited nonlinear viscoelastic behavior to the extent that there was a progressive decrease in ν during the time of the rheological measurement. This behavior (Fig. 3) indicates irreversible shear breakdown of the gel network. Analysis of the ν-time data using Guggenheim's method (8) showed that the breakdown obeyed first-order kinetics. The irreversibility of the process was evident from the fact that a sheared sample left between the plates of the rheogoniometer for 15 hr only recovered to ~5% of its original ν value on reshearing. The 1-dodecanol systems also exhibited syneresis when placed in the rheogoniometer at narrow gap widths.

To minimize this problem and to obtain comparative data, all samples were tested using the 0.05-cm gap. As a consequence of this behavior, it must be emphasized that G' data for the 8% (w/w) silica in 1-dodecanol gels (Fig. 2) have no absolute meaning since they are values calculated 1 min after shear. Nevertheless, the plot demonstrates that there was a progressive decrease in G' with increasing methyl salicylate concentration and no evidence of a maximum in the relationship.

The 1-dodecanol systems contained such an excess of hydroxyl groups relative to silanol groups that the probability of silanol–1-dodecanol interactions was higher than that of silanol–silanol interactions. This fact accounts for the much weaker network structure exhibited by these gels when compared with the n-dodecane systems. Methyl salicylate incorporated into the 1-dodecanol gels would act solely as a plasticizer and would reduce G', since it is not likely that any silanol groups would be available for hydrogen bond formation with the drug. The efficiency of the methyl salicylate molecule as a plasticizer is demonstrated by examining its effect on the kinetics of breakdown of the 1-dodecanol gel. The influence of the drug concentration on the first-order rate constant, k (Fig. 4), clearly demonstrates the disruptive effect of the drug on the interparticulate network structure.

In the n-dodecane systems, since there is no possibility of hydrogen bonding between silanol groups and the continuous phase, all silanol groups are available for interparticle or drug–particle interactions. Therefore, the initial increase in G' with methyl salicylate concentration

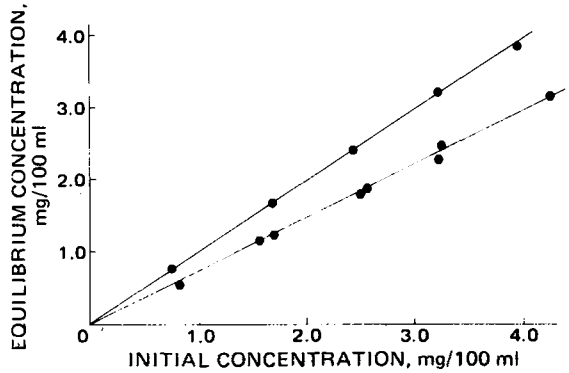

Figure 5—*Relation between initial and equilibrium methyl salicylate concentrations for systems containing 0.1 g of silica in 10 ml of* n-*dodecane (●) or 1-dodecanol (●) at 37°.*

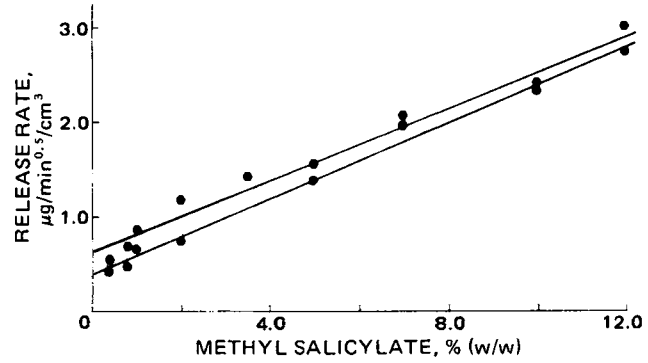

Figure 6—*Influence of continuous phase and methyl salicylate concentration on the release rate from gels containing 8% (w/w) silica at 37°. Key: ●, n-dodecane; and ●, 1-dodecanol.*

(Fig. 2) can be attributed to the drug acting as a cross-linking agent, *via* hydrogen bonds, and extending the network structure. Since there is a finite number of silanol groups in the gels, a point will be reached where they will all be involved in particle–particle or drug–particle interactions; upon further addition, methyl salicylate will act as a plasticizer and will reduce G' in a similar manner to that seen with the 1-dodecanol gels. A crude estimate of the drug concentration needed to produce saturation of the available silanol groups can be made from a knowledge of the specific surface area of the silica, its concentration in the gel, and the number of silanol groups in a given surface area.

According to the manufacturer's data (9), on average there are three silanol groups/100 Å^2 of silica surface. For this silica sample, the specific surface calculated using the Brunauer, Emmett, and Teller equation for adsorption (10) was 300 m^2/g. If the gross assumptions are made that all silanol groups are available and that each methyl salicylate molecule can react with a silanol group, then all groups will have interacted when approximately 2% (w/w) methyl salicylate is present. In practice, the correspondence ratio between methyl salicylate and silanol groups would probably be less than 1:1, and this would reduce the saturation concentration. Despite the crudity of the calculation, the result is in agreement with the experimentally observed maximum in G'.

The ability of methyl salicylate to bond to silanol groups in n-dodecane gels but not in 1-dodecanol systems also was demonstrated by the results of the adsorption studies (Fig. 5). If no bonding occurred, there would be a linear relation between initial and equilibrium methyl salicylate concentrations with a slope of unity. Bond formation, with consequent absorption, would result in an initial linear relation of a slope less than unity. Least-squares regression analysis gave slope values of 0.986 for 1-dodecanol systems and 0.744 for n-dodecane systems.

The differing effects on gel structure produced by addition of methyl salicylate to the two systems should be reflected in the drug release data. Preliminary work showed no significant drug adsorption to the cellophane membrane in the drug release experiments. Linear relations were obtained on plotting amounts released per unit area against (time)$^{0.5}$ after steady-state conditions had been attained.

Figure 6 shows the relation between the slope values for such plots and drug concentrations for the two systems. The experimental scatter reflects the difficulty in obtaining high quality data in this particular experiment. For this reason, no attempt was made to calculate effective diffusion coefficients. Statistically, there was no significant difference in the slopes of the two lines (p = 0.05), and this result parallels the similarity of the oil–pH 2.0 buffer partition coefficients for the two oily media (193.3 for n-dodecane and 184.4 for 1-dodecanol).

The conclusion to be drawn is that the amount of methyl salicylate bound in the n-dodecane gels is small with respect to the total drug concentration in the gels available for diffusion. Nevertheless, if the drug incorporated had been of high potency, its ability to bond to the silanol groups might seriously have reduced its availability. Further work is in progress on such systems; the continuous phase hydrogen bonding capability will be varied in a systematic manner to permit an investigation of the interaction thermodynamics.

REFERENCES

(1) K. Marshall and C. H. Rochester, *Faraday Discuss. Chem. Soc. No. 59.*, **1975**, 117.

(2) B. Warburton and S. S. Davis, *Rheol. Acta*, **8**, 205 (1969).

(3) S. S. Davis, *J. Pharm. Sci.*, **60**, 1351 (1971).

(4) K. Walters, "Rheometry," Chapman and Hall, London, England, 1975, pp. 151 *et seq.*
(5) K. Walters and R. A. Kemp, *Rheol. Acta*, **7**, 1 (1968).
(6) "Documenta Geigy," 7th ed., K. Diem and C. Lentner, Eds., J. R. Geigy, Basel, Switzerland, 1970, p. 208.
(7) T. E. R. Jones and K. Walters, *Rheol. Acta*, **10**, 365 (1971).
(8) E. A. Guggenheim, *Phil. Mag.*, **2**, 538 (1926).
(9) R. Bode, H. Ferch, and H. Fratzsher, *Kautsch. Gummi, Kunstst.*, **20**, 578 (1967).
(10) S. Brunauer, P. E. H. Emmett, and E. J. Teller, *J. Am. Chem. Soc.*, **60**, 309 (1938).

ACKNOWLEDGMENTS

A portion of this work was presented at the British Pharmaceutical Conference, St. Andrews, Scotland, 1976.

Quinazolines and 1,4-Benzodiazepines LXXXIX: Haptens Useful in Benzodiazepine Immunoassay Development

JAMES V. EARLEY, R. IAN FRYER ˣ, and ROBERT Y. NING

Received September 22, 1978, from the *Department of Chemical Research, Hoffmann-La Roche Inc., Nutley, NJ 07110.* Accepted for publication January 5, 1979.

Abstract □ The syntheses of some 1,4-benzodiazepines potentially useful as haptens are reported. These compounds are related to chlordiazepoxide, diazepam, nitrazepam, clonazepam, and some of their metabolites. The chemistry reported here is intended to support specific immunoassay development for these drugs.

Keyphrases □ Benzodiazepines—chemical synthesis, potentially useful haptens □ Tranquilizers—benzodiazepines, various, chemical synthesis, potentially useful haptens □ Haptens—benzodiazepines, chemical synthesis

Immunoassay (1, 2) is a powerful method for measuring drug levels in biological fluids. The extensive clinical use (3, 4) and continued development (4, 5) of benzodiazepines as a drug class make immunoassays for these compounds desirable. This paper reports some benzodiazepine hapten[1] syntheses. Many haptens reported here have been utilized (6–8) in the immunoassay development for clinically important benzodiazepines and their metabolites.

The synthetic compounds are presented in three groups. Where possible, the numerical sequence reflects the synthetic sequence. The end-products, XII–XXIV, in Group A are related to diazepam and metabolites of diazepam and chlordiazepoxide. Compounds XXXI–XXXVI in Group B are related to chlordiazepoxide. Group C contains compounds derived from nitrazepam, clonazepam, and their metabolites.

The synthetic methods are known either in the general art or in the special benzodiazepine chemistry described elsewhere (5, 9, 10). 5-Chloro-3-(4-hydroxyphenyl)-2,1-benzisoxazole (I) (11) and the corresponding 3-(4-aminophenyl) analog II (12–14) were the crucial starting materials for compounds in Groups A and B. All other compounds reported are new except for the following: IV (11, 15), VII (16), XXIV (6), XXV (17), XXXVIII (18), XXXVII (19), and XL (20). The preparation of VII, XXIV, and XL, however, is reported for the first time.

[1] Haptens are defined (1) as antigens that are coupled to larger molecules, usually proteins, to provoke an antibody response.

EXPERIMENTAL[2]

3-(4-Aminophenyl)-5-chloroanthranil (II) (12–14)—To a mixture of 100 g (0.662 mole) of *o*-nitrobenzaldehyde and 160 g (1.05 mole) of phosphorus oxychloride was added dropwise, with stirring, 100 g (1.08 moles) of aniline while the temperature was kept below 30°. After 3 hr at room temperature, the solution was heated at 75° for 18 hr and at 90° for 3 hr. (The reaction becomes exothermic when heated.)

The mixture was cooled, 200 ml of ethanol and 200 ml of concentrated hydrochloric acid were added, and the solution was heated to reflux for 3 hr with stirring. On cooling, the precipitate was collected and washed with acetone, resuspended in dilute ammonium hydroxide for 1 hr, and collected again. After crystallization from ethanol, 70 g (86%) of II was obtained. Recrystallization from ethanol gave orange rods, mp 208–211°.

4′-(5-Chloro-3-anthranilyl)-2,2,2-trifluoroacetanilide (III)—A mixture of 70 g (0.286 mole) of II, 75 g (0.357 mole) of trifluoroacetic anhydride, and 1 liter of tetrahydrofuran was heated to reflux for 30 min. After concentration to a small volume, ether (300 ml) was added. The solution was filtered to give 60 g of product and then was concentrated to give an additional 5 g. The filtrate was evaporated, and the residue was stirred with cold aqueous potassium carbonate solution and filtered.

The solid thus collected was dissolved in tetrahydrofuran and treated with charcoal. After filtration and concentration to a small volume, ether was added. A 10-g precipitate of III was collected to give a total yield of 75 g (77%). A sample recrystallized from tetrahydrofuran–hexane gave pale-yellow rods, mp 251–254°; IR (KBr): 3310 (NH) and 1705 (C=O) cm^{-1}.

Anal.—Calc. for $C_{15}H_8ClF_3N_2O_2$: C, 52.88; H, 2.37; N, 8.22. Found: C, 52.85; H, 2.32; N, 8.27.

2-Amino-5-chloro-4′-hydroxybenzophenone (IV) (11, 15)—To a solution of 83.7 g (0.34 mole) of 5-chloro-3-(4-hydroxyphenyl)-2,1-benzisoxazole (I) (11) in 1500 ml of acetic acid was added 45 g of iron filings. The mixture was stirred and heated on the steam bath for 20 min. Every 30 min, an additional 20 g of iron filings and 100 ml of water were added for 2.5 hr. After 30 min more, the reaction mixture was filtered while hot.

The collected precipitate was heated with acetic acid and filtered. The combined filtrates were diluted with ice water to precipitate 39.8 g (47%) of IV, mp 170–175°. Recrystallization from methanol–water gave yellow rods, mp 173–178°.

2-Amino -5- chloro-4′-(2,2,2-trifluoroacetamido)benzophenone

[2] Structural assignments are based on unambiguous spectral data and on related structures published elsewhere [R. I. Fryer, J. Blount, E. Reeder, E. J. Trybulski, and A. Walser, *J. Org. Chem.*, **43**, 4480 (1978)]. Only selected spectral data are presented here.

0022-3549/79/0700-0845$01.00/0
© 1979, American Pharmaceutical Association

(4) K. Walters, "Rheometry," Chapman and Hall, London, England, 1975, pp. 151 *et seq.*
(5) K. Walters and R. A. Kemp, *Rheol. Acta*, **7**, 1 (1968).
(6) "Documenta Geigy," 7th ed., K. Diem and C. Lentner, Eds., J. R. Geigy, Basel, Switzerland, 1970, p. 208.
(7) T. E. R. Jones and K. Walters, *Rheol. Acta*, **10**, 365 (1971).
(8) E. A. Guggenheim, *Phil. Mag.*, **2**, 538 (1926).
(9) R. Bode, H. Ferch, and H. Fratzsher, *Kautsch. Gummi, Kunstst.*, **20**, 578 (1967).
(10) S. Brunauer, P. E. H. Emmett, and E. J. Teller, *J. Am. Chem. Soc.*, **60**, 309 (1938).

ACKNOWLEDGMENTS

A portion of this work was presented at the British Pharmaceutical Conference, St. Andrews, Scotland, 1976.

Quinazolines and 1,4-Benzodiazepines LXXXIX: Haptens Useful in Benzodiazepine Immunoassay Development

JAMES V. EARLEY, R. IAN FRYER ˣ, and ROBERT Y. NING

Received September 22, 1978, from the *Department of Chemical Research, Hoffmann-La Roche Inc., Nutley, NJ 07110.* Accepted for publication January 5, 1979.

Abstract □ The syntheses of some 1,4-benzodiazepines potentially useful as haptens are reported. These compounds are related to chlordiazepoxide, diazepam, nitrazepam, clonazepam, and some of their metabolites. The chemistry reported here is intended to support specific immunoassay development for these drugs.

Keyphrases □ Benzodiazepines—chemical synthesis, potentially useful haptens □ Tranquilizers—benzodiazepines, various, chemical synthesis, potentially useful haptens □ Haptens—benzodiazepines, chemical synthesis

Immunoassay (1, 2) is a powerful method for measuring drug levels in biological fluids. The extensive clinical use (3, 4) and continued development (4, 5) of benzodiazepines as a drug class make immunoassays for these compounds desirable. This paper reports some benzodiazepine hapten[1] syntheses. Many haptens reported here have been utilized (6–8) in the immunoassay development for clinically important benzodiazepines and their metabolites.

The synthetic compounds are presented in three groups. Where possible, the numerical sequence reflects the synthetic sequence. The end-products, XII–XXIV, in Group A are related to diazepam and metabolites of diazepam and chlordiazepoxide. Compounds XXXI–XXXVI in Group B are related to chlordiazepoxide. Group C contains compounds derived from nitrazepam, clonazepam, and their metabolites.

The synthetic methods are known either in the general art or in the special benzodiazepine chemistry described elsewhere (5, 9, 10). 5-Chloro-3-(4-hydroxyphenyl)-2,1-benzisoxazole (I) (11) and the corresponding 3-(4-aminophenyl) analog II (12–14) were the crucial starting materials for compounds in Groups A and B. All other compounds reported are new except for the following: IV (11, 15), VII (16), XXIV (6), XXV (17), XXXVIII (18), XXXVII (19), and XL (20). The preparation of VII, XXIV, and XL, however, is reported for the first time.

[1] Haptens are defined (1) as antigens that are coupled to larger molecules, usually proteins, to provoke an antibody response.

EXPERIMENTAL[2]

3-(4-Aminophenyl)-5-chloroanthranil (II) (12–14)—To a mixture of 100 g (0.662 mole) of *o*-nitrobenzaldehyde and 160 g (1.05 mole) of phosphorus oxychloride was added dropwise, with stirring, 100 g (1.08 moles) of aniline while the temperature was kept below 30°. After 3 hr at room temperature, the solution was heated at 75° for 18 hr and at 90° for 3 hr. (The reaction becomes exothermic when heated.)

The mixture was cooled, 200 ml of ethanol and 200 ml of concentrated hydrochloric acid were added, and the solution was heated to reflux for 3 hr with stirring. On cooling, the precipitate was collected and washed with acetone, resuspended in dilute ammonium hydroxide for 1 hr, and collected again. After crystallization from ethanol, 70 g (86%) of II was obtained. Recrystallization from ethanol gave orange rods, mp 208–211°.

4′-(5-Chloro-3-anthranilyl)-2,2,2-trifluoroacetanilide (III)—A mixture of 70 g (0.286 mole) of II, 75 g (0.357 mole) of trifluoroacetic anhydride, and 1 liter of tetrahydrofuran was heated to reflux for 30 min. After concentration to a small volume, ether (300 ml) was added. The solution was filtered to give 60 g of product and then was concentrated to give an additional 5 g. The filtrate was evaporated, and the residue was stirred with cold aqueous potassium carbonate solution and filtered.

The solid thus collected was dissolved in tetrahydrofuran and treated with charcoal. After filtration and concentration to a small volume, ether was added. A 10-g precipitate of III was collected to give a total yield of 75 g (77%). A sample recrystallized from tetrahydrofuran–hexane gave pale-yellow rods, mp 251–254°; IR (KBr): 3310 (NH) and 1705 (C=O) cm^{-1}.

Anal.—Calc. for $C_{15}H_8ClF_3N_2O_2$: C, 52.88; H, 2.37; N, 8.22. Found: C, 52.85; H, 2.32; N, 8.27.

2-Amino-5-chloro-4′-hydroxybenzophenone (IV) (11, 15)—To a solution of 83.7 g (0.34 mole) of 5-chloro-3-(4-hydroxyphenyl)-2,1-benzisoxazole (I) (11) in 1500 ml of acetic acid was added 45 g of iron filings. The mixture was stirred and heated on the steam bath for 20 min. Every 30 min, an additional 20 g of iron filings and 100 ml of water were added for 2.5 hr. After 30 min more, the reaction mixture was filtered while hot.

The collected precipitate was heated with acetic acid and filtered. The combined filtrates were diluted with ice water to precipitate 39.8 g (47%) of IV, mp 170–175°. Recrystallization from methanol–water gave yellow rods, mp 173–178°.

2-Amino -5- chloro-4′-(2,2,2-trifluoroacetamido)benzophenone

[2] Structural assignments are based on unambiguous spectral data and on related structures published elsewhere [R. I. Fryer, J. Blount, E. Reeder, E. J. Trybulski, and A. Walser, *J. Org. Chem.*, **43**, 4480 (1978)]. Only selected spectral data are presented here.

0022-3549/79/0700-0845$01.00/0
© 1979, American Pharmaceutical Association

Structural Group A

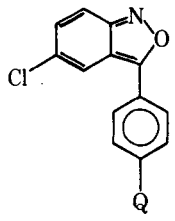

I: Q = OH
II: Q = NH_2
III: Q = $NHCOCF_3$

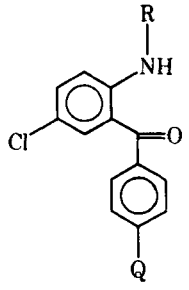

IV: Q = OH, R = H
V: Q = $NHCOCF_3$, R = H
VI: Q = $OCH_2CO_2CH_3$, R = H
VII: Q = OH, R = CH_3

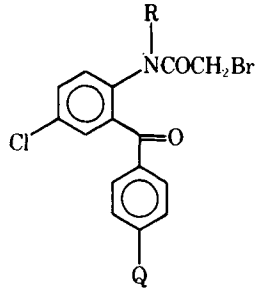

VIII: Q = OH, R = H
IX: Q = $NHCOCF_3$, R = H
X: Q = $OCH_2CO_2CH_3$, R = H
XI: Q = OH, R = CH_3

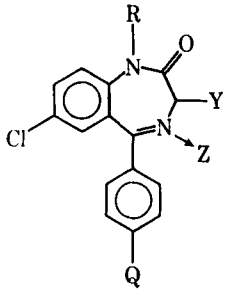

XII: Q = OH, R = H, Y = H
XIII: Q = $NHCOCF_3$, R = H, Y = H
XIV: Q = $OCH_2CO_2CH_3$, R = H, Y = H
XV: Q = OH, R = CH_3, Y = H
XVI: Q = OCH_3, R = CH_3, Y = H
XVII: Q = OCH_2CONH_2, R = H, Y = H
XVIII: Q = $OCH_2CONHNH_2$, R = H, Y = H
XIX: Q = $NHCOCF_3$, R = H, Y = H, Z = O
XX: Q = NH_2, R = H, Y = H, Z = O
XXI: Q = $NHCOCF_3$, R = H, Y = $OCOCH_3$
XXII: Q = NH_2, R = H, Y = OH

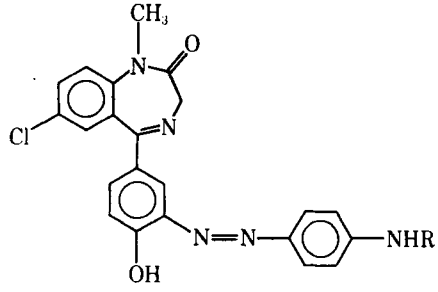

XXIII: R = $COCH_3$
XXIV: R = H

synthetic sequences

I, IV, VI, X, XIV–XVII, and XVIII
II, III, V, IX, XIII, XIX, XX, XXI, and XXII
IV, VIII, XII, and XV–XVI
XV, VII, XI, and XV
XV, XXIII, and XXIV

(V)—Following the procedure described for IV, III afforded V in an 88% yield. A sample was recrystallized from methanol to give yellow needles, which crystallized as a methanolate, mp 65–75°, reset 148–149°; IR ($CHCl_3$): 3500, 3420 (NH_2), 1740, and 1634 (2 C=O) cm^{-1}.

Anal.—Calc. for $C_{15}H_{10}ClF_3N_2O_2 \cdot CH_3OH$: C, 51.28; H, 3.77; N, 7.48. Found: C, 51.19; H, 3.71; N, 7.35.

2-[4-(2-Amino-5-chlorobenzoyl)phenoxy]acetic Acid (VI)—A solution of 30 g (0.12 mole) of IV in 75 ml of dry dimethylformamide under nitrogen was cooled in an ice bath, and 5.5 g (1.3 moles) of 57% sodium hydride in mineral oil was added with stirring. After 20 min, 24.5 g (0.16 mole) of methyl bromoacetate was added dropwise. The reaction mixture was allowed to stand at room temperature for 18 hr and then was poured into ice water. The precipitate was collected, dried, and recrystallized from methylene chloride–hexane to give VI as yellow needles (25.1 g, 65%), mp 144–147°; IR ($CHCl_3$): 3500, 3375 (NH_2), 1760, and 1638 (2 C=O) cm^{-1}.

Anal.—Calc. for $C_{16}H_{14}ClNO_4$: C, 60.10; H, 4.41; N, 4.38; Found: C, 60.03; H, 4.38; N, 4.28.

5-Chloro-4'-hydroxy-2-methylaminobenzophenone (VII) (16)—The 4.5 g of the XV–XVI mixture described under XV was heated on a steam bath for 2 hr with 70 ml of 48% hydrobromic acid and then at reflux for 1 hr. The reaction mixture was cooled, made basic with 3 *N* NaOH, and washed with 100 ml of ether. The water layer was acidified with hydrochloric acid and extracted with methylene chloride (2 × 100 ml). The methylene chloride extract was dried and evaporated. The residue was crystallized and recrystallized from aqueous methanol to give 2.9 g of VII as yellow rods, mp 163–164°.

Anal.—Calc. for $C_{14}H_{12}ClNO_2$: C, 64.25; H, 4.62; Cl, 13.55. Found: C, 64.03; H, 4.37; Cl, 13.50.

2-Bromo-4'-chloro-2'-(4-hydroxybenzoyl)acetanilide (VIII)[3]—A solution of 41 g (0.165 mole) of IV in 800 ml of ether and 200 ml of water was cooled to 5°. The mixture was stirred while 20 ml (0.277 mole) of bromoacetyl bromide and a 20% solution of sodium carbonate were added alternately, keeping the solution slightly basic. After 20 min, the reaction mixture was filtered to collect 60 g (~100%) of VIII, mp 201–202°. Recrystallization from ethanol gave colorless prisms, mp 201–203°.

Anal.—Calc. for $C_{15}H_{11}BrClNO_3$: C, 48.87; H, 3.01, total halides, 31.30. Found: C, 49.17; H, 3.34; total halides, 30.84.

2-(Bromoacetamido) - 5-chloro-4'-(2,2,2-trifluoroacetamido)-benzophenone (IX)—Following the procedure described for VIII but with sodium bicarbonate instead of sodium carbonate, V afforded IX in a 96% yield. Recrystallization of IX from methylene chloride–methanol–petroleum ether gave off-white rods, mp 198–201°; IR (KBr): 1750, 1663, and 1640 (3 C=O) cm^{-1}.

Anal.—Calc. for $C_{17}H_{11}BrClF_3N_2O_3$: C, 44.03; H, 2.39; N, 6.04. Found: C, 44.22; H, 2.56; N, 6.03.

2-Bromo - 4'-chloro-2'-(4-methoxycarbonylmethoxybenzoyl)-acetanilide (X)—To a stirring solution of 16 g (0.05 mole) of VI in 350 ml of methylene chloride was added 6.3 g (0.075 mole) of sodium bicarbonate, followed dropwise by 12.1 g (0.06 mole) of bromoacetyl bromide. After 18 hr, 125 ml of water was added; the organic layer was separated, dried, and evaporated. Crystallization of the residue from methylene chloride–methanol afforded 19 g (86%) of X as colorless needles, mp 124–126°; IR ($CHCl_3$): 3300 (NH), 1760, 1682, and 1640 (3 C=O) cm^{-1}.

Anal.—Calc. for $C_{18}H_{15}BrClNO_5$: C, 49.06; H, 3.43; N, 3.18. Found: C, 48.96; H, 3.31; N, 3.05.

2-Bromo-4'-chloro-2'-(*p*-hydroxybenzoyl)-*N*-methylacetanilide (XI)[3]—To a solution of 2.9 g (0.011 mole) of VII in 100 ml of methylene chloride were added 2.4 g (0.012 mole) of bromoacetyl bromide, 1 g (0.012 mole) of sodium bicarbonate, and 25 ml of water. The reaction was stirred for 18 hr. The water layer was separated and extracted with 50 ml of methylene chloride. The combined organic layers were dried and evaporated. Crystallization of the residue from methanol and recrystallization from acetone–hexane gave 2.2 g (52%) of XI as colorless prisms, mp 187–189°.

[3] This compound was first prepared by Dr. A. Stempel of these laboratories.

Structural Group B

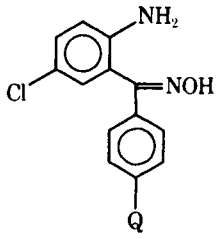

XXV: Q = OH
XXVI: Q = NHCOCF$_3$

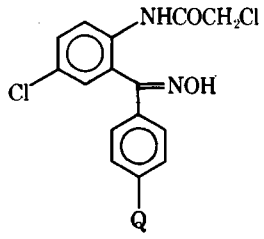

XXVII: Q = OH
XXVIII: Q = NHCOCF$_3$

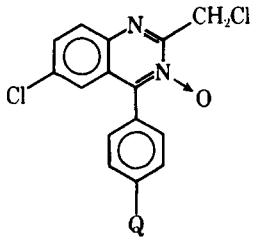

XXIX: Q = OH
XXX: Q = NHCOCF$_3$

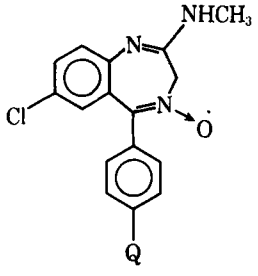

XXXI: Q = OH
XXXII: Q = NH_2
XXXIII: Q = $OCH_2CO_2CH_3$
XXXIV: Q = $OCH_2CONHNH_2$
XXXV: Q = $O(CH_2)_3NHCO_2CH_2C_6H_5$
XXXVI: Q = $O(CH_2)_3NH_2$

synthetic sequences

IV, XXV, XXVII, XXIX, XXXI, XXXIII, and XXXIV
XXXI, XXXV, and XXXVI
V, XXVI, XXVIII, XXX, and XXXII

Anal.—Calc. for $C_{16}H_{13}BrClNO_3$: C, 50.22; H, 3.42. Found: C, 50.09; H, 3.73.

7-Chloro - 1,3-dihydro-5-(4-hydroxyphenyl)-2*H*-1,4-benzodiazepin-2-one (XII)—To 350 ml of liquid ammonia was added 60 g (0.163 mole) of VIII. After refluxing for 3 hr, the ammonia was allowed to evaporate. The residue was heated to reflux in 400 ml of ethanol for 3 hr. Ethanol was evaporated, and 800 ml of acetone was added. This suspension was heated and filtered to remove inorganic salts. Concentration of the acetone filtrate gave 31.5 g (67%) of XII, mp 271–272°.

Anal.—Calc. for $C_{15}H_{11}ClN_2O_2$: C, 62.84; H, 3.87; N, 9.77. Found: C, 62.52; H, 4.13; N, 9.92.

7-Chloro - 1,3-dihydro-5-[4-(2,2,2-trifluoroacetamidophenyl)]-2*H*-1,4-benzodiazepin-2-one (XIII)—A solution of 90 g (0.194 mole) of IX in a mixture of 900 ml of tetrahydrofuran and 900 ml of ethyl acetate was stirred in an ice bath and saturated with a stream of ammonia gas over 1 hr. The mixture was allowed to stand overnight at room temperature and then filtered. The filtrate was evaporated, and the residue was partitioned between methylene chloride and water.

The product mixture from evaporation of the methylene chloride layer was heated to reflux in 400 ml of ethanol for 3 hr. The solution was concentrated, cooled, and filtered to give 32 g (43%) of XIII. A sample was recrystallized from methylene chloride–ether to give colorless prisms, which reset on heating to form needles, mp 273–276°; IR (KBr): 1730 and 1678 (2 C=O) cm^{-1}.

Anal.—Calc. for $C_{17}H_{11}ClF_3N_3O_2$: C, 53.49; H, 2.90; N, 11.00. Found: C, 53.63; H, 2.92; N, 10.85.

7-Chloro - 1,3-dihydro-5-(4-methoxycarbonylmethoxyphenyl)-2*H*-1,4-benzodiazepin-2-one (XIV) and 5-(4-Carbamoylmethoxyphenyl) -7- chloro -1,3- dihydro-2*H*-1,4-benzodiazepin -2- one (XVII)—A solution of 14.3 g (32.5 mmoles) of X in 100 ml of dioxane and 150 ml of methanol was added to 150 ml of a saturated solution of ammonia in methanol. After 5 hr, the reaction mixture was neutralized with acetic acid and evaporated to dryness. The residue was partitioned between 150 ml of methylene chloride and 100 ml of dilute ammonium hydroxide. After a few minutes, filtration gave 4.5 g (41%) of XVII. A sample was recrystallized from chloroform–ethanol to give off-white prisms, mp 272–275°; IR (KBr): 3440, 3210 (NH_2), and 1695 (2 C=O) cm^{-1}.

Anal.—Calc. for $C_{17}H_{14}ClN_3O_3$: C, 59.40; H, 4.11; N, 12.22. Found: C, 59.06; H, 3.99; N, 11.89.

The methylene chloride layer was separated, dried, and filtered through activated magnesium silicate. Elution with ether and then ethyl acetate and recrystallization of these two fractions gave 2.2 g (19%) of XIV as pale-yellow prisms, mp 235–243°; IR (KBr): 1762 and 1680 (2 C=O) cm^{-1}.

Anal.—Calc. for $C_{18}H_{15}ClN_2O_4$: C, 60.26; H, 4.21; N, 7.81. Found: C, 60.39; H, 4.36; N, 7.83.

7-Chloro - 1,3-dihydro-5-(4-hydroxyphenyl)-1-methyl-2*H*-1,4-benzodiazepin-2-one (XV)[3] and 7-Chloro-1,3-dihydro-5-(4-methoxyphenyl)-1-methyl-2*H*-1,4-benzodiazepin-2-one (XVI)—To a solution of 6.5 g (0.022 mole) of XII in 40 ml of dimethylformamide was added 11.6 ml (0.055 mole) of 4.74 *M* sodium methoxide in methanol. After 90 min, the mixture was cooled in an ice bath and 9.4 g (0.066 mole) of methyl iodide was added dropwise with stirring. After 18 hr at room temperature, the reaction mixture was acidified with acetic acid and partitioned between 100 ml of methylene chloride and 100 ml of water.

The water layer was extracted once more with methylene chloride. The combined extracts were evaporated to dryness. The residual product mixture was separated on an activated magnesium silicate column. The column was eluted with methylene chloride, ether, and then ethyl acetate. The ethyl acetate fraction was evaporated and crystallized from methanol to give 0.40 g (6%) of XV as colorless prisms, mp 255–259°.

Anal.—Calc. for $C_{16}H_{13}ClN_2O_2$: C, 63.90; H, 4.35; N, 9.31. Found: C, 63.89; H, 4.29; N, 9.46.

The filtrates and the other fractions from the column were combined and evaporated to give 4.5 g of a XV–XVI mixture.

Compound XV from XI—A solution of 2.2 g (5.7 mmoles) of XI in a mixture of 90 ml of methylene chloride and 20 ml of tetrahydrofuran was added to 175 ml of liquid ammonia. After 18 hr, 100 ml of methylene chloride was added and the reaction mixture was dried and evaporated to dryness. The residual oil was crystallized from methanol to give 1.45 g (85%) of XV as colorless prisms, mp 254–260°.

7-Chloro -1,3- dihydro -5- (4-hydrazinocarbonylmethoxyphenyl)-2*H*-1,4-benzodiazepin-2-one Hemitetrahydrofuranate (XVIII)—To a solution of 0.50 g (1.3 mmoles) of XIV in a mixture of 25 ml of methanol and 30 ml of tetrahydrofuran was added 5 ml of hydrazine hydrate (85% in water). After 1 hr, the solution was evaporated under reduced pressure and 25 ml of methylene chloride and 20 ml of water were added. After standing overnight, the solution was filtered and the solid was recrystallized from tetrahydrofuran–hexane to give 0.30 g (59%) of colorless prisms, mp 180–185°, resets 210–220°; IR (KBr): 1700 and 1680 (C=O) cm^{-1}.

Anal.—Calc. for $C_{17}H_{15}ClN_4O_3 \cdot 0.5\ C_4H_8O$: C, 57.80; H, 4.88; N, 14.19. Found: C, 57.59; H, 4.79; N, 14.10.

7-Chloro - 1,3-dihydro-5-[4-(2,2,2-trifluoroacetamido)phenyl]-2*H*-1,4-benzodiazepin-2-one 4-Oxide (XIX)—To a mixture of 31.5 g (0.0825 mole) of XIII in 1.8 liters of methylene chloride was added, with stirring, 30 g (0.147 mole) of 85% *m*-chloroperbenzoic acid. After 18 hr, 500 ml of cold water was added and the solution was made basic with ammonium hydroxide. The crystalline XIX was collected on a filter. The

Structural Group C

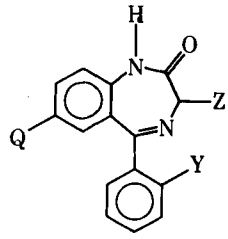

XXXVII: Q = NO_2, Y = H, Z = OH
XXXVIII: Q = NO_2, Y = H, Z = $OCOCH_2CH_2CO_2H$
XXXIX: Q = NH_2, Y = H, Z = $OCOCH_2CH_2CO_2H$
XL: Q = NO_2, Y = Cl, Z = OH
XLI: Q = NO_2, Y = Cl, Z = $OCOCH_2CH_2CO_2H$
XLII: Q = NH_2, Y = Cl, Z = $OCOCH_2CH_2CO_2H$

synthetic sequences

XXXVII, XXXVIII, XXXIX; XL, XLI, and XLII

methylene chloride was concentrated for a second crop, giving a total yield of 21.5 g (66%). Recrystallization from methylene chloride–methanol gave off-white rods, mp 295–297° dec.; IR (KBr): 1698 (broad 2 C=O) cm^{-1}.

Anal.—Calc. for $C_{17}H_{11}ClF_3N_3O_3$: C, 51.33; H, 2.79; N, 10.57. Found: C, 51.32; H, 2.57; N, 10.44.

5-(4-Aminophenyl) - 7-chloro-1,3-dihydro-2*H*-1,4-benzodiazepin-2-one 4-Oxide (XX)—To a solution of 1.0 g (2.51 mmoles) of XIX in 25 ml of methanol was added 20 ml (20 mmoles) of 1 *N* NaOH. After 15 min, 20 ml of water was added. The reaction mixture was allowed to stand for 3 hr and was then acidified with acetic acid; methanol was removed *in vacuo*. The mixture was made basic with ammonium hydroxide and filtered. Recrystallization from tetrahydrofuran–methanol gave 0.30 g (39%) of pale-yellow rods, mp 256–258°; IR (KBr): 3415, 3350, 3245 (NH_2, NH), and 1700 (C=O) cm^{-1}; mass spectrum: *m/e* 301 (M^+).

Anal.—Calc. for $C_{15}H_{12}ClN_3O_2$: C, 59.71; H, 4.10; N, 13.93. Found: C, 59.52; H, 4.02; N, 13.73.

3-Acetoxy - 7-chloro-1,3-dihydro-5-[4-(2,2,2-trifluoroacetamido)phenyl]-2*H*-1,4-benzodiazepin-2-one (XXI)—A mixture of 14 g (0.0352 mole) of XIX in 200 ml of tetrahydrofuran and 400 ml of acetic anhydride was heated on the steam bath for 2 hr. The mixture was evaporated under reduced pressure. Crystallization of the residue from methanol afforded 8.3 g of XXI. A second crop of 5.3 g was obtained from ether–hexane, giving a total yield of 13.5 g (87.7%).

Recrystallization from a mixture of tetrahydrofuran, methylene chloride, and hexane gave white prisms, mp 257–262°; IR (KBr): 1740, 1720, and 1688 (3 C=O) cm^{-1}; mass spectrum: *m/e* 439 (M^+).

Anal.—Calc. for $C_{19}H_{13}ClF_3N_3O_4$: C, 51.89; H, 2.98; N, 9.56. Found: C, 51.36; H, 2.99; N, 9.23.

5-(4-Aminophenyl) -7- chloro-1,3-dihydro -3- hydroxy-2*H*-1,4-benzodiazepin-2-one (XXII)—To a solution of 0.60 g (1.3 mmoles) of XXI in 25 ml of methanol was added 20 ml of 1 *N* NaOH, followed by the addition of 20 ml of water after 1 hr. The reaction mixture was filtered after 3 hr. The filtrate was acidified with acetic acid and then made slightly basic with ammonium hydroxide. It was extracted with methylene chloride (2 × 100 ml), which was dried and concentrated to a small volume.

Compound XXII, which crystallized, was collected. Recrystallization from tetrahydrofuran–methanol afforded 0.20 g (50%) of yellow prisms, mp >350°; IR (KBr): 3455, 3375 (NH_2, NH), 3225, 3160 (OH), 1713, and 1698 (split C=O) cm^{-1}; NMR (dimethyl sulfoxide-d_6): δ 10.60 (s, 1H, NH), 6.02 (d, 1H, OH), 5.58 (s, 2H, NH_2), and 4.64 (d, 1H, CH); mass spectrum: *m/e* 301 (M^+).

Anal.—Calc. for $C_{15}H_{12}ClN_3O_2$: C, 59.71; H, 4.00; N, 13.93. Found: C, 59.33; H, 4.46; N, 14.03.

5-[3-(4-Acetamidophenylazo)-4 - hydroxyphenyl]-7-chloro-1,3-dihydro-1-methyl-2*H*-1,4-benzodiazepin-2-one (XXIII)—To a mixture of 1.2 ml (15 mmoles) of concentrated hydrochloric acid and 5 g of ice was added 0.90 g (6 mmoles) of *p*-aminoacetanilide, followed by the dropwise addition of a solution of 0.45 g (6.2 mmoles) of sodium nitrite in 5 ml of water. To a separate solution of 0.5 g (1.67 mmoles) of XV in 25 ml of tetrahydrofuran were added 1 ml (12 mmoles) of 1 *N* NaOH and 20 g of ice. The diazonium salt solution was added rapidly with stirring to the basic solution.

The mixture was refrigerated at 5° for 2.5 days. The precipitate was collected and recrystallized from methylene chloride–methanol to give 0.60 g (70%) of XXIII as red prisms. Recrystallization from methylene chloride–petroleum ether gave yellow rods, mp 276–278°; IR (KBr): broad 1700 (2 C=O) cm^{-1}.

Anal.—Calc. for $C_{24}H_{20}ClN_5O_3$: C, 62.41; H, 4.36; N, 15.16. Found: C, 62.24; H, 4.31; N, 14.97.

5-[3-(4-Aminophenylazo)-4-hydroxyphenyl]-7-chloro-1,3-dihydro-1-methyl-2*H*-1,4-benzodiazepin-2-one (XXIV)—A solution of 0.60 g (1.3 mmoles) of XXIII in 50 ml of methanol and 10 ml of concentrated hydrochloric acid was heated for 10 min on a steam bath. After 2 hr at room temperature, the methanol was evaporated. The solution was made basic with ammonium hydroxide and extracted with 50 ml of methylene chloride. The organic layer was dried and evaporated. Crystallization of the residue from methanol and recrystallization from methylene chloride–methanol gave 0.25 g (45%) of brown prisms, mp 262–268°; IR (KBr): 3450, 3350 (NH_2), and 1682 (C=O) cm^{-1}.

Anal.—Calc. for $C_{22}H_{18}ClN_5O_2$: C, 62.93; H, 4.32; N, 16.68. Found: C, 62.96; H, 4.49; N, 16.47.

2-Amino-5-chloro-4'-hydroxybenzophenone Oxime (XXV)—The preparation of XXV from IV was described in Ref. 17.

2-Amino-5-chloro-4'-(2,2,2-trifluoroacetamido)benzophenone Oxime (XXVI)—A mixture of 3.1 g (8.27 mmoles) of V and 2.5 g (36 mmoles) of hydroxylamine hydrochloride in 100 ml of ethanol was heated under reflux for 66 hr and then concentrated. The residue was partitioned between 100 ml of methylene chloride and 75 ml of water. The organic layer was concentrated, cooled, and filtered to give 1.0 g of XXVI. An additional 0.6 g was obtained from the filtrates for a yield of 1.6 g (53%). Recrystallization from methylene chloride–hexane gave off-white prisms, mp 179–183°; IR (KBr): 3440, 3340, and 3280 (NH, NH_2, OH) cm^{-1}.

Anal.—Calc. for $C_{15}H_{11}ClF_3N_3O_2$: C, 50.37; H, 3.10; N, 11.75. Found: C, 50.31; H, 2.93; N, 11.72.

2,4' - Dichloro-2' - (4-hydroxybenzoyl)acetanilide Oxide (XXVII)—See Ref. 17.

2,4' - Dichloro-2'-(4-trifluoroacetamido-α-hydroxyiminobenzyl)acetanilide (XXVIII)—To a solution of 1.6 g (4.4 mmoles) of XXVI in 50 ml of ether was added 20 ml of water. The mixture was cooled to 5°, and 0.54 g (4.8 mmoles) of chloroacetyl chloride and a 5% solution of sodium bicarbonate were added alternately, keeping the solution slightly basic. After 1 hr, the ether layer was separated and the water layer was extracted with 50 ml of ether.

The combined ether layers were dried and evaporated. The residue was crystallized from methylene chloride–hexane to give 1.8 g (95%) of colorless prisms. A sample recrystallized for analysis from ether–methylene chloride melted at 210–214°; IR (KBr): 3420, 3300, 3200 (NH, OH), and 1700 (2 C=O) cm^{-1}.

Anal.—Calc. for $C_{17}H_{12}Cl_2F_3N_3O_3$: C, 47.03; H, 2.78; N, 9.58. Found: C, 46.94; H, 2.70; N, 9.48.

6-Chloro-2-chloromethyl-4-(4-hydroxyphenyl)quinazoline 3-Oxide (XXIX)[3]—A solution of 40.5 g (0.12 mole) of XXVII in 750 ml of dry dioxane and 40.5 ml (0.329 mole) of boron trifluoride etherate was heated to reflux. After 5 hr, it was cooled and 200 ml of water was added. The dioxane was removed by distillation, and the reaction mixture was made basic with a 5% sodium bicarbonate solution. The solid was collected, heated in methanol at reflux for a few minutes, cooled, and collected to give, in two crops, 21.3 g (56%) of XXIX. An analytical sample recrystallized from methanol melted at 226–227° dec.

Anal.—Calc. for $C_{15}H_{10}Cl_2N_2O_2$: C, 56.10; H, 3.14; N, 8.72. Found: C, 56.26; H, 2.81; N, 9.02.

6-Chloro - 2-chloromethyl-4-[4-(2,2,2-trifluoroacetamido)phenyl]quinazoline 3-Oxide (XXX)—Following the procedure described for XXIX, XXVIII was isolated by methylene chloride extraction. The residue from evaporation was crystallized from methanol and recrystallized from methylene chloride–methanol to give 1.0 g (62%) of pale-yellow rods, mp 244–248°. A good elemental analysis could not be obtained because of solvents in the crystals; IR (KBr): 1730 (C=O) cm^{-1}; mass spectrum: *m/e* 415 (M^+).

7-Chloro - 5-(4-hydroxyphenyl)-2-methylamino-3*H*-1,4-benzodiazepine 4-Oxide (XXXI)[3]—To a saturated methylamine solution in 600 ml of methanol in an ice bath was added 19.2 g (0.60 mole) of XXIX. The solution was stirred for 7 hr in an ice bath and for 10 hr at room temperature and then was evaporated under reduced pressure. The residue was acidified with dilute acetic acid, stirred with ether, and filtered to give 19 g of product. Recrystallization for analysis from ethyl acetate gave colorless plates, mp 278–279° dec.

Anal.—Calc. for $C_{16}H_{14}ClN_3O_2$: C, 60.86; H, 4.47; N, 13.30. Found: C, 61.23; H, 4.74; N, 13.14.

5-(4-Aminophenyl)-7 - chloro-2-methylamino-3*H*-1,4-benzodiazepine 4-Oxide (XXXII)—To 100 ml of methanol saturated with methylamine in an ice bath was added 1.6 g (3.8 mmoles) of XXX. After 18 hr at room temperature, the solution was evaporated to dryness. Crystallization of the residue from methanol followed by recrystallization from methylene chloride–methanol gave yellow prisms, mp 180–185°, reset 288–290°.

The filtrates were partitioned between 1 *N* HCl and ether. The acid layer was made basic with sodium hydroxide and filtered. The solids collected were recrystallized from methylene chloride–methanol to give 0.60 g (50%) of XXXII. A good elemental analysis was not obtained due to occlusion of solvents in the crystal; IR (KBr): 3250 (broad) and 1625 cm^{-1}; mass spectrum: *m/e* 314 (M^+).

7-Chloro - 5-(*p*-methoxycarbonylmethoxyphenyl)-2-methylamino-3*H*-1,4-benzodiazepine 4-Oxide (XXXIII)—A solution of 5.00 g (0.0158 mole) of XXXI in 25 ml of dry dimethylformamide under nitrogen was stirred and cooled in an ice bath. To the reaction was added 0.75 g (0.0174 mole) of 57% sodium hydride in mineral oil; after 45 min, 3.0 g (0.205 mole) of methyl bromoacetate was added dropwise. After 64 hr at room temperature, the mixture was poured into ice water.

The precipitate was collected and dissolved in 150 ml of methylene chloride, which was washed with water, dried, and evaporated. Crystal-

lization from methylene chloride–hexane gave 3.6 g (59%) of colorless prisms, mp 106–110°; IR ($CHCl_3$): 3460 (NH) and 1760 (C=O) cm^{-1}. An additional 1.6 g of crude XXXIII was obtained from the filtrates.

Anal.—Calc. for $C_{19}H_{18}ClN_3O_4$: C, 58.84; H, 4.68; N, 10.84. Found: C, 58.61; H, 4.56; N, 10.96.

7-Chloro - 5-(4-hydrazinocarbonylmethoxyphenyl)-2-methylamino-3*H*-1,4-benzodiazepine 4-Oxide (XXXIV)—A solution of 1.0 g (2.6 mmoles) of XXXIII in 125 ml of methanol was treated with 6 ml of 85% hydrazine hydrate. After stirring for 2 hr, the solution was concentrated to a small volume under reduced pressure and cooled. The precipitate was collected, triturated with ethanol, filtered, and recrystallized from dimethylformamide–methanol–water to give 0.90 g (90%) of colorless prisms, mp 254–256°; IR (KBr): 3300, 3240 (NH, NH_2), 1668 (C=O), 1635 (C=N), and 1250 (ether) cm^{-1}.

Anal.—Calc. for $C_{18}H_{18}ClN_5O_3$: C, 55.75; H, 4.68; N, 18.06. Found: C, 55.62; H, 4.58; N, 18.28.

7-Chloro -2- methylamino-5-[4-[(3-benzyloxycarbonylamino)-propoxy]phenyl]-3*H*-1,4-benzodiazepine 4-Oxide (XXXV)—A solution of 0.50 g (1.58 mmoles) of XXXI in 5 ml of dry dimethylformamide under nitrogen was treated with 0.080 g (1.9 mmoles) of 54.7% sodium hydride in mineral oil. After 20 min, 0.54 g (2 mmoles) of *N*-carbobenzyloxy-3-bromopropylamine and 0.10 g (0.29 mmole) of tetrabutylammonium hydrogen sulfate were added with stirring. After 18 hr, the reaction mixture was stirred with ice water, which was then decanted.

The remaining oil was dissolved in 25 ml of methylene chloride, washed with 15 ml of water, dried, and filtered over a pad of activated magnesium silicate. The pad was eluted with methylene chloride, ether, and then ethyl acetate. The ethyl acetate fraction was evaporated and purified by preparative TLC using five silica gel plates (20 cm × 20 cm × 1.5 mm), which were developed in benzene–acetone (1:1). The material having R_f 0.4–0.5 was eluted from the silica gel with methanol. Crystallization from methylene chloride–ether gave 0.15 g (19%) of colorless prisms, mp 103–106°; IR ($CHCl_3$): 3460 (NH) and 1720 (C=O) cm^{-1}; mass spectrum: *m/e* 506 (M^+).

Anal.—Calc. for $C_{27}H_{27}ClN_4O_4$: C, 63.97; H, 5.37; N, 11.05. Found: C, 63.87; H, 5.42; N, 10.80.

7-Chloro - 2-methylamino-5-[4-(3-amino)propoxy]phenyl-3*H*-1,4-benzodiazepine 4-Oxide Dihydrochloride (XXXVI)—To a stirring solution of 4 ml of 30% hydrogen bromide in acetic acid was added 0.10 g (0.197 mmole) of XXXV. After 40 min, 20 ml of ether was added. The precipitate was collected and partitioned between 30 ml of methylene chloride and 10 ml of dilute ammonium hydroxide. The organic layer was dried and evaporated, and excess ethanolic hydrogen chloride was added. After concentration, the oil was crystallized from isopropanol and recrystallized from a mixture of methanol and isopropanol to give 70 mg (80%) of colorless prisms, mp 211–215° dec.; IR (KBr): 3400 (broad NH, NH_2) and 1688 (C=O) cm^{-1}.

Anal.—Calc. for $C_{19}H_{21}ClN_4O_2 \cdot 2HCl$: C, 51.19; H, 5.20; N, 12.57. Found: C, 50.85; H, 5.49; N, 12.24.

1,3-Dihydro-3-hemisuccinyloxy - 7-nitro-5-phenyl-2*H*-1,4-benzodiazepin-2-one (XXXVIII) (18)—To a suspension of 6.60 g (22 mmoles) of 1,3-dihydro-3-hydroxy-7-nitro-5-phenyl-2*H*-1,4-benzodiazepin-2-one (XXXVII) (19) in 400 ml of tetrahydrofuran (dried by passing over a bed of activated alumina) was added 1.2 g of a 50% suspension of sodium hydride in mineral oil (27 mmoles hydride). After stirring for 0.5 hr at room temperature under a nitrogen atmosphere, a clear solution formed. Succinic anhydride (3.35 g, 33 mmoles) was added in one portion, and stirring was continued. After 1 hr, tetrahydrofuran was evaporated *in vacuo*.

The residual mixture was slurried with 200 ml of water, acidified with acetic acid, and extracted with 300 ml of methylene chloride. The acidification and extraction were performed rapidly enough so that the product did not crystallize out of solution. After drying over anhydrous sodium sulfate, the solution was concentrated to half of its volume. Hexane addition afforded 8.3 g of XXXVIII, mp 187–190° dec. After recrystallization from tetrahydrofuran–methylene chloride–hexane, 5.6 g (64%) of colorless needles was obtained, mp 183–185° dec.

An analytical sample obtained from recrystallization with methylene chloride–hexane melted at 187–190° dec.; IR (KBr): unresolved carbonyl bands at 1690–1760 cm^{-1}; UV λ_{max} (2-propanol): 219 (ε 24,500), 264 (17,100), and 305 (10,900) nm; NMR (dimethyl sulfoxide-d_6): δ 2.51–2.65 (m, 2, CH_2), 2.69–2.83 (m, 2, CH_2), 5.89 (s, 1, 3-H), 7.45–7.62 (m, 6, C_6H_5 and 9-H), 8.06 (d, *J* = 2.5 Hz, 1,6-H), and 8.48 (q, *J* = 2.5 and 9.0 Hz, 1, 8-H) ppm.

Anal.—Calc. for $C_{19}H_{15}N_3O_7$: C, 57.43; H, 3.81; N, 10.58. Found: C, 57.47; H, 3.87; N, 10.30.

7-Amino-1,3-dihydro-3-hemisuccinyloxy-5-phenyl-2*H*-1,4-benzodiazepin-2-one (XXXIX)—A solution of 397 mg (1.0 mmole) of XXXVIII in 25 ml of tetrahydrofuran containing 500 mg of Raney nickel was hydrogenated under a hydrogen atmosphere at room temperature for 2 hr. Removal of the catalyst and solvent followed by recyrstallizations from tetrahydrofuran–methylene chloride–hexane afforded 175 mg (48%) of XXXIX as yellow microprisms, melting point indefinite, gradually shrinking above 190°; UV λ_{max} (2-propanol): 243 (ε 31,100) and 354 (2700) nm; NMR (dimethylsulfoxide-d_6): δ 6.44 (d, *J* = 2.5 Hz, 1, 6-H), 6.80 (dd, *J* = 2.5 and 9.0 Hz, 1,8-H), and 6.94 (d, *J* = 9.0 Hz, 1,9-H) ppm.

Anal.—Calc. for $C_{19}H_{17}N_3O_5$: C, 62.12; H, 4.66; N, 11.44. Found: C, 62.20; H, 4.96; N, 11.17.

5-(2-Chlorophenyl)-1,3-dihydro-3-hydroxy - 7-nitro-2*H*-1,4-benzodiazepin-2-one (XL) (20)—A solution of 27 g (81 mmoles) of 5-(2-chlorophenyl)-1,3-dihydro-7-nitro-2*H*-1,4-benzodiazepin-2-one 4-oxide [prepared in 64% from clonazepam (V), the desoxy precursor, by oxidation with *m*-chloroperbenzoic acid and obtained from ethanol as colorless flakes, mp 254° dec.] in 300 ml of acetic anhydride was heated on a steam bath for 2 hr. After acetic anhydride was removed *in vacuo*, the residue was crystallized from benzene to afford 14 g of 3-acetoxy-5-(2-chlorophenyl)-1,3-dihydro-7-nitro-2*H*-1,4-benzodiazepin-2-one, mp 279–281°.

To a solution of the 3-acetoxy compound (14 g) in 400 ml of dioxane was added 160 ml of 1 *N* NaOH. The mixture was stirred at room temperature for 0.5 hr and then neutralized with 1 *N* HCl. Water (2 liters) was added, and the mixture was extracted with methylene chloride. The organic layer was washed with water, dried, and evaporated to dryness. Crystallization from acetone afforded XL, which, on recrystallization from acetone, yielded 8.7 g (30% overall) of a hemiacetonate of XL as colorless prisms, mp 159–160°; IR (KBr): 3200, 3140, 1700 (broad), 1530, and 1345 cm^{-1}.

Anal.—Calc. for $C_{15}H_{10}ClN_3O_4 \cdot 0.5C_3H_6O$: C, 54.93; H, 3.63; N, 11.65. Found: C, 55.14; H, 3.70; N, 11.47.

5-(2-Chlorophenyl)-1,3-dihydro-3 - hemisuccinyloxy-7-nitro-2*H*-1,4-benzodiazepin-2-one (XLI)—The 3-hydroxy compound (XL) was succinylated, as in the preparation of XXXVIII, in a 67% yield. Colorless prisms (tetrahydrofuran–methylene chloride–heptane) were obtained, mp 172–180° dec.; IR (KBr): 1770–1700 (strong unresolved), 1530, and 1350 cm^{-1}; UV λ_{max} (2-propanol): 215 (ε 32,800), 248 (16,500), and 308 (12,000) nm.

Anal.—Calc. for $C_{19}H_{14}ClN_3O_7$: C, 52.75; H, 3.08; N, 9.75. Found: C, 52.85; H, 3.27; N, 9.73.

7-Amino-5-(2-chlorophenyl)-1,3-dihydro - 3-hemisuccinyloxy-2*H*-1,4-benzodiazepin-2-one (XLII)—Catalytic hydrogenation of XLI in the manner described in the preparation of XXXIX afforded XLII in a 70% yield as a light-yellow amorphous solid from tetrahydrofuran–methylene chloride–hexane, melting point indefinite, beginning at 130°; IR (KBr): 3500–2800 and 1680–1760 (unresolved), 1620, 1505, and 1160 cm^{-1}.

Anal.—Calc. for $C_{19}H_{16}ClN_3O_5$: C, 56.80; H, 4.01; Cl, 8.82. Found: C, 57.06; H, 4.34; Cl, 8.54.

REFERENCES

(1) J. Landon and A. C. Moffat, *Analyst*, **101**, 225 (1976).

(2) V. P. Butler, Jr., *J. Immunol. Methods*, **7**, 1 (1975).

(3) D. J. Greenblatt and R. I. Shader, "Benzodiazepines in Clinical Practice," Raven, New York, N.Y., 1974.

(4) "The Benzodiazepines," S. Garattini, E. Mussini, and L. O. Randall, Eds., Raven, New York, N.Y., 1973.

(5) L. O. Randall, W. Schallek, L. H. Sternbach, and R. Y. Ning, in "Psychopharmacological Agents," vol. III, M. Gordon, Ed., Academic, New York, N.Y., 1974, p. 175.

(6) B. Peskar and S. Spector, *J. Pharmacol. Exp. Ther.*, **186**, 167 (1973).

(7) W. R. Dixon, J. Earley, and E. Postma, *J. Pharm. Sci.*, **64**, 937 (1975).

(8) W. R. Dixon, R. L. Young, R. Ning, and A. Liebman, *Pharmacologists*, **17**, 251 (1975).

(9) L. H. Sternbach and E. Reeder, *J. Org. Chem.*, **26**, 1111 (1961).

(10) L. H. Sternbach, R. I. Fryer, W. Metlesics, E. Reeder, G. Sach, G. Saucy, and A. Stempel, *ibid.*, **27**, 3788 (1962).

(11) J. D. Loudon and G. Tennant, *J. Chem. Soc.*, **1962**, 3092.

(12) I. Tanasescu, C. Anghel, and A. Popescu, *Stud. Univ. Babes-Bolyai, Ser. Chem.*, **9**, 89 (1964); through *Chem. Abstr.*, **61**, 16004 (1964).

(13) S. Secareanu and A. Silberg, *Bull. Soc. Chim. Fr.*, **3**, 1777 (1936).

(14) I. Tanasescu and M. Sugiu, *ibid.*, **3**, 1753 (1936).
(15) G. N. Walker, *J. Org. Chem.*, **27**, 1929 (1962).
(16) G. Jommi, P. Mannito, and M. Silanos, *Arch. Biochem. Biophys.*, **108**, 334 (1964).
(17) A. Stempel, I. Douvan, E. Reeder, and L. H. Sternbach, *J. Org. Chem.*, **32**, 2417 (1967).
(18) S. A. Ravizza, German pat. 2131158 (1971).
(19) E. Reeder, A. Stempel, and L. H. Sternbach, Belgian pat. 629,227 (1963); through *Chem. Abstr.*, **60**, 13261d (1964).
(20) E. Eschenhof, *Arzneim.-Forsch.*, **23**, 390 (1973).

ACKNOWLEDGMENTS

The authors acknowledge the initiation of this project and continued participation by Dr. W. R. Dixon, Dr. R. Davis, Dr. S. Spector, and their coworkers.

Benoxaprofen, a New Anti-Inflammatory Agent: Particle-Size Effect on Dissolution Rate and Oral Absorption in Humans

A. S. RIDOLFO ˣ, L. THOMPKINS, L. D. BECHTOL, and R. H. CARMICHAEL

Received September 7, 1978, from the *Lilly Laboratory for Clinical Research, Lilly Research Laboratories, and Dry Products Development, Indianapolis, IN 46202.* Accepted for publication December 28, 1978.

Abstract □ The particle-size effect of benoxaprofen, a new nonsteroidal anti-inflammatory agent, on the *in vitro* dissolution rate and oral absorption in humans was evaluated. Ten normal subjects participated in a randomized crossover-designed absorption study with two sieved particle-size formulations: one with crystals larger than 60 mesh (mean equivalent spherical diameter = 640 μm) and the other with crystals smaller than 100 mesh (mean equivalent spherical diameter = 67 μm). Plasma drug concentrations and urinary drug excretion were used to determine the relative absorption of the two formulations. The standard USP procedure was used for the dissolution study. Particle size had a dramatic effect on both the *in vitro* drug dissolution and its oral absorption in humans. *In vitro*, the smaller crystals dissolved more rapidly and more efficiently than the larger crystals. *In vivo*, the smaller crystals produced higher plasma concentrations, more rapid peak concentration attainment, and more drug excreted in the urine.

Keyphrases □ Benoxaprofen—effect of particle size on dissolution rate and oral absorption in humans □ Dissolution rate—benoxaprofen, effect of particle size □ Absorption, oral—benoxaprofen, effect of particle size □ Anti-inflammatory agents—benoxaprofen, effect of particle size on dissolution rate and oral absorption in humans

The particle size of sparingly soluble drugs (drugs that are practically insoluble in aqueous fluids at physiological pH) can affect their dissolution rate *in vitro* (1–7). Similarly, the rate and extent of drug absorption can be reduced *in vivo* when dissolution in GI fluids is limited by particle size (2, 8–11). In several cases, rank correlations were obtained between sparingly soluble drug dissolution *in vitro* and absorption *in vivo* (12). In several instances, drug dissolution improved when particle size was reduced, probably because an increased surface area was available for dissolution.

Certain physicochemical properties of the experimental anti-inflammatory compound benoxaprofen, *dl*-2-(4-chlorophenyl)-α-methyl-5-benzoxazoleacetic acid, indicate that its dissolution *in vitro* and its absorption *in vivo* might be affected by altering its crystal particle size. It is a crystalline solid at room temperature. The pKa in 66% dimethylformamide is 6.9, and its solubilities at 25° in phosphate buffer at pH 5.0, 6.0, 7.0, and 7.6 are 4.4, 21, 207, and 835 μg/ml, respectively[1].

Because of benoxaprofen's low aqueous solubility and its largely unionized, lipoid-soluble form in the GI tract, a rate-limiting step in oral absorption could be drug dissolution in the GI fluids. This report describes the relationship between drug particle sizes and dissolution rates *in vitro* and the effect of particle sizes on oral bioavailability in humans.

EXPERIMENTAL

Dosage Preparation—GLC showed benoxaprofen[2] to be 99.9% pure. Two particle-size fractions were isolated using U.S. standard mesh sieves. One fraction contained particles larger than 60 mesh (mean diameter = 640 μm), and one contained particles less than 100 mesh (mean diameter = 67 μm). The individual fractions were mixed with corn starch USP in a laboratory blender[3]. The blends were hand filled into size 2 gelatin capsules, each containing 100 mg of benoxaprofen and 180 mg of starch.

Dissolution Study—The assembly and conditions used to study the dissolution rate and extent of the two drug particle sizes are described in USP XIX (13). The dissolution assembly consisted of four variable-speed stirring motors attached to four basket and shaft assemblies with a three-blade stainless steel propeller mounted on each basket shaft immediately above each basket, four 3-liter beakers, and a water bath at 37 ± 0.5°. The dissolution medium for each determination was 2 liters of pH 7.6 phosphate buffer. One capsule was placed in each basket and rotated at 100 rpm. Four capsules from each formulation were tested.

Five-milliliter aliquots were withdrawn at 20, 60, and 120 min using a pipet fitted with a suitable filter. Aliquots withdrawn were not replaced with corresponding volumes of the dissolution medium[4]. After the 120-min sample withdrawal, the basket contents were quantitatively transferred to the remaining dissolution medium, a stirring bar was added, and the mixture was magnetically stirred (at >500 rpm) for ~1 hr. A final aliquot was then taken. The benoxaprofen content in each specimen was measured spectrophotometrically.

Clinical Study—In humans, the benoxaprofen availability from the dosage forms containing the two different particle sizes was compared on the basis of plasma unchanged drug concentration and of urinary excretion of the unchanged drug and its glucuronide conjugate.

Twelve healthy males participated in the study after being informed of the objectives, potential risks, and procedures. The subjects were 21–33 years and within an acceptable weight range (14). According to a randomized crossover design, each subject received a single oral 100-mg drug capsule. Two weeks elapsed between the single doses of the two parti-

[1] The pKa and solubilities of benoxaprofen were determined at the Lilly Research Laboratories, Indianapolis, Ind., by Dr. R. F. Childers, Jr. (unpublished data).

[2] Synthesized at the Lilly Research Centre in England.
[3] Twin-Shell.
[4] Corrections were made for changes in dissolution volume in calculations of the percent of drug released at each period.

0022-3549/79/0700-0850$01.00/0
© 1979, American Pharmaceutical Association

(14) I. Tanasescu and M. Sugiu, *ibid.*, **3**, 1753 (1936).
(15) G. N. Walker, *J. Org. Chem.*, **27**, 1929 (1962).
(16) G. Jommi, P. Mannito, and M. Silanos, *Arch. Biochem. Biophys.*, **108**, 334 (1964).
(17) A. Stempel, I. Douvan, E. Reeder, and L. H. Sternbach, *J. Org. Chem.*, **32**, 2417 (1967).
(18) S. A. Ravizza, German pat. 2131158 (1971).
(19) E. Reeder, A. Stempel, and L. H. Sternbach, Belgian pat. 629,227 (1963); through *Chem. Abstr.*, **60**, 13261d (1964).
(20) E. Eschenhof, *Arzneim.-Forsch.*, **23**, 390 (1973).

ACKNOWLEDGMENTS

The authors acknowledge the initiation of this project and continued participation by Dr. W. R. Dixon, Dr. R. Davis, Dr. S. Spector, and their coworkers.

Benoxaprofen, a New Anti-Inflammatory Agent: Particle-Size Effect on Dissolution Rate and Oral Absorption in Humans

A. S. RIDOLFO ˣ, L. THOMPKINS, L. D. BECHTOL, and R. H. CARMICHAEL

Received September 7, 1978, from the *Lilly Laboratory for Clinical Research, Lilly Research Laboratories, and Dry Products Development, Indianapolis, IN 46202.* Accepted for publication December 28, 1978.

Abstract □ The particle-size effect of benoxaprofen, a new nonsteroidal anti-inflammatory agent, on the *in vitro* dissolution rate and oral absorption in humans was evaluated. Ten normal subjects participated in a randomized crossover-designed absorption study with two sieved particle-size formulations: one with crystals larger than 60 mesh (mean equivalent spherical diameter = 640 μm) and the other with crystals smaller than 100 mesh (mean equivalent spherical diameter = 67 μm). Plasma drug concentrations and urinary drug excretion were used to determine the relative absorption of the two formulations. The standard USP procedure was used for the dissolution study. Particle size had a dramatic effect on both the *in vitro* drug dissolution and its oral absorption in humans. *In vitro*, the smaller crystals dissolved more rapidly and more efficiently than the larger crystals. *In vivo*, the smaller crystals produced higher plasma concentrations, more rapid peak concentration attainment, and more drug excreted in the urine.

Keyphrases □ Benoxaprofen—effect of particle size on dissolution rate and oral absorption in humans □ Dissolution rate—benoxaprofen, effect of particle size □ Absorption, oral—benoxaprofen, effect of particle size □ Anti-inflammatory agents—benoxaprofen, effect of particle size on dissolution rate and oral absorption in humans

The particle size of sparingly soluble drugs (drugs that are practically insoluble in aqueous fluids at physiological pH) can affect their dissolution rate *in vitro* (1–7). Similarly, the rate and extent of drug absorption can be reduced *in vivo* when dissolution in GI fluids is limited by particle size (2, 8–11). In several cases, rank correlations were obtained between sparingly soluble drug dissolution *in vitro* and absorption *in vivo* (12). In several instances, drug dissolution improved when particle size was reduced, probably because an increased surface area was available for dissolution.

Certain physicochemical properties of the experimental anti-inflammatory compound benoxaprofen, *dl*-2-(4-chlorophenyl)-α-methyl-5-benzoxazoleacetic acid, indicate that its dissolution *in vitro* and its absorption *in vivo* might be affected by altering its crystal particle size. It is a crystalline solid at room temperature. The pKa in 66% dimethylformamide is 6.9, and its solubilities at 25° in phosphate buffer at pH 5.0, 6.0, 7.0, and 7.6 are 4.4, 21, 207, and 835 μg/ml, respectively[1].

Because of benoxaprofen's low aqueous solubility and its largely unionized, lipoid-soluble form in the GI tract, a rate-limiting step in oral absorption could be drug dissolution in the GI fluids. This report describes the relationship between drug particle sizes and dissolution rates *in vitro* and the effect of particle sizes on oral bioavailability in humans.

EXPERIMENTAL

Dosage Preparation—GLC showed benoxaprofen[2] to be 99.9% pure. Two particle-size fractions were isolated using U.S. standard mesh sieves. One fraction contained particles larger than 60 mesh (mean diameter = 640 μm), and one contained particles less than 100 mesh (mean diameter = 67 μm). The individual fractions were mixed with corn starch USP in a laboratory blender[3]. The blends were hand filled into size 2 gelatin capsules, each containing 100 mg of benoxaprofen and 180 mg of starch.

Dissolution Study—The assembly and conditions used to study the dissolution rate and extent of the two drug particle sizes are described in USP XIX (13). The dissolution assembly consisted of four variable-speed stirring motors attached to four basket and shaft assemblies with a three-blade stainless steel propeller mounted on each basket shaft immediately above each basket, four 3-liter beakers, and a water bath at 37 ± 0.5°. The dissolution medium for each determination was 2 liters of pH 7.6 phosphate buffer. One capsule was placed in each basket and rotated at 100 rpm. Four capsules from each formulation were tested.

Five-milliliter aliquots were withdrawn at 20, 60, and 120 min using a pipet fitted with a suitable filter. Aliquots withdrawn were not replaced with corresponding volumes of the dissolution medium[4]. After the 120-min sample withdrawal, the basket contents were quantitatively transferred to the remaining dissolution medium, a stirring bar was added, and the mixture was magnetically stirred (at >500 rpm) for ~1 hr. A final aliquot was then taken. The benoxaprofen content in each specimen was measured spectrophotometrically.

Clinical Study—In humans, the benoxaprofen availability from the dosage forms containing the two different particle sizes was compared on the basis of plasma unchanged drug concentration and of urinary excretion of the unchanged drug and its glucuronide conjugate.

Twelve healthy males participated in the study after being informed of the objectives, potential risks, and procedures. The subjects were 21–33 years and within an acceptable weight range (14). According to a randomized crossover design, each subject received a single oral 100-mg drug capsule. Two weeks elapsed between the single doses of the two parti-

[1] The pKa and solubilities of benoxaprofen were determined at the Lilly Research Laboratories, Indianapolis, Ind., by Dr. R. F. Childers, Jr. (unpublished data).

[2] Synthesized at the Lilly Research Centre in England.
[3] Twin-Shell.
[4] Corrections were made for changes in dissolution volume in calculations of the percent of drug released at each period.

0022-3549/79/0700-0850$01.00/0
© 1979, American Pharmaceutical Association

Table I—Analyses of Variance (Mean Squares)

Source	*df*	Plasma Concentrations 0.5 hr	1 hr	1.5 hr	2 hr	3 hr	6 hr	9 hr	12 hr
Subject	9	0.67	2.80	4.40	5.58	2.65	3.50	3.50	2.66
Day	1	0.04	0.90	0.02	5.33	0.08	0.56	0.13	0.11
Mesh	1	6.44[a]	62.92[b]	156.75[b]	349.39[b]	342.09[b]	80.10[b]	44.00[b]	47.63[b]
Residual	8	0.95	3.90	6.15	4.09	1.39	1.23 (7 *df*)	2.75 (7 *df*)	0.97

Source	*df*	Plasma Concentrations 24 hr	48 hr	72 hr	96 hr	Peak	Time of Peak	Area	Urine
Subject	9	1.20	0.60	0.36	0.22	4.47	4.87	5,842.13	85.16
Day	1	0.04	0.04	0.33	0.07	1.28	1.52	726.19	0.02
Mesh	1	16.28[b]	2.86[b]	0.60[a]	0.13	208.03[b]	41.42[b]	95,631.95[b]	938.56
Residual	8	0.45	0.14	0.11	0.04	5.21	2.70	1,931.58	14.49

[a] $p < 0.05$. [b] $p < 0.01$.

cle-size formulations. This period represents about 10–12 plasma disappearance half-lives of the unchanged drug.

All subjects fasted overnight (at least 8 hr) before dosing. No food or liquid, except water, was permitted for at least 2 hr after the study dose, when a standard light meal was offered. Water, *ad libitum*, was permitted during this period. All doses were taken with 180 ml of water. After dosing, subjects remained ambulatory or sitting for at least 2 hr.

Blood samples (10 ml) were obtained by venipuncture at 0, 0.5, 1, 1.5, 2, 3, 6, 9, 12, 24, 48, 72, and 96 hr after dosing. The samples were heparinized and centrifuged; the plasma was collected and frozen until assayed. Total urine samples were collected every 6 hr for 24 hr and then daily through Day 4; the volume was measured and aliquots were frozen until assayed.

The plasma benoxaprofen concentration was determined by GLC after extraction and derivatization. Fifty micrograms of the mass internal standard, 2-(3,5-dichlorophenyl)-α-methyl-5-benzoxazoleacetic acid, in 1 ml of 0.01 *M* NaOH was added to 1 ml of plasma. The plasma proteins were precipitated with 2 ml of 10% trichloroacetic acid, and the mixture was extracted with 9 ml of 20% (v/v) hexane in ethyl acetate. The organic phase containing the drug and the internal standard was back-extracted into 5 ml of 0.3 *M* Na_3PO_4. The aqueous phase was recovered, made acidic with 2 ml of 1 *M* HCl, and reextracted with 5 ml of methylene chloride.

The organic phase was recovered and evaporated to dryness at 50° under a nitrogen stream, and the residue was treated with diazomethane in methylene chloride containing 10% (v/v) methanol. After evaporation, the derivatized material was dissolved in a small volume of methanol and analyzed by GLC using a 0.61-m × 3-mm i.d. glass column of 80–100-mesh Chromosorb W-HP coated with 2% OV-7. Chromatographic conditions were: injection temperature, 250°; column oven temperature, 235°; and flame-ionization detector temperature, 275°. Quantitation was by electronic integration.

The urine benoxaprofen concentration was measured as the sum of the unchanged free form plus the amount resulting from glucuronide conjugate hydrolysis (15). The analytical technique was the same as for plasma, except that the urine plus the added internal standard was treated with β-glucuronidase[5] before extraction to hydrolyze the glucuronide metabolite to the free drug and glucuronic acid.

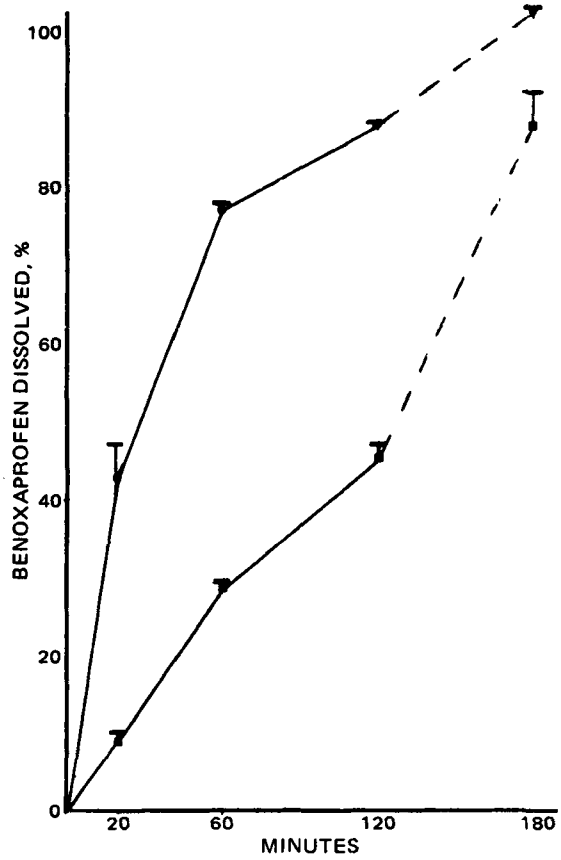

Figure 1—*Dissolution of two benoxaprofen particle-size formulations using the standard (USP XIX) 2-hr* in vitro *procedure. Key:* ■, *crystals larger than 60 mesh;* ●, *crystals smaller than 100 mesh; and* - - -, *results of vigorous magnetic stirring for an additional 1 hr. Each data point represents the mean of four assays with standard error.*

RESULTS AND DISCUSSION

The *in vitro* dissolution of the two benoxaprofen particle sizes is illustrated in Fig. 1. Twice as much benoxaprofen dissolved from the small particle formulation at each sampling time as from the large particle formulation, except the final sampling after an additional hour of vigorous stirring (>500 rpm with stirring bar). Since the medium would be only 6% of saturation if the 100 mg of drug dissolved, it was expected that both particle sizes would dissolve completely during this additional period of vigorous stirring. Instead, even under these relatively extreme conditions, the large particles dissolved relatively poorly.

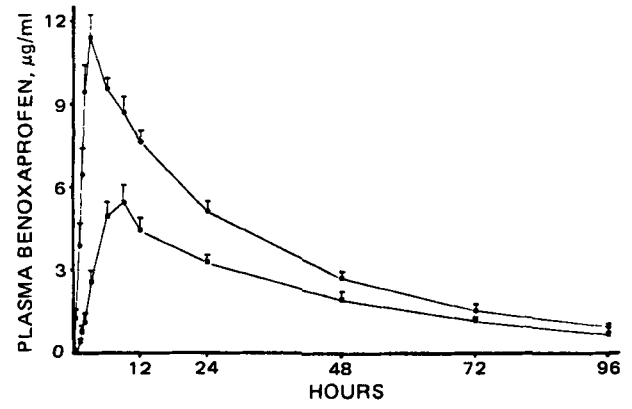

Figure 2—*Plasma unchanged benoxaprofen concentrations after oral dosing with 100 mg of two particle-size formulations. Key:* ■, *crystals larger than 60 mesh; and* ●, *crystals smaller than 100 mesh. Each data point represents the mean of 10 subjects with standard error.*

[5] Ketodase, General Diagnostics, Morris Plains, N.J.

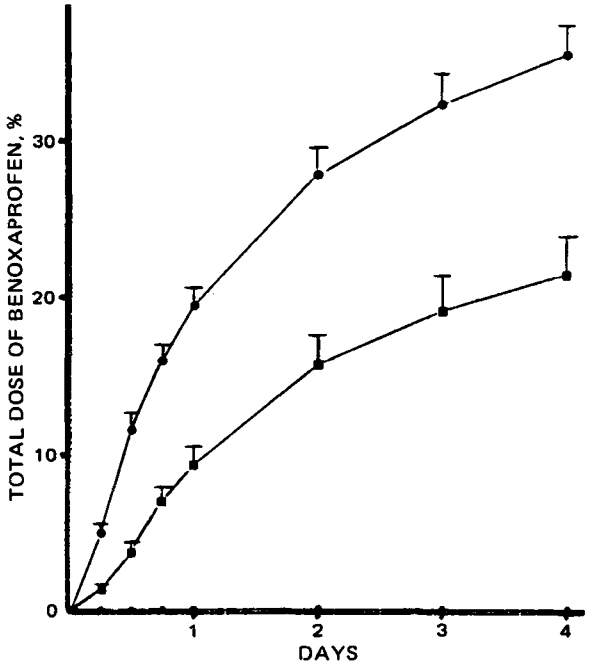

Figure 3—*Cumulative urinary benoxaprofen excretion (unchanged plus glucuronide metabolite) after oral dosing with 100 mg of two particle-size formulations. Key: ■, crystals larger than 60 mesh; and ●, crystals smaller than 100 mesh. Each data point represents the mean of 10 subjects with standard error.*

The average large particle dissolution after vigorous stirring was 87% of the drug in the capsules; the corresponding value for the small particles was 102%. Large particle dissolution also was more variable than dissolution of the small particles. Relative standard deviations for the average 20-, 60-, and 120-min large particle dissolution values were 26.7, 9.0, and 9.4, respectively; the corresponding determinations for the small particles were 25.6, 4.1, and 1.8.

These *in vitro* studies show that the dissolution of the two sieved benoxaprofen fractions containing particles with an ~10-fold difference in mean diameter was significantly different.

In the clinical study, two subjects withdrew after one dose for reasons other than those relating to drug dosing. The plasma data from the 10 subjects who completed the study are depicted in Fig. 2. Particle size dramatically affected both the rate and extent of GI benoxaprofen absorption. The calculated mean peak plasma concentration (12.0 μg/ml) for the small particle sizes was twice that for the large ones (5.5 μg/ml). Differences were also reflected in the calculated mean time to peak, 3.2 *versus* 6.2 hr, and the area under the mean plasma concentration–time curve, 357 *versus* 213 μg/hr/ml (0–96 hr).

The difference in benoxaprofen absorption from the two formulations also was reflected in the urinary drug and metabolite excretion (Fig. 3). An average of ~20% of the drug in the small particle formulation was excreted in the first 24 hr as the free plus glucuronide form compared to about 9% with the large particle formulation. Total drug excreted in the urine during the 96-hr collection averaged 35 and 21 mg, respectively.

That the differences in absorption noted were due to particle size is supported by analyses of variance (Table I) on the timed plasma levels, peak values, time to peak, area under plasma concentration–time curve, and total urinary drug excretion. The p value was <0.01 for all variables except the 0.5-, 72-, and 96-hr plasma levels.

REFERENCES

(1) J. M. Newton and G. J. Rowley, *J. Pharm. Pharmacol.*, **22**, 1635 (1970).

(2) G. Levy, *Am. J. Pharm.*, **135**, 78 (1963).

(3) A. J. Aquiar, L. M. Wheeler, S. Fusari, and J. E. Zelmer, *J. Pharm. Sci.*, **57**, 1844 (1968).

(4) A. T. Florence, E. G. Salole, and J. B. Stenlake, *J. Pharm. Pharmacol.*, **26**, 479 (1974).

(5) G. J. Eide, *Acta Pharm. Suec.*, **10**, 229 (1973).

(6) J. G. Wagner, "Biopharmaceutics and Relevant Pharmacokinetics," 1st ed., Drug Intelligence Publications, Hamilton, Ill., 1971, p. 115.

(7) F. J. Hailey and H. W. Glascock, *Curr. Ther. Res., Clin. Exp.*, **9**, 600 (1967).

(8) J. G. Reingold, F. J. Phillips, and H. F. Flippin, *Am. J. Med. Sci.*, **210**, 141 (1945).

(9) R. M. Atkinson, C. Bedford, K. J. Child, and E. G. Tomich, *Antibiot. Chemother.*, **12**, 232 (1962).

(10) T. R. Bates, J. A. Sequeira, and A. V. Tembo, *Clin. Pharmacol. Ther.*, **16**, 63 (1974).

(11) T. R. D. Shaw, J. E. Carless, M. Howard, and K. Raymond, *Lancet*, **2**, 209 (1973).

(12) J. G. Wagner, "Biopharmaceutics and Relevant Pharmacokinetics," 1st ed., Drug Intelligence Publications, Hamilton, Ill., 1971, p. 125.

(13) "The United States Pharmacopeia" 19th rev., Mack Publishing Co., Easton, Pa., 1974, p. 651.

(14) "Scientific Tables," 7th ed., Ciba-Geigy Ltd. Documenta, Basel, Switzerland, 1970, p. 712.

(15) G. L. Smith, R. A. Goulbourn, R. A. P. Burt, and D. H. Chatfield, *Br. J. Clin. Pharmacol.*, **4**, 585 (1977).

Interaction of Streptonigrin with Metals and with DNA

KOPPAKA V. RAO

Received August 28, 1978, from the *Department of Pharmaceutical Chemistry, College of Pharmacy, J. Hillis Miller Health Center, University of Florida, Gainesville, FL 32610.* Accepted for publication January 10, 1979.

Abstract □ The antitumor antibiotic, streptonigrin, interacted with zinc, copper, and manganese but not with calcium or magnesium, as indicated by spectral shifts and difference spectra. The titration data showed the formation of 1:1 complexes, and further titration continued to show spectral shifts until a molar ratio for zinc to streptonigrin of 5–10 to 1 was reached. Streptonigrin interacted with DNA only in the presence of a metal ion such as zinc. Streptonigrin titration with DNA at varying zinc molar equivalents revealed that one antibiotic molecule required 5–7 moles of zinc and 20–25 moles of DNA-phosphorus for complexation. Similar values were obtained from gel permeation chromatography.

Keyphrases □ Streptonigrin–interaction with metals and with DNA, complexation, spectrophotometry, gel permeation chromatography □ Antibiotics—streptonigrin, interaction with metals and with DNA □ Antineoplastic agents—streptonigrin, interaction with metals and with DNA □ DNA—interaction with streptonigrin and with metals □ Metals—complexation with streptonigrin and with DNA

Streptonigrin (I), an antitumor antibiotic and a *Streptomyces flocculus* metabolite (1, 2), shows high activity against various experimental neoplasms (3–5). Extensive clinical trials showed that it was active against certain lymphomas (6), and a double-blind comparison with chlorambucil showed comparable activity, with I being slightly more toxic in the GI tract (7).

Strong streptonigrin involvement in DNA metabolism in various cellular systems manifests itself in chromosomal aberration and fragmentation and in drug absorption by nuclear fractions (8–10). Mizuno and Gilboe (11), who studied the *in vitro* interaction of I and DNA, showed that two complexes were formed, one unstable to dialysis and the other stable, with a stoichiometry of 1:2000 for streptonigrin–DNA nucleotides. However, a sedimentation behavior, melting-profile, and gel permeation chromatography study (12) indicated that no complex was formed between streptonigrin and DNA. In that study, I showed no inhibition of DNA-dependent RNA polymerase, unlike other DNA-interacting antibiotics such as actinomycin or daunomycin. Thus, streptonigrin binding to DNA is controversial; this behavior would be somewhat unusual in view of its demonstrated involvement in DNA metabolism.

The complexing ability of streptonigrin toward certain metal ions was explored in this laboratory. Preliminary spectrophotometric studies showed that I readily formed complexes with ions such as Zn^{2+}, Cu^{2+}, and Mn^{2+} but not with Ca^{2+} or Mg^{2+}. Streptonigrin–metal complexes readily interacted with DNA to form clearly demonstrable and relatively stable complexes. This paper describes some characteristics of the interaction of I with metals such as Zn^{2+} and of the complexes such as streptonigrin–zinc with DNA.

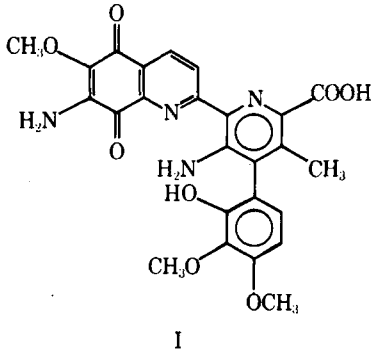

I

EXPERIMENTAL

Tromethamine buffer (0.01 *M*) of appropriate pH was used. Streptonigrin was dissolved in dioxane, approximately three equivalents of sodium bicarbonate were added, and the solution was diluted with water to $2–5 \times 10^{-4}$ *M*. Since I solutions made in tromethamine buffer (pH 7) decomposed gradually, the experiment was completed within 1 hr after the dilution with tromethamine.

Calf thymus DNA (sodium salt, highly polymerized, 8% phosphorus) was purchased[1]. A weighed sample was dissolved in water by gentle stirring with a magnetic stirrer at room temperature for 2–3 hr and was diluted to $1.0–1.5 \times 10^{-2}$ *M* solutions, based on DNA–phosphorus. The solutions were dispensed in 2–4-ml portions in test tubes and kept frozen until use.

The complexation was followed by a recording spectrophotometer[2] with silica cells of 1-cm path length. Metal complexes were studied in alcoholic and in aqueous solutions. For obtaining a Job plot, various molar mixtures of I and the metal ion with constant total molarity were prepared and their spectra were recorded. Corresponding reference solutions with I, but without the metal, also were prepared and their spectra were recorded. The difference in the absorbance between the two at the λ_{max} was plotted against the mole fraction.

Titrations were carried out by adding the metal-ion solution from a microburet[3] to the sample taken in the cell containing a magnetic stirring bar. The spectra were recorded against a distilled water (or alcohol) blank. In an alternative procedure, a I solution was taken in both the reference and sample cells, and the sample cell was titrated with the metal-ion solution. The spectra so obtained were the "difference spectra." Correction for the volume change was made by the addition of an identical volume of water to the reference cell.

DNA complexation was studied in aqueous solution with or without a buffer. Both titration methods, using either water or streptonigrin–Zn^{2+} solution as reference, were employed for measuring complexation.

Complex formation also was demonstrated through gel permeation chromatography by direct mixture chromatography and by an adaptation of the Hummel–Dreyer method (13). A cross-linked dextran[4] column (8 × 600 mm) was prepared and equilibrated with the streptonigrin–Zn^{2+} solution (4×10^{-5} *M* with respect to I and 4×10^{-4} *M* with respect to Zn^{2+}). The DNA sample (6.4×10^{-3} *M*, DNA–phosphorus) was diluted with the appropriate amount of the ligand–metal solution and applied to the column, which was then developed by more of the same solution. Fractions (3 ml) were collected, and their absorbance was read at 385 nm.

RESULTS AND DISCUSSION

In Fig. 1, curve A is a portion of the spectrum (300–450 nm) of 4×10^{-5} *M* I in 0.01 *M* tromethamine buffer, pH 7.5, with λ_{max} 363 nm and ϵ = 15,000. Curve B shows the shift of the λ_{max} to 385 nm (ϵ = 17,000) in the presence of 4×10^{-4} *M* Zn^{2+}. Curve C is the spectrum of a solution of I (4×10^{-5} *M*), Zn^{2+} (4×10^{-4} *M*), and DNA (3.2×10^{-3} *M*) with λ_{max} 410 nm and ϵ = 16,300. An identical solution, but without Zn^{2+}, gave curve

[1] ICN Pharmaceuticals, Cleveland, Ohio.
[2] Beckman model 25.
[3] Micrometric Instrument Co., Cleveland, Ohio.
[4] Sephadex G50, Pharmacia Fine Chemicals.

0022-3549/79/0700-0853$01.00/0
© 1979, American Pharmaceutical Association

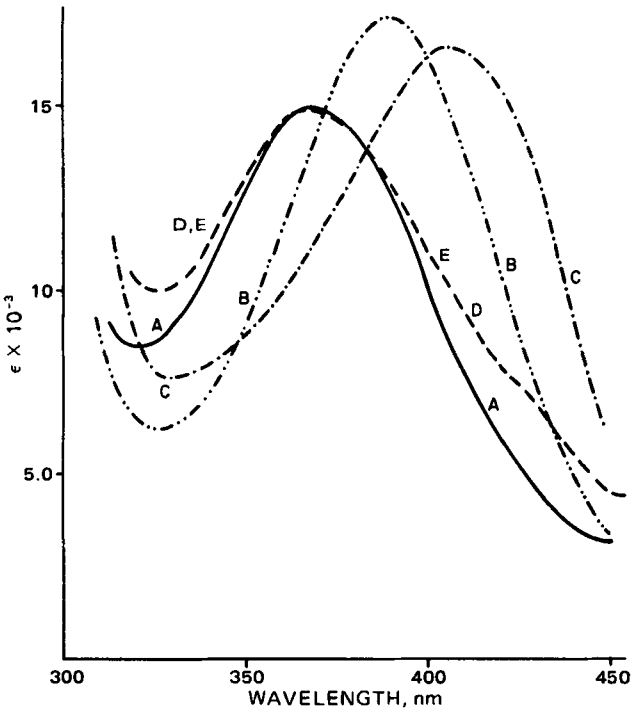

Figure 1—*Effects of Zn^{2+} and DNA on the absorption spectrum of I. Key: A, spectrum of I (4×10^{-5} M) in 0.01 M tromethamine buffer, pH 7.5; B, A + Zn^{2+} (4×10^{-4} M); C, A + B + DNA (3.2×10^{-3} M); D, A + DNA (3.2×10^{-3} M); and E, C + edetate sodium.*

D with λ_{max} and ϵ values essentially the same as those of I. To demonstrate that Zn^{2+} was essential for the I complexation with DNA, the solution that gave curve C was treated with edetate sodium, which produced a spectrum similar to that of D. Without zinc, DNA caused a slight spectral shift in the 410–450-nm region.

The complexation could be observed in two other ways. The reddish-brown I solutions essentially remained unchanged when treated with either Zn^{2+} or DNA separately; but when both were present, the color changed to brownish yellow. Addition of edetate sodium to this solution brought back the original reddish-brown color. In the second method, ethanol addition (5–6 volumes) to a I-DNA solution gave a white stringy DNA precipitate. Similar addition to streptonigrin-Zn^{2+}-DNA gave a dark-brown stringy precipitate even with 2–3 volumes of ethanol. The precipitate, after being washed with the solvent, gave the characteristic complex spectrum (curve C).

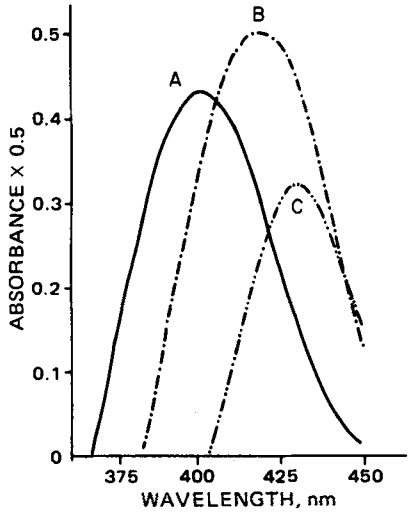

Figure 2—*Difference spectra. Key: A, spectrum of streptonigrin-Zn^{2+} complex read against a reference of streptonigrin; B, streptonigrin-Zn^{2+}-DNA complex read against a reference of streptonigrin-DNA; and C, streptonigrin-Zn^{2+}-DNA complex read against a reference of streptonigrin-Zn^{2+}.*

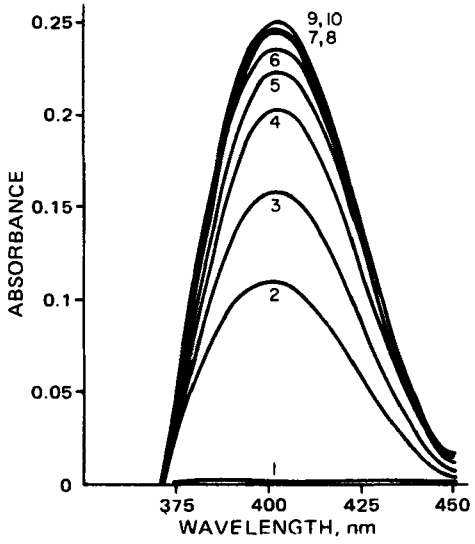

Figure 3—*Difference spectra similar to Fig. 2A resulting from titration of I with Zn^{2+}. The numbers 1–10 represent the zinc-streptonigrin molar ratios.*

Figure 2 shows the difference spectra.

Results with Cu^{2+} and Mn^{2+} were similar to those with Zn^{2+}. No spectral shifts were observed when I solutions were treated with Mg^{2+} or Ca^{2+} ions or when DNA was added in the presence of these ions in the pH 6.0–8.0 range.

Metal Complexation—I titration with Zn^{2+} solution, in the presence or absence of a buffer, gave difference spectra of increasing intensity (Fig. 3). A plot of the difference spectrum intensity against the I mole fraction is shown in Fig. 4. The slope change occurring at mole fraction 0.5 shows the existence of a 1:1 complex. The same result was obtained with the continuous variation (Job) method (Fig. 5). The experiments with Zn^{2+}, Cu^{2+}, and Mn^{2+} were carried out in aqueous as well as in ethanolic solutions with the same results shown in Fig. 3. Values from these experiments were used to calculate the formation constants for the complexation reaction shown in Table I according to Scheme I:

$$\text{streptonigrin} + Zn^{2+} \rightleftharpoons \text{streptonigrin-}Zn^{2+}$$

Scheme I

where the formation constant K = [streptonigrin-Zn^{2+}]/([streptonigrin]/[Zn^{2+}]). The concentration of each component was obtained from the spectrophotometric data according to the relationship:

$$K = \frac{(\epsilon_l - \epsilon_c)}{C_M(\epsilon_c - \epsilon_l) - (A - \epsilon_c C_l)} \qquad \text{(Eq. 1)}$$

where ϵ_c and ϵ_l were the absorptivities of the complex (which was the absorptivity at very high DNA/streptonigrin-Zn^{2+} ratios) and of the ligand, respectively; C_M and C_l were the total initial Zn^{2+} and streptonigrin

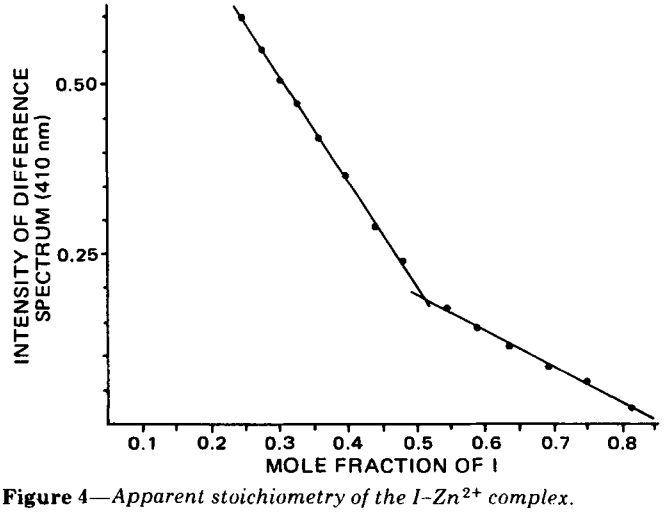

Figure 4—*Apparent stoichiometry of the I-Zn^{2+} complex.*

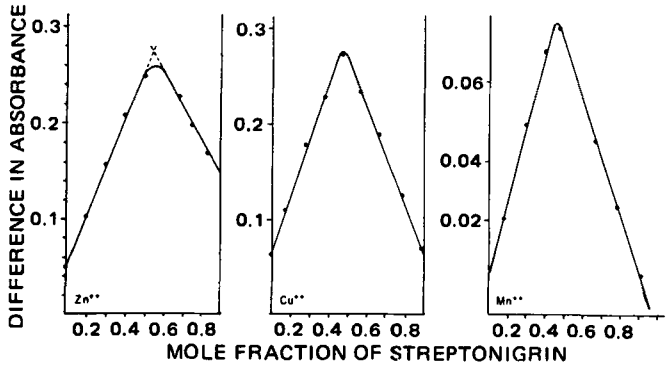

Figure 5—*Job plots of streptonigrin–metal complexes. The ordinates represent the difference between the absorbance of streptonigrin and that of the complex at the mole fraction value represented in the abscissa. The total molarity (ligand plus metal) was constant.*

concentrations, respectively; and A was the observed absorbance value.

Although a 1:1 complex could be demonstrated readily in the preceding experiments, further I titration with Zn^{2+} showed progressive increases in the difference spectrum intensity. The increase rate showed a slope change at a 5–10-mole ratio for Zn^{2+} to streptonigrin. This continued until a 20–25-mole ratio was reached, beyond which point it remained constant. This unusual metal to ligand ratio is difficult to rationalize merely on the basis of the streptonigrin structure. To assess the ionic strength influence on the metal complexation, a titration was carried out in the presence of sodium chloride (0.1 M). This lowered the end-point, with the constant value being obtained at a mole ratio of 10–15:1 for Zn^{2+} to streptonigrin.

The streptonigrin structure has many potential sites for complexation with zinc: the picolinic acid system, the 2,2-pyridylquinoline system, the aminoquinone system, the 2-(3-amino-2-pyridyl)quinoline system, and the amino and phenolic functions of rings C and D. The strongest are probably the first two. However, they cannot all be involved in complexation at the same time because some atoms or functions taking part in complexation are common to several systems. Also, after one proton has been displaced to form a complex, additional proton removal is a more difficult operation. A more likely explanation for the observed large metal–ligand ratios is in terms of mass action; *i.e.*, a sufficiently large metal ion excess must be present to form a relatively stable complex involving more than one metal atom. The term "apparent stoichiometry" is used in expressing this relationship until a more detailed picture of the interactions emerges.

DNA Complexation—Although the necessity for zinc was clearly demonstrated for streptonigrin binding with DNA, stoichiometry determination must consider the variable metal to ligand ratios indicated. For this reason, I titration with DNA was carried out at various Zn^{2+} to streptonigrin ratios (Fig. 6A). In the absence of Zn^{2+}, the difference spectrum was nonexistent. In the presence of varying Zn^{2+}, spectrophotometric titrations with DNA could be carried out to stable end-

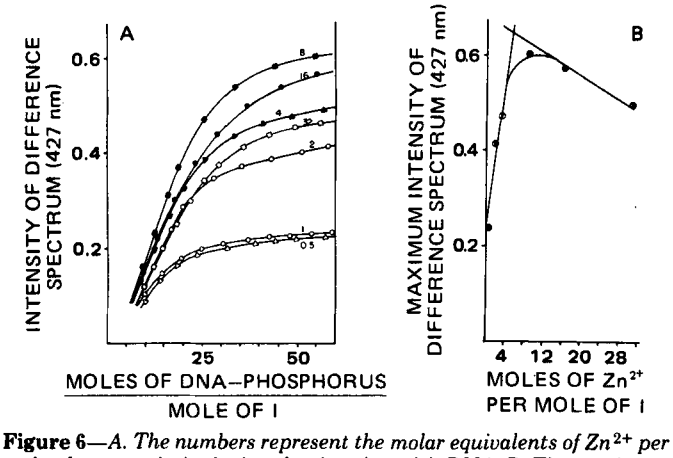

Figure 6—*A. The numbers represent the molar equivalents of Zn^{2+} per mole of streptonigrin during the titration with DNA. B. The maximum intensity values from Fig. 6A are plotted against the molar ratio of Zn^{2+}-streptonigrin.*

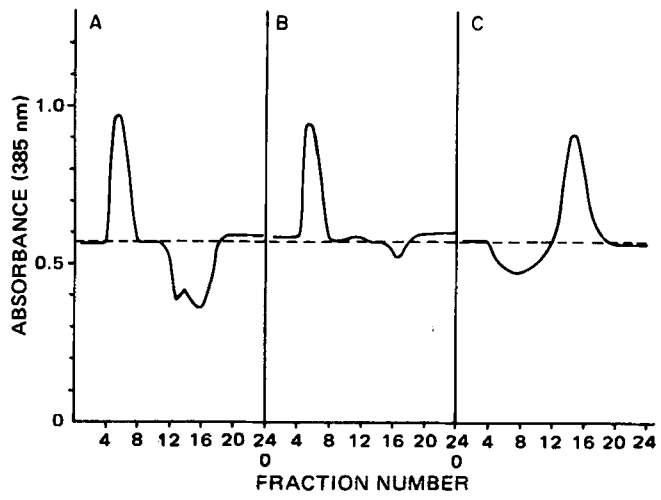

Figure 7—*Gel-chromatography of I-DNA in the presence (A and B) and absence (C) of Zn^{2+}. A. The column was equilibrated with streptonigrin–zinc (4×10^{-5} M and 4×10^{-4} M, respectively) and the DNA sample (6.4×10^{-3} M of DNA-phosphorus) was added. Elution was with the same streptonigrin–Zn^{2+} solution. B. Same as A but the DNA sample contained 3.2×10^{-4} M of streptonigrin. C. Same as A but without Zn^{2+}.*

points. At Zn^{2+} to streptonigrin ratios of 0.5:1 and 1:1, the curves were of the same order of magnitude. They showed that complexation took place between DNA and 1:1 streptonigrin–Zn^{2+}. At higher metal to ligand ratios, the difference spectrum intensity increased progressively until a maximum was reached at a zinc to streptonigrin ratio of 8:1. At still higher ratios, the difference spectrum intensity began to decrease.

In Fig. 6B, the maximum difference spectrum intensity was plotted against the Zn^{2+} to streptonigrin ratio. Extrapolation of the linear portions gave an intersection point that corresponded to a ratio of 6–7:1 for Zn^{2+} and streptonigrin. This value gave the maximum difference spectrum intensity change, suggesting that at this ratio of Zn^{2+} to streptonigrin, complexation with DNA was at the maximum. Titration of I with DNA at what appears to be an optimum Zn^{2+}-streptonigrin ratio of 7:1 showed the pattern commonly seen during complex formation, and titration could be performed to a relatively stable end-point. From several titrations, a value of 20–25 was obtained for the apparent stoichiometry, *i.e.*, 1 mole of streptonigrin/20–25 moles of DNA-phosphorus in the presence of 7 moles of Zn^{2+}. Thus, the interaction of I and DNA in the presence of Zn^{2+} parallels that of I and Zn^{2+}, where several moles of metal ion per mole of I were required for maximum interaction, as judged by the spectral shifts and intensity changes.

The streptonigrin–Zn^{2+}–DNA complex prepared in a 1:7:25 ratio could be diluted up to 10-fold without appreciable dissociation (as shown by the Beer's law plot). The complex was stable to dialysis for 4 days at 5°. The presence of Zn^{2+} in the complex was readily demonstrable by the λ_{max} (405–410 nm), as well as through the shift induced by edetate sodium to 365 nm.

Gel permeation chromatography was used for further characterization. When a I-DNA mixture was chromatographed on a cross-linked dextran column, the two appeared as sharp bands at their appropriate elution volumes. In the presence of Zn^{2+} (10 molar excess), two bands representing bound and free I could be seen during initial column development. However, as the elution progressed, they emerged as a very broad band. This behavior was not unexpected because of the continuous equilibrium alteration during elution.

The existence of the complex between streptonigrin and Zn^{2+} and DNA could be seen more clearly by the chromatographic procedure described previously (13) (Fig. 7A). As the DNA emerged from the column, the peak represented not only DNA but also the apparent stoichiometric amount of streptonigrin–Zn^{2+}. Since the introduced sample did not have the

Table I—I-Metal Complex Formation Constants

Complex	K at 22°
I-Zn^{2+}	$1.45 \pm 0.5 \times 10^5\ M^{-1}$
I-Cu^{2+}	$1.27 \pm 0.5 \times 10^5\ M^{-1}$
I-Mn^{2+}	$2.03 \pm 0.5 \times 10^4\ M^{-1}$

required ligand–metal complex concentration, it must have been taken up by the DNA from the surrounding solution. The negative peak that followed the DNA peak represented the ligand–metal complex removed from the solution. The two peak areas were equal.

Figure 7B shows the behavior when an additional 20 equivalents of streptonigrin–Zn^{2+} were introduced with the DNA sample. The negative peak was nearly absent, although the positive peak height due to the complex was the same as before. The apparent stoichiometry determined from several such elution curves, in which the negative peak was nearly absent, was 1 mole of streptonigrin/20–25 moles of DNA–phosphorus in the presence of 7 *M* equivalents of Zn^{2+}.

The column behavior in the absence of Zn^{2+} is shown in Fig. 7C. The initial negative peak suggested that the DNA displaced I from its position on the column and emerged first. The displaced streptonigrin appeared as the subsequent positive peak. This finding further indicates that complexation did not occur in the absence of Zn^{2+}.

REFERENCES

(1) K. V. Rao and W. P. Cullen *Antibiot. Annu.*, **1959–60**, 950.

(2) K. V. Rao, K. Biemann, and R. B. Woodward, *J. Am. Chem. Soc.*, **85**, 2532 (1963).

(3) J. J. Oleson, L. A. Caldarella, K. J. Mjos, A. R. Reith, R. S. Thie, and I. Toplin, *Antibiot. Chemother.*, **11**, 158 (1961).

(4) H. C. Reilly and K. Sigiura, *ibid.*, **1961**, 174.

(5) T. J. McBride, J. J. Oleson, and D. A. Wolff, *Cancer Res.*, **26A**, 727 (1966).

(6) D. S. Martin, P. E. Hayworth, and R. A. Guzman, *ibid.*, **30**, 709 (1970).

(7) D. T. Kuang, R. M. Wittington, H. E. Spencer, and M. E. Patno, *Cancer*, **23**, 597, 1280 (1969).

(8) A. Kihlman and G. Odmark, *Mutation Res.*, **2**, 494 (1965).

(9) N. S. Mizuno, *Biochim. Biophys. Acta*, **108**, 395 (1965).

(10) D. S. Miller, J. Laszlo, K. S. McCarty, W. R. Guild, and P. Hochstein, *Cancer Res.*, **27**, 632 (1967).

(11) N. S. Mizuno and D. P. Gilboe, *Biochim. Biophys. Acta*, **224**, 319 (1970).

(12) Y. V. Dudnik, G. G. Gauze, V. L. Karpova, V. I. Kozmyan, and E. Padron, *Antibiotiki*, **18**, 968 (1973); through *Chem. Abstr.*, **80**, 10500e (1974).

(13) J. P. Hummel and W. J. Dreyer, *Biochim. Biophys. Acta*, **63**, 530 (1962).

ACKNOWLEDGMENTS

The author thanks Mr. John L. Davenport for financial support, Dr. John Douros of the National Cancer Institute for the streptonigrin, and Dr. Stephen G. Schulman, College of Pharmacy, University of Florida, for many valuable discussions. The author also thanks Lederele Laboratories, Division of American Cyanamid Co., for the "Lederle Pharmaceutical Faculty Award" for 1977 based on the subject of this paper.

3-Quinuclidinyl Benzilate Hydrolysis in Dilute Aqueous Solution

LARRY A. HULL, DAVID H. ROSENBLATT, and JOSEPH EPSTEIN ˣ

Received March 9, 1977, from the *Environmental Research Division, Chemical Systems Laboratory, Department of the Army, Aberdeen Proving Ground, MD 21010.* Accepted for publication January 9, 1979.

Abstract □ The hydrolysis kinetics of 3-quinuclidinyl benzilate were determined over the pH 0–14 range at different temperatures in solutions buffered to a constant pH. Analysis of data extrapolated to zero buffer concentrations permitted construction of an overall rate expression for pH 0–14 and 0–100°. Reaction mechanisms are discussed.

Keyphrases □ Quinuclidinyl benzilate—hydrolysis in dilute aqueous solution, kinetics, pH, temperature □ Aminoalcohol esters—quinuclidinyl benzilate, hydrolysis in dilute aqueous solution, kinetics □ Hydrolysis kinetics—quinuclidinyl benzilate in dilute aqueous solution, pH, temperature

3-Quinuclidinyl benzilate (I), like atropine, is a muscarinic cholinergic antagonist of considerable pharmacological interest (1). Among the properties of greatest pharmaceutical significance is its hydrolytic behavior in dilute aqueous solution. In the present research, sufficient information was gained to permit hydrolysis rate prediction in the absence of high general base or salt concentrations at any desired temperature (0–100°) or pH (0–14).

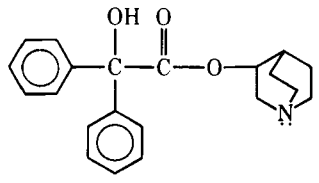

I

EXPERIMENTAL

Reagents and Materials—Technical grade I was dissolved in chloroform, decolorized with charcoal, and extracted into aqueous hydrochloric acid. The acidic solution was made slightly basic and back-extracted with chloroform. Solvent evaporation left a solid residue, which was recrystallized twice from ethyl acetate to give a product of at least 98% purity.

Anal.—Calc. for: C, 74.75; H, 6.87; N, 4.15; O, 14.23. Found: C, 74.6; H, 7.1; N, 4.3; O, 14.4.

Compound I-HCl was prepared by addition of hydrogen chloride-saturated ether to a chloroform solution of I; the crystalline precipitate was dried carefully. All solutions were made with carbon dioxide-free distilled water. Commercial grade buffers were used without additional purification. Ether was purified of peroxide by filtration through an alumina column.

Instrumentation—A spectrophotometer[1] with 1-cm quartz cells or 10-cm silica cells was used for absorptiometric determinations. The pH was determined with a pH meter[2]. Solvent contamination with stopcock grease was avoided through the use of separators with polytef stopcocks for liquid–liquid extractions. The reaction solutions were kept at a constant temperature with water baths[3], or, in some cases, the reacting mixtures were sealed in glass vials immersed in appropriate refluxing solvents that kept the temperature constant.

Procedure—Products were isolated from a pH 11.5 reaction mixture that was kept 4 hr at 60°. Only benzilic acid and 3-quinuclidinol were found; these compounds were identical to authentic samples according to IR and melting-point analyses.

[1] Beckman DK-2.
[2] Beckman model G.
[3] Forma 2095S and Aminco 4-8600.

0022-3549/79/0700-0856$01.00/0

© 1979, American Pharmaceutical Association

required ligand–metal complex concentration, it must have been taken up by the DNA from the surrounding solution. The negative peak that followed the DNA peak represented the ligand–metal complex removed from the solution. The two peak areas were equal.

Figure 7B shows the behavior when an additional 20 equivalents of streptonigrin–Zn^{2+} were introduced with the DNA sample. The negative peak was nearly absent, although the positive peak height due to the complex was the same as before. The apparent stoichiometry determined from several such elution curves, in which the negative peak was nearly absent, was 1 mole of streptonigrin/20–25 moles of DNA–phosphorus in the presence of 7 *M* equivalents of Zn^{2+}.

The column behavior in the absence of Zn^{2+} is shown in Fig. 7C. The initial negative peak suggested that the DNA displaced I from its position on the column and emerged first. The displaced streptonigrin appeared as the subsequent positive peak. This finding further indicates that complexation did not occur in the absence of Zn^{2+}.

REFERENCES

(1) K. V. Rao and W. P. Cullen *Antibiot. Annu.*, **1959–60**, 950.

(2) K. V. Rao, K. Biemann, and R. B. Woodward, *J. Am. Chem. Soc.*, **85**, 2532 (1963).

(3) J. J. Oleson, L. A. Caldarella, K. J. Mjos, A. R. Reith, R. S. Thie, and I. Toplin, *Antibiot. Chemother.*, **11**, 158 (1961).

(4) H. C. Reilly and K. Sigiura, *ibid.*, **1961**, 174.

(5) T. J. McBride, J. J. Oleson, and D. A. Wolff, *Cancer Res.*, **26A**, 727 (1966).

(6) D. S. Martin, P. E. Hayworth, and R. A. Guzman, *ibid.*, **30**, 709 (1970).

(7) D. T. Kuang, R. M. Wittington, H. E. Spencer, and M. E. Patno, *Cancer*, **23**, 597, 1280 (1969).

(8) A. Kihlman and G. Odmark, *Mutation Res.*, **2**, 494 (1965).

(9) N. S. Mizuno, *Biochim. Biophys. Acta*, **108**, 395 (1965).

(10) D. S. Miller, J. Laszlo, K. S. McCarty, W. R. Guild, and P. Hochstein, *Cancer Res.*, **27**, 632 (1967).

(11) N. S. Mizuno and D. P. Gilboe, *Biochim. Biophys. Acta*, **224**, 319 (1970).

(12) Y. V. Dudnik, G. G. Gauze, V. L. Karpova, V. I. Kozmyan, and E. Padron, *Antibiotiki*, **18**, 968 (1973); through *Chem. Abstr.*, **80**, 10500e (1974).

(13) J. P. Hummel and W. J. Dreyer, *Biochim. Biophys. Acta*, **63**, 530 (1962).

ACKNOWLEDGMENTS

The author thanks Mr. John L. Davenport for financial support, Dr. John Douros of the National Cancer Institute for the streptonigrin, and Dr. Stephen G. Schulman, College of Pharmacy, University of Florida, for many valuable discussions. The author also thanks Lederele Laboratories, Division of American Cyanamid Co., for the "Lederle Pharmaceutical Faculty Award" for 1977 based on the subject of this paper.

3-Quinuclidinyl Benzilate Hydrolysis in Dilute Aqueous Solution

LARRY A. HULL, DAVID H. ROSENBLATT, and JOSEPH EPSTEIN ˣ

Received March 9, 1977, from the *Environmental Research Division, Chemical Systems Laboratory, Department of the Army, Aberdeen Proving Ground, MD 21010.* Accepted for publication January 9, 1979.

Abstract □ The hydrolysis kinetics of 3-quinuclidinyl benzilate were determined over the pH 0–14 range at different temperatures in solutions buffered to a constant pH. Analysis of data extrapolated to zero buffer concentrations permitted construction of an overall rate expression for pH 0–14 and 0–100°. Reaction mechanisms are discussed.

Keyphrases □ Quinuclidinyl benzilate—hydrolysis in dilute aqueous solution, kinetics, pH, temperature □ Aminoalcohol esters—quinuclidinyl benzilate, hydrolysis in dilute aqueous solution, kinetics □ Hydrolysis kinetics—quinuclidinyl benzilate in dilute aqueous solution, pH, temperature

3-Quinuclidinyl benzilate (I), like atropine, is a muscarinic cholinergic antagonist of considerable pharmacological interest (1). Among the properties of greatest pharmaceutical significance is its hydrolytic behavior in dilute aqueous solution. In the present research, sufficient information was gained to permit hydrolysis rate prediction in the absence of high general base or salt concentrations at any desired temperature (0–100°) or pH (0–14).

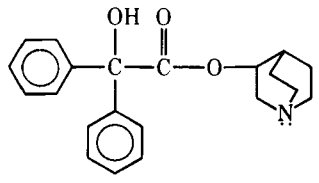

I

EXPERIMENTAL

Reagents and Materials—Technical grade I was dissolved in chloroform, decolorized with charcoal, and extracted into aqueous hydrochloric acid. The acidic solution was made slightly basic and back-extracted with chloroform. Solvent evaporation left a solid residue, which was recrystallized twice from ethyl acetate to give a product of at least 98% purity.

Anal.—Calc. for: C, 74.75; H, 6.87; N, 4.15; O, 14.23. Found: C, 74.6; H, 7.1; N, 4.3; O, 14.4.

Compound I-HCl was prepared by addition of hydrogen chloride-saturated ether to a chloroform solution of I; the crystalline precipitate was dried carefully. All solutions were made with carbon dioxide-free distilled water. Commercial grade buffers were used without additional purification. Ether was purified of peroxide by filtration through an alumina column.

Instrumentation—A spectrophotometer[1] with 1-cm quartz cells or 10-cm silica cells was used for absorptiometric determinations. The pH was determined with a pH meter[2]. Solvent contamination with stopcock grease was avoided through the use of separators with polytef stopcocks for liquid–liquid extractions. The reaction solutions were kept at a constant temperature with water baths[3], or, in some cases, the reacting mixtures were sealed in glass vials immersed in appropriate refluxing solvents that kept the temperature constant.

Procedure—Products were isolated from a pH 11.5 reaction mixture that was kept 4 hr at 60°. Only benzilic acid and 3-quinuclidinol were found; these compounds were identical to authentic samples according to IR and melting-point analyses.

[1] Beckman DK-2.
[2] Beckman model G.
[3] Forma 2095S and Aminco 4-8600.

0022-3549/79/0700-0856$01.00/0

© 1979, American Pharmaceutical Association

To determine the I hydrolysis rates, concentration analyses were made at appropriate intervals. The reaction solutions were buffered to a constant pH, adjusted to 0.055 ionic strength with sodium chloride, and thermostated to within ±2°. Kinetic experiments above pH 9 were performed under a nitrogen atmosphere to reduce carbon dioxide absorption.

Because of the limited solubility of I at high pH, two analytical procedures were employed. Each reaction mixture for studies below pH 7 was at an initial I-HCl concentration of 0.0023 *M*. Ten-milliliter aliquots of the reaction mixture were taken at appropriate intervals, mixed with 2 ml of 1.3 *M* H_2SO_4, and extracted with 10 ml of ether to remove benzilic acid. The aqueous extraction layer was collected and analyzed spectrophotometrically for I (as the protonated species, $I{\cdot}H^+$) at 258 nm using a 1-cm light path cell.

For kinetic studies above pH 9, initial concentrations of 0.00026 *M* I-HCl were used. Forty-milliliter aliquots of the reaction mixtures were extracted with mixtures of 40 ml of ether and 8 ml of 1.3 *M* H_2SO_4. Aqueous layers were analyzed spectrophotometrically as already described with 10-cm light path silica cells.

No appreciable error was introduced in the analyses due to I hydrolysis after extraction of the acidified mixtures since the molar absorptivities of I and benzilic acid were not significantly different. The molar absorptivities at 258 nm were 479 and 481, respectively. Also, the hydrolysis reaction in acid at 25° was extremely slow. There was a slight shift in the spectrum when benzilic acid was converted to the benzilate ion, but this shift was not noticeable at 258 nm.

Data Analysis—The linearity of semilogarithmic I absorbance plots (and, hence, of concentration) invariably indicated first-order kinetics. The pseudo-first-order rate constants, k_{obs}, were calculated from these lines by a least-squares treatment. The k_{obs} values determined at three different buffer concentrations were extrapolated back to zero buffer concentration to eliminate buffer effects and to obtain the first-order rate constants for the water species, *i.e.*, H_3O^+, OH^-, and H_2O. The intercept of each plot was designated k_0. The kinetic runs gave pseudo-first-order reactions with respect to the I disappearance rate because of the large excess or constancy of the water species, whether OH^-, H_3O^+, or H_2O.

Initial data inspection led to the assumption, later confirmed by theoretical curves, that the important reactions were analogous to those observed by Hussain and Schurman (2) with 2-dimethylaminoethanethiol propionate, *i.e.*:

$$I{\cdot}H^+ + H_3O^+ \xrightarrow{k_1} \text{products}$$

Scheme I

$$\text{rate} = k_1[I{\cdot}H^+][H_3O^+] \qquad \text{(Eq. 1)}$$

$$I{\cdot}H^+ + H_2O \xrightarrow{k_2} \text{products}$$

Scheme II

$$\text{rate} = k_2[I{\cdot}H^+][H_2O] \qquad \text{(Eq. 2)}$$

$$I{\cdot}H^+ + OH^- \xrightarrow{k_3} \text{products}$$

Scheme III

$$\text{rate} = k_3[I{\cdot}H^+][OH^-] \qquad \text{(Eq. 3}a\text{)}$$

or:

$$I + H_2O \xrightarrow{k_{3'}} \text{products}$$

Scheme IV

$$\text{rate} = k_{3'}[I][H_2O] \qquad \text{(Eq. 3}b\text{)}$$

and:

$$I + OH^- \xrightarrow{k_4} \text{products}$$

Scheme V

$$\text{rate} = k_4[I][OH^-] \qquad \text{(Eq. 4)}$$

Although Eqs. 3*a* and 3*b* are kinetically equivalent, Eq. 3*b* was ruled out effectively by several authors for related reactions (2–5). The rigid structure of I cannot be contorted to give the intermediate required by Bruice and Mautner (6), who would favor Eq. 3*b*. Equation 3*a* represents the important reaction in the present instance. Also, since the hydrogen-ion concentration is quite low in the region where the free base form (I) is significant, the following reaction was not considered:

$$I \xrightarrow{H^+} \text{products}$$

Scheme VI

The dissociation constant for $I{\cdot}H^+$, $K_a = [I][H_3O^+]/[I{\cdot}H^+]$, and the protolysis constant for water, $K_w = [H^+][OH^-]$, were utilized in an overall rate expression:

$$k_0 = \frac{k_3K_w + k_4K_aK_w/[H_3O^+] + k_1[H_3O^+]^2 + k_2[H_2O][H_3O^+]}{[H_3O^+] + K_a} \qquad \text{(Eq. 5)}$$

Values of K_w at 0.055 ionic strength were calculated according to the equations of Harned and Owen (7), assuming the electrolyte to be sodium chloride, where $K_{w0.055} = K_{w0.0}\,(\alpha_{H_2O}/\gamma_{H^+}\gamma_{OH^-})$. Values of k_4 were obtained from experiments above pH 11, where $k_4 = k_0/[OH^-]$. The individual values of k_4 were fitted to an Arrhenius equation by a least-squares plot.

The value of K_a could not be determined directly by potentiometric titration owing to solubility problems and to hydrolysis during titration. Therefore, at 25°, a least-squares data plot for pH 6.8, 8.1, and 9.05 was used to calculate k_3 and K_a. The resulting equation derived from Eq. 5, with omission of terms in k_1 and k_2, was:

$$k_0[H_3O^+] = k_3K_w + \{(k_4K_w/[H_3O^+]) - k_0\}K_a \qquad \text{(Eq. 6)}$$

The ordinate $k_0[H_3O^+]$ was plotted against the abscissa $(k_4K_w/[H_3O^+]) - k_0$ to give K_a as the slope and k_3K_w as the intercept. In this calculation, the average k_4 value at 25°, 155 M^{-1} hr^{-1}, was used.

Approximate k_3 values were calculated from 45 and 87° data at pH 6.86, which were used along with the 25° value for an initial Arrhenius plot of k_3. The Arrhenius plot values were used to calculate K_a at four temperatures; in turn, these values were used to correct the preliminary values of k_3, *i.e.*:

$$k_3 = \left\{k_0/[OH^-] - k_4\left(\frac{K_a}{[H_3O^+] + K_a}\right)\right\}\left(\frac{[H_3O^+] + K_a}{[H_3O^+]}\right) \qquad \text{(Eq. 7)}$$

The corrections were small. The final Arrhenius plot of k_3 (25, 45, and 87°) provided the necessary input for refined K_a calculations.

The reaction of $I{\cdot}H^+$ with water at 25° in the pH range of minimum reaction, ~pH 3.6, was too slow for a direct rate determination. Therefore, the value for k_2 was estimated by means of a Bronsted plot (8) of log k_B/q *versus* log $(p/q)K_a$, where k_B is the catalytic constant of the base and K_a is the dissociation constant of the aminomethane, HPO_4^{2-}, and acetate. This plot was extrapolated to the log of $(p/q)K_a$ for water (9), *i.e.*, 1.744, to obtain k_2, which is also k_B for water.

Values of k_B for each base were determined as follows. First, values of k_{Bi} for three of the bases that had been used to establish the k_0 values ($H_2BO_3^-$, tromethamine, and HPO_4^{2-}) were calculated from the slopes of:

$$k_{obs} = k_{Bi}[\text{buffer base}] + k_0 \qquad \text{(Eq. 8)}$$

where the buffer base concentration was taken as one-half of the total buffer concentration since the acid to base ratio was always 1:1. Then, k_B was calculated from k_{Bi} by correcting for the dissociation of $I{\cdot}H^+$ to I and assuming that the reactivity of I was 1/29 (*i.e.*, $k_3 = 29k_4$) as great as that of $I{\cdot}H^+$. (See *Appendix* for details.) The value of k_B for hydroxide ion was taken as equal to k_3, and the dissociation constant for water, the conjugate acid of hydroxide ion, was taken as 1.8×10^{-16}.

To obtain k_B for acetate ion, which was run at pH = pKa of acetic acid, the calculation required that the water reaction be included:

$$k_B = \frac{k_{obs} - k_3[OH^-] - k_2[H_2O]}{[\text{acetate ion}]} \qquad \text{(Eq. 9)}$$

Thus, on the first round, k_2 was considered to be zero in the calculation of acetate k_B, which was used in determining an approximate value of k_2. This value, in turn, was used to refine the acetate k_B and so on in a rapidly convergent iterative process.

For determining k_2 at 100°, an aqueous $I{\cdot}H^+$ solution was adjusted with hydrochloric acid to pH 3.6 and ionic strength 0.055. From the relative densities of water at 25 and 100° and the molar water concentration at 25°, the molar water concentration at 100° is 53.4. The value of k_{obs} was corrected by subtraction of $k_3[OH^-]$ to obtain k_0. The rate was then:

$$k_2 = k_0/[H_2O] = k_0/53.4 \qquad \text{(Eq. 10)}$$

At the pH in question, correcting k_2 for $k_1[H_3O^+]$ was unnecessary.

From the values of k_2 at 25 and 100°, an Arrhenius equation was derived.

The calculation of k_1 involved the assumption that ionic strength has little effect. [This assumption was necessary because the reaction rate at 0.055 ionic strength, *i.e.*, 0.055 *N* HCl, and 25 or 45° is so low. From data for 1 and 0.5 *N* HCl at 25°, one may estimate that the rate increase due to the ionic strength of 1 *N* HCl over the rate at ionic strength 0.055

Table I—Kinetic Data for Hydrolysis of 3-Quinuclidinyl Benzilate (I) in 0.055 Ionic Strength Aqueous Solutions

Buffer[a]	Total Molar Concentration	K_{obs}, hr^{-1}	pH
	15°		
Boric acid	0.02	0.01545	9.15
	0.04	0.01664	9.15
	0.06	0.01781	9.15
		0.01427[b]	9.15
NaOH	0.01243	0.8572	—
	0.00268	0.2012	—
	25°		
HCl	0.03	0.0001077	1.40
	0.5[c]	0.0003783	0.30
	1.0[c]	0.0007820	0.00
CH_3CO_2H	0.03	0.00006065	4.62
NaH_2PO_4 plus	0.010	0.0006177	6.75
Na_2HPO_4	0.018	0.0007639	6.84
	0.026	0.0009833	6.88
		0.000377[b]	6.80
Tromethamine	0.006	0.009007	8.01
	0.02	0.010427	8.08
	0.04	0.011004	8.10
		0.008899[b]	8.10
Boric acid	0.006	0.03956	0.97
	0.02	0.04171	9.03
	0.04	0.05105	9.05
	0.06	0.05213	9.08
		0.3796[b]	9.05
NaOH	0.00237	0.3956	—
	0.00593	0.8546	—
	0.01185	1.819	—
	35°		
Boric acid	0.02	0.1351	8.90
	0.04	0.1324	8.85
		0.1386	8.90
		0.1319[b]	8.90
NaOH	0.00248	0.7213	—
	0.01243	3.203	—
	45°		
HCl	1.03[c]	0.004146	−0.01
NaH_2PO_4 plus	0.010	0.00528	6.86
Na_2HPO_4[d]	0.015	0.00623	6.86
	0.02	0.00673	6.86
		0.0039[b]	6.86
Boric acid	0.02	0.3124	8.83
	0.04	0.3038	8.82
	0.06	0.3669	8.83
		0.2732[b]	8.83
NaOH	0.00248	1.224	—
	65.5°		
$Na_2B_4O_7 \cdot$	0.01	1.416	8.94
$10H_2O$[d]	0.015	1.495	8.94
	0.02	1.643	8.94
		1.178[b]	8.94
	87°		
NaH_2PO_4 plus	0.01	0.5026	6.86
Na_2HPO_4[d]	0.015	0.6109	6.86
	0.02	0.6535	6.86
		0.3627[b]	6.86
	100°		
HCl		0.001566	3.60

[a] Buffers other than NaOH and HCl consisted of equal concentrations of the buffer base and its conjugate acid. [b] Calculated k_0 for buffer concentration. [c] Ionic strength same as molar concentration. [d] The pH for these experiments was estimated from the pKa of the buffer at the given temperature. [H. W. Robinson, *J. Biol. Chem.*, **82**, 775 (1969). R. G. Bates, "Electronic pH Determinations," Wiley, New York, N.Y., 1954, p. 86. R. P. Bell, "Acid-Base Catalysis," Oxford University Press, London, England, 1941, pp. 11-35.]

is about 12%. According to Aksnes and Prue (10), it might have been higher.] The calculation was:

$$k_1 = k_{obs} - k_2[H_2O] \qquad \text{(Eq. 11)}$$

The values of k_1 at 25 and 45° were incorporated in an Arrhenius equation.

RESULTS AND DISCUSSION

Kinetic Rate Data and Equilibria—Kinetic rate data and associated pH values are summarized in Table I. Data used for the Bronsted plot to estimate k_2 at 25° are shown in Table II. A plot of log $k_{B/q}$ *versus* log $(p/q)K_a$ using the values in Table II was linear ($r = 0.9996$) with a slope of 0.58, supporting the contention that I hydrolysis is subject to general base catalysis.

Table II—General Base Catalysis Data for Hydrolysis of 3-Quinuclidinyl Benzilate (Protonated Species)

Base	p/q	K_a	k_B[a]
Water	1/1	55.5	2.94×10^{-7}
Acetate	1/2	2.399×10^{-5}	0.00272
Phosphate	2/3	1.585×10^{-5}	0.0460
Tromethamine	1/1	7.943×10^{-9}	0.1257
Borate	3/1	8.913×10^{-10}	1.0036
Hydroxide	1/1	1.80×10^{-16}	4514

[a] k_B calculated from:

$$k_B = \frac{k_{obs} - k_0}{[\text{buffer base}]} \left[\frac{[H_3O^+] + K_a}{[H_3O^+] + K_a/29} \right]$$

The temperature-related equations for the hydrolysis rate constants in units of M^{-1} hr^{-1} and the acid dissociation constant of I are:

$$\log_{10} k_1 = (-3388.2/T) + 8.2477 \qquad \text{(Eq. 12)}$$

$$\log_{10} k_2 = (-2717.5/T) + 2.5827 \qquad \text{(Eq. 13)}$$

$$\log_{10} k_3 = (-2379.6/T) + 11.5558 \qquad \text{(Eq. 14)}$$

$$\log_{10} k_4 = (-2531.6/T) + 10.6599 \qquad \text{(Eq. 15)}$$

and:

$$\log_{10} K_a = (-2455.8/T) - 1.0647 \qquad \text{(Eq. 16)}$$

where T is in °K.

In Table III, the values of k_0 for nine experiments are compared with those obtained by use of Eq. 5 with the constants calculated from Eqs. 12–16. The predicted values were generally within 35% of the experimental values.

The pH of maximum stability in water at 25° containing little or no basic anions is 3.64 (11). From Eq. 5, the observed rate at this pH is 1.66×10^{-5} hr^{-1}. The water reaction accounts for ~98% of the reaction at this pH. At pH 3, the rate is only 1.71×10^{-5} hr^{-1}, with the water reaction accounting for 95% of the overall reaction. At pH 4.5, the water reaction accounts for 93% of the total reaction.

Thus, the left side of the pH profile of I hydrolysis (Fig. 1) shows a decreasing rate with increasing pH; the change of the rate initially is 10-fold per pH unit but diminishes as the pH nears 3. The rate over pH

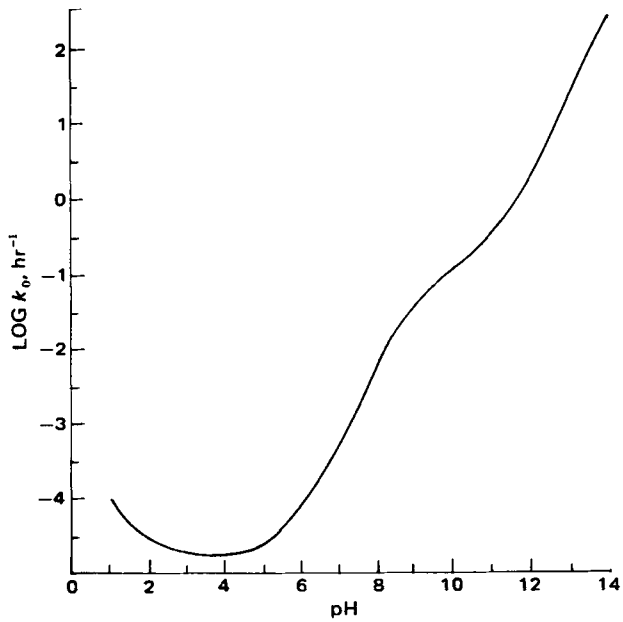

Figure 1—*Hydrolysis rates of 3-quinuclidinyl benzilate from pH 1–14 at t = 25° and μ = 0.055.*

Table III—Calculated *versus* Experimental k_0 Values for 3-Quinuclidinyl Benzilate (I) Hydrolysis in Buffer Solutions

Temperature	pH	k_0[a], hr^{-1} Calculated	Found
15°	9.15	0.0142	0.0143
25°	6.80	0.000356	0.000377
25°	8.10	0.00677	0.00890
25°	9.05	0.0428	0.0380
35°	8.90	0.102	0.132
45°	6.86	0.00522	0.00391
45°	8.83	0.253	0.273
65.5°	8.94	1.428	1.178
87°	6.86	0.522	0.363

[a] Values of k_0 calculated from:

$$k_0 = \frac{k_3K_w + K_4K_aK_w/[H_3O^+] + k_1[H_3O^+]^2 + k_2[H_2O][H_3O^+]}{[H_3O^+] + K_a}$$

3–4.5 is, to all intents, constant and is due to the reaction of $I{\cdot}H^+$ with water molecules. Above pH 4.5, the rate increases in the manner shown in Fig. 1.

The hydrolysis of I in the absence of buffers lowers the aqueous solution pH since hydrolysis produces benzilic acid. Thus, an unbuffered I solution that is initially slightly basic (the pKa of $I{\cdot}H^+$ is 9.3) will hydrolyze at a rate calculable from Eq. 5 but will produce acid, lower the pH, and thus produce an environment where the hydrolysis rate is less than it was initially.

Comparison with Hydrolysis of Related Compounds—The hydrolysis kinetics of amino alcohol (and amino mercaptan) esters in which the nitrogen is separated from the alcohol oxygen by two or three carbons was studied as early as 1950 (12). In general, reactivity with hydroxide ion is in the order: protonated tertiary amine > quaternary ammonium > tertiary amine. Values of k_4 (the hydroxide-ion rate constant with the unprotonated species) tend to remain fairly close to one another under a given set of conditions (4, 13–15), as well as to values for esters containing no nitrogen (4, 14, 15). Nitrogen proximity to the carbonyl carbon is unimportant (4, 13, 15).

Nitrogen quaternization by alkylation inductively increases these rate constants up to 32-fold (2, 4, 6, 12, 13, 15). Protonation, however, increases the reactivity up to 40,000-fold (2, 4, 6, 13, 14, 16). The higher increase, therefore, cannot be ascribed only to an inductive effect of the positive charge. The large increases are found in cases where the proton can participate in intramolecular hydrogen bonds with the acyl carbonyl oxygens (4, 17). When rigidity prevents intramolecular hydrogen bonding, the protonated species are not much more reactive than the quaternized species. Thus, in the case of 3-quinuclidinyl acetate, the factor is less than 2 (13, 18). The k_3/k_4 ratio of 29 in this work appears entirely reasonable.

Significance of Present Study—Amino alcohol ester hydrolytic stability has been of concern in the pharmaceutical field, and several pH profile determinations are on record (2–6, 16, 19, 20). These usually have ignored both the water reaction (k_2), which is generally slow enough to present experimental difficulties, and the acid-catalyzed hydrolysis (k_1). The present study provides the means for calculating the hydrolysis rate over wide temperature and pH ranges with all four rate-determining reactions considered.

APPENDIX

For the calculations of K_B from K_{Bi}:

$$k_{Bi} = \frac{[I{\cdot}H^+]k_B}{[I] + [I{\cdot}H^+]} + \frac{[I]k_B}{29([I] + [I{\cdot}H^+])} \qquad \text{(Eq. A1)}$$

Since:

$$\frac{[I{\cdot}H^+]}{[I] + [I{\cdot}H^+]} = \frac{[H_3O^+]}{[H_3O^+] + K_a} \qquad \text{(Eq. A2)}$$

and:

$$\frac{[I]}{[I] + [I{\cdot}H^+]} = \frac{K_a}{[H_3O^+] + K_a} \qquad \text{(Eq. A3)}$$

it follows that:

$$k_B = k_{Bi} \div \left(\frac{[H_3O^+]}{[H_3O^+] + K_a} + \frac{K_a/29}{[H_3O^+] + K_a}\right) \qquad \text{(Eq. A4)}$$

or:

$$k_B = k_{Bi}\left(\frac{[H_3O^+] + K_a}{[H_3O^+] + K_a/29}\right) \qquad \text{(Eq. A5)}$$

REFERENCES

(1) S. H. Snyder, K. J. Chang, M. J. Kuhar, and H. I. Yamamura, *Fed. Proc., Fed. Am. Soc. Exp. Biol.*, **34**, 1915 (1975).

(2) A. Hussain and P. Schurman, *J. Pharm. Sci.*, **58**, 687 (1969).

(3) J. A. Zaslowsky and E. Fisher, *J. Phys. Chem.*, **67**, 959 (1963).

(4) B. Hansen, *Acta Chem. Scand.*, **16**, 1927 (1962).

(5) Y. I. Tur'yan, F. G. Ignat'eva, and M. A. Korshunov, *Zh. Obshchei Khim.*, **38**, 2405 (1968).

(6) P. Y. Bruice and H. G. Mautner, *J. Am. Chem. Soc.*, **95**, 1582 (1973).

(7) H. S. Harned and B. B. Owen, "The Physical Chemistry of Electrolytic Solutions," 3rd ed., American Chemical Society Monograph Series, Reinhold, New York, N.Y., 1963, pp. 638–645.

(8) R. P. Bell, "The Proton in Chemistry," Cornell University Press, Ithaca, N.Y., 1959, p. 159.

(9) *Ibid.*, pp. 92, 188.

(10) G. Aksnes and J. E. Prue, *J. Chem. Soc.*, **1959**, 103.

(11) R. P. Bell, "Acid–Base Catalysis," Clarendon Press, Oxford, England, 1941, p. 7.

(12) W. Davis and W. C. J. Ross, *J. Chem. Soc.*, **1950**, 3056.

(13) A. K. Cho, D. J. Jenden, and S. I. Lamb, *J. Med. Chem.*, **15**, 391 (1972).

(14) L. A. Kundryutskova, S. V. Bogatkov, and E. M. Cherkasova, *Zh. Org. Khim.*, **7**, 1862 (1971).

(15) S. G. Kuznetsov and E. V. Roginskaya, *Zh. Obshchei Khim.*, **32**, 2026 (1962).

(16) T. Higuchi, A. Havinga, and L. W. Busse, *J. Am. Pharm. Assoc., Sci. Ed.*, **39**, 405 (1950).

(17) G. Aksnes and P. Frøven, *Acta Chem. Scand.*, **20**, 1451 (1966).

(18) B. Hansen and A. Flormark, *ibid.*, **17**, 1481 (1963).

(19) P. Zvirblis, I. Socholitsky, and A. A. Kondritzer, *J. Am. Pharm. Assoc., Sci. Ed.*, **45**, 450 (1956).

(20) A. Ågren, U. Hedsten, and B. Jonsson, *Acta Chem. Scand.*, **15**, 1532 (1961).

Controlled Drug Dissolution by Radiation-Induced Polymerization in the Presence of Dimethylaminoethyl Methacrylate–Methyl Methacrylate Copolymer or Methacrylic Acid–Methyl Acrylate Copolymer

MASARU YOSHIDA, MINORU KUMAKURA, and ISAO KAETSU ˣ

Received July 24, 1978, from the *Takasaki Radiation Chemistry Research Establishment, Japan Atomic Energy Research Institute, Takasaki, Gunma, Japan.* Accepted for publication January 11, 1979.

Abstract □ Polymer-containing tablet preparation was studied using radiation-induced polymerization of glass-forming monomers at low temperatures in the presence of dimethylaminoethyl methacrylate–methyl methacrylate copolymer or methyl acrylate–methacrylic acid copolymer. Drug dissolution from tablets was in the pH 3.0–8.0 range. A copolymer contained in the tablets dissolved in the dissolution medium at a specific pH. Drug dissolution from tablets took place rapidly at pH >6.0 in the presence of methyl acrylate–methacrylic acid copolymer and at pH <5.0 in the presence of dimethylaminoethyl methacrylate–methyl methacrylate copolymer. The polymers had fibrous or capillary pore structures in contrast to the spherical pore structures formed in the presence of polyethylene glycol 600.

Keyphrases □ Dosage forms—controlled-release delivery devices, radiation-induced polymerization of glass-forming monomers, low temperature, in the presence of dimethylaminoethyl methacrylate–methyl methacrylate or methacrylic acid–methyl acrylate copolymers, for various drugs, dissolution rate from tablets □ Tablets—drug dissolution rate, radiation-induced polymerization of glass-forming monomers in the presence of dimethylaminoethyl methacrylate–methyl methacrylate or methacrylic acid–methyl acrylate copolymers, various drugs □ Copolymers—anionic and cationic, controlled-release tablets, dissolution rate, various drugs □ Dissolution rates—various drugs, tablets containing radiation-induced polymers of glass-forming monomers in the presence of cationic and anionic copolymers

Recent studies reported enzyme immobilization by polymer entrapment (1–3). Controlled drug dissolution by polymer entrapment is attractive due to durable and moderately controlled pharmaceutical effects (4–6).

Radiation-induced polymerization using glass-forming monomers (7) at low temperatures for the preparation of polymer matrixes containing biofunctional substances (8–10) such as enzymes, microbial cells, and drugs has been reported. Glass-forming monomers are a suitable entrapping matrix because they supercool to highly viscous liquids or amorphous solid at low temperatures and because they polymerize even at low temperatures. The polymer matrixes produced by this method were characteristic in porous structure due to crystallized solvent or crystallized water in the matrix at low temperatures; this porous structure facilitates substrate or drug diffusion in and out of the matrix.

However, controlled drug dissolution often requires dissolution of a drug in a solvent within a specific pH range. The entrapping method permits the mixing of various additives with drugs and polymer in the matrix. This paper describes drug dissolution from solid tablets prepared by radiation-induced polymerization in the presence of dimethylaminoethyl methacrylate–methyl methacrylate copolymer or methacrylic acid–methyl acrylate copolymer for controlled dissolution at pH 3.0–8.0.

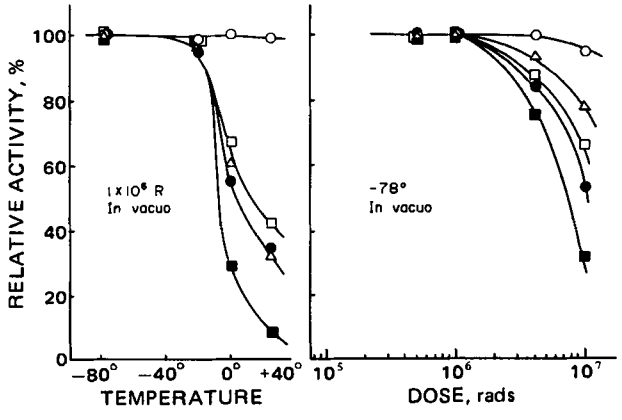

Figure 1—*Effect of irradiation conditions on native drug activity. Drug was dissolved in distilled water (pH 6.0) and put into a glass ampul. The ampul was sealed under a vacuum of 10^{-3} mm Hg. Irradiation was carried out at 1 × 10^6 rads (R)/hr* in vacuo. *The native drug activity was taken ds 100%. Key (drug concentration): ○, 60 μg of potassium chloride/ml; □, 25 μg of salicylic acid/ml; △, 8 μg of sulfanilamide/ml; ●, 60 μg of aspirin/ml; and ■, 20 μg of colchicine/ml.*

EXPERIMENTAL

Monomers—2-Hydroxyethyl methacrylate[1], hydroxyethyl acrylate[1], and glycidyl methacrylate[1] were used.

Drugs—Aspirin[2], sulfanilamide[3], salicylic acid[3], colchicine[3], and potassium chloride[4] were used.

Copolymers—Copolymer[5] of dimethylaminoethyl methacrylate–methyl methacrylate (cation-type copolymer) and copolymer[6] of methacrylic acid–methyl acrylate (anion-type copolymer) were used. The cation-type copolymer was dissolved only in a medium corresponding to the gastric juice at pH <5.0; the anion-type copolymer was dissolved in a medium corresponding to the intestinal juice at pH >6.0.

Porous Polymer–Drug Tablet Preparation—Polymer tablets containing drugs were made as follows. Drug, 600 mg, was put in a flat-bottom glass ampul, 14 mm i.d., and then 0.5 ml of the copolymers–glass-forming monomer mixture was added. Powdered copolymers, such as anion- and cation-type copolymers, completely dissolved at 30–80° in glass-forming monomers such as 2-hydroxyethyl methacrylate, hydroxyethyl acrylate, and glycidyl methacrylate. The ampul was sealed under a vacuum of 10^{-3} mm Hg at −196° (liquid nitrogen) and was irradiated for 2 hr at 5 × 10^5 rads/hr at −78° with γ-rays from a ^{60}Co source. After irradiation, the polymer–drug matrix was obtained as a homogeneous tablet, 14 mm in diameter and 4 mm thick.

Drug Dissolution from Tablets—The dissolution test was made with the dissolution apparatus[7] at 37° at a rate of 100 rpm according to USP XIX. The basket containing the tablet was immersed in 1000 ml of dissolution medium at various pH values. At time intervals over 480 min, 5 ml of the dissolution medium was sampled. The dissolved drug was

[1] Tokyo Kasei Kogyo Co., Ltd. Monomers were purified by distillation according to conventional methods.
[2] Nipponkayaku Co.
[3] Kanto Chemical Co.
[4] Otsuka Pharmaceuticals Co. (~48-mesh powder).
[5] Eudragit E, Röhm Pharma GMBH.
[6] Eudragit L, Röhm Pharma GMBH.
[7] Model TR-5S, Toyama Sangyo.

0022-3549/79/0700-0860$01.00/0
© 1979, American Pharmaceutical Association

Table I—Parameters for Drug Dissolution from Polymer Tablets, 14 mm in Diameter and 4 mm Thick, in the Presence of Anion-Type Copolymer

Sample	Composition, wt. % Anion-Type Copolymer	Monomer	Drug (mol. wt.)	W, %	k, $\times 10^{-3}$ min^{-1}
1	—	100% Hydroxyethyl methacrylate	Aspirin (180.16)	31.2	0.89
2	5	95% Hydroxyethyl methacrylate	Aspirin (180.16)	34.9	1.24
3	10	90% Hydroxyethyl methacrylate	Aspirin (180.16)	39.3	1.99
4	20	80% Hydroxyethyl methacrylate	Aspirin (180.16)	47.4	3.41
5	10	90% Hydroxyethyl acrylate	Aspirin (180.16)	57.9	7.26
6	10	90% Glycidyl methacrylate	Aspirin (180.16)	7.2	0.50
7	10	90% Hydroxyethyl methacrylate	Potassium chloride (74.55)	37.6	4.31
8	10	90% Hydroxyethyl methacrylate	Salicylic acid (138.12)	40.1	2.88
9	10	90% Hydroxyethyl methacrylate	Sulfanilamide (172.21)	37.2	2.36
10	10	90% Hydroxyethyl methacrylate	Colchicine (399.45)	38.6	1.00

assayed spectrophotometrically[8] at 460 nm by a mercury thiocyanate method for potassium chloride (11), at 258 nm for sulfanilamide, at 296 nm for salicylic acid, at 273 nm for aspirin, and at 353 nm for colchicine.

Measurement of Tablet Porosity—Polymer–drug matrix porosity was observed by scanning electron microscopy[9].

The polymer–drug matrix water content (W) was defined as:

$$W\ (\%) = \frac{W_w}{W_p + W_w} \times 100 \qquad \text{(Eq. 1)}$$

where W_w and W_p are the weights of water absorbed in the polymer and of dried polymer, respectively.

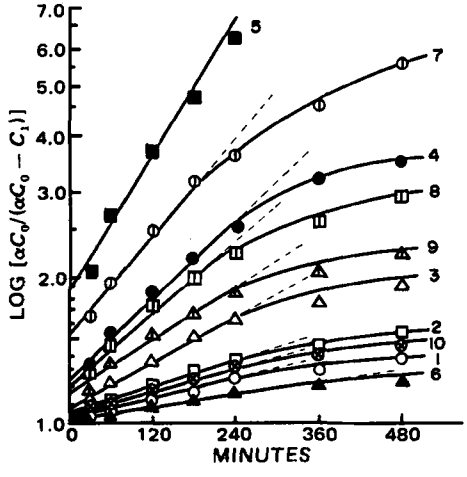

Figure 2—*Semilogarithmic relationship between $\alpha C_0/(\alpha C_0 - C_1)$ and dissolution time for polymer tablets in the presence of an anion-type copolymer. Sample number refers to compositions in Table I. The dissolution medium was at pH 8.0. Key (tablet system and drug): ○, 100% hydroxyethyl methacrylate (aspirin); □, 95% hydroxyethyl methacrylate–5% anion-type copolymer (aspirin); △, 90% hydroxyethyl methacrylate–10% anion-type copolymer (aspirin); ●, 80% hydroxyethyl methacrylate–20% anion-type copolymer (aspirin); ■, 90% hydroxyethyl acrylate–10% anion-type copolymer (aspirin); ▲, 90% glycidyl methacrylate–10% anion-type copolymer (aspirin); ⊙, 90% hydroxyethyl methacrylate–10% anion-type copolymer (potassium chloride); ⊡, 90% hydroxyethyl methacrylate–10% anion-type copolymer (salicylic acid); ◭, 90% hydroxyethyl methacrylate–10% anion-type copolymer (sulfanilamide); and ⊗, 90% hydroxyethyl methacrylate–10% anion-type copolymer (colchicine).*

[8] Shimazu double-beam spectrophotometer, model UV-200.

[9] Model JSM-03, Japan Electron Optics Laboratory Co.

RESULTS AND DISCUSSION

Effect of Irradiation on Drugs—It was necessary to know the irradiation effect on drug activity before polymer tablet preparation. The relation between native drug relative activity and the irradiation conditions used in experimental tablet preparation is shown in Fig. 1. Under the present experimental temperature, energy, and irradiation duration, there was no detectable drug decomposition. Since drug radiation damage is enhanced in the presence of oxygen, the irradiation in a vacuum is desirable.

Drug Dissolution–Time Curves of Tablets in Presence of Anion-Type Copolymer—Potassium chloride, salicylic acid, sulfanilamide, aspirin, or colchicine was entrapped in the polymer matrix by radiation-induced polymerization of a glass-forming monomer at low temperature in the presence of an anion-type copolymer. The dissolved drug in the dissolution medium at pH 8.0 was measured at certain time intervals.

First-order drug dissolution kinetics were investigated using the Noyes–Whitney equation (12, 13). The rate constant for dissolution (k) and the drug concentration at time t were expressed as:

$$kt = \ln \frac{\alpha C_0}{(\alpha C_0 - C_1)} \qquad \text{(Eq. 2)}$$

where α represents V/V_0, V and V_0 are the volumes of tablet per unit weight and medium used for dissolution, C_1 is the drug concentration in the dissolution medium, C_0 is the initial drug concentration in the tablet, and k is the dissolution rate constant.

The relation between t and $\alpha C_0/(\alpha C_0 - C_1)$ in tablets of various anion-type copolymer concentrations and various polymer matrixes and drug components is shown in Fig. 2. The dissolution rate constant (k) was calculated from the initial slope of linear graphs (Table I).

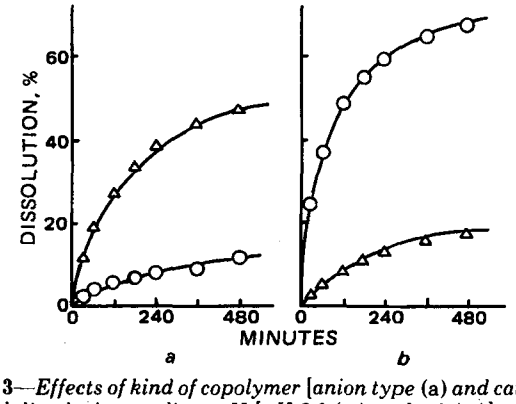

Figure 3—*Effects of kind of copolymer [anion type (a) and cation type (b)] and dissolution medium pH [pH 3.0 (○) and 8.0 (△)] on aspirin dissolution from polyhydroxyethyl methacrylate tablet. Tablet composition was 90% hydroxyethyl methacrylate–10% copolymer.*

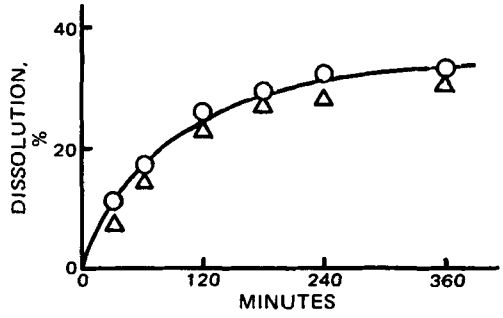

Figure 4—*Effect of dissolution medium pH [pH 3.0 (○) and 8.0 (△)] on aspirin dissolution from polyhydroxyethyl methacrylate tablet in the presence of polyethylene glycol 600.*

For Samples 1–4 (Fig. 2), aspirin dissolution from the tablet increased with anion-type copolymer concentration. This increase was attributed to anion-type copolymer dissolution in the tablet at pH 8.0, although the copolymer barely dissolved in 2-hydroxyethyl methacrylate monomer at concentrations above 30%. The results for Samples 3, 5, and 6 in Fig. 2, showing aspirin dissolution from various polymer tablets, depended on the kind of glass-forming monomer or matrix. This dissolution was related to the hydrophilic property of the matrix, which is indicated in Table I in relation to the polymer matrix water content (W).

Drug dissolution from tablets in the presence of a 10% anion-type copolymer is shown for Samples 3 and 7–10 in Fig. 2. Dissolution decreased in the order potassium chloride, salicylic acid, sulfanilamide, aspirin, and colchicine, perhaps due to differences in drug molecular weights (Table I). The larger the molecular weight of the trapped substances, the smaller was the dissolution rate from the matrix.

The intersections of the straight lines and the axis of the ordinates show values higher than unity (Fig. 2). This deviation was probably due to the rapid dissolution of drugs and anion- or cation-type copolymers trapped on the matrix surface by polymer swelling.

Effect of Medium pH on Aspirin Dissolution from Polyhydroxyethyl Methacrylate Tablet—The anion-type copolymer dissolved in the medium only at pH >6.0, while the cation-type copolymer dissolved only at pH <5.0. Aspirin dissolution from tablets containing various copolymers was investigated for dissolution media at various pH values (14, 15) (Fig. 3). The dissolution rate at pH 8.0 was larger than that at pH 3.0 for anion-type copolymer tablets, while the pH dependency of dissolution in the presence of the cation-type copolymer was the opposite to that in the presence of the anion-type copolymer. Therefore, dissolution of the formulation was markedly influenced by pH in the presence of a copolymer.

Aspirin dissolution from a porous polyhydroxyethyl methacrylate tablet prepared with polyethylene glycol 600 instead of with a copolymer also was investigated. Dissolution of the formulation was hardly influenced by dissolution medium pH (Fig. 4).

Porous Structure—Polymer tablet structure was observed by scanning electron microscopy after complete removal of additives such as aspirin, polyethylene glycol 600, and copolymers (Fig. 5). Since the porous structure is hardly observable in Fig. 5*a*, it must have been a consequence of the dissolution of copolymers or polyethylene glycol 600. The porous polymer matrix obtained in the presence of a copolymer is shown in Figs. 5*b* and 5*c*, and the porous polymer matrix obtained in the presence of polyethylene glycol 600 is shown in Fig. 5*d*. The porous structures in Figs. 5*b* and 5*c* are quite similar but are different from the structure in Fig. 5*d*. The reason may be the difference in dispersion form of those additives (copolymer and polyethylene glycol 600) in hydroxyethyl methacrylate monomer before polymerization. That is, the anion- or cation-type copolymer may be dispersed in the monomer in the fibrous molecular form, and the pore structure forms in the polymer after polymerization as shown in Figs. 5*b* and 5*c*. On the other hand, polyethylene glycol 600 may be dispersed in the monomer in the spherical form owing to its crystallization at low temperatures, and then the pore structure in Fig. 5*d* forms. Consequently, porous structure in the tablets can be controlled by varying the kinds of additives and their concentrations.

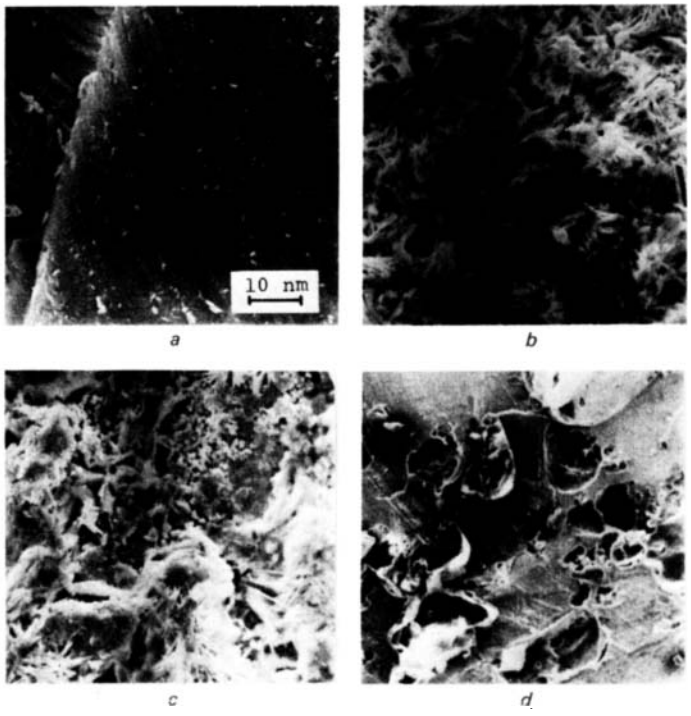

Figure 5—*Scanning electron microphotographs of porous structure of polyhydroxyethyl methacrylate tablets containing aspirin in the presence of various additives. The specimens were dried for 4 days at room temperature* in vacuo *(10^{-4} mm Hg) and then fractured at room temperature. The fractured surface was coated by gold in a vacuum evaporator. Key:* a, *tablet in the presence of 10% anion-type copolymer before treatment with dissolution medium;* b, *tablet in the presence of 10% anion-type copolymer after treatment with dissolution medium at pH 8.0;* c, *tablet in the presence of 10% cation-type copolymer after treatment with dissolution medium at pH 3.0; and* d, *tablet in the presence of 10% polyethylene glycol 600 after treatment with dissolution medium at pH 3.0.*

REFERENCES

(1) C. J. H. Melrose, *Rev. Pure Appl. Chem.*, **21**, 83 (1971).

(2) H. Maeda, H. Suzuki, and A. Yamauchi, *Biotech. Bioeng.*, **17**, 119 (1975).

(3) G. Manecke and H. G. Vogt, *Makromol. Chem.*, **177**, 725 (1976).

(4) J. C. Fu, C. Hagemeir, and D. L. Moyer, *J. Biomed. Mater. Res.*, **10**, 743 (1976).

(5) S. Borodkin and F. E. Tucker, *J. Pharm. Sci.*, **64**, 1289 (1975).

(6) K. Juni, M. Nakano, and Y. Arita, *Yakuzaigaku*, **36**, 129 (1976).

(7) I. Kaetsu, H. Okubo, A. Ito, and K. Hayashi, *J. Polym. Sci.*, **A1**, 2203 (1972).

(8) M. Yoshida, M. Kumakura, and I. Kaetsu, *Polym. Preprints, Jpn.*, **26**, 698 (1977).

(9) I. Kaetsu, M. Kumakura, M. Yoshida, and M. Asano, 26th IUPAC Congress, Tokyo, Japan, 1977, p. 262.

(10) M. Yoshida, M. Kumakura, and I. Kaetsu, *Kobunshi Ronbunshu*, **36**, 35 (1979).

(11) W. Uchiumi, *Nippon Kagaku Zasshi*, **73**, 835 (1952).

(12) A. A. Noyes and W. R. Whitney, *J. Am. Chem. Soc.*, **19**, 930 (1897).

(13) Y. Nozawa, T. Ushikawa, T. Yonezawa, and F. Higashide, *Yakuzaigaku*, **36**, 7 (1976).

(14) T. Saito, S. Suzuki, N. Nanbu, S. Sakurai, and T. Nagai, *ibid.*, **36**, 111 (1976).

(15) H. Kishi, S. Nishii, A. Yamaji, and E. Hiraoka, *Biyoin Yakugaku*, **3**, 150 (1977).

ACKNOWLEDGMENTS

The authors thank Dr. T. Seguchi for help with electron microscopy.

Cefoxitin Sodium: Solution and Solid-State Chemical Stability Studies

EARL R. OBERHOLTZER and GERALD S. BRENNER ˣ

Received July 31, 1978, from *Merck Sharp & Dohme Research Laboratories, West Point, PA 19486.* Accepted for publication January 16, 1979.

Abstract □ Studies were undertaken to provide the basic physicochemical information necessary for preparing a suitable parenteral formulation of cefoxitin sodium. Emphasis was placed on the physicochemical properties of the compound in solution and in the solid state. Cefoxitin sodium is very soluble in water and exhibits apparent first-order decomposition in this medium at pH 3–9. Maximum stability in water is at pH 5–7. Under these pH conditions, cefoxitin sodium loses about 10% of its activity in 2 days at 25°. Thermal decomposition rates for amorphous and crystalline cefoxitin sodium samples were determined. Amorphous cefoxitin sodium was considerably less stable than its corresponding crystalline form. Solid-state decomposition plots are biphasic, displaying initial rapid losses followed by a slower decay period. The extent of loss in the crystalline solid at the end of the more rapid initial phase can be correlated with the water content of the solid.

Keyphrases □ Cefoxitin sodium—chemical stability, amorphous and crystalline solids, water content □ Antibiotics—cefoxitin sodium, chemical stability, amorphous and crystalline solids, water content □ Stability—cefoxitin sodium, amorphous and crystalline solids, water content

Cefoxitin sodium[1] (I), the sodium salt of 3-(hydroxymethyl)-7α-methoxy-8-oxo-7-[2-(2-thienyl)acetamido] -5- thia-1-azabicyclo[4.2.0]oct-2-ene-2-carboxylate carbamate (ester), is a semisynthetic derivative of a new class of β-lactam antibiotics, the cephamycins. It is chemically unique in that the cephem nucleus is substituted with a 7α-methoxy and 3-carbamoyloxymethyl group. Cefoxitin is active against Gram-positive and Gram-negative bacteria (1) and is therapeutically important because of its resistance to destruction by bacterial β-lactamase (2, 3).

This paper describes preformulation studies undertaken to provide the basic physicochemical information necessary for preparing a suitable parenteral formulation of this antibiotic. Emphasis was placed on the physicochemical properties of the compound in solution and in the solid state. Findings from these preformulation studies are reported herein.

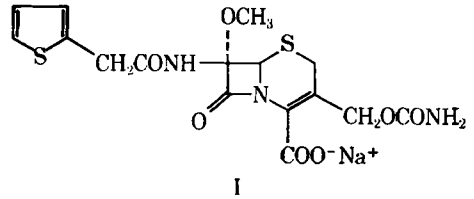

I

EXPERIMENTAL

Materials—Amorphous and crystalline cefoxitin sodium samples were laboratory samples[2] used as received. A selected lot of cefoxitin free acid was used as a reference standard. All other chemicals and solvents were reagent grade and were used without further purification.

Kinetic Procedures—*Solution Studies*—Buffer solutions for kinetic studies were prepared by adding 1.0 *N* NaOH sufficient to attain the desired pH to 50 ml of solutions 0.5 *M* each in acetic, phosphoric, and boric acids and diluting to 250 ml with water (modified Britton–Robinson buffer). In this manner, buffers were prepared at pH 3, 5, 7, or 9, 0.1 *M* in each of the previously named acids.

Aliquots of an aqueous stock solution (5% w/v) of cefoxitin sodium were diluted with sufficient buffer to make 0.5 or 1% solutions. These solutions were stored at 25.0 ± 0.5° in glass-stoppered volumetric flasks, and aliquots were withdrawn periodically for analysis. Aliquots of reaction solutions and reference standard cefoxitin acid were diluted for UV spectrophotometric assay with 1% pH 6.0 phosphate buffer prepared as directed in the USP (4). Each aliquot was diluted to a nominal concentration of 40 μg/ml with 1% pH 6.0 phosphate buffer. For the standard solution, cefoxitin acid was dissolved in 1% pH 6.0 phosphate buffer and diluted to about 40 μg/ml. Absorbances of sample and standard solutions were determined at 262 nm. The true absorbance at 262 nm was obtained by applying a suitable baseline correction.

The reaction solution pH was checked initially and at the end of the 10-day period and did not change significantly during that time.

Solid-State Studies—Individual samples of about 50 mg each of amorphous and crystalline cefoxitin sodium were stored in tightly closed glass vials in constant-temperature ovens. Separate individual samples were removed periodically for each assay point.

Characterization of Crystalline Form—The primary tool for the differentiation of amorphous and crystalline cefoxitin sodium was a commercial X-ray powder diffractometer[3] supplying CuKα radiation. Solid-state IR spectroscopy, differential scanning calorimetry, and optical

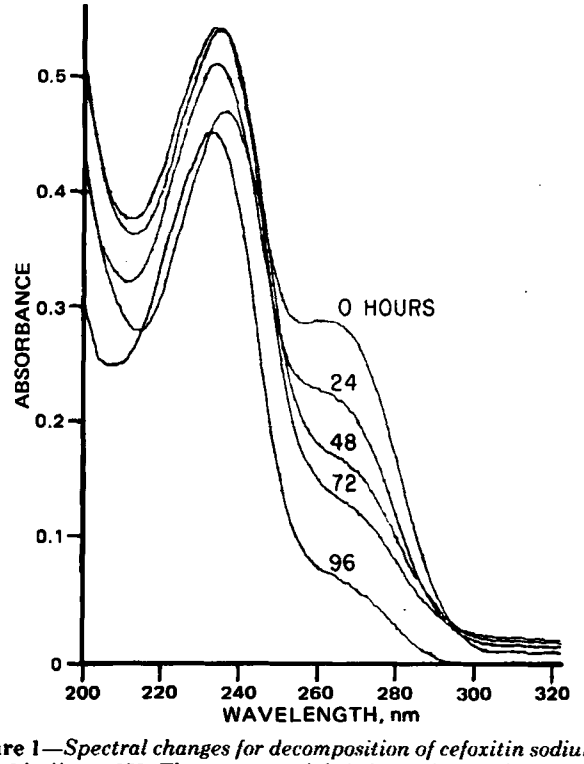

Figure 1—*Spectral changes for decomposition of cefoxitin sodium in pH 9.0 buffer at 25°. The curves are labeled as to hours after the start of the reaction.*

[1] Mefoxin, Merck Sharp and Dohme.
[2] Merck Sharp and Dohme Research Laboratories.
[3] Phillips Electronic Instruments model 12045 full-wave constant potential unit with vertical diffractometer and scintillation counter detector.

0022-3549/79/0700-0863$01.00/0
© 1979, American Pharmaceutical Association

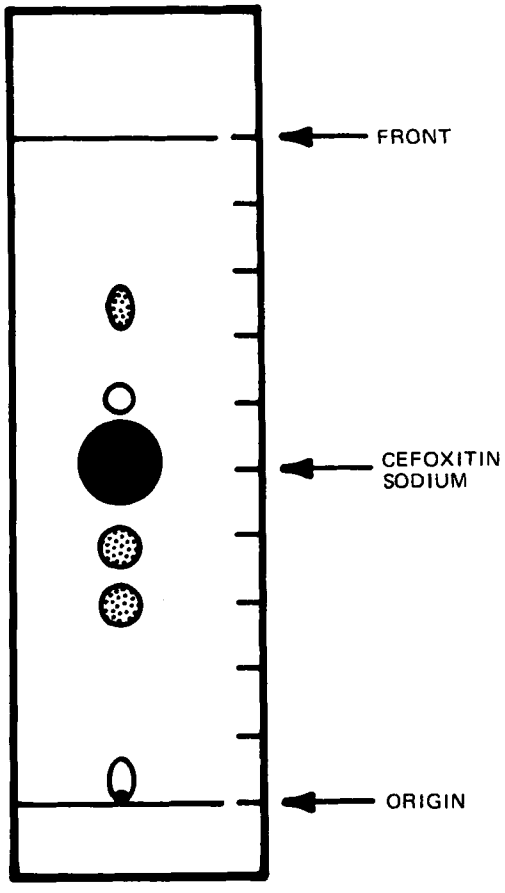

Figure 2—*Thin-layer chromatogram of a 1% solution of cefoxitin sodium following storage at 25° for 72 hr.*

microscopy with polarized light were also employed to determine crystallinity.

Analytical Procedures—Cefoxitin sodium stability studies in solution and in the solid state were monitored by UV spectrophotometry, iodometric titration, microbiological assay, high-performance liquid chromatography (HPLC), and TLC.

UV Spectrophotometry—Intact cefoxitin sodium exhibits a UV absorption band near 262 nm attributed to the O=CNC=C linkage in the molecule. β-Lactam ring opening leads to disappearance of this absorption band. Periodic monitoring of UV spectra of stability samples was carried out to follow the extent of this transformation. This UV spectrophotometric method, with appropriate baseline corrections, yielded assay values essentially identical to those obtained by HPLC and iodometric methods.

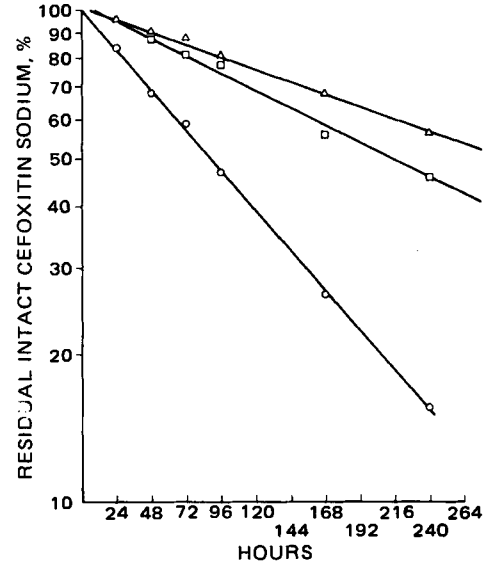

Figure 3—*Apparent first-order plots followed by UV spectrophotometry for decomposition of 0.5 and 1% solutions of cefoxitin sodium at 25° and various pH values. Key: △, pH 5 and 7; □, pH 3; and ○, pH 9.*

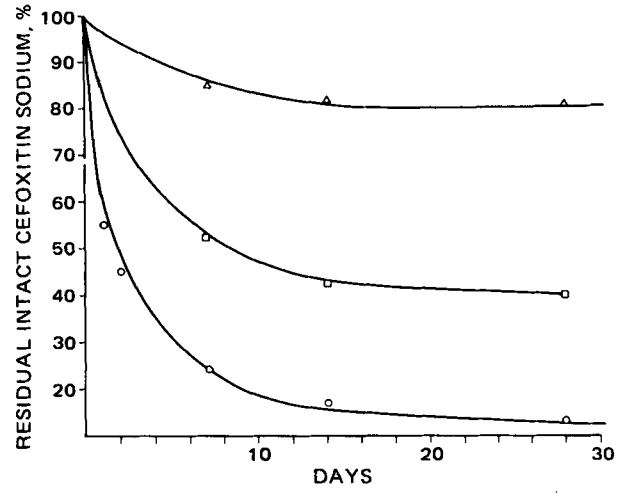

Figure 4—*Typical plots of solid-state decomposition of amorphous cefoxitin sodium at various temperatures. Key: △, 40°; □, 60°; and ○, 80°.*

Spectral changes as a function of time for the decomposition of a cefoxitin sodium solution at pH 9 are illustrated in Fig. 1.

Iodometric Titration—The well-established iodometric titration for β-lactam antibiotics is applicable to the determination of the integrity of the β-lactam moiety in cefoxitin sodium. The procedure used in these studies is a modification of the "Code of Federal Regulations" method (5).

Microbiological Assay—Cefoxitin sodium potency was determined by an agar-diffusion (plate) assay with *Staphylococcus aureus* (NRRL-B11034) as the test organism.

HPLC—HPLC was used to follow cefoxitin sodium decomposition. The liquid chromatograph[4] employed was equipped with a variable-wavelength UV detector[5] set at 254 nm; the separation was carried out on a 30-cm, 10-μm, microporous, octadecylsilane stationary phase[6] with an acetonitrile–water–acetic acid (20:80:1) mobile phase. The column pressure was 800–900 psig, and the column temperature was controlled at 25°. The sample load on the column was 10 μl of a 1-mg/ml solution.

TLC—Solution and solid degraded samples (100 μg) were evaluated qualitatively by TLC. Cefoxitin sodium was chromatographed using butanol–acetic acid–water (4:1:1) with precoated silica gel plates containing a fluorescent indicator[7]. Visualization was accomplished by fluorescence quenching under shortwave UV light or by iodine staining.

RESULTS AND DISCUSSION

The results of experimental studies with cefoxitin indicated that crystalline cefoxitin sodium has properties that make it a suitable chemical and physical form of the antibiotic for use as a sterile powder for reconstitution prior to parenteral administration.

Physical Properties—Crystalline and amorphous cefoxitin sodium forms are colorless to off-white solids with a slight characteristic odor. The compound is optically active and, as a 1% solution in methanol, exhibits a specific rotation of $[\alpha]^{25°}_{589\,nm}$ +210°, calculated on a water and solvent-free basis. The UV spectrum in pH 7.0 phosphate buffer is characterized by maxima at 235 and 262 nm with approximate log ε values of 4.17 and 3.97, respectively.

Solution Properties—*Aqueous Solubility*—Cefoxitin sodium is soluble in water in excess of 1000 mg/ml. This value more than satisfies

[4] Dupont model 841 with model 833 flow controller.
[5] Perkin-Elmer model LC-55.
[6] Waters Associates μBondapak C_{18}.
[7] Quantum Industries QIF.

Table I—Apparent First-Order Constants, $T_{10\%}$, and $T_{50\%}$ for 0.5 and 1.0% Solutions of Cefoxitin Sodium at 25° and Various pH Values

pH	$K_{obs} \times 10^3$, hr^{-1}	$T_{10\%}$, hr	$T_{50\%}$, hr
3.0	3.42	40	212
5.0	2.44	50	291
7.0	2.46	49	288
9.0	7.83	14	89

the required solubility for use in injection products based on the intended dose and desired volumes for administration.

Solution Stability—The β-lactam ring of cefoxitin sodium undergoes cleavage in water. Subsequent fragmentation of the β-lactam hydrolysis product yields a complex product mixture, as evidenced by the TLC hydrolysis product pattern (Fig. 2).

As with other β-lactam antibiotics, long-term solution stability at 25° is not sufficient at pH 3–9 to permit formulation of cefoxitin sodium as a preconstituted solution (Table I). However, these studies established the viability of a formulation consisting of a readily soluble sterile solid for the extemporaneous preparation of a solution for injection. As the data indicate, such solutions, under proper pH control, exhibit about a 10% loss ($T_{10\%}$) in potency when maintained at 25° for 48 hr.

The studies summarized in Table I and Fig. 3 establish the pH–rate profile for cefoxitin sodium at 25°. The semilogarithmic data plots obtained at various pH values were reasonably linear (Fig. 3), indicating that cefoxitin sodium degradation follows first-order kinetics. The apparent first-order rate constants, K_{obs} (Table I), were calculated from the slopes of log percent remaining cefoxitin sodium concentration–time data by means of a computer-programmed least-squares regression analysis. The β-lactam hydrolysis rate was nearly identical at pH 5.0 and 7.0. Under these pH conditions, the time for 10% loss ($T_{10\%}$) was approximately 50 hr at 25° and the half-life ($T_{50\%}$) was about 290 hr. Reactivity of the β-lactam was significantly greater under basic conditions. At pH 9.0, the half-life was approximately 89 hr. Sensitivity to acid was less pronounced than to base, as evidenced by the degradation rate at pH 3.0 which was not dramatically greater than the rate in the pH 5.0–7.0 range.

No adverse physical changes, other than some yellowing, were observed in the solutions employed for solution stability studies. All solutions remained free of precipitates during the study.

Solid-State Properties—*Physical Forms*—An amorphous and a crystalline form of cefoxitin sodium were evaluated during preformulation studies. The amorphous material was the first form investigated during preclinical and initial clinical studies. As solid-state stability deficiencies in the amorphous material became apparent, attention was directed toward preparation of a more highly ordered structure, a crystalline solid. When this goal was accomplished, the properties of the crystalline solid were investigated and compared to the amorphous materials.

The amorphous form is a white to off-white solid and does not exhibit any well-defined thermal transitions by differential scanning calorimetry below 350°. Gradual solid decomposition is observed by differential scanning calorimetry as temperatures increase over 150°. The amorphous form shows no distinct X-ray powder diffraction pattern and is nonbirefringent when examined microscopically under polarized light.

Crystalline cefoxitin sodium is a white to off-white solid and exhibits a characteristic X-ray powder diffraction pattern and a decomposition exotherm by differential scanning calorimetry at approximately 190–200°. The solid is birefringent when examined microscopically under polarized light.

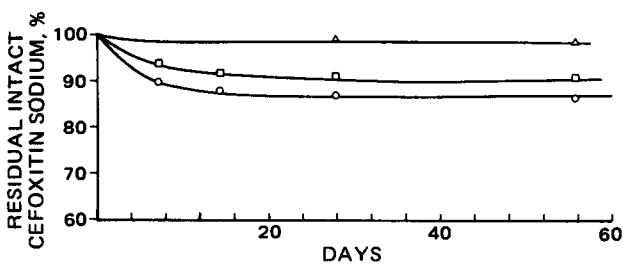

Figure 5—*Typical plots of solid-state decomposition of crystalline cefoxitin sodium at various temperatures. Key: △, 40°; □, 60°; and ○, 80°.*

Solid-State Stability—Accelerated chemical and physical stability testing of amorphous and crystalline cefoxitin sodium solids was carried out as part of a screening program to guide selection of the proper physical form for use in a formulation. Both solid forms, when exposed to elevated temperature and subsequently examined qualitatively by TLC, revealed degradation to a complex mixture of decomposition products. The complexity of the degradation pattern also was reflected in quantitative studies. Typical data plots from these studies used to determine reaction order indicate that degradation did not follow a simple kinetic relationship. A rough reaction order screening was carried out by data plotting. If the amount of intact cefoxitin is plotted as a function of time, a straight line does not result for zero- or first-order plots.

The amount of intact cefoxitin sodium in the two different solid forms as a function of time and temperature is depicted graphically in Figs. 4 and 5. Both solids exhibited a biphasic decomposition pattern typified by an initial accelerated decomposition period followed by a slower decay period. This trend suggests that cefoxitin sodium exhibits two or more parallel decomposition pathways, one or more of which is rapid and the others slower. The initial more rapid degradation rate of crystalline material at elevated temperature and of amorphous material at low temperatures to a level of ~85–90% of the initial concentration is consistent with partial solid hydrolysis; the hydrolysis apparently is limited only by the concentration of water, an exhaustible solid constituent. Thermal degradation reactions occurring at a slower rate most likely account for the additional losses in the subsequent slow decay period.

In cefoxitin sodium decomposition by hydrolysis, water is consumed when the β-lactam, R-CO-N-R′R″, is opened to RCOOH + HNR′R″. Since the cefoxitin sodium samples studied contained about 0.5% water, which corresponded to approximately 12 mole % water, about 12% of the drug could be expected to decompose by hydrolysis. In fact, as the data in Fig. 5 indicate, crystalline cefoxitin sodium subjected to 60 and 80° thermal stress suffered drug loss to that extent in the initial more rapid phase of its decomposition. Drug loss to that extent also occurred in crystalline material at 40° when the study was extended to periods beyond those shown in Fig. 5 and to samples of amorphous solid maintained at 40° as indicated in Fig. 4. The fact that the loss in the initial phase of accelerated studies on the amorphous solid at 60 and 80° is more extensive suggests that the decomposition pathway for this material is not the same as for the crystalline solid at higher temperatures and that the observed rates must reflect a substantial contribution from nonhydrolytic reactions. The activation energy for these thermal, nonhydrolytic processes is most likely considerably less for amorphous materials than for their corresponding crystalline forms.

A comparison of the thermal decomposition data for amorphous and crystalline cefoxitin sodium demonstrates that crystalline material is more stable. While an increasing water content generally increased the net decomposition rate of both forms, it could be shown by maintaining equivalent water levels that stability differences between the two forms did not reflect differences in water content. The data in Figs. 4 and 5 were obtained for samples of approximately equal water content (0.5%).

It is concluded that the stability differences noted between the solids relate to differences in the degree of crystallinity. Stability differences between crystalline and amorphous solids have been the subject of prior publications. Among β-lactam antibiotics, amorphous forms of penicillin potassium (6), epicillin (7), and a number of cephalosporins (8, 9) are less stable chemically than their crystalline counterparts.

In addition to chemical stability differences between amorphous and crystalline forms of cefoxitin sodium solids, physical stability differences have been noted. Upon aging, amorphous cefoxitin sodium develops considerably more color than its crystalline counterparts, as reflected in both solid-state and solution color measurements.

Crystalline cefoxitin sodium is thus both chemically and physically more stable than the amorphous form.

REFERENCES

(1) H. R. Onishi, D. R. Daoust, S. B. Zimmerman, D. Hendlin, and E. O. Stapley, "Abstracts, XII Interscience Conference on Antimicrobial Agents and Chemotherapy," Atlantic City, N.J., 1972, p. 77 and preceding two abstracts.

(2) H. R. Onishi, D. R. Daoust, S. B. Zimmerman, D. Hendlin, and E. O. Stapley, *Antimicrob. Agents Chemother.*, **5**, 38 (1974).

(3) H. C. Neu, *ibid.*, **6**, 170 (1974).

(4) "The United States Pharmacopeia," 19th rev., Mack Publishing

Co., Easton, Pa., 1975, p. 596.
(5) "Code of Federal Regulations," U.S. Government Printing Office, Washington, D.C., Title 21, 436.204, Apr. 1, 1977 Revision, p. 241.
(6) A. G. Mathews, C. J. Schram, and D. Minty, *Nature*, **211**, 959 (1966).
(7) J. P. Hou and A. Restivo, *J. Pharm. Sci.*, **64**, 710 (1975).
(8) R. Pfeiffer, G. L. Engel, and D. Coleman, *Antimicrob. Agents Chemother.*, **9**, 848 (1976).
(9) M. J. Pikal, A. L. Lukes, and J. E. Lang, *J. Pharm. Sci.*, **66**, 1312 (1977).

Synthesis and Evaluation of Benzylfluorenyl and 1-Arylethyl Quaternary Ammonium Salts for Antimicrobial and Antineoplastic Activities

J. R. DIMMOCK *x, P. J. SMITH ‡, and S. K. TSUI ‡

Received September 11, 1978, from the **College of Pharmacy and the* ‡*Department of Chemistry and Chemical Engineering, University of Saskatchewan, Saskatoon, Saskatchewan, S7N 0W0, Canada.* Accepted for publication January 18, 1979.

Abstract □ A number of substituted benzyldimethyl-9-fluorenylammonium bromides (II) and 9-benzylfluorenyl-9-trimethylammonium bromides (IV) were synthesized and examined for antimicrobial and anticancer activities. Series IV showed greater antimicrobial activity than Series II while some corresponding acyclic fluorene analogs were bereft of antimicrobial activities. Significant antineoplastic activity was not found in Series II and IV. Representative fluorenes subjected to a preliminary screen for various pharmacological activities revealed marked anti-inflammatory and analgesic properties coupled with some antihistaminic activities. The acyclic quaternary ammonium compounds demonstrated substantial pressor activities.

Keyphrases □ Benzylfluorene—quaternary ammonium derivatives, synthesis, antimicrobial and antineoplastic activity, structure-activity relationships □ Arylethylamines—quaternary ammonium derivatives, synthesis, antimicrobial and antineoplastic activity, structure-activity relationships □ Antimicrobial agents—benzylfluorene, arylethylamines, quaternary ammonium derivatives □ Antineoplastic agents—benzylfluorene, arylethylamines, quaternary ammonium derivatives

As a continuation of studies on new antimicrobial (1–4) and antineoplastic (5–8) agents, it was decided to examine the biological activities of some novel substituted fluorenes, representatives of which have demonstrated antimicrobial (9–11) and anticancer (12–14) activities. Since quaternary ammonium compounds are known to possess antiseptic properties, especially when bulkyl groups are attached to the quadrivalent nitrogen center, which may reduce adsorption onto serum proteins (15), the preparation of fluorenes attached to a quaternary nitrogen atom was contemplated.

The reactivity of benzylic derivatives is documented clearly (16); in the two planned structural isomer series (Scheme I), a benzyl group was attached either to a quaternary nitrogen atom (II) or directly to the fluorene ring (IV). In both cases, facile proton loss from the benzylic methylene group may occur. Furthermore, in Series II, the 9-fluorenyl proton may be considered labile. Thus, both II and IV have the potential for forming carbanions, which would be available for electrophilic attack by biological macromolecules.

In addition, it was proposed to synthesize some fluorene II and IV analogs so that structural requirements for bioactivities might be discerned. In the case of V, which is similar in structure to antifungal 9-fluorenol (9), both the benzyl and quaternary ammonium groups were removed. The quaternary ammonium compound VI was an analog of IV with the benzyl function replaced by a methyl group. Previous investigations compared the antimicrobial activities of flexible acyclic analogs of more rigid cyclic structures with the corresponding cyclic compounds (1–4). For this reason, the synthesis of several quaternary ammonium compounds derived from 1-arylethylamines (VII and VIII) was contemplated.

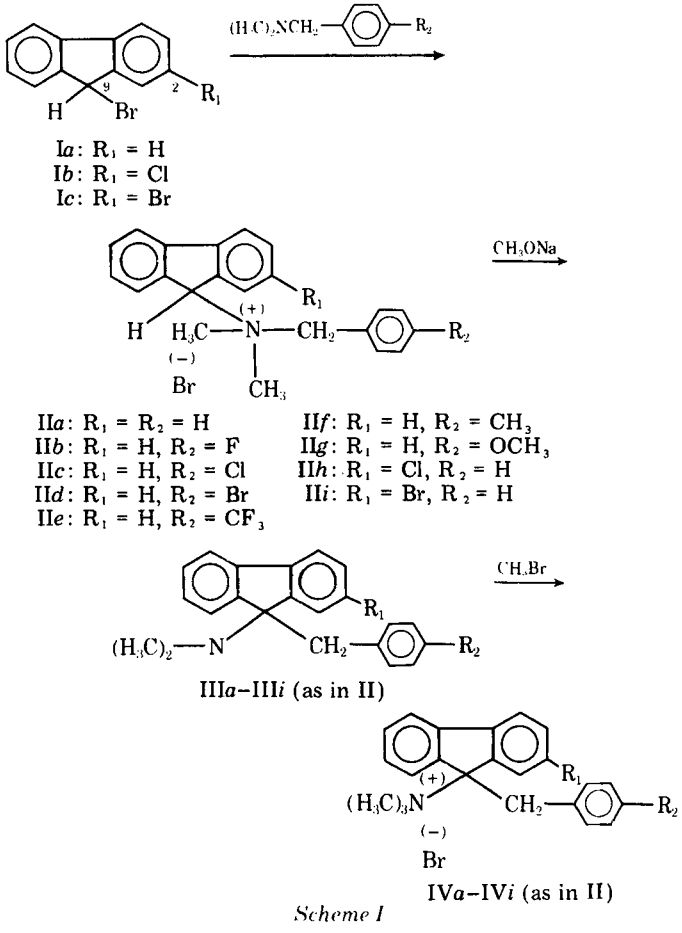

Scheme I

RESULTS AND DISCUSSION

The synthetic pathway for the prepared fluorenes is illustrated in Scheme I. The appropriate *N,N*-dimethylated benzylamines, prepared by the Eschwieler-Clark procedure, were quaternized with 9-bro-

0022-3549/79/0700-0866$01.00/0
© 1979, American Pharmaceutical Association

Co., Easton, Pa., 1975, p. 596.
(5) "Code of Federal Regulations," U.S. Government Printing Office, Washington, D.C., Title 21, 436.204, Apr. 1, 1977 Revision, p. 241.
(6) A. G. Mathews, C. J. Schram, and D. Minty, *Nature*, **211**, 959 (1966).
(7) J. P. Hou and A. Restivo, *J. Pharm. Sci.*, **64**, 710 (1975).
(8) R. Pfeiffer, G. L. Engel, and D. Coleman, *Antimicrob. Agents Chemother.*, **9**, 848 (1976).
(9) M. J. Pikal, A. L. Lukes, and J. E. Lang, *J. Pharm. Sci.*, **66**, 1312 (1977).

Synthesis and Evaluation of Benzylfluorenyl and 1-Arylethyl Quaternary Ammonium Salts for Antimicrobial and Antineoplastic Activities

J. R. DIMMOCK *x, P. J. SMITH ‡, and S. K. TSUI ‡

Received September 11, 1978, from the **College of Pharmacy and the* ‡*Department of Chemistry and Chemical Engineering, University of Saskatchewan, Saskatoon, Saskatchewan, S7N 0W0, Canada.* Accepted for publication January 18, 1979.

Abstract □ A number of substituted benzyldimethyl-9-fluorenylammonium bromides (II) and 9-benzylfluorenyl-9-trimethylammonium bromides (IV) were synthesized and examined for antimicrobial and anticancer activities. Series IV showed greater antimicrobial activity than Series II while some corresponding acyclic fluorene analogs were bereft of antimicrobial activities. Significant antineoplastic activity was not found in Series II and IV. Representative fluorenes subjected to a preliminary screen for various pharmacological activities revealed marked anti-inflammatory and analgesic properties coupled with some antihistaminic activities. The acyclic quaternary ammonium compounds demonstrated substantial pressor activities.

Keyphrases □ Benzylfluorene—quaternary ammonium derivatives, synthesis, antimicrobial and antineoplastic activity, structure-activity relationships □ Arylethylamines—quaternary ammonium derivatives, synthesis, antimicrobial and antineoplastic activity, structure-activity relationships □ Antimicrobial agents—benzylfluorene, arylethylamines, quaternary ammonium derivatives □ Antineoplastic agents—benzylfluorene, arylethylamines, quaternary ammonium derivatives

As a continuation of studies on new antimicrobial (1–4) and antineoplastic (5–8) agents, it was decided to examine the biological activities of some novel substituted fluorenes, representatives of which have demonstrated antimicrobial (9–11) and anticancer (12–14) activities. Since quaternary ammonium compounds are known to possess antiseptic properties, especially when bulkyl groups are attached to the quadrivalent nitrogen center, which may reduce adsorption onto serum proteins (15), the preparation of fluorenes attached to a quaternary nitrogen atom was contemplated.

The reactivity of benzylic derivatives is documented clearly (16); in the two planned structural isomer series (Scheme I), a benzyl group was attached either to a quaternary nitrogen atom (II) or directly to the fluorene ring (IV). In both cases, facile proton loss from the benzylic methylene group may occur. Furthermore, in Series II, the 9-fluorenyl proton may be considered labile. Thus, both II and IV have the potential for forming carbanions, which would be available for electrophilic attack by biological macromolecules.

In addition, it was proposed to synthesize some fluorene II and IV analogs so that structural requirements for bioactivities might be discerned. In the case of V, which is similar in structure to antifungal 9-fluorenol (9), both the benzyl and quaternary ammonium groups were removed. The quaternary ammonium compound VI was an analog of IV with the benzyl function replaced by a methyl group. Previous investigations compared the antimicrobial activities of flexible acyclic analogs of more rigid cyclic structures with the corresponding cyclic compounds (1–4). For this reason, the synthesis of several quaternary ammonium compounds derived from 1-arylethylamines (VII and VIII) was contemplated.

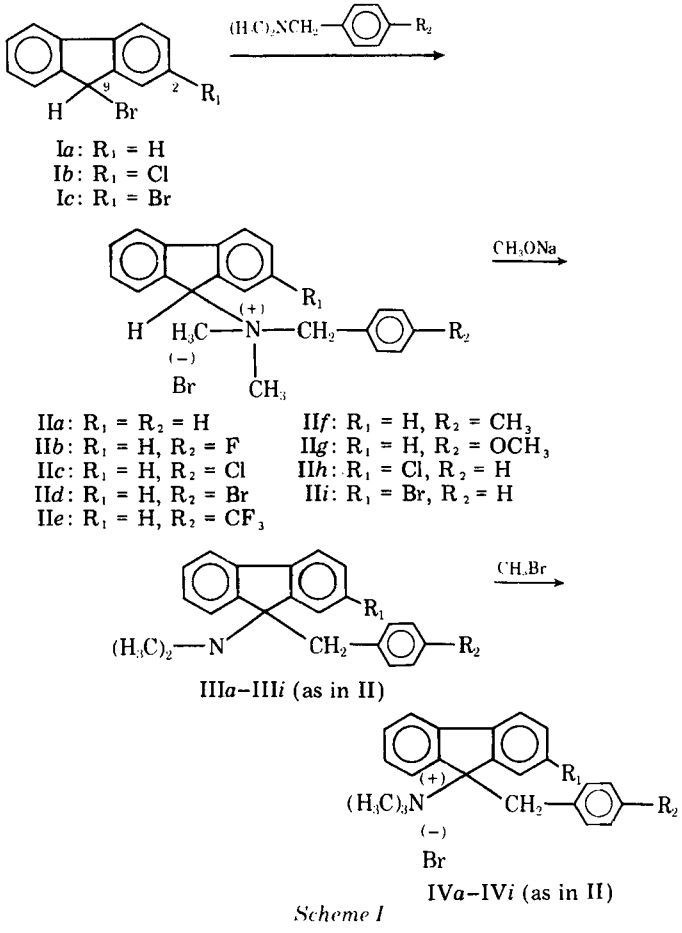

Scheme I

RESULTS AND DISCUSSION

The synthetic pathway for the prepared fluorenes is illustrated in Scheme I. The appropriate *N,N*-dimethylated benzylamines, prepared by the Eschwieler-Clark procedure, were quaternized with 9-bro-

0022-3549/79/0700-0866$01.00/0
© 1979, American Pharmaceutical Association

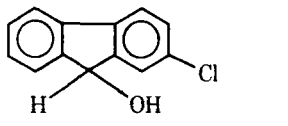

V

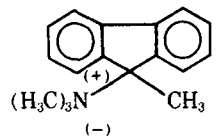

VI

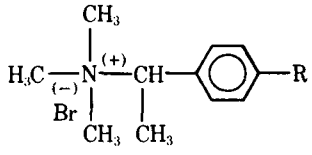

VII*a*: R = H
VII*b*: R = Cl
VII*c*: R = CF_3
VII*d*: R = OCH_3

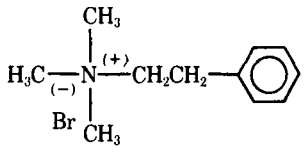

VIII

mofluorene (I), which was prepared by reduction of the appropriate 9-fluorenone followed by bromination. The quaternary ammonium salts II, having acidic hydrogen atoms alpha to the positively charged nitrogen atoms, underwent the Stevens rearrangement to the *N,N*-dimethyl-9-benzylfluorenylamines (III). The amines III were quaternized readily with bromomethane to produce the required salts IV.

Compound VI was prepared by a synthetic route in which methyl magnesium iodide was reacted with 9-fluorenone, and the resultant 9-fluorenol was brominated and treated with trimethylamine. The acyclic quaternary ammonium compounds VII were prepared by the action of methyl magnesium iodide on the substituted benzaldehyde, and the resultant carbinol was brominated and treated with trimethylamine.

The antimicrobial screening results are summarized in Table I. The quaternary ammonium compounds in Series II and IV showed the best activities; the tertiary amines III*a* and III*i*, the fluorenol V, and the 9-methylfluorene VI were either bereft of antimicrobial activity or possessed only marginal potencies. In Series II, with the exception of II*h*, the compounds had approximately the same activity. In Series IV, the halogenated compounds had higher potencies than the unsubstituted compound, which, in turn, was more active than IV*f* and IV*g*, which have electron-repelling groups in the phenyl ring. The average antimicrobial activity in Series IV was 175 compared to 120 in Series II.

The open chain quaternary ammonium compounds VII, which like Series II have one carbon atom separating the substituted phenyl ring from the quaternary nitrogen, were devoid of antimicrobial activity at the highest concentration examined (500 μg/ml). Furthermore, VIII, which may be regarded as an open chain IV*a* analog, was similarly devoid of antimicrobial activity.

The most susceptible bacteria to the compounds were species of *Staphylococci* and *Streptococci* as well as *Bacillus subtilis*. Approximately half of the compounds demonstrated low antifungal activity against *Microsporum gypseum* and *Saccharomyces uvarum*. With the exception of II*c*, II*d*, and IV*d*, all compounds in Table I were inactive at 10 μg/ml against the protozoan *Entamoeba histolytica*. Against *Trichomonas foetus*, the compounds listed in Table I, except II*c*, IV*e*–IV*g*, and VI, were devoid of antiprotozoal activity at the maximum concentration employed, 50 μg/ml.

All compounds listed in Table I plus III*h* were assessed for anticancer activity, except IV*e*–IV*g* and VI. The animal tumor model was the L-1210 lymphoid leukemia system in mice except for II*d* and IV*h*. In those two cases, the screen was conducted *versus* murine P-388 lymphocytic leukemia. No compounds achieved the criterion for activity, namely a 25% increase in mean survival time. The quaternary ammonium compounds II and IV showed murine toxicity at 100 mg/kg (either zero or one survivor out of six after 5 days of injections), but there were no mortalities on Day 5 when the dose was reduced to 50 mg/kg. The only exception to this observation was II*a;* in a screen *versus* Sarcoma 180 in mice, II*a* showed murine toxicity at 2 mg/kg, and there were no mortalities when the dose was reduced to 0.50 mg/kg.

The tertiary amines III*h* and III*i* showed no toxicity at 400 mg/kg, while III*a* showed marginal toxicity at 225 mg/kg (four out of six survivors on Day 5), which disappeared at 200 mg/kg. The *in vitro* KB screen conducted on II*h*, II*c*, III*h*, IV*a*, and IV*i* showed 50% inhibition of human nasopharyngeal epidermoid carcinoma at 25, 44, 100, 9.7, and 15 ppm, respectively, and thus fell short of the 4-ppm established criterion for activity.

The primary screen permitted the assessment of representative compounds for various pharmacological activities (Table II). Since the

Table I—Antimicrobial Evaluation of the Benzylfluorenyl Quaternary Ammonium Bromides [a] (II–VI)

Organism	II*a*	II*b*	II*c*	II*d*	II*h*	II*i*	III*a*	III*i*	IV*a*	IV*b*	IV*c*	IV*d*	IV*e*	IV*f*	IV*g*	IV*h*	IV*i*	V	VI
Escherichia coli (ATCC 8739)	>500	>500	>500	>500	>500	>500	>500	>500	>500	>500	250	500	>500	>500	>500	>500	>500	>500	>500
Pseudomonas aeruginosa (ATCC 10145)	>500	>500	>500	>500	>500	>500	>500	>500	>500	>500	>500	>500	>500	>500	>500	>500	>500	>500	>500
Klebsiella pneumoniae (ATCC 4352)	500	250	>500	>500	250	250	>500	>500	>500	>500	250	500	250	>500	>500	>500	500	>500	>500
Salmonella typhimurium (ATCC 13311)	>500	>500	>500	>500	>500	>500	>500	>500	>500	>500	500	500	>500	>500	>500	>500	>500	>500	>500
Haemophilus influenzae (ATCC 19418)	500	>500	>500	>500	>500	>500	>500	>500	>500	>500	250	500	>500	>500	>500	>500	500	>500	>500
Staphylococcus aureus (ATCC 6538)	250	100	100	100	250	250	>500	>500	100	50	100	50	50	100	100	50	50	>500	500
Streptococcus pyogenes (hospital isolate)	250	250	100	100	250	100	>500	>500	250	250	100	50	100	500	500	250	50	>500	>500
Streptococcus pneumoniae (ATCC 6303)	250	250	250	250	250	250	>500	>500	>500	250	100	100	100	500	500	250	50	>500	>500
Streptococcus faecalis (ATCC 8030)	250	250	500	250	500	250	>500	>500	>500	500	100	250	250	>500	>500	250	100	>500	>500
Bacillus subtilis (ATCC 6633)	500	250	250	250	500	250	>500	>500	500	250	50	50	50	250	250	250	50	>500	>500
Trichophyton mentagrophytes (ATCC 9533)	>500	>500	>500	>500	>500	>500	>500	>500	>500	>500	>500	250	>500	>500	>500	>500	>500	>500	>500
Microsporum gypseum (ATCC 14683)	>500	>500	250	250	>500	250	500	>500	500	>500	500	100	>500	>500	>500	250	>500	>500	>500
Aspergillus niger (ATCC 10535)	>500	>500	500	>500	>500	>500	>500	>500	>500	>500	>500	>500	>500	>500	>500	>500	>500	>500	>500
Candida albicans (ATCC 10231)	>500	>500	500	>500	>500	500	>500	>500	>500	>500	>500	>500	>500	>500	>500	>500	>500	>500	>500
Saccharomyces uvarum (ATCC 9080)	100	>500	100	500	>500	250	100	>500	500	>500	250	>500	>500	>500	>500	>500	250	>500	>500
Average antimicrobial activity[b]	107	100	160	127	67	160	40	0	67	113	267	320	227	60	60	133	327	0	7

[a] The figures in the table are the minimum inhibitory concentrations of the compounds in micrograms per milliliter. [b] Figures were calculated from the following expression: (combined antimicrobial activity × 100)/number of microorganisms in the screen. The combined antimicrobial activity was determined by giving the following scores at the lowest concentration of the compound required to inhibit microbial growth: 500: 1; 250: 2; 100: 5; and 50: 10.

Table II—Screening Data on Benzylfluorenyl and 1-Arylethyl Quaternary Ammonium Bromides [a] (IV, VI, VII, and VIII)

Compound	Analgesic Activity		Anti-Inflammatory Activity			Antianaphylactic Activity		Antihistaminic Activity		Antidepressant Activity			Cardiovascular Screen [b]		
		Reduction in Writhes,		Effect, %			Inhibition,		Change in Contractile		Protection, %			Change in Blood Pressure,	Change in Heart Rate,
	Dose	%	Dose	3 hr	5 hr	Dose	%	Dose	Force, %	Dose	1.5 hr	3 hr	Dose	%	%
IV*a*	64	78	64	67	83	2[d]	AN	0.1	38	64	67	50	0.1	−7	+7
	32	100											1.0	−31	+10
	16	22											2.0	−42	+10
	8[c]	Algesic													
IV*b*	64	13	64	17	83	2	0	0.1	44	64	21	0	0.1	−7	+2
													1.0	−31	0
													2.0	−52	+4
IV*e*	64	66	64	67	100	4	0	0.1	38	64	38	17	0.1	−22	+3
	32	82											1.0	−12	+1
													2.0	−5	−3
IV*f*	32[c]	Algesic	64	67	83	1	28	0.1	20	32	29	0	0.1	−1	+6
													1.0	−13	+18
													2.0	−20	+15
IV*g*	64	87	64	50	100	2[d]	AN	0.1	24	64	29	4	0.1	−5	+3
													1.0	+8	+8
													2.0	0	+12
VI	8	27	16	0	0	0.5	0	0.1	48	16	21	0	0.1	−21	−3
													1.0	−26	+4
													2.0	−17	+7
VII*a*	16	66	16	0	0	0.5	20	0.1	38	16	0	0	0.1	+14	+4
													1.0	+44	+9
													2.0	+64	+16
VII*b*	16	18	16	0	0	1	20	0.1	22	16	13	4	0.1	+32	+5
													1.0	+50	+6
													2.0	+80	+19
VII*c*	32	69	32	0	17	2	67	0.1	16	16	17	0	0.1	+49	+5
													1.0	+79	+21
													2.0	Respiratory arrest	
VII*d*	16	43	16	0	0	1	20	0.1[e]	Stimulatory effect	16	4	0	0.1	+31	+16
													1.0	+8	+12
													2.0	Respiratory arrest	
VIII	16	5	16	0	50	1	0	0.1	11	16	17	0	0.1	+14	+4
						2	0						1.0	+44	+9
													2.0	+86	+5
Reference compound[f]	50	50	32	17	83	100	91	0.01	100	8	100	100		+30[g]	+30[g]

[a] The doses in all screens are in milligrams per kilogram except for the antihistaminic screen in which the dose is in milligrams per milliliter. [b] The + indicates an increase in blood pressure or heart rate, and the − indicates a fall in either blood pressure or heart rate. [c] At these dose levels, IV*a* and IV*f* increased the number of writhes by 22 and 19%, respectively. [d] Compounds IV*a* and IV*g* increased the wheal formation by 20% in both compounds at the dose levels indicated. [e] Compound VII*d* increased the contractile force of the isolated guinea pig ileum preparation by 6%. [f] The reference compounds for the analgesic, anti-inflammatory, antianaphylactic, antihistaminic, and antidepressant screens were aspirin, indomethacin, disodium chromoglycate, diphenhydramine, and tranylcypromine sulfate, respectively. The criteria for activity in the analgesic, anti-inflammatory, antianaphylactic, and antihistaminic screens were changes of 50, 50, 50, and 20%, respectively; in the antidepressant screen, a compound had to show 30% protection at the end of 1.5 hr and 10% protection after 3 hr for it to be considered active. [g] In addition to increasing the blood pressure and heart rate by 30%, a compound should exert its action considerably in excess of 5 min.

compounds were screened at various dose levels and ED_{50} values were not obtained, a potency comparison was not possible. However, the fluorenes that demonstrated analgesia had marked anti-inflammatory activities, with the exception of VI. Antihistaminic potency as well as a small, but perceptible, heart rate elevation coupled with a decrease in blood pressure was found with the fluorenes. The cardiovascular effects were generally of less than 5-min duration, and in no case was action over 10 min observed. No noteworthy effects were seen by the fluorenes in the antianaphylactic and antidepressant screens.

The acyclic quaternary ammonium compounds VII and VIII were subjected to the primary screens. Analgesic activity was found with VII*a* and VII*c* but, in contrast to the fluorenes, there was an absence of anti-inflammatory activity. The cardiovascular screen showed that all compounds had marked pressor activity; VII*c* showed the maximum activity at the 1.0-mg/kg dose level. The duration of action was generally less than 5 min, and none of the compounds displayed an effect on blood pressure or heart rate for greater than 10 min. No compounds in Table II displayed hypoglycemic activity at 100 mg/kg.

In conclusion, the study showed that some fluorenes with a quaternary ammonium group at position 9 have antibacterial activities against three species of *Streptococcus* and also against *Staphylococcus aureus* and *B. subtilis*, coupled with moderate potency against two fungi. Some related open chain analogs displayed a complete absence of antimicrobial activity. While several useful anticancer drugs were chemically reactive, the quaternary ammonium compounds II and IV displayed murine toxicity but did not produce noteworthy increased mean survival times in mice with leukemia. Preliminary pharmacological tests showed anti-inflammatory analgesia as well as some effect in the cardiovascular screen to be present with a number of the fluorenes in contrast to the open chain analogs VII and VIII, which were devoid of anti-inflammatory and analgesic properties but had potent pressor activities.

EXPERIMENTAL[1]

Melting points and boiling points are uncorrected. Organic extracts were washed with water and dried over anhydrous sodium sulfate. The solvent was removed using a water aspirator. The 60-Hz NMR spectra[2] were determined in deuterochloroform with tetramethylsilane as the internal standard.

Substituted 9-Bromofluorenes (I) and 2-Chloro-9-fluorenol (V)—9-Bromofluorene[3] (I*a*) was used without further purification. 9-Bromo-2-chlorofluorene (I*b*) was prepared as follows. Reaction of 9-fluorenone[3] with *N*-chlorosuccinimide according to a literature method (17) gave 2-chloro-9-fluorenone in a 44% yield, mp 121–122° [lit. (17) mp 122°], which was reduced with lithium aluminum hydride by a reported procedure (18) to give 2-chloro-9-fluorenol (V) in a 50% yield, mp 140–141° [lit. (18) mp 140–141°]. Treatment of V with acetyl bromide using a literature method (19) gave I*b* in a 57% yield, mp 125–127° [lit. (19) mp 126–128°].

[1] Elemental analyses were carried out by Mr. R. E. Teed, Department of Chemistry and Chemical Engineering, University of Saskatchewan, and by Galbraith Laboratories Inc., Knoxville, Tenn.

[2] Varian T 60 spectrophotometer, Varian Associates of Canada Ltd., Georgetown, Ontario, L7G 2J4, Canada.

[3] Aldrich Chemical Co., Milwaukee, WI 53233.

2,9-Dibromofluorene (Ic) was prepared in an 80% yield by the reaction of 2-bromofluorene[3] with *N*-bromosuccinimide using a reported procedure (20). It had a melting point of 127–128° [lit. (20) mp 127°].

Benzyldimethyl-9-fluorenyl Ammonium Bromides (II)—The benzyldimethylamines were prepared as follows. Four of the required substituted benzylamines were treated with formic acid and formalin using a literature method (21) to give *p*-fluorobenzyldimethylamine in an 80% yield, bp 50–51°/2 mm [lit. (22) bp 61–62°/6.5 mm], *p*-chlorobenzyldimethylamine in a 79% yield, bp 100–105°/12 mm [lit. (23) bp 90–95°/9–11 mm], *p*-methylbenzyldimethylamine in an 82% yield, bp 197–198°/750 mm [lit. (23) bp 196–197°/760 mm], and *p*-methoxybenzyldimethylamine in an 80% yield, bp 104–106°/12 mm [lit. (23) bp 105–119°/10 mm].

p-Trifluoromethylbenzyl bromide, bp 93–94°/20 mm [lit. (24) bp 65–66°/5 mm], was prepared in a 61% yield from *p*-trifluoromethyl benzoic acid[3] using a literature synthetic sequence (24). A solution of *p*-trifluoromethylbenzyl bromide (0.05 mole) and anhydrous dimethylamine (0.10 mole) in nitromethane (50 ml) stood at room temperature for 4 hr and then was poured into water (100 ml). The reaction mixture was extracted with ether (2 × 50 ml), and removal of the solvent *in vacuo* gave an oil. On distillation, this oil afforded *p*-trifluoromethylbenzyldimethylamine, bp 107–110°/61 mm, in a 68% yield; the NMR spectrum was in accordance with the proposed structure. *p*-Bromobenzyldimethylamine, bp 130–132°/22 mm [lit. (25) bp 121–122°/20 mm], was prepared similarly from *p*-bromobenzyl bromide[3]. Benzyldimethylamine was obtained commercially[3].

A 0.1 *M* solution of Ia or of the 2-substituted bromofluorenes (Ib or Ic) in nitromethane (10 ml) was added to the appropriate benzyldimethylamine (0.2 mole), and the mixture was stirred at room temperature overnight. The product was precipitated by ether and purified by recrystallization from ether–ethanol. The melting points and yields of the benzyldimethyl-9-fluorenyl ammonium bromides were: II*a*, 154–156° [lit. (20) mp 155–156°], 88%; II*b*, 148–150°, 82%; II*c*, 153°, 84%; II*d*, 148°, 80%; II*e*, 153–154°, 85%; II*f*, 158°, 60%; II*h*, 149°, 50%; and II*i*, 155–156°, 85%. NMR spectra of the benzyldimethyl-9-fluorenyl ammonium bromides were consistent with the structures proposed. In the case of II*g*, ether failed to precipitate the compound from the reaction mixture and it was extracted with water (20 ml). The water was removed to give the crude product, which was not purified further.

9-Benzylfluorenyl-9-dimethylamines (III)—The appropriate benzyldimethyl-9-fluorenyl ammonium bromide (2.0 g) was dissolved in sodium methoxide solution, which was prepared by dissolving sodium (0.5 g) in methanol (7 ml). The reaction mixture stood at room temperature overnight with occasional shaking, and then water (100 ml) was added. The reaction mixture was extracted with ether (60 ml), and removal of the ether gave the crude amine III. With III*a*, III*b*, III*i*, and III*h*, the compounds were recrystallized from nitromethane unless otherwise stated.

9-Benzylfluorenyl-9-dimethylamine (III*a*) was prepared in an 81% yield, mp 98–99° [lit. (26) mp 98.5–99°]. The NMR spectrum of III*a* was consistent with the proposed structure. 9-(*p*-Fluorobenzyl)-fluorenyl-9-dimethylamine (III*b*), mp 55°, was recrystallized from petroleum ether (bp 100°).

Anal.—Calc. for $C_{22}H_{20}FN$: C, 83.24; H, 6.35; N, 4.41. Found: C, 84.00; H, 6.43; N, 4.38.

2-Chloro-9-benzylfluorenyl-9-dimethylamine (III*h*) melted at 108–109°.

Anal.—Calc. for $C_{22}H_{20}ClN$: C, 79.15; H, 6.04; N, 4.20. Found: C, 78.48; H, 6.00; N, 4.19.

2-Bromo-9-benzylfluorenyl-9-dimethylamine (III*i*) melted at 129°.

Anal.—Calc. for $C_{22}H_{20}BrN$: C, 69.84; H, 5.33; N, 3.70. Found: C, 69.71; H, 5.17; N, 3.63.

The remaining derivatives (III*c*–III*g*) were isolated as oils that could not be induced to crystallize. TLC of the products on silica gel with benzene as the solvent showed a single spot, and further purification was not undertaken.

9-Benzylfluorenyl-9-trimethylammonium Bromides (IV)—The 9-benzylfluorenyl-9-dimethylamine (0.01 mole) was dissolved in nitromethane (10 ml) containing bromomethane (0.065 mole), and the resultant solution stood at room temperature overnight. The product, obtained from the reaction mixture by the addition of ether, was recrystallized from ether–ethanol. The physical data for the salts (IV) are summarized in Table III.

9-Methylfluorenyl-9-trimethylammonium Bromide (VI)—A solution of 9-fluorenone[3] (0.035 mole) in anhydrous ether (100 ml) was added slowly to methyl magnesium iodide (0.035 mole), prepared from magnesium (0.85 g) and methyl iodide (5.0 g) in anhydrous ether (50 ml).

Table III—9-Benzylfluorenyl-9-trimethylammonium Bromides (IV)

Compound	Yield, %	Melting Point	Formula		Analysis, % Calc.	Found
IV*a*	80	178°[a]	$C_{23}H_{24}BrN$	C	70.05	70.21
				H	6.13	6.05
				N	3.55	3.55
IV*b*	80	179°	$C_{23}H_{23}BrFN$	C	66.99	66.61
				H	5.62	5.77
				N	3.40	3.38
IV*c*	80	172°	$C_{23}H_{23}BrClN$	C	64.42	64.36
				H	5.40	5.32
				N	3.27	3.25
IV*d*	81	192°	$C_{23}H_{23}Br_2N$	C	58.37	58.05
				H	4.90	4.70
				N	2.96	2.84
IV*e*	85	174°	$C_{24}H_{23}BrF_3N$	C	62.34	62.34
				H	5.01	5.00
				N	3.03	3.00
IV*f*	77	178°	$C_{24}H_{26}BrN$	C	70.58	70.63
				H	6.42	6.35
				N	3.43	3.25
IV*g*	72	175°	$C_{24}H_{26}BrNO$	C	67.92	67.88
				H	6.18	6.01
				N	3.30	3.25
IV*h*	61	180°	$C_{23}H_{23}BrClO$	C	64.42	64.19
				H	5.40	5.63
				N	3.27	3.25
IV*i*	66	190°	$C_{23}H_{23}Br_2N$	C	58.37	58.13
				H	4.90	5.03
				N	2.96	2.94

[a] Lit. (26) mp 175°.

The resultant mixture stood at room temperature overnight and then was poured onto a mixture of crushed ice (100 g) and 10% HCl (100 ml). The aqueous phase was extracted with ether. Solvent evaporation gave the crude product, which on recrystallization from benzene gave 9-methyl-9-fluorenol in a 58% yield, mp 176° [lit. (27) mp 176–177°].

Acetyl bromide (0.035 mole) was added to a solution of 9-methyl-9-fluorenol (0.025 mole) in chloroform (20 ml), and the reaction mixture was shaken. After the vigorous reaction had subsided, acetic acid and chloroform were removed under reduced pressure. The crude bromide was dissolved in nitromethane (20 ml) and added to a solution of trimethylamine in nitromethane (10%). The reaction mixture was kept at 0° for 2 days, and the separated product was recrystallized from absolute ethanol to give VI in a 20% yield, mp 170°.

Anal.—Calc. for $C_{17}H_{20}BrN$: C, 64.15; H, 6.33; N, 4.40. Found: C, 63.63; H, 6.55; N, 4.40.

1-Phenylethyltrimethylammonium Bromides (VII and VIII)—The following three-step synthesis was used for VII. A solution of the appropriate *para*-substituted benzaldehyde (0.03 mole) in anhydrous ether (25 ml) was added slowly to methyl magnesium iodide (0.035 mole), prepared from magnesium (1.0 g) and methyl iodide (5.0 g) in anhydrous ether (50 ml). The reaction mixture stood at room temperature overnight and, after being poured onto a mixture of crushed ice (100 g) and hydrochloric acid (10% v/v, 100 ml), was then extracted with ether. The solvent was removed and the required 1-phenylethanols were purified by distillation to give the *p*-chloro derivative in an 88% yield, bp 130–132°/15 mm [lit. (28) bp 110–120°/9 mm], the *p*-trifluoromethyl derivative in a 90% yield, bp 116–118°/20 mm [lit. (29) bp 106–107°/18 mm], and the *p*-methoxy derivative in an 85% yield, bp 130–132°/20 mm [lit. (30) bp 104°/3 mm].

Acetyl bromide (0.034 mole) was added quickly to the appropriate 1-phenylethanol (0.025 mole). After the vigorous reaction had subsided, acetic acid and acetyl bromide excess were removed under reduced pressure. The residue was dissolved in benzene (50 ml) and shaken with aqueous sodium bicarbonate solution (10% w/v). Solvent removal gave the crude 1-phenylethyl bromide as a pale-red oil. A crude bromide solution (0.016 mole) in nitromethane (10 ml) was added to a trimethylamine solution in nitromethane (10% w/v, 20 ml) at room temperature, and the reaction mixture was left overnight. Ether addition gave the required 1-phenylethyltrimethylammonium bromides, which were recrystallized from ether–ethanol. 1-Phenylethyltrimethylammonium bromide (VII*a*), mp 197–198° [lit. (31) mp 198–200°], was obtained in a 60% yield. 1-(*p*-Chlorophenyl)ethyltrimethylammonium bromide (VII*b*), mp 199°, was obtained in an 80% yield.

Anal.—Calc. for $C_{11}H_{17}BrClN$: C, 47.41; H, 6.15; N, 5.03. Found: C, 47.78; H, 6.53; N, 4.91.

1-(*p*-Methoxyphenyl)ethyltrimethylammonium bromide (VII*d*), mp 165–166°, was prepared in a 60% yield.

Anal.—Calc. for $C_{12}H_{20}BrNO$: C, 52.56; H, 7.35; N, 5.11. Found: C, 52.80; H, 7.58; N, 5.10.

1-(*p*-Trifluoromethylphenyl)ethyltrimethylammonium bromide (VII*c*) was prepared as follows. 1-(*p*-Trifluoromethylphenyl)ethanol (0.067 mole) was added to phosphorus bromide (0.067 mole). After standing at room temperature overnight, the reaction mixture was poured onto ice and extracted with benzene. The organic extracts were washed with aqueous sodium bicarbonate solution (10% w/v), and solvent removal gave the crude bromide. A solution of the crude bromide (3.2 g) in methanol (10 ml) was added to a triethylamine solution in absolute alcohol (10% v/v, 20 ml) to yield VII*c*, mp 218–219°, in a 58% yield.

Anal.—Calc. for $C_{12}H_{17}BrF_3N$: C, 46.17; H, 5.49; N, 4.49. Found: C, 45.47; H, 5.48; N, 4.48.

2-Phenylethyltrimethylammonium bromide (VIII) was prepared by the method described previously (32).

Screening[4] of Compounds—In the antimicrobial screen, the compounds were dissolved in water or dimethyl sulfoxide and diluted serially to various concentrations. The stock solutions were prepared in such a way that when 0.5 ml was added to 15 ml of agar, the desired final concentrations were obtained. The bacterial growth medium was trypticase soy agar with 5% defibrinated rabbit blood added for the growth of *Haemophilus influenzae*, *Streptococcus pyogenes*, and *Streptococcus pneumonia*. Modified Sabouraud agar was employed for the fungi.

The test organisms were grown previously for 2 days at 35° for bacteria and yeasts and for 1 week at 24° for fungi on slants of the media mentioned above. The agar plates were streaked with a loopful of cell suspension, which had been washed off from the slants and diluted to approximately 10^5 organisms/ml. The plates were incubated for 2–14 days at 24° for fungi and at 35° for bacteria. The results (Table I) indicated the minimal inhibitory concentration of the compound that prevented visible growth in the media.

The antiprotozoal screen utilized the tube dilution technique previously described (33). The test organisms were *E. histolytica* (ATCC 30015) grown in a TP-S-1 monophasic medium devised by Diamond (34) and *T. foetus* (ATCC 30003) grown in modified TYM basal media (34). Activity was defined as the minimal concentration that inhibited 90% of the protozoal growth at 10 and 50 μg/ml for *E. histolytica* and *T. foetus*, respectively.

Unless otherwise stated, the same numbers of animals were used as controls and for the evaluation of various pharmacological activities. The screen for examining analgesic activity was the phenylquinone writhing test (35). Five male Swiss albino mice, 18–22 g, were used for each compound except IV*g*, IV*e* (at the 64-mg/kg dose level), VII*a*, and VII*c*, in which cases 10 animals were used.

The anti-inflammatory screen measured the antagonism of the test compound to carrageenan-induced rat paw edema (36). Six female Sprague–Dawley rats, 120–160 g, were used for each compound, and the edema volume was recorded at the end of 3 and 5 hr.

The antianaphylactic screen measured passive cutaneous anaphylaxis inhibition in rats (37). Four female Sprague–Dawley rats were used for each compound except IV*f*, VII*c*, and disodium chromoglycate, in which cases eight rats were employed. Two rats were used for VIII at both dose levels.

The compounds were examined for antihistaminic activity using two guinea pig ileum preparations (38), except in the cases of IV*a*, IV*b*, and IV*f* where three preparations were used and VII*d* where one preparation was used.

The antidepressant screen measured the antagonism of tetrabenazine-induced ptosis in mice (39, 40). Six male Swiss albino mice were used for each compound.

In the cardiovascular screen, a Sprague–Dawley rat of either sex, 250–400 g, was anesthetized by intraperitoneal urethan (1.9 g/kg). After femoral vein cannulation, the blood pressure was monitored *via* a pressure transducer[5] connected to a cannula in the left carotid artery. The arterial blood pressure and heart rate were recorded on a polygraph[6]. After the preparation had stabilized, the test compound was dissolved in saline and/or polysorbate 80[7] (1%) and administered in a volume of 0.01–0.05 ml. The changes recorded in blood pressure and heart rate were expressed as percentage differences between the pre- and postdrug values. Two determinations at each dose level using one rat were made for each compound.

The screen for hypoglycemic activity involved the measurement of blood glucose in rats (41). Four male Sprague–Dawley rats were used for each compound at a dose of 100 mg/kg. A 20% decrease in blood glucose concentration was required for a compound to be considered active.

The anticancer screening was carried out by the Drug Research and Development Division of the National Cancer Institute according to their protocols (42). The compounds were administered to $B_6D_2F_1$ or CD_2F_1 mice by intraperitoneal injection either daily or every 4 days, except in the case of II*a versus* Sarcoma 180 in Swiss mice where injections were made twice daily for a total of 14 injections. The compound showed no activity.

[4] All screens, except for the assessment for anticancer activities, were carried out by Bio-Research Laboratories Ltd., Montreal, Quebec, Canada.

[5] Statham.

[6] Gass.

[7] Tween 80, Atlas Chemical Industries, Wilmington, DE 19899.

REFERENCES

(1) J. R. Dimmock, D. K. Kowal, W. A. Turner, P. J. Smith, L. M. Noble, and W. J. Pannekoek, *J. Pharm. Sci.*, **67**, 401 (1978).

(2) J. R. Dimmock, A. M. Qureshi, L. M. Noble, P. J. Smith, and H. A. Baker, *ibid.*, **65**, 38 (1976).

(3) J. R. Dimmock, W. A. Turner, and H. A. Baker, *ibid.*, **64**, 995 (1975).

(4) J. R. Dimmock and W. A. Turner, *Can. J. Pharm. Sci.*, **9**, 33 (1974).

(5) J. R. Dimmock, P. J. Smith, L. M. Noble, and W. J. Pannekoek, *J. Pharm. Sci.*, **67**, 1536 (1978).

(6) A. J. Repta, J. R. Dimmock, B. Kreilgard, and J. J. Kaminski, *ibid.*, **66**, 1501 (1977).

(7) J. R. Dimmock, N. W. Hamon, K. W. Hindmarsh, A. P. Sellar, W. A. Turner, G. H. Rank, and A. J. Robertson, *ibid.*, **65**, 538 (1976).

(8) J. R. Dimmock, G. B. Baker, and R. G. Sutherland, *Can. J. Pharm. Sci.*, **10**, 53 (1975).

(9) F. Gorssmann, H. Buchenauer, and B. Jank, *Tagungsber, Dtsch. Akad. Landwirtschafswiss. Berlin*, **1971**, 173; through *Chem. Abstr.*, **77**, 44161x (1972).

(10) S. Horiguchi, I. Takeda, M. Mizuno, and T. Sugawara, Japan. Kokai 7,461,332, (June 14, 1974); through *Chem. Abstr.*, **82**, 120059r (1975).

(11) H. S. Lowrie, U.S. pat. 3,843,657 (Oct. 22, 1974); through *Chem. Abstr.*, **82**, 125178p (1975).

(12) S. T. Yancey and W. A. Bleyer, *Cancer Res.*, **34**, 1866 (1974).

(13) A. R. Rhoads, W. L. West, and H. P. Morris, *Res. Commun. Chem. Pathol. Pharmacol.*, **6**, 741 (1973).

(14) M. W. Rana, H. Pinkerton, and A. Rankin, *Proc. Soc. Exp. Biol. Med.*, **150**, 32 (1975).

(15) A. Albert, "Selective Toxicity," 5th ed., Chapman and Hall, London, England, 1973, p. 314.

(16) J. Packer and J. Vaughan, "A Modern Approach to Organic Chemistry," Oxford, London, England, 1958, p. 594.

(17) F. Dewhurst and P. K. J. Shah, *J. Chem. Soc., C*, **1970**, 1737.

(18) G. G. Smith and R. P. Bayer, *Tetrahedron*, **18**, 323 (1962).

(19) D. Bethell, A. F. Cockerill, and O. B. Frankham, *J. Chem. Soc., B*, **1967**, 1287.

(20) J. D. Dickenson and C. Eaborn, *J. Chem. Soc.*, **1959**, 2337.

(21) R. N. Inke, B. B. Wisegarver, and G. A. Alles, in "Organic Syntheses," coll. vol. III, E. C. Horning, Ed., Wiley, New York, N.Y., 1955, p. 723.

(22) F. N. Jones and C. R. Hauser, *J. Org. Chem.*, **27**, 4020 (1962).

(23) E. L. Eliel, T. N. Ferdinand, and M. E. Herrman, *ibid.*, **19**, 1693 (1954).

(24) H. B. Haas and M. L. Bender, *J. Am. Chem. Soc.*, **71**, 1767 (1949).

(25) K. C. Dewkirst and D. J. Cram, *ibid.*, **80**, 3115 (1958).

(26) G. Wittig and G. Felletschin, *Ann.*, **555**, 133 (1944).

(27) V. V. Korshak and N. G. Matveeva, *Izv. Akad. Nauk SSSR, Otd. Khim. Nauk*, **1953**, 542; through *Chem. Abstr.*, **48**, 9918h (1954).

(28) E. Matsui, *J. Soc. Chem. Ind. Jpn.*, **45**, 412 (1942).

(29) E. T. McBee, S. Resconich, L. R. Belohlov, and H. P. Braendlin, *J. Org. Chem.*, **28**, 3579 (1963).

(30) J. Grundy, *J. Chem. Soc.*, **1957**, 5087.

(31) G. S. Dyson, Ph.D. thesis, University of Saskatchewan, Saskatoon, Canada, 1975, p. 127.

(32) P. J. Smith and A. N. Bourns, *Can. J. Chem.*, **52**, 749 (1974).

(33) L. S. Diamond and I. L. Burtgis, *Arch. Invest. Med., Suppl.*, **2** (1971).

(34) L. S. Diamond, *J. Parisitol.*, **54**, 1047 (1968).

(35) H. O. Collier, L. C. Dinneen, C. A. Johnson, and C. Schneider, *Br.*

J. Pharmacol. Chemother., **32**, 295 (1968).
(36) C. A. Winter, in "International Symposium on Non-Steroidal Anti-Inflammatory Drugs," S. Garattini and M. N. G. Dukes, Eds., Excerpta Medica Foundation, Amsterdam, The Netherlands, 1965, pp. 190–202.
(37) J. Goose and A. M. J. N. Blair, *Immunology*, **16**, 749 (1969).
(38) W. L. M. Perry, "Pharmacological Experiments on Isolated Preparations," Livingstone, Edinburgh, Scotland, 1968, pp. 58–68.
(39) B. Rubin, H. H. Malone, M. H. Waugh, and J. C. Burke, *J. Pharmacol. Exp. Ther.*, **120**, 125 (1957).
(40) A. Barnett and R. T. Taber, in "Screening Methods in Pharmacology," vol. II, P. A. Turner and P. Hebborn, Eds., Academic, New York, N.Y., 1971, pp. 203–208.
(41) G. F. Holland, D. A. Jaeger, R. L. Wagner, G. D. Laubach, W. M. McLamore, and S. Y. P'an, *J. Med. Pharm. Chem.*, **3**, 99 (1961).
(42) R. I. Geran, N. H. Greenberg, M. M. MacDonald, A. M. Schumacker, and B. J. Abbott, *Cancer Chemother. Rep. (Part 3)*, **3** (2) (Sept. 1972).

ACKNOWLEDGMENTS

The authors thank Dr. H. B. Wood, Jr., for arranging for some compounds to be assessed for antineoplastic activities and also Bio-Research Laboratories which undertook the remainder of the screening.

Separation and Determination of Testosterone and Testosterone Esters in Selected Pharmaceutical Formulations

R. E. GRAHAM *x, E. R. BIEHL ‡, and C. T. KENNER ‡

Received October 20, 1978, from the **Food and Drug Administration, Dallas, TX 75204*, and the ‡*Department of Chemistry, Southern Methodist University, Dallas, TX 75275.* Accepted for publication January 26, 1979.

Abstract □ A rapid quantitative procedure is presented for the separation of testosterone esters from their hydrolysis products through the use of the acetonitrile–infusorial earth column. The method was applied to testosterone cypionate, testosterone enanthate, and testosterone propionate. Recovery and replication of reference standard testosterone and its three esters through the proposed method ranged from 99.1 to 100.3%, and the percent relative standard deviation ranged from 0.6 to 1.0%. Two samples can be separated into testosterone and testosterone ester fractions in about 1.5 hr. The analyses of 20 injectable and one buccal tablet formulations made by 12 different manufacturers are reported.

Keyphrases □ Chromatography, column—analysis, testosterone and testosterone esters, various pharmaceuticals, acetonitrile–infusorial earth column □ Testosterone—analysis, acetonitrile–infusorial earth column chromatography, separation from testosterone esters, various pharmaceuticals □ Testosterone esters—analysis, acetonitrile–infusorial earth column chromatography, separation from testosterone esters, various pharmaceuticals

The "American Drug Index" (1) lists 57 different drug products that contain testosterone esters; they are mostly injectables and are made by 27 different manufacturers. The active ingredients are testosterone cypionate in 11 formulations, testosterone enanthate in 34, testosterone ketolaurate in one, and testosterone propionate in 11.

The official assay procedure in the USP (2) for testosterone drug substance and injection requires GLC analysis. Cleanup of testosterone propionate oil injectables by reversed-phase chromatography has been described (3), and this method is the basis for the modified cleanup procedure in USP XIX (4) for testosterone cypionate and testosterone propionate injectables. These USP procedures measure total testosterone plus esters. The final determinative step for these two compounds is spectrophotometric measurement of their isoniazid hydrazones, a procedure that is slightly altered from that originally described (5).

The USP–NF (6) presents a high-pressure liquid chromatographic (HPLC) method for testosterone propionate tablets. Other steroid separation methods include column adsorption chromatography (7), GLC (8, 9), TLC (10), paper chromatography (11), HPLC (4), column partition chromatography (12), and use of an acetonitrile–infusorial earth column (13).

This paper reports a relatively rapid quantitative analytical procedure for the separation of testosterone from its cypionate, enanthate, and propionate esters using an acetonitrile–infusorial earth column. The final determinative step compares the standard and sample isoniazid hydrazones. The proposed procedure was applied to the analysis of 21 pharmaceutical formulations made by 12 different manufacturers.

EXPERIMENTAL

Apparatus—The following were used: UV–visible recording spectrophotometers[1] with 1-cm stoppered quartz cells, a high-pressure liquid chromatograph[2] (sensitivity of 0.005 absorbance unit full scale with a 254-nm UV detector[3] and a reversed phase column[4]), glass chromatographic columns for partition chromatography (2.2 × 25 cm, constricted at one end to 0.4 × 5 cm), an aluminum tamping rod, an electrobalance[5], and TLC[6] equipment. Volumetric flasks and pipets were either NBS calibrated or Class A glassware.

Materials—Alcohol USP, distilled-in-glass grade[7] acetonitrile, chloroform, *n*-heptane, absolute methanol, and reagent grade acetic acid were used along with acid-washed infusorial earth[8]. Also used were USP reference standard testosterone cypionate, testosterone enanthate, and testosterone propionate and NF reference standard testosterone.

Reagents—Mutually saturated acetonitrile–*n*-heptane was prepared as follows. Acetonitrile, 30 ml, was mixed with 500 ml of *n*-heptane (sufficient for two determinations) in a separator, agitated vigorously for 2 min, and allowed to stand until both layers were clear. These mutually saturated solutions were used whenever acetonitrile or *n*-heptane was called for in these directions.

Sample Preparation—*Tablets*—Twenty tablets were weighed,

[1] Cary models 15 and 17.
[2] Waters model 6000 pump.
[3] Waters 440 detector.
[4] Separations Group, Vidac TP.
[5] Cahn models G-2 and 25.
[6] TLC plates 6060, Eastman Organic Chemicals.
[7] Burdick & Jackson.
[8] Celite 545, Johns-Manville Product Corp.

0022-3549/79/0700-0871$01.00/0
© 1979, American Pharmaceutical Association

J. Pharmacol. Chemother., **32**, 295 (1968).
(36) C. A. Winter, in "International Symposium on Non-Steroidal Anti-Inflammatory Drugs," S. Garattini and M. N. G. Dukes, Eds., Excerpta Medica Foundation, Amsterdam, The Netherlands, 1965, pp. 190–202.
(37) J. Goose and A. M. J. N. Blair, *Immunology*, **16**, 749 (1969).
(38) W. L. M. Perry, "Pharmacological Experiments on Isolated Preparations," Livingstone, Edinburgh, Scotland, 1968, pp. 58–68.
(39) B. Rubin, H. H. Malone, M. H. Waugh, and J. C. Burke, *J. Pharmacol. Exp. Ther.*, **120**, 125 (1957).
(40) A. Barnett and R. T. Taber, in "Screening Methods in Pharmacology," vol. II, P. A. Turner and P. Hebborn, Eds., Academic, New York, N.Y., 1971, pp. 203–208.
(41) G. F. Holland, D. A. Jaeger, R. L. Wagner, G. D. Laubach, W. M. McLamore, and S. Y. P'an, *J. Med. Pharm. Chem.*, **3**, 99 (1961).
(42) R. I. Geran, N. H. Greenberg, M. M. MacDonald, A. M. Schumacker, and B. J. Abbott, *Cancer Chemother. Rep. (Part 3)*, **3** (2) (Sept. 1972).

ACKNOWLEDGMENTS

The authors thank Dr. H. B. Wood, Jr., for arranging for some compounds to be assessed for antineoplastic activities and also Bio-Research Laboratories which undertook the remainder of the screening.

Separation and Determination of Testosterone and Testosterone Esters in Selected Pharmaceutical Formulations

R. E. GRAHAM *x, E. R. BIEHL ‡, and C. T. KENNER ‡

Received October 20, 1978, from the **Food and Drug Administration, Dallas, TX 75204*, and the ‡*Department of Chemistry, Southern Methodist University, Dallas, TX 75275.* Accepted for publication January 26, 1979.

Abstract □ A rapid quantitative procedure is presented for the separation of testosterone esters from their hydrolysis products through the use of the acetonitrile–infusorial earth column. The method was applied to testosterone cypionate, testosterone enanthate, and testosterone propionate. Recovery and replication of reference standard testosterone and its three esters through the proposed method ranged from 99.1 to 100.3%, and the percent relative standard deviation ranged from 0.6 to 1.0%. Two samples can be separated into testosterone and testosterone ester fractions in about 1.5 hr. The analyses of 20 injectable and one buccal tablet formulations made by 12 different manufacturers are reported.

Keyphrases □ Chromatography, column—analysis, testosterone and testosterone esters, various pharmaceuticals, acetonitrile–infusorial earth column □ Testosterone—analysis, acetonitrile–infusorial earth column chromatography, separation from testosterone esters, various pharmaceuticals □ Testosterone esters—analysis, acetonitrile–infusorial earth column chromatography, separation from testosterone esters, various pharmaceuticals

The "American Drug Index" (1) lists 57 different drug products that contain testosterone esters; they are mostly injectables and are made by 27 different manufacturers. The active ingredients are testosterone cypionate in 11 formulations, testosterone enanthate in 34, testosterone ketolaurate in one, and testosterone propionate in 11.

The official assay procedure in the USP (2) for testosterone drug substance and injection requires GLC analysis. Cleanup of testosterone propionate oil injectables by reversed-phase chromatography has been described (3), and this method is the basis for the modified cleanup procedure in USP XIX (4) for testosterone cypionate and testosterone propionate injectables. These USP procedures measure total testosterone plus esters. The final determinative step for these two compounds is spectrophotometric measurement of their isoniazid hydrazones, a procedure that is slightly altered from that originally described (5).

The USP–NF (6) presents a high-pressure liquid chromatographic (HPLC) method for testosterone propionate tablets. Other steroid separation methods include column adsorption chromatography (7), GLC (8, 9), TLC (10), paper chromatography (11), HPLC (4), column partition chromatography (12), and use of an acetonitrile–infusorial earth column (13).

This paper reports a relatively rapid quantitative analytical procedure for the separation of testosterone from its cypionate, enanthate, and propionate esters using an acetonitrile–infusorial earth column. The final determinative step compares the standard and sample isoniazid hydrazones. The proposed procedure was applied to the analysis of 21 pharmaceutical formulations made by 12 different manufacturers.

EXPERIMENTAL

Apparatus—The following were used: UV–visible recording spectrophotometers[1] with 1-cm stoppered quartz cells, a high-pressure liquid chromatograph[2] (sensitivity of 0.005 absorbance unit full scale with a 254-nm UV detector[3] and a reversed phase column[4]), glass chromatographic columns for partition chromatography (2.2 × 25 cm, constricted at one end to 0.4 × 5 cm), an aluminum tamping rod, an electrobalance[5], and TLC[6] equipment. Volumetric flasks and pipets were either NBS calibrated or Class A glassware.

Materials—Alcohol USP, distilled-in-glass grade[7] acetonitrile, chloroform, *n*-heptane, absolute methanol, and reagent grade acetic acid were used along with acid-washed infusorial earth[8]. Also used were USP reference standard testosterone cypionate, testosterone enanthate, and testosterone propionate and NF reference standard testosterone.

Reagents—Mutually saturated acetonitrile–*n*-heptane was prepared as follows. Acetonitrile, 30 ml, was mixed with 500 ml of *n*-heptane (sufficient for two determinations) in a separator, agitated vigorously for 2 min, and allowed to stand until both layers were clear. These mutually saturated solutions were used whenever acetonitrile or *n*-heptane was called for in these directions.

Sample Preparation—*Tablets*—Twenty tablets were weighed,

[1] Cary models 15 and 17.
[2] Waters model 6000 pump.
[3] Waters 440 detector.
[4] Separations Group, Vidac TP.
[5] Cahn models G-2 and 25.
[6] TLC plates 6060, Eastman Organic Chemicals.
[7] Burdick & Jackson.
[8] Celite 545, Johns-Manville Product Corp.

0022-3549/79/0700-0871$01.00/0
© 1979, American Pharmaceutical Association

Table I—Recovery Replication of Steroid Esters (Percent Recovered) through the Proposed Procedure

Run	Testosterone Cypionate			Testosterone Enanthate			Testosterone Propionate			Testosterone,
	Fraction 1[a]	Fraction 2[b]	Total	Fraction 1[a]	Fraction 2[b]	Total	Fraction 1[a]	Fraction 2[b]	Total	Fraction 2[b]
1	98.8	1.2	100.0	100.3	0.4	100.7	100.0	0.6	100.6	98.5
2	98.0	1.1	99.1	99.3	0.3	99.6	97.9	0.6	98.5	99.3
3	98.3	1.1	99.4	99.4	0.3	99.7	99.1	0.6	99.7	99.2
4	99.5	1.1	100.6	101.2	0.5	101.7	98.7	0.9	99.6	99.4
5	98.3	1.3	99.6	100.8	0.4	101.2	98.3	0.4	98.7	100.4
6	98.7	1.5	100.2	101.2	0.4	101.6	97.8	1.0	98.8	101.5
7	98.5	1.4	99.9	99.8	0.6	100.4	98.1	0.7	98.8	99.3
8	97.5	1.5	99.0	97.9	0.8	98.7	98.1	0.4	98.5	99.9
9	98.1	1.3	99.4	98.3	0.8	99.1	98.5	0.4	98.9	100.2
Average		1.3	99.7		0.5	100.3		0.6	99.1	99.7
RSD[c]			0.6			1.0			0.7	1.0

[a] Elution fraction 1. [b] Elution fraction 2. [c] Relative standard deviation calculated from the range by the method of Dean and Dixon (14).

ground to pass through a 60-mesh sieve, and mixed thoroughly. Then a sample containing ~12.5 mg of steroid was accurately weighed and transferred to a 50-ml volumetric flask, diluted to volume with methanol, and mixed. Two 5-ml aliquots, each containing ~1.25 mg of steroid, were evaporated just to dryness. The sample residues were dissolved in 1.5 ml each of acetonitrile and *n*-heptane for cleanup as directed under *Column Preparation*.

Injectables—The contents of several containers were well mixed, and duplicate 2.0-ml sample portions were diluted accurately with chloroform so that aliquots of the final sample solution containing ~1.25 mg of testosterone ester could be evaporated just to dryness on the steam bath. The sample residues were dissolved in 1.5 ml each of acetonitrile and *n*-heptane for cleanup as directed under *Column Preparation*.

Column Preparation—A glass wool plug was inserted in the bottom of a chromatographic column. Then a 4-g portion of infusorial earth, thoroughly mixed with 4 ml of acetonitrile, was transferred to the column and packed firmly with a tamping rod.

The sample solution, prepared as directed, was mixed thoroughly with 3 g of infusorial earth to yield a light fluffy mixture. This mixture was transferred to the column above the acetonitrile layer and packed firmly. The sample beaker, tamping rod, spatula, and funnel were dry washed with about 1 g of infusorial earth, which was added to the column. The same equipment was dry washed with glass wool, which was placed on top of the sample layer plus washings and packed firmly.

Column Elution of Steroids—The sample beaker was washed with 250 ml of *n*-heptane in small portions, which were transferred to the column to maintain a liquid head approximately 12 cm above the column bed. About 60 ml of *n*-heptane eluate was collected in the first fraction, the beakers were changed, and about 190 ml was collected in the second fraction. The last wash was allowed to drain completely from the column, the tip was rinsed with alcohol, and both effluents were saved for further analysis.

The first 60-ml *n*-heptane fraction was diluted accurately to volume with chloroform to give a final concentration of ~0.012 mg of steroid ester/ml. This solution was allowed to come to room temperature and was readjusted to volume before further dilution or taking of aliquots. The second 190-ml *n*-heptane fraction was carefully evaporated just to dryness on the steam bath. The residues were dissolved and diluted accurately to a volume with absolute methanol to yield a concentration of ~0.012 mg of steroid/ml. In every case, aliquots were taken carefully just to dryness for the isoniazid determination.

Isoniazid Method—The procedure of Umberger (5) was used, except that the hydrochloric acid concentration was doubled to increase the sensitivity.

UV Method—Aliquots of testosterone fractions 1 and 2 were taken carefully to dryness on the steam bath. The residues were dissolved and diluted with methanol to ~0.010 mg of testosterone/ml or 0.012 mg of testosterone esters/ml and scanned spectrophotometrically from 360 to 220 nm *versus* the same solvent. They were compared with a reference standard solution of steroid of about the same concentration.

Completeness of Testosterone Elution—After column elution with 250 ml of *n*-heptane in accordance with the proposed method, an additional step was employed to check the completeness of testosterone elution in all method development studies. The sample beaker was washed with 125 ml of chloroform in several portions, which were added to the column to maintain the liquid level close to the column top. The last portion was allowed to drain completely, the tip was rinsed with alcohol, and the eluate was taken carefully just to dryness. When dissolved and reacted with 4 ml of isoniazid, the residues gave no visible color.

Elution Studies—Approximately 2 mg, accurately weighed, of reference standard testosterone and each of the three testosterone esters were dissolved in 1.5 ml each of acetonitrile and *n*-heptane and placed on the column as described. These compounds were eluted at a rate of ~7 ml/min with 300 ml of *n*-heptane and collected in 15-ml portions for analysis. A second determination was made of testosterone with the rate of elution set at about 1 ml/min. Each 15-ml portion of the eluate was taken carefully just to dryness. Each residue was dissolved in and diluted with methanol and spectrophotometrically scanned in the UV region. Elution curves were plotted for each experiment.

Replication Studies of Recoveries of Testosterone and Its Esters—Reference standard testosterone and its esters, equivalent to ~10 mg (accurately weighed) of testosterone, were dissolved and diluted to 50 ml with methanol. Nine 5-ml aliquots of each steroid were taken carefully just to dryness. The residues were dissolved in 1.5 ml each of *n*-heptane and acetonitrile, placed on the column, and eluted according to the described procedure.

For testosterone esters, the 60-ml fraction of *n*-heptane was diluted to 100 ml with chloroform, and 5-ml aliquots were evaporated carefully

Table II—Replication and Separation of Testosterone (Percent Recovered) from Its Esters by the Proposed Procedure

Run	Testosterone Enanthate, Isoniazid	Testosterone, Isoniazid	Testosterone Cypionate		Testosterone		Testosterone Propionate		Testosterone	
			Isoniazid	UV	Isoniazid	UV	Isoniazid	UV	Isoniazid	UV
1	99.8	103.7	99.4	100.4	101.5	99.7	97.1	98.0	103.3	100.2
2	99.0	102.3	99.6	100.6	99.1	96.8	98.6	99.2	99.8	96.8
3	101.1	101.1	99.4	100.6	100.2	97.7	99.8	100.7	99.5	94.5
4	100.0	103.5	99.2	100.4	100.1	100.9	97.9	98.5	99.4	99.7
5	100.6	100.4	99.2	100.7	101.1	100.6	99.3	99.8	98.9	98.8
6	100.2	99.6[a]	98.3	99.8	100.3	100.6	98.9	99.5	99.7	101.1
7	100.5	98.4[a]	98.9	98.0	99.3	99.3	97.3	99.5	100.7	100.7
8	98.8	98.1[a]	100.8	98.3	99.8	100.2	100.2	98.8	97.4	102.0
9	99.3	101.2[a]	ND[b]	ND[b]	ND[b]	ND[b]	98.2	99.0	100.3	100.4
10	97.9	103.4[a]	ND[b]	ND[b]	ND[b]	ND[b]	ND[b]	ND[b]	ND[b]	ND[b]
Average	99.7	101.2	99.4	99.8	100.2	99.5	98.6	99.2	99.9	99.4
RSD[c]	1.1	1.8	0.9	0.9	0.8	1.4	1.0	0.9	1.9	2.5

[a] Testosterone eluted from column with 125 ml of chloroform following elution of the ester. [b] Not determined. [c] Relative standard deviation calculated from the range by the method of Dean and Dixon (14).

Table III—Recoveries of Testosterone Esters from the Acetonitrile Column

Testosterone Cypionate			Testosterone Enanthate			Testosterone Propionate		
Amount, mg	Percent Recovered		Amount, mg	Percent Recovered		Amount, mg	Percent Recovered	
	UV	Isoniazid[a]		UV	Isoniazid[a]		UV	Isoniazid[a]
2.757[b]	99.6	97.1 (1.1)	2.769	102.0	98.9 (0.3)	2.585[b]	100.1	100.1 (0.8)
4.165[b]	98.8	97.9 (2.1)	4.216	102.8	100.7 (0.3)	3.634[b]	100.5	99.7 (0.5)
4.216	99.3	97.8 (1.4)	5.627	100.4	99.8 (0.4)	3.655	100.3	101.4 (0.2)
5.541	100.6	98.0 (1.3)	—	—	—	4.834[b]	100.1	99.3 (0.7)
5.603[b]	98.5	96.8 (2.1)	—	—	—	5.015	101.3	101.2 (0.2)
Average	99.4	97.5 (1.6)		101.7	99.8 (0.3)		100.5	100.3 (0.5)

[a] The values in parentheses represent the percent of testosterone found in fraction 2. [b] Fraction 1 was evaporated to dryness and diluted with absolute methanol as required for determination by UV and isoniazid.

Table IV—Volatility Study (Percent Recovered by Isoniazid Method)

Minutes	Testosterone, Live Steam	Testosterone Cypionate		Testosterone Enanthate		Testosterone Propionate	
		Steam Bath	Live Steam	Steam Bath	Live Steam	Steam Bath	Live Steam
10	—	99.4	—	97.9	—	89.5	—
20	—	98.9	—	96.2	—	87.6	—
40	80.0	97.4	100.0	96.5	97.2	83.3	81.0
60	78.2	99.8	98.0	96.5	98.8	63.5	80.1

Table V—Base Degradation of Steroids (Percent Recovered by Isoniazid Method)

Hours[a]	Testosterone Cypionate		Testosterone Enanthate		Testosterone Propionate	
	Fraction 1	Fraction 2	Fraction 1	Fraction 2	Fraction 1	Fraction 2
1	94.5	2.0	97.5	0.7	91.1	2.9
2	ND[b]	ND	96.8	1.5	93.8	4.8
4	92.4	6.1	95.4	3.9	90.1	8.6
8	85.9	10.4	93.3	6.7	82.1	16.7
24	72.2	25.6	80.9	15.3	ND	ND
48	52.7	43.5	ND	ND	ND	ND
78	ND	ND	ND	ND	18.6	76.9

[a] Time of exposure of testosterone ester to base. [b] Not determined.

to dryness and used for the isoniazid determination. The 190-ml *n*-heptane fraction containing testosterone was evaporated to a small volume, made up to 100 ml with chloroform, and mixed; then 5-ml aliquots were taken carefully just to dryness for the isoniazid reaction. Results of this study (Table I) ranged from 99.1 to 100.3% recovery, and the relative standard deviations calculated from the range (14) were 0.6–1.0%.

Recovery and Replication Studies of Testosterone and Testosterone Ester Separation—About 10 mg of testosterone standard (accurately weighed) and the equivalent weight of its cypionate, enanthate, and propionate ester standards were dissolved and diluted to 50 ml with chloroform. Several 10-ml aliquots were taken carefully just to dryness on the steam bath. The residues were dissolved in 1.5 ml each of acetonitrile and *n*-heptane, placed on the column, and separated using the procedure described.

The first and second *n*-heptane fractions were taken carefully just to dryness on the steam bath. In some cases, the column was eluted with 60 ml of *n*-heptane and 125 ml of chloroform (instead of 190 ml of *n*-heptane), and the chloroform fraction was taken carefully just to dryness. All residues were dissolved in absolute methanol and diluted to 100 ml. Selected samples were determined by UV spectrophotometry, and 5-ml aliquots of all samples were evaporated just to dryness for colorimetric determination by isoniazid.

Results of this study (Table II) showed that recoveries ranged from 94.5 to 103.7% for testosterone and from 97.1 to 101.1% for its esters and that the values obtained by the UV and isoniazid methods compared favorably. Relative standard deviations of separated steroids calculated from the range were 0.8–2.5%.

TLC and HPLC determinations of Samples 5–8 (Table III) for the separation of testosterone and testosterone cypionate showed no cross-contamination. An 80:20 acetonitrile–water mixture was used to elute testosterone cypionate in 10.5 min, and a 40:60 acetonitrile–water system was used to elute testosterone by HPLC. TLC of testosterone and its cypionate on silica gel G with chloroform gave R_f values of 0.35 and 0.7, respectively.

Recovery Study of Large Quantities of Testosterone Esters—Three accurately weighed portions of each testosterone ester standard, ranging from 2 to 6 mg, were dissolved in 1.5-ml aliquots of acetonitrile and *n*-heptane and placed on columns using the procedure described. The first fractions from several columns were taken carefully to dryness on the steam bath. The residues were dissolved and diluted with absolute methanol to obtain a concentration of ~0.012 mg/ml for UV and isoniazid determinations.

For other selected samples, the first fraction was diluted to 100 ml with chloroform, and appropriate aliquots were taken just to dryness by evaporation for UV and isoniazid determinations. Each residue was treated with 4 ml of isoniazid reagent to develop the color. The results (Table III) showed that as much as 5.6 mg of testosterone esters could be recovered satisfactorily in fraction 1.

Solvent Volatility Study—About 1.25 mg, accurately weighed, of each testosterone ester was dissolved and diluted to 100 ml with methanol. Five-milliliter aliquots were placed in 100-ml beakers and evaporated just to dryness on the steam bath. Replicate residues were left on the steam bath for selected periods after dryness. The residues were dissolved and diluted to volume, and aliquots were taken for the isoniazid reaction.

The experiment was repeated with replicate aliquots of testosterone and its esters but with the beakers placed over the openings on the steam bath to allow heating by live steam for 40 and 60 min. The residues were dissolved and diluted to volume with methanol for determination by isoniazid. Table IV shows that significant testosterone and testosterone propionate losses occurred when they were exposed to steam temperatures for extended periods after solvent volatilization.

Base Degradation Study—About 12.5 mg, accurately weighed, of each testosterone ester was dissolved in ~25 ml of methanol. Then 0.5 ml of 10% aqueous tetramethylammonium hydroxide was added. The mixture was diluted to 50 ml with methanol and mixed. At selected times, 5-ml aliquots were removed and 0.5 ml of acetic acid was added to each aliquot. The acidified methanol aliquots were evaporated carefully just to dryness on the steam bath.

Each residue was dissolved in 1.5 ml each of acetonitrile and *n*-heptane, and the mixture was placed on the column and treated as already described. The results (Table V) showed that testosterone ester hydrolysis by tetramethylammonium hydroxide in methanol proceeded at a fairly

Table VI—Analysis of Typical Pharmaceutical Formulations

Sample[a]	Active Ingredient	Other Ingredients[b]	Amount Declared, mg/ml	Percent of Declared (by Isoniazid)	
				Steroid Ester	Testosterone
1	Testosterone enanthate	(2) (7)	100	100.4, 100.4	1.3, 1.3
2	Testosterone enanthate	(2) (7)	200	100.0, 100.5	1.3, 1.1
3	Testosterone enanthate	(2) (7)	200	82.4, 81.3	13.5, 12.9
4	Testosterone enanthate	(2) (7)	100	103.2, 103.4	1.7, 1.8
5	Testosterone enanthate	(2) (6) (7)	180	100.1, 100.4	1.9, 1.9
6	Testosterone enanthate	(2) (7)	100	104.6, 105.3	0.3, 0.2
7	Testosterone enanthate	(2) (6) (7)	90	99.3, 100.6	1.2, 1.4
8	Testosterone enanthate	(2) (7)	100	99.4, 100.0	1.1, 0.9
9	Testosterone enanthate	(2) (7)	200	100.7, 100.9	1.3, 1.2
10	Testosterone enanthate	(2) (3) (7)	200	97.3, 98.0	1.6, 1.7
11	Testosterone enanthate	(2) (3) (7)	200	98.4, 97.4	1.6, 1.6
12	Testosterone enanthate	(2) (7)	100	101.0, 100.6	1.0, 1.1
13	Testosterone enanthate	(2) (4) (7)	100	98.1, 97.9	1.5, 1.4
14	Testosterone cypionate	(2) (3) (5)	200	100.3, 100.3	0.3, 0.2
15	Testosterone cypionate	(2) (3) (5)	200	98.7, 97.3	0.4, 0.5
16	Testosterone cypionate	(2) (3) (5)	200	97.2, 97.5	0.1, 0.1
17	Testosterone cypionate	(2) (5)	100	98.4, 99.4	0.5, 0.4
18	Testosterone cypionate	(2) (5) (9)	100	103.0, 102.3	0.4, 0.4
19	Testosterone propionate	(8) (10) (11)	50	100.6, 100.3	3.6, 3.9
20	Testosterone propionate	(1) (2) (4) (11)	100	87.3, 86.3	2.1, 2.8
21[c]	Testosterone propionate		10[d]	97.6, 96.7	0.1, 0.1
22	Testosterone		100	0.1, 0.1	101.1, 101.6
23	Testosterone		25	0.2, 0.2	99.0, 98.6

[a] Samples 1–20 were injectables, Sample 21 was a tablet, and Samples 22 and 23 were suspensions. [b] (1) = absolute alcohol, (2) = benzyl alcohol, (3) = benzyl benzoate, (4) = chlorobutanol, (5) = cottonseed oil, (6) = estradiol valerate, (7) = ethyl oleate, (8) = methylparaben, (9) = oxystearin, (10) = propylparaben, and (11) = sesame oil. [c] Analysis of duplicate samples by UV: 96.0 and 96.6% of declared. [d] Amount is in milligrams per tablet.

rapid rate at room temperature and that the undecomposed steroid ester and testosterone could be separated and recovered by the proposed method.

RESULTS AND DISCUSSION

The effects of various hydrocarbon solvents and flow rates on testosterone elution from acetonitrile–infusorial earth columns have been studied (13). *n*-Heptane was selected as a solvent for use in the column chromatography because it gives optimum separation of testosterone from its esters. Symmetrical elution curves for testosterone and the three esters studied showed that testosterone enanthate required 20 ml, testosterone cypionate required 23 ml, and testosterone propionate required 45 ml of *n*-heptane for complete elution.

A 7-ml/min normal flow rate of *n*-heptane eluted 2 mg of testosterone from the acetonitrile column in a band between 88 and 195 ml. A 1-ml/min flow rate of *n*-heptane eluted the same amount of testosterone in a band between 105 and 184 ml. While the faster elution rate resulted in band broadening, adequate separations between testosterone and its esters were obtained. Testosterone propionate elution was completed at 45 ml of *n*-heptane, and elution of testosterone from the column did not occur before 88 ml. The recommended cut-off volume at 60 ml of *n*-heptane provided an adequate safety factor and resulted in pure fractions.

The values reported for all determinations represent an average of two isoniazid color developments.

Table I shows 0.3–1.3% hydrolysis of the testosterone ester reference standards. TLC confirmed the presence of testosterone in the second *n*-heptane fraction of all three esters. Both HPLC and TLC of portions of the final diluted solutions after separation on the acetonitrile column showed no testosterone cross-contamination with its esters in either *n*-heptane fraction. The agreement between the results obtained by the UV and isoniazid methods (Table II) was well within the expected range and recoveries obtained for testosterone by eluting the column with an additional 190 ml of *n*-heptane or with 125 ml of chloroform. Fewer manipulations were required if chloroform was used to elute testosterone from the acetonitrile column, but less sample interference resulted from elution with 190 ml of *n*-heptane.

Table III shows that up to 5.6 mg of the three testosterone esters could be eluted completely in the first 60 ml of *n*-heptane collected from the acetonitrile column. It also shows that the results of chloroform dilution of the first *n*-heptane fraction and evaporation of small aliquots to dryness were in agreement with the results obtained by evaporating the *n*-heptane (fraction 1) carefully just to dryness, dissolving the residue in absolute methanol for UV measurement, and carrying subsequent aliquots to dryness for isoniazid determination.

The solvent volatility study (Table IV) showed that when the samples were evaporated carefully just to dryness under air on the steam bath, no steroid loss occurred. However, significant losses of 10–30% of testosterone and testosterone propionate resulted when the sample residues were left on the steam bath for extended periods after the solvent had been volatilized.

The rate of testosterone ester hydrolysis by tetramethylammonium hydroxide (Table V) was faster for testosterone cypionate than for testosterone enanthate and fastest for testosterone propionate. At 8 hr, the hydrolysis rate for testosterone enanthate was ~0.8%/hr; for testosterone cypionate, it was ~1.3%/hr; and for testosterone propionate, it was ~2.1%/hr. TLC and IR spectrophotometry confirmed the presence of enanthic acid in the chloroform fraction from the acetonitrile column.

Analyses of typical pharmaceutical formulations, mostly injectables, by the proposed method are reported in Table VI. Good replication of sample analysis was obtained. The amount of testosterone found varied from 0.1 to 13.5% of the declared amount of testosterone ester, with only three of the 21 products analyzed showing more than 2.0%. Sample 14, analyzed in duplicate by direct dilution and the isoniazid method, gave 123.8 and 125.1%, while Sample 15 gave 121.6 and 120.0% of the declared amount. These results, when compared with those shown in Table VI, showed that a 20–25% interference was removed by the proposed cleanup procedure. Apparently the cleanup procedure is applicable to injectables containing a wide variety of excipients (Table VI) including cottonseed and sesame oils.

The samples that contained benzyl alcohol could not be cleaned up by the proposed procedure for determination by UV spectrophotometry since it eluted in the first *n*-heptane fraction along with the testosterone esters. While benzyl alcohol interfered with the UV spectrum of the testosterone esters, there was no interference when isoniazid was used as the final determinative step.

Samples 22 and 23 (Table VI) for testosterone suspensions are included to show the versatility of the acetonitrile column.

The proposed procedure is relatively rapid and is specific for testosterone ester determination. Two samples can be prepared for analysis, placed on separate columns, and separated into two fractions containing testosterone ester and testosterone in 1.5 hr. The results of the duplicate analyses of 21 different pharmaceutical formulations showed that the proposed procedure provided adequate sample cleanup with satisfactory accuracy and replication of the analytical data. This method can be used to assess hydrolytic degradation of testosterone esters in pharmaceutical formulations by measuring intact testosterone ester and/or testosterone present in the sample.

REFERENCES

(1) C. O. Wilson and T. E. Jones, "American Drug Index," Lippincott, Philadelphia, Pa., 1973, pp. 629, 630.

(2) "The United States Pharmacopeia," 19th rev., Mack Publishing Co., Easton, Pa., 1975, pp. 489, 490.

(3) E. Smith, *J. Pharm Sci.*, **56**, 630 (1967).
(4) "The United States Pharmacopeia," 19th rev., Mack Publishing Co., Easton, Pa., 1975, pp. 490–492.
(5) E. J. Umberger, *Anal. Chem.*, **27**, 768 (1955).
(6) "The United States Pharmacopeia," 19th rev., 4th suppl., United States Pharmacopeial Convention, Rockville, Md., 1978, p. 168.
(7) G. Cavina, G. Moretti, A. Mollica, and R. Antonina, *Farmaco, Ed. Prat.*, **26**, 275 (1971).
(8) A. N. Akolaev, V. P. Pakhomov, and S. D. Sokolov, *Farmatsiya*, **24**, 66 (1975); through *Chem. Abstr.*, 152426 V (1975).
(9) M. Delaforge, B. F. Maume, and P. Bournot, *J. Chromatogr. Sci.*, **12**, 545 (1974).
(10) T. Bican-Fister, *J. Chromatogr.*, **27**, 465 (1966).
(11) M. Sterescu and N. Cain, *Rev. Chim.*, **13**, 172 (1962).
(12) J. Carol, *J. Assoc. Off. Agric. Chem.*, **36**, 1001 (1953).
(13) R. E. Graham and C. T. Kenner, *J. Pharm. Sci.*, **62**, 1845 (1973).
(14) R. B. Dean and W. J. Dixon, *Anal. Chem.*, **23**, 636 (1951).

Application of Thermochromism in Spectrophotometric Analysis: Selective Determination of Berberine in Pharmaceuticals by Solvent Extraction

TADAO SAKAI

Received May 3, 1978, from the *Department of Chemistry, Gifu College of Dentistry, Gifu, Japan.* Accepted for publication January 19, 1979.

Abstract □ A solvent extraction and spectrophotometric method for selective determination of berberine in pharmaceuticals is proposed. Berberine forms an ion associate with tetrabromophenolphthalein ethyl ester, which is extracted into ethylene dichloride. Secondary and tertiary amines and alkaloids are coextracted with the berberine and complicate the berberine determination. The absorbance of the secondary and tertiary amines and alkaloids into ethylene dichloride, however, decreases nearly to zero when the temperature is elevated from 25 to 60°. Thus, berberine can be determined successfully in the presence of the secondary and tertiary amines and alkaloids by using thermochromism.

Keyphrases □ Berberine—analysis, solvent extraction, spectrophotometric method using thermochromism, various pharmaceuticals □ Thermochromism—analysis, berberine in various pharmaceuticals, solvent extraction, spectrophotometry □ Spectrophotometry, solvent extraction—analysis, berberine in various pharmaceuticals, using thermochromism □ Antibacterial agents—berberine, analysis in various pharmaceuticals, solvent extraction, spectrometry, using thermochromism

Bromthymol blue, bromcresol green, and bromphenol blue usually are used for the solvent extraction and spectrophotometric determination of thiamine (1), quaternary ammonium compounds (2), and quinine ethylcarbonate (3), respectively. These dyes are diprotic acids with a narrow optimum pH range and poor extractability of the ion associates into organic solvents.

Tetrabromophenolphthalein ethyl ester anion (I) is a monoprotic acid and can form ion associates (II) with quaternary ammonium cations (III) and charge transfer complexes (IV) with amines (V), which are effectively extracted into organic solvents through a wide pH range (4). Tetrabromophenolphthalein ethyl ester shows a high sensitivity for quaternary ammonium cations and amines, but the absorption spectra overlap each other. Thus, it is difficult to determine spectrophotometrically the quaternary ammonium salts and amines separately when they coexist. An attempt was made to separate the amine procaine from the quaternary ammonium salt benzethonium by solvent extraction, but it was difficult to remove the amine completely (5).

The author found, however, that the color of the charge transfer complex in ethylene dichloride reversibly disappeared with the elevation of temperature. Even at 60°, the red complex was rarely found while the absorbance of the ion associate at 610 nm was unchanged at 60°. Thus, a quaternary ammonium salt could be determined spectrophotometrically at 60° without the disturbance of amines.

This paper describes the extraction and spectrophotometric determination of berberine in pharmaceuticals after the temperature is increased to 60° to eliminate the effect of the coexisting amines.

EXPERIMENTAL

Apparatus—A double-beam spectrophotometer[1] attached to a temperature-controlled cell holder was used to measure absorbances at a constant temperature using quartz 1-cm cells with stoppers. An x–y recorder[2] was used for the spectra. Constant cell temperature was maintained by circulating constant-temperature water through the temperature-controlled cell holder by means of a temperature-controlled circulator[3]. The solvent temperature in the cell was checked by dipping a thermoelement of a thermometer[4] in the solvent. A pH meter, a shaker, and a centrifuge were also used.

Reagents—*Standard Berberine Solution*—A stock solution of 1×10^{-3} M berberine was prepared by dissolving 0.4075 g of berberine hydrochloride[5] (dried at 105°) in distilled water and diluting to 1 liter with distilled water. The stock solution was standardized by the official method (6). The solution was used after accurate dilution.

Tetrabromophenolphthalein Ethyl Ester Solution—A 2.0×10^{-3} M solution of tetrabromophenolphthalein ethyl ester was prepared by dissolving 0.1400 g of tetrabromophenolphthalein ethyl ester potassium salt[6] in ethanol to give a 100-ml solution.

Buffer Solution (pH 8.5)—The borate–phosphate buffer was prepared by adding 1 N H_2SO_4 or 1 N NaOH to the 0.3 M potassium dihydrogen phosphate containing 0.1 M sodium borate.

Procaine[7], ephedrine[8], quinine[9], papaverine[9], eserine[10], and emetine[5] were used as the hydrochloride and the sulfate. Ethylene dichloride was used as the extractant. All chemicals were reagent grade.

[1] Hitachi model 556.
[2] Hitachi model 057.
[3] Komatsu-Yamato model CTE-240.
[4] Anritsu model HP-4F.
[5] Nakarai Kagaku Yakuhin Co., Kyoto, Japan.
[6] Tokyo Kasei Kogyo Co., Tokyo, Japan.
[7] Daiichi Seiyaku Co., Tokyo, Japan.
[8] Sanwa Kagaku Co., Nagoya, Japan.
[9] Katayama Kagaku Kogyo Co., Osaka, Japan.
[10] E. Merck, Darmstadt, West Germany.

0022-3549/79/0700-0875$01.00/0
© 1979, American Pharmaceutical Association

(3) E. Smith, *J. Pharm Sci.*, **56**, 630 (1967).
(4) "The United States Pharmacopeia," 19th rev., Mack Publishing Co., Easton, Pa., 1975, pp. 490–492.
(5) E. J. Umberger, *Anal. Chem.*, **27**, 768 (1955).
(6) "The United States Pharmacopeia," 19th rev., 4th suppl., United States Pharmacopeial Convention, Rockville, Md., 1978, p. 168.
(7) G. Cavina, G. Moretti, A. Mollica, and R. Antonina, *Farmaco, Ed. Prat.*, **26**, 275 (1971).
(8) A. N. Akolaev, V. P. Pakhomov, and S. D. Sokolov, *Farmatsiya*, **24**, 66 (1975); through *Chem. Abstr.*, 152426 V (1975).
(9) M. Delaforge, B. F. Maume, and P. Bournot, *J. Chromatogr. Sci.*, **12**, 545 (1974).
(10) T. Bican-Fister, *J. Chromatogr.*, **27**, 465 (1966).
(11) M. Sterescu and N. Cain, *Rev. Chim.*, **13**, 172 (1962).
(12) J. Carol, *J. Assoc. Off. Agric. Chem.*, **36**, 1001 (1953).
(13) R. E. Graham and C. T. Kenner, *J. Pharm. Sci.*, **62**, 1845 (1973).
(14) R. B. Dean and W. J. Dixon, *Anal. Chem.*, **23**, 636 (1951).

Application of Thermochromism in Spectrophotometric Analysis: Selective Determination of Berberine in Pharmaceuticals by Solvent Extraction

TADAO SAKAI

Received May 3, 1978, from the *Department of Chemistry, Gifu College of Dentistry, Gifu, Japan.* Accepted for publication January 19, 1979.

Abstract □ A solvent extraction and spectrophotometric method for selective determination of berberine in pharmaceuticals is proposed. Berberine forms an ion associate with tetrabromophenolphthalein ethyl ester, which is extracted into ethylene dichloride. Secondary and tertiary amines and alkaloids are coextracted with the berberine and complicate the berberine determination. The absorbance of the secondary and tertiary amines and alkaloids into ethylene dichloride, however, decreases nearly to zero when the temperature is elevated from 25 to 60°. Thus, berberine can be determined successfully in the presence of the secondary and tertiary amines and alkaloids by using thermochromism.

Keyphrases □ Berberine—analysis, solvent extraction, spectrophotometric method using thermochromism, various pharmaceuticals □ Thermochromism—analysis, berberine in various pharmaceuticals, solvent extraction, spectrophotometry □ Spectrophotometry, solvent extraction—analysis, berberine in various pharmaceuticals, using thermochromism □ Antibacterial agents—berberine, analysis in various pharmaceuticals, solvent extraction, spectrometry, using thermochromism

Bromthymol blue, bromcresol green, and bromphenol blue usually are used for the solvent extraction and spectrophotometric determination of thiamine (1), quaternary ammonium compounds (2), and quinine ethylcarbonate (3), respectively. These dyes are diprotic acids with a narrow optimum pH range and poor extractability of the ion associates into organic solvents.

Tetrabromophenolphthalein ethyl ester anion (I) is a monoprotic acid and can form ion associates (II) with quaternary ammonium cations (III) and charge transfer complexes (IV) with amines (V), which are effectively extracted into organic solvents through a wide pH range (4). Tetrabromophenolphthalein ethyl ester shows a high sensitivity for quaternary ammonium cations and amines, but the absorption spectra overlap each other. Thus, it is difficult to determine spectrophotometrically the quaternary ammonium salts and amines separately when they coexist. An attempt was made to separate the amine procaine from the quaternary ammonium salt benzethonium by solvent extraction, but it was difficult to remove the amine completely (5).

The author found, however, that the color of the charge transfer complex in ethylene dichloride reversibly disappeared with the elevation of temperature. Even at 60°, the red complex was rarely found while the absorbance of the ion associate at 610 nm was unchanged at 60°. Thus, a quaternary ammonium salt could be determined spectrophotometrically at 60° without the disturbance of amines.

This paper describes the extraction and spectrophotometric determination of berberine in pharmaceuticals after the temperature is increased to 60° to eliminate the effect of the coexisting amines.

EXPERIMENTAL

Apparatus—A double-beam spectrophotometer[1] attached to a temperature-controlled cell holder was used to measure absorbances at a constant temperature using quartz 1-cm cells with stoppers. An x–y recorder[2] was used for the spectra. Constant cell temperature was maintained by circulating constant-temperature water through the temperature-controlled cell holder by means of a temperature-controlled circulator[3]. The solvent temperature in the cell was checked by dipping a thermoelement of a thermometer[4] in the solvent. A pH meter, a shaker, and a centrifuge were also used.

Reagents—*Standard Berberine Solution*—A stock solution of 1×10^{-3} M berberine was prepared by dissolving 0.4075 g of berberine hydrochloride[5] (dried at 105°) in distilled water and diluting to 1 liter with distilled water. The stock solution was standardized by the official method (6). The solution was used after accurate dilution.

Tetrabromophenolphthalein Ethyl Ester Solution—A 2.0×10^{-3} M solution of tetrabromophenolphthalein ethyl ester was prepared by dissolving 0.1400 g of tetrabromophenolphthalein ethyl ester potassium salt[6] in ethanol to give a 100-ml solution.

Buffer Solution (pH 8.5)—The borate–phosphate buffer was prepared by adding 1 N H_2SO_4 or 1 N NaOH to the 0.3 M potassium dihydrogen phosphate containing 0.1 M sodium borate.

Procaine[7], ephedrine[8], quinine[9], papaverine[9], eserine[10], and emetine[5] were used as the hydrochloride and the sulfate. Ethylene dichloride was used as the extractant. All chemicals were reagent grade.

[1] Hitachi model 556.
[2] Hitachi model 057.
[3] Komatsu-Yamato model CTE-240.
[4] Anritsu model HP-4F.
[5] Nakarai Kagaku Yakuhin Co., Kyoto, Japan.
[6] Tokyo Kasei Kogyo Co., Tokyo, Japan.
[7] Daiichi Seiyaku Co., Tokyo, Japan.
[8] Sanwa Kagaku Co., Nagoya, Japan.
[9] Katayama Kagaku Kogyo Co., Osaka, Japan.
[10] E. Merck, Darmstadt, West Germany.

0022-3549/79/0700-0875$01.00/0
© 1979, American Pharmaceutical Association

Table I—Effect of Foreign Substances on Berberine Determination [a]

Substance	Mole Ratio	Berberine Recovery, % 25°	60°
Glucose	1:1000	100	—
Lactose	1:1000	98	—
Ammonium sulfate	1:1000	101	—
Calcium chloride	1:1000	100	—
Sodium carbonate	1:1000	98	—
Sodium chloride	1:1000	102	—
Sodium nitrate	1:1000	101	—
Sodium acetate	1:1000	101	—
Sodium citrate	1:1000	100	—
Sodium salicylate	1:1000	99	—
Starch, 0.4%	—	101	—
Thiamine	1:1	102	—
Triethanolamine	1:500	105	105
Caffeine	1:100	101	—
Benzethonium	1:1	185	185
Neostigmine	1:0.1	111	111
Diphenhydramine	1:0.3	107	102
	1:0.5	112	104
Procaine	1:2	129	102
	1:4	159	106
Emetine	1:1	113	102
	1:2	130	106
Papaverine	1:10	105	98
	1:20	114	101
Pilocarpine	1:30	106	101
Eserine	1:1	111	100
	1:2	126	102
Chlorophenylamine	1:0.3	115	104
	1:0.5	128	106

[a] The berberine taken was 1×10^{-6} *M*, the wavelength was 610 nm, and the pH was 8.5.

Recommended Procedure—Berberine solution, 0.5–5 ml (2.5×10^{-5} *M*), 2 ml of tetrabromophenolphthalein ethyl ester (2×10^{-3} *M*), and 5 ml of borate–phosphate buffer (pH 8.5) were pipetted into a 100-ml separator. The mixture was diluted with water to 50 ml and shaken with 10 ml of ethylene dichloride for 5 min mechanically.

The organic layer was transferred into a stoppered test tube and centrifuged to remove water droplets. The absorbance (610 nm) of the organic phase was measured at 25° in the temperature-controlled cell holder against the reagent blank. The temperature was raised to 60° with the cell remaining in the holder, and the absorbance of the same phase was measured.

The calibration curves were straight, starting at the origin, over 0.25–2.5 $\times 10^{-6}$ *M* berberine aqueous solution. The molar absorptivities at 25 and 60° in ethylene dichloride were 9.80×10^4 and 9.24×10^4 mole^{-1} cm^{-1} liter, respectively. The precision was checked by 10 measurements, and the variation coefficient was ±1% at each temperature.

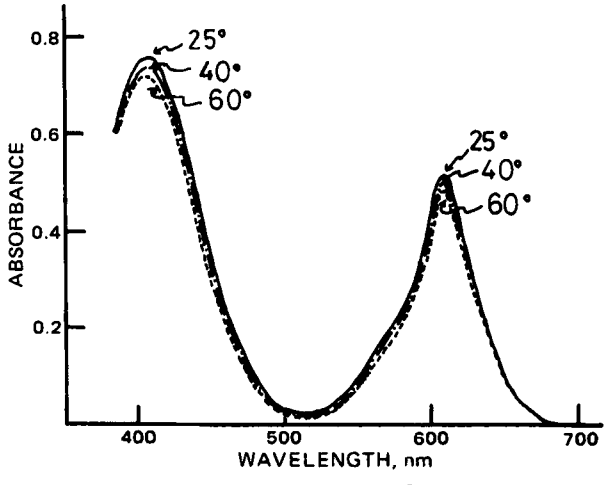

Figure 1—*Absorption spectra of 6.4 × 10^{-6} M tetrabromophenolphthalein ethyl ester–1 × 10^{-6} M berberine at different temperatures and pH 8.5. The shaking time was 5 min, and the reference was water.*

Table II—Berberine Analysis in Practical Samples

Sample	Amount Manifested, mg	Amount Found, mg 25°	60°
1[a]	75	81	76
2[b]	50	53.5	51
3[c]	100	105	101

[a] Also contained thiamine hydrochloride (5 mg), diphenhydramine hydrochloride (10 mg), and methylephedrine hydrochloride (15 mg). [b] Also contained diphenhydramine hydrochloride (10 mg), papaverine hydrochloride (5 mg), and thiamine hydrochloride (5 mg). [c] Also contained chlorpheniramine maleate (15 mg), thiamine hydrochloride (10 mg), and papaverine hydrochloride (20 mg).

RESULTS AND DISCUSSION

Extraction Mechanism with Tetrabromophenolphthalein Ethyl Ester—Tetrabromophenolphthalein ethyl ester anion (I) reacted with quaternary ammonium salts such as berberine, tetraethylammonium, benzethonium (7), and sparteine to form blue-color ion associates, which were extracted into ethylene dichloride. Secondary and tertiary amines such as ephedrine, quinine (4), papaverine, procaine (5), and emetine also reacted with I to form reddish complexes, which were extracted into ethylene dichloride. The ratio of I to the compounds of both the blue ion associates and the reddish complexes in ethylene dichloride was 1:1, as determined by the continuous variation method.

The electric conductivities of the dye molecule (VI), of the ion associate with berberine, and of the complex with procaine in ethylene dichloride were measured. The solutions containing 10^{-4} *M* VI and its charge transfer complex with procaine did not show conductivity when measured at various temperatures from 20 to 50°. The solutions containing 10^{-4} *M* of the ion associate with berberine showed some small conductivity (micro-ohms per centimeter): 20°, 6.14; 30°, 6.78; 40°, 7.29; and 50°, 8.0.

Accordingly, the following extraction scheme is presented. The subscripts *o* and *w* refer to the organic and aqueous phases, respectively.

$$\underset{\text{blue}}{I_w} + H_w^+ \rightleftarrows \underset{\text{yellow } (\lambda_{max} = 410 \text{ nm})}{VI_0}$$

Scheme I—Extraction of tetrabromophenolphthalein ethyl ester

$$I_w + III_w \rightleftarrows \underset{\text{blue}}{I\text{-}III_0(II)} \rightleftarrows \underset{\text{blue } (\lambda_{max} = 610 \text{ nm})}{I_0 + III_0}$$

Scheme II—Extraction of ion associate

$$I_w + H_w^+ + V_w \rightleftarrows \underset{\text{red } (\lambda_{max} = 545 - 585 \text{ nm})}{I\text{-}H\text{-}V_0(IV_0)}$$

Scheme III—Extraction of charge transfer complex

Thermochromism of Ion Associate and Charge Transfer Complex with I—The absorption spectra of the I–berberine ion associate and the

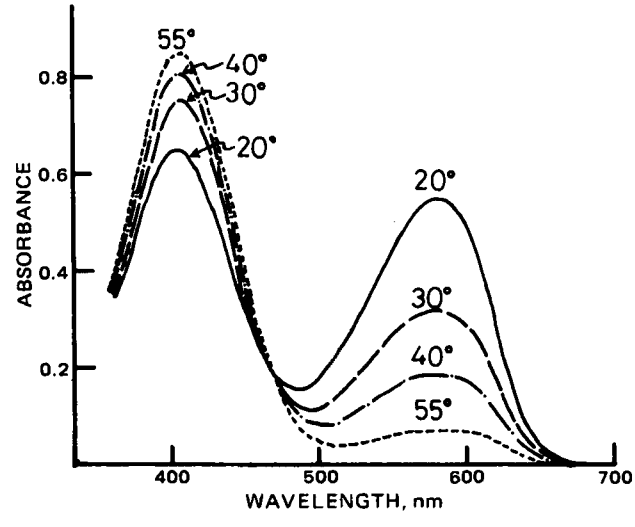

Figure 2—*Changes in absorption spectra of the charge transfer complex by thermochromism. The amine was 2.5 × 10^{-5} M procaine with 1.28 × 10^{-5} M tetrabromophenolphthalein ethyl ester at pH 8.5. The reference was water.*

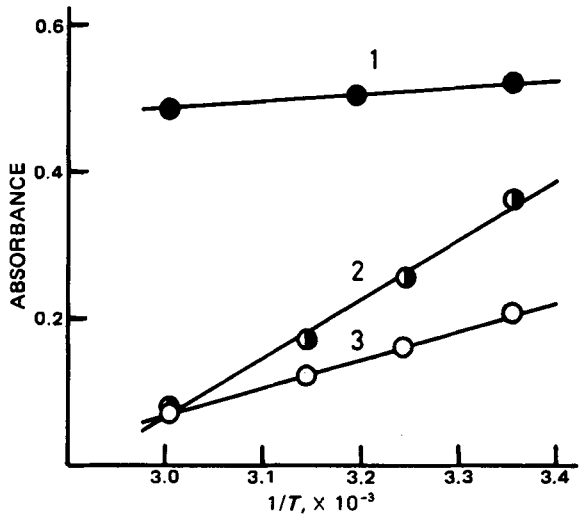

Figure 3—*Effect of temperature on tetrabromophenolphthalein ethyl ester–berberine and amines. Key: 1, 1 × 10⁻⁶ M berberine with 8 × 10⁻⁵ M tetrabromophenolphthalein ethyl ester at 610 nm; 2, 2.0 × 10⁻⁵ M papaverine with 1.6 × 10⁻⁴ M tetrabromophenolphthalein ethyl ester at 572 nm; and 3, 1.0 × 10⁻⁶ M procaine with 1.6 × 10⁻⁴ M tetrabromophenolphthalein ethyl ester. The reference was water.*

VI–procaine complex in ethylene dichloride at various temperatures are shown in Figs. 1 and 2, respectively. The absorption spectrum of the I–berberine ion associate was scarcely affected by the temperature change. The slight decrease in absorbance with a rise in temperature depended on the expansion of ethylene dichloride.

On the other hand, the VI–procaine complex absorption spectrum in ethylene dichloride was greatly influenced by temperature. When the temperature was elevated, the absorbance at 585 nm decreased and the absorbance at 410 nm increased. The isosbestic point in this absorption spectrum was 465 nm.

Thus, Scheme IV is presented.

$$\underset{\text{red}}{IV_0} \underset{\text{cool}}{\overset{\text{warm}}{\rightleftharpoons}} \underset{\text{yellow}}{VI_0} + \underset{\text{colorless}}{V_0}$$

Scheme IV

The absorbances of the I–berberine ion associate at 610 nm, of the VI–procaine complex at 585 nm, and of the VI–papaverine complex at 572 nm were plotted against $1/T$(T = absolute temperature) (Fig. 3). The absorbance change of the I–berberine ion associate is attributed to solvent expansion, and the absorbance decreases of the VI–papaverine and the VI–procaine complexes with increased temperature are due to complex dissociation according to Scheme IV. At 60°, the absorbances of the VI–procaine complex at 585 nm and of the VI–papaverine complex at 572 nm were almost the same as the reagent blank.

When berberine (1×10^{-6} M) was extracted into ethylene dichloride with I, the absorbance at 610 nm was 0.520 at 25° and 0.484 at 60°, with water as a reference. When berberine (1×10^{-6} M) and eserine (1×10^{-6} M) coexisted, the absorbance at 610 nm was 0.577 at 25° and 0.485 at 60°. When the eserine concentration was doubled, the absorbance was 0.655 at 25° and 0.493 at 60°. Therefore, the berberine concentration can be determined successfully at 60° without hindrance from coexisting amines. The other amines such as emetine, papaverine, procaine, and pilocarpine were tested, with the same results as eserine.

Effect of Foreign Substances—Various foreign substances were added to a solution containing 1×10^{-6} M berberine, and their influences were examined by the recommended procedure (Table I). Glucose, lactose, and inorganic ions such as ammonium, calcium, sodium, chloride, and sulfate did not interfere with the determination of berberine. Quaternary ammonium salts such as benzethonium and neostigmine severely affected the determination, with positive errors even at 60°. Amines such as emetine, papaverine, pilocarpine, and eserine interfered with the determination at 25° but not at 60°.

Analysis of Practical Samples—Commercial samples were analyzed according to the proposed method (Table II). Of the coexisting substances, diphenhydramine, methylephedrine, and chlorophenylamine gave some interference at 25°; at the elevated temperature, their influences were suppressed by thermochromism. As a result, this thermochromism method is more selective, sensitive, and accurate than the official methods of determining berberine in pharmaceuticals.

REFERENCES

(1) V. D. Gupta and D. E. Cadwallader, *J. Pharm. Sci.*, **57**, 112 (1968).

(2) H. M. N. H. Irving and J. J. Markham, *Anal. Chim. Acta*, **39**, 7 (1967).

(3) T. Inoue, M. Tatsuzawa, and N. Nakagome, *Bunseki Kagaku*, **19**, 766 (1970).

(4) T. Sakai, I. Hara, and M. Tsubouchi, *Chem. Pharm. Bull.*, **24**, 1254 (1976).

(5) T. Sakai, I. Ogawa, M. Tsubouchi, and T. Kamada, *Eisei Kagaku*, **21**, 199 (1975).

(6) "The Japanese Pharmacopoeia," IX ed., Hirokawa Publishing, Tokyo, Japan, 1976, c-312.

(7) M. Tsubouchi, *Bull. Chem. Soc. Jpn.*, **44**, 1560 (1971).

ACKNOWLEDGMENTS

The author thanks Professor K. Toei of Okayama University and Professor Y. Yamamoto of Hiroshima University for their valuable advice.

High-Pressure Liquid Chromatographic Determination of Saccharin in Artificial Sweeteners and Pharmaceuticals

PHILIP J. PALERMO ˣ **and PETER SHI-FU TSAI**

Received January 20, 1978, from *Norwich-Eaton Pharmaceuticals, Norwich, NY 13815.* Accepted for publication January 22, 1979.

Abstract □ A high-pressure liquid chromatographic procedure is presented for determining saccharin in various formulations. The method is fast, precise, and accurate and is specific for saccharin in the presence of its most likely impurities and degradation products. Reversed-phase chromatography on a micro-C_{18} column is utilized with an internal standard, and detection is by UV absorption at 280 nm.

Keyphrases □ High-pressure liquid chromatography—analysis, saccharin in various artificial sweeteners and pharmaceuticals, stability indicating □ Saccharin—analysis, high-pressure liquid chromatographic, in various artificial sweeteners and pharmaceuticals, stability indicating □ Stability—saccharin, various artificial sweeteners and pharmaceuticals, high-pressure liquid chromatography

Current literature is abundant in techniques for saccharin determination. Spectrophotometry (1, 2), gravimetry (3, 4), polarography (5), partitioning (6), and specific ion electrode (7, 8) techniques are available but lack the specificity needed for a stability-indicating assay. TLC techniques (9, 10) have a limited and unknown specificity and accuracy. GLC techniques (11–15) require isolation of the saccharin in the dry state and derivatization as either the methyl or trimethylsilyl derivative, and their specificity usually is not stated.

A liquid chromatographic procedure using an ion-exchange column has been described (16). This method was applied to soft drinks and foods, but its specificity for saccharin is unknown. Another liquid chromatographic procedure (17) using a μBondapak C_{18} column and aqueous acetic acid was not applied to pharmaceuticals. Its specificity for saccharin and, therefore, its use as a stability-indicating assay are questionable.

This paper describes the development of a high-pressure liquid chromatographic procedure for saccharin or saccharin sodium determination in artificial sweeteners. With modifications in sample handling, this procedure is applicable to a wide range of pharmaceutical preparations containing saccharin. The specificity and speed of this method allow its use as both a stability-indicating and a quality control assay.

EXPERIMENTAL

Apparatus—The high-pressure liquid chromatograph was equipped with a 280-nm absorbance detector. A 30-cm × 3.9-mm μBondapak C_{18} column of 10-μm average particle size was used with an eluent flow rate of 1.5 ml/min. Peak areas were determined by a computerized laboratory data system, but calculations may be performed using peak heights if desired.

Materials and Reagents—Saccharin and saccharin sodium equivalent to USP specifications and theophylline[1] of USP purity were used. All other reagents and chemicals were ACS reagent grade or equivalent.

Mobile Phase Preparation—Ten milliliters of acetic acid was added to 600 ml of methanol and diluted to 2 liters with distilled water. The eluent was filtered through a 0.5-μm cellulose acetate filter and degassed prior to use.

Internal Standard Solution—Theophylline, 0.35 ± 0.05 g, was dissolved in ~250 ml of eluent.

Saccharin Standard Solution—About 0.7 g of reference standard saccharin sodium or 0.6 g of reference standard saccharin was weighed accurately and diluted to 100.0 ml with 50% methanol–water.

Standard Solution for Injection—Ten milliliters of internal standard solution was combined with 10.0 ml of saccharin solution, and about 30 ml of eluent was added.

Procedure for Artificial Sweetener—Depending on the dosage level, the amount of ground sample equivalent to ~50 mg of saccharin was weighed into a flask. Ten milliliters of internal standard and ~40 ml of eluent were added. After dissolution and filtration, the sample was ready for injection.

General Procedure for Other Pharmaceutical Preparations—A sample size equivalent to 1–10 mg of saccharin was reacted with 50 ml of 5% HCl. The solution was extracted with a total of 100 ml of ether in several portions. The ether portions were combined and taken to near dryness with heat and a nitrogen stream. An aliquot of internal standard solution was added commensurate to the saccharin level in the sample. This solution was injected without further dilution.

TLC—Solution volumes of standards and samples corresponding to ~200 μg of saccharin were spotted onto 20 × 20-cm fluorescent silica gel (0.25 mm) plates. After drying, the plates were developed in chloroform–methanol–ammonia (70:30:0.5 v/v) to about a 15-cm solvent migration. The saccharin spots were excised with the aid of UV light and taken up in 4 ml of 2% ammonia in methanol. After centrifugation, the UV absorbances were measured at 269 nm.

RESULTS

Individual stock solutions of saccharin and theophylline were prepared, and aliquots of each were combined in different ratios for injection to determine the response linearity. Thus, for this experiment, both the saccharin and theophylline contents were varied simultaneously. The response ratios (both areas and peak heights) were plotted *versus* the weight ratios injected over 0–4 μg of saccharin and 0–1.6 μg of theophylline injected. The results of the least-squares linear regression analysis (Table I) indicated very good linearity by both peak height and area measurements. A typical chromatogram is shown in Fig. 1. The amounts injected were 2.9 μg of saccharin and 0.6 μg of theophylline.

Laboratory-prepared synthetic samples of the artificial sweetener were assayed to determine the accuracy of the method. Three groups of five samples each in which the placebo was held constant while the sodium saccharin was varied at 80, 100, and 125% of label were assayed by the procedure (Table II). The data indicated no bias in the method and statistically no difference in the groups by F and t tests. The calculation is:

$$\text{mg of saccharin sodium/g of sample} = \frac{R_{\text{sample}}}{R_{\text{standard}}} \times \frac{\text{mg of saccharin sodium standard}}{\text{sample weight}} \quad \text{(Eq. 1)}$$

where the R's are the saccharin to theophylline response ratios. The method was validated for peak height and area ratios.

A manufactured sample was assayed 15 times, varying the sample weights from 80 to 120% recommended. The relative standard deviation of the assay was ±0.3%. The solutions for injection were stable for many weeks as demonstrated by a lack of change in the response ratios.

The method was challenged directly by the presence of seven possible impurities and degradation products documented in the literature (1, 18–20). Figure 2 shows a chromatogram of a typical saccharin and theophylline sample solution after quantities of seven of these compounds, each equal to the amount of saccharin present, were added. The identities of the peaks are: 1, 1,5-naphthalenedisulfonic acid; 2, ammonium-*o*-sulfobenzoate; 3, 2-(aminosulfonyl)benzoic acid; 4, *p*-carboxyben-

[1] Mallinckrodt.

0022-3549/79/0700-0878$01.00/0
© 1979, American Pharmaceutical Association

Table I—Linear Regression of Response Ratio *versus* Weight Ratio, Saccharin to Theophylline

Weight Ratio	Area Ratio	Peak Height Ratio
2.0	0.319	0.519
3.2	0.518	0.843
4.0	0.648	1.018
5.0	0.804	1.343
6.0	0.966	1.569
8.0	1.300	2.065
Slope	0.163	0.258
Correlation coefficient	0.999	0.999
Standard error of estimate	0.02	0.01
Percent variation	2.0	0.7

zenesulfonamide; 5, salicylic acid; and 6, *o*- and *p*-toluenesulfonamides. All of the peaks were well resolved from both saccharin and theophylline, and none of these compounds at reasonable levels interfered in the method.

The artificial sweetener was subjected to stress conditions for an attempted forced degradation study. The samples showed no measurable degradation at 100° for 1 month and also were unaffected by 2 weeks of exposure to strong fluorescent and incandescent light. However, a sample stored at 75° at very high humidity gave a low assay and the formation of a new peak in the chromatogram. The assay value by the liquid chromatographic procedure was 44.9% of initial. This new peak had a retention time corresponding to 2-(aminosulfonyl)benzoic acid, the alkaline hydrolysis product, which was suspected to be the most likely first degradation product. This sample was assayed by TLC, and the result was 42.8% of initial.

Table II—Synthetic Samples (n = 5)

Group, %	Recovery, %	*RSD*, %
80	100.5	0.51
100	100.1	0.46
125	100.1	0.30

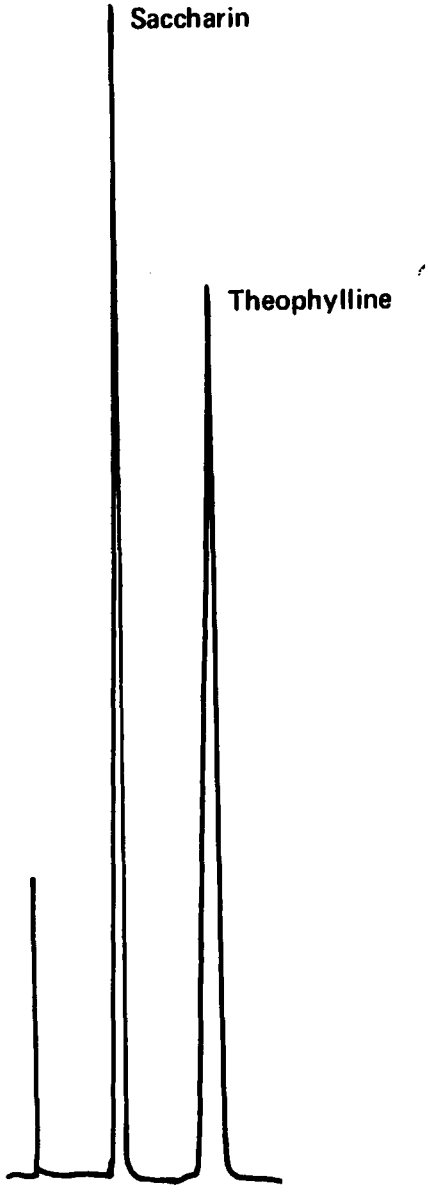

Figure 1—*Chromatogram of saccharin and theophylline.*

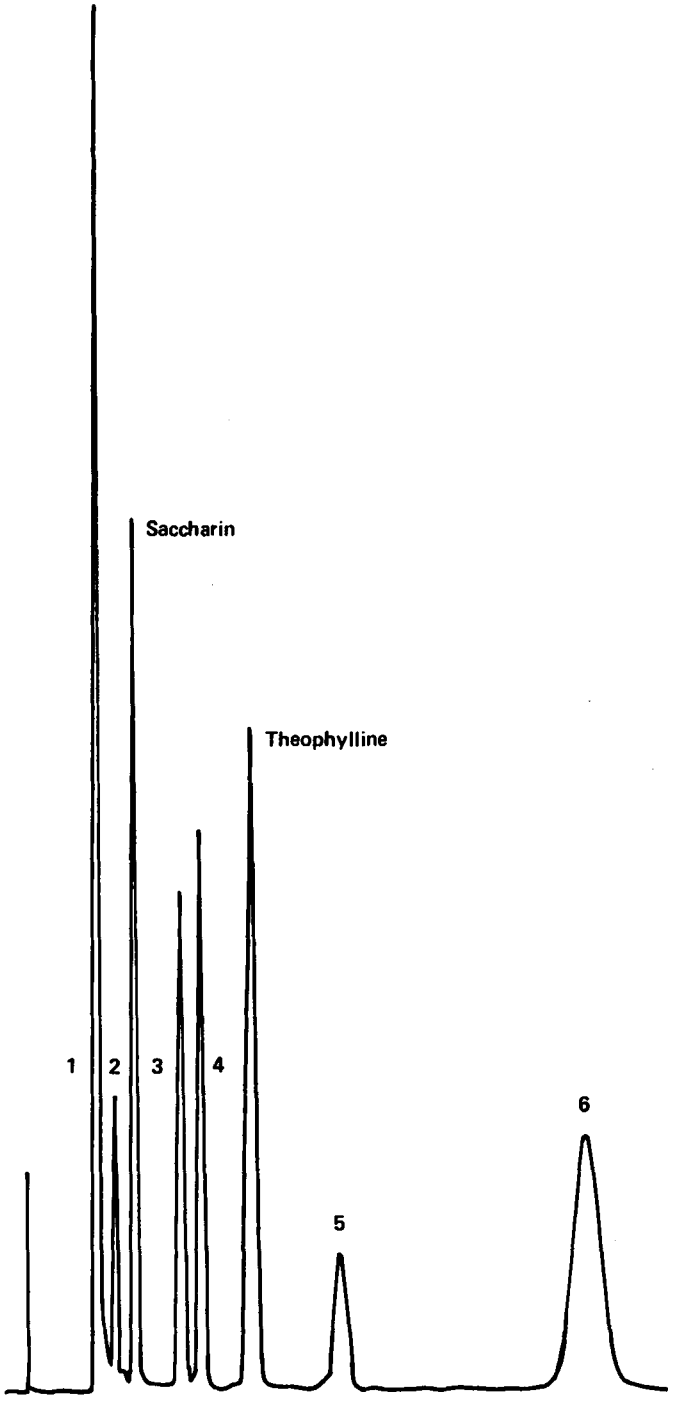

Figure 2—*Chromatogram of saccharin, theophylline, and postulated impurities and degradation products. (See text.)*

DISCUSSION

The artificial sweetener consists of saccharin sodium and sodium bicarbonate. Acetic acid in the eluent neutralizes both. Acetic acid in the eluent increases the retention (capacity factor) of saccharin by suppressing ionization and also results in a much sharper peak. If saccharin is allowed to elute in its ionic form, very little retention occurs and little use is made of the separating capabilities of the column.

Before an assay can be considered qualified for a stability-indicating program, its specificity characteristics must be proven. Specificity in this method is provided mainly by the liquid chromatographic column. It is clearly not proper to assume specificity simply because a chromatographic process is involved. For this study, the proposed method was challenged in three ways.

First, a literature search was conducted to determine the documented impurities and degradation products of the active drug saccharin. These compounds were subjected to the column under the assay conditions and were all innocuous to the assay. These compounds must be added directly to the sample solution so that possible matrix effects are eliminated.

Second, a forced degraded sample of the actual product was assayed for two reasons: (*a*) the actual decomposition products in the drug matrix may be different from those postulated in the literature and (*b*) interferences by degradation products of the excipients are possible. When the assay passes these conditions, it is more likely to prevail during the shelflife of the product.

Third, the forced degraded sample assay, whenever possible, should be compared with a completely independent assay based on different analytical principles. If possible, this reference method should be of demonstrated accuracy. When the results of the two methods agree within the expressed objectives, the method developer can be confident of the reliability of the new method. These three approaches are by no means completely rigorous but can be regarded as minimum criteria for a proposed stability-indicating method.

The general procedure given for other pharmaceutical preparations was applied to mouthwashes, analgesic liquids, and antidiarrhetics. Occasionally, such samples can be injected after dilution, addition of the internal standard, and clarification. Generally, however, ether extraction is required because of the low saccharin levels in the formulations. The ether extraction technique also is preferable because of the added selectivity of the extraction step and the extended column life resulting from injection of a cleaned-up sample solution.

Because of pharmaceutical formulation diversity, components other than saccharin are frequently extracted and the resulting chromatograms are less simple than those of the artificial sweetener. However, interferences often may be eliminated by proper pH and methanol adjustments in the eluent. The selectivity of the chromatographic process provides enough resolution so that the saccharin assay can be carried out in the presence of other ingredients such as salicylic acid and alkyl parabens. Injections can be made every 5 min, and about 30 samples of artificial sweetener can be analyzed per 8-hr day. Fewer samples of the other pharmaceutical formulations can be analyzed because of the lengthier sample-handling procedure, but this procedure is necessary for almost any technique.

In summary, this reversed-phase liquid chromatographic system provides a precise, accurate, and specific saccharin assay with high sample throughput. The procedure is applicable to a wide range of pharmaceuticals, especially for a stability-indicating program.

REFERENCES

(1) *Anal. Abstr.*, **26**, 3261 (June 1974).

(2) I. K. Shih and F. W. Teare, *Can. J. Pharm. Sci.*, **1**, 35 (1966).

(3) J. R. Markus, *J. Assoc. Off. Anal. Chem.*, **56**, 162 (1973).

(4) S. P. Mukherji, *Analyst*, **85**, 25 (1960).

(5) A. M. Lasheen, *Proc. Am. Soc. Hortic. Sci.*, **77**, 135 (1961).

(6) T. Korbelak, *J. Assoc. Off. Anal. Chem.*, **52**, 487 (1969).

(7) N. Hazemoto, N. Kamo, and Y. Kobatake, *ibid.*, **57**, 1205 (1974).

(8) H. Jacobson, *Ann. N.Y. Acad. Sci.*, **153**, 486 (1968).

(9) *Anal. Abstr.*, **30**, 6E43 (June 1976).

(10) *Ibid.*, **14**, 7864 (Dec. 1967).

(11) E. M. Ratchip and V. Viswanathan, *J. Pharm. Sci.*, **64**, 133 (1975).

(12) H. B. S. Conacher and R. C. O'Brien, *J. Assoc. Off. Anal. Chem.*, **54**, 1135 (1971).

(13) R. J. Daun, *ibid.*, **54**, 1140 (1971).

(14) R. Gerstl and K. Ranfft, *Z. Anal. Chem.*, **258**, 110 (1972).

(15) M. W. Couch, N. P. Das, K. N. Scott, C. M. Williams, and R. L. Foltz, *Biochem. Med.*, **8**, 362 (1973).

(16) J. J. Nelson, *J. Chromatogr. Sci.*, **11**, 28 (1973).

(17) D. S. Smyly, B. S. Woodward, and E. C. Conrad, *J. Assoc. Off. Anal. Chem.*, **59**, 14 (1976).

(18) B. Stavric, R. Lacombe, J. R. Watson, and I. C. Munro, *ibid.*, **57**, 678 (1974).

(19) R. E. King and J. S. Wragg, *J. Pharm. Pharmacol. Suppl.*, **18**, 22 (1966).

(20) M. N. Kazennova, *Optikomekh. Prom.* (12), 42 (1972); through *Anal. Abstr.*, **26**, 3261 (June 1974).

High-Performance Liquid Chromatographic Assay for the Anthelmintic Agent Mebendazole in Human Plasma

K. B. ALTON ˣ, J. E. PATRICK, and J. L. McGUIRE

Received June 30, 1976, from the *Drug Disposition Section, Ortho Pharmaceutical Corporation, Raritan, NJ 08869.* Accepted for publication January 16, 1979.

Abstract □ A rapid and specific high-performance liquid chromatographic (HPLC) assay for quantitative plasma mebendazole determination is described. After a simple extraction, the compound was analyzed by HPLC using a reversed-phase column and a UV detector (313 nm). Quantitation was accomplished using an internal standard; peak area ratios were determined with an integrating computer. The average mebendazole recovery over a concentration range of 0.01–0.20 μg/ml was 75.9 ± 3.8% *SD*, and the maximum assay sensitivity was ~10 ng/ml.

Keyphrases □ High-performance liquid chromatography—analysis, mebendazole in human plasma □ Mebendazole—analysis, high-performance liquid chromatography, in human plasma □ Anthelmintic agents—mebendazole, high-performance liquid chromatographic analysis in human plasma

Mebendazole[1] (I), methyl 5-benzoyl-2-benzimidazolecarbamate, is a broad spectrum anthelmintic agent (1–3). Initial absorption studies in humans (1) suggested that 6–10% of the radioactivity was recovered in the urine following 5–7 mg po of ^{14}C-mebendazole (18.5–22.7 μCi). Approximately 2.5% of this urinary radioactivity was unconjugated mebendazole, about 20% was the decarbamated metabolite, and 75% was of undetermined identity. Plasma radioactivity levels remained low throughout the study. There are no published methods sensitive enough to

[1] Vermox tablets, Ortho Pharmaceutical Corp.

0022-3549/79/0700-0880$01.00/0

© 1979, American Pharmaceutical Association

DISCUSSION

The artificial sweetener consists of saccharin sodium and sodium bicarbonate. Acetic acid in the eluent neutralizes both. Acetic acid in the eluent increases the retention (capacity factor) of saccharin by suppressing ionization and also results in a much sharper peak. If saccharin is allowed to elute in its ionic form, very little retention occurs and little use is made of the separating capabilities of the column.

Before an assay can be considered qualified for a stability-indicating program, its specificity characteristics must be proven. Specificity in this method is provided mainly by the liquid chromatographic column. It is clearly not proper to assume specificity simply because a chromatographic process is involved. For this study, the proposed method was challenged in three ways.

First, a literature search was conducted to determine the documented impurities and degradation products of the active drug saccharin. These compounds were subjected to the column under the assay conditions and were all innocuous to the assay. These compounds must be added directly to the sample solution so that possible matrix effects are eliminated.

Second, a forced degraded sample of the actual product was assayed for two reasons: (*a*) the actual decomposition products in the drug matrix may be different from those postulated in the literature and (*b*) interferences by degradation products of the excipients are possible. When the assay passes these conditions, it is more likely to prevail during the shelflife of the product.

Third, the forced degraded sample assay, whenever possible, should be compared with a completely independent assay based on different analytical principles. If possible, this reference method should be of demonstrated accuracy. When the results of the two methods agree within the expressed objectives, the method developer can be confident of the reliability of the new method. These three approaches are by no means completely rigorous but can be regarded as minimum criteria for a proposed stability-indicating method.

The general procedure given for other pharmaceutical preparations was applied to mouthwashes, analgesic liquids, and antidiarrhetics. Occasionally, such samples can be injected after dilution, addition of the internal standard, and clarification. Generally, however, ether extraction is required because of the low saccharin levels in the formulations. The ether extraction technique also is preferable because of the added selectivity of the extraction step and the extended column life resulting from injection of a cleaned-up sample solution.

Because of pharmaceutical formulation diversity, components other than saccharin are frequently extracted and the resulting chromatograms are less simple than those of the artificial sweetener. However, interferences often may be eliminated by proper pH and methanol adjustments in the eluent. The selectivity of the chromatographic process provides enough resolution so that the saccharin assay can be carried out in the presence of other ingredients such as salicylic acid and alkyl parabens. Injections can be made every 5 min, and about 30 samples of artificial sweetener can be analyzed per 8-hr day. Fewer samples of the other pharmaceutical formulations can be analyzed because of the lengthier sample-handling procedure, but this procedure is necessary for almost any technique.

In summary, this reversed-phase liquid chromatographic system provides a precise, accurate, and specific saccharin assay with high sample throughput. The procedure is applicable to a wide range of pharmaceuticals, especially for a stability-indicating program.

REFERENCES

(1) *Anal. Abstr.*, **26**, 3261 (June 1974).

(2) I. K. Shih and F. W. Teare, *Can. J. Pharm. Sci.*, **1**, 35 (1966).

(3) J. R. Markus, *J. Assoc. Off. Anal. Chem.*, **56**, 162 (1973).

(4) S. P. Mukherji, *Analyst*, **85**, 25 (1960).

(5) A. M. Lasheen, *Proc. Am. Soc. Hortic. Sci.*, **77**, 135 (1961).

(6) T. Korbelak, *J. Assoc. Off. Anal. Chem.*, **52**, 487 (1969).

(7) N. Hazemoto, N. Kamo, and Y. Kobatake, *ibid.*, **57**, 1205 (1974).

(8) H. Jacobson, *Ann. N.Y. Acad. Sci.*, **153**, 486 (1968).

(9) *Anal. Abstr.*, **30**, 6E43 (June 1976).

(10) *Ibid.*, **14**, 7864 (Dec. 1967).

(11) E. M. Ratchip and V. Viswanathan, *J. Pharm. Sci.*, **64**, 133 (1975).

(12) H. B. S. Conacher and R. C. O'Brien, *J. Assoc. Off. Anal. Chem.*, **54**, 1135 (1971).

(13) R. J. Daun, *ibid.*, **54**, 1140 (1971).

(14) R. Gerstl and K. Ranfft, *Z. Anal. Chem.*, **258**, 110 (1972).

(15) M. W. Couch, N. P. Das, K. N. Scott, C. M. Williams, and R. L. Foltz, *Biochem. Med.*, **8**, 362 (1973).

(16) J. J. Nelson, *J. Chromatogr. Sci.*, **11**, 28 (1973).

(17) D. S. Smyly, B. S. Woodward, and E. C. Conrad, *J. Assoc. Off. Anal. Chem.*, **59**, 14 (1976).

(18) B. Stavric, R. Lacombe, J. R. Watson, and I. C. Munro, *ibid.*, **57**, 678 (1974).

(19) R. E. King and J. S. Wragg, *J. Pharm. Pharmacol. Suppl.*, **18**, 22 (1966).

(20) M. N. Kazennova, *Optikomekh. Prom.* (12), 42 (1972); through *Anal. Abstr.*, **26**, 3261 (June 1974).

High-Performance Liquid Chromatographic Assay for the Anthelmintic Agent Mebendazole in Human Plasma

K. B. ALTON ˣ, J. E. PATRICK, and J. L. McGUIRE

Received June 30, 1976, from the *Drug Disposition Section, Ortho Pharmaceutical Corporation, Raritan, NJ 08869.* Accepted for publication January 16, 1979.

Abstract □ A rapid and specific high-performance liquid chromatographic (HPLC) assay for quantitative plasma mebendazole determination is described. After a simple extraction, the compound was analyzed by HPLC using a reversed-phase column and a UV detector (313 nm). Quantitation was accomplished using an internal standard; peak area ratios were determined with an integrating computer. The average mebendazole recovery over a concentration range of 0.01–0.20 μg/ml was 75.9 ± 3.8% *SD*, and the maximum assay sensitivity was ~10 ng/ml.

Keyphrases □ High-performance liquid chromatography—analysis, mebendazole in human plasma □ Mebendazole—analysis, high-performance liquid chromatography, in human plasma □ Anthelmintic agents—mebendazole, high-performance liquid chromatographic analysis in human plasma

Mebendazole[1] (I), methyl 5-benzoyl-2-benzimidazolecarbamate, is a broad spectrum anthelmintic agent (1–3). Initial absorption studies in humans (1) suggested that 6–10% of the radioactivity was recovered in the urine following 5–7 mg po of ^{14}C-mebendazole (18.5–22.7 μCi). Approximately 2.5% of this urinary radioactivity was unconjugated mebendazole, about 20% was the decarbamated metabolite, and 75% was of undetermined identity. Plasma radioactivity levels remained low throughout the study. There are no published methods sensitive enough to

[1] Vermox tablets, Ortho Pharmaceutical Corp.

0022-3549/79/0700-0880$01.00/0

© 1979, American Pharmaceutical Association

measure plasma levels of the parent compound following oral administration of mebendazole tablets.

This report describes a simple and specific high-performance liquid chromatographic (HPLC) method for the rapid determination of plasma mebendazole. This assay may have the sensitivity (~0.01 μg/ml) and precision needed to measure unchanged drug levels after chronic high-dose administration of mebendazole to patients being treated for *Echinococcus multilocularis* cysts.

EXPERIMENTAL

Apparatus—Analyses were performed on a liquid chromatograph[2] operated at ambient temperature and equipped with a differential UV (313 nm) detector[3]. Separations were performed on a 300 × 3.0-mm (i.d.) reversed-phase column[4]. Samples were introduced onto the column through a septumless injector[5] with a 25-μl syringe[6]. Chromatograms were traced on a strip-chart recorder[7], and peak area integration was performed by an integrating computer[8] interfaced with the detector by an analog–digital converter[9]. Analog signal modification to reduce noise from the UV detector was achieved with an electronic filter[10].

Reagents and Solvents—Mebendazole (I), three known human urinary metabolites of mebendazole [2-amino-5-benzoylbenzimidazole (II), 5-benzoyl-2-hydroxybenzimidazole (III), and methyl 5-(α-hydroxybenzyl)-2-benzimidazolecarbamate (IV)], and the internal standard methyl 5-(4-fluorobenzoyl)-2-benzimidazolecarbamate (V, flubendazole) were used as received[11]. All chemicals and reagents except acetonitrile[12] were reagent grade.

Chromatographic Conditions—The mobile phase was 0.05 *M* KH_2PO_4–NaOH buffer (pH 6.0)–acetonitrile (73:27 v/v), and the flow rate was adjusted to 2.5 ml/min (~2500 psi). The solvent mixture was prepared daily and degassed under reduced pressure before use. A stainless steel precolumn[13] (3 × 0.32 cm o.d.) was used to minimize the detrimental effect of any irreversibly adsorbed plasma-extracted material on the performance of the microparticulate reversed-phase column.

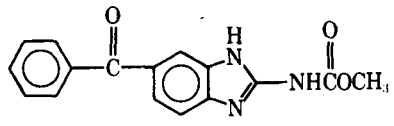

I

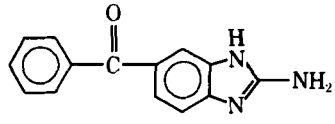

II

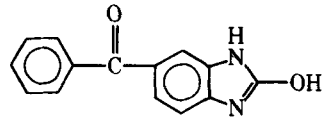

III

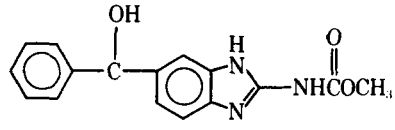

IV

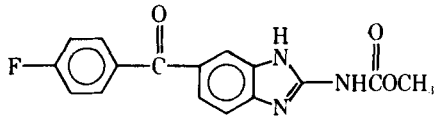

V

Table I—Recovery of Mebendazole from Human Plasma at Various Concentrations

Theoretical Plasma Concentration, μg/ml	Average Observed Plasma Concentration, μg/ml	*n*	Average Recovery[a], %
0.010	0.0757	7	75.7 ± 9.3
0.025	0.0187	6	74.9 ± 5.1
0.050	0.0389	9	77.9 ± 1.9
0.100	0.0754	13	75.4 ± 1.4
0.200	0.151	6	75.4 ± 1.5
		$\bar{x}$	75.9 ± 3.8[b]

[a] $\bar{x} \pm SD$. [b] $\overline{CV}$ = 5.09%.

Extraction Procedure—Aliquots (2.0 ml) of plasma were transferred to 15-ml test tubes (16 × 125 mm) fitted with polytef-lined screw caps, diluted with 2.0 ml of 0.05 *M* KH_2PO_4–NaOH buffer (pH 7.0), and extracted with 7.0 ml of ethyl acetate. The mixture was shaken vigorously, and the phases were separated by centrifugation (2 min at ~1500×*g*). The organic layer was removed with a Pasteur pipet and transferred to another 15-ml screw-capped tube. A second extraction was performed similarly. The ethyl acetate layers were pooled for each sample and taken to dryness under a nitrogen stream in a water bath (55°). An aliquot (2.0 ml) of 0.001 *N* HCl was added to the ethyl acetate residue and mixed with a vortex mixer. The hydrochloric acid solution was then extracted twice with 6.0 ml of petroleum ether (bp 30–60°) and centrifuged to obtain a clear supernate, and the upper layers were discarded after aspiration. The remaining aqueous fraction was alkalinized with 2.0 ml of 0.01 *N* NaOH, and this mixture was extracted twice with ethyl acetate.

The final residues were transferred with ethyl acetate to 2.5-ml glass conical centrifuge tubes and concentrated with two ethyl acetate washings under a nitrogen stream in a water bath (55°). The resulting residue was dissolved in 60 μl of ethyl acetate, and aliquots (20 μl) were injected onto the chromatograph for analyses.

Extraction Efficiency—Venous blood from several untreated volunteers was drawn into heparinized containers[14] and centrifuged to generate a plasma pool. The efficiency of extracting the drug from plasma was established using the following procedure. Known amounts of mebendazole and of the internal standard, flubendazole, both of which were dissolved in methanol–formic acid (described later), were added to drug-free plasma samples (15–25 ml each) to achieve mebendazole concentrations of 0.01, 0.025, 0.05, 0.10, and 0.20 μg/ml and a constant flubendazole concentration of 0.15 μg/ml for each sample. Aliquots (2.0 ml) of each plasma sample were transferred to 15-ml test tubes and stored frozen (−20°) until extracted as described.

All samples ($n \geq 6$) at each concentration were analyzed in duplicate. Mebendazole quantitation was accomplished by use of the described internal standard method.

Calibration and Standard Preparation—Mebendazole (25.0 mg) was dissolved in ~10 ml of formic acid (98%) and diluted to volume with methanol in a 25.0-ml volumetric flask to yield a concentration of 1.0 μg/μl. Three additional standard solutions containing 0.10, 0.01, and 0.001 μg/μl of mebendazole were prepared by serial dilution of the 1.0-μg/μl stock solution with methanol. Standard solutions of flubendazole (1.0, 0.1, and 0.01 μg/μl) were prepared in the same manner.

The internal standard method contained in the software section of the computer is predicated on a linear relationship between micrograms of mebendazole injected and the peak area ratio of mebendazole to the internal standard. Calibration solutions were prepared in the following manner. Aliquots (100, 71, 50, 33, and 25 μl) of the 0.1-μg/μl internal standard solution were transferred to glass vials and taken to dryness. These samples were diluted with 1.0 ml of the mebendazole standard solution (0.001 μg/μl) so that a constant amount of flubendazole (0.05 μg) and 0.005, 0.007, 0.01, 0.015, and 0.02 μg of mebendazole were delivered in 5, 7, 10, 15, and 20 μl of solution. The linearity of the calibration curve was initially evaluated by repeated ($n \geq 5$) injections of each solution. Thereafter, an average calibration response factor was established by the computer following triplicate injections (15 μl) of a calibration

[2] Model ALC 202/204, Waters Associates, Milford, Mass.
[3] Model 440, Waters Associates, Milford, Mass.
[4] μBondapak C-18, Waters Associates, Milford, Mass.
[5] Model U6K, Waters Associates, Milford, Mass.
[6] Pressure-Lok B-110, Precision Sampling Corp., Baton Rouge, La.
[7] Model 300, Linear Instruments, Irvine, Calif.
[8] Model 3352B, Hewlett-Packard, Avondale, Pa.
[9] Model 18652A, Hewlett-Packard, Avondale, Pa.
[10] Model 1021 A, Spectrum Scientific Corp., Newark, Del.
[11] Mebendazole, flubendazole, and metabolite standards were synthesized and supplied by Janssen Pharmaceutica, Beerse, Belgium.
[12] Glass distilled, Burdick & Jackson Laboratories, Muskegon, Mich.
[13] Packed with C-18 Corasil II, Waters Associates, Milford, Mass.
[14] Vacutainers, Becton Dickenson, Rutherford, N.J.

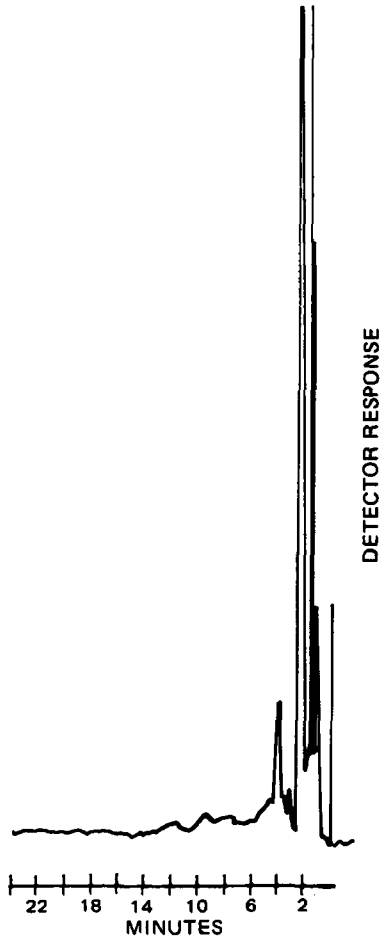

Figure 1—*Liquid chromatogram of an extract from drug-free plasma. The mobile phase consisted of 0.05 M KH_2PO_4–NaOH buffer (pH 6.0)–acetonitrile (73:27 v/v) with the flow rate adjusted to 2.5 ml/min.*

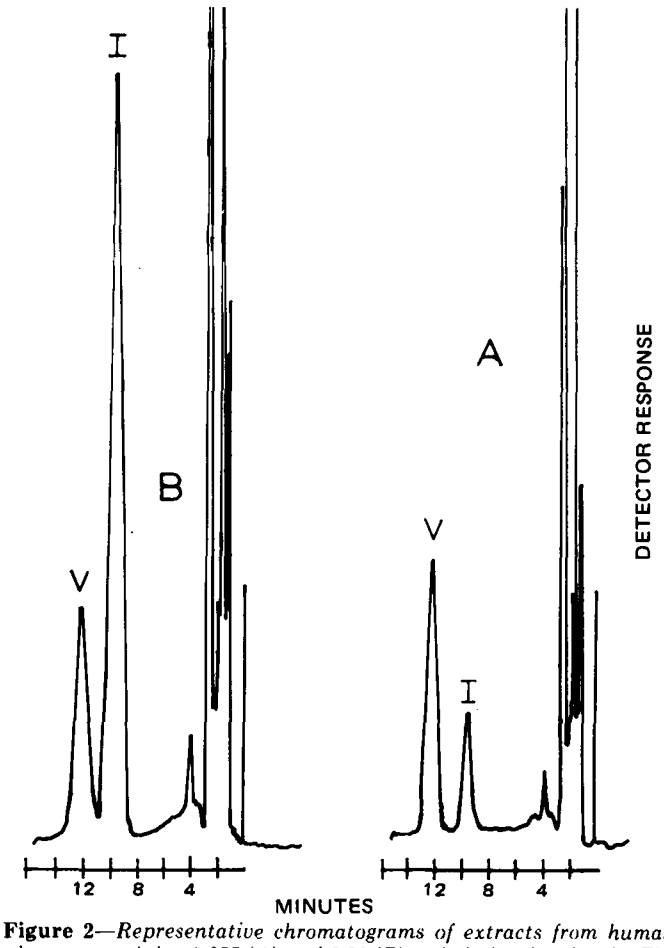

Figure 2—*Representative chromatograms of extracts from human plasma containing 0.025 (A) and 0.20 (B) μg/ml of mebendazole. The amount of the internal standard added to the plasma was 0.15 μg/ml. The detector response was at 0.005 aufs.*

solution containing 0.015 μg of mebendazole and 0.05 μg of the internal standard.

Specificity—Assay specificity was determined by injecting solutions of mebendazole (I) and its potential metabolites, II, III, and IV (~0.1 μg/μl in methanol), onto the HPLC column. A portion of an ethyl acetate extract (20 μl/60 μl) from a drug-free plasma sample also was chromatographically evaluated for the presence of any ethyl acetate-extractable, UV-absorbing (313 nm) material that might interfere with the measurement of mebendazole or flubendazole.

RESULTS AND DISCUSSION

The average drug recovery from plasma samples to which mebendazole had been added was 75.9 ± 3.8% *SD* (Table I) with an average precision (*CV*) of 5.09%. Linear regression analysis of percent recovery *versus* plasma concentration revealed no statistically significant ($p = 0.7143$) slope (β). One-way analysis of variance of the recovery data from each mebendazole concentration demonstrated no significant differences among the groups. These data suggest that extraction efficiencies are not concentration dependent over the investigated plasma drug range. The average internal standard recovery was 94.1 ± 2.88% *SD* with a coefficient of variation equal to 3.06%.

Even though the λ_{max} observed for mebendazole in methanol was 246 nm, detection at 313 nm was particularly advantageous since the ethyl acetate extracts from drug-free plasma were free of interfering UV-absorbing peaks (313 nm) (Fig. 1). Extraction of the acidified residue with petroleum ether aided in eliminating lipophilic material, which might otherwise become highly bound to the column and interfere with analyses.

Baseline resolution between mebendazole (I) and the internal standard, flubendazole (V), was achieved under the chromatographic conditions described. Compounds II, III, and IV, although not well separated from each other, were separated completely from I and V. The observed retention times (t_r) for I, II, III, IV, and V were 10.03, 5.61, 4.89, 4.89, and 12.64 min, respectively. Representative chromatograms of extracts from plasma containing 0.025 and 0.20 μg/ml of mebendazole are shown in Fig. 2.

Linear regression analysis of the curve described by plotting the area ratio (*y*-axis) of mebendazole over flubendazole *versus* micrograms of mebendazole injected (*x*-axis) demonstrated linearity ($r^2 = 0.9803$) over the concentration range evaluated (0.005–0.02 μg/injection). The slope of the line was calculated to be 21.908 μg^{-1}, and the *y*-intercept was calculated to be 0.021. The calculated *x*-intercept was equivalent to −0.96 ng of mebendazole/injection. This value was used as a background correction factor in mebendazole recovery calculations. Over a 2-month period of analyses, the slope of this line demonstrated little change ($CV = 4.8\%$, $n = 56$).

In summary, an assay was developed that can be used to measure plasma mebendazole levels as low as 0.01 μg/ml. The method is both rapid and specific, and its sensitivity indicates that it might be suitable for measuring unchanged drug levels after chronic administration of mebendazole tablets to patients being treated for *E. multilocularis* cysts.

REFERENCES

(1) J. P. Brugmans, D. Thienpont, I. Van Wijngaarden, O. F. Vanparijs, V. L. Schuermans, and H. L. Lauwers, *J. Am. Med. Assoc.*, **217**, 313 (1971).

(2) E. Fierlafijn, *Bruxelles-Med.*, **51**, 605 (1971).

(3) J. F. F. Callear and R. M. S. Neave, *Br. Vet. J.*, **127**, XLI (1971).

ACKNOWLEDGMENTS

The authors thank Dr. J. Heykants of Janssen Pharmaceutica, Beerse, Belgium, for providing samples of mebendazole, flubendazole, and metabolite standards. They also thank Mr. J. A. Shigo for technical assistance and Mr. R. Chen for statistical services.

Antitumor Agents XXXIV: Mechanism of Action of Bruceoside A and Brusatol on Nucleic Acid Metabolism of P-388 Lymphocytic Leukemia Cells

I. H. HALL ˣ, K. H. LEE, S. A. ElGEBALY, Y. IMAKURA, Y. SUMIDA, and R. Y. WU

Received October 13, 1978, from the *Division of Medicinal Chemistry, School of Pharmacy, University of North Carolina at Chapel Hill, Chapel Hill, NC 27514.* Accepted for publication January 8, 1979.

Abstract □ The quassinoids bruceantin, brucein D, brucein E, bruceoside A, and brusatol significantly inhibited P-388 lymphocytic leukemic cell RNA and protein synthesis in tissue culture. However, DNA synthesis inhibition seemed to correlate more directly with the antineoplastic activity of these compounds in the *in vivo* P-388 survival system. *In vitro*, brusatol and bruceoside A marginally inhibited 10-day P-388 lymphocytic leukemia DNA polymerase, RNA polymerase, thymidylate synthetase, dihydrofolate reductase, phosphoribosyl pyrophosphate aminotransferase, and cathepsin protease activities. *In vivo* studies demonstrated similar inhibition and elevated cyclic AMP levels, correlating positively with the antineoplastic activity of individual compounds. Purine synthesis was inhibited drastically by brusatol *in vivo*, and one key inhibition site in purine synthesis was at phosphoribosyl pyrophosphate aminotransferase, the regulatory enzyme. Histone phosphorylation and ribonucleotide reductase activity also were inhibited marginally by brusatol.

Keyphrases □ Antineoplastic agents—bruceoside A and brusatol, effect on cultured P-388 lymphocytic leukemia cell nucleic acid metabolism □ Quassinoids—antineoplastic activity, effect on cultured P-388 lymphocytic leukemia cell nucleic acid metabolism □ Leukemia, lymphocytic—*in vitro* P-388 cells, effect of quassinoids on nucleic acid metabolism □ Nucleic acid synthesis, tumor—effect of quassinoids on P-388 lymphocytic leukemia cells

The structure of bruceantin (I), a quassinoid isolated from *Brucea antidysenterica*, was elucidated previously (1). Subsequently, bruceantin was active at 1 mg/kg/day against P-388 lymphocytic leukemia (T/C = 197) and at 2 mg/kg/day against B16 melanoma (T/C = 178) in mice. Brucein D (II), brucein E (III), and bruceoside A (IV) were isolated from *Brucea javanica* and characterized by Lee *et al.* (2)[1].

Studies with HeLa cells (3) demonstrated that bruceantin inhibited protein synthesis >90% at 2 μM, whereas DNA synthesis was only inhibited ~60%. RNA synthesis was marginally inhibited (~15%). Protein synthesis was blocked 79% in rabbit reticulocytes by bruceantin at 0.1 mM during the initiation events of translocation. In *Saccharomyces cereviseae*, bruceantin did not inhibit the initiation event but blocked peptide bond formation during chain elongation by binding to the free ribosome P site, resulting in 90% inhibition at 0.01 mM (4).

This paper reports the effects of brusatol and bruceoside A on P-388 lymphocytic leukemia cell metabolism.

EXPERIMENTAL

Materials—Bruceantin (I) was obtained in small quantities from the National Cancer Institute. Brucein D (II), brucein E (III), and bruceoside A (IV) were extracted from *B. javanica* according to the exact literature technique (2), and brusatol (V) was obtained by treating bruceoside A with 3 N H_2SO_4–methanol (1:1) to hydrolyze the glycosidic linkage (2).

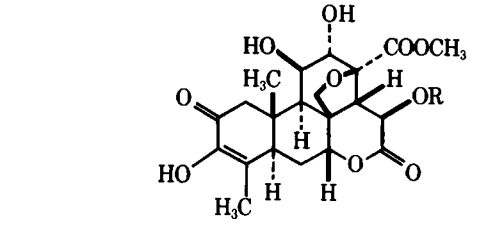

I: R = —COCH=C(CH$_3$)—CH(CH$_3$)$_2$

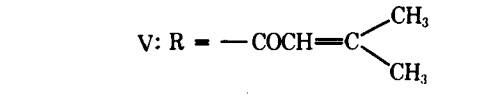

V: R = —COCH=C(CH$_3$)$_2$

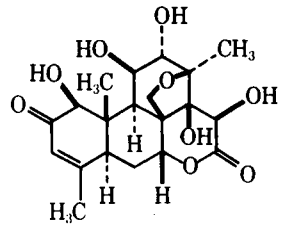

II: brucein D

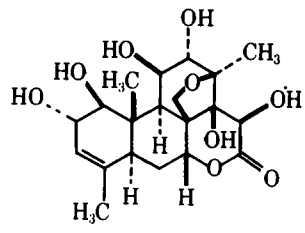

III: brucein E

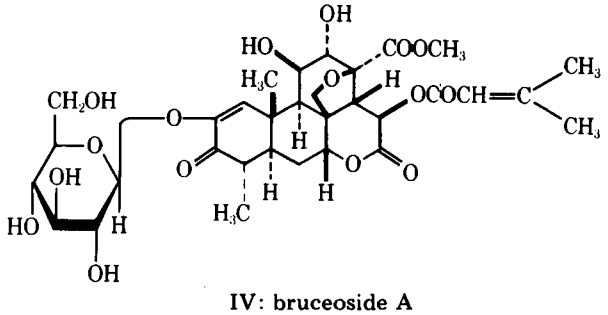

IV: bruceoside A

P-388 Lymphocytic Leukemia Antitumor Screen—DBA/2 male mice (~25 g) were administered 10^6 P-388 lymphocytic leukemia cells intraperitoneally on Day 0. Test compounds were homogenized in 0.05% polysorbate 80 and administered on Days 1–14 intraperitoneally. The average days survived for each group was determined, and T/C (treated/control) values were calculated (5). Fluorouracil was used as a positive standard.

P-388 Lymphocytic Leukemia Cell Metabolism Studies—DBA/2 male mice were innoculated with 10^6 P-388 lymphocytic leukemia cells on Day 0. On Days 7, 8, and 9, brusatol, 100 μg/kg/day, or bruceoside A, at 5 mg/kg/day, was administered intraperitoneally. On Day 10, P-388 cells were harvested from the peritoneal cavity. The number of tumor cells per milliliter and the 0.4% trypan blue uptake were determined with a hemocytometer (6). Thymidine incorporation into DNA was determined by a literature method (7). One hour prior to the animal's sacrifice, 10 μCi of [^{14}C-*methyl*]-thymidine (47.5 mCi/mmole) was injected intraperitoneally.

[1] See K. H. Lee, Y. Imakura, Y. Sumida, R. Y. Wu, I. H. Hall, and H. C. Huang, *J. Org. Chem.*, in press.

0022-3549/79/0700-0883$01.00/0
© 1979, American Pharmaceutical Association

Table I—P-388 Lymphocytic Leukemia Screen in DBA/2 Male Mice (~25 g)

Compound (n = 6)	Dose, μg/kg/day	Average Days Survived	T/C[a]
I[b]	1,000	22.7/11.5	197
	500	16.8/11.5	146
	250	15.0/11.5	130
	125	14.3/11.5	124
II	125	10.3/9.5	108
III	500[c]	8.5/9.5	89
	250	10.8/9.5	114
	125	10.8/9.5	114
IV	6,000	15.6/10.0	156
	250	11.5/9.5	121
	125	10.0/9.5	105
V	500[c]	12.5/9.5	132
	250	14.5/9.5	153
	125	15.0/9.5	158
Fluorouracil	25,000	19.7/10.6	186

[a] T/C ≥ 125 is required for significant activity. [b] Bruceantin was tested by the National Cancer Institute in CDF_1 mice. [c] Toxic at this dose.

The DNA was isolated, and the carbon-14 content was determined in two parts of toluene, one part of octoxynol, 0.4% 2,5-diphenyloxazole, and 0.01% 1,4-bis[2-(5-phenyloxazolyl)]benzene scintillation fluid and corrected for quenching. The DNA concentration was determined by UV spectrophotometry at 260 nm with calf thymus DNA as a standard. Uridine incorporation into RNA was determined in an analogous manner with 10 μCi of 5-^{3}H-uridine (24.2 Ci/mmole). RNA was extracted by a literature method (8). Leucine incorporation into protein was determined by the Sartorelli (9) method with 5 μCi of ^{14}C-leucine (54.4 Ci/mmole).

The P-388 tissue culture cells were maintained according to literature methods (10). Fetal calf serum (10%) was added to the medium 24 hr prior to studies. The P-388 cells were diluted to 1.6×10^6 cells/ml, and ^{14}C-thymidine (0.086 μCi), ^{3}H-uridine (0.08 μCi), or ^{14}C-leucine (0.0845 μCi) was added to 1 ml of cells (3). The synthesis rates, after 1 hr, of DNA, RNA, or protein were measured as the uptake of labeled precursors into cold trichloroacetic acid-insoluble material. DNA was collected on glass fiber paper (GF/F) by vacuum suction. RNA and protein were collected on nitrocellulose membrane filters.

The P-388 lymphocytic cells from 10-day DBA/2 mice also were collected for *in vitro* studies. The drug effects on the transport of precursor radiolabeled thymidine, uridine, or leucine across membranes were determined using whole cells and cell homogenates. Labeled macromolecules were collected on the appropriate filters after 1 hr of incubation (3).

In the *in vitro* studies, bruceantin and bruceoside A were present at 0.015 m*M* concentrations and brusatol was present at 0.015 and 0.005 m*M* final concentrations.

Emzymatic Studies—Nuclear DNA polymerase activity was determined on isolated P-388 lymphocytic leukemia cell nuclei (11). The incubation medium was that of Sawada *et al.* (12), except that 2-^{14}C-deoxyribothymidine triphosphate (45 mCi/mmole) was used; the insoluble nucleic acids were collected on glass fiber paper (GF/F). Messenger RNA polymerase activity was measured by literature methods (13, 14) with 5,6-^{3}H-uridine 5′-triphosphate (35 Ci/mmole). Insoluble RNA was collected on nitrocellulose filters.

Deoxythymidine kinase, deoxythymidylate monophosphate kinase, and deoxythymidylate diphosphate kinase activities were measured by a literature method (15) based on the disappearance of 0.1 μmole of reduced nadide (nicotinamide adenine dinucleotide) at 340 nm in 2 min. Thymidylate synthetase activity was assayed by a literature method (16), utilizing a postmitochondrial (9000×*g* for 10 min) supernate and 5 μCi of 5′-^{3}H-deoxyuridine monophosphate (11 Ci/mmole). Dihydrofolate reductase activity was determined by a literature method (17) based on the disappearance of 0.1 μmole of reduced nadide phosphate at 340 nm for 1 hr. *S*-Adenosylmethionine transferase activity was determined by a literature method (18) with 0.05 μCi of $^{14}CH_3$-*S*-adenosyl-L-methionine (53 mCi/mmole).

Ribonucleotide reductase activity was determined by the method of Moore and Hurlbert (19). Deoxyribonucleotides were separated from ribonucleotides by poly(ethyleneimine) cellulose TLC (20). ^{14}C-Formate incorporation into purines was measured by a reported method (21), using 0.5 μCi of ^{14}C-formic acid (4.95 mCi/mmole). Purine separation was carried out on silica gel TLC plates eluted with *n*-butanol–acetic acid–water (4:1:5). The plates were scraped and radioactivity was determined.

Table II—Relative Incorporation of Radiolabeled Precursors into P-388 Tissue Culture Cells during 1 hr with the Incubation Test Drugs (0.015 m*M*)

Compound	Percent Control (dpm)		
	^{14}C-Thymidine Incorporation into DNA	^{3}H-Uridine Incorporation into RNA	^{14}C-Leucine Incorporation into Protein
I (0.015 m*M*)	63 ± 7[a]	68 ± 9[b]	38 ± 5[a]
II (0.015 m*M*)	81 ± 5	45 ± 5[a]	26 ± 9[a]
III (0.015 m*M*)	76 ± 8	43 ± 3[a]	35 ± 13[a]
IV (0.015 m*M*)	67 ± 9[a]	45 ± 5[a]	35 ± 15[a]
V (0.015 m*M*)	16 ± 9[a]	38 ± 3[a]	14 ± 8[a]
0.05% Polysorbate 80	100 ± 7	100 ± 3	100 ± 14

[a] $p = 0.001$. [b] $p = 0.005$.

Phosphoribosyl pyrophosphate aminotransferase activity was determined by a method (22) based on the reduction of 0.6 μmole of nadide at 340 nm for 30 min.

Carbamyl phosphate synthetase activity was determined with ornithine and ornithine transcarbamylase present by the method of Kalman *et al.* (23). The colorimetric determination of citrulline was performed according to the Archibald method (24). Aspartate carbamyl transferase activity was carried out by a literature method (23) in the presence of aspartate transcarbamylase. The colorimetric determination of carbamyl aspartate was carried out according to a literature method (25).

To determine if purine synthesis inhibition was the reason for decreased ^{14}C-thymidine incorporation into DNA, P-388 lymphocytic leukemia cells were incubated *in vitro* with 0.05 μCi of [^{14}C-*methyl*]-thymidine and deoxyguanosine triphosphate, deoxycytosine triphosphate, and deoxyadenosine triphosphate in buffer for 1 hr. A second experiment was performed after dosing with brusatol on Days 7, 8, and 9 at 100 μg/kg/day to determine if the actual purine content had been altered *in vivo*. Purines were extracted (21) and determined by UV analysis at 258 nm.

Histone phosphorylation was determined by injecting intraperitoneally 10 μCi of γ-^{32}P-adenosine triphosphate (18.8 Ci/mmole). The nuclei were isolated 1 hr later, and the histone chromatin protein was extracted by a literature method (26). Nonhistone chromatin phosphorylation by nuclei protein kinase was determined on isolated nuclei (11), utilizing 2 nmoles of γ-^{32}P-adenosine triphosphate. Chromatin protein was collected on nitrocellulose membrane filters (27).

Cyclic AMP levels were determined by a literature method (28) with the ^{3}H(G)-adenosine 3′,5′-cyclic phosphate (39.8 Ci/mmole) radioimmunoassay. The drug effect on hydrolytic enzymatic activity was measured also. Deoxyribonuclease activity was measured at pH 5.0 by a modification of the deDuve method (29). Ribonuclease activity and acid cathepsin activity were determined at pH 5.0 by a literature method (30).

In vitro UV binding studies (6) were conducted with brusatol or bruceoside A (7.8 μg/ml) with DNA or deoxyguanosine monophosphate (38 μg/ml) in 0.1 *M* phosphate buffer, pH 7.2, over 200–340 nm for 24 hr. Protein concentration was determined by the method of Lowry *et al.* (31).

RESULTS

Bruceantin was active against the P-388 lymphocytic leukemia cell survival system in the 250–1000-μg/kg/day range. Brucein D and brucein E were inactive. Bruceoside A was active against the P-388 survival system at 6 mg/kg/day, and brusatol was active at 125–500 μg/kg/day (Table I). Incorporation of radiolabeled precursors into P-388 tissue culture cell macromolecules showed that thymidine, uridine, and leucine were incorporated at the rates of 5559, 3381, and 1646 dpm/10^6 cells, respectively, for the control.

All five compounds reduced protein and RNA syntheses significantly at 0.015 m*M* (Table II). Brusatol caused the highest inhibition, resulting in 86% suppression of protein synthesis and 62% suppression of RNA synthesis of P-388 lymphocytic leukemia tissue culture cells. DNA synthesis was inhibited 37% by bruceantin, 19% by brucein D, 24% by brucein E, 33% by bruceoside A, and 84% by brusatol at 0.15 m*M*. Since brucein D and brucein E were inactive in the P-388 lymphocytic leukemia survival system, it appeared that suppression of RNA and protein was not the critical event resulting in tumor cell death. DNA synthesis inhibition appeared to correlate more directly with antitumor activity. For this reason, it was decided to examine specific events in DNA synthesis.

Table III—*In Vitro* Effect of Brusatol (0.005 m*M*) and Bruceantin (0.015 m*M*) on Whole Cells and Homogenates of 10-Day P-388 Lymphocytic Leukemia Cells (n = 5)

	Whole Cells			Homogenized		
	Control	Brusatol[a]	Bruceantin[a]	Control	Brusatol[a]	Bruceantin[a]
Thymidine incorporation into DNA	100 ± 12	62 ± 5[b]	63 ± 7[b]	100 ± 9	46 ± 7[b]	50 ± 8[b]
Uridine incorporation into RNA	100 ± 15	56 ± 7[b]	68 ± 9[c]	100 ± 8	55 ± 5[b]	—
Leucine incorporation into protein	100 ± 14	40 ± 6[b]	38 ± 5[b]	100 ± 5	25 ± 3[b]	33 ± 4[b]
Thymidine incorporation in presence of deoxyriboguanine, cytosine, and adenosine triphosphates	—	—	—	100 ± 11	86 ± 10	—

[a] Percent of control. [b] p = 0.001. [c] p = 0.005.

Table IV—*In Vitro* Effects of Test Drugs on 10-Day P-388 Lymphocytic Leukemia Cell Metabolism of DBA/2 Mice at 0.015 *M* Final Concentration

	Percent Control					
Enzyme Assayed	Control	Bruceantin	Brucein D	Brucein E	Bruceoside A	Brusatol
Thymidine kinase	100 ± 5	—	—	—	104 ± 5	107 ± 6
Thymidylate monophosphate kinase	100 ± 4	—	102 ± 5	97 ± 5	105 ± 11	106 ± 5
Thymidylate diphosphate kinase	100 ± 5	—	95 ± 7	93 ± 8	98 ± 7	97 ± 4
DNA polymerase	100 ± 10	—	105 ± 17	88 ± 12	85 ± 10	79 ± 3[a]
Thymidylate synthetase	100 ± 6	—	103 ± 10	99 ± 13	87 ± 6[b]	68 ± 18[c]
Dihydrofolate reductase	100 ± 12	—	73 ± 18[b]	75 ± 15[b]	69 ± 17[c]	64 ± 11[d]
Deoxyribonuclease	100 ± 3	—	81 ± 5[d]	42 ± 4[d]	100 ± 3	99 ± 5
Ribonuclease	100 ± 9	—	55 ± 8[d]	63 ± 7[d]	96 ± 9	73 ± 6[d]
Cathepsin	100 ± 21	—	6 ± 3[d]	18 ± 5[d]	7 ± 6[d]	38 ± 13[d]
RNA polymerase	100 ± 18	—	—	83 ± 15	68 ± 12[b]	88 ± 17
Phosphoribosyl pyrophosphate aminotransferase	100 ± 8	96 ± 4	103 ± 9	104 ± 13	100 ± 8	61 ± 7[d]

[a] p = 0.005. [b] p = 0.025. [c] p = 0.010. [d] p = 0.001.

Whole cells harvested from 10-day P-388 lymphocytic leukemia-bearing mice and cells homogenized four times showed that brusatol at 0.005 m*M* and bruceantin at 0.015 m*M* did not retard ^{14}C-thymidine transport across the tumor membrane. In fact, both brusatol and bruceantin were more effective inhibitors of protein and DNA syntheses in homogenates (Table III). Untreated 10-day P-388 lymphocytic leukemia cells demonstrated changes in absorbance of 0.500 optical density (O.D.) unit/min/mg of protein for thymidine kinase activity, of 0.489 O.D. unit/min/mg of protein for thymidylate monophosphate kinase activity, and of 0.566 O.D. unit/min/mg of protein for thymidylate diphosphate kinase activity. Compounds II–V at 0.015 m*M* had no effect on the nucleotide kinases tested (Table IV). DNA polymerase activity for 10-day P-388 cells was 27,368 dpm/mg of nuclear protein. Brusatol caused 21% inhibition of polymerase activity. Thymidylate synthetase activity in 10-day P-388 cells was 1,645,840 dpm/mg of protein, which brusatol reduced 32%. Dihydrofolate reductase activity for 10-day P-388 cells was 2192 O.D. units/hr/mg of protein. At 0.015 m*M*, dihydrofolate reductase activity was reduced 27% by brucein D, 25% by brucein E, 31% by bruceoside A, and 36% by brusatol. At 0.005 m*M*, brusatol and methotrexate reduced dihydrofolate reductase activity by 28 and 59%, respectively.

Hydrolytic enzymatic activity was not increased due to the drugs; therefore, increased hydrolytic activity of deoxyribonuclease, ribonuclease, or cathepsin protease could not account for the reduction of radiolabeled precursors into macromolecules of P-388 cells. Deoxyribonuclease activity for 10-day cells was 1.718 μg of DNA hydrolyzed/min/mg of protein. Brucein D reduced the activity by 19% and brucein E reduced it by 58%. Ribonuclease activity for 10-day P-388 cells was 7.236 μg of RNA hydrolyzed/min/mg of protein. Brucein D reduced the activity by 45%, brucein E by 37%, and brusatol by 27%. Cathepsin activity for 10-day P-388 cells was 65.7 μg of azocasein hydrolyzed/min/mg of protein, which was suppressed significantly by brusatol, bruceoside A, brucein D, and brucein E.

In vitro messenger RNA polymerase activity also was measured in 10-day P-388 cells and was 76,088 dpm/mg of protein. The presence of brucein E reduced RNA polymerase activity by 17%; bruceoside A and brusatol reduced it by 32 and 12%, respectively. Phosphoribosyl pyrophosphate aminotransferase was inhibited by brusatol by 39%.

In the *in vivo* experiments, DBA/2 mice were treated with brusatol and bruceoside A on Days 7, 8, and 9 and the cells were harvested on Day 10. ^{14}C-Thymidine incorporation into DNA for the control was 75,098 dpm/mg of DNA, which was reduced 77% by brusatol and 48% by bruceoside A (Table V). ^{3}H-Uridine incorporation into RNA for the control was 386,004 dpm/mg of RNA, which was reduced 68% by brusatol and 55% by bruceoside A. ^{14}C-Leucine incorporation for the control was 22,666 dpm/mg of protein, which was reduced 86% by brusatol and 41% by bruceoside A. The number of tumor cells at Day 10 for the control was 142 × 10^6 cells/ml, which was reduced 79% by brusatol and 65% by bruceoside A after 3 days of administration.

Cyclic AMP in the control animals was 1.01 pmoles/10^6 P-388 cells. *In vivo* brusatol treatment increased cyclic AMP to 12.69 pmoles/10^6 cells. A single dose of brusatol (100 μg/kg) on Day 10 increased cyclic AMP by 167% after 1 hr. Bruceoside A for 3 days increased cyclic AMP only to 2.74 pmoles/10^6 cells. Bruceantin caused an increase to 5.49 pmoles of cyclic AMP/10^6 cells. Histone phosphorylation by ATP for the 10-day P-388 cells was 241 cpm/mg of protein, which was reduced 36% by brusatol. Nonhistone phosphorylation for the 10-day P-388 cells was 6246 cpm/mg of protein, which was reduced 8% by brusatol.

^{14}C-Formate incorporation into purine for the 10-day P-388 cells was 19,807 dpm/mg of protein. Brusatol treatment reduced purine synthesis 50%, whereas bruceoside A reduced it only 4%. Phosphoribosyl pyrophosphate aminotransferase activity for the 10-day P-388 cells was 0.285 O.D. unit/min/mg of protein, which was reduced 43% by brusatol. Carbamyl phosphate synthetase activity for 10-day P-388 cells was 1.8 mg of carbamyl phosphate formed/hr/mg of protein, which was unaffected by brusatol. Aspartate carbamyl transferase activity for 10-day P-388 cells was 44.4 mg of carbamyl aspartate formed/hr/mg of protein, which was reduced 7% by brusatol.

In vivo dihydrofolate reductase activity was reduced 30% by brusatol. Ribonucleotide reductase activity of 10-day P-388 cells was 517,053 dpm/mg of protein, which was reduced 14% by brusatol. *S*-Adenosyl-L-methionine transferase activity of 10-day P-388 cells was 251 dpm/mg of protein, which was unaffected by brusatol. Purine and pyrimidine base concentration after 3 days of brusatol treatment was reduced 17%. *In vitro* incorporation of ^{14}C-thymidine into DNA of 10-day P-388 cells in the presence of deoxyguanosine triphosphate, deoxyadenosine triphosphate, deoxycytidine triphosphate, and 0.005 *M* brusatol was inhibited only 14% (Table III). *In vivo* DNA polymerase activity was inhibited 16% by brusatol.

UV spectral studies demonstrated that brusatol had absorption peaks at 219 and 279 nm. Bruceoside A had an absorption peak at 270 nm. DNA had absorption peaks at 260 and 220 nm. Deoxyguanosine monophosphate had absorption peaks at 270 and 253 nm. Since these spectra overlapped, it was difficult to determine if binding occurred between nucleotides and drugs. However, when the drug was present, the absorption was higher for DNA and for deoxyguanosine monophosphate than would be expected for two single species in solution. The areas under the curves indicated that a combination of brusatol and DNA resulted in a 29% higher absorption than the calculated absorbances of both species added together. Brusatol and deoxyguanosine monophosphate combinations resulted in a 40% higher absorbance than the calculated

Table V—*In Vivo* Effects of Brusatol and Bruceoside A on P-388 Lymphocytic Leukemia Cell Metabolism of DBA/2 Mice ($n = 6$)

	Control	Percent Control: Brutasol, 100 μg/kg/day	Percent Control: Bruceoside A, 5 mg/kg/day
^{14}C-Thymidine incorporation into DNA	100 ± 17	23 ± 15[a]	52 ± 7[a]
^{3}H-Uridine incorporation into RNA	100 ± 16	32 ± 11[a]	45 ± 10[a]
^{14}C-Leucine incorporation into protein	100 ± 26	14 ± 2[a]	59 ± 21[b]
Number of tumor cells × 10^6/ml	100 ± 6	21 ± 5[a]	35 ± 9[a]
3′,5′-Cyclic adenosine monophosphate levels	100 ± 8	1269 ± 60[a]	271 ± 2[a]
γ-^{32}P-Adenosine triphosphate incorporation into histone proteins	100 ± 20	64 ± 17[b]	—
γ-^{32}P-Adenosine triphosphate incorporation into nonhistone proteins	100 ± 11	92 ± 27	99 ± 10
^{14}C-Formate incorporation into purines	100 ± 10	50 ± 12[a]	96 ± 24
Phosphoribosyl pyrophosphate aminotransferase activity	100 ± 12	57 ± 11[a]	—
Carbamyl phosphate synthetase activity	100 ± 7	107 ± 6	—
Aspartate carbamyl transferase activity	100 ± 5	93 ± 16	—
Dihydrofolate reductase activity	100 ± 12	70 ± 11[c]	—
Deoxynucleic acid polymerase activity	100 ± 7	84 ± 5[c]	—
Ribonucleotide reductase activity	100 ± 5	86 ± 3[a]	—
S-Adenosyl-L-methionine transferase activity	100 ± 10	100 ± 13	—
Purine concentration	100 ± 3	83 ± 2[a]	—

[a] $p = 0.001$. [b] $p = 0.025$. [c] $p = 0.005$.

absorbances. With DNA and deoxyguanosine monophosphate, bruceoside A likewise showed 73 and 18% higher absorbances, respectively, than the calculated absorbances of both species added together.

The Student t test was used to calculate the probable (p) significant difference in Tables II–V. Data are expressed as percent of control of the average mean and standard deviation; n equals the number of animals per group.

DISCUSSION

The effects of five quassinoids on P-388 lymphocytic leukemia metabolism are diverse. Although bruceantin, brucein D, brucein E, bruceoside A, and brusatol cause drastic inhibition of protein and RNA synthesis of cultured P-388 leukemic cells, these effects could not be correlated directly with cell death. Of these agents, Liao *et al.* (3) observed that compounds that did not contain the quassinoid ester side chain caused less protein synthesis reduction in HeLa cells and rabbit reticulocytes. These investigators postulated that the ester side chain at C-15 was necessary for drug transport across the cell membrane. Studies with P-388 cells do not support this postulate; brucein D and brucein E both inhibited protein synthesis. Actually the P-388 tumor cell membrane appears to retard transport of brusatol and bruceantin into the cell.

The inhibition of DNA synthesis showed the strongest correlation with antitumor activity in the P-388 lymphocytic leukemia survival system. DNA template activity, as observed through DNA polymerase activity, both *in vitro* and *in vivo* and RNA polymerase activity *in vitro* were inhibited marginally by the quassinoids. The nucleotide UV spectral studies showed absorbance increases in the presence of brusatol or bruceoside A above the calculated absorbance of the two individual species in solution, which may reflect partial or limited drug binding to the template and suppression of polymerase template activity. *In vitro* thymidylate synthetase inhibition correlated with antitumor activity for the quassinoids. Dihydrofolate reductase also was inhibited marginally by the quassinoids, with brusatol having the most activity. However, brusatol was only one-half as active as methotrexate at the same concentration. The nucleotide kinases did not appear to be a site of metabolism inhibition by the quassinoids.

In vivo quassinoid effects on P-388 lymphocytic leukemia cells at Day 10 were similar to the effects on DNA, RNA, and protein syntheses after 3 days of dosing. Brusatol required a dose of 100 μg/kg/day to bring about the same magnitude of inhibition as an *in vitro* concentration of 0.015 mM, whereas bruceoside A required a dose of 5 mg/kg/day. The *in vivo* doses correlated positively with doses required for antineoplastic activity in the P-388 survival system. The observation that brusatol was more active *in vivo* than bruceoside A raised the question whether brusatol is bioactivated *in vivo* to the active species, which is not fully seen in the *in vitro* studies.

Elevated cyclic AMP levels correlated with antineoplastic activity, brusatol > bruceantin > bruceoside A. Elevated levels of cyclic AMP reverse malignant states to a more normal cell (33, 34) and are correlated with less phosphorylation of the regulatory H-1 histone fraction, thereby reducing cell proliferation (35). Brusatol treatment moderately reduced histone phosphorylation, whereas nonhistone phosphorylation was unaffected. Cancer cells are also known to have a high proteolytic activity on the membrane surface. The quassinoids effectively blocked P-388 cathepsin proteolytic activity. Purine synthesis was significantly inhibited by brusatol but not by bruceoside A. The regulatory enzyme of purine synthesis, phosphoribosyl pyrophosphate aminotransferase, was a major site of brusatol inhibition. The enzyme was less affected by brusatol *in vitro* at 0.015 mM, again possibly indicating *in vivo* drug bioactivation.

Early steps in pyrimidine synthesis were not affected by brusatol. One carbon transfer from *S*-adenosyl-L-methionine also was unaffected by brusatol. Purine in the P-388 cells after 3 days of treatment also was reduced. A drastic purine reduction was not seen, which may have been due to the salvage pathway of purine from already synthesized nucleic acid. When DNA polymerase was assayed in the presence of added triphosphate deoxyribonucleotide, only marginal inhibition by brusatol *in vitro* was observed. One means of determining if the lack of purine for DNA synthesis was the prime factor in inhibition of ^{14}C-thymidine incorporation was to add nucleotide to the medium. In the presence of ample purine and pyrimidine, thymidine incorporation was inhibited only 14%, which probably reflects brusatol inhibition of DNA polymerase. Lack of purine would also explain the reduction in RNA synthesis. The reduction of ribose to deoxyribose nucleotide also was marginally inhibited in brusatol.

From these studies, it can be concluded that brusatol and bruceoside A have multiple sites of action on P-388 lymphocytic cells. Brusatol appeared to be more potent and effectively blocked a number of metabolic sites necessary for nucleic acid synthesis. Quassinoid effects on protein synthesis are currently being investigated. Preliminary data support the observation of Fresno *et al.* (4) that the elongation process of protein synthesis is the site of brusatol and bruceoside A inhibition.

REFERENCES

(1) S. M. Kupchan, R. W. Britton, J. A. Lacadie, M. F. Ziegler, and C. W. Sigel, *J. Org. Chem.*, **40**, 648 (1975).

(2) K. H. Lee, Y. Imakura, and H. C. Huang, *J. Chem. Soc. Chem. Commun.*, **1977**, 69.

(3) L.-L. Liao, S. M. Kupchan, and S. B. Howitz, *Mol. Pharmacol.*, **12**, 167 (1976).

(4) M. Fresno, A. Gonales, D. Vazquez, and A. Jimenez, *Biochim. Biophys. Acta*, **518**, 104 (1978).

(5) R. I. Geran, N. H. Greenberg, M. M. MacDonald, A. M. Schumacher, and B. J. Abbott, *Cancer Chemother. Rep.*, **3**, 9 (1972).

(6) I. H. Hall, K. H. Lee, E. C. Mar, C. O. Starnes, and T. G. Waddell, *J. Med. Chem.*, **20**, 333 (1977).

(7) C. B. Chae, J. L. Irvin, and C. Piantadosi, *Proc. Am. Assoc. Cancer Res.*, **9**, 44 (1968).

(8) R. G. Wilson, R. H. Bodner, and G. E. MacHorter, *Biochim. Biophys. Acta*, **378**, 260 (1975).

(9) A. C. Sartorelli, *Biochem. Biophys. Res. Commun.*, **27**, 26 (1967).

(10) J. L. Toohey, *Proc. Natl. Acad. Sci. USA*, **72**, 73 (1975).

(11) W. C. Hymer and E. L. Kuff, *J. Histochem. Cytochem.*, **12**, 359 (1964).

(12) H. Sawada, K. Tatsumi, M. Sasada, S. Shirakawa, T. Nakumura,

and G. Wakisaka, *Cancer Res.*, **34**, 3341 (1974).
(13) K. M. Anderson, I. S. Mendelson, and G. Guzik, *Biochim. Biophys. Acta*, **383**, 56 (1975).
(14) I. H. Hall, G. L. Carlson, G. S. Abernethy, and C. Piantadosi, *J. Med. Chem.*, **17**, 1253 (1974).
(15) F. Maley and S. Ochoa, *J. Biol. Chem.*, **233**, 1538 (1958).
(16) A. Kampf, R. L. Barfknecht, P. J. Schaffer, S. Osaki, and M. P. Mertes, *J. Med. Chem.*, **19**, 903 (1976).
(17) M. K. Ho, T. Hakalo, and S. F. Zakrzwski, *Cancer Res.*, **32**, 1023 (1972).
(18) R. T. Borchardt, J. A. Huber, and Y. S. Wu, *J. Med. Chem.*, **19**, 1094 (1976).
(19) E. C. Moore and R. B. Hurlbert, *J. Biol. Chem.*, **241**, 4802 (1966).
(20) K. Randerath, *Biochim. Biophys. Acta*, **76**, 622 (1963).
(21) M. K. Spassova, G. C. Russev, and E. V. Golovinsky, *Biochem. Pharmacol.*, **25**, 923 (1976).
(22) J. B. Wyngaarden and D. M. Ashton, *J. Biol. Chem.*, **234**, 1492 (1959).
(23) S. M. Kalman, P. H. Duffield, and T. Brzozowski, *Am. Biol. Chem.*, **24**, 1871 (1966).
(24) R. M. Archibald, *J. Biol. Chem.*, **156**, 121 (1944).
(25) S. B. Koritz and P. P. Cohen, *ibid.*, **209**, 145 (1954).
(26) A. Raineri, R. C. Simsiman, and R. K. Boutwell, *Cancer Res.*, **33**, 134 (1973).
(27) Y. M. Kish and L. J. Kleinsmith, *Methods Enzymol.*, **40**, 201 (1975).
(28) A. C. Gilman, *Proc. Natl. Acad. Sci., USA*, **67**, 305 (1970).
(29) I. H. Hall, K. S. Ishaq, and C. Piantadosi, *J. Pharm. Sci.*, **63**, 625 (1974).
(30) Y. S. Cho-Chung and P. M. Gullino, *J. Biol. Chem.*, **248**, 4743 (1973).
(31) O. H. Lowry, N. J. Rosebrough, A. L. Farr, and R. J. Randall, *ibid.*, **193**, 265 (1951).
(32) G. W. Snedecor, "Statistical Methods," Iowa State College Press, Ames, Iowa, 1956, sec. 2.
(33) T. Posternak, *Annu. Rev. Pharmacol.*, **14**, 23 (1974).
(34) Y. S. Cho-Chung and P. M. Gullino, *Science*, **183**, 87 (1974).
(35) C. S. Rubin and O. M. Roseau, *Annu. Rev. Biochem.*, **44**, 81 (1975).

ACKNOWLEDGMENTS

Adapted in part from a dissertation submitted by S. A. ElGebaly to the Graduate School, University of North Carolina at Chapel Hill, in partial fulfillment of the Doctor of Philosophy requirements.

Supported by American Cancer Society Grant CH-19 and National Cancer Institute Grant CA-22929 to K. H. Lee.

The authors thank Dr. Matthew Suffness, Plant and Animal Product Section, National Cancer Institute, for the bruceantin.

Antitumor Agents XXXV: Effects of Brusatol, Bruceoside A, and Bruceantin on P-388 Lymphocytic Leukemia Cell Respiration

S. A. ElGEBALY, I. H. HALL ˣ, K. H. LEE, Y. SUMIDA, Y. IMAKURA, and R. Y. WU

Received October 28, 1978, from the *Division of Medicinal Chemistry, School of Pharmacy, University of North Carolina at Chapel Hill, Chapel Hill, NC 27514.* Accepted for publication January 9, 1979.

Abstract □ Brusatol, a quassinoid with potent antineoplastic activity against P-388 lymphocytic leukemia cell proliferation, significantly inhibited P-388 cell hexokinase, phosphofructokinase, malic dehydrogenase, and succinic dehydrogenase. Mitochondrial oxidative phosphorylation, basal, and adenosine diphosphate-stimulated respiration, utilizing succinate and α-ketoglutarate as the substrate, was suppressed significantly by *in vivo* treatment with brusatol. However, brusatol treatment had no effect on liver oxidative phosphorylation. Brusatol greatly increased P-388 cyclic AMP levels but had no effect on liver cyclic nucleotides. Similar inhibitory effects on P-388 cell oxidative phosphorylation were found *in vitro* with brusatol, bruceoside A, and bruceantin. Brusatol had no effect on adenosine triphosphatase activity or on uncoupling of oxidative phosphorylation. Rather, brusatol appeared to increase the concentration of reduced mitochondrial electron-transport cofactors, thereby blocking aerobic respiration. A proposed mechanism of action is discussed.

Keyphrases □ Antineoplastic agents—brusatol, bruceoside A, bruceantin, effect on cellular respiration of P-388 leukemia cells, *in vivo, in vitro* □ Quassinoids—antineoplastic activity, effect on cellular respiration of P-388 leukemia cells, *in vivo, in vitro* □ Leukemia, P-388—effect of quassinoids on cellular respiration, *in vivo, in vitro* □ Cellular respiration—P-388 leukemia cells, effect of various quassinoids

Numerous quassinoids have been isolated recently, *e.g.*, bruceantin (I) from *Brucea antidysenterica* (1), bruceoside A (II) from *Brucea javanica* (2), and its subsequent hydrolysis product brusatol (III). All three agents are active in the P-388 lymphocytic leukemia survival system. Bruceantin has a T/C = 197 at 1 mg/kg/day, bruceoside A has a T/C = 156 at 6 mg/kg/day, and brusatol has a T/C = 158 at 125 μg/kg/day (3). At a concentration of 0.015 m*M*,

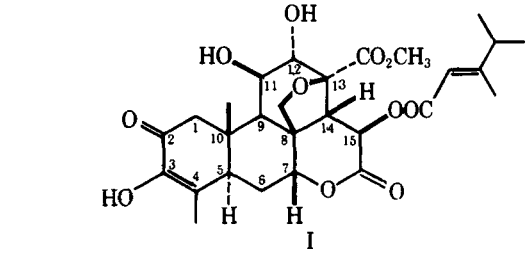

I

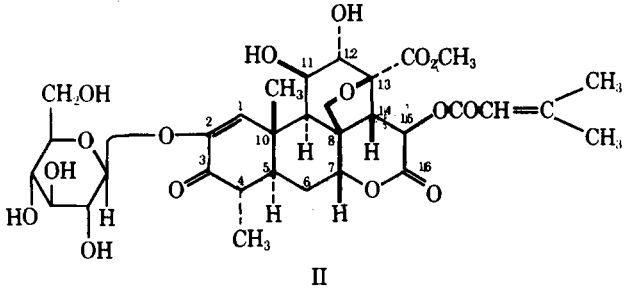

II

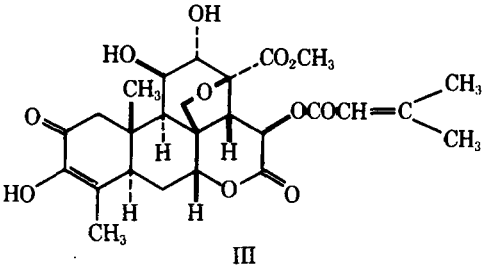

III

© 1979, American Pharmaceutical Association

and G. Wakisaka, *Cancer Res.*, **34**, 3341 (1974).
(13) K. M. Anderson, I. S. Mendelson, and G. Guzik, *Biochim. Biophys. Acta*, **383**, 56 (1975).
(14) I. H. Hall, G. L. Carlson, G. S. Abernethy, and C. Piantadosi, *J. Med. Chem.*, **17**, 1253 (1974).
(15) F. Maley and S. Ochoa, *J. Biol. Chem.*, **233**, 1538 (1958).
(16) A. Kampf, R. L. Barfknecht, P. J. Schaffer, S. Osaki, and M. P. Mertes, *J. Med. Chem.*, **19**, 903 (1976).
(17) M. K. Ho, T. Hakalo, and S. F. Zakrzwski, *Cancer Res.*, **32**, 1023 (1972).
(18) R. T. Borchardt, J. A. Huber, and Y. S. Wu, *J. Med. Chem.*, **19**, 1094 (1976).
(19) E. C. Moore and R. B. Hurlbert, *J. Biol. Chem.*, **241**, 4802 (1966).
(20) K. Randerath, *Biochim. Biophys. Acta*, **76**, 622 (1963).
(21) M. K. Spassova, G. C. Russev, and E. V. Golovinsky, *Biochem. Pharmacol.*, **25**, 923 (1976).
(22) J. B. Wyngaarden and D. M. Ashton, *J. Biol. Chem.*, **234**, 1492 (1959).
(23) S. M. Kalman, P. H. Duffield, and T. Brzozowski, *Am. Biol. Chem.*, **24**, 1871 (1966).
(24) R. M. Archibald, *J. Biol. Chem.*, **156**, 121 (1944).
(25) S. B. Koritz and P. P. Cohen, *ibid.*, **209**, 145 (1954).
(26) A. Raineri, R. C. Simsiman, and R. K. Boutwell, *Cancer Res.*, **33**, 134 (1973).
(27) Y. M. Kish and L. J. Kleinsmith, *Methods Enzymol.*, **40**, 201 (1975).
(28) A. C. Gilman, *Proc. Natl. Acad. Sci., USA*, **67**, 305 (1970).
(29) I. H. Hall, K. S. Ishaq, and C. Piantadosi, *J. Pharm. Sci.*, **63**, 625 (1974).
(30) Y. S. Cho-Chung and P. M. Gullino, *J. Biol. Chem.*, **248**, 4743 (1973).
(31) O. H. Lowry, N. J. Rosebrough, A. L. Farr, and R. J. Randall, *ibid.*, **193**, 265 (1951).
(32) G. W. Snedecor, "Statistical Methods," Iowa State College Press, Ames, Iowa, 1956, sec. 2.
(33) T. Posternak, *Annu. Rev. Pharmacol.*, **14**, 23 (1974).
(34) Y. S. Cho-Chung and P. M. Gullino, *Science*, **183**, 87 (1974).
(35) C. S. Rubin and O. M. Roseau, *Annu. Rev. Biochem.*, **44**, 81 (1975).

ACKNOWLEDGMENTS

Adapted in part from a dissertation submitted by S. A. ElGebaly to the Graduate School, University of North Carolina at Chapel Hill, in partial fulfillment of the Doctor of Philosophy requirements.

Supported by American Cancer Society Grant CH-19 and National Cancer Institute Grant CA-22929 to K. H. Lee.

The authors thank Dr. Matthew Suffness, Plant and Animal Product Section, National Cancer Institute, for the bruceantin.

Antitumor Agents XXXV: Effects of Brusatol, Bruceoside A, and Bruceantin on P-388 Lymphocytic Leukemia Cell Respiration

S. A. ElGEBALY, I. H. HALL ˣ, K. H. LEE, Y. SUMIDA, Y. IMAKURA, and R. Y. WU

Received October 28, 1978, from the *Division of Medicinal Chemistry, School of Pharmacy, University of North Carolina at Chapel Hill, Chapel Hill, NC 27514.* Accepted for publication January 9, 1979.

Abstract □ Brusatol, a quassinoid with potent antineoplastic activity against P-388 lymphocytic leukemia cell proliferation, significantly inhibited P-388 cell hexokinase, phosphofructokinase, malic dehydrogenase, and succinic dehydrogenase. Mitochondrial oxidative phosphorylation, basal, and adenosine diphosphate-stimulated respiration, utilizing succinate and α-ketoglutarate as the substrate, was suppressed significantly by *in vivo* treatment with brusatol. However, brusatol treatment had no effect on liver oxidative phosphorylation. Brusatol greatly increased P-388 cyclic AMP levels but had no effect on liver cyclic nucleotides. Similar inhibitory effects on P-388 cell oxidative phosphorylation were found *in vitro* with brusatol, bruceoside A, and bruceantin. Brusatol had no effect on adenosine triphosphatase activity or on uncoupling of oxidative phosphorylation. Rather, brusatol appeared to increase the concentration of reduced mitochondrial electron-transport cofactors, thereby blocking aerobic respiration. A proposed mechanism of action is discussed.

Keyphrases □ Antineoplastic agents—brusatol, bruceoside A, bruceantin, effect on cellular respiration of P-388 leukemia cells, *in vivo, in vitro* □ Quassinoids—antineoplastic activity, effect on cellular respiration of P-388 leukemia cells, *in vivo, in vitro* □ Leukemia, P-388—effect of quassinoids on cellular respiration, *in vivo, in vitro* □ Cellular respiration—P-388 leukemia cells, effect of various quassinoids

Numerous quassinoids have been isolated recently, *e.g.*, bruceantin (I) from *Brucea antidysenterica* (1), bruceoside A (II) from *Brucea javanica* (2), and its subsequent hydrolysis product brusatol (III). All three agents are active in the P-388 lymphocytic leukemia survival system. Bruceantin has a T/C = 197 at 1 mg/kg/day, bruceoside A has a T/C = 156 at 6 mg/kg/day, and brusatol has a T/C = 158 at 125 μg/kg/day (3). At a concentration of 0.015 m*M*,

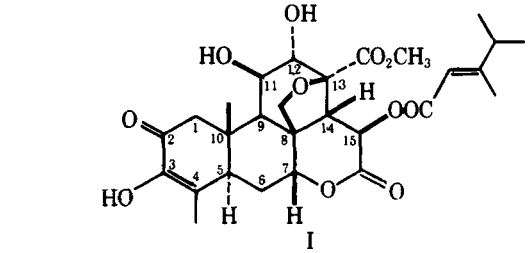

I

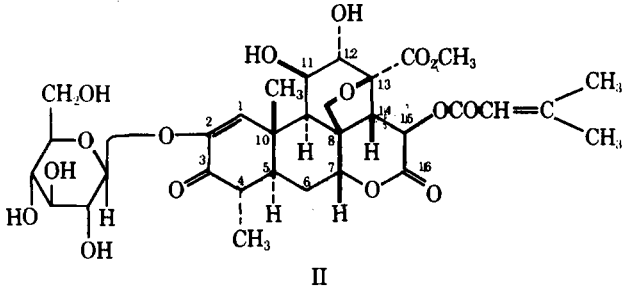

II

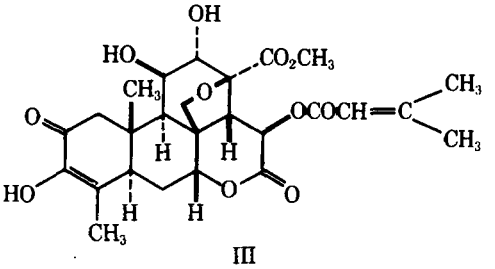

III

© 1979, American Pharmaceutical Association

Table I—Effects of Brusatol on Aerobic and Anaerobic Processes of DBA/2 Mice

Process	Control	Brusatol, 100 μg/kg/day on Days 7, 8, and 9, % of control
	P-388 Lymphocytic Leukemia Cells (n = 6)	
Hexokinase activity	100 ± 21	62 ± 17[a]
Phosphofructokinase activity	100 ± 16	54 ± 11[b]
Lactic dehydrogenase activity	100 ± 9	97 ± 13
Malic dehydrogenase activity	100 ± 16	43 ± 15[b]
Succinic dehydrogenase activity	100 ± 15	25 ± 3[b]
Adenosine triphosphatase activity	100 ± 6	107 ± 11
Cyclic AMP	100 ± 8	1269 ± 60[b]
Oxidative phosphorylation		
With succinate: state 4	100 ± 13	22 ± 6[b]
With succinate: state 3	100 ± 7	18 ± 5[b]
With α-ketoglutarate: state 4	100 ± 6	26 ± 5
With α-ketoglutarate: state 3	100 ± 11	29 ± 13
	Liver from Nontumor-Bearing Animals (n = 5)	
Cyclic AMP levels	100 ± 22	111 ± 14
Oxidative phosphorylation		
With succinate: state 4	100 ± 12	96 ± 5
With succinate: state 3	100 ± 8	102 ± 8
With α-ketoglutarate: state 4	100 ± 11	97 ± 10
With α-ketoglutarate: state 3	100 ± 13	93 ± 15

[a] p = 0.025. [b] p = 0.001.

all of these quassinoids significantly inhibited DNA, RNA, and protein syntheses in P-388 cells.

A positive correlation between aerobic respiration inhibition and antitumor–antimitotic activity has been observed for a number of nonrelated compounds, *e.g.*, a podophyllotoxin derivative, ellipticine, 4,6-diaminotriazines, methotrexate, naphthoquinone derivatives, tritylthioalanine, carminomycin, piperazinedione (4), 5-fluorinated pyrimidine-6-carboxyaldehydes (5), benzamalecene, triparanol (6), and sesquiterpene lactones (7). Sesquiterpene lactone antineoplastic agents also have been observed to suppress tumor cell glycolytic and Krebs cycle dehydrogenase activity enzymes (8). This paper reports the effect of quassinoids on P-388 lymphocytic leukemia aerobic and anaerobic cell metabolism.

EXPERIMENTAL

Materials—Bruceantin (I) was obtained in small quantities from the National Cancer Institute. Bruceoside A (II) was extracted from *B. javanica* according to the literature technique (2), and brusatol (III) was obtained by treating II with 3 *N* sulfuric acid–methanol (1:1) to hydrolyze the glycosidic linkage (2).

P-388 Lymphocytic Leukemia Cell Metabolism Studies—DBA/2 male mice (~25 g) were inoculated with 10^6 P-388 lymphocytic leukemia cells intraperitoneally on Day 0. For the *in vitro* studies, P-388 lymphocytic leukemia cells were harvested from the peritoneal cavity on Day 10. For the *in vivo* studies, the mice were treated on Days 7, 8, and 9 with 100 μg/kg/day ip of brusatol or 5 mg/kg/day ip of bruceoside A. Drugs were prepared by homogenization in 0.05% polysorbate 80 and water.

The number of tumor cells per milliliter and the 0.4% trypan blue uptake were determined with a hemocytometer (9). Phosphofructokinase activity of 10-day cells was determined by a literature method (10) based on the absorbance change of 1.125 μmoles of reduced nadide (nicotinamide adenine dinucleotide) at 340 nm. Hexokinase activity was assayed by a literature method (11) based on the absorbance change of 500 μmoles of nadide phosphate at 340 nm. Lactic dehydrogenase activity was determined by a literature method (12) based on absorbance changes of 0.12 μmole of reduced nadide at 340 nm.

Succinic dehydrogenase activity was determined by a literature method (13) based on the reduction of potassium ferric cyanide to the ferrous ion at 455 nm. Malic dehydrogenase activity was measured by a literature technique (14) based on absorption changes of 15 μmoles of reduced nadide. Protein concentrations were determined by the method of Lowry *et al.* (15).

In vitro respiration studies were carried out on 10-day P-388 lymphocytic leukemia cells. Oxygen consumption was measured with an electrode[1] connected to an oxygraph[2]. The reaction vessel typically contained 55 μmoles of sucrose, 22 μmoles of monobasic potassium phosphate, 22 μmoles of potassium chloride, 90 μmoles of succinate or 60 μmoles of α-ketoglutarate as the substrate, 22 μmoles of adenosine triphosphate, and 0.015 or 0.005 μmole of test drugs in a total volume of 1.8 ml at 37°. After the basal metabolic level (state 4) was obtained, 0.257 μmole of adenosine diphosphate was added to obtain the adenosine diphosphate-stimulated respiration rate (state 3) (7).

In vivo studies were conducted on 10-day cells after treatment of the DBA/2 mice. The method of Lindahl and Oberg (16) was used to determine if oxidative phosphorylation was uncoupled with 0.2 μmole of 2,4-dinitrophenol as an internal standard. The reaction medium contained, in 2 ml, 50 μmoles of phosphate buffer, 10 μmoles of magnesium chloride, 2 μmoles of diphosphate, 80 μmoles of glucose, excess hexokinase, 60 μmoles of pyruvate or succinate, and P-388 isolated mitochondria. Studies were carried out using the oxygraph. Measurement of individual electron-transport system components was carried out by a literature method (17) by recording differences in spectral absorption after incubating the P-388 lymphocytic leukemia mitochondrial suspensions (9000×*g* × 10 min) at pH 7.4 with 50 m*M* tromethamine hydrochloride, 50 m*M* potassium chloride, 50 m*M* sucrose, 10 m*M* inorganic phosphate, and either 4.2 m*M* glutarate plus 4.2 m*M* malate or 1.3 m*M* succinate as the substrate.

Nadide was measured at 340 and 374 nm, flavin adenine dinucleotide was measured at 455 and 500 nm, cytochrome b was measured at 410 and 430 nm, cytochrome c and c_1 was measured at 540 and 550 nm, and cytochrome oxidase was measured at 603 and 605 nm. The difference was obtained by calculating the difference between the reduced and oxidized cofactor forms, which was expressed as percent of the control. *In vitro* spectral studies were carried out by incubating 3.16 μmoles of nadide with 0.005 μmole of brusatol in phosphate buffer, pH 7.2, and measuring the appearance of the reduced form at 340 nm. Cytochrome c at 0.1 μmole was also incubated with brusatol, and the appearance of the reduced form was measured at 550 nm over 48 hr. Reduced nadide (6.5 μmoles) and brusatol (10 μmoles) were incubated at room temperature in 1 ml of 0.067 *M* phosphate buffer at pH 7.2 for 72 hr. The reaction medium was subjected to preparative TLC separation on silica gel plates eluted with chloroform–methanol (10:1). Spots were identified by UV absorption. Individual spots were scraped off the plate. An unknown spot was separated from the silica gel by column chromatography, which was eluted with acetone. Silica gel TLC showed a single spot at R_f 0.55 as compared to brusatol at R_f 0.64 whereas the cofactor remained at the origin.

Adenosine triphosphatase activity was measured in P-388 leukemia cells by the method of Suolinna *et al.* (18), and inorganic phosphate released was measured by the method of Chen *et al.* (19). Cyclic AMP levels were measured by a literature radioimmunoassay (20), using ^{3}H(G)-cyclic

[1] Clark.
[2] Gilson.

Table II—*In Vitro* Effects of Quassinoids on Oxidative Phosphorylation Process of P-388 Lymphocytic Leukemia Cells and DBA/2 Mouse Liver Homogenates

Substrate	0.05% Polysorbate 80,%	Percent Control: Bruceantin (0.015 μmole)	Bruceoside A (0.015 μmole)	Brusatol (0.005 μmole)	2,4-Dinitrophenol (0.2 μmole)
		P-388 Oxidative Phosphorylation Processes (n = 6)			
Succinate					
State 4	100 ± 13	50 ± 7[a]	54 ± 7[a]	50 ± 9[a]	—
State 3	100 ± 7	57 ± 10[a]	55 ± 10[a]	50 ± 7[a]	—
α-Ketoglutarate					
State 4	100 ± 6	60 ± 7[a]	58 ± 10[a]	59 ± 9[a]	—
State 3	100 ± 11	52 ± 6[a]	66 ± 5[a]	61 ± 11[a]	—
		Liver Oxidative Phosphorylation Processes (n = 5)			
Succinate					
State 4	100 ± 12	102 ± 14	105 ± 20	105 ± 19	—
State 3	100 ± 12	95 ± 14	86 ± 9	98 ± 17	—
α-Ketoglutarate					
State 4	100 ± 13	74 ± 13[b]	89 ± 19	101 ± 8	—
State 3	100 ± 21	70 ± 3[b]	105 ± 30	95 ± 28	—
		Isolated Mitochondria from P-388 Cells			
Pyruvate: state 3	100 ± 8	—	—	71 ± 7[a]	21 ± 5[a]
Succinate: state 3	100 ± 8	—	—	51 ± 6[a]	15 ± 4[a]

[a] p = 0.001. [b] p = 0.025.

AMP (39.8 Ci/mmole). Liver oxidative phosphorylation studies were carried out on nontumor-bearing DBA/2 male mice. The liver was excised, and a 10% homogenate in 0.25 *M* sucrose and 0.001 *M* edetic acid was prepared (21). Respiration was carried out on 0.1 ml of the homogenate in the reaction vessel. Cyclic AMP levels also were measured on the 10% homogenate.

RESULTS

Brusatol treatment of P-388 lymphocytic leukemia-bearing mice significantly reduced the activity of the glycolytic pathway regulatory enzymes of P-388 cells (Table I). Ten-day P-388 cells demonstrated a hexokinase activity as an absorbance change of 0.300 optical density (O.D.) unit/min/mg of protein, which brusatol reduced 38%. The phosphofructokinase activity for 10-day P-388 cells was 0.270 O.D. unit/min/mg of protein, which was reduced 46% by brusatol treatment. Krebs cycle dehydrogenase enzymes were also suppressed by brusatol. Malic dehydrogenase activity for control P-388 cells was 135.7 O.D. units/min/mg of protein, which brusatol reduced 57%. Succinic dehydrogenase activity for 10-day P-388 cells was 0.145 O.D. unit/min/mg of protein. Brusatol inhibited succinic dehydrogenase activity 75%.

In vitro oxidative phosphorylation studies showed that 0.015 μmole of bruceantin, bruceoside A, or brusatol at 0.015 and 0.005 μmole reduced states 3 and 4 respiration significantly (Table II). Basal respiration (state 4) with succinate as the substrate resulted in 11.44 μl of oxygen consumed/min/mg of protein. Adenosine diphosphate-stimulated respiration (state 3) with succinate was 20.76 μl of oxygen consumed/min/mg of protein. Basal respiration using α-ketoglutarate as the substrate resulted in 10.01 μl of oxygen consumed/min/mg of protein. State 3 consumption resulted in 19.17 μl of oxygen consumed/min/mg of protein.

Brusatol at 0.005 μmole *in vitro* caused a 50% inhibition of state 4 and state 3 with succinate as the substrate. Brusatol with α-ketoglutarate as the substrate caused a 41% inhibition of state 4 and a 39% inhibition of state 3. Both concentrations of brusatol, *i.e.*, 0.005 and 0.015 μmole, caused the same degree of suppression. Bruceoside A with succinate caused a 46% inhibition of state 4 and a 45% of inhibition of state 3. With α-ketoglutarate, bruceoside A caused a 42% inhibition of state 4 and a 34% inhibition of state 3. Bruceantin caused a 50% inhibition of state 4 and a 43% inhibition of state 3 with succinate and a 40% inhibition of state 4 and a 48% inhibition of state 3 with α-ketoglutarate.

At 100 μg/kg/day, brusatol suppressed *in vivo* state 4 basal respiration 78% and adenosine diphosphate respiration (state 3) 82% in the presence of succinate (Table I). α-Ketoglutarate basal respiration was suppressed 74% by brusatol treatment, and state 4 respiration was inhibited 71%. Bruceoside A treatment *in vivo* at 5 mg/kg/day caused a 7% inhibition of state 4 respiration and a 31% inhibition of state 3 with succinate. State 4 with α-ketoglutarate was inhibited 18% and state 3 was inhibited 25% by bruceoside A.

In vitro and *in vivo* studies with liver homogenates of nontumor-bearing animals demonstrated no changes in states 4 and 3 with either succinate or α-ketoglutarate as the substrate. *In vitro* state 3 studies with P-388 lymphocytic leukemia mitochondria with 0.005 μmole of brusatol showed that respiration was inhibited 29% with pyruvate and 49% with succinate as the substrate, respectively (Table II). 2,4-Dinitrophenol addition further suppressed state 3 respiration by 79% with pyruvate and 85% with succinate, indicating that oxidative phosphorylation was not uncoupled by brusatol. Adenosine triphosphatase activity after brusatol treatment was within normal limits (Table I).

Examination of the different spectra of cofactors of the electron-transport system showed that *in vivo* administration of brusatol increased the concentration of all reduced forms of the chain cofactors. Incubation with malate showed a 24% increase in reduced nadide, a 7% increase in reduced flavin adenine dinucleotide, a 13% increase in reduced cytochrome b, a 110% increase in reduced cytochrome c_1 and c, and a 100% increase in reduced cytochrome $\alpha_1 + \alpha_3$. Incubation with succinate resulted in a 198% increase in reduced flavin adenine dinucleotide, a 49% increase in reduced cytochrome b, a 216% increase in reduced cytochromes c_1 and c, and a 100% increase in reduced cytochrome $\alpha_1 + \alpha_3$.

In vitro studies showed the same trends but not as markedly. When brusatol was incubated with isolated nadide for 24 hr, there was a 26% increase in the reduced form; there was a 35% increase in reduced nadide after 40 hr, indicating that brusatol chemically reacted with the cofactor. When cytochrome c was incubated with brusatol, there was a 21% increase in reduced cytochrome c after 24 hr; after 48 hr, there was a 13% increase in reduced cytochrome c. Incubation of brusatol with reduced nadide demonstrated that the two agents chemically interacted to give a product that did not have the same R_f value as the two starting materials, suggesting the formation of an adduct between brusatol and the cofactor.

DISCUSSION

Brusatol treatment of P-388 lymphocytic leukemia-bearing mice significantly reduced the activities of enzymes of the Embden-Meyerhoff cycle and of the Krebs cycle. The key regulatory enzymes, hexokinase and phosphofructokinase, were significantly depressed by brusatol treatment. Krebs cycle dehydrogenase activities of malate and succinate were also significantly reduced. Succinate, which is a flavin adenine dinucleotide-linked dehydrogenase, was more severely depressed than malate dehydrogenase, which is a nadide-linked dehydrogenase. Oxidative phosphorylation processes of P-388 lymphocytic leukemia cells were significantly reduced by the quassinoids tested. With succinate as the substrate, both basal respiration (state 4) and adenosine diphosphate-stimulated respiration (state 3) were suppressed slightly more than with α-ketoglutarate as the substrate. Brusatol *in vivo* was more effective in reducing states 4 and 3 respiration with succinate or α-ketoglutarate.

Brusatol *in vivo*, however, did not affect normal liver respiration processes, nor did any of the quassinoids affect *in vitro* liver respiration at 0.015 μmole. The mitochondria studies showed that brusatol did not uncouple oxidative phosphorylation like 2,4-dinitrophenol does. Nor did brusatol treatment stimulate mitochondrial adenosine triphosphatase activity, which would facilitate the uncoupling of mitochondrial oxidative phosphorylation. Rather, brusatol appeared to act on the mitochondrial

electron-transport chain. *In vivo* studies showed drastic increases in the reduced forms of chain cofactors with either malate or succinate as the substrate. *In vivo* brusatol effects were more striking than *in vitro* effects on reducing cofactors, which may explain the observed increased effects of brusatol on *in vivo* states 4 and 3 respiration after 3 days of treatment as compared to *in vitro* effects. UV *in vitro* studies showed that brusatol chemically interacted with nadide increasing the reduced form absorbance at 340 nm. Cytochrome c, a heme, also was reduced in the presence of brusatol to the ferrous form with an increase in absorbance at 550 nm.

Although separation of the brusatol adduct and reduced nadide has not been achieved to date, incubation of the two agents showed that a possible reaction product existed. Nucleophilic attack of reduced nadide on the diosphenol ring A of brusatol may be postulated. If such an attack occurs, then complexation or alkylation of cofactor or functional groups of enzymes could account for the inhibitory effects of brusatol on P-388 lymphocytic leukemia cell metabolism with respect to the suppression of tumor cell anaerobic and aerobic respiration.

REFERENCES

(1) S. M. Kupchan, R. W. Britton, J. A. Lacadie, M. F. Ziegler, and C. W. Sigel, *J. Org. Chem.*, **40**, 648 (1975).

(2) K. H. Lee, Y. Imakura, and H. C. Huang, *J. Chem. Soc. Chem. Commun.*, **1977**, 69.

(3) I. H. Hall, K. H. Lee, S. A. ElGebaly, Y. Imakura, Y. Sumida, and R. Y. Wu, *J. Pharm. Sci.*, **68**, 883 (1979).

(4) M. Gosalvez, B. Blauco, and J. Hunter, *Eur. J. Cancer*, **10**, 567 (1974).

(5) C. Piantadosi, C. S. Kim, and J. L. Irvin, *J. Pharm. Sci.*, **58**, 821 (1969).

(6) I. Ananonson, *Proc. Soc. Exp. Biol. Med.*, **136**, 61 (1971).

(7) I. H. Hall, K. H. Lee, C. O. Starnes, S. A. ElGebaly, T. Ibuka, Y. S. Wu, T. Kimura, and K. Haruna, *J. Pharm. Sci.*, **67**, 1235 (1978).

(8) I. H. Hall, K.H. Lee, and S. A. ElGebaly, *ibid.*, **67**, 552 (1978).

(9) I. H. Hall, K. H. Lee, E. C. Mar, C. O. Starnes, and T. G. Waddell, *J. Med. Chem.*, **20**, 333 (1977).

(10) T. E. Mansour, in "Methods in Enzymology," vol. 9, W. A. Wood, Ed., Academic, New York, N.Y., 1967, p. 430.

(11) D. G. Walker and J. J. Parry, in *ibid.*, p. 381.

(12) M. K. Schwartz and O. Bodansky, in *ibid.*, p. 294.

(13) D. V. DerVartanian and C. Veerger, *Biochim. Biophys. Acta*, **92**, 233 (1964).

(14) S. Ochoa, A. H. Mehler, and A. Kornberg, *J. Biol. Chem.*, **174**, 979 (1948).

(15) O. H. Lowry, N. J. Rosebrough, A. L. Farr, and R. J. Randall, *ibid.*, **193**, 265 (1951).

(16) P. E. Lindahl and K. E. Oberg, *Nature*, **187**, 784 (1960).

(17) B. Chance and G. Hollinger, *J. Biol. Chem.*, **278**, 418 (1963).

(18) E. M. Suolinna, R. N. Buchsbaum, and E. Racker, *Cancer Res.*, **35**, 1865 (1975).

(19) P. S. Chen, T. Y. Toribara, and H. Warner, *Anal. Chem.*, **28**, 1756 (1956).

(20) A. C. Gilman, *Proc. Natl. Acad. Sci., USA*, **67**, 305 (1970).

(21) I. Hall and G. L. Carlson, *J. Med. Chem.*, **19**, 1257 (1976).

(22) G. W. Snedecor, "Statistical Methods," Iowa State College Press, Ames, Iowa, 1956, section 2.

ACKNOWLEDGMENTS

Adapted in part from a dissertation submitted by S. A. ElGebaly to the Graduate School, University of North Carolina at Chapel Hill, in partial fulfillment of the Doctor of Philosophy degree requirements.

Supported by American Cancer Society Grant CH-19 and National Cancer Institute Grants CA-22929 and CA 17625 (in part) to K. H. Lee.

The authors thank Dr. Matthew Suffness, Developmental Therapeutics Program, Chemotherapy, National Cancer Institute, for the bruceantin.

^{13}C-NMR Spectra of α-Adrenergic Blocking Agents

SHIVA P. SINGH *, SURENDRA S. PARMAR *x, SYLVIA A. FARNUM ‡, and VIRGIL I. STENBERG ‡

Received October 13, 1978, from the *Departments of *Physiology and ‡Chemistry, University of North Dakota, Grand Forks, ND 58202.* Accepted for publication January 17, 1979.

Abstract □ The natural abundance ^{13}C-NMR spectra of five α-adrenergic blocking agents, tolazoline, dibenamine, azapetine, phenoxybenzamine, and phentolamine, are reported. The chemical shifts of various carbon resonances were assigned on the basis of chemical shift theory, multiplicities observed in single-frequency off-resonance-decoupled spectra, relaxation times, and comparisons with the chemical shifts of model compounds.

Keyphrases □ NMR spectroscopy—analysis, tolazoline, dibenamine, azapetine, phenoxybenzamine, phentolamine □ α-Adrenergic blocking agents—analysis, NMR spectroscopy

Earlier studies reporting the ^{13}C-NMR spectra of antimalarials (1, 2), anti-inflammatory agents (3, 4), antipyretic analgesics (5), and central nervous system acting agents (6–10) prompted the assignments of the natural abundance ^{13}C-NMR chemical shifts of α-adrenergic blocking agents, 2-benzyl-2-imidazolone (I) (tolazoline), *N,N*-dibenzyl-β-chloroethylamine (II) (dibenamine), 6,7-dihydro-6-(2-propenyl)-5*H*-dibenz[*c,e*]azepine (III) (azapetine), *N*-(2-chloroethyl)-*N*-(1-methyl-2-phenoxyethyl)benzenemethanamine (IV) (phenoxybenzamine), and 3-[[(4,5-dihydro-1*H*-imidazol-2-yl)methyl](4-methylphenyl)amino]phenol (V) (phentolamine). The ^{13}C-NMR spectra of these therapeutic agents are of theoretical as well as of biological interest.

Both the proton noise-decoupled and single-frequency off-resonance-decoupled (SFORD) spectra of I–V were recorded using the Fourier transform technique. The proton noise-decoupled spectra of these compounds gave the chemical shifts of various carbon resonances, while the SFORD spectra provided the distinction of methyl, methylene, methine, and nonprotonated carbons. Furthermore, the relaxation time measurements differentiated nonprotonated carbons from protonated carbons.

The assignments of various carbon-13 signals were made on the basis of chemical shift theory (11), multiplicities observed in the SFORD spectra, percent integration of the signals in the proton noise-decoupled spectra, relaxation times, and chemical shifts of the corresponding carbons of model compounds (12).

0022-3549/79/0700-0890$01.00/0

© 1979, American Pharmaceutical Association

electron-transport chain. *In vivo* studies showed drastic increases in the reduced forms of chain cofactors with either malate or succinate as the substrate. *In vivo* brusatol effects were more striking than *in vitro* effects on reducing cofactors, which may explain the observed increased effects of brusatol on *in vivo* states 4 and 3 respiration after 3 days of treatment as compared to *in vitro* effects. UV *in vitro* studies showed that brusatol chemically interacted with nadide increasing the reduced form absorbance at 340 nm. Cytochrome c, a heme, also was reduced in the presence of brusatol to the ferrous form with an increase in absorbance at 550 nm.

Although separation of the brusatol adduct and reduced nadide has not been achieved to date, incubation of the two agents showed that a possible reaction product existed. Nucleophilic attack of reduced nadide on the diosphenol ring A of brusatol may be postulated. If such an attack occurs, then complexation or alkylation of cofactor or functional groups of enzymes could account for the inhibitory effects of brusatol on P-388 lymphocytic leukemia cell metabolism with respect to the suppression of tumor cell anaerobic and aerobic respiration.

REFERENCES

(1) S. M. Kupchan, R. W. Britton, J. A. Lacadie, M. F. Ziegler, and C. W. Sigel, *J. Org. Chem.*, **40**, 648 (1975).

(2) K. H. Lee, Y. Imakura, and H. C. Huang, *J. Chem. Soc. Chem. Commun.*, **1977**, 69.

(3) I. H. Hall, K. H. Lee, S. A. ElGebaly, Y. Imakura, Y. Sumida, and R. Y. Wu, *J. Pharm. Sci.*, **68**, 883 (1979).

(4) M. Gosalvez, B. Blauco, and J. Hunter, *Eur. J. Cancer*, **10**, 567 (1974).

(5) C. Piantadosi, C. S. Kim, and J. L. Irvin, *J. Pharm. Sci.*, **58**, 821 (1969).

(6) I. Ananonson, *Proc. Soc. Exp. Biol. Med.*, **136**, 61 (1971).

(7) I. H. Hall, K. H. Lee, C. O. Starnes, S. A. ElGebaly, T. Ibuka, Y. S. Wu, T. Kimura, and K. Haruna, *J. Pharm. Sci.*, **67**, 1235 (1978).

(8) I. H. Hall, K.H. Lee, and S. A. ElGebaly, *ibid.*, **67**, 552 (1978).

(9) I. H. Hall, K. H. Lee, E. C. Mar, C. O. Starnes, and T. G. Waddell, *J. Med. Chem.*, **20**, 333 (1977).

(10) T. E. Mansour, in "Methods in Enzymology," vol. 9, W. A. Wood, Ed., Academic, New York, N.Y., 1967, p. 430.

(11) D. G. Walker and J. J. Parry, in *ibid.*, p. 381.

(12) M. K. Schwartz and O. Bodansky, in *ibid.*, p. 294.

(13) D. V. DerVartanian and C. Veerger, *Biochim. Biophys. Acta*, **92**, 233 (1964).

(14) S. Ochoa, A. H. Mehler, and A. Kornberg, *J. Biol. Chem.*, **174**, 979 (1948).

(15) O. H. Lowry, N. J. Rosebrough, A. L. Farr, and R. J. Randall, *ibid.*, **193**, 265 (1951).

(16) P. E. Lindahl and K. E. Oberg, *Nature*, **187**, 784 (1960).

(17) B. Chance and G. Hollinger, *J. Biol. Chem.*, **278**, 418 (1963).

(18) E. M. Suolinna, R. N. Buchsbaum, and E. Racker, *Cancer Res.*, **35**, 1865 (1975).

(19) P. S. Chen, T. Y. Toribara, and H. Warner, *Anal. Chem.*, **28**, 1756 (1956).

(20) A. C. Gilman, *Proc. Natl. Acad. Sci., USA*, **67**, 305 (1970).

(21) I. Hall and G. L. Carlson, *J. Med. Chem.*, **19**, 1257 (1976).

(22) G. W. Snedecor, "Statistical Methods," Iowa State College Press, Ames, Iowa, 1956, section 2.

ACKNOWLEDGMENTS

Adapted in part from a dissertation submitted by S. A. ElGebaly to the Graduate School, University of North Carolina at Chapel Hill, in partial fulfillment of the Doctor of Philosophy degree requirements.

Supported by American Cancer Society Grant CH-19 and National Cancer Institute Grants CA-22929 and CA 17625 (in part) to K. H. Lee.

The authors thank Dr. Matthew Suffness, Developmental Therapeutics Program, Chemotherapy, National Cancer Institute, for the bruceantin.

^{13}C-NMR Spectra of α-Adrenergic Blocking Agents

SHIVA P. SINGH *, SURENDRA S. PARMAR *x, SYLVIA A. FARNUM ‡, and VIRGIL I. STENBERG ‡

Received October 13, 1978, from the *Departments of *Physiology and ‡Chemistry, University of North Dakota, Grand Forks, ND 58202.* Accepted for publication January 17, 1979.

Abstract □ The natural abundance ^{13}C-NMR spectra of five α-adrenergic blocking agents, tolazoline, dibenamine, azapetine, phenoxybenzamine, and phentolamine, are reported. The chemical shifts of various carbon resonances were assigned on the basis of chemical shift theory, multiplicities observed in single-frequency off-resonance-decoupled spectra, relaxation times, and comparisons with the chemical shifts of model compounds.

Keyphrases □ NMR spectroscopy—analysis, tolazoline, dibenamine, azapetine, phenoxybenzamine, phentolamine □ α-Adrenergic blocking agents—analysis, NMR spectroscopy

Earlier studies reporting the ^{13}C-NMR spectra of antimalarials (1, 2), anti-inflammatory agents (3, 4), antipyretic analgesics (5), and central nervous system acting agents (6–10) prompted the assignments of the natural abundance ^{13}C-NMR chemical shifts of α-adrenergic blocking agents, 2-benzyl-2-imidazolone (I) (tolazoline), *N,N*-dibenzyl-β-chloroethylamine (II) (dibenamine), 6,7-dihydro-6-(2-propenyl)-5*H*-dibenz[*c,e*]azepine (III) (azapetine), *N*-(2-chloroethyl)-*N*-(1-methyl-2-phenoxyethyl)benzenemethanamine (IV) (phenoxybenzamine), and 3-[[(4,5-dihydro-1*H*-imidazol-2-yl)methyl](4-methylphenyl)amino]phenol (V) (phentolamine). The ^{13}C-NMR spectra of these therapeutic agents are of theoretical as well as of biological interest.

Both the proton noise-decoupled and single-frequency off-resonance-decoupled (SFORD) spectra of I–V were recorded using the Fourier transform technique. The proton noise-decoupled spectra of these compounds gave the chemical shifts of various carbon resonances, while the SFORD spectra provided the distinction of methyl, methylene, methine, and nonprotonated carbons. Furthermore, the relaxation time measurements differentiated nonprotonated carbons from protonated carbons.

The assignments of various carbon-13 signals were made on the basis of chemical shift theory (11), multiplicities observed in the SFORD spectra, percent integration of the signals in the proton noise-decoupled spectra, relaxation times, and chemical shifts of the corresponding carbons of model compounds (12).

0022-3549/79/0700-0890$01.00/0

© 1979, American Pharmaceutical Association

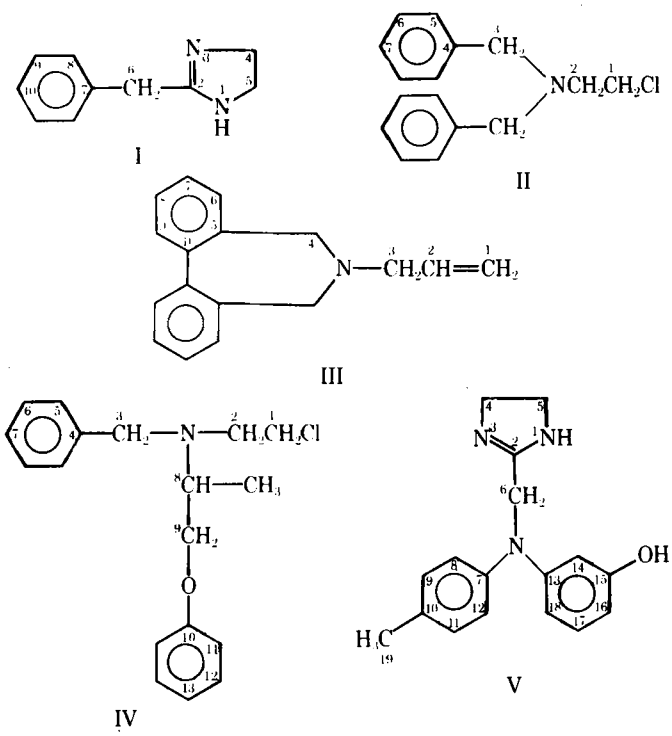

I II III IV V

EXPERIMENTAL

The ^{13}C-NMR spectra of I–V were obtained on a spectrometer[1] operating at 15.00 kHz with tetramethylsilane as a reference. The samples were run in a 10-mm tube with deuterochloroform (30% w/v) as an internal lock and solvent for I–IV and deuterated dimethyl sulfoxide (30% w/v) as an internal lock and solvent for V. The spectrometer settings were: spectral width, 4 kHz; pulse width, 12 μsec (60°); and data points, 4 K. Relaxation time (T_1) measurements of all compounds were carried out in undegassed solutions and were calculated automatically by the computer by least-squares analysis (13) of the plot of ln $(I - I_t)$ *versus* T.

Azapetine phosphate and the hydrochlorides of tolazoline, dibenamine, phenoxybenzamine, and phentolamine, were converted into the corresponding free bases prior to the determination of their ^{13}C-NMR spectra.

RESULTS AND DISCUSSION

Tolazoline (I)—The chemical shifts and relaxation times of various I carbon resonances are recorded in Table I. The SFORD spectrum of I showed two singlets, two doublets, and two triplets. The two singlets farthest downfield having longer relaxation time are due to C-2 and C-7. Since the methyl substituent in the benzene nucleus causes an 8.9-ppm downfield shift to the *ipso*-carbon (11), the singlets at 136.1 and 166.5 ppm are assigned to C-7 and C-2, respectively.

The C-10 chemical shift could be differentiated from the C-8 and C-9 chemical shifts by its shorter relaxation time (T_1). In I, C-10 is *para* to the methylene substituent of the benzene nucleus. It should have a shorter T_1 value compared to C-8 and C-9 due to the anisotropic motion along the preferred long molecular axis, *i.e.*, from C-6 to C-10, where C-8 and C-9 show more motion, resulting in longer T_1 values due to less favorable dipole–dipole interaction (11). Also, methyl substituents in the benzene ring produce 0.1- and 2.9-ppm upfield shifts to *meta*- and *para*-carbons, respectively, and a 0.7-ppm downfield shift to the *ortho*-carbon (11). On this basis and the percent integration of signals, the doublet centered at 126.7 ppm is assigned to C-10 and the doublet at 128.5 ppm is assigned to both C-8 and C-9. These assignments compare well with their calculated values.

Table I—^{13}C-Chemical Shifts of Tolazoline

Assignment[a]	Multiplicity[b]	Relaxation Time[c]	Chemical Shift[d]
C-2	s	15.20	166.5
C-7	s	26.10	136.1
C-8, C-9	d	3.21	128.5
C-10	d	1.68	126.7
C-4, C-5	t	1.02	49.5
C-6	t	2.40	35.7

[a] Numbering of the carbons is shown in the structure. [b] Signal multiplicity obtained from SFORD spectrum; s = singlet, d = doublet, t = triplet, and q = quartet. [c] Relaxation time was measured in undegassed solution. [d] Chemical shifts are expressed in parts per million relative to tetramethylsilane.

[1] Jeol FX 60.

Table II—^{13}C-Chemical Shifts of Dibenamine

Assignment[a]	Multiplicity[b]	Relaxation Time[c]	Chemical Shift[d]
C-4	s	7.68	138.9
C-5[e]	d	1.02	128.5
C-6[e]	d	1.03	128.1
C-7	d	0.75	126.9
C-3	t	0.60	58.3
C-2	t	0.60	55.1
C-1	t	0.98	41.6

[a–d] See Table I. [e] May be interchanged.

The C-4 and C-5 of the I imidazole ring are directly attached to the nitrogen atom and are in the same environment, so the signals due to these carbons should be observed at the same place. On this basis and the percent integration of the signals, the triplet centered at 35.7 ppm is assigned to C-6 and the triplet at 49.5 ppm is assigned to both C-4 and C-5.

Dibenamine (II)—As is evident from Table II, one singlet and three doublets in the downfield region and three triplets in the upfield region are observed in the ^{13}C-NMR spectrum of II; these signals account for all 16 carbon resonances. The four signals in the downfield region represent the 12 aromatic carbon resonances due to the plane of symmetry. The farthest downfield singlet at 138.9 ppm having a longer relaxation time is attributed to C-4. Considering the effect of a methyl substituent on the benzene nucleus (11) and the relaxation times of C-5, C-6, and C-7, where C-7 should have a shorter T_1 value compared to C-5 and C-6 (11), the doublets centered at 128.5, 128.1, and 126.9 ppm are assigned to C-5, C-6, and C-7, respectively. The assignments of C-5 and C-6 could be interchanged. Furthermore, these assignments compare well with the chemical shifts of the corresponding carbons of I and VI (12).

Previous studies reported that the amino group in aliphatic amines exhibits 20- and 2-ppm downfield shifts to α- and β-carbons, respectively (11). Also, chlorine in alkyl chlorides causes 23- and 2-ppm downfield shifts to α- and β-carbons, respectively (11). Both α- and β-carbons cause an ~9-ppm downfield shift while the γ-carbon produces a 2-ppm upfield shift (11). The chemical shift of the methyl group carbon resonance in toluene is 21.2 ppm (12). The C-3 is directly attached to the nitrogen atom and has two β- and one γ-carbons. Thus, the triplet centered at 58.3 ppm is best assigned to C-3. The C-1 has one α-chlorine, one α- and two γ-carbons, and one β-nitrogen; C-2 has one α- and two β-carbons, one α-nitrogen, and one β-chlorine. Considering these effects on the base peak of ethane (11), the triplets centered at 55.1 and 41.6 ppm are attributed to C-2 and C-1, respectively.

Azapetine (III)—The chemical shifts of the carbon resonances of III obtained from its ^{13}C-NMR spectrum and their relaxation times are recorded in Table III. The structure of III indicates that there is a plane of symmetry that reduces half of the aromatic carbon resonances. The signals at 140.9 and 134.4 ppm, observed as singlets in the SFORD spectrum of III and having longer relaxation times, must be due to C-5 and C-10. A phenyl substituent in the benzene ring produces a 13.1-ppm downfield shift to the *ipso*-carbon and a 1.1-ppm upfield shift to the *ortho*-carbon, and a methyl group causes 8.9- and 0.7-ppm downfield shifts to *ipso*- and *ortho*-carbons, respectively (11). The singlets at 140.9 and 134.3 ppm are assigned to C-10 and C-5, respectively.

The chemical shift of the ethylene carbon resonance is 123.3 ppm (11). The vinylic carbon C-2 has one α- and two γ-carbons and one β-nitrogen while C-1 has one α′- and two γ′-carbons and one β′-nitrogen. The α- and γ′-carbons cause 10.6- and 1.5-ppm downfield shifts, respectively, while γ and α′ produce 1.5- and 7.9-ppm upfield shifts, respectively, in alkenes (11). The β-nitrogen exhibits a 2-ppm downfield shift (11). On this basis, the doublet centered at 136.1 ppm and the triplet centered at 117.7 ppm

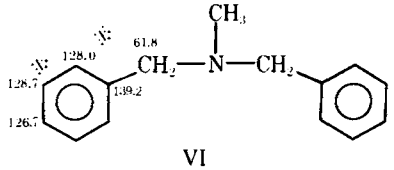

VI

Table III—^{13}C-Chemical Shifts of Azapetine

Assignment[a]	Multiplicity[b]	Relaxation Time[c]	Chemical Shift[d]
C-10	s	21.30	140.9
C-2	d	1.80	136.1
C-5	s	15.00	134.3
C-6	d	1.20	129.5
C-7[e]	—	0.87	127.7
C-8[e], C-9[e]	—	1.10	127.4
C-1	t	0.92	117.7
C-3	t	0.75	58.2
C-4	t	0.68	54.5

[a-d] See Table I. [e] See Table II.

are assigned to C-2 and C-1, respectively. The signals at 129.5 and 127.7 ppm are assigned to C-6 and C-7, respectively, and the signal at 127.4 ppm is assigned to both C-8 and C-9 on the basis of chemical shift theory and percent integration of the signals. The assignments of C-7, C-8, and C-9 may be interchanged.

The upfield triplets centered at 58.2 and 54.5 ppm are assigned to C-3 and C-4, respectively, on the basis of chemical shift theory and signal intensity observed in the proton noise-decoupled spectrum of III.

Phenoxybenzamine (IV)—The chemical shifts and relaxation times of the various carbon resonances of IV are recorded in Table IV. Thirteen separate signals in the proton noise-decoupled spectrum account for the 18 carbon resonances of IV. The carbon resonances of C-4 and C-10 could be easily separated from the others due to their longer relaxation times and multiplicities in the SFORD spectrum. Since methoxy and methyl substituents in the benzene nucleus exhibit 31.4- and 8.9-ppm downfield shifts to the *ipso*-carbon (11), respectively, the singlet at 158.7 ppm is assigned to C-10 and the singlet at 140.1 ppm is assigned to C-4. The benzene ring methoxy group causes a 1-ppm downfield shift to the *meta*-carbon and 14.4- and 7.7-ppm upfield shifts to *ortho*- and *para*-carbons, respectively (11). The chemical shift due to the methyl substituent in the benzene ring was already mentioned in the assignment of I carbon resonances. Thus, on the basis of signal intensities, multiplicities in the SFORD spectrum, and effects of methyl and methoxy substituents on the benzene ring, the doublets centered at 129.2, 128.2, 126.9, 120.5, and 114.3 ppm are attributed to C-12, both C-5 and C-6, C-7, C-13, and C-11, respectively. Furthermore, the assignments of C-4, C-5, C-6, and C-7 are in agreement with the corresponding carbon chemical shifts of II.

The farthest upfield quartet centered at 13.1 ppm could be easily assigned to C-14 on the basis of multiplicity and chemical shift theory. The signals at 42.9, 54.5, and 55.6 ppm are assigned to C-1, C-2, and C-3, respectively. These assignments are based on chemical shift theory and comparisons with the corresponding carbon chemical shifts of II. The chemical shift of C-3 is observed upfield compared to C-3 of II because C-3 of IV has two more γ-carbons, which produce about a 2-ppm upfield shift. The C-9 has one α-, one β-, and two γ-carbons, one α-oxygen, and one β-nitrogen while C-8 has two α-, two β-, and one γ-carbons, one α-nitrogen, and one β-oxygen. Considering the chemical shifts caused by carbon, nitrogen, and oxygen atoms (11), the triplet centered at 70.0 ppm is assigned to C-9 and the signal at 52.9 ppm is assigned to C-8.

Phentolamine (V)—The chemical shifts and relaxation times of the V various carbon resonances are shown in Table V. The SFORD spectrum gave five singlets, five doublets, two triplets, and one quartet. The singlets were confirmed by their longer relaxation times. The farthest downfield

Table IV—^{13}C-Chemical Shifts of Phenoxybenzamine

Assignment[a]	Multiplicity[b]	Relaxation Time[c]	Chemical Shift[d]
C-10	s	12.10	158.7
C-4	s	6.80	140.1
C-12	d	0.92	129.2
C-5, C-6	d	0.76	128.2
C-7	d	0.46	126.9
C-13	d	0.48	120.5
C-11	d	1.00	114.3
C-9	t	0.35	70.0
C-3	—	0.43	55.6
C-2	—	0.62	54.5
C-8	—	0.38	52.9
C-1	t	0.57	42.9
C-14	q	0.84	13.1

[a-d] See Table I.

Table V—^{13}C-Chemical Shifts of Phentolamine

Assignment[a]	Multiplicity[b]	Relaxation Time[c]	Chemical Shift[d]
C-2	s	2.60	165.9
C-15	s	2.00	158.3
C-13	s	3.10	149.6
C-7	s	3.70	145.0
C-10	s	2.80	132.2
C-9, C-11, C-17	d	0.34	129.7
C-8, C-12	d	0.31	123.9
C-18	d	0.14	108.2
C-16	d	0.12	107.2
C-14	d	0.18	104.9
C-6	t	0.10	51.1
C-4, C-5	t	0.13	49.1
C-19	q	0.92	20.4

[a-d] See Table I.

singlet at 165.9 ppm is assigned to C-2 by comparing the chemical shift of C-2 in I. Considering the chemical shifts caused by amino, hydroxy, and methyl substituents on the benzene ring (11), the singlets at 158.3, 149.6, 145.0, and 132.2 ppm are assigned to C-15, C-13, C-7, and C-10, respectively. The doublet centered at 129.7 ppm is assigned to C-9, C-11, and C-17, and the doublet at 123.9 ppm is assigned to C-8 and C-12. The remaining doublets at 108.2, 107.2, and 104.9 ppm are assigned to C-18, C-16, and C-14, respectively. The assignments are made on the basis of chemical shift theory (11) and signal intensity.

The quartet centered at 20.4 ppm is attributed to C-19, which agrees well with the toluene methyl carbon chemical shift (12). The triplet centered at 49.1 ppm is assigned to C-4 and C-5 on the basis of signal intensity and chemical shift theory. Furthermore, this assignment is supported by the corresponding carbon chemical shifts of I. The remaining triplet centered at 51.1 ppm is assigned to C-6.

REFERENCES

(1) S. P. Singh, S. S. Parmar, and V. I. Stenberg, *J. Heterocycl. Chem.*, **15**, 9 (1978).

(2) S. P. Singh, S. S. Parmar, V. I. Stenberg, and S. A. Farnum, *Spectrosc. Lett.*, **11**, 59 (1978).

(3) *Ibid.*, **10**, 1001 (1977).

(4) S. P. Singh, S. S. Parmar, V. I. Stenberg, and S. A. Farnum, *J. Heterocycl. Chem.*, **15**, 13 (1978).

(5) S. P. Singh, S. A. Farnum, V. I. Stenberg, and S. S. Parmar, *J. Pharm. Sci.*, **68**, 470 (1979).

(6) V. I. Stenberg, N. K. Narain, and S. P. Singh, *J. Heterocycl. Chem.*, **14**, 225 (1977).

(7) V. I. Stenberg, N. K. Narain, S. P. Singh, R. H. Obenauf, and M. J. Albright, *ibid.*, **14**, 407 (1977).

(8) S. P. Singh, S. S. Parmar, V. I. Stenberg, and T. K. Akers, *ibid.*, **15**, 53 (1978).

(9) S. P. Singh, S. S. Parmar, S. A. Farnum, and V. I. Stenberg, *ibid.*, in press.

(10) S. P. Singh, V. I. Stenberg, S. S. Parmar, and S. A. Farnum, *J. Pharm. Sci.*, **68**, 89 (1979).

(11) G. C. Levey and G. L. Nelson, "Carbon-13 Nuclear Magnetic Resonance for Organic Chemists," Wiley-Interscience, New York, N.Y., 1972, pp. 38, 47, 60, 63, 65, 81, 188, 189.

(12) L. F. Johnson and W. C. Jankowski, "Carbon-13 NMR Spectra," Wiley-Interscience, New York, N.Y., 1972, pp. 243, 465.

(13) K. Mullen and P. S. Pregosin, "Fourier Transform NMR Techniques: A Practical Approach," Academic, New York, N.Y., 1976, p. 65.

ACKNOWLEDGMENTS

Supported in part by a research grant from the American Parkinson Disease Association, New York, N.Y., and National Science Foundation Grant CHE 76-05678 for the partial purchase of the ^{13}C-NMR spectrometer.

The authors thank Dr. R. G. Severson and Dr. S. J. Brumleve for their advice and encouragement. Grateful acknowledgment is made to Smith Kline and French Laboratories for the generous gift of tolazoline, dibenamine, and phenoxybenzamine hydrochlorides; Hoffmann-La Roche for azepetine phosphate; Ciba-Geigy Corp. for Regitine (phentolamine) hydrochloride; and the Northwest Area Foundation, St. Paul, Minn., for providing a Hill Professorship to S. S. Parmar.

Synthesis of Phenyl-3- and Phenyl-5-acetamidosalicylates as Potential Analgesics

KHALID SABIH A. RAZZAK

Received April 24, 1978, from the *College of Pharmacy, University of Baghdad, Baghdad, Iraq.* Accepted for publication January 17, 1979.

Abstract □ Phenylsalicylate was nitrated to obtain two nitro isomers, which were separated and reduced to the corresponding amines followed by acetylation to give phenyl-5- or phenyl-3-acetamidosalicylate. Phenyl-5-acetamidosalicylate displayed analgesic activity comparable to that of aspirin and phenacetin at doses of 25–50 mg/kg sc and was much less toxic than the latter compounds. Phenyl-3-acetamidosalicylate, however, was ineffective at a similar dose range and caused restlessness at larger doses.

Keyphrases □ Phenylsalicylates—synthesis of phenyl-3- and phenyl-5-acetamidosalicylates, analgesic activity □ Analgesics—phenylsalicylates, derivatives, synthesis, tested for analgesic activity □ Antitubercular agents, potential—phenylsalicylates, synthesis, analgesic activity

Phenylsalicylate (I) has been used as an analgesic and as an enteric coating material for oral dosage forms (1). It also has several other industrial uses (2). However, it has been replaced by more potent and safer analgesic–antipyretic drugs such as aspirin and acetaminophen (II). Aminosalicylic acid (III), phenyl-*p*-aminosalicylate (IV), and their corresponding acetyl derivatives have been used for the treatment of tuberculosis (3–6) in conjunction with other antitubercular agents.

This report describes the synthesis of some new phenylsalicylate derivatives (V–X) as potential analgesic–antipyretic agents with possible antitubercular activity. Compound VIII is a combination of phenylsalicylate and acetaminophen in one molecule. Furthermore, VII–X are isomers of phenyl-4-amino- or phenyl-4-acetamidosalicylates, which are used as antitubercular agents.

EXPERIMENTAL[1]

Phenyl-3- and Phenyl-5-nitrosalicylates (V and VI)—A solution of 40 g (0.184 mole) of phenylsalicylate[2] in acetic acid was treated with 50 ml of nitric acid (68%) in acetic acid (1:1) dropwise with stirring and cooling in an ice bath for 20 min. The temperature was raised to 30–35°

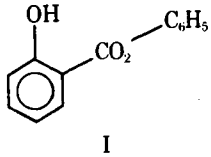

I

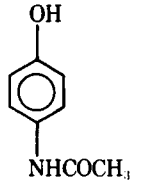

II

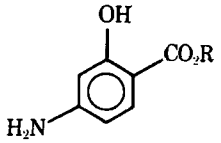

III: R = H
IV: R = C_6H_5

and maintained for 5–6 min, during which time the reaction mixture turned deep orange. The mixture was poured over 200 g of crushed ice. Upon stirring, an orange solid material separated. This material was filtered, washed with alcohol, and dried to give 45 g of nitrated salol.

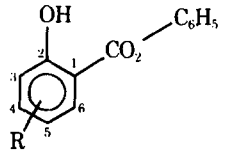

V: R = 5-nitro
VI: R = 3-nitro
VII: R = 5-amino
VIII: R = 5-acetamido
IX: R = 3-amino
X: R = 3-acetamido

Compounds V and VI were separated by fractional crystallization from ethanol; V crystallized immediately from the hot alcoholic solution. Further recrystallization of this fraction from alcohol gave 20 g (0.078 mole, 42%) of white needle-like crystals, mp 148–150°. Compound VI was obtained upon standing and cooling of the alcoholic mother liquor to give colorless crystals, mp 87–89°. Further recrystallization of this fraction from alcohol gave 22 g (0.097 mole, 52%) of VI, mp 99–100°.

The mass spectra of V and VI showed identical molecular ions at *m/e* 259 ($C_{13}H_9NO_5$); IR of V ($CHCl_3$): ν_{max} 3250–3090, 3010, 1690, 1630, 1530, 1350, and 840 cm^{-1}; NMR of V ($CDCl_3$): δ 11.18 (1H, s), 9.04 (1H at C-6, d, J = 2.6 Hz), 8.42 (1H at C-4, dd, J = 9.4 and 2.6 Hz), 7.16 (1H at C-3, d, J = 9.6 Hz), and 7.6–7.18 (5H, complex m) (one replaceable proton); IR of VI ($CHCl_3$): ν_{max} 3250–3090, 3010, 1690, 1630, 1530, 1350, 900, 860, and 840 cm^{-1}; NMR of VI ($CDCl_3$): δ 11.71 (1H, s), 8.32 (1H at C-4, dd, J = 8 and 1.7 Hz), 8.22 (1H at C-6, dd, J = 8.2 and 1.7 Hz), and 7.6–7.01 (6H, complex m) (one replaceable proton).

Nitro Derivative Reduction—A sample of 13 g of V or VI (0.05 mole) was dissolved in a minimum amount of chloroform and mixed with 200 ml of methanol or ethanol, 0.3 g of platinum oxide or palladium, and 1–2 g of activated charcoal. The mixture was placed in a hydrogenator[3], and hydrogenation of the nitro derivatives was allowed to proceed until no more hydrogen was absorbed. The reduction yield was based on the amount of hydrogen absorbed by the nitro derivatives.

In both cases, complete reduction was obtained, as indicated by the absorption of 3.4 liters (3 equivalents) of hydrogen in each reduction process. The reduction mixture was filtered, and the residue was washed with ~50 ml of alcohol. The combined filtrate and washings were taken to dryness under vacuum, and the residue was dissolved in 5% HCl. The amine hydrochloride was used for the next step without further purification.

Amine Acetylation—The aqueous solution of the hydrochloride of VII or IX was heated to 50° and mixed with 60 ml of acetic anhydride. A freshly prepared solution of 100 g of sodium acetate in 100 ml of water was heated to 50° and added to the mixture with stirring and cooling in an ice bath for 30 min. The acetamido derivatives were filtered and purified by recrystallization from ethanol or ethanol–water. Compound VIII was obtained in an 84% yield, and X was obtained in an 80% yield. The physical constants of VIII and X are shown in Table I.

Compound VIII was white to slightly pink needle-like crystals, mp 174–177°. Its mass spectrum showed a molecular ion at *m/e* 271; IR ($CHCl_3$): ν_{max} 3430, 3250, 3010, 1680, 1670, 1610, 1360, 1270, and 1050 cm^{-1}; NMR ($CDCl_3$): δ 2.17 (3H, s), 6.98 (1H at C-3, d, J = 8.8 Hz), 7.12–7.54 (5H, complex m), 7.62 (1H at C-4, dd, J = 8.5 and 2.4 Hz), and 8.22 (1H at C-6, d, J = 2.6 Hz).

Compound X was white to slightly greenish flakes, mp 165–166°. Its mass spectrum showed a molecular ion at *m/e* 271; IR ($CHCl_3$): ν_{max} 3420, 3180, 3010, 1680, 1670, 1610, 1360, 1280, 1060, and 980 cm^{-1}; NMR ($CDCl_3$): δ 2.23 (3H, s), 6.98 (1H at C-5, t, J = 8 Hz), 7.15–7.58 (5H, complex m), 7.78 (1H at C-4, dd, J = 8 and 1.5 Hz), and 8.65 (1H at C-6, dd, J = 8 and 1.5 Hz).

[1] Melting points were determined using a Büchi apparatus and are uncorrected. The structures of all compounds were confirmed by IR, NMR, and mass spectra. IR spectra were recorded on IR-257 and IR-221 spectrophotometers (Perkin-Elmer). NMR spectra were determined as solutions in deuterochloroform, with tetramethylsilane as the internal standard, on a WH-90 instrument (Bruker). The WH-90 instrument was connected to a computer (model B-NC 12) with a FINMR V 51218 program.

Mass spectra were recorded by Morgan-Schaffer Corp., Montreal, Canada. The spectra of V, VI, and VIII were recorded on a Hitachi Perkin-Elmer mass spectrometer (model RMU-6D) by introducing the samples by direct probe at 40° with an ionization voltage of 70 ev. The mass spectra of VIII and X were recorded on a CH-5 mass spectrometer (Varian MAT) by direct probe at 110° and 70 ev. TLC was performed on 0.25-mm precoated silica gel plates (Merck silica gel 60 F-254 or silica gel F-254). Materials on plates were detected with a UV lamp. NMR data are expressed in δ. Microanalyses were performed by Dr. Daessle, Organic Micro-Analysis Laboratories, Montreal, Canada.

[2] Fluka, Buchs, Switzerland.

[3] Hyna.

0022-3549/79/0700-0893$01.00/0
© 1979, American Pharmaceutical Association

Table I—Nitro- and Acetamidophenylsalicylates

Compound	R	Melting Point	Recrystallization Solvent	Yield, %	Formula		Analysis, % Calc.	Found	R_f Values[a] Chloroform	Benzene	Ethyl Acetate
V	5-NO_2	148–150°[b]	Ethanol	42	$C_{13}H_9NO_5$	C	60.10	59.89	0.496	0.256	—
						H	3.47	3.68	0.690	0.536	—
						N	5.78	5.52			
VI	3-NO_2	92–93°[c]	Ethanol	52	$C_{13}H_9NO_5 \cdot H_2O$	C	56.32	56.62	0.423	0.146	—
						H	3.97	3.58	0.560	0.330	—
						N	5.05	4.87			
VIII	5-$NHCOCH_3$	174–176°	Ethanol or ethanol–water	84	$C_{15}H_{13}NO_4$	C	66.42	66.36	0.023	0.013	0.631
						H	4.79	5.04	0.073	—[d]	0.877
						N	5.16	5.29			
X	3-$NHCOCH_3$	165–166°	Ethanol or ethanol–water	80	$C_{15}H_{13}NO_4$	C	66.42	66.27	0.122	0.013	0.821
						H	4.79	5.08	0.303	0.043	0.922
						N	5.16	5.32			

[a] Two R_f values are reported for each compound in different solvents. The first value represents the R_f on silica gel 60 F-254 (slow moving); the second value represents the R_f on silica gel F-254 (fast moving). [b] Lit. (7, 8) mp 150–151°. [c] Lit. (8) mp 101–102° for anhydrous. The compound was dried after analysis to give mp 99–100°. [d] The compound did not move.

Biological Testing of VIII and X—Solutions of VIII or X in dimethyl sulfoxide or propylene glycol or suspensions in 1% methylcellulose were administered to groups of six, eight, or 10 albino MRI female or male mice weighing 18–20 g. The doses were 25, 50, 100, 200, 300, 400, and 500 mg/kg. Twenty minutes later, the mice were given, intraperitoneally, 0.2 ml of a 0.02% solution of phenyl-*p*-quinone in water containing 5% alcohol.

The mice for each dose were placed in separate cages and observed for 20 min. Those that showed signs of writhing were removed from the cage. The ED_{50} data of VIII are shown in Table II. Compound X was ineffective at doses of 50 and 200 mg/kg.

RESULTS AND DISCUSSION

Chemistry—Several nitro derivatives of phenylsalicylate have been made by treatment of nitrosalicylic acid and phenol with phosphorus oxychloride or by treatment of salicylic acid and nitrophenol with phosphorus oxychloride (7–9). Other investigators (10) nitrated salicylic acid and salicylamide by treatment of these compounds with nitric acid to obtain the corresponding 3- and 5-nitro derivatives. Our approach to the synthesis of V and VI also involved direct nitration of I with nitric acid. This procedure achieved almost complete conversion of I into V and VI.

Evidence for structural identification of V and VI was obtained from mass spectral (Table III) and NMR studies. Both compounds had a molecular ion at *m/e* 259 with relative intensities of 95% for V and 76.5% for VI. These data indicate that one nitro group is introduced in both compounds and that the molecular ion of V is more stable than that of VI[4] (11). Isotopic analysis gave good agreement with the theoretical value for $C_{13}H_9NO_5$ (Table IV). The mass spectra of both compounds were similar except for the quantitative differences in the relative peak intensities.

Both V and VI showed peaks at *m/e* 166 (100%) upon electron impact. This peak may be represented by ion *a* (Scheme I), which indicated the introduction of the nitro group onto the salicylate ring of I.

The peak at *m/e* 229 may be represented by ion *b* (M − NO). This ion may result from the rearrangement of the nitro group prior to loss of the NO group (12–16). The intensity difference of this peak in the mass spectra of V and VI can be attributed to the differences in the nitro group position in the two molecules (12–16). Such rearrangement has been reported for several *para*- and *meta*-substituted nitrobenzene derivatives. The *ortho*-derivatives lack such rearrangement or show peaks of very low intensity corresponding to ions resulting from this rearrangement. This type of rearrangement was also observed for ion *a* (Scheme II and Table III).

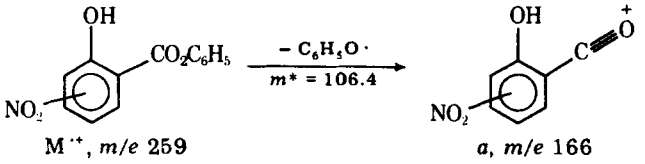

Scheme I

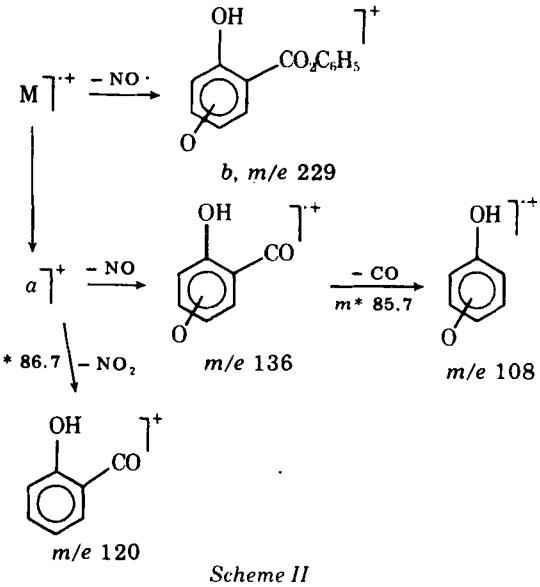

Scheme II

The IR spectra of various V and VI concentrations also were studied to reveal the effect of the nitro group on hydrogen bonding in phenylsalicylate. Both compounds showed broad absorption bands at 3300–3090 cm^{-1} in concentrations ranging between 2.5 and 12.5% in chloroform. No shift was observed in the absorption band of the hydroxyl group in this region. This result may indicate that the nitro group position in the salicylate ring had no effect on the intramolecular hydrogen bond that exists in I (17–19) between the hydroxyl group and the carboxyl group.

The mass spectral data for V and VI suggest that the former compound may have a 1,2,5-substitution and that the latter may have a 1,2,3-substitution. NMR and decoupling studies confirmed this evidence. At the low field end of the aromatic region of the NMR spectrum of V, there was a doublet at δ 9.04 with splitting of 2.6 Hz. The chemical shift indicated the resonance of the proton at C-6 with the two *ortho*-positions occupied by electron-withdrawing groups. The *J* value indicated the presence of a *meta*-proton (20–23), indicating the presence of a proton at C-4 whose signal appeared as two doublets at 8.42 with splitting of 9.4 and 2.6 Hz. This finding indicated the presence of *meta*- (at C-6) and *ortho*- (at C-3) protons. The signal of the latter appeared as a doublet at 7.16 with

Table II—Biological Testing Data of VIII

Dose, mg/kg	Number of Mice	Percent Protection
25	8	37.50
50	6, 6, 8[a]	50.00
100	8, 8, 10[a]	66.60
200	6	83.30
300	6	83.30
500	6, 8[a]	100.00

[a] The experiment was repeated using the number of animals shown, and percent protection represents the average.

[4] R. Schaffer, Morgan-Schaffer Corp., Montreal, Canada, 1977, personal communication.

Table III—Mass Spectral Data of V and VI

m/e	Percent V	Percent VI
92	64.4	22.4
108	11.2	3.0
120	81.4	69.2
121	15.0	10.0
166	100.0	100.0
229	11.9	3.3
259	95.1	76.5
260	43.9	17.0
261	6.3	2.9

splitting of 9.6 Hz, which indicated the presence of an *ortho*-proton (at C-4). The decoupling study confirmed this assignment since irradiation of H-3 removed the *ortho*-coupling to H-4, which appeared as a doublet with *meta*-splitting. Irradiation of H-4 removed the *ortho*-coupling to H-3, which appeared as a singlet, and the *meta*-coupling to H-6, which also appeared as a singlet. Irradiation of H-6 removed the *meta*-coupling to H-4, which appeared as a doublet with *ortho*-splitting only. These data indicate that the salicylate ring protons in V have a 1,2,4-relationship.

The NMR spectrum of VI showed a two-doublet signal at δ 8.32 with splitting of 8 and 1.7 Hz, characteristic of *ortho*- and *meta*-splitting, respectively (20–23). This signal was assigned to the proton at C-4. The signal representing the C-6 proton of the salicylate ring also appeared as a doublet at δ 8.21 with splitting of 8.2 and 1.7, which indicated the presence of *ortho*- and *meta*-protons at C-5 and C-4, respectively. However, the signal representing C-5 proton was included in the complex multiplet at δ 7.60–7.01. The decoupling study confirmed this assignment since H-5 irradiation removed the *ortho*-splitting with H-4 and H-6 and both appeared as doublets with *meta*-splitting to each other. Irradiation of H-4 or H-6 removed the *meta*-splitting to each other, and their signals appeared as doublets with *ortho*-splitting. These data indicate that the nitro group occupies the 3-position and that the protons in VI have a 1,2,3-relationship.

Reduction of the isomeric nitro salols was achieved by simple catalytic hydrogenation in very high yields. The corresponding amines were acetylated by treatment of the amines with acetic anhydride to produce the corresponding acetamido derivatives (VIII and X) in high yields. In contrast to the IR spectra of V and VI, the IR spectra of VIII and X showed a clear difference in the hydroxyl group absorption band. The hydroxyl absorption band in the IR spectrum of X appeared at 3180 cm^{-1}; in the IR spectrum of VIII, it appeared at 3250 cm^{-1}. This difference may be based upon the different types of hydrogen bonding the molecules undergo.

The mass spectra of VIII and X also were similar (Table V), and the fragmentation pattern was comparable to that of the nitro derivatives. The appearance of a peak at *m/e* 178 (100%) may have arisen from the loss of a phenoxide radical from the molecular ion (*m/e* 271), as shown in Scheme III together with the other important fragmentations.

The NMR spectra of VIII and X and the decoupling study were consistent with the positional assignment of the acetamido group (Table VI).

Biological Testing and Toxicity—Compounds VIII and X were tested for analgesic activity in the writhing test (24). Compound VIII had comparable analgesic activity to that of aspirin and phenacetin. The ED_{50} of VIII under the experimental conditions was 56 mg/kg (27–122) when the writhing material was injected 20 min after treatment of the mice. However, X was ineffective at 50 mg/kg and caused restlessness at 200 mg/kg upon injection of the writhing material. Compound VIII was nontoxic at doses of 1 and 2 g/kg sc and caused 10% death of the mice at 3 g/kg ip during 24 hr.

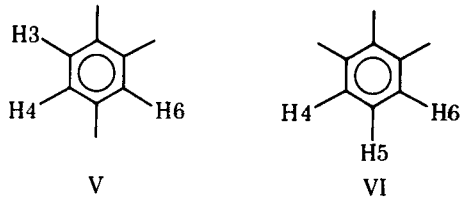

V VI

Table IV—Mass Spectral Isotopic Analysis [a] of V and VI

Compound	m/e	$C_{13}H_9NO_5$ Theoretical	$C_{13}H_9NO_5$ Found
V	259	100.00	100.00
	260	14.77	14.70
	261	2.01	2.09
VI	259	100.00	100.00
	260	14.77	14.79
	261	2.01	2.05

[a] Analysis performed by Morgan-Schaffer Corp., Montreal, Canada.

Table V—Mass Spectral Data of VIII and X

m/e	Percent VIII	Percent X
107	4.8	11.0
108	9.0	16.5
134	3.6	58.3
135	9.6	47.2
177	11.4	20.0
178	100.0	100.0
179	10.8	1.6
271	43.4	72.7
272	8.4	13.8
273	1.2	1.6

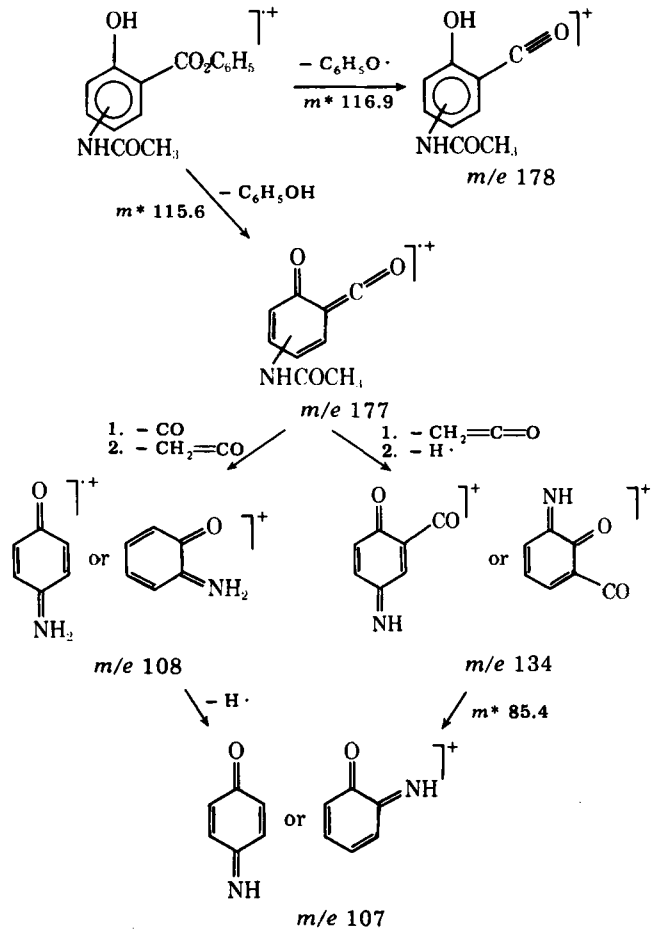

Scheme III

Table VI—NMR Data of VIII and X

Proton	δ	J_{meta}, Hz	J_{ortho}, Hz
Compound VIII			
H3	6.98 d	—	8.8
H4	7.62 dd	2.4	8.5
H6	8.22 d	2.6	—
Compound X			
H4	7.78 dd	1.5	8.0
H5	6.98 dd [a]		
H6	8.65 dd	1.5	8.0

[a] Collapsed into triplet at J = 8.0 Hz.

REFERENCES

(1) "Remington's Pharmaceutical Sciences," 15th ed., A. Osol and J. B. Hoover, Eds., Mack Publishing Co., Easton, Pa., 1975, p. 1269.

(2) J. T. Miyahara and R. Karler, *Biochem. J.*, **97**, 194 (1965).

(3) J. T. Sheehan, *J. Am. Chem. Soc.*, **70**, 1665 (1948).

(4) E. Wenis and T. S. Gardner, *J. Am. Pharm. Assoc., Sci. Ed.*, **38**, 9 (1949).

(5) U.S. pat. 2,604,488 to Rhom-Poulenc (Merck Index, 8th ed., Merck and Co., Rahway, N.J., 1968).

(6) S. Maruyama and H. Imamura, *J. Am. Chem. Soc.*, **74**, 2589 (1952).

(7) G. V. Jadhav and R. N. Thakkar, *J. Univ. Bombay, Sec. A*, **18**, 29 (1949); through *Chem. Abstr.*, **44**, 5845i (1950).

(8) Beilsteins Band X, System No. 1051–1054 (1927).

(9) N. G. Gaylord and P. N. Kamath, *Org. Synth. Coll. Vol.*, **4**, 178 (1967).

(10) A. N. Meldrum and N. W. Hirve, *J. Indian Chem. Soc.*, **5**, 95 (1928); through *Chem. Abstr.*, **22**, 4514 (1928).

(11) J. H. Beynon, R. A. Saunders, and A. E. Williams, *Ind. Chim. Belge*, **1964**, 311.

(12) M. M. Bursey and F. W. McLafferty, *J. Am. Chem. Soc.*, **88**, 5023 (1966).

(13) J. H. Beynon, G. R. Lester, and A. E. Williams, *ibid.*, **63**, 1861 (1959).

(14) S. Meyerson, I. Puskas, and E. K. Fields, *ibid.*, **88**, 4974 (1966).

(15) J. H. Beynon, "Mass Spectrometry and Its Application to Organic Chemistry," Elsevier, Amsterdam, The Netherlands, 1960, p. 268.

(16) J. H. Beynon, R. A. Saunders, A. Tapham, and A. E. Williams, *J. Chem. Soc.*, **1965**, 6403.

(17) W. Gardy, *J. Chem. Phys.*, **7**, 163 (1939); through *Chem. Abstr.*, **33**, 3262[5] (1939).

(18) R. A. Nyquist, *Spectrochim. Acta*, **19**, 1655 (1963).

(19) V. S. Korbkov, *Opt. Spektrosk.*, **17**, 938 (1964); through *Chem. Abstr.*, **62**, 11302c (1965).

(20) J. D. Swalen, "Progress in NMR Spectroscopy," vol. 1, Pergamon, New York, N.Y., 1966, p. 240.

(21) F. Scheinmann," An Introduction to Spectroscopic Methods for the Identification of Organic Compounds," vol. 1, Pergamon, New York, N.Y., 1970, p. 69.

(22) D. J. Pasto and C. R. Johnson," Organic Structure Determination," Prentice-Hall, Englewood Cliffs, N.J., 1969, p. 183.

(23) J. R. Dyer, "Application of Absorption Spectroscopy of Organic Compounds," Prentice-Hall, Englewood Cliffs, N.J., 1965, p. 58.

(24) A. Burger, "Selected Pharmacological Testing Methods," Dekker, New York, N.Y., 1963, p. 100.

ACKNOWLEDGMENTS

The author is indebted to the Deutscher Akademischer Austauschdienst and to Professor H. Oelschlager, Director of the Pharmaceutical Chemistry Institute, for their invitation to perform this project at the University of Frankfurt, West Germany. The author also thanks Professor H. Linde for his assistance in interpretation of the NMR spectra, Miss Cramer and Miss Ross for carrying out the mass and NMR spectra, Dr. M. Ewert for his assistance in the hydrogenation, and Professor E. Mutschler and Dr. G. Lambrecht for their assistance in the biological testing.

Conductivity and Hardness Changes in Aged Compacts

RAJKUMAR P. BHATIA * and NICHOLAS G. LORDI ˣ

Received August 8, 1978, from the *College of Pharmacy, Rutgers—The State University, Piscataway, NJ 08854.* Accepted for publication January 28, 1979. *Present address: Alcon Laboratories, Fort Worth, TX 76133.

Abstract □ Batches of sodium, potassium, and ammonium chloride tablets containing no excipients and spray-dried lactose tablets containing 0.5% magnesium stearate were stored at 20 and 76% relative humidity. Electrical resistance and hardness measurements were made within 1 hr after compression and at intervals during a 45-day period. Hardness values of sodium, potassium, and ammonium chloride tablets stored at 20% relative humidity increased from 70 to 200% at 45 days, while conductances decreased 10-fold. Tablets stored at 76% relative humidity showed no increases or slight decreases in hardness with slight increases in conductance. Lactose tablets decreased slightly in hardness with corresponding increases in conductance.

Keyphrases □ Conductivity, electrical—effect of aging and humidity, various compressed tablets □ Hardness—effect of aging and humidity, various compressed tablets □ Tablets, compressed—effect of aging and humidity on electrical conductivity and hardness

The effect of aging on the physical characteristics of tablets has been discussed by several investigators. Increased hardness was reported in hydrochlorothiazide tablets formulated with acacia (1). Dibasic calcium phosphate dihydrate tablets displayed no significant changes in hardness over a 4-month period but showed significant increases in disintegration and dissolution times when stored at 25° and 50% relative humidity (RH) (2).

The crushing strength of sodium chloride compacts prepared from dried samples doubled 1 hr after compaction (3). No significant changes in crushing strength were observed when compacts were stored for longer periods at low humidities. This phenomenon was attributed to time-dependent relaxations, resulting in stress release within the compacts which increased interparticulate contact and bonding. Compacts with higher moisture content possessed low tensile strength compared to those with lower moisture content, which was attributed to weakening of interparticulate bonding by trace moisture (3).

Significant increases in hardness were observed in sodium chloride tablets stored for several days (4). These changes correlated with changes in electrical conductances calculated from measured dissipation factors.

The electrical conductance of a compact is determined in part by the number of interparticulate contact points and the effective internal surface area resulting from microscopic cracks and imperfections (5). Hardness changes in compacts should be associated with conductance changes that reflect changes in the contact area and internal surface. Increases in compact strength should be correlated with decreases in electrical conductance, measured under conditions in which there is no substantial increase in compact moisture content.

This study was designed to verify the expected relationship between conductance and hardness changes in compacts and to establish the role of moisture in affecting these changes in compacts of directly compressible salts.

0022-3549/79/0700-0896$01.00/0

© 1979, American Pharmaceutical Association

REFERENCES

(1) "Remington's Pharmaceutical Sciences," 15th ed., A. Osol and J. B. Hoover, Eds., Mack Publishing Co., Easton, Pa., 1975, p. 1269.

(2) J. T. Miyahara and R. Karler, *Biochem. J.*, **97**, 194 (1965).

(3) J. T. Sheehan, *J. Am. Chem. Soc.*, **70**, 1665 (1948).

(4) E. Wenis and T. S. Gardner, *J. Am. Pharm. Assoc., Sci. Ed.*, **38**, 9 (1949).

(5) U.S. pat. 2,604,488 to Rhom-Poulenc (Merck Index, 8th ed., Merck and Co., Rahway, N.J., 1968).

(6) S. Maruyama and H. Imamura, *J. Am. Chem. Soc.*, **74**, 2589 (1952).

(7) G. V. Jadhav and R. N. Thakkar, *J. Univ. Bombay, Sec. A*, **18**, 29 (1949); through *Chem. Abstr.*, **44**, 5845i (1950).

(8) Beilsteins Band X, System No. 1051–1054 (1927).

(9) N. G. Gaylord and P. N. Kamath, *Org. Synth. Coll. Vol.*, **4**, 178 (1967).

(10) A. N. Meldrum and N. W. Hirve, *J. Indian Chem. Soc.*, **5**, 95 (1928); through *Chem. Abstr.*, **22**, 4514 (1928).

(11) J. H. Beynon, R. A. Saunders, and A. E. Williams, *Ind. Chim. Belge*, **1964**, 311.

(12) M. M. Bursey and F. W. McLafferty, *J. Am. Chem. Soc.*, **88**, 5023 (1966).

(13) J. H. Beynon, G. R. Lester, and A. E. Williams, *ibid.*, **63**, 1861 (1959).

(14) S. Meyerson, I. Puskas, and E. K. Fields, *ibid.*, **88**, 4974 (1966).

(15) J. H. Beynon, "Mass Spectrometry and Its Application to Organic Chemistry," Elsevier, Amsterdam, The Netherlands, 1960, p. 268.

(16) J. H. Beynon, R. A. Saunders, A. Tapham, and A. E. Williams, *J. Chem. Soc.*, **1965**, 6403.

(17) W. Gardy, *J. Chem. Phys.*, **7**, 163 (1939); through *Chem. Abstr.*, **33**, 3262[5] (1939).

(18) R. A. Nyquist, *Spectrochim. Acta*, **19**, 1655 (1963).

(19) V. S. Korbkov, *Opt. Spektrosk.*, **17**, 938 (1964); through *Chem. Abstr.*, **62**, 11302c (1965).

(20) J. D. Swalen, "Progress in NMR Spectroscopy," vol. 1, Pergamon, New York, N.Y., 1966, p. 240.

(21) F. Scheinmann," An Introduction to Spectroscopic Methods for the Identification of Organic Compounds," vol. 1, Pergamon, New York, N.Y., 1970, p. 69.

(22) D. J. Pasto and C. R. Johnson," Organic Structure Determination," Prentice-Hall, Englewood Cliffs, N.J., 1969, p. 183.

(23) J. R. Dyer, "Application of Absorption Spectroscopy of Organic Compounds," Prentice-Hall, Englewood Cliffs, N.J., 1965, p. 58.

(24) A. Burger, "Selected Pharmacological Testing Methods," Dekker, New York, N.Y., 1963, p. 100.

ACKNOWLEDGMENTS

The author is indebted to the Deutscher Akademischer Austauschdienst and to Professor H. Oelschlager, Director of the Pharmaceutical Chemistry Institute, for their invitation to perform this project at the University of Frankfurt, West Germany. The author also thanks Professor H. Linde for his assistance in interpretation of the NMR spectra, Miss Cramer and Miss Ross for carrying out the mass and NMR spectra, Dr. M. Ewert for his assistance in the hydrogenation, and Professor E. Mutschler and Dr. G. Lambrecht for their assistance in the biological testing.

Conductivity and Hardness Changes in Aged Compacts

RAJKUMAR P. BHATIA * and NICHOLAS G. LORDI ˣ

Received August 8, 1978, from the *College of Pharmacy, Rutgers—The State University, Piscataway, NJ 08854.* Accepted for publication January 28, 1979. *Present address: Alcon Laboratories, Fort Worth, TX 76133.

Abstract □ Batches of sodium, potassium, and ammonium chloride tablets containing no excipients and spray-dried lactose tablets containing 0.5% magnesium stearate were stored at 20 and 76% relative humidity. Electrical resistance and hardness measurements were made within 1 hr after compression and at intervals during a 45-day period. Hardness values of sodium, potassium, and ammonium chloride tablets stored at 20% relative humidity increased from 70 to 200% at 45 days, while conductances decreased 10-fold. Tablets stored at 76% relative humidity showed no increases or slight decreases in hardness with slight increases in conductance. Lactose tablets decreased slightly in hardness with corresponding increases in conductance.

Keyphrases □ Conductivity, electrical—effect of aging and humidity, various compressed tablets □ Hardness—effect of aging and humidity, various compressed tablets □ Tablets, compressed—effect of aging and humidity on electrical conductivity and hardness

The effect of aging on the physical characteristics of tablets has been discussed by several investigators. Increased hardness was reported in hydrochlorothiazide tablets formulated with acacia (1). Dibasic calcium phosphate dihydrate tablets displayed no significant changes in hardness over a 4-month period but showed significant increases in disintegration and dissolution times when stored at 25° and 50% relative humidity (RH) (2).

The crushing strength of sodium chloride compacts prepared from dried samples doubled 1 hr after compaction (3). No significant changes in crushing strength were observed when compacts were stored for longer periods at low humidities. This phenomenon was attributed to time-dependent relaxations, resulting in stress release within the compacts which increased interparticulate contact and bonding. Compacts with higher moisture content possessed low tensile strength compared to those with lower moisture content, which was attributed to weakening of interparticulate bonding by trace moisture (3).

Significant increases in hardness were observed in sodium chloride tablets stored for several days (4). These changes correlated with changes in electrical conductances calculated from measured dissipation factors.

The electrical conductance of a compact is determined in part by the number of interparticulate contact points and the effective internal surface area resulting from microscopic cracks and imperfections (5). Hardness changes in compacts should be associated with conductance changes that reflect changes in the contact area and internal surface. Increases in compact strength should be correlated with decreases in electrical conductance, measured under conditions in which there is no substantial increase in compact moisture content.

This study was designed to verify the expected relationship between conductance and hardness changes in compacts and to establish the role of moisture in affecting these changes in compacts of directly compressible salts.

0022-3549/79/0700-0896$01.00/0

© 1979, American Pharmaceutical Association

Table I—Conductance and Hardness (±*SD*) of Aged Sodium Chloride Compacts

Storage Period, days	20% RH: Apparent[a] Specific Conductance, $ohms^{-1}\ cm^{-1} \times 10^9$	20% RH: W/T[b] Ratio, g/cm	20% RH: Hardness, kg	76% RH: Apparent Specific Conductance, $ohms^{-1}\ cm^{-1} \times 10^9$	76% RH: W/T Ratio, g/cm	76% RH: Hardness, kg
Initial	1.238 (0.098)	2.566 (0.008)	2.54 (0.91)	1.260 (0.0.98)	2.586 (0.024)	2.65 (0.01)
2	0.818 (0.067)	2.544 (0.007)	3.44 (0.04)	1.159 (0.088)	2.589 (0.036)	3.20 (0.08)
7	0.141 (0.041)	2.541 (0.011)	5.01 (0.11)	0.862 (0.067)	2.597 (0.049)	3.36 (0.06)
15	0.073 (0.008)	2.544 (0.009)	6.22 (0.09)	1.144 (0.046)	2.588 (0.006)	3.25 (0.01)
30	0.055 (0.003)	2.571 (0.062)	6.36 (0.05)	1.144 (0.056)	2.589 (0.008)	2.91 (0.04)
45	0.049 (0.006)	2.600 (0.011)	6.42 (0.04)	1.190 (0.049)	2.595 (0.032)	2.66 (0.09)

[a] Average of five observations. [b] Weight to thickness.

Table II—Conductance and Hardness (±*SD*) of Aged Potassium Chloride Compacts

Storage Period, days	20% RH: Apparent[a] Specific Conductance, $ohms^{-1}\ cm^{-1} \times 10^9$	20% RH: W/T[b] Ratio, g/cm	20% RH: Hardness, kg	76% RH: Apparent Specific Conductance, $ohms^{-1}\ cm^{-1} \times 10^9$	76% RH: W/T Ratio, g/cm	76% RH: Hardness, kg
Initial	0.219 (0.034)	2.338 (0.006)	3.52 (0.02)	0.207 (0.028)	2.332 (0.008)	3.50 (0.06)
2	0.081 (0.021)	2.342 (0.005)	4.32 (0.04)	0.186 (0.018)	2.338 (0.008)	3.54 (0.02)
7	0.042 (0.008)	2.351 (0.008)	4.95 (0.06)	0.172 (0.034)	2.344 (0.006)	3.63 (0.05)
15	0.028 (0.008)	2.334 (0.005)	6.12 (0.03)	0.194 (0.038)	2.333 (0.005)	3.52 (0.02)
30	0.017 (0.004)	2.337 (0.008)	7.61 (0.04)	0.225 (0.031)	2.346 (0.010)	3.37 (0.01)
45	—	2.333 (0.006)	8.59 (0.03)	0.230 (0.072)	2.254 (0.028)	3.13 (0.02)

[a] Average of five observations. [b] Weight to thickness.

Table III—Conductance and Hardness (±*SD*) of Aged Ammonium Chloride Compacts

Storage Period, days	20% RH: Apparent[a] Specific Conductance, $ohms^{-1}\ cm^{-1} \times 10^9$	20% RH: W/T[b] Ratio, g/cm	20% RH: Hardness, kg	76% RH: Apparent Specific Conductance, $ohms^{-1}\ cm^{-1} \times 10^9$	76% RH: W/T Ratio, g/cm	76% RH: Hardness, kg
Initial	3.090 (0.120)	1.896 (0.012)	3.40 (0.05)	3.280 (0.083)	1.895 (0.009)	3.37 (0.03)
2	0.513 (0.063)	1.899 (0.018)	3.59 (0.05)	3.710 (0.112)	1.889 (0.006)	3.40 (0.04)
7	0.220 (0.041)	1.898 (0.021)	4.20 (0.07)	2.560 (0.086)	1.897 (0.012)	3.48 (0.03)
15	0.124 (0.033)	1.876 (0.008)	4.86 (0.03)	3.641 (0.041)	1.878 (0.008)	3.33 (0.01)
30	0.081 (0.018)	1.876 (0.006)	5.44 (0.03)	3.855 (0.132)	1.876 (0.006)	3.45 (0.03)
45	0.064 (0.008)	1.902 (0.011)	5.53 (0.04)	3.758 (0.098)	1.875 (0.010)	3.28 (0.02)

[a] Average of five observations. [b] Weight to thickness.

EXPERIMENTAL

Materials—Since different lots of the same material show variations in electrical properties (6), single lots of USP grade sodium chloride, potassium chloride, ammonium chloride[1], and spray-dried lactose[2] were studied. Saturated solutions of sodium acetate (analytical reagent) and potassium acetate (analytical reagent) were used to maintain ~20 and 76% RH in 5-liter desiccators. The chloride salts were screened to isolate the 40–50-mesh fractions, which were dried at 65° for 24 hr before compaction.

Preparation and Treatment of Compacts—Batches of compacts were prepared from the 40–50-mesh fraction of unlubricated sodium, potassium, and ammonium chlorides and spray-dried lactose blended with 0.5% magnesium stearate. The latter was included as an example of a formulation that showed no significant hardness changes on aging. Tablets were compressed manually, using a 1.27-cm diameter punch and die assembly, on a single-punch tablet press[3].

Compacts of suitable weight, thickness, and hardness were produced and stored in the 20 and 76% humidity chambers. Resistance and hardness values were determined within 1 hr of compression and after 2, 7, 15, 30, and 45 days of storage. The 20 and 76% RH conditions were selected to observe the effect of drying and atmospheric moisture on compact conductance and hardness.

In some experiments, sodium chloride compacts were stored at 76% RH for 10 days and then transferred to 20% RH. Resistance and hardness values were measured at the time of transfer and after up to 45 days of storage at 20% RH.

A small batch of sodium chloride compacts was prepared using the 1.27-cm punch and die assembly on a hydraulic press[4] at 1800-, 2700-, and 3600-kg gauge pressures. Pressure was applied for at least 15 sec. Compacts were stored at 20% RH until subject to resistance and hardness measurements.

Conductance Measurements—The complete system for measurement of the electrical resistance of compacts was described previously (7). Compacts were placed on a grounded steel plate attached to the lower stage of the hydraulic press. A 2.5-cm diameter shielded tablet punch, which was fixed to the upper stage of the press through an insulating acrylic[5] block, served as the active electrode. A shielded cable connected the punch to an electrometer[6]. The lower stage of the press was raised until the tablet contacted the punch face.

A minimal pressure (<50 kg) was applied to minimize contact resistance. Stable resistance values were attained within 1 min and recorded. The thickness and weight of each compact were measured before testing for hardness. Specific conductances were calculated from the measured resistance and dimensions. This procedure was repeated on five different compacts to obtain each experimental point.

Hardness Measurements—A 1.27-cm diameter standard concave punch was fastened to the platform of a motorized linear drive[7] so that it was exactly centered beneath an indentation probe. The latter consisted

[1] Fisher Scientific Co., Springfield, N.J.
[2] Foremost-McKesson, Appleton, Wis.
[3] Manesty model E2, Key Industries, Farmingdale, N.J.
[4] Model C, Fred S. Carver, Menomonee Falls, Wis.
[5] Lucite.
[6] Model 610C, Keithley Instruments, Cleveland, Ohio.
[7] Model LTCM, John Chatillon and Sons, New York, N.Y.

Table IV—Conductance and Hardness (±*SD*) of Aged 40–50-Mesh Sodium Chloride Compacts Stored under 76% RH for 7 Days and then Transferred to 20% RH

Storage Period, days	Apparent[a] Specific Conductance, $ohms^{-1}\ cm^{-1} \times 10^9$	W/T[b] Ratio, g/cm	Hardness, kg
Initial[c]	0.800 (0.041)	2.589 (0.007)	3.24 (0.02)
2	0.477 (0.028)	2.570 (0.009)	3.59 (0.01)
7	0.165 (0.013)	2.558 (0.010)	4.46 (0.02)
15	0.076 (0.008)	2.556 (0.009)	6.14 (0.02)
30	0.057 (0.008)	2.560 (0.007)	6.36 (0.01)
45	0.052 (0.004)	2.553 (0.006)	6.45 (0.01)

[a] Average of five observations. [b] Weight to thickness. [c] Represents 7 days of storage at 76% RH.

of an 0.4-cm diameter stainless steel ball bearing fixed to a threaded shaft, which was fastened to a 22.7-kg (50-lb) load cell[8]. The output of the load cell was amplified[9] and recorded[10]. The motorized drive was operated at a platform speed of 0.5 cm/min.

Compacts were placed on edge on the punch face, and the identation probe was driven diametrically into the compact, which split into two equal halves. Figure 1 shows a plot of measured force on the tablet as a function of time. Point A represents the onset of stress; point B represents the maximum stress the compact experienced prior to splitting, shown by line BC, which represents the sudden release in stress. In Fig. 1, AC represents the degree of indentation required to split the tablet. Hardness values were expressed in terms of the maximum force in kilograms required to split the compact.

RESULTS AND DISCUSSION

Tables I–III summarize observed conductance and hardness values of sodium, potassium, and ammonium chloride compacts stored at 20 and 76% RH for 45 days. Figure 2 shows relative changes in hardness compared to initial values as a function of time. Sodium and potassium chloride compacts stored at 20% RH exhibited marked increases in hardness along with significant decreases in specific conductance. Constant hardness and conductance values were observed after 15 days with

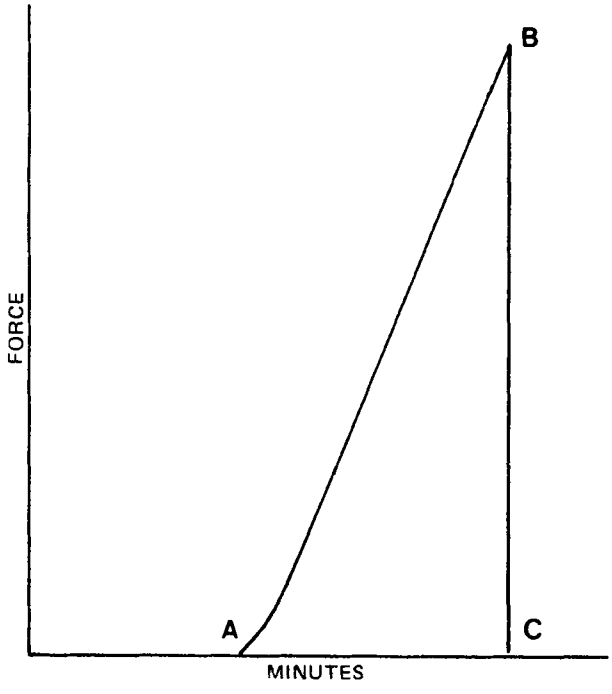

Figure 1—*Typical force-time plot observed in indentation testing of tablet hardness (see text).*

[8] Models UC3 and UL4-50, Statham Instruments, Los Angeles, Calif.
[9] Model UR3, Statham Instruments, Los Angeles, Calif.
[10] Model 680 recorder, Hewlett-Packard, Palo Alto, Calif.

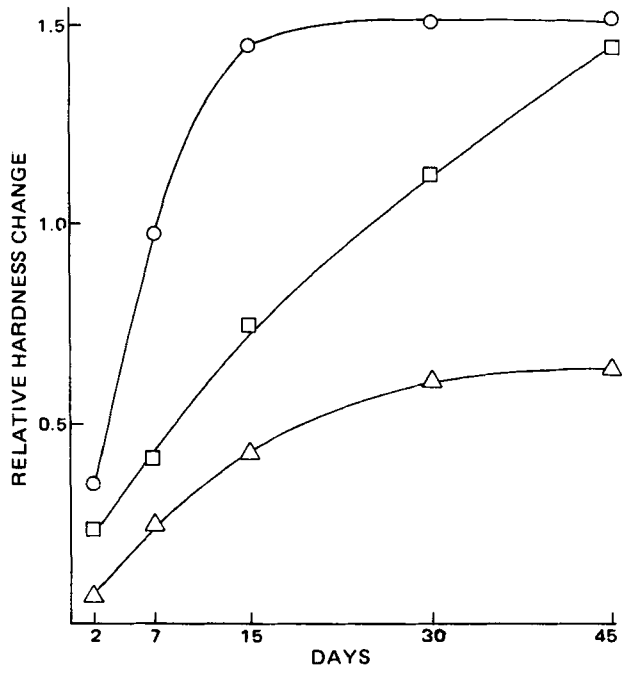

Figure 2—*Relative hardness changes observed in sodium (○), potassium (□), and ammonium chloride (△) compacts stored at 20% RH.*

sodium chloride and after 45 days with ammonium chloride. However, potassium chloride compacts continued to increase in hardness after 45 days. Measurements were made on compacts of equal density, as indicated by the constancy of the weight to thickness ratio.

No significant changes in hardness or conductance were observed in compacts stored at 76% RH, except for sodium chloride where hardness increased and conductance decreased slightly in the first 7 days of storage. Table IV summarizes observations made on sodium chloride compacts stored at 76% RH for 7 days before transfer to 20% RH. The same degree of conductance and hardness changes was observed as for compacts stored at 20% RH initially.

Table V summarizes conductance and hardness values for sodium chloride compacts prepared on the hydraulic press and stored at 20% RH. While the initial values varied as expected with the pressure used to form the compacts, essentially the same conductance and hardness values were observed after 30 days of storage. These data suggest that maximum bonding was attained in all three batches of sodium chloride compacts at the same time.

The observed significant increases in hardness of sodium, potassium, and ammonium chloride compacts when stored under low humidity is evidence of strong interparticulate bond formation during storage. Rees and Shotton (3) reported a doubling of the strength of sodium chloride compacts prepared from sodium chloride dried at 110° within 1 hr after compression with negligible changes after 140 hr. They also reported that exposure of salt compacts to 76% RH prevented the hardness increase. It was not possible to prepare satisfactory compacts from completely dried salts in the pressure ranges available on the single-punch press. The traces of moisture present in the materials used in this study contributed to the delayed hardening in contrast to Rees and Shotton's data, which may also reflect increased crystal defects owing to the higher temperatures required to dry the salt completely.

Not all of the potential bond strength developed immediately at the time of compression. Some of the bonded areas formed during compression might have broken during tablet elastic recovery when pressure was released. Sufficient bonding remained to permit the compacts to maintain their shape while new, stronger interparticulate bonding developed.

The data suggest that the principal mechanism of hardening occurs because of a loss of moisture traces at low humidities. This conclusion is supported by the observations summarized in Table IV since compacts stored at 76% RH increased in hardness when transferred to a significantly lower humidity. The amount of moisture involved did not significantly contribute to compact weight.

Rees and Shotton (3) also observed that sodium chloride compacts with a high moisture content had lower tensile strengths than those with a low moisture content. At high humidities, loss of moisture, which results in

Table V—Conductance and Hardness (±*SD*) of Aged Sodium Chloride Compacts Produced at Different Compaction Pressures and Stored at 20% RH

Storage Period, days	1800 kg			2700 kg			3600 kg		
	Apparent[a] Specific Conductance, $ohms^{-1}\ cm^{-1} \times 10^9$	W/T[b] Ratio, g/cm	Hardness, kg	Apparent Specific Conductance, $ohms^{-1}\ cm^{-1} \times 10^9$	W/T Ratio, g/cm	Hardness, kg	Apparent Specific Conductance, $ohms^{-1}\ cm^{-1} \times 10^9$	W/T Ratio, g/cm	Hardness, kg
Initial	0.998 (0.069)	2.470 (0.005)	3.17 (0.11)	0.856 (0.053)	2.488 (0.008)	3.32 (0.008)	0.836 (0.021)	2.481 (0.009)	3.46 (0.03)
2	0.560 (0.030)	2.469 (0.007)	4.28 (0.11)	0.343 (0.069)	2.468 (0.006)	4.39 (0.10)	0.307 (0.028)	2.465 (0.013)	4.46 (0.02)
7	0.095 (0.021)	2.466 (0.009)	5.35 (0.09)	0.076 (0.023)	2.477 (0.002)	5.60 (0.09)	0.073 (0.080)	2.471 (0.011)	5.64 (0.06)
15	0.063 (0.008)	2.476 (0.005)	6.52 (0.09)	0.060 (0.031)	2.473 (0.007)	6.32 (0.09)	0.056 (0.003)	2.478 (0.008)	6.66 (0.04)
30	0.054 (0.021)	2.472 (0.004)	6.70 (0.10)	0.052 (0.004)	2.486 (0.008)	6.68 (0.06)	0.052 (0.008)	2.472 (0.006)	6.73 (0.02)
45	0.053 (0.011)	2.473 (0.005)	6.72 (0.10)	0.052 (0.003)	2.474 (0.011)	6.76 (0.04)	0.051 (0.003)	2.473 (0.011)	6.78 (0.04)

[a] Average of five observations. [b] Weight to thickness.

Table VI—Conductance and Hardness (±*SD*) of Aged Spray-Dried Lactose Compacts Containing 0.5% Magnesium Stearate and Stored under 20% RH

Storage Period, days	Apparent[a] Specific Conductance, $ohms^{-1}\ cm^{-1} \times 10^9$	W/T[b] Ratio, g/cm	Hardness, kg
Initial	0.630 (0.018)	1.668 (0.005)	2.99 (0.12)
2	0.610 (0.022)	1.697 (0.009)	2.95 (0.13)
7	0.641 (0.028)	1.674 (0.006)	2.88 (0.11)
15	0.682 (0.031)	1.673 (0.008)	2.53 (0.18)
30	0.736 (0.042)	1.664 (0.011)	2.46 (0.11)
45	0.781 (0.038)	1.674 (0.016)	2.41 (0.13)

[a] Average of five observations. [b] Weight to thickness.

the deposition of salt around existing contact regions, is inhibited. The differences observed between the different chloride salts is related to the different tendencies of the salts to pick up moisture at 76% RH, which is the critical deliquescence point for sodium chloride. Potassium and ammonium chlorides are more deliquescent at this humidity.

Compacts prepared from spray-dried lactose containing lubricant showed a slight decrease in hardness with an increase in conductance at 20% RH (Table VI). Previous investigators (8) suggested that consolidation in lactose occurs mainly by brittle fracture, in contrast to plastic deformation in sodium chloride. Compacts stored at reduced humidity lose traces of moisture; at a reduced moisture content, magnesium stearate decreases hardness.

The data in this study support the expected relationship between conductance and hardness changes. In all cases, increased hardness was accompanied by more than 10-fold decreases in conductance. Conductance values were stable if hardness was stable. These effects were most pronounced in ionic materials whose electrical resistance was directly measurable. Compacted spray-dried lactose represented the upper limit of resistance measurement with the equipment employed.

REFERENCES

(1) A. S. Alan and E. L. Parrott, *J. Pharm. Sci.*, **60**, 263 (1971).

(2) J. M. Lausier, C.-W. Chiang, H. A. Zompa, and C. T. Rhodes, *ibid.*, **66**, 1636 (1977).

(3) J. E. Rees and E. Shotton, *J. Pharm. Pharmacol., Suppl.*, **22**, 17S (1970).

(4) E. J. Hanus, Ph.D. thesis, Rutgers—The State University, New Brunswick, N.J., 1967.

(5) W. Bollmann, "Crystal Defects and Crystalline Interfaces," 1st ed., Springer-Verlag, New York, N.Y., 1970.

(6) K. Marshall, *J. Pharm. Pharmacol.*, **15**, 413 (1963).

(7) R. P. Bhatia and N. G. Lordi, *J. Pharm. Sci.*, **68**, 222 (1979).

(8) E. T. Cole, J. E. Rees, and J. A. Hersey, *Pharm. Acta Helv.*, **50** (12), 28 (1975).

ACKNOWLEDGMENTS

Presented at the Basic Pharmaceutics Section, APhA Academy of Pharmaceutical Sciences, New York meeting, May 1977.

Abstracted in part from a thesis submitted by R. P. Bhatia to Rutgers—The State University in partial fulfillment of the Doctor of Philosophy degree requirements.

R. P. Bhatia was supported by Bevier and Gillette Fellowships.

Cytotoxic Saponins from the Chinese Herbal Drug Yunnan Bai Yao

P. R. RAVIKUMAR, PAUL HAMMESFAHR, and CHARLES J. SIH ˣ

Received August 14, 1978, from the *School of Pharmacy, University of Wisconsin, Madison, WI 53706.* Accepted for publication January 19, 1979.

Abstract □ Two cytotoxic saponins were isolated from the acetone extracts of the herbal preparation "Yunnan Bai Yao" by column chromatography. They were identified as 3-{[α-L-rhamnopyranosyl(1_{Rha} → 2_{Glu})]-[α-L-arabinofuranosyl(1_{Ara} → 4_{Glu})]-β-D-glucopyranosyl}-25(*R*)-spirost-5-en-3β-ol (I) and 3-{[α-L-rhamnopyranosyl(1_{Rha} → 4_{Rha})-α-L-rhamnopyranosyl(1_{Rha} → 4_{Glu})]-[α-L-rhamnopyranosyl(1_{Rha} → 2_{Glu})]-β-D-glucopyranosyl}-25(*R*)-spirost-5-en-3β-ol (VI). Both saponins exhibited significant cytotoxicity in the standard P-388, L-1210, and 9KB tissue culture screens.

Keyphrases □ Folk medicine—Yunnan Bai Yao, Chinese herbal, cytotoxic activity of isolated saponins □ Yunnan Bai Yao—analysis, cytotoxic saponins, Chinese herbal □ Antineoplastic agents, potential—Yunnan Bai Yao, Chinese herbal, cytotoxic activity of isolated saponins □ Hemostatic agents—Yunnan Bai Yao, cytotoxic activity of isolated saponins, Chinese herbal

The Chinese herbal preparation "Yunnan Bai Yao" was formulated with indigenous medicinal plants about 50 years ago in the Yunnan province. This powdered herbal mixture has been used primarily as a hemostatic agent and gained wide acceptance during the Sino-Japanese War (1937–1945) (1). Claims regarding its efficacy in promoting wound healing and relieving pain also have been made.

In recent years, rumors have circulated among the overseas Chinese that Yunnan Bai Yao could be used in cancer therapy (2). Since extracts of Yunnan Bai Yao exhibited a confirmed level of activity (3–5) in the National Cancer Institute's P-388, L-1210, and 9KB tissue culture screens, the cytotoxic components of this herbal preparation were of interest.

EXPERIMENTAL

Melting points were determined in open capillary tubes[1] and are uncorrected. Optical rotations were measured with a polarimeter[2]. NMR spectra[3] were determined in deuterochloroform containing tetramethylsilane as the internal standard. Mass spectra[4] were recorded at an ionizing voltage of 70 ev. Descending paper chromatography was carried out on Whatman No. 1 paper, which was developed for 48 hr in *n*-butanol–ethanol–water (4:1:5, upper phase). Sugars were visualized with alkaline silver nitrate spray.

Silica gel[5] was used for column chromatography. A gas chromatograph[6], equipped with a 3.66-m column (2.16 mm i.d.) of 5% SE-30 on Chromosorb and operated at 190°, was used for the separation of trimethylsilyl ethers (6) of the sugars. The carrier nitrogen gas flow was 40 ml/min. For the separation of methylated and partially methylated methyl glycosides, a 1.83-m column of 15% butanediol succinate (7) on Chromosorb W-AW (2.16 mm i.d.) at 175° was used instead. Monoglucoside and maltoside of 25(*R*)-spirost-5-en-3β-ol (II) were prepared by known methods (8).

Herbal Preparation of Yunnan Bai Yao—Commercially[7] available

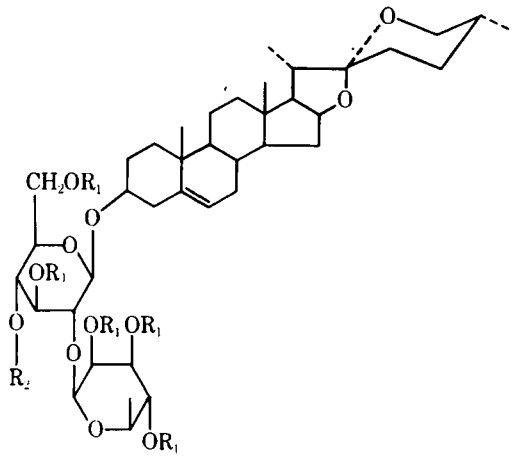

I: R_1 = H, R_2 = $HOCH_2$

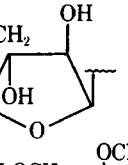

III: R_1 = CH_3, R_2 = CH_3OCH_2

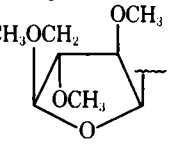

IV: R_1 = R_2 = H

V: R_1 = R_2 = CH_3

VI: R_1 = H, R_2 =

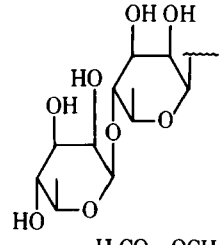

VII: R_1 = CH_3, R_2 =

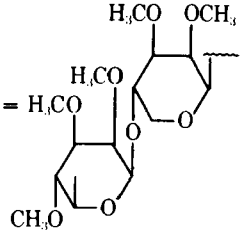

VIII: R_1 = CH_3, R_2 = H

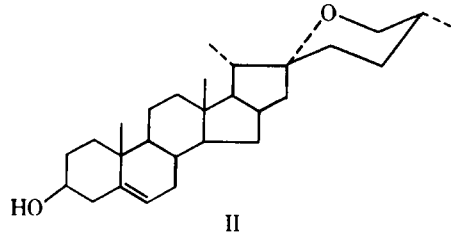

II

[1] Thomas-Hoover apparatus.
[2] Perkin-Elmer model 241.
[3] Varian model EM-390.
[4] AEI MS-9.
[5] MN-Kieselgel, 70-270 mesh ASTM.
[6] Varian Aerograph model 1860-1.
[7] Manufactured in Kuming, Yunnan, China, and purchased in Hong Kong.

0022-3549/79/0700-0900$01.00/0
© 1979, American Pharmaceutical Association

Yunnan Bai Yao was used. The preparation and its chemical constituents were described previously (2).

Fractionation and Isolation of I and VI (Scheme I)—A total of 1.3 kg of Yunnan Bai Yao was extracted successively with 10 liters of benzene for 24 hr, followed by 10 liters of acetone for 48 hr. After solvent evaporation *in vacuo*, 31 g of cytotoxic residue was obtained from the acetone extract. This residue (31 g) was chromatographed on a silica gel (2-kg) column (72 × 9.4 cm). The column was eluted with chloroform–methanol–water (65:25:10), and 900-ml fractions were collected. After solvent evaporation *in vacuo* from fractions 11–16, 5.15 g of a white solid was obtained. Crystallization from 95% ethanol afforded pure 3-{[α-L-rhamnopyranosyl(1_{Rha} → 2_{Glu})]-[α-L-arabinofuranosyl(1_{Ara} → 4_{Glu})]-β-D-glucopyranosyl}-25(*R*)-spirost-5-en-3β-ol (I), mp 242–248°; $[\alpha]_D^{25}$ −118.6° (c, 0.51, methanol); IR (KBr): 3550–3110, 981, 912, 894, and 862 cm^{-1}.

Anal.—Calc. for $C_{44}H_{70}O_{16}\cdot 2H_2O$: C, 59.32; H, 8.31. Found: C, 59.55; H, 8.39.

Fractions 24–33 were combined to afford 2.57 g of 3-{[α-L-rhamnopyranosyl(1_{Rha} → 4_{Rha})-α-L-rhamnopyranosyl(1_{Rha} → 4_{Glu})]-[α-L-rhamnopyranosyl(1_{Rha} → 2_{Glu})]-β-D-glucopyranosyl}-25(*R*)-spirost-5-en-3β-ol (VI), mp 203–210°; $[\alpha]_D^{25}$ −110° (c, 0.50, 95% ethanol); IR (KBr): 3600–3100, 976, 908, 890, and 860 cm^{-1}.

Anal.—Calc. for $C_{51}H_{82}O_{20}\cdot 4H_2O$: C, 56.35; H, 8.28. Found: C, 56.50; H, 8.42.

Hydrolysis of I—The saponin I (100 mg) was heated with 2 *N* H_2SO_4 (4 ml) and dioxane (2 ml) at 100° for 10 hr. It was then diluted with 75 ml of water, and the mixture was extracted with ethyl acetate (4 × 75 ml). The organic layer was washed successively with sodium bicarbonate solution and water. After drying over sodium sulfate, the solvent was evaporated *in vacuo* to give 42 mg of II, mp 205–206°; $[\alpha]_D^{25}$ −115.7° (c, 0.53, chloroform).

The aqueous portion of the hydrolysate was neutralized with anion-exchange resins (carbonate form). After filtration and evaporation, a syrup resulted (52 mg); paper chromatography demonstrated spots corresponding to D-glucose, L-arabinose, and L-rhamnose. The identification of these sugars was further confirmed by reacting 5 mg each of the sugars with hexamethyldisilazane (0.4 ml) and trimethylsilyl chloride (0.2 ml) in pyridine (0.5 ml). After removal of the pyridine *in vacuo*, a hexane solution of the silylated sugars was subjected to GLC analyses.

Methylation of I (9)—Sodium hydride (500 mg, washed three times with hexane) in 40 ml of dimethyl sulfoxide was heated at 70° for 30 min under nitrogen with stirring. A solution of 500 mg of I in 25 ml of dimethyl sulfoxide was added. After stirring for 30 min, methyliodide (10 ml) was added. After stirring for 60 min, the reaction mixture was diluted with 400 ml of water and extracted with ether (4 × 100 ml).

The ethereal extract was washed with water (6 × 100 ml), dried over sodium sulfate, and evaporated to dryness to yield 504 mg of crude III. This procedure was repeated three times to obtain 497 mg of III, mp 159–161°; $[\alpha]_D^{25}$ − 92.5° (c, 1.03, chloroform).

Methanolysis of III (7)—After 350 mg of III was refluxed with methanolic hydrogen chloride (3 *N*, 75 ml) for 10 hr, the mixture was kept overnight at 25° and then evaporated *in vacuo*. Anhydrous methanol (100 ml) was added and again evaporated. After the addition of 75 ml of water, the aqueous layer was neutralized with anion-exchange resin (carbonate form) and then evaporated to yield 170 g of mixed methyl glycosides, which was subjected to GLC.

The methyl glycosides also were separated by column (2 × 23.5 cm) chromatography on silica gel (20 g). The column was eluted with a gradient system consisting of 200 ml of chloroform–methanol (99.5:0.5) in the mixing flask and 200 ml of chloroform–methanol (98:2) in the reservoir flask, and 10-ml fractions were collected. Fractions 12–16 afforded 41 mg of methyl 2,3,4-tri-*O*-methyl-L-rhamnopyranoside (III*a*). Fractions 18–29 gave 36 mg of methyl 2,3,5-tri-*O*-methyl-L-arabinofuranoside (III*b*). Fractions 37–48 yielded 42 mg of methyl 3,6-di-*O*-methyl-D-glucopyranoside (III*c*). These methyl glycosides were identified by mass spectral analyses (10).

Partial Hydrolysis of I—After 250 mg of I was heated with 10 ml of dioxane and 20 ml of 2 *N* H_2SO_4 at 75° for 1 hr, the mixture was diluted with 30 ml of water and neutralized with anion-exchange resin (carbonate form). The mixture was then filtered through a bed of Dowex 1 × 4 resin (carbonate form). The resin was washed successively with 200 ml of methanol followed by 200 ml of methanol–chloroform (1:1).

The filtrate and the washings were combined and evaporated *in vacuo* to yield 246 mg of residue, which was chromatographed on a silica gel (65 g) column (2.2 × 36.5 cm). The column was eluted with chloroform–methanol–water (65:25:10, organic phase), and 4-ml fractions were collected. Fractions 22–27 afforded 28 mg of 3-[β-D-glucopyranosyl]-25(*R*)-spirost-5-en-3β-ol (IV), mp 246–251°, $[\alpha]_D^{25}$ −87.9° (c, 0.52, methanol). Fractions 43–61 gave 120 mg of the prosapogenin (IV), mp 215° dec.; $[\alpha]_D^{25}$ −98.4° (c, 0.51, methanol).

Table I—Calculated and Experimental Molecular Rotations of Glycosides

Glycoside	$[M]_D$ Found	$[M]_D$ Calc.
3-[β-D-Glucopyranosyl]-25(*R*)-spirost-5-en-3β-ol	−572	−656
3-[α-L-Rhamnopyranosyl(1 → 2)-β-D-glucopyranosyl]-25(*R*)-spirost-5-en-3β-ol	−889	−853
3-{[α-L-Rhamnopyranosyl(1 → 2)]-[α-L-arabinofuranosyl(1 → 4)]-β-D-glucopyranosyl}-25(*R*)-spirost-5-en-3β-ol	−1034	−1064

Permethylation of IV—With the same procedure as described for the methylation of I, 120 mg of IV afforded 123 mg of crude V. Purification by column chromatography yielded 8.6 mg of pure V, mp 97–100°; $[\alpha]_D^{25}$ −101.5° (c, 0.8, chloroform).

Methanolysis of V—After 70 mg of V was treated with 30 ml of 2 *N* methanolic hydrogen chloride, the procedure used was the same as that described for III. A total of 30 mg of methyl glycoside was obtained, which was chromatographed on a silica gel (3-g) column (0.5 × 16.5 cm). The column was eluted with benzene–ethyl acetate (7:3), and 3-ml fractions were collected. Fractions 27–29 gave 8 mg of III*a*, and fractions 49–56 afforded 7.6 mg of methyl 3,4,6-tri-*O*-methyl-D-glucopyranoside (V*a*).

Hydrolysis of VI—Hydrolysis of VI (100 mg), carried out in the same manner as for I, yielded 39 mg of II. The sugars were identified by paper chromatography as L-rhamnose and D-glucose.

Methylation of VI—Following the methylation procedure for I, 750 mg of VI afforded 703 mg of VII, mp 116–118°; $[\alpha]_D^{25}$ −86° (c, 1.0, chloroform).

Methanolysis of VII—A mixture of 259 mg of methyl glycosides was obtained from methanolysis of 470 mg of VII. These glycosides were analyzed by GLC and further separated by column chromatography on silica gel with the same solvent system as described for the isolation of methyl glycosides from III. Fractions 13–19 gave 70 mg of III*a*, fractions 23–31 afforded 52 mg of methyl 2,3-di-*O*-methyl-L-rhamnopyranoside (VII*a*), and fractions 38–45 yielded 48 mg of III*c*.

Partial Hydrolysis of VII—After 190 mg of VII was refluxed with 0.5 *N* HCl in 40 ml of methanol for 3 hr, the mixture was evaporated, and 50 ml of water was added. The mixture was extracted with ethyl acetate (4 × 30 ml), and the ethyl acetate layer was washed with water, dried over sodium sulfate, and evaporated to yield 98 mg of residue. This residue was subjected to preparative TLC (20 × 20 cm, Kieselgel 60 F-256) using chloroform–acetone (85:15) as the solvent system. Compound VIII (R_f 0.46) was isolated and, upon methylation, yielded V.

RESULTS AND DISCUSSION

Acid hydrolysis of the saponin I afforded II, D-glucose, L-rhamnose, and L-arabinose. GLC analyses of the trimethylsilyl derivatives of these sugars revealed that they were present in a 1:1:1 ratio. The mass spectrum of I showed prominent peaks at *m/e* 133, 147, 414, 576, and 722. The peaks at *m/e* 133 and 147 correspond to arabinosyl and rhamnosyl ions, respectively, suggesting that these sugars are present in I as terminal units in branched chain fashion.

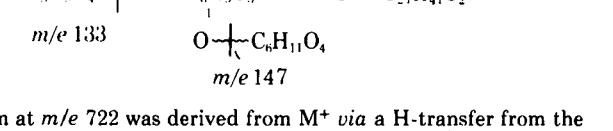

The ion at *m/e* 722 was derived from M^+ *via* a H-transfer from the arabinosyl group, accompanied by its concomitant elimination (Scheme I). In turn, the ion at *m/e* 576 originated from the ion at *m/e* 722 by a similar H-transfer from the terminal rhamnosyl group, accompanied by its elimination. The ion at *m/e* 414 was formed from the ion with *m/e* 576 by a H-transfer from the glucosyl group, followed by its elimination (11, 12), indicating that glucose was directly attached to the aglycone.

This proposed branched sugar sequence was further substantiated by the mass spectrum of the permethylated derivative (III), which gave prominent peaks at *m/e* 175 and 189, corresponding to terminal tri-*O*-methylarabinosyl and tri-*O*-methylrhamnosyl ions. The peak at *m/e* 435 may be rationalized by assuming that the terminal tri-*O*-methylrham-

Table II—Cytotoxic Activity of Natural and Synthetic Saponins [a]

Glycoside	ED_{50}, μg/ml P-388	L-1210	KB
I	0.94	0.14	0.16
VI	0.22	0.43	0.029
Synthetic 3-[glucosyl]-25(*R*)-spirost-5-en-3β-ol	23.9	65.7	12
Synthetic 3-[maltosyl]-25(*R*)-spirost-5-en-3β-ol	30.8	58.9	29

[a] For the P-388 and L-1210 tissue cultures, 1-(2-chloroethyl)-3-(4-methylcyclohexyl)-1-nitrosourea (NSC 95441) was used as the positive control compound, tested at 10, 5, 2.5, 1.25, and 0.625 μg/ml. For synthetic compounds, an ED_{50} value of ≤ 4 μg/ml is considered to be significant cytotoxic activity. For the KB tissue culture test system, mercaptopurine monohydrate was used as the standard.

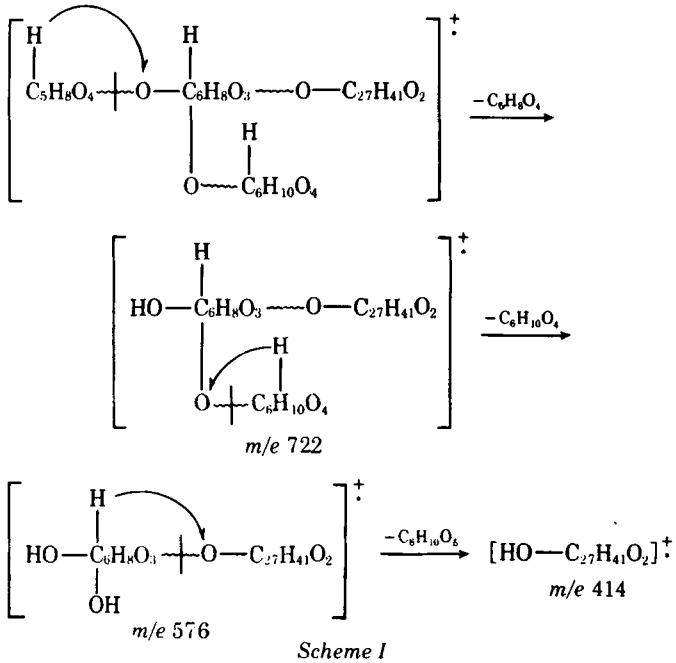

Scheme I

nosyl and tri-*O*-methylarabinosyl groups are attached to the C-2′ and C-4′ positions of the D-glucose moiety.

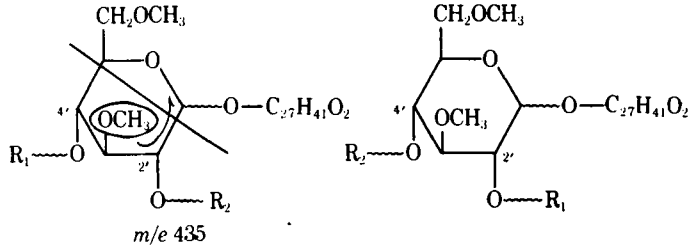

R_1 = tri-*O*-methyl-L-arabinosyl
R_2 = tri-*O*-methyl-L-rhamnosyl

The position of the sugar linkage was established by GLC analyses (7) of the methyl glycosides derived from methanolysis of III, which showed the presence of IIIa–IIIc. The identification of these methyl glycosides was made by comparison of their GLC retention times and mass spectra (10) with samples synthesized by published procedures (13, 14). These results were consistent with the supposition that rhamnose is attached to either the C-2′ or C-4′ position of glucose.

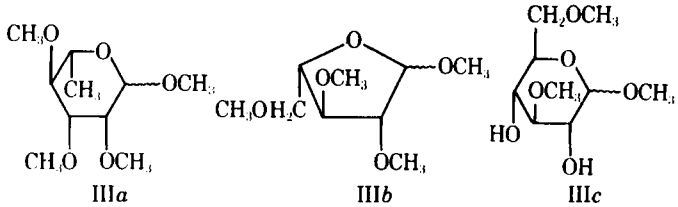

IIIa IIIb IIIc

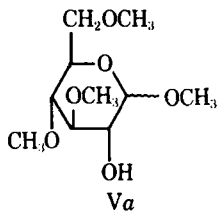

Va

The exact locations of the sugar linkages in I were deduced by the partial acid hydrolysis of I, which afforded 3-[β-D-glucopyranosyl]-25(*R*)-spirost-5-en-3β-ol and the prosapogenin IV. Paper chromatographic analysis of the sugars in the acid hydrolysate of IV showed only D-glucose and L-rhamnose, indicating that L-arabinose had been cleaved off during the partial hydrolysis of I. Permethylation of IV afforded V. Methanolysis of V gave two methyl glycosides, which were separated by column chromatography and characterized as IIIa and, more importantly, Va. This identification was accomplished by comparison of GLC retention times and mass spectral data with synthetic samples prepared by published procedures (10).

These experimental data can only be interpreted to mean that rhamnose is attached to the glucose C-2′ position. Hence, the arabinosyl unit must be attached to the glucose C-4′ in I.

With the sugar linkage sites established, the stereochemistry of the glycosidic linkages in I was then studied. The NMR spectrum of V showed signals at 4.26 (d, 1H, J = 7 Hz) and 5.15 (s, 1H) ppm. The former signal corresponds to the axial anomeric proton of the tri-*O*-methyl-D-glucopyranosyl moiety, and the latter corresponds to the equatorial anomeric proton of the tri-*O*-methyl-L-rhamnopyranosyl moiety. Thus, D-glucose is linked to II *via* a β-glycosidic bond, whereas L-rhamnose is linked to D-glucose *via* an α-glycosidic linkage.

The NMR spectrum of III exhibited signals at 4.36 (d, 1H, J = 7 Hz), 5.15 (s, 1H), and 5.18 (s, 1H) ppm. The signal at 5.15 ppm is characteristic of the equatorial anomeric proton in the tri-*O*-methyl-L-arabinosyl moiety, confirming that L-arabinose is attached to C-4′ of the D-glucose unit *via* an α-glycosidic linkage. The calculated and experimental molecular rotation values (16) for IV and I are in good agreement (Table I), further substantiating the stereochemical assignment.

Hydrolysis of the saponin VI afforded II, D-glucose, and L-rhamnose. GLC analyses of the trimethylsilyl derivatives of these sugars revealed that D-glucose and L-rhamnose were present in a 1:3 ratio. The mass spectrum of VI showed prominent peaks at *m/e* 147, 414, 576, and 722. The ions at *m/e* 414 and 576 indicated that D-glucose was linked directly to II as 3L-rhamnose–D-glucose–II.

Methanolysis of the permethylated derivative VII gave three types of methyl sugars, which were identified as IIIa, methyl 2,3-di-*O*-methyl-L-rhamnopyranoside (VIIa), and IIIc. Thus, VII may be represented by one of the following structures.

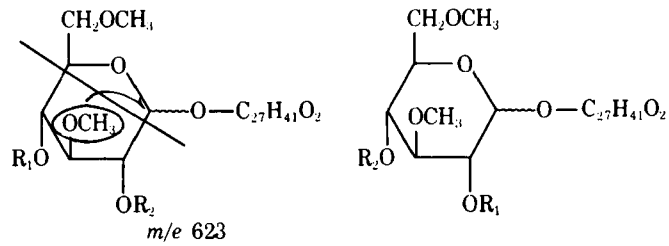

R_1 = tri-*O*-methyl-L-rhamnopyranosyl
R_2 = tri-*O*-methyl-L-rhamnopyranosyl(1→4)-di-*O*-methyl-L-rhamnopyranosyl

The mass spectrum of VII gave prominent ions at *m/e* 189, 363, and 623, in accord with this assignment. The peak at *m/e* 189 may be rationalized in terms of the two terminal tri-*O*-methyl-L-rhamnopyranosyl units; the ion at *m/e* 363 corresponds to the tri-*O*-methyl-L-rhamnopyranosyl(1 → 4)-di-*O*-methyl-L-rhamnopyranosyl ion. The ion at *m/e* 623 strongly suggests C-2′ and C-4′ substitutions of the D-glucosyl unit.

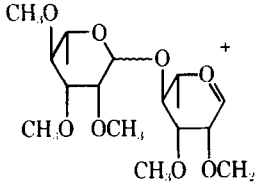

m/e 363

Partial acid hydrolysis of VII afforded VIII, whose mass spectrum gave prominent ions at *m/e* 189, 379 and 796 (M^+), indicating that a tri-*O*-methyl-L-rhamnopyranosyl(1 → 4)-di-*O*-methyl-L-rhamnopyranosyl group was cleaved during hydrolysis. Since methylation of VIII afforded V, one may logically conclude that the L-rhamnopyranosyl(1 → 4)-L-rhamnopyranosyl group must be attached to C-4′ and that the L-rhamnopyranosyl group may be attached to C-2′ of the D-glucopyranosyl moiety of VII.

The NMR spectrum of VII showed a doublet at 4.4 ppm (1H, J = 7 Hz) and two broad singlets at 5.03 (1H) and 5.21 (2H) ppm. The doublet corresponds to the axial anomeric proton of D-glucose, and the singlets correspond to the equatorial anomeric protons of the three L-rhamnose units. Thus, the D-glucose unit is attached to II *via* a β-glycosidic linkage and to the three L-rhamnose residues *via* α-glycosidic bonds, and the chemical structure of this tetraglycoside is represented by VI.

The cytotoxic activities of I and VI are shown in Table II. Both saponins were quite effective against P-388, L-1210, and 9KB tissue culture systems. To demonstrate that this cytotoxic activity is not simply due to a detergent effect, glucoside and maltoside of II were prepared and evaluated in these test systems. Since both synthetic saponins were much less active, it appears that some unique structural features are required for optimal cytotoxic activity.

Extracts of *Dioscorea* have been widely used for the treatment of a variety of tumors in China, India, South America, and Southeast Asia (17). After completion of these studies, it was noted that I and VI had been isolated from the dried rhizomes of *Paris polyphylla* SM. obtained in a market of Katmandu, Nepal (18).

REFERENCES

(1) K. H. Hsu, "Common Chinese Herbal Drugs," 2nd ed., Commercial Press, Hong Kong, 1974, pp. 98–100.

(2) J. Polesuk, J. M. Amodeo, and T. S. Ma, *Mikrochim. Acta*, **4**, 507 (1973).

(3) National Cancer Institute Protocol 1.800, National Institutes of Health, Bethesda, Md., 1978.

(4) National Cancer Institute Protocol 1.700, National Institutes of Health, Bethesda, Md., 1978.

(5) R. I. Geran, N. H. Greenberg, M. M. Macdonald, A. M. Schumacher, and B. J. Abbott, *Cancer Chemother. Rep.*, **3**, 17 (1972).

(6) M. Kumura, Y. Hattori, I. Yoshizawa, and M. Johma, *Chem. Pharm. Bull.*, **16**, 613 (1968).

(7) G. O. Aspinall, *J. Chem. Soc.*, **1963**, 1676.

(8) R. E. Marker and J. Krueger, *J. Am. Chem. Soc.*, **62**, 3349 (1940).

(9) S. Hakomori, *J. Biochem. (Tokyo)*, **55**, 205 (1964).

(10) K. Heyns, K. R. Sperling, and H. F. Grutzmacher, *Carbohydr. Res.*, **9**, 79 (1969).

(11) P. Brown, F. Brüschweiler, G. R. Pettit, and T. Reichstein, *J. Chem. Soc.*, **92**, 4470 (1970).

(12) P. Brown, F. Brüschweiler, G. R. Pettit, and T. Reichstein, *Org. Mass Spectrom.*, **5**, 573 (1971).

(13) E. L. Hirst and A. K. Macbeth, *J. Chem. Soc.*, **1926**, 22.

(14) D. J. Bell, *ibid.*, **1935**, 175.

(15) E. A. Sofowora and R. Hardman, *Lloydia*, **39**, 141 (1976).

(16) W. Klyne, *Biochem. J.*, **47**, xli (1950).

(17) J. L. Hartwell, *Lloydia*, **32**, 102 (1969).

(18) T. Nohara, H. Yabuta, M. Suenobu, R. Hida, K. Miyahara, and T. Kawasaki, *Chem. Pharm. Bull.*, **21**, 1240 (1973).

ACKNOWLEDGMENTS

Supported in part by National Institutes of Health Grant AM 04874. The authors thank Professor David Perlman for the cytotoxic testing.

NOTES

Phosphodiesterase Inhibition by Succinic and Related Acid Biphenylalkyl Monoesters

M. E. ROGERS ˣ, S. G. BOOTS *, and M. R. BOOTS

Received September 22, 1978, from the *Department of Pharmaceutical Chemistry, School of Pharmacy, Virginia Commonwealth University, Richmond, VA 23298.* Accepted for publication December 7, 1978.

*Present address: Department of Chemistry, Stanford University, Stanford, Calif.

Abstract □ Biphenylalkyl monoesters of succinic and related acids represent a potent new class of cyclic AMP phosphodiesterase inhibitors. The biphenyl group is necessary for potent inhibition. The spatial relationship of the carboxyl and ester groups and alkyl chain length are important to inhibitory potency.

Keyphrases □ Succinic acid biphenylalkyl monoesters—phosphodiesterase inhibition, synthesis, structure–activity relationships □ Cyclic AMP phosphodiesterase—inhibitors, succinic acid biphenylalkyl monoesters, synthesis, structure–activity relationships □ Phosphodiesterase inhibitors—succinic acid biphenylalkyl monoesters, synthesis, structure–activity relationships

Tissue cyclic AMP levels appear to be regulated by two enzymes, adenylate cyclase and phosphodiesterase, and by cellular extrusion. Phosphodiesterase catalyzes the hydrolysis of cyclic AMP to 5′-AMP. Because phosphodiesterase inhibitors can increase tissue cyclic AMP levels, these compounds are of interest as biochemical tools and as potential therapeutic agents (1–3).

Most potent cyclic AMP phosphodiesterase inhibitors are nitrogen-containing heterocycles, *i.e.*, theophylline, 3-isobutyl-1-methylxanthine, papaverine, and 4-(3-butoxy-4-methoxyphenyl)-2-imidazolidinone[1], and most contain either a 6,5- or 6,6-fused heterocyclic ring (4–6). Only a few reports described the effects of organic acids on phosphodiesterase. Citrate at high concentrations (12 m*M*) inhibited the enzyme (7). Ethacrynic acid was reported to be one-half as potent as theophylline against the enzyme from beef heart (8). Recently, acidic anti-inflammatory agents were reported to inhibit phosphodiesterase (9–11). Enzyme activation by the lipoidal organic acid, stearic acid, was observed (12), as was inhibition by unsaturated fatty acids (13).

1-(4-Biphenylyl)pentyl hydrogen succinate is a hypo-

[1] Ro 20-1724.

0022-3549/79/0700-0903$01.00/0

© 1979, American Pharmaceutical Association

Partial acid hydrolysis of VII afforded VIII, whose mass spectrum gave prominent ions at *m/e* 189, 379 and 796 (M^+), indicating that a tri-*O*-methyl-L-rhamnopyranosyl(1 → 4)-di-*O*-methyl-L-rhamnopyranosyl group was cleaved during hydrolysis. Since methylation of VIII afforded V, one may logically conclude that the L-rhamnopyranosyl(1 → 4)-L-rhamnopyranosyl group must be attached to C-4′ and that the L-rhamnopyranosyl group may be attached to C-2′ of the D-glucopyranosyl moiety of VII.

The NMR spectrum of VII showed a doublet at 4.4 ppm (1H, J = 7 Hz) and two broad singlets at 5.03 (1H) and 5.21 (2H) ppm. The doublet corresponds to the axial anomeric proton of D-glucose, and the singlets correspond to the equatorial anomeric protons of the three L-rhamnose units. Thus, the D-glucose unit is attached to II *via* a β-glycosidic linkage and to the three L-rhamnose residues *via* α-glycosidic bonds, and the chemical structure of this tetraglycoside is represented by VI.

The cytotoxic activities of I and VI are shown in Table II. Both saponins were quite effective against P-388, L-1210, and 9KB tissue culture systems. To demonstrate that this cytotoxic activity is not simply due to a detergent effect, glucoside and maltoside of II were prepared and evaluated in these test systems. Since both synthetic saponins were much less active, it appears that some unique structural features are required for optimal cytotoxic activity.

Extracts of *Dioscorea* have been widely used for the treatment of a variety of tumors in China, India, South America, and Southeast Asia (17). After completion of these studies, it was noted that I and VI had been isolated from the dried rhizomes of *Paris polyphylla* SM. obtained in a market of Katmandu, Nepal (18).

REFERENCES

(1) K. H. Hsu, "Common Chinese Herbal Drugs," 2nd ed., Commercial Press, Hong Kong, 1974, pp. 98–100.

(2) J. Polesuk, J. M. Amodeo, and T. S. Ma, *Mikrochim. Acta*, **4**, 507 (1973).

(3) National Cancer Institute Protocol 1.800, National Institutes of Health, Bethesda, Md., 1978.

(4) National Cancer Institute Protocol 1.700, National Institutes of Health, Bethesda, Md., 1978.

(5) R. I. Geran, N. H. Greenberg, M. M. Macdonald, A. M. Schumacher, and B. J. Abbott, *Cancer Chemother. Rep.*, **3**, 17 (1972).

(6) M. Kumura, Y. Hattori, I. Yoshizawa, and M. Johma, *Chem. Pharm. Bull.*, **16**, 613 (1968).

(7) G. O. Aspinall, *J. Chem. Soc.*, **1963**, 1676.

(8) R. E. Marker and J. Krueger, *J. Am. Chem. Soc.*, **62**, 3349 (1940).

(9) S. Hakomori, *J. Biochem. (Tokyo)*, **55**, 205 (1964).

(10) K. Heyns, K. R. Sperling, and H. F. Grutzmacher, *Carbohydr. Res.*, **9**, 79 (1969).

(11) P. Brown, F. Brüschweiler, G. R. Pettit, and T. Reichstein, *J. Chem. Soc.*, **92**, 4470 (1970).

(12) P. Brown, F. Brüschweiler, G. R. Pettit, and T. Reichstein, *Org. Mass Spectrom.*, **5**, 573 (1971).

(13) E. L. Hirst and A. K. Macbeth, *J. Chem. Soc.*, **1926**, 22.

(14) D. J. Bell, *ibid.*, **1935**, 175.

(15) E. A. Sofowora and R. Hardman, *Lloydia*, **39**, 141 (1976).

(16) W. Klyne, *Biochem. J.*, **47**, xli (1950).

(17) J. L. Hartwell, *Lloydia*, **32**, 102 (1969).

(18) T. Nohara, H. Yabuta, M. Suenobu, R. Hida, K. Miyahara, and T. Kawasaki, *Chem. Pharm. Bull.*, **21**, 1240 (1973).

ACKNOWLEDGMENTS

Supported in part by National Institutes of Health Grant AM 04874. The authors thank Professor David Perlman for the cytotoxic testing.

NOTES

Phosphodiesterase Inhibition by Succinic and Related Acid Biphenylalkyl Monoesters

M. E. ROGERS ˣ, S. G. BOOTS *, and M. R. BOOTS

Received September 22, 1978, from the *Department of Pharmaceutical Chemistry, School of Pharmacy, Virginia Commonwealth University, Richmond, VA 23298.* Accepted for publication December 7, 1978.

*Present address: Department of Chemistry, Stanford University, Stanford, Calif.

Abstract □ Biphenylalkyl monoesters of succinic and related acids represent a potent new class of cyclic AMP phosphodiesterase inhibitors. The biphenyl group is necessary for potent inhibition. The spatial relationship of the carboxyl and ester groups and alkyl chain length are important to inhibitory potency.

Keyphrases □ Succinic acid biphenylalkyl monoesters—phosphodiesterase inhibition, synthesis, structure–activity relationships □ Cyclic AMP phosphodiesterase—inhibitors, succinic acid biphenylalkyl monoesters, synthesis, structure–activity relationships □ Phosphodiesterase inhibitors—succinic acid biphenylalkyl monoesters, synthesis, structure–activity relationships

Tissue cyclic AMP levels appear to be regulated by two enzymes, adenylate cyclase and phosphodiesterase, and by cellular extrusion. Phosphodiesterase catalyzes the hydrolysis of cyclic AMP to 5′-AMP. Because phosphodiesterase inhibitors can increase tissue cyclic AMP levels, these compounds are of interest as biochemical tools and as potential therapeutic agents (1–3).

Most potent cyclic AMP phosphodiesterase inhibitors are nitrogen-containing heterocycles, *i.e.*, theophylline, 3-isobutyl-1-methylxanthine, papaverine, and 4-(3-butoxy-4-methoxyphenyl)-2-imidazolidinone[1], and most contain either a 6,5- or 6,6-fused heterocyclic ring (4–6). Only a few reports described the effects of organic acids on phosphodiesterase. Citrate at high concentrations (12 m*M*) inhibited the enzyme (7). Ethacrynic acid was reported to be one-half as potent as theophylline against the enzyme from beef heart (8). Recently, acidic anti-inflammatory agents were reported to inhibit phosphodiesterase (9–11). Enzyme activation by the lipoidal organic acid, stearic acid, was observed (12), as was inhibition by unsaturated fatty acids (13).

1-(4-Biphenylyl)pentyl hydrogen succinate is a hypo-

[1] Ro 20-1724.

0022-3549/79/0700-0903$01.00/0

© 1979, American Pharmaceutical Association

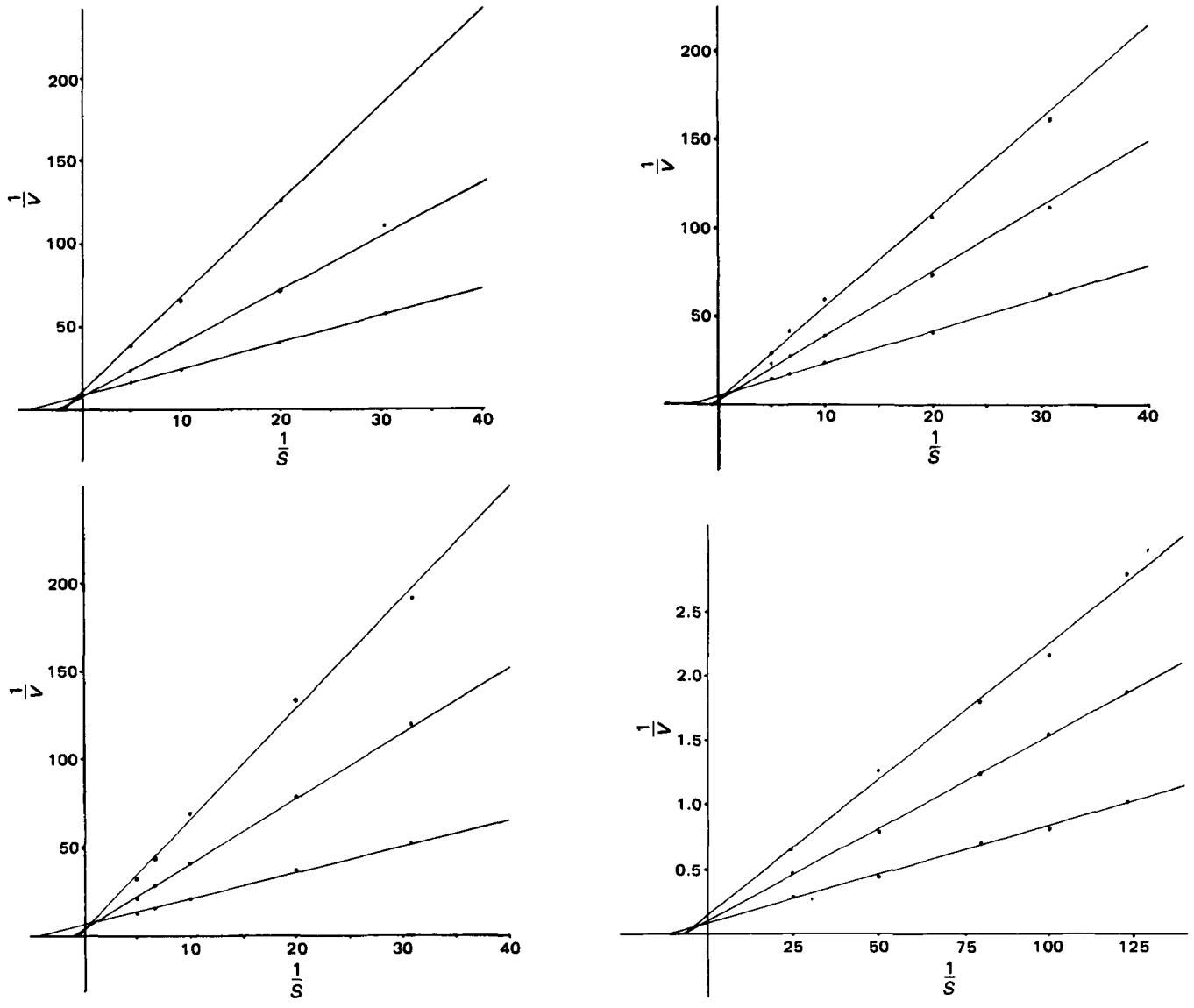

Figure 1—*Double reciprocal plots (micromoles^{-1} minute milligram of protein* versus *molarity^{-1} × 10^{-3}) at high substrate concentrations for 150 and 300 μM Ib (upper left), 70 and 110 μM Ie (upper right), and 350 and 500 μM Id (lower left) and at a low substrate concentration for 50 and 100 μM Ib (lower right).*

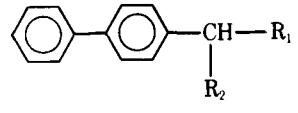

Ia: R_1 = —OC(=O)$CH_2CH_2CO_2H$, R_2 = methyl
Ib: R_1 = —OC(=O)$CH_2CH_2CO_2H$, R_2 = *n*-butyl
Ic: R_1 = —OC(=O)$CH_2CH_2CO_2H$, R_2 = *n*-hexyl
Id: R_1 = —OC(=O)CH=$CHCO_2H$ (*cis*), R_2 = *n*-butyl
Ie: R_1 = —OC(=O)CH=$CHCO_2H$ (*trans*), R_2 = *n*-butyl
If: R_1 = —OC(=O)CH=$CHCO_2H$ (*trans*), R_2 = *n*-hexyl

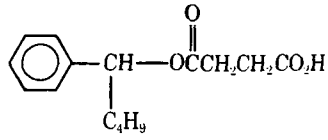

II

cholesterolemic agent previously reported to inhibit β-hydroxy-β-methylglutaryl coenzyme A reductase (14). The purpose of this investigation was to examine the phosphodiesterase inhibition by *Ib* and related acids.

RESULTS AND DISCUSSION

Compound *Ib* was a potent beef heart phosphodiesterase[2] inhibitor (Table I). Closely related *Ia*, *Ic*–*Ie*, and II were also examined for effects on the enzyme[3]. Lineweaver–Burke plots were obtained for *Ib*, *Id*, and *Ie* (Fig. 1). The I_{50} values were determined at substrate concentrations of 100 and 1 μ*M* for *Ia*–*Ie*. Most phosphodiesterase preparations, including bovine heart phosphodiesterase, contain both high and low affinity enzymes or enzyme forms (5, 6). The preparations could be assayed at a low cyclic AMP concentration to observe effects on the high affinity form and at high substrate concentrations (actually, this high concentration reflected total enzyme activity) to observe effects on the low affinity enzyme. Additionally, miscellaneous acids were examined for effects on phosphodiesterase to substantiate *Ib*–*Ie* specificity. Finally, structure–activity relationship analysis of *Ia*–*Ie* led to the synthesis of *If*, the most potent inhibitor yet uncovered in this series.

The discovery that *Ib* inhibited phosphodiesterase raised the following question: Would other organic acids, especially arylalkyl organic acids, in view of the known acidic anti-inflammatory agent effect, inhibit the enzymes? The failure of all eight diverse acids to inhibit phosphodiesterase indicated that this is not a general organic acid effect (Table I).

[2] Sigma Chemical Co.

[3] These results did not correlate with the potency of these compounds as inhibitors of β-hydroxy-β-methylglutaryl coenzyme A reductase (14, 15).

Table I—Phosphodiesterase Inhibition [a]

Compound [b]	I_{50}, μM	
	1 μM Cyclic AMP [c]	100 μM Cyclic AMP [c]
Ia	514 ± 56 [d]	1215 ± 103
Ib	64 ± 2	205 ± 6
Ic	49 ± 2	95 ± 7
Id	121 ± 15	402 ± 27
Ie	29 ± 2	93 ± 10
If	16 ± 2	25 ± 3
II	823 ± 68	>1000 [e]
Theophylline	306 ± 24	917 ± 25
3-Isobutyl-1-methyl-xanthine	10 ± 1	52 ± 1

[a] Bovine heart phosphodiesterase was used. [b] The following acids at 5×10^{-4} M, using 100 μM cyclic AMP, showed less than 5% enzyme inhibition: *p*-chlorophenoxyacetic, cinnamic, *p*-hydroxyphenylacetic, monomethyl adipate, α-naphthylacetic, α-phenylbutyric, phenylpropionic, and 2-pyridylacetic. [c] Substrate concentration. [d] Data are expressed as the mean ± *SE* of three determinations. [e] Sixteen-percent inhibition at 1000 μM; a solubility problem was encountered at higher concentrations.

Additional specificity evidence was indicated by the lack of succinate analog activity where biphenyl was replaced by phenyl (II) and where the *n*-butyl chain was replaced by methyl (Ia, Table I). Furthermore, if the inhibition was *via* an enzyme–inhibitor complex, there should be a variation in potency among stereoisomers. In fact, the fumarate (*trans*-isomer) analog Ie was four times as potent as the maleate (*cis*-isomer) analog Id, with the succinate Ib intermediate between the two.

Attempts to establish the inhibition type *via* Lineweaver–Burke plots were not definitive (Fig. 1). Beef heart phosphodiesterase inhibition by Ib appeared to be competitive or partially competitive at both low and high substrate concentrations. Replotting the data using Hofstee plots did not improve identification of the inhibition type. The inability to obtain definitive curves may have been due to assay error, enzyme preparation crudeness, or the presence of additional enzyme forms.

The most striking structure–activity relationships for this series (Table I) can be summarized as follows: the biphenyl moiety is necessary (Ib *versus* II), a *trans*-configuration of the carboxyl and ester groups is optimal (Ie > Ib > Id), and an increased alkyl chain length is advantageous (Ic > Ib > Ia). These results suggested the synthesis of If[4].

Compound If is almost equipotent with the very potent, standard phosphodiesterase inhibitor 3-isobutyl-1-methylxanthine against the high affinity enzyme and is more potent against the low affinity enzyme. The ability of these compounds to inhibit cyclic AMP phosphodiesterase should be considered when interpreting pharmacological studies.

EXPERIMENTAL

Chemistry[5]—Compounds Ia–Ic and II were prepared as previously described (15). Compounds Id and Ie were synthesized as previously described (14).

Compound If, mp 82–84°, was prepared using the method described for Ie (14); NMR: δ 0.60–2.20 [broad, 13H, $CH_3(CH_2)_5$], 5.90 (t, J = 6 Hz, 1H, HCO_2C–), 6.95 [s, 2H, —CH=CH—], 7.20–7.80 [m, 9H, aromatic], and 8.45 [s, 1H, CO_2H] ppm.

Anal.—Calc. for $C_{23}H_{26}O_4$: C, 75.4; H, 7.1. Found: C, 75.1; H, 7.4.

Enzyme Studies—The assay (16) was used as previously described (17) employing bovine heart phosphodiesterase[2].

[4] Further chain elongation would likely reduce solubility beyond workable limits.

[5] Melting points were determined with a Thomas–Hoover apparatus and are uncorrected. Elemental analyses were obtained from Atlantic Microlab Inc., Atlanta, Ga. NMR spectra were determined using a Perkin-Elmer R-24 spectrometer in deuterochloroform with tetramethylsilane as the internal reference.

REFERENCES

(1) M. S. Amer and G. R. McKinney, *Life Sci.*, **13**, 753 (1974).

(2) B. Weiss and W. N. Hait, *Ann. Rev. Pharmacol. Toxicol.*, **17**, 441 (1977).

(3) B. Weiss and R. Fertel, *Adv. Pharmacol. Chemother.*, **14**, 189 (1977).

(4) M. M. Appleman, W. J. Thompson, and T. R. Russell, *Adv. Cycl. Nucl. Res.*, **3**, 65 (1973).

(5) M. S. Amer and W. E. Kreighbaum, *J. Pharm. Sci.*, **64**, 1 (1975).

(6) M. Chasin and D. N. Harris, *Adv. Cycl. Nucl. Res.*, **7**, 225 (1976).

(7) W. Y. Cheung, *Biochemistry*, **6**, 1079 (1967).

(8) G. Sonft, K. Munske, G. Schultz, and M. Hoffman, *Naunyn Schmiedebergs Arch. Pharmacol. Exp. Pathol.*, **259**, 344 (1968).

(9) V. Stefanovich, *Res. Commun. Chem. Pathol. Pharmacol.*, **7**, 573 (1974).

(10) D. S. Newcombe, N. M. Thanassi, and C. P. Ciosek, Jr., *Life Sci.*, **14**, 505 (1974).

(11) J. W. Hon and F. C. Kauffman, *Pharmacologist*, **16**, 330 (1974).

(12) D. J. Wolff and C. O. Brostrom, *Arch. Biochem. Biophys.*, **173**, 720 (1976).

(13) S. Hirose, T. Asano, and H. Hidaka, *Thrombosis Res.*, **12**, 701 (1978).

(14) K. E. Guyer, S. G. Boots, P. E. Marecki, and M. R. Boots, *J. Pharm. Sci.*, **65**, 548 (1976).

(15) M. R. Boots, S. G. Boots, C. M. Noble and K. E. Guyer, *ibid.*, **62**, 952 (1973).

(16) C. B. Klee, *Biochemistry*, **16**, 1017 (1977).

(17) R. A. Glennon, M. E. Rogers, R. G. Bass, and S. B. Ryan, *J. Pharm. Sci.*, **67**, 1762 (1978).

ACKNOWLEDGMENTS

Supported in part by a grant from the Cancer Center, Medical College of Virginia, Virginia Commonwealth University.

The authors thank Mr. Anthony Burke for assistance.

Molecular Connectivity Analysis of Hallucinogenic Mescaline Analogs

R. A. GLENNON *x, **L. B. KIER** *, and **A. T. SHULGIN** ‡

Received June 9, 1978, from the *Department of Pharmaceutical Chemistry, School of Pharmacy, Medical College of Virginia, Virginia Commonwealth University, Richmond, VA 23298, and ‡1483 Shulgin Road, Lafayette, CA 94549. Accepted for publication December 20, 1978.

Abstract □ The hallucinogenic (psychotomimetic) potency of 10 mescaline analogs was examined by molecular connectivity analysis. Potencies could be described by a two-term relating equation, which explained 94% of the variance in activity, on the basis of structural variation. 2,5-Dimethoxy substitution as well as the nature of the 4-position substituent played an important role in determining hallucinogenic potency. With the relating equation, reasonable potency predictions were made for six compounds not included in the initial investigation.

Keyphrases □ Mescaline analogs—hallucinogenic activity, structure—activity relationships, molecular connectivity analysis □ Hallucinogenic agents—mescaline, analogs, hallucinogenic activity, structure-activity relationships, molecular connectivity analysis □ Structure-activity relationships—mescaline analogs, molecular connectivity analysis

Molecular connectivity analysis was used recently in studies of the structure–activity relationships of hallucinogenic phenylisopropylamine (amphetamine) analogs (1). Hallucinogenic activity could be related to three structural descriptors (χ terms) by an equation that accounted for greater than 80% of the variance in hallucinogenic potency. The relating equation, generated from the amphetamine data, was used to predict the hallucinogenic potency of six phenethylamine derivatives (mescaline analogs) (1).

One χ term in the original equation encodes the presence of the α-methyl group of the amphetamine side chain. Being devoid of this α-methyl group, the phenethylamines were predicted correctly to be of lower hallucinogenic potency (1). The correct prediction of the six phenethylamine derivative activities may have been fortuitous since only one of these six compounds was experimentally more active than mescaline in humans.

Recently, data became available on additional phenethylamines with potency six to 35 times that of mescaline. In light of these findings and of the newly available active compounds, it was of interest to reexamine the phenethylamines as a separate hallucinogenic class.

EXPERIMENTAL

Molecular structures can be analyzed in terms of the number of atoms, kinds of atoms, bonding types, and adjacency environment by the molecular connectivity method (2). The method used in this investigation was described previously (2) and has given good results in correlating biological activity with the structures of, for example, hallucinogenic amphetamine derivatives (1) and lysergide analogs (3). Molecular connectivity indexes or descriptors (χ terms) have been computed for each compound in this study. A multivariable search of connectivity terms was conducted in a regression analysis using a program that considers all variable combinations. The number of terms employed was limited necessarily by the molecular size and the number of observations and was governed by statistical considerations.

Psychotomimetic or hallucinogenic activity measurement is necessarily only semiquantitative. Hallucinogenic agent potencies are measured relative to a total dose of 350 mg of mescaline. For example, the dose of V required to produce an effect similar to that of 350 mg of mescaline is 40–60 mg (4); thus, for an average 50-mg dose, V is calculated to have a potency seven times that of mescaline, or 7 mescaline units. The variance in mescaline-unit data has been estimated as ~25% (5). Therefore, although V might possess an activity of ~5–9 mescaline units, a value of 7 mescaline units was used to perform the regression analysis.

Compounds I and IX are reported to possess an activity of "less than" 1 and 5 mescaline units, respectively (5). Again, to perform the regression, certain assumptions must be made. Thus, activities midway between inactivity and the reported activity (*i.e.*, 0.5 and 2.5 mescaline units, respectively) were assumed for these compounds. Although II has an activity of less than 1 mescaline unit, one study (6) reported an activity of 0.2 mescaline unit, and this latter value was used in the regression analysis.

RESULTS AND DISCUSSION

The relative hallucinogenic potencies of the 10 phenethylamine derivatives can be described by:

$$\text{mescaline units} = 129\ {}^{3}\chi_c^{v} - 4.45\ {}^{4}\chi_p - 14.54 \qquad \text{(Eq. 1)}$$

$$n = 10 \quad s = 3.02 \quad r = 0.97$$

Although the correlation is significant and explains 94% of the variation in hallucinogenic activity, the variation in biological activity measurement should be called to attention again.

The two molecular connectivity indexes important in the equation are weighted counts of structural fragments. The ${}^{3}\chi_c^{v}$ index describes a structural feature of three bonds converging at one atom (cluster). The v denotes the index valence form; that is, the atom δ assignments are based on the atomic valence rather than on the simple degree of adjacency. The ${}^{4}\chi_p$ index describes a structural feature of four contiguous bonds in which the atom δ values are based on the degree of adjacency. Several detailed descriptions of the molecular connectivity method and the calculation of the indexes were published recently (2).

From the relating equation, several generalizations can be derived about the impact of structural variation on activity. The ${}^{3}\chi_c^{v}$ term suggests that increasing the number of nuclear substituents will generally increase potency; compare the activities of I and II with those of III and IV. This is in accord, biologically, with previous findings (7) that those phenethylamines with high methoxylation serve less well as substrates for enzymatic degradation. In addition, the presence of the ${}^{3}\chi_c^{v}$ term implies that the lower the δ^{v} in the substituent, the higher the potency; *i.e.*, Br > CH_3 > OCH_3 (compare III, VII, and VIII).

The ${}^{4}\chi_p$ term is related to the phenethylamine ring substitution pattern. Because the coefficient for this term in the relating equation is negative, the greater the value of the term, the lower is the potency of the compound. In the monosubstituted phenethylamines, an *ortho*-substituent contributes two additional terms and a *meta*-substituent contributes one additional term as compared to a *para*-substituent. Therefore, the position of the substituent would be expected to enhance activity in the order: *ortho* < *meta* < *para*.

For phenethylamines with more than one nuclear substituent, the ${}^{4}\chi_p$ term indicates that activity is enhanced when two substituents are *para* to one another (*para* > *meta* > *ortho*). Such substitution can only be realized, in disubstituted molecules for example, when the phenethylamine is 2,5-disubstituted.

These statements, which can be quantified using the χ terms, echo those structure–activity relationships that have evolved in a qualitative manner by inspection of a phenethylamine series. Shulgin (4) reported that if the *p*-methoxy group is replaced with another substituent (higher alkoxy, methyl, or halo), there is an unquestioned increase in potency. Shulgin (4) commented further that 2,4,5-orientation appears to be more effective than 3,4,5-orientation, although there are too few examples to establish this generality.

Investigations of structure–activity relationships can highlight those structural features that influence activity. However, because hallucino-

0022-3549/79/0700-0906$01.00/0
© 1979, American Pharmaceutical Association

Table I—Chi Terms and Activities of Various Phenethylamine Analogs

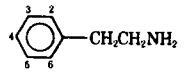

Compound	Position 2	3	4	5	6	$^3\chi_c^v$	$^4\chi_p$	Mescaline Units Obs.	Calc.
I			OCH_3			0.186	2.34	<1	0–2.0
II		OCH_3	OCH_3			0.236	3.13	<1	0–4.9
III	OCH_3		OCH_3	OCH_3		0.279	3.77	1	1.9–7.9
IV		OCH_3	OCH_3	OCH_3		0.287	3.94	1	1.6–7.6
V		OCH_3	OCH_2CH_3	OCH_3		0.287	4.07	7	1.3–7.3
VI		OCH_3	$OCH_2CH_2CH_3$	OCH_3		0.287	4.18	6	0.9–6.9
VII	OCH_3		CH_3	OCH_3		0.364	3.47	20	14–20
VIII	OCH_3		Br	OCH_3		0.509	3.47	35	33–39
IX	OCH_3	—O—CH_2—O—				0.263	4.34	<5	0–3.7
X		OCH_3	—O—CH_2—O—			0.287	4.22	2	0.6–6.6
XI[a]		—O—CH_2—O—				0.236	3.47	~1	0–3.5
XII[a]	OCH_3	OCH_3	OCH_3			0.236	4.06	<1	0–4.3
XIII[a]	OCH_3	OCH_3	OCH_3	OCH_3	OCH_3	0.344	5.69	—[b]	1.5–7.5
XIV[a]	OCH_3		I	OCH_3		0.593	3.47	44	42–48
XV[a]	OCH_3		C_2H_5	OCH_3		0.322	3.77	18	7–13
XVI[a]		OCH_3	SCH_3	OCH_3		0.383	3.94	12	14–20

[a] Not used to derive the relating equation; activities were predicted using the equation. [b] Effective human intoxication levels have not been evaluated fully.

genic activity cannot be measured with great accuracy and because mescaline units do not reflect the route of administration, time of onset, and duration of action, one cannot expect to predict hallucinogenic potency confidently. Furthermore, the potencies used in the regression analysis span more than two orders of magnitude (from 0.2 mescaline unit for II to 35 mescaline units for VIII). In addition, several activities have been reported in uncertain terms, *i.e.*, "less than." This uncertainty is reflected by the standard deviations and results in broad ranges of predicted activity, particularly for compounds that are only weakly active. Conversely, compounds that are the most active and, subsequently, those from which the most information might be gleaned should be predicted rather well (*e.g.*, VII and VIII).

Application of the relating equation should, nevertheless, afford a relative prediction of activity. To test the relating equation, data from several compounds that have not yet been fully evaluated in humans and/or were not used in generating the relating equation were compared with their predicted potencies. Compounds XI and XII are relatively weak hallucinogenic agents with potencies similar to mescaline. Both compounds are predicted by the relating equation to possess low hallucinogenic activity.

Previous investigators (8), employing a modified Bovet-Gatti profile, found that 2,3,4,5,6-pentamethoxyphenethylamine (XIII) is behaviorally active in animal models with a potency about eight times that of mescaline. With the relating equation, XIII is predicted to have a potency of ~4.5 mescaline units. As another example, an iodinated derivative, 4-iodo-2,5-dimethoxyphenethylamine (XIV), recently was titrated in humans, but effective intoxication levels have not been explored fully. The iodo group, which is *para* to the side chain, possesses a δ^v that is even lower than that of a bromo group. In addition, this molecule possesses two methoxy groups *para* to one another (*i.e.*, 2,5-dimethoxy). On this basis, XIV is predicted by the relating equation to be ~42–48 times more active than mescaline. Shulgin[1] found that the threshold effects of XIV were clear at a total dose of 8 mg; this amount corresponds to an activity of ~44 mescaline units.

Compounds XV and XVI are an order of magnitude more potent than mescaline[1] but less active than XIV. Table I reveals that their activity was predicted reasonably well.

The indexes encode structural information about features contributing to hallucinogenic potency. When applied to several examples not included in the analysis, the relating equation gives reasonable predictions. The structural information derived from this analysis contributes to an understanding of structural influence on hallucinogenic potency.

[1] A. T. Shulgin, unpublished observations.

REFERENCES

(1) L. B. Kier and L. H. Hall, *J. Med. Chem.*, **20**, 1631 (1977).

(2) L. B. Kier and L. H. Hall, "Molecular Connectivity in Chemistry and Drug Research," Academic, New York, N.Y., 1976.

(3) R. A. Glennon and L. B. Kier, *Eur. J. Med. Chem.*, **13**, 219 (1978).

(4) A. T. Shulgin, in "Handbook of Psychopharmacology," vol. 11, L. L. Iverson, S. D. Iverson, and S. H. Snyder, Eds., Plenum, New York, N.Y., 1978, pp 243–333.

(5) A. Shulgin, J. Sargent, and C. Narenjo, *Nature*, **221**, 537 (1969).

(6) M. Vojtechovsky and D. Krus, *Acta Neurol. Suppl.*, **1967**, 391.

(7) L. C. Clarke, F. Benington, and R. D. Morin, *J. Med. Chem.*, **8**, 353 (1965).

(8) J. R. Smythies, R. J. Bradley, V. S. Johnson, F. Benington, M. D. Morin, and L. Clarke, *Psychopharmacologia*, **10**, 379 (1967).

ACKNOWLEDGMENTS

Supported in part by U.S. Public Health Service Grants DA-02046 and DA-01642.

High-Pressure Liquid Chromatographic Evaluation of Aqueous Vehicles for Preparation of Prednisolone and Prednisone Liquid Dosage Forms

V. DAS GUPTA

Received July 10, 1978, from the *Department of Pharmaceutics, College of Pharmacy, University of Houston, Houston, TX 77004.* Accepted for publication December 19, 1978.

Abstract □ A high-pressure liquid chromatographic method was developed that separates prednisolone from prednisone, prednisone from methylprednisolone succinate sodium, and hydrocortisone from hydrocortisone acetate or cortisone acetate. The common liquid dosage preservatives methylparaben, propylparaben, and sodium benzoate do not interfere with quantitative prednisolone, prednisone, and hydrocortisone determinations. The method was used to study prednisolone and prednisone stability in five aqueous vehicles (water, citrate buffer USP, 50% glycerin, 50% sorbitol, and 50% sucrose) containing 10% (v/v) ethanol. Prednisone crystallized out in all vehicles except glycerin, in which it appeared to be stable for at least 92 days. Prednisolone did not crystallize in any vehicle but decomposed quickly in citrate buffer. Sorbitol and glycerin appeared to be the best vehicles for prednisolone. The developed method was applied successfully to the quantitative determinations of prednisolone, prednisone, and hydrocortisone in commercial tablets.

Keyphrases □ Prednisolone—analysis, high-pressure liquid chromatography, liquid dosage forms, separation from prednisone □ Prednisone—analysis, high-pressure liquid chromatography, liquid dosage forms, separation from prednisolone □ High-pressure liquid chromatography—analysis, prednisolone and prednisone in liquid dosage forms □ Dosage forms, liquid—prednisolone and prednisone, separation by high-pressure liquid chromatography

A number of drugs are not available commercially in liquid dosage forms due to stability problems. However, physicians often prescribe some of these drugs for infants and small children who cannot swallow tablets or capsules. Furthermore, liquid dosage forms may be required for administration to adults through nasal gastric tubes.

BACKGROUND

The effect of some solid buffering agents, *e.g.*, antacids, aluminum hydroxide, calcium carbonate, magnesium carbonate, magnesium oxide, and magnesium trisilicate, on prednisolone stability in aqueous suspensions was reported previously (1). The steroid was adsorbed by magnesium trisilicate and decomposed in the presence of magnesium carbonate. The other antacids had no effect on the stability. A later article (2) on base-catalyzed prednisolone decomposition reported that the steroid exhibited first-order degradation kinetics. A kinetic study (3) on fluprednisolone acetate stability in aqueous solution (pH 7.2) also indicated that the steroid could not be stabilized in a neutral aqueous solution.

Prednisone may change to prednisolone on standing in an aqueous solution[1]. Before vehicle evaluation, therefore, it was important to develop an appropriate analytical method to separate prednisolone from prednisone. The previously developed high-pressure liquid chromatographic (HPLC) technique for hydrocortisone (4) was not suitable since it did not separate prednisolone from prednisone. In this procedure, a column of semipolar packing material consisting of a monomolecular layer of cyanopropylsilane permanently bonded to silica was used.

The purposes of this study were to develop an appropriate analytical procedure to separate prednisone from prednisolone and to evaluate the effect of some aqueous vehicles [ethanol, citrate buffer USP (5), 50% glycerin, 50% sorbitol, and 50% sucrose] on prednisone and prednisolone stability.

[1] J. T. Slattery, School of Pharmacy, University of New York at Buffalo, Buffalo, N.Y., *personal communication*

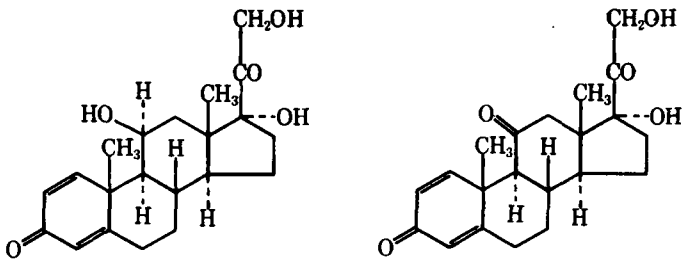

I

II

EXPERIMENTAL

Chemicals and Reagents—All chemicals and reagents were USP, NF, or ACS grade and were used without further purification. Prednisolone[2] (I), prednisone[2] (II), hydrocortisone[2], hydrocortisone acetate[3], and cortisone acetate[4] were used as received. Methylprednisolone succinate sodium[2] powder for injection USP also was used without further treatment.

Apparatus—The high-pressure liquid chromatograph[5] was equipped with a fixed wavelength (254 nm) detector, a recorder[6], and an integrator[7].

Column—The nonpolar prepacked column[8] consisted of a mono-

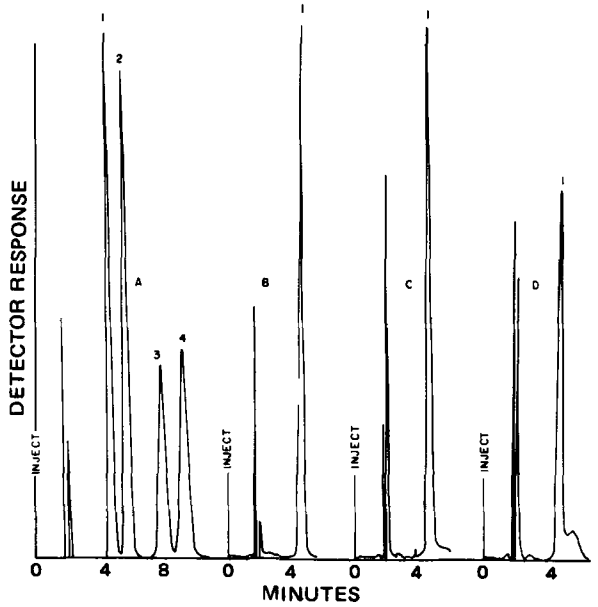

Figure 1—*Sample chromatograms. Key: peaks 1–4 in A, prednisone, prednisolone, methylprednisolone succinate sodium, and hydrocortisone acetate, respectively; and peak 1 in B–D, prednisone in a standard solution, in 50% glycerin (92 day old), and in 50% sugar (92 day old), respectively. For chromatographic conditions, see text.*

[2] The Upjohn Co., Kalamazoo, Mich.
[3] Premo Pharmaceutical Laboratories, South Hackensack, N.J.
[4] Merck & Co., Rahway, N.J.
[5] Waters ALC 202 equipped with U6K universal injector.
[6] Omniscribe 5213-12 equipped with an integrator.
[7] Autolab Minigrator, Spectra-Physics, Santa Clara, Calif.
[8] Waters μBondapak/C_{18}.

0022-3549/79/0700-0908$01.00/0
© 1979, American Pharmaceutical Association

Table I—Assay Results and pH Values of Aqueous Solutions

Vehicle	Active Ingredient	Percent Retained after 2 Days	30 Days	61 Days	92 Days	pH (±0.05) Initial	Final
Water	I	100.6	99.6	99.8	96.5	6.1	6.2
Citrate buffer	I	99.8	84.4	77.7	62.9	4.5	4.4
50% Glycerin	I	99.3	100.1	100.0	99.6	5.5	5.5
50% Sorbitol	I	98.9	99.5	99.5	99.0	5.4	5.3
50% Sucrose	I	100.4	99.3	93.9	93.3	6.0	6.0
Water	II	66.3[a]	—	—	—	6.0	—
Citrate buffer	II	62.8[a]	—	—	—	4.4	—
50% Glycerin	II	100.6	99.4	99.6	99.7	5.5	5.7
50% Sorbitol	II	81.6[a]	—	—	—	5.5	—
50% Sucrose	II	101.2	83.3[a]	—	69.3[a,b]	6.0	—

[a] Prednisone crystallized and, therefore, was not followed. [b] Done only to determine if II had changed to I (see Fig. 1D and *Discussion*).

molecular layer of octadecyltrichlorosilane permanently bonded to silica (30 cm and 4 mm i.d.).

Chromatographic Conditions—The solvent was 0.01 *M* KH_2PO_4 in water containing 50% (v/v) methanol. The temperature was ambient, the flow rate was 1.6 ml/min, and the chart speed was 30.5 cm/hr. The attenuation unit for full-scale deflection was 0.04.

Standard Solutions—The stock solution of each hormone was prepared by dissolving 100.0 mg of hormone in enough ethanol to make 100.0 ml. The standard solutions were prepared by diluting 2.0 ml of the stock solution to 100.0 ml with water. For tablet analysis, the standard solution was prepared by diluting with ethanol. A standard solution containing the four hormones, I, II, methylprednisolone succinate sodium, and hydrocortisone acetate, also was prepared by diluting with water.

Aqueous Solutions of I and II—Five aqueous solutions each of I and II were prepared. The stock solutions of I and II were prepared by dissolving 500.0 mg of drug in enough ethanol to make 100.0 ml. A 10.0-ml quantity of a stock solution was brought to volume (100.0 ml) either with water or with another appropriate solution, a 50% aqueous solution of glycerin (v/v), a 50% solution of sorbitol in water, a 50% solution of sucrose in water, or citrate buffer USP (5). The citrate buffer pH was 4.4. All solutions contained 0.1% sodium benzoate as a preservative.

Assay Solutions—A 2.0-ml quantity of the aqueous solution was diluted to 50.0 ml with water.

Assay Solutions from Commercial Tablets—Ten tablets were weighed and ground to a fine powder. A quantity of the powder representing 2.0 mg of the active ingredient was weighed accurately and transferred to a 150-ml beaker. Then 80 ml of ethanol was added, and the mixture was heated just to boiling. The mixture was cooled, brought to 100.0 ml with ethanol, and filtered. The first 20 ml of the filtrate was rejected, and then samples were collected for analysis.

After the initial assays using the method discussed below and the determination of pH values (after diluting 1:10 with water), the aqueous solutions of I and II were stored at room temperature. After appropriate storage periods, the aqueous solutions were assayed again and pH values also were determined.

Assay—Twenty microliters of the assay solution was injected into the chromatograph using the described conditions. For comparison, an identical volume of the standard solution was injected after the assay was eluted.

Since preliminary investigations on each hormone indicated that Beer's law was followed in the 0.2–2.5-μg range, the results were calculated as follows:

$$\frac{A_a}{A_s} \times 100 = \text{percent of label claim} \qquad \text{(Eq. 1)}$$

where A_a is the peak area of the assay solution and A_s is the peak area of the standard solution (Figs. 1 and 2 and Tables I and II).

Table II—Tablet Results

Tablet	Active Ingredient per Tablet	Color	Assay Results, % of claim HPLC Method	Blue Tetrazolium Method
1	5 mg of I	Yellow	100.5	295.3
2	5 mg of II	White	101.3	348.6
3	5 mg of hydrocortisone	White	99.8	>386

For comparison, the commercial tablets were also assayed (Table II) using the USP blue tetrazolium method (6). For this method, the same assay solution as already described was used.

DISCUSSION

The developed HPLC method separated I from II (Fig. 1A) efficiently. Other systems tried without success were[9]: (*a*) 0.01 *M* KH_2PO_4 in water containing 20% (v/v) methanol; (*b*) same as *a* with 2% (v/v) acetic acid (final pH 2.6); (*c*) same as *b* with 0.005 *M* heptanesulfonic acid sodium; (*d*) 0.01 *M* KH_2PO_4 in water containing 20% (v/v) ethanol (pH 7.8 adjusted with 1:100 phosphoric acid in water); (*e*) 0.005 *M* $(NH_4)_2HPO_4$ in 20% (v/v) ethanol in water; (*f*) 0.005 *M* tetrabutylammonium hydroxide in 20% (v/v) ethanol in water (pH 7.8 adjusted with 1:100 phosphoric acid in water); and (*g*) 0.005 *M* $(NH_4)_2HPO_4$ in water containing 10% (v/v) methanol, acetonitrile, or a combination of both (5% each).

The HPLC method separated I from its salt, methylprednisolone succinate sodium (Fig. 1A). It also separated hydrocortisone from hydrocortisone acetate and from cortisone acetate. Hydrocortisone did not separate from I, and hydrocortisone acetate did not separate from cortisone acetate. The common preservatives methylparaben, propylparaben, and sodium benzoate did not interfere with the determinations of I, II, and hydrocortisone. The relative percent standard deviations based on five injections of the standard solutions were 0.64, 0.84, and 1.8 for I, II, and hydrocortisone, respectively.

Due to the poor solubility of II, partial crystallization occurred in all of the vehicles except 50% (v/v) glycerin. In glycerin, there was no II decomposition (Table I) in 92 days. Chromatograms from a standard so-

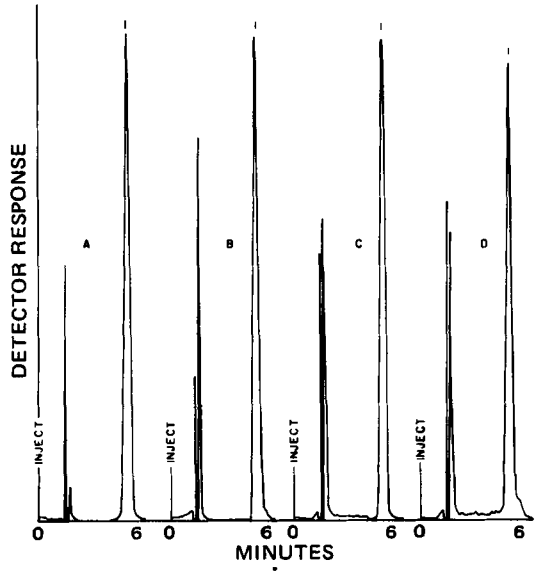

Figure 2—*Sample chromatograms from prednisolone. Key: peak 1 in A–D, prednisolone in a standard solution, in 50% glycerin, in 50% sorbitol, and in 50% sucrose, respectively; and B, C, and D, 92-day-old samples. For chromatographic conditions, see text.*

[9] Using Waters μBondapak/CN.

lution (Fig. 1B) and from a glycerin solution (Fig. 1C) were similar. In the presence of sugar, besides crystallization (Fig. 1B), II may be partially reduced to I (Figs. 1B and 1D).

Prednisolone did not crystallize in any vehicle investigated. It decomposed fast in the presence of citrate buffer. The percent retained after 92 days was 62.9 (Table I). Some decomposition also was recorded in water and in 50% aqueous sucrose (Table I and Fig. 2D). Both 50% (v/v) glycerin in water and 50% aqueous sorbitol appear to be excellent I vehicles (Table I). The peak obtained from a I solution in sorbitol (Fig. 2C) compared better with the standard (Fig. 1A) than did the peak from a glycerin solution (Fig. 2B), which had a slight shoulder, perhaps a sign of slight decomposition. All solutions studied contained 10% (v/v) ethanol and 0.1% sodium benzoate.

The developed method also was suitable for the quantitative determinations of I, II, and hydrocortisone in commercial tablets (Table II). The results obtained with the blue tetrazolium method were very high, presumably due to interference from some inactive ingredients. When the active ingredients were extracted with ethanol without heat, inconsistent and sometimes low results were obtained. Therefore, the mixture was heated to extract the active ingredient quantitatively.

REFERENCES

(1) T. Chulski and A. A. Forist, *J. Am. Pharm. Assoc., Sci. Ed.*, **47**, 553 (1958).

(2) D. E. Guttman and P. D. Meister, *ibid.*, **47**, 773 (1958).

(3) E. H. Jensen and D. J. Lamb, *J. Pharm. Sci.*, **53**, 402 (1964).

(4) V. D. Gupta, *ibid.*, **67**, 299 (1978).

(5) "The United States Pharmacopeia," 19th rev., Mack Publishing Co., Easton, Pa., 1975, p. 458.

(6) *Ibid.*, p. 238.

ACKNOWLEDGMENTS

The author thanks The Upjohn Co. for the generous supply of prednisolone and prednisone powders.

Fluorometric Determination of Chlorzoxazone in Tablets and Biological Fluids

JAMES T. STEWART ˣ **and CHE W. CHAN**

Received December 4, 1978, from the *Department of Medicinal Chemistry, School of Pharmacy, University of Georgia, Athens, GA 30602.* Accepted for publication December 27, 1978.

Abstract □ A fluorometric determination for chlorzoxazone was developed based on the intrinsic drug fluorescence in chloroform using excitation and emission wavelengths of 286 and 310 nm, respectively. A calibration curve for chlorzoxazone in chloroform gave a linear working range of 0.027–2.3 μg/ml (r = 0.9999) with the minimum detectability at 27 ng/ml. The procedure was applied to chlorzoxazone analysis in spiked plasma and urine samples. Minimum detectable drug levels in these samples were 60 and 130 ng/ml, respectively. Data revealed that chlorzoxazone could be determined in plasma and urine even in the presence of 20-fold molar excesses of its major metabolite, 6-hydroxychlorzoxaxone, and acetaminophen. The method also was applicable to chlorzoxazone analysis in a commercial dosage form containing acetaminophen.

Keyphrases □ Chlorzoxazone—analysis, fluorometry, in commercial tablets and biological fluids, in presence of hydroxychlorzoxazone and acetaminophen □ Fluorometry—analysis, chlorzoxazone in commercial tablets and biological fluids, in presence of hydroxychlorzoxazone and acetaminophen □ Muscle relaxants—chlorzoxazone, fluorometric analysis in commercial tablets and biological fluids, in presence of hydroxychlorzoxazone and acetaminophen

Chlorzoxazone (I) is one of the most useful skeletal muscle relaxants in the treatment of painful muscle spasm, especially in combination with acetaminophen, a product that has been among the top 100 drug products in the United States in recent years. Studies of chlorzoxazone metabolism in humans have shown that its major metabolite is 6-hydroxychlorzoxazone (II) (1, 2). The drug is rapidly absorbed from the GI tract and essentially disappears from the blood in 7–8 hr. Less than 1% of the intact drug is excreted in the urine.

Among the analytical methods reported for I analysis have been spectrophotometry (1), titrimetry (3), and GLC and TLC (4–6). Direct application of many procedures to the determination of the drug in biological fluids is lacking. In other instances, parameters such as accuracy, linearity, sensitivity, and detection limit were not evaluated for the reported methodology.

In this paper, the intrinsic fluorescence of I is presented as a suitable analytical technique for the determination of the drug in biological fluids. The method also is useful for analysis of I in tablets. The method described is sensitive for I in the nanogram per milliliter range and is free from interference from II and acetaminophen. A previous report examined the analysis of I using derivatization with various fluorogenic reagents (7).

EXPERIMENTAL

Apparatus—Fluorescence measurements were made with a spectrophotofluorometer[1] equipped with a corrected spectra accessory. The following settings were used: excitation and emission slits, 10 nm; amplifier sensitivity coarse, 0.1; and measurement mode in true emission. Clear fused quartz cells (12.5 × 45 mm) were used as sample cells for dosage form analysis. Quartz microcells[2] (path length 5 mm) were used for the biological fluid assays.

Reagents and Chemicals—Chlorzoxazone[3], 6-hydroxychlorzoxazone[3], and acetaminophen[4] were obtained as pure powders and were used without further purification in the preparation of stock solutions. All other reagents and chemicals were commercially available and were used as received.

Determination of Chlorzoxazone in Dosage Form—A tablet[5] containing 250 mg of chlorzoxazone and 300 mg of acetaminophen was suspended in 15 ml of distilled water contained in a 50-ml centrifuge tube. After 25 ml of ethyl acetate was added, the solution was mixed[6] for 5 min. An aliquot of the ethyl acetate extract corresponding to 100 mg of chlorzoxazone was transferred to a 50-ml volumetric flask and diluted to volume with ethyl acetate. One milliliter of this solution was trans-

[1] Model MPF-4, Perkin-Elmer Corp., Norwalk, Conn.
[2] Part No. 018-0056, Hitachi, Ltd., Tokyo, Japan.
[3] McNeil Pharmaceuticals, Fort Washington, Pa.
[4] Eastman Organic Chemicals, Rochester, N.Y.
[5] Parafon-Forte, McNeil Pharmaceuticals, Fort Washington, Pa.
[6] Vortex-Genie mixer, Scientific Industries, Bohemia, N.Y.

0022-3549/79/0700-0910$01.00/0

© 1979, American Pharmaceutical Association

lution (Fig. 1B) and from a glycerin solution (Fig. 1C) were similar. In the presence of sugar, besides crystallization (Fig. 1B), II may be partially reduced to I (Figs. 1B and 1D).

Prednisolone did not crystallize in any vehicle investigated. It decomposed fast in the presence of citrate buffer. The percent retained after 92 days was 62.9 (Table I). Some decomposition also was recorded in water and in 50% aqueous sucrose (Table I and Fig. 2D). Both 50% (v/v) glycerin in water and 50% aqueous sorbitol appear to be excellent I vehicles (Table I). The peak obtained from a I solution in sorbitol (Fig. 2C) compared better with the standard (Fig. 1A) than did the peak from a glycerin solution (Fig. 2B), which had a slight shoulder, perhaps a sign of slight decomposition. All solutions studied contained 10% (v/v) ethanol and 0.1% sodium benzoate.

The developed method also was suitable for the quantitative determinations of I, II, and hydrocortisone in commercial tablets (Table II). The results obtained with the blue tetrazolium method were very high, presumably due to interference from some inactive ingredients. When the active ingredients were extracted with ethanol without heat, inconsistent and sometimes low results were obtained. Therefore, the mixture was heated to extract the active ingredient quantitatively.

REFERENCES

(1) T. Chulski and A. A. Forist, *J. Am. Pharm. Assoc., Sci. Ed.*, **47**, 553 (1958).

(2) D. E. Guttman and P. D. Meister, *ibid.*, **47**, 773 (1958).

(3) E. H. Jensen and D. J. Lamb, *J. Pharm. Sci.*, **53**, 402 (1964).

(4) V. D. Gupta, *ibid.*, **67**, 299 (1978).

(5) "The United States Pharmacopeia," 19th rev., Mack Publishing Co., Easton, Pa., 1975, p. 458.

(6) *Ibid.*, p. 238.

ACKNOWLEDGMENTS

The author thanks The Upjohn Co. for the generous supply of prednisolone and prednisone powders.

Fluorometric Determination of Chlorzoxazone in Tablets and Biological Fluids

JAMES T. STEWART ˣ **and CHE W. CHAN**

Received December 4, 1978, from the *Department of Medicinal Chemistry, School of Pharmacy, University of Georgia, Athens, GA 30602.* Accepted for publication December 27, 1978.

Abstract □ A fluorometric determination for chlorzoxazone was developed based on the intrinsic drug fluorescence in chloroform using excitation and emission wavelengths of 286 and 310 nm, respectively. A calibration curve for chlorzoxazone in chloroform gave a linear working range of 0.027–2.3 μg/ml (r = 0.9999) with the minimum detectability at 27 ng/ml. The procedure was applied to chlorzoxazone analysis in spiked plasma and urine samples. Minimum detectable drug levels in these samples were 60 and 130 ng/ml, respectively. Data revealed that chlorzoxazone could be determined in plasma and urine even in the presence of 20-fold molar excesses of its major metabolite, 6-hydroxychlorzoxaxone, and acetaminophen. The method also was applicable to chlorzoxazone analysis in a commercial dosage form containing acetaminophen.

Keyphrases □ Chlorzoxazone—analysis, fluorometry, in commercial tablets and biological fluids, in presence of hydroxychlorzoxazone and acetaminophen □ Fluorometry—analysis, chlorzoxazone in commercial tablets and biological fluids, in presence of hydroxychlorzoxazone and acetaminophen □ Muscle relaxants—chlorzoxazone, fluorometric analysis in commercial tablets and biological fluids, in presence of hydroxychlorzoxazone and acetaminophen

Chlorzoxazone (I) is one of the most useful skeletal muscle relaxants in the treatment of painful muscle spasm, especially in combination with acetaminophen, a product that has been among the top 100 drug products in the United States in recent years. Studies of chlorzoxazone metabolism in humans have shown that its major metabolite is 6-hydroxychlorzoxazone (II) (1, 2). The drug is rapidly absorbed from the GI tract and essentially disappears from the blood in 7–8 hr. Less than 1% of the intact drug is excreted in the urine.

Among the analytical methods reported for I analysis have been spectrophotometry (1), titrimetry (3), and GLC and TLC (4–6). Direct application of many procedures to the determination of the drug in biological fluids is lacking. In other instances, parameters such as accuracy, linearity, sensitivity, and detection limit were not evaluated for the reported methodology.

In this paper, the intrinsic fluorescence of I is presented as a suitable analytical technique for the determination of the drug in biological fluids. The method also is useful for analysis of I in tablets. The method described is sensitive for I in the nanogram per milliliter range and is free from interference from II and acetaminophen. A previous report examined the analysis of I using derivatization with various fluorogenic reagents (7).

EXPERIMENTAL

Apparatus—Fluorescence measurements were made with a spectrophotofluorometer[1] equipped with a corrected spectra accessory. The following settings were used: excitation and emission slits, 10 nm; amplifier sensitivity coarse, 0.1; and measurement mode in true emission. Clear fused quartz cells (12.5 × 45 mm) were used as sample cells for dosage form analysis. Quartz microcells[2] (path length 5 mm) were used for the biological fluid assays.

Reagents and Chemicals—Chlorzoxazone[3], 6-hydroxychlorzoxazone[3], and acetaminophen[4] were obtained as pure powders and were used without further purification in the preparation of stock solutions. All other reagents and chemicals were commercially available and were used as received.

Determination of Chlorzoxazone in Dosage Form—A tablet[5] containing 250 mg of chlorzoxazone and 300 mg of acetaminophen was suspended in 15 ml of distilled water contained in a 50-ml centrifuge tube. After 25 ml of ethyl acetate was added, the solution was mixed[6] for 5 min. An aliquot of the ethyl acetate extract corresponding to 100 mg of chlorzoxazone was transferred to a 50-ml volumetric flask and diluted to volume with ethyl acetate. One milliliter of this solution was trans-

[1] Model MPF-4, Perkin-Elmer Corp., Norwalk, Conn.
[2] Part No. 018-0056, Hitachi, Ltd., Tokyo, Japan.
[3] McNeil Pharmaceuticals, Fort Washington, Pa.
[4] Eastman Organic Chemicals, Rochester, N.Y.
[5] Parafon-Forte, McNeil Pharmaceuticals, Fort Washington, Pa.
[6] Vortex-Genie mixer, Scientific Industries, Bohemia, N.Y.

0022-3549/79/0700-0910$01.00/0

© 1979, American Pharmaceutical Association

Table I—Determination of Chlorzoxazone in a Commercial Tablet [a]

Labeled Content in Aliquot, μg	Found, μg[b]	Percent of Theory
6.24	6.15 ± 0.23	98.61 ± 3.71
3.12	3.14 ± 0.12	100.75 ± 3.83
1.56	1.55 ± 0.07	99.57 ± 4.37
Average mean ± *SD*		99.64 ± 3.57
RSD, %		3.58

[a] Parafon-Forte, McNeil Laboratories, Fort Washington, Pa. [b] Based on triplicate samples.

ferred to a 25-ml volumetric flask, and the solution was adjusted to volume with ethyl acetate.

Individual aliquots of 19.5, 39, and 78 μl were each transferred to 5-ml volumetric flasks and evaporated to dryness with nitrogen. Chloroform, 5 ml, was added to redissolve each residue, and the chloroform solution fluorescence was determined using excitation and emission wavelengths of 286 and 310 nm, respectively. A calibration curve for chlorzoxazone in the 0.1–1.50-μg/ml range was determined concurrently using dilutions obtained from a stock solution of chlorzoxazone in chloroform. Slope and intercept data from the calibration data regression analysis were used to solve for the drug concentration in individual aliquots: fluorescence = (slope × concentration) + intercept.

Assay of Chlorzoxazone in Plasma or Urine—One milliliter of plasma or urine containing chlorzoxazone was added to a 15-ml centrifuge tube containing 0.5 ml of pH 2.5 phosphate buffer. Six milliliters of petroleum ether containing 1.5% isoamyl alcohol was added, followed by mixing[6] for 2 min and centrifugation for 5 min at 2000 rpm. Five milliliters of the organic phase was transferred to a clean 15-ml centrifuge tube, followed by the addition of 2.25 ml of 0.5 *N* NaOH. After mixing[6] (1 min) and centrifugation (3 min), the organic phase was aspirated and 1.25 ml of 1 *N* HCl and 5 ml of chloroform were added. The solution was mixed[6] for 1 min, and the aqueous phase was aspirated.

Anhydrous sodium sulfate (1 g) was added to the chloroform layer, and the mixture was centrifuged for 3 min. The chloroform was decanted into a clear 15-ml centrifuge tube and evaporated to dryness with a nitrogen stream. Chloroform, 1 ml, was added to redissolve the residue. Fluorescence measurements were made using excitation and emission wavelengths of 286 and 310 nm, respectively. A calibration curve for chlorzoxazone was performed concurrently using spiked plasma or urine samples[7] in the 1–10-μg/ml concentration range. Slope and intercept data from regression analysis of the calibration data were used to solve for the drug concentration in each sample: fluorescence = (slope × concentration) + intercept.

RESULTS AND DISCUSSION

Fluorometric examination of I in water at pH 2–14 showed maximum fluorescence at pH < 6 using excitation and emission wavelengths of 286 and 310 nm, respectively. The fluorescence was essentially quenched at pH ≧ 10. A comparison of chlorzoxazone fluorescence in various organic solvents (water, ethanol, isobutanol, tetrahydrofuran, ethyl acetate, chloroform, carbon tetrachloride, and petroleum ether containing 1.5% isoamyl alcohol or 2% isobutanol) indicated that the drug was more fluorescent in the polar solvents. However, sensitivity was limited by the influence of Raman scatter of the various solvents, especially at low I concentrations.

Data showed that the chloroform Raman peak was less intense than those of the other solvents studied. Chloroform also gave less interference at the I emission wavelength while showing adequate solubility for the drug. Thus, chloroform was selected as the solvent for the fluorescence measurements. A calibration curve for I in chloroform showed a linear working range from 0.027 to 2.3 μg/ml (r = 0.9999) with minimum detection at 27 ng/ml (signal/noise = 2).

Chlorzoxazone was extracted from water samples using various organic solvents. The percent recovery of I from water using chloroform was 100.0 ± 4.4% (n = 6). Optimal extraction was at pH < 7. Other solvents such as ethyl acetate, isobutyl or isoamyl alcohol, ethyl acetate–isobutanol (3:2), and petroleum ether containing 1.5% isoamyl alcohol or 2% isobutanol also were useful extraction solvents. However, when these solvents were applied to chlorzoxazone extraction in plasma or urine samples, petroleum ether containing 1.5% isoamyl alcohol yielded the highest percent recovery in terms of chlorzoxazone fluorescence in chloroform.

Inclusion of isoamyl alcohol in petroleum ether serves two purposes: (*a*) it increases the solvent system polarity, and (*b*) it prevents drug adsorption on the glass walls of the containers (8). Increasing the isoamyl alcohol concentration in the petroleum ether from 1.5 to 10% or adding isobutanol (2–10%) did not significantly increase the percent recovery of I but gave higher blank readings. In general, higher blank readings were obtained for biological fluids extracted with polar solvents, probably due to extraction of endogenous plasma and urine components that absorb strongly at 280 nm in the vicinity of the I fluorescence excitation wavelength. Such substances also could reduce chlorzoxazone fluorescence, a phenomenon known as the inner-filter effect (9).

The petroleum ether–isoamyl alcohol extraction solvent minimized these interferences as well as those of II and acetaminophen, potentially interfering substances likely to be present with I in biological samples. Calculated percent recoveries of II and acetaminophen from aqueous solution using the solvent mix were 0.2 and 0.12%, respectively. Little or no interference in the chlorzoxazone assay in plasma or urine was observed even in the presence of a 20-fold excess of II and/or acetaminophen (Table II).

In the assay for I in biological fluids, chlorzoxazone extraction with

Table II—Typical Analysis of Chlorzoxazone at 1.7 μg/ml in Spiked Plasma and Urine Samples [a]

Mixture	Amount Found[b], μg/ml		Percent of Theory	
	Plasma	Urine	Plasma	Urine
Chlorzoxazone and hydroxychlorzoxazone[c]	1.698 ± 0.035	1.735 ± 0.028	99.88 ± 2.19	102.06 ± 1.72
Chlorzoxazone and hydroxychlorzoxazone[d]	1.733 ± 0.042	1.679 ± 0.010	101.94 ± 2.45	98.76 ± 0.01
Chlorzoxazone and hydroxychlorzoxazone[e]	1.614 ± 0.092	1.597 ± 0.026	97.62 ± 1.61	93.94 ± 1.67
Chlorzoxazone and acetaminophen[e]	1.63 ± 0.020	1.70 ± 0.095	97.03 ± 1.80	100.06 ± 5.66

[a] Samples were spiked by addition of microliter aliquots of stock chlorzoxazone, hydroxychlorzoxazone, and acetaminophen solutions in ethanol to 1.0-ml blank plasma or urine samples. [b] Based on quadruplicate samples. [c] Hydroxy metabolite was present in equimolar concentration to that of chlorzoxazone. [d] Hydroxy compound present in fourfold molar excess. [e] Compound present in 20-fold molar excess.

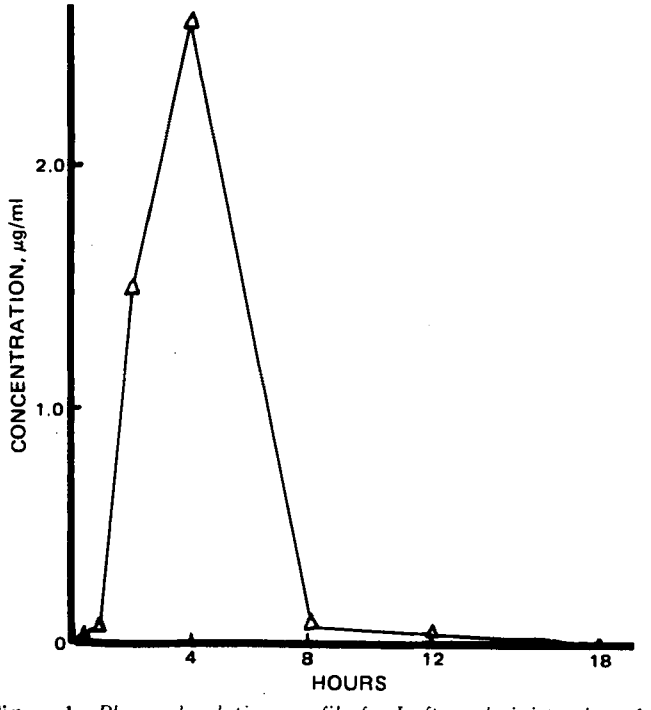

Figure 1—*Plasma level–time profile for I after administration of a single 300-mg oral dose to a healthy adult male.*

[7] Samples were spiked by addition of 2.5, 5.0, 10.0, and 20.0 μl of a 3.4-mg/10-ml ethanolic solution of I to 1.0 ml of blank plasma or urine samples.

petroleum ether–isoamyl alcohol is followed by a reextraction of the drug into aqueous sodium hydroxide, adjustment to pH 6.8 with acid, and extraction into chloroform for the final fluorometric measurement. With this procedure, percent recoveries of chlorzoxazone from plasma and urine compared to unextracted drug were 86.63 ± 1.66 (n = 8) and 95.37 ± 2.42 (n = 8), respectively. The linear working ranges for I in plasma and urine were 0.06–3.2 (r = 0.9993) and 0.13–3.0 (r = 0.9995) μg/ml, respectively, with minimum detectable levels at 60 and 130 ng/ml, respectively.

To demonstrate the application of the fluorometric I analysis, drug determinations in a commercial dosage form and in spiked plasma and urine samples were performed (Tables I and II). Plasma and urine data for spiked samples of I at 0.85, 3.4, and 6.8 μg/ml in the presence of varying concentrations of II and acetaminophen gave similar results. In addition, a plasma level–time profile for I (Fig. 1) illustrated the utility of the assay in determining plasma drug levels after oral administration of a single 300-mg dose to a healthy adult male. The peak plasma I level was obtained within 4 hr, with the drug essentially disappearing from plasma in 8 hr. Analysis of I in urine samples taken over 24 hr revealed that 116 μg of unchanged drug (<0.1% of administered dose) was excreted. These findings are comparable to those of previous metabolic studies (2).

REFERENCES

(1) A. H. Conney, N. Trousof, and J. J. Burns, *J. Pharmacol. Exp. Ther.*, **128**, 33 (1960).

(2) A. H. Conney and J. J. Burns, *ibid.*, **128**, 340 (1960).

(3) H. Beral, V. Gamentzy, and I. Bucur, *Rev. Chim. (Bucharest)*, **16**, 322 (1965).

(4) K. D. Parker, C. R. Fortan, and P. L. Kirk, *Anal. Chem.*, **34**, 757 (1962).

(5) B. Kaempe, *Arch. Pharm. Chem., Sci. Ed.*, **2**, 145 (1974).

(6) I. Ullah, D. E. Cadwallader, and I. L. Honigberg, *J. Chromatogr.*, **46**, 211 (1970).

(7) J. T. Stewart and C. W. Chan, *Anal. Lett.*, **B11**, 667 (1978).

(8) E. O. Titus, in "Fundamentals of Drug Metabolism and Drug Disposition," B. N. LaDu, H. G. Mandel, and E. L. Way, Eds., Williams & Wilkins, Baltimore, Md., 1971, p. 419.

(9) C. A. Parker and W. T. Rees, *Analyst*, **87**, 83 (1962).

ACKNOWLEDGMENTS

Abstracted in part from a thesis submitted by C. W. Chan to the University of Georgia in partial fulfillment of the Master of Science degree requirements.

Acetazolamide Binding to Two Carbonic Anhydrase Isoenzymes in Human Erythrocytes

W. F. BAYNE, L.-C. CHU, and F. THEEUWES ˣ

Received July 13, 1978, from *Alza Corporation, Palo Alto, CA 94304.* Accepted for publication August 18, 1978.

Abstract □ Acetazolamide binding to high activity and low activity carbonic anhydrase isoenzymes in red blood cells was studied. Inhibitory constants of 0.041 and 2.72 μ*M* and maximum binding capacities of 17.2 and 155 μ*M*, respectively, were found.

Keyphrases □ Acetazolamide—binding to two carbonic anhydrase isoenzymes, human erythrocytes, *in vitro* □ Carbonic anhydrase inhibitors—acetazolamide, binding to two carbonic anhydrase isoenzymes, human erythrocytes, *in vitro* □ Erythrocytes—acetazolamide binding to two carbonic anhydrase isoenzymes, *in vitro*

Acetazolamide, a carbonic anhydrase inhibitor widely used in the treatment of glaucoma, acts directly on the carbonic anhydrase in secretory cells of the ciliary body to reduce aqueous production and to lower intraocular pressure (1). The decrease in aqueous humor formation is thought to result from a decrease in bicarbonate flux from secretory cells (2, 3). Acetazolamide also acts indirectly to lower intraocular pressure by eliciting systemic acidosis (1). With the administration of therapeutic acetazolamide doses, renal carbonic anhydrase is inhibited, decreasing reabsorption of renally excreted bicarbonate (4).

BACKGROUND

Most carbonic anhydrase is in the red blood cells, with extravascular sources contributing an additional 10% or less (1). Two types of carbonic anhydrase have been identified: high activity type C and low activity type B (5). Extravascular carbonic anhydrase, including that found in the ciliary body, is generally the high activity type C isoenzyme (5). In humans, red blood cells are the major source of low activity type B isoenzyme (4). The ratio of low activity isoenzyme to high activity isoenzyme in human erythrocytes was reported as 6:1 (6).

Acetazolamide binding to human erythrocytes was studied previously (7). Intracellular and extracellular acetazolamide concentrations were determined by GLC following drug equilibration between the red blood cells and the external medium (either plasma or buffered saline). Rosenthal plots were constructed from the bound intracellular and extracellular concentrations to obtain the dissociation constants (inhibitory constant) of the enzyme–drug complex and the maximum binding capacity of the enzyme.

The inhibitory constant reported for the high activity isoenzyme was approximately an order of magnitude larger than that reported for the low activity isoenzyme (5, 6). Therefore, if *in vitro* binding studies are performed such that a wide range of intracellular acetazolamide concentrations is obtained, a definite curvature in the Rosenthal plot should be seen. Resolution of the curved plot into linear segments should permit the determination of maximum binding capacities and inhibitory constants for both isoenzymes.

Rosenthal plots constructed from *in vitro* equilibration studies performed in this laboratory exhibit a pronounced curvature. Inhibitory constants determined from the resolution of the curve were used as parameters in a nonlinear pharmacokinetic model for acetazolamide described previously (8).

EXPERIMENTAL

Human blood was drawn into heparinized tubes and immediately centrifuged to isolate the red blood cells. The cells were washed twice with two volumes of pH 7.4 buffered saline (0.15 *M* NaCl and 0.01 *M* phosphate), which were discarded. The cells were then suspended in the same buffered saline, and the hematocrit of the reconstituted red blood cell suspension was determined.

Acetazolamide was dissolved in methanol (0.5 μg/μl), and aliquots containing 1–200 μg of the drug were added to 20-ml disposable vials. Methanol was evaporated with a nitrogen stream. Red blood cell suspension was added to the vials (6 ml to vials containing <6 μg of acetazolamide and 3 ml to vials containing >6 μg of drug). The contents were incubated for 2 hr at 37° with gentle swirling in a reciprocating shaker. All incubations were performed using the suspension prepared from cells obtained from a single subject.

After incubation, the artificial blood medium was centrifuged. The acetazolamide concentration in 1–3-ml aliquots of the supernate was determined using a previously described high-pressure liquid chromatographic (HPLC) method (9).

0022-3549/79/0700-0912$01.00/0

© 1979, American Pharmaceutical Association

petroleum ether–isoamyl alcohol is followed by a reextraction of the drug into aqueous sodium hydroxide, adjustment to pH 6.8 with acid, and extraction into chloroform for the final fluorometric measurement. With this procedure, percent recoveries of chlorzoxazone from plasma and urine compared to unextracted drug were 86.63 ± 1.66 (n = 8) and 95.37 ± 2.42 (n = 8), respectively. The linear working ranges for I in plasma and urine were 0.06–3.2 (r = 0.9993) and 0.13–3.0 (r = 0.9995) μg/ml, respectively, with minimum detectable levels at 60 and 130 ng/ml, respectively.

To demonstrate the application of the fluorometric I analysis, drug determinations in a commercial dosage form and in spiked plasma and urine samples were performed (Tables I and II). Plasma and urine data for spiked samples of I at 0.85, 3.4, and 6.8 μg/ml in the presence of varying concentrations of II and acetaminophen gave similar results. In addition, a plasma level–time profile for I (Fig. 1) illustrated the utility of the assay in determining plasma drug levels after oral administration of a single 300-mg dose to a healthy adult male. The peak plasma I level was obtained within 4 hr, with the drug essentially disappearing from plasma in 8 hr. Analysis of I in urine samples taken over 24 hr revealed that 116 μg of unchanged drug (<0.1% of administered dose) was excreted. These findings are comparable to those of previous metabolic studies (2).

REFERENCES

(1) A. H. Conney, N. Trousof, and J. J. Burns, *J. Pharmacol. Exp. Ther.*, **128**, 33 (1960).

(2) A. H. Conney and J. J. Burns, *ibid.*, **128**, 340 (1960).

(3) H. Beral, V. Gamentzy, and I. Bucur, *Rev. Chim. (Bucharest)*, **16**, 322 (1965).

(4) K. D. Parker, C. R. Fortan, and P. L. Kirk, *Anal. Chem.*, **34**, 757 (1962).

(5) B. Kaempe, *Arch. Pharm. Chem., Sci. Ed.*, **2**, 145 (1974).

(6) I. Ullah, D. E. Cadwallader, and I. L. Honigberg, *J. Chromatogr.*, **46**, 211 (1970).

(7) J. T. Stewart and C. W. Chan, *Anal. Lett.*, **B11**, 667 (1978).

(8) E. O. Titus, in "Fundamentals of Drug Metabolism and Drug Disposition," B. N. LaDu, H. G. Mandel, and E. L. Way, Eds., Williams & Wilkins, Baltimore, Md., 1971, p. 419.

(9) C. A. Parker and W. T. Rees, *Analyst*, **87**, 83 (1962).

ACKNOWLEDGMENTS

Abstracted in part from a thesis submitted by C. W. Chan to the University of Georgia in partial fulfillment of the Master of Science degree requirements.

Acetazolamide Binding to Two Carbonic Anhydrase Isoenzymes in Human Erythrocytes

W. F. BAYNE, L.-C. CHU, and F. THEEUWES ˣ

Received July 13, 1978, from *Alza Corporation, Palo Alto, CA 94304.* Accepted for publication August 18, 1978.

Abstract □ Acetazolamide binding to high activity and low activity carbonic anhydrase isoenzymes in red blood cells was studied. Inhibitory constants of 0.041 and 2.72 μ*M* and maximum binding capacities of 17.2 and 155 μ*M*, respectively, were found.

Keyphrases □ Acetazolamide—binding to two carbonic anhydrase isoenzymes, human erythrocytes, *in vitro* □ Carbonic anhydrase inhibitors—acetazolamide, binding to two carbonic anhydrase isoenzymes, human erythrocytes, *in vitro* □ Erythrocytes—acetazolamide binding to two carbonic anhydrase isoenzymes, *in vitro*

Acetazolamide, a carbonic anhydrase inhibitor widely used in the treatment of glaucoma, acts directly on the carbonic anhydrase in secretory cells of the ciliary body to reduce aqueous production and to lower intraocular pressure (1). The decrease in aqueous humor formation is thought to result from a decrease in bicarbonate flux from secretory cells (2, 3). Acetazolamide also acts indirectly to lower intraocular pressure by eliciting systemic acidosis (1). With the administration of therapeutic acetazolamide doses, renal carbonic anhydrase is inhibited, decreasing reabsorption of renally excreted bicarbonate (4).

BACKGROUND

Most carbonic anhydrase is in the red blood cells, with extravascular sources contributing an additional 10% or less (1). Two types of carbonic anhydrase have been identified: high activity type C and low activity type B (5). Extravascular carbonic anhydrase, including that found in the ciliary body, is generally the high activity type C isoenzyme (5). In humans, red blood cells are the major source of low activity type B isoenzyme (4). The ratio of low activity isoenzyme to high activity isoenzyme in human erythrocytes was reported as 6:1 (6).

Acetazolamide binding to human erythrocytes was studied previously (7). Intracellular and extracellular acetazolamide concentrations were determined by GLC following drug equilibration between the red blood cells and the external medium (either plasma or buffered saline). Rosenthal plots were constructed from the bound intracellular and extracellular concentrations to obtain the dissociation constants (inhibitory constant) of the enzyme–drug complex and the maximum binding capacity of the enzyme.

The inhibitory constant reported for the high activity isoenzyme was approximately an order of magnitude larger than that reported for the low activity isoenzyme (5, 6). Therefore, if *in vitro* binding studies are performed such that a wide range of intracellular acetazolamide concentrations is obtained, a definite curvature in the Rosenthal plot should be seen. Resolution of the curved plot into linear segments should permit the determination of maximum binding capacities and inhibitory constants for both isoenzymes.

Rosenthal plots constructed from *in vitro* equilibration studies performed in this laboratory exhibit a pronounced curvature. Inhibitory constants determined from the resolution of the curve were used as parameters in a nonlinear pharmacokinetic model for acetazolamide described previously (8).

EXPERIMENTAL

Human blood was drawn into heparinized tubes and immediately centrifuged to isolate the red blood cells. The cells were washed twice with two volumes of pH 7.4 buffered saline (0.15 *M* NaCl and 0.01 *M* phosphate), which were discarded. The cells were then suspended in the same buffered saline, and the hematocrit of the reconstituted red blood cell suspension was determined.

Acetazolamide was dissolved in methanol (0.5 μg/μl), and aliquots containing 1–200 μg of the drug were added to 20-ml disposable vials. Methanol was evaporated with a nitrogen stream. Red blood cell suspension was added to the vials (6 ml to vials containing <6 μg of acetazolamide and 3 ml to vials containing >6 μg of drug). The contents were incubated for 2 hr at 37° with gentle swirling in a reciprocating shaker. All incubations were performed using the suspension prepared from cells obtained from a single subject.

After incubation, the artificial blood medium was centrifuged. The acetazolamide concentration in 1–3-ml aliquots of the supernate was determined using a previously described high-pressure liquid chromatographic (HPLC) method (9).

0022-3549/79/0700-0912$01.00/0

© 1979, American Pharmaceutical Association

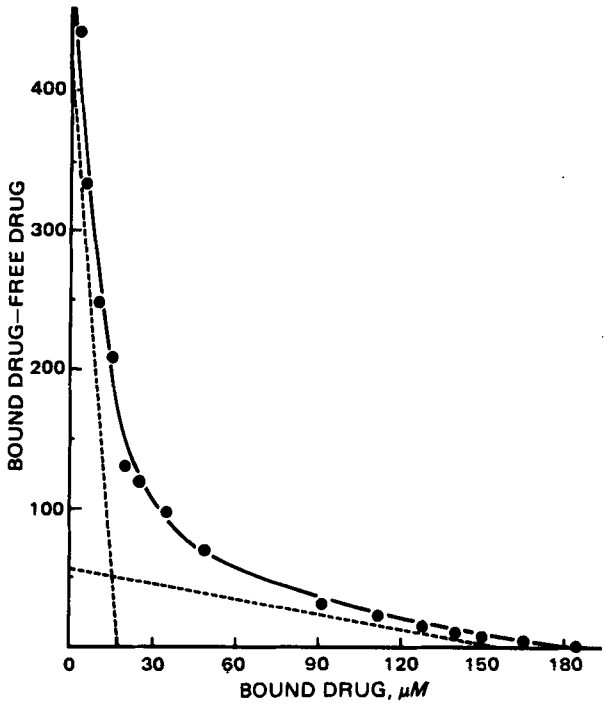

Figure 1—*Theoretical curve (—) that approximates the data points. The linear segment representing isoenzyme C has a negative reciprocal slope of 0.041 μM and an intercept on the abscissa of 17.2 μM; the linear segment representing isoenzyme B has a negative reciprocal slope of 2.71 μM and an intercept on the abscissa of 155 μM.*

The starting acetazolamide concentration in the artificial blood medium was assumed to be equivalent to the amount of acetazolamide added to each vial divided by the volume of the added suspension.

The total acetazolamide concentration in the red blood cells was calculated using:

$$C_{T,AB} = \frac{C_{AB} - (1-H)C_{ECF}}{H} \qquad \text{(Eq. 1)}$$

where C_{AB} is the concentration in the artificial blood, C_{ECF} is the concentration in the supernate or extracellular fluid, and H is the hematocrit.

RESULTS AND DISCUSSION

The acetazolamide concentration bound to carbonic anhydrase was calculated as the total intracellular concentration minus the product of the extracellular concentration times the cell water volume. The free drug concentration in the cell water was assumed to be equivalent to the extracellular concentration at equilibrium. The calculated bound drug concentration was expressed relative to the total cell volume, as was the measured total intracellular concentration.

A Rosenthal plot (Fig. 1) was constructed by plotting the ratio of the bound concentration to the intracellular free concentration *versus* the bound concentration. Except at bound concentrations that approached the total carbonic anhydrase concentration (intercept on abscissa), all intracellular drug essentially was bound (high bound to free ratio). The curvilinear plot was resolved into two linear segments by a graphic procedure (10). The negative reciprocal of the slope of each line is the inhibitory constant, and the intercept on the abscissa is the maximal binding capacity for the respective isoenzyme. The inhibitory constants were 0.041 and 2.72 μM and the maximum binding capacities were 17.2 and 155 μM for the high activity and low activity isoenzymes, respectively. Since there is one binding site per carbonic anhydrase molecule for the sulfonamides (11), the maximum binding capacity for a particular isoenzyme is the intracellular concentration of that isoenzyme.

The total carbonic anhydrase concentration in the human erythrocyte was reported to be 156 μM, of which 20 μM was the high activity isoenzyme and 136 μM was the low activity isoenzyme (6).

Previous studies (7) also showed that the carbonic anhydrase concentration (presumably type B) is variable in the human erythrocyte. Maren *et al.* (1) reported that the total carbonic anhydrase concentration is highly variable (range of 130–200 μM). Thus, the total carbonic anhydrase concentration in this study (172 μM) is within the range of previously reported values.

The inhibitory constant (2.72 μM) determined for the low activity isoenzyme in the present study agrees well with the inhibitory constant determined by previous investigators (7) (2 μM) using the *in vitro* equilibrium uptake technique. An inhibitory constant of 1 μM at 37° was reported for the low activity isoenzyme using kinetic measurements (6). The value reported at 37° in that study actually was extrapolated from measurements at lower temperatures.

Anions have been shown to inhibit carbonic anhydrase. For example, Maren *et al.* (5) showed that the low activity isoenzyme is much more sensitive to anion inhibition than the high activity isoenzyme (5). In particular, intracellular chloride and bicarbonate concentrations reduce the activity of the low activity isoenzyme to 8% of that in the absence of the anions. The intracellular chloride and bicarbonate anions probably compete with acetazolamide for binding sites in the uptake studies. Thus, the apparent inhibitory constant determined in studies may be larger than the true dissociation constant of the enzyme–drug complex in the absence of anions.

Intracellular red blood cell concentrations of chloride and bicarbonate are 85 and 15 mM, respectively (5). Chloride- and bicarbonate-ion concentrations that reduce the enzyme-catalyzed hydration of carbon dioxide by one-half (I_{50}) were reported to be 26 and 12 mM, respectively; these values approximate the inhibitory constants (5). Thus, the inhibitory constant of 2.72 μM, as determined in the present uptake study, becomes 0.18 μM in the absence of chloride and bicarbonate anions.

Maren *et al.* (1) reported an I_{50} value of 0.25 μM for acetazolamide using the low activity isoenzyme. These kinetic measurements were conducted using a barbital buffer to minimize carbonic anhydrase inhibition by anions in conventional buffer systems. Thus, there is agreement between the inhibitory constants determined by kinetic measurements and uptake studies if competition by intracellular anions is taken into account.

Since anions are present in the physiological situation, the inhibitory constants determined from uptake studies, rather than kinetic measurements, are more representative of the parameters to be used in describing drug disposition.

The I_{50} value reported for acetazolamide, using the high activity isoenzyme and the barbital buffer system, was 0.017 μM (1). This value compares favorably with the inhibitory constant (0.04 μM) determined from the uptake study. The similarity in these values is a manifestation of the negligible competition of intracellular anions with acetazolamide for the binding site on this isoenzyme. The negligible inhibition of the high activity isoenzyme by anions was demonstrated using kinetic measurements (5).

REFERENCES

(1) T. H. Maren, J. R. Haywood, S. K. Chapman, and T. J. Zimmerman, *Invest. Ophthalmol.*, **16**, 730 (1977).

(2) T. H. Maren, *ibid.*, **13**, 479 (1974).

(3) T. J. Zimmerman, L. C. Gang, B. P. Vough, and T. H. Maren, *J. Pharmacol. Exp. Ther.*, **196**, 510 (1967).

(4) T. H. Maren, *Physiol. Rev.*, **47**, 595 (1967).

(5) T. H. Maren, C. S. Rayburn, and N. E. Lidell, *Science*, **191**, 469 (1976).

(6) P. J. Wistrand and P. Baathe, *Acta Pharmacol. Toxicol.*, **26**, 145 (1968).

(7) S. M. Wallace and S. Riegelman, *J. Pharm. Sci.*, **66**, 739 (1977).

(8) R. G. Buckles and W. F. Bayne, Proceedings of Sixth International Congress of Pharmacology, Helsinki, Finland, 1975.

(9) W. F. Bayne, G. Rogers, and N. Crisologo, *J. Pharm. Sci.*, **64**, 402 (1975).

(10) H. F. Rosenthal, *Anal. Biochem.*, **20**, 522 (1967).

(11) J. E. Coleman, *Annu. Rev. Pharmacol.*, **15**, 221 (1975).

Modified Fluorometric Quantitation of Pancuronium Bromide and Metabolites in Human Maternal and Umbilical Serums

LEMUEL B. WINGARD, Jr. *‡x, EZZAT ABOULEISH ‡¶, DANIEL C. WEST *, and THOMAS J. GOEHL §

Received June 7, 1978, from the *Departments of *Pharmacology and ‡Anesthesiology, School of Medicine, and the §Department of Medicinal Chemistry, School of Pharmacy, University of Pittsburgh, Pittsburgh, PA 15261, and the ¶Magee-Women's Hospital, Pittsburgh, PA 15213.* Accepted for publication December 29, 1978.

Abstract □ The procedure for pancuronium bromide ion-pair extraction into chloroform using rose bengal and subsequent fluorometric measurement was modified by changing the extraction pH and eliminating phenol, ethanol, and acetone to give easier operation and enhanced fluorescence stability. Precision, accuracy, and sensitivity were evaluated over 0.14–0.82 μg/ml (CV = 14; relative error = 9%) and 0.05–0.17 μg/ml (CV = 19; relative error = 21%). Following a dose of 0.1 mg/kg for cesarean section in humans, the mean maternal arterial and umbilical venous serum concentrations of pancuronium bromide and metabolites were 0.52 and 0.12 μg/ml, respectively, at delivery (mean of 13 min after injection).

Keyphrases □ Muscle relaxants—pancuronium bromide, analysis, fluorometry, maternal arterial and umbilical venous serum □ Fluorometry—analysis, pancuronium bromide in maternal arterial and umbilical venous serum □ Pancuronium bromide—analysis, fluorometry, maternal arterial and umbilical venous serum, transplacental transfer □ Transplacental transfer—pancuronium bromide

Pancuronium bromide is used as a muscle relaxant during anesthesia for cesarean section (1). Therefore, the quantitation of maternal and fetal serum pancuronium bromide concentrations is important for evaluating transplacental drug transfer (2).

Pancuronium is a bisquaternary ammonium steroid that contains acetate ester groups at the 3- and 17-positions. Drug metabolism produces the 3-hydroxy, 17-hydroxy, and 3,17-dihydroxy derivatives through ester hydrolysis. A sensitive fluorometric quantitation procedure for pancuronium bromide and its metabolites in human plasma was described (3), and an initial modification to stabilize the fluorescence was reported (4). However, a higher intensity and more stable fluorescence signal was still desirable. In addition, a rigorous evaluation of the precision, accuracy, and sensitivity of the fluorometric plasma or serum pancuronium bromide determination has not appeared, although a minimum 0.02-μg/ml sensitivity, using 1 ml of plasma, was reported (3, 4).

Two reports on transplacental pancuronium bromide transfer have appeared (5, 6). In the earlier study (5), conclusions were based on the detection of pancuronium bromide and its metabolites in fetal urine using a limited sensitivity (0.6 μg/ml) spectrophotometric procedure. The second study (6) was based on maternal and umbilical cord blood samples taken during cesarean section delivery and assayed for pancuronium bromide using the fluorometric procedure; however, despite predosing with succinylcholine, no consideration was given to possible interferences in the pancuronium bromide assay due to succinylcholine or its metabolites.

In the present study, the fluorometric method was modified, and precision and accuracy were evaluated over the expected fetal and maternal concentration ranges. Serum, rather than plasma, was selected to facilitate the measurement of γ-globulin, to which pancuronium binds (7). The method was used to measure pancuronium bromide concentrations in maternal and umbilical cord blood samples obtained at cesarean section delivery.

EXPERIMENTAL

Chemicals and Reagents—Crystalline pancuronium bromide[1] was used as received. Rose bengal[2] was purified by washing six times with ethyl acetate[3] and three times with chloroform[4] and was desiccated (8). All other materials were reagent grade. All glassware was cleaned in 15% nitric acid. The centrifuge tubes were coated with dimethyldichlorosilane[5], rinsed with toluene[3], methanol[3], water, and acetone[3], and air dried. Pooled human serum[6] from normal subjects was used for the standard curves. The buffer was prepared by adding 0.2 M sodium bicarbonate to 0.2 M sodium carbonate until pH 10.5 was attained.

Previous Assay—To a 25-ml glass-stoppered centrifuge tube were added 7 ml of chloroform containing 2.5% phenol and 5% ethanol, 1 ml of serum, 1 ml of 0.1 M pH 7.8 phosphate buffer, and 0.5 ml of 0.2 mg of rose bengal/ml of 0.45 M dibasic potassium phosphate. The mixture was shaken 2 min on a vortex mixer followed by 30 min on a rotary mixer. The samples were centrifuged 10 min at 1500×g, and the aqueous layer was aspirated. An aliquot (0.5 ml) of the chloroform–phenol layer was added to 3.5 ml of acetone and vortexed. The relative fluorescence intensity was determined at 570 nm with excitation at 546 nm.

Modified Assay—To a 15-ml screw-capped (polytef-lined caps) centrifuge tube were added 1 ml of serum, 1 ml of 0.2 M sodium bicarbonate–carbonate buffer (pH 10.5), 0.5 ml of 0.5 mg of rose bengal/ml of 0.45 M dibasic potassium phosphate, and 7 ml of chloroform, with vortexing after each addition. After 30 min on a reciprocating horizontal shaker at 185 oscillations/min, the samples were centrifuged for 10 min at 1500×g; the aqueous layer was aspirated.

About 3 ml of the chloroform layer was transferred to a 1-cm silica cell. The relative fluorescence intensity was measured at 570 nm, with excitation at 546 nm, using a spectrofluorometer[7]. The instrument was adjusted daily to the same relative fluorescence intensity with 1 μg of quinine sulfate/ml of 0.1 N H_2SO_4 at 450 nm, with excitation at 350 nm. The blood samples were held for 2 hr at 0–4° and then centrifuged[8] for 10 min at 6000 rpm for serum preparation. All samples were assayed within 6 hr of blood sampling.

Standardization Procedure—To compensate for normal daily fluctuations in the spectrofluorometer xenon lamp output, a five-point linear least-squares fitted calibration curve was prepared each day using freshly prepared pancuronium bromide in serum over the range of 0–0.8 μg/ml. To establish precision, accuracy, and sensitivity, replicate pancuronium bromide samples in serum were prepared over the ranges of ~0.05–0.2 and 0.1–0.8 μg/ml. The resulting relative fluorescence intensity *versus* concentration data were fit by linear least squares; the coefficient of variation and the percentage deviation of each point (percent error) from the fitted line were calculated.

Human Study Protocol—Patients undergoing elective cesarean section delivery gave informed consent. The patients weighed 67 ± 10 (SD) kg and received 0.75 mg of hydroxyzine/kg im, 0.4 mg of atropine iv, 4 mg of thiamylal sodium/kg iv, 0.1 mg of pancuronium bromide/kg iv, and nitrous oxide–oxygen anesthesia. Blood samples included ma-

[1] Organon Inc., West Orange, N.J.
[2] Fisher, Pittsburgh, Pa.
[3] Certified ACS grade, Fisher, Pittsburgh, Pa.
[4] No. 4440, Mallinckrodt, St. Louis, Mo.
[5] Sigma, St. Louis, Mo.
[6] Immunopathology Laboratory, University Health Center, Pittsburgh, Pa.
[7] Aminco-Bowman model 4-8202.
[8] Sorvall RC2-B with SS-34 rotor.

0022-3549/79/0700-0914$01.00/0
© 1979, American Pharmaceutical Association

ternal predrug control, maternal arterial at delivery, and fetal venous from the clamped umbilical cord.

RESULTS AND DISCUSSION

A previous study in adults undergoing nonobstetric surgery showed that pancuronium concentrations ranged from 0.12 to 0.79 μg/ml during the 20-min interval after intravenous injection of ~0.1 mg/kg (9). Since pancuronium is a positively charged quaternary ammonium compound, its transfer rate across the placental membranes into the fetal blood would be slow; so fetal pancuronium concentrations would be much less than those in adults. For example, for the similar quaternary ammonium muscle relaxant metocurine, the human fetal plasma concentration was about one-tenth the maternal plasma concentration (10). Since the estimated fetal pancuronium bromide concentrations were near the lower limit for quantitation by the fluorometric method, its precision, accuracy, and sensitivity had to be evaluated.

In this laboratory, the relative fluorescence intensity varied by ±90% from the mean for four 1-μg/ml samples using the original (3) or modified (4) fluorometric assay. Since this variation was too great for the present study, the following changes were made: the extraction pH was increased from 7.8 to 10.5, phenol was eliminated from the extraction, and acetone and most of the ethanol were eliminated from the fluorescence measurement step.

The higher extraction pH increased the relative fluorescence from 0.27 ± 0.006 (*SD*) at pH 7.8 to 0.52 ± 0.03 (*SD*) at pH 10.5 for three samples of 0.5 μg of pancuronium bromide/ml of serum. The fluorescence decreased by 10% if the extraction was done at pH 12 instead of 10.5. This improvement could be expected if the rose bengal phenolic groups ionized to a greater extent at the higher pH. This would give a higher negative charge and improve complexation with the positively charged pancuronium ion. To obtain this desired pH change, a different buffer system (carbonate) was employed.

The phenol had been added in the extraction step to reduce emulsion formation during analysis (3, 8); however, there was still considerable emulsion formed. Unfortunately, the phenol also quenched the fluorescence (8). With the modifications, no advantage was observed from phenol addition; therefore, the phenol was omitted. Similarly, the ethanol used in the earlier procedures to stabilize the pancuronium–rose bengal complex fluorescence in acetone (3, 8) was omitted since the pancuronium–rose bengal–chloroform solutions without acetone showed only 3% change in fluorescence intensity over 30 min. The chloroform used in the present studies contained 0.75% ethanol as preservative; this amount was negligible compared with the 5% by volume in the chloroform–phenol solution used previously. Apparently, the combination of the higher pH, less alcohol, and no phenol minimized the emulsion formation by an unknown mechanism.

In these studies, the enhanced fluorescence obtained by mixing one volume of the pancuronium–rose bengal–chloroform solution with seven volumes of acetone was less than the loss in fluorescence due to dilution. For example, at 0.5 μg of pancuronium/ml, the relative fluorescence intensity was 0.52 ± 0.03 (*SD*) (n = 3) without acetone and only 0.19 ± 0.07 (*SD*) (n = 3) with acetone. Therefore, the acetone was omitted, which greatly helped to stabilize the fluorescence since the acetone fluorescence enhancement was transitory (4).

Precision and accuracy were evaluated by using serum to which known pancuronium bromide amounts were added. These samples were assayed as described. The standard curve was linear over the 0.14–0.82-μg/ml range, but some scatter was evident over the 0.05–0.17-μg/ml range. Representative results for the mean percent relative standard deviation (*CV*) and the mean relative error for each concentration range are shown in Table I. For the 0.05–0.14-μg/ml range, the validation was done on three separate groups (Table I). The averages of the *CV* for the high and low concentration ranges were 14 and 19, respectively; the averages of the mean relative error were 9% and 21% for the high and low ranges, respectively.

The mean fluorescence intensity at 0.05 μg/ml was three times the mean fluorescence intensity of the serum samples without added pancuronium bromide. Therefore, the minimum detectable level, defined as two times the blank fluorescence value, was less than 0.05 μg/ml. However, based on the *CV* values, the precision would be too poor to use at concentrations <0.05 μg/ml. Patient data with serum blanks that deviated more than 3 *SD* from the mean were omitted.

An evaluation to see if samples could be stored for later assay demonstrated that the fluorescence readings were significantly lower if the serum samples were not assayed promptly. In this evaluation, a solution of 0.5 μg of pancuronium bromide/ml of serum was prepared and divided into 15 1-ml aliquots. Three samples were assayed on the same day with a result of 0.49 μg/ml. The other samples were frozen. Three tubes were thawed and assayed after the days shown with the following results: 1 day, 0.42 μg/ml; 2 days, 0.41 μg/ml; 7 days, 0.28 μg/ml; and 13 days, 0.37 μg/ml. In addition, an umbilical cord sample assayed as described and again 24 hr later showed an apparent 30% decrease in pancuronium concentration.

Whether this change in fluorescence intensity was due to drug instability or to some other factor is not known. However, the results showed clearly that samples could not be stored and assayed later. Therefore, all samples were assayed within 4–6 hr after blood sampling. This finding raises an additional question concerning the data obtained in the previous placental transfer study of pancuronium using the fluorometric assay since the samples were frozen and assayed later (6). However, in that study, heparinized plasma rather than serum was used; pancuronium stability in heparinized plasma has not been reported.

The modified assay was utilized to determine the mean maternal arterial and umbilical vein concentrations in 15 patients undergoing elective cesarean section delivery. A preinduction maternal blood sample was used as a control. To test for possible interference in the pancuronium assay due to the other drugs used during cesarean section, the maximum maternal serum concentrations of the other drugs, except gaseous nitrous oxide, were estimated and added to samples of 0.5 μg of pancuronium bromide/ml of serum. The drugs, their concentrations, and the relative fluorescence following assay for pancuronium were: hydroxyzine hydrochloride, 50 μg/ml, 0.51 ± 0.04 (*SD*) (n = 3); atropine, 0.08 μg/ml, 0.49 ± 0.04 (*SD*) (n = 3); thiamylal sodium, 56 μg/ml, 0.44 ± 0.02 (*SD*) (n = 3); and control, 0.46 ± 0.05 (*SD*) (n = 9). It was concluded that no interference existed at the concentrations tested.

The mean maternal arterial and umbilical venous pancuronium concentrations were 0.52 ± 0.14 and 0.12 ± 0.04 μg/ml, respectively. All samples were obtained at delivery, which occurred at a mean time of 13 ± 4 min after the pancuronium injection. The resulting fetal to maternal ratio of the pancuronium concentrations at delivery was 0.23. This ratio was similar to the mean ratio of 0.24 reported earlier (6) for a smaller dose of pancuronium bromide but with a possible question concerning the absolute concentration values in the earlier study.

Table I—Representative Results for Precision and Accuracy Evaluation over Two Concentration Ranges [a]

Pancuronium Bromide Added, μg/ml	n	Calculated Experimental Mean (Range), μg/ml	*CV*	Relative Error, %
		Part 1: High Range		
0.14	4	0.14 (0.11–0.17)	24	17
0.38	3	0.40 (0.34–0.45)	15	12
0.82	4	0.81 (0.78–0.84)	3	3
		Part 2: Low Range		
0.05	3	0.04 (0.03–0.04)	15	18
0.06	6	0.06 (0.04–0.08)	22	22
0.07	4	0.11 (0.09–0.12)	11	47
0.12	5	0.10 (0.08–0.13)	22	20
0.14	5	0.14 (0.09–0.16)	20	13
0.15	3	0.13 (0.10–0.14)	16	16

[a] Unknown "test" and known "standard" samples of pancuronium in serum were prepared and assayed to give relative fluorescence values. All samples were randomized. The standard samples duplicated those used in preparing the daily reference curve and were used to plot a relative fluorescence intensity *versus* concentration reference curve. This curve was used to convert fluorescence intensity to concentration for the test samples. The results in this table are for the test samples.

REFERENCES

(1) J. B. Neeld, Jr., P. D. Seabrook, Jr., G. M. Chastain, and E. L. Frederickson, *Anesth. Analg.*, **53**, 7 (1974).

(2) L. B. Wingard, Jr., and D. R. Cook, *Clin. Pharmacokinet.*, **2**, 330 (1977).

(3) U. K. Kersten, D. K. F. Meijer, and S. Agoston, *Clin. Chim. Acta*, **44**, 59 (1973).

(4) M. J. Watson and K. McLeod, *ibid.*, **79**, 511 (1977).

(5) I. Speirs and A. W. Sim, *Br. J. Anaesth.*, **44**, 370 (1972).

(6) P. N. Booth, M. J. Watson, and K. McLeod, *Anesthesia*, **32**, 320 (1977).

(7) J. M. Thompson, *ibid.*, **31**, 219 (1976).
(8) E. N. Cohen, *J. Lab. Clin. Med.*, **61**, 338 (1963).
(9) S. Agoston, G. A. Vermeer, U. W. Kersten, and D. K. F. Meijer, *Acta Anaesth. Scand.*, **17**, 267 (1973).
(10) I. Kivalo and S. Saarikoski, *Br. J. Anaesth.*, **44**, 557 (1972).

ACKNOWLEDGMENTS

Supported by Organon Inc., West Orange, N.J.
The use of the Prophet computer system of the National Institutes of Health is acknowledged.

Isolation and Identification of 3,3′,5,5′-Tetrabis(*tert*-butyl)stilbenequinone from Polyethylene Closures Containing Titanium Dioxide and Butylated Hydroxytoluene

I. JAGNANDAN *x, H. DAUN, T. J. AMBROSIO *, and S. G. GILBERT

Received October 3, 1977, from the *Department of Food Science, Rutgers—The State University, New Brunswick, NJ 08903.* Accepted for publication December 28, 1978. *Present address: Research and Development, Schering Corp., Bloomfield, NJ 07003.

Abstract □ A yellow compound was isolated from commercially available, discolored, polyethylene ophthalmic closures containing titanium dioxide and butylated hydroxytoluene (I). This compound was present at 7.46 ppm (w/w). It was identified by UV, IR, and mass spectra as 3,3′,5,5′-tetrabis(*tert*-butyl)stilbenequinone (II), a dimer of I. Further structural confirmation was obtained by NMR. Formation of II is catalyzed by titanium dioxide.

Keyphrases □ Tetrabis(*tert*-butyl)stilbenequinone—analysis, isolation from polyethylene closures, synthesis from butylated hydroxytoluene catalyzed by titanium dioxide □ Butylated hydroxytoluene—conversion to tetrabis(*tert*-butyl)stilbenequinone in polyethylene closures, catalyzed by titanium dioxide □ Polyethylene—drug packaging, discoloration, butylated hydroxytoluene conversion to tetrabis(*tert*-butyl)stilbenequinone catalyzed by titanium dioxide □ Titanium dioxide—in polyethylene closures, catalysis of butylated hydroxytoluene discoloration reaction

Polymers are widely used in industry as packaging materials for food and drugs. As they age, they undergo oxidation *via* a free radical mechanism initiated by heat, light, or radiation. One result is scission or branching in the polymer chain, leading to eventual degradation in the mechanical properties of the polymer.

Antioxidants are added to the polymer in small amounts to prevent degradation. These substances can inhibit free radical formation and may become degraded instead of the polymer. Some antioxidants can convert to colored substances.

The oxidation products of antioxidants have been linked to the discoloration of polyethylene (1). An oxidation product of I caused a marked yellow discoloration of clear polyethylene (2). This colored compound was 3,3′,5,5′-tetrabis(*tert*-butyl)stilbenequinone (II). It has been isolated from cooking oil to which I was added (3). The corresponding yellowing of pigmented polyethylene caused by I has not been reported. The pigment, titanium dioxide, is used extensively as an opacifier for food and drug packaging.

This work was undertaken to isolate and identify the yellow discoloration product in titanium dioxide-pigmented polyethylene in which I is the antioxidant and to evaluate the titanium dioxide role in the discoloration reaction.

EXPERIMENTAL

Closures—Commercially available, opaque, ophthalmic, 15-mm closures, consisting of polyethylene with 1.5% titanium dioxide as the pigment and I as the antioxidant, were used. Each closure weighed ~0.2922 g with a specific gravity of 0.931.

Extraction—Extraction was performed using a soxhlet extractor under defined reproducible conditions.

Separation and Purification of II—*Column Chromatography*—The silica gel column was purged with hexane, toluene, and chloroform. The yellow band was removed using hexane and concentrated by blowing nitrogen on it at room temperature.

TLC—Hexane–toluene (80:20, v/v) was used as the developing medium on silica gel 60 F 254, 25-mm glass plates. On separation, the yellow band was scraped off and reeluted for further purification.

Spectrophotometry—A spectrophotometer was used to determine spectra in the visible and UV regions. IR spectrophotometric analysis was performed with a beam condenser in conjunction with an ultramicro liquid cell.

Mass Spectrometry—A mass spectrometer with a single-focusing magnetic mass analyzer was used. Temperature programming was such that spectra were obtained rapidly at increasing temperatures. All samples were analyzed at 70 ev.

NMR—An NMR spectrometer analyzed the sample in deuterated chloroform with tetramethylsilane as the internal marker. The sample was run at ambient temperature at 100.1 MHz in the Fourier transfer mode using a computer. Chemical shift was expressed as δ (delta) in parts per million.

GLC—GLC analysis was at 200° using a 3.08-m column (0.64 cm in diameter) with 10% SE-30 on 90–100-mesh packing. Nitrogen was the carrier gas with a flow rate of 60 ml/min.

Quantification—The amount of I injected *versus* response was generated using the gas chromatograph. Twelve solutions of I in acetone ranging from 1.0×10^{-5} to 12.0×10^{-5} g were prepared by linear stepwise dilution to quantify I in the 250–500-ppm region. Chloroform was unsuitable because both spectral and analytical grades produced a response at the same retention time as I around or below 9.0×10^{-8} g. With identical extraction conditions, the amount of I extracted per hour from nondiscolored caps was determined.

RESULTS AND DISCUSSION

At room temperature, the yellow material was slightly soluble in chloroform. A total of 913 closures, weighing 266.7786 g, was placed in this solvent. After the extraction procedure, they weighed 265.0773 g, a difference of 1.7013 g. A 10-μl injection of the concentrated crude extract into the gas chromatograph revealed 29 distinct substances.

Spectrophotometric examination of an aliquot of the extract showed major absorption bands at 418 and 442 nm and two minor absorption bands at 396 and 218–233 nm.

0022-3549/79/0700-0916$01.00/0
© 1979, American Pharmaceutical Association

(7) J. M. Thompson, *ibid.*, **31**, 219 (1976).
(8) E. N. Cohen, *J. Lab. Clin. Med.*, **61**, 338 (1963).
(9) S. Agoston, G. A. Vermeer, U. W. Kersten, and D. K. F. Meijer, *Acta Anaesth. Scand.*, **17**, 267 (1973).
(10) I. Kivalo and S. Saarikoski, *Br. J. Anaesth.*, **44**, 557 (1972).

ACKNOWLEDGMENTS

Supported by Organon Inc., West Orange, N.J.
The use of the Prophet computer system of the National Institutes of Health is acknowledged.

Isolation and Identification of 3,3′,5,5′-Tetrabis(*tert*-butyl)stilbenequinone from Polyethylene Closures Containing Titanium Dioxide and Butylated Hydroxytoluene

I. JAGNANDAN *x, H. DAUN, T. J. AMBROSIO *, and S. G. GILBERT

Received October 3, 1977, from the *Department of Food Science, Rutgers—The State University, New Brunswick, NJ 08903.* Accepted for publication December 28, 1978. *Present address: Research and Development, Schering Corp., Bloomfield, NJ 07003.

Abstract □ A yellow compound was isolated from commercially available, discolored, polyethylene ophthalmic closures containing titanium dioxide and butylated hydroxytoluene (I). This compound was present at 7.46 ppm (w/w). It was identified by UV, IR, and mass spectra as 3,3′,5,5′-tetrabis(*tert*-butyl)stilbenequinone (II), a dimer of I. Further structural confirmation was obtained by NMR. Formation of II is catalyzed by titanium dioxide.

Keyphrases □ Tetrabis(*tert*-butyl)stilbenequinone—analysis, isolation from polyethylene closures, synthesis from butylated hydroxytoluene catalyzed by titanium dioxide □ Butylated hydroxytoluene—conversion to tetrabis(*tert*-butyl)stilbenequinone in polyethylene closures, catalyzed by titanium dioxide □ Polyethylene—drug packaging, discoloration, butylated hydroxytoluene conversion to tetrabis(*tert*-butyl)stilbenequinone catalyzed by titanium dioxide □ Titanium dioxide—in polyethylene closures, catalysis of butylated hydroxytoluene discoloration reaction

Polymers are widely used in industry as packaging materials for food and drugs. As they age, they undergo oxidation *via* a free radical mechanism initiated by heat, light, or radiation. One result is scission or branching in the polymer chain, leading to eventual degradation in the mechanical properties of the polymer.

Antioxidants are added to the polymer in small amounts to prevent degradation. These substances can inhibit free radical formation and may become degraded instead of the polymer. Some antioxidants can convert to colored substances.

The oxidation products of antioxidants have been linked to the discoloration of polyethylene (1). An oxidation product of I caused a marked yellow discoloration of clear polyethylene (2). This colored compound was 3,3′,5,5′-tetrabis(*tert*-butyl)stilbenequinone (II). It has been isolated from cooking oil to which I was added (3). The corresponding yellowing of pigmented polyethylene caused by I has not been reported. The pigment, titanium dioxide, is used extensively as an opacifier for food and drug packaging.

This work was undertaken to isolate and identify the yellow discoloration product in titanium dioxide-pigmented polyethylene in which I is the antioxidant and to evaluate the titanium dioxide role in the discoloration reaction.

EXPERIMENTAL

Closures—Commercially available, opaque, ophthalmic, 15-mm closures, consisting of polyethylene with 1.5% titanium dioxide as the pigment and I as the antioxidant, were used. Each closure weighed ~0.2922 g with a specific gravity of 0.931.

Extraction—Extraction was performed using a soxhlet extractor under defined reproducible conditions.

Separation and Purification of II—*Column Chromatography*—The silica gel column was purged with hexane, toluene, and chloroform. The yellow band was removed using hexane and concentrated by blowing nitrogen on it at room temperature.

TLC—Hexane–toluene (80:20, v/v) was used as the developing medium on silica gel 60 F 254, 25-mm glass plates. On separation, the yellow band was scraped off and reeluted for further purification.

Spectrophotometry—A spectrophotometer was used to determine spectra in the visible and UV regions. IR spectrophotometric analysis was performed with a beam condenser in conjunction with an ultramicro liquid cell.

Mass Spectrometry—A mass spectrometer with a single-focusing magnetic mass analyzer was used. Temperature programming was such that spectra were obtained rapidly at increasing temperatures. All samples were analyzed at 70 ev.

NMR—An NMR spectrometer analyzed the sample in deuterated chloroform with tetramethylsilane as the internal marker. The sample was run at ambient temperature at 100.1 MHz in the Fourier transfer mode using a computer. Chemical shift was expressed as δ (delta) in parts per million.

GLC—GLC analysis was at 200° using a 3.08-m column (0.64 cm in diameter) with 10% SE-30 on 90–100-mesh packing. Nitrogen was the carrier gas with a flow rate of 60 ml/min.

Quantification—The amount of I injected *versus* response was generated using the gas chromatograph. Twelve solutions of I in acetone ranging from 1.0×10^{-5} to 12.0×10^{-5} g were prepared by linear stepwise dilution to quantify I in the 250–500-ppm region. Chloroform was unsuitable because both spectral and analytical grades produced a response at the same retention time as I around or below 9.0×10^{-8} g. With identical extraction conditions, the amount of I extracted per hour from nondiscolored caps was determined.

RESULTS AND DISCUSSION

At room temperature, the yellow material was slightly soluble in chloroform. A total of 913 closures, weighing 266.7786 g, was placed in this solvent. After the extraction procedure, they weighed 265.0773 g, a difference of 1.7013 g. A 10-μl injection of the concentrated crude extract into the gas chromatograph revealed 29 distinct substances.

Spectrophotometric examination of an aliquot of the extract showed major absorption bands at 418 and 442 nm and two minor absorption bands at 396 and 218–233 nm.

0022-3549/79/0700-0916$01.00/0
© 1979, American Pharmaceutical Association

Column chromatography separated the extract into a yellow band and a white polymeric band.

After 10 TLC separations for purification, the yellow substance exhibited an IR spectrum identical to that obtained by Bohn and Campbell (4).

Mass spectra were obtained at various temperatures. Below 110°, poor fragmentation occurred. Above 160°, the compound disintegrated. The ideal conditions for obtaining mass spectra were 110–160° and 70 ev. The mass spectrum obtained was similar to that obtained previously (2).

The NMR spectrum was similar to that reported for II (6). Values of 1.30 and 1.33 ppm resulted from *tert*-butyl groups. Peaks at 6.90 and 7.52 ppm were due to the aromatic CH's. Peaks at 7.08 and 7.18 ppm were due to the olefinic CH's.

Based on the IR, mass, and NMR spectra, the yellow substance was assigned a quinoid structure with empirical formula $C_{30}H_{42}O_2$. Based on these spectral data, the structure of the isolated compound is:

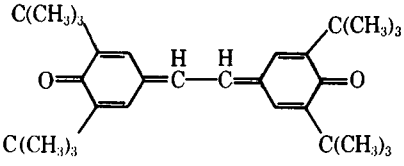

II

For quantification, 334.7895 g of discolored caps was extracted. The amount of I still present after discoloration was 47.7 ppm. After purification, 2.5 mg or 7.46 ppm of II was obtained.

Synthesis of Authentic Yellow Compound—The synthesis of the authentic yellow compound was carried out by a literature method (7). Compound I was put in an oven at 100° for 2 weeks. The yellow material obtained was purified by column chromatography and TLC. The isolation and purification procedures were identical to those used for II extracted from the closures.

IR and mass spectra were recorded. The sample was smeared with mineral oil and sandwiched between two salt blocks to obtain the IR spectrum, which was similar to that obtained for II. The mass spectrum was similar to that obtained for the unknown yellow substance.

The mass spectrum exhibited base peaks at *m/e* 435, 436, and 57. This compound was identical to that isolated from the polyethylene closures.

Synthesis of Yellow Compound by Catalytic Action of Titanium Dioxide—3,3′,5,5′-Tetrabis(*tert*-butyl)stilbenequinone was obtained by adding 1.5 g of rutile titanium dioxide powder to 100 g of I. Yellowing was obtained within 24 hr at 100° in an oven. The yellow compound was purified by the methods used for II and identified by IR and mass spectral analyses. The IR and mass spectra were similar to those reported previously (2, 4, 7). Under identical conditions but without titanium dioxide, discoloration of I to form II only occurred after 2 weeks.

REFERENCES

(1) R. S. Solvik, W. C. L. Wu, and L. J. Krebaum, *Mod. Plastic* (1974).

(2) H. Daun, S. G. Gilbert, and J. Giacin, *J. Assoc. Off. Anal. Chem.*, **51**, 404 (1974).

(3) B. Leventhal, H. Daun, and S. G. Gilbert, *J. Food Sci.*, **41**, 457 (1976).

(4) C. R. Bohn and T. W. Campbell, *J. Org. Chem.*, **22**, 458 (1957).

(5) J. Heiss, K. P. Zeller, and A. Rieker, *Org. Mass Spectrom.*, **2**, 1325 (1969).

(6) S. Brownstein and K. U. Ingold, *J. Am. Chem. Soc.*, **84** (1962).

(7) S. K. Zykova and B. V. Stolyarov, *Theor. Prikel. Khim.*, **25**, 1871 (1962).

Dihydroquinidine Contamination of Quinidine Raw Materials and Dosage Forms: Rapid Estimation by High-Performance Liquid Chromatography

PREM K. NARANG and WILLIAM G. CROUTHAMEL *x

Received October 3, 1978, from the *Department of Pharmacy, School of Pharmacy, University of Maryland, Baltimore, MD 21201.* Accepted for publication December 28, 1978.

*Present address: Department of Biochemistry and Drug Metabolism, Hoffmann-La Roche Inc., Nutley, NJ 07110.

Abstract □ Dihydroquinidine is a commonly encountered contaminant in quinidine raw materials. The USP allows 0–20% dihydroquinidine in quinidine products, but the assays used to quantitate dihydroquinidine have been lengthy or have required sophisticated equipment. The present method separates dihydroquinidine from quinidine and provides rapid, precise quantitation of both dihydroquinidine and quinidine. The clinical importance of dihydroquinidine contamination of quinidine dosage forms remains unanswered.

Keyphrases □ Hydroquinidine—analysis, high-performance liquid chromatography, as contaminant in quinidine raw materials and dosage forms □ Quinidine—analysis, high-performance liquid chromatography, hydroquinidine contamination in raw materials and dosage forms □ High-performance liquid chromatography—analysis, hydroquinidine contamination of quinidine raw materials and dosage forms

Quinidine raw materials and dosage forms routinely contain dihydroquinidine as a contaminant. The amount of the dihydro derivative varies from 0 to 25% (1), although dosage form dihydroquinidine content is limited to 20% by the USP (2). Many methods reported for quinidine quantitation do not separate the dihydroquinidine contaminant from quinidine. Previous methods for dihydroquinidine quantitation in dosage forms and raw materials include TLC (3), NMR (4), chemical-ionization mass spectrometry (5), and normal phase high-performance liquid chromatography (HPLC) (3). These methods are time consuming or tedious or require expensive equipment. The described HPLC method separates the dihydroquinidine contaminant from quinidine and allows rapid, precise quantitation of both compounds.

EXPERIMENTAL

Apparatus—The high-performance liquid chromatograph was equipped with a multiwavelength UV detector[1] and a microparticulate C-18 column[2]. A filter[3] with a 1.2-μm pore size was used for solution filtration prior to injection.

[1] Model 711 solvent delivery system with a Spectromonitor II detector, Laboratory Data Control, Riviera Beach, Fla.
[2] Waters Associates, Milford, Mass.
[3] Millipore Corp., Bedford, Mass.

0022-3549/79/0700-0917$01.00/0

© 1979, American Pharmaceutical Association

Column chromatography separated the extract into a yellow band and a white polymeric band.

After 10 TLC separations for purification, the yellow substance exhibited an IR spectrum identical to that obtained by Bohn and Campbell (4).

Mass spectra were obtained at various temperatures. Below 110°, poor fragmentation occurred. Above 160°, the compound disintegrated. The ideal conditions for obtaining mass spectra were 110–160° and 70 ev. The mass spectrum obtained was similar to that obtained previously (2).

The NMR spectrum was similar to that reported for II (6). Values of 1.30 and 1.33 ppm resulted from *tert*-butyl groups. Peaks at 6.90 and 7.52 ppm were due to the aromatic CH's. Peaks at 7.08 and 7.18 ppm were due to the olefinic CH's.

Based on the IR, mass, and NMR spectra, the yellow substance was assigned a quinoid structure with empirical formula $C_{30}H_{42}O_2$. Based on these spectral data, the structure of the isolated compound is:

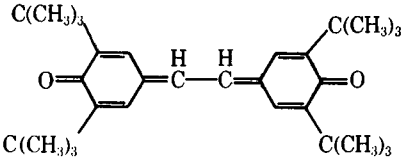

II

For quantification, 334.7895 g of discolored caps was extracted. The amount of I still present after discoloration was 47.7 ppm. After purification, 2.5 mg or 7.46 ppm of II was obtained.

Synthesis of Authentic Yellow Compound—The synthesis of the authentic yellow compound was carried out by a literature method (7). Compound I was put in an oven at 100° for 2 weeks. The yellow material obtained was purified by column chromatography and TLC. The isolation and purification procedures were identical to those used for II extracted from the closures.

IR and mass spectra were recorded. The sample was smeared with mineral oil and sandwiched between two salt blocks to obtain the IR spectrum, which was similar to that obtained for II. The mass spectrum was similar to that obtained for the unknown yellow substance.

The mass spectrum exhibited base peaks at *m/e* 435, 436, and 57. This compound was identical to that isolated from the polyethylene closures.

Synthesis of Yellow Compound by Catalytic Action of Titanium Dioxide—3,3′,5,5′-Tetrabis(*tert*-butyl)stilbenequinone was obtained by adding 1.5 g of rutile titanium dioxide powder to 100 g of I. Yellowing was obtained within 24 hr at 100° in an oven. The yellow compound was purified by the methods used for II and identified by IR and mass spectral analyses. The IR and mass spectra were similar to those reported previously (2, 4, 7). Under identical conditions but without titanium dioxide, discoloration of I to form II only occurred after 2 weeks.

REFERENCES

(1) R. S. Solvik, W. C. L. Wu, and L. J. Krebaum, *Mod. Plastic* (1974).

(2) H. Daun, S. G. Gilbert, and J. Giacin, *J. Assoc. Off. Anal. Chem.*, **51**, 404 (1974).

(3) B. Leventhal, H. Daun, and S. G. Gilbert, *J. Food Sci.*, **41**, 457 (1976).

(4) C. R. Bohn and T. W. Campbell, *J. Org. Chem.*, **22**, 458 (1957).

(5) J. Heiss, K. P. Zeller, and A. Rieker, *Org. Mass Spectrom.*, **2**, 1325 (1969).

(6) S. Brownstein and K. U. Ingold, *J. Am. Chem. Soc.*, **84** (1962).

(7) S. K. Zykova and B. V. Stolyarov, *Theor. Prikel. Khim.*, **25**, 1871 (1962).

Dihydroquinidine Contamination of Quinidine Raw Materials and Dosage Forms: Rapid Estimation by High-Performance Liquid Chromatography

PREM K. NARANG and WILLIAM G. CROUTHAMEL *x

Received October 3, 1978, from the *Department of Pharmacy, School of Pharmacy, University of Maryland, Baltimore, MD 21201.* Accepted for publication December 28, 1978.

*Present address: Department of Biochemistry and Drug Metabolism, Hoffmann-La Roche Inc., Nutley, NJ 07110.

Abstract □ Dihydroquinidine is a commonly encountered contaminant in quinidine raw materials. The USP allows 0–20% dihydroquinidine in quinidine products, but the assays used to quantitate dihydroquinidine have been lengthy or have required sophisticated equipment. The present method separates dihydroquinidine from quinidine and provides rapid, precise quantitation of both dihydroquinidine and quinidine. The clinical importance of dihydroquinidine contamination of quinidine dosage forms remains unanswered.

Keyphrases □ Hydroquinidine—analysis, high-performance liquid chromatography, as contaminant in quinidine raw materials and dosage forms □ Quinidine—analysis, high-performance liquid chromatography, hydroquinidine contamination in raw materials and dosage forms □ High-performance liquid chromatography—analysis, hydroquinidine contamination of quinidine raw materials and dosage forms

Quinidine raw materials and dosage forms routinely contain dihydroquinidine as a contaminant. The amount of the dihydro derivative varies from 0 to 25% (1), although dosage form dihydroquinidine content is limited to 20% by the USP (2). Many methods reported for quinidine quantitation do not separate the dihydroquinidine contaminant from quinidine. Previous methods for dihydroquinidine quantitation in dosage forms and raw materials include TLC (3), NMR (4), chemical-ionization mass spectrometry (5), and normal phase high-performance liquid chromatography (HPLC) (3). These methods are time consuming or tedious or require expensive equipment. The described HPLC method separates the dihydroquinidine contaminant from quinidine and allows rapid, precise quantitation of both compounds.

EXPERIMENTAL

Apparatus—The high-performance liquid chromatograph was equipped with a multiwavelength UV detector[1] and a microparticulate C-18 column[2]. A filter[3] with a 1.2-μm pore size was used for solution filtration prior to injection.

[1] Model 711 solvent delivery system with a Spectromonitor II detector, Laboratory Data Control, Riviera Beach, Fla.
[2] Waters Associates, Milford, Mass.
[3] Millipore Corp., Bedford, Mass.

0022-3549/79/0700-0917$01.00/0

© 1979, American Pharmaceutical Association

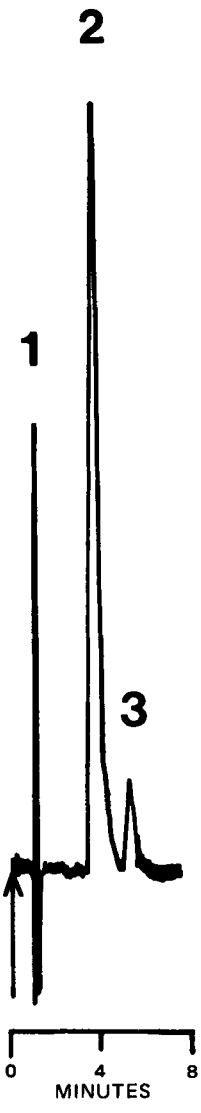

Figure 1—*Typical chromatogram for quinidine and dihydroquinidine in a tablet dosage form. Key: 1, solvent front; 2, quinidine peak; and 3, dihydroquinidine peak. Arrow indicates sample injection time.*

Reagents—All chemicals and reagents were analytical grade unless otherwise indicated. Quinidine sulfate[4,5], quinidine[5,6], and dihydroquinidine[7] were used as obtained. Glass-distilled methanol was used for the mobile phase[8]. Quinidine sulfate tablets from three different suppliers[9] were obtained from a local pharmacy.

Procedure—A quinidine sulfate tablet was weighed accurately, crushed carefully using a mortar and pestle, and added (25 mg) to a 100-ml volumetric flask. Then 5 ml of methanol was added to the powder, and the solution was diluted to 100 ml with acetic acid–water (1:1). This solution was shaken, and an aliquot was diluted 10 times with acetic acid–water (1:1). Then the solution was filtered[3] to remove suspended matter, and a 10-μl aliquot was injected into the chromatograph under the following conditions: flow rate, 2 ml/min; detection, 254 nm; and mobile phase, methanol–acetic acid–water (25:4:71).

The retention times for quinidine and dihydroquinidine under these conditions were 3.83 and 4.86 min, respectively. The assay sensitivity was a function of injection volume; at 10 μl, the dihydroquinidine sensitivity was 0.25 μg/ml, but larger injection volumes or smaller dilutions increased the sensitivity.

Dihydroquinidine standards were prepared in water or acetic acid–water (1:1). Both vehicles gave the same peak height results. Dihydroquinidine concentration was estimated by comparing the peak heights to a standard curve. Theobromine (10 μg/ml) could be added as an internal standard to correct for injection volume errors. Theobromine retention time was 2.25 min under these conditions.

To estimate the dihydroquinidine concentration in various raw materials, quinidine base and quinidine sulfate solutions (20 μg of quinidine/ml) were made as described.

[4] Sample KK, K&K Laboratories, Plainview, N.Y
[5] Sample ME, Merck & Co., Rahway, N.J.
[6] Sample MA, Mallinckrodt Chemical, New York, N.Y.
[7] Pfaltz & Bauer, Stamford, Conn.
[8] Burdick & Jackson Laboratories, Muskegon, Mich.
[9] Product PP, Purepac Pharmaceutical Co., Elizabeth, N.J.; Product PD, Parke-Davis and Co., Detroit, Mich.; and Product PR, Philips Roxane, Columbus, Ohio.

Table I—Dihydroquinidine Content in Three Marketed Quinidine Sulfate Tablet Formulations

Tablet	Dihydroquinidine, %		
	Product PD[a]	Product PP	Product PR
1	9.81[b]	3.19	6.50
2	9.49	3.80	6.57
3	9.09	3.38	6.25
	—	—	—
Mean	9.47 ± 0.52	3.49 ± 0.39	6.44 ± 0.24

[a] For product identification, see *Experimental*. [b] Each value represents the mean of four determinations.

RESULTS

Figure 1 shows a typical chromatogram for quinidine and dihydroquinidine in a tablet. No interfering peaks due to excipients were observed in the quinidine tablets. Slight variations in retention times could be seen from day to day.

The standard quinidine and dihydroquinidine curves for peak height *versus* concentration are linear over a wide concentration range and pass through the origin. Quinidine and dihydroquinidine concentration can be estimated accurately over 0–75 μg/ml, which encompasses the range used in this assay.

All quinidine raw materials contained dihydroquinidine, but no other cinchona alkaloids were detected. Samples from different commercial sources contained 3–29% dihydroquinidine. The mean dihydroquinidine concentration in the two quinidine sulfate raw materials varied from 3 to 16% whereas the content ranged from 25 to 29% in the two quinidine base materials. The percent of dihydroquinidine in the quinidine sulfate samples was (mean ± *SD*): Sample ME, 3.19 ± 0.13%; and Sample KK, 15.7 ± 1%. Similar values for quinidine base samples were (mean ± *SD*): Sample ME, 27.2 ± 1.9%; and Sample MA, 29.3 ± 1.1%. Each reported value is a mean of four determinations from the same sample.

Table I shows the dihydroquinidine content in three commercial quinidine sulfate tablets. Each reported value represents the mean of four determinations from the same solution. The mean dihydroquinidine content varied from 3.19 to 9.81%. Dihydroquinidine content was least in Product PP (3.49%), maximum in Product PD (9.47%), and intermediate in Product PR (6.44%).

DISCUSSION

No significant differences were observed in concentration when estimating dihydroquinidine and quinidine content from filtered or nonfiltered solutions. Thus, there was no significant adsorption to the filter[3]. Filters should be soaked in distilled water for at least 0.5 hr prior to use to remove any surfactant that might interfere with the assay.

The USP monograph for quinidine (2) allows dihydroquinidine concentrations up to 20% of the quinidine concentration, and the content uniformity requirement allows a tablet range of ±15%. Thus, a 200-mg quinidine sulfate tablet could contain as little as 148 mg of quinidine sulfate and 37 mg of dihydroquinidine sulfate (185-mg tablet) or 215 mg of quinidine sulfate with no dihydroquinidine. The three quinidine sulfate tablet formulations tested ranged from 3.4 to 9.5% dihydroquinidine. The sulfate raw materials contained 3.2 and 15.7% dihydroquinidine, and the two base samples contained 27 and 29%.

Quinidine in tablets was quantitated employing the quinidine peak height and the standard curve. All three tablet formulations met the USP content uniformity test; *e.g.*, the quinidine content was 87.5, 94.5, and 95.8% for Products PD, PR, and PP, respectively. The quinidine content of raw materials varied from 84 to 96% for the sulfate and 100–103% for the two base samples.

However, the question of differences between quinidine and dihydroquinidine persists. Previous studies showed that dihydroquinidine has a lower partition coefficient (4) and a slower dissolution rate from formulations (6) than quinidine. In a recent study in rats (7), quinidine and dihydroquinidine had similar efficacy and toxicity when given intravenously, but dihydroquinidine had a 40% higher oral LD_{50}. This

finding is in agreement with a study conducted in humans (8) where quinidine gluconate gave higher blood levels than dihydroquinidine gluconate after single and maintenance doses. These studies suggest that the cardiovascular activities of quinidine and dihydroquinidine are similar but that differences may exist when these two components are incorporated into dosage forms. For these reasons, monitoring of the dihydroquinidine content in quinidine raw materials and dosage forms may have practical importance.

REFERENCES

(1) T. Huynh-Ngoc and B. Sirois, *Pharm. Acta Helv.*, **49**, 37 (1974).

(2) "The United States Pharmacopeia," 18th rev., Mack Publishing Co., Easton, Pa., 1970, pp. 581, 582.

(3) E. Smith, S. Barken, B. Ross, M. Maienthal, and J. Levine, *J. Pharm. Sci.*, **62**, 1151 (1973).

(4) T. Huynh-Ngoc and G. Sirois, *ibid.*, **62**, 1334 (1973).

(5) W. A. Garland, W. F. Trager, and S. D. Nelson, *Biomed. Mass Spectrom.*, **1**, 124 (1974).

(6) T. Huynh-Ngoc and G. Sirois, *J. Pharm. Belg.*, **30**, 273 (1975).

(7) V. K. Dietmann, W. Bartsch, and M. Gutekunst, *Arzneim.-Forsch.*, **27**, 589 (1977).

(8) W. M. Goldberg and S. G. Chakrabarti, *Can. Med. Assoc. J.*, **91**, 991 (1964).

ACKNOWLEDGMENTS

The authors thank Ms. Gail Bird for technical assistance.

Controlled Drug Release by Polymer Dissolution II: Enzyme-Mediated Delivery Device

J. HELLER ˣ **and P. V. TRESCONY**

Received November 14, 1978, from the *Polymer Sciences Department, SRI International, Menlo Park, CA 94025.* Accepted for publication January 9, 1979.

Abstract □ A novel, closed-loop drug delivery system was developed where the presence or absence of an external compound controls drug delivery from a bioerodible polymer. In the described delivery system, hydrocortisone was incorporated into a *n*-hexyl half-ester of a methyl vinyl ether–maleic anhydride copolymer, and the polymer–drug mixture was fabricated into disks. These disks were then coated with a hydrogel containing immobilized urease. In a medium of constant pH and in the absence of external urea, the hydrocortisone release was that normally expected for that polymer at the given pH. With external urea, ammonium bicarbonate and ammonium hydroxide were generated within the hydrogel, which accelerated polymer erosion and drug release. The drug delivery rate increase was proportional to the amount of external urea and was reversible; that is, when external urea was removed, the drug release rate gradually returned to its original value.

Keyphrases □ Dosage forms—controlled-release delivery devices, *n*-hexyl half-ester of a methyl vinyl ether–maleic anhydride copolymer, urease, pH-controlled hydrocortisone release □ Hydrocortisone—controlled-release delivery, pH controlled, *n*-hexyl half-ester of a methyl vinyl ether–maleic anhydride copolymer, urease □ Copolymers—controlled-release delivery devices, *n*-hexyl half-ester of a methyl vinyl ether–maleic anhydride, urease, pH-controlled hydrocortisone release □ Urease—controlled-release delivery devices, pH-controlled hydrocortisone release □ Corticosteroids—hydrocortisone, controlled-release delivery device

Drug formulations that deliver an active agent to a specific body site in precisely regulated amounts are superior to those that indiscriminately flood the whole body with a therapeutic agent. Consequently, sustained drug release is receiving great attention (1).

However, even precisely controlled sustained delivery is not always the optimum therapeutic regimen. In many applications, a better delivery system is one that delivers the active agent only when needed. The essential ingredients of such a system are a sensing mechanism that can detect minute amounts of a specific compound in a complex mixture such as blood and some means of transferring this information to a delivery device that can then modify therapeutic agent delivery. While electromechanical devices that use microelectronics and enzyme probes to control miniaturized pumps are possible, this study centers on purely chemical methods.

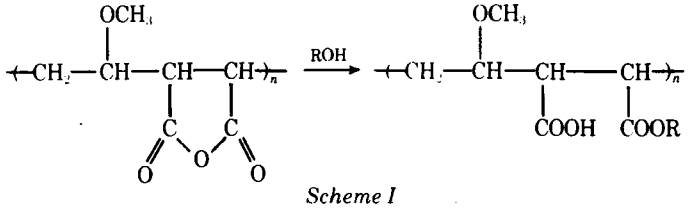

Scheme I

BACKGROUND

A previous paper (2) described the dissolution and concomitant drug release from partially esterified copolymers of methyl vinyl ether and maleic anhydride prepared as shown in Scheme I. Two notable features of these polymer systems were: (*a*) their ability to undergo surface erosion and, hence, to release an incorporated drug by zero-order kinetics, and (*b*) an extraordinary sensitivity of the erosion rate to the surrounding aqueous environment pH. These systems also exhibited a characteristic pH above which they were completely soluble and below which they were completely insoluble. This pH was very sharp and depended on the size of the alkyl group in the copolymer ester. Consequently, polymer erosion behavior can be tailored to fit any desired pH environment; even very small pH variations will have a major effect on the erosion rate and, thus, on drug release.

Any sensing mechanism that can convert the presence of a specific compound in the external environment to a pH change can be used to control polymer dissolution and therapeutic agent delivery. Enzymes almost ideally fit this requirement because their mode of action is highly specific; in many cases, enzyme–substrate reaction products are acidic or alkaline compounds.

For this study, an enzyme was needed that, after reaction with a substrate, liberated an alkaline product so that the net effect of the enzyme–substrate reaction would be a pH increase at the polymer–water interface. The enzyme urease, which interacts with urea as shown (3), was selected (Scheme II).

$$(NH_2)_2CO + 3H_2O \xrightarrow{\text{urease}} HCO_3^- + 2NH_4^+ + OH^-$$

Scheme II

The purpose of this study was to develop a system in which urea in an external environment would affect the release of hydrocortisone incor-

0022-3549/79/0700-0919$01.00/0

© 1979, American Pharmaceutical Association

finding is in agreement with a study conducted in humans (8) where quinidine gluconate gave higher blood levels than dihydroquinidine gluconate after single and maintenance doses. These studies suggest that the cardiovascular activities of quinidine and dihydroquinidine are similar but that differences may exist when these two components are incorporated into dosage forms. For these reasons, monitoring of the dihydroquinidine content in quinidine raw materials and dosage forms may have practical importance.

REFERENCES

(1) T. Huynh-Ngoc and B. Sirois, *Pharm. Acta Helv.*, **49**, 37 (1974).

(2) "The United States Pharmacopeia," 18th rev., Mack Publishing Co., Easton, Pa., 1970, pp. 581, 582.

(3) E. Smith, S. Barken, B. Ross, M. Maienthal, and J. Levine, *J. Pharm. Sci.*, **62**, 1151 (1973).

(4) T. Huynh-Ngoc and G. Sirois, *ibid.*, **62**, 1334 (1973).

(5) W. A. Garland, W. F. Trager, and S. D. Nelson, *Biomed. Mass Spectrom.*, **1**, 124 (1974).

(6) T. Huynh-Ngoc and G. Sirois, *J. Pharm. Belg.*, **30**, 273 (1975).

(7) V. K. Dietmann, W. Bartsch, and M. Gutekunst, *Arzneim.-Forsch.*, **27**, 589 (1977).

(8) W. M. Goldberg and S. G. Chakrabarti, *Can. Med. Assoc. J.*, **91**, 991 (1964).

ACKNOWLEDGMENTS

The authors thank Ms. Gail Bird for technical assistance.

Controlled Drug Release by Polymer Dissolution II: Enzyme-Mediated Delivery Device

J. HELLER ˣ **and P. V. TRESCONY**

Received November 14, 1978, from the *Polymer Sciences Department, SRI International, Menlo Park, CA 94025.* Accepted for publication January 9, 1979.

Abstract □ A novel, closed-loop drug delivery system was developed where the presence or absence of an external compound controls drug delivery from a bioerodible polymer. In the described delivery system, hydrocortisone was incorporated into a *n*-hexyl half-ester of a methyl vinyl ether–maleic anhydride copolymer, and the polymer–drug mixture was fabricated into disks. These disks were then coated with a hydrogel containing immobilized urease. In a medium of constant pH and in the absence of external urea, the hydrocortisone release was that normally expected for that polymer at the given pH. With external urea, ammonium bicarbonate and ammonium hydroxide were generated within the hydrogel, which accelerated polymer erosion and drug release. The drug delivery rate increase was proportional to the amount of external urea and was reversible; that is, when external urea was removed, the drug release rate gradually returned to its original value.

Keyphrases □ Dosage forms—controlled-release delivery devices, *n*-hexyl half-ester of a methyl vinyl ether–maleic anhydride copolymer, urease, pH-controlled hydrocortisone release □ Hydrocortisone—controlled-release delivery, pH controlled, *n*-hexyl half-ester of a methyl vinyl ether–maleic anhydride copolymer, urease □ Copolymers—controlled-release delivery devices, *n*-hexyl half-ester of a methyl vinyl ether–maleic anhydride, urease, pH-controlled hydrocortisone release □ Urease—controlled-release delivery devices, pH-controlled hydrocortisone release □ Corticosteroids—hydrocortisone, controlled-release delivery device

Drug formulations that deliver an active agent to a specific body site in precisely regulated amounts are superior to those that indiscriminately flood the whole body with a therapeutic agent. Consequently, sustained drug release is receiving great attention (1).

However, even precisely controlled sustained delivery is not always the optimum therapeutic regimen. In many applications, a better delivery system is one that delivers the active agent only when needed. The essential ingredients of such a system are a sensing mechanism that can detect minute amounts of a specific compound in a complex mixture such as blood and some means of transferring this information to a delivery device that can then modify therapeutic agent delivery. While electromechanical devices that use microelectronics and enzyme probes to control miniaturized pumps are possible, this study centers on purely chemical methods.

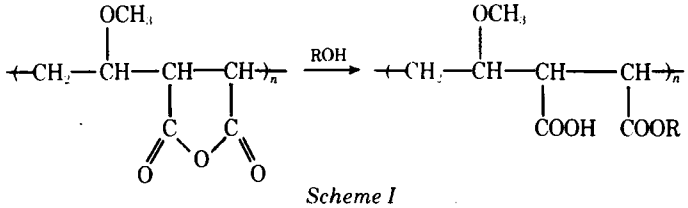

Scheme I

BACKGROUND

A previous paper (2) described the dissolution and concomitant drug release from partially esterified copolymers of methyl vinyl ether and maleic anhydride prepared as shown in Scheme I. Two notable features of these polymer systems were: (*a*) their ability to undergo surface erosion and, hence, to release an incorporated drug by zero-order kinetics, and (*b*) an extraordinary sensitivity of the erosion rate to the surrounding aqueous environment pH. These systems also exhibited a characteristic pH above which they were completely soluble and below which they were completely insoluble. This pH was very sharp and depended on the size of the alkyl group in the copolymer ester. Consequently, polymer erosion behavior can be tailored to fit any desired pH environment; even very small pH variations will have a major effect on the erosion rate and, thus, on drug release.

Any sensing mechanism that can convert the presence of a specific compound in the external environment to a pH change can be used to control polymer dissolution and therapeutic agent delivery. Enzymes almost ideally fit this requirement because their mode of action is highly specific; in many cases, enzyme–substrate reaction products are acidic or alkaline compounds.

For this study, an enzyme was needed that, after reaction with a substrate, liberated an alkaline product so that the net effect of the enzyme–substrate reaction would be a pH increase at the polymer–water interface. The enzyme urease, which interacts with urea as shown (3), was selected (Scheme II).

$$(NH_2)_2CO + 3H_2O \xrightarrow{\text{urease}} HCO_3^- + 2NH_4^+ + OH^-$$

Scheme II

The purpose of this study was to develop a system in which urea in an external environment would affect the release of hydrocortisone incor-

0022-3549/79/0700-0919$01.00/0

© 1979, American Pharmaceutical Association

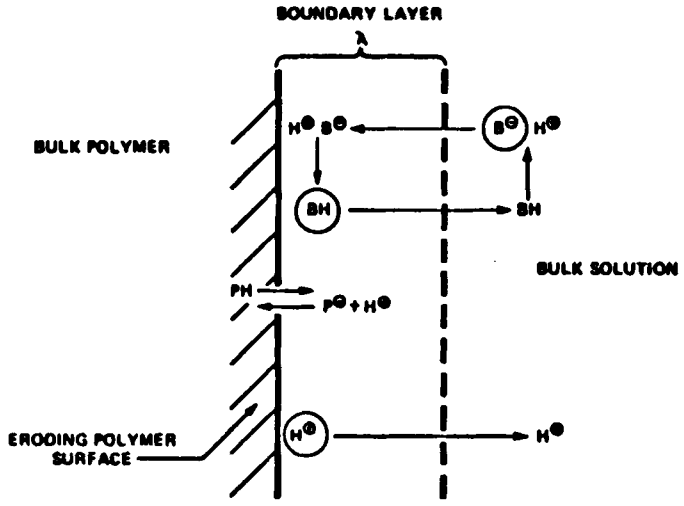

Figure 1—*Model for polymer erosion mechanism.*

porated into a polymer matrix. Such a system serves as a model; it has no obvious therapeutic application. More useful systems are being developed.

EXPERIMENTAL

***n*-Hexyl Half-Ester of a Methyl Vinyl Ether–Maleic Anhydride[1] Copolymer (50:50)**—A three-necked 2000-ml, round-bottom flask equipped with a mechanical stirrer, a heating oil bath, a condenser, and a nitrogen inlet and exit was charged with 109.30 g of the copolymer (1.400 equivalent) and 794.82 g of 1-hexanol (7.779 moles). The alcohol, present in an 11:1 molar excess, was sufficient to produce a 20% (w/w) solution of the half-ester product.

After the flask was purged with nitrogen, the reactants were vigorously stirred and heated over 0.5 hr to 145°. The reaction was followed by IR analysis of the carbonyl peaks associated with residual cyclic anhydride in the copolymer and with the formed ester linkage in the half-ester product. The reaction was judged complete after 2.5 hr at 145°. The solution was cooled to room temperature with an ice bath and precipitated in 8 liters of methanol–water (1:1 v/v). The precipitated polymer was dissolved in 2 liters of acetone and precipitated in 8 liters of methanol–water (1:2 v/v). This step was repeated twice. The product was dried in a forced-air oven for 3 days at 50°. A tough, clear-to-slightly-hazy material (148.10 g) was collected in an 82% yield.

Test Specimens—*Film Casting*—The polymer and micronized hydrocortisone[2] were added to 2-ethoxyethyl acetate–isopropylacetone (7:3 w/w) to produce a 9% polymer solution containing 10 parts of dispersed hydrocortisone/100 parts of resin. A homogeneous solution was obtained by using a jar mill. Films were cast by pouring this solution into level polytef-lined molds. The molds were then partially covered and, to prevent bubble formation in the film, were dried slowly for 8 days. They were further dried in a forced-air oven at 35° for 1 day and then *in vacuo* for 1 day.

Disks, 9.5 mm in diameter, were cut from the film using a drill press and hole cutter. The disks were weighed after being placed in a vacuum oven for 48 hr at room temperature and then being equilibrated to a constant weight in air. The disks selected for release-rate testing weighed 47.5–52.5 mg and were ~0.75 mm thick.

Enzyme Coating—Initial attempts to incorporate the enzyme urease into the polymer matrix involved dissolving the enzyme and polymer in acetone, dispersing micronized hydrocortisone in the solution, casting films, and gently drying at room temperature. However, considerable enzyme denaturation took place.

Subsequent successful urease coupling with the polymer matrix was based on the work of Mascini and Guibault (4). A small locking forceps was affixed to the edge of each polymer disk so that it could be manipulated without touching the surfaces during the immobilized enzyme-coating procedure. A 30% aqueous solution of bovine serum albumin was prepared, and 1 g of urease was added to 10 ml of this solution. After quick stirring until the urease had dissolved, the solution was chilled in an ice

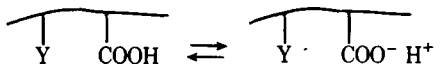

water insoluble water soluble

Scheme III

bath. Each disk was held horizontally by the attached forceps, and 1 drop of the albumin–urease solution was added to the upper disk face. The disk was quickly rotated, and a drop was added to the opposite face. Similarly, 1 drop of 25% aqueous glutaraldehyde was added to each face. One minute after the glutaraldehyde addition, the coating had gelled sufficiently to allow the disks to be hung vertically.

After standing in air for 15 min, the coated disks were immersed in cold, deionized water for 15 min, in 0.1 *M* glycine for 15 min, and in pH 5.75 phosphate buffer for 2 hr. Finally, they were immersed in fresh pH 5.75 phosphate buffer for 4 hr.

Release Rate Measurements—The coated disks were heat sealed in polypropylene mesh bags having 0.5-mm openings. Care was taken to apply heat only to the edges of the bags and to avoid applying heat to the disks. The mesh bags were attached to 10-gauge stainless steel wires and moved vertically up and down at ~140 cm/min in test tubes[3], as described previously (2). Hydrocortisone release was followed spectrophotometrically at 242 nm.

RESULTS AND DISCUSSION

A previous paper (2) described the erosion behavior of a hydrophobic polymer system where dissolution occurred by carboxyl group ionization. This solubilization behavior has been represented generally as shown in Scheme III (COOH is a solubilizing group and Y is a hydrophobic substituent). The dissolution behavior also was rationalized in terms of the model shown in Fig. 1. In this model, the erosion rate is principally determined by the rate at which hydrogen ions are neutralized within the boundary layer, so the induced pH change in that layer will significantly affect polymer erosion and, hence, drug release.

In the system described, a hydrophobic *n*-hexyl half-ester of a methyl vinyl ether–maleic anhydride copolymer containing hydrocortisone was surrounded by a hydrogel consisting of the enzyme urease immobilized in bovine serum albumin by crosslinking with glutaraldehyde. In the absence of external urea, the polymer dissolution and hydrocortisone release occur by the mechanism shown in Fig. 1, *i.e.*, hydrogen-ion neutralization by external buffer and diffusion of hydrogen ions away from the eroding polymer.

When urea is in the external environment, it diffuses into the hydrogel layer and is converted to ammonium bicarbonate and ammonium hydroxide by the immobilized urease. These basic species neutralize hy-

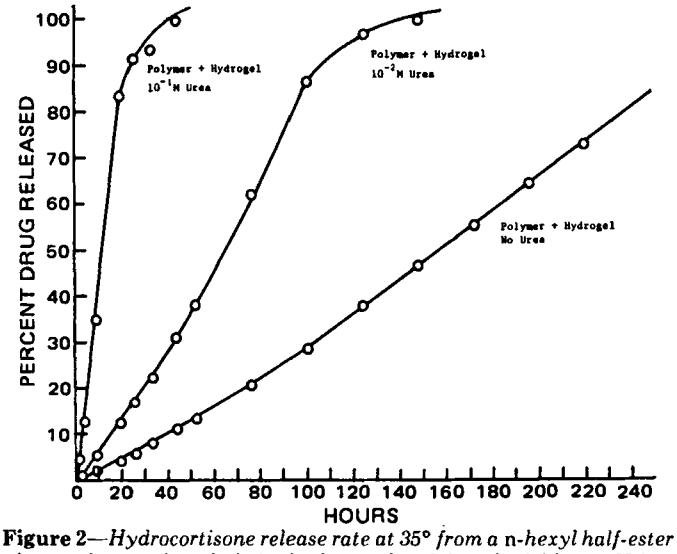

Figure 2—*Hydrocortisone release rate at 35° from a* n*-hexyl half-ester of a copolymer of methyl vinyl ether and maleic anhydride at pH 6.25 in the absence and presence of external urea. The stirring rate was ~140 cm/min*[3].

[1] Gantrez AN-169, GAF Corp., New York, N.Y.
[2] The Upjohn Co., Kalamazoo, Mich.

[3] Approximately 18.4 cycles/min at a total sample travel distance of 7.62 cm/cycle.

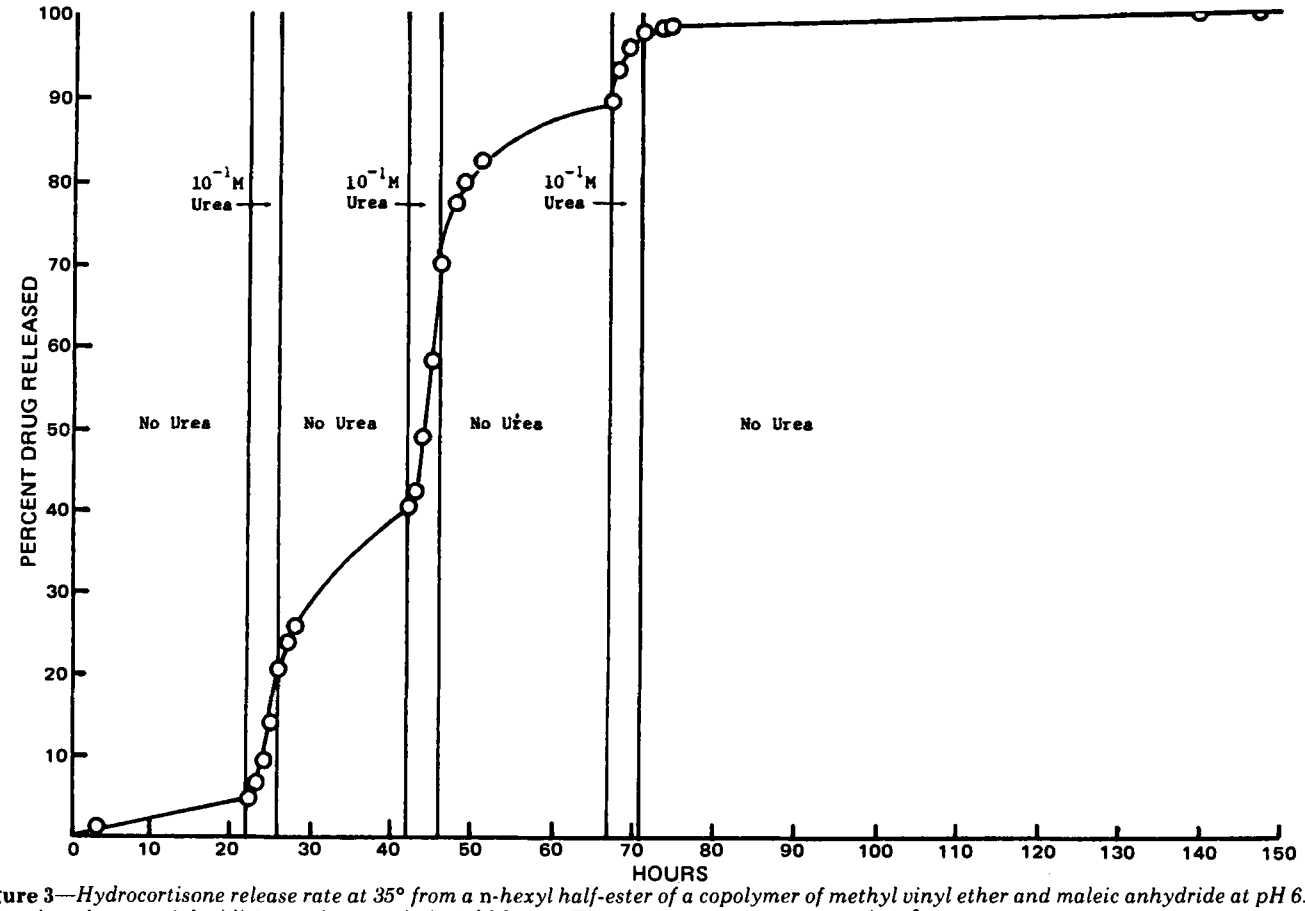

Figure 3—*Hydrocortisone release rate at 35° from a* n*-hexyl half-ester of a copolymer of methyl vinyl ether and maleic anhydride at pH 6.25 as a function of sequential addition and removal of* 10^{-1} M *urea. The stirring rate was ~140 cm/min*[3].

drogen ions generated by the eroding polymer, thus accelerating the process. Consequently, urea in the external environment should lead to accelerated drug release, and this acceleration should be directly proportional to the external urea concentration. Data in Fig. 2 corroborate these expectations.

While care was taken to maintain a constant pH in the external environment, this goal was accomplished only with 10^{-2} *M* urea. In the presence of 10^{-1} *M* urea, basic species generation was so rapid that the external medium buffering capacity was exceeded and a pH increase of ~0.25 occurred. Furthermore, the polymer dissolution rate was such that when the solubilized polymer chains diffused through the hydrogel, presumably through open pores, they precipitated again when exposed to the lower external pH. Because of the considerable difference in polymer dissolution rates between the hydrogel and the bulk solution, the devices gradually acquired a significant thickness of precipitated gelatinous polymer. Nevertheless, even though a rigorous comparison between no urea and urea is possible only in the 10^{-2} *M* case, the device definitely delivers hydrocortisone significantly faster in the presence of 10^{-1} *M* urea than in the presence of 10^{-2} *M* urea.

Data in Fig. 2 illustrate a situation where a device had a fixed and constant drug delivery rate that increased in response to the presence and concentration of external urea. The next question was whether this situation was reversible; that is, whether the drug delivery rate would return to its original value when urea was removed from the external environment.

Results illustrating this situation are shown in Fig. 3. As in the previous experiments, polymer erosion in the presence of 10^{-1} *M* urea was so rapid that the polymer precipitated around the device. Nevertheless, when the device was removed from a buffer solution without urea and placed in a buffer solution with 10^{-1} *M* urea, a significant increase in delivery immediately took place. When the device was next removed from that solution and again placed in a solution without urea, a delivery rate decrease took place.

The decrease in delivery was not abrupt but showed a first-order dependence. This first-order dependence was a consequence of the relatively water-insoluble hydrocortisone being trapped in the hydrogel layer and in the precipitated polymer around the device from which it was slowly released by a diffusional mechanism when the device was in the low rate erosion regimen. In the high rate delivery regimen, a zero-order delivery was noted because the slow diffusional release was masked by the rapid erosional release.

REFERENCES

(1) R. W. Baker and H. K. Lonsdale, *Chemtech*, **5**, 668 (1975).

(2) J. Heller, R. W. Baker, R. M. Gale, and J. O. Rodin, *J. Appl. Polym. Sci.*, **22**, 1991 (1978).

(3) R. C. Balkeley, J. A. Hinds, H. E. Kunze, E. C. Webb, and B. Zerner, *Biochemistry*, **8**, 1991 (1969).

(4) M. Mascini and G. G. Guibault, *Anal. Chem.*, **49**, 795 (1977).

ACKNOWLEDGMENTS

Supported by the World Health Organization.

Stability-Indicating Sulfa Drug Analysis Using High-Performance Liquid Chromatography

H. UMAGAT, P. F. McGARRY, and R. J. TSCHERNE ˣ

Received October 16, 1978, from the *Quality Control Department, Hoffmann-La Roche Inc., Nutley, NJ 07110.* Accepted for publication January 8, 1979.

Abstract □ Sensitive and efficient methods for sulfonamide determination as single entities and in combination with other drug substances in pharmaceutical dosage formulations were developed using high-performance liquid chromatography. These stability-indicating procedures involved a nitrile bonded phase column and nonaqueous mobile phases having diverse polarities. Sample potency was determined using peak height measurements. The methods may be used to determine trace sulfonamide quantities because detection limits are in the nanogram range.

Keyphrases □ High-performance liquid chromatography—analysis, sulfonamides in various pharmaceutical formulations, stability indicating □ Sulfonamides, various—analysis, high-performance liquid chromatography, various pharmaceutical formulations, stability indicating □ Dosage forms, various—analysis, sulfonamides, high-performance liquid chromatography, stability indicating

Methods for sulfonamide determination include potentiometric (1) or nonaqueous (2) titrations as well as direct spectrophotometric measurement (3). When sulfonamides are formulated in combination with other drug substances, the analysis of all components often requires more than one procedure, none being stability indicating. An interest in determining the active constituents of multicomponent sulfa drugs utilizing a single analytical method led to the development of a high-performance liquid chromatographic (HPLC) procedure.

BACKGROUND

Several studies were published on sulfonamide separation and determination using HPLC. Sulfonamides varying widely in pKa and hydrophobicity were separated using ion-pair partition chromatography (4). Liquid chromatographic sulfonamide separation also was accomplished using an "ether" bonded phase packing (5). Sulfonamides, including sulfisoxazole, sulfamethoxazole, *N'*-acetylsulfisoxazole, and sulfisoxazole diolamine, were separated on a strong anion-exchange column using a 0.01 *M* sodium borate mobile phase containing varying amounts of sodium nitrate (6).

Retention volume data for various sulfonamides on a pellicular-bonded reversed-phase packing, a pellicular packing coated with squalene, or a pellicular packing coated with octanol were reported (7). The partition coefficients, pKa values, and biological activity of each compound were correlated with retention volume.

Trace level quantitation of sulfamethazine residue in bovine tissue was reported (8). With this method, 0.07 ppm of sulfamethazine in tissue could be detected.

This paper describes a sensitive and efficient HPLC procedure for sulfonamide determination in pharmaceutical formulations. The assays involve a nitrile bonded phase column and nonaqueous mobile phases of varying polarity. The assays are stability indicating because precursors and decomposition products can be determined simultaneously with the drugs. Furthermore, compounds present in combination drug formulations are quantitated.

EXPERIMENTAL

Apparatus—A high-performance liquid chromatograph equipped with a UV detector[1] was used to monitor the eluted compounds at 254 nm. Separation was obtained on an alkylnitrile bonded phase column[2].

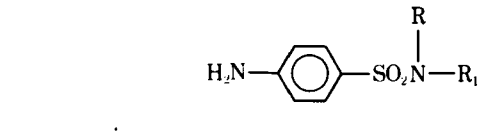

sulfanilamide: R = —H, R_1 = —H

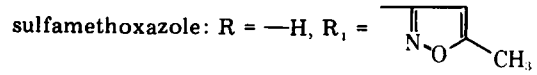

sulfamethoxazole: R = —H, R_1 =

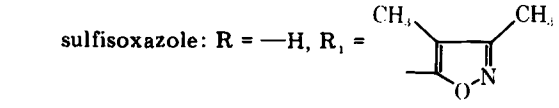

sulfisoxazole: R = —H, R_1 =

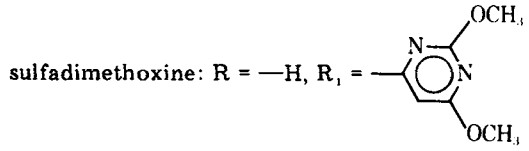

sulfadimethoxine: R = —H, R_1 =

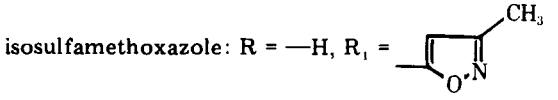

isosulfamethoxazole: R = —H, R_1 =

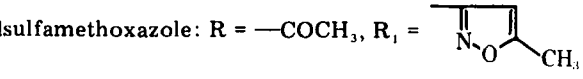

acetylsulfamethoxazole: R = —$COCH_3$, R_1 =

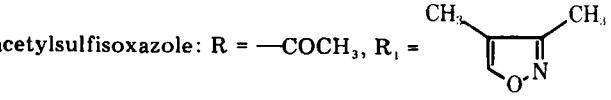

acetylsulfisoxazole: R = —$COCH_3$, R_1 =

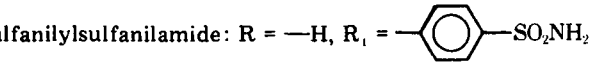

sulfanilylsulfanilamide: R = —H, R_1 =

Reagents and Chemicals—The methanol, methylene chloride, and ethyl acetate were ACS reagent grade. "Distilled-in-glass" heptane[3] was used. The diethylamine and hydrochloric acid were reagent grade. Released lots of sample material and in-house reference standards were used[4].

Mobile Phases—A mobile phase of methanol–methylene chloride–heptane (10:15:75) was used for sulfamethoxazole, *N'*-acetylsulfisoxazole, sulfisoxazole, and sulfadimethoxine analyses as well as for samples containing phenazopyridine hydrochloride in combination with sulfamethoxazole or sulfisoxazole.

A mobile phase of diethylamine–ethyl acetate–methanol–heptane (1:8:16:75) was used for samples containing trimethoprim or ormetoprim in combination with sulfamethoxazole or sulfadimethoxine, respectively.

Internal Standard Solution—Sulfanilylsulfanilamide was prepared by the Bauer (9) procedure and used as an internal standard. Approximately 600 mg of this material was accurately weighed into a 100-ml volumetric flask and diluted to volume with methanol (internal standard solution).

Sample Solution—Each sulfa drug solution was prepared by dissolving 100 mg in 100 ml of methanol except when in combination with

[1] Model 830, E. I. du Pont de Nemours & Co., Wilmington, Del.

[2] MicroPak CN-10 (25 cm × 2 mm i.d.), Varian Associates, Sunnyvale, Calif.

[3] Burdick & Jackson Laboratories, Muskegon, Mich.

[4] Hoffmann-La Roche, Nutley, N.J.

0022-3549/79/0700-0922$01.00/0
© 1979, American Pharmaceutical Association

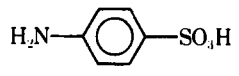

sulfanilic acid

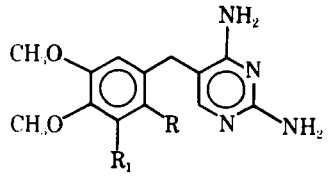

trimethoprim: R = —H, R_1 = —OCH_3
ormetoprim: R = —CH_3, R_1 = —H

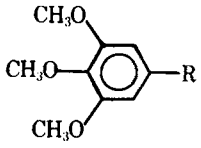

trimethoprim
precursor A: R = —CH_2—CH(CN)—CH(OCH_3)(OCH_3)

trimethoprim
precursor B: R = —C≡C—CH_2OCH_3 (CN)

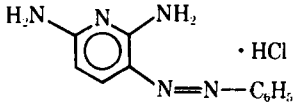

phenazopyridine hydrochloride

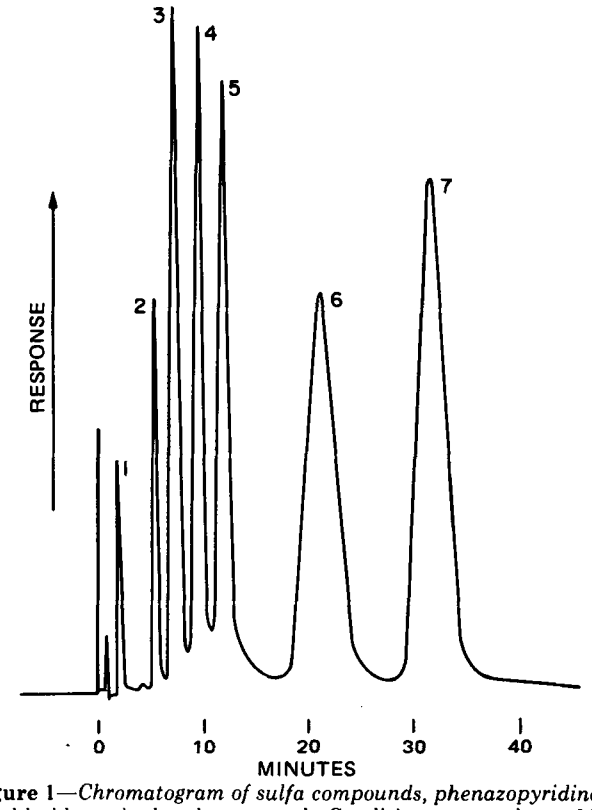

Figure 1—*Chromatogram of sulfa compounds, phenazopyridine hydrochloride, and related compounds. Conditions were: column, Micro-Pak CN-10; mobile phase, methanol–methylene chloride–heptane (10:15:75); and flow rate, 1.0 ml/min. Key: 1, phenazopyridine hydrochloride; 2, N′-acetylsulfamethoxazole; 3, sulfamethoxazole; 4, sulfisoxazole; 5, sulfanilamide; 6, isosulfamethoxazole; and 7, sulfanilylsulfanilamide.*

trimethoprim or ormetoprim, where 0.1 *N* HCl in methanol was used as the solvent. Four milliliters of the clear solution was pipetted into a 10-ml volumetric flask containing 2 ml of the internal standard solution and diluted to volume with methanol (working sample solution).

Reference Standard Solution—Reference standard solutions were prepared by diluting reference standard materials to a concentration similar to that of the samples with the same solvent (working reference standard solution).

Procedure—Five microliters of working sample and working reference standard solutions were alternately injected into the liquid chromatograph to determine the retention volumes for the compounds. Duplicate standards and samples were chromatographed, and the respective responses were determined using peak height measurements.

Calculations—Relative response ratios (*RR*) were calculated for the working reference standard solution using the chromatographic data. Calculation of drug potency for each tablet was made using:

$$\text{mg of drug/tablet} = \frac{(H_{spl})(W_{int})(\text{A.W.T.})(0.5)}{(H_{int})(W_{spl})(RR)} \qquad \text{(Eq. 1)}$$

where:

H_{spl} = sample peak height
H_{int} = internal standard in sample solution peak height
W_{int} = internal standard weight (milligrams)
W_{spl} = sample weight (milligrams)
RR = response ratio
0.5 = dilution factor
A.W.T. = average tablet weight (milligrams)

Formulas for calculating potency for other dosage forms (suspensions, solutions, creams, *etc.*) were adjusted to fit the particular dosage form.

RESULTS AND DISCUSSION

The sulfa drugs sulfamethoxazole, sulfisoxazole, *N′*-acetylsulfisoxazole, and sulfadimethoxine, both as single entities and in combination with ormetoprim, trimethoprim, and phenazopyridine hydrochloride, were analyzed successfully using normal phase partition HPLC. Two different mobile phases and a nitrile-bonded phase column were used to separate and determine all compounds of interest within a reasonable time. Typical chromatograms are shown in Figs. 1 and 2.

While the sulfa drugs could be chromatographed using either mobile phase, trimethoprim and ormetoprim did not elute in a reasonable time in the mobile phase without diethylamine. Sulfanilamide and sulfanilic acid, which are sulfonamide degradation products, were well resolved

Table I—Comparison of HPLC with Wet Chemical Results

Dosage Form	Compound Determined	Results for Various Lots, % claim HPLC	Wet Chemical
Tablet	Sulfisoxazole	100.1	102.1
		100.6	102.3
	Sulfamethoxazole	99.1	103.6
		100.6	101.6
	Sulfadimethoxine	100.8	104.4
		101.9	105.6
	Phenazopyridine hydrochloride	103.2	100.6
		100.0	100.0
	Trimethoprim	98.5	101.1
		101.3	99.9
	Ormetoprim	103.0	100.0
		105.0	102.0
Suspension	Acetylsulfisoxazole	99.7	102.0
		100.8	102.0
	Sulfamethoxazole	99.7	104.0
		98.0	101.6
	Trimethoprim	102.8	104.5
Cream	Sulfisoxazole	100.4	99.0
		99.3	98.0
Solution	Sulfisoxazole	105.5	106.0
		102.0	102.8

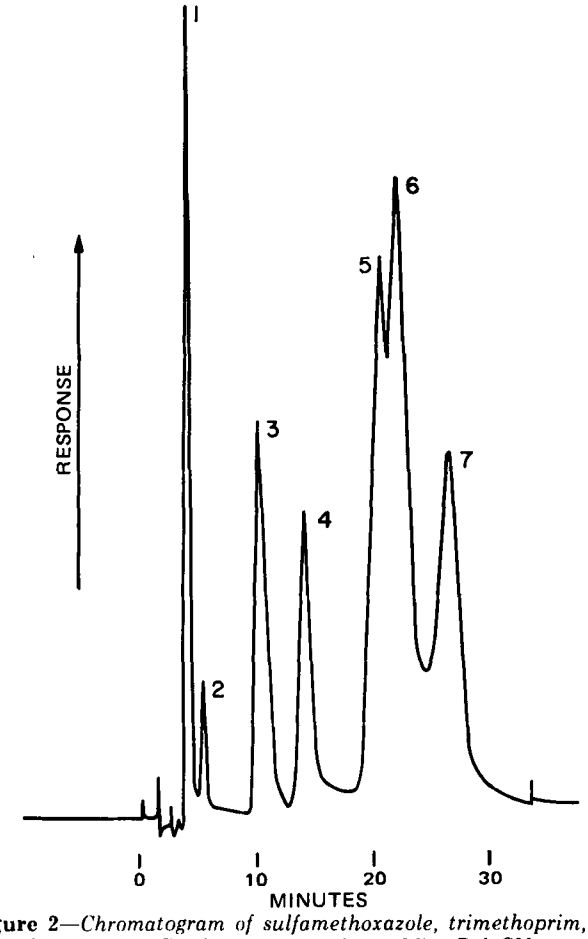

Figure 2—*Chromatogram of sulfamethoxazole, trimethoprim, and related compounds. Conditions were: column, MicroPak CN-10; mobile phase, methanol–ethyl acetate–diethylamine–heptane (16.8:1:75); and flow rate, 1.0 ml/min. Key: 1, trimethoprim precursor A; 2, trimethoprim precursor B; 3, trimethoprim; 4, N'-acetylsulfamethoxazole; 5, sulfanilamide; 6, sulfamethoxazole; and 7, isosulfamethoxazole.*

from the compounds of interest using the system without diethylamine; sulfanilic acid was eluted after all of the other sulfa compounds.

In some instances, 0.1 *N* HCl in methanol was chosen as the extraction solvent to ensure complete extraction of the drug substances from the matrix. Comparison of the HPLC results with results obtained using wet chemical procedures is made in Table I. Peak height responses *versus* amounts injected were linear for the formulation ranges for all components; however, deviations from linearity were found for many constituents when very high amounts were injected. Using the procedures described in this report, detection limits in the nanogram range were obtained. The determination of any compound tested in Table I, alone or in combination with another active drug substance, had a relative standard deviation of ±1.2%. An exception was found for the determination of trimethoprim and sulfamethoxazole formulated together, where the relative standard deviation was ±2.5%.

To ensure column-to-column duplication of the separation, three columns from the same supplier were evaluated. Differences in component retention times were noted with these columns, but only a slight modification in the mobile phase ratio was needed to effect resolution within a reasonable time.

In summary, the HPLC method presented was reliable, reproducible, rapid, and specific and should be useful for sulfa drug determinations in tablets, solutions, creams, and suspensions.

REFERENCES

(1) B. C. Rudy and B. Z. Senkowski, in "Analytical Profiles of Drug Substances," vol. 2, K. Florey, Ed., Academic, New York, N.Y., 1973, pp. 467–486.

(2) "The United States Pharmacopeia," 18th rev., Mack Publishing Co., Easton, Pa., 1970, p. 699.

(3) B. C. Rudy and B. Z. Senkowski, in "Analytical Profiles of Drug Substances," vol. 2, K. Florey, Ed., Academic, New York, N.Y., 1973, pp. 487–506.

(4) S. C. Sic., A. V. Hartkopf, and B. Karger, *J. Chromatogr.*, **119**, 523 (1976).

(5) J. J. Kirkland and J. J. DeStafano, *J. Chromatogr. Sci.*, **8**, 309 (1970).

(6) T. C. Kram, *J. Pharm. Sci.*, **61**, 254 (1972).

(7) D. Henry, J. Block, J. Anderson, and G. Carlson, *J. Med. Chem.*, **19**, 619 (1976).

(8) K. L. Joynson, D. T. Jeter, and R. C. Clairborne, *J. Pharm. Sci.*, **64**, 1657 (1975).

(9) H. Bauer, *J. Am. Chem. Soc.*, **61**, 613 (1939).

Antibacterial Activity of *Artemisia herba-alba*

JACOB YASHPHE *x, RUTH SEGAL ‡, AVIVA BREUER ‡, and GABI ERDREICH-NAFTALI ‡

Received July 31, 1978, from the **Department of Microbiological Chemistry, The Hebrew University—Hadassah Medical School, Jerusalem, Israel,* and the ‡*Department of Pharmacognosy, School of Pharmacy, The Hebrew University, Jerusalem, Israel.* Accepted for publication January 12, 1979.

Abstract □ The antibacterial activity of *Artemisia herba-alba* was investigated. Only its essential oil was active against some Gram-positive and Gram-negative bacteria. The essential oil was fractionated by column chromatography, and these fractions were tested for antibacterial activity. The principal component of the most active fraction was santolina alcohol.

Keyphrases □ *Artemisia herba-alba*—antibacterial activity, essential oil, column chromatography □ Antibacterial activity—evaluated for *Artemisia herba-alba* essential oil, column chromatography □ Folk medicine—*Artemisia herba-alba*, antibacterial activity of essential oil

Artemisia herba-alba Asso.[1], known as the desert wormwood, is a dwarf shrub growing in North Africa and the Middle East. This plant is used by the local population as an anthelmintic and for other purposes in folk medicine such as relief of coughing, intestinal disturbances, colds, measles, and muscle weakness.

Recently, several compounds were isolated from the aerial parts of this plant and their structures were established. These compounds were the sesquiterpene lactones

[1] Plant material was collected and identified as *Artemisia herba-alba* Asso. (Compositae) by Dr. Avinoam Danin, Department of Botany, The Hebrew University, Jerusalem, Israel. A voucher specimen (AHA-1) representing material collected for this investigation is available for inspection at the Department of Pharmacognosy (Dr. R. Segal), School of Pharmacy, The Hebrew University, Jerusalem, Israel.

0022-3549/79/0700-0924$01.00/0
© 1979, American Pharmaceutical Association

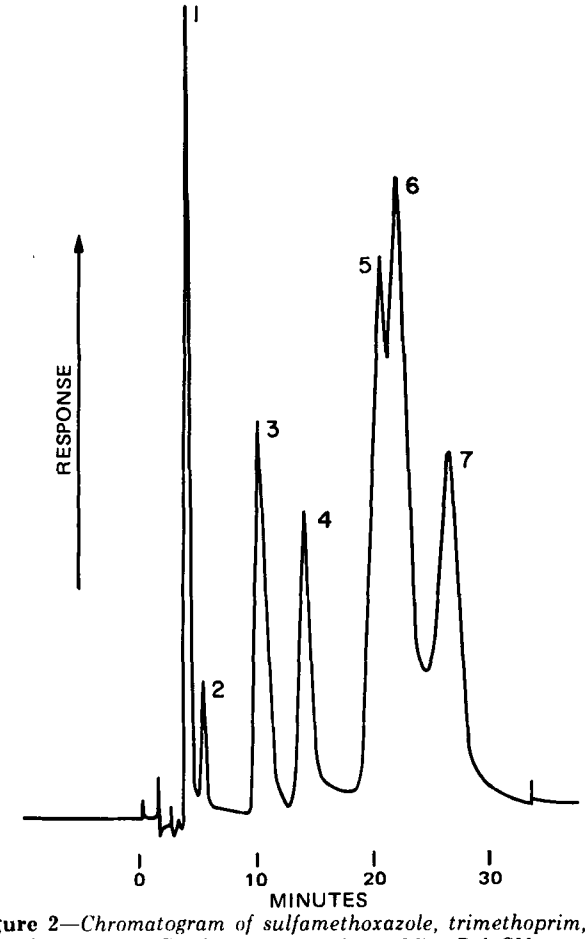

Figure 2—*Chromatogram of sulfamethoxazole, trimethoprim, and related compounds. Conditions were: column, MicroPak CN-10; mobile phase, methanol–ethyl acetate–diethylamine–heptane (16.8:1:75); and flow rate, 1.0 ml/min. Key: 1, trimethoprim precursor A; 2, trimethoprim precursor B; 3, trimethoprim; 4, N'-acetylsulfamethoxazole; 5, sulfanilamide; 6, sulfamethoxazole; and 7, isosulfamethoxazole.*

from the compounds of interest using the system without diethylamine; sulfanilic acid was eluted after all of the other sulfa compounds.

In some instances, 0.1 *N* HCl in methanol was chosen as the extraction solvent to ensure complete extraction of the drug substances from the matrix. Comparison of the HPLC results with results obtained using wet chemical procedures is made in Table I. Peak height responses *versus* amounts injected were linear for the formulation ranges for all components; however, deviations from linearity were found for many constituents when very high amounts were injected. Using the procedures described in this report, detection limits in the nanogram range were obtained. The determination of any compound tested in Table I, alone or in combination with another active drug substance, had a relative standard deviation of ±1.2%. An exception was found for the determination of trimethoprim and sulfamethoxazole formulated together, where the relative standard deviation was ±2.5%.

To ensure column-to-column duplication of the separation, three columns from the same supplier were evaluated. Differences in component retention times were noted with these columns, but only a slight modification in the mobile phase ratio was needed to effect resolution within a reasonable time.

In summary, the HPLC method presented was reliable, reproducible, rapid, and specific and should be useful for sulfa drug determinations in tablets, solutions, creams, and suspensions.

REFERENCES

(1) B. C. Rudy and B. Z. Senkowski, in "Analytical Profiles of Drug Substances," vol. 2, K. Florey, Ed., Academic, New York, N.Y., 1973, pp. 467–486.

(2) "The United States Pharmacopeia," 18th rev., Mack Publishing Co., Easton, Pa., 1970, p. 699.

(3) B. C. Rudy and B. Z. Senkowski, in "Analytical Profiles of Drug Substances," vol. 2, K. Florey, Ed., Academic, New York, N.Y., 1973, pp. 487–506.

(4) S. C. Sic., A. V. Hartkopf, and B. Karger, *J. Chromatogr.*, **119**, 523 (1976).

(5) J. J. Kirkland and J. J. DeStafano, *J. Chromatogr. Sci.*, **8**, 309 (1970).

(6) T. C. Kram, *J. Pharm. Sci.*, **61**, 254 (1972).

(7) D. Henry, J. Block, J. Anderson, and G. Carlson, *J. Med. Chem.*, **19**, 619 (1976).

(8) K. L. Joynson, D. T. Jeter, and R. C. Clairborne, *J. Pharm. Sci.*, **64**, 1657 (1975).

(9) H. Bauer, *J. Am. Chem. Soc.*, **61**, 613 (1939).

Antibacterial Activity of *Artemisia herba-alba*

JACOB YASHPHE *x, RUTH SEGAL ‡, AVIVA BREUER ‡, and GABI ERDREICH-NAFTALI ‡

Received July 31, 1978, from the **Department of Microbiological Chemistry, The Hebrew University—Hadassah Medical School, Jerusalem, Israel,* and the ‡*Department of Pharmacognosy, School of Pharmacy, The Hebrew University, Jerusalem, Israel.* Accepted for publication January 12, 1979.

Abstract □ The antibacterial activity of *Artemisia herba-alba* was investigated. Only its essential oil was active against some Gram-positive and Gram-negative bacteria. The essential oil was fractionated by column chromatography, and these fractions were tested for antibacterial activity. The principal component of the most active fraction was santolina alcohol.

Keyphrases □ *Artemisia herba-alba*—antibacterial activity, essential oil, column chromatography □ Antibacterial activity—evaluated for *Artemisia herba-alba* essential oil, column chromatography □ Folk medicine—*Artemisia herba-alba*, antibacterial activity of essential oil

Artemisia herba-alba Asso.[1], known as the desert wormwood, is a dwarf shrub growing in North Africa and the Middle East. This plant is used by the local population as an anthelmintic and for other purposes in folk medicine such as relief of coughing, intestinal disturbances, colds, measles, and muscle weakness.

Recently, several compounds were isolated from the aerial parts of this plant and their structures were established. These compounds were the sesquiterpene lactones

[1] Plant material was collected and identified as *Artemisia herba-alba* Asso. (Compositae) by Dr. Avinoam Danin, Department of Botany, The Hebrew University, Jerusalem, Israel. A voucher specimen (AHA-1) representing material collected for this investigation is available for inspection at the Department of Pharmacognosy (Dr. R. Segal), School of Pharmacy, The Hebrew University, Jerusalem, Israel.

0022-3549/79/0700-0924$01.00/0
© 1979, American Pharmaceutical Association

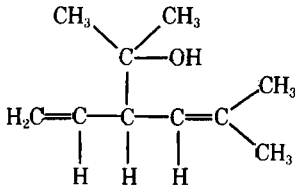

I

santonin (2), herbolides A, B, and C (3), and a flavone derivative (4). Santonin is well known as a "vermifuge" (5) and is probably responsible for the anthelmintic activity of *A. herba-alba*. No other biological activities of *A. herba-alba* or of compounds isolated from it have been reported.

Because the plant extracts were never contaminated with microorganisms, even after staying at room temperature for very long periods, the antibiotic activity of *A. herba-alba* was investigated.

EXPERIMENTAL

Extraction of Plant Material—*A. herba-alba* was collected near Sde-Boker (Negev desert), Israel. The dried flowers, leaves, and small stems (5 g) were crushed and extracted with methanol in a soxhlet apparatus. The waxy materials, which precipitated after cooling, were filtered and discarded. The methanol was evaporated, and the dark-green residue was dissolved in methanol to a defined concentration.

Steam Distillation of Plant Material—The dried flowers, leaves, and small stems (100 g) of *Artemisia* were crushed and steam distilled. The oil yield was about 1%. The plant material left after steam distillation was filtered, dried at 40°, and extracted with methanol as described.

Column Chromatography of Distillate—The volatile oil (200 mg) was chromatographed on a 10-g silica gel column and eluted with methylene chloride. The column was monitored by TLC, and five crude fractions were collected. These fractions were screened for antibiotic activities without further purification.

Bacterial Strains—The bacterial strains[2] used were: *Staphylococcus aureus*[3], *Escherichia coli*[4], *Salmonella typhosa*[5], *Shigella sonnei*[6], and *Streptococcus hemolyticus*[7].

Antibacterial Activity Detection by Disk Method—The essential oil and its fractions were diluted with methanol to a concentration (per milliliter) that was 100-fold the amount applied on the disks. Paper disks[8] of 6-mm diameter were impregnated with 0.01 ml of these solutions. The tested bacterial strains (0.1 ml of a log phase suspension of 10^9 cells/ml) were spread on petri plates containing nutrient agar[9]. The dried impregnated disks were placed on the inoculated plates. The plates were incubated at 37° for 24 hr, and the inhibition zones were measured.

Antibacterial Activity Assay in Liquid Cultures—The preparations were dispersed in 2% dimethyl sulfoxide (5 mg/ml), and 15 ml of this solution was added to 7.5 ml of sterile nutrient broth[9]. Further dilutions were made by the transfer of 4.5 ml of the solution to 4.5 ml of sterile nutrient broth. Similar dilutions were made from 2% dimethyl sulfoxide as a control. The suspension (0.1 ml) of the tested bacterial strains (10^4 log phase cells/ml) was added to each tube, and the cultures were incubated at 37° for 24 hr. Turbidity was measured by a photometer[10] at 420 nm. The absorption of the uninoculated control was subtracted.

[2] Taken from the strain collection of the Department of Clinical Bacteriology, The Hebrew University-Hadassah Medical School, Jerusalem, Israel.
[3] Identified as Gram-positive cocci, which fermented mannitol and coagulated plasma.
[4] Identified as motile Gram-negative rods, which fermented lactose, produced acid from glucose (methyl red test) and indole from tryptophan, utilized citrate, and did not produce acetoin (Voges-Prosqauer test).
[5] Identified as motile Gram-negative rods, which did not ferment lactose, produced acid but no gas from glucose and mannose, and produced hydrogen sulfide from thiosulfate.
[6] Identified as nonmotile Gram-negative rods, which fermented mannitol and lactose.
[7] Identified as Gram-positive cocci, which produced β-hemolysis on blood agar.
[8] Whatman, 3M.
[9] Difco.
[10] Klett-Summerson photoelectric colorimeter, Klett Manufacturing Co., New York, N.Y.

Table I—Antibacterial Activity of Various Plant Fractions Tested by the Disk Method

Fraction	Diameter of Growth Inhibition[a], mm	
	S. aureus	*E. coli*
Whole plant extract	14[b]	11
Essential oil (2.5 mg)	18	13
Residue extract[c] (2.5 mg)	6[d]	6

[a] Including 6-mm diameter of the disk. [b] By an amount extracted from 1 g of dry plant material as described. [c] Extract of the residual material after steam distillation. [d] Lack of activity.

Table II—Inhibition[a] of Growth of Various Bacterial Strains in Liquid Cultures by the Essential Oil

Essential Oil Concentration, mg/ml	*S. aureus*	*E. coli*	*Sal. typhosa*	*Sh. sonnei*	*St. hemolyticus*
0.8	100	50	100	78	100
0.4	40	26	73	67	100
0.2	0	16	64	55	73
0.1	0	6	45	45	46
0.05	0	0	45	45	36

[a] Inhibition was determined by the dilution method described and is expressed as percentage of decrease in culture turbidity from the turbidity of the control culture.

Table III—Antibacterial Activity of Essential Oil Fractions against *S. aureus* Tested by the Disk Method

Fraction	Diameter of Growth Inhibition[a], mm
1	6[b]
2	14
3	56
4	16
5	16

[a] Including 6-mm diameter of the disk. Each disk contained 1 mg of material. [b] Lack of activity.

RESULTS AND DISCUSSION

The aerial parts of *A. herba-alba* were tested for antibacterial activities. The antibiotic activity observed for the whole plant extract was concentrated in the essential oil (Table I). The oil inhibited the growth of five bacterial strains (Table II), both Gram positive (*S. aureus* and *St. hemolyticus*) and Gram negative (*E. coli, Sal. typhosa,* and *Sh. sonnei*). *St. hemolyticus* was slightly more sensitive to the oil than were the other tested organisms.

For the detection of the active antibacterial principle, the oil was subjected to column chromatography. Five fractions were collected according to their polarity and were tested for antibiotic activity by the disk method. *E. coli* and *S. aureus* were selected as representatives from Gram-negative and Gram-positive bacteria. The results (Table III) indicate that only fraction 3 possessed significant antibiotic activity, so the chemical composition of this fraction was investigated. Repeated column chromatography yielded a pure compound, which was identified as santolina alcohol (I) by its optical rotation value and IR and NMR spectra (6).

REFERENCES

(1) A. Danin, "The Vegetation of the Negev North of Nahal Paran," Sifriat Hapoalim, Tel-Aviv, Israel, 1977.

(2) S. M. Khafagy, S. A. Gharbo, and T. M. Sarg, *Planta Med.*, **20**, 90 (1971).

(3) R. Segal, S. Sokoloff, B. Haran, D. V. Zaitschek, and D. Lichtenberg, *Phytochemistry*, **16**, 1237 (1977).

(4) R. Segal, D. Cohen, S. Sokoloff, and D. V. Zaitschek, *Lloydia*, **36**, 103 (1973).

(5) B. Wichmann, *Pharmazie*, **13**, 487 (1958).

(6) Y. Chretien-Bessiere, *Bull. Soc. Chim. Fr.*, **1968**, 2018.

Quantitative Dexamethasone and Dexamethasone Sodium Phosphate Determinations in Pharmaceutical Dosage Forms by High-Pressure Liquid Chromatography

V. DAS GUPTA

Received August 28, 1978, from the *College of Pharmacy, University of Houston, Houston, TX 77004.* Accepted for publication January 5, 1979.

Abstract □ A high-pressure liquid chromatographic procedure for quantitative dexamethasone and dexamethasone sodium phosphate determinations in all types of commercially available pharmaceutical dosage forms was developed. The method also separates dexamethasone from its phosphate salt and separates dexamethasone or its salt from a number of inactive ingredients such as benzoic acid, benzyl alcohol, some colors, creatinine, and parabens. Inactive ingredient concentrations may be estimated without additional cost. Part of the parabens present in the commercial injections may be adsorbed by the rubber closures.

Keyphrases □ High-pressure liquid chromatography—analysis, dexamethasone and dexamethasone sodium phosphate, various pharmaceutical dosage forms □ Dexamethasone—analysis, high-pressure liquid chromatography, various pharmaceutical dosage forms □ Dexamethasone sodium phosphate—analysis, high-pressure liquid chromatography, various pharmaceutical dosage forms

The USP methods (1) for quantitative dexamethasone (I) and dexamethasone sodium phosphate (II) determinations in pharmaceutical dosage forms (elixir, injections, ointment, ophthalmic solution, and tablets) are tedious and time consuming. The USP methods involve many different preliminary extraction procedures and then reactions with blue tetrazolium at room temperature for 45 min or with phenylhydrazine at 60° for 2 hr. For testing the injection, a 2-hr preliminary treatment with alkaline phosphatase is required to free the base before reacting with blue tetrazolium.

Obviously, the analyst has to use different techniques to analyze similar active ingredients. Moreover, determining the presence of dexamethasone base in dexamethasone phosphate salt involves an additional and different method.

A high-pressure liquid chromatographic (HPLC) procedure for quantitative dexamethasone determination in creams and ointments was reported (2). In this method, the mobile phase was 0.2% acetonitrile in hexane, and the column was β,β'-oxydipropionitrile on Zipax (2). Application of this method to other pharmaceutical dosage forms, such as an elixir containing colors and benzoic acid and creams and injections containing dexamethasone sodium phosphate and parabens, was not reported.

Another HPLC procedure for quantitative dexamethasone determination in milk (3) involved a complicated preliminary extraction. The HPLC method reported (4) for quantitative plasma dexamethasone determination also involved complicated preliminary extraction. Furthermore, these methods (3, 4) were not investigated to determine their applicability to pharmaceutical dosage forms with numerous inactive ingredients.

This paper describes a simple HPLC procedure for the quantitation of dexamethasone and its phosphate salt in all pharmaceutical dosage forms available commercially which also separates dexamethasone base from its salt. The HPLC procedure was preferred because it can often assay some inactive ingredients without additional cost.

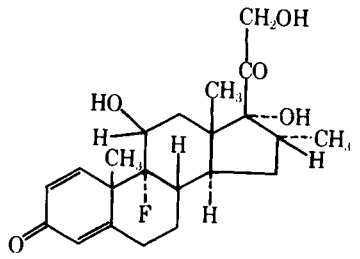

I

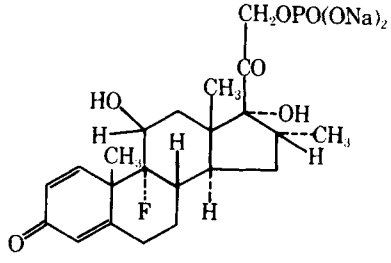

II

EXPERIMENTAL

Chemicals and Reagents—All chemicals and reagents were USP, NF, and ACS grade and were used without further purification. Dexamethasone[1] (I) and dexamethasone sodium phosphate[1] (II) were used as received.

Apparatus—The high-pressure liquid chromatograph[2] was equipped with a fixed wavelength (254 nm) detector, a recorder[3], and an integrator[4].

Column—The nonpolar prepacked column[5] consisted of a monomolecular layer of octadecyltrichlorosilane permanently bonded to silica (30 cm long and 4 mm i.d.).

Chromatographic Conditions—The chromatographic solvent was 0.01 *M* KH_2PO_4 in water containing 50% (v/v) methanol. The temperature was ambient, the flow rate was 1.6 ml/min, and the chart speed was 30.5 cm/hr. The attenuation units for full-scale deflection were 0.04 for I and 0.1 for dexamethasone phosphate (III), which was made using an equivalent quantity of II.

Assay Solutions—The elixir (label claim of 0.1 mg of I/ml) was diluted from 5.0 to 25.0 ml with water. Injections (label claim of 4 mg of III/ml from an equivalent amount of II) were diluted from 2.0 to 100.0 ml with water. The ophthalmic solution (label claim of 0.1% of III) was diluted from 8.0 to 100 ml with water.

Extraction of III from Ointment (Label Claim of 0.05% of III)—Ointment (0.8 g) was dissolved in 25 ml of methylene chloride in a separator and extracted with 25.0 ml of water. The clear water layer was

[1] Merck Sharp & Dohme, West Point, Pa.
[2] Waters ALC 202 equipped with U6K universal injector.
[3] Omniscribe 5213-12 equipped with an integrator.
[4] Autolab Minigrator, Spectra-Physics, Santa Clara, Calif.
[5] μBondapak C_{18}, Waters Associates, Milford, Mass.

0022-3549/79/0700-0926$01.00/0
© 1979, American Pharmaceutical Association

Table I—Assay Results

Product	Results, % of label claim
Synthetic injection 1 with parabens	100.5
Synthetic injection 2 with benzyl alcohol	99.8
Commercial injections	
1	99.6[a]
2	100.1[b]
3	99.1[c]
Commercial elixir[d]	99.8
Commercial ointment[e]	106.9[f]
Ophthalmic drops[g]	109.3[h]
Commercial tablets	
1 (0.75 mg/tablet, blue)	98.3[i]
2 (4.0 mg/tablet, white)	99.4[i]

[a] With parabens similar to synthetic solution 1. The results on parabens were estimated to be only ~80% of the claim. To estimate parabens, the attenuated units for full-scale deflection were 0.2 for methylparaben and 0.04 for propylparaben. [b] Same as footnote *a*, except that the results on parabens were about 76% of the label claim. [c] With benzyl alcohol similar to synthetic solution 2. The result on benzyl alcohol was estimated (using peak 1 in Fig. 1C) to be 99.2% of the label claim. [d] Also contained red color and 0.1% benzoic acid as preservative. [e] White petrolatum and mineral oil base. [f] The result using the blue tetrazolium method as provided by the manufacturer was 105.0%. [g] Also contained creatinine, sodium borate, sodium citrate, sodium bisulfite (0.32%), phenylethyl alcohol (0.25%), and benzalkonium chloride (0.02%). [h] The result using the blue tetrazolium method as provided by the manufacturer was 110.0%. [i] The results with the blue tetrazolium method were between 302 and 425%.

assayed using attenuation units for full-scale deflection of 0.04 instead of 0.1. The standard solution contained 16 μg of III/ml.

Extraction of I from Tablets (Label Claim of Sample 1, 0.75 mg of I/Tablet; Label Claim of Sample 2, 4 mg of I/Tablet)—Ten tablets were weighed and ground to a fine powder. Powder representing 2.0 mg of the active ingredient was weighed accurately and transferred to a 150-ml beaker. Ethanol (80 ml) was added, heated just to boiling, cooled, and brought to volume (100.0 ml) with alcohol. The solution was filtered, the first 20 ml of filtrate was rejected, and a sample was collected for analysis.

Standard Solutions—Two milliliters of a stock I solution (1 mg/ml) in alcohol was diluted to 100.0 ml with water for the elixir or with alcohol for the tablets. Ten milliliters of a stock II solution (contained an equivalent amount of 0.8 mg of III/ml of water) was diluted to 100.0 ml

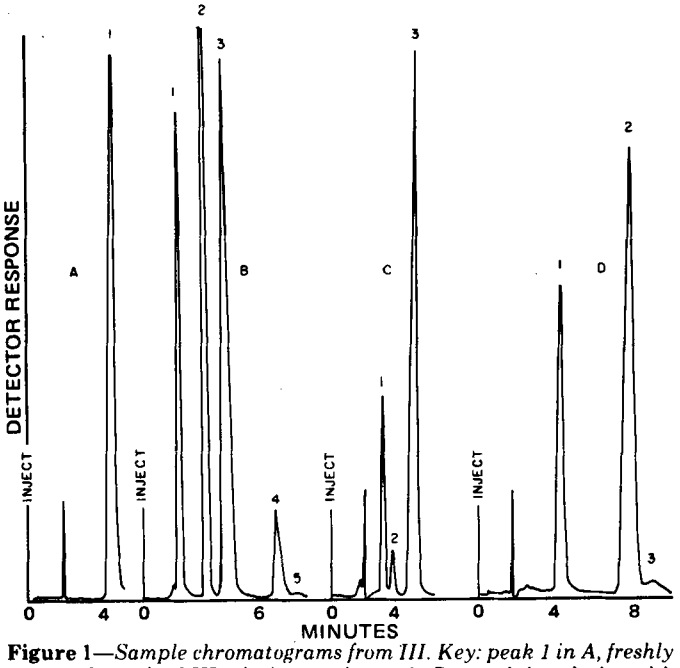

Figure 1—*Sample chromatograms from III. Key: peak 1 in A, freshly prepared standard III solution; peaks 1–5 in B, creatinine eluting with the solvent, methylparaben (out of scale when using 0.1 aufs), III, propylparaben, and a small quantity of a decomposition product, respectively (the chromatogram was obtained from a commercial injection sample); peaks 1 and 2 in C, benzyl alcohol present in a commercial injection from a different manufacturer; peak 3 in C, III; peak 1 in D, III in a 53-day-old aqueous solution of III (160 μg/ml); and peaks 2 and 3 in D, decomposition products. For chromatographic conditions, see text.*

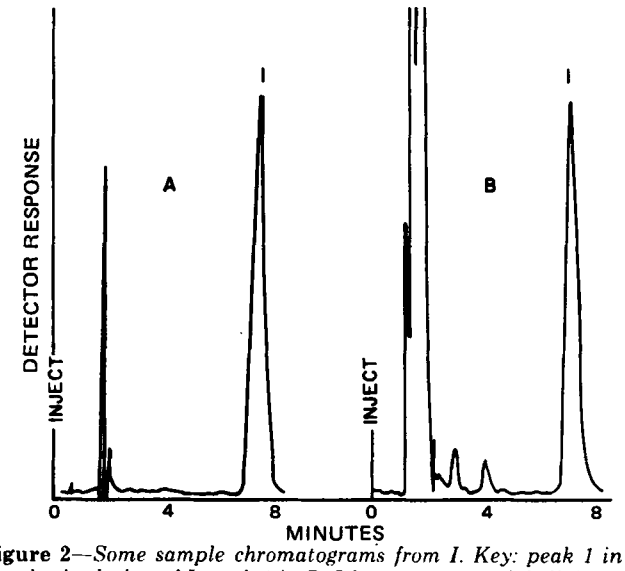

Figure 2—*Some sample chromatograms from I. Key: peak 1 in A, standard solution of I; peak 1 in B, I from a commercial elixir; other peaks, red color and benzoic acid (which comes out with the solvent). For chromatographic conditions, see text.*

with water. For the ointment, it was diluted further, 10.0 ml to 50.0 ml with water. Fresh II solutions were prepared every 4 hr.

Solutions Similar to Two Commercial Injections—One solution contained, per milliliter, 4.0 mg of III, 8 mg of creatinine, 10 mg of sodium citrate, 1.0 mg of sodium bisulfite, 1.5 mg of methylparaben, and 0.2 mg of propylparaben. The second contained, per milliliter, 4.0 mg of III, 1.0 mg of sodium sulfite, and 10 mg of benzyl alcohol. These solutions were diluted from 2.0 to 100.0 ml with water for quantitative analysis.

Assay—An aliquot (20.0 μl) was injected into the chromatograph as described. For comparison, an identical standard solution volume was injected after the sample was eluted.

Since preliminary investigations indicated that peak areas were directly related to concentrations (range of 0.2–0.6 μg for I, 0.5–2.0 μg for III for injections and ophthalmic solutions, and 0.1–0.4 μg of III for ointment), the results were calculated using the following equation:

$$\frac{A_a}{A_s} \times 100 = \text{percent of label claim} \qquad \text{(Eq. 1)}$$

where A_a is the assay solution peak area and A_s is the standard solution peak area. The results are presented in Figs. 1 and 2 and Table I.

For comparison, the commercial tablets also were assayed by the blue tetrazolium method as described in the USP (5) using the assay solution described (Table I).

DISCUSSION

The results indicate (Table I) that a single and simple assay can be used for the quantitative determinations of I and III in elixir, injections, ointment, ophthalmic solution, and tablets. The relative percent standard deviations based on five standard solution injections were 2.3 and 2.1 for I and III, respectively.

The USP assay methods (1) involve different preliminary treatments depending on the dosage form. These treatments are tedious and time consuming. After the preliminary treatment, color development by reaction with either blue tetrazolium or phenylhydrazine is also time consuming.

The standard III solution must be prepared fresh since it decomposes on standing. The single wash procedure with methylene chloride recommended in the USP to remove I from III extracted only ~97% of the total I present. The mixture contained 120 μg of III/ml and 40 μg of I/ml in water. A 10.0-ml quantity of the aqueous solution was extracted with 25 ml of methylene chloride. This estimation was possible since the developed procedure separates I and III very efficiently (see Figs. 1A and 2A for retention times).

There was no interference from: (*a*) red color and benzoic acid present in the elixir (Fig. 2B); (*b*) creatinine, parabens, and benzyl alcohol present in the injections (Figs. 1B and 1C); (*c*) phenylethyl alcohol present in ophthalmic solution; and (*d*) blue color and other inactive ingredients present in the tablets. With the tablets, there was significant interference

with the blue tetrazolium procedure (Table I, footnote *i*), presumably due to the heat used to extract the active ingredient. An extraction procedure using cold alcohol gave inconsistent and sometimes low results.

Another advantage of the developed method is that some inactive ingredients can be estimated without additional cost. For example, in commercial injections, parabens were estimated to be only between 76 and 80% of the label claim (Table I, footnotes *a* and *b*). This finding is presumably due to paraben adsorption onto the rubber closures. This problem was not recorded with benzyl alcohol (Table I, footnote *c*) as the preservative.

REFERENCES

(1) "The United States Pharmacopeia," 19th rev., Mack Publishing Co., Easton, Pa., 1975, pp. 122–126.

(2) J. A. Mollica and R. F. Strusz, *J. Pharm. Sci.*, **61**, 444 (1972).

(3) A. M. DePaolis, G. Schnabel, S. E. Katz, and J. D. Rosen, *J. Assoc. Off. Anal. Chem.*, **60**, 210 (1977).

(4) J. C. K. Loo and N. Jordan, *J. Chromatogr.*, **143**, 314 (1977).

(5) "The United States Pharmacopeia," 19th rev., Mack Publishing Co., Easton, Pa., 1975, p. 138.

ACKNOWLEDGMENTS

The author thanks Merck Sharp & Dohme for the generous supply of dexamethasone and dexamethasone sodium phosphate powders.

Terpenoid Biotransformation in Mammals II: Biotransformation of *dl*-Camphene in Rabbits

T. ISHIDA *[x], Y. ASAKAWA [‡], T. TAKEMOTO [‡], and T. ARATANI [§]

Received September 28, 1978, from the **Hiroshima Institute of Technology, Itsukaichi, Hiroshima 738, Japan*, the [‡]*Institute of Pharmacognosy, Tokushima-Bunri University, Tokushima 770, Japan*, and the [§]*Faculty of Integrated Arts and Sciences, Hiroshima University, Hiroshima 730, Japan.* Accepted for publication January 11, 1979.

Abstract □ The biotransformation of *dl*-camphene in rabbits was investigated. Four neutral metabolites, 6-*exo*-hydroxycamphene, 10-hydroxycamphene, and diastereoisomers of camphene-2,10-glycol, were identified and two alcohols, 7-hydroxycamphene and 3-hydroxytricyclene, were estimated by IR, UV, NMR, and mass spectra and chemical degradations. The formation of these compounds can be explained through a homoallylic oxidation or an epoxide formation.

Keyphrases □ Camphene—biotransformation in rabbits, four urinary metabolites identified by spectrometry and chemical degradations □ Biotransformation—camphene in rabbits, four urinary metabolites identified by spectrometry and chemical degradations □ Choleretic activity—camphene, biotransformation in rabbits, four urinary metabolites identified by spectrometry and chemical degradations

During investigations into terpenoid detoxification in mammals, the biotransformation of 3-carene and α- and β-pinenes having a *gem*-dimethyl group on the three- or four-membered ring, respectively, was reported (1). In this paper, the biotransformation of camphene in rabbits is reported. Camphene has a *gem*-dimethyl group on the five-membered ring.

Camphene is found in the essential oils of most plants, and conifers containing this compound are often damaged worldwide by field animals. The choleretic activity of camphene in rats has been studied (2). The present investigation was carried out to clarify camphene biotransformation in mammals with respect to xenobiotics.

RESULTS

Characterization and Identification of Free Neutral Metabolites—TLC and GLC revealed the products in the urinary extracts as shown in Fig. 1. The metabolites were column chromatographed on silica gel in *n*-hexane with gradually increasing amounts of ethyl acetate. When necessary, metabolites were isolated by preparative GLC.

Metabolites 1-3 (M-I–M-III)—Peak 2 was isolated preparatively by GLC as one component (TLC and GLC) and had a fragrant odor; mass spectrum: *m/e* (%) 152 (M^+, $C_{10}H_{16}O$, 3), 134 (9), 119 (24), 108 (base), 93 (67), 72 (21), and 66 (28); IR: ν ($CHCl_3$) 3625, 3450, and 890 cm^{-1}. Its NMR spectrum showed two kinds of metabolites (M-I and M-II) in a 2:1 ratio. The major signal group assigned was: δ ($CDCl_3$) 4.84 and 4.63 (each 1H, s, *endo*-methylene), 3.80 [1H, q, $J_{5\text{-}exo\text{-}6\text{-}endo} = 7$, $J_{5\text{-}endo\text{-}6\text{-}endo} = 3$ Hz, —C*H*(OH)], 2.62 (1H, b, bridge head), 2.21 (1H, octet, $J_{5\text{-}exo\text{-}5\text{-}endo} = 13$, $J_{5\text{-}exo\text{-}6\text{-}endo} = 7$, $J_{5\text{-}exo\text{-}4} = 2$ Hz, *exo*-5), 1.89 (1H, b, *endo*-5), 1.63 (2H, b), and 0.98 and 1.04 (each 3H, *gem*-dimethyl). All of these M-I signals agreed well with those of the synthetic 6-*exo*-hydroxycamphene (I) (3).

The Jones oxidation of I yielded 6-oxocamphene [ν ($CHCl_3$) 1740 and 890 cm^{-1}] (4) with a minor ketone; mass spectrum (minor ketone): *m/e* (%) 150 (M^+, $C_{10}H_{14}O$, 25), 135 (12), 121 (15), 108 (41), 107 (98), 93 (base), 91 (54), and 79 (41); IR: ν ($CHCl_3$) 1740 and 890 cm^{-1}; NMR: δ ($CDCl_3$) 4.98 and 4.76 (each 1H, s), 3.08 (1H, b), and 1.16 and 1.07 (each 3H, s). These spectra revealed the minor ketone to be 7-oxocamphene. Therefore, 7-hydroxycamphene (II) (M-II) was estimated as the camphene metabolite.

The minor signal group found in the I NMR spectrum can be attributed to II: δ ($CDCl_3$) 4.73 and 4.48 (each 1H, s), 4.24 (1H, bs), 2.68 (1H, bs), and 1.04 (6H, s). The other minor ketone was obtained as the Jones oxidation product from M-III following M-I. Its spectra were considerably different from those of the above-mentioned ketones; mass spectrum: *m/e* (%) 150 (M^+, $C_{10}H_{14}O$, 7), 122 (16), 107 (base), 105 (12), 91 (28), and 79 (14); IR: ν ($CHCl_3$) 1740 cm^{-1}; NMR: δ ($CDCl_3$) 1.21, 1.04, and 1.00 (each 3H, s). Disappearance of the *endo*-methylene group suggests some camphene rearrangement. Accordingly, this ketone was assigned as 3-ketotricyclene

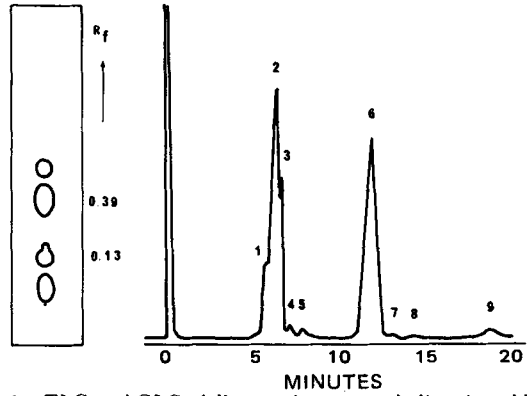

Figure 1—*TLC and GLC of* dl-*camphene metabolites in rabbits. The TLC solvent system was benzene–n-hexane–ethyl acetate (14:5:6); GLC utilized an SE-30 (5%) column.*

0022-3549/79/0700-0928$01.00/0

© 1979, American Pharmaceutical Association

with the blue tetrazolium procedure (Table I, footnote *i*), presumably due to the heat used to extract the active ingredient. An extraction procedure using cold alcohol gave inconsistent and sometimes low results.

Another advantage of the developed method is that some inactive ingredients can be estimated without additional cost. For example, in commercial injections, parabens were estimated to be only between 76 and 80% of the label claim (Table I, footnotes *a* and *b*). This finding is presumably due to paraben adsorption onto the rubber closures. This problem was not recorded with benzyl alcohol (Table I, footnote *c*) as the preservative.

REFERENCES

(1) "The United States Pharmacopeia," 19th rev., Mack Publishing Co., Easton, Pa., 1975, pp. 122–126.

(2) J. A. Mollica and R. F. Strusz, *J. Pharm. Sci.*, **61**, 444 (1972).

(3) A. M. DePaolis, G. Schnabel, S. E. Katz, and J. D. Rosen, *J. Assoc. Off. Anal. Chem.*, **60**, 210 (1977).

(4) J. C. K. Loo and N. Jordan, *J. Chromatogr.*, **143**, 314 (1977).

(5) "The United States Pharmacopeia," 19th rev., Mack Publishing Co., Easton, Pa., 1975, p. 138.

ACKNOWLEDGMENTS

The author thanks Merck Sharp & Dohme for the generous supply of dexamethasone and dexamethasone sodium phosphate powders.

Terpenoid Biotransformation in Mammals II: Biotransformation of *dl*-Camphene in Rabbits

T. ISHIDA *[x], Y. ASAKAWA [‡], T. TAKEMOTO [‡], and T. ARATANI [§]

Received September 28, 1978, from the **Hiroshima Institute of Technology, Itsukaichi, Hiroshima 738, Japan*, the [‡]*Institute of Pharmacognosy, Tokushima-Bunri University, Tokushima 770, Japan*, and the [§]*Faculty of Integrated Arts and Sciences, Hiroshima University, Hiroshima 730, Japan.* Accepted for publication January 11, 1979.

Abstract □ The biotransformation of *dl*-camphene in rabbits was investigated. Four neutral metabolites, 6-*exo*-hydroxycamphene, 10-hydroxycamphene, and diastereoisomers of camphene-2,10-glycol, were identified and two alcohols, 7-hydroxycamphene and 3-hydroxytricyclene, were estimated by IR, UV, NMR, and mass spectra and chemical degradations. The formation of these compounds can be explained through a homoallylic oxidation or an epoxide formation.

Keyphrases □ Camphene—biotransformation in rabbits, four urinary metabolites identified by spectrometry and chemical degradations □ Biotransformation—camphene in rabbits, four urinary metabolites identified by spectrometry and chemical degradations □ Choleretic activity—camphene, biotransformation in rabbits, four urinary metabolites identified by spectrometry and chemical degradations

During investigations into terpenoid detoxification in mammals, the biotransformation of 3-carene and α- and β-pinenes having a *gem*-dimethyl group on the three- or four-membered ring, respectively, was reported (1). In this paper, the biotransformation of camphene in rabbits is reported. Camphene has a *gem*-dimethyl group on the five-membered ring.

Camphene is found in the essential oils of most plants, and conifers containing this compound are often damaged worldwide by field animals. The choleretic activity of camphene in rats has been studied (2). The present investigation was carried out to clarify camphene biotransformation in mammals with respect to xenobiotics.

RESULTS

Characterization and Identification of Free Neutral Metabolites—TLC and GLC revealed the products in the urinary extracts as shown in Fig. 1. The metabolites were column chromatographed on silica gel in *n*-hexane with gradually increasing amounts of ethyl acetate. When necessary, metabolites were isolated by preparative GLC.

Metabolites 1-3 (M-I–M-III)—Peak 2 was isolated preparatively by GLC as one component (TLC and GLC) and had a fragrant odor; mass spectrum: *m/e* (%) 152 (M^+, $C_{10}H_{16}O$, 3), 134 (9), 119 (24), 108 (base), 93 (67), 72 (21), and 66 (28); IR: ν ($CHCl_3$) 3625, 3450, and 890 cm^{-1}. Its NMR spectrum showed two kinds of metabolites (M-I and M-II) in a 2:1 ratio. The major signal group assigned was: δ ($CDCl_3$) 4.84 and 4.63 (each 1H, s, *endo*-methylene), 3.80 [1H, q, $J_{5\text{-}exo\text{-}6\text{-}endo} = 7$, $J_{5\text{-}endo\text{-}6\text{-}endo} = 3$ Hz, —C*H*(OH)], 2.62 (1H, b, bridge head), 2.21 (1H, octet, $J_{5\text{-}exo\text{-}5\text{-}endo} = 13$, $J_{5\text{-}exo\text{-}6\text{-}endo} = 7$, $J_{5\text{-}exo\text{-}4} = 2$ Hz, *exo*-5), 1.89 (1H, b, *endo*-5), 1.63 (2H, b), and 0.98 and 1.04 (each 3H, *gem*-dimethyl). All of these M-I signals agreed well with those of the synthetic 6-*exo*-hydroxycamphene (I) (3).

The Jones oxidation of I yielded 6-oxocamphene [ν ($CHCl_3$) 1740 and 890 cm^{-1}] (4) with a minor ketone; mass spectrum (minor ketone): *m/e* (%) 150 (M^+, $C_{10}H_{14}O$, 25), 135 (12), 121 (15), 108 (41), 107 (98), 93 (base), 91 (54), and 79 (41); IR: ν ($CHCl_3$) 1740 and 890 cm^{-1}; NMR: δ ($CDCl_3$) 4.98 and 4.76 (each 1H, s), 3.08 (1H, b), and 1.16 and 1.07 (each 3H, s). These spectra revealed the minor ketone to be 7-oxocamphene. Therefore, 7-hydroxycamphene (II) (M-II) was estimated as the camphene metabolite.

The minor signal group found in the I NMR spectrum can be attributed to II: δ ($CDCl_3$) 4.73 and 4.48 (each 1H, s), 4.24 (1H, bs), 2.68 (1H, bs), and 1.04 (6H, s). The other minor ketone was obtained as the Jones oxidation product from M-III following M-I. Its spectra were considerably different from those of the above-mentioned ketones; mass spectrum: *m/e* (%) 150 (M^+, $C_{10}H_{14}O$, 7), 122 (16), 107 (base), 105 (12), 91 (28), and 79 (14); IR: ν ($CHCl_3$) 1740 cm^{-1}; NMR: δ ($CDCl_3$) 1.21, 1.04, and 1.00 (each 3H, s). Disappearance of the *endo*-methylene group suggests some camphene rearrangement. Accordingly, this ketone was assigned as 3-ketotricyclene

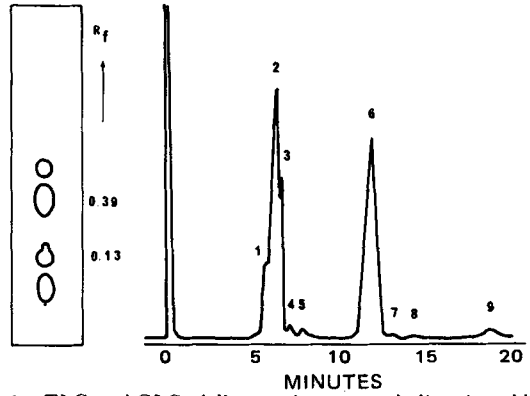

Figure 1—*TLC and GLC of* dl-*camphene metabolites in rabbits. The TLC solvent system was benzene–n-hexane–ethyl acetate (14:5:6); GLC utilized an SE-30 (5%) column.*

0022-3549/79/0700-0928$01.00/0

© 1979, American Pharmaceutical Association

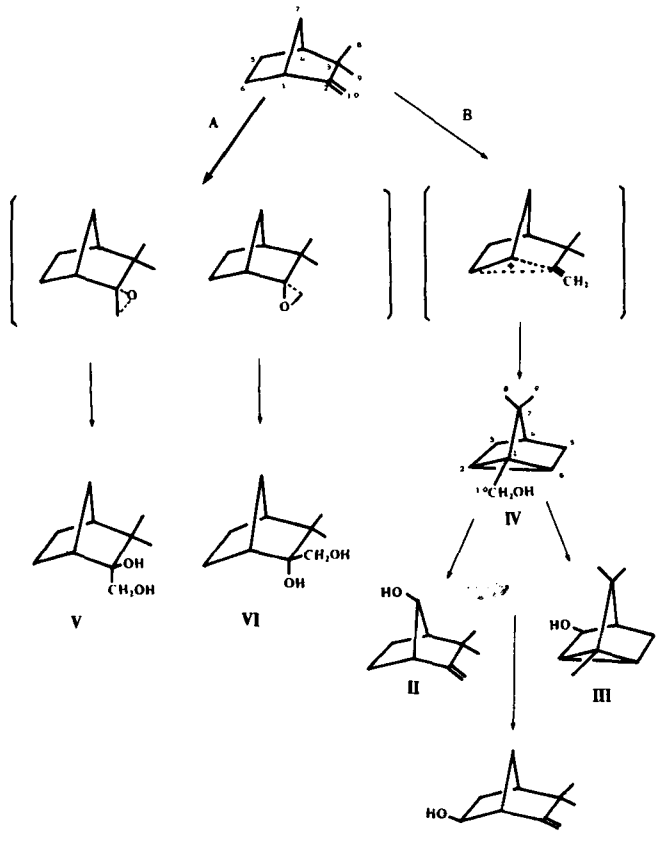

Scheme I—Proposed dl-*camphene metabolic pathway in rabbits. Pathway A is camphene epoxidation followed by cleavage of the oxirane ring by hydration. Pathway B consists of the formation of the nonclassical cation and cation rearrangement followed by hydroxylation.*

from those spectra. The corresponding alcohol, 3-hydroxytricyclene (III) (M-III), might be produced from camphene in rabbits. The peak 2 fragrance was due to I.

Metabolite 4 (M-IV)—Peak 1 also was isolated by preparative GLC. The mass spectrum of M-IV was: *m/e* (%) 152 (M^+, $C_{10}H_{16}O$, 35), 121 (49), 108 (base), 85 (72), and 79 (65); IR: ν ($CHCl_3$) 3640, 3455, 3070, and 850 cm^{-1}; NMR: δ ($CDCl_3$) 3.75 (2H, ss), A_2B_2 at 1.79, 1.68, 1.17, and 1.05 (each 1H, s); NMR: δ (dimethyl sulfoxide-d_6) 4.71 (t, J = 5 Hz, 1H, a primary hydroxyl). From these results, M-IV was identified as 10-hydroxytricyclene (IV).

Metabolite 5 (M-V)—The R_f 0.1 spot was in accord with peak 6, which was isolated by column chromatography. The mass spectrum of M-V was: *m/e* (%) 170 (M^+, $C_{10}H_{18}O_2$, 27), 152 (6), 139 (base), 121 (13), 101 (50), and 87 (60); IR: ν ($CHCl_3$) 3450 cm^{-1}. The NMR spectrum of the M-V acetate showed signals at δ 4.20 (in chloroform-d_1, methylene group adjacent to acetoxyl) and 3.27 (in dimethyl sulfoxide-d_6, s, *tert*-hydroxyl group) and clarified that M-V is a primary-tertiary diol.

This diol was oxidized by sodium periodate with sulfuric acid in ethanol and gave a ketone, camphenylon (VIII); IR: ν ($CHCl_3$) 1740 cm^{-1}. The NMR spectrum of VII showed only two signals of *gem*-dimethyl at δ 1.07 and 1.05. On the other hand, the spectrum of M-V showed four tertiary methyls [δ 1.02 and 0.98 (each 3H) and 0.96 (6H)] and two kinds of hydroxymethylene groups at δ 3.64 and 3.59. From these observations, it was decided that M-V consisted of two C-2 epimers (1:1) as shown in V and VI. The presence of diastereoisomers also was demonstrated by the remarkable melting-point difference; camphene-2,10-glycol obtained from rabbit urine had a melting point of 111–112° whereas that of 2-*exo*-hydroxycamphene glycol was reported as 196–198° (5).

DISCUSSION

The following camphene metabolic pathway (Scheme I) in rabbits can be proposed from the metabolites.

On the basis of the good glycol yields (260 mg), pathway A was assumed to be the main route. Glycol formation through epoxides has been demonstrated in many other metabolic pathways (6). The homoallylic camphene oxidation products (I–IV) apparently were formed through the nonclassical cation as the intermediate, as shown in pathway B. The ketone (VII) showed the negative optical rotation, $[\alpha]_D$ −8°, and the negative circular dichroism curve ($\Delta\epsilon$ −0.12) (Fig. 2*a*). On the other hand, the synthetic (+)-camphenylon was reported to give the positive circular dichroism curve ($\Delta\epsilon$ +0.50) (7).

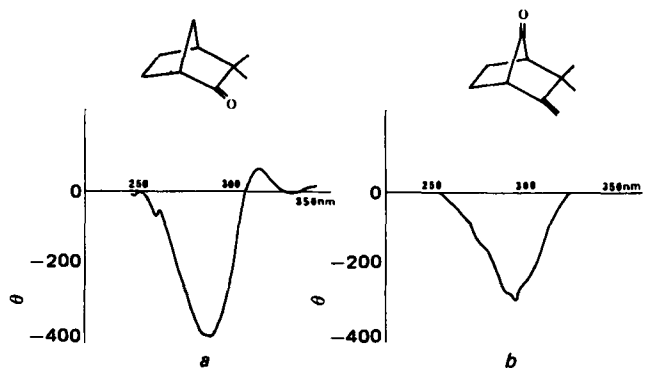

Figure 2—*Circular dichroism curves of camphenylon* (a) *and 7-oxocamphene* (b). *The concentrations were 3.77 × 10^{-2} M in ethanol* (a) *and 6.07 × 10^{-2} M in chloroform* (b).

Based on these results, the ratio was calculated as (−)/(+) = 0.6:0.4. Formation of the (−)-enantiomer from (−)-camphene was assumed to be more likely than formation of the (+)-enantiomer from (+)-camphene. Therefore, it was surmised that the degradation of (+)-camphene is faster than that of (−)-camphene and/or that the conversion of (+)-camphene into (−)-camphene may partly occur in rabbits just as in cicroprofen metabolism in rats (8). The negative circular dichroism curve of 7-oxocamphene (Fig. 2*b*) supports the proposal. The hydroxyl group orientation in II is considered to be *anti*- to the *gem*-dimethyl due to the steric factor.

EXPERIMENTAL[1]

Animals and Dosing—Five male albino rabbits[2], 2–3 kg, were starved for 2 days before the experiments. Camphene (10 g) was dissolved in water (90 ml) containing polysorbate[3] (0.1 g) and homogenized for 20 min. This solution (20 ml), followed by water (20 ml), was administered to each rabbit through a stomach tube. This camphene dose corresponds to 800 mg/kg, and the total amount of camphene fed to all rabbits equaled 8 g.

The animals were housed in individual stainless steel metabolism cages and were allowed rabbit food[4] and water *ad libitum*. The urine was collected daily for 3 days after drug administration and stored at 0–5° until use.

Extraction and Fractionation of Free Neutral Metabolites—The urine was centrifuged at under 3000 rpm at 0° to remove feces and hairs, and the supernate was used for experiments. The urine was adjusted to pH 4.7 with acetate buffer and then incubated with β-glucuronidase–arylsulfatase (3 ml/1000 ml of the fresh urine) at 37° for 48 hr followed by continuous ether extraction for 48 hr. The ether extracts were washed with 5% $NaHCO_3$ and 5% NaOH to remove the acidic and phenolic fractions, respectively, and dried over magnesium sulfate. Ether was evaporated under reduced pressure to give free neutral metabolites (1.471 g).

---

[1] *dl*-Camphene (above 90%) (Tokyo Kasei Kogyo), β-glucuronidase–arylsulfatase (Boehringer Manheim), Wako gel 200, and reagent grade solvents (Wako Chemicals) were used. A Shimadzu GC-6A gas chromatograph was equipped with a hydrogen flame-ionization detector and a thermal conductive detector. For neutral metabolite detection, the following were used: a 2-m × 2.6-mm i.d. glass column, 5% SE-30 or 5% OV-1 on Diasolid L (60–80 mesh); an injector at 250°; an oven programmed at 100–250° at 10°/min; a detector at 250°; and a nitrogen flow rate of 40 ml/min. For preparative use, the same size glass column of 5% DEGS on Diasolid L (60–80 mesh, AW-DMCS) (Japan Chromato) was employed under the same conditions.

TLC plates (20 × 20 cm) were glass, precoated with silica gel 60 F-254, and were 0.25 cm thick (Merck). The solvent system was benzene–ethyl acetate–*n*-hexane (14:5:6 v/v). The chromatograms were visualized with iodine vapor and under UV light (254 nm). NMR spectra were recorded on a Hitachi R-22 or a Varian T-60 spectrometer. IR spectra were run in chloroform using a Hitachi 215 spectrometer. Mass spectra were obtained on a Shimadzu LKB-9000B. UV spectra were obtained on a Shimadzu US 200S. Circular dichroism spectra were recorded on a JASCO ORD/UV-5 spectrometer with a circular dichroism attachment.

[2] Japanese White, Miyamoto Jikken Dobutsu.

[3] Tween 80.

[4] Oriental RC-4.

6-Oxocamphene from M-I—M-I (9 mg) was dissolved in acetone (1 ml). Anhydrous chromic acid (1.33 g) was added to the dilute sulfuric acid (1.15 g in 2 ml of water) and well stirred. This oxidant (0.1 ml) was added by drops to the acetone solution at 0°, and the reaction mixture was shaken for 20 min. After 13 hr, R_f 0.41 of M-I changed to 0.58. The reaction mixture was neutralized with 5% NaOH, extracted with methylene chloride (1 ml), and dried over magnesium sulfate. Evaporation of this solvent gave 6-oxocamphene (2.4 mg); mass spectrum: *m/e* (%) 150 (M^+, 54), 135 (24), 107 (base), 106 (78), 93 (40), 91 (60), 79 (34), and 77 (21); NMR: δ ($CDCl_3$) 5.07 and 4.82 (each 1H, s), 3.09 (1H), and 1.21 and 1.11 (each 3H, s).

Camphene-2,10-glycol 10-Acetate from M-V—Acetylation of M-V (100 mg) with acetic anhydride and pyridine gave its monoacetate (84.7 mg); mass spectrum: *m/e* (%) 214 (M^+, 4), 194 (13), 171 (82), 152 (78), 137 (53), 109 (base), and 43 (77); IR: ν ($CHCl_3$) 3550 and 1730 cm^{-1}; NMR: δ ($CDCl_3$) 4.20 (2H, s), 2.08 (3H, s), and 1.03 and 0.93 (each 3H, s); NMR: δ (dimethyl sulfoxide-d_6) 4.03 (2H, s), 2.03 (3H, s), 0.93 and 0.88 (each 3H, s), and 3.27 (1H, s, exchanged with deuterium oxide). The anhydrous ethereal solution (10 ml) of lithium aluminum hydride (38.8 mg) was added to the ethereal solution (20 ml) of the monoacetate (80 mg) under a nitrogen atmosphere and stirred at room temperature for 4 hr. Decomposition of the excess lithium aluminum hydride with ethyl acetate, filtration through a short column packed with magnesium sulfate, and evaporation of the solvent recovered camphene-2,10-glycols.

Camphenylon (VII) from M-V—The ethanol solution (5 ml) of M-V (100 mg) was added to the sodium periodate (130 mg)–1 *N* sulfuric acid solution (6 ml) at 40° and stirred for 13 hr until it became transparent (9). The reaction mixture was neutralized with 5% $NaHCO_3$, extracted with ether, and dried over magnesium sulfate. Evaporation of the solvent gave camphenylon (VII) (23.0 mg); mass spectrum: *m/e* (%) 138 (M^+, 28), 95 (10), 81 (5), 72 (14), 69 (base), 67 (67), and 41 (31); UV: λ_{max} (ethanol) 287 (ε 24) and 240 (21) nm; $[\alpha]_D$ −8.3° (c 2.4, $CHCl_3$).

REFERENCES

(1) T. Ishida, Y. Asakawa, M. Okano, and T. Aratani, *Tetrahedron Lett.*, **1977**, 2437.

(2) K. Moersdorf, *Chim. Ther.*, **1966**, 442.

(3) M. Julia, D. Mansuy, and P. Detraz, *Tetrahedron Lett.*, **1976**, 2141.

(4) Y. Uchio, thesis.

(5) P. Hirsjarvi, D. Klenberg, M. Patala, and P. Eenila, *Suom. Kemistil.*, **34B**, 152 (1961).

(6) J. W. Regan and L. F. Bjeldane, *J. Agr. Food Chem.*, **24**, 377 (1976). R. P. Hopkins, C. J. W. Brooks, and L. Young, *Biochem. J.*, **82**, 457 (1962). R. Miura, S. Honmura, and M. Nakazaki, *Tetrahedron Lett.*, **1968**, 5271.

(7) C. Coulombeau and A. Rassat, *Bull. Soc. Chim. Fr.*, **1966**, 3752.

(8) A. V. Dean, S. J. Lan, K. J. Kripalani, L. T. Difazio, and E. C. Schreiber, *Xenobiotica*, **7**, 549 (1977).

(9) L. F. Fieser and M. Fieser, "Reagents for Organic Synthesis," Wiley, New York, N.Y., 1967, p. 815.

ACKNOWLEDGMENTS

The authors thank Dr. Y. Hirose, Institute of Food Chemistry, for the mass spectra and Dr. M. Julia, Centre National de la Recherche Scientifique, for the NMR spectrum of 6-*exo*-hydroxycamphene.

New Compounds: Arylsulfonylhydrazones Derived from Various Heterocycles

RICHARD JUNEAU *x, SCOTT MITCHELL *, and GARY WOLGAMOTT ‡

Received November 20, 1978, from the **Department of Medicinal Chemistry, School of Pharmacy, and the* ‡*Department of Microbiology, Southwestern Oklahoma State University, Weatherford, OK 73096.* Accepted for publication January 24, 1979.

Abstract □ Ten arylsulfonylhydrazones were prepared from various heterocycles. The antimicrobial activity of these compounds was investigated, as was the cytotoxic activity of one of them.

Keyphrases □ Arylsulfonylhydrazones—derived from various heterocycles, antimicrobial and cytotoxic activity □ Hydrazine—derivatives, various heterocycles, antimicrobial and cytotoxic activity □ Antineoplastic agents, potential—arylsulfonylhydrazones, derived from various heterocycles, antimicrobial and cytotoxic activity

Arylsulfonylhydrazones of 2-formylpyridine and its oxide have been investigated as cytotoxic agents (1). Since studies involving the preparation and biological properties of arylsulfonylhydrazones derived from aromatic heterocycles other than pyridine and quinoline are not numerous, the synthesis and antibacterial screening of the compounds listed in Table I were attempted.

DISCUSSION

Chemistry—The compounds listed in Table I were synthesized by standard procedures, consisting of reaction between hydrazine and *p*-toluenesulfonyl chloride or α-toluenesulfonyl chloride followed by condensation with the appropriate heterocyclic 2-carboxaldehyde (Scheme I). For IV and IX, the requisite 5-nitrofurfural was obtained by the acid hydrolysis of 5-nitrofurfurylidene diacetate according to a literature method (2). Compounds IV, VIII, and IX are not new compounds and were reported previously (3–5).

The hydrazone linkage in the synthesized compounds allows geometric isomers to be formed. Attempts to detect *E*- and *Z*-isomers by TLC in several solvent systems were successful only with III and VII. Compounds III and VII demonstrated the presence of a trace amount of a second compound. However, only in the case of III were the two compounds nonoverlapping and amenable to dry column chromatography.

The IR and NMR spectra of III*a* and III*b* were practically superimposable and offered no aid in configurational assignments. Compound III*a* showed a bathochromic shift in the UV spectrum of only 3 nm (285–288) in going from a polar to a nonpolar solvent (ethanol to benzene), whereas III*b* showed a bathochromic shift of 10 nm (272–282). These data suggest the *Z*-configuration for III*b*, the trace component and more mobile compound on TLC (silica gel, chloroform), and the *E*-configu-

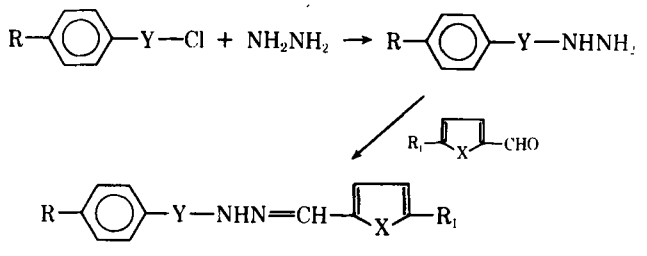

R = H, CH_3; Y = SO_2, CH_2SO_2;
X = O, N, S; R_1 = H, NO_2

Scheme I

0022-3549/79/0700-0930$01.00/0

© 1979, American Pharmaceutical Association

6-Oxocamphene from M-I—M-I (9 mg) was dissolved in acetone (1 ml). Anhydrous chromic acid (1.33 g) was added to the dilute sulfuric acid (1.15 g in 2 ml of water) and well stirred. This oxidant (0.1 ml) was added by drops to the acetone solution at 0°, and the reaction mixture was shaken for 20 min. After 13 hr, R_f 0.41 of M-I changed to 0.58. The reaction mixture was neutralized with 5% NaOH, extracted with methylene chloride (1 ml), and dried over magnesium sulfate. Evaporation of this solvent gave 6-oxocamphene (2.4 mg); mass spectrum: *m/e* (%) 150 (M^+, 54), 135 (24), 107 (base), 106 (78), 93 (40), 91 (60), 79 (34), and 77 (21); NMR: δ ($CDCl_3$) 5.07 and 4.82 (each 1H, s), 3.09 (1H), and 1.21 and 1.11 (each 3H, s).

Camphene-2,10-glycol 10-Acetate from M-V—Acetylation of M-V (100 mg) with acetic anhydride and pyridine gave its monoacetate (84.7 mg); mass spectrum: *m/e* (%) 214 (M^+, 4), 194 (13), 171 (82), 152 (78), 137 (53), 109 (base), and 43 (77); IR: ν ($CHCl_3$) 3550 and 1730 cm^{-1}; NMR: δ ($CDCl_3$) 4.20 (2H, s), 2.08 (3H, s), and 1.03 and 0.93 (each 3H, s); NMR: δ (dimethyl sulfoxide-d_6) 4.03 (2H, s), 2.03 (3H, s), 0.93 and 0.88 (each 3H, s), and 3.27 (1H, s, exchanged with deuterium oxide). The anhydrous ethereal solution (10 ml) of lithium aluminum hydride (38.8 mg) was added to the ethereal solution (20 ml) of the monoacetate (80 mg) under a nitrogen atmosphere and stirred at room temperature for 4 hr. Decomposition of the excess lithium aluminum hydride with ethyl acetate, filtration through a short column packed with magnesium sulfate, and evaporation of the solvent recovered camphene-2,10-glycols.

Camphenylon (VII) from M-V—The ethanol solution (5 ml) of M-V (100 mg) was added to the sodium periodate (130 mg)–1 *N* sulfuric acid solution (6 ml) at 40° and stirred for 13 hr until it became transparent (9). The reaction mixture was neutralized with 5% $NaHCO_3$, extracted with ether, and dried over magnesium sulfate. Evaporation of the solvent gave camphenylon (VII) (23.0 mg); mass spectrum: *m/e* (%) 138 (M^+, 28), 95 (10), 81 (5), 72 (14), 69 (base), 67 (67), and 41 (31); UV: λ_{max} (ethanol) 287 (ε 24) and 240 (21) nm; $[\alpha]_D$ −8.3° (c 2.4, $CHCl_3$).

REFERENCES

(1) T. Ishida, Y. Asakawa, M. Okano, and T. Aratani, *Tetrahedron Lett.*, **1977**, 2437.

(2) K. Moersdorf, *Chim. Ther.*, **1966**, 442.

(3) M. Julia, D. Mansuy, and P. Detraz, *Tetrahedron Lett.*, **1976**, 2141.

(4) Y. Uchio, thesis.

(5) P. Hirsjarvi, D. Klenberg, M. Patala, and P. Eenila, *Suom. Kemistil.*, **34B**, 152 (1961).

(6) J. W. Regan and L. F. Bjeldane, *J. Agr. Food Chem.*, **24**, 377 (1976). R. P. Hopkins, C. J. W. Brooks, and L. Young, *Biochem. J.*, **82**, 457 (1962). R. Miura, S. Honmura, and M. Nakazaki, *Tetrahedron Lett.*, **1968**, 5271.

(7) C. Coulombeau and A. Rassat, *Bull. Soc. Chim. Fr.*, **1966**, 3752.

(8) A. V. Dean, S. J. Lan, K. J. Kripalani, L. T. Difazio, and E. C. Schreiber, *Xenobiotica*, **7**, 549 (1977).

(9) L. F. Fieser and M. Fieser, "Reagents for Organic Synthesis," Wiley, New York, N.Y., 1967, p. 815.

ACKNOWLEDGMENTS

The authors thank Dr. Y. Hirose, Institute of Food Chemistry, for the mass spectra and Dr. M. Julia, Centre National de la Recherche Scientifique, for the NMR spectrum of 6-*exo*-hydroxycamphene.

New Compounds: Arylsulfonylhydrazones Derived from Various Heterocycles

RICHARD JUNEAU *x, SCOTT MITCHELL *, and GARY WOLGAMOTT ‡

Received November 20, 1978, from the **Department of Medicinal Chemistry, School of Pharmacy, and the* ‡*Department of Microbiology, Southwestern Oklahoma State University, Weatherford, OK 73096.* Accepted for publication January 24, 1979.

Abstract □ Ten arylsulfonylhydrazones were prepared from various heterocycles. The antimicrobial activity of these compounds was investigated, as was the cytotoxic activity of one of them.

Keyphrases □ Arylsulfonylhydrazones—derived from various heterocycles, antimicrobial and cytotoxic activity □ Hydrazine—derivatives, various heterocycles, antimicrobial and cytotoxic activity □ Antineoplastic agents, potential—arylsulfonylhydrazones, derived from various heterocycles, antimicrobial and cytotoxic activity

Arylsulfonylhydrazones of 2-formylpyridine and its oxide have been investigated as cytotoxic agents (1). Since studies involving the preparation and biological properties of arylsulfonylhydrazones derived from aromatic heterocycles other than pyridine and quinoline are not numerous, the synthesis and antibacterial screening of the compounds listed in Table I were attempted.

DISCUSSION

Chemistry—The compounds listed in Table I were synthesized by standard procedures, consisting of reaction between hydrazine and *p*-toluenesulfonyl chloride or α-toluenesulfonyl chloride followed by condensation with the appropriate heterocyclic 2-carboxaldehyde (Scheme I). For IV and IX, the requisite 5-nitrofurfural was obtained by the acid hydrolysis of 5-nitrofurfurylidene diacetate according to a literature method (2). Compounds IV, VIII, and IX are not new compounds and were reported previously (3–5).

The hydrazone linkage in the synthesized compounds allows geometric isomers to be formed. Attempts to detect *E*- and *Z*-isomers by TLC in several solvent systems were successful only with III and VII. Compounds III and VII demonstrated the presence of a trace amount of a second compound. However, only in the case of III were the two compounds nonoverlapping and amenable to dry column chromatography.

The IR and NMR spectra of III*a* and III*b* were practically superimposable and offered no aid in configurational assignments. Compound III*a* showed a bathochromic shift in the UV spectrum of only 3 nm (285–288) in going from a polar to a nonpolar solvent (ethanol to benzene), whereas III*b* showed a bathochromic shift of 10 nm (272–282). These data suggest the *Z*-configuration for III*b*, the trace component and more mobile compound on TLC (silica gel, chloroform), and the *E*-configu-

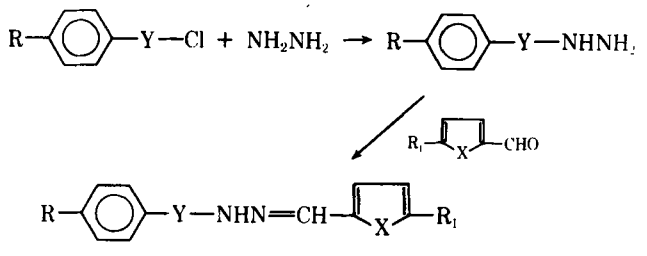

R = H, CH_3; Y = SO_2, CH_2SO_2;
X = O, N, S; R_1 = H, NO_2

Scheme I

0022-3549/79/0700-0930$01.00/0

© 1979, American Pharmaceutical Association

Table I—Arylsulfonylhydrazones

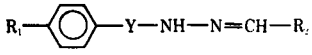

Compound[a]	R_1	Y	R_2	Formula	Melting Point	Analysis, %		
							Calc.	Found
I	H	$-CH_2SO_2-$		$C_{12}H_{13}N_3O_2S$	169–173°	C	54.74	54.77
						H	4.98	5.04
						N	15.96	16.00
II	H	$-CH_2SO_2-$		$C_{12}H_{12}N_2O_2S_2$	144–146°	C	51.41	51.50
						H	4.31	4.30
						N	9.99	10.03
IIIa and IIIb	H	$-CH_2SO_2-$		$C_{12}H_{12}N_2O_3S$	108–109°	C	54.53	54.46
					110–112°	H	4.58	4.61
						N	10.59	10.43
IV	H	$-CH_2SO_2-$		$C_{12}H_{11}N_3O_5S$	180–182°	C	46.60	46.48
						H	3.59	3.48
						N	13.59	13.58
V	H	$-CH_2SO_2-$	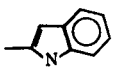	$C_{16}H_{15}N_3O_2S$	188–190°	C	61.33	61.23
						H	4.82	4.96
						N	13.41	13.43
VI	CH_3	$-SO_2-$		$C_{12}H_{13}N_3O_2S$	175–180°	C	54.74	54.80
						H	4.98	5.01
						N	15.96	15.94
VII	CH_3	$-SO_2-$		$C_{12}H_{12}N_2O_3S$	110–112°	C	54.53	54.53
						H	4.58	4.66
						N	10.60	10.52
VIII	CH_3	$-SO_2-$		$C_{12}H_{12}N_2O_2S_2$	140–141°	C	51.41	51.42
						H	4.31	4.30
						N	9.99	9.96
IX	CH_3	$-SO_2-$		$C_{12}H_{11}N_3O_5S$	149–150°	C	46.60	46.71
						H	3.59	3.62
						N	13.59	13.61
X	CH_3	$-SO_2-$	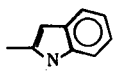	$C_{16}H_{15}N_3O_2S$	174–176°	C	61.33	61.20
						H	4.82	4.92
						N	13.41	13.39

[a] All compounds were recrystallized from alcohol, except IIIa and IIIb which were recrystallized from ether.

ration for IIIa in analogy to previously prepared thiosemicarbazones (6).

Biological—Compounds I–X were screened for antibacterial activity against *Staphylococcus aureus* and *Escherichia coli* and were inactive except for the weak inhibitory activity by IV. Because VII is the pyrrole analog of the active arylsulfonylhydrazone derived from 2-formylpyridine (1), it was chosen for antineoplastic screening, but it was devoid of activity.

EXPERIMENTAL[1]

General Synthetic Procedure—The heterocyclic 2-carboxaldehyde, 0.01 mole, was dissolved in 20 ml of methanol and maintained at ice bath temperatures. To this well-stirred solution was added dropwise the sulfonylhydrazide (0.01 mole) in 20 ml of methanol. After addition, the mixture was stirred for an additional 1 hr and placed in the refrigerator overnight. Then the solvent was removed under vacuum to yield semicrystalline solids. The solids were recrystallized from solvents (Table I) and were easily characterized by their NMR and IR spectra.

Biological Screening—The standard filter paper disk method on an agar culture medium was used to screen for antimicrobial activity against *S. aureus* and *E. coli*[2]. The disk was saturated with a methanol solution of the sulfonylhydrazone, and solutions as concentrated as 100 mg/ml were used before inactivity was pronounced.

Compound VII was screened against P-388 leukemia in CDF-1 mice. The compound was administered intraperitoneally as a suspension in polysorbate 80 and 5% ethanol. Doses as high as 120 mg/kg failed to show increased survival time relative to controls.

[1] Melting points were taken with a Thomas-Hoover Uni-Melt apparatus and are uncorrected. IR spectra were determined with a Beckman AccuLab spectrophotometer. NMR spectra were obtained with a Varian model 360-A spectrometer relative to an internal standard of tetramethylsilane with deuterochloroform or deuterated dimethyl sulfoxide as the solvent. UV spectra were determined with a Beckman model 25 spectrophotometer. TLC was performed on silica gel (Eastman chromagram) and visualized with either iodine vapors or UV light. Dry column chromatography was performed on silica gel Woelm (ICN Pharmaceuticals) with chloroform as the solvent. Elemental analyses were performed by Galbraith Laboratories, Knoxville, Tenn.

[2] The bacterial cells employed in the screening test were stock cultues originally derived from Midwest Culture Service (Terre Haute, Ind.) and currently designated as *Staphylococcus aureus* (SW43) and *Escherichia coli* (SW17).

REFERENCES

(1) A. C. Sartorelli, K. C. Agrawal, B. A. Booth, J. Pittman, D. G. Bartholomew, and A. D. Broom, *J. Med. Chem.*, **19**, 830 (1976).

(2) H. Gilman and G. F. Wright, *J. Org. Chem.*, **52**, 2550 (1930).

(3) F. K. Kirchner, U.S. pat. 3,651,057 (Mar. 21, 1972); through *Chem. Abstr.*, **77**, 48212n (1972).

(4) B. W. Mueller, *Helv. Chim. Acta*, **61**, 325 (1978).

(5) W. Hoyle, *J. Chem. Soc. C*, **1967**, 690.

(6) T. L. Lemke, T. W. Shek, L. A. Cates, and L. K. Smith, *J. Med. Chem.*, **20**, 1351 (1977).

ACKNOWLEDGMENTS

The authors are indebted to Dr. Krishna Agrawal, Department of Pharmacology, Tulane University School of Medicine, for providing the anticancer screening.

S. Mitchell is an undergraduate research participant.

Mathematical Treatment of Linear Mammillary Models Using Inverse Laplace Transforms

Keyphrases □ Mammillary models, linear—mathematics, inverse Laplace transforms □ Laplace transforms—inverse, in mathematical treatment of linear mammillary models □ Mathematics—inverse Laplace transforms in linear mammillary models

To the Editor:

In discussing linear mammillary models, Benet (1) used Laplace transform methods to solve the differential equations describing the compartmental exchanges of drug. Several investigators (2–5) described this method and gave it broader application and understanding relative to this type of pharmacokinetic modeling. However, none of these authors indicated a mathematical correction in the use of the Laplace transform to derive Eqs. 12 and 23 (1). In this article, we attempt to identify previous mathematical oversights and to offer a corrected derivation of the equations describing this model.

Equation 12 (1):

$$a_{s,1} = \frac{k^0(s + E_2)(s + E_3)(1 - e^{-bs})}{s(s + \alpha)(s + \beta)(s + \gamma)} \quad \text{(Eq. 1)}$$

is the Laplace transform for the amount of drug in the central compartment, Compartment 1, in a three-compartment model for an intravenous infusion over the time interval $0 \leq t \leq b$. The given equation is correct but, in determining the inverse Laplace transform of $a_{s,1}$, the numerator $k^0(s + E_2)(s + E_3)(1 - e^{-bs})$ has been misinterpreted as a polynomial in the variable s and, therefore, the General Partial Fraction Theorem has been misapplied. The presence of the factor $(1 - e^{-bs})$ destroys the polynomial character of the numerator, so neither the General Partial Fraction Theorem nor the Heaviside expansion immediately pertains (6).

The following modifications should be made:

$$a_{s,1} = \frac{k^0(s + E_2)(s + E_3)}{s(s + \alpha)(s + \beta)(s + \gamma)} - \frac{k^0(s + E_2)(s + E_3)}{s(s + \alpha)(s + \beta)(s + \gamma)} e^{-bs} \quad \text{(Eq. 2)}$$

The first term in this difference is the quotient of two polynomials, so the Heaviside expansion applies as follows:

$$L^{-1}\left\{\frac{k^0(s + E_2)(s + E_3)}{s(s + \alpha)(s + \beta)(s + \gamma)}\right\} = \frac{k^0(E_2)(E_3)}{\alpha\beta\gamma} + \frac{k^0(E_2 - \alpha)(E_3 - \alpha)}{-\alpha(\beta - \alpha)(\gamma - \alpha)} e^{-\alpha t} + \frac{k^0(E_2 - \beta)(E_3 - \beta)}{-\beta(\alpha - \beta)(\gamma - \beta)} e^{-\beta t} + \frac{k^0(E_2 - \gamma)(E_3 - \gamma)}{-\gamma(\alpha - \gamma)(\beta - \gamma)} e^{-\gamma t} \quad \text{(Eq. 3)}$$

To compute the inverse Laplace transform of the second term, a shift theorem should be used. Let $H(t - b)$ be a function defined by the expression

$$H(t - b) = \begin{cases} 0 & t < b \\ 1 & t > b \end{cases} \quad \text{(Eq. 4)}$$

This function is usually called the unit-step function or the Heaviside function (7). With $H(t - b)$, the needed shift theorem is easily stated. Let $b > 0$ and let the Laplace transforms of $F(t)$, $L\{F(t)\}$, exist. Then:

$$L\{F(t - b)H(t - b)\} = e^{-bs}L\{F(t)\} \quad \text{(Eq. 5)}$$

By applying this theorem under the assumption that:

$$F(t) = L^{-1}\left\{\frac{k^0(s + E_2)(s + E_3)}{s(s + \alpha)(s + \beta)(s + \gamma)}\right\} \quad \text{(Eq. 6)}$$

it is found that:

$$L^{-1}\left\{\frac{k^0(s + E_2)(s + E_3)}{s(s + \alpha)(s + \beta)(s + \gamma)} e^{-bs}\right\} = \left\{\frac{k^0E_2E_3}{\alpha\beta\gamma} + \frac{k^0(E_2 - \alpha)(E_3 - \alpha)}{-\alpha(\beta - \alpha)(\gamma - \alpha)} e^{-\alpha(t-b)} + \frac{k^0(E_2 - \beta)(E_3 - \beta)}{-\beta(\alpha - \beta)(\gamma - \beta)} e^{-\beta(t-b)} + \frac{k^0(E_2 - \gamma)(E_3 - \gamma)}{-\gamma(\alpha - \gamma)(\beta - \gamma)} e^{-\gamma(t-b)}\right\} H(t - b) \quad \text{(Eq. 7)}$$

When Eqs. 3 and 7 are combined, the solution becomes:

$$a_1 = k^0\left[\frac{E_2E_3}{\alpha\beta\gamma} - \frac{(E_2 - \alpha)(E_3 - \alpha)}{\alpha(\beta - \alpha)(\gamma - \alpha)} e^{-\alpha t} - \frac{(E_2 - \beta)(E_3 - \beta)}{\beta(\alpha - \beta)(\gamma - \beta)} e^{-\beta t} - \frac{(E_2 - \gamma)(E_3 - \gamma)}{\gamma(\alpha - \gamma)(\beta - \gamma)} e^{-\gamma t}\right] \quad \text{(Eq. 8)}$$

in the time interval $0 \leq t \leq b$ and:

$$a_1 = k^0\left[\frac{(E_2 - \alpha)(E_3 - \alpha)(e^{\alpha b} - 1)}{\alpha(\beta - \alpha)(\gamma - \alpha)} e^{-\alpha t} + \frac{(E_2 - \beta)(E_3 - \beta)(e^{\beta b} - 1)}{\beta(\alpha - \beta)(\gamma - \beta)} e^{-\beta t} + \frac{(E_2 - \gamma)(E_3 - \gamma)(e^{\gamma b} - 1)}{\gamma(\alpha - \gamma)(\beta - \gamma)} e^{-\gamma t}\right] \quad \text{(Eq. 9)}$$

in the time interval $t > b$. This solution coincides exactly with that of Benet (1) for $t > b$ and gives a more explicit solution for $0 \leq t \leq b$. It is a fact that if the constant b is allowed to vary while infusion continues, *i.e.*, $b = t$ in Ref. 1, one can simplify Benet's solution to the one proposed. However, changing constants to variables in the middle of a derivation confuses the reader and the simplification requires very tedious calculations. The proposed approach is more direct and leaves b as a fixed constant in the model.

With Eq. 23 (1):

$$a_{s,3} = \frac{k_{13}k^0(s + E_2)(1 - e^{-bs})}{s^2(s + \alpha)(s + \beta)} \quad \text{(Eq. 10)}$$

Benet wished to demonstrate how to handle a partial fraction decomposition in which the denominator has a repeated root. However, the numerator is misread as a polynomial in s. The term $a_{s,3}$ may be written as follows:

$$a_{s,3} = k_{13}k^0\left\{\frac{s + E_2}{s^2(s + \alpha)(s + \beta)} - \frac{(s + E_2)e^{-bs}}{s^2(s + \alpha)(s + \beta)}\right\} \quad \text{(Eq. 11)}$$

Then, by using the expansion described by Benet in the Appendix (1) and the shift theorem quoted above, the following expression is obtained from Eq. 11:

$$L^{-1}\{a_{s,3}\} = k_{13}k^0\left[\frac{1 - (\alpha + \beta)E_2}{\alpha\beta} + \frac{tE_2}{\alpha\beta} + \frac{(E_2 - \alpha)e^{-\alpha t}}{\alpha^2(\beta - \alpha)} + \frac{(E_2 - \beta)}{\beta^2(\alpha - \beta)} e^{-\beta t}\right] \quad \text{(Eq. 12)}$$

0022-3549/79/0700-0932$01.00/0
© 1979, American Pharmaceutical Association

for $0 \leq t \leq b$ and:

$$L^{-1}\{a_{s,3}\} = k_{13}k^0\left[\frac{E_2 b}{\alpha\beta} + \frac{(E_2-\alpha)(1-e^{\alpha b})e^{-\alpha t}}{\alpha^2(\beta-\alpha)} + \frac{(E_2-\beta)(1-e^{\beta b})e^{-\beta t}}{\beta^2(\alpha-\beta)}\right] \quad \text{(Eq. 13)}$$

for $t > b$. Equation 13 coincides with Eq. 24 (1), which is valid for the model only after infusion has ceased. Equation 12 gives a very explicit form of the solution during the infusion time.

It is hoped that the corrections made in this article can contribute to the broader application and understanding of the method proposed by Benet.

(1) L. Z. Benet, *J. Pharm. Sci.*, **61**, 536 (1972).

(2) D. P. Vaughan and A. Trainor, *J. Pharmacokinet. Biopharm.*, **3**, 203 (1975).

(3) D. P. Vaughan, D. J. H. Mallard, A. Trainor, and M. Mitchard, *Eur. J. Clin. Pharmacol.*, **8**, 141 (1975).

(4) M. Gibaldi and D. Perrier, "Pharmacokinetics," Dekker, New York, N.Y., 1975, pp. 273–279.

(5) J. G. Wagner, "Fundamentals of Clinical Pharmacokinetics," Drug Intelligence Publications, Hamilton, Ill., 1975, pp. 231–246.

(6) R. V. Churchill, "Operational Mathematics," 3rd ed., McGraw-Hill, New York, N.Y., 1972, pp. 1–84.

(7) W. R. Derrick and S. I. Grossman, "Elementary Differential Equations with Applications," Addison-Wesley, Reading, Mass., 1976, pp. 214–254.

George E. Haborak
Department of Mathematics
College of Charleston
Charleston, SC 29401

Joseph D. Benmaman ˣ
James W. Warren, Jr.
College of Pharmacy
Medical University of South Carolina
Charleston, SC 29403

Received November 20, 1978.
Accepted for publication April 12, 1979.

Mathematical Treatment of Linear Mammillary Models Using Inverse Laplace Transforms: A Reply

Keyphrases □ Mammillary models, linear—mathematics, inverse Laplace transforms □ Laplace transforms—inverse, in mathematical treatment of linear mammillary models □ Mathematics—inverse Laplace transforms in linear mammillary models

To the Editor:

The impetus for preparing my 1972 paper on the general treatment of linear mammillary models as used in pharmacokinetics (1) was a sense of frustration with the pages of mathematical derivation included as part of each pharmacokinetic paper that appeared in print up to that time. As I stated in the introduction (1): "This paper intends to present some very simplified general treatments which will allow workers to derive equations for any linear mammillary compartment model with any first- or zero-order input process." I believed then, as I believe now, that pharmacokinetic compartment models are useful only as a convenient means to describe and predict the time course of measurable body fluid compartments such as plasma, blood, and urine following single and multiple doses. I did not consider the possibility of input into a peripheral compartment or the general derivation for such a treatment, as was described by Vaughan and Trainor (2), since I believe this use of compartment models is inappropriate, *i.e.*, defining one compartment in the model as specifically describing an organ in the body such as the liver. Such a combination of compartment and perfusion models requires exponential terms that are not needed to fit the minimal compartment model adequately and leads to difficulties in interpreting "absorption" rate constants for such a system.

Haborak *et al.* (3) questioned the solution of two equations in my earlier paper, stating: "The presence of the factor $(1 - e^{-bs})$ destroys the polynomial character of the numerator, so neither the General Partial Fraction Theorem nor the Heaviside expansion immediately pertains." They are correct. However, the correct solution is also obtained using the one-step method that I proposed (1, 4). Apparently, the restriction concerning the polynomial character of the numerator may be relaxed when exponential functions appear in the numerator due to the inclusion of a zero-order input function. Since I am no mathematician, I shall leave the proof of this exception to others. However, I have tested the one-step method and found that it gives the correct equations for the usual multicompartment pharmacokinetic models with zero-order input into the central or peripheral compartments.

The authors of the preceding article (3) were most disturbed by the fact that I proposed the use of a single equation to describe the time course of drug in the central compartment during infusion *and* when infusion has ceased. Although I did explain, following Eq. 13 (1), that this approach was equivalent to using two independent variables, t = clock time and b = infusion time, Haborak *et al.* (3) stated that "changing constants to variables in the middle of a derivation confuses the reader . . .." I must admit that this point has led to questions by a number of readers over the years. Perhaps the preceding note and this reply will help readers to understand the appropriate use of Eqs. 13 and 24 in the 1972 paper (1).

Haborak *et al.* (3) also stated that my use of a single equation "requires very tedious calculations." This statement I do not understand; it certainly would be quicker to calculate A_1 values in Eq. 13 on any programmable calculator using a single equation with two inputs during the infusion phase than it would be using two different equations. But "calculation" is not the important functional use for Eq. 13. In 1972, I was concerned that investigators were fitting data from the postinfusion phase separately from the infusion phase. This procedure is inappropriate, as I stated previously (1). In 1972, many of the computer programs used to fit pharmacokinetic data, particularly the BMD series (5), only allowed the investigator to fit one function at a time. However, I stated then (1) that: "All the least-squares nonlinear fitting programs usually utilized in pharmacokinetic treatments have the ability to fit data to Eq. 13. . . ."

In conclusion, the previous article (3) points out the detailed solution for the Laplace derivation when an exponential operator term appears in the numerator of the

0022-3549/79/0700-0933$01.00/0

© 1979, American Pharmaceutical Association

for $0 \leq t \leq b$ and:

$$L^{-1}\{a_{s,3}\} = k_{13}k^0\left[\frac{E_2 b}{\alpha\beta} + \frac{(E_2-\alpha)(1-e^{\alpha b})e^{-\alpha t}}{\alpha^2(\beta-\alpha)} + \frac{(E_2-\beta)(1-e^{\beta b})e^{-\beta t}}{\beta^2(\alpha-\beta)}\right] \quad \text{(Eq. 13)}$$

for $t > b$. Equation 13 coincides with Eq. 24 (1), which is valid for the model only after infusion has ceased. Equation 12 gives a very explicit form of the solution during the infusion time.

It is hoped that the corrections made in this article can contribute to the broader application and understanding of the method proposed by Benet.

(1) L. Z. Benet, *J. Pharm. Sci.*, **61**, 536 (1972).

(2) D. P. Vaughan and A. Trainor, *J. Pharmacokinet. Biopharm.*, **3**, 203 (1975).

(3) D. P. Vaughan, D. J. H. Mallard, A. Trainor, and M. Mitchard, *Eur. J. Clin. Pharmacol.*, **8**, 141 (1975).

(4) M. Gibaldi and D. Perrier, "Pharmacokinetics," Dekker, New York, N.Y., 1975, pp. 273–279.

(5) J. G. Wagner, "Fundamentals of Clinical Pharmacokinetics," Drug Intelligence Publications, Hamilton, Ill., 1975, pp. 231–246.

(6) R. V. Churchill, "Operational Mathematics," 3rd ed., McGraw-Hill, New York, N.Y., 1972, pp. 1–84.

(7) W. R. Derrick and S. I. Grossman, "Elementary Differential Equations with Applications," Addison-Wesley, Reading, Mass., 1976, pp. 214–254.

George E. Haborak
Department of Mathematics
College of Charleston
Charleston, SC 29401

Joseph D. Benmaman ˣ
James W. Warren, Jr.
College of Pharmacy
Medical University of South Carolina
Charleston, SC 29403

Received November 20, 1978.
Accepted for publication April 12, 1979.

Mathematical Treatment of Linear Mammillary Models Using Inverse Laplace Transforms: A Reply

Keyphrases □ Mammillary models, linear—mathematics, inverse Laplace transforms □ Laplace transforms—inverse, in mathematical treatment of linear mammillary models □ Mathematics—inverse Laplace transforms in linear mammillary models

To the Editor:

The impetus for preparing my 1972 paper on the general treatment of linear mammillary models as used in pharmacokinetics (1) was a sense of frustration with the pages of mathematical derivation included as part of each pharmacokinetic paper that appeared in print up to that time. As I stated in the introduction (1): "This paper intends to present some very simplified general treatments which will allow workers to derive equations for any linear mammillary compartment model with any first- or zero-order input process." I believed then, as I believe now, that pharmacokinetic compartment models are useful only as a convenient means to describe and predict the time course of measurable body fluid compartments such as plasma, blood, and urine following single and multiple doses. I did not consider the possibility of input into a peripheral compartment or the general derivation for such a treatment, as was described by Vaughan and Trainor (2), since I believe this use of compartment models is inappropriate, *i.e.*, defining one compartment in the model as specifically describing an organ in the body such as the liver. Such a combination of compartment and perfusion models requires exponential terms that are not needed to fit the minimal compartment model adequately and leads to difficulties in interpreting "absorption" rate constants for such a system.

Haborak *et al.* (3) questioned the solution of two equations in my earlier paper, stating: "The presence of the factor $(1 - e^{-bs})$ destroys the polynomial character of the numerator, so neither the General Partial Fraction Theorem nor the Heaviside expansion immediately pertains." They are correct. However, the correct solution is also obtained using the one-step method that I proposed (1, 4). Apparently, the restriction concerning the polynomial character of the numerator may be relaxed when exponential functions appear in the numerator due to the inclusion of a zero-order input function. Since I am no mathematician, I shall leave the proof of this exception to others. However, I have tested the one-step method and found that it gives the correct equations for the usual multicompartment pharmacokinetic models with zero-order input into the central or peripheral compartments.

The authors of the preceding article (3) were most disturbed by the fact that I proposed the use of a single equation to describe the time course of drug in the central compartment during infusion *and* when infusion has ceased. Although I did explain, following Eq. 13 (1), that this approach was equivalent to using two independent variables, t = clock time and b = infusion time, Haborak *et al.* (3) stated that "changing constants to variables in the middle of a derivation confuses the reader . . .." I must admit that this point has led to questions by a number of readers over the years. Perhaps the preceding note and this reply will help readers to understand the appropriate use of Eqs. 13 and 24 in the 1972 paper (1).

Haborak *et al.* (3) also stated that my use of a single equation "requires very tedious calculations." This statement I do not understand; it certainly would be quicker to calculate A_1 values in Eq. 13 on any programmable calculator using a single equation with two inputs during the infusion phase than it would be using two different equations. But "calculation" is not the important functional use for Eq. 13. In 1972, I was concerned that investigators were fitting data from the postinfusion phase separately from the infusion phase. This procedure is inappropriate, as I stated previously (1). In 1972, many of the computer programs used to fit pharmacokinetic data, particularly the BMD series (5), only allowed the investigator to fit one function at a time. However, I stated then (1) that: "All the least-squares nonlinear fitting programs usually utilized in pharmacokinetic treatments have the ability to fit data to Eq. 13. . . ."

In conclusion, the previous article (3) points out the detailed solution for the Laplace derivation when an exponential operator term appears in the numerator of the

© 1979, American Pharmaceutical Association

Laplace transform. Hopefully, that paper and this response will allow the uninitiated reader to understand better the use of such functions. However, once the reader becomes initiated (*i.e.*, not confused), I suggest he or she define b as the time of infusion rather than the time when infusion ends and use the anti-Laplace techniques and equations presented in my 1972 publication. They really are easier to use.

(1) L. Z. Benet, *J. Pharm. Sci.*, **61**, 536 (1972).
(2) D. P. Vaughan and A. Trainor, *J. Pharmacokinet. Biopharm.*, **3**, 203 (1975).
(3) G. E. Haborak, J. D. Benmaman, and J. W. Warren, Jr., *J. Pharm. Sci.*, **68**, 932 (1979).
(4) L. Z Benet and J. S. Turi, *ibid.*, **60**, 1593 (1971).
(5) P. Sampson, in "BMD Biomedical Computer Programs," W. J. Dixon, Ed., Health Sciences Computer Facility, University of California, Los Angeles, Calif., 1970, pp. 387–396.

Leslie Z. Benet
Department of Pharmacy
School of Pharmacy
University of California
San Francisco, CA 94143

Received December 27, 1978.
Accepted for publication April 12, 1979.

Time-Dependent Kinetics VI: Direct Relationship between Equations for Drug Levels during Induction and Those Involving Constant Clearance

Keyphrases □ Pharmacokinetics—time dependent, equations for drug levels during induction and during constant clearance □ Models, pharmacokinetic—equations for drug levels during induction and during constant clearance

To the Editor:

In a previous report (1), equations were derived to describe the time course of drug levels during enzyme induction under various drug input conditions: single-dose intravenous (Case I) and oral (Case II) administration, constant rate intravenous infusion (Case III), and multiple-dose intravenous (Case IV) and oral (Case V) administration. These equations were based on the following assumptions:

1. Drug distribution is instantaneous (one compartment of volume V).
2. Drug is excreted unchanged by first-order processes.
3. Metabolism occurs by several first-order pathways, with one being controlled by a single inducible enzyme.
4. Metabolic clearance (pre- and postinduction) approaches intrinsic clearance.
5. Total body drug clearance increases during induction from a preinduction value $Q(t \leq \lambda)$ to a maximum Q' according to (2):

$$Q(t) = Q' - (Q' - Q)\exp[-k'(t - \lambda)] \qquad \text{(Eq. 1)}$$

where k' represents the first-order degradation rate constant of the induced enzyme, $k' < 0.1\ Q'/V$, and λ is the time at which induction begins.

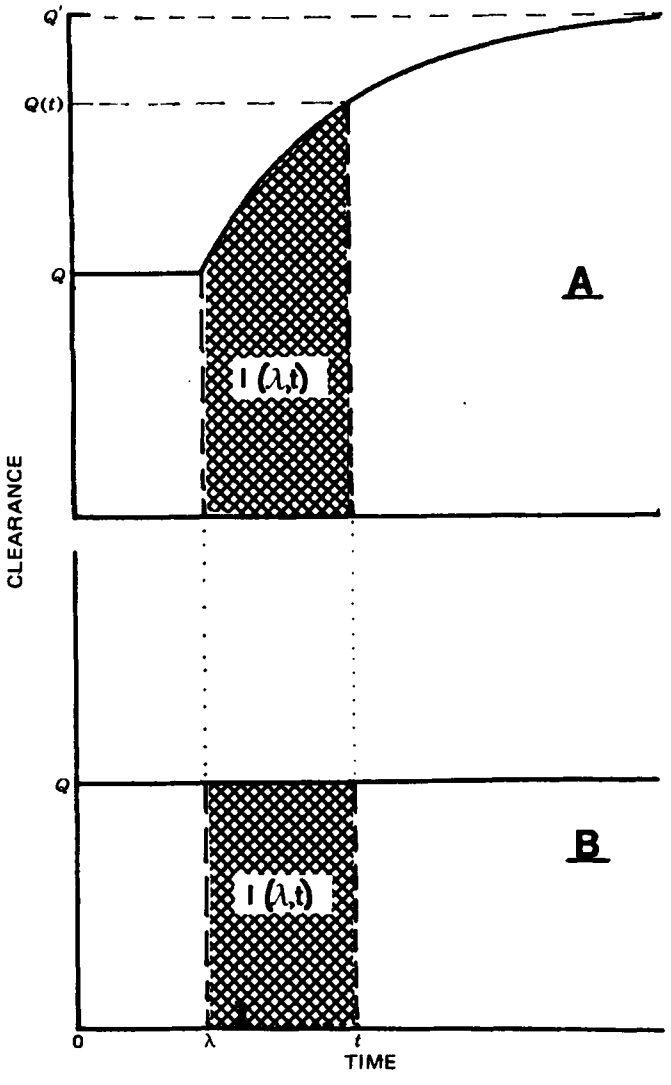

Figure 1—*Exponent* I(λ, t) *in time-dependent kinetics (A) and in linear kinetics (B). Whereas in linear kinetics (constant clearance) the area term* I(λ, t) *increases proportionately with time, in time-dependent kinetics the increase in area is more than proportional.*

To date, equations based on an exponentially increasing clearance have been validated only to the extent that the time course of blood levels that they predict is compatible with some experimental observations (3–7). In this report, a mathematical proof is presented to show that these equations are consistent with the corresponding equations of the classical one-compartment model with constant clearance. In fact, the latter represent a particular case of the former.

Table I presents solutions for Cases I–V with corresponding solutions for the one compartment with constant clearance.

Figure 1 is a plot of $Q(t)$ *versus* time. The term $I(\lambda, t)$ in every equation involving a time-dependent clearance (Table I) is defined as:

$$I(\lambda, t) = \int_{\lambda}^{t} Q(u)\,du \qquad \text{(Eq. 2)}$$

and, therefore, represents the area under the $Q(t)$ *versus*

0022-3549/79/0700-0934$01.00/0
© 1979, American Pharmaceutical Association

Laplace transform. Hopefully, that paper and this response will allow the uninitiated reader to understand better the use of such functions. However, once the reader becomes initiated (*i.e.*, not confused), I suggest he or she define b as the time of infusion rather than the time when infusion ends and use the anti-Laplace techniques and equations presented in my 1972 publication. They really are easier to use.

(1) L. Z. Benet, *J. Pharm. Sci.*, **61**, 536 (1972).
(2) D. P. Vaughan and A. Trainor, *J. Pharmacokinet. Biopharm.*, **3**, 203 (1975).
(3) G. E. Haborak, J. D. Benmaman, and J. W. Warren, Jr., *J. Pharm. Sci.*, **68**, 932 (1979).
(4) L. Z Benet and J. S. Turi, *ibid.*, **60**, 1593 (1971).
(5) P. Sampson, in "BMD Biomedical Computer Programs," W. J. Dixon, Ed., Health Sciences Computer Facility, University of California, Los Angeles, Calif., 1970, pp. 387–396.

Leslie Z. Benet
Department of Pharmacy
School of Pharmacy
University of California
San Francisco, CA 94143

Received December 27, 1978.
Accepted for publication April 12, 1979.

Time-Dependent Kinetics VI: Direct Relationship between Equations for Drug Levels during Induction and Those Involving Constant Clearance

Keyphrases □ Pharmacokinetics—time dependent, equations for drug levels during induction and during constant clearance □ Models, pharmacokinetic—equations for drug levels during induction and during constant clearance

To the Editor:

In a previous report (1), equations were derived to describe the time course of drug levels during enzyme induction under various drug input conditions: single-dose intravenous (Case I) and oral (Case II) administration, constant rate intravenous infusion (Case III), and multiple-dose intravenous (Case IV) and oral (Case V) administration. These equations were based on the following assumptions:

1. Drug distribution is instantaneous (one compartment of volume V).
2. Drug is excreted unchanged by first-order processes.
3. Metabolism occurs by several first-order pathways, with one being controlled by a single inducible enzyme.
4. Metabolic clearance (pre- and postinduction) approaches intrinsic clearance.
5. Total body drug clearance increases during induction from a preinduction value $Q(t \leq \lambda)$ to a maximum Q' according to (2):

$$Q(t) = Q' - (Q' - Q)\exp[-k'(t - \lambda)] \qquad \text{(Eq. 1)}$$

where k' represents the first-order degradation rate constant of the induced enzyme, $k' < 0.1\ Q'/V$, and λ is the time at which induction begins.

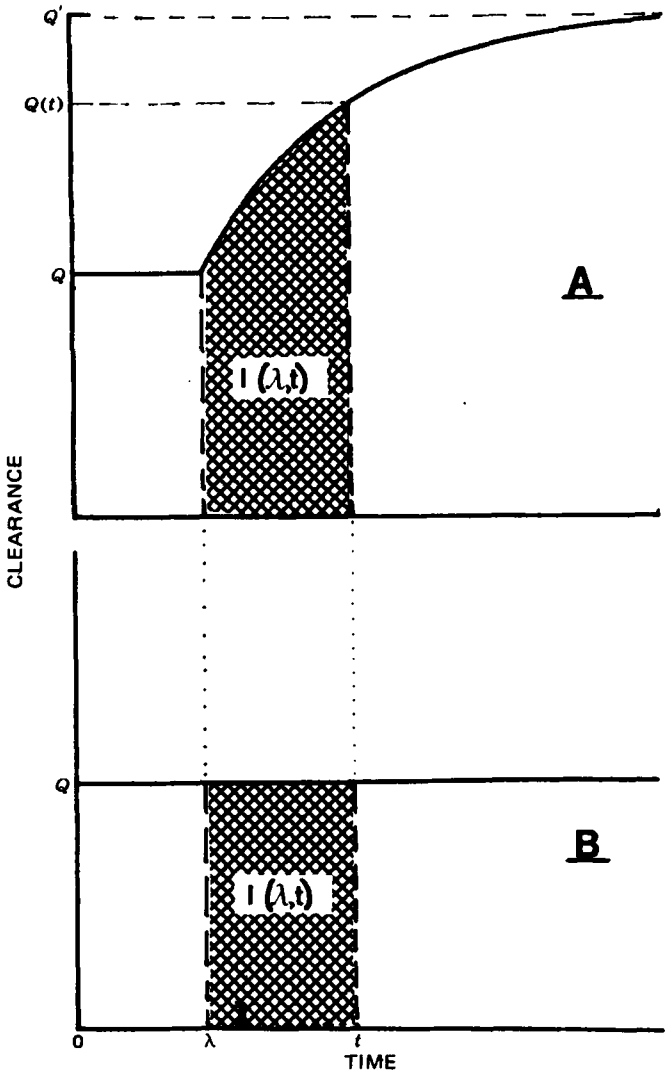

Figure 1—*Exponent* I(λ, t) *in time-dependent kinetics (A) and in linear kinetics (B). Whereas in linear kinetics (constant clearance) the area term* I(λ, t) *increases proportionately with time, in time-dependent kinetics the increase in area is more than proportional.*

To date, equations based on an exponentially increasing clearance have been validated only to the extent that the time course of blood levels that they predict is compatible with some experimental observations (3–7). In this report, a mathematical proof is presented to show that these equations are consistent with the corresponding equations of the classical one-compartment model with constant clearance. In fact, the latter represent a particular case of the former.

Table I presents solutions for Cases I–V with corresponding solutions for the one compartment with constant clearance.

Figure 1 is a plot of $Q(t)$ *versus* time. The term $I(\lambda, t)$ in every equation involving a time-dependent clearance (Table I) is defined as:

$$I(\lambda, t) = \int_{\lambda}^{t} Q(u)\,du \qquad \text{(Eq. 2)}$$

and, therefore, represents the area under the $Q(t)$ *versus*

0022-3549/79/0700-0934$01.00/0
© 1979, American Pharmaceutical Association

Table I—Equations [a] for Blood Concentration at Any Time When Clearance Increases Exponentially (A) and When Clearance Is Constant (B)

Case	A. Time-Dependent Clearance	B. Constant Clearance
I: Intravenous single dose	$C = \frac{X_0}{V}\exp\{-[Q\lambda + I(\lambda, t)]/V\}$ (Eq. I-1)	$C = \frac{X_0}{V}\exp(-Qt/V)$ (Eq. I-2)
II: Oral single dose	$C = \frac{FX_0k_a}{k_aV - Q}\exp\{-[Q\lambda + I(\lambda, t)]/V\} - \frac{FX_0k_a}{k_aV - Q(t)}\exp(-k_at)$ (Eq. II-1)	$C = \frac{FX_0k_a}{Vk_a - Q}\left[\exp\left(-\frac{Qt}{V}\right) - \exp(-k_at)\right]$ (Eq. II-2)
III: Constant rate infusion	$C = \frac{R}{Q(t)} - \frac{R}{Q}\exp\{-[Q\lambda + I(\lambda, t)]/V\}$ (Eq. III-1)	$C = \frac{R}{Q} - \frac{R}{Q}\exp(-Qt/V)$ (Eq. III-2)
IV: Intravenous multiple dose	$C = \frac{X_0}{V}\left\{\left[\frac{1 - \exp(-Q\lambda/V)}{1 - \exp(-Q\tau/V)}\right]\exp\{-[Q\tau + I(\lambda, t)]/V\} + \sum_{j=m}^{n-1}\exp[-I(j\tau, t)/V]\right\}$ (Eq. IV-1)	$C = \frac{X_0}{V}\left[\frac{1 - \exp(-n\tau Q/V)}{1 - \exp(-Q\tau/V)}\exp(-Qt'/V)\right]$ (Eq. IV-2)
V: Oral multiple dose	$C = \frac{FX_0k_a}{Vk_a - Q}\frac{1 - \exp(-Q\lambda/V)}{1 - \exp(-\tau Q/V)}\exp\{-[Q\tau + I(\lambda, t)]/V\} + \frac{FX_0k_a}{V}\left[\sum_{j=m}^{n-1}\frac{\exp[-I(j\tau, t)/V]}{k_a - Q(j\tau)/V} - \frac{\exp(-k_at')[1 - \exp(-n\tau k_a)]}{k_a - Q(t)/V[1 - \exp(-k_a\tau)]}\right]$ (Eq. V-1)	$C = \frac{FX_0k_a}{Vk_a - Q}\left[\frac{1 - \exp(-n\tau Q/V)}{1 - \exp(-\tau Q/V)}\exp(-Qt'/V) - \frac{1 - \exp(n\tau k_a)}{1 - \exp(-\tau k_a)}\exp(-k_at')\right]$ (Eq. V-2)

[a] X_0 = dose, V = single-compartment volume of distribution, F = fraction of dose absorbed, k_a = first-order absorption rate constant, τ = fixed dosing interval, n = number of doses, and:

$$I(\lambda, t) = Q'(t - \lambda) - \frac{(Q' - Q)}{k'}\{1 - \exp[-k'(t - \lambda)]\}$$

$$I(j\tau, t) = Q'\{t' + [n - (j + 1)]\tau\} - \frac{(Q' - Q)}{k'}(\exp[-(j - m)\tau k'] - \exp[-k'\{t' + [n - (m + 1)]\tau\}])$$

All other symbols are as defined in the text.

time plot between λ and t (Fig. 1A). The term $Q\lambda + I(\lambda, t)$ is equal to the total area under the $Q(t)$ *versus* time plot from 0 to t.

When $Q(t)$ is defined by Eq. 1, $I(\lambda, t)$ is given by:

$$I(\lambda, t) = Q'(t - \lambda) - \frac{(Q' - Q)}{k'}\{1 - \exp[-k'(t - \lambda)]\} \quad \text{(Eq. 3)}$$

For the one-compartment model with a constant clearance Q, the term $I(\lambda, t)$ as defined in Eq. 2 becomes:

$$I(\lambda, t) = \int_\lambda^t Q\,du = Q(t - \lambda) \quad \text{(Eq. 4)}$$

In this latter case, $I(\lambda, t)$ is equal to the area under the rectangle with height Q and width $t - \lambda$ (Fig. 1B).

For Case I, the term Qt in Eq. I-2 (Table I) can be written as:

$$Qt = Q\lambda + Q(t - \lambda) \quad \text{(Eq. 5)}$$

Using the definition of $I(\lambda, t)$ in Eq. 4, Qt becomes:

$$Qt = Q\lambda + I(\lambda, t) \quad \text{(Eq. 6)}$$

and, therefore:

$$C = \frac{X_0}{V}\exp(-Qt/V) = \frac{X_0}{V}\exp\{-[Q\lambda + I(\lambda, t)]/V\} \quad \text{(Eq. 7)}$$

Similarly in Case II, Eq. II-1 reduces to Eq. II-2 by substitution of Qt for $[Q\lambda + I(\lambda, t)]$ in the first term and Q for $Q(t)$ in the second term. In Case III also, Eq. III-1 reduces to Eq. III-2 by substitution of Q for $Q(t)$ in the first term and Qt for $[Q\lambda + I(\lambda, t)]$ in the second term.

In Cases IV and V, the relationships between Eqs. IV-1 and V-1 and between Eqs. V-1 and V-2 become apparent only after a few substitutions:

1. The term $I(j\tau, t)$, which appears in Eqs. IV-1 and V-1, is also defined by Eq. 2 with $j\tau$ as the lower bound of the integral ($\lambda \leq j\tau \leq t$). When the clearance is constant, it is given by:

$$I(j\tau, t) = Q(t - j\tau) = Q\{t' + [n - (j + 1)]\tau\} \quad \text{(Eq. 8)}$$

where $t' = t - (n - 1)\tau$.

2. The term $Q\tau + I(\lambda, t)$ can also be expressed in terms of t':

$$Q\tau + I(\lambda, t) = Q(t' + n\tau - \lambda) = Q[t' + (n - m)\tau] \quad \text{(Eq. 9)}$$

where $\lambda = m\tau$.

3. By using Eqs. 8 and 9, Eq. IV-1 can be written as:

$$C = \frac{X_0}{V}\exp(-Qt'/V)\frac{\exp[-(n - m)\tau Q/V] - \exp(-n\tau Q/V)}{1 - \exp(-Q\tau/V)} + \frac{X_0}{V}\sum_{j=m}^{n-1}\exp(-Q\{t' + [n - (j + 1)]\tau\}/V) \quad \text{(Eq. 10)}$$

4. The second term in Eq. 10 is a geometric series and, therefore, multiplication by:

$$1 = \frac{1 - \exp(-Q\tau/V)}{1 - \exp(-Q\tau/V)}$$

results in the following expression for Eq. IV-1:

$$C = \frac{X_0}{V}\exp(-Qt'/V)\left[\frac{\exp[-(n - m)\tau Q/V] - \exp(-n\tau Q/V)}{1 - \exp(-Q\tau/V)}\right] + \frac{X_0}{V}\exp(-Qt'/V)\left[\frac{1 - \exp[-(n - m)\tau Q/V]}{1 - \exp(-Q\tau/V)}\right] \quad \text{(Eq. 11)}$$

Equation 11 yields Eq. IV-2 after addition of its two terms.

5. Substitution of Q for $Q(j\tau)$ in Eq. V-1 shows that the sum of its first two terms becomes identical to Eq. IV-1, except for the difference between $FX_0k_a/(Vk_a - Q)$ and X_0/V. Correspondingly, the first term in Eq. V-2 is equal to Eq. IV-2 (except for $X_0/V \neq FX_0k_a/(Vk_a - Q)$. The third term in Eq. V-1 becomes the second term in Eq. V-2 after substitution of Q for $Q(t)$.

Thus, it appears that for all of the input modes considered, the equations commonly used for the one-compartment model with constant clearance represent only particular cases of the corresponding equations involving a time-dependent clearance. This direct correspondence provides further validation of the equations proposed to describe drug levels when metabolic clearance increases exponentially.

(1) R. H. Levy, M. S. Dumain, and J. L. Cook, *J. Pharmacokinet. Biopharm.*, in press.

(2) R. H. Levy, A. A. Lai, and M. S. Dumain, *J. Pharm. Sci.*, **68**, 398 (1979).

(3) W. H. Pitlick, R. H. Levy, A. S. Troupin, and J. R. Green, *ibid.*, **65**, 462 (1976).

(4) R. H. Levy, W. H. Pitlick, A. S. Troupin, and J. R. Green, in "The Effect of Disease States on Drug Pharmacokinetics," L. Z. Benet, Ed., American Pharmaceutical Association, Washington, D.C., 1976, pp. 87–95.

(5) W. H. Pitlick and R. H. Levy, *J. Pharm. Sci.*, **66**, 647 (1977).

(6) A. A. Lai, R. H. Levy, and R. E. Cutler, *Clin. Pharmacol. Ther.*, **34**, 316 (1978).

(7) A. A. Lai and R. H. Levy, *J. Pharm. Sci.*, **68**, 416 (1979).

René H. Levy ˣ
Martin S. Dumain
Departments of Pharmaceutical Sciences and Neurological Surgery
Schools of Pharmacy and Medicine
University of Washington
Seattle, WA 98195

Received February 26, 1979.
Accepted for publication April 18, 1979.
Supported by National Institutes of Health Research Grants N01-NS-1-2282 and N01-NS-6-2341.

Cetaben Sodium, an Antiatherosclerotic Agent

Keyphrases □ Cetaben sodium—synthesis, antiatherosclerotic activity □ Antiatherosclerotic agents—cetaben sodium, synthesis □ Sodium 4-(hexadecylamino)benzoate—synthesis, antiatherosclerotic activity

To the Editor:

We wish to report the synthesis of cetaben sodium [sodium 4-(hexadecylamino)benzoate], a substance that shows promise as an antiatherosclerotic agent.

Ethyl 4-(hexadecylamino)benzoate (mp 85–86°) was prepared (yield 65–85%) from hexadecyl bromide or mesylate and 2 moles of ethyl 4-aminobenzoate at 135° in hexamethylphosphoric amide. Of the liquid amides, hexamethylphosphoric amide was the best reaction solvent (faster rate and fewer by-products); however, some dialkylation did occur. With dimethylformamide or *N,N*-dimethylacetamide at 135–150° as solvents, *N*-formyl and *N*-acetyl products were obtained as well as some 4-(hexadecylamino)-*N,N*-dimethylbenzamide by-product. Among various alternative synthetic methods, the diborane reduction of ethyl 4-(hexadecanoylamino)benzoate gave ethyl 4-(hexadecylamino)benzoate in good yield and can be used for preparing various isomers and analogs.

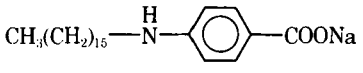

cetaben sodium

Cetaben sodium can be obtained directly from the quantitative alkaline hydrolysis of the ester but is generally prepared from 4-(hexadecylamino)benzoic acid (double mp 108–110 and 126–128°) since the latter is more easily purified. This salt, which is moderately soluble (about 2%) in 75% alcohol, is crystallized from a solution of the acid and a slight sodium hydroxide excess in aqueous ethanol in 95% yield.

The 4-(alkylamino)benzoic acids (1) are substantially less toxic and more hypolipidemic than the 4-alkoxybenzoic acids (2, 3) and 4-alkylbenzoic acids (3). Extensive studies have elucidated the structure–activity relationships in the aminobenzoic acid series, which are different from those in the alkoxybenzoic acids. The tabulated data show the hypolipidemic activity of representative aminobenzoic acids as well as of clofibrate under the same test conditions (Table I). The hypocholesterolemic activity falls off as the alkyl chain is increased to 20 or decreased to eight carbon atoms (1). However, the hypotriglyceridemic activity is relatively unaffected by the alkyl chain length. Cetaben is also the most effective member of the series in inhibiting ^{14}C-acetate and ^{3}H-glycerol incorporation into liver triglycerides, phospholipids, and cholesterol in rats. It is not esterogenic, and its hypocholesterolemic mechanism of action does not involve inhibition of a late stage in cholesterol biosynthesis. Hypocholesterolemic activity has been demonstrated also in the rabbit and monkey.

The considerable therapeutic potential of cetaben is suggested by its activity in two experimental atherosclerosis models in laboratory animals. First, cetaben sodium was shown to possess antiatherosclerotic activity in a rabbit model (4). Average reductions of 32–73% in the incidence of atherosclerotic lesions and of 24–28% in abdominal aortic cholesterol accumulation were observed in treated animals at doses below those that were hypolipidemic[1]. The reductions in aortic cholesterol were essentially all due to the decreases in cholesterol ester.

Second, Hollander *et al.* (5) reported on the antiatherosclerotic activity of cetaben sodium in the cynomolgus monkey. Serum cholesterol concentrations were reduced by 37% in the treated animals as compared to controls fed the atherogenic diet alone. This change was reflected in an altered lipoprotein distribution with decreases in very low density lipoproteins (by 30%) and low density lipoproteins (by 38%) but an increase in high density lipoproteins (by 96%). Such a shift in lipoprotein concentrations in humans is considered to be antiatherogenic (6, 7). Antiatherosclerotic activity was manifested by changes in the disease incidence and severity as well as in the chemical composition of the lesions present in the drug-treated monkeys.

[1] A. S. Katocs, Jr., and S. A. Schaffer, unpublished results.

0022-3549/79/0700-0936$01.00/0
© 1979, American Pharmaceutical Association

Equation 11 yields Eq. IV-2 after addition of its two terms.

5. Substitution of Q for $Q(j\tau)$ in Eq. V-1 shows that the sum of its first two terms becomes identical to Eq. IV-1, except for the difference between $FX_0k_a/(Vk_a - Q)$ and X_0/V. Correspondingly, the first term in Eq. V-2 is equal to Eq. IV-2 (except for $X_0/V \neq FX_0k_a/(Vk_a - Q)$. The third term in Eq. V-1 becomes the second term in Eq. V-2 after substitution of Q for $Q(t)$.

Thus, it appears that for all of the input modes considered, the equations commonly used for the one-compartment model with constant clearance represent only particular cases of the corresponding equations involving a time-dependent clearance. This direct correspondence provides further validation of the equations proposed to describe drug levels when metabolic clearance increases exponentially.

(1) R. H. Levy, M. S. Dumain, and J. L. Cook, *J. Pharmacokinet. Biopharm.*, in press.

(2) R. H. Levy, A. A. Lai, and M. S. Dumain, *J. Pharm. Sci.*, **68**, 398 (1979).

(3) W. H. Pitlick, R. H. Levy, A. S. Troupin, and J. R. Green, *ibid.*, **65**, 462 (1976).

(4) R. H. Levy, W. H. Pitlick, A. S. Troupin, and J. R. Green, in "The Effect of Disease States on Drug Pharmacokinetics," L. Z. Benet, Ed., American Pharmaceutical Association, Washington, D.C., 1976, pp. 87–95.

(5) W. H. Pitlick and R. H. Levy, *J. Pharm. Sci.*, **66**, 647 (1977).

(6) A. A. Lai, R. H. Levy, and R. E. Cutler, *Clin. Pharmacol. Ther.*, **34**, 316 (1978).

(7) A. A. Lai and R. H. Levy, *J. Pharm. Sci.*, **68**, 416 (1979).

René H. Levy ˣ
Martin S. Dumain
Departments of Pharmaceutical Sciences and Neurological Surgery
Schools of Pharmacy and Medicine
University of Washington
Seattle, WA 98195

Received February 26, 1979.
Accepted for publication April 18, 1979.
Supported by National Institutes of Health Research Grants N01-NS-1-2282 and N01-NS-6-2341.

Cetaben Sodium, an Antiatherosclerotic Agent

Keyphrases □ Cetaben sodium—synthesis, antiatherosclerotic activity □ Antiatherosclerotic agents—cetaben sodium, synthesis □ Sodium 4-(hexadecylamino)benzoate—synthesis, antiatherosclerotic activity

To the Editor:

We wish to report the synthesis of cetaben sodium [sodium 4-(hexadecylamino)benzoate], a substance that shows promise as an antiatherosclerotic agent.

Ethyl 4-(hexadecylamino)benzoate (mp 85–86°) was prepared (yield 65–85%) from hexadecyl bromide or mesylate and 2 moles of ethyl 4-aminobenzoate at 135° in hexamethylphosphoric amide. Of the liquid amides, hexamethylphosphoric amide was the best reaction solvent (faster rate and fewer by-products); however, some dialkylation did occur. With dimethylformamide or *N,N*-dimethylacetamide at 135–150° as solvents, *N*-formyl and *N*-acetyl products were obtained as well as some 4-(hexadecylamino)-*N,N*-dimethylbenzamide by-product. Among various alternative synthetic methods, the diborane reduction of ethyl 4-(hexadecanoylamino)benzoate gave ethyl 4-(hexadecylamino)benzoate in good yield and can be used for preparing various isomers and analogs.

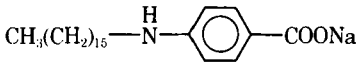

cetaben sodium

Cetaben sodium can be obtained directly from the quantitative alkaline hydrolysis of the ester but is generally prepared from 4-(hexadecylamino)benzoic acid (double mp 108–110 and 126–128°) since the latter is more easily purified. This salt, which is moderately soluble (about 2%) in 75% alcohol, is crystallized from a solution of the acid and a slight sodium hydroxide excess in aqueous ethanol in 95% yield.

The 4-(alkylamino)benzoic acids (1) are substantially less toxic and more hypolipidemic than the 4-alkoxybenzoic acids (2, 3) and 4-alkylbenzoic acids (3). Extensive studies have elucidated the structure–activity relationships in the aminobenzoic acid series, which are different from those in the alkoxybenzoic acids. The tabulated data show the hypolipidemic activity of representative aminobenzoic acids as well as of clofibrate under the same test conditions (Table I). The hypocholesterolemic activity falls off as the alkyl chain is increased to 20 or decreased to eight carbon atoms (1). However, the hypotriglyceridemic activity is relatively unaffected by the alkyl chain length. Cetaben is also the most effective member of the series in inhibiting ^{14}C-acetate and ^{3}H-glycerol incorporation into liver triglycerides, phospholipids, and cholesterol in rats. It is not esterogenic, and its hypocholesterolemic mechanism of action does not involve inhibition of a late stage in cholesterol biosynthesis. Hypocholesterolemic activity has been demonstrated also in the rabbit and monkey.

The considerable therapeutic potential of cetaben is suggested by its activity in two experimental atherosclerosis models in laboratory animals. First, cetaben sodium was shown to possess antiatherosclerotic activity in a rabbit model (4). Average reductions of 32–73% in the incidence of atherosclerotic lesions and of 24–28% in abdominal aortic cholesterol accumulation were observed in treated animals at doses below those that were hypolipidemic[1]. The reductions in aortic cholesterol were essentially all due to the decreases in cholesterol ester.

Second, Hollander *et al.* (5) reported on the antiatherosclerotic activity of cetaben sodium in the cynomolgus monkey. Serum cholesterol concentrations were reduced by 37% in the treated animals as compared to controls fed the atherogenic diet alone. This change was reflected in an altered lipoprotein distribution with decreases in very low density lipoproteins (by 30%) and low density lipoproteins (by 38%) but an increase in high density lipoproteins (by 96%). Such a shift in lipoprotein concentrations in humans is considered to be antiatherogenic (6, 7). Antiatherosclerotic activity was manifested by changes in the disease incidence and severity as well as in the chemical composition of the lesions present in the drug-treated monkeys.

[1] A. S. Katocs, Jr., and S. A. Schaffer, unpublished results.

0022-3549/79/0700-0936$01.00/0
© 1979, American Pharmaceutical Association

Table I—Hypolipidemic Effect of 4-(*n*-Alkylamino)benzoic Acids and Clofibrate in Normal Rats

n-Alkyl Group	Oral Dose in Diet[a], mg/kg/day	Percent Lowering[b] of Serum	
		Sterol	Triglyceride
C_{12}	86	11[c]	68[d]
	47	20[e]	60[d]
	25	14[f]	49[d]
C_{14}	82	9	47[d]
	46	9	49[d]
	23	9	36[d]
C_{16} (cetaben)	89	44[d]	69[d]
	64	30[d]	48[f]
	42	26[d]	40[f]
	22	27[d]	38[f]
	10	27[d]	29[d]
C_{18}	91	18[g]	40[e]
	48	6	28[c]
	23	14[f]	29[c]
Clofibrate	375	26[d]	43[c]
	106	5	30
	33	0	32

[a] The method used was described in detail in Ref. 2. Oral dosing was by normal rat chow containing drug; 0.05% in the diet corresponds to a measured average daily dosage of 46 mg/kg, *etc.* [b] Percent lowering of the mean serum concentrations relative to the mean values in control animals in the same test; control groups averaged 75 ± 3 mg % sterol and 85 ± 6 mg % triglyceride. The significant level (p), determined by the Student t test, is denoted by the appropriate footnote. Numbers without a footnote are not statistically significant lowerings. [c] $p < 0.05$. [d] $p < 0.001$. [e] $p < 0.005$. [f] $p < 0.02$. [g] $p < 0.01$.

Most important was the presence of only half as much luminal narrowing in four major coronary arteries (5). Accompanying this effect on lumen size were increases in myocardial blood flow in the nonstressed and stressed heart. In the stressed heart, regional blood flow toward the endocardium was improved as well. Reductions in luminal narrowing and incidence of atherosclerotic lesions also were seen in several major peripheral arteries. In the aortas of treated monkeys, average 48% reductions in cholesterol accumulation resulted predominantly from decreases in esterified cholesterol. Additionally, there was complete prevention of a 2.5-fold calcium increase in the aortic wall and a 70% inhibition of the increase in aortic fibrous connective tissue. Up to now, such pronounced therapeutic effects on this atherosclerosis model (5, 8, 9) have not been reported with any other drug.

The reduced cholesterol ester content in the rabbit and monkey aortas may result from cetaben inhibition of the cholesterol-esterifying enzyme in the aortic wall. With a cell-free preparation of fatty acyl-CoA: cholesterol acyl transferase (ACAT) from rabbit aortas, cetaben sodium substantially inhibited the enzyme at therapeutically obtainable concentrations[1] (~5 μg/ml). This effect is especially significant in view of the greater proportion of esterified to free cholesterol in atheromatous lesions in humans (10) as well as the lower experimental reversibility of ester deposition in rabbits (11).

In a series of papers, we shall fully report on the biological activity described here and elaborate the structure–activity relationships of alkyl size; branching, cyclization, substitution, and unsaturation of the alkyl group; further substitution of the amino nitrogen and its position isomers; additional substitution on the benzene ring and its replacement with other rings; and carboxyl group derivatization, modification, and extension.

Effective atherosclerosis therapy probably will require drugs that have several modes of action such as those displayed by cetaben sodium. Cetaben sodium is now undergoing clinical trials as an antiatherosclerotic agent in humans.

(1) E. E. Largis, A. S. Katocs, Jr., L. W. Will, D. K. McClintock, and S. A. Schaffer, *J. Am. Oil Chem. Soc.*, **53**, 140A (1976).

(2) V. G. DeVries, D. B. Moran, G. R. Allen, Jr., and S. J. Riggi, *J. Med. Chem.*, **19**, 946 (1976).

(3) R. A. Parker, T. Kariya, J. M. Grisar, and V. Petrow, *ibid.*, **20**, 781 (1977).

(4) A. S. Katocs, Jr., E. E. Largis, L. Will, D. K. McClintock, and S. J. Riggi, *Artery*, **2**, 38 (1976).

(5) W. Hollander, S. Prusty, S. Nagraj, B. Kirkpatrick, J. Paddock, and M. Colombo, *Atherosclerosis*, **31**, 307 (1978).

(6) N. E. Miller, D. S. Thelle, O. H. Forde, and O. D. Mjos, *Lancet*, **1**, 965 (1977). G. M. B. Berger, *S. Afr. Med. J.*, **54**, 689 (1978).

(7) C. E. Day, *Annu. Rep. Med. Chem.*, **13**, 184 (1978).

(8) W. Hollander, S. Prusty, B. Kirkpatrick, J. Paddock, and S. Nagraj, *Circ. Res. (Suppl. I)*, **40**, 170 (1977).

(9) M. R. Malinow, P. McLaughton, L. Papworth, H. K. Naito, L. Lewis, and W. P. McNulty, *Adv. Exp. Med. Biol.*, **67**, 3 (1976).

(10) C. W. M. Adams, O. B. Bayliss, R. W. R. Baker, Y. H. Abdulla, and C. J. Hunter-Craig, *Atherosclerosis*, **19**, 429 (1974).

(11) G. Bondjers and S. Bjorkerud, *ibid.*, **15**, 273 (1972).

J. Donald Albright
Sheldon A. Schaffer
Robert G. Shepherd ˣ

Metabolic Disease Research Section
Medical Research Division
American Cyanamid Company
Lederle Laboratories
Pearl River, NY 10965

Received March 26, 1979.
Accepted for publication May 2, 1979.

pKa of 2-Methylamino-5-chlorobenzophenone, a Diazepam Hydrolysis Product

Keyphrases □ Methylaminochlorobenzophenone—pKa, diazepam hydrolysis product, structure–activity relationships □ Diazepam—hydrolysis products, methylaminochlorobenzophenone, pKa, structure–activity relationships □ Structure–activity relationships—diazepam hydrolysis products, pKa

To the Editor:

The compound 2-methylamino-5-chlorobenzophenone (I) is the aromatic product of diazepam (II) hydrolysis in acidic aqueous solution (1). It was of interest to estimate the pKa of I because of its importance in kinetic stability and analytical studies of prazepam (2) and II (1, 3–8).

The pKa of I[1] was determined spectrophotometrically[2] at 25° at 415 nm in a concentration of 4.07×10^{-5} *M* (10 μg/ml). All samples contained 7% (v/v) ethanol. The pH was varied by preparing samples in 0.02–0.40 *N* HCl. The spectrum of the conjugate acid was obtained in 60% (w/w) H_2SO_4 ($H_0 = -4.4$), and that of the nonionized base was obtained in buffers of pH 7.20 and 9.23. The conjugate acid species showed no absorbance at 415 nm, and the base had an absorbance of 0.23. The other spectral characteristics included decreasing absorbance at 410–420 nm and a hypsochromic shift from ~268 to 238 nm with increasing

[1] Ro 5-4365, lot PP-4 Hoffmann-La Roche, Nutley, N.J.
[2] Beckman DB-GT grating spectrophotometer, Beckman Instruments, Fullerton, Calif.

0022-3549/79/0700-0937$01.00/0

© 1979, American Pharmaceutical Association

Table I—Hypolipidemic Effect of 4-(*n*-Alkylamino)benzoic Acids and Clofibrate in Normal Rats

n-Alkyl Group	Oral Dose in Diet[a], mg/kg/day	Percent Lowering[b] of Serum	
		Sterol	Triglyceride
C_{12}	86	11[c]	68[d]
	47	20[e]	60[d]
	25	14[f]	49[d]
C_{14}	82	9	47[d]
	46	9	49[d]
	23	9	36[d]
C_{16} (cetaben)	89	44[d]	69[d]
	64	30[d]	48[f]
	42	26[d]	40[f]
	22	27[d]	38[f]
	10	27[d]	29[d]
C_{18}	91	18[g]	40[e]
	48	6	28[c]
	23	14[f]	29[c]
Clofibrate	375	26[d]	43[c]
	106	5	30
	33	0	32

[a] The method used was described in detail in Ref. 2. Oral dosing was by normal rat chow containing drug; 0.05% in the diet corresponds to a measured average daily dosage of 46 mg/kg, *etc.* [b] Percent lowering of the mean serum concentrations relative to the mean values in control animals in the same test; control groups averaged 75 ± 3 mg % sterol and 85 ± 6 mg % triglyceride. The significant level (p), determined by the Student t test, is denoted by the appropriate footnote. Numbers without a footnote are not statistically significant lowerings. [c] $p < 0.05$. [d] $p < 0.001$. [e] $p < 0.005$. [f] $p < 0.02$. [g] $p < 0.01$.

Most important was the presence of only half as much luminal narrowing in four major coronary arteries (5). Accompanying this effect on lumen size were increases in myocardial blood flow in the nonstressed and stressed heart. In the stressed heart, regional blood flow toward the endocardium was improved as well. Reductions in luminal narrowing and incidence of atherosclerotic lesions also were seen in several major peripheral arteries. In the aortas of treated monkeys, average 48% reductions in cholesterol accumulation resulted predominantly from decreases in esterified cholesterol. Additionally, there was complete prevention of a 2.5-fold calcium increase in the aortic wall and a 70% inhibition of the increase in aortic fibrous connective tissue. Up to now, such pronounced therapeutic effects on this atherosclerosis model (5, 8, 9) have not been reported with any other drug.

The reduced cholesterol ester content in the rabbit and monkey aortas may result from cetaben inhibition of the cholesterol-esterifying enzyme in the aortic wall. With a cell-free preparation of fatty acyl-CoA: cholesterol acyl transferase (ACAT) from rabbit aortas, cetaben sodium substantially inhibited the enzyme at therapeutically obtainable concentrations[1] (~5 μg/ml). This effect is especially significant in view of the greater proportion of esterified to free cholesterol in atheromatous lesions in humans (10) as well as the lower experimental reversibility of ester deposition in rabbits (11).

In a series of papers, we shall fully report on the biological activity described here and elaborate the structure–activity relationships of alkyl size; branching, cyclization, substitution, and unsaturation of the alkyl group; further substitution of the amino nitrogen and its position isomers; additional substitution on the benzene ring and its replacement with other rings; and carboxyl group derivatization, modification, and extension.

Effective atherosclerosis therapy probably will require drugs that have several modes of action such as those displayed by cetaben sodium. Cetaben sodium is now undergoing clinical trials as an antiatherosclerotic agent in humans.

(1) E. E. Largis, A. S. Katocs, Jr., L. W. Will, D. K. McClintock, and S. A. Schaffer, *J. Am. Oil Chem. Soc.*, **53**, 140A (1976).

(2) V. G. DeVries, D. B. Moran, G. R. Allen, Jr., and S. J. Riggi, *J. Med. Chem.*, **19**, 946 (1976).

(3) R. A. Parker, T. Kariya, J. M. Grisar, and V. Petrow, *ibid.*, **20**, 781 (1977).

(4) A. S. Katocs, Jr., E. E. Largis, L. Will, D. K. McClintock, and S. J. Riggi, *Artery*, **2**, 38 (1976).

(5) W. Hollander, S. Prusty, S. Nagraj, B. Kirkpatrick, J. Paddock, and M. Colombo, *Atherosclerosis*, **31**, 307 (1978).

(6) N. E. Miller, D. S. Thelle, O. H. Forde, and O. D. Mjos, *Lancet*, **1**, 965 (1977). G. M. B. Berger, *S. Afr. Med. J.*, **54**, 689 (1978).

(7) C. E. Day, *Annu. Rep. Med. Chem.*, **13**, 184 (1978).

(8) W. Hollander, S. Prusty, B. Kirkpatrick, J. Paddock, and S. Nagraj, *Circ. Res. (Suppl. I)*, **40**, 170 (1977).

(9) M. R. Malinow, P. McLaughton, L. Papworth, H. K. Naito, L. Lewis, and W. P. McNulty, *Adv. Exp. Med. Biol.*, **67**, 3 (1976).

(10) C. W. M. Adams, O. B. Bayliss, R. W. R. Baker, Y. H. Abdulla, and C. J. Hunter-Craig, *Atherosclerosis*, **19**, 429 (1974).

(11) G. Bondjers and S. Bjorkerud, *ibid.*, **15**, 273 (1972).

J. Donald Albright
Sheldon A. Schaffer
Robert G. Shepherd ˣ

Metabolic Disease Research Section
Medical Research Division
American Cyanamid Company
Lederle Laboratories
Pearl River, NY 10965

Received March 26, 1979.
Accepted for publication May 2, 1979.

pKa of 2-Methylamino-5-chlorobenzophenone, a Diazepam Hydrolysis Product

Keyphrases □ Methylaminochlorobenzophenone—pKa, diazepam hydrolysis product, structure–activity relationships □ Diazepam—hydrolysis products, methylaminochlorobenzophenone, pKa, structure–activity relationships □ Structure–activity relationships—diazepam hydrolysis products, pKa

To the Editor:

The compound 2-methylamino-5-chlorobenzophenone (I) is the aromatic product of diazepam (II) hydrolysis in acidic aqueous solution (1). It was of interest to estimate the pKa of I because of its importance in kinetic stability and analytical studies of prazepam (2) and II (1, 3–8).

The pKa of I[1] was determined spectrophotometrically[2] at 25° at 415 nm in a concentration of 4.07×10^{-5} *M* (10 μg/ml). All samples contained 7% (v/v) ethanol. The pH was varied by preparing samples in 0.02–0.40 *N* HCl. The spectrum of the conjugate acid was obtained in 60% (w/w) H_2SO_4 ($H_0 = -4.4$), and that of the nonionized base was obtained in buffers of pH 7.20 and 9.23. The conjugate acid species showed no absorbance at 415 nm, and the base had an absorbance of 0.23. The other spectral characteristics included decreasing absorbance at 410–420 nm and a hypsochromic shift from ~268 to 238 nm with increasing

[1] Ro 5-4365, lot PP-4 Hoffmann-La Roche, Nutley, N.J.
[2] Beckman DB-GT grating spectrophotometer, Beckman Instruments, Fullerton, Calif.

0022-3549/79/0700-0937$01.00/0

© 1979, American Pharmaceutical Association

Table I—pKa Values of Some Aniline Derivatives

Substance	Substituent	Position	pKa[a]
Aniline	—	—	4.60[b]
Aniline	Benzoyl	4	2.2[c]
Aniline	Chloro	4	3.98[b]
N-Methylaniline	—	—	4.85[b]
N-Methylaniline	Chloro	4	3.9[c]

[a] At 25°. [b] References 10 and 11. [c] Reference 11.

absorbance, both in relation to the increasing sample acidity. The I pKa was calculated from Eq. 1 (9) to be 1.45 ± 0.04[3]:

$$\text{pKa} = \text{pH} + \log (A_b - A/A - A_i) \qquad \text{(Eq. 1)}$$

where A_b, A_i, and A = the absorbances of the nonionized base, the conjugate acid, and the various samples, respectively.

The pKa values of substituted anilines such as I are lowered more by an *ortho*- than by a *meta*- or *para*-electron-withdrawing substituent (10, 11). Thus, the inductive effect of 2-benzoyl and 4-chloro groups on *N*-methylaniline (*i.e.*, I) as regards the pKa of the anilino nitrogen atom would be predicted to exceed that of the sum of these substituents at the 4-position. From Table I, the pKa differences among anilines substituted with *N*-methyl, 4-benzoyl, and 4-chloro groups are 0.25, −2.4, and −0.62 units, respectively. The arithmetic sum of these differences is −2.77 units, thereby predicting a pKa of ~1.8 (*i.e.*, 4.6 − 2.8) for I. However, the pKa lowering caused by a 4-chloro substituent is 0.1 unit greater for *N*-methylaniline than for aniline. Therefore, the observed anilino pKa decrements (Table I), augmented by the expected superior electron-inducing capability of a 2-benzoyl (*ortho*) over that of a 4-benzoyl *N*-methylaniline substituent, appear to be in reasonable agreement with the pKa estimate of 1.4–1.5 for I.

(1) J. A. F. de Silva, M. A. Schwartz, V. Stefanovic, J. Kaplan, and L. D'Arconte, *Anal. Chem.*, **36**, 2099 (1964).

(2) L. Chafetz and C. A. Gaglia, Jr., *J. Pharm. Sci.*, **56**, 1681 (1967).

(3) J. T. Carstensen, K. S. E. Su, P. Maddrell, J. B. Johnson, and H. N. Newmark, *Bull. Parenteral Drug Assoc.*, **25**, 193 (1971).

(4) J. B. Johnson and V. S. Venturella, *ibid.*, **25**, 239 (1971).

(5) W. Mayer, S. Erbe, G. Wolf, and R. Voigt, *Pharmazie*, **27**, 700 (1974).

(6) W. W. Han, G. J. Yakatan, and D. D. Maness, *J. Pharm. Sci.*, **66**, 573 (1977).

(7) D. W. Newton, *ibid.*, **67**, 550 (1978).

(8) P. J. G. Cornelissen, G. M. J. Beijersbergen Van Henegouwen, and K. W. Gerritsma, *Int. J. Pharm.*, **1**, 173 (1978).

(9) A. Albert and E. P. Serjeant, "The Determination of Ionization Constants," 2nd ed., Chapman and Hall, London, England, 1971, pp. 44, 45.

(10) *Ibid.*, p. 94.

(11) D. D. Perrin, "Dissociation Constants of Organic Bases in Aqueous Solution," Butterworths, London, England, 1965, pp. 58–87.

David W. Newton

Department of Pharmaceutics
Massachusetts College of Pharmacy
Boston, MA 02115

Received April 9, 1979.

Accepted for publication May 8, 1979.

The author thanks Dr. W. E. Scott, Hoffmann-La Roche, Nutley, N.J., for donating the sample of I.

[3] Average of five values in the pH range of pKa ± 1 unit.

Drug Dissolution within a Cascade Barrier Bed

Keyphrases □ Dissolution—test apparatus, cascade barrier bed □ Pharmacokinetics—drug dissolution tests, apparatus, cascade barrier bed □ Cascade barrier bed—for testing drug dissolution

To the Editor:

When dissolution limits the rate of drug absorption, *in vitro* dissolution tests are useful for quality control or in formulation development only if they correlate well with *in vivo* drug levels. Where satisfactory correlations have not been found, differences in solubility behavior among the polydisperse particles produced during dosage unit disintegration may be a factor. Where the relative intrinsic solubilities of particles are size dependent and sensitive to formulation variables, a single dissolution test method cannot be relied upon. Depending on the desired degree of resolution among formulations, at least two procedures are needed that produce linearly independent functional relationships between particle size and dissolution hydrodynamics. To accomplish this result, they must control the dissolution fluid mechanics as a function of particle size.

This communication discusses a cascade barrier bed test method, which complements existing procedures by providing distinctly different dissolution conditions. It differs from the USP–NF (1, 2), stationary basket–rotating filter (3), and flowthrough cell (4, 5) methods by favoring the dissolution of small particles over large.

The device consists of a vertical cylindrical cell (Fig. 1). It is partially filled with discrete layers, B, of uniformly sized, silanized glass balls. The ball size of each layer is successively increased from the bottom to the top of the bed. The prototype tested contained five layers, each 6.25 cm in height and composed of 0.25-, 0.56-, 1-, 2-, and 4-mm balls. The cell was 50 cm in height × 1.9 cm i.d.

In preparation for a run, solvent was introduced through the efflux chamber, C, to the top of the previously loaded bed so as to preclude air entrapment. The powder was then placed on top of the bed; the solvent receiving chamber, A, was filled with solvent; and flow was initiated. Flow was controlled and maintained by hydrostatic pressure; solvent flowed from an elevated reservoir through Tygon tubing to the receiving chamber, A. Samples of effluent were collected through tubing attached to chamber C and assayed. A sintered-glass frit, D, retained and supported the bed within the cell.

In operation, drug particles are carried into the bed by viscous drag forces and by gravity to a level where they are trapped. Their location is determined by drug particle size and the pore size characteristic of each layer in the bed. Particles from polydispersed systems are thus separated into various size fractions within the bed.

Although fluid flow fields in this type of packed bed are complicated, the hydrodynamics within the various layers are simply related. With column and ball diameters in a practical range for dissolution testing, random packing fractions of uniform spheres are size independent. For a constant column cross-sectional area, the average linear velocity of the solvent also will be constant throughout the bed for incompressible fluids. Voids and pores are geo-

0022-3549/79/0700-0938$01.00/0
© 1979, American Pharmaceutical Association

Table I—pKa Values of Some Aniline Derivatives

Substance	Substituent	Position	pKa[a]
Aniline	—	—	4.60[b]
Aniline	Benzoyl	4	2.2[c]
Aniline	Chloro	4	3.98[b]
N-Methylaniline	—	—	4.85[b]
N-Methylaniline	Chloro	4	3.9[c]

[a] At 25°. [b] References 10 and 11. [c] Reference 11.

absorbance, both in relation to the increasing sample acidity. The I pKa was calculated from Eq. 1 (9) to be 1.45 ± 0.04[3]:

$$\text{pKa} = \text{pH} + \log (A_b - A/A - A_i) \qquad \text{(Eq. 1)}$$

where A_b, A_i, and A = the absorbances of the nonionized base, the conjugate acid, and the various samples, respectively.

The pKa values of substituted anilines such as I are lowered more by an *ortho*- than by a *meta*- or *para*-electron-withdrawing substituent (10, 11). Thus, the inductive effect of 2-benzoyl and 4-chloro groups on *N*-methylaniline (*i.e.*, I) as regards the pKa of the anilino nitrogen atom would be predicted to exceed that of the sum of these substituents at the 4-position. From Table I, the pKa differences among anilines substituted with *N*-methyl, 4-benzoyl, and 4-chloro groups are 0.25, −2.4, and −0.62 units, respectively. The arithmetic sum of these differences is −2.77 units, thereby predicting a pKa of ~1.8 (*i.e.*, 4.6 − 2.8) for I. However, the pKa lowering caused by a 4-chloro substituent is 0.1 unit greater for *N*-methylaniline than for aniline. Therefore, the observed anilino pKa decrements (Table I), augmented by the expected superior electron-inducing capability of a 2-benzoyl (*ortho*) over that of a 4-benzoyl *N*-methylaniline substituent, appear to be in reasonable agreement with the pKa estimate of 1.4–1.5 for I.

(1) J. A. F. de Silva, M. A. Schwartz, V. Stefanovic, J. Kaplan, and L. D'Arconte, *Anal. Chem.*, **36**, 2099 (1964).

(2) L. Chafetz and C. A. Gaglia, Jr., *J. Pharm. Sci.*, **56**, 1681 (1967).

(3) J. T. Carstensen, K. S. E. Su, P. Maddrell, J. B. Johnson, and H. N. Newmark, *Bull. Parenteral Drug Assoc.*, **25**, 193 (1971).

(4) J. B. Johnson and V. S. Venturella, *ibid.*, **25**, 239 (1971).

(5) W. Mayer, S. Erbe, G. Wolf, and R. Voigt, *Pharmazie*, **27**, 700 (1974).

(6) W. W. Han, G. J. Yakatan, and D. D. Maness, *J. Pharm. Sci.*, **66**, 573 (1977).

(7) D. W. Newton, *ibid.*, **67**, 550 (1978).

(8) P. J. G. Cornelissen, G. M. J. Beijersbergen Van Henegouwen, and K. W. Gerritsma, *Int. J. Pharm.*, **1**, 173 (1978).

(9) A. Albert and E. P. Serjeant, "The Determination of Ionization Constants," 2nd ed., Chapman and Hall, London, England, 1971, pp. 44, 45.

(10) *Ibid.*, p. 94.

(11) D. D. Perrin, "Dissociation Constants of Organic Bases in Aqueous Solution," Butterworths, London, England, 1965, pp. 58–87.

David W. Newton

Department of Pharmaceutics
Massachusetts College of Pharmacy
Boston, MA 02115

Received April 9, 1979.

Accepted for publication May 8, 1979.

The author thanks Dr. W. E. Scott, Hoffmann-La Roche, Nutley, N.J., for donating the sample of I.

[3] Average of five values in the pH range of pKa ± 1 unit.

Drug Dissolution within a Cascade Barrier Bed

Keyphrases □ Dissolution—test apparatus, cascade barrier bed □ Pharmacokinetics—drug dissolution tests, apparatus, cascade barrier bed □ Cascade barrier bed—for testing drug dissolution

To the Editor:

When dissolution limits the rate of drug absorption, *in vitro* dissolution tests are useful for quality control or in formulation development only if they correlate well with *in vivo* drug levels. Where satisfactory correlations have not been found, differences in solubility behavior among the polydisperse particles produced during dosage unit disintegration may be a factor. Where the relative intrinsic solubilities of particles are size dependent and sensitive to formulation variables, a single dissolution test method cannot be relied upon. Depending on the desired degree of resolution among formulations, at least two procedures are needed that produce linearly independent functional relationships between particle size and dissolution hydrodynamics. To accomplish this result, they must control the dissolution fluid mechanics as a function of particle size.

This communication discusses a cascade barrier bed test method, which complements existing procedures by providing distinctly different dissolution conditions. It differs from the USP–NF (1, 2), stationary basket–rotating filter (3), and flowthrough cell (4, 5) methods by favoring the dissolution of small particles over large.

The device consists of a vertical cylindrical cell (Fig. 1). It is partially filled with discrete layers, B, of uniformly sized, silanized glass balls. The ball size of each layer is successively increased from the bottom to the top of the bed. The prototype tested contained five layers, each 6.25 cm in height and composed of 0.25-, 0.56-, 1-, 2-, and 4-mm balls. The cell was 50 cm in height × 1.9 cm i.d.

In preparation for a run, solvent was introduced through the efflux chamber, C, to the top of the previously loaded bed so as to preclude air entrapment. The powder was then placed on top of the bed; the solvent receiving chamber, A, was filled with solvent; and flow was initiated. Flow was controlled and maintained by hydrostatic pressure; solvent flowed from an elevated reservoir through Tygon tubing to the receiving chamber, A. Samples of effluent were collected through tubing attached to chamber C and assayed. A sintered-glass frit, D, retained and supported the bed within the cell.

In operation, drug particles are carried into the bed by viscous drag forces and by gravity to a level where they are trapped. Their location is determined by drug particle size and the pore size characteristic of each layer in the bed. Particles from polydispersed systems are thus separated into various size fractions within the bed.

Although fluid flow fields in this type of packed bed are complicated, the hydrodynamics within the various layers are simply related. With column and ball diameters in a practical range for dissolution testing, random packing fractions of uniform spheres are size independent. For a constant column cross-sectional area, the average linear velocity of the solvent also will be constant throughout the bed for incompressible fluids. Voids and pores are geo-

0022-3549/79/0700-0938$01.00/0
© 1979, American Pharmaceutical Association

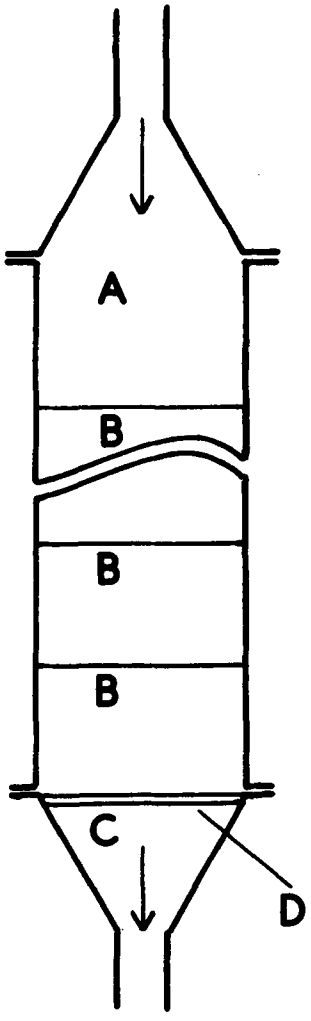

Figure 1—*Cascade barrier bed cell. Key: A, solvent receiving chamber; B, layers of monodisperse silanized glass balls; C, solvent efflux chamber; and D, sintered-glass frit for bed support.*

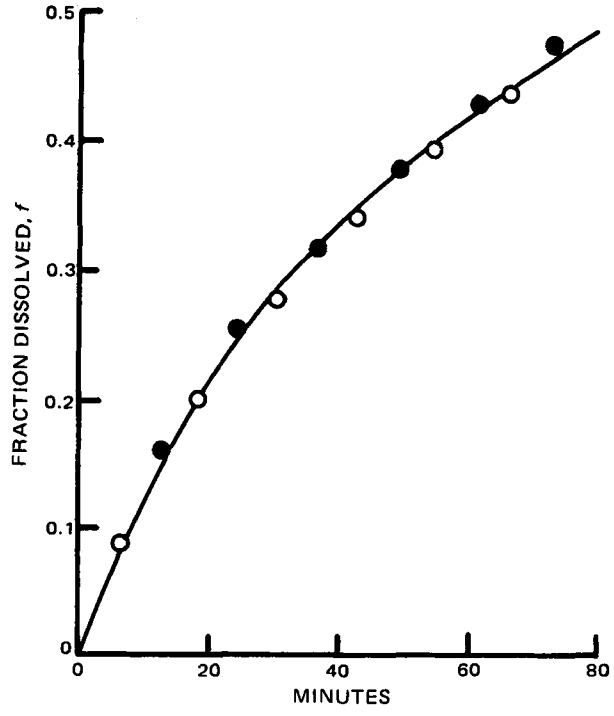

Figure 2—*Sulfadiazine dissolution data from cascade barrier bed method. Key: ○, 10-mg mixture of equal weights of fine and coarse powders; and ●, sum of fraction dissolved from separate runs of 5 mg of the individual, unmixed fine and coarse powders.*

metrically similar among the various bed layers and have dimensions in direct proportion to ball size. Therefore, solvent laminar flow shear rates are inversely proportional to ball size at equivalent locations within the voids and pores of various layers. This result is a direct consequence of the principle of geometric similarity from dimensional analysis of fluid mechanics (6). Under these conditions, shear rate gradients are inversely proportional to the square of ball dimension. No loss of solubility rate dependency on particle size will occur in going from sink to nonsink conditions, provided significant saturation does not occur in a single pass of solvent through the cell.

Table I—Regression Coefficients for Sulfadiazine Dissolution by Cascade Barrier Bed (CBB) and USP Basket Methods

Method	Sulfadiazine, mg	Particle Size, mesh	Linear Coefficient, $b \times 10^3$, min^{-1}	Quadric Coefficient, $c \times 10^5$, min^{-2}
CBB	10	100/200[a]	21.0	31.4
	10	30/50[a]	2.7	1.6
	5, 5	100/200[b], 30/50	14.5	19.7
USP	10	100/200[a]	11.1	9.1
	10	30/50[a]	2.5	2.6
	5, 5	100/200[b], 30/50	7.1	5.4

[a] Average of duplicate runs. [b] Average of triplicate runs.

It is apparent that the size and quantity of balls comprising the layers, B, the desirable number of such layers, and the solvent selected will depend on the size distribution, the amount of multiparticulate material, excipients, and drug solubility. The preliminary experiments reported were designed to test the operation of the fluid mechanical principle, which is the basis of the method.

The prototype cell was tested using deaerated 0.01 N H_2SO_4 at a flow rate of 30 ml/min under sink conditions. For comparison, the USP–NF rotating-basket method was run at 120 rpm using the same solvent, essentially under sink conditions due to low saturation levels. Sulfadiazine USP powder was compressed into tablets, coarsely ground in a mortar, and screened through U.S. standard sieves. Two size fractions were used as test materials: those passing a 30-mesh and retained on a 50-mesh sieve and those passing a 100-mesh and retained on a 200-mesh sieve.

The nondisintegrating powders were placed either on top of the bed or in the basket[1], depending on the apparatus, at the start of each run. All experiments were conducted at 25 ± 0.1°, and samples withdrawn at 3–5-min intervals were assayed by UV absorption at 243 nm. The cumulative fraction dissolved, f, was fitted to the equation $f = bt - ct^2$ by the method of least squares. Results are shown in Table I. Equally satisfactory cleaning of the cell following a run was obtained by simply continuing solvent flow or by disassembly and washing with solvent.

The ratio of the initial dissolution rate of the small particles to that of the large particles can be taken as the

[1] Hanson Research Corp., Northridge, CA 91324.

ratio of the corresponding b values. These ratios are 7.7 and 4.4 for the cascade barrier bed and USP methods, respectively. If a uniform size distribution for each powder fraction is assumed, the finer powder should have approximately four times the specific surface area of the coarse powder. Thus, the initial dissolution rate per unit surface area of the fine powder is nearly twice that of the coarse powder for the cascade barrier bed method and is comparable to the coarse powder for the USP method. These observations conform to expectations based on apparatus design and fluid mechanical theory.

Figure 2 shows the cascade barrier bed dissolution behavior of a mixture of 5 mg each of the fine and coarse sulfadiazine powders. For comparison, results of separate cascade barrier bed runs of 5 mg of the individual powder grades were added and the sum was plotted. The two plots closely correspond and indicate independent dissolution behavior of the two powder fractions within the bed.

These findings do not indicate the superiority of one *in vitro* dissolution apparatus over another. Instead, they suggest that, where particle-size effects prevent useful correlations with *in vivo* drug levels, parallel use of two such contrasting methods is necessary.

(1) "The United States Pharmacopeia," 19th rev., Mack Publishing Co., Easton, Pa., 1975, p. 651.

(2) "Fourth Supplement to USP XIX and NF XIV," The United States Pharmacopeial Convention, Rockville, Md., 1978, pp. 194, 195.

(3) A. C. Shah, C. B. Peot, and J. F. Ochs, *J. Pharm. Sci.*, **62**, 671 (1973).

(4) F. Langenbucher, *ibid.*, **58**, 1265 (1969).

(5) J. E. Tingstad and S. Riegelman, *ibid.*, **59**, 692 (1970).

(6) W.-H. Li and S.-H. Lam, "Principles of Fluid Mechanics," Addison-Wesley, Reading, Mass., 1964, p. 18.

Edward G. Rippie ˣ
Abu S. M. S. Huq
Department of Pharmaceutics
College of Pharmacy
University of Minnesota
Minneapolis, MN 55455

Received January 8, 1979.
Accepted for publication April 20, 1979.

BOOKS

REVIEWS

Analytical Profiles of Drug Substances, Volume 7. Edited by KLAUS FLOREY. Academic, 111 Fifth Ave., New York, NY 10003. 1978. ix + 504 pp. 15 × 23 cm.

Volume 7 of this series includes individual drug monographs dealing with supplementary information that is not listed in the official compendia. The entire series of volumes was undertaken as a cooperative venture by the Pharmaceutical Analysis and Control Section, Academy of Pharmaceutical Sciences. The profiles of drug substances in each volume are submitted by contributors and checked by selected reviewers. A typical profile includes such topics as a description of the compound (name, formula, molecular weight, color, odor, and salts), physical properties (IR, NMR, UV, and mass spectra, melting or boiling point, solubility, partition coefficient, and dissociation constant), syntheses, stability, analysis methods, and metabolism and pharmacokinetic data.

The monographs include up-to-date references, and many contributors state that their references are complete through a certain year, a worthwhile piece of information for the reader. Among the drugs covered in Volume 7 are allopurinol, amoxicillin, chlorpheniramine maleate, dihydroergotoxine methanesulfonate, diphenoxylate hydrochloride, droperidol, epinephrine, ethambutol hydrochloride, fluoxymesterone, hexetidine, hydroflumethiazide, hydroxyzine dihydrochloride, 6-mercaptopurine, phenobarbital, sulfamethazine, thiostrepton, trimethoprim, and tubocurarine chloride.

The entire series should be included in school of pharmacy library reading rooms and in university science libraries. They contain important drug data that have not been available previously in one single reference source. The series is not meant to be used as a textbook but can be employed effectively as reference material for any pharmaceutical or medicinal chemistry course.

Reviewed by James T. Stewart
School of Pharmacy
University of Georgia
Athens, GA 30602

NOTICES

Acta Facultatis Pharmaceuticae. Universitatis Comenianae. XXX. 1977. 221 pp. 17 × 24 cm.

Advances in Modern Toxicology. Vol. 1. New Concepts in Safety Evaluation, Part 2. Edited by MYRON A. MEHLMAN, RAYMOND E. SHAPIRO, and HERBERT BLUEMENTHAL. Wiley, One Wiley Drive, Somerset, NJ 08873. 1979. 191 pp. 14 × 23 cm.

The Aqueous Cytoplasm. Contemporary Bio-physics Series, Vol. 1. Edited by ALEC D. KEITH. Dekker, 270 Madison Ave., New York, NY 10016. 1979. 230 pp. 14 × 23 cm. Price $27.50.

Clinical Laboratory Statistics. 2nd Ed. By ROY N. BARNETT. Little, Brown, 34 Beacon St., Boston, MA 02106. 1978. 237 pp. 15 × 23 cm.

Comparative Endocrinology of Prolactin. By D. M. ENSOR. Wiley, 605 Third Ave., New York, NY 10016. 1978. 309 pp. 15 × 23 cm. Price $45.00.

Drugs and the Special Child. Edited by MICHAEL JAY COHEN. Wiley, One Wiley Drive, Somerset, NJ 08873. 1979. 258 pp. 15 × 23 cm. Price $18.95.

Environmental Health Criteria 5: Nitrates, Nitrites, and N-Nitroso Compounds. Published under the joint sponsorship of the United Nations Environment Programme and the World Health Organization, Geneva, Switzerland. 1978. 207 pp. 13 × 21 cm. Price $5.00.

Evaluation and Optimization of Laboratory Methods and Analytical Procedures. A Survey of Statistical and Mathematical Techniques. By DESIRÉ L. MASSART, AUKE DIJKSTRA, and LEONARD KAUFMAN. Elsevier/North-Holland Inc., 52 Vanderbilt Ave., New York, NY 10017. 1978. 596 pp. 16 × 24 cm.

Computers in the Clinical Laboratory: An Introduction. Clinical and Biochemical Analysis: A Series of Monographs and Textbooks, Vol. 8. By E. CLIFFORD TOREN, Jr., and ARTHUR A. EGGERT. Dekker, 270 Madison Ave., New York, NY 10016. 1978. 166 pp. 15 × 23 cm. Price $19.75.

Cutting's Handbook of Pharmacology. The Actions and Uses of Drugs, 6th Ed. By T. Z. CSKAY. Appleton-Century-Crofts, 292 Madison Ave., New York, NY 10017. 1978. 697 pp. 14 × 23 cm.

ratio of the corresponding b values. These ratios are 7.7 and 4.4 for the cascade barrier bed and USP methods, respectively. If a uniform size distribution for each powder fraction is assumed, the finer powder should have approximately four times the specific surface area of the coarse powder. Thus, the initial dissolution rate per unit surface area of the fine powder is nearly twice that of the coarse powder for the cascade barrier bed method and is comparable to the coarse powder for the USP method. These observations conform to expectations based on apparatus design and fluid mechanical theory.

Figure 2 shows the cascade barrier bed dissolution behavior of a mixture of 5 mg each of the fine and coarse sulfadiazine powders. For comparison, results of separate cascade barrier bed runs of 5 mg of the individual powder grades were added and the sum was plotted. The two plots closely correspond and indicate independent dissolution behavior of the two powder fractions within the bed.

These findings do not indicate the superiority of one *in vitro* dissolution apparatus over another. Instead, they suggest that, where particle-size effects prevent useful correlations with *in vivo* drug levels, parallel use of two such contrasting methods is necessary.

(1) "The United States Pharmacopeia," 19th rev., Mack Publishing Co., Easton, Pa., 1975, p. 651.

(2) "Fourth Supplement to USP XIX and NF XIV," The United States Pharmacopeial Convention, Rockville, Md., 1978, pp. 194, 195.

(3) A. C. Shah, C. B. Peot, and J. F. Ochs, *J. Pharm. Sci.*, **62**, 671 (1973).

(4) F. Langenbucher, *ibid.*, **58**, 1265 (1969).

(5) J. E. Tingstad and S. Riegelman, *ibid.*, **59**, 692 (1970).

(6) W.-H. Li and S.-H. Lam, "Principles of Fluid Mechanics," Addison-Wesley, Reading, Mass., 1964, p. 18.

Edward G. Rippie ˣ
Abu S. M. S. Huq
Department of Pharmaceutics
College of Pharmacy
University of Minnesota
Minneapolis, MN 55455

Received January 8, 1979.
Accepted for publication April 20, 1979.

BOOKS

REVIEWS

Analytical Profiles of Drug Substances, Volume 7. Edited by KLAUS FLOREY. Academic, 111 Fifth Ave., New York, NY 10003. 1978. ix + 504 pp. 15 × 23 cm.

Volume 7 of this series includes individual drug monographs dealing with supplementary information that is not listed in the official compendia. The entire series of volumes was undertaken as a cooperative venture by the Pharmaceutical Analysis and Control Section, Academy of Pharmaceutical Sciences. The profiles of drug substances in each volume are submitted by contributors and checked by selected reviewers. A typical profile includes such topics as a description of the compound (name, formula, molecular weight, color, odor, and salts), physical properties (IR, NMR, UV, and mass spectra, melting or boiling point, solubility, partition coefficient, and dissociation constant), syntheses, stability, analysis methods, and metabolism and pharmacokinetic data.

The monographs include up-to-date references, and many contributors state that their references are complete through a certain year, a worthwhile piece of information for the reader. Among the drugs covered in Volume 7 are allopurinol, amoxicillin, chlorpheniramine maleate, dihydroergotoxine methanesulfonate, diphenoxylate hydrochloride, droperidol, epinephrine, ethambutol hydrochloride, fluoxymesterone, hexetidine, hydroflumethiazide, hydroxyzine dihydrochloride, 6-mercaptopurine, phenobarbital, sulfamethazine, thiostrepton, trimethoprim, and tubocurarine chloride.

The entire series should be included in school of pharmacy library reading rooms and in university science libraries. They contain important drug data that have not been available previously in one single reference source. The series is not meant to be used as a textbook but can be employed effectively as reference material for any pharmaceutical or medicinal chemistry course.

Reviewed by James T. Stewart
School of Pharmacy
University of Georgia
Athens, GA 30602

NOTICES

Acta Facultatis Pharmaceuticae. Universitatis Comenianae. XXX. 1977. 221 pp. 17 × 24 cm.

Advances in Modern Toxicology. Vol. 1. New Concepts in Safety Evaluation, Part 2. Edited by MYRON A. MEHLMAN, RAYMOND E. SHAPIRO, and HERBERT BLUEMENTHAL. Wiley, One Wiley Drive, Somerset, NJ 08873. 1979. 191 pp. 14 × 23 cm.

The Aqueous Cytoplasm. Contemporary Bio-physics Series, Vol. 1. Edited by ALEC D. KEITH. Dekker, 270 Madison Ave., New York, NY 10016. 1979. 230 pp. 14 × 23 cm. Price $27.50.

Clinical Laboratory Statistics. 2nd Ed. By ROY N. BARNETT. Little, Brown, 34 Beacon St., Boston, MA 02106. 1978. 237 pp. 15 × 23 cm.

Comparative Endocrinology of Prolactin. By D. M. ENSOR. Wiley, 605 Third Ave., New York, NY 10016. 1978. 309 pp. 15 × 23 cm. Price $45.00.

Drugs and the Special Child. Edited by MICHAEL JAY COHEN. Wiley, One Wiley Drive, Somerset, NJ 08873. 1979. 258 pp. 15 × 23 cm. Price $18.95.

Environmental Health Criteria 5: Nitrates, Nitrites, and N-Nitroso Compounds. Published under the joint sponsorship of the United Nations Environment Programme and the World Health Organization, Geneva, Switzerland. 1978. 207 pp. 13 × 21 cm. Price $5.00.

Evaluation and Optimization of Laboratory Methods and Analytical Procedures. A Survey of Statistical and Mathematical Techniques. By DESIRÉ L. MASSART, AUKE DIJKSTRA, and LEONARD KAUFMAN. Elsevier/North-Holland Inc., 52 Vanderbilt Ave., New York, NY 10017. 1978. 596 pp. 16 × 24 cm.

Computers in the Clinical Laboratory: An Introduction. Clinical and Biochemical Analysis: A Series of Monographs and Textbooks, Vol. 8. By E. CLIFFORD TOREN, Jr., and ARTHUR A. EGGERT. Dekker, 270 Madison Ave., New York, NY 10016. 1978. 166 pp. 15 × 23 cm. Price $19.75.

Cutting's Handbook of Pharmacology. The Actions and Uses of Drugs, 6th Ed. By T. Z. CSKAY. Appleton-Century-Crofts, 292 Madison Ave., New York, NY 10017. 1978. 697 pp. 14 × 23 cm.

ratio of the corresponding b values. These ratios are 7.7 and 4.4 for the cascade barrier bed and USP methods, respectively. If a uniform size distribution for each powder fraction is assumed, the finer powder should have approximately four times the specific surface area of the coarse powder. Thus, the initial dissolution rate per unit surface area of the fine powder is nearly twice that of the coarse powder for the cascade barrier bed method and is comparable to the coarse powder for the USP method. These observations conform to expectations based on apparatus design and fluid mechanical theory.

Figure 2 shows the cascade barrier bed dissolution behavior of a mixture of 5 mg each of the fine and coarse sulfadiazine powders. For comparison, results of separate cascade barrier bed runs of 5 mg of the individual powder grades were added and the sum was plotted. The two plots closely correspond and indicate independent dissolution behavior of the two powder fractions within the bed.

These findings do not indicate the superiority of one *in vitro* dissolution apparatus over another. Instead, they suggest that, where particle-size effects prevent useful correlations with *in vivo* drug levels, parallel use of two such contrasting methods is necessary.

(1) "The United States Pharmacopeia," 19th rev., Mack Publishing Co., Easton, Pa., 1975, p. 651.

(2) "Fourth Supplement to USP XIX and NF XIV," The United States Pharmacopeial Convention, Rockville, Md., 1978, pp. 194, 195.

(3) A. C. Shah, C. B. Peot, and J. F. Ochs, *J. Pharm. Sci.*, **62**, 671 (1973).

(4) F. Langenbucher, *ibid.*, **58**, 1265 (1969).

(5) J. E. Tingstad and S. Riegelman, *ibid.*, **59**, 692 (1970).

(6) W.-H. Li and S.-H. Lam, "Principles of Fluid Mechanics," Addison-Wesley, Reading, Mass., 1964, p. 18.

Edward G. Rippie ˣ
Abu S. M. S. Huq
Department of Pharmaceutics
College of Pharmacy
University of Minnesota
Minneapolis, MN 55455

Received January 8, 1979.
Accepted for publication April 20, 1979.

BOOKS

REVIEWS

Analytical Profiles of Drug Substances, Volume 7. Edited by KLAUS FLOREY. Academic, 111 Fifth Ave., New York, NY 10003. 1978. ix + 504 pp. 15 × 23 cm.

Volume 7 of this series includes individual drug monographs dealing with supplementary information that is not listed in the official compendia. The entire series of volumes was undertaken as a cooperative venture by the Pharmaceutical Analysis and Control Section, Academy of Pharmaceutical Sciences. The profiles of drug substances in each volume are submitted by contributors and checked by selected reviewers. A typical profile includes such topics as a description of the compound (name, formula, molecular weight, color, odor, and salts), physical properties (IR, NMR, UV, and mass spectra, melting or boiling point, solubility, partition coefficient, and dissociation constant), syntheses, stability, analysis methods, and metabolism and pharmacokinetic data.

The monographs include up-to-date references, and many contributors state that their references are complete through a certain year, a worthwhile piece of information for the reader. Among the drugs covered in Volume 7 are allopurinol, amoxicillin, chlorpheniramine maleate, dihydroergotoxine methanesulfonate, diphenoxylate hydrochloride, droperidol, epinephrine, ethambutol hydrochloride, fluoxymesterone, hexetidine, hydroflumethiazide, hydroxyzine dihydrochloride, 6-mercaptopurine, phenobarbital, sulfamethazine, thiostrepton, trimethoprim, and tubocurarine chloride.

The entire series should be included in school of pharmacy library reading rooms and in university science libraries. They contain important drug data that have not been available previously in one single reference source. The series is not meant to be used as a textbook but can be employed effectively as reference material for any pharmaceutical or medicinal chemistry course.

Reviewed by James T. Stewart
School of Pharmacy
University of Georgia
Athens, GA 30602

NOTICES

Acta Facultatis Pharmaceuticae. Universitatis Comenianae. XXX. 1977. 221 pp. 17 × 24 cm.

Advances in Modern Toxicology. Vol. 1. New Concepts in Safety Evaluation, Part 2. Edited by MYRON A. MEHLMAN, RAYMOND E. SHAPIRO, and HERBERT BLUEMENTHAL. Wiley, One Wiley Drive, Somerset, NJ 08873. 1979. 191 pp. 14 × 23 cm.

The Aqueous Cytoplasm. Contemporary Bio-physics Series, Vol. 1. Edited by ALEC D. KEITH. Dekker, 270 Madison Ave., New York, NY 10016. 1979. 230 pp. 14 × 23 cm. Price $27.50.

Clinical Laboratory Statistics. 2nd Ed. By ROY N. BARNETT. Little, Brown, 34 Beacon St., Boston, MA 02106. 1978. 237 pp. 15 × 23 cm.

Comparative Endocrinology of Prolactin. By D. M. ENSOR. Wiley, 605 Third Ave., New York, NY 10016. 1978. 309 pp. 15 × 23 cm. Price $45.00.

Drugs and the Special Child. Edited by MICHAEL JAY COHEN. Wiley, One Wiley Drive, Somerset, NJ 08873. 1979. 258 pp. 15 × 23 cm. Price $18.95.

Environmental Health Criteria 5: Nitrates, Nitrites, and N-Nitroso Compounds. Published under the joint sponsorship of the United Nations Environment Programme and the World Health Organization, Geneva, Switzerland. 1978. 207 pp. 13 × 21 cm. Price $5.00.

Evaluation and Optimization of Laboratory Methods and Analytical Procedures. A Survey of Statistical and Mathematical Techniques. By DESIRÉ L. MASSART, AUKE DIJKSTRA, and LEONARD KAUFMAN. Elsevier/North-Holland Inc., 52 Vanderbilt Ave., New York, NY 10017. 1978. 596 pp. 16 × 24 cm.

Computers in the Clinical Laboratory: An Introduction. Clinical and Biochemical Analysis: A Series of Monographs and Textbooks, Vol. 8. By E. CLIFFORD TOREN, Jr., and ARTHUR A. EGGERT. Dekker, 270 Madison Ave., New York, NY 10016. 1978. 166 pp. 15 × 23 cm. Price $19.75.

Cutting's Handbook of Pharmacology. The Actions and Uses of Drugs, 6th Ed. By T. Z. CSKAY. Appleton-Century-Crofts, 292 Madison Ave., New York, NY 10017. 1978. 697 pp. 14 × 23 cm.

A publication of the
American Pharmaceutical Association—
the National Professional Society
of Pharmacists

JOURNAL OF PHARMACEUTICAL SCIENCES

INDEX TO AUTHORS
INDEX TO SUBJECTS

VOLUME 68
JANUARY TO DECEMBER, 1979

Published monthly under the supervision of the Board of Trustees

MARY H. FERGUSON
Editor

SHELLY ELLIOTT
Production Editor

MARCIA GARTRELL
Copy Editor

NICOLETTE TRIANTAFELLU
Copy Editor

EDWARD G. FELDMANN
Contributing Editor

SAMUEL W. GOLDSTEIN
Contributing Editor

BELLE R. BECK
Editorial Secretary

DAVID BOHARDT
Director of Publications

L. LUAN CORRIGAN
Assistant Director of Publications

EDITORIAL ADVISORY BOARD

John Autian
Norman R. Farnsworth
William O. Foye
William J. Jusko
Herbert A. Lieberman
David E. Mann, Jr.
Gerald J. Papariello
Edward G. Rippie

AUGUST 1979
VOLUME 68 NUMBER 8

JOURNAL OF PHARMACEUTICAL SCIENCES

MARY H. FERGUSON
Editor

SHELLY ELLIOTT
Production Editor

MARCIA GARTRELL
Copy Editor

EDWARD G. FELDMANN
Contributing Editor

SAMUEL W. GOLDSTEIN
Contributing Editor

BELLE R. BECK
Editorial Secretary

DAVID BOHARDT
Director of Publications

L. LUAN CORRIGAN
Assistant Director of Publications

EDITORIAL ADVISORY BOARD

JOHN AUTIAN	HERBERT A. LIEBERMAN
NORMAN R. FARNSWORTH	DAVID E. MANN, JR.
WILLIAM O. FOYE	GERALD J. PAPARIELLO
WILLIAM J. JUSKO	EDWARD G. RIPPIE

The *Journal of Pharmaceutical Sciences* (ISSN 0022-3549) is published monthly by the American Pharmaceutical Association (APhA) at 2215 Constitution Ave., N.W., Washington, DC 20037. Second-class postage paid at Washington, D.C., and at additional mailing office.

All expressions of opinion and statements of supposed fact appearing in articles or editorials carried in this journal are published on the authority of the writer over whose name they appear and are not to be regarded as necessarily expressing the policies or views of APhA.

Offices—Editorial, Advertising, and Subscription: 2215 Constitution Ave., N.W., Washington, DC 20037. Printing: 20th & Northampton Streets, Easton, PA 18042.

Annual Subscriptions—United States and foreign, industrial and government institutions $50, educational institutions $50, individuals *for personal use only* $30; single copies $5. All foreign subscriptions add $5 for postage. Subscription rates are subject to change without notice. Members of APhA may elect to receive the *Journal of Pharmaceutical Sciences* as a part of their annual $70 (foreign $75) APhA membership dues.

Claims—Missing numbers will not be supplied if dues or subscriptions are in arrears for more than 60 days or if claims are received more than 60 days after the date of the issue, or if loss was due to failure to give notice of change of address. APhA cannot accept responsibility for foreign delivery when its records indicate shipment was made.

Change of Address—Members and subscribers should notify at once both the Post Office and APhA of any change of address.

Photocopying—The code at the foot of the first page of an article indicates that APhA has granted permission for copying of the article beyond the limits permitted by Sections 107 and 108 of the U.S. Copyright Law provided that the copier sends the per copy fee stated in the code to the Copyright Clearance Center, Inc., P.O. Box 8891, Boston, MA 02114. Copies may be made for personal or internal use only and not for general distribution.

Microfilm—Available from University Microfilms International, 300 N. Zeeb Road, Ann Arbor, MI 48106.

© Copyright 1979, American Pharmaceutical Association, 2215 Constitution Ave., N.W., Washington, DC 20037; all rights reserved.

PHARMACEUTICAL EXCIPIENTS COME OF AGE

For a great variety of reasons, but all with the objective of serving the needs of its membership specifically and the needs of the profession of pharmacy and the health care community in general, APhA has embarked on a broad publication program which now includes a complete spectrum of journals, pamphlets, workbooks, textbooks, audio-visual aids, newsletters, and so on. If it is true that *"Heinz has pickles,"* then it can equally be said that *"APhA has publications!"*

Given the fact that the Association is knee-deep in the products of its publications program, something really special would need to come along for us to devote this column to a discussion of just one of these literary undertakings. Moreover, if the end-product of that undertaking is still a couple of years off, then it needs to be more than special but even extra-special. And, in our opinion, the prospective item we have in mind looks as if it will be just that.

For many years, pharmaceutical scientists have devoted considerable time, attention, and effort to devising definitions, tests, standards, assays, specifications, and the like for drug entities and drug dosage forms. Indeed, they did such a good job that Congress legally recognized two products of this activity—the *United States Pharmacopeia* and the *National Formulary*—as "official compendia," and mandated that bulk drug substances and marketed drug dosage forms comply with the standards or be subject to enforcement actions on legal grounds of misbranding or adulteration.

In formulating drug dosage forms, pharmaceutical research and development staff will generally utilize a variety of substances that are intended to transform the simple drug active ingredient into a pharmaceutically elegant dosage form. These substances are broadly referred to as pharmaceutical excipients, aids, or adjuncts, and while contributing to the overall quality of the product, they are not intended to have any physiological effect of their own. They impart improved properties such as appearance, flavor, stability, ease of administration, and convenience.

Although standards, specifications, and the like have also been devised for some of these excipients, neither the breadth nor the depth of these efforts has compared to that devoted to the drug entities and dosage forms. Moreover, no concerted effort has been made to pull all this information together in a single reference source where it would be conveniently available as well as presented in a uniform and consistent format. Finally, the *kinds* of information most useful to a pharmaceutical scientist involved in product formulation are often quite different from those that may be appropriate for an excipient which is recognized in a compendium of tests and standards.

Given this background, a pharmacist and pharmaceutical scientist with a long background in drug product formulation, research, development, analysis, and specifications concluded that the time was over-ripe for someone to respond to this need. The man of vision in this case is Jack Cooper, a person who has been long active in APhA, its old Scientific Section and Industrial Pharmacy Section, and then the initial Past President when the APhA Academy of Pharmaceutical Sciences was created in the mid-1960's.

Approximately three years ago, Mr. Cooper conceived of the idea of developing a *Handbook of Pharmaceutical Excipients*, and then went about the job, virtually single-handedly, of convincing others of the value and need for such a compilation. In this process, he took his proposal to the APhA Academy of Pharmaceutical Sciences, and he won their endorsement, support, and agreement to take on the task as an Academy-sponsored project. He also recruited some 120 pharmaceutical scientists for service as volunteer collaborators on the various committees to identify and select excipients for inclusion, to ascertain and compile information currently known about those excipients, to develop new information in order to fill gaps in what is known, to verify literature values and data, and to prepare the resultant information in an orderly, organized monograph format.

Presently, Mr. Cooper reports that the project is moving steadily along, but it is still too early to predict a completion date. We do, however, wish to take this opportunity to congratulate the APS for taking on the sponsorship of this important project, and to salute Jack Cooper for his vision, determination, and dedication in undertaking immediate responsibility for its development. At the same time, we would encourage any of our readers with an interest in this subject to volunteer their efforts. As Project Chairman, Mr. Cooper can use all the assistance he can get. In his own words, "*. . . it has become increasing clear that a direct relationship exists between the amount of technical data in the monographs and the potential value of the book to pharmaceutical scientists.*"

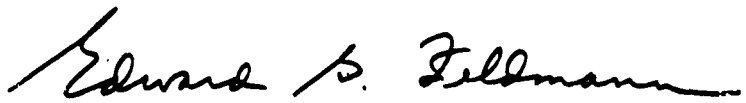

Hospital Pharmacy and the CGMP

Doctor Feldmann's editorial in the May issue[1] charges FDA with requiring hospital pharmacists to comply with the revised current Good Manufacturing Practice Regulations (CGMP).

Not so.

The quotation in this editorial comes from paragraph 43 of the preamble to the CGMP's[2] in which FDA responded to the general comments received from the public on the proposed amendments. Retrospectively, it is apparent that paragraph 43 is not as clear as it should be. Nevertheless, we can state unequivocally that FDA is not interested in, and has *never* asserted jurisdiction over, a hospital pharmacy that limits its activities to serving the hospital of which it is a part. We would only consider the hospital pharmacy to be a repacker if the unit dose packages that it prepares are marketed outside the hospital. Even then, if it shares its unit dose services with other hospitals, we have special, separate guidelines covering such services.

FDA's position is best expressed by the Commissioner's endorsement of the unit dose repackaging guidelines prepared by The American Society of Hospital Pharmacists and published in the December 1977 issue of the *American Journal of Hospital Pharmacy*. Dr. Kennedy said:

> *"We applaud the American Society of Hospital Pharmacists for preparing this important guide to a better quality control system for drugs repackaged by hospital pharmacists for use in a unit dose drug distribution system. We recognize it as a major step forward in assuring that patients receive safe and efficacious drugs. In our judgment it is an excellent example of what a professional society can do to improve patient care in hospitals."*

It is FDA's view that the ASHP guidelines are suitable equivalents to our CGMP's for normal hospital pharmacy practice.

J. Joseph Belson, Director
Division of Drug Product Quality
Bureau of Drugs
Food and Drug Administration
Rockville, MD 20852

Bernard T. Loftus, Director
Division of Drug Manufacturing
Bureau of Drugs
Food and Drug Administration
Rockville, MD 20852

Received May 25, 1979.

[1] E. G. Feldmann, *J. Pharm. Sci.*, **68** (5), I (1979).
[2] *Fed. Regist.* (Sept. 29, 1978).

Hospital Pharmacy and the CGMP: A Response

We appreciate this response from Mr. Belson and Mr. Loftus and their effort to clarify the FDA intent of the current GMP regulations.

Our May editorial was originally stimulated by a series of discussions between APhA (and ASHP) staff on the one side and FDA staff on the other side during the 1977–1978 period. The background facts, as we were told them, differ from those described in the Belson–Loftus letter.

Specifically, FDA *did* attempt to assert jurisdiction over hospital pharmacy *via* challenges to certain operating procedures pertaining to unit dose repackaging. These challenges took several forms, one of which was directed at an arrangement whereby a "contract repackager" would bring unit dose repackaging equipment to the hospital and operate it to fulfill the current repackaging needs of the hospital. Under these arrangements, the operation (*a*) took place at the pertinent hospital, (*b*) functioned under the direct supervision of the hospital pharmacist, and (*c*) was limited to producing unit dose packages exclusively for use within that hospital. But, nevertheless, FDA did assert jurisdiction in at least several such instances, thereby causing significant problems and generally hassling the various parties involved.

After considerable skirmishing, an unwritten "truce" eventually emerged, and both sides appeared content to leave the matter rest—although basically unresolved, the issue was not actively pursued further.

But the wording of the September 1978 *Federal Register* preamble—plus pharmacist West's correspondence—made it appear to us that FDA was again preparing to flex its muscle.

Upon receipt of the Belson–Loftus letter, we checked once more to ensure that we had correctly stated our recollection of the situation and its past history. One of the APhA staff members familiar with the situation stated that: "FDA is now trying to do a disappearing act." And an ASHP staff member pointed out that in this letter the operable word is "asserted"; that is, even here, FDA is not conceding any lack of jurisdiction over such pharmacy practice in the hospital setting, but only that it is not presently asserting such jurisdiction.

Nevertheless, both of these staff members also added that this Belson–Loftus letter was far less equivocating than past FDA statements on this issue. Furthermore, had FDA actually followed the policy described in this letter in the past, the entire controversy would never have arisen in the first place!

Edward G. Feldmann
American Pharmaceutical Association
Washington, DC 20037

Received June 19, 1979.

Amphetamine Analogs

The recent article on "Heterocyclic Analogs of Amphetamine . . ." by W. O. Foye and S. Tovivich[1] listed two pyridine compounds without reference to previous work. β-(6-Methyl-2-pyridyl)-isopropylamine was reported by A. Burger and G. E. Ullyot [*J. Org. Chem.*, **12**, 342 (1947)], and β-(3-pyridyl)isopropylamine was reported by A. Burger and C. R. Walter, Jr. [*J. Am. Chem. Soc.*, **72**, 1988 (1950)].

Alfred Burger
Professor Emeritus
Department of Chemistry
University of Virginia
Charlottesville, VA 22901

Received June 14, 1979.

[1] W. O. Foye and S. Tovivich, *J. Pharm. Sci.*, **68**, 591 (1979).

Hospital Pharmacy and the CGMP

Doctor Feldmann's editorial in the May issue[1] charges FDA with requiring hospital pharmacists to comply with the revised current Good Manufacturing Practice Regulations (CGMP).

Not so.

The quotation in this editorial comes from paragraph 43 of the preamble to the CGMP's[2] in which FDA responded to the general comments received from the public on the proposed amendments. Retrospectively, it is apparent that paragraph 43 is not as clear as it should be. Nevertheless, we can state unequivocally that FDA is not interested in, and has *never* asserted jurisdiction over, a hospital pharmacy that limits its activities to serving the hospital of which it is a part. We would only consider the hospital pharmacy to be a repacker if the unit dose packages that it prepares are marketed outside the hospital. Even then, if it shares its unit dose services with other hospitals, we have special, separate guidelines covering such services.

FDA's position is best expressed by the Commissioner's endorsement of the unit dose repackaging guidelines prepared by The American Society of Hospital Pharmacists and published in the December 1977 issue of the *American Journal of Hospital Pharmacy*. Dr. Kennedy said:

> *"We applaud the American Society of Hospital Pharmacists for preparing this important guide to a better quality control system for drugs repackaged by hospital pharmacists for use in a unit dose drug distribution system. We recognize it as a major step forward in assuring that patients receive safe and efficacious drugs. In our judgment it is an excellent example of what a professional society can do to improve patient care in hospitals."*

It is FDA's view that the ASHP guidelines are suitable equivalents to our CGMP's for normal hospital pharmacy practice.

J. Joseph Belson, Director
Division of Drug Product Quality
Bureau of Drugs
Food and Drug Administration
Rockville, MD 20852

Bernard T. Loftus, Director
Division of Drug Manufacturing
Bureau of Drugs
Food and Drug Administration
Rockville, MD 20852

Received May 25, 1979.

[1] E. G. Feldmann, *J. Pharm. Sci.*, **68** (5), I (1979).
[2] *Fed. Regist.* (Sept. 29, 1978).

Hospital Pharmacy and the CGMP: A Response

We appreciate this response from Mr. Belson and Mr. Loftus and their effort to clarify the FDA intent of the current GMP regulations.

Our May editorial was originally stimulated by a series of discussions between APhA (and ASHP) staff on the one side and FDA staff on the other side during the 1977–1978 period. The background facts, as we were told them, differ from those described in the Belson–Loftus letter.

Specifically, FDA *did* attempt to assert jurisdiction over hospital pharmacy *via* challenges to certain operating procedures pertaining to unit dose repackaging. These challenges took several forms, one of which was directed at an arrangement whereby a "contract repackager" would bring unit dose repackaging equipment to the hospital and operate it to fulfill the current repackaging needs of the hospital. Under these arrangements, the operation (*a*) took place at the pertinent hospital, (*b*) functioned under the direct supervision of the hospital pharmacist, and (*c*) was limited to producing unit dose packages exclusively for use within that hospital. But, nevertheless, FDA did assert jurisdiction in at least several such instances, thereby causing significant problems and generally hassling the various parties involved.

After considerable skirmishing, an unwritten "truce" eventually emerged, and both sides appeared content to leave the matter rest—although basically unresolved, the issue was not actively pursued further.

But the wording of the September 1978 *Federal Register* preamble—plus pharmacist West's correspondence—made it appear to us that FDA was again preparing to flex its muscle.

Upon receipt of the Belson–Loftus letter, we checked once more to ensure that we had correctly stated our recollection of the situation and its past history. One of the APhA staff members familiar with the situation stated that: "FDA is now trying to do a disappearing act." And an ASHP staff member pointed out that in this letter the operable word is "asserted"; that is, even here, FDA is not conceding any lack of jurisdiction over such pharmacy practice in the hospital setting, but only that it is not presently asserting such jurisdiction.

Nevertheless, both of these staff members also added that this Belson–Loftus letter was far less equivocating than past FDA statements on this issue. Furthermore, had FDA actually followed the policy described in this letter in the past, the entire controversy would never have arisen in the first place!

Edward G. Feldmann
American Pharmaceutical Association
Washington, DC 20037

Received June 19, 1979.

Amphetamine Analogs

The recent article on "Heterocyclic Analogs of Amphetamine . . ." by W. O. Foye and S. Tovivich[1] listed two pyridine compounds without reference to previous work. β-(6-Methyl-2-pyridyl)-isopropylamine was reported by A. Burger and G. E. Ullyot [*J. Org. Chem.*, **12**, 342 (1947)], and β-(3-pyridyl)isopropylamine was reported by A. Burger and C. R. Walter, Jr. [*J. Am. Chem. Soc.*, **72**, 1988 (1950)].

Alfred Burger
Professor Emeritus
Department of Chemistry
University of Virginia
Charlottesville, VA 22901

Received June 14, 1979.

[1] W. O. Foye and S. Tovivich, *J. Pharm. Sci.*, **68**, 591 (1979).

Hospital Pharmacy and the CGMP

Doctor Feldmann's editorial in the May issue[1] charges FDA with requiring hospital pharmacists to comply with the revised current Good Manufacturing Practice Regulations (CGMP).

Not so.

The quotation in this editorial comes from paragraph 43 of the preamble to the CGMP's[2] in which FDA responded to the general comments received from the public on the proposed amendments. Retrospectively, it is apparent that paragraph 43 is not as clear as it should be. Nevertheless, we can state unequivocally that FDA is not interested in, and has *never* asserted jurisdiction over, a hospital pharmacy that limits its activities to serving the hospital of which it is a part. We would only consider the hospital pharmacy to be a repacker if the unit dose packages that it prepares are marketed outside the hospital. Even then, if it shares its unit dose services with other hospitals, we have special, separate guidelines covering such services.

FDA's position is best expressed by the Commissioner's endorsement of the unit dose repackaging guidelines prepared by The American Society of Hospital Pharmacists and published in the December 1977 issue of the *American Journal of Hospital Pharmacy*. Dr. Kennedy said:

> *"We applaud the American Society of Hospital Pharmacists for preparing this important guide to a better quality control system for drugs repackaged by hospital pharmacists for use in a unit dose drug distribution system. We recognize it as a major step forward in assuring that patients receive safe and efficacious drugs. In our judgment it is an excellent example of what a professional society can do to improve patient care in hospitals."*

It is FDA's view that the ASHP guidelines are suitable equivalents to our CGMP's for normal hospital pharmacy practice.

J. Joseph Belson, Director
Division of Drug Product Quality
Bureau of Drugs
Food and Drug Administration
Rockville, MD 20852

Bernard T. Loftus, Director
Division of Drug Manufacturing
Bureau of Drugs
Food and Drug Administration
Rockville, MD 20852

Received May 25, 1979.

[1] E. G. Feldmann, *J. Pharm. Sci.*, **68** (5), I (1979).
[2] *Fed. Regist.* (Sept. 29, 1978).

Hospital Pharmacy and the CGMP: A Response

We appreciate this response from Mr. Belson and Mr. Loftus and their effort to clarify the FDA intent of the current GMP regulations.

Our May editorial was originally stimulated by a series of discussions between APhA (and ASHP) staff on the one side and FDA staff on the other side during the 1977–1978 period. The background facts, as we were told them, differ from those described in the Belson–Loftus letter.

Specifically, FDA *did* attempt to assert jurisdiction over hospital pharmacy *via* challenges to certain operating procedures pertaining to unit dose repackaging. These challenges took several forms, one of which was directed at an arrangement whereby a "contract repackager" would bring unit dose repackaging equipment to the hospital and operate it to fulfill the current repackaging needs of the hospital. Under these arrangements, the operation (*a*) took place at the pertinent hospital, (*b*) functioned under the direct supervision of the hospital pharmacist, and (*c*) was limited to producing unit dose packages exclusively for use within that hospital. But, nevertheless, FDA did assert jurisdiction in at least several such instances, thereby causing significant problems and generally hassling the various parties involved.

After considerable skirmishing, an unwritten "truce" eventually emerged, and both sides appeared content to leave the matter rest—although basically unresolved, the issue was not actively pursued further.

But the wording of the September 1978 *Federal Register* preamble—plus pharmacist West's correspondence—made it appear to us that FDA was again preparing to flex its muscle.

Upon receipt of the Belson–Loftus letter, we checked once more to ensure that we had correctly stated our recollection of the situation and its past history. One of the APhA staff members familiar with the situation stated that: "FDA is now trying to do a disappearing act." And an ASHP staff member pointed out that in this letter the operable word is "asserted"; that is, even here, FDA is not conceding any lack of jurisdiction over such pharmacy practice in the hospital setting, but only that it is not presently asserting such jurisdiction.

Nevertheless, both of these staff members also added that this Belson–Loftus letter was far less equivocating than past FDA statements on this issue. Furthermore, had FDA actually followed the policy described in this letter in the past, the entire controversy would never have arisen in the first place!

Edward G. Feldmann
American Pharmaceutical Association
Washington, DC 20037

Received June 19, 1979.

Amphetamine Analogs

The recent article on "Heterocyclic Analogs of Amphetamine . . ." by W. O. Foye and S. Tovivich[1] listed two pyridine compounds without reference to previous work. β-(6-Methyl-2-pyridyl)-isopropylamine was reported by A. Burger and G. E. Ullyot [*J. Org. Chem.*, **12**, 342 (1947)], and β-(3-pyridyl)isopropylamine was reported by A. Burger and C. R. Walter, Jr. [*J. Am. Chem. Soc.*, **72**, 1988 (1950)].

Alfred Burger
Professor Emeritus
Department of Chemistry
University of Virginia
Charlottesville, VA 22901

Received June 14, 1979.

[1] W. O. Foye and S. Tovivich, *J. Pharm. Sci.*, **68**, 591 (1979).

JOURNAL OF PHARMACEUTICAL SCIENCES

AUGUST 1979
VOLUME 68 NUMBER 8

RESEARCH ARTICLES

In Vivo Methotrexate Transport in Murine Lewis Lung Tumor

K. H. YANG *, W. P. FUNG *, R. J. LUTZ ‡, R. L. DEDRICK ‡, and D. S. ZAHARKO *x

Received November 29, 1978, from the **Laboratory of Chemical Pharmacology, National Cancer Institute, and the* ‡*Biomedical Engineering and Instrumentation Branch, Division of Research Services, National Institutes of Health, Bethesda, MD 20014.* Accepted for publication February 5, 1979.

Abstract □ Methotrexate uptake by murine Lewis lung tumor was measured *in vivo* over a wide dose range. The data were analyzed according to a model previously developed for tissues in which methotrexate uptake is rate limited by transport across the cell membrane. Methotrexate transport in this tumor followed Michaelis–Menten kinetics with a rate constant for permeability (k/K) of 0.012 min^{-1}. The methotrexate binding capacity of dihydrofolate reductase in the tumor was not exceeded at any dose studied. A low membrane permeability in conjunction with a high dihydrofolate reductase level explains the resistance of this tumor to methotrexate.

Keyphrases □ Methotrexate—transport in murine Lewis lung tumor, *in vivo*, dihydrofolate reductase binding, tumor resistance □ Antineoplastic agents—methotrexate, transport in murine Lewis lung tumor, *in vivo*, dihydrofolate reductase binding, tumor resistance □ Lung neoplasms—Lewis, methotrexate transport, dihydrofolate reductase binding, *in vivo*

A previous study (1) found that when mice bearing Lewis lung tumor were infused with methotrexate to maintain a 0.01-μg/ml plasma level, the incorporation of ^{3}H-deoxyuridine into DNA was nearly completely blocked in the small intestine but virtually unaffected in the tumor. This difference was thought to occur because tumor cells contain a higher dihydrofolate reductase level and are less permeable to methotrexate than are intestinal cells. Subsequent measurements of this enzyme showed that its level in tumor cells is about six times higher than that in intestinal cells (2).

The question of membrane permeability remained. It is well known that many solid tumors are resistant to standard chemotherapeutic treatments (3). A relatively low permeability was recently demonstrated *in vivo* for methotrexate in spontaneous canine lymphosarcoma (4). The Lewis lung tumor, a solid metastasizing carcinoma insensitive to many chemotherapeutic agents (5), has been used as a valuable experimental tumor model (6, 7). Therefore, the membrane permeability of this tumor to methotrexate *in vivo* was examined to gain insights into the nature of tumor resistance through model simulations.

THEORETICAL

A general model was described (8) for methotrexate uptake in normal tissues, in which the uptake rate is limited by the membrane permeability. This model is now applied to the Lewis lung tumor tissue (Fig. 1). Implicit in this tumor model are the assumptions that: (*a*) the capillary membrane offers no barrier to passage, (*b*) no methotrexate binding occurs in the extracellular compartment, whereas saturable binding to dihydrofolate reductase occurs in the intracellular compartment, and (*c*) instantaneous, complete mixing takes place in the extracellular compartment. For such a model, the following equations apply:

$$\left(\frac{V_e}{V}\right)\frac{dC_e}{dt} = \left(\frac{Q}{V}\right)(C_p - C_e) - \frac{jA}{V} \qquad \text{(Eq. 1)}$$

$$\left(1 - \frac{V_e}{V}\right)\frac{dq_i}{dt} = \frac{jA}{V} \qquad \text{(Eq. 2)}$$

$$dq_i = C_i + \frac{aC_i}{E + C_i} \qquad \text{(Eq. 3)}$$

where C is the free methotrexate concentration, Q is the blood flow rate, jA is the net transport rate of methotrexate over total area A, q is the total intracellular methotrexate concentration, a is the maximum dihydrofolate reductase binding capacity for methotrexate, E is the dissociation constant of the dihydrofolate reductase–methotrexate complex, and V

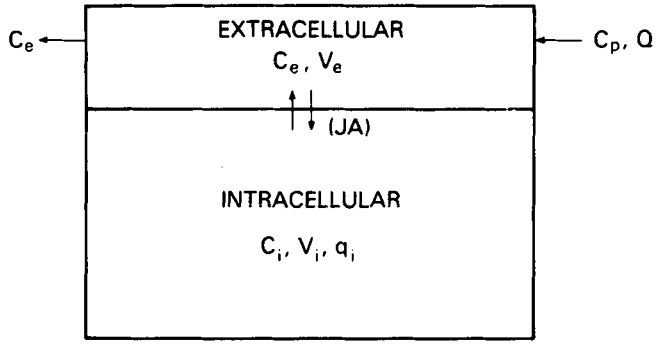

Figure 1—*Diagram of tumor model. See text for notations.*

0022-3549/79/0800-0941$01.00/0
© 1979, American Pharmaceutical Association

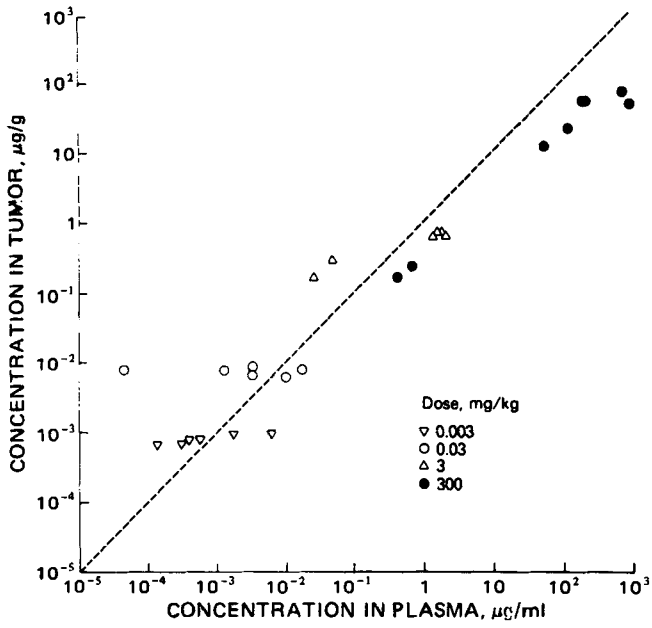

Figure 2—*Methotrexate distribution between plasma and Lewis lung tumor of mice at several doses and various times after dosing.*

is the total tissue volume. The subscripts e, i, and p denote extracellular, intracellular, and plasma, respectively.

Methotrexate transport across most normal and tumor cell membranes is generally assumed to be a carrier-mediated process (9, 10). At high concentrations, passive diffusion may play a role (11). With the assumption that the efflux and influx of the facilitated process are characterized by the same parameters, the net methotrexate transport rate into the cells is given by:

$$\frac{jA}{V} = \frac{kC_e}{K + C_e} - \frac{kC_i}{K + C_i} + b(C_e - C_i) \qquad \text{(Eq. 4)}$$

where k is the maximum transport rate per unit volume, K is the Michaelis constant for the transport, and b is the passive permeability coefficient per unit volume. At doses low enough so that virtually all methotrexate entering the cells becomes tightly bound to dihydrofolate reductase (*i.e.*, $C_i = 0$) and where the passive process is relatively insignificant compared with the facilitated process (*i.e.*, $b = 0$), Eq. 4 reduces to:

$$\frac{jA}{V} = \frac{kC_e}{K + C_e} \qquad \text{(Eq. 5)}$$

For low doses where $C_e \ll K$, Eq. 5 becomes:

$$\frac{jA}{V} = \left(\frac{k}{K}\right) C_e \qquad \text{(Eq. 6)}$$

Since $C_e \simeq C_p$, Eq. 6 predicts a linear increase of jA with C_p. For a time τ sufficiently large such that $C_e V_e \ll q_i V_i$, Eq. 6 leads to:

$$\left(\frac{k}{K}\right) \simeq \frac{C_T(\tau)}{\int_0^\tau C_p(t)\,dt} \qquad \text{(Eq. 7)}$$

where C_T is the average concentration of methotrexate in tumor cells and is given by:

$$C_T = (C_e V_e + q_i V_i)/V \qquad \text{(Eq. 8}a\text{)}$$

$$C_T = q_i + (V_e/V)(C_e - q_i) \qquad \text{(Eq. 8}b\text{)}$$

Equation 7 then gives a first estimate of k/K from $C_T(t)$ and $C_p(t)$, both of which can be determined experimentally. The resolution of the k/K ratio into its components was discussed in detail previously (4, 8). Based on the parameters k, K, Q/V, V_e/V, a, and E, the time course of methotrexate uptake in the tumor cell can be simulated through Eqs. 1–4.

EXPERIMENTAL

Lewis Lung Tumor-Bearing Mice—CDF_1 male mice, 18 ± 2 g, were transplanted subcutaneously with Lewis lung tumor of ~2 mm^3 in size.

Table I—Percentage of Radioactivity Associated with Methotrexate in Plasma and Tumor Samples of CDF_1 Mice Given ^{3}H-Methotrexate Intravenously

Sample	Dose, mg/kg	Percentage[a] of Radioactivity Associated with Methotrexate after 30 min	180 min
Plasma[b]	0.03	82	10
	3	89	29
	300	—	24
Tumor[c]	0.03	—	93
	3	—	76
	300	—	32

[a] Based on the total radioactivity put on the column. [b] In control experiments, where ^{3}H-methotrexate was added to the pooled blood from the tumor-bearing mice and identical preparative procedures were followed, nearly 100% of the radioactivity was associated with methotrexate. [c] In control experiments, where ^{3}H-methotrexate was mixed with the homogenizing medium and added to the pooled tumors, the radioactivity associated with methotrexate was 96%.

Three weeks later, these tumor-bearing mice were used in the study. At this time, the primary tumors weighed 0.5–1.0 g.

Drug Solution Purification and Preparation—3′,5′,9′(*n*)-Methotrexate[1] was purified by diethylaminoethylcellulose chromatography (12) each time before use. The sodium salt of ^{3}H-methotrexate, 250 μCi, was taken up with 0.75 ml of 0.1 *M* ammonium bicarbonate buffer and applied onto a 0.7 × 9-cm column. The column was then eluted at 18 ml/hr with a linear gradient of the buffer at pH 8.3 from 0.1 to 0.4 *M*. The fractions containing methotrexate were pooled and lyophilized.

The lyophilized ^{3}H-methotrexate was reconstructed into a solution of the desired concentration with unlabeled methotrexate dissolved in an aqueous solution of 0.25% $NaHCO_3$ and 0.9% NaCl. The unlabeled methotrexate, of which the purity was checked by the column chromatography, was relatively free of impurities and was used without further purification. The specific activity of the solution, determined from measurements of its optical density at 302 nm and its disintegrations per milliliter, ranged from 1.6 to 17 μCi/μg.

Uptake Study—The tumor-bearing mice were injected with the drug solution *via* the tail vein at doses of 0.003, 0.03, 3, and 300 mg/kg. Then the animals were killed by decapitation at specified times. Blood samples were collected in heparinized tubes and centrifuged to separate the plasma. The tumors were removed surgically.

Aliquots of the plasma and of the nonnecrotic portion of the tumor were digested in a tissue solubilizer[2] and counted[3] for tritium in a counting cocktail consisting of 0.01% 1,4-bis[2-(5-phenyloxazolyl)]benzene[4] and 0.3% 2,5-diphenyloxazole[4] in methanol–toluene (6:14). The counting error was <5%. Appropriate corrections for quenching were made using the automatic external standard ratio method.

Two control mice, which received no drug, were processed for each dose.

Plasma and Tumor Sample Radiopurity—The radiopurity of the plasma and tumor samples was determined at several doses and time points by column chromatography. Six tumor-bearing mice were used for each time point. The drug solution was administered as in the uptake studies. Pooled plasma samples were heated in a boiling water bath for 10 min and centrifuged. An aliquot of the supernate thus obtained was applied onto the same column system described in the purification procedure and eluted similarly, starting, however, with a 0.05 *M* buffer. Each 0.75-ml fraction was collected, mixed with 15 ml of a scintillation cocktail[5], and counted for tritium content with appropriate corrections for quench. Pooled tumors weighing 1.5 g were homogenized with 2 ml of an ice-cold aqueous solution of 0.25% $NaHCO_3$ and 0.9% NaCl. The homogenate was treated similarly to the pooled plasma samples.

All procedures were carried out under minimal incandescent light to prevent the photodecomposition of these pteridine derivatives. The total radioactivity obtained from fractions that coincided with the absorbance of the coeluted methotrexate, which was added to the sample before fractionation as a marker, divided by the total radioactivity put on the column gave the fraction of remaining methotrexate in the samples. The radioactivity from these boiled plasma or tumor tissue extracts accounted

[1] NCS, Amersham/Searle.
[2] From Drug Research and Development Branch, National Cancer Institute.
[3] Packard Tri-Carb liquid scintillation spectrometer, model 3390.
[4] Packard.
[5] Aquasol, New England Nuclear.

for greater than 90% of the radioactivity as determined by digested and counted aliquots of similar tissues. Control experiments, in which the purified ^{3}H-methotrexate solution was added either to the blood pooled from the tumor-bearing mice receiving no drug or to the homogenizing medium for tumors from control mice, were also performed.

RESULTS AND DISCUSSION

Plasma and Tumor Sample Radioactivity—Methotrexate is significantly metabolized in rodents by the host intestinal bacteria (13–15). Thus, the measured radioactivity is the sum of the radioactivity associated with both methotrexate and its metabolites. The radioactivity fraction associated with methotrexate in the samples, however, will vary with the dose given, the administration route, and the time after injection, as was observed in this study.

As can be seen in Table I, at times shorter than 30 min, methotrexate remained largely intact regardless of the dose. By 3 hr, only 10–20% of the radioactivity measured in the plasma (depending on the dose) was associated with methotrexate; the remainder was associated with metabolites and, in a few cases (plasma sample at 3 hr and 300 mg/kg; tumor sample at 3 hr and 300 mg/kg), with ^3H_2O. However, nearly all tritium measured in the tumor at 0.03 mg/kg at 3 hr was in methotrexate. The same result is to be expected for the 0.003-mg/kg dose. The lower percentage found in the tumor sample at 3 mg/kg can be attributed to the relatively significant amount of metabolite in the extracellular compartment, which is insignificant at lower doses. At 300 mg/kg, most of the radioactivity in both samples came from ^3H_2O, which largely accounted for the low percentages associated with methotrexate. These findings were used to make corrections in the uptake studies.

Membrane Transport as Rate-Limiting Step—After corrections were made in accordance with Table I, the methotrexate concentrations in tumors at different time points for all doses were plotted against the corresponding concentrations in plasma (Fig. 2). The tumor methotrexate concentration was not a unique function of its concentration in the plasma, which would be expected if the uptake were flow limited. The dependence of the tumor methotrexate concentration on the dose given as well as on the plasma concentration strongly suggests that membrane resistance can be a rate-limiting factor for methotrexate uptake in this tumor. Similar observations were made with such tissues as the small intestine, spleen, and bone marrow of the rat (8) and lymphosarcoma of the dog (4).

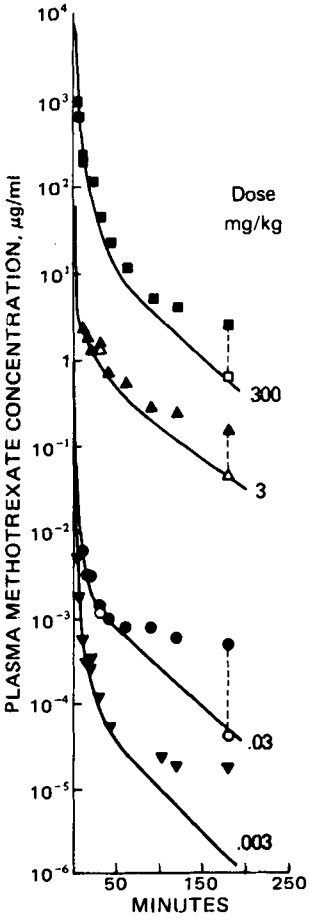

Figure 3—*Plasma methotrexate concentrations* versus *time following several intravenous doses. Dark symbols are experimental data. Open symbols are corrected data. Solid lines represent triexponential curve fitted as described in the text. Each point is from one mouse.*

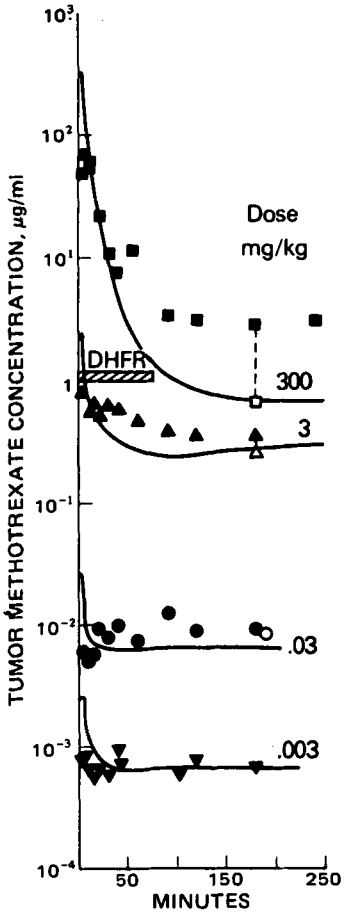

Figure 4—*Average tumor methotrexate concentrations* versus *time following several intravenous doses. Dark symbols are experimental data. Open symbols are corrected data. Solid lines represent model simulations. Shaded bar represents dihydrofolate reductase level. Each point is from one mouse.*

Plasma Data—The plasma methotrexate concentrations obtained for each dose up to 3 hr are shown in Fig. 3. Corrections for tritium not associated with methotrexate were made in accordance with Table I. For the lowest dose, a correction was made at 3 hr in proportion to that made for 0.03 mg/kg. Based on these points and with the assumption of 100% radiopurity at time zero, a linear interpolation provided the points between 30 min and 3 hr. The resulting corrected plasma data sets for each dose were then curve fitted (16) with the following triexponential equation:

$$C_p(t) = a_1 \exp(-b_1 t) + a_2 \exp(-b_2 t) + a_3 \exp(-b_3 t) \quad \text{(Eq. 9)}$$

where $C_p(0)$ for each dose was obtained from the whole animal model developed earlier (17). These equations thus served to evaluate the denominator in Eq. 7 and as input functions for tumor model simulations.

Tumor Data—The measured tumor methotrexate concentrations as a function of time are plotted for each dose in Fig. 4. Also shown are the corrections made in accordance with Table I. The tumor methotrexate concentrations were indeed proportional to the doses at the two lowest doses, indicating the validity of Eq. 6. As the dose increased, the tumor concentration did not increase proportionally, and the transport mechanism apparently became saturated.

The data obtained at either of the two lowest doses were then used, together with the corresponding plasma data, in Eq. 7 to estimate k/K. Equations 1, 2, 6, and 8 can be solved simultaneously on a digital computer for C_T as a function of time for the two lowest doses, using the estimated value of k/K once V_e/V and Q/V are determined. The value of V_e/V was conveniently evaluated from Fig. 2, where $V_e/V \simeq C_T/C_p$ at short times following the highest dose when most of the drug is confined in the extracellular space due to transport saturation. To evaluate Q/V, it is noted that the change in C_T during the first few minutes following the highest dose can be approximated by:

$$\frac{dC_T}{dt} \simeq \left(\frac{Q}{V}\right)(C_p - C_T) \quad \text{(Eq. 10)}$$

Table II—Model Parameters for Murine Lewis Lung Tumor

Parameter	Value
Q/V, flow rate for unit volume, min^{-1}	0.1
V_e/V, fractional extracellular volume	0.2
a, maximum binding capacity, μg/ml	1.0[a]
E, dissociation constant, μg/ml	0.00001[b]
k, maximum transport rate for unit volume, μg/ml/min	0.0036
K, Michaelis constant for transport, μg/ml	0.3

[a] Reference 2. [b] Reference 8.

An approximate value of Q/V was thus found from the best fit of Eq. 10 to the experimental data under such conditions. Since the uptake is not flow limited, a precise knowledge of Q is not required. These parameters, along with other model parameters, are given in Table II. The predicted C_T values were made to best fit the experimental data at the two lowest doses by slightly adjusting the initial k/K estimate. The final k/K value was compared to that of the small intestine in Table III.

The nonresponsiveness of the Lewis lung tumor to methotrexate clearly results from a combination of at least two factors: higher dihydrofolate reductase and lower membrane permeability. With drug doses that are not lethal to the mouse, there is probably always free dihydrofolate reductase present in the tumor to produce sufficient coenzymes for the utilization of nucleotides in DNA and RNA synthesis. The molecular mechanism of decreased tumor permeability as compared to normal tissues certainly cannot be elucidated from this study alone. As an indication, however, it is seen in Table III that since the K's are the same for different tissues, the difference in the permeability thus reflects the difference in k's as shown. Acceptance of the hypothesis of a carrier-mediated transport (18) suggests that the carrier quantity and/or accessibility is less in the tumor cell membrane than in the normal cell membrane.

Model Simulation—The simulations of the average methotrexate concentrations in tumors for all doses are shown in Fig. 4. The model simulates the experimental data over a wide concentration range, spanning six logarithms. The tight binding (19) of methotrexate to dihydrofolate reductase was recently shown to be ionic in nature (20), and the overwhelmingly high dihydrofolate reductase content of this tumor ensures a sink condition within the tumor cell and a one-way

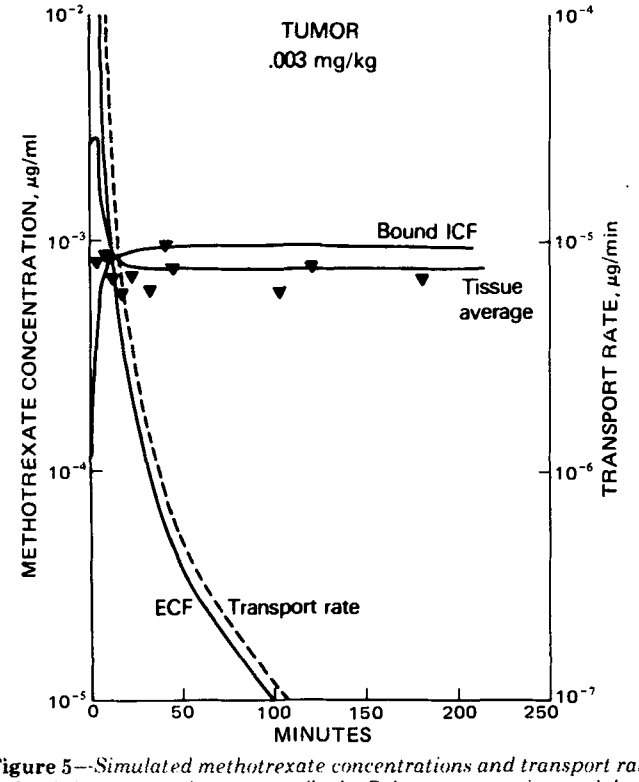

Figure 5—*Simulated methotrexate concentrations and transport rate in Lewis lung tumor for 0.003 mg/kg iv. Points are experimental data. ECF = extracellular fluid. ICF = intracellular fluid. The level of dihydrofolate reductase is at 1 μg of methotrexate equivalents/ml.*

Table III—Transport Parameters and Enzyme (Dihydrofolate Reductase) Activity for Murine Lewis Lung Tumor as Compared to the Small Intestine

Tissue	Permeability (k/K), min^{-1}	k, μg/ml/min	K, μg/ml	Enzyme Activity[a], nmoles of dihydrofolate/hr/mg of protein
Lewis lung tumor	0.012	0.0036	0.3	97
Small intestine	0.024[b]	0.0072[b]	0.3[b]	16

[a] Reference 2. [b] Bile-diverted mice (R. J. Lutz, D. S. Zaharko, K. H. Yang, and R. L. Dedrick, to be published).

transport involving influx only. This condition greatly simplifies the experimental system and may account for the apparent success of the simple model used here. Therefore, the conformity of the model predictions with the data should not be construed as indicating that the influx and efflux parameters of the transport system in the present case are indeed identical. The contrary, in fact, was suggested in some other tumor lines (21–23).

The events that take place are illustrated in Figs. 5 and 6 for 0.003 and 300 mg/kg, respectively. Figure 5 shows that methotrexate enters the cell quickly and binds to dihydrofolate reductase. With the extracellular concentration rapidly decreasing, very little methotrexate enters after 15 min; from then on, the measured tissue averages closely represent the bound intracellular concentrations. The transport rate is directly proportional to the extracellular concentration.

In Fig. 6, for the highest dose, the extracellular concentration dominates the measured concentration for the first 30 min. Only after ~3 hr does the intracellular concentration become significant. More impor-

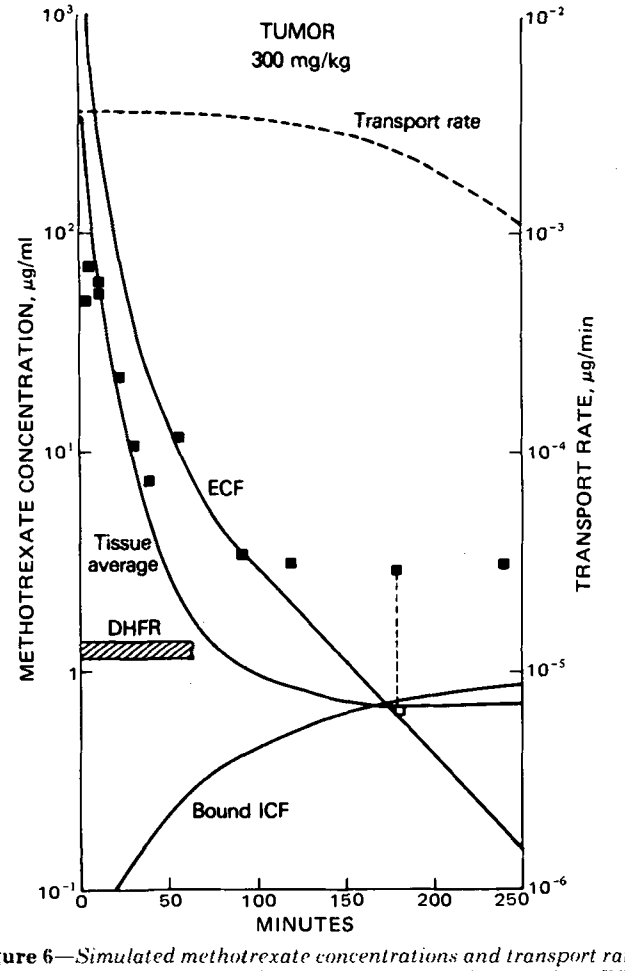

Figure 6—*Simulated methotrexate concentrations and transport rate in Lewis lung tumor for 300 mg/kg iv. Points are experimental data. ECF = extracellular fluid. ICF = intracellular fluid. The level of dihydrofolate reductase (DHFR) is at 1 μg of methotrexate equivalents/ml.*

tantly, there is insufficient methotrexate entering the cell to saturate all the dihydrofolate reductase present and, therefore, little free methotrexate exists inside the cell at any time. It has been demonstrated (24, 25), however, that the persistence of the free intracellular methotrexate accounts for its cytotoxic action. Thus, through model simulations, the measured concentrations in tumors are shown to consist almost entirely of extracellular and bound intracellular concentrations in various proportions, depending on the time and the dose. Since the transport rate has already reached its maximal value at this high dose (Fig. 6), a further increase in the dose would only shift the extracellular curve and, correspondingly, the tissue average curve upwards without a large concomitant increase in the intracellular concentration during the first 2–3 hr. The transport rate would be near the maximum level, only dropping at a later time.

These predictions will be altered, however, if a passive process plays an increasingly significant role as the dose is increased further. This role is still largely unknown at the present time. Nevertheless, what happens at even higher doses is probably of theoretical interest only. In practice, there is a limit to which the dose can be further increased; the LD_{50} of the drug in mice is 350 mg/kg (26).

REFERENCES

(1) D. S. Zaharko, R. L. Dedrick, A. L. Peale, J. C. Drake, and R. J. Lutz, *J. Pharmacol. Exp. Ther.*, **189**, 585 (1974).

(2) D. S. Zaharko, "Pharmacokinetics and Cancer Chemotherapy," Proceedings of the 7th International Congress of Pharmacology, Paris, France, July 1978.

(3) G. Zubrod, *Cancer*, **30**, 1474 (1972).

(4) R. J. Lutz, R. L. Dedrick, J. A. Straw, M. M. Hart, P. Klubes, and D. S. Zaharko, *J. Pharmacokinet. Biopharm.*, **3**, 77 (1975).

(5) J. G. Mayo, *Cancer Chemother. Rep., Part 2*, **3**, 325 (1972).

(6) J. M. Venditti, in "Pharmacological Basis of Cancer Chemotherapy, 27th Annual Symposium on Fundamental Cancer Research," Williams & Wilkins, Baltimore, Md., 1975, p. 245.

(7) T. Giraldi, P. J. Houghton, D. M. Taylor, and L. Nisi, *Cancer Treat. Rep.*, **62**, 721 (1978).

(8) R. L. Dedrick, D. S. Zaharko, and R. J. Lutz, *J. Pharm. Sci.*, **62**, 882 (1973).

(9) I. D. Goldman, *Ann. N.Y. Acad. Sci.*, **186**, 400 (1971).

(10) M. T. Hakala, in "Antineoplastic and Immunosuppressive Agents, Part 1," A. C. Sartorelli and D. G. Johns, Eds., Springer-Verlag, Berlin, Germany, 1974, p. 240.

(11) D. Kessel, T. C. Hall, and D. Roberts, *Cancer Res.*, **28**, 564 (1968).

(12) V. T. Oliverio, *Anal. Chem.*, **33**, 263 (1961).

(13) D. S. Zaharko and V. T. Oliverio, *Biochem. Pharmacol.*, **19**, 2923 (1970).

(14) D. M. Valerino, D. G. Johns, D. S. Zaharko, and V. T. Oliverio, *ibid.*, **21**, 821 (1972).

(15) R. E. Kates and T. N. Tozer, *J. Pharm. Sci.*, **62**, 2056 (1973).

(16) J. E. Fletcher and R. I. Shrager, "Users Guide to Least Squares Model Fitting," Technical Report No. 1, Division of Computer Research and Technology, National Institutes of Health, Washington, D.C., 1968.

(17) K. B. Bischoff, R. L. Dedrick, D. S. Zaharko, and J. A. Longstreth, *J. Pharm. Sci.*, **60**, 1128 (1971).

(18) W. D. Stein, "The Movement of Molecules Across Cell Membranes," Academic, New York, N.Y., 1967, p. 148.

(19) W. C. Werkheiser, *J. Biol. Chem.*, **236**, 888 (1961).

(20) D. S. Saperstein, A. J. Rein, M. Poe, and M. F. Leahy, *J. Am. Chem. Soc.*, **100**, 4296 (1978).

(21) I. D. Goldman, N. S. Lichenstein, and V. T. Oliverio, *J. Biol. Chem.*, **243**, 5007 (1968).

(22) M. Dembo and F. M. Sirotnak, *Biochim. Biophys. Acta*, **448**, 505 (1976).

(23) F. M. Sirotnak and R. C. Donsbach, *Cancer Res.*, **36**, 1151 (1976).

(24) I. D. Goldman, *Mol. Pharmacol.*, **10**, 257 (1974).

(25) J. C. White and I. D. Goldman, *ibid.*, **12**, 711 (1976).

(26) D. S. Zaharko, in "Pharmacological Basis of Cancer Chemotherapy, 27th Annual Symposium on Fundamental Cancer Research," Williams & Wilkins, Baltimore, Md., 1975, p. 69.

ACKNOWLEDGMENTS

Presented in part at the Basic Pharmaceutics Section, APhA Academy of Pharmaceutical Sciences, Phoenix meeting, November 1977.

Effect of Enzyme-Inducing and Enzyme-Inhibiting Agents on Drug Absorption II: Influence of Proadifen on 3-*O*-Methylglucose Transport in Rats

WILLIAM R. RAVIS * and STUART FELDMAN ‡×

Received September 5, 1978, from the **School of Pharmacy, Auburn University, Auburn, AL 36830*, and the ‡*Department of Pharmaceutics, College of Pharmacy, University of Houston, Houston, TX 77004.* Accepted for publication January 22, 1979.

Abstract □ Studies utilizing the *in vitro* everted rat jejunum were performed to investigate the effects of proadifen pretreatment and fasting on active and passive intestinal transfer of 3-*O*-methylglucose. Animals were pretreated 24 hr prior to the experiments with 100 mg of proadifen/kg ip. With mucosal concentrations of 0.1 m*M* 3-*O*-methylglucose and ^{14}C-3-*O*-methylglucose, transfer to the sugar-free serosal buffer after pretreatment with proadifen was 50% greater than controls after a 24-hr fast and 120% greater than controls after a 48-hr fast. Everted intestinal segments obtained from unfasted control animals showed diminished ability to transfer the sugar derivative, with transfer rates approximately 50% less than those of segments obtained from 24-hr fasted control animals. Wet and dry tissue weights for 24- and 48 hr-fasted groups increased following proadifen pretreatment. The results suggest that proadifen enhances 3-*O*-methylglucose transport across the rat jejunum and also increases intestinal tissue weight.

Keyphrases □ Enzyme induction—effect of proadifen on intestinal methylglucose transport, rats, fasting □ Enzyme inhibition—effect of proadifen on intestinal methylglucose transport, rats, fasting □ Methylglucose—effect of proadifen on intestinal transport, rats, fasting □ Proadifen—effect on intestinal methylglucose transport, rats, fasting

Several monosaccharides, amino acids, vitamins, and clinically employed drugs are absorbed from the intestinal lumen by carrier-mediated processes. A 3-*O*-methyl derivative of *d*-glucose has been shown to be absorbed across the mucosal epithelia by an active transport mechanism (1, 2). Since this derivative is not utilized by animal tissue (1), as is *d*-glucose, it is a useful agent for specific examination of active sugar transport by intestinal tissue.

Chemical agents capable of altering cell metabolism influence active absorption processes in the intestine (3–8).

0022-3549/79/0800-0945$01.00/0

© 1979, American Pharmaceutical Association

tantly, there is insufficient methotrexate entering the cell to saturate all the dihydrofolate reductase present and, therefore, little free methotrexate exists inside the cell at any time. It has been demonstrated (24, 25), however, that the persistence of the free intracellular methotrexate accounts for its cytotoxic action. Thus, through model simulations, the measured concentrations in tumors are shown to consist almost entirely of extracellular and bound intracellular concentrations in various proportions, depending on the time and the dose. Since the transport rate has already reached its maximal value at this high dose (Fig. 6), a further increase in the dose would only shift the extracellular curve and, correspondingly, the tissue average curve upwards without a large concomitant increase in the intracellular concentration during the first 2–3 hr. The transport rate would be near the maximum level, only dropping at a later time.

These predictions will be altered, however, if a passive process plays an increasingly significant role as the dose is increased further. This role is still largely unknown at the present time. Nevertheless, what happens at even higher doses is probably of theoretical interest only. In practice, there is a limit to which the dose can be further increased; the LD_{50} of the drug in mice is 350 mg/kg (26).

REFERENCES

(1) D. S. Zaharko, R. L. Dedrick, A. L. Peale, J. C. Drake, and R. J. Lutz, *J. Pharmacol. Exp. Ther.*, **189**, 585 (1974).

(2) D. S. Zaharko, "Pharmacokinetics and Cancer Chemotherapy," Proceedings of the 7th International Congress of Pharmacology, Paris, France, July 1978.

(3) G. Zubrod, *Cancer*, **30**, 1474 (1972).

(4) R. J. Lutz, R. L. Dedrick, J. A. Straw, M. M. Hart, P. Klubes, and D. S. Zaharko, *J. Pharmacokinet. Biopharm.*, **3**, 77 (1975).

(5) J. G. Mayo, *Cancer Chemother. Rep., Part 2*, **3**, 325 (1972).

(6) J. M. Venditti, in "Pharmacological Basis of Cancer Chemotherapy, 27th Annual Symposium on Fundamental Cancer Research," Williams & Wilkins, Baltimore, Md., 1975, p. 245.

(7) T. Giraldi, P. J. Houghton, D. M. Taylor, and L. Nisi, *Cancer Treat. Rep.*, **62**, 721 (1978).

(8) R. L. Dedrick, D. S. Zaharko, and R. J. Lutz, *J. Pharm. Sci.*, **62**, 882 (1973).

(9) I. D. Goldman, *Ann. N.Y. Acad. Sci.*, **186**, 400 (1971).

(10) M. T. Hakala, in "Antineoplastic and Immunosuppressive Agents, Part 1," A. C. Sartorelli and D. G. Johns, Eds., Springer-Verlag, Berlin, Germany, 1974, p. 240.

(11) D. Kessel, T. C. Hall, and D. Roberts, *Cancer Res.*, **28**, 564 (1968).

(12) V. T. Oliverio, *Anal. Chem.*, **33**, 263 (1961).

(13) D. S. Zaharko and V. T. Oliverio, *Biochem. Pharmacol.*, **19**, 2923 (1970).

(14) D. M. Valerino, D. G. Johns, D. S. Zaharko, and V. T. Oliverio, *ibid.*, **21**, 821 (1972).

(15) R. E. Kates and T. N. Tozer, *J. Pharm. Sci.*, **62**, 2056 (1973).

(16) J. E. Fletcher and R. I. Shrager, "Users Guide to Least Squares Model Fitting," Technical Report No. 1, Division of Computer Research and Technology, National Institutes of Health, Washington, D.C., 1968.

(17) K. B. Bischoff, R. L. Dedrick, D. S. Zaharko, and J. A. Longstreth, *J. Pharm. Sci.*, **60**, 1128 (1971).

(18) W. D. Stein, "The Movement of Molecules Across Cell Membranes," Academic, New York, N.Y., 1967, p. 148.

(19) W. C. Werkheiser, *J. Biol. Chem.*, **236**, 888 (1961).

(20) D. S. Saperstein, A. J. Rein, M. Poe, and M. F. Leahy, *J. Am. Chem. Soc.*, **100**, 4296 (1978).

(21) I. D. Goldman, N. S. Lichenstein, and V. T. Oliverio, *J. Biol. Chem.*, **243**, 5007 (1968).

(22) M. Dembo and F. M. Sirotnak, *Biochim. Biophys. Acta*, **448**, 505 (1976).

(23) F. M. Sirotnak and R. C. Donsbach, *Cancer Res.*, **36**, 1151 (1976).

(24) I. D. Goldman, *Mol. Pharmacol.*, **10**, 257 (1974).

(25) J. C. White and I. D. Goldman, *ibid.*, **12**, 711 (1976).

(26) D. S. Zaharko, in "Pharmacological Basis of Cancer Chemotherapy, 27th Annual Symposium on Fundamental Cancer Research," Williams & Wilkins, Baltimore, Md., 1975, p. 69.

ACKNOWLEDGMENTS

Presented in part at the Basic Pharmaceutics Section, APhA Academy of Pharmaceutical Sciences, Phoenix meeting, November 1977.

Effect of Enzyme-Inducing and Enzyme-Inhibiting Agents on Drug Absorption II: Influence of Proadifen on 3-*O*-Methylglucose Transport in Rats

WILLIAM R. RAVIS * and STUART FELDMAN ‡×

Received September 5, 1978, from the **School of Pharmacy, Auburn University, Auburn, AL 36830*, and the ‡*Department of Pharmaceutics, College of Pharmacy, University of Houston, Houston, TX 77004.* Accepted for publication January 22, 1979.

Abstract □ Studies utilizing the *in vitro* everted rat jejunum were performed to investigate the effects of proadifen pretreatment and fasting on active and passive intestinal transfer of 3-*O*-methylglucose. Animals were pretreated 24 hr prior to the experiments with 100 mg of proadifen/kg ip. With mucosal concentrations of 0.1 m*M* 3-*O*-methylglucose and ^{14}C-3-*O*-methylglucose, transfer to the sugar-free serosal buffer after pretreatment with proadifen was 50% greater than controls after a 24-hr fast and 120% greater than controls after a 48-hr fast. Everted intestinal segments obtained from unfasted control animals showed diminished ability to transfer the sugar derivative, with transfer rates approximately 50% less than those of segments obtained from 24-hr fasted control animals. Wet and dry tissue weights for 24- and 48 hr-fasted groups increased following proadifen pretreatment. The results suggest that proadifen enhances 3-*O*-methylglucose transport across the rat jejunum and also increases intestinal tissue weight.

Keyphrases □ Enzyme induction—effect of proadifen on intestinal methylglucose transport, rats, fasting □ Enzyme inhibition—effect of proadifen on intestinal methylglucose transport, rats, fasting □ Methylglucose—effect of proadifen on intestinal transport, rats, fasting □ Proadifen—effect on intestinal methylglucose transport, rats, fasting

Several monosaccharides, amino acids, vitamins, and clinically employed drugs are absorbed from the intestinal lumen by carrier-mediated processes. A 3-*O*-methyl derivative of *d*-glucose has been shown to be absorbed across the mucosal epithelia by an active transport mechanism (1, 2). Since this derivative is not utilized by animal tissue (1), as is *d*-glucose, it is a useful agent for specific examination of active sugar transport by intestinal tissue.

Chemical agents capable of altering cell metabolism influence active absorption processes in the intestine (3–8).

0022-3549/79/0800-0945$01.00/0

© 1979, American Pharmaceutical Association

Dicumarol in mucosal solutions inhibited galactose active uptake by the rat small intestine (3). Cardiac glycosides such as strophantidin (4) and ouabain (5) reduced active sugar absorption, possibly due to influence on Na^+-K^+ ATPase, an apparently important component of the translocation mechanism. On the other hand, pretreatment of rats with parathion, a widely used insecticide, elevated intestinal glucose transport, as shown by increases in serosal–mucosal gradients (6). Subcutaneous phenobarbital in rats increased active bile salt ileal absorption (7) and enhanced the ability of duodenal tissue to take up ^{59}Fe-iron sulfate (8).

Previous studies demonstrated that 24-hr pretreatment of rats with 100 mg of proadifen/kg ip increased intestinal transport capabilities for 3-*O*-methylglucose (2). Phenobarbital and 3,4-benzo[*a*]pyrene treatment schedules had no significant influence on 3-*O*-methylglucose transport. In addition, proadifen possessed spasmolytic activity on the small intestine since 24-hr fasting periods prior to the experiments were insufficient to render the lumen free of food and fecal materials.

The present investigation was undertaken to distinguish the nonfasting effects on active 3-*O*-methylglucose absorption from the proadifen pretreatment effects.

EXPERIMENTAL

Animals and Treatment—Male Sprague-Dawley rats[1], 176–255 g, were maintained on regular rat chow and water *ad libitum*. Prior to preparation of *in vitro* everted sacs, the rats were fasted for 24 or 48 hr, depending on the experiment. Water was allowed *ad libitum*.

Proadifen hydrochloride[2]-pretreated animals received 100 mg of drug/kg ip either 24 or 48 hr prior to the experiment. The necessary proadifen hydrochloride dose was administered in <0.5 ml of water, with control animals receiving 0.4 ml of water.

Preparation of Everted Jejunal Sacs—While anesthesia was maintained with ether, a midline incision was made; the small intestine was removed carefully and then rinsed several times with cool saline. The first 15 cm distal to the pylorus was discarded, and the remaining intestine was everted over a glass rod.

Ten-centimeter segments of everted intestine were prepared as everted ligated sacs as described previously (9) or were cannulated (10). Both the serosal and mucosal bathing buffers consisted of pH 7.4 Krebs–Henseleit buffer with the pH determined before and after incubation in the tissue preparation. The serosal buffers were bubbled with 95% oxygen–5% carbon dioxide before installation into the sacs; the mucosal buffers were bubbled prior to and during the experiment. Temperature over the incubation period was maintained at 37 ± 0.2° by a circulating water bath[3].

Uptake and Transfer of ^{14}C-3-*O*-Methylglucose from 0.1 m*M* Mucosal Solutions—Everted ligated sacs from 24- and 48-hr fasted and unfasted animals were filled with 1.0 ml of buffer free of 3-*O*-methylglucose and incubated in 0.1 m*M* methylglucose in 10 ml of mucosal buffer. Sugar transfer and uptake were examined for sacs from both control and proadifen-pretreated animals under various fasting conditions, with one-half of all sacs incubated in 0.08 m*M* phlorizin[4] as well. All mucosal solutions contained initially 0.3 μCi of ^{14}C-3-*O*-methylglucose[5] with appropriate addition of unlabeled 3-*O*-methylglucose[6]. In separate studies, 10^{-3} *M* proadifen hydrochloride was incorporated into mucosal and serosal buffers of segments from control animals.

After 30 min of incubation, the sacs were emptied and the volumes were recorded with sequential dilution of 2 ml with water. One-tenth-milliliter serosal and mucosal samples were saved for liquid scintillation counting. Following rinsing and weighing of the sac tissue, the tissue was homogenized[7] with 2 ml of methanol and centrifuged. A portion of the methanol supernate was counted. Approximately 90% of the total initial label could be accounted for by the buffer and tissue samples.

Table I—Effects of Fasting and Proadifen Pretreatment on ^{14}C-3-*O*-Methylglucose[a] Transfer and Tissue Uptake across the Everted Rat Small Intestine

Condition	*n*	Amount Transferred to Serosal Fluid in 30 min[b], m*M* × 10^{-6}	30-min Tissue Uptake[b], m*M* × 10^{-6}
1-Day fast			
Untreated	19	21.82 ± 4.56	26.60 ± 3.74
Proadifen	8	33.09 ± 7.84[c]	33.64 ± 7.11[c]
2-Day fast			
Untreated	4	17.73 ± 2.64	26.68 ± 4.71
Proadifen	4	39.04 ± 8.40[c]	32.82 ± 3.29[c]
Unfasted			
Untreated	6	9.95 ± 1.25[d]	20.45 ± 0.99[d]

[a] Initial mucosal concentration = 0.1 m*M*. [b] Mean ± *SD*. [c] $p < 0.05$ compared to untreated of same fast period. [d] $p < 0.05$ compared to 1-day untreated.

Serosal to Mucosal Concentration Gradients—Cannulated sacs from 24-hr fasted treated and control animals as well as untreated unfasted animals were incubated with 1.0 m*M* 3-*O*-methylglucose in both mucosal and serosal buffers. The mucosal volume was 60 ml; the serosal volume was 2 ml. After 30 min, the concentration and amount of ^{14}C-3-*O*-methylglucose in the mucosal solution, the serosal solution, and the intestinal tissue were determined. Before the segments were homogenized with methanol, they were rinsed with 1 ml of water and their wet weights were recorded.

Transfer Rates of ^{14}C-3-*O*-Methylglucose as a Function of Incubation Time—Ten-centimeter everted segments from 24-hr fasted control and proadifen-pretreated animals were suspended in 60 ml of 10 m*M* 3-*O*-methylglucose buffer. Of the two segments utilized from each animal, one was randomly chosen for incubation with either 0.08 or 0.8 m*M* phlorizin. Two milliliters of sugar-free buffer was placed into the serosal compartment. Every 10 min over the 2-hr experiment, the 2 ml of buffer was withdrawn followed by a 2-ml serosal rinse and instillation of another 2 ml for the subsequent time interval. The rinse was combined with the initial sample for that 10-min period, and its radioactivity was determined.

Determination of Tissue Weights and Extracellular Space—In separate experiments, wet and dry intestinal tissue weights were recorded for 24- and 48-hr fasted control and pretreated animals. Wet weights were measured after segments were thoroughly rinsed and drained. The wet tissue was placed on tared slides, dried for 2 hr at 120°, and reweighed.

Extracellular space values were obtained for whole sac preparations. Five-centimeter ligated everted segments were incubated with serosal and mucosal buffers containing 0.625 μCi/ml of ^{14}C-carboxyinulin[5] (0.05 mCi/19.6 mg). The mucosal volume was 10 ml; the serosal volume was 0.5 ml. All buffers were gassed with the oxygen carbon dioxide mixture, and the preparations were incubated at 37° for 60 min.

Upon completion of the incubation, the sacs were rinsed, drained, and halved for weighing in tared vials. The tissue contents of the vials were then digested with 1.5 ml of alkaline digestant[8] at 45° until digestion was complete. Before neutralization with acetic acid, the vials were allowed to cool. Five milliliters of liquid scintillation cocktail[9] was added to each vial, and the radioactivity was determined. Values of extracellular space were calculated from the following relationship (11):

$$\text{extracellular space (ml/g)} = \frac{\text{cpm/g of tissue}}{\text{cpm/ml of mucosal inulin solution}} \quad \text{(Eq. 1)}$$

Assay—Samples of serosal buffers, mucosal buffers, and tissue extracts were placed in vials containing 7 ml of scintillant, and their radioactivity was determined with a liquid scintillation spectrometer[10]. Counts per minute were corrected for quenching by standardized quench curves.

RESULTS

These studies were designed to examine the effect of proadifen pretreatment and length of fast on active and passive 3-*O*-methylglucose

[1] Texas Inbred Mice Co., Houston, Tex.
[2] Supplied by Smith Kline and French Laboratories, Philadelphia, Pa.
[3] Blue M, model 1152.
[4] Sigma Chemical Co., St. Louis, Mo.
[5] New England Nuclear, Boston, Mass.
[6] Calbiochem, Los Angeles, Calif.
[7] Polytron model 125-C, Brinkmann Instruments.
[8] NCS, Amersham/Searle Corp., Arlington Heights, Ill.
[9] PCS, Amersham/Searle Corp., Arlington Heights, Ill.
[10] Packard Tri-Carb model 3326.

Table II—Effects of Fasting and Proadifen Pretreatment on ^{14}C-3-*O*-Methylglucose [a] Transfer and Tissue Uptake across Phlorizin [b]-Incubated Everted Rat Intestinal Sacs

Condition	n	Amount Transferred to Serosal Fluid in 30 min[c], mM × 10^{-6}	30-min Tissue Uptake[c], mM × 10^{-6}
1-Day fast			
Untreated	19	4.87 ± 1.22	7.85 ± 1.68
Proadifen	8	2.64 ± 0.81[d]	5.32 ± 1.53
2-Day fast			
Untreated	4	4.10 ± 0.52	7.93 ± 0.46
Proadifen	4	4.50 ± 1.24	7.88 ± 0.90
Unfasted			
Untreated	6	2.50 ± 0.62[e]	7.41 ± 0.64

[a] Initial mucosal concentration = 0.1 mM. [b] Concentration of phlorizin in mucosal and serosal buffer = 0.08 mM. [c] Mean ± SD. [d] $p < 0.05$ compared to untreated of same fast period. [e] $p < 0.05$ compared to 1-day fasted untreated.

transfer across everted rat intestinal segments. Following 24 hr pretreatment with proadifen, the lumens of the 24-hr fasted group were distended with fecal matter; 48-hr fasting provided lumens free of matter. Variation of fasting periods allowed an assessment of fasting and proadifen effects on the mucosal to serosal sugar transfer. By including phlorizin, a glucose transport inhibitor (12), in the incubation medium, passive 3-*O*-methylglucose transfer could be examined separately. Further studies were conducted to determine alterations in wet and dry intestinal tissue weight and whole tissue extracellular space as a result of fasting and proadifen pretreatment.

Study A: Uptake and Transfer of ^{14}C-3-*O*-Methylglucose from 0.1 m*M* Mucosal Solutions—To examine the effects of fasting and proadifin pretreatment on mucosal to serosal transfer and tissue uptake of the actively transported sugar, animals were divided into five groups: unfasted animals, 24- and 48-hr fasted control animals, and 24- and 48-hr fasted animals that were pretreated with proadifen 24 hr prior to segment preparation. Table I gives values for the amount of 3-*O*-methylglucose transferred to the initially sugar-free serosal buffer in 30 min. Everted segments from 24- and 48-hr fasted proadifen-pretreated animals transferred significantly greater amounts of the labeled sugar than the corresponding fasted controls, with increases approximating 52 and 120%, respectively. Segments obtained from unfasted animals transferred 54% less labeled 3-*O*-methylglucose in 30 min than the 24-hr fasted controls.

Tissue sugar levels were elevated in the proadifen-treated group while the sugar levels in the sacs from unfasted animals were significantly ($p < 0.05$) lower than the fasted controls. Due to measured increases in wet tissue weight for the pretreated group, no differences were noted between treated and control fasted groups when comparisons were made based on counts per gram of tissue. Counts per gram of tissue determined from sacs from unfasted animals were significantly ($p < 0.05$) less than the other experimental groups.

Of the two 10-cm intestinal segments utilized from each animal, one was chosen in an alternating pattern for incubation in a similar 3-*O*-methylglucose buffer containing 0.08 mM phlorizin. In experiments where the phlorizin concentration was varied, this inhibitor level provided maximum 3-*O*-methylglucose transport inhibition. Phlorizin dramatically reduced sugar mucosal to serosal transfer and tissue uptake in all experimental conditions, and this transfer was assumed to represent the

Table III—Effects of Unfasting and 1-Day Fasting of Controls and Proadifen-Pretreated Animals on Final ^{14}C-3-*O*-Methylglucose [a] Concentration Ratios and Tissue Levels (n = 6)

Parameter	Fasted[b]	Proadifen Treated[b]	Unfasted[b]
Final ratio, serosal-mucosal	1.152 ± 0.057	1.426 ± 0.094[c]	1.091 ± 0.173
Serosal gain[d], mM × 10^{-3}	0.184 ± 0.092	0.706 ± 0.190[c]	0.082 ± 0.340
Wet tissue weight	0.701 ± 0.102	0.859 ± 0.080[c]	0.897 ± 0.091[c]
Tissue concentration, mM × 10^{-3}/g	1.504 ± 0.307	1.729 ± 0.271	1.238 ± 0.463

[a] Initial mucosal and serosal concentration = 1.0 mM. [b] Mean ± SD. [c] $p < 0.05$ compared to 1-day fasted control. [d] Obtained by subtracting initial amount from final amount.

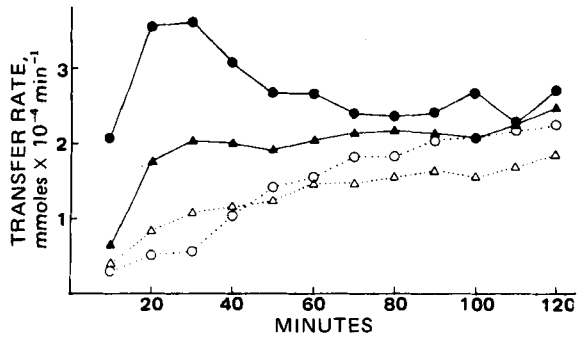

Figure 1—*Mean 10-min transfer rates of ^{14}C-3-O-methylglucose across the everted rat intestine of control and proadifen-pretreated animals* versus *incubation time in a 10 m*M *mucosal buffer. Key:* ●, *proadifen pretreated alone;* ▲, *control alone;* ○, *proadifen pretreated in the presence of phlorizin (0.08 m*M*); and* △, *control in the presence of phlorizin (0.08 m*M*).*

passive component of the sugar transfer. As can be seen in Table II, significantly less 3-*O*-methylglucose was transferred to the serosal compartment for unfasted and 24-hr fasted treated animals.

Study B: Serosal to Mucosal Concentration Gradients across Intestinal Segments from 1-Day Fasted Control, 1-Day Fasted Proadifen-Treated, and Unfasted Control Animals—The ability of everted segments from unfasted control, 24-hr fasted control, and 24-hr fasted proadifen-treated animals to generate concentration gradients for the sugar between mucosal and serosal buffers was examined. 3-*O*-Methylglucose, 1 mM, was incorporated into both the 60-ml mucosal buffers and the 2-ml serosal buffers followed by a 30-min incubation. Final concentration ratios, net serosal gains in 3-*O*-methylglucose, and wet tissue weights are presented in Table III. Segments from pretreated animals exhibited greater final gradients than those of the control and unfasted groups. Intestinal tissue from treated and unfasted animals was greater in wet tissue weight per length than that of 24-hr fasted controls.

Study C: ^{14}C-3-*O*-Methylglucose Transfer as a Function of Incubation Time—Cannulated everted intestinal sacs, prepared from 24-hr fasted control and pretreated animals, were utilized to examine active and passive transfer of 3-*O*-methylglucose across isolated segments over extended incubation periods. The sugar transfer rates at 10-min intervals as a function of incubation time appear in Fig. 1. With phlorizin excluded from the bathing solutions, marked increases in 3-*O*-methylglucose transfer to the serosal buffers were noted at 10, 20, and 30 min for segments obtained from pretreated animals, with percentage increases over controls of 120, 100, and 75% for the three time periods, respectively.

After 30 min, the average rate for the proadifen group progressively fell; rate values from 70 to 120 min were similar to those of the control sacs and phlorizin-incubated sacs of treated and untreated animals for the same time period. The fall in transfer rates and the similarity to passive rates may represent transport system deterioration in isolated segments with long incubation times.

For phlorizin-incubated sacs, the amount of labeled sugar appearing in the serosal buffers up to 30 min was reduced in the proadifen group compared to controls. Passive transfer rates in both control and treated groups progressively increased with incubation, possibly suggesting mucosal membrane barrier deterioration with extended incubation periods (13).

Study D: Uptake and Transfer of ^{14}C-3-*O*-Methylglucose by Intestinal Tissue following 40-hr Proadifen Pretreatment—Preliminary studies examining concentration gradients across ligated sacs from 24-hr fasted animals representing control, 12-hr proadifen pretreatment, and 24-hr proadifen pretreatment groups demonstrated only moderate increases in final concentration gradients following 12-hr pretreatment. To determine whether the effects noted after 24 hr were temporary or became more evident when longer intervals separated the time of injection and transfer measurements, a 40-hr interval between dosing and sacrifice was chosen.

The animals were fasted 24 hr prior to the experiment. Thirty-minute transfer and uptake were determined for ligated sacs in 0.1 mM 3-*O*-methylglucose buffers. No differences were observed between control and 40-hr treated animals, with serosal transfer values of 2.26 ± 0.50 × 10^{-5} and 2.75 ± 0.24 × 10^{-5} mM/10 cm/30 min, respectively. Likewise, tissue levels of the labeled sugar suggested no enhanced sugar uptake by

Table IV—Effects of *In Vitro* Proadifen on 10-min Serosal Transfer and Tissue Uptake of ^{14}C-3-*O*-Methylglucose [a] across the Everted Rat Small Intestine (n = 4)

Treatment	Amount Transferred to Serosal Fluid in 10 min [b], $mM \times 10^{-6}$		10-min Tissue Uptake [b], $mM \times 10^{-6}$	
	Phlorizin [c]	Control	Phlorizin [c]	Control
Untreated	1.454 ± 0.255	4.534 ± 0.220	6.302 ± 0.860	17.910 ± 6.259
Proadifen incubated	1.594 ± 0.333	5.133 ± 0.576	7.082 ± 0.933	17.838 ± 4.449

[a] Initial mucosal concentration = 0.1 m*M*. [b] Mean ± *SD*. [c] Phlorizin concentration in serosal and mucosal buffer = 0.08 m*M*.

the treated group, with a value of $2.68 \pm 0.24 \times 10^{-5}$ m*M*/10 cm/30 min for the 40-hr pretreated group.

Study E: Uptake and Transfer of ^{14}C-3-*O*-Methylglucose for Ligated Segments Incubated in 10^{-3} *M* Proadifen—Possible direct alterations of sugar transport by proadifen were investigated by dissolving 10^{-3} *M* proadifen in the incubation buffers. This concentration was based on reported alterations in the permeability of human erythrocytes (14) and rat hepatocytes (15) in the presence of 10^{-9}–10^{-4} *M* proadifen. *In vitro* drug incubation did not influence mucosal to serosal passive transfer of the sugar in the sac preparations (Table IV). Wet tissue weights were also similar.

Study F: Determination of Wet and Dry Intestinal Tissue Weights—To determine whether the larger values for wet tissue weight were the result of fluid accumulation or tissue proliferation, wet and dry intestinal tissue weights of 24-hr fasted control and treated animals as well as 48-hr fasted groups were recorded. While the lumens of 24-hr fasted proadifen-treated animals were filled with fecal matter, the lumens of the remaining three groups were clear. In both treated groups, the wet and dry tissue weight increased significantly over controls (Table V). Wet tissue weight determinations were greater by 23 and 32% and dry tissue weight determinations were greater by 30 and 27% for 24- and 48-hr fasts, respectively.

Study G: Determination of Whole Tissue Extracellular Space—Measurements of the intestinal tissue extracellular space of 24- and 48-hr fasted, control and treated groups were conducted with ^{14}C-carboxyinulin. No significant differences in whole tissue extracellular space were demonstrated (Table V).

DISCUSSION

As noted in Studies A and C, intestinal segments from unfasted and 24-hr fasted proadifen-treated animals displayed reduced mucosal to serosal passive transfer compared to fasted controls. These two groups coincided with those found to have fecal material in their lumens at the time of sac preparation. Literature reports suggest that differences exist between fasted and unfasted animals with respect to intestinal absorption (16, 17). Alterations in extracellular space as a result of fasting or drug treatment could influence the passive absorption of water-soluble drugs that transverse the mucosal epithelia by aqueous channels. Similar increases in passive transfer rates with incubation time, as seen with 3-*O*-methylglucose in Study C, were reported for water-soluble drugs that are believed to pass the mucosal epithelia by aqueous pathways (13). However, in the present study, no differences were observed in the estracellular space volume per gram of tissue. On the other hand, such measured values are based on whole tissue space and may not be useful in evaluating aqueous channel volume in the absorption-limiting mucosal epithelia (11).

In the present study, segments from unfasted animals displayed diminished serosal transfer when the active transport pathway was not inhibited. If active and passive transfer and uptake are additive, the lower transfer in the absence of phlorizin for unfasted segments cannot be accounted for solely by lower passive transfer rates but must represent the reduced ability of unfasted tissue to transport sugar actively. In contrast, Newey *et al.* (18) found that fasting for 72 hr reduced active D-glucose transport in hamsters. However, other investigators (19) reported elevations in glucose and histidine transport with fasting.

Transfer and tissue weight data indicate that an intestinal segment's transfer abilities are not correlated with segment weight. Proadifen elevated both the amount of 3-*O*-methylglucose transferred and the tissue weight. However, increased intestinal weights noted for the unfasted groups did not coincide with elevations in transfer rates but with reduced rates. Newey *et al.* (18) also showed the inappropriateness of direct comparisons of the amount of sugar transported per gram of tissue in hamsters.

Table V—Effects of 24-hr Proadifen Pretreatment on Rat Intestinal Tissue after 1- and 2-Day Fast [a]

Tissue	Control [b,c]	Treated [b,c]
1-Day fast		
Wet tissue weight, mg/cm	62.14 ± 7.58	76.30 ± 13.70 [d]
Dry tissue weight, mg/cm	7.04 ± 0.82	9.16 ± 1.84 [d]
Extracellular space, ml/g	44.15 ± 5.30	42.27 ± 2.56
2-Day fast		
Wet tissue weight, mg/cm	62.12 ± 1.94	82.10 ± 4.98 [d]
Dry tissue weight, mg/cm	7.30 ± 0.26	9.30 ± 0.48 [d]
Extracellular space, ml/g	41.58 ± 3.43	41.59 ± 3.84

[a] One- and 2-day fast studies performed on separate days. [b] Number of sacs = 8. [c] Mean ± *SD*. [d] $p < 0.05$ compared to control.

Despite the presence or absence of fecal material in the intestinal lumen as noted in Study A, proadifen pretreatment elevated mucosal to serosal transfer of the sugar derivative. Likewise, wet and dry tissue weights were greater in all pretreated groups than in controls of the same fast period. Both effects appeared to be caused by an indirect mechanism and/or *via* a proadifen metabolite since direct drug incubation did not alter sugar transfer (Study E). Of the three pretreatment periods in Study D, 24-hr pretreatment produced optimum enhancement.

Possible indirect mechanisms include the prolongation of the half-life of endogenous steroids (20) or stimulated pituitary hormone release (20) by proadifen or its metabolites. The hepatic microsomal enzyme inducer phenobarbital increased intestinal tissue weight following several days of administration (8). Further studies are necessary to clarify the mechanism of proadifen's effects on intestinal tissue and to evaluate possible alterations in drug absorption following exposure to enzyme-inducing and inhibiting agents.

In summary, enhanced 3-*O*-methylglucose transfer across *in vitro* everted intestinal sacs and increased wet and dry intestinal tissue weights were observed in 24-hr proadifen-pretreated rats. Both effects apparently were unrelated to the unfasted state of the lumen, resulting from proadifen's spasmolytic effects, since 48-hr fasting of treated animals provided material-free lumens with the same effects. Proadifen enhancement of sugar transport appeared to be indirect since drug incubation of segments produced no alterations. In control animals, 24- and 48-hr fasting decreased intestinal weight and increased mucosal to serosal sugar transport as determined by everted intestine techniques.

REFERENCES

(1) T. Z. Csaky, *Fed. Proc.*, **22**, 3 (1963).

(2) W. R. Ravis and S. Feldman, *J. Pharm. Sci.*, **67**, 245 (1978).

(3) E. Anselmi, R. Jordana, and J. Larralde, *Rev. Esp. Fisiol.*, **26**, 325 (1970).

(4) R. K. Crane, D. Miller, and I. Bihler, in "Membrane Transport and Metabolism," A. Kleinzeller and A. Kotyk, Eds., Academic, New York, N.Y., 1961, p. 439.

(5) T. S. Csaky, H. G. Hortzog, III, and G. W. Fernald, *Am. J. Physiol.*, **200**, 459 (1961).

(6) C. R. Robinson, J. K. Chai, and J. T. Pinto, *J. Pharm. Sci.*, **66**, 879 (1977).

(7) V. S. Ostrower, P. Coan, and F. Kern, *Gastroenterology*, **67**, 1162 (1974).

(8) F. B. Thomas, F. S. McCullough, and J. J. Greenberger, *ibid.*, **62**, 590 (1972).

(9) T. H. Wilson and G. Wiseman, *J. Physiol.*, **123**, 116 (1954).

(10) S. Feldman and M. Gibaldi, *J. Pharm. Sci.*, **58**, 425 (1969).

(11) M. Mayersohn, M. Gibaldi, and B. Grundhofer, *ibid.*, **60**, 1813 (1971).

(12) H. Newey, B. J. Parsons, and D. H. Smyth, *J. Physiol.*, **148**, 83 (1959).

(13) M. Gibaldi and B. Grundhofer, *Proc. Soc. Exp. Biol. Med.*, **141**, 564 (1972).

(14) I. P. Lee, H. I. Yamamura, and R. L. Dixon, *Biochem. Pharmacol.*, **17**, 1671 (1968).

(15) P. T. Henderson and J. H. Dewade, *ibid.*, **18**, 2087 (1969).

(16) J. M. Orr and L. Z. Benet, *Digest. Dis.*, **20**, 858 (1975).

(17) J. T. Doluisio, G. H. Tan, N. F. Billups, and L. Diamond, *J. Pharm. Sci.*, **58**, 1200 (1969).
(18) H. Newey, P. A. Sanford, and D. H. Smyth, *J. Physiol.*, **208**, 705 (1970).
(19) J. T. Hindmarsh, D. Kolby, B. Ross, and G. Wiseman, *ibid.*, **188**, 207 (1967).
(20) R. D. Magus, D. E. Rickert, and J. R. Fouts, *Biochem. Pharmacol.*, **17**, 2071 (1968).

Prostaglandin Prodrugs III: Synthesis and Biological Properties of C_9- and C_{15}-Monoesters of Dinoprost (Prostaglandin $F_{2\alpha}$)

W. MOROZOWICH ˣ, T. O. OESTERLING, W. L. MILLER, C. F. LAWSON, J. C. CORNETTE, J. R. WEEKS, and S. L. DOUGLAS

Received September 15, 1975, from the *Research Laboratories, The Upjohn Company, Kalamazoo, MI 49001.* Accepted for publication November 5, 1975.

Abstract □ Methods are described for the synthesis of dinoprost C_9- and C_{15}-monoesters using protective groups. Esters at C_9 were synthesized by acylation of dinoprost 11,15-bis(tetrahydropyran-2-yl)ether followed by acid-catalyzed protective group removal. Esters at C_{15} were synthesized by initial formation of the protected intermediate, dinoprost 9,11-*n*-butylboronate, followed by acylation and hydrolytic protective group removal. Many esters were active *in vivo* in the hamster antifertility screen. Plasma hydrolysis studies showed that the C_{15}-esters were more readily cleaved than the C_9-esters. *In vivo* studies in the rat showed that both the C_9- and C_{15}-esters resulted in urinary excretion of 5α,7α-dihydroxy-11-ketotetranorprosta-1,16-dioic acid in amounts comparable to those obtained after dosing with dinoprost, indicating that ester hydrolysis occurred *in vivo*.

Keyphrases □ Dinoprost—prodrugs, C_9- and C_{15}-monoesters, synthesis, bioactivity □ Prostaglandins—dinoprost, prodrugs, C_9- and C_{15}-monoesters, synthesis, bioactivity □ Prodrugs—dinoprost, C_9- and C_{15}-monoesters, synthesis, bioactivity

Previously, methods were described for the synthesis of aromatic and aliphatic prostaglandins C_1-esters, and the utility of these prodrugs in improving solid-state stability and oral absorption was reported (1, 2). This report describes synthetic routes for dinoprost C_9- and C_{15}-monoesters and an evaluation of ester bioactivity.

EXPERIMENTAL

Materials and Methods—Dinoprost and dinoprost 11,15-bis(tetrahydropyran-2-yl)ether (I)[1] (3) were pure by silica gel TLC. The acid chlorides were obtained commercially[2]. Pyridine (analytical reagent) was dried over molecular sieves[3] for 1 week prior to use. All other solvents were glass-distilled quality[4].

Column chromatography was conducted on 0.063–0.2-mm silica gel[5]. Silica gel TLC was conducted on 250-μm layer plates[6], and visualization was by spraying the developed plates with aqueous 15% ammonium sulfate followed by charring on a hot plate. Prostaglandin ester mass spectra were obtained[7] for (*a*) the trimethylsilyl derivative, (*b*) the C_1-methyl ester of the trimethylsilyl derivative, and (*c*) the nonderivatized compound. The methyl esters were obtained using diazomethane, and the trimethylsilyl derivatives were obtained with a mixture of hexamethyldisilazane – trimethylchlorosilane – bis(trimethylsilyl)acetamide–pyridine (2:2:1:5).

Synthesis—Representative ester syntheses are described. The other esters were synthesized similarly.

Dinoprost 9-n-Butyrate (*III*b)—A solution of 100 mg of I (3) in a mixture of 0.5 ml of butyric anhydride and 1 ml of pyridine was allowed to stand at room temperature for 24 hr. Upon solvent removal at 45° under vacuum, the residue was dissolved in 50 ml of acetone–acetic acid–water (1:1:1). After 24 hr at 40°, the solvent was removed and the residue was subjected to column chromatography on 75 g of silica gel. Elution was achieved with ethyl acetate–acetic acid (97:3), and the product fractions were identified by silica gel TLC with the same solvent system. Evaporation of the pooled product fractions gave 51 mg of a colorless oil, which was pure by TLC.

Dinoprost 15-Acetate (*VIII*a)—A solution of 48.4 mg (0.137 mmole) of IV and 24 mg (0.236 mmole) of *n*-butylboronic acid in 2 ml of dry pyridine was allowed to stand at room temperature for 1 hr. Acetic anhydride, 2 ml, was added; after 24 hr at room temperature, 3 ml of water was added and the solvent was removed at 45° under vacuum. The residual oil was dissolved in 50 ml of ethyl acetate and extracted with 50 ml of 0.2 *M* citrate buffer, pH 3.0.

The organic phase was dried over sodium sulfate; upon solvent removal, the residue was subjected to column chromatography on 50 g of silica gel. Elution was achieved with ethyl acetate–acetic acid (97:3). The product fractions were identified by TLC; upon solvent removal, 25.3 mg of a colorless oil was isolated.

Biological Activity—The ester activity was studied in the gerbil colon assay, the rat pressor blood pressure assay, and the hamster antifertility assay (subcutaneous administration) as described previously (1, 4).

Plasma Hydrolysis—Standard aqueous solutions (0.1 ml) of dinoprost, the 9-acetate (IIIa), the 15-acetate (VIIIa), the 9-*n*-butyrate (IIIb), and the 15-*n*-butyrate (VIIIc) containing quantities in terms of IV ranging from 5 to 20×10^3 ng/ml were incubated separately with 0.05 ml of each of the following: (*a*) saline solution, (*b*) heparinized rat plasma, (*c*) heparinized monkey plasma, and (*d*) heparinized human plasma. After 2 hr at 37°, the affinity of each incubated sample for anti-dinoprost serum was determined using a double antibody radioimmunoassay (5). Relative cross-reactivity was calculated by comparing the amount of the compound required to displace 50% of the label with the amount of IV required. Increased antibody affinity occurred as ester hydrolysis proceeded to yield IV.

***In Vivo* Metabolism**—Mature Sprague–Dawley female rats were injected subcutaneously with one of the following: I, IIIa, VIIIa, IIIb, VIIIc, and the vehicle as the control. The compounds were administered in amounts equivalent to 1 mg of IV dissolved in 0.5 ml of vehicle consisting of polyethoxylated vegetable oil[8]–ethanol–5% aqueous dextrose (1:1:8).

The animals were kept in metabolism cages, and total urine volumes

[1] Supplied by the Research Division, The Upjohn Co.
[2] Aldrich Chemical Co., Milwaukee, Wis., and Eastman Kodak Co., Rochester, N.Y.
[3] Beads, 10–16 mesh, 4 Å, Davison Chemical Co., Baltimore, Md.
[4] Burdick & Jackson Co., Muskegon, Mich.
[5] Silica gel 60, EM Laboratories, Elmsford, N.Y.
[6] Uniplate, Analtech Inc., Newark, Del.
[7] LKB 9000 mass spectrometer.
[8] Emulphor EL-620, GAF Corp., New York, N.Y.

0022-3549/79/0800-0949$01.00/0
© 1979, American Pharmaceutical Association

(17) J. T. Doluisio, G. H. Tan, N. F. Billups, and L. Diamond, *J. Pharm. Sci.*, **58**, 1200 (1969).
(18) H. Newey, P. A. Sanford, and D. H. Smyth, *J. Physiol.*, **208**, 705 (1970).
(19) J. T. Hindmarsh, D. Kolby, B. Ross, and G. Wiseman, *ibid.*, **188**, 207 (1967).
(20) R. D. Magus, D. E. Rickert, and J. R. Fouts, *Biochem. Pharmacol.*, **17**, 2071 (1968).

Prostaglandin Prodrugs III: Synthesis and Biological Properties of C_9- and C_{15}-Monoesters of Dinoprost (Prostaglandin $F_{2\alpha}$)

W. MOROZOWICH ˣ, T. O. OESTERLING, W. L. MILLER, C. F. LAWSON, J. C. CORNETTE, J. R. WEEKS, and S. L. DOUGLAS

Received September 15, 1975, from the *Research Laboratories, The Upjohn Company, Kalamazoo, MI 49001.* Accepted for publication November 5, 1975.

Abstract □ Methods are described for the synthesis of dinoprost C_9- and C_{15}-monoesters using protective groups. Esters at C_9 were synthesized by acylation of dinoprost 11,15-bis(tetrahydropyran-2-yl)ether followed by acid-catalyzed protective group removal. Esters at C_{15} were synthesized by initial formation of the protected intermediate, dinoprost 9,11-*n*-butylboronate, followed by acylation and hydrolytic protective group removal. Many esters were active *in vivo* in the hamster antifertility screen. Plasma hydrolysis studies showed that the C_{15}-esters were more readily cleaved than the C_9-esters. *In vivo* studies in the rat showed that both the C_9- and C_{15}-esters resulted in urinary excretion of 5α,7α-dihydroxy-11-ketotetranorprosta-1,16-dioic acid in amounts comparable to those obtained after dosing with dinoprost, indicating that ester hydrolysis occurred *in vivo*.

Keyphrases □ Dinoprost—prodrugs, C_9- and C_{15}-monoesters, synthesis, bioactivity □ Prostaglandins—dinoprost, prodrugs, C_9- and C_{15}-monoesters, synthesis, bioactivity □ Prodrugs—dinoprost, C_9- and C_{15}-monoesters, synthesis, bioactivity

Previously, methods were described for the synthesis of aromatic and aliphatic prostaglandins C_1-esters, and the utility of these prodrugs in improving solid-state stability and oral absorption was reported (1, 2). This report describes synthetic routes for dinoprost C_9- and C_{15}-monoesters and an evaluation of ester bioactivity.

EXPERIMENTAL

Materials and Methods—Dinoprost and dinoprost 11,15-bis(tetrahydropyran-2-yl)ether (I)[1] (3) were pure by silica gel TLC. The acid chlorides were obtained commercially[2]. Pyridine (analytical reagent) was dried over molecular sieves[3] for 1 week prior to use. All other solvents were glass-distilled quality[4].

Column chromatography was conducted on 0.063–0.2-mm silica gel[5]. Silica gel TLC was conducted on 250-μm layer plates[6], and visualization was by spraying the developed plates with aqueous 15% ammonium sulfate followed by charring on a hot plate. Prostaglandin ester mass spectra were obtained[7] for (*a*) the trimethylsilyl derivative, (*b*) the C_1-methyl ester of the trimethylsilyl derivative, and (*c*) the nonderivatized compound. The methyl esters were obtained using diazomethane, and the trimethylsilyl derivatives were obtained with a mixture of hexamethyldisilazane – trimethylchlorosilane – bis(trimethylsilyl)acetamide–pyridine (2:2:1:5).

Synthesis—Representative ester syntheses are described. The other esters were synthesized similarly.

Dinoprost 9-n-Butyrate (*III*b)—A solution of 100 mg of I (3) in a mixture of 0.5 ml of butyric anhydride and 1 ml of pyridine was allowed to stand at room temperature for 24 hr. Upon solvent removal at 45° under vacuum, the residue was dissolved in 50 ml of acetone–acetic acid–water (1:1:1). After 24 hr at 40°, the solvent was removed and the residue was subjected to column chromatography on 75 g of silica gel. Elution was achieved with ethyl acetate–acetic acid (97:3), and the product fractions were identified by silica gel TLC with the same solvent system. Evaporation of the pooled product fractions gave 51 mg of a colorless oil, which was pure by TLC.

Dinoprost 15-Acetate (*VIII*a)—A solution of 48.4 mg (0.137 mmole) of IV and 24 mg (0.236 mmole) of *n*-butylboronic acid in 2 ml of dry pyridine was allowed to stand at room temperature for 1 hr. Acetic anhydride, 2 ml, was added; after 24 hr at room temperature, 3 ml of water was added and the solvent was removed at 45° under vacuum. The residual oil was dissolved in 50 ml of ethyl acetate and extracted with 50 ml of 0.2 *M* citrate buffer, pH 3.0.

The organic phase was dried over sodium sulfate; upon solvent removal, the residue was subjected to column chromatography on 50 g of silica gel. Elution was achieved with ethyl acetate–acetic acid (97:3). The product fractions were identified by TLC; upon solvent removal, 25.3 mg of a colorless oil was isolated.

Biological Activity—The ester activity was studied in the gerbil colon assay, the rat pressor blood pressure assay, and the hamster antifertility assay (subcutaneous administration) as described previously (1, 4).

Plasma Hydrolysis—Standard aqueous solutions (0.1 ml) of dinoprost, the 9-acetate (IIIa), the 15-acetate (VIIIa), the 9-*n*-butyrate (IIIb), and the 15-*n*-butyrate (VIIIc) containing quantities in terms of IV ranging from 5 to 20×10^3 ng/ml were incubated separately with 0.05 ml of each of the following: (*a*) saline solution, (*b*) heparinized rat plasma, (*c*) heparinized monkey plasma, and (*d*) heparinized human plasma. After 2 hr at 37°, the affinity of each incubated sample for anti-dinoprost serum was determined using a double antibody radioimmunoassay (5). Relative cross-reactivity was calculated by comparing the amount of the compound required to displace 50% of the label with the amount of IV required. Increased antibody affinity occurred as ester hydrolysis proceeded to yield IV.

***In Vivo* Metabolism**—Mature Sprague–Dawley female rats were injected subcutaneously with one of the following: I, IIIa, VIIIa, IIIb, VIIIc, and the vehicle as the control. The compounds were administered in amounts equivalent to 1 mg of IV dissolved in 0.5 ml of vehicle consisting of polyethoxylated vegetable oil[8]–ethanol–5% aqueous dextrose (1:1:8).

The animals were kept in metabolism cages, and total urine volumes

[1] Supplied by the Research Division, The Upjohn Co.
[2] Aldrich Chemical Co., Milwaukee, Wis., and Eastman Kodak Co., Rochester, N.Y.
[3] Beads, 10–16 mesh, 4 Å, Davison Chemical Co., Baltimore, Md.
[4] Burdick & Jackson Co., Muskegon, Mich.
[5] Silica gel 60, EM Laboratories, Elmsford, N.Y.
[6] Uniplate, Analtech Inc., Newark, Del.
[7] LKB 9000 mass spectrometer.
[8] Emulphor EL-620, GAF Corp., New York, N.Y.

0022-3549/79/0800-0949$01.00/0
© 1979, American Pharmaceutical Association

Table I—Mass Spectral Data of Dinoprost Esters [a]

Compound	Formula	Derivative Employed for Mass Spectrometry[b]	Key Mass Spectral Ions (*m/e*)
IIIa	$C_{22}H_{36}O_6$	A	597 ($M^+ - CH_3$), 552 ($M^+ - CH_3COOH$), 537 ($M^+ - CH_3 - CH_3COOH$), 462 [$M^+ - CH_3COOH - (CH_3)_3SiOH$]
IIIb	$C_{24}H_{40}O_6$	A	625 ($M^+ - CH_3$), 552 ($M^+ - C_3H_7COOH$), 537 ($M^+ - CH_3 - C_3H_7COOH$), 462 [$M^+ - C_3H_7COOH - (CH_3)_3SiOH$]
IIIc	$C_{28}H_{48}O_6$	B	336 ($M^+ - C_7H_{15}COOH$), 318 ($M^+ - C_7H_{15}COOH - H_2O$)
IIId	$C_{32}H_{56}O_6$	A	752 (M^+), 737 ($M^+ - CH_3$), 681 ($M^+ - C_5H_{11}$), 662 [$M^+ - (CH_3)_3SiOH$]
VIIIa	$C_{22}H_{36}O_6$	A	612 (M^+), 552 ($M^+ - CH_3COOH$), 537 ($M^+ - CH_3 - CH_3COOH$), 462 [$M^+ - CH_3COOH - (CH_3)_3SiOH$]
VIIIb	$C_{23}H_{38}O_6$	B	336 ($M^+ - C_2H_5COOH$), 318 ($M^+ - C_2H_5COOH - H_2O$)
VIIIc	$C_{24}H_{40}O_6$	A	640 (M^+), 552 ($M^+ - C_3H_7COOH$), 537 ($M^+ - CH_3 - C_3H_7COOH$), 481 ($-C_3H_7COOH - C_5H_{11}$)
VIIId	$C_{25}H_{42}O_6$	B	336 ($M^+ - C_4H_9COOH$), 318 ($M^+ - C_4H_9COOH - H_2O$)
VIIIe	$C_{26}H_{44}O_6$	C	610 (M^+), 595 ($M^+ - CH_3$), 579 ($M^+ - OCH_3$), 520 [$M^+ - (CH_3)_3SiOH$], 494 ($M^+ - C_5H_{11}COOH$)
VIIIf	$C_{30}H_{52}O_6$	B	336 ($M^+ - C_9H_{19}COOH$), 318 ($M^+ - C_9H_{19}COOH - H_2O$), 300 ($M^+ - C_9H_{19}COOH - 2H_2O$)
VIIIg	$C_{36}H_{64}O_6$	B	318 ($M^+ - C_{15}H_{31}COOH - H_2O$), 300 ($M^+ - C_{15}H_{31}COOH - 2H_2O$)

[a] The compounds were liquids, except IIIc (mp 55.9–60.5°). [b] A = trimethylsilyl derivative, B = no derivatization, and C = C_1-methyl ester trimethylsilyl derivative.

were collected over 2 days. Each 24-hr urine sample was assayed for 5α,7α-dihydroxy-11-ketotetranorprosta-1,16-dioic acid (IX), an ultimate major urinary IV metabolite (6), using the radioimmunoassay and the antibody specific for this compound (7).

RESULTS AND DISCUSSION

Synthesis—Since selective monoesterification of dinoprost (IV) with acid anhydrides or acid chlorides in pyridine was not possible, protective groups were necessary (8).

The C_9-esters (III) were synthesized by reacting the 11,15-bis(tetrahydropyran-2-yl)ether (I) (3) with an acid anhydride or an acid chloride in pyridine at room temperature (Scheme I). Only the acetate ester could be synthesized *via* the acid anhydride in high yields (>90%) at room temperature in 24 hr, and acid chlorides were required for the synthesis of the higher esters at room temperature.

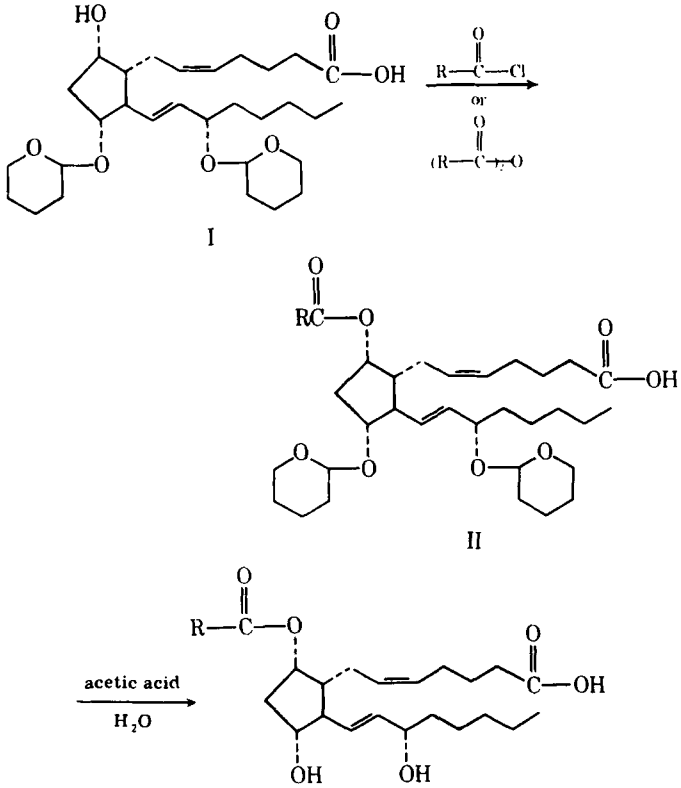

Scheme I

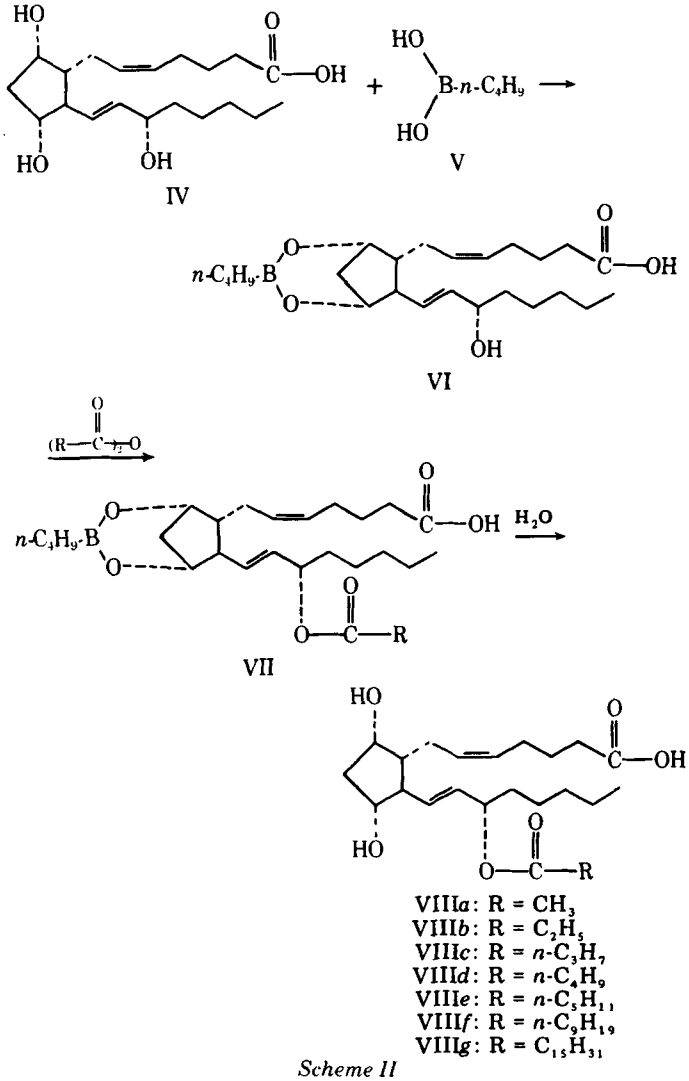

Scheme II

Tetrahydropyranyl protective group removal from ester II was achieved with aqueous acetic acid, and the resulting C_9-esters (III) were purified by column chromatography.

The C_{15}-esters (VIII) were synthesized by initial protection of the C_9- and C_{15}-hydroxyl groups with *n*-butylboronic acid (V) (9) (Scheme II). The reaction proceeded rapidly at room temperature (15–60 min) in the presence of a 1–2-mole excess of *n*-butylboronic acid to give the cyclic 9,11-boronate ester (VI).

Compound VI formation generally was quantitative, as evidenced by GLC upon trimethylsilylation of a reaction mixture aliquot. Occasionally,

Table II—Biological Activity of Dinoprost Esters

Compound	Hamster Antifertility[a] Percent Non-pregnant	Dose, μg/animal	Gerbil Colon[b]	Rat Blood Pressure (Depressor)[c]
IIIa	50	125	0.03–0.1	0.01–0.03
IIIb	75	125	0.03–0.1	0.01–0.03
IIIc	100	200	<0.001	0.003–0.01
IIId	17	100	0.01–0.03	0.03–0.1
VIIIa	75	125	0.1–0.3	0.3–1
VIIIb	0	100	0.01–0.3	0.3–1
VIIIc	83	125	0.03–0.1	0.3–1
VIIId	17	100	0.1–0.3	0.3–1
VIIIe	33	100	0.01–0.03	0.3–1
VIIIf	0	100	0.03–0.1	0.3–1
VIIIg	0	100	0.001–0.003	0.3–1

[a] Administered subcutaneously. The minimum effective dose for 100% inhibition of pregnancy was 100 μg of IV/animal. [b] The dinoprost (IV) activity score in this assay was 2. Prostaglandin E_1 = 1. [c] Dinoprost = 1.

a larger (3–5 mole) excess of *n*-butylboronic acid had to be employed to provide a quantitative reaction, presumably due to the inhibition by trace moisture contamination. Silica gel TLC was ineffective in monitoring the reaction since severe streaking occurred due to apparent VI hydrolysis during chromatography.

Compound VI esterification with an acid anhydride proceeded smoothly to give the protected C_{15}-esters (VII). After hydrolysis with water, the C_{15}-esters (VIII) were isolated by column chromatography.

All C_9- and C_{15}-esters were isolated as oily liquids, except C_9-*n*-octanoate (IIIc), which was a solid, mp 55.9–60.5°. The ester structures were confirmed by mass spectral analysis of the trimethylsilyl derivatives, and the fragmentation patterns supported the structures (Table I).

Biological Activity—The biological activity of the esters in three test systems (1, 4) is summarized in Table II. In the hamster antifertility assay, the minimum effective dose for 100% pregnancy inhibition was 100 μg/animal for IV; the assay results indicate significant C_9-ester activity at the dosage level tested. In the C_{15}-ester series, VIIIa and VIIIc–VIIIe showed significant activity; VIIIb, VIIIf, and VIIIg were inactive.

In the gerbil colon assay, IV had an activity score of 2. The biological data show that the C_9- and C_{15}-esters displayed activities significantly less than the parent compound.

In the rat blood pressure assay, the pressor activity of VIIIa–VIIIg approached that of IV whereas IIIa–IIId were significantly less active.

***In Vitro* and *In Vivo* Hydrolysis**—The cleavage of the acetate and *n*-butyrate esters IIIa, IIIb, VIIIa, and VIIIc was studied both *in vitro* and *in vivo*. The *in vitro* studies were conducted by equilibrating the esters with rat, monkey, and human plasma for 2 hr at 37°. Hydrolysis was measured by the radioimmunoassay using the antibody specific for IV (5). The percent hydrolysis was determined by comparing the assay response of the esters to that of an equimolar amount of IV treated similarly. The results (Table III) showed that the 9-acetate (IIIa) and 9-butyrate (IIIb) esters were resistant to cleavage by the three plasma samples.

Table III—Plasma Hydrolysis (Percent in 2 hr at 37°) of Dinoprost Esters[a]

Compound	Saline Control	Rat Plamsa	Monkey Plasma	Human Plasma
IIIa	1.0	0.9	1.0	0.6
IIIb	1.3	1.5	0.7	0.5
VIIIa	22.0	50.8	28.6	9.1
VIIIc	5.0	40.0	6.7	2.6

[a] Solutions of the compounds in 0.1 ml of water diluted with 0.05 ml of plasma or saline control. The amount of IV liberated was determined by the radioimmunoassay.

Table IV—Total Daily Urinary Metabolite IX Excretion (Micrograms) in Rats Dosed Subcutaneously[a]

Compound	Day 1	Day 2
(Vehicle control)	(0.8)	(0.8)
IV	138	1.4
IIIa	116	2.5
IIIb	155	5.0
VIIIa	195	5.0
VIIIc	132	1.6

[a] Determined by the radioimmunoassay.

The 15-acetate (VIIIa) and 15-butyrate (VIIIc) esters were appreciably hydrolyzed by rat plasma but less efficiently by monkey plasma. Compound VIIIa hydrolysis by human plasma was unusual since partial hydrolysis occurred in the saline control, presumably due to the esterases present in the antiserum; C_{15}-ester hydrolysis did not occur in water at 37° for 2 hr. The decreased hydrolysis by human plasma may be due to an hydrolysis-inhibiting component present in human plasma or to extensive ester protein binding.

In vivo ester hydrolysis was studied in rats by monitoring the urinary excretion of the major urinary IV metabolite, 5α,7α-dihydroxy-11-ketotetranorprosta-1,16-dioic acid (IX) (6), using the radioimmunoassay (7). The esters were injected subcutaneously in rats, and the daily urinary IX excretion was determined using the antibody specific for this compound. Thus, if ester hydrolysis occurred *in vivo*, the resulting IV would be converted to IX.

Table IV shows that the acetate and butyrate esters at both the 9- and 15-positions yielded approximately the same amount of urinary metabolite IX as was found upon administration of IV, indicating complete ester hydrolysis *in vivo*. The data imply that all four esters should be as active as IV in the antifertility assay, but IIIa was somewhat less active. *In vivo* IIIa hydrolysis probably occurs competitively with metabolism at C_1 or C_{15}, and the low antifertility activity of this ester could be due to preferential metabolism to yield an inactive ester metabolite. Ultimate ester hydrolysis and metabolism to IX would account for the full bioavailability of the metabolite from IIIa.

REFERENCES

(1) W. Morozowich, T. O. Oesterling, W. L. Miller, C. F. Lawson, J. R. Weeks, R. G. Stehle, and S. L. Douglas, *J. Pharm. Sci.*, **68**, 833 (1979).

(2) W. Morozowich, T. O. Oesterling, W. L. Miller, and S. L. Douglas, *ibid.*, **68**, 836 (1979).

(3) E. J. Corey, T. K. Schaaf, W. Huber, U. Koelliker, and N. M. Weinshenker, *J. Am. Chem. Soc.*, **92**, 397 (1970).

(4) J. R. Weeks, D. W. DuCharme, W. E. Magee, and W. L. Miller, *J. Pharmacol. Exp. Ther.*, **186**, 67 (1973).

(5) J. C. Cornette, K. T. Kirton, K. L. Barr, and A. D. Forbes, in "The Prostaglandins: Clinical Application in Human Reproduction," E. M. Southern, Ed., Futura, Mount Kisco, N.Y., 1972, p. 243.

(6) E. Granström and B. Samuelsson, *Eur. J. Biochem.*, **10**, 411 (1969).

(7) J. C. Cornette, K. T. Kirton, W. P. Schneider, F. F. Sun, R. A. Johnson, and E. G. Nidy, *Prostaglandins*, **9**, 323 (1975).

(8) E. J. Corey, K. C. Nicolaou, and L. S. Melvin, Jr., *J. Am. Chem. Soc.*, **97**, 653 (1975).

(9) C. Pace-Asciak and L. S. Wolfe, *J. Chromatogr.*, **56**, 129 (1971).

ACKNOWLEDGMENTS

The authors thank Mr. F. H. Lincoln and Mr. J. F. Kinner for providing samples of dinoprost and dinoprost 11,15-bis(tetrahydropyran-2-yl)ether, Mr. L. H. Humphrey for mass spectral analyses, and Miss M. J. Sutton and Mr. A. T. Soule for technical assistance.

Bioavailability and Dissolution Parameters of Seven Lithium Carbonate Products

T. E. NEEDHAM *x, **P. JAVID** ‡, **and W. BROWN** §

Received November 7, 1978, from the *Department of Pharmaceutics, School of Pharmacy, University of Georgia, Athens, GA 30602.* Accepted for publication January 26, 1979. *Present address: Baxter Travenol Laboratories, Morton Grove, Ill. ‡Present address: University of Tehran, Tehran, Iran. §University Health Service, Gilbert Health Center, Athens, GA 30602.

Abstract □ Seven commercial products and a standard powder of lithium carbonate were administered to healthy human volunteers in a crossover study. An analysis of variance of saliva levels and urinary excretion as well as an analysis of variance of peak concentration and the area under the curve from 0 to 24 hr for the saliva levels showed no significant difference between the powder and products, but a significant difference between subjects. A significant difference was found between the time of peak saliva levels, which was attributed to faster powder absorption. A dissolution study using the USP basket method at 50 and 100 rpm and the Levy beaker at 50 rpm also showed no significant difference between products after the lag time for the capsule dosage forms. With a regression analysis, a significant correlation was found between the saliva levels of the products at 2 hr and dissolution in the USP basket at 50 rpm at 4 min.

Keyphrases □ Lithium carbonate—bioavailability and dissolution, various commercial products, powder, humans □ Bioavailability—lithium carbonate, various commercial products, powder, humans □ Dissolution rate—lithium carbonate, various commercial products, powder, humans □ Antidepressants—lithium carbonate, bioavailability and dissolution, various commercial products, powder, humans

Lithium salts have been used extensively in the management of the manic episodes in manic–depressive illness (1–3). Lithium carbonate is the salt form of choice and is used in most oral products available in this country.

The therapeutic plasma range (0.5–1.5 mEq/liter) and the toxic plasma levels (>1.6 mEq/liter) are very close (4). This critical proximity in combination with large variability in patient drug response requires careful plasma level monitoring during lithium therapy.

Lithium carbonate pharmacokinetics have been defined, and the bioavailabilities of several different products have been investigated (5–10). Shepherd *et al.* (11) investigated the dissolution of three lithium carbonate capsule dosage forms and one tablet product and found a large difference in *in vitro* drug release. The USP later required a dissolution standard for lithium carbonate products of 60% dissolved in 30 min at 100 rpm using the basket method (12).

The purpose of this study was to investigate the bioavailabilities of the seven oral lithium carbonate products currently available in this country and to compare *in vitro* drug release as a function of dissolution methods and their defined parameters.

EXPERIMENTAL

Dosage Forms—Seven commercial dosage forms containing 300 mg of lithium carbonate/tablet or capsule were used[1]. Lithium carbonate powder was used as received from the manufacturer.

***In Vivo* Studies**—Seven healthy male subjects, 22–48 years old and within 90–110% of their ideal weight (13), volunteered for this study. Informed written consent was obtained from each subject. Each volunteer was given a general physical examination including a chest X-ray, an ECG, and normal blood and urine profiles prior to initiation of the study. All were within normal limits. Volunteers were asked to refrain from taking any medications or alcohol prior to and during the study.

Following an overnight fast, each subject was instructed to void and to drink 250 ml of water. An hour later, the zero-time urine and saliva samples were taken and 600 mg of drug was administered. The powder was administered as a suspension in water. Cumulative urine samples were subsequently taken at 1, 2, 3, 4, 6, 8, 12, and 24 hr. Fifteen to 20 ml of urine and the saliva samples were refrigerated immediately. Each subject was instructed to drink 250 ml of water after each urine collection for the first 2 hr. Subjects were allowed to eat after the 2-hr sample.

Urine samples were diluted and analyzed, with appropriate blanks, at 670.8 nm using an atomic absorption spectrophotometer[2]. Results are expressed in terms of percent drug excreted. Saliva samples were taken simultaneously with urine samples. All subjects produced saliva freely in amounts from 1 to 6 ml. Saliva samples were diluted with water, homogenized by shaking for 30 min, and analyzed.

The seven products and the powder were administered to the seven volunteers according to an 8 (formulations) × 7 (subjects) crossover design.

***In Vitro* Studies**—Two dissolution apparatuses were used, the USP basket (12) and the modified Levy beaker method (14–16). A stirring rate

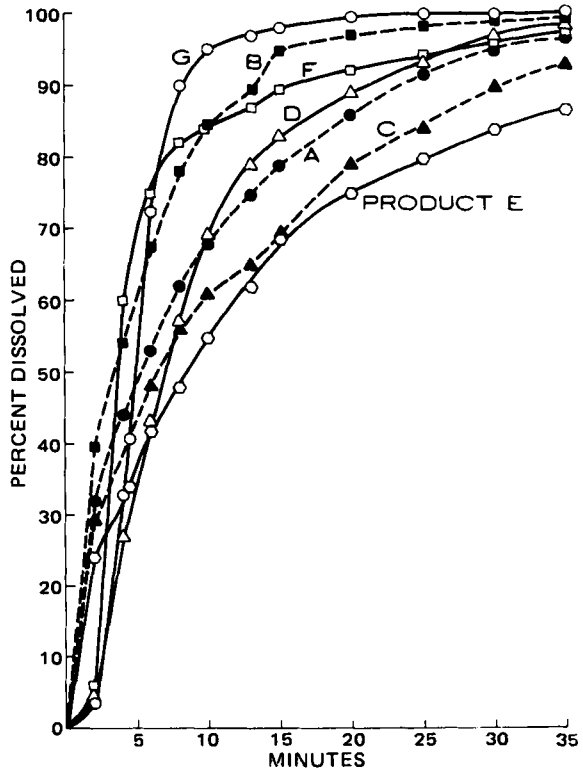

Figure 1—*Average percent dissolved for seven lithium carbonate products in the USP basket at 50 rpm.*

[1] Product A (lot 760475, tablet), Philips Roxane Laboratories, Columbus, OH 43216; Product B (lot 106J07, capsule), Smith Kline and French Laboratories, Philadelphia, PA 19101; Product C (tablet), Pfizer Inc., New York, NY 10017; Product D (lot 760074, capsule), Philips Roxane Laboratories; Product E (lot 62202, tablet), Roerig Division of Pfizer, New York, NY 10017; Product F (lot 59666, capsule), Rowell Laboratories, Baudette, MN 56623; Product G (lot 61631, tablet), Rowell Laboratories; and Product H (lot 76-18, powder), Philips Roxane Laboratories.

[2] Model 360, Perkin-Elmer, Norwalk, Conn.

0022-3549/79/0800-0952$01.00/0
© 1979, American Pharmaceutical Association

Table I—Cumulative Urinary Excretion [a] of the Seven Lithium Carbonate Dosage Forms and the Powder [b]

Hours	Dosage Form A	B	C	D	E	F	G	Powder
1	3.12	2.59	3.08	2.58	2.88	2.24	3.38	4.90
	(2.69)[c]	(1.31)	(2.05)	(1.55)	(2.57)	(1.48)	(2.22)	(2.47)
2	7.77	7.31	8.03	8.58	7.71	6.91	9.17	11.94
	(3.97)	(2.94)	(3.35)	(4.39)	(4.69)	(2.53)	(3.94)	(4.64)
3	10.14	13.08	12.88	12.85	13.41	12.49	15.24	18.53
	(4.48)	(3.65)	(4.27)	(5.31)	(6.34)	(3.92)	(4.66)	(6.69)
4	14.32	18.78	17.38	17.30	18.60	17.59	19.62	21.98
	(6.58)	(4.90)	(5.13)	(5.76)	(7.48)	(4.88)	(5.39)	(7.28)
6	25.27	24.98	24.20	23.06	27.51	26.72	28.02	28.38
	(18.42)	(6.55)	(6.32)	(7.96)	(7.77)	(7.94)	(6.39)	(8.58)
8	31.23	30.02	30.26	30.20	33.76	32.84	32.66	34.49
	(10.52)	(6.55)	(7.92)	(7.28)	(9.24)	(9.93)	(7.59)	(9.90)
12	39.07	39.93	38.32	38.02	41.40	41.64	42.18	41.26
	(11.73)	(7.15)	(8.42)	(6.12)	(10.77)	(11.39)	(8.94)	(9.43)
24	56.19	50.12	53.77	53.87	58.67	60.67	59.96	58.00
	(17.23)	(8.46)	(13.01)	(5.58)	(12.91)	(15.01)	(10.89)	(10.89)

[a] Percent of dose excreted. [b] Average of seven subjects. [c] Standard deviation.

Table II—Saliva Lithium Concentration [a] as a Function of Time

Hours	Dosage Form A	B	C	D	E	F	G	Powder
1	0.262	0.319	0.329	0.306	0.265	0.499	0.317	0.972
	(0.152)[b]	(0.081)	(0.257)	(0.170)	(0.115)	(0.588)	(6.180)	(1.262)
2	0.438	0.424	0.499	0.493	0.483	0.749	0.494	0.867
	(1.83)	(0.111)	(0.347)	(0.211)	(0.200)	(0.820)	(0.288)	(0.865)
3	0.456	0.510	0.682	0.579	0.511	0.916	0.624	0.647
	(0.174)	(0.233)	(0.620)	(0.269)	(0.285)	(0.950)	(0.434)	(0.681)
4	0.398	0.391	0.408	0.361	0.374	0.620	0.349	0.468
	(0.170)	(0.176)	(0.281)	(0.200)	(0.232)	(0.550)	(0.143)	(0.521)
6	0.298	0.287	0.294	0.267	0.277	0.479	0.291	0.341
	(0.139)	(0.120)	(0.161)	(0.137)	(0.178)	(0.465)	(0.135)	(0.322)
8	0.213	0.219	0.222	0.224	0.206	0.374	0.220	0.279
	(0.111)	(0.087)	(0.126)	(0.09)	(0.139)	(0.375)	(0.109)	(0.303)
12	0.155	0.157	0.142	0.161	0.137	0.251	0.160	0.100
	(0.070)	(0.076)	(0.061)	(0.051)	(0.092)	(0.272)	(0.072)	(0.153)
24	0.099	0.100	0.075	0.093	0.053	0.158	0.085	0.107
	(0.434)	(0.050)	(0.041)	(0.034)	(0.028)	(0.196)	(0.046)	(0.086)

[a] Average in micrograms per milliliter for seven subjects. [b] Standard deviation.

Table III—C_{pk} [a] and t_{pk} [a] of Lithium in Saliva

Subject	A		B		C		D		E		F		G		Powder	
	t_{pk}	C_{pk}	t_{pk}	C_{pk}	t_{pk}	C_{pk}	t_{pk}	C_{pk}	t_{pk}	C_{pk}	t_{pk}	C_{pk}	t_{pk}	C_{pk}	t_{pk}	C_{pk}
1	2.5	0.30	2.5	0.32	3	0.70	3	0.43	2	0.59	3	0.92	2.2	0.74	1	0.49
2	4	0.56	2	0.47	3	0.53	3	0.53	2	0.70	2	0.49	2	0.34	1	0.56
3	3	0.67	3	0.72	3	0.30	3	1.72	3	0.70	3	0.84	3	0.70	2	1.23
4	3	0.26	3.2	0.34	3	0.40	3	0.38	3	0.34	3	0.22	3	0.45	2	0.32
5	2	0.68	3	0.90	3	2.08	2.5	0.98	3	1.02	3	3.0	3	1.56	1	3.78
6	2.5	0.37	2.2	0.38	3.2	0.30	2	0.50	2	0.20	3	0.40	3	0.26	2	0.38
7	2.5	0.68	2.2	0.64	2.5	0.64	3	0.43	3	0.58	3	0.56	3	0.37	2	0.55

[a] Peak concentration in milliequivalents per liter and time in hours.

of 50 rpm was used for the modified Levy beaker, and rates of 50 and 100 rpm were used for the USP basket method. Temperature was controlled at 37.0 ± 0.5°. Six hundred milliliters of potassium biphthalate buffer (pH 3.0) was used as the dissolution medium.

At appropriate times, a 1-ml sample was withdrawn and an equal volume of medium was added to maintain a constant volume. Samples were filtered, diluted, and analyzed at 670.8 nm using the atomic absorption spectrophotometer.

RESULTS AND DISCUSSION

***In Vivo* Studies**—Table I shows the cumulative percent of dose excreted in the urine for the seven lithium carbonate products and powder as a function of time. There was little apparent difference in urinary excretion among all eight doses during the 24 hr of sampling. Comparison of these results with work previously reported (8) shows an excellent agreement in cumulative excretion of lithium at 4, 8, and 24 hr.

An analysis of variance using a repeated measures design was employed at each sampling time. This analysis showed no significant difference in drug excretion between brands ($p = 0.05$) during any sampling time up to 24 hr. However, a significant difference was found among subjects at all time intervals. These results aptly illustrate the wide variability mentioned previously and the need to monitor individual patients during drug administration.

Since it has been reported that the saliva/plasma lithium concentration ratio is constant and reproducible for a given individual (17), the saliva lithium concentration also was determined for the dosage forms and the powder for all seven subjects (Table II). Very little difference was apparent, although the average drug concentration produced by the powder seemed to be higher at 1.0 and 2.0 hr. However, the repeated-measures analysis of variance at each sample time showed no significant difference between the products or the powder ($p = 0.05$). Again, the difference among subjects was significant at all sample times.

The constant plasma/saliva lithium ratio makes feasible a comparison of the saliva peak drug level (C_{pk}), the peak level time (t_{pk}), and the area under the saliva level curve (AUC) as a means of measuring the bio-

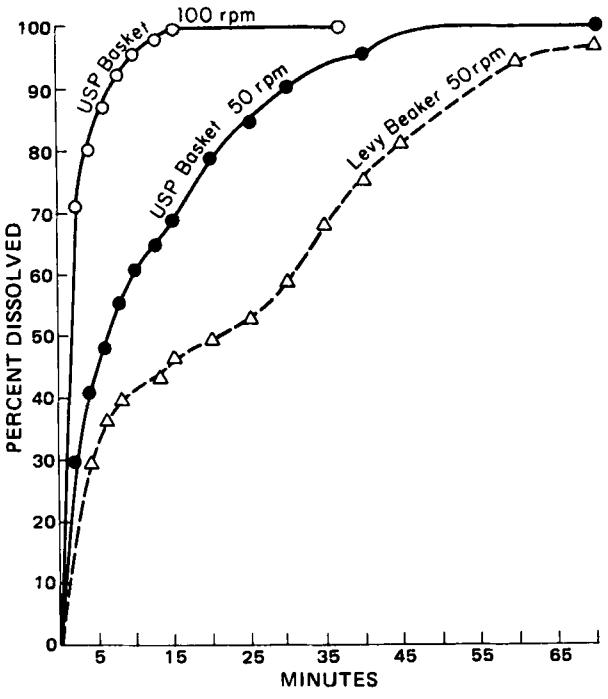

Figure 2—*Dissolution profiles for Product C using the three different dissolution methods/agitation speeds.*

availability of the seven products and powder. Table III shows the C_{pk} and t_{pk} values for each administered dose in each subject. The peak level time is presented as an estimate based on saliva data interpolation.

A two-way analysis of variance for peak concentration to include seven subjects and eight dose administrations produced an F value (7, 42) of 1.16 for the between-brands comparison and an F value (6, 42) of 9.08 among these subjects. These results indicated that no significant differences ($p = 0.05$) existed among the peak saliva concentrations for the seven different lithium carbonate brands and the powder. Significant differences existed among the subjects.

A further analysis of variance of the time required to reach the peak saliva lithium concentration was performed. An F value (7, 42) of 6.80 was calculated for the between-brands comparison. This result indicated a significant difference ($p = 0.05$). A Newman–Keuls (18) analysis was performed to determine which of the t_{pk} means of the administered brands or powder was significantly different. The powder, with an average t_{pk} of 1.57 hr, was different from all of the commercial products. No significant difference was found among any of the remaining seven lithium carbonate products. Interestingly, the calculated F value (6, 42) of 1.84 indicated no significant difference ($p = 0.05$) among subjects for t_{pk}.

The area under the saliva level curve for 0–24 hr was calculated using the trapezoidal rule with average AUC values of 4.406 (Brand E), 4.823 (Brand A), 4.962 (Brand C), 4.972 (Brand D), 4.981 (Brand G), 4.992 (Brand B), 6.789 (powder), and 8.020 (Brand F). A two-way analysis of variance for the AUC *versus* subjects produced an F value (7, 42) of 1.02 for the between-brands comparison, which was not significant ($p = 0.05$). The calculated F value (7, 42) of 6.13 for the between-subjects comparison was significant.

***In Vitro* Dissolution Studies**—The seven lithium carbonate brands were dissolved using three systems: a modified Levy beaker method at 50 rpm and the USP basket method at 50 and 100 rpm.

Figure 1 illustrates the average percent dissolved for all seven products in the USP basket at 50 rpm. This method and agitation speed illustrate the behavior seen in both the USP basket at 100 rpm and the Levy beaker.

These results were compared using an analysis of variance. The percent of drug dissolved was transformed using a log arc sine transformation to ensure homogeneity of variance and additivity of effects (19). Since previous work had determined that an analysis of variance across time produces significant interaction effects (20), a 7 (brands) × 3 (methods/rpm) with five replications repeated-measures analysis of variance at each sample time was performed. This analysis showed a significant difference between brands ($p = 0.05$) in drug dissolution from the dosage forms at 2 and 4 min. Comparison of the average percent dissolved showed that these differences were due to capsule dosage forms Brands B, D, and F, which displayed the expected lag time. However, the analysis of variance showed a significant difference in the dissolution between methods at all sample times. Figure 2 illustrates an example comparison, using Product C, of the average percent dissolved for each method and agitation speed. The order of decreasing rate of dissolution was USP 100 rpm, USP 50 rpm, and Levy 50 rpm for all brands at all sampling times.

All products adhered to the USP regulation that 60% of drug dissolve in 30 min at 100 rpm in the USP basket. In fact, the time to achieve 60% dissolution ranged from <2 min for Brands C and E to <8 min for Brand F.

A correlation of the *in vivo* saliva concentrations of the different lithium carbonate brands with the *in vitro* drug release from the dosage forms at all possible combinations of sample times was attempted using a regression analysis. A significant correlation at the 0.95 level was found for the Levy 50-rpm and USP 50-rpm methods at the 2-min sample time *versus* the *in vivo* time of 1 hr. However, comparison of the presented results showed that this correlation occurred during the only *in vitro* sample time that showed a significant difference between brands and at the *in vivo* sampling time that had no difference between brands. Apparently, the regression analysis produced a mathematical correlation of little practical significance.

A second significant correlation was found at the 0.99 level for the USP basket at 50 rpm at 4 min with the *in vivo* sample time of 2 hr. In this comparison, the significance level was higher. The analysis of variance of both the *in vivo* and *in vitro* data for the USP basket at 50 rpm showed no significant difference between brands, and the dosage forms were in that phase of absorption and dissolution where drug release was significant. This finding seems important since the assumption inherent in *in vivo–in vitro* correlation requires a comparison based on drug release from dosage form, manifested as dissolution or as absorption. To determine the practicality of this means of correlation as a control method, further work employing dosage forms designed to produce diverse drug concentration levels is necessary.

REFERENCES

(1) M. Shou, N. Juel-Neilson, E. Stromgreen, and H. Voldby, *J. Neurol. Neurosurg. Psychiatry*, **17**, 25 (1954).

(2) S. Gerslan and A. Yarvilder, *J. Neuropsychiatry*, **1**, 210 (1966).

(3) P. C. Bustraf and M. Sehou, *Arch. Gen. Psychiatry*, **16**, 162 (1967).

(4) R. F. Prien, E. M. Caffer, and C. J. Klett, *Dis. Nerv. Syst.*, **32**, 521 (1971).

(5) H. C. Caldwell, W. J. Westlake, S. M. Conner, and J. Planajan, *J. Clin. Pharmacol.*, **11**, 349 (1971).

(6) R. W. Mason, E. G. McQueen, P. J. Keary, and N. Mcl. James, *Clin. Pharmacokinet.*, **3**, 241 (1978).

(7) V. Otto, L. Paalzow, and G. Suren, *Acta Pharm. Suec.*, **9**, 595 (1972).

(8) E. T. Sugita, J. W. Stokes, A. Frazer, P. Grof, J. Mendels, F. J. Goldstein, and P. J. Niebergal, *J. Clin. Pharmacol.*, **13**, 264 (1973).

(9) P. Grof, M. C. Saxena, L. Dagli, and M. Prior, *J. Neuropsychiatry*, **9**, 313 (1976).

(10) R. I. Poust, A. Mallinger, J. Mallinger, J. M. Himmelholh, J. F. Neil, and I. Hanin, *J. Pharm. Sci.*, **66**, 609 (1977).

(11) R. E. Shepherd, J. C. Price, and L. A. Luzzi, *ibid.*, **61**, 1152 (1972).

(12) "The United States Pharmacopeia," 18th rev., Mack Publishing Co., Easton, Pa., 1970.

(13) "Scientific Tables," 7th ed., K. Diem and C. Lentner, Eds., Geigy Pharmaceuticals, Ardsley, N.Y., 1970, p. 712.

(14) G. Levy and B. A. Hayes, *N. Engl. J. Med.*, **262**, 1053 (1961).

(15) G. Levy, *J. Pharm. Sci.*, **52**, 1039 (1963).

(16) G. Levy and B. Sahli, *ibid.*, **51**, 58 (1962).

(17) C. Neu, A. Dimascio, and D. Williams, *Am. J. Psychiatry*, **132**, 66 (1976).

(18) G. W. Snedecor and W. G. Cochran, "Statistical Methods," 6th ed., Iowa State University Press, Ames, Iowa, 1967, p. 273.

(19) C. A. Bennett and N. L. Franklin, "Statistical Analysis in Chemistry and the Chemical Industry," Wiley, New York, N.Y., 1954, p. 355.

(20) T. E. Needham, K. Shah, J. Kotzan, and H. Zia, *J. Pharm. Sci.*, **67**, 1070 (1978).

Synthesis of Substituted 2-Aminopyrrole Analogs of Lidocaine II

RONALD W. JOHNSON *, THOMAS H. KEENAN ‡, JOSEPH W. KOSH, and J. WALTER SOWELL, Sr. ˣ

Received December 18, 1978, from the *College of Pharmacy, University of South Carolina, Columbia, SC 29208.* Accepted for publication January 30, 1979. *Present address: Medical University of South Carolina, Charleston, S.C. ‡Present address: Purdue University, West Lafayette, Ind.

Abstract □ The synthesis and local anesthetic and antiarrhythmic properties of eight substituted 2-diethylaminoacetamido-3-carbamyl-4-methylpyrroles are described. Three compounds showed significant local anesthetic activity by the guinea pig wheal test, and four showed antiarrhythmic activity against chloroform-induced ventricular arrhythmias in mice.

Keyphrases □ Lidocaine analogs—synthesis of 2-diethylaminoacetamido-3-carbamyl-4-methylpyrroles, local anesthetic activity, antiarrhythmic activity, structure–activity relationships □ Structure–activity relationships—lidocaine analogs, local anesthetic activity, antiarrhythmic activity □ Local anesthetic agents—lidocaine analogs, synthesis, structure–activity relationships □ Antiarrhythmic agents—lidocaine analogs, synthesis, structure–activity relationships

The synthesis and local anesthetic and antiarrhythmic properties of a series of substituted 2-diethylaminoacetamido-3-cyano-4-methylpyrrole (I) analogs of lidocaine (II) were reported previously (1). The biological activity exhibited by members of I prompted further research on heteroaromatic pyrrole analogs of II.

This report describes the synthesis and preliminary pharmacological evaluation for local anesthetic and antiarrhythmic activities of a series of substituted 2-diethylaminoacetamido-3-carbamyl-4-methylpyrroles (III).

DISCUSSION

Chemistry—The utilization of substituted 2-amino-3-cyano-4-methylpyrroles (IV*a*–IV*h*) (2–4) as precursors to substituted 2-chloroacetamido-3-cyano-4-methylpyrroles (V*a*–V*h*) was reported previously (1). In the present work, V*a*–V*h* were utilized as intermediates in the synthesis of III (Scheme I).

Nitrile hydrolysis proceeded smoothly, by heating V*a*–V*h* in 85% phosphoric acid, to yield the corresponding substituted 2-chloroacetamido-3-carbamyl-4-methylpyrroles (VI*a*–VI*h*). The lower molecular weight analogs (V*a* and V*b*) and analogs possessing polar R groups (V*d* and V*g*) were hydrolyzed easily in 85% phosphoric acid at 120–125° for 5–10 min. The higher molecular weight analogs with nonpolar R groups (V*e*, V*f*, and V*h*) required more drastic conditions for hydrolysis. These conditions included more phosphoric acid, a temperature of 135–140°, and a total hydrolysis time of 10 min. With V*d*, the more drastic reaction conditions resulted in a decreased yield of VI*d*.

In general, the hydrolyzed compounds VI*a*–VI*h* were less soluble in organic solvents than their immediate precursors V*a*–V*h*. The decreased solubility can be explained, in part, by the increased potential for intramolecular hydrogen bonding. NMR and IR spectra were consistent with the assigned structures. Elemental analysis and TLC were used in determining chloroacetamide purity (Table I).

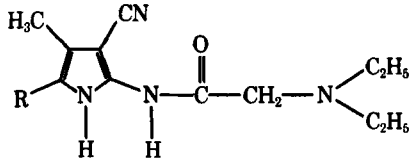

I

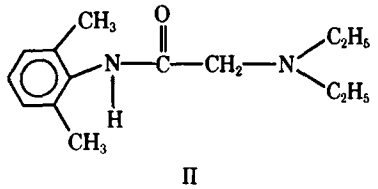

II

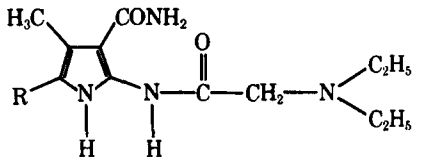

III

The substituted 2-diethylaminoacetamido-3-carbamyl-4-methylpyrroles (VII*a*–VII*h*) were obtained by refluxing a suspension of the corresponding chloroacetamide (VI*a*–VI*h*) in methanol or ethanol with

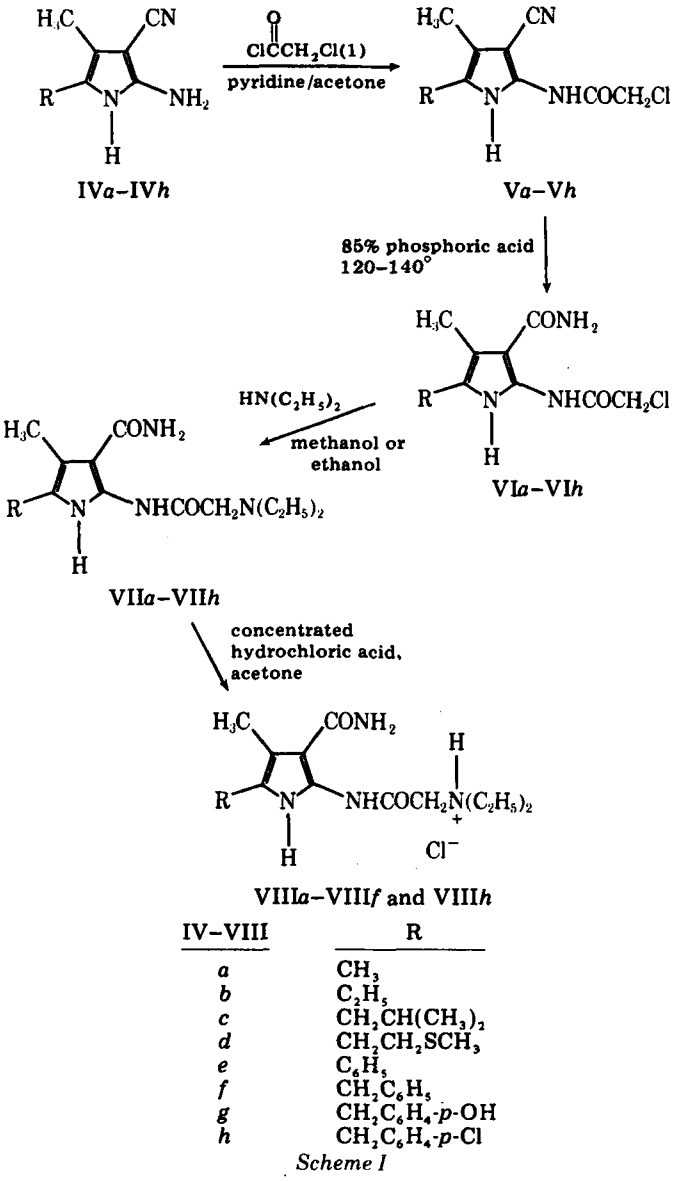

IV–VIII	R
a	CH_3
b	C_2H_5
c	$CH_2CH(CH_3)_2$
d	$CH_2CH_2SCH_3$
e	C_6H_5
f	$CH_2C_6H_5$
g	$CH_2C_6H_4$-*p*-OH
h	$CH_2C_6H_4$-*p*-Cl

Scheme I

0022-3549/79/0800-0955$01.00/0
© 1979, American Pharmaceutical Association

Table I—Substituted 2-Chloroacetamido-3-carbamyl-4-methylpyrroles

Compound	Yield, %	Melting Point	R_f[a]	Recrystallization Solvent	Formula	Analysis, %	Calc.	Found
VI*a*	96.9	210–211° dec.	0.46	Methanol	$C_9H_{12}ClN_3O_2$	C	47.06	47.10
						H	5.27	5.29
						Cl	15.44	15.36
						N	18.30	18.26
VI*b*	81.3	195–196° dec.	0.47	Ethanol	$C_{10}H_{14}ClN_3O_2$	C	49.28	49.33
						H	5.79	5.82
						Cl	14.55	14.61
						N	17.24	17.22
VI*c*	89.6	210–211° dec.	0.35	Ethanol	$C_{12}H_{18}ClN_3O$	C	53.04	52.99
						H	6.68	6.71
						Cl	13.05	13.04
						N	15.46	15.44
VI*d*	73.0	195.5–196° dec.	0.41	Ethanol	$C_{11}H_{16}ClN_3O_2S$	C	45.59	45.75
						H	5.57	5.67
						Cl	12.24	12.06
						N	14.50	14.43
						S	11.07	11.20
VI*e*	89.7	215–216° dec.	0.47	Ethanol	$C_{14}H_{14}ClN_3O_2$	C	57.64	57.72
						H	4.84	4.88
						Cl	12.16	12.07
						N	14.40	14.34
VI*f*	95.3	224.5–225° dec.	0.42	Ethanol–2-propanol–toluene	$C_{15}H_{16}ClN_3O_2$	C	58.92	58.96
						H	5.28	5.31
						Cl	11.60	11.65
						N	13.74	13.75
VI*g*	84.4	231–232° dec.	0.36	Methanol–ethanol–benzene	$C_{15}H_{16}ClN_3O_3$	C	55.99	55.84
						H	5.01	5.09
						Cl	11.02	11.01
						N	13.06	12.99
VI*h*	88.1	209.5–210.5° dec.	0.41	Ethanol	$C_{15}H_{15}Cl_2N_3O_2$	C	52.95	52.92
						H	4.44	4.44
						Cl	20.84	20.74
						N	12.35	12.37

[a] Ethyl acetate.

excess diethylamine. During the reactions, solutions were achieved within 0.5–3 hr. An exception was observed for the synthesis of VII*h*; a solution was not achieved after refluxing for 9 hr. In general, the solutions were refluxed for an additional hour, the solvent and excess diethylamine were removed *in vacuo*, and the residues were dissolved in 10% HCl. Unreacted chloroacetamides were removed by filtration, and the amines were precipitated by the addition of 5% aqueous NaOH. Yields, melting points, and purification data are given in Table II.

All amine hydrochlorides were prepared by treating an acetone solution of the free amine (VII*a*–VII*e*) or an acetone suspension of the free amine (VII*f* and VII*h*) with concentrated hydrochloric acid. Compound VIII*g* separated from acetone as a red oil when this procedure was employed for salt formation. IR spectra of the amine hydrochlorides (VIII*a*–VIII*f* and VIII*h*) exhibited typical N–H stretching absorption bands between 3500 and 3100 cm^{-1} and broad absorption in the 3100–2600-cm^{-1} region for the amine salts. Two intense carbonyl absorption bands at 1690–1680 and 1645–1640 cm^{-1} were observed for each compound.

NMR spectra of the amine hydrochlorides in dimethyl sulfoxide-d_6 exhibited a typical triplet and quartet for the methyl and methylene of the diethylamino group, respectively. Chemical shifts for the triplet ranged from 1.15 to 1.20 ppm, and those for the quartet ranged from 3.10 to 3.15 ppm. The triplet and quartet integrated for three protons and two protons, respectively. A singlet in the 2.00–2.15-ppm region, integrating for three protons, was assigned to the methyl group at the C-4 position. In the 4.05–4.15-ppm region, the spectra exhibited a singlet, integrating for two protons, which was assigned to the methylene located alpha to the carbonyl. A broad singlet at 6.55–6.85 ppm, integrating for two protons, was assigned to the carbamyl function protons.

The salt NH proton was observed as a broad singlet, integrating for one proton, in the 9.8–10.5-ppm region. Two additional broad singlets, one in the 10.7–11.0-ppm region and the other in the 10.95–11.0-ppm region, were assigned to the amide and pyrrole ring NH protons. Miscellaneous absorptions for the various hydrochloride salts were consistent with their structure. The purity of VIII*a*–VIII*f* and VIII*h* was determined by elemental analysis and TLC (Table III).

Pharmacology—*Antiarrhythmic Activity*—Cardiac rates less than the mean rate of 200 beats/min were used as an index of protection from arrhythmia at 70 mg/kg. Compounds VIII*a*, VIII*b*, VIII*d*, and VIII*e* (Table IV) showed activity at this dosage. Compounds VIII*c* and VIII*f* also may be effective if the standard error of the mean is considered.

Local Anesthetic Activity—Compounds VIII*c* and VIII*e*–VIII*g* possessed local anesthetic activity at all three solution concentrations whereas the remaining compounds possessed weak activity only at the highest solution concentration. Compounds VIII*e* and VIII*f* were the most active, having activity comparable to that of lidocaine (Table V).

EXPERIMENTAL[1]

Chemistry—*2-Chloroacetamido-3-carbamyl-4,5-dimethylpyrrole (VI*a*)*—The procedure for the synthesis of VI*a* is given as representative for VI*b*–VI*h*. A suspension of 2-chloroacetamido-3-cyano-4,5-dimethylpyrrole (V*a*) (15.0 g, 0.07 mole) (1) in 100 ml of 85% phosphoric acid was stirred at room temperature for 5 min. The vessel was placed into an oil bath preheated to 120° and stirred vigorously for 10 min. During this time, solution was achieved, and some of the product precipitated on the stirring solution surface. The vessel was removed from the oil bath and cooled to room temperature. The resulting semisolid was diluted with 300 ml of water and stirred for 10 min.

The crude product was collected by filtration, washed with water, and air dried. One gram of the pale-yellow product (15.6 g, 96.9%) was recrystallized twice from absolute methanol to yield yellow needle-shaped crystals (homogeneous on TLC, ethyl acetate, R_f 0.46), mp 210–211° dec.; IR (KBr): 3520, 3350, 3160, 1680, 1645, 1600, 1570, 1460, 1445, 1400, 1385, 1280, 1215, 790, 735, and 625 cm^{-1}; NMR (dimethyl sulfoxide-d_6): δ 1.95 (s, 6H, $-CH_3$ at C_4 and C_5), 4.20 (s, 2H, $-CH_2-$), 6.42 (broad s, 2H, $-CONH_2$ at C_3), 10.72 (broad s, 1H, NH of amide at C_2 or N_1H), and 10.89 (broad s, 1H, N_1H or NH of amide at C_2) ppm. (See Table I for analyses.)

*2-Diethylaminoacetamido-3-carbamyl-4,5-dimethylpyrrole (VII*a*)*—The procedure for the synthesis of VII*a* is given as representative for VII*b*–VII*h*. A suspension of VI*a* (9.2 g, 0.04 mole) in 125 ml of methanol

[1] IR spectral data were determined on a Beckman IR-20A grating spectrophotometer using the potassium bromide techniques. NMR spectra were determined on a Hitachi Perkin-Elmer R24 high-resolution spectrophotometer with tetramethylsilane as the internal reference. Melting points were obtained using a Thomas-Hoover capillary apparatus and are uncorrected. Carbon, hydrogen, chlorine, and nitrogen values were obtained from analysis performed by Atlantic Microlab, Inc., Atlanta, Ga. TLC was performed using Eastman chromatogram sheets, type 6060 (silica gel), and the sheets were developed in an iodine chamber.

Table II—Substituted 2-Diethylaminoacetamido-3-carbamyl-4-methylpyrroles

Compound	Yield, %	Melting Point	Reaction Solvent[a]	Recrystallization Solvent	Formula
VII*a*	98.9	160.5–162°	Methanol	Methanol–water (4:1)	$C_{13}H_{22}N_4O_2$
VII*b*	90.2	164–166°	Ethanol	Methanol–water (4:1)	$C_{14}H_{24}N_4O_2$
VII*c*	74.6	116.5–117°	Ethanol	Methanol–water (4:1)	$C_{16}H_{28}N_4O_2$
VII*d*	93.4	130.5–131.5°	Ethanol	Methanol–water (4:1)	$C_{15}H_{26}N_4O_2S$
VII*e*	96.2	60–62°	Methanol	Methanol–water (4:1)	$C_{18}H_{24}N_4O_2$
VII*f*	59.2	202–204°	Methanol	—[b]	$C_{19}H_{26}N_4O_2$
VII*g*[c]	81.7	161–163°[d]	Methanol	Methanol–water (4:1)	$C_{19}H_{26}N_4O_3$
VII*h*	89.0	218–219.5°	Ethanol	—[d]	$C_{19}H_{25}ClN_4O_2$

[a] Absolute. [b] Crude product washed with cold acetone. [c] Calc. for: C, 63.67; H, 7.31; N, 15.63. Found: C, 63.40; H, 7.39; N, 15.73. [d] Crude product was boiled with 100 ml of methanol and filtered while hot. The insoluble amine was suitable for hydrochloride salt formation.

Table III—Substituted 2-Diethylaminoacetamido-3-carbamyl-4-methylpyrrole Hydrochlorides

Compound	Yield, %	Recrystallization Solvent	R_f[a]	Melting Point	Formula	Analysis, %	Calc.	Found
VIII*a*	97.3	Methanol–acetone	0.40	244–245° dec.	$C_{13}H_{23}ClN_4O_2$	C	51.56	51.32
						H	7.66	7.66
						Cl	11.71	11.55
						N	18.50	18.44
VIII*b*	94.7	—[b]	0.39	241.5–242.5° dec.	$C_{14}H_{25}ClN_4O_2$	C	53.07	53.10
						H	7.95	7.99
						Cl	11.19	11.22
						N	17.68	17.67
VIII*c*	82.6	—[b]	0.37	225.5–226.5° dec.	$C_{16}H_{29}ClN_4O_2$	C	55.72	55.62
						H	8.48	8.52
						Cl	10.28	10.18
						N	16.25	16.23
VIII*d*	84.9	—[b]	0.36	224–225° dec.	$C_{15}H_{27}ClN_4O_2S$	C	49.64	49.66
						H	7.50	7.50
						Cl	9.77	9.72
						N	15.44	15.47
						S	8.84	8.81
VIII*e*	79.9	Methanol–acetone–chloroform	0.44	260.5–261° dec.	$C_{18}H_{25}ClN_4O_2$	C	59.25	59.05
						H	6.91	6.94
						Cl	9.72	9.65
						N	15.36	15.32
VIII*f*	83.3	Methanol–acetone	0.44	247.5–248° dec.	$C_{19}H_{27}ClN_4O_2$	C	60.22	60.27
						H	7.18	7.22
						Cl	9.36	9.35
						N	14.79	14.84
VIII*g*[c]	—	—	—	Oil	—	—	—	—
VIII*h*	83.6	Ethanol	0.42	226–226.5° dec.	$C_{19}H_{26}Cl_2N_4O_2$	C	55.21	55.27
						H	6.34	6.40
						Cl	17.16	17.20
						N	13.56	13.57

[a] Ethyl acetate. [b] Salt obtained was analytically pure. [c] Salt obtained was a red oil; therefore, elemental analysis was determined on the free base (VII*g*).

and diethylamine (30 g, 0.4 mole) was refluxed, with stirring, until complete solution was achieved (0.5–3 hr). Then the solution was refluxed for an additional 1 hr, the excess diethylamine and solvent were removed *in vacuo*, and the residue was dissolved in 100 ml of 10% HCl.

The solution was filtered and poured over 300 g of crushed ice. The amine was precipitated by the addition of 5% aqueous NaOH. The solid was collected by filtration, washed with distilled water, and air dried. The crude product (9.09 g, 98.9%) was recrystallized from methanol–water (4:1) to yield fine off-white crystals (mp 160.5–162°), which were suitable for hydrochloride salt formation. (See Table II for analogs.)

Table IV—Antiarrhythmic Activity of Substituted 2-Diethylaminoacetamido-3-carbamyl-4-methylpyrrole Hydrochlorides[a]

Compound	40 mg/kg	70 mg/kg	100 mg/kg
Lidocaine	242 ± 13	141 ± 23	116 ± 6
VIII*a*	236 ± 12	182 ± 8	158 ± 9
VIII*b*	232 ± 6	175 ± 5	133 ± 5
VIII*c*	196 ± 10	202 ± 6	187 ± 13
VIII*d*	218 ± 11	193 ± 13	217 ± 5
VIII*e*	244 ± 8	174 ± 10	157 ± 6
VIII*f*	208 ± 13	203 ± 12	200 ± 8
VIII*g*	255 ± 11	214 ± 8	211 ± 3
VIII*h*	248 ± 4	217 ± 17	214 ± 8
Control	351 ± 8	—	—

[a] Data represent cardiac rates following arrhythmias induced in mice by exposure to chloroform vapor (n = 6).

2-Diethylaminoacetamido-3-carbamyl-4,5-dimethylpyrrole Hydrochloride (*VIII*a)—The procedure for the synthesis of VIII*a* is given as representative for VIII*b*–VIII*f* and VIII*h*. A stirred solution of VII*a* (10.0 g, 0.03 mole) in 225 ml of acetone was treated with 4 ml of concentrated hydrochloric acid. After stirring for 5 min at room temperature, the vessel was sealed and placed in a freezer for 2 hr. The salt was collected by filtration, washed with 50 ml of cold acetone, and air dried.

The crude product (10.8 g, 97.3%) was recrystallized from methanol–

Table V—Local Anesthetic Activity of Substituted 2-Diethylaminoacetamido-3-carbamyl-4-methylpyrrole Hydrochlorides[a]

Compound	Concentration, % 1	0.5	0.2
VIII*a*	19	—	—
VIII*b*	19	—	—
VIII*c*	26	25	7
VIII*d*	5	—	—
VIII*e*	70	53	16
VIII*f*	70	59	16
VIII*g*	72	33	10
VIII*h*	20	—	—
Lidocaine	68	41	17
0.9% NaCl	0	0	0

[a] Data represent the number of pinpricks failing to elicit a twitch response following intradermal injection in guinea pigs (n = 2).

acetone to yield light-tan crystals (homogeneous on TLC, ethyl acetate, R_f 0.40), mp 244–245° dec.; IR (KBr): 3420, 3340, broad absorption from 3200 to 2600, 1675, 1635, 1600, 1570, 1545, 1470, 1435, 1380, 1370, 1355, 1270, 1240, 1155, 955, 805, and 630 cm^{-1}; NMR (dimethyl sulfoxide-d_6): δ 1.19 (t, 6H, $-CH_3$ of diethylamino), 2.08 (s, 6H, $-CH_3$ at C_4 and C_5), 3.14 (q, 4H, methylenes of diethylamino), 4.05 (broad s, 2H, $COCH_2$), 6.55 (broad s, 2H, $CONH_2$), 9.90–10.50 (broad s, 1H, N^+H), 10.70 (broad s, NH of amide at C_2 or N_1H), and 10.95 (broad s, 1H, N_1H or NH of amide at C_2) ppm. (See Table III for analyses.)

Pharmacology—*Antiarrhythmic Activity*—With the method of Lawson (5), fibrillations were induced in 20–30-g male mice by exposure to chloroform vapor until respiration ceased. The heart was exposed, and the cardiac rate was determined with a binocular microscope. Mice with cardiac rates >200 beats/min were considered unprotected (Table IV).

Local Anesthetic Activity—The guinea pig wheal method of Bülbring and Wajda (6) was used to determine the activity. The back of the guinea pig was shaved 1 day prior to the test, and 0.25 ml of the aqueous drug solution was administered intradermally at two sites along the midline. The resulting wheals were tested by pricking the area six times with a pin at 5-min intervals for 1 hr. Local anesthesia was present if the pinprick did not elicit a skin twitch. The number of pinpricks that failed to elicit a response was then recorded at each time interval (Table V).

REFERENCES

(1) R. W. Johnson, T. H. Keenan, J. W. Kosh, and J. W. Sowell, Sr., *J. Pharm. Sci.*, **68**, 317 (1979).

(2) R. Gewald, *Z. Chem.*, **1**, 349 (1961).

(3) R. W. Johnson, R. J. Mattson, and J. W. Sowell, Sr., *J. Heterocycl. Chem.*, **14**, 383 (1977).

(4) V. I. Shvedov, M. V. Mezentseva, and A. N. Grinev, *Khim. Geterotsikl. Soedin.*, **9**, 1219 (1975); through *Chem. Abstr.*, **84**, 59299 (1976).

(5) J. W. Lawson, *J. Pharmacol. Exp. Ther.*, **160**, 22 (1968).

(6) E. Bülbring and I. Wajda, *ibid.*, **85**, 78 (1945).

ACKNOWLEDGMENTS

Adapted in part from theses submitted by R. W. Johnson and T. H. Keenan to the Graduate School, University of South Carolina, in partial fulfillment of the Master of Science degree requirements.

Comparative Pharmacokinetics of Coumarin Anticoagulants XLI: Effect of Phenobarbital on Systemic Availability of Orally Administered Dicumarol in Rats

JAMES W. CROW, MILO GIBALDI, and GERHARD LEVY ×

Received December 8, 1978, from the *Department of Pharmaceutics, School of Pharmacy, State University of New York at Buffalo, Amherst, NY 14260.* Accepted for publication January 26, 1979.

Abstract □ The purpose of this investigation was to determine the effect of phenobarbital on the systemic availability of orally administered dicumarol in rats. Adult male Sprague–Dawley rats, matched for dicumarol free fraction in serum, received either phenobarbital sodium, 75 mg/kg, or saline solution, orally or intravenously, daily for 7 days. On Day 6, they also received ^{14}C-dicumarol, 2 mg/kg iv, and unlabeled dicumarol, 50 mg/kg po, in aqueous suspension. Venous blood samples were obtained serially over 32 hr through an indwelling cannula. Systemic dicumarol availability was determined from the dose-normalized ratio of areas under the plasma concentration–time curves. Phenobarbital treatment almost doubled the total clearance of dicumarol and the intrinsic clearance of free dicumarol, with no significant difference between the inductive effects of oral and intravenous doses of phenobarbital. Systemic dicumarol availability in control rats (mean ± *SD*) was 84 ± 8% (n = 10) and 84 ± 10% (n = 6) in the oral and intravenous phenobarbital studies, respectively. The systemic dicumarol availability in phenobarbital-treated rats was appreciably lower: 48 ± 7% (n = 10) and 61 ± 12% (n = 6) for orally and intravenously treated animals, respectively. The effect of oral phenobarbital on systemic dicumarol availability was more pronounced than that of intravenous phenobarbital ($p < 0.025$). The apparent first-order absorption rate constants for the fraction of the dose available systemically were similar for control and treated animals. There was a positive correlation between systemic dicumarol availability and total dicumarol clearance in control animals ($p < 0.001$). Proper matching of control and treated animals is, therefore, important for this type of study. The rat appears to be a good model for investigating the mechanism of the inhibitory effect of phenobarbital on dicumarol absorption observed previously in humans.

Keyphrases □ Phenobarbital—effect on systemic availability of oral dicumarol, comparison of oral and intravenous doses □ Bioavailability—dicumarol in rats, effect of oral and intravenous phenobarbital □ Dicumarol—bioavailability, effect of oral and intravenous phenobarbital □ Anticoagulants—dicumarol, effect of oral and intravenous phenobarbital on systemic availability

The bioavailability of orally administered dicumarol in humans is reduced by pretreatment of the subjects with an orally administered barbiturate (1). Similar effects have been observed with respect to two other poorly water-soluble drugs, griseofulvin and diethylstilbestrol. The bioavailability of orally administered griseofulvin in humans is reduced by pretreatment with orally administered phenobarbital (2). Such a reduction in griseofulvin bioavailability has also been observed in rats (3). Pretreatment with phenobarbital has been reported to decrease diethylstilbestrol absorption from the rat intestine (4).

Little is known about the mechanism of the barbiturate effect on drug absorption. A study was designed to determine the effect of orally and intravenously administered phenobarbital on GI absorption of dicumarol in rats. The results of this investigation have bearing not only on the specific interaction under study but also on the design of studies to determine the bioavailability of drugs that are subject to enzyme induction and that exhibit pronounced interindividual differences in pharmacokinetic characteristics.

EXPERIMENTAL

The studies were carried out on adult male Sprague–Dawley rats weighing 250–375 g. Groups of animals were screened for plasma free fraction values of dicumarol, using serum obtained from ~5 ml of blood withdrawn from the tail artery under light ether anesthesia. The free fraction determinations were performed in duplicate by dialyzing, to

0022-3549/79/0800-0958$01.00/0

© 1979, American Pharmaceutical Association

acetone to yield light-tan crystals (homogeneous on TLC, ethyl acetate, R_f 0.40), mp 244–245° dec.; IR (KBr): 3420, 3340, broad absorption from 3200 to 2600, 1675, 1635, 1600, 1570, 1545, 1470, 1435, 1380, 1370, 1355, 1270, 1240, 1155, 955, 805, and 630 cm^{-1}; NMR (dimethyl sulfoxide-d_6): δ 1.19 (t, 6H, $-CH_3$ of diethylamino), 2.08 (s, 6H, $-CH_3$ at C_4 and C_5), 3.14 (q, 4H, methylenes of diethylamino), 4.05 (broad s, 2H, $COCH_2$), 6.55 (broad s, 2H, $CONH_2$), 9.90–10.50 (broad s, 1H, N^+H), 10.70 (broad s, NH of amide at C_2 or N_1H), and 10.95 (broad s, 1H, N_1H or NH of amide at C_2) ppm. (See Table III for analyses.)

Pharmacology—*Antiarrhythmic Activity*—With the method of Lawson (5), fibrillations were induced in 20–30-g male mice by exposure to chloroform vapor until respiration ceased. The heart was exposed, and the cardiac rate was determined with a binocular microscope. Mice with cardiac rates >200 beats/min were considered unprotected (Table IV).

Local Anesthetic Activity—The guinea pig wheal method of Bülbring and Wajda (6) was used to determine the activity. The back of the guinea pig was shaved 1 day prior to the test, and 0.25 ml of the aqueous drug solution was administered intradermally at two sites along the midline. The resulting wheals were tested by pricking the area six times with a pin at 5-min intervals for 1 hr. Local anesthesia was present if the pinprick did not elicit a skin twitch. The number of pinpricks that failed to elicit a response was then recorded at each time interval (Table V).

REFERENCES

(1) R. W. Johnson, T. H. Keenan, J. W. Kosh, and J. W. Sowell, Sr., *J. Pharm. Sci.*, **68**, 317 (1979).

(2) R. Gewald, *Z. Chem.*, **1**, 349 (1961).

(3) R. W. Johnson, R. J. Mattson, and J. W. Sowell, Sr., *J. Heterocycl. Chem.*, **14**, 383 (1977).

(4) V. I. Shvedov, M. V. Mezentseva, and A. N. Grinev, *Khim. Geterotsikl. Soedin.*, **9**, 1219 (1975); through *Chem. Abstr.*, **84**, 59299 (1976).

(5) J. W. Lawson, *J. Pharmacol. Exp. Ther.*, **160**, 22 (1968).

(6) E. Bülbring and I. Wajda, *ibid.*, **85**, 78 (1945).

ACKNOWLEDGMENTS

Adapted in part from theses submitted by R. W. Johnson and T. H. Keenan to the Graduate School, University of South Carolina, in partial fulfillment of the Master of Science degree requirements.

Comparative Pharmacokinetics of Coumarin Anticoagulants XLI: Effect of Phenobarbital on Systemic Availability of Orally Administered Dicumarol in Rats

JAMES W. CROW, MILO GIBALDI, and GERHARD LEVY ×

Received December 8, 1978, from the *Department of Pharmaceutics, School of Pharmacy, State University of New York at Buffalo, Amherst, NY 14260.* Accepted for publication January 26, 1979.

Abstract □ The purpose of this investigation was to determine the effect of phenobarbital on the systemic availability of orally administered dicumarol in rats. Adult male Sprague–Dawley rats, matched for dicumarol free fraction in serum, received either phenobarbital sodium, 75 mg/kg, or saline solution, orally or intravenously, daily for 7 days. On Day 6, they also received ^{14}C-dicumarol, 2 mg/kg iv, and unlabeled dicumarol, 50 mg/kg po, in aqueous suspension. Venous blood samples were obtained serially over 32 hr through an indwelling cannula. Systemic dicumarol availability was determined from the dose-normalized ratio of areas under the plasma concentration–time curves. Phenobarbital treatment almost doubled the total clearance of dicumarol and the intrinsic clearance of free dicumarol, with no significant difference between the inductive effects of oral and intravenous doses of phenobarbital. Systemic dicumarol availability in control rats (mean ± *SD*) was 84 ± 8% (n = 10) and 84 ± 10% (n = 6) in the oral and intravenous phenobarbital studies, respectively. The systemic dicumarol availability in phenobarbital-treated rats was appreciably lower: 48 ± 7% (n = 10) and 61 ± 12% (n = 6) for orally and intravenously treated animals, respectively. The effect of oral phenobarbital on systemic dicumarol availability was more pronounced than that of intravenous phenobarbital ($p < 0.025$). The apparent first-order absorption rate constants for the fraction of the dose available systemically were similar for control and treated animals. There was a positive correlation between systemic dicumarol availability and total dicumarol clearance in control animals ($p < 0.001$). Proper matching of control and treated animals is, therefore, important for this type of study. The rat appears to be a good model for investigating the mechanism of the inhibitory effect of phenobarbital on dicumarol absorption observed previously in humans.

Keyphrases □ Phenobarbital—effect on systemic availability of oral dicumarol, comparison of oral and intravenous doses □ Bioavailability—dicumarol in rats, effect of oral and intravenous phenobarbital □ Dicumarol—bioavailability, effect of oral and intravenous phenobarbital □ Anticoagulants—dicumarol, effect of oral and intravenous phenobarbital on systemic availability

The bioavailability of orally administered dicumarol in humans is reduced by pretreatment of the subjects with an orally administered barbiturate (1). Similar effects have been observed with respect to two other poorly water-soluble drugs, griseofulvin and diethylstilbestrol. The bioavailability of orally administered griseofulvin in humans is reduced by pretreatment with orally administered phenobarbital (2). Such a reduction in griseofulvin bioavailability has also been observed in rats (3). Pretreatment with phenobarbital has been reported to decrease diethylstilbestrol absorption from the rat intestine (4).

Little is known about the mechanism of the barbiturate effect on drug absorption. A study was designed to determine the effect of orally and intravenously administered phenobarbital on GI absorption of dicumarol in rats. The results of this investigation have bearing not only on the specific interaction under study but also on the design of studies to determine the bioavailability of drugs that are subject to enzyme induction and that exhibit pronounced interindividual differences in pharmacokinetic characteristics.

EXPERIMENTAL

The studies were carried out on adult male Sprague–Dawley rats weighing 250–375 g. Groups of animals were screened for plasma free fraction values of dicumarol, using serum obtained from ~5 ml of blood withdrawn from the tail artery under light ether anesthesia. The free fraction determinations were performed in duplicate by dialyzing, to

0022-3549/79/0800-0958$01.00/0

© 1979, American Pharmaceutical Association

Table I—Pharmacokinetic Constants for Dicumarol in Adult Male Sprague–Dawley Rats Used to Determine the Effect of Oral Phenobarbital on Dicumarol Absorption

Pharmacokinetic Constant[a]	Control Animals	Phenobarbital-Treated Animals	Control–Phenobarbital Ratio	Statistical Significance of Difference (p)[c]
Total clearance, ml/hr/kg	18.6 ± 4.9[b]	31.4 ± 13.2	0.655 ± 0.242	<0.025
Apparent volume of distribution, ml/kg	150 ± 20	153 ± 71	1.16 ± 0.47	N.S.
β, hr^{-1}	0.123 ± 0.026	0.214 ± 0.054	0.593 ± 0.119	<0.001
Intrinsic clearance of free drug, ml/hr/kg × 10^{-4}	12.4 ± 7.3	21.9 ± 12.8	0.596 ± 0.226	<0.005
Serum free fraction × 10^4	2.09 ± 1.27[d]	1.89 ± 1.17[d]	1.12 ± 0.14	—[e]

[a] Based on ^{14}C-dicumarol injected intravenously. [b] All data are mean ± SD, n = 10. [c] Paired two-tailed t-test. [d] Determined before phenobarbital and dicumarol administration. [e] Not analyzed statistically because animals were matched with respect to serum free fraction.

Table II—Pharmacokinetic Constants for Dicumarol in Adult Male Sprague–Dawley Rats Used to Determine the Effect of Intravenous Phenobarbital on Dicumarol Absorption

Pharmacokinetic Constant[a]	Control Animals	Phenobarbital-Treated Animals	Control–Phenobarbital Ratio	Statistical Significance of Difference (p)[c]
Total clearance, ml/hr/kg	19.5 ± 6.5[b]	38.6 ± 11.1	0.513 ± 0.138	<0.005
Apparent volume of distribution, ml/kg	189 ± 42	190 ± 57	1.03 ± 0.18	N.S.
β, hr^{-1}	0.102 ± 0.016	0.206 ± 0.031	0.512 ± 0.168	<0.005
Intrinsic clearance of free drug, ml/hr/kg × 10^{-4}	13.1 ± 9.3	24.4 ± 16.4	0.518 ± 0.128	<0.025
Serum free fraction × 10^4	2.00 ± 0.96[d]	2.02 ± 0.92[d]	0.993 ± 0.107	—[e]

[a] Based on ^{14}C-dicumarol injected intravenously. [b] All data are mean ± SD, n = 6. [c] Paired two-tailed t-test. [d] Determined before phenobarbital and dicumarol administration. [e] Not analyzed statistically because animals were matched with respect to serum free fraction.

equilibrium (20–24 hr), 1-ml samples of serum with 30 μg of added ^{14}C-dicumarol[1] against an equal volume of isotonic Sorensen phosphate buffer, pH 7.4, at 37° (5). The serum and buffer phases were assayed after selective extraction (6).

Each group of 20 rats yielded, on the average, four pairs of animals, with the members of any one pair having similar serum free fraction values. One member of each pair was assigned to the control group, and the other was assigned to the treatment group. Treatment with either normal saline solution or phenobarbital was started 1–2 weeks after screening. Phenobarbital sodium, 75 mg/kg, or saline solution was administered intravenously or orally daily for 7 days. The volumes of the intravenous and oral solutions were 0.75 and 1.8 ml/kg, respectively. Rats that received intravenous treatments had the solutions injected through a right femoral vein catheter exteriorized at the back of the neck, which was implanted 1 day before the treatment period. On the 5th day of the treatment period, the right external jugular vein was cannulated (7) to facilitate blood withdrawal, and the rats were placed in individual metabolism cages in a room maintained at 21°. Food, but not water, was withdrawn for 24 hr, starting that evening at about 9 pm.

On the 6th day at about 9 am, the animals received an intravenous injection of ^{14}C-dicumarol (2 mg/kg in Sorensen buffer solution containing 1.3 mg/ml) and an oral dose of dicumarol[2], 50 mg/kg in aqueous suspension, by gastric tube. On the day of dicumarol administration, the daily phenobarbital dose was given immediately after the anticoagulant.

Dicumarol suspensions were prepared with 0.25% aqueous methylcellulose[3] solution. The solution was made by sprinkling the suspending agent on the water, refrigerating, and gently stirring the cold solution with a glass rod. Dicumarol was incorporated on the day of dosing by making a paste with a small volume of the solution and then adding the remaining solution. This was done with a spatula in a beaker, and care was taken not to grind the dicumarol particles. Pairs of control and phenobarbital-treated animals always received the same lot of dicumarol suspension.

Blood samples (0.5 ml) were obtained from the intravenous cannula at about 0.5, 2, 4, 6, 8, 10, 14, 16, 18, 24, 28, and 36 hr and were transferred to heparinized micro-blood collecting tubes. These tubes were centrifuged, and duplicate 0.1-ml plasma samples were collected and quick frozen pending assay.

Plasma was assayed simultaneously for radiolabeled and nonlabeled dicumarol (6, 8). Duplicate 0.1-ml plasma portions were adjusted to pH 3.1 and extracted into heptane. One portion of the extract was added to scintillation fluid and counted. The other portion was extracted into sodium hydroxide solution, which was assayed spectrophotometrically. The concentration of unlabeled dicumarol was determined by subtracting the concentration of radiolabeled drug, determined by scintillation spectrometry, from the concentration determined by spectrophotometry.

Pharmacokinetic constants were obtained in the usual manner (5, 9, 10) from the ^{14}C-dicumarol (intravenous) concentrations in plasma. Intrinsic clearance of free drug was calculated by dividing total clearance by the serum free fraction of dicumarol. The area under the nonlabeled (orally administered) dicumarol plasma concentration–time curve (AUC) was obtained by the trapezoidal method (11). The area beyond the last concentration point was obtained by two methods: (a) extrapolating the apparently exponential concentration decay phase to zero concentration (Method I), and (b) dividing the last concentration by the β value obtained concomitantly in the same animal from the plasma ^{14}C-dicumarol concentrations (Method II). Systemic availability was calculated by dividing AUC_{oral} by AUC_{iv} after multiplying the latter by the oral/intravenous dose ratio. The cumulative fraction of the oral dose absorbed as a function of time was determined by a literature method (12) modified such that the denominator was $\beta \cdot AUC_{iv}$ (oral dose/intravenous dose).

RESULTS

Initial screening of a large group of rats yielded 17 pairs with similar dicumarol serum free fraction values in any given pair. Eleven pairs were assigned to the experiment with orally administered phenobarbital, and the other six pairs were assigned to the experiment with intravenous phenobarbital. One member of the 11-pair group was lost during the study, so the reported results for the experiment with orally administered phenobarbital are based on 10 pairs of animals.

The serum free fraction values for the group of 10 pairs ranged from 7.24×10^{-5} to 4.40×10^{-4}, and the correlation coefficient between free fraction values for members of each pair was 0.99 ($p < 0.001$). The range of serum free fraction values in the group of six pairs was 8.08×10^{-5}–3.39×10^{-4}, with a correlation coefficient of 0.96 ($p < 0.001$). In view of the excellent match of serum free fraction values in any one pair and the consequent similarity of dicumarol total clearance within each pair [total clearance of dicumarol is proportional to the drug's free fraction in serum (13)], statistical analyses of observed differences in pharmacokinetic parameters due to phenobarbital treatment were performed by paired t-test.

Figures 1 and 2 show typical results obtained when ^{14}C-dicumarol was injected intravenously and unlabeled dicumarol in an aqueous suspension was administered orally to control and phenobarbital-treated rats. Prolonged absorption was often evident in both control and treated animals during the entire experimental period (*i.e.*, for more than 30 hr), as reflected by the difference in the log concentration *versus* time slopes of ^{14}C-dicumarol and unlabeled drug in plasma.

Pharmacokinetic constants for dicumarol disposition were determined from plasma concentrations of ^{14}C-dicumarol following intravenous injection of that drug (Tables I and II). Phenobarbital caused approxi-

[1] ^{14}C-Dicumarol, 71.4 μCi/mg, labeled in the methylene position, radiochemical purity > 98%, New England Nuclear Corp., Boston, Mass.

[2] Lot 4210, particle diameter 0.002–0.01 mm, Nutritional Biochemical Corp., Cleveland, Ohio.

[3] Methylcellulose 60 HG, Premium, 4000 cps, Dow Chemical Corp., Midland, Mich.

Table III—Effect of Oral Phenobarbital on Systemic Availability of Oral Dicumarol in Adult Male Sprague-Dawley Rats

Rat Pair	Systemic Availability, % of dose					
	Control Animals			Phenobarbital-Treated Animals		
	Method I[a]	Method II[b]	I–II Ratio	Method I	Method II	I–II Ratio
1	0.78	0.78	1.00	0.41	0.39	1.05
2	0.78	0.78	1.00	0.50	0.50	1.00
3	0.79	0.78	1.01	0.60	0.59	1.02
4	0.81	0.81	1.00	0.48	0.42	1.14
5	0.91	0.89	1.02	0.57	0.49	1.06
6	0.79	0.78	1.01	0.41	0.41	1.00
7	0.90	0.87	1.03	0.45	0.45	1.00
8	0.75	0.75	1.00	0.54	0.48	1.12
9	0.91	0.91	1.00	0.39	0.38	1.03
10	0.97	0.97	1.00	0.51	0.49	1.04
Mean	0.84	0.83	1.01	0.48[c]	0.46[c]	1.05
SD	0.08	0.07		0.07	0.06	

[a] Method I = area under plasma concentration–time curve of orally administered drug (AUC_{oral}) determined by extrapolation of apparently exponential concentration decay phase from last data point to zero concentration. [b] Method II = AUC_{oral} determined by assuming that concentrations after the last data point decline at the same relative rate as the postdistribution concentrations of ^{14}C-dicumarol administered intravenously. [c] Significantly different from the appropriate control value ($p < 0.05$).

Table IV—Effect of Intravenously Administered Phenobarbital on Systemic Availability of Oral Dicumarol in Adult Male Sprague-Dawley Rats

Rat Pair	Systemic Availability, % of dose					
	Control Animals			Phenobarbital-Treated Animals		
	Method I[a]	Method II[b]	I–II Ratio	Method I	Method II	I–II Ratio
1	0.74	0.74	1.00	0.49	0.48	1.02
2	0.71	0.71	1.00	0.52	0.52	1.00
3	0.83	0.83	1.00	0.56	0.53	1.06
4	0.92	0.89	1.03	0.80	0.79	1.01
5	0.87	0.82	1.06	0.68	0.59	1.15
6	0.97	0.94	1.03	0.59	0.59	1.00
Mean	0.84	0.82	1.02	0.61[c]	0.58[c]	1.04
SD	0.10	0.09		0.12	0.11	

[a,b] See Table III. [c] Significantly different from the appropriate control value by paired two-tailed t-test ($p < 0.005$).

mately twofold increases in total clearance, β, and in intrinsic clearance but had no significant effect on the apparent distribution volume. There was no statistically significant difference between the total and intrinsic clearance ratios, control/phenobarbital, of dicumarol in the oral and intravenous phenobarbital studies. Thus, the enzyme inductive effect of intravenous and oral phenobarbital was of similar magnitude.

Figure 3 shows the average time course of dicumarol absorption by control rats and by rats pretreated orally with phenobarbital. The individual dicumarol systemic availability data obtained in that experiment are listed in Table III. Calculation of the *AUC* of unlabeled plasma dicumarol was complicated by prolonged absorption. Two methods were used for the extrapolation of the plasma concentration *versus* time curve from the last assayed concentration (36 hr) to infinity. Method I involved the extrapolation of the apparently exponential terminal concentration decay phase. This implied that absorption was continuing in a predictable manner until the dicumarol concentration approached zero. Method II involved extrapolation of postexperimental plasma concentrations such that these concentrations declined at the same relative rate as the post-

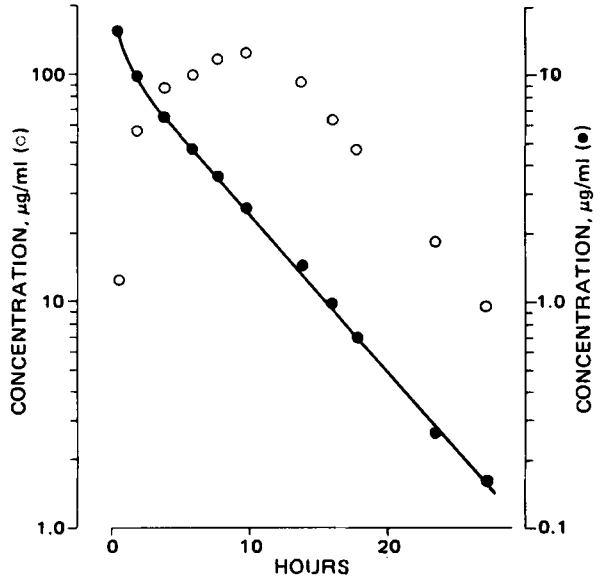

Figure 1—*Plasma dicumarol concentrations as a function of time after simultaneous administration of 50 mg/kg po (○) and 2 mg/kg iv (●) to a control rat. ^{14}C-Labeled drug was used for the intravenous injection.*

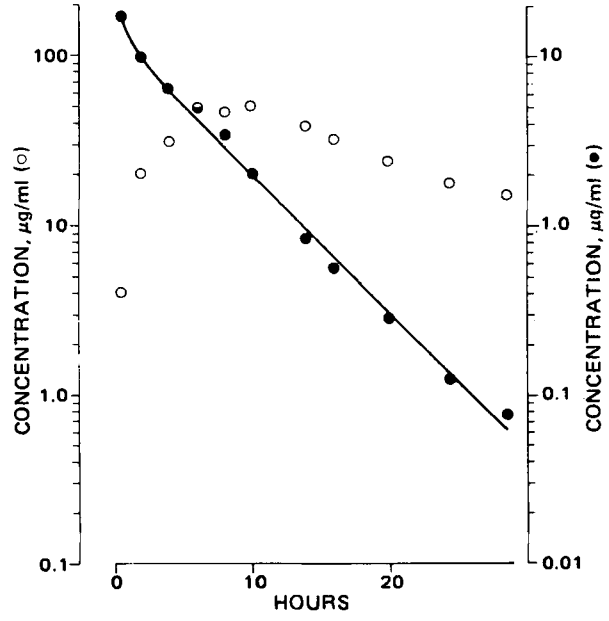

Figure 2—*Plasma dicumarol concentrations as a function of time after simultaneous administration of 50 mg/kg po (○) and 2 mg/kg iv (●) to a rat treated with phenobarbital sodium, 75 mg/kg/day iv, beginning 5 days before dicumarol administration. ^{14}C-Labeled drug was used for the intravenous injection.*

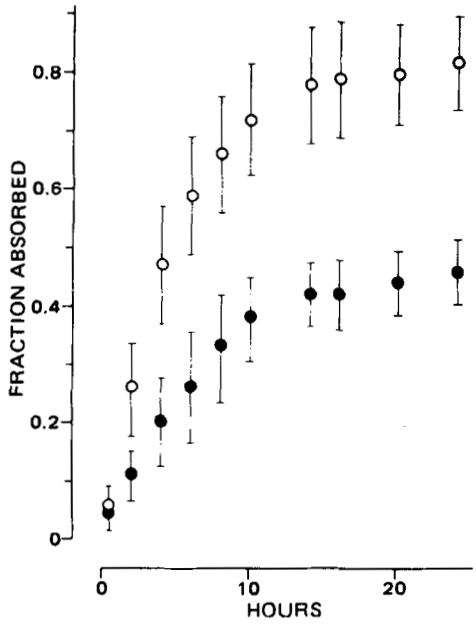

Figure 3—*Time course of dicumarol absorption after administration of 50 mg/kg po to control rats (○) and to rats treated with phenobarbital sodium, 75 mg/kg/day po, beginning 5 days before dicumarol administration (●). Points are means ± SD of 10 control and 10 phenobarbital-treated animals.*

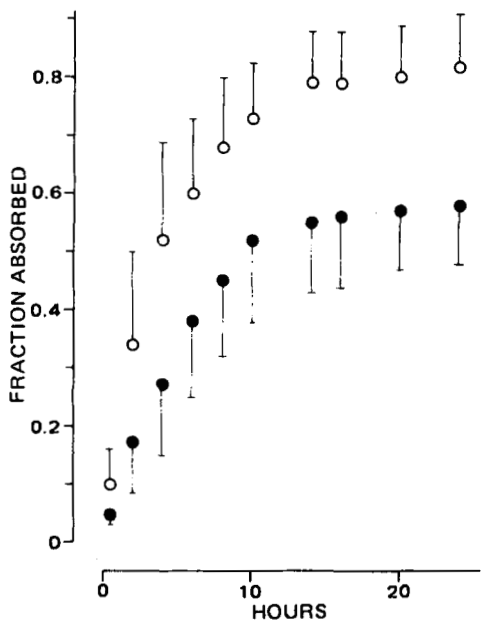

Figure 5—*Time course of dicumarol absorption after administration of 50 mg/kg po to control rats (○) and to rats treated with phenobarbital sodium, 75 mg/kg/day, iv beginning 5 days before dicumarol administration (●). Points are means ± SD (in one direction) of six animals each.*

distribution concentrations of intravenously injected ^{14}C-dicumarol. As evident from Table III, the results from the two methods were virtually identical.

Oral phenobarbital treatment reduced the absorption of orally administered dicumarol from 84% (control animals) to 48% on the average. While phenobarbital treatment reduced the amount of dicumarol absorbed, it had little or no effect on absorption kinetics. The drug was absorbed by apparent first-order kinetics, and the absorption rate constant *for the amount absorbed* apparently was not affected by phenobarbital (Fig. 4).

Figure 5 shows the time course of dicumarol absorption in control rats and in rats treated with intravenous phenobarbital. Individual systemic availability data for this experiment are listed in Table IV. Like the control animals for the oral phenobarbital experiment, the intravenous controls absorbed 84% of the oral dicumarol dose on the average. Intravenous phenobarbital reduced the extent of absorption to 61% of the dose, *i.e.*, to a lesser degree than the 48% average following oral phenobarbital. This difference is statistically significant ($p < 0.005$). Again, phenobarbital treatment had no apparent effect on the dicumarol absorption kinetics (Fig. 6).

Additional examination of the data revealed a statistically significant positive correlation ($r = 0.76$; $p < 0.001$) between the systemic availability and the total dicumarol clearance in control animals but not in phenobarbital-treated animals (Fig. 7).

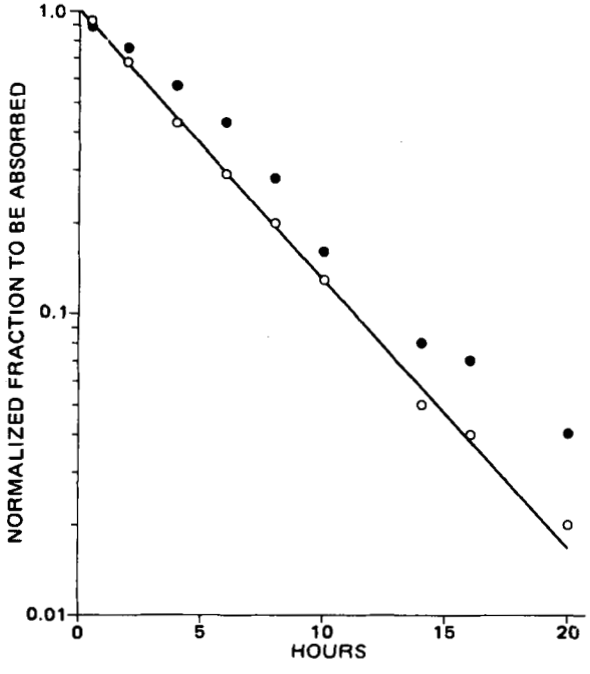

Figure 4—*Apparent first-order dicumarol absorption kinetics in 10 control (○) and 10 oral phenobarbital-treated rats (●). Plotted on the ordinate is the fraction of the total amount of dicumarol eventually absorbed that is remaining to be absorbed at various times after a 50-mg/kg po dose.*

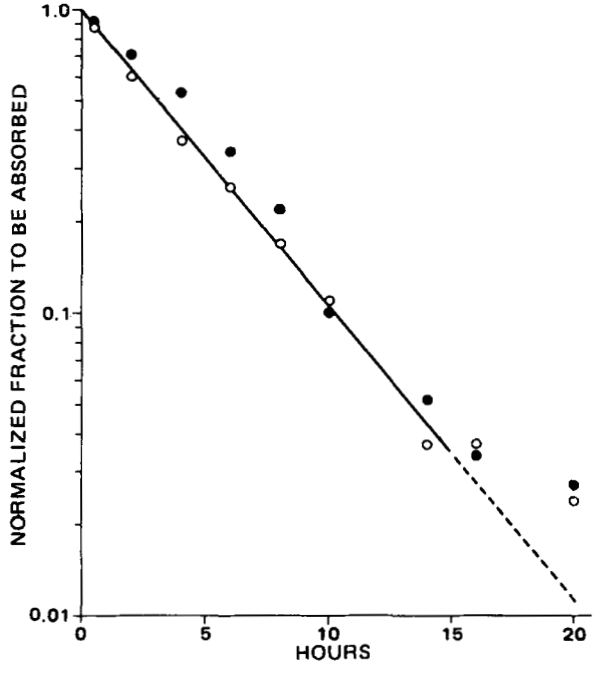

Figure 6—*Apparent first-order dicumarol absorption kinetics in six control (○) and six intravenous phenobarbital-treated rats (●). See Fig. 4 for further explanation.*

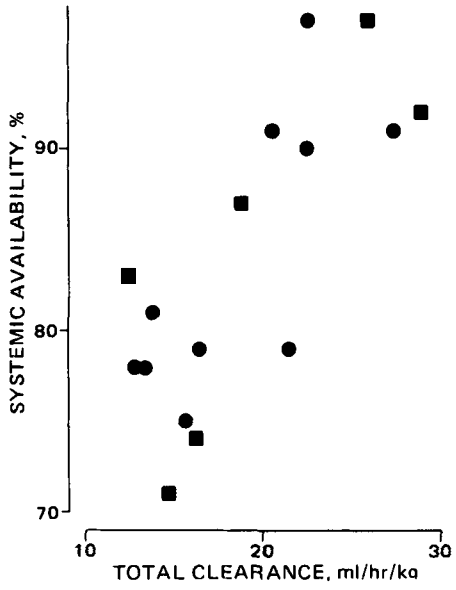

Figure 7—*Relationship between total clearance of intravenous dicumarol and systemic availability of oral dicumarol in 16 rats. Ten rats were control animals in the oral phenobarbital study (●), and six rats were control animals in the intravenous phenobarbital study (■). Correlation coefficient = 0.76, p < 0.001.*

DISCUSSION

Assessment of the effect of phenobarbital on the systemic availability of orally administered dicumarol requires consideration of numerous experimental design variables. There are pronounced interindividual differences in dicumarol pharmacokinetics in rats (5, 14) and humans (15). Phenobarbital is an enzyme inducer known to enhance dicumarol elimination (16). This enzyme induction may be prolonged, making crossover studies in rats difficult if not impossible. In addition, the results of the present investigation reveal that the systemic dicumarol availability in control rats increases with increasing total clearance. The reason for this correlation is not known.

To deal with these complicating factors, the systemic availability of orally administered dicumarol was determined by simultaneous administration of unlabeled dicumarol orally and ^{14}C-dicumarol intravenously as an "internal standard." Since crossover studies could not be performed, the control and phenobarbital-treated groups were matched with respect to their serum free fraction values of dicumarol. It was found previously that serum protein binding is the major determinant of interindividual differences in dicumarol elimination by rats (13).

A problem encountered in the pharmacokinetic assessment of dicumarol systemic availability was the very prolonged drug absorption, which had been observed also in humans (1). This prolonged absorption complicated calculations of the *AUC* values of orally administered drug. Fortunately, plasma concentrations were monitored long enough to encompass most of the *AUC*. Consequently, extrapolations based on the assumption of two different limiting cases yielded essentially identical *AUC* and systemic availability estimates.

The slow and prolonged absorption of dicumarol can cause "flip-flop" kinetics (11) in animals that eliminate the drug rather rapidly. This may have been the case in a recent study (17), which was commented upon subsequently (18, 19).

Plasma dicumarol concentrations decline triexponentially with time after rapid intravenous injection (10). However, the so-called distribution phase is so small that the apparent volume of distribution estimated by the area method and by the intercept ("single-compartment") method are almost identical [159 *versus* 166 ml/kg in a recent study (10) on 10 animals]. The data obtained in the present study were insufficient for a multiexponential characterization of the time course of dicumarol elimination (Figs. 1 and 2) because the number of blood samples during the first hours after drug administration had to be minimized to permit blood withdrawals for 36 hr without serious depletion of the blood volume. Therefore, absorption kinetics were estimated by the Wagner–Nelson method, which is based on the assumption of monoexponential elimination kinetics. The error introduced by that data treatment probably is minor.

Phenobarbital had a pronounced inductive effect on dicumarol elimination kinetics. It was established previously that phenobarbital treatment does not affect the serum protein binding of dicumarol in rats (20). There was no significant difference in the inductive effect of identical intravenous and oral phenobarbital doses.

Consistent with previous observations in humans (1), phenobarbital had a pronounced inhibitory effect on dicumarol absorption from an oral aqueous suspension in rats. The effect of oral phenobarbital was somewhat greater than that of intravenous phenobarbital, perhaps due to greater exposure of gut tissue to the orally administered drug. Little or no phenobarbital is excreted as such in the bile of rats (21); thus, intravenous phenobarbital-treated animals have little or no phenobarbital in their GI tracts. Considering this fact and the absorption inhibition by intravenous phenobarbital, it is our opinion that the inhibition of dicumarol absorption is unlikely to be the result of a direct physicochemical interaction between dicumarol and phenobarbital.

An "hepatic first-pass" effect on dicumarol in the rat can be excluded (16). However, the possibility must be considered that phenobarbital caused induction of dicumarol metabolizing enzyme systems in the gut wall. The results obtained in the present study are consistent with dissolution rate-limited absorption and subsequent partial biotransformation of some absorbed drug as it passes through the intestinal wall. However, studies in humans have shown that the amount of unmetabolized dicumarol found in the stool after oral administration of the anticoagulant increased following treatment with a barbiturate (1). It cannot be excluded, in our view, that some of the drug found in the stool of humans was derived from the hydrolysis of a conjugate formed by, or excreted into, the intestine.

Phenobarbital treatment affects bile flow (22) and, particularly in the large doses used in this study, may affect GI motility. The role of these variables cannot be determined from the present investigation. The possible role of bile in dicumarol absorption will be examined in a subsequent report.

REFERENCES

(1) P. M. Aggeler and R. A. O'Reilly, *J. Lab. Clin. Med.*, **74**, 229 (1969).

(2) S. Riegelman, M. Rowland, and W. L. Epstein, *J. Am. Med. Assoc.*, **213**, 426 (1970).

(3) F. Jamali and J. E. Axelson, *J. Pharm. Sci.*, **67**, 466 (1978).

(4) J. L. Lasker and D. E. Richert, *Pharmacologist*, **18**, 8 (1976).

(5) A. Yacobi, C.-M. Lai, and G. Levy, *J. Pharm. Sci.*, **64**, 1995 (1975).

(6) L. B. Wingard and G. Levy, *J. Pharmacol. Exp. Ther.*, **184**, 253 (1973).

(7) J. R. Weeks and J. D. Davis, *J. Appl. Physiol.*, **19**, 540 (1964).

(8) R. Nagashima, G. Levy, and E. Nelson, *J. Pharm. Sci.*, **57**, 58 (1968).

(9) E. Jähnchen, L. B. Wingard, and G. Levy, *J. Pharmacol. Exp. Ther.*, **187**, 176 (1973).

(10) A. Yacobi, C.-M. Lai, and G. Levy, *J. Pharm. Sci.*, **66**, 1741 (1977).

(11) M. Gibaldi and D. Perrier, "Pharmacokinetics," Dekker, New York, N.Y., 1975.

(12) J. G. Wagner and E. Nelson, *J. Pharm. Sci.*, **53**, 1392 (1964).

(13) C.-M. Lai and G. Levy, *ibid.*, **66**, 1739 (1977).

(14) *Ibid.*, **67**, 337 (1978).

(15) E. S. Vesell and J. G. Page, *J. Clin. Invest.*, **47**, 2657 (1968).

(16) C.-M. Lai, A. Yacobi, and G. Levy, *J. Pharmacol. Exp. Ther.*, **199**, 74 (1976).

(17) L. Putcha, P. Nandiwada, S. Feldman, J. V. Bruckner, and W. G. Kramer, *Res. Commun. Chem. Pathol. Pharmacol.*, **19**, 67 (1978).

(18) G. Levy, *ibid.*, **20**, 609 (1978).

(19) S. Feldman, *ibid.*, **20**, 611 (1978).

(20) A. Yacobi, J. T. Slattery, and G. Levy, *J. Pharm. Sci.*, **66**, 941 (1977).

(21) C. D. Klaassen, *Br. J. Pharmacol.*, **43**, 161 (1971).

(22) C. D. Klaassen, *J. Pharmacol. Exp. Ther.*, **176**, 743 (1971).

ACKNOWLEDGMENTS

Supported in part by Grant GM 20852 and by postdoctoral fellowship 5 F32 GM05653 (J. W. Crow) from the National Institute of General Medical Sciences, National Institutes of Health.

For the previous paper in this series, see A. Jain, F. G. McMahon, J. T. Slattery, and G. Levy, *Clin. Pharmacol. Ther.*, **25**, 61 (1979).

Short-Term Effects on *Artemia salina* of Aponin and *Gomphosphaeria aponina* in Unialgal Cultures and in Mixed Cultures with *Gymnodinium breve*

DAVID L. ENG-WILMOT * **and DEAN F. MARTIN** ˣ

Received August 19, 1977, from the *Department of Chemistry, University of South Florida, Tampa, FL 33620.* Accepted for publication January 26, 1979. *Present address: Department of Chemistry, University of Oklahoma, Norman, OK 73019.

Abstract □ Previous investigations showed that the natural marine substance aponin, produced by the blue-green alga *Gomphosphaeria aponina*, was cytolytic toward Florida's red tide organism, *Gymnodinium breve*. As part of a study of the aponin–alga biological interactions, the effects of unialgal (*G. aponina*) and mixed cultures (*G. aponina* + *G. breve*) on the viability of *Artemia salina* were investigated. Two contrasting effects were observed in mixed cultures: survival of *A. salina* was promoted in low *G. aponina* populations, while enhanced toxicity of *G. breve* to *A. salina* occurred at higher culture populations. Unialgal *G. aponina* cultures exerted no adverse effects on *A. salina*. The apparent protective effect is thought to result from the observed change in *G. breve* morphology (motile to sessile); toxicity was the result of enhanced toxin release by cytolyzed *G. breve* cells. In dose–response studies, aponin exhibited no adverse effect on *A. salina* at concentrations (1 unit) that were deleterious to *G. breve*. However, at higher applied levels (4–6 units), mortality was substantial (>70%) after 48 hr of incubation. Probit analysis yielded an apparent LD_{50} of 2.3 units, where 1 unit was that amount required to cytolyze 50% of the *G. breve* cells (2000 cells/ml) after 20 hr of incubation.

Keyphrases □ Aponin—effect on *Artemia salina*, unialgal and mixed cultures with *Gomphosphaeria aponina* and *Gymnodinium breve*, potential biological control agent □ *Gymnodinium breve*—effect of aponin, *Gomphosphaeria aponina*, unialgal and mixed cultures, potential biological control □ *Artemia salina*—effect of aponin, bioassay method □ Biological control—*Gymnodinium breve*, effect of aponin and *Gomphosphaeria aponina* in unialgal and mixed cultures, *Artemia salina* bioassay

Interest in localized management measures for the ichthyotoxic blooms of Florida's red tide organism, *Gymnodinium breve* (an unarmored dinoflagellate), was rekindled with the isolation and partial purification of a biologically active natural marine product, aponin, from cultures of the blue-green alga, *Gomphosphaeria aponina* (1, 2). Earlier reports (3, 4) described aponin cytolysis of *G. breve* cells; presumably, this action results from either a direct lytic interaction with the cell membrane or a perturbation/inhibition of a vital cellular function, causing cell degeneration. The aponin effect on *G. breve* cells is rapid (<24 hr), irreversible, and dosage dependent. Further aponin purification is underway and should provide a better understanding of its structural, chemical, and biological properties.

BACKGROUND

Additional evidence for aponin cytolysis of *G. breve* was demonstrated in mixed culture studies with *G. aponina* (4). *G. breve* cultures incubated with various amounts of log-phase *G. aponina* cells declined linearly with the number of blue-green alga cells present after 10 days of growth. This effect was not attributed to organism–organism competition for a growth-limiting nutrient; freeze-dried *G. aponina* cells also were cytolytic toward *G. breve* cells (4). The incubation period required prior to the initiation of *G. breve* degeneration (8–10 days) and the growth response of *G. aponina* were in good agreement with the time of maximum aponin elaboration (6–8 days) and inocula size–growth rate relationships observed in unialgal cultures of the blue-green alga (5).

In contrast to the neurologic (6) and hemolytic (7) properties exhibited by components of the ichthyotoxin associated with *G. breve*, aponin has not been shown to possess any short-term (25 hr) ichthyotoxic activity when applied at high levels (about 15 units, or 7.5 times the amount required to cytolyze all *G. breve* cells) to several fish species. A 25-hr test period corresponds to 83 times the standard death time of fish exposed to *G. breve* toxin (8). An increase in the mean survival time of *Poecilia spenops* and *Mollienesia latipinna* was observed when aponin was incubated at low concentration with *G. breve* cells for 25 hr; enhanced ichthyotoxicity of *G. breve* cultures toward these species also was noted at higher aponin dosages, resulting from the anticipated *G. breve* cell degeneration and subsequent toxin release into the test vessels (2, 4).

Aponin possesses nine significant characteristics that are favorable for its use as a biocontrol agent for Florida's red tide organism, including thermal stability and slow activity loss in alkaline solutions (base labile) (3). The problems of aponin specificity and of its effects on biological systems other than *G. breve* cells have been addressed only recently. This paper considers findings on short-term effects of aponin (cytolytic factor) and *G. aponina* on *Artemia salina* (brine shrimp) in unialgal and in mixed cultures with *G. breve*.

A. salina may not be widely used in biological assays, but ample precedent exists, including the assay of ciguatera (9), *G. breve* (10), fungal toxins (11), and insecticides (12). The importance of *A. salina* in tropical food chains and its commercial value as a potential food source in shrimp and fish mari-culture (13) render *A. salina* an important organism for consideration. However, *A. salina* is more tolerant to *G. breve* toxin than are fish (10), which may mitigate against its use in some bioassays. For example, one *A. salina* (6 mg) could tolerate more than 10 times the amount of *G. breve* toxin than a 60-mg *Gambusia affinis* fish could withstand (10). Such tolerance has been attributed to medium detoxification by chemical absorption or metabolic means and would suggest that a population effect should be considered in the interpretation of bioassay results (10).

EXPERIMENTAL

Organism Source and Culture—Unialgal *G. breve*[1] cultures were maintained as axenic stock cultures in artificial sea water medium enriched with modified Wilson's B-5 supplements (14). *G. aponina*, isolated as detailed previously (1), were maintained as bacteria-free unialgal stock cultures, as described elsewhere (15). *A. salina* (mean dimensions: length = 7 ± 0.8 mm and wet weight = 2 mg) were obtained through local sources, and the stock organisms were maintained in artificial sea water.

The crustacea were nourished periodically with a few drops of Baker's yeast solution and aerated continuously (~250 ml/min). Stock cultures of the three organisms were maintained under similar salinity (34‰), pH (7.8), and temperature (24 ± 1°) conditions and under continuous illumination (approximately 2000 lux) provided by 40-w cool-white fluorescent lamps with lead shielded cathodes (16).

Organism Enumeration—Microorganism cultures were routinely sampled, and populations were enumerated with an electronic particle counter[2] using the electronic and threshold settings reported elsewhere (17). Organisms also were examined microscopically with an inverted binocular microscope.

A. salina cultures were observed and counted visually. Individual crustacean mortality was defined as the cessation of all peleopod locomotor activity for no less than 5 min.

Isolation and Bioassay of Aponin—Aponin was isolated from the

[1] Obtained through the courtesy of W. B. Wilson and S. M. Ray, Texas A&M Marine Institute, Galveston, Tex.

[2] Model B or ZB_i fitted with a 100-μm aperture and equipped with a C-1000 Channelyzer, Coulter Electronics, Hialeah, Fla.

0022-3549/79/0800-0963$01.00/0
© 1979, American Pharmaceutical Association

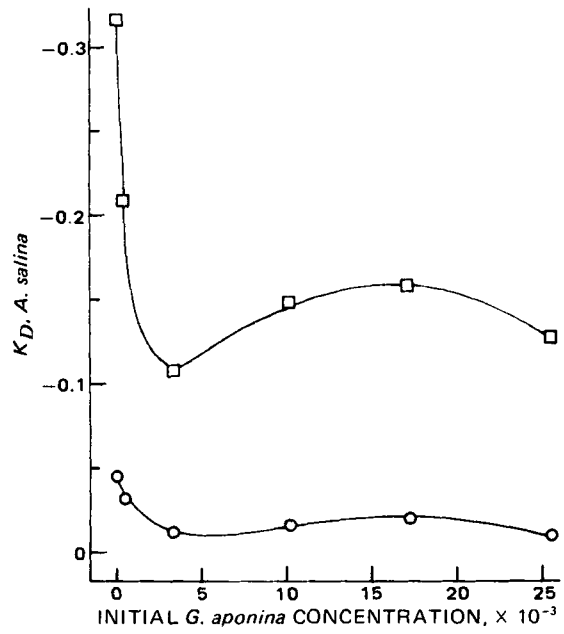

Figure 1—*Influence of various initial* G. aponina *populations in unialgal* (○) *and in mixed* (□) *culture with* G. breve *on* A. salina *mortality.*

10-day-old *G. aponina* cultures using the procedure of McCoy (2). *G. aponina* cells were cultured in a large-scale (20-liter) continuous culture system (18) and were harvested by continuous centrifugation using a Szent-Gyorgi apparatus[3]. The cell-free centrifugate was extracted for 24 hr with redistilled chloroform (50 ml/liter of centrifugate). The chloroform layer was then evaporated to dryness by rotary evaporation, and the residues were redissolved in a known chloroform volume.

Cytolytic activity of the crude aponin extract was determined using a modification of the bioassay described previously (2). In triplicate, serial volumes of the crude preparation were placed in 15-ml test tubes, and the chloroform was removed in an evacuated oven (41°). Ten milliliters of well-mixed *G. breve* culture[4] were pipetted carefully into each assay tube, and the cultures were mixed gently for 1 hr. After 20 hr of incubation, the *G. breve* cells remaining were counted and viability was checked microscopically.

One (relative) unit of aponin activity was defined as that amount of material required to produce 50% mortality of *G. breve* cells, at an initial concentration of 2000 cells/ml, after 20 hr of incubation (2000 lux, 25 ± 2°).

Unialgal and Mixed Culture Studies—Six pairs of sterile culture vessels (500-ml Fleaker flasks fitted with foam stoppers and aeration ports) were prepared; one set was designated as the unialgal (U) cultures, and the other was designated as the mixed (M) cultures. Into each U flask was placed 400 ml of sterile artificial sea water (34‰) enriched with the modified B-5 supplements; 400 ml of *G. breve* culture (cell counts >1400/ml) were introduced into the M flasks. Equal volumes of log-phase *G. aponina* cell concentrate and B-5 medium were pipetted into corresponding pairs of vessels.

The final volume of each culture was adjusted to 450 ml with artificial sea water medium and then both organisms were counted. After 24 hr of incubation (constant illumination of ~2000 lux) and aeration (~6 ml/min), *A. salina* (25–30 organisms in 15 ml of medium) were introduced into each vessel. Survival of *A. salina* individuals was monitored continuously for the initial 24 hr and regularly (3–6 hr) thereafter. *G. breve* and *G. aponina* were sampled and enumerated periodically, and cell viability was observed.

Aponin Toxicity—The protocol to test the toxicity of aponin on *A. salina* was similar to the bioassay procedure described. In triplicate, serial aponin solution volumes (in chloroform) were pipetted into 50-ml test tubes. Solvent and medium controls also were prepared. After the solvent was evaporated, 35 ml of modified B-5 medium (filtered, sterilized artificial sea water, 34‰) were placed into each tube, and the solutions were mixed for 24 hr at 25°.

Following mixing, five healthy *A. salina* (in 5 ml of medium) were added gently to the cultures, which were illuminated (2000 lux) and aerated (6 ml/min) continuously. *A. salina* survival was monitored hourly for the first 12 hr and periodically (3–4 hr) thereafter. To establish dosage levels applied to the organisms, a bioassay of the same aponin preparation with *G. breve* was run concurrently.

RESULTS

Three approaches were used to assess aponin and *G. aponina* effects on *A. salina* survival: direct presentation (surviving *A. salina* as a function of time), kinetic treatment (calculation of the zero-order mortality constant, K_D, where $K_D = m$, the slope of the linear portion of the direct presentation plot), and probit transformation[5]. These approaches were used appropriately with three groups of studies.

First, preliminary unialgal (*G. aponina* + *A. salina*) studies (Fig. 1) revealed two interesting results. *A. salina* survival (adults and larvae) was promoted in the presence of *G. aponina* relative to controls (B-5 medium without *G. aponina* and mixed culture systems). A threefold (1.3–4.3×) reduction in mortality constant values, K_D, for unialgal cultures of *G. aponina* (flasks U_2–U_6) was noted relative to control values (U_1, artificial sea water only). In addition, a twofold reduction in K_D values was observed for mixed culture systems (flasks M_2–M_6) relative to *G. breve* controls (M_1, 1400 cells/ml initially). These results also were confirmed by statistically significant (*t* test, $p < 0.001$) differences in the percent brine shrimp surviving for 90 hr in unialgal (80%) *versus* mixed (30%) cultures.

No apparent increase in the mixed culture toxicity to *A. salina* was noted, as anticipated for cultures containing high initial *G. aponina* populations. However, the *G. breve* cells used were relatively old (early stationary phase). Although *G. breve* cell numbers were sufficient to cause ichthyotoxic mortality, reported as populations greater than 250,000 cells/liter (20), the toxicity of this particular culture may have been reduced by enzymatic or physicochemical toxin degradation or by reduced toxin biosynthesis during the stationary phase of culture growth (21).

In contrast, at low initial *G. aponina* concentrations, a definite protective influence was exerted, as evidenced by the reduced *A. salina* mortality constants at these levels. This result may have been due in part to feeding of the brine shrimp on *G. aponina*, as suggested from inspection of fecal remains. Microscopic examination of the mixed cultures revealed sessile *G. breve* forms in cultures M_2–M_4 after 10 days; motile forms were observed in M_1 (*G. breve* only), and a few motile cells and cell debris were observed in cultures M_5 and M_6.

A second group of unialgal and mixed culture studies confirmed the original observations with a few notable exceptions (Table I). In these studies, log-phase *G. breve* cells (3 weeks old, 1900 cells/ml initially) were used. Enhanced *A. salina* mortality rates were observed in mixed cultures with high initial *G. aponina* populations, resulting from the expected cytolytic action exerted on *G. breve* cells. Furthermore, increased *A. salina* survival was noted at low initial *G. aponina* concentrations (cultures M_2 and M_3).

Aeration had no adverse effect on *G. breve* (viability or morphology), as evidenced by an increase in cell counts and size distributions. However, sessile *G. breve* forms were noted only in the latter mentioned cultures; cell debris and a few motile forms were found in M_4–M_6, and motile cells were observed in M_1. These differences in morphology also were reflected in culture population size distributions. Motile cells had morphologies as described previously (22), with cell volumes ranging from 3608 to 6220 μm^3, while sessile forms similar to those described previously (23) had volumes of 2240–4168 μm^3.

No significant deleterious short-term effect of unialgal *G. aponina* cultures on *A. salina* viability was found; *G. aponina* promoted brine shrimp survival, although the mortality rate increased slightly at intermediate initial cell populations. In addition, *G. aponina* cultures exerted no obvious effect on larval maturation or viability. Hatchlings were observed in the unialgal cultures and survived the duration of the experiment. In the mixed cultures, however, larvae did not persist for more than 3–4 days after hatching. Death of *A. salina* individuals in cultures containing *G. breve* followed a period of confused hyperactivity, disorientation, and contortions (curling) (10). These symptoms were not noted in the unialgal *G. aponia* cultures, where more subtle signs of death were

[3] Centrifugation was carried out at 12,000×*g* in a SS-3 centrifuge (DuPont-Sorvall); the flow rate was 100 ml/min.

[4] A stock culture was swirled for 30 min at 120 rpm on a G-22 Gyrotory shaker bath (New Brunswick Scientific).

[5] The probit transformation converts a sigmoidal relationship (percent killed *versus* dose) to a linear one (probits *versus* $\log_e$ dose); a probit of 5 corresponds to 50% killed (19).

Table I—Unialgal and Mixed Culture Interactions with *A. salina*

Culture [a]	Initial [b] *G. aponina*	$-K_D \pm SD$ [c]	*A. salina* Surviving [d], %	Percent *G. breve* Decrease	Percent *G. aponina* Increase
Unialgal					
U_1	0	0.161 ± 0.007	8	—	—
U_2	474	0.085 ± 0.008	28	—	+484
U_3	1,836	0.078 ± 0.007	40	—	+958
U_4	5,629	0.107 ± 0.008	44	—	+365
U_5	8,637	0.122 ± 0.011	44	—	+295
U_6	14,068	0.059 ± 0.004	52	—	+167
Mixed					
M_1	0	2.08 ± 0.09	0	+26.3	—
M_2	474	1.36 ± 0.05	0	−3.4	—
M_3	1,836	1.87 ± 0.16	0	−37.8	—
M_4	5,629	1.85 ± 0.04	0	−69.5	—
M_5	8,629	2.07 ± 0.14	0	−51.5	—
M_6	14,068	2.73 ± 0.21	0	−72.8	—

[a] Unialgal (*G. aponina*) and mixed (*G. aponina* + *G. breve*, initial concentration of 1910 ± 80 cells/ml) cultures, maintained at a salinity of 34‰ and 25 ± 2° with continuous aeration (milliliters per minute) and illumination (2000 lux). [b] Serial dilution of log-phase cell concentrate in cells per 10-sec flow. [c] Zero-order rate constant of *A. salina* mortality in organisms per hour. [d] Duration of experiment was 246 hr.

Table II—Effect of Crude Aponin on *A. salina* Viability

Crude Aponin Applied per 10 ml of Media, ml	Units of Aponin Applied [a]	Percent *G. breve* Mortality	K_D of *A. salina* (Organisms/hr)	Time for 100% Mortality, hr
0.00	0.02 ± 0.01	2.2 ± 1.2	−0.20 ± 0.02	113 ± 45
0.10	0.29 ± 0.02	35.2 ± 2.1	−0.17 ± 0.02	73 ± 21
0.20	0.57 ± 0.04	70.3 ± 4.6	−0.19 ± 0.01	77 ± 13
0.40	0.79 ± 0.01	96.0 ± 0.5	−0.25 ± 0.03	71 ± 19
0.80	1.6 [b]	99.2 ± 1.8	−0.43 ± 0.03	39 ± 9
1.0 $CHCl_3$	0.04 ± 0.02	4.5 ± 1.8	−0.21 ± 0.03	140 ± 41

[a] One aponin unit (relative) is defined as that amount required to cause 50% mortality in *G. breve* culture of 2000 cells/ml: units = 2 × fraction cells killed × [cells per milliliter used/(2000 cells/ml)]. [b] Estimation based on volumetric dilution.

noted: a slow, prolonged loss of motor-related activity associated with the peleopods, which ceased at death.

A third group of studies, involving crude aponin and *A. salina* (Table II), revealed two significant results. First, aponin concentrations (up to 0.8 unit of aponin) had little adverse effect on either adults or larvae, at least as indicated by the mortality constant, K_D. Second, higher concentrations exhibited adverse effects. For example, the K_D for 1.6 units was 72% greater than the value for 0.8 unit, and the time for 100% mortality decreased by a similar amount (82%).

Little or no aponin effect on *A. salina* was noted at concentrations less than 1 unit, as compared with control organisms (artificial sea water enriched with the B-5 supplements, and chloroform), which survived without loss of any individuals up to 60 hr. *A. salina* mortality at higher aponin levels (4 and 6 units) was observed within 24 hr. Probit analysis performed on percent *A. salina* killed after 48 hr yielded a linear relation and gave an apparent aponin LD_{50} for *A. salina* of 2.3 units (Fig. 2). Larvae survived the duration of the experiment (96 hr), except at the higher doses (4 and 6 units) where none survived. Aponin produced signs of death similar to those described for *G. aponina*.

DISCUSSION

The present study of the short-term effect on *A. salina* viability of the cytolytic factor aponin and of *G. aponina* in unialgal and mixed cultures with the toxic dinoflagellate *G. breve* suggested the following:

1. Although relatively high aponin concentrations accelerated brine shrimp (*A. salina*) mortality, these concentrations were at or beyond those levels required to cause complete cytolysis of *G. breve* cells. In addition, test conditions were unrealistically stressful in the sense of being static.

2. In unialgal cultures, the crustacea (adults and larvae) were relatively unaffected by the presence of, or variations in, *G. aponina* populations. In fact, *G. aponina* enhanced the *A. salina* viability, presumably due to grazing, as compared to control cultures.

3. In mixed cultures with *G. breve*, *G. aponina* exerted two contrasting effects on *A. salina* viability. At high blue-green alga concentrations, adult and larval *A. salina* mortality was accelerated, at rates comparable to or greater than the mortality rates of *G. breve* cultures. In contrast, at lower *G. aponina* populations, mortality was reduced.

The noted toxicity to *A. salina* of mixed *G. breve* cultures incubated with large numbers of *G. aponina* is attributed to the additional endotoxin released from cytolyzed *G. breve* cells. Similar enhancements of *G. breve* toxicity were reported for two fish species when incubated with large doses (15–30 units) of aponin (2, 4). However, the apparent protective effect (increased survival) exerted by *G. aponina* toward *A. salina* when incubated in low populations with the dinoflagellate is more complex and not well defined. *A. salina* grazing on the blue-green algae was observed and would account for the decline in mortality rates of indi-

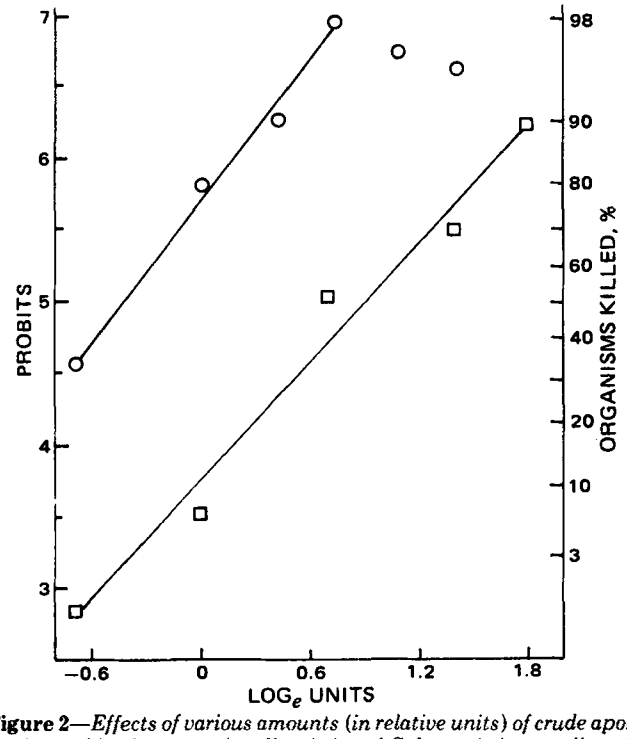

Figure 2—*Effects of various amounts (in relative units) of crude aponin on the probit of percent* A. salina (○) *and* G. breve (□) *mortality after 48 and 20 hr of incubation, respectively. Corresponding percent killed is given.*

viduals observed in unialgal cultures compared to controls. Feeding in mixed cultures also occurred, although ingestions of *G. breve* cells would enhance mortality of *A. salina* individuals, as was observed when compared with unialgal systems. However, feeding might not be directly responsible for the protective effect inasmuch as increases in the survival times of two fish species were noted when *G. breve* cells were incubated with small amounts (<1 unit) of aponin (4).

The appearance of sessile *G. breve* forms in certain mixed cultures would indicate that their presence might be related to the increased *A. salina* survival. Little is known about the nature and toxicity of the sessile or "resting" *G. breve* stage. In laboratory studies, high light intensities and spurious radiation from fluorescent lamps (16), as well as agitation and swirling (23), will initiate their formation. Agitation (aeration and periodic swirling) had no effect on *G. breve* viability or morphology in these experiments. Moreover, the fluorescent lamp cathodes were shielded, and illumination intensities were considerably less (2000 lux) than those thought to initiate sessile formation [10,000 lux (12)].

If such subtle external perturbations as those mentioned induce sessile formation, then other phenomena might also initiate such a change. One factor to consider is competition between organisms for a vital nutrient such as iron, which would result in rapid growth and dominance of one species (15). Equally important is biochemical "conditioning" of the medium by elaborated substances of one organism that are deleterious to the other. At low *G. aponina* populations, sufficient aponin may not be present to cause cytolysis, but perhaps enough is present to initiate a change in *G. breve* morphology. If, indeed, the *G. breve* sessile phase is a protective one or an intermediate of the encysted form, then it is reasonable that toxin release by *G. breve* would be reduced. Recent reports (24) demonstrated that benthic cysts of a New England red tide organism, *Gonyaulax tameranesis*, were highly toxic to shellfish and crustacea. However, preliminary fish assays (5) indicated that in laboratory cultures the sessile *G. breve* form exhibited less toxicity to *Gambusia affinis* than did motile organisms of the same age and concentration.

CONCLUSION

The cytolytic factor, aponin, did not adversely affect or significantly increase the mortality of adult and larval *A. salina* incubated at aponin concentrations (1 unit) that cause *G. breve* cytolysis. However, at application levels (4–6 units) considerably higher than those that might realistically be used for red tide control, >70% mortality was observed after 48 hr.

In addition, two contrasting effects on *A. salina* were observed in mixed cultures of the dinoflagellate and the blue-green alga, *G. aponina:* (*a*) survival was promoted at low *G. aponina* populations, a result of the presence of sessile *G. breve* forms; and (*b*) enhanced mortality was observed at high *G. aponina* populations, caused by toxin released from cytolyzed *G. breve* cells. Unialgal *G. aponina* cultures exerted no adverse effect on adult and larval *A. salina*, as compared to controls.

Despite the obvious need for an environmentally and economically practical control measure for the red tide (25), it is too early to judge the utility of aponin without additional scrutiny of its broad biological implications. Nonetheless, these studies indicated its potential use as a biocontrol agent.

REFERENCES

(1) E. C. Kutt and D. F. Martin, *Environ. Lett.*, **9**, 195 (1975).

(2) L. F. McCoy, Jr., Ph.D. dissertation, University of South Florida, Tampa, Fla., 1977.

(3) D. F. Martin and B. B. Martin, *J. Environ. Sci. Health*, **A11** (10 and 11), 613 (1976).

(4) L. F. McCoy, Jr., and D. F. Martin, *Chem. Biol. Interact.*, **17**, 17 (1977).

(5) D. L. Eng-Wilmot, Ph.D. dissertation, University of South Florida, Tampa, Fla., 1978.

(6) J. J. Sasner, Jr., M. Ikawa, F. Thurberg, and M. Alam, *Toxicon*, **10**, 163 (1972).

(7) Y. S. Kim, J. R. Linton, and D. F. Martin, *ibid.*, **12**, 439 (1974).

(8) M. T. Doig, III, and D. F. Martin, *Environ. Lett.*, **3**, 278 (1972).

(9) H. R. Grande, P. C. Cheng, and N. J. Doorenbos, *J. Pharm. Sci.*, **65**, 1414 (1976).

(10) N. M. Trieff, M. McShan, D. Grajcer, and M. Alam, *Tex. Rep. Biol. Med.*, **31**, 409 (1973).

(11) J. Harwig and P. M. Scott, *Appl. Microbiol.*, **21**, 1011 (1971).

(12) A. S. Michael, C. G. Thompson, and M. Abramovitz, *Science*, **123**, 464 (1956).

(13) J. F. Wickins, ICES, Fisheries Improvement Committee, Doc. E. 6., Fisheries Experimental Station, Conway, England, 1970.

(14) G. A. Brydon, D. F. Martin, and W. K. Olander, *Environ. Lett.*, **1**, 235 (1971).

(15) D. L. Eng-Wilmot and D. F. Martin, *Microbios*, **19**, 167 (1978).

(16) D. F. Martin and M. H. Gonzalez, *J. Environ. Sci. Health*, **A11** (6), 385 (1976).

(17) D. L. Eng-Wilmot, W. S. Hitchcock, and D. F. Martin, *Mar. Biol.*, **41**, 71 (1977).

(18) D. L. Eng-Wilmot and D. F. Martin, *Fla. Sci.*, **40**, 193 (1977).

(19) D. J. Finney, "Probit Analysis," University Press, Cambridge, England, 1962.

(20) K. A. Steidinger, *CRC Crit. Rev. Microbiol*, **3**, 49 (1973).

(21) W. B. Wilson, S. M. Ray, and D. V. Aldrich, in "Proceeding of the First International Conference on Toxic Dinoflagellate Blooms," V. R. Lo Cicero, Ed., Massachusetts Science and Technology Foundation, Wakeford, Mass., 1975, p. 127.

(22) C. C. Davis, *Bot. Gaz.*, **109**, 358 (1948).

(23) H. D. Baldridge and M. Klein, *Environ. Lett.*, **7**, 31 (1972).

(24) B. Dale, C. M. Yentsch, and J. W. Hurst, *Science*, **201** 1223 (1978).

(25) D. F. Martin and B. B. Martin, *J. Chem. Educ.*, **53**, 614 (1976).

ACKNOWLEDGMENTS

The authors gratefully acknowledge the financial support and encouragement of the National Institute of Environmental Health Sciences. They also thank Dr. L. F. McCoy, Jr., for technical assistance.

Automated Analysis of Chlorthalidone

MARTHA M. JOHNSTON ˣ, MARC ROSENBERG, and BURDE KAMATH *

Received October 20, 1978, from the *Biochemistry and Drug Disposition Department, USV Pharmaceutical Corporation, Tuckahoe, NY 10707.* Accepted for publication January 31, 1979. *Present address: Arnar-Stone Laboratories, Mount Prospect, Ill.

Abstract □ Chlorthalidone inhibition of the enzymatic hydrolysis rate of *p*-nitrophenyl acetate by bovine erythrocyte carbonic anhydrase was used as a basis for chlorthalidone determination in plasma and urine. For urinary samples, a completely automated, continuous flow system was developed to extract the samples and perform the enzymatic reaction. Over 100 samples per day could be assayed by one person. The assay had a sensitivity of 0.5 μg/ml and thus could determine urinary concentrations after a therapeutic chlorthalidone dose. To determine plasma concentrations after a therapeutic dose, a manual extraction procedure was used in combination with a second continuous flow system for the enzymatic reaction. This system was optimized to detect the lowest chlorthalidone concentration allowed by the enzymatic inhibition constant and could detect 25 ng/ml.

Keyphrases □ Chlorthalidone—analysis, automated, plasma and urine, carbonic anhydrase inhibition, humans □ Diuretic agents—chlorthalidone, automated analysis, plasma and urine, carbonic anhydrase inhibition, humans □ Automated analysis—chlorthalidone, plasma and urine, carbonic anhydrase inhibition, humans

Previously (1), a method was described in which urinary chlorthalidone was determined by measuring the amount of inhibition of carbonic anhydrase caused by the chlorthalidone. This method was partially automated; the chlorthalidone extraction from the urine was done manually, but the inhibition measurement was automated using continuous flow equipment[1]. The present paper describes a completely automated method by which one person can analyze over 100 urinary samples per day.

Additionally, a partially automated method for plasma sample analysis is described. Since plasma chlorthalidone concentrations after a therapeutic dose (2) are lower than urinary concentrations (1), a method for plasma requires a greater sensitivity than a method for urinary samples. Neither the previous method (1) for urinary chlorthalidone nor the fully automated method described here have sufficient sensitivity for plasma analysis; however, a manual extraction procedure combined with an optimized automated system for the enzymatic reaction was sensitive enough for plasma analysis after therapeutic doses.

EXPERIMENTAL

Reagents for Automated Analysis System—The buffer was 0.1 *M* tromethamine[2], pH 8.0. The enzyme solution contained 40 mg of bovine erythrocyte carbonic anhydrase[2]/liter of buffer plus 0.1% surfactant[3]. The substrate solution was 2.0 m*M* *p*-nitrophenyl acetate[2] in polyethylene glycol 200[4]. The butanol[5] was saturated by shaking five volumes of it with two volumes of glass-distilled, deionized water. Solutions of 0.01 *N* NaOH[5] and 0.1 *N* HCl[5] were used.

Chlorthalidone Standards—A 100-μg/ml stock solution was prepared by dissolving 10.0 mg of chlorthalidone[6] in 10.0 ml of dioxane[7] and diluting to 100 ml with buffer. For urinary standards, the stock solution was diluted volumetrically with normal human urine to concentrations of 0.5, 1.0, 2.5, 4.0, 5.0, 6.0, and 7.5 μg/ml. For plasma standards, the stock solution was diluted with control plasma[8] to concentrations of 0.05, 0.10, 0.15, 0.20, and 0.25 μg/ml. The standards were extracted by the same procedures as were used for the unknown samples.

Automated Procedure for Urine Samples—Figure 1 is a diagram of the continuous flow system[9,10] for urinary chlorthalidone for extraction and analysis. Absorbance chart paper was used for the recorder. The spectrophotometer was used in the inverse mode in which decreases in absorbance are recorded as positive differences on the chart paper. In this mode, the baseline was set to zero with all reagents pumped through their respective lines and the buffer pumped through the sample line. Substrate solution was kept in an ice bath. The standard calibration of the spectrophotometer was adjusted so that a 5.0-μg/ml standard chlorthalidone sample gave a reading of 50 absorbance units.

Samples were assayed using a 40/hr cam with a 3:1 sample–wash ratio. After each 15 samples, the baseline was checked using a buffer sample, and the calibration point was checked using a 5.0-μg/ml standard. For unknown samples, the absorbance units were read directly off the chart and divided by 10 to obtain the chlorthalidone concentration. Samples beyond the linear range, >60 absorbance units, were diluted and reassayed.

Automated Procedure for Plasma Samples—The continuous flow system[9,11] in Fig. 2 was used for plasma samples because it diluted samples less and thus was able to measure lower chlorthalidone concentrations. The spectrophotometer was used in the direct mode. The baseline was adjusted to zero with the buffer pumped through the sample and enzyme lines and the other reagents pumped through their respective lines. The enzyme line was switched to the enzyme solution.

After the large increase in absorbance was recorded, indicating that the enzyme solution had traversed the entire system, the standard calibration of the spectrophotometer was adjusted so that the enzymatic baseline was between 50 and 60 relative absorbance units (*RA*) on the chart. After the enzymatic baseline was established, the sampler was started, and the inhibition of carbonic anhydrase by the samples was determined by measuring the decrease in relative absorbance (Δ*RA*). Standards were run before and after every 15 unknown samples. The chlorthalidone concentrations of the unknown samples were calculated from a standard Δ*RA versus* concentration curve.

Plasma and urine samples introduced to the carbonic anhydrase and *p*-nitrophenyl acetate reaction decreased the rate of *p*-nitrophenol formed, which decreased the absorbance at 400 nm. In the system for urine samples, these decreases were translated into positive recorder deflections by using the spectrophotometer in the inverse mode. To minimize plasma sample dilution, the spectrophotometer was used in

Table I—Chlorthalidone Standards in Plasma

Chlorthalidone Concentration, ng/ml	Δ*RA*, Mean ± *SD*[a]
0	0.2 ± 0.6
50	6.3 ± 1.3
100	11.5 ± 0.4
150	15.9 ± 0.8
200	20.7 ± 2.5
250	23.5 ± 2.0
300	28.1 ± 0.8

[a] Quadruplicate samples were extracted from plasma and analyzed.

[1] AutoAnalyzer, Technicon Industrial Systems, Tarrytown, N.Y.
[2] Sigma Chemical Co., St. Louis, Mo.
[3] Triton X-405, Rohm and Haas Co., Philadelphia, Pa.
[4] J. T. Baker Chemical Co., Phillipsburg, N.J.
[5] Fisher Scientific Co., Pittsburgh, Pa.
[6] USV Pharmaceutical Corp., Tuckahoe, N.Y.
[7] Mallinckrodt, St. Louis, Mo.
[8] Monitrol, American Hospital Supply Corp., Miami, Fla.
[9] AutoAnalyzer II, sampler IV, proportioning pump III, UV spectrophotometer, and recorder, Technicon Industrial Systems, Tarrytown, N.Y.
[10] AutoAnalyzer heating bath with 40-ft coil, Technicon Industrial Systems, Tarrytown, N.Y.
[11] GCA circulating system, Precision Scientific, Chicago, Ill.

0022-3549/79/0800-0967$01.00/0
© 1979, American Pharmaceutical Association

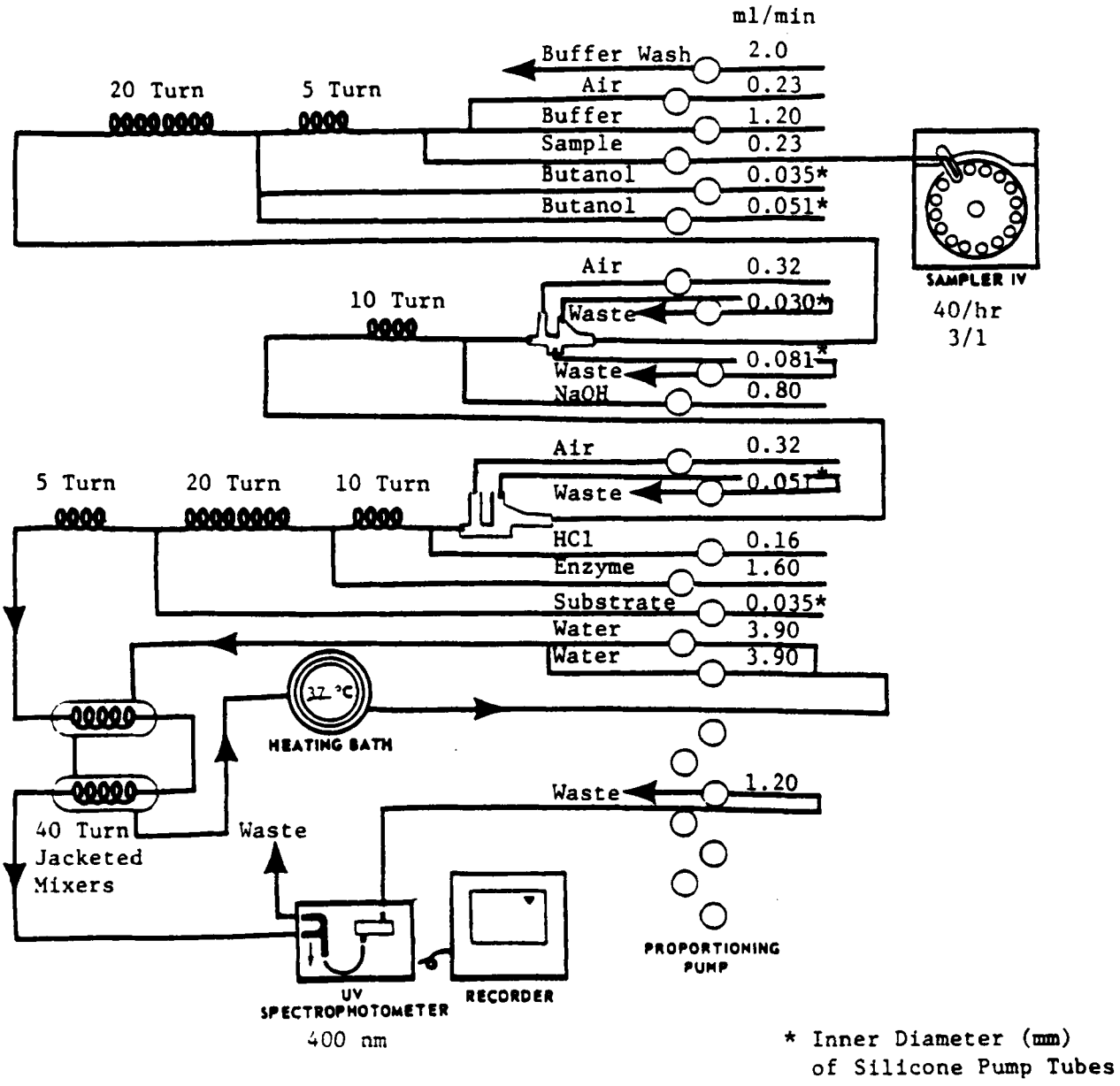

Figure 1—*Continuous flow system for urinary chlorthalidone analysis.*

the direct mode in which the decreases in absorbance (ΔRA) were recorded as shown in Fig. 3.

Extraction Procedure—Plasma was prepared by centrifugation from blood containing either citrate[7] or oxalate as an anticoagulant. Plasma, 1.0 ml, was mixed with 5.0 ml of 0.04 *M* sodium tungstate[7] in 0.09 *M* HCl[5] and extracted twice with 5.0 ml of ether[5]. The ether extracts were combined, and the chlorthalidone was back-extracted with 2.0 ml of 0.1 *M* NaOH[5].

The phases were separated, and the aqueous phase was neutralized with 2.0 ml of 0.1 *M* HCl, buffered with 2.0 ml of 0.1 *M* tromethamine[2] (pH 8.0), and extracted twice with 5.0 ml of ether. The ether extracts were combined and evaporated to dryness, and the residue was dissolved in 2.0 ml of buffer.

Table II—Analysis of Clinical Urinary Samples Containing Chlorthalidone

Sample	Chlorthalidone Concentration, μg/ml: Partially Automated Method (1)	Fully Automated Method
17	6.96	6.36
25	4.97	4.93
36	3.51	3.52
44	4.50	3.95
52	5.15	5.07
63	11.76	11.70
71	6.67	6.13
78	3.22	3.52
90	13.98	13.40
98	3.92	3.57

RESULTS

Standard Curves—The response of the automated system for urine samples to a series of standard chlorthalidone concentrations in urine was linear up to 6.0 μg/ml. Between 6.0 and 10.0 μg/ml, the response was a nonlinear function of the concentration. Linear regression analysis of urine standards from 0 to 6.0 μg/ml, analyzed 16 times over 2 days, yielded a regression coefficient of $r = 0.999$ and a standard error in chlorthalidone concentration of ±0.12 μg/ml.

Figure 3 shows the response of the system for plasma samples to a series of chlorthalidone standards after extraction from plasma. A plot of ΔRA *versus* chlorthalidone concentration yielded a function that was slightly curved, a phenomenon that had been observed earlier (1). In Table I, the mean and standard deviation values are reported for a series of quadruplicate standards extracted from plasma and analyzed. The sensitivity

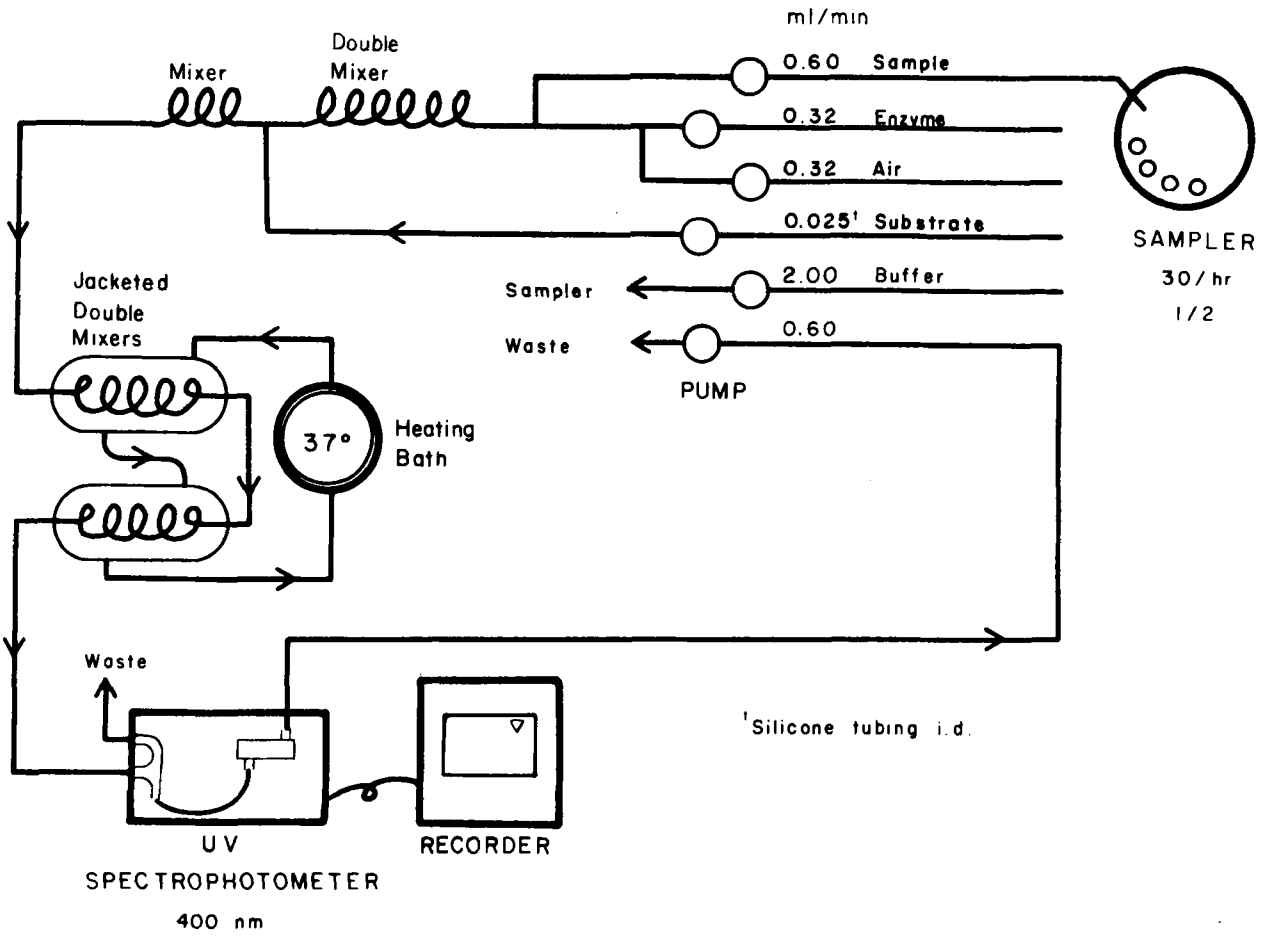

Figure 2—*Continuous flow system for plasma chlorthalidone analysis.*

of the assay was ~25 ng/ml. The extraction procedure efficiency was 50–55% throughout the concentration range.

Clinical Samples—Urinary samples from a subject who had received a therapeutic chlorthalidone dose were analyzed by the previous reported method (1) and by the fully automated procedure described here. Table II shows that both procedures yielded the same results within experimental error. Plasma samples from subjects who had received 100-mg tablets were analyzed, and the concentration–time curves were similar to those obtained by other authors (2, 3) who used GLC methods.

DISCUSSION

Using the fully automated system for urinary samples, one person could analyze 100 or more unknown samples a day. The assay specificity was discussed previously (1). Unknown samples were assayed by both methods, and the results were the same within experimental error. The method is reproducible (±0.12 μg/ml) and is sensitive enough to determine chlorthalidone concentrations after a therapeutic dose (1). Because of these factors, especially speed, this automated method appears to be ideally suited for the analysis of a large number of samples, as would be encountered in a clinical bioavailability or bioequivalency study.

An assay for plasma samples needs to be more sensitive than one for urinary samples because plasma chlorthalidone concentrations after a therapeutic dose are lower than urinary concentrations (2, 3). Since this assay depends on carbonic anhydrase inhibition by chlorthalidone, the ultimate sensitivity of the method is dependent on the inhibition constant, $K_I = 3 \times 10^{-7}\ M$ (4). Thus, a 10% decrease in enzymatic velocity (a detectable decrease) would be observed with a chlorthalidone concentration of $3.3 \times 10^{-8}\ M$ in the reaction mixture.

To obtain this maximum sensitivity, the continuous flow system shown in Fig. 2 was designed to minimize sample dilution between the sampler and the substrate addition that starts the reaction. This optimization was discussed in detail previously (5). From the inhibitor concentration at 10% inhibition ($I_{10} = 3.3 \times 10^{-8}\ M$), the chlorthalidone molecular weight (339 g/mole), the dilution in the continuous flow system (0.60 ml sample/1.15 ml total), and the extraction efficiency (0.55), an approximate sensitivity of 38 ng/ml was calculated:

$$\text{sensitivity} = \frac{339\ \text{g/mole} \times 3.3 \times 10^{-8}\ M}{(0.60/1.15) \times 0.55} = 38\ \text{ng/ml} \quad \text{(Eq. 1)}$$

The experimental limit as estimated from Table I is 25 ng/ml, probably a result of detecting less than a 10% change in enzymatic velocity. Automation of the extraction procedure for plasma samples was considered but is probably not possible since continuous flow system mechanics involve sampling only part of a desired phase, which would result in lower recovery, greater dilution, and loss of the necessary sensitivity.

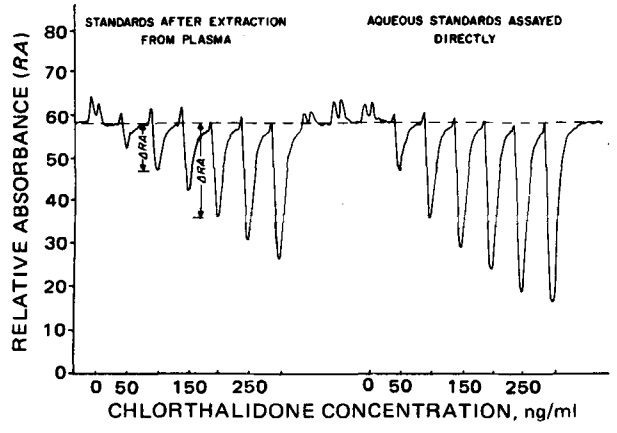

Figure 3—*Typical recording from standard samples analyzed on the continuous flow system (Fig. 2). The samples on the left were extracted from plasma, as described in the text, before introduction into the system. The samples on the right were prepared as known chlorthalidone concentrations in buffer for sampling by the system.*

For clinical studies, especially bioavailability or bioequivalency studies, collection and analysis of urine samples rather than plasma samples may be preferable (6). The distribution of chlorthalidone between plasma and erythrocytes is not instantaneous, so it is difficult to obtain a blood sample and to prepare the plasma quickly enough so that the determined chlorthalidone concentration is the same as the plasma concentration *in vivo* (7). The analysis of urinary samples can be accomplished rapidly with the fully automated system.

REFERENCES

(1) M. M. Johnston, H. Li, and D. Mufson, *J. Pharm. Sci.*, **66**, 1735 (1977).

(2) P. Collste, M. Garle, M. D. Rawlins, and F. Sjöqvist, *Eur. J. Clin. Pharmacol.*, **9**, 319 (1976).

(3) H. L. J. Fleuren and J. M. van Rossum, *J. Pharmacokinet. Biopharm.*, **5**, 359 (1977).

(4) K. H. Beyer and J. E. Baer, *Pharmacol. Rev.*, **13**, 517 (1961).

(5) M. Rosenberg, H. Li, and M. M. Johnston, in "Advances in Automated Analysis, Technicon International Congress," vol. 2, E. C. Barton, A. Conetta, M. J. F. Du Cros, F. J. Kabot, R. K. Love, C. Maddix, J. F. Murdock, and L. Perlman, Eds., Mediad, Tarrytown, N.Y., 1977, pp. 279–283.

(6) W. Riess, U. C. Dubach, D. Burckhardt, W. Theobald, P. Vuillard, and M. Zimmerli, *Eur. J. Clin. Pharmacol.*, **12**, 375 (1977).

(7) H. L. J. M. Fleuren and J. M. van Rossum, *J. Chromatogr.*, **152**, 41 (1978).

ACKNOWLEDGMENTS

Presented in part at the 7th Technicon International Congress, December 1976, and at the APhA Academy of Pharmaceutical Sciences, Phoenix meeting, November 1977.

The authors thank Mr. M. Patel for excellent technical assistance.

Progestin Permeation through Polymer Membranes IV: Mechanism of Steroid Permeation and Functional Group Contributions to Diffusion through Hydrogel Films

G. M. ZENTNER, J. R. CARDINAL ˣ, J. FEIJEN, and SUK-ZU SONG

Received September 7, 1978, from the *Department of Pharmaceutics, College of Pharmacy, University of Utah, Salt Lake City, UT 84112.* Accepted for publication January 26, 1979.

Abstract □ Hydrogel films were prepared from hydroxyethyl methacrylate, both with (Film II) and without (Film I) 5.25 mole % of ethylene glycol dimethacrylate. Permeation, diffusion, and partition coefficients for progesterone, testosterone, nandrolone, norethindrone, 17α-hydroxyprogesterone, estradiol, and hydrocortisone were determined. A solute permeation model was proposed based on the separation of a domain (B) composed of "bulk-like" water and a domain (A) composed of polymer, interfacial water, and bound water present in the films. The separate contributions from the "pore" and "solution–diffusion" mechanisms to the total permeability were calculated from the model. Steroid permeabilities through Films I and II were analyzed in accordance with this model. Permeation of Film II occurred *via* the solution–diffusion mechanism. Permeation of Film I occurred predominately by the pore mechanism with a small contribution (~20%) from the solution–diffusion mechanism. The latter contribution was dependent on the solubility of the solute within the A domains of the hydrogel film. Functional group contributions to permeation of Film II were ascribed to either steric or hydrogen bonding effects.

Keyphrases □ Progesterone—permeation through hydrogel films, models, structure–activity relationships, steroids □ Hydrogel films—progesterone permeation, structure–activity relationships, steroids, models □ Structure–activity relationships—steroid permeation through hydrogel films □ Models—steroid permeation through hydrogel films

In previous reports from this laboratory (1, 2), the permeation mechanisms of a model hydrophobic drug, progesterone, through poly(hydroxyalkyl methacrylate) films were examined. The importance of film hydration was emphasized. Similar conclusions were drawn by others (3–5) for hydrophilic solute permeation through hydrogel films. Several investigators (2, 4, 5) indicated that, depending on the hydrogel composition, either a "pore" or a "solution–diffusion" mechanism may dominate permeation. For polymers prepared from various comonomers or from hydroxyethyl methacrylate without added cross-linking agents, the pore mechanism dominates. At high concentrations of the cross-linking agent, ethylene glycol dimethacrylate and possibly tetraethylene glycol dimethacrylate, the solution–diffusion mechanism appears to dominate permeation. These results were found for both hydrophobic (2) and hydrophilic (4, 5) solutes.

These conclusions are tenuous without further investigation. One problem is the partition coefficient reported for the hydrophobic solute progesterone (2). This value, which is >100, appears to be inconsistent with a pore mechanism in which transport presumably occurs within water-filled pores or microchannels present in the film. For permeation within these channels, partition coefficients close to one are expected. Hydrophilic solutes in hydrogels generally exhibit partition coefficients close to this value (6).

For this reason, the permeation mechanism of hydrophobic solutes through hydrogel films was examined in greater detail. The permeation characteristics for several steroids that have systematic structural differences were determined in films prepared from hydroxyethyl methacrylate, both with and without 5.25 mole % of ethylene glycol dimethacrylate as a cross-linking agent. The results substantiate previous conclusions concerning the two mechanisms for solute permeation in hydrogel films, provide an explanation for the proposed pore-type permeation mechanism for solutes having high hydrogel–water partition coefficients, and demonstrate the effects of steroid structural differences on permeation rates through hydrogel films.

0022-3549/79/0800-0970$01.00/0

© 1979, American Pharmaceutical Association

For clinical studies, especially bioavailability or bioequivalency studies, collection and analysis of urine samples rather than plasma samples may be preferable (6). The distribution of chlorthalidone between plasma and erythrocytes is not instantaneous, so it is difficult to obtain a blood sample and to prepare the plasma quickly enough so that the determined chlorthalidone concentration is the same as the plasma concentration *in vivo* (7). The analysis of urinary samples can be accomplished rapidly with the fully automated system.

REFERENCES

(1) M. M. Johnston, H. Li, and D. Mufson, *J. Pharm. Sci.*, **66**, 1735 (1977).

(2) P. Collste, M. Garle, M. D. Rawlins, and F. Sjöqvist, *Eur. J. Clin. Pharmacol.*, **9**, 319 (1976).

(3) H. L. J. Fleuren and J. M. van Rossum, *J. Pharmacokinet. Biopharm.*, **5**, 359 (1977).

(4) K. H. Beyer and J. E. Baer, *Pharmacol. Rev.*, **13**, 517 (1961).

(5) M. Rosenberg, H. Li, and M. M. Johnston, in "Advances in Automated Analysis, Technicon International Congress," vol. 2, E. C. Barton, A. Conetta, M. J. F. Du Cros, F. J. Kabot, R. K. Love, C. Maddix, J. F. Murdock, and L. Perlman, Eds., Mediad, Tarrytown, N.Y., 1977, pp. 279–283.

(6) W. Riess, U. C. Dubach, D. Burckhardt, W. Theobald, P. Vuillard, and M. Zimmerli, *Eur. J. Clin. Pharmacol.*, **12**, 375 (1977).

(7) H. L. J. M. Fleuren and J. M. van Rossum, *J. Chromatogr.*, **152**, 41 (1978).

ACKNOWLEDGMENTS

Presented in part at the 7th Technicon International Congress, December 1976, and at the APhA Academy of Pharmaceutical Sciences, Phoenix meeting, November 1977.

The authors thank Mr. M. Patel for excellent technical assistance.

Progestin Permeation through Polymer Membranes IV: Mechanism of Steroid Permeation and Functional Group Contributions to Diffusion through Hydrogel Films

G. M. ZENTNER, J. R. CARDINAL ˣ, J. FEIJEN, and SUK-ZU SONG

Received September 7, 1978, from the *Department of Pharmaceutics, College of Pharmacy, University of Utah, Salt Lake City, UT 84112.* Accepted for publication January 26, 1979.

Abstract □ Hydrogel films were prepared from hydroxyethyl methacrylate, both with (Film II) and without (Film I) 5.25 mole % of ethylene glycol dimethacrylate. Permeation, diffusion, and partition coefficients for progesterone, testosterone, nandrolone, norethindrone, 17α-hydroxyprogesterone, estradiol, and hydrocortisone were determined. A solute permeation model was proposed based on the separation of a domain (B) composed of "bulk-like" water and a domain (A) composed of polymer, interfacial water, and bound water present in the films. The separate contributions from the "pore" and "solution–diffusion" mechanisms to the total permeability were calculated from the model. Steroid permeabilities through Films I and II were analyzed in accordance with this model. Permeation of Film II occurred *via* the solution–diffusion mechanism. Permeation of Film I occurred predominately by the pore mechanism with a small contribution (~20%) from the solution–diffusion mechanism. The latter contribution was dependent on the solubility of the solute within the A domains of the hydrogel film. Functional group contributions to permeation of Film II were ascribed to either steric or hydrogen bonding effects.

Keyphrases □ Progesterone—permeation through hydrogel films, models, structure–activity relationships, steroids □ Hydrogel films—progesterone permeation, structure–activity relationships, steroids, models □ Structure–activity relationships—steroid permeation through hydrogel films □ Models—steroid permeation through hydrogel films

In previous reports from this laboratory (1, 2), the permeation mechanisms of a model hydrophobic drug, progesterone, through poly(hydroxyalkyl methacrylate) films were examined. The importance of film hydration was emphasized. Similar conclusions were drawn by others (3–5) for hydrophilic solute permeation through hydrogel films. Several investigators (2, 4, 5) indicated that, depending on the hydrogel composition, either a "pore" or a "solution–diffusion" mechanism may dominate permeation. For polymers prepared from various comonomers or from hydroxyethyl methacrylate without added cross-linking agents, the pore mechanism dominates. At high concentrations of the cross-linking agent, ethylene glycol dimethacrylate and possibly tetraethylene glycol dimethacrylate, the solution–diffusion mechanism appears to dominate permeation. These results were found for both hydrophobic (2) and hydrophilic (4, 5) solutes.

These conclusions are tenuous without further investigation. One problem is the partition coefficient reported for the hydrophobic solute progesterone (2). This value, which is >100, appears to be inconsistent with a pore mechanism in which transport presumably occurs within water-filled pores or microchannels present in the film. For permeation within these channels, partition coefficients close to one are expected. Hydrophilic solutes in hydrogels generally exhibit partition coefficients close to this value (6).

For this reason, the permeation mechanism of hydrophobic solutes through hydrogel films was examined in greater detail. The permeation characteristics for several steroids that have systematic structural differences were determined in films prepared from hydroxyethyl methacrylate, both with and without 5.25 mole % of ethylene glycol dimethacrylate as a cross-linking agent. The results substantiate previous conclusions concerning the two mechanisms for solute permeation in hydrogel films, provide an explanation for the proposed pore-type permeation mechanism for solutes having high hydrogel–water partition coefficients, and demonstrate the effects of steroid structural differences on permeation rates through hydrogel films.

0022-3549/79/0800-0970$01.00/0

© 1979, American Pharmaceutical Association

EXPERIMENTAL

Materials—Hydroxyethyl methacrylate[1] was a highly purified sample containing the following levels of impurities[1]: methacrylic acid, 0.06%; ethylene glycol dimethacrylate, 0.024%; and diethylene glycol methacrylate, 0.24%. Ethylene glycol dimethacrylate[2] was purified by base extraction and distillation. Azobis(methylisobutyrate) was prepared by the method of Mortimer (7).

Hydrocortisone[3], 17α-hydroxyprogesterone[3], progesterone[3], testosterone[3], nandrolone[3], estradiol[3], norethindrone[4], 6,7-^{3}H-estradiol[5], and 1,2-^{3}H-progesterone[6] were used as received. TLC analysis, with 20% (v/v) ethyl acetate in toluene and 5% (v/v) methanol in chloroform as developing reagents, indicated that all steroids were pure. In all cases, a single UV-detectable spot was observed. Radiolabeled steroids had the same R_f values as the unlabeled counterparts, with >95% of the detectable activity associated with the primary spot. The remaining radioactivity was distributed evenly throughout the remainder of the plate.

Methods—Hydrogel films were prepared by polymerization between sealed polyethylene plates at 60° for 24 hr. Azobis(methylisobutyrate) (7.84 mmoles/liter of monomer) was the initiator.

Film I was prepared from a mixture of hydroxyethyl methacrylate and 40% (v/v) deionized water. Film II was prepared from a mixture of hydroxyethyl methacrylate with 5.25 mole % ethylene glycol dimethacrylate as the cross-linking agent and 40% (v/v) ethanol as the solvent. These mixtures were homogeneous before and after polymerization. Subsequent to polymerization, the films were soaked in water (changed repeatedly) for 3–4 weeks prior to use.

The diffusion experiments were performed at room temperature (24 ± 1°) in an all-glass cell described previously (1). An aqueous solution of 17α-hydroxyprogesterone, progesterone, testosterone, nandrolone, norethindrone, estradiol (~5 μg/ml), or hydrocortisone (~250 μg/ml) was placed into one chamber. The second chamber was filled with deionized water. The concentration increase was followed in the initially steroid-free chamber by UV spectrophotometry[7] or by liquid scintillation counting of the radiolabeled compounds using scintillation fluid[8] and a scintillation counter[9].

Partition coefficients, defined as the ratio of the concentrations in the film and in the bulk aqueous phase, were determined by a solution depletion technique (1) in which 50 ml of a steroid solution was allowed to equilibrate with a known volume of polymer. Adsorption of the steroids onto glass was checked and was not a problem. The steroid equilibrium concentration in the bulk aqueous solutions was obtained as described previously.

Film thicknesses (~0.03 cm) were measured on the water-swollen films using a lightwave micrometer[10].

RESULTS AND DISCUSSION

Permeability and diffusion coefficients for steroids in hydrogel films were calculated using:

$$\ln\left\{\frac{C_0V - (2V + K_dV_m)C_4}{C_0V - (2V + K_dV_m)C_2}\right\} = -\frac{2AU}{Vl}(t_{ss} - t_{oss}) \qquad \text{(Eq. 1)}$$

where:

C_0 = initial drug concentration in Compartment I
V = compartment volumes (176 ml)
K_d = partition coefficient
V_m = membrane volume
C_2 = concentration in Compartment II at the onset of steady state (t_{oss})
C_4 = concentration in Compartment II at the time t_{ss}
A = membrane area (14.2 cm^2)
l = wet membrane thickness
$U = DK_d$
D = diffusion coefficient
t_{ss} = any time during steady state

[1] Courtesy of Hydron Laboratories, New Brunswick, N.J.
[2] Monomer Polymer Laboratories, Philadelphia, Pa.
[3] Steraloids Inc., Pauling, N.Y.
[4] Sigma Chemical Co., St. Louis, Mo.
[5] Amersham Corp., Arlington Heights, Ill.
[6] New England Nuclear, Boston, Mass.
[7] Cary model 15, Varian Instruments, Palo Alto, Calif.
[8] Formula 950-A, New England Nuclear, Boston, Mass.
[9] Model 3385, Packard Instrument Co., Downers Grove, Ill.
[10] Van Kueren Co., Watertown, Mass.

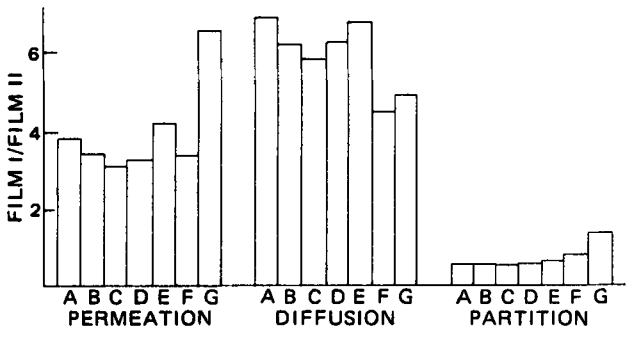

Figure 1—*Relative comparison of steroid permeation, diffusion, and partition coefficients in Films I and II. Key: A, testosterone; B, norethindrone; C, nandrolone; D, progesterone; E, 17α-hydroxyprogesterone; F, estradiol; and G, hydrocortisone.*

The values of U, D, and K_d for the various steroids in Films I and II are given in Table I. The relative values for each steroid in these films are shown in Fig. 1. Except for hydrocortisone and possibly estradiol, the relative permeation factors for all steroids were the same. This finding suggests that similar mechanisms control the permeation of these solutes.

Equation 1 differs somewhat from that used previously (Eq. A15, *Appendix*) (1, 2, 8). An assumption implicit in the previous work is that the amount of drug within the polymer film during steady-state diffusion is small (9). However, the K_d values in Tables I and II suggest that, during steady-state diffusion, a significant portion of the initial drug load added to Compartment I of the diffusion cell will be associated with the polymer film. In effect, this association of drug with the film reduces the concentration gradient between the aqueous compartments and results in permeability coefficients that are too low if the amount of drug in the film is assumed to be small. The magnitude of the effect depends on K_d. For example, with progesterone, which has a K_d of 129, Eq. 1 yields a value of 8.44×10^{-7} cm^2/sec for the permeability in polyhydroxyethyl methacrylate, whereas the equation used in previous work (Eq. A15, *Appendix*) provides a value of 5.62×10^{-7} cm^2/sec for progesterone in the same film. The difference in the calculated permeability coefficients for hydrocortisone, $K_d = 27$, is much less for the same film, *i.e.*, 2.39×10^{-7} cm^2/sec *versus* 2.32×10^{-7} cm^2/sec.

Equation 1 is derived on the assumptions that the drug partitions into the film in accordance with its equilibrium partition coefficient and that the partition coefficient is concentration independent. Experiments with several steroids over a wide concentration range suggest that this assumption is valid for the hydrogels. The derivation of Eq. 1 from Fick's first law is given in the *Appendix*.

These results raise questions with respect to the validity of conclusions reached in previous work (1, 2, 8) on the effects of various factors on the permeability of hydrogel films to progesterone. The conclusions reached depended primarily on relative changes in permeability and/or diffusion coefficients. All previously reported values of U and D were recalculated according to the methods outlined in the present paper. The new values are consistent with the conclusions stated in those papers.

Steroid Permeation through Hydrogel Films—Solute permeation through polymeric films is normally described in terms of either a "pore" or a "solution-diffusion" mechanism. In the pore mechanism, transport occurs *via* diffusion through solvent present within microchannels or pores. The K_d values are usually less than one and reflect solute distribution between the membrane solvent and bulk solvent. Solution-diffusion transport occurs *via* dissolution and diffusion of the solute within the segments making up the polymer matrix. The K_d values for this mechanism vary widely but usually are much greater than one.

For progesterone diffusion through hydrogel films, previous work (2) indicated that the solution-diffusion mechanism dominates in Film II whereas the pore mechanism dominates in Film I. These conclusions are based on an analysis of permeation data according to methods outlined by other investigators (4, 5).

The data in Table I indicate that the K_d values for both Films I and II are much greater than one. These high K_d values for Film I appear to be inconsistent with the pore mechanism for solute transport. The possibility remains, however, that K_d is dominated by the high solute solubility within the hydrophobic regions of the hydrogel (10) whereas permeation is dominated by diffusion within "fluctuating pores" (11) or microchannels within this film.

Separation of pore and solution-diffusion contributions to total per-

Table I—Permeation Parameters for Steroids in Hydrogel Films

Steroid	Film I			Film II			K_d^I/K_d^{II}
	Permeability Coefficients, $U \times 10^7$ cm²/sec	Diffusion Coefficients, $D \times 10^9$ cm²/sec	Partition Coefficients, K_d	Permeability Coefficients, $U \times 10^7$ cm²/sec	Diffusion Coefficients, $D \times 10^9$ cm²/sec	Partition Coefficients, K_d	
Testosterone	9.05	18.8	48	2.40	2.70	89	0.54
Norethindrone	9.47	13.5	70	2.83	2.16	131	0.54
Nandrolone	7.56	20.4	37	2.45	3.45	71	0.52
Progesterone	8.44	7.04	129	2.61	1.12	232	0.56
17α-Hydroxyprogesterone	8.78	10.6	83	2.02	1.53	132	0.63
Estradiol	9.69	5.48	177	2.85	1.21	235	0.75
Hydrocortisone	2.39	8.86	27	0.36	1.78	20	1.35

meation is necessary to determine the dominant mechanism in Film I. The following discussion concerns the development of a model for diffusion within hydrogels that will provide for the calculation of these separate contributions from the data in Table I. This model is based on the physical–chemical properties of hydrogels and, in particular, on the water distribution within these films.

Macroscopically, hydrogel films are homogeneous single-phase systems having water and polymer as components. Microscopically, the polymer and water can be visualized as separate dispersed phases.

Jhon and Andrade (12) hypothesized that water can exist in at least three different environments within synthetic hydrogel films in a fashion analogous to that proposed (13) for biological membranes. These environments include hydration or bound water, interfacial water, and normal or "bulk-like" water. The bound water is strongly associated with the polymer, probably as water hydrating the hydrophilic polymer groups. Interfacial water is not well defined but may be associated with hydrophobic interactions between the polymer segments. Bulk-like water is similar to bulk water in aqueous solutions.

Sung (14) defined the concentrations of these various water types within poly(hydroxyethyl methacrylate) films, prepared with and without 1 mole % of ethylene glycol dimethacrylate. The amount of bulk-like water is highly dependent on the total hydrogel water content. Films cross-linked with ethylene glycol dimethacrylate have a lower percentage of bulk-like water than hydrogels prepared without cross-linker at equal total water contents. Interpolation of Sung's data is possible with the assumption that the distribution of water into bound, interfacial, and bulk-like fractions is similar in a 1-mole % ethylene glycol dimethacrylate cross-linked gel containing the same weight fraction of total water (nonequilibrium value) as a 5.25-mole % cross-linked gel that is equilibrated with water.

The equilibrium weight fraction of water in Film II is 0.35. A 1-mole % cross-linked gel contains less than 5 volume % of bulk-like water at this weight fraction. From this value, it may be inferred that the volume percent of bulk-like water in Film II approaches zero. A value of 22.8 volume % of bulk-like water is obtained for hydrogel films prepared without cross-linker having a total water weight fraction of 0.43 (Film I).

These results, together with other data (2–6) on solute permeation through hydrogel films, provide the basis for the model of solute permeation through these films.

In this model, the hydrogel films prepared without cross-linker are composed of two domains, A and B. Domain A is composed of polymer segments that associate by hydrophobic interactions and are surrounded by bound and interfacial water. Domain B is bulk-like water and forms the fluctuating pores described previously (11). Increasing the mole percent of cross-linker increases the amount of A and reduces the amount of B. A hydrogel such as Film II, having no bulk-like water, is assumed to be composed entirely of A-type domains. Although the relative amounts of Domains A and B change as the mole percent of cross-linker is changed, the inherent permeabilities of the domains are assumed to remain constant. Therefore, the total permeability of a hydrogel film is a summation of the individual permeabilities of Domains A and B and varies in accordance with the volume percent of bulk-like water present.

Transport in the hydrogel A domains occurs through the bound and interfacial water, through the hydrophobic regions, or through some combination of these. Irrespective of the specific transport region, permeation in the A regions occurs by the solution–diffusion mechanism as previously defined. The K_d values for transport in the A regions vary widely, depending on the solute solubility characteristics.

Transport in the B domains occurs by simple diffusion in bulk-like water. The K_d values must be precisely one since the solute is simply partitioning from bulk water into hydrogel domains of bulk-like water.

Film II, having no bulk-like water, is a diffusion barrier composed exclusively of A-type domains. As postulated in the model, solute transport occurs only by the solution–diffusion mechanism in such a film.

Several lines of evidence support this contention and are consistent for both hydrophobic and hydrophilic solutes:

1. It is supported by the cited data, which indicate that films containing high cross-linker concentrations have little or no bulk-like water.

2. Past work has shown that both hydrophobic (2) and hydrophilic (4, 5) solutes exhibit limiting values for the diffusion coefficient as the cross-linking agent concentration increases. This result is inconsistent with a pore mechanism since, if this mechanism is operative, the diffusion

Table II—Model Analysis of Steroid Permeation Data

Steroid	Partial Molar Volume[a], cm³/mole	Diffusion Coefficient in Water, $D_0 \times 10^6$ cm²/sec	Diffusion Coefficient in Bulk-Like Water of Film I, $D_B \times 10^7$ cm²/sec	ln (D_B/D_0)	D_B/P_T
Testosterone	237.4	6.04	7.20	−2.13	0.80
Norethindrone	252.0	5.83	7.29	−2.08	0.77
Nandrolone	218.1	6.35	5.67	−2.42	0.75
Progesterone	269.8	5.59	6.43	−2.16	0.76
17α-Hydroxyprogesterone	272.1	5.56	7.22	−2.04	0.82
Estradiol	214.9	6.41	7.49	−2.15	0.77
Hydrocortisone	273.6	5.55	2.11	−3.27	0.88

[a] Calculated from group contributions, Ref. 24.

coefficients must decrease with increasing cross-linker content due to a reduction in the average pore size as a consequence of reduced polymer chain mobility.

3. Film II was nearly impermeable to hydrophilic solutes such as inositol and sucrose (6). Since sucrose is of approximately the same molecular weight as the steroids used in the present study, its diffusion coefficient should be similar to the steroids if the pore mechanism is operative in Film II.

4. The conclusion that transport occurs by the solution-diffusion mechanism in Film II is consistent with the high partition coefficients obtained for the steroids used in the present study.

5. The disproportionately large decrease in the permeability coefficient of hydrocortisone, a relatively water-soluble steroid, in Film II compared with Film I, coupled with a lower partition coefficient in Film II than in Film I, suggests a dependence on bulk water not seen with the more hydrophobic steroids yet consistent with the pattern exhibited by the sugars.

Film I contains 22.8% of bulk-like water making up the B domains; the remainder is designated as A-type domains. Based on the proposed model and using the data in Table I, it is possible to estimate the contribution of each domain to the total permeability. Total Film I permeability can be represented as a summation of the individual domain contributions:

$$P_T = P_A + P_B \qquad \text{(Eq. 2)}$$

where:

P_T = total permeability in Film I
P_A = permeability coefficient in the A domains
P_B = permeability coefficient in the B domains

The P_A value is obtained from the relation $P_A = (\phi_A)P_T^{II}$, where P_T^{II} is the permeability coefficient of the solute in Film II and ϕ_A is the volume fraction of A-type domains in Film I. The ϕ_A value is given by $\phi_A = 1 - \phi_B$, where ϕ_B is the volume fraction of bulk-like water present in Film I (0.228).

Equation 2 may be rewritten as:

$$P_T - (\phi_A)P_T^{II} = P_B \qquad \text{(Eq. 3)}$$

The calculated P_B values represent the total permeability attributable to the pore mechanism in Film I. By definition, the partition coefficient in the B domains equals one. Therefore, P_B quantitatively equals the diffusion coefficient, D_B, using $P_B = K_d D_B$. These values are given in Table II along with the ratio D_B/P_T, which is the percent pore-type permeation in Film I. This ratio is approximately 0.77 for all of the steroids investigated except hydrocortisone, which is 0.88. This finding indicates that the pore contribution to transport in Film I is similar for the more hydrophobic steroids, with the relatively water-soluble steroid hydrocortisone permeating *via* pores to a greater extent. This result is consistent with the proposed model. The relatively high values of D_B/P_T for all steroids suggest that permeation through Film I is dominated by the pore mechanism, a result consistent with previous work (2).

The high K_d values with Film I are consistent with the model. Although permeation is dominated by the pore mechanism, Film I is composed primarily of A-type domains, which dominate the partitioning of hydrophobic solutes but make little contribution to permeability.

An implicit assumption of the model is that the A domains are similar in Films I and II. Were this strictly true, the partition coefficients, which are dominated by A-type domains, in Film I should be related to those in Film II according to the volume fraction of A-type domains present in Film I (0.772). These values are given in Table I as the ratio K_d^I/K_d^{II}. The estradiol value is in close agreement with the predicted value. However, for the other steroids, except hydrocortisone, this ratio is approximately 0.54. Thus, qualitative agreement with the predicted value is found, but the quantitative agreement is not good. This finding implies that differences exist between the A domains of Films I and II. This conclusion is expected based on the high cross-linker content in Film II. The corrections that must be made to overcome this deficiency in the model are not readily apparent.

Sufficient data were available from previous work (2) to test the model in predicting progesterone permeation in gels containing intermediate concentrations of the cross-linking agent ethylene glycol dimethacrylate. From the data of Sung (14), the volume percent of bulk-like water in a film prepared from 0.75 mole % of cross-linker is approximately 0.15. Based on this value, the permeability coefficient for progesterone in this cross-linked gel can be calculated from Eq. 3 by assuming that the total permeation arising from transport in the B regions is given by $P_B = \beta D_B$; β is defined by the ratio ϕ_B^I/ϕ_B, where ϕ_B^I is the volume fraction of bulk-like water in the cross-linked film. By using the values found in Tables I and II for P_T^{II} and D_B, 0.15 for ϕ_B^I, 0.228 for ϕ_B, and 0.85 for ϕ_A, the total permeability for a film containing 0.75 mole % cross-linker is calculated to be 6.45×10^{-7} cm²/sec. This value is in good agreement with the experimental value of 5.64×10^{-7} cm²/sec (2).

A theoretical treatment of solute permeability in hydrated polymer films was developed by Yasuda *et al.* (15). This treatment examines solute diffusion as a function of the free volume of the water–polymer system and predicts a linear correlation for plots of ln (D/D_0) *versus* the square of the cross-sectional solute radius; D is the diffusion coefficient in the polymer film and D_0 is the diffusion coefficient in bulk water. All solutes should correlate with a single straight line for a given polymer film provided the free volumes accessible to the various solutes are equal or can be resolved into equivalent contributions.

Wisniewski and Kim (6) examined the permeabilities of ions and various other hydrophilic solutes in Film I-type hydrogels. A plot of ln (D/D_0) *versus* the square of the cross-sectional radius was linear, with partition coefficients approximately equivalent to the volume fraction of bulk-like water in the film. This information suggested (6) that these solutes are restricted to permeation through the free volume of bulk-like water that is located in the B-type domains proposed in the present study. The D_B values obtained in the present study represent the diffusion coefficients of hydrophobic steroids in the bulk-like water and, therefore, should correlate with the previous data (6). The values of ln (D_B/D_0) are given in Table II. The D_0 values were calculated by a literature method (16).

Lacey and Cowsar (17) showed that the minimal cross-sectional area for steroids of the type investigated in the present study is about 36 Å². When using this value to determine the minimal cross-sectional radius, a value of −2.7 for ln (D_B/D_0) is required for an exact correlation with the data of Wisniewski and Kim (6). The data given in Table II are, in general, somewhat more positive than this value. Thus, as with the comparison with the K_d values in Films I and II discussed previously, the model presented here fits the expected value qualitatively but not quantitatively. The somewhat larger values of ln (D_B/D_0) compared to the predicted value arise from D_B values that are too large. This result indicates that the model predicts a contribution from pore-type permeation that is too large. This discrepancy probably arises from the assumption that A-type domains have similar permeation characteristics in Films I and II. The A domains are probably more permeable in Film I due to a lower cross-link density, leading to increased values for $\phi_A P_T^{II}$. Therefore, the observed deviations are in the right direction.

Table III—Functional Group Contributions to Diffusivity

Pair	Functional Group Changes		Relative Molecular Volume	Relative Diffusivity Factor
1	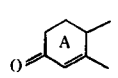 Nandrolone	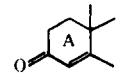 Testosterone	1.09	0.78
2	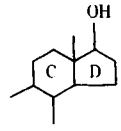 Nandrolone	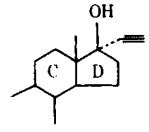 Norethindrone	1.16	0.63
3	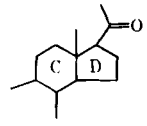 Progesterone	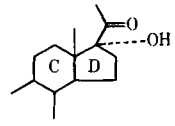 17α-Hydroxyprogesterone	1.01	1.37
4	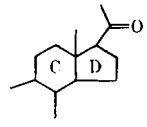 Progesterone	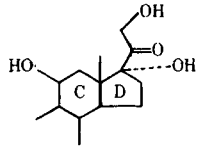 Hydrocortisone	1.01	1.59
5	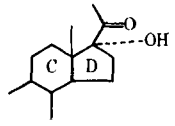 17α-Hydroxyprogesterone	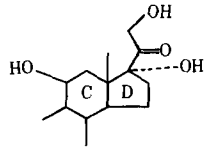 Hydrocortisone	1.01	1.16
6	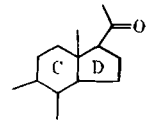 Progesterone	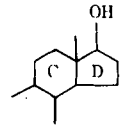 Testosterone	0.88	2.41
7	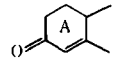 Nandrolone	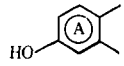 Estradiol	0.99	0.35

Effect of Steroid Structure on Permeation through Hydrogel Films—Previous work (1, 2, 18–23) demonstrated that hydrogels are excellent candidates for use in controlled-release drug delivery systems. The major advantages of these polymers for this purpose are biocompatibility (24, 25) and the potential for controlling permeation characteristics through modifications in the hydrogel composition. Several studies using hydrophobic (2) and hydrophilic (4, 5, 20, 21) solutes indicated that permeability coefficients can be varied by more than an order of magnitude by changing either the cross-link density or the monomer composition.

Several studies (6, 26) demonstrated effects of molecular structure on solute permeation in films prepared without added cross-linker. The importance of the solute molecular volume on the permeation characteristics has been demonstrated. However, no studies have considered the effects of molecular structure on permeability in films containing high cross-linker concentrations. Studies on the permeation characteristics of these films are of interest since intermolecular interactions between the solute and polymer segments are expected to increase and should dominate the overall permeability of these films.

For poly(dimethyl siloxane), a film in which solutes permeate by the solution-diffusion mechanism, small changes in steroidal structure can lead to variations in the diffusion coefficients of more than two orders of magnitude (17). These dramatic changes in the diffusion coefficients in the solution-diffusion-type poly(dimethyl siloxane) films are not observed with Film II, a solution-diffusion-type hydrogel. Changes in permeability coefficients are even less, indicating the importance of solute partitioning in the overall film permeation characteristics. Specific effects of solute structure on the diffusion coefficients in Film II are demonstrated more clearly by the comparisons made in Table III. In this table, relative diffusivity factors, defined as the ratio of diffusion coefficients for steroids that differ by one structural feature, have been calculated. From the results in this table, the following conclusions were obtained:

1. The addition of a C-19 angular methyl group decreases diffusivity by a small factor (0.78) due to steric hindrance (relative K_d values are independent of cross-linker content).
2. The same effect is seen on the addition of a C-17 ethynyl group, where diffusivity decreases by a factor of 0.63.
3. The addition of hydroxyl groups increases diffusivity by rather substantial factors, as seen from Comparisons 3–6 in Table III. However, the effect of the first hydroxyl group is proportionately greater than the second and third hydroxyl groups (Table III, Comparisons 3 and 5).
4. Changing the A ring of the steroid nucleus from an alicyclic (nandrolone) to an aromatic (estradiol) ring produces a decrease in diffusivity by a factor of 0.35. This decrease occurs in spite of the change from a keto to a hydroxy function at the 3-position of the steroid nucleus, which should increase diffusivity (Table III, Comparison 6).

The outlined group contributions to diffusivity should be valuable in predicting approximate diffusion coefficients for other steroids. For example, the diffusion coefficient of testosterone may be approximated as follows. Beginning with progesterone, the effect of removing the side chain at C-17 may be approximated by a factor of 1/0.63 (*i.e.*, the inverse of the effect noted for the addition of a C-17 ethynyl group to nandrolone) times a factor of 1.37 (the effect of the addition of a C-17 hydroxyl group to progesterone). The result of this calculation gives 2.42×10^{-9} cm^2/sec for the diffusion coefficient of testosterone in Film II, a result that compares favorably with the experimental value of 2.70×10^{-9} cm^2/sec.

CONCLUSIONS

Steroid permeation in poly(hydroxyethyl methacrylate) films is complex. However, to a first approximation, the total observed permeability can be separated into pore and solution-diffusion components by applying a model describing the polymer films in terms of domains. Such an analysis supports the contentions of Film I being a pore-type and Film II being a solution-diffusion-type barrier for both hydrophilic and hydrophobic solutes.

As expected from the inherent nature of solution-diffusion permeation, structural alterations in steroidal solutes affect diffusion. Decreases in molecular volume and increases in hydrogen bonding capacity increase diffusivity. By quantifying these effects for specific functional groups, it is possible to predict diffusion coefficients.

APPENDIX

When a linear concentration gradient exists within a barrier film, the instantaneous concentration gradient within the film may be expressed as:

$$-\frac{dC}{dl} = \frac{C_I' - C_{II}'}{l} \qquad \text{(Eq. A1)}$$

where C_I' and C_{II}' represent the surface concentrations of the diffusant in the membrane at the donor (I) and receptor (II) sides of the film and l represents the thickness of the film. Provided that the partition coefficient, K_d, is independent of the solute concentration, this equation may be rewritten as:

$$-\frac{dC}{dl} = \frac{K_d(C_I - C_{II})}{l} \qquad \text{(Eq. A2)}$$

where C_I and C_{II} are the donor and receptor phase concentrations, respectively. The flux of solute within the film can be described by Fick's first law as:

$$J = -D\frac{dC}{dl} = -D\frac{(C_I' - C_{II}')}{l} \qquad \text{(Eq. A3)}$$

which can be rewritten as:

$$J = \frac{DK_d}{l}(C_I - C_{II}) = \frac{U}{l}(C_I - C_{II}) \qquad \text{(Eq. A4)}$$

where the permeability $U = DK_d$.

During steady state, the flux out of Compartment I equals the flux into Compartment II, which also equals the flux within the film barrier. This may be expressed as:

$$-J = \frac{V}{A}\frac{dC_I}{dt} \qquad \text{(Eq. A5)}$$

and:

$$J = \frac{V}{A}\frac{dC_{II}}{dt} \qquad \text{(Eq. A6)}$$

where V is the compartment volume and A is the film area. Subtracting Eq. A6 from Eq. A5 and equating to Eq. A4 give:

$$\frac{d(C_I - C_{II})}{dt} = -\frac{2UA}{lV}(C_I - C_{II}) \qquad \text{(Eq. A7)}$$

Equation A7 is valid only during steady-state flux. Under these conditions, the concentrations of solute in Compartments I and II are C_1 and C_2 at t_{oss} (onset of steady state) and C_3 and C_4 at t_{ss} (any time during steady state). When using these concentrations and times for the limits of integration, Eq. A7 gives:

$$\ln\left\{\frac{C_3 - C_4}{C_1 - C_2}\right\} = \frac{-2UA}{lV}(t_{ss} - t_{oss}) \qquad \text{(Eq. A8)}$$

Steady-state mass balance gives:

$$C_0V = C_1V + C_2V + C_mV_m \qquad \text{(Eq. A9)}$$

$$C_0V = C_3V + C_4V + C_mV_m \qquad \text{(Eq. A10)}$$

where C_0 is the initial concentration in the donor phase, C_m is the solute concentration within the film, and V_m is the film volume. The film concentration may be defined as:

$$C_m = K_d\frac{(C_1 + C_2)}{2} = K_d\frac{(C_3 + C_4)}{2} \qquad \text{(Eq. A11)}$$

Substitution of Eq. A11 into Eqs. A9 and A10 and rearranging give:

$$C_1 = \frac{2}{2V + K_dV_m}\left(C_0V - C_2V - \frac{K_dC_2V_m}{2}\right) \qquad \text{(Eq. A12)}$$

and:

$$C_3 = \frac{2}{2V + K_dV_m}\left(C_0V - C_4V - \frac{K_dC_4V_m}{2}\right) \qquad \text{(Eq. A13)}$$

Substituting Eqs. A12 and A13 into Eq. A8 and rearranging give:

$$\ln\left\{\frac{C_0V - (2V + K_dV_m)C_4}{C_0V - (2V + K_dV_m)C_2}\right\} = -\frac{2UA}{lV}(t_{ss} - t_{oss}) \qquad \text{(Eq. A14)}$$

In the limit where K_d is small and t_{oss} approaches zero, C_2 also approaches zero and Eq. A14 may be written as:

$$\ln\left\{1 - \frac{2C_4}{C_0}\right\} = -\frac{2UAt}{lV} \qquad \text{(Eq. A15)}$$

Equation A15 was developed (9) for the case of quasi-steady-state diffusion in a film, assuming that the amount of solute in the film is negligible.

REFERENCES

(1) G. M. Zentner, J. R. Cardinal, and S. W. Kim, *J. Pharm. Sci.*, **67**, 1347 (1978).

(2) *Ibid.*, **67**, 1352 (1978).

(3) H. Yasuda, C. E. Lamaze, and A. Peterlin, *J. Polym. Sci., Part A-2*, **9**, 1117 (1971).

(4) R. Y. S. Chen, *Polym. Preprints*, **15** (2), 387 (1974).

(5) S. J. Wisniewski, D. E. Gregonis, S. W. Kim, and J. D. Andrade, in "Hydrogels for Medical and Related Applications," J. D. Andrade, Ed., American Chemical Society Symposium Series 31, 1976, p. 80.

(6) S. J. Wisniewski and S. W. Kim, "Abstracts of 25th Meeting of Academy of Pharmaceutical Sciences," American Pharmaceutical Association, Washington, D.C., 1978.

(7) G. A. Mortimer, *J. Org. Chem.*, **30**, 1632 (1964).

(8) G. M. Zentner, J. R. Cardinal, and D. E. Gregonis, *J. Pharm. Sci.*, **68**, 794 (1979).

(9) G. L. Flynn, S. H. Yalkowsky, and T. J. Roseman, *ibid.*, **63**, 479 (1974).

(10) M. F. Refojo, *J. Polym. Sci., Part A-1*, **5**, 3103 (1967).

(11) H. Yasuda, C. E. Lamaze, and L. D. Ikenberry, *Makromol. Chem.*, **118**, 19 (1968).

(12) M. S. Jhon and J. D. Andrade, *J. Biomed. Mater. Res.*, **7**, 509 (1973).

(13) R. J. Scheuplein, *Biophys. J.*, **6**, 1 (1966).

(14) Y. K. Sung, Ph.D. thesis, University of Utah, Salt Lake City, Utah, 1978.

(15) H. Yasuda, A. Peterlin, C. K. Colton, K. A. Smith, and E. W. Merrill, *Makromol. Chem.*, **126**, 177 (1969).

(16) C. R. Wilke and P. Chang, *Am. Inst. Chem. Eng.*, **1**, 264 (1955).

(17) R. E. Lacey and D. R. Cowsar, *Adv. Exp. Med. Biol.*, **47**, 117 (1974).

(18) M. Tollar, M. Stol, and K. Kliment, *J. Biomed. Mater. Res.*, **3**, 305 (1969).

(19) V. Majkus, F. Horakova, F. Vymola, and M. Stol, *ibid.*, **3**, 443 (1969).

(20) J. M. Anderson, T. Koinis, T. Nelson, M. Horst, and D. S. Love, in "Hydrogels for Medical and Related Applications," J. D. Andrade, Ed., American Chemical Society Symposium Series 31, 1976, p. 167.

(21) D. R. Cowsar, O. R. Tarwater, and A. C. Tanquary, in *ibid.*, p. 180.

(22) J. Drobnik, P. Spacek, and O. Wichterle, *J. Biomed. Mater. Res.*, **8**, 45 (1974).

(23) R. A. Abrahams and S. H. Ronel, *ibid.*, **9**, 355 (1975).

(24) J. D. Andrade, *Med. Instrum.*, **1**, 110 (1973).

(25) B. D. Ratner and A. S. Hoffman, in "Hydrogels for Medical and Related Applications," J. D. Andrade, Ed., American Chemical Society Symposium Series 31, 1976, p. 1.

(26) K. H. Lee, J. G. Lee, M. S. Jhon, and T. Ree, *J. Bioeng.*, **2**, 269 (1978).

ACKNOWLEDGMENTS

Presented in part at the APhA Academy of Pharmaceutical Sciences, Hollywood, Fla., meeting, November 1978.

Supported by NIH Grant HD-09791-03.

The authors thank Dr. S. W. Kim, Dr. D. E. Gregonis, and Dr. J. D. Andrade for their contributions to this work.

Simple Field Test for Marijuana

C. A. LAU-CAM ˣ and V. PIZZITOLA

Received October 30, 1978, from the *Department of Pharmaceutical Sciences, College of Pharmacy and Allied Health Professions, St. John's University, Jamaica, NY 11439.* Accepted for publication February 2, 1979.

Abstract □ A simple, rapid, sensitive, and specific field test for marijuana and its products is described. The test employs an extracting-eluting solvent and an inert adsorbent microcolumn coated with Fast Blue B salt as the reagent. One milligram or less of the suspect material can be tested within 1 min. Of >80 nonmarijuana plant samples tested, only nutmeg and its mace responded similarly to marijuana initially. A differentiation was possible by careful evaluation of the colored microcolumn and of the elution behavior of the colored products. The test also provides for a confirmatory step, based on spectrophotometric analysis of the colored eluates. The reagent microcolumn was very stable to environmental factors such as moisture, light, and air.

Keyphrases □ Marijuana—analysis, microcolumn, field test, compared to other plant substances □ Chromatography, microcolumn—analysis, marijuana, field test, compared to other plant substances

With the recent relaxation of the laws governing marijuana use and possession in several states, the illicit market will increase. Consequently, there is a pressing need for a field test that will enable law enforcement agents, custom officers, and other responsible personnel readily to obtain presumptive evidence on suspected sample identity.

BACKGROUND

Fast Blue B salt (3,3'-dimethoxybiphenyl-4,4'-bis-diazonium chloride) is probably the most widely used reagent for marijuana detection and identification. In addition to high sensitivity and characteristic chromogenic reaction with several cannabinoids, Fast Blue B also is reasonably selective for these substances. Its low cost and ready availability further contribute to its popularity.

Marijuana samples were field tested on pieces of filter paper by means of a solid Fast Blue B reagent (1, 2). Although quite specific, this method requires special precautions in reagent preparation, reaction performance, and interpretation of results (1, 3). A very specific field test for hashish was reported, which utilized a suspension of Fast Blue B in chloroform in conjunction with aqueous sodium hydroxide (4). However, this method requires a large apparatus and two liquid reagents.

A "breathanalyzer" for the breath analysis of marijuana smokers was described (5). The suspect was required to breathe onto pieces of filter paper or tissue freshly dampened with aqueous Fast Blue B. The reagent was unstable, and the color response was slow. Hashish also was detected with filter paper strips pretreated with methanolic Fast Blue B (6). The reagent papers were unstable and decreased in sensitivity upon long storage (3, 6).

This paper describes a marijuana field test that circumvents many problems encountered with existing procedures. In addition to using a stable Fast Blue B color reagent, it requires few steps, one liquid reagent, and little apparatus. The test capability to differentiate false-positive responses also was investigated.

EXPERIMENTAL

Reagents—Fast Blue B salt[1], neutral alumina for chromatography[2], analytical reagent grade solvents[2] (petroleum ether, bp 60–90°; methanol; and chloroform), collodion USP[2], and microcrystalline cellulose[3] were used as obtained from commercial sources.

Apparatus—Spectrophotometric curves were recorded using 1-cm semimicro quartz cells on a double-beam recording spectrophotometer[4] equipped with a digital readout accessory and a strip-chart recorder.

Reagent Preparation—Neutral alumina–microcrystalline cellulose (3:1) was intimately mixed by manual stirring and bottle tumbling. For every 12 g of this mixture, a suspension of 0.2 g of Fast Blue B salt in 25 ml of chloroform was added with stirring. The smooth slurry was transferred to a large glass petri dish and allowed to air dry inside a hood. The dry residue was homogenized to a fine powder and stored in an amber glass container.

Microcolumn Preparation—A small glass wool or absorbent cotton pledget was placed at the bottom of a glass tube (3 × 0.7 cm), approximately 3 mm away from one end. Small portions of the reagent were introduced into the tube with gentle tapping until an ~2-cm high column was obtained. The upper end of this column was closed with another glass wool or cotton pledget. A 1-cm space remained over the packed reagent column. Both ends of the glass tube were sealed by immersion into collodion followed by air drying.

The microcolumns were stored in an amber glass container.

Extracting-Eluting Solvent Preparation—Isopropanol, 10 ml, was added, with stirring, to 80 ml of petroleum ether, bp 60–90°, and 20 ml of anhydrous methanol. The solution was stored in a dropping bottle.

Field Test—The collodion seals were removed from both ends of a microcolumn. A small amount of suspect material, preferably powdered, was layered ~2 mm high on top of the microcolumn. The extracting-eluting solvent was added dropwise until the liquid reached the bottom of the microcolumn. The color that developed along the microcolumn within 1 min was recorded. A red, purple-red, or burgundy-red color, deepening with time and rapidly spreading downward, was interpreted as a positive test.

Differential Test—To a still wet or to a dry colored microcolumn, sufficient extracting-eluting solvent was added until the colored product emerged at the lower end of the tube and could be collected. A rapidly eluting red, purple-red, or burgundy-red liquid signified a positive test.

Spectral Analysis—The colored eluate from the differential step was transferred to a semimicro spectrophotometric cell, and its visible absorption spectrum was recorded against the extracting-eluting solvent serving as the blank. If the eluate separated into two phases, the addition of 1–2 drops of chloroform reestablished the single phase.

RESULTS AND DISCUSSION

Microcolumn—Several common chromatographic support media were tested for suitability in the microcolumn preparation. Among those investigated were microcrystalline cellulose, infusorial earth, neutral alumina, silica gel, nylon, and methylcellulose. Selection criteria were: (*a*) inertness toward Fast Blue B, (*b*) rate at which solvents such as petroleum ether, chloroform, and petroleum ether–methanol eluted when

Table I—Samples Tested

Part Tested	Name
Bark	*Cascara sagrada*, cinchona, cinnamon, quassia, sassafras, wild cherry
Fruit	Anise, black pepper, capsicum, caraway, cardamom, coriander, fennel, juniper, paprika, star anise
Leaf	Basil, belladonna, boldo, buchu, catnip, digitalis, eucalyptus, hamamelis, henna, hyoscyamus, jaborandi, marijuana (Mexican, New York), oregano, parsley, rosemary, rumex, sage, savory, senna, spearmint, stramonium
Root, rhizome	Aconite, aspidium, belladonna, gentian, ginger, golden seal, hellebore (American), ipecac, jalap, licorice, orris, rauwolfia, rhubarb, rumex, sarsaparilla
Seed	Betel, cacao, coffee (decaffeinated, ground, instant), colchicum, cumin, kola, mace, mustard (black), nutmeg, *Nux vomica*, strophanthus
Miscellaneous	Aloe, clove, curry, ergot, gum benzoin, gum kino, gum myrrh, nutgall, squill, tolu, turmeric

[1] Sigma Chemical Co., St. Louis, Mo.
[2] J. T. Baker Chemical Co., Phillipsburg, N.J.
[3] Avicel PH-105, FMC Corp., Newark, Del.
[4] Model DB-GT, Beckman Instruments, Fullerton, Calif.

0022-3549/79/0800-0976$01.00/0
© 1979, American Pharmaceutical Association

Table II—Differentiation of Samples Giving Similar Colors in the Field Test

Sample	Color on Microcolumn	Characteristics of Colored Product	Absorption Maxima, nm[a]
Marijuana	Red to burgundy red	Elutes very rapidly, red eluate	295 (300, 305), 475
Mace	Red to burgundy red	Remains at top of microcolumn, beige to light-orange eluate	343 (330), 390 (sh), 485 (490) (sh)[b]
Nutmeg	Red to burgundy red	Remains at top of microcolumn, beige to light-orange eluate	340, 390 (400) (sh), 485 (490) (sh)[b]
Coffee, decaffeinated	Lavender to light violet	Elutes very rapidly, lavender to light-violet eluate	335, 425 (sh), 480 (sh)
Coffee, ground	Lavender to light violet	Elutes very rapidly, lavender to light-violet eluate	313, 335 (sh), 485
Cascara sagrada	Red	Remains at top of microcolumn, yellow to greenish-yellow eluate	Not recorded
Rhubarb	Red	Remains at top of microcolumn, yellow eluate	Not recorded

[a] Values in parentheses indicate absorption maxima recorded for a different sample. [b] Eluted with chloroform–methanol (7:3)

Table III—Absorption Maxima of Fast Blue B–Marijuana and Fast Blue B–Cannabinoid Colored Products

Sample[a]	Absorption Maxima, nm[b]
Marijuana	295 (300, 305), 475
I	298 (300), 450 (465)
II	292 (295), 500 (495)
III	295, 460
I + II + III (1:1:1)	295, 475
I + II (2:1)	307, 480
I + II (1:2)	300 (305), 467 (470)
I + III (1:1)	306, 465
II + III (1:1)	298 (305), 490 (492)

[a] Values in parentheses indicate approximate ratios in the mixture. [b] Values in parentheses indicate absorption maxima recorded for a different sample.

passed through a microcolumn, (*c*) ease of handling and packing, and (*d*) provision of contrasting background for the color reaction interpretation.

Neutral alumina best fulfilled the requirements. However, to promote a better interaction between the cannabinoids contained in the mobile phase and the Fast Blue B present on the microcolumn, the elution rate was decreased by admixing the alumina with microcrystalline cellulose (3:1).

Extracting-Eluting Solvent—The solvents investigated were those commonly used for cannabinoid extraction from marijuana samples, *i.e.*, petroleum ether, chloroform, benzene, and toluene. None of these solvents by themselves produced a color reaction following incorporation into a microcolumn loaded with marijuana, probably due to the insolubility of the Fast Blue B in the liquid phase. Addition of a small amount of methanol to the solvents brought about azo dye solubilization and interaction with the cannabinoids. Based on cost, organoleptic properties, and human safety, petroleum ether was the most satisfactory solvent. Furthermore, mixtures of methanol with chloroform, benzene, and toluene were less selective in extracting exclusively cannabinoids than were the corresponding mixtures with petroleum ether.

Petroleum ethers of bp 30–75°, 60–90°, and 90–120° were admixed with methanol in 9:1, 8:2, and 7:3 (v/v) ratios, respectively. A 9:1 ratio was inadequate in producing readily discernible marijuana color reactions. A 7:3 ratio yielded the strongest colors but at the same time produced more false-positive reactions with samples other than marijuana. Of the three petroleum ethers, the lower boiling solvent was the only one completely miscible with methanol in the stated ratios; those with higher boiling points gave a two-phase system. The former, however, occasionally separated from methanol upon storage. The possibility that the field test would be carried out in hot climates also discouraged further testing of this type of petroleum ether.

Perfect and stable solutions of methanol in petroleum ether of bp 60–90 or 90–120° in an 8:2 ratio could be obtained by the addition of a small quantity of isopropanol. Petroleum ether (bp 60–90°)–methanol–isopropanol (8:2:1) was preferred over a similar combination containing petroleum ether of bp 90–120°, because the former was more compatible with methanol. Mixtures of any of these two petroleum ethers with the alcohols in a 7:3:1 ratio invariably separated into two phases upon storage. On the other hand, combinations of all three types of petroleum ether with isopropanol in 9:1, 8:2, and 7:3 ratios did not produce distinguishable color reactions.

Test Selectivity—Table I lists the plant samples tested by the proposed field test. A positive reaction was when red, purple-red, or burgundy-red zones developed almost immediately at the top of the microcolumn and, on further addition of extracting–eluting solvent, rapidly moved downward as a red band. Of the >80 samples investigated, only those listed in Table II were initially confused with marijuana, but they were ultimately differentiated by careful evaluation of the colored microcolumn characteristics. For example, nutmeg and its mace gave red zones in a hue almost identical with those obtained for marijuana samples. Nevertheless, on repeated addition of the extracting–eluting solvent mixture, the colored products barely moved downward and the eluate emerging at the other end was colored light brown to light orange.

Rhubarb and *Cascara sagrada* also yielded red bands, even when Fast Blue B was absent from the microcolumn, due to extraction of certain red to brown-red constituents by the mobile phase. Their eluates were usually yellow to greenish yellow in contrast to the red tones recorded for marijuana. Various ground and instant coffees gave lavender to light-violet zones, which could be eluted rapidly out of the microcolumn as lavender to light-violet solutions.

Spectrophotometric Analysis—When a more conclusive identification of the field-tested material is needed, a confirmatory step may be added. The colored product may be eluted into a spectrophotometric cell, and the visible absorption spectrum may be recorded. Tables II and III summarize the spectral characteristics of those samples submitted to the spectrophotometric analysis. Marijuana samples typically exhibited two absorption maxima, at ~300 and ~475 nm. Entirely different spectral patterns were recorded for coffee, nutmeg, and mace, which initially approximated the marijuana chromogenic response.

The absorption spectra of the three main cannabinoids, *i.e.*, cannabi-

Table IV—Comparison of Various Field Tests for Marijuana Using Fast Blue B Salt

Characteristic	de Faubert Maunder (Refs. 1 and 2)	Watanabe (Ref. 4)	Woodhouse (Ref. 6)	McCarthy and van Zyl (Ref. 5)	Proposed
Number of reagents	3	2	3	1	2
Number of liquid reagents	2	2	2	1	1
Steps required:					
Extraction	+	+	+	–	+
Filtration	+	–	–	–	–
Addition of color reagent	+	–	–	–	–
Addition of alkali	+	+	+	–	–
Differential step	None	None	None	None	Included
Interferences reported	2	None	Several	None	None
Stability of Fast Blue B reagent	Stable	Stable	Unstable	Unstable	Stable

diol (I), cannabinol (II), and tetrahydrocannabinol (II), demonstrated that the marijuana absorption curve was primarily contributed by a combination of these three substances (Table III) rather than by any single cannabinoid or cannabinoid pair. The fact that these constituents occur only in marijuana confers high specificity and diagnostic value on the spectrophotometric analysis.

Test Comparison—Table IV compares the proposed field test with those reported in the literature in terms of reagent requirements, steps involved, and reported interferences.

CONCLUSIONS

The proposed field test was rapid, simple, sensitive and selective. It required only one liquid reagent, which served as the extracting-eluting solvent. Color development and sample extraction were accomplished simultaneously. Colors appeared almost immediately and were easy to interpret against the white background of the microcolumn. The use of a dry absorbent such as alumina offered several advantages since it acted as a diluent for the color reagent and as a medium for the color reaction, and, more importantly, provided a means for differentiating marijuana from other plant materials such as nutmeg and its mace, rhubarb, and *C. sagrada*, whose colored products remained tightly adsorbed to the microcolumn and were not eluted by petroleum ether–methanol mixtures.

The dry microcolumn formulation of Fast Blue B resulted in a reagent that remained stable to ambient conditions such as light and air for periods over 6 months. Since both ends of the glass tube enclosing the microcolumn could be sealed with collodion, adverse effects from moisture, air, and contaminated atmospheres were avoided. The inclusion of differential and confirmatory steps improved the test from a simply presumptive one to a tool with diagnostic capability. None of the plant samples tested by this procedure was confused with marijuana.

REFERENCES

(1) M. J. de Faubert Maunder, *J. Assoc. Public Anal.*, **7**, 24 (1969).

(2) M. J. de Faubert Maunder, *Bull. Narc.*, **21**, 37 (1969).

(3) *Ibid.*, **26**, 19 (1974).

(4) K. Watanabe, *Eisei Kagaku*, **16**, 101 (1970); through *Chem. Abstr.*, **73**, 69772 (1970).

(5) T. J. McCarthy and J. D. van Zyl, *J. Pharm. Pharmacol.*, **24**, 489 (1972).

(6) E. J. Woodhouse, Tech. Rep. LWL-CR-08072, Midwest Research Institute, Kansas City, Mo., 1972.

ACKNOWLEDGMENTS

Presented at the Natural Products Section, APhA Academy of Pharmaceutical Sciences, Montreal meeting, May 1978.

Metabolic Performance and GI Function in Magnesium-Deficient Rats

WENDELL E. LANDIN, FRANCIS M. KENDALL, and MARTIN F. TANSY ˣ

Received January 5, 1979, from the *Department of Physiology and Biophysics, Temple University, Philadelphia, PA 19140.* Accepted for publication February 6, 1979.

Abstract □ A quantitative evaluation of the mass balance and GI motor effects of dietary magnesium deficiency in the adult male Sprague–Dawley rat is described. Seventy-seven animals were used. Both sham control and experimental groups were maintained on a commercial stock laboratory diet *ad libitum* for 30 days, after which the experimental rats were switched for 30 days to the magnesium-deficient diet *ad libitum*, containing a magnesium concentration of 16.2 ppm. Ten rats were used to determine the acetylcholine responsiveness of duodenal muscle segments *in vitro*. In all cases, the segments from the deficient rats were hyperresponsive to a fixed acetylcholine dose. Forty-six rats were used to determine the average intestinal transit rate, which increased significantly in 30-day magnesium-deficient rats. A final series employed 21 rats who were housed in individual metabolic cages. After 5 days on the deficient diet, the average daily fecal pellet counts and fecal weights were significantly reduced. It is concluded that chronic magnesium deficiency is associated with altered GI motor function in the adult male rat.

Keyphrases □ Magnesium deficiency—GI motility, metabolism, rats □ GI tract—magnesium deficiency, motility, metabolism, rats □ Nutritional disorders—magnesium deficiency, GI motility, metabolism, rats

With few exceptions, most of the existing literature concerning the effects of chronic magnesium deficiency in the rat considers the GI tract only as a defective intake route: magnesium deficiency resulting from malabsorption, failure of magnesium conservation in the gut, and loss of fluid and ions *via* the intestines.

Curiously, the effect of magnesium deficiency on the functioning of the GI tract itself was not considered until the motor effects from exposure of the small intestines of rats (1) and humans (2–4) to ionizing radiation were significantly associated with hypomagnesemia. The data also indicated that prophylactic administration of soluble magnesium salts prior to exposure had a mitigating effect in both cases. These observations led to the proposal that the GI symptomatology defined by the acute intestinal radiation syndrome in the rat was the result of acute hypomagnesemia (5, 6).

Another interesting relationship is that between magnesium deficiency and the GI secretory apparatus. The effect of magnesium on gastric structure and function has received some attention, but reported results have been inconsistent. Recent observations (7) showed that dietary magnesium deficiency in rats alters the ratio of chief to parietal cells. Additional evidence (8) indicated that rats treated with parathyroid hormone for 2 weeks exhibited a reduced basal gastric acid secretory rate associated with nonspecific gastric mucosal damage. Veilleux (9) demonstrated that mast cells increase in the duodenum and kidney of magnesium-deficient rats. Unfortunately, these latter studies were not extended to the gastric mucosa. The foregoing results and the finding that the inhibition of calcium-induced acid secretion by magnesium may be caused by blockade of a calcium effect directly on the parietal cell (10) preclude any simple explanation of the effect of magnesium on gastric secretion.

Practically speaking, sufficient attention has not been directed to the effect of magnesium on the GI system. Therefore, the purpose of this study was to determine whether the GI motor functions of rats maintained on a magnesium-deficient diet were different from similar functions in control animals.

0022-3549/79/0800-0978$01.00/0

© 1979, American Pharmaceutical Association

diol (I), cannabinol (II), and tetrahydrocannabinol (II), demonstrated that the marijuana absorption curve was primarily contributed by a combination of these three substances (Table III) rather than by any single cannabinoid or cannabinoid pair. The fact that these constituents occur only in marijuana confers high specificity and diagnostic value on the spectrophotometric analysis.

Test Comparison—Table IV compares the proposed field test with those reported in the literature in terms of reagent requirements, steps involved, and reported interferences.

CONCLUSIONS

The proposed field test was rapid, simple, sensitive and selective. It required only one liquid reagent, which served as the extracting-eluting solvent. Color development and sample extraction were accomplished simultaneously. Colors appeared almost immediately and were easy to interpret against the white background of the microcolumn. The use of a dry absorbent such as alumina offered several advantages since it acted as a diluent for the color reagent and as a medium for the color reaction, and, more importantly, provided a means for differentiating marijuana from other plant materials such as nutmeg and its mace, rhubarb, and *C. sagrada*, whose colored products remained tightly adsorbed to the microcolumn and were not eluted by petroleum ether–methanol mixtures.

The dry microcolumn formulation of Fast Blue B resulted in a reagent that remained stable to ambient conditions such as light and air for periods over 6 months. Since both ends of the glass tube enclosing the microcolumn could be sealed with collodion, adverse effects from moisture, air, and contaminated atmospheres were avoided. The inclusion of differential and confirmatory steps improved the test from a simply presumptive one to a tool with diagnostic capability. None of the plant samples tested by this procedure was confused with marijuana.

REFERENCES

(1) M. J. de Faubert Maunder, *J. Assoc. Public Anal.*, **7**, 24 (1969).

(2) M. J. de Faubert Maunder, *Bull. Narc.*, **21**, 37 (1969).

(3) *Ibid.*, **26**, 19 (1974).

(4) K. Watanabe, *Eisei Kagaku*, **16**, 101 (1970); through *Chem. Abstr.*, **73**, 69772 (1970).

(5) T. J. McCarthy and J. D. van Zyl, *J. Pharm. Pharmacol.*, **24**, 489 (1972).

(6) E. J. Woodhouse, Tech. Rep. LWL-CR-08072, Midwest Research Institute, Kansas City, Mo., 1972.

ACKNOWLEDGMENTS

Presented at the Natural Products Section, APhA Academy of Pharmaceutical Sciences, Montreal meeting, May 1978.

Metabolic Performance and GI Function in Magnesium-Deficient Rats

WENDELL E. LANDIN, FRANCIS M. KENDALL, and MARTIN F. TANSY ˣ

Received January 5, 1979, from the *Department of Physiology and Biophysics, Temple University, Philadelphia, PA 19140.* Accepted for publication February 6, 1979.

Abstract □ A quantitative evaluation of the mass balance and GI motor effects of dietary magnesium deficiency in the adult male Sprague–Dawley rat is described. Seventy-seven animals were used. Both sham control and experimental groups were maintained on a commercial stock laboratory diet *ad libitum* for 30 days, after which the experimental rats were switched for 30 days to the magnesium-deficient diet *ad libitum*, containing a magnesium concentration of 16.2 ppm. Ten rats were used to determine the acetylcholine responsiveness of duodenal muscle segments *in vitro*. In all cases, the segments from the deficient rats were hyperresponsive to a fixed acetylcholine dose. Forty-six rats were used to determine the average intestinal transit rate, which increased significantly in 30-day magnesium-deficient rats. A final series employed 21 rats who were housed in individual metabolic cages. After 5 days on the deficient diet, the average daily fecal pellet counts and fecal weights were significantly reduced. It is concluded that chronic magnesium deficiency is associated with altered GI motor function in the adult male rat.

Keyphrases □ Magnesium deficiency—GI motility, metabolism, rats □ GI tract—magnesium deficiency, motility, metabolism, rats □ Nutritional disorders—magnesium deficiency, GI motility, metabolism, rats

With few exceptions, most of the existing literature concerning the effects of chronic magnesium deficiency in the rat considers the GI tract only as a defective intake route: magnesium deficiency resulting from malabsorption, failure of magnesium conservation in the gut, and loss of fluid and ions *via* the intestines.

Curiously, the effect of magnesium deficiency on the functioning of the GI tract itself was not considered until the motor effects from exposure of the small intestines of rats (1) and humans (2–4) to ionizing radiation were significantly associated with hypomagnesemia. The data also indicated that prophylactic administration of soluble magnesium salts prior to exposure had a mitigating effect in both cases. These observations led to the proposal that the GI symptomatology defined by the acute intestinal radiation syndrome in the rat was the result of acute hypomagnesemia (5, 6).

Another interesting relationship is that between magnesium deficiency and the GI secretory apparatus. The effect of magnesium on gastric structure and function has received some attention, but reported results have been inconsistent. Recent observations (7) showed that dietary magnesium deficiency in rats alters the ratio of chief to parietal cells. Additional evidence (8) indicated that rats treated with parathyroid hormone for 2 weeks exhibited a reduced basal gastric acid secretory rate associated with nonspecific gastric mucosal damage. Veilleux (9) demonstrated that mast cells increase in the duodenum and kidney of magnesium-deficient rats. Unfortunately, these latter studies were not extended to the gastric mucosa. The foregoing results and the finding that the inhibition of calcium-induced acid secretion by magnesium may be caused by blockade of a calcium effect directly on the parietal cell (10) preclude any simple explanation of the effect of magnesium on gastric secretion.

Practically speaking, sufficient attention has not been directed to the effect of magnesium on the GI system. Therefore, the purpose of this study was to determine whether the GI motor functions of rats maintained on a magnesium-deficient diet were different from similar functions in control animals.

0022-3549/79/0800-0978$01.00/0

© 1979, American Pharmaceutical Association

Table I—Composition of the Magnesium-Deficient Diet

Ingredient	Amount, g/kg
Casein	250
Corn oil	50
Cellulose fiber	50
Magnesium-free salt	49.23
Vitamin mixture[a]	20
DL-Methionine	2.99
Dextrose	572.94
Choline chloride	4.84

[a] Standard fortification mix. Produced by Bioserv Inc., Frenchtown, N.J.

EXPERIMENTAL

Animals—The Sprague–Dawley rat was chosen as the experimental animal because a large portion of the relevant literature employed this breed (7, 9, 10). To obviate variations due to body size and estrus stage, only adult male rats weighing 125–150 g were used. The rats were acclimatized in the laboratory for 7 or more days before use. They were kept two per cage in an air-conditioned room under constant temperature (22°) and light cycles and were fed pelleted stock laboratory diet and water *ad libitum*. Some rats were housed in colony cages accommodating six animals. When necessary, coprophagy was minimized by employing cages with wire mesh false bottoms.

Magnesium-Deficient Diet—The basal magnesium-deficient diet[1] (Table I) was assayed[2] to contain ~16.2 ppm of magnesium. The magnesium content of the stock diet was reported by the manufacturer to be 2400 ppm.

Gross Metabolic Behavior—The first series of experiments was designed to determine whether magnesium-deficient rats would show any significant differences in gross metabolic behavior. Twenty-one adult rats were divided into two groups: an experimental group of 11 rats fed the magnesium-deficient diet and a control group of 10 rats fed the stock laboratory diet. With a week of preliminary conditioning, both groups became adjusted to a small individual cage, to a water bottle, and to a pelleted ration.

Both groups were then placed in individual plastic metabolism cages[3] where they consumed individual rations of pelleted stock diet and tap water *ad libitum*. An additional 30 days was allowed for the rats to adjust to the metabolism cages. The experimental group was then switched to the magnesium-deficient diet.

All animals, identified by coded ears, were weighed daily. The unconsumed water and food and urine and feces were collected daily. Water was supplied *ad libitum*, and water intake was measured by recording the water bottle contents. Food intake was more difficult to determine because of spillage. Feeders with narrow openings that permitted only the snout to enter reduced spillage. Food spillage could be further minimized by not filling the attached food containers to maximum capacity.

The usual food supply was 40 g of pelletized chow and 100 ml of water. Both quantities were sufficient for >2 days. Daily food and water intake

Figure 1—*Gross appearance of magnesium-deficient rat.*

[1] Bioserv Inc., Frenchtown, N.J.
[2] Technological Resources, Camden, N.J.
[3] Econo cage 110 with chrome extenders and conventional urinary-fecal separators, Maryland Plastics, New York, N.Y.

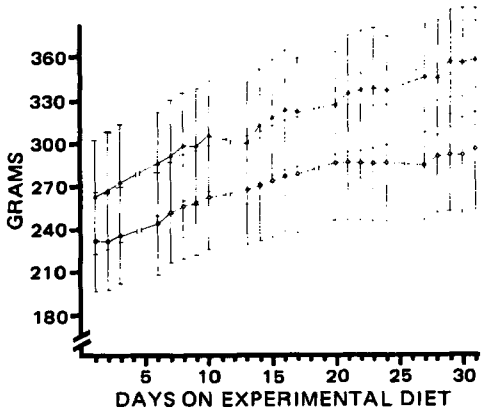

Figure 2—*Time courses of mean body weights from sham control* (▲) *and magnesium-deficient* (○) *rats.*

were determined by differences in the weights and volumes that were supplied the previous day. The collected feces from each animal were counted, weighed, and dried in an oven at 55° over 24 hr. The dry fecal weight was defined as net solid output. The loss in weight of the dry feces represented the fecal moisture weight. Net fluid output was obtained by adding the difference between wet and dry fecal weight in grams to the urine volume excreted in milliliters.

Corrected values for solid and fluid intake were made by subtracting a fixed percentage of the weight in grams of food consumed and directly adding this value to the volume of water consumed in milliliters. For such computations, the manufacturer of the magnesium-deficient diet specified the water content as being 6% by weight. The stock diet water content was 10.5% by weight. Utilization of these percentages and the requirement that weights in grams of water be numerically equal to volumes in milliliters at room temperature contributed to less absolute error than that produced by the inherent variability of the raw data collected.

***In Vitro* and *In Vivo* Intestinal Motor Activities**—The second series of experiments determined whether magnesium deficiency was associated with a change in overall small intestinal peristaltic activity in the rat. Two procedures were used. The classical contractile force measurement of isolated intestinal muscle segments in a tissue bath was used as a screening procedure. This measurement indicates muscular activity at a localized bowel region. The propulsive motility technique, which measures actual transit of intestinal contents over a given period, was used to assess overall small bowel activity.

The *in vitro* experiments were performed on 10 rats after 4 weeks on the diets. Each animal was fasted overnight. The animals were sacrificed by decapitation, followed quickly by the removal of 2–3-cm segments of the duodenum, jejunum, ileum, and descending colon. The responses of small and large intestinal segments to test drugs were recorded isometrically[4]. The particular segments were mounted in parallel in an isolated organ-tissue bath[5] with Tyrodes solution of the following composition (percent): NaCl, 0.8; KCl, 0.02; $CaCl_2$, 0.02; $MgCl_2$, 0.01; $NaHCO_3$, 0.1; NaH_2PO_4, 0.005; and glucose, 0.1. The solution was gassed with 95% oxygen and 5% carbon dioxide and maintained at 38 ± 1°. The pH of the solution varied between 7.4 and 7.6.

Comparison between the reactivity of two uneverted bowel segments was made simultaneously in parallel sets, with the respective segments mounted aborally from top to bottom in the bath chamber. The free proximal portion of the bowel segment was attached to a strain-gauge transducer, with the distal end fixed to the bottom of the bath. The bowel segment was attached by thread so that it was completely submerged in the Tyrodes solution, yet closed at each end so that the lumen was not bathed by the bath solution. No undue tension was applied to the segments during the mounting procedure.

System response amplitude was the measured variable and was always calibrated initially to the same value by means of an initial lever displacement, which was effected by hanging the same calibrating weight on each transducer system in turn. To avoid any differences due to the lever systems–transducers–polygraph channels, the two tested segments were alternated in successive experiments with the corresponding isometric lever force transducer and polygraph channel. The contraction height of the bowel segments after addition of fixed acetylcholine doses

[4] Grass polygraph, Grass Instrument Co., Quincy, Mass.
[5] Phipps and Bird, Richmond, Va.

Table II—Sham Control Regression Equations of Metabolic Performance as a Function of Time [a]

Variable	n	b	$\hat{Y}$	S_b	$S^2_{y \cdot x}$
Food intake					
Days 1–28	14	−0.046	11.42	0.0378	1.3821
Days 29–58	17	−0.084	11.34	0.0240	0.7822
Net water intake					
Days 1–28	14	−0.201	22.70	0.0633	3.8801
Days 29–58	17	−0.114	18.48	0.0404	2.2178
Number of fecal pellets					
Days 1–28	14	−0.836	42.12	0.0875	7.4153
Days 29–58	17	−0.307	27.74	0.0335	1.5212
Fecal wet weight					
Days 1–28	14	−0.021	6.613	0.0225	0.4013
Days 29–58	17	−0.095	8.613	0.0134	0.2460
Fecal dry weight					
Days 1–28	14	+0.033	2.44	0.0180	0.3134
Days 29–58	16	−0.046	4.35	0.0112	0.1599
Net fluid output					
Days 1–28	14	−0.053	11.69	0.0437	1.8437
Days 29–58	16	−0.1041	12.23	0.0129	0.2119

[a] n = number of observations, b = sample regression coefficient, $\hat{Y}$ = zero intercept, S_b = sample standard deviation, and $S^2_{y \cdot x}$ = mean square deviation from regression.

was taken as a measure of the segment's responsiveness. After the segment had contracted in response to acetylcholine, the medium was rinsed once or twice and replaced with fresh Tyrodes. After such procedures, the preparation was allowed to equilibrate for a few minutes before further stimulant was added.

All contraction measurements refer to maximum contraction amplitude observed on the polygram within a few seconds of drug addition to the bath. Acetylcholine was prepared immediately before use by dilution with the same physiological solution used in the bath and was added directly into the bath.

Intestinal transit measurement was made by the procedure of Macht as cited by VanLiere *et al.* (11). Briefly, 1 ml of a standard test meal, consisting of 10% charcoal suspended in an aqueous solution of 10% gum acacia, was fed by intragastric tube to 19, 48-hr fasted magnesium-deficient rats and 27 comparably fasted sham controls. The experimental rats, which had been fed the deficient diet for 30 days, were killed by decapitation in groups of 10 and 9 at 15 and 30 min, respectively, following intubation. The sham control groups for the 15- and 30-min intervals consisted of 13 and 14 rats, respectively.

Following sacrifice, the stomach and intestines were removed. The total small intestine length from pylorus to cecum was measured. The net distance that the charcoal had traversed from the pylorus was measured at the same time. Transit was defined as the distance traversed divided by the total intestine length.

Histopathology—Complete necropsies were done on sacrificed animals. The entire visceral contents were inspected visually to determine the presence of such obvious pathology as focal or generalized lesions and hemorrhage. The following organs and tissues were subjected to microscopic examination: stomach, representative segments of the small and large intestines, liver, heart, kidneys, and skeletal muscle from the thigh. Tissue samples were fixed in formaldehyde solution and embedded in paraffin. Sections were cut at 6 μm and stained with hematoxylin–eosin for routine histopathologic examination. All microscopic examinations were on a blind basis.

Reduction of Data and Interpretation of Results—All recorded values for the metabolic performance studies were normalized to 100 g of body weight to reduce the variations caused by differences in weights. The daily mean of the individual normalized values for each variable studied was plotted for the sham control and experimental groups, and least-squares linear regression lines were fitted through the points. Then, a pooled variances t test of the difference between regression coefficients was performed. This test only allows a determination of the significance of differences between average rates of change of metabolic performance; but if the difference between the rates is significant, it can be assumed that the metabolic performances of the two groups with respect to the variable being studied are not the same.

An F test to check for homogeneity of variance between the two least-squares lines to be compared was performed utilizing the mean square deviation from regression ($S^2_{y \cdot x}$) for each group. The appropriate degrees of freedom associated with each $S^2_{y \cdot x}$ are $n - 2$. If variance homogeneity could be assumed, the following pooled variances t test was used to compare the two regression coefficients:

$$t = \frac{b_1 - b_2}{\sqrt{S^2_{y \cdot x_{pooled}} \left(\frac{1}{S_{y \cdot x_1}} + \frac{1}{S_{y \cdot x_2}} \right)}} \quad \text{(Eq. 1)}$$

with $(n_1 + n_2 - 4)$ degrees of freedom, and where:

$$S^2_{y \cdot x_{pooled}} = \frac{S_{y \cdot x_{pooled}}}{n_1 + n_2 - 4} \quad \text{(Eq. 2)}$$

and:

$$S_{y \cdot x_{pooled}} = S_{y \cdot x_1} + S_{y \cdot x_2} \quad \text{(Eq. 3)}$$

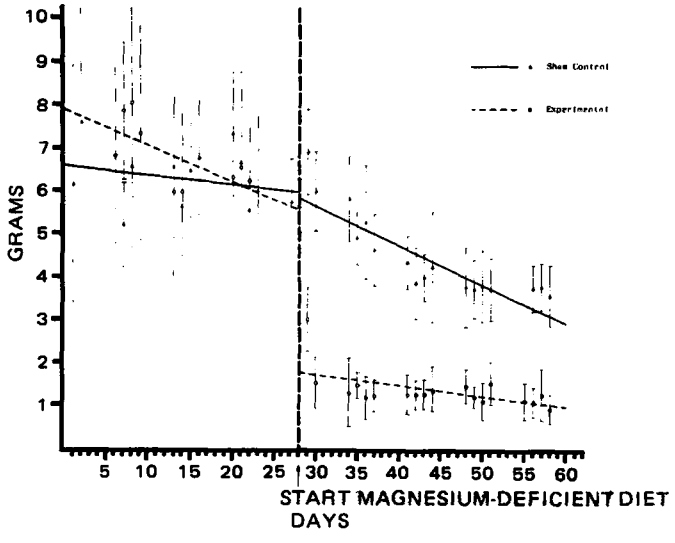

Figure 3—*Time courses of mean fecal wet weights from sham control and magnesium-deficient rats.*

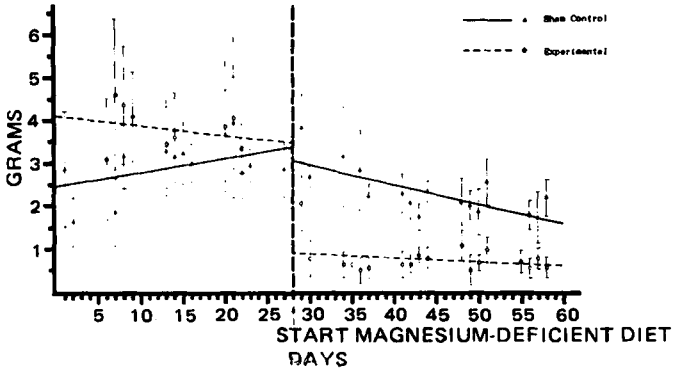

Figure 4—*Time courses of mean fecal dry weights from sham control and magnesium-deficient rats.*

Table III—Magnesium-Deficient Regression Equations of Metabolic Performance as a Function of Time [a]

Variable	n	b	$\hat{Y}$	S_b	$S^2_{y \cdot x}$
Food intake					
Days 1–28	10	−0.165	14.38	0.0983	4.2088
Days 29–58	18	−0.058	9.29	0.0165	0.4064
Net water intake					
Days 1–28	10	−0.209	24.24	0.2692	31.5779
Days 29–58	18	−0.116	16.89	0.0398	2.3490
Number of fecal pellets					
Days 1–28	10	−1.262	53.09	0.2167	20.4579
Days 29–58	18	−0.094[b]	11.59	0.0305	1.3833
Fecal wet weight					
Days 1–28	9	−0.081	7.89	0.0355	0.4042
Days 29–58	18	−0.025[b]	2.47	0.0099	0.1453
Fecal dry weight					
Days 1–28	9	−0.018	4.07	0.0290	0.2696
Days 29–58	18	−0.013[b]	1.32	0.0092	0.1260
Net fluid output					
Days 1–28	9	−0.0743	12.74	0.0511	0.8366
Days 29–58	18	−0.0989	10.844	0.0275	1.1212

[a] n = number of observations, b = sample regression coefficient, $\hat{Y}$ = zero intercept, S_b = sample standard deviation, and $S^2_{y \cdot x}$ = mean square deviation from regression. [b] Statistically significant difference when compared to corresponding values in Table II ($p \leq 0.05$).

Table IV—Effect of a 30-Day Magnesium-Deficient Diet on Small Intestinal Transit Performance and Related Data in 48-hr Fasted Rats [a]

Parameter	Sham Control Group		Experimental Group	
	15 min	30 min	15 min	30 min
Body weight, g	173.69 ± 18.42 (13)	174.32 ± 13.26 (14)	184.30 ± 26.45 (10)	197.56 ± 22.95[b] (9)
Length of small intestine, cm	119.15 ± 11.55	124.07 ± 5.68	116.80 ± 6.66	119.33 ± 4.00[b]
Normalized small intestinal length, cm/100 g of body weight	68.81 ± 4.97	71.53 ± 5.92	64.44 ± 9.25	61.19 ± 7.96[b]
Length of small intestine traversed, cm	54.92 ± 13.62	81.64 ± 12.18	83.00 ± 15.39[b]	90.00 ± 12.48
Percentage of small intestine traversed	46.02 ± 10.02	65.80 ± 9.35	70.83 ± 11.20[b]	75.33 ± 9.40[b]

[a] The ± indicates 1 *SD*; parentheses contain number of animals. [b] Statistically significant difference when compared with the mean values of sham control rats ($p \leq 0.05$).

Pooling increases the degrees of freedom and sensitivity of the test and is possible if the ratios of the mean square deviation from regression are satisfactorily homogeneous. If the F test showed that the ratios of the mean square deviation from regression were not satisfactorily homogeneous, a modified Welch test to test the significance of difference between slopes was used. The following formula expresses this test:

$$t' = \frac{b_1 - b_2}{\sqrt{\frac{S^2_{y \cdot x_1}}{x_1^2} + \frac{S^2_{y \cdot x_2}}{x_2^2}}} \qquad \text{(Eq. 4)}$$

The approximate degrees of freedom for t' was calculated using the following formula:

$$df = \frac{\left(\frac{S^2_{y \cdot x_1}}{x_1^2} + \frac{S^2_{y \cdot x_2}}{x_2^2}\right)^2}{\left(\frac{1}{df_1}\right)\left(\frac{S^2_{y \cdot x_1}}{x_1^2}\right)^2 + \left(\frac{1}{df_2}\right)\left(\frac{S^2_{y \cdot x_2}}{x_2^2}\right)^2} \qquad \text{(Eq. 5)}$$

For propulsive motility, a simple Student t test was used to compare the significance of the mean differences. In all statistical tests, significance was tested at the 5% level.

RESULTS

The progressive magnesium deficiency syndrome was observed in the deficient animals: hyperemia of the skin, nose, ears, footpads, and tail appeared on the 5th day and progressed to weeping, crusting lesions (Fig. 1).

The magnesium-deficient rats were inactive but irritable when stimulated with a blast of air. At the end of the 2nd week, the appetite of the animals improved considerably, although irritability became increasingly prominent. The weight curves of the sham control and magnesium-deficient groups are given in Fig. 2. The deficient group rats lagged in the rate of weight increase compared to the sham control group until the 3rd week, when they ceased to gain weight.

Results of changes in food intake, net water intake, and fecal and urinary excretions are given as daily average values for the rats fed the magnesium-deficient diet. After 5 days, the average daily wet fecal weight (Fig. 3), dry fecal weight (Fig. 4), and fecal pellet count (Fig. 5) were significantly less for the magnesium-deficient animals. At no time could it be concluded that differences existed in daily average food intake (Fig. 6), net water intake (Fig. 7), or net fluid output (Fig. 8). The regression equations fitted to the data points in Figs. 2–7 are presented in Tables II and III.

In all cases, muscle strips from the small intestine of magnesium-deficient animals showed a greatly increased contraction strength in response to a test acetylcholine dose (Fig. 9). This response was present 4 weeks following initiation of the magnesium-deficient regimen. Although not depicted, muscle segments from the colons of magnesium-deficient

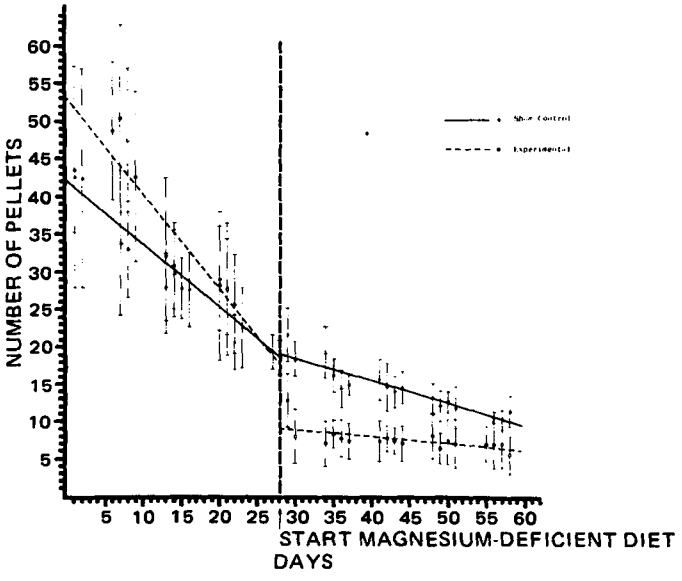

Figure 5—*Time courses of mean fecal pellet outputs from sham control and magnesium-deficient rats.*

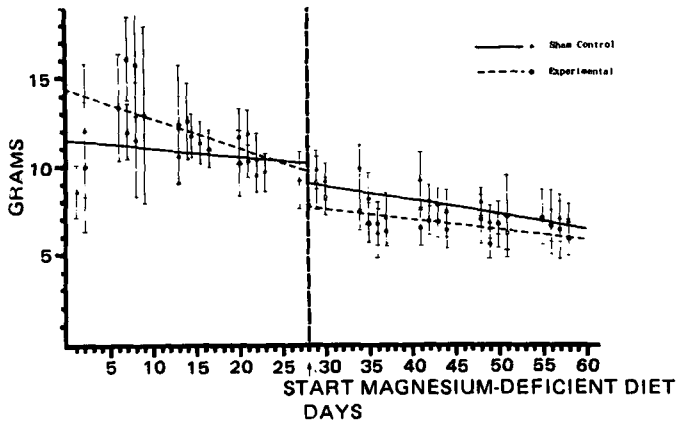

Figure 6—*Time courses of mean daily food intakes from sham control and magnesium-deficient rats.*

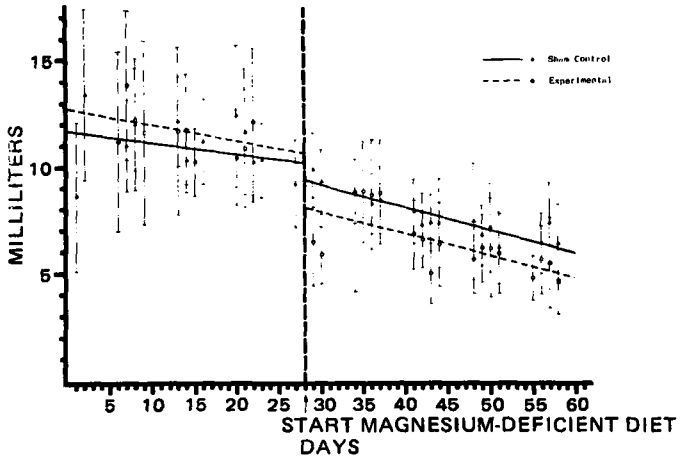

Figure 8—*Time courses of mean net fluid outputs from sham control and magnesium-deficient rats.*

animals either failed to show increased contractile force to acetylcholine or showed a decreased response. As seen in Table IV, statistically significant increases in the small intestinal transit rate were noted in the 4-week magnesium-deficient animals when contrasted to the sham controls. The mass transit data indicate that the effects noted in isolated duodenal muscle segments probably are generalized to other regions of the small intestine as well.

All animals carried for 30 days on the magnesium-deficient diet displayed significant morphological differences from the sham controls in the heart, liver, skeletal muscle, kidney, and gastric mucosa. In all magnesium-deficient rats of this group, there were focal degenerative and inflammatory changes in the myocardium. In the liver, areas of focal degeneration and increased vacuolization were noted. In the magnesium-deficient group, degenerative and inflammatory changes appeared in the voluntary muscles. The lesions consisted chiefly of a degenerative change and associated muscle bundle swelling, with an accompanying loss of sarcolemmal nuclei.

In the stomach, alterations were seen in the mucosa. These changes included occasional dilation and engorgement of small vessels and enlargement of gastric pits. Elsewhere, chief cells appeared reduced in number and compressed by swollen adjacent parietal cells. However, the most consistent abnormalities noted were in the kidneys. The kidneys of all magnesium-deficient rats showed large calcium deposits in the medullary tubule lumina, with a preponderance near the corticomedullary junction. These deposits were laminated, the affected tubules were dilated, and their epithelium was flattened.

DISCUSSION

The pathophysiological findings of magnesium deficiency in the rat were in good agreement with numerous previous studies (12–16). Hyperexcitability, cutaneous hyperemia, general fur loss, shaggy coat, ringed eye dermatitis, encrusted nostrils, and signs of early diarrhea were consistent findings. Histological findings also were in agreement with previously reported data to an extent that they confirmed that hypomagnesemia existed in the experimental rats (15).

However, certain metabolic effects were not found. For example, unlike the findings of Orent *et al.* (17), the average weight of the magnesium-deficient group never fell below the initial average weight of this parameter; and although the average rate of weight increase was less than that of the control group, the difference was not significant. Such inconsistencies may have been due to the use of different strains and ages of rats and to variations in the formulations of the deficient diets, particularly in earlier days when it was more difficult to make an accurately defined diet with simple magnesium deficiency alone.

Fecal wet weight and pellet count performance of the deficient group were reduced while the mean small intestinal transit fraction increased. These results are in agreement with *in vitro* studies which showed that isolated duodenal muscle segments were hyperreactive to a cholinergic stimulus, while no differences in acetylcholine reactivity were apparent in the colons of the deficient group. Upon necropsy, the colons of the magnesium-deficient rats were visually observed to be enlarged.

It is concluded that, in the rat, GI motor activity and, to some degree, excretory performance are affected by chronic magnesium deficiency. Frank liver damage suggests that the function of this organ may become impaired. Thus, the function of the digestive system is affected to such an extent that it cannot be regarded merely as a conduit for magnesium intake, excretion, and conservation.

The increased small intestinal transit rate in the deficient state suggests that a regeneratively destructive response may exist in this organ in response to magnesium deficiency: intake restriction results in impaired ability to absorb and/or conserve magnesium in the small bowel. The visual appearance of distended colons in deficient rats is consistent with the reduction in fecal water content in these animals; a condition of partial constipation would be consistent with efforts to conserve magnesium by increasing colonic residence time. This hypothesis is attractive in the particular case of the rat where, under normal circumstances, approximately 70% of the total magnesium absorption occurs in the cecum and ascending colon (18).

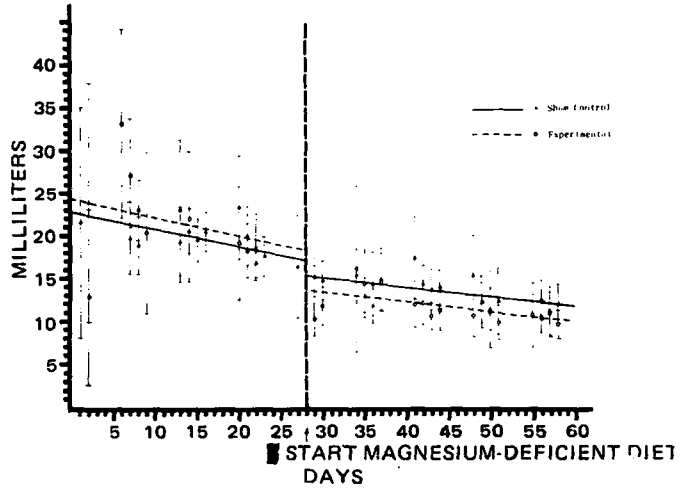

Figure 7—*Time courses of mean net water intakes from sham control and magnesium-deficient rats.*

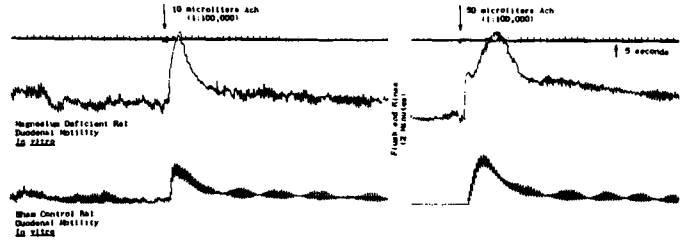

Figure 9—In vitro *motility responses of small intestinal muscle strips from sham control and magnesium-deficient rats.*

REFERENCES

(1) M. F. Tansy, in "Intestinal Absorption of Metal Ions, Trace Elements and Radionuclides," S. C. Skoryna and D. Waldron-Edward, Eds., Pergamon, Oxford, England, 1970.

(2) B. L. Vallee, W. E. C. Wacker, and D. D. Ulmer, *N. Engl. J. Med.*, **262**, 155 (1960).

(3) M. F. Tansy, F. M. Nichini, H. W. Baker, and J. Chrzyanowski, *J. Surg. Res.*, **11**, 213 (1971).

(4) F. M. Nichini, M. F. Tansy, and F. M. Kendall, *Radiology*, **108**, 413 (1973).

(5) M. F. Tansy, F. M. Kendall, and F. M. Nichini, *IRCS Letters to the Editor*, July (1973).

(6) M. F. Tansy, W. E. Landin, and L. Salkin, presented at 2nd International Symposium on Magnesium, Montreal, Canada, 1976.

(7) M. Artizzu and B. Messier, *Br. J. Exp. Pathol.*, **52**, 70 (1971).

(8) B. Frenning, P. Johansson, and P. G. Ohrn, *Upsala J. Med. Sci.*, **79**, 90 (1974).

(9) R. Veilleux, *Lab. Invest.*, **33**, 80 (1975).

(10) J. Christiansen, J. F. Rehfeld, and F. Stadil, *Gastroenterology*, **68**, 1140 (1975).

(11) E. J. VanLiere, J. Stickney, and D. W. Northrup, *ibid.*, **5**, 37 (1945).

(12) H. D. Kruse, E. R. Orent, and E. V. McCollum, *J. Biol. Chem.*, **96**, 519 (1932).

(13) E. R. Orent, H. D. Kruse, and E. V. McCollum, *ibid.*, **106**, 573 (1934).

(14) E. Lowenkaupt, M. P. Schulman, and D. M. Greenberg, *Arch. Pathol.*, **49**, 427 (1950).

(15) L. A. Goldsmith, *J. Nutr.*, **93**, 87 (1967).

(16) B. S. W. Smith and D. I. Nisbet, *J. Comp. Pathol.*, **78**, 149 (1968).

(17) E. R. Orent, H. D. Kruse, and E. V. McCollum, *Am. J. Physiol.*, **101**, 454 (1932).

(18) J. G. Chutkow, *J. Lab. Clin. Med.*, **63**, 71 (1964).

ACKNOWLEDGMENTS

Presented at the 27th Annual Fall Meeting of the American Physiological Society, Philadelphia, Pa., August 1976 [*Physiologist*, **19**, 263 (1976) (Abstract)].

Abstracted in part from a thesis submitted by W. E. Landin to Temple University in partial fulfillment of the Master of Science degree requirements.

Absorption and Penetration of Dinoprost (Prostaglandin $F_{2\alpha}$) and Dinoprost Methyl Ester into Perfused Mesenteric Circulation in Rats

BRUCE M. TAYLOR ˣ and FRANK F. SUN

Received March 6, 1978, from *Experimental Biology, The Upjohn Company, Kalamazoo, MI 49001.* Accepted for publication February 6, 1979.

Abstract □ The absorption of dinoprost (prostaglandin $F_{2\alpha}$) and its methyl ester in rat jejunum was studied. A 22-cm segment of rat jejunum was cannulated at both ends and connected to an oscillating perfusion pump system. The mesenteric vasculature supplying this isolated segment also was cannulated and perfused with Kreb's bicarbonate buffer with dextran. Solutions of ^{3}H-dinoprost or its methyl ester were introduced into the lumen and oscillated through the segment. The disappearance of radioactivity from the lumen and the appearance of radioactivity in the vascular perfusate were monitored. The metabolite patterns in the vascular perfusate were analyzed by TLC. A lag between the time the drug disappeared from the lumen and the time it appeared in the mesenteric circulation was detected. This lag was longer for the methyl ester than for the free acid, even though the ester disappears from the lumen faster than does the free acid. Upon removal of dinoprost from the gut lumen, a gradual decrease in the amount of drug appearing in the mesenteric circulation could be detected. However, with the ester, a slight increase could be observed for ~0.5 hr, followed by a decrease. Metabolism by the gut wall appears to be greater for the ester than for the acid. The results suggest that, although the ester disappears from the lumen more quickly than does the acid, it actually penetrates to the blood at a slower rate and undergoes greater metabolism.

Keyphrases □ Dinoprost—absorption and penetration, mesenteric circulation, rats, metabolism □ Dinoprost—methyl ester, absorption and penetration, mesenteric circulation, rats, metabolism □ Pharmacokinetics—dinoprost and dinoprost methyl ester, mesenteric circulation, rats □ Prostaglandins—dinoprost, dinoprost methyl ester, absorption and penetration, mesenteric circulation, rats, metabolism

Prostaglandins have been viewed as potential panaceas almost since the moment of their discovery. Much research has been devoted to their endogenous and exogenous functions in various organs and tissues, and various roles have been assigned to this family of compounds. Because of their ubiquity and functional diversity, prostaglandins are appealing prospects as therapeutic agents for many conditions. However, before this potential can be realized, a practical administration route must be developed. The most desirable route would be oral. When dinoprost (prostaglandin $F_{2\alpha}$) or its methyl ester are administered orally, the major absorption site appears to be the small intestine since there is little absorption from the stomach[1]; although there can be some absorption by the large intestine, most of the compound disappears before reaching this area (1).

The present study was designed to gain insight into intestinal absorption of prostaglandins: their disappearance from the intestinal lumen, their appearance in the mesentric circulation, and the extent of their metabolism in the intestinal wall. Investigations into the rates of prostaglandin disappearance from the intestinal lumen (1, 2) have been based on studies of prostaglandin disappearance from the mucosal side of the intestine. From such studies, Ho and coworkers (3, 4) proposed that dinoprost absorption is diffusion dependent and that its metabolism may affect the absorption rate. In addition, previous work[2] showed that the lymphatic system does not play a role in the transport of orally administered prostaglandins.

This study looked at the serosal side of the intestine *via*

[1] E. Daniels and R. VanEyk, The Upjohn Co., Kalamazoo, MI 49001, personal communication.

[2] L. Compton and J. Weeks, The Upjohn Co., Kalamazoo, MI 49001, personal communication.

0022-3549/79/0800-0983$01.00/0

© 1979, American Pharmaceutical Association

REFERENCES

(1) M. F. Tansy, in "Intestinal Absorption of Metal Ions, Trace Elements and Radionuclides," S. C. Skoryna and D. Waldron-Edward, Eds., Pergamon, Oxford, England, 1970.

(2) B. L. Vallee, W. E. C. Wacker, and D. D. Ulmer, *N. Engl. J. Med.*, **262**, 155 (1960).

(3) M. F. Tansy, F. M. Nichini, H. W. Baker, and J. Chrzyanowski, *J. Surg. Res.*, **11**, 213 (1971).

(4) F. M. Nichini, M. F. Tansy, and F. M. Kendall, *Radiology*, **108**, 413 (1973).

(5) M. F. Tansy, F. M. Kendall, and F. M. Nichini, *IRCS Letters to the Editor*, July (1973).

(6) M. F. Tansy, W. E. Landin, and L. Salkin, presented at 2nd International Symposium on Magnesium, Montreal, Canada, 1976.

(7) M. Artizzu and B. Messier, *Br. J. Exp. Pathol.*, **52**, 70 (1971).

(8) B. Frenning, P. Johansson, and P. G. Ohrn, *Upsala J. Med. Sci.*, **79**, 90 (1974).

(9) R. Veilleux, *Lab. Invest.*, **33**, 80 (1975).

(10) J. Christiansen, J. F. Rehfeld, and F. Stadil, *Gastroenterology*, **68**, 1140 (1975).

(11) E. J. VanLiere, J. Stickney, and D. W. Northrup, *ibid.*, **5**, 37 (1945).

(12) H. D. Kruse, E. R. Orent, and E. V. McCollum, *J. Biol. Chem.*, **96**, 519 (1932).

(13) E. R. Orent, H. D. Kruse, and E. V. McCollum, *ibid.*, **106**, 573 (1934).

(14) E. Lowenkaupt, M. P. Schulman, and D. M. Greenberg, *Arch. Pathol.*, **49**, 427 (1950).

(15) L. A. Goldsmith, *J. Nutr.*, **93**, 87 (1967).

(16) B. S. W. Smith and D. I. Nisbet, *J. Comp. Pathol.*, **78**, 149 (1968).

(17) E. R. Orent, H. D. Kruse, and E. V. McCollum, *Am. J. Physiol.*, **101**, 454 (1932).

(18) J. G. Chutkow, *J. Lab. Clin. Med.*, **63**, 71 (1964).

ACKNOWLEDGMENTS

Presented at the 27th Annual Fall Meeting of the American Physiological Society, Philadelphia, Pa., August 1976 [*Physiologist*, **19**, 263 (1976) (Abstract)].

Abstracted in part from a thesis submitted by W. E. Landin to Temple University in partial fulfillment of the Master of Science degree requirements.

Absorption and Penetration of Dinoprost (Prostaglandin $F_{2\alpha}$) and Dinoprost Methyl Ester into Perfused Mesenteric Circulation in Rats

BRUCE M. TAYLOR ˣ and FRANK F. SUN

Received March 6, 1978, from *Experimental Biology, The Upjohn Company, Kalamazoo, MI 49001.* Accepted for publication February 6, 1979.

Abstract □ The absorption of dinoprost (prostaglandin $F_{2\alpha}$) and its methyl ester in rat jejunum was studied. A 22-cm segment of rat jejunum was cannulated at both ends and connected to an oscillating perfusion pump system. The mesenteric vasculature supplying this isolated segment also was cannulated and perfused with Kreb's bicarbonate buffer with dextran. Solutions of ^{3}H-dinoprost or its methyl ester were introduced into the lumen and oscillated through the segment. The disappearance of radioactivity from the lumen and the appearance of radioactivity in the vascular perfusate were monitored. The metabolite patterns in the vascular perfusate were analyzed by TLC. A lag between the time the drug disappeared from the lumen and the time it appeared in the mesenteric circulation was detected. This lag was longer for the methyl ester than for the free acid, even though the ester disappears from the lumen faster than does the free acid. Upon removal of dinoprost from the gut lumen, a gradual decrease in the amount of drug appearing in the mesenteric circulation could be detected. However, with the ester, a slight increase could be observed for ~0.5 hr, followed by a decrease. Metabolism by the gut wall appears to be greater for the ester than for the acid. The results suggest that, although the ester disappears from the lumen more quickly than does the acid, it actually penetrates to the blood at a slower rate and undergoes greater metabolism.

Keyphrases □ Dinoprost—absorption and penetration, mesenteric circulation, rats, metabolism □ Dinoprost—methyl ester, absorption and penetration, mesenteric circulation, rats, metabolism □ Pharmacokinetics—dinoprost and dinoprost methyl ester, mesenteric circulation, rats □ Prostaglandins—dinoprost, dinoprost methyl ester, absorption and penetration, mesenteric circulation, rats, metabolism

Prostaglandins have been viewed as potential panaceas almost since the moment of their discovery. Much research has been devoted to their endogenous and exogenous functions in various organs and tissues, and various roles have been assigned to this family of compounds. Because of their ubiquity and functional diversity, prostaglandins are appealing prospects as therapeutic agents for many conditions. However, before this potential can be realized, a practical administration route must be developed. The most desirable route would be oral. When dinoprost (prostaglandin $F_{2\alpha}$) or its methyl ester are administered orally, the major absorption site appears to be the small intestine since there is little absorption from the stomach[1]; although there can be some absorption by the large intestine, most of the compound disappears before reaching this area (1).

The present study was designed to gain insight into intestinal absorption of prostaglandins: their disappearance from the intestinal lumen, their appearance in the mesentric circulation, and the extent of their metabolism in the intestinal wall. Investigations into the rates of prostaglandin disappearance from the intestinal lumen (1, 2) have been based on studies of prostaglandin disappearance from the mucosal side of the intestine. From such studies, Ho and coworkers (3, 4) proposed that dinoprost absorption is diffusion dependent and that its metabolism may affect the absorption rate. In addition, previous work[2] showed that the lymphatic system does not play a role in the transport of orally administered prostaglandins.

This study looked at the serosal side of the intestine *via*

[1] E. Daniels and R. VanEyk, The Upjohn Co., Kalamazoo, MI 49001, personal communication.

[2] L. Compton and J. Weeks, The Upjohn Co., Kalamazoo, MI 49001, personal communication.

0022-3549/79/0800-0983$01.00/0

© 1979, American Pharmaceutical Association

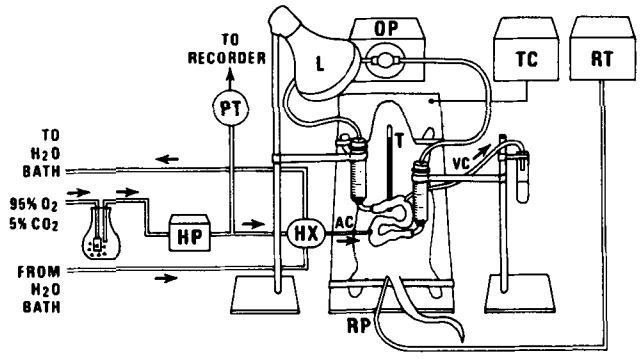

Figure 1—*Diagram of experimental setup. Key: HP, parastaltic pump; PT, pressure transducer; L, warming lamp; HX, heat exchanger; AC and VC, arterial cannula and venous cannula; OP, oscillating pump; TC, platform temperature controller; RP, rectal probe; RT, radio thermometer; and T, thermometer.*

the mesenteric circulation to obtain a more complete intestinal absorption profile. Since it has been proposed that prostaglandin esters are absorbed faster and achieve greater circulating levels than the free acids (2, 5), the differences in absorption between dinoprost and its methyl ester were examined.

EXPERIMENTAL

Materials[3]—[9(*N*)-^{3}H]-Dinoprost was commercially prepared[4]. ^{3}H-Dinoprost methyl ester was produced by reacting ^{3}H-dinoprost with diazomethane.

Methods—Several techniques have been developed for studying intestinal absorption and transfer into the mesenteric circulation (6–10). The experimental technique employed for this study was an expansion of Ho's modified Doluisio absorption method (5) (Fig. 1).

Male Sprague–Dawley rats, 600–800 g (these larger animals were chosen because the mesenteric blood vessels were much easier to cannulate), were anesthetized with cyclopal sodium and placed on a temperature control platform[5] to maintain body temperature at 37°; body temperature was monitored with a rectal probe. The abdomen was opened, and branches of the superior mesenteric artery and vein supplying the superior jejunum were cannulated with polyethylene tubing[6].

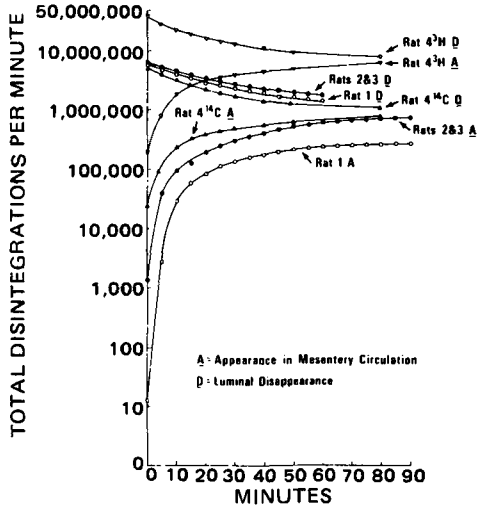

Figure 2—*Dinoprost disappearance and appearance curves.*

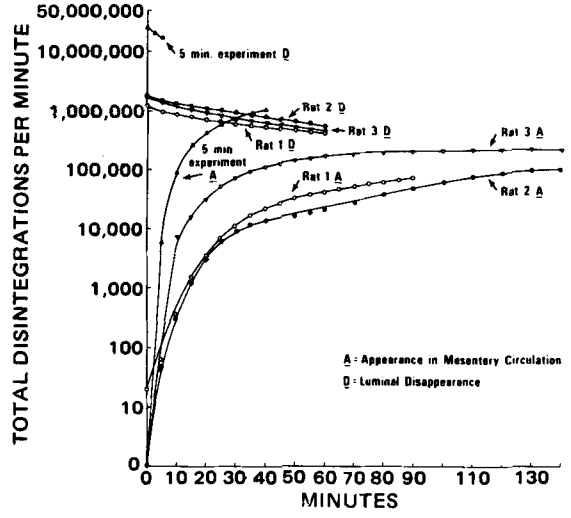

Figure 3—*Dinoprost methyl ester disappearance and appearance curves.*

The vasculature was perfused with an oxygenated solution of Kreb's bicarbonate buffer (pH 7.4) with 10% dextran and 150 IU of heparin/ml *via* a parastaltic pump[7]. Perfusion pressure was monitored by a pressure transducer[8]. Perfusate passed from the arterial cannula[6] through the vasculature and into the venous cannula[6], where it drained into collecting tubes. Next, a 22-cm section of jejunum supplied by the perfused vasculature was laid out in a S pattern and washed free of fecal matter. Cannulas were inserted at each end such that syringe barrels could be inserted into the cannulas and secured.

The exposed gut temperature was monitored (thermometer) and regulated with a lamp. Radiolabeled drug solution[9] (2 ml) containing 10 μg of prostaglandin in pH 6 buffer was placed in the gut, and a reversible pump[10] was connected to the syringe barrels, allowing the solution to be oscillated slowly through the gut (0.75 ml/min). [Moving the solution is reported to reduce the thickness of the aqueous diffusion layer (4).] The drug solution was prepared in isoosmotic pH 6.0 phosphate buffer (prepared by diluting 9.07 g of anhydrous monobasic potassium phosphate and 11.93 g of potassium sulfate to 1 liter with water). The pH was adjusted with 1 *N* NaOH (11). This buffer produces no water flux into or out of the gut in experiments with ^{14}C-polyethylene glycol.

Two minutes was allowed for mixing before the first luminal fluid sample was taken, followed by sampling at 5-min intervals. Effluent from

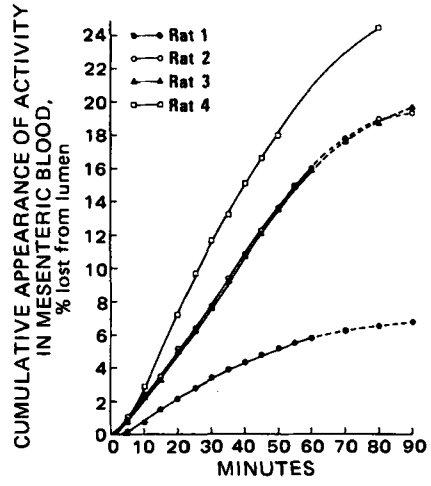

Figure 4—*Dinoprost appearance in mesenteric circulation. Dotted lines indicate time after drug removal from lumen.*

[3] Metabolite standards were provided by Frank Lincoln, Experimental Chemistry, The Upjohn Co., Kalamazoo, MI 49001.
[4] New England Nuclear, Boston, MA 02118.
[5] Narco Biosystems, Houston, Tex.
[6] PE-50 Intramedic, Clay Adams, Division of Becton, Dickinson and Co., Parsippany, NJ 07054.
[7] Model 911 Holter Roller Pump, Extracorporal Medical Specialities, King of Prussia, PA 19406.
[8] Harvard Apparatus Co., Millis, MA 02054.
[9] Two milliliters of drug solution had the same disappearance half-life in these large rats as was demonstrated in the smaller rats used by Ho (5).
[10] FMI lab pump, Fluid Metering Inc., Oyster Bay, NY 11771.

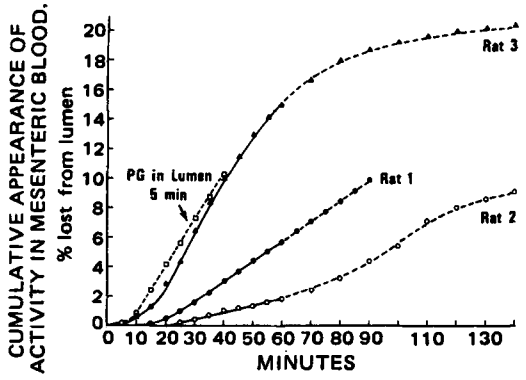

Figure 5—*Dinoprost methyl ester appearance in mesenteric circulation. Dotted lines indicate time after drug removal from lumen.*

the venous cannula was collected in separate tubes for each sampling interval. The drug solution remained in the gut for the designated time—usually 60 min—and was then removed; the gut was then washed free of drug. The vascular perfusion was continued for an additional period to check for drug holdup in the intestinal wall and to follow drug release. Upon completion of the perfusion, the experimental intestine section was removed, and the amount of radioactivity remaining in the wall was determined.

Analysis—The radioactivity in the luminal samples and that in the vascular perfusate were determined by direct counting of small aliquots in a scintillation counter[11]. These and all other counting data were corrected for quench. Intestinal wall tissue was homogenized[12] and oxidized with an oxidizer[11], and the oxidation products were counted to determine the residual radioactivity in the gut wall.

The metabolism data were obtained by pooling the vascular perfusate samples into three portions (0–30 min, 35–60 min, and 65 min–end), extracting with ethyl acetate, and subjecting the extract to TLC. TLC was carried out on silica gel plates[13] in chloroform–methanol–water (40:10:1) and then chloroform–methanol–acetic acid (40:2.5:5). The plates were scraped, and the areas where the various standards ran were noted and counted.

RESULTS AND DISCUSSION

Several intestinal absorption parameters were determined from the data collected: (*a*) the amount of drug lost from the lumen, (*b*) the amount and pattern of drug appearance in the mesenteric circulation, (*c*) the amount of drug held up in the gut wall, and (*d*) the extent and pattern of intestinal metabolism. In addition, the esterase activity in the gut lumen was determined for the experiments with dinoprost methyl ester[14].

Figure 2 shows dinoprost disappearance from the intestinal lumen and the appearance of the label in the mesenteric circulation plotted on a log scale of the total disintegratious per minute *versus* time. By the time that the zero sample was taken (after a 2-min delay), activity had already begun to appear in the circulation and continued to increase until the drug was removed from the gut. After removal of the drug solution from the lumen, the rate of increase of radioactivity appearing in the mesenteric circulation slowly leveled off; after 30 min, the slope approached zero.

Figure 3 shows the disappearance and appearance of dinoprost methyl ester. Ester disappearance studies are complicated by the presence of a luminal esterase, which converts the ester to the free acid at a highly variable rate. TLC of the luminal extract demonstrated that the only radioactive species present were dinoprost and dinoprost methyl ester and, therefore, indicated no back-diffusion of prostaglandin metabolites into the lumen.

Some differences between the free acid and the ester should be noted. First, there is a delay between the time the drug disappears from the lumen and the time it appears in the circulation since most plots start from zero. Second, radioactivity continues to increase in the circulation

[11] Packard Tri-Carb, Packard Instrument Co., Downers Grove, IL 60515.
[12] Polytron homogenizer, Brinkmann Instruments, Westbury, NY 11590.
[13] Analtech.
[14] G. Tarpley and F. Sun, The Upjohn Co., Kalamazoo, MI 49001, 1976, unpublished data.

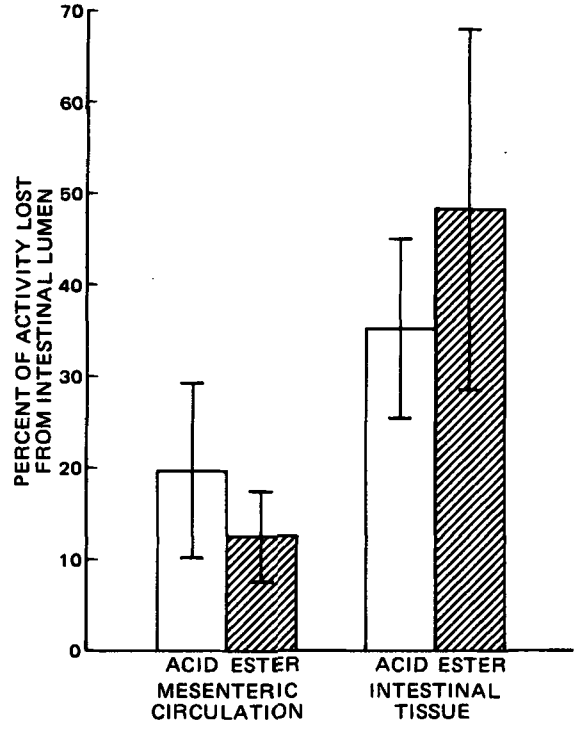

Figure 6—*Dinoprost and dinoprost methyl ester activity distribution. Vertical line indicates standard deviation.*

after the drug is removed from the lumen; *i.e.*, the slope remains positive. The slope of the appearance curve for Rat 3 more closely resembles the slopes for dinoprost because the esterases, as measured by the ester to acid ratio in the luminal fluid, were not as active in Rats 1 and 2 as in Rat 3.

The percent of the total activity lost from the lumen appearing in the mesenteric circulation for dinoprost *versus* time is shown in Fig. 4. The broken line indicates the time after drug was removed from the lumen. The radioactivity appeared immediately in the mesenteric circulation, and the slope began to level off shortly after drug removal. A similar plot for dinoprost methyl ester is shown in Fig. 5. There was an apparent delay before radioactivity began to appear, and the slope continued to rise even after drug removal, which was especially apparent when the drug solution was removed after only 5 min in the lumen.

Figure 6 shows the activity distribution in the two compartments, tissue and blood (plotted mean ± *SD*). These results, along with those showing

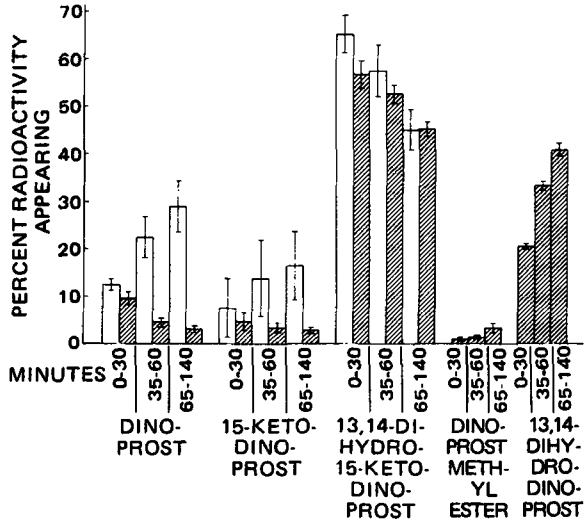

Figure 7—*Metabolites appearing in mesenteric circulation. Key:* □, *dinoprost in intestinal lumen; and* □, *dinoprost methyl ester in intestinal lumen.*

a delay between disappearance from the lumen and appearance in the blood, are in agreement with previous studies (12), which indicate that the greater a compound's lipophilicity, the longer will be its holdup in the intestinal wall and the less will penetrate to the serosal side of the membrane.

Finally, as is expected with longer holdup, the ester is more extensively metabolized than is the acid, as indicated by TLC. With dinoprost, the main metabolites are 15-ketodinoprost and 13,14-dihydro-15-ketodinoprost. As the experiment progressed, the metabolism decreased (Fig. 7). With the ester, four main metabolites are seen: dinoprost, 15-ketodinoprost, 13,14-dihydro-15-ketodinoprost, and 13,14-dihydrodinoprost. Although the amount of intact ester entering the blood increased slightly as the experiment progressed, the total metabolism increased, as indicated by the increase in 13,14-dihydrodinoprost in the circulation.

In summary, intestinal prostaglandin absorbed appears to have at least three phases. First, prostaglandins appear to diffuse rapidly from the gut lumen into the intestinal wall. Second, once in the gut wall, time is required for the compound to reach the other side of the cell. During this transcellular movement, the compound appears to be extensively, although not completely, metabolized. The duration of this second phase appears to be directly related to lipophilicity. Third, the compound and its metabolites are released into the mesenteric circulation. Prostaglandin esters apparently are released slower and over a longer period than the parent acids; however, they also undergo more extensive metabolism.

This study demonstrated differences in dinoprost and dinoprost methyl ester absorption patterns in the rat. However, these differences were not in agreement with the hypothesis that prostaglandin esters are absorbed faster than the parent prostaglandins in this species.

REFERENCES

(1) W. Magee, S. Armour, and O. Miller, *Biochim. Biophys. Acta*, **306**, 270 (1973).

(2) A Robert, W. Magee, O. Miller, and J. Nezamis, *ibid.*, **348**, 269 (1974).

(3) N. F. H. Ho and W. Higuchi, *J. Pharm. Sci.*, **63**, 686 (1974).

(4) N. Ho, J. Park, W. Morozowich, and W. Higuchi, *J. Theoret. Biol.*, **61**, 185 (1976).

(5) J. Y. Park, thesis, University of Michigan, Ann Arbor, Mich., 1977.

(6) F. Jacobs and M. Luper, *J. Appl. Physiol.*, **11**(I), 136 (1957).

(7) P. Jacobs, F. H. Bothwell, and R. Charlton, *Am. J. Physiol.*, **210**, 694 (1966).

(8) H. Kavin, N. Levin, and M. Stanley, *J. Appl. Physiol.*, **22**, 604 (1967).

(9) J. Lee, *Am. J. Physiol.*, **200**, 979 (1961).

(10) J. Lee and K. Duncan, *Gastroenterology*, **54**, 559 (1968).

(11) K. J. Desai, thesis, University of Michigan, Ann Arbor, Mich., 1977.

(12) V. Houston, D. Upshall, and J. Bridges, *J. Pharmacol. Exp. Ther.*, **189**, 244 (1974).

ACKNOWLEDGMENTS

Special thanks are extended to Dr. N. F. H. Ho, Department of Pharmaceutical Chemistry, University of Michigan, Ann Arbor, Mich., for advice and consultation during this work.

Conjugated Estrogens Bioinequivalence: Comparison of Four Products in Postmenopausal Women

WALLACE P. ADAMS *x, JUN HASEGAWA *, RAYMOND N. JOHNSON ‡, and RONALD C. HARING ‡

Received November 6, 1978, from the **Pharmacy Research and Development Department and the* ‡*Analytical Research and Development Department, Ayerst Laboratories Inc., Rouses Point, NY 12979.* Accepted for publication February 7, 1979.

Abstract □ The bioequivalence of four conjugated estrogens tablets USP was compared by measurement of seven estrogens or estrogen metabolites in the urine during steady-state dosing in postmenopausal women. Two studies compared three generic products with the innovator's product. The urinary excretion of 17α-dihydroequilin, 17α-dihydroequilenin, and 17α-estradiol were significantly greater in all cases with the innovator's product than with the generic products. Statistically significant differences between products were observed occasionally for other components. The generic products thus were bioinequivalent to the innovator's product, although all products essentially met current compendial specifications. A third study observed no significant differences between three batches of the innovator's product for the seven components. Total conjugated estrogens excretion of all products at the steady state was essentially equal and correlated with neither disintegration time nor dissolution half-time. Bioinequivalence between products is discussed in relation to the need for an improved USP conjugated estrogens monograph. Evidence suggesting the metabolism of a fraction of dosed estrone, equilin, and 17α-dihydroequilin to 17β-estradiol, 17β-dihydroequilin, and 17α-dihydroequilenin, respectively, is presented.

Keyphrases □ Estrogens, conjugated—bioinequivalence of generic and proprietary products, postmenopausal women □ Bioequivalence—conjugated estrogens, bioinequivalence of generic and proprietary products, postmenopausal women □ Product substitution—estrogens, conjugated, bioinequivalence of generic and proprietary products, postmenopausal women

Conjugated estrogens of natural origin are composed of at least nine different estrogens or estrogen metabolites, each present in a different amount. The USP monograph for conjugated estrogens (1) contains specifications for total conjugated estrogens and for the two most abundant components, sodium estrone sulfate and sodium equilin sulfate. The sodium estrone sulfate specification is 50–65% and the sodium equilin sulfate specification is 20–35% of the total conjugated estrogens content. The monograph does not contain quantitative specifications for additional components, although an identification test (2) requires the presence of a prominent GLC peak for 17α-dihydroequilin and additional peaks for 17α-estradiol, 17β-dihydroequilin, equilenin, 17β-estradiol, and 9-dehydroestrone.

Broad content ranges are specified for sodium estrone sulfate and sodium equilin sulfate. The content of the third major component, sodium 17α-dihydroequilin sulfate, which by GLC is 15% of the total estrogens in the innovator's product, is unspecified; the specification for this component is an imprecise and nonquantitative identification test. A similar requirement is made for minor components.

Pharmaceutical equivalents are defined (3) as "drug products that contain identical amounts of the identical active drug ingredient. . . ." Drug product compliance with compendial standards is generally assumed to assure pharmaceutical equivalence (4). A consequence of the broad or nonquantitative specifications for both major and minor components is that compendial standards may not

0022-3549/79/0800-0986$01.00/0

© 1979, American Pharmaceutical Association

a delay between disappearance from the lumen and appearance in the blood, are in agreement with previous studies (12), which indicate that the greater a compound's lipophilicity, the longer will be its holdup in the intestinal wall and the less will penetrate to the serosal side of the membrane.

Finally, as is expected with longer holdup, the ester is more extensively metabolized than is the acid, as indicated by TLC. With dinoprost, the main metabolites are 15-ketodinoprost and 13,14-dihydro-15-ketodinoprost. As the experiment progressed, the metabolism decreased (Fig. 7). With the ester, four main metabolites are seen: dinoprost, 15-ketodinoprost, 13,14-dihydro-15-ketodinoprost, and 13,14-dihydrodinoprost. Although the amount of intact ester entering the blood increased slightly as the experiment progressed, the total metabolism increased, as indicated by the increase in 13,14-dihydrodinoprost in the circulation.

In summary, intestinal prostaglandin absorbed appears to have at least three phases. First, prostaglandins appear to diffuse rapidly from the gut lumen into the intestinal wall. Second, once in the gut wall, time is required for the compound to reach the other side of the cell. During this transcellular movement, the compound appears to be extensively, although not completely, metabolized. The duration of this second phase appears to be directly related to lipophilicity. Third, the compound and its metabolites are released into the mesenteric circulation. Prostaglandin esters apparently are released slower and over a longer period than the parent acids; however, they also undergo more extensive metabolism.

This study demonstrated differences in dinoprost and dinoprost methyl ester absorption patterns in the rat. However, these differences were not in agreement with the hypothesis that prostaglandin esters are absorbed faster than the parent prostaglandins in this species.

REFERENCES

(1) W. Magee, S. Armour, and O. Miller, *Biochim. Biophys. Acta*, **306**, 270 (1973).

(2) A Robert, W. Magee, O. Miller, and J. Nezamis, *ibid.*, **348**, 269 (1974).

(3) N. F. H. Ho and W. Higuchi, *J. Pharm. Sci.*, **63**, 686 (1974).

(4) N. Ho, J. Park, W. Morozowich, and W. Higuchi, *J. Theoret. Biol.*, **61**, 185 (1976).

(5) J. Y. Park, thesis, University of Michigan, Ann Arbor, Mich., 1977.

(6) F. Jacobs and M. Luper, *J. Appl. Physiol.*, **11**(I), 136 (1957).

(7) P. Jacobs, F. H. Bothwell, and R. Charlton, *Am. J. Physiol.*, **210**, 694 (1966).

(8) H. Kavin, N. Levin, and M. Stanley, *J. Appl. Physiol.*, **22**, 604 (1967).

(9) J. Lee, *Am. J. Physiol.*, **200**, 979 (1961).

(10) J. Lee and K. Duncan, *Gastroenterology*, **54**, 559 (1968).

(11) K. J. Desai, thesis, University of Michigan, Ann Arbor, Mich., 1977.

(12) V. Houston, D. Upshall, and J. Bridges, *J. Pharmacol. Exp. Ther.*, **189**, 244 (1974).

ACKNOWLEDGMENTS

Special thanks are extended to Dr. N. F. H. Ho, Department of Pharmaceutical Chemistry, University of Michigan, Ann Arbor, Mich., for advice and consultation during this work.

Conjugated Estrogens Bioinequivalence: Comparison of Four Products in Postmenopausal Women

WALLACE P. ADAMS *x, JUN HASEGAWA *, RAYMOND N. JOHNSON ‡, and RONALD C. HARING ‡

Received November 6, 1978, from the **Pharmacy Research and Development Department and the* ‡*Analytical Research and Development Department, Ayerst Laboratories Inc., Rouses Point, NY 12979.* Accepted for publication February 7, 1979.

Abstract □ The bioequivalence of four conjugated estrogens tablets USP was compared by measurement of seven estrogens or estrogen metabolites in the urine during steady-state dosing in postmenopausal women. Two studies compared three generic products with the innovator's product. The urinary excretion of 17α-dihydroequilin, 17α-dihydroequilenin, and 17α-estradiol were significantly greater in all cases with the innovator's product than with the generic products. Statistically significant differences between products were observed occasionally for other components. The generic products thus were bioinequivalent to the innovator's product, although all products essentially met current compendial specifications. A third study observed no significant differences between three batches of the innovator's product for the seven components. Total conjugated estrogens excretion of all products at the steady state was essentially equal and correlated with neither disintegration time nor dissolution half-time. Bioinequivalence between products is discussed in relation to the need for an improved USP conjugated estrogens monograph. Evidence suggesting the metabolism of a fraction of dosed estrone, equilin, and 17α-dihydroequilin to 17β-estradiol, 17β-dihydroequilin, and 17α-dihydroequilenin, respectively, is presented.

Keyphrases □ Estrogens, conjugated—bioinequivalence of generic and proprietary products, postmenopausal women □ Bioequivalence—conjugated estrogens, bioinequivalence of generic and proprietary products, postmenopausal women □ Product substitution—estrogens, conjugated, bioinequivalence of generic and proprietary products, postmenopausal women

Conjugated estrogens of natural origin are composed of at least nine different estrogens or estrogen metabolites, each present in a different amount. The USP monograph for conjugated estrogens (1) contains specifications for total conjugated estrogens and for the two most abundant components, sodium estrone sulfate and sodium equilin sulfate. The sodium estrone sulfate specification is 50–65% and the sodium equilin sulfate specification is 20–35% of the total conjugated estrogens content. The monograph does not contain quantitative specifications for additional components, although an identification test (2) requires the presence of a prominent GLC peak for 17α-dihydroequilin and additional peaks for 17α-estradiol, 17β-dihydroequilin, equilenin, 17β-estradiol, and 9-dehydroestrone.

Broad content ranges are specified for sodium estrone sulfate and sodium equilin sulfate. The content of the third major component, sodium 17α-dihydroequilin sulfate, which by GLC is 15% of the total estrogens in the innovator's product, is unspecified; the specification for this component is an imprecise and nonquantitative identification test. A similar requirement is made for minor components.

Pharmaceutical equivalents are defined (3) as "drug products that contain identical amounts of the identical active drug ingredient. . . ." Drug product compliance with compendial standards is generally assumed to assure pharmaceutical equivalence (4). A consequence of the broad or nonquantitative specifications for both major and minor components is that compendial standards may not

0022-3549/79/0800-0986$01.00/0

© 1979, American Pharmaceutical Association

Table I—Estrogens Content Determined by USP XIX Assay Method, Disintegration Times, and Dissolution Half-Times of Conjugated Estrogens Tablets USP [a]

Product or Batch	Sodium Estrogen Sulfate Content, mg/tablet			Disintegration Time, min		Dissolution Half-Time, min	
	Estrone	Equilin	Total Conjugated Estrogens	Mean	Range	Mean	Range
			Study I				
P1	0.70	0.38	1.29	23.0	19–29	24.5	23.4–25.9
A	0.82	0.34	1.24	28.2	25–31	55.5	48.4–64.7
			Study II				
P2	0.69	0.35	1.31	41.3	36–49	119	101–138
B	0.74	0.33	1.18	22.5	18–30	89.1	54.3–123
C	0.75	0.34	1.20	74.5	69–81	—[b]	—[b]
			Study III				
P3	0.66	0.36	1.27	56.2	49–67	224	186–287
P4	0.67	0.38	1.28	38.9	33–44	164	148–175
P5	0.69	0.37	1.30	41.8	38–52	241	199–284

[a] The assay for estrogens content, disintegration times, and dissolution half-times used 20, six, and three tablets, respectively, except the disintegration times for P3, P4, and P5, which used 24 tablets. [b] Tablets were unavailable for dissolution half-time determination.

assure the pharmaceutical equivalence of conjugated estrogens products.

A previous publication (5) presented a sensitive and specific method to quantitate seven estrogens or estrogen metabolites in the urine of postmenopausal subjects after dosing to the steady state. The usefulness of the urinary excretion profile in assessing the bioinequivalence of conjugated estrogens products from multiple sources was discussed. The present investigation examined the bioinequivalence of four conjugated estrogens products based on their urinary excretion profiles. The innovator's product and three generic products, all of which meet or nearly meet current compendial specifications, were studied. The purpose of this study was to investigate the extent to which adherence of these products to compendial specifications assures their bioequivalence.

EXPERIMENTAL

The results of Studies I–III, conducted at intervals of 1 year, are reported.

Subjects—Eleven, 12, and eight postmenopausal women were selected for Studies I, II, and III, respectively. A physical examination and medical history were obtained for each subject. The postmenopausal syndrome was established by documented physiological or surgical menopause of long duration and anestrogenism was established by colpocytogram. Each subject in Studies II and III was requested to take no medication other than the conjugated estrogens. Each subject signed a voluntary informed consent form.

Study I—The two physiologically menopausal subjects' ages were 51 and 54 years, and the nine surgically menopausal subjects' average age was 50 years (range 44–61). The average weight of all subjects was 65 kg (range 54–91). Serum biochemistry tests[1] and urinalyses[2] (pH, glucose, and protein) were conducted to assure normal liver and kidney function. Nine subjects were concomitantly receiving thyroid replacement hormones, digoxin, or an oral hypoglycemic agent.

Study II—The eight physiologically menopausal subjects' average age was 52 years (range 50–57), and the four surgically menopausal subjects' average age was 44 years (range 37–54). The average weight of all subjects was 62 kg (range 54–73). All subjects were in good health, established by physical examination, serum biochemistry tests[1], and urinalyses[2] (pH, glucose, and protein).

Study III—The four physiologically menopausal subjects' average age was 53 years (range 51–56), and the four surgically menopausal subjects' average age was 35 years (range 29–38). The average weight of all subjects was 65 kg (range 51–94). The good health of the subjects was established as in Study II.

[1] SMA 12/60.
[2] Combistix, Ames Co., Elkhart, Ind.

Protocol—*Study I*—The study was divided into four consecutive phases of 28, 21, 14, and 21 days. The first phase was a washout period to permit urinary estrogen levels of those subjects previously taking estrogen medication to return to baseline levels. At the end of this phase, a 24-hr urine sample was collected from each subject.

During the second phase, each subject received a 2.5-mg dose (as two 1.25-mg tablets) of conjugated estrogens daily for 21 days. Each subject received Treatments P1[3] and A (generic product) in a randomized two-way crossover design. Each subject was instructed to select a time for dosing each morning and to take the dose at the same time each morning. On any day between Days 16 and 20 inclusive, a 24-hr urine sample was collected from each subject beginning at the time of dosing. The third phase was a washout period; a 24-hr urine sample was collected on any day between Days 11 and 13 inclusive. The fourth phase was the second half of the crossover design.

Diet was unrestricted throughout the three studies.

Study II—The study was divided into four consecutive 28-day phases. The first phase was a washout period; a 24-hr urine sample was collected from each subject during the latter part of the 4th week. Each subject received two 1.25-mg tablets of conjugated estrogens daily for 21 days during the last three phases. Each subject received Treatments P2[4], B (generic product), and C (generic product) in a randomized three-way crossover design. Each subject was instructed to select a time for dosing each morning and to take the dose at the same time each morning. On Days 17–19, three consecutive 24-hr urine samples were collected from each subject, beginning at the time of dosing. In accord with the recommended cyclic dosing schedule, no medication was administered during the last 7 days of the last three phases.

Study III—The study design was similar to that of Study II. Six subjects were common to Studies II and III. A shorter washout phase of at least 18 days was allowed for these six subjects. Each subject received Treatments P3[5], P4[6], and P5[7] in a randomized three-way crossover design.

***In Vitro* Tests**—The content and disintegration times of each product and batch were determined for conformity to USP specifications. Sodium estrone sulfate, sodium equilin sulfate, and total conjugated estrogens were determined by the spectrophotometric method described in the USP. Disintegration times were determined by the procedure for plain coated tablets described in the USP (6). The content of nine individual sodium estrogen sulfates was determined by a GLC method (7).

Dissolution half-times were determined utilizing USP Dissolution Method II (8). The dissolution medium was simulated gastric fluid TS, 1000 ml, and the stirring speed was 150 rpm. Based upon preliminary studies, at least six 10-ml samples were withdrawn at times above and below the dissolution half-times for each product or batch. The dissolution medium was not replaced after sampling. Results were determined

[3] Premarin conjugated estrogens tablets USP, batch 108984, Ayerst Laboratories, Montreal, Quebec, Canada.
[4] Premarin conjugated estrogens tablets USP, batch D403 WXA, Ayerst Laboratories, New York, N.Y.
[5] Premarin conjugated estrogens tablets USP, batch E124 BFA, Ayerst Laboratories, New York, N.Y.
[6] Premarin conjugated estrogens tablets USP, batch A176 AFP, Ayerst Laboratories, New York, N.Y.
[7] Premarin conjugated estrogens tablets USP, batch J203 CLB, Ayerst Laboratories, New York, N.Y.

Table II—GLC Analysis of Conjugated Estrogens Tablets USP

Sodium Estrogen Sulfate	Product or Batch, μg/tablet							
	P1	P2	P3	P4	P5	A	B	C
Estrone	715	730	720	687	720	846	806	853
Equilin	308	352	326	327	314	351	348	371
Equilenin	42	37	29	31	38	46	40	46
17α-Estradiol	45	48	46	60	59	11	11	11
17β-Estradiol	11	10	8	10	10	3	2	3
17α-Dihydroequilin	211	220	216	220	214	37	54	53
17β-Dihydroequilin	35	27	31	33	29	4	7	5
17α-Dihydroequilenin	29	20	19	24	23	4	8	12
17β-Dihydroequilenin	9	8	7	9	8	—[a]	—[a]	—[a]
Total	1405	1452	1402	1401	1415	1302	1276	1354

[a] Approximately 1 μg of 17β-dihydroequilenin was present in Products A–C; accurate quantitation was prevented by an interfering peak in the chromatogram.

by interpolation after correction for the drug and dissolution medium removed by sampling.

Assay—Seven estrogens or estrogen metabolites in the urine were determined using enzyme hydrolysis of urine samples, extraction and purification, and GLC (5). An initial version of the method, in which urine samples were frozen prior to assay and the GLC derivatization reagent contained 1% trimethylchlorosilane catalyst, was used for Study I. Studies II and III used the published method, which specifies refrigerated sample storage and a 10% catalyst level.

Aliquots of each 24-hr urine sample from the three studies were assayed for creatinine (9, 10).

Calculations—Urinary excretion differences between treatments were examined based on the 1-day levels (Study I) or on the 3-day mean levels (Studies II and III) of each estrogen (11–13). Attainment of the steady state in Studies II and III was examined by multivariate analysis of the Day 18 minus Day 17 and Day 19 minus Day 18 differences (14). When significant treatment differences were observed in Study II, differences between individual treatments were evaluated by a Student t test, with the Bonferroni adjustment for multiple comparisons.

RESULTS AND DISCUSSION

Tablet Assays—The total conjugated estrogens content of all products (Table I) was within USP specifications (6) and ranged from 1.18 to 1.31 mg/tablet or from 94.4 to 104.8% of the labeled amount. Sodium estrone sulfate ranged from 52.0 to 62.7% of the total conjugated estrogens content in seven products or batches; Product A exceeded the USP specification range (1) of 50.0–65.0% by 1.1%. Sodium equilin sulfate was within USP specifications (1) in all cases and ranged from 26.7 to 29.7% of the total conjugated estrogens content.

The content in all products of nine individual sodium estrogen sulfates and their total was determined by GLC analysis (Table II).

Disintegration and Dissolution—The disintegration times of all products (Table I) were within the 90 min specified by the USP and ranged from 22.5 to 74.5 min. No correlation was observed between the disintegration times and the amounts of total conjugated estrogens excreted per 24 hr at the steady state.

The USP conjugated estrogens tablets monograph does not contain a dissolution rate requirement. A study was performed to investigate the possible relationship between dissolution rate and estrogens excretion. Mean dissolution half-times ranged from 24.5 to 241 min (Table I); a correlation between these values and mean disintegration times was observed ($r = 0.84$, $p < 0.025$). No correlation between dissolution rate and estrogens excretion was observed.

The correlation was based on data obtained from separate disintegration time and dissolution rate experiments. A previous study[8] of the disintegration times of two batches of the innovator's product and four generic products in simulated gastric fluid TS and assay of conjugated estrogens dissolved in this fluid during tablet disintegration demonstrated no significant difference between disintegration times and times to 90% dissolution. These results, combined with those of the present study, indicate that, for the representative products examined, water-soluble sodium estrogen sulfate dissolution is rate limited by disintegration. Since the total conjugated estrogens excretion of all products was essentially equal, as will be discussed in a subsequent section, and individual tablet disintegration times ranged only up to 81 min, the validity of the 90-min USP disintegration time limit (6) in assuring equal extent of absorption could not be examined.

[8] R. N. Johnson and R. P. Neil, Ayerst Laboratories, Rouses Point, N.Y., unpublished results.

Bioinequivalence Method—Bioequivalent drug products are defined (3) as "pharmaceutical equivalents or pharmaceutical alternatives whose rate and extent of absorption do not show a significant difference . . . ." The present experimental design precluded rate measurements. Equal extent of urinary excretion is a necessary, but not sufficient, condition for bioequivalency. However, unequal urinary excretion is a sufficient condition for bioinequivalence. Therefore, the present method permits assessment of bioinequivalence of conjugated estrogens products if those products differ in the extent of absorption.

Improvements in sample storage and analytical procedure, which resulted in the improved recovery values reported previously, were made after Study I. The subject population was different in all three studies, although six subjects were common to Studies II and III. Therefore, absolute values between studies must be compared cautiously. Mean endogenous urinary estrogen levels (Tables III–V) generally were near, but greater than, the estimated minimum quantifiable levels reported previously.

The frequent occurrence of endogenous estrogens below the minimum quantifiable levels in some subjects increased the uncertainty in their estimation. However, the mean values were considered sufficiently reliable for each study to estimate true increases in excretion by subtraction

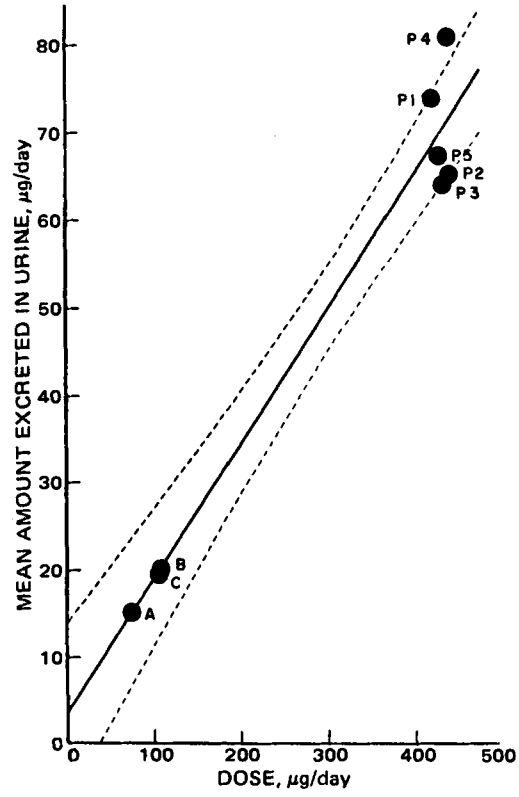

Figure 1—*Correlation between the daily sodium 17α-dihydroequilin sulfate dose and the amount of 17α-dihydroequilenin, expressed as the sodium estrogen sulfate, excreted in the urine per day* ($r = 0.98$, $p < 0.001$) *for each product or batch. Values corrected for endogenous levels. Key: P1–P5, five batches of the innovator's product; A–C, three generic products; ---, 95% confidence limits about the regression line.*

Table III—Mean Steady-State Urinary Estrogen Levels Over 24 hr for 11 Subjects Receiving Treatments P1 and A Conjugated Estrogens Tablets (Study I)

	Sodium Estrogen Sulfate[a]							
	17α-ED	17β-ED	17α-DHEQ	17β-DHEQ	17α-DHEQN	ES	EQ	Total
Mean endogenous levels[b], μg/24 hr	7.0	10.9	1.5	2.0	3.5	10.0	5.9	40.8
Treatment means[b,c], μg/24 hr								
P1	22.8	102.2	23.0	32.3	77.5[d]	339.1	25.0	621.9
A	9.2	86.9	1.5	25.2	18.7[d]	406.7	28.1	576.3
Probability of difference between treatment averages	$p = 0.064$	N.S.[e]	$p < 0.01$	N.S.	$p < 0.001$	$p < 0.05$	N.S.	—

[a] Abbreviations are as follows: 17α-ED, 17α-estradiol; 17β-ED, 17β-estradiol; 17α-DHEQ, 17α-dihydroequilin; 17β-DHEQ, 17β-dihydroequilin; 17α-DHEQN, 17α-dihydroequilenin; ES, estrone; and EQ, equilin. [b] Values are uncorrected for analytical losses (Tables III–V). [c] Values are uncorrected for endogenous levels (Tables III–V). [d] Values represent the data of 10 subjects only. [e] Not statistically significant at $p < 0.05$ (Tables III–V).

Table IV—Mean Steady-State Urinary Estrogen Levels over Three Consecutive 24-hr Periods for 12 Subjects Receiving Treatments P2, B, and C Conjugated Estrogens Tablets (Study II)

	Sodium Estrogen Sulfate[a]							
	17α-ED	17β-ED	17α-DHEQ	17β-DHEQ	17α-DHEQN	ES	EQ	Total[b]
Mean endogenous levels, μg/24 hr	10.0	9.2	1.6	1.3	3.9	8.1	3.4	37.5
Treatment means, μg/24 hr								
P2 Day 17	32.7	65.8	26.6	28.1	72.2	330.2	15.0	549.3
Day 18	30.3	69.1	20.2	25.5	66.5	341.0[c]	13.3[c]	565.7
Day 19	32.0	67.6	25.2	28.5	69.4	319.9[c]	14.5[c]	545.1
Mean	31.7	67.5	24.0	27.4	69.4	330.4	14.3	553.4
B Day 17	19.8	68.4	6.2	26.5	21.5	349.6	11.0	507.5
Day 18	18.2	69.4	3.9	26.8	26.7	353.7	13.0	507.6
Day 19	15.5	78.6	4.1	28.3	24.2	357.5	9.3	523.1
Mean	17.8	72.1	4.7	27.2	24.1	353.6	11.1	512.7
C Day 17	20.0	89.2	6.6	30.4	26.3	427.5	10.0	608.8
Day 18	20.0	85.4	3.4	27.8	24.5	390.2	12.6	566.4
Day 19	21.3	82.0	13.2	25.8	20.0	330.2	9.4	503.1
Mean	20.4	85.5	7.7	28.0	23.6	382.6	10.7	559.4
Probability of differences among treatment averages	$p < 0.01$	$p < 0.01$	$p < 0.01$	N.S.	$p < 0.01$	N.S.	N.S.	—
Student t test[d]								
P2 *versus* B	$p < 0.01$	N.S.	$p < 0.01$	—	$p < 0.01$	—	—	—
P2 *versus* C	$p < 0.01$	$p < 0.05$	$p < 0.01$	—	$p < 0.01$	—	—	—

[a] See footnote *a* of Table III. [b] Totals for the treatment means represent the data of 11 subjects only. [c] Values represent the data of 11 subjects only. [d] With the Bonferroni adjustment for multiple comparisons.

Table V—Mean Steady-State Urinary Estrogen Levels over Three Consecutive 24-hr Periods for Eight Subjects Receiving Treatments P3, P4, and P5 Conjugated Estrogens Tablets (Study III)

	Sodium Estrogen Sulfate[a]							
	17α-ED	17β-ED	17α-DHEQ	17β-DHEQ	17α-DHEQN	ES	EQ	Total
Mean endogenous levels, μg/24 hr	24.6	30.9	—[b]	—[b]	5.1	7.7	5.4	—
Treatment means, μg/24 hr								
P3 Day 17	41.9	81.0	26.5	32.3	70.3	375.4	11.5	639.0
Day 18	46.4	74.7	24.9	27.8	66.5	341.7	12.4	594.3
Day 19	43.4	85.5	24.8	30.0	70.9	379.2	13.6	647.4
Mean	43.9	80.4	25.4	30.0	69.2	365.4	12.5	626.9
P4 Day 17	53.3	82.6	36.7	36.2	85.9	382.9	15.4	692.9
Day 18	45.6	70.2	31.3	31.4	80.0	360.5	10.9	629.8
Day 19	45.6	76.6	32.9	32.8	92.5	369.0	11.7	661.1
Mean	48.2	76.5	33.6	33.5	86.1	370.8	12.7	661.3
P5 Day 17	47.5	89.2	31.1	32.0	73.4	384.6	11.3	669.1
Day 18	48.5	93.2	32.8	33.0	75.1	375.3	12.1	669.9
Day 19	47.1	82.1	33.5	34.7	69.4	401.3	10.5	678.6
Mean	47.7	88.2	32.5	33.2	72.6	387.1	11.3	672.5
Probability of differences among treatment averages	N.S.	N.S.	N.S.	N.S.	N.S.	N.S.	N.S.	—

[a] See footnote *a* of Table III. [b] The 17α-DHEQ region was masked in six of eight Phase I samples; the 17β-DHEQ region was masked in five of eight samples. Correction for endogenous levels is made using the values obtained in Study II.

of endogenous levels. In this manner, absolute comparisons of excreted estrogens as a function of dose could be made for the combined studies. The absence of information about the specific conjugate estrogen forms excreted does not allow determination of pertinent percentage recovery data. Therefore, the values reported in Tables III–V and subsequent values calculated from these data are not corrected for analytical losses.

The primary advantage of steady-state bioinequivalence studies for the conjugated estrogens is the ability to obtain the highest possible estrogen levels in the biological samples with normal doses while adhering to the recommended cyclic drug dosing schedule. Inadequate knowledge of the elimination pathways and their rates for each estrogen prohibited estimating the time of attainment of the steady state upon daily dosing. Therefore, samples were collected late in the normal 21-day dosing cycle, on a single day between Days 16 and 20 inclusive (Study I) or on Days 17–19 (Studies II and III).

The daily changes in excreted amounts of each estrogen or estrogen metabolite (Day 18 minus Day 17 and Day 19 minus Day 18) were not significantly different from zero. Therefore, the steady state was reached by Day 17, and each study was performed under steady-state conditions.

Metabolic Interconversions—Although metabolism studies were not an objective of the present work, the excretion of three of the seven components in greater than dosed amounts permitted tentative assignment of their conjugated estrogens origin. The high levels of 17β-estradiol in the urine appear to reflect the well-established metabolic reduction of estrone in humans (15). The amount of 17β-dihydroequilin found in the urine was essentially constant among all products tested and independent of the 17β-dihydroequilin content of these products. Also, levels of 17β-dihydroequilin in the urine exceeded the dosed amounts of this component in the generic products and the dosed amounts of 17β-dihydroequilenin in all products. The apparently constant excretion suggests

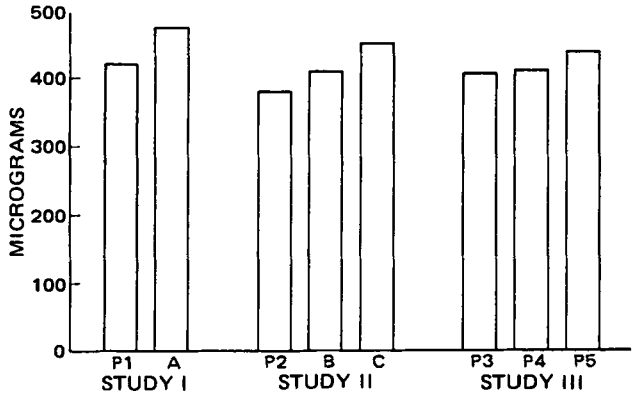

Figure 2—*Summation of estrone and 17β-estradiol, expressed as the sodium estrogen sulfates, excreted in the urine per day at the steady state during daily dosing with two 1.25-mg conjugated estrogens tablets USP. Values are corrected for endogenous levels. Key: see Fig. 1.*

origin from equilin, the tablet content of which was relatively constant for all products. This metabolic conversion is analogous to the reduction of estrone to 17β-estradiol, the only structural difference being the presence of a double bond in the B ring of equilin and 17β-dihydroequilin. The reduction of equilin to 17β-dihydroequilin was observed previously in dogs[9].

The amounts of 17α-dihydroequilenin excreted in the urine are generally greater than the dosed amounts. Possible sources of this compound are 17α-dihydroequilin, equilin, and equilenin. The equilin and equilenin content of all products is relatively constant, whereas the content of 17α-dihydroequilin is much greater in the reference product than in the generic products. A highly significant correlation was observed between the 17α-dihydroequilin dose and the amount of 17α-dihydroequilenin excreted (Fig. 1). Approximately 12% of 17α-dihydroequilin in urine samples is oxidized to 17α-dihydroequilenin during assay (5). This amount would not account for the observed recovery of 17α-dihydroequilenin in the urine and suggests oxidative metabolism of a portion of the dosed 17α-dihydroequilin.

Product Bioinequivalence—The mean endogenous estrogen levels and levels of seven estrogens and estrogen metabolites and their totals excreted during dosing are presented in Tables III–V. Analyses of variance revealed no significant differences in urinary excretion among Treatments P3, P4, and P5 for the seven estrogens (Table V). These three treatments were three batches of the innovator's product manufactured in March, June, and September of 1976 and represented production over a full raw material collection season.

Analyses of variance revealed significant differences in urinary estrogen levels between the innovator's product and the generic products for certain estrogens or estrogen metabolites (Tables III and IV). Levels of

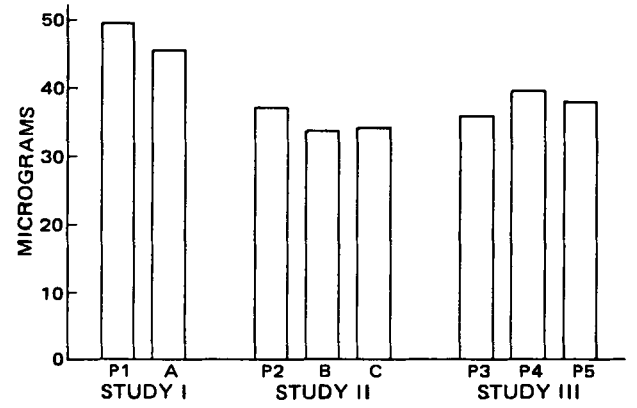

Figure 3—*Summation of equilin and 17β-dihydroequilin, expressed as the sodium estrogen sulfates, excreted in the urine per day at the steady state during daily dosing with two 1.25-mg conjugated estrogens tablets USP. Values are corrected for endogenous levels. Key: see Fig. 1.*

[9] K. Sestanj and D. Dvornik, Ayerst Laboratories, Montreal, Quebec, Canada, unpublished results.

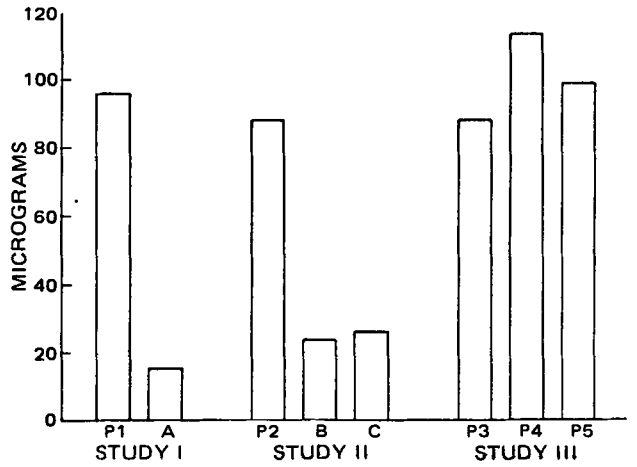

Figure 4—*Summation of 17α-dihydroequilin and 17α-dihydroequilenin, expressed as the sodium estrogen sulfates, excreted in the urine per day at the steady state during daily dosing with two 1.25-mg conjugated estrogens tablets USP. Values are corrected for endogenous levels. Key: see Fig. 1.*

17α-estradiol after dosing with the three generic products were significantly lower than after dosing with the reference product ($p = 0.064$, Treatment A; $p < 0.01$, Treatments B and C). Levels of 17α-dihydroequilin and 17α-dihydroequilenin were also significantly lower with the generic products ($p < 0.01$, Treatments A–C, 17α-dihydroequilin; $p < 0.001$, Treatment A, $p < 0.01$, Treatments B and C, 17α-dihydroequilenin). Levels of estrone were significantly higher after dosing with Treatment A than after dosing with the reference product ($p < 0.05$). Levels of 17β-estradiol were significantly higher after dosing with Treatment C than after dosing with the reference product ($p < 0.05$).

The discussed metabolic relationships provided a basis for separating the urinary excretion of the conjugated estrogens components into groups (Figs. 2–4). Exceedingly small amounts of 17α-estradiol were observed in the urine of a premenopausal woman (16), possibly as a consequence of estrone metabolism. In the present study, the absence of a correlation with dosed estrone, the good correlation with dosed 17α-estradiol, and the mean recovery of only 24.2% of the dose suggest that dosed 17α-estradiol is the source of the excreted compound. Thus, 17α-estradiol was categorized separately (Fig. 5).

Figure 2 indicates relatively small differences between products in the summation of estrone and 17β-estradiol. Of the six instances in which differences between the reference and generic products are possible for these compounds, only two comparisons were statistically significant. Similarly, relatively small differences between products were observed in the equilin plus 17β-dihydroequilin group (Fig. 3). No significant differences between products were observed within this group. In these two groups, variations between the mean urinary estrogen excretion of the reference product and of the generic product(s) within Studies I and II were less than 20%. Similarly, variations between the mean urinary estrogen excretion of the five batches of the reference product and each generic product were less than 20%.

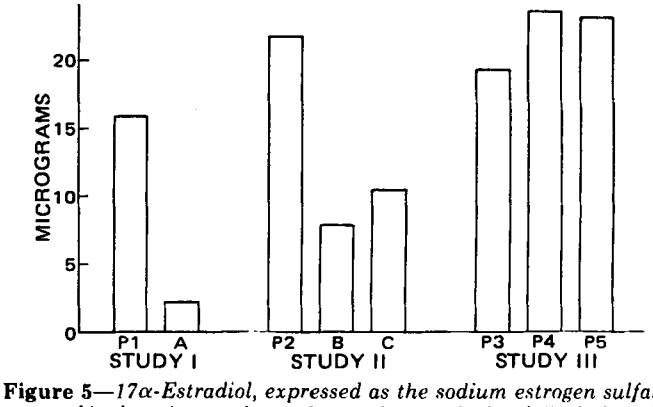

Figure 5—*17α-Estradiol, expressed as the sodium estrogen sulfate, excreted in the urine per day at the steady state during daily dosing with two 1.25-mg conjugated estrogens tablets USP. Values are corrected for endogenous levels. Key: see Fig. 1.*

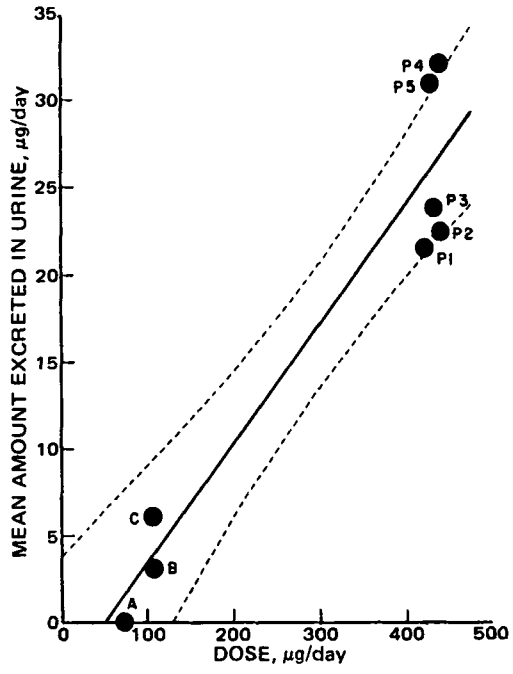

Figure 6—*Correlation between the daily dose of sodium 17α-dihydroequilin sulfate and the amount of 17α-dihydroequilin, expressed as the sodium estrogen sulfate, excreted in the urine per day (r = 0.95, p < 0.001) for each product or batch. Values are corrected for endogenous levels. Key: see Fig. 1.*

Urinary excretion of the 17α-dihydroequilin and 17α-dihydroequilenin group (Fig. 4) and of 17α-estradiol (Fig. 5) was markedly different between the innovator's product and the generic products. In every case, the greater excretion of these components after dosing with the innovator's product was statistically significant compared to dosing with the generic products. The excretion of 17α-dihydroequilin plus 17α-dihydroequilenin of generic Products A, B, and C relative to the reference product was 15.9, 26.5, and 29.4%, respectively. Comparable values for 17α-estradiol excretion from the three generic products relative to the reference product were 13.9, 35.9, and 47.9%, respectively.

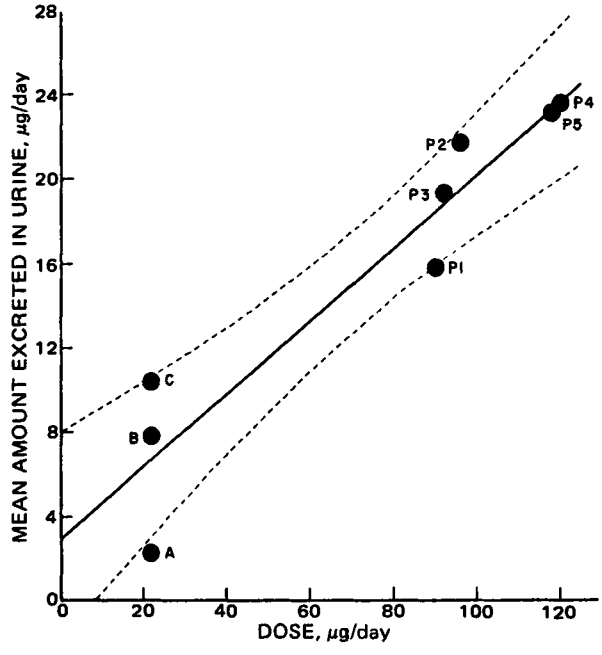

Figure 7—*Correlation between the daily dose of sodium 17α-estradiol sulfate and the amount of 17α-estradiol, expressed as the sodium estrogen sulfate, excreted in the urine per day (r = 0.94, p < 0.001) for each product or batch. Values are corrected for endogenous levels. Key: see Fig. 1.*

If urinary estrogen excretion were a measure of relative extent of absorption, there should be a linear relationship between dose and urinary excretion. This relationship was previously established by demonstrating that at the 1.25- and 2.5-mg dose levels, constant percentages of the individual estrogens were excreted. In the present study, highly significant correlations between the four- to fivefold differences in the dose of 17α-dihydroequilin and 17α-estradiol among the four products and their excretion in the urine were observed (Figs. 6 and 7). These correlations confirm previous findings.

Total estrogen recoveries from all products were similar. Expressed as a percentage of the daily dose and calculated as previously described, the mean total recovery for all treatments was 19.9 ± 1.2 (*SD*) %. The extent of absorption and metabolic fate of the conjugated estrogens are unknown. However, when solutions of 4-^{14}C-estrone sulfate (6-mg dose) and 6,9-^{3}H-equilin sulfate (7-mg dose) were simultaneously ingested by two premenopausal volunteers (21 and 22 years old), a total of 70–88% of the administered radioactivity was recovered in the urine after 5 days[10]. These findings, together with the results of the present study, indicate that these estrogens are both well absorbed and highly metabolized.

The results from Tables III and IV and Figs. 4 and 5 clearly indicate that the three generic conjugated estrogens products studied are bioinequivalent to the innovator's product. This bioinequivalence occurs primarily as a result of large differences in the urinary 17α-hydroxy estrogen levels. As shown in Figs. 6 and 7, the bioinequivalence of the generic conjugated estrogens products relative to the innovator's product is due to differences in estrogens composition among products (Table II). The absence of significant differences between batches of the innovator's product (Table V) is due to the similar composition of each batch. Thus, the bioinequivalence that occurs among conjugated estrogens products is attributable to their pharmaceutical inequivalence. The broad content ranges for sodium estrone sulfate and sodium equilin sulfate and the inadequate specifications for other components suggest the need for more rigorous specifications in the USP conjugated estrogens monograph.

REFERENCES

(1) "The United States Pharmacopeia," 19th rev., Mack Publishing Co., Easton, Pa., 1975, pp. 181, 182.

(2) "Fourth Supplement to USP XIX and NF XIV," Mack Publishing Co., Easton, Pa., Jan. 31, 1978, pp. 74, 75.

(3) *Fed. Regist.*, **42**, 1624 (Jan. 7, 1977), Title 21, subchapter D, part 320.

(4) M. I. Blake, *U.S. Pharmacist*, **3**, 66 (1978).

(5) R. N. Johnson, R. P. Masserano, B. T. Kho, and W. P. Adams, *J. Pharm. Sci.*, **67**, 1218 (1978).

(6) "The United States Pharmacopeia," 19th rev., Mack Publishing Co., Easton, Pa., 1975, pp. 182, 183, 650.

(7) R. Johnson, R. Masserano, R. Haring, B. Kho, and G. Schilling, *J. Pharm. Sci.*, **64**, 1007 (1975).

(8) "Fourth Supplement to USP XIX and NF XIV," Mack Publishing Co., Easton, Pa., Jan. 31, 1978, pp. 194, 195.

(9) S. Pino, J. Benotti, and H. Gardyna, *Clin. Chem.*, **11**, 664 (1965).

(10) M. G. Metcalf and E. G. Hunt, *Clin. Biochem.*, **9**, 75 (1976).

(11) J. E. Grizzle, *Biometrics*, **21**, 467 (1965).

(12) P. W. John, "Statistical Design and Analysis of Experiments," Macmillan, New York, N.Y., 1971, pp. 115–117.

(13) B. J. Winer, "Statistical Principles in Experimental Design," 2nd ed., McGraw-Hill, New York, N.Y., 1971, pp. 240–244.

(14) D. S. Morrison, "Multivariate Statistical Methods," 2nd ed., McGraw-Hill, New York, N.Y., 1976, chap. 5.

(15) C. Longcope, D. S. Layne, and J. F. Tait, *J. Clin. Invest.*, **47**, 93 (1968).

(16) H. Adlercreutz, M. J. Tikkanen, and D. H. Hunneman, *J. Steroid Biochem.*, **5**, 211 (1974).

ACKNOWLEDGMENTS

The authors acknowledge the assistance of Mr. C. F. Boudreau and Mr. M. T. Gaffney with the statistical analyses, Mr. N. G. Nash with the tablet dissolution studies, Ms. S. S. MackNair and Mrs. I. B. Matott with clinical aspects of the studies, and Dr. J. B. Southwick with medical supervision of the subjects.

[10] K. Sestanj, E. Langenbach, and D. Dvornik, Ayerst Laboratories, Montreal, Quebec, Canada, unpublished results.

Kinetics and Mechanism of Chlorambucil Hydrolysis

W. R. OWEN and P. J. STEWART ˣ

Received June 20, 1977, from the *Pharmacy Department, University of Queensland, St. Lucia, Australia.* Accepted for publication February 7, 1979.

Abstract □ The kinetics and mechanism of hydrolysis of the cytotoxic drug chlorambucil were investigated. A study of the reaction order and of the pH, dielectric constant, and ionic strength effects on the reaction rate revealed that the hydrolysis was a limiting unimolecular nucleophilic substitution, the rate-determining step being the ionization of the first 2-chloroethylamine chlorine. The hydrolysis rate was markedly dependent on the protonation degree of the chlorambucil basic group, indicating that a cyclic ethyleneimmonium ion may be involved in the rate-determining step.

Keyphrases □ Chlorambucil—hydrolysis, kinetics and mechanism, reaction order, pH, dielectric constant, ionic strength □ Antineoplastic agents—chlorambucil, hydrolysis, kinetics and mechanism, reaction order, pH, dielectric constant, ionic strength □ Hydrolysis—chlorambucil, kinetics and mechanism

The cytotoxic drug chlorambucil has been used clinically in the treatment of malignant conditions associated with white blood cell proliferation (follicular lymphoma, Hodgkin's disease, *etc.*) and ovarian carcinoma (1–3). Dosage forms include intravenous injections and perfusion fluids. In these aqueous media, chlorambucil, an aromatic nitrogen mustard, undergoes hydrolysis by nucleophilic substitution. The hydrolytic pathway involves several consecutive steps. Previous stability studies (4–8) were semiquantitative or revealed little information regarding the kinetics and mechanism of hydrolysis in conditions appropriate to formulation.

The formation of a cyclic ethyleneimmonium ion has been proposed as an intermediate in aliphatic nitrogen mustard hydrolysis (7). A cyclic intermediate has not been suggested for aromatic nitrogen mustards but would seem highly probable by analogy with the aliphatic series. However, in aromatic compounds, such an intermediate would probably be less favored since the availability of the lone electron pair on the nitrogen would be reduced somewhat by resonance with the π-electrons of the aromatic ring. Therefore, this investigation was undertaken to elucidate the reaction mechanism under conditions appropriate to formulation.

EXPERIMENTAL

Materials—Chlorambucil BP (mp 65.8–66.0°) was recrystallized from a light petroleum (bp 40–60°, dried over sodium)–benzene (fractionated and dried over sodium) mixture. Silver chloride was prepared by potentiometrically titrating silver nitrate (25 ml, 0.1 *M*) and nitric acid (1 ml) with sodium chloride (0.1 *M*) to the exact end-point using an automatic titrimeter. The supernatant liquid was decanted, and the silver chloride precipitate was washed six times with oxygen-free distilled water. The following buffers were used: boric acid (0.1 *M*) in potassium nitrate (0.1 *M*)–sodium hydroxide (0.1 *M*) for pH 10.1–7.8, and sodium acetate (0.1 *M*)–nitric acid (0.1 *M*) for pH 5.5–1.63. Other chemicals were reagent grade.

The silver–silver chloride electrodes were prepared electrolytically (9, 10) and possessed asymmetric potentials of $< \pm 0.02$ mv.

Kinetic Methods—*Potentiometric*—An alcoholic solution of chlorambucil (1 ml, 10 mg/ml) was added to the buffer (500 ml) in the reaction half-cell of the silver–silver chloride concentration cell (Fig. 1). The concentration cell was equilibrated previously in a water bath (25.00 ± 0.01°). The pH was measured[1] (±0.002 pH unit) initially and on completion of the kinetic run (pH difference was within ±0.05 pH unit in all experiments). The temperature was monitored throughout the experiment. Throughout the hydrolysis, the electromotive force (emf) and time were monitored on a data logging unit[2]. Selection of the appropriate range and sensitivity multiplier ensured maximum accuracy in the electromotive force measurement.

The silver–silver chloride concentration cell allowed continuous monitoring of the liberated chloride. At low chloride-ion concentrations and constant ionic strength, the electromotive force of the concentration cell was related to the liberated chloride by the following equation (10):

$$E = E' + 2.303RT/nF \log [c_A/2 + \sqrt{K_S + (c_A/2)^2}] \quad \text{(Eq. 1)}$$

where E is the electromotive force of the concentration cell; E' is the standard potential of the concentration cell, dependent on the reference half-cell potential and the activity coefficient correction term; R is the gas constant (8.314 J mole^{-1} deg^{-1}); T is the absolute temperature (°K), F is the Faraday constant (96,487 coulomb equivalents^{-1}); n is the number of electrons transferred per ion; c_A is the liberated chloride; and K_S is the silver chloride solubility product.

Preliminary electrode response calibrations showed that the concentration cell operated in a theoretical and reproducible manner. Use of E', slope ($2.303RT/nF$), and K_S, derived by a nonlinear parameter estimation (11) for each ionic strength, allowed calculation of the liberated chloride concentration. The first-order rate constants were determined by a linear least-squares regression–orthogonal polynomial analysis (12), using the c_∞ derived from all of the data by a nonlinear parameter estimation (10).

Conductimetric—An alcoholic chlorambucil solution was added to

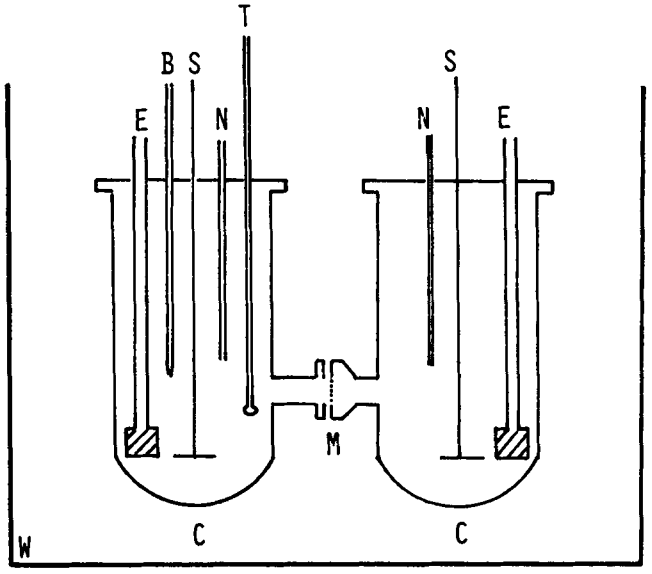

Figure 1—*Silver–silver chloride concentration cell for chloride determination. Key: W, thermostated water bath (±0.01°) containing the concentration cell (C); M, Millipore sintered-glass filter separating the half-cells of the concentration cell; E, silver–silver chloride electrodes; B, buret tip; S, mechanical stirrer; N, nitrogen inlet/outlet; and T, thermometer (0–50°).*

[1] Radiometer (pHM26).

[2] Solartron command range unit (EC 1475), digital voltmeter (LM 1420.2), punch drive (LU 1967), digital clock (LU 1963), scanner (LU 1461), and Facit paper tape punch (model 4070).

0022-3549/79/0800-0992$01.00/0
© 1979, American Pharmaceutical Association

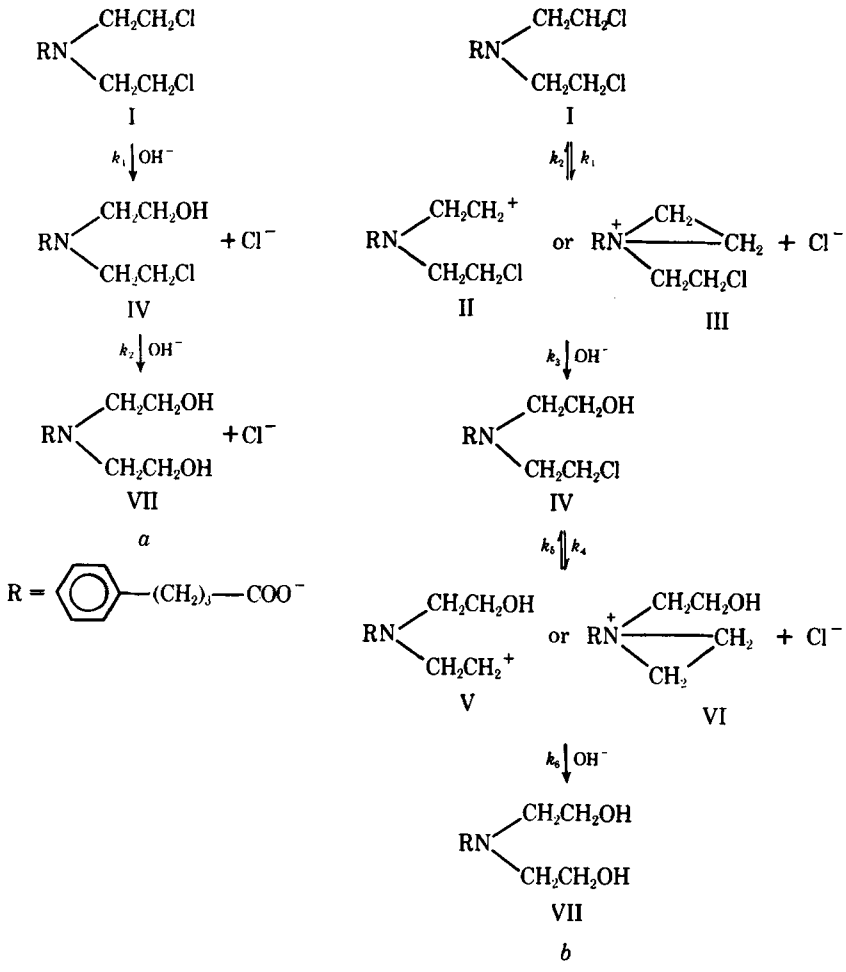

Scheme I—Alternative hydrolytic pathways for chlorambucil. Key: a, *bimolecular nucleophilic substitution; and* b, *unimolecular nucleophilic substitution.*

the reaction medium (500 ml) in a stoppered reaction vessel previously equilibrated in a water bath (25.00 ± 0.01°). The conductance was measured[3] at predetermined times with a platinized conductance cell (13). The temperature and pH were monitored throughout the experiment.

The ionized chlorambucil decomposition products (mainly chloride) were monitored conductimetrically. Preliminary experiments showed that the conductance–chloride-ion response calibrations were linear over the chloride concentration range required for the kinetic study. Rate constants were determined as in the potentiometric method, using conductance instead of concentration terms.

RESULTS AND DISCUSSION

Order of Reaction—The general shape of the chloride concentration–time curve (Fig. 2) typified first-order behavior. Fitting the data to the first-order model:

$$\log [(c_\infty - c_0)/(c_\infty - c)] = kt/2.303 \qquad \text{(Eq. 2)}$$

where c is the concentration of chloride at time t, c_0 is the initial concentration of chloride at time $t = 0$, c_∞ is the concentration of chloride at infinity, and k is the first-order rate constant (seconds^{-1}), and testing the linearity of this model (12) confirmed first-order behavior (Fig. 2). Attempts to fit more complex models were unrewarding and did not improve the fit.

The infinite chloride concentration in Fig. 2 was indicative of the hydrolysis of both chloroethyl chains (*i.e.*, 0.114×10^{-3} *M* compared to 0.120×10^{-3} *M*). This situation was typical of all kinetic runs. Therefore, the rate-determining step must be the hydrolysis of the first chlorine, because a consecutive pathway involving the hydrolysis of the chlorohydrin as the rate-determining step would result in a nonlinear first-order plot. This result was consistent with previous reports (5). For a first-order reaction, the hydrolysis mechanism of the first chlorine must be either limiting unimolecular ($k_1 \gg k_2$ and $k_3 \gg k_1$), with the rate-determining step being the ionization of the first chlorine (Scheme I*b*), or limiting bimolecular ($k_1 \ll k_2$), with the rate-determining step being the reaction of chlorambucil with H_2O or OH^- (Scheme I*a*).

pH Effect—Duplicate rate determinations for chlorambucil hydrolysis were made over pH 1.63–10.10 using the potentiometric method (Fig. 3).

Two discrete sections of the profile were obvious. First, at pH 5–10, the chlorambucil reaction rate with the amino group unionized [*i.e.*, pKa = 2.499 (10)] was independent of hydroxide ion, and a bimolecular substitution with the poorly nucleophilic water molecule seemed unlikely (14). Therefore, a unimolecular hydrolytic mechanism is suggested. Second, below pH 5, a decrease in the reaction rate occurred with a decrease in pH, *i.e.*, with increased protonation of the chlorambucil amino group. The decreased availability of the lone pair of nitrogen electrons should have little effect on conventional S_N1 or S_N2 reaction rates owing to the two-carbon separation from the chlorine. If any influence did occur in a bimolecular solvolysis, the decreased inductive effect should promote the reaction rate.

The lone pair, however, is essential for the formation of the cyclic ethyleneimmonium ion as the intermediate in a unimolecular pathway (Scheme I). Amino group protonation will greatly affect the reaction rate by decreasing the "effective" species concentration. The formation of a cyclic ethyleneimmonium ion would adequately explain the rate dependence on the availability of a free lone pair on the nitrogen atom.

Proposed Kinetic Models—While the primary chlorambucil decomposition pathway was the limiting unimolecular hydrolysis of the unprotonated basic species, the possibility of a secondary parallel reaction mechanism, which could become dominant as the ratio of the protonated to unprotonated species increased, must be considered. Two possible secondary mechanisms emerge.

[3] Cambridge conductance bridge L-380287.

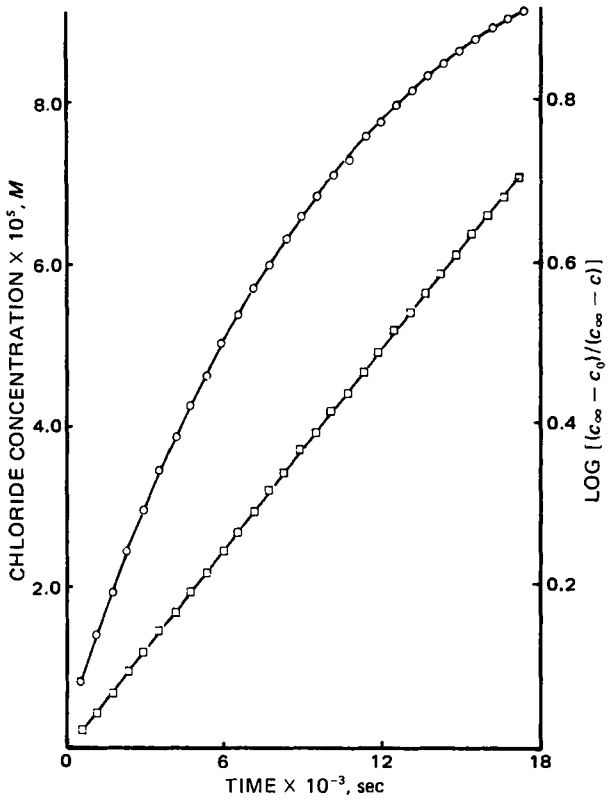

Figure 2—*Chlorambucil hydrolysis in borate buffer (pH 9.0, μ = 0.05) at 25.0° showing first-order behavior. Key:* ○, *chloride concentration;* □, *log* $[(c_\infty - c_0)/(c_\infty - c)]$; —, *linear least-squares regression;* c_0, *0.214* × 10^{-5} M; *and* c_∞, *0.114* × 10^{-5} M.

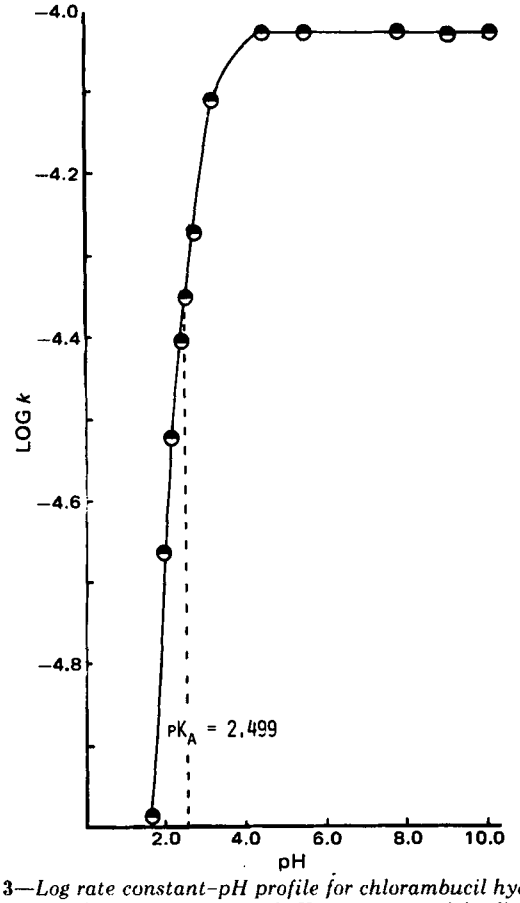

Figure 3—*Log rate constant–pH profile for chlorambucil hydrolysis in aqueous solution (μ = 0.1) at 25.0°. Key:* ⊖, *mean of duplicate rate determinations.*

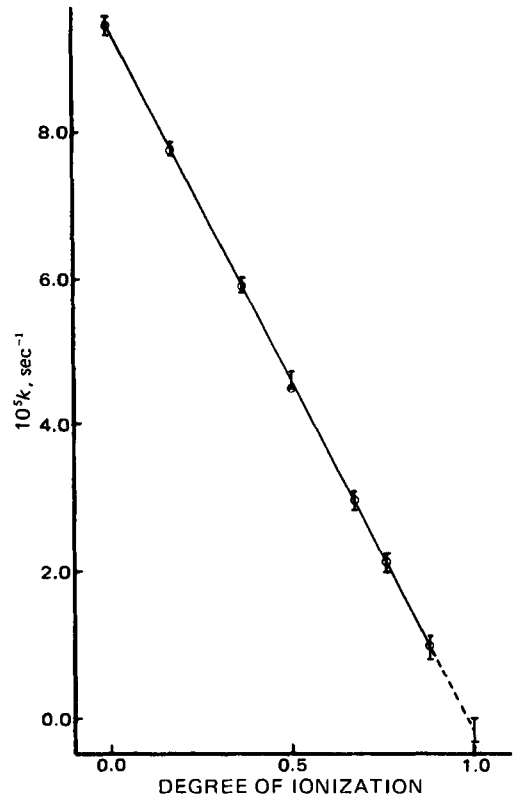

Figure 4—*Regression of rate constant* versus *the degree of ionization (basic group) for chlorambucil hydrolysis in an aqueous solution at 25.0°. Key:* ○, *mean of replicate rate determinations;* —, *fitted linear least-squares regression with the confidence limits of the calculated rate constants* (p = 0.95); *and* ---, *extrapolated regression to* α = 1.

Unimolecular Ionized Base Hydrolysis Involving Noncyclic Carbonium Ion—

$$dc_T/dt = k_A c_A + k_{AH} c_{AH} \quad \text{(Eq. 3)}$$

where c_T is the total chlorambucil concentration equal to the sum of the unionized concentration (c_A) and the ionized concentration (c_{AH}), k_A is the unimolecular rate constant for free base decomposition, and k_{AH} is the unimolecular rate constant for ionized base decomposition.

$$\therefore dc_T/dt = k_A(1 - \alpha)c_T + k_{AH}\alpha c_T$$

$$= kc_T \quad \text{(Eq. 4)}$$

where k is the observed first-order rate constant and equals $k_A(1 - \alpha) + k_{AH}\alpha$ and α is the degree of ionization.

Therefore, the model (Model A) to be tested is:

$$k = k_A + (k_{AH} - k_A)\alpha \quad \text{(Eq. 5)}$$

Bimolecular Hydrolysis for Ionized Base Involving Noncyclic Intermediate—

$$dc_T/dt = k_A c_A + k_{AH} c_{AH} c_{OH} \quad \text{(Eq. 6)}$$

where k_{AH} is the bimolecular rate constant for decomposition of the ionized base and c_{OH} is the concentration of hydroxyl ions.

$$\therefore dc_T/dt = [k_A(1 - \alpha) + k_{AH}\alpha c_{OH}]c_T \quad \text{(Eq. 7)}$$

For pseudo-first-order kinetics at constant pH:

$$k = k_A(1 - \alpha) + k_{AH}\alpha c_{OH} \quad \text{(Eq. 8)}$$

where k = observed first-order rate constant (seconds^{-1}).

$$\therefore k = (k_A K_a + k_{AH} K_w)/(K_a + c_H) \quad \text{(Eq. 9)}$$

where c_H is the hydrogen-ion concentration, K_a is the dissociation constant for the basic group of chlorambucil, and K_w is the water dissociation constant.

Therefore, the model (Model B) becomes:

$$\log k = \log (k_A K_a + k_{AH} K_w) - \log (K_a + c_H) \quad \text{(Eq. 10)}$$

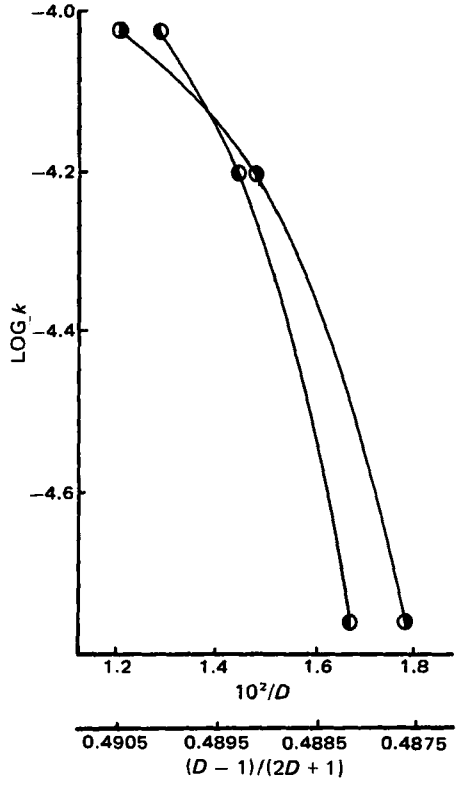

Figure 5—*Solvent effect on the chlorambucil hydrolysis rate in aqueous-alcohol solutions at 25.0°. Key:* ◑, *dielectric constant function* = (D − 1)/(2D + 1); *and* ◐, *dielectric constant function* = 1/D. *Each point is the mean of three replicates.*

Model A was tested by regressing the observed rate constant (k) against the degree of ionization (α) (Fig. 4). An analysis of variance showed no significant deviations from linearity ($p > 0.2$). Thus, the data can be adequately interpreted by this model; *i.e.*, the reaction proceeds by a unimolecular hydrolysis of the free base *via* a cyclic intermediate in parallel with a similar unimolecular hydrolysis of the ionized base.

The magnitude of the two parallel mechanisms can be determined by calculation of the rate constants k_A and k_{AH}. Linear regression analysis provided the following results:

$$k_A = 9.436 \times 10^{-5} \pm 0.988 \times 10^{-6} \quad (p = 0.95) \qquad \text{(Eq. 11)}$$

$$k_{AH} = -0.210 \times 10^{-5} \pm 0.225 \times 10^{-5} \quad (p = 0.95) \qquad \text{(Eq. 12)}$$

The hypothesis that k_{AH} does not differ significantly from zero cannot be rejected [t test: $p(t = 1.93, 22\ df) = 0.1$–$0.05$]. Under these circumstances, the rate constant k_{AH} must be extremely small or zero. Hence, the decomposition occurred substantially by unimolecular hydrolysis of the free base. Hydrolysis of the ionized base was insignificant. Therefore, the data can be adequately represented by the model:

$$k = k_A(1 - \alpha) \qquad \text{(Eq. 13)}$$

In addition, since there was no significant departure from linearity shown by the analysis of variance, nonlinear terms such as $k_{AH}\alpha c_{OH}$ in the bimolecular Model B were unnecessary. Consequently, testing of Model B was irrelevant.

Solvent Effects—Replicate rate determinations were made in 0.0, 20.0, and 40.0% (v/v) ethanol in water at zero ionic strength by the conductimetric method. The effect of the dielectric constant on the hydrolysis rate is shown in Fig. 5, where log k is plotted as a function of the dielectric constant (15), *i.e.*, log k *versus* $1/D$ (Amis theory) or log k *versus* $(D - 1)/(2D + 1)$ (Laidler and Eyring theory). The chlorambucil reaction rate increased markedly with the solvent dielectric constant. For a unimolecular mechanism, this finding reflected the increased solvation (and, therefore, stabilization) of the transition state (*i.e.*, ethyleneimmonium ion) with respect to the uncharged reactant (14). In contrast, for a bimolecular reaction, an increase or decrease could be expected depending on whether the attacking nucleophile is uncharged or charged and, therefore, on the degree of charge dispersion in the transition state (14). The results obtained are thus consistent with the proposed unimolecular model but do not provide absolute proof of the reaction pathway.

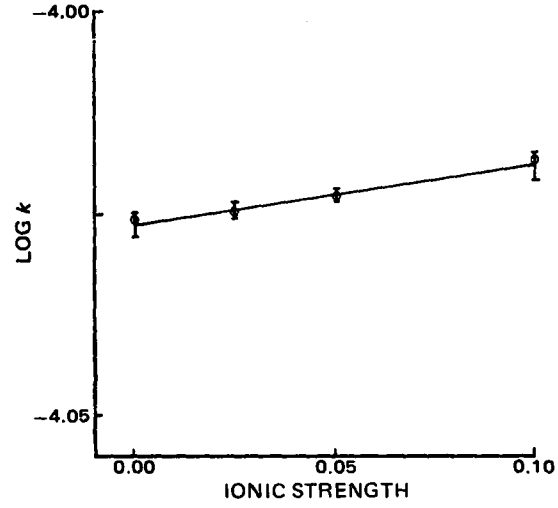

Figure 6—*Ionic strength effect on the chlorambucil hydrolysis rate in borate buffer (pH 9.0) at 25.0°. Key:* ○, *mean of three replicate rate determinations; and* —, *fitted linear least-squares regression with the confidence limits* (p = 0.95).

Neither kinetic model provided a linear representation of the data. However, nonelectrostatic effects in the Laidler–Eyring and Amis models were assumed to be negligible. Therefore, specific effects such as hydrogen bonding and van der Waal's forces of interaction between the solvent and reactant, which may be prevalent in chlorambucil hydrolysis in a hydroalcoholic solution, could modify the efficiency of the solvent in promoting the reaction rate. If so, linearity of the log k–dielectric constant function cannot be expected (16).

Salt Effects—The effect of common ions (chloride) on the reaction rate could not be ascertained since the required added chloride concentrations markedly reduced the sensitivity of the silver–silver chloride electrode. However, the effect of noncommon ions (*e.g.*, acetate, borate, and nitrate used in the study of pH effect) on the reaction rate was negligible, as evidenced by the pH-independent region of the log k–pH profile in Fig. 3. The results are indicative of a unimolecular substitution where the rate-determining step is independent of nucleophilicity. For a bimolecular mechanism, however, the reaction rate would be markedly dependent on the concentration and nucleophilic character of the attacking species (14).

The general ionic strength effect also was studied. Replicate rate determinations using the potentiometric method were performed for chlorambucil hydrolysis in borate buffer (pH 9.0, 0.01 M), adjusted to ionic strengths 0.100, 0.050, and 0.025 with potassium nitrate. Rate constant determinations at zero ionic strength were performed conductimetrically. Log k is regressed against the ionic strength (16) in Fig. 6. An increase in ionic strength caused a small acceleration of chlorambucil hydrolysis, which reflected the greater solvation and stabilization of the transition state at higher solvent polarity. For both the unimolecular and bimolecular pathways, an increase in the reaction rate with an increase in ionic strength would be expected (14). The small degree of acceleration of the observed rate was indicative of a reaction in a high dielectric constant solvent.

REFERENCES

(1) D. A. G. Galton, L. G. Israels, J. D. N. Nabarro, and M. Till, *Br. Med. J.*, **11**, 1172 (1955).

(2) L. G. Israels, D. A. G. Galton, M. Till, and E. Wiltshaw, *Ann. N.Y. Acad. Sci.*, **68**, 915 (1958).

(3) J. G. Masterson, R. J. Calame, and J. Nelson, *Am. J. Obstet. Gynecol.*, **79**, 1002 (1960).

(4) L. G. Israels and J. H. Linford, *Proc. Can. Cancer Res. Conf.*, **5**, 399 (1962).

(5) W. C. J. Ross, *J. Chem. Soc.*, **1949**, 183.

(6) J. L. Everett, J. J. Roberts, and W. C. J. Ross, *ibid.*, **1953**, 2386.

(7) W. C. J. Ross, "Biological Alkylating Agents," Butterworths, London, England, 1962, p. 13.

(8) L. S. Yaguzhinskii and A. D. Chinaeva, *Zh. Obshch. Khim.*, **36**, 671 (1966).

(9) G. L. Janz, "Reference Electrodes—Theory and Practice," Aca-

demic, New York, N.Y., 1961, p. 179.
(10) P. J. Stewart, Ph.D. thesis, University of Queensland, St. Lucia, Australia, 1975.
(11) D. W. Marquardt, *J. Soc. Ind. Appl. Math.*, 11, 431 (1963).
(12) P. J. Davis, in "Survey of Numerical Analysis," J. Todd, Ed., McGraw-Hill, New York, N.Y., 1962, pp. 347, 363.
(13) L. Meites and H. C. Thomas, "Advanced Analytical Chemistry," McGraw-Hill, New York, N.Y., 1958, pp. 129, 131.
(14) C. K. Ingold, "Structure and Mechanism in Organic Chemistry," Cornell University Press, Ithaca, N.Y., 1953, pp. 306, 418.
(15) E. S. Amis, "Solvent Effects on Reaction Rates and Mechanisms," Academic, New York, N.Y., 1966, pp. 59, 69.
(16) A. A. Frost and R. G. Pearson, "Kinetics and Mechanism," 2nd ed., Wiley, New York, N.Y., 1961, pp. 123, 157.

ACKNOWLEDGMENTS

Abstracted in part from a thesis submitted by P. J. Stewart to the University of Queensland in partial fulfillment of the Doctor of Philosophy degree requirements.

The authors thank Burroughs Wellcome & Co. for the chlorambucil used in this research.

Effects of Aspirin on ^{14}C-Pirprofen Disposition in Rats

THOMAS A. THOMPSON ˣ, CORNELIUS H. BORMAN, ROSALIND S. GOODBLATT, and WILLIAM J. ROTH, III

Received December 18, 1978, from the *Research Department, Pharmaceuticals Division, Ciba-Geigy Corporation, Ardsley, NY 10502.* Accepted for publication February 8, 1979.

Abstract □ The effects of aspirin on ^{14}C-pirprofen disposition in the rat were studied. An oral 60-mg/kg dose of aspirin significantly reduced plasma radioactivity during the 1–8-hr interval after an intravenous 5-mg/kg injection of ^{14}C-pirprofen. The aspirin-treated group had only 69% as much area under the radioactivity curve as the control group. The radioactive material in plasma consisted almost entirely of ^{14}C-pirprofen, as shown by GLC. The plasma clearance of ^{14}C-pirprofen was 7.4 ml/hr for the aspirin-treated group and 5.1 ml/hr for the control group, while the volumes of distribution were 0.32 and 0.20 liter/kg, respectively. The apparent elimination half-life was unchanged at 5.9 hr. ^{14}C-Pirprofen was approximately 98.6% bound to plasma proteins, and the binding decreased to an average of 97.2% in the presence of salicylate. Binding to blood cellular constituents was insignificant. Rats given ^{14}C-pirprofen by intravenous injection without aspirin secreted 36.0–42.8% of the dose radioactivity into bile during 4 hr while a comparable group given 60 mg of aspirin/kg secreted 46.4–70.8%. TLC and GLC demonstrated that the radioactivity in rat bile was 80–90% conjugated ^{14}C-pirprofen. The increased radioactive material secretion into bile was compensated in the intact rat by reabsorption, since the total radioactive material excreted in urine was not changed by aspirin administration.

Keyphrases □ Aspirin—effect on pirprofen disposition, rats □ Pirprofen—disposition, effect of aspirin, rats □ Anti-inflammatory agents—pirprofen, disposition, effect of aspirin, rats

Pirprofen, 2-[3-chloro-4(3-pyrrolinyl)-phenyl] propionic acid, is a new anti-inflammatory drug of the arylalkanoic acid type (1).

Salicylate has been reported to reduce the plasma concentration of various arylalkanoic acid compounds including indomethacin (2), fenoprofen (3, 4), naproxen (5, 6), and diclofenac (7) in animals and humans. Pirprofen concentrations in human plasma as well as that bound to plasma proteins were reduced by salicylate[1], and the present study was undertaken to examine salicylate effects on the biological disposition of pirprofen in the rat.

EXPERIMENTAL

Radioactive Pirprofen—^{14}C-Pirprofen (I), with the radioactive atom in position three of the propionic acid moiety, was used[2]. The specific

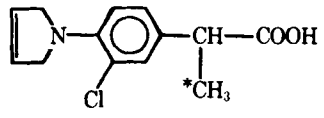

I

activity was 13 μCi/mg. The labeled compound was examined by TLC using the procedures described later. The major constituent chromatographed like authentic pirprofin, and the only impurity was a substance comprising about 5% of the radioactivity.

Animal Procedures—Young adult male Wistar rats[3], ~200 g, were used.

^{14}C-Pirprofen dosage solutions were prepared in 0.2 *M* $NaHCO_3$ to provide 5 mg/kg and 3 μCi/animal in volumes of 0.3 ml for injection and 1.0 ml for intubation. Aspirin[4] was administered as a 60-mg/kg aqueous dose by intubation.

Blood samples were obtained by anesthetizing the rats with ether, opening the abdominal cavity, and exsanguinating *via* the abdominal aorta into a heparinized 10-ml syringe. Blood plasma was frozen pending analysis.

Bile duct cannulations were done under ether anesthesia for rats that were to receive intravenous ^{14}C-pirprofen, and these rats were confined in restraining cages[5] during bile collection. Rats receiving ^{14}C-pirprofen orally were anesthetized with urethan[4] rather than ether to preclude the necessity for restraint. A 25% solution of urethan in water was administered as a 1.25-g/kg ip dose.

Radioactivity Measurements—A solubilizer–phosphore solution was prepared by mixing one volume of a commercial solubilizer[6] with four volumes of toluene containing 0.5% 2,5-diphenyloxazole[7] and 0.01% *p*-bis(*o*-methylstyryl)benzene[8]. The solubilizer–phosphore solution (15 ml) was mixed with 10 μl of injection solutions, 50 μl of ultrafiltrates, or 0.1 ml of plasma, bile, or urine prior to duplicate sample counting in a liquid scintillation spectrometer[9]. Counting efficiency was measured by external standardization.

Whole blood (0.1 ml) was pipetted onto 2.5-cm circles of filter paper and dried before combustion[10]. The resulting carbon dioxide was absorbed in 4 ml of ethanolamine to which 9 ml of methanol and 6 ml of scintillator solution, containing 15.0 g of 2,5-diphenyloxazole and 1.0 g of *p*-bis(*o*-methylstyryl)benzene/liter of toluene, were added for counting.

TLC—Aliquots (20 μl) of bile or an equivalent amount of hydrolyzate

[1] To be published.
[2] The material was synthesized by Dr. Naba K. Chaudhuri and coworkers at Ciba-Geigy Corp., Ardsley, NY 10502.
[3] Charles River C.D. or Marland Farms.
[4] Merck and Co., West Point, PA 19486.
[5] Aerospace Industries, Garnerville, NY 10923.
[6] Bio-Solv BBS-3, Beckman Instruments, Fullerton, CA 92634.
[7] Eastman Kodak Co., Rochester, NY 14650.
[8] Packard Instrument Co., Downers Grove, IL 60515.
[9] Intertechnique SL-40, IN/US Service Corp., Fairfield, NJ 07006.
[10] Model 305 oxidizer, Packard Instrument Co., Downers Grove, IL 60515.

0022-3549/79/0800-0996$01.00/0
© 1979, American Pharmaceutical Association

demic, New York, N.Y., 1961, p. 179.
(10) P. J. Stewart, Ph.D. thesis, University of Queensland, St. Lucia, Australia, 1975.
(11) D. W. Marquardt, *J. Soc. Ind. Appl. Math.*, 11, 431 (1963).
(12) P. J. Davis, in "Survey of Numerical Analysis," J. Todd, Ed., McGraw-Hill, New York, N.Y., 1962, pp. 347, 363.
(13) L. Meites and H. C. Thomas, "Advanced Analytical Chemistry," McGraw-Hill, New York, N.Y., 1958, pp. 129, 131.
(14) C. K. Ingold, "Structure and Mechanism in Organic Chemistry," Cornell University Press, Ithaca, N.Y., 1953, pp. 306, 418.
(15) E. S. Amis, "Solvent Effects on Reaction Rates and Mechanisms," Academic, New York, N.Y., 1966, pp. 59, 69.
(16) A. A. Frost and R. G. Pearson, "Kinetics and Mechanism," 2nd ed., Wiley, New York, N.Y., 1961, pp. 123, 157.

ACKNOWLEDGMENTS

Abstracted in part from a thesis submitted by P. J. Stewart to the University of Queensland in partial fulfillment of the Doctor of Philosophy degree requirements.

The authors thank Burroughs Wellcome & Co. for the chlorambucil used in this research.

Effects of Aspirin on ^{14}C-Pirprofen Disposition in Rats

THOMAS A. THOMPSON ˣ, CORNELIUS H. BORMAN, ROSALIND S. GOODBLATT, and WILLIAM J. ROTH, III

Received December 18, 1978, from the *Research Department, Pharmaceuticals Division, Ciba-Geigy Corporation, Ardsley, NY 10502.* Accepted for publication February 8, 1979.

Abstract □ The effects of aspirin on ^{14}C-pirprofen disposition in the rat were studied. An oral 60-mg/kg dose of aspirin significantly reduced plasma radioactivity during the 1–8-hr interval after an intravenous 5-mg/kg injection of ^{14}C-pirprofen. The aspirin-treated group had only 69% as much area under the radioactivity curve as the control group. The radioactive material in plasma consisted almost entirely of ^{14}C-pirprofen, as shown by GLC. The plasma clearance of ^{14}C-pirprofen was 7.4 ml/hr for the aspirin-treated group and 5.1 ml/hr for the control group, while the volumes of distribution were 0.32 and 0.20 liter/kg, respectively. The apparent elimination half-life was unchanged at 5.9 hr. ^{14}C-Pirprofen was approximately 98.6% bound to plasma proteins, and the binding decreased to an average of 97.2% in the presence of salicylate. Binding to blood cellular constituents was insignificant. Rats given ^{14}C-pirprofen by intravenous injection without aspirin secreted 36.0–42.8% of the dose radioactivity into bile during 4 hr while a comparable group given 60 mg of aspirin/kg secreted 46.4–70.8%. TLC and GLC demonstrated that the radioactivity in rat bile was 80–90% conjugated ^{14}C-pirprofen. The increased radioactive material secretion into bile was compensated in the intact rat by reabsorption, since the total radioactive material excreted in urine was not changed by aspirin administration.

Keyphrases □ Aspirin—effect on pirprofen disposition, rats □ Pirprofen—disposition, effect of aspirin, rats □ Anti-inflammatory agents—pirprofen, disposition, effect of aspirin, rats

Pirprofen, 2-[3-chloro-4(3-pyrrolinyl)-phenyl] propionic acid, is a new anti-inflammatory drug of the arylalkanoic acid type (1).

Salicylate has been reported to reduce the plasma concentration of various arylalkanoic acid compounds including indomethacin (2), fenoprofen (3, 4), naproxen (5, 6), and diclofenac (7) in animals and humans. Pirprofen concentrations in human plasma as well as that bound to plasma proteins were reduced by salicylate[1], and the present study was undertaken to examine salicylate effects on the biological disposition of pirprofen in the rat.

EXPERIMENTAL

Radioactive Pirprofen—^{14}C-Pirprofen (I), with the radioactive atom in position three of the propionic acid moiety, was used[2]. The specific

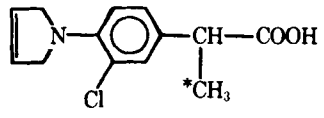

I

activity was 13 μCi/mg. The labeled compound was examined by TLC using the procedures described later. The major constituent chromatographed like authentic pirprofin, and the only impurity was a substance comprising about 5% of the radioactivity.

Animal Procedures—Young adult male Wistar rats[3], ~200 g, were used.

^{14}C-Pirprofen dosage solutions were prepared in 0.2 *M* $NaHCO_3$ to provide 5 mg/kg and 3 μCi/animal in volumes of 0.3 ml for injection and 1.0 ml for intubation. Aspirin[4] was administered as a 60-mg/kg aqueous dose by intubation.

Blood samples were obtained by anesthetizing the rats with ether, opening the abdominal cavity, and exsanguinating *via* the abdominal aorta into a heparinized 10-ml syringe. Blood plasma was frozen pending analysis.

Bile duct cannulations were done under ether anesthesia for rats that were to receive intravenous ^{14}C-pirprofen, and these rats were confined in restraining cages[5] during bile collection. Rats receiving ^{14}C-pirprofen orally were anesthetized with urethan[4] rather than ether to preclude the necessity for restraint. A 25% solution of urethan in water was administered as a 1.25-g/kg ip dose.

Radioactivity Measurements—A solubilizer–phosphore solution was prepared by mixing one volume of a commercial solubilizer[6] with four volumes of toluene containing 0.5% 2,5-diphenyloxazole[7] and 0.01% *p*-bis(*o*-methylstyryl)benzene[8]. The solubilizer–phosphore solution (15 ml) was mixed with 10 μl of injection solutions, 50 μl of ultrafiltrates, or 0.1 ml of plasma, bile, or urine prior to duplicate sample counting in a liquid scintillation spectrometer[9]. Counting efficiency was measured by external standardization.

Whole blood (0.1 ml) was pipetted onto 2.5-cm circles of filter paper and dried before combustion[10]. The resulting carbon dioxide was absorbed in 4 ml of ethanolamine to which 9 ml of methanol and 6 ml of scintillator solution, containing 15.0 g of 2,5-diphenyloxazole and 1.0 g of *p*-bis(*o*-methylstyryl)benzene/liter of toluene, were added for counting.

TLC—Aliquots (20 μl) of bile or an equivalent amount of hydrolyzate

[1] To be published.
[2] The material was synthesized by Dr. Naba K. Chaudhuri and coworkers at Ciba-Geigy Corp., Ardsley, NY 10502.
[3] Charles River C.D. or Marland Farms.
[4] Merck and Co., West Point, PA 19486.
[5] Aerospace Industries, Garnerville, NY 10923.
[6] Bio-Solv BBS-3, Beckman Instruments, Fullerton, CA 92634.
[7] Eastman Kodak Co., Rochester, NY 14650.
[8] Packard Instrument Co., Downers Grove, IL 60515.
[9] Intertechnique SL-40, IN/US Service Corp., Fairfield, NJ 07006.
[10] Model 305 oxidizer, Packard Instrument Co., Downers Grove, IL 60515.

0022-3549/79/0800-0996$01.00/0
© 1979, American Pharmaceutical Association

Table I—Effect of Salicylate on ^{14}C-Pirprofen Radioactivity in Rat Plasma

Hours Postdose[a]	Concentration, average μg/ml[b] ± SD		
	Apparent ^{14}C-Pirprofen		
	Without Aspirin	With Aspirin	Salicylate
0.1	35.9 ± 1.6	31.0 ± 1.4	114 ± 8
0.25	31.1 ± 4.8	24.1 ± 4.0	127 ± 10
0.5	25.8 ± 2.0	19.9 ± 3.8	111 ± 6
0.75	24.2 ± 2.4	17.5 ± 1.2	121 ± 12
1.0	22.0 ± 1.4	13.3 ± 1.0	118 ± 8
2.0	18.6 ± 2.8	10.7 ± 2.2	113 ± 8
4.0	16.1 ± 1.2	10.3 ± 1.4	91 ± 26
6.0	11.3 ± 0.4	6.4 ± 1.0	66 ± 22
8.0	9.8 ± 1.6	5.7 ± 1.0	63 ± 16
11.0	4.1 ± 0.8	3.6 ± 0.2	11 ± 14
14.0	4.1 ± 1.2	3.0 ± 0.4	2 ± 0
17.0	2.3 ± 0.8	2.1 ± 0.8	—

[a] Rats were intubated with 60 mg of aspirin/kg in solution or with an equal volume of water and injected intravenously 1 hr later with 5 mg of ^{14}C-pirprofen/kg. [b] Four rats at each time point, except the aspirin-treated group at 4 hr which had three.

were spotted on silica gel plates[11] and developed in chloroform–methanol–formic acid (70:30:1) or benzene–ethanol–formic acid (90:10:1). The dried plates were examined under UV light and scanned for radioactivity[12].

Pirprofen Analysis—Pirprofen was determined quantitatively (8), using 3.0-ml aliquots of rat plasma containing 0–120 μg of pirprofen. The conjugated pirprofen in bile was hydrolyzed before analysis. Bile (0.2 ml) was mixed with 50 μl of 0.5 *N* KOH and stored 15 min at room temperature. The reaction mixture was neutralized with hydrochloric acid, and 1.0 ml of 0.4 *M*, pH 5.4 acetate buffer was added. Pirprofen was extracted by adding 2.0 ml of 20% methylene chloride in ether and rotating[13] for 20 min. The extraction was repeated, and the combined extracts were processed as described previously (8).

Protein Binding Measurement—Cellulose dialyzer tubing[14] was soaked 0.5 hr in water, and excess water was removed by blotting. A 20-cm length of tubing was formed into a U-shape, 2.0 ml of plasma was introduced, and the tubing was placed into a 2.8 × 10-cm polypropylene centrifuge tube containing eight or 10 0.5-cm diameter glass beads. A cork was used to close the tube and wedge the ends of the tubing with the bottom of the loop supported on the beads. Centrifugation at 1100×*g* for 30 min produced ~100 μl of ultrafiltrate, and 50-μl aliquots were taken for radioactivity counting.

Salicylate Analysis—Plasma (0.5 ml) was mixed with 1.0 ml of water, 0.3 ml of 6 *N* HCl, and 20 ml of methylene chloride. The tubes were rotated 30 min and centrifuged. The aqueous phase was aspirated off, and 10.0 ml of organic phase was mixed with 10.0 ml of 1 *N* NaOH. After rotating for 25 min and centrifuging, the aqueous phase fluorescence was measured[15] at an excitation wavelength of 310 nm and an emission wavelength of 400 nm.

RESULTS

The radioactivity concentrations found in the plasma of control and aspirin-treated rats are shown in Table I, expressed as the average and standard deviation for micrograms of apparent ^{14}C-pirprofen per milliliter. Lower apparent pirprofen concentrations were found for the aspirin-treated rats. Table I also contains the mean and standard deviation for the salicylate concentrations. Selected plasma samples from the same experiment also were analyzed for unbound radioactivity (Table II). For the aspirin-treated animals, binding was decreased slightly until the plasma salicylate concentrations declined to low values, at which point the binding had returned to the control value.

The radioactivity concentration in a few whole blood samples also was measured. No association of radioactive material with the cellular blood constituents was found.

A separate experiment was done to obtain sufficient plasma for quantitative pirprofen determination by GLC. As shown in Table III, very good agreement was found by radiometric and chromatographic analyses.

Table II—Effect of Aspirin on Binding of ^{14}C-Pirprofen by Rat Plasma Proteins *In Vivo*[a]

Time after ^{14}C-Pirprofen, 5 mg/kg iv	Plasma ^{14}C-Pirprofen, mean μg/ml ± SD	Plasma Salicylate, mean μg/ml ± SD	Binding, % ± SD
Controls—no aspirin			
5 min	35.9 ± 1.6	—	98.8 ± 0.4
6 hr	11.3 ± 0.4	—	98.6 ± 0.4
14 hr	4.1 ± 1.2	—	99.6 ± 0.2
Aspirin, 60 mg/kg po			
5 min	31.0 ± 1.4	114 ± 8	96.6 ± 1.4
6 hr	6.4 ± 1.0	66 ± 22	96.5 ± 1.2
14 hr	3.0 ± 0.4	2 ± 0	99.6 ± 0.2

[a] Four rats at each time point.

The binding of ^{14}C-pirprofen to rat plasma proteins also was measured in the presence and absence of salicylate in an *in vitro* experiment. ^{14}C-Pirprofen (17 μg/ml) was added to pooled plasma from control rats, and sodium salicylate (100 μg/ml) was added to half of the plasma aliquots prior to a 30-min equilibration and binding measurements. All three control samples showed 98.6% binding. Samples containing salicylate had values of 97.6, 97.7, and 97.6%.

The urinary radioactivity excretion after 5 mg of ^{14}C-pirprofen/kg iv was measured after intubation with 60 mg of aspirin/kg or an equal volume of water. As shown in Table IV, the amount and time course for urinary radioactivity excretion were not altered by aspirin administration under these conditions.

The effect of aspirin on biliary secretion of radioactivity from ^{14}C-pirprofen was examined in bile duct-cannulated rats. Rats were given 60 mg of aspirin in aqueous solution/kg or an equal volume of water by intubation. The bile ducts were cannulated. One hour after the aspirin or water intubation, the animals were given 5 mg of ^{14}C-pirprofen/kg by tail vein injection or by intubation. The bile volume collected each hour was not different for the aspirin and water-treated rats. The radioactivity secretion into bile was much greater for the aspirin-treated rats than for the control rats (Fig. 1). Similar results were seen after oral rather than intravenous ^{14}C-pirprofen administration.

TLC of rat bile collected within 2 hr of oral ^{14}C-pirprofen administration showed one major constituent, which comprised 80–90% of the radioactivity. Four or five minor, unknown metabolites also were present. None of these constituents was identical to pirprofen. Base treatment

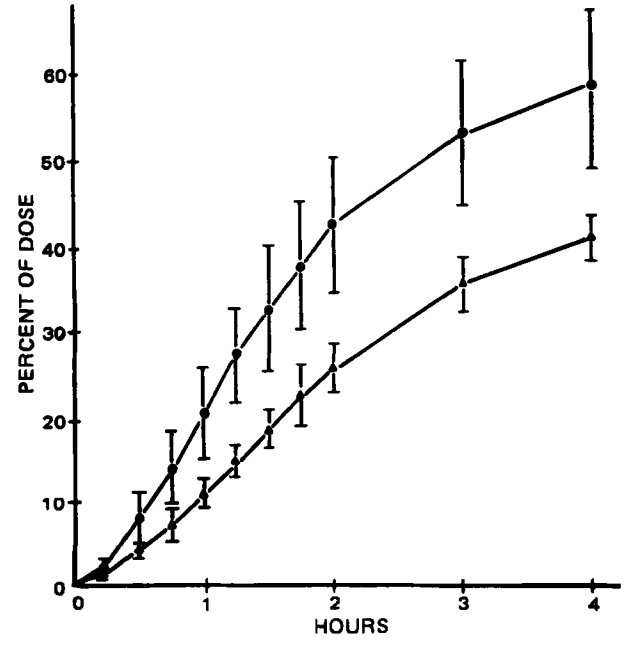

Figure 1—*Effect of 60 mg of aspirin/kg po on biliary radioactivity in rats after 5 mg of ^{14}C-pirprofen/kg iv, showing mean and standard deviation for five rats per treatment. Key: ●, aspirin-treated rats; and ▲, control rats.*

[11] E. Merck, 0.25-mm type 60 F-254 plates, EM Laboratories, Elmsford, NY 10523.
[12] Berthold radioscanner, Varian Instrument Division, Palo Alto, CA 94303.
[13] Rugged rotator model RD-250, Kraft Apparatus, South Richmond Hill, NY 11419.
[14] Catalog No. 3787-D22, 1.5-cm diameter, Arthur Thomas Co., Philadelphia, PA 19105.
[15] Model MPF-2A spectrofluorometer, Perkin-Elmer Corp., Norwalk, CT 06856.

Table III—Radioactivity and Pirprofen in Rat Plasma after 5 mg of ^{14}C-Pirprofen/kg iv

Hours Postdose	Concentration, μg/ml[a] Liquid Scintillation Counting	GLC Analysis
0.25	23.6	28.6
0.25	25.6	22.2
1	19.4	19.4
1	16.4	14.8
3	10.6	9.6
3	8.2	7.3
6	8.7	6.0
6	5.9	4.6
12	2.4	2.0
12	1.1	1.2
18	0.8	0.6
18	0.2	0.9
24	0.4	<0.1

[a] Plasma from three rats was pooled and analyzed in duplicate by the two methods.

of bile resulted in a change in the TLC pattern. The major radioactive constituent was converted to a material that behaved like pirprofen on TLC in two different solvent mixtures. Quantitative analysis by GLC confirmed that the hydrolyzed material was pirprofen.

DISCUSSION

Oral administration of aspirin (60 mg/kg) to rats 1 hr before intravenous ^{14}C-pirprofen administration (5 mg/kg) resulted in markedly reduced radioactive material in plasma, and GLC analysis showed the radioactive material to be unchanged ^{14}C-pirprofen. The effect was significant ($p = 0.01$) during the 1–8-hr interval and decreased as salicylate concentrations declined to average values of 11 μg/ml or less (Table I). Comparison of area under the curve (*AUC*) values, calculated from time zero to infinity, showed the aspirin group to have 69% as much area as the control group.

Accordingly, pirprofen is another example of an arylalkanoic acid for which concentrations in plasma are reduced by salicylate. Yesair *et al.* (2) found that salicylate altered indomethacin disposition in the rat, resulting in reduced concentrations in plasma, decreased excretion in urine, and increased elimination *via* the bile and feces. For pirprofen, aspirin had no effect on the amount of radioactivity excreted in urine. Four rats excreted 74.9 ± 4.5% of the radioactivity from a dose of 5 mg of ^{14}C-pirprofen/kg iv in urine during 48 hr when given 60 mg of aspirin/kg po. This finding can be compared to 77.4 ± 2.3% for four rats given ^{14}C-pirprofen without aspirin (Table IV).

A similar situation was described by Rubin *et al.* (3) for fenoprofen in humans. The fenoprofen concentration in plasma and the *AUC* were reduced by concomitant aspirin administration without a change in the total amount of material excreted in urine. This finding could result from increased clearance by the liver if the rate with which metabolites are released into blood by the liver is greatly exceeded by renal metabolite clearance. The metabolites will be present in plasma only in low concentrations and will contribute little to the *AUC* for radioactive material, while the bile serves as a depot due to increased recycling.

Aspirin administration with ^{14}C-pirprofen greatly affected biliary radioactivity in rats. Five rats given intravenous ^{14}C-pirprofen without aspirin secreted 40.5 ± 2.7% of the dose radioactivity into bile during 4 hr, while a comparable aspirin-treated group secreted 58.6 ± 9.6% (Fig. 1). The bile production rate was similar for the aspirin-treated and the control animals, precluding increased choleresis as a factor. Similar results were obtained on administration of ^{14}C-pirprofen by intubation rather than by intravenous injection.

The major radioactive constituent (80–90%) in bile of both the aspirin-treated and the control animals was a material that was converted on alkaline hydrolysis to a product indistinguishable from pirprofen by TLC and GLC. In the intact rat, reabsorption compensated for the increased secretion into bile caused by aspirin, as indicated by unaltered urinary excretion.

Calculation of plasma clearance according to the equation:

$$\text{clearance} = \frac{\text{dose}}{AUC} \qquad \text{(Eq. 1)}$$

Table IV—Effect of Aspirin on Urinary Excretion of Radioactivity by Rats after an Intravenous Dose of ^{14}C-Pirprofen

Postdose[a], hr	Average ± *SD* for Cumulated Percent of Dose[b] Control Rats	Aspirin-Treated Rats
1	6.0 ± 1.7	4.9 ± 4.4
2	11.7 ± 4.7	13.0 ± 1.8
3	19.3 ± 5.8	18.2 ± 3.1
4	21.4 ± 6.2	25.5 ± 4.3
6	34.5 ± 4.8	37.8 ± 7.0
8	42.0 ± 7.2	44.6 ± 9.4
10	51.7 ± 8.4	51.3 ± 7.0
24	74.3 ± 3.9	70.2 ± 7.1
48	77.4 ± 2.3	74.9 ± 4.5

[a] Rats were intubated with 60 mg of aspirin/kg in 10 ml of aqueous solution or with an equal volume of water and injected intravenously 1 hr later with 5 mg of ^{14}C-pirprofen/kg. [b] Each group contained four rats.

gave values of 5.1 ml/hr for control rats and 7.4 ml/hr for aspirin-treated rats. The apparent volumes of distribution were 0.20 liter/kg for the control group and 0.32 liter/kg for the aspirin group. As a result of the compensatory changes in plasma clearance and apparent volume of distribution, no change in half-life resulted from aspirin administration; half-life values of 5.9 hr were found for both the aspirin and control groups.

Rubin *et al.* (4) reported that the fenoprofen half-life in humans was decreased by aspirin, but the change only became apparent after repeated fenoprofen and aspirin administration. A short study reported in the same publication showed no change in either the half-life or the *AUC* for indomethacin in humans, although the indomethacin concentrations were reduced by aspirin in the early part of the plasma curve.

Binding of ^{14}C-pirprofen to plasma proteins in the rat was extensive and reduced slightly by salicylate. Binding of 98.6% was reduced by salicylate to an average value of 97.2% in the *in vivo* and *in vitro* experiments. This modest decrease in binding represents a marked increase in the unbound drug availability. Binding to the blood cellular constituents did not occur in either the presence or absence of salicylate.

Pirprofen, indomethacin (9), naproxen (5, 6), and fenoprofen (3) are all highly bound to plasma proteins, and all except fenoprofen are displaced by salicylate. Chaplin (5) suggested that the mechanism by which aspirin reduced plasma naproxen concentrations was by increasing the unbound naproxen availability for transformation or excretion. Evidently, this factor is not the sole causative mechanism for decreasing the plasma concentrations of all arylalkanoic acids, because Rubin *et al.* (3) found that fenoprofen was not displaced. An additional factor such as altered hepatic extraction or increased splanchnic blood flow may be involved.

In conclusion, concomitant administration of aspirin and ^{14}C-pirprofen to rats reduced plasma concentrations and reduced *AUC* values of radioactive material. No change in half-life was found, due to increases in both the plasma clearance and the volume of distribution. Binding to plasma proteins decreased slightly. Urinary radioactivity excretion was unchanged by aspirin administration. Secretion of pirprofen metabolite(s) into bile was increased but was compensated by reabsorption.

REFERENCES

(1) R. W. J. Carney, J. J. Chart, R. Goldstein, N. Howie, and J. Wojtkunski, *Experientia*, **29**, 938 (1973).

(2) D. W. Yesair, L. Remington, M. Callahan, and C. J. Kensler, *Biochem. Pharmacol.*, **19**, 1591 (1970).

(3) A. Rubin, P. Warrick, R. L. Wolen, S. M. Chernish, A. S. Ridolfo, and C. M. Gruber, Jr., *J. Pharmacol. Exp. Ther.*, **183**, 449 (1972).

(4) A. Rubin, B. E. Rodda, P. Warrick, C. M. Gruber, Jr., and A. S. Ridolfo, *Arthritis Rheum.*, **16**, 635 (1973).

(5) M. D. Chaplin, *Biochem. Pharmacol.*, **22**, 1589 (1973).

(6) E. J. Segre, M. Chaplin, E. Forchielli, R. Runkel, and H. Sevelius, *Clin. Pharmacol. Ther.*, **15**, 374 (1974).

(7) F. O. Muller, H. K. L. Hundt, and D. G. Muller, *Int. J. Clin. Pharmacol.*, **15**, 397 (1977).

(8) R. C. Luders, M. B. Maggio-Cavaliere, H. Egger, O. B. Gum, O. Resnick, M. F. Bartlett, M. J. Gaito, A. Soo, and C. Li, *Clin. Pharmacol. Ther.*, **21**, 721 (1977).

(9) R. W. Mason, and E. G. McQueen, *Pharmacology (Basle)*, **12**, 12 (1974).

Doxycycline Determination in Human Serum and Urine by High-Performance Liquid Chromatography

ANDRÉ P. De LEENHEER ˣ **and HANS J. C. F. NELIS**

Received October 6, 1978, from the *Laboratoria voor Medische Biochemie en voor Klinische Analyse, Faculteit van de Farmaceutische Wetenschappen, Rijksuniversiteit Gent, 135 De Pintelaan, B-9000 Gent, Belgium.* Accepted for publication February 8, 1979.

Abstract □ A reversed-phase high-performance liquid chromatographic method for quantitative doxycycline determination in human serum and urine is described. The drug was extracted from buffered (pH 6.1) serum or urine into ethyl acetate. A structural analog, demeclocycline, was added as the internal standard. A 10-cm × 2-mm i.d., 5-μm Lichrosorb RP8 column with acetonitrile–0.1 *M* citric acid as the eluent was used. The effluent was monitored at 350 nm. The extraction recovery from spiked serum was 87.8 ± 4.3% (mean ± *SD*, $n = 11$); for urine, a value of 92.2 ± 2.0% (mean ± *SD*, $n = 10$) was found. Within-run and within-day relative standard deviations averaged 1.80% ($\bar{x} = 2.5$ μg/ml, $n = 10$) and 4.75% ($\bar{x} = 2.6$ μg/ml, $n = 9$), respectively. The detection limit was estimated at 50 ng/ml of serum. No significant extra peaks were observed in chromatograms obtained on serum or urine extracts, suggesting the probable absence of metabolic processes *in vivo*.

Keyphrases □ Doxycycline—analysis, human serum and urine, high-performance liquid chromatography □ High-performance liquid chromatography—analysis, doxycycline in human serum and urine □ Antibiotics—doxycycline, high-performance liquid chromatographic analysis, human serum and urine

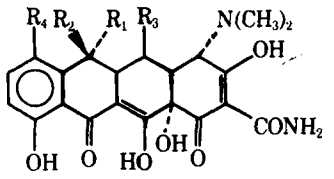

	R_1	R_2	R_3	R_4
oxytetracycline	CH_3	OH	OH	H
tetracycline	CH_3	OH	H	H
demeclocycline	H	OH	H	Cl
chlortetracycline	CH_3	OH	H	Cl
methacycline	$=CH_2$		OH	H
doxycycline	CH_3	H	OH	H

The disposition of the antibiotic doxycycline in the human body has been the subject of numerous investigations. Owing to its stronger lipophilicity, this drug has a higher absorption rate and a longer half-life than the other tetracyclines (I). Although the absence of metabolites *in vivo* has been postulated (1), this has not been proven due to the lack of specific assay methods.

The existing fluorometric (2–4) and microbiological (5, 6) procedures provide good sensitivity but are unable to differentiate doxycycline from its analogs, including possible metabolites. In addition, the latter technique only allows estimation of total biological activity without correlation to the chemical structure of the substance. It also overlooks possible metabolites without antimicrobial activity.

Therefore, the incorporation of a suitable chromatographic step in the analysis is highly desirable. Several TLC methods allow the separation and densitometric quantitation of tetracyclines in pure solutions (7–10). However, no attempt has been made to investigate their potential for analysis in biological materials.

High-performance liquid chromatography (HPLC) combines a fast and reliable chromatographic technique with the relatively high sensitivity of on-line UV detection. A few papers (11–13) report its use for tetracycline, oxytetracycline, and chlortetracycline determination in serum and urine. However, none of these systems was applied to doxycycline. Disadvantages include the poor efficiency of some chromatographic separations (11, 13), the lack of an internal standard (11, 12), and bad detection limits (12, 13).

During some preliminary work, an HPLC system capable of separating doxycycline from several analogs in pure solutions was developed (14). A new system is now reported for quantitative doxycycline determination in human serum and urine. The procedure described involves a simple one-step solvent extraction followed by reversed-phase HPLC, using a structural analog as an internal standard.

EXPERIMENTAL

Reagents—All chemicals were analytical grade[1]. Acetonitrile and distilled water were used without further purification for the preparation of the chromatographic eluent. A pH 6.1 phosphate sulfite buffer was prepared by dissolving 27.6 g of monobasic sodium phosphate and 25.2 g of sodium sulfite in 100 ml of water to give a final concentration of 2 *M* for each salt. Stock solutions of doxycycline hydrochloride[2] and demeclocycline (demethylchlortetracycline) hydrochloride[3] were prepared by dissolving the compounds in methanol–0.1 *M* HCl. All glassware was silanized using a 10% (v/v) solution of hexamethyldisilazane in toluene.

Apparatus and Operating Conditions—The basic liquid chromatographic unit consisted of a single pumping system[4] and a sampling valve[5] with a 20-μl loop. A variable-wavelength detector[6] was used to monitor the column effluent at 350 nm. Chromatography was performed on a homemade 10-cm × 2-mm i.d., 5-μm Lichrosorb RP8[1] column with acetonitrile–0.1 *M* citric acid (24:76 v/v) as the mobile phase. The flow rate was 0.5 ml/min (9.65 MPa or 1400 psi). A filtration device was assembled by pressing a filter disk[7] in a pasteur pipet.

Column Preparation—The column was slurry packed using a modified version of the viscosity method (15). A 9% (w/v) slurry was prepared in glycerol–methanol (20:80 v/v) and introduced into a 4.1-ml reservoir directly assembled on top of the column. A pressure of 34.47 MPa (5000 psi) was applied by pumping acetonitrile through the column, using the maximum flow rate setting of the pump[4]. This procedure allowed reproducible packing of some 30 columns, which were all of the required standard, *i.e.*, 2000 theoretical plates or more under the working conditions described.

Extraction Procedure—A 0.5-ml sample of human serum, 50 μl of a 6% (w/v) aqueous ascorbic acid solution, 50 μl of the internal standard stock solution, and 1 ml of the pH 6.1 phosphate sulfite buffer were combined in a screw-capped polytef-lined tube. After mixing[8] for 30 sec, 6 ml of ethyl acetate was added. The tube was placed for 10 min on a rotating mixer[9] and centrifuged for 6 min at 3000 rpm.

[1] E. Merck Co., Darmstadt, West Germany.
[2] Pfizer Inc., Brussels, Belgium.
[3] Lederle Laboratories, Brussels, Belgium.
[4] Model 8500, Varian Associates, Palo Alto, Calif.
[5] Model CV-6-UHPa-N60, Valco Instruments Co., Houston, Tex.
[6] Varichrom, Varian, Palo Alto, Calif.
[7] Type AP 40, pore size "prefilter," Millipore Corp., Bedford, Mass.
[8] Super mixer 1291, Lab-Line Instruments, Melrose Park, Ill.
[9] Rotary mixer, Cenco Instruments, Breda, The Netherlands.

0022-3549/79/0800-0999$01.00/0
© 1979, American Pharmaceutical Association

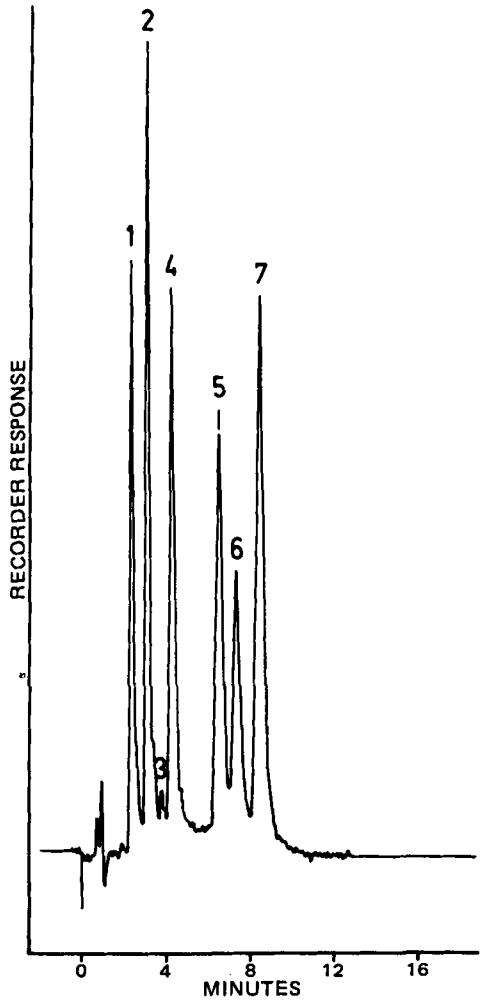

Figure 1—*Separation of seven tetracyclines. Key: 1, oxytetracycline; 2, tetracycline; 3, unidentified by-product of doxycycline; 4, demeclocycline; 5, chlortetracycline; 6, methacycline; and 7, doxycycline. The column was 10-cm × 2-mm Lichrosorb RP8 (5 μm), the mobile phase was acetonitrile–0.1 M citric acid (24:76 v/v), the flow rate was 0.5 ml/min, and the temperature was ambient.*

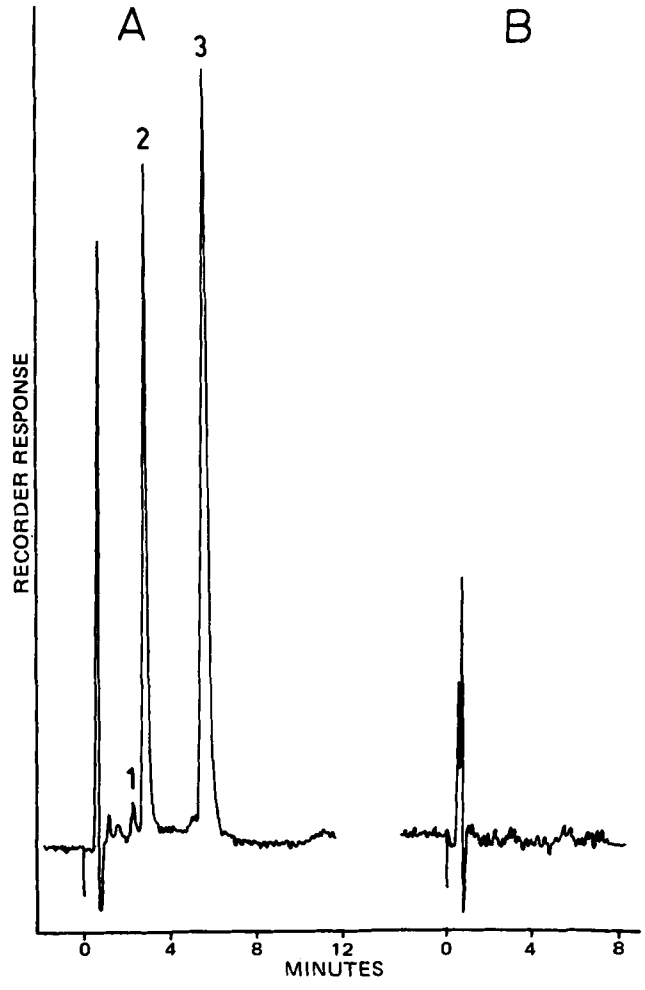

Figure 2—*Chromatograms of serum containing 3 μg of doxycycline/ml (dose of 200 mg iv) (A) and of blank serum (B). Key: 1, unidentified by-product of doxycycline; 2, demeclocycline (internal standard); and 3, doxycycline. Conditions were as in Fig. 1 except for the temperature (30°); detector sensitivity was 0.02 aufs.*

The organic layer was transferred to a conical evaporation tube containing 100 μl of a 0.2% (w/v) methanolic ascorbic acid solution. The mixture was evaporated[10] to dryness at room temperature by applying vacuum under continuous vortexing of the tubes. The residue was finally dissolved in 200 μl of the chromatographic eluent. After mixing[8], the solution was filtered and kept in ice until a 20-μl aliquot was injected into the chromatograph.

A procedure identical to the plasma assay was followed for urine extraction, except that a 100-μl sample, 0.4 ml of buffer, and 3 ml of ethyl acetate were used.

Calculations—Standard curves were constructed by analyzing serum samples containing known drug amounts and plotting peak height ratios (doxycycline/internal standard) *versus* the corresponding doxycycline concentration.

RESULTS AND DISCUSSION

Chromatography—The excellent selectivity of the chromatographic system for the separation of seven tetracyclines is illustrated in Fig. 1. A previously used 25-cm × 4.6-mm i.d. RP8 column (14) was replaced by a short narrow-bore column to improve the detection limit. The extremely small void volume reduces dilution in the column (16) but requires severe precautions to minimize extracolumn band broadening, which especially occurs in the connecting tubes and the detector cell. In addition, injection of components in a solvent that is stronger than the eluent, *e.g.*, methanol, must be strictly avoided since such solvents cause a severe loss of column efficiency due to a secondary solvent effect.

On the basis of this elution pattern, as well as its structural analogy, demeclocycline was chosen as the internal standard. Both other closely eluting derivatives, *i.e.*, chlortetracycline and methacycline, were unsuitable. The former showed a pronounced chemical instability, and low extraction yields (5–10%) were obtained for the latter.

Extraction—The development of a suitable extraction step for this very polar, amphoteric, and labile compound involved various problems. A few techniques, used as a part of some fluorometric assay methods for tetracyclines in general, have been reported (2, 3, 17, 18). Only medium polar organic solvents, *i.e.*, ethyl acetate, amyl acetate, *n*-butanol, and 1-pentanol, can be considered for the isolation of these compounds from a weakly acidic medium (2, 17). Several authors also used chelate extraction performed with divalent cations in a strong alkaline medium (3, 4, 12, 13, 18). However, subsequent concentration of the organic extract proved inconvenient; a dense salt residue prevented redissolution of the compounds in a limited aqueous solvent volume.

The isolation procedure is a modification of a previously described method (2). Amyl acetate was replaced by ethyl acetate to accelerate the final evaporation step. Partition into the organic solvent was particularly favored by salting out the compounds in the nearly saturated phosphate sulfite buffer. Three different buffers consisting of 3, 2, and 1 *M* sodium dihydrogen phosphate and 1, 2, and 2 *M* sodium sulfite gave corresponding pH values of ~5.4, 6.1, and 6.5, respectively. The second buffer system was chosen because it provided the least aggressive medium and gave slightly superior extraction yields. In fact, all tetracyclines are subject to a reversible epimerization process of the C_4-dimethylamino group, occurring preferentially in various buffers over a pH 2–6 range (19, 20).

[10] Rotary Evapo-Mix, Büchler Instruments, Fort Lee, N.J.

Table I—Analytical Recovery of Doxycycline from Human Serum

Added, μg/ml	Measured, μg/ml	Recovery[a], %
3.07	2.69	87.6
3.07	2.73	88.9
3.07	2.80	91.2
3.07	2.63	85.7
3.07	2.60	84.7
6.18	5.27	85.3
6.18	5.55	89.8
6.18	5.25	85.0
6.18	5.75	93.0
6.18	5.93	96.0
6.18	5.40	87.4
6.18	4.92	79.6

[a] Mean ± *SD* = 87.8 ± 4.3.

Despite these precautions, the internal standard, unlike doxycycline, initially deteriorated when serum extracts in ethyl acetate were evaporated at 60°. The additional peak appearing in the chromatogram was identified as 4-epidemethylchlortetracycline on the basis of its retention time and UV characteristics (absorption rate method). No degradation occurred when a standard solution of demeclocycline in ethyl acetate was taken to dryness at 60°. However, considerable epimerization took place even when the compound was added to the organic layer after the extraction of a blank serum sample. Apparently, one or more coextracted

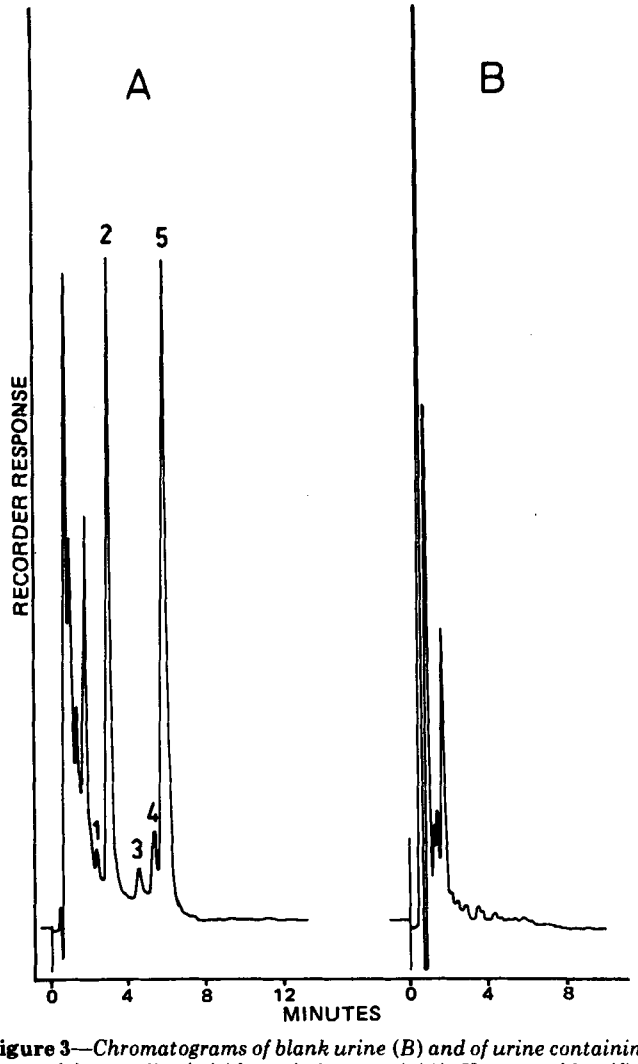

Figure 3—*Chromatograms of blank urine (B) and of urine containing 15 μg of doxycycline/ml (dose of 100 mg po) (A). Key: 1, unidentified by-product of doxycycline; 2, demeclocycline (internal standard); 3 and 4, unidentified peaks; and 5, doxycycline. Conditions were as in Fig. 2; detector sensitivity was 0.02 aufs.*

Table II—Analytical Recovery of Doxycycline from Human Urine

Added, μg/ml	Measured, μg/ml	Recovery[a], %
26.15	24.35	93.1
26.15	23.85	91.2
26.15	25.20	96.4
26.15	24.70	94.5
26.15	23.91	91.4
52.30	47.40	90.6
52.30	46.70	89.3
52.30	48.10	92.0
52.30	48.10	92.0
52.30	48.00	91.8

[a] Mean ± *SD* = 92.2 ± 2.0.

serum component(s) act as a catalyst to this effect. Doxycycline itself was more stable under the same conditions. As previously suggested (20), a hydroxyl group at position 5 of the molecule should prevent epimerization by forming an intramolecular hydrogen bond with the dimethylamino group at carbon 4.

Mild evaporation conditions (room temperature, vacuum) and addition of a little ascorbic acid to the ethyl acetate eliminated the epimerization reaction. Although other tetracycline-stabilizing properties of ascorbic acid are reported (21), its action in suppressing the epimerization was somewhat surprising.

Dissolution of the residue in the chromatographic eluent was adopted for column efficiency. It also served as an ultimate purification step. Most of the coextracted lipids and yellow serum pigments finally remained undissolved in this medium and were filtered off. Colorless and cleaner extracts were thus injected. This practice contributed markedly in prolonging the column life. If loss of column efficiency is occasionally noticed, a simple replacement of the PTFE inlet filter will restore most of the original efficiency.

Extraction Recovery—Recovery studies were carried out by extracting samples containing known drug amounts and adding the internal standard after the extraction was completed. An external calibration curve for this experiment was constructed from the direct analysis (without extraction) of mixtures of doxycycline and the internal standard. Results for serum and urine are summarized in Tables I and II.

Linearity, Sensitivity, and Reproducibility—Linear relationships were observed up to concentrations of 6 μg/ml for serum and 100 μg/ml for urine. The amounts covered the entire anticipated therapeutic range. A pooled standard curve for serum, based on 30 values (0–6 μg/ml) obtained on 12 different days, had a slope of 0.305, an intercept of +0.008, and a correlation coefficient of 0.9995. A similar curve constructed for urine (0–100 μg/ml) yielded 0.073, + 0.002, and 0.9999, respectively. The detection limit in serum is estimated at 50 ng/ml, a value much lower than the concentrations occurring at usual dosage regimens. A within-run relative standard deviation for serum at the 2.5-μg/ml level of 1.8% (n = 10) was obtained. Long-term reproducibility was evaluated over a 20-day period (n = 9) at a concentration of 2.6 μg/ml and yielded a value of 4.75%.

Applications—The assay method presented has been used routinely in this laboratory to monitor serum drug levels in patients receiving doxycycline therapy (130 samples, 38 subjects). Levels after 2–3 hr ranged from 2 to 9 μg/ml after a single intravenous dose of 200 mg.

Figure 2A shows a typical HPLC record of a human serum extract containing doxycycline and the internal standard. Capacity ratios (k') of both compounds were 4.5 and 9.6, respectively. No interfering peaks were observed in a blank serum extract (Fig. 2B).

Chromatograms of a blank urine extract (B) and of a urine extract (A) from a patient who received 100 mg of doxycycline are shown in Fig. 3.

No large extra peaks were present in serum or in urine extracts. The small unidentified peak (Figs. 2 and 3) was probably due to a doxycycline degradation product since it was found in freshly prepared standard solutions and in serum and urine samples from patients receiving doxycycline therapy. Because metabolites are generally more polar than the parent compound, they should elute earlier than doxycycline from a reversed-phase column. Therefore, it is noteworthy that no such metabolites could be detected.

Furthermore, the method can be valuable for determining the pharmacokinetic parameters of the drug to optimize its dosage scheme. Its application to other biological materials requires a few modifications and is presently under study.

REFERENCES

(1) F. Ritzl, M. Schoog, A. Höck, and F. E. Feinendegen, *Proc. Int. Congr. Chemother. 7th*, **1**, 35 (1972).

(2) M. Lever, *Biochem. Med.*, **6**, 216 (1972).

(3) D. M. Wilson, M. Lever, E. A. Brosnan, and A. Stillwell, *Clin. Chim. Acta*, **36**, 260 (1972).

(4) G. Bessard, J.-M. Mallion, H. Morena, and M. Gavend, *Grenoble Med.-Chir.*, **9**, 653 (1971).

(5) E. J. Stokes, "Clinical Bacteriology," 3rd ed., Arnold, London, England, 1969, p. 207.

(6) M. F. Michel, J. P. van Waardhuizen, and K. F. Kerrebijn, *Chemotherapy*, **18**, 77 (1973).

(7) C. Radecka and W. L. Wilson, *J. Chromatogr.*, **57**, 297 (1971).

(8) E. Ragazzi and G. Veronese, *Farmaco Ed. Prat.*, **29**, 372 (1974).

(9) E. Ragazzi and G. Veronese, *J. Chromatogr.*, **132**, 105 (1977).

(10) A. Szabó, M. Kovács Nagy, and E. Tömörkény, *ibid.*, **151**, 256 (1978).

(11) I. Nilsson-Ehle, T. T. Yoshikawa, M. C. Schotz, and L. B. Guze, *Antimicrob. Ag. Chemother.*, **9**, 754 (1976).

(12) J. P. Sharma, E. G. Perkins, and R. F. Bevill, *J. Chromatogr.*, **134**, 441 (1977).

(13) J. P. Sharma, G. D. Koritz, E. G. Perkins, and R. F. Bevill, *J. Pharm. Sci.*, **66**, 1319 (1977).

(14) A. P. De Leenheer and H. J. C. F. Nelis, *J. Chromatogr.*, **140**, 293 (1977).

(15) C. F. Simpson, "Practical High Performance Liquid Chromatography," Heyden and Son, London, England, 1976, p. 295.

(16) B. L. Karger, M. Martin, and G. Guiochon, *Anal. Chem.*, **46**, 1640 (1974).

(17) K. H. Ibsen, R. L. Saunders, and M. R. Urist, *Anal. Biochem.*, **5**, 505 (1963).

(18) H. Poiger and C. Schlatter, *Analyst (London)*, **101**, 808 (1976).

(19) J. R. D. McCormick, S. M. Fox, L. L. Smith, B. A. Bitler, J. Reichenthal, V. E. Origoni, W. H. Muller, R. Winterbottom, and A. P. Doerschuk, *J. Am. Chem. Soc.*, **79**, 2849 (1957).

(20) D. A. Hussar, P. J. Niebergall, E. T. Sugita, and J. T. Doluisio, *J. Pharm. Pharmacol.*, **20**, 539 (1968).

(21) L. J. Leeson and J. F. Weidenheimer, *J. Pharm. Sci.*, **58**, 355 (1969).

ACKNOWLEDGMENTS

Supported by the National Research Foundation (NFWO) through a grant to one of the authors.

The authors acknowledge the generous gift of doxycycline standard from Dr. Gordts, Medical Department, Pfizer Inc., Brussels, Belgium.

Examination of Blood Clobazam Levels and Several Pupillary Measures in Humans

JEFFREY A. KOTZAN ˣ, THOMAS E. NEEDHAM, IRVING L. HONIGBERG, JOSEPH J. VALLNER, JAMES T. STEWART, WALTER J. BROWN, and HUNG W. JUN

Received January 23, 1978, from *Biological Group Studies, School of Pharmacy, University of Georgia, Athens, GA 30602.* Accepted for publication February 7, 1979.

Abstract □ The State–Trait Anxiety Inventory was administered to 15 subjects before initiation of the experiment. Three subgroups of five subjects were defined by computing the unweighted sum of the state and trait anxiety scores. A 40-mg dose of clobazam, a 1,5-benzodiazepine, was administered to each subject and repeated with two additional dosage forms following a 2-week washout period. Blood samples were withdrawn, and blood levels were determined by fluorometric analysis. Additionally, pupillary measures of critical flicker fusion, constriction, and dilation in response to a cognitive task were obtained at 0, 2, 4, and 6 hr. A repeated measures analysis of variance revealed that blood levels were, as expected, statistically different over time and dosage form. The pupillary constriction mirrored the blood levels in statistical patterns. The pupillary measure of cognition related to the anxiety state after the performance effects of the cognitive task were statistically removed. The results suggest that clobazam has less immediate human effect than does diazepam.

Keyphrases □ Clobazam—analysis, fluorometry, blood levels, effect on pupillary constriction, and anxiety level □ Pupillary constriction—clobazam effect, blood level, and anxiety level □ Tranquilizers, minor—clobazam, fluorometric analysis, blood levels, effect on pupillary constriction, and anxiety level

Clobazam, a 1,5-benzodiazepine, is effective in the treatment of anxiety neurosis (1, 2). The immediate and long-term effects of the benzodiazepines on human performance ability likewise have been demonstrated. Generally, the benzodiazepines decrease human ability to perform complex tasks (3–5). Additionally, the benzodiazepine drug class affects physiological measures such as auditory reaction times and complex visual reaction times (6–8).

Pupillometrics is defined as the aspect of psychology that deals with the assessment of pupillary alterations elicited by any stimulus other than light (9). Pupil dilation in response to complex cognitive tasks can be observed with proper instrumentation and experimental controls (10). A sensitive means of generating pupillary cognition curves by verbally presenting randomized digits to subjects was described (11, 12). Furthermore, diazepam consumption was shown to alter the pupil cognition curves and recall ability (12).

The objective of this research was to determine if clobazam consumption related to pupillometry involving human cognition and two noncognitive pupillary measures. Critical flicker fusion and miotic effect of the drug were selected as noncognitive measures.

EXPERIMENTAL

Fifteen male volunteers were recruited and subjected to the State–Trait Anxiety Inventory (13). A high anxiety subgroup, consisting of five members, was defined operationally by a combined state–trait anxiety score of >72.0. A five-membered, low anxiety group was defined by a combined score of <64.0. The remaining five subjects were assigned to the middle anxiety group.

A randomized Latin-square design was employed to assign the subjects to a three-level dosage form treatment group. Each subject received separate 40-mg doses by tablet, solution, and capsule dosage forms in randomized and matched sequences. Blood samples were obtained for up to 144 hr following ingestion (14). The blood levels were determined by a fluorometric assay, which did not distinguish between the drug and its active major metabolite, the *N*-desmethyl compound (15).

0022-3549/79/0800-1002$01.00/0

© 1979, American Pharmaceutical Association

REFERENCES

(1) F. Ritzl, M. Schoog, A. Höck, and F. E. Feinendegen, *Proc. Int. Congr. Chemother. 7th*, **1**, 35 (1972).

(2) M. Lever, *Biochem. Med.*, **6**, 216 (1972).

(3) D. M. Wilson, M. Lever, E. A. Brosnan, and A. Stillwell, *Clin. Chim. Acta*, **36**, 260 (1972).

(4) G. Bessard, J.-M. Mallion, H. Morena, and M. Gavend, *Grenoble Med.-Chir.*, **9**, 653 (1971).

(5) E. J. Stokes, "Clinical Bacteriology," 3rd ed., Arnold, London, England, 1969, p. 207.

(6) M. F. Michel, J. P. van Waardhuizen, and K. F. Kerrebijn, *Chemotherapy*, **18**, 77 (1973).

(7) C. Radecka and W. L. Wilson, *J. Chromatogr.*, **57**, 297 (1971).

(8) E. Ragazzi and G. Veronese, *Farmaco Ed. Prat.*, **29**, 372 (1974).

(9) E. Ragazzi and G. Veronese, *J. Chromatogr.*, **132**, 105 (1977).

(10) A. Szabó, M. Kovács Nagy, and E. Tömörkény, *ibid.*, **151**, 256 (1978).

(11) I. Nilsson-Ehle, T. T. Yoshikawa, M. C. Schotz, and L. B. Guze, *Antimicrob. Ag. Chemother.*, **9**, 754 (1976).

(12) J. P. Sharma, E. G. Perkins, and R. F. Bevill, *J. Chromatogr.*, **134**, 441 (1977).

(13) J. P. Sharma, G. D. Koritz, E. G. Perkins, and R. F. Bevill, *J. Pharm. Sci.*, **66**, 1319 (1977).

(14) A. P. De Leenheer and H. J. C. F. Nelis, *J. Chromatogr.*, **140**, 293 (1977).

(15) C. F. Simpson, "Practical High Performance Liquid Chromatography," Heyden and Son, London, England, 1976, p. 295.

(16) B. L. Karger, M. Martin, and G. Guiochon, *Anal. Chem.*, **46**, 1640 (1974).

(17) K. H. Ibsen, R. L. Saunders, and M. R. Urist, *Anal. Biochem.*, **5**, 505 (1963).

(18) H. Poiger and C. Schlatter, *Analyst (London)*, **101**, 808 (1976).

(19) J. R. D. McCormick, S. M. Fox, L. L. Smith, B. A. Bitler, J. Reichenthal, V. E. Origoni, W. H. Muller, R. Winterbottom, and A. P. Doerschuk, *J. Am. Chem. Soc.*, **79**, 2849 (1957).

(20) D. A. Hussar, P. J. Niebergall, E. T. Sugita, and J. T. Doluisio, *J. Pharm. Pharmacol.*, **20**, 539 (1968).

(21) L. J. Leeson and J. F. Weidenheimer, *J. Pharm. Sci.*, **58**, 355 (1969).

ACKNOWLEDGMENTS

Supported by the National Research Foundation (NFWO) through a grant to one of the authors.

The authors acknowledge the generous gift of doxycycline standard from Dr. Gordts, Medical Department, Pfizer Inc., Brussels, Belgium.

Examination of Blood Clobazam Levels and Several Pupillary Measures in Humans

JEFFREY A. KOTZAN ˣ, THOMAS E. NEEDHAM, IRVING L. HONIGBERG, JOSEPH J. VALLNER, JAMES T. STEWART, WALTER J. BROWN, and HUNG W. JUN

Received January 23, 1978, from *Biological Group Studies, School of Pharmacy, University of Georgia, Athens, GA 30602.* Accepted for publication February 7, 1979.

Abstract □ The State–Trait Anxiety Inventory was administered to 15 subjects before initiation of the experiment. Three subgroups of five subjects were defined by computing the unweighted sum of the state and trait anxiety scores. A 40-mg dose of clobazam, a 1,5-benzodiazepine, was administered to each subject and repeated with two additional dosage forms following a 2-week washout period. Blood samples were withdrawn, and blood levels were determined by fluorometric analysis. Additionally, pupillary measures of critical flicker fusion, constriction, and dilation in response to a cognitive task were obtained at 0, 2, 4, and 6 hr. A repeated measures analysis of variance revealed that blood levels were, as expected, statistically different over time and dosage form. The pupillary constriction mirrored the blood levels in statistical patterns. The pupillary measure of cognition related to the anxiety state after the performance effects of the cognitive task were statistically removed. The results suggest that clobazam has less immediate human effect than does diazepam.

Keyphrases □ Clobazam—analysis, fluorometry, blood levels, effect on pupillary constriction, and anxiety level □ Pupillary constriction—clobazam effect, blood level, and anxiety level □ Tranquilizers, minor—clobazam, fluorometric analysis, blood levels, effect on pupillary constriction, and anxiety level

Clobazam, a 1,5-benzodiazepine, is effective in the treatment of anxiety neurosis (1, 2). The immediate and long-term effects of the benzodiazepines on human performance ability likewise have been demonstrated. Generally, the benzodiazepines decrease human ability to perform complex tasks (3–5). Additionally, the benzodiazepine drug class affects physiological measures such as auditory reaction times and complex visual reaction times (6–8).

Pupillometrics is defined as the aspect of psychology that deals with the assessment of pupillary alterations elicited by any stimulus other than light (9). Pupil dilation in response to complex cognitive tasks can be observed with proper instrumentation and experimental controls (10). A sensitive means of generating pupillary cognition curves by verbally presenting randomized digits to subjects was described (11, 12). Furthermore, diazepam consumption was shown to alter the pupil cognition curves and recall ability (12).

The objective of this research was to determine if clobazam consumption related to pupillometry involving human cognition and two noncognitive pupillary measures. Critical flicker fusion and miotic effect of the drug were selected as noncognitive measures.

EXPERIMENTAL

Fifteen male volunteers were recruited and subjected to the State–Trait Anxiety Inventory (13). A high anxiety subgroup, consisting of five members, was defined operationally by a combined state–trait anxiety score of >72.0. A five-membered, low anxiety group was defined by a combined score of <64.0. The remaining five subjects were assigned to the middle anxiety group.

A randomized Latin-square design was employed to assign the subjects to a three-level dosage form treatment group. Each subject received separate 40-mg doses by tablet, solution, and capsule dosage forms in randomized and matched sequences. Blood samples were obtained for up to 144 hr following ingestion (14). The blood levels were determined by a fluorometric assay, which did not distinguish between the drug and its active major metabolite, the *N*-desmethyl compound (15).

0022-3549/79/0800-1002$01.00/0

© 1979, American Pharmaceutical Association

Table I—Analysis of Variance of Blood Clobazam Levels (Nanograms per Milliliter)

Source	Degrees of Freedom	*F*	P
Anxiety	2	N.S.[a]	
Dosage form	2	5.0818	0.014
Dosage form–anxiety	4	2.8937	0.044
Time	3	461.5114	0.001
Time–anxiety	6	N.S.	
Dosage form–time	6	2.6644	0.022
Dosage form–time–anxiety	12	N.S.	

[a] Not significant.

Table II—Analysis of Variance of Pupillary Diameter (Millimeters)

Source	Degrees of Freedom	*F*	P
Anxiety	2	N.S.[a]	
Dosage form	2	7.0835	0.004
Dosage form–anxiety	4	N.S.	
Time	3	9.3013	0.001
Time–anxiety	6	N.S.	
Dosage form–time	6	N.S.	
Dosage form–time–anxiety	12	N.S.	

[a] Not significant.

Pupillary measures were obtained for all subjects and all doses immediately preceding ingestion of the 40-mg dose. Additional pupillary observations were obtained immediately preceding the 2-, 4-, and 6-hr blood samplings.

The total pupillary recordings required approximately 7 min for each subject–dosage form–time set. The subjects entered an experiment room illuminated at 5 foot-candles, and critical flicker fusion measures were obtained. Ascending and descending measures were recorded individually for each eye. The flicker fusion apparatus was calibrated to balanced maximum brightness, a neutral density wedge setting of 3, and 15% light[1].

The cognitive task methodology outlined previously (11, 12) was employed after determination of the critical flicker fusion rates. Thus, the subject's pupils were accommodated to the experimental room illumination level before the cognition recordings commenced. The subjects were required to remember the exact order of seven randomized digits between zero and nine. The digits were presented in monotone fashion at 1-sec intervals. The pupillary dilation pattern was simultaneously recorded[2] and continued for several seconds following the presentation of the seventh digit, which permitted the subjects to resort the numbers and finalize their thought processes. Each trial covered 14 sec, and two trials were executed at each subject–dosage form–time interval and averaged to reduce variability. Finally, a measure of satisfactory completion of the cognitive task was obtained by recording the number of digits correctly recalled at each trial.

All pupillary and blood level data were reduced to machine-readable form. To isolate the pupillary cognition curve from the constriction effect of the drug, the initially recorded diameter at the 1st sec of the cognitive task was subtracted from that at each remaining second of the cognitive curve. In this manner, a constriction factor was created. A program was written that computed the areas under the "cleansed" cognition curves, employing the trapezoidal rule (16).

Thus, the final data base contained 15 subjects categorized into one of three anxiety levels. Each subject's file contained fluorometric blood level recordings, pupillary constriction measures, pupillary cognitive area under the curve measures, a recording of the correct number of responses, and critical flicker fusion measures. All measures were repeated at 0, 2, 4, and 6 hr and further repeated using three dosage forms of tablet, solution, and capsule. The data were analyzed by means of an analysis of variance and covariance (17). The anxiety level was input as the grouping factor.

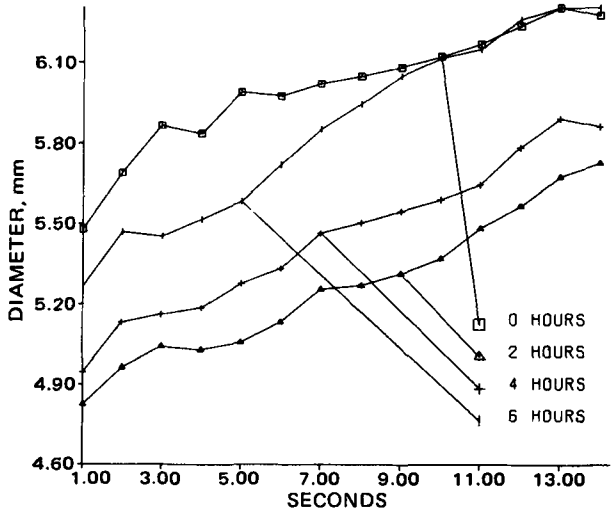

Figure 1—*Average pupil cognition curves for 15 male subjects following consumption of 4 × 10-mg clobazam tablets.*

[1] Control model 12025 and (viewing chamber) model 12024, Lafayette Instrument Co., West Lafayette, Ind.

[2] Polymetric model V11651R, U. S. Testing Co., Hoboken, N.J.

RESULTS

The ability of the random digit task to stimulate pupil dilation was substantiated. Figures 1–3 display the average pupil dilation pattern for the three dosage forms and four time levels. It was immediately apparent that the pupil-constricting effect of clobazam was substantial.

The blood levels were highly significant for the time and dosage form factors, as expected (Table I). The anxiety level did not relate to the blood level, but the dosage form–anxiety interaction proved significant. In a similar pattern, the pupil-constricting effect of the drug proved highly significant for the time and dosage form factors. Table II displays the analysis of variance of the constriction measures, and Table III compares the mean blood levels and pupillary constriction at each time level, summing over the three dosage forms. The pupil was constricted to the greatest degree at the 2-hr point, at which time the greatest average blood level was recorded. The pupil diameter returned to the baseline at the 6-hr point, but the blood level of the parent compound and the metabolites exceeded 350 ng/ml. The factors of critical flicker fusion and number of correct responses proved insignificant for the time factor, which was not anticipated.

An initial analysis of variance of the cognition curves over time and dosage forms proved significant for the anxiety and dosage form factors. However, the variance terms were not homogeneous, and previous research indicated that the ability of subjects to recall randomized digits correctly affects the cognition curves (11, 12). Therefore, the number of digits correctly recalled was input in the analysis as covariates, and the analysis of variance was repeated. In such a manner, the effect of recalling all, or less than all, of the randomized digits was removed from the pupillary cognition curves.

The results of the combined analysis of variance and covariance are presented in Table IV. Only the anxiety factor remained statistically significant in terms of the area under the cognition curve. The covariates removed the statistical significance from the dosage form factor. The

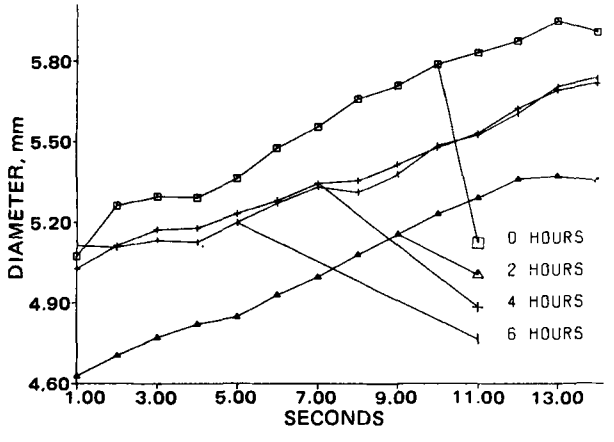

Figure 2—*Average pupil cognition curves for 15 male subjects following consumption of 4 × 10-mg clobazam capsules.*

Table III—Comparison between Blood Levels and Pupil Diameter at Four Time Levels for All Dosage and Anxiety Levels

Hours	Pupil Diameter, mm	Blood Level, ng/ml
0	5.3567	3.2444
2	4.8289	436.4221
4	5.0711	363.9110
6	5.3622	352.3110

mean areas under the cognition curves, corrected for accuracy of recall, were 5.9631, 4.1535, and 7.1379 mm-sec for the low, medium, and high anxiety groups (n = 5), respectively.

CONCLUSIONS

The major conclusion of this study was that the drug and its metabolite reduced the diameter of the pupil when blood levels peaked. However, pupil diameters did not remain constricted at the 6-hr point when blood levels exceeded 350 ng/ml. These results are similar to reports that many psychomotor functions such as coordination tests, tracing tests, sorting tests, and letter cancellation tests returned to baseline values 5 hr after subjects consumed 20 mg of diazepam (18). However, the average blood diazepam level exceeded 300 ng/ml at the 5-hr point. Furthermore, at 105 min, blood diazepam levels exceeded 800 ng/ml and most psychomotor functions were impaired (18). Thus, the benzodiazepines clobazam and diazepam appear to produce a detectable human response at higher blood levels.

Anxiety state proved to be significantly related to the area under the cognition curve after correction was made for recall ability. The low and high anxiety subgroups generated greater areas under the curve than did the middle anxiety group at all times and with all dosage forms. Apparently, anxiety is partly related to the nonresponsive phenomenon, and the nonsensitive subjects were assigned to one of the three groups. The anxiety results manifest the high degree of intersubject pupillary variation in response to the cognitive task.

Some evidence suggests considerable variance among the benzodiazepines in their ability to alter human performance. In fact, clobazam demonstrated little effect on adaptive tracking and reaction times when compared to diazepam and chlordiazepoxide (3). However, the results of this experiment demonstrated a measurable alteration in human pupillary response at higher blood levels of clobazam and its metabolites.

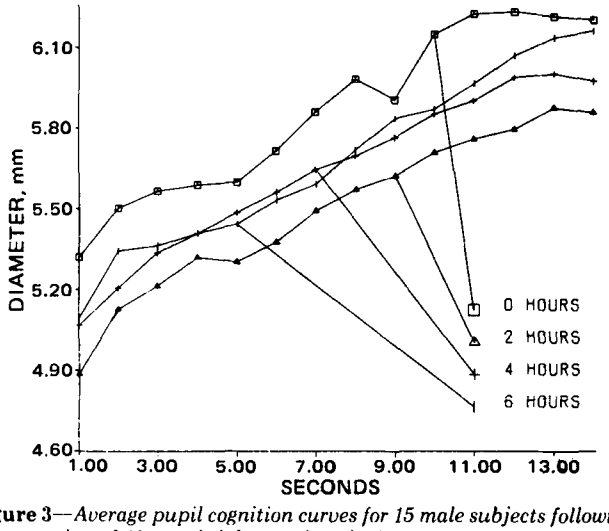

Figure 3—*Average pupil cognition curves for 15 male subjects following consumption of 40 mg of clobazam in solution.*

Table IV—Analysis of Variance and Covariance of Area under Cognition Curve (Millimeters per Second)

Source	Degrees of Freedom	F	P
Anxiety	2	4.9656	0.040
Recall covariate time 0 hr	1	8.2676	0.021
Recall covariate time 2 hr	1	N.S.[a]	
Recall covariate time 4 hr	1	5.5813	0.046
Recall covariate time 6 hr	1	N.S.	
Dosage form	2	N.S.	
Dosage form–anxiety	4	N.S.	
Recall covariate time 0 hr	1	4.0503	0.058
Recall covariate time 2 hr	1	N.S.	
Recall covariate time 4 hr	1	N.S.	
Recall covariate time 6 hr	1	N.S.	
Time	3	N.S.	
Time–anxiety	6	N.S.	
Dosage form–time	6	N.S.	
Dosage form–time–anxiety	12	N.S.	

[a] Not significant.

REFERENCES

(1) S. Devanthan, and S. M. Channabasavanna, *Curr. Ther. Res.*, **21**, 361 (1977).

(2) K. Sandler, D. Brunswick, J. Digiacomo, and J. Mendels, *ibid.*, **21**, 114 (1977).

(3) R. G. Borland and A. N. Nicholson, *Br. J. Clin. Pharmacol.*, **2**, 215 (1974).

(4) R. Saario, M. Linnoila, and M. J. Mattila, *ibid.*, **3**, 843 (1976).

(5) R. G. Borland and A. N. Nicholson, *ibid.*, **2**, 9 (1975).

(6) M. Ransella, O. Siciliani, L. Burti, and M. Schiavon, *Psychopharmacologia*, **41**, 81 (1975).

(7) A. J. Bond and M. H. Lader, *ibid.*, **32**, 223 (1973).

(8) S. M. Luria, H. M. Paulson, J. S. Kinney, C. L. McKay, M. S. Strauss, and A. P. Ryann, "Naval Submarine Medical Research Laboratory Report," No. 808, Bureau of Medicine and Surgery, Navy Department, Groton, Conn., 1975.

(9) E. H. Hess and H. M. Plott, *Science*, **132**, 349 (1960).

(10) B. C. Goldwater, *Psychol. Bull.*, **77**, 340 (1972).

(11) S. W. Peavler, *Psychophysiology*, **11**, 559 (1975).

(12) J. A. Kotzan, *J. Pharm. Sci.*, **67**, 956 (1978).

(13) C. D. Spielberger, R. L. Gorsuch, and R. E. Lushene, "STAI Manual," Psychologists Press, Palo Alto, Calif., 1970.

(14) T. E. Needham, J. J. Vallner, H. W. Jun, I. L. Honigberg, J. T. Stewart, J. A. Kotzan, and W. J. Brown, in *Abstracts, APhA Academy Pharm. Sci.*, **7**, 119 (1977).

(15) I. L. Honigberg, J. T. Stewart, W. J. Brown, H. W. Jun, J. A. Kotzan, T. E. Needham, and J. J. Vallner, in *ibid.*, **7**, 165 (1977).

(16) M. Gibaldi and D. Perrier, "Pharmacokinetics," Dekker, New York, N.Y., 1975, p. 293.

(17) "Biomedical Computer Programs—P," W. J. Dixon, Ed., University of California Press, Berkeley, Calif., 1975 (rev. Feb. 1976).

(18) J. F. Haffner, J. Morland, J. Setekleiv, C. E. Stromsather, A. Danielson, P. T. Frivik, and F. Dybing, *Acta Pharmacol. Toxicol.*, **32**, 161 (1973).

ACKNOWLEDGMENTS

Supported by Hoeschst-Roussel Pharmaceuticals, Inc., Somerville, N.J.

The authors thank Dr. Henry Fraser for support and advice.

Physical Characterization of Solid Iopanoic Acid Forms

WILLIAM C. STAGNER and J. KEITH GUILLORY ˣ

Received December 1, 1978, from the *Division of Pharmaceutics, College of Pharmacy, University of Iowa, Iowa City, IA 52242.* Accepted for publication February 9, 1979.

Abstract □ Three solid forms of iopanoic acid were characterized by X-ray diffraction, differential scanning calorimetry, scanning electron microscopy, thermal microscopy, IR spectroscopy, and dissolution studies. X-ray analysis demonstrated that two solid forms were crystalline and that the third was amorphous. The amorphous form had been reported previously as crystalline. Enthalpies and entropies of transition were calculated using differential scanning calorimetry. A fourth form, a benzene solvate, also was isolated but proved to be too unstable at room temperature to permit conclusive characterization. The amorphous form demonstrated a 10-fold greater intrinsic dissolution rate than the commercially available form (Form I). Form II's intrinsic dissolution rate was 1.5 times greater than that of Form I. In powder dissolution studies, the peak solubilities of the different forms followed the same rank order as their intrinsic dissolution rates. Form II was relatively stable in aqueous saturated solutions, but the amorphous form was rapidly converted to Form I under similar conditions.

Keyphrases □ Iopanoic acid—solid forms, physical characterization, polymorphism, thermal behavior □ Polymorphism—iopanoic acid, physical characterization, thermal behavior □ Radiopaque media—iopanoic acid, solid forms, physical characterization, polymorphism, thermal behavior

Gallbladder disease, a commonly occurring medical problem, is most frequently diagnosed through the use of oral radiographic agents. Over 2,000,000 patients in the United States alone undergo oral cholecystography each year (1). The agent most commonly prescribed to produce gallbladder opacification is iopanoic acid[1] (I), an iodinated organic acid poorly soluble in water; it is administered orally in tablet form.

However, in approximately 25–50% of patients with apparently normal gallbladders, iopanoic acid reaches the gallbladder in insufficient concentration to permit radiographic opacification (1, 2). Consequently, a second examination with another dose of contrast material is often required. Nevertheless, iopanoic acid continues to be widely used because of its ability to permit accurate visualization of gallstones and because of its relatively low toxicity.

BACKGROUND

Inadequate normal gallbladder visualization on initial examination is a complex problem. Ingestion of an insufficient amount of contrast medium, faulty dosing instructions, changes in gastric pH, and decreases in bile flow associated with dietary control are often mentioned as causes for initial nonvisualization. In 1971, Evens *et al.* (3) postulated that poor visualization of normal gallbladders on initial examination was due to incomplete absorption of the radiocontrast medium. They observed large amounts of coarse radiopaque residue on abdominal radiographs of normal patients for whom poor gallbladder opacification had been obtained. Subsequent investigators (4) reported that iopanoic acid exhibited dissolution rate-limited absorption.

Numerous studies (5–8) showed that the sodium salt of iopanoic acid is more rapidly and completely absorbed than the free acid. Sodium iopanoate may react with hydrochloric acid in the stomach to precipitate the free acid as an amorphous material. In a recent investigation, Goldberger *et al.* (9) isolated the precipitated iopanoic acid immediately following acid addition to an aqueous solution of the sodium salt. The dissolution rate of the "freshly precipitated" acid was compared to that of the "dried precipitate," which was assumed to be analogous to the commercially supplied compound. Marked differences in the dissolution rates of the two forms were observed. On examination of the commercial acid, the recent precipitate, and the dried precipitate by oil immersion light microscopy and electron microscopy, the authors concluded that all three forms are crystalline. Consequently, they noted that use of the term "amorphous" to describe the recently precipitated material is not justified.

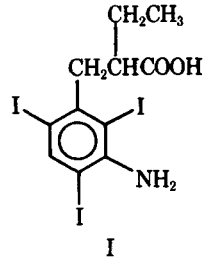

I

The purposes of the present study were: (*a*) to characterize further the previously reported crystalline iopanoic acid forms, and (*b*) to crystallize the material from various solvent systems in an attempt to isolate a polymorph with a rapid dissolution rate that might be stable in the solid state for a reasonable period.

EXPERIMENTAL

Solid Forms—Attempts were made to prepare polymorphs of iopanoic acid by crystallization from various solvent systems using the customary (10) techniques of shock cooling, crystallization at room temperature, and slow crystallization at elevated temperatures. Some 30 samples of crystalline material were examined by thermal microscopy, differential scanning calorimetry, IR spectroscopy, and other techniques, but only in the instances described here were unique crystalline forms obtained.

Commercial iopanoic acid[2] (Form I) was used in the preparation of three other solid forms. A free acid precipitate was obtained by a procedure similar to that described by Goldberger *et al.* (9). Iopanoic acid (3–5 g) was dissolved in 0.1 *N* NaOH, and the final solution pH was adjusted to ~12.5. Nitrogen was bubbled into the solution, and mixing was by a magnetic stirrer. Hydrochloric acid, 0.1 *N*, was added at a rate of 15 ml min^{-1} until the pH reached 2.15. The precipitate was vacuum filtered and stored *in vacuo* (380 mm Hg) for 12 hr at 35°.

In the preparation of Form II, a warm solution of commercial iopanoic acid in analytical reagent grade benzene was frozen rapidly in a dry ice–acetone mixture and then slowly allowed to melt at room temperature. Crystals obtained by filtration of this mixture were identified as a benzene solvate of iopanoic acid. Form II, free of benzene, was obtained when these crystals were stored *in vacuo* (380 mm Hg) for 12 hr at 70°.

X-Ray Analysis—All X-ray data were collected on an automated diffractometer[3] with monochromatized CuKα (λ = 1.5413 Å) radiation. The diffractometer was equipped with a 2θ compensating slit and a graphite monochromator. The instrument was calibrated to within ±0.02° 2θ using the quartz peak at 26.66°. The patterns were recorded both from 2 to 60° 2θ at a scanning speed of 2.4° 2θ min^{-1} and from 6 to 46° 2θ at a scanning speed of 6° 2θ min^{-1}.

Differential Scanning Calorimetry—A thermal analyzer[4], equipped with a differential scanning calorimeter cell, was used to record transition temperatures and heats. Thermograms were recorded simultaneously on an *x–y* recorder[4] and on an external time-base recorder equipped with a mechanical integrator[5]. A 10° min^{-1} heating rate was employed, and a nitrogen purge was maintained throughout each run.

[1] Telepaque, Winthrop Laboratories, New York, N.Y.

[2] Sterling-Winthrop Research Institute, Rensselaer, N.Y.

[3] Phillips APD 3500.

[4] DuPont 900.

[5] Servo/Riter II, Texas Instruments Inc.

0022-3549/79/0800-1005$01.00/0
© 1979, American Pharmaceutical Association

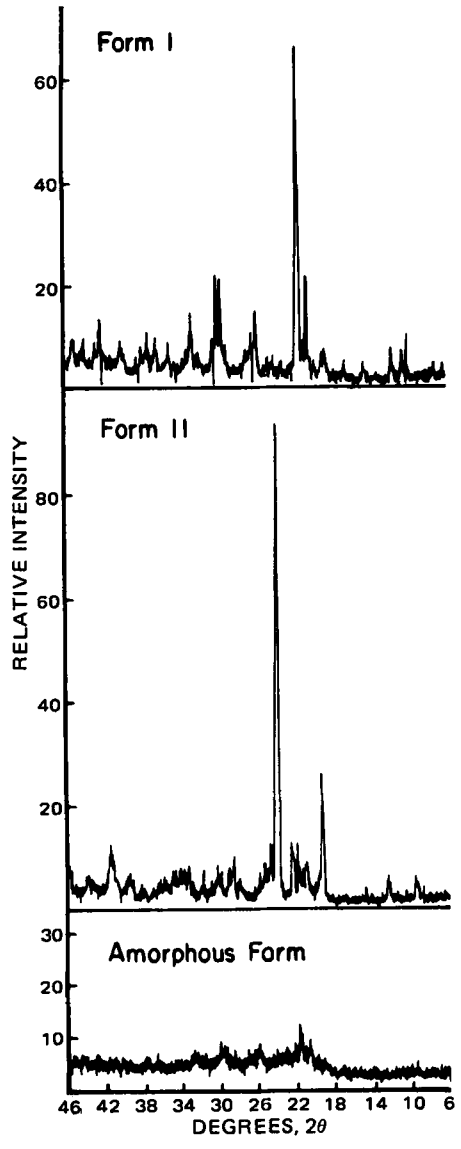

Figure 1—*X-ray powder diffraction patterns of solid iopanoic acid forms.*

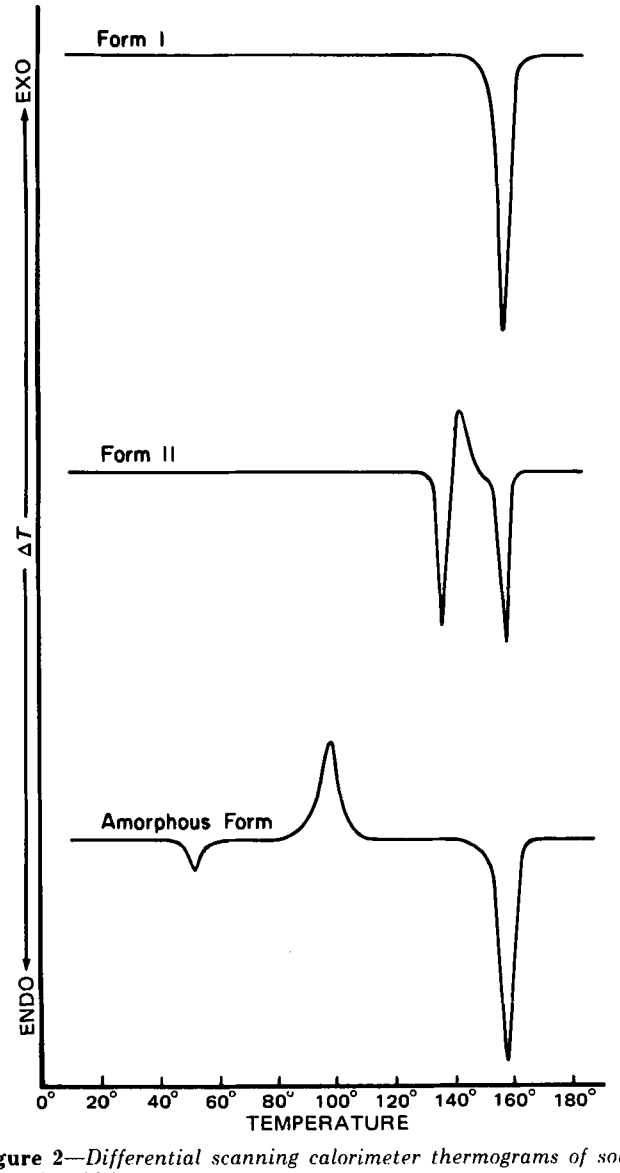

Figure 2—*Differential scanning calorimeter thermograms of solid iopanoic acid forms.*

Area measurements were obtained either by planimetry[6] or from the mechanical integrator trace. When areas were measured by planimetry, a line was drawn from the point at which the thermogram first departed from the baseline to the point, following the transition peak, at which the baseline was resumed.

Benzophenone[7] [ΔH_{fus} 23.5 cal g^{-1}; mp 48.2° (11)], stearic acid[8] (99+%) [ΔH_{fus} 47.5 cal g^{-1}; mp 69.0° (11)], and indium[9] (99.99%) [ΔH_{fus} 6.97 cal g^{-1} (12); mp 156.4° (11)] were used to prepare the calibration curve and to calibrate the temperature axis. The benzophenone was recrystallized twice from absolute alcohol. The stearic acid and indium were used without further purification. All samples were weighed on an electrobalance[10] to the nearest 0.001 mg. Peak area measurements, when performed by planimetry, were repeated with a precision approaching 0.1%. The relative standard deviation for the area measurements ranged from 3.16% for indium fusion to 1.70% for stearic acid fusion.

Thermal Microscopy—Thermal microscopic examinations of the samples were performed on a Kofler micro hot stage[11]. A few sample particles were placed on a microscope slide and examined between crossed Nicols. A heating rate of 1° min^{-1} was used to determine transition temperatures. Known melting-point standards were utilized to check the thermometer calibration and the technique used. The magnification employed was 100×, and the numerical aperture was 0.25.

Scanning Electron Microscopy—Scanning electron micrographs[12] were obtained for each iopanoic acid form. Solid samples were coated with a thin gold film and maintained under a vacuum of 1×10^{-5} mm Hg. A 100-μm aperture was used to obtain magnifications of 1000–6000×.

IR Spectroscopy—Spectra of solid samples, prepared as potassium bromide[13] pellets in a miniature press[14], were recorded on a double-beam IR spectrophotometer[15]. A polystyrene film was used to check the spectrophotometer wavelength calibration. After the spectra were obtained, thermograms of the triturated and compressed samples were recorded to detect possible alterations in crystalline form due to the grinding operations and the pressures used.

Dissolution Studies—Powder dissolution profiles were obtained for each solid iopanoic acid form. A quantity of solute approximately equivalent to twice the saturation solubility was employed. No attempt was made to control particle size. The powder was added to 500 ml of preheated 0.02 *M* phosphate buffer solution, pH 6.50. The dissolution medium was stirred at 228 rpm with a stainless steel propeller, which was positioned 3 cm from the bottom of a USP dissolution flask. All experiments were performed at 37.0 ± 0.1°.

Fifteen-milliliter samples were withdrawn periodically through a me-

[6] Model 620005, Keuffel & Esser Co.
[7] MC & B Manufacturing Chemists, Norwood, Ohio.
[8] Supelco, Inc., Bellefonte, Pa.
[9] Fisher Scientific Co., Fair Lawn, N.J.
[10] Cahn G-2.
[11] Arthur H. Thomas Co.
[12] Stereoscan S4, Cambridge Instrument Co.
[13] Harshaw Chemical Co.
[14] Wilk's minipress.
[15] Perkin-Elmer 267.

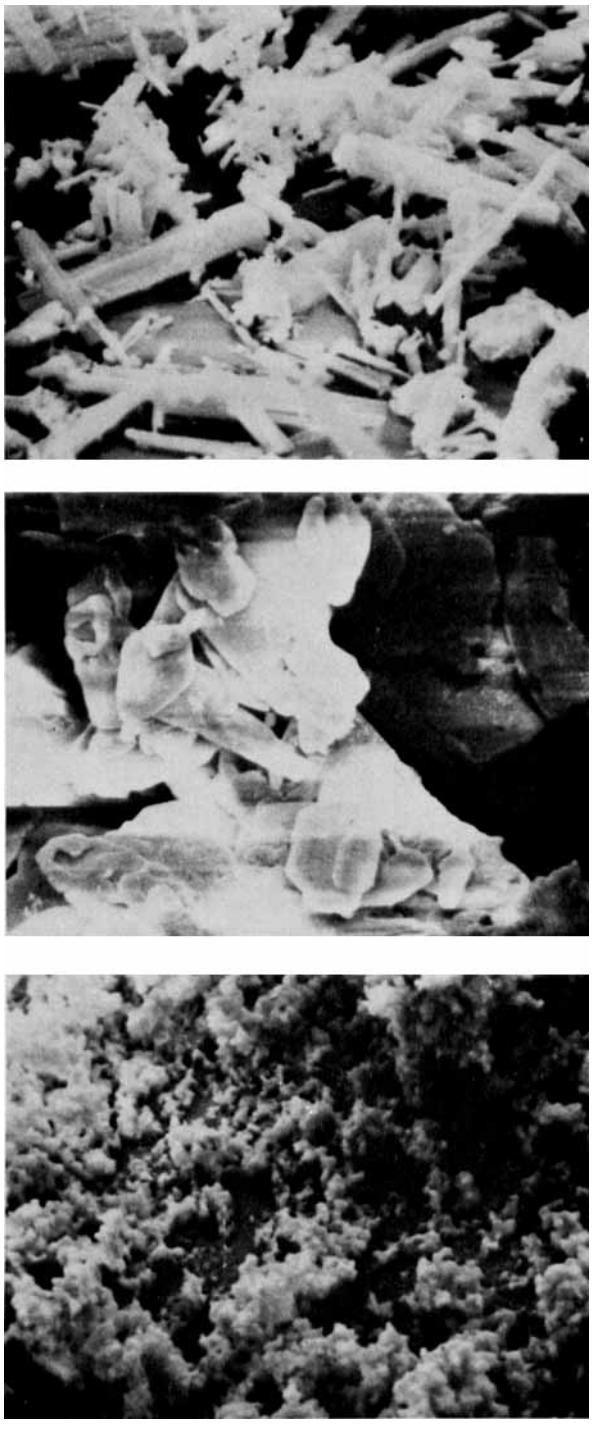

Figure 3 *Scanning electron micrographs of solid iopanoic acid forms. Key:* a, *Form I, magnification 1050×;* b, *Form II, magnification 1080×; and* c, *amorphous form, magnification 1200×.*

dium fritted glass disk, 3 cm in diameter. The volume withdrawn was immediately replaced with a equal volume of thermally equilibrated buffer. After appropriate dilution, samples were analyzed spectrophotometrically[16] at 230 nm, and a correction (13) was applied for the amount of solute removed during sampling.

Intrinsic dissolution rates also were determined. Approximately 500 mg of powder was placed in a 1.27-cm diameter flat-faced punch and die set and compressed under vacuum for 1 min with an applied load of 4545 kg[17]. The disk was removed from the die and mounted, with epoxy glue, in a glass tube, 2 cm in height and 1.27 cm in diameter, so as to expose only the upper surface of the pellet to the dissolution medium. Four extenders were attached to the bottom of the glass tube to stabilize the holder when it was placed in the dissolution medium. The intrinsic dissolution studies were carried out under sink conditions. All other experimental conditions and procedures were identical with those used in the powder dissolution studies.

[16] Cary model 14 or Gilford model 240.
[17] Carver laboratory press, model C.

RESULTS AND DISCUSSION

Three crystalline iopanoic acid forms and an amorphous form were obtained. With only one exception, all solvent systems used and all crystallization techniques attempted produced crystals identical with those of commercially available iopanoic acid (Form I). Crystals obtained by shock cooling a warm, saturated solution of iopanoic acid in benzene were identified as benzene solvate crystals. These crystals rapidly lost solvent when stored in air at room temperature.

Because the benzene solvate loses solvent to the atmosphere so quickly under ordinary temperature and pressure conditions, it is virtually impossible to obtain reproducible physical data on this form. Thermograms of the solvate are affected markedly by sample size and history, by heating rate, and by the tightness of the seal used on the sample pans. The typical thermogram of this form, however, is very similar to that of Form II, except for a broad, dual peak centered around 80°, the approximate benzene boiling point. When solvate crystals, after having been stored under a benzene atmosphere since preparation, are subjected to X-ray diffraction analysis, their X-ray pattern is essentially superimposable on that of Form II.

X-ray diffraction patterns of Forms I and II and of the amorphous form are shown in Fig. 1. The patterns indicate that the commercially available iopanoic acid (Form I) and Form II are both crystalline and that they are distinctly different. Peak positions and relative intensities for these forms are listed in Table I. Differences in peak positions and intensities can be attributed to alterations in the crystal lattice molecular arrangement. The X-ray pattern of the precipitated form, on the other hand, is characteristic of an amorphous solid. Identical patterns were obtained from "recently precipitated" iopanoic acid and from precipitated iopanoic acid that had been stored in a desiccator for more than 1 year. This observation is in contrast to that of Goldberger *et al.* (9), who reported that the dried precipitate is crystalline.

When longer radiation times and higher sensitivities were employed, peaks of low intensity were observed in some precipitated samples. Further analysis indicated that the peaks can be attributed to contamination of the largely amorphous material by Form I crystals. The degree of crystallinity in the precipitated samples is apparently a function of the iopanoic acid precipitation rate.

Thermograms of three solid forms are reproduced in Fig. 2. Sample weights of Form I and of the amorphous form varied from 12 to 17 mg, but smaller samples (7–9 mg) of Form II were used. Form I exhibits a single endothermic peak at 153.8°. The reported melting range for iopanoic acid is 152–158° (14). The Form II thermogram has a sharp endothermic peak at 132.6°, an exothermic peak at 141.2°, and a melting peak at 153.4°. The amorphous solid demonstrates a relatively small endothermic glass transition peak at 54.9°, a broad exothermic peak at 99.9°, and a melting peak at 153.2°. Over a two-year storage period, samples of both the amorphous form and of Form II underwent gradual transformations, which were reflected in minor changes in their thermograms.

Interpretation of the differential scanning calorimetry thermograms is facilitated by observations from thermal microscopy. Form I crystals are needle shaped; when examined between crossed Nicols, they exhibit a wide color spectrum. They begin to liquefy at 147°, and melting is complete at 155°. Kuhnert-Brandstatter (15), who employed a similar technique, reported a melting range of 148–155° for iopanoic acid.

Form II is plate-like and demonstrates birefringence when viewed between crossed polars. At 131°, its crystals begin to soften; in some samples, total liquefaction occurs at 135°. As the temperature is increased further, birefringent, needle-like crystals are formed, which eventually melt at 155°.

The amorphous powder is extremely electrostatic, and it is difficult to separate individual particles so that they can be examined microscopically. However, no distinct crystalline habit can be detected. As the temperature is increased to 50°, the centers of the particles become somewhat translucent, so that they acquire a donut-like appearance. At ~80°, the outer edges of the particles also become translucent. At >80°, there is virtually no change in appearance until melting occurs. No polarization of colors can be observed during the heating process.

Scanning electron micrographs of three solid forms are illustrated in

Table I—X-Ray Diffraction Patterns of Iopanoic Acid Forms I and II

Form I		Form II	
d, Å	I/I_1	d, Å	I/I_1
8.429	11.63	4.577	23.65
7.608	15.54	4.235	13.99
4.344	23.46	4.160	12.69
4.258	13.63	4.069	19.52
4.145	100.00	3.940	16.62
3.472	14.02	3.688	100.00
3.046	21.55	3.590	15.38
3.004	20.89	3.112	13.05
2.421	15.80	2.932	13.83
2.139	17.78	2.175	15.54

Fig. 3. The crystalline habits of Forms I and II can clearly be distinguished in these photomicrographs. The precipitated iopanoic acid, on the other hand, appears to be amorphous. Even at 6000-fold magnification, there is no evidence of crystallinity.

Differences in peak positions and in absorption intensities can be observed in the IR spectra of the various forms. Spectra of Form II and of the amorphous form are quite similar, with the largest difference being in the 910–940-cm^{-1} region, which is representative of carboxylic acid -OH out-of-plane bending (16). The two peaks at 1211 and 1295 cm^{-1} are both more intense in spectra of Forms I and II than in the spectrum of the amorphous form. These peaks have been attributed (16) to coupled -OH bending and C–O stretching of the carboxylic acid dimer and to C–N stretching, respectively. In addition, the NH symmetric stretching frequency at 3345 cm^{-1} can be used to distinguish Form I from the two other solid forms.

Results of the calorimetric studies are collected in Table II. The heats of transition were calculated from the equation:

$$\Delta H = \frac{K(A)}{m} \qquad \text{(Eq. 1)}$$

where ΔH is the enthalpy of transition, K is a calibration coefficient that is a function of temperature, A is the area of the transition peak, and m is the sample mass. The calibration coefficient is obtained by plotting $\Delta Hm/A$ *versus* the transition temperature for substances with known transition enthalpies (11). The precision reported here is comparable to that achieved by other authors employing similar techniques (17–19). Entropy changes associated with the transitions were obtained by dividing the transition enthalpy by the temperature in degrees Kelvin.

From the temperatures at which Form II and the amorphous form melt,

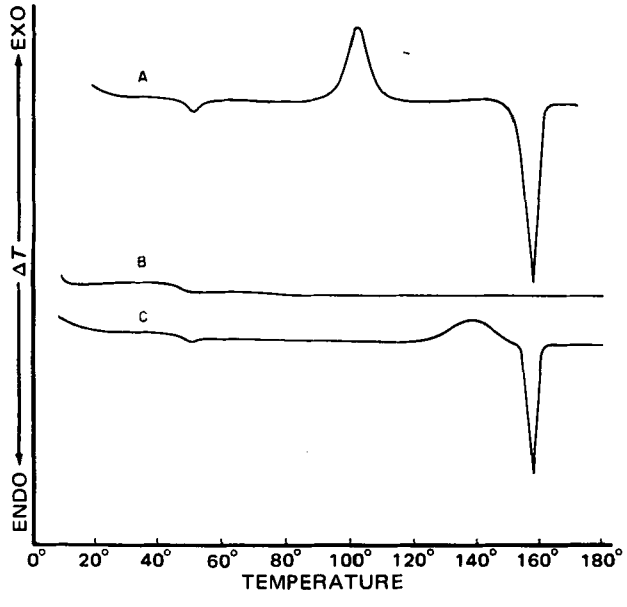

Figure 4—*Effect of thermal history and presence of seed crystals on differential scanning calorimeter thermograms for iopanoic acid. Key: A, typical thermogram of amorphous iopanoic acid; B, thermogram of the resolidified melt of the amorphous form; C, thermogram of the resolidified melt of the amorphous form following cooling in a dry ice–acetone mixture.*

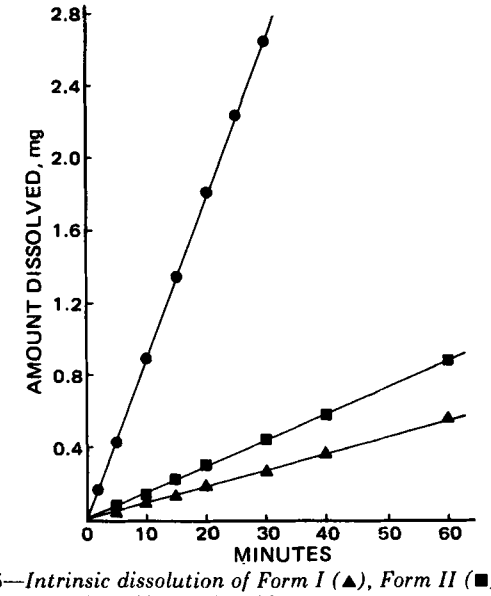

Figure 5—*Intrinsic dissolution of Form I (▲), Form II (■), and the amorphous form (●) of iopanoic acid.*

one can conclude that each is converted to Form I prior to final melting. However, a statistical test of the three ΔH_{fus} values at the 95% confidence level demonstrates a significant difference between the fusion enthalpy of Form II and of the two other forms. This discrepancy can be explained on the basis of incomplete Form I crystallization. The temperature at which the transition from Form II to Form I occurs is so close to the Form I melting point that, at the heating rates employed in this study, the transformation is incomplete when melting begins. This interpretation is corroborated by thermal microscopic observations.

Figure 4 illustrates the influence that seed crystals and thermal history can have on the transition temperature and on the exothermic peak observed in amorphous iopanoic acid thermograms. The top curve is a typical thermogram for the amorphous form heated from room temperature to beyond its melting point. Obviously, no seed crystals remain in this sample; when it is cooled, a glass forms. Curve B demonstrates the thermal behavior of the glass. A change in heat capacity is observed at approximately 48°; however, the typical exotherm and melt transition

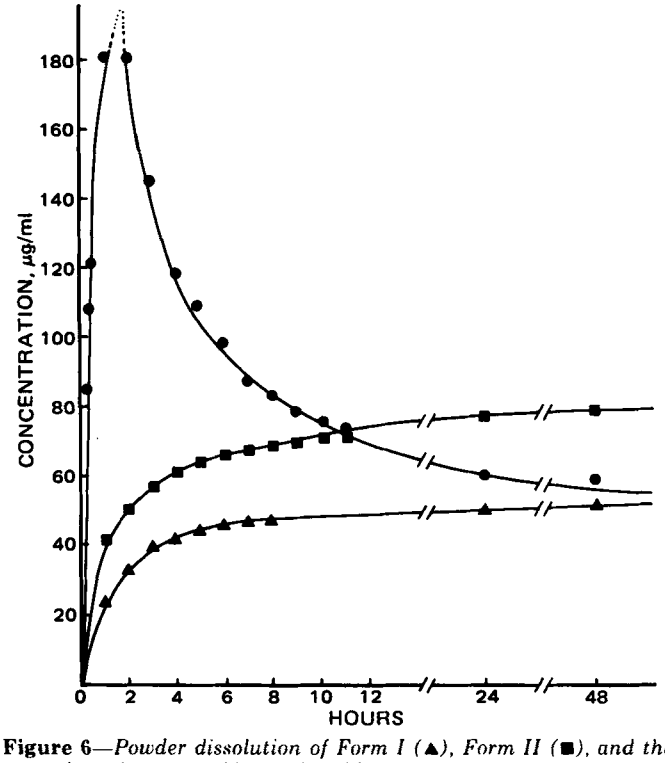

Figure 6—*Powder dissolution of Form I (▲), Form II (■), and the amorphous form (●) of iopanoic acid.*

Table II—Thermodynamic Data for Three Solid Iopanoic Acid Forms [a]

Form	Enthalpic Transition Type: Endothermic Temperature	Endothermic ΔH, kcal mole^{-1}	Endothermic ΔS, eu	Exothermic Temperature	Exothermic ΔH, kcal mole^{-1}	Exothermic ΔS, eu	Melt Temperature	Melt ΔH, kcal mole^{-1}	Melt ΔS, eu
Form I	—	—	—	—	—	—	153.8°	6.62	15.5
							±0.2°	±0.09	±0.2
Form II	132.6°	4.96	12.2	141.2°	−3.61	−8.71	153.4°	4.61	10.8
	±0.2°	±0.08	±0.2	±0.1°	±0.15	±0.15	±0.2°	±0.05	±0.1
Amorphous	54.9°	0.662	2.02	99.9°	−3.60	−9.65	153.2°	6.85	16.1
	±0.1°	±0.079	±0.02	±0.5°	±0.09	±0.23	±0.3°	±0.23	±0.5

[a] Values reported represent the mean and standard error of the mean of five to eight samples.

are not observed. When the glass is cooled in dry ice, it again exhibits an endothermic and exothermic transition, as well as the usual melting peak (curve C). In this case, however, the exotherm due to crystallization of Form I is broader and occurs at a higher temperature than in the original sample.

The results of the intrinsic dissolution rate studies are shown in Fig. 5. Assuming the dissolution rate is diffusion controlled, one can describe the process by:

$$\frac{1}{A}\frac{dW}{dt} = \frac{D}{h}(C_s - C) \qquad \text{(Eq. 2)}$$

where A is the surface area of the dissolving solid, W is the solute mass at time t, D is the diffusion coefficient, h is the diffusion layer thickness, C_s is the solubility of the substance, and C is its concentration in the bulk solution at time t. In the initial stages of the dissolution process, *i.e.*, when sink conditions prevail, $C_s \gg C$, and the equation reduces to:

$$\frac{1}{A}\frac{dW}{dt} = \frac{DC_s}{h} \qquad \text{(Eq. 3)}$$

All three solid iopanoic acid forms can be characterized by the same D and h values. In addition, the surface area of the dissolving disk is essentially constant, so Eq. 3 may be rewritten in a simpler form:

$$\frac{dW}{dt} = kC_s \qquad \text{(Eq. 4)}$$

where the constant k now includes the terms A, D, and h. Integration from time 0 to t yields:

$$W = kC_s t \qquad \text{(Eq. 5)}$$

Thus, a plot of amount dissolved as a function of time should be linear for the initial dissolution stages. Intrinsic dissolution rates (kC_s/A) can be calculated from the slopes of the three straight lines in Fig. 5. They are 0.00739 mg cm^{-2} min^{-1} for Form I, 0.0117 mg cm^{-2} min^{-1} for Form II, and 0.0703 mg cm^{-2} min^{-1} for the amorphous form. So the intrinsic dissolution rate for Form II is 1.5 times greater, whereas the dissolution rate for the amorphous form is an order of magnitude greater than that of the commercially available form.

Typical dissolution profiles for the three forms are shown in Fig. 6. The peak solubilities of the different forms follow the same rank order as their intrinsic dissolution rates, as predicted by Eq. 5. Form II is relatively stable in saturated aqueous solutions. The excess solid iopanoic acid remaining in the sample containers at the end of a dissolution run was predominantly Form II. With the amorphous form, on the other hand, there was appreciable conversion to Form I after only 2 hr, and conversion was essentially complete at the end of 12 hr of exposure to the dissolution medium.

Aguiar and Zelmer (20) employed the saturation concentrations obtained from powder dissolution profiles to predict whether a given metastable polymorph will demonstrate enhanced bioavailability. According to their hypothesis, differences in human absorption observed following administration of chloramphenicol polymorphs A and B can be explained on the basis of the relatively large (−774 cal mole^{-1}) free energy difference between the two forms. On the basis of the much smaller free energy difference (−231 cal mole^{-1}) between polymorphs I and II of mefenamic acid, the authors predicted that there would be no significant differences in the absorption of these two forms. Their prediction was borne out in subsequent *in vivo* tests.

By applying the Aguiar–Zelmer hypothesis to iopanoic acid, the free energy difference, ΔG, between two solid forms (*e.g.*, A and B) of the same compound can be obtained from:

$$\Delta G = RT \ln \frac{C_s \text{ Form B}}{C_s \text{ Form A}} \qquad \text{(Eq. 6)}$$

Since the saturation solubility, C_s, of each solid form, measured at the same temperature, is directly proportional to its intrinsic dissolution rate, the dissolution rate ratio can be substituted for the ratio of solubilities in Eq. 6. In the case of iopanoic acid, $\Delta G_{\text{II}\rightarrow\text{I},\,37°}$ is −284 cal mole^{-1}, and $\Delta G_{\text{amorphous}\rightarrow\text{I},\,37°}$ is −1390 cal mole^{-1}. Based on these calculations, it seems likely that the bioavailability of Form II should not be appreciably greater than that of Form I. In contrast, the bioavailability of the amorphous form should be considerably greater than that of the stable polymorph. While many other factors affect the optimal opacification of the bladder, it would be of interest to determine whether these thermodynamic data can be quantitatively correlated with bioavailabilities of the three forms.

REFERENCES

(1) H. J. Burhenne and W. G. Obata, *N. Engl. J. Med.*, **292**, 627 (1975).

(2) P. M. Loeb, R. N. Berk, J. O. James, L. Perkin, and J. Moore, *Radiology*, **126**, 395 (1978).

(3) R. G. Evens, C. Schroer, and P. R. Koehler, *ibid.*, **98**, 365 (1971).

(4) R. N. Berk, P. M. Loeb, L. E. Goldberger, and J. Sokoloff, *N. Engl. J. Med.*, **290**, 204 (1974).

(5) E. Gunnarson, *Acta Radiol.*, **52**, 289 (1959).

(6) K. Holmdahl and H. Lodin, *ibid.*, **51**, 247 (1959).

(7) P. Virtama, *ibid.*, **52**, 308 (1959).

(8) R. Peterhoff, *ibid.*, **46**, 719 (1956).

(9) L. E. Goldberger, R. N. Berk, J. H. Lang, and P. M. Loeb, *Invest. Radiol.*, **9**, 16 (1974).

(10) S. S. Yang and J. K. Guillory, *J. Pharm. Sci.*, **61**, 26 (1972).

(11) W. W. Wendlandt, "Thermal Methods of Analysis," 2nd ed., vol. 19 of "Chemical Analysis," P. J. Elving and I. M. Kolthoff, Eds., Wiley–Interscience, New York, N.Y., 1974, pp. 178–184.

(12) M. J. Richardson and N. G. Savill, *Thermochim. Acta*, **12**, 221 (1975).

(13) E. Nelson, *J. Am. Pharm. Assoc., Sci. Ed.*, **46**, 607 (1957).

(14) "The United States Pharmacopeia," 19th ed., Mack Publishing Co., Easton, Pa., 1975, p. 261.

(15) M. Kuhnert-Brandstätter, "Thermomicroscopy in the Analysis of Pharmaceuticals," Pergamon, New York, N.Y., 1971, p. 409.

(16) K. Nakanishi and P. H. Solomon, "Infrared Absorption Spectroscopy," 2nd ed., Holden-Day, San Francisco, Calif., 1977, p. 39.

(17) J. Y. C. Chu, *J. Phys. Chem.*, **79**, 119 (1975).

(18) M. J. Vold, H. Funakoshi, and R. D. Vold, *ibid.*, **80**, 1753 (1976).

(19) K. Konkoly-Thege, I. Ruff, S. O. Adeosun, and S. J. Sime, *Thermochim. Acta*, **24**, 89 (1978).

(20) A. J. Aguiar and J. E. Zelmer, *J. Pharm. Sci.*, **58**, 983 (1969).

ACKNOWLEDGMENTS

Presented in part at the Basic Pharmaceutics Section, APhA Academy of Pharmaceutical Sciences, Anaheim meeting, April 1979.

Iopanoic acid was generously provided by Dr. F. C. Nachod of the Sterling-Winthrop Research Institute. The authors thank Dr. Ching-Yuan Shih, Department of Botany, University of Iowa, who supervised the electron microscopy, and Dr. George R. McCormick, Department of Geology, University of Iowa, in whose laboratory the X-ray analysis was performed.

W. C. Stagner is a Charles J. Lynn Memorial Fellow, American Foundation for Pharmaceutical Education.

Guanabenz Degradation Products and Stability Assay

CHARLES M. SHEARER ˣ **and NICHOLAS J. DeANGELIS**

Received October 20, 1977, from the *Pharmacy Research and Development Division, Wyeth Laboratories, Inc., Radnor, PA 19087.* Accepted for publication February 9, 1979.

Abstract □ Guanabenz, [(2,6-dichlorobenzylidene)amino]guanidine, acetate was shown to be the *E*-isomer. It decomposed to form the *Z*-isomer, 2,6-dichlorobenzaldehyde, aminoguanidine, and 2,6-dichlorobenzaldehyde semicarbazone. A stability-indicating assay for the intact drug in the presence of all of its decomposition products by the use of UV spectroscopy is presented.

Keyphrases □ Guanabenz—degradation products, stability, UV spectroscopic analysis □ Antihypertensive agents—guanabenz, degradation products, stability, UV spectroscopic analysis □ Spectroscopy, UV—analysis, guanabenz degradation products □ Stability—guanabenz, degradation products

Guanabenz, [(2,6-dichlorobenzylidene)amino]guanidine, acetate is being evaluated as an antihypertensive agent. To develop a stability-indicating assay, the drug was decomposed by all meaningful modes, *i.e.*, hydrolytic, thermal (dry heat), and photolytic, and all degradation products were isolated and identified. This paper describes the isolation and identification of these degradation products and the development of a rapid spectrophotometric assay specific for guanabenz in their presence.

EXPERIMENTAL

Guanabenz Degradation—Sufficient degradation products for characterization were obtained by using accelerated conditions. The hydrolysates were prepared by refluxing a guanabenz acetate solution in equal volumes of 2 *N* NaOH and ethanol for 8 hr or in 1 *N* HCl for 5 days. These products were separated from the intact drug by a biphase extraction into chloroform from aqueous acid.

Thermal degradation was studied by storing the drug substance at 100 and 75° for several weeks.

The photolytic degradation product was formed by exposing a 1% guanabenz solution in ethanol to UV light in a closed quartz vessel[1] for 1 week. The photolytic product was separated from guanabenz by column chromatography using silica gel[2] as the adsorbent and increasing methanol concentrations in chloroform containing 1% ammonium hydroxide as the eluent.

TLC—TLC was used to determine the purity of the isolated degradation products and to help establish their identity. Silica gel TLC plates with a fluorescent indicator[3] and an eluting solvent of chloroform–methanol–ammonium hydroxide (48.5:50:1.5) were used. Visualization was by shortwave UV light.

For quantitative TLC, 100-μg quantities were applied to the plate; after elution, the silica gel containing the intact guanabenz was scraped off and extracted from the silica gel with 10 ml of 10% 0.1 *N* NaOH in ethanol. The guanabenz concentration was determined by comparing the absorbance of the resulting solution at 305 nm to the absorbance of a standard carried through the same procedure.

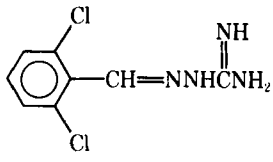

I

Spectrophotometric Analysis—UV spectra[4] were obtained using 1-cm path length silica cells and the described solvents. To obtain IR spectra[5], samples were presented in the form of potassium bromide pellets. NMR spectra[6] were obtained by preparing solutions of the samples in deuterated dimethyl sulfoxide containing tetramethylsilane as the internal marker. Mass spectra[7] were obtained using an energy beam of 70 ev with the sample probe at 150°.

Stability-Indicating Assay—*Solvents*—For the pH 4.5 buffer, a 0.2 *M* aqueous monobasic sodium phosphate solution was diluted with an equal volume of methanol.

For the pH 10.8 buffer, a 0.1 *M* aqueous dibasic sodium phosphate solution was adjusted to pH 10.8 with 5 *N* NaOH. Two volumes of this buffer were diluted with one volume of methanol.

Procedure—The sample was quantitatively weighed or diluted into each solvent to obtain a concentration of ~0.01 mg of guanabenz/ml. The method was applicable in the range of 0.004–0.015 mg of guanabenz/ml. If the addition of the sample to the buffer solvent changed the pH by >0.1 unit, the sample was neutralized with acid or base as necessary.

The absorbance of each solution was determined at 265 and 305 nm in a 1-cm silica cell *versus* a solvent blank. The guanabenz concentration (c) in the final solutions was calculated using the following equation:

$$c = \frac{(A_2^{S1} - A_2^{S2}) - 1.32(A_1^{S1} - A_1^{S2})}{78.9} \qquad \text{(Eq. 1)}$$

where A_2^{S1} is the absorbance in pH 4.5 buffer at 265 nm, A_2^{S2} is the absorbance in pH 10.8 buffer at 265 nm, A_1^{S1} is the absorbance in pH 4.5 buffer at 305 nm, and A_1^{S2} is the absorbance in pH 10.8 buffer at 305 nm.

RESULTS AND DISCUSSION

Degradation Product Identification—Guanabenz was synthesized (1) as the acetate by the condensation reaction of 2,6-dichlorobenzaldehyde with aminoguanidine in the presence of acetic acid. Possible degradation hydrolysis routes were: (*a*) the reverse reaction of the synthesis, and (*b*) the replacement of the amino group on the guanidine by oxygen to give 2,6-dichlorobenzaldehyde semicarbazone. Both reactions occurred under reflux conditions in strong acid or base, based on a comparison of TLC R_f values of the degradation products to those of the known compounds.

For further proof of the reactions, the semicarbazone was isolated from the refluxed basic solution and identified by comparison of its IR spectrum with that of an authentic sample prepared from 2,6-dichlorobenzaldehyde and semicarbazide hydrochloride using the classical method (2). The 2,6-dichlorobenzaldehyde was similarly obtained in appreciable quantities from the refluxed acidic solution. No attempt was made to isolate and characterize the aminoguanidine found along with the 2,6-dichlorobenzaldehyde. TLC of the guanabenz-containing layers of the biphase extractions in both refluxed solutions showed a small amount of an additional degradation product, characterized as *Z*-2,6-dichlorophenylmethyleneaminoguanidine and later shown by TLC to be the same as the photoproduct.

In the thermal study, no degradation product was observed by TLC for samples of guanabenz acetate stored at 75 or 100° for 4 weeks. The sample stored at 100° did lose a portion of the acetic acid associated with it, as verified by titrimetric analysis (3) in 50% methanol–water.

The photolytic degradation product was not as readily identified as were the hydrolytic products. Guanabenz in mildly acidic, neutral, or mildly basic solutions undergoes a reversible reaction in the presence of light. The reaction reversibility was established by starting with the photoproduct and allowing it to convert to guanabenz. The same reversible reaction occurred in the dark but only in acidic solution.

[1] A 10-cm pathlength spectrophotometric cell.
[2] Silica gel grade 923, mesh 100–200, Grace & Co., Davison Chemical Division, Baltimore, Md.
[3] Silica gel GF, Analtech Inc., Newark, Del.
[4] Cary model 14.
[5] Perkin-Elmer model 537.
[6] Varian model XL-100.
[7] AE1-MS-902.

0022-3549/79/0800-1010$01.00/0
© 1979, American Pharmaceutical Association

Table I—Absorptivities of Guanabenz *E*- and *Z*-Isomers

Wavelength, nm	*E*-Isomer		*Z*-Isomer	
	pH 10.8	pH 4.5	pH 10.8	pH 4.5
305	55.2	14.8	18.2	0.2
265	28.3	53.9	40.1	16.2

The reaction reversibility immediately suggested that the two compounds were isomers. The photoproduct structure proved to be like that of the intact guanabenz by many classical structure elucidation methods. The mass spectra of the two compounds were the same (*m/e* 230), as were the elemental analyses (guanabenz: C, 41.29; H, 3.61; Cl, 30.84; N, 23.99; photoproduct: C, 41.57; H, 3.60; Cl, 30.39; N, 24.35). The equivalent weights, as determined by nonaqueous titrations, were the same and were in agreement with the mass spectrometric molecular weight. The ionization constants were 8.3. These were determined spectrophotometrically, thus assuring that changes in the spectra were due to ionization and not to interconversion of guanabenz and the photoproduct. These data and the reversibility of the reaction support the contention that the two compounds are isomers.

IR spectra of guanabenz and the photoproduct were distinctly different, but no useful information could be derived from these differences. NMR spectra showed four nonexchangeable protons. Three of these protons were aromatic and, although the spectra of the two compounds in the aromatic region were slightly different, these differences are not readily interpreted. The singlet peak for the other proton associated with the imino carbon was at 8.22 ppm for guanabenz and at 7.21 ppm for the photoproduct.

Previous investigators (4–9) extensively studied the NMR spectra of *Z*- and *E*-isomers about imino and similar bonds. In all cases, the signal from the *E*-isomer was downfield from that of the *Z*-isomer. A comparison of these data with those for guanabenz and the photoproduct indicated that the photoproduct is the *Z*-isomer and that guanabenz is the *E*-isomer. However, only aliphatic compounds were studied previously (4–9).

UV spectrophotometry was most important in proving the structure of the two compounds. Other investigators (10) found that phenyl ketone semicarbazones were categorized into two types by their UV spectra. One group had a maximum absorbance around 280 nm, and the second group showed a maximum absorbance only at lower wavelengths, if at all. Stenberg *et al.* (11) reported that *Z*-phenyl acetophenone semicarbazone had no peak in its UV spectrum above 230 nm while the *E*-isomer had a maximum at about 270 nm. When the UV spectra for guanabenz and the photoproduct (Fig. 1) were compared with these observations, it became evident that guanabenz was the *E*-isomer and that the photoproduct was the *Z*-isomer.

Differences in the UV spectra of the two isomers can be explained on the basis of steric hindrance. In an examination of a molecular model, a restricted rotation of the dichlorophenyl group in the *Z*-isomer is apparent. The π orbital of the imino bond is nearly perpendicular to the π orbital of the phenyl ring. The π orbital system for the *E*-isomer is nearly parallel throughout the molecule. Thus, the *E*-isomer, with a longer conjugated π electron system, will have a maximum absorbance at a longer wavelength than the *Z*-isomer.

Well-documented *cis–trans* isomerizations of semicarbazones and similar molecules occur under photolytic conditions as well as acidic conditions. Previous investigators (11) reported the photoisomerization of semicarbazones and gave evidence that the photoproduct of acetophenone semicarbazone, when dissolved in an ether solution, isomerized to the starting semicarbazone on exposure to anhydrous hydrogen chloride. Earlier work (12, 13) showed that *Z*- and *E*-isomers of semicarbazones could be interconverted by UV light.

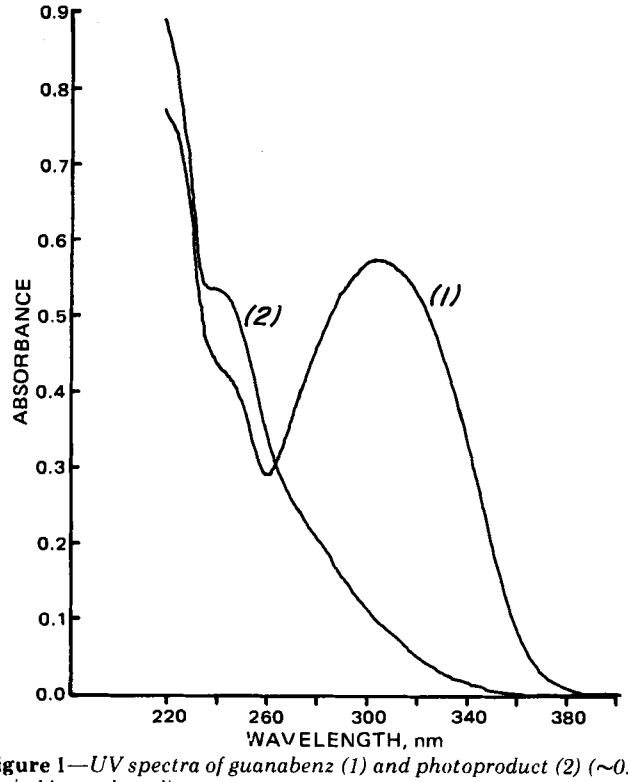

Figure 1—*UV spectra of guanabenz (1) and photoproduct (2) (~0.01 mg/ml in methanol).*

The *cis–trans* photoisomerization of aromatic Schiff bases has been studied (14). Aldehyde 2,4-dinitrophenylhydrazones underwent isomer equilibration in acid solution (15). Methylene bromide solutions of acetaldehyde 2,4-dinitrophenylhydrazone did not reach equilibrium after standing at room temperature for 10 days, while the addition of traces of sulfuric acid effected equilibration in less than a day. Another report (7) gave evidence for acid-catalyzed isomerization of several phenylhydrazones, semicarbazones, and thiosemicarbazones. 2,4-Dinitrophenylhydrazones of α-bromoacetophenone and α-bromobutyrophenone underwent *cis–trans* isomerization when refluxed in an organic solvent in the presence of a trace of hydrochloric acid (16).

Assay Development—The difference in the UV spectra of guanabenz and the *Z*-isomer, as well as the change in spectra with pH as related to the determination of the ionization constant, has been discussed. Figures 2 and 3 present the spectra of the neutral and the protonated species of

Table II—Analysis of Synthetic Samples of Decomposed Guanabenz Acetate

Micrograms per Milliliter					
Z-Isomer	2,6-Dichlorobenzaldehyde Semicarbazone	2,6-Dichlorobenzaldehyde	Guanabenz Acetate	Guanabenz Acetate, mg/ml found	Recovery, %
0.0	0.0	0.0	0.0269	0.0270	100
0.0	0.0	0.0	0.0242	0.0243	100
0.0	0.0	0.0	0.0215	0.0217	101
0.0	0.0	0.0	0.0188	0.0188	100
0.0018	0.0	0.0	0.0242	0.0242	100
0.0	0.0021	0.0	0.0242	0.0244	101
0.0	0.0	0.0018	0.0252	0.0249	99
0.0007	0.0004	0.0004	0.0252	0.0255	101
0.0	0.0012	0.0	0.0252	0.0255	101
0.0007	0.0	0.0008	0.0252	0.0255	101
0.0	0.0	0.0	0.0269	0.0271	100
0.0006	0.0	0.0	0.0263	0.0262	100
0.0011	0.0	0.0	0.0258	0.0260	100
0.0021	0.0	0.0	0.0241	0.0246	100
0.0033	0.0	0.0	0.0236	0.0235	100
0.0054	0.0	0.0	0.0215	0.0217	101

Table III—Comparison of Stability Assay and Quantitative TLC for Decomposed Guanabenz Acetate

Condition for Degradation	Intact Guanabenz Acetate Found, %	
	Stability Assay	Quantitative TLC
5 weeks at 60° in water	89	92
5 weeks in direct sunlight in water	50	50
5 weeks at 60° in 0.1 *N* HCl	76	73
5 weeks in direct sunlight in 0.1 *N* HCl	80	76
5 weeks in direct shortwave UV light (solid)	99	98
3 days at 170° (solid)	72	69

guanabenz and the *Z*-isomer, respectively. Aminoguanidine has no appreciable UV spectrum. The spectra of the two UV-absorbing hydrolysates, 2,6-dichlorobenzaldehyde and 2,6-dichlorobenzaldehyde semicarbazone, do not change between pH 4.5 and 10.8. Thus, only guanabenz and the *Z*-isomer have spectral differences at these two pH values.

By utilizing these differences, a simple stability-indicating assay was developed. The procedure can be considered to be a two-component spectral method; but rather than using the predetermined absorptivities of the two species, this method uses the differences in the absorptivities (Table I) at two wavelengths and the two pH values. Thus, this method combines the concepts of $\Delta\epsilon$ values described by Aulin-Erdtman (17) and Vieroidt's method (18) for two-component mixtures.

Method Validation—To determine the accuracy and specificity of this method, solutions were prepared containing varying amounts of guanabenz and the degradation products (Table II). Solutions containing only small percentages (≤20%) of the decomposition products were prepared since this is the range of interest.

To evaluate this assay procedure further, guanabenz acetate was decomposed in solution and as a dry drug substance under various conditions. These samples were analyzed by the stability-indicating assay, and the results of these analyses were compared with the results of quantitative TLC. The conditions for the degradation and the results are given in Table III.

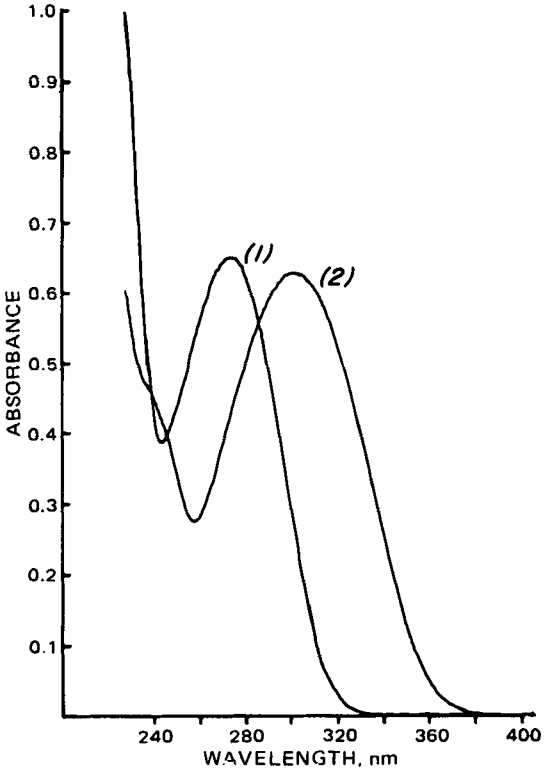

Figure 2—*UV spectra of guanabenz (E-isomer) in pH 4.4 buffer (1) and pH 10.8 buffer (2).*

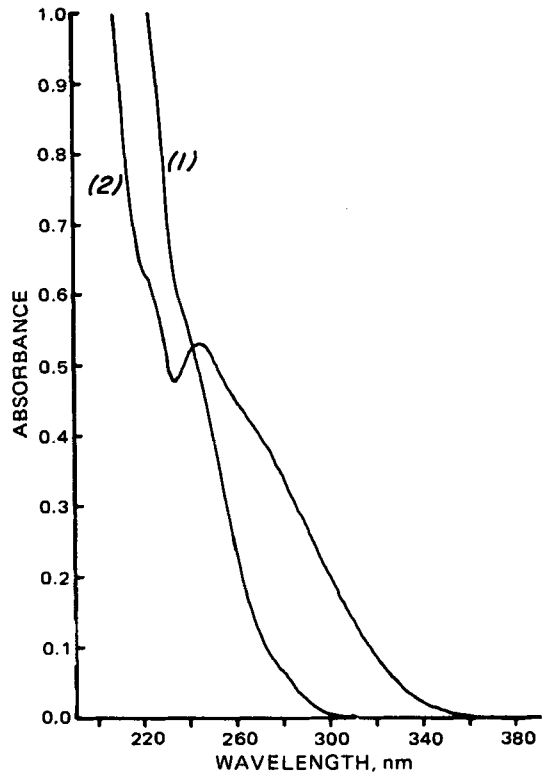

Figure 3—*UV spectra of photoproduct (Z-isomer) in pH 4.4 buffer (1) and pH 10.8 buffer (2).*

REFERENCES

(1) W. F. Bruce and T. Baum, Ger. Offen. 1,802,394.

(2) R. L. Shriner and R. C. Fuson, "The Systematic Identification of Organic Compounds," 3rd ed., Wiley, New York, N.Y., 1948, p. 170.

(3) T. V. Parke and W. W. Davis, *Anal. Chem.*, **26,** 642 (1954).

(4) G. J. Karabatsos and R. A. Taller, *Tetrahedron*, **24,** 3347 (1968).

(5) G. J. Karabatsos and C. E. Osborne, *ibid.*, **24,** 3361 (1968).

(6) G. J. Karabatsos and R. A. Taller, *J. Am. Chem. Soc.*, **85,** 3624 (1963).

(7) G. J. Karabatsos, F. M. Vane, R. A. Taller, and N. Hsi, *J. Am. Chem. Soc.*, **86,** 3351 (1964).

(8) G. J. Karabatsos and N. Hsi, *Tetrahedron*, **23,** 1079 (1967).

(9) G. J. Karabatsos and R. A. Taller, *ibid.*, **24,** 3557 (1968).

(10) M. Ramart-Lucas and M. Bruzau, *Bull. Soc. Chem. Fr.*, **1,** 119 (1934).

(11) V. I. Stenberg, P. A. Barks, D. Bays, D. D. Hammargren, and D. V. Rao, *J. Org. Chem.*, **33,** 4402 (1968).

(12) I. M. Heilbron and F. J. Wilson, *J. Chem. Soc.*, **101,** 1482 (1912).

(13) F. J. Wilson and R. M. Macaulay, *ibid.*, **125,** 841 (1925).

(14) G. Wettermark and E. Wallstrom, *Acta Chem. Scand.*, **22,** 675 (1968).

(15) G. J. Karabatsos, B. L. Shapiro, F. M. Vane, J. S. Fleming, and J. S. Ratka, *J. Am. Chem. Soc.*, **85,** 2784 (1963).

(16) F. Raimirez and A. F. Kirby, *ibid.*, **75,** 6026 (1953).

(17) G. Aulin-Erdtman, *Chem. Ind.*, **1955,** 581.

(18) A. E. Gillam and E. S. Stern, "An Introduction to Electronic Absorption Spectroscopy in Organic Chemistry," Edward Arnold Ltd., London, England, 1958, pp. 214–217.

Structural Biochemistry XIII: Synthesis of Luteinizing Hormone-Releasing Hormone Modification [Trp^8]-LH-RH

GEORGE R. PETTIT ˣ **and THOMAS H. SMITH**

Received February 28, 1978, from the *Cancer Research Institute and Department of Chemistry, Arizona State University, Tempe, AZ 85281.* Accepted for publication August 3, 1978.

Abstract □ A fragment condensation method was utilized for synthesis of the Trp^8-substituted luteinizing hormone-releasing hormone (LH-RH). *tert*-Butoxycarbonyl protection was employed for the α-amino positions, and benzyl protection was used for the phenol group of Tyr and the imidazole nitrogen of His. Peptide bond-forming reactions were performed using *N*-hydroxysuccinimide (for Trp), dicyclohexylcarbodiimide-1-hydroxybenzotriazole, 1-ethyl-3-(3′-dimethylaminopropyl)-carbodiimide hydrochloride, or mixed carbonic anhydride methods. Biological evaluation of [Trp^8]-LH-RH indicated no luteinizing hormone-releasing activity or inhibition of luteinizing hormone release over the dose ranges studied.

Keyphrases □ Luteinizing hormone-releasing hormone—derivatives, synthesis, structure-activity relationships □ Chemical synthesis—luteinizing hormone-releasing hormone derivatives, structure-activity relationships □ Hormones—luteinizing hormone-releasing hormone, derivatives, synthesis, structure-activity relationships □ Structure-activity relationships—luteinizing hormone-releasing hormone derivatives

In humans, 1 μg of the hypothalamus decapeptide luteinizing hormone-releasing hormone (LH-RH, I) stimulates the pituitary to synthesize and release the luteinizing hormone (LH). Isolation of this decapeptide hormone from porcine hypothalami was first reported in 1971 (1, 2). This discovery has impressive potential for solving certain medical problems, from overcoming a cause of female sterility to opening new approaches to contraception. Therefore, synthetic efforts directed at the decapeptide hormone and related substances have been undertaken and presently underlie the major effort in decapeptide chemistry (3–15).

BACKGROUND

One facet of the LH-RH potential that seemed particularly attractive was that a suitable modification of this hormone might inhibit certain cancer types, *e.g.*, of the ovary. In 1968, certain tryptophan dipeptides were observed[1] to have antineoplastic activity. This discovery led to attempts to modify LH-RH by replacement of Arg at position 8 with Trp. This amino acid replacement modification also was selected because the hypothalamus growth hormone release-inhibiting tetradecapeptide hormone, somatostatin (16–18), contains Trp at position 8. In addition, LH-RH activity was known to be profoundly affected by modification at the Arg position (19–21).

Decapeptide synthesis was performed by a fragment condensation, as outlined in Scheme I. The *tert*-butoxycarbonyl (Boc) group was used for α-amino protection, and its removal was performed employing 50% trifluoroacetic acid in methylene chloride. With peptides containing a Trp unit, 2-mercaptoethanol was added to prevent oxidative degradation (22). The phenolic group of Tyr was protected as the *O*-benzyl ether, and the imidazole nitrogen of His was protected as the benzylamine derivative. In both cases, deprotection was achieved by hydrogenolysis using palladium-on-carbon.

Methyl ester saponification was effected employing aqueous sodium hydroxide in methanol. Peptide bond-forming reactions were efficiently realized employing the *N*-hydroxysuccinimide (NHS) active ester for coupling Trp (II → III), and either dicyclohexylcarbodiimide 1-hydroxybenzotriazole (DCCI-HBT), 1-ethyl-3-(3′-dimethylaminopropyl)carbodiimide hydrochloride (EDCI), or mixed carbonic anhydride (MCA) techniques at the other positions (13). By this combination of methods, the protected decapeptide was obtained in reasonable yield. After hydrogenolysis, [Trp^8]-LH-RH was isolated and evaluated[2].

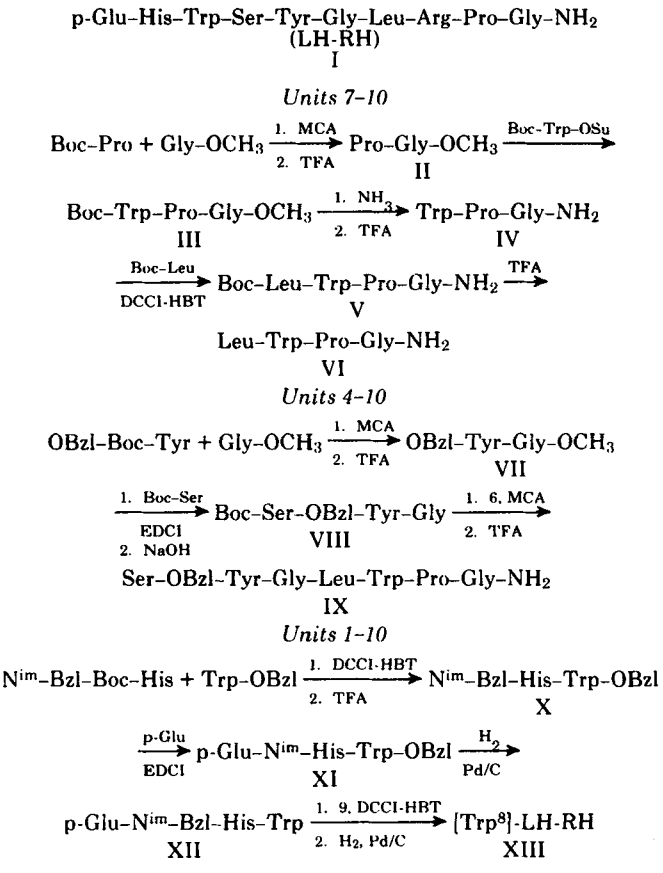

Scheme I

The luteinizing hormone-releasing biological assay was performed with 200-g female rats, which were ovariectomized and allowed to rest 6 weeks. Three days following treatment with progesterone and estradiol benzoate, the animals were treated intravenously with 10–1000-ng doses of [Trp^8]-LH-RH with standard LH-RH as a control. Samples were collected 15 min later and analyzed for luteinizing hormone content. While the standard LH-RH produced significant dose-related luteinizing hormone release as expected, the [Trp^8]-LH-RH showed no significant luteinizing hormone release over the same dose range. Also, at doses of 50–200 μg, [Trp^8]-LH-RH showed no inhibition of luteinizing hormone release when given to 25-day-old male rats (23).

Based on these results, preparation of a modified LH-RH decapeptide bearing D-Trp at positions 8 and/or 2 is of interest with respect (24) to influencing luteinizing hormone release (5, 8, 9). Unfortunately, the limited amount of [Trp^8]-LH-RH available did not allow a definitive assessment of antineoplastic activity.

EXPERIMENTAL

All of the precursor L-amino acids and derivatives were employed as

[1] G. R. Pettit and S. K. Gupta, unpublished results.

[2] Dr. B. H. Vickery, Institute of Biological Sciences, Syntex, Palo Alto, Calif.

0022-3549/79/0800-1013$01.00/0
© 1979, American Pharmaceutical Association

received[3]. Solvent extracts containing completely protected peptides were washed consecutively with water, 0.5 *M* citric acid, water, 5% aqueous sodium bicarbonate, and saturated aqueous sodium chloride. Each extract was dried over anhydrous sodium sulfate, and the solvent was removed under reduced pressure at 35–40° using a rotating evaporator. Dimethylformamide was distilled (under reduced pressure) from calcium oxide, while tetrahydrofuran was distilled from lithium aluminum hydride just prior to use.

All melting points were recorded using a hot-stage apparatus[4] and are uncorrected. Each analytical specimen gave one spot on TLC and gave IR, PMR, and mass spectral data in accord with the assigned structure[5].

Boc-Pro-Gly-OCH_3—A solution of Boc-Pro (10.75 g, 50 mmoles) in tetrahydrofuran (250 ml) was cooled to −15°, and *N*-methylmorpholine (5.5 ml, 50 mmoles) followed by isobutyl chlorocarbonate (6.95 ml, 50 mmoles) was added. Before Gly-OCH_3 hydrochloride (6.6 g, 50 mmoles) and *N*-methylmorpholine (5.5 ml, 50 mmoles) were added, the mixture was stirred for 15 min at −15°. Stirring was continued for 2 hr at 0° and for 48 hr at 23°. The solvent was removed, and the residue was dissolved in ethyl acetate, washed, and dried. Solvent evaporation yielded a pink solid, which was recrystallized from ether to afford 11.8 g (78%), mp 70–72°; $[\alpha]_D^{25}$ −138° (methanol).

Anal.—Calc. for $C_{13}H_{22}N_2O_5$: C, 54.53; H, 7.74; N, 9.78. Found: C, 54.40; H, 7.86; N, 9.85.

Pro-Gly-OCH_3 (II) Hydrochloride—After 1 hr at room temperature, the solvent was removed from a solution of Boc-Pro-Gly-OCH_3 (102.8 mg, 0.358 mmole) in 50% trifluoroacetic acid (TFA)–methylene chloride (4 ml). The oily residue was treated with cold ethereal hydrogen chloride to form an oily precipitate. The solvent was removed, and the residue was dissolved in water (5 ml) and chromatographed on a column of XAD-2 resin (75 ml). Elution with water (300 ml), concentration to 15 ml, and lyophilization yielded 79.5 mg (100%) of the dipeptide II as a viscous oil.

Boc-Trp-Pro-Gly-OCH_3 (III)—A solution of Pro-Gly-OCH_3 hydrochloride (0.82 g, 3.71 mmoles), Boc-Trp-OSu (1.49 g, 3.71 mmoles), *N*-methylmorpholine (0.41 ml, 3.71 mmoles), and dimethylformamide (6 ml) was stirred at 23° for 8 hr. Ethyl acetate was added, and the mixture was washed and dried. The solvent was removed, and the residue was purified by column chromatography on silica gel (100 g, elution with ethyl acetate) and crystallized from ether–ligroin to afford 0.98 g (56%) of the tripeptide III, mp 86–88°; $[\alpha]_D^{25}$ −112° (methanol).

Anal.—Calc. for $C_{24}H_{32}N_4O_6$: C, 61.00; H, 6.83; N, 11.86. Found: C, 60.86; H, 7.00; N, 11.67.

Boc-Trp-Pro-Gly-NH_2—Boc-Trp-Pro-Gly-OCH_3 (0.82 g, 1.73 mmoles) was dissolved in methanol (40 ml) and cooled to 0°. Ammonia was passed into the solution for 1.5 hr. The reaction flask was tightly stoppered and allowed to stand at room temperature for 24 hr. Following solvent removal, the residue was crystallized from ethyl acetate–ligroin to afford 0.788 g (100%) of amide, mp 120–121°; $[\alpha]_D^{25}$ −49° (methanol).

Anal.—Calc. for $C_{23}H_{31}N_5O_5 \cdot H_2O$: C, 57.98; H, 6.93; N, 14.71. Found: C, 58.38; H, 6.66; N, 14.86.

Trp-Pro-Gly-NH_2 (IV) Trifluoroacetate—A solution of Boc-Trp-Pro-Gly-NH_2 (0.65 g, 1.42 mmoles) in 50% trifluoroacetic acid–methylene chloride (20 ml) containing 1% 2-mercaptoethanol was maintained at room temperature for 1 hr. The solvent was removed, and the residue was triturated with ether. The colorless precipitate was collected, and this hygroscopic solid was dissolved in water (20 ml) and lyophilized to yield 0.65 g (97%) of the amide IV as the trifluoroacetate.

Boc-Leu-Trp-Pro-Gly-NH_2 (V)—Dicyclohexylcarbodiimide (1.33 g, 6.48 mmoles) was added to a solution prepared from Trp-Pro-Gly-NH_2 trifluoroacetate (2.77 g, 5.89 mmoles), Boc-Leu (1.37 g, 5.89 mmoles)[1], 1-hydroxybenzotriazole (1.59 g, 11.8 mmoles), and *N*-methylmorpholine (0.66 ml, 5.89 mmoles) in tetrahydrofuran (80 ml) cooled to 0°. The mixture was stirred at 0° for 1 hr and at 23° for 3 hr. The solution was filtered, the solvent was removed, and the residue was dissolved in ethyl acetate, washed, and dried. After the solvent was evaporated, the residue was recrystallized from ethyl acetate ligroin to afford 2.37 g (70%) of the tetrapeptide amide V, mp 119–120°; $[\alpha]_D^{25}$ −37° (methanol).

Anal.—Calc. for $C_{29}H_{42}N_6O_6 \cdot H_2O$: C, 59.18; H, 7.48; N, 14.29. Found: C, 59.04; H, 7.52; N, 14.48.

Leu-Trp-Pro-Gly-NH_2 (VI) Trifluoroacetate—Cleavage of the protecting group from Boc-Leu-Trp-Pro-Gly-NH_2 (26.8 mg, 0.047 mmole) was conducted with 50% trifluoroacetic acid–methylene chloride (4 ml) containing 1% 2-mercaptoethanol as described for preparation of IV to yield 32.8 mg (84%) of the amide VI as the trifluoroacetate.

OBzl-Boc-Tyr-Gly-OCH_3—To a solution of OBzl-Boc-Tyr (5.0 g, 16.2 mmoles) in tetrahydrofuran (90 ml), cooled to −15°, was added *N*-methylmorpholine (1.81 ml, 16.2 mmoles) and isobutyl chlorocarbonate (2.11 ml, 16.2 mmoles). Before Gly-OCH_3 hydrochloride (2.02 g, 16.2 mmoles) and *N*-methylmorpholine (1.81 ml, 16.2 mmoles) were added, the mixture was stirred for 15 min at −15°. Then the mixture was stirred for 2 hr at 0° and for 26 hr at 23°. The solvent was removed, and a solution of the residue in ethyl acetate was washed, dried, and concentrated to a solid. The solid was recrystallized from ether to provide 5.70 g (92%) of the dipeptide, mp 118–120°; $[\alpha]_D^{25}$ −11° (methanol). The dipeptide VII was previously prepared in a 90% yield (mp 118–120°) by a *p*-nitrophenyl ester peptide bond-forming method (25).

Anal.—Calc. for $C_{24}H_{30}N_2O_6$: C, 65.11; H, 6.78; N, 6.35. Found: C, 64.90; H, 6.96; N, 6.32.

OBzl-Tyr-Gly-OCH_3 (VII) Hydrochloride—Removal of the Boc group from OBzl-Boc-Tyr-Gly-OCH_3 (3.65 g, 8.26 mmoles) was achieved using 50% trifluoroacetic acid–methylene chloride (30 ml, for 1 hr at 23°). The solvent was removed, and the residue was treated with cold ethereal hydrogen chloride. The colorless precipitate was collected and washed with ether. The hygroscopic solid was dissolved in water (20 ml) and lyophilized to yield 3.02 g (97%) of dipeptide ester VII as the hydrochloride.

Boc-Ser-OBzl-Tyr-Gly-OCH_3—A solution prepared from Boc-Ser (0.27 g, 1.31 mmoles), OBzl-Tyr-Gly-OCH_3 hydrochloride (VII, 0.497 g, 1.31 mmoles), and *N*-methylmorpholine (0.15 ml, 1.31 mmoles) in ethyl acetate–dimethylformamide (2:1, 15 ml) was cooled to 0°. Following addition of 1-ethyl-3-(3′-dimethylaminopropyl)carbodiimide hydrochloride (0.27 g, 1.43 mmoles), the mixture was stirred at 0° for 1 hr and at 23° for 20 hr. The reaction mixture was diluted with ethyl acetate, washed, and dried; the solvent was removed to yield a yellow oil. The crude product was purified by column chromatography on silica gel (100 g, elution with 1:1 ethyl acetate–chloroform) and recrystallized from ethyl acetate–ligroin to afford 0.49 g (72%) of the tripeptide, mp 104–105°; $[\alpha]_D^{25}$ −26° (methanol).

Anal.—Calc. for $C_{27}H_{35}N_3O_8$: C, 61.25; H, 6.62; N, 7.94. Found: C, 61.15; H, 6.75; N, 8.07.

Boc-Ser-OBzl-Tyr-Gly (VIII)—Boc-Ser-OBzl-Tyr-Gly-OCH_3 (0.71 g, 1.34 mmoles) was dissolved in a solution of 0.86 *N* NaOH in 90% aqueous methanol (15 ml). After 45 min at room temperature, the methanol was removed and the residue was diluted with water (25 ml) and extracted with ether (10 ml). The aqueous layer was acidified with 1 *N* HCl, saturated with sodium chloride, and extracted with ethyl acetate (3 × 20 ml). The combined extract was concentrated to dryness, and the residue was recrystallized from ethyl acetate–ligroin to give 0.61 g (87%) of tripeptide VIII, mp 88–90°; $[\alpha]_D^{25}$ −24° (methanol).

Anal.—Calc. for $C_{26}H_{33}N_3O_8$: C, 60.57; H, 6.45; N, 8.15. Found: C, 60.44; H, 6.35; N, 8.29.

Boc-Ser-OBzl-Tyr-Gly-Leu-Trp-Pro-Gly-NH_2—By means of the mixed carbonic anhydride procedure described for the preparation of the dipeptide IV, Boc-Ser-OBzl-Tyr-Gly (VIII, 0.27 g, 0.521 mmole) was allowed to react in tetrahydrofuran (15 ml) with *N*-methylmorpholine (58 μl, 0.521 mmole) and isobutyl chlorocarbonate (75 μl, 0.573 mmole) followed by Leu-Trp-Pro-Gly-NH_2 trifluoroacetate (0.30 g, 0.521 mmole) and *N*-methylmorpholine (58 μl, 0.521 mmole) in tetrahydrofuran (2 ml). The product was recrystallized from chloroform–ligroin to afford 0.47 g (94%) of the heptapeptide amide, mp 136–138°; $[\alpha]_D^{25}$ −35° (methanol).

Anal.—Calc. for $C_{50}H_{65}N_9O_{11} \cdot H_2O$: C, 60.91; H, 6.80; N, 12.80. Found: C, 60.56; H, 6.61; N, 12.70.

Ser-OBzl-Tyr-Gly-Leu-Trp-Pro-Gly-NH_2 (IX) Hydrochloride—A solution of Boc-Ser-OBzl-Tyr-Gly-Leu-Trp-Pro-Gly-NH_2 (0.71 g, 0.735 mmole) in 50% trifluoroacetic acid–methylene chloride (40 ml) containing 1% 2-mercaptoethanol was allowed to remain for 1 hr at 23°. Solvent was removed, and the residue was treated with cold ethereal hydrochloric acid to form a colorless precipitate. The precipitate was collected, washed with ether, and dried to yield 0.55 g (85%) of the heptapeptide amide IX, mp 149–150°.

N^{im}-Bzl-Boc-His-Trp-OBzl—A solution prepared from N^{im}-Bzl-Boc-His (5.10 g, 14.8 mmoles) (26), Trp-OBzl hydrochloride (4.87 g, 14.8 mmoles) (27), 1-hydroxybenzotriazole (3.95 g, 29.6 mmoles), *N*-methylmorpholine (1.66 ml, 14.8 mmoles), and dimethylformamide (100 ml) was cooled to 0°, and dicyclohexylcarbodiimide (3.34 g, 16.3 mmoles)

[3] Nutritional Biochemicals Corp. or Koch-Light.

[4] Kofler.

[5] The amino acid analyses provided by Dr. R. H. Ode and Dr. J. Cronin were determined with a Beckman-Spinco 121 amino acid analyzer. Elemental microanalytical data were determined by Dr. A. Bernhardt, Mikroanalytisches Laboratorium, 5251 Elbach über Engelskirchen, West Germany.

was added. The mixture was stirred at 0° for 1 hr and at 23° for 16 hr. The solution was filtered, the solvent was removed, and the residue was triturated with chloroform. The chloroform solution was filtered, and the filtrate was washed, dried, and concentrated to dryness. Recrystallization of the residue from chloroform–ligroin afforded 6.27 g (68%) of the dipeptide, mp 67–68°; $[\alpha]_D^{25}$ +3° (methanol).

Anal.—Calc. for $C_{36}H_{39}N_5O_5$: C, 69.73; H, 6.28; N, 11.27. Found: C, 69.49; H, 6.18; N, 11.12.

N^{im}-Bzl-His-Trp-OBzl (X) Hydrochloride—Elimination of the Boc protecting group was realized as described for preparation of VII hydrochloride employing N^{im}-Bzl-Boc-His-Trp-OBzl (55.8 mg, 0.090 mmole) in 50% trifluoroacetic acid–methylene chloride (8 ml) containing 1% 2-mercaptoethanol. The hygroscopic product was dissolved in water (15 ml) and lyophilized to yield 45.9 mg (91%) of the dipeptide ester (X) hydrochloride.

p-Glu-N^{im}-Bzl-His-Trp-OBzl (XI)—To a dimethylformamide (40 ml) solution of p-Glu (0.45 g, 3.51 mmoles), N^{im}-Bzl-His-Trp-OBzl hydrochloride (1.95 g, 3.51 mmoles), and *N*-methylmorpholine (0.39 ml, 3.51 mmoles), cooled to 0°, was added 1-ethyl-3-(3′-dimethylaminopropyl)carbodiimide hydrochloride (0.74 g, 3.86 mmoles). The mixture was stirred at 0° for 1 hr and at 23° for 12 hr. After concentration to 15 ml, the solution was poured into ice–5% sodium bicarbonate (100 ml). The solid was collected, washed with water, and recrystallized from dimethylformamide–water to afford 1.66 g (75%) of the tripeptide XI, mp 235–237°; $[\alpha]_D^{25}$ +13° (dimethylformamide).

Anal.—Calc. for $C_{36}H_{36}N_6O_5 \cdot H_2O$: C, 66.46; H, 5.85; N, 12.91. Found: C, 65.70; H, 5.64; N, 12.64.

p-Glu-N^{im}-Bzl-His-Trp (XII)—A mixture of p-Glu-N^{im}-Bzl-His-Trp-OBzl (XI, 1.55 g, 2.42 mmoles), 5% palladium-on-charcoal (1.0 g), and methanol–acetic acid (80 ml) (3:2) was stirred under 1 atmosphere of hydrogen at 23° for 8 hr. The solution was filtered through diatomaceous earth, and solvent was removed from the filtrate. The residue was recrystallized from methanol–ether to provide 0.64 g (48%) of the tripeptide XII, mp 165–167°; $[\alpha]_D^{25}$ +19° (methanol).

p-Glu-His-Trp-Ser-OBzl-Tyr-Gly-Leu-Trp-Pro-Gly-NH_2 ([Trp^8]-LH-RH) (XIII)—A dimethylformamide (30 ml) solution of XII (0.335 g, 0.617 mmole), Ser-OBzl-Tyr-Gly-Leu-Trp-Pro-Gly-NH_2 hydrochloride (0.55 g, 0.617 mmole), 1-hydroxybenzotriazole (0.17 g, 1.23 mmoles), and *N*-methylmorpholine (69 μl, 0.617 mmole) was cooled to 0°, and dicyclocarbodiimide (0.14 g, 0.679 mmole) was added. The mixture was stirred at 0° for 1 hr and at 23° for 7 hr. Then the solution was filtered and poured into ice–5% sodium bicarbonate (100 ml). Following collection of the solid and trituration with hot methanol, the resulting solution was filtered. The solvent was removed, and the residue was dissolved in acetic acid (20 ml) and lyophilized to yield 0.60 g (71%) of the protected decapeptide as a powder. Recrystallization from methylethyl ether gave a specimen of p-Glu-N^{im}-Bzl-His-Trp-Ser-OBzl-Tyr-Gly-Leu-Trp-Pro-Gly-NH_2, mp 245–248° dec.; $[\alpha]^{25}$ −19° (acetic acid).

A mixture composed of the decapeptide (89.7 mg, 0.0645 mmole), 5% palladium-on-charcoal (0.10 g), and methanol–acetic acid (40 ml) (4:1) was stirred under 1 atmosphere of hydrogen at 23° for 40 hr. The solution was filtered through diatomaceous earth, and the solvent was evaporated to a solid. The solid was purified by preparative TLC on silica gel with methanol–ethyl acetate (7:3) as the mobile phase. The product was eluted with methanol–acetic acid, dissolved in acetic acid, and lyophilized to yield 55.4 mg (71%) of [Trp^8]-LH-RH (XIII).

The decapeptide XIII (5 mg) was dissolved in 6 *N* HCl and hydrolyzed at 110° for 20 hr in a sealed tube. The solution was freeze dried, and the residue was dissolved in citrate buffer (1 ml). A 500-μl aliquot was diluted to 10.0 ml with the same buffer, and a 1-ml sample of this solution was used for amino acid analysis, which showed: His (0.6), Ser (1.0), Glu (1.0), Pro (1.0), Gly (2.0), Leu (1.0), and Tyr (1.0). Repeated amino acid analyses gave essentially the same results for His. Similar low values for this amino acid were noted with several other modified LH-RH decapeptides (6).

REFERENCES

(1) A. V. Schally, R. M. G. Nair, T. W. Redding, and A. Arimura, *J. Biol. Chem.*, **246**, 7230 (1971).

(2) H. Matsuo, Y. Baba, R. M. G. Nair, A. Arimura, and A. V. Schally, *Biochem. Biophys. Res. Commun.*, **43**, 1334 (1971).

(3) D. J. Schafer, A. D. Black, and J. D. Bower, *J. Med. Chem.*, **18**, 613 (1975).

(4) D. H. Coy, Y. Hirotsu, T. W. Redding, E. J. Coy, and A. V. Schally, *ibid.*, **18**, 948 (1975).

(5) R. W. A. Rees, T. J. Foell, S. Y. Chai, and N. Grant, *ibid.*, **17**, 1016 (1974).

(6) H. Immer, V. R. Nelson, C. Revesz, K. Sestanj, and M. Götz, *ibid.*, **17**, 1060 (1974).

(7) J. Rivier, M. Amoss, C. Rivier, and W. Vale, *ibid.*, **17**, 230 (1974).

(8) J. Humphries, G. Fisher, Y.-P. Wan, and K. Folkers, *ibid.*, **17**, 569 (1974).

(9) M. Fujino, T. Fukuda, S. Shinagawa, S. Kobayashi, I. Yamazaki, and R. Nakayama, *Biochem. Biophys. Res. Commun.*, **60**, 406 (1974).

(10) J. Humphries, Y.-P. Wan, G. Fisher, and K. Folkers, *ibid.*, **57**, 675 (1974).

(11) Y. Okada, H. Horikoshi, and Y. Baba, *Chem. Pharm. Bull.*, **22**, 721 (1974).

(12) B. L. Currie, K. N. G. Johansson, and K. Folkers, *Biochem. Biophys. Res. Commun.*, **50**, 20 (1973).

(13) K. Folkers, N.-G. Johansson, F. Hooper, B. Currie, H. Sievertsson, J.-K. Chang, and C. Y. Bowers, *Angew. Chemie. Int. Ed. Engl.*, **12**, 255 (1973).

(14) G. R. Pettit, "Synthetic Peptides," vol. 3, Academic, New York, N.Y., 1975, p. 309.

(15) G. R. Pettit, "Synthetic Peptides," vol. 4, Elsevier Scientific Publishing, Amsterdam, The Netherlands, 1976.

(16) J. Rivier, P. Brazeau, W. Vale, and R. Guillemin, *J. Med. Chem.*, **18**, 123 (1975).

(17) H. U. Immer, K. Sestanj, V. R. Nelson, and M. Götz, *Helv. Chim. Acta*, **57**, 730 (1974).

(18) P. Brazeau and R. Guillemin, *N. Engl. J. Med.*, **290**, 963 (1974).

(19) J.-K. Chang, R. H. Williams, A. J. Humphries, N.-G. Johansson, K. Folkers, and C. Y. Bowers, *Biophys. Res. Commun.*, **47**, 727 (1972).

(20) J.-K. Chang, H. Sievertsson, B. L. Currie, C. Bogentoft, K. Folkers, and C. Y. Bowers, *J. Med. Chem.*, **15**, 623 (1972).

(21) N. Yanaihara, C. Yanaihara, T. Hashimoto, Y. Kenmochi, T. Kaneko, H. Oka, S. Saito, A. V. Schally, and A. Arimura, *Biochem. Biophys. Res. Commun.*, **49**, 1280 (1972).

(22) J. Blake and C. H. Li, *J. Am. Chem. Soc.*, **90**, 5882 (1968).

(23) J. Sandow, A. V. Schally, H. G. Schröder, T. W. Redding, W. Heptner, and H. G. Vogel, *Arzneim-Forsch.*, **22**, 1718 (1972).

(24) J. A. Vilchez-Martinez, A. V. Schally, D. H. Coy, E. J. Coy, C. M. Miller, and A. Arimura, *Endocrinology*, **96**, 1130 (1975).

(25) G. R. Flouret, W. H. Arnold, J. W. Cole, R. L. Morgan, W. F. White, M. T. Hedlund, and R. H. Rippel, *J. Med. Chem.*, **16**, 369 (1973).

(26) E. Schnabel, *Ann. Chem.*, **702**, 188 (1967).

(27) M. Wilchek and A. Patchornik, *J. Org. Chem.*, **28**, 1874 (1963).

ACKNOWLEDGMENTS

Abstracted in part from a dissertation submitted by T. H. Smith to Arizona State University in partial fulfillment of the Doctor of Philosophy degree requirements.

Supported by Syntex, Inc., the Fannie E. Rippel Foundation, Mrs. Mary Dell Pritzlaff, the Phoenix Coca-Cola Bottling Co., and Public Health Service Research Grants CA-16049-02 and CA-16049-03 from the National Cancer Institute.

The authors thank Dr. T. R. Kasturi, Dr. Christine Tai, and Dr. T. Harvey for assistance with preliminary experiments and Dr. H. J. Ringold for valuable contributions.

For Part XII of this series, see G. R. Pettit, S. K. Gupta, and R. H. Ode, *J. Chem. Soc., Perkin Trans.*, 1, 950 (1973).

Pharmacokinetic Model for Procaine in Humans during and following Intravenous Infusion

RANDOLPH H. SMITH *x, DANIEL H. HUNT ‡, ASTRIDE B. SEIFEN *, ALFREDO FERRARI *, and DOLA S. THOMPSON *

Received September 1, 1978, from the **Department of Anesthesiology and the* ‡*Department of Pharmacology, University of Arkansas for Medical Sciences, Little Rock, AR 72201.* Accepted for publication February 9, 1979.

Abstract □ A multicompartment pharmacokinetic model is presented to describe procaine distribution in humans during and following intravenous infusion. The model, based on a general perfusion model, relates individual characteristics such as sex, age, weight, height, infusion rate and duration, and hematocrit to general parameters such as drug metabolism, protein binding, ion-trapping effects, and tissue–plasma distribution coefficients to provide an individualized distribution prediction. Experimentally observed kinetics of blood procaine levels collected during intravenous procaine infusion as an adjunct to surgical anesthesia and blood lidocaine levels obtained from the literature compared very well with the model simulation.

Keyphrases □ Pharmacokinetics—procaine in humans, intravenous infusion, drug interactions □ Procaine—pharmacokinetics, intravenous infusion, humans, drug interactions □ Local anesthetics—procaine, pharmacokinetics, intravenous infusion, humans, drug interactions □ Models, pharmacokinetic—procaine, intravenous infusion, humans, drug interactions

Local anesthetics are given intravenously for various clinical purposes. Intravenous procaine is now being studied as a supplement or adjunct to general anesthesia, whereas in the past it has been used for local anesthesia, for intravenous regional anesthesia, and in cardiac arrhythmia treatment.

In these clinical applications, there are potential dangers to the patient such as cardiovascular depression and central nervous system toxicity. The ability to predict drug concentrations in various body organs as the result of intravenous infusion rates could aid the clinician's choice of an infusion rate and thereby offer additional safety in drug administration. Additionally, the clinical application of intravenous local anesthetics is usually simultaneous with the application of other drugs. Therefore, a potential for interaction between the various drugs exists. These interactions can change significantly the degree of pharmacological action expressed by the drugs individually.

This project was undertaken in order to describe and simulate the pharmacokinetics of intravenous procaine used as an adjuvant drug for surgical anesthesia.

BACKGROUND

In traditional pharmacokinetic studies, the drug concentration in the blood is used as an index because the clinical sampling procedure for blood is easier and more convenient than the sampling of other tissues and fluids. The traditional pharmacokinetic approach (1–3) is to correlate the drug concentration in blood data by using one or several exponential terms, with each exponential term representing a compartment, to describe the data. The distribution volumes, rate constant, *etc.*, in the pharmacokinetic model are determined from the parameters of the exponential equation describing the drug concentration in blood (4).

The traditional approach utilizing the pharmacokinetic distribution based on these data alone may not provide sufficient information for adequate therapy when such drugs as ultrashort-acting barbiturates, some cardiovascular drugs, especially cancer chemotherapeutic agents, and local anesthetics are employed. An additional knowledge of the drug distribution in various organs and tissues as well as in the blood may be necessary to provide optimal drug concentrations in areas targeted for treatment without undue risk.

Previous investigators (5–7) developed an entirely different approach to pharmacokinetic modeling to make *a priori* prediction of drug distributions in the body. Included were parameters such as blood flow rates, lipid solubility, protein binding, and metabolism based on *in vitro* studies of well-documented physiological parameters. The model described here is an extension of this perfusion model approach with additional parameters that improve the scaling to different body sizes based on fat-free proportions as well as account for erythrocyte ion trapping.

EXPERIMENTAL

Arterial blood samples were collected from human volunteers undergoing intravenous procaine infusion as an adjuvant to surgical anesthesia along with thiamylal and nitrous oxide. These samples were collected before, during, and after the infusion. An inhibitor of plasma butyrylcholinesterase (pseudocholinesterase) was added to preserve the procaine for analysis. A flame-ionization GLC technique (8) was used to determine the blood concentrations. Additional parameters such as age, weight, height, sex, hematocrit, and other drugs administered were collected for use in the simulation. The exact infusion rates and duration were determined also.

THEORETICAL

The model can be thought of as an interactive blood–drug–tissue system. To describe such a system, previous investigators (5–7) used a four-compartment model with the body divided into the blood pool, the viscera, the lean tissue, and the adipose tissue. They utilized this scheme to describe the pharmacokinetics of several drugs such as thiopental and methotrexate.

This study of clinical intravenous procaine use focuses on the drug concentration in the brain because of anesthetic and potential convulsive effects. The blood pool was divided into separate arterial and venous pools with a lung compartment added to provide a mixing and time delay between the arterial and venous pools since procaine is hydrolyzed very rapidly by the plasma cholinesterases. Additional compartments were added to describe procaine metabolism in the liver and the ion-trapping effect due to the lower pH within the GI tract. The model (Fig. 1) contains nine compartments and adequately describes intravenous procaine pharmacokinetics, although consideration could be given to separating the blood from tissue for the highly perfused organs due to borderline adherence to the basic assumption of instantaneous mixing or flow-limitation of the system.

Each compartment equation describes a material (drug mass) balance between the incoming and outgoing drug rates. For example, blood flowing into a compartment transports an amount of drug at an incoming rate equal to the volume flow times the total concentration. Summation of all incoming and outgoing rates yields a net accumulation rate within the compartment. The free (unbound) concentration of drug leaving a compartment is assumed to equal (is in equilibrium with) the free concentration within that compartment.

This assumption may not be valid for a compartment that is a combination of blood and tissue and is highly perfused (such as viscera). If the drug does not diffuse into and out of the tissue at a rate faster than the transport by blood flow, the assumption also is not correct. Hence, the viscera might be described more accurately as a viscera tissue compartment and a viscera blood compartment. Furthermore, an equation (statement of material balance) written for one compartment contains concentration values from other compartments and, therefore, all compartment equations are interdependent (as are the body functions they describe) and must be solved together.

The venous blood pool compartment is given first, and the terms are

0022-3549/79/0800-1016$01.00/0
© 1979, American Pharmaceutical Association

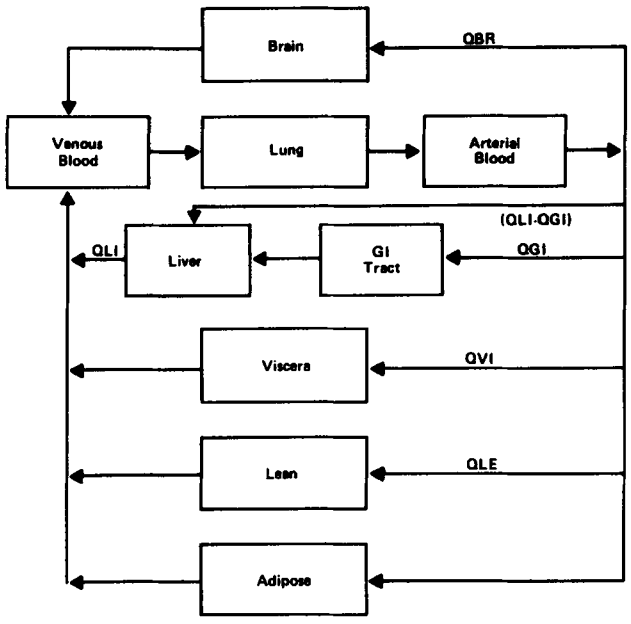

Figure 1—*Body compartments important in procaine distribution.*

elucidated for better understanding of the entire model before stating the other compartment equations.

Venous Blood: Compartment 1—

$$TRAPC(HMT)V_{Vb}F_{W,e}\frac{dC_{Vb}}{dt} + (1 - HMT)V_{Vb}F_{W,Pl}\frac{dC_{Vb}}{dt} + (1 - HMT)V_{Vb}C_{M,Pl}\frac{dX_{Vb}}{dt} = Q_{BR}[TRAPC(HMT)F_{W,e}C_{BR} + (1 - HMT)(F_{W,Pl}C_{BR} + C_{M,Pl}X_{BRb})] + Q_{LI}[TRAPC(HMT)F_{W,e}C_{LI} + (1 - HMT)(F_{W,Pl}C_{LI} + C_{M,Pl}X_{LIb})] + Q_{VI}[TRAPC(HMT)F_{W,e}C_{VI} + (1 - HMT)(F_{W,Pl}C_{VI} + C_{M,Pl}X_{VIb})] + Q_{LE}[TRAPC(HMT)F_{W,e}C_{LE} + (1 - HMT)(F_{W,Pl}C_{LE} + C_{M,Pl}X_{LEb})] + Q_{AD}[TRAPC(HMT)F_{W,e}C_{AD} + (1 - HMT)(F_{W,Pl}C_{AD} + C_{M,Pl}X_{ADb})] - Q[TRAPC(HMT)F_{W,e}C_{Vb} + (1 - HMT)(F_{W,Pl}C_{Vb} + C_{M,Pl}X_{Vb})] - (1 - HMT)V_{Vb}R_{MET,b} + Q_{INF}(BWT) \quad \text{(Eq. 1)}$$

where:

C_i = free (unbound concentration in compartment i) water (micromoles per liter)
Vb = venous blood
LE = lean
AD = adipose
VI = viscera
BR = brain
Ab = arterial blood
LI = liver
LG = lung
e = erythrocyte
Pl = plasma
Q = blood flow rate (liters per minute)
V = volume of the compartment (liters)
HMT = hematocrit of erythrocyte (fraction)
$C_{M,Pl}$ = effective plasma binding protein concentration (kilograms per liter)
$F_{W,Z}$ = fraction water in compartment Z
X = bound concentration (micromoles per kilogram of protein)
$R_{MET,b}$ = metabolism [hydrolysis rate, micromoles per liter (plasma)-minutes]
Q_{INF} = infusion rate [micromoles per kilogram (body)-minutes]
BWT = body mass (kilograms)
$TRAPC$ = ion-trapping constant

Since a compartment contains "free" and "bound" concentrations of drug, summation of these concentrations gives the total concentration. In general, the free drug is assumed to be in the water phase of the compartment, and the bound drug exists in physical attachment to protein or large macromolecules. However, not all protein is effective or available for binding. Therefore, an effective protein concentration as described previously (9) is used to determine the bound drug concentration. The total concentration for a compartment is described as:

$$C_{tot} = F_{W,Z}C + C_{M,Z}X \quad \text{(Eq. 2)}$$

where:

C_{tot} = total concentration (micromoles per liter)
C = free concentration (micromoles per liter)
X = bound concentration (micromoles per liter)
$F_{W,Z}$ = fraction water (W) in region Z
$C_{M,Z}$ = effective protein macromolecule (M) concentrations (kilograms of protein per liter)

For the venous plasma pool, the total plasma drug concentration is of the form:

$$C_{Pl} = F_{W,Pl}C_{Vb} + C_{M,Pl}X_{Vb} \quad \text{(Eq. 3)}$$

However, for total blood, the amount sequestered within the erythrocytes must be included (10). Due to the erythrocyte ion-trapping effect at a slightly lower intracellular pH (erythrocyte water, pH 7.26) as opposed to extracellular medium pH (plasma water, pH 7.40), the concentration ratio can be calculated as:

$$TRAPC = \frac{C_{eW}}{C_{PW}} = \frac{1 + 10^{pKa\text{-}pH_{eW}}}{1 + 10^{pKa\text{-}pH_{PW}}} \quad \text{(Eq. 4)}$$

where:

C = free concentration (micromoles per liter)
pKa = negative logarithm of acid dissociation constant = 8.92 (procaine base)
eW = erythrocyte water
PW = plasma water

The calculation yields a concentration ratio, $C_{eW}/C_{PW} = 1.37$. However, a study (11) of procaine uptake in human platelets, although they are smaller than erythrocytes, showed that the highest concentration ratio occurred at pH 7.4 with $C_{medium} = 100$ mg/liter and was 2.85 ± 0.78. High uptake also was found (12) for several anilide-type local anesthetics. Therefore, it could be concluded that binding was present, but no definitive binding relationship was noted other than a dependence on pH. Hence, in this work, the concentration ratio is only calculated from the ion-trapping effects as per Eq. 4. Additionally, since no difference in uptake was reported (12) from 5 min to 24 hr, a rapid establishment of equilibrium may be assumed.

The drug concentration in erythrocytes as a fraction of blood is determined from the hematocrit (HMT), the erythrocyte water fraction ($F_{W,e}$), the trapping ratio ($TRAPC$), and the plasma water concentration. Combination of the erythrocyte concentration with the total plasma concentration gives the total blood concentration:

$$C_{t,VB} = TRAPC(HMT)F_{W,e}C_{Vb} + (1 - HMT)(F_{W,Pl}C_{Vb} + C_{M,Pl}X_{Vb}) \quad \text{(Eq. 5)}$$

The protein or macromolecular drug binding has a major influence on the concentration relationship (12, 13). The general form for the relationship is:

$$r = \sum_{i=1}^{n}\frac{N_iK_iC}{1 + K_iC} \quad \text{(Eq. 6)}$$

where:

r = moles of bound drug per mole of protein macromolecule (moles per mole of protein)
N_i = average number of type i binding sites per protein macromolecule (moles per mole of protein)
K_i = intrinsic association constant of type i binding site (liters per mole)

A bound concentration of micromoles bound per kilogram of macromolecule is used instead of a mole per mole basis, and the general form of the relationship can be simplified to only one binding site. Therefore:

$$X = \frac{BKC}{1 + KC} \quad \text{(Eq. 7)}$$

where:

X = bound concentration (micromoles per kilogram)
C = free concentration (micromoles per liter)

B = binding site constant (micromoles per kilogram)
K = intrinsic association constant (liters per micromole)

This relationship is sufficient in the presence of a single drug. The presence of two or more drugs may cause competition for a binding site, and the equation describing the binding relationship must take this competitive binding into account (14). The following describes the competition between two drugs for a single site on the protein complex:

$$P + C \underset{K_2}{\overset{K_1}{\rightleftarrows}} PC$$

Scheme I

$$K_c = \frac{K_1}{K_2} = \frac{(PC)}{(P)(C)} \qquad \text{(Eq. 8a)}$$

$$P + D \underset{K_4}{\overset{K_3}{\rightleftarrows}} PD$$

Scheme II

$$K_D = \frac{K_3}{K_4} = \frac{(PD)}{(P)(D)} \qquad \text{(Eq. 8b)}$$

$$r = \frac{(PC)}{(P)} = \frac{N_t K_t C}{1 + K_D D + K_C C} \qquad \text{(Eq. 9)}$$

and:

$$X = \frac{B_C K_C C}{1 + K_D D + K_C C} \qquad \text{(Eq. 10)}$$

where:

B_C = binding site constant for drug C (micromoles per kilogram)
K_C = intrinsic association constant for drug C (liters per micromole)
C = free drug C concentration (micromoles per liter)
D = free inhibitor drug D concentration (micromoles per liter)

The use of the binding equation requires an estimation of the inhibitor drug concentration. A one-compartment model approximation *via* exponential decay of the initial concentration may be sufficient if the inhibitor drug has a half-life much longer than the drug of interest. In this case, the inhibitor drug concentration changes relatively slowly and can be assumed to act in one compartment uniformly throughout the body. Hence, thiamylal, an ultrashort-acting barbiturate having a half-life of at least 2 hr, which is much longer (~20 times) than that of procaine, was handled as a one-compartment drug in this study. In the clinical situation being simulated, thiamylal is given several minutes before procaine so the equation describing the thiamylal concentration would be:

$$C_{th} = C_{tho} \exp \frac{-(T + TD)0.693}{T^1/_2} \qquad \text{(Eq. 11)}$$

where:

C_{th} = thiamylal concentration (micromoles per liter)
$C_{tho} = D_{th}/V_{th}$ = initial concentration
D_{th} = dose (micromoles per kilogram)
V_{th} = volume of distribution (liters per kilogram)
TD = time delay between thiamylal and procaine administration

Another important function of the blood pool with regard to procaine is the metabolism *via* circulating enzymes, procainesterases (assumed to be plasma cholinesterases). The reaction rate has been well investigated (15–17) and is suited to description by the Michaelis–Menten-type equation of the form:

$$R_{MET} = \frac{V_{max} C}{C_{half} + C} \qquad \text{(Eq. 12)}$$

where:

R_{MET} = reaction rate [micromoles per liter (plasma)-minutes]
V_{max} = maximum reaction rate (micromoles per liter-minutes)
C_{half} = free drug concentration (micromoles per liter)

As with protein binding competition, it is necessary to account for the inhibition or competitive effect of other drugs, particularly in the clinical setting where many drugs are administered concurrently. In this work, one such drug of special significance is succinylcholine, a muscle relaxant, which is metabolized by the plasma cholinesterases (18). The derivation and design of the competitive inhibition phenomena for a chemical reaction are almost identical to those for protein binding, differing only in the final form of the equation. The Michaelis–Menten equation becomes:

$$R_{MET} = \frac{V_{max} C}{C_{half}\left(1 + \frac{I}{K_I}\right) + C} \qquad \text{(Eq. 13)}$$

where:

I = free inhibitor concentration (micromoles per liter)
$K_I = K_m$ value or half maximal I concentration (micromoles per liter)

Obviously, the inhibitor increases the value of C_{half}.

Calculation of the final reaction rate requires estimation of the drug I concentration, which in this case is succinylcholine (suxamethonium) (17). Since succinylcholine is very water soluble and sparingly soluble in organic media, it will be assumed that the distribution volume is approximately equal to the extracellular fluid volume. If the intravenously administered dose is eliminated solely by its reaction with plasma cholinesterase, the succinylcholine concentration can be estimated as follows:

$$CSD = \frac{\text{dose} - \frac{VSD(CSD)T}{CKSD(1 - C/C_{half}) + CSD}(1 - HMT)V_b}{V_{EX}} \qquad \text{(Eq. 14)}$$

where:

CSD = free concentration of succinylcholine (micromoles per liter)
VSD = maximum reaction rate [micromoles per liter (plasma)-minutes]
$CKSD$ = K_m value for succinylcholine (micromoles per liter)
V_{EX} = extracellular fluid volume (liters)
V_b = blood volume (liters)
HMT = hematocrit
C = free procaine concentration (micromoles per liter)
C_{half} = K_m value for procaine (micromoles per liter)
dose = intravenous succinylcholine dose (micromoles)
T = time (minutes)

Essentially, the complexity of this model is exhibited in the blood equation. However, the various tissue compartments must be described with particular emphasis on the tissue macromolecular drug binding. Since no literature description of a relationship as a function of free concentration is available for tissue, the plasma binding relationship parameter was assumed to be valid. It remained to determine the effective tissue macromolecule concentration. Values for the partitioning of drug into tissue from plasma are available (10, 19–21). A tissue–plasma partition ratio can be calculated for brain, as an example, as follows:

$$P_{BR} = \frac{F_{W,BRt} C_{BR} + C_{M,BRt} X_{BRt}}{F_{W,Pl} C_{BR} + C_{M,Pl} X_{BRb}} = \frac{\text{plasma}}{\text{tissue}} \qquad \text{(Eq. 15)}$$

The unknown value of $C_{M,BRt}$ (effective macromolecule concentration in brain tissue) can be determined since $F_{W,BRt}$ is available from the literature and the other terms have been previously determined. A slightly different approach to the formulation is needed to handle adipose tissue where the fatty tissue concentration may be approximated by using a Henry's law relationship (21):

$$X_{ADt} = B_{ADt} C_{AD} \qquad \text{(Eq. 16)}$$

where B_{ADt} is Henry's law constant for procaine. Hence, the partition equation becomes:

$$P_{AD} = \frac{F_{W,ADt} C_{AD} + C_{M,ADt} B_{ADt} C_{AD}}{F_{W,Pl} C_{AD} + C_{M,Pl} X_{ADb}} \qquad \text{(Eq. 17)}$$

Even if B_{ADt} is not known, the combination $C_{M,Adt} B_{ADt}$ is sufficient for the descriptive equation since X_{ADb} in the plasma is calculated from Eq. 10. Now the other compartments can be expressed quantitatively.

Lean: Compartment 2—

$$TRAPC(HMT)V_{LEb}F_{W,e}\frac{dC_{LE}}{dt} + (1 - HMT)V_{LEb}F_{W,Pl}\frac{dC_{LE}}{dt}$$
$$+ (1 - HMT)V_{LEb}C_{M,Pl}\frac{dX_{LEb}}{dt} + V_{LEt}F_{W,LEt}\frac{dC_{LE}}{dt}$$

Table I—Model Parameters for Standard 70-kg Man [a]

Parameter	Compartment								
	Arterial Blood	Venous Blood	Brain	Viscera	Liver	Lean	GI Tract	Adipose	Lung
Tissue volume, liters	—	—	1.50	0.64	1.50	3.92	1.50	12.2	0.60
Flow rate, liters/min	5.54	5.54	0.76	1.66	1.58	1.28	1.20	0.26	5.54
Fraction water	0.714	0.94	0.76	0.78	0.73	0.77	0.74	0.19	0.90
Blood volume, liters	0.58	1.16	0.47	1.05	0.37	0.52	1.05	0.16	0.46

[a] Values modified from Refs. 22 and 25.

$$+ V_{LEt}C_{M,LEt}\frac{dX_{LEt}}{dt} = Q_{LE}[TRAPC(HMT)F_{W,e}C_{Vb} + (1 - HMT)(F_{W,Pl}C_{Vb} + C_{M,Pl}X_{Vb}) - TRAPC(HMT)F_{W,e}C_{LE} + (1 - HMT)(F_{W,Pl}C_{LE} + C_{M,Pl}X_{LEb})] - (1 - HMT)V_{LEb}R_{MET,LEb} \quad \text{(Eq. 18)}$$

Adipose: Compartment 3—

$$TRAPC(HMT)V_{ADb}F_{W,e}\frac{dC_{AD}}{dt} + (1 - HMT)V_{ADb}F_{W,Pl} \times \frac{dC_{AD}}{dt} + (1 - HMT)V_{ADb}C_{M,Pl}\frac{dX_{ADb}}{dt} + V_{ADt}F_{W,ADt}\frac{dC_{AD}}{dt} + V_{ADt}C_{M,ADt}\frac{dX_{ADt}}{dt} = Q_{AD}[TRAPC(HMT)F_{W,e}C_{Vb} + (1 - HMT)(F_{W,Pl}C_{Vb} + C_{M,Pl}X_{Vb}) - TRAPC(HMT)F_{W,e}C_{AD} + (1 - HMT)(F_{W,Pl}C_{AD} + C_{M,Pl}X_{ADb})] - (1 - HMT)V_{ADb}R_{MET,ADb} \quad \text{(Eq. 19)}$$

Because of the highly perfused nature of the brain, heart, and kidneys as well as some other organs, the assumption that mass transfer with each compartment is flow limited, *i.e.*, at the normal blood flow rate, incoming drug is instantly mixed with surrounding tissue and the outgoing free drug concentration is equal to the total compartment free concentration, should be considered. For high lipid-soluble drugs, this assumption is valid; but for less soluble ones, it is not. This subject is treated thoroughly in the literature (5–7).

Instead of a transfer coefficient equal to infinity, a transfer value for procaine equal to the flow rate of the compartment could be used for lack of a more exact determination. It is significant to account for this phenomenon since the rate of procaine appearance into cerebrospinal fluid is less than the ratio of blood flow to tissue volume (19). Conversely, in the lean and adipose compartments, the flow to volume ratio is much less than the transfer rate into tissue, and the uniformity is still assumed to be valid.

The viscera, brain, liver, GI tract, and lung compartments could be described with plasma and tissue separated, where the transfer between plasma and tissue is dependent on the free concentration difference. However, the following description ignores the finite plasma-tissue transfer and combines plasma and tissue into one compartment for simplicity.

Viscera: Compartment 4—

$$TRAPC(HMT)V_{VIb}F_{W,e}\frac{dC_{VI}}{dt} + (1 - HMT)V_{VIb}F_{W,Pl} \times \frac{dC_{VI}}{dt} + (1 - HMT)V_{VIb}C_{M,Pl}\frac{dX_{VI}}{dt} + V_{VIt}F_{W,VIt}\frac{dC_{VIb}}{dt} + V_{VIt}C_{M,VIt}\frac{dX_{VIb}}{dt} = Q_{VI}[TRAPC(HMT)F_{W,e}C_{Ab} + (1 - HMT)(F_{W,Pl}C_{Ab} + C_{M,Pl}X_{Ab}) - TRAPC(HMT)F_{W,e}C_{VIb} + (1 - HMT)(F_{W,Pl}C_{VIb} + C_{M,Pl}X_{VIb})] - (1 - HMT)V_{VIb}R_{MET,VIb} - RC(C_{VIb}) \quad \text{(Eq. 20)}$$

where RC is the renal clearance rate (liters per minute).

Brain: Compartment 5—

$$TRAPC(HMT)V_{BRb}F_{W,e}\frac{dC_{BR}}{dt} + (1 - HMT)V_{BRb}F_{W,Pl} \times \frac{dC_{BR}}{dt} + (1 - HMT)V_{BRb}C_{M,Pl}\frac{dX_{BRb}}{dt} + V_{BRt}F_{W,BRt}\frac{dC_{BR}}{dt} + V_{BRt}C_{M,BRt}\frac{dX_{BRt}}{dt} = Q_{BR}[TRAPC(HMT)F_{W,e}C_{Ab} + (1 - HMT)(F_{W,Pl}C_{Ab} + C_{M,Pl}X_{Ab}) - TRAPC(HMT)F_{W,e}C_{BR} + (1 - HMT)(F_{W,Pl}C_{BR} + C_{M,Pl}X_{BR})] - (1 - HMT)V_{BRb}R_{MET,BRb} \quad \text{(Eq. 21)}$$

Liver: Compartment 6—

$$TRAPC(HMT)V_{LIb}F_{W,e}\frac{dC_{LI}}{dt} + (1 - HMT)V_{LIb}F_{W,Pl}\frac{dC_{LI}}{dt} + (1 - HMT)V_{LIb}C_{M,Pl}\frac{dX_{LIb}}{dt} + V_{LIt}F_{W,LIt}\frac{dC_{LI}}{dt} + V_{LIt}C_{M,LIt}\frac{dX_{LIt}}{dt} = (Q_{LI} - Q_{GI})[TRAPC(HMT)F_{W,e}C_{Ab} + (1 - HMT)(F_{W,Pl}C_{Ab} + C_{M,Pl}X_{Ab})] + Q_{GI}[TRAPC(HMT)F_{W,e}C_{GI} + (1 - HMT)(F_{W,Pl}C_{GI} + C_{M,Pl}X_{GIb})] - Q_{LI}[TRAPC(HMT)F_{W,e}C_{LI} + (1 - HMT)(F_{W,Pl}C_{LI} + C_{M,Pl}X_{LIb})] - (1 - HMT)V_{LIb}R_{MET,LIb} - (V_{LIt}R_{LIt}C_{LIb})/(C_{half} + C_{LIb}) \quad \text{(Eq. 22)}$$

where R_{LIt} is the reaction rate constant for liver metabolism of procaine (minutes^{-1}).

GI Tract: Compartment 7—

$$TRAPC(HMT)V_{GIb}F_{W,e}\frac{dC_{GI}}{dt} + (1 - HMT)_{GIb}F_{W,Pl}\frac{dC_{GI}}{dt} + (1 - HMT)V_{GIb}C_{M,Pl}\frac{dX_{GIb}}{dt} + V_{GIt}F_{W,GIt}\frac{dC_{GI}}{dt} + V_{GIt}C_{M,GIt}\frac{dX_{GIt}}{dt} = Q_{GI}[TRAPC(HMT)F_{W,e}C_{Ab} + (1 - HMT)(F_{W,Pl}C_{Ab} + C_{M,Pl}X_{Ab}) - TRAPC(HMT)F_{W,e}C_{GIb} + (1 - HMT)(F_{W,Pl}C_{GIb} + C_{M,Pl}X_{GIb})] - (1 - HMT)V_{GIb}R_{MET,GIb} \quad \text{(Eq. 23)}$$

Lungs: Compartment 8—

$$TRAPC(HMT)V_{LGb}F_{W,e}\frac{dC_{LG}}{dt} + (1 - HMT)V_{LGb}\frac{dC_{LG}}{dt} + (1 - HMT)V_{LGb}C_{M,Pl}\frac{dX_{LGb}}{dt} + V_{LGt}F_{W,LGt}\frac{dC_{LG}}{dt} + V_{LGt}C_{M,LGt}\frac{dX_{LGt}}{dt} = Q_b[TRAPC(HMT)F_{W,e}C_{Vb} + (1 - HMT)(F_{W,Pl}C_{Vb} + C_{M,Pl}X_{Vb} - TRAPC(HMT)F_{W,e}C_{LG} + (1 - HMT)(F_{W,Pl}C_{LG} + C_{M,Pl}X_{LGb})] - V_{LGb}(1 - HMT)R_{MET,LGb} \quad \text{(Eq. 24)}$$

Arterial Blood: Compartment 9—

$$TRAPC(HMT)V_{Ab}F_{W,e}\frac{dC_{Ab}}{dt} + (1 - HMT)V_{Ab}F_{W,Pl}\frac{dC_{Ab}}{dt} + (1 - HMT)V_{Ab}C_{M,Pl}\frac{dX_{Ab}}{dt} = Q_B[TRAPC(HMT)F_{W,e}C_{LG} + (1 - HMT)(F_{W,Pl}C_{LG} + C_{M,Pl}X_{LGb}) - TRAPC(HMT)F_{W,e}C_{Ab} + (1 - HMT)(F_{W,Pl}C_{Ab} + C_{M,Pl}X_{Ab})] - (1 - HMT)V_{Ab}R_{MET,Ab} \quad \text{(Eq. 25)}$$

The physiological and anatomical parameters were based on those of a standard 70-kg man but were scaled, to simulate each individual studied, on the basis of basal energy metabolism (BEM) which is a

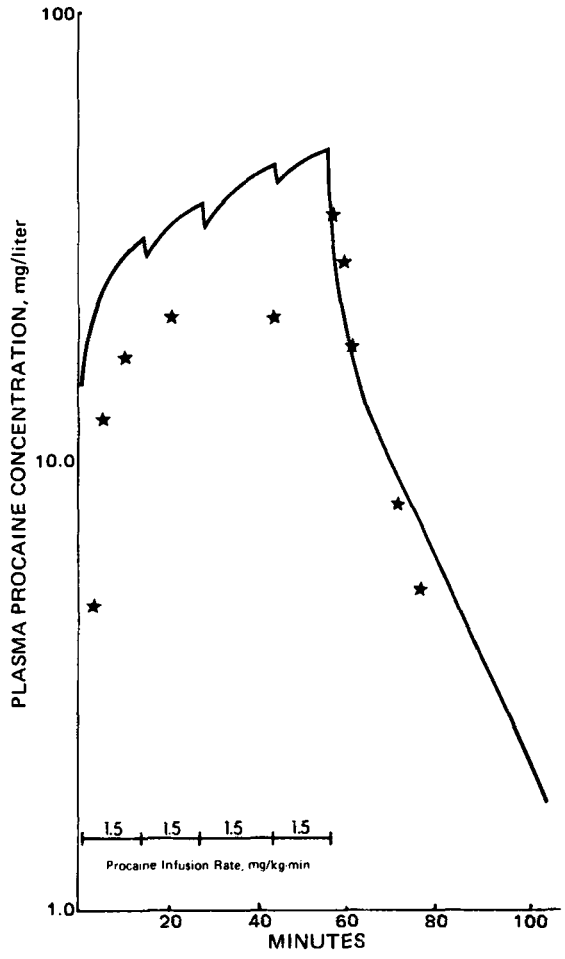

Figure 2—*Model predictions of plasma procaine concentrations* versus *experimental results for a female (age 34, weight 58.7 kg, height 177.8 cm, and hematocrit 35.0) with infusion rates and duration as shown.*

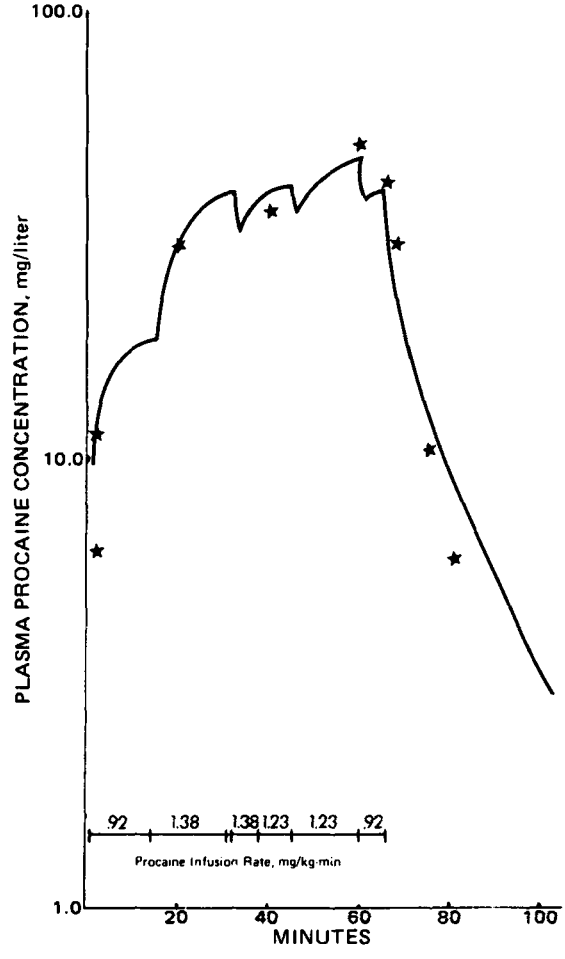

Figure 3—*Model predictions of plasma procaine concentrations* versus *experimental results for a female (age 24, weight 65 kg, height 165 cm, and hematocrit 36.8) with infusion rates and duration as shown.*

function of age, sex, height, and weight. This value was estimated by calculating the body surface area as:

$$S = 0.007184\ (Wt^{0.425})(Ht^{0.725}) \qquad \text{(Eq. 26)}$$

where Wt is weight (kilograms) and Ht is height (centimeters). Then, based on the tables relating age, surface area, and basal energy metabolism (22), for males 18–25 years:

$$BEM = [40.5 - (age - 18) \times 0.3](S)/60 \qquad \text{(Eq. 27}a\text{)}$$

for males over 25 years:

$$BEM = [38.4 - (age - 25) \times 0.11](S)/60 \qquad \text{(Eq. 27}b\text{)}$$

for females 20–40 years:

$$BEM = [35.3 - (age - 20) \times 0.05](S)/60 \qquad \text{(Eq. 27}c\text{)}$$

and for females over 40 years:

$$BEM = [34.3 - (age - 40) \times 0.10](S)/60 \qquad \text{(Eq. 27}d\text{)}$$

The fraction fat can be estimated from the tables (22) by:

$$FRFAT = 1.04 + 0.4\ (Wt - 50)/30 - BEM \qquad \text{(Eq. 28)}$$

Since the standard 70-kg man is considered to contain approximately 17.4% fat, the anatomical scaling was based on the body weight minus the fat contents by:

$$ANA = Wt(1 - FRFAT)/57.8 \qquad \text{(Eq. 29)}$$

where ANA is the scale factor.

RESULTS AND DISCUSSION

Analytical solution of the simultaneous differential equations was not feasible because of the nonlinearities caused by the binding terms. Therefore, the equations were solved by the fourth-order Runge–Kutta numerical method. The model stability was tested by comparing the numerical results from the standard values in Tables I and II with those from variations of the standard value for each of the following parameters:

1. ±10% variation of the volume of any body region
2. ±10% variation of the volume and the blood flow rate of any body region
3. ±10% variation of the water volume fraction of any body region
4. ±10% variation of the lipid solubility constant, BAT
5. ±10% of the binding constant, B
6. ±10% of the metabolism constants, VSD and C_{half}
7. ±10% variation of the effective binding macromolecule concentration of any body region

Figures 2 and 3 compare the model simulation with experimental values for two cases with a wide variation of physiological parameters as well as different infusion rates. The model was designed to account for both variations in the infusion rate and interruptions in the infusion continuity. This flexibility permitted a close simulation of the actual clinical application of the procaine infusion. As shown in the figures, due to rapid procaine hydrolysis in the blood, the rapid decline in concentration resulting from very short interruptions in the infusion can be very pronounced and will result in a substantial error in the simulated prediction of the concentration if it is not accounted for in the model design.

Figure 2 shows the experimental kinetic data of plasma procaine levels (symbol) and the model-predicted kinetics (solid line) for a 1.5-mg/kg/min intravenous infusion in a female. The results are in agreement within the range of measurement accuracy of the experimental data. Similar results are shown in Fig. 3 for a varied infusion rate in a female.

Figure 4 demonstrates the predicted procaine concentrations in the

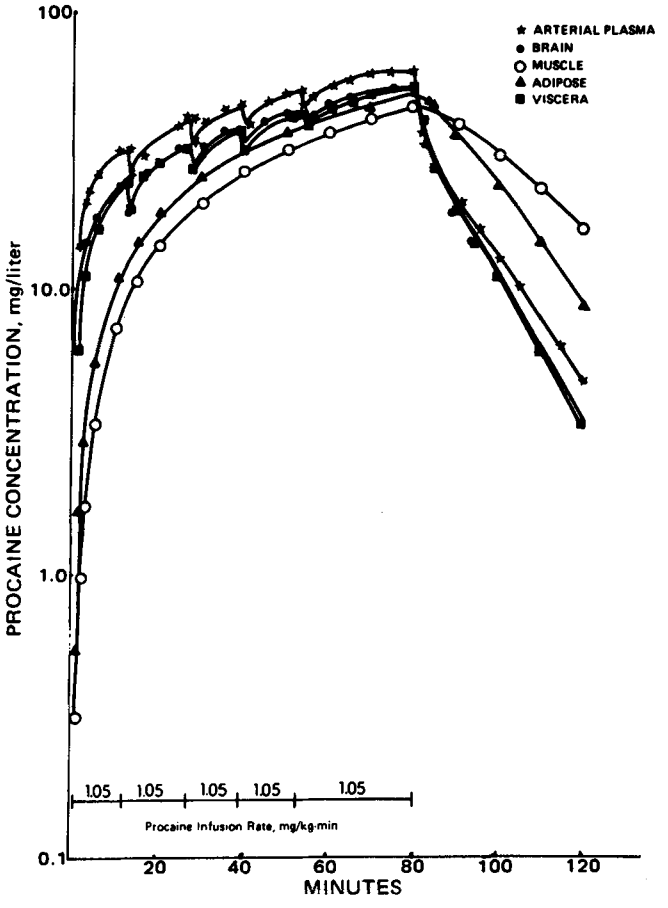

Figure 4—*Model predictions for various compartments (arterial plasma, brain, viscera, adipose, and muscle) for a female (age 25, weight 87.4, height 165 cm, and hematocrit 35.3) with infusion rates and duration as shown.*

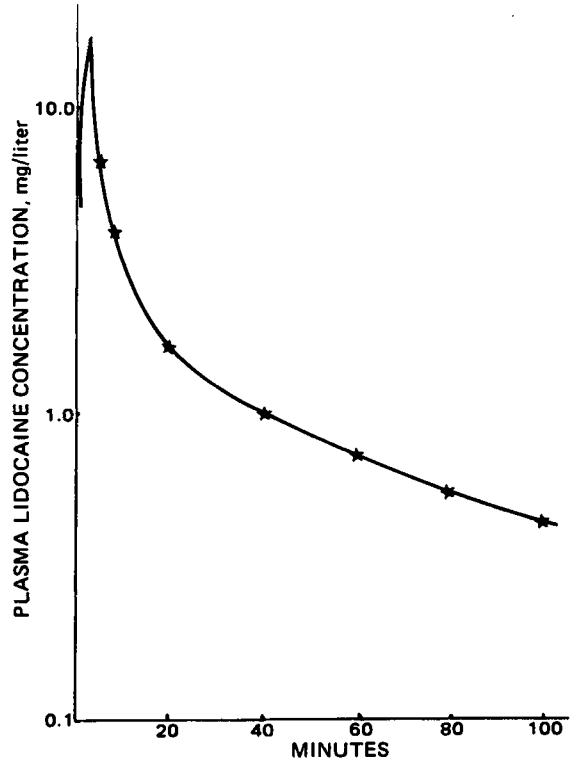

Figure 5—*Model predictions of plasma lidocaine concentrations* versus *literature values (12).*

Table II—Binding and Metabolism Parameters

Parameter	Procaine	Lidocaine[a]
Effective binding macromolecule concentration, kg/liter		
Brain	0.00079[b]	0.00135
Plasma	0.000945[b]	0.000945
Liver	0.0115[b]	0.000485
GI tract	0.0142[b]	0.00319
Viscera	0.0115[b]	0.00233
Lean	0.00167[b]	0.00052
Lung	0.00238[b]	0.00418
Adipose	0.01	0.0481
Binding factors		
Binding site constants, moles/liter	29,500.0[c]	28,571.0
Intrinsic association constant, liters/μmole	0.00314[c]	0.101
pKa	8.92[c]	7.86
Lipid solubility constant	12.0[c]	100.0
Maximum reaction rate, μmoles/liter (plasma)-min	70.0[d]	0.0
Free concentration reaction rate, μmoles/liter	28.0[d]	6.0
Renal clearance, liters/min	0.2	0.1

[a] Calculated based on Refs. 12 and 23. [b] Calculated based on Ref. 19. [c] Calculated based on Refs. 13 and 23. [d] Calculated based on Ref. 16.

various body regions for an infusion rate of 1.05 mg/kg/min. Since it was not possible to analyze samples from body regions other than the blood compartments, the basic model was further tested using literature data for lidocaine infusions (1, 20). With the appropriate lidocaine parameters (Table II), several simulations were made (one is shown in Fig. 5). The results of the simulation kinetics and the experimental kinetics are very similar and thus indicate the accuracy of the basic model.

CONCLUSIONS

Knowledge of the kinetic behavior of a drug in blood or plasma may not provide sufficient information for appropriate therapy; additional kinetic information of drug levels in specific organs, tissues, or body regions may be required for the development of improved dosage regimens. The pharmacokinetic model presented can predict detailed distribution in humans of intravenous infusion of local anesthetics, procaine and lidocaine, not only in blood or plasma but also in brain, liver, and other tissues or body regions.

Based on a general perfusion model, this model relates individual characteristics such as sex, age, weight, height, infusion rate, and hematocrit to general parameters such as metabolism, protein binding, ion-trapping effects, and tissue–plasma distribution coefficients to provide an individualized distribution prediction. Since each equation (compartment) in the system contains terms (concentrations) from other compartments and, therefore, all equations are interdependent, changes in any compartment influence the other compartments. This feature of the model has an important application in clinical pharmacokinetics.

Experimentally observed kinetics of blood procaine levels collected during procaine intravenous infusion as an adjunct to surgical anesthesia and blood levels of lidocaine obtained from the literature compared very well with the model simulation. While it was not possible in this study to collect experimental data in any organs or tissues other than the blood to support the predicted drug level, information from the literature derived from animal studies of tissue levels tends to verify the accuracy of the model. Until appropriate data for procaine concentrations are available for comparison with the predicted values, the predictions must be considered only to offer an approximation of what the physiological and pharmacological parameters indicate should occur. However, one application of this model is the comparison of drug levels obtained within a body region as a result of different infusion conditions such as rate changes, addition of thiamylal or succinylcholine, and variations in metabolism without the potential drastic effects an individual might experience under the same conditions. As more conditions are tested, the successful predictions should clarify the pharmacokinetics being described.

REFERENCES

(1) G. T. Tucker and R. A. Boas, *Anesthesiology*, **34**, 538 (1971).
(2) M. Ehrnebo, *J. Pharm Sci.*, **63**, 1114 (1974).
(3) D. D. Breimer, *Br. J. Anaesth.*, **48**, 643 (1976).

(4) J. C. K. Loo and S. Riegelman, *J. Pharm. Sci.*, **59**, 53 (1970).
(5) K. B. Bischoff, R. L. Dedrick, D. S. Zaharko, and J. A. Longstreth, *ibid.*, **60**, 1128 (1971).
(6) K. B. Bischoff and R. L. Dedrick, *ibid.*, **57**, 1346 (1968).
(7) K. B. Bischoff and R. L. Dedrick, *Chem. Eng. Prog. Symp. Ser.*, **64**, 32 (1968).
(8) R. H. Smith, M. A. Brewster, J. A. MacDonald, and D. S. Thompson, *Clin. Chem.*, **24**, 1599 (1978).
(9) D. Shen and M. Gibaldi, *J. Pharm. Sci.*, **63**, 1698 (1974).
(10) L. S. Schanker, P. A. Nafpliotis, and J. M. Johnson, *J. Pharmacol. Exp. Ther.*, **133**, 325 (1961).
(11) H. M. Soloman and P. D. Zieve, *ibid.*, **155**, 112 (1967).
(12) G. T. Tucker, R. N. Boyes, P. O. Bridenbough, and D. C. Moore, *Anesthesiology*, **33**, 287 (1970).
(13) V. S. Sawinski and G. W. Rapp, *J. Dental Res.*, **42**, 1429 (1963).
(14) A. Goldstein, L. Aronaw, and S. M. Kalman, "The Basis of Pharmacology," 2nd ed., Wiley, New York, N.Y., 1974.
(15) B. B. Brodie, P. A. Lief, and R. Poet, *J. Pharmacol. Exp. Ther.*, **94**, 359 (1948).
(16) W. Kalow, *ibid.*, **104**, 122 (1952).
(17) N. Kvisselgaard and F. Moya, *Acta Anaesth. Scand.*, **5**, 1 (1961).
(18) L. B. Hersh, P. P. Raj, and D. Ohlweiler, *J. Pharmacol. Exp. Ther.*, **189**, 544 (1974).
(19) J. E. Usubiaga, F. Moya, J. A. Wikinski, R. Wikinski, and L. E. Usubiaga, *Br. J. Anaesth.*, **39**, 943 (1967).
(20) J. B. Keenaghan and R. N. Boyes, *J. Pharmacol. Exp. Ther.*, **180**, 454 (1972).
(21) J. Buchi and X. Perlia, "International Encyclopedia of Pharmacology and Therapeutics," sect. 8, vol. 1, Pergamon, Elmsford, N.Y., 1971, chaps. 1, 2, 5, 39.
(22) W. S. Spector, "Handbook of Biological Data," Saunders, Philadelphia, Pa., 1956.
(23) C. Sung and A. P. Truant, *J. Pharmacol. Exp. Ther.*, **112**, 432 (1954).
(24) A. P. Truant and B. Takman, *Anesth. Anal.*, **38**, 478 (1959).
(25) W. W. Mapleson, *J. Appl. Physiol.*, **18**, 197 (1963).

Myoinositol Uptake by Rat Hepatocytes *In Vitro*

CHI-PO CHEN ˣ and VAN T. VU

Received November 27, 1978, from the *Section of Pharmacology and Toxicology, School of Pharmacy, University of Connecticut, Storrs, CT 06268.* Accepted for publication February 12, 1979.

Abstract □ Myoinositol uptake by rat hepatocytes *in vitro* was studied. Adult rat hepatocytes were prepared by digestion of the perfused liver with collagenase. Cell suspensions were incubated with tritium-labeled myoinositol in pH 7.4 Krebs bicarbonate solution containing 1% gelatin at 37°. ^{14}C-Carbon-labeled polyethylene glycol was used as a marker of adherent extracellular fluid volume. Myoinositol uptake was demonstrable after 5 min of incubation, but no intracellular concentration in excess of that in the incubation medium was observed after 60 min of incubation. Uptake saturation over a wide myoinositol concentration range could not be demonstrated. Neither the omission of sodium ions nor the inclusion of ouabain suppressed the distribution ratio significantly. Metabolic inhibitors and lower temperatures also showed no effect. Hexoses, phlorizin or mannitol, exerted no observable effect on myoinositol uptake. The results indicated that myoinositol uptake by rat hepatocytes is probably a passive process.

Keyphrases □ Myoinositol—uptake by hepatocytes, *in vitro*, rats, pharmacokinetics □ Hepatocytes—myoinositol uptake, pharmacokinetics, *in vitro*, rats □ Liver—myoinositol uptake, *in vitro*, pharmacokinetics, rats

The liver plays a predominant role in lipid metabolism. Under normal conditions, the influx of nonesterified fatty acids into the liver from the serum is counterbalanced by the formation of lipoprotein, which is transported back to the blood. The whole process requires myoinositol. In myoinositol-deficient animals, fatty livers often can be observed since the rate of fatty acid transport to the liver from the adipose tissue exceeds the capacity of the liver to mobilize the lipid and to transport it back to the plasma (1, 2). The administration of myoinositol to myoinositol-deficient animals often can alleviate the fatty liver condition.

BACKGROUND

Myoinositol has long been considered to be a lipotropic agent because of its ability to prevent and remove fat deposits in the liver (3, 4). This lipotropic action is thought to be due to stimulation of hepatic transferable phosphatidylinositol synthesis. Once formed, the phosphorylated myoinositol can be utilized in β-lipoprotein production in the endoplasmic reticulum. The newly synthesized β-lipoprotein is transported from the liver to the blood (4). In addition, exogenous myoinositol inhibits any further deposition of either liver triglycerols or cholesterol and causes the removal of the lipids deposited during the myoinositol-deficiency period (5–7).

Although there is much evidence that myoinositol is transported into the small intestine (8), kidney (9–12), central nervous system (13–16), and crystalline lens (17–19) *via* a specific carrier-mediated system, hepatic uptake of myoinositol has not been studied in spite of its well-known lipotropic activity. Hauser (11) reported that the radioactive myoinositol distribution ratio in liver slices is less than one-half of the radioactivity in the incubation medium, while the hepatic myoinositol concentration *in vivo* is similar to that of plasma; higher hepatic than blood myoinositol concentrations also were observed (20, 21).

In recent years, the use of isolated hepatocytes for various biochemical and pharmacological studies has gained wide acceptance (22). Studies with isolated liver cells can clarify certain molecular aspects of the transport system, such as binding and metabolism, while cellular integrity is maintained.

The purpose of this study was to investigate hepatic myoinositol uptake using liver cells freshly isolated from normal adult rats.

EXPERIMENTAL

Male rats[1], 200–300 g, were housed in groups in wire-bottomed cages in an air-conditioned room (23°). They received regular laboratory chow and water without restriction.

The methods of liver perfusion and cell isolation were described previously (23, 24). Cell viability was determined by the exclusion of 0.2% trypan blue from the cells and was frequently checked by incubating the cells with α-aminoisobutyric acid, which is actively accumulated by the hepatocytes (23). Cell pellets, following the final wash of the isolation procedure, were resuspended in 10 volumes of pH 7.4 Krebs–Ringer bicarbonate buffer containing 1% gelatin.

Uptake studies were performed by placing 5 ml of the final cell suspension (50–80 mg wet weight/ml of suspension) into 25-ml plastic erlenmeyer flasks. Under control conditions, the cell suspensions contained a trace amount of [2-^{3}H(N)]-myoinositol[2] (3 μCi/nmole/100 ml of suspension) with or without 0.1 μmole of nonlabeled myoinositol/ml. In

[1] Charles River Breeding Laboratory, Wilmington, Mass.
[2] New England Nuclear Corp., Boston, Mass.

0022-3549/79/0800-1022$01.00/0
© *1979, American Pharmaceutical Association*

(4) J. C. K. Loo and S. Riegelman, *J. Pharm. Sci.*, **59**, 53 (1970).
(5) K. B. Bischoff, R. L. Dedrick, D. S. Zaharko, and J. A. Longstreth, *ibid.*, **60**, 1128 (1971).
(6) K. B. Bischoff and R. L. Dedrick, *ibid.*, **57**, 1346 (1968).
(7) K. B. Bischoff and R. L. Dedrick, *Chem. Eng. Prog. Symp. Ser.*, **64**, 32 (1968).
(8) R. H. Smith, M. A. Brewster, J. A. MacDonald, and D. S. Thompson, *Clin. Chem.*, **24**, 1599 (1978).
(9) D. Shen and M. Gibaldi, *J. Pharm. Sci.*, **63**, 1698 (1974).
(10) L. S. Schanker, P. A. Nafpliotis, and J. M. Johnson, *J. Pharmacol. Exp. Ther.*, **133**, 325 (1961).
(11) H. M. Soloman and P. D. Zieve, *ibid.*, **155**, 112 (1967).
(12) G. T. Tucker, R. N. Boyes, P. O. Bridenbough, and D. C. Moore, *Anesthesiology*, **33**, 287 (1970).
(13) V. S. Sawinski and G. W. Rapp, *J. Dental Res.*, **42**, 1429 (1963).
(14) A. Goldstein, L. Aronaw, and S. M. Kalman, "The Basis of Pharmacology," 2nd ed., Wiley, New York, N.Y., 1974.
(15) B. B. Brodie, P. A. Lief, and R. Poet, *J. Pharmacol. Exp. Ther.*, **94**, 359 (1948).
(16) W. Kalow, *ibid.*, **104**, 122 (1952).
(17) N. Kvisselgaard and F. Moya, *Acta Anaesth. Scand.*, **5**, 1 (1961).
(18) L. B. Hersh, P. P. Raj, and D. Ohlweiler, *J. Pharmacol. Exp. Ther.*, **189**, 544 (1974).
(19) J. E. Usubiaga, F. Moya, J. A. Wikinski, R. Wikinski, and L. E. Usubiaga, *Br. J. Anaesth.*, **39**, 943 (1967).
(20) J. B. Keenaghan and R. N. Boyes, *J. Pharmacol. Exp. Ther.*, **180**, 454 (1972).
(21) J. Buchi and X. Perlia, "International Encyclopedia of Pharmacology and Therapeutics," sect. 8, vol. 1, Pergamon, Elmsford, N.Y., 1971, chaps. 1, 2, 5, 39.
(22) W. S. Spector, "Handbook of Biological Data," Saunders, Philadelphia, Pa., 1956.
(23) C. Sung and A. P. Truant, *J. Pharmacol. Exp. Ther.*, **112**, 432 (1954).
(24) A. P. Truant and B. Takman, *Anesth. Anal.*, **38**, 478 (1959).
(25) W. W. Mapleson, *J. Appl. Physiol.*, **18**, 197 (1963).

Myoinositol Uptake by Rat Hepatocytes *In Vitro*

CHI-PO CHEN ˣ and VAN T. VU

Received November 27, 1978, from the *Section of Pharmacology and Toxicology, School of Pharmacy, University of Connecticut, Storrs, CT 06268.* Accepted for publication February 12, 1979.

Abstract □ Myoinositol uptake by rat hepatocytes *in vitro* was studied. Adult rat hepatocytes were prepared by digestion of the perfused liver with collagenase. Cell suspensions were incubated with tritium-labeled myoinositol in pH 7.4 Krebs bicarbonate solution containing 1% gelatin at 37°. ^{14}C-Carbon-labeled polyethylene glycol was used as a marker of adherent extracellular fluid volume. Myoinositol uptake was demonstrable after 5 min of incubation, but no intracellular concentration in excess of that in the incubation medium was observed after 60 min of incubation. Uptake saturation over a wide myoinositol concentration range could not be demonstrated. Neither the omission of sodium ions nor the inclusion of ouabain suppressed the distribution ratio significantly. Metabolic inhibitors and lower temperatures also showed no effect. Hexoses, phlorizin or mannitol, exerted no observable effect on myoinositol uptake. The results indicated that myoinositol uptake by rat hepatocytes is probably a passive process.

Keyphrases □ Myoinositol—uptake by hepatocytes, *in vitro*, rats, pharmacokinetics □ Hepatocytes—myoinositol uptake, pharmacokinetics, *in vitro*, rats □ Liver—myoinositol uptake, *in vitro*, pharmacokinetics, rats

The liver plays a predominant role in lipid metabolism. Under normal conditions, the influx of nonesterified fatty acids into the liver from the serum is counterbalanced by the formation of lipoprotein, which is transported back to the blood. The whole process requires myoinositol. In myoinositol-deficient animals, fatty livers often can be observed since the rate of fatty acid transport to the liver from the adipose tissue exceeds the capacity of the liver to mobilize the lipid and to transport it back to the plasma (1, 2). The administration of myoinositol to myoinositol-deficient animals often can alleviate the fatty liver condition.

BACKGROUND

Myoinositol has long been considered to be a lipotropic agent because of its ability to prevent and remove fat deposits in the liver (3, 4). This lipotropic action is thought to be due to stimulation of hepatic transferable phosphatidylinositol synthesis. Once formed, the phosphorylated myoinositol can be utilized in β-lipoprotein production in the endoplasmic reticulum. The newly synthesized β-lipoprotein is transported from the liver to the blood (4). In addition, exogenous myoinositol inhibits any further deposition of either liver triglycerols or cholesterol and causes the removal of the lipids deposited during the myoinositol-deficiency period (5–7).

Although there is much evidence that myoinositol is transported into the small intestine (8), kidney (9–12), central nervous system (13–16), and crystalline lens (17–19) *via* a specific carrier-mediated system, hepatic uptake of myoinositol has not been studied in spite of its well-known lipotropic activity. Hauser (11) reported that the radioactive myoinositol distribution ratio in liver slices is less than one-half of the radioactivity in the incubation medium, while the hepatic myoinositol concentration *in vivo* is similar to that of plasma; higher hepatic than blood myoinositol concentrations also were observed (20, 21).

In recent years, the use of isolated hepatocytes for various biochemical and pharmacological studies has gained wide acceptance (22). Studies with isolated liver cells can clarify certain molecular aspects of the transport system, such as binding and metabolism, while cellular integrity is maintained.

The purpose of this study was to investigate hepatic myoinositol uptake using liver cells freshly isolated from normal adult rats.

EXPERIMENTAL

Male rats[1], 200–300 g, were housed in groups in wire-bottomed cages in an air-conditioned room (23°). They received regular laboratory chow and water without restriction.

The methods of liver perfusion and cell isolation were described previously (23, 24). Cell viability was determined by the exclusion of 0.2% trypan blue from the cells and was frequently checked by incubating the cells with α-aminoisobutyric acid, which is actively accumulated by the hepatocytes (23). Cell pellets, following the final wash of the isolation procedure, were resuspended in 10 volumes of pH 7.4 Krebs–Ringer bicarbonate buffer containing 1% gelatin.

Uptake studies were performed by placing 5 ml of the final cell suspension (50–80 mg wet weight/ml of suspension) into 25-ml plastic erlenmeyer flasks. Under control conditions, the cell suspensions contained a trace amount of [2-^{3}H(N)]-myoinositol[2] (3 μCi/nmole/100 ml of suspension) with or without 0.1 μmole of nonlabeled myoinositol/ml. In

[1] Charles River Breeding Laboratory, Wilmington, Mass.
[2] New England Nuclear Corp., Boston, Mass.

0022-3549/79/0800-1022$01.00/0
© *1979, American Pharmaceutical Association*

Table I—Time Course of Myoinositol Uptake as the Distribution Ratio between Intracellular Fluid and Medium [a]

Minutes	Nonlabeled Myoinositol (*M*)	
	0	1×10^{-4}
5	0.66 ± 0.04	0.92 ± 0.08
15	0.83 ± 0.09	0.89 ± 0.11
30	0.90 ± 0.09	0.96 ± 0.18
45	1.24 ± 0.20	—
60	1.10 ± 0.16	1.06 ± 0.04
90	1.14 ± 0.20	0.91 ± 0.14

[a] Hepatocytes were incubated at 37°. Incubations were terminated at different times. Values are means ± *SD* ($n = 4$).

experiments with a sodium-free medium, tromethamine buffer[3] was used and sodium chloride was replaced by tromethamine chloride (23, 24). The flasks were shaken in a metabolic shaker at 37° under an atmosphere of 95% O_2–5% CO_2 for various times.

At the end of the incubation period, 1 ml of the cell suspension was removed, placed into a preweighed microcentrifuge tube[4], and centrifuged for 30 sec in a microcentrifuge[5]. The supernate was removed, and the tube was weighed. The cell pellets were resuspended in 150 μl of distilled water, transferred into an 8-ml counting vial, and digested at room temperature with 0.5 ml of tissue solubilizer[6] for 16–24 hr or until a clear solution was obtained. Absolute methanol, 250 μl, was added with mixing, and then 5 ml of scintillation cocktail[7] was added.

An aliquot of the supernate was placed into an 8-ml scintillation vial containing 6 ml of scintillation fluid[8]. The extracellular aqueous volume was determined by incubating hepatocytes in the presence of ^{14}C-polyethylene glycol[2] for varying times. The ^{14}C- and ^{3}H-radioactivity was measured in a liquid scintillation counter[9] using methods for double-isotope counting that correct for quenching and ^{14}C-activity appearing in the ^{3}H-channel. Results were corrected on this basis to account for extracellular myoinositol trapping. The distribution ratio (I/M) is referred to as the ratio of intracellular to medium (or extracellular) concentrations.

The extent of macromolecular myoinositol binding was estimated by the following procedures. At the end of 5 and 60 min of incubation, 10 ml of cell suspension was centrifuged at 1000 rpm[10] for 1 min; the supernate was removed by pipet. The cell pellets were washed with 10 volumes of ice-cold Krebs bicarbonate buffer, resuspended in an equal volume of 0.05 *M* phosphate buffer (pH 7.2), and sonicated. Then 0.5 ml of the cell extract was placed on a 0.9 × 8-cm column[11], equilibrated with 0.05 *M* phosphate buffer (pH 7.2), and eluted with the same buffer. One-half-milliliter fractions were collected and counted in 6 ml of scintillation fluid.

Formation of myoinositol metabolites during the transport process was tested by TLC using an acetone–water (9:1) solvent system (25). The sonicated solution was deproteinized with five volumes of absolute

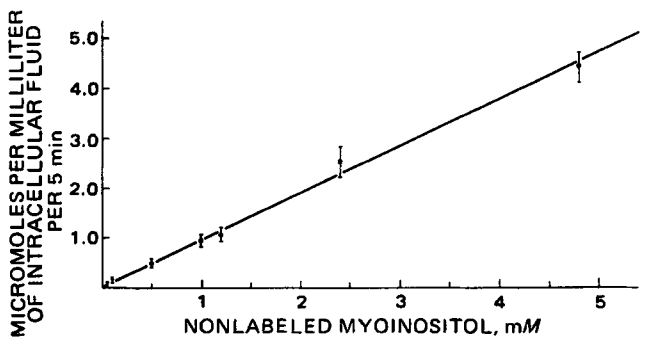

Figure 1—*Effect of myoinositol concentration on 5-min in vitro myoinositol uptake into hepatocytes. Data are expressed as means* ± SD. *Each point is the mean of four determinations.*

[3] Tris(hydroxymethyl)aminomethane, Sigma Chemical Co., St. Louis, Mo.
[4] Brinkmann Instruments, Westbury, N.Y.
[5] Centrifuge 3200, Brinkmann Instruments, Westbury, N.Y.
[6] Unisol, Isolab, Akron, Ohio.
[7] Unisol-complement, Isolab, Akron, Ohio.
[8] Scintisol, Isolab, Akron, Ohio.
[9] Model 3375, Packard Instrument Co., Chicago, Ill.
[10] Sorval GLC-1, Dupont Instruments, Newtown, Conn.
[11] Bio-Gel P-2, Bio-Rad Laboratories, Richmond, Calif.

Table II—Effect of Inhibitors Added *In Vitro* on Myoinositol Uptake [a]

Inhibitor	Concentration, *M*	Percent of Control
None	—	100.0 ± 6.1 [b]
Sodium free	—	98.0 ± 12.2
Ouabain	1×10^{-4}	103.3 ± 2.1
2,4-Dinitrophenol	1×10^{-4}	107.7 ± 25.5
Potassium cyanide	1×10^{-3}	95.1 ± 6.1
	5×10^{-3}	100.0 ± 6.1
N-Ethylmaleimide	1×10^{-4}	93.9 ± 2.4

[a] Hepatocytes were incubated at 37° for 30 min in the presence of various inhibitors or the omission of sodium. [b] Each value is expressed as the mean ± *SD* from three to four determinations. All values were not significantly different from the control ($p > 0.05$).

methanol. The methanol solution was concentrated under an air stream and placed on the instant thin-layer plate[12] (5 × 20 cm). After development, the nonsprayed chromatogram was cut into strips (1 cm wide), and the radioactivity of each strip was measured by counting it with 6 ml of scintillation fluid. Authentic myoinositol was cochromatographed with all samples tested.

RESULTS

When isolated liver cells were incubated under normal conditions with radioactive myoinositol, the initial uptake rate was rapid. Uptake was demonstrable after 5 min of incubation; however, the entry rate decreased over time (Table I). Equilibrium was reached after 30 min of incubation, and further incubation did not increase the intracellular myoinositol concentration. When 0.1 m*M* of nonlabeled myoinositol was added to the incubation medium, the initial entry rate increased significantly while the distribution ratio remained unchanged after prolonged incubation.

The concentration dependence of myoinositol uptake also was investigated. There was no evidence of uptake saturation over a wide myoinositol concentration range (0.1–4.8 m*M*) (Fig. 1).

To test whether hepatic myoinositol uptake is energy dependent, isolated hypatocytes were incubated in the presence of various metabolic inhibitors. Myoinositol uptake was not altered significantly by such inhibitors (Table II).

The specificity of myoinositol uptake by isolated liver cells also was examined. The addition of glucose or galactose (5 m*M*) did not appreciably affect the distribution ratio (Table III). Similarly, phlorizin (0.1 m*M*) or mannitol (5 m*M*) produced no measurable effect on myoinositol uptake.

The extent of myoinositol and tissue binding is depicted in Fig. 2.

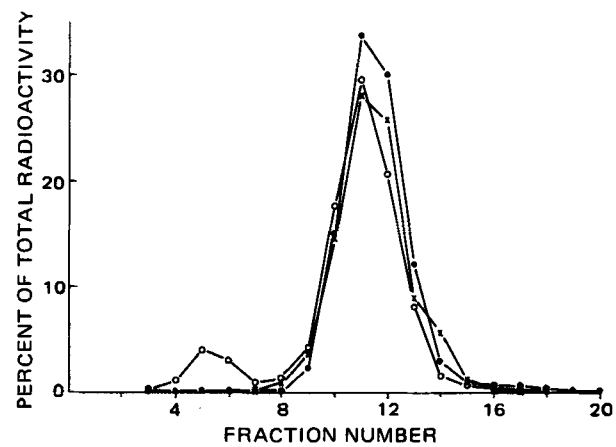

Figure 2—*Chromatographic identification of free and bound myoinositol. Radioactivity found in the aqueous hepatocyte extract after 5 and 60 min of incubation with labeled myoinositol was chromatographed on 0.9 × 8-cm Bio-Gel P-2 columns equilibrated with 0.05* M *phosphate buffer (pH 7.2) and eluted with the same solvent. Authentic ^{3}H-myoinositol was cochromatographed as a control. Key:* ●, *myoinositol standard;* ×, *after 5 min; and* ○, *after 60 min.*

[12] Gelman Instrument Co., Ann Arbor, Mich.

Table III—Effects of Sugars and Analogs on the Myoinositol Uptake [a]

Addition	Concentration, M	I/M [b]	Percent of Control
None	—	0.91 ± 0.04	100.0 ± 4.4
Glucose	5×10^{-3}	0.95 ± 0.22	104.4 ± 24.2
Galactose	5×10^{-3}	0.79 ± 0.19	86.8 ± 20.9
Mannitol	5×10^{-3}	0.91 ± 0.07	100.0 ± 7.7
Phlorizin	1×10^{-4}	0.81 ± 0.17	89.0 ± 18.7

[a] Hepatocytes were incubated with 1×10^{-4} M myoinositol at 37° for 30 min in the presence of various agents. [b] Distribution ratio between intracellular and medium concentration. Each value is the mean of four determinations with the standard deviation. All values were not significantly different from the control ($p > 0.05$).

Cellular extracts were chromatographed on small columns. Only a small portion of the transported molecules was associated with the cellular macromolecules while most myoinositol existed in a free state. Some metabolic myoinositol alterations apparently took place during the experimental period (Fig. 3).

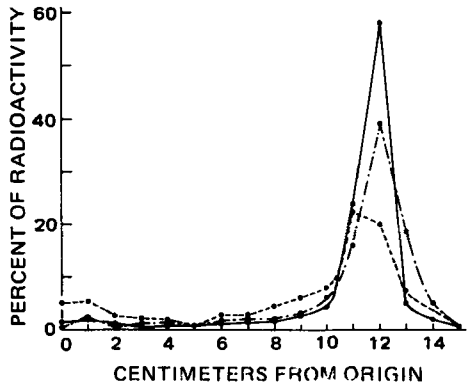

Figure 3—*Chromatographic identification of myoinositol and its metabolites. The aqueous hepatocyte extracts after 20 (●---●) and 30 (●---●) min of incubation with labeled myoinositol were chromatographed on thin-layer plates with an acetone–water (9:1) solvent system. Authentic myoinositol was cochromatographed as a control (●—●).*

DISCUSSION

Although numerous studies demonstrated that isolated rat liver cells can transport various substances into the cellular compartment by a specific carrier-mediated process (22–24), the present study indicated that myoinositol probably enters the hepatocytes by a nonenergy-requiring, noncarrier-mediated process. The nature of hepatic myoinositol uptake appeared to be different from the transport systems for myoinositol in various biological systems (8–19, 26–31).

The failure of hepatocytes to establish a concentration gradient after prolonged incubation demonstrated that hepatic myoinositol uptake is not cumulative. Although demonstrable amounts of intracellular myoinositol were observed after 5 min of incubation, the distribution ratio (I/M) rose slowly with time and reached unity after 30 min of incubation. The I/M ratio remained around one throughout the experimental period. Addition of nonlabeled myoinositol (0.1 mM) did not change the distribution ratio significantly. The absence of saturation kinetics (Fig. 2) in the present study suggested a passive diffusion process.

Myoinositol uptake also was not dependent on metabolic energy. As shown in Table II, inclusion of an uncoupling agent (2,4-dinitrophenol), a cellular respiration poison (potassium cyanide), or sulfhydryl blocking agents (iodoacetic acid and N-ethylmaleimide) in the incubation medium did not cause any significant inhibition. Likewise, ouabain, a "sodium-pump" inhibitor, also showed no effect. Replacement of sodium ions also did not inhibit cellular myoinositol uptake.

The competitive inhibition of hexoses and phlorizin on the transport of myoinositol has been reported in various biological systems (8, 10, 13, 16, 18). The present experiment (Table III), which demonstrated that hepatic myoinositol uptake was not inhibited by monosaccharides or a sugar-carrier inhibitor (phlorizin), also strongly suggests that hepatic myoinositol uptake is not a carrier-mediated process.

Although myoinositol plays an important role in lipoprotein formation in experimental animals (5–7), the present study could not demonstrate significant myoinositol binding to hepatocyte macromolecules, nor was myoinositol metabolized significantly during the experimental periods. There are similar findings in the choroid plexus (13, 16) and the crystalline lens (17).

The results obtained with ouabain, sodium-free medium, metabolic inhibitors, and a lack of saturation all lead to the suggestion that myoinositol uptake into the hepatic parenchymal cells is probably by a passive mechanism.

REFERENCES

(1) E. Hayashi, T. Maeda, and T. Tomita, *Biochim. Biophys. Acta*, **360**, 134 (1974).

(2) *Ibid.*, **360**, 146 (1974).

(3) E. R. Weidlein, Jr., "The Biochemistry of Inositol," Mellon Institute, Pittsburgh, Pa., 1951, chap. 7.

(4) T. Posternak, "The Cyclitols," Holden-Day, San Francisco, Calif., 1965, chap. 16.

(5) K. Yagi and A. Kotaki, *Ann. N.Y. Acad. Sci.*, **165**, 710 (1969).

(6) I. Nishigaki, S. H. Hasan, A. Kotaki, K. Yagi, S. Okuyama, S. Ito, K. Yamada, and K. Yamashita, *J. Vitaminol. (Tokyo)*, **17**, 112 (1971).

(7) S. H. Hasan, Y. Nakagana, I. Nishigaki, and K. Yagi, *ibid.*, **17**, 159 (1971).

(8) W. F. Caspary and R. K. Crane, *Biochim. Biophys. Acta*, **203**, 308 (1970).

(9) G. Hauser, *Biochem. Biophys. Res. Commun.*, **19**, 696 (1965).

(10) G. Hauser, *Biochim. Biophys. Acta*, **173**, 257 (1969).

(11) *Ibid.*, **173**, 267 (1969).

(12) G. Hauser, *Ann. N.Y. Acad. Sci.*, **165**, 630 (1969).

(13) C. P. Chen, Ph.D. dissertation, University of Kentucky, Lexington, Ky., 1973.

(14) R. Spector and A. V. Lorenzo, *Am. J. Physiol.*, **228**, 1510 (1975).

(15) R. Spector, *J. Neurochem.*, **27**, 229 (1976).

(16) T. Z. Csaky, in "Intestinal Permeation," M. Kramer and F. Lauterbach, Eds., Excerpta Medica, Amsterdam, The Netherlands, 1977, p. 209.

(17) E. Cotlier, *Invest. Ophthalmol.*, **9**, 681 (1970).

(18) V. N. Reddy, S. D. Varma, and B. Chakrapani, *ibid.*, **9**, 785 (1970).

(19) S. D. Varma, B. Chakrapani, and V. N. Reddy, *ibid.*, **9**, 794 (1970).

(20) G. Hauser and V. N. Fenelli, *J. Biol. Chem.*, **238**, 3224 (1963).

(21) L. M. Lewin, Y. Y. S. Sulimovici, and P. F. Kracier, *Biochem. J.*, **156**, 375 (1976).

(22) H. A. Krebs, in "Use of Isolated Liver Cells and Kidney Tubules in Metabolic Studies," J. M. Tager, H. D. Soling, and J. R. Williamson, Eds., North-Holland Publishing, Amsterdam, The Netherlands, 1976, p. 465.

(23) C. P. Chen and R. H. Lee, *Life Sci.*, **21**, 577 (1977).

(24) C. P. Chen, *J. Nutr. Sci. Vitaminol.*, **24**, 351 (1978).

(25) M. K. Gaitonde and M. Griffiths, *Anal. Biochem.*, **15**, 532 (1966).

(26) R. M. Johnstone and C. P. Sung, *Biochim. Biophys. Acta*, **135**, 1052 (1967).

(27) J. Deshusses and G. Reber, *ibid.*, **274**, 598 (1972).

(28) J. Deshusses, *Experientia*, **30**, 996 (1974).

(29) J. Deshusses and G. Reber, *Eur. J. Biochem.*, **72**, 87 (1977).

(30) *Ibid.*, **72**, 101 (1977).

(31) G. Reber, M. Belet, and J. Deshusses, *J. Bacteriol.*, **131**, 872 (1977).

ACKNOWLEDGMENTS

Presented in part at the Basic Pharmaceutics Section, APhA Academy of Pharmaceutical Sciences, Montreal meeting, May 1978.

Supported by Grant 35-252 from the University of Connecticut Research Foundation.

Binding of Mono- and Bis-*N*-substituted Benzoquinolinium Halides to Butyrylcholinesterase: Fluorescence Measurements

WEN-SHERNG CHEN, GEORGE H. COCOLAS ˣ, and CHESTER J. CAVALLITO

Received October 23, 1978, from the *Division of Medicinal Chemistry, School of Pharmacy, University of North Carolina at Chapel Hill, Chapel Hill, NC 27514.* Accepted for publication February 13, 1979.

Abstract □ The dissociation constants (K_{diss}) of mono- and bis-*N*-substituted benzoquinolinium salts from butyrylcholinesterase were determined by the disappearance of the fluorescence of the free ligand. The K_{diss} value determined by this method agreed closely with the dissociation constants ($K_{I,s}$) of the free enzyme obtained by steady-state kinetic studies. The results indicate that the *N*-substituted benzoquinolinium salts with a strong binding ability to butyrylcholinesterase also are potent inhibitors of the esterolytic properties of the enzyme. Enzyme binding is favored by the coplanar structure and does not require a high concentration of charge on the onium function. The shape of the hydrophobic structures markedly influences binding.

Keyphrases □ Benzoquinolinium halides—binding to butyrylcholinesterase, spectrophotofluorometric analysis □ Spectrophotofluorometry—analysis, benzoquinolinium halides, binding to butyrylcholinesterase □ Butyrylcholinesterase—binding to benzoquinolinium halides, spectrophotofluorometric analysis

A series of mono- and bisquaternary ammonium compounds was reported (1) to be reversible inhibitors of butyrylcholinesterase. The most potent inhibitors were characterized by a large nitrogen-containing conjugated heterocycle such as phenanthridine or acridine. Lineweaver–Burk plots of the enzymatic hydrolysis data showed mixed competitive–noncompetitive inhibition kinetics. Since many potential binding sites are present on the enzyme (2), these mono- and bisquaternary onium compounds were studied to determine if their anticholinesterase activity was produced by binding to sites that affect the esterolytic properties of the enzyme.

EXPERIMENTAL

Horse serum butyrylcholinesterase[1] was purified by gel filtration, using a Sephadex G-200 column (2 × 90 cm) developed with pH 7.5 25 m*M* sodium phosphate, and by ion-exchange chromatography, using a diethylaminoethyl cellulose column (2 × 85 cm) developed with a 1-liter linear gradient of 1.0 *M* NaCl in pH 7.5 25 m*M* sodium phosphate. Protein concentrations (milligrams per milliliter) were determined by the method of Lowry *et al.* (3). Enzyme activities were measured by the continuous automatic titration method, using a pH stat (1). The butyrylcholinesterase solution normality was determined by a titration method using echothiophate iodide (4).

Table I—Quenching of Hexamethylene-1,6-bisacridinium Diiodide (50 n*M*) Fluorescence by Butyrylcholinesterase

E, N	F	$F_0 - F$	α	$10^{-8} I$, M	R	$10^8 R/I$
0	40 (F_0)					
5.5×10^{-9}	37.0	3.0	0.1	4.50	0.91	0.20
2.0×10^{-8}	29.8	10.2	0.34	3.30	0.85	0.26
3.8×10^{-8}	24.0	16.0	0.53	2.35	0.70	0.30
5.5×10^{-8}	18.7	21.3	0.71	1.45	0.65	0.45
7.5×10^{-8}	16.3	23.7	0.79	1.05	0.53	0.51
1.1×10^{-7}	13.3	26.7	0.89	0.55	0.40	0.73
2.5×10^{-7}	11.2	28.8	0.96	0.20	0.19	0.95
4.5×10^{-7}	10.6	29.4	0.98	0.10	0.11	1.10
1.1×10^{-6}	10 (F_e)	30.0				

[1] Worthington Biochemical Corp.

Inhibitors were prepared as described previously (1). The inhibitors, butyrylcholinesterase, and bovine serum albumin were dissolved in 10 m*M* sodium phosphate buffer containing 100 m*M* NaCl and 20 m*M* $MgCl_2$. The enzyme solution was diluted to give concentrations of 50 μN–5.5 n*N*. For the fluorescence measurements, each solution was mixed with an equal volume of inhibitor solution whose concentration was near its $K_{I,s}$ value. UV absorption spectra of the inhibitor solutions (5 μM) in the presence of varying amounts of butyrylcholinesterase or bovine serum albumin were measured on a double-beam spectrophotometer[2].

Disappearance of the fluorescence of the inhibitors in the presence of butyrylcholinesterase or bovine serum albumin was measured on a spectrophotofluorometer[3] equipped with a 150-w xenon lamp and a 1P 21 photomultiplier tube. Excitation at 360 nm caused fluorescence maxima of *N*-substituted acridinium halides at 490 nm, of phenanthridinium halides at 420 nm, of 5,6-benzoquinolinium halides at 440 nm, and of 7,8-benzoquinolinium halides at 460 nm. Fluorescence intensity measurements were made at 25° and were reproducible within 0.5%.

The disappearance of the fluorescence spectra of benzoquinolinium salts in the presence of butyrylcholinesterase was used to determine the dissociation constants (K_{diss}) of the enzyme–benzoquinolinium salt complex. The binding to butyrylcholinesterase or bovine serum albumin can be expressed according to Scatchard *et al.* (5) by:

$$\frac{R}{[I]} = \frac{n}{K_{diss}} - \frac{R}{K_{diss}} \qquad \text{(Eq. 1)}$$

where R is the number of inhibitor molecules bound per subunit (equivalent to 1 mole of echothiophate iodide) of butyrylcholinesterase or per molecule of bovine serum albumin at a free inhibitor concentration, $[I]$, and n is the number of binding sites on a butyrylcholinesterase subunit or a bovine serum albumin molecule. Both R and $[I]$ were determined by utilizing the disappearance of inhibitor fluorescence intensities while being bound by butyrylcholinesterase (6, 7).

The relative intensities, F, of the fluorescence inhibitor were determined for a series of enzyme and inhibitor mixtures of different compositions containing a constant total inhibitor concentration. The expressions for the relative fluorescence intensities in the absence and in an excess of butyrylcholinesterase are $F_0 = r[I]_t$ and $F_e = r'[I]_t$, respectively; $[I]_t$ is the total inhibitor concentration, r is the intensity coefficient of the free inhibitor, and r' is the intensity coefficient of the bound inhibitor (EI) whose concentration is equal to the total free inhibitor concentration when an excess of enzyme is added. It is assumed that all inhibitor molecules are bound in the presence of excess enzyme.

The relative fluorescence intensity of butyrylcholinesterase is much less than that of the inhibitor itself and can be neglected while making enzyme blank measurements. Thus, relative fluorescence at varying butyrylcholinesterase concentrations is expressed by $F = r[I] + r'[EI]$. The fraction of total inhibitor bound, α, is expressed by:

$$\alpha = \frac{F_0 - F}{F_0 - F_e} = \frac{r[I]_t - r[I] - r'[EI]}{r[I]_t - r'[I]_t} = \frac{[EI]}{[I]_t} \qquad \text{(Eq. 2)}$$

The free inhibitor concentration is expressed by:

$$[I] = [I]_t(1 - \alpha) \qquad \text{(Eq. 3)}$$

and if $[E]_t$ is the amount of butyrylcholinesterase used, then:

$$R = \frac{[EI]}{[E]_t} = \frac{\alpha[I]_t}{[E]_t} \qquad \text{(Eq. 4)}$$

Data for the disappearance of the fluorescence of hexamethylene-1,6-bisacridinium diiodide (I) in the presence of butyrylcholinesterase are shown in Table I. The K_{diss} value is the reciprocal value of the Scatchard

[2] Model 15, Cary Instrument Co.
[3] Aminco-Bowman.

0022-3549/79/0800-1025$01.00/0
© 1979, American Pharmaceutical Association

Table II—Binding of Some Quaternary Ammonium Salts to Butyrylcholinesterase

	Compound	Butyrylcholinesterase K_{diss}, μM	Butyrylcholinesterase $K_{I,s}$, μM[a]
I[b]	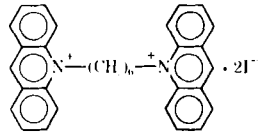	0.0083 ± 0.0002[c]	0.0073 ± 0.0002
II	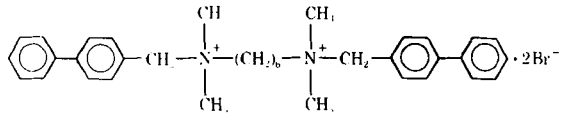	2.01 ± 0.06[d]	1.5 ± 0.2
III	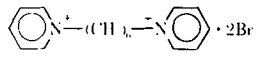	210 ± 40[d]	120 ± 10
IV[b]	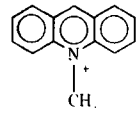	0.14 ± 0.04[c]	0.24 ± 0.03
V	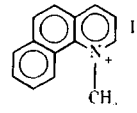	21 ± 3[c]	32 ± 1
VI	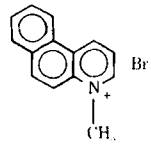	6.7 ± 0.5[c]	5.4 ± 0.2
VII	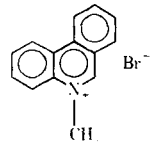	1.2 ± 0.5[c]	1.10 ± 0.02

[a] Determined by steady-state enzyme kinetic studies (1). [b] The K_{diss} values of I and IV *versus* bovine serum albumin, determined by the disappearance of the free ligand fluorescence, were 15 ± 4 and 87 ± 5 μM, respectively. [c] Determined by the disappearance of the free ligand fluorescence. [d] Determined by a fluorescence probe technique (8).

plot slope of $R/[I]$ *versus* R (Fig. 1) and was calculated by fitting the values of $R/[I]$ and R to the least-squares computer program.

The same procedure was used for measuring the binding of the nonfluorescent inhibitor, hexamethylene-1,6-bis-*p*-phenylbenzyl ammonium dibromide (II), with butyrylcholinesterase by the addition of a fluorescent probe (A) such as I (1). The dissociation constant (K_B) of the nonfluorescent inhibitor (B) which competes with A for sites on the enzyme can be determined according to a literature method (8) and expressed by:

$$K_B = (K_A)\left(\frac{\alpha}{1-\alpha}\right)\left(\frac{[B]_t - S}{S}\right) \qquad \text{(Eq. 5)}$$

where K_A is the dissociation constant of the fluorescent probe, $[B]_t$ is the total concentration of the nonfluorescent inhibitor, and S is the bound nonfluorescent inhibitor in moles per liter. The value of S can be calculated by:

$$S = n[E]_t - \alpha[A]_t - \frac{\alpha K_A}{1-\alpha} \qquad \text{(Eq. 6)}$$

where $[A]_t$ is the total fluorescent probe concentration. A Scatchard plot for the probe–enzyme complex in the presence of a nonfluorescent inhibitor is shown in Fig. 2.

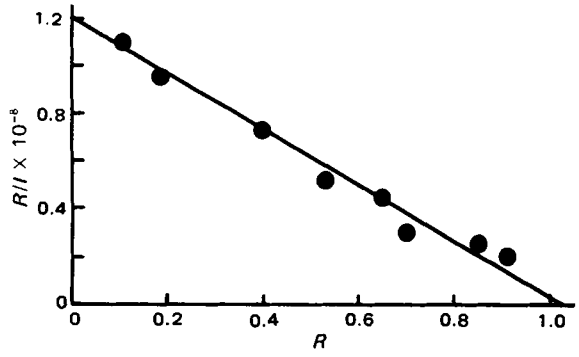

Figure 1—*Scatchard plot for I (50 nM) binding to various concentrations (5.5 nN–1.1 μN) of butyrylcholinesterase by spectrofluorometry.*

RESULTS AND DISCUSSION

The addition of butyrylcholinesterase to aqueous solutions of mono- and bisquaternary ammonium salts that are potent reversible enzyme inhibitors caused a hypochromic shift in their UV spectrum. The UV absorbance of a 5 μM solution of I was altered from maxima at 251 and 258 nm to a single maximum at 253 nm with a decrease of the extinction coefficient as the butyrylcholinesterase concentration was increased from 2.2 to 18 μN (Fig. 3). Similar mixtures of I solutions and bovine serum albumin in concentrations from 0.29 to 72 μM did not cause any significant change in the UV absorption spectrum of I. The acridinium compound spectral changes, which occurred following enzyme addition but not following addition of the same or even higher bovine serum albumin concentrations, suggest a specific and extensive binding by the inhibitor to butyrylcholinesterase.

Dissociation constants (K_{diss}) of mono- and bisonium salts complexed with butyrylcholinesterase were measured by disappearance of the heterocyclic moiety fluorescence spectra in the presence of butyrylcholinesterase (Table II). The K_{diss} of I from butyrylcholinesterase was 8.3 ± 0.2 nM and compared favorably with the inhibition constant ($K_{I,s}$ = 7.3 ± 0.2 nM) determined by the kinetics of the hydrolysis rate inhibition under Michaelis–Menten conditions (1). The dissociation constant of I from bovine serum albumin determined by free ligand fluorescence disappearance showed less affinity by at least 10^3.

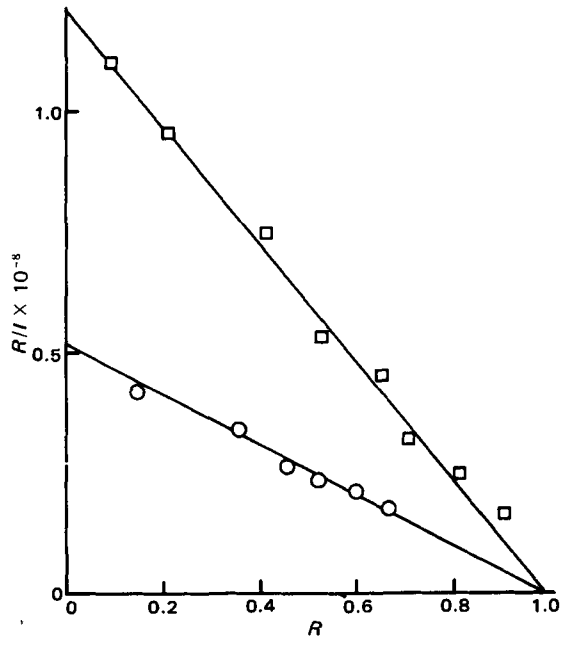

Figure 2—*Scatchard plots for the probe-enzyme complex of I (50 nM) and varying concentrations (5.5 nN–1.1 μN) of butyrylcholinesterase in the absence (□) and presence (○) of hexamethylene-1,6-bisbiphenyl ammonium dibromide (1.0 μM).*

N-Methylacridinium (IV) had a smaller binding affinity than I for butyrylcholinesterase when calculated from fluorescence measurements ($K_{diss} = 0.14 \pm 0.04\ \mu M$) or enzyme kinetic data ($K_{I,s} = 0.24 \pm 0.03\ \mu M$). Binding of IV to bovine serum albumin was also weaker than that of I. The additional acridinium moiety in I undoubtedly contributes to the stronger binding properties on both butyrylcholinesterase and bovine serum albumin. Since butyrylcholinesterase has a single anionic site at the active center (9–12), the enhancement of the binding force of the bis compound to both butyrylcholinesterase and bovine serum albumin could result from the hydrophobic binding of the additional onium moiety to the hydrophobic area adjacent to the anionic site of the enzyme.

The other *N*-methyl benzoquinolinium salts, 7,8-benzoquinolinium (V), 5,6-benzoquinolinium (VI), and 3,4-benzoquinolinium (VII), gave K_{diss} values that were comparable to the $K_{I,s}$ values obtained from enzyme kinetic data. A parallel can be seen between the data from the dissociation constants as determined by fluorescence measurements and by enzyme kinetics. All compounds appeared to bind in a similar manner to the enzyme with binding energies depending on their lipophilic and steric properties. The Scatchard plots showed that both mono- and bis-*N*-substituted benzoquinolinium compounds bound stoichiometrically to the enzyme (*i.e.*, one molecule of inhibitor bound per subunit of enzyme). The esterolytic function was affected proportionately to the intensity of inhibitor binding.

Among these compounds, the onium group probably serves primarily as a carrier to deliver the hydrophobic structure to the active site. The positive charge in these heterocyclic structures may be delocalized by either internal resonance or pseudobase formation (1). Together with the hydrophobic nature of the hydrocarbon mass and the lack of hydrogen bonding substituents, these compounds would be unfavorable to solvation but would probably influence the structure of neighboring water, either in bulk solution or as the inhibitor–enzyme complex.

The effects of hydrocarbon-substituted ammonium salts on water structure were reported to vary with the hydrophobic mass of the substituents, the concentration, and the temperature (13–16). It would be

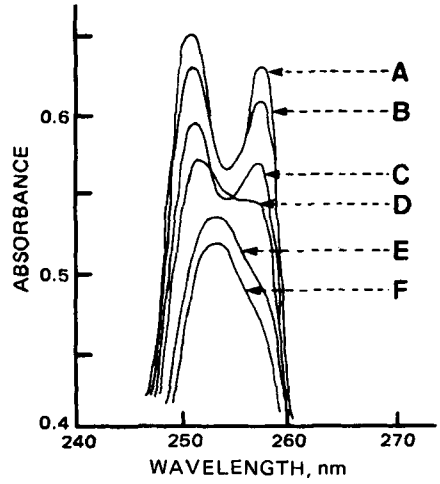

Figure 3—*Hypochromic effect of the UV spectra of I (5.0 μM) in the presence of different butyrylcholinesterase concentrations: A, 0; B, 2.3 μN; C, 4.6 μN; D, 9.2 μN; E, 14 μN; and F, 18 μN.*

of interest to determine the effect of structure of these isomeric monoquaternaries on the structure of the surrounding water. The hydrophobic mass structure may contribute to potency by influencing the difficulty with which other molecules and ions in solution can displace the inhibitor from the inhibitor–enzyme complex.

REFERENCES

(1) W. S. Chen, G. H. Cocolas, C. J. Cavallito, and K. J. Chai, *J. Med. Chem.*, **20**, 1617 (1977).

(2) K. B. Augustinsson, *Handb. Exp. Pharmakol.*, **15**, 89 (1963).

(3) O. H. Lowry, N. J. Rosebrough, A. L. Farr, and R. J. Randall, *J. Biol. Chem.*, **193**, 265 (1951).

(4) L. E. Tammelin, *Acta Chem. Scand.*, **11**, 1340 (1957).

(5) G. Scatchard, J. S. Coleman, and A. L. Shen, *J. Am. Chem. Soc.*, **79**, 12 (1957).

(6) G. Mooser, H. Schulman, and D. S. Sigman, *Biochemistry*, **11**, 1595 (1972).

(7) A. R. Peacocke and J. N. H. Skerrett, *Trans. Faraday Soc.*, **52**, 261 (1956).

(8) I. M. Klotz, H. Triwush, and F. M. Walker, *J. Am. Chem. Soc.*, **70**, 2935 (1948).

(9) D. H. Adams and V. P. Whittaker, *Biochim. Biophys. Acta*, **4**, 543 (1950).

(10) F. Bergman, *Discuss. Faraday Soc.*, **20**, 126 (1955).

(11) K. B. Augustisson, *Biochim. Biophys. Acta*, **128**, 351 (1966).

(12) M. T. Kabachnik, A. P. Brestkin, N. M. Godovikov, J. J. Michelson, E. V. Rozengart, and V. I. Rozengart, *Pharmacol. Rev.*, **22**, 355 (1970).

(13) A. De Trobriand, M. Ceccaldi, M. Henry, M. M. Manning-Rousselot, and M. Lucas, *C.R. Acad. Sci., Ser. C*, **274**, 919 (1972).

(14) M. Lucas and A. De Trobriand, *ibid.*, **274**, 1757 (1972).

(15) K. Schwabe, *Croat. Chem. Acta*, **44**, 27 (1972); through *Chem. Abstr.*, **77**, 39808j (1972).

(16) M. C. R. Symons, *Philos. Trans. R. Soc. London, Ser. B*, **272**, 13 (1975).

ACKNOWLEDGMENTS

Supported in part by U.S. Public Health Service Grant NS-09088.

The authors thank Ayerst Laboratories for supplying the echothiophate iodide.

Osmolality of Parenteral Solutions

H. E. HUBER ˣ, WILLIAM H. STRENG, and HETTY G. H. TAN

Received June 19, 1978, from *Merrell-National Laboratories, Division of Richardson-Merrell Inc., Cincinnati, OH 45215.* Accepted for publication February 14, 1979.

Abstract □ Osmolality–concentration profiles for individual and mixed solute systems are presented. Linear relationships between osmolality and concentration held true in all systems examined at concentrations below 0.2 molal levels. At higher concentrations, linearity existed only in select systems. Deviations from linearity can be greater or less than extrapolated values. In view of the need to determine an osmolarity conversion factor for each parenteral formulation and the many errors possible in the use of these values, adoption of osmolality values for labeling parenteral products rather than osmolarity, as stipulated in USP XIX–NF XIV third supplement, is strongly recommended.

Keyphrases □ Osmolality—parenteral solutions, compared to osmolarity, calculations □ Osmolarity—parenteral solutions, compared to osmolality, calculations □ Parenteral solutions—osmolality and osmolarity compared, calculations

Use of the terms osmolality and osmolarity was once confined largely to clinical laboratories and hospital pharmacies; however, the terms are now being applied to parenteral solutions. The third supplement of USP XIX–NF XIV (1) requires that pharmacopeial solutions providing intravenous replenishment of fluid, nutrients, or electrolytes, as well as the osmotic diuretic mannitol injection, state the osmolar concentration.

These terms are not familiar to many; and with the compendial requirements for labeling, it seems appropriate to discuss them at length. The purposes of this manuscript are to review the important theoretical considerations of osmolality and osmolarity and to present a few experimentally obtained osmolality–concentration profiles to illustrate the interrelation of some representative solutes utilized in parenteral formulas. This information serves as a basis for a recommendation on parenteral labeling.

BACKGROUND

Labeling—In 1975, USP XIX required sodium chloride injection labeling to state the total osmolarity of the solution, expressed in milliosmoles per liter. Since label components of a quantitative nature usually require some analytical method to demonstrate the label claim within limits, it was considered reasonable to determine what production experience would show in lot-to-lot variation.

As some investigators discovered, instrumentation measures the osmolality of a solution, milliosmoles per kilogram of solvent, not the osmolarity, milliosmoles per liter of solution. To be precise for labeling purposes, a search was undertaken for a mathematical expression to relate these two entities. Little was found in the literature or textbooks to equate these two terms. The problems in this area were recognized previously and reviewed at length (2). Previous investigators also attempted to equate the two expressions to resolve the problem and pointed out that solution measurements can be carried out only in terms of osmolality. In the physical chemistry discipline, osmolality is used and is well defined in terms of basic concepts. In pharmaceutical practice, a definition of osmolarity has been developed, but a derivation of the basic relationship between osmolality and osmolarity was not found.

Streng *et al.* (3) carried out this mathematical exercise and determined that osmolarity was not measurable as a defined parameter. The conversion of osmolality measurements to osmolarity requires determination of the partial molal volume of the solute(s) at infinite dilution and the density of the pure solvent. In simple one-solute aqueous systems, this determination is not difficult, and a single conversion factor can be determined for all concentrations. For more complex systems such as hyperalimentation fluids, conversion factor determination becomes more complex and questionable.

The alternative to such a dilemma would be to label the products in osmolality terms, directly measurable by instrumentation, provided the concentrations are within the 100–2000-milliosmoles/kg range usually measurable with commercially available osmometers.

Osmolarity Calculations—Pharmacists over the years have used gravimetric measurements for solids and volumetric measurements for liquids. The preparation of solutions by weighing the liquid occurs primarily in industry. This practice of bringing solutions to volume rather than using a specific solvent weight has led to the term osmolarity.

Although one cannot measure osmolarity (osmoles or milliosmoles per liter of solution), it is commonly assumed the numerical values do not differ significantly from those of osmolality (milliosmoles per kilogram of solvent) and that the two can be used interchangeably. This assumption may be reasonable in some cases. However, these terms must be fully understood so that they can be used correctly and, perhaps, interchangeably where the error is negligible or insignificant.

Calculations in the pharmaceutical literature that utilize osmolality or osmolarity values assume that the values change in direct proportion to the change in solute(s) concentration. The literature also teaches that the osmolality/osmolarity values for individual solute systems can be used

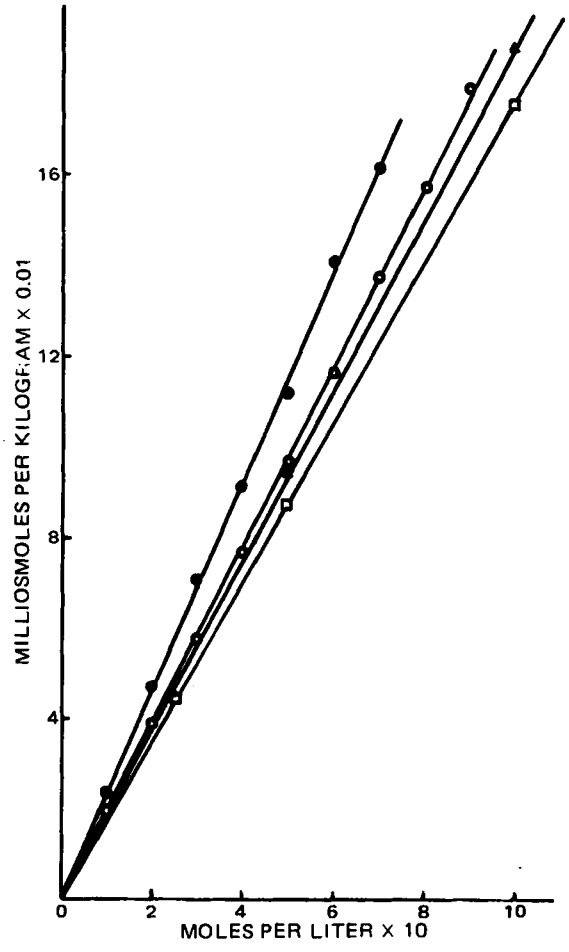

Figure 1—*Osmolality–molar concentration profiles of sodium chloride (△), potassium chloride (□), sodium acetate (○), and sodium tartrate (●) aqueous solutions.*

0022-3549/79/0800-1028$01.00/0
© 1979, American Pharmaceutical Association

Table I—Osmotic Coefficients for Sodium Chloride and Calcium Chloride Aqueous Solutions at 25°

Molal Concentration (m)	Molar Concentration (M^a)		Osmotic Coefficient at 25° (φ^{25})		Osmolality, mOs/kg	
	Sodium Chloride	Calcium Chloride	Sodium Chloride	Calcium Chloride	Sodium Chloride	Calcium Chloride
0.100	0.098	0.098	0.9324	0.854	186.5	256.2
0.200	0.196	0.197	0.9245	0.862	369.8	517.2
0.300	0.294	0.296	0.9215	0.876	552.9	788.4
0.400	0.391	0.394	0.9203	0.894	736.2	1072
0.500	0.488	0.494	0.9209	0.917	920	1375
0.600	0.587	0.592	0.9230	0.940	1109	1692
0.700	0.685	0.690	0.9257	0.963	1295	2022
0.800	0.783	0.786	0.9288	0.988	1486	2371
0.900	0.881	0.880	0.9320	1.017	1677	2745
1.000	0.978	0.974	0.9355	1.046	1871	3138

[a] Calculated from $m = 1000 \times M/C_w$. The C_w values were obtained from Ref. 6.

additively to calculate the value for a solution containing two or more solutes.

In reality, few solutions exhibit a linear relationship between osmolality and concentration except in dilute solutions, and the linear concentration range varies from one substance to another. The assumption of an additive property was tested and found to hold for all solutions tested at less than 0.2 molal concentrations. The results constitute the following experimental section.

Basic Principles—Before proceeding further, a review of basic principles should be extended to clarify the terminology. A solution can be characterized by what is referred to in physical chemistry as its colligative properties: (*a*) freezing point, (*b*) boiling point, (*c*) vapor pressure, and (*d*) osmotic pressure. All of these measurable parameters are related to the same physical property: the ratio of solute "particles" to molecules of water or mole fraction of water.

Osmolality is defined as that mass of solute which, when dissolved in 1 kg of water, will exert an osmotic pressure equal to that exerted by a gram-molecular weight of an ideal unionized substance dissolved in 1 kg of water. Osmolarity is defined as that mass of solute which, when dissolved in 1 liter of solution, will exert an osmotic pressure equal to that exerted by a gram-molecular weight of an ideal unionized substance dissolved in 1 liter of solution.

From the derivations of Streng *et al.* (3), osmolality can be described by:

$$\xi_m = \nu m \varphi \frac{\bar{v}_1^0}{\bar{v}_1} \qquad \text{(Eq. 1)}$$

where:

ξ_m = osmolality
ν = number of ions into which the solute theoretically dissociates
m = molality of the solution
φ = osmotic coefficient
$\frac{\bar{v}_1^0}{\bar{v}_1}$ = ratio of the partial molal volumes for the solvent at infinite dilution and in the solution

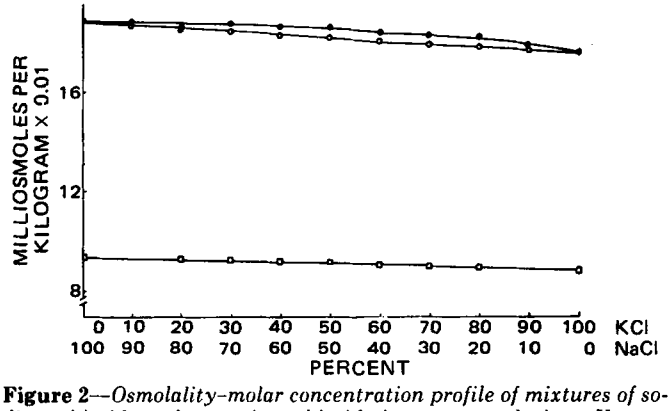

Figure 2—*Osmolality-molar concentration profile of mixtures of sodium chloride and potassium chloride in aqueous solutions. Key:* ●, *measured osmolality values for aqueous solutions containing a mixture of sodium chloride and potassium chloride totaling 1.0* M *concentrations;* O, *calculated osmolality values determined by summing values for each component at its respective concentration; and* □, *measured osmolality and calculated osmolality values for solutions containing mixtures of sodium chloride and potassium chloride at 0.5* M *total concentration.*

For the concentration ranges normally considered, the ratio $(\bar{v}_1^0/\bar{v}_1)$ has a value close to one[1].

Osmolarity is described by:

$$\xi_c = \nu m \varphi [d_1^0(1 - 0.001\bar{v}_2^0)] \qquad \text{(Eq. 2)}$$

where:

ξ_c = osmolarity
d_1^0 = density of the pure solvent
$\bar{v}_2^0$ = partial molal volume of the solute

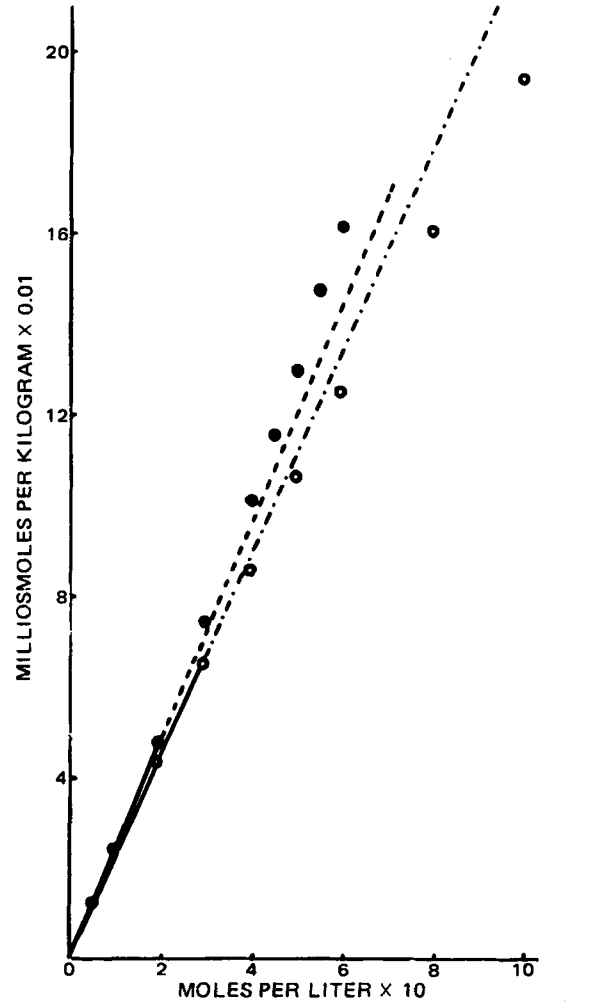

Figure 3—*Osmolality-molar concentration profile for aqueous solutions of calcium chloride* (●) *and sodium sulfate* (O).

[1] The ratio $(\bar{v}_1^0/\bar{v}_1)$ is dependent upon the solute system. There is, however, little difference in this ratio between simple salt solutions. Sodium chloride solution has a value of 1.001 for a 1 molal concentration.

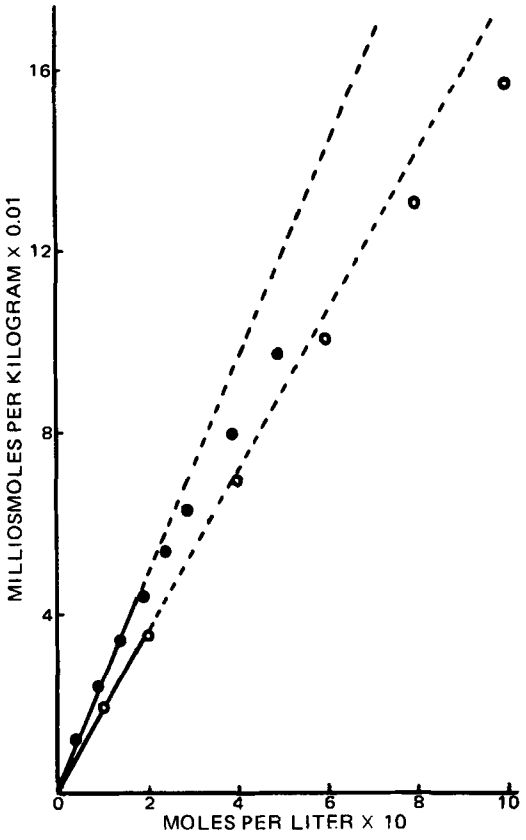

Figure 4—*Osmolality–molar concentration profile for aqueous solutions of dibasic sodium phosphate (●) and monobasic sodium phosphate (○).*

Thus, osmolarity can be calculated from osmolality measurements by:

$$\xi_c = \xi_m[d_1^0(1 - 0.001\bar{v}_2^0)] \qquad \text{(Eq. 3)}$$

The conversion factor $[d_1^0(1 - 0.001\bar{v}_2^0)]$ for sodium chloride solutions is 0.98049; for potassium chloride solutions, it is 0.97041(3).

Partial molal volumes are available in the literature for some solutes; however, for most pharmaceutical compounds, it is necessary to determine these values experimentally.

Table I shows the osmotic coefficients and osmolality values for sodium chloride and calcium chloride solutions taken from the literature (4).

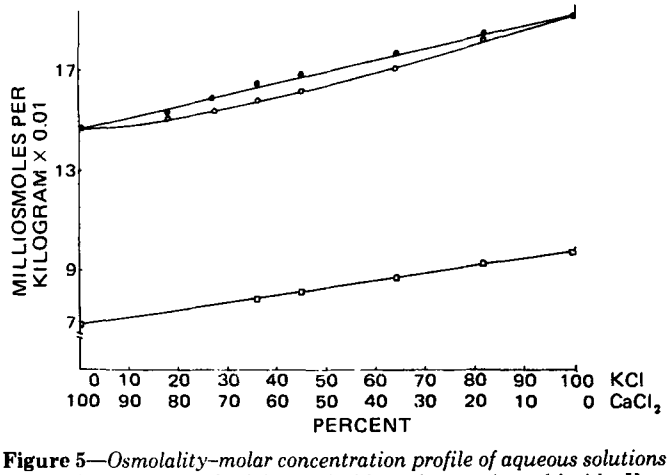

Figure 5—*Osmolality–molar concentration profile of aqueous solutions containing mixtures of calcium chloride and potassium chloride. Key: ○, measured osmolality values for mixtures of calcium chloride and potassium chloride totaling 1.1 M chloride concentration; ●, calculated osmolality values determined by summing values for each component at its respective concentration; and □, measured osmolality and calculated osmolality values for mixtures of calcium chloride and potassium chloride at 0.55 total chloride concentration.*

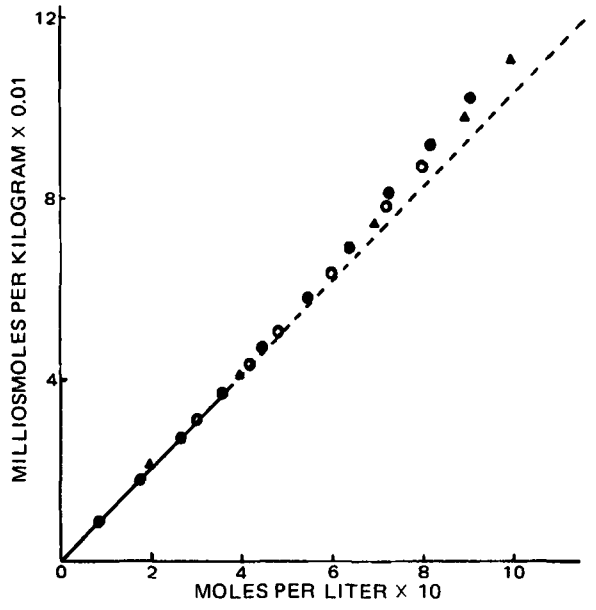

Figure 6—*Osmolality–molar concentration profiles for aqueous solutions of dextrose (●), mannitol (○), and sorbitol (△).*

Osmotic coefficients can be found in these tables for many electrolytes and for a few nonelectrolytes. However, coefficients for most pharmaceutical compounds need to be determined. Examination of Table I shows that deviation from linearity is small for sodium chloride in terms of milliosmoles per kilogram up to a 1.0 molal concentration. For calcium chloride solutions, the deviation becomes much greater. In the case of a twofold dilution of a 0.8 molal solution, the value is about 100 mOs/kg less than expected. For the same dilution with sodium chloride solution, the value is only 7 mOs/kg less than expected. A 0.9% sodium chloride solution is ~0.15 molal.

EXPERIMENTAL

Experiments were carried out to determine the extent of change in the osmolality as a function of concentration for various solutes and for mixtures of these solutes in aqueous solutions.

Solutions were prepared, in the usual manner, on a molar rather than molal basis; a concentration–osmolality profile was obtained for each solute as well as for solute combinations in aqueous solution. Any concentration representation could have been used, such as milligrams per milliliter or molality. All molar concentrations were calculated on an anhydrous basis.

A vapor pressure osmometer[2] was used to measure the osmolality (milliosmoles per kilogram) of each solution. Prior to use, the instrument was calibrated with the appropriate sodium chloride reference standard[3]. A minimum of three readings was taken for each solution, and the standard deviations fell well within the areas of the open or solid geometric forms used in the graphs.

Profiles of the experimental solutions for sodium chloride, potassium chloride, sodium acetate, calcium chloride, sodium sulfate, dibasic sodium phosphate, and monobasic sodium phosphate were checked against calculated profiles obtained by using the osmotic coefficients reported in the literature (4) for the solutes in solutions at 25° ($\xi_m = \nu m\varphi^{25}$). In all cases except calcium chloride, the experimental osmolality values did not differ significantly from the calculated values. For calcium chloride, the values were slightly less than expected, indicating that the material contained water and was not completely anhydrous. Due to the hygroscopic nature of anhydrous calcium chloride, this finding was not surprising.

Profiles for dextrose, mannitol, and sorbitol sugars were also determined. These compounds are used in parenterals and are representative of nonionizing substances. Similar profiles for some of these components were reported previously (2).

[2] Wescor, 5100.

[3] Reference standards were obtained from Wescor, Inc., and prepared by New England Reagent Laboratories (Rhode Island) on a molal basis according to Fiske (5).

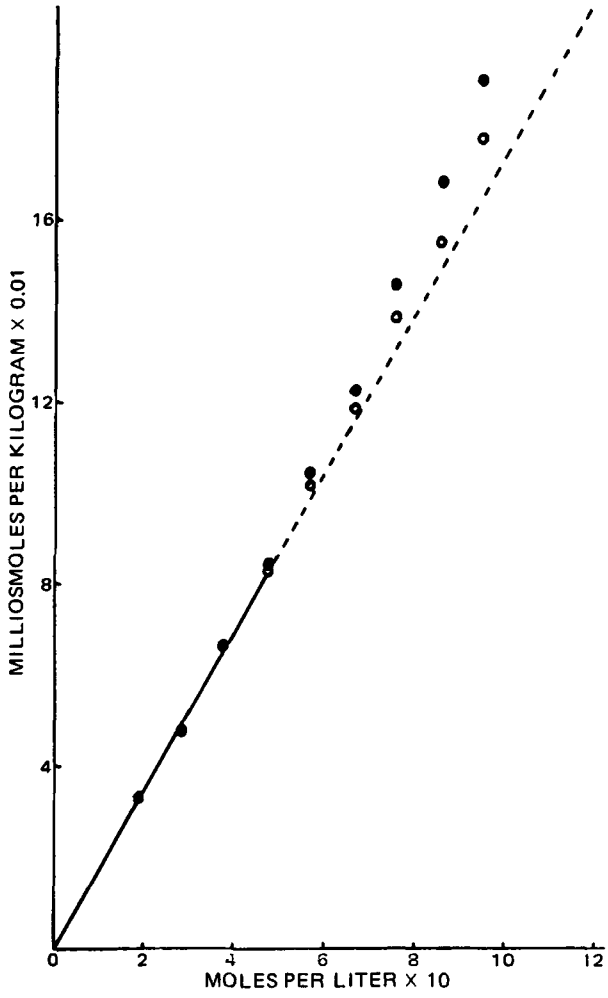

Figure 7—*Osmolality–molar concentration profile for aqueous solutions containing equal molar amounts of calcium chloride and dextrose. Key: ●, measured osmolality values for mixtures of calcium chloride and dextrose; and ○, calculated osmolality values determined by summing values for each component at its respective concentration.*

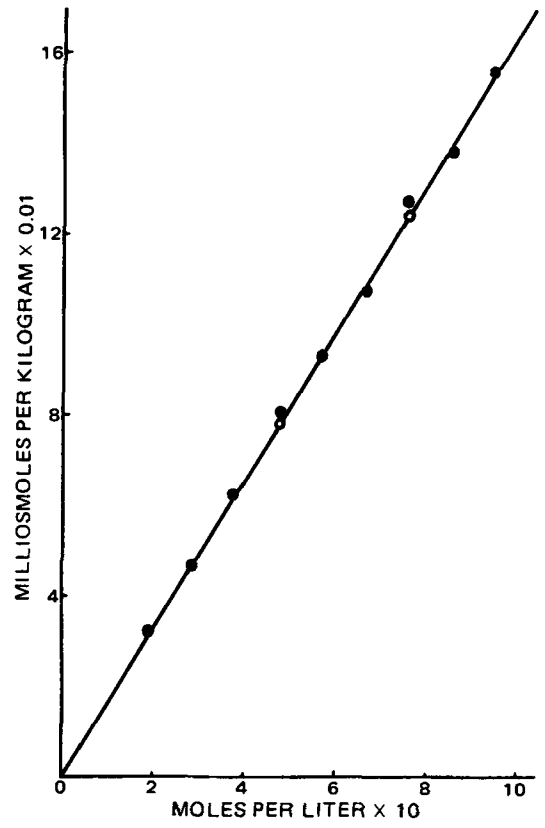

Figure 8—*Osmolality–molar concentration profile for aqueous solutions containing equal molar amounts of sodium sulfate and dextrose. Key: ●, measured osmolality values for mixtures of sodium sulfate and dextrose; and ○, calculated osmolality values determined by summing values for each component at its respective concentration.*

To determine the resulting osmolality values for combinations of these components, solutions with various compositions and concentrations were measured as a function of concentration. The values obtained were then compared to calculated values, assuming additive relationships for each component, as is common practice.

RESULTS

Monovalent Solutes—Figure 1 shows the approximately linear response between osmolality and concentration, up to 1.0 *M*, for sodium chloride, potassium chloride, sodium acetate, and sodium tartrate. Figure 2 shows the measured osmolality values for sodium chloride–potassium chloride mixtures made in different ratios at 1 *M* and diluted to 0.5 *M* total concentrations. The measured osmolality value for each mixture differed or agreed with the sum of the experimentally obtained values for each compound as shown. For the mixed salts at 1 *M* concentration, the values differed by as much as 50 mOs/kg in the region where ratios between 40:60 and 60:40 were used. Upon dilution to 0.5 *M*, these same solutions gave measured results identical to calculated values.

Polyvalent Solutes—Figure 3 shows the values obtained for calcium chloride and sodium sulfate. With calcium chloride, the osmotic coefficient values increased as the concentration increased from 0.1 to 1.0 molal; with sodium sulfate, the coefficient decreased over this same range. The result is a positive deviation (higher values) with increased concentration for calcium chloride solutions but negative deviation (lower values) with increased concentration for sodium sulfate solutions.

Figure 4 illustrates a negative deviation for the phosphate salt (dibasic sodium phosphate and monobasic sodium phosphate) solutions. Although not as obvious as in a plot using molal concentrations *versus* osmolality, the greater negative deviation from linearity of dibasic sodium phosphate solutions over monobasic sodium phosphate solutions is apparent since the number of ions, ν, for dibasic sodium phosphate is three and that for monobasic sodium phosphate is two.

Solutions containing mixtures of potassium chloride and calcium chloride in varying ratios to give 1.1 *M* chloride concentrations were studied in the same manner as potassium chloride and sodium chloride. The difference between the calculated and measured values for 1.1 *M* solutions can be seen in Fig. 5. Again, dilution to 0.55 *M* concentration gave the same calculated values as observed values.

Nonionic Sugar Solutes—Figure 6 shows the relationships obtained for the nonionizing sugars dextrose, mannitol, and sorbitol. All three showed a positive deviation from linearity above 0.4 *M* concentrations, and the osmolality values agreed very closely with each other for the same molar concentrations. For a point of comparison, a 5% dextrose solution is ~0.3 *M* and a 20% solution is ~1 *M*.

Solutions of Ionic and Nonionic Solutes—Finally, solutions prepared with an ionic salt and nonionic dextrose gave the results shown in Figs. 7–9. In the first experiment, calcium chloride and dextrose, both positive deviating solutes, were combined in solution to give the results shown in Fig. 7. A positive deviation greater than that calculated for the contribution of each solute was found for total concentrations above ~0.4 *M*.

Combination of the negatively deviating solute sodium sulfate with dextrose, a positively deviating solute, gave the results shown in Fig. 8. The calculated sum of the values from each single solute system was in close agreement with the measured values. In addition, combination of these two solutes in equal amounts resulted in a linear profile up to 1.0 *M* total concentration.

A combination of equal molar concentrations of sodium chloride and dextrose gave a linear response in total concentrations up to 0.9 *M* and a positive deviation at concentrations above 1 *M* (Fig. 9). For this combination, summation of the osmolality values obtained for each component was on the low side, and the error appeared to increase as the total concentration progressed above 1 *M*.

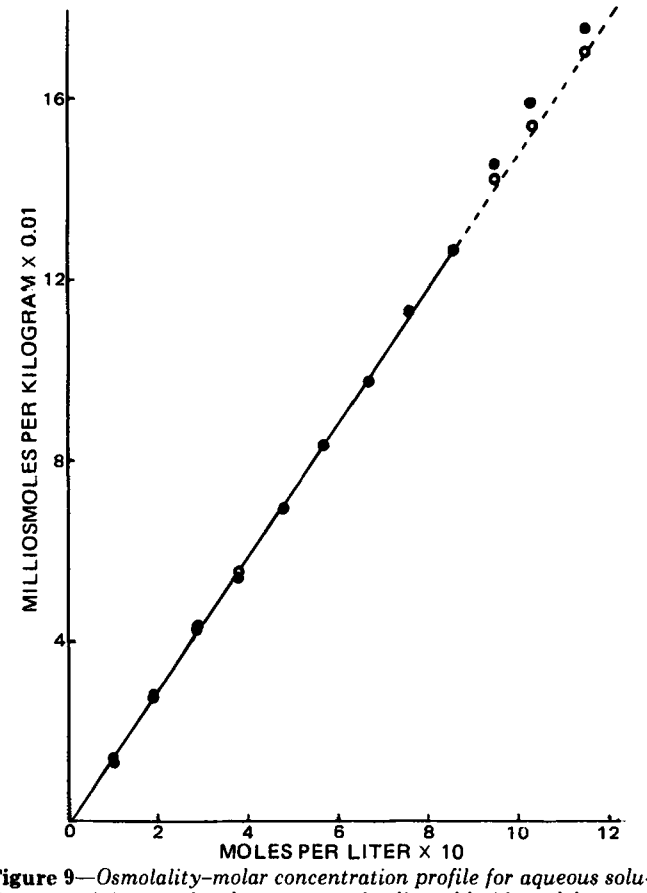

Figure 9—*Osmolality–molar concentration profile for aqueous solutions containing equal molar amounts of sodium chloride and dextrose. Key: ●, measured osmolality values for mixtures of sodium chloride and dextrose; and ○, calculated osmolality values determined by summing values for each component at its respective concentration.*

DISCUSSION

These studies demonstrated that the measured osmolality values for solute mixtures above 0.2–0.4 *M* concentrations differed from calculated values by amounts that were dependent on the total solute concentration and the specific combination of solutes. In general terms, if the osmolality of the solution exceeded 500–800 mOs/kg, a difference between measured and calculated values could be expected. The deviations also could be greater or less than calculated values, depending on the solutes.

Although these experiments were carried out with volumetrically formulated solutions, it would have been well to have used molal concentrations and weighed the solvent as well as the solutes. Recalculation of the molar solutions to molal equivalents in order to compare experimental results with literature values was tedious and not possible in some cases.

Measurement of solution colligative properties is based on the molal relationship; use of molar concentrations makes calculations more difficult or, possibly, incorrect if the molar concentration is assumed to be the same as a molal concentration. Although it may be more convenient to formulate by volumetric measurement, for accuracy and meaningful data interpretation, this practice should be abandoned when carrying out research in this area. There is also the added advantage of avoiding the errors introduced when incorrectly calibrated volumetric equipment is used or when the solution temperature is not controlled.

Based on these considerations, it is recommended that osmolality values be used in labeling parenteral products and that the term osmolarity be avoided. This practice would eliminate the need to determine a conversion factor for each parenteral system. In some cases, it may be impossible to calculate a conversion factor and only osmolality values can be obtained.

REFERENCES

(1) "The United States Pharmacopeia XIX and National Formulary XIV, 3rd Supplement," Mack Publishing Co., Easton, Pa., 1977, pp. 99, 131, 168, 169.

(2) B. S. R. Murty, J. N. Kapoor, and P. P. DeLuca, *Am. J. Hosp. Pharm.*, **33**, 546 (1976).

(3) W. H. Streng, H. E. Huber, and J. T. Carstensen, *J. Pharm. Sci.*, **67**, 384 (1978).

(4) R. A. Robinson and R. H. Stokes, "Electrolyte Solutions," 2nd ed. (rev.), Butterworths, London, England, 1970, pp. 476–478.

(5) R. B. Johnson and H. Hoch, in "Standard Methods of Clinical Chemistry," vol. 5, S. Meites, Ed., Academic, New York, N.Y., 1965, p. 159.

(6) "CRC Handbook of Chemistry and Physics," 49th ed., Chemical Rubber Co., Cleveland, Ohio, 1968.

Nuclear-Substituted Styryl Ketone Analogs: Effects on Neoplasms, Microorganisms, and Mitochondrial Respiration of Tumorous and Normal Cells

J. R. DIMMOCK ˣ, N. W. HAMON, L. M. NOBLE, and D. E. WRIGHT

Received October 31, 1978, from the *College of Pharmacy, University of Saskatchewan, Saskatoon, Saskatchewan, Canada, S7N 0W0.* Accepted for publication February 15, 1979.

Abstract □ Analogs of some antineoplastic and cytotoxic Mannich bases derived from conjugated styryl ketones were prepared and evaluated for activity in the P-388 lymphocytic leukemia screen. Most of the new compounds had lower antineoplastic and murine toxicity than the parent compounds. Antimicrobial evaluation of some oximes and alcohols related to the Mannich bases revealed activity against certain Gram-positive bacteria and fungi. Primary pharmacological evaluation showed that some compounds containing a dimethylaminomethyl group displayed analgesic and antihistaminic properties. Five of the Mannich bases were evaluated as respiratory inhibitors in mitochondria derived from hepatic tumors, liver tissue from tumor-bearing animals, and normal rat liver. No statistical difference between the sensitivity of the three tissues to the compounds was obtained.

Keyphrases □ Styryl ketones, nuclear substituted—effects on neoplasms, microorganisms, mitochondrial respiration in normal and tumor cells, structure–activity relationships □ Antineoplastic agents, potential—nuclear-substituted styryl ketones, effects on neoplasms, microorganisms, mitochondrial respiration in normal and tumor cells, structure–activity relationships □ Mitochondria—effect of nuclear-substituted styryl ketones on respiration, normal and tumor cells □ Mannich bases—derivatives, effects on neoplasms, microorganisms, mitochondrial respiration in normal and tumor cells, structure–activity relationships

Numerous Mannich bases derived from conjugated styryl ketones (I) have shown promising levels of antineoplastic activity accompanied by murine toxicity (1). The activity of these compounds is due, in part at least, to interference with mitochondrial function (2); examination of the effect of representative compounds on the electron transport chain of rat liver cells showed that competition with coenzyme Q_{10} is an important site of action (3). In addition, various studies revealed that Mannich bases have antimicrobial activity (4–7) as well as other bioactivities (8, 9), including analgesia in both Mannich bases (10) and their derivatives (11).

BACKGROUND

The aim of the present investigation was twofold. First, a study was contemplated involving a systematic modification of the lead compounds (I) to see if antineoplastic activity could be retained while toxicity was diminished. The assessment of the new derivatives for other bioactivities was also of interest. Second, this study compared the effects of representative Mannich bases on the mitochondrial electron transport chain derived from normal rat liver cells and from hepatomas. A structure–activity relationship to antineoplastic activity would permit the rational design of novel anticancer agents.

The modification of the Mannich bases (Ia–If) was through systematic alterations of the basic center, then of the lipophilic pentamethylene chain, and finally of the carbonyl group. Reaction of Ic and If with methyl iodide produced IIa and IIb, which are quaternary ammonium salts, representatives of which are known to cause lysis of cytoplasmic membranes (12). Furthermore, the addition of one bulky group onto the quadrivalent nitrogen atom (IIa and IIb) may reduce absorption onto serum proteins (13).

The activity of certain Mannich bases may be due to deamination to the corresponding conjugated carbonylene (14, 15), and thus IIc and IId may be breakdown products of the precursor derivatives Ic, If, IIa, and IIb *in vivo*. A comparison of the antitumor efficacies of these six compounds may allow certain conclusions about the active species. Compounds IIc and IId, while retaining the conjugated styryl ketone function permitting biological alkylation to occur (16–18), were expected to have considerably lower aqueous solubility than the precursor compounds. By contrast, Mannich bases IIIa and IIIb, in which the lipophilic pentamethylene chain of Ia had been removed, were predicted to have greater aqueous solubility than Ia. Recently, the biological activity of α,β-unsaturated ketones has been attributed partially to a judicious balance between their hydrophilic and hydrophobic portions (19).

The final series of alkylating agents related to I involved ketone modification. Oximes may be ketone prodrugs (20), and the formation of IVa and IVb might allow selective release of the precursor ketones in tumorous tissue due to the acid lability of oximes (21); the claim has been made that the extracellular fluid of certain tumors is more acidic than

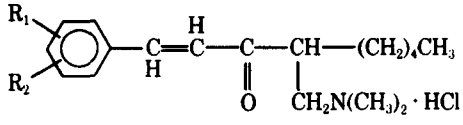

Ia: $R_1 = R_2 = H$
Ib: R_1 = 2-Cl, $R_2 = H$
Ic: R_1 = 4-Cl, $R_2 = H$
Id: R_1 = 2-Cl, R_2 = 4-Cl
Ie: R_1 = 2-Cl, R_2 = 6-Cl
If: R_1 = 3-Cl, R_2 = 4-Cl

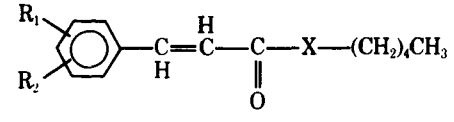

IIa: R_1 = 4-Cl, $R_2 = H$, X = $CH(CH_2\overset{+}{N}(CH_3)_3\ \bar{I})$
IIb: R_1 = 3-Cl, R_2 = 4-Cl, X = $CH(CH_2\overset{+}{N}(CH_3)_3\ \bar{I})$
IIc: R_1 = 4-Cl, $R_2 = H$, X = 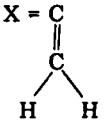
IId: R_1 = 3-Cl, R_2 = 4-Cl, X = 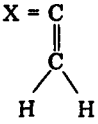

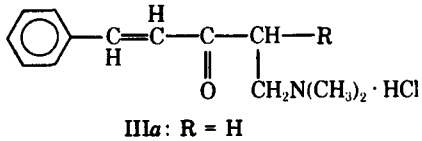

IIIa: R = H
IIIb: R = CH_3

0022-3549/79/0800-1033$01.00/0
© 1979, American Pharmaceutical Association

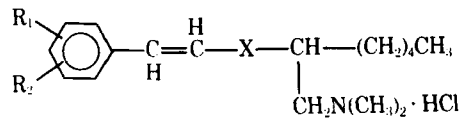

IV*a*: R_1 = 2-Cl, R_2 = H, X = C(=NOH)

IV*b*: R_1 = 3-Cl, R_2 = 4-Cl, X = C(=NOH)

IV*c*: R_1 = 2-Cl, R_2 = H, X = CH(OH)
IV*d*: R_1 = 4-Cl, R_2 = H, X = CH(OH)
IV*e*: R_1 = 2-Cl, R_2 = 4-Cl, X = CH(OH)
IV*f*: R_1 = 3-Cl, R_2 = 4-Cl, X = CH(OH)

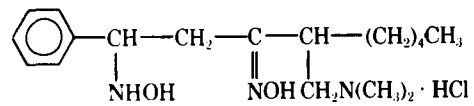

V

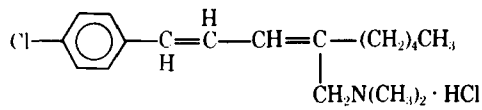

VI

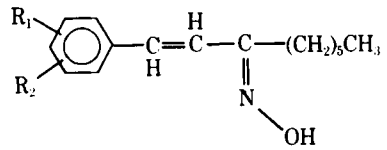

VII*a*: R_1 = R_2 = H
VII*b*: R_1 = 2-Cl, R_2 = H
VII*c*: R_1 = 4-Cl, R_2 = H
VII*d*: R_1 = 2-Cl, R_2 = 6-Cl
VII*e*: R_1 = 3-Cl, R_2 = 4-Cl
VII*f*: R_1 = 4-N(CH$_3$)$_2$, R_2 = H

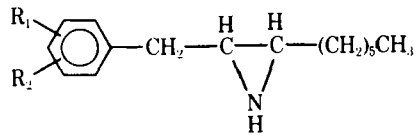

VIII*a*: R_1 = R_2 = H
VIII*b*: R_1 = 2-Cl, R_2 = H
VIII*c*: R_1 = 4-Cl, R_2 = H
VIII*d*: R_1 = 3-Cl, R_2 = 4-Cl

normal extracellular fluid (22, 23). In addition, an oxime derived from an α,β-unsaturated ketone had a ninefold increase in aqueous solubility over the precursor ketone (24). Reduction of the Mannich base ketone function would produce the substituted allyl alcohols IV*c*–IV*f*, expected to have alkylating properties due to the stability of the carbonium ion. In the case of these aryl-substituted alcohols, the carbonium ion would be expected to be further destabilized by delocalization of the positive charge on the ring. The murine toxicity of I may be associated with the dimethylaminomethyl function. Hence, nitrogenous analogs of conjugated styryl ketones that were not Mannich bases, were synthesized, namely the oximes VII as well as the aziridines VIII, representatives of which have displayed anticancer activities (25).

The second phase of the investigation involved comparing the effects of certain compounds on mitochondria derived from normal and from tumorous cells. Since the Mannich bases I*a* and I*d*–I*f* interfere with certain processes in the hepatocyte mitochondrial electron transport chain (3), an experimental rat hepatoma model was sought in which to examine the effects of these compounds on mitochondria from nontumorous tissue from normal and tumor-bearing rats.

Since 1960, various Morris hepatomas have become available (26). The 5123 TCH hepatoma chosen has a high mitochondria titer and is a highly differentiated stable growing tumor with an intermediate growth rate. This hepatoma grows in the pelvic region of the Buffalo rat strain, and the tumors develop within 4–5 weeks. Thus, by isolating the mitochondria from these three sources, the effects of I*a*, I*d*–I*f*, and III*a* in the presence of various substrates may permit conclusions about a mitochondrial sensitivity to the cytotoxic and antineoplastic Mannich bases.

RESULTS AND DISCUSSION

The first phase involved the synthesis and screening of derivatives I–VIII. In these compounds, the olefinic double bond of the styryl group was shown by ^{1}H-NMR and IR spectroscopy to have the (*E*)-configuration; ^{1}H and ^{13}C-NMR spectroscopy revealed that allyl alcohols IV*c* and IV*e* had the *threo*-configuration, while IV*f* was a 60:40 mixture of *erythro*- and *threo*-isomers. Purification of IV*d* led to the isolation of the *threo*-isomer (IV*d'*). After considerable difficulty, a small quantity of the *erythro*-isomer (IV*d"*) was isolated as the maleate salt. In the reaction between I*a* and hydroxylamine, the only product isolated was the hydroxylamino derivative, V. An attempt was made to form the IV*d* phosphate ester since the claim has been made that certain cancers contain high phosphatase (27). However, the product showed that IV*d* dehydration had occurred, producing the diolefin VI. NMR spectroscopy (100 MHz) showed that the aziridines VIII had the *cis*-configuration.

The activity of I–VIII against P-388 lymphocytic leukemia and their murine toxicity is summarized in Table I. The Mannich bases (I) increased the survival time in mice by an average 18%, and the related

Table I—Evaluation against P-388 Lymphocytic Leukemia and Murine Toxicity of Some Conjugated Styrenoid Ketones and Related Compounds

Compound	Maximum Increase in Mean Survival Time (dose in milligrams per kilogram)[a]	Murine Toxicity of Compound (dose in milligrams per kilogram)[b]	KB[c]
I*a*	105 (100)	0 (200), 6 (100)	1.5
I*b*	104 (6.25)	0 (200), 5 (100), 6 (50)	5.1
I*c*	113 (50)	0 (100), 6 (50)	1.7
I*d*	130 (18)	0 (200), 2 (100), 6 (50)	1.0
I*e*	115 (28)	2 (100), 6 (50)	2.8
I*f*	142 (6.25)	0 (55), 1 (35), 6 (12.5)	1.2
II*a*	113 (6.25)	0 (200), 4 (100), 6 (50)	2.1
II*b*	119 (12.5)	0 (200), 3 (50), 6(25)	—
II*c*	118 (400)	6 (200)	2.3
II*d*	109 (50)	0 (100), 6 (50)	5.0
III*a*	108 (50)	0 (200), 2 (100), 6 (50)	11
III*b*	109 (37.5)	0 (170), 3 (115), 6 (75)	1.2
IV*a*	112 (100)	2 (200), 6 (100)	—
IV*b*	116 (50)	1 (200), 5 (100), 6 (50)	—
IV*c*	117 (50)	0 (200), 3 (100), 6 (50)	3.2
IV*d'*	127 (25)	6 (50)[d]	2.6
IV*d"*	112 (25)	6 (50)[e]	2.5
IV*e*	108 (12.5)	0 (100), 5 (50), 6 (25)	—
IV*f*	109 (12.5)	0 (100), 3 (50), 6 (25)	—
V	106 (50)	2 (200), 6 (100)	—
VI	111 (50)	1 (200), 6 (100)	—
VII*a*	122 (50)	6 (200)	—
VII*b*	105 (200)	5 (200), 6 (100)	—
VII*c*	108 (100)	6 (200)	—
VII*d*	118 (400)	6 (400)	—
VII*e*	120 (200)	6 (200)	—
VII*f*	93 (100)	6 (400)	—
VIII*a*	115 (4.5)	0 (100), 5 (18), 6 (9)	—

[a] Figures are the ratios of the survival times of treated animals to those of control animals, expressed as a percentage. A compound is considered to be active if it increases the mean survival time by 25%. The data for I*d*–I*f* and III*b* are from Ref. 1 and are reproduced with permission of the copyright owner. [b] The murine toxicity of the compound is measured by the number of survivors out of six on the 5th day after the dosage schedule commenced. The data for Compounds I*a*, I*b* (200- and 100-mg/kg doses), I*d*–I*f*, II*a* (200- and 100-mg/kg doses), II*c*, III*b*, and IV*c* are from Ref. 1, and the data for II*d* (50-mg/kg dose) are from Ref. 2. These results are reproduced with permission of the copyright owner. [c] The figures, in micrograms per milliliter, in the KB cell culture screen indicate the dose inhibiting 50% of the growth of human epidermoid carcinoma of the nasopharynx in Eagle's medium. A compound is considered to be active if it inhibits 50% of the growth of this tumor at a concentration of 4 μg/ml. The data for I*c*–I*f*, II*a*, II*c*, III*b*, and IV*c* are from Ref. 1, and the result for III*a* is from Ref. 2. This information is reproduced with permission of the copyright owner. [d] The maximum dose administered with this compound was 50 mg/kg. [e] At 400 mg/kg, there were no deaths when the compound was administered twice on Days 2 and 6 to three animals.

Table II—Antimicrobial Evaluations of Some Oximes and Alcohols Derived from Conjugated Styryl Ketones [a]

Organism	IV*a*	IV*b*	IV*d'*	IV*e*	VII*a*	VII*b*	VII*c*	VII*d*	VII*e*	VII*f*
Escherichia coli (ATCC 8739)	>500	>500	>500	>500	>500	>500	>500	>500	>500	>500
Pseudomonas aeruginosa (ATCC 10145)	>500	>500	>500	>500	>500	>500	>500	>500	>500	>500
Klebsiella pneumoniae (ATCC 4352)	<100	<100	<100	<100	>500	>500	>500	>500	>500	>500
Haemophilus influenzae (ATCC 19418)	—	—	—	—	>500	>500	>500	—	>500	—
Staphylococcus aureus (ATCC 6538)	<100	<100	<100	<100	10	10	>500	<100	>500	>500
Streptococcus pyogenes (hospital isolate)	—	—	—	—	100	10	>500	—	>500	—
Streptococcus pneumoniae (ATCC 6303)	—	—	—	—	>500	10	>500	—	>500	—
Streptococcus faecalis (ATCC 8030)	<100	<100	<100	<100	100	10	250	<100	>500	>500
Bacillus subtilis (ATCC 6633)	<100	<100	<100	<100	10	10	10	<100	>500	>500
Salmonella typhimurium (G46)	<100	>500	>500	>500	>500	>500	>500	>500	>500	>500
Bordetella bronchiseptica (ATCC 4617)	<100	<100	<500	<100	—	—	—	>500	—	>500
Trichophyton mentagrophytes (ATCC 9533)	>500	<100	<100	<100	>500	>500	>500	<100	>500	<500
Microsporum gypseum (ATCC 14683)	>500	<100	<100	<100	>500	>500	>500	<100	>500	<500
Aspergillus niger (ATCC 10535)	>500	<500	<500	<500	>500	>500	>500	>500	>500	>500
Candida albicans (ATCC 10231)	>500	<500	<500	<500	>500	>500	>500	>500	>500	>500
Saccharomyces carlbergensis (ATCC 9080)	>500	<500	<500	<500	>500	>500	>500	>500	>500	>500
Average antimicrobial activity[b]	231	292	262	292	100	167	40	192	0	15

[a] Figures are the minimum inhibitory concentrations of the compounds in micrograms per milliliter. [b] Figures were calculated from (combined antimicrobial activity × 100)/number of microorganisms in the screen. The combined antimicrobial activity was determined by giving the following scores at the highest potency of the compound against the microorganisms: <500:1, 100:2.5, and <100:5.

synthons (II–VIII) caused an average 13% increase. Thus, antineoplastic activity was retained, albeit diminished. In general, murine toxicity also was retained but reduced except for the VII oximes, which did not contain the dimethylaminomethyl function. The oximes VII had an average 11% increase in mean survival time but were virtually bereft of murine toxicity.

All compounds examined in the *in vitro* KB screen displayed cytotoxicity. Quaternization of Ic gave IIa with similar effect in the P-388 screen and murine toxicity; the possible metabolite of both compounds, the $\alpha,\beta,\alpha',\beta'$-diolefinic ketone IIc, retained activity and decreased host toxicity. Quaternization of the highly active Mannich base If gave IIb with lower antineoplastic activity and lower murine toxicity, while the deaminated IId was virtually devoid of antileukemic potency, even though host toxicity was lower than in If. A comparison of the data for the unsubstituted Mannich bases Ia, IIIa, and IIIb revealed that while a similar low activity level in the P-388 screen was observed, murine toxicity increased as the chain length was shortened. While the average increase in mean survival time for Ib and If was 23%, the related oximes IVa and IVb increased survival time by 14% and host toxicity was reduced. The *threo*-isomeric allyl alcohol IV*d'* increased the mean survival time by twice that of either the *erythro*-isomer IV*d''* or the precursor Mannich base Ic.

The dichlorinated alcohols IVe and IVf had markedly inferior antineoplastic activity compared to the related Mannich bases Id and If. While three oximes, VIIa, VIId, and VIIe, showed an average 20% increase in the lifespan of the mice unaccompanied by host toxicity at the maximum doses administered, the aziridines VIIIa–VIIId proved lethal at 100 mg/kg. A representative aziridine, VIIIa, was examined further, but an increase of only 15% in mean survival time was found at the optimum dose level.

Some Mannich base derivatives were screened for antimicrobial activity (4, 5) and other pharmacological activities (11). Since α,β-unsaturated ketones have shown significant mammalian toxicity, it was felt that evaluating some related alcohols and oximes, in which the carbonylene group is masked, might lead to a greater chance of clinical acceptability if antimicrobial or pharmacological activity is found.

The antimicrobial results of 10 of the alcohols and oximes are listed in Table II. The results indicated that compounds containing a dimethylaminomethyl group, namely the oximes IVa and IVb and the alcohols IV*d'* and IVe, had the greatest activity and were virtually equipotent. In the VII series of oximes, the *o*-chloro and 2,6-dichloro oximes VIIb and VII*d* showed the greatest activity. The most sensitive bacteria to these compounds were the Gram-positive organisms *Staphylococcus aureus*, *Streptococcus faecalis*, and *Bacillus subtilis*. Compounds IVb, IV*d'*, and IVe all showed the same activity against the five fungi in contrast to IVa, which was inactive. The VII oximes were virtually devoid of antifungal activity.

Some Mannich bases have demonstrated analgesia (10), and the data generated from the primary pharmacological screening (Table III) indicate that the oximes and alcohols derived from these compounds have this property. Numerous narcotic analgesics have a common structural unit linked together, namely a tertiary nitrogen atom, a two-carbon chain, and a quaternary carbon atom to which an aryl ring is attached (28). The compounds bear some similarity to the general formula of narcotic analgesics, although a styryl group and not an aryl ring is attached to the quaternary carbon atom. The overlap of π-orbitals in this group of

Table III—Evaluation of Some Oximes and Alcohols Derived from Conjugated Styryl Ketones for Analgesic, Anti-Inflammatory, and Antihistaminic Activities

	Analgesic Activity[a]				Anti-Inflammatory Activity[b]			
	Percentage Protection[c]					Percentage Protection		
Compound	32	64	128	ED_{50}	Dose, mg/kg	3 hr	5 hr	Antihistaminic Activity[d]
IVa	75[e]	100	—	22	64	17	0	100[f]
IVb	7	42	96	64	—	—	—	79
IV*d'*	74	91	91	18	128	39	17	100[f]
					256	87	17	
IVe	52[e]	98	—	30	128	0	0	100[f]
VIIa	—	—	Algesic[g]	—	64	0	0	29
VIIb	—	—	Algesic[g]	—	64	25	50	13
VIIc	—	—	Algesic[g]	—	64	0	0	12
VII*d*	—	38	54	—	128	0	0	15
VIIe	—	—	6	—	64	0	0	7
VIIf	49	58	96	42	128	0	0	31

[a] Analgesic activity was measured by the percentage protection in the phenylquinone writhing test. Under these conditions, aspirin gave 50% protection at 52 mg/kg. A compound displaying an effect >50% is considered to be active. [b] Anti-inflammatory activity was measured by the percentage protection afforded by the compound to carrageenin-induced edema. The reference compound, indomethacin, gave 50% protection at 12 mg/kg under these conditions. Compounds showing >50% protection are considered active. [c] Dose levels in milligrams per kilogram. [d] Figures indicate the percentage protection of the compound at 0.1 mg/ml against a standard histamine dose. A compound is considered active if 20% protection is obtained. The reference compound, diphenylhydramine, gave 100% protection at 0.01 mg/ml. [e] Percentage protections at 16 mg/kg for IVa and IVe were 42 and 10, respectively. [f] At a dose level of 0.01 mg/ml, IVa, IV*d'*, and IVe inhibited the histamine action by 52, 70, and 100%, respectively. At 0.001 mg/ml, IVa, IV*d'*, and IVe inhibited the action of histamine by 29, 18, and 52%, respectively. [g] Percentage increases in the number of writhes for VIIa, VIIb, and VIIc were 18, 31, and 6, respectively.

Table IV—Inhibition of Respiration of Mitochondria Obtained from the Hepatic Tumor 5123 TCH, from the Liver of the Tumor-Bearing Animal, and from Normal Rat Liver by the Mannich Bases Ia, Id–If, and IIIa Using Succinate as the Substrate

Compound	Concentration, μmoles	Hepatic Tumor 5123 TCH				Hepatic Tissue from Tumor-Bearing Animal				Normal Rat Liver			
		Inhibition, %	SE	Increase in Respiration[a], %	SE	Inhibition, %	SE	Increase in Respiration[a], %	SE	Inhibition, %	SE	Increase in Respiration[a], %	SE
Ia	5.0	96.69	1.07	−0.61	2.43	96.62	1.72	2.40	0.80	85.10	1.68	2.98	2.63
	2.5	66.35	6.15	2.44	6.38	84.27	2.88	−4.49	2.41	85.00	5.77	−4.74	2.34
	0.5	4.70	4.64	10.83	54.92	−4.57	12.30	−30.20	46.99	−25.42	22.71	−0.58	28.70
Id	5.0	97.38	1.00	−2.75	1.06	97.35	1.62	−1.87	1.21	94.27	2.26	−2.01	0.96
	2.5	95.62	1.52	−0.58	1.81	96.18	1.43	−1.00	1.13	91.47	2.99	−4.65	2.14
	0.5	85.09	3.05	11.96	2.36	83.26	2.84	10.29	2.98	71.08	6.26	2.59	2.53
	0.1	21.05	3.99	−4.62	41.17	51.06	10.70	−13.10	19.77	23.29	27.08	−12.37	7.97
Ie	5.0	97.14	1.06	−1.79	0.55	94.34	2.20	−2.37	1.93	97.49	1.64	0.21	0.38
	2.5	101.6	3.35	−1.05	0.94	89.69	2.08	−4.78	1.34	95.85	2.00	0.049	0.75
	0.5	83.29	4.07	14.53	3.71	74.40	3.92	2.10	0.97	74.44	6.59	8.81	4.20
	0.1	22.61	7.58	47.98	17.09	6.57	12.31	−29.02	23.33	21.92	13.24	7.37	10.42
If	5.0	95.60	2.12	−0.88	0.88	97.55	1.53	1.55	1.02	95.00	1.30	−3.73	1.45
	2.5	84.69	8.78	5.30	3.31	95.22	3.08	−1.20	1.03	94.27	1.85	−1.59	1.52
	0.5	90.78	4.24	5.81	3.59	78.68	8.47	3.45	1.49	76.76	5.37	−5.78	6.21
	0.1	44.53	17.23	−32.25	21.27	36.21	20.18	−37.64	15.16	49.92	8.81	−17.97	9.54
IIIa	5.0	10.83	4.50	−64.41	28.39	−10.08	7.02	−52.87	45.27	1.86	12.17	−44.33	31.12

[a] The percentage increase in respiration indicates the change in respiration after ubiquinone addition.

compounds may not preclude alignment at a nonpolar portion of the receptor, which is normally occupied by the aryl ring. The IV*a* and IV*d'* monochloro derivatives had, on the average, approximately 2.4 times the potency of IV*b* and IV*e*, which have two chlorine atoms in the aromatic ring and may exert some steric impedance to binding at a receptor. Codeine analgesia, expressed as an ED_{50} value, is 14.2 mg/kg in the hot plate test (29); and although the compounds listed in Table III were evaluated by the phenylquinone writhing test, it may be considered that IV*a* and IV*d'* are similar in potency to codeine, while IV*e* and IV*b* are approximately one-half and one-fifth as active as this widely used drug.

The VII oximes displayed a wide spectrum of response in the analgesia screen, ranging from algesia (VII*a*–VII*c*) to weak analgesic activity (VII*d* and VII*e*) to VII*f*, which had approximately one-third of the activity of codeine. The demonstration of analgesia by certain of these compounds would be enhanced if anti-inflammatory properties were also found in the active compounds. Table III indicates that none of the derivatives met the criterion for activity at 3 and 5 hr.

Table III indicates that all of the compounds examined in the antihistaminic screen displayed activity, with maximum potency shown by the dimethylaminomethyl compounds IV*a*, IV*b*, IV*d'*, and IV*e*. These derivatives are related structurally to the propylamine group of antihistaminics, in which halogenation of the aromatic ring enhances activity (30). Both of the alcohols IV*d'* and IV*e* as well as the oxime IV*a* showed histamine-inhibiting properties at a concentration as low as 0.001 mg/ml. None of the compounds listed in Table III demonstrated activity in the cardiovascular, hypoglycemic, and antianaphylactic screens, except IV*e* which inhibited passive cutaneous anaphylaxis in rats by 75% at a dose of 75 mg/kg.

The second phase of the work involved the examination of the effect of the Mannich bases Ia, Id–If, and IIIa on respiration of mitochondria obtained from the 5123 TCH hepatic tumor and from the tumor-bearing animal as well as from normal rat liver using different substrates (Tables IV–VII). Statistical evaluation showed no difference (at $p = 0.05$, analysis of variance) in sensitivity of the three types of tissue to the Mannich bases.

In summary, this work has shown that molecular modification of the Mannich bases (I) produced compounds of lower murine toxicity, generally accompanied by reduced anticancer activity. The results of mitochondrial respiration inhibition studies likewise showed that five of the compounds were not selective for mitochondria from tumor cells.

Table V—Inhibition of Respiration of Mitochondria Obtained from the Hepatic Tumor 5123 TCH, from the Liver of the Tumor-Bearing Animal, and from Normal Rat Liver by the Mannich Bases Ia, Id–If, and IIIa Using Glutamate as the Substrate

Compound	Concentration, μmoles	Hepatic Tumor 5123 TCH				Hepatic Tissue from Tumor-Bearing Animal				Normal Rat Liver			
		Inhibition, %	SE	Increase in Respiration[a], %	SE	Inhibition, %	SE	Increase in Respiration[a], %	SE	Inhibition, %	SE	Increase in Respiration[a], %	SE
Ia	5.0	75.54	5.93	1.01	5.44	83.59	4.58	−6.83	6.51	89.16	1.03	−2.77	4.21
	2.5	67.39	3.85	−15.16	7.02	75.36	6.24	−8.14	3.66	61.30	3.54	−0.61	1.41
	0.5	42.88	9.81	1.44	11.85	7.17	9.36	19.77	26.91	31.44	11.22	−11.47	17.10
Id	5.0	81.78	4.33	−8.17	4.65	88.74	2.58	−1.22	2.79	84.19	4.11	−1.06	4.60
	2.5	77.24	2.90	−13.55	4.95	87.44	2.47	−5.86	2.77	81.64	2.02	−0.58	1.62
	0.5	50.05	3.11	−24.80	11.49	85.91	0.68	−1.89	1.83	73.77	4.72	6.45	9.52
	0.1	23.40	11.67	−13.39	6.74	78.58	3.16	−5.36	2.99	−22.38	30.43	−11.56	20.53
Ie	5.0	90.06	3.47	0.096	6.72	83.70	4.32	−4.90	2.90	81.69	4.41	−1.27	3.71
	2.5	75.73	3.22	−11.52	9.87	89.91	3.75	−0.46	1.91	81.22	2.61	−2.17	3.97
	0.5	68.45	2.50	−16.04	7.90	82.37	2.29	−2.78	3.19	75.23	2.48	−6.37	6.51
	0.1	44.42	9.06	−1.73	13.31	68.68	7.77	−9.82	1.52	29.12	23.30	−25.05	17.93
If	5.0	86.61	3.08	0.36	7.91	92.82	3.23	2.95	4.62	91.76	2.81	3.44	5.00
	2.5	80.06	6.89	−13.42	15.30	88.83	3.34	1.49	2.18	85.47	2.39	−3.71	2.70
	0.5	57.18	4.49	−27.68	5.91	81.08	3.65	−0.39	2.71	81.92	6.06	−5.89	2.13
	0.1	47.77	13.65	−24.71	8.95	78.09	4.93	−3.05	2.76	72.41	5.36	−7.14	3.36
IIIa	5.0	6.87	3.62	−78.15	17.10	18.75	12.85	7.54	13.21	4.45	11.14	−46.67	46.67

[a] The percentage increase in respiration indicates the change in respiration after ubiquinone addition.

Table VI—Inhibition of Respiration of Mitochondria Obtained from the Hepatic Tumor 5123 TCH, from the Liver of the Tumor-Bearing Animal, and from Normal Rat Liver by the Mannich Bases Ia, Id–If, and IIIa Using 3-Hydroxybutyrate as the Substrate

Compound	Concentration, μmoles	Hepatic Tumor 5123 TCH				Hepatic Tissue from Tumor-Bearing Animal				Normal Rat Liver			
		Inhibition, %	SE	Increase in Respiration[a], %	SE	Inhibition, %	SE	Increase in Respiration[a], %	SE	Inhibition, %	SE	Increase in Respiration[a], %	SE
Ia	5.0	95.16	2.75	−1.38	1.13	94.89	2.07	−2.99	1.38	92.49	0.67	−2.20	1.16
	2.5	92.59	2.59	−4.47	2.39	96.06	2.00	−1.90	1.66	93.43	1.35	−0.19	1.70
	0.5	23.20	12.14	−125.9	31.37	−21.82	38.68	−8.55	5.13	−26.75	15.98	−19.23	17.44
Id	5.0	97.57	1.32	−1.72	1.36	92.79	2.22	−6.38	2.26	96.64	1.71	−1.27	1.14
	2.5	97.83	3.09	−0.73	2.53	95.28	2.24	0.64	2.14	94.73	2.00	−1.58	1.28
	0.5	93.72	3.01	−7.80	4.44	92.41	4.88	−8.92	6.95	98.02	0.80	−1.37	1.13
	0.1	54.19	10.61	−51.62	19.46	90.42	4.11	3.14	3.43	33.10	29.67	−1.54	1.54
Ie	5.0	99.70	0.27	0.27	0.27	96.15	1.51	−2.34	0.96	91.90	2.19	−2.67	1.68
	2.5	97.11	1.85	−0.51	3.51	94.53	1.47	−3.49	1.56	96.47	1.87	−1.81	1.05
	0.5	92.99	3.49	−3.33	1.65	95.74	2.40	−1.54	2.52	96.41	1.28	−0.94	0.95
	0.1	69.17	13.79	−20.79	12.11	93.79	1.65	−3.46	1.02	−55.73	28.36	−24.56	17.88
If	5.0	93.90	2.03	−4.07	2.28	97.76	0.84	−1.17	0.53	98.75	1.25	−0.33	0.33
	2.5	93.22	1.72	−6.47	1.85	97.56	0.99	−1.90	0.78	97.11	1.23	−1.87	1.90
	0.5	89.01	3.37	−4.90	3.82	97.67	0.83	−0.89	0.67	97.91	1.91	−1.70	1.70
	0.1	58.21	2.24	−52.97	21.57	95.56	1.09	−3.59	1.37	76.45	22.02	0.16	0.16
IIIa	5.0	18.27	8.18	−36.35	10.08	14.46	9.59	−81.10	27.19	−21.91	8.63	−16.77	12.37

[a] The percentage increase in respiration indicates the change in respiration after ubiquinone addition.

Table VII—Inhibition of Respiration of Mitochondria Obtained from the Hepatic Tumor 5123 TCH, from the Liver of the Tumor-Bearing Animal, and from Normal Rat Liver by the Mannich Bases Ia, Id–If, and IIIa Using Palmitylcarnitine as the Substrate

Compound	Concentration, μmoles	Hepatic Tumor 5123 TCH				Hepatic Tissue from Tumor-Bearing Animals				Normal Rat Liver			
		Inhibition, %	SE	Increase in Respiration[a], %	SE	Inhibition, %	SE	Increase in Respiration[a], %	SE	Inhibition, %	SE	Increase in Respiration[a], %	SE
Ia	5.0	87.97	6.02	2.05	9.84	88.84	2.23	4.22	2.75	89.04	4.39	19.86	5.11
	2.5	51.85	7.01	−29.37	12.39	77.88	10.15	−17.67	16.74	−30.02	33.32	−24.37	19.51
	0.5	−26.17	8.35	10.16	6.30	−61.49	17.48	51.99	24.57	−51.86	16.34	23.18	38.94
Id	5.0	85.24	4.29	−0.05	5.31	89.21	3.42	−7.13	4.15	82.12	5.54	−1.16	2.58
	2.5	81.74	5.07	−8.94	10.42	91.26	2.71	−1.44	4.49	77.65	5.87	−2.85	4.09
	0.5	2.38	16.93	−71.21	29.14	83.99	2.80	−9.38	2.96	−18.53	28.21	−31.67	20.80
	0.1	−25.77	4.74	79.23	28.93	−19.96	8.24	−55.53	37.91	−57.76	30.49	−128.4	61.18
Ie	5.0	89.35	3.71	−0.09	2.62	86.80	2.03	−1.77	2.15	71.89	6.02	−1.84	4.43
	2.5	86.70	4.67	−0.48	2.23	87.44	2.20	−1.28	2.45	61.85	7.40	−2.11	12.53
	0.5	22.93	11.17	−36.30	28.82	56.24	12.88	−14.94	12.11	−16.31	21.19	−11.41	28.94
	0.1	−20.13	6.02	74.52	18.14	−46.65	23.45	3.88	10.05	−69.09	9.42	64.25	10.90
If	5.0	96.45	1.60	3.07	1.60	96.13	2.13	−3.51	2.59	95.00	2.89	−2.62	2.48
	2.5	81.48	2.48	−4.46	6.38	90.93	0.57	−3.01	2.33	91.24	1.39	2.03	5.69
	0.5	74.67	8.74	−12.51	9.94	65.81	25.86	4.37	10.04	59.62	8.40	−31.72	14.01
	0.1	−68.39	13.27	71.82	60.09	−50.89	47.13	−9.36	674.6	−83.61	55.68	−19.41	45.80
IIIa	5.0	12.80	10.58	−56.56	47.96	−39.03	5.07	14.01	20.58	−57.71	30.26	−64.10	45.30

[a] The percentage increase in respiration indicates the change in respiration after ubiquinone addition.

EXPERIMENTAL

Compound Preparation—The preparation of Ia–If, IIa, and IIc was described previously (31). Compounds IIb, IId, and IIIa were prepared by the literature methodology (2) as was IIIb (1). The synthesis of IVa, IVb, IVe, IVf, and V–VIII was accomplished using a reported procedure (32), and the alcohols IVc and IVd were prepared by the method described previously (33). Compounds IVc and IVe possessed the *threo*-configuration; IVd was obtained as the pure *threo*-isomer, IVd′ (33), and a small quantity of the *erythro*-isomer (IVd″) was isolated as the maleate salt (33). The alcohol IVf was shown by spectroscopic means to consist of a 60:40 mixture of the *erythro*- and *threo*-isomers (32).

Compound Screening—The data summarized in Table I were generated by the Drug Research and Development Division of the National Cancer Institute, using their protocols (34). The compounds were administered in saline (Ia, Ib, Id, If, IIb, IIIa, IIIb, IVa–IVd′, IVe, and IVf), saline with polysorbate 80[1] (Ic, VIId, VIIf, and VIIIa–VIIId), hydroxypropylcellulose (Ie, IIa, IIc, IVd″, V, VI, VIIa–VIIc, and VIIe), and an unspecified solvent (IId) by the intraperitoneal route. The CD_2F_1 strain of mice was used for all compounds except Ie, If, IIa, IIc, IIIb, IVc, IVd′, and IVd″, in which cases the $B_6D_2F_1$ strain of mice was employed.

Injections were made daily for 9 consecutive days, except in the following cases. The maximum increase in mean survival times recorded in Table I for Ie was obtained by making three injections every 4 days; for IIa and IIc, only one injection was made. In addition, the murine toxicity data found in Table I for Id were obtained when three injections were made every 4 days, and the toxicity of IIa at the 50-mg/kg dose level was found when one injection was made. The toxicity data for IIb and IId at the 200- and 100-mg/kg dose levels, respectively, were derived from two injections separated by a 4-day period. The toxicity data for IVc at the 200-mg/kg dose level were obtained by making three injections every 4 days.

For the antimicrobial screen[2], the compounds were dissolved in water or dimethyl sulfoxide and diluted serially to various concentrations. The concentrations of stock solutions were prepared such that when 0.5 ml

[1] Tween 80, Atlas Chemical Industries, Wilmington, DE 19899.

[2] The antimicrobial and pharmacological screens were carried out by Bio-Research Laboratories Ltd., Montreal, Quebec, Canada.

was added to 15 ml of agar medium, the desired final concentrations were obtained. The growth medium for the bacteria was trypticase soy agar with 5% defibrinated rabbit blood added for the growth of *Haemophilus influenzae*, *Streptococcus pyogenes*, and *Streptococcus pneumoniae*. Modified Sabouraud agar was employed for the growth of the fungi. The test organisms were grown previously for 2 days at 35° for bacteria and yeast and for 1 week at 24° for fungi on slants of the same media. The agar plates were streaked with a loopful of cell suspension, which had been washed off the slants and diluted to approximately 10^5 organisms/ml. The plates were incubated for 2–14 days at 24° for fungi and at 35° for bacteria. The results in Table II indicate the minimal inhibitory concentration of the compound that prevents visible growth in the media.

Unless otherwise stated, the same number of animals was used for controls as for pharmacological evaluation of the compound. The screen employed for examining the compounds for analgesic activity was the phenylquinone writhing test (35). Five male Swiss albino mice, 18–22 g, were used for each dose for each compound. The ED_{50} values for five of the compounds listed in Table III were obtained by using five mice at doses of 16, 32, and 64 mg/kg for IV*a* and IV*e* and at 32, 64, and 128 mg/kg for IV*b*, IV*d'*, and VII*f*.

The anti-inflammatory screen measured the antagonism of the test compound to carrageenin-induced rat paw edema (36). Six female Sprague–Dawley rats, 120–160 g, were used for the compounds listed in Table III, except for VII*a*–VII*c* and VII*e* where four animals were used. The edema volume was recorded at the end of 3 and 5 hr. The compounds were examined for antihistaminic activity using four guinea pig ileum preparations (37). The antianaphylactic screen measured the potential of a compound to inhibit passive cutaneous anaphylaxis in rats (38). Four female Sprague–Dawley rats were used for each compound. Compounds were administered intravenously at 125 mg/kg for IV*a*, 100 mg/kg for IV*b* and VII*d*, 25 mg/kg for IV*d'* and IV*e*, 128 mg/kg for VII*a*–VII*c* and VII*e*, and 50 mg/kg for VII*f*. A compound was considered active if it reduced wheal formation by 50%. The reference compound, chromolyn sodium, reduced the wheal area by 90% at a dose of 100 mg/kg.

The antidepressant screen measured the antagonism of a compound to tetrabenazine-induced ptosis in mice (39, 40). Six male Swiss albino mice were used for each compound; the compounds were administered subcutaneously, except VII*a*–VII*c* and VII*e*, which were given intraperitoneally. A dose of 128 mg/kg was used for all compounds except IV*a* and IV*e*, where the dose was 64 mg/kg. A compound should antagonize the tetrabenazine effect by 30% after 30 min and by 10% after 60 min to be considered active. The reference compound, amitriptyline, caused an antagonism of 90 and 50% after 30 and 60 min, respectively, at a dose of 8 mg/kg.

In the cardiovascular screen, a Sprague–Dawley rat of either sex, 250–400 g, was anesthetized by intraperitoneal urethan injection (1.9 g/kg). After cannulation of the femoral vein, the blood pressure was monitored *via* a pressure transducer[3] connected to a cannula in the left carotid artery. The arterial blood pressure and heart rate were recorded on a polygraph[4]. After the preparation had stabilized, the test compound was dissolved in saline and/or polysorbate 80[1] (1%) and administered in a volume of 0.01–0.05 ml. The changes in blood pressure and heart rate were expressed as percentage differences between the pre- and postdrug values. One or two determinations using one rat for each compound were made at the following dose levels: IV*a*, IV*b*, and VII*d* at 20 mg/kg; IV*d'*, IV*e*, and VII*f* at 10 mg/kg; and VII*a*–VII*c* and VII*e* at both 1 and 5 mg/kg. A compound should increase the blood pressure and heart rate by 30% for a time period considerably in excess of 5 min to be considered active.

The screen for hypoglycemic activity involved the measurement of blood sugar concentration in rats (41). Four male Sprague–Dawley rats were used for each compound. Compounds IV*b*, IV*d'*, IV*e*, VII*d*, and VII*f* were administered at a dose of 128 mg/kg po. A dose of 64 mg/kg po was employed for IV*a*. Compounds VII*a*–VII*c* and VII*e* were administered at 100 mg/kg iv. A 20% decrease in blood sugar concentration is required for a compound to be considered active in this screen.

Inhibition of Respiration in Mitochondria Obtained from Hepatic Tumor 5123 TCH and from Rat Liver—The inoculation of the hepatic tumor 5123 TCH into rats proceeded as follows. Adult, male Buffalo strain rats[5] containing a 4–5-week-old tumor[6] were sacrificed and the tumors were removed. The healthy tumor tissue was dissected from the remainder of the neoplasm. A 10% suspension of the tumor tissue in normal saline was prepared and placed in a glass hand homogenizer[7], after which two or three thrusts with a glass pestle were undertaken. The suspension (1 ml) was injected subcutaneously into each side of the inguinal regions of a male Buffalo rat, 100 g.

The mitochondrial pellet containing tumorous tissue was prepared as follows. Adult, male Buffalo rats containing a 4–5-week-old 5123 TCH tumor were sacrificed by decapitation and the tumors were removed. The healthy tumor tissue (5 g) was dissected from the remaining tumor mass and made into a 25% suspension using ice-cold 3.4 m*M* tromethamine hydrochloride[8] buffer (pH 7.40 at room temperature). The 3.4 m*M* tromethamine hydrochloride buffer contained 0.25 *M* sucrose and 1.0 m*M* ethylene glycol-bis(aminoethyl)tetraacetate. All of the following procedures were carried out at 0°.

The tumor tissue was homogenized with 15–20 thrusts with a pestle in a glass homogenizer[7] and then diluted to a 10% homogenate with buffer. The mitochondrial pellet, prepared from the homogenate using the reported methodology (3), was suspended in cold buffer (10 ml) to give a protein concentration of approximately 6 mg/ml; 0.5 ml of this suspension was used in each determination. Homogenates from 10 g of liver from tumor-bearing animals and normal Buffalo rats were prepared in a similar manner and suspended in 10 ml of buffer. One milliliter of this suspension was diluted with 4 ml of buffer, giving a suspension with a protein concentration of ~5 mg/ml; 0.5 ml of this suspension was used in each determination.

The media and methodology for measuring the effect of the Mannich bases on mitochondrial respiration were reported previously (3). The percentage increase in respiration was measured by adding 5 μl of a solution of ubiquinone (9 nmoles) in ethanol to the cell approximately 2 min after the addition of the Mannich base and noting the effect on respiration. The results in Tables IV–VII represent the mean values of five to eight separate determinations. In every case that mitochondria were used, the protein content was determined by a modification (42) of the previously described procedure (43). Results were evaluated statistically by the analysis of variance using the SPSS-Anova program (44) and a computer[9].

REFERENCES

(1) J. R. Dimmock and W. G. Taylor, *J. Pharm. Sci.*, **64**, 241 (1975).

(2) J. R. Dimmock, N. W. Hamon, K. W. Hindmarsh, D. G. Mills, L. E. Negrave, G. H. Rank, and A. J. Robertson, *ibid.*, **65**, 482 (1976).

(3) N. W. Hamon, D. L. Bassendowski, D. E. Wright, J. R. Dimmock, and L. M. Noble, *ibid.*, **67**, 1539 (1978).

(4) J. R. Dimmock, W. A. Turner, and H. A. Baker, *ibid.*, **64**, 995 (1975).

(5) J. R. Dimmock, D. K. Kowal, W. A. Turner, P. J. Smith, L. M. Noble, and W. J. Pannekoek, *ibid.*, **67**, 401 (1978).

(6) E. D. Taylor and W. L. Nobles, *J. Am. Pharm. Assoc., Sci. Ed.*, **49**, 317 (1960).

(7) R. S. Varma and W. L. Nobles, *J. Med. Chem.*, **11**, 195 (1968).

(8) M. Tramontini, *Synthesis*, **1973**, 703.

(9) R. S. Varma, B. Ali, S. S. Parmar, and W. L. Nobles, *J. Med. Chem.*, **13**, 147 (1970), and references cited therein.

(10) P. B. J. Janssen, U.S. pat. 3,030,372 (Apr. 12, 1962); through *Chem. Abstr.*, **59**, 2780g (1963).

(11) N. J. Harper, A. F. Casy, and J. R. Dimmock, *J. Chem. Soc.*, **1964**, 4280.

(12) A. Albert, "Selective Toxicity", 5th ed., Chapman and Hall, London, England, 1973, p. 473.

(13) *Ibid.*, p. 314.

(14) P. N. Gordon, J. D. Johnston, and A. R. English, in "Antimicrobial Agents and Chemotherapy," G. L. Hobby, Ed., American Society for Microbiology, Ann Arbor, Mich., 1965, p. 165.

(15) H. Schönenberger, T. Bastug, L. Bindl, A. Adam, D. Adam, A. Petter, and W. Zwez, *Pharm. Acta Helv.*, **44**, 691 (1969).

(16) C. E. Lough, D. J. Currie, and H. L. Holmes, *Can. J. Chem.*, **46**, 771 (1968).

(17) S. M. Kupchan, D. C. Fessler, M. A. Eakin, and T. J. Giacobbe, *Science*, **168**, 376 (1970).

[3] Statham.
[4] Gass.
[5] Simonsen Laboratories, Gilroy, Calif.
[6] Dr. R. A. Hickie, Department of Pharmacology, College of Medicine, University of Saskatchewan, Saskatoon, Saskatchewan, Canada, S7N 0W0.
[7] Dounce (40 ml size with large pestle A), Kontes Glass Co., Vineland, NJ 08360.
[8] Sigma Chemical Co., St. Louis, MO 63178.
[9] IBM 370/158.

(18) F. W. Menger and J. H. Smith, *J. Am. Chem. Soc.*, **91**, 4211 (1969).
(19) A. Burger, *J. Med. Chem.*, **21**, 1 (1978).
(20) R. T. Williams, "Detoxification Mechanisms," 2nd ed., Wiley, New York, N.Y., 1959, p. 166.
(21) H. J. E. Loewenthal, in "Protective Groups in Organic Chemistry," J. F. W. McOmie, Ed., Plenum, London, England, 1973, p. 341.
(22) H. Kahler and W. B. Robertson, *J. Natl. Cancer Inst.*, **3**, 495 (1943).
(23) P. M. Guillino, F. H. Grantham, S. H. Smith, and A. C. Haggerty, *ibid.*, **34**, 857 (1965).
(24) L. J. Fischer and S. Riegelman, *J. Pharm. Sci.*, **56**, 469 (1967).
(25) J. A. Stock, in "Drug Design," vol. II, E. J. Ariens, Ed., Academic, London, England, 1971, p. 541.
(26) H. P. Morris and L. J. Slaughter, in "Morris Hepatomas: Mechanisms of Regulation," H. P. Morris and W. E. Criss, Eds., Plenum, New York, N.Y., 1978, p. 1.
(27) H. Druckrey and S. Raabe, *Klin. Wochenschr.*, **30**, 882 (1952).
(28) O. L. Salerni, "Natural and Synthetic Organic Medicinal Compounds," C. V. Mosby, St. Louis, Mo., 1976, p. 43.
(29) N. B. Eddy and D. Leimbach. *J. Pharmacol. Exp. Ther.*, **107**, 385 (1953).
(30) O. L. Salerni, "Natural and Synthetic Organic Medicinal Compounds", C. V. Mosby, St. Louis, Mo., 1976, p. 87.
(31) J. R. Dimmock and W. G. Taylor, *J. Pharm. Sci.*, **63**, 69 (1974).
(32) J. R. Dimmock, P. J. Smith, L. M. Noble, and W. J. Pannekoek, *ibid.*, **67**, 1536 (1978).
(33) W. G. Taylor and J. R. Dimmock, *Can. J. Chem.*, **52**, 2522 (1974).
(34) R. I. Geran, N. H. Greenberg, M. M. MacDonald, A. M. Schumacher, and B. J. Abbott, *Cancer Chemother. Rep. (Part 3)*, **3** (2) (Sept. 1972).
(35) H. O. Collier, L. C. Dinneen, C. A. Johnson, and C. Schneider, *Br. J. Pharmacol. Chemother.*, **32**, 295 (1968).
(36) C. A. Winter, in "International Symposium on Non-Steroidal Anti-inflammatory Drugs," S. Garattini and M. N. G. Dukes, Eds., Excerpta Medica Foundation, Amsterdam, The Netherlands, 1965, pp. 190–202.
(37) J. Goose and A. M. J. N. Blair, *Immunology*, **16**, 749 (1969).
(38) W. L. M. Perry, "Pharmacological Experiments on Isolated Preparations," Livingstone, Edinburgh, Scotland, 1968, pp. 58–68.
(39) B. Rubin, H. H. Malone, M. H. Waugh, and J. C. Burke, *J. Pharmacol. Exp. Ther.*, **120**, 125 (1957).
(40) A. Barnett and R. T. Taber, in "Screening Methods in Pharmacology," vol. II, P. A. Turner and P. Hebborn, Eds., Academic, New York, N.Y., 1971, pp. 203–208.
(41) G. F. Holland, D. A. Jaeger, R. L. Wagner, G. D. Laubach, W. M. McLamore, and S. Y. P'an, *J. Med. Pharm. Chem.*, **3**, 99 (1961).
(42) G. L. Miller, *Anal. Chem.*, **31**, 964 (1959).
(43) O. H. Lowry, N. J. Rosebrough, L. Fair, and R. J. Randall, *J. Biol. Chem.*, **193**, 265 (1951).
(44) J.-O. Kim and F. J. Kohout, in "Statistical Package for the Social Sciences," 2nd ed., N. H. Nie, C. H. Hull, J. G. Jenkins, K. Steinbrenner, and D. H. Brent, Eds., McGraw-Hill, New York, N.Y., 1975, p. 398.

ACKNOWLEDGMENTS

The authors thank the Medical Research Council of Canada for the award of an operating grant (MA 5538) to J. R. Dimmock and for funds provided under the Summer Undergraduate Research Scholarship program to D. E. Wright. The assistance of Dr. R. A. Hickie and M. R. Novokowsky of the Department of Pharmacology, College of Medicine, University of Saskatchewan, in regard to the inoculation and excision of malignant hepatic tissue is gratefully acknowledged. In addition, Dr. S. M. Wallace of the College of Pharmacy, University of Saskatchewan, offered constructive assistance concerning the statistical evaluation of experiments involving mitochondrial respiration.

The authors also thank Dr. H. B. Wood, Jr., for the antineoplastic assessment of the compounds and Dr. F. Fried, Dr. B. G. Procter, and Dr. R. B. Rastogi of Bio-Research Laboratories for arranging the antimicrobial and pharmacological evaluations of a number of the derivatives. The technical assistance of Mrs. D. L. Bassendowski is gratefully acknowledged.

Preparation of Diastereomeric Urethane Derivatives of Atropine and *l*-Hyoscyamine Using (−)-1-Phenylethylisocyanate

W. O. LANDEN, Jr. *[x], and DRURY S. CAINE [‡]

Received December 27, 1978, from the **Food and Drug Administration, Atlanta, GA 30309,* and the [‡]*School of Chemistry, Georgia Institute of Technology, Atlanta, GA 30332.* Accepted for publication February 20, 1979.

Abstract □ Diastereomeric urethane derivatives of atropine (*d,l*-hyoscyamine) and *l*-hyoscyamine were prepared by reacting the alkaloids with (−)-1-phenylethylisocyanate. The derivatives, as the picrate ion-pairs, were characterized by their melting points, optical rotations, elemental analyses, and IR, NMR, and UV–visible spectra.

Keyphrases □ Diastereomers—atropine and *l*-hyoscyamine urethane derivatives, chemical synthesis □ Atropine—derivatives, urethane diastereomers, chemical synthesis □ Hyoscyamine—derivatives, urethane diastereomers, chemical synthesis

In an investigation designed to develop a procedure for the quantitation of *d*-hyoscyamine and *l*-hyoscyamine at therapeutic levels in finished drug dosage forms, a method for the preparation and isolation of stable diastereomeric urethane picrate derivatives was found. The derivatives were prepared by reacting the chiral isocyanate reagent (−)-1-phenylethylisocyanate with *l*-hyoscyamine and atropine (*d,l*-hyoscyamine).

The preparation of suitable alcohol derivatives generally is based on ester formation by reactions with acid chlorides or acid anhydrides (1–3) or on urethane formation by reaction with isocyanates (4–6). Little use of optically active isocyanates for the racemic mixture resolution has been reported in the literature. The reaction of (−)-menthylisocyanate with alcohols (7), the use of (−)-menthylisocyanate to prepare derivatives with *tert*-butyl alcohol, lactic acid, and amino acids (8), and the reaction of α-phenylethylisocyanates with amines, alcohols, and Grignard reagents (9) have been studied. Optical activity was retained during these reactions, and the respective derivatives possessed a larger optical rotation than the reagent itself.

Other investigators (10) reported that (−)-1-phenylethylisocyanate does not polymerize and can be stored for long periods, neat or in solution, without a change in the optical rotation value. GLC has been used (11) for the

0022-3549/79/0800-1039$01.00/0
© 1979, American Pharmaceutical Association

(18) F. W. Menger and J. H. Smith, *J. Am. Chem. Soc.*, **91**, 4211 (1969).
(19) A. Burger, *J. Med. Chem.*, **21**, 1 (1978).
(20) R. T. Williams, "Detoxification Mechanisms," 2nd ed., Wiley, New York, N.Y., 1959, p. 166.
(21) H. J. E. Loewenthal, in "Protective Groups in Organic Chemistry," J. F. W. McOmie, Ed., Plenum, London, England, 1973, p. 341.
(22) H. Kahler and W. B. Robertson, *J. Natl. Cancer Inst.*, **3**, 495 (1943).
(23) P. M. Guillino, F. H. Grantham, S. H. Smith, and A. C. Haggerty, *ibid.*, **34**, 857 (1965).
(24) L. J. Fischer and S. Riegelman, *J. Pharm. Sci.*, **56**, 469 (1967).
(25) J. A. Stock, in "Drug Design," vol. II, E. J. Ariens, Ed., Academic, London, England, 1971, p. 541.
(26) H. P. Morris and L. J. Slaughter, in "Morris Hepatomas: Mechanisms of Regulation," H. P. Morris and W. E. Criss, Eds., Plenum, New York, N.Y., 1978, p. 1.
(27) H. Druckrey and S. Raabe, *Klin. Wochenschr.*, **30**, 882 (1952).
(28) O. L. Salerni, "Natural and Synthetic Organic Medicinal Compounds," C. V. Mosby, St. Louis, Mo., 1976, p. 43.
(29) N. B. Eddy and D. Leimbach. *J. Pharmacol. Exp. Ther.*, **107**, 385 (1953).
(30) O. L. Salerni, "Natural and Synthetic Organic Medicinal Compounds", C. V. Mosby, St. Louis, Mo., 1976, p. 87.
(31) J. R. Dimmock and W. G. Taylor, *J. Pharm. Sci.*, **63**, 69 (1974).
(32) J. R. Dimmock, P. J. Smith, L. M. Noble, and W. J. Pannekoek, *ibid.*, **67**, 1536 (1978).
(33) W. G. Taylor and J. R. Dimmock, *Can. J. Chem.*, **52**, 2522 (1974).
(34) R. I. Geran, N. H. Greenberg, M. M. MacDonald, A. M. Schumacher, and B. J. Abbott, *Cancer Chemother. Rep. (Part 3)*, **3** (2) (Sept. 1972).
(35) H. O. Collier, L. C. Dinneen, C. A. Johnson, and C. Schneider, *Br. J. Pharmacol. Chemother.*, **32**, 295 (1968).
(36) C. A. Winter, in "International Symposium on Non-Steroidal Anti-inflammatory Drugs," S. Garattini and M. N. G. Dukes, Eds., Excerpta Medica Foundation, Amsterdam, The Netherlands, 1965, pp. 190–202.
(37) J. Goose and A. M. J. N. Blair, *Immunology*, **16**, 749 (1969).
(38) W. L. M. Perry, "Pharmacological Experiments on Isolated Preparations," Livingstone, Edinburgh, Scotland, 1968, pp. 58–68.
(39) B. Rubin, H. H. Malone, M. H. Waugh, and J. C. Burke, *J. Pharmacol. Exp. Ther.*, **120**, 125 (1957).
(40) A. Barnett and R. T. Taber, in "Screening Methods in Pharmacology," vol. II, P. A. Turner and P. Hebborn, Eds., Academic, New York, N.Y., 1971, pp. 203–208.
(41) G. F. Holland, D. A. Jaeger, R. L. Wagner, G. D. Laubach, W. M. McLamore, and S. Y. P'an, *J. Med. Pharm. Chem.*, **3**, 99 (1961).
(42) G. L. Miller, *Anal. Chem.*, **31**, 964 (1959).
(43) O. H. Lowry, N. J. Rosebrough, L. Fair, and R. J. Randall, *J. Biol. Chem.*, **193**, 265 (1951).
(44) J.-O. Kim and F. J. Kohout, in "Statistical Package for the Social Sciences," 2nd ed., N. H. Nie, C. H. Hull, J. G. Jenkins, K. Steinbrenner, and D. H. Brent, Eds., McGraw-Hill, New York, N.Y., 1975, p. 398.

ACKNOWLEDGMENTS

The authors thank the Medical Research Council of Canada for the award of an operating grant (MA 5538) to J. R. Dimmock and for funds provided under the Summer Undergraduate Research Scholarship program to D. E. Wright. The assistance of Dr. R. A. Hickie and M. R. Novokowsky of the Department of Pharmacology, College of Medicine, University of Saskatchewan, in regard to the inoculation and excision of malignant hepatic tissue is gratefully acknowledged. In addition, Dr. S. M. Wallace of the College of Pharmacy, University of Saskatchewan, offered constructive assistance concerning the statistical evaluation of experiments involving mitochondrial respiration.

The authors also thank Dr. H. B. Wood, Jr., for the antineoplastic assessment of the compounds and Dr. F. Fried, Dr. B. G. Procter, and Dr. R. B. Rastogi of Bio-Research Laboratories for arranging the antimicrobial and pharmacological evaluations of a number of the derivatives. The technical assistance of Mrs. D. L. Bassendowski is gratefully acknowledged.

Preparation of Diastereomeric Urethane Derivatives of Atropine and *l*-Hyoscyamine Using (−)-1-Phenylethylisocyanate

W. O. LANDEN, Jr. *[x], and DRURY S. CAINE [‡]

Received December 27, 1978, from the **Food and Drug Administration, Atlanta, GA 30309,* and the [‡]*School of Chemistry, Georgia Institute of Technology, Atlanta, GA 30332.* Accepted for publication February 20, 1979.

Abstract □ Diastereomeric urethane derivatives of atropine (*d,l*-hyoscyamine) and *l*-hyoscyamine were prepared by reacting the alkaloids with (−)-1-phenylethylisocyanate. The derivatives, as the picrate ion-pairs, were characterized by their melting points, optical rotations, elemental analyses, and IR, NMR, and UV–visible spectra.

Keyphrases □ Diastereomers—atropine and *l*-hyoscyamine urethane derivatives, chemical synthesis □ Atropine—derivatives, urethane diastereomers, chemical synthesis □ Hyoscyamine—derivatives, urethane diastereomers, chemical synthesis

In an investigation designed to develop a procedure for the quantitation of *d*-hyoscyamine and *l*-hyoscyamine at therapeutic levels in finished drug dosage forms, a method for the preparation and isolation of stable diastereomeric urethane picrate derivatives was found. The derivatives were prepared by reacting the chiral isocyanate reagent (−)-1-phenylethylisocyanate with *l*-hyoscyamine and atropine (*d,l*-hyoscyamine).

The preparation of suitable alcohol derivatives generally is based on ester formation by reactions with acid chlorides or acid anhydrides (1–3) or on urethane formation by reaction with isocyanates (4–6). Little use of optically active isocyanates for the racemic mixture resolution has been reported in the literature. The reaction of (−)-menthylisocyanate with alcohols (7), the use of (−)-menthylisocyanate to prepare derivatives with *tert*-butyl alcohol, lactic acid, and amino acids (8), and the reaction of α-phenylethylisocyanates with amines, alcohols, and Grignard reagents (9) have been studied. Optical activity was retained during these reactions, and the respective derivatives possessed a larger optical rotation than the reagent itself.

Other investigators (10) reported that (−)-1-phenylethylisocyanate does not polymerize and can be stored for long periods, neat or in solution, without a change in the optical rotation value. GLC has been used (11) for the

0022-3549/79/0800-1039$01.00/0
© 1979, American Pharmaceutical Association

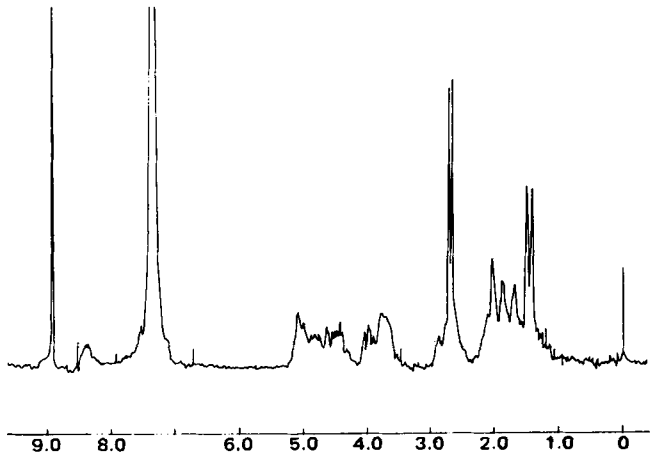

Figure 1—*NMR spectrum of I in deuterochloroform with 0.1% tetramethylsilane as reference (frequency, 99.539 MHz; single pulse width, 4 μsec; repetition, 5 sec; data points, 8k; number of scans, 1001).*

separation of diastereomers of (*R*)-(+)-1-phenylethylurethanes of secondary alcohols.

EXPERIMENTAL

Apparatus—The reaction apparatus was assembled from stock items with 24/40 joints: round-bottom flask, 150 ml, three neck; dropping funnel, 25 ml; reflux condenser, water jacketed; glass inlet tubing with stopcock for nitrogen introduction; heating mantle with rheostat; and rotary vacuum evaporator with dry ice–acetone cold trap and high vacuum pump. NMR spectrometers for operation at 60 MHz[1] and 100 MHz[2] were used. Tetramethylsilane in deuterochloroform was the internal reference for chemical shift measurements.

Reagents—Benzene was analytical reagent grade, thiophene free, dried by refluxing over sodium, and distilled just prior to use. The ether[3] was anhydrous grade, and all other reagents were analytical reagent grade. The nitrogen gas was highly purified, anhydrous grade. *l*-Hyoscyamine and atropine[4] were dried in a vacuum desiccator over silica gel. (−)-1-Phenylethylisocyanate[5], 97% purity, was received in a sealed ampul and maintained under a nitrogen atmosphere after opening.

Procedure—The glass reaction apparatus was assembled with the water condenser in place. The reaction flask was flame dried while the system was purged with nitrogen, and the system was allowed to cool to room temperature while a nitrogen atmosphere was maintained.

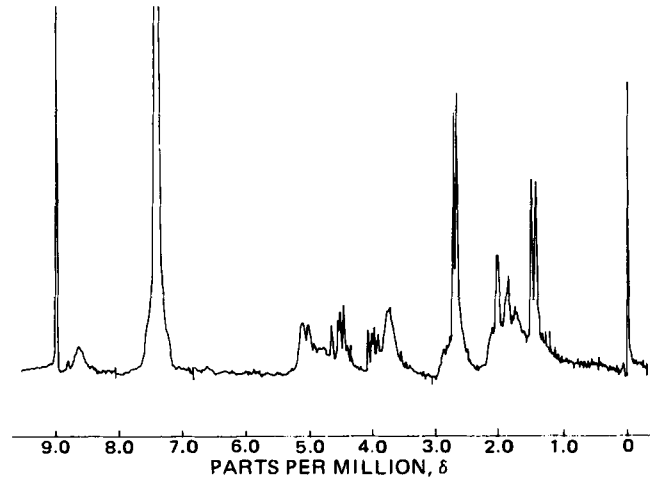

Figure 2—*NMR spectrum of II in deuterochloroform with 0.1% tetramethylsilane as reference. For instrument parameters, see Fig. 1.*

[1] Varian T-60, Varian Instrument, Palo Alto, Calif.
[2] Jeol Ft-100 (Fourier transformation), Jeol Analytical Instruments, Cranford, N.J.
[3] Fisher Scientific Co., Fair Lawn, N.J.
[4] Sigma Chemical Co., St. Louis, Mo.
[5] Tridom Chemical, Hauppauge, N.Y.

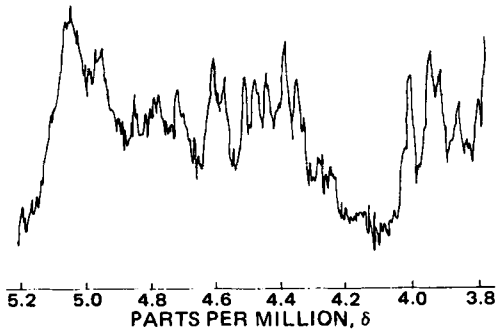

Figure 3—*Expansion of Fig. 1, 3.8–5.2-ppm region.*

To assure anhydrous conditions, the alkaloids (300 mg) were dissolved in 10 ml of benzene in a 50-ml glass stoppered flask, followed by the addition of 2 g of anhydrous magnesium sulfate. This preparation was allowed to stand 2 hr with intermittent stirring and was transferred to the dried reaction flask after filtering.

While a nitrogen atmosphere was maintained, 300 μl of (−)-1-phenylethylisocyanate reagent was added to give a 2:1 molar ratio of reagent to alkaloid. The heating mantle temperature was slowly adjusted to bring the solution to a gentle boil with stirring by a small magnetic stirring bar. After refluxing 2 hr under nitrogen, the reaction flask (intact system) was lowered into a water bath maintained at 5°. The water condenser was removed, and the dropping funnel containing picric acid solution was attached to the system. (The picric acid solution was prepared by dissolving 500 mg of picric acid in 10 ml of benzene; 5 g of anhydrous magnesium sulfate was added and, after standing for 48 hr, the solution was filtered into the dropping funnel.)

The picric acid solution was added dropwise, with stirring, over a 25-min period to the reaction flask maintained at 5°. Ten milliliters of dry benzene was used to wash the dropping funnel and to assure the quantitative addition of the picric acid solution.

All connections were removed from the reaction flask, and the flask was attached to a vacuum rotary evaporator. Glass stoppers (24/40 joint) were used to close the other openings.

The flask was rotated in a water bath at 25°, and the solvent was removed by reduced pressure. The unreacted reagent was removed by maintaining a vacuum (<1 mm Hg) for 4 hr at 25° after the solvent was removed.

The residue was dissolved in 5 ml of methylene chloride and transferred dropwise to a flask containing 300 ml of ether. Crystals formed on cooling the solution to −19°. The solution was allowed to stand for 24 hr before filtering. Crystallization from ether was repeated prior to the characterization studies.

RESULTS AND DISCUSSION

The initial investigation for the preparation of diastereomeric derivatives involved the formation of esters by the reaction of the alkaloids individually with both camphor-*d*-sulfonyl chloride and α-methoxy-α-trifluoromethylphenyl acid chloride (Mosher's acid chloride) in pyri-

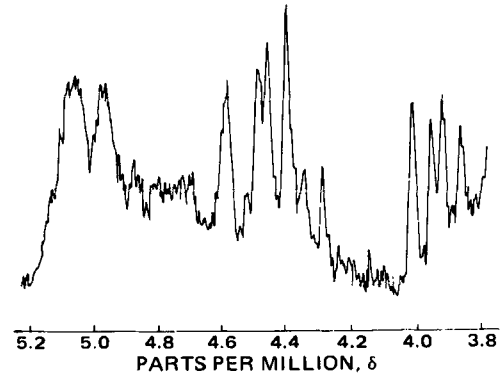

Figure 4—*Expansion of Fig. 2, 3.8–5.2-ppm region.*

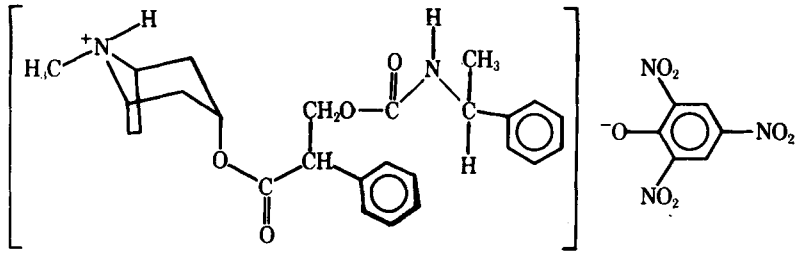

I
II

dine at 10°. The acid produced during the reaction formed salts with the derivatives. However, since these salts could not be induced to crystallize, isolation of the free amine derivatives was attempted. Unfortunately, this attempt was unsuccessful because partial elimination occurred to give apoatropine, which was identified by comparison of the NMR spectrum with a published spectrum (12).

Since the alkaloid reaction with an isocyanate would give the free amine derivatives directly, derivatization with a chiral isocyanate reagent was investigated next. The (−)-1-phenylethylurethane derivatives of l-hyoscyamine and atropine were prepared by reacting the alkaloids with (−)-1-phenylethylisocyanate in benzene. Both the free amine (−)-1-phenylethylurethane derivative and the corresponding hydrochlorides were oils at room temperature. To aid in characterization of these derivatives, a stable crystalline solid was needed. Picrate derivatives of tropane alkaloids are stable solids. Thus, the picrate salts of the diastereomeric derivatives were prepared using picric acid in benzene.

A high-performance liquid chromatographic (HPLC) procedure (13), using the derivatives as the picrate ion-pairs, indicated that less than 2% of the underivatized alkaloids remained in the crude reaction mixtures prepared according to the reaction conditions given under *Experimental*.

The NMR spectra at 60 MHz of atropine (−)-1-phenylethylurethane picrate (I) and *l*-hyoscyamine (−)-1-phenylethylurethane picrate (II) revealed minor differences in chemical shifts for the proton absorbances in the 3.84–4.64-ppm region.

However, more dramatic differences were observed when these NMR spectra were determined at 100 MHz using Fourier transformation.

Table I—Elemental Analyses and Melting Points of I and II

Compound	Trial	Melting[a] Point	Analysis[b], %	Calc.	Found
I	1	148–149°	C	57.74	57.65
			H	5.30	5.33
			N	10.52	10.51
I	2	148–149°	C	—	57.86
			H	—	5.35
			N	—	10.56
II	1	169–170°	C	57.74	57.50
			H	5.30	5.40
			N	10.52	10.47
II	2	169–170°	C	—	57.62
			H	—	5.32
			N	—	10.54

[a] Capillary melting-point apparatus, Arthur H. Thomas Co., Philadelphia, Pa.
[b] Atlantic Microlab, Atlanta, Ga.

Table II—UV and Visible Absorptivity Values for I and II

Compound	Wavelength, nm	Absorptivity
I	405	11.3
	345	21.7
	242	18.5
II	405	11.1
	345	21.5
	242	18.9

Figures 1 and 2 compare the complete 100-MHz spectra (0–10 ppm) determined on individual solutions having 10 mg of I and II in 0.5 ml of deuterochloroform containing 0.1% tetramethylsilane. Figures 3 and 4 show expansions (fivefold) of the 3.8–5.2-ppm regions of I and II, respectively. These spectra better demonstrate the differences in the chemical shifts of the absorptions of the methine proton (3.84–4.04-ppm region) and the methylene protons (4.22–4.64-ppm region) of the tropic acid moiety. The absorptions for the tropane ring C-3 proton and for the urethane moiety methine and nitrogen atom protons overlap and occur in the 4.54–5.20-ppm region. These absorptions overlap the lower field peaks for the methylene protons. By preparing various mixtures of I and II, rough diastereomeric composition estimates could be made from the NMR spectra in the 4.22–4.64-ppm region.

The derivatives, as the picrate ion pairs, were characterized by determination of melting points, optical rotations, elemental analyses, and IR, NMR, and UV–visible spectra. Table I contains elemental analysis data and melting points as determined on duplicate preparations of I and II.

In line with the original goal of this project, several HPLC systems were investigated for resolution of the diastereomeric mixture. However, satisfactory resolution was not achieved using various ion-exchange, reversed-phase partitioning, and ion-pairing techniques.

The optical rotations were determined on I and II in chloroform using a recording polarimeter[6]. The specific rotations were calculated for each derivative: I, $[\alpha]_D^{25} = -25.4°$, 0.965; and II, $[\alpha]_D^{25} = -51.2°$, 0.702.

The IR[7] spectra of I and II were identical and gave absorbance bands in agreement with their structure.

The UV and visible[8] absorptivity values for I and II in chloroform are recorded in Table II.

REFERENCES

(1) J. A. Dale, D. L. Dull, and H. S. Mosher, *J. Org. Chem.*, **34**, 2543 (1969).

(2) J. A. Dale and H. S. Mosher, *ibid.*, **35**, 4002 (1970).

(3) M. S. Biernbaum and H. S. Mosher, *ibid.*, **36**, 3168 (1971).

(4) B. T. Dewey and N. F. Witt, *Ind. Eng. Chem., Anal. Ed.*, **12**, 459 (1940).

(5) *Ibid.*, **14**, 648 (1942).

(6) W. M. Hearon, J. D. Hiatt, and C. R. Fordyce, *Am. Soc.*, **66**, 995 (1944).

(7) A. Neville and R. H. Pickard, *J. Chem. Soc.*, **85**, 685 (1904).

(8) C. Valee, *Ann. Chim.*, **15**, 410 (1908).

(9) A. P. Terent'ev, R. A. Gracheva, and V. T. Bezruchko, *Dokl. Akal. Nauk SSSR*, **172**, 622 (1967) (Russian).

(10) R. A. Gracheva, A. P. Terent'ev, and V. T. Bezruchko, *Zh. Org. Khim.*, **5**, 1058 (1969) (Russian).

(11) W. Pereira, V. A. Bacon, W. Patton, D. Halpern, and G. E. Pollock, *Anal. Lett.*, **3**, 23 (1970).

(12) "Sadtler Standard Spectra," Sadtler Research Laboratories, Philadelphia, Pa., Spectrum 4443 M.

(13) W. Santi, J. M. Huen, and R. W. Frei, *J. Chromatogr.*, **115**, 423 (1975).

[6] Bendix Ericsson automatic type 143A, Bendix Corp., Lewisburg, W.Va.
[7] Model 180, Perkin-Elmer Corp., Norwalk, Conn.
[8] Model 5260, Beckman Instruments, Fullerton, Calif.

Ionization Kinetics of the Carbon Acid Phenindione

V. J. STELLA ˣ **and R. GISH**

Received December 14, 1978, from the *Department of Pharmaceutical Chemistry, University of Kansas, Lawrence, KS 66045.* Accepted for publication February 20, 1979.

Abstract □ The ionization kinetics of carbon acids are slow relative to those of classical acids and bases. Phenindione (2-phenyl-1,3-indandione) is a 1,3-diketone carbon acid of macroscopic experimental pKa 4.09 at 25° and ionic strength 0.1. The ionization kinetics of phenindione were determined at an ionic strength of 0.1 and 25° using stopped-flow spectrophotometry and a pH jump technique. A log k'_{obs}–pH profile for the approach to the ionization equilibrium was determined, and a mechanism consistent with the profile was postulated. The percent enol *versus* diketo form of phenindione and the pKa_{enol} and pKa_{diketo} were calculated from the kinetic data. Phenindione acid deprotonation kinetics by various oxygen and nitrogen bases suggested that, with bases of pKa 4.7–8.5 and in the pH 5–8.5 range, the acidic phenindione proton was ~45% transferred in the rate-determining transition state.

Keyphrases □ Phenindione—ionization kinetics, stopped-flow spectrophotometric and pH analysis, model □ Anticoagulants—phenindione, ionization kinetics, pH □ Kinetics, ionization—phenindione

Phenindione (I) (2-phenyl-1,3-indandione) is an anticoagulant used in patients where the more popular anticoagulants are contraindicated. It is a 1,3-diketone carbon acid [lit. pKa 4.13 (1), 4.10 (2), 5.4 (3)]. Recent work (4, 5) suggested that some of the nonclassical phase transport behavior of another carbon acid, phenylbutazone, might be accounted for by its relatively slow ionization rate. Noninstantaneous ionization is a characteristic of some carbon acids (6–10).

The ionization kinetics of phenindione have not been studied previously, although the ionization kinetics of other carbon acids of much higher pKa's than those of phenindione and phenylbutazone have been well documented in the chemical literature (6–24). The immediate objective of this study was to determine the kinetics and mechanism of ionization of phenindione and to compare its behavior to that of phenylbutazone. Studying the kinetics and mechanism of ionization of a number of carbon acids of varying acidity might permit accurate prediction of the ionization kinetics of other pharmaceutically significant carbon acids. The ultimate objective is to use this information, combined with current ongoing mass transport studies, to predict the effect of noninstantaneous ionization kinetics on the mass transport behavior of carbon acids.

EXPERIMENTAL

Materials—Phenindione[1] was used as received. All reactions and pKa determinations were carried out in double-deionized, carbon dioxide-free water, freshly deoxygenated with oxygen-free nitrogen. The sodium chloride used to adjust the ionic strength was analytical reagent quality and was used without further purification. Hydrochloric acid, acetic acid–acetate, phosphate, and imidazole buffers were prepared with analytical grade components without further purification.

Pyridine, 3-methylpyridine (3-picoline), and morpholine were freshly purified by fractional distillation from potassium hydroxide pellets and stored over molecular sieves. A buffer component, 4-methoxypyridine, was prepared by the catalytic reduction of 4-methoxypyridine-*N*-oxide[2] using a literature method (25) for the reduction of 4-ethoxypyridine-*N*-oxide to 4-ethoxypyridine.

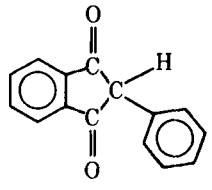

I

pKa Determination—The pKa of phenindione was determined spectrophotometrically[3] (26) at 326 nm and the same temperature and ionic strength conditions as in the kinetic studies, *i.e.*, 25 ± 0.2° and μ = 0.1 (sodium chloride). The pKa's of the various buffers used in the kinetic studies were determined potentiometrically using a pH meter[4] standardized with a standard buffer to a pH near the expected buffer component pKa (26).

Kinetic Studies—The procedures used to follow phenindione ionization kinetics were similar to those previously described for phenylbutazone (4). The reactions were followed at 326 nm, and the initial phenindione concentration was 1×10^{-4} *M*. At a pH where the primary reaction was the protonation of the mesomeric phenindione anion to phenindione acid, phenindione at pH ~7 was jumped to acidic pH (hydrochloric acid buffer or acetate buffer). At a pH where the primary reaction was the phenindione acid deprotonation to the mesomeric anion, phenindione in an aqueous solution of μ = 0.1 and with pH adjusted to ~4 with hydrochloric acid was jumped to the final pH by mixing with a buffer of desired final pH but double the desired final concentration.

The pH values after solution mixing were determined independently by mixing equal volumes of the phenindione solution and the buffer component. In most cases, the final pH was identical to that of the buffer solution. The exceptions were the most dilute morpholine buffer concentrations (see *Results and Discussion*), the hydrochloride acid buffer (final hydrochloric acid concentration was half the initial concentration), and one study where an unbuffered phenindione solution (pH ~4) was mixed with a very dilute sodium hydroxide solution (2×10^{-4} *M*). In this last case, the final pH was 8.91, even though the pH was expected to be closer to 10. The pH's used to construct the pH profile (Fig. 1) for the hydrochloric acid solutions and the sodium hydroxide solution were those measured experimentally.

RESULTS AND DISCUSSION

Figure 2 shows the phenindione UV spectrum under basic as well as acidic conditions, 0.1 *M* NaOH and 0.1 *M* HCl, respectively. The strong bathochromic shift from acidic to basic pH conditions is due to the extended conjugation on ionization, *i.e.*, coupling of the two phenindione phenyl rings through the enolate double bond (1). The macroscopic dissociation constant of phenindione was determined by observing the change in absorbance of a 1×10^{-4} *M* phenindione solution (25° and μ = 0.1) at pH 1 (0.1 *M* HCl), in the pH 2–6 range (acetate buffer), and at pH 13 (0.1 *M* NaOH).

The K_a was determined from a plot of $(A - A_0)[H^+]$ *versus* A as described previously (4), where A is the phenindione absorbance at a given hydrogen-ion concentration, $[H^+]$, and A_0 is the phenindione absorbance under acid conditions, *i.e.*, with the ionization completely suppressed (0.1 *M* HCl). The K_a under the experimental conditions was 8.13×10^{-5}, giving a pKa of 4.09. This value compares favorably with the literature pKa values (1–3) when differences in ionic strength and solvent composition are considered.

Table I gives the observed rate constants, k_{obs} (sec^{-1}), for phenindione ionization kinetics under various pH and buffer concentrations. All observed rate constants are the mean of three or more determinations. Also

[1] Pfaltz and Bauer, Flushing, N.Y.
[2] Aldrich Chemical Co., Milwaukee, Wis.
[3] Cary 15, Cary Instruments, Monrovia, Calif.
[4] Model 701, Orion Research, Cambridge, Mass.

0022-3549/79/0800-1042$01.00/0
© 1979, American Pharmaceutical Association

Table I—Effect of pH and Buffers on the Ionization Kinetics of Phenindione at 25 ± 0.2° and μ = 0.1 with Sodium Chloride

pH[a]	Buffer (pKa; Concentration Range; Number of Concentrations Studied)	k'_{obs}, sec^{-1}	k_{CAT}, M^{-1} sec^{-1}
1.62	Hydrochloric acid (NA[b]; 0.024 *M*; NA)	262	NA
1.65	Hydrochloric acid (NA; 0.022 *M*; NA	258	NA
2.04	Hydrochloric acid (NA; 0.009 *M*; NA)	198	NA
2.05	Hydrochloric acid (NA; 0.009 *M*; NA)	206	NA
2.05	Hydrochloric acid (NA; 0.009 *M*; NA)	190	NA
2.58	Hydrochloric acid (NA; 0.0026 *M*; NA)	112	NA
2.66	Hydrochloric acid (NA; 0.0025 *M*; NA)	97	NA
2.94	Hydrochloric acid (NA; 0.00115 *M*; NA)	63	NA
3.06	Hydrochloric acid (NA; 0.00087 *M*; NA)	54	NA
3.09	Hydrochloric acid (NA; 0.00081 *M*; NA)	50	NA
3.45	Hydrochloric acid (NA; 0.00035 *M*; NA)	28	NA
5.00	Acetate (4.70; 0–0.05 *M*; 4)	6.3	938 ± 48
6.00	Acetate (4.70; 0–0.05 *M*; 4)	6.0	845 ± 18
6.50	3-Methylpyridine (5.75; 0–0.05 *M*; 4)	7.1	4475 ± 128
7.00	3-Methylpyridine (5.75; 0.03 *M*; 3)	6.8	4900 ± 56
5.00	Pyridine (5.28; 0–0.05 *M*; 3)	8.1	803 ± 10
6.00	Pyridine (5.28; 0–0.05 *M*; 4)	6.9	2489 ± 54
6.20	4-Methoxypyridine (6.64; 0–0.04 *M*; 4)	6.9	1797 ± 58
6.80	4-Methoxypyridine (6.64; 0–0.04 *M*; 4)	7.0	3694 ± 127
7.00	Imidazole (7.10; 0–0.05 *M*; 3)	9.1	2407 ± 94
7.50	Imidazole (7.10; 0–0.025 *M*; 5)	4.7	4310 ± 131
7.00	Morpholine (8.53; 0–0.035 *M*; 3)	7.5	122 ± 61
7.50	Morpholine (8.53; 0–0.035 *M*; 3)	6.0	3660 ± 1
8.00	Morpholine (8.53; 0–0.01 *M*; 5)	13.2	12150 ± 240
8.50	Morpholine (8.53; 0–0.008 *M*; 4)	26	26500 ± 288
7.00	Phosphate (6.75; 0–0.0165 *M*; 3)	5.0	2271 ± 216
7.50	Phosphate (6.75; 0–0.0165 *M*; 3)	7.9	2615 ± 26
8.91	Sodium hydroxide (NA; 1 × 10^{-4} *M*; NA)	61	NA

[a] Experimentally measured final pH. [b] NA = not applicable.

included in this table are the observed rate constants extrapolated to zero buffer concentrations, k'_{obs} (sec^{-1}), obtained from plots of k_{obs} *versus* total buffer concentration. Figure 1 is a plot of log k_{obs} *versus* pH from the phenindione ionization.

A possible model for phenindione ionization kinetics is given in Scheme I, where K is the diketo form of phenindione and the predominant neutral form of phenindione in aqueous solution (1), E is the enol form of phenindione, and E^- is the so-called mesomeric anion (7). The macroscopic dissociation constant for phenindione is defined by:

$$K_a = \frac{[E^-][H^+]}{[K] + [E]} \qquad \text{(Eq. 1)}$$

which can be rearranged to:

$$\frac{1}{K_a} = \frac{1}{K_{a,diketo}} + \frac{1}{K_{a,enol}} \qquad \text{(Eq. 2)}$$

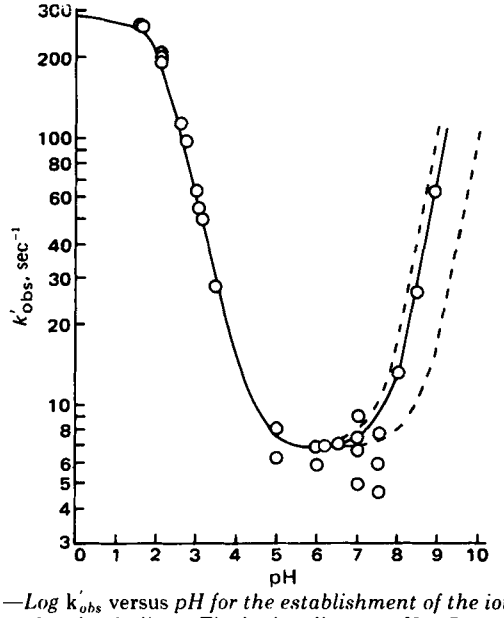

Figure 1—*Log* k'_{obs} versus *pH for the establishment of the ionization equilibrium for phenindione. The broken lines at pH > 7 represent* k_3 *having the limits of* 10^6–10^7 M^{-1} sec^{-1}. *The lack of reproducibility of the data at pH > 8 precludes placing an accurate value on* k_3.

Equation 2 shows the relationship between the macroscopic dissociation constant, K_a, and the microscopic constants, $K_{a,diketo}$ and $K_{a,enol}$. The percent enol present in aqueous solution will be defined by the relative values of $K_{a,diketo}$ and $K_{a,enol}$. The percent enol is defined by:

$$\% \text{ enol} = \frac{[E]}{[K] + [E]} (100) \qquad \text{(Eq. 3)}$$

which can be rearranged to:

$$\% \text{ enol} = \frac{K_{a,diketo}}{K_{a,diketo} + K_{a,enol}} \left(\frac{100}{1}\right) \qquad \text{(Eq. 4)}$$

The assumption can be made that the equilibrium defined by $K_{a,enol}$ is rapid and instantaneous[5] (7). The rate constant k_1 represents the water-catalyzed phenindione deprotonation, k_3 is the hydroxide-ion-catalyzed deprotonation rate constant, and k_{GB} is the general base-catalyzed deprotonation rate constant. The constant k_2 represents the hydronium-catalyzed protonation constant, *i.e.*, the addition of a proton at C-2 of the mesomeric anion; k_4 is the water or spontaneous protonation rate constant, and k_{GA} is the general acid-catalyzed protonation rate constant.

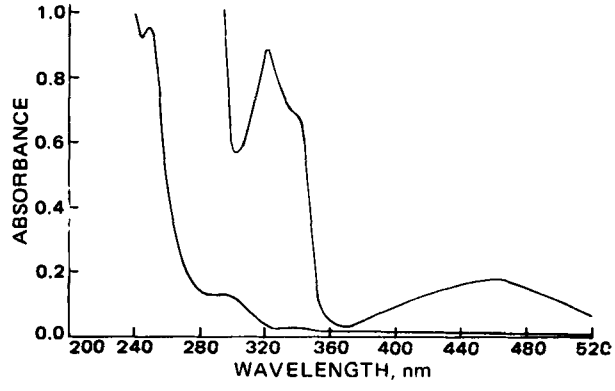

Figure 2—*Phenindione (1 × 10⁻⁴ M) UV spectrum in 0.1 M NaOH (upper curve) and in 0.1 M HCl (lower curve).*

[5] The word instantaneous is used to describe phenomena taking place at rates near the diffusion-controlled limit.

Table II—Final pH after Mixing Equal Volumes of the Initial Morpholine Buffer Solution (Double the Final Concentration) with the Phenindione Solution [a]

Initial Buffer pH	Buffer Concentration (after Mixing), M	Measured Final pH
8.00	2×10^{-3}	7.80[b]
8.00	4×10^{-3}	7.94
8.00	6×10^{-3}	7.98
8.00	8×10^{-3}	8.00
8.00	10×10^{-3}	8.00
8.50	2×10^{-3}	8.44[b]
8.50	4×10^{-3}	8.49
8.50	6×10^{-3}	8.50
8.50	8×10^{-3}	8.50
8.50	10×10^{-3}	8.50

[a] Aqueous phenindione solution of $\mu = 0.1$ with sodium chloride and added hydrochloric acid sufficient to give a pH of ~4. [b] As expected, both of these buffers gave negative deviations in plots of k_{obs} *versus* $[buffer]_T$ so neither was used in the k_{CAT} calculations.

With the assumption of Scheme I, an equation for the approach to the ionization equilibrium can be derived for any perturbation of that equilibrium (4):

$$k'_{obs} = k_1 + k_3[OH^-] + \frac{k_2[H^+]K_{a,enol}}{K_{a,enol} + [H^+]} + \frac{k_4 K_{a,enol}}{K_{a,enol} + [H^+]} \quad \text{(Eq. 5)}$$

For example, if a pH ~ 7 phenindione solution is perturbed rapidly (in the stopped-flow apparatus) to pH ~ 2, the first reaction is the instantaneous protonation of the mesomeric anion to the enol, E, and eventually (at equilibrium) to a mixture of the enol and diketo phenindione forms. Similarly, an acidic phenindione solution perturbed to alkaline pH involves primarily the deprotonation of the diketo phenindione and the small fraction of enol to the mesomeric anion. The observed buffer independent rate constant for the attainment of equilibrium, k'_{obs}, is the sum of both the forward and reverse rate constants because the system under study is a reversible reaction.

UV spectroscopic studies (1) showed that phenindione exists predominantly in its diketo form in aqueous solution. This means (Eq. 4) that $pKa_{diketo} \gg pKa_{enol}$ so that $pKa_{diketo} \sim pKa$ and $pKa_{enol} \ll 4.09$. From Fig. 1, phenindione deprotonation to form the anion, *i.e.*, pH > pKa_{diketo}, the k'_{obs} can be given by:

$$k'_{obs} = k_1 + \frac{k_4 K_{a,enol}}{K_{a,enol} + [H^+]} + k_3[OH^-] \quad \text{(Eq. 6)}$$

and since $K_{a,enol} \gg [H^+]$ at the pH's in question, Eq. 6 simplifies to:

$$k'_{obs} = (k_1 + k_4) + k_3[OH^-] \quad \text{(Eq. 7)}$$

As discussed previously (4), k_4 is negligible relative to k_1, so the plateau seen in Fig. 1 in the pH 5–7.5 range is essentially due to k_1. The constant k_1 calculated as the mean values of k'_{obs} in the pH 6.0–7.0 range was 6.9 sec^{-1}.

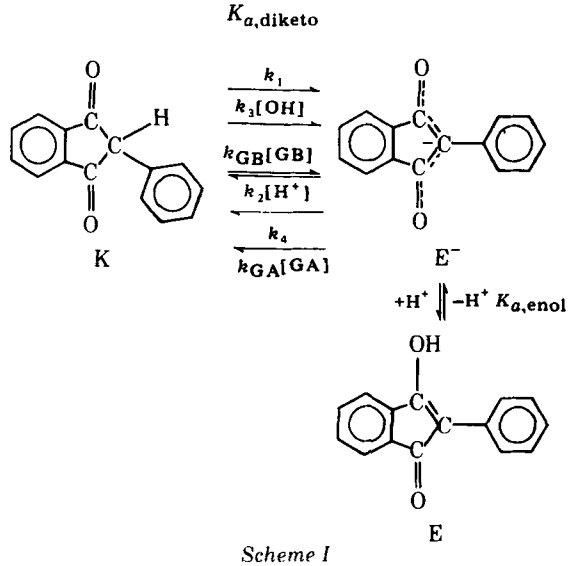

Scheme I

Table III—Kinetic and Equilibrium Constants for Phenindione Ionization at 25° and $\mu = 0.1$ with Sodium Chloride

Parameter	Value
k_1	$6.9\ sec^{-1}$
k_2	$6.5 \times 10^4\ M^{-1}\ sec^{-1}$
k_3	$\sim 6 \times 10^6\ M^{-1}\ sec^{-1}$
k_4	$\sim 5.5 \times 10^{-4}\ sec^{-1}$
$K_{a,enol}$	4.24×10^{-3} ($pKa_{enol} = 2.37$)
$K_{a,diketo}$	1.06×10^{-4} (pKa = 3.97)
K_a	1.03×10^{-4} (pKa = 3.99[a])
	8.13×10^{-5} (pKa = 4.09[b])
% enol	2.4

[a] Determined kinetically. [b] Determined spectrophotometrically.

The limited number of points and the questionable accuracy of the unbuffered hydroxide-ion solution reaction given on the last line of Table I allow only a crude k_3 estimate of between 10^6 and $10^7\ M^{-1}\ sec^{-1}$. For the sake of fitting the observed data to Eq. 5, $6 \times 10^6\ M^{-1}\ sec^{-1}$ was used for k_3. In an earlier study with phenylbutazone (4), borate buffers, which are poor proton-abstracting agents, were used at pH 8.5–9.5. Recent papers and some earlier work suggested that the ionization kinetics of borate buffers themselves are slow (27–33). This then raises the question as to what was the microscopic pH upon perturbing an acid solution of the carbon acid to an alkaline pH maintained with a borate buffer.

In the present study, when a borate buffer study was undertaken in the pH 8.5–9.5 range, an estimate of k_3 of closer to $1 \times 10^6\ M^{-1}\ sec^{-1}$ was made. This would suggest that the earlier k_3 estimate for phenylbutazone deprotonation by hydroxide ion may be low. Unfortunately, other techniques for following fast reactions cannot be applied to the deprotonation reactions in question. Even though k_{obs} is in the measurable range (by stopped-flow spectrophotometry) at pH 8–9, the pH after mixing must be maintained with a buffer of sufficient buffer capacity. Normally, the buffer concentration is varied and plots of k_{obs} *versus* buffer concentrations are extrapolated to zero buffer concentration to obtain k'_{obs}. This approach was attempted with morpholine buffer at pH 8.00 and 8.50 (Table I) and concentrations after mixing of below $1 \times 10^{-2}\ M$.

Table II gives the final pH values after the morpholine buffers were mixed with the phenindione solution (pH ~ 4 with hydrochloric acid). At the low buffer concentrations, significant pH alterations, affecting both the hydroxide-ion concentration and the fraction of total morpholine present in the the unionized state, occurred. Higher buffer concentrations or stronger bases could not be used because the deprotonation reaction became too rapid to be followed by stopped-flow spectrophotometry. The phenindione solution had to be somewhat acidic so that sufficient spectral alteration would occur as a result of the pH perturbation to allow the reaction to be followed spectrophotometrically.

At pH < 8, the $k_3[OH^-]$ term is negligible and, since k_4 is small relative to all other terms:

$$k'_{obs} = k_1 + \frac{k_2[H^+]K_{a,enol}}{K_{a,enol} + [H^+]} \quad \text{(Eq. 8)}$$

which can be rearranged to:

$$\frac{1}{k'_{obs} - k_1} = \frac{1}{k_2[H^+]} + \frac{1}{k_2 K_{a,enol}} \quad \text{(Eq. 9)}$$

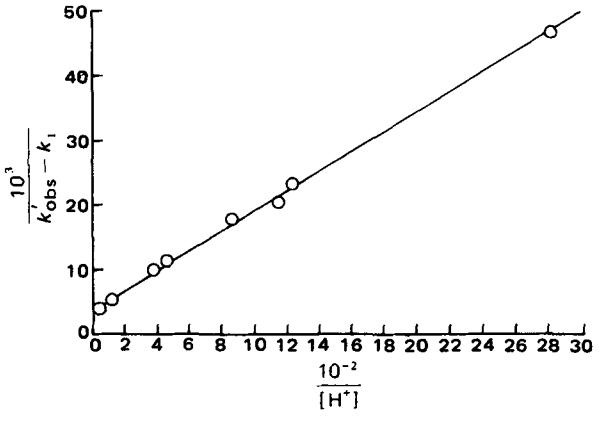

Figure 3—*Plot used to determine* k_2 *and* $K_{a,enol}$ *for phenindione ionization (Eq. 9 and Scheme I).*

predicting that a plot of the left side of Eq. 9 against $1/[H^+]$ should give a straight line of slope $1/k_2$ and intercept $1/k_2K_{a,enol}$, thus allowing both k_2 and $K_{a,enol}$ to be calculated. Such a plot for phenindione is shown in Fig. 3. The calculated values of k_2 and $K_{a,enol}$ are $6.5 \times 10^4\ M^{-1}\ sec^{-1}$ and $4.24 \times 10^{-3}\ M$, respectively ($pK_{a_{enol}} = 2.37$).

According to Scheme I, the equilibrium ionization constant for diketo phenindione is:

$$K_{a,diketo} = \frac{k_1}{k_2} = \frac{6.9}{6.5 \times 10^4} = 1.06 \times 10^{-4}\ M \qquad \text{(Eq. 10)}$$

Having determined $K_{a,enol}$ and $K_{a,diketo}$ and using Eq. 4, the enol was calculated at 2.4%.

Table III summarizes the kinetic and equilibrium constants calculated. The values for rate constants from Table III were placed into Eq. 5 to generate a theoretical curve for phenindione ionization kinetics at various pH's, assuming the mechanism shown in Scheme I. The solid line drawn in Fig. 1 is the line generated by Eq. 5 and the appropriate values in Table III. Apparently, Eq. 5 and Scheme I adequately describe the observed values, although other mechanisms may be possible (4).

A comparison of the values of k_1 and k_2, the two most accurately determined rate constants for both phenylbutazone and phenindione, highlights some interesting points. The lower pKa of phenindione relative to phenylbutazone, 3.99 *versus* 4.33, is due to changes in both k_1 and k_2. *A priori*, based on the strength of the acids, k_1 for phenindione (the stronger acid) would be expected to be greater than that for phenylbutazone. Such is not the case. The constant k_1 has a value of 6.9 sec^{-1} for phenindione compared to 10.1 sec^{-1} for phenylbutazone. The small differences in k_1, ~30%, are more than compensated by the differences in k_2. The constant k_2 has a value of $6.5 \times 10^4\ M^{-1}\ sec^{-1}$ for phenindione relative to $2.1 \times 10^5\ M^{-1}\ sec^{-1}$ for phenylbutazone. The greater acidity of phenindione relative to phenylbutazone is controlled not by how readily the acid gives up its proton but by the ability of its base form to accept a proton.

Equation 5 appears to describe adequately phenindione protonation and deprotonation kinetics in the absence of buffer species capable of acting as general acids and bases. In the presence of acids and bases other than the water species, the observed rate constant for the approach to the ionization equilibrium after a pH perturbation would be given by:

$$k_{obs} = k'_{obs} + k_{GB}[GB] + \frac{k_{GA}[GA]K_{a,enol}}{[H^+] + K_{a,enol}} \qquad \text{(Eq. 11)}$$

and since at pH > 4, $K_{a,enol} \gg [H^+]$, Eq. 11 reduces to:

$$k_{obs} = k'_{obs} + k_{GB}[GB] + k_{GA}[GA] \qquad \text{(Eq. 12)}$$

$$k_{obs} = k'_{obs} + k_{CAT}\,[buffer]_T \qquad \text{(Eq. 13)}$$

where k_{CAT} is the observed catalytic rate constant for any buffer at any given pH value. This is equal to:

$$k_{CAT} = k_{GB}f + k_{GA}(1 - f) \qquad \text{(Eq. 14)}$$

$$k_{CAT} = f(k_{GB} - k_{GA}) + k_{GA} \qquad \text{(Eq. 15)}$$

where f is equal to the fraction of total buffer species in the base form and $(1 - f)$ is the fraction of total buffer species in its acid form at any given pH. For any given singly dissociating buffer species with a known dissociation constant, f can be calculated from:

$$f = \frac{[H^+]}{K'_a + [H^+]} \qquad \text{(Eq. 16)}$$

where K'_a is the dissociation constant of the conjugate acid form of the buffer. Equation 13 predicts that a plot of k_{obs} *versus* total buffer concentrations, $[buffer]_T$, would be linear with slope k_{CAT} and intercept k'_{obs}. A plot of k_{CAT} *versus* f is predicted from Eq. 15 to be linear with an intercept at $f = 0$ of k_{GA} and an intercept at $f = 1$ of k_{GB}. With the buffers studied, acetate, phosphate, pyridine, 3-methylpyridine, 4-methoxypyridine, imidazole, and morpholine, all plots of k_{obs} *versus* total buffer concentration were linear. From plots of k_{CAT} *versus* f, for all cases except acetic acid, k_{GA} was negligible relative to k_{GB}. When a small or even slightly negative intercept at $f = 0$ was seen from plots of k_{CAT} *versus* f, k_{GB} was calculated from k_{CAT}/f and the mean values of k_{GB} for the various bases calculated at different pH's are recorded in Table IV. Table IV is a compilation of the calculated k_{GA} and k_{GB} values for all of the buffers and water species.

A Brønsted plot (19, 23, 34) of log k_{GB} *versus* the pKa''s of the various buffers is given in Fig. 4. When studying a limited number of bases (acetate through morpholine in the present study) for a reaction catalyzed by general bases, apparent linear Brønsted plots usually result (19, 23).

Table IV—Calculated k_{GA} and k_{GB}

Buffer (pKa)	k_2, k_4, or k_{GA}, $M^{-1}\ sec^{-1}$	k_1, k_3, or k_{GB}, $M^{-1}\ sec^{-1}$
H_3O^+ (−1.74)	6.5×10^4	—
H_2O (−1.74 and 15.74)[a]	1×10^{-5} (5.5 $\times 10^{-4}$/55.5)[b]	1.24×10^{-1} (6.9/55.5)[b]
Acetic acid (4.70)	1161	828
Pyridine (5.28)	263	3635
3-Methylpyridine (5.75)	—[c]	5210[c]
4-Methoxypyridine (6.64)	—[c]	6458[c]
Imidazole (7.10)	—[c]	5728[c]
Morpholine (8.53)	—[c]	48123[c]
Phosphoric acid (2.12)	1223[d]	1223[d]
Phosphoric acid (6.75)	—	2861[d]
OH^- (15.74)	—	6×10^6

[a] When H_2O is acting as a base, its conjugate acid is H_3O^+. When H_2O is acting as an acid, its conjugate base is OH^-. [b] From the kinetic study, it was possible to calculate the rate constants for H_2O acting both as an acid and a base. [c] Plots of k_{CAT} *versus* gave either negligible k_{GA} values or slightly negative values. Therefore, k_{GB} was calculated as the mean value for k_{CAT}/f for each pH studied. [d] This refers to $H_2PO_4^-$ acting as either a general acid or a general base. Because of this ambiguity, the point for $H_2PO_4^-$ was not included in Fig. 4. It is not possible to determine in what capacity $H_2PO_4^-$ is acting. Although HPO_4^{2-} is capable of acting either as an acid or a base, it is more likely acting as a base.

It is becoming increasingly obvious that over a more extensive range of bases, nonlinear Brønsted plots, especially for the ionization kinetics of carbon acids, are more the rule than the exception (6, 7, 19, 23). The reason behind the nonlinearity was first discussed by Eigen (7) and quantitated recently by the Marcus theory (23, 35).

The Marcus theory of general base catalysis suggests that a quadratic fit to the Brønsted plot is more accurate and reflects more closely the mechanism of such catalysis. The solid curved line drawn through the points in Fig. 4 is the quadratic fit[6] to the data. The number of bases studied in the present work was limited by the speed of the reaction. Of course, the catalytic effect of water acting as a base could be determined because of its high intrinsic concentration (55.5 *M*), and hydroxide-ion catalysis could be approximately determined because its effective concentration could be determined from pH measurements.

The solid curved line in Fig. 4 is described by:

$$\log k_{GB} = -1.36 \times 10^{-2}\,pKa'^2 + 6.25 \times 10^{-1}\,pKa' + 2.76 \times 10^{-1} \qquad \text{(Eq. 17)}$$

Differentiation of Eq. 17 would give the slope of the line at any point and is described by Eq. 18. For a Brønsted plot, the slope for general base-catalyzed reactions is given the designation β:

$$\beta = \frac{d(\log k_{GB})}{d(pKa')} = -2.72 \times 10^{-2}\,pKa' + 0.625 \qquad \text{(Eq. 18)}$$

The Brønsted plot resulting from the present study could just as easily be described by a linear plot, with the H_2O term and the OH^- term giving

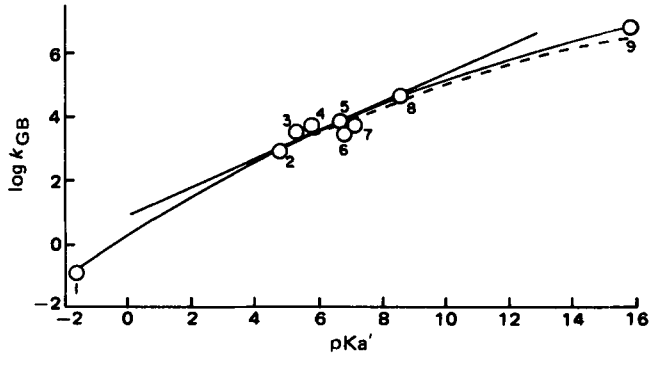

Figure 4—*Log* k_{GB} versus *pKa' for phenindione deprotonation by various general bases of varying pKa. Key: 1, water; 2, acetate; 3, pyridine; 4, 3-methylpyridine; 5, 4-methoxypyridine; 6, monohydrogen phosphate; 7, imidazole; 8, morpholine; and 9, hydroxide ion.*

[6] Least-squares analysis; TI59 programmable calculator utilizing the solid-state statistic module.

negative deviations from the linear plot. Such a plot would be given by the solid straight line in Fig. 4. The slope of the line is 0.45.

The Marcus theory states that when the pKa′ of the general base is equal to the carbon acid pKa, β, the slope of the Brønsted plot, should be equal to 0.5. Substitution of 3.99 for the phenindione pKa into Eq. 18 gives a β value of 0.52. Kresge (23) and Hupe and Wu (19) recently attempted to interpret the nonlinear Brønsted plots often seen for the ionization of various carbon acids. The Marcus theory (35) for such curvature relates the free energy of activation, $\Delta G^{\neq}$, for the proton transfer process to the energy required to bring the reactants together, Wr, and the intrinsic energy involved in the proton transfer, $(1 + \Delta G_0/4\Delta G_0^{\neq})^2\Delta G_0^{\neq}$, as defined by Eq. 19. The term ΔG_0 is the free energy for proton transfer at equilibrium, and $\Delta G_0^{\neq}$ is the free energy of activation for the proton transfer when $\Delta G_0 = 0$. That is, ΔG_0 is equal to zero when the pKa′ of the general base is equal to the pKa of the carbon acid:

$$\Delta G^{\neq} = (1 + \Delta G_0/4\Delta G_0^{\neq})^2\Delta G_0^{\neq} + Wr \qquad \text{(Eq. 19)}$$

The term ΔG_0 can be calculated from:

$$\Delta G_0 = -RT \ln(K_a'/K_a) \qquad \text{(Eq. 20)}$$

From the quadratic fit to the general base data (Eq. 17), k_{GB} at pKa′ 3.99 was calculated to be 357 M^{-1} sec^{-1}; $\Delta G^{\neq}$, calculated by solving for $\Delta G^{\neq}$ from:

$$k_{GB} = 10^{12.74} e^{-\Delta G^{\neq}/RT} \qquad \text{(Eq. 21)}$$

is equal to 13,899 cal/mole (~13,900 cal/mole). It is possible to relate the first coefficient (pKa′^{2} term) of Eq. 17, a, directly to the term $\Delta G_0^{\neq}$ through (23):

$$a = \frac{2.303RT}{16\Delta G_0^{\neq}} \qquad \text{(Eq. 22)}$$

thus allowing $\Delta G_0^{\neq}$ to be calculated. A value of ~6300 cal/mole was thus determined for $\Delta G_0^{\neq}$. Having calculated $\Delta G_0^{\neq}$ as ~6300 cal/mole and $\Delta G^{\neq}$ as ~13,900 cal/mole, at pKa′ = pKa, Wr can be estimated as ~7600 cal/mole. By using the values for $\Delta G_0^{\neq}$ of 6300 cal/mole and Wr of 7600 cal/mole, $\Delta G^{\neq}$ from the full range of bases (H_2O–OH^-) can be calculated and compared to the quadratic fit to Eq. 17. The broken line in Fig. 4 is the line generated from Eqs. 19 and 21. Note that the broken line was generated from Eqs. 19 and 21 using the information that, at pKa′ 3.99, the two lines should have intersected. That is, the solid curved line and the curved broken line intersect at pKa′ 3.99.

The interpretation of these observations is that carbon acid deprotonation involves two processes: (*a*) a work term, which includes desolvation of the incoming base and alteration in the solvation around the reaction center as well as getting the molecule in the correct configuration for proton abstraction, and (*b*) the energy required for breaking the carbon–hydrogen bond. The Wr term in Eq. 19, which is considered to be the work required to bring the two reacting molecules together, has an energy requirement of 7600 cal/mole, which is a little more than the energy required to break a hydrogen bond (36). Similarly, the standard free energy of activation, $\Delta G_0^{\neq}$, which is related to the intrinsic barrier to the breaking of the carbon–hydrogen bond, also has an energy requirement that is a little more than that required to break a weak carbon hydrogen bond (36).

In the past, the apparent negative deviation of hydroxide ion in linear Brønsted plots was always interpreted as the "anomolous" behavior of hydroxide ion. A study involving proton abstraction from a weak carbon acid (19) recently showed that hydroxide-ion behavior is not "anomalous" when other weak oxygen acids are included; *i.e.*, hydroxide ion acted as predicted for a base of pKa 15.74. The Brønsted plot curvature was interpreted as a change in the rate-determining step in going from weak bases to strong bases such as hydroxide ions. That is, with weak bases, the major rate-determining factor is the carbon–hydrogen bond breaking (first term in Eq. 19 is dominant) while with stronger bases the work term, Wr, begins to dominate. The reverse of this step (protonation of the mesomeric anion by a water molecule) has shown similarly anomalous kinetic behavior, suggesting that solvent reorganization around the reaction center may contribute to the rate-determining step (4, 37). As discussed previously (19), the alternative mechanism of a gradual change only in the degree of proton transfer in going from weak to stronger bases does *not* appear to be reasonable for the nonlinear Brønsted plot, although this mechanism cannot be totally ruled out.

If the Brønsted slope, β, *does* approximate the degree of a proton transfer over a limited pKa′ range for weak bases (23), it can be seen from Fig. 4 that a Brønsted slope of 0.45 is calculated for bases with a pKa′ of 4.7–8.53. An interpretation of this result is that the phenindione proton is 45% transferred in the rate-determining transition state for proton abstraction by these bases. A way of testing the hypothesis that a change is occurring at the reaction center in going from proton abstraction by a very weak base (water) to stronger bases (buffers used in present study) to very strong bases (hydroxide ion) would be to study the effects of electron-withdrawing and electron-donating groups on both the pKa and ionization kinetics of 4′-substituted 2-phenyl-1,3-indandiones. Such a study will be reported separately (38).

In summary, the ionization kinetics of phenindione in aqueous solution appear to be qualitatively similar to those of phenylbutazone, but quantitative differences do occur. A study of the effect of various bases in promoting proton abstraction from phenindione has led to some insights into possible rate-determining transition states for the deprotonation reaction. The various rate constants calculated for proton donation and abstraction during phenindione ionization are substantially slower than the diffusion-limited constants for the ionization of normal or classical acids such as carboxylic, phenolic, and nitrogen acids. The ionization kinetics generated from this work will be used along with ongoing mass transport studies to predict the effect of noninstantaneous ionization kinetics on the mass transport behavior of carbon acids.

REFERENCES

(1) Y. Linaberg, O. Neiland, A. Veis, A. N. Latv, and G. Vanag, *Dokl. Akad. SSSR*, **154**, 1385 (1964); *Engl. Transl.*, **154**, 184 (1964).

(2) W. Sztark, *Diss. Pharm. Pharmacol.*, **19**, 429 (1968).

(3) J. G. Lombardino and E. H. Wiseman, *J. Med. Chem.*, **11**, 342 (1968).

(4) V. J. Stella and J. D. Pipkin, *J. Pharm. Sci.*, **65**, 1161 (1976).

(5) V. Stella, *ibid.*, **64**, 706 (1975).

(6) M. L. Bender, "Mechanisms of Homogeneous Catalysis from Protons to Proteins", Wiley–Interscience, New York, N.Y. 1971, chap. 2.

(7) M. Eigen, *Angew. Chem. Int. Ed.*, **3**, 1 (1964).

(8) J. R. Jones, *Prog. Phys. Org. Chem.*, **9**, 241 (1972).

(9) A. J. Kresge, *Acc. Chem. Res.*, **8**, 354 (1975).

(10) R. P. Bell and S. Grainger, *J. Chem. Soc. Perkin Trans. II*, **1976**, 1367.

(11) T. Riley and F. A. Long, *J. Am. Chem. Soc.*, **84**, 522 (1962).

(12) R. F. Pratt and T. C. Bruice, *J. Org. Chem.*, **37**, 3563 (1972).

(13) F. G. Bordwell and W. J. Boyle, Jr., *J. Am. Chem. Soc.*, **97**, 3447 (1975).

(14) *Ibid.*, **93**, 512 (1971).

(15) F. G. Bordwell, W. J. Boyle, Jr., J. A. Hautala, and K. C. Lee, *J. Am. Chem. Soc.*, **91**, 4002 (1969).

(16) F. G. Bordwell, W. J. Boyle, Jr., and K. C. Lee, *ibid.*, **92**, 5926 (1970).

(17) F. G. Bordwell and W. J. Boyle, Jr., *ibid.*, **93**, 511 (1971).

(18) *Ibid.*, **94**, 3907 (1972).

(19) D. J. Hupe and D. Wu, *J. Am. Chem. Soc.*, **99**, 7653 (1977).

(20) A. J. Kresge, D. A. Drake, and Y. Chang, *Can. J. Chem.*, **52**, 1889 (1974).

(21) J.-H. Kim and K. T. Leffek, *ibid.*, **52**, 592 (1974).

(22) D. J. Barnes and R. P. Bell, *Proc. R. Soc. London A*, **318**, 421 (1970).

(23) A. J. Kresge, *Chem. Soc. Rev.*, **2**, 475 (1973).

(24) R. P. Bell and R. G. Pearson, *J. Chem. Soc.*, **1953**, 3443.

(25) H. J. den Hertog and W. P. Combé, *Recueil*, **70**, 589 (1951).

(26) A. Albert and E. P. Serjeant, "Ionization Constants of Acids and Bases," Metheun, London, England, 1962.

(27) O. Kajimoto, T. Saeki, Y. Nagaoka, and T. Fueno, *J. Phys. Chem.*, **81**, 1712 (1977).

(28) J. L. Anderson, E. M. Eyring, and M. P. Whittaker, *ibid.*, **68**, 1128 (1964).

(29) R. K. Momu and N. H. Nachtrieb, *Inorg. Chem.*, **6**, 1189 (1967).

(30) N. Ingri, G. Lagerstrom, M. Frydman, and L. G. Sillén, *Acta Chem. Scand.*, **11**, 1034 (1957).

(31) N. Ingri, *ibid.*, **16**, 439 (1962).

(32) *Ibid.*, **17**, 573 (1963).

(33) *Ibid.*, **17**, 581 (1963).

(34) J. N. Brønsted and K. Pederson, *Z. Phys. Chem.*, **108**, 185 (1924).

(35) R. A. Marcus, *J. Phys. Chem.*, **72**, 891 (1968).
(36) G. C. Pimentel and A. L. McClellan, "The Hydrogen Bond," W. H. Freeman, San Francisco, Calif. 1960, chap. 6.
(37) G. S. Rork and I. H. Pitman, *J. Am. Chem. Soc.*, **96**, 4654 (1974).
(38) V. J. Stella and R. Gish, *J. Pharm. Sci.*, **68**, 1047 (1979).

ACKNOWLEDGMENTS

Supported by Grant GM 22357 from the National Institutes of Health.

The authors thank Dr. R. Schowen for valuable discussions and assistance.

Kinetics and Mechanism of Ionization of the Carbon Acids 4′-Substituted 2-Phenyl-1,3-indandiones

V. J. STELLA ˣ and R. GISH

Received December 14, 1978, from the *Department of Pharmaceutical Chemistry, University of Kansas, Lawrence, KS 66045.* Accepted for publication February 20, 1979.

Abstract □ The ionization kinetics of 1,3-diketone carbon acids are slow relative to those of classical acids and bases. The ionization kinetics of three 4′-substituted 2-phenyl-1,3-indandiones, 4′-chloro-, 4′-methoxy-, and 2-phenyl-1,3-indandione itself, were studied at 25° and ionic strength 0.1 using stopped-flow spectrometry and a pH jump technique. A log k'_{obs}–pH profile for the approach to the ionization equilibrium was consistent with a reaction scheme postulated earlier for the ionization of another carbon acid, phenylbutazone. The percent enol *versus* diketo form of the acids and the pKa_{enol} and pKa_{diketo} were calculated from the kinetic data. Hammett plots of the various kinetic and equilibrium constants supported a mechanism for acid deprotonation consistent with proton abstraction being the predominant process when very weak bases such as water were the proton acceptors. Desolvation effects and the work required to get the two reacting molecules together in the correct configurations predominated when the proton abstraction was by stronger proton acceptors.

Keyphrases □ Carbon acids—ionization kinetics, stopped-flow spectrophotometric and pH jump analysis □ Ionization kinetics—carbon acids, anisindione, phenindione, clorindione □ Anticoagulants—anisindione, phenindione, clorindione, ionization kinetics

The objective of this study was to compare the kinetics and ionization of the 1,3-diketone carbon acids anisindione (I), phenindione (II), and clorindione (III). All three compounds are used clinically as anticoagulants. The ionization kinetics of phenindione and phenylbutazone, two carbon acids of pharmaceutical interest, were reported previously (1, 2). Kinetic data for the deprotonation of various carbon acids have appeared in the chemical literature, but few studies of the effects of electron-withdrawing and electron-donating groups on the ionization kinetics and mechanism have been reported. The reported chemical studies have concerned acids of fairly high pKa (3, 4) or substituted nitromethane carbon acids (3, 5–12).

The objectives of this work were to study the effects of electron-withdrawing and electron-donating substituents

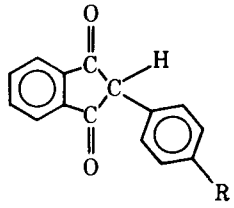

I: R = OCH_3
II: R = H
III: R = Cl

on ionization kinetics of I–III and to determine whether the results supported a model proposed previously for phenindione ionization (1).

EXPERIMENTAL

Phenindione[1] and anisindione[2] were used as received. Clorindione was prepared by the reaction of phthalide and *p*-chlorobenzaldehyde in a sodium ethoxide–ethanol solution using a literature procedure (13) for the synthesis of various 2-phenyl-1,3-indandiones. All other materials, kinetic procedures, conditions, and methods of pKa determination were identical to those described previously (1).

RESULTS AND DISCUSSION

The macroscopic dissociation constants for I–III, determined spectrophotometrically in aqueous solution at 25° and $\mu = 0.1$, are given in Table I. These values compare favorably with the literature values for the pKa's when solvent differences are considered.

Figure 1 is a plot of log k'_{obs} *versus* pH for the approach to ionization equilibrium for I–III. The rate constant k'_{obs} is the pseudo-first-order observed rate constant for the approach to ionization equilibrium extrapolated to zero buffer concentration. A possible model for the ionization kinetics of I–III is given in Scheme I. This model is identical to the scheme postulated previously for phenylbutazone ionization (2).

The predominant neutral form of I–III in aqueous solution is the diketo species, K, rather than the enol species, E (14). The dissociated form of I–III is the so-called mesomeric anion, E^- (17). The macroscopic dissociation constant K_a, the percent enol, and k'_{obs} for the approach to ionization equilibrium in the absence of buffers are best described by Eqs. 1–3 (2):

$$\frac{1}{K_a} = \frac{1}{K_{a,enol}} + \frac{1}{K_{a,diketo}} \quad \text{(Eq. 1)}$$

$$\% \text{ enol} = \frac{K_{a,diketo}}{K_{a,enol} + K_{a,diketo}}\left(\frac{100}{1}\right) \quad \text{(Eq. 2)}$$

$$k'_{obs} = k_1 + k_3[OH^-] + \frac{k_2[H^+]K_{a,enol}}{K_{a,enol} + [H^+]} + \frac{k_4 K_{a,enol}}{K_{a,enol} + [H^+]} \quad \text{(Eq. 3)}$$

Table I—Macroscopic Ionization Constants for Anisindione, Phenindione, and Clorindione Determined Spectrophotometrically at 25 ± 0.1° and $\mu = 0.1$ with Sodium Chloride

Compound, Wavelength Used, nm	pKa	Literature pKa Values
Anisindione, 330	4.13	4.09 (14), 4.25 (15), 5.6 (16)
Phenindione, 326	4.09	4.10 (14), 4.13 (15), 5.4 (16)
Clorindione, 284	3.59	3.54 (14), 3.72 (15), 4.8 (16)

[1] Pfaltz and Bauer, Flushing, N.Y.
[2] Schering Corp., Bloomfield, N.J.

0022-3549/79/0800-1047$01.00/0
© 1979, American Pharmaceutical Association

(35) R. A. Marcus, *J. Phys. Chem.*, **72**, 891 (1968).
(36) G. C. Pimentel and A. L. McClellan, "The Hydrogen Bond," W. H. Freeman, San Francisco, Calif. 1960, chap. 6.
(37) G. S. Rork and I. H. Pitman, *J. Am. Chem. Soc.*, **96**, 4654 (1974).
(38) V. J. Stella and R. Gish, *J. Pharm. Sci.*, **68**, 1047 (1979).

ACKNOWLEDGMENTS

Supported by Grant GM 22357 from the National Institutes of Health.

The authors thank Dr. R. Schowen for valuable discussions and assistance.

Kinetics and Mechanism of Ionization of the Carbon Acids 4′-Substituted 2-Phenyl-1,3-indandiones

V. J. STELLA ˣ and R. GISH

Received December 14, 1978, from the *Department of Pharmaceutical Chemistry, University of Kansas, Lawrence, KS 66045.* Accepted for publication February 20, 1979.

Abstract □ The ionization kinetics of 1,3-diketone carbon acids are slow relative to those of classical acids and bases. The ionization kinetics of three 4′-substituted 2-phenyl-1,3-indandiones, 4′-chloro-, 4′-methoxy-, and 2-phenyl-1,3-indandione itself, were studied at 25° and ionic strength 0.1 using stopped-flow spectrometry and a pH jump technique. A log k'_{obs}–pH profile for the approach to the ionization equilibrium was consistent with a reaction scheme postulated earlier for the ionization of another carbon acid, phenylbutazone. The percent enol *versus* diketo form of the acids and the pKa_{enol} and pKa_{diketo} were calculated from the kinetic data. Hammett plots of the various kinetic and equilibrium constants supported a mechanism for acid deprotonation consistent with proton abstraction being the predominant process when very weak bases such as water were the proton acceptors. Desolvation effects and the work required to get the two reacting molecules together in the correct configurations predominated when the proton abstraction was by stronger proton acceptors.

Keyphrases □ Carbon acids—ionization kinetics, stopped-flow spectrophotometric and pH jump analysis □ Ionization kinetics—carbon acids, anisindione, phenindione, clorindione □ Anticoagulants—anisindione, phenindione, clorindione, ionization kinetics

The objective of this study was to compare the kinetics and ionization of the 1,3-diketone carbon acids anisindione (I), phenindione (II), and clorindione (III). All three compounds are used clinically as anticoagulants. The ionization kinetics of phenindione and phenylbutazone, two carbon acids of pharmaceutical interest, were reported previously (1, 2). Kinetic data for the deprotonation of various carbon acids have appeared in the chemical literature, but few studies of the effects of electron-withdrawing and electron-donating groups on the ionization kinetics and mechanism have been reported. The reported chemical studies have concerned acids of fairly high pKa (3, 4) or substituted nitromethane carbon acids (3, 5–12).

The objectives of this work were to study the effects of electron-withdrawing and electron-donating substituents

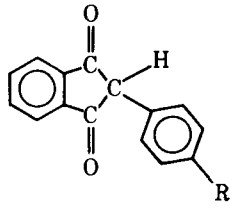

I: R = OCH_3
II: R = H
III: R = Cl

on ionization kinetics of I–III and to determine whether the results supported a model proposed previously for phenindione ionization (1).

EXPERIMENTAL

Phenindione[1] and anisindione[2] were used as received. Clorindione was prepared by the reaction of phthalide and *p*-chlorobenzaldehyde in a sodium ethoxide–ethanol solution using a literature procedure (13) for the synthesis of various 2-phenyl-1,3-indandiones. All other materials, kinetic procedures, conditions, and methods of pKa determination were identical to those described previously (1).

RESULTS AND DISCUSSION

The macroscopic dissociation constants for I–III, determined spectrophotometrically in aqueous solution at 25° and $\mu = 0.1$, are given in Table I. These values compare favorably with the literature values for the pKa's when solvent differences are considered.

Figure 1 is a plot of log k'_{obs} *versus* pH for the approach to ionization equilibrium for I–III. The rate constant k'_{obs} is the pseudo-first-order observed rate constant for the approach to ionization equilibrium extrapolated to zero buffer concentration. A possible model for the ionization kinetics of I–III is given in Scheme I. This model is identical to the scheme postulated previously for phenylbutazone ionization (2).

The predominant neutral form of I–III in aqueous solution is the diketo species, K, rather than the enol species, E (14). The dissociated form of I–III is the so-called mesomeric anion, E^- (17). The macroscopic dissociation constant K_a, the percent enol, and k'_{obs} for the approach to ionization equilibrium in the absence of buffers are best described by Eqs. 1–3 (2):

$$\frac{1}{K_a} = \frac{1}{K_{a,enol}} + \frac{1}{K_{a,diketo}} \quad \text{(Eq. 1)}$$

$$\% \text{ enol} = \frac{K_{a,diketo}}{K_{a,enol} + K_{a,diketo}}\left(\frac{100}{1}\right) \quad \text{(Eq. 2)}$$

$$k'_{obs} = k_1 + k_3[OH^-] + \frac{k_2[H^+]K_{a,enol}}{K_{a,enol} + [H^+]} + \frac{k_4 K_{a,enol}}{K_{a,enol} + [H^+]} \quad \text{(Eq. 3)}$$

Table I—Macroscopic Ionization Constants for Anisindione, Phenindione, and Clorindione Determined Spectrophotometrically at 25 ± 0.1° and $\mu = 0.1$ with Sodium Chloride

Compound, Wavelength Used, nm	pKa	Literature pKa Values
Anisindione, 330	4.13	4.09 (14), 4.25 (15), 5.6 (16)
Phenindione, 326	4.09	4.10 (14), 4.13 (15), 5.4 (16)
Clorindione, 284	3.59	3.54 (14), 3.72 (15), 4.8 (16)

[1] Pfaltz and Bauer, Flushing, N.Y.
[2] Schering Corp., Bloomfield, N.J.

0022-3549/79/0800-1047$01.00/0
© 1979, American Pharmaceutical Association

Table II—Kinetic and Equilibrium Constants for the Ionization of I–III at 25° and μ = 0.1 with Sodium Chloride

Parameter	I	II	III	ρ^a
σ^b	−0.11	0	+0.23	
k_1, sec^{-1}	5	6.9	13	1.22
k_2, M^{-1} sec^{-1}	6.7×10^4	6.5×10^4	3.5×10^4	−0.88
k_3, M^{-1} sec^{-1}	10^6–10^7	10^6–10^7	10^6–10^7	—[c]
k_4, sec^{-1}	10^{-3}–10^{-4}	10^{-3}–10^{-4}	10^{-3}–10^{-4}	—[c]
$K_{a,enol}$	7.1×10^{-3}	4.2×10^{-3}	1.2×10^{-2}	1.77
$K_{a,diketo}$	7.5×10^{-5}	1.1×10^{-4}	3.7×10^{-4}	2.08
$pK_{a_{enol}}$	2.52	2.34	1.92	—
$pK_{a_{diketo}}$	4.12	3.96	3.43	—
$pK_{a_{calc}}$	4.14	3.97	3.44	—
$pK_{a_{exp}}$	4.13	4.09	3.59	—
% enol	2.4	2.6	3.0	—

[a] The ρ value refers to the slope of log k *versus* σ for I–III and is a measure of the relative sensitivity of the parameter k to electron-donating and electron-withdrawing groups. [b] The σ value refers to the Hammett σ value for the various substituents, R. The σ values used were those for the ionization of phenols. G. B. Barlin and D. D. Perrin, *Q. Rev.*, **20**, 75 (1966). [c] Because of the inaccuracy in the values of these two rate constants, Hammett σ plots were not attempted.

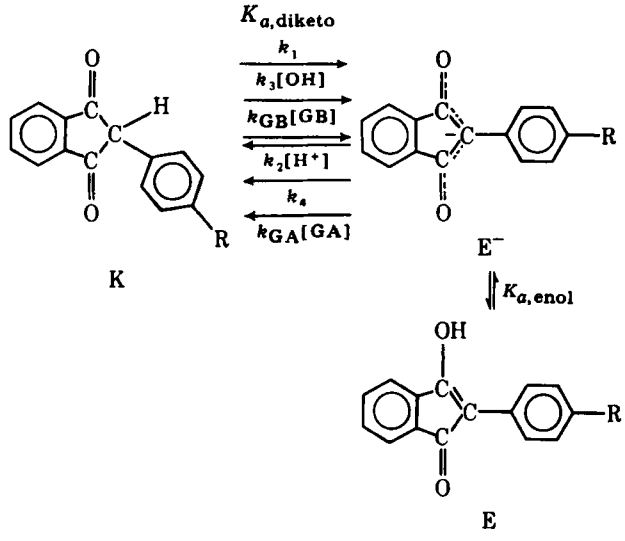

Scheme I

Treatment of the k_{obs} data as previously described (1) allows estimates of the constants k_1, k_2, k_3, k_4, $K_{a,diketo}$, and $K_{a,enol}$ as well as k_{GB} and k_{GA} for those buffers used in the study. Table II summarizes the calculated buffer-independent kinetic and equilibrium constants. The values for the constants placed into Eq. 3 were used to generate the solid lines in Fig. 1. Apparently, Eq. 3 and Scheme I adequately describe the observed values, although, as discussed previously (1, 2), alternative mechanisms and schemes may be possible. The pKa values determined from the kinetic data compare favorably to those determined experimentally.

Unfortunately, little confidence can be placed on the k_3 values given in Table II since the pH range where the hydroxide-ion-catalyzed proton abstraction begins to be significant is also the region where stronger bases, buffers of high pKa′, must be used to control the pH. Normally the buffer concentration is varied while the pH is maintained constant and plots of k_{obs} *versus* buffer concentration are extrapolated to zero buffer concentration to obtain k'_{obs}. The constant k_{GB} can be calculated from the slopes (1). With stronger bases like morpholine, the plots have such a large slope that intercept values become very inaccurate. The use of lower buffer concentrations is not possible because the desired final pH cannot be maintained. All k_3 values appear to be between 10^6 and 10^7 M^{-1} sec^{-1} for I–III. Similarly, the accuracy of the k_4 values, which are calculated from k_3 and $k_{a,diketo}$, is limited by the accuracy of the k_3 values.

Although Eq. 3 appears to describe adequately the protonation and deprotonation kinetics of I–III in the absence of acids and bases other than water, analysis of kinetic data in the presence of general acids (GA) and bases (GB) (buffer components) requires a more complex equation. The observed pseudo-first-order rate constant for the approach to ionization equilibrium at constant pH could be described by Eq. 4 (1):

$$k_{obs} = k'_{obs} + k_{GB}[GB] + k_{GA}[GA] \qquad \text{(Eq. 4)}$$

The constants k_{GA} and k_{GB} can be determined for various buffer species if the ionization kinetics of I–III are determined at various buffer concentrations and pH values (1). Table III is a compilation of some calculated k_{GB} values for all buffer and water species studied for I–III. The conjugate acids of these bases did not show any significant general acid catalysis.

Table III—Values of k_{GB} for Various General Bases as well as Water and Hydroxide Ion for the Deprotonation at 25° and μ = 0.1 for I–III

General Base (pKa′)	k'_1, k_3, or k_{GB}, M^{-1} sec^{-1} I	II	III	ρ^a
H_2O (−1.74)	9.0×10^{-2} [b]	1.24×10^{-1} [b]	2.34×10^{-1} [b]	1.22
Pyridine (5.28)	2.7×10^3	3.6×10^3	3.8×10^3	0.39
3-Methylpyridine (5.75)	4.6×10^3	5.2×10^3	7.1×10^3	0.56
4-Methoxypyridine (6.64)	5.7×10^3	6.5×10^3	1×10^4	0.73
Imidazole (7.10)	5.2×10^3	5.7×10^3	8.0×10^3	0.56
Morpholine (8.53)	5.0×10^4	4.8×10^4	7.6×10^4	0.59
OH^- (15.74)	10^6–10^7	10^6–10^7	10^6–10^7	—[c]

[a] The ρ values have the same meaning as that described in Table II. The σ values used for substituents R also were the same. [b] These numbers are equal to $k_1/55.5 = k'_1$; *i.e.*, k_1 is a pseudo-first-order rate constant that has to be corrected for the water concentration, 55.5 M, to convert it to the second-order rate constant k'_1. [c] Because of the k_3 inaccuracy, Hammett plots were not attempted.

The effects of various electron-donating or electron-withdrawing substituents on any kinetic or equilibrium constant are best quantitated by linear free energy relations such as the Hammett equation:

$$\log k/k_0 = \rho\sigma \qquad \text{(Eq. 5)}$$

Equation 5 assumes that a free energy difference in any rate or equilib-

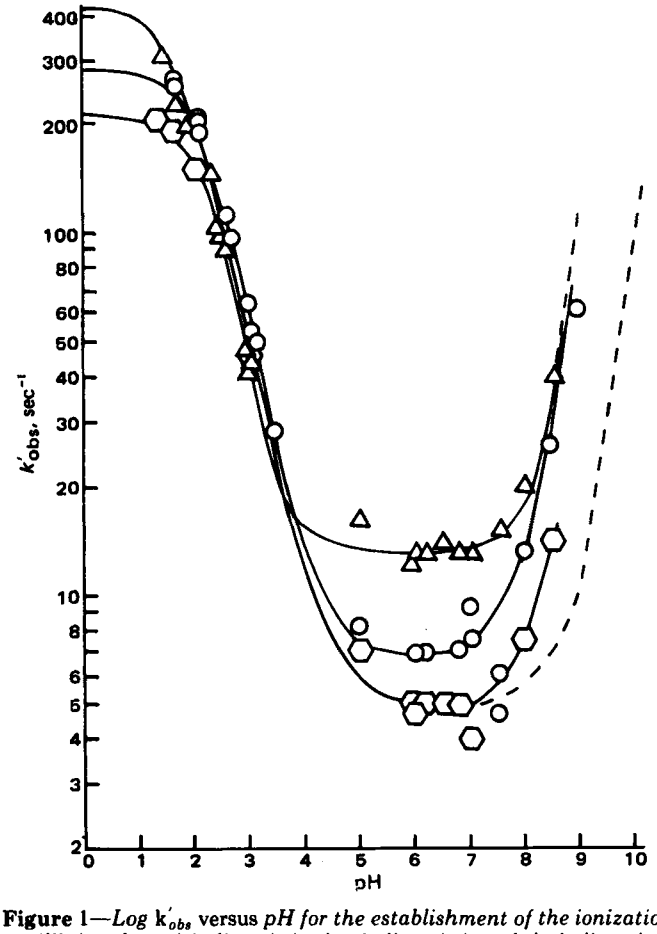

Figure 1—*Log* k'_{obs} versus *pH for the establishment of the ionization equilibrium for anisindione* (○), *phenindione* (○), *and clorindione* (△). *The broken lines at pH > 7 represent* k_3 *having the limits of* 10^6–10^7 M^{-1} *sec*$^{-1}$. *The lack of reproducibility of the data at pH > 8 precludes placing an accurate value on* k_3. *The solid lines drawn at pH > 7–8 are simply the best eyeball fit.*

rium process (given by $\log k/k_0$) between two compounds that differ only by a substituent is a linear function of some property of that substituent group. In Eq. 5, σ, the substituent constant, refers to the relative electron-donating (negative) or electron-withdrawing (positive) power of the substituent and ρ, the reaction constant, is a measure of the sensitivity of the constants, k, to changes in σ values of the substituents (18). The constant k_0 refers to the constant (rate or equilibrium constant) where the substituent is a hydrogen atom, *e.g.*, II.

In the present case, any proton abstraction reaction leading to a buildup of negative charge on the 2-position of the phenylindandiones will be stabilized by electron-withdrawing groups in the 4'-position (R), while electron-donating groups in the 4'-position will destabilize the transition state by increasing electron density at the 2-position. For example, k_1 of Scheme I refers to the pseudo-first-order rate constant for proton abstraction by the base, water. A plot of $\log k_1$ *versus* σ was linear with a slope, ρ, equal to 1.22. The reverse reaction, proton donation to the 2-position by hydronium ion, H_3O^+, represented by k_2 gave a ρ value of −0.88. This finding suggests that the R groups on the 4'-position of the phenylindandiones were having a greater effect on k_1 than on k_2.

The effects of the substituents on $K_{a,\text{enol}}$ and $K_{a,\text{diketo}}$ are also interesting. The $K_{a,\text{diketo}}$ term describes the equilibrium acidity constant associated with proton abstraction from the 2-position of the phenylindandiones. It would be expected to be more sensitive to substituent effects than $K_{a,\text{enol}}$, which represents proton abstraction from the enol form of the phenylindandiones, because the enol proton is further removed from the substituent. The measured ρ values of 2.08 for $K_{a,\text{diketo}}$ *versus* 1.77 for $K_{a,\text{enol}}$ are consistent with this hypothesis.

In an earlier paper (1), it was hypothesized from Brønsted data that the deprotonation rate of phenindione (II) was determined largely by the free energy of the proton abstraction step when weak bases were the proton acceptors, while with the stronger bases the deprotonation was significantly affected by the work necessary to get the molecules into the correct configuration and solvation state for reaction. If this were the case, these effects should be seen in the ρ value of a Hammett plot. Table III lists the ρ values for proton abstraction by various bases. The rate constant for proton abstraction by a weak base like water (pKa' = −1.74), ρ = 1.22, was more sensitive to substituent effects than the rate constants for proton abstraction by various other stronger bases, pyridine through morpholine (pKa' = 5.28–8.53), ρ = 0.39–0.74. The rather small ρ values for this latter group suggest that a smaller negative charge was formed on the 2-carbon of the phenylindandiones in the rate-determining proton abstraction transition state, which supports the hypothesis that the work required to desolvate and bring the two reacting species together probably contributes significantly to the free energy of reaction.

Eigen (17) and others (19) have suggested that proton abstraction from strong carbon acids should be relatively insensitive to pKa differences between the carbon acids. The present study supports this hypothesis when the proton abstracting base is a relatively strong base, *i.e.*, ρ is small. However, if the proton abstracting base is very weak, *e.g.*, water, the proton abstraction step can be sensitive to the pKa differences between the carbon acids; *i.e.*, substituent effects are significant, as measured by larger ρ values.

REFERENCES

(1) V. J. Stella and R. Gish, *J. Pharm. Sci.*, **68**, 1042 (1979).

(2) V. J. Stella and J. D. Pipkin, *ibid.*, **65**, 1161 (1976).

(3) R. G. Pearson and R. L. Dillon, *J. Am. Chem. Soc.*, **75**, 2439 (1953).

(4) R. P. Bell and S. Grainger, *J. Am. Chem. Soc. Perkin Trans., II*, **1976**, 1367.

(5) F. G. Bordwell and W. J. Boyle, Jr., *J. Am. Chem. Soc.*, **97**, 3447 (1975).

(6) F. G. Bordwell, W. J. Boyle, Jr., and K. C. Yee, *ibid.*, **92**, 5926 (1970).

(7) F. G. Bordwell and W. J. Boyle, Jr., *ibid.*, **93**, 512 (1971).

(8) F. G. Bordwell, J. E. Bartmess, and J. A. Hautala, *J. Org. Chem.*, **43**, 3095 (1978).

(9) F. G. Bordwell and J. E. Bartmess, *ibid.*, **43**, 3101 (1978).

(10) *Ibid.*, **43**, 3107 (1978).

(11) *Ibid.*, **43**, 3113 (1978).

(12) F. G. Bordwell and J. A. Hautala, *J. Org. Chem.*, **43**, 3116 (1978).

(13) C. F. Koelsch, *J. Am. Chem. Soc.*, **58**, 1331 (1936).

(14) Y. Linaberg, O. Neiland, A. Veis, A. N. Latu, and G. Vanag, *Dokl. Akad. SSSR*, **154**, 1385 (1964); *Engl. Transl.*, **154**, 184 (1964).

(15) W. Sztark, *Diss. Pharm. Pharmacol.*, **19**, 429 (1968).

(16) J. G. Lombardino and E. H. Wiseman, *J. Med. Chem.*, **65**, 1161 (1976).

(17) M. Eigen, *Angew. Chem. Int. Ed.*, **3**, 1 (1964).

(18) L. P. Hammett, "Physical Organic Chemistry," McGraw-Hill, New York, N.Y., 1940, chap. 7.

(19) M. L. Bender, "Mechanisms of Homogeneous Catalysis from Protons to Proteins," Wiley-Interscience, New York, N.Y., 1971, chap. 2.

ACKNOWLEDGMENTS

Supported by Grant GM 22357 from the National Institutes of Health.

The authors thank Dr. R. Schowen for valuable discussions and assistance.

TLC Differentiation of Butyrophenone and Diphenylbutylpiperidine Compounds from Phenothiazine Derivatives

ACHILLE PLUYM

Received August 7, 1978, from the *Analytical Department, Janssen Pharmaceutica, B-2340 Beerse, Belgium.* Accepted for publication January 26, 1979.

Abstract □ A procedure is described for TLC detection and differentiation of the butyrophenone–diphenylbutylpiperidine group and phenothiazine derivatives at the microgram level. A two-dimensional TLC method to separate butyrophenone and diphenylbutylpiperidine compounds is reported. A variety of possible detection reagents were examined. The solvent systems and spray reagents described should be useful for the identification of these drugs in various dosage forms.

Keyphrases □ Butyrophenones—analysis, TLC, differentiation from phenothiazine derivatives □ Diphenylbutylpiperidines—analysis, TLC, differentiation from phenothiazine derivatives □ TLC—analysis, butyrophenones, diphenylbutylpiperidines, phenothiazine derivatives

Butyrophenones, diphenylbutylpiperidines, and the pharmacologically analogous phenothiazines are currently used for the treatment of various psychotic disorders. A rapid detection and identification method is needed for screening pharmaceutical formulations for these drugs.

Numerous investigators (1–13) described various solvent systems for chromatography of psychotropic drugs, mainly phenothiazine derivatives. However, none of these systems completely separates the two groups of neuroleptic compounds. In the proposed analytical system, group differentiation depends on R_f values and on color reactions to spray reagents. Identification of the butyrophenone or diphenylbutylpiperidine compounds can be accomplished with the described two-dimensional TLC method.

Table I—Guide R_f Values for Phenothiazine Derivatives (Eluent A)

Compound	R_f[a]	RR_f[b]
Acepromazine	0.23	0.72
Acetophenazine	0.20	0.62
Alimemazine (trimeprazine)	0.35	1.09
Chlorpromazine	0.32	1
Dixyrazine	0.31	0.97
Fluphenazine	0.33	1.03
Levomepromazine (methotrimeprazine)	0.36	1.12
Perazine	0.18	0.56
Perphenazine	0.31	0.97
Piperacethazine	0.18	0.56
Prochlorperazine	0.29	0.90
Promazine	0.23	0.72
Promethazine	0.37	1.16
Propericiazine (pericyazine)	0.30	0.94
Prothipendyl	0.17	0.53
Thiopropazate	0.71	2.22
Thioproperazine	0.23	0.72
Thioridazine	0.32	1
Triethylperazine	0.30	0.94
Trifluoperazine	0.33	1.03
Trifluopromazine	0.36	1.12

[a] Mean of six values. [b] Relative R_f value with chlorpromazine as standard.

EXPERIMENTAL

Adsorbent—Precoated TLC silica gel 60 F 254[1] plates were used.

Eluent Systems—Solvents were analytical grade and were used as received from commercial sources[1]. Eluent A consisted of ethyl acetate–chloroform–methanol–0.1 *M* sodium acetate buffer (pH 4.7) (54:23:18:5). Eluent B consisted of chloroform–ethanol (90:10).

Detection—The following spray reagents were used:

Reagent A—To 250 mg of vanadium pentoxide, 40 ml of concentrated sulfuric acid was added. The mixture was diluted with distilled water to 500 ml (12).

Reagent B—To 5 ml of 5% aqueous iron(III) chloride, 45 ml of 20% perchloric acid and 50 ml of 50% nitric acid were added (12, 13).

Reagent C—Five grams of *p*-dimethylaminobenzaldehyde was dissolved in 100 ml of 18 *N* H_2SO_4 (13).

Reagent D—A 40% (v/v) aqueous sulfuric acid solution was used. After spraying, the TLC plate was heated at 110° for 5–10 min (14).

Reagent E—To 0.1% ethanolic bromcresol purple solution were added a few drops of a 10% ammonia solution until the color changed (15, 16).

Reagent F—Forty milligrams of bromcresol green was dissolved in 100 ml of ethanol, and 0.1 *N* NaOH was added until a blue color appeared (15, 16).

Reagent G—Aconitic acid, 250 mg, was dissolved in 40 ml of acetic anhydride by heating; the mixture was diluted with toluene to 100 ml. After spraying, the TLC plate was heated at 100° for 30 min (17, 18).

Drug Solutions—Ten milligrams of the pure drug reference standards[2] were dissolved in 10 ml of chloroform–methanol (7:3). The compounds investigated are summarized in Tables I and II.

Procedure—*Rapid Group Detection*—Volumes of 10 μl, corresponding to 10 μg of a compound, were applied to a precoated silica gel plate with a syringe[3]. The chromatoplate was developed over 15 cm using Eluent A in a tank[4] without filter paper lining. Use of a saturated paper-lined development tank resulted in a poor separation because of the lower R_f values of all compounds and because many of the phenothiazine derivatives did not migrate from the application point.

The plate was air dried at room temperature and viewed under shortwave UV light[5]. The spots were outlined with a pencil. Finally, the plate was sprayed with one detection reagent for group identification.

Identification of Butyrophenones and Diphenylbutylpiperidines—When the rapid detection method showed the presence of a neuroleptic compound of the butyrophenone–diphenylbutylpiperidine group, identification of this compound could be confirmed using two-dimensional TLC. With a 10-μl syringe, the butyrophenone–diphenylbutylpiperidine mixture was applied to the three corners of a TLC plate prepared as shown in Fig. 1.

After development over 15 cm using Eluent A in a tank without paper lining, the TLC plate was removed and air dried at room temperature. The plate was then developed for 15 cm at right angles to the first run in a second tank containing Eluent B and saturated by lining the walls with filter paper moistened with the mobile phase. The chromatogram

[1] Merck, Darmstadt, West Germany.

[2] Pure drug samples were supplied by Janssen Pharmaceutica (all butyrophenones and diphenylbutylpiperidines), Farmitalia, Searle, Schering, Rhône-Poulenc, Smith Kline & French, Sandoz, Clin-Byla, Pitman-Moore, Promonta, and Homburg and Union Chimique Belge (phenothiazine derivatives).

[3] Hamilton, Bonaduz, Switzerland.

[4] Desaga, Heidelberg, West Germany.

[5] Chromato-vue cabinet CC-20, Ultra-Violet Products, San Gabriel, Calif.

0022-3549/79/0800-1050$01.00/0
© 1979, American Pharmaceutical Association

Table II—Guide R_f Values for Butyrophenone and Diphenylbutylpiperidine Compounds

Compound	Eluent A			Eluent B	
	R_f[a]	RR_f[b]	RR_f[c]	R_f[a]	RR_f[c]
Butyrophenones					
Benperidol	0.55	1.72	1	0.29	1
Droperidol	0.63	1.97	1.14	0.37	1.27
Fluanisone	0.76	2.37	1.38	0.62	2.14
Haloperidol	0.44	1.37	0.80	0.16	0.55
Pipamperone	0.22	0.69	0.40	0.06	0.21
Trifluperidol	0.47	1.47	0.85	0.16	0.55
Diphenylbutylpiperidines					
Fluspirilene	0.67	2.09	1.22	0.43	1.48
Penfluridol	0.77	2.40	1.40	0.37	1.27
Pimozide	0.75	2.34	1.36	0.52	1.79

[a] Mean of four values. [b] Relative R_f value with chlorpromazine as standard. [c] Relative R_f value with benperidol as standard.

was air dried at room temperature and evaluated by quenching the 254-nm-induced fluorescence.

RESULTS

Guide R_f values for the examined compounds are summarized in Tables I and II.

The described one-dimensional TLC method with Eluent A allows almost a complete differentiation of the phenothiazine group and the butyrophenone–diphenylbutylpiperidine group. With this solvent system, nearly all compounds of the latter group were located between R_f 0.44 and 0.76. Pipamperone (R_f 0.22) was the only compound that did not migrate into this region. Fluanisone, penfluridol, and pimozide were not separated with this eluent. The phenothiazine thiopropazate (R_f 0.71) interfered with these three compounds. All other phenothiazines migrated into the R_f 0.18–0.37 region where pipamperone interference was possible.

Combination of R_f values and the color reactions can facilitate the identification of the compounds. All compounds investigated quenched the 254-nm-induced fluorescence. Group differentiation was possible with different reagents (Table III).

The phenothiazine group reacted positively with Reagents A–D, whereas no color reaction was seen for the butyrophenones and diphenylbutylpiperidines. Reagents C and D gave more intense colors than did Reagents A and B. All compounds examined reacted with Reagents E and F to give lightly bluish-colored spots. Reagent G reacted with butyrophenones and diphenylbutylpiperidines, but spot intensities were so light that identification was very difficult.

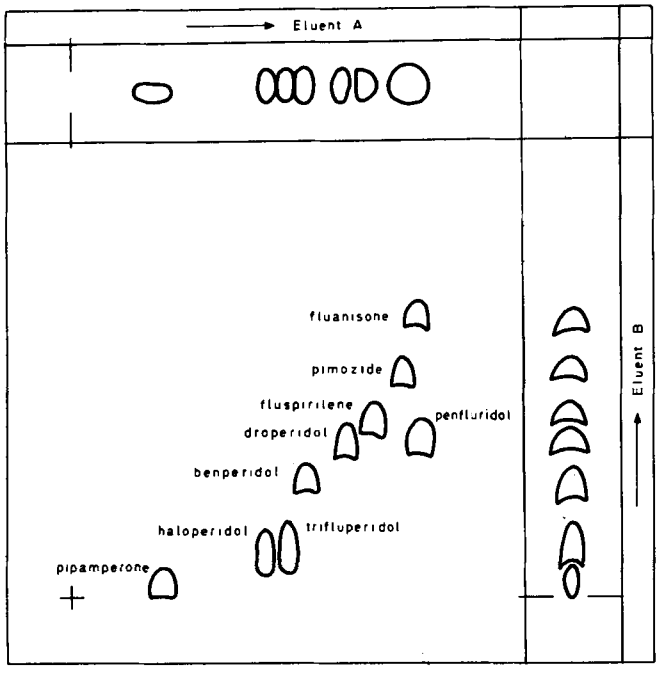

Figure 1—*Type chromatogram of the two-dimensional identification test for butyrophenones and diphenylbutylpiperidines.*

Table III—Color Reaction to Various Spray Reagents

Compound	UV, 254 nm	Detection Reagent[a]						
		A	B	C	D	E	F	G
Phenothiazines								
Acepromazine	+	RO	R	RO	RB	BL	BL	–
Acetophenazine	+	R	R	R	R	BL	BL	–
Alimemazine	+	RO	RO	RO	RB	BL	BL	–
Chlorpromazine	+	R	R	R	R	BL	BL	–
Dixyrazine	+	RO	R	R	R	BL	BL	–
Fluphenazine	+	O	O	O	O	BL	BL	–
Levomepromazine	+	P	P	BL	BL	BL	BL	–
Perazine	+	RO	R	R	R	BL	BL	–
Perphenazine	+	R	R	R	R	BL	BL	–
Piperacethazine	+	R	R	R	R	BL	BL	–
Prochlorperazine	+	R	R	R	R	BL	BL	–
Promazine	+	RO	RO	RO	RB	BL	BL	–
Promethazine	+	BO	B	B	RB	BL	BL	–
Propericiazine	+	RO	R	R	RO	BL	BL	–
Prothipendyl	+	O	Y	Y	B	BL	BL	–
Thiopropazate	+	WR	WR	R	R	BL	BL	–
Thioproperazine	+	R	R	R	R	BL	BL	–
Thioridazine	+	P	P	BL	BL	BL	BL	–
Triethylperazine	+	P	P	BL	BL	BL	BL	–
Trifluoperazine	+	O	O	O	O	BL	BL	–
Trifluopromazine	+	O	O	O	O	BL	BL	–
Butyrophenones								
Benperidol	+	–	–	–	–	BL	BL	W+
Droperidol	+	–	–	–	–	BL	BL	W+
Fluanisone	+	–	–	–	–	BL	BL	W+
Haloperidol	+	–	–	–	–	BL	BL	W+
Pipamperone	+	–	–	–	–	BL	BL	W+
Trifluperidol	+	–	–	–	–	BL	BL	W+
Diphenylbutylpiperidines								
Fluspirilene	+	–	–	–	–	BL	BL	W+
Penfluridol	+	–	–	–	–	BL	BL	W+
Pimozide	+	–	–	–	–	BL	BL	W+

[a] B = brown, BL = blue, O = orange, P = purple, R = red, Y = yellow, W = weak, + = detectable, and – = not detectable.

The color of a compound after TLC and spraying is generally dependent on the concentration of the substance in the sample, on the mode of reagent application, and on the amount of reagent used for detection. In this TLC procedure, identification depends on R_f values (or relative R_f values with, for example, chlorpromazine as a standard) and on color. Neither is an absolute.

Identity of the butyrophenone or diphenylbutylpiperidine compound can be accomplished by the described two-dimensional TLC method. Guide R_f values of the compounds for the two solvent systems are summarized in Table II. A two-dimensional chromatogram is shown in Fig. 1. Because of the great similarity in chemical structure of the butyrophenones and diphenylbutylpiperidines, it is very difficult to find a specific reagent for each compound of this group. Therefore, unspecific detection such as shortwave UV light was used.

Iodine vapors or the Munier–Macheboeuf modification of Dragendorff's reagent can be used also. The use of unspecific detecting agents, however, makes identification dependent on R_f values, which are influenced by numerous parameters. Comparison with reference samples would be absolutely necessary.

REFERENCES

(1) A. Hulshoff and J. H. Perrin, *J. Chromatogr.*, **129,** 249 (1976).

(2) M. L. Bastos, G. E. Kananen, R. M. Young, J. R. Monforte, and I. Sunshine, *Clin. Chem.*, **16,** 931 (1970).

(3) J. A. Vinson and J. E. Hooyman, *J. Chromatogr.*, **105,** 416 (1975).

(4) W. N. French, F. F. Matsui, D. L. Robertson, and S. J. Smith, *ibid.*, **97,** 223 (1974).

(5) S. Thunnell, *ibid.*, **130,** 209 (1977).

(6) D. C. Fenimore, C. J. Meyer, C. M. Davis, F. Hsu, and A. Zlatkis, *ibid.*, **142,** 399 (1977).

(7) W. W. Fike, *Anal. Chem.*, **38,** 1697 (1966).

(8) A. C. Moffat and K. W. Smalldon, *J. Chromatogr.*, **90,** 9 (1974).

(9) S. N. Tewari, *Z. Anal. Chem.*, **275,** 31 (1975).

(10) K. K. Kaistha, R. Tadrus, and R. Janda, *J. Chromatogr.*, **107,** 359 (1975).

(11) H. Gänshirt, in "Dünnschichtchromatographie," E. Stahl, Ed.,

Springer-Verlag, Berlin, Germany, 1967, p. 483.
(12) A. De Leenheer, *J. Chromatogr.*, **75**, 79 (1973).
(13) A. Noirfalise, *ibid.*, **20**, 61 (1965).
(14) "Phenothiazine Separations," Tech. Bull. 526, Kontes, Vineland, N.J., 1977.
(15) P. J. A. W. Demoen, *J. Pharm. Sci.*, **50**, 350 (1961).
(16) K. G. Krebs, in "Dünnschichtchromatographie," E. Stahl, Ed., Springer-Verlag, Berlin, Germany, 1967, p. 819.
(17) H. Soep, *J. Chromatogr.*, **6**, 122 (1961).
(18) S. Sass, J. J. Kaufman, A. A. Cordenas, and J. J. Martin, *Anal. Chem.*, **30**, 529 (1958).

ACKNOWLEDGMENTS

The author thanks Dr. W. Van Bever and Mr. J. Van Rompay for critically reading and Mrs. A. Claessens for typing the manuscript.

High-Pressure Liquid Chromatographic Analysis of Antipyrine in Small Plasma Samples

LEON SHARGEL ˣ, WAI-MAN CHEUNG, and ANDREW B. C. YU

Received August 28, 1978, from the *College of Pharmacy and Allied Health Professions, Northeastern University, Boston, MA 02115.* Accepted for publication January 31, 1979.

Abstract □ A high-pressure liquid chromatographic (HPLC) method was developed for the assay of antipyrine in small (0.1-ml) plasma samples using aminopyrine as the internal standard and a reversed-phase microparticulate column. The assay sensitivity (1 μg/ml) permits development of a plasma level–time curve using a single rat. The mean (± *SE*) plasma elimination half-life in rats was 1.28 ± 0.14 hr. A comparison of the spectrophotometric method with the HPLC method yielded a correlation coefficient of 0.98. The HPLC assay for antipyrine is rapid and precise and can be used for hepatic drug metabolism study in a single animal.

Keyphrases □ Antipyrine—analysis, high-pressure liquid chromatography, plasma, rats □ High-pressure liquid chromatography—analysis, antipyrine, plasma, rats □ Analgesics—antipyrine, high-pressure liquid chromatographic assay, plasma, rats

The plasma antipyrine elimination rate is commonly used to study hepatic drug metabolism *in vivo* (1–5). Antipyrine is metabolized almost completely by the liver enzymes (6), and protein binding of the drug is minimal (7).

BACKGROUND

The spectrophotometric assay of Brodie *et al.* (8) generally is used for measuring plasma antipyrine levels. The spectrophotometric method is tedious and may yield high blank values. Furthermore, the method requires 1–2 ml of plasma, which precludes obtaining multiple samples from a small animal such as the rat.

GLC analyses of antipyrine also have been reported (3, 9). Although these methods appear to be more precise than the spectrophotometric method, they still require a 1.0-ml plasma sample and drug extraction. Another assay for plasma antipyrine using ^{14}C-label drug (4) is very sensitive but requires expensive equipment and involves the hazards of radioactivity.

High-pressure liquid chromatography (HPLC) has been applied to the separation and quantitation of many drugs. A sensitive HPLC procedure for antipyrine using a silica gel column was reported (10). This procedure requires 0.5 ml of plasma for drug extraction. A rapid, sensitive method was needed that utilizes smaller blood samples, 0.1–0.2 ml, so that an antipyrine pharmacokinetic profile can be obtained in a single laboratory animal such as the rat. Recently, HPLC procedures utilizing reversed-phase chromatography were developed for drug analysis in biological tissues (11). The advantage of reversed-phase HPLC is that minimal sample cleanup is required prior to chromatography; therefore, smaller tissue samples may be used.

This report describes a rapid HPLC procedure which is more precise than the spectrophotometric method and utilizes small plasma sample volumes.

EXPERIMENTAL

Materials—Antipyrine NF and aminopyrine NF were used as standards[1]. All other reagents, analytical grade or better, were purchased from commercial sources.

Animals—Adult, male, Sprague–Dawley strain rats[2], 200–350 g, were used.

Plasma Assay and Animal Dosing—For standard curves, heparinized blood samples were removed from the abdominal aorta of nonmedicated ether-anesthetized rats, placed into centrifuge tubes, and centrifuged to obtain the plasma fraction. Plasma aliquots (0.1 ml) were pipetted into 1.5-ml microtest tubes[3] and spiked with 10 μl of concentrated antipyrine solutions to yield final drug concentrations corresponding to 0, 1.5, 3, 4.5, 6, 12, 25, and 50 μg/ml of plasma.

To each microtest tube was added 0.05 ml of 20% (w/v) $ZnSO_4 \cdot 7H_2O$ in 50% (v/v) methanol–water containing aminopyrine, 100 μg/ml, as the internal standard. The mixture was mixed on a vortex mixer. Then 0.05 ml of saturated barium hydroxide solution was added to the mixture. The final mixture was vortexed and centrifuged for 10 min. A 10-μl sample of the supernate was removed and subjected to HPLC.

Rats were given 100 mg of antipyrine/kg ip (injection volume of 0.5 ml/200 g). Blood samples of approximately 250–300 μl were removed from the tail vein at 0, 2, 3, 4, 5, and 6 hr. The samples were placed into heparinized microcentrifuge tubes and centrifuged to obtain the plasma fraction. Plasma aliquots, 0.1 ml, were processed along with the spiked plasma standards described.

HPLC—Samples were chromatographed on a high-pressure liquid chromatograph[4] equipped with a universal liquid chromatographic injector, a UV (254-nm) absorbance detector, and a strip-chart recorder[5]. The deproteinated plasma samples (10 μl) were chromatographed at room temperature on a microparticulate[6] reversed-phase HPLC column, 4 mm × 30 cm, with an eluting mobile phase of methanol–water (50% v/v). The mobile phase flow rate was adjusted to 1 ml/min with an inlet pressure of ~1750 psig. The chart speed was 0.25 cm/min.

A standard curve was obtained by comparing the peak height ratio of antipyrine to aminopyrine and the spiked plasma antipyrine concentration. Unknown plasma sample concentrations were calculated by comparing the peak height ratios of the samples to the processed standards.

Correlation with Spectrophotometric Assay—Ten plasma samples obtained from nonmedicated rats were spiked with antipyrine at con-

[1] Merck & Co., Rahway, N.J.
[2] Charles River CD.
[3] Eppendorf, Brinkmann Instrument, Westbury, N.Y.
[4] Model ALC/GPC 204, Waters Associates, Milford, Mass.
[5] Fisher Recordall, series 500, Fisher Scientific Co., Pittsburgh, Pa.
[6] μBondapak C_{18}, Waters Associates, Milford, Mass.

0022-3549/79/0800-1052$01.00/0
© 1979, American Pharmaceutical Association

Springer-Verlag, Berlin, Germany, 1967, p. 483.
(12) A. De Leenheer, *J. Chromatogr.*, **75**, 79 (1973).
(13) A. Noirfalise, *ibid.*, **20**, 61 (1965).
(14) "Phenothiazine Separations," Tech. Bull. 526, Kontes, Vineland, N.J., 1977.
(15) P. J. A. W. Demoen, *J. Pharm. Sci.*, **50**, 350 (1961).
(16) K. G. Krebs, in "Dünnschichtchromatographie," E. Stahl, Ed., Springer-Verlag, Berlin, Germany, 1967, p. 819.
(17) H. Soep, *J. Chromatogr.*, **6**, 122 (1961).
(18) S. Sass, J. J. Kaufman, A. A. Cordenas, and J. J. Martin, *Anal. Chem.*, **30**, 529 (1958).

ACKNOWLEDGMENTS

The author thanks Dr. W. Van Bever and Mr. J. Van Rompay for critically reading and Mrs. A. Claessens for typing the manuscript.

High-Pressure Liquid Chromatographic Analysis of Antipyrine in Small Plasma Samples

LEON SHARGEL ˣ, WAI-MAN CHEUNG, and ANDREW B. C. YU

Received August 28, 1978, from the *College of Pharmacy and Allied Health Professions, Northeastern University, Boston, MA 02115.* Accepted for publication January 31, 1979.

Abstract □ A high-pressure liquid chromatographic (HPLC) method was developed for the assay of antipyrine in small (0.1-ml) plasma samples using aminopyrine as the internal standard and a reversed-phase microparticulate column. The assay sensitivity (1 μg/ml) permits development of a plasma level–time curve using a single rat. The mean (± *SE*) plasma elimination half-life in rats was 1.28 ± 0.14 hr. A comparison of the spectrophotometric method with the HPLC method yielded a correlation coefficient of 0.98. The HPLC assay for antipyrine is rapid and precise and can be used for hepatic drug metabolism study in a single animal.

Keyphrases □ Antipyrine—analysis, high-pressure liquid chromatography, plasma, rats □ High-pressure liquid chromatography—analysis, antipyrine, plasma, rats □ Analgesics—antipyrine, high-pressure liquid chromatographic assay, plasma, rats

The plasma antipyrine elimination rate is commonly used to study hepatic drug metabolism *in vivo* (1–5). Antipyrine is metabolized almost completely by the liver enzymes (6), and protein binding of the drug is minimal (7).

BACKGROUND

The spectrophotometric assay of Brodie *et al.* (8) generally is used for measuring plasma antipyrine levels. The spectrophotometric method is tedious and may yield high blank values. Furthermore, the method requires 1–2 ml of plasma, which precludes obtaining multiple samples from a small animal such as the rat.

GLC analyses of antipyrine also have been reported (3, 9). Although these methods appear to be more precise than the spectrophotometric method, they still require a 1.0-ml plasma sample and drug extraction. Another assay for plasma antipyrine using ^{14}C-label drug (4) is very sensitive but requires expensive equipment and involves the hazards of radioactivity.

High-pressure liquid chromatography (HPLC) has been applied to the separation and quantitation of many drugs. A sensitive HPLC procedure for antipyrine using a silica gel column was reported (10). This procedure requires 0.5 ml of plasma for drug extraction. A rapid, sensitive method was needed that utilizes smaller blood samples, 0.1–0.2 ml, so that an antipyrine pharmacokinetic profile can be obtained in a single laboratory animal such as the rat. Recently, HPLC procedures utilizing reversed-phase chromatography were developed for drug analysis in biological tissues (11). The advantage of reversed-phase HPLC is that minimal sample cleanup is required prior to chromatography; therefore, smaller tissue samples may be used.

This report describes a rapid HPLC procedure which is more precise than the spectrophotometric method and utilizes small plasma sample volumes.

EXPERIMENTAL

Materials—Antipyrine NF and aminopyrine NF were used as standards[1]. All other reagents, analytical grade or better, were purchased from commercial sources.

Animals—Adult, male, Sprague–Dawley strain rats[2], 200–350 g, were used.

Plasma Assay and Animal Dosing—For standard curves, heparinized blood samples were removed from the abdominal aorta of nonmedicated ether-anesthetized rats, placed into centrifuge tubes, and centrifuged to obtain the plasma fraction. Plasma aliquots (0.1 ml) were pipetted into 1.5-ml microtest tubes[3] and spiked with 10 μl of concentrated antipyrine solutions to yield final drug concentrations corresponding to 0, 1.5, 3, 4.5, 6, 12, 25, and 50 μg/ml of plasma.

To each microtest tube was added 0.05 ml of 20% (w/v) $ZnSO_4 \cdot 7H_2O$ in 50% (v/v) methanol–water containing aminopyrine, 100 μg/ml, as the internal standard. The mixture was mixed on a vortex mixer. Then 0.05 ml of saturated barium hydroxide solution was added to the mixture. The final mixture was vortexed and centrifuged for 10 min. A 10-μl sample of the supernate was removed and subjected to HPLC.

Rats were given 100 mg of antipyrine/kg ip (injection volume of 0.5 ml/200 g). Blood samples of approximately 250–300 μl were removed from the tail vein at 0, 2, 3, 4, 5, and 6 hr. The samples were placed into heparinized microcentrifuge tubes and centrifuged to obtain the plasma fraction. Plasma aliquots, 0.1 ml, were processed along with the spiked plasma standards described.

HPLC—Samples were chromatographed on a high-pressure liquid chromatograph[4] equipped with a universal liquid chromatographic injector, a UV (254-nm) absorbance detector, and a strip-chart recorder[5]. The deproteinated plasma samples (10 μl) were chromatographed at room temperature on a microparticulate[6] reversed-phase HPLC column, 4 mm × 30 cm, with an eluting mobile phase of methanol–water (50% v/v). The mobile phase flow rate was adjusted to 1 ml/min with an inlet pressure of ~1750 psig. The chart speed was 0.25 cm/min.

A standard curve was obtained by comparing the peak height ratio of antipyrine to aminopyrine and the spiked plasma antipyrine concentration. Unknown plasma sample concentrations were calculated by comparing the peak height ratios of the samples to the processed standards.

Correlation with Spectrophotometric Assay—Ten plasma samples obtained from nonmedicated rats were spiked with antipyrine at con-

[1] Merck & Co., Rahway, N.J.
[2] Charles River CD.
[3] Eppendorf, Brinkmann Instrument, Westbury, N.Y.
[4] Model ALC/GPC 204, Waters Associates, Milford, Mass.
[5] Fisher Recordall, series 500, Fisher Scientific Co., Pittsburgh, Pa.
[6] μBondapak C_{18}, Waters Associates, Milford, Mass.

0022-3549/79/0800-1052$01.00/0
© 1979, American Pharmaceutical Association

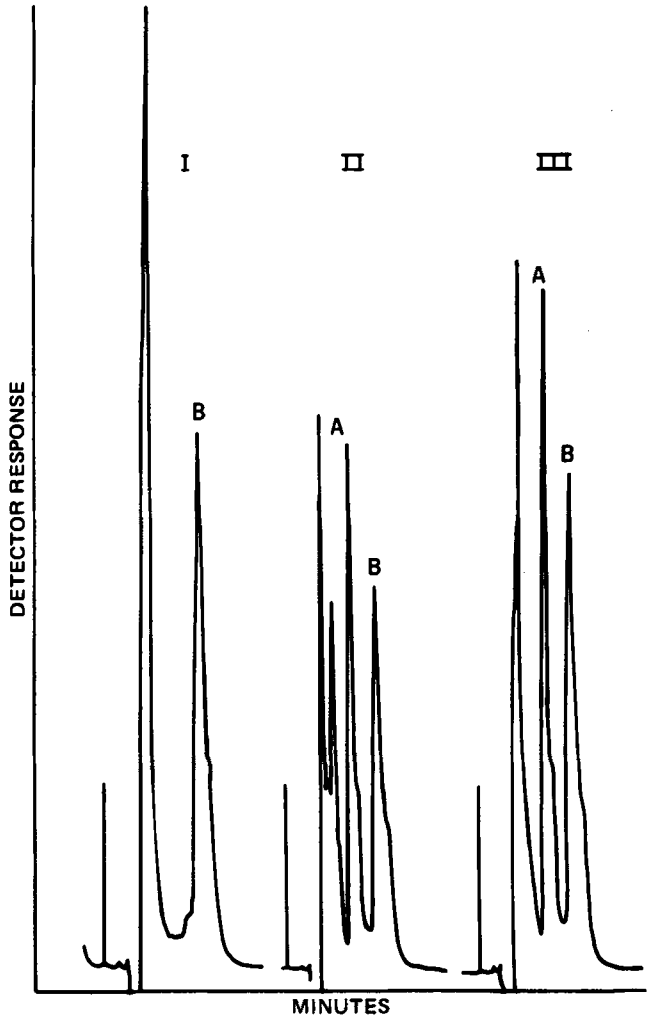

Figure 1—*High-pressure liquid chromatograms of blank plasma with 50 μg of aminopyrine/ml (B) as the internal standard (I), rat plasma collected 2 hr after the intraperitoneal injection of 100 mg of antipyrine/kg (A) containing 50 μg of aminopyrine/ml (B) (II), and processed standards in control rat plasma containing 37.5 μg of antipyrine/ml (A) and 50 μg of aminopyrine/ml (B) (III).*

centrations of 0, 5, 10, 20, and 40 μg/ml of plasma. The samples were split; one portion was assayed by the precipitation procedure of Brodie *et al.* (8), and the second portion was assayed by HPLC. The two assays were compared to obtain a correlation coefficient.

RESULTS

Chromatograms of plasma samples containing antipyrine demonstrated no interfering peaks with normal plasma constituents (Fig. 1). Retention times for antipyrine and aminopyrine were 5.6 and 8.7 min, respectively. Processed standard curves of antipyrine plasma samples were linear to 50 μg/ml, and the assay sensitivity was ~1.0 μg/ml. Standards were processed in triplicate, and the regression line slope was calculated as 27.1 with a correlation coefficient of 0.99, demonstrating excellent linearity. The assay sensitivity was ~1.0 μg of antipyrine/ml of plasma.

A comparison of the HPLC and spectrophotometric assays demonstrated excellent correlation. A correlation coefficient of 0.98 and a slope of 0.97 were obtained.

To demonstrate the application of the HPLC method *in vivo*, three rats were given 100 mg of antipyrine/kg ip. The plasma elimination of antipyrine for each rat was first order (Fig. 2). The mean (± *SE*) plasma elimination half-life for antipyrine was 1.28 ± 0.14 hr, which agrees with the reported value of 85 min (2).

DISCUSSION

The main advantage of the HPLC assay of antipyrine over previous

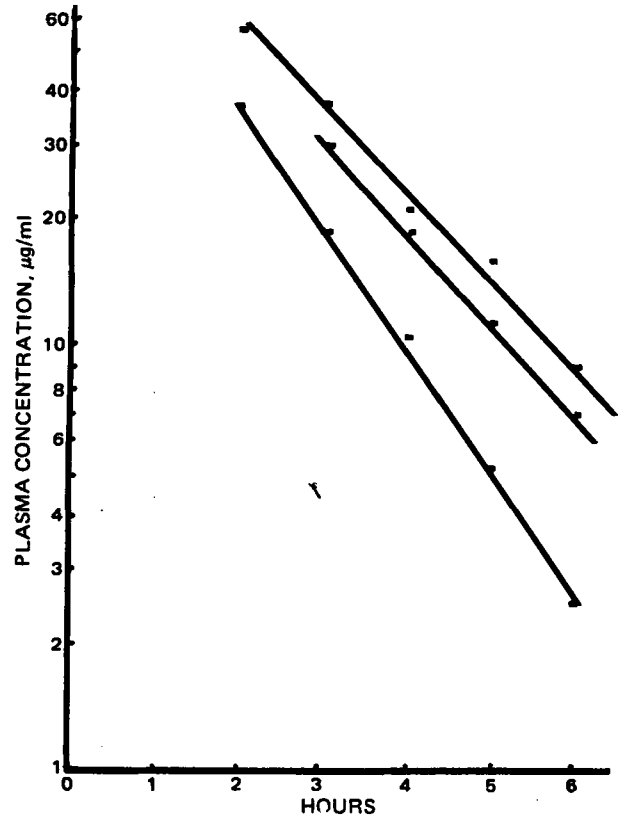

Figure 2—*Plasma antipyrine levels in individual rats. Each rat was given 100 mg of antipyrine/kg ip. Plasma samples were assayed for antipyrine according to the described HPLC procedure.*

methods is that a complete plasma concentration *versus* time curve may be obtained from a single rat. Previously, investigators performing pharmacokinetic and drug metabolism studies *in vivo* with the rat as the animal model needed many rodents to obtain sufficient data points to describe accurately the plasma elimination of antipyrine (2). This micromethod for antipyrine measurement allows the use of the rat as its own control since very small (0.1 ml) plasma samples are used. Although the assay sensitivity is only 1.0 μg/ml, enough data points describing antipyrine elimination kinetics may be obtained quickly and accurately. The assay sensitivity probably could be improved by further sample cleanup and injection of larger sample volumes on the chromatograph.

The *in vivo* data demonstrated that reasonable elimination half-lives for antipyrine may be obtained by this HPLC method. Therefore, this method should be useful for studying the effects of environmental factors of various xenobiotics on hepatic drug metabolism activity in the rat *in vivo* using antipyrine pharmacokinetics as one parameter.

In comparison to the popular spectrophotometric method for antipyrine (8), the HPLC assay is simple, rapid, and precise. Moreover, there is no need for involved separation and purification techniques. Since results of the HPLC method agree well with those of the spectrophotometric method, as shown by a correlation coefficient of 0.98, the HPLC assay offers a reasonable alternative for antipyrine measurement.

REFERENCES

(1) E. S. Vesell, C. J. Lee, G. T. Passanati, and C. A. Shively, *Pharmacology*, **10**, 217 (1973).

(2) E. A. Sotaniemi, *ibid.*, **10**, 306 (1973).

(3) D. H. Huffman, D. W. Shoeman, and D. L. Azarnoff, *Biochem. Pharmacol.*, **23**, 197 (1974).

(4) O. M. Bakke, M. Bending, J. Arabakke, and D. S. Davies, *Acta Pharmacol. Toxicol.*, **35**, 91 (1974).

(5) J. L. Miller, C. R. Clark, S. J. Gee, and R. I. Krieger, *Pharmacology*, **16**, 279 (1978).

(6) B. B. Brodie and J. Axelrod, *J. Pharmacol. Exp. Ther.*, **98**, 97 (1950).

(7) R. Soberman, B. B. Brodie, B. B. Levy, J. Axelrod, V. Hollender, and J. M. Steele, *J. Biol. Chem.*, **179**, 31 (1949).

(8) B. B. Brodie, J. Axelrod, R. Soberman, and B. B. Levy, *ibid.*, **179**, 25 (1949).

(9) L. F. Prescott, K. K. Adjepon-Yamoah, and E. Roberts, *J. Pharm. Pharmacol.*, **25**, 205 (1973).

(10) M. Eichelbaum and N. Spannbrucker, *J. Chromatogr.*, **140**, 288 (1977).

(11) J. Orcutt, P. Kozak, S. Gillman, and L. Cummins, *Clin. Chem.*, **23**, 599 (1977).

Metabolic Fate of N^6-Benzyladenosine and N^6-Benzyladenosine-5′-phosphate in Rats

G. B. CHHEDA ˣ, C. I. HONG *, S. K. GURWARA ‡, and A. MITTELMAN

Received February 10, 1978, from the *Department of General Surgery and the Department of Biophysics, Roswell Park Memorial Institute, Buffalo, NY 14263.* Accepted for publication December 8, 1978. *Present address: Department of Neurosurgery, Roswell Park Memorial Institute, Buffalo, NY 14263. ‡Present address: Invenex Pharmaceuticals, Grand Island, NY 14072.

Abstract □ The radiolabeled antitumor nucleoside (^{14}C-8)-N^6-benzyladenosine and its (^{14}C-8)-5′-phosphate were administered to rats intravenously, and their metabolic fate was studied. Twenty-nine percent of the radioactivity was recovered in the 48-hr urine collection after (^{14}C-8)-N^6-benzyladenosine administration. The following metabolites were isolated: unchanged N^6-benzyladenosine (20%), adenine (12%), uric acid (5%), and N^6-benzyladenine (0.3%). In the case of (^{14}C-8)-N^6-benzyladenosine-5′-phosphate, a total of 28% of the radioactivity was recovered in the 48-hr urine collection and the following metabolites were isolated: N^6-benzyladenosine (40%), uric acid (12%), adenine (trace), and unidentified urea derivatives (30%). Metabolism of N^6-benzyladenosine appears to involve N-debenzylation to some extent, followed by conversion to adenine and uric acid. N^6-Benzyladenosine and its 5′-phosphate differ from other adenosine analogs in being retained in significant amounts by the animals.

Keyphrases □ Benzyladenosine—metabolism, rats □ Benzyladenosine phosphate—metabolism, rats □ Antineoplastic agents—benzyladenosine, metabolism, rats

Since N^6-(Δ^2-isopentenyl)adenosine (1) exhibited growth inhibitory activity in mammalian cell lines as well as *in vivo*, several 6-substituted adenosines were synthesized and their antitumor activities were determined (2, 3). Among them, N^6-benzyladenosine (I) was of particular interest since it exhibited a significant growth inhibitory activity against mouse L-1210 leukemia (2). In rats, N^6-benzyladenosine, like N^6-(Δ^2-isopentenyl)adenosine, inhibited the incorporation of precursors into DNA, RNA, and protein (4). More recently, this nucleoside underwent a clinical trial as an antitumor agent (5). Subsequently, because of the poor solubility of N^6-benzyladenosine, a more water-soluble derivative, N^6-benzyladenosine-5′-phosphate (II) (6), was prepared and used instead. Since initial metabolism studies indicated that N^6-benzyladenosine did not behave like other N^6-substituted adenosines (7, 8), investigations were undertaken to determine the metabolic fate of N^6-benzyladenosine and its 5′-phosphate in rats.

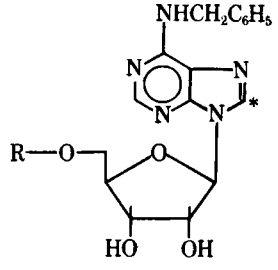

I: R = H

II: R = $-P(=O)-(OH)_2$

* = ^{14}C

EXPERIMENTAL

Materials and Methods—(^{14}C-8)-N^6-Benzyladenosine[1] (I) was synthesized by reacting (^{14}C-8)-adenosine[2] (100 μCi, 2 μmoles), adenosine (10 μmoles), benzyl bromide (20 μl), and dimethylformamide at 40° for 24 hr, followed by heating with 14 N ammonium hydroxide (1 ml) and water (2 ml) at 95° for 3 hr (2). The yield was 9.8 μmoles (81.7%), the total radioactivity was 62.3 μCi, and the specific radioactivity was 6.3 μCi/μmole. (^{14}C-8)-N^6-Benzyladenosine-5′-phosphate (II) was synthesized by phosphorylation of (^{14}C-8)-N^6-benzyladenosine, prepared from (^{14}C-8)-adenosine (130 μCi, 10 μmoles), phosphorus oxychloride (50 μl), and triethyl phosphate (1 ml) (6). The yield was 5.1 μmoles (51%), the total radioactivity was 44.93 μCi, and the specific radioactivity 8.81 μCi/μmole.

Chromatography—Paper chromatograms were developed in a descending manner on 3 MM filter paper during initial preparative stages and on acid-washed (No. 1) filter paper when purifications and comparative identification were required[3]. The following solvent systems were utilized for paper chromatography: A, isopropanol–concentrated ammonium hydroxide–water (7:1:2), B, ethyl acetate–2-ethoxyethanol–16% formic acid (4:1:2), upper phase; C, n-butanol–water–concentrated ammonium hydroxide (86:14:5), upper phase; D, n-propanol–concentrated ammonium hydroxide–water (11:2:7); and E, ethyl acetate–n-propanol–water (4:1:2), upper phase. Chromatograms were viewed under a shortwave UV lamp at 254 nm. All UV-absorbing areas were eluted and analyzed in a UV spectrophotometer[4].

Radioactivity Determination—The liquid samples (100–250 μl) were counted for radioactivity in scintillation vials containing 10 ml of the scintillation fluid[5]. The solid samples (feces and organs) were homogenized, aliquots corresponding to 0.5 g were placed in a gelatin capsule and burned in a sample oxidizer[6], and the radioactive carbon dioxide was counted.

Labeled Compound Administration—Two Sprague–Dawley rats (male, 200 g) were given aqueous (^{14}C-8)-N^6-benzyladenosine (0.18 mg,

[1] Aqueous solutions of (^{14}C-8)-N^6-benzyladenosine should be stored frozen at −70° or below. When being kept at −20° for 2 months, 5% of the labeled compound underwent degradation to (^{14}C-8)-N^6-benzyladenine.

[2] Specific radioactivity, 50 mCi/mmole; Schwartz Bio-Research, Orangeburg, NY 10962.

[3] Whatman filter papers were used for paper chromatography.

[4] Beckman Acta V.

[5] Five percent Bio-Solv (BBS-3) solubilizer (Beckman Instruments, Fullerton, CA 92634) in diluted Permafluor III (Packard Instrument Co., Downers Grove, IL 60515).

[6] Packard Tri-Carb model 306. The $^{14}CO_2$ was trapped in Carbo-Solv (Packard Instrument Co.).

0022-3549/79/0800-1054$01.00/0
© 1979, American Pharmaceutical Association

(8) B. B. Brodie, J. Axelrod, R. Soberman, and B. B. Levy, *ibid.*, **179**, 25 (1949).

(9) L. F. Prescott, K. K. Adjepon-Yamoah, and E. Roberts, *J. Pharm. Pharmacol.*, **25**, 205 (1973).

(10) M. Eichelbaum and N. Spannbrucker, *J. Chromatogr.*, **140**, 288 (1977).

(11) J. Orcutt, P. Kozak, S. Gillman, and L. Cummins, *Clin. Chem.*, **23**, 599 (1977).

Metabolic Fate of N^6-Benzyladenosine and N^6-Benzyladenosine-5′-phosphate in Rats

G. B. CHHEDA ˣ, C. I. HONG *, S. K. GURWARA ‡, and A. MITTELMAN

Received February 10, 1978, from the *Department of General Surgery and the Department of Biophysics, Roswell Park Memorial Institute, Buffalo, NY 14263.* Accepted for publication December 8, 1978. *Present address: Department of Neurosurgery, Roswell Park Memorial Institute, Buffalo, NY 14263. ‡Present address: Invenex Pharmaceuticals, Grand Island, NY 14072.

Abstract □ The radiolabeled antitumor nucleoside (^{14}C-8)-N^6-benzyladenosine and its (^{14}C-8)-5′-phosphate were administered to rats intravenously, and their metabolic fate was studied. Twenty-nine percent of the radioactivity was recovered in the 48-hr urine collection after (^{14}C-8)-N^6-benzyladenosine administration. The following metabolites were isolated: unchanged N^6-benzyladenosine (20%), adenine (12%), uric acid (5%), and N^6-benzyladenine (0.3%). In the case of (^{14}C-8)-N^6-benzyladenosine-5′-phosphate, a total of 28% of the radioactivity was recovered in the 48-hr urine collection and the following metabolites were isolated: N^6-benzyladenosine (40%), uric acid (12%), adenine (trace), and unidentified urea derivatives (30%). Metabolism of N^6-benzyladenosine appears to involve N-debenzylation to some extent, followed by conversion to adenine and uric acid. N^6-Benzyladenosine and its 5′-phosphate differ from other adenosine analogs in being retained in significant amounts by the animals.

Keyphrases □ Benzyladenosine—metabolism, rats □ Benzyladenosine phosphate—metabolism, rats □ Antineoplastic agents—benzyladenosine, metabolism, rats

Since N^6-(Δ^2-isopentenyl)adenosine (1) exhibited growth inhibitory activity in mammalian cell lines as well as *in vivo*, several 6-substituted adenosines were synthesized and their antitumor activities were determined (2, 3). Among them, N^6-benzyladenosine (I) was of particular interest since it exhibited a significant growth inhibitory activity against mouse L-1210 leukemia (2). In rats, N^6-benzyladenosine, like N^6-(Δ^2-isopentenyl)adenosine, inhibited the incorporation of precursors into DNA, RNA, and protein (4). More recently, this nucleoside underwent a clinical trial as an antitumor agent (5). Subsequently, because of the poor solubility of N^6-benzyladenosine, a more water-soluble derivative, N^6-benzyladenosine-5′-phosphate (II) (6), was prepared and used instead. Since initial metabolism studies indicated that N^6-benzyladenosine did not behave like other N^6-substituted adenosines (7, 8), investigations were undertaken to determine the metabolic fate of N^6-benzyladenosine and its 5′-phosphate in rats.

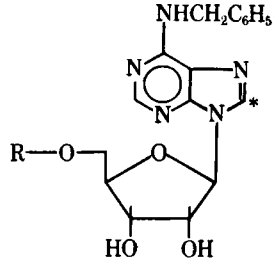

I: R = H

II: R = $-P(=O)-(OH)_2$

* = ^{14}C

EXPERIMENTAL

Materials and Methods—(^{14}C-8)-N^6-Benzyladenosine[1] (I) was synthesized by reacting (^{14}C-8)-adenosine[2] (100 μCi, 2 μmoles), adenosine (10 μmoles), benzyl bromide (20 μl), and dimethylformamide at 40° for 24 hr, followed by heating with 14 N ammonium hydroxide (1 ml) and water (2 ml) at 95° for 3 hr (2). The yield was 9.8 μmoles (81.7%), the total radioactivity was 62.3 μCi, and the specific radioactivity was 6.3 μCi/μmole. (^{14}C-8)-N^6-Benzyladenosine-5′-phosphate (II) was synthesized by phosphorylation of (^{14}C-8)-N^6-benzyladenosine, prepared from (^{14}C-8)-adenosine (130 μCi, 10 μmoles), phosphorus oxychloride (50 μl), and triethyl phosphate (1 ml) (6). The yield was 5.1 μmoles (51%), the total radioactivity was 44.93 μCi, and the specific radioactivity 8.81 μCi/μmole.

Chromatography—Paper chromatograms were developed in a descending manner on 3 MM filter paper during initial preparative stages and on acid-washed (No. 1) filter paper when purifications and comparative identification were required[3]. The following solvent systems were utilized for paper chromatography: A, isopropanol–concentrated ammonium hydroxide–water (7:1:2), B, ethyl acetate–2-ethoxyethanol–16% formic acid (4:1:2), upper phase; C, n-butanol–water–concentrated ammonium hydroxide (86:14:5), upper phase; D, n-propanol–concentrated ammonium hydroxide–water (11:2:7); and E, ethyl acetate–n-propanol–water (4:1:2), upper phase. Chromatograms were viewed under a shortwave UV lamp at 254 nm. All UV-absorbing areas were eluted and analyzed in a UV spectrophotometer[4].

Radioactivity Determination—The liquid samples (100–250 μl) were counted for radioactivity in scintillation vials containing 10 ml of the scintillation fluid[5]. The solid samples (feces and organs) were homogenized, aliquots corresponding to 0.5 g were placed in a gelatin capsule and burned in a sample oxidizer[6], and the radioactive carbon dioxide was counted.

Labeled Compound Administration—Two Sprague–Dawley rats (male, 200 g) were given aqueous (^{14}C-8)-N^6-benzyladenosine (0.18 mg,

[1] Aqueous solutions of (^{14}C-8)-N^6-benzyladenosine should be stored frozen at −70° or below. When being kept at −20° for 2 months, 5% of the labeled compound underwent degradation to (^{14}C-8)-N^6-benzyladenine.

[2] Specific radioactivity, 50 mCi/mmole; Schwartz Bio-Research, Orangeburg, NY 10962.

[3] Whatman filter papers were used for paper chromatography.

[4] Beckman Acta V.

[5] Five percent Bio-Solv (BBS-3) solubilizer (Beckman Instruments, Fullerton, CA 92634) in diluted Permafluor III (Packard Instrument Co., Downers Grove, IL 60515).

[6] Packard Tri-Carb model 306. The $^{14}CO_2$ was trapped in Carbo-Solv (Packard Instrument Co.).

0022-3549/79/0800-1054$01.00/0
© 1979, American Pharmaceutical Association

Table I—Radiactivity Excretion in Rat 48-hr Urine and Feces Collection after Intravenous (^{14}C-8)-N^6-Benzyladenosine (I) and (^{14}C-8)-N^6-Benzyladenosine-5′-phosphate (II) [a]

Labeled Compound	Amount Administered, mg (dpm × 10^6)	Radioactivity Excreted, dpm × 10^6	Recovery, %
I	0.18 (7.167)	Urine: 2.08	29.0
		Feces: 0.51	7.1
		Total: 2.59	36.1
II	0.17 (7.583)	Urine: 2.128	28.1
		Feces: 0.857	11.3
		Total: 2.985	39.4

[a] A separate experiment was conducted for determining the excretion of radioactivity beyond 48 hr. About 2% of additional radioactivity was excreted in 6 more days.

7.167 × 10^6 dpm) or (^{14}C-8)-N^6-benzyladenosine-5′-phosphate (0.17 mg, 7.585 × 10^6 dpm) through the tail vein.

Each pair of rats was then placed in a metabolic cage, and urine and feces were collected up to 48 hr postadministration. Precautions were taken to avoid contamination of feces by urine. All materials obtained were subjected to radioactivity measurement to determine excretion levels.

Isolation, Purification, and Identification of Urinary Metabolites—Prior to paper chromatography, the rat urine sample was filtered under 35 psi nitrogen pressure through a membrane filter with a molecular weight retention of ≥1000 with respect to spherical product[7]. After filtration, two generous water washings were employed, and the combined filtrates were evaporated to dryness. The residue was dissolved in minimal water and streaked on four 3 MM filter papers[3] (23 × 57 cm) along with the following markers: N^6-benzyladenine, N^6-benzyladenosine, N^6-benzyladenosine-5′-phosphate, adenine, adenosine, hypoxanthine, inosine, and uric acid.

The paper chromatographic purification was performed first with Solvent A, and major materials were subjected to further purification for the isolation and identification of the radioactive metabolites. Metabolites were identified by comparison of their paper chromatographic mobilities and UV spectra with those of the authentic samples.

RESULTS AND DISCUSSION

The metabolism studies showed that N^6-benzyladenosine behaved differently from some other N^6-substituted adenosines such as N^6-(Δ^2-isopentenyl)adenosine (7) as well as N-(purine-6-ylcarbamoyl)-L-threonine ribonucleoside (8). Fifty percent of N^6-(Δ^2-isopentenyl)-adenosine was metabolized to non-UV-absorbing compounds, and most of the administered radioactivity was excreted in the first 5 hr. N-(Purine-6-ylcarbamoyl)-L-threonine ribonucleoside also was excreted relatively rapidly from the body; however, it usually did not undergo purine ring or side-chain catabolism.

In the case of N^6-benzyladenosine, 36% of the administered radioactivity of I was excreted over 48 hr; 29% was in the urine and 7% was in the feces (Table I). Significant radioactivity was retained in the animal beyond 48 hr. The additional activity excreted was <2.5% during the 6 days after the initial 2 days.

Table II—Radioactivity Distribution in Rat Organs 48 hr after Intravenous (^{14}C-8)-N^6-Benzyladenosine

Organ	Disintegrations per Minute × 10^3	Percent of Administered
Liver	701.6	9.8
Kidney	44.2	0.61
Pancreas	25.9	0.36
Spleen	10.0	0.13
Adrenal	2.0	0.02
Brain	0.7	0.01
Muscle[a]	2313	32.3
Bone[a]	123	1.7
Plasma[a]	2.5	0.03
Red cells[a]	28.4	0.4

[a] These calculations are based on the total of 90 g of muscle, 13 g of bone, 6 ml of plasma, and 6 ml of red cells in an average rat. Actually, the disintegrations per minute values were determined on a weighed sample of muscle and bone and a per milliliter sample of plasma and red cells. Thus, 81.5% of the radioactivity can be accounted for when urine and fecal activities are added.

Table III—Urinary Metabolites Isolated from Urine 48 hr after Intravenous (^{14}C-8)-N^6-Benzyladenosine (I) and (^{14}C-8)-N^6-Benzyladenosine-5′-phosphate (II)

Metabolite	Percent of Total I Radioactivity	Percent of Total II Radioactivity
N^6-Benzyladenosine-5′-phosphate	Not detected	Not detected
N^6-Benzyladenosine	20	40
Benzyladenine	0.3	—
Adenine	12	0.1
Uric acid	5	12
Unidentified compounds (urea test positive)	43	30
Other unidentified compounds	5	6
Losses	15	12

The rats were sacrificed 48 hr after administration, and various organs and tissues were removed and checked for radioactivity (Table II). Among the organs, the liver contained the highest radioactivity (10%). The kidney and pancreas showed less than 1% of the administered radioactivity, and muscle accounted for 32% of the activity. Red cells also retained some radioactivity after 48 hr. The activity in the urine, feces, and organs added up to 81% of the administered radioactivity.

Chromatographic and UV spectral analysis of the radioactivity found in urine revealed that 20% of the excreted radioactivity was in the unchanged parent nucleoside while ~0.3% was in benzyladenine, the free base (Table III). Adenine constituted 12%, and uric acid contained 5% of the activity. Since N^6-benzyladenosine is not a substrate for the enzyme adenosine deaminase (3), formation of adenine and uric acid (Table III) probably takes place after N-debenzylation of the nucleoside. No metabolites with the hydroxylated phenyl nucleus were observed.

Significant radioactivity was found in the unidentified compounds, for which the urea color test was positive[8]. Since N^6-benzyladenosine is a substrate for adenosine kinase and also gets phosphorylated in cultured cells (9), some of it may possibly be converted to the 5′-mono-, di-, and triphosphates *in vivo* in rats. In the studies reported here, however, the tissues were not analyzed for these phosphorylated derivatives. Urine sample analysis did not reveal any 5′-phosphates.

In the case of N^6-benzyladenosine-5′-phosphate, a total of 39% of the administered activity of II was excreted over 48 hr, 20% in the urine and 11% in the feces (Table I). In terms of radioactivity disposition and metabolism studies of the 5′-phosphate, the overall picture was not much different from that of the parent nucleoside. N^6-Benzyladenosine-5′-phosphate was converted to N^6-benzyladenosine *in vivo* and was excreted as the major metabolite (40%); no 5′-phosphate could be detected in the urine. Twelve percent of the radioactivity was excreted as uric acid, and ~35% was excreted as unidentified compounds.

Preliminary studies in humans indicated that this nucleoside (I) and its 5′-phosphate (II) are retained in the body for a long period. Only ~20% of the radioactivity was excreted in urine in 48 hr. The nucleotide is converted into the nucleoside, and the former may serve as a soluble and sustained-release form for the latter (10). Unchanged N^6-benzyladenosine and uric acid are the major urinary metabolites in humans.

REFERENCES

(1) J. T. Grace, Jr., M. T. Hakala, R. H. Hall, and J. Blackeslee, *Proc. Am. Assoc. Cancer Res.*, 8, 87 (1967).

(2) M. H. Fleysher, A. Bloch, M. T. Hakala, and C. A. Nichol, *J. Med. Chem.*, 12, 1056 (1969).

(3) S. P. Dutta, G. L. Tritsch, C. Cox, and G. B. Chheda, *ibid.*, 18, 780 (1975).

(4) Y. Rustom, T. Al-Hussainy, C. Simpson, and E. Mihich, *Proc. Am. Assoc. Cancer Res.*, 14, 60 (1973).

(5) A Mittelman, J. T. Evans, and G. B. Chheda, *Ann. N.Y. Acad. Sci.*, 255, 255 (1975).

[7] Amicon TCF-10 apparatus with a UM-2 membrane filter was used for filtration. Both were obtained from Amicon Corp., Lexington, MA 02173.

[8] *p*-Dimethylaminobenzaldehyde and *p*-dimethylaminocinnamaldehyde were used for the two urea tests.

(6) C. I. Hong, G. L. Tritsch, A. Mittelman, P. Hebborn, and G. B. Chheda, *J. Med. Chem.*, **18**, 465 (1975).
(7) G. B. Chheda and A. Mittelman, *Biochem. Pharmacol.*, **21**, 27 (1972).
(8) C. I. Hong, G. B. Chheda, G. P. Murphy, and A. Mittelman, *ibid.*, **22**, 1927 (1973).
(9) A. Y. Divekar and M. T. Hakala, *Mol. Pharmacol.*, **7**, 663 (1971).
(10) G. A. LePage, S. R. Naik, S. B. Katakkar, and A. Khaliq, *Cancer Res.*, **35**, 3036 (1975).

ACKNOWLEDGMENTS

Supported by U.S. Public Health Service Grant CA 14185.
The authors thank Mr. C. F. Piskorz for technical assistance and Dr. E. D. Holyoke for interest and encouragement.

Differential Potentiometric Method for Determining Dissociation Constants of Very Slightly Water-Soluble Drugs Applied to the Sulfonamide Diuretic Chlorthalidone

H. L. J. FLEUREN ˣ, C. A. M. van GINNEKEN, and J. M. van ROSSUM

Received December 26, 1978, from the *Department of Pharmacology, University of Nijmegen, 6500 HB Nijmegen, The Netherlands.* Accepted for publication February 6, 1979.

Abstract □ A renewed application of potentiometric acid–base titrations is described, by which dissociation constants of practically water-insoluble drugs can be measured accurately. The method uses the difference in the amount of titrant between a suitable aqueous solvent and a solution of the drug in that solvent. Such potentiometric difference titrations were conducted on a 3.7×10^{-4} *M* solution of chlorthalidone in 0.1 *M* aqueous KCl in the pH 3.5–10.6 range at 25°. Nonlinear least-squares regression analysis was applied to the data. From four determinations, a value of 9.24 ± 0.02 (mean ± *SEM*) resulted for the apparent dissociation constant of the first chlorthalidone acid group. The thermodynamic dissociation constant was calculated at pKa_1 = 9.35 (25°) by using a correction for activity.

Keyphrases □ Chlorthalidone—analysis, differential potentiometry, dissociation constants □ Potentiometry, differential—analysis, chlorthalidone dissociation constants, ibuprofen dissociation constant □ Ibuprofen—analysis, differential potentiometry, dissociation constant

A drug's dissociation constant is an important parameter in pharmacokinetic and pharmacodynamic investigations. Once the pKa is known, the degree of compound dissociation at physiological pH is derived easily; and since only unionized molecules generally pass readily across biological membranes (1), predictions concerning the access to tissue sites of interest can be made. The pKa also has value in the estimation of the lipiphilicity of a compound from its partitioning between an organic solvent and water; if the pKa is known, true partition coefficients can be calculated from the apparent values at any arbitrary pH.

BACKGROUND

Chlorthalidone[1] (I) contains two weakly acidic groups: one sulfonamide and one oxoisoindolin (acid amide) moiety. Although the latter was not expected to contribute to drug dissociation at acid or neutral pH, the former could influence back-resorption of the drug in the renal tubules when pH 8 urine is produced. In this situation, a pH-dependent urinary excretion should become evident. This aspect gains quantitative importance because normally ~70% of an available chlorthalidone dose is excreted unchanged in the urine (2). The present study was undertaken because no chlorthalidone pKa value was available from the literature.

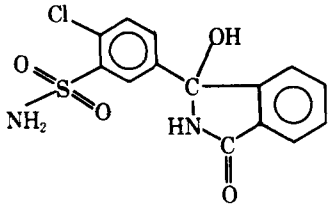

I

Various methods to determine acid and base dissociation constants are used. They were comprehensively evaluated by Albert and Serjeant (3). These authors stated that both potentiometry and UV spectrophotometry produce accurate results, although the latter method is more laborious (3).

One premise for a conventional potentiometric titration is that the weak acid or base concentration must be so high that the amount of titrant needed to titrate the solvent is negligible in comparison with the amount necessary to protonate or deprotonate the dissolved compound. This condition could not be fulfilled at present, because maximum chlorthalidone solubility in neutral aqueous solutions was reported as ~0.12 mg/ml (4), equivalent to 3.45×10^{-4} *M*. In such a case, a difference titration can be conducted, provided that the amounts of strong acid and base, with which the solution of the compound with an unknown pKa and its blank (solvent alone) are titrated, are measured accurately.

Moreover, the pH measurement must be of high precision and very reproducible. To meet this requirement, use was made of automatic potentiometric titration equipment containing a precisely operating, motor-driven microburet and a high-resolution digital voltmeter connected to a low-drift pH meter. The apparatus was used previously to determine pKa values and numbers of titratable groups of purified proteins (5, 6).

EXPERIMENTAL

An aqueous solution of 0.1 *M* KCl served as the blank. A saturated chlorthalidone solution in this solvent was prepared by vigorously stirring ~8 mg of the crystalline drug in 50 ml of solvent at room temperature overnight. After filtration, the concentration, determined in triplicate by GLC (7), was 125.2 ± 0.7 μg/ml (mean ± *SD*), equivalent to 3.695×10^{-4} *M*. Aqueous hydrochloric acid and sodium hydroxide solutions, 0.0604 *M*, were diluted by weighing with four volumes of distilled water and bubbled with nitrogen gas to remove carbon dioxide.

The titrant was added stepwise, using a microburet[2], at 0.01 ml/min with an accuracy of ±0.1%. The titrations were conducted on the chlor-

[1] Hygroton, Ciba-Geigy, Basel, Switzerland.

[2] Metrohm, Zürich, Switzerland.

0022-3549/79/0800-1056$01.00/0
© 1979, American Pharmaceutical Association

(6) C. I. Hong, G. L. Tritsch, A. Mittelman, P. Hebborn, and G. B. Chheda, *J. Med. Chem.*, **18**, 465 (1975).
(7) G. B. Chheda and A. Mittelman, *Biochem. Pharmacol.*, **21**, 27 (1972).
(8) C. I. Hong, G. B. Chheda, G. P. Murphy, and A. Mittelman, *ibid.*, **22**, 1927 (1973).
(9) A. Y. Divekar and M. T. Hakala, *Mol. Pharmacol.*, **7**, 663 (1971).
(10) G. A. LePage, S. R. Naik, S. B. Katakkar, and A. Khaliq, *Cancer Res.*, **35**, 3036 (1975).

ACKNOWLEDGMENTS

Supported by U.S. Public Health Service Grant CA 14185.
The authors thank Mr. C. F. Piskorz for technical assistance and Dr. E. D. Holyoke for interest and encouragement.

Differential Potentiometric Method for Determining Dissociation Constants of Very Slightly Water-Soluble Drugs Applied to the Sulfonamide Diuretic Chlorthalidone

H. L. J. FLEUREN ˣ, C. A. M. van GINNEKEN, and J. M. van ROSSUM

Received December 26, 1978, from the *Department of Pharmacology, University of Nijmegen, 6500 HB Nijmegen, The Netherlands.* Accepted for publication February 6, 1979.

Abstract □ A renewed application of potentiometric acid–base titrations is described, by which dissociation constants of practically water-insoluble drugs can be measured accurately. The method uses the difference in the amount of titrant between a suitable aqueous solvent and a solution of the drug in that solvent. Such potentiometric difference titrations were conducted on a 3.7×10^{-4} *M* solution of chlorthalidone in 0.1 *M* aqueous KCl in the pH 3.5–10.6 range at 25°. Nonlinear least-squares regression analysis was applied to the data. From four determinations, a value of 9.24 ± 0.02 (mean ± *SEM*) resulted for the apparent dissociation constant of the first chlorthalidone acid group. The thermodynamic dissociation constant was calculated at pKa_1 = 9.35 (25°) by using a correction for activity.

Keyphrases □ Chlorthalidone—analysis, differential potentiometry, dissociation constants □ Potentiometry, differential—analysis, chlorthalidone dissociation constants, ibuprofen dissociation constant □ Ibuprofen—analysis, differential potentiometry, dissociation constant

A drug's dissociation constant is an important parameter in pharmacokinetic and pharmacodynamic investigations. Once the pKa is known, the degree of compound dissociation at physiological pH is derived easily; and since only unionized molecules generally pass readily across biological membranes (1), predictions concerning the access to tissue sites of interest can be made. The pKa also has value in the estimation of the lipiphilicity of a compound from its partitioning between an organic solvent and water; if the pKa is known, true partition coefficients can be calculated from the apparent values at any arbitrary pH.

BACKGROUND

Chlorthalidone[1] (I) contains two weakly acidic groups: one sulfonamide and one oxoisoindolin (acid amide) moiety. Although the latter was not expected to contribute to drug dissociation at acid or neutral pH, the former could influence back-resorption of the drug in the renal tubules when pH 8 urine is produced. In this situation, a pH-dependent urinary excretion should become evident. This aspect gains quantitative importance because normally ~70% of an available chlorthalidone dose is excreted unchanged in the urine (2). The present study was undertaken because no chlorthalidone pKa value was available from the literature.

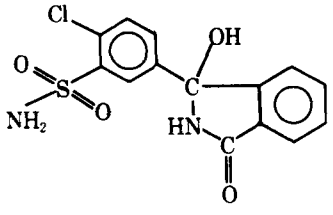

I

Various methods to determine acid and base dissociation constants are used. They were comprehensively evaluated by Albert and Serjeant (3). These authors stated that both potentiometry and UV spectrophotometry produce accurate results, although the latter method is more laborious (3).

One premise for a conventional potentiometric titration is that the weak acid or base concentration must be so high that the amount of titrant needed to titrate the solvent is negligible in comparison with the amount necessary to protonate or deprotonate the dissolved compound. This condition could not be fulfilled at present, because maximum chlorthalidone solubility in neutral aqueous solutions was reported as ~0.12 mg/ml (4), equivalent to 3.45×10^{-4} *M*. In such a case, a difference titration can be conducted, provided that the amounts of strong acid and base, with which the solution of the compound with an unknown pKa and its blank (solvent alone) are titrated, are measured accurately.

Moreover, the pH measurement must be of high precision and very reproducible. To meet this requirement, use was made of automatic potentiometric titration equipment containing a precisely operating, motor-driven microburet and a high-resolution digital voltmeter connected to a low-drift pH meter. The apparatus was used previously to determine pKa values and numbers of titratable groups of purified proteins (5, 6).

EXPERIMENTAL

An aqueous solution of 0.1 *M* KCl served as the blank. A saturated chlorthalidone solution in this solvent was prepared by vigorously stirring ~8 mg of the crystalline drug in 50 ml of solvent at room temperature overnight. After filtration, the concentration, determined in triplicate by GLC (7), was 125.2 ± 0.7 μg/ml (mean ± *SD*), equivalent to 3.695×10^{-4} *M*. Aqueous hydrochloric acid and sodium hydroxide solutions, 0.0604 *M*, were diluted by weighing with four volumes of distilled water and bubbled with nitrogen gas to remove carbon dioxide.

The titrant was added stepwise, using a microburet[2], at 0.01 ml/min with an accuracy of ±0.1%. The titrations were conducted on the chlor-

[1] Hygroton, Ciba-Geigy, Basel, Switzerland.

[2] Metrohm, Zürich, Switzerland.

0022-3549/79/0800-1056$01.00/0
© 1979, American Pharmaceutical Association

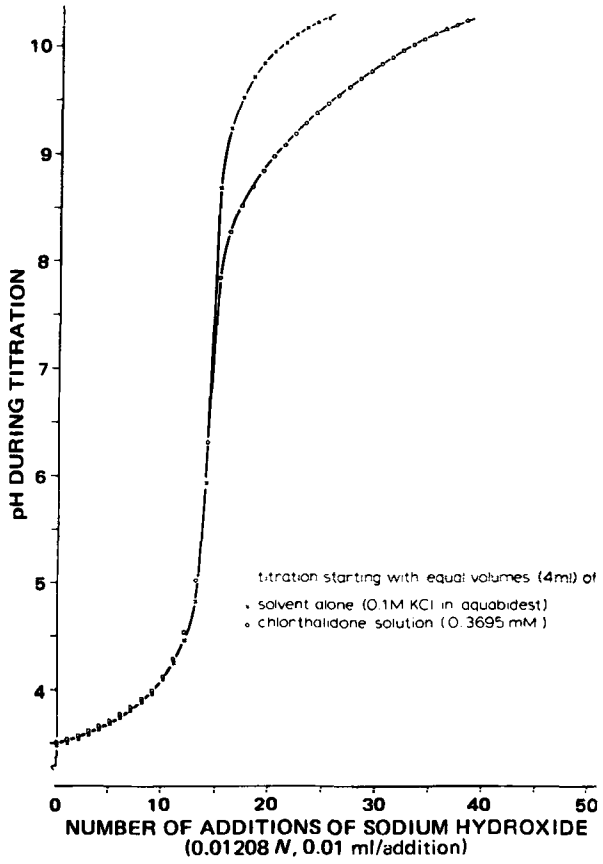

Figure 1—*Acid-base titration of the very slightly water-soluble drug chlorthalidone by measurement of the difference in titrant between samples with and without the substance.*

thalidone solution (4.00 ml) and on the solvent alone (4.00 ml), at 25° and under nitrogen, in both directions of the pH 3.5–10.6 range. Two runs with hydrochloric acid (Experiments B and D) and two with sodium hydroxide (Experiments A and C) were carried out. The actual pH ranges were 3.47–10.28 in A, 8.55–10.58 in B, 8.10–10.50 in C, and 6.61–10.45 in D. A pH meter[3] in combination with a glass[4] and a calomel[5] electrode was used.

A high-resolution digital voltmeter[6] was connected with the pH meter. The pH was measured 10 times after each addition of hydrochloric acid or sodium hydroxide, and the mean of these readings was taken. In this way, very reproducible values, including the third decimal figure, were obtained (8). Detailed descriptions of this automatic potentiometric equipment were published (6, 8). To calibrate the pH meter, phthalate buffer (pH 4.008) and phosphate buffer (pH 6.865) were used.

RESULTS AND DISCUSSION

Typical titration curves are shown in Fig. 1. Equal volumes of 0.1 *M* KCl, with and without chlorthalidone, were titrated with dilute sodium hydroxide from pH 3.5 to 10.3. A larger number of additions of alkali was needed to increase the pH of the drug solution in the region where the drug becomes deprotonated. The difference at each pH value between the number of additions of the two titration runs clearly represents the quantity necessary for titration of the drug itself. When these differences are plotted *versus* the pH, a difference titration curve is obtained. For a weak acid, the titration curve obeys the familiar Henderson–Hasselbalch equation:

$$\mathrm{pH} = \mathrm{pKa}' + \log\frac{\alpha}{1-\alpha} \qquad \text{(Eq. 1)}$$

where α represents the degree of acid group dissociation and pKa′ is its apparent dissociation constant, which becomes equal to the thermodynamic dissociation constant, pKa, at infinite dilution. At higher ionic strength, the following relationship is valid:

$$\mathrm{pKa} = \mathrm{pKa}' - \log\frac{\gamma A^-}{\gamma HA} \qquad \text{(Eq. 2)}$$

in which γA^- and γHA are the activity coefficients of the ionized and unionized forms of the acid, respectively. The activity coefficients can be calculated according to the Debye-Hückel equation (3); for log $\gamma A^-/\gamma HA$, a value of −0.11 was obtained. By using this correction, the pKa_1 is readily obtained if the experimental pKa_1' value is known.

When a strong base is added, an equivalent amount of protons is lost by the weak acid. Then α can be written as $\alpha = Z/A$, where Z represents the amount of strong base added at any moment of the titration and A is the amount added at the titration end-point. Polyacid titration produces the relation:

$$Z = \sum_{i=1}^{n} A_i\alpha_i \qquad \text{(Eq. 3)}$$

where i denotes the identity of a specific weak acid group and n is the total number of classes of weak acid groups.

Chlorthalidone contains two acidic moieties, one sulfonamide and one oxoisoindolin group, potentially dissociating in the pH range under study. Therefore, $A_1 = A_2$ and:

$$Z = A_1(\alpha_1 + \alpha_2) \qquad \text{(Eq. 4)}$$

By applying Eq. 1, one can write:

$$Z = A_1\left(\frac{10^{\mathrm{pH}-\mathrm{pKa}_1'}}{1+10^{\mathrm{pH}-\mathrm{pKa}_1'}} + \frac{10^{\mathrm{pH}-\mathrm{pKa}_2'}}{1+10^{\mathrm{pH}-\mathrm{pKa}_2'}}\right) \qquad \text{(Eq. 5)}$$

The titration data were analyzed by means of a nonlinear least-squares regression analysis program[7]. In every curve-fitting procedure, the correct assignment of independent and dependent variables is essential to obtaining unbiased estimates of the unknown parameters (9). The pH was chosen as the independent variable, because its measurement was highly reproducible (see *Experimental*), such that there existed, apart from a potential calibration error that could influence only the absolute pH scale, a very small error within each experiment. For the dependent variable Z, a constant error of 0.1, expressed as additions of strong base, was taken since this value was the read-off uncertainty of the differences between titration curves of the chlorthalidone solution and the blank (Fig. 1).

At first, the data points were fitted according to the first term of Eq. 5 only, with the assumption that the dissociation of the second acid group was negligible (if pH ≪ pKa_2', the second term approximates zero). Much better fits were obtained when the second term also was considered. For this purpose, the value for pKa_2' was not left free in the least-squares regression analysis, because too few data points were available in the high pH region, only up to pH 10.6, which would introduce large errors in the estimates of the other parameters, A_1 and pKa_1'. Preset values of pKa_2' were systemically changed until the minimum of the sum of weighed

Table I—Superiority of Computer Fits of Difference Titration Curves of Chlorthalidone when the Dissociation of Two Weak Acid Groups Instead of One Is Included[a]

Experiment	Two Titratable Groups Involved in Curve Fitting				One Titratable Group Involved in Curve Fitting		
	pKa_1'	A_1	k_2	χ^2	pKa_1'	A_1	χ^2
A	9.228	12.15	10.94	12.6	9.35	14.43	96.6
B	9.287	12.33	11.11	14.3	9.56	14.16	210
C	9.210	13.27	11.55	8.1	9.27	14.17	67.5
D	9.235	12.67	11.95	6.1	9.26	12.96	11.1
Mean ± *SEM* (n = 4)	9.24 ± 0.02						

[a] pKa_1' = apparent first dissociation constant, A_1 = total amount of base at first titration end-point, k_2 = optimally fixed value for the dissociation of the second acid group, and χ^2 = sum of weighed squared deviations of the experimental data from the fitted curve. The χ^2 (5%) value, the tabulated level of significance at p = 0.05, was 39, 44, 40, and 37 in Experiments A, B, C, and D, respectively. The thermodynamic dissociation constant, pKa_1, is larger than the pKa_1' by a factor of 0.11 due to the contribution of activity coefficients. Therefore, pKa_1 = 9.35 ± 0.02 (mean ± *SEM*).

[3] Type PHM 26, Radiometer, Copenhagen, Denmark.
[4] Type G202B, Radiometer, Copenhagen, Denmark.
[5] Type K401, Radiometer, Copenhagen, Denmark.
[6] Type LM 1867, Solartron, Peekel, Rotterdam, The Netherlands.

[7] Formfit, a digital computer program in use at the Computer Center of the University of Nijmegen. Details are available upon request.

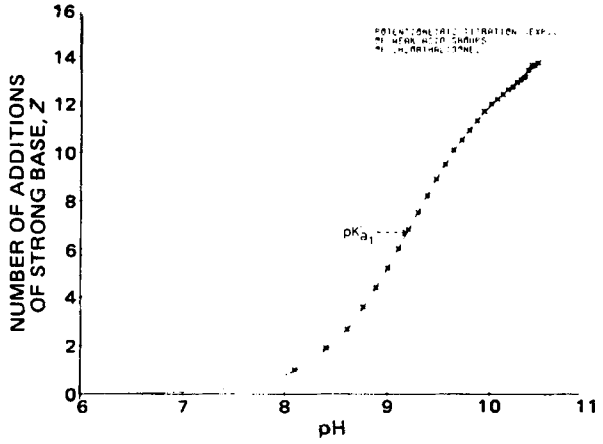

Figure 2—*Computer-fitted difference titration curve of chlorthalidone. From four experiments, the following estimates resulted for* pKa_1': *9.228 (A), 9.287 (B), 9.210 (C), and 9.235 (D), yielding a mean apparent dissociation constant of 9.24 ± 0.02 (±SEM) at 0.1 ionic strength and 25°.*

squared deviations was found. The results of these calculations are included in Table I (pKa_2' has been denoted k_2).

For A_1, the best estimate was sought by the fitting procedure. When this parameter was fixed at its theoretically calculated value (12.24 additions of strong base), it influenced the pKa_1' estimate, with possible errors in the concentration and pipetted volume of the chlorthalidone solution and in the normality and volume of the titrant.

Figure 2 shows a typical difference titration curve, fitted according to Eq. 5 (at fixed optimal pKa_2' values). The decision in favor of such a fit over that based on ionization of only one acid group was made using several criteria: (*a*) visual plot inspection, (*b*) symmetry of the residuals around the fitted curves, and (*c*) calculation of the sum of weighed squared residuals (as χ^2). Table I compares the χ^2 values for both procedures and indicates the superiority of curve fitting according to two titratable groups in all four experiments. In addition, the scatter of the pKa_1' estimates in the left part is much smaller than that in the right part. Also, the A_1 estimates at the left correspond better with the value calculated on the basis of total chlorthalidone in the titration vessel (equivalent to 12.24 additions of strong base), indicating that actually one proton-donor group was dissociated completely at this stage.

The variance of the four pKa_1' estimates exceeds the within-experiment error (the computer-estimated relative errors ranged from 0.0 to 0.1%). This finding points to minor systematic differences between the four experiments caused, for example, by the pH meter calibration. However, the differences are small enough that the pKa_1' (25°) = 9.24 ± 0.02 (mean ± *SEM*) can be treated as a reliable operational ionization constant, suitable for use as a physicochemical parameter in pharmacological studies. When the correction for ionic strength is carried out with Eq. 2, the thermodynamic dissociation constant is calculated at pKa = 9.35 (25°).

Determination of very slightly water-soluble drug dissociation constants appears to be convenient and reproducible by the method described, and no corrections for titrant consumption by the solvent are needed. The technique was applied also to the analgesic ibuprofen[8] in the laboratory (10), indicating that potentiometric difference titrations can be conducted in a wide area of pharmaceutical substances.

REFERENCES

(1) A. Goldstein, L. Aronow, and S. Kalman, "Principles of Drug Action," 2nd ed., Wiley, New York, N.Y., 1974.

(2) H. L. J. Fleuren, T. A. Thien, C. P. W. Verwey-van Wissen, and J. M. van Rossum, *Eur. J. Clin. Pharmacol.*, **15**, 35 (1979).

(3) A. Adrien and E. P. Serjeant, "Ionization Constants of Acids and Bases," Methuen, London, England, 1962, pp. 10, 58.

(4) E. G. Stenger, H. Wirz, and R. Pulver, *Schweiz. Med. Wochenschr.*, **89**, 1126 (1959).

(5) S. H. de Bruin, L. H. M. Janssen, and G. A. J. van Os, *Biochim. Biophys. Acta*, **188**, 207 (1969).

(6) L. H. M. Janssen, S. H. de Bruin, and G. A. J. van Os, *ibid.*, **221**, 214 (1970).

(7) H. L. J. Fleuren and J. M. van Rossum, *J. Chromatogr.*, **152**, 41 (1978).

(8) G. A. J. van Os, S. H. de Bruin, and L. H. M. Janssen, *J. Electroanal. Chem.*, **37**, 303 (1972).

(9) J. H. Perrin, J. J. Vallner, and S. Wold, *Biochim. Biophys. Acta*, **371**, 482 (1974).

(10) C. A. M. van Ginneken, Ph.D. thesis, University of Nijmegen, Nijmegen, The Netherlands, 1976, p. 93.

ACKNOWLEDGMENTS

Supported by a grant from the Netherlands Organization for the Advancement of Pure Research (ZWO/FUNGO).

The technical assistance of Mr. J. J. M. Joordens, Miss C. W. J. Prinse, and Ir. G. G. M. van Beek as well as the discussion by Dr. S. H. de Bruin (all members of the Department of Biophysical Chemistry, University of Nijmegen, Nijmegen, The Netherlands) is greatly appreciated. The authors also thank Mrs. C. P. W. Verwey-van Wissen for assistance, Mrs. E. L. Klok-Huyser for skillful operation of the Formfit computer program, and Mrs. M. P. M. Klumpkens-Janssen for typing the manuscript.

[8] Preliminary estimate of pKa ~ 4.4.

Improvements of Dissolution Characteristics and Chemical Stability of 16,16-Dimethyl-*trans*-Δ^2-prostaglandin E_1 Methyl Ester by Cyclodextrin Complexation

KANETO UEKAMA *x, **FUMITOSHI HIRAYAMA** *, **YOSHITSUGU YAMADA** *, **KOJI INABA** ‡, and **KEN IKEDA** §

Received July 31, 1978, from the *Faculty of Pharmaceutical Sciences, Kumamoto University, Kumamoto, 862, Japan, ‡Ono Pharmaceutical Co. Ltd., Osaka, 537, Japan, and the §Faculty of Pharmaceutical Sciences, Nagoya City University, Nagoya, 467, Japan. Accepted for publication February 6, 1979.

Abstract □ Inclusion complexation of 16,16-dimethyl-*trans*-Δ^2-prostaglandin E_1 methyl ester (I), which is effective in early pregnancy termination, with cyclodextrins in water was ascertained by a solubility study. A solid complex of I-β-cyclodextrin in a 1:2 molar ratio was obtained, and its dissolution behavior and chemical stability were examined. The results indicated that the complex may have great utility as a rapidly dissolving form of I with prolonged storage time.

Keyphrases □ Prostaglandin E_1 derivatives—cyclodextrin complexation, dissolution, stability □ Cyclodextrin—complexation with prostaglandin E_1, dissolution, stability □ Complexation—prostaglandin E_1 with cyclodextrin, dissolution, stability

Some naturally occurring prostaglandins such as prostaglandins E_1, E_2, and $F_{2\alpha}$ (dinoprost) have clinical applications (1). 16,16-Dimethyl-*trans*-Δ^2-prostaglandin E_1 methyl ester[1] (I), a prostaglandin E_1 derivative, induced uterine contraction in rats with an efficacy 10 times that of prostaglandin $F_{2\alpha}$ (2, 3). This compound is more acceptable for early pregnancy termination than prostaglandin $F_{2\alpha}$ because it produces fewer side effects. However, the solubility and chemical instability of the prostaglandins, including I, in aqueous solution have limited dosage form development and resulted in a substantial challenge to the pharmaceutical scientist.

Cyclodextrins form inclusion complexes with various drug molecules (4–8). Since I is essentially a methyl ester of long chain unsaturated fatty acids, the relatively hydrophobic cyclodextrin cavity is expected to attract I as an adequate guest molecule (9–11). Thus, the present study dealt with inclusion complexation of I with α- and β-cyclodextrins in anticipation of improved solubilization and stabilization of I.

EXPERIMENTAL

Materials—Compound I[1], α-cyclodextrin[2], and β-cyclodextrin[2] were used as supplied. All other materials and solvents were analytical reagent grade. Deionized, double-distilled water was used.

Solubility and Dissolution Studies—Solubility measurement and analytical methods for I were essentially those reported previously (9).

Table I—Thermal Stabilities of I and Its β-Cyclodextrin Complex at 60°

Compound	Decomposition of I, % 1 Day	3 Days	8 Days	14 Days
I	2.2	8.8	30.2	54.0
Complex	0.1	0.5	2.5	4.0

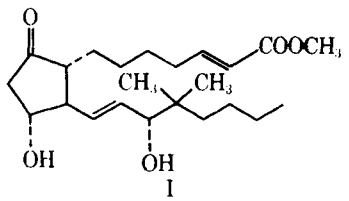

I

The dissolution behaviors of I and its β-cyclodextrin complex in water were compared at the same I concentration according to the dispersed amount method (12). A 120-mg sample of a I-β-cyclodextrin complex as a 100–200-mesh powder was weighed and put in a dissolution cell. Because I is a viscous oil, an ether solution containing 18 mg of I was placed in the dissolution cell and evaporated to dryness. The dissolution medium (25 ml) was maintained at 25° and stirred at 93 rpm. At an appropriate interval, 0.5 ml of solution was sampled by a pipet with a cotton filter. The assay procedure for I was the same as that used in the solubility study (9).

Stability Studies—Stability tests for I and its β-cyclodextrin complex were conducted at 60° in a moisture-free environment. Intact I was quantitatively determined by high-performance liquid chromatography (HPLC). The liquid chromatograph[3] (20-cm column[4]) was operated at a flow rate of 0.5 ml/min, and the mobile phase consisted of acetonitrile–methanol–water (2:8:3). Under these conditions, the disappearance of the I peak was followed by a UV detector[5] at 215 nm.

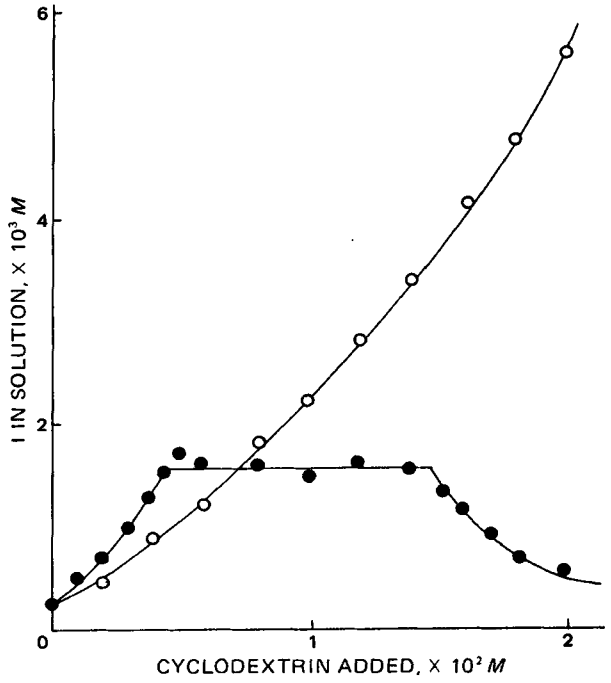

Figure 1—*Solubility of I as a function of cyclodextrin concentration in water at 25°. Key:* ○, *α-cyclodextrin; and* ●, *β-cyclodextrin.*

[1] 9-Oxo-11α,15α-dihydroxy-16,16-dimethyl-2-*trans*,13-*trans*-prostadienoic acid methyl ester (ONO-802). Supplied by Ono Pharmaceutical Co. Ltd., Osaka, Japan.

[2] Teijin Ltd., Tokyo, Japan.

[3] Model FLC-A700, Jasco, Tokyo, Japan.

[4] Packed with LiChrosorb RD-18, E. Merck, Darmstadt, West Germany.

[5] Model UVIDEC-1M, Jasco, Tokyo, Japan.

0022-3549/79/0800-1059$01.00/0
© 1979, American Pharmaceutical Association

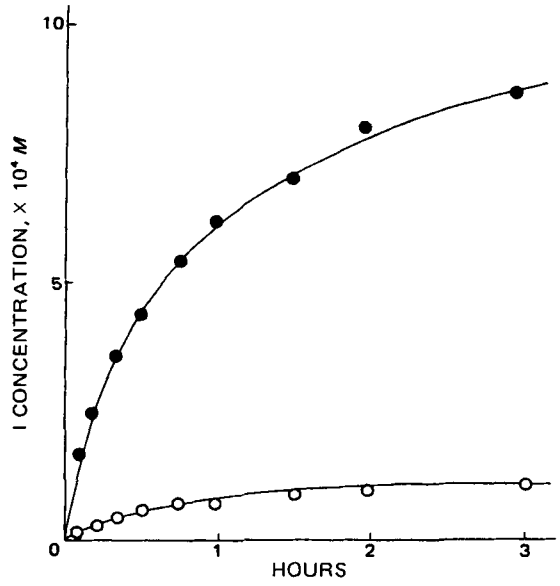

Figure 2—*Dissolution behavior of I* (○) *and its β-cyclodextrin complex* (●) *at the same I concentration in water at 25°.*

RESULTS AND DISCUSSION

The equilibrium phase solubility diagrams obtained for I with α- and β-cyclodextrins in water are shown in Fig. 1. In both of these systems, the solubility of I increased following cyclodextrin addition, and the solubility curves of α- and β-cyclodextrins can be generally classified as types A_p and B_s (13), respectively. According to Higuchi and Kristiansen (14), the stability constants for 1:1 (SL) and 1:2 (SL_2) complexes (S = I, and L = cyclodextrin) were calculated from ascending positive curvatures in Fig. 1. The stability constants for α- ($K_{1:1}$ = 820 M^{-1}, and $K_{1:2}$ = 260 M^{-1}) and β- ($K_{1:1}$ = 1600 M^{-1}, and $K_{1:2}$ = 370 M^{-1}) cyclodextrin complexes were obtained.

The β-cyclodextrin system deposited a crystalline complex of I–β-cyclodextrin (1:2) at high β-cyclodextrin concentrations. Stoichiometry based on the data in the plateau region (13) in Fig. 1 was in good agreement with that obtained by isolation and analysis of the crystalline complex. In sharp contrast, the α-cyclodextrin system did not give any solid complex, a smaller cavity size apparently allowing little penetration of the bulky guest molecule.

The dissolution behavior and chemical stability of the isolated β-cyclodextrin complex were examined. The dissolution rate of the complex in powder was extremely large compared with that of I in water (Fig. 2), indicating an improved bioavailability. As shown in Table I, the decomposition of I was significantly retarded by inclusion complex formation. Thus, the increased dissolution rate, together with improved chemical stability, suggested that the β-cyclodextrin–I complex may have great utility in the development of fast dissolving dosage forms with prolonged storage time.

Furthermore, thermal gravimetric analysis[6] showed that the volatility of I was extremely depressed by binding to β-cyclodextrin. The crystallinity of the complex should facilitate drug formulation, which is difficult with uncomplexed I because it occurs as a viscous oil.

REFERENCES

(1) "The Prostaglandins: Clinical Application in Human Reproduction," E. M. Southern, Ed., Futura Publishing, Mount Kisco, N.Y., 1972.

(2) S. Takagi, H. Sakata, T. Yoshida, S. Nakazawa, T. K. Fujita, Y. Tomida, K. Itoh, and R. Matsukawa, *Prostaglandins*, **14**, 791 (1977).

(3) S. Takagi, H. Sakata, T. Yoshida, K. Den, T. K. Fujita, H. Amemiya, and M. Tomita, *ibid.*, **15**, 913 (1978).

(4) J. L. Lach and J. Cohen, *J. Pharm. Sci.*, **52**, 137 (1963).

(5) A. L. Thakkar, P. B. Kuehn, J. H. Perrin, and W. L. Wilham, *ibid.*, **61**, 1841 (1972).

(6) M. Otagiri, J. H. Perrin, K. Uekama, K. Ikeda, and K. Takeo, *Pharm. Acta Helv.*, **51**, 343 (1976).

(7) Y. Hamada, N. Nambu, and T. Nagai, *Chem. Pharm. Bull.*, **23**, 1205 (1975).

(8) K. H. Frömming and I. Weyerman, *Arzneim.-Forsch.*, **23**, 424 (1973).

(9) K. Uekama, F. Hirayama, K. Ikeda, and K. Inaba, *J. Pharm. Sci.*, **66**, 706 (1977).

(10) K. Uekama, F. Hirayama, S. Yamasaki, M. Otagiri, and K. Ikeda, *Chem. Lett.*, **1977**, 679.

(11) K. Uekama and F. Hirayama, *Chem. Pharm. Bull.*, **26**, 1195 (1978).

(12) H. Nogami, T. Nagai, and T. Yotsuyanagi, *ibid.*, **17**, 499 (1969).

(13) T. Higuchi and K. A. Connors, *Adv. Anal. Chem. Instr.*, **4**, 117 (1965).

(14) T. Higuchi and H. Kristiansen, *J. Pharm. Sci.*, **58**, 661 (1969).

ACKNOWLEDGMENTS

Supported by a Grant-in-Aid for Scientific Research from the Ministry of Education, Science and Culture, Japan.

[6] Model DT-20B thermal analyzer, Shimadzu, Osaka, Japan.

Differential Pulse Polarography of Tetracycline: Determination of Complexing Tendencies of Tetracycline Analogs in the Presence of Cations

T. JOCHSBERGER ˣ, A. CUTIE, and J. MILLS

Received October 18, 1978, from the *Arnold & Marie Schwartz College of Pharmacy and Health Sciences of Long Island University, Brooklyn, NY 11201.* Accepted for publication February 8, 1979.

Abstract □ The complexation tendencies, stoichiometries, and stability constants for tetracycline, minocycline, and demeclocycline with the metallic ions calcium(II), magnesium(II), zinc(II), aluminum(III), iron(II), and iron(III) were evaluated using a polarographic technique. Changes in pulse peak heights for each tetracycline derivative were measured as a function of cation concentration. The method provides an *in vitro* method of evaluating the selectivity of particular metal ions for different tetracycline analogs.

Keyphrases □ Tetracycline analogs—complexation, effect of cations, differential pulse polarography □ Tetracycline—complexation, effect of cations, differential pulse polarography □ Minocycline—complexation, effect of cations, differential pulse polarography □ Demeclocycline—complexation, effect of cations, differential pulse polarography □ Differential pulse polarography—tetracycline analogs, complexation, effect of cations

The phenomenon of complex formation between tetracycline analogs and various cations is well documented (1–3). This study reports the application of differential pulse polarography in determining the apparent complexation parameters for tetracycline, minocycline, and demeclocycline with Fe(II), Fe(III), and Al(III). The effect of other cations on the polarograms of the various tetracyclines was also examined.

EXPERIMENTAL

Apparatus—All polarograms were recorded on a polarograph[1] equipped with a three-electrode system and an *x–y* recorder[2]. The working electrode consisted of a dropping mercury electrode with a 1-sec drop time, which was controlled by a mechanical drop knocker. A commercial calomel electrode was used as the reference electrode, and a platinum wire was used as the auxiliary electrode. The electrolysis cell[3] had a 25-ml total volume, and the tetracycline derivative concentrations were 10^{-4}–10^{-5} *M*. Potential sweeps of 1 or 2 mv/sec and pulse modulations of 10 or 25 mv were employed.

Deaeration was performed by passing a stream of highly purified nitrogen through the solutions for ≥10 min. All experiments were carried out at room temperature, and potentials are reported with respect to the saturated calomel electrode.

Reagents—All salts (ferrous sulfate heptahydrate, ferric nitrate monohydrate, aluminum chloride hexahydrate, magnesium sulfate heptahydrate, calcium nitrate tetrahydrate, and potassium chloride) were reagent grade and used without purification. Compendial grade samples[4] of demeclocycline hydrochloride, minocycline hydrochloride, and tetracycline hydrochloride were utilized without further purification. Acetate buffers were freshly prepared from reagent grade materials.

Procedure—Complexation parameters were determined by measuring the polarograms of the cations in 0.1 *N* KCl in the absence and in the presence of added tetracycline derivative. The shifts in peak potential were determined as a function of concentration (Table I), and the complexation parameters (Table II) were calculated as described later.

In another set of experiments, the effect of successive additions of a given cation on the polarograms of the various tetracycline analogs was determined. In both sets of experiments, the standard addition technique was employed.

[1] Princeton Applied Research model 174 polarographic analyzer.
[2] Princeton Applied Research model 9002A.
[3] Princeton Applied Research model 9301.
[4] Provided by Lederle Laboratories, Pearl River, N.Y.

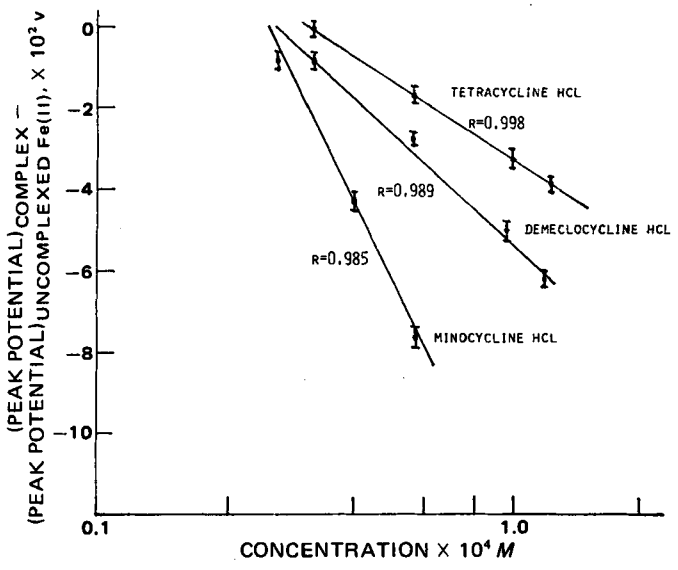

Figure 1—*Effect of tetracycline derivative concentration on Fe(II) peak potential (in 0.1 N KCl).*

RESULTS AND DISCUSSION

The polarography of complexed ions is well documented (4). The basic relationship between potential shifts and concentrations may be expressed by Lingane's equation (5):

$$E^{c}_{1/2} - E_{1/2} = \frac{-0.0591}{n} \log K_f - \frac{0.0591p}{n} \log M_L \qquad \text{(Eq. 1)}$$

where $E^{c}_{1/2}$ is the half-wave potential of a metal ion in the presence of M_L moles per liter of ligand, $E_{1/2}$ is the half-wave potential in the absence of ligand, n is the number of electrons gained in the reduction, K_f is the

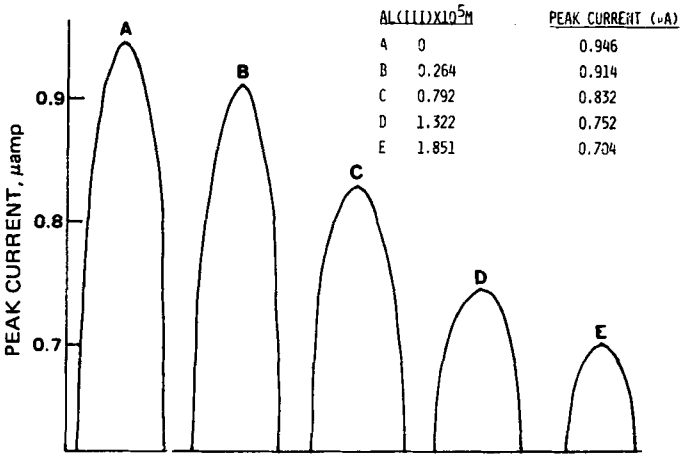

Figure 2—*Effect of aluminum ion on tetracycline hydrochloride polarograms (1.872×10^{-5} M) at a peak potential of −1.342 v.*

0022-3549/79/0800-1061$01.00/0
© 1979, American Pharmaceutical Association

Table I—Peak Potentials of Al(III), Fe(II), and Fe(III) as a Function of Tetracycline Derivative Concentration

Tetracycline Hydrochloride, $\times 10^4$ M	E_p, v	Minocycline Hydrochloride, $\times 10^4$ M	E_p, v	Demeclocycline Hydrochloride, $\times 10^4$ M	E_p, v
		Al(III)			
0	−1.788	0	−1.784	0	−1.786
0.661	−1.762	0.157	−1.660	0.322	−1.764
1.32	−1.726	0.314	−1.606	0.643	−1.746
1.98	−1.702	0.471	−1.560	0.965	−1.736
2.31	−1.696			1.29	−1.722
		Fe(II)			
0	−1.366	0	−1.366	0	−1.364
0.326	−1.368	0.265	−1.376	0.329	−1.374
0.651	−1.386	0.398	−1.404	0.657	−1.396
0.977	−1.400	0.530	−1.440	0.986	−1.414
1.30	−1.406			1.31	−1.432
		Fe(III)			
0	−1.614	0	−1.610	0	−1.606
0.648	−1.636	0.278	−1.576	0.629	−1.636
0.972	−1.652	0.417	−1.560	0.943	−1.672
1.30	−1.662	0.556	−1.546	1.26	−1.684

Table II—Complexation Parameters for Cation-Tetracycline Derivative Complexes

Cation	Derivative	Log K_f	Apparent Coordination Number of Cation
Al(III)	Tetracycline	14.5	3
Al(III)	Minocycline	34.5	6
Al(III)	Demeclocycline	10.8	2
Fe(II)	Tetracycline	6.9	2
Fe(II)	Minocycline	17.8	4
Fe(II)	Demeclocycline	10.2	3
Fe(III)	Tetracycline	14.0	4
Fe(III)	Minocycline	20.2	4
Fe(III)	Demeclocycline	20.6	6

apparent formation constant, and p is the complex coordination number. There have been few attempts to apply differential pulse polarography to the study of complexation. Since the peak potential observed with the technique is identical to the half-wave potential (6), Eq. 1 can be modified to:

$$E_p^c - E_p = \frac{-0.0591}{n} \log K_f - \frac{0.0591p}{n} \log M_L \qquad \text{(Eq. 2)}$$

where E_p^c is the peak potential of the ion in the presence of M_L moles per liter of ligand and E_p is the peak potential in the absence of ligand. The other symbols have the same meaning as in Eq. 1.

Equation 2 indicates that plots of peak potential shift *versus* the logarithm of the ligand concentration should be linear. The slopes of these plots can be used to determine the complex coordination number, and the intercepts yield values for the formation constants. Figure 1 shows representative plots for ferrous ion and the various tetracyclines analogs. Slopes and intercepts were computed by linear regression, and correlation coefficients ranged from ±0.982 to ±0.999. Apparent complexation parameters determined utilizing this technique are presented in Table II.

The data indicate that minocycline forms more stable complexes with Al(III), Fe(III), and Fe(II) than do the other analogs. Since the exact point of attachment between the cations and the tetracyclines has not been elucidated, it is difficult to assess the precise basis of this greater stability. However, previous investigators (1) suggested the dimethylamino group as one coordinating group of tetracycline; the existence of two such groups on minocycline could account for the increased stability of its complexes. The data indicate that in the presence of Fe(II) and Al(III) ions, the apparent coordination number toward minocycline is twice that of tetracycline; this finding further supports the idea that complexing is *via* the dimethylamino groups.

Apparently, Ca(II) and Mg(II) do not complex as strongly with minocycline as they do with tetracycline and demeclocycline. Due to the close proximity of their reduction potential to that of potassium ion, it was not possible to obtain quantitative data in the form of complexation parameters for Ca(II) and Mg(II). However, these two ions had no effect on the polarogram of minocycline (Table III). The lack of an apparent interaction between Ca(II) and minocycline is consistent with the low effect of dairy products on the *in vivo* availability of this analog compared to tetracycline and other derivatives (7). This effect may also be indicative of an interaction between Ca(II) and Mg(II) and the various tetracyclines that is different from that of other cations (1).

The general effect of cation addition on tetracycline, minocycline, and demeclocycline solutions was to decrease the peak current in the polarograms (Table III and Fig. 2). This effect was not uniform. Al(III), Fe(III), and Fe(II) had significant effects on all three derivatives studied. With Fe(III) and tetracycline, the effect was observable at a peak potential of −1.04 v but not at −1.35 v. Ca(II) had a significant effect on the tetracycline and demeclocycline polarograms but not, as noted, on those of minocycline. Again the Ca(II)-tetracycline interaction appeared at a peak potential of −1.04 v but not at −1.35 v.

The dependence of the observed effect on peak potential is possibly related to the point of attachment between the cation and the tetracycline molecule. The present data, however, do not permit any definitive conclusion about that relationship. Zn(II) had no effect on the −1.35-v peak of the tetracycline polarogram. It was not possible to determine if an interaction occurred in the −1.0-v region due to the reduction of the cation itself. The interaction between Al(III) and the three tetracycline derivatives appears to be somewhat different from that of Fe(II) and Fe(III). The tetracycline and demeclocycline complexes of both iron salts and the minocycline-Fe(II) complex exhibited more negative peak potentials than the uncomplexed species, which is the usual observation with complexed species (8). However, Al(III) complexes exhibited a positive shift in peak potential with increasing ligand concentration.

The relative magnitude of the formation constants (Table II) for the three cations studied is consistent with previous observations made under different experimental conditions (2). The values for the coordination numbers determined by this technique (Table II) are generally consistent with those reported for tetracycline derivative complexes (1, 2). However, both significant clinical effects (9) and spectrophotometric changes occur

Table III—Relative Effect [a] of Cations on Peak Currents in Tetracycline Derivative Polarograms

Derivative	Al(III)	Fe(III)	Fe(II)	Ca(II)	Mg(II)	Zn(II)
Tetracycline	++	++[b]	++	++[b]	++	0[b]
Minocycline	++	++	++	0	0	—[c]
Demeclocycline	++	++	++	++	+	—[c]

[a] 0 = no effect, + = moderate effect, and ++ = significant effect. [b] Effect depends on peak potential. [c] No data.

at equimolar ratios of tetracycline to cation[5] (3). Therefore, even partial complexing can have important effects on both *in vivo* and *in vitro* tetracycline interactions.

REFERENCES

(1) J. T. Doluisio and A. N. Martin, *J. Med. Chem.*, **6**, 16 (1963).
(2) A. Albert and C. W. Rees, *Nature*, **177**, 433 (1956).
(3) T. Chin and J. L. Lach, *Am. J. Hosp. Pharm.*, **32**, 625 (1975).
(4) D. R. Crow and J. V. Westwood, "Polarography," Methuen, London, England, 1968, pp. 63–79.
(5) J. J. Lingane, *Chem. Rev.*, **29**, 1 (1941).
(6) L. Meites, "Polarographic Techniques," 2nd ed., Interscience, New York, N.Y., 1965, p. 571 ff.
(7) "Physicians' Desk Reference," Medical Economics Co., Oradell, N.J., 1978, pp. 956, 1285.
(8) D. A. Skoog and D. M. West, "Fundamentals of Analytical Chemistry," 3rd ed., Holt, Rinehart and Winston, New York, N.Y., 1976, p. 469.
(9) R. H. Harris, in "Handbook of Drug Interactions," 2nd ed., E. A. Hartshorn, Ed., Drug Intelligence Publications, Hamilton, Ill., 1973, p. 158.

[5] A. Cutie and T. Jochsberger, unpublished results.

ACKNOWLEDGMENTS

Presented at the APhA Academy of Pharmaceutical Sciences, Montreal meeting, May 1978.

Photolytic Decomposition of Indapamide

REG DAVIS *x, CLIFFORD H. J. WELLS *, and ALBERT R. TAYLOR ‡

Received December 20, 1978, from the **School of Chemical and Physical Sciences, Kingston Polytechnic, Kingston upon Thames KT1 2EE, England,* and ‡*Servier Laboratories, Ltd., Greenford, Middlesex UB6 7PW, England.* Accepted for publication February 7, 1979.

Abstract □ Photolytic decomposition of indapamide (I) in nitrogen-flushed methanol yields 3-sulfamoyl-4-chlorobenzamide (II), 2-methylindoline (III), semicarbazide (IV), and 1-(*N*-formamido)-2-methylindoline (V); in oxygen-flushed methanol, II–V, 1-aminocarboxymethyl-2-methylindoline (VI), 3-sulfamoyl-4-chlorobenzoic acid (VII), methyl-3-sulfamoyl-4-chlorobenzoate (VIII), and 2-(*N*-acetamido)-benzoic acid (IX) are formed. A comparison is made with thermal decomposition of I.

Keyphrases □ Indapamide—photolytic decomposition, thermal decomposition, decomposition products identified □ Photolysis—indapamide, products identified □ Thermolysis—indapamide, products identified □ Diuretics—indapamide, photolytic and thermal decomposition, products identified

There has recently been a growth in drug photosensitization studies. Numerous drugs have photosensitizing properties (1), and these properties appear to show a correlation with *in vivo* photosensitivity. In particular, the saluretic furosemide exhibits a high affinity for oxygen under UV irradiation, and this affinity may be related to the reported skin rash reaction among patients taking the drug (2).

As part of detailed studies of indapamide [*N*-(3-sulfamoyl-4-chlorobenzamido)-2-methylindole] (I), a compound with prolonged saluretic action (3), a study of the photolytic decomposition of this compound was conducted. In contrast to earlier studies (1), the products of *in vitro* photolytic decomposition were identified prior to *in vivo* experiments.

EXPERIMENTAL[1]

Indapamide (I) was supplied as a pure compound[2]. 2-Methylindoline (III), semicarbazide (IV), and 2-(*N*-acetamido)benzoic acid (IX) were supplied as pure reference compounds[3].

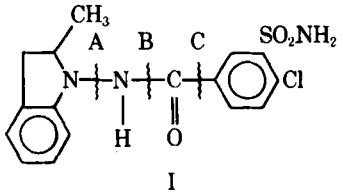

I

Photolytic decompositions were performed on 2.7×10^{-3} *M* I solutions in nitrogen- or oxygen-flushed methanol. The reactant solutions were contained in the inner well of a cylindrical quartz reaction vessel, which was mounted vertically before a 1000-w Hanovia medium-pressure mercury lamp. A filter solution of saturated aqueous copper sulfate was pumped through the annular space (4-mm i.d.) surrounding the inner well of the reaction vessel and also was pumped through a heat-exchanger to maintain the reactant solution at 293°K. The filter solution had a short wavelength cutoff at 300 nm. After photolysis for 12 hr, the solution was evaporated to dryness under reduced pressure. The residue was dissolved in a small volume of redistilled methanol prior to spotting on TLC plates.

Thermal decompositions were performed by heating samples in an automatic thermo-recording balance[4]. A 1-g sample of I was heated either at a constant rate of 5°K/min from ambient temperature to 453°K until the weight loss rate stabilized or at 453°K for 12 hr while the sample underwent a regular and continuous weight loss. The solids were dissolved in redistilled methanol prior to spotting on TLC plates.

Preparative TLC was performed using 20 × 20-cm plates coated with a 1-mm layer of silica gel[5]. Two solvent systems were used for plate development: 1, 100% dimethyl carbonate; and 2, the top layer obtained after vigorously shaking pentan-1-ol (85 cm^3) and ammonia (specific gravity 0.880, 15 cm^3) together and then allowing them to stand. All solvent systems were prepared fresh daily, and not more than two developments were carried out in any one preparation.

After development, reactant and product spots were visualized under UV light, scraped off the plates, and extracted into a small volume of redistilled methanol, which was evaporated to dryness under reduced pressure. The residual material was identified spectroscopically.

RESULTS AND DISCUSSION

The results relating to the identification of the products formed by I photolysis are summarized in Table I. These products arise principally as a result of bond cleavages in the N–NH–CO–C linkage.

[1] Mass spectra were recorded on an A.E.I. MS9 spectrometer, IR spectra were recorded on a Perkin-Elmer 257 spectrophotometer, NMR spectra were recorded on a Perkin-Elmer R.10 spectrometer, and UV spectra were recorded on a Unicam SP 8000 spectrophotometer.
[2] Les Laboratories, Servicer, Gidy, France.
[3] Servier Laboratories, Greenford, Middlesex, England.
[4] Stanton.
[5] Merck GF_{254}.

0022-3549/79/0800-1063$01.00/0

© 1979, American Pharmaceutical Association

at equimolar ratios of tetracycline to cation[5] (3). Therefore, even partial complexing can have important effects on both *in vivo* and *in vitro* tetracycline interactions.

REFERENCES

(1) J. T. Doluisio and A. N. Martin, *J. Med. Chem.*, **6**, 16 (1963).
(2) A. Albert and C. W. Rees, *Nature*, **177**, 433 (1956).
(3) T. Chin and J. L. Lach, *Am. J. Hosp. Pharm.*, **32**, 625 (1975).
(4) D. R. Crow and J. V. Westwood, "Polarography," Methuen, London, England, 1968, pp. 63–79.
(5) J. J. Lingane, *Chem. Rev.*, **29**, 1 (1941).
(6) L. Meites, "Polarographic Techniques," 2nd ed., Interscience, New York, N.Y., 1965, p. 571 ff.
(7) "Physicians' Desk Reference," Medical Economics Co., Oradell, N.J., 1978, pp. 956, 1285.
(8) D. A. Skoog and D. M. West, "Fundamentals of Analytical Chemistry," 3rd ed., Holt, Rinehart and Winston, New York, N.Y., 1976, p. 469.
(9) R. H. Harris, in "Handbook of Drug Interactions," 2nd ed., E. A. Hartshorn, Ed., Drug Intelligence Publications, Hamilton, Ill., 1973, p. 158.

[5] A. Cutie and T. Jochsberger, unpublished results.

ACKNOWLEDGMENTS

Presented at the APhA Academy of Pharmaceutical Sciences, Montreal meeting, May 1978.

Photolytic Decomposition of Indapamide

REG DAVIS *x, CLIFFORD H. J. WELLS *, and ALBERT R. TAYLOR ‡

Received December 20, 1978, from the **School of Chemical and Physical Sciences, Kingston Polytechnic, Kingston upon Thames KT1 2EE, England,* and ‡*Servier Laboratories, Ltd., Greenford, Middlesex UB6 7PW, England.* Accepted for publication February 7, 1979.

Abstract □ Photolytic decomposition of indapamide (I) in nitrogen-flushed methanol yields 3-sulfamoyl-4-chlorobenzamide (II), 2-methylindoline (III), semicarbazide (IV), and 1-(*N*-formamido)-2-methylindoline (V); in oxygen-flushed methanol, II–V, 1-aminocarboxymethyl-2-methylindoline (VI), 3-sulfamoyl-4-chlorobenzoic acid (VII), methyl-3-sulfamoyl-4-chlorobenzoate (VIII), and 2-(*N*-acetamido)-benzoic acid (IX) are formed. A comparison is made with thermal decomposition of I.

Keyphrases □ Indapamide—photolytic decomposition, thermal decomposition, decomposition products identified □ Photolysis—indapamide, products identified □ Thermolysis—indapamide, products identified □ Diuretics—indapamide, photolytic and thermal decomposition, products identified

There has recently been a growth in drug photosensitization studies. Numerous drugs have photosensitizing properties (1), and these properties appear to show a correlation with *in vivo* photosensitivity. In particular, the saluretic furosemide exhibits a high affinity for oxygen under UV irradiation, and this affinity may be related to the reported skin rash reaction among patients taking the drug (2).

As part of detailed studies of indapamide [*N*-(3-sulfamoyl-4-chlorobenzamido)-2-methylindole] (I), a compound with prolonged saluretic action (3), a study of the photolytic decomposition of this compound was conducted. In contrast to earlier studies (1), the products of *in vitro* photolytic decomposition were identified prior to *in vivo* experiments.

EXPERIMENTAL[1]

Indapamide (I) was supplied as a pure compound[2]. 2-Methylindoline (III), semicarbazide (IV), and 2-(*N*-acetamido)benzoic acid (IX) were supplied as pure reference compounds[3].

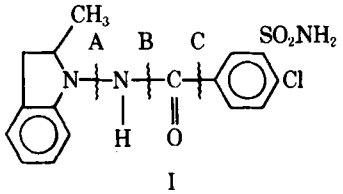

I

Photolytic decompositions were performed on 2.7×10^{-3} *M* I solutions in nitrogen- or oxygen-flushed methanol. The reactant solutions were contained in the inner well of a cylindrical quartz reaction vessel, which was mounted vertically before a 1000-w Hanovia medium-pressure mercury lamp. A filter solution of saturated aqueous copper sulfate was pumped through the annular space (4-mm i.d.) surrounding the inner well of the reaction vessel and also was pumped through a heat-exchanger to maintain the reactant solution at 293°K. The filter solution had a short wavelength cutoff at 300 nm. After photolysis for 12 hr, the solution was evaporated to dryness under reduced pressure. The residue was dissolved in a small volume of redistilled methanol prior to spotting on TLC plates.

Thermal decompositions were performed by heating samples in an automatic thermo-recording balance[4]. A 1-g sample of I was heated either at a constant rate of 5°K/min from ambient temperature to 453°K until the weight loss rate stabilized or at 453°K for 12 hr while the sample underwent a regular and continuous weight loss. The solids were dissolved in redistilled methanol prior to spotting on TLC plates.

Preparative TLC was performed using 20 × 20-cm plates coated with a 1-mm layer of silica gel[5]. Two solvent systems were used for plate development: 1, 100% dimethyl carbonate; and 2, the top layer obtained after vigorously shaking pentan-1-ol (85 cm^3) and ammonia (specific gravity 0.880, 15 cm^3) together and then allowing them to stand. All solvent systems were prepared fresh daily, and not more than two developments were carried out in any one preparation.

After development, reactant and product spots were visualized under UV light, scraped off the plates, and extracted into a small volume of redistilled methanol, which was evaporated to dryness under reduced pressure. The residual material was identified spectroscopically.

RESULTS AND DISCUSSION

The results relating to the identification of the products formed by I photolysis are summarized in Table I. These products arise principally as a result of bond cleavages in the N–NH–CO–C linkage.

[1] Mass spectra were recorded on an A.E.I. MS9 spectrometer, IR spectra were recorded on a Perkin-Elmer 257 spectrophotometer, NMR spectra were recorded on a Perkin-Elmer R.10 spectrometer, and UV spectra were recorded on a Unicam SP 8000 spectrophotometer.
[2] Les Laboratories, Servicer, Gidy, France.
[3] Servier Laboratories, Greenford, Middlesex, England.
[4] Stanton.
[5] Merck GF_{254}.

0022-3549/79/0800-1063$01.00/0

© 1979, American Pharmaceutical Association

Table I—Products from Photolytic and Thermal Decomposition of Indapamide

Photochemical Decomposition in N_2-Flushed Methanol	Photochemical Decomposition in O_2-Flushed Methanol	Thermal Decomposition	Product R_f Value[a]	Method of Structure Assignment[b]
II	II	II	0.19[c]	NMR, IR, UV, and mass spectra
III	III	III[d]	0.68	Comparison of IR, UV, and mass spectra with those of a reference sample
		IV	0.75	Comparison of IR, UV, and mass spectra with those of a reference sample
		V[d]	0.26	UV and mass spectra
VI	VI	VI	0.19[c]	NMR, IR, UV, and mass spectra
VII[e]	VII[e]		0.35	Mass spectrum[f]
	VIII[e]		0.45, 0.44*	Mass spectrum[f]
	IX		0.12*	Comparison of IR, UV, and mass spectra with those of a reference sample
	X		0.65	NMR, IR, UV, and mass spectra
	XI[e]		0.27*	Mass spectrum[f]

[a] The R_f values refer to qualitative TLC plates developed in Solvent System 1, except for those marked with an asterisk, which refer to Solvent System 2. [b] Unless otherwise stated, spectra were obtained for products isolated from each of the three decomposition systems. [c] The product at R_f 0.19 was a mixture of II and VI. Compound VI was sublimed out of the mixture and obtained as a white crystalline compound. [d] Product only observed in those thermal decomposition samples maintained at 453°K for 12 hr. [e] Minor product as judged by quantity of material isolated from TLC plates as compared to other products. [f] Only sufficient material could be isolated for a mass spectrum to be recorded.

Type A cleavage leads to 3-sulfamoyl-4-chlorobenzamide (II and III), type B cleavage leads to 3-sulfamoyl-4-chlorobenzoic acid, and type C cleavage yields 1-(*N*-formamido)-2-methylindoline (V) and 1-aminocarboxymethyl-2-methylindoline (VI). Methyl-3-sulfamoyl-4-chlorobenzoate (VIII) presumably arises as a consequence of esterification of VII by the solvent, while IX arises as a consequence of indoline ring oxidative cleavage in species such as III or I. At present, the origin of IV is not clear.

Thermal decomposition of I yields only II–IV besides 2-methylindole (X) and *N*-(3-sulfamoyl-4-chlorobenzamido)-2-methylindole (XI). Thus, type A cleavage can occur from vibrationally excited levels of the ground (S_0) state, and II and III can arise by this mechanism in photolytic reactions. Such species could be generated by internal conversion from the photolytically generated S_1 state. Presumably, the appropriate S_0 levels for dehydrogenation are not accessible *via* internal conversion. Type B and C cleavages only occur under photolysis and must, therefore, arise from the first excited states. Since such reactions are not inhibited by oxygen, which is known to quench triplet-state molecules (4), the S_1 state is implicated.

Thus, the study has demonstrated the complexity of photolysis of a simple pharmaceutical and has shown the wide range of compounds to be screened in photosensitization tests of such molecules.

REFERENCES

(1) D. E. Moore, *J. Pharm. Sci.*, **66**, 1282 (1977).

(2) H. J. Dargie and C. T. Dollery, in "Meyler's Side Effects of Drugs," vol. 8, M. N. G. Dukes, Ed., Excerpta Medica, Amsterdam, The Netherlands, 1975, p. 484.

(3) J. Kynel, K. Oheim, T. Seki, and A. Solles, *Arzneim.-Forsch.*, **25**, 1491 (1975).

(4) S. P. McGlynn, T. Azumi, and M. Kinoshita, "Molecular Spectroscopy of the Triplet State," Prentice-Hall, Englewood Cliffs, N.J., 1969.

ACKNOWLEDGMENTS

The authors thank Mr. D. Sen for experimental assistance.

Improved Spectrophotometric Determination of Glycerol and Its Comparison with an Enzymatic Method

ROY J. STURGEON ˣ, ROBERT L. DEAMER, and HARRY A. HARBISON

Received November 9, 1978, from *McGaw Laboratories, Irvine, CA 92714.* Accepted for publication February 5, 1979.

Abstract □ A chemical method for the determination of glycerol was developed and compared to an enzymatic assay for sensitivity and reproducibility. The chemical assay is based on glycerol oxidation to formaldehyde and subsequent reaction with chromotropic acid to yield a colored product. With this method, as little as 5 μg of glycerol/ml can be detected. The enzymatic assay is based on enzymatic glycerol phosphorylation followed by glycerol phosphate dehydrogenation by nadide (nicotinamide adenine dinucleotide). The reduced nadide is used to reduce iodonitrotetrazolium violet to its colored formazan product. The enzymatic method can be used to determine 50 μg of glycerol/ml in aqueous samples.

Keyphrases □ Glycerol—analysis, spectrophotometry, comparison with enzymatic method □ Spectrophotometry—analysis, glycerol, comparison with enzymatic method

Glycerol is widely used in pharmaceuticals as a vehicle, sweetening agent, emollient, and humectant. Various analysis methods for glycerol have been reported (1–5), but they are usually nonspecific and are limited to a narrow concentration range that gives linear results. Enzymatic methods (2, 4, 5) for glycerol and glycerol-releasing compounds (*i.e.*, triglycerides) have been used widely but are usually expensive and require rigid temperature control and timing of reagent addition to obtain reproducible results.

Chemical methods (1, 3) usually utilize glycerol oxidation to formaldehyde and subsequent reaction with a chromogenic reagent. These methods generally have been shown to produce linear results over a very limited concentration range. The present investigations were undertaken to develop a chemical analysis for glycerol with improved reaction conditions and to compare this method with a standard enzymatic assay.

EXPERIMENTAL

Instrumentation—All absorbance measurements were taken on a

0022-3549/79/0800-1064$01.00/0

© 1979, American Pharmaceutical Association

Table I—Products from Photolytic and Thermal Decomposition of Indapamide

Photochemical Decomposition in N_2-Flushed Methanol	Photochemical Decomposition in O_2-Flushed Methanol	Thermal Decomposition	Product R_f Value[a]	Method of Structure Assignment[b]
II	II	II	0.19[c]	NMR, IR, UV, and mass spectra
III	III	III[d]	0.68	Comparison of IR, UV, and mass spectra with those of a reference sample
		IV	0.75	Comparison of IR, UV, and mass spectra with those of a reference sample
		V[d]	0.26	UV and mass spectra
VI	VI	VI	0.19[c]	NMR, IR, UV, and mass spectra
VII[e]	VII[e]		0.35	Mass spectrum[f]
	VIII[e]		0.45, 0.44*	Mass spectrum[f]
	IX		0.12*	Comparison of IR, UV, and mass spectra with those of a reference sample
	X		0.65	NMR, IR, UV, and mass spectra
	XI[e]		0.27*	Mass spectrum[f]

[a] The R_f values refer to qualitative TLC plates developed in Solvent System 1, except for those marked with an asterisk, which refer to Solvent System 2. [b] Unless otherwise stated, spectra were obtained for products isolated from each of the three decomposition systems. [c] The product at R_f 0.19 was a mixture of II and VI. Compound VI was sublimed out of the mixture and obtained as a white crystalline compound. [d] Product only observed in those thermal decomposition samples maintained at 453°K for 12 hr. [e] Minor product as judged by quantity of material isolated from TLC plates as compared to other products. [f] Only sufficient material could be isolated for a mass spectrum to be recorded.

Type A cleavage leads to 3-sulfamoyl-4-chlorobenzamide (II and III), type B cleavage leads to 3-sulfamoyl-4-chlorobenzoic acid, and type C cleavage yields 1-(*N*-formamido)-2-methylindoline (V) and 1-aminocarboxymethyl-2-methylindoline (VI). Methyl-3-sulfamoyl-4-chlorobenzoate (VIII) presumably arises as a consequence of esterification of VII by the solvent, while IX arises as a consequence of indoline ring oxidative cleavage in species such as III or I. At present, the origin of IV is not clear.

Thermal decomposition of I yields only II–IV besides 2-methylindole (X) and *N*-(3-sulfamoyl-4-chlorobenzamido)-2-methylindole (XI). Thus, type A cleavage can occur from vibrationally excited levels of the ground (S_0) state, and II and III can arise by this mechanism in photolytic reactions. Such species could be generated by internal conversion from the photolytically generated S_1 state. Presumably, the appropriate S_0 levels for dehydrogenation are not accessible *via* internal conversion. Type B and C cleavages only occur under photolysis and must, therefore, arise from the first excited states. Since such reactions are not inhibited by oxygen, which is known to quench triplet-state molecules (4), the S_1 state is implicated.

Thus, the study has demonstrated the complexity of photolysis of a simple pharmaceutical and has shown the wide range of compounds to be screened in photosensitization tests of such molecules.

REFERENCES

(1) D. E. Moore, *J. Pharm. Sci.*, **66**, 1282 (1977).

(2) H. J. Dargie and C. T. Dollery, in "Meyler's Side Effects of Drugs," vol. 8, M. N. G. Dukes, Ed., Excerpta Medica, Amsterdam, The Netherlands, 1975, p. 484.

(3) J. Kynel, K. Oheim, T. Seki, and A. Solles, *Arzneim.-Forsch.*, **25**, 1491 (1975).

(4) S. P. McGlynn, T. Azumi, and M. Kinoshita, "Molecular Spectroscopy of the Triplet State," Prentice-Hall, Englewood Cliffs, N.J., 1969.

ACKNOWLEDGMENTS

The authors thank Mr. D. Sen for experimental assistance.

Improved Spectrophotometric Determination of Glycerol and Its Comparison with an Enzymatic Method

ROY J. STURGEON ˣ, ROBERT L. DEAMER, and HARRY A. HARBISON

Received November 9, 1978, from *McGaw Laboratories, Irvine, CA 92714.* Accepted for publication February 5, 1979.

Abstract □ A chemical method for the determination of glycerol was developed and compared to an enzymatic assay for sensitivity and reproducibility. The chemical assay is based on glycerol oxidation to formaldehyde and subsequent reaction with chromotropic acid to yield a colored product. With this method, as little as 5 μg of glycerol/ml can be detected. The enzymatic assay is based on enzymatic glycerol phosphorylation followed by glycerol phosphate dehydrogenation by nadide (nicotinamide adenine dinucleotide). The reduced nadide is used to reduce iodonitrotetrazolium violet to its colored formazan product. The enzymatic method can be used to determine 50 μg of glycerol/ml in aqueous samples.

Keyphrases □ Glycerol—analysis, spectrophotometry, comparison with enzymatic method □ Spectrophotometry—analysis, glycerol, comparison with enzymatic method

Glycerol is widely used in pharmaceuticals as a vehicle, sweetening agent, emollient, and humectant. Various analysis methods for glycerol have been reported (1–5), but they are usually nonspecific and are limited to a narrow concentration range that gives linear results. Enzymatic methods (2, 4, 5) for glycerol and glycerol-releasing compounds (*i.e.*, triglycerides) have been used widely but are usually expensive and require rigid temperature control and timing of reagent addition to obtain reproducible results.

Chemical methods (1, 3) usually utilize glycerol oxidation to formaldehyde and subsequent reaction with a chromogenic reagent. These methods generally have been shown to produce linear results over a very limited concentration range. The present investigations were undertaken to develop a chemical analysis for glycerol with improved reaction conditions and to compare this method with a standard enzymatic assay.

EXPERIMENTAL

Instrumentation—All absorbance measurements were taken on a

0022-3549/79/0800-1064$01.00/0

© 1979, American Pharmaceutical Association

Table I—Effect of Sulfuric Acid Volume on Absorbance (300 μg of Glycerol/ml, 0.5 ml of 10% Chromotropic Acid)

Sulfuric Acid, ml	Absorbance (570 nm)
0	0.00
1	0.37
2	0.50
4	0.52
5	0.54
7	0.52

double-beam spectrophotometer[1] using 1-cm quartz cells.

Reagents—All inorganic reagents were analytical reagent grade, were used without further purification, and were prepared in distilled deionized water. These reagents included sodium metaperiodate, sulfuric acid, sodium sulfite, and hydrochloric acid[2]. Glycerol[2] was obtained as the analytical reagent and was used without further purification.

Sodium 1,8-dihydroxynaphthalene-3,6-disulfonate[3] (chromotropic acid) was recrystallized several times from water–isopropyl alcohol by dissolution in hot water and then slow addition of an equivalent volume of alcohol until precipitation. The crystals were collected and dried overnight in a vacuum oven.

ATP[4] (8.9×10^{-3} *M*) and nadide (nicotinamide adenine dinucleotide)[4] (1.56×10^{-2} *M*) were obtained as a mixture and reconstituted with distilled water just prior to use. Iodonitrotetrazolium violet[4] and *N*-methylphenazonium methosulfate[4] were supplied in solution as analytical reagents. Glycerol kinase[4] (1780 units) and glycerol phosphate dehydrogenase[4] (150,000 units) were supplied in solution and mixed with the ATP–nadide solution immediately prior to use.

Procedures—*Chemical Assay*—The standard, 2.0 ml, or appropriately prepared sample containing 0–1000 μg of glycerol/ml was pipetted into a 16 × 100-mm test tube. One milliliter of 1% $NaIO_4$ was added and mixed thoroughly, and the mixture was allowed to stand at room temperature for ~15 min. Then 1 ml of 5% Na_2SO_3 was added and mixed, and the mixture was allowed to stand for 5 min.

One milliliter of this solution was pipetted into a 100-ml volumetric flask, and 0.50 ml of a 10% chromotropic acid solution was added. Then 5.0 ml of concentrated H_2SO_4 was added slowly, and the solution was heated at 100° in a water bath for 30 min. After heating for 30 min, air was bubbled through the solution for ~20 min. Distilled water was added to raise the volume to 90%. The solution was allowed to cool to room temperature and raised to volume with distilled water. The solution absorbance was measured at 570 nm.

Enzymatic Assay—Fifty microliters of the standard or appropriately prepared sample was pipetted into a 16 × 100-mm test tube. Glycerol kinase–glycerol phosphate dehydrogenase, 0.5 ml, was added, and the solution was placed in a 37° water bath. Exactly 10 min after the addition of the enzyme mixture, the test tube was removed from the water bath, 0.5 ml of 0.03% iodonitrotetrazolium violet and 0.005% *N*-methylphenazonium methosulfate was added, the test tube was returned immediately to the water bath.

Exactly 10 min after the last addition, the test tube was removed from the water bath, and 2.0 ml of 0.1 *N* HCl was added and mixed. Then the test tube was allowed to stand for 5 min. Within 30 min, the solution absorbance was measured at 505 nm.

Special care must be taken to ensure exact time intervals and proper temperature controls.

RESULTS AND DISCUSSION

After glycerol oxidation to formaldehyde by sodium periodate, the formaldehyde reacts with chromotropic acid in the presence of excess acid to yield a colored product (6). This reaction produces a product that follows Beer's law in the range of 5–1000 μg of glycerol/ml. Several investigators (7–9) have dealt with the optimization of the formaldehyde reaction with chromotropic acid. The critical factors found in the chemical assay procedure reported in this paper are: (*a*) the sulfuric acid concentration in the reaction mixture, (*b*) the chromotropic acid to glycerol concentration ratio, and (*c*) the time of heating at 100°.

Table I contains the results of varying the sulfuric acid concentration during the reaction with a sample originally containing 300 μg of glycerol/ml and after addition of the 0.50 ml of 10% chromotropic acid. The results indicate that 5.0 ml of sulfuric acid is an appropriate volume. Table II indicates that a chromotropic acid–glycerol ratio by weight of at least 50:1 should be used. These data were generated for 500-μg of glycerol/ml samples and 5.0 ml of sulfuric acid. From Table III, it can be seen that the reaction mixture using 300-μg of glycerol/ml samples, 0.5 ml of chromotropic acid, and 5.0 ml of sulfuric acid should be heated approximately 30 min. The color developed in this manner is stable for at least 48 hr. Other references for the reaction of formaldehyde with chromotropic acid (7, 10) have reported very limited concentration ranges over which the reaction will yield linear results. The sodium chromotropate recrystallization is essential to obtain reproducible results and greatly extends the linearity range.

Table II—Effect of Chromotropic Acid Concentration (5 ml of Sulfuric Acid, 500 μg of Glycerol/ml)

10% Chromotropic Acid, ml	Absorbance (570 nm)
0	0.00
0.1	0.67
0.2	0.81
0.5	0.84
1.0	0.83
2.0	0.86

Table III—Effect of Heating Time at 100° (5 ml of Sulfuric Acid, 300 μg of Glycerol/ml)

Minutes	Absorbance
0	0.288
5	0.478
10	0.522
15	0.520
30	0.543
45	0.532

Table IV—Day-to-Day Reproducibility of the Chemical and Enzymatic Assays Using 300-μg of Glycerol/ml Samples

Day	Absorbance	
	Chemical Assay	Enzymatic Assay
1	0.525, 0.526	0.271, 0.23
2	0.527, 0.526	0.230, 0.250
3	0.523, 0.523	0.249, 0.210
4	0.532, 0.525	0.230, 0.235
5	0.526, 0.526	0.260, 0.230
Mean	0.526	0.235
SD	0.0025	0.025
CV, %	0.48	7.46

Thus, glycerol in concentrations as low as 5 μg and as high as 1000 μg/ml was determined. The chemical method yields a linear relationship between the glycerol concentration and absorbance, with a correlation coefficient of 0.997. The results from two determinations per day for 5 days of 300-μg of glycerol/ml samples are listed in Table IV and give a standard deviation of 1.4 μg/ml and a coefficient of variance of 0.48%.

In the enzyme assay, following glycerol phosphorylation and glycerol phosphate dehydrogenation by nadide, the reduced nadide reduces iodonitrotetrazolium violet to a colored product (11). This procedure yields a product that follows Beer's law from 50 to 600 μg of glycerol/ml. Of critical importance in enzyme assays is the maintenance of temperature at 37° during the reaction and the time intervals at which reagents are added. The time intervals and temperature were already optimized for triglyceride testing (12) and were not investigated further.

In this method, as low as 50 μg and as high as 600 μg of glycerol/ml were determined. The enzymatic methods yields a linear relationship between the concentration of glycerol and absorbance, with a correlation coefficient of 0.975. As can be seen in Table IV, 10 determinations (two per day for 5 days) of 300-μg of glycerol/ml samples yielded a standard deviation of 22.4 μg/ml and a coefficient of variance of 7.5%.

Both the chemical and enzymatic assays are linear over the regions analyzed, with the working curve slopes being statistically different. The average response factor over the region analyzed in the chemical assay was $1.73 \pm 0.095 \times 10^{-3}$ absorbance unit/μg of glycerol/ml, with a coefficient of variance of 5.5%. The average response factor for the enzymatic assay was $8.3 \pm 1.5 \times 10^{-4}$ absorbance unit/μg of glycerol/ml, with a coefficient of variance of 18.2%. The chemical assay method is more sensitive due to a greater response per unit change in concentration and shows a wider linear concentration range than the enzymatic assay.

[1] Beckman model 25.
[2] Mallinckrodt, St. Louis, Mo.
[3] Eastman Kodak Co., Rochester, N.Y.
[4] Hycel Inc., Houston, Tex.

The reproducibility of the chemical assay (on a day to day basis) is superior to the enzyme assay, as seen by comparing the standard deviations and coefficients of variance from the data obtained from five consecutive test periods. The need for rigid controls of temperature and timing and the low reproducibility of the enzyme assay dictate that a standard working curve be generated each time numerous samples are run. The chemical assay offers a significant improvement in reproducibility and requires only an initial standard curve. The chemical assay described in this paper offers an easy, inexpensive, and reproducible method of determining glycerol in aqueous samples.

REFERENCES

(1) M. Pays, P. Malangaeu, and R. Bourdon. *Ann. Pharm. Fr.*, **25**, 29 (1967).

(2) P. B. Schneider, *J. Lipid Res.*, **18**, 396 (1977).

(3) R. Schwarzenbach, *J. Chromatogr.*, **140**, 304 (1977).

(4) A. R. MacRae, *Clin. Biochem.*, **10**, 16 (1977).

(5) D. G. Cramp, *J. Med. Lab. Technol.*, **27**, 359 (1970).

(6) M. S. Karawya and M. G. Ghourab, *J. Assoc. Off. Anal. Chem.*, **55**, 1180 (1972).

(7) C. E. Bricker and H. R. Johnson, *Ind. Eng. Chem. Anal. Ed.*, **17**, 400 (1945).

(8) A. S. Olansky and S. N. Deming, *Anal. Chim. Acta*, **83**, 241 (1976).

(9) B. Klein and M. Weissman, *Anal. Chem.*, **25**, 771 (1953).

(10) C. E. Bricker and W. A. Vail, *ibid.*, **22**, 720 (1950).

(11) C. P. Vogel and S. M. F. Lartillot, *Fr. Demande*, **2**, 314, 497.

(12) M. Eggstein and, F. H. Kreutz, *Klin. Wochenschr.*, **44**, 262 (1966).

Clearance Constants in Physiologically Based Pharmacokinetic Models

HSIAO-SHENG GEORGE CHEN and JOSEPH F. GROSS ˣ

Received December 18, 1978, from the *Departments of Chemical Engineering and Internal Medicine, University of Arizona, Tucson, AZ 85721.* Accepted for publication February 14, 1979.

Abstract □ The intrinsic clearance of an organ is usually approximated by the apparent clearance from that organ in the development of a physiologically based pharmacokinetic model. In this study, the exact relationship between the two clearances was derived and analyzed. When the extraction ratio of the drug was small (<0.05), the approximation was reasonable. However, when the extraction ratio was high (>0.2), serious errors could be made by using the approximation. These errors could be as much as 50% reduction in the estimated extraction ratio and as much as an order-of-magnitude difference in the intrinsic clearance.

Keyphrases □ Pharmacokinetics—drug clearance through an organ, estimation □ Drug clearance—estimation of clearance through an organ, pharmacokinetics □ Antineoplastic agents—estimation of clearance through an organ, pharmacokinetics

In a typical linear physiologically based pharmacokinetic model (1), the drug concentration in an organ such as the kidney is governed by the differential equation:

$$V\frac{dC}{dt} = Q\left(C_p - \frac{C}{R}\right) - K\frac{C}{R} \qquad \text{(Eq. 1)}$$

where C and C_p are the drug concentrations in the organ and plasma (or blood), respectively; V is the physiological volume of the organ; Q is the plasma (or blood) flow rate through the organ; R is the equilibrium partition coefficient for drug distribution between the organ tissue and its venous plasma, and the constant K is a clearance term for drug elimination from the organ.

The development of a physiological model for predicting drug concentration–time histories requires the estimation of V, Q, R, and K. The parameters V and Q are the physiological volumes and blood flow rates through the organs for the subject to be simulated; R can be estimated from animal experiments and calculated according to a recently developed method (2). The clearance K is usually assumed to be equal to K_{app}, the apparent drug clearance from the organ. For example, if the organ is the kidney, K is usually calculated from:

$$K = K_{app} \equiv \text{total urinary excretion} \Big/ \int_0^\infty C_p\,dt \qquad \text{(Eq. 2)}$$

Several questions can be posed regarding K and its significance. What is its physical meaning? Is it equal to the apparent drug clearance from the organ? Can it be greater than Q, the plasma flow rate through the organ? How can K be estimated from experimental data? These questions will be discussed in the present paper.

THEORETICAL

Without loss of generality, the typical organ to be studied will be the kidney. The total cumulative urinary excretion, U, is then given as:

$$\frac{dU}{dt} = K\frac{C}{R} \qquad \text{(Eq. 3)}$$

or:

$$U = \frac{K}{R}\int_0^T C\,dt \qquad \text{(Eq. 4)}$$

where T is the urine collection time interval. Chen and Gross (2) showed recently that the drug concentration in the organ is related to the plasma drug level by:

$$C = \frac{QRC_p}{Q + K - \beta VR} \qquad \text{(Eq. 5)}$$

during the terminal elimination phase after intravenous bolus injection and that:

$$C = \frac{QRC_p}{Q + K} \qquad \text{(Eq. 6)}$$

at steady state after a constant-rate infusion. The parameter β is the apparent elimination rate constant for the terminal phase after intravenous injection. Therefore, Eq. 4 may be approximated as:

$$U = \frac{QK}{Q + K}\int_0^T C_p\,dt \qquad \text{(Eq. 7)}$$

for all modes of drug administration if $K + Q \gg \beta VR$ and if the tissue

0022-3549/79/0800-1066$01.00/0

© 1979, American Pharmaceutical Association

The reproducibility of the chemical assay (on a day to day basis) is superior to the enzyme assay, as seen by comparing the standard deviations and coefficients of variance from the data obtained from five consecutive test periods. The need for rigid controls of temperature and timing and the low reproducibility of the enzyme assay dictate that a standard working curve be generated each time numerous samples are run. The chemical assay offers a significant improvement in reproducibility and requires only an initial standard curve. The chemical assay described in this paper offers an easy, inexpensive, and reproducible method of determining glycerol in aqueous samples.

REFERENCES

(1) M. Pays, P. Malangaeu, and R. Bourdon. *Ann. Pharm. Fr.*, **25**, 29 (1967).

(2) P. B. Schneider, *J. Lipid Res.*, **18**, 396 (1977).

(3) R. Schwarzenbach, *J. Chromatogr.*, **140**, 304 (1977).

(4) A. R. MacRae, *Clin. Biochem.*, **10**, 16 (1977).

(5) D. G. Cramp, *J. Med. Lab. Technol.*, **27**, 359 (1970).

(6) M. S. Karawya and M. G. Ghourab, *J. Assoc. Off. Anal. Chem.*, **55**, 1180 (1972).

(7) C. E. Bricker and H. R. Johnson, *Ind. Eng. Chem. Anal. Ed.*, **17**, 400 (1945).

(8) A. S. Olansky and S. N. Deming, *Anal. Chim. Acta*, **83**, 241 (1976).

(9) B. Klein and M. Weissman, *Anal. Chem.*, **25**, 771 (1953).

(10) C. E. Bricker and W. A. Vail, *ibid.*, **22**, 720 (1950).

(11) C. P. Vogel and S. M. F. Lartillot, *Fr. Demande*, **2**, 314, 497.

(12) M. Eggstein and, F. H. Kreutz, *Klin. Wochenschr.*, **44**, 262 (1966).

Clearance Constants in Physiologically Based Pharmacokinetic Models

HSIAO-SHENG GEORGE CHEN and JOSEPH F. GROSS ˣ

Received December 18, 1978, from the *Departments of Chemical Engineering and Internal Medicine, University of Arizona, Tucson, AZ 85721.* Accepted for publication February 14, 1979.

Abstract □ The intrinsic clearance of an organ is usually approximated by the apparent clearance from that organ in the development of a physiologically based pharmacokinetic model. In this study, the exact relationship between the two clearances was derived and analyzed. When the extraction ratio of the drug was small (<0.05), the approximation was reasonable. However, when the extraction ratio was high (>0.2), serious errors could be made by using the approximation. These errors could be as much as 50% reduction in the estimated extraction ratio and as much as an order-of-magnitude difference in the intrinsic clearance.

Keyphrases □ Pharmacokinetics—drug clearance through an organ, estimation □ Drug clearance—estimation of clearance through an organ, pharmacokinetics □ Antineoplastic agents—estimation of clearance through an organ, pharmacokinetics

In a typical linear physiologically based pharmacokinetic model (1), the drug concentration in an organ such as the kidney is governed by the differential equation:

$$V\frac{dC}{dt} = Q\left(C_p - \frac{C}{R}\right) - K\frac{C}{R} \qquad \text{(Eq. 1)}$$

where C and C_p are the drug concentrations in the organ and plasma (or blood), respectively; V is the physiological volume of the organ; Q is the plasma (or blood) flow rate through the organ; R is the equilibrium partition coefficient for drug distribution between the organ tissue and its venous plasma, and the constant K is a clearance term for drug elimination from the organ.

The development of a physiological model for predicting drug concentration–time histories requires the estimation of V, Q, R, and K. The parameters V and Q are the physiological volumes and blood flow rates through the organs for the subject to be simulated; R can be estimated from animal experiments and calculated according to a recently developed method (2). The clearance K is usually assumed to be equal to K_{app}, the apparent drug clearance from the organ. For example, if the organ is the kidney, K is usually calculated from:

$$K = K_{app} \equiv \text{total urinary excretion} \Big/ \int_0^\infty C_p\,dt \qquad \text{(Eq. 2)}$$

Several questions can be posed regarding K and its significance. What is its physical meaning? Is it equal to the apparent drug clearance from the organ? Can it be greater than Q, the plasma flow rate through the organ? How can K be estimated from experimental data? These questions will be discussed in the present paper.

THEORETICAL

Without loss of generality, the typical organ to be studied will be the kidney. The total cumulative urinary excretion, U, is then given as:

$$\frac{dU}{dt} = K\frac{C}{R} \qquad \text{(Eq. 3)}$$

or:

$$U = \frac{K}{R}\int_0^T C\,dt \qquad \text{(Eq. 4)}$$

where T is the urine collection time interval. Chen and Gross (2) showed recently that the drug concentration in the organ is related to the plasma drug level by:

$$C = \frac{QRC_p}{Q + K - \beta VR} \qquad \text{(Eq. 5)}$$

during the terminal elimination phase after intravenous bolus injection and that:

$$C = \frac{QRC_p}{Q + K} \qquad \text{(Eq. 6)}$$

at steady state after a constant-rate infusion. The parameter β is the apparent elimination rate constant for the terminal phase after intravenous injection. Therefore, Eq. 4 may be approximated as:

$$U = \frac{QK}{Q + K}\int_0^T C_p\,dt \qquad \text{(Eq. 7)}$$

for all modes of drug administration if $K + Q \gg \beta VR$ and if the tissue

0022-3549/79/0800-1066$01.00/0

© 1979, American Pharmaceutical Association

to plasma concentration ratio can be approximated by Eq. 6 during the entire study period.

Comparison of Eq. 7 with the definition of apparent clearance, K_{app}, given by Eq. 2 yields:

$$K_{app} = \frac{QK}{Q+K} \quad \text{(Eq. 8)}$$

and:

$$K = \frac{QK_{app}}{Q-K_{app}} \quad \text{(Eq. 9)}$$

These equations apply to all organs except the lung where all the venous blood from all organs converges. A similar derivation for the lung gives:

$$(K_{app})_{lung} = K_{lung}(Q_{plasma} + K_{plasma})/Q_{plasma} \quad \text{(Eq. 10)}$$

and:

$$K_{lung} = \frac{(Q_{plasma})(K_{app})_{lung}}{Q_{plasma} + K_{plasma}} \quad \text{(Eq. 11)}$$

The reason for the difference is based on the definition of K_{app}; K_{app} is defined as the blood (or plasma) volume from which drug is completely removed in a unit time. For the other organs, the blood flows from the pooled plasma compartment into each individual organ. For the lung, the blood exits from the lung compartment into the plasma pool.

RESULTS AND DISCUSSION

Equation 8 shows that, as Q increases and approaches infinity, K_{app} approaches K. It is clear, then, that K is the true capacity of the organ to eliminate the drug. In other words, K is the intrinsic clearance, a concept developed for hepatic drug clearance (3). In fact, Eq. 8 reduces to the equation for hepatic clearance but is more general and applicable to all drug-eliminating organs except the lung.

In view of Eq. 8, which can be rewritten as:

$$K_{app} = K\left(1 - \frac{K}{Q+K}\right) = Q\left(1 - \frac{Q}{Q+K}\right) \quad \text{(Eq. 12)}$$

the apparent clearance K_{app} is always smaller than K or Q. However, there will be no upper limit for the intrinsic clearance K. Once the value of K_{app} is obtained from experiment using Eq. 2, K can be calculated from Eq. 9 by using the blood flow rate Q through that particular organ.

The alternative to this approach is to rearrange Eq. 12 to yield:

$$K = \frac{K_{app}}{1-E} \quad \text{(Eq. 13)}$$

where:

$$E = \frac{K}{Q+K} = \frac{K_{app}}{Q} \quad \text{(Eq. 14)}$$

is the steady-state extraction ratio, defined as the amount of drug eliminated divided by the amount of drug entering the organ at steady state. The approximation of K by K_{app} is valid only when the extraction ratio E is very small ($E < 0.05$). Most anticancer drugs have small E values, and this approximation is reasonable. However, when E is high and closer to unity, serious error of as much as an order-of-magnitude difference in K and as much as 50% in the estimated E may result from the approximation of K by K_{app}. Therefore, for drugs that have high hepatic extraction ratios such as doxorubicin ($E = 0.6$) (1), fluorodeoxyuridine ($E = 0.95 \sim 0.98$) (4), and fluorouracil [$E = 0.9$ in one study (5) and $E = 0.2$–0.5 in another (4)], Eq. 9 or 13 always should be used to calculate the intrinsic clearance.

REFERENCES

(1) P. A. Harris and J. F. Gross, *Cancer Chemother. Rep. Part 1*, **59**, 819 (1975).

(2) H.-S. G. Chen and J. F. Gross, *J. Pharmacokinet. Biopharm.*, **7**, 117 (1979).

(3) G. R. Wilkinson and D. G. Shand, *Clin. Pharmacol. Ther.*, **18**, 377 (1975).

(4) W. Ensmihger, A. Rosowsky, V. Rass, and D. Levin, *Proc. Am. Assoc. Cancer Res.* (Abstract), **19** (639), 100 (1978).

(5) W. Sadee, C. Finn, H.-J. Schwandt, L. Yale, Y.-T. Lee, and J. R. Bateman, *ibid.* (Abstract), **16** (No. 745), 187 (1975).

ACKNOWLEDGMENTS

Supported by Grant CA-17094 from National Cancer Institute.

COMMUNICATIONS

New Calculation Method for Mean Apparent Drug Volume of Distribution and Application to Rational Dosage Regimens

Keyphrases □ Drug distribution volume—calculations, arithmetic mean method, harmonic mean method □ Dosage regimens—design, calculation of drug distribution volume, arithmetic mean method, harmonic mean method

To the Editor:

One important purpose of clinical pharmacokinetic studies is to obtain mean pharmacokinetic data to be used as an initial guide for drug therapy. The apparent volume of distribution (V_d) of a drug is a useful pharmacokinetic parameter in the one-compartment open-model system, which is often adequate clinically for the characterization of drug disposition kinetics (1–5). For example, the product of the mean V_d ($\overline{V}_d$) obtained from several subjects and the desired plasma level ($\overline{C}_p$) of the drug could be equal theoretically to the *mean* priming dose recommended for the same type of patient.

The mean V_d of test subjects has been calculated almost exclusively to date by the arithmetic mean method. In this method, the individual V_d values (V_{d1}, V_{d2}, ..., V_{dn}) estimated by various standard or approximate (3) methods are added and the sum is divided by the total number of test subjects (n). The purposes of this communication are to propose a new method for calculating the mean V_d and to point out the potential shortcoming of the conventional arithmetic mean method in predicting rational dosage regimens.

If the test subjects are representative of the mean patient population, one should expect that the recommended mean dose ($\overline{V}_d\overline{C}_p$) when applied to the original test subjects should *ideally* result in an arithmetic mean plasma level of all the test subjects *exactly* equal to the originally targeted $\overline{C}_p$ value. In other words:

0022-3549/79/0800-1067$01.00/0

© 1979, American Pharmaceutical Association

to plasma concentration ratio can be approximated by Eq. 6 during the entire study period.

Comparison of Eq. 7 with the definition of apparent clearance, K_{app}, given by Eq. 2 yields:

$$K_{app} = \frac{QK}{Q+K} \quad \text{(Eq. 8)}$$

and:

$$K = \frac{QK_{app}}{Q-K_{app}} \quad \text{(Eq. 9)}$$

These equations apply to all organs except the lung where all the venous blood from all organs converges. A similar derivation for the lung gives:

$$(K_{app})_{lung} = K_{lung}(Q_{plasma} + K_{plasma})/Q_{plasma} \quad \text{(Eq. 10)}$$

and:

$$K_{lung} = \frac{(Q_{plasma})(K_{app})_{lung}}{Q_{plasma} + K_{plasma}} \quad \text{(Eq. 11)}$$

The reason for the difference is based on the definition of K_{app}; K_{app} is defined as the blood (or plasma) volume from which drug is completely removed in a unit time. For the other organs, the blood flows from the pooled plasma compartment into each individual organ. For the lung, the blood exits from the lung compartment into the plasma pool.

RESULTS AND DISCUSSION

Equation 8 shows that, as Q increases and approaches infinity, K_{app} approaches K. It is clear, then, that K is the true capacity of the organ to eliminate the drug. In other words, K is the intrinsic clearance, a concept developed for hepatic drug clearance (3). In fact, Eq. 8 reduces to the equation for hepatic clearance but is more general and applicable to all drug-eliminating organs except the lung.

In view of Eq. 8, which can be rewritten as:

$$K_{app} = K\left(1 - \frac{K}{Q+K}\right) = Q\left(1 - \frac{Q}{Q+K}\right) \quad \text{(Eq. 12)}$$

the apparent clearance K_{app} is always smaller than K or Q. However, there will be no upper limit for the intrinsic clearance K. Once the value of K_{app} is obtained from experiment using Eq. 2, K can be calculated from Eq. 9 by using the blood flow rate Q through that particular organ.

The alternative to this approach is to rearrange Eq. 12 to yield:

$$K = \frac{K_{app}}{1-E} \quad \text{(Eq. 13)}$$

where:

$$E = \frac{K}{Q+K} = \frac{K_{app}}{Q} \quad \text{(Eq. 14)}$$

is the steady-state extraction ratio, defined as the amount of drug eliminated divided by the amount of drug entering the organ at steady state. The approximation of K by K_{app} is valid only when the extraction ratio E is very small ($E < 0.05$). Most anticancer drugs have small E values, and this approximation is reasonable. However, when E is high and closer to unity, serious error of as much as an order-of-magnitude difference in K and as much as 50% in the estimated E may result from the approximation of K by K_{app}. Therefore, for drugs that have high hepatic extraction ratios such as doxorubicin ($E = 0.6$) (1), fluorodeoxyuridine ($E = 0.95 \sim 0.98$) (4), and fluorouracil [$E = 0.9$ in one study (5) and $E = 0.2$–0.5 in another (4)], Eq. 9 or 13 always should be used to calculate the intrinsic clearance.

REFERENCES

(1) P. A. Harris and J. F. Gross, *Cancer Chemother. Rep. Part 1*, **59**, 819 (1975).

(2) H.-S. G. Chen and J. F. Gross, *J. Pharmacokinet. Biopharm.*, **7**, 117 (1979).

(3) G. R. Wilkinson and D. G. Shand, *Clin. Pharmacol. Ther.*, **18**, 377 (1975).

(4) W. Ensmihger, A. Rosowsky, V. Rass, and D. Levin, *Proc. Am. Assoc. Cancer Res.* (Abstract), **19** (639), 100 (1978).

(5) W. Sadee, C. Finn, H.-J. Schwandt, L. Yale, Y.-T. Lee, and J. R. Bateman, *ibid.* (Abstract), **16** (No. 745), 187 (1975).

ACKNOWLEDGMENTS

Supported by Grant CA-17094 from National Cancer Institute.

COMMUNICATIONS

New Calculation Method for Mean Apparent Drug Volume of Distribution and Application to Rational Dosage Regimens

Keyphrases □ Drug distribution volume—calculations, arithmetic mean method, harmonic mean method □ Dosage regimens—design, calculation of drug distribution volume, arithmetic mean method, harmonic mean method

To the Editor:

One important purpose of clinical pharmacokinetic studies is to obtain mean pharmacokinetic data to be used as an initial guide for drug therapy. The apparent volume of distribution (V_d) of a drug is a useful pharmacokinetic parameter in the one-compartment open-model system, which is often adequate clinically for the characterization of drug disposition kinetics (1–5). For example, the product of the mean V_d ($\overline{V}_d$) obtained from several subjects and the desired plasma level ($\overline{C}_p$) of the drug could be equal theoretically to the *mean* priming dose recommended for the same type of patient.

The mean V_d of test subjects has been calculated almost exclusively to date by the arithmetic mean method. In this method, the individual V_d values (V_{d1}, V_{d2}, ..., V_{dn}) estimated by various standard or approximate (3) methods are added and the sum is divided by the total number of test subjects (n). The purposes of this communication are to propose a new method for calculating the mean V_d and to point out the potential shortcoming of the conventional arithmetic mean method in predicting rational dosage regimens.

If the test subjects are representative of the mean patient population, one should expect that the recommended mean dose ($\overline{V}_d\overline{C}_p$) when applied to the original test subjects should *ideally* result in an arithmetic mean plasma level of all the test subjects *exactly* equal to the originally targeted $\overline{C}_p$ value. In other words:

0022-3549/79/0800-1067$01.00/0

© 1979, American Pharmaceutical Association

Table I—Reported Apparent Volumes of Distribution of Gentamicin in 11 Patients and Simulated Initial Serum Gentamicin Levels after Intravenous Bolus Doses Calculated Based on the Arithmetic and Harmonic Mean Methods for the Calculation of Mean Volume of Distribution and Initial Mean Targeted Level of 10 mg/liter

Patient	V_d, liter/kg	$C_{p(ari)}$, mg/liter	$C_{p(har)}$, mg/liter
1	0.19	12.94	12.11
2	0.19	12.94	12.11
3	0.22	11.18	10.45
4	0.25	9.84	9.20
5	0.20	12.30	11.50
6	0.29	8.48	7.93
7	0.20	12.30	11.50
8	0.49	5.02	4.69
9	0.22	11.18	10.45
10	0.25	9.84	9.20
11	0.21	11.71	10.95
Arithmetic mean	0.246	10.70	10.00

$$\overline{C}_p = (C_{p1} + C_{p2} + \ldots + C_{pn})/n \qquad \text{(Eq. 1)}$$

where $C_{p1}, C_{p2}, \ldots, C_{pn}$ are the resultant individual plasma levels for the n subjects, respectively. Since:

$$C_{pi} = \frac{\text{dose}}{V_{di}} = \frac{\overline{V}_d \overline{C}_p}{V_{di}} \qquad \text{(Eq. 2)}$$

combination of Eqs. 1 and 2 would result in:

$$\frac{1}{\overline{V}_d} = \frac{1}{n}\left(\frac{1}{V_{d1}} + \frac{1}{V_{d2}} + \ldots + \frac{1}{V_{dn}}\right) \qquad \text{(Eq. 3)}$$

This equation clearly shows that for the purpose of predicting a *correct* mean dosage, the mean V_d must be calculated by Eq. 3, which is commonly referred to as the harmonic mean method.

When different doses are used on the test subjects, Eq. 3 becomes:

$$\frac{1}{\overline{V}_d} = \frac{1}{n}\left(\frac{C'_{p1}}{\text{dose}_1} + \frac{C'_{p2}}{\text{dose}_2} + \ldots + \frac{C'_{pn}}{\text{dose}_n}\right) \qquad \text{(Eq. 4)}$$

where $C'_{p1}, C'_{p2}, \ldots, C'_{pn}$ are the resulting plasma levels for the n subjects, respectively. The plasma level from each subject can be corrected further based on the same total dose or some dose per unit of body weight or body surface area:

$$\frac{1}{\overline{V}_d} = \frac{1}{(n)(\text{dose})}(C^*_{p1} + C^*_{p2} + \ldots + C^*_{pn}) \qquad \text{(Eq. 5)}$$

Therefore:

$$\overline{V}_d = \frac{\text{dose}}{(C^*_{p1} + C^*_{p2} + \ldots + C^*_{pn})/n} \qquad \text{(Eq. 6)}$$

$$\overline{V}_d = \frac{\text{dose}}{\text{arithmetic mean plasma level}} \qquad \text{(Eq. 7)}$$

In other words, the mean V_d can be calculated also by dividing the dose (corrected to the same amount for all of the test subjects) by the arithmetic mean plasma level of the test subjects. This method will be referred to as the arithmetic mean–plasma level method. Obviously, these analyses can be applied equally well to the calculation of the mean apparent volume of the central compartment or the mean initial apparent volume of drug distribution in the multicompartment open model or the polyexponential plasma level decay system.

Table II—Reported Apparent Volumes of the Central Compartment of Theophylline in Nine Cirrhotic Patients and Simulated Initial Plasma Theophylline Levels after Intravenous Bolus Doses Calculated Based on Arithmetic and Harmonic Mean Methods for the Calculation of the Mean Central Compartment Volume and Initial Mean Targeted Level of 10 mg/liter

Patient	V_p, liter/kg	$C_{p(ari)}$, mg/liter	$C_{p(har)}$, mg/liter
1	0.448	7.37	4.44
2	0.144	22.92	13.82
3	0.781	4.23	2.55
4	0.095	34.74	20.95
5	0.157	21.02	12.68
6	0.163	20.25	12.21
7	0.146	22.60	13.63
8	0.282	11.70	7.06
9	0.753	4.38	2.64
Arithmetic mean	0.330	16.58	10.00

Literature examples on gentamicin, theophylline, and propranolol will be used to illustrate the differences in the mean volume of distribution and the initial plasma level that might result from the use of the two different methods for the volume of distribution calculation.

The data on the apparent volume of distribution of gentamicin in 11 burn patients (Table I) were reported by Sawchuk and Zaske (6). Their mean V_d based on the arithmetic mean method was 0.246 liter/kg. The mean V_d will be reduced to 0.230 liter/kg if the harmonic mean method is used. The data on the apparent volume of the central compartment (V_p) of theophylline in nine cirrhotic patients (Table II) were taken from a study of Piafsky *et al.* (7). The mean V_p reported, based on the arithmetic mean method, was 0.330 liter/kg. Based on the harmonic mean method, the mean V_p is 0.199 liter/kg. The arithmetic mean V_p of propranolol in three normal subjects was reported by Gomeni *et al.* (8) as 0.867 liter/kg. The mean V_p is, however, only 0.591 liter/kg based on the harmonic mean method. Different methods for calculating the mean V_d or V_p for these three drugs produce discrepancies ranging from 6.96 to 65.8% (Table III).

If the mean doses based on the two methods to achieve a mean serum or plasma level of 10 mg/liter for gentamicin or theophylline were used in these same patients, variations in the same manner in both individual or mean arithmetic mean serum or plasma levels would result (Tables I and II).

Although the arithmetic mean method for the mean volume of distribution calculation appears to be mathematically correct and the information obtained is useful, the harmonic mean or arithmetic mean–plasma level method reported here is the superior or perhaps the only correct method when the mean volume of distribution data

Table III—Summary of the Mean Apparent Volume of Distribution of Gentamicin and Mean Volumes of the Central Compartment of Theophylline and Propranolol in Human Subjects Estimated by Arithmetic and Harmonic Mean Methods

Method	Gentamicin, liter/kg	Theophylline, liter/kg	Propranolol, liter/kg
Arithmetic mean	0.246	0.330	0.867
Harmonic mean	0.230	0.199	0.591
Percent difference based on harmonic mean method as a reference	6.96	65.8	46.7

from the clinical trial are intended for designing a rational dosage regimen. The mean volume of distribution calculated from the test subjects should accurately predict their own plasma levels, even if the information is not intended for designing a rational dosage regimen.

In some studies, all individual plasma or serum data from the test subjects were grouped together and the pharmacokinetic analysis was performed based on these arithmetical *averaged* plasma or serum data (9). In intravenous bolus studies, the calculated mean initial volume of distribution obviously will be identical to the value calculated by the harmonic mean method and different from that calculated by the arithmetic mean method. This fact, which has probably not been pointed out before, might contribute to the difference in values reported from different studies.

In an earlier study (10) on clinical theophylline pharmacokinetics, the investigators reported that, depending on the methods used to calculate the mean total body clearance, as much as a 25–30% difference in the recommended infusion rate could occur. This phenomenon was considered as "unfortunate" (10). This author has made a similar analysis as presented in this communication and concluded that the best method for calculating the mean total body clearance in designing a rational dosage regimen is the harmonic mean method. Details of analyses will be reported later.

The preceding discussion is based on the assumption that the arithmetic mean method be used for the calculation of the mean plasma level. This approach was justified because the arithmetic mean method has been used almost exclusively for averaging peak, trough, steady-state, or mean steady-state plasma levels of drugs or metabolites in pharmacokinetic studies. This is probably also the case with mean levels of endogenous substances such as creatinine and urea reported in the literature. Statistically speaking, if the geometric, harmonic, or other mean method can be shown to be the best method for averaging plasma level data, then a different conclusion regarding the proper method for averaging the apparent volume of distribution can be obtained. The method proposed here can be applied to the calculation of other mean volumes of distribution such as the distribution volume at steady state.

In estimating the apparent volume of distribution of drugs after oral administration, the potential hepatic and pulmonary first-pass effects are often ignored. Appropriate equations are available for correcting for such effects (11–13). The harmonic mean method has been recommended for the calculation of the mean biological half-life of drugs (14).

(1) W. L. Chiou and F. H. Hsu, *J. Clin. Pharmacol.*, **15**, 427 (1975).

(2) W. L. Chiou and F. H. Hsu, *Res. Commun. Chem. Pathol. Pharmacol.*, **10**, 315 (1975).

(3) W. L. Chiou, G. W. Peng, and R. L. Nation, *J. Clin. Pharmacol.*, **18**, 266 (1978).

(4) W. L. Chiou, M. A. F. Gadalla, and G. W. Peng, *J. Pharmacokinet. Biopharm.*, **6**, 135 (1978).

(5) W. L. Chiou, S. M. Huang, and Y. C. Huang, *Int. J. Clin. Pharmacol. Biopharm.*, in press.

(6) R. J. Sawchuk and D. E. Zaske, *J. Pharmacokinet. Biopharm.*, **4**, 183 (1976).

(7) K. M. Piafsky, D. S. Sitar, R. E. Rangno, and R. I. Ogilvie, *N. Engl. J. Med.*, **296**, 1495 (1977).

(8) R. Gomeni, G. Bianchetti, R. Sega, and P. L. Morselli, *J. Pharmacokinet. Biopharm.*, **5**, 183 (1977).

(9) D. C. Hobbs, T. M. Twomey, and R. F. Palmer, *J. Clin. Pharmacol.*, **18**, 402 (1978).

(10) F. A. Chrzanowski, P. J. Niebergall, R. L. Mayock, J. M. Taubin, and E. T. Sugita, *Clin. Pharmacol. Ther.*, **22**, 188 (1977).

(11) W. L. Chiou, *Res. Commun. Chem. Pathol. Pharmacol.*, **7**, 679 (1974).

(12) W. L. Chiou, *J. Pharmacokinet. Biopharm.*, **3**, 193 (1975).

(13) W. L. Chiou, *J. Pharm. Sci.*, **67**, 1776 (1978).

(14) F. B. Eatman, W. A. Colburn, H. G. Boxenbaum, H. N. Posmanter, R. E. Weinfeld, R. Ronfeld, L. Weissman, J. D. Moore, M. Gibaldi, and S. A. Kaplan, *J. Pharmacokinet. Biopharm.*, **5**, 481 (1977).

W. L. Chiou

Clinical Pharmacokinetics Laboratory
and Department of Pharmacy
College of Pharmacy
University of Illinois at the Medical Center
Chicago, IL 60612

Received February 5, 1979.
Accepted for publication May 29, 1979.

Prostaglandin Prodrugs IV: Empirical Relationship between Functional Group Contributions and Melting Points of C_1-Esters

Keyphrases □ Prostaglandins—influence of functional group on melting points, dinoprostone and dinoprost C_1-esters □ Prodrugs—prostaglandins, influence of functional group on melting points, dinoprostone and dinoprost C_1-esters □ Dinoprost and dinoprostone C_1-esters—influence of functional group on melting points

To the Editor:

Many prostaglandins occur as viscous liquids at room temperature, which presents problems in various pharmaceutical processes such as weighing and formulation. We recently showed that certain crystalline esters of the E-series prostaglandins are remarkably more stable than the parent prostaglandins (1). Now, based on melting-point data of numerous dinoprostone (I) and dinoprost (II) C_1-esters accumulated in our laboratories, we present a functional group contribution analysis of the influence of structure on melting points.

In principle, the melting point (T_m) of a substance can be calculated from:

$$T_m = \frac{\Delta H_f}{\Delta S_f} \qquad \text{(Eq. 1)}$$

where ΔH_f and ΔS_f are the heat and the entropy of fusion,

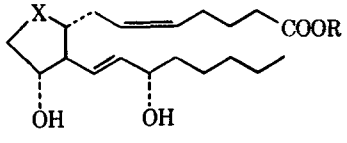

I: C_1-ester, X = >C=O

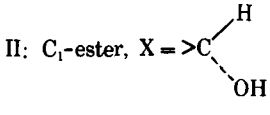

II: C_1-ester, X = >C

© 1979, American Pharmaceutical Association

from the clinical trial are intended for designing a rational dosage regimen. The mean volume of distribution calculated from the test subjects should accurately predict their own plasma levels, even if the information is not intended for designing a rational dosage regimen.

In some studies, all individual plasma or serum data from the test subjects were grouped together and the pharmacokinetic analysis was performed based on these arithmetical *averaged* plasma or serum data (9). In intravenous bolus studies, the calculated mean initial volume of distribution obviously will be identical to the value calculated by the harmonic mean method and different from that calculated by the arithmetic mean method. This fact, which has probably not been pointed out before, might contribute to the difference in values reported from different studies.

In an earlier study (10) on clinical theophylline pharmacokinetics, the investigators reported that, depending on the methods used to calculate the mean total body clearance, as much as a 25–30% difference in the recommended infusion rate could occur. This phenomenon was considered as "unfortunate" (10). This author has made a similar analysis as presented in this communication and concluded that the best method for calculating the mean total body clearance in designing a rational dosage regimen is the harmonic mean method. Details of analyses will be reported later.

The preceding discussion is based on the assumption that the arithmetic mean method be used for the calculation of the mean plasma level. This approach was justified because the arithmetic mean method has been used almost exclusively for averaging peak, trough, steady-state, or mean steady-state plasma levels of drugs or metabolites in pharmacokinetic studies. This is probably also the case with mean levels of endogenous substances such as creatinine and urea reported in the literature. Statistically speaking, if the geometric, harmonic, or other mean method can be shown to be the best method for averaging plasma level data, then a different conclusion regarding the proper method for averaging the apparent volume of distribution can be obtained. The method proposed here can be applied to the calculation of other mean volumes of distribution such as the distribution volume at steady state.

In estimating the apparent volume of distribution of drugs after oral administration, the potential hepatic and pulmonary first-pass effects are often ignored. Appropriate equations are available for correcting for such effects (11–13). The harmonic mean method has been recommended for the calculation of the mean biological half-life of drugs (14).

(1) W. L. Chiou and F. H. Hsu, *J. Clin. Pharmacol.*, **15**, 427 (1975).

(2) W. L. Chiou and F. H. Hsu, *Res. Commun. Chem. Pathol. Pharmacol.*, **10**, 315 (1975).

(3) W. L. Chiou, G. W. Peng, and R. L. Nation, *J. Clin. Pharmacol.*, **18**, 266 (1978).

(4) W. L. Chiou, M. A. F. Gadalla, and G. W. Peng, *J. Pharmacokinet. Biopharm.*, **6**, 135 (1978).

(5) W. L. Chiou, S. M. Huang, and Y. C. Huang, *Int. J. Clin. Pharmacol. Biopharm.*, in press.

(6) R. J. Sawchuk and D. E. Zaske, *J. Pharmacokinet. Biopharm.*, **4**, 183 (1976).

(7) K. M. Piafsky, D. S. Sitar, R. E. Rangno, and R. I. Ogilvie, *N. Engl. J. Med.*, **296**, 1495 (1977).

(8) R. Gomeni, G. Bianchetti, R. Sega, and P. L. Morselli, *J. Pharmacokinet. Biopharm.*, **5**, 183 (1977).

(9) D. C. Hobbs, T. M. Twomey, and R. F. Palmer, *J. Clin. Pharmacol.*, **18**, 402 (1978).

(10) F. A. Chrzanowski, P. J. Niebergall, R. L. Mayock, J. M. Taubin, and E. T. Sugita, *Clin. Pharmacol. Ther.*, **22**, 188 (1977).

(11) W. L. Chiou, *Res. Commun. Chem. Pathol. Pharmacol.*, **7**, 679 (1974).

(12) W. L. Chiou, *J. Pharmacokinet. Biopharm.*, **3**, 193 (1975).

(13) W. L. Chiou, *J. Pharm. Sci.*, **67**, 1776 (1978).

(14) F. B. Eatman, W. A. Colburn, H. G. Boxenbaum, H. N. Posmanter, R. E. Weinfeld, R. Ronfeld, L. Weissman, J. D. Moore, M. Gibaldi, and S. A. Kaplan, *J. Pharmacokinet. Biopharm.*, **5**, 481 (1977).

W. L. Chiou

Clinical Pharmacokinetics Laboratory
and Department of Pharmacy
College of Pharmacy
University of Illinois at the Medical Center
Chicago, IL 60612

Received February 5, 1979.
Accepted for publication May 29, 1979.

Prostaglandin Prodrugs IV: Empirical Relationship between Functional Group Contributions and Melting Points of C_1-Esters

Keyphrases □ Prostaglandins—influence of functional group on melting points, dinoprostone and dinoprost C_1-esters □ Prodrugs—prostaglandins, influence of functional group on melting points, dinoprostone and dinoprost C_1-esters □ Dinoprost and dinoprostone C_1-esters—influence of functional group on melting points

To the Editor:

Many prostaglandins occur as viscous liquids at room temperature, which presents problems in various pharmaceutical processes such as weighing and formulation. We recently showed that certain crystalline esters of the E-series prostaglandins are remarkably more stable than the parent prostaglandins (1). Now, based on melting-point data of numerous dinoprostone (I) and dinoprost (II) C_1-esters accumulated in our laboratories, we present a functional group contribution analysis of the influence of structure on melting points.

In principle, the melting point (T_m) of a substance can be calculated from:

$$T_m = \frac{\Delta H_f}{\Delta S_f} \qquad \text{(Eq. 1)}$$

where ΔH_f and ΔS_f are the heat and the entropy of fusion,

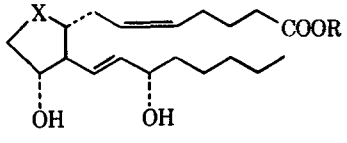

I: C_1-ester, X = >C=O

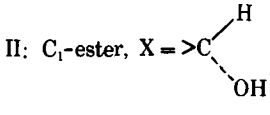

II: C_1-ester, X = >C

© 1979, American Pharmaceutical Association

Table I—Group Contribution Values to Heat of Sublimation [a]

Group	$\Delta H_s°$, kcal/mole	Group	$\Delta H_s°$, kcal/mole
$-CH_3$	2.45	—O—, aliphatic	1.55
$-C_2H_5$	4.28	—O—, aromatic	1.0
$-CH_2-$	2.0	—OH, aliphatic	8.2
$=CH-$	2.0	—OH, aromatic	6.8
Phenyl	$8.4 + \frac{1.6^b}{N}$	>C=O, aliphatic	5.6
Naphthyl	15.0	>C=O, aromatic	3.6
$-NH_2$ (aliphatic)	6.35	>C=O, hetero-aromatic	6.0
$-NH_2$ (aromatic)	6.5	—F, aromatic	1.9
—NH (aliphatic)	4.5	—O—C(=O), aliphatic	4.4
—NH (aromatic)	6.5[c]	—Br, aliphatic	3.34
$-NO_2$ (aliphatic)	9.6	—Br, aromatic	4.28
$-NO_2$ (aromatic)	6.8	—I, aromatic	5.03

[a] See Ref. 2 for more extensive data. [b] Number of carbon atoms in the ring substituents. [c] Approximated value.

respectively. When a given substance undergoes an isothermal process, thermodynamic parameters associated with the process such as ΔH_f and ΔS_f can be approximated as the sum of the contributions of each functional group present in the molecule. For an ester, we would like to consider the values of ΔH_f and ΔS_f as the sum of the contributions by the prostaglandin (PG) and the ester alkyl or aryl (R) moieties. Thus, Eq. 1 becomes:

$$T_m = \frac{\Delta H_f^{PG} + \Delta H_f^{R}}{\Delta S_f^{PG} + \Delta S_f^{R}} \qquad \text{(Eq. 2)}$$

The prostaglandin group contribution should be constant for a series of prostaglandin C_1-esters, whereas the R group contribution varies depending on the structure. This group contribution approach appears to be quite valid for a series of dinoprostone C_1-phenyl esters in which the melting points are well correlated with those of the parent phenols (1).

In the present analysis, instead of handling both the heat and the entropy contributions, we are making a key assumption that the overall entropy of fusion is constant for the following two reasons. First, the group entropy contribution of the prostaglandin group is expected to predominate, mainly because the molecular size of these esters is largely determined by the prostaglandin group rather than the R group. The molecular weights of the esters are rather constant (570 ± 100). In this context, the entropy of fusion is considered to consist of two components: that due to the volume change and that due to the true entropy change upon fusion at constant volume (2). Thus:

$$\Delta S_f^{PG} + \Delta S_s^{R} \cong \Delta S_f^{PG} = \text{constant} \qquad \text{(Eq. 3)}$$

Second, we can approximate ΔS_f^{PG} to be constant if ΔS_f^{R} cannot be neglected with respect to ΔS_f^{PG}:

$$\Delta S_f^{R} = \Delta S_s^{R} - \Delta S_v^{R} \qquad \text{(Eq. 4)}$$

where ΔS_s^{R} and ΔS_v^{R} are the entropies of sublimation and vaporization, respectively. The entropy of sublimation is relatively constant for organic compounds of moderately constant size. For example, of 136 compounds for which ΔS_s values were compiled (3), over 100 compounds showed ΔS_s values within 50 ± 15 eu. As expected, extreme deviations are reported when the compounds become very

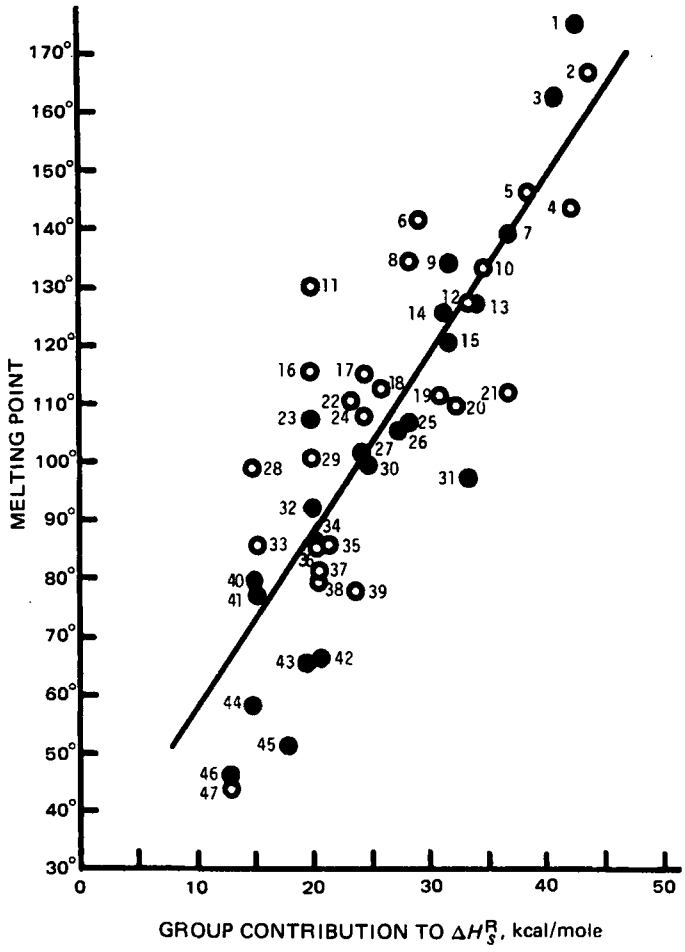

Figure 1—*Plot of melting points of dinoprostone (●) and dinoprost (○) C_1-esters* versus *the group contribution of the alcoholic portion of the ester (R) to the heat of sublimation (ΔH_s^R). The following dinoprostone C_1-esters were derived from the stated parent phenols (1): 1, p,p'-benzamidophenol; 3, N-benzoyl-L-tryosine amide; 7, N-acetyl-L-tyrosine amide; 9, p-benzamidophenol; 14, p-hydroxybenzaldehyde semicarbazone; 23, p-hydroxybenzamide; 25, p-hydroxyphenylurea; 27, acetaminophen; 31, p-tritylphenol; 32, p-phenylphenol; 40, 2-naphthol; and 41, phenyl acetate. The other compounds will be identified in future articles.*

large or very small; *e.g.*, the ΔS_s values for nonadecanoic acid and acetic acid are 151.2 and 25.7 eu, respectively (3). On the other hand, following Trouton's rule, we approximate $\Delta S_v \sim 21$ eu for pure liquids. Thus:

$$\Delta S_f^{R} = \text{constant} \qquad \text{(Eq. 5a)}$$

or:

$$\Delta S_f^{PG} + \Delta S_f^{R} = \text{constant} \qquad \text{(Eq. 5b)}$$

In reality, the combination of these two independent considerations supports the assumption that ΔS_f in Eq. 1 is constant for these esters. Now Eq. 2 becomes:

$$T_m = \alpha + \beta \sum_{i=1}^{n} \Delta H_i \qquad \text{(Eq. 6)}$$

where the summation operates over each functional group present in the R group.

Since no extensive group contribution data on ΔH_f are available in the literature and since ΔH_f is approximately proportional to the heat of sublimation (ΔH_s) in a series of compounds (2), we explored a relationship between the melting points of prostaglandin C_1-esters consisting of

Table II—Prednisolone C_{21}-Esters of

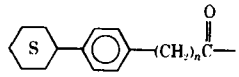

n	Melting Point
0	242°
1	202–203°
2	190–191°
3	160–162°

para-substituted phenyl and substituted alkyl moieties and the sum of ΔH_s contributions of each functional group present in the R moiety in the ester. Some important ΔH_s values used in our study are shown in Table I (2). A straightforward additivity rule was applied in calculating ΔH_s contributions from the R group. For instance, for the *p*-benzamidophenyl ester of dinoprostone, the ΔH_s contribution of the phenolic moiety is the sum of 2 × 10.0 for phenyl, 6.5 for >C=O, and 5.6 for —NH—, giving 32.1 kcal/mole.

The relationship between the melting points of 22 dinoprostone C_1-esters and 25 dinoprost C_1-esters and the ΔH_s contribution of the R groups is shown in Fig. 1. A least-squares analysis resulted in a slope of 3.04°/kcal/mole of ΔH_s and an intercept, the physically meaningless melting point of the prostaglandins without a proton at C_1, of 26.7°. Although the melting points of dinoprostone (63.4°) and dinoprost (~35°) are rather removed, visual inspection of the plot gives no indication of two separate relationships. The correlation coefficient was 0.851, which is surprisingly good considering all of the assumptions and approximations involved.

The reasonably good correlation observed appears to reflect the validity of our basic assumption that the prostaglandin group contribution to the melting point is constant. Both the E and F series of prostaglandins have substantial intramolecular interactions between two alkyl chains in the solid state (4) and the C_1-substituents probably do not disturb this basic molecular conformation, resulting in a rather constant crystal packing arrangement of the esters.

Of the C_1-esters prepared, about 20% of the liquid esters are predicted to be solids. Since it was difficult to crystallize many of the esters (up to 2 weeks of manipulation was sometimes required), many of these liquid esters possibly could be crystallized under proper conditions. Although we attribute the deviations observed largely to assumptions in the analysis, they could originate from polymorph formation. All of the esters were carefully purified by silica gel column chromatography, and it is unlikely that the deviations were due to impurities.

The present analysis applies mainly to terminally substituted prodrugs such as the prostaglandin C_1-esters. Application of the additivity principle may not hold for other prodrugs where the modification is at an internal position. Under these conditions, the assumption that ΔS_f is constant is not warranted due to a significantly higher entropy contribution (mainly rotational) brought about by modification at an internal position. This situation is illustrated by the *decrease* in melting points observed in some prodrug series using internal homologation (Table II). This decrease probably is due to an additional increase in entropy, which would lower T_m (Eq. 1). Therefore, our group contribution approach is not applicable in this case.

Cautious application of the treatment to terminally substituted prodrugs of relatively constant size should be of great use in analyzing the influence of structure on melting points. In these special prodrug series, the melting points may now allow *a priori* estimates of the influence of structure on other related physical properties.

(1) W. Morozowich, T. O. Oesterling, W. L. Miller, C. F. Lawson, J. R. Weeks, R. G. Stehle, and S. L. Douglas, *J. Pharm. Sci.*, **68**, 833 (1979).

(2) A. Bondi, "Physical Properties of Molecular Crystals, Liquids, and Glasses," Wiley, New York, N.Y., 1968, pp. 139–196, 452–488.

(3) "Handbook of Chemistry and Physics," 49th ed., R. C. Weast, Ed., Chemical Rubber Co., Cleveland, Ohio, 1968, p. C-686.

(4) J. W. Edmonds and W. L. Daux, *Prostaglandins*, **5**, 275 (1974). *J. Am. Chem. Soc.*, **97**, 413 (1975) and references cited therein.

(5) G. Carenini, M. Carissimi, R. D'Ambrosio, and R. Ravenna, *Farmaco Ed. Sci.*, **30**, 167 (1975).

M. J. Cho ˣ
W. Morozowich
Pharmacy Research Unit
The Upjohn Company
Kalamazoo, MI 49001

Received July 5, 1975.
Accepted for publication August 11, 1975.

Noncompartmental Determination of the Steady-State Volume of Distribution

Keyphrases □ Volume of distribution—steady state, noncompartmental determination, calculations □ Pharmacokinetics—steady-state volume of distribution, noncompartmental determination, calculations

To the Editor:

Up to the present time, the use in pharmacokinetics of the steady-state volume of distribution (Vd_{ss}) has been limited to specific compartmental mammillary models. However, mathematical methods usually associated in medicine with the use of indicator dilution curves to determine cardiac output and with the determination of mean residence time of endogenous substances following radiolabeled tracer injection permit Vd_{ss} determination without the assumption of a specific compartment model (or its analog, the assumption of a specific number of exponential functions).

Riggs (1) introduced the use of an overall volume of distribution term, Vd_{ss}, defined specifically with respect to the two-compartment open model, with elimination taking place from the central compartment:

$$Vd_{ss} = \left(1 + \frac{k_{12}}{k_{21}}\right) V_1 \qquad \text{(Eq. 1)}$$

The steady-state volume of distribution, as defined by Riggs (1), equals the total quantity of drug in the body divided by the concentration in the reference region of the central compartment when these measurements are taken when the tissue compartment contains the maximum amount of drug. Riegelman *et al.* (2) presented an exten-

0022-3549/79/0800-1071$01.00/0
© 1979, American Pharmaceutical Association

Table II—Prednisolone C_{21}-Esters of

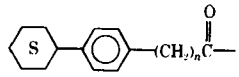

n	Melting Point
0	242°
1	202–203°
2	190–191°
3	160–162°

para-substituted phenyl and substituted alkyl moieties and the sum of ΔH_s contributions of each functional group present in the R moiety in the ester. Some important ΔH_s values used in our study are shown in Table I (2). A straightforward additivity rule was applied in calculating ΔH_s contributions from the R group. For instance, for the *p*-benzamidophenyl ester of dinoprostone, the ΔH_s contribution of the phenolic moiety is the sum of 2 × 10.0 for phenyl, 6.5 for >C=O, and 5.6 for —NH—, giving 32.1 kcal/mole.

The relationship between the melting points of 22 dinoprostone C_1-esters and 25 dinoprost C_1-esters and the ΔH_s contribution of the R groups is shown in Fig. 1. A least-squares analysis resulted in a slope of 3.04°/kcal/mole of ΔH_s and an intercept, the physically meaningless melting point of the prostaglandins without a proton at C_1, of 26.7°. Although the melting points of dinoprostone (63.4°) and dinoprost (~35°) are rather removed, visual inspection of the plot gives no indication of two separate relationships. The correlation coefficient was 0.851, which is surprisingly good considering all of the assumptions and approximations involved.

The reasonably good correlation observed appears to reflect the validity of our basic assumption that the prostaglandin group contribution to the melting point is constant. Both the E and F series of prostaglandins have substantial intramolecular interactions between two alkyl chains in the solid state (4) and the C_1-substituents probably do not disturb this basic molecular conformation, resulting in a rather constant crystal packing arrangement of the esters.

Of the C_1-esters prepared, about 20% of the liquid esters are predicted to be solids. Since it was difficult to crystallize many of the esters (up to 2 weeks of manipulation was sometimes required), many of these liquid esters possibly could be crystallized under proper conditions. Although we attribute the deviations observed largely to assumptions in the analysis, they could originate from polymorph formation. All of the esters were carefully purified by silica gel column chromatography, and it is unlikely that the deviations were due to impurities.

The present analysis applies mainly to terminally substituted prodrugs such as the prostaglandin C_1-esters. Application of the additivity principle may not hold for other prodrugs where the modification is at an internal position. Under these conditions, the assumption that ΔS_f is constant is not warranted due to a significantly higher entropy contribution (mainly rotational) brought about by modification at an internal position. This situation is illustrated by the *decrease* in melting points observed in some prodrug series using internal homologation (Table II). This decrease probably is due to an additional increase in entropy, which would lower T_m (Eq. 1). Therefore, our group contribution approach is not applicable in this case.

Cautious application of the treatment to terminally substituted prodrugs of relatively constant size should be of great use in analyzing the influence of structure on melting points. In these special prodrug series, the melting points may now allow *a priori* estimates of the influence of structure on other related physical properties.

(1) W. Morozowich, T. O. Oesterling, W. L. Miller, C. F. Lawson, J. R. Weeks, R. G. Stehle, and S. L. Douglas, *J. Pharm. Sci.*, **68**, 833 (1979).

(2) A. Bondi, "Physical Properties of Molecular Crystals, Liquids, and Glasses," Wiley, New York, N.Y., 1968, pp. 139–196, 452–488.

(3) "Handbook of Chemistry and Physics," 49th ed., R. C. Weast, Ed., Chemical Rubber Co., Cleveland, Ohio, 1968, p. C-686.

(4) J. W. Edmonds and W. L. Daux, *Prostaglandins*, **5**, 275 (1974). *J. Am. Chem. Soc.*, **97**, 413 (1975) and references cited therein.

(5) G. Carenini, M. Carissimi, R. D'Ambrosio, and R. Ravenna, *Farmaco Ed. Sci.*, **30**, 167 (1975).

M. J. Cho ˣ
W. Morozowich
Pharmacy Research Unit
The Upjohn Company
Kalamazoo, MI 49001

Received July 5, 1975.
Accepted for publication August 11, 1975.

Noncompartmental Determination of the Steady-State Volume of Distribution

Keyphrases □ Volume of distribution—steady state, noncompartmental determination, calculations □ Pharmacokinetics—steady-state volume of distribution, noncompartmental determination, calculations

To the Editor:

Up to the present time, the use in pharmacokinetics of the steady-state volume of distribution (Vd_{ss}) has been limited to specific compartmental mammillary models. However, mathematical methods usually associated in medicine with the use of indicator dilution curves to determine cardiac output and with the determination of mean residence time of endogenous substances following radiolabeled tracer injection permit Vd_{ss} determination without the assumption of a specific compartment model (or its analog, the assumption of a specific number of exponential functions).

Riggs (1) introduced the use of an overall volume of distribution term, Vd_{ss}, defined specifically with respect to the two-compartment open model, with elimination taking place from the central compartment:

$$Vd_{ss} = \left(1 + \frac{k_{12}}{k_{21}}\right) V_1 \qquad \text{(Eq. 1)}$$

The steady-state volume of distribution, as defined by Riggs (1), equals the total quantity of drug in the body divided by the concentration in the reference region of the central compartment when these measurements are taken when the tissue compartment contains the maximum amount of drug. Riegelman *et al.* (2) presented an exten-

0022-3549/79/0800-1071$01.00/0
© 1979, American Pharmaceutical Association

sive discussion of the steady-state volume of distribution and the advantages of using this term when describing multicompartment distribution of drug in the body. They preferred the use of steady-state volume of distribution because this term (Eq. 1) is independent of the elimination rate constant. However, Benet and Ronfeld (3) pointed out that Vd_{ss} is independent of the elimination rate constant only when elimination occurs exclusively from the central compartment.

Gibaldi (4) showed that under steady-state conditions, as in a zero-order infusion, Vd_{ss} may be calculated without establishing the appropriate model or determining the distribution and elimination rate constants if plasma concentrations are measured from time zero until steady state is reached and then following termination of the infusion until no drug remains in the body. Once again, this determination is only valid when elimination occurs exclusively from the central compartment of a multicompartmental model (3). In practice, Vd_{ss} determinations in the literature (at least up to 1977) have been based on calculations involving microconstants and the volume of the central compartment such as is given in Eq. 1 for a two-compartment model.

Wagner (5) and van Ginneken (6) showed that Vd_{ss} may be determined directly from the coefficients and exponents of a polyexponential equation fit to the plasma concentration time data:

$$Vd_{ss} = \frac{\text{dose} \sum \left(\frac{A_i}{\lambda_i^2}\right)}{\left(\sum \frac{A_i}{\lambda_i}\right)^2} \qquad \text{(Eq. 2)}$$

where A_i defines the coefficients and λ_i defines the exponents in a polyexponential equation such as Eq. 3, an example for data requiring three exponential terms to describe the plasma concentration–time curve:

$$C_p = A_1 e^{-\lambda_1 t} + A_2 e^{-\lambda_2 t} + A_3 e^{-\lambda_3 t} \qquad \text{(Eq. 3)}$$

Wagner (5) stated that the Vd_{ss} value calculated using Eq. 2 applies only to the general model where elimination occurs exclusively from the central compartment. He suggested: "However, because of the dilemma of not knowing from which compartment there are exit rate constants to outside the body, use of Equation 2 will at least make all authors homogeneous in their approach." However, when the distribution constants for the model are determined as was done previously for calculations of Vd_{ss} (2) or when the coefficients and exponentials of a polyexponential equation are utilized (5, 6), the investigator is still required to propose some model and to determine a number of constants and coefficients either by graphical means or through the use of a nonlinear least-squares computer program. We describe a noncompartmental method of determining Vd_{ss} utilizing area under the curve determinations exclusively.

In indicator dilution studies, basic mathematical methodology is based on the Stewart–Hamilton theorems for flow and volume (7, 8). Perl and Samuel (9) generalized these theorems to the case of multiple input channels with partially labeled input in a study of the input rate and traced mass of body cholesterol. More recently, Oppenheimer *et al.* (10, 11) adapted these principles to facilitate calculation of conventionally used parameters in the study of iodothyronine metabolism and distribution. In these endocrinology studies (9, 10), the basic parameter determined using noncompartmental analysis is the mean residence time, $\bar{t}$, following an intravenous bolus dose:

$$\bar{t} = \frac{\int_0^\infty t C_p \, dt}{\int_0^\infty C_p \, dt} = \frac{AUMC_{0\to\infty}}{AUC_{0\to\infty}} \qquad \text{(Eq. 4)}$$

The denominator of Eq. 4 is the familiar (in pharmacokinetic terms) area under the plasma concentration–time curve (AUC) from time zero to infinity. The numerator is the area under the first moment of the plasma curve ($AUMC$), *i.e.*, the area under the curve of the product of time, t, and plasma concentration, C_p, from time zero to infinity.

Oppenheimer *et al.* (10) defined the mean residence time in terms of a rate constant, k, designated as the fraction of the total pool of iodothyronine irreversibly removed per unit of time:

$$k_{ss} = 1/\bar{t} \qquad \text{(Eq. 5)}$$

We have added a subscript to this rate constant to indicate that it is a constant *defined at steady state*. This k_{ss} should not be confused with either the rate constant describing elimination from the plasma compartment of a pharmacokinetic model or the rate constant describing the terminal plasma disappearance curve in a multicompartment model.

At steady state, the product of the rate constant k_{ss} and the volume Vd_{ss} may be defined as the total body clearance:

$$\text{total body clearance} = k_{ss} Vd_{ss} \qquad \text{(Eq. 6)}$$

since clearance may be defined as a product of the rate constant describing the total drug fraction irreversibly removed from the body as a function of time, multiplied by the volume of distribution on which that rate constant is operating. That is, Eq. 6 is identical to other definitions of total body clearance such as $k_{10}V_1$ and βVd_β (5). The total body clearance is a model-independent term and may be calculated for an intravenous injection as dose divided by the area under the plasma concentration–time curve from time zero to infinity. Substituting this quotient into Eq. 6, substituting the area relations for k_{ss} defined in Eq. 4 and 5, and rearranging yield the noncompartmental method for determining the steady-state volume of distribution:

$$Vd_{ss} = \frac{\text{dose}\left[\int_0^\infty t C_p \, dt\right]}{\left[\int_0^\infty C_p \, dt\right]^2} = \frac{\text{dose}[AUMC_{0\to\infty}]}{[AUC_{0\to\infty}]^2} \qquad \text{(Eq. 7)}$$

This calculation will be valid only when the underlying assumptions discussed by Perl and Samuel (9) are valid. In terms of pharmacokinetic analysis, the two most important of these assumptions are: (*a*) the system must respond linearly, *i.e.*, follow first-order kinetics, and (*b*) the exit of tracer or drug from the body must be directly from the measured site, *i.e.*, the plasma or central compartment

Table I—Sample Noncompartmental Vd_{ss} Calculation

Hours	C_p, μg/ml	tC_p, μg hr/ml	$\int_0^t C_p\,dt$ $[AUC_{0\to t}]$, μg hr/ml	$\int_0^t tC_p\,dt$ $[AUMC_{0\to t}]$, μg hr²/ml
0.0	100.00	0		
0.0833	78.90	6.57	7.40[a]	0.3[a]
0.1667	65.01	10.83	13.4	1.0
0.25	55.86	13.97	18.4	2.1
0.5	43.14	21.57	30.6	6.5
0.75	39.28	29.46	40.9	12.9
1.0	37.92	37.92	50.5	21.3
1.5	36.83	55.24	69.2	44.6
2.0	36.08	72.16	87.4	76.5
3.0	34.68	104.04	122.8	164.6
5.0	32.04	160.22	189.5	428.8
7.0	29.61	207.27	251.2	796.3
9.0	27.36	246.23	308.1	1249.8
12.0	24.30	291.61	385.6	2056.6
18.0	19.17	345.07	515.6	3982.9
24.0	15.12	362.97	618.5	6107.0
36.0	9.41	338.84	763.7	10360.0
48.0	5.86	281.18	855.3	14080.1
72.0	2.27	163.36	947.8	19372.2
96.0	0.88	84.37	985.6	22344.9
120.0	0.34	40.85	1000.2	23847.5
∞	0.0	0.0	1008.8	25099.1

[a] All integrals approximated by using the linear trapezoidal rule. Vd_{ss} = (dose $[AUMC_{0\to\infty}]/[AUC_{0\to\infty}]^2$) = 12,332 ml.

in a pharmacokinetic analysis. However, these are the same assumptions necessary to calculate Vd_{ss} by the methods described previously (Eqs. 1 and 2).

Wagner (5) compared Vd_{ss} calculation by Eq. 2 with Eq. 1 by simulating a bolus intravenous injection of a drug following two-compartment kinetics with elimination exclusively from the central compartment. Equation 8 contains the coefficients and exponentials utilized by Wagner to describe plasma concentrations following an intravenous 500-mg bolus dose (5):

$$C_p = 60.9545e^{-5.0605t} + 39.0459e^{-0.03952t} \qquad \text{(Eq. 8)}$$

Using Eq. 8, we calculated plasma concentration values over a 120-hr period (Table I). Column 1 indicates time in hours; column 2 is plasma concentration in micrograms per milliliter; column 3 is the product of columns 1 and 2. The linear trapezoid rule was utilized to calculate areas under the curve. Column 4 tabulates area under the plasma concentration *versus* time curve, and column 5 tabulates the values under the moment curve. The area under the plasma concentration–time curve from $C_{p_{last}}$ until time infinity was estimated using:

$$\int_{t_{last}}^{\infty} C_p\,dt = \frac{C_{p_{last}}}{\lambda_2} \qquad \text{(Eq. 9)}$$

where λ_2 is the terminal rate constant, *i.e.*, $-0.03952\ hr^{-1}$ in Eq. 8. Likewise, the area under the concentration–moment curve from $C_{p_{last}}$ to time infinity is given by Eq. 10 (11):

$$\int_{t_{last}}^{\infty} tC_p\,dt = \frac{t_{last}C_{p_{last}}}{\lambda_2} + \frac{C_{p_{last}}}{(\lambda_2)^2} \qquad \text{(Eq. 10)}$$

By using the coefficients and exponents of Eq. 8 to calculate AUC (*i.e.*, $A_1/\lambda_1 + A_2/\lambda_2$) and $AUMC$ (*i.e.*, $A_1/\lambda_1^2 + A_2/\lambda_2^2$), values of 1000.0 and 25,002.5 are obtained (5). The difference between these values and the summations in columns 4 and 5 of Table I results from the errors inherent in estimating areas using the linear trapezoid rule. If the logarithmic trapezoid rule (12, 13), Eq. 11[1], is used to estimate AUC, then a value of 1000.5 is obtained:

$$AUC_{t_1\to t_2} = \frac{(y_1 - y_2)\,\Delta t}{\ln (y_1/y_2)} \qquad \text{(Eq. 11)}$$

When the time infinity values for AUC and $AUMC$ from Table I are substituted into Eq. 7 with a dose of 500,000 μg, Vd_{ss} is calculated to be 12,332 ml, which is ~1.3% less than the actual 12,500-ml value. (Use of the logarithmic AUC calculation results in a value of 12,537 for Vd_{ss}.) These Vd_{ss} calculations were carried out using simple area under the curve determinations, independent of the assignment of a particular compartment model or a multiexponential computer data fit. Unfortunately, if plasma level measurements are not carried out to characterize accurately the area determinations or the terminal rate constant (as necessary in Eqs. 9 and 10), this simple method to determine Vd_{ss} is just as inaccurate as the classical methods under those conditions. A future publication will discuss the theoretical basis for the method as well as an error analysis. We have been utilizing this method in our recent pharmacokinetic work (14–16).

(1) D. S. Riggs, "The Mathematical Approach to Physiological Problems," Williams & Wilkins, Baltimore, Md., 1963, chaps. 7 and 8.

(2) S. Riegelman, J. C. K. Loo, and M. Rowland, *J. Pharm. Sci.*, **57**, 128 (1968).

(3) L. Z. Benet and R. A. Ronfeld, *ibid.*, **58**, 639 (1969).

(4) M. Gibaldi, *ibid.*, **58**, 327 (1969).

(5) J. G. Wagner, *J. Pharmacokinet. Biopharm.*, **4**, 443 (1976).

(6) C. A. M. van Ginneken, "Pharmacokinetics of Antipyretic and Anti-Inflammatory Analgesics," Stichting Studentenpers, Nijmegen, The Netherlands, 1976.

(7) G. N. Stewart, *Am. J. Physiol.*, **58**, 20 (1921).

[1] This equation is only appropriate for decreasing plasma concentrations with time. When calculating AUC for curves that increase to a maximum, the linear trapezoid rule should be used for concentrations up to the peak. Again, Eq. 11 is just an approximation since theoretically the logarithmic trapezoid rule should only give a correct area estimation during the terminal log-linear portion of the plasma–time curve.

(8) W. F. Hamilton, J. W. Moore, J. M. Kinsman, and R. G. Spurling, *ibid.*, **99**, 534 (1931).
(9) W. Perl and P. Samuel, *Circ. Res.*, **25**, 191 (1969).
(10) J. H. Oppenheimer, J. L. Schwartz, and M. I. Surks, *J. Clin. Endocrinol. Metab.*, **41**, 319 (1975).
(11) *Ibid.*, **41**, 1172 (1975).
(12) K. C. Yeh and K. C. Kwan, *J. Pharmacokinet. Biopharm.*, **6**, 79 (1978).
(13) W. L. Chiou, *ibid.*, **6**, 539 (1978).
(14) N. S. Aziz, J. G. Gambertoglio, E. T. Lin, H. Grausz, and L. Z. Benet, *ibid.*, **6**, 153 (1978).
(15) J. Ham, R. D. Miller, L. Z. Benet, R. S. Matteo, and L. L. Roderick, *Anesthesiology*, **49**, 324 (1978).
(16) R. Platzer, R. L. Galeazzi, G. Karlaganis, and J. Bircher, *Eur. J. Clin. Pharmacol.*, **14**, 293 (1978).

Leslie Z. Benet ˣ
Department of Pharmacy
University of California
San Francisco, CA 94143
Renato L. Galeazzi
Department of Medicine
University of Bern
Bern, Switzerland

Received February 5, 1979.
Accepted for publication June 1, 1979.
Presented in part at the Basic Pharmaceutics Section, APhA Academy of Pharmaceutical Sciences, New York meeting, May 1977.
Supported in part by National Institutes of Health Grant GM 26551.

BOOKS

REVIEWS

Methods in Pharmacology, Vol. 4B, Renal Pharmacology. Edited by MANUEL MARTINEZ-MALDONADO. Plenum, 227 W. 17th St., New York, NY 10011. 1978. 403 pp. 15 × 25 cm. Price $39.50.

This volume aptly fills a gap in the literature. Although the book was apparently intended for researchers in this area, each topic is treated such that even pharmacologists and physiologists not active in renal research can gain a better understanding of and appreciation for the technology discussed. In addition to the clear treatment of each topic, all chapters are well referenced. This book should be made available to all students of pharmacology, physiology, and medicine.

The first chapter deals with morphological methods for studying the kidney, including fixation methods, light microscopy, and EM procedures. The second and third chapters deal with renal dynamics, including clearance methods and intrarenal blood flow measurements. Chapter 4 deals with micropuncture techniques, while the fifth chapter is concerned with microanalytical methods for analyzing samples obtained by the methods discussed in the previous chapter.

In Chapter 6, methods measuring glomerular dynamics are described, and mathematical models of glomerular ultrafiltration are discussed.

Chapters 7 and 8 provide detailed descriptions of the apparatus used in microelectrode studies; Chapter 7 has to do with electrical potential measurement, and Chapter 8 concerns pH measurement. Chapter 9 is especially interesting, providing methods for dissection and perfusion of isolated tubules.

Chapters 10–12 deal with renal biochemistry: Na–K-ATPase, adenylate cyclase, and intermediary metabolism. The last three chapters describe the methodology used in studying isolated perfused kidney in the dog (*in vitro* and *in vivo*) and the rat (*in vitro*).

The effectiveness of the book would have been greatly enhanced by including with each chapter a brief description of several experiments using the methods described. Including examplary experimental drug application protocols and some typical data obtained by the methods would have provided the pharmacologist reader with a much clearer understanding of how the method might be applied.

In addition, it would probably be helpful for many readers if the names and addresses of manufacturers of critical equipment and supplies had been provided with each chapter.

I have personally experienced a need for such information in my previous experience with other volumes of *Methods in Pharmacology*.

These two shortcomings are the only major problems I see in this volume, and I view it generally as a very informative and useful contribution to the scientific literature.

Reviewed by W. M. Bourn
College of Pharmacy and Health Sciences
Northeast Louisiana University
Monroe, LA 71209

Cocaine: 1977 National Institute on Drug Abuse (Research Monograph Series 13). Edited by R. C. PETERSON and R. C. STILLMAN. Superintendent of Documents, U.S. Government Printing Office, Washington, DC 20402. Price $3 (paper cover).

The National Institute on Drug Abuse (NIDA) has been publishing monographs on specific substances of abuse. The monograph on cocaine follows a pattern similar to earlier monographs. There are 10 chapters by 13 authors with 350 references dating from 1884 to 1977. There is an adequate author and subject index.

The information in the book could be classified according to history, pharmacology and toxicology, abuse, use, behavioral aspects, and legal aspects.

This book and the others in the series are useful to anyone involved in the area of substance abuse. Their rather low price makes the entire series inviting.

Reviewed by Charles L. Winek
School of Pharmacy
Duquesne University
Pittsburgh, PA 15219

NOTICES

Disposition of Toxic Drugs and Chemicals in Man. Vol. 1. Centrally-Acting Drugs. By RANDALL C. BASELT. Biomedical Publications, P.O. Box 368, Canton, CT 06019. 1978. 306 pp. 15 × 23 cm. Price $22.50.

Handbook of Experimental Pharmacology, Vol. 51. Uric Acid. By WILLIAM N. KELLEY and IRWIN M. WEINER. Springer-Verlag New York Inc., 175 Fifth Ave., New York, NY 10010. 1978. 639 pp. 16 × 24 cm. Price $159.50

IARC Monographs on the Evaluation of the Carcinogenic Risk of Chemicals to Humans. Some N-Nitroso Compounds. (Vol. 17). International Agency for Research on Cancer, distributed by World Health Organization. 1978. 165 pp. 17 × 24 cm. Price $25.00; 50 fr.

IARC Monographs on the Evaluation of the Carcinogenic Risk of Chemicals to Humans. Vol. 18. Polychlorinated Biphenyls and Polybrominated Biphenyls. International Agency for Research on Cancer, distributed by World Health Organization. 1978. 140 pp. 18 × 24 cm. Price 20 fr.

The International Challenge of Drug Abuse: NIDA Research Monograph 19. By ROBERT C. PETERSEN. National Institute on Drug Abuse, Division of Research, 5600 Fishers Lane, Rockville, MD 20857. 1978. 349 pp. 14 × 23 cm.

Methods in Cancer Research, Vol. XVII. Cancer Drug Development, Part B. Edited by VINCENT T. DeVITA, Jr., and HARRIS BUSCH. Academic, 111 Fifth Ave., New York, NY 10003. 1979. 356 pp. 15 × 23 cm. Price $37.00.

(8) W. F. Hamilton, J. W. Moore, J. M. Kinsman, and R. G. Spurling, *ibid.*, **99**, 534 (1931).
(9) W. Perl and P. Samuel, *Circ. Res.*, **25**, 191 (1969).
(10) J. H. Oppenheimer, J. L. Schwartz, and M. I. Surks, *J. Clin. Endocrinol. Metab.*, **41**, 319 (1975).
(11) *Ibid.*, **41**, 1172 (1975).
(12) K. C. Yeh and K. C. Kwan, *J. Pharmacokinet. Biopharm.*, **6**, 79 (1978).
(13) W. L. Chiou, *ibid.*, **6**, 539 (1978).
(14) N. S. Aziz, J. G. Gambertoglio, E. T. Lin, H. Grausz, and L. Z. Benet, *ibid.*, **6**, 153 (1978).
(15) J. Ham, R. D. Miller, L. Z. Benet, R. S. Matteo, and L. L. Roderick, *Anesthesiology*, **49**, 324 (1978).
(16) R. Platzer, R. L. Galeazzi, G. Karlaganis, and J. Bircher, *Eur. J. Clin. Pharmacol.*, **14**, 293 (1978).

Leslie Z. Benet ˣ
Department of Pharmacy
University of California
San Francisco, CA 94143
Renato L. Galeazzi
Department of Medicine
University of Bern
Bern, Switzerland

Received February 5, 1979.
Accepted for publication June 1, 1979.
Presented in part at the Basic Pharmaceutics Section, APhA Academy of Pharmaceutical Sciences, New York meeting, May 1977.
Supported in part by National Institutes of Health Grant GM 26551.

BOOKS

REVIEWS

Methods in Pharmacology, Vol. 4B, Renal Pharmacology. Edited by MANUEL MARTINEZ-MALDONADO. Plenum, 227 W. 17th St., New York, NY 10011. 1978. 403 pp. 15 × 25 cm. Price $39.50.

This volume aptly fills a gap in the literature. Although the book was apparently intended for researchers in this area, each topic is treated such that even pharmacologists and physiologists not active in renal research can gain a better understanding of and appreciation for the technology discussed. In addition to the clear treatment of each topic, all chapters are well referenced. This book should be made available to all students of pharmacology, physiology, and medicine.

The first chapter deals with morphological methods for studying the kidney, including fixation methods, light microscopy, and EM procedures. The second and third chapters deal with renal dynamics, including clearance methods and intrarenal blood flow measurements. Chapter 4 deals with micropuncture techniques, while the fifth chapter is concerned with microanalytical methods for analyzing samples obtained by the methods discussed in the previous chapter.

In Chapter 6, methods measuring glomerular dynamics are described, and mathematical models of glomerular ultrafiltration are discussed.

Chapters 7 and 8 provide detailed descriptions of the apparatus used in microelectrode studies; Chapter 7 has to do with electrical potential measurement, and Chapter 8 concerns pH measurement. Chapter 9 is especially interesting, providing methods for dissection and perfusion of isolated tubules.

Chapters 10–12 deal with renal biochemistry: Na–K-ATPase, adenylate cyclase, and intermediary metabolism. The last three chapters describe the methodology used in studying isolated perfused kidney in the dog (*in vitro* and *in vivo*) and the rat (*in vitro*).

The effectiveness of the book would have been greatly enhanced by including with each chapter a brief description of several experiments using the methods described. Including examplary experimental drug application protocols and some typical data obtained by the methods would have provided the pharmacologist reader with a much clearer understanding of how the method might be applied.

In addition, it would probably be helpful for many readers if the names and addresses of manufacturers of critical equipment and supplies had been provided with each chapter.

I have personally experienced a need for such information in my previous experience with other volumes of *Methods in Pharmacology*.

These two shortcomings are the only major problems I see in this volume, and I view it generally as a very informative and useful contribution to the scientific literature.

Reviewed by W. M. Bourn
College of Pharmacy and Health Sciences
Northeast Louisiana University
Monroe, LA 71209

Cocaine: 1977 National Institute on Drug Abuse (Research Monograph Series 13). Edited by R. C. PETERSON and R. C. STILLMAN. Superintendent of Documents, U.S. Government Printing Office, Washington, DC 20402. Price $3 (paper cover).

The National Institute on Drug Abuse (NIDA) has been publishing monographs on specific substances of abuse. The monograph on cocaine follows a pattern similar to earlier monographs. There are 10 chapters by 13 authors with 350 references dating from 1884 to 1977. There is an adequate author and subject index.

The information in the book could be classified according to history, pharmacology and toxicology, abuse, use, behavioral aspects, and legal aspects.

This book and the others in the series are useful to anyone involved in the area of substance abuse. Their rather low price makes the entire series inviting.

Reviewed by Charles L. Winek
School of Pharmacy
Duquesne University
Pittsburgh, PA 15219

NOTICES

Disposition of Toxic Drugs and Chemicals in Man. Vol. 1. Centrally-Acting Drugs. By RANDALL C. BASELT. Biomedical Publications, P.O. Box 368, Canton, CT 06019. 1978. 306 pp. 15 × 23 cm. Price $22.50.

Handbook of Experimental Pharmacology, Vol. 51. Uric Acid. By WILLIAM N. KELLEY and IRWIN M. WEINER. Springer-Verlag New York Inc., 175 Fifth Ave., New York, NY 10010. 1978. 639 pp. 16 × 24 cm. Price $159.50

IARC Monographs on the Evaluation of the Carcinogenic Risk of Chemicals to Humans. Some N-Nitroso Compounds. (Vol. 17). International Agency for Research on Cancer, distributed by World Health Organization. 1978. 165 pp. 17 × 24 cm. Price $25.00; 50 fr.

IARC Monographs on the Evaluation of the Carcinogenic Risk of Chemicals to Humans. Vol. 18. Polychlorinated Biphenyls and Polybrominated Biphenyls. International Agency for Research on Cancer, distributed by World Health Organization. 1978. 140 pp. 18 × 24 cm. Price 20 fr.

The International Challenge of Drug Abuse: NIDA Research Monograph 19. By ROBERT C. PETERSEN. National Institute on Drug Abuse, Division of Research, 5600 Fishers Lane, Rockville, MD 20857. 1978. 349 pp. 14 × 23 cm.

Methods in Cancer Research, Vol. XVII. Cancer Drug Development, Part B. Edited by VINCENT T. DeVITA, Jr., and HARRIS BUSCH. Academic, 111 Fifth Ave., New York, NY 10003. 1979. 356 pp. 15 × 23 cm. Price $37.00.

(8) W. F. Hamilton, J. W. Moore, J. M. Kinsman, and R. G. Spurling, *ibid.*, **99**, 534 (1931).
(9) W. Perl and P. Samuel, *Circ. Res.*, **25**, 191 (1969).
(10) J. H. Oppenheimer, J. L. Schwartz, and M. I. Surks, *J. Clin. Endocrinol. Metab.*, **41**, 319 (1975).
(11) *Ibid.*, **41**, 1172 (1975).
(12) K. C. Yeh and K. C. Kwan, *J. Pharmacokinet. Biopharm.*, **6**, 79 (1978).
(13) W. L. Chiou, *ibid.*, **6**, 539 (1978).
(14) N. S. Aziz, J. G. Gambertoglio, E. T. Lin, H. Grausz, and L. Z. Benet, *ibid.*, **6**, 153 (1978).
(15) J. Ham, R. D. Miller, L. Z. Benet, R. S. Matteo, and L. L. Roderick, *Anesthesiology*, **49**, 324 (1978).
(16) R. Platzer, R. L. Galeazzi, G. Karlaganis, and J. Bircher, *Eur. J. Clin. Pharmacol.*, **14**, 293 (1978).

Leslie Z. Benet ˣ
Department of Pharmacy
University of California
San Francisco, CA 94143
Renato L. Galeazzi
Department of Medicine
University of Bern
Bern, Switzerland

Received February 5, 1979.
Accepted for publication June 1, 1979.
Presented in part at the Basic Pharmaceutics Section, APhA Academy of Pharmaceutical Sciences, New York meeting, May 1977.
Supported in part by National Institutes of Health Grant GM 26551.

BOOKS

REVIEWS

Methods in Pharmacology, Vol. 4B, Renal Pharmacology. Edited by MANUEL MARTINEZ-MALDONADO. Plenum, 227 W. 17th St., New York, NY 10011. 1978. 403 pp. 15 × 25 cm. Price $39.50.

This volume aptly fills a gap in the literature. Although the book was apparently intended for researchers in this area, each topic is treated such that even pharmacologists and physiologists not active in renal research can gain a better understanding of and appreciation for the technology discussed. In addition to the clear treatment of each topic, all chapters are well referenced. This book should be made available to all students of pharmacology, physiology, and medicine.

The first chapter deals with morphological methods for studying the kidney, including fixation methods, light microscopy, and EM procedures. The second and third chapters deal with renal dynamics, including clearance methods and intrarenal blood flow measurements. Chapter 4 deals with micropuncture techniques, while the fifth chapter is concerned with microanalytical methods for analyzing samples obtained by the methods discussed in the previous chapter.

In Chapter 6, methods measuring glomerular dynamics are described, and mathematical models of glomerular ultrafiltration are discussed.

Chapters 7 and 8 provide detailed descriptions of the apparatus used in microelectrode studies; Chapter 7 has to do with electrical potential measurement, and Chapter 8 concerns pH measurement. Chapter 9 is especially interesting, providing methods for dissection and perfusion of isolated tubules.

Chapters 10–12 deal with renal biochemistry: Na–K-ATPase, adenylate cyclase, and intermediary metabolism. The last three chapters describe the methodology used in studying isolated perfused kidney in the dog (*in vitro* and *in vivo*) and the rat (*in vitro*).

The effectiveness of the book would have been greatly enhanced by including with each chapter a brief description of several experiments using the methods described. Including examplary experimental drug application protocols and some typical data obtained by the methods would have provided the pharmacologist reader with a much clearer understanding of how the method might be applied.

In addition, it would probably be helpful for many readers if the names and addresses of manufacturers of critical equipment and supplies had been provided with each chapter.

I have personally experienced a need for such information in my previous experience with other volumes of *Methods in Pharmacology*.

These two shortcomings are the only major problems I see in this volume, and I view it generally as a very informative and useful contribution to the scientific literature.

Reviewed by W. M. Bourn
College of Pharmacy and Health Sciences
Northeast Louisiana University
Monroe, LA 71209

Cocaine: 1977 National Institute on Drug Abuse (Research Monograph Series 13). Edited by R. C. PETERSON and R. C. STILLMAN. Superintendent of Documents, U.S. Government Printing Office, Washington, DC 20402. Price $3 (paper cover).

The National Institute on Drug Abuse (NIDA) has been publishing monographs on specific substances of abuse. The monograph on cocaine follows a pattern similar to earlier monographs. There are 10 chapters by 13 authors with 350 references dating from 1884 to 1977. There is an adequate author and subject index.

The information in the book could be classified according to history, pharmacology and toxicology, abuse, use, behavioral aspects, and legal aspects.

This book and the others in the series are useful to anyone involved in the area of substance abuse. Their rather low price makes the entire series inviting.

Reviewed by Charles L. Winek
School of Pharmacy
Duquesne University
Pittsburgh, PA 15219

NOTICES

Disposition of Toxic Drugs and Chemicals in Man. Vol. 1. Centrally-Acting Drugs. By RANDALL C. BASELT. Biomedical Publications, P.O. Box 368, Canton, CT 06019. 1978. 306 pp. 15 × 23 cm. Price $22.50.

Handbook of Experimental Pharmacology, Vol. 51. Uric Acid. By WILLIAM N. KELLEY and IRWIN M. WEINER. Springer-Verlag New York Inc., 175 Fifth Ave., New York, NY 10010. 1978. 639 pp. 16 × 24 cm. Price $159.50

IARC Monographs on the Evaluation of the Carcinogenic Risk of Chemicals to Humans. Some N-Nitroso Compounds. (Vol. 17). International Agency for Research on Cancer, distributed by World Health Organization. 1978. 165 pp. 17 × 24 cm. Price $25.00; 50 fr.

IARC Monographs on the Evaluation of the Carcinogenic Risk of Chemicals to Humans. Vol. 18. Polychlorinated Biphenyls and Polybrominated Biphenyls. International Agency for Research on Cancer, distributed by World Health Organization. 1978. 140 pp. 18 × 24 cm. Price 20 fr.

The International Challenge of Drug Abuse: NIDA Research Monograph 19. By ROBERT C. PETERSEN. National Institute on Drug Abuse, Division of Research, 5600 Fishers Lane, Rockville, MD 20857. 1978. 349 pp. 14 × 23 cm.

Methods in Cancer Research, Vol. XVII. Cancer Drug Development, Part B. Edited by VINCENT T. DeVITA, Jr., and HARRIS BUSCH. Academic, 111 Fifth Ave., New York, NY 10003. 1979. 356 pp. 15 × 23 cm. Price $37.00.

(8) W. F. Hamilton, J. W. Moore, J. M. Kinsman, and R. G. Spurling, *ibid.*, **99**, 534 (1931).
(9) W. Perl and P. Samuel, *Circ. Res.*, **25**, 191 (1969).
(10) J. H. Oppenheimer, J. L. Schwartz, and M. I. Surks, *J. Clin. Endocrinol. Metab.*, **41**, 319 (1975).
(11) *Ibid.*, **41**, 1172 (1975).
(12) K. C. Yeh and K. C. Kwan, *J. Pharmacokinet. Biopharm.*, **6**, 79 (1978).
(13) W. L. Chiou, *ibid.*, **6**, 539 (1978).
(14) N. S. Aziz, J. G. Gambertoglio, E. T. Lin, H. Grausz, and L. Z. Benet, *ibid.*, **6**, 153 (1978).
(15) J. Ham, R. D. Miller, L. Z. Benet, R. S. Matteo, and L. L. Roderick, *Anesthesiology*, **49**, 324 (1978).
(16) R. Platzer, R. L. Galeazzi, G. Karlaganis, and J. Bircher, *Eur. J. Clin. Pharmacol.*, **14**, 293 (1978).

Leslie Z. Benet ˣ
Department of Pharmacy
University of California
San Francisco, CA 94143
Renato L. Galeazzi
Department of Medicine
University of Bern
Bern, Switzerland

Received February 5, 1979.
Accepted for publication June 1, 1979.
Presented in part at the Basic Pharmaceutics Section, APhA Academy of Pharmaceutical Sciences, New York meeting, May 1977.
Supported in part by National Institutes of Health Grant GM 26551.

BOOKS

REVIEWS

Methods in Pharmacology, Vol. 4B, Renal Pharmacology. Edited by MANUEL MARTINEZ-MALDONADO. Plenum, 227 W. 17th St., New York, NY 10011. 1978. 403 pp. 15 × 25 cm. Price $39.50.

This volume aptly fills a gap in the literature. Although the book was apparently intended for researchers in this area, each topic is treated such that even pharmacologists and physiologists not active in renal research can gain a better understanding of and appreciation for the technology discussed. In addition to the clear treatment of each topic, all chapters are well referenced. This book should be made available to all students of pharmacology, physiology, and medicine.

The first chapter deals with morphological methods for studying the kidney, including fixation methods, light microscopy, and EM procedures. The second and third chapters deal with renal dynamics, including clearance methods and intrarenal blood flow measurements. Chapter 4 deals with micropuncture techniques, while the fifth chapter is concerned with microanalytical methods for analyzing samples obtained by the methods discussed in the previous chapter.

In Chapter 6, methods measuring glomerular dynamics are described, and mathematical models of glomerular ultrafiltration are discussed.

Chapters 7 and 8 provide detailed descriptions of the apparatus used in microelectrode studies; Chapter 7 has to do with electrical potential measurement, and Chapter 8 concerns pH measurement. Chapter 9 is especially interesting, providing methods for dissection and perfusion of isolated tubules.

Chapters 10–12 deal with renal biochemistry: Na–K-ATPase, adenylate cyclase, and intermediary metabolism. The last three chapters describe the methodology used in studying isolated perfused kidney in the dog (*in vitro* and *in vivo*) and the rat (*in vitro*).

The effectiveness of the book would have been greatly enhanced by including with each chapter a brief description of several experiments using the methods described. Including examplary experimental drug application protocols and some typical data obtained by the methods would have provided the pharmacologist reader with a much clearer understanding of how the method might be applied.

In addition, it would probably be helpful for many readers if the names and addresses of manufacturers of critical equipment and supplies had been provided with each chapter.

I have personally experienced a need for such information in my previous experience with other volumes of *Methods in Pharmacology*.

These two shortcomings are the only major problems I see in this volume, and I view it generally as a very informative and useful contribution to the scientific literature.

Reviewed by W. M. Bourn
College of Pharmacy and Health Sciences
Northeast Louisiana University
Monroe, LA 71209

Cocaine: 1977 National Institute on Drug Abuse (Research Monograph Series 13). Edited by R. C. PETERSON and R. C. STILLMAN. Superintendent of Documents, U.S. Government Printing Office, Washington, DC 20402. Price $3 (paper cover).

The National Institute on Drug Abuse (NIDA) has been publishing monographs on specific substances of abuse. The monograph on cocaine follows a pattern similar to earlier monographs. There are 10 chapters by 13 authors with 350 references dating from 1884 to 1977. There is an adequate author and subject index.

The information in the book could be classified according to history, pharmacology and toxicology, abuse, use, behavioral aspects, and legal aspects.

This book and the others in the series are useful to anyone involved in the area of substance abuse. Their rather low price makes the entire series inviting.

Reviewed by Charles L. Winek
School of Pharmacy
Duquesne University
Pittsburgh, PA 15219

NOTICES

Disposition of Toxic Drugs and Chemicals in Man. Vol. 1. Centrally-Acting Drugs. By RANDALL C. BASELT. Biomedical Publications, P.O. Box 368, Canton, CT 06019. 1978. 306 pp. 15 × 23 cm. Price $22.50.

Handbook of Experimental Pharmacology, Vol. 51. Uric Acid. By WILLIAM N. KELLEY and IRWIN M. WEINER. Springer-Verlag New York Inc., 175 Fifth Ave., New York, NY 10010. 1978. 639 pp. 16 × 24 cm. Price $159.50

IARC Monographs on the Evaluation of the Carcinogenic Risk of Chemicals to Humans. Some N-Nitroso Compounds. (Vol. 17). International Agency for Research on Cancer, distributed by World Health Organization. 1978. 165 pp. 17 × 24 cm. Price $25.00; 50 fr.

IARC Monographs on the Evaluation of the Carcinogenic Risk of Chemicals to Humans. Vol. 18. Polychlorinated Biphenyls and Polybrominated Biphenyls. International Agency for Research on Cancer, distributed by World Health Organization. 1978. 140 pp. 18 × 24 cm. Price 20 fr.

The International Challenge of Drug Abuse: NIDA Research Monograph 19. By ROBERT C. PETERSEN. National Institute on Drug Abuse, Division of Research, 5600 Fishers Lane, Rockville, MD 20857. 1978. 349 pp. 14 × 23 cm.

Methods in Cancer Research, Vol. XVII. Cancer Drug Development, Part B. Edited by VINCENT T. DeVITA, Jr., and HARRIS BUSCH. Academic, 111 Fifth Ave., New York, NY 10003. 1979. 356 pp. 15 × 23 cm. Price $37.00.

A publication of the
American Pharmaceutical Association—
the National Professional Society
of Pharmacists

JOURNAL OF PHARMACEUTICAL SCIENCES

INDEX TO AUTHORS
INDEX TO SUBJECTS

VOLUME 68
JANUARY TO DECEMBER, 1979

Published monthly under the supervision of the Board of Trustees

MARY H. FERGUSON
Editor

SHELLY ELLIOTT
Production Editor

MARCIA GARTRELL
Copy Editor

NICOLETTE TRIANTAFELLU
Copy Editor

EDWARD G. FELDMANN
Contributing Editor

SAMUEL W. GOLDSTEIN
Contributing Editor

BELLE R. BECK
Editorial Secretary

DAVID BOHARDT
Director of Publications

L. LUAN CORRIGAN
Assistant Director of Publications

EDITORIAL ADVISORY BOARD

John Autian
Norman R. Farnsworth
William O. Foye
William J. Jusko
Herbert A. Lieberman
David E. Mann, Jr.
Gerald J. Papariello
Edward G. Rippie

SEPTEMBER 1979
VOLUME 68 NUMBER 9

JOURNAL OF PHARMACEUTICAL SCIENCES

MARY H. FERGUSON
Editor

SHELLY ELLIOTT
Production Editor

MARCIA GARTRELL
Copy Editor

NICOLETTE TRIANTAFELLU
Copy Editor

EDWARD G. FELDMANN
Contributing Editor

SAMUEL W. GOLDSTEIN
Contributing Editor

BELLE R. BECK
Editorial Secretary

DAVID BOHARDT
Director of Publications

L. LUAN CORRIGAN
Assistant Director of Publications

EDITORIAL ADVISORY BOARD

JOHN AUTIAN
HERBERT A. LIEBERMAN
NORMAN R. FARNSWORTH
DAVID E. MANN, JR.
WILLIAM O. FOYE
GERALD J. PAPARIELLO
WILLIAM J. JUSKO
EDWARD G. RIPPIE

The *Journal of Pharmaceutical Sciences* (ISSN 0022-3549) is published monthly by the American Pharmaceutical Association (APhA) at 2215 Constitution Ave., N.W., Washington, DC 20037. Second-class postage paid at Washington, D.C., and at additional mailing office.

All expressions of opinion and statements of supposed fact appearing in articles or editorials carried in this journal are published on the authority of the writer over whose name they appear and are not to be regarded as necessarily expressing the policies or views of APhA.

Offices—Editorial, Advertising, and Subscription: 2215 Constitution Ave., N.W., Washington, DC 20037. Printing: 20th & Northampton Streets, Easton, PA 18042.

Annual Subscriptions—United States and foreign, industrial and government institutions $50, educational institutions $50, individuals *for personal use only* $30; single copies $5. All foreign subscriptions add $5 for postage. Subscription rates are subject to change without notice. Members of APhA may elect to receive the *Journal of Pharmaceutical Sciences* as a part of their annual $70 (foreign $75) APhA membership dues.

Claims—Missing numbers will not be supplied if dues or subscriptions are in arrears for more than 60 days or if claims are received more than 60 days after the date of the issue, or if loss was due to failure to give notice of change of address. APhA cannot accept responsibility for foreign delivery when its records indicate shipment was made.

Change of Address—Members and subscribers should notify at once both the Post Office and APhA of any change of address.

Photocopying—The code at the foot of the first page of an article indicates that APhA has granted permission for copying of the article beyond the limits permitted by Sections 107 and 108 of the U.S. Copyright Law provided that the copier sends the per copy fee stated in the code to the Copyright Clearance Center, Inc., P.O. Box 8891, Boston, MA 02114. Copies may be made for personal or internal use only and not for general distribution.

Microfilm—Available from University Microfilms International, 300 N. Zeeb Road, Ann Arbor, MI 48106.

©. Copyright 1979, American Pharmaceutical Association, 2215 Constitution Ave., N.W., Washington, DC 20037; all rights reserved.

CAUTION URGED IN RATIONING RESEARCH

Remember those long gasoline lines earlier this summer?

Perhaps some of our readers reside in places where the gas crunch didn't hit so badly, but those of us in the Washington, D.C. area were not so lucky. As a result, we won't quickly forget the long lines of frustrated, agonizing motorists. Undoubtedly, our keen recollection is at least in part due to the fact that we ourselves sat in those lines, and we personally underwent the experience involved.

This constituted a vivid, living example of the theory of supply and demand; supply went down and demand went up, with the delicately balanced system thrown completely awry. If the supply falls or can't be increased, and if the demand either continues or expands, then a shortage will result. And the best that anyone can suggest as a remedy is some sort of rationing plan.

All of this is an introduction to another area of "rationing." We had first heard this suggested only within the past year, but have seen it mentioned with increasing frequency in recent months. And that is the idea of "rationing" health care.

In late June of this year, United Press International reported on the release of a Brookings Institute study which stated that health care costs are rising rapidly at a time when the traditional governing control—namely, ability to pay—is being abandoned in favor of the growing belief that no one should have to forgo medical care because of inability to pay.

The author of the study was quoted as saying, *"We must accept the true nature of the cost problem. Once we decide that costs are rising too fast and that, in order to slow them, we are willing to modify the philosophy that costs should not be a consideration in medical care, the next question is, 'How do we want to accomplish the rationing that must take place?' "*

Recognizing that even the idea of rationing health care is an "explosive one" for the medical community as well as the general public, the study points out that only modest economies remain to be achieved by current attacks on waste and fraud. Meanwhile, the demand for care and the cost of care are both soaring.

We might have simply dismissed this Brookings study as some academic speculation and idle theorizing if it were not for several similar reports, projections, and conclusions appearing from other sources. The most startling of these was a full three-page discussion entitled "Is health care 'rationing' inevitable?" which appeared in the weekly newspaper of that bastion of conservatism, the American Medical Association.

This publication labeled the thought as "a somewhat alarming idea," but the message that came through was that ultimately some kind of rationing system will be applied to health care. To quote one of the discussants, *"At some point, society, quite independently of what you and I believe about medicine, will decide that 10% or 12% of the GNP is enough to spend on health care and decide that they aren't going to pay any more. Given that societal decision, then we'll have to decide what the appropriate balance should be between the present marketplace rationing system and the implicit and explicit rationing."*

What does all this have to do with pharmacy and the pharmaceutical sciences? Plenty! Drug products and pharmaceutical service are integral components of health care. Although they account for only a fraction of the health care dollar, they do represent significant costs. Moreover, when government agencies and legislators have looked for places to cut costs in the past, drugs and pharmaceutical services are among the first areas targeted. And when the budget for drug purchase goes down, the drug research budget ultimately is affected as well.

Although "rationing" *per se* would be a new development in the case of pharmaceuticals, we have had some related experiences in which restrictions have been applied or considered in drug development or distribution, due either to the cost or availability of drug products.

For example, each year the question of mass flu immunization programs centers around the cost of such programs *viś-à-viś* their anticipated or projected benefit in terms of health savings to the public. Regarding limited supplies, during World War II shortages of quinine to treat malaria and of the newly developed antibiotic, penicillin, to treat infections caused by battle wounds required a system of priority establishment that certainly approximated rationing. Subsequently, when polio vaccine first became available, the limited supplies required that choices be made as to whom it would be administered.

But in the quest for economy, we hope that the decision-makers recognize that carefully chosen and wisely selected research can often be the most effective route to major economies. For example, countless drugs are now available to use *via* chemical synthesis at a small fraction of their previous cost from biological or botanical sources. In other instances, research has led to the development of greatly improved and more effective agents.

Hence, we must remain vigilant to the need to ensure the continued viability of our drug research effort, so long as it is channeled toward truly productive goals and objectives.

—EGF

Isoproterenol-Induced Cardiac Arrhythmias

The October 1978 issue of the *Journal of Pharmaceutical Sciences* (p. 1390) contained a publication from the Department of Pharmaceutical Sciences, College of Pharmacy and Allied Health Professions, St. John's University, Jamaica, N.Y., entitled "Hemodynamic Alterations in Isoproterenol-Induced Cardiac Arrhythmias in Corticoid-Treated Rats," under the authorship of Michael A. Barletta, David Lehr, and Giancarlo Guideri.

This article was published by Dr. Barletta without approval or knowledge of the coauthors and did not contain any reference to the Department of Pharmacology, New York Medical College, Valhalla, N.Y., where the described studies had been performed and where both coauthors hold full-time positions. Neither coauthor has any association with St. John's University.

The data described in Dr. Barletta's publication were derived from his thesis research carried out from 1971 to 1974, in partial fulfillment of the requirements for a Ph.D. degree in Pharmacology at New York Medical College, under the sponsorship and guidance of Dr. Lehr and with the supervisory collaboration of Dr. Guideri.

Since Dr. Barletta's thesis had been completed early in 1974, the publication cited above does not encompass the current concepts of the coauthors, which are based on comprehensive additional studies carried out in the 5 intervening years. This is true, in particular, for work on the mechanism of sensitization of the corticoid-pretreated rat to ventricular arrhythmias and ventricular fibrillation by β-adrenergic agonists, as well as the role of α- and β-adrenergic stimulation in the elicitation of arrhythmias in the corticoid-pretreated rat and in the production of experimental myocardial necrosis. These aspects have been investigated by the coauthors in association with Ph.D. candidates Mark Green, Cynthia Healy, and Alison Brown[1-9].

An article representative of the present status of these investigations and focusing on data obtained by Mark Green in direct continuation of studies in the area of Dr. Barletta's thesis research has been submitted for publication.

David Lehr
Giancarlo Guideri
Department of Pharmacology
New York Medical College
Valhalla, NY 10595

Received March 5, 1979.

[1] G. Guideri, M. Green, and D. Lehr, *Res. Commun. Chem. Pathol. Pharmacol.*, **21**, 197 (1978).
[2] D. Lehr, in "Cardiac Toxicology," T. Balazs, Ed., CRC Press, in press.
[3] M. Green, G. Guideri, and D. Lehr, *Fed. Proc.*, **35**, 384 (1976).
[4] M. Green, G. Guideri, and D. Lehr, *Pharmacologist*, **18**, 145 (1976).
[5] C. Healy, G. Guideri, and D. Lehr, *Fed. Proc.*, **36**, 1013 (1977).
[6] M. Green, G. Guideri, and D. Lehr, *ibid.*, **37**, 817 (1978).
[7] G. Guideri, C. Healy, and D. Lehr, *ibid.*, **37**, 817 (1978).
[8] A. Brown, R. Blaiklock, and D. Lehr, *ibid.*, **38**, 694 (1979).
[9] G. Guideri, C. Healy, and D. Lehr, *Life Sci.*, **24**, 2385 (1979).

Quality Control in the Pharmaceutical Industry
Edited by MURRAY S. COOPER

This multi-volume treatise represents a convenient, practical and comprehensive guide to nearly every aspect of the quality control of pharmaceutical products. It encompasses the spectrum of relevant scientific disciplines—including biochemistry, analytical chemistry, physiology, and microbiology—as well as administrative matters such as the function of government agencies. The authors discuss each topic in sufficient detail to be of immediate practical value to pharmaceutical quality control managers and their technical staffs. In addition, the treatise will enable the scientist or administrator in the industry to broaden his knowledge of technical areas outside of his own speciality. This treatise will be a necessary addition to the libraries of technical and administrative personnel in the pharmaceutical industry.

VOLUME 3

CHAPTER HEADINGS: *A. S. Arambulo*, Interpretations of Current Good Manufacturing Practice Regulations. *A. J. Schmitz, Jr.*, The Auditing Function in the Total Control of Quality. *T. H. Meltzer and R.C. Lukaszewics*, Filtrative Sterilization with Porous Membranes *R. V. Smith and G. J. Yakatan*, Bioavailability Standards for Pharmaceutical Products. *P. B. Stones*, Quality Control of Poliomyelitis Vaccines. *J. D. Mullins and T. C. Fleming*, Quality Control of Ophthalmic Products. References appear at the end of each chapter.

1979, 312 pp., $29.50 ISBN: 0-12-187603-9

Analytical Profiles of Drug Substances

VOLUME 8

Edited by KLAUS FLOREY

Contributing Editors: NORMAN W. ATWATER, RAFIK BISHARA, GLENN A. BREWER, JR., LESTER CHAFETZ, HANS-GEORG LEEMANN, and BRUCE C. RUDY

CONTENTS: *K. Florey*, Aspirin. *D. A. Giron-Forest and W. D. Schönleber*, Bromocriptine Methanesulphonate. *E. Debesis*, Calcitriol. *G. Schwartzman et al.*, Chlortetracycline Hydrochloride. *R. H. Bishara and H. B. Long*, Dobutamine Hydrochloride. *W. L. Koch*, Erythromycin. *G. A. Brewer*, Gramicidin. *E. R. Townley*, Griseofulvin. *J. Kirschbaum*, Halcinonide. *C. E. Orzech et al.*, Hydralazine Hydrochloride. *L. O. Pont et al.*, Calcium Leucovorin *H. Y. Aboul-Enein and A. A. Al-Badr*, Methimazole. *P. E. Grubb*, Nalidixic Acid. *W. F. Heyes*, Neomycin. *S. A. Benezra and J. W. Rae*, Pseudoephedrine Hydrochloride. *S. A. Benezra and C.-H. Yang*, Triprolidine Hydrochloride. *Z. L. Chang*, Sodium Valproate and Valproic Acid.

1979, 576 pp., $28.00 ISBN: 0-12-260808-9

Continuation Orders authorize us to ship and bill each volume in a series, or "Advances" type publication automatically, immediately upon publication. This order will remain in effect until cancelled. Specify the volume number with which your order is to begin.

Send payment with order and save postage and handling charge. *Prices are subject to change without notice.*

ACADEMIC PRESS, INC.
A Subsidiary of Harcourt Brace Jovanovich, Publishers
111 FIFTH AVENUE, NEW YORK, N.Y. 10003
24-28 OVAL ROAD, LONDON NW1 7DX

JOURNAL OF PHARMACEUTICAL SCIENCES

SEPTEMBER 1979
VOLUME 68 NUMBER 9

RESEARCH ARTICLES

Effect of ^{60}Co-Irradiation on Penicillin G Procaine in Veterinary Mastitis Products

KIYOSHI TSUJI ˣ, JOHN F. GOETZ, and WILLIAM VANMETER

Received January 8, 1979, from *Control Analytical Research and Development, The Upjohn Company, Kalamazoo, MI 49001.* Accepted for publication March 2, 1979.

Abstract □ The effect of ^{60}Co-irradiation on penicillin G procaine in a peanut oil-based veterinary mastitis product was examined by reversed-phase high-performance liquid chromatography (HPLC). The HPLC method is capable of separating and quantifying procaine, penicillin G, and various degradation compounds. Penicillin G recovery from a placebo formulation was 100.4% with a relative standard deviation of <1%. When irradiated at 4.0 Mrads, the penicillin G in two product lots decreased slightly (~1–2%) with a corresponding increase in two compounds inherently present in bulk penicillin G powder. These compounds may be formed in abundance by treating penicillin G in an acidic solution. From the mass spectrometric analysis and the relative retention data with authentic compounds, these compounds were identified as benzylpenilloaldehyde and benzylpenaldic acid. Values obtained by the HPLC method on the product irradiated and stored at various temperatures correlated well with those of the microbiological assay. No significant decrease in the procaine was detected even after 4.0-Mrad irradiation. The HPLC method is applicable for analysis of other β-lactam antibiotics.

Keyphrases □ Penicillin G procaine—effect of cobalt irradiation, veterinary mastitis products, sterilization □ Cobalt irradiation—effect on penicillin G procaine, veterinary mastitis products, sterilization □ Sterilization—penicillin G procaine, veterinary mastitis products, cobalt irradiation

The Ministry of Agriculture, Food, and Fisheries in the United Kingdom has served notice that all new veterinary mastitis products to be marketed in the United Kingdom must be sterile. Moreover, sterility is required for existing veterinary mastitis products at their reregistration time. Since the efficacy and toxicity of ethylene oxide as a sterilization agent are being questioned by both the Food and Drug Administration (1) and the Environmental Protection Agency in the United States (2), ^{60}Co-irradiation was examined as a reliable and economical means to sterilize terminally a veterinary mastitis product. The ^{60}Co-irradiation has been recognized as the method of choice for sterilization of medical devices and has been accepted for terminal sterilization of ophthalmic ointments (3). In many countries, products irradiated at 2.5 Mrads by cobalt 60 may be released as sterile without the final sterility testing.

Although the official microbiological cylinder cup–agar diffusion assay may be used as a stability-indicating method for penicillin G (4), a more precise and accurate method is desirable for monitoring the effect of ^{60}Co-irradiation treatment. Since a reversed-phase high-performance liquid chromatographic (HPLC) assay of β-lactam antibiotics (5) was improved by use of a column packed with 5–10-μm particle size C_{18} (6) and used in this laboratory for many years, this method was selected to assess the effect of ^{60}Co-irradiation on procaine and penicillin G in a veterinary mastitis product. Similar HPLC assays for β-lactam antibiotics have appeared (7–16).

EXPERIMENTAL

Apparatus—A modular liquid chromatograph equipped with a 254-nm UV monitor[1], a high-pressure pump[2], and a 20-μl fixed-loop injector[3] were used. A low C_{18}-loaded reversed-phase column[4] with a stainless steel precolumn[5], 51 × 2.1 mm i.d., was used to separate procaine and penicillin G.

Reagents—For the mobile phase, acetonitrile–water–0.2 *M* ammonium acetate buffer (20:70:10) was used. The pH was adjusted to 6.0 with acetic acid. The 0.2 *M* ammonium acetate buffer was prepared by weighing 15.5 g of ammonium acetate into a 1-liter graduated cylinder and adding water to volume. The mobile phase was filtered through a membrane filter[5].

The mobile phase was pumped through the column at a flow rate of ~1.0 ml/min.

Reference Standard Solutions—*Penicillin G*—The USP penicillin G potassium reference standard was used "as is" at 1590 units/mg. Ap-

[1] Model 1203 UV monitor III, Laboratory Data Control, Riviera Beach, Fla.
[2] Model 6000 A chromatographic pump, Waters Associates, Milford, Mass.
[3] Model 70-10, Rheodyne, Berkeley, Calif.
[4] Partisil PXS 10/25 ODS, Whatman Inc., Clifton, N.J.
[5] Catalog No. FHLP04700 fluoropore filter, Millipore Corp., Bedford, Mass.

0022-3549/79/0900-1075$01.00/0
© 1979, American Pharmaceutical Association

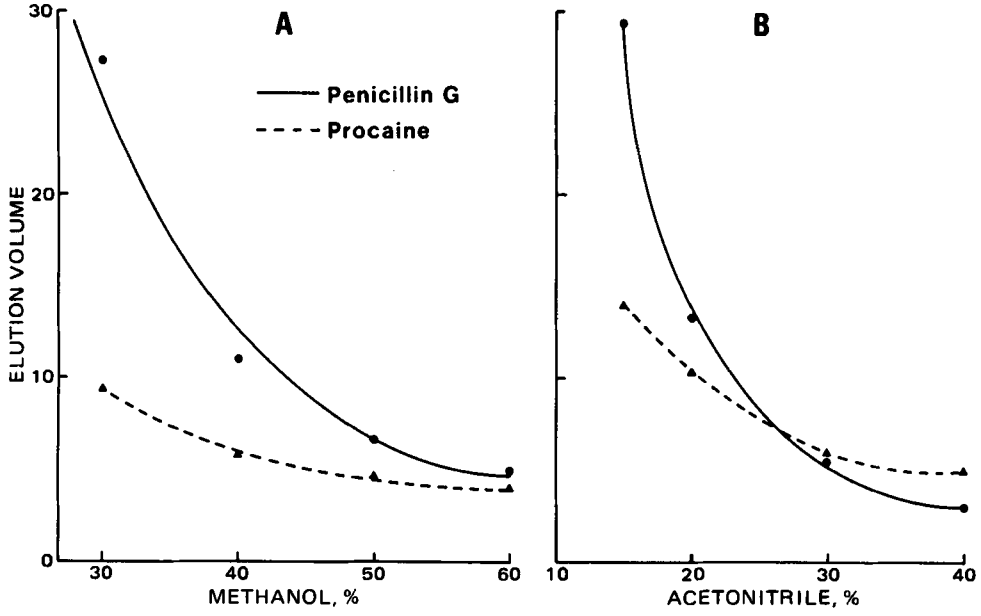

Figure 1—(*A*) *Effect of methanol concentration in the mobile phase on elution volumes of penicillin G and procaine using a μBondapak C_{18} column.* (*B*) *Effect of acetonitrile concentration in the mobile phase on elution volumes of penicillin G and procaine using a μBondapak C_{18} column.*

proximately 6.7 mg of the reference standard was weighed accurately[6] and placed in a 10-ml volumetric flask. The standard was dissolved and diluted to volume with the mobile phase. The reference standard solution thus prepared was transferred to a 35-ml disposable vial, and 10 ml of isooctane (2,2,4-trimethylpentane) was added. The vial was capped and shaken gently for 5 min on an automatic reciprocal shaker[7]. The top isooctane layer was aspirated off, and 5 ml of isooctane was again added. The vial was shaken again for 5 min and then centrifuged at 1000×*g* for 1 min. The top half of the sample was aspirated off, and the sample was sonicated just prior to chromatographic analysis.

Procaine—Approximately 4.5 mg of procaine hydrochloride USP was weighed accurately[6] and placed in a 50-ml volumetric flask. The standard was dissolved and diluted to volume with the mobile phase. The standard solution was transferred to a 125-ml separator containing 50 ml of isooctane. The flask was shaken gently for 5 min on an automatic reciprocal shaker[7].

The top isooctane layer was aspirated off, and 25 ml of isooctane was added. The flask was shaken again for 5 min. Approximately 10 ml of the lower phase was transferred into a 35-ml disposable vial and centrifuged at 1000×*g* for 1 min. The top half of the sample was aspirated off, and the sample was sonicated just prior to chromatographic analysis.

Sample Preparation—A plastet containing the peanut oil-based mastitis product was weighed. After the plastet was shaken vigorously, the contents were expelled into a 250-ml separator containing 100 ml of the mobile phase. The empty plastet was weighed to calculate by difference the weight of the content being assayed. Approximately 100 ml of isooctane was added, and the flask was shaken gently for 5 min on a reciprocal shaker[7].

Approximately 75% of the top layer was aspirated off, and 50 ml of isooctane was added. The flask was shaken again for 5 min. Approximately 10 ml of the lower phase was transferred into a 35-ml disposable vial and centrifuged for 1 min at 1000×*g*. The top half of the sample was aspirated off.

Table I—Precision of the HPLC Assay for Penicillin G in Peanut Oil-Based Mastitis Product

Net Weight of Product, g	Height of Penicillin G Peak, cm	Peak Height of Penicillin G/ Weight of Product[a]
8.16	27.0	3.31
8.21	27.0	3.29
8.19	27.2	3.32
8.25	27.6	3.35
8.36	28.2	3.37
8.33	28.0	3.36

[a] *RSD* = 0.94%.

[6] Model G electrobalance, Cahn Instrument Corp., Paramount, Calif.
[7] Eberbach, Ann Arbor, Mich.

Penicillin G—For the penicillin G assay, the sample solution was chromatographed.

Procaine—The sample solution was diluted 1:5 with the mobile phase and chromatographed.

Calculations—*Penicillin G*—The penicillin G content in a plastet was calculated from:

$$\text{penicillin G content} = \frac{P_{sm}}{W_{sm}} \times \frac{W_{std}}{P_{std}} \times \text{Sp.G.} \times 100 \times 1590 \quad \text{(Eq. 1)}$$

where P_{sm} is the peak height or peak area of the sample, W_{sm} is the weight of the sample in grams, W_{std} is the weight of the standard in milligrams per milliliter, P_{std} is the peak height or peak area of the reference standard, Sp.G. is the specific gravity of the mastitis product, and 1590 is the potency of the penicillin G USP reference standard (issue F).

Procaine—The procaine content per plastet may be calculated from:

$$\text{procaine content} = \frac{PK_{sm}}{W_{sm}} \times \frac{W_{std}}{PK_{std}} \times \frac{F_1}{F_2} \times F_3 \times F_4 \times F_5 \times \text{Sp.G.} \times P \quad \text{(Eq. 2)}$$

where PK_{sm} is the peak height or peak or peak area of the sample; W_{sm} is the weight of the sample; PK_{std} is the peak height or peak area of the reference standard; W_{std} is the weight of the standard; F_1, F_2, and F_3 are volumes of the sample solution, the reference standard solution, and the plastet, respectively; F_4 is the final volume of the sample; F_5 is the conversion factor from procaine hydrochloride to procaine base (0.866); Sp.G. is the specific gravity of the mastitis product; and P is the purity of the procaine USP reference standard.

RESULTS AND DISCUSSION

Factors Affecting Resolution of Penicillin G and Procaine Peaks—During the evaluation of several silica with bonded octadecylsilane[8] columns, the resolution of penicillin G from the procaine peak

Table II—Recovery of Penicillin G from Mastitis Product

Penicillin G Added, mg/plastet	Penicillin G Recovered, mg/plastet	Recovery, %
67.63	68.91	101.9
67.13	66.58	99.2
66.79	66.91	100.2
Average		100.4

[8] μBondapak C_{18}, Waters Associates, Milford, Mass.

Table III—HPLC Analysis of Penicillin G in Mastitis Product Irradiated with Cobalt 60

Lot	Penicillin G, units/plastet			
	0 Mrad	1.5 Mrads	2.5 Mrads	4.0 Mrads
A	112,400	109,200	107,600	108,500
	114,700	107,500	106,800	108,000
	108,400	108,800	107,500	107,900
	107,500	109,500	106,000	109,800
Average	110,800	108,800	107,000	108,600
B	117,300	115,300	115,500	113,600
	117,600	115,800	115,500	113,400
	110,500	112,300	112,400	112,400
	111,400	113,500	113,500	113,000
	114,400	114,400	112,900	112,900
	113,600	114,900	112,500	111,200
Average	114,100	114,400	113,700	112,800

was difficult to reproduce. Factors such as the acetonitrile and methanol concentrations in the mobile phase were examined to obtain the optimum resolution of the two compounds.

As shown in Fig. 1A, an increase in the methanol concentration decreased the elution volume of both the penicillin G and the procaine peaks. The effect on the penicillin G peak was more pronounced than on procaine. The peak elution order, however, remained the same.

Acetonitrile, on the other hand, drastically affected the penicillin G peak elution volume (Fig. 1B). The effect of the acetonitrile concentration on the procaine elution volume was less. In fact, the elution order of

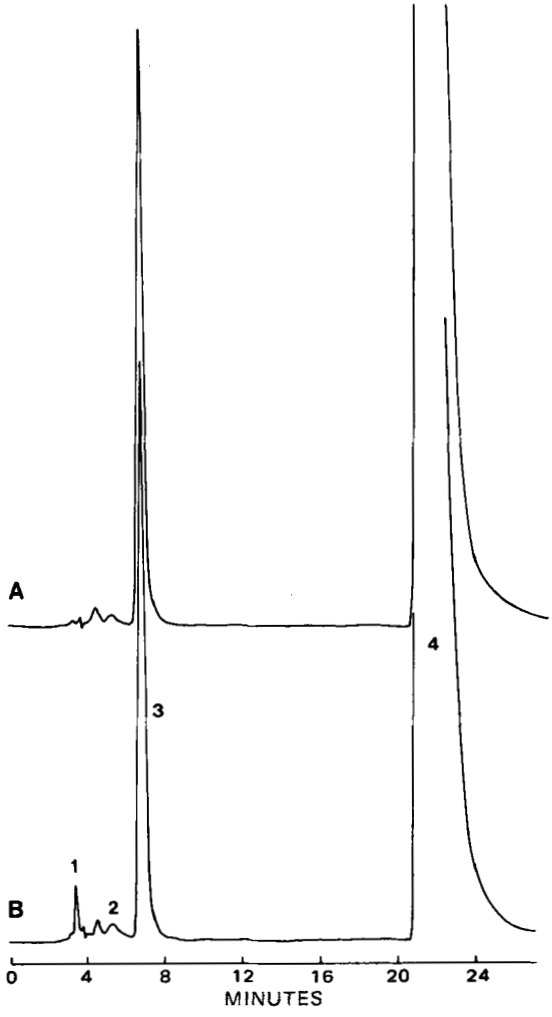

Figure 2—*HPLC analysis of penicillin G procaine irradiated at 0 Mrads (A) and 4.0 Mrads (B) in a mastitis product using a ODS-I column. The mobile phase was acetonitrile 0.2 M ammonium acetate–water (20: 10:70), pH 6.0. Key: 1, degradation compound I; 2, degradation compound II; 3, penicillin G; and 4, procaine.*

Table IV—HPLC Analysis of Procaine in Mastitis Product

Lot	Procaine Concentration, mg/plastet			
	0 Mrad	1.5 Mrads	2.5 Mrads	4.0 Mrads
A	45.0	43.1	44.3	43.5
	42.0	43.8	44.0	43.1
Average	43.5	43.5	44.2	43.3
B	43.5	43.7	43.3	43.1
	43.4	43.1	43.2	43.1
	43.8	43.7	43.5	43.0
	43.7	44.3	43.8	42.8
Average	43.6	43.7	43.5	43.0

penicillin G and procaine crossed over at the acetonitrile concentration of ~27–28%. This intersecting point varied from one column to the next. Since the majority of the penicillin G degradation compounds elute earlier than the penicillin G peak, the chromatographic conditions should be adjusted such that penicillin G elutes faster than the procaine peak.

This adjustment cannot always be reliably reproduced, however, especially between columns, and such attempts often caused the penicillin G peak to elute too close to the solvent front. Therefore, various commercially available C_{18} reversed-phase columns[9] were evaluated. In general, use of a highly C_{18} loaded column (more than 10%) resulted in near complete merger of the two peaks. Only a low C_{18} loaded column[4] (about 5%) consistently achieved a complete separation of the two peaks;

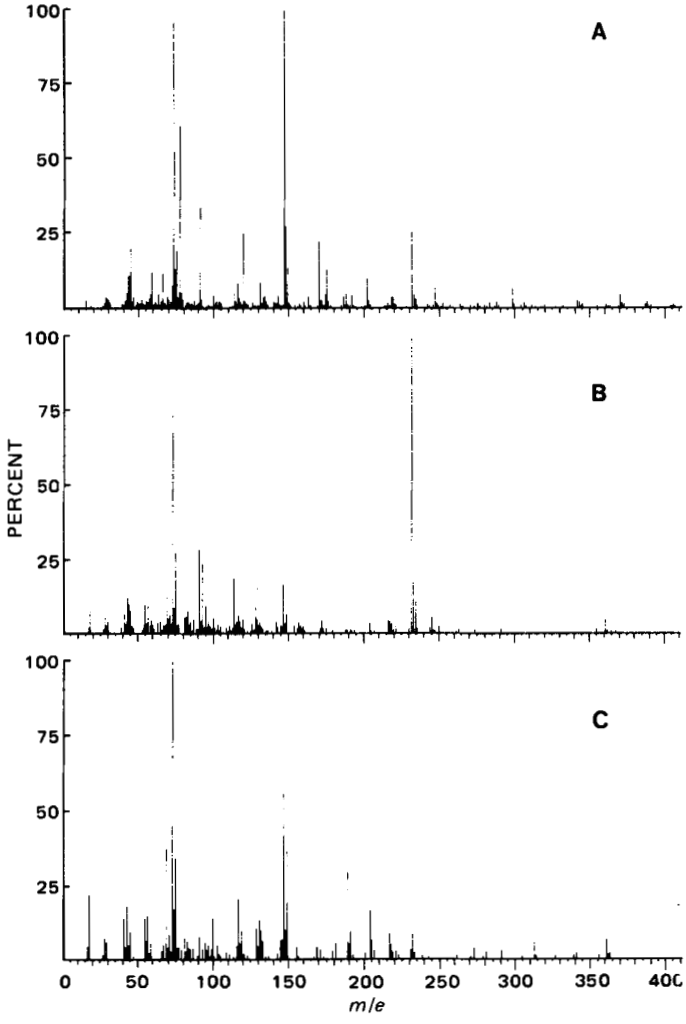

Figure 3—*Mass spectrum of silylated penicillin G and radiolytic compounds. Key: A, trimethylsilylpenicillin G; B, peak 1; and C, peak 2.*

[9] Waters C_{18}, Brown Lee RP-18, E. M. Merck RP-18, Varian C_{18}, Whatman ODS-I, and Whatman ODS-II.

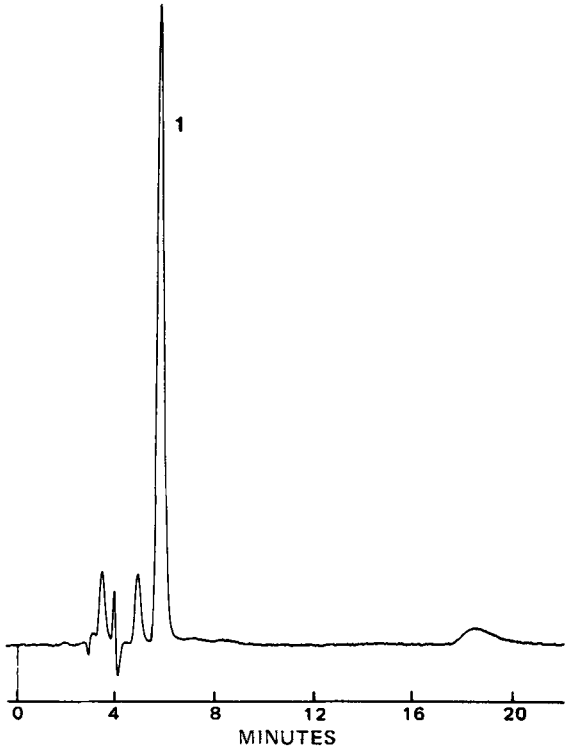

Figure 4—*HPLC analysis of ampicillin (1) in an oral formulation using a μBondapak C_{18} column. The mobile phase was acetonitrile–0.2 M ammonium acetate buffer–water (15:10:85), pH 6.0.*

more than 12 min of elution time separated the procaine and penicillin G peaks (Fig. 2A). It may be theorized that the underivatized hydroxyl groups on the silica column support exhibit strong affinity toward the procaine molecule, resulting in longer procaine retention and the separation of the two compounds.

Precision and Recovery of Penicillin G from Peanut Oil-Based Mastitis Product—Precision of the HPLC assay was evaluated by individually weighing and extracting six replicate mastitis product samples. The relative standard deviation of the HPLC method was <1% (Table I).

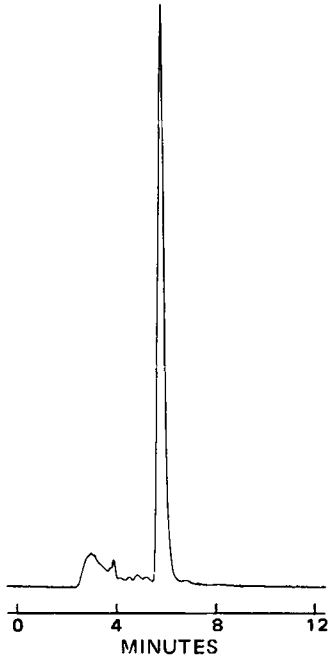

Figure 5—*HPLC analysis of penicillin O using a μBondapak C_{18} column. The mobile phase was acetonitrile–0.2 M ammonium acetate–water (25:10:65), pH 6.0.*

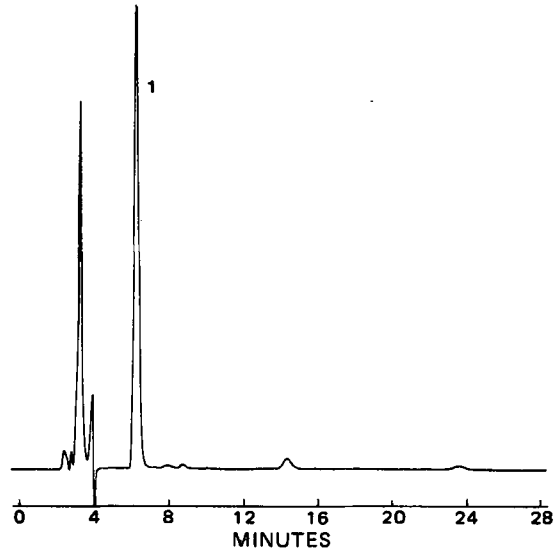

Figure 6—*HPLC analysis of penicillin V (1) in an oral formulation using a μBondapak C_{18} column. The mobile phase was acetonitrile–0.2 M ammonium acetate–water (30:10:60), pH 6.0.*

The extraction technique efficiency for penicillin G recovery from the product was evaluated by adding three independently weighed penicillin G USP reference standard samples to the product base. The penicillin G recovery from the product base was 100.4% (Table II).

Penicillin G Stability to ^{60}Co-Irradiation—Penicillin G in a peanut oil-based veterinary mastitis product was relatively stable to ^{60}Co-irradiation. Even after 4.0 Mrads irradiation, the maximum irradiation level targeted for product sterilization, penicillin G in two product lots showed decreases in potency of only 2.0 and 1.1% (Table III).

Although several impurity peaks were present in unirradiated penicillin G procaine (Fig. 2A), only two peaks were increased by ^{60}Co-irradiation (Fig. 2B). Since these degradation compounds are inherently present in the untreated penicillin G procaine powder, these compounds are not formed uniquely by ^{60}Co-irradiation. These degradation compounds can be formed in abundance when penicillin G powder is treated in a low pH solution (pH 3.0) at 37° for 1 hr.

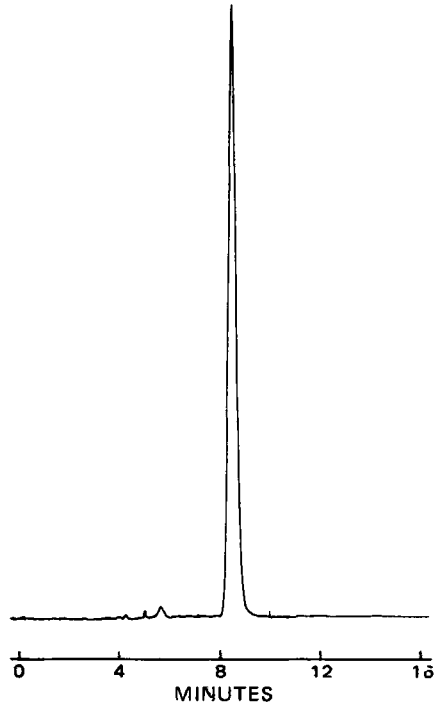

Figure 7—*HPLC chromatogram of cephalothin using a μBondapak C_{18} column. The mobile phase was acetonitrile–0.2 M ammonium acetate–water (25:10:65), pH 6.0.*

Table V—Correlation between HPLC and Microbiological Assay Methods for Penicillin G in Mastitis Product

Lot	Irradiation, Mrads	Storage	Penicillin G, units/plastet HPLC	Microbiological
A	0	Initial	100,500	108,000
		25°, 3 months	100,100	101,000
		40°, 3 months	54,300	41,000
	2.5	Initial	103,600	107,000
		25°, 3 months	99,100	103,000
		40°, 3 months	61,500	62,000
	4.0	Initial	104,600	109,000
		25°, 3 months	100,900	101,000
		40°, 3 months	59,500	34,000
B	0	Initial	105,100	111,000
		25°, 3 months	101,300	101,000
		40°, 3 months	64,200	65,000
	2.5	Initial	105,800	108,000
		25°, 3 months	99,700	104,000
		40°, 3 months	64,800	58,000
	4.0	Initial	106,400	97,000
		25°, 3 months	101,700	102,000
		40°, 3 months	61,600	53,000

Approximately an eightfold increase in degradation compound I (peak 1) was noted, with less than a twofold increase in peak 2, by 4 Mrads irradiation. Increase in the area under peaks 1 and 2 was too great to be accounted for by the decrease in the penicillin G peak. This discrepancy may be attributed to the difference in the molar absorptivity of these compounds at 254 nm.

Degradation Compound Identification—As stated previously, the impurity compounds (peaks 1 and 2) that were increased by ^{60}Co-irradiation also may be formed in abundance by treating a penicillin G powder in a pH 3.0, 0.02 *M* phosphate buffer at 37° for 1 hr. The fact that the retention of peak 2 is greatly influenced by change in the mobile phase

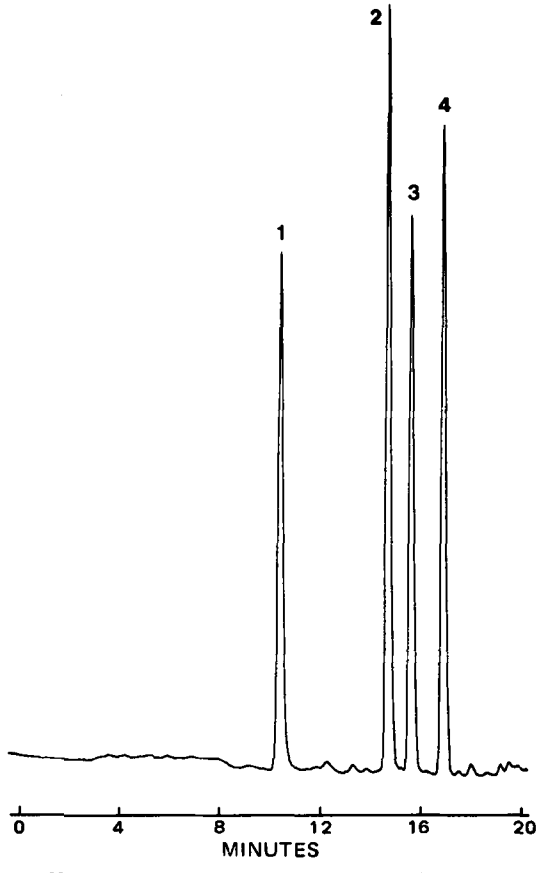

Figure 8—*HPLC gradient elution chromatogram for tentative identification of β-lactam antibiotics using a μBondapak C_{18} column. The linear gradient was from 10:10:80 (acetonitrile–0.2 M ammonium acetate–water), pH 6.0, to 50:10:40, pH 6.0, in 15 min. Key: 1, ampicillin; 2, penicillin O; 3, penicillin G; and 4, penicillin V.*

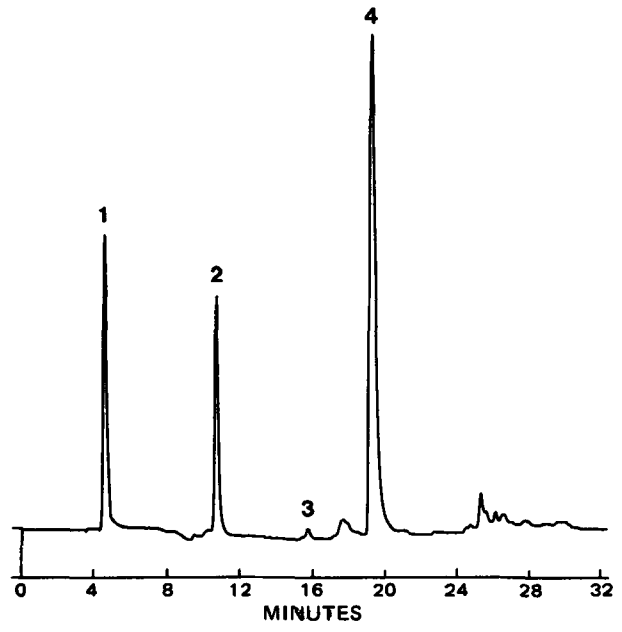

Figure 9—*HPLC gradient elution chromatogram indicating separation of an ampicillin prodrug, bacampicillin, from process intermediates. The convex gradient elution was from mobile phase A, 5:10:85 (acetonitrile–0.2 M ammonium acetate–water), pH 4.0, to mobile phase B, 80:10:10, pH 4.0, in 30 min. Key: 1, phenylglycine; 2, ampicillin; 3, penicillin G; and 4, bacampicillin.*

pH indicates the presence of acidic radical(s) in the molecule. The retention of peak 1 was not affected by the pH change.

Formation of benzylpenicilloic acid, benzylpenilloic acid, and hydroxybenzylpenicillin in an aqueous penicillin G solution irradiated by cobalt 60 has been reported (17). These radiolytic compounds also may be formed by an alkaline treatment (18). However, the relative retention of these alkaline (pH 10.0) hydrolyzed compounds failed to match the two peaks of interest.

To identify the two degradation compounds, a small preparative liquid chromatograph was constructed with a 122-cm × 7-mm i.d. stainless steel column packed with C_{18}[10].

About 30 mg of penicillin G sodium USP, irradiated at 6.0 Mrads, was dissolved in 10 ml of the mobile phase and introduced onto the column *via* a 100-μl loop injector. The column effluents corresponding to the two peaks were collected in 250-ml round-bottom flasks immersed in a methanol–dry ice bath. The procedure was repeated 10 times. The effluents were freeze dried overnight.

The submilligram quantities of samples thus collected were dissolved in acetonitrile, transferred into microreaction vials[11], and dried under a nitrogen stream. About 100 μl of bis(trimethylsilyl)trifluoroacetamide containing 1% trimethylchlorosilane[12] was added to the two dried samples and penicillin G powder and allowed to react 3 hr at room temperature. The silylated samples were placed in capillary glass tubings and dried under vacuum. The samples were analyzed by mass spectrometry using the electron-impact ionization mode.

The mass spectra of penicillin G and two degradation compounds are shown in Fig. 3. The penicillin G mass spectrum (Fig. 3A) showed that both *m/e* 478 [M^+, bis(trimethylsilyl)penicillin G] and 406 [mono(trimethylsilyl)penicillin G] were weak, indicating instability of the silylated compounds. Another weak peak was observed at *m/e* 306 [M − $C(CH_3)_2CHCO_2Si(CH_3)_3$]. Much stronger peaks were seen at *m/e* 463 (M − 15), 387 (M − $CH_3C_6H_5$), and 247. An intense peak was shown at *m/e* 232 (*m/e* 247 − CH_3).

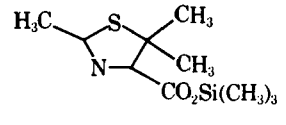

(*m/e* 247)

[10] Bondapak C_{18} Porasil B, Waters Associates, Milford, Mass.
[11] Reacti-Vial, Pierce Chemical Co., Rockford, Ill.
[12] Regisil RC-2, Regis Chemical Co., Morton Grove, Ill.

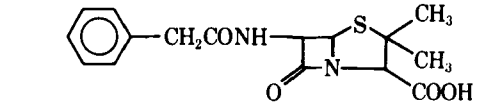

penicillin G (benzylpenicillin)

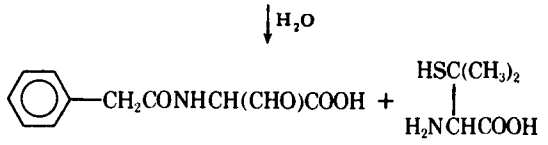

benzylpenaldic acid penicillamine

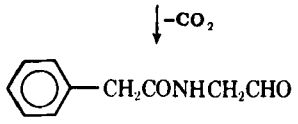

benzylpenilloaldehyde

Scheme I

The mass spectrum of the column effluent corresponding to peak 1 (Fig. 3B) is essentially identical to that of benzylpenilloaldehyde and showed the weak molecular ion at *m/e* 250 (M^+) and a strong peak at *m/e* 232 (M − 18). Weak peaks were found at *m/e* 158 (M − $CH_2C_6H_5$), 130 (M − $CH_2C_6H_5CO$), and 43 (M − $CH_2C_6H_5CONH$). A much stronger peak was observed at *m/e* 149 [M − $COSi(CH_3)_3$].

The mass spectrum of Compound II (Fig. 3C) is that of benzylpenaldic acid. The molecular ions at *m/e* 437 [tris(trimethylsilyl) derivative] and 291 [mono(trimethylsilyl) derivative] were relatively weak, indicating incomplete silylation. Much stronger peaks were shown at *m/e* 232 [M − $CH_2C_6H_5CONSi(CH_3)_3$] and 207 [M − CH(COO-trimethylsilyl)-$COSi(CH_3)_3$]. The presence of an acidic radical in this compound was indicated previously.

From the identification, it may be speculated that penicillin G may undergo a slight degradation by ^{60}Co-irradiation as shown in Scheme I. Penicillamine cannot be detected by monitoring at 254 nm.

Procaine Stability to ^{60}Co-Irradiation—The effect of ^{60}Co-irradiation on the stability of procaine is shown in Table IV. Although 0.5 and 1.5%, decreases were noted in two lots of the product irradiated at 4.0 Mrads, these decreases were not statistically significant. Careful examination of the chromatogram of procaine irradiated at 4.5 Mrads failed to detect any peak other than procaine.

Correlation between HPLC and Microbiological Methods—A correlation between the HPLC and the microbiological methods for the penicillin G assay was examined by use of two simulated product lots ^{60}Co-irradiated at 2.5 and 4.0 Mrads and stored at 25 and 40° for 3 months. The microbiological cylinder cup-agar diffusion assay used was as described in the Code of Federal Regulations (4) (Table V). A cross-classified analysis of variance was used to test for lot, radiation dosage, and time–temperature main effects and for all two-way interactions between the main effects. The analysis of variance showed that only the time–temperature effect was statistically significant ($p<0.05$) due to the instability of penicillin G at 40°.

Thus, the HPLC method correlated well with the microbiological assay and was stability indicating.

Other β-Lactam Antibiotics—With a slight modification of the mobile phase, the isocratic reversed-phase HPLC method is applicable to many β-lactam antibiotics (Figs. 4–7) with a relative standard deviation of ~1.0%.

The reversed-phase HPLC method using a gradient elution technique also is applicable for tentatively identifying β-lactam antibiotics (Fig. 8) and for assessing the stability of the prodrug, bacampicillin (Fig. 9).

REFERENCES

(1) *Fed. Regist.*, **43** (19), 4110 (1978).

(2) *Fed. Regist.*, **43** (19), 6560 (1978).

(3) R. A. Nash, *Bull. Parenter. Drug Assoc.*, **28**, 181 (1974).

(4) Code of Federal Regulations, Title 21, Food and Drug Administration, U.S. Government Printing Office, Washington, D.C., 1977.

(5) K. Tsuji and J. H. Robertson, *J. Pharm. Sci.*, **64**, 1942 (1975).

(6) K. Tsuji, in "GLC and HPLC Determination of Therapeutic Agents," part 2, K. Tsuji, Ed., Dekker, New York, N.Y., 1978, pp. 773–780.

(7) M. A. Carroll, E. R. White, Z. Jansik, and J. E. Zarembo, *J. Antibiot.*, **30**, 397 (1977).

(8) V. Hartman and M. Roediger, *Chromatographia*, **9**, 266 (1976).

(9) D. Herbst, *J. Pharm. Sci.*, **66**, 1646 (1977).

(10) J. H. Kennedy, *J. Chromatogr. Sci.*, **16**, 492 (1978).

(11) J. Konecny, E. Felber, and J. Gruner, *J. Antibiot.*, **26**, 135 (1973).

(12) J. H. Knox and A. Pryde, *J. Chromatogr.*, **112**, 171 (1975).

(13) S. Lam and E. Grushka, *J. Liq. Chromatogr.*, **1**, 33 (1978).

(14) R. D. Miller and N. Neuss, *J. Antibiot.*, **29**, 902 (1976).

(15) T. Nakagawa, J. Haginaka, K. Yamanoka, and T. Uno, *J. Antibiot.*, **31**, 769 (1978).

(16) E. R. White, M. A. Carroll, and J. E. Zarembo, *J. Antibiot.*, **30**, 811 (1977).

(17) D. M. Power, in "Sterilization of Medical Products by Ionizing Irradiation," vol. II, E. R. L. Ganghran and A. J. Goudie, Eds., Multiscience Publishing, Montreal, Canada, 1978, pp. 237–246.

(18) P. P. Regna, in "Antibiotics, Their Chemistry and Non-Medical Uses," H. S. Goldberg, Ed., D. Van Nostrand, New York, N.Y., 1959, pp. 59–66.

ACKNOWLEDGMENTS

The authors thank D. G. Pope for the supply of ^{60}Co-irradiated products, L. Baczynskyj for the mass spectrometric analysis, K. A. Gusciora for technical assistance, and A. R. Lewis for statistical analysis.

Quantitative Structure–Selectivity Relationships: Selective Drug Design

ALDO GARZIA *, ALBERTO VILLANTI ˣ, and GIANFRANCO TUCCINI

Received July 21, 1978, from *Tecnofarmaci S.p.A., Via Ardeatina Km. 21,000, 00040 Pomezia, Italy.* Accepted for publication February 23, 1979. *Present address: Istituto Chemioterapico Italiano, S. Grato, 20075 Lodi, Italy.

Abstract □ The concept of complex selectivity (S_c^n) permits the investigation of quantitative structure–selectivity relationships in the presence of n side effects; S_c^n permits differentiation of the most selective molecules rather than the most active ones in a congener series. Selectivity quantification in the presence of n side effects facilitates molecular comparisons. The information provided by S_c^n and its changes with increasing n is discussed. The proposed mathematical model is applied to the study of the selectivity of some antibiotics and antibacterial agents.

Keyphrases □ Structure–selectivity relationships—penicillins, alkylchlorophenols, drug design, bioavailability, structure–activity relationships □ Penicillins—structure–selectivity relationships, bioavailability □ Alkylchlorophenols—structure–selectivity relationships, bioavailability □ Drug design—structure–selectivity relationships, penicillins, alkylchlorophenols □ Antibacterials—structure–selectivity relationships, penicillins

Researchers working on quantitative structure–activity relationships have been mainly examining the most active compound, the one that produces the highest activity characteristic of a series of congeners. Insufficient care has been given to rational drug design.

Identification of the most active molecule is insufficient for therapeutically useful drug design. The ideal compound must be as specific and selective as possible, with minimal side effects. This aim can be achieved by generalizing some results obtained by previous investigators (1–3). These studies extended the multiparameter Hansch analysis (4) to the study of selectivity, taking only one side effect into account.

The purpose of this work was to extend this approach to the study of n side effects considered simultaneously with the main effect. With the proposed method, isolation of the most selective compounds rather than the most active ones in a series of molecules is possible.

This work is a contribution to the development of a general mathematical model for forecasting overall drug action and for quantifying biopharmacological activities in order to direct, *a priori*, the synthetic work toward molecules with optimal therapeutic characteristics.

THEORETICAL

In a series of pharmacologically active congener molecules, all producing the same range of effects but having different intensities from molecule to molecule, the overall effect, E_o, of each molecule can be expressed as a function of the combined single effects:

$$E_o = f(E_m, E_1, \ldots E_i, \ldots E_n) \qquad \text{(Eq. 1)}$$

where E_m is the main effect and E_i represents the n undesirable side effects.

The application of the Hansch approach to each single effect for the whole series gives:

$$E_m: \quad \log \frac{1}{C_m} = a_{0m} + \sum_{j=1}^{r_m} a_{jm}x_{jm} \qquad \text{(Eq. 2)}$$

$$E_1: \quad \log \frac{1}{C_1} = a_{01} + \sum_{j=1}^{r_1} a_{j1}x_{j1} \qquad \text{(Eq. 3)}$$

$$E_i: \quad \log \frac{1}{C_i} = a_{0i} + \sum_{j=1}^{r_i} a_{ji}x_{ji} \qquad \text{(Eq. 4)}$$

$$E_n: \quad \log \frac{1}{C_n} = a_{0n} + \sum_{j=1}^{r_n} a_{jn}x_{jn} \qquad \text{(Eq. 5)}$$

where $1 < i < n$ and r_i is the number of parameters in the ith equation.

The therapeutic index or selectivity, S_i, of each molecule relative to the ith side effect usually is described (5) as the quotient between a standard concentration, C_i, that produces a side effect, E_i, with a given intensity and an effective standard concentration, C_m, relative to the main effect, E_m:

$$S_i = \frac{C_i}{C_m} \qquad \text{(Eq. 6)}$$

A high selectivity, *i.e.*, a high S_i value, depends on a relatively large numerator and a small denominator of Eq. 6. By taking the logarithms, Eq. 6 becomes:

$$\log S_i = \log \frac{C_i}{C_m} \qquad \text{(Eq. 7)}$$

Enlarging a summation to the n selectivities gives:

$$\sum \log S_i = \sum_{i=1}^{n} \log \frac{C_i}{C_m} \qquad \text{(Eq. 8}a\text{)}$$

or:

$$\sum \log S_i = \log \frac{\prod_{i=1}^{n} C_i}{(C_m)^n} \qquad \text{(Eq. 8}b\text{)}$$

where the logarithmic fraction on the right side is the "complex selectivity" and is indicated by the symbol S_c^n where n is the number of side effects studied contemporaneously with the main effect. In this way, one can speak of first-, second-, . . . , nth-order complex selectivity according to the number of side effects simultaneously considered. Therefore, Eq. 8*b* can be rewritten:

$$\log S_c^n = \log \frac{\prod_{i=1}^{n} C_i}{(C_m)^n} \qquad \text{(Eq. 9}a\text{)}$$

or:

$$\log S_c^n = n \log \frac{1}{C_m} - \sum_{i=1}^{n} \log \frac{1}{C_i} \qquad \text{(Eq. 9}b\text{)}$$

If the various C_i's and C_m's in Eq. 9*b* are substituted by their functional expressions as represented by Eqs. 2–5, the following is obtained:

$$\log S_c^n = n\left(a_{0m} + \sum_{j=1}^{r_m} a_{jm}x_{jm}\right) - \sum_{i=1}^{n}\sum_{j=1}^{r_i} a_{ji}x_{ji} - \sum_{i=1}^{n} a_{0i} \qquad \text{(Eq. 10)}$$

The series of values of physicochemical parameters that maximizes $\log S_c^n$ should identify the molecule whose action is the best compromise between therapeutic activity and side effects. This calculus method of complex selectivity is based on the linear combination of the single linear combinations that correlate the main effect and the side effects with their relative physicochemical parameters. In synthesis, this calculus method of quantitative structure–selectivity relationships presumes knowledge of the structure–activity relationships.

A different approach may consist in direct analysis of the eventual correlation between all of the experimental data properly combined according to Eq. 9*a* or 9*b* in a series of $\log S_c^n$ values and the physicochemical parameters:

$$\log S_c^n = a_0 + \sum_{1}^{r} a_r x_r \qquad \text{(Eq. 11)}$$

Equation 11 is a generalization of Eq. 10.

0022-3549/79/0900-1081$01.00/0
© 1979, American Pharmaceutical Association

Table I—Penicillins: Compounds, Constants, Activities, and Observed and Calculated Values of Log S_c^n

	Compound	R_m^a	Activity[b] against *S. aureus*	Activity[b] against *E. coli*	Activity[b] against *T. pallidum*	Log S_c^2, Eq. 12[c] Obs.[f]	Log S_c^2, Eq. 12[c] Calc.	Log S_c^1, Eq. 13[d] Obs.[f]	Log S_c^1, Eq. 13[d] Calc.	Log S_c^1, Eq. 14[e] Obs.[f]	Log S_c^1, Eq. 14[e] Calc.
I	Dicloxacillin	1.63	4.23	0.66	4.89	2.91	3.43	3.57	3.95	−0.66	−0.52
II	Nafcillin	1.39	3.72	0.72	4.54	2.18	2.95	3.00	3.58	−0.82	−0.63
III	Cloxacillin	1.34	4.10	0.86	4.85	2.49	2.85	3.24	3.50	−0.75	−0.65
IV	Oxacillin	1.05	3.98	0.93	4.84	2.19	2.27	3.05	3.05	−0.86	−0.78
V	Phenethicillin	1.03	4.80	1.06	5.10	3.44	2.23	3.74	3.02	−0.30	−0.79
VI	Penicillin V	0.89	5.14	1.72	5.78	2.78	1.95	3.42	2.81	−0.64	−0.85
VII	Benzylpenicillin	0.55	4.85	2.09	5.76	1.85	1.27	2.76	2.28	−0.91	−1.01
VIII	Methicillin	0.47	3.15	0.85	4.50	0.95	1.11	2.30	2.15	−1.35	−1.04
IX	Ampicillin	0.08	4.35	3.10	5.43	0.17	0.33	1.25	1.55	−1.08	−1.22
X	Methylenampicillin	−0.29	3.87	2.94	5.14	−0.34	−0.41	0.93	0.98	−1.27	−1.38
XI	Carbenicillin	−0.46	3.45	3.12	5.16	−1.38	−0.75	0.33	0.71	−1.71	−1.46

[a] Chromatographic parameters. See Ref. 6, p. 513. [b] The biological activity is expressed as log $1/C$, where C is the molar (mM × 10^{-2}) concentration of each antibiotic that gives an inhibition diameter of 20 mm. See Ref. 6, p. 513. [c] Equation 12: log S_c^2 = 2.00 (±0.67) R_m + 0.17 (±0.65). [d] Equation 13: log S_c^1 = 1.55 (±0.47) R_m + 1.43 (±0.45). [e] Equation 14: log S_c^1 = 0.45 (±0.25) R_m − 1.25 (±0.24). [f] Equation 9*b*.

Table II—Alkylchlorophenols: Compounds, Constants, Activities, and Observed and Calculated Values of Log S_c^n

	Compound	Log P^a	Activity[b] Against *S. aureus*	Activity[b] Against *S. typhosa*	Activity[b] Against *S. hemolyticus*	Log S_c^2, Eq. 15[c] Obs.[b]	Log S_c^2, Eq. 15[c] Calc.	Log S_c^1, Eq. 17[d] Obs.[f]	Log S_c^1, Eq. 17[d] Calc.	Log S_c^1, Eq. 19[e] Obs.[b]	Log S_c^1, Eq. 19[e] Calc.
XII	4-Chloro	2.39	0.77	0.77	0.78	−0.01	0.16	0.00	0.08	−0.01	0.08
XIII	4-Chloro-2-methyl	2.89	1.28	1.28	1.23	0.05	−0.03	0.00	−0.08	0.05	0.05
XIV	4-Chloro-2-ethyl	3.39	1.76	1.68	1.72	0.12	−0.07	0.08	−0.09	0.04	0.02
XV	4-Chloro-2-*n*-propyl	3.89	2.23	2.23	2.15	0.08	0.06	0.00	0.05	0.08	0.01
XVI	4-Chloro-2-*n*-butyl	4.39	2.70	2.44	2.69	0.27	0.34	0.26	0.33	0.01	0.01
XVII	4-Chloro-2-*n*-amyl	4.89	3.03	2.52	3.07	0.47	0.79	0.51	0.77	−0.04	0.02
XVIII	4-Chloro-2-*sec*-amyl	4.69	2.82	2.00	2.82	0.82	0.59	0.82	0.58	0.00	0.01
XIX	4-Chloro-2-hexyl	5.39	3.45	1.72	3.48	1.70	1.39	1.73	1.35	−0.03	0.04
XX	2-Chloro	2.15	0.60	0.53	0.43	0.24	0.31	0.07	0.21	0.17	0.10
XXI	2-Chloro-4-methyl	2.65	1.06	0.98	0.93	0.21	0.04	0.08	−0.02	0.13	0.06
XXII	2-Chloro-4-ethyl	3.15	1.42	1.46	1.40	−0.02	−0.07	−0.04	−0.10	0.02	0.03
XXIII	2-Chloro-*n*-propyl	3.65	1.77	1.83	1.80	−0.09	−0.02	−0.06	−0.04	−0.03	0.02
XXIV	2-Chloro-4-*n*-butyl	4.15	2.27	2.23	2.24	0.07	0.19	0.04	0.18	0.03	0.01
XXV	2-Chloro-4-*n*-amyl	4.65	2.78	2.22	2.67	0.67	0.55	0.56	0.54	0.11	0.01
XXVI	2-Chloro-4-*tert*-amyl	4.33	2.42	1.83	2.47	0.54	0.30	0.59	0.29	−0.05	0.01
XXVII	4-Chloro-3-methyl	2.95	1.24	1.21	1.24	0.03	−0.04	0.03	−0.09	0.00	0.04
XXVIII	4-Chloro-3,5-dimethyl	3.51	1.63	1.70	1.66	−0.10	−0.05	−0.07	−0.07	−0.03	0.02
XXIX	4-Chloro-6-ethyl-3-methyl	3.95	1.96	2.07	2.00	−0.15	0.08	−0.11	0.07	−0.04	0.01
XXX	4-Chloro-6-*n*-propyl-3-methyl	4.45	2.60	2.42	2.54	0.24	0.39	0.18	0.38	0.06	0.01
XXXI	4-Chloro-6-isopropyl-3-methyl	4.25	2.47	2.32	2.43	0.19	0.25	0.15	0.24	0.04	0.01
XXXII	4-Chloro-2-ethyl-3,5-dimethyl	4.51	2.32	1.96	2.27	0.41	0.43	0.36	0.42	0.05	0.01
XXXIII	4-Chloro-6-*sec*-butyl-3-methyl	4.77	2.86	1.96	2.85	0.91	0.66	0.90	0.65	0.01	0.02
XXXIV	4-Chloro-2-isopropyl-3,5-dimethyl	4.81	2.82	2.24	2.82	0.58	0.70	0.58	0.69	0.00	0.02
XXXV	4-Chloro-6-diethylmethyl-3-methyl	5.25	3.19	1.78	3.10	1.50	1.20	1.41	1.17	0.09	0.03
XXXVI	4-Chloro-6-isopropyl-2-ethyl-3-methyl	5.25	2.66	2.11	2.60	0.61	1.20	0.55	1.17	0.06	0.03
XXXVII	4-Chloro-2-*sec*-butyl-3,5-dimethyl	5.31	3.11	1.81	3.10	1.31	1.28	1.30	1.25	0.01	0.03

[a] Octanol-water partition coefficients. See Ref. 7, p. 432. [b] The biological activity is expressed as log PC', where PC' is the phenol coefficient converted to a molar basis. See Ref. 7, pp. 431, 432. The biological activity is the minimum concentration effective in 10 min. See Ref. 8, p. 2577. [c] Equation 15: log S_c^2 = −2.07 (±0.81) log P + 0.32 (±0.10) (log P)^2 + 3.30 (±1.51). [d] Equation 17: log S_c^1 = 1.89 (±0.82) log P + 0.30 (±0.11) (log P)^2 + 2.90 (±1.52). [e] Equation 19: log S_c^1 = −0.18 (±0.20) log P + 0.02 (±0.03) (log P)^2 + 0.39 (±0.37). [f] Equation 9*b*.

Table III—Penicillins: Regression Equations Generated from Table I Data According to Eq. 11

	Equation[a]	r	s	EV	F	p
Main effect: against *S. aureus*	12. log S_c^2 = 2.00 (±0.67)R_m + 0.17 (±0.65)	0.91	0.66	0.81	43.82	<0.01
Side effect: against *E. coli*	13. log S_c^1 = 1.55 (±0.47)R_m + 1.43 (±0.45)	0.93	0.46	0.84	53.60	<0.01
Side effect: against *T. pallidum*	14. log S_c^1 = 0.45 (±0.25)R_m − 1.25 (±0.24)	0.80	0.25	0.60	15.68	<0.01

[a] n = 11.

When one considers only one side effect, *i.e.*, when n = 1, the meaning of log S_c^n is obvious; it expresses the relationship between the main effect and the side effect in a qualitative and quantitative way. If log S_c^n is positive, it means that the main effect prevails over the side effect and the value of log S_c^n indicates on a logarithmic scale to what extent the former is superior to the latter. If, on the contrary, log S_c^n is negative, the side effect is stronger than the main effect. When the value of log S_c^n is near zero, the effects are of similar intensities and, therefore, the molecules are hardly selective. The larger the absolute value of S_c^n, the greater is the prevalence of one effect over the other.

If $n > 1$, *i.e.*, if more than one side effect is considered at a time, the question becomes more complicated. If $n = 2$ and log $S_c^2 > 0$ starting from Eq. 9*b*, the following is obtained:

$$2 \log \frac{1}{C_m} > \left(\log \frac{1}{C_1} + \log \frac{1}{C_2} \right)$$

This relationship holds for three different situations. In Case A:

$$\log \frac{1}{C_m} > \log \frac{1}{C_1}$$

$$\log \frac{1}{C_m} > \log \frac{1}{C_2}$$

In Case B:

$$\log \frac{1}{C_m} > \log \frac{1}{C_1}$$

$$\log \frac{1}{C_m} < \log \frac{1}{C_2}$$

with:

$$\log \frac{1}{C_m} < \log \frac{1}{C_2} < \left(2 \log \frac{1}{C_m} - \log \frac{1}{C_1} \right)$$

Table IV—Alkylchlorophenols: Regression Equations Generated from Table II Data According to Eq. 11

	Equation[a]	r	s	EV	F	P
Main effect: against *S. aureus*	15. $\log S_c^2 = -2.07\ (\pm 0.81) \log P + 0.32\ (\pm 0.10)(\log P)^2 + 3.30\ (\pm 1.51)$	0.91	0.21	0.81	55.63	<0.01
	16. $\log S_c^2 = 0.39\ (\pm 0.15) \log P - 1.16\ (\pm 0.63)$	0.73	0.35	0.51	27.28	<0.01
Side effect: against *S. typhosa*	17. $\log S_c^1 = 1.89\ (\pm 0.82) \log P + 0.30\ (\pm 0.11)(\log P)^2 + 2.90\ (\pm 1.52)$	0.91	0.22	0.81	54.68	<0.01
	18. $\log S_c^1 = 0.40\ (\pm 0.15) \log P - 1.25\ (\pm 0.61)$	0.75	0.33	0.55	31.91	<0.01
Side effect: against *S. hemolyticus*	19. $\log S_c^1 = -0.18\ (\pm 0.20) \log P + 0.02\ (\pm 0.03)(\log P)^2 + 0.39\ (\pm 0.37)$	0.42	0.05	0.11	2.49	>0.1
	20. $\log S_c^1 = -0.02\ (\pm 0.02) \log P + 0.09\ (\pm 0.10)$	0.26	0.06	0.03	1.77	>0.1

[a] $n = 26$.

In Case C:

$$\log \frac{1}{C_m} < \log \frac{1}{C_1}$$

$$\log \frac{1}{C_m} > \log \frac{1}{C_2}$$

with:

$$\log \frac{1}{C_m} < \log \frac{1}{C_1} < \left(2 \log \frac{1}{C_m} - \log \frac{1}{C_2}\right)$$

Case A is the situation of a molecule whose main effect is stronger than the two side effects. In Cases B and C, the main effect is stronger than one side effect but not the other. Nevertheless, under the given conditions, the value of $\log S_c^2$ is greater than zero. In these cases, the sign of $\log S_c^2$ indicates that the main effect prevails over the sum of the two side effects. However, it is not possible to establish with certainty if the main effect is greater than one single side effect or if it is greater than both of them.

In an analogous way, it can be stated that the undesired side effects in their totality are more intense than the main effect when $\log S_c^2 < 0$, but the latter could be stronger than one of the former.

These considerations can be extended to cases where $n > 2$. Generally, with increasing n, one will obtain less information from $\log S_c^n$. Nevertheless, the absolute value and the sign of $\log S_c^n$ can give useful information about the prevalence of the main effect or of the total of the side effects.

During drug design such information should be able to direct the synthetic work toward molecules with the highest forecasted $\log S_c^n$ values. However, more detailed knowledge of the molecular action may require comparing each effect with the main effect by studying the trend of the corresponding series of $\log S_c^1$ values.

EXPERIMENTAL

The applicability of the proposed model was tested using literature data regarding a group of penicillins (6) and a larger group of alkylchlorophenols (7). Data on the activities of the pencillins against *Staphylococcus aureus, Escherichia coli,* and *Treponema pallidum* and of the alkylchlorophenols against *S. aureus, Salmonella typhosa,* and *Streptococcus hemolyticus* were available.

Methods—None of the activities produced by the two series of molecules could be considered strictly as side effects. Nevertheless, these examples were chosen because exact quantitative data on undesired side effects are often unavailable.

Moreover, the definition of a pharmacological activity as a side effect is not always univocal and absolute but can depend on contingent research requirements. Furthermore, the aim of this study was to focus on the separability of the single effects more than on their specific characteristics. Therefore, the cases illustrated have essentially a paradigmatic value and show how the mathematical model can be applied and what conclusions can be deduced from it.

In both cases, one of the activities was taken arbitrarily as the main effect and the others as side effects. By comparing contemporaneously the main effect with the two side effects, the observed $\log S_c^2$ and the relative regressions were obtained. The observed values of $\log S_c^1$ and the corresponding regressions were obtained by comparing the main effect with each single side effect.

Penicillins—The experimental data on the activities against *S. aureus, E. coli,* and *T. pallidum* and the values of the chromatographic parameter R_m were those published previously (6). The same paper (6) reported the methods of culturing and preparing the microorganisms for the tests. The activity arbitrarily considered as the main effect was the one against *S. aureus*. These data are given in Table I together with the observed and calculated values of $\log S_c^n$.

Alkylchlorophenols—The data on the activities aginst *S. aureus, S. typhosa,* and *S. hemolyticus* and the values of the physicochemical parameter $\log P$ were those provided in the literature (7, 8). The bacteriological techniques were the same as those used by the U.S. Department of Agriculture (9) and have been reported (10). As in the preceding example, the activity against *S. aureus* was arbitrarily chosen as the main effect. The biological data are given in Table II, together with the relative values of $\log S_c^n$.

Regression Analysis—The regression equations were generated by the least-squares method (11). The relative calculations and the statistics were performed by an HP-97 desk minicomputer.

The values of R_m and $\log P$ are given in Tables I and II, respectively. The reported statistics are r, s, the explained variance EV, F values, and p levels. The significance of the regression coefficients was tested at the $p < 0.05$ level by the t test.

RESULTS

The observed values of $\log S_c^n$ were obtained from Eq. 9*b*. These values were correlated directly with the physicochemical parameters according to Eq. 11.

The regressions used to calculated $\log S_c^n$ were generated from the data of Tables I and II are are reported in Table III for the penicillins and in Table IV for the alkylchlorophenols. In this last case, since the introduction of $(\log P)^2$ improved the statistics, the calculated values of $\log S_c^n$ reported in Table II are from Eqs. 15, 17, and 19 of Table IV.

DISCUSSION

The first point that can be deduced from the results is the possibility of correlating directly the selectivity of congener molecules, expressed as $\log S_c^n$, and the structural physicochemical parameters. This was clear from the regression statistics.

Second, the observed $\log S_c^2$ values identified the most selective molecules, even if they were not the most active ones. In fact, from Table I it is evident that I and V are the most selective compounds in their action against *S. aureus* whereas the most active molecule is VI, which is not as selective as the first two. Similarly, the least selective molecule is XI, whereas the least active one is VIII.

The values of $\log S_c^2$ calculated according to Eq. 12 confirm these conclusions with good approximation, even if there is some contradiction with the observed values. This example belongs to Case B (see *Theoretical*), where the main effect is stronger than one of the side effects but not as intense as the other one. This is indicated clearly by the trend of the observed and calculated values of $\log S_c^1$ relative to Eqs. 13 and 14. The values relative to Eq. 14 are all negative, indicating that the side effect against *T. pallidum* is more intense than the main effect against *S. aureus*.

Similar considerations may be deduced regarding the alkylchlorophenols, but in this example the set of the most selective molecules is the same as the most active ones. The less selective compounds, however, do not coincide with the less active ones.

The statistics of Eqs. 14, 19, and 20 indicated a significant worsening of the quality of these regressions compared with the others. This result could be explained by the fact that in these cases the compared activities were carried out on pairs of Gram-positive microorganisms. *S. aureus* and *S. hemolyticus* are Gram-positive; *T. pallidum,* although lacking a cell wall, is sensitive to the antibiotics in an analogous way to Gram-positive bacteria. The R_m and $\log P$ values express the lipophilicity of molecules and, therefore, their ability to cross the cell wall. It is, therefore, likely that these parameters do satisfactorily explain selectivity and its variance in the case of Gram-dissimilar bacteria but that they lead to worse results with Gram-similar bacteria.

CONCLUSIONS

In conclusion, within the limits discussed, the use of log S_c^n should make easier and faster the search for, and the identification of, the therapeutically best molecules. Log S_c^n permits selectivity forecasting by methods and techniques analogous to the ones (quantitative structure-selectivity relationships) utilized to forecast biological activity. Moreover, log S_c^n makes it easier and faster to compare the therapeutic characteristics of different molecules since it permits selectivity quantification in the presence of many side effects.

REFERENCES

(1) C. Hansch, A. R. Steward, and J. Iwasa, *Mol. Pharmacol.*, **1**, 87 (1965).

(2) A. Fujinami, A. Mine, and T. Fujita, *Agr. Biol. Chem.*, **38**, 1399 (1974).

(3) A. Fujinami, T. Satomi, A. Mine, and T. Fujita, *Pestic. Biochem. Physiol.*, **6**, 287 (1976).

(4) W. P. Purcell, G. E. Bass, and J. Clayton, "Strategy of Drug Design: A Guide to Biological Activity," Wiley, New York, N.Y., 1973.

(5) E. Fingl and D. M. Woodbury, in "The Pharmacological Basis of Therapeutics," 4th ed., L. S. Goodman and A. Gilman, Eds., Macmillan, London, England, 1970, pp. 21, 22.

(6) G. L. Biagi, M. C. Guerra, A. M. Barbaro, and M. F. Gamba, *J. Med. Chem.*, **13**, 511 (1970).

(7) E. J. Lien, C. Hansch, and S. M. Anderson, *ibid.*, **11**, 430 (1968).

(8) E. Klarmann, V. A. Shternov, and L. W. Gates, *J. Am. Chem. Soc.*, **55**, 2576 (1933).

(9) G. L. A. Ruehle and C. M. Brewer, "United States Food and Drug Administration Methods of Testing Antiseptics and Disinfectants," Circular 198, U.S. Department of Agriculture, Dec. 1931.

(10) E. Klarmann, V. A. Shternov, and L. W. Gates, *J. Lab. Clin. Med.*, **19**, 835 (1934).

(11) G. W. Snedecor and W. G. Cochran, "Statistical Methods," 6th ed., Iowa State University Press, Ames, Iowa, 1967.

ACKNOWLEDGMENTS

The authors thank Dr. William P. Purcell, University of Tennessee, Memphis, Tenn., for helpful comments.

Hydrodynamic Characterization of a Spin-Filter Dissolution Device

J. W. MAUGER ˣ, S. A. HOWARD, and A. KHWANGSOPHA

Received December 26, 1978, from the *School of Pharmacy, West Virginia University, Morgantown, WV 26506.* Accepted for publication March 1, 1979.

Abstract □ The spin-filter dissolution device was characterized using a two-dimensional convective diffusion model. Experimental model testing involved analysis of dissolution rates from nondisintegrating salicylic acid disks. The disks were prepared as double-layer tablets, with an ethylcellulose layer as a nondissolving surface. For each dissolution run, the disk was positioned so that the dissolving salicylic acid surface was parallel to the flow of the circulating fluid. Experimental variables included the stirring speed, the tablet radius, and the distance of the tablet from the stirring source. At the farthest distance from the stirring source, the average numerical exponents for stirring speed and tablet radius were 0.58 and 1.54, respectively, which compare favorably with the values of 0.50 and 1.50 from the model. When the dissolving salicylic acid surface was positioned closer to the stirring source, the numerical exponent for the stirring speed increased significantly, while the average numerical exponent for the tablet radius was lowered to 1.07, indicating a change in dissolution mechanism as a function of distance from the stirring source. These data indicate that dissolution rates are not necessarily proportional to surface area as predicted by the Nernst equation and that distance from the stirring source is significant.

Keyphrases □ Hydrodynamics—dissolution devices, spin filter, salicylic acid disks □ Models, hydrodynamic—dissolution devices, spin filter, salicylic acid disks □ Dissolution devices—spin filter, hydrodynamic analysis, models

Knowledge of critical operating variables for a dissolution device is important to the pharmaceutical scientist interested in product development, quality control, and research applications. A recent paper (1) discussed certain operating variables for the spin-filter dissolution device developed by Shah *et al.* (2). The results of this investigation indicate that the dissolution of a tablet placed in a basket is much more rapid from the face of the tablet resting on the bottom of the basket than from the face inside the basket. This effect was duplicated at stirring speeds of 300 and 500 rpm.

Understanding and predicting the dissolution performance for a given dissolution instrument require evaluating the instrument with a justifiable model. The purpose of the present study was to continue an evaluation of the spinning-filter device *via* a convective diffusion model based on a physically realistic and mathematically sound development.

THEORY

The model chosen is a classical one involving the flow of incompressible fluids past immersed bodies. For a nondissolving plate immersed in a fluid where the free stream velocity is U (centimeters per second), the velocity of the fluid in contact with the surface of the plate ($y = 0$) is assumed to be zero and frictional resistance retards the moving fluid in a thin layer near the wall. A property of the hydrodynamic boundary layer, h_1 (centimeters), is that its thickness is a function of the length of the plate. It is assumed that h_1 is zero at the leading edge of the plate ($x = 0$). A functional relationship between the hydrodynamic boundary layer, h_1, the free stream velocity, U, and the length of the plate, x, is:

$$h_1 = 4.64\left(\frac{\nu x}{U}\right)^{1/2} \qquad \text{(Eq. 1)}$$

Thus, h_1 increases as a function of the square root of the distance along the x axis of the plate and diminishes by a factor equal to the reciprocal square root of the free stream velocity. As Levich (3) emphasized, in reality h_1 is not a distinct distance. Instead, it represents a transition from viscous flow in the hydrodynamic boundary layer to inviscid flow in the main stream and is smooth and gradual. The thickness is commonly defined as the distance from the wall ($y = 0$) to a point where the velocity in the x direction is 90% of the free stream velocity.

A mass transfer model under conditions of forced convection can now be evaluated. Once again, visualize a plate immersed in a fluid stream.

0022-3549/79/0900-1084$01.00/0

© 1979, American Pharmaceutical Association

CONCLUSIONS

In conclusion, within the limits discussed, the use of log S_c^n should make easier and faster the search for, and the identification of, the therapeutically best molecules. Log S_c^n permits selectivity forecasting by methods and techniques analogous to the ones (quantitative structure-selectivity relationships) utilized to forecast biological activity. Moreover, log S_c^n makes it easier and faster to compare the therapeutic characteristics of different molecules since it permits selectivity quantification in the presence of many side effects.

REFERENCES

(1) C. Hansch, A. R. Steward, and J. Iwasa, *Mol. Pharmacol.*, **1**, 87 (1965).

(2) A. Fujinami, A. Mine, and T. Fujita, *Agr. Biol. Chem.*, **38**, 1399 (1974).

(3) A. Fujinami, T. Satomi, A. Mine, and T. Fujita, *Pestic. Biochem. Physiol.*, **6**, 287 (1976).

(4) W. P. Purcell, G. E. Bass, and J. Clayton, "Strategy of Drug Design: A Guide to Biological Activity," Wiley, New York, N.Y., 1973.

(5) E. Fingl and D. M. Woodbury, in "The Pharmacological Basis of Therapeutics," 4th ed., L. S. Goodman and A. Gilman, Eds., Macmillan, London, England, 1970, pp. 21, 22.

(6) G. L. Biagi, M. C. Guerra, A. M. Barbaro, and M. F. Gamba, *J. Med. Chem.*, **13**, 511 (1970).

(7) E. J. Lien, C. Hansch, and S. M. Anderson, *ibid.*, **11**, 430 (1968).

(8) E. Klarmann, V. A. Shternov, and L. W. Gates, *J. Am. Chem. Soc.*, **55**, 2576 (1933).

(9) G. L. A. Ruehle and C. M. Brewer, "United States Food and Drug Administration Methods of Testing Antiseptics and Disinfectants," Circular 198, U.S. Department of Agriculture, Dec. 1931.

(10) E. Klarmann, V. A. Shternov, and L. W. Gates, *J. Lab. Clin. Med.*, **19**, 835 (1934).

(11) G. W. Snedecor and W. G. Cochran, "Statistical Methods," 6th ed., Iowa State University Press, Ames, Iowa, 1967.

ACKNOWLEDGMENTS

The authors thank Dr. William P. Purcell, University of Tennessee, Memphis, Tenn., for helpful comments.

Hydrodynamic Characterization of a Spin-Filter Dissolution Device

J. W. MAUGER ˣ, S. A. HOWARD, and A. KHWANGSOPHA

Received December 26, 1978, from the *School of Pharmacy, West Virginia University, Morgantown, WV 26506.* Accepted for publication March 1, 1979.

Abstract □ The spin-filter dissolution device was characterized using a two-dimensional convective diffusion model. Experimental model testing involved analysis of dissolution rates from nondisintegrating salicylic acid disks. The disks were prepared as double-layer tablets, with an ethylcellulose layer as a nondissolving surface. For each dissolution run, the disk was positioned so that the dissolving salicylic acid surface was parallel to the flow of the circulating fluid. Experimental variables included the stirring speed, the tablet radius, and the distance of the tablet from the stirring source. At the farthest distance from the stirring source, the average numerical exponents for stirring speed and tablet radius were 0.58 and 1.54, respectively, which compare favorably with the values of 0.50 and 1.50 from the model. When the dissolving salicylic acid surface was positioned closer to the stirring source, the numerical exponent for the stirring speed increased significantly, while the average numerical exponent for the tablet radius was lowered to 1.07, indicating a change in dissolution mechanism as a function of distance from the stirring source. These data indicate that dissolution rates are not necessarily proportional to surface area as predicted by the Nernst equation and that distance from the stirring source is significant.

Keyphrases □ Hydrodynamics—dissolution devices, spin filter, salicylic acid disks □ Models, hydrodynamic—dissolution devices, spin filter, salicylic acid disks □ Dissolution devices—spin filter, hydrodynamic analysis, models

Knowledge of critical operating variables for a dissolution device is important to the pharmaceutical scientist interested in product development, quality control, and research applications. A recent paper (1) discussed certain operating variables for the spin-filter dissolution device developed by Shah *et al.* (2). The results of this investigation indicate that the dissolution of a tablet placed in a basket is much more rapid from the face of the tablet resting on the bottom of the basket than from the face inside the basket. This effect was duplicated at stirring speeds of 300 and 500 rpm.

Understanding and predicting the dissolution performance for a given dissolution instrument require evaluating the instrument with a justifiable model. The purpose of the present study was to continue an evaluation of the spinning-filter device *via* a convective diffusion model based on a physically realistic and mathematically sound development.

THEORY

The model chosen is a classical one involving the flow of incompressible fluids past immersed bodies. For a nondissolving plate immersed in a fluid where the free stream velocity is U (centimeters per second), the velocity of the fluid in contact with the surface of the plate ($y = 0$) is assumed to be zero and frictional resistance retards the moving fluid in a thin layer near the wall. A property of the hydrodynamic boundary layer, h_1 (centimeters), is that its thickness is a function of the length of the plate. It is assumed that h_1 is zero at the leading edge of the plate ($x = 0$). A functional relationship between the hydrodynamic boundary layer, h_1, the free stream velocity, U, and the length of the plate, x, is:

$$h_1 = 4.64\left(\frac{\nu x}{U}\right)^{1/2} \qquad \text{(Eq. 1)}$$

Thus, h_1 increases as a function of the square root of the distance along the x axis of the plate and diminishes by a factor equal to the reciprocal square root of the free stream velocity. As Levich (3) emphasized, in reality h_1 is not a distinct distance. Instead, it represents a transition from viscous flow in the hydrodynamic boundary layer to inviscid flow in the main stream and is smooth and gradual. The thickness is commonly defined as the distance from the wall ($y = 0$) to a point where the velocity in the x direction is 90% of the free stream velocity.

A mass transfer model under conditions of forced convection can now be evaluated. Once again, visualize a plate immersed in a fluid stream.

0022-3549/79/0900-1084$01.00/0

© 1979, American Pharmaceutical Association

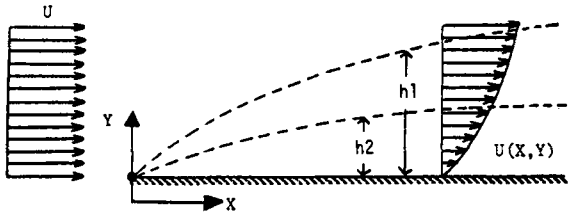

Figure 1—*Development of hydrodynamic boundary layer and diffusion layer.*

Now, however, the plate has a dissolving surface; as a fluid flows past the immersed solid, a hydrodynamic boundary layer, h_1, as well as a diffusion layer, h_2, forms (Fig. 1). The relative thickness of the two boundary layers is given by:

$$\frac{h_2}{h_1} = \left(\frac{D}{\nu}\right)^{1/3} \quad \text{(Eq. 2)}$$

where D is the diffusion coefficient (square centimeters per second) of the solute and ν is the kinematic viscosity (square centimeters per second) of the dissolution fluid. For dissolving solids of pharmaceutical interest, D is $\sim 10^{-6}$ and ν for water is $\sim 10^{-2}$. Therefore, h_2/h_1 is expected to be on the order of 0.05/1. The equation that relates h_2 and h_1 is:

$$h_2 = \left(\frac{D}{\nu}\right)^{1/3} (4.46) \left(\frac{\nu x}{U}\right)^{1/2} \quad \text{(Eq. 3)}$$

The diffusional flux, j (grams per second square centimeter), to the plate is:

$$j = -D\left(\frac{dc}{dy}\right) \quad \text{(Eq. 4)}$$

where (dc/dy) is the concentration gradient. We are interested in evaluating (dc/dy) at the wall, *i.e.*, where $y = 0$. Differentiating a particular concentration profile[1] that provides a functional relationship between c and y yields:

$$\left(\frac{dc}{dy}\right)_{y=0} = \frac{-1.5C_s}{h_2} \quad \text{(Eq. 5)}$$

Substituting the expression for h_2 from Eq. 3 gives the diffusional flux for the model shown in Fig. 1:

$$j = (0.32)(D)(C_s)\left(\frac{\nu}{D}\right)^{1/3}\left(\frac{U}{\nu x}\right)^{1/2} \quad \text{(Eq. 6)}$$

where C_s is the saturation solubility (grams per cubic centimeter). This equation expresses the physical situation where the diffusional flux decreases as the reciprocal of the square root of the distance from the leading edge of the plate. As Levich (3) pointed out, different points along the plate are not uniformly accessible to diffusion. Furthermore, Eqs. 3 and 6 express a physically and mathematically defined diffusion layer rather than allow it to be empirically defined according to the commonly used Nernst equation. The mechanistic inadequacy involved with the application of the Nernst theory was commented on previously (3, 5, 6).

The governing equations for the model shown in Fig. 1 recognize velocity components and concentration gradients for both the x and y axes (3). Under particular experimental conditions, the convection term in one axis and the diffusional term in another axis may be equated with zero (5). However, the present experimental design seeks to test a model that conforms with Fig. 1.

EXPERIMENTAL

The dissolution rates were determined in a modified rotating-filter–stationary basket dissolution device[2,3]. In place of the stationary basket, a nut and holder assembly was developed that would permit the dissolution from a constant area surface of a nondisintegrating tablet disk.

The compound selected for study was salicylic acid. Double-layer tablets of 0.624-cm radius consisted of 150 mg of salicylic acid and 150 mg of ethylcellulose; double-layer tablets of 0.451-cm radius consisted of 85 mg of salicylic acid and 85 mg of ethylcellulose. These two ingredients were compressed at 2273 kg of pressure for 15 sec on a hydraulic press[4]. All tablets were 0.194 cm thick. Epoxy glue was used to connect the nut and double-layer tablet for use with the holder device.

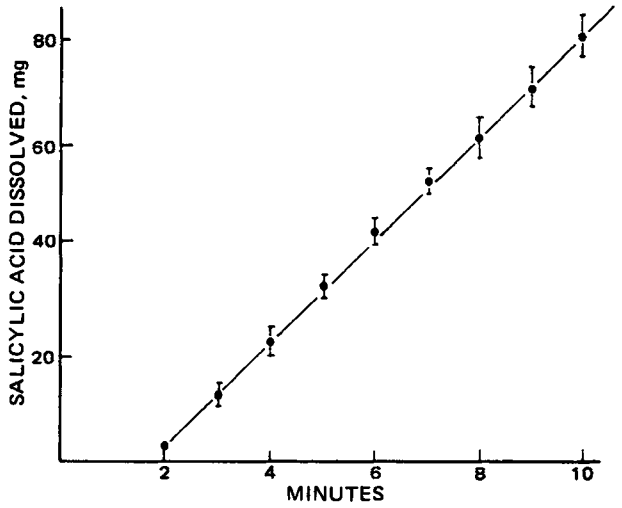

Figure 2—*Typical dissolution profile for the double-layer tablet: (tablet radius of 0.624 cm, position of 1.25 cm from the stirring source, and stirring speed of 400 rpm).*

The stirring speeds were controlled by a magnetic stirrer[3] with a tachometer, and a strobe light was used to check the speeds. A 0.5-μm stainless steel filter[3] was used in the spinning-filter device. Temperature was maintained at 37°. The dissolution medium consisted of an aqueous solution buffered to pH 1.2 with hydrochloric acid buffer, maintaining the dissolved drug in the unionized form.

The position of the tablet in the dissolution apparatus is important. The dissolution apparatus was set up as originally described (2) with the spinning filter in a vertical position at the center of the dissolution flask. The vertically located spinning filter represents the y axis. The vertical location of the tablet was kept constant at the vertical midpoint of the spinning filter. The horizontal distance of the tablet from the spinning filter along the x axis was varied; 2.58 cm from the center of the tablet holder to the edge of the spinning filter was the *farthest* distance studied, and 1.25 cm from the center of the tablet holder to the edge of the rotating filter was the *nearest* distance studied. The nondissolving ethylcellulose side of the tablet was placed up in relation to the bottom of the flask, and the dissolving salicylic acid side was placed down and parallel to the flask bottom.

The assay was conducted spectrophotometrically at 305 nm. All experiments were conducted in the same dissolution flask, thereby eliminating cell to cell variation. The ethylcellulose did not contribute to dissolution and showed no observable change after dissolution.

The spectrophotometer was allowed to warm up for ~20 min before the experiment was begun. Three runs were conducted for each stirring speed, and these studies were conducted using four stirring speeds: 200, 300, 400, and 500 rpm. Samples were withdrawn automatically at known time intervals and assayed on a spectrophotometer[5]. A calibration curve confirmed linearity throughout the absorbance range used.

RESULTS AND DISCUSSION

Dissolution experiments were done in triplicate for each experimental condition. A representative dissolution profile for a particular set of experimental conditions is provided in Fig. 2. Each point shown is the average of three experiments, and the associated standard deviation is indicated by the vertical line. As anticipated, all dissolution data plotted in this way were linear and reproducible. The dissolution rates, R, were calculated from the data in Fig. 2 and a series of similar curves. For a circular disk wetted on one side, Eq. 6 becomes:

$$R = (1.58)(D)(C_s)\left(\frac{\nu}{D}\right)^{1/3}\left(\frac{U}{\nu}\right)^{1/2}(r)^{1.5} \quad \text{(Eq. 7)}$$

where R is the dissolution rate (grams per second) and r is the disk radius (centimeters). A logarithmic transformation of this expression leads to:

$$\ln R = \ln A + \tfrac{1}{2}\ln U + 1.5 \ln r \quad \text{(Eq. 8)}$$

[1] The concentration profile chosen was $C/C_s = 1\ 1.5(y/h_2) + 0.5(y/h_2)^3$. Details concerning the concentration profile and analysis of two-dimensional heat (mass) transfer models *via* Von Karman integral method are provided in Ref. 4.

[2] Courtesy of The Upjohn Co., Kalamazoo, Mich.

[3] The Virtis Co., Gardiner, NY 12525.

[4] Model K, hydraulic equipment, Fred S. Carver Inc., Summit, N.J.

[5] Hitachi Ltd., Tokyo, Japan.

Table I—Dissolution Rates (Milligrams per Minute) for the Salicylic Acid Disks Positioned 2.58 cm from the Stirring Source

Stirring Speed, rpm	Tablet Radius, cm 0.451	0.624	Numerical Coefficient for Tablet Radius (0.624/0.451)
200	0.00400	0.00677	1.62
300	0.00485	0.00767	1.41
400	0.00591	0.01000	1.69
500	0.00687	0.01090	1.42
			1.54 ± 0.142

where:

$$A = (1.58)(D)^{2/3}(\nu)^{-1/6}(C_s) \qquad \text{(Eq. 9)}$$

Of initial interest is the relationship between the dissolution rate and the stirring speed. A graphical presentation of the data is given in Fig. 3, where the natural logarithm of the mean dissolution rate[6] is plotted *versus* the natural logarithm of the stirring speed. The salicylic acid disks in this case were positioned 2.58 cm from the stirring source, the *farthest* distance studied. According to Eq. 7, the expected slope of these data is 0.5. For a tablet with a 0.451-cm radius, the least-squares slope is 0.61 with an associated standard error of 0.029; for a tablet having a 0.624-cm radius, the least-squares slope is 0.55 with an associated standard error of 0.050.

The average numerical coefficients relating the dissolution rate with the stirring speed are 0.58 for the experimental data and 0.50 according to theory. A deviation of 16% from the theory requires explanation. One possible reason is that the theory is not perfect in explaining the flow patterns developed by the spinning-filter device. The physical picture of the free stream flow patterns inherent in the model is a unidirectional flow, which is laminar and which will develop a well-behaved hydrodynamic boundary layer. The flow actually developed from the spinning-filter device is tangential.

Figure 4 is a plot of the natural logarithm of the mean dissolution rate *versus* the natural logarithm of stirring speed. These dissolution rates were generated with the salicylic acid disk positioned 1.25 cm from the stirring source, the *nearest* distance studied. The distance from the stirring source is of interest in an agitated vessel where it is reasonable to anticipate that the power generated by the stirrer will not be equally distributed throughout the vessel. The intensity of stirring is expected to be greater closer to the agitator. Therefore, the stirring coefficient may be a function of the distance of the dissolving disk from the stirring device, and these data test this relationship. For a tablet with a 0.451-cm radius, the least-squares slope is 0.80 with a standard error of 0.058; the least-squares slope for a tablet with a 0.624-cm radius is 0.66 with a standard error of 0.036. The stirring coefficients for both tablet radii are considerably above the anticipated value of 0.5 and validate the idea that the coefficient is a function of the stirring intensity or the distance of the disk from the agitation source.

An analysis of heat transfer with turbulent flow parallel to a flat plate

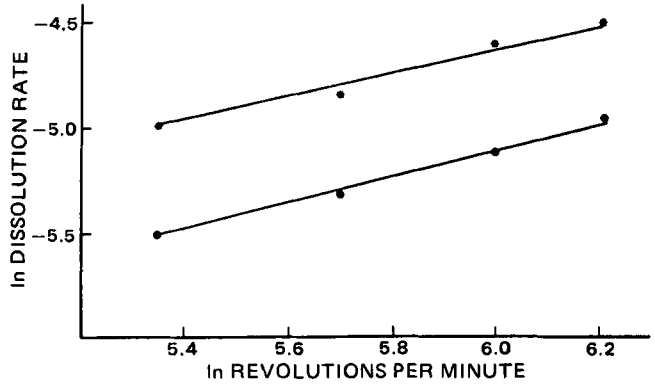

Figure 3—*Natural logarithm of dissolution rate* versus *natural logarithm of stirring speed for salicylic acid disks positioned 2.58 cm from the stirring device. Key (tablet radius):* ●, *0.451 cm; and* ∗, *0.624 cm.*

[6] Each point in Figs. 3 and 4 represents the average slopes from the dissolution profiles similar to those shown in Fig. 2.

Table II—Dissolution Rates (Milligrams per Minute) for the Salicylic Acid Disks Positioned 1.25 cm from the Stirring Source

Stirring Speed, rpm	Tablet Radius, cm 0.451	0.624	Numerical Coefficient for Tablet Radius (0.624/0.451)
200	0.00406	0.00640	1.40
300	0.00638	0.00860	0.920
400	0.00734	0.00980	0.890
500	0.00846	0.01190	1.05
			1.07 ± 0.234

(7) leads to a coefficient of 0.6–0.8. Therefore, the experimental stirring coefficients at closer distances may imply that a turbulent hydrodynamic boundary is present, with the result that the dissolution rate is more sensitive to the stirring speed. This finding is of practical importance because it indicates that one must be sensitive to the distance variable to generate reproducible dissolution data.

Further analysis shows that the average numerical coefficient relating the functional dependence of the dissolution rate with the tablet radius for a tablet positioned farthest from the stirring source is 1.54 (Table I). The expected value for the model is 1.5, and verification of this numerical coefficient is particularly important with regard to understanding the dissolution mechanism. As already discussed, the model expresses the fact that the dissolving plate is not uniformly accessible to diffusion.

This concept is inherent in the mathematical expressions given by Eqs. 3, 5, and 6 for the diffusion layer thickness. It is also important to compare this relationship with the commonly used Nernst theory, where one would expect the dissolution rate to be related to area and the expected numerical coefficient is 2 (area = πr^2). As Nelson and Shah (5, 6) verified, the Nernst theory does not provide for mechanistic insight under certain conditions of forced convection.

The data in Table II are for a tablet positioned closest to the stirring device and show that the average numerical coefficient for the tablet radius is 1.07, which is considerably lower than the expected value for the model of 1.5. More importantly, the coefficient varies with stirring speed. At 200 rpm, the coefficient is 1.40 and decreases noticeably at stirring speeds of 300, 400, and 500 rpm. Therefore, the original model is not successful in predicting the functional relationship between the dissolution rate and the tablet radius. The apparent lack of parallelism between the two curves shown in Fig. 4 leads one to believe that the original model must be modified to include an interaction term between the stirring speed and the tablet radius[7] to account for the apparent difference in flow patterns across the entire dissolution surface.

To learn more about the flow patterns, visualization studies were accomplished by adding phenolphthalein to the salicylic acid portion of the disk. The colored indicator appeared when the salicylic acid disk dissolved in an aqueous medium alkalinized with sodium hydroxide, thus allowing the flow pattern to be seen. In particular, patterns across the surface of the dissolving disk could be seen in detail. Colored photographs

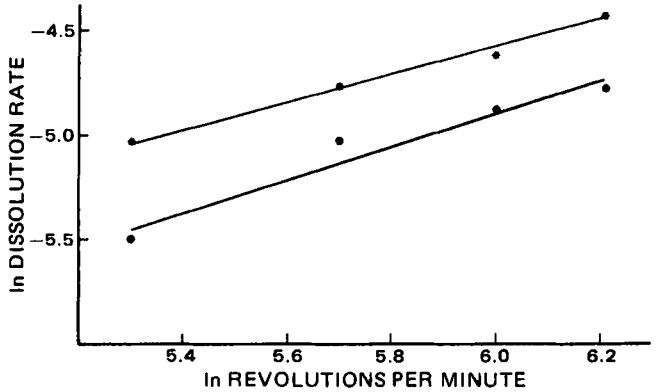

Figure 4—*Natural logarithm of dissolution rate* versus *natural logarithm of stirring speed for salicylic acid disks positioned 1.25 cm from the stirring device. Key (tablet radius):* ●, *0.451 cm; and* ∗, *0.624 cm.*

[7] From statistical analysis of the data, there is insufficient evidence to indicate that the two lines are not parallel at the 0.05 level of significance, but a lack of parallelism exists at the 0.10 level of significance.

were taken at the near and far positions with the filter turning at 300 rpm. These photographs showed that the flow at the tablet surface was uniform and parallel to the filter face with an even color distribution when the disk was at the far position from the stirring source. The tailing streams of color away from the tablet revealed the tangential nature of the stirring patterns. This overall visualization is reasonably close to that assumed by the model and is in keeping with the data analysis from the dissolution experiments.

For the near position, the colored photographs showed that the flow pattern at the surface was less uniform and in the direction of the spinning filter rather than parallel to it. Furthermore, a concentration of color appeared on the filter side of the tablet. The visualization procedure combined with dissolution data confirms that the flow pattern is influenced by the distance from the rotating stirring source. Dissolution rates measured from disintegrating tablets would presumably be influenced in a similar way, making basket placement a critical factor.

SUMMARY

At the farthest distance from the stirring source, the average numerical exponents for stirring speed and tablet radius were 0.58 and 1.54, respectively, which compares favorably with the theoretical values of 0.50 and 1.50. When the dissolving salicylic acid surface was positioned closer to the stirring source, the numerical exponent for the tablet radius was lowered to 1.07, indicating a change in dissolution as a function of distance from the stirring source. These data indicate that dissolution rates are not necessarily proportional to surface area, as predicted by the Nernst equation, and that distance from the stirring source is a significant factor. Convective diffusion models combined with easily accomplished visualization techniques provide the methodology needed to characterize various dissolution devices.

REFERENCES

(1) S. Howard, J. Mauger, A. Khwangsopha, and D. Pasquarelli, "Operating Variables for the Spin Filter Dissolution Device," presented at APhA Academy of Pharmaceutical Sciences, New York meeting, May 1977.

(2) A. C. Shah, C. B. Peot, and J. F. Ochs, *J. Pharm. Sci.*, **62**, 671 (1973).

(3) V. Levich, "Physiochemical Hydrodynamics," Prentice Hall, Englewood Cliffs, N.J., 1962.

(4) J. Knudsen and D. Katz, "Fluid Dynamics and Heat Transfer," McGraw-Hill, New York, N.Y., 1958, pp. 247–259, 473–481.

(5) K. G. Nelson and A. C. Shah, *J. Pharm. Sci.*, **64**, 610 (1975).

(6) A. C. Shah and K. G. Nelson, *ibid.*, **64**, 1519 (1975).

(7) J. Kestin and L. N. Persen, *Int. J. Heat Mass Transfer*, **5**, 355 (1962).

Linear Pharmacokinetics of Orally Administered Fenoprofen Calcium

J. F. NASH ˣ, L. D. BECHTOL, C. A. BUNDE *, R. J. BOPP, K. Z. FARID, and C. T. SPRADLIN

Received October 6, 1978, from the *Lilly Research Laboratories, Indianapolis, IN 46206.* Accepted for publication February 20, 1979.
*Present address: Cintest, Inc., Cincinnati, OH 45220.

Abstract □ The bioavailability of fenoprofen from three different fenoprofen calcium capsule formulations containing the equivalent of 60, 165, and 300 mg of fenoprofen was determined in two studies. In the first study, 12 subjects received one capsule of each formulation according to a three-period crossover design. The second study required each of 13 subjects to receive 300 mg of fenoprofen equivalent of the 60- and 300-mg capsules and 330 mg of the 165-mg capsule. The initial study provided information on the linearity of fenoprofen pharmacokinetics, and the second study established that the three capsule formulations were bioequivalent. The bioavailability parameters C_{max}, t_{max}, and $AUC_{0-12\ hr}$ for the drug in plasma were consistent with a linear pharmacokinetic model, as were the amounts of fenoprofen and hydroxyfenoprofen excreted in the urine. These data show linearity of kinetics for fenoprofen in plasma throughout the 60–300-mg dosage range after a single dose. Physical measurements of each capsule formulation drug content, weight variation, and dissolution showed the products to be uniform and readily soluble.

Keyphrases □ Fenoprofen—pharmacokinetics, oral administration, calcium salt □ Pharmacokinetics—fenoprofen calcium, oral administration □ Anti-inflammatory agents—fenoprofen calcium, pharmacokinetics, oral administration

Fenoprofen calcium[1] was shown to be a useful anti-inflammatory agent in osteoarthritis (1–4) and rheumatoid arthritis (5–16) in adults. To extend the therapeutic range of the compound, drug formulations containing 60–300 mg of fenoprofen equivalent as fenoprofen calcium[2] were selected for juvenile rheumatoid arthritis studies. This paper reports the linearity of fenoprofen pharmacokinetics, fenoprofen bioavailability, and the uniformity of drug excretion after a single-dose oral administration of capsules containing 60, 165, or 300 mg of fenoprofen equivalent in an adult population.

EXPERIMENTAL

Clinical Study Protocol—Healthy adult male volunteers, 18–50 years old, participated in the two studies. Their weight was ±10% of the ideal weight (17). The subjects had no history of significant GI disorder; hepatic, renal, hematological, or cardiovascular disease; or chronic alcoholism. Each subject underwent a urinalysis, hematology, and blood analysis[3] as well as a physical examination to ensure inclusion of only subjects in good health.

In the first bioavailability study, 12 subjects were placed into Groups I, II, and III. Each group consisted of four subjects, each of whom received a single capsule of 60, 165, or 300 mg of fenoprofen equivalent (Table I) on three consecutive occasions, with a 2-day washout period between each dose. Each subject was instructed to adhere to a standard protocol and

Table I—Fenoprofen Calcium Capsule Formulas [a]

Ingredient	Capsule[b], mg		
	60	165	300
Fenoprofen calcium	70.0	192.5	350.0
Silicone fluid 350 centistokes	3.0	8.2	15.0
Microcrystalline cellulose with carboxymethylcellulose sodium[c]	217.0	179.2	125.0

[a] Values in milligrams. [b] Fenoprofen equivalent. [c] Avicel RC-591 MCC, FMC Corp.

[1] Nalfon, Dista Products Co. (a Division of Eli Lilly and Co.).

[2] Drug weight is reported in this paper as fenoprofen equivalent of fenoprofen calcium.

[3] SMA 12/60.

0022-3549/79/0900-1087$01.00/0
© 1979, American Pharmaceutical Association

were taken at the near and far positions with the filter turning at 300 rpm. These photographs showed that the flow at the tablet surface was uniform and parallel to the filter face with an even color distribution when the disk was at the far position from the stirring source. The tailing streams of color away from the tablet revealed the tangential nature of the stirring patterns. This overall visualization is reasonably close to that assumed by the model and is in keeping with the data analysis from the dissolution experiments.

For the near position, the colored photographs showed that the flow pattern at the surface was less uniform and in the direction of the spinning filter rather than parallel to it. Furthermore, a concentration of color appeared on the filter side of the tablet. The visualization procedure combined with dissolution data confirms that the flow pattern is influenced by the distance from the rotating stirring source. Dissolution rates measured from disintegrating tablets would presumably be influenced in a similar way, making basket placement a critical factor.

SUMMARY

At the farthest distance from the stirring source, the average numerical exponents for stirring speed and tablet radius were 0.58 and 1.54, respectively, which compares favorably with the theoretical values of 0.50 and 1.50. When the dissolving salicylic acid surface was positioned closer to the stirring source, the numerical exponent for the tablet radius was lowered to 1.07, indicating a change in dissolution as a function of distance from the stirring source. These data indicate that dissolution rates are not necessarily proportional to surface area, as predicted by the Nernst equation, and that distance from the stirring source is a significant factor. Convective diffusion models combined with easily accomplished visualization techniques provide the methodology needed to characterize various dissolution devices.

REFERENCES

(1) S. Howard, J. Mauger, A. Khwangsopha, and D. Pasquarelli, "Operating Variables for the Spin Filter Dissolution Device," presented at APhA Academy of Pharmaceutical Sciences, New York meeting, May 1977.

(2) A. C. Shah, C. B. Peot, and J. F. Ochs, *J. Pharm. Sci.*, **62**, 671 (1973).

(3) V. Levich, "Physiochemical Hydrodynamics," Prentice Hall, Englewood Cliffs, N.J., 1962.

(4) J. Knudsen and D. Katz, "Fluid Dynamics and Heat Transfer," McGraw-Hill, New York, N.Y., 1958, pp. 247–259, 473–481.

(5) K. G. Nelson and A. C. Shah, *J. Pharm. Sci.*, **64**, 610 (1975).

(6) A. C. Shah and K. G. Nelson, *ibid.*, **64**, 1519 (1975).

(7) J. Kestin and L. N. Persen, *Int. J. Heat Mass Transfer*, **5**, 355 (1962).

Linear Pharmacokinetics of Orally Administered Fenoprofen Calcium

J. F. NASH ˣ, L. D. BECHTOL, C. A. BUNDE *, R. J. BOPP, K. Z. FARID, and C. T. SPRADLIN

Received October 6, 1978, from the *Lilly Research Laboratories, Indianapolis, IN 46206.* Accepted for publication February 20, 1979.
*Present address: Cintest, Inc., Cincinnati, OH 45220.

Abstract □ The bioavailability of fenoprofen from three different fenoprofen calcium capsule formulations containing the equivalent of 60, 165, and 300 mg of fenoprofen was determined in two studies. In the first study, 12 subjects received one capsule of each formulation according to a three-period crossover design. The second study required each of 13 subjects to receive 300 mg of fenoprofen equivalent of the 60- and 300-mg capsules and 330 mg of the 165-mg capsule. The initial study provided information on the linearity of fenoprofen pharmacokinetics, and the second study established that the three capsule formulations were bioequivalent. The bioavailability parameters C_{max}, t_{max}, and $AUC_{0-12\ hr}$ for the drug in plasma were consistent with a linear pharmacokinetic model, as were the amounts of fenoprofen and hydroxyfenoprofen excreted in the urine. These data show linearity of kinetics for fenoprofen in plasma throughout the 60–300-mg dosage range after a single dose. Physical measurements of each capsule formulation drug content, weight variation, and dissolution showed the products to be uniform and readily soluble.

Keyphrases □ Fenoprofen—pharmacokinetics, oral administration, calcium salt □ Pharmacokinetics—fenoprofen calcium, oral administration □ Anti-inflammatory agents—fenoprofen calcium, pharmacokinetics, oral administration

Fenoprofen calcium[1] was shown to be a useful anti-inflammatory agent in osteoarthritis (1–4) and rheumatoid arthritis (5–16) in adults. To extend the therapeutic range of the compound, drug formulations containing 60–300 mg of fenoprofen equivalent as fenoprofen calcium[2] were selected for juvenile rheumatoid arthritis studies. This paper reports the linearity of fenoprofen pharmacokinetics, fenoprofen bioavailability, and the uniformity of drug excretion after a single-dose oral administration of capsules containing 60, 165, or 300 mg of fenoprofen equivalent in an adult population.

EXPERIMENTAL

Clinical Study Protocol—Healthy adult male volunteers, 18–50 years old, participated in the two studies. Their weight was ±10% of the ideal weight (17). The subjects had no history of significant GI disorder; hepatic, renal, hematological, or cardiovascular disease; or chronic alcoholism. Each subject underwent a urinalysis, hematology, and blood analysis[3] as well as a physical examination to ensure inclusion of only subjects in good health.

In the first bioavailability study, 12 subjects were placed into Groups I, II, and III. Each group consisted of four subjects, each of whom received a single capsule of 60, 165, or 300 mg of fenoprofen equivalent (Table I) on three consecutive occasions, with a 2-day washout period between each dose. Each subject was instructed to adhere to a standard protocol and

Table I—Fenoprofen Calcium Capsule Formulas [a]

Ingredient	Capsule[b], mg		
	60	165	300
Fenoprofen calcium	70.0	192.5	350.0
Silicone fluid 350 centistokes	3.0	8.2	15.0
Microcrystalline cellulose with carboxymethylcellulose sodium[c]	217.0	179.2	125.0

[a] Values in milligrams. [b] Fenoprofen equivalent. [c] Avicel RC-591 MCC, FMC Corp.

[1] Nalfon, Dista Products Co. (a Division of Eli Lilly and Co.).

[2] Drug weight is reported in this paper as fenoprofen equivalent of fenoprofen calcium.

[3] SMA 12/60.

0022-3549/79/0900-1087$01.00/0
© 1979, American Pharmaceutical Association

Table II—*In Vitro* Tests of Fenoprofen Calcium Capsules

Property	Number of Measurements	Capsule, mg[a] 60[b]	165[b]	300[c]
Fenoprofen[d]	$\bar{x}_{10}$	58.8	160.3	307.0
equivalent, mg	Range	(55.9–62.9)	(154–168)	(303–313)
Weight, mg	$\bar{x}_{10}$	291.8	374.2	491.9
	Range	(282.8–303.2)	(368.7–385.7)	(489.6–505.7)
Dissolution in	$\bar{x}_6$	59.4	40.6	38.1
10 min[e], %	Range	(56.9–62.6)	(36.4–43.6)	(34.3–42.1)
Dissolution in	$\bar{x}_6$	89.5	72.0	72.9
30 min[e], %	Range	(85.8–94.3)	(66.6–78.5)	(70.7–74.8)
Dissolution in	$\bar{x}_6$	97.4	84.0	87.6
60 min[e], %	Range	(91.4–104.4)	(77.4–89.5)	(85.7–89.7)

[a] Fenoprofen equivalent. [b] Nalfon Capsules, representative production size lots. [c] Nalfon Pulvules, lot OCF84, 300 mg of fenoprofen equivalent as fenoprofen calcium. [d] One hundred milligrams of fenoprofen is equivalent to 116.7 mg of fenoprofen calcium. [e] USP XIX dissolution apparatus: 1000 ml of 0.05 *M* phosphate buffer at 37°, pH 4.5, ionic strength 0.3, and stirring at 50 rpm.

Table III—Mean Fenoprofen Bioavailability Parameters from Single Capsules

Bioavailability Parameter	Capsule 60 mg[a]	60-mg Data Adjusted[b] to 300 mg	165 mg[a]	165-mg Data Adjusted[b] to 300 mg	300 mg[a]
0 hr	0.0 (0.0)		0.0 (0.0)		0.1 (0.3)
0.25 hr	1.6 (1.2)		2.9 (2.7)		4.4 (4.4)
0.5 hr	4.0 (2.0)		10.4 (5.6)		15.8 (10.0)
0.75 hr	4.7 (1.9)		13.8 (5.0)		21.1 (7.8)
1.0 hr	4.8 (1.7)		13.8 (5.0)		22.2 (8.0)
1.5 hr	4.3 (1.0)		13.6 (3.9)		21.9 (6.9)
2.0 hr	4.8 (1.4)		11.2 (3.2)		22.1 (7.4)
2.5 hr	3.9 (1.1)		9.7 (2.4)		18.1 (5.4)
3.0 hr	2.9 (1.0)		7.9 (2.7)		15.4 (4.6)
4.0 hr	2.2 (0.7)		5.7 (1.8)		10.8 (3.2)
6.0 hr	1.0 (0.5)		3.1 (1.2)		7.0 (2.9)
8.0 hr	0.5 (0.3)		1.5 (0.7)		3.7 (2.0)
12.0 hr	0.2 (0.2)		0.5 (0.4)		1.5 (1.4)
$AUC_{0\text{-}12\ hr}$, μg-hr/ml	20.2 (4.0)	100.9	55.3 (12.7)	100.6	105.2 (21.8)
C_{max}, μg/ml	6.2 (1.1)	31.0	17.2 (3.0)	31.2	28.3 (7.9)
t_{max}, hr	1.4 (0.6)	—	1.3 (0.7)	—	1.8 (1.4)
Urinary excretion, 0–24 hr, mg					
Fenoprofen	19.9 (10.5)	99.3	66.1 (27.8)	120.3	89.2 (42.0)
Hydroxyfenoprofen	20.9 (11.1)	104.7	71.5 (31.9)	130.1	99.2 (44.4)
Total drug	40.8 (20.8)	204.0	137.6 (57.3)	250.4	188.4 (82.7)

[a] Mean plasma fenoprofen levels of 12 subjects in micrograms per milliliter (standard deviation). [b] Adjusted mean fenoprofen bioavailability parameters.

Table IV—Mean Fenoprofen Bioavailability Parameters from Multiple Capsules

Bioavailability Parameter	Capsule Five 60 mg	Two 165 mg	One 300 mg
0 hr	0.0[a] (0.0)	0.0 (0.0)	0.0 (0.0)
0.25 hr	9.5 (8.7)	4.7 (4.7)	5.2 (8.4)
0.5 hr	23.6 (8.6)	17.6 (11.5)	16.0 (12.5)
0.75 hr	26.7 (6.6)	24.3 (9.8)	19.0 (11.9)
1.0 hr	27.3 (6.4)	25.8 (9.0)	20.3 (9.3)
1.5 hr	24.8 (4.3)	23.3 (6.2)	21.6 (6.1)
2.0 hr	21.1 (2.7)	21.1 (6.1)	22.3 (4.1)
2.5 hr	17.2 (2.4)	19.9 (5.4)	19.3 (3.6)
3.0 hr	13.3 (2.0)	14.9 (3.8)	14.9 (2.9)
4.0 hr	9.2 (1.9)	10.3 (2.5)	10.1 (1.9)
6.0 hr	4.9 (1.2)	5.1 (1.6)	5.5 (1.6)
8.0 hr	2.5 (0.7)	2.7 (1.0)	2.8 (1.0)
12.0 hr	0.9 (0.4)	1.1 (0.5)	1.1 (0.6)
$AUC_{0\text{-}12\ hr}$, μg-hr/ml	99.6 (16.4)	100.6 (15.9)	97.2 (14.8)
C_{max}, μg/ml	31.2 (5.2)	31.0 (4.0)	28.4 (5.2)
t_{max}, hr	1.0 (0.5)	1.1 (0.6)	1.4 (0.8)
Urinary excretion, 0–24 hr, mg			
Fenoprofen	93.0 (35.7)	103.9 (36.9)	104.7 (25.4)
Hydroxyfenoprofen	117.6 (42.7)	146.3 (79.3)	130.0 (31.2)
Total drug	210.6 (55.7)	250.2 (87.5)	234.7 (40.2)

[a] Mean plasma fenoprofen levels of 13 subjects in micrograms per milliliter (standard deviation).

to abstain from taking any other medication 7 days preceding and 24 hr following the study drug administration. All subjects fasted for at least 8 hr prior to and 2 hr after medication. The subjects were given the capsules with 240 ml of water in the morning. After medication, they remained ambulatory or sitting for at least 2 hr.

Heparinized venous blood, 10 ml, was obtained at 0, 0.25, 0.5, 0.75, 1, 1.5, 2, 2.5, 3, 4, 6, 8, and 12 hr after medication. The blood samples were centrifuged within 1 hr, and the plasma was separated and frozen until assayed. Urine specimens were collected from 0 to 24 hr after medication. The collections were refrigerated as obtained. The specimens were mixed to ensure homogeneity, the volume was recorded, and a 50-ml aliquot was removed and frozen until assayed.

A second similar bioavailability study was conducted in which five capsules of 60 mg, two capsules of 165 mg, and one capsule of 300 mg of

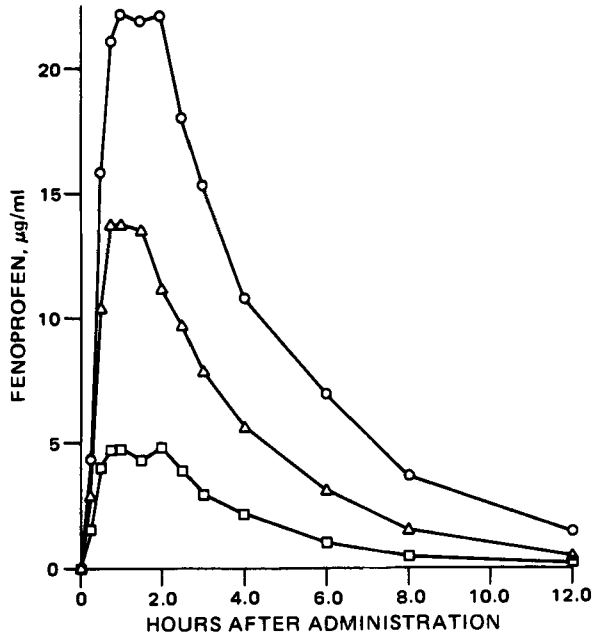

Figure 1—*Mean plasma fenoprofen levels of 12 subjects after administration of 60- (□), 165- (△), and 300- (○) mg capsules of fenoprofen equivalent as fenoprofen calcium.*

fenoprofen equivalent were administered to each of 13 subjects.

Assay of Plasma and Urine Samples—In the initial study, plasma samples were assayed for fenoprofen by GLC (18). In the second study, plasma samples were assayed by HPLC[4]. The total fenoprofen and 4-hydroxyfenoprofen (the free compounds and conjugates) in urine were determined by the following GLC procedure. A 100-μl urine sample was diluted with 200 μl of purified water and 50 μl of concentrated sulfuric acid. When thoroughly mixed, the sample was heated on a boiling water bath for 30 min. After cooling, 30 μg of *dl*-2-(4-phenoxyphenyl)valeric acid was added as an internal standard. The fenoprofen, hydroxyfenoprofen, and internal standard were extracted into 4 ml of ethylene dichloride. The ethylene dichloride was evaporated, and 50 μl of a 1:10 mixture of *N*-trimethylsilylimidazole–carbon disulfide was added to the residue. The silylated compounds were chromatographed under the same conditions as the plasma samples.

***In Vitro* Tests**—The USP XIX (19) capsule weight variation, the product assay, and the dissolution test results are reported in Table II.

RESULTS AND DISCUSSION

Plasma and Urine Drug Levels in Study 1—Table III summarizes the mean plasma fenoprofen level at each sampling time, along with the means of $AUC_{0\text{–}12\ hr}$, C_{max}, t_{max}, and 0–24-hr urinary recovery of fenoprofen and hydroxyfenoprofen. Figure 1 presents the mean plasma fenoprofen profiles graphically. Figure 2 shows the near linearity of the plots of dose *versus* $AUC_{0\text{–}12\ hr}$, C_{max}, and 0–24-hr urinary excretion. Linear regression analysis suggests that an increase of 1 mg of fenoprofen in a dose increases its $AUC_{0\text{–}12\ hr}$ by 0.35 μg-hr/ml, the C_{max} by 0.10 μg/ml, and the 0–24-hr urinary recovery by 0.68 mg.

Table III also contains $AUC_{0\text{–}12\ hr}$, C_{max}, and urinary recovery data adjusted so as to correspond to a single dose of 300 mg of fenoprofen equivalent under the hypothesis of pharmacokinetic linearity. An analysis of variance of these adjusted data indicated that there were no significant differences ($p > 0.05$) among the three capsule formulations with respect to adjusted *AUC*, adjusted C_{max}, and adjusted urinary drug recovery. An analysis of variance on unadjusted t_{max} estimates also failed to demonstrate any differences among the three capsule formulations.

Plasma and Urine Drug Levels in Study 2—Mean plasma fenoprofen levels, $AUC_{0\text{–}12\ hr}$, C_{max}, t_{max}, and 0–24-hr urinary recovery measurements from approximately equal doses of the 60-, 165-, and 300-mg capsules are reported in Table IV. The mean plasma fenoprofen profiles are presented in Fig. 3. Analyses of variance on these data indicated that there were no differences among the three capsule formulations

[4] To be published.

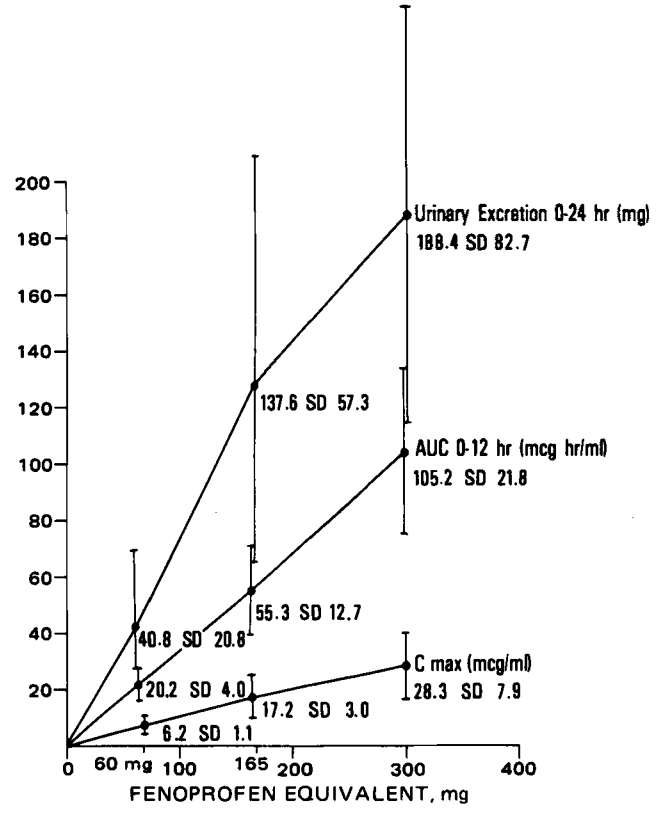

Figure 2—*Near linear plots of fenoprofen administered (60, 165, and 300 mg)* versus *means of* $AUC_{0\text{–}12\ hr}$, C_{max}, *and 0–24-hr urinary excretion.*

with respect to plasma levels at most sampling times, *AUC*, C_{max}, t_{max}, and urinary recovery.

Mean plasma levels from the one 300-mg capsule were significantly lower than those following five 60-mg capsules at 0.75 and 1 hr and significantly lower than those following two 165-mg capsules at 0.75 hr. The former differences may have been due to the apparently lower dissolution of the 300-mg capsules, as compared to the 60-mg capsules, while the

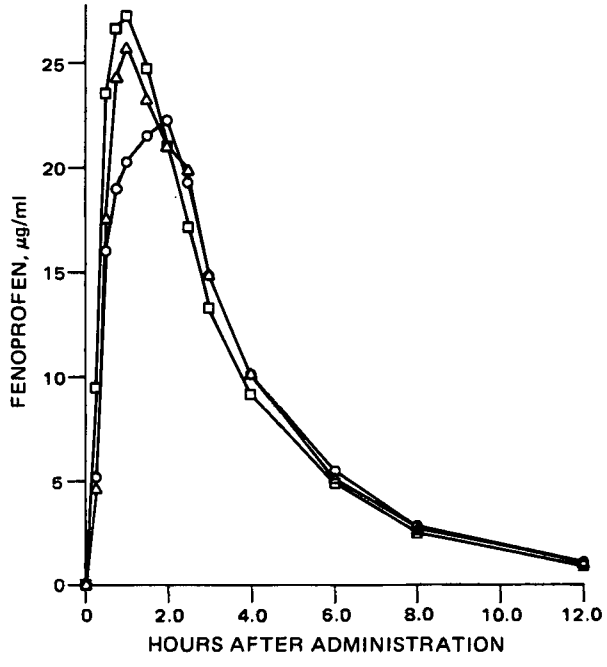

Figure 3—*Mean plasma fenoprofen levels of 13 subjects after administration of five 60- (□), two 165- (△), and one 300- (○) mg capsules of fenoprofen equivalent as fenoprofen calcium.*

latter may have been a result of the slightly larger dose of the 165-mg capsule. The equivalence of the capsule formulations with respect to all other variables suggests that any differences in the bioavailabilities of the three formulations are inconsequential.

According to previous reports (20, 21), fenoprofen pharmacokinetics after an oral or intravenous dose of 250 mg can be adequately represented by a two-compartment open model. Under such a model, plasma levels are a linear function of the dose administered (22).

The results of Study 1 are sufficient to corroborate linearity of orally administered fenoprofen pharmacokinetics in the 60–300-mg dose range only if nonlinearities are not obscured by bioinequivalencies of the three capsule formulations. Since Study 2 established that the three formulations are essentially bioequivalent, the differences among the formulations in Study 1 probably were due solely to differing doses. Since the Study 1 bioavailability parameters are proportional to the dose, as established by the analysis of variance of the adjusted variables, these experiments provide additional evidence that orally administered fenoprofen pharmacokinetics are linear over the 60–300-mg dose range.

A previous study (23) reported nonlinearity of plasma levels to high doses of another α-methylarylacetic acid, naproxen. The nonlinearity occurred at doses of >500 mg while lower doses two times a day yielded a linear dose–response curve. This fenoprofen study included single doses of 60–300 mg. Higher fenoprofen doses were not investigated.

REFERENCES

(1) J. A. Wojtulewski, *Curr. Med. Res. Opin.*, **2**, 551 (1974).
(2) H. S. Diamond, *J. Rheumatol., Suppl. 2*, **3**, 67 (1976).
(3) J. W. Brooke, *ibid.*, **3**, 71 (1976).
(4) F. G. McMahon, A. Jain, and A. Onel, *ibid.*, **3**, 76 (1976).
(5) E. C. Huskisson, *Curr. Med. Res. Opin.*, **2**, 545 (1974).
(6) P. M. Reynolds and P. J. Whorwell, *ibid.*, **2**, 461 (1974).
(7) R. Marcolongo, E. Camarri, M. Tocca, and E. Fanteria, *Clin. Ter.*, **75**, 449 (1975).
(8) J. Zuckner and R. J. Auclair, *J. Rheumatol., Suppl. 2*, **3**, 18 (1976).
(9) O. B. Gum, *ibid.*, **3**, 26 (1976).
(10) I. F. Duff, J. E. Neukom, and J. E. Himes, *ibid.*, **3**, 32 (1976).
(11) W. J. Blechman and S. Zane, *ibid.*, **3**, 38 (1976).
(12) S. H. Roth, D. W. Englund, and B. K. Harris, *ibid.*, **3**, 43 (1976).
(13) J. W. Sigler, A. S. Ridolfo, and G. B. Bluhm, *ibid.*, **3**, 49 (1976).
(14) J. F. Fries and M. C. Britton, *ibid.*, **3**, 61 (1976).
(15) M. Franke and G. Manz, *Curr. Ther. Res.*, **21**, 43 (1977).
(16) J. D. Davis, R. A. Turner, R. L. Collins, I. R. Ruchte, and J. S. Kaufman, *Clin. Pharmacol. Ther.*, **21**, 52 (1977).
(17) "Scientific Tables," 7th ed., Documenta Geigy, p. 712.
(18) J. F. Nash, R. J. Bopp, and A. Rubin, *J. Pharm. Sci.*, **60**, 1062 (1971).
(19) "The United States Pharmacopeia," 19th rev., Mack Publishing Co., Easton, Pa., 1975, p. 670.
(20) A. Rubin, B. E. Rodda, P. Warrick, A. S. Ridolfo, and C. M. Gruber, *J. Pharm. Sci.*, **61**, 739 (1972).
(21) *Ibid.*, **60**, 1797 (1971).
(22) J. G. Wagner, "Fundamentals of Clinical Pharmacokinetics," Drug Intelligence Publications, Hamilton, Ill., 1975, p. 57.
(23) R. Ruckel, E. Forchielli, K. Sevelius, M. Chaplin, and E. Segra, *Clin. Pharmacol. Ther.*, **15**, 261 (1974).

ACKNOWLEDGMENTS

The authors thank Dr. F. C. Blubaugh for preparation of the capsules and Mr. P. R. Page for analysis of the plasma and urine samples.

Cholesterol Solubility in Organic Solvents

G. L. FLYNN *x, Y. SHAH *, S. PRAKONGPAN *, K. H. KWAN *, W. I. HIGUCHI *, and A. F. HOFMANN ‡

Received August 9, 1977, from the **College of Pharmacy, University of Michigan, Ann Arbor, MI 48109,* and the ‡*School of Medicine, University of California, San Diego, CA 92103.* Accepted for publication March 1, 1979.

Abstract □ The 37° cholesterol solubilities in over 50 solvents, including the homologous *n*-alkanols through dodecanol and homologous ethyl carboxylates through the undecanoate, and the 37° β-sitosterol solubilities in the *n*-alkanols through decanol are reported. Additionally, solubility data for cholesterol at 7, 17, and 27° in the alcohol series were obtained. These measurements allowed the calculation of heats of solution for cholesterol in the alkanols, which range from 7.5 kcal for methanol to 4.3 kcal for decanol and which tend to decrease, although irregularly, with increasing alkanol chain length. A solubility maximum in all of these series for both solutes was observed between a chain length of six and seven. A surprisingly irregular, odd–even alternating solubility pattern was noted for cholesterol in the alkanols at all four temperatures. Experimental evidence indicated that this pattern was due to solvent-induced crystalline changes, presumably solvate formation, in each alkanol solvent through C_{10}. Overall, the solubility studies screened solvents for their utility in dissolving cholesterol and, thus, cholesterol gallstones. To these ends, some limited dissolution experiments were performed, which indicated that the solution rate is directly related to the measured solubility in organic solvents. The dissolution behavior is thus different from micellar bile salt solutions, in which a significant interfacial barrier controls kinetics.

Keyphrases □ Cholesterol—solubility in organic solvents, *n*-alkanols, ethyl carboxylates, structure–activity relationships □ β-Sitosterol—solubility in organic solvents, *n*-alkanols, structure–activity relationships □ Gallstones—cholesterol, solubility in organic solvents, treatment of stones retained in common bile duct □ Organic solvents—cholesterol dissolution, treatment of gallstones retained in common bile duct, structure–activity relationships

Cholesterol is an important biological membrane constituent and is the principal component of many gallstones. It also has been indicted as a causative agent in arteriosclerosis. The physicochemical properties of cholesterol are important to its necessary membrane functions, to its role as an initiator and component of gallstones, and to its presumed involvement in vascular diseases. Indeed, the understanding of cholesterol's natural and pathophysiological roles is dependent on a thorough knowledge of cholesterol's biochemistry and physical chemistry. Particularly important is cholesterol solubilization in the major aqueous biological fluids, blood and bile (1–3). Elucidation of cholesterol's biological solubility and deposition would be aided by an understanding of its solubility behavior *in vitro*.

BACKGROUND

A promising direct application of cholesterol solubility data is the dissolution of small cholesterol stones in the common bile duct of patients

0022-3549/79/0900-1090$01.00/0

© 1979, American Pharmaceutical Association

latter may have been a result of the slightly larger dose of the 165-mg capsule. The equivalence of the capsule formulations with respect to all other variables suggests that any differences in the bioavailabilities of the three formulations are inconsequential.

According to previous reports (20, 21), fenoprofen pharmacokinetics after an oral or intravenous dose of 250 mg can be adequately represented by a two-compartment open model. Under such a model, plasma levels are a linear function of the dose administered (22).

The results of Study 1 are sufficient to corroborate linearity of orally administered fenoprofen pharmacokinetics in the 60–300-mg dose range only if nonlinearities are not obscured by bioinequivalencies of the three capsule formulations. Since Study 2 established that the three formulations are essentially bioequivalent, the differences among the formulations in Study 1 probably were due solely to differing doses. Since the Study 1 bioavailability parameters are proportional to the dose, as established by the analysis of variance of the adjusted variables, these experiments provide additional evidence that orally administered fenoprofen pharmacokinetics are linear over the 60–300-mg dose range.

A previous study (23) reported nonlinearity of plasma levels to high doses of another α-methylarylacetic acid, naproxen. The nonlinearity occurred at doses of >500 mg while lower doses two times a day yielded a linear dose–response curve. This fenoprofen study included single doses of 60–300 mg. Higher fenoprofen doses were not investigated.

REFERENCES

(1) J. A. Wojtulewski, *Curr. Med. Res. Opin.*, **2**, 551 (1974).
(2) H. S. Diamond, *J. Rheumatol., Suppl. 2*, **3**, 67 (1976).
(3) J. W. Brooke, *ibid.*, **3**, 71 (1976).
(4) F. G. McMahon, A. Jain, and A. Onel, *ibid.*, **3**, 76 (1976).
(5) E. C. Huskisson, *Curr. Med. Res. Opin.*, **2**, 545 (1974).
(6) P. M. Reynolds and P. J. Whorwell, *ibid.*, **2**, 461 (1974).
(7) R. Marcolongo, E. Camarri, M. Tocca, and E. Fanteria, *Clin. Ter.*, **75**, 449 (1975).
(8) J. Zuckner and R. J. Auclair, *J. Rheumatol., Suppl. 2*, **3**, 18 (1976).
(9) O. B. Gum, *ibid.*, **3**, 26 (1976).
(10) I. F. Duff, J. E. Neukom, and J. E. Himes, *ibid.*, **3**, 32 (1976).
(11) W. J. Blechman and S. Zane, *ibid.*, **3**, 38 (1976).
(12) S. H. Roth, D. W. Englund, and B. K. Harris, *ibid.*, **3**, 43 (1976).
(13) J. W. Sigler, A. S. Ridolfo, and G. B. Bluhm, *ibid.*, **3**, 49 (1976).
(14) J. F. Fries and M. C. Britton, *ibid.*, **3**, 61 (1976).
(15) M. Franke and G. Manz, *Curr. Ther. Res.*, **21**, 43 (1977).
(16) J. D. Davis, R. A. Turner, R. L. Collins, I. R. Ruchte, and J. S. Kaufman, *Clin. Pharmacol. Ther.*, **21**, 52 (1977).
(17) "Scientific Tables," 7th ed., Documenta Geigy, p. 712.
(18) J. F. Nash, R. J. Bopp, and A. Rubin, *J. Pharm. Sci.*, **60**, 1062 (1971).
(19) "The United States Pharmacopeia," 19th rev., Mack Publishing Co., Easton, Pa., 1975, p. 670.
(20) A. Rubin, B. E. Rodda, P. Warrick, A. S. Ridolfo, and C. M. Gruber, *J. Pharm. Sci.*, **61**, 739 (1972).
(21) *Ibid.*, **60**, 1797 (1971).
(22) J. G. Wagner, "Fundamentals of Clinical Pharmacokinetics," Drug Intelligence Publications, Hamilton, Ill., 1975, p. 57.
(23) R. Ruckel, E. Forchielli, K. Sevelius, M. Chaplin, and E. Segra, *Clin. Pharmacol. Ther.*, **15**, 261 (1974).

ACKNOWLEDGMENTS

The authors thank Dr. F. C. Blubaugh for preparation of the capsules and Mr. P. R. Page for analysis of the plasma and urine samples.

Cholesterol Solubility in Organic Solvents

G. L. FLYNN *x, Y. SHAH *, S. PRAKONGPAN *, K. H. KWAN *, W. I. HIGUCHI *, and A. F. HOFMANN ‡

Received August 9, 1977, from the **College of Pharmacy, University of Michigan, Ann Arbor, MI 48109,* and the ‡*School of Medicine, University of California, San Diego, CA 92103.* Accepted for publication March 1, 1979.

Abstract □ The 37° cholesterol solubilities in over 50 solvents, including the homologous *n*-alkanols through dodecanol and homologous ethyl carboxylates through the undecanoate, and the 37° β-sitosterol solubilities in the *n*-alkanols through decanol are reported. Additionally, solubility data for cholesterol at 7, 17, and 27° in the alcohol series were obtained. These measurements allowed the calculation of heats of solution for cholesterol in the alkanols, which range from 7.5 kcal for methanol to 4.3 kcal for decanol and which tend to decrease, although irregularly, with increasing alkanol chain length. A solubility maximum in all of these series for both solutes was observed between a chain length of six and seven. A surprisingly irregular, odd–even alternating solubility pattern was noted for cholesterol in the alkanols at all four temperatures. Experimental evidence indicated that this pattern was due to solvent-induced crystalline changes, presumably solvate formation, in each alkanol solvent through C_{10}. Overall, the solubility studies screened solvents for their utility in dissolving cholesterol and, thus, cholesterol gallstones. To these ends, some limited dissolution experiments were performed, which indicated that the solution rate is directly related to the measured solubility in organic solvents. The dissolution behavior is thus different from micellar bile salt solutions, in which a significant interfacial barrier controls kinetics.

Keyphrases □ Cholesterol—solubility in organic solvents, *n*-alkanols, ethyl carboxylates, structure–activity relationships □ β-Sitosterol—solubility in organic solvents, *n*-alkanols, structure–activity relationships □ Gallstones—cholesterol, solubility in organic solvents, treatment of stones retained in common bile duct □ Organic solvents—cholesterol dissolution, treatment of gallstones retained in common bile duct, structure–activity relationships

Cholesterol is an important biological membrane constituent and is the principal component of many gallstones. It also has been indicted as a causative agent in arteriosclerosis. The physicochemical properties of cholesterol are important to its necessary membrane functions, to its role as an initiator and component of gallstones, and to its presumed involvement in vascular diseases. Indeed, the understanding of cholesterol's natural and pathophysiological roles is dependent on a thorough knowledge of cholesterol's biochemistry and physical chemistry. Particularly important is cholesterol solubilization in the major aqueous biological fluids, blood and bile (1–3). Elucidation of cholesterol's biological solubility and deposition would be aided by an understanding of its solubility behavior *in vitro*.

BACKGROUND

A promising direct application of cholesterol solubility data is the dissolution of small cholesterol stones in the common bile duct of patients

0022-3549/79/0900-1090$01.00/0

© 1979, American Pharmaceutical Association

Table I—Cholesterol Solubility in the Alkanols at Several Temperatures

Alcohol	Temperature	Solubility, mg/ml[a] Radiolabel Assay	Solubility, mg/ml[a] Spectrophotometric Assay
Methanol	7°	2.30 (2.35, 2.25)	1.96
	17°	3.37 (3.44, 3.30)	3.65
	27°	6.09 (6.03, 6.15)	5.21 (5.38, 5.03)
	37°	7.89 (3, 0.26)	6.19 (4, 0.75)
Ethanol (95%)	7°	11.5 (11.6, 11.4)	11.0
	17°	17.0 (17.2, 16.7)	17.0
	27°	23.7 (23.5, 23.8)	23.4 (22.6, 24.2)
	37°	32.5 (3, 0.58)	31.1 (4, 6.29)
n-Propanol	7°	28.6 (28.5, 28.7)	28.0
	17°	41.0 (41.1, 40.9)	47.2
	27°	58.6 (59.4, 57.8)	63.6 (69.7, 57.4)
	37°	92.7	94.4 (4, 1.63)
n-Butanol	7°	31.6 (31.5, 31.7)	28.5
	17°	44.6 (44.5, 44.7)	46.1
	27°	64.2 (65.2, 63.1)	70.8 (65.6, 75.9)
	37°	95.1 (92.3, 97.8)	97.8 (4, 5.74)
n-Pentanol	7°	54.7 (53.3, 56.0)	47.6
	17°	79.5 (80.0, 78.9)	87.3
	27°	107.2 (108.4, 106.0)	121.5 (112.5, 130.4)
	37°	157.1 (158.3, 155.9)	150.0 (4, 1.40)
	37° (water saturated)	—	124
n-Hexanol	7°	69.3	62.3
	17°	91.7 (90.7, 92.6)	100.5
	27°	122.3 (3, 2.75)	143.3 (149.1, 137.4)
	37°	165.7 (165.9, 165.5)	178.2 (4, 9.63)
	37° (water saturated)	—	150.8
n-Heptanol	7°	91.1 (90.7, 91.5)	89.3
	17°	126.9 (129.0, 124.8)	139.0
	27°	157.9 (161.9, 153.9)	197.7 (191.0, 204.4)
	37°	210.9 (208.7, 213.1)	200.4 (4, 13.36)
	37° (water saturated)	—	176.9
n-Octanol	7°	74.2 (73.5, 74.8)	68.4
	17°	101.4 (103.9, 98.8)	103.9
	27°	128.8 (128.1, 129.4)	154.9 (154.0, 155.8)
	37°	172.4 (174.2, 170.5)	180.0 (4, 6.16)
n-Nonanol	7°	72.6 (73.6, 71.5)	—
	17°	96.7 (98.2, 95.2)	94.5
	27°	119.0	150.0 (144.7, 155.8)
	37°	164.0 (166.5, 161.5)	177.6 (4, 8.71)
	37° (water saturated)	—	182.9
n-Decanol	7°	98.3 (98.6, 97.9)	—
	17°	143.7 (140.5, 146.8)	142.7
	27°	168.7 (165.8, 171.5)	147.7 (152.7, 142.7)
	37°	212.2 (216.3, 208.0)	215.6 (4, 20.89)
n-Undecanol	37°	—	233.7 (237.1, 230.3)
n-Dodecanol	37°	—	110.5
Isopropanol	37°	48.9 (39.6, 58.2)	—
Isobutanol	37°	96.3 (98.0, 94.5)	—
sec-Butanol	37°	123.4 (131.8, 115.0)	—
tert-Butanol	37°	19.9 (20.1, 19.6)	—

[a] The averaged result is reported where there were more than two determinations, followed by parentheses which indicate the number of determinations and the standard deviation. For two determinations, the average is followed by parentheses containing the individual values. A single determination is without parentheses.

who have undergone cholecystectomy. This occurs in up to 5% of patients after gallbladder surgery (4–6).

The common duct is often explored during cholecystectomy, and a T-tube is inserted into the common duct to keep it "decompressed" during healing. If stones are discovered before the T-tube is removed, various approaches are possible. Traditionally, the patient simply has been observed since such "retained" stones may pass or dissolve spontaneously and duct reexploration is dangerous. There also have been repeated reports of the direct instillation into the T-tube of organic solvents, such as ether or chloroform (7), which are excellent solvents for gallstones *in vitro*. This approach has been abandoned as too hazardous by most physicians.

In 1972, Way *et al.* (6) directly instilled a micellar sodium cholate solution into the common duct *via* the T-tube for stone dissolution, and this procedure has been used with moderate success in uncontrolled studies (8, 9). Some investigators reported success in uncontrolled studies with micellar sodium chenodeoxycholate solutions, and others have proposed the instillation of presumably less toxic solvents, such as polyoxyethylene hydrogenated castor oil (10), or *N*-alkylacetamides (11). Recently, direct stone aspiration by a Dormia basket catheter has been the treatment of choice. Nonetheless, direct physical extraction of retained common duct stones is not always possible, and a need persists for a solution that can be directly infused into the common duct and that will safely induce rapid gallstone dissolution.

The present study is concerned with the solubility of cholesterol "monohydrate," a model gallstone material, in several homologous solvent series and in other selected solvents, some of which are promising from the standpoint of physiological suitability for dissolving cholesterol stones. The homologous series were chosen to provide regular alteration of the physicochemical properties of the solvent. Initially, it was felt that, if the optimum solvent polarity for cholesterol could be put in terms of a maximum in solubility in a homologous series of solvents, a rational basis for solvent selection would materialize. In other words, it was anticipated that solvents of the same solubility parameter or polarity as the best homolog also would be efficient solubilizers.

This approach was viewed as more systematic than most previous investigations, which reported on cholesterol solubility in fats, oils, arbitrarily selected organic solvents, and modified bile solutions (1–3, 12). During the present investigations on the cholesterol solubility in the *n*-alkanols, there appeared a physicochemical curiosity, an odd–even alternation in solubility at chain lengths up to seven carbons. Resolution of this phenomenon is a principal feature of this report.

EXPERIMENTAL

Preparation of Cholesterol Monohydrate—Crude anhydrous cholesterol (25 g) was dissolved in 2 liters of 95% ethanol warmed to 60°

Table II—Cholesterol Solubility at 37° in Various Organic Solvents

Solvent	Solubility, mg/ml[a] Radiolabel Assay	Spectrophotometric Assay
Ethylene glycol	0.30 (0.35, 0.24)	—
Propylene glycol	1.79 (1.51, 2.06)	2.07 (1.26, 2.88)
1,3-Butylene glycol	1.57 (1.56, 1.58)	3.32 (3.36, 3.27)
1,4-Butylene glycol	—	2.15
2,3-Butylene glycol	6.33 (7.52, 5.13)	5.27
Formamide	—	1.41
N-Methylformamide	5.33 (5.72, 4.93)	—
N,N-Dimethylformamide	—	4.92
Propylene carbonate	1.75 (1.75, 1.75)	—
Polyethylene glycol 400	3.85 (3.98, 3.72)	3.53 (3, 0.37)
Diethylene glycol monoethyl ether	53.3 (3, 0.36)	50.0
Diethylene glycol monoethyl ether acetate	29.5	—
Diethylene glycol monobutyl ether	106.5	—
2-Methoxyethanol	27.1 (26.1, 28.1)	—
2-Ethoxyethanol	87.0 (89.3, 84.6)	—
2-Methoxyethyl acetate	28.5 (28.5, 28.5)	—
2-Ethoxyethyl acetate	43.2	—
2-(2-Ethoxyethoxy) ethyl acetate	30.3 (3, 0.85)	—
2-(2-*n*-Butoxyethoxy) ethanol	106.9 (106.5, 107.2)	—
Dipropylene glycol	25.6	29.7
Ethylene glycol diacetate	7.01 (3, 0.44)	6.90
Glyceryl triacetate (triacetin)	7.17	—
Methyl benzoate	107.9 (3, 1.82)	—
Glyceryl-1-monooctanoate (monooctanoin)	116.8	—
Glyceryl trioctanoate (tricapryline)	52.0 (3, 0.79)	—
Isopropyl myristate	67.4 (67.7, 67.1)	—
Oleic acid	146.2 (3, 8.45)	—

[a] The averaged result is reported where there were more than two determinations, followed by parentheses which indicate the number of determinations and the standard deviation. For two determinations, the average is followed by parentheses containing the individual values. A single determination is without parentheses.

and filtered through a paper filter[1] while warm. This mixture was allowed to return to room temperature and to crystallize by standing overnight. The formed crystals were collected in a sintered-glass funnel and dried 15–18 hr under vacuum. The material was crystallized a second time using the same procedure. The twice-crystallized cholesterol was stored in the dark in a desiccator containing water (100% humidity).

Radiolabeled cholesterol was prepared similarly. After the first crystallization, 25 g of cholesterol was dissolved in 2 liters of 95% ethanol at 65°, 10 μCi of ^{14}C-cholesterol in benzene (<1 ml) was added, and the recrystallization was carried out as with the cold material. The activity of the labeled cholesterol was 803 cpm/mg.

The other materials were organic solvents obtained commercially[2] in the purest form available and were used as received.

Sample Preparation—Excess cholesterol monohydrate was placed in screw-capped test tubes containing 3–4 ml of solvent. The tubes were sealed and placed in a thermostated bath (7, 17, 27, or 37°) equipped with a shaker and equilibrated for ≥3 days. In preliminary studies, this time was more than adequate to obtain equilibrium. Samples were taken using glass wool-tipped pipets preconditioned to the experimental temperature. The samples were appropriately diluted for the spectrophotometric procedure using 95% ethanol. In the radiolabel assay, the samples were added directly to the scintillation cocktail without further dilution.

Cholesterol solubility in water-saturated, water-immiscible *n*-alkanols was also determined (C_5 and above). In this case, excess cholesterol was added to a two-phase system containing several milliliters of an aqueous phase overlayered with several milliliters of the immiscible, water-saturated alkanol phase. The two-phase systems were equilibrated for ≥3 days with gentle agitation and allowed to reform into two clear, distinct layers. Samples were drawn carefully from the upper organic phase using glass wool-tipped pipets. These samples were assayed using the procedures employed with the pure solvents.

[1] Whatman.

[2] Aldrich; Baker; Eastman; Fisher; Matheson, Coleman, and Bell; and U.S. Industrial Chemicals.

Table III—Cholesterol Solubility in the Homologous Ethyl Carboxylates at 37°

Ethyl Carboxylate Solvent	Solubility[a], mg/ml (37°, Radiolabel Assay)
Ethyl acetate	76.4
Ethyl propionate	101.4 (101.3, 101.5)
Ethyl butyrate	103.0 (102.6, 103.3)
Ethyl pentanoate (valerate)	112.3
Isoamyl acetate	109.5 (109.9, 109.1)
Ethyl hexanoate	101.9 (3, 2.55)
Ethyl octanoate	99.2 (98.6, 99.7)
Ethyl nonanoate (pelargonate)	95.6 (3, 1.46)
Ethyl deconoate	88.5 (87.4, 89.5)
Ethyl undecanoate	102.9 (3, 3.72)
Ethyl dodecanoate (laurate)	85.2
Ethyl tetradecanoate (myristate)	78.5
Ethyl hexadecanoate (palmitate)	76.7

[a] The averaged result is reported where there were more than two determinations, followed by parentheses which indicate the number of determinations and the standard deviation. For two determinations, the average is followed by parentheses containing the individual values. A single determination is without parentheses.

Generally, duplicate samples were taken from each solute–solvent equilibrium mixture at separate times and were assayed independently. The initial studies were done using the spectrophotometric procedure. However, as can be seen from Tables I and II, this procedure was accompanied by substantial variability, so an alternative procedure involving radiolabeled cholesterol was adopted. This procedure proved to be far more precise, although the averaged results between procedures were in reasonable agreement for the alkanols and some other solvents. With few exceptions, replicate assays with the radiolabeled cholesterol agreed within 5%. Specific statistical data on the methods are given in Tables I–III. Percent coefficients of variation calculated from these data were typically between 1 and 5% and were smaller for the least viscous solvents, such as the low molecular weight alcohols.

Given the unusual solubility patterns observed for cholesterol in the *n*-alkanols, the solubilities of a structurally closely related steroid, β-sitosterol, in these normal alcohol solvents were determined also. This experiment was done to see if the peculiar solubility behavior was unique to cholesterol or was a more general phenomenon exhibited by this steroid class. The procedure was identical to that employed in the cholesterol analysis. Radiolabeled β-sitosterol was recrystallized from ethanol for the experiment.

Radiolabel Assay—Scintillation cocktail was made as follows: naphthalene, 60 g; 2,5-diphenyloxazole, 4 g; 1,4-bis[2-(5-phenyloxazolyl)]benzene, 0.2 g; absolute methanol, 100 ml; ethylene glycol, 20 ml; and dioxane, *qsad*, 1000 ml.

Aliquots of 0.1 ml were taken from the saturated solutions and diluted in 10 ml of the cocktail. In all cases, clear solutions were obtained. The vials were placed in a scintillation counter, and the disintegrations (counts) per minute were obtained. These values were compared against standard solutions prepared by taking 0.5 ml of a cholesterol solution in acetone containing 114.9 mg of labeled compound/50 ml, evaporating it to dryness, and dissolving the residue in 10 ml of the cocktail. It was unnecessary to add 0.1 ml of the particular solvent to simulate the sample composition. The solubility in milligrams per milliliter was calculated from the ratio of the sample counts to the standard counts, times the appropriate dilution factor.

Spectrophotometric Procedure—Cholesterol solubility in the *n*-alkanols and some other polar solvents was determined by a literature spectrophotometric procedure (13) (cold cholesterol) as well as by scintillation counting, which was used for most solvents. The spectrophotometric procedure was used for the initial work, but the data are presented here only as a cross-check on the scintillation method. The reader is referred to the literature for the details of this complex assay. Where both analytical procedures were employed, the results were in close agreement.

Differential Thermal Analysis—The equilibrium crystals in the *n*-alkanols were collected on a sintered-glass funnel and rinsed quickly with about 50 ml of cold hexane to remove residual alcohol. The crystals were transferred to a filter paper and allowed to dry overnight at room temperature. Several milligrams of cholesterol obtained from each alcohol was placed in glass capillaries, and differential thermal scans[3] were made. All tracings were repeated, and no significant differences appeared in the thermograms from run to run with a given compound.

[3] Du Pont 990 thermal analyzer.

Table IV—Cholesterol Solubilities in Binary Mixtures of *n*-Alkanols at 37° Adjusted to Fractional Chain Lengths

Fractional Chain Length	Alkanol Pair	Solubility, mg/ml: Radiolabel Assay	Solubility, mg/ml: Spectrophotometric Assay
2.5	Ethanol–propanol	—	67.0
3.5	Propanol–butanol	—	100.5
4.5	Butanol–pentanol	—	127.1
5.5	Pentanol–hexanol	—	189.9
6.1	Hexanol–heptanol	183.4	—
6.2	Hexanol–heptanol	192.9	—
6.3	Hexanol–heptanol	202.0	—
6.4	Hexanol–heptanol	212.0	—
6.5	Hexanol–heptanol	215.0	114.6 (?)[a]
6.6	Hexanol–heptanol	216.2	—
6.7	Hexanol–heptanol	219.9	—
6.8	Hexanol–heptanol	215.9	—
6.9	Hexanol–heptanol	214.2	—
7.5	Heptanol–octanol	—	198.3
8.5	Octanol–nonanol	—	206.5

[a] This data point was discarded as an anomaly.

RESULTS

Cholesterol solubilities in the *n*-alkanols from methanol to undecanol are given in Table I. These values were determined at 7, 17, 27, and 37° for most of the pure alkanols and at 37° in several water-saturated long chain alkanols. Both the spectrophotometric procedure and radiolabeled assay were used and gave results generally in accord.

The data for the alkanol solvents through chain length 10 at the four temperatures are plotted in Fig. 1. This profile is characterized by an odd–even alternation in solubility up to an alkanol solvent chain length of seven, followed by an erratic solubility pattern through the remainder of the series. The "staircase effect" is somewhat more pronounced at the higher temperatures.

The solubilities of cholesterol at 37° in a second homologous series, the ethyl carboxylates, were also determined (Table III). Data are not available for the C_7 compound, but otherwise the series is uninterrupted from C_2 to C_{11}; ethyl heptanoate was not available from the major

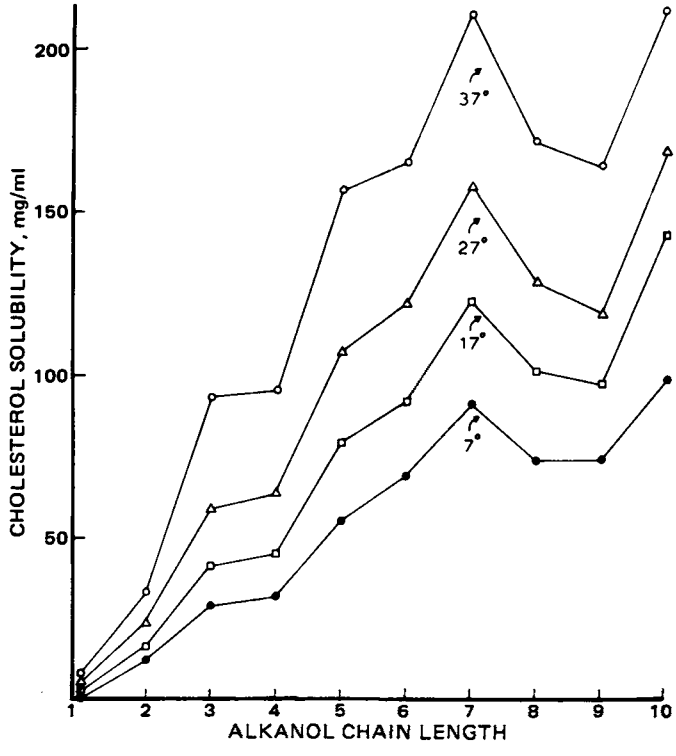

Figure 1—*Solubility profiles of cholesterol in the* n*-alkanols at 7, 17, 27, and 37°. The unusual feature of these plots is the odd–even alternation in solubility behavior from C_1 to C_7. It is apparent from thermal analysis data that the equilibrium crystals yielding these solubilities are not identical. The plotted data are those obtained with the radioassay.*

Table V—β-Sitosterol Solubilities in the *n*-Alkanols at 37°

Alcohol Solvent	Solubility, mg/ml[a] (Radiolabel Assay)
Methanol	5.39 (5.34, 5.44)
Ethanol	36.3 (37.0, 35.6)
n-Propanol	204.8 (209.0, 200.5)
n-Butanol	279.8 (294.4, 265.2)
n-Pentanol	318.6 (312.2, 324.9)
n-Hexanol	333.1 (326.2, 339.9)
n-Heptanol	312.1 (312.2, 312.0)
n-Octanol	315.1 (314.8, 315.3)
n-Nonanol	314.9 (318.2, 311.6)
n-Decanol	319.3 (314.6, 324.0)

[a] The parentheses indicate the values of the independent determinations.

chemical suppliers. The solubility of the isoamyl acetate is listed in the table under that of the comparable compound, ethyl valerate. These two compounds have the same molecular weight and empirical formula, $C_7H_{14}O_2$, and their solubilizing capacity for cholesterol is nearly identical.

The data found in Table III are also displayed in Fig. 2. Unlike the alkanols, the solubility–chain length profile is a smooth curve. The maximum in the plot is observed at a carboxyl chain length of five or total carbons, counting the ethyl ester group, of seven. The solubility varies only about 50% from the minimum to the maximum in the series.

The 37° solubilities of cholesterol in diverse additional solvents are given in Table II. These values are crudely grouped according to the type of solvent structure and are listed in rough progression from polar to nonpolar solvent character.

The cholesterol solubilities in binary *n*-alkanol mixtures combined so as to give a "fractional chain length" were also determined (Table IV) by mixing appropriate amounts of adjacent homologs to predetermined fractional molar compositions, usually half and half. A mixture containing equal molar amounts of ethanol and propanol, for instance, was considered to have an effective chain length of 2.5. Because of an initial analytical error, which indicated that the solubility of fractional chain length 6.5 was approximately one-half of the value expected based on the solubilities of pure hexanol or heptanol, the cholesterol solubility in binary solvent mixtures of these two alcohols was studied in detail (Fig. 3). There is a maximum in solubility at about fractional chain length 6.7, but the solubility in this mixture is only slightly greater than that observed in pure heptanol.

Lastly, the solubilities of β-sitosterol were also determined in the *n*-alkanols (Table V and Fig. 4). The solubility patterns observed are totally

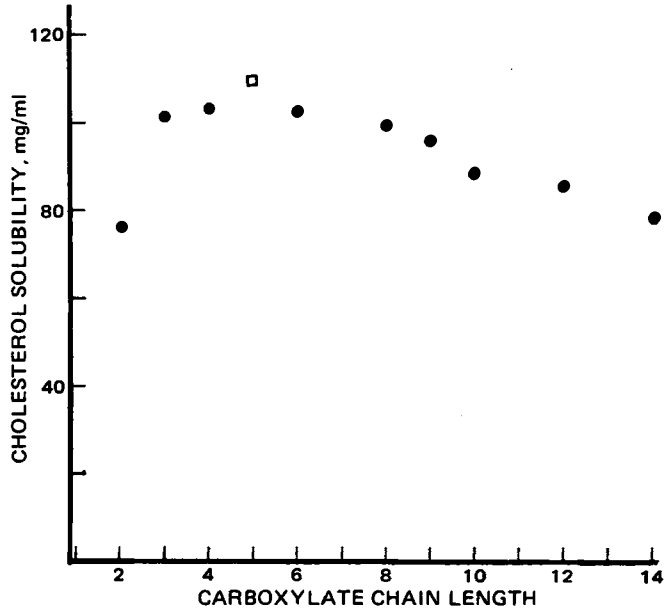

Figure 2—*Solubility at 37° of cholesterol monohydrate in the homologous ethyl carboxylates. Unlike the* n*-alkanols, the curve is without serious irregularities, suggesting that there are no solvent-induced crystalline changes in these solvents. Key: □, isoamyl acetate.*

Table VI—Heats of Solution of Cholesterol in the *n*-Alkanols through Decanol

Alcohol Solvent	Least-Squares Slope Arrhenius Plot[a]	Correlation Coefficient	Heat of Solution, ΔH_s, cal/mole
Methanol	-1.648×10^3	−0.9926	7540
Ethanol	-1.301×10^3	−0.9997	5950
n-Propanol	-1.464×10^3	−0.9961	6700
n-Butanol	-1.383×10^3	−0.9983	6330
n-Pentanol	-1.304×10^3	−0.9986	5970
n-Hexanol	-1.095×10^3	−0.9989	5010
n-Heptanol	-1.042×10^3	−0.9993	4770
n-Octanol	-1.045×10^3	−0.9991	4780
n-Nonanol	-0.9995×10^3	−0.9962	4570
n-Decanol	-0.9327×10^3	−0.9878	4270

[a] Slope = $(-\Delta H_s/2.303R)$.

unlike those seen for cholesterol and indicate that cholesterol is unique in the way it interacts with the homologous alcohols.

DISCUSSION

General Solubility Patterns—The 37° solubility data for cholesterol in the ethyl carboxylates (Table III and Fig. 2) and in the diverse solvents listed in Table II suggest some general solubility patterns. Not too surprisingly, cholesterol is relatively insoluble in the very polar solvents such as the glycols and formamides. The solubility in ethyl acetate of 76.4 mg/ml is the lowest observed in the ethyl carboxylate series, although it is not experimentally different from the solubility in ethyl myristate (78.5 mg/ml) and ethyl palmitate (76.7 mg/ml).

The solubility in the latter two solvents suggests that they are effectively more nonpolar than cholesterol and interact less strongly with this compound than the intermediate chain length esters. Since the intermolecular forces involved here would be primarily of the London dispersion and other van der Waals types, it can be qualitatively stated that the solubility parameter of the shortest and longest chain esters differs from that of cholesterol and that there is a significant activity coefficient correction based on the solubility parameter differential, in the direction of reducing the solubility. It is assumed here that there are no significant

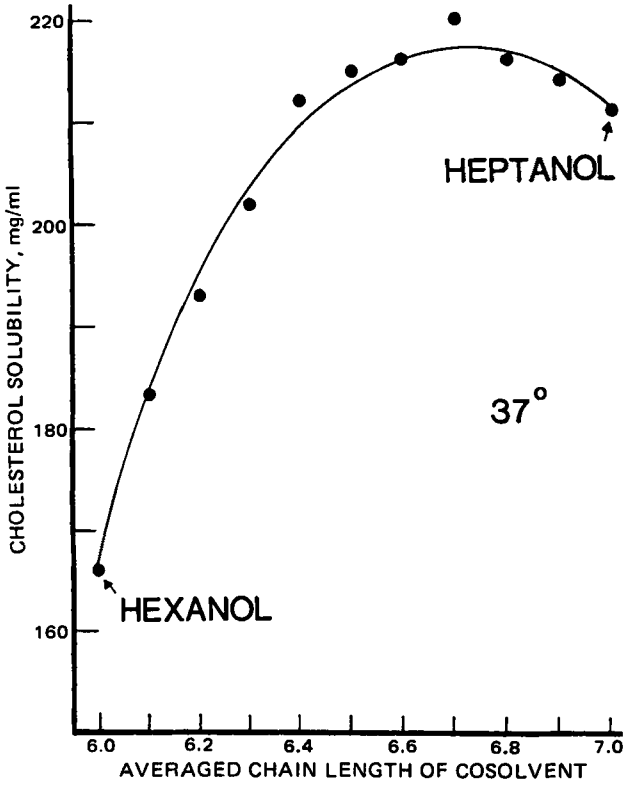

Figure 3—*Cholesterol solubilities in mixtures of hexanol and heptanol against the average chain length of the solvent pair. The extreme points are the solubilities in pure hexanol and heptanol.*

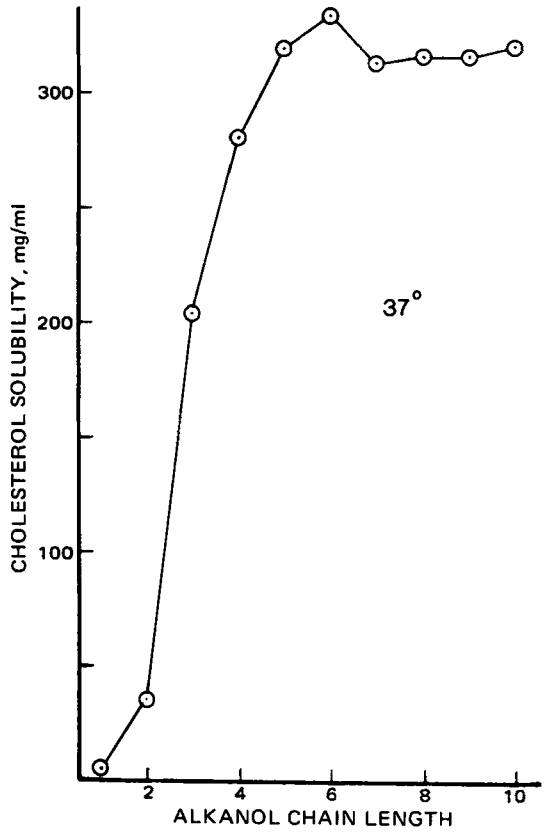

Figure 4—*Solubility of β-sitosterol in the n-alkanols. The behavior here is far more regular than that seen for cholesterol in these same solvents.*

crystalline changes in these solvents. Certainly, the smooth solubility profile (Fig. 2) strongly suggests this condition.

These general observations are fully consistent with those of previous investigators (2) who studied cholesterol solubility in various fats and oils and in a series of pure triglycerides. In general, they found the solubility in oils not to vary appreciably, as observed with the ethyl carboxylates, but they also found the solubility to be greatest in fats and oils containing relatively short chain (C_6–C_{12}) fatty acids. In the pure triglycerides, they observed a solubility maximum of 54.7 mg/ml for glyceryl tridecanoate (tricaprin). Solubilities were considerably less in short chain triglycerides and somewhat less in triolein and trilinolein, 37.7 and 34.1 mg/ml, respectively. The reported (12) very low solubility of cholesterol in mineral oil, an apolar solvent, of 13.9 mg/ml at 37° also is consistent with the observation that a moderate polarity favors solubility. The consistency of cholesterol solubility in ethyl valerate (112.3 mg/ml), isoamyl acetate (109.5 mg/ml), and methyl benzoate (107.9 mg/ml), which are all C_7 esters, further indicates a general cohesive energy effect because these esters would have similar solubility parameters.

Another factor affecting solubility, in addition to the general cohesive energy effect, is evident from consideration of several pairs of compounds. The cholesterol solubility in 2-(2-butoxyethoxy)ethanol (106.9 mg/ml) was more than threefold greater than that found for 2-(2-ethoxyethoxy) ethyl acetate (30.3 mg/ml). The same was true for diethylene glycol monobutyl ether (106.5 mg/ml). These two pairs have similar empirical formulas. Cholesterol solubility in glyceryl-1-monooctanoate was over twice that for glyceryl trioctanoate, which may be a solubility parameter effect. Solubility in diethylene glycol monoethyl ether was considerably greater than in diethylene glycol acetate, which is in the opposite direction from the general trend. Solubility in 2-ethoxyethanol was slightly greater than in ethyl acetate, which also runs contrary to the general polarity behavior.

In each pair, the better solubilizing solvent had a free hydroxyl group, two in the case of the glyceride, but the hydroxyls were esterified in the poorer solvent pair member. The presence of a free hydroxyl obviously favors solution. Whether the effect is due to enhanced intermolecular interaction in the solution phase or whether it is due to a change in the cholesterol crystal form occurring in the approach to equilibrium, or both, is undetermined. Energetic hydrogen bonding with the cholesterol hy-

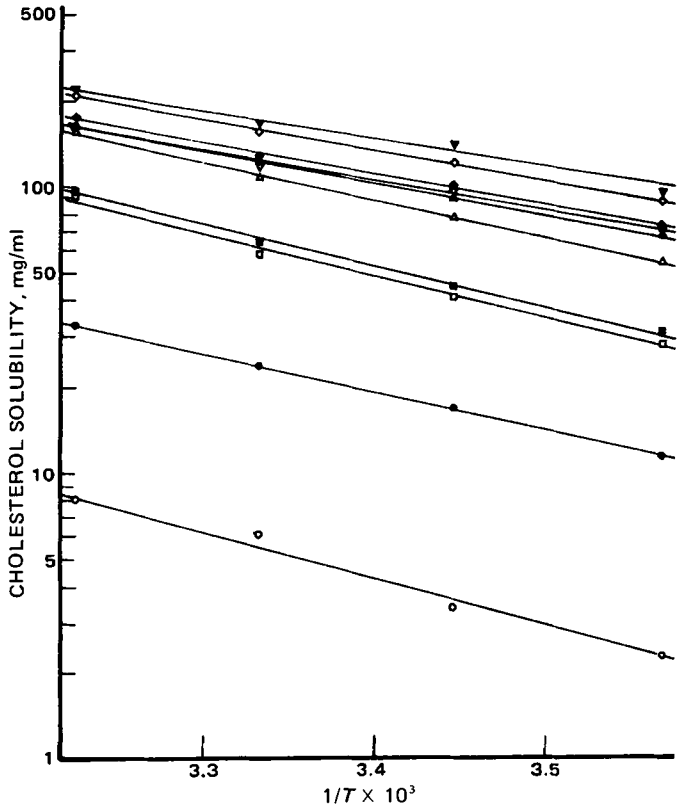

Figure 5—*Arrhenius-type plot of the solubilities of cholesterol in the n-alkanols. Key: ○, methanol; ●, ethanol; □, propanol; ■, butanol; △, pentanol; ▲, hexanol; ◇, heptanol; ◆, octanol; ▽, nonanol; and ▼, decanol.*

droxyl is certainly promoted by having free hydroxyl functions in the solvent structure. However, as will be demonstrated, some alcohols also change the nature of the crystalline phase.

In most solvents, even the poorer ones, cholesterol solubility exceeds that found in micellar bile acid solutions. Typically, the solubility in the latter systems is ~0.5–1.5 mg/ml (9). Given that the dissolution rate of an organic solid is generally directly proportional to its solubility in the solvent, this observation superficially suggests that organic solvents should be more efficient (in terms of rates) in dissolving gallstones. The superficiality of this statement resides in the fact that gallstone dissolution is controlled by an interfacial barrier, at least with respect to bile acid solubilization, and is not diffusion controlled and also in the fact that the dissolution process hydrodynamics have not been accounted for. If the solvent is viscous, the solution rates will be slowed because a thicker effective boundary layer will form around the stone and because the diffusivity in this layer may be significantly reduced. Nevertheless, cholesterol solubility in many of these solvents is sufficiently high to suggest that residual stones may be dissolved and removed relatively quickly by solvent dissolution.

Cholesterol Solubility in *n*-Alkanols—The introduction stated that the *n*-alkanols were chosen as model solvents to pinpoint an optimum solvent polarity for cholesterol, at least qualitatively, to put solvent selection for gallstone dissolution on a rational basis. These solvents show regular incremental increases in their physicochemical properties, such as boiling points, heats of vaporization, and water solubilities, all related to the alkyl chain length. The use of regularly altering physicochemical properties has proved fruitful in other studies involving organizing and interpreting solubilities of homologous solutes in a given solvent (14) and solubilities of a given solute in binary solvent mixtures (15). As can be seen in Fig. 1, cholesterol solubilities in the alkanols do not yield a smooth solubility trend as a function of solvent chain length. Rather, the solubility profile is irregular and exhibits odd–even alternations up to heptanol.

Heats of solution for each compound also were obtained from plots of the solubility logarithms *versus* reciprocal absolute temperature (Fig. 5). These values systematically decrease with increasing solvent alkyl chain length (Table VI), albeit irregularly. The value for ethanol, which

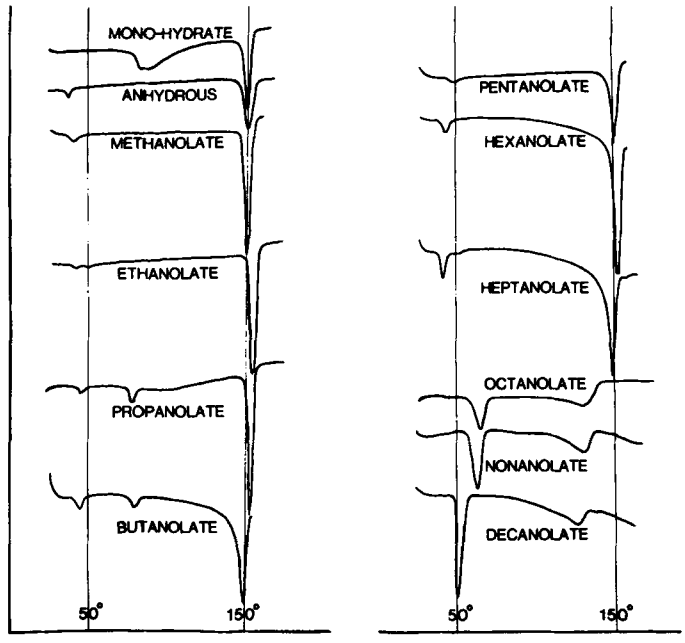

Figure 6—*Differential thermal analysis tracings of the equilibrium cholesterol crystals from the various n-alkanols as well as of the monohydrate and anhydrous forms. All curves were reproducible for a given solvent and decidedly different between solvents. The 50 and 150° reference points are given. The tracings are identified as if for true solvates but are for crystalline forms, which are not as yet fully characterized.*

appears to fall out of the overall trend, was obtained in 95% ethanol and not in the pure solvent.

It was reasoned that if the general solvent properties were sensitive to whether the alcohol was odd or even in carbon number, which would be over and above more general effects of increasing alkyl chain length, then the solubility behavior of closely related steroids should parallel that shown for cholesterol. Therefore, the solubility of β-sitosterol in the alkanols was examined. The data (Fig. 4) form a smooth profile, which plateaus at about 320 mg/ml between C_5 and C_{10}. While the very large solubilities at the longer chain lengths are unusual for this type of compound, clearly the behavior is dissimilar to that of cholesterol, ruling out a nonspecific solvent effect. Also, since the odd–even effect was seen at four temperatures, it was not the result of a solid phase transition known to occur at 37° (16).

The unusual solubility behavior was resolved by collecting the equilibrated cholesterol crystals in each alkanol and examining the solid by qualitative differential thermal analysis. Figure 6 shows thermogram tracings for cholesterol crystals obtained from saturated solutions of each alkanol along with a tracing of the starting material, cholesterol monohydrate. The fusion properties of the solvent-equilibrated crystalline phases are quite different. These data indicate that cholesterol "solvates" [4] of each alkanol are formed and, taken together with the solubilities, further suggest that the crystalline properties of the formed solvates exhibit alternations in the fusion energetics, which are effectively odd–even in character up to a chain length of seven. This phenomenon is typical of the fusion energetics of homologs (17) but apparently has never been demonstrated for solvates.

The thermogram tracing for the starting material, cholesterol monohydrate, was rerun multiple times and was never exactly the same. Its general features were a shallow endotherm beginning at about 80° with a double minimum. From run to run, the minimums shifted slightly on the temperature axis and alternated in relative magnitude. Furthermore, the major melting endotherm was double tipped in most cases with minimums at ~151 and 152.5°. There is a strong suggestion that this is not a pure crystal but a mixture of forms, probably, considering the re-

[4] The term "solvate" is used here with some liberty. The thermograms show the crystalline phases to be different, but the exact nature of the differences is unknown. However, the solubility patterns strongly suggest solvent participation in the crystalline form. Other data in the literature concerning cholesterol solid states support this idea (16).

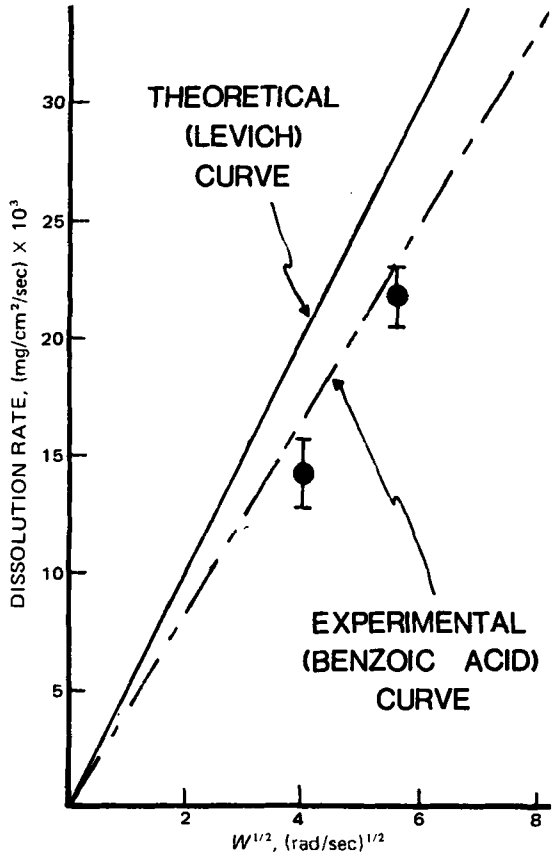

Figure 7—*Theoretical behavior for dissolution from a rotating flat surface according to Levich (—) and the expected behavior for the dissolution cell based on benzoic acid dissolution (- - -). The dissolution of cholesterol at 150 and 300 rpm falls very near the exact expectations for boundary layer control based on the benzoic acid "calibration."*

crystallization procedure and storage conditions, an ethanolate and a hydrate.

On cooling and remelting, the curve took a different form with a slight endotherm at 37° and a major melting endotherm at 151°. This curve has been associated with anhydrous cholesterol (16). The 37° endotherm is a solid phase transition known to occur with the anhydrous form (16). In methanol-equilibrated crystals, there is also an endotherm at ~40° (minimum) and the retracing on cooling is indistinguishable from that of the anhydrous form. In ethanol, there is a broad and very shallow endotherm beginning at ~40° and extending beyond 50°. In propanol, there is an initial shallow endotherm at 45° and a second shallow endotherm at ~78°. All three of these alkanols exhibit a major melting endotherm at 151°. All yield the same thermogram tracing after cooling and remelting, characteristic of the anhydrous form.

The thermograms for butanol-, pentanol-, hexanol-, and heptanol-equilibrated crystals exhibit differences in the magnitude and placement of the minor endotherm but all also melt essentially at 150°. In these solvates, there is no return to the anhydrous form based on thermogram retracings. For octanol, nonanol, and decanol, the entire thermogram shape is changed; in each case, the major endotherm is found below 70° or at 65, 63, and 50°, respectively. In each case, there also is a peculiarly shaped endotherm above 100°. The change in melting behavior seen at octanol and above corresponds with changes in solubility patterns seen in the solubility profile above C_7.

Just as in the case of the ethyl carboxylates (counting all carbons), there is a maximum in the alkanol solubility at C_7. The alcohols also provide a hydroxyl for intermolecular bonding with the cholesterol hydroxyl and, as seen in the previous analysis, this feature seems to be important in inducing solubilization. Thus, it appears that the larger cholesterol solubilities in the intermediate chain length alkanols can be attributed to the proper polarity, the presence of a free hydroxyl, and modifications in the crystal form in equilibrium with the saturated phase. From the data in Fig. 3, the ideal polarity appears to be slightly less than that of heptanol; a solubility maximum exists in binary mixtures of hexanol and heptanol. If the data are examined carefully, however, the fractional chain length solubilities are, without exception, larger than the average of the bracketing pure solvents, and this is probably attributable to mixed crystalline forms.

The study presented here, when considered in its entirety, suggests a general caution to investigators dealing with solubility analysis. Solubility data are often collected and analyzed with the assumption of solid phase stability. These experiences with cholesterol indicate that the solid phase for some compounds may be remarkably sensitive to the solvents used. Such effects were observed previously (18) for corticosteroids. Thus, before one can *quantitatively* analyze solubility data, the solid phase properties must be examined and shown to be invariant with the solvent system used. Otherwise, both crystalline energetics and solution phase energetics must be simultaneously accounted for. Other compounds with solvent-dependent crystalline forms probably will surface if the solid phases in equilibrium are examined routinely.

The ethyl carboxylates and glyceryl esters were studied because of their relative safety for use in the T-tube elution of cholesterol gallstones retained in the common bile duct. The ethyl carboxylates should be absorbed poorly due to their limited aqueous solubilities, and their hydrolysis products, ethanol and the respective long chain acids, also should be physiologically innocuous in moderate quantities. The glyceryl esters were presumed even more suited for this purpose from the toxicity standpoint. The solubilities in these solvents ranged from ~ 5% (w/v) to as much as 11% (w/v) for ethyl valerate and glyceryl monooctanoate. The latter was the most suitable for gallstone dissolution in view of its cholesterol-solubilizing capacity and its physiological compatibility.

The general approach followed with regard to solubility and its impact on cholesterol dissolution was based on the assumption that the solution rate is proportional to the solubility in the solvent, after due consideration to fluid hydrodynamics. Since this is not the case for cholesterol dissolution in bile acid solutions, in which a large rate-controlling interfacial barrier is operating (19), it seemed necessary to assess whether the presumed direct relationship between solubility and dissolution exists for organic solvents. Because of its apparent suitability for cholesterol stone dissolution in the common duct, a few dissolution experiments were performed with glyceryl monooctanoate. Compressed pellets of cholesterol monohydrate were used as the model cholesterol gallstone; the procedure, detailed in a previous paper (19), is based on dissolution from a rotating disk (20).

The dissolution apparatus was calibrated using benzoic acid, a substance known to follow diffusion layer-controlled dissolution kinetics. The kinematic viscosity of glyceryl monooctanoate and the diffusivity of cholesterol in glyceryl monooctanoate, both necessary for the analysis of the rotating disk dissolution experiment, were determined and estimated, respectively. The viscosity was 50.6 centipoises on a Cannon-Fenske-modified Ostwald viscometer. The density was 0.9954 g/cm^3, thus yielding a kinematic viscosity of 50.8 centistokes. The diffusivity was estimated to be 5.6×10^{-8} cm^2/sec using the Stokes–Einstein equation.

The data for the dissolution experiments are shown in Fig. 7, along with the experimental benzoic acid curve and the theoretical dissolution curve according to Levich (20). The data points for cholesterol dissolution in glyceryl monooctanoate at 150 and 300 rpm fall only slightly below the benzoic acid curve, indicating that cholesterol dissolution in this solvent is essentially diffusion layer controlled.

Since similar diffusion-controlled dissolution kinetics have been demonstrated for cholesterol monohydrate in a 63% ethanol–water mixture (21), it can be assumed that cholesterol dissolution in organic media is unlike that observed in micellar bile acid–lecithin media and generally will be diffusion layer controlled and predictably dependent on the solvent viscosity and the cholesterol solubility in the solvent. Thus, it seems reasonable to select solvents for T-tube perfusion of retained cholesterol stones on the basis of physiologic compatibility, capacity to solubilize cholesterol, and viscosity. Obviously, the greater the solubility and the smaller the kinematic viscosity, the faster is the dissolution rate.

REFERENCES

(1) J. A. Wilkens, J. A. deWit, and B. Bronte-Steward, *Can. J. Biochem. Physiol.*, **40**, 1091 (1962).

(2) D. Kritchevsky and S. H. Tepper, *Proc. Soc. Exp. Biol. Med.*, **116**, 104 (1964).

(3) R. D. Stauffer and F. Bischoff, *Clin. Chem.*, **12**, 206 (1966).

(4) C. Lansford, S. Mehta, and F. Kern, *Gut*, **15**, 48 (1974).

(5) F. Glenn, *Surg. Gynecol. Obstet.*, **134**, 249 (1972).
(6) L. Way, W. Admirand, and J. E. Dunphy, *Ann. Surg.*, **176**, 347 (1972).
(7) W. Walters and H. R. Wesson, *Surg. Gynecol. Obstet.*, **65**, 695 (1937).
(8) R. G. Danzinger, A. F. Hofmann, L. J. Schoenfield, and J. L. Thistle, *N. Engl. J. Med.*, **286**, 1 (1972).
(9) A. M. Molokhia, W. I. Higuchi, and A. F. Hofmann, *J. Pharm. Sci.*, **64**, 2029 (1975).
(10) T. Hisatsugu, H. Igimi, and M. Nishimura, *Jpn. J. Surg.*, **2**, 62 (1972).
(11) H. Igimi, *Igaku Kenkyu*, **42**, 55 (1972).
(12) L. D. Wright and J. A. Presberg, *Proc. Soc. Exp. Biol. Med.*, **115**, 497 (1964).
(13) W. M. Sperry and M. Webb, *J. Biol. Chem.*, **123**, 97 (1951).
(14) G. Saracco and E. S. Marchetti, *Ann. Chim.*, **48**, 1357 (1958).
(15) S. H. Yalkowsky, G. L. Flynn, and G. L. Amidon, *J. Pharm. Sci.*, **61**, 983 (1972).
(16) H. L. Spier and K. G. VanSenden, *Steroids*, **6**, 871 (1965).
(17) S. H. Yalkowsky, G. L. Flynn, and T. G. Slunick, *J. Pharm. Sci.*, **61**, 852 (1972).
(18) J. A. Ostrenga and C. Steinmetz, *ibid.*, **59**, 414 (1970).
(19) S. Prakongpan, W. I. Higuchi, K. H. Kwan, and A. M. Molokhia, *ibid.*, **65**, 685 (1976).
(20) V. G. Levich, "Physicochemical Hydrodynamics," Prentice-Hall, Englewood Cliffs, N.J., 1962.
(21) S. Prakongpan, Ph.D. thesis, University of Michigan, Ann Arbor, Mich., 1974.

Sensitive Fluorescence Assay for *d,l*-Methadone

CHRISTINA H. CHI and BALWANT N. DIXIT ˣ

Received February 9, 1976, from the *Department of Pharmacology, School of Pharmacy, University of Pittsburgh, Pittsburgh, PA 15261.* Accepted for publication February 28, 1979.

Abstract □ *d,l*-Methadone forms a fluorophore when reacted with paraformaldehyde in concentrated sulfuric acid. Based on this reaction, a fluorescence assay suitable for quantitative *d,l*-methadone analysis from plasma and other tissues was developed. *d,l*-Methadone was extracted at pH 9.2 from the deproteinized filtrate of plasma or of aqueous tissue homogenate into an organic phase of 25% isobutanol in ethylene dichloride. After an aliquot of the organic phase was evaporated to dryness at 50–55° with an air jet, paraformaldehyde (0.1%, in concentrated sulfuric acid) was added, and fluorescence was read at 450 nm with excitation at 275 nm. By this method, *d,l*-methadone can be assayed in the presence of its metabolites, morphine, diacetylmorphine (heroin), codeine, and cocaine; however, amphetamine, meperidine, and quinine interfere.

Keyphrases □ Methadone—analysis, fluorescence assay, lung, liver, brain, serum, rats □ Narcotic analgesics—methadone, fluorescence assay, lung, liver, brain, serum, rats □ Fluorometry—analysis, methadone in lung, liver, brain, serum, rats

During the past decade, *d,l*-methadone has been extensively used in maintenance and rehabilitation programs for chronic diacetylmorphine (heroin) users (1). Most of the work on its distribution and metabolic disposition (2–4) has involved complex assays requiring labeled methadone. Other available methods are not sensitive enough to study *d,l*-methadone distribution following therapeutic doses (5–9). Recently, a highly sensitive GLC method (10) was reported.

When *d,l*-methadone is reacted with paraformaldehyde in concentrated sulfuric acid by heating at 100°, a fluorophore is formed (11). The purpose of this paper is to report a fluorescence assay based on this observation. This assay is applicable for methadone analysis from biological tissues in nanogram concentrations.

EXPERIMENTAL

Reagents—All reagents were prepared from reagent grade chemicals.

Zinc Sulfate Solution, 5%—Fifty grams of $ZnSO_4 \cdot 7H_2O$ was dissolved in glass-distilled water to a final volume of 1000 ml. The solution was filtered to remove any turbidity.

Barium Hydroxide Solution, 4.5%—Forty-five grams of $Ba(OH)_2 \cdot 8H_2O$ was dissolved in glass-distilled water to a final volume of 1000 ml. The solution was filtered to remove any turbidity and stored in tightly stoppered bottles.

Borate Buffer, pH 9.6—Fifty milliliters of 0.1 *M* boric acid in 0.1 *M* KCl was mixed with 36.85 ml of 0.1 *M* NaOH.

25% Isobutanol in Ethylene Dichloride—Isobutanol, 250 ml, was mixed with 750 ml of ethylene dichloride.

0.1% Paraformaldehyde in Sulfuric Acid—Paraformaldehyde, 25 mg, was dissolved in 25 ml of concentrated sulfuric acid. This reagent was prepared fresh just prior to use.

Procedure—Rats were pretreated with *d,l*-methadone and sacrificed by decapitation. Blood and other tissues such as lung, liver, and brain were removed. Plasma or serum was separated by centrifugation. Tissue samples were frozen over powdered dry ice and stored at −20° until assayed.

Just prior to assay, tissues were weighed and homogenized in distilled water (1:3). A 2-ml aliquot of the homogenate or 1 ml of serum (or plasma) diluted to 2 ml with distilled water was used for the assay. One milliliter of zinc sulfate solution was added to each sample, and the contents were thoroughly mixed on a vortex mixer before the addition of 1 ml of barium hydroxide solution. After thorough mixing, samples were centrifuged at 1000×*g* for 6 min[1].

Two-milliliter aliquots of the clear supernate were transferred into 15-ml glass-stoppered centrifuge tubes, and 0.4 ml of pH 9.6 borate buffer was added to give the final pH of 9.2. Six milliliters of 25% isobutanol in ethylene dichloride was added, and the tubes were shaken on a reciprocating shaker[2] for a minimum of 10 min to facilitate methadone extraction into the organic phase. The samples were centrifuged for 6 min at 1000×*g*, and the aqueous layer was removed by aspiration and discarded.

Three milliliters, or any other suitable aliquot of the organic phase, was then transferred to a set of test tubes, and the contents were evaporated to dryness under an air jet. The air was passed sequentially through a column of water and concentrated sulfuric acid. The test tubes were kept in a water bath maintained at 50–55°. Paraformaldehyde reagent, 0.1 ml, was added to each sample, and the tubes were transferred to a boiling water bath for 15 min.

After the samples were removed from the bath, 7.1 ml of distilled water was added to adjust the normality of the solution to 0.5. The contents were mixed and left at room temperature. Thirty minutes later, the fluorescence was read on a spectrophotofluorometer[3] with the emission monochromator rotary slit at 5, the excitation wavelength at 275 nm, and the emission wavelength at 450 nm (uncorrected). Tissue blanks, using tissues of untreated animals, and a set of standards were run simultaneously with each set of unknowns.

[1] Model UV, International Equipment Co.
[2] Eberbach model S1103.
[3] Model SPF, American Instrument Co.

0022-3549/79/0900-1097$01.00/0
© 1979, American Pharmaceutical Association

(5) F. Glenn, *Surg. Gynecol. Obstet.*, **134**, 249 (1972).
(6) L. Way, W. Admirand, and J. E. Dunphy, *Ann. Surg.*, **176**, 347 (1972).
(7) W. Walters and H. R. Wesson, *Surg. Gynecol. Obstet.*, **65**, 695 (1937).
(8) R. G. Danzinger, A. F. Hofmann, L. J. Schoenfield, and J. L. Thistle, *N. Engl. J. Med.*, **286**, 1 (1972).
(9) A. M. Molokhia, W. I. Higuchi, and A. F. Hofmann, *J. Pharm. Sci.*, **64**, 2029 (1975).
(10) T. Hisatsugu, H. Igimi, and M. Nishimura, *Jpn. J. Surg.*, **2**, 62 (1972).
(11) H. Igimi, *Igaku Kenkyu*, **42**, 55 (1972).
(12) L. D. Wright and J. A. Presberg, *Proc. Soc. Exp. Biol. Med.*, **115**, 497 (1964).
(13) W. M. Sperry and M. Webb, *J. Biol. Chem.*, **123**, 97 (1951).
(14) G. Saracco and E. S. Marchetti, *Ann. Chim.*, **48**, 1357 (1958).
(15) S. H. Yalkowsky, G. L. Flynn, and G. L. Amidon, *J. Pharm. Sci.*, **61**, 983 (1972).
(16) H. L. Spier and K. G. VanSenden, *Steroids*, **6**, 871 (1965).
(17) S. H. Yalkowsky, G. L. Flynn, and T. G. Slunick, *J. Pharm. Sci.*, **61**, 852 (1972).
(18) J. A. Ostrenga and C. Steinmetz, *ibid.*, **59**, 414 (1970).
(19) S. Prakongpan, W. I. Higuchi, K. H. Kwan, and A. M. Molokhia, *ibid.*, **65**, 685 (1976).
(20) V. G. Levich, "Physicochemical Hydrodynamics," Prentice-Hall, Englewood Cliffs, N.J., 1962.
(21) S. Prakongpan, Ph.D. thesis, University of Michigan, Ann Arbor, Mich., 1974.

Sensitive Fluorescence Assay for *d,l*-Methadone

CHRISTINA H. CHI and BALWANT N. DIXIT ˣ

Received February 9, 1976, from the *Department of Pharmacology, School of Pharmacy, University of Pittsburgh, Pittsburgh, PA 15261.* Accepted for publication February 28, 1979.

Abstract □ *d,l*-Methadone forms a fluorophore when reacted with paraformaldehyde in concentrated sulfuric acid. Based on this reaction, a fluorescence assay suitable for quantitative *d,l*-methadone analysis from plasma and other tissues was developed. *d,l*-Methadone was extracted at pH 9.2 from the deproteinized filtrate of plasma or of aqueous tissue homogenate into an organic phase of 25% isobutanol in ethylene dichloride. After an aliquot of the organic phase was evaporated to dryness at 50–55° with an air jet, paraformaldehyde (0.1%, in concentrated sulfuric acid) was added, and fluorescence was read at 450 nm with excitation at 275 nm. By this method, *d,l*-methadone can be assayed in the presence of its metabolites, morphine, diacetylmorphine (heroin), codeine, and cocaine; however, amphetamine, meperidine, and quinine interfere.

Keyphrases □ Methadone—analysis, fluorescence assay, lung, liver, brain, serum, rats □ Narcotic analgesics—methadone, fluorescence assay, lung, liver, brain, serum, rats □ Fluorometry—analysis, methadone in lung, liver, brain, serum, rats

During the past decade, *d,l*-methadone has been extensively used in maintenance and rehabilitation programs for chronic diacetylmorphine (heroin) users (1). Most of the work on its distribution and metabolic disposition (2–4) has involved complex assays requiring labeled methadone. Other available methods are not sensitive enough to study *d,l*-methadone distribution following therapeutic doses (5–9). Recently, a highly sensitive GLC method (10) was reported.

When *d,l*-methadone is reacted with paraformaldehyde in concentrated sulfuric acid by heating at 100°, a fluorophore is formed (11). The purpose of this paper is to report a fluorescence assay based on this observation. This assay is applicable for methadone analysis from biological tissues in nanogram concentrations.

EXPERIMENTAL

Reagents—All reagents were prepared from reagent grade chemicals.

Zinc Sulfate Solution, 5%—Fifty grams of $ZnSO_4 \cdot 7H_2O$ was dissolved in glass-distilled water to a final volume of 1000 ml. The solution was filtered to remove any turbidity.

Barium Hydroxide Solution, 4.5%—Forty-five grams of $Ba(OH)_2 \cdot 8H_2O$ was dissolved in glass-distilled water to a final volume of 1000 ml. The solution was filtered to remove any turbidity and stored in tightly stoppered bottles.

Borate Buffer, pH 9.6—Fifty milliliters of 0.1 *M* boric acid in 0.1 *M* KCl was mixed with 36.85 ml of 0.1 *M* NaOH.

25% Isobutanol in Ethylene Dichloride—Isobutanol, 250 ml, was mixed with 750 ml of ethylene dichloride.

0.1% Paraformaldehyde in Sulfuric Acid—Paraformaldehyde, 25 mg, was dissolved in 25 ml of concentrated sulfuric acid. This reagent was prepared fresh just prior to use.

Procedure—Rats were pretreated with *d,l*-methadone and sacrificed by decapitation. Blood and other tissues such as lung, liver, and brain were removed. Plasma or serum was separated by centrifugation. Tissue samples were frozen over powdered dry ice and stored at −20° until assayed.

Just prior to assay, tissues were weighed and homogenized in distilled water (1:3). A 2-ml aliquot of the homogenate or 1 ml of serum (or plasma) diluted to 2 ml with distilled water was used for the assay. One milliliter of zinc sulfate solution was added to each sample, and the contents were thoroughly mixed on a vortex mixer before the addition of 1 ml of barium hydroxide solution. After thorough mixing, samples were centrifuged at 1000×*g* for 6 min[1].

Two-milliliter aliquots of the clear supernate were transferred into 15-ml glass-stoppered centrifuge tubes, and 0.4 ml of pH 9.6 borate buffer was added to give the final pH of 9.2. Six milliliters of 25% isobutanol in ethylene dichloride was added, and the tubes were shaken on a reciprocating shaker[2] for a minimum of 10 min to facilitate methadone extraction into the organic phase. The samples were centrifuged for 6 min at 1000×*g*, and the aqueous layer was removed by aspiration and discarded.

Three milliliters, or any other suitable aliquot of the organic phase, was then transferred to a set of test tubes, and the contents were evaporated to dryness under an air jet. The air was passed sequentially through a column of water and concentrated sulfuric acid. The test tubes were kept in a water bath maintained at 50–55°. Paraformaldehyde reagent, 0.1 ml, was added to each sample, and the tubes were transferred to a boiling water bath for 15 min.

After the samples were removed from the bath, 7.1 ml of distilled water was added to adjust the normality of the solution to 0.5. The contents were mixed and left at room temperature. Thirty minutes later, the fluorescence was read on a spectrophotofluorometer[3] with the emission monochromator rotary slit at 5, the excitation wavelength at 275 nm, and the emission wavelength at 450 nm (uncorrected). Tissue blanks, using tissues of untreated animals, and a set of standards were run simultaneously with each set of unknowns.

[1] Model UV, International Equipment Co.
[2] Eberbach model S1103.
[3] Model SPF, American Instrument Co.

0022-3549/79/0900-1097$01.00/0
© 1979, American Pharmaceutical Association

Table I—R_f Values of *d,l*-Methadone (M), Metabolite I (M-I), and Metabolite II (M-II) under Various Experimental Conditions [a]

Experimental Condition	R_f Value		
	d,l-Methadone	Metabolite I	Metabolite II
M + M-I + M-II	0.58	0.27	0.96
Lung homogenate (untreated) + M + M-I + M-II	0.58	0.27	0.97
Lung homogenate (treated, M, 20 mg/kg sc after 1 hr)	0.52	Not detected	Not detected
Liver homogenate (untreated) + M + M-I + M-II	0.46	0.21	0.98
Liver homogenate (treated, M, 20 mg/kg sc after 1 hr)	0.43	0.17	0.99
Ref. 14	0.55	0.15	0.95

[a] Gelman instant TLC media and a solvent system of *tert*-amyl alcohol–*n*-butyl ether–water (14:7:1) according to Ref. 14.

RESULTS AND DISCUSSION

Several homogenization media were evaluated, and the most desirable results were obtained with glass-distilled water. The aqueous homogenate or plasma was deproteinized by three different methods. When deproteinization was done with 5% $ZnSO_4$ and 4.5% $Ba(OH)_2$, the blank fluorescence values were the lowest and the recovery the highest and most consistent.

Individual organic solvents as well as solvent mixtures were tested for their ability to extract methadone from aqueous solutions at various pH levels. At pH 9.0–10.0, over 90% of methadone was extracted from the aqueous phase into chloroform, ether, a mixture of 10% isopropanol in chloroform, or a mixture of 25% isobutanol in ethylene dichloride. In this investigation, a mixture of 25% isobutanol in ethylene dichloride was used. With 25% isobutanol in ethylene dichloride, *d,l*-methadone was nearly completely transferred from the aqueous into the organic phase, and an extraction period of 10 min was satisfactory.

By using the systematic multiple fractional extraction procedure (12), it was possible to demonstrate that at pH 9.6 up to 96% of methadone was extracted from the aqueous into the organic phase. Evaporation of the organic solvent by air could be achieved at 20–55°; however, it was best performed at 50–55°. At higher temperatures, inconsistent results were obtained. The recovery of *d,l*-methadone (0–50 μg) added to the aqueous phase just prior to the extraction was about 96%, while the recovery of methadone from tissue homogenate was between 75 and 80%.

The amount of paraformaldehyde reagent was not critical. The addition of 0.1 ml of 0.1% reagent was satisfactory for *d,l*-methadone concentrations ranging from 0.005 to 100 μg. Over the range of 0–50 μg of *d,l*-methadone/sample, the fluorescence intensity increased linearly with increasing concentration. The formation of the *d,l*-methadone fluorophore was complete after ~15 min (Fig. 1), and it was stable for 1 hr at room temperature. During this period, the fluorescence intensity decreased only by ~10%, and the decrease was of the same magnitude in both standard and unknown samples.

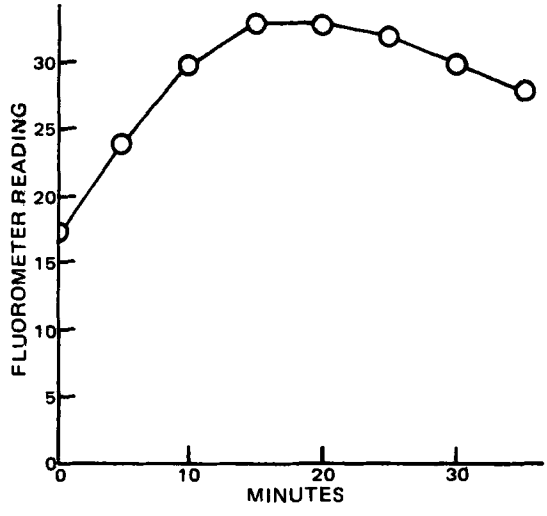

Figure 1—*Effect of heating time at 100° on the development of* d,l-*methadone fluorophore.*

Table II—Tissue *d,l*-Methadone Levels in Nontolerant Male Wistar Rats [a] after 20 mg/kg sc

Tissue	*d,l*-Methadone, μg/g of wet wt. (mean ± *SE*, *n* = 4)			
	0.5 hr	1 hr	2 hr	4 hr
Lung	54.2 ± 6.7	64.0 ± 6.7	52.6 ± 6.8	18.3 ± 4.1
Liver	25.1 ± 3.8	27.2 ± 4.5	20.0 ± 2.9	2.5 ± 0.2
Brain	4.1 ± 0.1	4.2 ± 0.2	3.0 ± 0.3	1.3 ± 0.3
Serum	1.3 ± 0.1	1.5 ± 0.04	0.9 ± 0.1	0.7 ± 0.1

[a] Average weight 200 g.

The last step, which consisted of diluting sulfuric acid with glass-distilled water up to 0.5 *N*, provided a way to measure *d,l*-methadone over concentrations from 0.005 to 50 μg/sample because the fluorescence output (arbitrary units per 100 ng of *d,l*-methadone) increased as the final sulfuric acid normality decreased. For example, at the final normality of 4.0, the fluorescence output was 0.8 unit/100 ng while at 0.5 *N* it was 83 units/100 ng.

The emission and excitation spectra of the "substance" extracted from the tissues of treated rats closely matched those obtained by using authentic *d,l*-methadone, indicating that the substance extracted was probably *d,l*-methadone.

Further confirmation of the identity was obtained by a method (13) that compares the distribution ratio patterns of a substance extracted at various pH levels from the biological samples to that of authentic chemical. If the distribution ratio patterns of the authentic and extracted substances are identical, then the two substances are considered to be identical. The distribution ratio pattern of "methadone" extracted from the tissues was compared to that of authentic *d,l*-methadone. In repeated experiments, the distribution ratios of authentic *d,l*-methadone and the material extracted from brain homogenate into 25% isobutanol in ethylene dichloride over pH 7.5–11.0 were almost identical (Fig. 2).

The third method used in the identification of the extracted substance was TLC as described previously (14). Comparison of pure methadone added to lung or liver homogenates and the substance extracted from treated tissues showed nearly identical R_f values (Table I). These data further support the claim that the substance assayed was *d,l*-methadone.

The two major methadone metabolites (2, 3) are 2-ethylidene-1,5-dimethyl-3,3-diphenylpyrrolidine (Metabolite I) and 2-ethyl-5-methyl-3,3-diphenyl-1-pyrroline (Metabolite II). TLC studies indicated

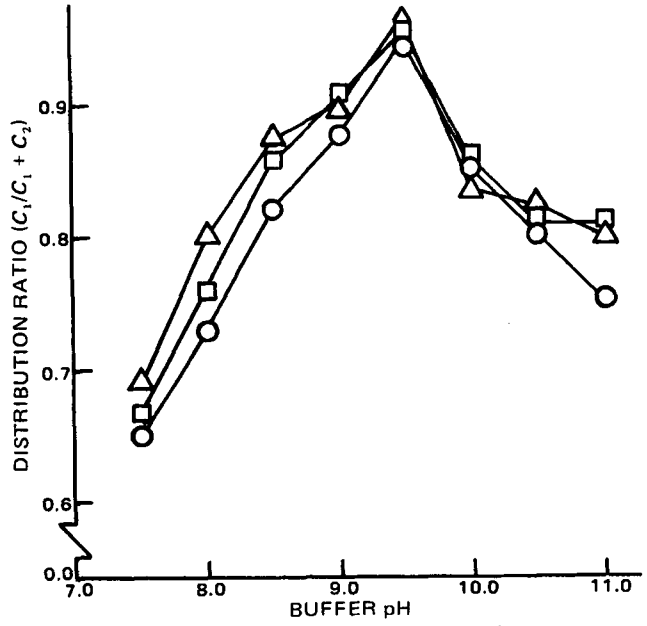

Figure 2—*Distribution ratios of 25 μg of* d,l-*methadone between borate buffer of various pH levels and 25% isobutanol in ethylene dichloride. Key:* ○, *tissue homogenate of treated animals;* △, d,l-*methadone added to tissue homogenate of untreated animals; and* □, d,l-*methadone from aqueous solution. Organic phase is* C_1, *and buffer phase is* C_2.

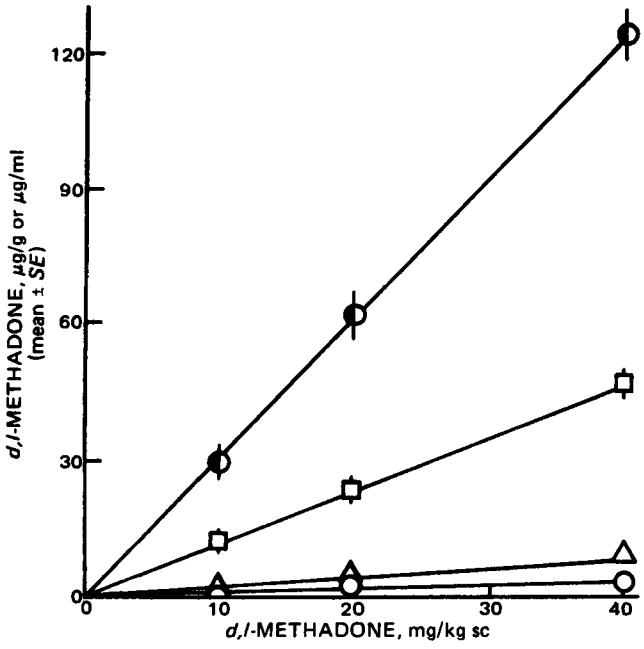

Figure 3—*Tissue* d,l-*methadone levels in the rat 60 min after subcutaneous administration of various* d,l-*methadone doses. Key:* ◐, *lung;* □, *liver;* △, *brain; and* ○, *serum.*

that these metabolites are extracted into the organic phase. However, they do not form fluorophores with paraformaldehyde. Also, morphine, diacetylmorphine (heroin), and codeine do not react with paraformaldehyde to form fluorophores. Cocaine forms a fluorophore but is not extracted from the aqueous phase (pH 9.2) under the conditions employed. Therefore, cocaine probably will not interfere in the methadone assay. Meperidine, amphetamine, and quinine form fluorophores with paraformaldehyde, and they are extracted into the organic phase. To remove the interference from these drugs, separation prior to their extraction into the organic phase is necessary.

Table II gives the levels of *d,l*-methadone in lung, liver, brain, and serum at various time intervals after 20 mg of *d,l*-methadone/kg was administered to rats subcutaneously. Figure 3 shows that the tissue levels were dose dependent.

REFERENCES

(1) V. P. Dole and M. E. Nyswander, *Br. J. Addict.*, **63**, 55 (1968).

(2) A. H. Beckett, M. Mitchard, and A. A. Shihab, *J. Pharm. Pharmacol.*, **23**, 347 (1971).

(3) A. Pohland, H. E. Boaz, and H. R. Sullivan, *J. Med. Chem.*, **14**, 194 (1971).

(4) A. L. Misra, S. J. Mule, R. Bloch, and N. L. Vadlamani, *J. Pharmacol. Exp. Ther.*, **185**, 287 (1973).

(5) A. E. Robinson and F. M. Williams, *J. Pharm. Pharmacol.*, **23**, 353 (1971).

(6) H. W. Elliott, F. N. H. Chang, I. A. Abdou, and H. H. Anderson, *J. Pharmacol. Exp. Ther.*, **95**, 494 (1949).

(7) J. C. Rickards, G. E. Boxer, and C. C. Smith, *ibid.*, **98**, 380 (1950).

(8) E. L. Way, C. Y. Sung, and W. P. McKelway, *ibid.*, **97**, 222 (1949).

(9) J. E. Wallace, H. E. Hamilton, J. T. Payte, and K. Blum, *J. Pharm. Sci.*, **61**, 1397 (1972).

(10) C. E. Inturrisi and K. Verebely, *J. Chromatogr.*, **65**, 361 (1972).

(11) E. J. McGonigle, *Anal. Chem.*, **43**, 966 (1971).

(12) M. T. Bush and P. M. Densen, *ibid.*, **20**, 121 (1948).

(13) B. B. Brodie and S. Udenfriend, *J. Biol. Chem.*, **158**, 705 (1945).

(14) A. L. Misra, N. L. Vadlamani, and S. J. Mule, *J. Chromatogr.*, **67**, 379 (1972).

ACKNOWLEDGMENTS

Supported by U.S. Public Health Service Training Grant GM-1217.

The advice and assistance of Dr. John D. Alvin are gratefully acknowledged.

Bioavailability of Chlorothiazide Tablets in Humans

ARTHUR B. STRAUGHN, ARMEN P. MELIKIAN *, and MARVIN C. MEYER ˣ

Received January 8, 1979, from the *Division of Biopharmaceutics and Pharmacokinetics, Department of Pharmaceutics, College of Pharmacy, University of Tennessee Center for the Health Sciences, Memphis, TN 38163.* Accepted for publication March 2, 1979. *Present address: Clinical Pharmacology Department, A. H. Robins Company, Richmond, VA 23220.

Abstract □ A urinary excretion bioavailability study was conducted in 12 healthy male subjects to evaluate three 250-mg and three 500-mg chlorothiazide tablet products. The study was a crossover design, and urine samples were collected 1, 2, 3, 4, 6, 8, 12, and 24 hr after administration of each dose. The resulting data were statistically analyzed for significant differences in cumulative percent of dose excreted at each sampling time, total drug recovery after 24 hr, maximum excretion rate, and time of maximum excretion rate. No statistically significant differences were found between the three 250-mg tablets tested. The urinary drug recovery after administration of one of the 500-mg products was significantly ($p < 0.05$) lower than that from the other two 500-mg tablets. The total mean recovery from each product ranged from only 11 to 20%, indicating that in general chlorothiazide was not well absorbed following oral administration. Attempts at correlating the urinary excretion data with the dissolution rate determinations were not successful.

Keyphrases □ Chlorothiazide—bioavailability, tablets, humans, urinary recovery □ Diuretics—chlorothiazide, tablets, bioavailability, humans □ Bioavailability—chlorothiazide tablets, humans

The Food and Drug Administration recently implemented a bioequivalence requirement for chlorothiazide tablets (1), and available information indicates that oral chlorothiazide dosage forms might exhibit bioavailability problems. The drug solubility is <1 mg/ml at pH ≤ 7 (2–4), and the usual oral dose is 0.5–1.0 g.

On the basis of urinary excretion studies, chlorothiazide appears to be incompletely absorbed from the GI tract of animals and humans (4–6). These studies reported 10–58% urinary recoveries of the oral dose administered to humans. The low urinary recovery of unchanged drug is not thought to be the result of other elimination routes since no metabolites have been identified and the urinary recovery of intravenously administered chlorothiazide approaches 100% (4, 6, 7).

In view of the potential for oral chlorothiazide dosage

0022-3549/79/0900-1099$01.00/0
© 1979, American Pharmaceutical Association

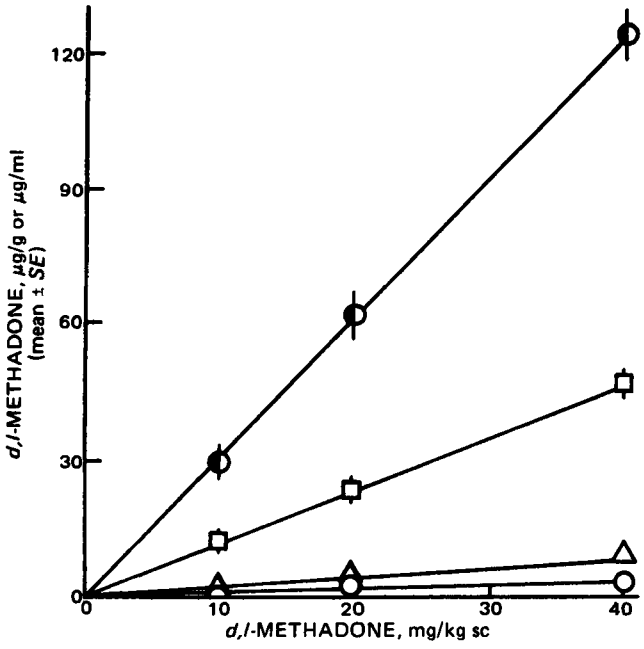

Figure 3—*Tissue* d,l-*methadone levels in the rat 60 min after subcutaneous administration of various* d,l-*methadone doses. Key:* ◐, *lung;* □, *liver;* △, *brain; and* ○, *serum.*

that these metabolites are extracted into the organic phase. However, they do not form fluorophores with paraformaldehyde. Also, morphine, diacetylmorphine (heroin), and codeine do not react with paraformaldehyde to form fluorophores. Cocaine forms a fluorophore but is not extracted from the aqueous phase (pH 9.2) under the conditions employed. Therefore, cocaine probably will not interfere in the methadone assay. Meperidine, amphetamine, and quinine form fluorophores with paraformaldehyde, and they are extracted into the organic phase. To remove the interference from these drugs, separation prior to their extraction into the organic phase is necessary.

Table II gives the levels of *d,l*-methadone in lung, liver, brain, and serum at various time intervals after 20 mg of *d,l*-methadone/kg was administered to rats subcutaneously. Figure 3 shows that the tissue levels were dose dependent.

REFERENCES

(1) V. P. Dole and M. E. Nyswander, *Br. J. Addict.*, **63**, 55 (1968).

(2) A. H. Beckett, M. Mitchard, and A. A. Shihab, *J. Pharm. Pharmacol.*, **23**, 347 (1971).

(3) A. Pohland, H. E. Boaz, and H. R. Sullivan, *J. Med. Chem.*, **14**, 194 (1971).

(4) A. L. Misra, S. J. Mule, R. Bloch, and N. L. Vadlamani, *J. Pharmacol. Exp. Ther.*, **185**, 287 (1973).

(5) A. E. Robinson and F. M. Williams, *J. Pharm. Pharmacol.*, **23**, 353 (1971).

(6) H. W. Elliott, F. N. H. Chang, I. A. Abdou, and H. H. Anderson, *J. Pharmacol. Exp. Ther.*, **95**, 494 (1949).

(7) J. C. Rickards, G. E. Boxer, and C. C. Smith, *ibid.*, **98**, 380 (1950).

(8) E. L. Way, C. Y. Sung, and W. P. McKelway, *ibid.*, **97**, 222 (1949).

(9) J. E. Wallace, H. E. Hamilton, J. T. Payte, and K. Blum, *J. Pharm. Sci.*, **61**, 1397 (1972).

(10) C. E. Inturrisi and K. Verebely, *J. Chromatogr.*, **65**, 361 (1972).

(11) E. J. McGonigle, *Anal. Chem.*, **43**, 966 (1971).

(12) M. T. Bush and P. M. Densen, *ibid.*, **20**, 121 (1948).

(13) B. B. Brodie and S. Udenfriend, *J. Biol. Chem.*, **158**, 705 (1945).

(14) A. L. Misra, N. L. Vadlamani, and S. J. Mule, *J. Chromatogr.*, **67**, 379 (1972).

ACKNOWLEDGMENTS

Supported by U.S. Public Health Service Training Grant GM-1217.

The advice and assistance of Dr. John D. Alvin are gratefully acknowledged.

Bioavailability of Chlorothiazide Tablets in Humans

ARTHUR B. STRAUGHN, ARMEN P. MELIKIAN *, and MARVIN C. MEYER ˣ

Received January 8, 1979, from the *Division of Biopharmaceutics and Pharmacokinetics, Department of Pharmaceutics, College of Pharmacy, University of Tennessee Center for the Health Sciences, Memphis, TN 38163.* Accepted for publication March 2, 1979. *Present address: Clinical Pharmacology Department, A. H. Robins Company, Richmond, VA 23220.

Abstract □ A urinary excretion bioavailability study was conducted in 12 healthy male subjects to evaluate three 250-mg and three 500-mg chlorothiazide tablet products. The study was a crossover design, and urine samples were collected 1, 2, 3, 4, 6, 8, 12, and 24 hr after administration of each dose. The resulting data were statistically analyzed for significant differences in cumulative percent of dose excreted at each sampling time, total drug recovery after 24 hr, maximum excretion rate, and time of maximum excretion rate. No statistically significant differences were found between the three 250-mg tablets tested. The urinary drug recovery after administration of one of the 500-mg products was significantly ($p < 0.05$) lower than that from the other two 500-mg tablets. The total mean recovery from each product ranged from only 11 to 20%, indicating that in general chlorothiazide was not well absorbed following oral administration. Attempts at correlating the urinary excretion data with the dissolution rate determinations were not successful.

Keyphrases □ Chlorothiazide—bioavailability, tablets, humans, urinary recovery □ Diuretics—chlorothiazide, tablets, bioavailability, humans □ Bioavailability—chlorothiazide tablets, humans

The Food and Drug Administration recently implemented a bioequivalence requirement for chlorothiazide tablets (1), and available information indicates that oral chlorothiazide dosage forms might exhibit bioavailability problems. The drug solubility is <1 mg/ml at pH ≤ 7 (2–4), and the usual oral dose is 0.5–1.0 g.

On the basis of urinary excretion studies, chlorothiazide appears to be incompletely absorbed from the GI tract of animals and humans (4–6). These studies reported 10–58% urinary recoveries of the oral dose administered to humans. The low urinary recovery of unchanged drug is not thought to be the result of other elimination routes since no metabolites have been identified and the urinary recovery of intravenously administered chlorothiazide approaches 100% (4, 6, 7).

In view of the potential for oral chlorothiazide dosage

0022-3549/79/0900-1099$01.00/0
© 1979, American Pharmaceutical Association

Table I—*In Vitro* Analysis of Chlorothiazide Tablets

Product[a]	Labeled Dose, mg	Assayed Percent of Label	Mean Disintegration Time, min[b]	Mean Time for Dissolution, min			
				30%	40%	50%	60%
1	250	105.8	1.7 (6)	4	10	34	72
2	500	99.4	0.5 (6)	10	57	110	>120
3	250	98.6	4.6 (12)	3	4	8	21
4	250	101.2	3.1 (6)	9	23	39	63
5	500	101.9	7.7 (6)	10	44	105	>120
6	500	93.5	16.4 (18)	6	19	47	>120

[a] Distributor (manufacturer if different from distributor) and lot numbers are as follows: 1, Merck Sharp & Dohme, S3420; 2, Merck Sharp & Dohme, T0972; 3, Econo-Rx (Bolar), 035437; 4, Columbia Medical Co. (Bolar), 015319; 5, Spencer Mead (Bolar), 065574; and 6, Econo-Rx (Bolar), 035438. [b] Tablets taking >30 min to disintegrate were averaged in as 30 min. Number in parentheses indicates number of tablets tested.

forms to exhibit incomplete or erratic absorption, a study was undertaken to evaluate the relative bioavailability of three lots of 250-mg and three lots of 500-mg chlorothiazide tablets manufactured by two companies. Attempts also were made to relate the *in vivo* data to the *in vitro* tablet disintegration and dissolution characteristics.

EXPERIMENTAL

Product Selection—Six products containing 250 or 500 mg of chlorothiazide were obtained through a local pharmacy. The six products (Table I) were from five different distributors but actually only represent two manufacturers. After the study was completed, it was learned that Products 3–6 had never been the subject of a New Drug Application.

***In Vitro* Studies**—Each product was evaluated for compliance with USP XIX (8) specifications for tablet content and disintegration. Although the USP XIX does not contain a chlorothiazide dissolution rate specification, dissolution testing was undertaken to provide *in vitro* data that might be useful for correlation with data from the *in vivo* studies.

The USP XIX rotating-basket apparatus was employed, using 900 ml of distilled water maintained at 37 ± 0.5° as the dissolution medium. The basket was rotated at 100 rpm, and 0.5-ml aliquots were removed every 5 min and diluted to 25 ml with distilled water. The resulting solutions were analyzed spectrophotometrically at 220 nm. The dissolution data were corrected for drug loss due to sample removal.

Clinical Study Protocol—Twelve adult males, between the ages of 23 and 28 years, volunteered to participate and provided written informed consent. Each subject was screened regarding general health and any known drug allergies. All subjects underwent a urine analysis and a hematologic and blood chemistry[1] analysis to ensure that they were in good health. The subjects ranged in height from 97 to 116 cm and in weight from 61.4 to 95.5 kg. Each subject was instructed to avoid any other medication during the study.

The 12 subjects received one of six different chlorothiazide tablets at weekly intervals for 6 weeks. The administration sequence was based on a crossover matrix to minimize any residual or cumulative effects of the preceding doses (9).

The tablets were administered in the morning following an overnight fast. No food or liquid other than water was permitted until 4 hr following dose ingestion. Just prior to dose administration the subjects voided a urine sample to be used as a blank. Following tablet administration, the subjects collected urine samples at 1, 2, 3, 4, 6, 8, 12, and 24 hr. The subjects were instructed to empty their bladders as completely as possible at each voiding. The sample volume was measured, and a portion was saved and frozen until analysis. Samples voided at other times were also measured and a portion was saved.

Data Analysis—Analysis of variance was used to determine significant differences ($p < 0.05$) between subjects, weeks, and drug products for cumulative percent of drug excreted at each sampling time, maximum excretion rate, time of maximum excretion rate, and cumulative drug excreted at 24 hr. The Newman–Keuls *a posteriori* test (10) was applied to evaluate where statistically significant differences occurred among the various parameters.

Urine Assay Methodology—All urine samples were analyzed in duplicate for chlorothiazide by a previously described spectrophotometric method (6) based on a modification of the procedure developed by Baer *et al.* (3).

[1] SMA 12/60.

RESULTS AND DISCUSSION

***In Vitro* Studies**—Table I summarizes the results of the *in vitro* tests. The analysis of a 20-tablet composite of each lot indicated that each product was within the 93–107% limits specified by the USP XIX for chlorothiazide tablets. Tablet disintegration tests were performed with and without disks in the disintegration chambers, even though USP XIX specifies that disks should be used. With the disks present, the six tablets of each product, except Product 1, disintegrated in less than 1 min; Product 1 disintegrated between 1.5 and 2.8 min. These times are well within the 30-min limit provided for in the USP.

When the disks were removed, there was greater variation in disintegration times among the products. Product 3 had one tablet out of 12 that did not disintegrate within 60 min. Seven of the 18 tablets tested for Product 6 did not disintegrate within 30 min, and two of the tablets did not disintegrate within 60 min. The mean disintegration time for the six products ranged from 0.5 (Product 2) to 16.4 (Product 6) min. When determining the average disintegration time, the maximum time utilized for any tablet was the USP limit of 30 min, even for tablets requiring more than 2 hr to disintegrate.

There was a large range in the tablet dissolution times as indicated in Table I. In view of the limited drug solubility, the 900 ml of water utilized as the dissolution medium probably was not sufficient to permit tablet dissolution under "sink conditions" (11). Therefore, even after 2 hr, the 500-mg tablets had not reached 60% dissolution.

Cumulative Percent of Dose Excreted—The mean cumulative percent of chlorothiazide excreted unchanged at each sampling time for the six products tested is illustrated in Fig. 1.

The mean cumulative 24-hr urinary recovery was quite low, ranging from 10.9% for Product 6 to 19.7% for Product 1. The greatest cumulative recovery observed in any one subject after single-dose administration

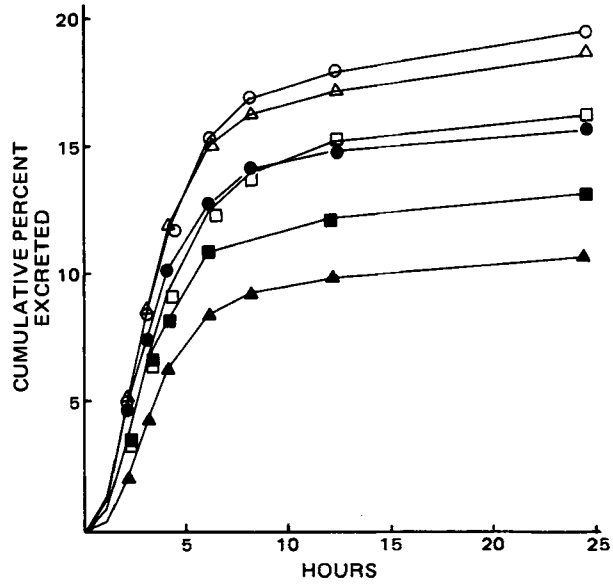

Figure 1—*Mean cumulative percent of chlorothiazide excreted following the oral administration of six tablet products. Each data point is the mean calculated for 12 subjects. Code numbers correspond to the products identified in Table I:* ○, *Product 1;* □, *Product 2;* △, *Product 3;* ●, *Product 4;* ■, *Product 5; and* ▲, *Product 6.*

Table II—Newman–Keuls *a Posteriori* Test for Significant Product Differences in Parameters Studied

Parameter	Product Ranking[a] (Lowest to Highest)					
Cumulative percent of dose excreted at:						
1 hr	6	4	2	5	1	3
2 hr	6	5	2	4	3	1
3 hr	6	5	2	4	3	1
4 hr	6	5	2	4	1	3
6 hr	6	5	2	4	3	1
8 hr	6	5	2	4	3	1
12 hr	6	5	4	2	3	1
24 hr	6	5	4	2	3	1
Total milligrams excreted	4	3	1	6	5	2
Maximum excretion rate, % of dose/hr	6	5	2	4	1	3
Time of maximum excretion rate	5	3	4	1	2	6

[a] Products underlined by a common line did not differ significantly ($p > 0.05$). See Table I for product identification.

was 33.3%, and recovery of more than 30% occurred only one other time. The cumulative 24-hr urinary recoveries also exhibited high coefficients of variation, ranging from 30% for Product 2 to 46% for Product 5. Such variability would be consistent with a poorly and erratically absorbed dosage form. These data may be contrasted to a recently completed study of 25- and 50-mg hydrochlorothiazide tablets in which ~75% of the administered dose was excreted as unchanged drug, and the mean values for the individual products exhibited coefficients of variation between 8 and 16% (12).

Table II summarizes the statistically significant differences among the products at each sampling time. There were differences ($p < 0.05$) at all sampling times in terms of cumulative percent of chlorothiazide excreted. Product 6 exhibited the lowest cumulative percent excreted at each sampling time, and Product 5 exhibited the next lowest recovery at all times except at the 1-hr sampling time.

In general, the three 500-mg chlorothiazide tablets (Products 2, 5, and 6) exhibited lower cumulative percent excretion than the 250-mg tablets at the various sampling times. Product 6 was significantly lower ($p < 0.05$) in cumulative percent excretion than one or more products at each sampling time. At 24 hr, the percent recovery for Products 5 and 6 was significantly lower ($p < 0.05$) than for Product 1, and the percent recovery for Product 6 also was significantly lower than for Products 2 and 3.

Other Urinary Excretion Parameters—Table III summarizes the mean values for maximum excretion rate, time of maximum excretion rate, and total milligrams of drug excreted after 24 hr. The results of the statistical analysis are presented in Table II.

The time of maximum excretion rate did not differ significantly among the six products ($p > 0.05$), although Product 6, which exhibited the lowest urinary recovery of drug, did require the longest time to achieve peak excretion. Since urine samples were collected only hourly during the first 4 hr of the study, the accuracy of the peak excretion time is limited.

As expected, the total chlorothiazide recovered in the urine after 24 hr indicated a greater recovery from the 500-mg tablets than from the 250-mg tablets. The drug recovered from Product 2 was significantly greater ($p < 0.05$) than from any other product, including the two other 500-mg tablets. The recovery from Product 6, a 500-mg tablet, did not differ significantly ($p > 0.05$) from that obtained with the three 250-mg products. On the basis of amount of drug excreted in 24 hr for Products 5 and 6, expressed as a percent relative to Product 2, the bioavailabilities of these two products were 81 and 66%, respectively. Furthermore, the recoveries from Products 5 and 6 did not differ significantly from the recovery from Product 2, which contained 50% as much drug. There was not a significant difference in urinary recovery among the three products containing 250 mg of chlorothiazide. The bioavailabilities of Products 3 and 4, based on the total amount of drug recovered expressed as a percent relative to Product 1, were 95 and 80%, respectively.

When the absorption and disposition processes operative for a drug exhibit linear kinetics, a proportionality between dose administered and amount of drug eliminated is expected. Thus, the percent of dose eliminated and the maximum excretion rate expressed as a percent of dose should be independent of the dose administered. The data obtained in the present study indicate that drug recovery after the 500-mg doses was not twice that after the 250-mg doses. The observed lack of proportionality between dose and urinary recovery could not be attributed to nonlinear elimination kinetics since previously reported studies involving intravenous administration of 500-mg chlorothiazide doses resulted in over 90% urinary recovery of unchanged drug (4, 6, 7).

Furthermore, a preliminary pilot study (6) involving the administration of 250 and 500-mg oral doses as a solution to two subjects resulted in an urinary recovery that was only 30% of the administered dose. Previous investigators (13), using a specific high pressure liquid chromatographic (HPLC) assay, also noted a lack of dose proportionality in the urinary recovery of chlorothiazide administered to dogs. The drug was quantitatively recovered after intravenous administration, but the recoveries declined from 70 to 26% as the oral dose was increased from 125 to 750 mg.

Following completion of the present study, a report (14) appeared which indicated that various modifications of the Bratton–Marshall assay for chlorothiazide may be subject to interferences from urinary constituents, which vary in concentration at each urine sampling time. In a noncrossover study (14) involving oral administration of 250- and 500-mg chlorothiazide tablets to two groups of two subjects, the colorimetric method employed in the present study underestimated by 1% the total 24-hr urinary chlorothiazide recovery in two subjects. In the other two subjects, the recovery was overestimated by 2 and 5.6% compared to recoveries determined using a HPLC assay. However, even with an HPLC assay, the reported 24-hr recoveries were only 5–10% for the 500-mg tablets and 14–20% for the 250-mg tablets. These workers (14) also observed that an additional 4–11% of the administered dose could be accounted for when the urinary collection was extended to 48 hr.

In the present study, less than 2% of the administered dose was recovered in the 12–24-hr collection period. Furthermore, the data shown in Fig. 1 suggest that extending the urine collection time would not have greatly increased the overall percent of administered drug recovered for each dosage form. In general, chlorothiazide apparently is not well absorbed following oral administration.

Subject and Week Differences—Analysis of variance indicated significant subject differences ($p < 0.05$) for each parameter examined, except for the time of maximum excretion rate. There were no significant differences ($p > 0.05$) among weeks.

***In Vitro–In Vivo* Relationships**—Attempts were made to correlate the *in vivo* data with the results of the disintegration time and dissolution rate determinations. Because of the large variability in the urinary excretion data at the early sampling times, only the 24-hr *in vivo* data were employed for correlation purposes. The time for 30% dissolution of the six products ranged from 3 to 10 min. The time for 60% dissolution ranged

Table III—Average Total Cumulative Milligrams, Maximum Excretion Rate, and Time of Maximum Excretion Rate[a]

Product[b]	Dose, mg	Maximum Excretion Rate, % of dose/hr	Time of Maximum Excretion Rate, hr	Total Milligrams Excreted in 24 hr
1	250	4.72 (41.8)	2.9 (46.8)	49.32 (36.45)
2	500	3.79 (31.6)	3.3 (41.4)	81.99 (29.91)
3	250	4.82 (44.5)	2.8 (35.3)	46.81 (42.32)
4	250	4.26 (42.4)	2.8 (31.4)	39.42 (32.15)
5	500	3.18 (55.4)	2.7 (39.3)	66.48 (46.11)
6	500	2.84 (38.3)	3.3 (26.6)	54.30 (31.10)

[a] Data presented as mean values for 12 subjects. Coefficient of variation (percent) is indicated in parentheses. [b] See Table I for product identification.

from 21 to 72 min for the three 250-mg tablets and was >2 hr for all three 500-mg tablets.

Because of the small range in 30% dissolution times and the excessively long 60% dissolution times, only the times for 40 and 50% dissolution were compared to the 24-hr cumulative percent recoveries. The correlation between dissolution time and urinary excretion was poor, although the attempt at correlation may have failed because of the previously cited lack of sink conditions during the dissolution rate determinations. The correlation coefficients, using the times for 40 and 50% dissolution, were only −0.352 and −0.399, respectively.

The disintegration times used for correlation with the urinary excretion data were determined without disks in the disintegration chambers, even though the USP XIX states that disks should be present. The data without disks were utilized because of the small range in disintegration times when the disks were present. In contrast to the correlation between dissolution and urinary excretion at 24 hr, the correlation between disintegration time and urinary excretion was considerably better, with a correlation coefficient of −0.829 ($p = 0.05$). However, the mean disintegration times employed for Products 3 and 6 were somewhat arbitrary because tablets requiring >30 min were averaged in as 30 min.

The results of these studies suggest that the present USP XIX disintegration specification should be revised to omit the use of disks in the apparatus. Moreover, a dissolution rate specification requiring 900 ml of distilled water as the dissolution medium apparently would not be useful in predicting the *in vivo* performance of chlorothiazide tablets.

REFERENCES

(1) *Fed. Regist.*, Jan. 7, 1977, Part III, V. 42, No. 5, 1649.

(2) W. F. Charnicki, F. A. Bacher, S. A. Freeman, and D. H. DeCesare, *J. Am. Pharm. Assoc., Sci. Ed.*, **48**, 656 (1959).

(3) J. E. Baer, H. L. Leidy, A. V. Brooks, and K. H. Beyer, *J. Pharmacol. Exp. Ther.*, **125**, 295 (1959).

(4) "Product Information Summary-Diuril," Merck Sharp and Dohme, West Point, Pa.

(5) R. E. Kauffman and D. L. Azarnoff, *Clin. Pharmacol. Ther.*, **14**, 886 (1973).

(6) M. C. Meyer and A. B. Straughn, *Curr. Ther. Res.*, **22**, 573 (1977).

(7) H. R. Brettell, J. K. Aikawa, and G. S. Gordon, *Arch. Intern. Med.*, **106**, 57 (1960).

(8) "The United States Pharmacopeia," 19th rev., Mack Publishing Co., Easton, Pa., 1975, p. 84.

(9) E. J. Williams, *Aust. J. Sci. Res. A*, **2**, 149 (1949).

(10) B. J. Winer, "Statistical Principles in Experimental Design," McGraw-Hill, New York, N.Y., 1971, pp. 185–196.

(11) M. Pernarowski, in "Dissolution Technology," L. J. Leeson and J. T. Carstensen, Eds., Industrial Pharmaceutical Technology Section of the Academy of Pharmaceutical Sciences, Washington, D.C., 1974, pp. 67–70.

(12) M. C. Meyer, A. P. Melikian, P. L. Whyatt, and G. W. A. Slywka, *Curr. Ther. Res.*, **17**, 570 (1975).

(13) D. E. Resetarits and T. R. Bates, "Abstracts," APhA Academy of Pharmaceutical Sciences, Hollywood, Fla., meeting, Nov. 12–16, 1978, p. 82, No. 26.

(14) V. P. Shah, P. Sojka, V. K. Prasad, and B. E. Cabana, "Abstracts," APhA Academy of Pharmaceutical Sciences, Montreal meeting, May 13–18, 1978, p. 195, No. 36.

ACKNOWLEDGMENTS

Supported in part by a contract from the Tennessee Department of Public Health and FDA Contract 223-74-3097.

The authors gratefully acknowledge the technical assistance of Ms. Ann Robinson and Ms. Donna Philips, the medical supervision of Dr. Philip Lieberman, the assistance of Ms. Ann McEachran in the statistical and computer data analysis, and the support of Mr. Herbert Bates, Jr., Pharmacist Consultant, Tennessee Department of Public Health.

Effect of Temperature and an Ion-Exchange Resin on Cation Diffusion through Silicone Polymer Tubing

DON P. CHRISTY, SUNG WAN KIM, and ROBERT V. PETERSEN ˣ

Received October 23, 1978, from the *Department of Pharmaceutics, College of Pharmacy, University of Utah, Salt Lake City, UT 84112.* Accepted for publication February 28, 1979.

Abstract □ Permeation of cations through silicone rubber tubing was measured, and the effect of an ion-exchange resin on the cation diffusion was determined. Silicone rubber has been used as a biomedical polymer and shows a very low solubility to ionizable species. Correlations between the calculated diffusion coefficients, with and without the resin, depended on the charge and number of waters of hydration for each cation. These increases ranged from 1.11 for potassium to 3.06 for iron, multiplied by the diffusion coefficient as a result of the resin. Solubilities of each cation in the polymer were temperature dependent. Activation energies were calculated for each cation by measuring the increased permeation with increasing temperature, with and without the resin. Decreasing magnitudes of activation energies ranged from 0.91 for sodium to 0.57 for iron when the resin was present. Correlations were established between the measured activation energies and reported free energy change for the hydration of each cation.

Keyphrases □ Cations—diffusion through silicone polymer tubing, effect of temperature and ion-exchange resin □ Temperature—effect on cation diffusion through silicone polymer tubing □ Ion-exchange resins—effect on cation diffusion through silicone polymer tubing □ Dosage forms, sustained release—silicone polymer tubing, effect of temperature and ion-exchange resin on cation diffusion

Because of the minimal body tissue response and relatively high diffusivities of hydrophobic solutes, polydimethylsilicone is an excellent candidate for sustained-release medication implantation devices. Hydrophobic solute diffusion through this polymer is well documented (1–6), showing high rates of diffusivity and polymer solubility.

BACKGROUND

Little information is available on the permeation of charged or uncharged solutes that show a low solubility in silicone films. In evaluating the function of silicone heart valves, a previous investigator (7) reported that hydrophobic dyes such as rhodamine diffused into the valve, while hydrophilic dyes such as methylene blue did not. Silicone capsules containing normal saline, 5% dextrose in water, sodium citrate, and a calcium-saturated solution of edetic acid showed a lack of permeation of these solutes through the polymer (8).

Permeation of both charged and uncharged solutes through silicone membranes has been measured (9). Silicone was not permeated by the charged organic molecules but was permeated by the uncharged organic molecules, which were lipophilic. Both atropine base and histamine diffused through silicone rubber tubes (10). Histamine is water soluble.

The limited permeability of charged or water-soluble solutes has re-

0022-3549/79/0900-1102$01.00/0

© 1979, American Pharmaceutical Association

from 21 to 72 min for the three 250-mg tablets and was >2 hr for all three 500-mg tablets.

Because of the small range in 30% dissolution times and the excessively long 60% dissolution times, only the times for 40 and 50% dissolution were compared to the 24-hr cumulative percent recoveries. The correlation between dissolution time and urinary excretion was poor, although the attempt at correlation may have failed because of the previously cited lack of sink conditions during the dissolution rate determinations. The correlation coefficients, using the times for 40 and 50% dissolution, were only −0.352 and −0.399, respectively.

The disintegration times used for correlation with the urinary excretion data were determined without disks in the disintegration chambers, even though the USP XIX states that disks should be present. The data without disks were utilized because of the small range in disintegration times when the disks were present. In contrast to the correlation between dissolution and urinary excretion at 24 hr, the correlation between disintegration time and urinary excretion was considerably better, with a correlation coefficient of −0.829 ($p = 0.05$). However, the mean disintegration times employed for Products 3 and 6 were somewhat arbitrary because tablets requiring >30 min were averaged in as 30 min.

The results of these studies suggest that the present USP XIX disintegration specification should be revised to omit the use of disks in the apparatus. Moreover, a dissolution rate specification requiring 900 ml of distilled water as the dissolution medium apparently would not be useful in predicting the *in vivo* performance of chlorothiazide tablets.

REFERENCES

(1) *Fed. Regist.*, Jan. 7, 1977, Part III, V. 42, No. 5, 1649.

(2) W. F. Charnicki, F. A. Bacher, S. A. Freeman, and D. H. DeCesare, *J. Am. Pharm. Assoc., Sci. Ed.*, **48**, 656 (1959).

(3) J. E. Baer, H. L. Leidy, A. V. Brooks, and K. H. Beyer, *J. Pharmacol. Exp. Ther.*, **125**, 295 (1959).

(4) "Product Information Summary-Diuril," Merck Sharp and Dohme, West Point, Pa.

(5) R. E. Kauffman and D. L. Azarnoff, *Clin. Pharmacol. Ther.*, **14**, 886 (1973).

(6) M. C. Meyer and A. B. Straughn, *Curr. Ther. Res.*, **22**, 573 (1977).

(7) H. R. Brettell, J. K. Aikawa, and G. S. Gordon, *Arch. Intern. Med.*, **106**, 57 (1960).

(8) "The United States Pharmacopeia," 19th rev., Mack Publishing Co., Easton, Pa., 1975, p. 84.

(9) E. J. Williams, *Aust. J. Sci. Res. A*, **2**, 149 (1949).

(10) B. J. Winer, "Statistical Principles in Experimental Design," McGraw-Hill, New York, N.Y., 1971, pp. 185–196.

(11) M. Pernarowski, in "Dissolution Technology," L. J. Leeson and J. T. Carstensen, Eds., Industrial Pharmaceutical Technology Section of the Academy of Pharmaceutical Sciences, Washington, D.C., 1974, pp. 67–70.

(12) M. C. Meyer, A. P. Melikian, P. L. Whyatt, and G. W. A. Slywka, *Curr. Ther. Res.*, **17**, 570 (1975).

(13) D. E. Resetarits and T. R. Bates, "Abstracts," APhA Academy of Pharmaceutical Sciences, Hollywood, Fla., meeting, Nov. 12–16, 1978, p. 82, No. 26.

(14) V. P. Shah, P. Sojka, V. K. Prasad, and B. E. Cabana, "Abstracts," APhA Academy of Pharmaceutical Sciences, Montreal meeting, May 13–18, 1978, p. 195, No. 36.

ACKNOWLEDGMENTS

Supported in part by a contract from the Tennessee Department of Public Health and FDA Contract 223-74-3097.

The authors gratefully acknowledge the technical assistance of Ms. Ann Robinson and Ms. Donna Philips, the medical supervision of Dr. Philip Lieberman, the assistance of Ms. Ann McEachran in the statistical and computer data analysis, and the support of Mr. Herbert Bates, Jr., Pharmacist Consultant, Tennessee Department of Public Health.

Effect of Temperature and an Ion-Exchange Resin on Cation Diffusion through Silicone Polymer Tubing

DON P. CHRISTY, SUNG WAN KIM, and ROBERT V. PETERSEN ˣ

Received October 23, 1978, from the *Department of Pharmaceutics, College of Pharmacy, University of Utah, Salt Lake City, UT 84112.* Accepted for publication February 28, 1979.

Abstract □ Permeation of cations through silicone rubber tubing was measured, and the effect of an ion-exchange resin on the cation diffusion was determined. Silicone rubber has been used as a biomedical polymer and shows a very low solubility to ionizable species. Correlations between the calculated diffusion coefficients, with and without the resin, depended on the charge and number of waters of hydration for each cation. These increases ranged from 1.11 for potassium to 3.06 for iron, multiplied by the diffusion coefficient as a result of the resin. Solubilities of each cation in the polymer were temperature dependent. Activation energies were calculated for each cation by measuring the increased permeation with increasing temperature, with and without the resin. Decreasing magnitudes of activation energies ranged from 0.91 for sodium to 0.57 for iron when the resin was present. Correlations were established between the measured activation energies and reported free energy change for the hydration of each cation.

Keyphrases □ Cations—diffusion through silicone polymer tubing, effect of temperature and ion-exchange resin □ Temperature—effect on cation diffusion through silicone polymer tubing □ Ion-exchange resins—effect on cation diffusion through silicone polymer tubing □ Dosage forms, sustained release—silicone polymer tubing, effect of temperature and ion-exchange resin on cation diffusion

Because of the minimal body tissue response and relatively high diffusivities of hydrophobic solutes, polydimethylsilicone is an excellent candidate for sustained-release medication implantation devices. Hydrophobic solute diffusion through this polymer is well documented (1–6), showing high rates of diffusivity and polymer solubility.

BACKGROUND

Little information is available on the permeation of charged or uncharged solutes that show a low solubility in silicone films. In evaluating the function of silicone heart valves, a previous investigator (7) reported that hydrophobic dyes such as rhodamine diffused into the valve, while hydrophilic dyes such as methylene blue did not. Silicone capsules containing normal saline, 5% dextrose in water, sodium citrate, and a calcium-saturated solution of edetic acid showed a lack of permeation of these solutes through the polymer (8).

Permeation of both charged and uncharged solutes through silicone membranes has been measured (9). Silicone was not permeated by the charged organic molecules but was permeated by the uncharged organic molecules, which were lipophilic. Both atropine base and histamine diffused through silicone rubber tubes (10). Histamine is water soluble.

The limited permeability of charged or water-soluble solutes has re-

0022-3549/79/0900-1102$01.00/0

© 1979, American Pharmaceutical Association

stricted the use of silicone as a potential drug delivery carrier for water-soluble or charged drugs. If an additional factor could be added to enhance the permeation of charged solutes through silicone rubber, new delivery systems could be devised for these drugs.

The use of charged nondiffusable polyelectrolytes to increase coion diffusion was suggested previously (11). Carboxymethylcellulose sodium greatly increased the diffusion of both penicillin and salicylate ions, more than doubling the observed transport rate and equilibrium distribution compared to the rate and distribution when the resin was not present. Similar results were obtained by investigators (12) who measured electrostatic forces between polyelectrolyte solutions and counterions and the effect of these forces on counterion diffusion. It has been observed in this laboratory (13) that a positively charged polyelectrolyte increases the diffusion rate and equilibrium concentrations of cations by its presence, based on the Donnan membrane effect.

The purpose of the work was to determine the effects of an anion-exchange resin on the diffusion rate of the cations through silicone polymer. It was postulated that the resin would provide an additional driving force due to electrostatic repulsion between the resin and the cations and would increase their diffusion rate.

EXPERIMENTAL

Materials—The diffusion species used were the chloride salts of potassium, sodium, calcium, and iron prepared from reagent grade chemicals. Silicone[1] polymer tubing and medical grade adhesive[2] were used throughout the experiment. The tubing sizes (inside diameter by outside diameter in centimeters) were: A, 0.335 × 0.465; B, 0.267 × 0.318; and C, 0.292 × 0.318. The anion-exchange resin[3] was a trimethylbenzylammonium chloride polymer. Deionized water was used in the preparation of all solutions.

Methods—Specific lengths of silicone polymer tubing were sealed at one end with the adhesive and allowed to cure. The tubes were filled with aqueous solutions of 1-mg/ml concentrations of each cation, leaving a small air space at the top of each tube, and then were sealed with the adhesive. Two tubes were prepared for each cation, one containing only the cation solution and the other containing the cation solution plus 10 mg of the resin/ml.

The filled polymer tubes were placed in glass tubes, and a deionized water receptor phase was added in a volume sufficient to immerse completely the polymer tube and leave only a small air space after the glass tube was stoppered. The prepared glass tubes were rotated end over end at a constant 16 rpm, which caused the air bubbles in the silicone tubes to traverse the entire length of the tube during each half-revolution. This procedure produced a uniform distribution of the resin and a continual solution mixing within the polymer tubes. This rotation also produced receptor phase mixing.

The receptor phase was changed weekly and analyzed for cation concentration by atomic absorption spectrophotometry[4]. The receptor phase for the 1st week was discarded because 4–6 days was required before any cations appeared in the receptor phase. Temperature regulation was maintained by placing the glass tubes in an incubator; all solutions and equipment were brought to the appropriate temperature before the experiments.

The solubility of each cation in the silicone polymer was determined by using a known polymer volume and measuring the ion depletion from a solution of known concentration and volume. The polymer was placed in each cation solution for 7 days, removed, and desorbed by deionized water for another 7 days. The membrane was used for cation solubility determinations after drying in an evacuated chamber to a constant weight.

RESULTS AND DISCUSSION

The mathematical relationship for the diffusion from a cylinder consists of a membrane diffusional component and a diffusional layer component. Research into the diffusion from polymeric systems (14) indicates that the rate-determining step is the membrane diffusional component and that the diffusion rate follows Fick's law. A modified form of the general case for diffusion through a cylinder, as obtained from the literature (15), is given by:

[1] Silastic, Dow Corning Corp., Midland, Mich.
[2] Silastic Type A, Dow Corning Corp., Midland, Mich.
[3] Dowex-1, Sigma Chemical Corp., St. Louis, Mo.
[4] Model 305-A, Perkin-Elmer Corp., Norwalk, Conn.

Table I—Cation Solubility in Silicone Rubber at Different Temperatures

Temperature	Potassium, $\mu g/cm^3$	Sodium, $\mu g/cm^3$	Calcium, $\mu g/cm^3$	Iron (Ferric), $\mu g/cm^3$
15°	1.44	1.37	1.38	1.20
25°	1.72	1.64	1.66	1.45
35°	1.98	1.96	1.98	1.74

$$J = 2\pi h D_m C_m / \ln\left(\frac{\text{o.d.}}{\text{i.d.}}\right) \qquad \text{(Eq. 1)}$$

where J is the flux, h is the cylinder length, D_m is the diffusion coefficient, C_m is the solubility of the diffusing species in the polymer, and o.d. and i.d. are the outer and inner wall diameters, respectively. Flux was determined by measuring the concentration of each ion as it appears in the receptor phase and calculating the cumulative release (micrograms) per centimeter of tube length over the measured time periods.

The relation of activation energies to the diffusion coefficients are shown by Eq. 2, a modified Arrhenius equation:

$$\ln\frac{D_2}{D_1} = \frac{E_a}{R}\frac{(T_2 - T_1)}{T_2 T_1} \qquad \text{(Eq. 2)}$$

where D_1 is the diffusion coefficient at temperature T_1, D_2 is the diffusion coefficient at temperature T_2, E_a is the activation energy, and R is the gas content; E_a was calculated from the slope of ln D *versus* $(1/t)$.

The filler used in silicone polymer reportedly (16–18) is high surface area fumed silica, which physically adsorbs many diffusing species. This adsorption may physically remove such species from the diffusion process or slow down the diffusion rate. Therefore, these adsorption sites would influence species solubility and diffusion lag times for each ion. This factor was the primary reason for presoaking the polymer in a solution of each ion before polymer solubilities were determined.

The solubilities of the four cations in silicone rubber are shown in Table I. Iron had the least solubility, sodium and calcium solubilities were nearly identical, and potassium showed the greatest solubility. The solubilities of all ions increased with temperature.

A typical concentration *versus* time plot is shown in Fig. 1. A cumulative total of micrograms of calcium that diffused through the silicone tubes, with and without the resin at 25°, is plotted against time. The effects of the resin are visible, as can be seen from the increasing slopes of the lines. The linearity of the plotted data is reasonable due to the differences in ion concentrations on each side of the polymer. Few ions

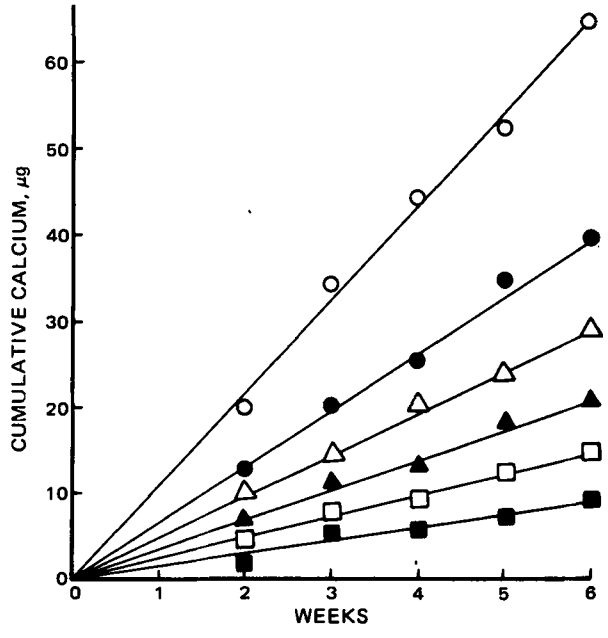

Figure 1—*Cumulative micrograms of calcium* versus *time at 25°. Key:* ○, *calcium plus resin for Tube C;* ●, *calcium for Tube C;* △, *calcium plus resin for Tube B;* ▲, *calcium for Tube B;* □, *calcium plus resin for Tube A; and* ■, *calcium for Tube A.*

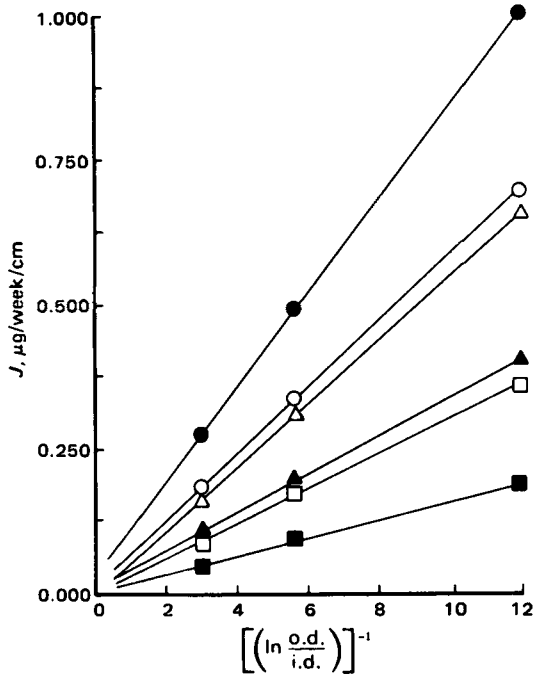

Figure 2—*Flux (J) for calcium permeation from Silastic polymer tubes versus [ln (o.d./i.d.)]$^{-1}$ for Tubes A–C. Key: ●, calcium plus resin at 35°; ○, calcium at 35°; △, calcium plus resin at 25°; ▲, calcium at 25°; □, calcium plus resin at 15°; and ■, calcium at 15°.*

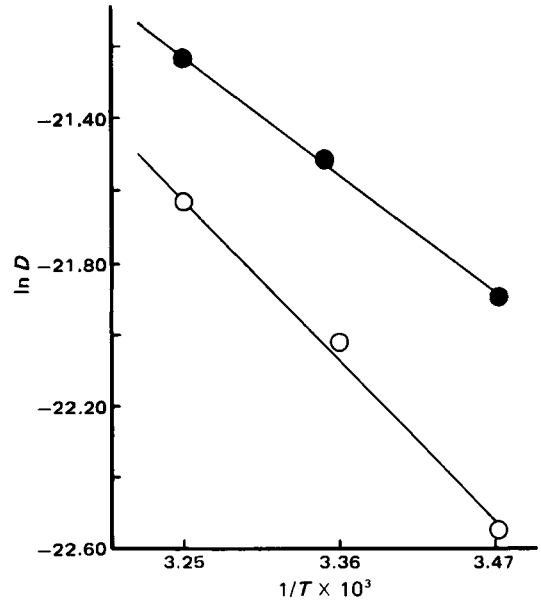

Figure 3—*Arrhenius plot of ln* D versus *1/*T *for calcium (○) and calcium plus resin (●).*

permeated the tubing relative to the ionic concentration within the tube, the latter being almost constant.

The diffusion results are shown in Fig. 2 for calcium, where the flux, J, is plotted against [ln (o.d./i.d.)]$^{-1}$ of each silicone tube. This figure depicts the data from the measured flux at three temperatures, with and without the resin. The effect of the resin on its diffusion through the polymer is in the order: iron > calcium > sodium > potassium.

Diffusion coefficients calculated from the slopes of these plots are given in Table II. Here D_m is the diffusion coefficient where no resin was present, and D_m^* is the diffusion coefficient where the resin was present. The correlation coefficients were greater than 0.99.

A comparison of D_m *versus* D_m^* was obtained from the ratio D_m^*/D_m at 25°: potassium, 1.11; sodium, 1.26; calcium, 1.62; and iron, 1.81. Because the increase in the diffusion rate due to the resin is based on the repulsion of like charges on the resin and the ions, for a given equal weight concentration the charge groups per unit volume for the ions is in the order: iron > calcium > sodium > potassium.

The calculated effect the resin would have on the increased diffusion rate for these ions using the Donnan equilibrium, times the diffusion where no resin was present, is: potassium, 1.46; sodium, 2.48; calcium, 2.85; and iron, 3.06. These figures were obtained by calculating the gram equivalent per liter of each cation present in a 1-mg/ml concentration and the electrical repulsion due to the resin in a 10-mg/ml concentration. Comparison of the calculated to actual increased diffusion rate caused by the resin demonstrates that the actual rate was less than the calculated rate. This finding could be due, in part, to the limited solubility of the ions in the polymer, which may be the rate-limiting step for the diffusion process.

Activation energies as calculated from the slopes of the lines of plots similar to Fig. 3 are given in Table III. Figure 3 is a plot of ln D *versus* $1/T$ for calcium. Decreased activation energies can be seen by the difference of the slopes for the resin and nonresin plots; E_a signifies that no resin was present, and E_a^* indicates that the resin was present in the silicone tube. Correlation coefficients all exceeded 0.99.

Activation energies decreased due to the resin in the same order and about to the same extent as the diffusion coefficients increased. Ratios of E_a^*/E_a are: potassium, 0.91; sodium, 0.81; calcium, 0.72; and iron, 0.57.

Table IV is a comparison of activation energy and various parameters obtained from the literature. In each case, the activation energy where no resin was present, as calculated from the results of this experiment, was only slightly larger than the free energy change for the ion hydration.

These data may suggest that the ions utilize dehydration energy for the initial movement into the membrane. Because of the hydrophobic nature of silicone rubber, the measured activation energies may be important in the hypothesis that only the dehydrated ion permeates these types of polymers. When the resin was present, the measured activation energies of the ions for diffusion were less than when no resin was present. The magnitude of decreased activation energies increased as the charge on the ion increased. This effect was due to the increased electrical re-

Table II—Measured Cation Diffusion Coefficients through Silicone Rubber

Cation	Temperature	$D_m \times 10^{10}$, cm^2/sec	$D_m^* \times 10^{10}$, cm^2/sec
Potassium	35°	4.34	4.61
	25°	3.12	3.46
	15°	1.93	2.21
Sodium	35°	3.71	4.41
	25°	2.62	3.30
	15°	1.58	2.20
Calcium	35°	4.03	5.97
	25°	2.80	4.54
	15°	1.59	3.06
Iron (ferric)	35°	3.70	5.94
	25°	2.44	4.42
	15°	1.17	3.08

Table III—Measured Cation Activation Energies

Cation	E_a, kcal/mole	E_a^*, kcal/mole
Potassium	7.3	6.7
Sodium	7.7	6.2
Calcium	8.4	6.1
Iron (ferric)	10.4	6.0

Table IV—Reported Values of the Radius of the Ions (r) (19), the Number of Waters of Hydration (N) (20), and the Free Energy of Hydration for the Ions (ΔG) (21) and E_a Values from Table III

Parameter	Potassium	Sodium	Calcium	Iron (Ferric)
r, Å	1.38	0.95	0.99	0.64
N	3	4	10	12
ΔG, kcal/mole	7.08	7.45	8.16	—
E_a	7.31	7.68	8.40	10.39

pulsion between the resin and the ion as the net charge difference increased. The resin introduced an additional driving force, which reduced the activation energy required for each ion to permeate the membrane.

REFERENCES

(1) P. J. Dziuk and B. Cook, *Endocrinology*, **78**, 208 (1966).

(2) P. J. Dziuk, B. Cook, G. D. Niswender, C. C. Kaltenbach, and B. B. Doane, *Am. J. Vet. Res.*, **29**, 2415 (1968).

(3) F. A. Kincl, G. Benagiano, and I. Angee, *Steroids*, **11**, 673 (1968).

(4) G. Levy and E. J. Mroszczak, *J. Pharm Sci.*, **57**, 235 (1968).

(5) R. H. Reuning and G. Levy, *ibid.*, **58**, 79 (1969).

(6) K. Sundaram and F. A. Kincl, *Steroids*, **12**, 517 (1968).

(7) D. M. Long, speech given at Naval Medical Research Institute, National Naval Medical Center, Bethesda, Md.

(8) J. Folkman and D. Long, *J. Surg. Res.*, **4**, 139 (1964).

(9) E. R. Garrett and P. B. Chemburkar, *J. Pharm. Sci.*, **57**, 944, 949, 1401 (1968).

(10) P. Bass, *Nature*, **208**, 591 (1965).

(11) T. Higuchi, R. Kuramoto, L. Kennon, T. Flanagan, and A. Polk, *J. Am. Pharm. Assoc., Sci. Ed.*, **43**, 646 (1954).

(12) E. Pefferkan and R. Varogui, *Eur. Polym. J.*, **6**, 663 (1970).

(13) D. P. Christy, S. W. Kim, and R. V. Petersen, *J. Pharm. Sci.*, in press.

(14) A. L. Tanquary and R. E. Lacey, in "Advances in Experimental Medicine and Biology," vol. 47, Plenum, New York, N.Y., 1974.

(15) J. Crank, "The Mathematics of Diffusion," Oxford University Press, London, England, 1964.

(16) C. F. Most, *J. Appl. Polym. Sci.*, **14**, 1019 (1970).

(17) W. Higuchi and T. Higuchi, *J. Am. Pharm. Assoc., Sci. Ed.*, **49**, 598 (1960).

(18) K. F. Finger, A. P. Lemberger, T. Higuchi, L. W. Busse, and D. E. Wurster, *ibid.*, **49**, 569 (1960).

(19) R. Noyes, *J. Am. Chem. Soc.*, **84**, 513 (1962).

(20) J. O'm Bockris, "Modern Electrochemistry," vol. 1, Plenum, New York, N.Y., 1970.

(21) M. Jhon, H. B. Lee, S. W. Kim, and J. Andrade, *J. Korean Chem. Soc.*, **20**, 448 (1976).

Antipyretic Effect of Acetaminophen Suppositories in Rats

ALBERT LOCK, BRENDA McALLISTER ECKMAN, and JAMES AYRES ˣ

Received October 24, 1978, from the *School of Pharmacy, Oregon State University, Corvallis, OR 97331.* Accepted for publication March 6, 1979.

Abstract □ An animal model used yeast-fevered rats to measure the relative antipyretic effects of different commercially available acetaminophen-containing suppositories. A laboratory-prepared acetaminophen-containing suppository and placebo suppositories also were investigated. Release from the suppositories was measured *in vitro*. All acetaminophen products containing 600 mg of drug elicited significant decreases in the rectal temperature of fever-induced rats.

Keyphrases □ Antipyretic agents—acetaminophen, suppositories, rats □ Acetaminophen—antipyretic effects, suppositories, rats □ Dosage forms, solid—suppositories, acetaminophen, antipyretic effects, rats

The antipyretic effect of acetaminophen is well known. However, formulation factors can influence the rate and extent of acetaminophen bioavailability from rectal dosage forms (1–5). Drug release from suppository vehicles is necessary before absorption can occur. Acetaminophen release from various polyethylene glycol vehicles appears to be related to its solubility in the vehicle, which, in turn, is related to vehicle dielectric properties (1, 2). Different formulations of polyethylene glycol suppositories show fairly wide variation in total urinary acetaminophen excretion due to differences in absorption patterns of the rectally administered acetaminophen (1).

The use of rectal suppositories for systemic acetaminophen administration has been the subject of recent studies in humans. The results from a well-controlled, double-blind study in humans indicated no significant differences in antipyretic effect between acetaminophen administration of a hospital pharmacy-prepared suppository and a commercially available tablet dosage form (4). However, large differences in acetaminophen bioavailability from suppositories prepared in two different hospitals were found when they were compared to a commercial rectal product in a urinary excretion study using human subjects (5). The large differences found in the relative bioavailability, peak excretion rates, and times of peak action between the hospital-manufactured acetaminophen suppositories themselves and the commercially obtained product prompted the investigator to suggest the need for *in vivo* testing of hospital-prepared suppositories (5).

The purpose of this study was to compare *in vivo* the antipyretic effects of five different generic acetaminophen suppository products purchased from different commercial sources with acetaminophen-containing and placebo suppositories prepared in this laboratory. The animal model used was a modified version of a previously reported *in vivo* method for measuring the antipyretic effect of aspirin in rats (6).

EXPERIMENTAL

Reagents and Equipment—Petrolatum[1], polyethylene glycol 1540[2], polyethylene glycol 6000[2], polyethylene glycol 400[2], acetaminophen[3], brewer's yeast[4], and ether[5] were used as supplied.

Acetaminophen suppositories, A–E[6], were obtained from commercial sources.

The equipment used included a rectal thermometer[7], thermistor probe[8], wound clip applier[9], and 9-mm wound clips[10].

[1] Matheson, Coleman and Bell, Norwood, OH 45212.
[2] J. T. Baker Chemical Co., Phillipsburg, NJ 08865.
[3] Lot 7032-LSR-43, S. B. Penick, Lyndhurst, NJ 07071.
[4] E. R. Squibb & Sons, Princeton, NJ 08540.
[5] Mallinckrodt, St. Louis, MO 63147.
[6] Product A, Westward, Inc., Eatontown, NJ 07724; Product B, American Quinine, Hospital Division of Natcon Chemicals, Plainview, NJ 11803; Product C, Consolidated Midland Corp., Brewster, NY 10509; Product D, Reiss Williams Co., Division of G & W Laboratories, Port Reading, NJ 07064; and Product E, Upsher-Smith Laboratories, Minneapolis, MN 55415.
[7] Model 47TD, Yellow Springs Instrument Co., Yellow Springs, Ohio.
[8] Series T2 605, Yellow Springs Instrument Co., Yellow Springs, Ohio.
[9] Model 7630, Clay Adams, Division of Becton, Parsippany, NJ 07054.
[10] Clay Adams, Parsippany, NJ 07054.

0022-3549/79/0900-1105$01.00/0

© 1979, American Pharmaceutical Association

pulsion between the resin and the ion as the net charge difference increased. The resin introduced an additional driving force, which reduced the activation energy required for each ion to permeate the membrane.

REFERENCES

(1) P. J. Dziuk and B. Cook, *Endocrinology*, **78**, 208 (1966).

(2) P. J. Dziuk, B. Cook, G. D. Niswender, C. C. Kaltenbach, and B. B. Doane, *Am. J. Vet. Res.*, **29**, 2415 (1968).

(3) F. A. Kincl, G. Benagiano, and I. Angee, *Steroids*, **11**, 673 (1968).

(4) G. Levy and E. J. Mroszczak, *J. Pharm Sci.*, **57**, 235 (1968).

(5) R. H. Reuning and G. Levy, *ibid.*, **58**, 79 (1969).

(6) K. Sundaram and F. A. Kincl, *Steroids*, **12**, 517 (1968).

(7) D. M. Long, speech given at Naval Medical Research Institute, National Naval Medical Center, Bethesda, Md.

(8) J. Folkman and D. Long, *J. Surg. Res.*, **4**, 139 (1964).

(9) E. R. Garrett and P. B. Chemburkar, *J. Pharm. Sci.*, **57**, 944, 949, 1401 (1968).

(10) P. Bass, *Nature*, **208**, 591 (1965).

(11) T. Higuchi, R. Kuramoto, L. Kennon, T. Flanagan, and A. Polk, *J. Am. Pharm. Assoc., Sci. Ed.*, **43**, 646 (1954).

(12) E. Pefferkan and R. Varogui, *Eur. Polym. J.*, **6**, 663 (1970).

(13) D. P. Christy, S. W. Kim, and R. V. Petersen, *J. Pharm. Sci.*, in press.

(14) A. L. Tanquary and R. E. Lacey, in "Advances in Experimental Medicine and Biology," vol. 47, Plenum, New York, N.Y., 1974.

(15) J. Crank, "The Mathematics of Diffusion," Oxford University Press, London, England, 1964.

(16) C. F. Most, *J. Appl. Polym. Sci.*, **14**, 1019 (1970).

(17) W. Higuchi and T. Higuchi, *J. Am. Pharm. Assoc., Sci. Ed.*, **49**, 598 (1960).

(18) K. F. Finger, A. P. Lemberger, T. Higuchi, L. W. Busse, and D. E. Wurster, *ibid.*, **49**, 569 (1960).

(19) R. Noyes, *J. Am. Chem. Soc.*, **84**, 513 (1962).

(20) J. O'm Bockris, "Modern Electrochemistry," vol. 1, Plenum, New York, N.Y., 1970.

(21) M. Jhon, H. B. Lee, S. W. Kim, and J. Andrade, *J. Korean Chem. Soc.*, **20**, 448 (1976).

Antipyretic Effect of Acetaminophen Suppositories in Rats

ALBERT LOCK, BRENDA McALLISTER ECKMAN, and JAMES AYRES ˣ

Received October 24, 1978, from the *School of Pharmacy, Oregon State University, Corvallis, OR 97331.* Accepted for publication March 6, 1979.

Abstract □ An animal model used yeast-fevered rats to measure the relative antipyretic effects of different commercially available acetaminophen-containing suppositories. A laboratory-prepared acetaminophen-containing suppository and placebo suppositories also were investigated. Release from the suppositories was measured *in vitro*. All acetaminophen products containing 600 mg of drug elicited significant decreases in the rectal temperature of fever-induced rats.

Keyphrases □ Antipyretic agents—acetaminophen, suppositories, rats □ Acetaminophen—antipyretic effects, suppositories, rats □ Dosage forms, solid—suppositories, acetaminophen, antipyretic effects, rats

The antipyretic effect of acetaminophen is well known. However, formulation factors can influence the rate and extent of acetaminophen bioavailability from rectal dosage forms (1–5). Drug release from suppository vehicles is necessary before absorption can occur. Acetaminophen release from various polyethylene glycol vehicles appears to be related to its solubility in the vehicle, which, in turn, is related to vehicle dielectric properties (1, 2). Different formulations of polyethylene glycol suppositories show fairly wide variation in total urinary acetaminophen excretion due to differences in absorption patterns of the rectally administered acetaminophen (1).

The use of rectal suppositories for systemic acetaminophen administration has been the subject of recent studies in humans. The results from a well-controlled, double-blind study in humans indicated no significant differences in antipyretic effect between acetaminophen administration of a hospital pharmacy-prepared suppository and a commercially available tablet dosage form (4). However, large differences in acetaminophen bioavailability from suppositories prepared in two different hospitals were found when they were compared to a commercial rectal product in a urinary excretion study using human subjects (5). The large differences found in the relative bioavailability, peak excretion rates, and times of peak action between the hospital-manufactured acetaminophen suppositories themselves and the commercially obtained product prompted the investigator to suggest the need for *in vivo* testing of hospital-prepared suppositories (5).

The purpose of this study was to compare *in vivo* the antipyretic effects of five different generic acetaminophen suppository products purchased from different commercial sources with acetaminophen-containing and placebo suppositories prepared in this laboratory. The animal model used was a modified version of a previously reported *in vivo* method for measuring the antipyretic effect of aspirin in rats (6).

EXPERIMENTAL

Reagents and Equipment—Petrolatum[1], polyethylene glycol 1540[2], polyethylene glycol 6000[2], polyethylene glycol 400[2], acetaminophen[3], brewer's yeast[4], and ether[5] were used as supplied.

Acetaminophen suppositories, A–E[6], were obtained from commercial sources.

The equipment used included a rectal thermometer[7], thermistor probe[8], wound clip applier[9], and 9-mm wound clips[10].

[1] Matheson, Coleman and Bell, Norwood, OH 45212.
[2] J. T. Baker Chemical Co., Phillipsburg, NJ 08865.
[3] Lot 7032-LSR-43, S. B. Penick, Lyndhurst, NJ 07071.
[4] E. R. Squibb & Sons, Princeton, NJ 08540.
[5] Mallinckrodt, St. Louis, MO 63147.
[6] Product A, Westward, Inc., Eatontown, NJ 07724; Product B, American Quinine, Hospital Division of Natcon Chemicals, Plainview, NJ 11803; Product C, Consolidated Midland Corp., Brewster, NY 10509; Product D, Reiss Williams Co., Division of G & W Laboratories, Port Reading, NJ 07064; and Product E, Upsher-Smith Laboratories, Minneapolis, MN 55415.
[7] Model 47TD, Yellow Springs Instrument Co., Yellow Springs, Ohio.
[8] Series T2 605, Yellow Springs Instrument Co., Yellow Springs, Ohio.
[9] Model 7630, Clay Adams, Division of Becton, Parsippany, NJ 07054.
[10] Clay Adams, Parsippany, NJ 07054.

0022-3549/79/0900-1105$01.00/0

© 1979, American Pharmaceutical Association

Table I—Antipyretic Effect [a] of Various Acetaminophen Suppository Products Administered Rectally in Yeast-Fevered Rats

Product	$\bar{X}$ Predrug Temperature	Time Postdrug 0.5 hr	1.0 hr	2.0 hr	3.0 hr	4.0 hr	5.0 hr	6.0 hr
A	39.38°	1.62 ± 0.259°	2.25* [b] ± 0.217°	1.95* ± 0.242°	1.37 ± 0.436°	0.983 ± 0.489°	0.695 ± 0.500°	0.261 ± 0.411°
B	39.49°	1.43* ± 0.076°	2.00* ± 0.166°	2.14* ± 0.109°	2.26* [b] ± 0.146°	1.64* ± 0.229°	1.13 ± 0.321°	1.05 ± 0.310°
C	39.33°	1.88* ± 0.109°	2.11* [b] ± 0.142°	2.01* ± 0.173°	1.35* ± 0.226°	1.15 ± 0.337°	0.943 ± 0.427°	0.990 ± 0.400°
D	39.49°	2.01* ± 0.264°	2.26* [b] ± 0.227°	2.10* ± 0.134°	1.66* ± 0.159°	1.26* ± 0.235°	0.880 ± 0.280°	0.992 ± 0.388°
E	39.34°	2.00* ± 0.368°	2.40* [b] ± 0.565°	2.28* ± 0.191°	1.87* ± 0.221°	1.56* ± 0.195°	1.13 ± 0.297°	0.998 ± 0.382°
F	39.38°	1.40 ± 0.228°	1.90* ± 0.226°	1.94* [b] ± 0.244°	1.63* ± 0.332°	1.19 ± 0.400°	0.934 ± 0.368°	0.590 ± 0.256°
Prestudy control	39.61°	0.946 ± 0.384°	0.710 ± 0.123°	0.710 ± 0.181°	0.500 ± 0.292°	0.378 ± 0.331°	0.368 ± 0.326°	0.448 ± 0.161°
Poststudy control	39.30°	0.563 ± 0.100°	0.526 ± 0.102°	0.155* ± 0.048°	0.036* ± 0.061°	0.008 ± 0.032°	0.071 ± 0.039°	0.081 ± 0.066°
Combined control	39.41°	0.737 ± 0.108°	0.610 ± 0.065°	0.407 ± 0.097°	0.247 ± 0.097°	0.167 ± 0.089°	0.206 ± 0.080°	0.248 ± 0.096°

[a] Values are mean decreases in temperature ± *SE*. The asterisk (*) indicates significant difference ($p = 0.05$) from prestudy control. [b] Maximum temperature decrease.

Pharmacology and Methodology—Male Sprague-Dawley rats, 300–400 g, in groups of six were used for each of the five commercially obtained acetaminophen suppositories as well as for the laboratory-manufactured acetaminophen and control suppositories. To examine the variations due to tests run on different days, the control suppositories were tested twice. The first group of control suppositories was tested prior to the main study; and the second control group was tested afterward. A rectal thermometer[7] was used to obtain rat rectal temperatures.

The ambient temperature of each rat was obtained before inducing fever by inserting a prewarmed (38°), lubricated thermistor rectal probe exactly 4 cm into the rectum for 45 sec. Accurate probe insertion to the exact distance was critical to obtain reproducible results. The animal was lightly anesthetized with ether[5]. Fever was induced by 20 ml/kg of a 20% aqueous suspension of brewer's yeast[4], which was injected subcutaneously into the back below the nape of the neck (6).

Food was then withheld from the animals, but water was available *ad libitum* for the rest of the experiment. Room temperature was maintained at 23°. Room lighting was maintained from 7:00 am to 7:00 pm and turned off from 7:00 pm to 7:00 am. Rectal temperatures were obtained at about the same time each day throughout this study. Twenty-four hours after the yeast injections, the rectal temperature was recorded for each rat. The rat was then anesthetized with ether, and the appropriate modified suppository was inserted rectally. A wound clip was applied to the rectal opening to prevent its expulsion.

The animal was returned to its cage between temperature recordings. Rectal temperature readings were obtained at 0.5 and 1 hr and hourly thereafter for 6 hr after administration of the modified suppository. Rectal temperatures were obtained as described previously, except that the thermistor probe was inserted from above or below the wound clip depending on which direction facilitated a more direct probe insertion. For each animal, the probe was inserted from the same direction for every temperature reading.

All commercially obtained suppositories (A–E) and those manufactured in the laboratory (F) were adult size; each contained 600 mg of acetaminophen. To test for antipyretic activity in rats, each suppository was reduced to one-fourth of its original size. It was quartered with a scalpel longitudinally and weighed. All quartered suppositories were within 25–27% of their original weight. The control placebo suppositories (G) contained no drug and were quartered in the same manner.

The laboratory-manufactured suppositories (F) were prepared by incorporating sufficient analytical grade acetaminophen into the vehicle so that each suppository contained 600 mg of drug. They were made by the fusion process using the double pour technique (7). The control suppositories (G) were prepared by the fusion process and contained no drug. The control suppository and the laboratory-manufactured suppository vehicle contained polyethylene glycol 1540 (34%), polyethylene glycol 6000 (46%), and polyethylene glycol 400 (20%).

RESULTS AND DISCUSSION

Subcutaneous injections of aqueous brewer's yeast suspensions induced fever in 60 rats, from a preinjection mean rectal temperature of 37.8° (*SE* = 0.049) to a 24-hr postinjection rectal temperature of 39.4° (*SE* = 0.034). The temperature elevations induced by the brewer's yeast injection agree with those reported previously (6).

The results (Table I and Fig. 1) on rat rectal temperatures were obtained when the five commercially obtained products (A–E) and the laboratory-manufactured acetaminophen suppositories (F) were compared to control placebo suppositories (G). Since each product was tested on a different day, the controls were tested both on a prestudy day and on a poststudy day to examine the influence of day-to-day variability (Table I).

There were no significant differences between the prestudy and poststudy controls at 0.5, 1, 4, 5, or 6 hr. At 2 or 3 hr, the poststudy controls exhibited smaller temperature decreases in the yeast-fevered rats than the prestudy controls. Use of the poststudy controls would have given a larger difference in temperature between the controls and the products tested. For this reason, the prestudy controls were used for statistical comparison to the products as a conservative estimate of significant antipyretic effect.

The Student *t* test was used to determine significant differences ($p < 0.05$) for the control *versus* the products. At 0.5 hr after drug administration, Products B–E elicited significant decreases in rat rectal temperatures but Products A and F did not. This finding indicates a slower onset of action for Products A and F since both differed significantly from controls at 1 hr after drug administration. At 1 and 2 hr, all products elicited significant decreases in rectal temperatures. At 3 hr, all products except A continued to maintain lowered rectal temperatures. At 4 hr, only B, D, and E still elicited significant lowering of rat rectal temperatures.

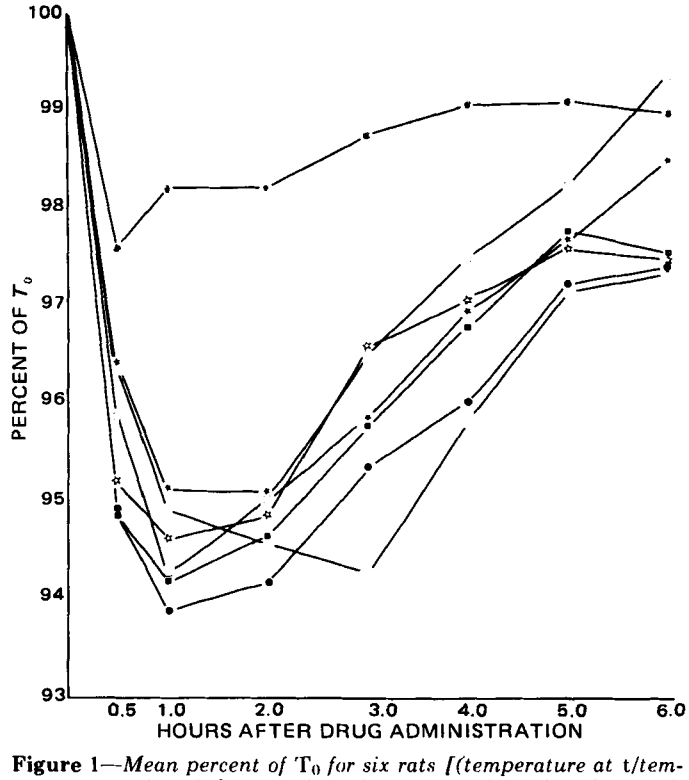

Figure 1—*Mean percent of* T_0 *for six rats [(temperature at t/temperature at* t_0*) × 100] versus time t in hours postinsertion of suppository. Key:* □, *Product A;* ○, *Product B;* ☆, *Product C;* ■, *Product D;* ●, *Product E;* ★, *Laboratory Product F; and* ⊙, *placebo control, G.*

By 5 and 6 hr, none of the products elicited any significant antipyretic effect.

When the various commercial acetaminophen suppositories (A–E) were compared to each other and to the laboratory-prepared product (F), no significant differences in antipyretic response were found at 0.5, 1, 2, 4, 5, and 6 hr. At 3 hr, there were no significant differences among Products C–F; however, Products A and B showed some differences. Product B showed its maximum effect at 3 hr (Table I) and exhibited the slowest onset of action; Product A was indistinguishable from the controls at 3 hr and thereafter, thus providing the shortest duration of action.

The magnitude of the variability, as indicated by the standard error (*SE*) (Table I), differed among products, with some showing more intraproduct variability than others. Because of the large variability when compared with other products, Product A was retested; the results were not significantly different from the original results. Product A showed a marked variability *via* visual examination in consistency and coloration when quartered longitudinally. Uniform drug distribution is essential for consistent absorption; and since only one-fourth of the suppository was inserted rectally into the animal, the lack of homogeneity and uniformity among Product A suppositories may account for the large variability in effect.

All five commercial products were stated to contain polyethylene glycol vehicles, but none listed the types or percentages of polyethylene glycol. Thus, a comparison of the differences in effect among formulations was not possible. The differences in the polyethylene glycol vehicle formulations, as well as other formulation factors, could account for the slight differences in the onset of action, duration of action, and time to reach peak antipyretic effect among the products tested.

All products were obtained from commercial sources and were tested within their expiration dates, but their shelftime prior to purchase was not known. The laboratory-manufactured acetaminophen and control suppositories were prepared and used within 1 month of manufacture. Stability of the vehicles is an important consideration in efficacy. Aging can influence the physical–chemical properties of the vehicle (3, 8) and may have contributed to the slight differences in effect among the products tested.

Correlation between *in vivo* and *in vitro* results was previously reported for benzocaine suppositories (9). Similar *in vitro* testing of acetaminophen suppositories A–F did not show any significant differences in drug release. The effects of aging, the polyethylene glycol composition, and other manufacturing and formulation factors all could account for the slight differences among products in this study. Nevertheless, all products tested, including the laboratory-manufactured product, did decrease the rectal temperatures of the yeast-fevered animals significantly. This animal model was a viable method for studying the efficacy of rectally administered antipyretic agents.

REFERENCES

(1) S. N. Pagay, R. I. Poust, and J. L. Colaizzi, *J. Pharm. Sci.*, **63**, 44 (1974).

(2) R. F. Shangraw and W. D. Walkling, *ibid.*, **60**, 600 (1971).

(3) S. Keinfinen, M. Hietula, S. Simila, and K. Kouvalainen, *Eur. J. Clin. Pharmacol.*, **12**, 77 (1977).

(4) J. J. Maron and A. C. Jekes, *Curr. Ther. Res.*, **20**, 45 (1976).

(5) S. Feldman, *Am. J. Hosp. Pharm.*, **32**, 1173 (1975).

(6) J. J. Loux, P. D. DePalma, and S. L. Yankell, *Toxicol. Appl. Pharmacol.*, **22**, 672 (1972).

(7) T. W. Schwartz, in "Sprowl's American Pharmacy," 7th ed., L. W. Dittert, Ed., Lippincott, Philadelphia, Pa., 1974, p. 296.

(8) A. Moes and F. Jaminet, *Pharm. Acta Helv.*, **51**, 5 (1976).

(9) J. W. Ayres, D. Lorskulsint, A. Lock, L. Kuhl, and P. A. Laskar, *J. Pharm. Sci.*, **65**, 832 (1976).

Species Difference in GI Motor Response to Somatostatin

MARTIN F. TANSY ˣ, JOHN S. MARTIN, WENDELL E. LANDIN, and FRANK M. KENDALL

Received January 29, 1979, from the *Department of Physiology and Biophysics, Health Sciences Center, Temple University, Philadelphia, PA 19140.* Accepted for publication March 2, 1979.

Abstract □ Acute experiments were performed on overnight fasted chloralose–urethan anesthetized dogs, cats, rabbits, and rats. Under these conditions, somatostatin practically abolished gastric contractions and decreased GI tonus in all species examined. The canine duodenum, jejunum, and ileum exhibited only a contractile response to somatostatin, whereas motor activities of the small intestines of the cat, rabbit, and rat were inhibited. In all instances and at all dosages, both the inhibitory and excitatory effects showed suggestions of tachyphylaxis. The data also indicate that excitatory or inhibitory effects were not dependent on the presence of long arc pathways. It is concluded that somatostatin exerts a direct stimulatory effect on the canine small intestine that is mediated by the muscularis mucosa.

Keyphrases □ Somatostatin—effect on GI motor activities, species specificity, dogs, cats, rabbits, rats □ GI motility—somatostatin effect, species specificity, dogs, cats, rabbits, rats □ Growth hormone inhibitors—somatostatin, effect on GI motor activities, species specificity, dogs, cats, rabbits, rats

Intravenous somatostatin administration to the anesthetized dog is associated with anatomically defined GI motor effects: gastric antrum relaxation and a generalized augmentation of the small intestine segmenting activities (1). Similar observations have been made in conscious dogs.

Because more recent abstracts (2, 3) documented similar observations for the canine small intestine, a series of experiments in four mammalian species was designed to determine the mechanism of the excitatory effect on the small bowel as well as its species specificity.

EXPERIMENTAL

Animals and General Procedure—Acute experiments were performed on 15 mongrel dogs, four cats, four rabbits, and four adult male Sprague–Dawley rats. Following an overnight fast with tap water *ad libitum*, all animals were anesthetized by the intravenous administration of a mixture of α-chloralose (5%, dissolved in polyethylene glycol 200) and urethan (50% in 0.9% saline). Each animal was individually titrated to a surgical plane of anesthesia using this mixture. Anesthesia was maintained by individual administration of the chloralose–urethan mixture.

Surgical and Recording Procedures—In all species, a tracheal cannula was inserted to ensure airway patency or, when necessary, to maintain artificial ventilation with a positive pressure pump. The femoral artery was cannulated to record blood pressure. The ipsilateral vein was cannulated to permit either bolus or infusion administration of drugs and fluids. A midline laparotomy was performed.

Recording balloons were inserted *via* the oral route for gastric recording and retrograde *via* a stab wound in the ileum for small intestinal recording. Motor activities of the large intestine were monitored by surgi-

0022-3549/79/0900-1107$01.00/0

© 1979, American Pharmaceutical Association

By 5 and 6 hr, none of the products elicited any significant antipyretic effect.

When the various commercial acetaminophen suppositories (A–E) were compared to each other and to the laboratory-prepared product (F), no significant differences in antipyretic response were found at 0.5, 1, 2, 4, 5, and 6 hr. At 3 hr, there were no significant differences among Products C–F; however, Products A and B showed some differences. Product B showed its maximum effect at 3 hr (Table I) and exhibited the slowest onset of action; Product A was indistinguishable from the controls at 3 hr and thereafter, thus providing the shortest duration of action.

The magnitude of the variability, as indicated by the standard error (*SE*) (Table I), differed among products, with some showing more intraproduct variability than others. Because of the large variability when compared with other products, Product A was retested; the results were not significantly different from the original results. Product A showed a marked variability *via* visual examination in consistency and coloration when quartered longitudinally. Uniform drug distribution is essential for consistent absorption; and since only one-fourth of the suppository was inserted rectally into the animal, the lack of homogeneity and uniformity among Product A suppositories may account for the large variability in effect.

All five commercial products were stated to contain polyethylene glycol vehicles, but none listed the types or percentages of polyethylene glycol. Thus, a comparison of the differences in effect among formulations was not possible. The differences in the polyethylene glycol vehicle formulations, as well as other formulation factors, could account for the slight differences in the onset of action, duration of action, and time to reach peak antipyretic effect among the products tested.

All products were obtained from commercial sources and were tested within their expiration dates, but their shelftime prior to purchase was not known. The laboratory-manufactured acetaminophen and control suppositories were prepared and used within 1 month of manufacture. Stability of the vehicles is an important consideration in efficacy. Aging can influence the physical–chemical properties of the vehicle (3, 8) and may have contributed to the slight differences in effect among the products tested.

Correlation between *in vivo* and *in vitro* results was previously reported for benzocaine suppositories (9). Similar *in vitro* testing of acetaminophen suppositories A–F did not show any significant differences in drug release. The effects of aging, the polyethylene glycol composition, and other manufacturing and formulation factors all could account for the slight differences among products in this study. Nevertheless, all products tested, including the laboratory-manufactured product, did decrease the rectal temperatures of the yeast-fevered animals significantly. This animal model was a viable method for studying the efficacy of rectally administered antipyretic agents.

REFERENCES

(1) S. N. Pagay, R. I. Poust, and J. L. Colaizzi, *J. Pharm. Sci.*, **63**, 44 (1974).

(2) R. F. Shangraw and W. D. Walkling, *ibid.*, **60**, 600 (1971).

(3) S. Keinfinen, M. Hietula, S. Simila, and K. Kouvalainen, *Eur. J. Clin. Pharmacol.*, **12**, 77 (1977).

(4) J. J. Maron and A. C. Jekes, *Curr. Ther. Res.*, **20**, 45 (1976).

(5) S. Feldman, *Am. J. Hosp. Pharm.*, **32**, 1173 (1975).

(6) J. J. Loux, P. D. DePalma, and S. L. Yankell, *Toxicol. Appl. Pharmacol.*, **22**, 672 (1972).

(7) T. W. Schwartz, in "Sprowl's American Pharmacy," 7th ed., L. W. Dittert, Ed., Lippincott, Philadelphia, Pa., 1974, p. 296.

(8) A. Moes and F. Jaminet, *Pharm. Acta Helv.*, **51**, 5 (1976).

(9) J. W. Ayres, D. Lorskulsint, A. Lock, L. Kuhl, and P. A. Laskar, *J. Pharm. Sci.*, **65**, 832 (1976).

Species Difference in GI Motor Response to Somatostatin

MARTIN F. TANSY ˣ, JOHN S. MARTIN, WENDELL E. LANDIN, and FRANK M. KENDALL

Received January 29, 1979, from the *Department of Physiology and Biophysics, Health Sciences Center, Temple University, Philadelphia, PA 19140.* Accepted for publication March 2, 1979.

Abstract □ Acute experiments were performed on overnight fasted chloralose–urethan anesthetized dogs, cats, rabbits, and rats. Under these conditions, somatostatin practically abolished gastric contractions and decreased GI tonus in all species examined. The canine duodenum, jejunum, and ileum exhibited only a contractile response to somatostatin, whereas motor activities of the small intestines of the cat, rabbit, and rat were inhibited. In all instances and at all dosages, both the inhibitory and excitatory effects showed suggestions of tachyphylaxis. The data also indicate that excitatory or inhibitory effects were not dependent on the presence of long arc pathways. It is concluded that somatostatin exerts a direct stimulatory effect on the canine small intestine that is mediated by the muscularis mucosa.

Keyphrases □ Somatostatin—effect on GI motor activities, species specificity, dogs, cats, rabbits, rats □ GI motility—somatostatin effect, species specificity, dogs, cats, rabbits, rats □ Growth hormone inhibitors—somatostatin, effect on GI motor activities, species specificity, dogs, cats, rabbits, rats

Intravenous somatostatin administration to the anesthetized dog is associated with anatomically defined GI motor effects: gastric antrum relaxation and a generalized augmentation of the small intestine segmenting activities (1). Similar observations have been made in conscious dogs.

Because more recent abstracts (2, 3) documented similar observations for the canine small intestine, a series of experiments in four mammalian species was designed to determine the mechanism of the excitatory effect on the small bowel as well as its species specificity.

EXPERIMENTAL

Animals and General Procedure—Acute experiments were performed on 15 mongrel dogs, four cats, four rabbits, and four adult male Sprague–Dawley rats. Following an overnight fast with tap water *ad libitum*, all animals were anesthetized by the intravenous administration of a mixture of α-chloralose (5%, dissolved in polyethylene glycol 200) and urethan (50% in 0.9% saline). Each animal was individually titrated to a surgical plane of anesthesia using this mixture. Anesthesia was maintained by individual administration of the chloralose–urethan mixture.

Surgical and Recording Procedures—In all species, a tracheal cannula was inserted to ensure airway patency or, when necessary, to maintain artificial ventilation with a positive pressure pump. The femoral artery was cannulated to record blood pressure. The ipsilateral vein was cannulated to permit either bolus or infusion administration of drugs and fluids. A midline laparotomy was performed.

Recording balloons were inserted *via* the oral route for gastric recording and retrograde *via* a stab wound in the ileum for small intestinal recording. Motor activities of the large intestine were monitored by surgi-

0022-3549/79/0900-1107$01.00/0

© 1979, American Pharmaceutical Association

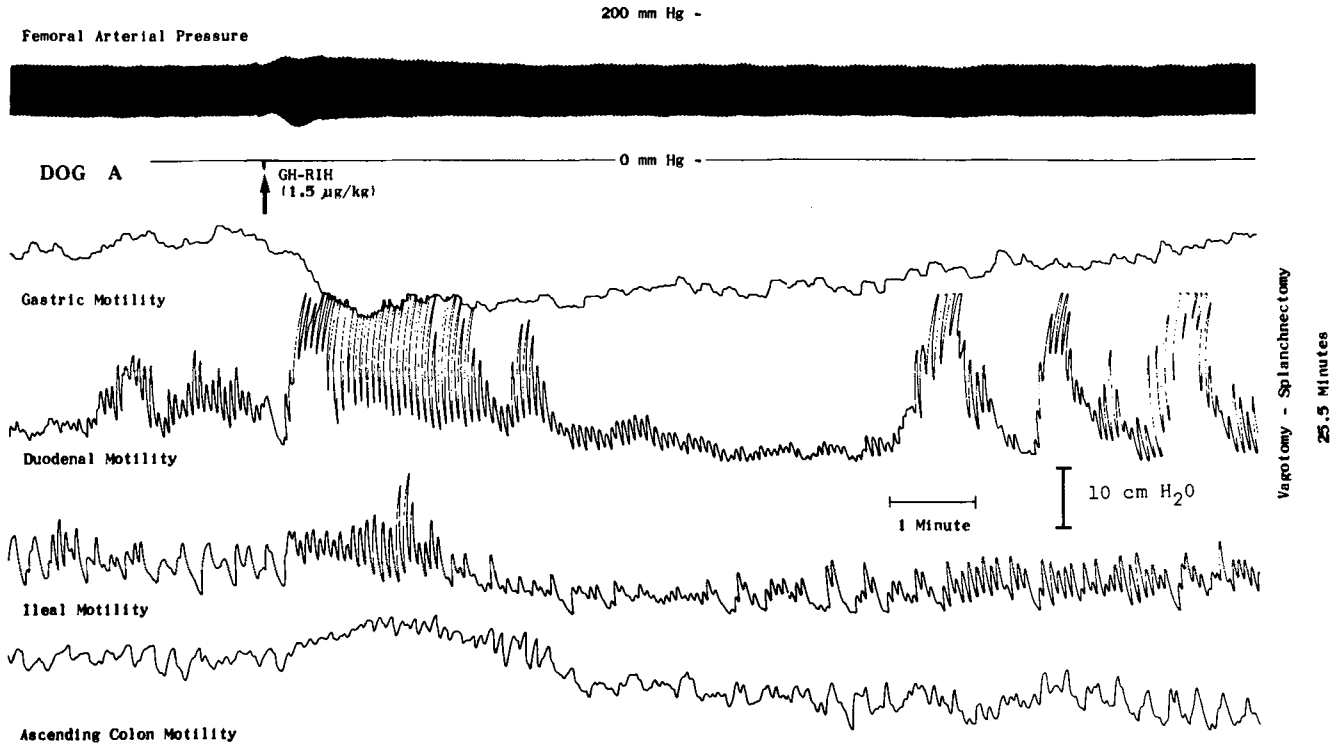

Figure 1—*Time courses of arterial blood pressure and various GI parameters showing the effects of intravenous somatostatin administered to an anesthetized dog. Stomach relaxation and increased motor activity of the intestinal tract are seen consistently. GH-RIH = growth hormone release inhibiting hormone (somatostatin).*

cally placed intraluminal water-filled balloons. Polygraphic control tracings were obtained before and at stated intervals after the physical and chemical stimulatory procedures in each group of animals. In all instances, intestinal pressure records were linked to a particular motility response on the basis of a visual observation that such a response occurred concurrently with the recorded events.

The following specific procedures were employed, depending on the particular canine experiment design. In some experiments, the vagus nerves were exposed cervically, and either the splanchnic nerves or the sympathetic chains were exposed at the T-9–T-10 level. In other experiments, the contractions of the mucosal musculature and of the longitudinal fibers of the small intestine tunica muscularis of the dog were recorded, both in excised surviving strips and in the living animal with the circulation intact according to a modified version (4) of a literature technique (5). Briefly, a small longitudinal incision was made through the entire wall of the intestinal segment opposite the mesenteric arcade attachment point. Two circular incisions were performed to create flaps such that the incisions or flap reflections did not interrupt the arcade blood vessels or innervation. The tunica muscularis was separated from the muscularis mucosa by blunt dissection and affixed by suture thread to a force transducer. It was then possible to monitor the muscularis mucosa activity by an intraluminal balloon.

Chemicals—In most experiments, drugs were administered intravenously through the femoral venous pressure cannula. Occasionally, intraarterial drug administration in the region of the denuded bowel segment was performed *via* a cannula inserted into a mesenteric artery,

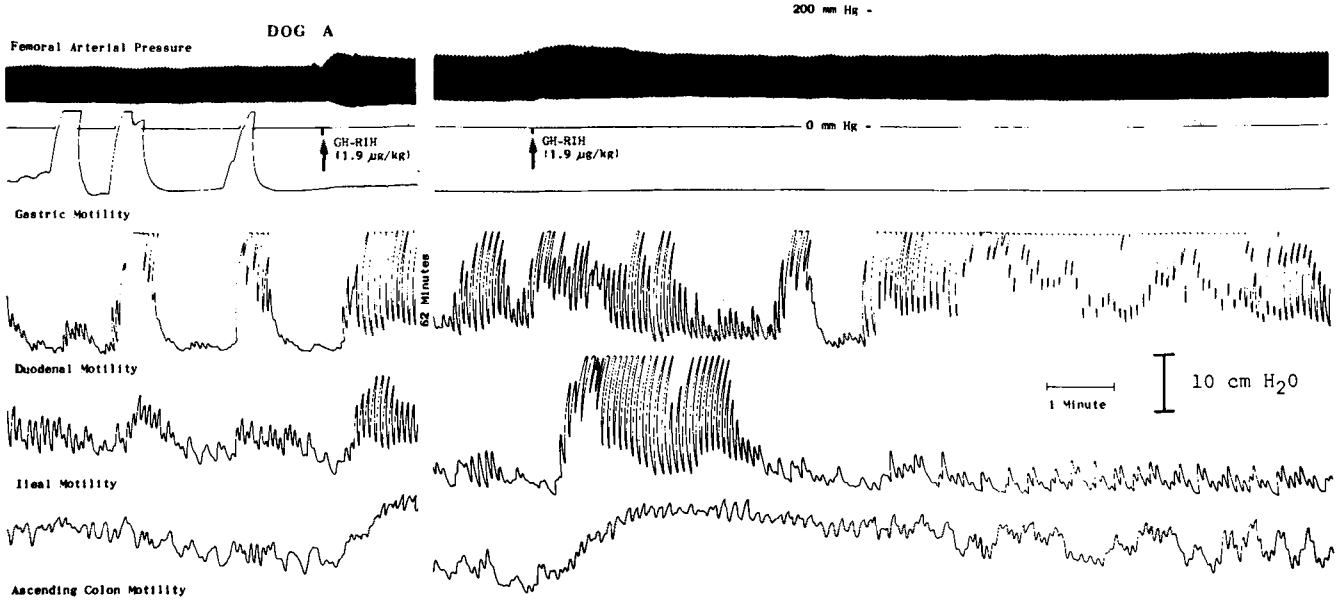

Figure 2—*Continuation of the experimental record depicted in Fig. 1 following bilateral cervical vagectomy and splanchnectomy. The same effects depicted in Fig. 1 continue with multiple subsequent intravenous somatostatin dosages.*

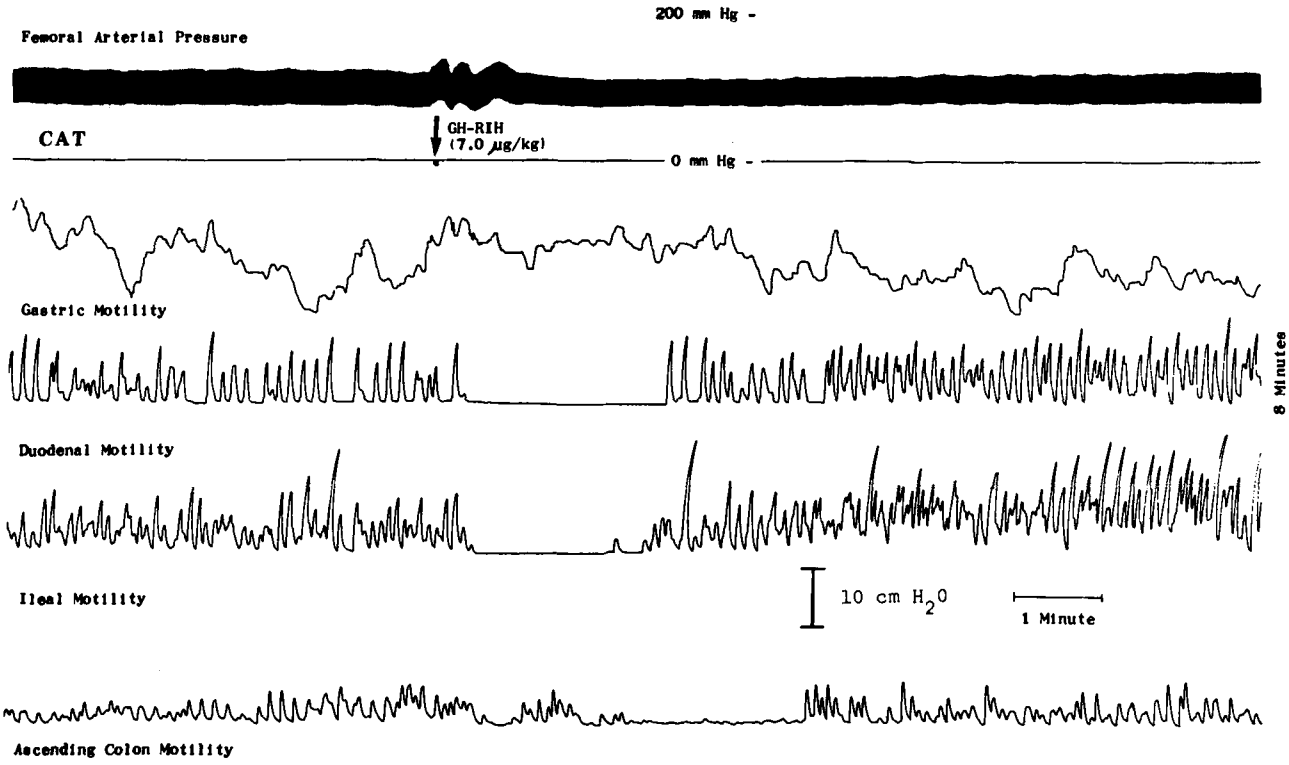

Figure 3—*Experimental record showing the effects of an intravenous bolus dosage of somatostatin administered to an anesthetized cat. In this case, there was a generalized intestinal motor activity inhibition, but spontaneous gastric motor activity was not affected.*

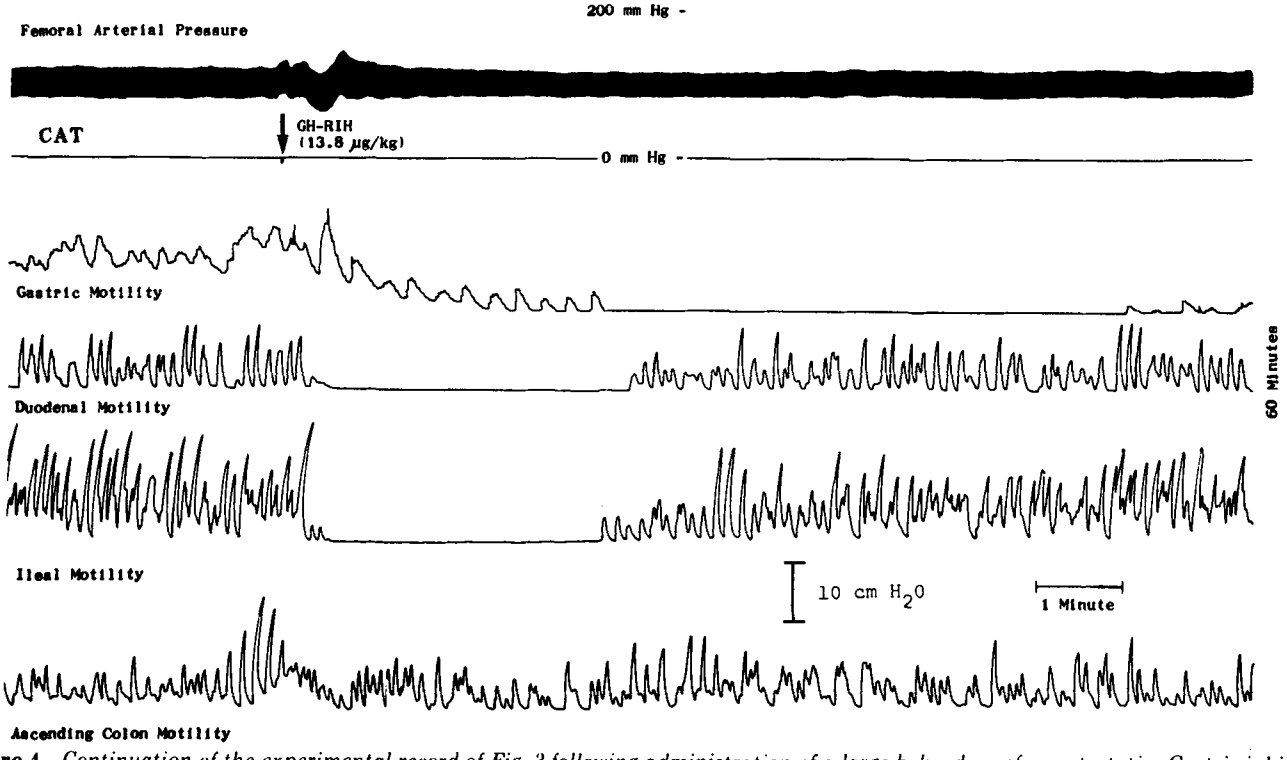

Figure 4—*Continuation of the experimental record of Fig. 3 following administration of a large bolus dose of somatostatin. Gastric inhibition accompanied small bowel inhibition, while the large intestine was no longer affected.*

which appeared to supply the immediate vicinity of the split bowel preparation. Intravenously administered agents were synthetic somatostatin (C-11873)[1], epinephrine hydrochloride[2], atropine sulfate[2], and tetraethylammonium chloride[3]. Somatostatin also was introduced into the arterial supply of the canine small intestine. The following drugs were used in the classical tissue bath: somatostatin, acetylcholine chloride[2], and epinephrine hydrochloride. The drug dose was specified as the final concentration of the active base present in the tissue bath.

[1] Wyeth Laboratories.
[2] Sigma.
[3] Etamon, Parke, Davis.

RESULTS AND DISCUSSION

As illustrated in Fig. 1, the canine stomach antrum exhibited a unan-

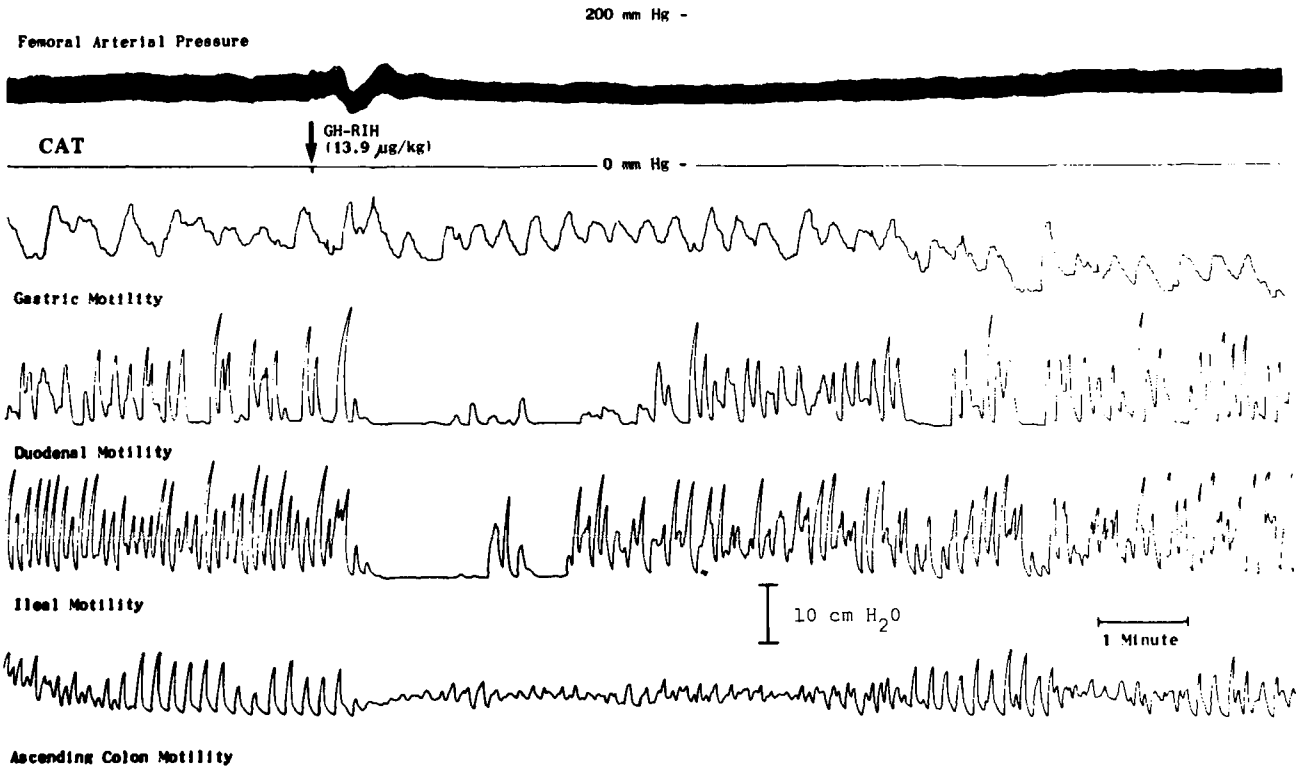

Figure 5—*Continuation of the experimental record of Fig. 4 following a 1-hr interval. A repeat administration of nearly the same bolus somatostatin dose resulted in shorter durations of inhibition of spontaneous small intestinal motor activity and no noticeable effect on gastric motor activity.*

imous relaxation response in 45 trials to a fixed bolus somatostatin dose, whereas the small bowel exhibited only a contractile response in all 15 animals, each to the same dose. Both responses showed dosage dependence and tachyphylaxis.

Gastric motor inhibition and augmented small intestinal segmenting activity always continued for a variable time (10–60 min) subsequent to the cessation of somatostatin administration. Somatostatin had minor and seemingly inconsistent excitatory effects on the ascending colon spontaneous motor activities. No effects on the descending colon were noted.

Figures 1 and 2 show that GI inhibitory and excitatory effects in response to somatostatin were not blocked in four surgically denervated

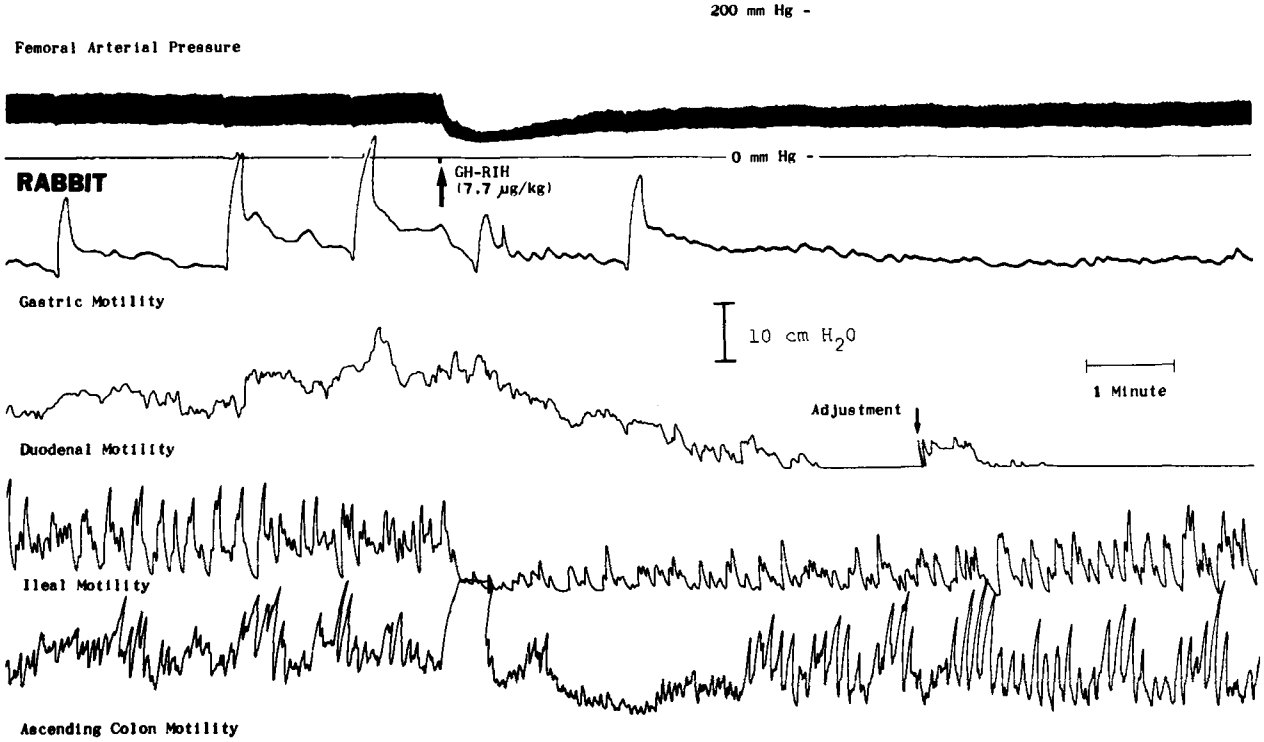

Figure 6—*Polygram depicting the time courses of arterial blood pressure and GI motor activities in an anesthetized rabbit following the intravenous somatostatin bolus dosage. Gastric and duodenal activities were noticeably inhibited, with marginal inhibition of the ileum and ascending colon.*

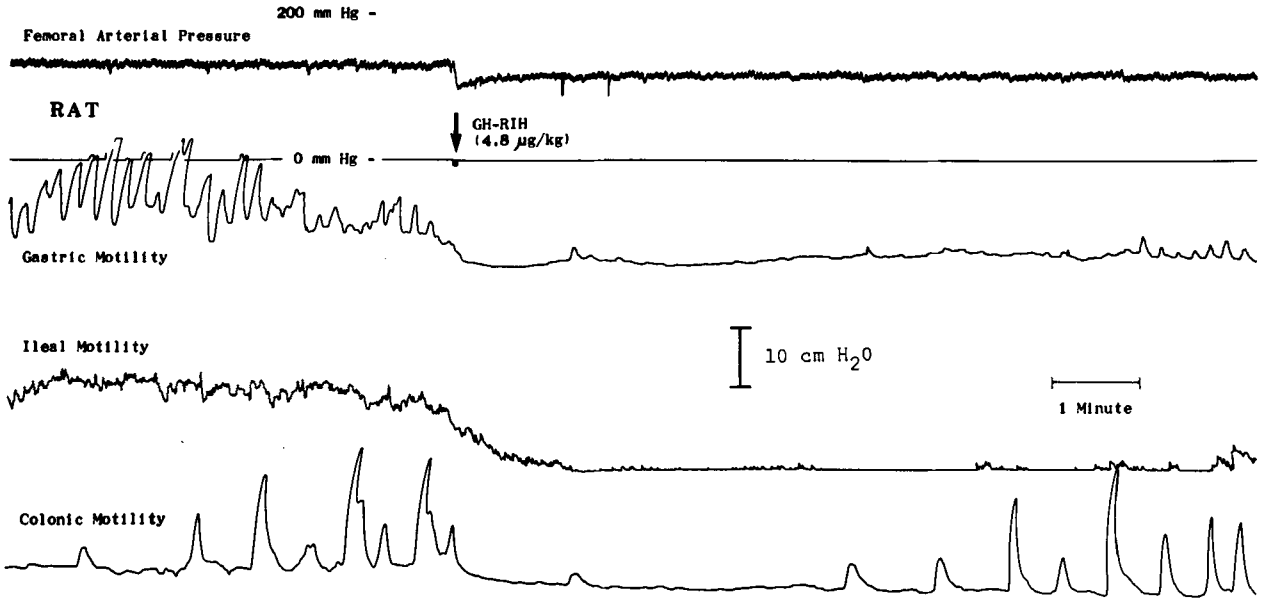

Figure 7—*Polygram from an anesthetized rat showing generalized GI motor inhibition by a single intravenous somatostatin bolus dosage.*

canine preparations. Although not depicted, the polygrams from four other dogs also revealed that the inhibitory and excitatory effects produced by somatostatin on the stomach and small intestinal tissues could not be blocked by prior intravenous administration of high doses (10 mg/kg) of the ganglionic blocking agent tetraethylammonium chloride.

Intravenous somatostatin infusions to three dogs resulted in essentially normal gastric activity following the initial depression, but small intestinal excitation (particularly in the duodenum) was maintained throughout the infusion period.

In all cases, low bolus intravenous somatostatin dosages to the cat promptly inhibited small intestinal motility but had no gastric effect (Fig. 3). Higher dosages inhibited gastric activity as well as small intestinal motor activity (Fig. 4). Repeated administration of high somatostatin dosages to the cat resulted in a loss of gastric inhibition and a reduction in the duration of small intestine inhibition (Fig. 5). In any event, stimulation of small intestinal activity was never observed in cats, regardless of the dosage or administration method.

Bolus dosages of intravenous somatostatin in four rabbits produced protracted gastric and duodenal inhibition and transient ileal inhibition (Fig. 6). There was no evidence of small intestinal stimulatory effects. Intravenous somatostatin also was effective in inhibiting GI motor activities in each instance in the rat, with even bolus dosages producing long inhibition periods (Fig. 7). No evidence of a small intestinal stimulatory effect was observed in the rat.

The excitatory effect of somatostatin on the dog small bowel was investigated in four animals by the split bowel preparation. Simultaneous recording indicated that ileal excitation to close intraarterial somatostatin was due to vigorous circular muscularis mucosa contractions while the longitudinal tunica muscularis was inhibited (Fig. 8). Results of *in vitro*

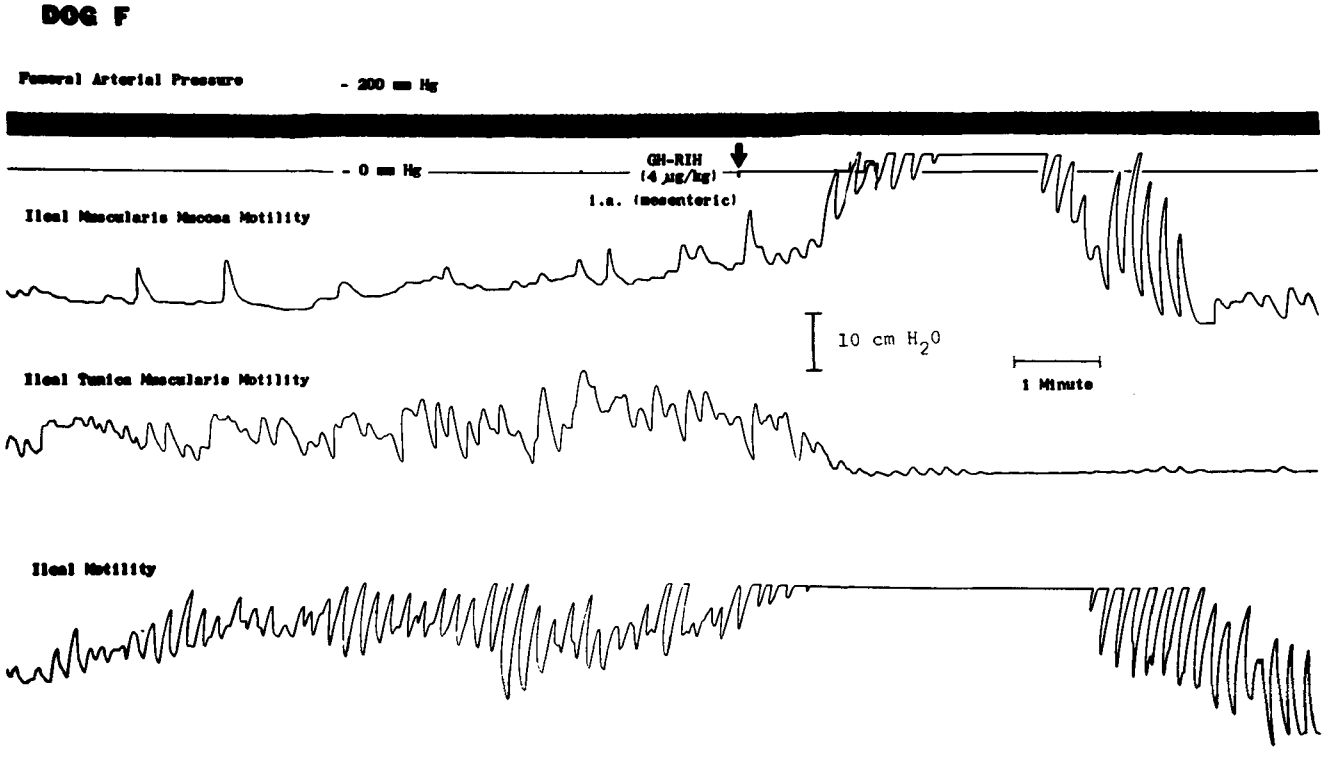

Figure 8—*Experimental record from an anesthetized dog showing mechanical responses of a small intestinal split bowel preparation to a close intraarterial bolus dosage of somatostatin. Tunica muscularis relaxation occurred in parallel with an increase in activity of the underlying muscularis mucosa. The overall effect, as recorded from an intraluminal balloon in an adjacent intact segment, was excitation.*

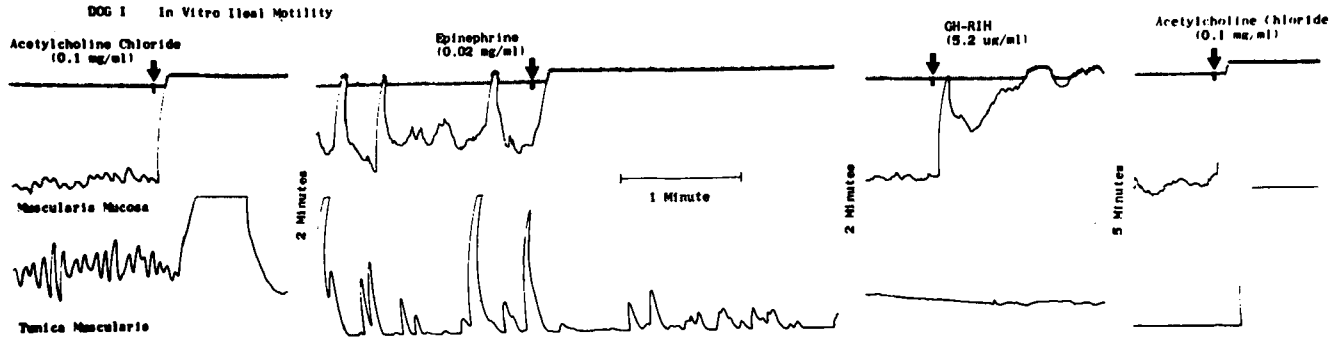

Figure 9—*Force records obtained* in vitro *from strips of canine muscularis mucosa and tunica muscularis showing the effects of somatostatin. Somatostatin produced an excitatory effect on the muscularis mucosa and an inhibitory effect on the tunica muscularis. In contrast, epinephrine excited the muscularis mucosa and inhibited the tunica muscularis; acetylcholine excited both.*

experiments on denuded canine small intestine segments supported the *in vivo* observations in the same animal. The *in vitro* pharmacological responsiveness of a circular strip of the muscularis mucosa and the outer tunica muscularis is depicted in the top and bottom traces of Fig. 9. Both ileal muscular components exhibited spontaneous motility, and they exhibited tonic contractions when challenged with acetylcholine.

As expected, epinephrine had opposite effects in different parts of the ileum of the same animal. As illustrated, the tunica muscularis portion of the ileum exhibited a relaxation response to epinephrine, whereas the muscularis mucosa portion exhibited only a tonic contractile response to the same dose of the catecholamine. Somatostatin produced a prolonged stimulation of ileal muscularis mucosa tone with no evidence of a stimulatory effect on the tunica muscularis.

This mechanistic explanation fits in well with the comparative histology of the small intestines of the species studied, viewed from the perspective of coupled mechano-effector systems. Although not depicted, only the dog small intestine has a well-developed circular component of the muscularis mucosa, and, aside from the dog, only the rabbit small intestine has any developed muscularis mucosa, albeit the orientation is longitudinal. The cat has a rudimentary longitudinal layer, and the rat has practically none.

It has been reported (6) that somatostatin acutely inhibits acetylcholine release by the guinea pig ileum myenteric plexus as in the *in vitro* preparation described previously (7). As suggested (6), the data may explain, at least in part, the ability of somatostatin to inhibit or decrease spontaneous or elicited gastric, gut, and gallbladder contractions.

In experiments to determine the effects of somatostatin on the myenteric plexus, Guillemin (6) observed tachyphylaxis, occasionally persisting for as long as 2 hr. This observation is in complete agreement with our findings on the duration of tachyphylaxis in feline preparations.

A review of the experiments by Guillemin (6) indicates that the guinea pig ileum failed to contract regardless of the somatostatin concentration in the bath. Interestingly enough, the guinea pig ileum has no circular muscularis mucosa and very little of the longitudinal components. Experiments in this laboratory have not produced an *in vitro* stimulatory effect on the rat small intestine, which is almost exclusively tunica muscularis (Fig. 10). Therefore, a mechanistic explanation for the anatomically specific canine responses probably can be advanced. The stimulatory effect is due to the action of the circular muscularis mucosa and cannot be produced in species that do not have this muscular component. The inhibitory effect probably is due to inhibition *via* the myenteric plexus of the tunica muscularis, which is the only significant muscle layer in the small intestines of the noncanine species studied.

In the dog stomach, where presumably both effector layers are present, the primary inhibitory effect may be due partly to the difference in ge-

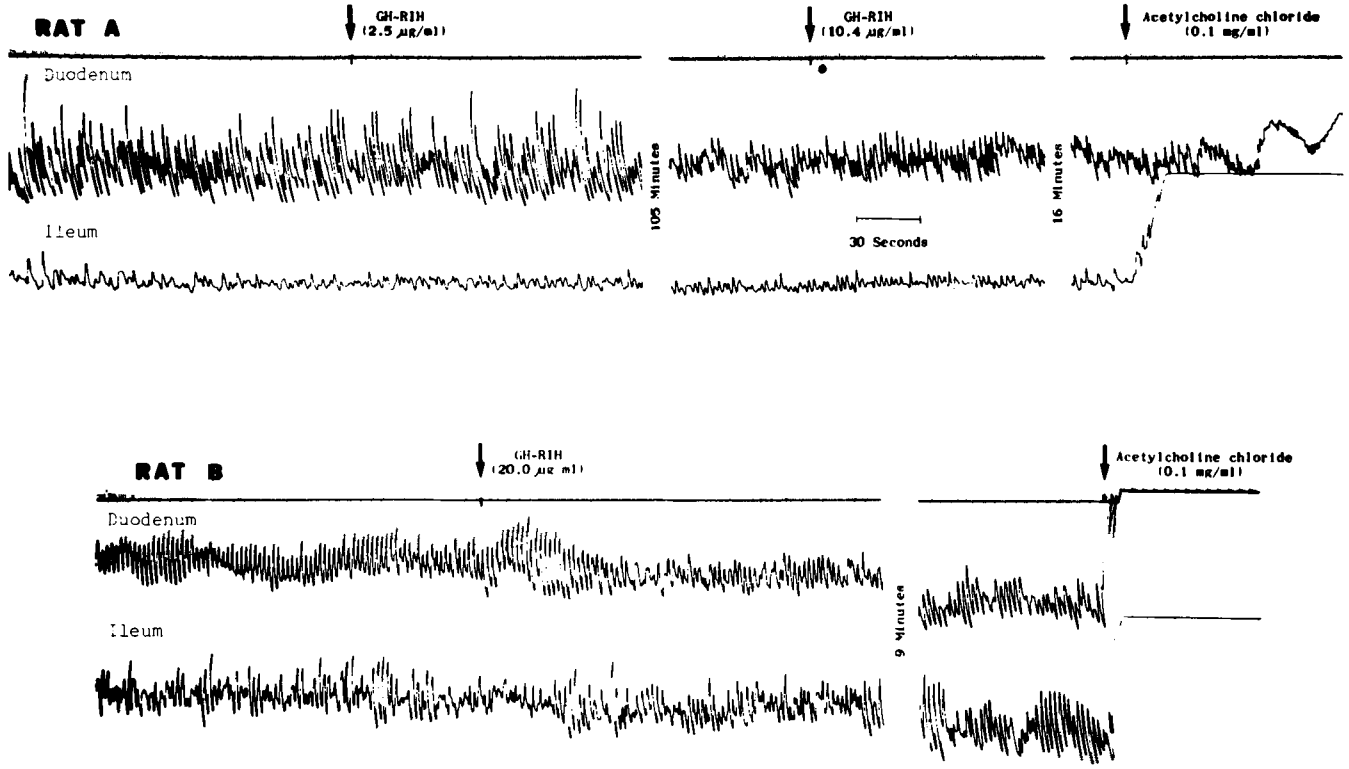

Figure 10—In vitro *force records of spontaneous muscle contractions in whole bowel segments from rats showing responses to challenges by somatostatin and acetylcholine.*

ometry. The stomach is neither circular nor does its average diameter approximate that of the small intestine. Consequently, there is no reason to expect that simultaneous excitation of the muscularis mucosa and inhibition of the tunica muscularis would increase intraluminal pressure sufficiently to register with a water-filled intraluminal recording balloon, and the contrary might well be the case if the external effector layers are indeed inhibited.

No acceptable adaptation of the split bowel preparation to the stomach appears practical, but indirect means are available to estimate at least the presence or absence of spontaneous motor activity. Such demonstrations will be necessary to determine whether the observed net inhibition of canine gastric motor activity is due to the relative geometries of coupled effector systems.

With the canine small intestine, paradoxical motor effects were observed by intraluminal pressure measurements, probably because the test agents had opposite effects on the two muscle layers. This is amply illustrated in Fig. 8, which shows the effect of somatostatin on the canine ileum. Clearly, the tunica muscularis is inhibited and the muscularis mucosa is stimulated, while an overall stimulatory effect is seen from an intraluminal balloon in an adjacent intact small bowel segment. These data confirm and explain the excitation mechanism reported by several investigators (1–3) in the somatostatin effect on the motor activity of the canine small intestine. These results also lead to the conclusion that the circular components of the canine small intestine muscularis mucosa possess physiologically significant contractile powers.

The overall significance of these findings is that both the canine and human small intestine constitute pharmacologically separate, but mechanically coupled, muscular systems, either one of which can show excitation when the coupled effects are measured by any system that does not differentiate the identity of the effector system involved. In the future, it will be necessary to evaluate motor effects of test agents on a separate basis. Those that have been reported to produce paradoxical effects should be reevaluated. Obviously, the use of the split bowel technique would not be appropriate for chronic preparations, but these results also suggest a cautious interpretation of the mechanisms from experimental data obtained from either open-ended catheters or intraluminal pressure telemetry capsules.

REFERENCES

(1) M. F. Tansy, J. S. Martin, W. E. Landin, and F. M. Kendall, *Metabolism*, **27**, 1353 (1978).

(2) G. Boden, H. Jacoby, and A. Staus, *Gastroenterology*, **70**, 961 (1976).

(3) H. Ormsbee, III, and S. Koehler, Jr., *Fed. Proc.*, **36**, 557 (1977).

(4) M. F. Tansy, J. S. Martin, W. E. Landin, and F. M. Kendall, *ibid.*, **37**, 373 (1978).

(5) C. E. King, L. C. Glass, and S. E. Townsend, *Am. J. Physiol.*, **148**, 667 (1947).

(6) R. Guillemin, *Endocrinology*, **99**, 1653 (1976).

(7) W. D. Paton and M. A. Zar, *J. Physiol. (London)*, **194**, 13 (1968).

ACKNOWLEDGMENTS

The authors are indebted to Dr. Harvey E. Alburn, Wyeth Laboratories, Philadelphia, Pa., for the generous supply of synthetic somatostatin.

High-Performance Liquid Chromatographic Microdetermination of Indoprofen in Human Milk

DUANE B. LAKINGS *x, CARLOS LIZARRAGA *, WILLIAM J. HAGGERTY *, and MARTIN J. WILLIAMSON ‡

Received August 30, 1978, from the **Chemical Sciences Division, Midwest Research Institute, Kansas City, MO 64110,* and ‡*Adria Laboratories, Inc., Columbus, OH 43216.* Accepted for publication March 6, 1979.

Abstract □ A previously reported high-performance liquid chromatographic (HPLC) method for indoprofen determination in physiological fluids was modified and extended to provide quantitative data on drug concentrations in human milk samples at a low nanogram per milliliter level. The reversed-phase HPLC technique was modified to give a better separation of the drug and milk components. To achieve the necessary cleanup for low level determination, the milk samples required protein precipitation, liquid–liquid drug extraction, and concentration. Excellent indoprofen recovery was obtained with this technique; the average recovery from 20 milk samples spiked with various nanogram drug levels was 95%. The analytical technique showed excellent reproducibility; the calibration solutions over 15 days had a relative standard deviation of 3.2%. Results for indoprofen levels in milk and plasma samples from seven subjects who received either a single or multiple oral drug dose are presented.

Keyphrases □ Indoprofen—analysis, high-performance liquid chromatography, human milk □ High-performance liquid chromatography—analysis, indoprofen, human milk □ Anti-inflammatory agents—indoprofen, high-performance liquid chromatographic analysis, human milk □ Milk, human—analysis, indoprofen, high-performance liquid chromatography

Indoprofen, 4-(1,3-dihydro-1-oxo-2*H*-isoindol-2-yl)-α-methylbenzeneacetic acid (I), has been reported to have analgesic activity in animals and humans (1–4). In an earlier report (5), a reversed-phase high performance liquid chromatographic (HPLC) method was presented for the quantitation of drug levels in plasma and urine samples. This method was very simple and had sufficient sensitivity for determination of microgram per milliliter levels. However, in certain cases, such as determinations in later plasma time point samples for pharmacokinetic studies or in physiological fluids such as milk where the drug level is expected to be low, a more sensitive technique is required. Therefore, a sample preparation procedure was developed that provides the necessary cleanup and sensitivity for low level analyses. The method has the necessary precision and accuracy to provide quantitative data for nanogram indoprofen levels in milk samples and may be applicable to other physiological fluids containing low drug levels.

EXPERIMENTAL

Apparatus and Reagents—The liquid chromatograph consisted of a high-pressure pump[1], a loop injector[2], a UV detector[3], and a strip-chart recorder[4]. The chromatographic column was μBondapak C_{18}[5] (300 × 4 mm i.d.).

[1] Model 6000A, Waters Associates, Milford, Mass.
[2] Model U6K, Waters Associates, Milford, Mass.
[3] Model 440, Waters Associates, Milford, Mass.
[4] Model SR-240, Heath/Schlumberger Instruments, Benton Harbor, Mich.
[5] Waters Associates, Milford, Mass.

0022-3549/79/0900-1113$01.00/0

© 1979, American Pharmaceutical Association

ometry. The stomach is neither circular nor does its average diameter approximate that of the small intestine. Consequently, there is no reason to expect that simultaneous excitation of the muscularis mucosa and inhibition of the tunica muscularis would increase intraluminal pressure sufficiently to register with a water-filled intraluminal recording balloon, and the contrary might well be the case if the external effector layers are indeed inhibited.

No acceptable adaptation of the split bowel preparation to the stomach appears practical, but indirect means are available to estimate at least the presence or absence of spontaneous motor activity. Such demonstrations will be necessary to determine whether the observed net inhibition of canine gastric motor activity is due to the relative geometries of coupled effector systems.

With the canine small intestine, paradoxical motor effects were observed by intraluminal pressure measurements, probably because the test agents had opposite effects on the two muscle layers. This is amply illustrated in Fig. 8, which shows the effect of somatostatin on the canine ileum. Clearly, the tunica muscularis is inhibited and the muscularis mucosa is stimulated, while an overall stimulatory effect is seen from an intraluminal balloon in an adjacent intact small bowel segment. These data confirm and explain the excitation mechanism reported by several investigators (1–3) in the somatostatin effect on the motor activity of the canine small intestine. These results also lead to the conclusion that the circular components of the canine small intestine muscularis mucosa possess physiologically significant contractile powers.

The overall significance of these findings is that both the canine and human small intestine constitute pharmacologically separate, but mechanically coupled, muscular systems, either one of which can show excitation when the coupled effects are measured by any system that does not differentiate the identity of the effector system involved. In the future, it will be necessary to evaluate motor effects of test agents on a separate basis. Those that have been reported to produce paradoxical effects should be reevaluated. Obviously, the use of the split bowel technique would not be appropriate for chronic preparations, but these results also suggest a cautious interpretation of the mechanisms from experimental data obtained from either open-ended catheters or intraluminal pressure telemetry capsules.

REFERENCES

(1) M. F. Tansy, J. S. Martin, W. E. Landin, and F. M. Kendall, *Metabolism*, **27**, 1353 (1978).

(2) G. Boden, H. Jacoby, and A. Staus, *Gastroenterology*, **70**, 961 (1976).

(3) H. Ormsbee, III, and S. Koehler, Jr., *Fed. Proc.*, **36**, 557 (1977).

(4) M. F. Tansy, J. S. Martin, W. E. Landin, and F. M. Kendall, *ibid.*, **37**, 373 (1978).

(5) C. E. King, L. C. Glass, and S. E. Townsend, *Am. J. Physiol.*, **148**, 667 (1947).

(6) R. Guillemin, *Endocrinology*, **99**, 1653 (1976).

(7) W. D. Paton and M. A. Zar, *J. Physiol. (London)*, **194**, 13 (1968).

ACKNOWLEDGMENTS

The authors are indebted to Dr. Harvey E. Alburn, Wyeth Laboratories, Philadelphia, Pa., for the generous supply of synthetic somatostatin.

High-Performance Liquid Chromatographic Microdetermination of Indoprofen in Human Milk

DUANE B. LAKINGS *x, CARLOS LIZARRAGA *, WILLIAM J. HAGGERTY *, and MARTIN J. WILLIAMSON ‡

Received August 30, 1978, from the **Chemical Sciences Division, Midwest Research Institute, Kansas City, MO 64110,* and ‡*Adria Laboratories, Inc., Columbus, OH 43216.* Accepted for publication March 6, 1979.

Abstract □ A previously reported high-performance liquid chromatographic (HPLC) method for indoprofen determination in physiological fluids was modified and extended to provide quantitative data on drug concentrations in human milk samples at a low nanogram per milliliter level. The reversed-phase HPLC technique was modified to give a better separation of the drug and milk components. To achieve the necessary cleanup for low level determination, the milk samples required protein precipitation, liquid–liquid drug extraction, and concentration. Excellent indoprofen recovery was obtained with this technique; the average recovery from 20 milk samples spiked with various nanogram drug levels was 95%. The analytical technique showed excellent reproducibility; the calibration solutions over 15 days had a relative standard deviation of 3.2%. Results for indoprofen levels in milk and plasma samples from seven subjects who received either a single or multiple oral drug dose are presented.

Keyphrases □ Indoprofen—analysis, high-performance liquid chromatography, human milk □ High-performance liquid chromatography—analysis, indoprofen, human milk □ Anti-inflammatory agents—indoprofen, high-performance liquid chromatographic analysis, human milk □ Milk, human—analysis, indoprofen, high-performance liquid chromatography

Indoprofen, 4-(1,3-dihydro-1-oxo-2*H*-isoindol-2-yl)-α-methylbenzeneacetic acid (I), has been reported to have analgesic activity in animals and humans (1–4). In an earlier report (5), a reversed-phase high performance liquid chromatographic (HPLC) method was presented for the quantitation of drug levels in plasma and urine samples. This method was very simple and had sufficient sensitivity for determination of microgram per milliliter levels. However, in certain cases, such as determinations in later plasma time point samples for pharmacokinetic studies or in physiological fluids such as milk where the drug level is expected to be low, a more sensitive technique is required. Therefore, a sample preparation procedure was developed that provides the necessary cleanup and sensitivity for low level analyses. The method has the necessary precision and accuracy to provide quantitative data for nanogram indoprofen levels in milk samples and may be applicable to other physiological fluids containing low drug levels.

EXPERIMENTAL

Apparatus and Reagents—The liquid chromatograph consisted of a high-pressure pump[1], a loop injector[2], a UV detector[3], and a strip-chart recorder[4]. The chromatographic column was μBondapak C_{18}[5] (300 × 4 mm i.d.).

[1] Model 6000A, Waters Associates, Milford, Mass.
[2] Model U6K, Waters Associates, Milford, Mass.
[3] Model 440, Waters Associates, Milford, Mass.
[4] Model SR-240, Heath/Schlumberger Instruments, Benton Harbor, Mich.
[5] Waters Associates, Milford, Mass.

0022-3549/79/0900-1113$01.00/0

© 1979, American Pharmaceutical Association

Table I—Indoprofen Recovery from Human Milk

Subject	Hours after Administration	Indoprofen Added, ng	Calculated Indoprofen/0.5 ml of Milk, ng		Recovery, %
			Neat	Spiked	
		Part A			
1	Baseline	10	ND[a]	11	110
2	Baseline	25	Tr[b]	33	102
3	Baseline	10	Tr	13	95
4	Baseline	50	20[c]	77[c]	—
5	Baseline	25	ND	25	100
6	Baseline	10	ND	10	100
7	Baseline	25	ND	23	92
				Average ± *SD*	100 ± 6
		Part B			
1	12	25	17	37	88
1	48	25	ND	20	80
2	12	25	96	124	112
2	24	25	Tr	23	92
3	2	200	39	225	94
3	12	25	99	117	96
3	24	25	11	30	83
4	26	25	229	239	94
5	26	50	137	171	91
5	50	50	211	246	94
6	26	50	86	138	102
6	50	50	68	118	100
7	50	50	109	152	96
				Average ± *SD*	94 ± 8
				Overall average	96

[a] ND = not detected. [b] Tr = trace, indoprofen level <10 ng/ml. [c] Subject 4 had an interfering milk component eluting 1 min before indoprofen, thus preventing recovery calculation.

Acetonitrile[6] was of "distilled in glass" purity. The water was first deionized and then distilled to remove contaminants. Hexane[7] and ethyl acetate[7] were of "nanograde" purity.

An indoprofen reference standard[8] was provided, and the internal standard was the pentanoic acid indoprofen homolog[8]. All calculations were made using the internal standard method and the relative weight response (*RWR*) of calibration solutions.

HPLC Conditions—The HPLC conditions used throughout consisted of a μBondapak C_{18} column, 300 × 4 mm i.d., and acetonitrile in 0.175 *M* acetic acid, 35:65 for milk samples and 40:60 for plasma determinations. The flow rate was maintained at 1.0 ml/min, and the temperature was ambient. A 280-nm filter was used in the UV detector since indoprofen has a λ_{max} at 282 nm. Injection volumes varied between 20 and 100 μl, depending on the drug concentration.

Sample Preparation Procedure—Since the indoprofen level in human milk samples was expected to be low, the analytical technique required sensitivity in the low nanogram per milliliter range. Studies were undertaken to define the optimal procedures for extracting the drug from milk and concentrating the extract to provide sufficient sensitivity.

The final method consisted of adding 0.1 ml of 0.1 *N* NaOH to the milk (0.5 ml) to ensure complete ionization of the drug. Then, acetonitrile (2.0 ml) containing the internal standard was added; the sample was mixed and allowed to stand for at least 1 hr at 4° to precipitate the protein. The sample was centrifuged at 2000 rpm for 15 min, and the supernate was transferred to a culture tube. The supernate was extracted with 3 × 3 ml of hexane, which was discarded. The solution was neutralized with 0.1 *N* HCl, and the drug was extracted with 1 × 4 ml, followed by 2 × 2 ml of ethyl acetate.

The extracts were combined and evaporated to dryness on a 50° hot plate under nitrogen stream. The residue was dissolved in 400 μl of the HPLC eluent and filtered through a 0.45-μm[9] filter. An aliquot was injected onto the HPLC column.

For the indoprofen determination in plasma samples, the method reported earlier (5) was used and consisted of precipitating the protein with acetonitrile and filtering the supernate prior to injection.

Samples and Sample Handling—Milk and plasma samples were obtained from seven subjects who received oral indoprofen doses. All subjects were in the early postpartum period. Three subjects received a single 200-mg dose in capsules, and the other four were given 2 × 100 mg of indoprofen every 6 hr for nine doses. A baseline milk sample was obtained from each subject before dosing to determine possible interfering components. Additional samples were obtained at 2.0, 12, 24, and 48 hr for the single-dose subjects and at 2.0, 26, and 50 hr after the initial dose for the multiple-dose subjects. Plasma samples from each subject were obtained at 2.0 hr after the initial drug dose and at 26 and 50 hr for subjects receiving multiple doses. All samples were frozen in dry ice immediately after collection and maintained at −80° until analysis.

Calculations—The calculations were based on an internal standard and the relative weight response of calibration solutions. The average relative weight response of standards was used to calculate indoprofen levels by the following equations:

$$RWR\ \text{std} = \frac{\text{PH I std}}{\text{PH II}} \times \frac{\text{wt II}}{\text{wt I std}} \qquad \text{(Eq. 1)}$$

$$\text{wt I} = \frac{\text{PH I}}{\text{PH II}} \times \frac{\text{wt II}}{RWR\ \text{std}} \qquad \text{(Eq. 2)}$$

where PH I and PH II are the peak heights and wt I and wt II are the weights of the drug and internal standard, respectively.

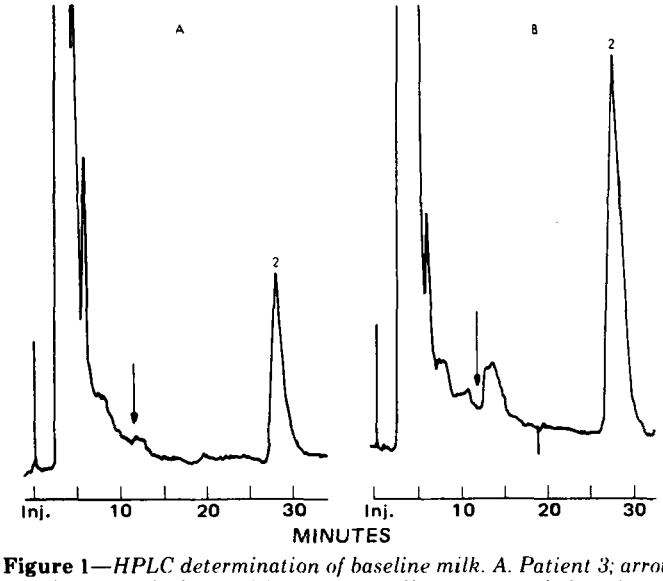

Figure 1—*HPLC determination of baseline milk. A. Patient 3; arrow = indoprofen elution position corresponding to 10.4 ng/ml, and peak 2 = internal standard, 206 ng. B. Patient 7; arrow = indoprofen elution position; and peak 2 = internal standard, 411 ng. Sample preparation and HPLC conditions are given in text.*

[6] Burdick & Jackson Laboratories, Muskegon, Mich.
[7] Mallinckrodt Chemical Works, St. Louis, Mo.
[8] Adria Laboratories, Columbus, Ohio.
[9] Floropore, Millipore Corp., Bedford, Mass.

Table II—Indoprofen in Milk and Plasma

Subject	Nanograms of Indoprofen per Milliliter of Milk, Time from First Dose, hr					Micrograms of Indoprofen per Milliliter of Plasma, Time from First Dose, hr		
	Baseline[a]	2.0	12	24	48	2.0	26	50
1	Tr	681	34	Tr	ND[b]	9.4	—	—
2	ND	Tr	192	Tr	Tr[c]	10.5	—	—
3	Tr	80	198	Tr	Tr	12.4	—	—
	Baseline[a]	2.0	26	50				
4	Tr	60	459	488		3.4	19.4	15.2
5	ND	41	273	422		3.5	5.6	11.3
6	ND	176	172	136		13.5	9.5	12.4
7	ND	Tr	184	219		0.8	6.6	23.8

[a] Calculated baseline level subtracted from other samples to obtain indoprofen level. [b] ND = not detected. [c] Tr = trace, <25 ng/ml.

Table III—Day-to-Day Precision of Relative Weight Response of Reference Standards[a]

Indoprofen Level, ng/ml	Run	Day						
		1	3	4	5	9	11	15
20	1	2.24	2.33	2.38	2.31	—	—	2.31
	2	2.21	—	—	2.42	—	—	—
50	1	2.16	2.22	2.26	2.39	2.18	2.28	2.25
	2	2.23	2.19	—	2.16	2.24	2.26	2.30
100	1	2.14	—	2.18	2.14	2.17	2.18	2.24
	2	2.22	—	2.20	—	2.24	2.24	2.31

[a] Average relative weight response = 2.24, $SD = \pm 0.07$, and $RSD = 3.2\%$.

The recovery of indoprofen added to samples to determine the procedure accuracy was calculated as follows:

$$\%R = \frac{\text{ng I "spiked" sample}}{\text{ng I added} + \text{ng I "unspiked" sample}} \times 100 \quad \text{(Eq. 3)}$$

where $\%R$ is the percent recovery and ng I is the nanograms of indoprofen calculated in the spiked and neat (unspiked) sample.

The analysis precision was determined by analyzing duplicate aliquots from each sample and calculating the standard deviation (SDP) and relative standard deviation ($RSDP$) of pairs:

$$SDP = (\sum |A - B|^2/2 \times P)^{1/2} \quad \text{(Eq. 4)}$$

$$RSDP = SDP/\text{average of all } A \text{ and } B \times 100 \quad \text{(Eq. 5)}$$

where A and B are values of duplicate determinations and P is the number of pairs.

RESULTS AND DISCUSSION

The previously developed HPLC analytical technique had sufficient sensitivity and selectivity to detect and measure nanogram quantities of indoprofen standards. However, prior to physiological fluid analysis at these levels, the sample required concentration and the removal of possible interfering components. This study was initiated to develop the necessary sample cleanup procedure and to determine indoprofen in human milk.

Initial experiments were conducted using cow's milk spiked with varying indoprofen levels. Many different parameters were evaluated, and the steps necessary to provide satisfactory drug recovery and sufficient sample cleanup were defined. The final cleanup procedure is outlined in the *Experimental* section. The indoprofen retention volume was increased by changing the acetonitrile content of the eluent from 40% (for plasma samples) to 35%. This eluent modification separated the drug from some major interfering milk components.

A final evaluation of the method was conducted by analyzing two or more milk samples spiked with 0, 10, 25, 50, 100, and 200 ng of drug/ml. Even with the eluent modification, a minor milk component was detected in the blank samples at the indoprofen retention volume. The level of this compound corresponded to 6.0 ng of indoprofen/ml, and this value was subtracted from the indoprofen levels in the spiked samples prior to recovery calculations. The average recovery for 15 spiked samples of cow's milk was 103% with a standard deviation of ±8.1.

Prior to using the method to determine indoprofen levels in human milk, the sample preparation procedure was further evaluated using the baseline milk samples from the seven subjects (Table I, Part A). Duplicate samples from each subject were prepared, one of which was spiked with 20, 50, or 100 ng of indoprofen/ml. Two analytical runs were made on a number of these samples to ensure technique reproducibility. An interfering milk component was observed in three baseline milk samples (Subjects 2–4) at an elution position near indoprofen. For Subjects 2 and 3, this component represented <10 ng of indoprofen/ml; however, for Subject 4, the peak was equivalent to 20 ng/ml and eluted 1 min before indoprofen. The interfering peak in Subjects 2 and 3 was subtracted from the drug level calculated in the corresponding spiked sample for recovery determination; Subject 4 was not included.

The average recovery for these analyses was 100% with a standard deviation of ±6. Thus, the cleanup technique provided excellent drug recovery and was able to give relatively clean chromatograms for nanogram determination. However, since some samples had interfering components, the method provided quantitative data on samples with drug levels greater than 25 ng/ml. Below that level, indoprofen levels were considered to be semiquantitative and were designated as trace (Tr) if a peak was calculated to be <10 ng/ml and as not detected (ND) if no peak was observed. Figure 1 presents representative chromatograms for two baseline milk samples.

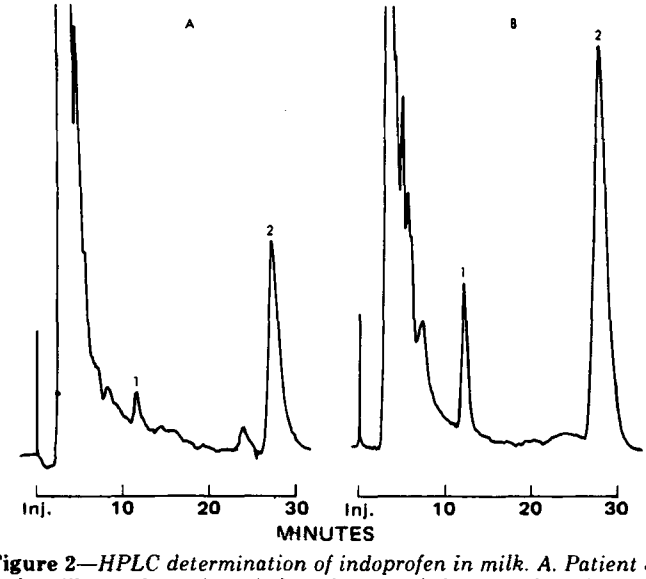

Figure 2—*HPLC determination of indoprofen in milk. A. Patient 3; 24-hr milk sample; peak 1 = indoprofen, 21 ng/ml; and peak 2 = internal standard, 206 ng. B. Patient 6; 24-hr milk sample; peak 1 = indoprofen, 136 ng/ml; and peak 2 = internal standard, 411 ng. Sample preparation and HPLC conditions are given in text.*

The analytical procedure was employed for the determination of indoprofen levels in human milk from seven subjects (Table II). All samples were analyzed in duplicate, and each value is the average of these determinations. The relative standard deviation of pairs was 5.1%. Subjects 1, 3, and 4 had detectable levels of a component in the baseline samples, and these values were subtracted to obtain the corrected indoprofen levels. The impurity level was similar to that observed previously (~10 ng/ml). This interfering compound was possibly present in all samples but was not completely removed in some during the sample preparation. Thirteen recovery samples were analyzed (Table I, Part B). The average recovery was 94% with a standard deviation of ±8. Representative indoprofen chromatograms in milk samples are presented in Fig. 2. For the 20 spiked samples analyzed, the average recovery was 96%.

Plasma samples were obtained at 2.0 hr after administration for the single-dose subjects and at 2.0, 26, and 50 hr after the first dose for multiple-dose subjects. Each plasma sample was analyzed in duplicate, and the averages are given in Table II. The precision of the plasma determinations was excellent, with a relative standard deviation of pairs of 5.1%.

Indoprofen calibration standards were analyzed after every fourth sample to determine the relative weight response for drug level calculations. New standards were prepared for each subject. A comparison of the relative weight responses obtained during milk sample analysis is given in Table III. During the 15-day period, the day-to-day variation in standards was very small, with a relative standard deviation of 3.2% for the relative weight response. Thus, the analytical system had excellent stability and provided quantitative data for extended periods.

REFERENCES

(1) A. Buttinoni, A. Cuttica, J. Franceschini, U. Mandelli, G. Orsini, N. Passerini, C. Turba, and R. Tommosini, *Arzneim.-Forsch.*, **23**, 1100 (1973).

(2) L. M. Fuccella, F. Conti, G. Corvi, U. Mandelli, M. Randelli, and G. Stefanelli, *Clin. Pharmacol. Ther.*, **17**, 277 (1975).

(3) U. Ventafridda, G. Martiro, U. Mandelli, and L. M. Fuccella, *J. Int. Med. Res.*, **3**, 16 (1975).

(4) L. M. Fuccella, G. C. Coldaniga, E. Moro, U. Tamassia, G. P. Tosolini, and G. Valzelli, *Eur. J. Clin. Pharmacol.*, **6**, 256 (1973).

(5) D. B. Lakings, W. J. Haggerty, G. Rehagen, and H. Barth, *J. Pharm. Sci.*, **67**, 831 (1978).

ACKNOWLEDGMENTS

Supported through a contract with Adria Laboratories, Columbus, OH 43216.

The authors express their appreciation to Ms. Gail Rehagen, Midwest Research Institute, and to Dr. W. Hausmann, Adria Laboratories, Inc., for helpful discussions and recommendations.

Simple Analogs of the Toxin Callicarpone

JAMES D. McCHESNEY *ˣ, POKAR M. KABRA, and PHILIP FRAHER

Received June 2, 1978, from the *Department of Medicinal Chemistry, School of Pharmacy, University of Kansas, Lawrence, KS 66045.* Accepted for publication March 14, 1979. *Present address: Department of Pharmacognosy, School of Pharmacy, University of Mississippi, University, MS 38677.

Abstract □ Callicarpone, a component 10 times as toxic to fish as rotenone, has been isolated from the leaves of *Callicarpa candicans*. It is reasonable to assume that callicarpone will act as an insecticidal agent as does rotenone. Therefore, the structure–activity relationship of callicarpone was examined by synthesizing a series of compounds having certain of its structural features. Those compounds were tested for insecticidal and antimicrobial activities. A study of synthetic analogs elucidated the functional group chemistry of callicarpone so that a synthesis might be undertaken. Piperitone oxide showed ~1/100th the activity of rotenone against *Daphnia magna*. 1-(α-Hydroxyisopropyl)-3-oxocyclohexene oxide showed activity against mycobacterium while 2,3,4,6,7,8-hexahydronaphthalene-1,4-dione showed inhibitory activity against the mycobacterium and two yeasts.

Keyphrases □ Callicarpone—analogs, structure–activity relationships, toxicity, antimicrobial activity □ Insecticides—callicarpone, analogs, structure–activity relationships, toxicity, antimicrobial activity □ Structure–activity relationships—callicarpone analogs, antimicrobial activity

The use of decoctions of various plants as fish poisons has been practiced for many centuries by native tribes in Africa, India, and South America. Usually, the poisonous plants were macerated with water, the decoction was poured into a selected body of water, and the fish that rose to the surface were collected. It was reasonable to assume that these poisonous plants should exhibit toxicity against organisms besides fish, and some of these plants have been found to contain useful insecticides.

A component toxic to fish has been isolated from the leaves of *Callicarpa candicans* (1). These leaves have long been used for stupefying fish by natives of Palau and the Philippine Islands. The active principle was named callicarpone (I). Callicarpone exhibited 10 times stronger toxicity against loach fish (*Misgurnus anguillicaudatus*) than did rotenone. The structure of callicarpone was deduced from spectral and chemical evidence.

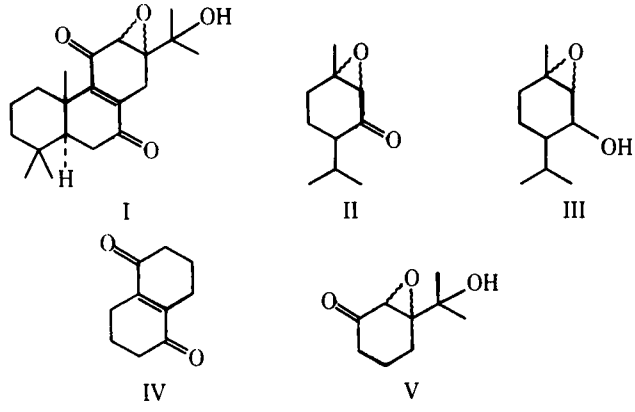

Since callicarpone possesses stronger toxicity against fish than does rotenone, it is reasonable to assume that callicarpone also might act as an insecticidal agent. Therefore, a study of the structure–activity relationship of callicarpone was initiated by synthesizing a series of compounds having certain of its structural features and by testing these compounds for their toxicity to *Daphnia magna* (a fresh water crustacean) (2). To determine if these functional groups might show a more general biological activity, the agents also were tested for antimicrobial activity. A study of synthetic analogs provided information about the functional group chemistry of callicarpone so that a synthesis might be undertaken.

Callicarpone possesses some unique structural and

0022-3549/79/0900-1116$01.00/0

© 1979, American Pharmaceutical Association

The analytical procedure was employed for the determination of indoprofen levels in human milk from seven subjects (Table II). All samples were analyzed in duplicate, and each value is the average of these determinations. The relative standard deviation of pairs was 5.1%. Subjects 1, 3, and 4 had detectable levels of a component in the baseline samples, and these values were subtracted to obtain the corrected indoprofen levels. The impurity level was similar to that observed previously (~10 ng/ml). This interfering compound was possibly present in all samples but was not completely removed in some during the sample preparation. Thirteen recovery samples were analyzed (Table I, Part B). The average recovery was 94% with a standard deviation of ±8. Representative indoprofen chromatograms in milk samples are presented in Fig. 2. For the 20 spiked samples analyzed, the average recovery was 96%.

Plasma samples were obtained at 2.0 hr after administration for the single-dose subjects and at 2.0, 26, and 50 hr after the first dose for multiple-dose subjects. Each plasma sample was analyzed in duplicate, and the averages are given in Table II. The precision of the plasma determinations was excellent, with a relative standard deviation of pairs of 5.1%.

Indoprofen calibration standards were analyzed after every fourth sample to determine the relative weight response for drug level calculations. New standards were prepared for each subject. A comparison of the relative weight responses obtained during milk sample analysis is given in Table III. During the 15-day period, the day-to-day variation in standards was very small, with a relative standard deviation of 3.2% for the relative weight response. Thus, the analytical system had excellent stability and provided quantitative data for extended periods.

REFERENCES

(1) A. Buttinoni, A. Cuttica, J. Franceschini, U. Mandelli, G. Orsini, N. Passerini, C. Turba, and R. Tommosini, *Arzneim.-Forsch.*, **23**, 1100 (1973).

(2) L. M. Fuccella, F. Conti, G. Corvi, U. Mandelli, M. Randelli, and G. Stefanelli, *Clin. Pharmacol. Ther.*, **17**, 277 (1975).

(3) U. Ventafridda, G. Martiro, U. Mandelli, and L. M. Fuccella, *J. Int. Med. Res.*, **3**, 16 (1975).

(4) L. M. Fuccella, G. C. Coldaniga, E. Moro, U. Tamassia, G. P. Tosolini, and G. Valzelli, *Eur. J. Clin. Pharmacol.*, **6**, 256 (1973).

(5) D. B. Lakings, W. J. Haggerty, G. Rehagen, and H. Barth, *J. Pharm. Sci.*, **67**, 831 (1978).

ACKNOWLEDGMENTS

Supported through a contract with Adria Laboratories, Columbus, OH 43216.

The authors express their appreciation to Ms. Gail Rehagen, Midwest Research Institute, and to Dr. W. Hausmann, Adria Laboratories, Inc., for helpful discussions and recommendations.

Simple Analogs of the Toxin Callicarpone

JAMES D. McCHESNEY *ˣ, POKAR M. KABRA, and PHILIP FRAHER

Received June 2, 1978, from the *Department of Medicinal Chemistry, School of Pharmacy, University of Kansas, Lawrence, KS 66045.* Accepted for publication March 14, 1979. *Present address: Department of Pharmacognosy, School of Pharmacy, University of Mississippi, University, MS 38677.

Abstract □ Callicarpone, a component 10 times as toxic to fish as rotenone, has been isolated from the leaves of *Callicarpa candicans*. It is reasonable to assume that callicarpone will act as an insecticidal agent as does rotenone. Therefore, the structure–activity relationship of callicarpone was examined by synthesizing a series of compounds having certain of its structural features. Those compounds were tested for insecticidal and antimicrobial activities. A study of synthetic analogs elucidated the functional group chemistry of callicarpone so that a synthesis might be undertaken. Piperitone oxide showed ~1/100th the activity of rotenone against *Daphnia magna*. 1-(α-Hydroxyisopropyl)-3-oxocyclohexene oxide showed activity against mycobacterium while 2,3,4,6,7,8-hexahydronaphthalene-1,4-dione showed inhibitory activity against the mycobacterium and two yeasts.

Keyphrases □ Callicarpone—analogs, structure–activity relationships, toxicity, antimicrobial activity □ Insecticides—callicarpone, analogs, structure–activity relationships, toxicity, antimicrobial activity □ Structure–activity relationships—callicarpone analogs, antimicrobial activity

The use of decoctions of various plants as fish poisons has been practiced for many centuries by native tribes in Africa, India, and South America. Usually, the poisonous plants were macerated with water, the decoction was poured into a selected body of water, and the fish that rose to the surface were collected. It was reasonable to assume that these poisonous plants should exhibit toxicity against organisms besides fish, and some of these plants have been found to contain useful insecticides.

A component toxic to fish has been isolated from the leaves of *Callicarpa candicans* (1). These leaves have long been used for stupefying fish by natives of Palau and the Philippine Islands. The active principle was named callicarpone (I). Callicarpone exhibited 10 times stronger toxicity against loach fish (*Misgurnus anguillicaudatus*) than did rotenone. The structure of callicarpone was deduced from spectral and chemical evidence.

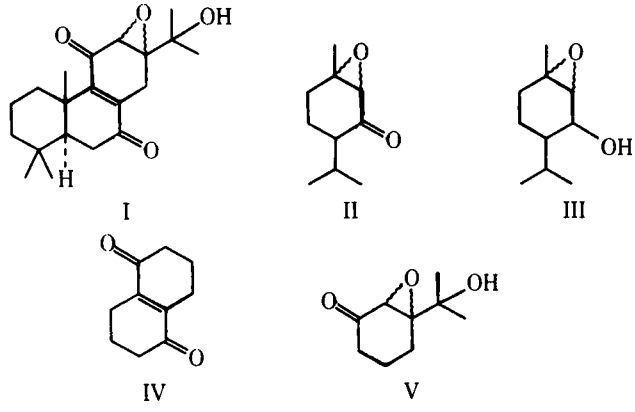

Since callicarpone possesses stronger toxicity against fish than does rotenone, it is reasonable to assume that callicarpone also might act as an insecticidal agent. Therefore, a study of the structure–activity relationship of callicarpone was initiated by synthesizing a series of compounds having certain of its structural features and by testing these compounds for their toxicity to *Daphnia magna* (a fresh water crustacean) (2). To determine if these functional groups might show a more general biological activity, the agents also were tested for antimicrobial activity. A study of synthetic analogs provided information about the functional group chemistry of callicarpone so that a synthesis might be undertaken.

Callicarpone possesses some unique structural and

0022-3549/79/0900-1116$01.00/0

© 1979, American Pharmaceutical Association

functional features, especially in rings B and C. To determine the structure–activity relationship, these structural and functional features were incorporated into compounds II–V.

DISCUSSION

Compound II possessed the α-epoxyketone functionality with a comparable substitution pattern around the epoxide ring and the carbonyl group as found in callicarpone. To determine the importance of the α-epoxyketone for biological potency, III also was synthesized; it incorporated all of the features of II, except that the carbonyl group was replaced by a hydroxyl group. This compound also allowed study, independently, of the activity of an α-hydroxy epoxide function, a system present in the parent callicarpone.

Compound IV possessed the 1,4-enedione functionality incorporated into a hexahydronaphthalene moiety as found in callicarpone. The importance of an α-hydroxyisopropyl group associated with the α-epoxyketone in callicarpone could be tested by synthesis of V, which incorporated the α-hydroxyisopropyl group in a comparable position to the α-epoxyketone as found in callicarpone.

The synthesis of piperitone oxide II was accomplished by treating piperitone VI with hydrogen peroxide and base according to the organic synthesis procedure (3). The II yield was low and erratic with the use of 6 *N* NaOH. A substantial amount of diol was recovered from the reaction mixture. The yield was significantly improved (to >75%) when the strength of the base was lowered to 4 *N* NaOH. A pure sample of II, whose physical properties were consistent with those reported (4), was recovered from the reaction mixture by distillation under vacuum.

The synthesis of III was initiated by reducing VI with sodium borohydride in methanol at room temperature according to a literature procedure (5). However, the reaction failed to yield any appreciable amount of VII. Lithium aluminum hydride reduction of piperitone, according to a literature procedure (6), resulted in the isolation of the desired alcohol (VII) in a 95% yield. The synthesis of III was accomplished by subjecting VII to *m*-chloroperbenzoic acid buffered with sodium acetate in methylene chloride at 0–5° (7). The pure epoxyalcohol (III) was obtained in a 70% yield from the reaction product by distillation under vacuum (Scheme I).

Campbell and Harris (8) reported the synthesis of 2,3,4,6,7,8-hexahydronaphthalene-1,5-dione (IV) in a <0.5% overall yield from Δ^{9-10} octalin. Alternatively, Johnson *et al.* (9) reported the synthesis of decalin-1,5-diones (X and XI) from naphthalene-1,5-diol (VIII) by reduction with Raney nickel at high temperature and pressure and subsequent oxidation. Since rhodium and ruthenium catalysts were unknown at the time of that work, an attempt was made to reduce the naphthalene-1,5-diol with 5% rhodium on alumina at 60 psi (10), which resulted in the isolation of the desired decalin-1,5-diols (IX) in a >90% yield (Scheme II).

The stereochemistry of the diols (IX) was not crucial for further transformations, so the mixture of stereoisomers was not separated at this juncture. The diols (IX) were subjected to modified Jones oxidation using chromium trioxide, benzene, sulfuric acid, and acetic acid at 0–5°. The *cis*- and *trans*-decalin-1,5-diones (X and XI) were obtained in a 2:3 ratio in an ~85% yield. These two compounds were separated by repeated fractional crystallization using benzene and petroleum ether (bp 60–65°). The physical properties of X and XI were consistent with those reported previously (9).

The mixture of *cis*- and *trans*-decalin-1,5-diones was refluxed with *N*-bromosuccinimide in carbon tetrachloride with irradiation with IR light (11). However, the anticipated monobromodecalin-1,5-dione was not obtained in a good yield. To improve the yield, the reflux time was increased to 48 hr. The isolated yellowish-brown solid, obtained in a 65% yield, was devoid of bromine. On repeated crystallization with petroleum ether (bp 60–65°), a light-yellow solid was obtained; it was characterized as IV on the basis of physical and spectral properties. Compound IV also could be obtained from the reaction product mixture by eluting it through

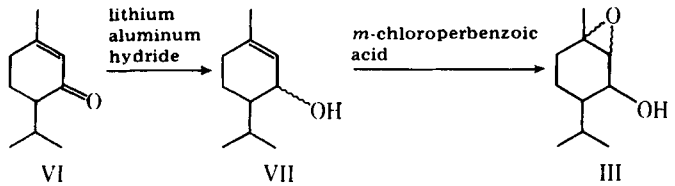

Scheme I

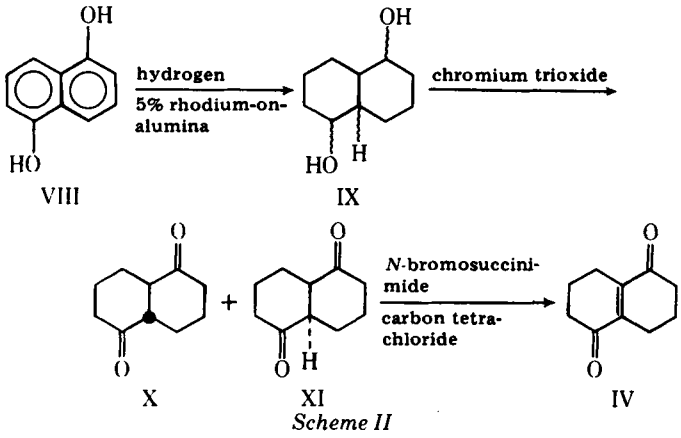

Scheme II

a short alumina column with cyclohexane or petroleum ether (bp 60–65°).

The synthesis of 1-(α-hydroxyisopropyl)-3-oxocyclohexene oxide (V) (Scheme III) was initiated from commercially available 2,3-dimethoxybenzaldehyde (XII), which was oxidized with aqueous potassium permanganate at steam bath temperature by an organic synthesis procedure (12) to 2,3-dimethoxybenzoic acid (XIII) in a >90% yield. The acid XIII was esterified by treatment with methanolic hydrogen chloride containing a trace of sulfuric acid prior to the cleavage of the methyl ethers (13).

Gero (14) used boron trichloride to cleave methyl ethers in the presence of an ester group. Application of this procedure to XIV, using a fourfold excess of boron trichloride in methylene chloride at −78°, gave the desired catechol (XV) in an 85–90% yield.

The synthesis of methyl-2,3-dihydroxycyclohexane carboxylate (XVI) was accomplished by the reduction of XV over 5% rhodium on alumina at 3 atmospheres of hydrogen pressure. Sodium methoxide treatment of XVI failed to provide the desired elimination product, methyl-3-hydroxycyclohex-1-ene carboxylate. A yellowish-brown solid obtained from the reaction could not be identified. Acetylation of XVI, using acetic anhydride in pyridine (XV), failed to give appreciable diacetate.

The synthesis of XVII was achieved by refluxing XVI with acetic anhydride in the presence of sodium acetate for 72 hr. A mixture of XVII and the diacetate of XVI was obtained in an ~70–75% yield. The two components were separated by chromatography on an alumina column. The formation of XVII could be explained by sodium acetate-catalyzed elimination of acetic acid from the diacetate. This hypothesis is supported

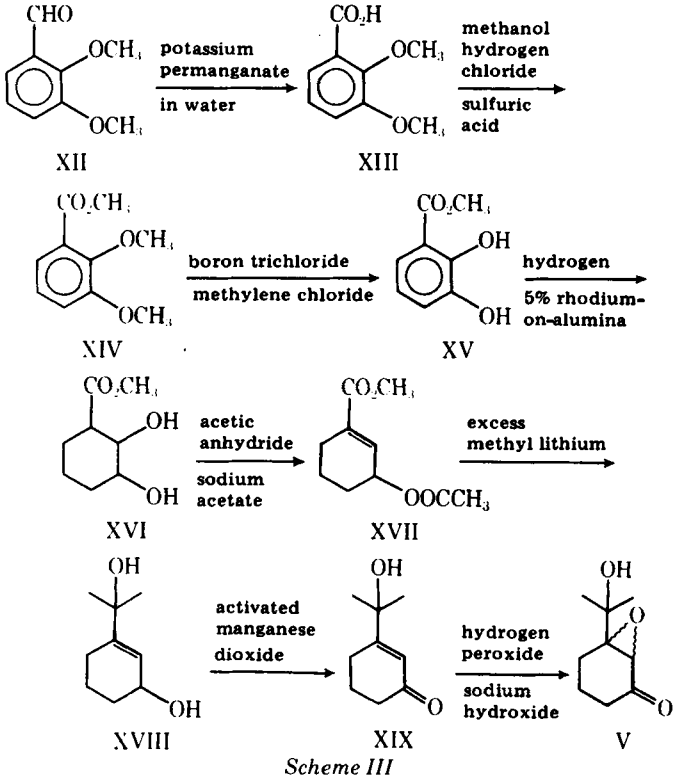

Scheme III

by the observation that the diacetate was transformed to XVII under these reaction conditions. Treatment of XVII with six equivalents of methyl lithium in ether at room temperature for 16 hr (15) produced XVIII in a good yield. Conversion of XVIII to XIX was performed in a 60% yield by treating XVIII with commercially available activated magnesium dioxide in hexane at room temperature for 96 hr (16).

The final step in the synthesis of V was achieved in a 65% yield by treating XIX with hydrogen peroxide and 4 *N* NaOH. The structure of V was established on the basis of spectral data. The IR spectrum showed an intense band at 1700 cm^{-1}, indicating the presence of a saturated six-membered alicyclic ketone. The PMR spectrum of V indicated the presence of the α-hydroxyisopropyl group at δ 1.4 ppm integrating for six protons. This signal was shifted downfield on the addition of trichloroacetyl isocyanate. The PMR spectrum also showed a sharp singlet integrating for one proton at δ 3.4 ppm, supporting the presence of the epoxide ring. The mass spectrum contained peaks at *m/e* 170 (M^+), 152, 137, 124, 83, and 82.

BIOLOGICAL RESULTS

Compounds II–V were assayed for antimicrobial activity[1] using the standard agar well-diffusion technique. Organisms included in the assay were *Staphylococcus aureus* (ATCC 6538), *Escherichia coli* (ATCC 10536), *Pseudomonas aeruginosa* (ATCC 15442), *Bacillus subtilis* (ATCC 6633), *Mycobacterium smegmatis* (ATCC 14468), *Aspergillus niger* (ATCC 11394), *Saccharomyces cereviseae* (ATCC 9763), and *Candida albicans* (ATCC 10231).

Stock cultures (except *A. niger*) were inoculated into 50 ml of culture broth (Eugon broth for bacteria and Mycophil broth for the yeasts) and incubated for 24 hr with shaking. The 24-hr cultures were diluted 1:50 in sterile distilled water, and agar plates (Eugon or Mycophil) were streaked (quadrant method) with the 1:50 dilution using a sterile dacron swab. For *A. niger*, a sterile water suspension of conidia was streaked on Mycophil agar.

Cylindrical plugs were removed from the agar plates using a sterile cork borer to produce wells having a diameter of 11 mm. Each 100 × 15-mm plate had two wells, one for the test solution and one for the solvent blank. With a micropipet, 100 μl of the test solution or solvent was added to each well. Compounds were tested routinely at a 2-mg/ml concentration in ethanol. A standard antibiotic for each organism was incorporated into the screen. Streptomycin sulfate (2 mg/ml) was used for the bacteria, and amphotericin B (250 μg/ml) was used for the fungi and yeasts. The results were read after 24 and 48 hr and are reported as the average radius of the inhibition zone measured in millimeters from the edge of the well to the edge of the inhibition zone.

Compounds II and III showed no inhibition of any organism. Compound IV showed slight inhibition of the two yeasts and the mycobacterium (Table I). Compound IV might distantly resemble the quinone compounds, which are so widely prevalent in biological systems, although it is premature to draw any conclusion regarding its mechanism of action. Compound V showed good inhibition (17 mm) of the mycobacterium but no inhibition of any other organism.

Compounds II–IV also were tested against *D. magna* (a fresh water organism). Solutions containing 80, 8, 0.8, or 0.08 mg of II, III, or IV/liter were tested against *D. magna* using a rotenone standard (2). Toxicity to the *Daphnia* from these compounds was observed every 30 min. Compound II was the most active of the compounds tested. It possessed ~1/100th the activity of rotenone. Compound III was devoid of any activity, while Compound IV was ~1/1000th as active as rotenone.

EXPERIMENTAL[2]

Piperitone Oxide (II)—In a 250-ml three-necked flask equipped with a mechanical stirrer, a dropping funnel, and a thermometer was placed a solution of 7.1 g (0.046 mole) of piperitone (VI) and 15 ml (0.12 mole) of 30% H_2O_2 in 50 ml of methanol. After the contents of the flask had been cooled to 15° by an ice–water bath, 15 ml (0.06 mole) of 4 *N* NaOH was added dropwise over 1 hr. During the addition, the temperature of the reaction mixture was maintained at 15–20° with the ice–water bath. After the addition was complete, the resulting mixture was stirred for 3 hr at room temperature.

The reaction mixture was poured into 100 ml of water and extracted with three 100-ml portions of ether. The ethereal extracts were combined, washed with water, dried over magnesium sulfate, concentrated, and distilled *in vacuo* to give 5.3 g (70%) of II, bp 63–65° (1 mm) [lit. (4) bp 66–67° (1 mm)]; IR (liquid film): 1705 (C=O) and 780 and 840 (epoxide) cm^{-1}; PMR ($CDCl_3$): 3.1 (s, 1, epoxide), 0.8–1.0 (dd, 6, CH_3CHCH_3), and 1.4 (s, 3, CH_3CCH); mass spectrum: 168 (M^+, 2% of base peak), 126 ($M^+ - C_3H_6$, 20% of base peak), 140 (M^+ – C=O, 5% of base peak), and 56 (base peak, 100%).

1-Methyl-4-isopropyl-Δ^1-cyclohexene-3-ol (VII)—In a 250-ml three-necked flask equipped with a magnetic stirrer, a dropping funnel, and a condenser was placed a solution of 8.0 g (0.053 mole) of VI in 100 ml of ether. Then a solution of 0.80 g (0.021 mole) of lithium aluminum hydride in 50 ml of ether was added during 30 min. The mixture was refluxed for 0.5 hr. Excess lithium aluminum hydride was decomposed with 5 ml of 50% ethanol followed by 10 ml of water until the precipitation of aluminum oxide had stopped. The ether layer was separated, washed with water, dried over magnesium sulfate, concentrated, and distilled to give 7.8 g (95%) of VII; IR (liquid film): 3400 (OH), 1640 (C=C), and 1380 (C—CH_3) cm^{-1}; PMR ($CDCl_3$): 5.5 (bs, 1, C=CH), 4.1 (m, 1, CHOH), and 1.8 (s, 3, vinylic methyl).

1-Methyl-3-hydroxy-4-isopropylcyclohexene Oxide (III)—In a 250-ml three-necked flask equipped with a stirrer, a dropping funnel, and a thermometer was placed a solution of 4.5 g (0.03 mole) of VII in 100 ml of methylene chloride. The solution was cooled to 20° by an ice–water bath. A solution of 9.5 g (0.045 mole) of 85% *m*-chloroperbenzoic acid, containing 1.5 g of sodium acetate in 50 ml of methylene chloride, was added dropwise in 15 min. The resulting mixture was stirred at room temperature for 20 hr. The contents of the flask were poured into 150 ml of water, the organic layer separated, and the aqueous layer was extracted with two 50-ml portions of methylene chloride.

The combined methylene chloride layers were washed with two 25-ml portions of 10% sodium carbonate and two 50-ml portions of water. The organic layer was dried over magnesium sulfate, concentrated, and distilled *in vacuo* to give 3.5 g (70%) of III; IR (liquid film): 3450 (hydroxyl), 1380 (C—CH_3), and 840 and 770 (epoxide) cm^{-1}; PMR ($CDCl_3$): 3.9 (m, 1, CHOH), 3.3 (bs, 1, C—CH), and 1.2 (s, 3, epoxide methyl); mass spectrum: 170 (M^+, 5% of base peak), 152 ($M^+ - H_2O$, 7% of base peak), 85 (15% of base peak), 84 (base peak, 100%), and 56 (30% of base peak).

Decalin-1,5-diol (IX)—A solution of 20 g of 1,5-dihydroxynaphthalene (VIII) in 500 ml of 95% ethanol was boiled with 4 g of activated charcoal for 15 min and filtered while hot. The filtrate was again boiled with 4 g of activated charcoal for 5 min and filtered while hot. Upon cooling to ice bath temperature, a first crop of VIII crystallized. The crystals were separated by filtration, and the filtrate was concentrated on the rotary evaporator, filtered, and chilled in the refrigerator. A second crop of VIII was obtained, yielding a total recovery of 11.5 g.

A solution of 10.0 g (0.063 mole) of VIII in 100 ml of methanol was hydrogenated in the presence of 5 g of 5% rhodium-on-alumina at an initial pressure of 65 psi. This sample was left until no additional fall in pressure was observed (usually 48 hr). The catalyst was removed by filtration, and the solvent was removed on the rotary evaporator. The residue was treated with 20 ml of 10% NaOH and 50 ml of benzene and shaken vigorously. A white solid material was separated, filtered, and washed twice with water and then with ether. A yield of 9.1 g (86%) of IX

Table I—Inhibition of Microorganisms by IV

Organism	Zone of Inhibition, mm
Yeasts and fungi	
A. niger	0
C. albicans	4
S. cereviseae	3
Mycobacteria	
M. smegmatis	2
Bacteria	
S. aureus	0
E. coli	0
P. aeruginosa	0
B. subtilis	0

[1] Department of Pharmacognosy, University of Mississippi, University, MS 39677.

[2] All melting points were taken on a Thomas-Hoover Unimelt apparatus and are corrected. Analyses were performed either by Midwest Microlab, Inc., Indianapolis, Ind., or on an F and M model 185 C, H, N analyzer at the University of Kansas. IR data were recorded on Beckman IR-8, IR-10, and IR-33 spectrophotometers. PMR data were recorded on Varian A-60, A-60A, and T-60 analytical spectrometers with tetramethylsilane as the internal standard. PMR data are reported as δ values (parts per million). Mass spectra were recorded on a Varian Atlas CH 5 at 70 ev at a resolution of ~4000.

was obtained, mp 208–209° [lit. (12) mp 210–211°]; IR (KBr disk): 3400 (hydroxyl), 1450 (methylene), and 1030–1050 (COH) cm^{-1}.

Decalin-1,5-diones (X and XI)—A suspension of 5.0 g (0.03 mole) of IX in 75 ml of benzene was cooled to 0–5° by cooling in an ice–water bath. To this suspension was added dropwise, with stirring, a cold solution of 7 g of sodium dichromate in 5.25 ml of glacial acetic acid, 9.5 ml of concentrated sulfuric acid, and 50 ml of water. During the addition, which required ~2 hr, the temperature of the reaction mixture was not allowed to exceed 5°.

After the addition was complete, the mixture was stirred for an additional 3 hr at 0–5° and then allowed to stand at room temperature overnight. The aqueous layer was separated and extracted with two 25-ml portions of benzene. The combined benzene layers were washed with water, with saturated sodium bicarbonate, and finally with water. The benzene was removed on the rotary evaporator to give 4.1 g (83%) of the *cis*- and *trans*-decalin-1,5-diones (X and XI). These compounds were separated from the mixture by fractional crystallization using benzene and petroleum ether (bp 60–65°), mp (X) 80–81° [lit. (12) mp 79–80°] and mp (XI) 165–166° [lit. (12) mp 166–167°]; IR (KBr disk): 1700 (C=O) and 1460 (methylene) cm^{-1}.

2,3,4,6,7,8-Hexahydronaphthalene-1,5-dione (IV)—A solution of 1.4 g (0.009 mole) of X and XI and 1.6 g (0.01 mole) of *N*-bromosuccinimide, recrystallized from water, in 50 ml of carbon tetrachloride was refluxed for 48 hr. The solution was irradiated intermittently with IR light. The floating succinimide residue was filtered and washed with carbon tetrachloride. The organic layer was concentrated to give 0.95 g (65%) of a yellow solid which, on recrystallization from petroleum ether, gave a light-yellow solid (IV), mp 110–111° [lit. (10) mp 112–113°]; IR (KBr disk): 2960 (CH), 1710, 1675 (C=O), and 1640 (C=C) cm^{-1}; PMR ($CDCl_3$): 2.5 (m, 6, allylic and methylenes alpha to carbonyl), and 2.0 (m, 4, methylene); mass spectrum: 164 (M^+, 40% of base peak), 136 (M^+ – C=O, 70% of base peak), and 84 (base peak, 100%).

2,3-Dimethoxybenzoic Acid (XIII)—A mixture of 2,3-dimethoxybenzaldehyde (XII) (100 g, 0.6 mole) and 1 liter of water was placed in a three-necked flask equipped with a mechanical stirrer, a dropping funnel, and a thermometer. The flask was placed on a steam bath, heated to 70–80°, and stirred. A solution of 150 g of $KMnO_4$ in 800 ml of water was allowed to flow into the emulsion of XII over 40–45 min. The stirring was continued for 90 min.

Sufficient 10% potassium hydroxide solution was added to make the reaction mixture alkaline, the mixture was filtered while hot, and the manganese dioxide was washed with two 200-ml portions of hot water. The filtrate was acidified with concentrated hydrochloric acid until no further precipitate formed. The resulting XIII was filtered, washed with cold water, and dried. The yield was 95 g (92%), mp 121° [lit. (17) mp 120–122°].

Methyl-2,3-dimethoxybenzoate (XIV)—A solution of XIII (90 g, 0.53 mole) in 500 ml of methanol saturated with dry hydrogen chloride gas was prepared. One milliliter of concentrated sulfuric acid was added, and the mixture was refluxed for 12 hr. The reaction mixture was concentrated on the rotary evaporator, the residue was extracted with ether, and the ethereal layer was washed with water, saturated sodium bicarbonate solution, and then water. It was then dried over magnesium sulfate and concentrated to give 81.5 g (85%) of XIV, mp 58–59° [lit. (18) mp 57–58°].

Methyl-2,3-dihydroxybenzoate (XV)—In a 1-liter three-necked flask equipped with a mechanical stirrer was placed a solution of 55 g (0.27 mole) of XIV in 400 ml of methylene chloride. Boron trichloride (90 g, 0.81 mole) was condensed into the solution at −78°. The reaction mixture was stirred at −78° for 90 min and then allowed to stir at room temperature overnight. The resulting boron trichloride complex was decomposed with careful addition of water, the organic layer separated, and the aqueous layer was extracted with two 100-ml portions of methylene chloride.

The methylene chloride layers were combined and washed with three 100-ml portions of water, saturated sodium bicarbonate solution, and then water. Then they were dried over magnesium sulfate and concentrated to yield 45 g (85%) of XV, mp 78–80°; PMR ($CDCl_3$): 7.0 (m, 3, aromatic), 5.9 (bs, 1, OH), 10.8 (s, 1, OH), and 3.9 (s, 3, $COOCH_3$).

Methyl-2,3-dihydroxycyclohexane Carboxylate (XVI)—A solution of 20.0 g (0.12 mole) of XV and methanol (200 ml) was hydrogenated in the presence of 5 g of 5% rhodium-on-alumina at an initial pressure of 60 psi for 24 hr. The catalyst was removed by filtration, and the solvent was removed on a rotary evaporator to give 19.8 g (96%) of an oil (XVI); IR (liquid film): 3450 (OH), 2960 (CH), and 1735 ($COOCH_3$) cm^{-1}; PMR ($CDCl_3$): 4.3 (m, 1, *H*—C—OH), 4.1 (m, 1, *H*—C—OH), 3.8 (s, 3, $COOCH_3$), and 1.6 (m, 8, methylene).

Methyl-3-acetoxy-Δ^1-cyclohexene Carboxylate (XVII)—A solution of 20.0 g (0.115 mole) of XVI in 250 ml of acetic anhydride, containing 6.5 g of anhydrous sodium acetate, was refluxed for 72 hr. The solution was filtered, excess acetic anhydride was distilled *in vacuo*, and the residue was poured into 150 ml of 10% sodium carbonate solution and kept overnight. The solution was extracted with three 100-ml portions of ether, and the ether layers were combined and washed with water, dried over magnesium sulfate, and concentrated to give 15.5 g of an oil containing a mixture of XVII and methyl-2,4-diacetoxycyclohexane carboxylate.

The crude mixture was adsorbed onto a neutral alumina column (activity grade II) and eluted with 20% ethyl acetate in cyclohexane. A yield of 8.5 g (35%) of pure XVII was eluted from the column; IR (liquid film): 2960 (CH), 1730 ($COOCH_3$ and acetate), 1650 (C=C), and 1370 ($C—CH_3$) cm^{-1}; PMR ($CDCl_3$): 6.8 (m, 1, C=CH), 5.4 (m, 1, $CHOOCH_3$), 3.8 (s, 3, $COOCH_3$), and 2.1 (s, 3, acetate).

1-(α-Hydroxyisopropyl)-Δ^1-cyclohexane-3-ol (XVIII)—In a 250-ml three-necked flask equipped with a stirrer and a dropping funnel was placed a solution of 4.0 g (0.02 mole) of XVII in 50 ml of ether under an atmosphere of argon gas. The solution was cooled to 0–5° by an ice bath. A 120-ml aliquot of a 1 *M* solution (0.12 mole) of methyl lithium in ether was added dropwise over 1 hr. The resulting solution was allowed to stir overnight at room temperature. The solution was poured into 100 ml of 5% ammonium bicarbonate, the ethereal layer separated, and the aqueous layer was extracted with two 50-ml portions of ether.

The combined ether layers were washed with water, dried over sodium sulfate, and concentrated to give 2.6 g (83%) of XVIII; IR (liquid film): 3400 (OH), 3000 (CH), 1660 (C=C), and 1370 and 1380 ($CH_3—C—CH_3$) cm^{-1}; PMR ($CDCl_3$): 5.8 (m, 1, C=CH), 3.9 (m, 1, *CH*—OH), and 1.32 [s, 6, $CH_3—C(—OH)—CH_3$].

1-(α-Hydroxyisopropyl)-Δ^1-cyclohexane-3-one (XIX)—A solution of 1.5 g (0.0098 mole) of XVIII in 50 ml of hexane, containing 5 g of activated manganese dioxide, was allowed to stir at room temperature for 96 hr. The solution was filtered, and the solvent was removed *in vacuo* to give 1.05 g (65%) of XIX; IR (liquid film): 3450 (OH), 1675 (C=O), and 1620 (C=C) cm^{-1}; PMR ($CDCl_3$): 6.15 (s, 1, C=C—H), 2.4 (m, 2, CH_2C=O), and 1.4 [s, 6, $CH_3—C(—OH)—CH_3$]; mass spectrum: 154 (M^+, 1% of base peak), 136 ($M^+ - H_2O$, 2% of base peak), 139 ($M^+ - CH_3$, 2% of base peak), and 83 (base peak, 100%).

1-(α-Hydroxyisopropyl)-3-oxocyclohexane Oxide (V)—In a 100-ml three-necked flask equipped with a mechanical stirrer and a dropping funnel was placed a solution of 0.77 g (0.002 mole) of XIX and 1.5 ml (0.012 mole) of 30% H_2O_2 in 40 ml of methanol. After the contents of the flask were cooled to 15° by an ice–water bath, 1 ml (0.006 mole) of 4 *N* NaOH was added. The resulting mixture was stirred at room temperature for 4 hr and poured into 50 ml of water. Then the aqueous layer was extracted with three 30-ml portions of ether.

The ethereal layers were combined, washed with water, dried over magnesium sulfate, and concentrated *in vacuo* to give 0.55 g (70%) of V; IR (liquid film): 3400 (OH), 1705 (C=O), and 825 and 780 (epoxide) cm^{-1}; PMR ($CDCl_3$): 3.4 (s, 1, C—CH), 2.2 (t, 2, $CH_2—C$=O), and 1.4 (s, 6, $CH_3—C—CH_3$); mass spectrum: 170 (M^+, 1% of base peak), 152 ($M^+ - H_2O$, 2% of base peak), 83 (base peak, 100%), and 82 (8% of base peak).

REFERENCES

(1) K. Kanwazu and T. Mitsui, *Tetrahedron Lett.*, **1966,** 3519.

(2) D. G. Crosby and R. K. Tucker, *Science*, **154,** 289 (1966).

(3) "Organic Synthesis," coll. vol. IV, N. Rabjohn, Ed., Wiley, New York, N.Y., 1963, p. 552.

(4) J. Rupe and M. Refardt, *Helv. Chim. Acta*, **25,** 836 (1942).

(5) W. S. Allen, S. Bernstein, and R. Littel, *J. Am. Chem. Soc.*, **76,** 6116 (1954).

(6) E. H. Eschinasi, *J. Org. Chem.*, **35,** 2010 (1970).

(7) "Organic Synthesis," coll. vol. IV, N. Rabjohn, Ed., Wiley, New York, N.Y., 1963, p. 860.

(8) W. P. Campbell and G. C. Harris, *J. Am. Chem. Soc.*, **63,** 2721 (1941).

(9) W. S. Johnson, C. D. Gutsche, and D. K. Banerjee, *J. Am. Chem. Soc.*, **73,** 5464 (1951).

(10) A. I. Meyers, W. Beverung, and G. Bargia-Munoz, *J. Org. Chem.*, **29,** 3427 (1964).

(11) C. Djerassi and C. R. Scholz, *Experientia*, **3,** 107 (1947).

(12) "Organic Synthesis," coll. vol. II, A. H. Blatt, Ed., Wiley, New York, N.Y., 1943, p. 538.

(13) "Organic Synthesis," coll. vol. IV, N. Rabjohn, Ed., Wiley, New York, N.Y., 1963, p. 635.
(14) S. D. Gero, *Tetrahedron Lett.*, **1966**, 591.
(15) L. F. Fieser and M. Fieser, "Reagents for Organic Synthesis," Wiley, New York, N.Y., 1967, p. 686.
(16) F. Sindheimer, O. Mancera, M. Vrguiza, and G. Posenkranz, *J. Am. Chem. Soc.*, **77**, 4145 (1955).
(17) L. F. Fieser, *J. Am. Chem. Soc.*, **75**, 4400 (1953).
(18) G. A. Edwards, W. H. Perkin, and F. W. Stoyle, *J. Chem. Soc.*, **127**, 195 (1925).

ACKNOWLEDGMENTS

Abstracted in part from a dissertation submitted by P. M. Kabra to the University of Kansas in partial fulfillment of the Doctor of Philosophy degree requirements.

Kinetic Parameter Estimation by Numerical Algorithms and Multiple Linear Regression: Application to Pharmacokinetics

K. C. YEH*x and K. C. KWAN

Received July 26, 1978, from *Merck Sharp & Dohme Research Laboratories, West Point, PA 19486.* Accepted for publication March 19, 1979. *Present address: College of Pharmacy and Allied Health Professions, St. John's University, Jamaica, NY 11439.

Abstract □ Two numerical examples are presented to illustrate the application of the proposed method of parameter estimation in pharmacokinetics. Results for a system exemplifying first-order kinetics indicate that parameters estimated by the proposed procedure compare favorably with those estimated by a nonlinear regression method. In a simulated example characterized by Michaelis–Menten elimination kinetics, the accuracy of the estimated parameters was comparable to that expected, verifying the validity of the method. The importance of the numerical approximation algorithms was demonstrated also.

Keyphrases □ Pharmacokinetics—estimation by numerical algorithms and multiple linear regression □ Numerical algorithms—estimation of kinetic parameters □ Multiple linear regression—estimation of kinetic parameters □ Statistics—numerical algorithms, multiple linear regression, estimation of kinetic parameters

A general approach suitable for parameter estimation was reported previously (1). The strategy is to obtain equivalent mathematical expressions in linear form. Briefly, the procedure involves data transformation, usually by numerical integration and/or differentiation, followed by multiple linear regression. The application of this technique in pharmacokinetics is illustrated in the present report.

ESTIMATION PROCEDURE

Linear Case—Many pharmacokinetic processes are linear, and their description can be approximated by multiexponential equations. In a two-compartment open model (2, 3), the observed drug concentration in the central compartment, C_i, after intravenous administration can be described by:

$$C_i = a\exp(-\alpha t_i) + b\exp(-\beta t_i) \qquad i = 1, 2, \ldots, n \qquad \text{(Eq. 1)}$$

where a, b, α, and β are unknown constants and n is the number of observations[1]. If the elimination is assumed to take place from the central compartment only, as depicted in Scheme I, the relationships between the four constants and the model parameters become:

$$\alpha = 0.5[(k_{12} + k_{21} + k_{10}) + \sqrt{(k_{12} + k_{21} + k_{10}) - 4k_{21}k_{10}}] \qquad \text{(Eq. 2)}$$

$$\beta = 0.5[(k_{12} + k_{21} + k_{10}) - \sqrt{(k_{12} + k_{21} + k_{10}) - 4k_{21}k_{10}}] \qquad \text{(Eq. 3)}$$

$$a = D(\alpha - k_{21})/V(\alpha - \beta) \qquad \text{(Eq. 4)}$$

[1] For simplicity, subscript i is omitted and implied in most of the equations.

$$T \underset{K_{21}}{\overset{K_{12}}{\rightleftharpoons}} B \xrightarrow{K_{10}} U$$

Scheme I—Linear two-compartment open model depicting the body as composed of the central compartment B *(including blood) and the peripheral compartment* T, *where* k_{12} *and* k_{21} *are first-order intercompartmental transfer rate constants,* k_{10} *is the first-order elimination rate constant, and* U *is the eliminating compartment. The drug dose* D *is introduced into the central compartment at zero time. The drug concentration in the central compartment is defined as* C = B/V, *where* V *is the volume of distribution of the central compartment.*

$$b = D(k_{21} - \beta)/V(\alpha - \beta) \qquad \text{(Eq. 5)}$$

$$V = D/(a + b) \qquad \text{(Eq. 6)}$$

By applying the procedure described earlier (1) and recognizing that concentration at time zero is not an observation for a given experiment, the biexponential equation can be transformed into the following linear expression, which contains four terms:

$$C = \sum_{j=1}^{4} A_j X_j \qquad \text{(Eq. 7)}$$

where:

$$A_1 = \frac{D}{V} + \frac{K_{21}D}{V}t_1 - (\alpha + \beta)\int_0^{t_1} C\,dt - (\alpha\beta)\int_0^{t_1}\int_0^{t_1} C\,dt^2 \qquad \text{(Eq. 8)}$$

$$A_2 = \frac{K_{21}D}{V} - (\alpha\beta)\int_0^{t_1} C\,dt \qquad \text{(Eq. 9)}$$

$$A_3 = -(\alpha + \beta) \qquad \text{(Eq. 10)}$$

$$A_4 = -(\alpha\beta) \qquad \text{(Eq. 11)}$$

$$X_1 = 1.0 \qquad \text{(Eq. 12)}$$

$$X_2 = t_i - t_1 \qquad \text{(Eq. 13)}$$

$$X_3 = \int_{t_1}^{t_i} C\,dt \qquad \text{(Eq. 14)}$$

$$X_4 = \int_{t_1}^{t_i} X_3\,dt \qquad \text{(Eq. 15)}$$

In deriving Eqs. 8 and 9, the following identities apply:

$$\int_0^{t_i} C\,dt = \int_0^{t_1} C\,dt + \int_{t_1}^{t_i} C\,dt \qquad \text{(Eq. 16)}$$

$$\int_0^{t_i}\int_0^{t_i} C\,dt^2 = \int_0^{t_1}\int_0^{t_1} C\,dt^2 + (t_i - t_1)\cdot\int_0^{t_1} C\,dt + \int_{t_1}^{t_i}\int_{t_1}^{t_i} C\,dt^2 \qquad \text{(Eq. 17)}$$

0022-3549/79/0900-1120$01.00/0
© 1979, American Pharmaceutical Association

(13) "Organic Synthesis," coll. vol. IV, N. Rabjohn, Ed., Wiley, New York, N.Y., 1963, p. 635.
(14) S. D. Gero, *Tetrahedron Lett.*, **1966**, 591.
(15) L. F. Fieser and M. Fieser, "Reagents for Organic Synthesis," Wiley, New York, N.Y., 1967, p. 686.
(16) F. Sindheimer, O. Mancera, M. Vrguiza, and G. Posenkranz, *J. Am. Chem. Soc.*, **77**, 4145 (1955).
(17) L. F. Fieser, *J. Am. Chem. Soc.*, **75**, 4400 (1953).
(18) G. A. Edwards, W. H. Perkin, and F. W. Stoyle, *J. Chem. Soc.*, **127**, 195 (1925).

ACKNOWLEDGMENTS

Abstracted in part from a dissertation submitted by P. M. Kabra to the University of Kansas in partial fulfillment of the Doctor of Philosophy degree requirements.

Kinetic Parameter Estimation by Numerical Algorithms and Multiple Linear Regression: Application to Pharmacokinetics

K. C. YEH*x and K. C. KWAN

Received July 26, 1978, from *Merck Sharp & Dohme Research Laboratories, West Point, PA 19486.* Accepted for publication March 19, 1979. *Present address: College of Pharmacy and Allied Health Professions, St. John's University, Jamaica, NY 11439.

Abstract □ Two numerical examples are presented to illustrate the application of the proposed method of parameter estimation in pharmacokinetics. Results for a system exemplifying first-order kinetics indicate that parameters estimated by the proposed procedure compare favorably with those estimated by a nonlinear regression method. In a simulated example characterized by Michaelis–Menten elimination kinetics, the accuracy of the estimated parameters was comparable to that expected, verifying the validity of the method. The importance of the numerical approximation algorithms was demonstrated also.

Keyphrases □ Pharmacokinetics—estimation by numerical algorithms and multiple linear regression □ Numerical algorithms—estimation of kinetic parameters □ Multiple linear regression—estimation of kinetic parameters □ Statistics—numerical algorithms, multiple linear regression, estimation of kinetic parameters

A general approach suitable for parameter estimation was reported previously (1). The strategy is to obtain equivalent mathematical expressions in linear form. Briefly, the procedure involves data transformation, usually by numerical integration and/or differentiation, followed by multiple linear regression. The application of this technique in pharmacokinetics is illustrated in the present report.

ESTIMATION PROCEDURE

Linear Case—Many pharmacokinetic processes are linear, and their description can be approximated by multiexponential equations. In a two-compartment open model (2, 3), the observed drug concentration in the central compartment, C_i, after intravenous administration can be described by:

$$C_i = a\exp(-\alpha t_i) + b\exp(-\beta t_i) \qquad i = 1, 2, \ldots, n \qquad \text{(Eq. 1)}$$

where a, b, α, and β are unknown constants and n is the number of observations[1]. If the elimination is assumed to take place from the central compartment only, as depicted in Scheme I, the relationships between the four constants and the model parameters become:

$$\alpha = 0.5[(k_{12} + k_{21} + k_{10}) + \sqrt{(k_{12} + k_{21} + k_{10}) - 4k_{21}k_{10}}] \qquad \text{(Eq. 2)}$$

$$\beta = 0.5[(k_{12} + k_{21} + k_{10}) - \sqrt{(k_{12} + k_{21} + k_{10}) - 4k_{21}k_{10}}] \qquad \text{(Eq. 3)}$$

$$a = D(\alpha - k_{21})/V(\alpha - \beta) \qquad \text{(Eq. 4)}$$

[1] For simplicity, subscript i is omitted and implied in most of the equations.

$$T \underset{K_{21}}{\overset{K_{12}}{\rightleftharpoons}} B \xrightarrow{K_{10}} U$$

Scheme I—Linear two-compartment open model depicting the body as composed of the central compartment B *(including blood) and the peripheral compartment* T, *where* k_{12} *and* k_{21} *are first-order intercompartmental transfer rate constants,* k_{10} *is the first-order elimination rate constant, and* U *is the eliminating compartment. The drug dose* D *is introduced into the central compartment at zero time. The drug concentration in the central compartment is defined as* C = B/V, *where* V *is the volume of distribution of the central compartment.*

$$b = D(k_{21} - \beta)/V(\alpha - \beta) \qquad \text{(Eq. 5)}$$

$$V = D/(a + b) \qquad \text{(Eq. 6)}$$

By applying the procedure described earlier (1) and recognizing that concentration at time zero is not an observation for a given experiment, the biexponential equation can be transformed into the following linear expression, which contains four terms:

$$C = \sum_{j=1}^{4} A_j X_j \qquad \text{(Eq. 7)}$$

where:

$$A_1 = \frac{D}{V} + \frac{K_{21}D}{V}t_1 - (\alpha + \beta)\int_0^{t_1} C\,dt - (\alpha\beta)\int_0^{t_1}\int_0^{t_1} C\,dt^2 \qquad \text{(Eq. 8)}$$

$$A_2 = \frac{K_{21}D}{V} - (\alpha\beta)\int_0^{t_1} C\,dt \qquad \text{(Eq. 9)}$$

$$A_3 = -(\alpha + \beta) \qquad \text{(Eq. 10)}$$

$$A_4 = -(\alpha\beta) \qquad \text{(Eq. 11)}$$

$$X_1 = 1.0 \qquad \text{(Eq. 12)}$$

$$X_2 = t_i - t_1 \qquad \text{(Eq. 13)}$$

$$X_3 = \int_{t_1}^{t_i} C\,dt \qquad \text{(Eq. 14)}$$

$$X_4 = \int_{t_1}^{t_i} X_3\,dt \qquad \text{(Eq. 15)}$$

In deriving Eqs. 8 and 9, the following identities apply:

$$\int_0^{t_i} C\,dt = \int_0^{t_1} C\,dt + \int_{t_1}^{t_i} C\,dt \qquad \text{(Eq. 16)}$$

$$\int_0^{t_i}\int_0^{t_i} C\,dt^2 = \int_0^{t_1}\int_0^{t_1} C\,dt^2 + (t_i - t_1)\cdot\int_0^{t_1} C\,dt + \int_{t_1}^{t_i}\int_{t_1}^{t_i} C\,dt^2 \qquad \text{(Eq. 17)}$$

0022-3549/79/0900-1120$01.00/0
© 1979, American Pharmaceutical Association

$$T \underset{K_{21}}{\overset{K_{12}}{\rightleftharpoons}} B \xrightarrow{V_m, K_m} U$$

Scheme II—Nonlinear disposition model obtained by modification of Scheme I. Conditions are identical for the two schemes except that the elimination is characterized by saturable Michaelis–Menten-type kinetics.

Equation 7 also can be independently derived from the following rate and mass-balance equations:

$$\dot{C} = -(k_{12} + k_{10})C + (k_{21}/V)T \quad \text{(Eq. 18a)}$$

$$\dot{U} = k_{10}VC \quad \text{(Eq. 18b)}$$

$$D = VC + T + U \quad \text{(Eq. 18c)}$$

From Eqs. 8–11, where A_1 and A_2 are simplified to:

$$A_1 = a \exp(-\alpha t_1) + b \exp(-\beta t_1) \quad \text{(Eq. 19)}$$

$$A_2 = a\beta \exp(-\alpha t_1) + b\alpha \exp(-\beta t_1) \quad \text{(Eq. 20)}$$

the four parameters can be calculated:

$$\alpha = 0.5[-A_3 + (A_3^2 + 4A_4)^{1/2}] \quad \text{(Eq. 21)}$$

$$\beta = 0.5[-A_3 - (A_3^2 + 4A_4)^{1/2}] \quad \text{(Eq. 22)}$$

$$K_{21} = \frac{\beta(A_2 - A_1\alpha)\exp(-\beta t_1) - \alpha(A_2 - A_1\beta)\exp(-\alpha t_1)}{(A_2 - A_1\alpha)\exp(-\beta t_1) - (A_2 - A_1\beta)\exp(-\alpha t_1)} \quad \text{(Eq. 23)}$$

$$V = \frac{D}{A_1(\alpha - \beta)}[(\alpha - k_{21})\exp(-\alpha t_1) + (k_{21} - \beta)\exp(-\beta t_1)] \quad \text{(Eq. 24)}$$

While four parameters are associated with the biexponential equation, only α and β are nonlinearly related. The other two constants, a and b, are linearly related and can be estimated by linear regression. Thus, the procedure is slightly modified so that regression Eq. 7 is used to obtain the two nonlinear parameters only. Once they are calculated from Eqs. 21 and 22, they are then substituted into Eq. 1 to obtain a and b by a second linear regression.

Nonlinear Case—A nonlinear pharmacokinetic model obtained by a simple modification of the previous one is shown in Scheme II. In this model, drug elimination from the central compartment is assumed to follow Michaelis–Menten kinetics. The rate and mass-balance equations are:

$$\dot{C} = -k_{12}C + (k_{21}/V)T - (V_m/V)C/(K_m + C) \quad \text{(Eq. 25a)}$$

$$\dot{U} = V_mC/(K_m + C) \quad \text{(Eq. 25b)}$$

$$D = VC + T + U \quad \text{(Eq. 25c)}$$

where V_m is the maximum rate and K_m is the Michaelis constant.

Although closed-form solutions explicit in t to this nonlinear model cannot be obtained, numerical solutions can be generated by using Runge–Kutta approximations.

The regression equation describing the time course of the drug concentration in the central compartment is:

$$C = \sum_{j=1}^{4} A_jX_j \quad \text{(Eq. 26)}$$

where:

$$A_1 = \frac{k_{21}D}{V(k_{12} + k_{21})} - \frac{k_{21}V_m}{V(k_{12} + k_{21})}\int_0^{t_1} \frac{C}{K_m + C}\,dt \quad \text{(Eq. 27)}$$

$$A_2 = -1/(k_{12} + k_{21}) \quad \text{(Eq. 28)}$$

$$A_3 = -V_m/V(k_{12} + k_{21}) \quad \text{(Eq. 29)}$$

$$A_4 = -k_{21}V_m/V(k_{12} + k_{21}) \quad \text{(Eq. 30)}$$

$$X_1 = 1.0 \quad \text{(Eq. 31)}$$

$$X_2 = \dot{C} \quad \text{(Eq. 32)}$$

$$X_3 = C/(K_m + C) \quad \text{(Eq. 33)}$$

$$X_4 = \int_{t_1}^{t_i} X_3\,dt \quad \text{(Eq. 34)}$$

The main difference between the two models is the presence of nonlinear parameter K_m. As described earlier (1), the best-fit K_m can be found by scanning the weighted sum of squared deviations, WSS, as a function of K_m. The minimum WSS is then located by iteration. The search should be confined to a range of values where K_m is numerically comparable to the observed C values. Otherwise, the system reduces to a linear model with either first-order ($K_m \gg C$) or zero-order ($K_m \ll C$) elimination.

Numerical Integration—To perform the regression analysis, numerical methods such as numerical integration and numerical differentiation are required to generate the necessary X_j values. Many numerical integrating algorithms, including the well-known trapezoidal rule, can be found in the literature (5). In a recent publication, algorithms based on Lagrange and spline functions were shown to be relatively free of systematic errors (6).

A slightly modified spline method is employed in the present work to minimize spurious oscillations near both ends of the curve. In the original procedure (6), the two end conditions are defined as $\ddot{Y}_2 = \ddot{Y}_3$ and $\ddot{Y}_{n-1} = \ddot{Y}_n$. In the modified version, the first condition is amended so that $\ddot{Y}_1 = 0$ if $Y_1 = 0$, with the constraint $\dot{Y}_1 \geq 0$. The second condition is changed to $\ddot{Y}_n = 0$; in the event that $Y_n = 0$, an additional constraint of $\dot{Y}_n = 0$ is also imposed. These two conditions, except for the constraints, were suggested previously (7). The modified procedure is especially useful if input data contain two or more consecutive zero Y values.

Numerical Differentiation—Numerical differentiation is required to generate the X_2 values in Eq. 32. In contrast to numerical integration, which tends to dampen noise, numerical differentiation tends to magnify the effect of input errors. If experimental data are of high precision, interpolating polynomials such as spline functions (6, 7) can be used. With noisy data, a possible solution is to use smoothing least-squares polynomials. The procedure is described here.

To obtain derivatives at each data point (t_i, C_i), the nearest five contiguous points are taken and fitted with a cubic polynomial, using an appropriate weighting scheme:

$$C = a_i + b_it + c_it^2 + d_it^3 \quad \text{(Eq. 35)}$$

The four coefficients are solved by the standard linear regression technique. Once they are obtained, the derivative of Eq. 35 is evaluated at t_i:

$$\dot{C}_i = b_i + 2c_it_i + 3d_it_i^2 \quad \text{(Eq. 36)}$$

This procedure is repeated successively for each i, $i = 3, 4, \ldots, n-2$. For $i = 1$ or 2, the derivative is calculated from the cubic polynomial fitted to the first five points. For $i = n-1$, it is calculated from the cubic polynomial fitted to the last five points. For $i = n$, it is calculated from the following equation, assuming monoexponential decay of C between t_{n-1} and t_n:

$$\dot{C}_n = C_n \ln (C_n/C_{n-1})/(t_n - t_{n-1}) \quad \text{(Eq. 37)}$$

Derivatives obtained in this procedure are less sensitive to the variation in the data than those obtained by the spline method. However, since a cubic polynomial allows one inflection point and two extrema, approximations are usually less accurate if experimental errors are high.

To improve the reliability, a second set of derivatives is calculated by repeating the entire procedure, using parabolic polynomials as the fitting function. The corresponding fitting polynomials and derivatives are:

$$C = a_i + b_it + c_it^2 \quad \text{(Eq. 38)}$$

$$\dot{C}_i = b_i + 2c_it_i \quad \text{(Eq. 39)}$$

The X_2 values as shown in Eq. 32 are obtained by taking the average of the two derivatives calculated from the above two series. This procedure is called the LEASQ method.

Weighting Scheme—Since there are diversified analytical techniques for obtaining pharmacokinetic data, experimental observations may not be homogeneous in variance at all times. These variances should be considered when devising a weighting scheme. In general, data are weighted in proportion to the inverse of their variances. Excellent discussions of data weighting can be found elsewhere (8).

Accuracy of Parameters—By analogy to a technique commonly used in nonlinear regression, the uncertainty associated with each estimated parameter can be evaluated as follows. If $\overline{D}$ is a square matrix of the weighted sum of cross-products of the approximate partial derivatives, then the approximate standard error, ASE, of parameter θ_j is:

$$ASE(\theta_j) = \sqrt{d_{jj}WSS/df} \quad \text{(Eq. 40)}$$

Table I—Comparison of the Present Results and Those Obtained by the Nonlinear Regression Program COMPT [a]

Parameter	Ref. 10	Present Results[b]		
		Spline	Lagrange	Trapezoidal
k_{12}, hr^{-1}	0.160	0.136	0.145	0.172
k_{21}, hr^{-1}	0.345	0.247	0.245	0.454
k_{10}, hr^{-1}	0.570	0.545	0.551	0.579
α, hr^{-1}	0.844	0.747 (0.115)	0.764 (0.111)	0.920 (0.220)
β, hr^{-1}	0.235	0.180 (0.020)	0.177 (0.019)	0.286 (0.013)
V, liters	7.59	7.83	7.74	7.62
V_p, liters/hr	4.35	4.27	4.27	4.41
a, μg/ml	53.94	56.32 (16.91)	57.08 (15.00)	48.23 (21.12)
b, μg/ml	11.96	7.52 (14.24)	7.51 (12.65)	17.41 (17.85)
A_1, μg/ml	—	56.31	56.61	57.05
A_2, μg/ml/hr	—	14.34	14.32	28.23
A_3, hr^{-1}	—	−0.927	−0.940	−1.206
A_4, hr^{-2}	—	−0.134	−0.135	−0.263
WSS	0.0245	0.0230	0.0242	0.0283

[a] Dose = 500 mg. [b] *ASE* values are given in parentheses.

Table II—Tabulation of Time-Dependent Variables, where X_3 and X_4 Values Were Generated by the Spline Method, for the Spectinomycin Data

i	t, hr	C, μg/ml	X_1	X_2, hr	X_3, μg hr/ml	X_4, μg hr^2/ml
1	0.1667	63.3	1.0	0	0	0
2	0.3333	50.6	1.0	0.1666	9.3864	0.7972
3	0.5	43.3	1.0	0.3333	17.1643	3.0314
4	1.0	31.0	1.0	0.8333	35.3746	16.4102
5	2.0	18.3	1.0	1.8333	59.3086	64.8208
6	4.0	6.9	1.0	3.8333	82.5641	210.5057
7	6.0	3.05	1.0	5.8333	91.6509	385.9920
8	8.0	1.95	1.0	7.8333	96.5691	574.4830

Table III—Summary of the Estimated Parameters for the Nonlinear Model, Using Derivatives Obtained by the Spline Method or by the LEASQ Method [a]

Parameter	True Value	Error-Free Data[b]		Corrupted Data[b]		
		Spline	LEASQ	Spline	LEASQ	Expected
K_m, μg/ml	4.0	4.095 (0.039)	2.192 (0.532)	3.786 (4.430)	2.277 (2.204)	4.0 (4.293)
V_m, mg/hr	40.0	40.592 (0.234)	29.491 (3.672)	38.499 (26.849)	28.774 (14.652)	40.0 (25.742)
V, liters	10.0	10.003 (0.004)	10.128 (0.118)	8.658 (0.558)	9.459 (0.448)	10.0 (0.453)
k_{12}, hr^{-1}	1.0	0.998 (0.001)	0.966 (0.023)	1.432 (0.214)	1.086 (0.104)	1.0 (0.105)
k_{21}, hr^{-1}	0.5	0.502 (0.001)	0.422 (0.027)	0.557 (0.155)	0.409 (0.096)	0.5 (0.125)
WSS	—	1.73×10^{-6}	1.56×10^{-3}	5.57×10^{-2}	3.01×10^{-2}	2.41×10^{-2}

[a] Dose = 200 mg. [b] *ASE* values are given in parentheses.

where d_{jj} is the jth diagonal element of the inverse matrix $\overline{D}^{-1}$ and df is the degree of freedom. By definition, the elements of the matrix $\overline{D}$ are:

$$a_{jl} = \sum_{i=1}^{n} W_i \cdot \frac{\partial C_i}{\partial \theta_j} \cdot \frac{\partial C_i}{\partial \theta_l} \qquad j,l = 1, 2, \ldots, p \qquad \text{(Eq. 41)}$$

where W_i is the weight of C_i, and p is the number of parameters. If Δ is small compared to θ_j, the partial derivatives can be approximated by:

Table IV—Comparison of X_2 Values (Micrograms per Milliliter per Hour) Calculated by the Spline or the LEASQ Method from Simulated Data Containing 10% Random Noise

t, hr	Theoretical	Spline	LEASQ
0.1	−20.1748	−30.6219	−22.7207
0.2	−17.4505	−24.6711	−19.2046
0.5	−11.3241	−10.1656	−10.8613
1.0	−5.5902	−4.3048	−5.9614
1.5	−2.8722	−4.1152	−3.2711
2.0	−1.6013	−0.5344	−1.9930
3.0	−0.7330	−1.4030	−1.1104
4.0	−0.5188	−0.5738	−0.6446
6.0	−0.3718	−0.2766	−0.3547
8.0	−0.2695	−0.2699	−0.2428
10.0	−0.1875	−0.1438	−0.1715
12.0	−0.1265	−0.1449	−0.1334
14.0	−0.0838	−0.0717	−0.0887
16.0	−0.0549	−0.0496	−0.0496

$$\frac{\partial C_i}{\partial \theta_j} = \frac{C_i(\theta_1, \ldots, \theta_j + \Delta, \ldots, \theta_p) - C_i(\theta_1, \ldots, \theta_j - \Delta, \ldots, \theta_p)}{2\Delta} \qquad \text{(Eq. 42)}$$

Equation 42, when applied to multiexponential functions of the form:

$$C_i = \sum_{k=1}^{m} a_k \exp(-\lambda_k t_i) \qquad \text{(Eq. 43)}$$

can be simplified to yield:

$$\frac{\partial C_i}{\partial a_k} = \exp(-\lambda_k t_i) \qquad \text{(Eq. 44)}$$

$$\frac{\partial C_i}{\partial \lambda_k} = \frac{-a_k t_i}{2\Delta}[e^{-(\lambda_k+\Delta)t_i} - e^{-(\lambda_k-\Delta)t_i}] \qquad \text{(Eq. 45)}$$

EXPERIMENTAL

Computation—A computer program, written in FORTRAN, was devoloped to make the necessary computations[2]. Briefly, the program contains several general subroutines to perform the following tasks: receive input, compute weights, numerically integrate and differentiate by the described procedures, compile matrix elements, compute determinant, obtain inverse matrix, calculate regression coefficients, solve a system of simultaneous linear equations, locate the minimum by qua-

[2] Detailed description of the program will be documented elsewhere.

Table V—Effect of K_m on *WSS* and Other Model Parameters Using Corrupted Data Set and X_2 Values Calculated by the LEASQ Method

K_m, μg/ml	K_{12}, hr^{-1}	K_{21}, hr^{-1}	V_m, mg/hr	V, liters	*WSS*
1.0	1.221	0.248	31.72	4.982	2.046
1.5	1.172	0.310	30.83	6.476	0.597
2.0	1.119	0.371	29.70	8.233	0.094
2.5	1.056	0.442	27.83	10.663	0.070
3.0	0.969	0.537	25.03	14.553	0.474
3.5	0.834	0.681	21.24	21.836	1.443
4.0	0.583	0.945	16.44	38.533	3.332
4.5	−0.062	1.604	—	—	—

dratic approximation, and compute *ASE* values associated with multiexponential equations. In addition, specific subroutines were developed to generate numerical solutions to Eqs. 25*a*–25*c* and to compute the associated *ASE* values. The value of Δ was arbitrarily taken to be $0.001\theta_j$.

Linear Case—A set of spectinomycin serum data, originally published by Wagner *et al.* (9), was used to demonstrate the estimation procedure and to compare the results with those reported in the literature. The same data were cited by Pfeffer (10) to illustrate the nonlinear regression program COMPT, assuming the model depicted in Scheme I.

To make the results comparable, the data were weighted by $1/C^2$ as in COMPT. The two-step regression procedure was repeated three times to test the effect of the numerical integrating algorithms (6) on the estimated parameter values.

In the first run, X_3 values were calculated by the log trapezoidal method and X_4 values were calculated by the linear trapezoidal method. In the second run, both were calculated by the Lagrange method. In the third run, both were calculated by the modified spline method.

Nonlinear Case—Two simulated data sets, one error free and the other corrupted with 10% random noise, were generated by the fourth-order Runge–Kutta technique to illustrate the iterative nonlinear estimation procedure. Two numerical differentiation algorithms, the spline method and the LEASQ method with weights defined in Eq. 46, were employed to generate the X_2 values so that the effect of data smoothing on parameter estimation could be examined. In all cases, the spline method was employed to generate X_4 values and data were weighted according to Eq. 46, where the sum of weights was equal to the number of data points (11):

$$W_i = (n/C_i^2) \Big/ \sum_{i=1}^{n} (1/C_i^2) \qquad \text{(Eq. 46)}$$

The *WSS* was first scanned as a function of K_m in the range of 1–10 μg/ml, with the constraint that all model parameters must be positive. The more precise location of the best-fit K_m was then refined by iteration. Convergence was assumed if, in two consecutive iterations, the change in K_m was less than 0.01% by quadratic approximation. At each iteration, the four linear parameters were calculated from the regression coefficients as follows:

$$k_{21} = -A_4/A_3 \qquad \text{(Eq. 47)}$$

$$k_{12} = -k_{21} - 1/A_2 \qquad \text{(Eq. 48)}$$

$$V = A_2 D \Big/ \left(A_3 \int_0^{t_1} \frac{C}{K_m + C}\, dt - A_1/k_{21} \right) \qquad \text{(Eq. 49)}$$

$$V_m = V(A_3/A_2) \qquad \text{(Eq. 50)}$$

where V was further adjusted to yield the lowest *WSS* value.

RESULTS AND DISCUSSION

Linear Case—Table I lists the results, including the four intermediate regression coefficients defined in Eqs. 8–11, of pharmacokinetic analysis for the spectinomycin data. The effect of numerical algorithm is obvious. While the estimated parameters and the corresponding *ASE* values are generally comparable by all three methods, a comparison of the *WSS* values suggests that the spline method gave the best fit, followed by the Lagrange method, and then by the trapezoidal method. These differences are related to the algorithm errors associated with the numerical integration procedures used. Listed in Table II are the X_3 and X_4 values and other time-dependent variables. Plotted in Fig. 1 are the interpolating spline functions for C and X_3. Evidently, no spurious oscillations occurred with this sample (6).

For comparison, results of nonlinear regression analysis on the same data used by Pfeffer (10) are listed in the second column of Table I. With the exception of V, parameter values by COMPT were intermediate between those of the trapezoidal method and those of the Lagrange method. On the basis of *WSS* values, the present method is either comparable to, or slightly better than, the nonlinear regression process, depending on the numerical integrating algorithm employed. The two-step regression procedure improved the fitting by reducing the effect of algorithm errors, as evidenced by comparing the present results with those reported earlier (12), and is applicable to other multiexponential equations. In some cases, either the trapezoidal or the Lagrange procedure may yield lower *WSS* values.

Nonlinear Case—Shown in Table III are the parameter values used in generating simulated data and the results of analysis in accordance with the nonlinear model. When employing collocative splines as the numerical differentiation tool, it is apparent that nearly perfect solutions were obtained with error-free data as the input. In contrast, solutions based on the LEASQ numerical differentiation algorithms were relatively poor, suggesting imprudence in trying to improve upon perfection.

Results for data corrupted with random noise are shown in columns 4 and 5 of Table III. On the basis of *WSS* values, the LEASQ algorithm appears to have yielded better solutions. This result is related to the basic differences between the two approximating procedures, the LEASQ method being more accurate in generating derivatives from data containing noise. Comparisons of the calculated X_2 values are given in Table IV.

The effect of K_m on *WSS* is exemplified in Table V. Corresponding values for other model parameters are also listed. As can be seen, increasing K_m caused the formation of a minimum in *WSS*. A further increase in K_m resulted in the formation of meaningless solutions.

With noisy data (Table III), neither algorithm produced solutions that were consistently closer to the expected true values. The uncertainty of the estimated parameters can be examined by comparing the *ASE* values with those predicted from the expected parameter values (13). The proximity of the actual to the predicted errors is a measure of the reli-

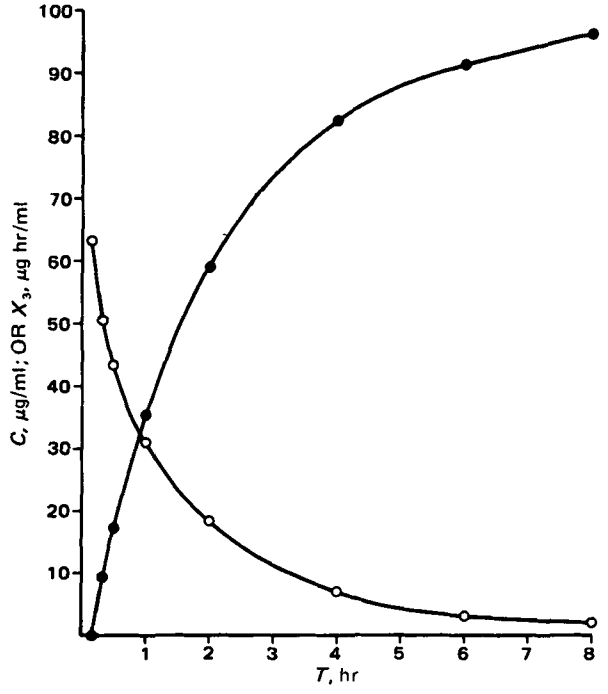

Figure 1—*Spline function interpolation of* C (○) *and* X_3 (●) *for spectinomycin data.*

Table VI—Comparison of the Predicted and Input Data

t, hr	Input[a]	Predicted by Spline[b]	Predicted by LEASQ[b]	Theoretical (Expected)[b]
0.1	18.68	19.7470 (−4.26)	18.7512 (−0.28)	17.8285 (3.40)
0.2	15.92	16.9891 (−5.01)	16.6838 (−3.58)	15.9506 (−0.14)
0.5	10.82	11.3095 (−3.37)	12.0142 (−8.23)	11.7020 (−6.08)
1.0	8.38	6.8147 (13.92)	7.5799 (7.12)	7.6489 (6.50)
1.5	5.57	5.0242 (7.30)	5.3858 (2.47)	5.6179 (−0.64)
2.0	4.83	4.2152 (9.49)	4.2544 (8.89)	4.5397 (4.48)
3.0	3.51	3.4274 (1.75)	3.2208 (6.14)	3.4777 (0.69)
4.0	2.59	2.8980 (−8.86)	2.6901 (−2.88)	2.8726 (−8.13)
6.0	1.92	2.0464 (−4.91)	1.9381 (−0.70)	1.9997 (−3.10)
8.0	1.29	1.4026 (−6.51)	1.3608 (−4.09)	1.3617 (−4.15)
10.0	0.92	0.9385 (−1.50)	0.9294 (−0.76)	0.9083 (0.95)
12.0	0.63	0.6176 (1.47)	0.6228 (0.85)	0.5977 (3.83)
14.0	0.39	0.4020 (−2.30)	0.4128 (−4.36)	0.3900 (−0.01)
16.0	0.27	0.2600 (2.77)	0.2721 (−0.59)	0.2533 (4.60)

[a] Simulated plasma levels containing 10% random noise. [b] Weighted residuals are given in parentheses ($\times 10^2$).

ability of the estimated parameters and of the efficiency of the estimation procedure. As can be seen in Table III, the errors associated with either the spline or the LEASQ results are in the same range as the expected error. Compared to the errors of the LEASQ solutions, the expected *ASE* values were greater but the expected *WSS* was smaller. The first observation suggests that the true parameters probably are irretrievable from corrupted input data. The second observation indicates that further improvement of the parameter estimates can be made by applying superior numerical algorithms. This conclusion is manifested in Table VI where the predicted and the observed (input) data are compared.

Conclusions—Two numerical examples have been described to illustrate the proposed method in the estimation of pharmacokinetic parameters. For a given model and weighting scheme, the reliability of the estimates is dependent on data accuracy as well as on the numerical algorithms employed. Obviously, when experimental errors are large, meaningful estimates are difficult, irrespective of algorithmic sophistication.

REFERENCES

(1) K. C. Yeh, *J. Pharm. Sci.*, **66**, 1688 (1977).

(2) S. Riegelman, J. C. K. Loo, and M. Rowland, *ibid.*, **57**, 117 (1968).

(3) D. W. Brown, paper presented at Third Annual Rocky Mountain Bioengineering Symposium, Boulder, Colo., May 1966.

(4) J. G. Wagner, *J. Pharmacokinet. Biopharm.*, **3**, 457 (1975).

(5) B. Carnahan, H. A. Luther, and J. O. Wilkes, "Applied Numerical Methods," Wiley, New York, N.Y., 1969.

(6) K. C. Yeh and K. C. Kwan, *J. Pharmacokinet. Biopharm.*, **6**, 79 (1978).

(7) T. N. E. Greville, in "Mathematical Methods for Digital Computers," vol. 2, A. Ralston and H. W. Wilf, Eds., Wiley, New York, N.Y., 1967, p. 156.

(8) J. H. Ottaway, *Biochem. J.*, **134**, 729 (1973).

(9) J. G. Wagner, E. Novak, L. G. Leslie, and C. M. Metzler, *Int. J. Clin. Pharmacol.*, **1**, 261 (1968).

(10) M. Pfeffer, *J. Pharmacokinet. Biopharm.*, **1**, 137 (1973).

(11) H. G. Boxenbaum, S. Riegelman, and R. M. Elashoff, *ibid.*, **2**, 123 (1974).

(12) K. C. Yeh and K. C. Kwan, paper presented at APhA Academy of Pharmaceutical Science, New Orleans meeting, Apr. 1976.

(13) J. Swartz and H. Bremerman, *J. Math. Biol.*, **1**, 241 (1975).

Impurities in Drugs III: Trihexyphenidyl

M. A. POIRIER, N. M. CURRAN, K. M. McERLANE, and E. G. LOVERING ˣ

Received January 17, 1979, from the *Drug Research Laboratories, Health Protection Branch, Tunney's Pasture, Ottawa, Ontario, K1A 0L2, Canada.* Accepted for publication March 16, 1979.

Abstract □ Two lots of trihexyphenidyl hydrochloride raw material, one lot of elixir, and 10 lots of tablets were examined for impurities by TLC. Impurities found were 1-phenyl-2-propenone, 3-piperidinopropiophenone, and 3-aminopropiophenone. Not all impurities were present in all lots, and none exceeded 1.9% of the label drug claim. Impurities were identified by mass spectrometry and by comparison of TLC R_f values and GLC retention times to those of synthesized specimens of the impurities.

Keyphrases □ Trihexyphenidyl—analysis, TLC, impurities in tablets and elixir □ Trihexyphenidyl, derivatives—1-phenyl-2-propenone, 3-piperidinopropiophenone, 3-aminopropiophenone, TLC analysis, impurities in tablets and elixir □ Drug impurities—trihexyphenidyl, tablets and elixir, TLC analysis

Impurities in drug raw materials and formulations may be intermediates or by-products of the synthetic process, products of degradation or drug–excipient interaction, or the result of contamination. The nature of impurities may depend on the synthetic route, the reagent purity, and the excipient quality. To obtain a good perspective of potential impurities, raw materials and formulations from as many sources as possible should be examined (1–4). This paper describes the impurities found in trihexyphenidyl (I) raw material and tablet and elixir products.

Trihexyphenidyl was synthesized first (5) by the addition of cyclohexylmagnesium bromide to 3-piperidinopropiophenone (II), obtained by the Mannich reaction with acetophenone (III), formaldehyde, and piperidine hydrochloride in acidic medium. Trihexyphenidyl hydrochloride raw material and tablets are official in the USP (6) and BP as benzhexol (7). An elixir is official in the USP only. The only impurity specification is that in the BP for 3-piperidinopropiophenone in drug raw material.

EXPERIMENTAL

Materials—All drugs and formulations were obtained from the

0022-3549/79/0900-1124$01.00/0

© 1979, American Pharmaceutical Association

Table VI—Comparison of the Predicted and Input Data

t, hr	Input[a]	Predicted by Spline[b]	Predicted by LEASQ[b]	Theoretical (Expected)[b]
0.1	18.68	19.7470 (−4.26)	18.7512 (−0.28)	17.8285 (3.40)
0.2	15.92	16.9891 (−5.01)	16.6838 (−3.58)	15.9506 (−0.14)
0.5	10.82	11.3095 (−3.37)	12.0142 (−8.23)	11.7020 (−6.08)
1.0	8.38	6.8147 (13.92)	7.5799 (7.12)	7.6489 (6.50)
1.5	5.57	5.0242 (7.30)	5.3858 (2.47)	5.6179 (−0.64)
2.0	4.83	4.2152 (9.49)	4.2544 (8.89)	4.5397 (4.48)
3.0	3.51	3.4274 (1.75)	3.2208 (6.14)	3.4777 (0.69)
4.0	2.59	2.8980 (−8.86)	2.6901 (−2.88)	2.8726 (−8.13)
6.0	1.92	2.0464 (−4.91)	1.9381 (−0.70)	1.9997 (−3.10)
8.0	1.29	1.4026 (−6.51)	1.3608 (−4.09)	1.3617 (−4.15)
10.0	0.92	0.9385 (−1.50)	0.9294 (−0.76)	0.9083 (0.95)
12.0	0.63	0.6176 (1.47)	0.6228 (0.85)	0.5977 (3.83)
14.0	0.39	0.4020 (−2.30)	0.4128 (−4.36)	0.3900 (−0.01)
16.0	0.27	0.2600 (2.77)	0.2721 (−0.59)	0.2533 (4.60)

[a] Simulated plasma levels containing 10% random noise. [b] Weighted residuals are given in parentheses ($\times 10^2$).

ability of the estimated parameters and of the efficiency of the estimation procedure. As can be seen in Table III, the errors associated with either the spline or the LEASQ results are in the same range as the expected error. Compared to the errors of the LEASQ solutions, the expected *ASE* values were greater but the expected *WSS* was smaller. The first observation suggests that the true parameters probably are irretrievable from corrupted input data. The second observation indicates that further improvement of the parameter estimates can be made by applying superior numerical algorithms. This conclusion is manifested in Table VI where the predicted and the observed (input) data are compared.

Conclusions—Two numerical examples have been described to illustrate the proposed method in the estimation of pharmacokinetic parameters. For a given model and weighting scheme, the reliability of the estimates is dependent on data accuracy as well as on the numerical algorithms employed. Obviously, when experimental errors are large, meaningful estimates are difficult, irrespective of algorithmic sophistication.

REFERENCES

(1) K. C. Yeh, *J. Pharm. Sci.*, **66**, 1688 (1977).

(2) S. Riegelman, J. C. K. Loo, and M. Rowland, *ibid.*, **57**, 117 (1968).

(3) D. W. Brown, paper presented at Third Annual Rocky Mountain Bioengineering Symposium, Boulder, Colo., May 1966.

(4) J. G. Wagner, *J. Pharmacokinet. Biopharm.*, **3**, 457 (1975).

(5) B. Carnahan, H. A. Luther, and J. O. Wilkes, "Applied Numerical Methods," Wiley, New York, N.Y., 1969.

(6) K. C. Yeh and K. C. Kwan, *J. Pharmacokinet. Biopharm.*, **6**, 79 (1978).

(7) T. N. E. Greville, in "Mathematical Methods for Digital Computers," vol. 2, A. Ralston and H. W. Wilf, Eds., Wiley, New York, N.Y., 1967, p. 156.

(8) J. H. Ottaway, *Biochem. J.*, **134**, 729 (1973).

(9) J. G. Wagner, E. Novak, L. G. Leslie, and C. M. Metzler, *Int. J. Clin. Pharmacol.*, **1**, 261 (1968).

(10) M. Pfeffer, *J. Pharmacokinet. Biopharm.*, **1**, 137 (1973).

(11) H. G. Boxenbaum, S. Riegelman, and R. M. Elashoff, *ibid.*, **2**, 123 (1974).

(12) K. C. Yeh and K. C. Kwan, paper presented at APhA Academy of Pharmaceutical Science, New Orleans meeting, Apr. 1976.

(13) J. Swartz and H. Bremerman, *J. Math. Biol.*, **1**, 241 (1975).

Impurities in Drugs III: Trihexyphenidyl

M. A. POIRIER, N. M. CURRAN, K. M. McERLANE, and E. G. LOVERING ˣ

Received January 17, 1979, from the *Drug Research Laboratories, Health Protection Branch, Tunney's Pasture, Ottawa, Ontario, K1A 0L2, Canada.* Accepted for publication March 16, 1979.

Abstract □ Two lots of trihexyphenidyl hydrochloride raw material, one lot of elixir, and 10 lots of tablets were examined for impurities by TLC. Impurities found were 1-phenyl-2-propenone, 3-piperidinopropiophenone, and 3-aminopropiophenone. Not all impurities were present in all lots, and none exceeded 1.9% of the label drug claim. Impurities were identified by mass spectrometry and by comparison of TLC R_f values and GLC retention times to those of synthesized specimens of the impurities.

Keyphrases □ Trihexyphenidyl—analysis, TLC, impurities in tablets and elixir □ Trihexyphenidyl, derivatives—1-phenyl-2-propenone, 3-piperidinopropiophenone, 3-aminopropiophenone, TLC analysis, impurities in tablets and elixir □ Drug impurities—trihexyphenidyl, tablets and elixir, TLC analysis

Impurities in drug raw materials and formulations may be intermediates or by-products of the synthetic process, products of degradation or drug–excipient interaction, or the result of contamination. The nature of impurities may depend on the synthetic route, the reagent purity, and the excipient quality. To obtain a good perspective of potential impurities, raw materials and formulations from as many sources as possible should be examined (1–4). This paper describes the impurities found in trihexyphenidyl (I) raw material and tablet and elixir products.

Trihexyphenidyl was synthesized first (5) by the addition of cyclohexylmagnesium bromide to 3-piperidinopropiophenone (II), obtained by the Mannich reaction with acetophenone (III), formaldehyde, and piperidine hydrochloride in acidic medium. Trihexyphenidyl hydrochloride raw material and tablets are official in the USP (6) and BP as benzhexol (7). An elixir is official in the USP only. The only impurity specification is that in the BP for 3-piperidinopropiophenone in drug raw material.

EXPERIMENTAL

Materials—All drugs and formulations were obtained from the

0022-3549/79/0900-1124$01.00/0

© 1979, American Pharmaceutical Association

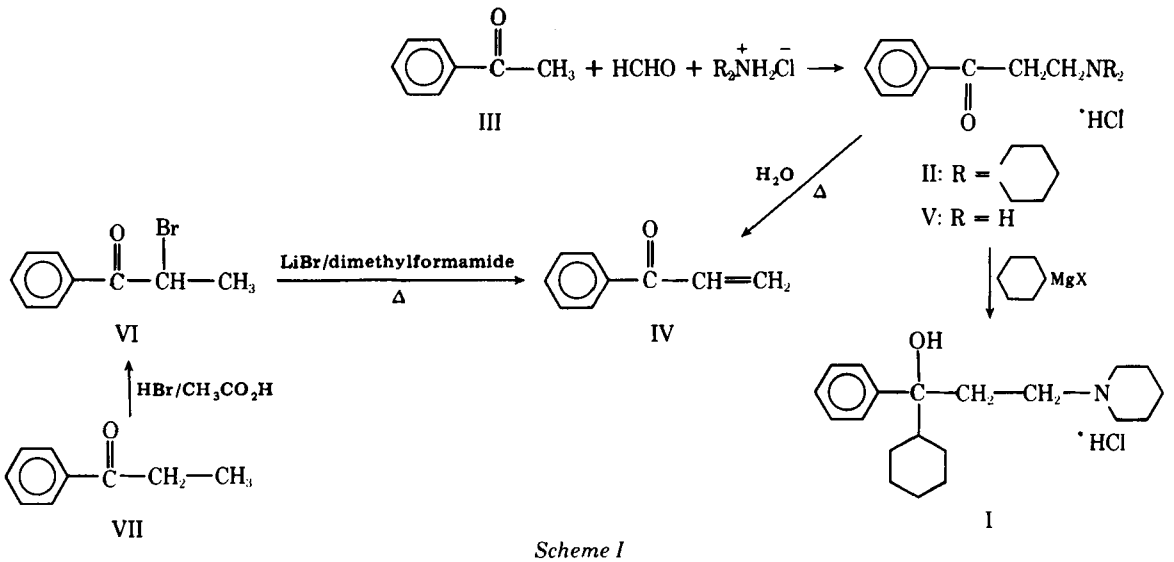

Scheme I

manufacturer. Acetophenone[1], 3-piperidinopropiophenone[1], formaldehyde 37% solution[2], ammonium chloride[2], lithium carbonate[3], lithium bromide[3], acetic acid[4], dimethylformamide[4], bromine[5], and hydrogen chloride gas[6] were obtained commercially. All solvents were analytical grade.

TLC plates were precoated with silica gel GF[7] (20 × 20 cm, 0.25 mm). The gas chromatograph[8] was equipped with flame-ionization detectors and 1.8-m × 0.4 cm i.d., U-shaped glass columns, packed with 3% OV-210 coated on acid-washed, dimethylchlorosilane-treated, high-performance flux-calcined diatomite support[9] (100–120 mesh).

Standard Solutions—For TLC, chloroform solutions contained 5 mg of trihexyphenidyl hydrochloride/ml and either 0.01 mg of 1-phenyl-2-propenone (IV)/ml or 0.04 mg of 3-aminopropiophenone (V)/ml. For GLC, a solution of 5.2 mg of 3-piperidinopropiophenone in 50 ml of chloroform was prepared.

TLC Systems—A neutral system of chloroform–methanol–ethyl acetate–acetone (20:20:20:40) and a basic system of chloroform–methanol–concentrated ammonium hydroxide (100:25:1) were used. Spots were visualized with UV light at 254 nm and with Dragendorff spray.

Extraction from Tablet Formulations—An amount of powdered tablet equivalent to 10 mg of trihexyphenidyl hydrochloride was weighed into a 10-ml screw-capped culture tube[5] and extracted by shaking[10] for 15 min with 2 ml of chloroform. After centrifuging, the solutions were filtered, and aliquots were applied to the TLC plates and injected into the gas chromatograph.

Extraction from Elixir Formulation—An amount (25 ml) equivalent to 10 mg of trihexyphenidyl hydrochloride in 15 ml of water was partitioned three times with 20 ml of chloroform. The chloroform portions were concentrated, and the volume was adjusted to 2 ml with chloroform. Aliquots of this solution were applied to the TLC plates or injected into the gas chromatograph.

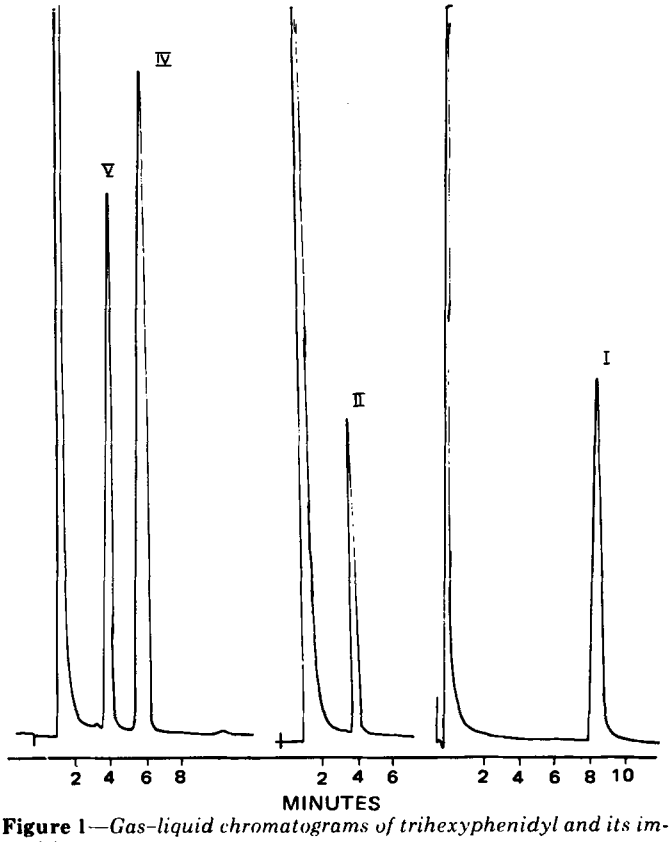

Figure 1—*Gas-liquid chromatograms of trihexyphenidyl and its impurities.*

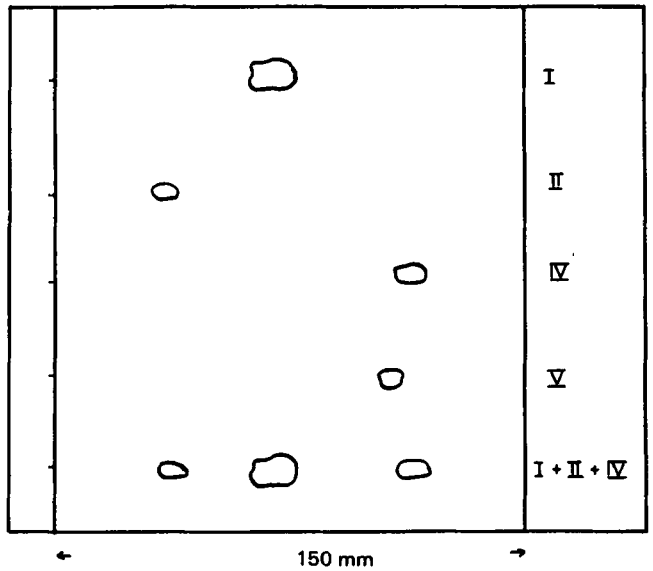

Figure 2—*TLC separations of trihexyphenidyl and its impurities using the neutral system.*

[1] Aldrich Chemical Co., Milwaukee, Wis.
[2] Anachemia Chemicals Ltd., Montreal, Canada.
[3] BDH Chemicals Ltd., Poole, England.
[4] J. T. Baker Chemical Co., Phillipsburg, N.J.
[5] Canlab Laboratories, Ottawa, Canada.
[6] Matheson, Toronto, Canada.
[7] Brinkmann Instruments, Toronto, Canada.
[8] Bendix 2500, Aviation Electric, Montreal, Canada.
[9] Chromosorb W, Chromatographic Specialties, Brockville, Canada.
[10] Horizontal shaker, Eberbach Corp., Ann Arbor, Mich.

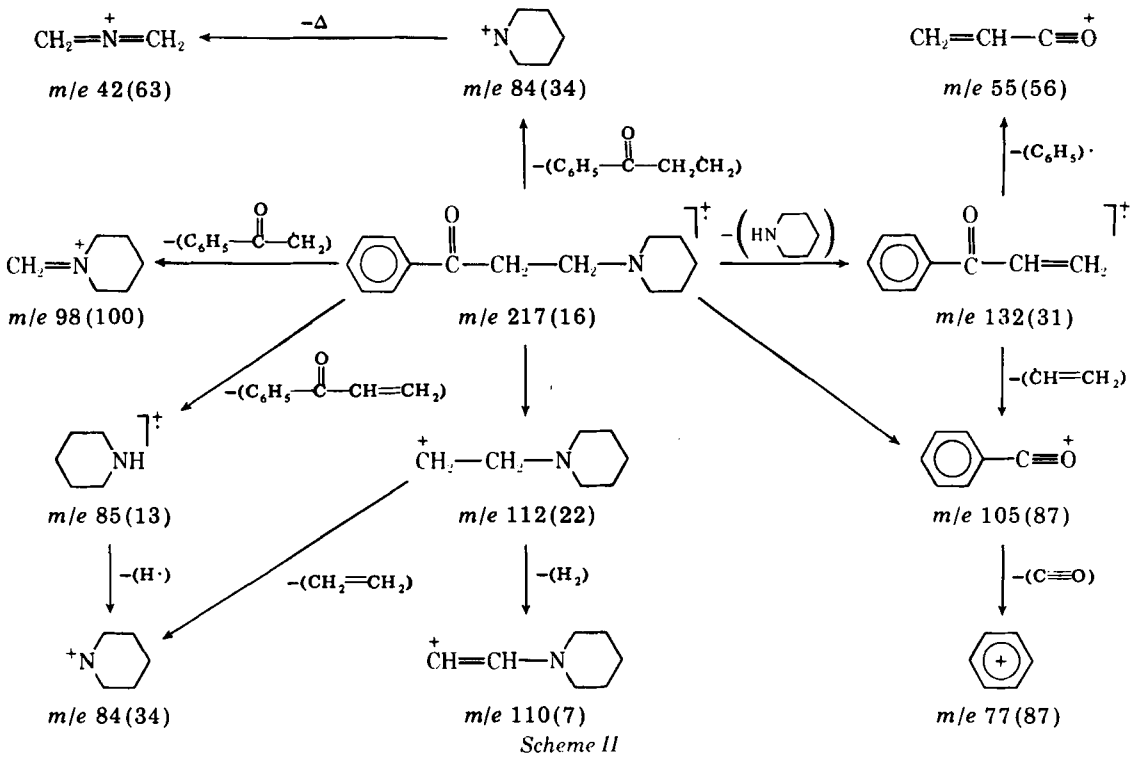

Scheme II

Screening for Impurities—The R_f values of the drug and of each impurity were determined in both TLC systems, and the lower detectability limit was established by serial dilutions of the stock solutions. Aliquots of 50 μl (250 μg) of the tablet extracts in chloroform were applied to the TLC plates. The concentration of impurities was approximated by comparison of the spot diameters and intensities to those of the corresponding spots from the standard solutions.

Aliquots, 5 μl, of the appropriate solution were injected into the gas chromatograph for quantification of the 3-piperidinopropiophenone. Quantification was done by peak height. To check for possible decomposition on the plate, each compound was subjected to two-dimensional TLC.

Isolation of Impurities—Impurities IV and V were isolated from Tablet Formulation B and Raw Material M, respectively. A chloroform extract containing 200 mg of the drug in ~6 ml of the solvent was applied in a narrow band to a 20 × 20-cm × 2-mm TLC plate[7] and developed in the neutral system. Impurities were visualized by UV light at 254 nm and by spraying a 1-cm band along each side of the plate with Dragendorff[1] spray. Impurity bands were scraped from the plate, stirred with 30 ml of methanol for 30 min, filtered, evaporated to dryness, redissolved in 20 ml of chloroform, and evaporated to dryness.

The purity of the isolated compound was checked by TLC and GLC. The injection port, detector block, and column temperatures were 250, 250, and 140°, respectively, and the flow rates of nitrogen, hydrogen, and air were 13, 50, and 400 ml/min, respectively. The impurities were subjected to GLC–mass spectral analysis[11].

Syntheses—Scheme I illustrates the syntheses of the following compounds.

Table I—Chromatographic Characteristics

Compound	TLC R_f[a]	TLC R_f[b]	TLC Detectability Limit[c], μg	GLC Retention Time, min
I	0.46	0.78	2.5	8.4[d]
II	0.24	0.74	2.5	4.2[e]
IV	0.75	0.84	0.25	6.0[e]
V	0.73	0.86	2.5	4.0[e]

[a] In the neutral system. [b] In the basic system. [c] Applied with 250 μg of the drug. [d] 3% OV-210, Chromosorb W (high performance), 100–120 mesh, 170°, nitrogen flow of 38 ml/min. [e] Same as footnote *d* except 140° and nitrogen flow of 13 ml/min.

[11] Hewlett-Packard model 5985 and Varian MAT 311A mass spectrometers with electron energy of 70 ev.

2-Bromopropiophenone (VI)—In a 250-ml, three-necked round-bottom flask, 17.4 g (0.13 mole) of propiophenone (VII) (8) was dissolved in 100 ml of glacial acetic acid. A 135-ml normal solution of bromine in glacial acetic acid was added at 0° by a dropping funnel over 30 min. The agitation was maintained for an additional 2 hr, and the mixture was diluted with water and extracted with ether.

The organic layer was washed, neutralized with sodium bicarbonate and dried over anhydrous sodium sulfate. The mixture was filtered and evaporated[12] at 30° to yield 25.3 g (92%) of VI, bp_{10} 125–128° [lit. (9) bp_{12} 130–132°]; IR (film): 1690 (C=O), 710, and 685 (C–Br) cm^{-1}.

1-Phenyl-2-propenone (IV)—In a 500-ml, round-bottom flask equipped with a condenser, 21.2 g (0.1 mole) of VI (10) was refluxed for 1 hr in 180 ml of dimethylformamide containing 10.7 g of lithium carbonate and 1.2 g of lithium bromide. The reaction mixture was diluted with water and extracted with ether, and the organic phase was washed with a saturated sodium carbonate solution. The ether phase was dried over anhydrous sodium carbonate, filtered, evaporated, and distilled to

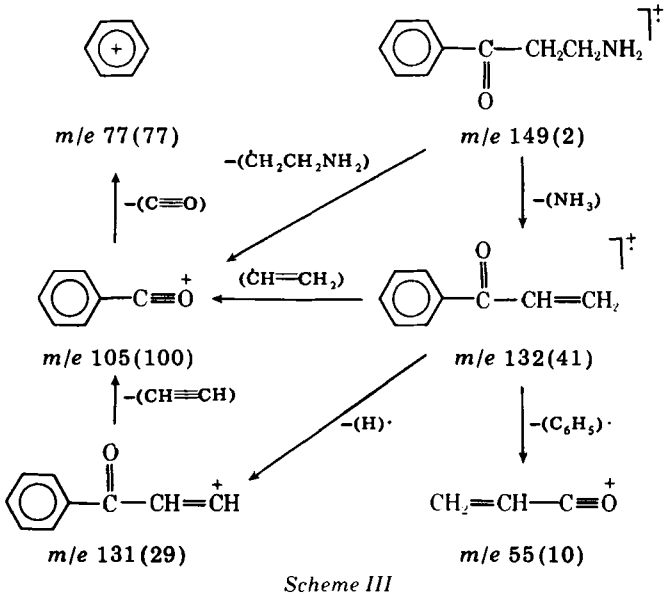

Scheme III

[12] Rotavapor-R, Büchi, Switzerland.

Table II—Impurities in Trihexyphenidyl Tablets

Lot	Dose, mg	Impurities[a], % II	IV	V
A	2	ND[b]	0.4	ND
B	5	Tr[c]	1.9	ND
C	2	1.0	0.2	ND
D	5	1.6	0.2	ND
E	2	ND	0.2	ND
F	5	0.1	ND	ND
G	2	0.1	ND	ND
H	5	0.1	0.1	ND
I	2	ND	ND	ND
J	5	ND	0.1	ND
K (elixir)	2/5 ml	ND	ND	1.0
Raw material	—	ND	ND	ND
Raw material	—	ND	ND	1.6

[a] Expressed as percentage of the label claim of drug in the hydrochloride form. [b] None detected. [c] Trace.

yield 5.3 g (40%) of crude IV, bp_3 75–79° [lit. (11) $bp_{2.5}$ 74–76°]; IR (film): 1680 (C=O) cm^{-1}.

3-Aminopropiophenone (V)—In a 300-ml, round-bottom flask, 5.3 g (0.1 mole) of ammonium chloride, 4.5 g (0.15 mole) of formaldehyde 37% solution, and 0.2 ml of concentrated hydrochloric acid were dissolved in 40 ml of ethanol (5). To this solution, 12.0 g (0.1 mole) of acetophenone (III) was added. The mixture was refluxed for 1.5 hr, another 9 ml of formaldehyde (37% solution) was added, and the mixture was refluxed for another 1.5 hr.

Compound V was extracted into ether as the free base. The ether phase was dried over sodium sulfate and filtered, and hydrogen chloride gas was passed through the solution. The yield of the hydrochloride salt was 5.0 g (33%) of V, mp (hydrochloride) 125–127° [lit. (11) mp 128°]; IR ($CHCl_3$): 1685 (C=O) and 3440 (NH_2 vibration) cm^{-1}.

RESULTS AND DISCUSSION

The identity of 3-piperidinopropiophenone (II), 1-phenyl-2-propenone (IV), and 3-aminopropiophenone (V) found in raw material and tablet formulations was established by comparison of TLC R_f values, GLC retention times, and mass spectral fragmentation patterns to those of synthetic samples. The authenticity of the synthetic samples was demonstrated by TLC, GLC, and mass spectra.

The structure postulated for the impurities is supported by the mass spectral results, which conform to the fragmentation diagrams presented in Schemes II and III. Detectability limits, R_f values, and GLC retention times for trihexyphenidyl, 3-piperidinopropiophenone, 1-phenyl-2-propenone, and 3-aminopropiophenone are listed in Table I (Figs. 1 and 2). Two lots of trihexyphenidyl hydrochloride, 10 lots of tablets, and one lot of elixir preparation from five manufacturers were screened for impurities (Table II). Five lots contained II at levels from 0.1 to 1.6%, and half of the lots contained IV at levels from 0.1 to 1.9%. Compound V was found in two lots from the same manufacturer at levels of 1.0 to 1.6%.

The presence of V may be the result of ammonium chloride in the piperidine hydrochloride used as a starting material in one synthetic process (5) (Scheme I). Compound II is an intermediate in the synthesis of trihexyphenidyl (5). The presence of IV, which was observed in low levels, may be due, according to previous investigators (12), to the hydrolysis of II or to an elimination reaction in the step involving the Grignard reagent (11).

REFERENCES

(1) G. R. Gordon, D. C. Ghoul, and J. H. Peters, *J. Pharm. Sci.*, **64**, 1205 (1975).

(2) D. C. Chatterji, A. G. Frazier, and J. F. Gallelli, *ibid.*, **67**, 622 (1978).

(3) K. M. McErlane, N. M. Curran, and E. G. Lovering, *ibid.*, **66**, 1015 (1977).

(4) K. M. McErlane, R. J. Wood, F. Matsui, and E. G. Lovering, *ibid.*, **67**, 958 (1978).

(5) J. J. Denton, W. B. Neier, and V. A. Lawson, *J. Am. Chem. Soc.*, **71**, 2053 (1949).

(6) "The United States Pharmacopeia," 19th rev., Mack Publishing Co., Easton, Pa., 1975.

(7) "British Pharmacopoeia 1973," Her Majesty's Stationery Office, London, England, 1973.

(8) E. J. Corey, T. H. Topie, and W. A. Wozniak, *J. Am. Chem. Soc.*, **77**, 5415 (1955).

(9) H. Bredereck, F. Effenberger, F. Marquez, and K. Ockewitz, *Chem. Ber.*, **93**, 2083 (1960).

(10) J. Warkentin and L. K. M. Lam, *Can. J. Chem.*, **42**, 1676 (1964).

(11) H. G. O. Becker and E. Fanghaenel, *J. Prakt. Chem.*, **26**, 58 (1964).

(12) A. C. B. Smith and W. Wilson, *J. Chem. Soc.*, **1955**, 1342.

ACKNOWLEDGMENTS

The authors are grateful to Mr. W. Miles and Mr. J. C. Ethier for determination of the mass spectra.

High-Pressure Liquid Chromatographic Assay for Griseofulvin in Plasma

MARVIN C. MEYER ˣ and GURSHARAN RAGHOW

Received January 17, 1979, from the *Division of Biopharmaceutics and Pharmacokinetics, Department of Pharmaceutics, College of Pharmacy, University of Tennessee Center for the Health Sciences, Memphis, TN 38163.* Accepted for publication March 14, 1979.

Abstract □ A high-pressure liquid chromatographic procedure was developed for griseofulvin assay in human plasma. The method utilized warfarin as an internal standard and easily quantitated griseofulvin plasma levels as low as 0.10 μg/ml. The method was compared to two fluorometric assay methods and was more specific for griseofulvin. Assay of 6-demethylgriseofulvin isolated from human urine demonstrated that this material was not responsible for the interferences apparent in the fluorometric procedures.

Keyphrases □ Griseofulvin—analysis, high-pressure liquid chromatography, human plasma, compared to fluorometric assays □ Antifungal agents—griseofulvin, high-pressure liquid chromatographic analysis, human plasma, compared to fluorometric assays □ Fluorometry—analysis, griseofulvin in human plasma, compared to high-pressure liquid chromatography

Griseofulvin is a poorly water-soluble, antifungal agent. This orally administered drug may be subject to reduced bioavailability, and particle-size reduction and preparation of polyethylene glycol dispersions have been employed to improve absorption from the GI tract (1, 2). In view of the potential for griseofulvin dosage forms to exhibit poor bioavailability, a convenient and specific assay method for intact drug measurement in the plasma of patients or volunteer subjects receiving griseofulvin is needed.

The most widely utilized analytical methods have em-

0022-3549/79/0900-1127$01.00/0

© 1979, American Pharmaceutical Association

Table II—Impurities in Trihexyphenidyl Tablets

Lot	Dose, mg	Impurities[a], % II	IV	V
A	2	ND[b]	0.4	ND
B	5	Tr[c]	1.9	ND
C	2	1.0	0.2	ND
D	5	1.6	0.2	ND
E	2	ND	0.2	ND
F	5	0.1	ND	ND
G	2	0.1	ND	ND
H	5	0.1	0.1	ND
I	2	ND	ND	ND
J	5	ND	0.1	ND
K (elixir)	2/5 ml	ND	ND	1.0
Raw material	—	ND	ND	ND
Raw material	—	ND	ND	1.6

[a] Expressed as percentage of the label claim of drug in the hydrochloride form. [b] None detected. [c] Trace.

yield 5.3 g (40%) of crude IV, bp_3 75–79° [lit. (11) $bp_{2.5}$ 74–76°]; IR (film): 1680 (C=O) cm^{-1}.

3-Aminopropiophenone (V)—In a 300-ml, round-bottom flask, 5.3 g (0.1 mole) of ammonium chloride, 4.5 g (0.15 mole) of formaldehyde 37% solution, and 0.2 ml of concentrated hydrochloric acid were dissolved in 40 ml of ethanol (5). To this solution, 12.0 g (0.1 mole) of acetophenone (III) was added. The mixture was refluxed for 1.5 hr, another 9 ml of formaldehyde (37% solution) was added, and the mixture was refluxed for another 1.5 hr.

Compound V was extracted into ether as the free base. The ether phase was dried over sodium sulfate and filtered, and hydrogen chloride gas was passed through the solution. The yield of the hydrochloride salt was 5.0 g (33%) of V, mp (hydrochloride) 125–127° [lit. (11) mp 128°]; IR ($CHCl_3$): 1685 (C=O) and 3440 (NH_2 vibration) cm^{-1}.

RESULTS AND DISCUSSION

The identity of 3-piperidinopropiophenone (II), 1-phenyl-2-propenone (IV), and 3-aminopropiophenone (V) found in raw material and tablet formulations was established by comparison of TLC R_f values, GLC retention times, and mass spectral fragmentation patterns to those of synthetic samples. The authenticity of the synthetic samples was demonstrated by TLC, GLC, and mass spectra.

The structure postulated for the impurities is supported by the mass spectral results, which conform to the fragmentation diagrams presented in Schemes II and III. Detectability limits, R_f values, and GLC retention times for trihexyphenidyl, 3-piperidinopropiophenone, 1-phenyl-2-propenone, and 3-aminopropiophenone are listed in Table I (Figs. 1 and 2). Two lots of trihexyphenidyl hydrochloride, 10 lots of tablets, and one lot of elixir preparation from five manufacturers were screened for impurities (Table II). Five lots contained II at levels from 0.1 to 1.6%, and half of the lots contained IV at levels from 0.1 to 1.9%. Compound V was found in two lots from the same manufacturer at levels of 1.0 to 1.6%.

The presence of V may be the result of ammonium chloride in the piperidine hydrochloride used as a starting material in one synthetic process (5) (Scheme I). Compound II is an intermediate in the synthesis of trihexyphenidyl (5). The presence of IV, which was observed in low levels, may be due, according to previous investigators (12), to the hydrolysis of II or to an elimination reaction in the step involving the Grignard reagent (11).

REFERENCES

(1) G. R. Gordon, D. C. Ghoul, and J. H. Peters, *J. Pharm. Sci.*, **64**, 1205 (1975).

(2) D. C. Chatterji, A. G. Frazier, and J. F. Gallelli, *ibid.*, **67**, 622 (1978).

(3) K. M. McErlane, N. M. Curran, and E. G. Lovering, *ibid.*, **66**, 1015 (1977).

(4) K. M. McErlane, R. J. Wood, F. Matsui, and E. G. Lovering, *ibid.*, **67**, 958 (1978).

(5) J. J. Denton, W. B. Neier, and V. A. Lawson, *J. Am. Chem. Soc.*, **71**, 2053 (1949).

(6) "The United States Pharmacopeia," 19th rev., Mack Publishing Co., Easton, Pa., 1975.

(7) "British Pharmacopoeia 1973," Her Majesty's Stationery Office, London, England, 1973.

(8) E. J. Corey, T. H. Topie, and W. A. Wozniak, *J. Am. Chem. Soc.*, **77**, 5415 (1955).

(9) H. Bredereck, F. Effenberger, F. Marquez, and K. Ockewitz, *Chem. Ber.*, **93**, 2083 (1960).

(10) J. Warkentin and L. K. M. Lam, *Can. J. Chem.*, **42**, 1676 (1964).

(11) H. G. O. Becker and E. Fanghaenel, *J. Prakt. Chem.*, **26**, 58 (1964).

(12) A. C. B. Smith and W. Wilson, *J. Chem. Soc.*, **1955**, 1342.

ACKNOWLEDGMENTS

The authors are grateful to Mr. W. Miles and Mr. J. C. Ethier for determination of the mass spectra.

High-Pressure Liquid Chromatographic Assay for Griseofulvin in Plasma

MARVIN C. MEYER ˣ and GURSHARAN RAGHOW

Received January 17, 1979, from the *Division of Biopharmaceutics and Pharmacokinetics, Department of Pharmaceutics, College of Pharmacy, University of Tennessee Center for the Health Sciences, Memphis, TN 38163.* Accepted for publication March 14, 1979.

Abstract □ A high-pressure liquid chromatographic procedure was developed for griseofulvin assay in human plasma. The method utilized warfarin as an internal standard and easily quantitated griseofulvin plasma levels as low as 0.10 μg/ml. The method was compared to two fluorometric assay methods and was more specific for griseofulvin. Assay of 6-demethylgriseofulvin isolated from human urine demonstrated that this material was not responsible for the interferences apparent in the fluorometric procedures.

Keyphrases □ Griseofulvin—analysis, high-pressure liquid chromatography, human plasma, compared to fluorometric assays □ Antifungal agents—griseofulvin, high-pressure liquid chromatographic analysis, human plasma, compared to fluorometric assays □ Fluorometry—analysis, griseofulvin in human plasma, compared to high-pressure liquid chromatography

Griseofulvin is a poorly water-soluble, antifungal agent. This orally administered drug may be subject to reduced bioavailability, and particle-size reduction and preparation of polyethylene glycol dispersions have been employed to improve absorption from the GI tract (1, 2). In view of the potential for griseofulvin dosage forms to exhibit poor bioavailability, a convenient and specific assay method for intact drug measurement in the plasma of patients or volunteer subjects receiving griseofulvin is needed.

The most widely utilized analytical methods have em-

0022-3549/79/0900-1127$01.00/0

© 1979, American Pharmaceutical Association

ployed plasma extraction followed by fluorescence detection (3, 4). The method of Schwarz *et al.* (3) is a modification of the earlier procedure of Shah *et al.* (4), but the two methods have not been compared directly. Schwarz *et al.* (3) also described a GLC method, using electron-capture detection. They compared their fluorometric and GLC procedures (3) and found that the assayed plasma griseofulvin levels were ~30% higher using the fluorometric method. These authors felt their data indicated an interference in the fluorometric assay by 6-demethylgriseofulvin, a griseofulvin metabolite.

More recent investigators (5) reported a high-pressure liquid chromatographic (HPLC) procedure for plasma griseofulvin levels. The method was very rapid, involving only a protein precipitation step prior to chromatographic analysis, but did not include an internal standard. The drug was quantitated using a fluorescent detector.

The present study investigated the potential interference of 6-demethylgriseofulvin in the fluorometric methods (3, 4). In addition, an HPLC method was developed to provide a procedure utilizing an internal standard that could be applied to the assay of plasma griseofulvin levels in humans.

EXPERIMENTAL

Reagents and Chemicals—The following were used: griseofulvin[1]; glass-distilled methanol[2], ether[2], and hexane[2]; and warfarin sodium[3].

Comparison of Fluorometric Procedures—Pooled plasma samples were prepared containing 0.1, 0.2, 0.4, 0.6, 0.8, and 1.0 μg/ml of griseofulvin. These plasma samples were assayed utilizing the procedures of Shah *et al.* (4) and Schwarz *et al.* (3). In both methods, the final fluorescence[4] reading was determined using 5 drops of sulfuric acid for complete sample quenching.

HPLC Method—The procedure utilized warfarin sodium as an internal standard. The extraction method was essentially that of Shah *et al.* (4), except that the plasma was adjusted to pH 5 with hydrochloric acid before extraction to facilitate warfarin removal. One-milliliter aliquots of pooled plasma were spiked with 1-ml aqueous griseofulvin solutions to simulate plasma griseofulvin levels of 0.1, 0.2, 0.4, 0.6, 0.8. 1.0, 1.5, and 2.0 μg/ml. To this mixture were added 1 ml of a 150-μg/ml aqueous warfarin sodium solution, 0.1 ml of 1 *N* HCl, and 10 ml of ether.

The mixture was extracted for 10 min in a 50-ml screw-capped centrifuge tube[5] and centrifuged at 3000 rpm at −10° for 15 min. The tube was then dipped into a dry ice–acetone bath until the aqueous phase was frozen. The ether layer was decanted into a 20-ml screw-capped centrifuge tube and evaporated under nitrogen at 40°. The residue was taken up in 50% methanol and shaken for 5 min with hexane. After centrifuging for 15 min at 3000 rpm and −10°, the hexane layer was removed and discarded. A 50-μl aliquot of the methanolic solution was injected into the chromatograph.

The HPLC system consisted of a sample injector[6]; a mobile phase pump[7] operated at 2.2 ml/min (pressure 2000 psi); a reversed-phase column[8]; a fluorescence detector[9], using 300 and 418 nm as the excitation and emission wavelengths, respectively, and a range setting of 1.0 μamp; and a variable-speed recorder[10] operated at 0.25 cm/min. The mobile phase consisted of 61.5% methanol and 38.5% of 0.5% acetic acid in water. Standard curves were obtained by plotting peak height ratio (griseofulvin/warfarin) *versus* griseofulvin concentration.

Griseofulvin Metabolite Isolation—A 24-hr urine collection was obtained from a volunteer who had ingested two 500-mg griseofulvin tablets[11]. The 2145 ml of urine was adjusted to pH 4 with hydrochloric acid and extracted in ~300-ml portions. Each urine aliquot was extracted twice with 300 ml of ether, and the combined ether extracts were evaporated under nitrogen. The ~100 ml of aqueous residue remaining after ether evaporation was then extracted four times with 100-ml portions of ether. The ~50 ml of aqueous residue remaining after evaporation of the 400 ml of ether extract was then extracted twice with 100 ml of ether. The ~25 ml of aqueous residue remaining after evaporation of the 200 ml of ether extract was further extracted with two 100-ml portions of ether. The 10 ml of aqueous residue remaining after evaporation of the 200 ml of ether extract was finally extracted five times with 50 ml of ether.

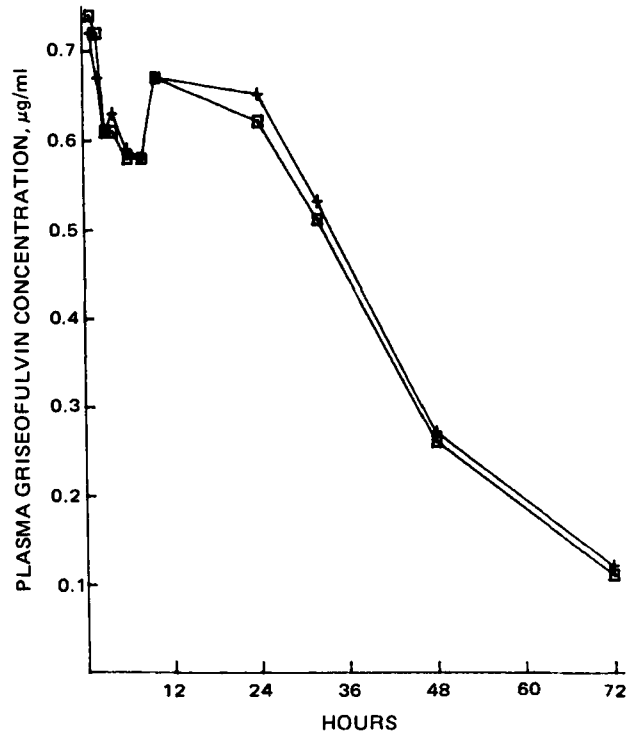

Figure 1—*Plasma griseofulvin levels for a subject receiving a 500-mg tablet. Fluorometric assays were performed using the method of Schwarz* et al. *(3)* (□) *and Shah* et al. *(4)* (+).

The 250 ml of ether was evaporated, and the ~5 ml of deep-red aqueous residue was utilized in the TLC separation. With a 10-μl pipet, the aqueous residue was applied as multiple spots to form a continuous streak on 11 TLC plates[12] (20 × 20 cm, 0.5 mm thick). The plates were developed for 2 hr, using a 1:4 mixture of acetone and chloroform. Even though the solvent front reached the top of the TLC plate before 2 hr, the longer development time was required for optimal separation. At least six well-separated fluorescent bands were observed on each plate when viewed under shortwave UV light. One relatively weak band corresponded to griseofulvin.

Since the fluorescence of 6-demethylgriseofulvin had been reported to be quenched at alkaline pH (6), the strongly fluorescent band that quenched upon exposure to ammonium hydroxide fumes was assumed to be 6-demethylgriseofulvin. This band was carefully scraped from each TLC plate, placed in a 50-ml centrifuge tube, and extracted five times with 30 ml of ether. A total of 87 mg of white powder was obtained after evaporation of the combined ether extracts.

The uncorrected melting point of the material was determined to be 280° with decomposition. The UV spectrum was determined[13] for the compound dissolved in 80% ethanol, to which was added 1% (v/v) of either 2 *N* HCl or 2 *N* NaOH. The fluorescence spectra[4] of the compound dissolved in methanol also were obtained, before and after the addition of 2 drops of ammonium hydroxide. A 5-μl portion of a methanol solution of the material also was spotted on a 0.25-mm TLC plate[14] along with a

[1] Sigma Chemical Co., St. Louis, Mo.
[2] Burdick & Jackson Laboratories, Muskegon, Mich.
[3] Lot R69-522m, provided by Endo Laboratories, Garden City, N.Y.
[4] Aminco-Bowman spectrophotofluorometer, American Instrument Co., Silver Spring, Md.
[5] No. 14-930-10J, Fisher Scientific, Pittsburgh, Pa.
[6] Model U6K, Waters Associates, Milford, Mass.
[7] Model M6000, Waters Associates, Milford, Mass.
[8] μBondapak C_{18}, Water Associates, Milford, Mass.
[9] Model FS 970, Schoeffel Instrument Corp., Westwood, N.J.
[10] Recordall series 5000, Fisher Scientific, St. Louis, Mo.
[11] Fulvicin-U/F, Schering Corp., Kenilworth, N.J.
[12] Silica gel G with calcium sulfate binder, Supelco, Inc., Bellefonte, Pa.
[13] DB-GT spectrophotometer, Beckman Instruments, Irvine, Calif.
[14] NEN-silica gel OF, 5 × 20 cm, 0.25 mm, New England Nuclear, Boston, Mass.

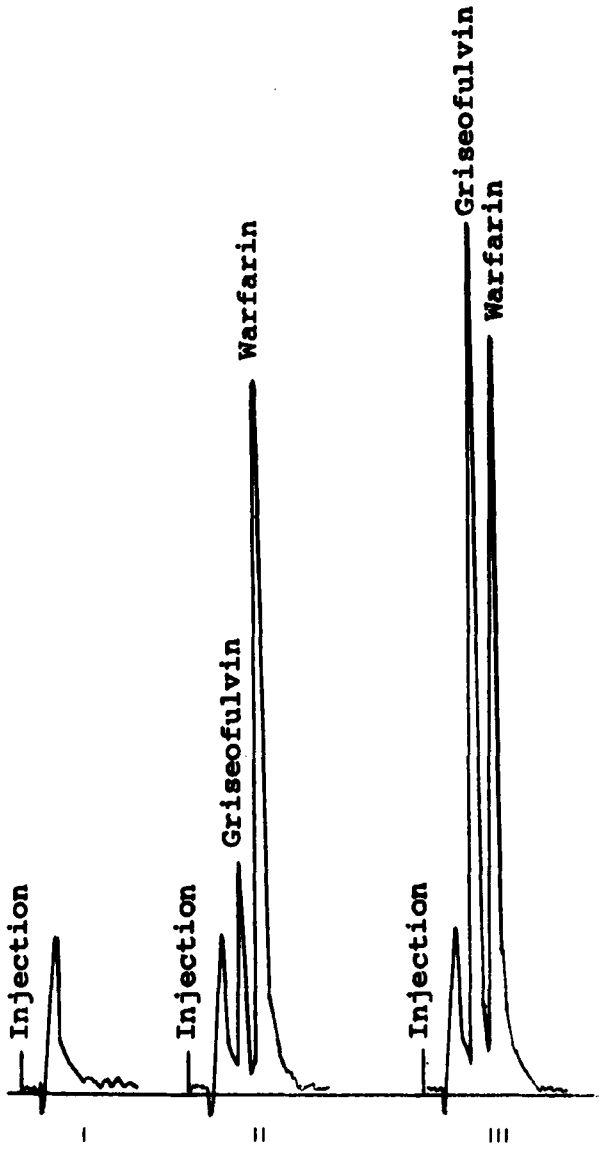

Figure 2—*Typical HPLC chromatograms for the assay of a blank human plasma sample (I) and plasma samples containing 0.1 μg/ml (II) and 0.4 μg/ml (III) of griseofulvin. Warfarin was added to plasma samples II and III as an internal standard.*

griseofulvin sample. The plate was developed for 25 min with acetone–chloroform (1:4).

After development, the plate was viewed under shortwave UV light, followed by exposure to ammonium hydroxide fumes. A diluted methanol solution of the compound also was injected into the chromatograph, using the parameters previously described for the HPLC plasma assay. Finally, the 270-MHz NMR spectra[15] were determined for the material, a sample of griseofulvin, and a sample of 4-demethylgriseofulvin[16]. Deuterated acetone was employed as the solvent for the NMR spectra.

Since interference by 6-demethylgriseofulvin has been suggested as the cause for higher plasma griseofulvin assay values for a fluorometric assay compared to a GLC procedure (3), pooled plasma samples were prepared containing either 1 μg of griseofulvin/ml or 5 μg of 6-demethylgriseofulvin/ml and both 1 μg of griseofulvin/ml and 5 μg of 6-demethylgriseofulvin/ml. These samples were carried through the extraction procedures of Schwarz *et al.* (3) and Shah *et al.* (4). The resulting extracts were assayed fluorometrically, and an aliquot was injected into the chromatograph, using the previously described HPLC system.

Plasma Level Studies—To obtain plasma samples for evaluation of the fluorometric and HPLC assay methods, a healthy male volunteer received a 500-mg griseofulvin tablet[11] on two different occasions, approximately 4 months apart. Ten-milliliter plasma samples were obtained just before and 1, 2, 3, 4, 6, 8, 10, 24, 32, 48, and 72 hr after the first administration. These samples were assayed using the two previously discussed fluorometric methods. Since the purpose of the second study was to provide plasma samples for a comparison of the HPLC method with the method of Shah *et al.* (4), 10-ml plasma samples were obtained just before and 2, 4, 8, 24, and 48 hr after the second administration. The doses were taken after an overnight fast, and no food or beverage other than water was permitted for 4 hr after dosing.

RESULTS AND DISCUSSION

Comparison of Fluorometric Procedures—In an earlier study (3), plasma griseofulvin levels assayed fluorometrically by the method of Schwarz *et al.* (3) were approximately 30% higher than those from a GLC assay. Since no direct comparison had been made of the two previously reported fluorometric methods (3, 4), it was of interest to determine if the procedures yielded comparable data. Calibration curves obtained for fluorescence intensity, corrected for blank plasma fluorescence, *versus* plasma griseofulvin concentration were essentially superimposable for plasma standards assayed by either method.

The least-squares slope, intercept, and correlation coefficient for one procedure (4) were 24.24, 0.24, and 0.999, respectively; the same values for the other method (3) were 23.88, −0.03, and 0.998, respectively. The recovery of griseofulvin from the plasma samples averaged ~90% for both methods. The blank plasma correction required with the method of Schwarz *et al.* (3) was generally four times that required with the method of Shah *et al.* (4). This difference appeared to be due to the hexane extraction step present in the latter method.

The data shown in Fig. 1 were obtained by assaying plasma samples from a subject who received a 500-mg griseofulvin tablet. The plasma levels at each sampling time differed by 5% or less by the two fluorometric methods.

HPLC Method—Since the two previously described fluorometric methods (3, 4) provided comparable assay data and since one of the methods had been shown earlier (3) apparently to lack suitable griseofulvin specificity, an HPLC assay was developed.

Typical chromatograms for pooled plasma containing 0, 0.1, and 0.4 μg of griseofulvin/ml and 150 μg of warfarin sodium/ml, carried through the extraction and HPLC assay, are shown in Fig. 2. The retention times for griseofulvin and warfarin were 3.1 and 4.3 min, respectively. An additional peak, which also appeared in blank plasma extracts, was well separated from griseofulvin and had a retention time of 2.2 min. No interferences were observed in blank plasma samples obtained from 12 human subjects who participated in a griseofulvin bioavailability study (to be reported later). However, plasma obtained from a subject who was administered three 0.33-g (5-gr) aspirin tablets exhibited a large interfering peak, which would have precluded detection of the griseofulvin peak.

The calibration curve of peak height ratio (griseofulvin/warfarin) *versus* griseofulvin concentration for the assay of pooled plasma samples containing 0–2.0 μg of griseofulvin/ml exhibited a slope of 2.91, an intercept of −0.01, and a correlation coefficient of 0.999. Griseofulvin recovery from plasma averaged 91%, compared to the direct HPLC analysis of methanolic standards. The lowest standard contained 0.1 μg of griseofulvin/ml of plasma. However, a greater sensitivity should be readily attainable by utilizing >1 ml of plasma, diluting the extract with <2 ml of 50% methanol, or injecting >50 μl of sample.

The HPLC assay was compared directly to the fluorometric method of Shah *et al.* (4), using plasma samples obtained from a human volunteer who had been administered a 500-mg griseofulvin tablet. The results of these determinations are shown in Fig. 3. The ratio of griseofulvin concentrations determined by the fluorometric assay divided by the HPLC assay averaged 1.22, which is in agreement with the mean ratio of 1.3 previously reported in a comparison of a fluorometric and a GLC assay method (3).

Griseofulvin Metabolite Isolation—6-Demethylgriseofulvin has been reported to be the primary griseofulvin metabolite in humans (6, 7). Thus, it is logical to assume that the major source of interference in the fluorometric assay procedures can be attributed to this metabolite.

The uncorrected melting point of the material isolated from the urine extracts was 280°, in reasonable agreement with the 273–275° melting point reported previously for 6-demethylgriseofulvin (7). The recovery of 87 mg of metabolite after the administration of the 1-g dose is similar to the reported 7% (8) and 10% (2) recoveries 24 hr after administration

[15] Recorded on a custom-built 270-MHz spectrometer, based on an Oxford Instruments solenoid, a Bruker-Nicolet console, and a Nicolet 1180 computer.

[16] Glaxo Laboratories, Greenford, Middlesex, England.

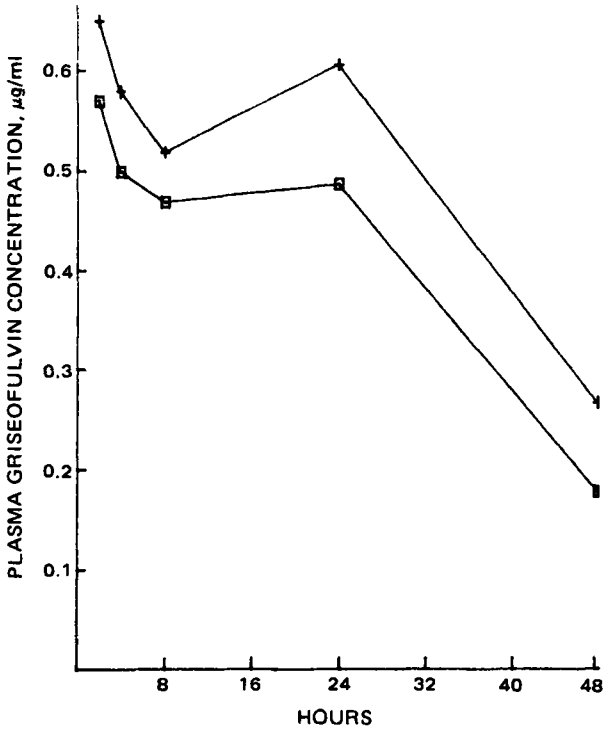

Figure 3—*Plasma griseofulvin levels for a subject receiving a 500-mg tablet. Determinations were carried out using the fluorometric method of Shah* et al. *(4) (+) and an HPLC method (□).*

of a 500-mg dose to a human subject. Similarly, 10.5% of a 1-g dose in a 24-hr urine sample was obtained from a human subject (7).

No attempt was made to recover 6-demethylgriseofulvin that might have been present as a glucuronide metabolite in the urine. The UV absorption maxima in alkaline solution were 250 and 300 nm, compared to previously reported values of 249.5 and 330 nm (7). Similarly, the maxima were 236 and 293.5 nm in acidic solution, compared to 235.5 and 293.5 nm. The excitation and emission fluorescence maxima were 320 and 425 nm, respectively, which were nearly identical to the maxima exhibited by griseofulvin. The fluorescence spectrum was totally quenched upon the addition of 2 drops of ammonium hydroxide. When the presumed 6-demethylgriseofulvin was spotted on a 0.25-mm TLC plate along with a sample of griseofulvin and the plates were developed for 25 min, only two distinct spots appeared under shortwave UV light. The R_f values were 0.23 and 0.44 for 6-demethylgriseofulvin and griseofulvin, respectively, and only the former spot quenched after exposure to ammonium hydroxide fumes. When a sample of presumed 6-demethylgriseofulvin was examined using the HPLC system described in the assay procedure, a single sharp peak resulted. The retention time of this peak was 2.2 min, compared to 3.1 min for griseofulvin.

The NMR spectra for griseofulvin, 4-demethylgriseofulvin, and the presumed 6-demethylgriseofulvin provided the final confirmation of structure. The data in Table I summarize the assignment of the protons in each spectra. The spectra of all three substances were quite similar, with the correct number of methoxyls being observed in each instance. The replacement of a methoxyl with a hydroxyl slightly shifted the ring proton and remaining methoxyl to a higher field. The methoxyl in 4-demethylgriseofulvin is adjacent to chlorine and is downfield from the methoxyl in 6-demethylgriseofulvin.

To assess the 6-demethylgriseofulvin interference in the fluorometric plasma assay for griseofulvin, samples spiked with griseofulvin and 6-demethylgriseofulvin were assayed by the methods of Shah *et al.* (4) and Schwarz *et al.* (3). With either method, plasma samples containing 5 µg of 6-demethylgriseofulvin/ml exhibited fluorescence values equal to those obtained with blank plasma samples. The fluorescence of plasma spiked with both 1 µg of griseofulvin/ml and 5 µg of 6-demethylgriseofulvin/ml was identical to that resulting from the assay of plasma containing only 1 µg of griseofulvin/ml. Furthermore, when the extracts of the plasma samples containing 6-demethylgriseofulvin were injected into the chromatograph, no peak corresponding to the retention time of 6-demethylgriseofulvin appeared.

Thus, it appears that the higher assay values resulting from the fluorometric assay of plasma samples obtained from subjects ingesting griseofulvin, compared to assay values determined with either a GLC (3) or an HPLC assay, could not be attributed to interference by 6-demethylgriseofulvin as proposed earlier (3). Since the material that interferes in the fluorometric procedures only appears in the plasma of subjects who have received griseofulvin, the material might represent an unidentified griseofulvin metabolite. However, whatever the identity of the interfering material, the use of the fluorometric assays for plasma griseofulvin results in falsely elevated values. The described HPLC procedure provides an alternative assay with good sensitivity and specificity.

Table I—Protons for 270-MHz Signals of Griseofulvin and Metabolites (δ, ppm)

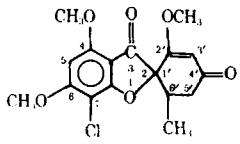

griseofulvin

Proton	Griseofulvin	4-Demethylgriseofulvin	6-Demethylgriseofulvin
2′-OCH_3	3.62	3.62	3.62
3′-H	5.48	5.48	5.48
5′-H	2.77	2.76	2.77
6′-H	2.27	2.28	2.28
6′-CH_3	0.83	0.84	0.84
4-OCH_3	3.93	—	3.80
5-H	6.49	6.49	6.29
6-OCH_3	4.04	3.94	—

REFERENCES

(1) M. Rowland, S. Riegelman, and W. L. Epstein, *J. Pharm. Sci.*, **57**, 984 (1968).

(2) W. L. Chiou and S. Riegelman, *ibid.*, **60**, 1376 (1971).

(3) H. J. Schwarz, B. A. Waldman, and V. Madrid, *ibid.*, **65**, 370 (1976).

(4) V. P. Shah, S. Riegelman, and W. L. Epstein, *ibid.*, **61**, 634 (1972).

(5) R. L. Nation, G. W. Peng, V. Smith, and W. L. Chiou, *ibid.*, **67**, 805 (1978).

(6) M. Rowland and S. Riegelman, *ibid.*, **62**, 2030 (1973).

(7) M. J. Barnes and B. Boothroyd, *Biochem. J.*, **78**, 41 (1961).

(8) P. Kabasakalian, M. Katz, B. Rosenkrantz, and E. Townley, *J. Pharm. Sci.*, **59**, 595 (1970).

ACKNOWLEDGMENTS

Supported in part by a contract from the Tennessee Department of Public Health and FDA Contract 223-77-3097.

The contributions of Dr. James Axelson, Dr. Frank Abbott, and Mr. Roland Burton of the University of British Columbia, in the running and interpretation of the NMR spectra, are gratefully acknowledged.

Mercaptoalkylamine Coordination Compounds of Platinum(II) and Palladium(II) and Their Anticancer Activity

WILLIAM O. FOYE [x] **and VALAPHA KAEWCHANSILP** [*]

Received November 24, 1978, from the *Samuel M. Best Research Laboratory, Massachusetts College of Pharmacy, Boston, MA 02115.* Accepted for publication March 16, 1979. *Present address: Department of Mineral Resources, Ground Water Division, Bangkok 4, Thailand.

Abstract □ A series of coordination compounds of platinum(II) and palladium(II) with several amino- and heterocyclic aminoalkyl mercaptans was synthesized, and their structures were determined by IR absorption and elemental analyses. Because of the tendency of the mercapto group to undergo oxidation on reaction with metals, as observed with copper(II), the complexes were obtained by use of the aminoalkylthiosulfates, which decomposed to the thiol in either acid or alkaline solution. Furthermore, palladium–sulfide complex formation by reaction with an aminoalkyltrithiocarbonate made it possible to distinguish between metal–sulfur and metal–nitrogen bonds in the 650–400-cm^{-1} region. Anticancer screening against L-1210 lymphoid leukemia in mice did not reveal positive activity among the compounds tested.

Keyphrases □ Platinum—mercaptoalkylamine coordination compounds, antineoplastic activity, structure–activity relationships □ Palladium—mercaptoalkylamine coordination compounds, antineoplastic activity, structure–activity relationships □ Antineoplastic agents, potential—platinum, palladium, mercaptoalkylamine coordination compounds, structure–activity relationships

cis-Dichlorodiammineplatinum(II) and a number of closely related diaminodichloro platinum(II) complexes have shown appreciable anticancer activity in several tumor systems (1, 2). This discovery resulted from the observation (3) that certain coordination compounds of platinum(II) inhibited bacterial cell division without inhibiting growth. It is now known that for anticancer activity with the platinum(II) complexes, two *cis*-monodentate (or one bidentate) leaving groups are required; the most active complexes have contained chloride, bromide, oxalate, or malonate ligands (4). In addition, the complexes should be neutral, their geometries should be either square planar or octahedral, and the ligands *trans* to the leaving groups should be strongly bonded and relatively inert amines.

Little work has been reported on platinum complexes having ligands with phosphorus, oxygen, or sulfur donor atoms. Lindoy *et al.* (5) reported the formation of some sulfur–nitrogen complexes containing ligands with platinum(II), palladium(II), nickel(II), copper(II), copper(I), silver(I), and mercury(II), but these complexes were not tested for anticancer activities.

With the assumptions that palladium(II) complexes are generally more reactive than platinum(II) complexes (6) and that sulfur-containing ligands should be bound more strongly than nitrogen-containing ligands, a series of complexes was prepared with sulfur–nitrogen ligands (mercaptoalkylamines) coordinated with both platinum(II) and palladium(II). Following a postulation of anticancer activity of the platinum(II) complexes that depends on dissociation of the complexes (7), such compounds could be expected to possess at least the same order anticancer activity as that of the known platinum(II) compounds. Attempts also were made to prepare corresponding nickel(II) and copper(II) complexes.

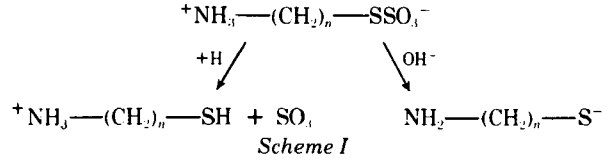

Scheme I

DISCUSSION

Palladium(II) and platinum(II) are sufficiently large that four ligands may fit on these metals with less repulsion in a square planar complex, regardless of whether the ligands are weak or strong field ligands. Ligands used in this study are considered to be strong field ligands: primary and secondary aliphatic amines, the sulfide ion, and the chloride ion. In the first transition series, only very strong field ligands can effect the spin pairing necessary for stabilization of the square planar arrangement. With heavier metals, however, low-spin square planar complexes can result even with weak field ligands. In the present series, with both large metals and strong field ligands, it can be assumed that square planar complexes exist.

The reaction of mercaptoethylamine with copper(II) resulted in an oxidation–reduction reaction, so a derivative of the thiol group was employed to avoid this reaction and to give mercaptoalkylamine complexes. Use of the aminoalkylthiosulfates provided a method of obtaining the desired ligands since the thiosulfates hydrolyze in either acidic or alkaline solution to give the thiol or thiol anion (8) (Scheme I). A cyclic or chelate complex should result, with chloride, water, or both filling the metal-ion coordination capacity. Complete loss of the S=O stretching frequency of the uncomplexed ligands at 1220–1190 cm^{-1} also confirmed that the thiosulfate group was not present in the metal complexes.

Since the sulfur ion is a class b (soft) base, it should coordinate with palladium(II) and platinum(II) (class b soft acids) prior to the amine group (class a hard base). A reaction that illustrates this situation occurs with the aminoalkyltrithiocarbonates. In this case, however, carbon disulfide is eliminated, and a metal–mercaptide complex may be isolated in acidic solution (9) (Scheme II). Here, there is no possibility that metal–nitrogen bonds may be formed since the amine groups are protonated. This reaction made it possible to distinguish Pd–S from Pd–N IR absorption bands, both of which occur in the 650–400-cm^{-1} region. Metal–sulfur stretching modes are also found in the 400–250-cm^{-1} region (10). Again, there is no possibility of confusion with metal–chloride stretching frequencies in the 350–300-cm^{-1} region since, in the palladium sulfide compound formation, no metal–chloride bond results.

The structures of the palladium(II) and platinum(II) complexes were determined by IR absorption spectra and elemental analyses. Where NH_2 groups were present, stretching frequencies of the coordinated amines were lowered by 100 cm^{-1} or more from those of the free NH_2 groups in the 3550–3330- and 3400–3250-cm^{-1} ranges. Observed frequencies for the NH_2 groups in the complexes were in the same range as those of Pd(II) complexes of methionine (3360–3090 cm^{-1}) (11). Frequencies for the Pd–N and Pt–N bonds were found in the 560–420-cm^{-1} range and could be distinguished from the Pd–S bonds, which were revealed from the reaction with the aminoalkyltrithiocarbonate.

Metal–sulfur stretching frequencies were located in the 390–355-cm^{-1} range (10). Also, one or two bands in the region between 650 and 600 cm^{-1} could be assigned to metal–sulfur coordination. Metal chloride bands were observed at 350–300 cm^{-1} (10), in the same region as for Pt(II)

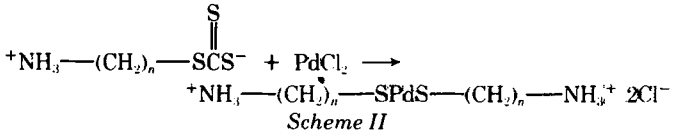

Scheme II

0022-3549/79/0900-1131$01.00/0
© 1979, American Pharmaceutical Association

Table I—IR Absorption Frequencies

Compound	Ligands	Frequencies (KBr), cm^{-1} O–H	N–H	Pd–N or Pt–N	Pd–S or Pt–S	Pd–Cl or Pt–Cl
		Palladium Complexes				
I	$NH_2CH_2CH_2S—, Cl^-, H_2O$	3500–3400	3190, 3100	510	650, 615, 380	335, 320
II	$NH_2CH_2CH_2CH_2S—, Cl^-, H_2O$	3500–3400	3200, 3150	485, 465	620, 390	330, 300
III		3550–3450		490, 465	625, 375	345, 320
IV	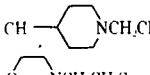	3550–3450		490, 470	650, 620, 370	300 (br)
V	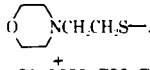	3550–3450		510, 480	650, 615, 360	300
VI	$2Cl^-\overset{+}{N}H_3CH_2CH_2S—$	3500–3400			650, 610, 355	
VII	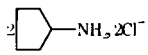	3480–3360	3200, 3120	435, 420		315, 300
VIII	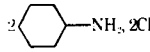	3480–3360	3200, 3100	450, 425		330, 315
IX	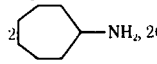	3460–3360	3200, 3110	460, 435		335, 320
X	$(NH_2CH_2CH_2S—)_2, Cl^-$	3480–3360	3220, 3170, 3080	505	650, 380	350
		Platinum Complexes				
XI	$Cl^-\overset{+}{N}H_3CH_2CH_2S—, Cl^-, 2H_2O$	3560–3400			620, 390	320
XII	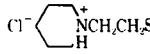	3600–3400			625, 420	320
XIII	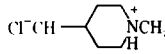	3560–3400			620, 590, 390	310 (br)
XIV	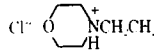	3600–3400			650, 610, 370	310 (br)
XV	$NH_2CH_2CH_2S—, Cl^-, H_2O$	3580–3400	3200, 3120	535	620, 590, 390	315 (br)
XVI	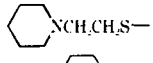	3540–3380		500	620, 590, 390	310 (br)
XVII	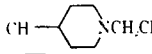	3560–3360		505	620, 590, 380	310 (br)
XVIII	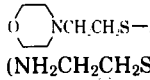	3560–3360		560	615, 590, 370	310 (br)
XIX	$(NH_2CH_2CH_2S—)_2, Cl^-$	3520–3340	3230, 3160, 3090	510	650, 390	355

Table II—Physical Constants

Compound	M	Ligands	Formula	Decomposition Point	Yield, %	Analysis, %	Calc.	Found
I	Pd	$NH_2CH_2CH_2S—, Cl^-, H_2O$	$C_2H_8ClNOPdS$	323°	34	C	10.18	10.52
						H	3.42	3.47
						Cl	15.13	15.13
						N	5.94	6.01
						S	13.59	13.47
II	Pd	$NH_2CH_2CH_2CH_2S—, Cl^-, H_2O$	$C_3H_{10}ClNOPdS$	285°	68	C	14.41	14.78
						H	4.03	3.73
						Cl	14.18	14.08
						N	5.60	5.97
						S	12.82	12.59
III	Pd	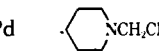	$C_7H_{16}ClNOPdS$	210°	78	C	27.64	27.57
						H	5.30	5.17
						Cl	11.66	11.42
						N	4.61	4.60
						S	11.54	11.20
IV	Pd	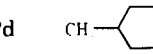	$C_8H_{18}ClNOPdS·H_2O$	213°	65	C	28.58	28.58
						H	5.98	5.80
						Cl	10.54	10.55
						N	4.17	4.20
						S	9.53	9.46
V	Pd	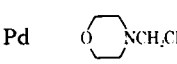	$C_6H_{14}ClNOPdS$	236°	74	C	23.54	23.78
						H	4.60	4.19
						Cl	11.58	11.51
						N	4.58	4.62
						S	10.45	9.95
VI	Pd	$2Cl^-\overset{+}{N}H_3CH_2CH_2S—$	$C_4H_{12}N_2PdS_2·2HCl·H_2O$	220°	63	C	13.90	13.73
						H	3.50	3.31
						N	8.10	7.89
						S	18.55	18.10
VII	Pd	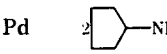	$C_{10}H_{22}Cl_2N_2Pd·6H_2O$	180°	30	C	26.36	26.50
						H	6.50	6.16
						Cl	15.56	15.19
						N	6.14	5.89
VIII	Pd	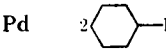	$C_{12}H_{26}Cl_2N_2Pd·6H_2O$	187°	77	C	29.79	29.46
						H	6.90	6.68
						Cl	14.66	14.21
						N	5.79	5.56

Table II—*Continued*

Compound	M	Ligands	Formula	Decomposition Point	Yield, %		Analysis, % Calc.	Found
IX	Pd	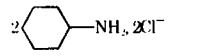	$C_{14}H_{30}Cl_2N_2Pd{\cdot}6H_2O$	180°	78	C	32.86	33.15
						H	7.26	6.90
						Cl	13.86	13.51
						N	5.47	5.52
X	Pd	$(NH_2CH_2CH_2S—)_2$, Cl^-	$C_4H_{12}Cl_2N_2PdS_2{\cdot}H_2O$	313°	27	C	13.82	13.70
						H	4.06	4.24
						Cl	20.39	19.90
						N	8.06	7.94
						S	18.44	17.98
XI	Pt	$Cl^-\overset{+}{N}H_3CH_2CH_2S—$, Cl^-, $2H_2O$	$C_2H_{10}ClNO_2PtS{\cdot}HCl$	330°	66	C	6.40	6.60
						H	2.90	2.72
						N	3.70	3.73
						S	8.46	8.50
XII	Pt	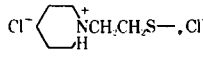	$C_7H_{18}ClNO_2PtS{\cdot}HCl$	232°	83	C	18.79	18.10
						H	4.27	3.90
						Cl	15.85	15.53
						N	3.13	2.97
						S	7.16	7.14
XIII	Pt	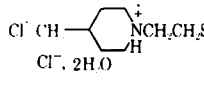	$C_8H_{20}ClNO_2PtS{\cdot}HCl{\cdot}H_2O$	240°	87	C	20.04	20.43
						H	4.83	4.53
						Cl	14.79	14.50
						N	2.92	2.81
						S	6.69	7.20
XIV	Pt	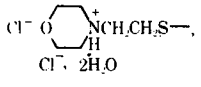	$C_6H_{16}ClNO_3PtS{\cdot}HCl$	265°	70	C	16.04	16.48
						H	3.80	3.12
						Cl	15.78	15.76
						N	3.11	3.07
						S	7.14	7.22
XV	Pt	$NH_2CH_2CH_2S—$, Cl^-, H_2O	$C_2H_8ClNOPtS{\cdot}H_2O$	340°	66	C	6.99	6.76
						H	2.93	2.46
						Cl	10.34	9.89
						N	4.07	3.80
						S	9.35	9.02
XVI	Pt		$C_7H_{16}ClNOPtS$	258°	67	C	21.41	21.42
						H	4.11	3.87
						Cl	9.03	8.86
						N	3.57	3.58
						S	8.16	8.33
XVII	Pt	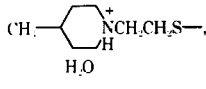	$C_8H_{18}ClNOPtS$	239°	49	C	23.57	23.16
						H	4.69	4.63
						N	3.44	3.82
						S	7.86	7.53
XVIII	Pt	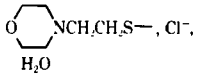	$C_6H_{14}ClNO_2PtS{\cdot}2H_2O$	280°	48	C	16.73	16.73
						H	4.17	3,80
						Cl	8.23	8.18
						N	3.25	3.25
						S	7.45	7.50
XIX	Pt	$(NH_2CH_2CH_2S—)_2$, Cl^-	$C_4H_{12}Cl_2N_2PtS_2{\cdot}8H_2O$	245°	24	C	8.54	8.70
						H	4.98	4.65
						N	4.97	4.73
						S	11.41	10.97

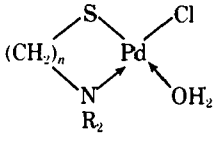

I

complexes of ethionine and *S*-methyl-L-cysteine with chloride ligands (10). Broad bands for water were shown in the 3600–3400-cm^{-1} region for many complexes. IR absorption frequencies for the various bonds observed are listed in Table I. Other physical constants for the complexes are listed in Table II.

Palladium(II) Complexes—The IR absorption spectra indicated clearly that the mercaptoamines derived from the thiosulfates acted as bidentate ligands, being coordinated to palladium(II) *via* the sulfur and nitrogen. Both chloride ion and water also were coordinated to give type I structures. Elemental analyses agreed with this structure.

For the palladium(II) complex of bis(2-aminoethyl) disulfide, however, IR absorption and elemental analyses indicated a type II structure. Polymeric complexes are not commonly found with palladium(II) and platinum(II) but are possible with halogen and sulfur ligands. Three strong bands for NH_2 stretching of the palladium–cystamine complex were exhibited at 3300–3090 cm^{-1}, and Pd–N stretching at 500 cm^{-1} showed coordination of both nitrogens. Strong C–S stretching frequencies at 1270–1220 cm^{-1} indicated that the disulfide linkage was intact, and Pd–S bands at 650 and 380 cm^{-1} showed coordination to sulfur. Pd–Cl bands appeared at 350 cm^{-1}, and a positive test for ionic chloride was given by the disulfide complex but not for the mercaptoamine complexes.

Cycloalkylamine complexes of palladium(II) were also prepared since *cis*-dichloro-bis(cycloalkylamine) platinum(II) complexes have shown promising anticancer activities (12). Elemental analyses and IR ab-

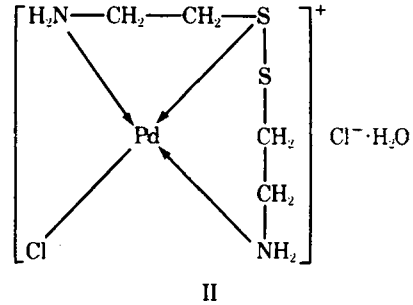

II

Table III—Antileukemic Activities in Mice [a]

Compound	Dose, mg/kg	Animal Weight Difference (T − C), g [b]	Survival (T − C), % [c]
I	200	−3.6	111
II	100	−2.4	103
III	100	−1.1	105
IV	25	−0.7	106
X	12.5	−0.6	101
XIII	12.5	−0.9	107
XV	200	−1.4	107
XVI	50	−1.5	98
XVIII	50	−0.6	102
XIX	100	−2.1	103

[a] Mice were infected with L-1210 lymphoid leukemia. Compounds were administered intraperitoneally every 4th day, for a total of three injections, beginning on the 1st day after tumor implantation. The vehicle was either saline or saline with polysorbate (Tween) 80. Six mice were used at each dosage level. [b] Average weight change of test group minus average weight change of control animals on Day 5. [c] Ratio of mean survival time of treated animals to that of control animals. Observations were made for 20 days.

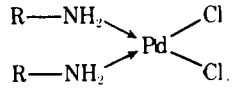

III

sorption for the cycloalkylamine complexes indicated type III structure, analogous to the previously determined cycloalkylamine complexes of Pt(II). Actually, there were two Pd–N bands at 495 and 476 cm^{-1} and two Pd–Cl bands at 327 and 306 cm^{-1} for the dichlorodiamminepalladium(II) *cis* structure but only one band of each type for the *trans* structure (13). The IR spectra showed, in general, two bands of each type and agreed closely with those for the *cis* structures. The *cis*-isomer of dichlorodiamminepalladium(II) isomerizes to the *trans* structure on standing, however (13).

Platinum(II) Complexes—Platinum(II) complexes were formed in both acidic and slightly alkaline media. In acidic solution, the thiosulfates were cleaved to the mercaptans and the amino groups remained protonated, so only Pt–S coordination took place. Pt–S bands around 650–590 and 420–370 cm^{-1} appeared, along with Pt–Cl bands at 320–310 cm^{-1}. The IR absorption spectra, combined with elemental analyses, indicated structures of type IV.

In slightly alkaline solution, both Pt–S and Pt–N coordination could take place and cyclic type I complexes were formed, as indicated by IR absorption. The NH_2 stretching frequencies at 3500–3300 cm^{-1} were lowered by about 100 cm^{-1} in the mercaptoethylamine complex. The Pt–N frequencies were at 560–500 cm^{-1}, and Pt–S bands appeared at 620–590 and 390–370 cm^{-1}. A broad Pt–Cl band was observed at 315–310 cm^{-1}, and water was recognized by absorption at 3600–3400 cm^{-1}. Elemental analyses were in agreement with this structure (I).

The platinum complex of cystamine was found to have a type II structure analogous to the palladium complex. Absorption bands for Pt–N, Pt–S, and Pt–Cl, as well as N–H stretching frequencies, were very similar for the platinum(II) and palladium(II) cystamine complexes.

Nickel(II) and Copper(II) Complexes—Attempts to prepare nickel (II) complexes by the procedures described here, in acidic and slightly alkaline solution, did not result in isolatable products. Jicha and Busch (14) reported the formation of two types of nickel(II) complexes of 2-mercaptoethylamine in alkaline solution, one the 2:1 chelate and the other having a structure of type $M(ML_2)_2Cl_2$.

Attempts to prepare copper(II) complexes by these methods also were unsuccessful.

Anticancer Tests—Anticancer screening was carried out[1] using mice infected with L-1210 lymphoid leukemia. Table III lists the most favorable dosage level of compound giving a measurable response in comparison to survival times and toxicities of control animals. None of the compounds tested produced survival times great enough in comparison to those of controls (T/C, %) to be listed as active.

Since the most active known platinum coordination compounds have a *cis*-dichloro function, the results presented here indicate that such a function is necessary for activity. Although a coordinated water molecule should be replaced equally as readily as a chloride ion (16), the biological replacing group may not replace a water molecule as readily or at all if it is ionic. If the anticancer mechanism of *cis*-dichlorodiammineplatinum depends upon binding to DNA (17, 18), then binding to ionic groups would appear to be favored.

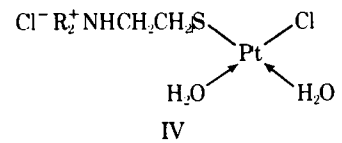

IV

EXPERIMENTAL[2]

The following procedures are representative.

***N,S*-(2-Aminoethanethio)chloroaquopalladium(II)**—2-Aminoethanethiosulfuric acid (0.1572 g, 0.001 mole) was dissolved in 35 ml of water, and the pH was adjusted to 8.0 with 0.04 *N* NaOH. A solution (10 ml) containing 0.1773 g (0.001 mole) of palladium(II) chloride in hot 0.04 *N* HCl was added dropwise with stirring. The solution became yellow, and the pH was maintained at 6.5–6.8 by the alternate dropwise addition of 0.04 *N* NaOH and the palladium chloride solution. Stirring was continued for 1 hr after addition was complete, and the yellow product was filtered, washed with water and ethanol, and dried at 60° for 2 days. The yield was 0.0611 g (34.5%) of product, which decomposed above 323°.

Anal.—Calc. for $C_2H_8ClNOPdS$: C, 10.18; H, 3.42; Cl, 15.13; N, 5.94; S, 13.59. Found: C, 10.52; H, 3.47; Cl, 15.13; N, 6.01; S, 13.47.

Bis-(*S*-2-aminoethanethio)palladium(II) Dihydrochloride—2-Aminoethanetrithiocarbonic acid (0.6132 g, 0.004 mole) was dissolved in 35 ml of *N*,*N*-dimethylformamide. A solution of palladium(II) chloride (0.3546 g, 0.002 mole) in 12 ml of hot 0.04 *N* HCl was added dropwise with stirring. A yellow precipitate appeared immediately, and the solution became red-yellow. After the addition was complete, the pH had decreased to 2.5, and the solution was stirred for 30 min. The precipitate was filtered, washed with water and ethanol, and dried in a desiccator. The dried product was brown and weighed 0.2238 g (63% yield); it decomposed above 220°.

Anal.—Calc. for $C_4H_{12}N_2PdS_2 \cdot 2HCl \cdot H_2O$: C, 13.90; H, 3.50; N, 8.10; S, 18.15. Found: C, 13.73; H, 3.31; N, 7.89; S, 18.10.

***cis*-Dichlorodi(cyclohexylamine)palladium(II)**—Solutions of potassium tetrachloropalladate(II) (0.3264 g, 0.001 mole) in 15 ml of water and cyclohexylamine (0.1984 g, 0.002 mole) in 5 ml of water were cooled to 1° and mixed, and light-brown crystals appeared immediately. The mixture was stored at 1° for 24 hr, and the product was filtered, washed with cold water, and dried. The yield was 0.2538 g (77.8%) of product, which decomposed above 187°.

Anal.—Calc. for $C_{12}H_{26}Cl_2N_2Pd \cdot 6H_2O$: C, 29.79; H, 6.90; Cl, 14.66; N, 5.79. Found: C, 29.46; H, 6.68; Cl, 14.21; N, 5.56.

Chloro-*N,N',S*-(cystamine)palladium(II) Chloride—Cystamine dihydrochloride (1.125 g, 0.005 mole) was dissolved in 70 ml of water, and the pH was adjusted to 8.0 using 0.04 *N* NaOH. A solution (50 ml) containing 0.8865 g (0.005 mole) of palladium(II) chloride in hot 0.04 *N* HCl was added dropwise with stirring along with sufficient alkali to maintain the pH at 6.5–7.0. A yellow precipitate appeared but dissolved on further addition and reappeared when the addition neared completion. Stirring was continued for 1 hr after the addition; the yellow product was filtered, washed with ethanol, and dried at 70° for 2 days. The yield was 0.2383 g (26.9%) of material, decomposing above 313°.

Anal.—Calc. for $C_4H_{12}Cl_2N_2PdS_2 \cdot H_2O$: C, 13.82; H, 4.06; Cl, 20.39; N, 8.06; S, 18.44. Found: C, 13.70; H, 4.24; Cl, 19.90; N, 7.94; S, 17.98.

***S*-(2-Aminoethanethio)chlorodiaquoplatinum(II) Hydrochloride**—To a solution of 2-aminoethanethiosulfuric acid (0.1572 g, 0.001 mole) in 25 ml of water was added dropwise with stirring a solution of 0.4151 g (0.001 mole) of potassium tetrachloroplatinate(II) in 10 ml of water. Stirring was continued for 1 hr after the addition; the yellow precipitate was filtered, washed with water, and dried at 70° overnight. The product weighed 0.2728 g (65.7%) and decomposed above 330°.

Anal.—Calc. for $C_2H_{11}Cl_2NO_2PtS$: C, 6.40; H, 2.90; N, 3.70; S, 8.46. Found: C, 6.60; H, 2.72; N, 3.73; S, 8.50.

[1] By the Division of Cancer Treatment, National Cancer Institute, in accordance with their protocol (15).

[2] Melting points were determined with a Mel-Temp capillary melting-point block and are uncorrected. IR spectra were obtained using a Perkin-Elmer model 457 A grating spectrophotometer and were corrected against polystyrene bands. Elemental analyses were done by Strauss Microanalytical Laboratory, Oxford, England.

Potassium tetrachloroplatinate(II) was a gift of Engelhard Minerals and Chemicals Co., supplied through the courtesy of Dr. Carl D. Keith. Palladium(II) chloride and potassium tetrachloropalladate(II) were obtained from Ventron Corp. The organic ligands were prepared by Dr. J. J. Lanzillo (19) and were recrystallized before use.

***N,S*-(2-Aminoethanethio)chloroaquoplatinum(II)** — 2-Aminoethanethiosulfuric acid (0.1572 g, 0.001 mole) was dissolved in 25 ml of water, and the pH was adjusted to 7.4 with 0.01 *N* NaOH. An aqueous solution (10 ml) of potassium tetrachloroplatinate(II) (0.4151 g, 0.001 mole) was added dropwise with stirring along with sufficient alkali to maintain a pH of 7.0–7.4. Stirring was continued for 1 hr after the addition; the yellow product was filtered, washed with water, and dried at 70° overnight, yielding 0.2742 g (66%), mp 340° dec.

Anal.—Calc. for $C_2H_8ClNOPtS \cdot H_2O$: C, 6.99; H, 2.93; Cl, 10.34; N, 4.07; S, 9.35. Found: C, 6.76; H, 2.46; Cl, 9.89; N, 3.80; S, 9.02.

Chloro-*N,N',S*-(cystamine)platinum(II) Chloride—Cystamine dihydrochloride (0.225 g, 0.001 mole) was dissolved in 35 ml of water, and the pH was adjusted to 7.4 with 0.01 *N* NaOH. A solution of 0.4151 g (0.001 mole) of potassium tetrachloroplatinate(II) in 10 ml of water was added dropwise with stirring, and stirring was continued for 2 hr after the addition. The yellow product was filtered, washed with water, and dried at 70° overnight. The yield was 0.42 g (52.6%) of material, which decomposed above 183°.

Anal.—Calc. for $C_4H_{12}Cl_2N_2PtS_2 \cdot 8H_2O$: C, 8.54; H, 4.98; N, 4.97; S, 11.41. Found: C, 8.70; H, 4.65; N, 4.73; S, 10.97.

REFERENCES

(1) B. Rosenberg, L. Van Camp, J. E. Trosko, and V. H. Mansour, *Nature*, **222**, 385 (1969).

(2) M. J. Cleare and J. D. Hoeschele, *Bioinorg. Chem.*, **2**, 187 (1973).

(3) B. Rosenberg, L. Van Camp, and T. Krigas, *Nature*, **205**, 698 (1965).

(4) M. J. Cleare and J. D. Hoeschele, *Platinum Met. Rev.*, **17**, 2 (1973).

(5) L. F. Lindoy, S. E. Livingstone, and T. N. Lockyer, *Aust. J. Chem.*, **20**, 471 (1967).

(6) F. Basolo, "Mechanisms of Inorganic Reactions," American Chemical Society, Washington, D.C., 1965.

(7) B. Rosenberg, *Cancer Chemother. Rep.*, **59**, 589 (1975).

(8) D. L. Klayman and R. J. Shine, *Qt. Rep. Sulfur Chem.*, **3**, 231 (1968).

(9) W. O. Foye and J. Mickles, *J. Pharm. Sci.*, **53**, 1030 (1964).

(10) S. E. Livingstone and J. D. Nolan, *Inorg. Chem.*, **7**, 1447 (1968).

(11) C. A. McAuliffe, *J. Chem. Soc.*, **1967**, 641.

(12) T. A. Connors, M. Jones, W. J. C. Ross, P. D. Braddock, A. R. Kokhar, and M. L. Tobe, *Chem.-Biol. Interact.*, **5**, 415 (1972).

(13) R. Layton, D. W. Sink, and J. R. Durig, *J. Inorg. Nucl. Chem.*, **28**, 1965 (1966).

(14) D. C. Jicha and D. H. Busch, *Inorg. Chem.*, **1**, 872 (1962).

(15) R. I. Geran, N. H. Greenberg, M. M. MacDonald, A. M. Schumacher, and B. J. Abbott, *Cancer Chemother. Rep., Part 3*, **3**, 1 (1972).

(16) J. E. Huheey, "Inorganic Chemistry: Principles of Structure and Reactivity," Harper and Row, New York, N.Y., 1972.

(17) S. Mansy, B. Rosenberg, and A. J. Thomson, *J. Am. Chem. Soc.*, **95**, 1633 (1973).

(18) T. A. Connors and J. J. Roberts, "Platinum Coordination Complexes in Cancer Chemotherapy," Springer Verlag, Berlin, Germany, 1974, p. 79.

(19) W. O. Foye, J. J. Lanzillo, Y. H. Lowe, and J. M. Kauffman, *J. Pharm. Sci.*, **64**, 211 (1975).

ACKNOWLEDGMENTS

Abstracted from a thesis submitted by V. Kaewchansilp to the Massachusetts College of Pharmacy in partial fulfillment of the Master of Science degree requirements.

Supported by funds from the John R. and Marie K. Sawyer Memorial Fund, Massachusetts College of Pharmacy.

Ion-Pair Liquid Chromatographic Assay of Decongestants and Antihistamines

THEODORE R. KOZIOL, JAMES T. JACOB, and RAJA G. ACHARI ˣ

Received February 5, 1979, from *Cooper Laboratories, Inc., Cedar Knolls, NJ 07927.* Accepted for publication March 21, 1979.

Abstract □ The quantitative determinations of combinations of antihistamine and decongestant drugs including phenylephrine, *dl*-ephedrine, ψ-ephedrine, phenylpropanolamine, pyrilamine, pheniramine, *l*-ephedrine, chlorpheniramine, brompheniramine, oxymetazoline, naphazoline, and antazoline contained in solid and liquid dosage forms are described. All active ingredients except the ephedrine optical isomers were separated from other ingredients with ion-paired high-pressure liquid chromatography. Manipulation of the mobile phase either by changing the hydroalcoholic ratio or by changing the alkyl chain length of the counterion (sulfonic acid) for achieving optimum separations is discussed. The method is simple, short, accurate, and precise.

Keyphrases □ Decongestants—analysis, ion-pair liquid chromatography, various cough and cold preparations, structure–activity relationships □ Antihistaminics—analysis, ion-pair liquid chromatography, various cough and cold preparations, structure–activity relationships □ Liquid chromatography, ion-pair—analysis, decongestants and antihistaminics in various cough and cold preparations, structure–activity relationships □ Structure–activity relationships—decongestants and antihistaminics, various cough and cold preparations

Combinations of decongestant and antihistamine pharmaceutical preparations are widely used for cough and cold treatment. Generally, such preparations contain one decongestant and one antihistamine, but several contain more than one decongestant. These combination preparations are made in various forms, *e.g.*, syrup, elixir, tablet, capsule, and timed-release tablet or capsule. Some liquid formulations may also contain preservative(s), dye(s), or flavor(s).

High-performance liquid chromatography (HPLC) has become useful for pharmaceutical preparation analysis. Decongestant and antihistamine compounds were analyzed using a strong cation-exchange column (1), and the separation of two decongestants and one antihistamine was demonstrated using a nonpolar reversed-phase column and heptanesulfonic acid as an ion-pairing agent (2, 3). This report describes a comprehensive analytical procedure applicable to numerous decongestants and antihistamines and discusses ways to achieve a desired separation by changing the alkyl chain length of sulfonic acid or by altering the hydroalcoholic composition of the mobile phase.

EXPERIMENTAL

Chemicals and Reagents—The following drugs and preservatives were used: phenylephrine (I), *dl*-ephedrine (II), ψ-ephedrine (III), phenylpropanolamine (IV), pyrilamine (V), pheniramine (VI), *l*-ephedrine (VII), chlorpheniramine (VIII), brompheniramine (IX), diphenhydra-

0022-3549/79/0900-1135$01.00/0

© 1979, American Pharmaceutical Association

***N,S*-(2-Aminoethanethio)chloroaquoplatinum(II)** — 2-Aminoethanethiosulfuric acid (0.1572 g, 0.001 mole) was dissolved in 25 ml of water, and the pH was adjusted to 7.4 with 0.01 *N* NaOH. An aqueous solution (10 ml) of potassium tetrachloroplatinate(II) (0.4151 g, 0.001 mole) was added dropwise with stirring along with sufficient alkali to maintain a pH of 7.0–7.4. Stirring was continued for 1 hr after the addition; the yellow product was filtered, washed with water, and dried at 70° overnight, yielding 0.2742 g (66%), mp 340° dec.

Anal.—Calc. for $C_2H_8ClNOPtS \cdot H_2O$: C, 6.99; H, 2.93; Cl, 10.34; N, 4.07; S, 9.35. Found: C, 6.76; H, 2.46; Cl, 9.89; N, 3.80; S, 9.02.

Chloro-*N,N',S*-(cystamine)platinum(II) Chloride—Cystamine dihydrochloride (0.225 g, 0.001 mole) was dissolved in 35 ml of water, and the pH was adjusted to 7.4 with 0.01 *N* NaOH. A solution of 0.4151 g (0.001 mole) of potassium tetrachloroplatinate(II) in 10 ml of water was added dropwise with stirring, and stirring was continued for 2 hr after the addition. The yellow product was filtered, washed with water, and dried at 70° overnight. The yield was 0.42 g (52.6%) of material, which decomposed above 183°.

Anal.—Calc. for $C_4H_{12}Cl_2N_2PtS_2 \cdot 8H_2O$: C, 8.54; H, 4.98; N, 4.97; S, 11.41. Found: C, 8.70; H, 4.65; N, 4.73; S, 10.97.

REFERENCES

(1) B. Rosenberg, L. Van Camp, J. E. Trosko, and V. H. Mansour, *Nature*, **222**, 385 (1969).

(2) M. J. Cleare and J. D. Hoeschele, *Bioinorg. Chem.*, **2**, 187 (1973).

(3) B. Rosenberg, L. Van Camp, and T. Krigas, *Nature*, **205**, 698 (1965).

(4) M. J. Cleare and J. D. Hoeschele, *Platinum Met. Rev.*, **17**, 2 (1973).

(5) L. F. Lindoy, S. E. Livingstone, and T. N. Lockyer, *Aust. J. Chem.*, **20**, 471 (1967).

(6) F. Basolo, "Mechanisms of Inorganic Reactions," American Chemical Society, Washington, D.C., 1965.

(7) B. Rosenberg, *Cancer Chemother. Rep.*, **59**, 589 (1975).

(8) D. L. Klayman and R. J. Shine, *Qt. Rep. Sulfur Chem.*, **3**, 231 (1968).

(9) W. O. Foye and J. Mickles, *J. Pharm. Sci.*, **53**, 1030 (1964).

(10) S. E. Livingstone and J. D. Nolan, *Inorg. Chem.*, **7**, 1447 (1968).

(11) C. A. McAuliffe, *J. Chem. Soc.*, **1967**, 641.

(12) T. A. Connors, M. Jones, W. J. C. Ross, P. D. Braddock, A. R. Kokhar, and M. L. Tobe, *Chem.-Biol. Interact.*, **5**, 415 (1972).

(13) R. Layton, D. W. Sink, and J. R. Durig, *J. Inorg. Nucl. Chem.*, **28**, 1965 (1966).

(14) D. C. Jicha and D. H. Busch, *Inorg. Chem.*, **1**, 872 (1962).

(15) R. I. Geran, N. H. Greenberg, M. M. MacDonald, A. M. Schumacher, and B. J. Abbott, *Cancer Chemother. Rep., Part 3*, **3**, 1 (1972).

(16) J. E. Huheey, "Inorganic Chemistry: Principles of Structure and Reactivity," Harper and Row, New York, N.Y., 1972.

(17) S. Mansy, B. Rosenberg, and A. J. Thomson, *J. Am. Chem. Soc.*, **95**, 1633 (1973).

(18) T. A. Connors and J. J. Roberts, "Platinum Coordination Complexes in Cancer Chemotherapy," Springer Verlag, Berlin, Germany, 1974, p. 79.

(19) W. O. Foye, J. J. Lanzillo, Y. H. Lowe, and J. M. Kauffman, *J. Pharm. Sci.*, **64**, 211 (1975).

ACKNOWLEDGMENTS

Abstracted from a thesis submitted by V. Kaewchansilp to the Massachusetts College of Pharmacy in partial fulfillment of the Master of Science degree requirements.

Supported by funds from the John R. and Marie K. Sawyer Memorial Fund, Massachusetts College of Pharmacy.

Ion-Pair Liquid Chromatographic Assay of Decongestants and Antihistamines

THEODORE R. KOZIOL, JAMES T. JACOB, and RAJA G. ACHARI ˣ

Received February 5, 1979, from *Cooper Laboratories, Inc., Cedar Knolls, NJ 07927.* Accepted for publication March 21, 1979.

Abstract □ The quantitative determinations of combinations of antihistamine and decongestant drugs including phenylephrine, *dl*-ephedrine, ψ-ephedrine, phenylpropanolamine, pyrilamine, pheniramine, *l*-ephedrine, chlorpheniramine, brompheniramine, oxymetazoline, naphazoline, and antazoline contained in solid and liquid dosage forms are described. All active ingredients except the ephedrine optical isomers were separated from other ingredients with ion-paired high-pressure liquid chromatography. Manipulation of the mobile phase either by changing the hydroalcoholic ratio or by changing the alkyl chain length of the counterion (sulfonic acid) for achieving optimum separations is discussed. The method is simple, short, accurate, and precise.

Keyphrases □ Decongestants—analysis, ion-pair liquid chromatography, various cough and cold preparations, structure–activity relationships □ Antihistaminics—analysis, ion-pair liquid chromatography, various cough and cold preparations, structure–activity relationships □ Liquid chromatography, ion-pair—analysis, decongestants and antihistaminics in various cough and cold preparations, structure–activity relationships □ Structure–activity relationships—decongestants and antihistaminics, various cough and cold preparations

Combinations of decongestant and antihistamine pharmaceutical preparations are widely used for cough and cold treatment. Generally, such preparations contain one decongestant and one antihistamine, but several contain more than one decongestant. These combination preparations are made in various forms, *e.g.*, syrup, elixir, tablet, capsule, and timed-release tablet or capsule. Some liquid formulations may also contain preservative(s), dye(s), or flavor(s).

High-performance liquid chromatography (HPLC) has become useful for pharmaceutical preparation analysis. Decongestant and antihistamine compounds were analyzed using a strong cation-exchange column (1), and the separation of two decongestants and one antihistamine was demonstrated using a nonpolar reversed-phase column and heptanesulfonic acid as an ion-pairing agent (2, 3). This report describes a comprehensive analytical procedure applicable to numerous decongestants and antihistamines and discusses ways to achieve a desired separation by changing the alkyl chain length of sulfonic acid or by altering the hydroalcoholic composition of the mobile phase.

EXPERIMENTAL

Chemicals and Reagents—The following drugs and preservatives were used: phenylephrine (I), *dl*-ephedrine (II), ψ-ephedrine (III), phenylpropanolamine (IV), pyrilamine (V), pheniramine (VI), *l*-ephedrine (VII), chlorpheniramine (VIII), brompheniramine (IX), diphenhydra-

0022-3549/79/0900-1135$01.00/0

© 1979, American Pharmaceutical Association

Table I—Detection Limit and Linear Detection Range at 254 nm of Various Drugs Tested

Drug	Minimum[a] Detection Limit, ng	Linear[a] Detection Range	Correlation Coefficient
Phenylephrine hydrochloride	40	40 ng–100 μg	0.9759
Ephedrine	60	60 ng–60 μg	0.9990
Phenylpropanolamine hydrochloride	140	140 ng–8 μg	0.9976
Pyrilamine maleate	18	18 ng–40 μg	0.9849
Pheniramine maleate	20	20 ng–50 μg	0.9991
Guaifenesin	40	40 ng–100 μg	0.9990
Pseudoephedrine hydrochloride	80	80 ng–60 μg	0.9972
Chlorpheniramine maleate	14	14 ng–20 μg	0.9996
Brompheniramine maleate	20	20 ng–20 μg	0.9949
Antazoline phosphate	18	18 ng–10 μg	0.9910
Naphazoline hydrochloride	24	24 ng–20 μg	0.9964
Oxymetazoline hydrochloride	280	280 ng–30 μg	0.9930

[a] Amount injected.

mine (X), guaifenesin (XI), caffeine (XII), aspirin (XIII), oxymetazoline (XIV), naphazoline (XV), antazoline (XVI), methylparaben (XVII), and propylparaben (XVIII). All were USP or NF quality and were used without further purification.

All sulfonic acids were received as their sodium salts except methanesulfonic acid, which was received as a free acid. All reagents were used as received[1]. The chromatographic solvents were distilled-in-glass quality[2].

Chromatography—The modular liquid chromatograph consisted of a constant flow pump of 6000 psi maximum operating pressure[3], a variable wavelength detector set at 254 nm[4], and a constant volume loop injector[5]. The chromatograms were recorded using a strip-chart recorder[6]. The column (moderately polar phenyl bonded) was purchased commercially[7].

Mobile Phase—The mobile phase was water–methanol–glacial acetic acid (55:44:1 v/v) containing enough heptanesulfonic acid sodium salt to yield a 0.005 *M* solution. The flow rate was 2.0 ml/min.

Sample Preparation—*Diluent*—The diluent was methanol–water (1:1 v/v).

Elixirs and Syrups—Three elixirs and two syrups were analyzed. Ten milliliters of elixir or syrup were diluted with the diluent to 50 ml in a volumetric flask.

Table II—Retention Data of Various Antihistamine and Sympathomimetic Drugs and Related Compounds

Drug	k'[a]	Tailing Factor[b]
Phenylephrine	1.2	100
dl-Ephedrine	2.2	100
Phenylpropanolamine	1.9	96
Pyrilamine	8.8	86
Pheniramine	4.4	91
l-Ephedrine	2.2	100
Guaifenesin	1.4	100
ψ-Ephedrine	2.2	100
Chlorpheniramine	8.8	86
Brompheniramine	10.5	86
Oxymetazoline	9.8	63
Naphazoline	4.6	90
Antazoline	11.0	73
Diphenhydramine	8.6	43
Methylparaben	2.2	100
Propylparaben	5.0	91
Caffeine	1.4	100
Aspirin	2.2	100

[a] k' is the capacity factor calculated as $(V_R - V_0)/V_0$, where V_R is the apparent retention volume and V_0 is the dead volume of the column. [b] Calculated by drawing a perpendicular line from the baseline to the peak maximum and then measuring the base width of the second half (y) of the chromatographic peak relative to the first half (x). Measurements were made at 10% of the peak maximum. Tailing factor = $x/y \times 100$.

[1] Eastman Kodak Co., Rochester, N.Y.
[2] Burdick & Jackson, Muskegon, Mich.
[3] Waters Associates, Milford, Mass.
[4] Schoeffel Instruments Corp., Westwood, N.J.
[5] Valco Instruments, Houston, Tex.
[6] Model 56, Perkin-Elmer.
[7] μBondapak phenyl (4 mm i.d. × 30 cm), Waters Associates, Milford, Mass.

Tablets—Four tablet preparations were assayed. Ten tablets were ground to a fine powder, and the powder equivalent to one tablet weight was transferred into a 50-ml volumetric flask. Approximately 30 ml of the diluent was added, and the flask was shaken for 15 min. The solution was diluted to volume with the diluent, and ~10 ml of this solution was filtered through a 0.45-μm filter for chromatographic analysis.

Timed-Release Capsules or Tablets—Three dosage forms were analyzed. The contents equivalent to one capsule or tablet were transferred to a 100-ml volumetric flask, and 10 ml of 1.0 *N* HCl was added. The flask was shaken for 15 min. Approximately 50 ml of diluent was added, and the flask was shaken for another 15 min. The solution was diluted to volume with the diluent, and ~10 ml was filtered through a 0.45-μm filter.

Quantitation—Standard curves for the appropriate compounds were established. A 20-μl sample was injected, and the peak response was measured (as peak height). The drug concentration was measured either directly from the standard curve or by regression analysis. The amount of drug present in the dosage form was calculated by:

$$\% \text{ label claim} = (C)(D)\left(\frac{100}{L}\right) \qquad \text{(Eq. 1)}$$

where C is the concentration of the sample (milligrams per milliliter) read from the standard curve, D is the total dilution (milliliters), and L is the label amount of drug in the dosage form (milligrams).

RESULTS AND DISCUSSION

All compounds previously mentioned were tested for linear detection range and minimum detection limit. The data were obtained using six to 10 calibration points (Table I).

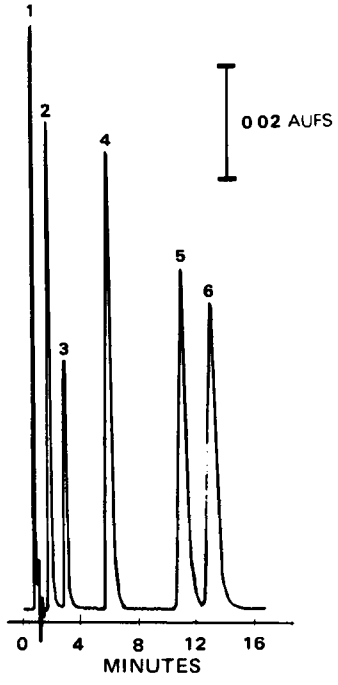

Figure 1—*Chromatogram of five common cough and cold drugs. Key: 1, maleic acid; 2, phenylephrine; 3, pseudoephedrine; 4, naphazoline; 5, chlorpheniramine; and 6, brompheniramine.*

Table III—Regression Analysis of the Relationship between Retention Volume and the Hydroalcoholic Composition of the Mobile Phase

Compound	Correlation Coefficient	Slope	Intercept
Chlorpheniramine	0.974	-6.7×10^{-3}	4.3×10^{-1}
Pheniramine	0.995	-7.1×10^{-3}	4.9×10^{-1}
ψ-Ephedrine	0.998	-6.7×10^{-3}	5.3×10^{-1}
Phenylephrine	0.997	-5.4×10^{-3}	5.3×10^{-1}

Table IV—Liquid Pharmaceutical Preparations Analyzed

Active Ingredient	Label, mg/5 ml	Assay, mg/5 ml
Elixir A[a]		
Pseudoephedrine hydrochloride	30.0	30.1
Chlorpheniramine maleate	2.0	2.0
Syrup B[b]		
Phenylpropanolamine hydrochloride	20.0	18.7
Phenylephrine hydrochloride	5.0	4.72
Phenyltoloxamine citrate[c]	7.5	—
Chlorpheniramine maleate	2.5	2.48
Syrup C		
Phenylephrine hydrochloride	2.5	1.9
Chlorpheniramine maleate	1.0	0.96
Elixir D[d]		
Brompheniramine maleate	4.0	4.2
Phenylephrine hydrochloride	5.0	5.3
Phenylpropanolamine hydrochloride	5.0	4.85
Elixir E[e]		
Phenylephrine hydrochloride	5.0	5.0
Chlorpheniramine maleate	1.0	1.0
Chloroform	13.5	—

[a] Deconamine elixir, Cooper Laboratories. [b] Naldecon syrup, Bristol Laboratories. [c] Could not be analyzed due to lack of reference standard. [d] Dimetapp elixir, A. H. Robins. [e] Novahistine elixir, Dow.

The chromatographic separation of five common drugs used for cough and cold treatment is shown in Fig. 1, and the chromatographic retention data are listed in Table II. The phenyl column, of moderate polarity, is capable of resolving almost all of the compounds listed except the stereoisomers such as *l*-ephedrine and *d*-ephedrine. A nonpolar hydrocarbon-bonded column[8] (C_{18} bonded) did not produce satisfactory results. For example, chlorpheniramine showed unacceptable peak tailing, and pyrilamine and pheniramine could not be separated (2).

The retention of compounds can be varied to obtain a desired separation. Four compounds of decreasing polarity (phenylephrine, ψ-ephedrine, pheniramine, and chlorpheniramine) were studied to show how a slight modification of the mobile phase can allow almost any desired separation. Two relationships were studied: (*a*) change in the hydroalcoholic composition, and (*b*) change in the alkyl chain length of the counterion, *i.e.*, alkylsulfonic acid.

Figure 2 shows the effect of changing the water–methanol ratio on the retention volume. The retention volumes of all compounds increased with the increased water ratio in the mobile phase. A linear relationship for each drug was obtained by plotting percent water in the mobile phase *versus* V_R^{-1}. This result is due to a decrease in the solubility (hydrophobicity) of the solute molecule in the mobile phase. The regression analyses of the data points are given in Table III.

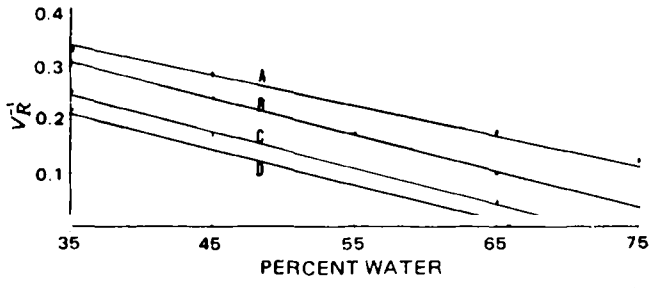

Figure 2—*Relationship between hydroalcoholic composition of mobile phase and drug retention volume. Key: A, θ, chlorpheniramine; B, O, pheniramine; C, ×, pseudoephedrine; and D, ■, phenylephrine.*

[8] μBondapak-C_{18}, Waters Associates, Milford, Mass.

Table V—Solid Dosage Forms Analyzed

Active Ingredient	Label, mg	Assay, mg
Tablet A[a]		
Pseudoephedrine hydrochloride	60.0	60.5
Chlorpheniramine maleate	4.0	4.02
Tablet B[b]		
Dexbrompheniramine maleate	2.0	2.01
d-Isoephedrine maleate	60.0	60.3
Tablet C[c]		
Phenylephrine hydrochloride	10.0	9.24
Chlorpheniramine maleate	2.0	1.85
Tablet D[d]		
Phenylpropanolamine hydrochloride	50.0	50.2
Phenindamine tartrate[e]	24.0	—
Chlorpheniramine maleate	4.0	4.15

[a] Deconamine tablets, Cooper Laboratories. [b] Disophrol tablets, Schering. [c] Novahistine Fortis, Dow. [d] Nolamine tablets, Carnrick. [e] Could not be analyzed due to lack of reference standard.

The effect on drug retention of changing the alkyl chain length of the counterion (sulfonic acid) in the mobile phase is shown in Fig. 3. The plot of the carbon number of the alkyl chain *versus* $\log_e$ retention volume shows a linear relationship for pheniramine and chlorpheniramine, but the plot for ψ-ephedrine and phenylephrine is dual sloped. This result is due to the fact that with pheniramine and chlorpheniramine, the increase in the carbon chain length of the counterion decreases the polarity of the "ion-paired" molecule as a whole, causing a linear increase in the retention volume in the reversed-phase system. However, there is very little change in polarity for ψ-ephedrine and phenylephrine when the counterion is methane through butanesulfonic acid. A linear increase in the retention is noticed ($\log_e V_R$ *versus* carbon number of the alkyl chain of the counterion) from pentane to octanesulfonic acid.

Thus, the point from which a change in polarity is noticed could be called the "polarity threshold" of each compound. Varying the carbon chain length of the counterion below the polarity threshold causes no significant variation of retention volumes. The concept of polarity threshold can be exploited to manipulate drug analyses, as shown by the following example.

A dosage form containing ψ-ephedrine and chlorpheniramine was analyzed using the solvent system described in the *Experimental* section. When heptanesulfonic acid was replaced by pentanesulfonic acid as the counterion, the retention volumes of both ψ-ephedrine and chlorpheniramine were reduced from 6.0 and 20.4 ml to 3.9 and 11.9 ml, respectively. Further replacement of pentanesulfonic acid by butanesulfonic acid selectively reduced the chlorpheniramine retention to 9.6 ml without affecting the ψ-ephedrine retention (3.8 ml) because of the polarity threshold.

Change of the alkyl chain of sulfonic acid also can be of advantage when the dosage form contains acidic molecules such as parabens or aspirin, which do not ion-pair with sulfonic acid. Naphazoline and propylparaben had a very similar k' (Table II) and could not be separated from each

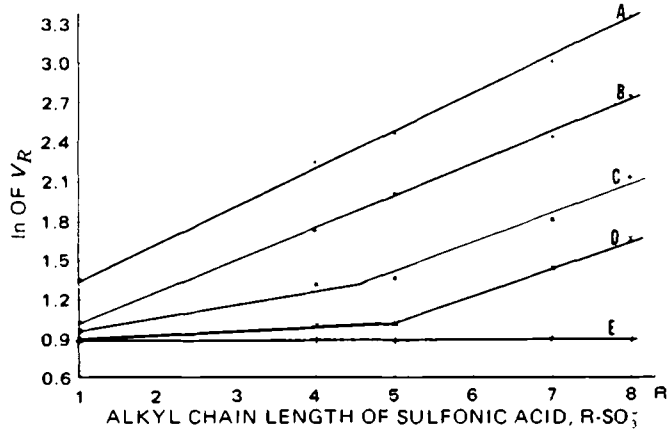

Figure 3—*Relationship between alkyl chain length of the counterion and drug retention volume. Key: A, ■, chlorpheniramine; B, O, pheniramine; C, *, pseudoephedrine; D, ×, phenylephrine; and E, +, maleate.*

Table VI—Timed-Release Dosage Forms Analyzed

Active Ingredient	Label, mg	Assay, mg
Capsule A[a]		
Pseudoephedrine hydrochloride	120.0	118.8
Chlorpheniramine maleate	8.0	7.8
Timed-Release Tablet B[b]		
Phenylpropanolamine hydrochloride	40.0	44.0
Phenylephrine hydrochloride	10.0	10.7
Chlorpheniramine maleate	5.0	4.8
Phenyltoloxamine citrate[c]	15.0	—
Capsule C[d]		
Chlorpheniramine maleate	8.0	7.43
Phenylephrine hydrochloride	15.0	20.4
Methscopolamine[c]	2.5	—

[a] Deconamine capsules, Cooper Laboratories. [b] Naldecon timed-release tablets, Bristol. [c] Could not be analyzed due to lack of reference standard. [d] Cosea-D capsules, Center.

other. By changing the counterion from heptanesulfonic acid to pentanesulfonic acid, the naphazoline retention was reduced without affecting the propylparaben retention, and a complete resolution of these compounds was possible.

To ensure the specificity of the proposed method, all drugs were artificially degraded. All drugs were well separated from their degradation products. Twelve pharmaceutical preparations were analyzed by this method. The versatility of the method was demonstrated by the analysis of various combination preparations (Tables IV–VI). The reproducibility of the method was excellent. Five replicate analyses of Liquid Preparation I (Table IV) had a coefficient of variation of 0.9%. The variation coefficients of five replicate analyses of two solid dosage forms (Preparation I, Table V; and Preparation I, Table VI) were 1.4 and 1.9%, respectively.

The proposed method is useful for assaying of cough and cold drugs. The method is simple, requires no elaborate sample preparation techniques, and is specific, accurate, and reproducible. Many separations can be achieved by proper manipulation of the mobile phase.

REFERENCES

(1) T. L. Sprieck, *J. Pharm. Sci.*, **63**, 591 (1974).
(2) V. D. Gupta and A. G. Ghanekar, *ibid.*, **66**, 895 (1977).
(3) A. Yacobi, Z. M. Look, and C.-M. Lai, *ibid.*, **67**, 1668 (1978).

ACKNOWLEDGMENTS

Presented at the Federation of Analytical Chemistry and Spectroscopy Society, Boston meeting, October 30–November 3, 1978.

Specific and Sensitive High-Performance Liquid Chromatographic Determination of Glyburide

WADE J. ADAMS ˣ and D. SCOTT KRUEGER

Received December 18, 1978, from the *Pharmaceutical Research and Development and Control Research and Development Laboratories, The Upjohn Company, Kalamazoo, MI 49001.* Accepted for publication March 21, 1979.

Abstract □ A specific and sensitive high-performance liquid chromatographic method has been developed for the rapid determination of intact glyburide in dog serum. With butylparaben as an internal standard, 1 ml of acid-buffered serum was extracted with toluene and an aliquot of the toluene was evaporated to dryness. The redissolved residue was chromatographed on a microparticulate reversed-phase column, and quantitation was achieved by monitoring the UV absorbance of the eluate at 228 nm. The response was linear, and the lower detection limit was ~20 ng/ml. Assay precision, as estimated by analyzing replicate samples of a laboratory standard, was better than 6% (*CV*). The utility of the analytical methodology for the determination of this highly potent sulfonylurea in pharmacokinetic studies in the dog was demonstrated.

Keyphrases □ Glyburide—analysis, high-performance liquid chromatography, dog serum □ Antidiabetic agents—glyburide, high-performance liquid chromatographic analysis, dog serum □ High-performance liquid chromatography—analysis, glyburide in dog serum

Glyburide[1] (I), 1-[[4-[2-(5-chloro-2-methoxybenzamido)ethyl]phenyl]sulfonyl]-3-cyclohexylurea, is a potent, orally active sulfonylurea for the management of maturity-onset diabetes mellitus (1). A number of analytical methods for the determination of glyburide in serum have been reported. These methods include procedures based on UV spectrophotometry, colorimetry following reaction with 2,4-dinitrofluorobenzene, fluorometry (2), and competitive protein binding (3, 4). However, only a recently developed radioimmunoassay (4) is sufficiently sensitive for monitoring blood levels following administration of

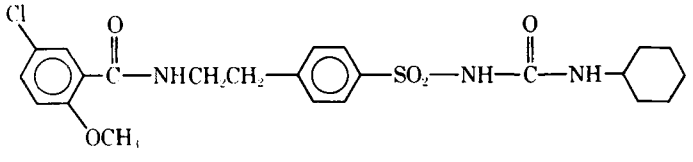

I

therapeutic doses (2.5–10 mg). Although this radioimmunoassay is highly sensitive, with the lower limit of detection being ~4 ng/ml of serum, the method lacks specificity because of cross-reactivity of the hydroxy metabolites of glyburide. In addition, it is necessary to prepare standard curves using pretreatment serum from each subject because the assay response is subject dependent (4).

GLC has been used extensively for the analysis of sulfonylureas in biological fluids (5–14). However, this technique requires a time-consuming derivatization step to form volatile, thermally stable derivatives unless on-column derivatization is employed with concomitant loss in reproducibility[2] (12). Furthermore, the technique frequently lacks specificity since the intact compound and its metabolites may form identical derivatives (14, 15). Finally, the high molecular weight and inherently low volatility of glyburide or its derivatives make GLC analysis difficult if not impossible.

[1] Micronase, The Upjohn Co., Kalamazoo, MI 49001.

[2] D. G. Kaiser, The Upjohn Co., Kalamazoo, MI 49001, personal communication.

0022-3549/79/0900-1138$01.00/0

© 1979, American Pharmaceutical Association

Table VI—Timed-Release Dosage Forms Analyzed

Active Ingredient	Label, mg	Assay, mg
Capsule A[a]		
Pseudoephedrine hydrochloride	120.0	118.8
Chlorpheniramine maleate	8.0	7.8
Timed-Release Tablet B[b]		
Phenylpropanolamine hydrochloride	40.0	44.0
Phenylephrine hydrochloride	10.0	10.7
Chlorpheniramine maleate	5.0	4.8
Phenyltoloxamine citrate[c]	15.0	—
Capsule C[d]		
Chlorpheniramine maleate	8.0	7.43
Phenylephrine hydrochloride	15.0	20.4
Methscopolamine[c]	2.5	—

[a] Deconamine capsules, Cooper Laboratories. [b] Naldecon timed-release tablets, Bristol. [c] Could not be analyzed due to lack of reference standard. [d] Cosea-D capsules, Center.

other. By changing the counterion from heptanesulfonic acid to pentanesulfonic acid, the naphazoline retention was reduced without affecting the propylparaben retention, and a complete resolution of these compounds was possible.

To ensure the specificity of the proposed method, all drugs were artificially degraded. All drugs were well separated from their degradation products. Twelve pharmaceutical preparations were analyzed by this method. The versatility of the method was demonstrated by the analysis of various combination preparations (Tables IV–VI). The reproducibility of the method was excellent. Five replicate analyses of Liquid Preparation I (Table IV) had a coefficient of variation of 0.9%. The variation coefficients of five replicate analyses of two solid dosage forms (Preparation I, Table V; and Preparation I, Table VI) were 1.4 and 1.9%, respectively.

The proposed method is useful for assaying of cough and cold drugs. The method is simple, requires no elaborate sample preparation techniques, and is specific, accurate, and reproducible. Many separations can be achieved by proper manipulation of the mobile phase.

REFERENCES

(1) T. L. Sprieck, *J. Pharm. Sci.*, **63**, 591 (1974).
(2) V. D. Gupta and A. G. Ghanekar, *ibid.*, **66**, 895 (1977).
(3) A. Yacobi, Z. M. Look, and C.-M. Lai, *ibid.*, **67**, 1668 (1978).

ACKNOWLEDGMENTS

Presented at the Federation of Analytical Chemistry and Spectroscopy Society, Boston meeting, October 30–November 3, 1978.

Specific and Sensitive High-Performance Liquid Chromatographic Determination of Glyburide

WADE J. ADAMS ˣ and D. SCOTT KRUEGER

Received December 18, 1978, from the *Pharmaceutical Research and Development and Control Research and Development Laboratories, The Upjohn Company, Kalamazoo, MI 49001.* Accepted for publication March 21, 1979.

Abstract □ A specific and sensitive high-performance liquid chromatographic method has been developed for the rapid determination of intact glyburide in dog serum. With butylparaben as an internal standard, 1 ml of acid-buffered serum was extracted with toluene and an aliquot of the toluene was evaporated to dryness. The redissolved residue was chromatographed on a microparticulate reversed-phase column, and quantitation was achieved by monitoring the UV absorbance of the eluate at 228 nm. The response was linear, and the lower detection limit was ~20 ng/ml. Assay precision, as estimated by analyzing replicate samples of a laboratory standard, was better than 6% (*CV*). The utility of the analytical methodology for the determination of this highly potent sulfonylurea in pharmacokinetic studies in the dog was demonstrated.

Keyphrases □ Glyburide—analysis, high-performance liquid chromatography, dog serum □ Antidiabetic agents—glyburide, high-performance liquid chromatographic analysis, dog serum □ High-performance liquid chromatography—analysis, glyburide in dog serum

Glyburide[1] (I), 1-[[4-[2-(5-chloro-2-methoxybenzamido)ethyl]phenyl]sulfonyl]-3-cyclohexylurea, is a potent, orally active sulfonylurea for the management of maturity-onset diabetes mellitus (1). A number of analytical methods for the determination of glyburide in serum have been reported. These methods include procedures based on UV spectrophotometry, colorimetry following reaction with 2,4-dinitrofluorobenzene, fluorometry (2), and competitive protein binding (3, 4). However, only a recently developed radioimmunoassay (4) is sufficiently sensitive for monitoring blood levels following administration of

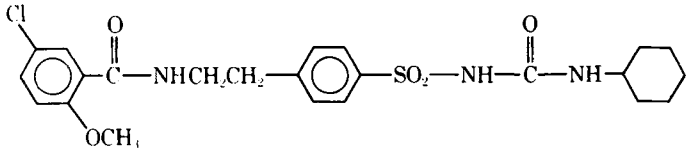

I

therapeutic doses (2.5–10 mg). Although this radioimmunoassay is highly sensitive, with the lower limit of detection being ~4 ng/ml of serum, the method lacks specificity because of cross-reactivity of the hydroxy metabolites of glyburide. In addition, it is necessary to prepare standard curves using pretreatment serum from each subject because the assay response is subject dependent (4).

GLC has been used extensively for the analysis of sulfonylureas in biological fluids (5–14). However, this technique requires a time-consuming derivatization step to form volatile, thermally stable derivatives unless on-column derivatization is employed with concomitant loss in reproducibility[2] (12). Furthermore, the technique frequently lacks specificity since the intact compound and its metabolites may form identical derivatives (14, 15). Finally, the high molecular weight and inherently low volatility of glyburide or its derivatives make GLC analysis difficult if not impossible.

[1] Micronase, The Upjohn Co., Kalamazoo, MI 49001.

[2] D. G. Kaiser, The Upjohn Co., Kalamazoo, MI 49001, personal communication.

0022-3549/79/0900-1138$01.00/0

© 1979, American Pharmaceutical Association

The utility of high-performance liquid chromatography (HPLC) for the determination of sulfonylureas in plasma and serum was demonstrated recently[3] (15–19), with quantitation of concentrations as low as 200 ng/ml (19). HPLC with UV detection represents a particularly sensitive technique for the determination of glyburide because of its high molar extinction coefficient at 228 nm (2). The present report describes a rapid, specific, and sensitive HPLC method for the determination of glyburide in dog serum.

EXPERIMENTAL

Reagents—Acetonitrile[4], toluene[4], monobasic ammonium phosphate[5], monobasic sodium phosphate[6], and butylparaben[7] were used as received. The inorganic reagents were prepared in distilled, deionized water. Glyburide[8] and synthetic samples of the major metabolites of glyburide in the dog (2), 3-*cis*-[1-[[4-[2-(2-methoxy-5-chlorobenzamido)ethyl]-phenyl]sulfonyl]ureido]cyclohexanol, 1-[[4-carboxyphenyl]sulfonyl]3-cyclohexylurea[9], and 2-methoxy-5-chlorobenzamide[8], were used without further purification.

Standard Solutions—A stock solution containing 10 μg of glyburide/ml was prepared by dissolving an accurately weighed sample of the reference standard material in 40 ml of acetonitrile containing 0.2 ml of blank dog serum and diluting to 100 ml with toluene. Appropriate dilutions were made with toluene to obtain calibration curve standards containing 1500, 1200, 900, 600, 300, 150, 75, and 37.5 ng of glyburide/ml. These solutions were stable for at least 2 months when stored at −15°.

A stock solution containing 300 μg of butylparaben/ml was prepared by dissolving an appropriate quantity of the compound in toluene. Two milliliters of the stock solution was diluted to 1 liter with toluene to provide a working internal standard solution containing 600 ng of butylparaben/ml.

Calibration Curves—Calibration curves were prepared each day samples were analyzed to establish the linearity and reproducibility of the assay. The calibration curve standards were prepared by adding 1-ml aliquots of the appropriate glyburide standards to 16 × 125-mm screw-capped culture tubes fitted with aluminum-lined caps[10] and containing 1 ml of blank serum. These standards were analyzed along with the samples.

Sample Analysis—One-milliliter aliquots of serum were added to 16 × 125-mm culture tubes fitted with aluminum-lined caps along with 1 ml of toluene. After 1 ml of working internal standard was added to all samples, including the calibration curve standards, 1 ml of 2.55 *M* NaH_2PO_4 and 8 ml of toluene were added. The samples were then extracted at 280 cpm on a two-speed reciprocating shaker[11] for 30 min. Following separation of the phases by centrifugation for 15 min at 1800 rpm, 8-ml aliquots of the organic phase were transferred to clean 16 × 125-mm culture tubes and evaporated to dryness at 40° using a gentle dry nitrogen stream[12].

The residues were redissolved in 300–600 μl of chromatographic mobile phase and thoroughly mixed on a high-speed vortex mixer[13], and 250-μl aliquots were chromatographed.

Chromatographic Analysis—The samples were chromatographed on a commercially prepared reversed-phase column[14] (25 cm × 4.6 mm) packed with 5-μm LiChrosorb RP-8[15] using a constant flow liquid chromatograph[16], a loop injection valve[17], and a variable-wavelength UV detector[18]. Separation of glyburide and the internal standard from coextracted endogenous components in the serum was accomplished using a mobile phase composed of 0.05 *M* $NH_4H_2PO_4$–acetonitrile (1:1 v/v) at a 1.2-ml/min flow rate (~1000 psig). The UV absorbance of the column eluate was monitored at 228 nm.

Under these chromatographic conditions, the internal standard and glyburide retention times were ~7.6 and 9.8 min, respectively. Slight changes in retention times were produced by small variations in the solvent composition.

Quantitation—Peak height ratios were calculated by dividing the glyburide peak height by the internal standard peak height. Calibration curves were constructed by plotting the peak height ratios of calibration curve standards *versus* their concentrations, expressed in nanograms per milliliter of serum. The glyburide concentration was calculated from the peak height ratio using the slope and intercept obtained by linear regression analysis of the calibration curve data.

***In Vivo* Studies**—Six beagle dogs, 12.2–16.3 kg, were fasted for 16 hr prior to and 4 hr after oral treatment with a 2.5- or a 10.0-mg compressed glyburide tablet. Blood was collected using 10-ml vacutainers[19] at 0, 1, 2, 3, 4, 6, 8, 12, and 24 hr. The blood was allowed to clot (~30 min) and centrifuged at 1800 rpm for 20 min, and the collected serum was stored frozen (−15°) until analysis.

Table I—Glyburide Assay Precision

Trial	Glyburide, ng/ml		
	Within Day		Between Day
1	1036.0	999.0	924.0
2	1065.0	1001.0	985.0
3	1009.0	966.0	906.0
4			870.0
5			1002.0
Average	1037.0	989.0	937.0
CV, %	2.7	2.0	5.9

RESULTS AND DISCUSSION

The high molecular weight, low volatility, and large molar extinction coefficient of glyburide make HPLC the technique of choice for the analyses of the bulk drug, compressed tablets (20), and biological fluids. The simplicity of the cited methodology for glyburide determination in dog serum, coupled with its high specificity and sensitivity, provides a particularly suitable analytical method for pharmacokinetic studies and monitoring the bioavailability/bioequivalence of pharmaceutical formulations.

Chromatographic Analysis—During assay development, commercially prepared reversed-phase columns from a number of manufacturers and a variety of mobile phases were investigated before adoption of the

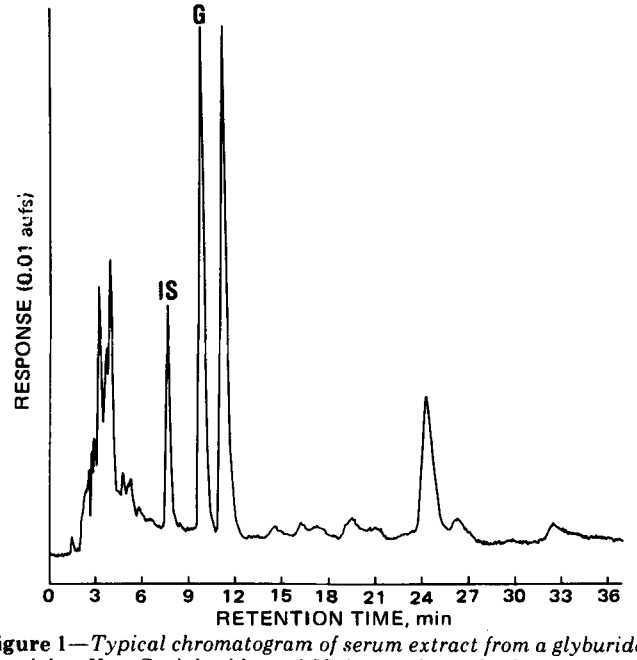

Figure 1—*Typical chromatogram of serum extract from a glyburide-dosed dog. Key: G, glyburide; and IS, internal standard.*

[3] Unpublished data.
[4] Burdick & Jackson Laboratories, Muskegon, Mich.
[5] Analytical reagent, J. T. Baker Chemical Co., Phillipsburg, N.J.
[6] Analytical reagent, Mallinckrodt, St. Louis, Mo.
[7] Eastman Kodak Co., Rochester, N.Y.
[8] Farbwerke Hoechst AG, Frankfurt, West Germany.
[9] The Upjohn Co., Kalamazoo, MI 49001.
[10] Brockway Glass Co., Parkersburg, W. Va.
[11] Eberbach and Sons, Ann Arbor, Mich.
[12] Organomation Associates, Shrewsburg, Mass.
[13] Lab-line Instruments, Melrose Park, Ill.
[14] Brownlee Labs RP-5A, Rheodyne, Inc., Berkeley, Calif.
[15] E. Merck, Darmstadt, West Germany.
[16] Model 100, Altex Scientific Inc., Berkeley, Calif.
[17] Model 70-10, Rheodyne, Inc., Berkeley, Calif.
[18] Altex/Hitachi model 155-40, Altex Scientific Inc., Berkeley, Calif.
[19] Fisher Scientific Co., Pittsburgh, Pa.

Table II—Selected Pharmacokinetic Parameters: Glyburide in Dogs

Dose, mg	Average Peak Serum Concentration, μg/ml	Average Half-Life, hr	*AUC*, (μg hr)[a]/ml
2.5	0.291	2.3	0.156
10.0	1.386	2.1	0.632

[a] Average area under the serum concentration–time curve, 0–24 hr.

described chromatographic conditions. Optimum chromatography was achieved using a reversed-phase column packed with 5-μm LiChrosorb RP-8 and a mobile phase of 0.05 *M* $NH_4H_2PO_4$–CH_3CN (1:1 v/v). A typical chromatogram of a serum extract is shown in Fig. 1. Baseline resolution of glyburide from the coextracted interference eluting at ~11.2 min was ordinarily achieved for all concentrations and animals studied. On occasion, a small interference having a retention time similar to that of glyburide (~10.5 min) was observed. Resolution of these peaks was nearly complete for low glyburide concentrations. Utilization of a precolumn[20] to protect the analytical column is recommended when large numbers of samples are analyzed.

Separation of glyburide from the major interference at ~11.2 min was sensitive to both the pH and percentage of acetonitrile in the mobile phase. Increasing the pH and/or the percentage of acetonitrile resulted in poorer resolution, or even coalescence, of these peaks. Above pH 6, the elution order was reversed.

Major glyburide metabolites in the dog (2), 3-*cis*-[1-[[4-[2-(2-methoxy-5- chlorobenzamido]ethyl]phenyl]sulfonyl]ureido]cyclohexanol, 1-[[4-carboxyphenyl]sulfonyl]-3-cyclohexylurea, and 2-methoxy-5-chlorobenzamide, elute prior to the internal standard and do not interfere. An additional proposed metabolite of glyburide in the dog is 1-[[4-[2-(2-methoxy-5-chlorobenzamido)ethylenyl]phenyl]sulfonyl] -3- cyclohexylurea (2). The structure of this metabolite has not yet been confirmed, and a synthetic sample was not available for chromatographic analysis. Evidence of its presence in dog serum following glyburide administration could not be found in chromatograms of serum extracts. The major metabolites of glyburide in humans (2) do not interfere.

Assay Recovery and Sensitivity—The absolute recovery of glyburide from serum containing 100, 400, 800, 1200, or 1600 ng/ml was determined by comparing the peak heights obtained when 250-μl aliquots of the redissolved serum residues and standards were chromatographed. No statistically significant differences in the recovery were found ($p = 0.38$), with the average recovery being 96 ± 5% (*SD*, $n = 19$).

Glyburide extraction from the acidified serum was essentially insensitive to the monobasic sodium phosphate buffer concentration; however, high ionic strength minimized the coextraction of endogenous components, which could potentially interfere. A small amount of serum was added to the stock standard glyburide solution because previous researchers (4) reported binding of glyburide to glass in the absence of serum. Preparation of glyburide in organic solvents, *e.g.*, acetonitrile, obviates the need for serum to prevent binding to glass. Comparable analytical results can be obtained by preparing glyburide standards in acetonitrile and evaporating the solvent under dry nitrogen prior to addition of control serum.

The lower glyburide detection limit was ~20 ng/ml of serum extracted. This concentration gave rise to a response equivalent to approximately three times the peak-to-peak noise level, or 2% of full-scale response at 0.01 absorbance unit full scale (aufs).

Assay Precision—Linear regression analyses of calibration curve data indicated no significant deviations from linearity for concentrations up to 1500 ng of glyburide/ml of serum. Coefficients of variation were better than 4.8% for all curves, with the average coefficient of variation being 2.8 ± 1.0% (*SD*) for standard curves run on 6 successive days.

The precision of the methodology was assessed further by analyzing replicate samples of a laboratory standard prepared by pooling serum collected from glyburide-dosed dogs. Triplicate samples were analyzed on 2 different days to establish within-day precision, and single samples were analyzed on 5 different days to establish between-day precision (Table I). Within-day coefficients of variation were comparable to the coefficients of variation of the standard curves. Not unexpectedly, the between-day coefficient of variation, 5.9%, was approximately equal to the standard deviation in the recovery of glyburide from serum, ±5%.

[20] LiChrosorb RP-8, 10 μm, 4.2 cm × 3.2 mm i.d., Altex Scientific Inc., Berkeley, Calif.

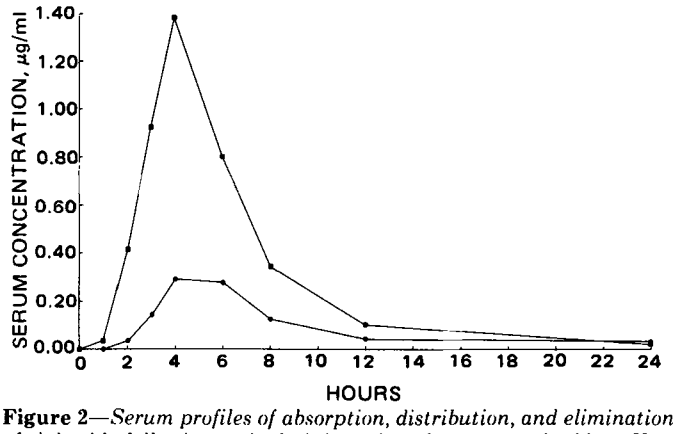

Figure 2—*Serum profiles of absorption, distribution, and elimination of glyburide following oral administration of compressed tablets. Key:* ●, *2.5 mg of glyburide; and* □, *10.0 mg of glyburide.*

Methodology Applicability—The utility of the analytical method for the determination of glyburide in pharmacokinetic studies was demonstrated by monitoring serum profiles in the dog in a pilot study. Average serum profiles for three beagle dogs, each dosed with a 2.5- or a 10-mg compressed tablet, are shown in Fig. 2. The average peak serum concentrations and areas under the average serum concentration–time curves were proportional to the administered dose (Table II). Peak serum concentrations occurred 4–5 hr after oral administration of the compressed tablets, essentially identical to the mean time of 4.3 ±1.4 hr (*SD*) found in a recent human study (21). Serum glyburide concentrations then decreased by apparent first-order kinetics, with average half-lives of 2.3 and 2.1 hr for the 2.5- and 10.0-mg compressed tablets, respectively.

REFERENCES

(1) *Drugs*, **1**, 116 (1971).

(2) P. Hajdú, K. F. Kohler, F. H. Schmidt, and H. Spingler, *Arzneim.-Forsch.*, **19**, 1381 (1969).

(3) P. Glogner, P. Burmeister, and N. Heni, *Klin. Wochenschr.*, **51**, 352 (1973).

(4) M. E. Royer, H. Ko, J. S. Evans, and K. T. Johnston, *Anal. Lett.*, **9**, 629 (1976).

(5) K. Sabih and K. Sabih, *J. Pharm. Sci.*, **59**, 782 (1970).

(6) J. A. F. Wickramasinghe and S. R. Shaw, *ibid.*, **60**, 1669 (1971).

(7) D. L. Simmons, R. J. Ranz, and P. Picotte, *J. Chromatogr.*, **71**, 421 (1972).

(8) L. F. Prescott and D. R. Redman, *J. Pharm. Pharmacol.*, **24**, 713 (1972).

(9) J. A. Taylor, *Clin. Pharmacol. Ther.*, **15**, 964 (1972).

(10) S. B. Matin and M. Rowland, *Anal. Lett.*, **6**, 865 (1973).

(11) S. B. Matin and M. Rowland, *J. Pharm. Pharmacol.*, **25**, 186 (1973).

(12) V. Aggarwal and I. Sunshine, *Clin. Chem.*, **20**, 200 (1974).

(13) F. J. E. Vagda, F. Williams, and D. S. Davies, *Med. J. Aust.*, **1**, 64 (1974).

(14) K. K. Midha, I. J. McGilveray, and C. Charette, *J. Pharm. Sci.*, **65**, 576 (1976).

(15) S. Sved, I. J. McGilveray, and N. Beaudoin, *ibid.*, **65**, 1356 (1976).

(16) D. J. Weber, *ibid.*, **65**, 1502 (1976).

(17) R. E. Hill and J. Crechiolo, *J. Chromatogr.*, **145**, 165 (1978).

(18) R. L. Nation, G. W. Peng, and W. L. Chiou, *ibid.*, **146**, 121 (1978).

(19) H. M. Hill and J. Chamberlain, *ibid.*, **149**, 349 (1978).

(20) W. F. Beyer, *Anal. Chem.*, **44**, 2656 (1972).

(21) H. Ko, M. E. Royer, and B. A. Molony, in "Micronase: Pharmacological and Clinical Evaluation," H. Rifkin, Ed., Excerpta Medica, Princeton, N.J., 1975.

ACKNOWLEDGMENTS

Presented in part at the Pharmaceutical Analysis and Control Section, APhA Academy of Pharmaceutical Sciences, Hollywood, Fla. meeting, 1978.

Helpful discussions with D. G. Kaiser, H. Ko, M. E. Royer, and A. C. Sarapu and the able assistance of J. L. Eddy and W. M. Kooyers in obtaining serum samples are gratefully acknowledged.

Solubility in Amide–Water Cosolvent Systems II: Cosolvent Excess at Solute Surface

RICHARD E. LINDSTROM

Received December 12, 1978, from the *School of Pharmacy, University of Connecticut, Storrs, CT 06268.* Accepted for publication March 19, 1979.

Abstract □ The solubility of methylparaben was determined at 25° in a series of amide–water cosolvent systems. The data were used to demonstrate the possibility of an amide excess at or near the ester solute over that in the bulk solvent. The analysis, stemming from an interfacial tension–solute area solubility model proposed by earlier workers, involved data obtained as a function of amide concentration and as a function of amide alkylation. Both sets of data support the basic contention of the paper.

Keyphrases □ Solubility—methylparaben in amide–water cosolvent systems, cosolvent excess □ Methylparaben—solubility in amide–water cosolvent systems, cosolvent excess □ Amide–water cosolvent systems—methylparaben solubility, cosolvent excess

An interesting approach to explaining the solubility of nonelectrolytes in polar solvents was proposed and tested by previous investigators (1–6). The idea stems from the concepts of regular solutions (7), and it describes the excess work of cohesion and adhesion in forming those solutions in terms of the tension and surface area at the solute–solvent interface. The apparent success of the model has prompted an extension of these relatively new concepts.

BACKGROUND

The mole fraction solubility of a solid nonelectrolyte, X_3, may be represented as:

$$\ln X_3 = -\left[\frac{\Delta H_f(T_m - T)}{RTT_m}\right] + [-V_3\phi_1^2(\delta_2 - \delta_1)^2/RT] \quad \text{(Eq. 1)}$$

where the first term on the right is the ideal solubility of the solid material in any solvent as calculated using the heat of fusion, ΔH_f, the melting point of the solid, T_m, and the temperature, T, at which the solubility is desired.

The second term on the right in Eq. 1 represents the natural logarithm of the activity coefficient, $\ln Y_3$, which adjusts for solute–solvent interactions. In that expression, V_3 is the molar volume of the solute, ϕ_1 is the volume fraction of solvent in the solution, and δ_1 and δ_2 are the solubility parameters for the solvent and solute, respectively. The latter are the subject of an excellent review (8). This approach to describing the activity coefficient is based on a summation of the energies associated with: (*a*) the removal of a solute molecule from the bulk solute, (*b*) creation of a hole or cavity in the solvent, and (*c*) subsequent adhesive interactions between the solute and the solvent.

Amidon *et al.* (2), using arguments of Langmuir (9) and Scatchard (10), suggested the following relationship as a workable alternative for the activity coefficient expression:

$$\ln Y_3 = -\gamma_{12}(SA_3) \quad \text{(Eq. 2)}$$

where γ_{12} is the tension at the interface between the solute molecule and the surrounding solvent, and (SA_3) is the surface area that the solute molecule presents to the solvent. According to this model, the nonideal energy of interaction is due to the creation of new surface, (SA_3), against the interfacial tension, γ_{12}.

Equation 2 has been discussed and tested in various forms, which permit some helpful analyses of solvent interactions with the polar and nonpolar portions of numerous nonelectrolyte solutes. One form of the expression particularly relevant to cosolvent systems is (4):

$$\log X_f = \log X_w + \sigma f_c \quad \text{(Eq. 3)}$$

in which X_f is the mole fraction solubility of the solute at volume fraction, f_c, of the cosolvent, and X_w is the mole fraction solubility of the solute in water. The term σ is defined as:

$$\sigma = \frac{C(\gamma_w^0 - \gamma_c^0)(HYSA_3)}{2.303kT} \quad \text{(Eq. 4)}$$

where γ_w^0 and γ_c^0 are the macroscopic interfacial tensions between tetradecane (a model hydrophobic surface) and water and between tetradecane and pure cosolvent, respectively. The hydrophobic surface area for the solute is $(HYSA_3)$, and C is a correction for the extremely small radius of curvature at the solute molecule surface. Tests using aqueous cosolvent mixtures with glycerin, propylene glycol, ethylene glycol, formamide, methanol, and ethanol over the range from pure water to pure cosolvent suggest that Eq. 4 is a reliable representation and that C has a relatively constant value near 0.5.

While there is general agreement that theory predicts a reduced surface tension at the solute–solvent interface because of the small radius of curvature, some disagreement exists (11) as to whether the reductions should be as great as 50%. Arguments for the curvature effects as they relate to cosolvent systems have assumed that the solvent mixture at the solute surface is of the same composition and character as it is in the bulk. Indeed, it was suggested (3, 4) that the thermal motion of the solute molecules and the already lowered tension at the curved interface with the solvent preclude the accumulation of cosolvent molecules at the solute surface over that in the bulk of the mixed solvent. These researchers (3, 4) showed compelling evidence that this hypothesis may be true in reporting rather constant values for C in Eq. 4 and σ in Eq. 3 for several cosolvent–solute systems.

In spite of the evidence, however, it seems reasonable to reconsider the possibility of a cosolvent excess at or near the solute. In this regard, one must ask if the shearing force on a diffusing semipolar solute is sufficient to overcome the van der Waal's interactions between it and the water and cosolvent molecules, as has been suggested (3, 4). These interactions, often referred to as nonspecific because they are nondirectional and lack a definite stoichiometry (12), can be significant. Thus, it is difficult to accept solute diffusion that is completely independent of some solvation shell or environment. Furthermore, it can be argued that the tendency for a cosolvent to partition to the molecule–solvent interface is not controlled so much by the existing tension at that interface as by the need to minimize the energy of the entire system. Thus, the lowered tension at the solute–solvent interface does not preclude cosolvent adsorption to that surface with consequent further tension lowering.

The latter contentions have significant possibilities with regard to cosolvency mechanisms. Accordingly, it seemed desirable to investigate the conditions further. The present paper is a supplemental and, perhaps, more detailed view of the solute–cosolvent microinterface in that it focuses on very water-rich systems where more characteristic cosolvent effects may be evident.

EXPERIMENTAL

The data used in the preparation of this paper were reported previously (13, 14). In brief, the procedures for obtaining these data entailed: (*a*) preparation of the amide–water solvent systems by careful weighing of the two ingredients, (*b*) equilibration of excess methylparaben with the cosolvents at 25.0°, and (*c*) determination of the ester concentration in the resulting solutions using a standard UV spectrophotometric procedure. The results pertinent to the present study are listed in Tables I and II.

The volume fraction values, f_a, shown in Tables I and II were calculated according to:

$$f_a = \frac{X_a\overline{V}_a}{X_a\overline{V}_a + X_w\overline{V}_w} \quad \text{(Eq. 5)}$$

where X and $\overline{V}$ refer to mole fractions and partial molar volumes, respectively, of the amide, a, and the water, w, in the binary mixtures. The

0022-3549/79/0900-1141$01.00/0
© 1979, American Pharmaceutical Association

Table I—Mole Fraction Solubility of Methylparaben, X_f, in Various Amide-in-Water Cosolvent Systems at 25°

Amide	X_a[a]	f_a[b]	$X_f \times 10^3$	$\log X_f$[c] $- \log X_w$	σ[d]
Formamide	0	0	0.246	—	—
	0.0100	0.0213	0.306	0.095	4.46
	0.0258	0.0573	0.368	0.175	3.26
	0.0506	0.1029	0.534	0.337	3.38
	0.0746	0.1483	0.712	0.462	3.12
	0.1002	0.1946	0.948	0.586	3.01
	0.1248	0.2371	1.23	0.699	2.95
	0.1490	0.2768	1.55	0.799	2.89
	0.1747	0.3169	1.84	0.874	2.76
	0.1997	0.3538	2.35	0.980	2.77
Methylformamide	0	0	0.246	—	—
	0.0100	0.0307	0.344	0.146	4.76
	0.0247	0.0734	0.523	0.328	4.47
	0.0497	0.1406	0.939	0.582	4.14
	0.0754	0.2036	1.61	0.816	4.01
	0.0998	0.2598	2.51	1.009	3.88
	0.1245	0.3105	3.83	1.192	3.84
	0.1490	0.3572	5.44	1.345	3.77
	0.1736	0.4011	8.29	1.528	3.81
	0.1981	0.4416	11.72	1.678	3.80
Dimethylformamide	0	0	0.246	—	—
	0.0100	0.0409	0.431	0.244	5.95
	0.0249	0.0969	0.830	0.528	5.45
	0.0499	0.1799	2.04	0.919	5.11
	0.0745	0.2513	4.57	1.269	5.05
	0.0992	0.3150	10.39	1.626	5.16
	0.1224	0.3686	22.07	1.953	5.30
	0.1440	0.4137	40.71	2.219	5.36
	0.1644	0.4534	61.07	2.395	5.28
	0.1833	0.4869	83.60	2.531	5.20

[a] Mole fraction of amide in the binary aqueous cosolvent system. [b] Volume fraction of amide in the binary aqueous cosolvent system. [c] Corresponding terms in Eq. 3. [d] Calculated according to Eq. 3.

partial molar values employed were those corresponding to the appropriate amide mole fraction. Measurements equivalent to density determinations to 1 ppm were the bases for these volume data (13).

DISCUSSION

The data in Table I report cosolvency effects produced by changes in cosolvent concentration. Those in Table II report the analogous effects as the hydrophobic nature of the cosolvent was varied. Both sets of data strongly suggest that an excess of cosolvent in these aqueous solutions may be found at or near the solute–solvent interface.

Table I presents the results of a study in which the solubility of methylparaben was determined in aqueous cosolvents of increasing formamide, methylformamide, or dimethylformamide concentration. The last column of the table lists the σ values calculated according to Eq. 3 for each solution system. The trends in all three data sets are similar. The σ value is highest at the low amide concentrations and decreases to a somewhat constant value which appears to be characteristic of the particular amide involved. This result contrasts with the findings and suggestions of Yalkowsky *et al.* (3, 4) indicating that σ would be a constant as described in Eq. 4.

Inspection of the parameters in Eq. 4 reveals little that may change to meet the present circumstance if one is to subscribe to the interfacial tension–solute surface area model for solubility predictions. Both γ_w^0 and γ_a^0, whatever their precise value against a suitable hydrophobic surface, are constants for the particular amide–water cosolvent systems; $HYSA_3$ is a constant for this study since only the solute methylparaben was used. The theoretical meaning and constancy of the curvature correction, C, are uncertain. Nevertheless, previous results involving numerous solvent systems strongly support a relatively constant, although empirical, value near 0.55 (4).

An additional point should be considered. If σ is in fact a constant, then theory may be reconciled with observation if the volume fraction of the amide in the cosolvent, f_a, is larger than that shown for the lower amide concentrations in Table I. Practically speaking, this can occur if the amide cosolvent accumulates at or near the solute molecules as an excess over that in the bulk. The result would be a higher "effective" cosolvent volume fraction, as well as a tendency toward the constant σ. Water–amide interactions and steric effects should limit this cosolvent excess and, in all probability, account for the decrease in the apparent σ to the characteristic and relatively constant values shown at higher amide concentrations in Table I. Moreover, no exception need be taken with the results of the earlier studies since the cosolvent concentrations employed were all undoubtedly high enough to be in the range where the σ values had plateaued.

Table II presents the results of a study in which the solubility of methylparaben was determined in several 0.01 mole fraction amide-in-water cosolvent systems. The amides used were relatively simple and differed only in the degree of alkylation on the nitrogen and on the carbonyl carbon.

Values for σ (not shown) were calculated according to Eq. 3. They varied from 3.40 for acetamide to 6.43 for dimethylpropionamide. The surface tensions of several of the pure amides against air were obtained from the literature (3, 15). While some correspondence between these values and an amide–tetradecane interfacial tension might be anticipated (3), there was no obvious correlation with the calculated σ.

An inspection of the data in Table II indicates that $(\log X_f - \log X_w)$ does bear some dependence on the degree of alkylation. This relation is seen more clearly in Fig. 1 where $(\log X_f - \log X_w)$ is plotted against the number of methylene groups in the various amides. The line in the figure is a linear least-squares representation of the data, having its origin at $(\log X_f - \log X_w)$ for formamide and a slope of 0.0495.

Since $(\log X_f - \log X_w)$ is the logarithm of the activity coefficient of the solute, the slope of the line in Fig. 1 permits the calculation of the standard partial molar free energy change, $\Delta\overline{G}_t^0$, accompanying the transfer of 1 mole of solute from a saturated solution in an amide–water cosolvent to a second saturated solution in which the amide cosolvent possesses an additional methylene group per molecule. The expression is given by:

$$\Delta\overline{G}_t^0 = -2.303RT\frac{(\log X_f/X_w)}{CH_2} \qquad \text{(Eq. 6)}$$

which, upon insertion of the least-squares slope on the right, gives $\Delta\overline{G}_t^0 = -1780$ cal/methylene group.

It is interesting to consider this free energy change in contrast with several possible events. For example, a straightforward application of the interfacial tension–solute area model, using 130 Å^2 as the approximate ($HYSA_3$) for methylparaben[1], would require a decrease in γ_a^0 of −9.4 dynes/cm as each methylene group is added to the amide cosolvent to produce the energy change. If a curvature correction of 0.55 is included, the required change in γ_a^0 becomes nearly 18. Intuition and the surface

[1] S. H. Yalkowsky, personal communication.

Table II—Mole Fraction Solubility of Methylparaben, X_f, in 0.01-Mole Fraction Amide-in-Water Cosolvent Systems at 25°

Amide	f_a[a]	$X_f \times 10^3$	$\log X_f$[b] $- \log X_w$	γ[c]
Formamide	0.0213	0.306	0.095	(58)
Methylformamide	0.0307	0.344	0.146	39 (40)
Ethylformamide	0.0394	0.388	0.198	—
Propylformamide	0.0466	0.455	0.257	—
Acetamide	0.0300	0.311	0.102	—
Methylacetamide	0.0394	0.389	0.199	35
Ethylacetamide	0.0477	0.427	0.239	—
Propylacetamide	0.0546	0.524	0.328	—
Propionamide	0.0384	0.362	0.168	
Methylpropionamide	0.0472	0.415	0.227	32
Ethylpropionamide	0.0548	0.442	0.254	—
Propylpropionamide	0.0624	0.512	0.318	—
Dimethylformamide	0.0409	0.431	0.244	35 (37)
Diethylformamide	0.0560	0.551	0.350	28
Dimethylacetamide	0.0473	0.481	0.291	33
Diethylacetamide	0.0628	0.669	0.281	—
Dipropylacetamide	0.0785	—[d]	—	—
Dimethylpropionamide	0.0549	0.554	0.353	—
Diethylpropionamide	0.0703	—[d]	—	—

[a] Volume fraction of amide in the cosolvent system. [b] Corresponding terms in Eq. 3. [c] Surface tension of pure liquid amides obtained from Ref. 15. Numbers in parentheses are the values of Yalkowsky *et al.* (3). [d] Separation into two phases on equilibration.

tension data shown in Table II indicate that neither change is probable. Complexation between the solute and the amides seems to be a remote possibility given the relatively low energy change and the fact that the change is related only to the degree of amide alkylation. This once again points to the possibility of an accumulation of excess cosolvent at or near the solute.

According to Traube's rule (16), the free energy of a system is reduced by 640 cal for every mole of methylene group that partitions to the air–water interface. While the reduction in the case of partitioning to a solvent–hydrophobic solute interface will undoubtedly be greater due to the enhanced dispersion interactions, this added effect probably would not triple the energy reduction needed to give the observed value. Obviously, factors other than, or in addition to, adsorption to an interface are involved.

The phase separations noted in Table II support the view that a cosolvent excess probably exists at the solute surface. Dipropylacetamide is miscible with water in all proportions, as is diethylpropionamide (13). However, the introduction of methylparaben at less than one-tenth the amide concentration leads to a separation of the otherwise stable water–amide mixtures into two systems. Again, no distinct explanation is apparent. Nevertheless, the largely hydrophobic ester indisputably provides a focus for the amide molecules in these solutions.

Presumably, the same type of amide–solvent, amide–solute, and amide–amide interactions that lead to the observed phase separations exist to varying degrees in each single-phase system obtained and studied in this work. Further investigation is necessary to characterize these interactions, which apparently promote the cosolvent excess.

SUMMARY

The solubility of methylparaben in various water-rich, amide–water cosolvent systems was studied. The findings cannot be explained on the basis of the interfacial energy–solubility model proposed by earlier workers. The present analysis finds evidence suggesting the existence of excess amide molecules near the dissolved ester over those in the bulk. Such an excess might explain the effects on solute–solvent interfacial tension and/or a decrease in the free energy of the systems through some cooperative hydrophobic effect. This matter is being studied.

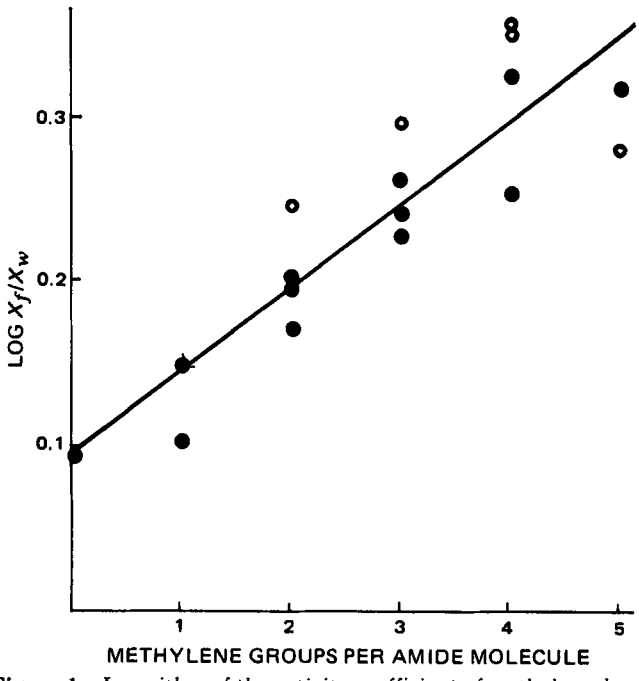

Figure 1—*Logarithm of the activity coefficient of methylparaben in its saturated solutions with 0.01-mole fraction amide-in-water cosolvents, log X_f/X_w, as a function of the number of methylene groups on the amide molecule in the respective cosolvent system. Key:* ●, *N-substituted amides; and* ○, *N,N_1-disubstituted amides.*

REFERENCES

(1) S. H. Yalkowsky, G. L. Flynn, and G. L. Amidon, *J. Pharm Sci.*, **61**, 983 (1972).

(2) G. L. Amidon, S. H. Yalkowsky, and S. Leung, *ibid.*, **63**, 1858 (1974).

(3) S. H. Yalkowsky, G. L. Amidon, G. Zografi, and G. L. Flynn, *ibid.*, **64**, 48 (1975).

(4) S. H. Yakowsky, S. C. Valvani, and G. L. Amidon, *ibid.*, **65**, 1488 (1976).

(5) G. L. Amidon, S. H. Yalkowsky, S. T. Anik, and S. C. Valvani, *J. Phys. Chem.*, **79**, 2239 (1975).

(6) S. C. Valvani, S. H. Yalkowsky, and G. L. Amidon, *ibid.*, **80**, 829 (1976).

(7) J. H. Hildebrand, J. M. Pransnitz, and R. L. Scott, "Regular and Related Solutions," Van Nostrand Reinhold, New York, N.Y., 1970.

(8) A. F. M. Barton, *Chem. Rev.*, **75**, 731 (1975).

(9) I. Langmuir, in "Third Colloid Symposium Monograph," Chemical Catalog Co., New York, N.Y., 1925, p. 3.

(10) G. Scatchard, *Chem. Rev.*, **8**, 321 (1931).

(11) J. T. Davies and E. K. Rideal, "Interfacial Phenomena," 2nd ed., Academic, New York, N.Y., 1963, p. 11.

(12) P. C. Hiemenz, "Principles of Colloid and Surface Chemistry," Dekker, New York, N.Y., 1977.

(13) A. Giaquinto, Ph.D. dissertation, University of Connecticut, Storrs, Conn., 1972 (No. 73-9827, University Microfilms, Ann Arbor, Mich.).

(14) A. R. Giaquinto, R. E. Lindstrom, J. Swarbrick, and A. LoSurdo, *J. Solution Chem.*, **6**, 687 (1977).

(15) R. Gopal and S. A. Rizvi, *J. Indian Chem. Soc.*, **43**, 179 (1966).

(16) G. Traube, *Justus Liebigs Ann. Chem.*, **265**, 27 (1891).

High-Performance Liquid Chromatographic Assay of Cyclophosphamide in Raw Material and Parenteral Dosage Forms

L. R. WANTLAND and S. D. HERSH ×

Received October 13, 1978, from *McGaw Laboratories, Irvine, CA 92714.* Accepted for publication March 26, 1979.

Abstract □ A simple, specific, high-performance liquid chromatographic method is described for the assay of cyclophosphamide as the raw material and in parenteral dosage forms. The assay involves dilution, addition of an internal standard (methyl 4-aminobenzoate), injection onto a reversed-phase C_{18} column, and quantitation with a UV detector at 200 nm. Sensitivity is ~40 μg/ml. Decomposition products elute at the void volume and do not interfere.

Keyphrases □ Cyclophosphamide—analysis, high-performance liquid chromatography, raw material, parenteral dosage forms □ Antineoplastic agents—cyclophosphamide, high-performance liquid chromatographic analysis, raw material, parenteral dosage forms □ High-performance liquid chromatography—analysis, cyclophosphamide, raw material, parenteral dosage forms

Cyclophosphamide[1], *N,N*-bis(2-chloroethyl)tetrahydro-2*H*-1,3,2-oxazaphosphorin-2-amine 2-oxide (I), is a commonly used antineoplastic drug. Initially, colorimetric (1), titrimetric (2, 3), and IR (4) assays were utilized for I dosage forms, but these methods lacked specificity.

BACKGROUND

A GLC assay for I dosage forms was developed (5) and later adapted by the USP (6). This method was used subsequently to study drug stability in parenteral solutions (7). However, during GLC, the underivatized I partially decomposed on the column, an occurrence reported by others (8, 9). These decomposition peaks were summed with the cyclophosphamide peak in the assay.

The major GLC decomposition product, a dehydrohalogenated compound, also has been proposed as an intermediate in the aqueous hydrolysis of I (10, 11). Therefore, in the analysis of I in aqueous solutions, the USP method might not differentiate the dehydrohalogenated product formed by aqueous hydrolysis from that formed by GLC degradation. Thus, the value of this method is limited, especially in the analysis of parenteral solutions.

More recently, I has been assayed in biological fluids by methods that are sensitive and specific but time consuming. In several methods, the drug is incompletely but quantitatively extracted, and the subsequently produced trifluoroacetyl derivative is analyzed by a gas–liquid chromatograph equipped with either a flame-ionization or an electron-capture detector (12) or by a chemical-ionization mass spectrometer (8, 13). A TLC procedure (14) suffers from the additional problems inherent in that technique.

Compound I also has been assayed in biological samples using a gas–liquid chromatograph equipped with a nitrogen–phosphorus selective detector (15). Again, an extraction was necessary; but even though the drug was underivatized, no mention was made of the on-column decomposition products.

Recently, the Food and Drug Administration proposed the compatibility testing of small-volume parenteral drugs, including I, in large-volume parenteral solutions packaged in plastic containers (16). This notice[2] requires rapid and specific assay methods.

The goal of this study was to develop an assay for I in intravenous solutions that is stability indicating and sufficiently brief to allow the analysis of 40 samples/8 hr. The reported method meets this goal but is not sensitive enough for biological samples. It involves the addition of an internal standard, methyl 4-aminobenzoate (II), to an aliquot of the intravenous solution admixture and subsequent analysis by a high-performance liquid chromatograph equipped with a variable UV detector set at 200 nm. This technique was also used to assay the raw material and cyclophosphamide for injection.

EXPERIMENTAL

Equipment—The microprocessor-controlled high-performance liquid chromatograph was equipped with a variable-volume injector[3], a variable-wavelength detector[4], and a 250-mm × 3.2-mm i.d. reversed-phase C_{18} column[5]. The UV spectrum of I in a 45% methanol solution was obtained[6] using 1-cm quartz cells.

Compounds and Reagents—Methanol[7] was filtered through a 1-μm filter[8]. Distilled water was passed through a deionization apparatus[9] and a 0.8-μm filter[10]. Compounds I[11] and II[12] and intravenous solutions[13] were used as received.

Internal Standard Stock Solution—A solution of II, 100 mg/500 ml of water, was prepared accurately with a sonicator.

Calibration—Calibration solutions were prepared in water to contain concentrations of I and II that were similar to the concentrations in the appropriate sample solutions. The calibration solution for the raw material and for cyclophosphamide for injection contained 4.4 mg of I/ml and 0.04 mg of II/ml. Fifty-microliter aliquots were injected in triplicate to calibrate the microprocessor.

The calibration solution for the intravenous solution admixture contained 0.44 mg of I/ml and 0.004 mg of II/ml. Aliquots (200 μl) were injected in triplicate to calibrate the microprocessor.

Sample Preparation—*Raw Material*—About 110 mg of the raw material, accurately weighed, and 5.0 ml of the internal standard stock solution were diluted to 25.0 ml with water. A 50-μl aliquot was injected into the appropriately calibrated chromatograph.

Cyclophosphamide for Injection (500 mg)—Water, 25.0 ml, was added to dissolve the powder. Exactly 10 ml of this solution and 10.0 ml of the internal standard stock solution were diluted to 50.0 ml with water. A 50-μl aliquot was injected into the appropriately calibrated chromatograph.

Intravenous Solution Admixture (500 mg of I/Liter)—Exactly 20 ml of the sample intravenous solution admixture and 3.0 ml of a 0.15 dilution

Table I—Cyclophosphamide for Injection, 500-mg Vial

Actual[a] Amount, mg	*n*	Mean Experimental Amount, mg	Mean Percent Recovery	*CV*, %
441.9	5	437.1	98.9	0.2
496.0	5	497.5	100.3	0.4
540.7	5	545.0	100.8	0.8

[a] Amounts expressed on an anhydrous basis. Quantities represent 90, 100, and 110% of label.

[1] CAS Reg. No. 6055-19-2.

[2] Codified as 21 CFR 310.509, effective Feb. 13, 1979.

[3] Model 1084A, Hewlett-Packard, Avondale, Pa.

[4] SF770 Spectroflow, Schoeffel, Westwood, N.J.

[5] Lichrosorb C_{18}, 10 μm, Altex, Berkeley, Calif.

[6] Acta MIV, Beckman, Fullerton, Calif.

[7] HPLC grade, Fisher, Fair Lawn, N.J.

[8] FALP 04700, Millipore, Bedford, Mass.

[9] Nanopure, Barnstead, Boston, Mass.

[10] AAWP04700, Millipore, Bedford, Mass.

[11] The authors are grateful to the Mead Johnson Research Center for the gift of cyclophosphamide monohydrate, which was used in sample preparations. USP reference standard cyclophosphamide monohydrate was used for standard preparations.

[12] Eastman, Rochester, N.Y.

[13] McGaw Laboratories, Irvine, Calif.

0022-3549/79/0900-1144$01.00/0
© 1979, American Pharmaceutical Association

Table II—Cyclophosphamide Intravenous Solution Admixtures

Intravenous Solution	n	Concentration[a], mg/liter	Mean Experimental Concentration, mg/liter	Mean Percent Recovery	CV, %
5% Dextrose injection USP	5	475.8	485.2	102.0	0.7
Sodium chloride injection USP	5	474.9	479.2	100.9	1.0
Lactated Ringer's injection USP	5	474.9	482.8	101.7	1.6
5% Dextrose in 0.9% sodium chloride USP	5	474.9	482.2	101.5	1.2
5% Dextrose in lactated Ringer's injection	4	480.5	488.5	101.7	1.4

[a] Concentrations expressed on an anhydrous basis.

of the internal standard stock solution were mixed, and a 200-μl aliquot was injected into the appropriately calibrated chromatograph.

High-Performance Liquid Chromatographic (HPLC) Conditions—The methanol and water were pumped from separate pumps to achieve a mobile phase of 45% (v/v) methanol at a flow rate of 1.0 ml/min. The oven temperature was maintained at 30°. The detector was set at 200 nm; the detector and microprocessor sensitivity was 0.1 au/cm.

Calculations—The microprocessor, operating in the internal standardization mode, automatically calculated the results, C_I, in terms of percent purity (raw material), milligrams of I per vial[14] (cyclophosphamide for injection), or milligrams of I per liter[14] (intravenous solution admixture). The general equation applied was:

$$C_I = \frac{R_I}{R_{II}} \frac{A_I}{A_{II}} C_{II} D F \qquad \text{(Eq. 1)}$$

where R_I is the concentration of I (hydrous basis) in the calibration solution divided by the area counts of peak I in the calibration graph; R_{II} is the concentration of II in the calibration solution divided by the area counts of peak II in the calibration graph; A_I is the area counts of peak I in the sample graph; A_{II} is the area counts of peak II in the sample graph; C_{II} is the concentration of II in the sample solution injected into the chromatograph; D is the dilution factor, which is 25 for the raw material, 125 for the vial, and 1.15 for the intravenous solution admixture; and F is the factor that converts to the anhydrous basis (F = 1 for the raw material and 0.936 for the other dosage forms).

Interference Study—To study the potential interference from degradation products, a 1% solution of I in water was heated to 83°. Aliquots were withdrawn at about 15-min intervals up to 4 hr and injected without the addition of an internal standard.

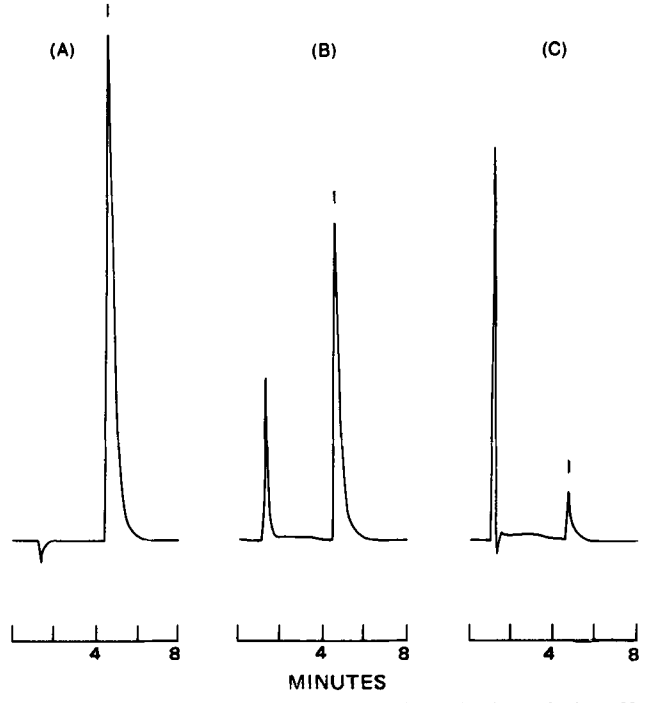

Figure 1—*Chromatograms of cyclophosphamide degradation. Key: A, zero time; B, 2 hr; and C, 3.5 hr.*

[14] Concentration of I expressed on an anhydrous basis.

RESULTS AND DISCUSSION

UV Spectrum—A solution of I in 45% methanol, 7.1 mg/25 ml, had a λ_{max} of 198 nm (ϵ = 464).

Interference Study—Selected chromatograms of the interference study are shown in Fig. 1. Once the temperature of 83° was reached, peak I decreased logarithmically with time, indicating first-order kinetics as previously reported (7). The peak at the void volume, representing the decomposition product(s), continually increased. No peaks eluted at the retention time of the internal standard. Therefore, it was concluded that decomposition products do not interfere.

The UV spectrum of the final reaction mixture exhibited a λ_{max} of 198 nm, the same maximum as for I.

Assays—The retention times of I and II were ~5.1 and ~3.3 min, respectively.

Two lots of raw material were assayed in quintuplicate against a USP reference standard. Lot 1 had a purity of 99.4% with a coefficient of variation (CV) of 0.7%; Lot 2 had a purity of 98.6% with a CV of 0.5% (Fig. 2A).

Simulated vials of cyclophosphamide for injection containing 90, 100, and 110% of the label amount of I were prepared by mixing I of known purity with sodium chloride. Each sample was assayed five times. HPLC recoveries of 98.9–100.8% and CV's of less than 1% were achieved (Table I). The chromatogram (Fig. 2B) is similar to that of the raw material. Separations were baseline. The calculated performance parameters for peak I were: N = 1850, k' = 2.6, and the asymmetry factor (17) at 10% of peak height = 2.8. The resolution was 4.6.

Admixtures were prepared by adding simulated vials of cyclophosphamide for injection to five different intravenous solutions at known concentrations of ~0.5 mg of I/ml. Each admixture was assayed four or five times. Mean recoveries ranged from 100.9 to 102.0% with CV's of

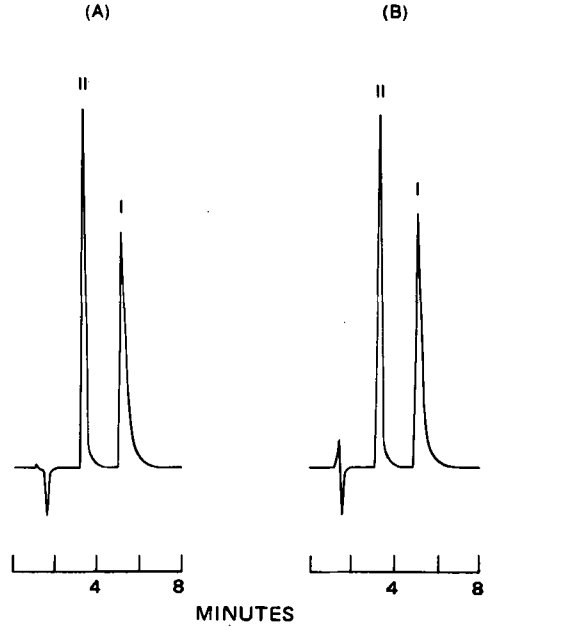

Figure 2—*Chromatograms of cyclophosphamide. Key: A, raw material; and B, cyclophosphamide for injection.*

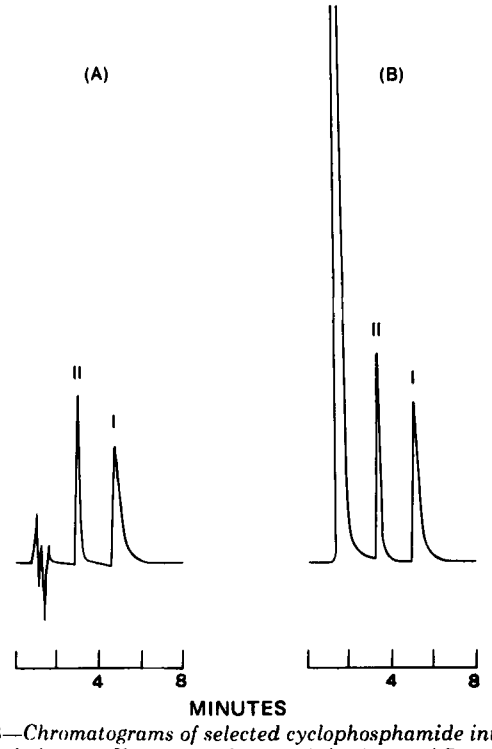

Figure 3—*Chromatograms of selected cyclophosphamide intravenous solution admixtures. Key: A, 5% dextrose injection; and B, 5% dextrose in lactated Ringer's injection.*

0.7–1.6% (Table II). In all admixtures, baseline separations were achieved. Chromatograms of selected admixtures are illustrated in Fig. 3. Peaks at the void volume are intravenous solution components and decomposition product(s), if present. The negative peaks in Fig. 3A represent the water used as the sample diluent. The minimum concentration that can be quantitated is ~0.2 mg/ml, and the detection limit is ~40 μg/ml (three times noise). This sensitivity is sufficient for parenteral solutions.

For all three sample types, blank solutions were prepared containing all appropriate ingredients (without I). In all cases, the chromatograms exhibited no peaks eluting after the peak due to the water used as the sample diluent.

In summary, the reported method is precise, accurate, specific, extremely brief, and applicable to dosage forms of I. It is particularly suited to the analysis of I in large-volume parenteral solutions.

REFERENCES[15]

(1) O. M. Friedman and E. Boger, *Anal. Chem.*, **33,** 906 (1961).

(2) "The British Pharmacopoeia," The Pharmaceutical Press, London, England, 1968, p. 275.

(3) V. Egerts, N. Ozolins, M. V. Shimanskaya, and A. Cebere, *Tsiklofosfan,* **1965,** 13; through *Chem. Abstr.*, **64,** 10404a (1966).

(4) "The National Formulary," 12th ed., Mack Publishing Co., Easton, Pa., 1965. "The United States Pharmacopeia," 18th rev., Mack Publishing Co., Easton, Pa., 1970.

(5) O. D. Boughton, R. D. Brown, R. Bryant, F. J. Burger, and C. M. Combs, *J. Pharm. Sci.*, **61,** 97 (1972).

(6) "The United States Pharmacopeia," 19th rev., 2nd supplement, Mack Publishing Co., Easton, Pa., 1976, p. 31.

(7) D. Brooke, R. J. Bequette, and R. E. Davis, *Am. J. Hosp. Pharm.*, **30,** 134 (1973).

(8) C. Pantarotto, A. Martini, G. Belvedere, M. G. Donelli, and A. Frigerio, *Cancer Treat. Rep.*, **60,** 493 (1976).

(9) J. H. Duncan, O. M. Colvin, and C. Fenselau, *Toxicol. Appl. Pharmacol.*, **24,** 317 (1973).

(10) O. M. Friedman, S. Bien, and J. K. Chakrabarti, *J. Am. Chem. Soc.*, **87,** 4978 (1965).

(11) O. M. Friedman, *Cancer Chemother. Rep.*, **51,** 327 (1967).

(12) C. Pantarotto, A. Rossi, G. Belvedere, A. Martini, M. G. Donelli, and A. Frigerio, *J. Pharm. Sci.*, **63,** 1554 (1974).

(13) I. Jardine, C. Fenselau, M. Appler, M.-N. Kan, R. B. Brundrett, and M. Colvin, *Cancer Res.*, **38,** 408 (1978).

(14) Von K. Norpoth, H. W. Addicks, U. Witting, G. Müller, and H. Raidt, *Arzneim.-Forsch.*, **25,** 1331 (1975).

(15) T. Facchinetti, M. D'Incalci, G. Martelli, L. Cantoni, G. Belvedere, and M. Salmona, *J. Chromatogr.*, **145,** 315 (1978).

(16) *Fed. Regist.*, **40,** 58557 (1978).

(17) D. L. Saunders, *J. Chromatogr. Sci.*, **15,** 372 (1977).

[15] While this report was being considered for publication, a similar article was published: T. T. Kensler, R. J. Behme, and D. Brooke, *J. Pharm. Sci.*, **68,** 172 (1979).

Controlled Release of Tetracycline I: *In Vitro* Studies with a Trilaminate 2-Hydroxyethyl Methacrylate–Methyl Methacrylate System

L. OLANOFF, T. KOINIS, and J. M. ANDERSON ˣ

Received October 30, 1978, from the *Departments of Biomedical Engineering and Macromolecular Science and Pathology, Case Western Reserve University, Cleveland, OH 44106.* Accepted for publication March 23, 1979.

Abstract □ A membrane-controlled drug delivery device was developed to release tetracycline at zero-order rates. The tetracycline delivery vehicle is a trilaminate disk consisting of core and coating membranes fabricated from a series of 2-hydroxyethyl methacrylate and methyl methacrylate copolymers. Appropriate adjustment of the monomer composition ratio imparts a hydrophobic nature to the copolymer outer coating membrane (relative to the core material), which serves as the rate-limiting membrane in drug diffusion. The trilaminate disks demonstrated a zero-order tetracycline release over 4 months *in vitro*. The zero-order release rate was a function of the general device geometry, coating membrane thickness, disk surface area, level of core reservoir drug loading, and membrane coating copolymer composition. Permeability parameters of tetracycline diffusion through a series of 2-hydroxyethyl methacrylate–methyl methacrylate copolymer membranes were determined by a flux–lag time method. Equilibrium hydration values of these membranes also were determined. The ability of trilaminate 2-hydroxyethyl methacrylate–methyl methacrylate devices to release tetracycline at constant rates over a prolonged period offers unique therapeutic and investigational possibilities.

Keyphrases □ Tetracycline—controlled-release dosage form, pharmacokinetics, hydroxyethyl methacrylate–methyl methacrylate copolymer, *in vitro* □ Antibacterial agents—tetracycline, controlled-release dosage form, pharmacokinetics, hydroxyethyl methacrylate–methyl methacrylate copolymer, *in vitro* □ Models, pharmacokinetic—tetracycline, controlled-release dosage form, *in vitro* □ Dosage forms, controlled release—tetracycline, hydroxyethyl methacrylate–methyl methacrylate copolymer, *in vitro*

Numerous drug–polymer delivery systems have been proposed with the expressed purpose of releasing a biologically active agent into the surrounding medium at a constant (zero-order) release rate. Attempts to achieve zero-order release rates have included infusion pumps (1), erodable matrixes (2), controlled geometries (3), and various membrane-enclosed reservoir devices (4–6). Unfortunately, many of these systems fall far short of their goal, suffering from prolonged burst effects, device breakdown, and constraints in design, fabrication, or material properties. The result is usually an exponential release pattern with time and a relatively limited period of constant release.

Previous experience with a hydrogel matrix–drug delivery system (7) led to the investigation of a membrane-controlled drug delivery device in which a hydrophilic polymer core is supersaturated with a given pharmaceutical. The core–drug mixture is coated with a drug-free polymer layer which, by its hydrophobic nature (relative to the core material), functions as the rate-limiting membrane in drug diffusion from the device. Membrane-enclosed drug delivery systems maintain a constant activity source of the permeating drug at the interface between the core and membrane-coating material. The result is a constant drug release rate that is proportional to the concentration gradient established over the diffusion rate-limiting outer membrane.

The described membrane-controlled drug delivery system is a trilaminate device consisting of core and outer membranes fabricated from a series of hydroxyethyl methacrylate and methyl methacrylate copolymers. Yasuda *et al.* (8, 9) reported on the permeability properties of sodium chloride and a number of water-soluble organic solutes through 2-hydroxyethyl methacrylate–methyl methacrylate copolymers of varying composition. Diffusive permeabilities were related to the equilibrium water content of the copolymer films, which increased as the 2-hydroxyethyl methacrylate content was increased. Thus, by varying the relative percentage of the hydrophilic and hydrophobic monomer components (2-hydroxyethyl methacrylate and methyl methacrylate, respectively) of a copolymer, the diffusivity of a given drug through the copolymer coating membrane can be varied over a sizable range. In addition, the drug release rate from a trilaminate delivery vehicle can be controlled by altering the coating membrane thickness and/or the device geometry. The control of diffusion properties in a similar trilaminate delivery device for the constant release of sodium fluoride was described previously (10).

Tetracycline, a middle molecular weight bacteriostatic antibiotic, was chosen as the diffusant species to be incorporated within the delivery device core. Previous (11, 12) controlled-release tetracycline preparations incorporated the drug in a cross-linked hydrogel matrix or in an erodable complex of polyvinylpyrrolidine, shellac, and a low solubility organic acid.

Tetracycline in an implantable controlled delivery form with long-term constant release rates offers numerous therapeutic and investigational applications. The purposes of this report are to evaluate the *in vitro* performance of the trilaminate device and to describe the effects of copolymer composition and device geometry on tetracycline permeability through various 2-hydroxyethyl methacrylate–methyl methacrylate copolymers.

EXPERIMENTAL

Copolymer Synthesis—Random copolymers of 2-hydroxyethyl methacrylate[1] and methyl methacrylate[2] were prepared by mixing varying molar weight percentages of the monomers (total of 25 g) in 475 ml of a 3:2 ethanol–water mixture. The reaction mixture was purged of oxygen by bubbling with nitrogen, and polymerization was initiated by the addition of 0.125 g of potassium persulfate and 0.25 g of sodium persulfate/liter of reaction mixture.

Ten days was allowed to carry the copolymerization reaction to completion, after which the copolymer was precipitated in an excess of water. After separation by filtration, the resultant copolymer was subjected to multiple washings with water and dried at 50° *in vacuo*. Reaction yields

[1] Hydron Labs, New Brunswick, N.J.
[2] Eastman Kodak, Rochester, N.Y.

0022-3549/79/0900-1147$01.00/0
© 1979, American Pharmaceutical Association

Table I—Polymer Composition and Diffusional Properties for 2-Hydroxyethyl Methacrylate–Methyl Methacrylate Copolymers

Feed Composition, mole ratio[a]	Copolymer Composition[a,b], mole ratio	Diffusion[c] Coefficient, D, $cm^2/sec \times 10^{-9}$	Partition[c] Coefficient, K_p, $\times 10^{-3}$
10:90	2:98	8.0 ± 4.7	6.8 ± 5.9
20:80	14:86	12.0 ± 2.1	16.4 ± 6.6
32:68	22:78	25.1 ± 11.0	30.7 ± 16.8
75:25	63:37	43.2 ± 8.9	126.7 ± 35.9

[a] 2-Hydroxyethyl methacrylate–methyl methacrylate. [b] As determined by NMR analysis. [c] Mean values ± SD.

were 72–95%. The 2-hydroxyethyl methacrylate–methyl methacrylate copolymers were prepared in the following molar feed ratios: 10:90, 20:80, 32:68, and 75:25.

Chemicals—[7-^{3}H]Tetracycline[3] was mixed with unlabeled tetracycline[4] to the desired specific activity by dissolving both drug forms in methanol (~100 mg of mixture/5 ml of solvent). The solvent was evaporated slowly at a temperature not exceeding 42° until a constant crystalline tetracycline weight was obtained. The drug mixture was stored at −4° until needed.

Copolymer Composition—Determination of the respective copolymer composition was performed by NMR analysis[5]. Copolymer specimens were analyzed in deuterochloroform–methanol with increasing amounts of d-4-methanol for copolymers of higher 2-hydroxyethyl methacrylate content. To determine the molar composition of the individual components, the area under the peak due to the methyl methacrylate methyl ester was compared to the area under the combined peaks attributable to the α-methyl hydrogens (representing total methacrylate content).

Tetracycline–Copolymer Device Fabrication—Disk-shaped trilaminate tetracycline devices were prepared by the following process. Copolymer material was dissolved in a cosolvent of 3:2 (v/v) acetone–dioxane (0.5 g/5 ml of solvent). Films were cast by pouring the copolymer solution onto a clean glass plate and adjusting the wet film thickness with a Gardner knife. The film was covered and allowed to dry for 15–30 min under ambient conditions. Subsequent films were cast and allowed to dry until the desired outer membrane-coating thickness was obtained.

After the total bottom coating film was cast, the core material was constructed by casting additional individual films of a copolymer–tetracycline mixture (either a solution or suspension, depending on the percent drug loading) over the coating membrane. When the core layer was complete, the top coating membrane was film cast in individual layers directly over the core layer. The completed trilaminate film was dried overnight in a 37° oven. The film was slightly swollen with an aerosol application of 95% ethanol, and disks were punched out with a cork borer. Residual alcohol was allowed to evaporate, and the disks were edge coated by brushing on two or three layers of the coating copolymer solution. The completed disks were stored in a desiccant jar at 4°.

Permeability Parameters and Hydration Studies—Drug-free copolymer films were cast as described for use in diffusion characterization and hydration studies. Permeability parameters were determined with a diffusion cell apparatus described in detail elsewhere (13). The permeation studies were designed to measure the steady-state flux of the penetrant molecule ([^{3}H]tetracycline) through the copolymer membrane according to the following principle:

$$Q = \frac{K_p D C_0}{l}\left(t - \frac{l^2}{6D}\right) \qquad \text{(Eq. 1)}$$

where:

Q = total amount of permeant species diffused through a unit area of membrane as a function of time
K_p = membrane–diffusant system partition coefficient
D = diffusion coefficient
C_0 = permeant concentration in reservoir solution
l = membrane thickness
t = time

Measurements were made on the cumulative diffusive transfer of tetracycline from the saturated reservoir solution through the copolymer film and into the effluent stream on the flow side of the diffusion cell. Cumulative drug transfer was plotted against time to determine the steady-state flux, Q/t, equal to the slope and the lag time, t_L, equal to the time intercept on the abscissa. Slope and intercept values were determined by linear regression techniques.

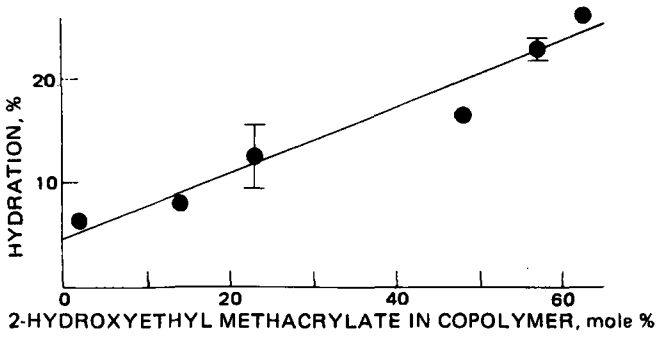

Figure 1—*Variation in percent hydration with copolymer composition (mean values ± SD). Copolymer membrane samples swelled in distilled water.*

By rearranging Eq. 1 and applying it to the region of steady-state mass transfer, the permeability parameters may be calculated:

$$K_p D = Ql/tC_0 \qquad \text{(Eq. 2)}$$

where:

$$D = l^2/6t_L \qquad \text{(Eq. 3)}$$

Hydration studies were performed by swelling films of predetermined dry weights in both Ringer's solution and distilled water at 37°. The wet films were quickly blotted to remove excess surface water and weighed. Percent hydration was expressed as:

$$\%\ \text{hydration} = (\text{wet weight} - \text{dry weight})/\text{wet weight} \qquad \text{(Eq. 4)}$$

***In Vitro* Diffusion Studies**—*In vitro* [^{3}H]tetracycline diffusion was followed by placing the trilaminate disks on a cellulose Millipore filter (0.65-μm pore diameter) sealed with acetone to the ground flat top of a 25-ml erlenmeyer flask with a glass side arm for sampling. The flask was filled with Ringer's solution, which served as the desorbing medium. A glass cap was fitted over the polymer disk and filter to provide a constant temperature and humidity environment. The diffusion flasks were maintained at 37°. At sampling, 1-ml aliquots were removed from the flask through the side arm. Volume was replaced by the addition of fresh Ringer's solution to keep the fluid level continuous with the bottom of the filter. All *in vitro* diffusion experiments were run in triplicate.

Tetracycline diffusion was measured in the permeation studies and *in vitro* diffusion experiments by analyzing for [^{3}H]tetracycline. One milliliter of the aqueous [^{3}H]tetracycline sample was added to 5 ml of a 1:1 nonionic surfactant[6]–toluene scintillation fluor (0.14 g of p-bis[2-(5-phenyloxazolyl)]benzene[7] and 5.34 g of 2,5-diphenyloxazole[7]/liter). The samples were counted in glass vials[8].

In vitro diffusion flask samples were obtained at the termination of the procedure and analyzed for pure tetracycline content and tetracycline breakdown products by a previously reported UV spectroscopic technique (14). The percent pure tetracycline content was calculated from the absorbance ratio of the solution read at 357 and 391 nm (Q:357:391) according to:

$$\%\ \text{tetracycline} = \frac{Q{:}357{:}391 - 0.23}{0.0367} \qquad \text{(Eq. 5)}$$

The pure tetracycline level in the diffusion samples (after 28 days) was 81.3% (original unlabeled drug = 100%).

RESULTS AND DISCUSSION

NMR Analysis—For the series of 2-hydroxyethyl methacrylate–methyl methacrylate copolymer membranes (Table I), NMR studies revealed that the actual mole percentage of methyl methacrylate in the polymer was higher (by 6–12%) than in the original feed. This result was

[3] New England Nuclear, Boston, Mass.
[4] Sigma Chemical Co., St. Louis, Mo.
[5] Dr. Donald Gregonis, Department of Pharmaceutics, University of Utah, Salt Lake City, Utah, personal communication.
[6] Triton X-100, Research Products International Corp., Elk Grove Village, Ill.
[7] Research Products International Corp., Elk Grove Village, Ill.
[8] Isocap liquid scintillation counter, Searle Analytic, Des Plaines, Ill.

Table II—2-Hydroxyethyl Methacrylate–Methyl Methacrylate Trilaminate Tetracycline Disks: *In Vitro* Diffusion Results

Disk Composition[a]					
Coating Co-polymer	Core Co-polymer	Surface Area, cm^2	Core Loading, mg of drug/ mg of core	Coating Thickness, cm × 10^{-2}	Steady-State Release Rate, μg of tetracycline/day
2:98	63:37	0.709	0.02	1.40	0.54
2:98	63:37	0.709	0.02	0.81	0.77
2:98	63:37	1.33	0.02	1.47	0.97
2:98	63:37	0.709	0.2	0.54	18.5
2:98	63:37	0.950	0.2	0.53	23.9
22:78	63:37	0.709	0.2	0.59	28.9

[a] 2-Hydroxyethyl methacrylate–methyl methacrylate.

due to the higher reactivity ratio of the methyl methacrylate monomer with respect to the 2-hydroxyethyl methacrylate monomer. The result of such a difference in reactivity ratios would lead to a skewed distribution of random copolymers in a particular polymerization batch.

Copolymer chains polymerizing during the initiation of the synthesis process would be expected to contain larger proportions of the more reactive methyl methacrylate monomer, depleting the methyl methacrylate monomer pool. Those copolymers synthesized later in the reaction would have increasing proportions of the remaining 2-hydroxyethyl methacrylate monomer in the chain. Multiple washings with water during the preparative procedure would lead to a greater relative loss of those copolymers with higher 2-hydroxyethyl methacrylate content (of associated higher water solubilities), effectively fractionating the copolymer batch and producing a copolymer whose final composition contains a higher mole percentage of the methyl methacrylate monomer than is reflected in the original monomer feed.

Hydration Studies—As expected, copolymer samples of increasing mole percent 2-hydroxyethyl methacrylate composition were more hydrophilic in nature, demonstrating greater degrees of equilibrium swelling (Fig. 1). There was no significant difference in hydration values obtained when the copolymer samples were swelled in distilled water or in Ringer's solution. In the 2-hydroxyethyl methacrylate composition range below 50 mole %, there was good general agreement in equilibrium swelling values between these samples and similar experimental 2-hydroxyethyl methacrylate–methyl methacrylate copolymers described by Cowsar *et al.* (10).

For samples of >50 mole % 2-hydroxyethyl methacrylate content, Cowsar *et al.* (10) reported no further increase in equilibrium water content, whereas the copolymers in the present study continued to increase in percent hydration with increased 2-hydroxyethyl methacrylate content. Cowsar *et al.* (10) failed to provide confirmation of their assumption that the final composition of their experimental copolymers was equal to the molar ratio of monomers in the original feed. Falsely high estimates of 2-hydroxyethyl methacrylate content in samples reported to be of 50 mole % 2-hydroxyethyl methacrylate or greater would explain the observed discrepancy in hydration values.

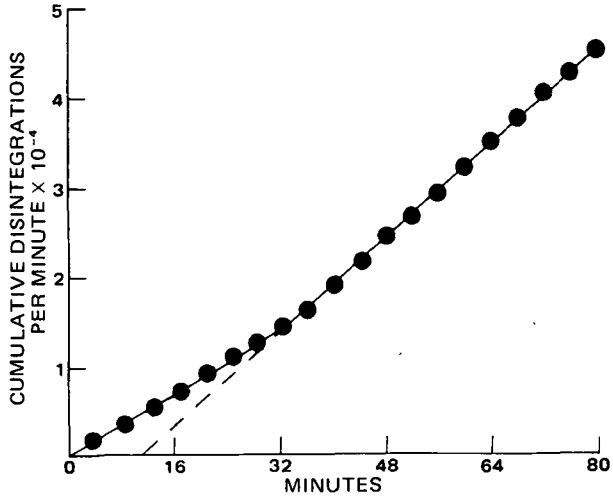

Figure 2—*Lag time method for determination of steady-state flux and diffusion coefficient of a 63:37 2-hydroxyethyl methacrylate–methyl methacrylate copolymer membrane. Flux (Q) is expressed as cumulative disintegrations per minute of labeled drug permeating through the membrane sample per unit time during steady-state period of diffusion. Lag time value (t_L) was taken at the intercept of the steady-state flux line (dashed line) with the time axis.*

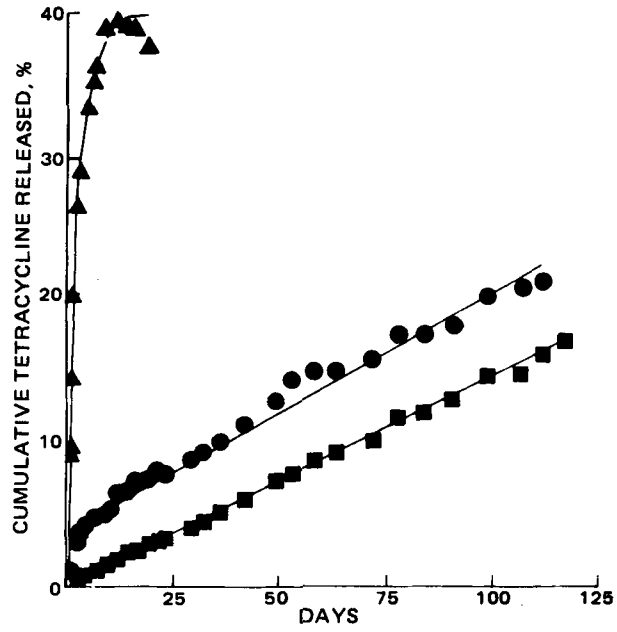

Figure 3—*Zero-order tetracycline release rates maintained by trilaminate membrane device over 4 months of testing* in vitro, *showing effect of copolymer coating composition on constant release rate. Key:* ■, *2:98 2-hydroxyethyl methacrylate–methyl methacrylate coating polymer;* ●, *14:86 2-hydroxyethyl methacrylate–methyl methacrylate coating copolymer; and* ▲, *rapid tetracycline release from 63:37 2-hydroxyethyl methacrylate–methyl methacrylate core material alone. Total average loading of trilaminate device equals 0.155 mg of tetracycline.*

Trilaminate disks, constructed of a core of 63:37 copolymer and coated with an equal total thickness of 22:78 copolymer, achieved 90% of their equilibrium water content after ~3 hr of swelling in Ringer's solution. In general, all copolymers exhibited rapid hydration, and equilibrium swelling was achieved in <6 hr.

Permeability Studies—Diffusion parameters for copolymer membranes of varying composition are presented in Table I. Each set of permeability parameters (D and K_p) represents an average of results obtained in at least five separate experiments, and an example of the data obtained using the flux–lag time experimental method is presented in Fig. 2. The slope of the line determined by linear regression techniques through the steady-state region of the curve provides an accurate measurement of the tetracycline flux through the copolymer film. The diffusion coefficient, D, was determined from the lag time measurement, t_L, equal to the intercept value on the abscissa.

The tetracycline permeability ($P = DK_p$) of the various copolymers increased in relationship to their increase in equilibrium water content. Plotting the log of the diffusion coefficients, D, *versus* the reciprocal of the equilibrium hydration values, $1/H$, for the series of copolymers produced a straight line. This result is consistent with an analysis of the free volume of diffusion theory presented by Yasuda *et al.* (8) who stated that a linear relationship would exist between the logarithm of the diffusion coefficient and the reciprocal hydration value. This relation assumes a linear variation of the free polymer volume with the diluent volume fraction (as expressed by the hydration value, H). The free polymer volume would consist of thermally transient random holes or voids in the polymer matrix, which would serve as the passage for diffusing molecules. This discussion provides an explanation of the tetracycline diffusion process in the membranes. The free volume available for tetracycline permeation in the copolymer would be directly related to the hydration volume of the membrane.

***In Vitro* Diffusion Studies**—Figure 3 demonstrates the ability of the trilaminate device to release tetracycline at constant (zero-order) rates over a 4-month period. The results of several diffusion studies with the trilaminate tetracycline disks are detailed in Table II. The effect of

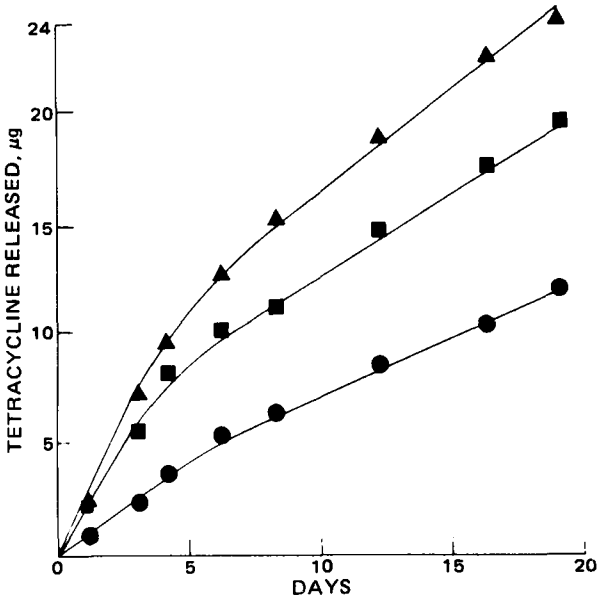

Figure 4—*Effect of trilaminate device geometry on steady-state tetracycline release rates. The 2:98 copolymer coating membrane had a thickness and surface area available for diffusion of 0.14 mm and 0.709 cm^2 (●), 0.081 mm and 0.709 cm^2 (■), and 0.14 mm and 1.33 cm^2 (▲), respectively.*

varying device geometry on the steady-state release is presented graphically in Fig. 4. Increasing surface areas available for diffusion by 1.88 times (0.709–1.33 cm^2) produced a proportionate increase in the release rate by 1.80 times (0.54–0.97 μg/day). Correspondingly, increasing the coating membrane thickness by 1.73 times (0.81–0.14 mm) while holding the surface area constant had an inverse effect on the release rate, decreasing the rate by 1.43 times.

Increasing the drug loading in the core material (expressed as milligrams of drug per milligram of total core weight) by an order of magnitude (0.02–0.2) increased the tetracycline release rate by 16.0 times when corrected for differences in membrane thickness. This higher-than-predicted increase in the release rate is probably the result of osmotic effects that become significant for core materials of higher drug loading. The effects of varying the coating membrane composition are also evident in Table II and Fig. 3.

These results are consistent with steady-state diffusion theory as presented in Eq. 2. In conclusion, the described membrane-controlled trilaminate drug delivery system demonstrated the ability to release tetracycline at constant rates over a prolonged period. The trilaminate device is constructed of a series of 2-hydroxyethyl methacrylate–methyl methacrylate copolymers, which control the tetracycline diffusion rate from the system by their characteristic properties of equilibrium hydration and solute permeability. Tetracycline release rates from the trilaminate device also are dependent on device geometry. The ability of the trilaminate device to deliver tetracycline at zero-order rates offers potential therapeutic and investigational applications. The *in vivo* release characteristics of the tetracycline trilaminate delivery system will be discussed in a separate article (15).

REFERENCES

(1) F. Theeuwes, *J. Pharm. Sci.*, **64**, 1987 (1975).

(2) D. L. Wise and H. Rosenkrantz, in "Drug Delivery Systems," H. L. Gabelnick, Ed., DHEW Publication (NIH)77-1238, 1976, p. 252.

(3) D. Brooke and R. J. Washkuhn, *J. Pharm. Sci.*, **66**, 159 (1977).

(4) S. Borodkin and F. E. Tucker, *ibid.*, **64**, 1289 (1975).

(5) J. W. Shell and R. W. Baker, *Ann. Ophthamol.*, **6**, 1037 (1974).

(6) A. Zaffaroni, *Acta Endocrinol., Suppl.*, **185**, 423 (1974).

(7) J. M. Anderson, T. Koinis, T. Nelson, M. Horst, and D. S. Love, in "Hydrogels for Medical and Related Applications," J. D. Andrade, Ed., American Chemical Society, Washington, D.C., 1976, p. 167.

(8) H. Yasuda, C. E. Lamaze, and L. D. Ikenberry, *Die Makromol. Chemie*, **118**, 19 (1968).

(9) H. Yasuda, L. D. Ikenberry, and C. E. Lamaze, *ibid.*, **125**, 108 (1969).

(10) D. R. Cowsar, O. R. Tarwater, and A. C. Tanquary, in "Hydrogels for Medical and Related Applications," J. D. Andrade, Ed., American Chemical Society, Washington, D.C., 1976, p. 180.

(11) K. Kliment, J. Vacik, Z. Ott, V. Majkus, M. Stol, V. Stoy, and O. Wichterle, U.S. pat. 3,689,634 (Sept. 5, 1972) and 3,551,556 (Dec. 29, 1970).

(12) M. E. Corn, U.S. pat. 3,499,959 (Mar. 10, 1970).

(13) L. Sogor and J. M. Anderson, in "Coatings and Plastic Preprints, ACS San Francisco Meeting," American Chemical Society, Washington, D.C., 1976, p. 1.

(14) M. Pernarowski, R. O. Searl, and J. Naylor, *J. Pharm. Sci.*, **58**, 470 (1969).

(15) L. Olanoff and J. M. Anderson, *ibid.*, **68**, 1151 (1979).

ACKNOWLEDGMENTS

L. Olanoff gratefully acknowledges support from the National Institutes of Health Medical Scientist Training Program, Grant GM-07250.

Controlled Release of Tetracycline II: Development of an *In Vivo* Flow-Limited Pharmacokinetic Model

L. OLANOFF and J. M. ANDERSON ˣ

Received October 30, 1978, from the *Departments of Biomedical Engineering and Macromolecular Science and Pathology, Case Western Reserve University, Cleveland, OH 44106.* Accepted for publication March 23, 1979.

Abstract □ Controlled delivery of pharmaceuticals at zero-order rates from a polymer implant vehicle offers a valuable means by which constant drug levels may be maintained in the plasma over prolonged periods. A 2-hydroxyethyl methacrylate–methyl methacrylate copolymer was applied in the fabrication of a membrane-controlled tetracycline delivery device with previously demonstrated *in vitro* zero-order release rates. The trilaminate tetracycline-releasing disks were evaluated *in vivo* by implantation in the peritoneal cavities of female Sprague–Dawley rats. The implanted disks were coated with copolymer membranes of either 2:98 or 22:78 2-hydroxyethyl methacrylate–methyl methacrylate composition. *In vivo* release rates of tetracycline were constant with time, as measured by the cumulative drug release from disks recovered over different implantation periods. Steady-state tetracycline release rates from the trilaminate devices—158 μg/day for the 22:78 2-hydroxyethyl methacrylate–methyl methacrylate copolymer-coated disks and 123 μg/day for the 2:98 2-hydroxyethyl methacrylate–methyl methacrylate-coated disks—were in excellent correlation with the steady-state total daily excretion of the drug (153 and 110 μg/day for the two systems, respectively) by the rats. Plasma tetracycline concentrations reached steady-state levels within 2–3 days of trilaminate disk implantation and remained constant over the 14-day implantation period. Steady-state tissue tetracycline concentrations averaged 10–12 μg/g in the bone; 3–4 μg/g in the liver, kidney, and GI tract; 2–3 μg/g in the muscle; and <1 μg/g in the fat tissue. A flow-limited pharmacokinetic model was constructed to simulate *in vivo* tetracycline delivery from the trilaminate disks and the subsequent drug distribution. Model predictions of tissue and plasma tetracycline concentrations based on the experimentally determined zero-order drug release rates were in good agreement with experimental measurements.

Keyphrases □ Tetracycline—controlled-release dosage form, pharmacokinetics, hydroxyethyl methacrylate—methyl methacrylate copolymer implant, rats, *in vivo* □ Antibacterial agents—tetracycline, controlled-release dosage form, pharmacokinetics, hydroxyethyl methacrylate–methyl methacrylate copolymer implant, rats, *in vivo* □ Models, pharmacokinetic—tetracycline controlled-release dosage form, rats, *in vivo* □ Dosage forms, controlled release—tetracycline, hydroxyethyl methacrylate–methyl methacrylate copolymer implant, rats, *in vivo*

Numerous studies (1–6) attempted to measure plasma and tissue tetracycline levels in animals following oral or parenteral administration of the antibiotic. These early reports dealt with short-term drug studies and failed to determine steady-state tetracycline disposition in the animal. Such information is necessary to understand the correlation of serum tetracycline levels with the drug's therapeutic efficacy and potential toxicities. To achieve true steady-state drug kinetics, a constant-rate drug delivery system such as a long-term infusion pump apparatus is necessary, and the difficulty of performing such experiments with small animals is readily appreciated. Multiple oral administrations fall far short of meeting steady-state drug delivery requirements, producing a typical sawtooth pattern of serum drug concentrations with time.

A practical alternative to this problem is controlled drug release with an implantable system that delivers the pharmaceutical at a constant rate. Steroid delivery polymer devices based on a matrix-controlled diffusional process have been developed and investigated *in vivo* (7–9). Matrix devices with a characteristic release profile that is initially high and decreases with time fail to deliver the drug at a constant rate. Winkler *et al.* (10) developed a matrix-controlled progesterone-releasing intravaginal matrix device which, due to the unequal lag times of the device's inner and outer surfaces, produced a pseudo-zero-order release profile *in vivo*.

Chien *et al.* (11) recently reported a zero-order rate device for deoxycorticosterone acetate delivery from subcutaneous implants in rats. This device, named the microsealed drug delivery system, provided constant drug release for studying the production of metacorticoid hypertension in rats.

A previous publication (12) detailed the development in this laboratory of a membrane-controlled drug delivery system designed to release tetracycline at a constant rate with time. *In vitro* testing demonstrated the zero-order release characteristics of the trilaminate device in which the release rate was adjustable by either varying the copolymer coating membrane composition or altering the coating membrane thickness and/or the device geometry.

The present report details the *in vivo* release characteristics of the trilaminate tetracycline device implanted intraperitoneally in rats. A flow-limited pharmacokinetic modeling approach, as previously reported (13), was used to correlate *in vivo* zero-order tetracycline release rates from the implanted trilaminate device with the subsequent steady-state drug distribution in the plasma and tissues. The flow-limited model is based on measurable anatomical and physiological parameters and is designed to provide a conceptual representation of the mass transfer and elimination of drugs and their metabolites between real organ compartments. This modeling approach was chosen to define steady-state tetracycline disposition and to confirm the zero-order release characteristics of the trilaminate device.

EXPERIMENTAL

Tetracycline–Copolymer Device Fabrication—Disk-shaped trilaminate tetracycline-releasing devices were prepared by a procedure outlined previously (12). In brief, [^{3}H]tetracycline is mixed with a 63:37 2-hydroxyethyl methacrylate–methyl methacrylate copolymer to form the core of the device (20% drug by weight loading). The core is enclosed by a uniform membrane layer constructed of either a 2:98 or a 22:78 2-hydroxyethyl methacrylate–methyl methacrylate copolymer which, by its reduced tetracycline permeability (relative to the core material), maintains a constant drug concentration gradient within the enclosure, providing for a constant steady-state tetracycline release rate. The implanted disks were 15 mm in diameter and had an average coating thickness of 0.055 mm.

Animals—All animals were virgin female Sprague–Dawley rats weighing 180–220 g. For the pharmacokinetic studies, the rats were housed individually in standard metabolic cages, permitting the collection

0022-3549/79/0900-1151$01.00/0
© 1979, American Pharmaceutical Association

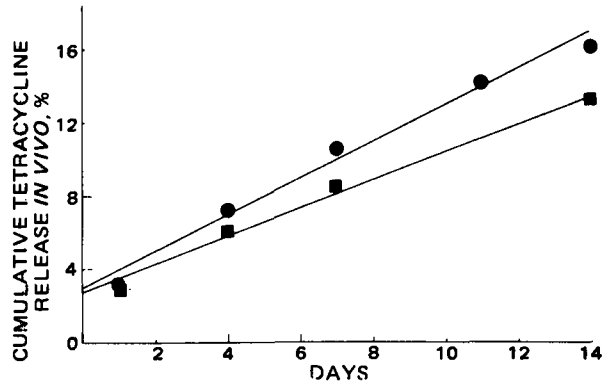

Figure 1—*Steady-state tetracycline release from trilaminate disks in 200-g rats. Percent release was determined by analysis of drug remaining in recovered disks. Key:* ■, *2:98 2-hydroxyethyl methacrylate–methyl methacrylate-coated trilaminate disks; and* ●, *22:78 2-hydroxyethyl methacrylate–methyl methacrylate-coated trilaminate disks.*

and quantitation of separate daily urine and fecal samples. The rats were fed[1] and provided with unrestricted water.

Biocompatibility Studies—Copolymer trilaminates (either containing tetracycline or with drug-free cores) were implanted subcutaneously in a pocket constructed by blunt dissection beneath the dorsal fascia layers and directly superficial to the spinotrapezius muscle. The incision was closed superficially with wound clips. Five rats received implants containing 1% tetracycline by weight in the cores, and an additional five rats received drug-free implants constructed in an otherwise identical manner to the tetracycline-containing implants. Before implantation, the trilaminate disks were washed in a small volume of sterile saline solution to remove surface contaminants.

At 1, 2, 4, 6, and 9 weeks following implantation, one rat from each group was sacrificed and the implant was removed carefully along with its surrounding tissue capsule. The tissue block containing the implant was fixed in formaldehyde for 24–48 hr. Paraffin sections were prepared and stained with hematoxylin and eosin and with trichrome dyes for histological investigation.

This procedure was repeated for a series of 10 intraperitoneal implants. The animals were laparotomized, and the saline-washed trilaminate disks were placed within the lower portion of the peritoneal cavity; the peritoneum and skin incisions then were closed separately with interrupted sutures. Recovered implants and tissue capsules were sectioned and stained as described previously.

Pharmacokinetic Studies—Trilaminate devices in the pharmacokinetic studies were implanted intraperitoneally, according to the outlined procedure, to minimize variations in implant drug release rates due to site-specific tissue capsule formation and associated inflammatory response. Ten rats received tetracycline–copolymer implants coated with a 22:78 2-hydroxyethyl methacrylate–methyl methacrylate copolymer membrane, and 10 rats received implants coated with a 2:98 2-hydroxyethyl methacrylate–methyl methacrylate copolymer membrane. Immediately prior to implantation, the trilaminate disks were washed with a saline solution and the saline wash solutions were analyzed for [^{3}H]-tetracycline. In all cases, the tetracycline loss into the saline wash was insignificant (always <0.01% of the original drug loading).

One day prior to surgery, a control blood sample was taken and the animals were placed in the metabolic cages to collect control fecal and urine samples. Blood was obtained from the jugular vein by puncture with a 1-ml tuberculin syringe fitted with a 26-gauge intradermal tip needle. Blood was drawn once a day from each rat up to and including the day the animal was sacrificed. Daily urine and feces from each animal were weighed and collected for [^{3}H]tetracycline analysis.

The urine sample was centrifuged to remove solids, and 0.2 ml was added with 0.5 ml of distilled water, to prevent salting out, to 10 ml of fluor[2] in a glass counting vial. A 100–150-mg sample of the daily fecal collection was prepared according to a modified oxidative procedure described in the literature (14). The dissolved fecal sample, to which 10 ml of fluor[3] was added, was allowed to equilibrate overnight before counting. Whole blood samples were centrifuged, 0.2 ml of plasma was

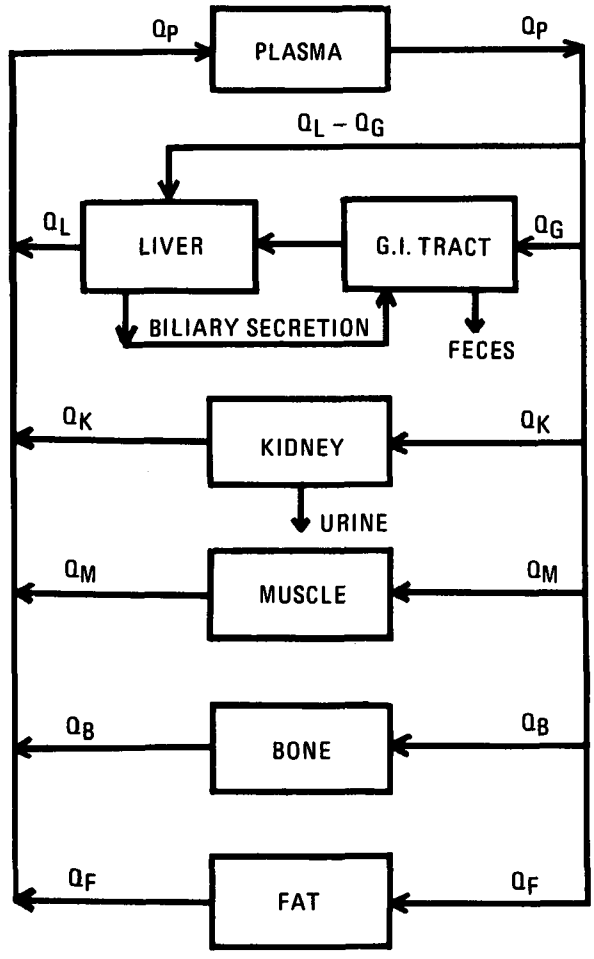

Figure 2—*Flow scheme and organ compartmental diagram utilized in pharmacokinetic model; Q represents plasma flow rate to indicated organs. Model parameter values are listed in Table I.*

added to a glass vial containing 10 ml of fluor[2], and concentrations were determined in a liquid scintillation counter[4].

Animal Sacrifice and Tissue Recovery—Rats were sacrificed (two from each series) on Days 1, 4, 7, 10, and 14 of implantation by cervical-spinal dislocation. Tissues and organs were removed carefully to prevent excess bleeding and blotted gently. Gut tissue was obtained from the upper small intestine. The kidneys were clamped at the renal arteries and removed *in toto*. A section of the liver from the upper right lobe was recovered. The tibia was dissected clean of muscle and connective tissue and crushed, and a muscle sample was removed from the lower thigh.

Sections of soft tissue (100–150 mg) were prepared by a tissue digestion technique (15). Minced tissue was weighed into glass vials to which 1.0 ml of a tissue solubilizer[5] was added. The vials were capped tightly and incubated at 55° for 16–24 hr until digestion was complete. Hydrogen peroxide (0.1 ml/sample) was added to decolorize the samples, the vials were cooled, and 10 ml of fluor[6] was added to each vial. Samples were allowed to equilibrate overnight before counting. Unlabeled tissue samples were processed in an identical manner to correct for background radiation and quenching effects.

Bone samples were prepared by a modified tetracycline extraction procedure (16). Clean bone samples fractured into small fragments were weighed and added to glass vials (~100–150 mg) containing 3 ml of 0.25 *N* HCl. The vials were sealed tightly and stored at 4° with daily shakings. After 1 week, the extract was removed; bone contents were washed with distilled water and transferred to new vials to repeat the procedure (a total of three times). The extract was centrifuged, and 1 ml of the supernate was assayed for [^{3}H]tetracycline by counting in 10 ml of fluor[2].

[1] Purina Rat Chow, Ralston Purina Co., St. Louis, Mo.
[2] Scintosol, Isolabs, Akron, Ohio.
[3] Biofluor, New England Nuclear, Boston, Mass.
[4] Isocap, Searle Analytic, Des Plaines, Ill.
[5] Protosol, New England Nuclear, Boston, Mass.
[6] Econofluor, New England Nuclear, Boston, Mass.

Table I—Physiological Parameters for Tetracycline Pharmacokinetic Model

Tissue[a]	Volume[b], V, ml	Plasma Flow[c], Q, ml/hr	Partition Coefficient, R_i	Literature Values for Tissue–Plasma Concentration Ratio
Plasma	9.0	1416.0	—	—
Liver	8.3	585.0	5.3	4.1[d]
Kidneys	2.0	487.0	4.8	3.3[d]
Bone	10.0[e]	40.0	12.5	8.95[f]
Muscle	100.0	292.0	2.9	1.2[d]
Fat	14.0[g]	19.2[g]	0.7	0[h], 1.5[d]
GI tract	16.0	463.0	4.4	3.1[i]

[a] Values given are for 200-g female rat. [b] Reference 18. [c] Reference 19. [d] Reference 1. [e] Calculated as 2.5 times bone marrow volume reported. [f] Reference 2; concentration was measured in mouse femur. [g] Reference 20; values were scaled down from those reported for a 250-g rat. [h] Reference 6. [i] Reference 14.

Implants recovered at sacrifice were blotted dry of surface fluid and weighed. Sections of the recovered implants and the original trilaminate film were dried to constant weight in a vacuum oven (2.1 kg/cm^2, 40°) and allowed to dissolve in 10 ml of dioxane over 2–3 weeks at 50–60°. Measured aliquots of the dioxane solution were analyzed on the liquid scintillation counter for [^{3}H]tetracycline. Tetracycline remaining in the recovered implant was calculated and expressed as a percentage of the original weight of drug loaded in the trilaminate film (Fig. 1).

Blood Volume Measurements—Organ blood volumes in five rats were measured by a standard ^{51}Cr-red blood cell labeling procedure (17). One milliliter of whole blood, obtained by jugular puncture from the animal to be tested, was added to 1.0 ml of citrate–dextrose solution, Strumia type, containing chromate 51 salt. After 20–30 min of incubation at room temperature, the whole blood solution was centrifuged at 2000×g for 10 min, the supernate was discarded, and 1.0 ml of fresh saline–plasma (5:1) solution was mixed with the suspended cells, after which the sample was recentrifuged. This procedure was repeated four to eight times until extracellular radionuclide levels were <0.1%.

After the final wash, 0.5 ml of the fresh saline–plasma solution was mixed with the suspended cells, and the total volume was injected by cardiac puncture into the rat. Heparinized whole blood samples were taken by jugular vein puncture at 10 and 20 min postinjection; the animal was then sacrificed by cervical-spinal dislocation. Tissues were removed exactly as already described in an effort to measure organ residual blood volumes best reflecting the tissue recovery techniques employed in the kinetic studies. In all cases, radionuclide levels in the whole blood were similar, to within 5%, at the 10- and 20-min sampling periods. Whole blood, saline wash solutions, and minced tissue samples were analyzed using an automatic gamma counter[7].

Pharmacokinetic Model—The pharmacokinetics of zero-order tetracycline delivery from controlled-release implants and tissue drug distribution were described by a mathematical model based on the blood flow-limited concept of drug transport. The relevant compartments and general blood flow scheme are depicted in Fig. 2. This model employs true physiological and anatomical parameters to generate a series of mass balance equations for seven organ compartments. An example of such a mass balance equation is presented for the hypothetical compartment i:

$$V_i \frac{dC_i}{dt} = Q_i C_P - Q_i \frac{C_i}{R_i} - K_i \frac{C_i}{R_i} \qquad \text{(Eq. 1)}$$

where C_i is the tissue drug concentration, V_i is the tissue volume, R_i is the equilibrium partition coefficient (tissue–plasma), K_i is the rate of drug elimination or clearance by the tissue, C_P is the plasma drug concentration, Q_P is the plasma flow rate, and t is time.

Organ volumes, blood plasma flow rates, and drug partition coefficients (determined by best fit analysis of the data) are listed in Table I. Total drug clearance was estimated from the total daily excretion rates and the steady-state plasma concentrations. Approximately 30% of the drug was excreted in the urine, while 70% of the drug was accounted for by fecal elimination. The biliary clearance was estimated from available literature data (21). For simplicity, the gut tissue and gut contents were combined as one compartment. Fecal tetracycline clearance calculations were adjusted by a factor equal to the approximate steady-state ratio of tetracycline concentration in the gut tissue and gut contents.

Tetracycline delivery was modeled as a zero-order input term into the plasma compartment. The magnitude of this input term was set equal to the zero-order release rate determined from the implant recovery analysis. The balance equation for the plasma is:

$$V_P \frac{dC_P}{dt} = K_0 + Q_L \frac{C_L}{R_L} + Q_G \frac{C_G}{R_G} + Q_K \frac{C_K}{R_K} + Q_M \frac{C_M}{R_M} + Q_B \frac{C_B}{R_B} + Q_F \frac{C_F}{R_F} - Q_P C_P \qquad \text{(Eq. 2)}$$

where subscripts L, K, M, B, F, P, and G denote liver, kidney, muscle, bone, fat, plasma, and GI tract, respectively; and K_0 is the zero-order input term.

Burst effects corresponding to experimentally measured values are incorporated into the K_0 term and into the clearance terms for the first 24 hr of implantation.

RESULTS AND DISCUSSION

Biocompatibility—Subcutaneous implant studies revealed no differences in fibrous capsule formation or general tissue response between the tetracycline-loaded trilaminate disks and the control trilaminate disks containing no drug in the core. Capsule thickness was maximal by 4–6 weeks implantation time, followed by further organization of the surrounding fibrous tissue. Early implant capsules (1–2 weeks) demonstrated mild inflammation with some surrounding tissue edema and loose granulation tissue with onset of fibrous capsule formation. There was little evidence of any chronic inflammatory processes in the long-term implants (4–9 weeks), the surrounding capsules consisting of well-organized, dense collagen fibrils with little cellular infiltration. These results agree with previous observations (22) concerning the tissue biocompatibility of methyl methacrylate polymers, indicating that the coating copolymer surface (containing 2% 2-hydroxyethyl methacrylate and 98% methyl methacrylate) was the controlling factor in the response of the surrounding tissue to the implanted device.

By comparison, fibrous capsule formation was essentially absent for both drug-loaded and control disks implanted in the peritoneal cavities of rats. Only a thin membrane formed over the intraperitoneal implants, and this membrane was easily disrupted upon implant recovery. In most cases, the implant lodged in the intraperitoneal fat near the site of the original laparotomy. In three cases, the implant migrated to the upper peritoneum, resting on either the dome of the lower left lobe of the liver or the omentum.

***In Vivo* Implant Hydration**—Equilibrium swelling was achieved for samples of both the 2:98 and 22:78 implant series retrieved on the 4th day of implantation. For these implant series, the equilibrium swelling values were 44.5 ± 2.6 and 44.8 ± 1.6%, respectively (mean ± SE taken over the entire implantation period). These similar values indicate that equilibrium hydration of the device is best represented by the swelling of the core component (63:37 copolymer) that makes up the bulk of the trilaminate disk.

The *in vivo* swelling measurement of 44–45% is higher than the equilibrium hydration value of 26.5% previously reported for blank 63:37 copolymer membranes measured *in vitro* (12). The observed difference in swelling values between the *in vivo* disks and the blank 63:37 membrane tested *in vitro* was likely due to the osmotic action of the drug contained in the core (20% drug, w/w) of the implanted device.

Cumulative Release and Excretion Data—Tetracycline release from the implanted trilaminate disks (Fig. 1) appeared constant with time and exhibited a zero-order release profile similar to that reported in the *in vitro* trials. The release rates of the 2:98 (123 μg/day) and the 22:78 (158 μg/day) copolymer coated disks differed significantly. The fact that both series demonstrated a nonzero intercept indicates an initial burst effect of 2–3% over the first 24 hr of release.

To confirm the observation of *in vivo* zero-order release from the implanted trilaminate disks, tetracycline levels were measured in fecal and urine samples. Total daily fecal and urine volumes were recorded over the implantation period. These values were employed to quantitate total daily tetracycline elimination in the excretion products. This method provides a reliable estimate of total physiological drug elimination since tetracycline is not metabolized by the rat (23). Over the steady-state drug release period (Days 2–14), the mean cumulative daily physiological elimination of tetracycline (Table II, measured as the sum of the total daily drug excretion in the steady-state fecal and urine outputs) was 110

[7] Model 1185, Searle Analytic, Des Plaines, Ill.

Table II—Comparison of Steady-State Cumulative Tetracycline Release and Elimination Rates

Coating Composition of Membrane Device	Zero-Order Release Rate[a], μg/day	Total Elimination by Rat[b], μg/day, Mean ± *SD*
2:98 series	123	110 ± 32
22:78 series	158	153 ± 42

[a] Determined from slope of cumulative release curve (Fig. 1). [b] Sum of urine and fecal tetracycline excretion per day over steady-state period (12 days).

μg/day for the 2:98 copolymer-coated implant series and 153 μg/day for the 22:78 copolymer-coated implant series.

These elimination rate values agree remarkably well with the steady-state, *in vivo* release rates. The initial drug release burst of 2–3% from the implants also was evident in the initial high drug elimination levels recorded over the first 1 or 2 days of implantation (~480 μg total for the first 2 days in the 22:78 implant series and 435 μg total for Days 1–3 in the 2:98 series, corresponding to 2.7–3.0% the initial drug loading in the disks). For both implant series, daily tetracycline elimination was ~31% in the urine and ~69% by the fecal route.

Without further data, it would be inappropriate to correlate *in vivo* release rates with the physiological drug elimination rate. However, given the evidence of near-constant plasma and tissue tetracycline levels over the same steady-state period (Figs. 3 and 4), a true mass balance is possible for the *in vivo* system. The analysis of drug release from recovered disks, daily tetracycline elimination rates, and steady-state drug levels in the blood and tissues provides indisputable experimental evidence that the implants are releasing tetracycline at a constant rate over the steady-state portion of the implantation period. This finding confirms the earlier *in vitro* observations on the zero-order release rate character of the copolymer trilaminate device.

Experimental Drug Levels in Blood and Tissue—Plasma tetracycline achieved near-constant levels within 2–4 days following implantation and remained stable during the experiment (Fig. 3). Experimental tissue tetracycline concentration values were corrected for residual blood content. Experimental values for residual blood volumes in individual organs were determined by a ^{51}Cr-red blood cell labeling technique (17). These results are compared to literature values given in Table III.

Minimum organ blood volumes reported by Sharpe *et al.* (24) were determined by a radiolabeled cell method in which the rats were anesthetized with ether and bled maximally from the abdominal aorta or inferior vena cava before the organs were recovered and analyzed for radiolabeled blood cell content. Organ blood volume values reported by Everett *et al.* (25) (Table III) were determined by achieving maximal recovery of residual blood in the respective tissues. In this method, the rats were injected with radiolabeled red blood cells or ^{135}I-serum albumin; after a suitable circulatory mixing period (3–15 min), the rats were sacrificed quickly by freezing in liquid nitrogen. Quick freezing of the animal's body fluids and tissues produced a rapid stasis of the blood, permitting dissection of the organs for radioassay without blood loss.

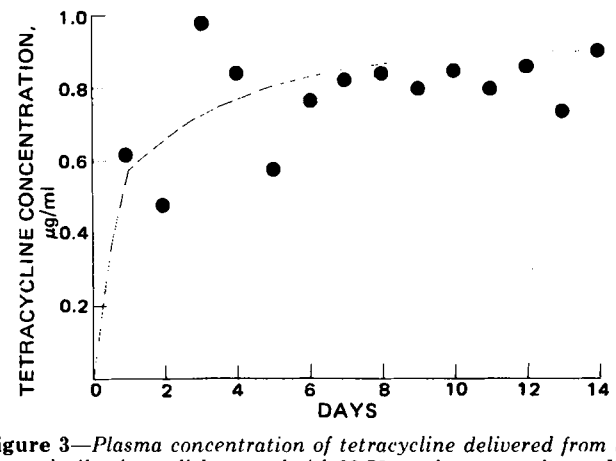

Figure 3—*Plasma concentration of tetracycline delivered from implanted trilaminate disks coated with 22:78 copolymer membrane. Key: ●, experimentally determined plasma tetracycline concentrations; and ---, model simulation results.*

Table III—Tissue Residual Blood Volumes (Milliliter of Whole Blood per Gram of Wet Tissue)

Tissue	Experimental Results[a], Mean ± *SD*	Reference Values: Minimum Volume[b]	Reference Values: Total Volume[c]
Liver	0.060 ± 0.012	0.047	0.265
Kidney	0.087 ± 0.027	0.049	0.154
Muscle	0.008 ± 0.002	0.004	0.023
Fat	0.006 ± 0.001	—	—
Gut	0.016 ± 0.004	—	0.035
Bone	0.028 ± 0.009	—	0.033

[a] As determined from five experiments employing ^{51}Cr-labeled red blood cells. [b] Data from Ref. 24. [c] Data from Ref. 25.

Residual blood volumes calculated in the present experiment are the result of a procedure designed to reflect the organ blood volumes remaining in the various tissues after the experimental dissection of the organs for analysis of drug content. As expected, these experimental values fall within the range of results presented by the more radical techniques. Previous investigations of differential tissue drug levels failed to correct for residual blood drug content. Depending on actual blood–tissue drug partitioning effects, the method of sacrifice, and the organ recovery techniques employed, failure to correct for the residual blood volume can lead to significant errors in experimental drug content analysis. The need for accurate tissue drug level determinations is critical when attempts are made to fit experimental data to pharmacokinetic models; false experimental values produce erroneous estimates of model transport and kinetic parameters.

The highest tissue tetracycline concentrations were recorded in the whole bone samples (Fig. 4). This result is in agreement with previous observations (26) on the deposition of high tetracycline levels in growing bone tissue. High tetracycline levels in the kidney and liver (Fig. 4) reflect the roles of these organs in tetracycline elimination through the urine and bile, respectively. The lowest tetracycline concentrations were measured in the fat tissue, which failed to concentrate the antibiotic above levels measurable in the plasma. Steady-state plasma and tissue levels were not significantly different in the two tetracycline delivery series. The difference in recorded release rates apparently contributed only to the observed differences in tetracycline elimination rates since the tissues reached similar equilibrium saturation levels early in the experiment for the observed range of drug delivery rates from the two implant series.

Pharmacokinetic Model—There was good general agreement between predictions based on the flow-limited pharmacokinetic model (Fig. 2) and the actual experimental measurements of the organ disposition of tetracycline and of tetracycline elimination. Experimental tetracycline concentrations in the plasma (Fig. 3) and individual tissues (Fig. 4) demonstrated levels consistent with model predictions based on the zero-order rate diffusional input determined from the slopes of the cumulative release curves (Fig. 1). The tissue–plasma equilibrium partition

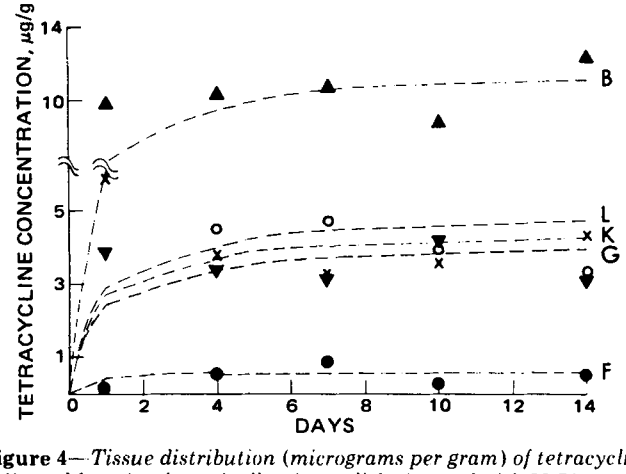

Figure 4—*Tissue distribution (micrograms per gram) of tetracycline delivered from implanted trilaminate disks (coated with 22:78 copolymer membranes). Key (experimentally determined values): ●, fat tissue; ▼, GI tissue; ×, kidney; ○, liver; and ▲, bone. The dashed lines (labeled at right) represent model simulation results for these tissues: F, fat tissue; G, GI tissues; K, kidney; L, liver; and B, bone.*

coefficients (Table I) were estimated initially from the results of earlier intravenous bolus studies with tetracycline (1, 2, 4, 6) and later were adjusted by trial and error to best fit the model predictions to the experimental tissue concentrations.

The ability of trilaminate controlled-release disks fabricated from 2-hydroxyethyl methacrylate–methyl methacrylate copolymers to deliver tetracycline at a constant release rate when implanted in rats has been demonstrated. A full range of *in vivo* zero-order release kinetics is attainable through variations in the copolymer composition of the diffusion-controlling coating membrane of the trilaminate disk. The ability of such a device to deliver a pharmaceutical at a desired constant release rate over a long period is extremely valuable both as a therapeutic and an investigational tool. This system may be extended to the study of other drugs where long-term constant delivery rates are desired.

A flow-limited pharmacokinetic model is presented that utilizes the ability of the trilaminate controlled-release device to deliver tetracycline at constant rates over a prolonged implantation period. Predictions based on this model are consistent with tissue tetracycline concentrations measured in experiments with these implant devices. The physiological pharmacokinetic model can be utilized to provide reliable predictions of tissue drug levels and is useful in studies of differential organ toxicities due to effects caused by the parent drug or its metabolites (27). The model also contributes information valuable for the design of proper drug dosing regimens and for the fabrication and placement of controlled drug delivery systems designed to deliver drugs to selected physiological target sites.

The coupling of the principles of controlled release from a zero-order rate device and long-term physiological pharmacokinetic modeling is a unique research concept and will be used in investigational systems where such drug delivery characteristics help elucidate physiological rate mechanisms.

REFERENCES

(1) T. Andre, *Acta. Radiol. Scand., Suppl.*, **142**, 1 (1956).

(2) A. L. Dunn, C. D. Eskelson, J. F. McLeay, R. E. Ogborn, and B. R. Walske, *Proc. Soc. Exp. Biol. Med.*, **104**, 12 (1960).

(3) E. I. Takesue, G. Tonelli, L. Alfano, and D. A. Buyske, *Int. J. Appl. Rad. Isotopes*, **8**, 52 (1960).

(4) J. F. Snell, R. Garkuscha, and E. L. Allen, in "Antibiotics Annual, 1957–1958," Medical Encyclopedia, New York, N.Y., pp. 502–506.

(5) R. G. Kelly and L. A. Kanegis, *Toxicol. Appl. Pharmacol.*, 11, 114 (1967).

(6) L. E. Bottiger, *Acta Med. Scand.*, **151**, 343 (1955).

(7) Y. W. Chien, S. E. Mares, J. Berg, S. Huber, H. J. Lambert, and K. F. King, *J. Pharm. Sci.*, **64**, 1775 (1975).

(8) Y. W. Chien and E. P. K. Lau, *ibid.*, **65**, 488 (1976).

(9) D. R. Kalkwarf, M. R. Sikov, L. Smith, and R. Gordon, *Contraception*, **6**, 423 (1972).

(10) V. W. Winkler, S. Borodkin, S. K. Webel, and J. T. Mannebach, *J. Pharm. Sci.*, **66**, 816 (1977).

(11) Y. W. Chien, L. F. Rozek, and H. J. Lambert, *ibid.*, **67**, 214 (1978).

(12) L. Olanoff, T. Koinis, and J. M. Anderson, *ibid.*, **68**, 1147 (1979).

(13) R. L. Dedrick and K. B. Bischoff, *Chem. Eng. Prog. Symp. Ser.*, **64**, 32 (1968).

(14) D. T. Mahin and R. T. Lofberg, *Anal. Biochem.*, **16**, 500 (1966).

(15) New England Nuclear, "Liquid Scintillation Counting, Procedures and Products," July 1977, p. 7.

(16) K. van Jackman, L. Klein, and S. H. Lacey, *Biochem. Med.*, **8**, 114 (1973).

(17) C. A. Owen, "Diagnostic Radioisotopes," Charles C Thomas, Springfield, Ill., 1959, pp. 157–168.

(18) R. L. Dedrick, D. S. Zaharko, and R. J. Lutz, *J. Pharm. Sci.*, **62**, 882 (1973).

(19) L. I. Harrison and M. Gibaldi, *ibid.*, **66**, 1138 (1977).

(20) D. B. Tuey and H. B. Matthews, *Drug Metab. Dispos.*, **5**, 444 (1977).

(21) J. Adir, *J. Pharm. Sci.*, **64**, 1847 (1975).

(22) E. O. Dillingham, N. Webb, W. H. Lawrence, and J. Autian, *J. Biomed. Mater. Res.*, **9**, 569 (1975).

(23) R. G. Kelly and D. A. Buyske, *J. Pharmacol. Exp. Ther.*, **130**, 144 (1960).

(24) L. M. Sharpe, G. C. Culbreth, and J. R. Klein, *Proc. Soc. Exp. Biol. Med.*, **74**, 681 (1950).

(25) N. B. Everett, B. Simmons, and E. P. Lasher, *Circ. Res.*, **4**, 419 (1956).

(26) D. A. Buyske, H. J. Eisner, and R. G. Kelly, *J. Pharmacol. Exp. Ther.*, **130**, 150 (1960).

(27) R. J. Lutz, R. L. Dedrick, H. B. Matthews, T. E. Eling, and M. W. Anderson, *Drug Metab. Dispos.*, **5**, 386 (1977).

ACKNOWLEDGMENTS

L. Olanoff gratefully acknowledges support from the National Institutes of Health Medical Scientist Training Program, Grant GM-07250.

Urinary Metabolites of 3a,4,5,6,7,7a-Hexahydro-3-(1-methyl-5-nitro-1H-imidazol-2-yl)-1,2-benzisoxazole in the Dog

W. J. A. VANDENHEUVEL *x, B. H. ARISON *, T. W. MILLER *, P. KULSA *, P. ESKOLA *, H. MROZIK *, A. K. MILLER ‡, H. SKEGGS ‡§, S. B. ZIMMERMAN ‡, and B. M. MILLER ‡

Received December 21, 1978, from *Merck Sharp & Dohme Research Laboratories and ‡Merck Institute for Therapeutic Research, Rahway, NJ 07065. Accepted for publication March 27, 1979. §Merck Sharp & Dohme Research Laboratories, West Point, PA 19486.

Abstract □ The antiprotozoal drug 3a,4,5,6,7,7a-hexahydro-3-(1-methyl-5-nitro-1H-imidazol-2-yl)-1,2-benzisoxazole (I), which exhibits activity against trypanosomiasis, is also antibacterial *in vivo*. Since the urine from a dog dosed with I showed a broader spectrum of antibacterial activity than I itself, metabolites from this urine were isolated and partially characterized. The metabolites were mono- and dihydroxy-substituted species with the hydroxyl groups on carbons 4–7 of the hexahydrobenzisoxazole ring. These observations led to the synthesis of several such hydroxy derivatives of I, and their properties fully supported the proposed positions of metabolic hydroxylation. One synthetic compound, the 6,7-*cis*-dihydroxy compound, exhibited higher antibacterial activity against *Salmonella schottmuelleri* in mice and greater trypanocidal activity *in vivo* against *Trypanosoma cruzi* (Brazil strain) than I.

Keyphrases □ 3a,4,5,6,7,7a - Hexahydro-3 - (1-methyl-5-nitro-1H-imidazol-2-yl)-1,2-benzisoxazole—urinary metabolites, antibacterial activity, antiprotozoal activity, dog □ Antiprotozoal agents—3a,4,5,6,7,7a-hexahydro -3- (1-methyl -5- nitro-1H-imidazol -2- yl)-1,2-benzisoxazole, urinary metabolites, antibacterial activity, antiprotozoal activity, dog □ Benzisoxazoles—3a,4,5,6,7,7a-hexahydro-3-(1-methyl-5-nitro-1H-imidazol-2-yl)-1,2-benzisoxazole, urinary metabolites, antibacterial activity, antiprotozoal activity, dog

3a,4,5,6,7,7a-Hexahydro-3-(1-methyl -5- nitro-1H-imidazol-2-yl)-1,2-benzisoxazole (MK-436, I) exhibits antiprotozoal activity (1), including activity against *Trypanosoma cruzi*[1]. The evaluation of I for mutagenicity was hampered by the fact that the compound was antibacterial in the host-mediated mouse test at levels of 200 mg/kg or higher but not at 10 mg/ml in the Ames *et al.* (2) spot test utilizing *Salmonella typhimurium* G46[2]. These results aroused the suspicion that antibacterial metabolites were produced by the mouse, especially since incubation of I with liver homogenate fraction S-9, prepared by reported procedures (3), produced antibacterial activity not observed with I alone. Since mouse and dog urine from animals dosed with I showed a broader antibacterial spectrum (and higher potency) than I, the present study was undertaken to characterize the canine urinary metabolites of I to allow their synthesis for biological testing.

EXPERIMENTAL

Dog urine was collected for metabolite isolation. The dog was dosed with I at 1000 mg/kg po in two divided doses per day for 2 days. This regimen was repeated 2 weeks later; the two 48-hr postdose urine collections were pooled to yield 2800 ml. The pooled urine was extracted twice with equal volumes of methylene chloride. The extracts were combined, concentrated to dryness under reduced pressure, dissolved in methanol, and centrifuged to remove insoluble components.

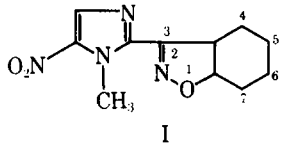

I

The methanol was removed *in vacuo*, and 150 mg of the residue was dissolved in benzene and chromatographed on a column containing 100 g of silica gel[3] packed in benzene. The column was developed with a stepwise gradient of methanol in benzene as follows: 400 ml of benzene, 800 ml of benzene containing 5% methanol (v/v), and then 600 ml of benzene containing 10% methanol. The column was developed at 5 ml/min, and 20-ml fractions were collected and assayed against a highly sensitive bacterium, *Bacillus subtilis* MB964.

The most active fractions occurred toward the end of the 5% methanol development, and they were pooled and concentrated to dryness to yield 68 mg of residue. The residue was dissolved in 1.7 ml of ethanol, and 100-μl portions were subjected to preparative TLC on silica gel plates[4]. The plates were developed with benzene–methanol (9:1) and then examined under shortwave UV light and by bioautography against *B. subtilis*. Ten distinct bands were observed under UV light, and five were active against *B. subtilis*. Four major bands [R_f 0.27 (active), 0.32 (inactive), 0.37 (active), and 0.42 (inactive)] were scraped off the plates and extracted with benzene–methanol (5:1). These extracts (designated Metabolite Fractions A–D) were examined by direct probe mass spectrometry, combined GLC–mass spectrometry, and NMR spectroscopy.

n-Butylboronate derivatives were prepared by allowing aliquots of samples dissolved in acetone to react with excess *n*-butylboronic acid[5] for 1 hr at room temperature. Trimethylsilylation was carried out by treating aliquots of samples with bis(trimethylsilyl)acetamide[6] or bis-(trimethylsilyl)acetamide-d_{18}[7] (to form the perdeutero derivatives) and pyridine (2:1) for 1 hr at 60°.

Mass spectra were obtained[8] using a 70-ev ionizing potential, a 3.5-kv accelerating potential, a 60-μamp trap current, and a 250° source temperature. GLC conditions were: 1.8-m × 3-mm i.d. spiral glass column at 205°; 3% OV-101 on 80–100-mesh acid-washed and silanized diatomaceous earth[9]; flash heater and molecular separator temperatures, 250°; and helium flow rate, 30 ml/min. NMR spectra were obtained[10] with samples dissolved in deuterochloroform.

The spent urine from the extraction was concentrated to 1150 ml under reduced pressure, adjusted to pH 4.5 with 1 *M* HCl, mixed with 30 ml of an enzyme preparation containing sulfatase and glucuronidase[11], and then incubated at 37° for 18 hr. This mixture was extracted with 2 liters and then with 1 liter of methylene chloride. The extracts were combined, concentrated to dryness under reduced pressure, dissolved in 15 ml of methanol, and centrifuged to remove insoluble components. Aliquots of this solution (Metabolite Fraction E) were examined also by mass spectrometric-based methods.

In vivo evaluations of I and 6,7-*cis*-dihydroxy-I (Compound G) were conducted by suspending the test compounds evenly in a 1% methylcellulose aqueous vehicle to the desired concentrations. Albino male mice[12]

[1] C. M. Malanga, J. Conroy, and A. C. Cuckler, Merck Sharp & Dohme Research Laboratories, Rahway, NJ 07065, personal communication.
[2] H. Skeggs, unpublished data.
[3] Silica gel G, Brinkmann.
[4] Quanta/Gram QIF plates, Quantum Industries.
[5] Applied Science Laboratories.
[6] Supelco.
[7] Merck Sharp & Dohme of Canada.
[8] LKB model 9000.
[9] Gas Chrom P, Applied Science Laboratories.
[10] Varian HA-100D equipped with a Fourier transform accessory.
[11] Glusulase, Endo Laboratories.
[12] Carworth Farms.

0022-3549/79/0900-1156$01.00/0
© 1979, American Pharmaceutical Association

Table I—Mass Spectrometric Behavior of I and Related Compounds

I		Dihydroxy Metabolite C			Dihydroxy Metabolite C *n*-BuB[c]		Monohydroxy Metabolite			6,7-*cis*-Dihydroxy Synthetic G		
Ion, *m/e*	Intensity[a]	Ion, *m/e*	Δ[b]	Intensity	Ion, *m/e*	Intensity	Ion, *m/e*	Δ	Intensity	Ion, *m/e*	Δ	Intensity
M, 250	100	M, 282	32	35	M, 348 (^{11}B) 347 (^{10}B)	100 25	M, 266	16	73	M, 282	32	61
M − 17, 233	42	M − 17, 265	32	30	M − 17, 331 (^{11}B)	19	M − 17, 249	16	61	M − 17, 265	32	43
		M − 35, 242	—	20						M − 35, 247	—	70
		M − 43, 239	—	6	M − 57, 291 (^{11}B)	73	M − 43, 223	—	25	M − 43, 239	—	22
M − 45, 205	17	M − 45, 237	32	5			M − 45, 221	16	11	M − 45, 237	32	8
							M − 61, 205	0	10			
M − 55, 195	36	M − 87, 195	0	90	M − 153, 195	57	M − 71, 195	0	83	M − 87, 195	0	89
169	21	169	0	8	169	13	169	0	21	169	0	16
153	70	153	0	100	153	64	153	0	100	153	0	100
107	18	107	0	22	107	11	107	0	30	107	0	31

[a] Relative to base peak (100). [b] Change in *m/e* relative to I. [c] *n*-Butylboronate derivative.

(CF-1 strain), 18–22 g, were inoculated subcutaneously with ~2 × 10^4 *T. cruzi* B[13]; the inoculum was parasitemic mouse blood diluted with Hoppe–Chapman solution (0.75% NaCl and sodium citrate plus 0.2% glucose).

Twenty-four hours after inoculation and for 3 successive days thereafter, each mouse was dosed by gavage with 0.2 ml of the test suspension at the desired concentration; there were two groups of five mice each per treatment. Infected, sham-treated (five groups), and sham-infected, sham-treated (two groups) controls were included. Mortality and percent with parasitemia were noted through Day 50 postinoculation. All infected controls became parasitemic, and 83% died.

For the mouse protection study, Charles River CDI female mice, 21 g, were injected intraperitoneally with 0.5 ml of a broth dilution of a 15-hr culture of *Salmonella schottmuelleri* MSD 3010. The challenge dose contained about 1 × 10^7 colony-forming units, estimated to be 11 times the number of organisms that should kill 50% of the infected, nontreated mice (LD_{50}). The test compounds were suspended evenly in 5% dimethylformamide and were administered by gavage immediately after injection and again 6 hr later. There were five mice at each of the fourfold drug concentrations tested. On the 7th day after infection, the test was considered complete; the survival records of that day were used to calculate the ED_{50} values, the amount of compound that should protect 50% of the infected, treated mice.

RESULTS AND DISCUSSION

Mass spectrometric data for I are presented in Table I. The molecular ion is the base peak with other intense, pertinent ions at *m/e* 233 (M − 17, possibly loss of hydroxyl from the adjacent methyl and nitro groups), 195 [M − 55, loss of C_4H_7 (C-4–C-7 with all but one of the associated hydrogen atoms)], and 153.

The canine metabolite fractions were subjected to direct probe mass spectrometry. Without exception, each appeared to contain a drug-related compound possessing a molecular weight of 282, suggesting introduction of two oxygen atoms into I. Mass spectrometric data for Metabolite Fraction C are presented in Table I. Based on a comparison with the fragmentation pattern of I, the metabolic transformations occurred on C-4–C-7 of the hexahydrobenzisoxazole or "cyclohexane" ring and did not involve either heterocyclic ring. Although the spectra from the four fractions all showed the same molecular ion (*m/e* 282), their relative intensity patterns varied significantly, suggesting that the four zones contain compounds in which two hydroxyl groups are substituted isomerically on positions C-4–C-7 of the cyclohexane ring.

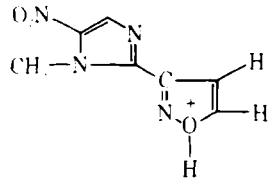

m/e 195

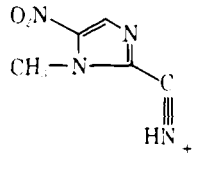

m/e 153

Each metabolite fraction also was subjected to derivatization using *n*-butylboronic acid (4, 5) followed by direct probe mass spectrometry (Table I). These products all exhibited *m/e* 348 as a molecular ion, with fragment ions of *m/e* 331 (M − 17), 291, 195, 169, 153, and 107; the relative intensities of the ions varied from isolate to isolate. The increases of 66 mass units in molecular weight and the $^{10}B/^{11}B$ ratio (1:4) at *m/e* 347/348 demonstrate formation of monocyclic boronate esters and require the presence of 1,2- or 1,3-(*cis*)-diol systems in the metabolites. The ion of *m/e* 291 (M − 57) arises *via* loss of the butyl radical (C_4H_9); prominent ions that do not contain boron (*m/e* 195, 169, 153, and 107) are also found in the spectra of I and underivatized metabolite fractions.

These data demonstrate that the compounds in the TLC zones are metabolites of I: isomeric, dihydroxy-substituted species in which the hydroxyl groups are present on positions 4–7[14]. GLC–mass spectrometry of the trimethyl- (and perdeuterotrimethyl-) silylated metabolite fractions not only supported the dihydroxylation proposal [molecular ions of 426/444 (d)[15]] but showed that each fraction is multicomponent in nature (Fig. 1 and Table II).

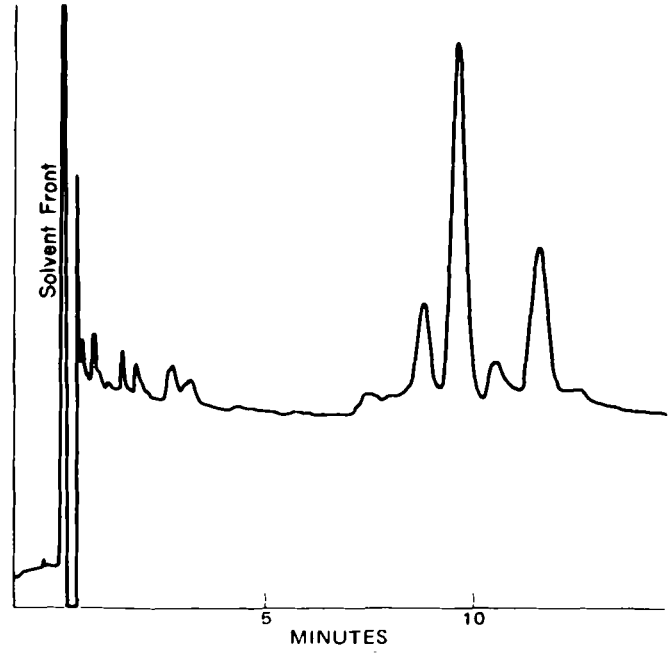

Figure 1—*Gas chromatogram of trimethylsilylated Metabolite Fraction C. Each of the four major peaks results from a metabolite of I. Column conditions are given in* Experimental *section.*

[13] Culture was isolated from a Brazilian patient in 1942 by T. S. Hauschka and maintained by mouse passage at the National Institutes of Health from which R. Hewitt (Lederle Laboratories) obtained subsequent passage material in March 1948. A passage culture was provided to the authors in 1969 and cryogenically preserved until use.

[14] Studies carried out on a methylene chloride extract of the urine of mice treated with I demonstrated that cyclohexane ring hydroxylation also occurred in this species.

[15] Value for trimethylsilyl-d_9 derivative.

Table II—GLC Retention Behavior of Metabolites of I and of Related Compounds

Sample	Retention Time[a]	Extent of Hydroxylation
A	0.92	Dihydroxy
	1.21	Dihydroxy
B	0.76	Dihydroxy
	0.90	Dihydroxy
	1.20	Dihydroxy
C	0.91	Dihydroxy
	1.00	Dihydroxy
	1.09	Dihydroxy
	1.21	Dihydroxy
D	0.97	Dihydroxy
E	0.70	Monohydroxy
	0.76	Dihydroxy
	0.81	Monohydroxy
	0.91	Dihydroxy
	0.97	Dihydroxy
	1.20	Dihydroxy
F[b]	1.19	Dihydroxy
G[c]	1.19	Dihydroxy

[a] Retention times (trimethylsilyl derivatives) relative to the major component of C. Column conditions are given in *Experimental* section. [b] 5,6-*cis*-Dihydroxy. [c] 6,7-*cis*-Dihydroxy.

NMR spectroscopy provided general support for the mass spectrometric conclusion that the metabolites were dihydroxylated on the cyclohexane ring. Although the isolates are admittedly multicomponent in nature and impure, the imidazole ring could be excluded as a possible hydroxylation site since the chemical shifts of the *N*-methyl and nuclear proton were essentially unchanged from those in the parent drug. Compared with the NMR spectrum of I, the metabolites showed new signals in the region associated with HC attached to oxygen. Only partial characterizations were attempted since the isolates were mixtures of two or more closely related isomeric structures.

Fraction E, containing metabolites originally present as conjugates, was examined by direct probe and GLC–mass spectrometry, free and also following trimethylsilylation (Table II). These studies demonstrated that it contained a mixture of mono- and dihydroxy (two and four, respectively) metabolites with the hydroxyl group(s) present on the cyclohexane ring. Mass spectrometric data for one of the two monohydroxy metabolites are presented in Table I. The molecular ion is *m/e* 266, 16 mass units greater than that of I. Many fragment ions in the spectrum possess the same *m/e* values (*i.e.*, 195, 169, 153, and 107) as those found in the spectra of I and its dihydroxy metabolites, indicating the hydroxylation occurred at C-4–C-7. As required, the molecular ions for the trimethylsilyl derivatives of the monohydroxy metabolites were found at *m/e* 338/347 (d). Mono- and dihydroxylation of the cyclohexane ring are reminiscent of the work by Elliott *et al.* (6), who reported that, in the rabbit, the urinary cyclohexane metabolites are the glucuronides of cyclohexanol and *trans*-cyclohexane-1,2-diol. Renwick and Williams (7) also demonstrated that these alcohols (free and conjugated) are cyclohexylamine metabolites in several species. The metabolic hydroxylation of cyclohexyl groups was discussed by Testa and Jenner (8).

Because of the large number of possible dihydroxy I isomers and the complicated nature of the metabolite fractions, complete structural elucidation of the metabolites was not undertaken. Based on available information, however, several dihydroxy I derivatives (Table II) were synthesized[16]. Their mass spectrometric and other physical properties demonstrated that the metabolic transformation of I does, indeed, involve hydroxylation of the hexahydrobenzisoxazole ring (Table I, comparison of the mass spectra of Metabolite Fraction C and Compound G[17]). Efficacious doses (no deaths; no parasitemia) of I and G against an experimental *T. cruzi* B infection in mice were 62.5 and 15.6 mg/kg po × 4 days, respectively. The ED_{50} values of I and G against *S. schottmuelleri* infections in mice were 3.0 and 1.25 mg/mouse (150 and 62.5 mg/kg × 2 doses), respectively. The approach chosen in this study—structural characterization of biologically active metabolites followed by synthesis of bioactive compounds based on this information—has been validated.

REFERENCES

(1) P. Kulsa and C. S. Rooney, U.S. pat. 3,711,495, (Jan. 16, 1973).

(2) B. N. Ames, W. E. Durston, E. Yamasaki, and F. D. Lee, *Proc. Natl. Acad. Sci., USA*, **70**, 2281 (1973).

(3) B. N. Ames, J. McCann, and E. Yamasaki, *Mut. Res.*, **31**, 347 (1975).

(4) G. M. Anthony, C. J. W. Brooks, I. Maclean, and I. Sangster, *J. Chromatogr. Sci.*, **7**, 623 (1969).

(5) M. T. M. Tulp and O. Hutzinger, *J. Chromatogr.*, **139**, 51 (1977).

(6) T. H. Elliott, D. V. Parke, and R. T. Williams, *Biochem. J.*, **72**, 13 (1958).

(7) A. G. Renwick and R. T. Williams, *ibid.*, **129**, 857 (1972).

(8) B. Testa and P. Jenner, *J. Pharm. Pharmacol.*, **28**, 731 (1976).

[16] Unpublished data.

[17] Although the GLC and mass spectrometric data for several metabolites and the synthesized dihydroxy compounds are similar, it is not possible now to state unequivocally whether there are cases of identity.

Analysis of Nitrosamines in Aqueous and Biological Fluids Based on Measurement of Photochemically Liberated Nitrite

DONALD G. MUSSON and LARRY A. STERNSON ˣ

Received November 14, 1978, from the *Department of Pharmaceutical Chemistry, University of Kansas, Lawrence, KS 66045.* Accepted for publication March 27, 1979.

Abstract □ A method is described for the analysis of nitrosamines in aqueous solution and in biological fluids (blood, plasma, and rat liver microsomal suspensions). The method is based on photochemical degradation of the nitrosamine in a controlled environment to yield the corresponding amine and nitrite ion, and the latter is subsequently used to form a chromophoric or fluorescent product. The analysis scheme is a modular three-component system consisting of a column to remove contaminating nitrite prior to photolysis, a photochemical reactor, and a chemical reactor. Additional modules are used to accommodate biological samples or large-volume (5–50 ml) aqueous samples. In this study, *N*-nitrosopyrrolidine, *N*-nitrosodimethylamine, and *N*,*N*-diethanolnitrosamine were utilized as substrates. Because of intersubstrate variability in the photochemical decomposition rate and overall nitrite yield, the structure (*i.e.*, photochemical behavior) of the particular nitrosamine in the sample must be known prior to analysis. With a colorimetric readout, the sensitivity for analysis of *N*-nitrosopyrrolidine was 800 ng/ml for a 5-ml sample and the measurement precision was ±6% in the biological fluids. Fluorometric analysis improved sensitivity to 4 ng/ml with a precision of ±10% in biological media.

Keyphrases □ Nitrosamines—analysis, chromophoric or fluorescent products of photochemical degradation, aqueous suspensions, biological fluids, rats, humans □ Carcinogens—nitrosamines, analysis, chromophoric or fluorescent products of photochemical degradation, aqueous suspensions, biological fluids, rats, humans □ Colorimetry—analysis, nitrosamines, aqueous suspensions, biological fluids □ Fluorometry—analysis, nitrosamines, aqueous suspensions, biological fluids

Nitrosamines are highly carcinogenic compounds (1). They are receiving considerable attention and concern because of their ubiquitous occurrence in the environment (2), food (3), cosmetics (4), and other matrixes. To evaluate the hazards of nitrosamines, adequate analytical methods are needed for their detection and quantitation. Such methods must be extremely sensitive, must give unequivocal and reproducible results, and must be applicable to a wide range of nitrosamines of varying physicochemical properties and in various matrixes.

Nitrosamines are monitored routinely by mass spectrometry (5) or thermal energy analysis (6, 7) after isolation by GLC or high-performance liquid chromatography (HPLC). In these cases, extensive cleanup has been required prior to chromatography. Nitrosamines also have been detected by polarography (8) or spectrophotometry after chemical derivatization (3, 9). These methods also have required extensive cleanup and enrichment and were not specific when applied to complex mixtures.

This report describes a method for nitrosamine analysis at nanograms per milliliter levels in various complex matrixes including water, human plasma, and liver homogenates. Analysis is based on the method described by Daiber and Preussmann (10), in which the nitrosamine is photochemically cleaved to yield an amine and nitrite ion; the nitrite is detected spectrophotometrically after diazotization of an amine and conversion of the resulting diazonium salt to an azo dye.

In this paper, emphasis is on cleanup and enrichment of samples containing nitrosamines to achieve selectivity and high sensitivity. *N*-Nitrosopyrrolidine, *N*,*N*-diethanolnitrosamine, and *N*-nitrosodimethylamine were used as model compounds.

EXPERIMENTAL

Reagents—*N*-Nitrosopyrrolidine[1], 2,6-diaminopyridine[1], *p*-chloroaniline[1], 1-decanol[2], *N*-(1-naphthyl)ethylenediamine dihydrochloride[2], and sulfanilamide[2] were used as received. *N*-Nitrosodimethylamine (11) and diethanolnitrosamine (1, 12) were synthesized by condensation of dimethylamine and diethanolamine with nitrous acid.

Column Preparation—XAD-2 beads[3] (20–50 mesh) were purified by 30-min successive washes with 5.25% sodium hypochlorite, double-distilled water (distilled from alkaline permanganate), 3 *M* HCl, water, and acetone. Fractured beads were removed from the acetone solution by decantation, and the remaining beads were isolated by filtration. Forty-five milliliters of the purified beads was slurried with acetone containing 3 ml of 1-decanol as described previously (13). The acetone was removed under reduced pressure on a rotary evaporator, and the beads (coated with decanol) were packed into a column made from a disposable pipet (14.6 cm × 7.6 mm o.d.).

Sample Purification—A sample of human plasma or rat liver homogenate (14) containing nitrosamine was subjected to ultrafiltration[4] at 1000×*g* for 30 min to deproteinize the mixture. The resulting ultrafiltrate was either passed directly through a column packed with anion-exchange resin (0.5 g AgI, 200–400 mesh, HO^-) or the pH of the ultrafiltrate was adjusted to 1.7 with 6 *N* H_2SO_4 and the mixture was passed through an XAD-2/decyl alcohol column (13).

The eluent was adjusted to pH 5–7, if necessary, and added to quartz vessels. These vessels were placed 16 cm from a 15-w, 46-cm germicidal lamp[5] (maximum output at 250 nm), and the mixtures were irradiated for 15 min. The freed nitrite could be detected colorimetrically or fluorometrically. Alternatively, the nitrite in the irradiated samples could first be concentrated on an XAD-2/decyl alcohol column (13), and the resulting decyl nitrite could be monitored colorimetrically or fluorometrically after its elution from the column with 1.2 ml of acetone.

Nitrite Detection—*Colorimetry (15)*—Sulfanilamide (0.15–0.50 ml of a 5% solution) was added to the acetone eluate (containing the decyl nitrite) or directly to the photolysis mixture (after acidification to pH 1.7) containing the liberated nitrous acid. The solution was mixed thoroughly and allowed to stand for 1 min. An equal volume of *N*-(1-naphthyl)ethylenediamine (0.25% solution) was added, and the absorbance of the final solution was measured[6] at 545 nm (a_m 4×10^{-5}) after 2 min was allowed for complete color development.

Fluorometry—Nitrite or decyl nitrite was monitored using a modification of the Dombrowski and Pratt procedure (16), in which either the photolysis mixture containing nitrous acid (after pH adjustment to 1.7) or the decyl nitrite (eluted from the XAD-2/decyl alcohol column with acetone) was used to diazotize *p*-chloroaniline (0.3 ml of a 0.06% solution in 0.1 *M* HCl). Samples in which the diazonium salt was formed from decyl nitrite were extracted with benzene (6 ml) to remove decyl alcohol.

All samples were reacted with ammonium sulfamate (0.3 ml of a 4%

[1] Aldrich Chemical Co., Milwaukee, Wis.
[2] Eastman Chemical Co., Rochester, N.Y.
[3] Rohm & Haas Co., Philadelphia, Pa.
[4] CF-50A conical filters, Amicon Corp.
[5] General Electric Corp.
[6] Cary model 118 spectrophotometer, Varian Associates, Palo Alto, Calif.

0022-3549/79/0900-1159$01.00/0
© 1979, American Pharmaceutical Association

Table I—Kinetics for Photochemical Nitrosamine Decomposition and Yield of Nitrite Formed [a]

Compound	Fluid	Rate Constant ± SD[b], min^{-1}	Yield of Nitrite[c] ± SD[b], %
N-Nitrosopyrrolidine	Distilled water	0.291 ± 0.029	45.3 ± 5.57
	0.1 *M* H_2SO_4	0.513 ± 0.149	9.7 ± 2.20
	0.1 *M* NaOH	0.275 ± 0.007	51.1 ± 5.23
	Buffer pH 3[d]	0.443 ± 0.081	32.7 ± 3.93
	Buffer pH 5[d]	0.360 ± 0.014	34.8 ± 3.87
	Buffer pH 7[e]	0.274 ± 0.073	40.8 ± 2.86
	Buffer pH 9[e]	0.266 ± 0.084	34.3 ± 0.85
	Plasma[f]	0.18 ± 0.084	33.3 ± 8.7
	Liver microsomes[g]	0.24 ± 0.056	28.5 ± 3.1
N-Nitrosodimethylamine	Distilled water	0.154 ± 0.017	59.8 ± 0.83
	Buffer pH 7[e]	0.382 ± 0.014	56.3 ± 3.12
	Plasma[f]	0.140 ± 0.014	31.9 ± 2.53
	Liver microsomes[g]	0.067 ± 0.008	30.3 ± 2.63
N,N-Diethanolnitrosamine	Distilled water	0.411 ± 0.033	41.6 ± 1.40
	Buffer pH 7[e]	0.529 ± 0.017	41.9 ± 6.22
	Plasma[f]	0.140 ± 0.014	35.4 ± 0.30
	Liver microsomes[g]	0.134 ± 0.040	31.2 ± 0.30

[a] Reaction carried out as described under *Experimental.* [b] Values represent the mean ± *SD* for three determinations. [c] Yield was determined spectrophotometrically at 545 nm and arose from the azo compound produced by successive reaction of nitrite with sulfanilamide and *N*-(1-naphthyl)ethylenediamine. [d] Acetate buffer (0.5 *M*). [e] Britton-Robinson buffer. [f] Obtained from the Kansas City Blood Bank and used as received. [g] Prepared from rat liver as previously described (14).

solution) followed by 2,6-diaminopyridine (0.05% solution prepared in 1 *M* acetate buffer, pH 5). The reaction was continued for 15 min, and the resulting azo dye was extracted with benzene (6 ml) and washed with water (6 ml). The benzene layer was evaporated to dryness under a nitrogen stream. The yellow residue was redissolved in water (2 ml), ammoniacal cupric sulfate (0.4 ml of a 0.725 *M* aqueous solution) was added, and the solution was heated in boiling water for 30 min. The mixture was acidified with 0.4 ml of 6 *M* HCl to yield a triazole, which was monitored fluorometrically[7] at 420 nm ($\lambda_{excitation}$ = 360 nm).

RESULTS AND DISCUSSION

Analysis of nitrosamines in water and biological fluids (human plasma and rat liver microsomal suspensions) will be described as a modular system (Scheme I) requiring at least three components: (*a*) a column packed with either anion-exchange resin or XAD-2 beads coated with decyl alcohol to remove any nitrite contaminants, (*b*) a photochemical reactor to convert nitrosamines to the corresponding amine and nitrite ion, and (*c*) a chemical reactor to transform the liberated nitrite into a readily monitored product. In this system, the nitrite was used to diazotize a primary aromatic amine and the diazonium salt was coupled with a reactive arene to yield a product that could be measured colorimetrically or fluorometrically, depending on the amine-coupling agent pair chosen.

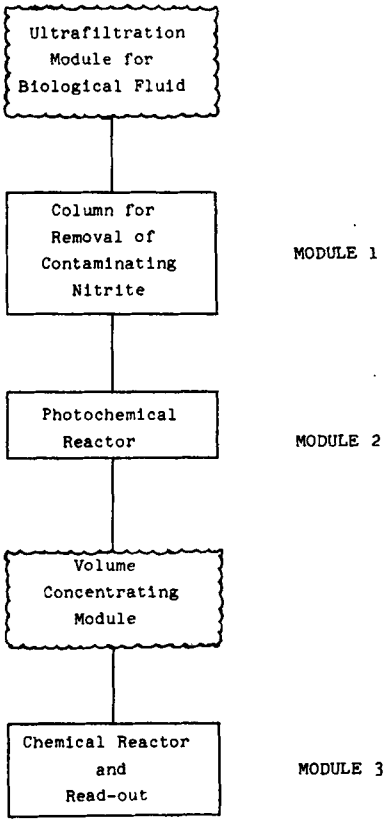

Scheme I—Modular nitrosamine analysis system (〰, optional modules)

If nitrosamines are to be analyzed in biological fluid (human plasma rat liver microsomal suspensions), an ultrafiltration module must be introduced into the modular system (Scheme I). Biological samples were initially deproteinized by centrifugal ultrafiltration and then processed through Modules 1–3. For nitrosamine analysis in large-volume (>5 ml) aqueous samples, a second column packed with XAD-2 beads coated with decyl alcohol was introduced after the photolysis step to concentrate the liberated nitrite by extractive alkylation (13) prior to diazotization. Where sample size was restricted (<5 ml), sample concentration and cleanup were carried out primarily after diazotization.

Sample Purification—Samples of biological fluid containing *N*-nitrosopyrrolidine, *N*-nitrosodimethylamine, or *N,N*-diethanolnitrosamine (1–2000 ng/ml) were deproteinized by centrifugal ultrafiltration through membranes that excluded material of molecular weight ≥50,000. This procedure removed ≥98% of the protein, *i.e.*, material responsive to the biuret or Lowry assays (17). When aqueous buffer samples containing these nitrosamines (10–10,000 ng/ml) were carried through analysis before and after ultrafiltration, no statistical difference in nitrosamine levels was observed, indicating that the nitrosamine was not retained by the filter. Deproteinized samples were carried through the analysis scheme as described for aqueous samples.

Because the final analysis of nitrosamines in all matrixes was based on measuring liberated nitrite, it was necessary to ensure that any residual, contaminating nitrite was removed prior to photolysis. This elimination could be accomplished by passing the ultrafiltrate or aqueous sample through a column packed with an anion-exchange resin or through a column containing XAD-2 beads coated with decyl alcohol. Failure to deproteinize biological samples prior to applying samples to these columns resulted in erratic and incomplete (<35%) nitrite removal.

The anion-exchange resin quantitatively removed added nitrite from the solution (as well as other anions such as nitrate); however, some nitrosamine was also retained by the resin (Fig. 1). Total nitrite retention by the column was observed, even at the 5-μg/ml concentration when nitrite was present in a 500-fold *M* excess with respect to nitrosamine. The amount of nitrosamine held by the resin was a function of the amounts of nitrosamine and resin present. The amount of resin was optimized so that nitrite was quantitatively removed, but the loss of nitrosamine was minimized. With the assumption of nitrosamine concentrations of 1–1000 ng/ml and nitrite levels of 5 μg/ml, 0.5 g (wet weight) of anion exchanger gave optimum response: quantitative removal of nitrite and 25 ± 4% loss of nitrosamine.

When nitrite decontamination was carried out by passing the sample through a column packed with XAD-2 beads coated with decyl alcohol, the nitrite removed from the solution was inversely proportional to the

[7] Model MPF-2A spectrofluorometer, Perkin-Elmer Corp., Norwich, Conn.

Table II—Colorimetric Assay[a] for *N*-Nitrosopyrrolidine

Fluid	Standard Curve[b] Slope	Intercept	Regression Coefficient	Sensitivity, ng/ml	Precision[c], %
		Method I			
Water	0.057	0.048	0.998	800	5.7
Plasma[d]	0.065	0.023	0.997	800	9.8
		Method II			
Water (10-ml sample)	0.049	0.065	0.997	200	6.6
Water (100-ml sample)[e]	0.017	0.124	0.993	15	4.3

[a] As described under *Experimental*. [b] Standard curve was prepared from five 5-ml samples of *N*-nitrosopyrrolidine dissolved in the indicated fluid in the concentration range of 0.75–20 μg/ml and carried through the described assay. Each sample was assayed in triplicate. [c] Values represent the precision at the minimum sensitivity and represent the average for four determinations. [d] Obtained from the Kansas City Blood Bank and used as received. [e] Standard curve was prepared from five 5-ml samples of *N*-nitrosopyrrolidine dissolved in the indicated fluid in the concentration range of 1–50 ng/ml and carried through the described assay. Each sample was assayed in triplicate.

Table III—Fluorometric Assay[a] for *N*-Nitrosopyrrolidine (Method I)

Fluid	Standard Curve[b] Slope	Intercept	Regression Coefficient	Sensitivity, ng/ml	Precision[c], %
Water	4.26	7.4	0.99	4	9.9
Plasma[d]	0.21	25.0	0.99	40	9.6
Liver microsomes[e]	0.20	8.0	1.00	80	12.0

[a] As described under *Experimental*. [b] Standard curve was prepared from five 5-ml samples of *N*-nitrosopyrrolidine dissolved in the indicated fluid in the concentration range of 1–250 ng/ml and carried through the described assay. Each sample was assayed in triplicate. [c] Values represent the precision at the minimum sensitivity and are the average of four determinations. [d] Obtained from the Kansas City Blood Bank and used as received. [e] Prepared from rat liver as previously described (14).

flow rate through the column, as previously discussed (13). At a flow rate of 44 ml/hr, solutions containing *N*-nitrosopyrrolidine (1–20 μg/ml) were cleared of 70 ± 2% of added nitrite (4.6 μg/ml) (Fig. 1), with no detectable loss of nitrosamine from solution. Thus, the anion exchanger is a more efficient medium for removing contaminating nitrite but suffers from the disadvantage of retaining some nitrosamine. The XAD-2 column does not retain any nitrosamine but, unfortunately, incompletely removes nitrite contaminants.

Varying combinations of ion-exchange resin and XAD-2 beads coated with decyl alcohol did not improve nitrosamine recovery and concomitant nitrite removal. The major difficulty was the dependency of on-column nitrosation on an acidic (pH ≤3) environment and ion-exchange removal of nitrite optimally requiring a medium of pH ≥ 5.

In all cases, ion-exchange and XAD-2 columns were not reused, so problems with residuals were not encountered.

Nitrite Liberation from Nitrosamine—Initial studies were carried out to determine the feasibility of cleaving nitrosamines to amines and nitrous acid with acid (18). However, when *N*-nitrosopyrrolidine and *N*-nitrosodimethylamine were heated in a sealed vial with acid (hydrochloric, hydrobromic, or sulfuric), inconsistent (±20%) and low (≤40%) yields of nitrous acid were obtained (monitored colorimetrically). In separate experiments under acid hydrolysis conditions, nitrite was consumed as a function of time, perhaps through oxidation by a contaminant in the acid.

A more satisfactory method for liberating nitrite from nitrosamines involved photolysis (10). The formation rate and yield of nitrite were functions of the particular substrate being analyzed, light intensity, wavelength, pH, and photolyzed sample matrix. As shown in Table I, the nitrite formation rate was faster at low pH than at neutral or high pH; however, the nitrite recovery was poorer from acidic solutions and improved at higher pH values. Conditions were chosen that produced the maximum nitrite yield, *i.e.*, pH 6–7. The nitrite liberation rate was sufficiently rapid over the pH 1–13 range to suggest that the reaction speed could be sacrificed in favor of maximum conversion to nitrite.

The nitrite yield from photolysis of aqueous nitrosamine solutions varied among the three model compounds studied; however, the reproducibility of the nitrite yield from sample to sample for a given nitrosamine was high (±3%). This variability in nitrite yield, however, precluded nitrosamine analysis of samples containing more than one nitrosamine or nitrosamines whose response to photolysis was unknown. The nitrite yield from biological fluid samples (blood plasma or liver microsomal homogenates) containing nitrosamine did not show as much variability among the three model substrates as did the water samples. An average of 31.9 ± 2.6% nitrite was obtained from photolysis of plasma and liver microsomal suspensions containing dimethyl-, diethanol-, or pyrrolidinenitrosamine. The nitrite yield from nitrosamines present in ultrafiltrates from biological samples was ~50–80% of that obtained in buffers of similar pH to the ultrafiltrate. The nitrite production was also somewhat slower in ultrafiltrate than in buffer. This finding may have been due to extraneous material in the ultrafiltrate lowering the photon flux available for reaction with the nitrosamine. The lamp output and the distance between the lamp and sample cell were chosen to give maximum nitrite recovery. A lamp with maximum intensity at 250 nm placed 16 cm from the quartz reaction vessel gave the optimum rate and nitrite yield.

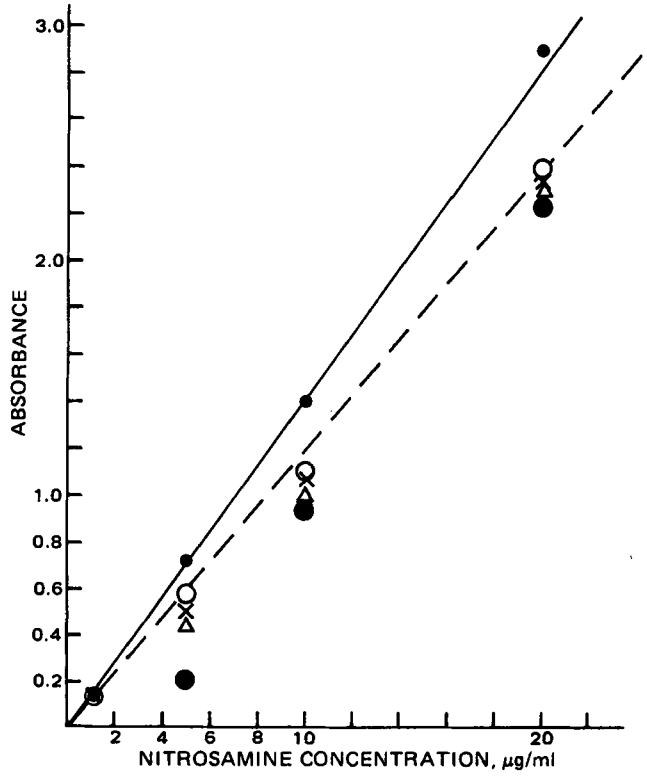

Figure 1—*Loss of nitrosamine to the anion-exchange column during removal of background nitrite prior to photolysis. Loss was determined as a function of total amount of exchange resin. Key: ●, no resin; ○, 0.25 g of wet weight; ×, 0.5 g of wet weight; △, 1 g of wet weight; and ●, 2 g of wet weight.*

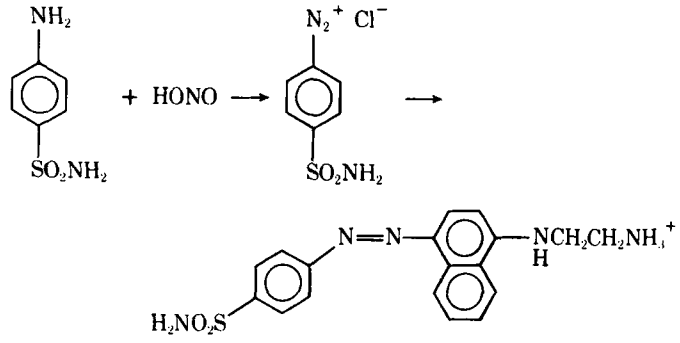

Scheme II

Detection of Liberated Nitrite—*Method I*—When the available sample size was limited (≤5 ml, *e.g.*, biological samples), liberated nitrite was reacted immediately with an aromatic amine under acid conditions to produce a diazonium salt, which was then coupled with an arene to yield either a chromophoric or a fluorescent product (Scheme II). The colorimetric assay was based on diazotization of sulfanilamide and coupling with *N*-(1-naphthyl)ethylenediamine. The reaction proceeded rapidly and could be carried out with minimum sample manipulation. The sensitivity attained using this method was ~800 ng of nitrosamine/ml of solution (Table II).

Sensitivity could be improved greatly by fluorometric monitoring of liberated nitrite (Scheme III). In this case, the nitrite was reacted with *p*-chloroaniline and the resulting diazonium salt was coupled with 2,6-diaminopyridine. This resulting azo compound was extracted into benzene, the benzene was removed by evaporation, and the residue was redissolved in water. The azo dye was oxidized to a fluorescent thiazole with ammoniacal cupric sulfate. Conversion to this fluorescent species permitted detection of nitrosamines at levels of 4 ng/ml in aqueous solution, 40 ng/ml in plasma, and 80 ng/ml in liver microsomes. In biological fluid, a precision of ±10% was readily attainable. The limitation preventing nitrosamine detection at lower levels by the fluorescence method was the appreciable background fluorescence (note the large intercept observed in standard curves constructed for fluorescence analysis of nitrosamine samples of varying concentration; Table III).

For both fluorescence and colorimetric analysis, quantitation was based on comparing detector response with a standard curve constructed for each nitrosamine in the matrix. The curve was prepared by carrying samples containing known amounts of the nitrosamine through the entire assay. The disadvantages of the fluorescence procedure were: (*a*) the extensive sample preparation required for fluorescence analysis and (*b*) the background fluorescence inherent in the method at low nanogram per milliliter concentrations.

Method II—For samples where sample volume was not limited (*e.g.*, water samples, pharmaceutical preparations, and food), nitrite, liberated by photolysis of nitrosamines, was first concentrated on a column packed with XAD-2 beads coated with decyl alcohol before being processed through the chemical reactor module (Scheme I). It was demonstrated

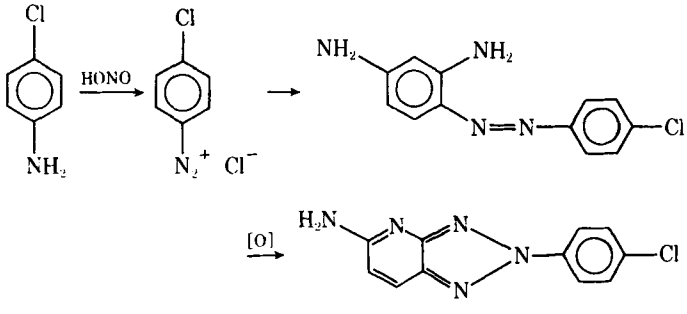

Scheme III

previously (13) that when an aqueous solution of nitrous acid is passed through such columns, the nitrous acid is extracted into the decyl alcohol phase as decyl nitrite, formed on-column. An optimum flow rate of 44 ml/hr was reached at which 70 ± 2% of the nitrite present in a photolyzed sample (5–50-ml volumes) was retained on the column. With sample volumes >75 ml, however, the percent of nitrite retained by the column decreased in a nonlinear fashion, as discussed previously (13). Therefore, sample size was maintained below 100 ml.

The nitrite concentrated on-column in the form of decyl nitrite was eluted from the resin with 1.2 ml of acetone passed through the bed. The decyl nitrite present in the acetone eluate was then used to diazotize a primary aryl amine, as described for nitrous acid. Thus, a 50-ml aqueous sample can be concentrated to <2 ml, providing a 15-fold increase in sensitivity over that obtained when the XAD-2 decyl alcohol column module is not used. Some nitrite loss did take place with this column since only 70% of the nitrite passed through it was retained on-column as decyl nitrite, thus accounting for the observation that a decrease in sample volume by a factor of 25 only increased sensitivity by a factor of 15 (Tables II and III).

In conclusion, an analytical method has been described for the analysis of nitrosamines in aqueous solutions and biological fluids. No highly sophisticated instrumentation is required, and the methodology is adaptable to automation. The procedure is described as a modular system requiring a minimum of three components, but it can accommodate biological samples or large-volume aqueous samples by the introduction of additional modules. Sensitivity is adequate for many quality control applications.

REFERENCES

(1) H. Druckrey, R. Preussmann, S. Ivankovic, and D. Schmahl, *Z. Krebsforsch.*, **69**, 103 (1967).

(2) D. H. Fine, D. P. Founbehler, E. D. Pellizzari, J. E. Pellizzari, J. E. Bunch, R. W. Berkley, J. McCrae, J. T. Bursey, E. Sawicki, K. Krost, and G. A. DeMarrais, *Bull. Environ. Contam. Toxicol.*, **15**, 739 (1976).

(3) L. Ceh and F. Ender, *Food Cosmet. Toxicol.*, **16**, 117 (1978).

(4) T. Y. Fan, U. Goff, D. H. Fine, G. P. Arenault, and K. Biemann, *ibid.*, **15**, 423 (1977).

(5) R. Goodhead and T. A Gough, *ibid.*, **13**, 307 (1975).

(6) D. H. Fine, D. P. Rounbehler, and P. E. Oetinger, *Anal. Chim. Acta*, **78**, 383 (1975).

(7) D. H. Fine, D. Lieb, and D. P. Rounbehler, *Anal. Chem.*, **47**, (1975).

(8) K. Hasebe and J. Osteryoung, *ibid.*, **47**, 2412 (1975).

(9) T. Y. Fan and S. R. Tannenbaum, *J. Agr. Food Chem.*, **19**, 1267 (1971).

(10) D. Daiber and R. Preussmann, *Z. Anal. Chem.*, **206**, 344 (1964).

(11) A. Vogel, "Elementary Practical Organic Chemistry", 3rd impression, Longman Group Ltd., London, England, 1970.

(12) T. Y. Fan, V. Goff, L. Song, and D. H. Fine, *Cosmet. Toxicol.*, **15**, 423 (1977).

(13) M. C. K. Chao, T. Higuchi, and L. A. Sternson, *Anal. Chem.*, **50**, 1670 (1978).

(14) R. A. Wiley, L. A. Sternson, H. A. Sasame, and J. R. Gillette, *Biochem. Pharmacol.*, **21**, 3235 (1972).

(15) M. Shinn, *Ind. Prac. Org. Chem.*, **13**, 33 (1941).

(16) L. J. Dombrowski and E. J. Pratt, *Anal. Chem.*, **44**, 2268 (1972).

(17) S. J. Bannister, L. A. Sternson, and A. J. Repta, *Clin. Chem.*, **23**, 1258 (1977).

(18) R. Zahradmik, *Collect. Czech. Chem. Commun.*, **23**, 1529 (1958).

ACKNOWLEDGMENTS

Supported in part by National Institutes of Health Grant CA-09242 awarded by the National Cancer Institute.

Loss of Nitroglycerin from Aqueous Solution into Plastic Intravenous Delivery Systems

PUI-HO YUEN, SANDRA L. DENMAN, THEODORE D. SOKOLOSKI ˣ, and ALLAN M. BURKMAN

Received September 28, 1978, from the *Divisions of Pharmaceutics and Pharmaceutical Chemistry and Pharmacology, College of Pharmacy, Ohio State University, Columbus, OH 43210.* Accepted for publication March 22, 1979.

Abstract □ The mechanism of potential loss of nitroglycerin stored in plastic and glass containers was studied from an equilibrium and kinetic approach. Plastic strips equilibrated with dilute aqueous solutions of neat nitroglycerin showed that the drug was lost by absorption. Drug loss was followed by an electron-capture GLC assay. The same assay of control solutions in glass showed no drug loss in 48 hr at pH 5.7. The kinetics of nitroglycerin absorption and desorption were determined using synthesized ^{14}C-labeled drug. Absorption can be quantified using a diffusion model, where the concentration in the aqueous phase falls with time. Curve fitting yielded an average diffusion coefficient in plastic of 2.05×10^{-9} cm^2/sec and a partition coefficient of 104 (plastic–water) at 30°. Temperature-dependence studies of absorption showed that the diffusion coefficient followed an Arrhenius relationship with an energy requirement of 19.6 kcal/mole, whereas effects on the partition coefficient were negligible. Nitroglycerin desorption from plastic disks under sink conditions into water can be quantified by assuming a diffusion model where the concentration at the surface of a plane sheet remains constant. Nonlinear least-squares curve fitting generated a diffusion coefficient of 1.14×10^{-9} cm^2/sec for the desorption process at 30°.

Keyphrases □ Nitroglycerin—intravenous delivery systems, loss from aqueous solution into plastics □ Plastics—loss of nitroglycerin from aqueous solution into intravenous delivery system components □ Drug delivery systems, intravenous—loss of nitroglycerin from aqueous solution into plastics

Nitroglycerin in tableted dosage forms has been studied extensively from the standpoint of stability and packaging (1–7). In the past few years, considerable interest has centered on the clinical use of intravenous nitroglycerin solutions for myocardial infarction and in open heart surgery (8, 9). The intravenous solutions are prepared extemporaneously by pharmacists, usually from sublingual tablets. Two recent studies (9, 10) raised questions concerning the potency and stability of such solutions.

An editorial pointed out that there are certain agreements in the results of these studies but that there are also certain significant differences (8). Both papers reported some nitroglycerin loss from intravenous solutions stored in glass and plastic containers and suggested that the drug loss might be consistent with sorption to container or delivery units. However, the two studies differed in those results concerned with the apparent actual drug chemical stability and the relative amounts of drug lost to plastic containers. Two letters appearing subsequent to these studies corroborated nitroglycerin loss from intravenous solution to plastic (11, 12).

The purposes of this study were to define the mechanism of nitroglycerin loss to a plastic intravenous container material[1] using equilibrium and kinetic studies and to reevaluate nitroglycerin stability in glass containers. This information seemed to be a necessary requisite to an understanding of factors affecting the potency and stability of intravenous nitroglycerin solutions. Solutions were prepared using freshly synthesized nitroglycerin to obviate any effects of adjuvants present in formulations. This possibility was pointed out by Pikal *et al.* (7). Potential adjuvant effect is another complicating factor in comparing the results of previous studies. Moreover, the assays used in this study for nitroglycerin were different from those used previously and provide an additional basis for evaluation of stability and potency problems associated with intravenous nitroglycerin solutions.

EXPERIMENTAL

In equilibrium studies, strips of a plastic[1] intravenous container (17.88 × 4.98 × 0.04075 cm; volume 3.63 cm^3) were equilibrated with 200 ml of normal saline solutions[2] containing various initial nitroglycerin concentrations (8–90 μg/ml). The dilute solutions were kept in aluminum foil-stoppered 250-ml erlenmeyer flasks at 35 ± 1° [3]. The solution pH was ~5.7 and remained constant throughout the study. Separate studies over a 2-week period showed that equilibrium essentially occurred in 2 days.

The nitroglycerin was synthesized using the method of Dean and Baun (13), where the ratio of reactants was varied to increase the nitroglycerin yield[4]. A 1.05% stock solution of the synthesized nitroglycerin in ethyl acetate was used as a nitroglycerin source for the solutions in this study. The stock solution was standardized using the phenol disulfonic acid method of Dean and Baun (13).

The nitroglycerin content of the aqueous phase in equilibrium with plastic was determined using a GLC procedure[5] based on the work of Rosseel and Bogaert (14). The assay is stability indicating, since hydrolysis products of nitroglycerin are separated and detected. Isosorbide dinitrate was used as the internal standard[6]. Standard curves for nitroglycerin were constructed by plotting the ratio of the area under the nitroglycerin chromatogram to that of isosorbide dinitrate as a function of the nitroglycerin concentration. These standard curves were used to determine the nitroglycerin concentration initially and after equilibrium with plastic in the following way. A 100-μl sample was taken and extracted with 500 μl of benzene containing a known amount of isosorbide dinitrate. The extraction removed 98+% of both nitrates. After extraction, the organic layer was removed and refrigerated until a portion of it was injected on the column. The nitroglycerin concentration was determined from the ratio of nitroglycerin areas to standard isosorbide chromatograms.

Control studies were conducted at the same time as the equilibrium studies under identical conditions. The only difference was the absence of plastic.

In kinetic sorption studies, two strips cut from plastic intravenous containers[1] (4 × 4 × 0.04075 cm; volume 0.652 cm^3) were placed in a 100-ml water jacketed beaker, kept at constant temperature[7], containing

[1] Viaflex, lot HP05 × 7, Travenol.

[2] Lot G446 × 4A, Travenol.

[3] Water controlled shaker bath, Research Specialties model 2156, operated at 25 rpm.

[4] Sulfuric acid (2.17 moles) and nitric acid (2.27 moles) were cooled to 25°. Then 0.130 mole of glycerin (Eaton-Colby) was slowly added, keeping the temperature below 16°. The mixture was then added to 1.5 liters of distilled water at 10°, and the congealed nitroglycerin was collected and purified by repeated washing with water. Purity was established by TLC and GLC (9).

[5] Hewlett-Packard model 5730A with a ^{63}Ni-electron-capture detector. A glass column (1.8 m × 2 mm i.d.) was used with 3.5% QF-1 on Gas Chrom Q (Supelco D3550). The carrier gas (argon–methane, 95:5) had a flow rate of 30 ml/min; the injection port and detector were at 200°, and the column was at 120°.

[6] Stuart Pharmaceuticals AN00983, 25% adsorbate on lactose. The isosorbide dinitrate was extracted with hot acetone, and the acetone was then removed over a nitrogen stream. Standard solutions were prepared by accurately weighing known amounts and dissolving them in chromatographic grade benzene.

[7] Haake model FK circulating water bath at 30, 35, 40, and 45 ± 0.5°.

0022-3549/79/0900-1163$01.00/0
© 1979, American Pharmaceutical Association

Table I—Recovery of Initial Concentration of Nitroglycerin Stored in Glass at 35° in Normal Saline Solution, pH 5.7

Initial Concentration, μg/ml	Percent Found	
	24 hr	48 hr
95	99	104
15	104	107
15	98	107
3.8	87	105
3.6	101	107
0.2	90	87
Average	96.5	102.8

aqueous solutions of constant labeled[8] drug (61.06 μg/ml, 38,212 dpm/ml) together with nonlabeled drug in various total concentrations. In studies at 30°, four different initial concentrations were used (61–473 μg/ml), and each concentration study was run in duplicate. Temperature-dependence studies (30–45°) were run in duplicate with a single initial concentration of 473 μg/ml.

The solutions were prepared from ethanol stock solutions of both labeled and nonlabeled drug. The cold stock solution contained 205.91 mg of nitroglycerin/ml, and the labeled drug stock solution contained 152.65 mg/ml[9]. At appropriate time intervals, 50 μl of aqueous sample was placed in a vial containing 10 ml of counting cocktail[10] and 4 ml of water. The radioactivity was determined by liquid scintillation counting[11] for 20 min (counting efficiency 86.35%, background 46 cpm).

The initially clear strips became opaque when exposed to water. To determine if the imbibed water affected sorption, the following experiment was run. Plastic strips were presoaked in distilled water for more than a day and immediately immersed in a solution of the radioactive drug (473 μg/ml total, 61.06 μg/ml labeled, 38,212 dpm/ml). Sorption studies using the presoaked strips were carried out as were those described for nonpresoaked strips.

In desorption studies, 40 disks cut from the same plastic intravenous bags (1.503 cm in diameter, 0.0407 cm thick; volume 0.0723 cm^3) were equilibrated 1 week with 300 ml of a 442-μg/ml (43.19 dpm/μg) nitroglycerin solution. Two disks were collected and counted to determine the initial amount of nitroglycerin sorbed (1652.1 and 1644.9 μg/disk were found). The desorption studies, run in duplicate, were conducted at 30° using 19 disks in 300 ml of stirred water. Sink conditions were maintained by replacing the water at a rate of 5 ml/min with a peristaltic pump[12].

In the desorption studies, a disk was removed from solutions in the jacketed beaker at appropriate intervals, rinsed in water, blotted on paper, and placed in a counting vial containing 10 ml of cocktail. The disk was allowed to stand in the cocktail for a few hours to enhance the leaching of ^{14}C-nitroglycerin, thus increasing counting efficiency. Four milliliters of water was then added to form a gel, permitting suspension of the disk horizontally and halfway from the bottom of the vial. The radioactivity was determined by liquid scintillation counting for 20 min.

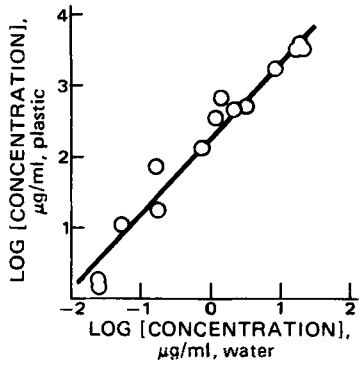

Figure 1—*Log-log relationship between nitroglycerin equilibrium concentration (micrograms per milliliter) in plastic and concentration in normal saline solution at 35°. The circles are experimental values, and the line was generated by least-squares regression, giving a slope of 1.09 ± 0.07 SD.*

[8] Prepared from 500 μCi of 1,3-^{14}C-glycerol (New England Nuclear, 1.64 mg/10 ml, specific activity 55.7 mCi/mmole). Water in the labeled sample was removed by storage over phosphorus pentoxide for 1 day. One gram of cold glycerin was added, and nitroglycerin was synthesized as indicated in footnote 4. The yield was 70%, and the product had a specific activity of 69.02 μCi/mmole.

[9] The initial concentrations were determined by an HPLC method (15) using a DuPont model 830 chromatograph with a Tracor model 970 variable-wavelength detector at a wavelength of 210 nm. A 25-cm Partisil ODS (Whatman) column was used. The assay separates and detects hydrolysis products of nitroglycerin.

[10] PCS cocktail, Amersham/Searle.

[11] Beckman model 345.

[12] Harvard model 500 1200.

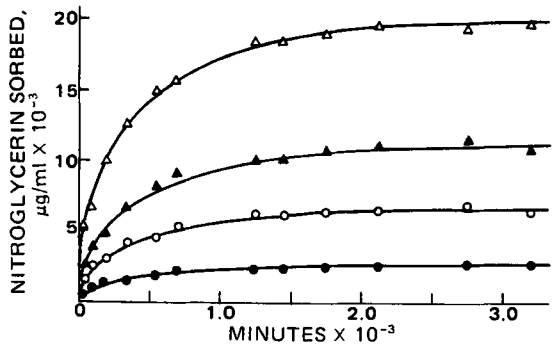

Figure 2—*Relationship between the amount (micrograms per cubic centimeter) of nitroglycerin adsorbed by plastic strips and time from a solution initially at 61 (●), 143 (○), 267 (△), and 472 (▲) μg of nitroglycerin/ml at 30°. The symbols are experimental data, and the line was generated by nonlinear least-squares fitting based on Eq. 1.*

RESULTS AND DISCUSSION

In the studies where plastic strips were permitted to equilibrate with aqueous nitroglycerin solutions, the amount of drug in the plastic was calculated from the difference between the measured initial concentration and the concentration found at equilibrium in the aqueous phase. The concentration in plastic was calculated using the measured volume of the strip. The calculation is valid because control studies showed no drug loss through either hydrolysis or sorption to glass in 48 hr.

Table I presents the nitroglycerin recovery from solutions stored in aluminum foil-stoppered 250-ml erlenmeyer flasks at 35°. Over a concentration range of 0.2–95 μg/ml, assay of the solution showed 97% nitroglycerin remaining after 24 hr and 103% after 48 hr. The drug is apparently stable over a 2-day period in aqueous solution. This finding is in agreement with the results of many investigators (12–18) but not with those of others (9, 10). Sturek *et al.* (9) found a 13% loss after 50 hr, which may have been the result of adjuvants in the sublingual tablets used to prepare the solutions. It is difficult to speculate about the 25% loss in 5 hr reported by Ludwig and Ueda (10) since the contents of their nitroglycerin stock solution are not known.

When the logarithm of the concentration found in plastic at equilibrium is plotted as a function of the logarithm of the concentration in the aqueous phase at equilibrium, a linear relation is found (Fig. 1) with a slope of 1.09 ± 0.15 (95% confidence limit) as generated by linear regression. This result shows that nitroglycerin loss to plastic is an absorption or partitioning process and that the role of adsorption, if present, is minor. When the apparent partition coefficient is calculated from the slope of a regression of concentration in plastic on the concentration in the aqueous phase at equilibrium, the value obtained is 166 ± 14. There is little doubt that nitroglycerin preferentially distributes into the plastic from its aqueous solution.

In kinetic sorption studies, the amount of nitroglycerin taken up by

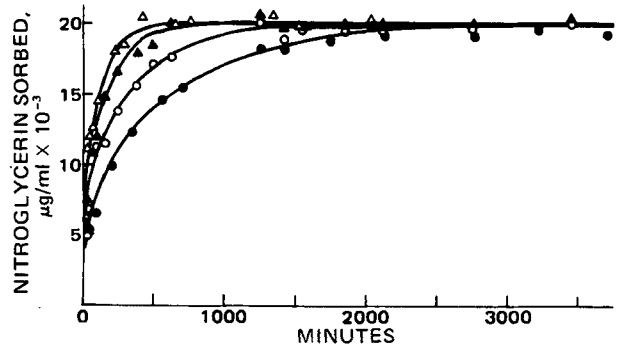

Figure 3—*Relationship between the amount of nitroglycerin adsorbed per cubic centimeter of plastic strips and time from solutions initially at 473.0 μg/ml at 45° (△), 40° (▲), 35° (○), and 30° (●). The symbols are experimental data, and the lines were generated by nonlinear least-squares fitting of Eq. 1.*

Table II—Amount Adsorbed, Diffusion Coefficient, Partition Coefficient, and Time for 0.5 Fractional Sorption for Nitroglycerin in Solution at Different Initial Concentrations Exposed to Plastic Strips at 30°

Initial Concentration, μg/ml	Amount Adsorbed at Equilibrium, M_∞, μg/cm³	Diffusion Coefficient[a], D, cm²/sec × 10⁹ (±SD × 10¹⁰)	Partition Coefficient	Time for 0.5 Fractional Sorption, min[b]
61.1	2,404.0	1.75 (1.58)	91.3	180
61.1	2,690.8	1.88 (1.30)	111.1	200
143.4	5,876.2	2.01 (1.74)	96.9	210
158.7	6,703.5	1.96 (1.29)	101.6	175
266.9	11,300.8	2.06 (1.23)	105.7	200
266.9	11,674.8	1.83 (1.47)	106.4	220
470.9	21,359.7	2.68 (2.25)	111.2	190
470.9	19,956.6	2.22 (1.31)	103.8	175

[a] Obtained by nonlinear least-squares fitting of amount adsorbed by plastic (micrograms per cubic centimeter) at time t (M_t) and the time using Eq. 1. [b] Interpolated from nitroglycerin sorbed-time profiles (Fig. 2).

the plastic strips was followed by measuring the solution loss of radioactivity as a function of time. Since equilibrium studies indicated that a sorption process was taking place, the data were treated using a model describing sorption by a plane sheet immersed in a limited volume of solution where the solute concentration in an aqueous solution falls as the solute enters the sheet. In such a system, the equation relating fractional equilibration, M_t/M_∞, and time is (19):

$$\frac{M_t}{M_\infty} = 1 - \sum_{n=1}^{\infty} \frac{2\alpha(1+\alpha)}{1+\alpha+\alpha^2 q_n^2} \exp(-Dq_n^2 t/h^2) \qquad \text{(Eq. 1)}$$

where M_t is the total amount of solute in the sheet at time t, M_∞ is the corresponding amount after infinite time, h is the half film thickness, and D is the diffusion coefficient. The value of α is the ratio of the final concentration to the total concentration drop in the aqueous solution (initial concentration, C_0, minus final concentration, C_∞):

$$\alpha = \frac{C_\infty}{C_0 - C_\infty} \qquad \text{(Eq. 2)}$$

The values of q_n are the nonzero positive roots of:

$$\tan q_n = -\alpha q_n \qquad \text{(Eq. 3)}$$

and can be obtained from published tables (19) or with a suitable programmable hand calculator.

The amount of nitroglycerin adsorbed by the plastic at time t, M_t (micrograms per disk), was fitted to Eq. 1 using a nonlinear least-squares fitting technique[13] (NONLIN). The values for α ranged from 0.69 to 0.82, and six terms under the summation were used. The total amount of nitroglycerin in the strips at infinite time, M_∞ (micrograms per cubic centimeter), and the diffusion coefficient (square centimeters per second) were estimated by the computer program. Figure 2 represents the fit obtained for data at initial concentrations of 61–473 μg/ml at 30°. The symbols are data points, and the line was generated by nonlinear least-squares fitting.

Table II lists the values of M_∞, the diffusion coefficient, the partition coefficient calculated from M_∞ and C_∞, and the time for 0.5 fractional attainment of sorption at the four different initial solution concentrations used. The studies were run in duplicate. The accuracy obtained, as reflected in the standard deviation for the diffusion coefficient, was good and the precision between duplicate runs was ±5% or better. Because of the constant half-life for sorption (Table II) at the several concentrations used, it is concluded that the diffusion coefficient is independent of concentration over a 61–473-μg/ml range, giving an average value of 2.05×10^{-9} ($SD = 0.29 \times 10^{-9}$) cm²/sec at 30°. The average partition coefficient obtained from the kinetic studies, 103.5 (SD = 6.82), is of the same order of magnitude as that found in the equilibrium studies run at 35° in normal saline solution. A log–log plot of the concentration in plastic *versus* aqueous concentration at equilibrium agrees well with the conclusion reached from the equilibrium studies that absorption, and not adsorption, is the major cause for nitroglycerin loss.

Data obtained from sorption kinetic studies using presoaked plastic strips were also fitted to Eq. 1 and showed excellent conformance. The diffusion coefficients generated, 2.27×10^{-9} ($SD = 0.163 \times 10^{-9}$) and 1.76×10^{-9} ($SD = 0.132 \times 10^{-9}$) cm²/sec, are not significantly different from those found using nonpresoaked strips.

In absorption temperature-dependence studies, the initial nitroglycerin solution concentration bathing the strips was held constant at 473 μg/ml and the temperature was held constant at 30, 35, 40, or 45°. The relation between the amount of nitroglycerin taken up per cubic centimeter of strip and the time at each temperature is presented in Fig. 3. The figure gives data for one of the duplicate trials used. When the data are fitted to Eq. 1, the result obtained is given by the solid lines in Fig. 3, showing excellent compliance with the diffusional model selected. The computer-generated diffusion coefficients for nitroglycerin in the plastic as well as the amount of nitroglycerin taken up at equilibrium are given in Table III for both experimental trials. The diffusion coefficient is dependent on temperature. Plotting the diffusion coefficient–temperature data in the Arrhenius manner:

$$D = D_0 e^{-E/RT} \qquad \text{(Eq. 4)}$$

gives an excellent linear relation between the logarithm of the diffusion coefficient, D, and the reciprocal of absolute temperature, $1/T$. The energy term, E, has a value of 19.6 kcal/mole (1.59 SD), and the preexponential term, D_0, is 3.24×10^5 cm²/sec.

Although the diffusion coefficient is temperature sensitive, the calculated partition coefficient does not change with temperature (Table III).

Studies directed toward measuring the desorption kinetics of nitroglycerin from the container material were intended to establish the reversibility of the interaction. The amount of nitroglycerin remaining per disk under sink conditions was measured by scintillation counting over 8000 min. The nitroglycerin lost per disk, L_t, at each sampling time was determined by taking the difference between the amount initially present (1652 and 1645 μg/disk in two trials) and the amount found at each time.

The relation between the amount lost and time for one trial is given in Fig. 4. The symbols represent experimental values, and the line joining them was generated by NONLIN[13] from a diffusion model describing diffusion through a plane sheet where the concentration throughout the sheet is initially uniform and where the concentration at the surface remains constant during the time course of desorption (19). The relation between fractional loss, L_t/L_∞, and time, t, under these conditions is:

$$\frac{L_t}{L_\infty} = 1 - \sum_{n=0}^{\infty} \frac{8}{(2n+1)^2\pi^2} \exp[-D(n+\tfrac{1}{2})^2\pi^2 t/h^2] \qquad \text{(Eq. 5)}$$

where L_∞ is the amount lost at long time (equal to the amount present initially), D is the diffusion coefficient, and h is the half thickness of the

Table III—Effect of Temperature on the Diffusion Coefficient and Partition Coefficient of Nitroglycerin Sorption from Aqueous Solution by a Plastic Intravenous Container Material

Temperature	Amount Adsorbed at Equilibrium, M_∞, μg/cm³	Diffusion Coefficient[a], D, cm²/sec × 10⁹ (±SD × 10¹⁰)	Partition Coefficient
30°	21,359.7	2.68 (2.25)	111.2
30°	19,956.6	2.22 (1.31)	103.8
35°	18,154.6	4.53 (2.86)	92.4
35°	19,982.9	4.28 (2.80)	102.4
40°	20,118.2	8.61 (6.30)	94.6
40°	19,774.2	8.06 (5.46)	93.8
45°	21,718.3	9.82 (9.74)	106.7
45°	21,818.3	11.8 (13.8)	104.1

[a] Obtained by nonlinear least-squares fitting of amount adsorbed by plastic at time t (M_t) and the time using Eq. 1.

[13] Unit 7292, The Upjohn Co., Kalamazoo, Mich.

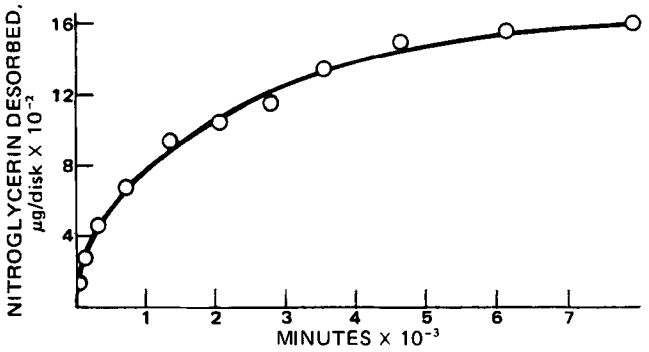

Figure 4—*Relationship between the amount of nitroglycerin lost from a plastic disk initially containing 1652 μg and time under sink conditions at 30°. The symbols are experimental data, and the line was that generated by nonlinear least-squares fitting of Eq. 4.*

sheet. Equation 5 is a reduced form of the more general Eq. 1, where α equals ∞ and where the roots of Eq. 3 are:

$$q_n = (n + \tfrac{1}{2})\pi \qquad \text{(Eq. 6)}$$

Equation 5 was used by Pikal *et al.* (7) in describing nitroglycerin desorption from two packaging materials. The computer-generated values for the diffusion coefficient using Eq. 5 are 1.17×10^{-9} (4.63×10^{-11} *SD*) and 1.10×10^{-9} (4.62×10^{-11} *SD*) cm²/sec at the two initial amounts of nitroglycerin per disk used (1652 and 1645 μg/ml, respectively). These values agree well with each other and with those generated in sorption studies at 30°: 2.05×10^{-9} cm²/sec (average value from Table II) and 2.45×10^{-9} cm²/sec (average value from Table III). Thus, the loss of nitroglycerin to the plastic intravenous container apparently is a reversible sorption process.

SUMMARY

Under the experimental conditions used, both equilibrium and kinetic studies showed that nitroglycerin is removed from aqueous solution by the plastic container material through an absorption process. The partition coefficient of nitroglycerin between plastic and aqueous solutions is ~104 at 30°. The time course for the absorption can be described as diffusion through a sheet where the concentration in the aqueous solution phase falls with time, with a diffusion coefficient of about 2.1×10^{-9} cm²/sec. Nitroglycerin loss from aqueous solution does not occur through hydrolysis since solutions stored in glass containers at pH 5.7 and 35° retained potency for at least 48 hr.

Although the experimental data support the thesis that the uptake of nitroglycerin is migration of the drug into the plastic matrix, this finding does not exclude the possible adsorption of the drug on the surface. Conceivably, the quantity of solute adsorbed may be insignificant when compared with the amount absorbed and the rate of adsorption may be much faster than the rate of absorption, with the result that any adsorption is obscured. Thus, the experimental conditions employed as well as the physical and chemical properties of the drug molecule and the plastic could affect conclusions reached regarding the rate-limiting mechanisms and the equilibrium distribution of drugs exposed to plastic.

REFERENCES

(1) D. Banes, *J. Pharm. Sci.*, **57**, 893 (1968).

(2) B. Edelman, A. M. Contractor, and R. Shangraw, *J. Am. Pharm. Assoc.*, **NS11**, 30 (1971).

(3) S. A. Fusari, *J. Pharm. Sci.*, **62**, 122 (1973).

(4) S. A. Fusari, *ibid.*, **62**, 2012 (1973).

(5) B. Dorsch and R. Shangraw, *Am. J. Hosp. Pharm.*, **32**, 795 (1975).

(6) M. J. Pikal, A. L. Lukes, and L. F. Ellis, *J. Pharm. Sci.*, **65**, 1278 (1976).

(7) M. J. Pikal, D. A. Bibler, and B. Rutherford, *ibid.*, **66**, 1293 (1977).

(8) H. L. Fung, *Am. J. Hosp. Pharm.*, **35**, 528 (1978).

(9) J. K. Sturek, T. D. Sokoloski, W. T. Winsley, and P. E. Stach, *ibid.*, **35**, 537 (1978).

(10) D. J. Ludwig and C. T. Ueda, *ibid.*, **35**, 541 (1978).

(11) W. G. Crouthamel, B. Dorsch, and R. Shangraw, *N. Engl. J. Med.*, **299**, 262 (1978).

(12) J. C. Boylan, R. L. Robison, and P. M. Terrill, *Am. J. Hosp. Pharm.*, **35**, 1031 (1978).

(13) T. W. Dean and D. C. Baun, *Am. J. Hosp. Pharm.*, **32**, 1036 (1975).

(14) M. T. Rosseel and M. G. Bogaert, *J. Pharm. Sci.*, **62**, 754 (1973).

(15) W. G. Crouthamel and B. Dorsch, in "Abstracts of APhA Academy of Pharmaceutical Sciences," Phoenix meeting, Nov. 1977, p. 162.

(16) M. C. Crew and F. J. DiCarlo, *J. Chromatogr.*, **35**, 506 (1968).

(17) U. Amschler, *Pharm. Ztg.*, **119**, 1077 (1974).

(18) S. K. Yap, C. T. Rhodes, and H. L. Fung, *Am. J. Hosp. Pharm.*, **32**, 1039 (1975).

(19) J. Crank, "The Mathematics of Diffusion," Clarendon Press, Oxford, England, 1975, pp. 57, 58, 379.

ACKNOWLEDGMENTS

Presented at the APhA Academy of Pharmaceutical Sciences, Hollywood, Fla., meeting, November 1978.

Supported in part by a grant from Eli Lilly Co. and the Public Health Service, National Heart, Lung, and Blood Institute (1R01 HL 23303-01).

Isolation of Salicylsalicylic Acid, Acetylsalicylsalicylic Acid, and Acetylsalicylic Anhydride from Aspirin Tablets by Extraction and High-Pressure Liquid Chromatography

JOHN C. REEPMEYER [x] **and ROSS D. KIRCHHOEFER**

Received March 1, 1979, from the *National Center for Drug Analysis, Food and Drug Administration, St. Louis, MO 63101.* Accepted for publication March 29, 1979.

Abstract □ Aspirin and four salicylate impurities of aspirin (salicylic acid, acetylsalicylsalicylic acid, acetylsalicylic anhydride, and salicylsalicylic acid) were resolved by silica gel TLC and by high-pressure liquid chromatography (HPLC) on a reversed-phase C_{18} column. Care was necessary in the choice of a column because a similar column failed to resolve these five compounds. Salicylsalicylic acid was isolated from aspirin tablets by extraction, followed by reversed-phase C_{18} HPLC. The structure of this compound was confirmed by comparison with an authentic sample of salicylsalicylic acid by HPLC, TLC, IR and UV spectrophotometry, and mass spectrometry. Two other compounds, acetylsalicylic anhydride and acetylsalicylsalicylic acid, which had been previously identified by chromatography as impurities in aspirin, were isolated and further characterized.

Keyphrases □ Aspirin—impurities in tablets, salicylsalicylic acid, acetylsalicylsalicylic acid, acetylsalicylic anhydride, isolation by extraction and high-pressure liquid chromatography □ Aspirin, derivatives—isolated as impurities from tablets, extraction, high-pressure liquid chromatography □ Analgesics—aspirin, isolation of derivatives from tablets, extraction, high-pressure liquid chromatography □ High-pressure liquid chromatography—analysis, aspirin derivatives in tablets

In recent years, two salicylate derivatives, acetylsalicylic anhydride (I) (1) and acetylsalicylsalicylic acid (II) (2), have been detected as impurities in aspirin tablets. These two compounds were reported (1, 3, 4) to be immunogenic substances capable of inducing the formation of acetylsalicyloyl- or salicyloyl-specific antibodies. According to these reports, allergic reactions to commercial aspirin preparations are due to these antibodies and, therefore, are caused by the aspirin impurities rather than by aspirin itself[1]. The clinical significance of these *in vivo* findings has been disputed (6). Demonstration of the potential immunogenic activity of these salicylate derivatives has emphasized the significance of their presence in pharmaceutical aspirin preparations even at low concentrations. Two papers (7, 8) reported the use of high-pressure liquid chromatography (HPLC) in the determination of salicylic acid, I, and II in aspirin.

A third salicylate derivative, salicylsalicylic acid (III), was found to undergo aminolysis to *N*-salicyloyl derivatives by reaction with amino acids (4) and to be an intermediate in the aminolysis of II, an alleged immunogenic agent (3). *In vivo* tests demonstrated the immunogenicity of I–III in guinea pigs (4). Although Bundgaard and DeWeck (4) did not find III in various aspirin samples, III was detected in most of the commercial aspirin tablets analyzed by HPLC in the present studies.

This paper reports the detection and identification of III as an impurity in aspirin and aspirin tablets. Methods for separation of aspirin and four salicylate impurities by TLC and HPLC are described. The isolation of I–III from aspirin tablets by extraction and HPLC and the possible confusion of III with I in reversed-phase HPLC are discussed.

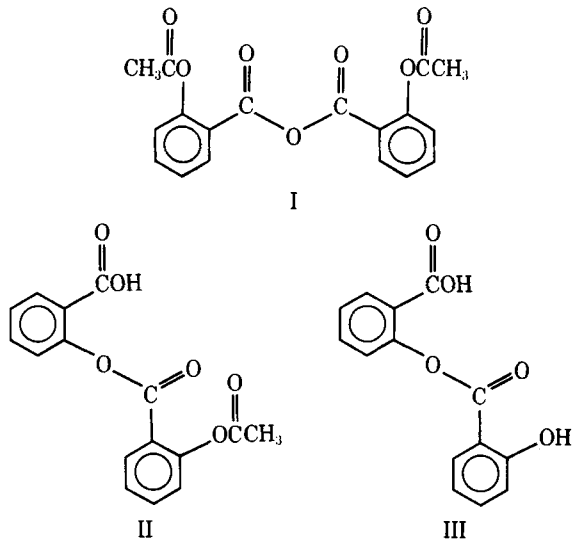

I

II

III

EXPERIMENTAL

Instruments—All samples for IR spectral analysis were prepared as potassium bromide pellets, and the spectra were recorded on a grating IR spectrophotometer[2]. Melting points were taken in a capillary melting-point apparatus[3] and are uncorrected. NMR spectra were recorded on a 60-MHz spectrometer[4] with tetramethylsilane as an internal reference standard. UV spectra were recorded on a double-beam UV–visible spectrophotometer[5]. A high-pressure liquid chromatograph[6] with a UV detector set at 254 nm was used.

Reagents and Chemicals—Acetylsalicylic anhydride was synthesized according to a literature procedure (9). Recrystallization (95% ethanol) provided a white crystalline solid, mp 83.5–84.5°; IR: ν 1790, 1765, and 1730 cm^{-1} (ester and anhydride carbonyl stretching frequencies), identical to a published I spectrum (10); NMR ($CDCl_3$): δ 8.05 (d of d, J = 7.5 and 2 Hz, 2H, protons *ortho* to each anhydride carbonyl), 7.83–7.02 (m, 6H, aromatic protons other than the protons *ortho* to the anhydride carbonyl), and 2.27 (s, 6H, methyl protons). This compound is referred to throughout as reference standard I.

Acetylsalicylsalicylic acid was prepared by acetylation of salicylsalicylic acid[7] with acetic anhydride in cold aqueous sodium hydroxide according to a literature procedure (11). Recrystallization (twice) from aqueous ethanol (charcoal) gave white crystals, mp 163.5–164.5°; IR: ν 1748 with a shoulder at 1752 (two ester carbonyl stretching frequencies) and 1690 (acid carbonyl stretching frequency) cm^{-1}; NMR (CD_3OD): δ 8.36–7.84 (m, 2H, aromatic protons *ortho* to the carbonyl groups), 7.84–7.02 (m, 6H, aromatic protons other than those *ortho* to the carbonyl groups), and 2.22 (s, 3H, methyl protons). This compound is referred to throughout as reference standard II.

[1] An alternative theory is that aspirin itself is responsible for the formation of an antigenic determinant by initially undergoing an intramolecular rearrangement to a mixed anhydride, which, in turn, reacts with a protein amino function (5).

[2] Model 337, Perkin-Elmer Corp., Norwalk, Conn.
[3] Thomas-Hoover, Arthur H. Thomas Co., Philadelphia, Pa.
[4] Model T-60A, Varian Associates, Palo Alto, Calif.
[5] Cary model 219, Varian Associates, Palo Alto, Calif.
[6] Chromatronix model 3500B, Spectra-Physics, Santa Clara, Calif.
[7] K & K Laboratories, Plainview, N.Y.

0022-3549/79/0900-1167$01.00/0
© 1979, American Pharmaceutical Association

Acetylsalicylic acid[8], salicylic acid[8], salicylsalicylic acid[7], and methylacetylsalicylate[9] were used as obtained. Glass-distilled benzene[10], methanol[11], and cyclohexane[11] were used. All other chemicals and reagents were USP, ACS, or chromatographic grade. Deionized water was used for preparation of aqueous solutions.

Phosphate buffer (0.5 *M*, pH 8) was prepared from 2 *N* NaOH (120 ml), monobasic potassium phosphate (34 g), and water (to 500 ml). Phosphate buffer (0.5 *M*, pH 11.3) was prepared from 2 *N* NaOH (380 ml), monobasic potassium phosphate (68 g), and water (to 1000 ml).

α-Benzamidocinnamate–pyridine reagent, used in the spectrophotometric analysis of I, was prepared according to Bundgaard and Bundgaard (9). Sodium α-benzamidocinnamate was synthesized by the following route: benzaldehyde + hippuric acid → 4-benzylidene-2-phenyloxazoline-5-one (12) → α-benzamidocinnamic acid (12) → sodium α-benzamidocinnamate (9).

HPLC Parameters—The analytical HPLC system was operated with a flow rate of 1.6 ml/min and a chart speed of 30.48 cm (12 in.)/hr. The mobile phase was prepared by adding 12.5 ml of acetic acid to 450 ml of water and diluting with methanol to 1000 ml. This solvent mixture was filtered through a 0.6-μm filter[12] before use. Two different analytical reversed-phase C_{18} columns, A[13] and B[14], were used.

For the isolation of aspirin impurities, a semipreparative HPLC system was used with the following parameters: an 8-mm (i.d.) × 250-mm (length) stainless steel column packed with a reversed-phase C_{18} stationary phase[15]; a 1-ml loop injector; a chart speed of 30.48 cm/hr; a flow rate of 7 ml/min; and a mobile phase of acetic acid (11.5 ml), water (540 ml), and methanol (to 1000 ml).

Qualitative TLC—A single TLC system, one that has been employed successfully in separating I from aspirin (1, 13), separated aspirin and its four salicylate impurities. Samples were spotted on silica gel plates containing a fluorescent indicator[16] and developed in 2-butanone–cyclohexane (1:1) by ascending chromatography. Due to the instability of I on silica gel, the chromatogram was developed immediately after this compound was spotted. The compounds were detected by a UV hand lamp (254 nm). The R_f values for salicylic acid, aspirin, II, III, and I were 0.27, 0.34, 0.38, 0.44, and 0.51, respectively. Salicylic acid was fluorescent.

Isolation of I–III from Aspirin Tablets—One hundred 324-mg (5 gr) aspirin tablets were triturated in a mortar and pestle, and the powder was added to a cold biphasic mixture of benzene (130 ml) and phosphate buffer solution (650 ml, 0.5 *M*, pH 11.3). The mixture was stirred with a magnetic stirrer for 5 min and poured into a separator. The benzene layer was separated, dried over magnesium sulfate, and saved for isolation of I. The aqueous solution, pH 8 following neutralization of the original buffer solution with aspirin, was acidified with 2 *N* HCl (~300 ml) to pH 1–2 and filtered to remove the excipients and precipitated aspirin. The filtrate was extracted with 300 ml of benzene.

At this point, after all of the salicylates were in benzene solution, attention was directed toward the final isolation of I, since this compound undergoes decomposition. The first benzene extract (containing I) was filtered and concentrated to ~3 ml under reduced pressure at a bath temperature not exceeding 35°. Since TLC showed the presence of aspirin as well as I, the benzene solution was extracted with an equal amount of phosphate buffer (0.5 *M*, pH 8). The benzene solution, which now showed only I, was dried over magnesium sulfate, filtered, and evaporated under a dry nitrogen stream. This isolated I sample was compared to the reference standard I by UV (cyclohexane), TLC, and the α-benzamidocinnamate–pyridine test (9).

The second benzene extract, containing all salicylates except I, was extracted with four 100-ml portions of 0.1 *N* HCl to concentrate the remaining salicylate impurities relative to aspirin. Solvent benzene was removed under reduced pressure. The residue was dissolved in 4 ml of methanol, and an equal volume of water containing 1% acetic acid was added. This solution was passed through a 0.6-μm filter[12] before injection onto the semipreparative HPLC column. Fractions corresponding in retention times to II and III were collected. Solvents were evaporated under reduced pressure at 35°, with last traces being removed with a vacuum pump. Benzene (1 ml) was added to the isolated II sample; the solution was filtered and evaporated. The isolated II and III samples were compared to their reference standards by HPLC, IR, UV (95% ethanol), and TLC.

To demonstrate that III did not result from hydrolysis of II during the extraction procedure, reference standard II was subjected to the described extraction process; no evidence of III was found.

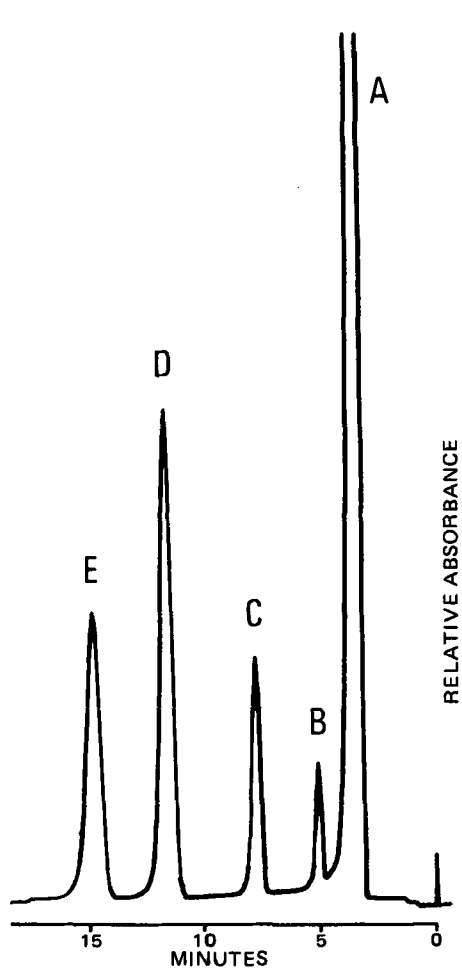

Figure 1—*HPLC on Column A of a synthetic mixture of aspirin (A) containing 1% each of salicylic acid (B), acetylsalicylsalicylic acid (C), acetylsalicylic anhydride (D), and salicylsalicylic acid (E). For the mobile phase, 12.5 ml of acetic acid was added to 450 ml of water and diluted to 1000 ml with methanol.*

RESULTS AND DISCUSSION

Aspirin and four salicylate impurities were adequately resolved by HPLC on Column A (Fig. 1). However, on Column B, another reversed-phase C_{18} column, I and III had almost identical retention times. Changes in the methanol–water ratio of the mobile phase or changes in the flow rate did not significantly change the difference between the retention times of these two compounds on Column B. The lack of resolution of these two compounds on one column emphasizes the precautions that must be taken in the HPLC analysis of aspirin for these compounds and the uncertainty of identifying them by HPLC alone.

HPLC of solutions obtained by extraction of aspirin or aspirin tablets with the mobile phase showed II, III, and salicylic acid in most samples tested. Although I generally was present in the aspirin samples and could be quantitated by the α-benzamidocinnamate–pyridine reagent[17] (9),

[8] Sigma Chemical Co., St. Louis, Mo.
[9] Aldrich Chemical Co., Milwaukee, Wis.
[10] Nanograde, Mallinckrodt, St. Louis, Mo.
[11] Burdick & Jackson Laboratories, Muskegon, Mich.
[12] Type BD, 0.6-μm pore size, Millipore Corp., Bedford, Mass.
[13] LiChrosorb RP-18, 10-μm particle size, 250 mm (length) × 4.6 mm (i.d.), EM Laboratories Inc., Elmsford, N.Y.
[14] μBondapak C_{18}, 10-μm particle size, 30 cm (length) × 3.9 mm (i.d.), Waters Associates, Milford, Mass.
[15] Corasil, 37–50 μm, Waters Associates, Milford, Mass.
[16] Precoated TLC plates, silica gel 60 F-254, EM Laboratories Inc., Elmsford, N.Y.

[17] We have determined that aspirin itself will react with the α-benzamidocinnamate–pyridine reagent, although at a slower rate than I. When present in the benzene extract at a concentration even as low as that of I, aspirin will interfere seriously with the analysis of I. The presence of interfering amounts of aspirin in this analysis can be determined by following the reaction over time. Absorbance resulting from I reaches a plateau in 20–30 min, whereas it continues to show a gradual increase past 30 min when aspirin is present.

detection and quantitation of I by HPLC was difficult because of its instability in the mobile phase and its presence in low concentration.

One feature that distinguishes I from III and the other salicylates mentioned is its high susceptibility to solvolysis. When reference standard I was dissolved in mobile phase (1 mg/ml) and examined by successive injection on Column A, the compound underwent solvolysis at room temperature to give rise to two new compounds with retention times corresponding to aspirin and methyl acetylsalicylate[18]. After 4 hr, <5% of the anhydride remained. The observed rate constant for the anhydride hydrolysis in 10% dioxane–90% water containing 0.57 *M* acetic acid at pH 2.59 and 25.1° has been reported as 6.0×10^{-4} sec^{-1} (14), from which the half-life is calculated to be 19 min. This rate was much faster than the rate of aspirin hydrolysis and was in general agreement with our observations. The salicylates other than acetylsalicylic anhydride were relatively stable in the mobile phase and showed no decomposition under the analytical conditions.

In a recent report (15) on aspirin impurities, it was tentatively assumed that III was present as an impurity in some aspirin samples based on its retention time by silica gel HPLC. The present study confirmed the presence of III in aspirin samples by isolation and identification of the compound; it is recognized that this compound is a commonly occurring impurity in aspirin and commercial aspirin preparations. The isolation of this compound from aspirin tablets by extraction and HPLC, as described, provided a sample that was identical to the reference standard III[7] by TLC and by HPLC on Columns A and B.

The UV spectrum (λ_{max}, relative absorbance) in 95% ethanol of the isolated III sample (234 nm, 1; 308 nm, 0.313) was comparable to that of reference standard III (234 nm, 1; 308 nm, 0.310). The IR spectrum of the isolated III showed maximum absorbance at frequencies of 3455 (phenolic OH stretching) and 1740 and 1690 (carbonyl stretching) cm^{-1}; this spectrum, including the fingerprint region, was identical to an IR spectrum of the reference standard. The structure was confirmed by an electron-impact mass spectrum[19], which provided a parent ion (*m/e* 258) and gave a breakdown pattern similar to that of the reference standard III.

Two other salicylate impurities found in aspirin, I and II, whose characterization by chromatographic methods was previously reported (1, 2, 7, 8), were isolated by extraction and HPLC and were characterized further. The isolated II sample was identical to its reference standard by HPLC, TLC, IR, and UV (95% ethanol). The isolated I gave a positive test for I with the α-benzamidocinnamate–pyridine reagent. The UV (cyclohexane) and TLC characteristics were the same as those for the reference standard I. When dissolved in mobile phase and monitored by HPLC on Column A, the isolated anhydride, like the reference standard, underwent hydrolysis and methanolysis at ambient temperature to give aspirin and methyl acetylsalicylate.

In the analysis of 176 samples of commercial aspirin tablets, the III concentration varied from below detectable limits (0.001%) to 0.25% of the amount of aspirin present. Of the samples tested, 70% contained levels that were detectable by HPLC (≥0.001%). Details of the quantitative analysis of aspirin impurities in aspirin and aspirin tablets will be the subject of a future report.

[18] The retention time of methyl acetylsalicylate was similar to that of salicylic acid under these conditions. To differentiate between these two compounds, the mobile phase was changed to one consisting of methanol (46 ml), acetic acid (1.2 ml), and water (to 100 ml) after I had decreased to about 5% of its original concentration.

[19] Varian MAT 311 mass spectrometer, Varian Associates, Palo Alto, Calif.

REFERENCES

(1) A. L. DeWeck, *Int. Arch. Allergy Appl. Immunol.*, **41**, 393 (1971).

(2) S. Patel, J. H. Perrin, and J. J. Windheuser, *J. Pharm. Sci.*, **61**, 1794 (1972).

(3) H. Bundgaard, *J. Pharm. Pharmacol.*, **26**, 18 (1974).

(4) H. Bundgaard and A. L. DeWeck, *Int. Arch. Allergy Appl. Immunol.*, **49**, 119 (1975).

(5) M. A. Schwartz and G. L. Amidon, *J. Pharm. Sci.*, **55**, 1464 (1966).

(6) P. Kallos and H. D. Schlumberger, *J. Pharm. Pharmacol.*, **30**, 67 (1978).

(7) S. L. Ali, *J. Chromatogr.*, **126**, 651 (1976).

(8) S. O. Jansson and I. Andersson, *Acta Pharm. Suec.*, **14**, 161 (1977).

(9) H. Bundgaard and C. Bundgaard, *J. Pharm. Pharmacol.*, **25**, 593 (1973).

(10) O. R. Sammul, W. L. Brannon, and A. L. Hayden, *J. Assoc. Off. Anal. Chem.*, **47**, 932 (1964).

(11) F. D. Chattaway, *J. Chem. Soc.*, **1931**, 2495.

(12) H. B. Gillespie and H. R. Snyder, in "Organic Synthesis Collective Volume II," A. H. Blatt, Ed., Wiley, New York, N.Y., 1943, p. 489.

(13) H. D. Spitz, *J. Chromatogr.*, **140**, 131 (1977).

(14) E. R. Garrett, *J. Am. Chem. Soc.*, **82**, 711 (1960).

(15) H. Bundgaard, *Arch. Pharm. Chem. Sci. Ed.*, **4**, 103 (1976).

ACKNOWLEDGMENTS

The authors are grateful to Walter R. Benson and Robert P. Barron, Division of Drug Chemistry, Food and Drug Administration, Washington, D.C., for mass spectral data.

Lyophilization of Pharmaceutical Injections: Theoretical Physical Model

N. F. H. HO * and T. J. ROSEMAN ‡x

Received December 28, 1978, from the *College of Pharmacy, University of Michigan, Ann Arbor, MI 48109, and ‡Pharmacy Research, The Upjohn Company, Kalamazoo, MI 49001. Accepted for publication March 28, 1979.

Abstract □ A physical model for the lyophilization kinetics of parenteral formulations is presented. Mathematical relationships are derived, which involve the simultaneous change in the receding boundary of the ice–vapor interface with time as well as water vapor diffusion across the dry porous matrix and boundary layer. Heat from an external heat source is transferred across the frozen solution to the receding ice surface. The model predicts that the water lost and the receding boundary distance are linearly related to the square root of time when lyophilization is matrix controlled. The mathematical descriptions are predictive of the physicochemical and transport events and can lead to the design of quantitative experiments to relate theory to formulation design.

Keyphrases □ Lyophilization—physicochemical model, parenteral formulations □ Models, physicochemical—lyophilization, parenteral formulations □ Dosage forms, parenteral—lyophilization, physicochemical model

Lyophilization, commonly called freeze drying, involves the removal of water from a frozen substance by sublimation and mass transfer under vacuum conditions and at temperatures less than the eutectic temperature of the multicomponent aqueous solution. Its importance and usage as a drying process are well known in the pharmaceutical and food industries and in biological laboratories (1–4). The lyophilization of parenteral products is not problem free. Rejection rates are attributed to melt-backs or nonuniformity in the color of the dried drug matrix, which is not necessarily accompanied by decreased potency. The total drying cycles are often long, ranging from 24 to 48 hr, and approaches toward optimizing the drying cycle and time of complete drying are generally empirical.

Much interest in theoretical kinetic models and their application to the freeze drying of foods and model systems is found in the literature (2, 5–8). These models have addressed both the mass transfer process and the heat transfer problem, including the physical factors governing the kinetics.

DeLuca and Lachman (9), in reporting on the freeze drying of pharmaceutical products, emphasized the theory and method of determining eutectic temperatures of drug formulations and also the influence of the eutectic temperature on practical lyophilization cycles. They investigated the effect of various metal trays on heat transfer during lyophilization (10). Effects of additives in preformulation systems on melting behavior and eutectic temperatures have been investigated (11). The macroscopic appearance of frozen solutions and dried samples has been studied (12).

This paper describes a physical model for lyophilization. The model is based on the principles of physical chemistry and on the laws of transport with accompanying mathematics and is described in a manner amenable to well-designed experimental approaches, mechanistic interpretation, quantitation of physically relevant parameters, and predictiveness. The lyophilization of parenteral products is one area of pharmaceutical processing that presents nearly an ideal situation for relating theory and practice. With a basic understanding about lyophilization and the rate-determining physicochemical conditions, a rational approach to optimizing the formulation and process conditions can evolve.

THEORY

Physical Model—The physical model describing lyophilization of a frozen aqueous solution containing drug and a matrix-building substance (*e.g.*, mannitol or lactose) should be analogous to the well-known model for drug release from an inert and insoluble matrix (13, 14). As shown in Fig. 1, it involves the simultaneous change in the receding boundary with time, phase transition at the ice–vapor interface, and water vapor diffusion across both the pore path length of the matrix and the diffusional boundary layer just outside the matrix. No unusual water vapor accumulation is assumed here, *i.e.*, sink conditions.

It is taken that the matrix pores are continuous and fairly uniform, with no significant presence of end pores and isolated ice pockets; hence, the receding boundary is sharp. The freezing rates have marked influence on the distribution, quality, and sizes of the pores and, consequently, on the overall lyophilization kinetics (15, 16). In the general situation, water vapor transport occurs by ordinary (viscous) and free molecular flow according to well-established laws of kinetic motion of gases in pores. The general case also includes water vapor adsorption on polar surfaces with surface diffusion.

Throughout the following sections, the definitions of various terms with their corresponding units are presented so that the paired set of units will yield the correct calculations.

Flux Expressions—The mass transport of water vapor across the boundary layer at the matrix surface is expressed by:

$$J = \frac{DC_0}{H} = (\mathrm{PC})(C_0) \qquad \text{(Eq. 1)}$$

where:

J = flux per unit of cross-sectional area
D = diffusion coefficient of the water vapor, square centimeters per second
H = boundary layer thickness
PC = permeability coefficient of the boundary layer, centimeters per second
C_0 = concentration of vapor at the matrix surface at $x = 0$

The flux per unit of cross-sectional area across the matrix pores for the viscous, molecular, and surface diffusion mechanism is:

$$J_M = \frac{\epsilon}{\tau} D_p \frac{dC}{dx} + \frac{\epsilon}{\tau} D^* \frac{dC^*}{dx} \qquad \text{(Eq. 2)}$$

where:

J_M = flux per unit of area
D_p = effective diffusion coefficient for viscous and molecular flow
D^* = surface diffusion coefficient
ϵ = volume fraction of water in the total system
τ = tortuosity factor ≥ 1.0 and usually 3.0
C = concentration of vapor in the pores
C^* = concentration of vapor molecules adsorbed on the matrix surface in the pores

According to the Langmuir adsorption isotherm:

$$C^* = \frac{k_1 k_2 C}{1 + k_1 C} \qquad \text{(Eq. 3)}$$

0022-3549/79/0900-1170$01.00/0
© 1979, American Pharmaceutical Association

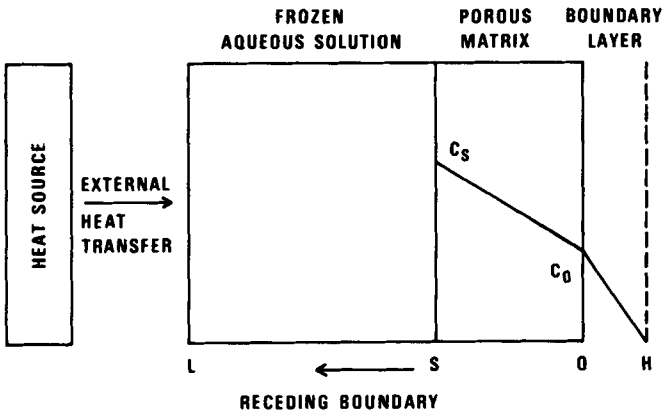

Figure 1—*Physical model for lyophilization involving simultaneous receding boundary of ice-vapor interface and water vapor diffusion across porous matrix and boundary layer and into sink with time. Heat from an external heat source is transferred across frozen solution to receding ice surface.*

where k_1 is the adsorption coefficient and k_2 is the maximum surface concentration of adsorption sites.

Utilizing the chain rule, one gets:

$$\frac{dC^*}{dx} = \left(\frac{dC^*}{dC}\right)\left(\frac{dC}{dx}\right) \quad \text{(Eq. 4)}$$

whereupon:

$$\frac{dC^*}{dx} = \frac{k_1 k_2}{(1 + k_1 C)^2}\left(\frac{dC}{dx}\right) \quad \text{(Eq. 5)}$$

With the condition of $k_1 C \ll 1$, Eq. 5 is simplified considerably to:

$$\frac{dC^*}{dx} = k\frac{dC}{dx} \quad \text{(Eq. 6)}$$

where $k = k_1 k_2$. This assumption in the Henry's law region of the adsorption isotherm is reasonable because of the low vapor pressure conditions employed in lyophilization. It follows that:

$$J_M = \left(\frac{\epsilon}{\tau}\right)(D_p + kD^*)\left(\frac{dC}{dx}\right) \quad \text{(Eq. 7)}$$

and, allowing for linear concentration gradients:

$$J_M = \frac{(D_e)(C_s - C_0)}{S} \quad \text{(Eq. 8)}$$

where:

$$D_e = \left(\frac{\epsilon}{\tau}\right)(D_p + kD^*) \quad \text{(Eq. 9)}$$

and S is the receding boundary distance and C_s is the concentration of water vapor at the ice surface.

The continuity of mass flow at $x = 0$ is given by:

$$J = J_M \quad \text{(Eq. 10)}$$

Accordingly, one readily gets:

$$J_M = \frac{C_s}{\frac{S}{D_e} + \frac{1}{PC}} \quad \text{(Eq. 11)}$$

and, in turn:

$$J_M = \frac{dQ}{dt} \quad \text{(Eq. 12)}$$

where Q is the amount of water released from the system per unit area and t is time.

Change in Receding Boundary in Matrix and Amount of Water Released with Time—By using a linear approximation, it can be seen in Fig. 1 that:

$$Q = S(A - n\epsilon C_s) \quad \text{(Eq. 13)}$$

where A is the amount of water per unit volume of the system and n is a constant whereby $0.5 \leq n < 1.0$. If sink conditions exist at $x = 0$, *i.e.*, there is no appreciable water vapor accumulation at the matrix surface, $n = 0.5$; otherwise, $n > 0.5$. As will be seen in the next section, A will be much greater than $n\epsilon C_s$ such that:

$$Q = AS \quad \text{(Eq. 14)}$$

Thus:

$$\frac{dQ}{dt} = A\frac{dS}{dt} \quad \text{(Eq. 15)}$$

By combining Eqs. 11, 12, and 15 and integrating between the limits of $S(0) = 0$ and $S(t)$, the change in the receding boundary with time is:

$$S^2 + \frac{2D_e S}{PC} = \frac{2D_e C_s t}{A} \quad \text{(Eq. 16)}$$

$$S = -\frac{D_e}{PC} + \sqrt{\left(\frac{D_e}{PC}\right)^2 + \frac{2D_e C_s t}{A}} \quad \text{(Eq. 17)}$$

With Eqs. 11 and 14, the change in the amount of water released per unit of cross-sectional area is given by the quadratic expression:

$$Q^2 + \frac{2AD_e Q}{PC} = 2AD_e C_s t \quad \text{(Eq. 18)}$$

$$Q = A\left[-\frac{D_e}{PC} + \sqrt{\left(\frac{D_e}{PC}\right)^2 + \frac{2D_e C_s t}{A}}\right] \quad \text{(Eq. 19)}$$

It is readily observed in Eqs. 17 and 18 that when the transport rate is controlled by the matrix, the kinetics directly follow the square root of time relationship. Thus:

$$S = \sqrt{\frac{2D_e C_s t}{A}} \quad \text{(Eq. 20)}$$

$$\frac{dS}{dt} = \sqrt{\frac{D_e C_s}{2At}} \quad \text{(Eq. 21)}$$

$$Q = \sqrt{2D_e AC_s t} \quad \text{(Eq. 22)}$$

$$\frac{dQ}{dt} = \sqrt{\frac{D_e AC_s}{2t}} \quad \text{(Eq. 23)}$$

It is explicit in the development of the theory that C_s is constant throughout time; in other words, the vapor pressure and temperature at the ice surface are constant.

Surface Concentration of Water Vapor and Pressure—The water vapor concentration at the ice surface, C_s in grams per cubic centimeter, may be approximated by the ideal gas law:

$$C_s = \frac{P_s M}{1000RT_s} \quad \text{(Eq. 24)}$$

where:

P_s = vapor pressure of ice, atmospheres
R = gas constant, 0.08205 liter atm $°K^{-1}$ $mole^{-1}$
T_s = absolute temperature at the ice surface
M = molecular weight of water

The vapor pressure on ice, P_{mm} in millimeters of mercury, is given by the following relationship (18) or in critical tables:

$$\log P_{mm} = -\frac{2445.5656}{T} + 8.2312 \log T - 1677.006 \times 10^{-5} T + 120514 \times 10^{-10} T^2 - 6.757169 \quad \text{(Eq. 25)}$$

It can be determined that at −20°, P_s is 1.02×10^{-3} atm and C_s is 8.88×10^{-7} g/cm^3; at −10°, P_s and C_s are 2.56×10^{-3} atm and 2.14×10^{-6} g/cm^3, respectively. Accordingly, the cited condition of $A \gg n\epsilon C_s$ is justified since the amount of water per cubic centimeter, A, is generally ≥ 0.5 g/cm^3.

Diffusivity of Water Vapor in Porous Matrix—According to the kinetic theory of gases, the flow of vapor molecules in fine pores depends on the mean free path relative to the pore radius (18, 19). The Knudsen number, Kn, is defined by:

$$Kn = \frac{\lambda}{r_e} \quad \text{(Eq. 26)}$$

where λ is mean free path in centimeters and r_e is the effective pore radius in centimeters. The mean free path, the distance a molecule travels before

Table I—Estimates of the Water Vapor Diffusion Coefficients at Low Temperatures and Vapor Pressures for Different Effective Pore Sizes [a]

T_s	P_s, mm Hg	r_e, μm	Diffusion Coefficient × 10^{-2} cm²/sec			Knudsen Number
			D_v	D_K	D_{pore}	
−20°	0.779	25	2.68	0.91	0.68	10.2
		50	2.68	1.82	1.08	5.1
		100	2.68	3.64	1.54	2.5
		200	2.68	7.28	1.96	1.27
−30°	0.293	25	6.78	0.89	0.79	27.6
		50	6.78	1.78	1.41	13.8
		100	6.78	3.57	2.34	6.9
		200	6.78	7.14	3.48	3.5

[a] Values used were: M = 18, P_{out} = 10^{-3} mm, σ_{H_2O} = 2.641, Ω_D = 2.613 at −20° and 2.662 at −30°, and λ = 254 μm at − 20° and 690 μm at −30°.

colliding with another one, is further given by:

$$\lambda = \frac{1}{\sqrt{2}(\pi d^2 N)} \qquad \text{(Eq. 27)}$$

where d is the molecular diameter of water vapor (3.46 Å) and N is the number of molecules per cubic centimeter. In turn:

$$N = \frac{PN_{Av}}{1000RT} \qquad \text{(Eq. 28)}$$

where N_{Av} is Avogadro's number, P is pressure, and the other terms are as defined previously. As can be seen, λ is inversely proportional to the vapor concentration or pressure.

Gas flow in pores is generally divided into four regimes (20): (*a*) $Kn < 0.01$, viscous flow; (*b*) $0.01 < Kn < 0.1$, viscous slip flow; (*c*) $0.1 < Kn < 3.0$, transition; and (*d*) $3.0 < Kn$, free molecular flow. As the vapor pressure approaches near-vacuum conditions, the character of the vapor flow progressively changes from viscous to free molecular flow. In viscous flow, the diffusional resistance arises from intermolecular collisions; at the other extreme, the diffusional resistance in free molecular flow is due to the collision of gas molecules with the pore surface. At pressures below the viscous limit previously indicated, the viscous flow must be corrected for slip flow about the pore walls.

At this point, it is useful to determine the flow regime under which lyophilization (low pressures and low temperatures below the eutectic temperature) generally occurs. For example, when the average pressure in the pores is equal to one-half the vapor pressure of ice at −20°, λ is 1.27 × 10^{-2} cm or 127 μm by Eqs. 25, 27, and 28; at −30°, λ is 345 μm. Since the effective pore radius is expected to be <1000 μm, Kn will be >0.1. Accordingly, the pore transport of vapor will occur most likely within the transition of viscous to free molecular flow regimes.

In the Knudsen region of free molecular flow, the water vapor diffusion coefficient (19, 21) is:

$$D_K = \left(\frac{2r_e}{3}\right)\left(\frac{8RT}{\pi M}\right)^{1/2} \qquad \text{(Eq. 29)}$$

When the following parameters are defined with the units indicated, *i.e.*, r_e is the effective pore radius in centimeters, R is the gas constant taken as 8.315 × 10^7 ergs deg^{-1} mole^{-1}, M is the molecular weight, and T is the average absolute temperature in the pores, then D_K will have units of square centimeters per second. Here, λ is much larger than r_e so that the collision of gas molecules with the walls is more probable than that between molecules.

In viscous flow, the ordinary diffusion coefficient for gases, allowing for mutual interaction, may be employed (22):

$$D_v = \frac{0.002627T^{3/2}}{\sigma^2_{H_2O}\Omega_D P_{ave} M^{1/2}} \qquad \text{(Eq. 30)}$$

where:

D_v = diffusion coefficient for viscous flow, square centimeters per second

P_{ave} = average pressure in the pores in atmospheres with respect to the vapor pressure of ice and the pressure outside the porous matrix
$= (P_s - P_0)/2$

σ_{H_2O} = Lennard–Jones force constant for water

Ω_D = temperature-dependent collision integral

The σ_{H_2O} (= 2.641 Å) and Ω_D constants are found in various sources (22–24). The values of Ω_D are 2.613 at −20° and 2.662 at −30°. As can be seen, D_v can be rather large at low pressures.

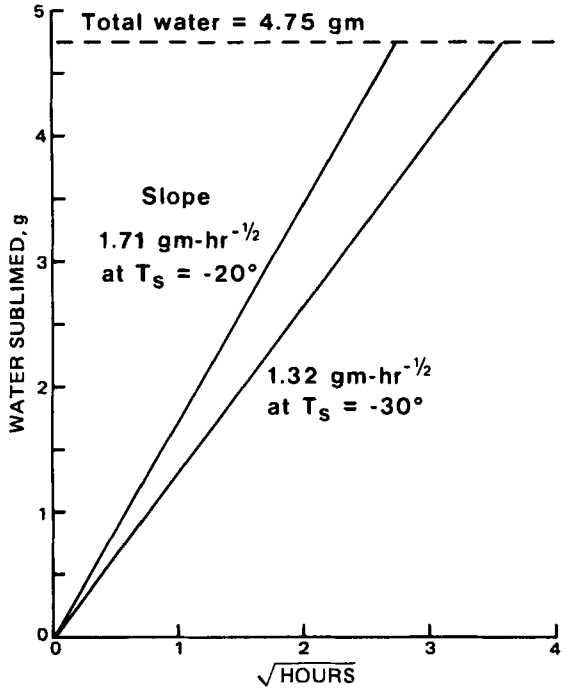

Figure 2—*Changes in amount of water lyophilized with time for two surface temperatures at the receding front. Theoretical plots are based on parameter values in Table II.*

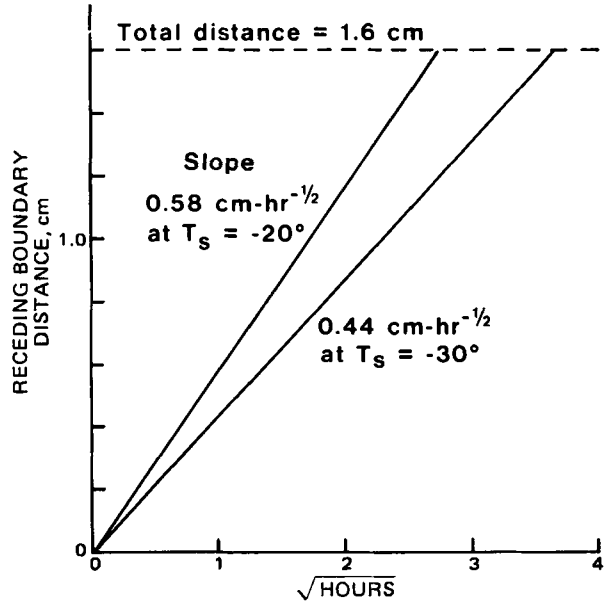

Figure 3—*Receding boundary distance changes with time for two surface temperatures at the receding front. Theoretical plots are based on parameter values in Table II.*

Table II—Physical Parameters Used in Theoretical Computations of Lyophilization Rates[a]

T_s	P_s, mm Hg	r_e, μm	D_v, cm²/sec	D_κ, cm²/sec	A, g/ml	ϵ	τ
−20°	0.779	100	2.68×10^2	3.64×10^2	0.95	0.95	3.0
−30°	0.293	100	6.78×10^2	3.57×10^2	0.95	0.95	3.0

[a] A 5-ml sample was in a 2.0-cm i.d. vial. Total amount of water was 4.75 g.

The transition of viscous to Knudsen's free molecular flow is not precise. While the former is pressure dependent, the latter is not. For practical purposes, Pollard and Present (25) provided an approximate expression:

$$D_P = \frac{1}{1/D_v + 1/D_K} \qquad \text{(Eq. 31)}$$

Although the mathematical form implies a physical situation (which is not real here) whereby the pore resistance due to viscous flow is in series with the pore resistance due to free molecular flow, the expression does allow an adequately smooth transition for computational purposes. When $D_v \gg D_K$, Knudsen diffusion will be the rate-controlling mechanism.

Table I gives estimates of the diffusion coefficients of water vapor at low temperatures and pressures for different pore radii. At −20° where the vapor pressure of ice is 0.779 mm Hg and the outside pressure is 10^{-3} mm Hg, the D_{pore} is 0.68–1.96 × 10^2 cm²/sec for average pore radii of 25–200 μm. When the average pore radius (r_e) is 25 μm, the vapor transport is ~ 75% controlled by Knudsen diffusion; when r_e = 200 μm, the transport is largely controlled by viscous flow. At the low surface temperature condition of −30°, Knudsen flow kinetics prevail.

Owing to the presence of the many hydroxyl groups in lactose and mannitol, usually employed as matrix builders, water adsorption is likely, *e.g.*, the water vapor adsorption on standard cellulose and cotton cellulose (26), for the latter of which the heat of adsorption is 15.7 kcal/mole. At low vapor densities, the mobility of adsorbed molecules occurs mechanistically by two-dimensional "random walk" (27):

$$D^* = \frac{\lambda_s^2}{4\tau^*} \qquad \text{(Eq. 32)}$$

where D^* is the surface diffusion coefficient in square centimeters per second, λ_s is the distance between adsorption sites (3 × 10^{-8} cm), and τ^* is the average residence time between lateral jumps in seconds.

With:

$$\tau^* = \tau_0^{\cdot} e^{E^*/RT} \qquad \text{(Eq. 33)}$$

where:

$\tau_0^{\cdot}$ = residence time related to the vibrational frequency of the solid surface atoms
$\nu^* = 1/\tau_0^{\cdot}$, the jump frequency being ~10^{12} sec^{-1}
E^* = activation energy for surface diffusion
RT = thermal energy

Eq. 32 becomes:

$$D^* = \frac{\lambda_s^2 \nu^*}{4} e^{-E^*/RT} \qquad \text{(Eq. 34)}$$

It is assumed that the surface is isotropic and that the vapor pressure is low. At higher pressures, viscous surface diffusion becomes increasingly important due to collision with adsorbed molecules. Gilliland *et al.* (28) let E^* vary linearly with the differential heat of adsorption, with the result that more strongly adsorbed molecules are less mobile. For physically adsorbed molecules, D^* values are 10^{-2}–10^{-5} cm²/sec; for chemically adsorbed species, they range from 10^{-5} to 10^{-13} cm²/sec (29).

Final Expressions of Matrix-Controlled Lyophilization Kinetics—When the diffusional rate is controlled by the matrix, it is expected to follow the square root of time law. Replacing C_s in Eqs. 20 and 22 with 24 and expanding D_e, one gets for the receding boundary:

$$S = \left[\frac{\epsilon}{\tau}\left(\frac{1}{1/D_v + 1/D_K} + kD^*\right)\left(\frac{MP_s}{500ART_s}\right)(t)\right]^{1/2} \qquad \text{(Eq. 35)}$$

Likewise, the amount of water released per unit of cross-sectional area is:

$$Q = \left[\frac{\epsilon}{\tau}\left(\frac{1}{1/D_v + 1/D_K} + kD^*\right)\left(\frac{AMP_s}{500RT_s}\right)(t)\right]^{1/2} \qquad \text{(Eq. 36)}$$

Interrelation of Heat and Mass Transfer—The steady-state rate of heat transfer from an external heat source and across the frozen region to supply the necessary sublimation energy at the ice front (Fig. 1) is:

$$\frac{dU}{dt} = (h_{ex})(T_{ex} - T_L) = \left(\frac{\kappa}{L - S}\right)(T_L - T_s) \qquad \text{(Eq. 37)}$$

or:

$$\frac{dU}{dt} = \frac{(T_{ex} - T_s)}{\frac{1}{h_{ex}} + \frac{L}{\kappa} - \frac{S}{\kappa}} \qquad \text{(Eq. 38)}$$

and, in turn, it is related to the lyophilization rate by:

$$\left.\frac{dU}{dt}\right|_{x=-S} = \Delta H_{sub}\frac{dQ}{dt} \qquad \text{(Eq. 39)}$$

where:

dU/dt = heat flux per unit of area, calories per second per square centimeter
h_{ex} = external heat transfer coefficient, calories per second per square centimeter per degree
κ = thermal conductivity, calories per second per centimeter per degree
S = receding boundary, centimeters
T_{ex} = temperature of the external heat source
T_L = temperature at $x = -L$ of the frozen region
T_s = temperature of the ice–vapor interface
ΔH_{sub} = heat of sublimation, 600–700 cal/g
dQ/dt = lyophilization rate per square centimeter

It can be seen in Eq. 38 that when $\kappa/L \gg h_{ex}$, the supply of heat to the receding ice front will be controlled by the external heat transfer system (geometry, method of heating, heat transfer mechanism, *etc.*).

Combining Eqs. 11, 38, and 39 and assuming that T_s does not change with time[1], one obtains:

$$S = -\beta\kappa + \sqrt{(\beta\kappa)^2 + \frac{(2\kappa)(T_{ex} - T_s)(t)}{A\,\Delta H_{sub}}} \qquad \text{(Eq. 40)}$$

$$Q = -A\beta\kappa + \sqrt{(A\beta\kappa)^2 + \frac{(2A\kappa)(T_{ex} - T_s)(t)}{\Delta H_{sub}}} \qquad \text{(Eq. 41)}$$

with:

$$\beta = \frac{1}{h_{ex}} + \frac{L}{\kappa} \qquad \text{(Eq. 42)}$$

From the linear portion of a Q or S *versus* $\sqrt{t}$ plot, one can estimate the thermal conductivity, κ, of the frozen system once T_{ex} and T_s are known.

In the region where Eq. 41 is applicable, the lyophilization rates are affected not only by external heat transfer factors due to the equipment but also by internal thermal factors characteristic of the material being dried. In contrast, the derived rates as described previously (*e.g.*, Eqs. 35 and 36) focus attention on the frozen system formulation, the ice–vapor interface, and the mass transfer processes within the growing dry matrix.

DISCUSSION

To demonstrate the predictions of the model, the lyophilization of a 5% solution in which 5 ml is frozen in a 2-cm diameter cylinder is used as an example. Let the solid additives (drug and matrix builder) and water have a density of unity. Therefore, the amount of water per unit volume is 0.95 and the porosity, approximated by the volume fraction of water, is also 0.95. The total amount of water is 4.75 g. The tortuosity and the pore radius are taken to be 3.0 and 100 μm, respectively. Wall effects are assumed to be negligible. Two surface temperature cases are considered: −20 and −30°.

[1] When the temperature at the ice–vapor interface changes with the receding boundary, it can be evaluated from Eq. 37; thus:

$$T_s = T_L - \left(\frac{h_{ex}}{\kappa}\right)(T_{ex} - T_L)(L - S)$$

Here, T_s increases with the receding boundary thickness until $S = L$, whereby $T_s = T_L$. If $h_{ex}/\kappa \ll 1.0$, then $T_s \simeq T_L$.

The physical parameters for these conditions are summarized in Table II. Figure 2 shows the amount of water lyophilized *versus* square root of time curves generated by the steady-state expression described in Eq. 36, whereby the surface diffusion consideration is neglected. As can be seen, the lyophilization rates are faster at −20° than at −30°. Lyophilization is completed in 7.7 hr at the surface temperature of −20° and in 13 hr at −30°. The linear profiles of the receding boundary with the square root of time according to Eq. 35 are observed in Fig. 3.

Future studies will be directed toward the experimental verification of the interdependence of the variables described in this paper.

REFERENCES

(1) E. Flosdorf, "Freeze Drying," Reinhold, New York, N.Y., 1949.

(2) C. J. King, "Freeze Drying of Foods," CRC Press, Cleveland, Ohio, 1971.

(3) R. Noyes, "Freeze Drying of Foods and Biologicals," Noyes Development Corp., Park Ridge, N.J., 1968.

(4) S. A. Goldblith, L. Rey, and W. W. Rothmayr, "Freeze Drying and Advanced Food Technology," Academic, New York, N.Y., 1975.

(5) L. Rey, "Advances in Freeze Drying," Hermann, Paris, France, 1966, pp. 39, 55, 75.

(6) J. L. Stephenson, *Bull. Math. Biophys.*, **15**, 411 (1953).

(7) D. F. Dyer and J. E. Sunderland, *J. Heat Trans.*, **90**, 379 (1968).

(8) *Ibid.*, **93**, 427 (1971).

(9) P. DeLuca and L. Lachman, *J. Pharm. Sci.*, **54**, 617, 1411 (1965).

(10) P. DeLuca and L. Lachman, *Bull. Parenter. Drug Assoc.*, **20**, 65 (1966).

(11) R. M. Patel and A. Hurwitz, *J. Pharm. Sci.*, **61**, 1806 (1972).

(12) K. Ito, *Chem. Pharm. Bull.*, **18**, 1509, 1519 (1970).

(13) T. Higuchi, *J. Pharm. Sci.*, **52**, 1145 (1963).

(14) S. J. Desai, P. Singh, A. P. Simonelli, and W. I. Higuchi, *ibid.*, **55**, 1224, 1230 (1966).

(15) A. P. MacKenzie, *Bull. Parenter. Drug Assoc.*, **20**, 101 (1966).

(16) D. G. Quast and M. Karel, *J. Food Sci.*, **33**, 170 (1968).

(17) N. E. Dorsey, "Properties of Ordinary Water Substance," Reinhold, New York, N.Y., 1940, p. 598.

(18) E. H. Kennard, "Kinetic Theory of Gases," McGraw-Hill, New York, N.Y., 1938, p. 291.

(19) S. Dushman, in "Scientific Foundations of Vacuum Technique," 2nd ed., J. M. Lafferty, Ed., Wiley, New York, N.Y., 1965, chap. 2.

(20) M. J. Zucrow and J. Hoffman, "Gas Dynamics," vol. I, Wiley, New York, N.Y., 1976, p. 12.

(21) T. K. Sherwood, R. L. Pigford, and C. R. Wilke, "Mass Transfer," McGraw-Hill, New York, N.Y., 1975, p. 39.

(22) *Ibid.*, p. 17.

(23) J. O. Hirshfelder, C. F. Curtis, and R. B. Bird, "Molecular Theory of Gases and Liquids," Wiley, New York, N.Y., 1954.

(24) R. B. Bird, W. E. Stewart, and E. N. Lightfoot, "Transport Phenomena," Wiley, New York, N.Y., 1960, p. 744.

(25) W. G. Pollard and R. D. Present, *Phys. Rev.*, **73**, 762 (1948).

(26) S. Dushman, in "Scientific Foundations of Vacuum Technique," 2nd ed., J. M. Lafferty, Ed., Wiley, New York, N.Y., 1965, p. 500.

(27) J. R. Dacey, in "Chemistry and Physics of Interfaces," D. E. Gushee, Ed., American Chemical Society, Washington, D.C., 1965, p. 151.

(28) E. R. Gilliland, R. F. Baddour, G. P. Perkinson, and K. J. Sladek, *Ind. Eng. Chem., Fundam.*, **13**, 95 (1974).

(29) K. J. Sladek, E. R. Gilliland, and R. E. Baddour, *ibid.*, **13**, 100 (1974).

NOTES

Flame-Ionization GLC Assay for Fluorouracil in Plasma of Cancer Patients

A. P. De LEENHEER ˣ and M. Cl. COSYNS-DUYCK

Received December 21, 1978, from the *Laboratoria voor Medische Biochemie en voor Klinische Analyse, Faculteit van de Farmaceutische Wetenschappen, Rijksuniversiteit, Academisch Ziekenhuis, 135 De Pintelaan, 9000-Gent, Belgium.* Accepted for publication February 20, 1979.

Abstract □ A rapid and specific flame-ionization GLC method was developed for the determination of plasma fluorouracil. The chloro analog is used as the internal standard. The method involves the isolation of both the drug and the internal standard from plasma on a strong anion-exchange column at pH 10. Elution is performed with acetic acid in methanol. The evaporated eluate is dissolved in tetrahexylammonium hydroxide. An aliquot of the resulting solution is introduced directly into the gas chromatograph, where conversion to the bishexyl derivatives and subsequent separation take place. The extraction recovery from blank plasma, to which fluorouracil was added, was 96.8 ± 2.4% (*SD*). Linearity was proven in the range from 0 to 25 μg/ml, whereas the detection limit of the method was estimated at about 2 μg/ml of plasma. The within-run precision was determined at three different fluorouracil levels. To demonstrate method applicability, plasma samples obtained from cancer patients to whom 1 g of fluorouracil had been administered intravenously were analyzed.

Keyphrases □ GLC, flame ionization—analysis, fluorouracil, human plasma, *in vivo* □ Antineoplastic agents—fluorouracil, flame-ionization GLC analysis, human plasma, *in vivo* □ Fluorouracil—analysis, flame-ionization GLC, human plasma, *in vivo*

Fluorouracil has been used for several years in the chemotherapeutic treatment of breast, stomach, and colon carcinoma. Different investigators administer fluorouracil in accordance with their own experience, using various dosage schedules (1–4). Systematic observation of fluorouracil disposition as a function of dosage schedule and route of administration in several patients would be valuable. Therefore, a rapid, sensitive, analytical method for fluorouracil determination in numerous biological samples is needed.

Besides the microbiological bioassays (5, 6), few chemical methods have been published. The spectrophotometric assay for fluorouracil (5) lacks specificity and sensitivity. GLC methods were reported using flame-ionization detection (7, 8), electron-capture detection (9), and multiple-ion detection (10–12). Most of these methods are based

0022-3549/79/0900-1174$01.00/0

© 1979, American Pharmaceutical Association

The physical parameters for these conditions are summarized in Table II. Figure 2 shows the amount of water lyophilized *versus* square root of time curves generated by the steady-state expression described in Eq. 36, whereby the surface diffusion consideration is neglected. As can be seen, the lyophilization rates are faster at −20° than at −30°. Lyophilization is completed in 7.7 hr at the surface temperature of −20° and in 13 hr at −30°. The linear profiles of the receding boundary with the square root of time according to Eq. 35 are observed in Fig. 3.

Future studies will be directed toward the experimental verification of the interdependence of the variables described in this paper.

REFERENCES

(1) E. Flosdorf, "Freeze Drying," Reinhold, New York, N.Y., 1949.

(2) C. J. King, "Freeze Drying of Foods," CRC Press, Cleveland, Ohio, 1971.

(3) R. Noyes, "Freeze Drying of Foods and Biologicals," Noyes Development Corp., Park Ridge, N.J., 1968.

(4) S. A. Goldblith, L. Rey, and W. W. Rothmayr, "Freeze Drying and Advanced Food Technology," Academic, New York, N.Y., 1975.

(5) L. Rey, "Advances in Freeze Drying," Hermann, Paris, France, 1966, pp. 39, 55, 75.

(6) J. L. Stephenson, *Bull. Math. Biophys.*, **15**, 411 (1953).

(7) D. F. Dyer and J. E. Sunderland, *J. Heat Trans.*, **90**, 379 (1968).

(8) *Ibid.*, **93**, 427 (1971).

(9) P. DeLuca and L. Lachman, *J. Pharm. Sci.*, **54**, 617, 1411 (1965).

(10) P. DeLuca and L. Lachman, *Bull. Parenter. Drug Assoc.*, **20**, 65 (1966).

(11) R. M. Patel and A. Hurwitz, *J. Pharm. Sci.*, **61**, 1806 (1972).

(12) K. Ito, *Chem. Pharm. Bull.*, **18**, 1509, 1519 (1970).

(13) T. Higuchi, *J. Pharm. Sci.*, **52**, 1145 (1963).

(14) S. J. Desai, P. Singh, A. P. Simonelli, and W. I. Higuchi, *ibid.*, **55**, 1224, 1230 (1966).

(15) A. P. MacKenzie, *Bull. Parenter. Drug Assoc.*, **20**, 101 (1966).

(16) D. G. Quast and M. Karel, *J. Food Sci.*, **33**, 170 (1968).

(17) N. E. Dorsey, "Properties of Ordinary Water Substance," Reinhold, New York, N.Y., 1940, p. 598.

(18) E. H. Kennard, "Kinetic Theory of Gases," McGraw-Hill, New York, N.Y., 1938, p. 291.

(19) S. Dushman, in "Scientific Foundations of Vacuum Technique," 2nd ed., J. M. Lafferty, Ed., Wiley, New York, N.Y., 1965, chap. 2.

(20) M. J. Zucrow and J. Hoffman, "Gas Dynamics," vol. I, Wiley, New York, N.Y., 1976, p. 12.

(21) T. K. Sherwood, R. L. Pigford, and C. R. Wilke, "Mass Transfer," McGraw-Hill, New York, N.Y., 1975, p. 39.

(22) *Ibid.*, p. 17.

(23) J. O. Hirshfelder, C. F. Curtis, and R. B. Bird, "Molecular Theory of Gases and Liquids," Wiley, New York, N.Y., 1954.

(24) R. B. Bird, W. E. Stewart, and E. N. Lightfoot, "Transport Phenomena," Wiley, New York, N.Y., 1960, p. 744.

(25) W. G. Pollard and R. D. Present, *Phys. Rev.*, **73**, 762 (1948).

(26) S. Dushman, in "Scientific Foundations of Vacuum Technique," 2nd ed., J. M. Lafferty, Ed., Wiley, New York, N.Y., 1965, p. 500.

(27) J. R. Dacey, in "Chemistry and Physics of Interfaces," D. E. Gushee, Ed., American Chemical Society, Washington, D.C., 1965, p. 151.

(28) E. R. Gilliland, R. F. Baddour, G. P. Perkinson, and K. J. Sladek, *Ind. Eng. Chem., Fundam.*, **13**, 95 (1974).

(29) K. J. Sladek, E. R. Gilliland, and R. E. Baddour, *ibid.*, **13**, 100 (1974).

NOTES

Flame-Ionization GLC Assay for Fluorouracil in Plasma of Cancer Patients

A. P. De LEENHEER ˣ and M. Cl. COSYNS-DUYCK

Received December 21, 1978, from the *Laboratoria voor Medische Biochemie en voor Klinische Analyse, Faculteit van de Farmaceutische Wetenschappen, Rijksuniversiteit, Academisch Ziekenhuis, 135 De Pintelaan, 9000-Gent, Belgium.* Accepted for publication February 20, 1979.

Abstract □ A rapid and specific flame-ionization GLC method was developed for the determination of plasma fluorouracil. The chloro analog is used as the internal standard. The method involves the isolation of both the drug and the internal standard from plasma on a strong anion-exchange column at pH 10. Elution is performed with acetic acid in methanol. The evaporated eluate is dissolved in tetrahexylammonium hydroxide. An aliquot of the resulting solution is introduced directly into the gas chromatograph, where conversion to the bishexyl derivatives and subsequent separation take place. The extraction recovery from blank plasma, to which fluorouracil was added, was 96.8 ± 2.4% (*SD*). Linearity was proven in the range from 0 to 25 μg/ml, whereas the detection limit of the method was estimated at about 2 μg/ml of plasma. The within-run precision was determined at three different fluorouracil levels. To demonstrate method applicability, plasma samples obtained from cancer patients to whom 1 g of fluorouracil had been administered intravenously were analyzed.

Keyphrases □ GLC, flame ionization—analysis, fluorouracil, human plasma, *in vivo* □ Antineoplastic agents—fluorouracil, flame-ionization GLC analysis, human plasma, *in vivo* □ Fluorouracil—analysis, flame-ionization GLC, human plasma, *in vivo*

Fluorouracil has been used for several years in the chemotherapeutic treatment of breast, stomach, and colon carcinoma. Different investigators administer fluorouracil in accordance with their own experience, using various dosage schedules (1–4). Systematic observation of fluorouracil disposition as a function of dosage schedule and route of administration in several patients would be valuable. Therefore, a rapid, sensitive, analytical method for fluorouracil determination in numerous biological samples is needed.

Besides the microbiological bioassays (5, 6), few chemical methods have been published. The spectrophotometric assay for fluorouracil (5) lacks specificity and sensitivity. GLC methods were reported using flame-ionization detection (7, 8), electron-capture detection (9), and multiple-ion detection (10–12). Most of these methods are based

0022-3549/79/0900-1174$01.00/0

© 1979, American Pharmaceutical Association

Table I—Fluorouracil Assay Precision

Plasma Level, μg/ml	$\bar{x}$, μg/ml	CV, %	n
10	10.16	4.79	24
4	4.27	9.97	16
2	2.72	10.53	20

on the chromatography of silyl drug derivatives (7–10) and on the use of internal standards such as anthracene (8) and thymine (9, 11). These standards are structurally unrelated to the compound to be assayed, and thymine is a possible endogenous compound. The mass fragmentographic method allows determination of plasma fluorouracil levels down to 2 ng/ml (12) but requires expensive apparatus.

The present work describes a simple and specific method for the determination of plasma fluorouracil levels. The procedure can be performed on a routine basis for clinical studies of patients receiving fluorouracil therapy.

EXPERIMENTAL

Reagents—A pH 10 carbonate buffer (ionic strength 0.1) was prepared by mixing 25.0 ml of 1 *M* $NaHCO_3$ with 50.0 ml of 0.5 *M* Na_2CO_3 and diluting to 1000 ml with double-distilled water.

A 0.2 *M* tetrahexylammonium hydroxide solution in methanol was prepared as described previously (13).

All other chemicals and solvents were analytical reagent grade.

Extraction from Plasma—Blood samples were collected in heparinized tubes, mixed, and centrifuged to allow plasma separation. The plasma was frozen until assayed. An aliquot of 1.0 ml of plasma, 100 μl of internal standard solution (20.0 mg of chlorouracil[1]/100 ml of methanol), and 4.0 ml of pH 10 carbonate buffer were mixed in a 15-ml centrifuge tube. The sample was transferred to a glass column packed with anion-exchange resin[2] (2 cm × 0.6 cm i.d.).

Prior to use, the column was washed with 10 ml of 0.3 *M* acetic acid in methanol, and the resin was equilibrated with 10 ml of pH 10 carbonate buffer. The entire sample was put through the resin bed. The column was consecutively washed with 10 ml of water and 10 ml of methanol. Both the drug and the internal standard were eluted with 10 ml of 0.3 *M* acetic acid in methanol. The eluate was evaporated to dryness in a water bath at 50° under a nitrogen stream.

Derivatization—The residue obtained after evaporation was dissolved into 25 μl of 0.2 *M* tetrahexylammonium hydroxide in methanol. An aliquot was introduced in the gas chromatograph[3] injection port.

GLC and Quantitation—The hexyl derivatives were chromatographed on a silanized glass column (1.8 m × 0.2 cm i.d.) packed with 3% Dexsil-300[4] on 80–100-mesh Gas Chrom Q. A flame-ionization detector was used. Nitrogen was the carrier gas at a linear velocity of 7 cm/sec.

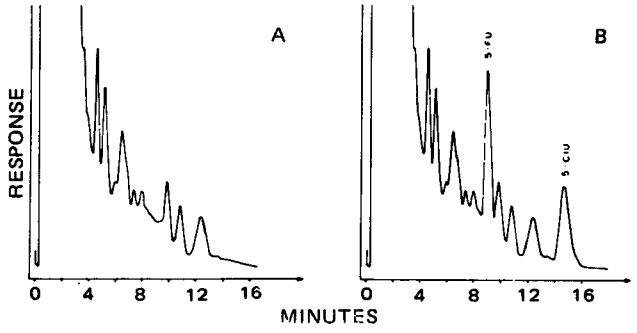

Figure 1—*GLC of 1 ml of drug-free plasma (A) and of 1 ml of plasma spiked with 10 μg of fluorouracil (B).*

[1] Calbiochem A. G., Lucerne, Switzerland.
[2] AG 1-X4 (Cl^-), 100–200 mesh, Bio-Rad, Richmond, Va.
[3] Hewlett-Packard model 5750G.
[4] Supelco Inc., Bellefonte, Pa.

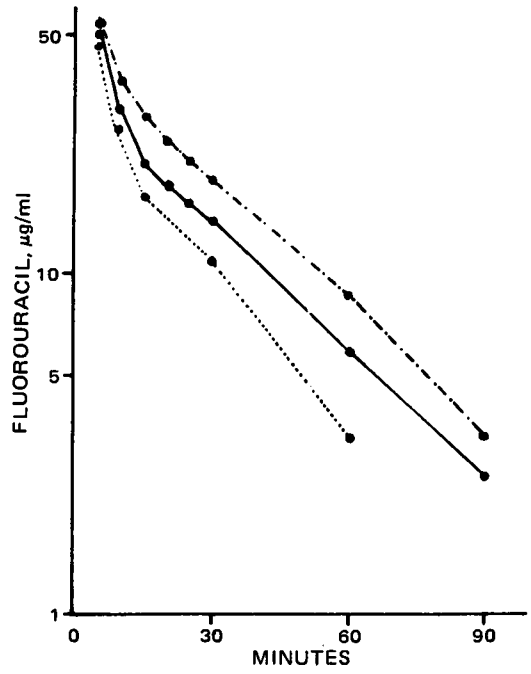

Figure 2—*Plasma fluorouracil concentration in Patient B (—), Patient VH (. . .) and Patient VW (---) after administration of a single 1-g intravenous dose.*

Hydrogen and air flows were adjusted to optimum sensitivity. The injection port, oven, and detector temperatures were 270, 230, and 250°, respectively.

Quantitation was accomplished by using calibration curves obtained from standard fluorouracil[5] solutions in methanol or from blank plasma to which known amounts of fluorouracil[5] had been added.

RESULTS AND DISCUSSION

The problems concerning the isolation of fluorouracil, floxuridine, and fluorouridine from aqueous solutions and the anion-exchange extraction procedure were discussed in previous papers (12, 14, 15).

Flash alkylation, based on the Hofmann degradation (16), converted both fluorouracil and chlorouracil into hexyl derivatives suitable for GLC analysis. The derivatives were identified by combined GLC–mass spectrometric[6] analysis as *N,N'*-dihexyl derivatives; the spectral characteristics for the fluorouracil derivative were: *m/e* (relative intensity) 298 (7.1) M^+, 215 (54.1) $C_{10}H_{16}N_2O_2F^+$ or $M - C_6H_{13} + 2H$, and 131 (65.5), $C_4H_4N_2O_2F^+$ or $M - 2C_6H_{13} + 3H$.

Figure 1 shows the gas chromatograms obtained from 1 ml of drug-free plasma (A) and from 1 ml of the same plasma to which 10 μg of fluorouracil (5-FU) and 10 μg of chlorouracil (5-ClU) had been added (B). Because of interference from endogenous compounds, the detection limit in plasma was ~2 μg/ml.

Blank plasma samples to which 0–25 μg of fluorouracil/ml had been added were taken through the entire procedure. A linear relationship existed between the peak height ratios of fluorouracil to chlorouracil and the plasma fluorouracil concentration (regression line: $y = 0.113x + 0.036$, $r = 0.9996$).

The extraction recovery was determined by analyzing plasma samples spiked with a known amount of fluorouracil and adding the internal standard to the column eluate. The fluorouracil concentration was calculated from a calibration curve obtained from standard fluorouracil and chlorouracil solutions in methanol and submitted to flash hexylation under the circumstances outlined. An extraction recovery of 96.8 ± 2.4% (*SD*) was calculated.

Three plasma pools containing various amounts of fluorouracil were analyzed on the same day (Table I). The values for the coefficients of variation (*CV*) indicate that the overall method reproducibility is satisfactory.

[5] Sigma Chemical Co., St. Louis, Mo.
[6] LKB model 9000S; 3% Dexsil-300 (1.8 m × 0.2 cm i.d.) Gas Chrom Q (100–120 mesh); helium flow, 30 ml/min; 20 ev; injector, oven, and separator temperatures of 260, 230, and 275°, respectively.

Method accuracy was checked by analyzing some samples with the GLC method and with a previously described UV method (17). The results were plotted against each other and correlation analysis revealed a correlation coefficient, r, of 0.9960 (regression line: $y = 1.028x + 0.203$).

Plasma samples collected at different time intervals from six cancer patients to whom 1 g of fluorouracil had been administered intravenously were analyzed. Control runs with plasma blanks, collected before the drug administration, showed no major interfering peaks eluting in the regions corresponding to the drug or to the internal standard.

Figure 2 shows data obtained from three representative patients. In all cases, the fluorouracil concentration leveled off rapidly, with no measurable plasma levels occurring after 60 min and for three patients after 90 min. After an extremely short distribution phase, the drug appears to be eliminated by a logarithmic linear phase. The applicability of the method to these patients indicates that the procedure is suitable for clinical pharmacological studies on fluorouracil.

REFERENCES

(1) F. J. Ansfield, *J. Am. Med. Assoc.*, **190**, 686 (1964).

(2) E. M. Jacobs, W. J. Reeves, D. A. Wood, R. Pugh, J. Braunwald, and J. R. Bateman, *Cancer*, **27**, 1302 (1971).

(3) S. R. Lahiri, G. Boileau, and T. C. Hall, *ibid.*, **28**, 902 (1971).

(4) F. J. Ansfield, J. Klotz, T. Nealon, G. Ramirez, J. Minton, G. Hill, W. Wilson, H. Davis, and G. Cornell, *ibid.*, **39**, 34 (1977).

(5) B. Clarkson, A. O'Connor, L. Winston, and D. Hutchison, *Clin. Pharmacol. Ther.*, **5**, 581 (1964).

(6) E. R. Garrett, G. H. Hurst, and J. R. Green, *J. Pharm. Sci.*, **66**, 1422 (1977).

(7) J. J. Windheuser, J. L. Sutter, and E. Auen, *ibid.*, **61**, 301 (1972).

(8) J. L. Cohen and P. B. Brenan, *ibid.*, **62**, 572 (1973).

(9) H. W. Van Den Berg, R. F. Murphy, R. Hunter, and D. T. Elmore, *J. Chromatogr.*, **145**, 311 (1978).

(10) C. Finn and W. Sadée, *Cancer Chemother. Rep.*, **59**, 279 (1975).

(11) B. L. Hillcoat, M. Kawai, P. B. McCulloch, J. Rosenfeld, and C. K. O. Williams, *Br. J. Clin. Pharmacol.*, **3**, 135 (1976).

(12) A. P. De Leenheer, R. R. Roncucci, and C. Van Peteghem, "Quantitative Mass Spectrometry in Life Sciences II, Proceedings of the Second International Symposium on Quantitative Mass Spectrometry in Life Sciences" (Gent, June 13–16, 1978), Elsevier, New York, N.Y., 1978, p. 399.

(13) T. J. Giovanniello and J. Pecci, *Clin. Chim. Acta*, **67**, 7 (1976).

(14) A. P. De Leenheer and C. F. Gelijkens, *J. Pharm. Sci.*, **67**, 417 (1978).

(15) A. P. De Leenheer and C. F. Gelijkens, *J. Chromatogr. Sci.*, **16**, 552 (1978).

(16) A. W. Hofmann, *Ber. Dsch. Chem. Ges.*, **14**, 494 (1881).

(17) A. P. De Leenheer, M. C. Cosyns-Duyck, and P. M. Van Vaerenbergh, *J. Pharm. Sci.*, **66**, 1190 (1977).

ACKNOWLEDGMENTS

Supported by the National Medical Research Foundation (F.G.W.O.) through Grants 20 452 and 3.0004.76.

The authors are grateful to Dr. A. A. M. Cruyl from the N.F.W.O. for running the mass spectra.

Influence of Cetylpyridinium Chloride on Corneal Permeability to Penicillin

RENEE E. W. GODBEY *, KEITH GREEN *‡ˣ, and DAVID S. HULL *

Received January 12, 1979, from the **Department of Ophthalmology and the* ‡*Department of Physiology, Medical College of Georgia, Augusta, GA 30901.* Accepted for publication March 14, 1979.

Abstract □ The epithelial surface or the deepithelialized anterior stromal surface of isolated rabbit corneas was perfused for 3 hr with ^{14}C-penicillin in 25 m*M* Ringer–bicarbonate solution with or without 1% albumin and with or without 0.02% cetylpyridinium chloride. The intact epithelium acted as a barrier to penicillin and impeded the flux rate by 66% when compared to the flux rate across the deepithelialized cornea. The presence of 0.02% cetylpyridinium chloride increased the penicillin flux rate across corneas with an intact epithelial layer to that of deepithelialized corneas. Cetylpyridinium chloride, 0.02%, had no effect on penicillin flux across deepithelialized corneas. The penicillin flux rate across corneas, with or without epithelium, was increased slightly following the inclusion of 1.0% albumin in the bathing solution. The flux rates across deepithelialized corneas in the presence of albumin, with or without cetylpyridinium chloride, were similar to fluxes found in the absence of albumin. Albumin–penicillin "binding" was not a significant factor in impeding penicillin flux, and this binding apparently was not altered by cetylpyridinium chloride. The surfactant appeared to alter epithelial permeability physiologically.

Keyphrases □ Cetylpyridinium chloride—effect on corneal permeability to penicillin, effect on epithelium □ Surfactants—cetylpyridinium chloride, effect on corneal permeability to penicillin, effect on epithelium □ Benzylpenicillin—corneal permeability, effect of cetylpyridinium chloride

The penetration efficiency of most topically applied drugs is very small, but penicillin penetration is especially poor (1, 2). Poor intraocular drug levels have been attributed (3) both to rapid drug removal by tears and to drug binding to the tear protein, thus rendering the drug biologically unavailable. Inclusion of 0.02% cetylpyridinium chloride with pilocarpine nitrate when applied topically to the rabbit eye caused 10 times the miotic effect of the same amount of pilocarpine without cetylpyridinium chloride. Previous investigators (4) hypothesized that cetylpyridinium chloride was a competitive inhibitor of pilocarpine protein binding and that the cetylpyridinium chloride allowed a higher percentage of drug to be unbound and bioavailable.

Cetylpyridinium chloride, when applied to the cornea, increased fluorescein penetration across the cornea; transmission electron microscopy revealed increased intercellular spaces in the superficial epithelial layer and lysis of the outermost cell membranes (5). Scanning electron microscopy revealed a loss of epithelial microvilli and microplicae, a process accompanied by surface pitting, which exposed deeper epithelial cells (6).

The purpose of this investigation was to delineate further the mechanism of cetylpyridinium chloride in increasing drug penetration into the eye by examining its effects on the corneal flux rate of a known albumin-bound drug.

0022-3549/79/0900-1176$01.00/0

© 1979, American Pharmaceutical Association

Method accuracy was checked by analyzing some samples with the GLC method and with a previously described UV method (17). The results were plotted against each other and correlation analysis revealed a correlation coefficient, r, of 0.9960 (regression line: $y = 1.028x + 0.203$).

Plasma samples collected at different time intervals from six cancer patients to whom 1 g of fluorouracil had been administered intravenously were analyzed. Control runs with plasma blanks, collected before the drug administration, showed no major interfering peaks eluting in the regions corresponding to the drug or to the internal standard.

Figure 2 shows data obtained from three representative patients. In all cases, the fluorouracil concentration leveled off rapidly, with no measurable plasma levels occurring after 60 min and for three patients after 90 min. After an extremely short distribution phase, the drug appears to be eliminated by a logarithmic linear phase. The applicability of the method to these patients indicates that the procedure is suitable for clinical pharmacological studies on fluorouracil.

REFERENCES

(1) F. J. Ansfield, *J. Am. Med. Assoc.*, **190**, 686 (1964).

(2) E. M. Jacobs, W. J. Reeves, D. A. Wood, R. Pugh, J. Braunwald, and J. R. Bateman, *Cancer*, **27**, 1302 (1971).

(3) S. R. Lahiri, G. Boileau, and T. C. Hall, *ibid.*, **28**, 902 (1971).

(4) F. J. Ansfield, J. Klotz, T. Nealon, G. Ramirez, J. Minton, G. Hill, W. Wilson, H. Davis, and G. Cornell, *ibid.*, **39**, 34 (1977).

(5) B. Clarkson, A. O'Connor, L. Winston, and D. Hutchison, *Clin. Pharmacol. Ther.*, **5**, 581 (1964).

(6) E. R. Garrett, G. H. Hurst, and J. R. Green, *J. Pharm. Sci.*, **66**, 1422 (1977).

(7) J. J. Windheuser, J. L. Sutter, and E. Auen, *ibid.*, **61**, 301 (1972).

(8) J. L. Cohen and P. B. Brenan, *ibid.*, **62**, 572 (1973).

(9) H. W. Van Den Berg, R. F. Murphy, R. Hunter, and D. T. Elmore, *J. Chromatogr.*, **145**, 311 (1978).

(10) C. Finn and W. Sadée, *Cancer Chemother. Rep.*, **59**, 279 (1975).

(11) B. L. Hillcoat, M. Kawai, P. B. McCulloch, J. Rosenfeld, and C. K. O. Williams, *Br. J. Clin. Pharmacol.*, **3**, 135 (1976).

(12) A. P. De Leenheer, R. R. Roncucci, and C. Van Peteghem, "Quantitative Mass Spectrometry in Life Sciences II, Proceedings of the Second International Symposium on Quantitative Mass Spectrometry in Life Sciences" (Gent, June 13–16, 1978), Elsevier, New York, N.Y., 1978, p. 399.

(13) T. J. Giovanniello and J. Pecci, *Clin. Chim. Acta*, **67**, 7 (1976).

(14) A. P. De Leenheer and C. F. Gelijkens, *J. Pharm. Sci.*, **67**, 417 (1978).

(15) A. P. De Leenheer and C. F. Gelijkens, *J. Chromatogr. Sci.*, **16**, 552 (1978).

(16) A. W. Hofmann, *Ber. Dsch. Chem. Ges.*, **14**, 494 (1881).

(17) A. P. De Leenheer, M. C. Cosyns-Duyck, and P. M. Van Vaerenbergh, *J. Pharm. Sci.*, **66**, 1190 (1977).

ACKNOWLEDGMENTS

Supported by the National Medical Research Foundation (F.G.W.O.) through Grants 20 452 and 3.0004.76.

The authors are grateful to Dr. A. A. M. Cruyl from the N.F.W.O. for running the mass spectra.

Influence of Cetylpyridinium Chloride on Corneal Permeability to Penicillin

RENEE E. W. GODBEY *, KEITH GREEN *‡ˣ, and DAVID S. HULL *

Received January 12, 1979, from the **Department of Ophthalmology and the* ‡*Department of Physiology, Medical College of Georgia, Augusta, GA 30901.* Accepted for publication March 14, 1979.

Abstract □ The epithelial surface or the deepithelialized anterior stromal surface of isolated rabbit corneas was perfused for 3 hr with ^{14}C-penicillin in 25 m*M* Ringer–bicarbonate solution with or without 1% albumin and with or without 0.02% cetylpyridinium chloride. The intact epithelium acted as a barrier to penicillin and impeded the flux rate by 66% when compared to the flux rate across the deepithelialized cornea. The presence of 0.02% cetylpyridinium chloride increased the penicillin flux rate across corneas with an intact epithelial layer to that of deepithelialized corneas. Cetylpyridinium chloride, 0.02%, had no effect on penicillin flux across deepithelialized corneas. The penicillin flux rate across corneas, with or without epithelium, was increased slightly following the inclusion of 1.0% albumin in the bathing solution. The flux rates across deepithelialized corneas in the presence of albumin, with or without cetylpyridinium chloride, were similar to fluxes found in the absence of albumin. Albumin–penicillin "binding" was not a significant factor in impeding penicillin flux, and this binding apparently was not altered by cetylpyridinium chloride. The surfactant appeared to alter epithelial permeability physiologically.

Keyphrases □ Cetylpyridinium chloride—effect on corneal permeability to penicillin, effect on epithelium □ Surfactants—cetylpyridinium chloride, effect on corneal permeability to penicillin, effect on epithelium □ Benzylpenicillin—corneal permeability, effect of cetylpyridinium chloride

The penetration efficiency of most topically applied drugs is very small, but penicillin penetration is especially poor (1, 2). Poor intraocular drug levels have been attributed (3) both to rapid drug removal by tears and to drug binding to the tear protein, thus rendering the drug biologically unavailable. Inclusion of 0.02% cetylpyridinium chloride with pilocarpine nitrate when applied topically to the rabbit eye caused 10 times the miotic effect of the same amount of pilocarpine without cetylpyridinium chloride. Previous investigators (4) hypothesized that cetylpyridinium chloride was a competitive inhibitor of pilocarpine protein binding and that the cetylpyridinium chloride allowed a higher percentage of drug to be unbound and bioavailable.

Cetylpyridinium chloride, when applied to the cornea, increased fluorescein penetration across the cornea; transmission electron microscopy revealed increased intercellular spaces in the superficial epithelial layer and lysis of the outermost cell membranes (5). Scanning electron microscopy revealed a loss of epithelial microvilli and microplicae, a process accompanied by surface pitting, which exposed deeper epithelial cells (6).

The purpose of this investigation was to delineate further the mechanism of cetylpyridinium chloride in increasing drug penetration into the eye by examining its effects on the corneal flux rate of a known albumin-bound drug.

0022-3549/79/0900-1176$01.00/0

© 1979, American Pharmaceutical Association

Table I—Penicillin Fluxes across Rabbit Cornea [a]

Group I	
Intact epithelium (n = 6, 36)	$0.043 \pm 0.001^{b,c}$
Deepithelialized (n = 6, 36)	$0.126 \pm 0.004^{b,c}$
Group II	
Intact epithelium (n = 5, 30)	$0.053 \pm 0.004^{b,c}$
Deepithelialized (n = 5, 30)	$0.179 \pm 0.016^{b,c}$
Group III	
Intact epithelium (n = 5, 30)	0.130 ± 0.005
Deepithelialized (n = 5, 30)	0.130 ± 0.005
Group IV	
Intact epithelium (n = 6, 36)	0.123 ± 0.004
Deepithelialized (n = 6, 36)	0.133 ± 0.004

[a] Values (10^{-9} mole/cm^2/hr) are the means ± *SEM*; n = number of corneas, number of experimental determinations. [b] $p < 0.001$, comparing flux rate of corneas with epithelium intact to flux rate of deepithelialized corneas within a given group. [c] $p < 0.05$, comparing flux rate of epithelialized corneas in the presence and absence of albumin (*cf.*, Groups I and II); also comparing flux rate of deepithelialized corneas in the presence and absence of albumin (*cf.*, Groups I and II).

EXPERIMENTAL

Forty-four adult albino rabbits of either sex, ~3 kg, were sacrificed with an overdose of pentobarbital sodium. Each eye was proptosed, and the epithelium was removed from one eye by scraping with a Gill corneal knife. The epithelium of the opposite eye was left intact and protected from abrasions during mounting. The corneas were removed and mounted in corneal flux chambers, using the specular microscope mounting system; this system permits the mounting of corneas without trauma to the corneal epithelium (7, 8).

Ringer–bicarbonate (2.5×10^{-2} *M*) solution (pH 7.35) containing reduced glutathione (0.092 g/liter) and adenosine (0.134 g/liter) with an osmolarity of 300 mOsm bathed both corneal surfaces (7–10). The volume of the endothelial (posterior) chamber was 0.45 ml, and that of the stromal or epithelial (anterior) chamber was 1.20 ml. The anterior chamber contained a polytef-coated magnetic stirring bar driven by an external magnet at 400 rpm.

Four epithelial surface perfusion solutions containing ^{14}C-penicillin G potassium[1] were prepared in Ringer solution to make a final concentration of 8×10^{-9} *M* ^{14}C-penicillin/ml. Group I corneas were perfused with penicillin in Ringer solution. Group II corneas were perfused with penicillin and 1% bovine serum albumin in Ringer solution; the mixture was stirred with a magnetic bar for 30 min prior to instillation into the flux chamber to allow maximal penicillin protein binding to occur (11).

Group III corneas were perfused with a Ringer solution containing penicillin, 1% bovine serum albumin, and 0.02% cetylpyridinium chloride (also stirred for 30 min prior to use). The penicillin and cetylpyridinium chloride were added simultaneously to allow any competitive inhibition of the protein binding sites by cetylpyridinium chloride to occur. Group IV corneas were perfused with penicillin and 0.02% cetylpyridinium chloride in Ringer solution.

All groups contained paired corneas, one epithelialized and the other deepithelialized. The endothelial surface was bathed with normal Ringer solution at all times.

The anterior flux chamber was filled with one of the radioactive penicillin solutions (Group I, II, III, or IV) immediately after mounting and allowed to equilibrate for 1 hr. Sample collection and quantitation of the penicillin flux by a liquid scintillation technique were performed as described previously (7) every 30 min over an additional 3-hr period, thus providing six sample periods for each cornea.

RESULTS

In Group I, the penicillin flux across deepithelialized corneas was three times greater than across corneas with an intact epithelium, indicating that the intact epithelial membrane provided a very significant barrier, $p < 0.001$ (Table I). This finding was confirmed by the data for Group II in the presence of 1% bovine serum albumin. In Group II, a small but significant increase in penicillin flux across both epithelialized and deepithelialized corneas also was noted in the presence of 1% bovine serum albumin when compared to the respective epithelialized and deepithelialized corneas in Group I that were perfused without albumin, $p < 0.05$ (Table I).

Penicillin penetration was the same for corneas in the presence or absence of epithelium when cetylpyridinium chloride was present (Groups III and IV). Cetylpyridinium chloride increased the penicillin flux across epithelialized corneas so that it equaled the flux across untreated deepithelialized corneas (Groups I and IV). This finding demonstrated that cetylpyridinium chloride converted the cornea with an intact epithelium into a physiologically deepithelialized cornea. The presence or absence of albumin made no difference in the cetylpyridinium chloride-evoked response (Table I, Groups I and IV *versus* Groups II and III).

Comparison of penicillin fluxes in Groups I and II reveals some puzzling trends. In both the epithelialized and deepithelialized corneas, penicillin penetration was increased by approximately one-fourth ($p < 0.05$) by the presence of 1% albumin. Such a difference was not noted between Groups III and IV, where again the only difference was the presence or absence of albumin.

DISCUSSION

The corneal epithelial barrier impeded the penicillin flux rate to one-third that of the flux rate across deepithelialized corneas. Cetylpyridinium chloride chemically converted the penetration characteristics of the epithelialized cornea into those of a deepithelialized cornea; *i.e.*, it increased its permeability so that both deepithelialized corneas and cetylpyridinium chloride-perfused epithelialized corneas showed equal penicillin fluxes.

An unexplained finding was that the penicillin flux significantly increased when 1% bovine serum albumin was present in the solutions perfusing the anterior corneal surface. Albumin apparently enhances the corneal permeability (across both the normal and deepithelialized corneas) in the absence of cetylpyridinium chloride, despite the known 60–65% binding of penicillin by albumin (11). Such a difference was not noted in the presence of cetylpyridinium chloride. The reason for this albumin-enhanced permeability is unknown.

The penicillin fluxes across deepithelialized corneas (Groups I and II) and cetylpyridinium chloride-treated normal and deepithelialized corneas (Groups III and IV), with and without bovine serum albumin, were of the same general magnitude. These results illustrate that cetylpyridinium chloride increases corneal permeability to penicillin by its action on the epithelium and that albumin does not retard penicillin flux across the cornea. The permeability increase induced by cetylpyridinium chloride in the normal cornea is similar to that found in the deepithelialized cornea. There was no indication of either an increased or decreased penicillin protein binding caused by cetylpyridinium chloride.

These findings are in contrast to the findings of Mikkelson *et al.* (3, 4), especially to their hypothesis that competitive inhibition of protein binding of drugs by cetylpyridinium chloride makes more drug bioavailable in the unbound form. The current experiments confirm the concept that cetylpyridinium chloride increases drug penetration by reducing the epithelial barrier effect. In view of the present findings and those noted previously that indicated an effect of cetylpyridinium chloride on the epithelial ultrastructure (5, 6), it is not surprising that drugs placed on the surface of the eye in the presence of cetylpyridinium chloride would penetrate the cornea better and have a greater pharmacological effect.

In summary, cetylpyridinium chloride apparently enhances penicillin penetration across the cornea in a manner similar to that found for benzalkonium chloride both *in vitro* and *in vivo* (5, 12, 13); there is a direct effect on the epithelium, which causes disorganization of the normal structure and breakdown of the physiological barrier.

[1] Amersham Corp., Arlington Heights, Ill.

REFERENCES

(1) W. H. Havener, "Ocular Pharmacology," 3rd ed., Mosby, St. Louis, Mo., 1974.

(2) S. H. Witzel, I. Z. Fielding, and H. L. Ormsby, *Am. J. Ophthalmol.*, **42**, 89 (1956).

(3) T. J. Mikkelson, S. S. Chrai, and J. R. Robinson, *J. Pharm. Sci.*, **62**, 1648 (1973).

(4) *Ibid.*, **62**, 1942 (1973).

(5) K. Green and A. M. Tønjum, *Am. J. Ophthalmol.*, **72**, 897 (1971).

(6) K. Green, *Acta Ophthalmol.*, **54**, 145 (1976).

(7) D. S. Hull, K. Green, M. Boyd, and H. R. Wynn, *Invest. Ophthalmol.*, **16**, 883 (1977).

(8) S. Dikstein and D. M. Maurice, *J. Physiol.*, **221**, 29 (1972).

(9) E. I. Anderson, J. Fischbarg, and A. Spector, *Exp. Eye Res.*, **19**,

1 (1973).
(10) B. E. McCarey, H. F. Edelhauser, and D. L. Van Horn, *Invest. Ophthalmol.*, **12**, 410 (1973).
(11) "The Pharmacological Basis of Therapeutics," 5th ed., L. S. Goodman and A. Gilman, Eds., Macmillan, New York, N.Y., 1975.
(12) K. Green and S. Downs, *Invest. Ophthalmol.*, **13**, 316 (1974).
(13) K. Green and A. M. Tønjum, *Acta Ophthalmol.*, **53**, 348 (1975).

ACKNOWLEDGMENTS

Supported in part by Research Grants EY 02386 (D. S. Hull) and EY 01413 (K. Green) from the National Eye Institute, in part by a research grant from the Georgia Lions Lighthouse Foundation, Inc., in part by the Lions Club of Augusta, Ga., and in part by the J. H. Hall Eye Foundation. A Wang 2200 computer, used for statistical data evaluation, was provided through a Research to Prevent Blindness, Inc., grant.

Renal Actions of Oxyphenbutazone

HAROLD E. WILLIAMSON ˣ, GARY R. GAFFNEY, and WILLIAM A. BOURLAND

Received January 8, 1979, from the *Department of Pharmacology, College of Medicine, University of Iowa, Iowa City, IA 52242.* Accepted for publication February 28, 1979.

Abstract □ Oxyphenbutazone decreased the renal excretion of sodium and water in anesthetized dogs. As these excretions decreased, the drug also produced a decrease in renal blood flow and in the glomerular filtration rate. Blood pressure increased slightly. These changes are consistent with an inhibition of renal prostaglandin synthesis and could explain why oxyphenbutazone is reported to produce weight gain and edema when used clinically.

Keyphrases □ Oxyphenbutazone—effect on renal sodium and water excretion, renal blood flow, glomerular filtration rate, blood pressure, prostaglandin synthesis ■ Anti-inflammatory agents—oxyphenbutazone, renal effects ■ Kidney—effect of oxyphenbutazone

Oxyphenbutazone[1] is an analog of phenylbutazone[2] and, like the latter compound, is employed as an anti-inflammatory agent. Both agents produce edema and weight gain as side effects (1). A possible renal mechanism has been suggested for phenylbutazone since this agent markedly reduced renal blood flow and decreased the glomerular filtration rate at the time that urinary volume and sodium excretion were reduced (2). In this study, the effect of oxyphenbutazone on several renal functions was determined.

EXPERIMENTAL

Mongrel dogs of either sex, 13–16 kg, were anesthetized with pentobarbital sodium (30 mg/kg iv), and the trachea was intubated to maintain an open airway. Mean arterial blood pressure was monitored with a pressure transducer[3] *via* a femoral artery catheter. A femoral vein was catheterized for administration of a 0.9% NaCl infusion (4 ml/min) during preparation of the animals and throughout the experiments. Inulin was added to the infusion to estimate the glomerular filtration rate.

The left kidney was exposed *via* a retroperitoneal flank incision, and a flow probe was placed around the renal artery and connected to a square wave electromagnetic flowmeter[4] to monitor renal blood flow. Blood pressure and renal blood flow were recorded[5] continuously. Urine was collected at timed intervals by a cannula placed in the left ureter. Arterial blood samples were obtained from the femoral artery catheter. After stabilization of the preparation, control urine collections (10-min periods) and blood samples at the midpoint of alternate urine collection periods were obtained. Oxyphenbutazone was administered intravenously over 3 min, and urine collections were continued for several periods.

[1] Tanderil, Ciba-Geigy Corp., Summit, N.J.
[2] Butazolidin, Ciba-Geigy Corp., Summit, N.J.
[3] Model P23AA, Statham, Hato Rey, Puerto Rico.
[4] Carolina Medical Electronics, King, N.C.
[5] Dynograph (type R), Beckman Instruments, Fullerton, Calif.

Table I—Effect of Oxyphenbutazone (5 mg/kg iv) on Renal Function

Parameter	Control Period[a]	Oxyphenbutazone Period[b]	Difference
Blood pressure, mm Hg	115	128	+13 ± 5[c]
Renal blood flow, ml/min	262	220	−42 ± 5[c]
Urine volume, ml/min	1.1	0.4	−0.7 ± 0.2[c]
Glomerular filtration rate, ml/min	33	23	−10 ± 4[c]
Sodium excretion, μEq/min	136	77	−59 ± 1.9[c]

[a] Values are from the clearance period preceding oxyphenbutazone administration. [b] Values are from the clearance period 10–20 min after oxyphenbutazone administration. [c] Significant difference ($p < 0.05$); Student paired t test; $n = 7$.

Urinary and plasma inulin levels were determined by a reported method (3). Urinary sodium concentrations were measured with a flame photometer[6]. Data were analyzed using the Student paired t test (4); a $p < 0.05$ was the significance criterion.

RESULTS AND DISCUSSION

The effect of oxyphenbutazone on renal blood flow and blood pressure is shown in Fig. 1. Following oxyphenbutazone administration, 5 mg/kg iv, blood pressure increased slightly while renal blood flow decreased gradually. These effects, as well as effects on other renal functions, are summarized in Table I. At 20 min after oxyphenbutazone administration, blood pressure was increased while renal blood flow, the glomerular filtration rate, urinary volume, and sodium excretion were decreased. All changes were statistically significant. These changes also were present at 60 min.

Since similar changes were reported with phenylbutazone (2) and since both agents are similar structurally, it seems reasonable that these two agents act by the same mechanism. Both oxyphenbutazone and phenylbutazone have been reported to be inhibitors of prostaglandin syn-

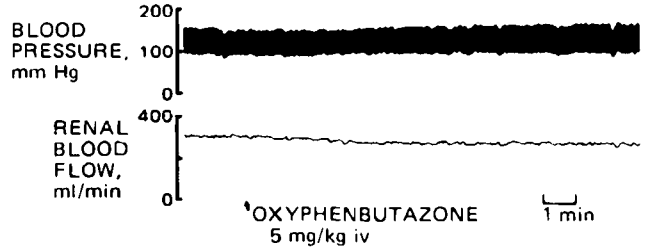

Figure 1—*Effect of oxyphenbutazone, 5 mg/kg iv, on blood pressure and renal blood flow.*

[6] Instrumentation Laboratories, Lexington, Mass.

0022-3549/79/0900-1178$01.00/0
© 1979, American Pharmaceutical Association

1 (1973).
(10) B. E. McCarey, H. F. Edelhauser, and D. L. Van Horn, *Invest. Ophthalmol.*, **12**, 410 (1973).
(11) "The Pharmacological Basis of Therapeutics," 5th ed., L. S. Goodman and A. Gilman, Eds., Macmillan, New York, N.Y., 1975.
(12) K. Green and S. Downs, *Invest. Ophthalmol.*, **13**, 316 (1974).
(13) K. Green and A. M. Tønjum, *Acta Ophthalmol.*, **53**, 348 (1975).

ACKNOWLEDGMENTS

Supported in part by Research Grants EY 02386 (D. S. Hull) and EY 01413 (K. Green) from the National Eye Institute, in part by a research grant from the Georgia Lions Lighthouse Foundation, Inc., in part by the Lions Club of Augusta, Ga., and in part by the J. H. Hall Eye Foundation. A Wang 2200 computer, used for statistical data evaluation, was provided through a Research to Prevent Blindness, Inc., grant.

Renal Actions of Oxyphenbutazone

HAROLD E. WILLIAMSON ˣ, GARY R. GAFFNEY, and WILLIAM A. BOURLAND

Received January 8, 1979, from the *Department of Pharmacology, College of Medicine, University of Iowa, Iowa City, IA 52242.* Accepted for publication February 28, 1979.

Abstract □ Oxyphenbutazone decreased the renal excretion of sodium and water in anesthetized dogs. As these excretions decreased, the drug also produced a decrease in renal blood flow and in the glomerular filtration rate. Blood pressure increased slightly. These changes are consistent with an inhibition of renal prostaglandin synthesis and could explain why oxyphenbutazone is reported to produce weight gain and edema when used clinically.

Keyphrases □ Oxyphenbutazone—effect on renal sodium and water excretion, renal blood flow, glomerular filtration rate, blood pressure, prostaglandin synthesis ■ Anti-inflammatory agents—oxyphenbutazone, renal effects ■ Kidney—effect of oxyphenbutazone

Oxyphenbutazone[1] is an analog of phenylbutazone[2] and, like the latter compound, is employed as an anti-inflammatory agent. Both agents produce edema and weight gain as side effects (1). A possible renal mechanism has been suggested for phenylbutazone since this agent markedly reduced renal blood flow and decreased the glomerular filtration rate at the time that urinary volume and sodium excretion were reduced (2). In this study, the effect of oxyphenbutazone on several renal functions was determined.

EXPERIMENTAL

Mongrel dogs of either sex, 13–16 kg, were anesthetized with pentobarbital sodium (30 mg/kg iv), and the trachea was intubated to maintain an open airway. Mean arterial blood pressure was monitored with a pressure transducer[3] *via* a femoral artery catheter. A femoral vein was catheterized for administration of a 0.9% NaCl infusion (4 ml/min) during preparation of the animals and throughout the experiments. Inulin was added to the infusion to estimate the glomerular filtration rate.

The left kidney was exposed *via* a retroperitoneal flank incision, and a flow probe was placed around the renal artery and connected to a square wave electromagnetic flowmeter[4] to monitor renal blood flow. Blood pressure and renal blood flow were recorded[5] continuously. Urine was collected at timed intervals by a cannula placed in the left ureter. Arterial blood samples were obtained from the femoral artery catheter. After stabilization of the preparation, control urine collections (10-min periods) and blood samples at the midpoint of alternate urine collection periods were obtained. Oxyphenbutazone was administered intravenously over 3 min, and urine collections were continued for several periods.

[1] Tanderil, Ciba-Geigy Corp., Summit, N.J.
[2] Butazolidin, Ciba-Geigy Corp., Summit, N.J.
[3] Model P23AA, Statham, Hato Rey, Puerto Rico.
[4] Carolina Medical Electronics, King, N.C.
[5] Dynograph (type R), Beckman Instruments, Fullerton, Calif.

Table I—Effect of Oxyphenbutazone (5 mg/kg iv) on Renal Function

Parameter	Control Period[a]	Oxyphenbutazone Period[b]	Difference
Blood pressure, mm Hg	115	128	+13 ± 5[c]
Renal blood flow, ml/min	262	220	−42 ± 5[c]
Urine volume, ml/min	1.1	0.4	−0.7 ± 0.2[c]
Glomerular filtration rate, ml/min	33	23	−10 ± 4[c]
Sodium excretion, μEq/min	136	77	−59 ± 1.9[c]

[a] Values are from the clearance period preceding oxyphenbutazone administration. [b] Values are from the clearance period 10–20 min after oxyphenbutazone administration. [c] Significant difference ($p < 0.05$); Student paired t test; $n = 7$.

Urinary and plasma inulin levels were determined by a reported method (3). Urinary sodium concentrations were measured with a flame photometer[6]. Data were analyzed using the Student paired t test (4); a $p < 0.05$ was the significance criterion.

RESULTS AND DISCUSSION

The effect of oxyphenbutazone on renal blood flow and blood pressure is shown in Fig. 1. Following oxyphenbutazone administration, 5 mg/kg iv, blood pressure increased slightly while renal blood flow decreased gradually. These effects, as well as effects on other renal functions, are summarized in Table I. At 20 min after oxyphenbutazone administration, blood pressure was increased while renal blood flow, the glomerular filtration rate, urinary volume, and sodium excretion were decreased. All changes were statistically significant. These changes also were present at 60 min.

Since similar changes were reported with phenylbutazone (2) and since both agents are similar structurally, it seems reasonable that these two agents act by the same mechanism. Both oxyphenbutazone and phenylbutazone have been reported to be inhibitors of prostaglandin syn-

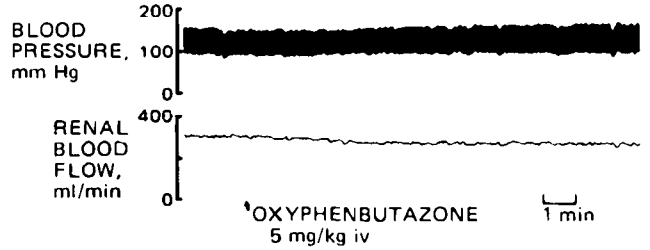

Figure 1—*Effect of oxyphenbutazone, 5 mg/kg iv, on blood pressure and renal blood flow.*

[6] Instrumentation Laboratories, Lexington, Mass.

0022-3549/79/0900-1178$01.00/0
© 1979, American Pharmaceutical Association

thesis (5). The latter compound also has been shown to decrease prostaglandin E synthesis at the time that it decreases renal blood flow and the glomerular filtration rate (2). Since a prostaglandin synthesis reduction can reduce renal blood flow by removing prostaglandin E, an endogenous vasodilator (6), the reduction in renal blood flow by oxyphenbutazone could be due to such a mechanism.

A reduction in sodium and water excretion can occur as a result of such a hemodynamic change. Early and Schrier (7) showed that a decrease in renal blood flow can alter the distribution of blood flow or physical factors to enhance sodium and water reabsorption.

A decrease in the glomerular filtration rate would also be expected to reduce sodium and water excretion. Whether the decrease in the glomerular filtration rate is a consequence of the inhibition of prostaglandin synthesis, as is the decrease in renal blood flow and the increase in blood pressure (8), or a separate action is not clear. Previous studies with prostaglandin synthesis inhibitors showed variable effects on the glomerular filtration rate (2, 8).

Thus, these experiments demonstrate that oxyphenbutazone reduces renal blood flow and the glomerular filtration rate during the time that it decreases sodium and water excretion. A decrease in renal blood flow and the glomerular filtration rate could cause or contribute to the decrease in water and sodium excretion produced by oxyphenbutazone.

REFERENCES

(1) "The Pharmacological Basis of Therapeutics," 5th ed., L. S. Goodman and A. Gilman, Eds., Macmillan, New York, N.Y., 1975, pp. 339–341.

(2) H. E. Williamson, G. R. Gaffney, W. A. Bourland, D. B. Farley, and D. E. Van Orden, *J. Pharmacol. Exp. Ther.*, **204**, 130 (1978).

(3) G. E. Schreiner, *Proc. Soc. Exp. Biol. Med.*, **74**, 117 (1950).

(4) G. W. Snedecor, "Statistical Methods," 5th ed., Iowa State College Press, Ames, Iowa, 1956, pp. 35–65.

(5) D. S. Newcombe, N. M. Thanassi, and C. P. Crosek, *Life Sci.*, **14**, 505 (1974).

(6) A. J. Lonigro, H. D. Itskovitz, K. Crowshaw, and J. C. McGiff, *Circ. Res.*, **32**, 712 (1973).

(7) L. E. Early and R. W. Schrier, in "Handbook of Physiology, Renal Physiology," J. Orloff and R. W. Berliner, Eds., American Physiological Society, Washington, D.C., 1973, pp. 721–762.

(8) L. P. Feigen, E. Klainer, B. M. Chapnick, and P. J. Kadowitz, *J. Pharmacol. Exp. Ther.*, **198**, 457 (1976).

ACKNOWLEDGMENTS

Supported in part by an Iowa Heart Association grant.

Effects of Pyridoxine Hydrochloride (Vitamin B_6) on Chlorpromazine-Induced Serum Prolactin Rise in Male Rats

JACK M. ROSENBERG *x, CESAR A. LAU-CAM, and HOWARD McGUIRE ‡

Received December 14, 1978, from the *Department of Pharmaceutical Sciences, St. John's University College of Pharmacy and Allied Health Professions, Jamaica, NY 11439.* Accepted for publication March 7, 1979.

*Present address: Arnold and Marie Schwartz College of Pharmacy and Health Sciences, Brooklyn, NY 11201. ‡Present address: Long Island University at the Brooklyn Center, Brooklyn, NY 11201.

Abstract □ To investigate if vitamin B_6 inhibits prolactin release and to compare this effect to that of bromocriptine, a known suppressor of prolactin release, a study was conducted in male rats. Animals were pretreated with pyridoxine hydrochloride, pyridoxal hydrochloride, saline, or bromocriptine 30 min prior to receiving varying doses of chlorpromazine hydrochloride. Blood samples were obtained 90 min later and analyzed for serum prolactin by a double-antibody radioimmunoassay. Another study involved pyridoxal hydrochloride and saline pretreatments 30 min prior to doses of chlorpromazine hydrochloride. Blood samples collected 60 min later were also analyzed for serum prolactin. Pyridoxine hydrochloride significantly suppressed the chlorpromazine-induced prolactin rise ($p < 0.01$). However, the suppression was significantly less than that produced by bromocriptine ($p < 0.01$). Pyridoxal hydrochloride, another natural form of vitamin B_6, failed to suppress prolactin under the conditions of both studies. This investigation may lend support to the concept that pyridoxine hydrochloride partially inhibits prolactin by a mechanism not involving dopamine.

Keyphrases □ Pyridoxine—effect on chlorpromazine-induced serum prolactin rise, rats □ Chlorpromazine—induction of serum prolactin rise, effect of pyridoxine, rats □ Prolactin—chlorpromazine-induced rise, effect of pyridoxine, rats

In 1973, Foukas (1) suggested that oral pyridoxine suppressed lactation within 7 days in 95% of postpartum women. This finding was supported by Marcus (2) but not by other investigators (3–6). Pyridoxine reduction of serum prolactin levels in the galactorrhea–amenorrhea syndrome has been reported (7, 8). Other studies showed that pyridoxine has no effect on elevated plasma prolactin levels due to various causes, including two subjects with chlorpromazine-induced hyperprolactinemia and galactorrhea (9, 10). However, Reiter and Root (11) observed a significant decrease in plasma prolactin in children following intravenous pyridoxine.

An *in vitro* investigation indicated that pyridoxine possessed some inhibitory effect on prolactin release from whole rat pituitary culture (12). Harris *et al.* (13) demonstrated that pyridoxine suppressed the plasma prolactin rise associated with proestrus and thyrotropin-releasing hormone stimulation in the rat. More recently, Husami *et al.* (14) presented evidence that high pyridoxine doses affected neither prolactin secretion nor lactation in humans, monkeys, and rats, including animals stimulated with thyrotropin-releasing hormone.

The present study was undertaken to determine the effects of pyridoxine and pyridoxal, two natural forms of vitamin B_6, on chlorpromazine-induced prolactin secretion in rats (15) and to compare the inhibition by these vitamins with the effects of bromocriptine, a known potent inhibitor of prolactin release (16).

EXPERIMENTAL

Two hundred and forty male Sprague–Dawley adult rats[1], 245–280 g, were divided into four equal groups. The rats were housed for 21 days prior to the study in a temperature-controlled (23 ± 3°) artificially illuminated (lights on from 7:00 am to 7:00 pm daily) room. The animals were given food[2] and water *ad libitum*. Each group was intraperitoneally in-

[1] Taconic Farms, Germantown, N.Y.
[2] Purina Lab Chow, Ralston Purina Co., St. Louis, Mo.

0022-3549/79/0900-1179$01.00/0

© 1979, American Pharmaceutical Association

thesis (5). The latter compound also has been shown to decrease prostaglandin E synthesis at the time that it decreases renal blood flow and the glomerular filtration rate (2). Since a prostaglandin synthesis reduction can reduce renal blood flow by removing prostaglandin E, an endogenous vasodilator (6), the reduction in renal blood flow by oxyphenbutazone could be due to such a mechanism.

A reduction in sodium and water excretion can occur as a result of such a hemodynamic change. Early and Schrier (7) showed that a decrease in renal blood flow can alter the distribution of blood flow or physical factors to enhance sodium and water reabsorption.

A decrease in the glomerular filtration rate would also be expected to reduce sodium and water excretion. Whether the decrease in the glomerular filtration rate is a consequence of the inhibition of prostaglandin synthesis, as is the decrease in renal blood flow and the increase in blood pressure (8), or a separate action is not clear. Previous studies with prostaglandin synthesis inhibitors showed variable effects on the glomerular filtration rate (2, 8).

Thus, these experiments demonstrate that oxyphenbutazone reduces renal blood flow and the glomerular filtration rate during the time that it decreases sodium and water excretion. A decrease in renal blood flow and the glomerular filtration rate could cause or contribute to the decrease in water and sodium excretion produced by oxyphenbutazone.

REFERENCES

(1) "The Pharmacological Basis of Therapeutics," 5th ed., L. S. Goodman and A. Gilman, Eds., Macmillan, New York, N.Y., 1975, pp. 339–341.

(2) H. E. Williamson, G. R. Gaffney, W. A. Bourland, D. B. Farley, and D. E. Van Orden, *J. Pharmacol. Exp. Ther.*, **204**, 130 (1978).

(3) G. E. Schreiner, *Proc. Soc. Exp. Biol. Med.*, **74**, 117 (1950).

(4) G. W. Snedecor, "Statistical Methods," 5th ed., Iowa State College Press, Ames, Iowa, 1956, pp. 35–65.

(5) D. S. Newcombe, N. M. Thanassi, and C. P. Crosek, *Life Sci.*, **14**, 505 (1974).

(6) A. J. Lonigro, H. D. Itskovitz, K. Crowshaw, and J. C. McGiff, *Circ. Res.*, **32**, 712 (1973).

(7) L. E. Early and R. W. Schrier, in "Handbook of Physiology, Renal Physiology," J. Orloff and R. W. Berliner, Eds., American Physiological Society, Washington, D.C., 1973, pp. 721–762.

(8) L. P. Feigen, E. Klainer, B. M. Chapnick, and P. J. Kadowitz, *J. Pharmacol. Exp. Ther.*, **198**, 457 (1976).

ACKNOWLEDGMENTS

Supported in part by an Iowa Heart Association grant.

Effects of Pyridoxine Hydrochloride (Vitamin B_6) on Chlorpromazine-Induced Serum Prolactin Rise in Male Rats

JACK M. ROSENBERG *x, CESAR A. LAU-CAM, and HOWARD McGUIRE ‡

Received December 14, 1978, from the *Department of Pharmaceutical Sciences, St. John's University College of Pharmacy and Allied Health Professions, Jamaica, NY 11439.* Accepted for publication March 7, 1979.

*Present address: Arnold and Marie Schwartz College of Pharmacy and Health Sciences, Brooklyn, NY 11201. ‡Present address: Long Island University at the Brooklyn Center, Brooklyn, NY 11201.

Abstract □ To investigate if vitamin B_6 inhibits prolactin release and to compare this effect to that of bromocriptine, a known suppressor of prolactin release, a study was conducted in male rats. Animals were pretreated with pyridoxine hydrochloride, pyridoxal hydrochloride, saline, or bromocriptine 30 min prior to receiving varying doses of chlorpromazine hydrochloride. Blood samples were obtained 90 min later and analyzed for serum prolactin by a double-antibody radioimmunoassay. Another study involved pyridoxal hydrochloride and saline pretreatments 30 min prior to doses of chlorpromazine hydrochloride. Blood samples collected 60 min later were also analyzed for serum prolactin. Pyridoxine hydrochloride significantly suppressed the chlorpromazine-induced prolactin rise ($p < 0.01$). However, the suppression was significantly less than that produced by bromocriptine ($p < 0.01$). Pyridoxal hydrochloride, another natural form of vitamin B_6, failed to suppress prolactin under the conditions of both studies. This investigation may lend support to the concept that pyridoxine hydrochloride partially inhibits prolactin by a mechanism not involving dopamine.

Keyphrases □ Pyridoxine—effect on chlorpromazine-induced serum prolactin rise, rats □ Chlorpromazine—induction of serum prolactin rise, effect of pyridoxine, rats □ Prolactin—chlorpromazine-induced rise, effect of pyridoxine, rats

In 1973, Foukas (1) suggested that oral pyridoxine suppressed lactation within 7 days in 95% of postpartum women. This finding was supported by Marcus (2) but not by other investigators (3–6). Pyridoxine reduction of serum prolactin levels in the galactorrhea–amenorrhea syndrome has been reported (7, 8). Other studies showed that pyridoxine has no effect on elevated plasma prolactin levels due to various causes, including two subjects with chlorpromazine-induced hyperprolactinemia and galactorrhea (9, 10). However, Reiter and Root (11) observed a significant decrease in plasma prolactin in children following intravenous pyridoxine.

An *in vitro* investigation indicated that pyridoxine possessed some inhibitory effect on prolactin release from whole rat pituitary culture (12). Harris *et al.* (13) demonstrated that pyridoxine suppressed the plasma prolactin rise associated with proestrus and thyrotropin-releasing hormone stimulation in the rat. More recently, Husami *et al.* (14) presented evidence that high pyridoxine doses affected neither prolactin secretion nor lactation in humans, monkeys, and rats, including animals stimulated with thyrotropin-releasing hormone.

The present study was undertaken to determine the effects of pyridoxine and pyridoxal, two natural forms of vitamin B_6, on chlorpromazine-induced prolactin secretion in rats (15) and to compare the inhibition by these vitamins with the effects of bromocriptine, a known potent inhibitor of prolactin release (16).

EXPERIMENTAL

Two hundred and forty male Sprague–Dawley adult rats[1], 245–280 g, were divided into four equal groups. The rats were housed for 21 days prior to the study in a temperature-controlled (23 ± 3°) artificially illuminated (lights on from 7:00 am to 7:00 pm daily) room. The animals were given food[2] and water *ad libitum*. Each group was intraperitoneally in-

[1] Taconic Farms, Germantown, N.Y.
[2] Purina Lab Chow, Ralston Purina Co., St. Louis, Mo.

0022-3549/79/0900-1179$01.00/0

© 1979, American Pharmaceutical Association

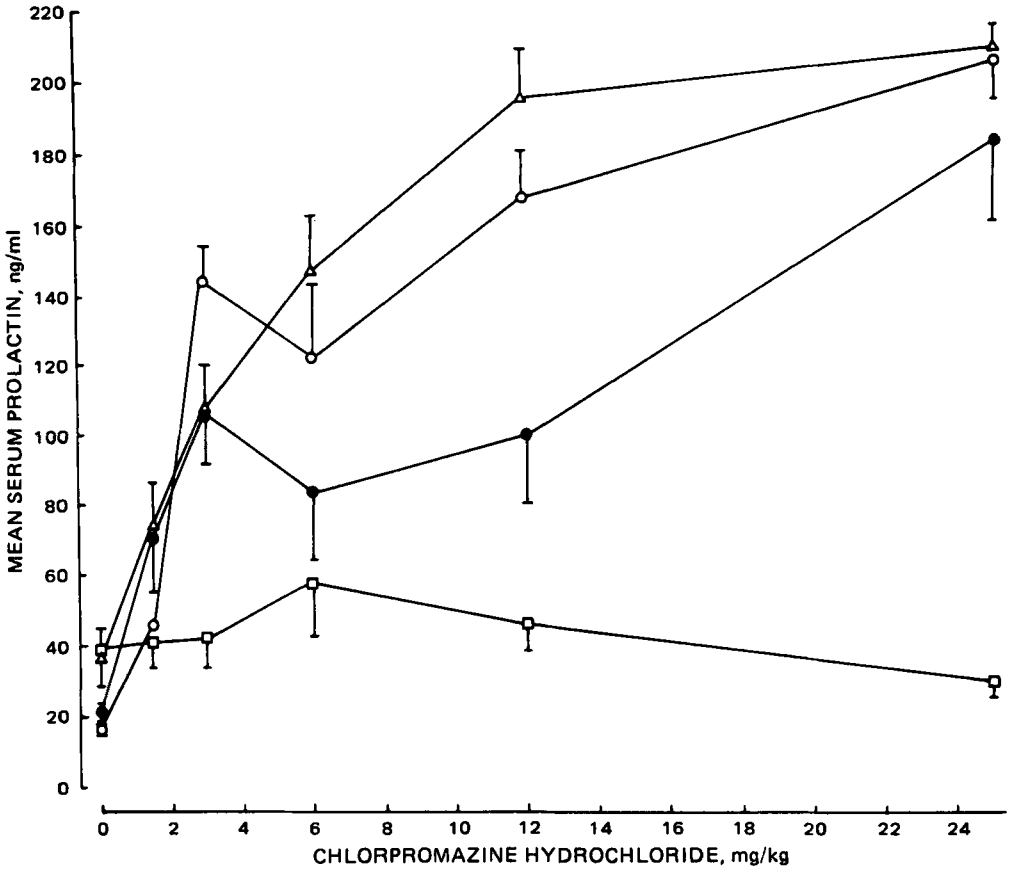

Figure 1—*Effects of intraperitoneal pyridoxine hydrochloride (75 mg, ●), pyridoxal hydrochloride (75 mg, ○), bromocriptine (1 mg, □), and saline (△) administered 30 min prior to intraperitoneal saline or chlorpromazine hydrochloride (1.25–25 mg/kg). Serum prolactin determinations were made on blood samples collected 90 min after chlorpromazine treatment. Each point represents the mean value for 10 animals. Vertical lines show standard errors of the mean.*

jected between 12:30 pm and 2:00 pm with 0.5 ml of aqueous solution containing 75 mg of pyridoxine hydrochloride[3], 75 mg of pyridoxal hydrochloride[3], 1 mg of bromocriptine[4], or normal saline[5].

Thirty minutes following pretreatment of each group, serial dilutions of chlorpromazine hydrochloride[6], ranging from 25 to 1.25 mg/kg, were administered intraperitoneally to five subgroups of 10 animals each; the remaining 10 animals received normal saline. Blood samples were obtained by decapitation from the trunk portion 90 min later, previously determined as the time of peak serum prolactin response to intraperitoneal chlorpromazine hydrochloride[7].

A further study under similar experimental conditions involved 12 animals, 245–280 g. Six animals received intraperitoneally 0.5 ml of an aqueous solution containing 75 mg of pyridoxal hydrochloride; the other six received an equal volume of normal saline. Thirty minutes later, five of the six animals from each group received one of five serial chlorpromazine hydrochloride dilutions ranging from 25 to 1.25 mg/kg ip, and the other animal received normal saline. Blood samples were obtained by decapitation from the trunk portion 60 min later.

Serum samples for both studies were separated and analyzed for prolactin by a double-antibody radioimmunoassay[8] based on the principle first described by Yallow and Berson (17). All results are expressed in terms of National Institute of Arthritis, Metabolism, and Digestive Diseases (NIAMDD)-rat prolactin. Each serum sample was assayed in duplicate, and the average was taken as representative of the true prolactin concentration. Statistical significance was determined by a two-way fixed analysis of variance, the Student t test, and linear trend analysis (18).

RESULTS

Figure 1 shows the effects of the different pretreatments on serum prolactin levels at 90 min following varied chlorpromazine hydrochloride doses. Replicate 2 × 6 analyses of variance to compare the drugs against normal saline showed that serum prolactin was significantly suppressed ($F_{1,108} = 9.799$, $p < 0.01$) by pyridoxine hydrochloride but not by pyridoxal hydrochloride ($F_{1,108} = 0.026$). In a 2 × 6 analysis of variance, bromocriptine suppressed prolactin ($F_{1,108} = 39.534$, $p < 0.01$) to a much greater extent than did pyridoxine hydrochloride. Trend analysis of pyridoxine hydrochloride and pyridoxal hydrochloride revealed that the effects of increasing drug concentrations were significantly linear ($F_{1,54} = 29.89$, $p < 0.01$, and $F_{1,54} = 118.24$, $p < 0.001$, respectively).

While pyridoxal hydrochloride was not significantly different from normal saline, it resembled the more effective pyridoxine hydrochloride in its concentration effects. In a further study to compare the effects of pyridoxal hydrochloride and normal saline pretreatments on serum prolactin levels at 60 min following varied chlorpromazine hydrochloride doses, the mean serum prolactin levels of both groups were not significantly different [135.4 ± 40.8 (*SE*) *versus* 72.7 ± 29.7 (*SE*) ng/ml, respectively; $t = 1.14$, $df = 10$].

DISCUSSION

Serum prolactin levels are largely controlled by a hypothalamic prolactin-inhibiting factor related to dopamine and, indeed, may be dopamine, and, to a lesser extent, by a prolactin-releasing factor also hypothalamic in origin (19). Pharmacological agents that reduce serum prolactin levels include dopamine agonists such as bromocriptine and dopamine-replenishing agents such as levodopa (20). Although both bromocriptine and levodopa also may transiently increase the prolactin clearance from plasma by stimulating its uptake into peripheral receptor sites, their exact inhibition mechanisms are not fully known (21).

Pyridoxine hydrochloride, in a pharmacological dose, exhibited some inhibitory effect on the serum prolactin rise induced by varied chlorpromazine hydrochloride doses. This suppression was significantly less than that produced by bromocriptine. On the other hand, its biologically equivalent form, pyridoxal hydrochloride, did not significantly alter prolactin secretion.

The manner by which pyridoxine hydrochloride exerts its prolactin inhibitory effect cannot be determined from the present data. It has been suggested that pyridoxine enhances hypothalamic dopamine synthesis through its metabolism to pyridoxal phosphate, the coenzyme for the conversion of dopa to dopamine by dopa decarboxylase (1, 2, 7, 8). This

[3] Sigma Chemical, St. Louis, Mo.
[4] Sandoz Laboratories, East Hanover, N.J.
[5] Abbott Laboratories, Chicago, Ill.
[6] Smith Kline & French Co., Carolina, Puerto Rico.
[7] Unpublished data.

theory is based on the widely quoted explanation of Duvoisin *et al.* (22) for their finding that pyridoxine reduces or abolishes the antiparkinsonian effect of levodopa. They suggested that pyridoxine, in the form of pyridoxal phosphate, increases decarboxylase activity so that more levodopa is converted to dopamine in the periphery and less is available to penetrate into the central nervous system. However, this mechanism was refuted by Johnson *et al.* (23), who found no evidence of decarboxylase facilitation in levodopa-treated Parkinsonian patients receiving pyridoxine. These investigators offered the formation of a Schiff's base complex between pyridoxal phosphate and dopamine (24, 25) and other mechanisms (26) as alternative explanations.

Harris *et al.* (13) suggested that pyridoxine hydrochloride directly inhibits prolactin release and that dopamine involvement is unlikely. The present results may support the concept of direct prolactin inhibition by pyridoxine hydrochloride since pyridoxal hydrochloride also can be readily metabolized to the active form of the vitamin that serves as the coenzyme in the conversion of dopa to dopamine. In addition, although studies with radioactive tracers showed that an equilibrium between all active vitamin B_6 forms is established in the mammalian organism, this equilibrium does not result when large doses are given (27, 28). Even though the effects of pyridoxal hydrochloride on chlorpromazine hydrochloride-induced prolactin secretion were tested at two different time intervals, a different sampling time may reveal a prolactin-suppressant effect for this form of the vitamin.

Clarification of the mechanism(s) by which pyridoxine hydrochloride partially inhibits prolactin secretion requires further study.

REFERENCES

(1) M. D. Foukas, *J. Obstet. Gynaecol. Br. Commonw.*, **80**, 718 (1973).

(2) R. G. Marcus, *S. Afr. Med. J.*, **49**, 2155 (1975).

(3) H. E. del Pozo, R. B. Del Re, M. Hinselmann, and H. Wyss, *Arch. Gynaecol.*, **219**, 469 (1975).

(4) H. N. MacDonald, Y. D. Collins, M. J. W. Tobin, and D. N. Wijayaratne, *Br. J. Obstet. Gynaecol.*, **83**, 54 (1976).

(5) E. S. Canales, J. Soria, A. Zarate, M. Mason, and M. Molina, *Br. J. Gynaecol.*, **83**, 387 (1976).

(6) G. Tolis, R. Laliberte, H. Guyda, and F. Naftolin, *J. Clin. Endocrinol. Metab.*, **44**, 1197 (1977).

(7) E. N. MacIntosh, *ibid.*, **42**, 1192 (1976).

(8) G. Delitala, A. Masala, S. Alagna, and L. Devilla, *ibid.*, **42**, 603 (1976).

(9) A. M. Spiegel, S. W. Rosen, B. D. Weintraub, and S. P. Marynick, *ibid.*, **46**, 686 (1978).

(10) J. M. DeWaal, A. F. Steyn, J. H. K. Harms, C. F. Slabber, and P. R. Pannall, *S. Afr. Med. J.*, **53**, 293 (1978).

(11) E. O. Reiter and A. W. Root, *J. Clin. Endocrinol. Metab.*, **47**, 689 (1978).

(12) R. M. MacLeod and J. E. Lehmeyer, in "Lactogenic Hormones," G. E. W. Wolstenholme and J. Knight, Eds., Ciba Foundation, Associated Scientific Publishers, New York, N.Y., 1972, p. 53.

(13) A. R. C. Harris, M. S. Smith, S. Alex, H. A. Salhanick, A. G. Vagenakis, and L. E. Braverman, *Endocrinology*, **102**, 362 (1978).

(14) N. Husami, W. Idriss, R. Jewelewicz, M. Ferin, and R. L. VandeWiele, *Fertil. Steriol.*, **30**, 393 (1978).

(15) "The Pharmacological Basis of Therapeutics," 5th ed., L. S. Goodman and A. Gilman, Eds., Macmillan, New York, N.Y., 1975, p. 1556.

(16) W. H. Utian, G. Begg, A. I. Vinik, M. Paul, and L. Shuman, *Br. J. Obstet. Gynaecol.*, **82**, 755 (1975).

(17) R. S. Yallow and S. A. Berson, *J. Clin. Invest.*, **39**, 1157 (1960).

(18) B. J. Winer, "Statistical Principles in Experimental Design," 2nd ed., McGraw-Hill, New York, N.Y., p. 471.

(19) C. H. Mortimer and G. M. Besser, in "Recent Advances in Medicine," 17th ed., D. N. Baron, N. Compston, and A. M. Dawson, Eds., Churchill Livingstone, London, England, 1977, p. 441.

(20) D. C. Evered and W. B. A. Tunbridge, in "Textbook of Adverse Reactions," vol. 1., D. M. Davis, Ed., Oxford University Press, Oxford, England, 1977, p. 206.

(21) E. E. Muller, A. E. Panerai, D. Cocchi, and P. Mantegazza, *Life Sci.*, **21**, 1545 (1977).

(22) R. C. Duvoisin, M. D. Yahr, and L. D. Cote, *Trans. Am. Neurol. Assoc.*, **94**, 81 (1969).

(23) R. D. Johnson, C. R. J. Ruthven, B. L. Goodwin, and M. Sandler, *J. Neural Transm.*, **38**, 181 (1976).

(24) D. B. Calne and M. Sandler, *Nature*, **226**, 21 (1970).

(25) G. A. R. Johnstone, *Lancet*, **2**, 220 (1972).

(26) M. Sandler, in "Handbook of Experimental Pharmacology," vol. 33, H. Blaschko and E. Muscholl, Eds., Springer, New York, N.Y., 1972, p. 845.

(27) S. Johansson, S. Lindstedt, and U. Register, *Am. J. Physiol.*, **210**, 1086 (1966).

(28) S. Johansson, S. Lindstedt, and H. G. Tiselius, *Biochemistry*, **7**, 2327 (1968).

ACKNOWLEDGMENTS

The authors thank the National Institute of Arthritis, Metabolism, and Digestive Diseases Rat Pituitary Hormone Distribution Program and Dr. A. F. Parlow for their gift of radioimmunoassay materials.

Resolution of (±)-Propranolol

YUL YOST *x and JORDAN L. HOLTZMAN *‡

Received July 17, 1978, from the **Research Service, Veterans Administration Hospital, Minneapolis, MN 55417,* and the ‡*Departments of Medicine and Pharmacology, University of Minnesota, Minneapolis, MN 55455.* Accepted for publication March 1, 1979.

Abstract □ Two improvements in propranolol resolution were developed. Both the (+)- and (−)-di-(*p*-toluoyl)tartaric acids were used as the resolving agents. This procedure reduced the number of crystallizations needed to obtain a pure product. Furthermore, synthesis of the resolving agent was improved.

Keyphrases □ Propranolol—racemic mixtures, resolution of enantiomers, (+)- and (−)-di-(*p*-toluoyl)tartaric acids used as resolving agents □ Enantiomers—propranolol, resolving agents

Propranolol (I) [1-isopropylamino-3-(1-naphthoxy)-2-propanol], the principal commercially available β-adrenergic blocking agent, is usually supplied as the racemic compound[1]. The (−)-isomer has as much as 60 times greater β-blocking activity than the (+)-isomer (1). Not only can there be significant differences in the pharmacological activity of the enantiomers, but, as has been shown for other drugs, there also can be significant metabolic differences (2, 3).

DISCUSSION

There is only one preliminary report on the metabolism of propranolol enantiomers (4). In preparation for a metabolic study in humans, two improvements in the overall procedure for resolution of these enantiomers were made. First, preparation of the resolving agent [di-(*p*-toluoyl)tartaric acid (II)] was modified. In contrast to the original report (5), the agent was found to be insoluble in pure benzene. Moreover, the customary spectral data were not reported and are included here.

Second, in the original report on racemic propranolol resolution (1), only the (−)-di-(*p*-toluoyl)tartaric acid was used to resolve both enan-

[1] Available as (±)-propranolol hydrochloride (Inderal).

0022-3549/79/0900-1181$01.00/0

© 1979, American Pharmaceutical Association

theory is based on the widely quoted explanation of Duvoisin *et al.* (22) for their finding that pyridoxine reduces or abolishes the antiparkinsonian effect of levodopa. They suggested that pyridoxine, in the form of pyridoxal phosphate, increases decarboxylase activity so that more levodopa is converted to dopamine in the periphery and less is available to penetrate into the central nervous system. However, this mechanism was refuted by Johnson *et al.* (23), who found no evidence of decarboxylase facilitation in levodopa-treated Parkinsonian patients receiving pyridoxine. These investigators offered the formation of a Schiff's base complex between pyridoxal phosphate and dopamine (24, 25) and other mechanisms (26) as alternative explanations.

Harris *et al.* (13) suggested that pyridoxine hydrochloride directly inhibits prolactin release and that dopamine involvement is unlikely. The present results may support the concept of direct prolactin inhibition by pyridoxine hydrochloride since pyridoxal hydrochloride also can be readily metabolized to the active form of the vitamin that serves as the coenzyme in the conversion of dopa to dopamine. In addition, although studies with radioactive tracers showed that an equilibrium between all active vitamin B_6 forms is established in the mammalian organism, this equilibrium does not result when large doses are given (27, 28). Even though the effects of pyridoxal hydrochloride on chlorpromazine hydrochloride-induced prolactin secretion were tested at two different time intervals, a different sampling time may reveal a prolactin-suppressant effect for this form of the vitamin.

Clarification of the mechanism(s) by which pyridoxine hydrochloride partially inhibits prolactin secretion requires further study.

REFERENCES

(1) M. D. Foukas, *J. Obstet. Gynaecol. Br. Commonw.*, **80**, 718 (1973).

(2) R. G. Marcus, *S. Afr. Med. J.*, **49**, 2155 (1975).

(3) H. E. del Pozo, R. B. Del Re, M. Hinselmann, and H. Wyss, *Arch. Gynaecol.*, **219**, 469 (1975).

(4) H. N. MacDonald, Y. D. Collins, M. J. W. Tobin, and D. N. Wijayaratne, *Br. J. Obstet. Gynaecol.*, **83**, 54 (1976).

(5) E. S. Canales, J. Soria, A. Zarate, M. Mason, and M. Molina, *Br. J. Gynaecol.*, **83**, 387 (1976).

(6) G. Tolis, R. Laliberte, H. Guyda, and F. Naftolin, *J. Clin. Endocrinol. Metab.*, **44**, 1197 (1977).

(7) E. N. MacIntosh, *ibid.*, **42**, 1192 (1976).

(8) G. Delitala, A. Masala, S. Alagna, and L. Devilla, *ibid.*, **42**, 603 (1976).

(9) A. M. Spiegel, S. W. Rosen, B. D. Weintraub, and S. P. Marynick, *ibid.*, **46**, 686 (1978).

(10) J. M. DeWaal, A. F. Steyn, J. H. K. Harms, C. F. Slabber, and P. R. Pannall, *S. Afr. Med. J.*, **53**, 293 (1978).

(11) E. O. Reiter and A. W. Root, *J. Clin. Endocrinol. Metab.*, **47**, 689 (1978).

(12) R. M. MacLeod and J. E. Lehmeyer, in "Lactogenic Hormones," G. E. W. Wolstenholme and J. Knight, Eds., Ciba Foundation, Associated Scientific Publishers, New York, N.Y., 1972, p. 53.

(13) A. R. C. Harris, M. S. Smith, S. Alex, H. A. Salhanick, A. G. Vagenakis, and L. E. Braverman, *Endocrinology*, **102**, 362 (1978).

(14) N. Husami, W. Idriss, R. Jewelewicz, M. Ferin, and R. L. VandeWiele, *Fertil. Steriol.*, **30**, 393 (1978).

(15) "The Pharmacological Basis of Therapeutics," 5th ed., L. S. Goodman and A. Gilman, Eds., Macmillan, New York, N.Y., 1975, p. 1556.

(16) W. H. Utian, G. Begg, A. I. Vinik, M. Paul, and L. Shuman, *Br. J. Obstet. Gynaecol.*, **82**, 755 (1975).

(17) R. S. Yallow and S. A. Berson, *J. Clin. Invest.*, **39**, 1157 (1960).

(18) B. J. Winer, "Statistical Principles in Experimental Design," 2nd ed., McGraw-Hill, New York, N.Y., p. 471.

(19) C. H. Mortimer and G. M. Besser, in "Recent Advances in Medicine," 17th ed., D. N. Baron, N. Compston, and A. M. Dawson, Eds., Churchill Livingstone, London, England, 1977, p. 441.

(20) D. C. Evered and W. B. A. Tunbridge, in "Textbook of Adverse Reactions," vol. 1., D. M. Davis, Ed., Oxford University Press, Oxford, England, 1977, p. 206.

(21) E. E. Muller, A. E. Panerai, D. Cocchi, and P. Mantegazza, *Life Sci.*, **21**, 1545 (1977).

(22) R. C. Duvoisin, M. D. Yahr, and L. D. Cote, *Trans. Am. Neurol. Assoc.*, **94**, 81 (1969).

(23) R. D. Johnson, C. R. J. Ruthven, B. L. Goodwin, and M. Sandler, *J. Neural Transm.*, **38**, 181 (1976).

(24) D. B. Calne and M. Sandler, *Nature*, **226**, 21 (1970).

(25) G. A. R. Johnstone, *Lancet*, **2**, 220 (1972).

(26) M. Sandler, in "Handbook of Experimental Pharmacology," vol. 33, H. Blaschko and E. Muscholl, Eds., Springer, New York, N.Y., 1972, p. 845.

(27) S. Johansson, S. Lindstedt, and U. Register, *Am. J. Physiol.*, **210**, 1086 (1966).

(28) S. Johansson, S. Lindstedt, and H. G. Tiselius, *Biochemistry*, **7**, 2327 (1968).

ACKNOWLEDGMENTS

The authors thank the National Institute of Arthritis, Metabolism, and Digestive Diseases Rat Pituitary Hormone Distribution Program and Dr. A. F. Parlow for their gift of radioimmunoassay materials.

Resolution of (±)-Propranolol

YUL YOST *x and JORDAN L. HOLTZMAN *‡

Received July 17, 1978, from the **Research Service, Veterans Administration Hospital, Minneapolis, MN 55417,* and the ‡*Departments of Medicine and Pharmacology, University of Minnesota, Minneapolis, MN 55455.* Accepted for publication March 1, 1979.

Abstract □ Two improvements in propranolol resolution were developed. Both the (+)- and (−)-di-(*p*-toluoyl)tartaric acids were used as the resolving agents. This procedure reduced the number of crystallizations needed to obtain a pure product. Furthermore, synthesis of the resolving agent was improved.

Keyphrases □ Propranolol—racemic mixtures, resolution of enantiomers, (+)- and (−)-di-(*p*-toluoyl)tartaric acids used as resolving agents □ Enantiomers—propranolol, resolving agents

Propranolol (I) [1-isopropylamino-3-(1-naphthoxy)-2-propanol], the principal commercially available β-adrenergic blocking agent, is usually supplied as the racemic compound[1]. The (−)-isomer has as much as 60 times greater β-blocking activity than the (+)-isomer (1). Not only can there be significant differences in the pharmacological activity of the enantiomers, but, as has been shown for other drugs, there also can be significant metabolic differences (2, 3).

DISCUSSION

There is only one preliminary report on the metabolism of propranolol enantiomers (4). In preparation for a metabolic study in humans, two improvements in the overall procedure for resolution of these enantiomers were made. First, preparation of the resolving agent [di-(*p*-toluoyl)tartaric acid (II)] was modified. In contrast to the original report (5), the agent was found to be insoluble in pure benzene. Moreover, the customary spectral data were not reported and are included here.

Second, in the original report on racemic propranolol resolution (1), only the (−)-di-(*p*-toluoyl)tartaric acid was used to resolve both enan-

[1] Available as (±)-propranolol hydrochloride (Inderal).

0022-3549/79/0900-1181$01.00/0

© 1979, American Pharmaceutical Association

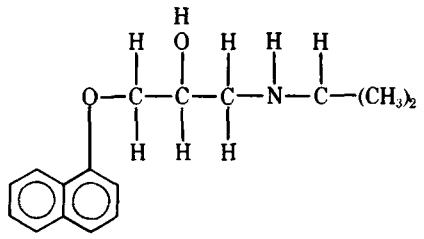

I

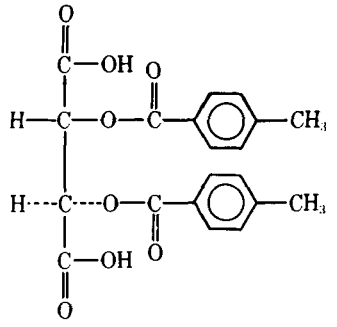

II

tiomers. In the present work, (−)- and (+)-di-(*p*-toluoyl)tartaric acids were employed in the resolution. This procedure required fewer recrystallizations to achieve optical purity. In particular, the (−)-propranolol was best isolated with (+)-di-(*p*-toluoyl)tartaric acid. Pure compounds were obtained after only one to five recrystallizations; in the original study, pure compounds were obtained "by a tedious fractional crystallization" (1).

In the original study (1), the optical rotations of propranolol enantiomers were reported to be +10.6 and −10.2°, with a melting point of 72°. The values obtained here are +8.34 and −8.32°, with a melting point of 72°. Despite the discrepancy between these rotations and those previously reported, the present values are apparently correct since the optical rotations of the respective hydrochloride derivatives obtained here (−23.82 and +22.85°) agree well with those reported (−22.7 and +22.2°). Furthermore, a sample of the (−)-enantiomer hydrochloride[2] gave a specific rotation of −23.80°. The metabolic studies will be published elsewhere.

EXPERIMENTAL

(−)-Di-(*p*-toluoyl)tartaric Acid (II)—(+)-Tartaric acid (31.6 g, 0.21 mole) and *p*-toluoyl chloride (108 g, 0.699 mole) were heated in an oil bath until the reaction mixture solidified (140°); it was then kept at that temperature for 2 hr. The cooled solid was triturated with benzene (70 ml), collected by filtration, and washed with benzene. The material was dissolved in refluxing toluene (480 ml), the mixture was filtered hot, and the filtrate was cooled to 18° to yield the II anhydride (65 g, 84%). It was recrystallized from refluxing ethyl acetate (500 ml), mp 206°, $[\alpha]_D^{18}$ +183° (c, 0.33 in acetone) and −135°, after a 1% mixture was heated in 95% ethanol; IR: ν_{max} (KBr) OH, none, 1890, 1810, 1740, and 1710 (C=O) cm^{-1} [lit. (5) mp 198° and [α] +195° (c, 0.5 in acetone)].

The anhydride (44 g, 0.12 mole) was refluxed for 2 hr in 5% aqueous acetone (250 ml). The solvent was removed, and the residue was recrystallized from a solution of 5% acetone in benzene (130 ml) to yield II (36 g, 78%), mp 173°, $[\alpha]_D^{18}$ −136.5° (c, 0.33 in ethanol); UV: λ_{max} (in ethanol) 240 (ε 28,200) nm; IR: λ_{max} (KBr) 3400–2500 (OH) and 1730 (C=O) cm^{-1} [lit. (4) mp 172° and $[\alpha]_D^{18}$ −140° (c, 1.0 in ethanol)].

Racemic Propranolol Resolution—(+)-Di-(*p*-toluoyl)tartaric acid (5.79 g, 15.0 mmoles), prepared from (−)-tartaric acid as just described, and (±)-propranolol (3.88 g, 15.0 mmoles) were dissolved in methanol (55 ml). The solution volume was reduced to 40 ml by boiling and then allowed to cool to 18°.

The resulting first crop of crystals (6 g) was redissolved in boiling methanol (70 ml). The procedure was repeated until the salt gave a constant optical rotation, $[\alpha]_D^{18}$ +63.06°.

To obtain the free base, the tartarate was decomposed with 0.5 *N* NaOH and the precipitated product was extracted with ether. The organic phase was dried (magnesium sulfate), the ether was evaporated off, and the residue was recrystallized from cyclohexane to yield (−)-propranolol, mp 72°, $[\alpha]_D^{18}$ −8.32° (c, 1.0 in ethanol); UV: λ_{max} (in 95% ethanol) 293 (ε 6000) nm [lit. (1) mp 72° and [α] −10.2° (c, 1.02)].

Treatment of (−)-propranolol (1.7 g) in ether (100 ml) with dry hydrogen chloride yielded (−)-propranolol hydrochloride, mp 196°, $[\alpha]_D^{18}$ −23.82° (c, 1.0 in ethanol) [lit. (1) mp 192° and [α] −22.7°]. An aliquot was recrystallized by suspending the material in hot benzene and then adding dropwise anhydrous ethanol to clear the suspension, mp 196°, [α] −23.45° (c, 1.0 in ethanol).

(+)-Propranolol was obtained by the identical procedure but with II as the resolving agent. In one series, after five recrystallizations the tartarate salt had an optical rotation of −63.27°. Table I shows a sequence of typical experiments beginning with equimolar amounts (15 mmoles) of racemic propranolol and the resolving agent in methanol (70 ml).

(+)-Propranolol was then isolated as described for its enantiomer, mp 72°, $[\alpha]_D^{18}$ +8.34° (c, 1.0 ethanol) [lit. (1) mp 73° and [α] +10.6°]. The (+)-propranolol hydrochloride had a melting point of 196°, $[\alpha]_D^{18}$ +22.97° (c, 1.0 in ethanol) [lit. (1) mp 192° and [α] +22.2°].

In another experiment, partially resolved propranolol, [α] +3.67° (4.00 g, 15.4 mmoles), was complexed with II (4.28 g, 11.0 mmoles), *i.e.*, an amount equivalent to the percent of the (+)-isomer. After two crystallizations from boiling methanol (55 ml), the optically pure complex was obtained (2.80 g), mp 163–165°, [α] −64.64°. It gave the free base, $[\alpha]_D^{18}$ +7.82° (c, 1.0 ethanol), which with hydrochloric acid gave (+)-propranolol hydrochloride, $[\alpha]_D^{18}$ +22.85° (c, 1.0 ethanol).

Propranolol hydrochloride for use in humans was not recrystallized from benzene. It was assayed for the presence of di-(*p*-toluoyl)tartaric acid spectrophotometrically as follows. The ratio of ε at λ_{max} (in ethanol) 290 (ε 5950) and of ε at λ_{min} 245 (ε 760) of racemic propranolol hydrochloride prepared from propranolol, which had not been treated with the resolving agent, was compared with the ratio of $\epsilon\lambda_{max}/\epsilon\lambda_{min}$ of resolved propranolol hydrochloride. Since (+)- and (−)-di-(*p*-toluoyl)tartaric acids have an ε of 25,000 at 245 nm, even a 0.1% contamination would cause a detectable alteration in the absorbance ratio at 290 and 245 nm. No contamination was detected in either propranolol enantiomer.

Table I—Fractional Crystallization of Salt of Equimolar Amounts of Racemic Propranolol and (−)-Di-(*p*-toluoyl)tartaric Acid in 70 ml of Methanol

Step	Methanol, ml	Yield of Complex: Millimoles	Yield of Complex: Percent Theoretical[a]	Melting Point	$[\alpha]_D^{18}$
1	70	8.79	117	156–164°	−68.2°
2	70	6.20	83	160–165°	−65.4°
3	65	4.96	66	162–165°	−64.4°
4	60	3.25	43	162–165°	−63.6°
5	55	2.94	39	163–165°	−62.9°

[a] Given as percent of maximal yield (7.5 mmoles).

REFERENCES

(1) R. Howe and R. G. Shanks, *Nature*, **210**, 1336 (1966). R. Howe and R. G. Shanks, British pat. 1,069,343/67 (1967).

(2) A. Breckenridge, H. Orme, H. Messeling, R. J. Lewis, and R. Gibbons, *Clin. Pharmacol. Ther.*, **15**, 424 (1974).

(3) J. L. Holtzman and J. A. Thompson, *Drug Metab. Dispos.*, **3**, 113 (1975).

(4) C. F. George, T. Fenyvesi, M. E. Conolly, and C. T. Dollery, *Eur. J. Clin. Pharmacol.*, **4**, 74 (1974).

(5) A. Stoll and A. Hofmann, *Helv. Chim. Acta*, **26**, 922 (1943).

ACKNOWLEDGMENTS

Supported by the General Medical Research Service of the Veterans Administration Hospital, Minneapolis, MN 55417.

[2] Supplied by Ayerst Laboratories.

Dissolution Rates of Doxycycline Free Base and Hydrochloride Salts

JOSEPH B. BOGARDUS ˣ **and ROBERT K. BLACKWOOD, Jr.**

Received November 7, 1978, from *Pharmaceutical Research and Development, Pfizer Central Research, Groton, CT 06340.* Accepted for publication February 26, 1979.

Abstract □ The dissolution rates of doxycycline monohydrate, hyclate, and hydrochloride dihydrate crystal forms were investigated using the static pellet method. Solubility product equilibria with chloride ion strongly suppressed the dissolution rate of the hydrochloride dihydrate salt. This form dissolved about fourfold slower in 0.1 *N* HCl than in water, which was consistent with its solubility in these media. Specificity for chloride was demonstrated by the rapid dissolution rate for the hydrochloride dihydrate in 0.1 *N* methanesulfonic acid. The dissolution rates of the hyclate, a solvated hydrochloride salt, and the free base were not sensitive to chloride ion. The results show that common ion equilibria with chloride can strongly reduce the dissolution rate of a thermodynamically stable hydrochloride salt form, while the free base or a metastable hydrochloride salt are not similarly affected.

Keyphrases □ Doxycycline—dissolution rates, free base and hydrochloride salts □ Dissolution rates—doxycycline free base and hydrochloride salts □ Antibacterials—doxycycline, dissolution rates of free base and hydrochloride salts

Aqueous solubilities of doxycycline monohydrate (Ia), hyclate (Ib), and hydrochloride dihydrate (Ic) crystal forms have been studied (1). Solubility product equilibria involving chloride ion and self-association were major factors affecting the aqueous solubility of the hydrochloride dihydrate salt (Ic). Common ion effects also influenced the solubilities and dissolution rates of the hydrochloride salts of chlortetracycline, demeclocycline, and methacycline (2). Evidence was presented for greater bioavailability from the chlortetracycline and methacycline free bases compared to the hydrochloride salts (3).

In contrast with other tetracyclines, several studies have found doxycycline to be well absorbed orally (4–8). In a crossover study, a suspension of Ia had a significantly more rapid absorption rate but equivalent area under the curve values compared to capsules and an oral solution containing Ib (4). Serum doxycycline levels were less affected by food than those of tetracycline or demeclocycline (5, 6).

The purposes of the present investigation were to examine factors affecting the intrinsic dissolution rate of doxycycline forms (Ia–Ic) in various media and to correlate these findings with previously reported solubility behavior (1).

EXPERIMENTAL

Materials—Compounds Ia and Ib were USP grade and were used as received[1]. Compound Ic was prepared as described previously (1) and ground in a mortar and pestle before compression. Buffer materials were reagent grade. Water was deionized and double distilled.

Dissolution Rate Determination—The static pellet method was used (9). Pellets were prepared by directly compressing 500 mg of powder in a 1.27-cm diameter die. A laboratory press[2] was used at 211 kg/cm² (3000 psi) for 20 sec. After the lower side was masked, the die with the pellet was positioned facing up in the bottom of a water-jacketed beaker containing 800 ml of dissolution medium at 25.0 ± 0.2°. The solution was stirred[3] by a paddle rotating at 50 rpm.

Samples were withdrawn at appropriate intervals and assayed spectrophotometrically[4] at 345 nm. Filtration was not necessary since significant pellet disintegration did not occur. The I concentration (free base equivalent) was determined from Beer's law plots prepared using Ib in the solvent of the dissolution experiment. The results are reported as the average of two or more runs.

RESULTS AND DISCUSSION

Dissolution curves for Ia–Ic under several conditions are shown in Figs. 1 and 2. Dissolution rate constants given in Table I were calculated as linear regression slopes. In several cases, the dissolution medium solubility is not meaningful since conversion to a more stable crystalline form occurred during the equilibration period. For example, solutions of the hyclate salt (Ib) in 0.1 *N* HCl will ultimately crystallize as the more stable hydrochloride salt form (Ic). Similarly, addition of sufficient Ic to pH 4.0 or 7.0 buffers results in its conversion to the less soluble free base (Ia), assuming sufficient buffer capacity. Thus, the original crystalline form, for which a solubility value was desired, does not exist at equilibrium.

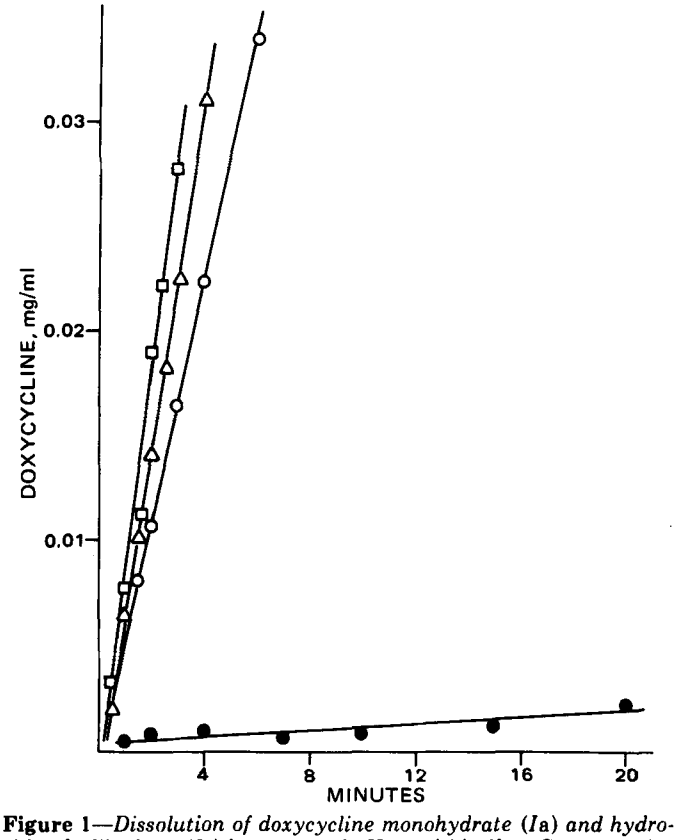

Figure 1—*Dissolution of doxycycline monohydrate (Ia) and hydrochloride dihydrate (Ic) in water and pH 4 and 7 buffers. Concentration is expressed as free base equivalent. Key: □, Ic in 0.1 M acetate buffer, pH 4.0; △, Ic in 0.1 M sodium phosphate buffer, pH 7.0; ○, Ic in water (pH 6.8–7.0 during run); and ●, Ia in 0.1 M acetate buffer, pH 4.0. Buffers did not contain chloride ion.*

[1] Pfizer Inc.
[2] Carver.
[3] Servodyne, Cole-Palmer.
[4] Model 240, Gilford.

0022-3549/79/0900-1183$01.00/0
© 1979, American Pharmaceutical Association

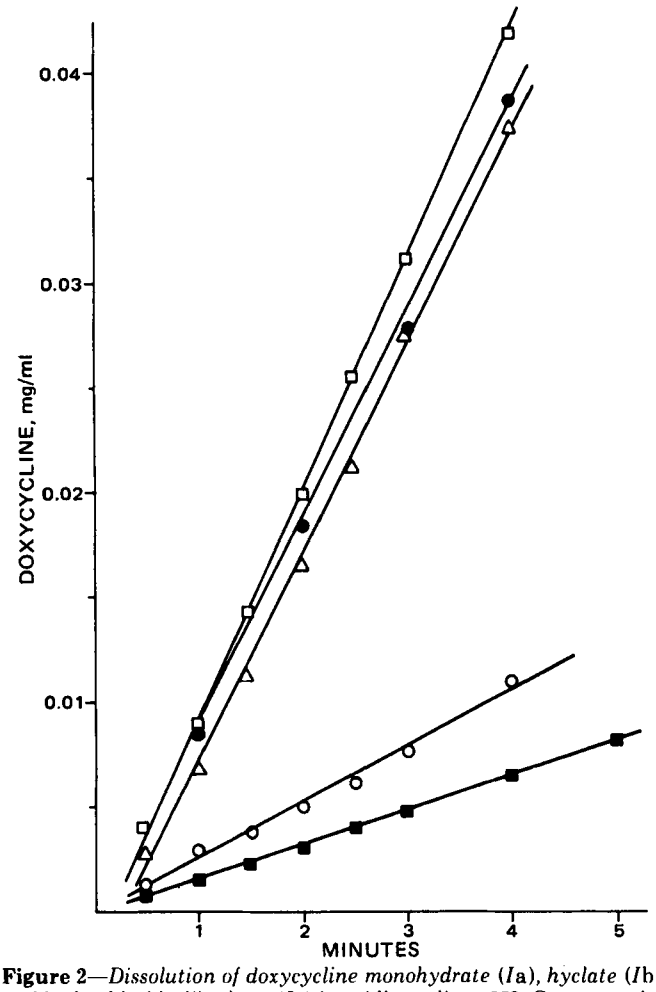

Figure 2—*Dissolution of doxycycline monohydrate (Ia), hyclate (Ib), and hydrochloride dihydrate (Ic) in acidic media at 25°. Concentration is expressed as free base equivalent. Key: □, Ib in 0.1 N HCl; ●, Ia in 0.1 N HCl; △, Ic in 0.1 N CH_3SO_3H; ○, Ic in 0.05 N HCl; and ■, Ic in 0.1 N HCl.*

Compound Ic dissolved rapidly in water and pH 4.0 and 7.0 buffers (Fig. 1), whereas Ia dissolved approximately 100-fold slower at pH 4. Precipitation of Ia could occur on the pellet surface during Ic dissolution in pH 4.0 or 7.0 buffers. A phenomenon of this type resulted in nonlinear dissolution rates for tolazamide sodium in phosphate buffers due to apparent surface conversion to the acid form (10). The good linearity and rapid dissolution rates in Fig. 1 indicate that significant conversion to Ia did not occur during dissolution of Ic.

The dissolution rate order of Ic > Ia applicable to neutral pH values was reversed in dilute hydrochloric acid (Fig. 2). The common ion effect of chloride inhibited dissolution of the thermodynamically stable form (Ic). In 0.1 *N* HCl, Ic dissolved four- to sixfold slower than in water and pH 4 or 7 buffers. Reduction of hydrochloric acid from 0.1 to 0.05 *N* caused a 70% increase in the dissolution rate. The expected chloride-ion specificity was confirmed by measurement of the dissolution rate of Ic in 0.1 *N* CH_3SO_3H. In this medium of similar acidity but without chloride, the Ic dissolution rate was equivalent to that found for Ia or Ib in 0.1 *N* HCl. The solubility product equilibrium of Ic with chloride ion was reported with a K^0_{sp} value of $1.8 \times 10^{-3}\ M^2$ (1). Compound Ic was about fivefold less soluble in 0.1 *N* HCl than in water, consistent with the dissolution rate data.

The dissolution rates of Ia and Ib in hydrochloric acid were apparently insensitive to chloride ion, indicating that conversion to Ic did not occur on the pellet surface. Doxycycline solubility is complicated by self-association in relatively concentrated solutions to form a dimer and higher order forms (1). Therefore, self-association in the diffusion layer probably prevents Ic crystallization during the dissolution experiments.

When an acid–base reaction occurs between buffer species and the dissolving substance, dissolution rates cannot be compared with solubilities. A study of the benzoic acid dissolution rate in basic and buffered media showed that the dissolution rate was dependent on the strength, diffusivity, and concentration of the basic-buffer species (11). Examples of similar dissolution behavior from the present data are Ia in 0.1 *N* HCl, Ic in pH 4.0 buffer, and Ic in pH 7.0 buffer. The rapid dissolution of Ia in 0.1 *N* HCl compared to pH 4.0 buffer is analogous to the acid–buffer interaction already discussed. The hydrochloric acid strength and diffusivity are largely responsible for the rapid dissolution of poorly water-soluble Ia (11, 12). The more rapid dissolution rate for Ic in pH 4.0 and 7.0 buffers compared to water is due to the rate-increasing effects of the basic buffer components.

Table I—Dissolution Rates and Solubilities of Doxycycline Forms at 25°

Doxycycline Form	Medium	Dissolution Rate, mg/(min cm²)	Equilibrium Solubility, mg/ml
Ia	0.1 *N* HCl	6.3	—[a]
Ib	0.1 *N* HCl	6.9	—[a]
Ic	0.1 *N* HCl	1.0	9.9[b]
Ic	0.05 *N* HCl	1.7	23.5[b]
Ic	0.1 *N* CH_3SO_3H	6.3	—
Ic	pH 4.0 buffer	6.3	—[a]
Ic	pH 7.0 buffer	5.0	—[a]
Ic	Water (pH 6.8–7.0)	3.8	50[b]
Ia	pH 4.0 buffer	0.05	0.75[b]

[a] No value is given since the solubility of the stated crystalline form is not measurable in this medium. Conversion to a thermodynamically more stable form occurs. [b] Reference 1.

The hyclate salt (Ib) is a solvated hydrochloride containing 0.5 mole each of ethanol and water. Without consideration of common ion effects, the intrinsic dissolution rate of this metastable salt form should be greater than that of the stable form (Ic) due to its higher thermodynamic activity (13). In the present system, Ib had the significant advantage of not taking part in a common ion equilibrium with chloride ion. This difference may be important in oral dosage forms due to the high chloride level in human gastric juice, 0.07–0.16 *M* (14). This amount of chloride is sufficient to alter markedly the dissolution properties of Ic but not of Ia or Ib. Under identical conditions of pH and chloride concentration, Ia–Ic all must yield the same equilibrium solubility in dilute hydrochloric acid, *i.e.*, that of the thermodynamically stable form (Ic).

The results of this study indicate that solubility product equilibria can be a major factor affecting dissolution of hydrochloride salts in chloride-containing media. In such cases, selection of an alternative salt form or "less soluble" free base may improve dissolution and bioavailability.

REFERENCES

(1) J. B. Bogardus and R. K. Blackwood, Jr., *J. Pharm. Sci.*, **68**, 188 (1979).

(2) S. Miyazaki, M. Nakano, and T. Arita, *Chem. Pharm. Bull.*, **23**, 1197 (1975).

(3) *Ibid.*, **23**, 2151 (1975).

(4) E. J. Antal, J. M. Jaffe, R. I. Poust, and J. L. Colaizzi, *J. Pharm. Sci.*, **64**, 2015 (1975).

(5) P. G. Welling, P. A. Koch, C. C. Lau, and W. A. Craig, *Antimicrob. Agents Chemother.*, **11**, 462 (1977).

(6) J. E. Rosenblatt, J. E. Barrett, J. L. Brodie, and W. M. M. Kirby, *ibid.*, **1966**, 134.

(7) J. D. Arcilla, J. L. Fiore, Jr., O. Resnick, J. W. Nadelmann, J. L. Huth, and W. M. Troetal, *Curr. Ther. Res.*, **16**, 1126 (1974).

(8) M. Schach von Wittenau, *Int. Z. Klin. Pharmakol. Ther. Toxikol.*, **2**, 52 (1969).

(9) W. I. Higuchi, S. Prakongpan, and F. Young, *J. Pharm. Sci.*, **62**, 945 (1973).

(10) W. I. Higuchi, N. A. Mir, A. P. Parker, and W. E. Hamlin, *ibid.*, **54**, 8 (1965).

(11) W. I. Higuchi, E. L. Parrott, D. E. Wurster, and T. Higuchi, *J. Am. Pharm. Assoc., Sci. Ed.*, **47**, 376 (1958).

(12) W. E. Hamlin and W. I. Higuchi, *J. Pharm. Sci.*, **55**, 205 (1966).

(13) E. Shefter and T. Higuchi, *ibid.*, **52**, 781 (1963).

(14) "Scientific Tables", 7th ed., K. Diem and C. Lentner, Eds., Ciba-Geigy, Basel, Switzerland, 1970, p. 649.

ACKNOWLEDGMENTS

R. K. Blackwood, Jr., was a National Pharmaceutical Council Summer Pharmacy Intern, 1977.

High-Performance Liquid Chromatography of Benzodiazepines I: Stability-Indicating Assay of Diazepam Tablets

MARGARET EMERY ˣ **and JUNE KOWTKO**

Received January 17, 1979, from the *Quality Control Department, Hoffmann-La Roche Inc., Nutley, NJ 07110.* Accepted for publication March 20, 1979.

Abstract □ A high-performance liquid chromatographic procedure was developed for diazepam tablet analysis. This procedure separates the manufacturing intermediate, 7-chloro-1,3-dihydro-5-phenyl-2*H*-1,4-benzodiazepin-2-one, and the decomposition products, 3-amino-6-chloro-1-methyl-4-phenylcarbostyril and 2-methylamino-5-chlorobenzophenone, from diazepam. The liquid chromatographic procedure is superior to the USP UV assay because it is stability indicating. The method is simple, accurate, and fast, involving only one extraction step. A reversed-phase column and a methanol–water mobile phase were used. Under these conditions, 0.1% of the decomposition products was detectable. Typical samples of diazepam tablets showed no degradation.

Keyphrases □ Diazepam—analysis, high-performance liquid chromatography, stability, tablets □ High-performance liquid chromatography—analysis, diazepam tablets, stability indicating □ Sedatives—diazepam, high-performance liquid chromatographic analysis, tablets, stability indicating

1,4-Benzodiazepines are widely used as tranquilizers and muscle relaxants, and this wide use has prompted extensive literature on the analysis of these compounds. Diazepam[1] (I) is no exception. Most of the published literature on the use of high-performance liquid chromatography (HPLC) for I analysis describes methods for the quantitation and identification of I and its metabolites in biological samples for both pharmacological and clinical applications (1–5). Several liquid chromatographic separations of a benzodiazepine series including I (6–8) and of I from drugs of abuse (9, 10) have been reported. Liquid chromatography has also been used to quantitate I as a ketazolam decomposition product (11).

The current compendial (12) procedure for I analysis in tablets is a spectrophotometric method. In this procedure, the tablet mass is extracted three times with chloroform. The extracts are combined, brought to volume, and washed with a borate buffer solution. The chloroform layer is passed through anhydrous sodium sulfate; an aliquot is taken, evaporated to dryness, and dissolved in acidic alcohol. The absorbance of this solution is measured and compared to that of a USP standard.

This report describes the development of an HPLC procedure for the analysis of I in tablets. The liquid chromatographic procedure separates I from its manufacturing precursor, 7-chloro-1,3-dihydro-5-phenyl-2*H*-1,4-benzodiazepin-2-one (II), and the decomposition products 3-amino-6-chloro-1-methyl-4-phenylcarbostyril (III) and 2-methylamino-5-chlorobenzophenone (IV) and is both specific and stability indicating.

The sample workup is minimal, involving the addition of an internal standard to the weighed tablet mass, extraction of the active compound into methanol, and injection into the liquid chromatograph.

Table I—Retention Volume (Milliliters)

Compound	Water–Methanol 350:650	Water–Methanol 400:600	Water–Acetonitrile 350:650	Water–Acetonitrile 400:600	Water with 0.1% NH_4CO_3–Methanol, 300:700
I	8.3	11.7	5.7	6.6	8.3
II	7.4	9.8	4.8	5.3	7.3
III	14.8	23.3	7.6	9.1	13.6
IV	19.1	31.3	9.6	12.4	14.6

EXPERIMENTAL

Instrumental Conditions—A high-performance liquid chromatograph equipped with a 254-nm UV detector[2] and a reversed-phase C_{18} column[3] was used. Three-microliter injections were made with a 5-μl high-pressure syringe[4]. The flow rate was set at 0.5–0.6 ml/min, which

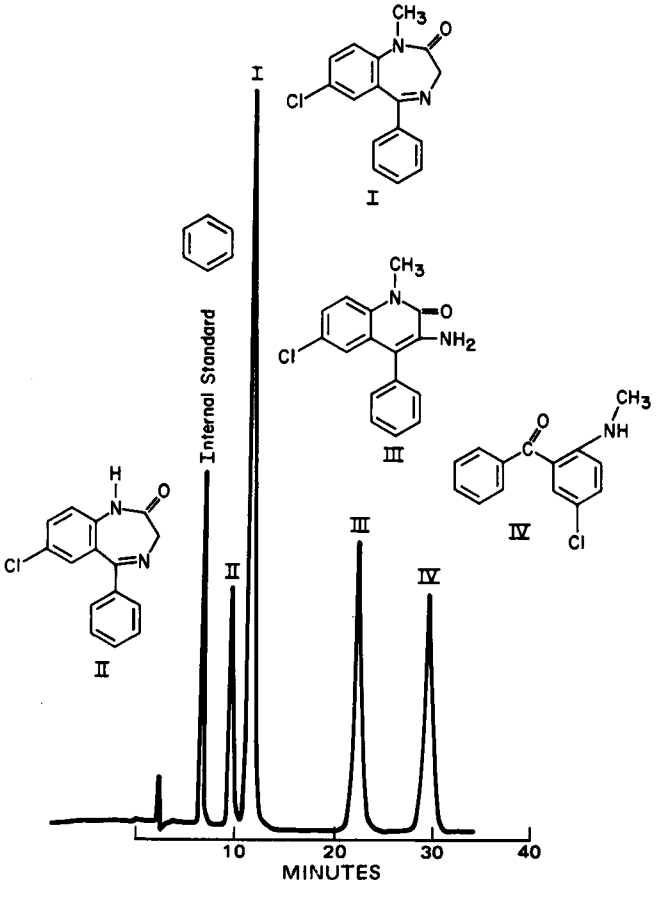

Figure 1—*Chromatogram of a synthetic mixture of the internal standard and I–IV.*

[1] Valium, Hoffmann-La Roche Inc.

[2] Model 830, du Pont Instrument Co., Wilmington, Del.
[3] μBondapak C_{18}, Waters Associates, Milford, Mass.
[4] Model HP305N, Hamilton Co., Reno, Nev.

0022-3549/79/0900-1185$01.00/0
© 1979, American Pharmaceutical Association

Table II—Second-Day Reproducibility Data

	2-mg Tablets		5-mg Tablets		10-mg Tablets	
	Day 1, mg/ tablet	Day 2, mg/ tablet	Day 1, mg/ tablet	Day 2, mg/ tablet	Day 1, mg/ tablet	Day 2, mg/ tablet
Mean	2.01	2.02	4.97	4.99	10.01	10.08
SD	0.02	0.03	0.05	0.04	0.03	0.1
CV, %	1.3	1.3	0.9	0.7	0.3	1.0
USP	2.00		4.95		10.1	

required pressures of 600–1000 psi, depending on the age of the column. The column was at ambient temperature, the electrometer setting was 8, and the recorder chart speed was 3.9 min/cm. Quantitation was by peak height measurement.

Mobile Phase—Various mixtures of water and methanol or water and acetonitrile were tried to optimize the separation. The quantitative results were obtained with a 65:35 methanol–water mobile phase.

Internal Standard—The internal standard stock solution was prepared by pipetting 25 ml of benzene into a 1000-ml volumetric flask and bringing to volume with methanol.

Standard Diazepam Solutions—The standard stock solution was prepared by accurately weighing ~100 mg of I into a 100-ml volumetric flask and diluting to volume with methanol. The standard for the 2-mg diazepam tablet was made by pipetting 2 ml of the standard stock solution and 2 ml of the internal standard solution into a 10-ml volumetric flask and diluting to volume with methanol. The standard solution for the 5-mg diazepam tablets was prepared by pipetting 5 ml of the standard stock solution and 5 ml of the internal standard solution into a 25-ml volumetric flask and diluting to volume with methanol. For the standard solution for the 10-mg diazepam tablets, 10 ml of the standard stock solution and 10 ml of the internal standard solution were pipetted into a 50-ml volumetric flask and diluted with methanol to volume.

Preparation of Sample Solutions of Diazepam Tablets—*2-mg Tablets*—Approximately 170 mg of ground tablet mass was weighed accurately into a 10-ml volumetric flask, and 2 ml of internal standard solution was added. The flask was half filled with methanol and shaken for 0.5 hr on a wrist-action shaker. The contents were brought to volume with methanol, shaken, transferred to a plastic syringe, and filtered without vacuum through a 0.6-μm polyvinyl chloride filter[5].

5-mg Tablets—Approximately 170 mg of ground tablet mass was weighed accurately into a 25-ml volumetric flask, 5 ml of internal standard solution was added, and the procedure for the 2-mg tablets was followed.

10-mg Tablets—Approximately 170 mg of ground tablet mass was weighed accurately into a 50-ml volumetric flask, 10 ml of internal standard solution was added, and the procedure for the 2-mg tablets was followed.

RESULTS AND DISCUSSION

Several mobile phases can be employed to obtain the desired separation. Mixtures of water–acetonitrile, water–methanol, and methanol–water with 0.1% ammonium carbonate were tried. Table I gives the retention volumes of the four experimental compounds with the different mobile phases.

A 350:650 mixture of water–methanol was chosen because the analysis time was reasonable and the solvents are readily available. The preliminary work was done with a mobile phase of water with 0.1% ammonium carbonate and methanol. However, since it was thought that the ammonium carbonate might contribute to column deterioration and since the ammonium carbonate was not necessary, a change was made to water–methanol.

Figure 1 shows the separation of a synthetic mixture of benzene, II, I, III, and IV. Benzene is used as the internal standard for the quantitative work, II is the manufacturing intermediate, and III and IV are the I decomposition products.

Quantitative Determination of Diazepam—All variables in the quantitative procedure were validated to ensure that errors could not be introduced inadvertently. The linearity of peak height ratios of I *versus* two possible internal standards, benzene and *p*-xylene, was verified over the range of possible concentrations of I. Benzene was the internal standard used for the quantitative work. However, *p*-xylene elutes just after I and before II and is an alternative.

[5] Type BD filter, Millipore Corp., Bedford, Mass.

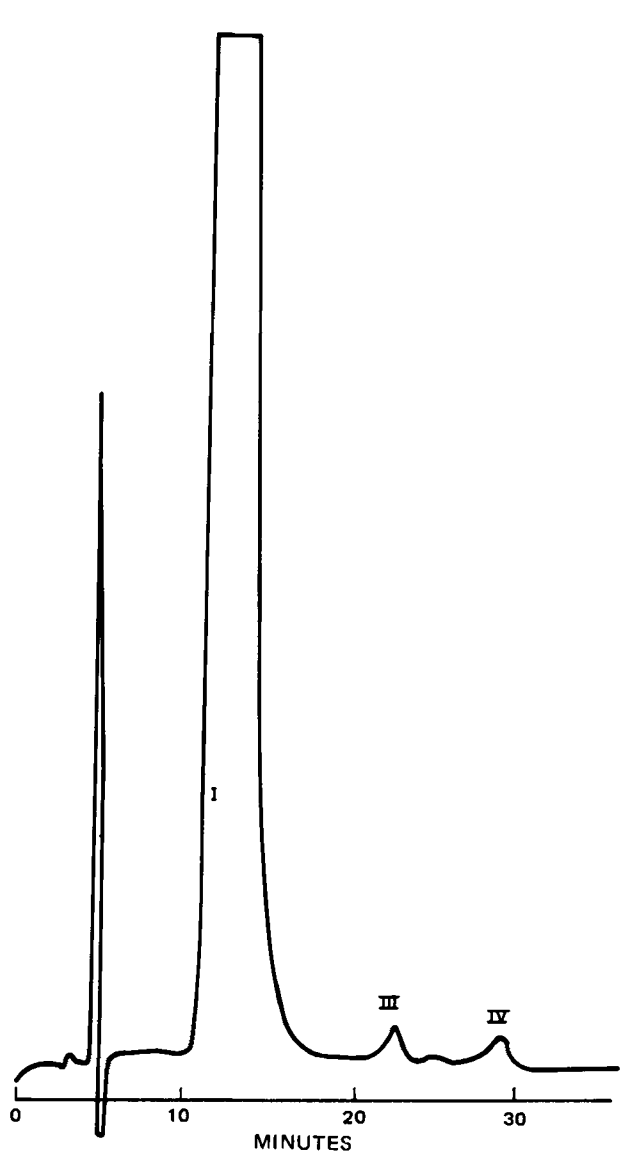

Figure 2—*Chromatogram of a synthetic mixture representing 0.1% decomposition of I to III and IV.*

The linear relationship of the amount of I *versus* sample weight was verified also. These measurements, made in triplicate, show that the method is valid for a large range of sample sizes.

The required extraction time was determined also. Samples of 2-mg tablets were analyzed in triplicate using 10, 20, 30, and 40 min on the shaker. There was no difference within the experimental error for samples shaken for different times. This finding indicates that the timing of the shaking is not critical. The results of a 2-day reproducibility study for each strength tablet as well as the USP spectrophotometric method are given in Table II. The mean value is for 10 samples.

Determination of Degradation Products—A synthetic mixture of I, III, and IV representing the analysis of a diazepam tablet with 0.1% decomposition is shown in Fig. 2. This figure indicates that if the decomposition products were present, the limit of detection would be 0.1%. However, expired manufactured lots of diazepam tablets were analyzed and no decomposition was detected.

REFERENCES

(1) A. Bugge, *J. Chromatogr.*, **128**, 111 (1976).

(2) M. D. Osselton, M. D. Hammond, and P. J. Twitchett, *J. Chromatogr. Pharmacol.*, **29**, 460 (1977).

(3) P. M. Kabra, G. L. Stevens, and L. J. Marton, *J. Chromatogr.*, **150**, 355 (1978).

(4) R. R. Brodie, L. F. Chasseaud, and T. Taylor, *ibid.*, **150**, 361 (1978).

(5) R. J. Perchalski and B. J. Wilder, *Anal. Chem.*, **50**, 554 (1978).
(6) C. G. Scott and P. Bommer, *J. Chromatogr. Sci.*, **8**, 446 (1970).
(7) D. H. Rogers, *ibid.*, **12**, 742 (1974).
(8) K. Macek and V. Rehak, *J. Chromatogr.*, **105**, 182 (1975).
(9) M. L. Chan, C. Whetsell, and J. D. McChesney, *J. Chromatogr. Sci.*, **12**, 512 (1974).
(10) I. Jane, *J. Chromatogr.*, **111**, 227 (1975).
(11) D. J. Weber, *J. Pharm. Sci.*, **61**, 1797 (1972).
(12) "The United States Pharmacopeia," 19th rev., Mack Publishing Co., Easton, Pa., 1975.

ACKNOWLEDGMENTS

Presented in part at the Pharmaceutical Analysis and Control Section, APhA Academy of Pharmaceutical Sciences, Orlando meeting, November 1976.

The authors thank Dr. S. A. Moros for many helpful discussions.

Quantitative Flash-Methylation Analysis of Phenobarbital

KOUICHI KURATA ˣ, MASASHI TAKEUCHI, and KEIKO YOSHIDA

Received October 18, 1978, from the *Department of Neuropsychiatry, School of Medicine, Kanazawa University, 13-1 Takara-Machi, Kanazawa 920, Japan.* Accepted for publication February 26, 1979.

Abstract □ In phenobarbital measurement by GLC with the flash-methylation technique, using trimethylanilinium hydroxide as a methylating reagent, a small amount of water decomposed phenobarbital and interfered with the quantitative analysis. Thus, both the sample and the methylating reagent must be sufficiently dehydrated to attain quantitative analyses. The hydrolysis decomposition product of phenobarbital was *N*-methyl-2-phenylbutyramide, as shown by its mass spectrum. The sum of methylated phenobarbital and *N*-methyl-2-phenylbutyramide (if observed in the spectrum) can be used for an accurate phenobarbital assay in the present flash-methylation technique.

Keyphrases □ Phenobarbital—analysis, flash-methylation GLC, degradates □ GLC, flash methylation—analysis, phenobarbital in biological fluids, degradates □ Mass spectrometry—analysis, phenobarbital in biological fluids, degradates

GLC determination of anticonvulsant drugs in biological fluids has been widely adopted in clinical laboratories. Phenytoin and phenobarbital have usually been assayed with the flash-methylation technique, using trimethylanilinium hydroxide as a methylating reagent. Some authors (1, 2) described the common errors in the assay of phenobarbital due to its decomposition by hydrolysis, and the GLC peak derived from the decomposition product has been called "early phenobarbital" (3); its structure has been speculated to be *N*-methyl-2-phenylbutyramide (III) (4, 5).

In the present work, the authors identified the decomposition product as III by mass spectrometry and found that its formation was due to the basic phenobarbital hydrolysis caused in pretreating the sample with basic methylation reagent and the subsequent methylation of the resulting 2-phenylbutyramide (I) in the GLC unit. Several problems in the assay of the anticonvulsant drugs by flash methylation are discussed here also.

EXPERIMENTAL

Methylation—Various concentrations of trimethylanilinium hydroxide in methanol were prepared as described previously (6) and stored at 4°. A 10-μg sample of phenobarbital was dissolved in 30 μl of trimethylanilinium hydroxide–methanol solution (the reagent must be used within 2 weeks of preparation), and the mixture was kept standing for 5 min. Each 3-μl sample obtained was then subjected to GLC.

GLC—The gas–liquid chromatograph[1] was equipped with a dual flame-ionization detector and columns for linear temperature programming. The glass columns, 200 cm long × 4.0 mm i.d., were packed with an equal amount of either 1.5% QF-1 on 60–80-mesh Chromosorb W or 3% OV-17 on 80–100-mesh Shimalite[2]. The analysis was performed under the following conditions for 1.5% QF-1: injection temperature, 245°; detector temperature, 245°; and column temperature, initial 150° and programmed to 215° at 6°/min. For 3% OV-17, the injection temperature

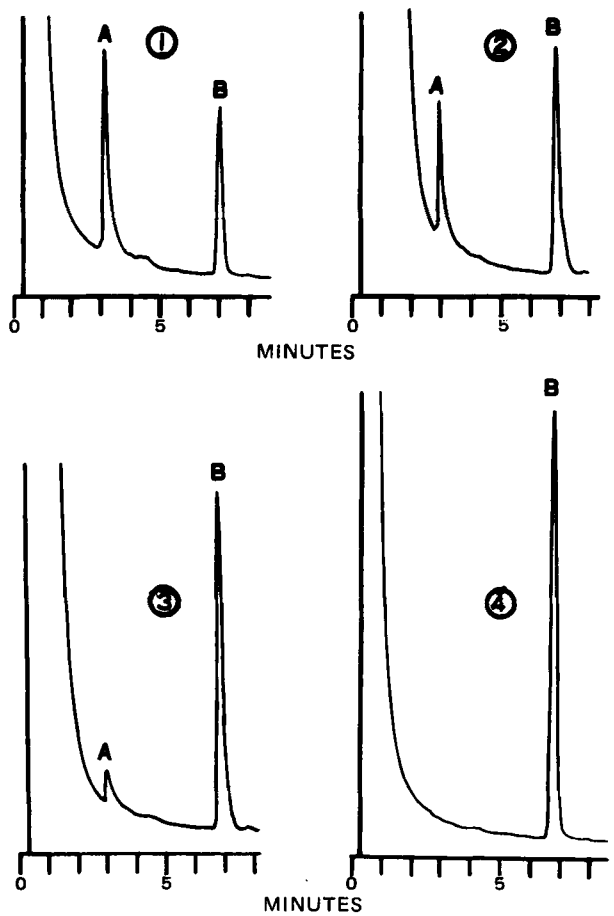

Figure 1—*Gas chromatograms of phenobarbital treated with various trimethylanilinium hydroxide concentrations. Phenobarbital was analyzed with 1.5% QF-1 in 0.20 (①), 0.10 (②), 0.05 (③), and 0.025 (④) M trimethylanilinium hydroxide solution. A 10-μg sample of phenobarbital was dissolved in 30 μl of trimethylanilinium hydroxide solution; after 5 min, a 3-μl sample was injected into the chromatograph.*

[1] Shimadzu GC-4CMPF, Shimadzu Ltd., Japan.

[2] Wako Chemical Industries Ltd., Japan.

0022-3549/79/0900-1187$01.00/0
© 1979, American Pharmaceutical Association

(5) R. J. Perchalski and B. J. Wilder, *Anal. Chem.*, **50**, 554 (1978).
(6) C. G. Scott and P. Bommer, *J. Chromatogr. Sci.*, **8**, 446 (1970).
(7) D. H. Rogers, *ibid.*, **12**, 742 (1974).
(8) K. Macek and V. Rehak, *J. Chromatogr.*, **105**, 182 (1975).
(9) M. L. Chan, C. Whetsell, and J. D. McChesney, *J. Chromatogr. Sci.*, **12**, 512 (1974).
(10) I. Jane, *J. Chromatogr.*, **111**, 227 (1975).
(11) D. J. Weber, *J. Pharm. Sci.*, **61**, 1797 (1972).
(12) "The United States Pharmacopeia," 19th rev., Mack Publishing Co., Easton, Pa., 1975.

ACKNOWLEDGMENTS

Presented in part at the Pharmaceutical Analysis and Control Section, APhA Academy of Pharmaceutical Sciences, Orlando meeting, November 1976.

The authors thank Dr. S. A. Moros for many helpful discussions.

Quantitative Flash-Methylation Analysis of Phenobarbital

KOUICHI KURATA ˣ, MASASHI TAKEUCHI, and KEIKO YOSHIDA

Received October 18, 1978, from the *Department of Neuropsychiatry, School of Medicine, Kanazawa University, 13-1 Takara-Machi, Kanazawa 920, Japan.* Accepted for publication February 26, 1979.

Abstract □ In phenobarbital measurement by GLC with the flash-methylation technique, using trimethylanilinium hydroxide as a methylating reagent, a small amount of water decomposed phenobarbital and interfered with the quantitative analysis. Thus, both the sample and the methylating reagent must be sufficiently dehydrated to attain quantitative analyses. The hydrolysis decomposition product of phenobarbital was *N*-methyl-2-phenylbutyramide, as shown by its mass spectrum. The sum of methylated phenobarbital and *N*-methyl-2-phenylbutyramide (if observed in the spectrum) can be used for an accurate phenobarbital assay in the present flash-methylation technique.

Keyphrases □ Phenobarbital—analysis, flash-methylation GLC, degradates □ GLC, flash methylation—analysis, phenobarbital in biological fluids, degradates □ Mass spectrometry—analysis, phenobarbital in biological fluids, degradates

GLC determination of anticonvulsant drugs in biological fluids has been widely adopted in clinical laboratories. Phenytoin and phenobarbital have usually been assayed with the flash-methylation technique, using trimethylanilinium hydroxide as a methylating reagent. Some authors (1, 2) described the common errors in the assay of phenobarbital due to its decomposition by hydrolysis, and the GLC peak derived from the decomposition product has been called "early phenobarbital" (3); its structure has been speculated to be *N*-methyl-2-phenylbutyramide (III) (4, 5).

In the present work, the authors identified the decomposition product as III by mass spectrometry and found that its formation was due to the basic phenobarbital hydrolysis caused in pretreating the sample with basic methylation reagent and the subsequent methylation of the resulting 2-phenylbutyramide (I) in the GLC unit. Several problems in the assay of the anticonvulsant drugs by flash methylation are discussed here also.

EXPERIMENTAL

Methylation—Various concentrations of trimethylanilinium hydroxide in methanol were prepared as described previously (6) and stored at 4°. A 10-μg sample of phenobarbital was dissolved in 30 μl of trimethylanilinium hydroxide–methanol solution (the reagent must be used within 2 weeks of preparation), and the mixture was kept standing for 5 min. Each 3-μl sample obtained was then subjected to GLC.

GLC—The gas–liquid chromatograph[1] was equipped with a dual flame-ionization detector and columns for linear temperature programming. The glass columns, 200 cm long × 4.0 mm i.d., were packed with an equal amount of either 1.5% QF-1 on 60–80-mesh Chromosorb W or 3% OV-17 on 80–100-mesh Shimalite[2]. The analysis was performed under the following conditions for 1.5% QF-1: injection temperature, 245°; detector temperature, 245°; and column temperature, initial 150° and programmed to 215° at 6°/min. For 3% OV-17, the injection temperature

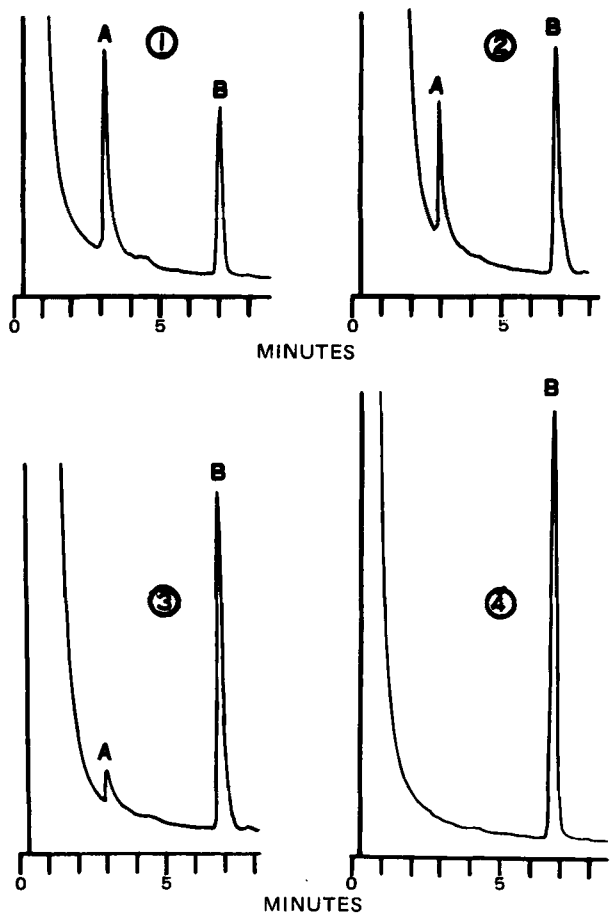

Figure 1—*Gas chromatograms of phenobarbital treated with various trimethylanilinium hydroxide concentrations. Phenobarbital was analyzed with 1.5% QF-1 in 0.20 (①), 0.10 (②), 0.05 (③), and 0.025 (④) M trimethylanilinium hydroxide solution. A 10-μg sample of phenobarbital was dissolved in 30 μl of trimethylanilinium hydroxide solution; after 5 min, a 3-μl sample was injected into the chromatograph.*

[1] Shimadzu GC-4CMPF, Shimadzu Ltd., Japan.

[2] Wako Chemical Industries Ltd., Japan.

0022-3549/79/0900-1187$01.00/0
© 1979, American Pharmaceutical Association

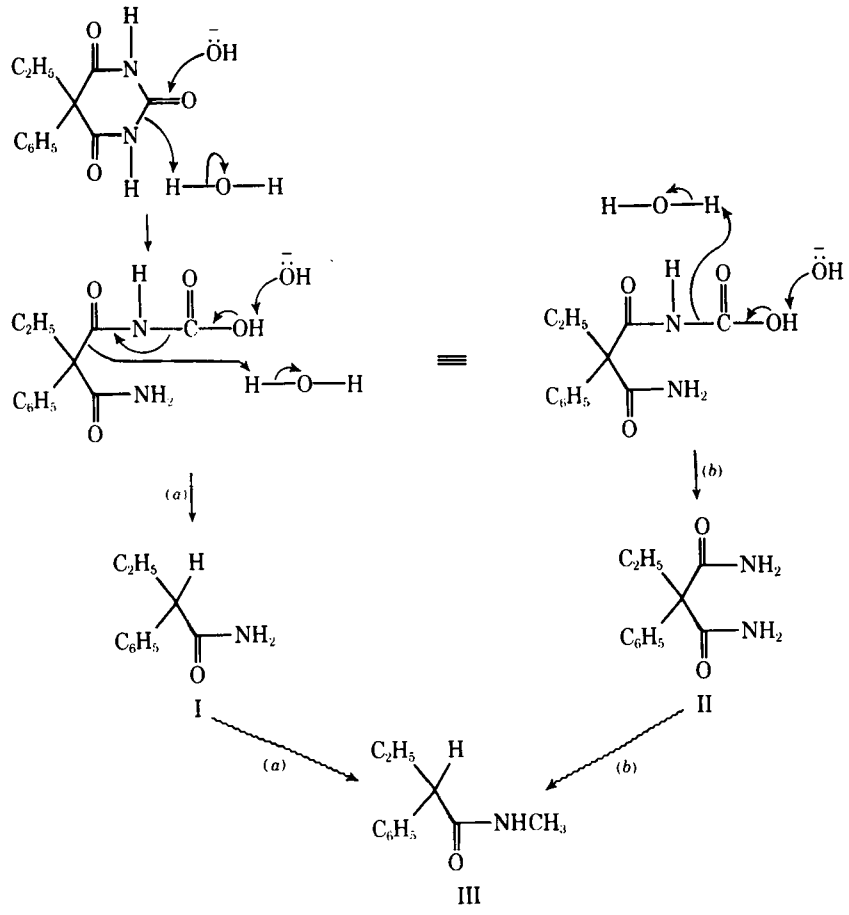

Scheme I—Mechanistic consideration through which N-*methyl-2-phenylbutyramide (III) should be derived from phenobarbital by basic hydrolysis and methylation. The hydrolyzed product should be considered as 2-phenylbutyramide [path* a *(I)] or 2-ethyl-2-phenylmalondiamide [path* b *(II)].*

was 300°, the detector temperature was 300°, and the column temperature was 150–275°, programmed to rise at 10°/min. The gas flows were: hydrogen, 50 ml/min; air, 800 ml/min; and nitrogen (as a carrier), 50 ml/min.

Mass Spectrometry—For detailed analysis of each methylation product, a GLC mass spectrometer[3] was used with the flash heater temperature at 245°. The glass column, 200 cm × 4.0 mm, was packed with 1.5% QF-1. The column temperature was 130–190°, programmed to rise at 5°/min. Helium flow was 27 ml/min. For the mass fragmentometry, a total ion detector was used. The ionization voltage was 70 ev.

RESULTS

Figure 1 shows the chromatograms analyzed with 1.5% QF-1 resulting from phenobarbital methylation using various concentrations of trimethylanilinium hydroxide. At low trimethylanilinium concentrations, only the B peak was observed; at higher concentrations, the A peak appeared and the B peak decreased. In the analysis using the two columns (1.5% QF-1 and 3% OV-17), two peaks were generally observed. The A peak was the one previously called "early phenobarbital." The sum of the A and B amplitudes was almost constant (Fig. 1) in each analysis.

The influence of water on the methylation was investigated. In Fig. 2, Chart 1 corresponds to the chromatogram of phenobarbital treated with 30 μl of 0.10 *M* trimethylanilinium hydroxide dehydrated with anhydrous sodium sulfate; Chart 2 shows the chromatogram resulting from the methylation of phenobarbital treated with 30 μl of trimethylanilinium hydroxide containing 3 μl of water. The A′ and B′ peaks showed the same retention times as A and B (Fig. 1) under identical GLC and, therefore, were identified with A and B. Only the B′ peak is observed in Chart 1, while two peaks, A′ and B′, appeared in Chart 2. This result suggests clearly that phenobarbital was decomposed through the hydrolysis in the latter case (Chart 2). However, as already described, the sum of the amplitudes of the A′ and B′ peaks is almost the same in Charts 1 and 2.

Both A and B peaks were characterized by GLC–mass spectrometry. Each molecular weight of the compounds corresponding to the A and B peaks indicated *m/e* 177 and 260. The B peak was identified as methylated phenobarbital by comparison with the mass spectrum of the authentic sample The structure of the A peak was determined as *N*-methyl-2-phenylbutyramide by reasonable fragmentation of its spectrum, and this conclusion was supported by the mechanism of its formation from phenobarbital under the basic condition (*vide infra*).

DISCUSSION

The simultaneous measurement of many anticonvulsant drugs by GLC has been adopted in many clinical laboratories. Drugs such as phenytoin and phenobarbital usually have been measured with the flash methylation technique. However, in the measurement of phenobarbital with this technique, some authors (1, 2, 7) have suggested that phenobarbital has not quantitatively changed into its methylated derivatives and have demonstrated that the longer the time spent in the pretreatment stage (before injection), the more phenobarbital decomposed (2). In accordance with this conclusion, it was demonstrated (Fig. 2) that a small amount of water contaminant decomposed phenobarbital. Hence, the decomposition (Fig. 1) might reasonably be caused by moisture contaminating the trimethylanilinium hydroxide solution.

The more trimethylanilinium hydroxide used, the more phenobarbital was decomposed. Hence, it is very important that the sample and trimethylanilinium hydroxide solution should be sufficiently dehydrated for quantitative phenobarbital analysis. However, moisture, which inevitably contaminates during operation, sufficiently decomposes phenobarbital at high trimethylanilinium hydroxide concentrations. Therefore, it is desirable that phenobarbital might be treated with a low trimethylanilinium hydroxide concentration (*e.g.*, 0.025 *M*). However,

[3] Shimadzu GCMS-7000, Shimadzu Ltd., Japan.

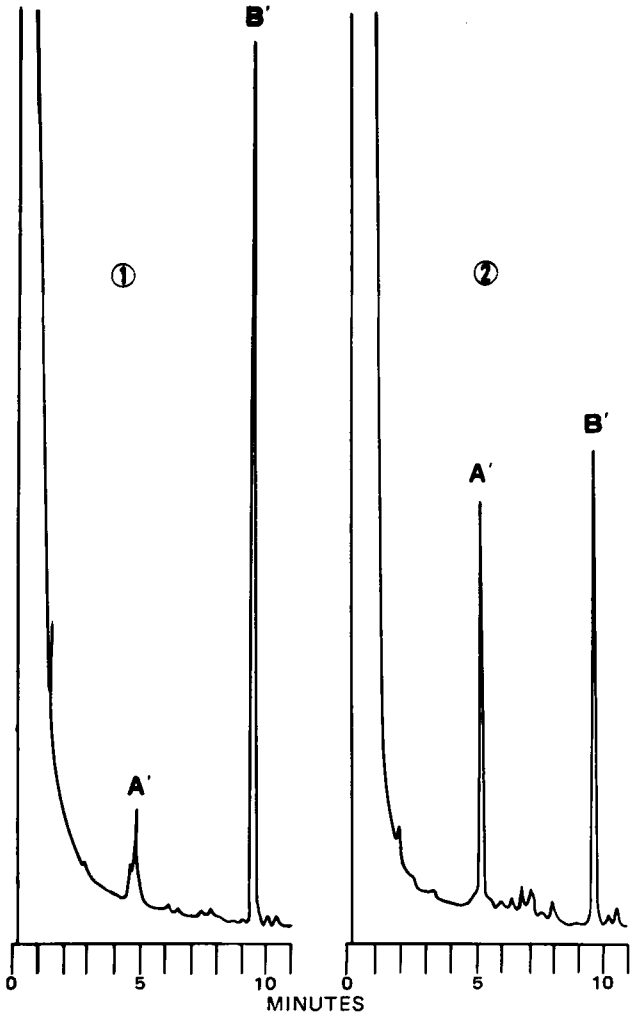

Figure 2—*Gas chromatograms of phenobarbital treated with dehydrated (Chart 1) and watered (Chart 2) trimethylanilinium hydroxide solution, analyzed with 3% OV-17. A 10-μg sample of phenobarbital was treated with 30 μl of 0.10* M *trimethylanilinium hydroxide solution dehydrated by anhydrous sodium sulfate (Chart 1) and by 0.10* M *trimethylanilinium hydroxide containing 3 μl of water (Chart 2).*

phenytoin sometimes was insufficiently methylated in 0.025 *M* because of contamination from biological fluids.

In the simultaneous measurement of phenytoin and phenobarbital, a higher concentration (0.10–0.20 *M*) of trimethylanilinium hydroxide is required for sufficient methylation. In this case, phenobarbital is frequently decomposed even if these precautions are taken. Therefore, for the quantitative analysis, operators must first check whether the A peak is present in the spectrum. When the A peak is observed, the sum of the A′ and B′ peaks should be considered as being formed from phenobarbital. Even if phenobarbital is decomposed, a peak height ratio of the sum of these two peaks to cholestane (as an internal standard) gives the accurate assay of phenobarbital.

The A peak was analyzed by GLC–mass spectrometry and showed its molecular ion at *m/e* 177, together with fragment ions at 149 ($M^+ - C_2H_4$), 120 ($C_6H_5CH_2CHO$), 91 ($C_6H_5 - CH_2^+$), and 58 ($CONHCH_3^+$). Careful mass spectrogram analysis and mechanistic considerations of its fragmentation pattern suggested this product to be *N*-methyl-2-phenylbutyramide (4, 5). Scheme I shows the reasonable mechanism of its formation from phenobarbital. Thus, phenobarbital should be first decomposed to 2-phenylbutyramide (I) through basic hydrolysis, and then this hydrolyzed product should be changed into *N*-methyl-2-phenylbutyramide (III) on column methylation (Scheme I, path *a*). Such analysis does not exclude the possibility that the A peak is *N*-formyl-*N*-methylphenylacetamide. However, from the mechanistic viewpoint, this species can be ruled out because its formation is not expected from phenobarbital by basic hydrolysis.

An alternative path of III formation also is possible (Scheme I, path *b*). Some authors (2, 8) proposed that a possible phenobarbital degradation product in alkaline solution was 2-ethyl-2-phenylmalondiamide (II). However, since the molecular ion of the A peak (*m/e* 177) fit neither that of the malondiamide (*m/e* 206) nor that of its methylated derivatives, the latter product could not be the same as the A peak. However, II could give III (A peak) by flash methylation. The study of these two paths (*a* and *b*) is now in progress.

REFERENCES

(1) C. E. Pippenger, *Clin. Chem.*, **19**, 666 (1973).

(2) J. C. Van Meter, *ibid.*, **19**, 359 (1973).

(3) G. O. Kananen, R. Osiewicz, and I. Sunshine, *J. Chromatogr.*, **10**, 283 (1972).

(4) A. Wu, *Clin. Chem.*, **20**, 630 (1974).

(5) R. Osievicz, V. Aggarwal, M. R. Young, and I. Sunshine, *J. Chromatogr.*, **88**, 157 (1974).

(6) E. Brochmann-Hanssen and T. O. Oke, *J. Pharm. Sci.*, **58**, 370 (1969).

(7) H. J. Kupferberg and C. E. Pippenger, in "Clinical Pharmacology of Antiepileptic Drugs," H. Schneider, D. Janz, C. Gardner-Thorpe, H. Meinerdi, and A. L. Sherwin, Eds., Springer-Verlag, New York, N.Y., 1975, p. 339.

(8) R. J. Perchalski and B. J. Wilder, *Clin. Chem.*, **19**, 788 (1973).

ACKNOWLEDGMENTS

The authors thank Professor N. Yamaguchi of this faculty and Professor C. Kaneko, Faculty of Pharmaceutical Sciences, Kanazawa University, for helpful discussions.

Pharmacokinetics and Bioavailability of Pyridinol Carbamate in Humans

JEAN SASSARD *x, NICOLE BERNARD *, JACQUES LEGHEAND *, GUY CUISINAUD *, and JULES TRAEGER ‡

Received November 14, 1978, from the **Department of Physiology and Clinical Pharmacology, Faculty of Pharmacy, University of Lyon, Lyon 69008, France,* and the *‡Nephrology Clinic and Inserm U80, Lyon, France.* Accepted for publication March 30, 1979.

Abstract □ The pharmacokinetics of two pyridinol carbamate formulations were studied after a single oral administration in 10 healthy volunteers. An open one-compartment model described the evolution of plasma concentrations as a function of time. Pyridinol carbamate was rapidly absorbed (mean lag time from 0.36 to 0.38 hr). Its elimination half-life ranged from 3.3 to 7.9 hr. The two formulations were bioequivalent.

Keyphrases □ Pyridinol carbamate—pharmacokinetics, bioavailability, comparison of two tablet formulations, humans □ Antiarteriosclerotic agents—pyridinol carbamate, pharmacokinetics, bioavailability, comparison of two tablet formulations, humans □ Anti-inflammatory agents—pyridinol carbamate, pharmacokinetics, bioavailability, comparison of two tablet formulations, humans □ Pharmacokinetics—pyridinol carbamate, humans

The human pharmacokinetics of pyridinol carbamate, a widely used antiatheromatous agent (1, 2), have been studied in only a small number of patients and with a nonspecific analytical procedure (3, 4).

In the present work, a new sensitive and specific high-pressure liquid chromatographic (HPLC) method (5) was applied to determine the pharmacokinetics and to compare the bioavailabilities of two pyridinol carbamate formulations.

EXPERIMENTAL

Subjects—After giving informed consent, 10 healthy male volunteers (25–35 years and 58–80 kg) each received, in a randomized order, a single oral 1-g dose of two different pyridinol carbamate formulations. There was a 14-day interval between the two treatments.

Treatments—The two formulations used, A[1] and B[2], were tablets containing 250 mg of pyridinol carbamate.

Protocol—One hour after a liquid breakfast, each subject received at 8:00 am four tablets of A or B with 150 ml of water. During the following 25 hr, 12 heparinized venous blood samples (5 ml) were drawn. The first standardized meal was allowed 4 hr after drug administration.

Analytical Method—Each blood sample was centrifuged within 30 min. The separated plasma was kept frozen (−80°) until assayed. Nonmetabolized pyridinol carbamate was specifically measured by using a previously described HPLC technique (5).

Calculations—The relevant pharmacokinetic parameters were computed for the two forms of pyridinol carbamate according to an open one-compartment linear model. The plot of log plasma concentrations (C, micrograms per milliliter) *versus* time (t, hours) allowed a rough determination of the absorption (k_a, hours^{-1}) and the elimination rate constants (k_e, hours^{-1}) by using the peeling method. These empirical values were used to calculate the parameters of the most probable curve:

$$C = f(t) = -Ae^{-k_{at}} + Be^{-k_{et}} \qquad \text{(Eq. 1)}$$

This calculation was achieved by an iterative program using the least-squares principle devised for a computer[3]. The lag time (T_L, hours) before the appearance of pyridinol carbamate in plasma was calculated as follows:

$$T_L = \frac{\ln A/B}{(k_a - k_e)} \qquad \text{(Eq. 2)}$$

The relative volume of distribution (V/F, liters), which is the ratio of the volume of the compartment (V) to the absolute bioavailability factor

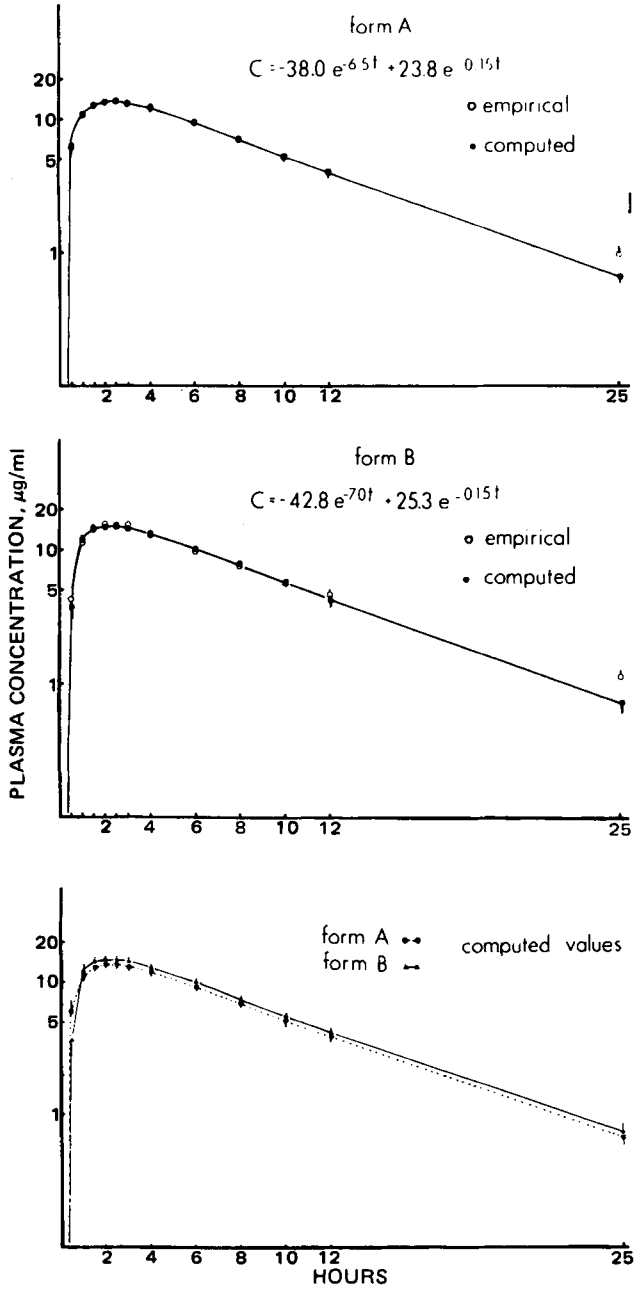

Figure 1—*Plasma concentration–time curves for pyridinol carbamate after the oral administration of 1 g of Formulations A and B in 10 healthy volunteers.*

[1] Medoxal, Allard Laboratories, Paris, France.
[2] Angioxine, Roussel Laboratories, Paris, France.
[3] Model SR 60, Texas Instruments, Almelö, Holland.

0022-3549/79/0900-1190$01.00/0
© 1979, American Pharmaceutical Association

Table I—Pharmacokinetic Parameters of Two Formulations (*A* and *B*) of Pyridinol Carbamate after a Single Oral Administration in Healthy Volunteers

Subject	Form	T_L, hr	t_{max}, hr	C_{max}, μg/ml	k_a, hr^{-1}	k_e, hr^{-1}	*A*	*B*	$t_{1/2}$, hr	$(V/F)/BW$, liters/kg	*AUC*, μg/hr/ml	AUC_{cor}, 10^{-4} μg/hr/ml	$F_{A/B}$
1	A	0.52	3.36	16.2	0.605	0.182	−53.53	42.96	3.8	0.52	149.94	1.91	1.51
	B	0.45	1.91	14.6	1.934	0.141	−46.25	20.75	4.9	0.79	127.74	1.26	
2	A	0.50	3.07	14.3	0.680	0.194	−46.38	36.45	3.5	0.73	121.63	1.37	1.23
	B	0.47	1.37	16.8	3.717	0.150	−114.38	21.50	4.6	0.90	128.22	1.11	
3	A	0.34	2.34	9.7	1.26	0.132	−21.71	14.79	5.2	1.27	95.95	0.78	0.54
	B	0.44	2.82	16.0	0.898	0.152	−41.07	9.65	4.5	0.70	152.00	1.43	
4	A	0.38	2.87	14.2	0.865	0.142	−33.79	15.73	4.8	0.73	143.49	1.36	1.04
	B	0.28	2.50	14.4	1.053	0.138	−30.45	23.54	5.0	0.76	142.05	1.31	
5	A	−0.64	1.47	15.9	1.408	0.087	−8.26	19.29	7.9	0.77	220.56	1.30	0.86
	B	0.26	1.35	19.7	3.223	0.107	−52.93	23.59	6.4	0.66	207.14	1.51	
6	A	0.36	1.09	14.0	5.025	0.145	−98.63	16 98	4.7	1.03	107.84	0.97	0.83
	B	0.50	0.61	18.6	—	0.145	−1.41	20.37	4.7	0.85	130.61	1.17	
7	A	−0.01	1.78	12.9	1.339	0.162	−19.40	19.69	4.2	0.77	107.34	1.30	0.72
	B	0.49	2.85	14.6	0.752	0.209	−48.21	36.86	3.3	0.55	114.96	1.80	
8	A	0.46	0.58	16.5	—	0.137	−1.92	18.00	5.0	0.87	122.45	1.14	0.84
	B	0.12	1.91	16.7	1.687	0.099	−26.08	21.51	7.0	0.73	202.95	1.36	
9	A	0.41	1.40	14.8	3.087	0.170	−66.26	20.01	4.0	0.71	103.68	1.41	0.90
	B	0.38	2.69	12.6	0.831	0.188	−34.78	27.20	3.6	0.64	104.05	1.56	
10	A	0.19	2.06	16.2	1.375	0.135	−30.04	23.81	5.1	0.80	154.85	1.25	0.99
	B	0.23	2.51	13.7	0.850	0.186	−32.62	28.05	3.7	0.79	113.10	1.26	
Mean	A[a]	0.38	2.00	14.5	1.738	0.149	−37.99	23.77	4.8	0.82	132.77	1.28	0.95
±*SEM*		0.06	0.29	0.6	0.477	0.010	9.23	2.87	0.4	0.06	11.69	0.09	±0.09
Mean	B[a]	0.36	2.05	15.8	1.660	0.151	−42.82	25.30	4.8	0.74	142.28	1.38	
±*SEM*		0.04	0.24	0.70	0.370	0.011	9.18	1.64	1.2	0.03	11.35	0.04	

[a] Not significant when Formulation A is compared with B.

(*F*), was obtained by using:

$$\frac{V}{F} = \left(\frac{D}{A}\right)\left(\frac{k_a}{(k_a - k_e)}\right) e^{-k_a T_L} = \left(\frac{D}{B}\right)\left(\frac{k_a}{(k_a - k_e)}\right) e^{-k_e T_L} \quad \text{(Eq. 3)}$$

where *D* is the administered dose. This parameter was corrected for body weight (*BW*, kilograms) and expressed as:

$$\frac{V}{(F)(BW)}$$

The area under the curve (*AUC*, micrograms per hour per milliliter) was calculated by integrating the equation $C = f(t)$ from $t = T_L$ to infinity:

$$AUC = -\frac{A}{k_a} e^{-k_a T_L} + \frac{B}{k_e} e^{-k_e T_L} \quad \text{(Eq. 4)}$$

This value was corrected (AUC_{cor}) for the administered dose, *BW*, and k_e relative to each subject and for the mean of these two last variables ($\overline{BW}$ and $\overline{k_e}$) for the group of volunteers as follows:

$$AUC_{cor} = AUC\left(\frac{BW}{\overline{BW}}\right)\left(\frac{k_e}{\overline{k_e}}\right) \quad \text{(Eq. 5)}$$

The plasma half-life ($t_{1/2}$, hours) was derived from k_e. The time (t_{max}, hours) needed to obtain the maximal plasma concentration (C_{max}) was obtained by:

$$t_{max} = \frac{\ln (Ak_a/Bk_e)}{(k_a - k_e)} \quad \text{(Eq. 6)}$$

The relative bioavailability factor of the two formulations ($F_{A/B}$) was calculated as follows:

$$F_{A/B} = \frac{AUC_{cor}\ \text{Form A}}{AUC_{cor}\ \text{Form B}} \quad \text{(Eq. 7)}$$

Results were expressed as means ± *SEM*. Statistical analysis of the differences between Forms A and B was carried out by a threeway analysis of variance in which the nature and the order of treatments were the two variables.

RESULTS AND DISCUSSION

The empirical and computed log plasma concentration–time curves are shown in Fig. 1, and the pharmacokinetic parameters are listed in Table I.

After oral administration, pyridinol carbamate appeared in the blood after a mean lag time of 0.36–0.38 hr. Its absorption was regular, as shown by the small interindividual variations in the plasma concentrations. No distribution phase could be detected from the plasma concentration–time curves. This finding indicates that the drug rapidly reached a relative distribution volume of 0.52–1.27 liters/kg.

Drug elimination was characterized by a plasma half-life of 3.32–7.96 hr.

These results vary with those of Mallein *et al.* (3) who reported slower absorption, higher peak plasma concentrations, and longer plasma half-lives. All of these differences could be explained by the nonspecificity of their analytical method (4) for plasma of pyridinol carbamate metabolites.

Finally, due to the absence of significant differences between the AUC_{cor} obtained after administration of the two forms and to a relative bioavailability factor ($F_{A/B}$) of 0.95 ± 0.09, it was concluded that the two pyridinol carbamate formulations were bioequivalent.

REFERENCES

(1) T. Shimamoto, F. Numaro, and T. Fujita, *Am. Heart J.*, **71**, 216 (1966).

(2) T. Shimamoto, H. Maezawa, H. Yamazaki, T. Atsumi, T. Fujita, T. Ishioka, and T. Suraga, *ibid.*, **71**, 297 (1966).

(3) R. Mallein, J. Rondelet, M. Boucherat, and H. Avenue, *Thérapie*, **28**, 115 (1973).

(4) H. Maezawa, T. Atsumi, N. Sagawa, T. Sano, and T. Odakura, *The Ochanomizu Med. J.*, **13**, 289 (1965).

(5) N. Bernard, J. L. Brazier, and J. Sassard, *J. Chromatogr.*, **152**, 260 (1978).

ACKNOWLEDGMENTS

The authors gratefully acknowledge Dr. H. Saby for supplying the drug used and Mrs. M. Seccia for technical assistance.

Correlations of Parotid Saliva and Plasma Lidocaine Concentrations in Rats

G. JOHN DiGREGORIO ˣ, ANTHONY J. PIRAINO, and EILEEN RUCH

Received August 31, 1978, from the *Department of Pharmacology, Hahnemann Medical College, Philadelphia, PA 19102.* Accepted for publication March 30, 1979.

Abstract □ The concentration ratios of parotid saliva to plasma lidocaine were determined in rats after a single dose (10 mg of lidocaine/kg) and constant infusion (60 μg of lidocaine/kg/min). Parotid saliva and plasma samples were obtained at 10, 20, and 30 min after single-dose lidocaine administration and at 70, 80, and 90 min after the initiation of a lidocaine infusion. The saliva/plasma concentration ratios for lidocaine after single-dose administration decreased from 1.13 ± 0.03 at 10 min to 0.51 ± 0.06 at 30 min, whereas the ratios determined during the lidocaine infusion remained constant (0.43 ± 0.03, 0.45 ± 0.03, and 0.43 ± 0.04) over the time period tested. The variable saliva/plasma concentration ratios obtained after single-dose administration may be associated with rapid drug distribution between the plasma and peripheral compartments and variation in lidocaine binding to plasma proteins. However, during constant lidocaine infusion, a steady-state concentration was achieved within 70 min, as demonstrated by the constant saliva/plasma concentration ratios.

Keyphrases □ Lidocaine—concentration in parotid saliva and in blood, single dose and continuous infusion, rats □ Anesthetics, local—lidocaine, concentration in parotid saliva and in blood, single dose and continuous infusion, rats □ Saliva—lidocaine concentration after single dose and continuous infusion, compared to serum □ Serum—lidocaine concentration after single dose and continuous infusion, compared to saliva

The secretion of pharmacological agents into saliva has been the subject of several investigations in animals and humans. Drugs such as synthetic opium derivatives (1), barbiturates (2, 3), ethanol (4), and procainamide (5) have been detected and quantitated in saliva. Little or no information is available, however, concerning the salivary excretion patterns of other antiarrhythmic agents including lidocaine. The work presented here reports the detection and quantitation of lidocaine in parotid saliva and plasma samples simultaneously collected from rats. Experiments were divided into two phases: single-dose lidocaine administration and constant lidocaine infusion.

The saliva/plasma lidocaine concentration ratios were calculated in each experiment, and comparisons were made to determine whether parotid salivary secretion of lidocaine directly reflects plasma concentrations.

EXPERIMENTAL

Male Wistar rats, 200–230 g, were surgically prepared for drug administration and parotid saliva collection by a reported method (6). The rats were anesthetized with pentobarbital (50 mg/kg ip), and tracheotomies were performed. With a dissecting microscope, both parotid ducts, the left femoral vein, the femoral artery, and the brachial artery were surgically exposed for cannulation.

The parotid duct was opened by puncturing the duct membrane with the tip of a 23-gauge needle; a polyethylene cannula (~275–0.015 mm i.d. × ~0.600–0.150 mm o.d.) was inserted into the duct. A calibrated collecting cannula (PE 60) was placed over the free end of the parotid cannula for measurement of salivary flow rates. The collecting cannula was interchangeable so that sequential collections could be obtained.

The brachial artery, the femoral artery, and the femoral vein were cannulated with polyethylene tubes (PE 50). The brachial artery was used primarily for the constant pilocarpine infusion (0.06 mg/min), and the femoral vein was available as the administration route for a single bolus dose or constant infusion of lidocaine. The femoral artery was used for blood sample collection.

Saliva samples collected in this manner were transferred to appropriate vessels by flushing the calibrated collecting cannula with a syringe containing distilled water. In the first experiment (single lidocaine dose), pilocarpine (0.2 mg/ml) was infused over 30 min to induce salivary secretion into the brachial artery at a rate of 0.3 ml/min. At the beginning of the pilocarpine infusion, a single lidocaine dose (10 mg/kg) was administered intravenously into the femoral vein. Samples were collected 10, 20, and 30 min after lidocaine administration. Blood was collected simultaneously with saliva collection into heparinized capillary tubes and centrifuged, and the plasma was removed. Saliva was collected into precalibrated capillary tubes and stored for analysis (Fig. 1a).

In the second experiment, lidocaine was infused at a rate of 60 μg/kg/min through the femoral vein. After 1 hr of lidocaine infusion, a pilocarpine infusion (0.2 mg/ml) was started at a rate of 0.3 ml/min. Both the pilocarpine infusion and the lidocaine infusion proceeded coincidentally without interruption for the remaining 30 min of this experi-

Table I—Rat Plasma and Parotid Saliva Concentration Ratios of Lidocaine after a Single Dose and after Constant Infusion

Minutes[a]	Saliva/Plasma Concentration Ratios: Constant Infusion[b]	Saliva/Plasma Concentration Ratios: Single Dose[c]
10 (70)	0.43 ± 0.03	1.13 ± 0.03
20 (80)	0.45 ± 0.03	0.68 ± 0.07
30 (90)	0.43 ± 0.04	0.51 ± 0.06

[a] Time intervals in parentheses refer to the collection periods employed in the constant 90-min lidocaine infusion; $n = 9$. [b] During administration of a constant lidocaine infusion (60 μg/kg/min). [c] After the administration of a single bolus dose of lidocaine (10 mg/kg).

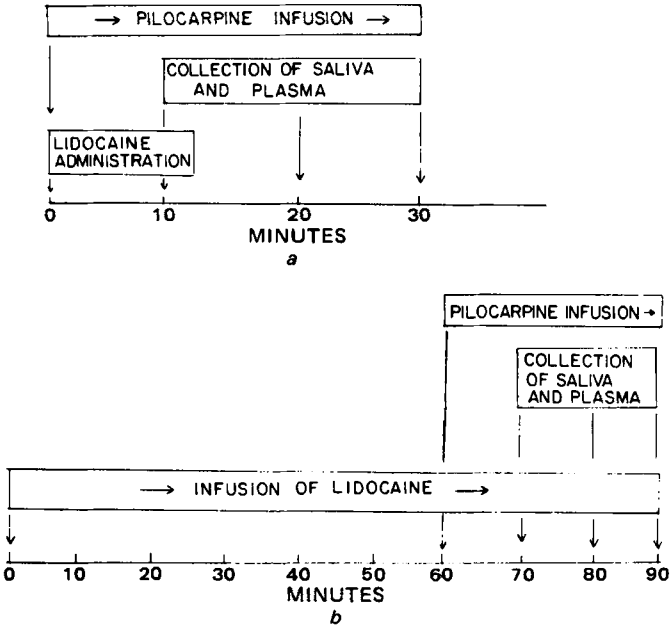

Figure 1—*Experimental approach in determining blood and parotid saliva lidocaine concentrations utilizing single-dose lidocaine administration (10 mg/kg) (a) and constant lidocaine infusion (60 μg/kg/min) (b) in the rat model.*

0022-3549/79/0900-1192$01.00/0
© 1979, American Pharmaceutical Association

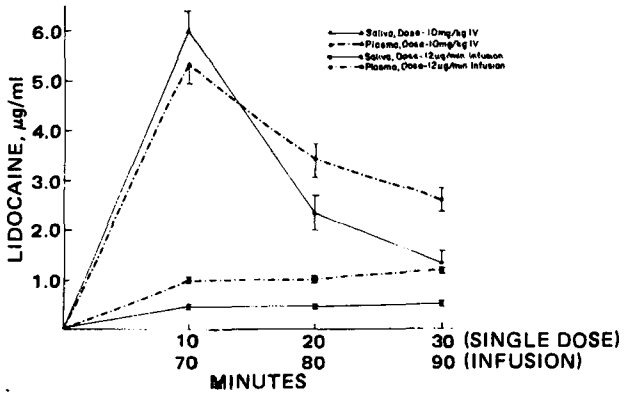

Figure 2—*Mean rat plasma and saliva concentrations (±SEM) of lidocaine. Each concentration is the mean of nine individual rat experiments. Key: ▲, plasma and saliva concentrations after single dose; and ●, plasma and saliva concentrations after constant infusion.*

ment. Total lidocaine infusion did not exceed 2.7 ml over 90 min. Saliva and blood samples were collected at 70, 80, and 90 min after the initiation of lidocaine infusion (Fig. 1*b*).

Lidocaine analysis was accomplished utilizing a commercially available enzyme multiplier immunoassay technique kit[1].

RESULTS AND DISCUSSION

Following a single lidocaine dose (10 mg/kg), the 10-, 20-, and 30-min mean (±*SEM*) plasma concentrations were 5.30 ± 0.42, 3.40 ± 0.35, and 2.57 ± 0.28 μg/ml, respectively (Fig. 2). The corresponding parotid saliva concentrations were 6.00 ± 0.40, 2.30 ± 0.37, and 1.34 ± 0.25 μg/ml. The mean saliva/plasma concentration ratios were 1.13 ± 0.03, 0.68 ± 0.07, and 0.51 ± 0.06 at these three time periods (Table I).

During a constant lidocaine infusion (60 μg/kg/min), the mean (±*SEM*) plasma concentrations obtained at 70, 80, and 90 min were 0.99 ± 0.08, 1.00 ± 0.08, and 1.18 ± 0.15 μg/ml, respectively (Fig. 2). The corresponding parotid saliva concentrations were 0.43 ± 0.03, 0.45 ± 0.03, and 0.51 ± 0.03 μg/ml, respectively. The mean saliva/plasma concentration ratios were 0.43 ± 0.03, 0.45 ± 0.03, and 0.43 ± 0.04 at these times (Table I).

In single-dose lidocaine experiments, the saliva/plasma ratios were not constant over 30 min. At the initial 10-min sample collection, the saliva lidocaine concentration was significantly higher than that in plasma. The saliva lidocaine concentrations fell below the plasma concentrations, however, during subsequent sample collection periods. These results indicate that salivary lidocaine secretion was markedly greater during the first 10 min than at the later two collection periods.

This particular finding is best explained by this drug's rapid distribution and redistribution among various tissues in the body. This hypothesis is supported by distribution studies using ^{14}C-lidocaine (7). Following administration, lidocaine distributed quickly within the first 10 min to the liver, gut, kidney, muscle, and adipose tissue (7). In the first 10 min of the present study, the parotid salivary concentration exceeded plasma levels and then decreased. Because of the dynamic changes occurring during this period, the saliva/plasma concentration ratios were not constant. However, the saliva/plasma concentration ratio at 30 min was 0.51 ± 0.06. Concentration ratios for the single lidocaine dose were not estimated beyond this 30-min period. If samples had been obtained at later times (in the postdistributive phase), the saliva/plasma ratio might have tended to be constant and might have approached values of 0.43–0.45 as occurred during the constant infusion.

During a constant (90-min) lidocaine infusion, the saliva/plasma concentration ratios remained unchanged at 70-, 80-, and 90-min sample collection periods, indicating that a steady state was achieved. The mean saliva/plasma concentration ratio was 0.44. Thus, about 44% of the plasma lidocaine concentration could be found in the parotid saliva at any time during the 30-min sample collection period.

Tucker *et al.* (8) performed *in vitro* studies indicating that lidocaine is protein bound and that the degree of binding to human plasma proteins is dependent on the plasma lidocaine concentration. At a 5-μg/ml plasma concentration, only 45% was present as unbound drug and the remainder was bound to plasma proteins. In the present study during constant lidocaine infusion, a plasma concentration of ~1.0 μg/ml yielded a parotid saliva concentration that corresponded to 44% of the total plasma concentration. If one accepts the premise that the parotid salivary drug concentration reflects the free form of a drug in plasma, then the percentage of lidocaine unbound in rat plasma, at 1 μg/ml of plasma, appears to be about 44%. This value compares favorably with the results of Tucker *et al.* (8) and suggests that saliva reflects the free (nonprotein-bound) drug concentration in the plasma.

[1] EMIT system, Syva Co., Palo Alto, Calif.

REFERENCES

(1) J. C. Munch, *J. Am. Pharm. Assoc., Sci. Ed.*, **24**, 557 (1935).

(2) A. J. Piraino, G. J. DiGregorio, and B. T. Nagle, *J. Dent. Res.*, **55**, 43 (1976).

(3) G. J. DiGregorio, A. J. Piraino, B. T. Nagle, and E. K. Kniaz, *ibid.*, **56**, 502 (1977).

(4) G. J. DiGregorio, A. J. Piraino, and E. Ruch, *Drug Alcohol Depend.*, **3**, 43 (1978).

(5) J. R. Koup, W. J. Jusko, and A. L. Goldfarb, *J. Pharm. Sci.*, **64**, 2008 (1975).

(6) G. J. DiGregorio and E. K. Kniaz, *Drug Alcohol Depend.*, **1**, 377 (1976).

(7) J. Katz, *Anesthesiology*, **29**, 249 (1968).

(8) G. T. Tucker, R. N. Boyes, P. O. Bridenbaugh, and D. C. Moore, *ibid.*, **33**, 287 (1970).

Separation and Spectral Properties of Diisopropylphosphate, the Major Decomposition Product of Isoflurophate

JAMES ARTHUR RYAN [x], WHITCOMB RILEY McGAUGHRAN [*], CARL JOSEPH LINDEMANN, and ANTHONY GABRIEL ZACCHEI [‡]

Received November 15, 1978, from the *Department of Pharmaceutical Research and Development, Merck Sharp and Dohme Research Laboratories, Division of Merck and Co., Inc., West Point, PA 19486.* Accepted for publication March 22, 1979. *Present address: 1636 Clearbrook Road, Lansdale, PA 19446. [‡]Present address: Merck Institute for Therapeutic Research, West Point, Pa.

Abstract □ The reaction of water with isoflurophate to form diisopropylphosphate was examined and confirmed. Isolation of this decomposition product from an antiglaucoma drug formulation is described. A known reference compound was isolated from a commercial mixture also containing the monoisopropyl ester. The isolation, purification, and molecular spectroscopic and elemental confirmation of structure are described. IR, NMR, and mass spectra are included. Additionally, a GLC procedure and parameters used to identify diisopropylphosphate in a degraded peanut oil formulation of isoflurophate are reported. Reaction mixtures of this drug with water and sodium hydroxide were analyzed by GLC with the expected results.

Keyphrases □ Diisopropylphosphate—analysis, IR, NMR, mass spectra, GLC, isolation as degradation product from peanut oil isoflurophate formulation □ Isoflurophate—degradation products, diisopropylphosphate, analysis, peanut oil formulation □ GLC—analysis, diisopropylphosphate, isolation as degradation product from peanut oil isoflurophate formulation □ Antiglaucoma agents—isoflurophate, degradation products, diisopropylphosphate isolated from peanut oil formulation, GLC

Isoflurophate (I) is an important and highly potent drug in glaucoma treatment and is a well-known inhibitor of acetylcholinesterase and other enzymes (1). It reacts with moisture with concurrent loss of activity and formation of hydrofluoric acid and diisopropylphosphate (II) (1). Ion-specific electrodes were used to detect ionic fluoride resulting from this hydrolysis. Analytically, a poor correlation with the degree of hydrolysis was noted.

Several reports (2–4) indicated that the major hydrolytic decomposition product of I was II, but no confirmatory qualitative evidence was presented. The presumed chemical hydrolysis is shown in Scheme I. The present work was undertaken to obtain this necessary qualitative information. Lindemann developed an assay for intact I using GLC, which is described in USP XIX (5). This paper provides associated general analytical information for II including isolation, purification, and spectral data.

$$\underset{\text{I}}{[(CH_3)_2CHO]_2P(O)F} + H_2O \rightarrow \underset{\text{II}}{[(CH_3)_2CHO]_2P(O)OH} + 1/2H_2F_2$$

Scheme I

EXPERIMENTAL

Reagents and Chemicals—Compound II was not available commercially in pure form. A reference material was obtained by separation from a 1:1 mixture of II with the monoisopropyl ester[1]. Petroleum ether[2], used in the isolation of II, was analytical reagent grade. Compound I[3] was used in the hydrolysis experiments.

GLC—All GLC retention time data were obtained on a gas chromatograph equipped for flame-ionization detection[4]. Samples were reacted with excess diazomethane in ether, the ether was evaporated, and the residue was dissolved in carbon disulfide prior to injection. Separation was conducted on a 1.52-m long × 4-mm i.d. glass column containing 4% QF-1 on 80–100-mesh Gas Chrom Q. The column temperature was 105°, the flow rate was 40 ml/min, the inlet temperature was 225°, and the detector temperature was 295°. The chart speed was 38 cm/hr. A 1-mv recorder was used.

NMR—An NMR spectrometer equipped with a proton probe[5] and a 5-mm sample tube was used (Fig. 1).

Mass Spectrometry—An authentic II sample was derivatized with *N,O*-bis(trimethysilyl)acetamide in pyridine (for 30 min at 60°) to form the trimethylsilyl derivative. All mass spectra were obtained on a mass spectrometer[6] using a direct probe. The ionizing and accelerating potentials were 70 ev and 3.5 kv, respectively. The ion source temperature was 270°. The mass spectrum of the derivative is presented in Fig. 2.

IR Spectrophotometry—The IR spectrum of authentic II (Fig. 3) was run as a capillary film of the neat liquid between potassium bromide windows. The IR spectrophotometer[7] was set for linear frequency measurement and equipped with a wide Nernst glower. Parameters were: slits, programmed at 1000; gain, normal; scan speed, 32; attenuator speed, 1100; and source, 0.78 amp.

Isolation of Major Decomposition Product of I—A 10-year-old sample of 1% I in mineral oil was selected for isolation of the major decomposition product. The sample had been stored in a wide-mouth bottle enclosed in a metal can at ambient conditions near 24° during this period. No other protection against moisture uptake was in evidence. The sample assayed 0% I by GLC (5). An immiscible phase in the mineral oil was removed by centrifugation and subjected to IR analysis.

Isolation of Authentic II—Pure II was isolated utilizing the low solubility of the monoisopropyl compound in petroleum ether. Fifty grams of the 1:1 mixture in a 500-ml erlenmeyer flask was diluted to 300 ml with petroleum ether. After thorough shaking, the mixture was allowed to separate and the petroleum ether phase was decanted[8] into a large calibrated beaker. Second and third elutions were made in this manner, and the petroleum ether phases were combined by decantation[8] and evaporated without heat; decantations were performed when 450-, 350-, and 200-ml volumes were reached. The solution was allowed to stand until clear. Materials not remaining in the petroleum ether were discarded.

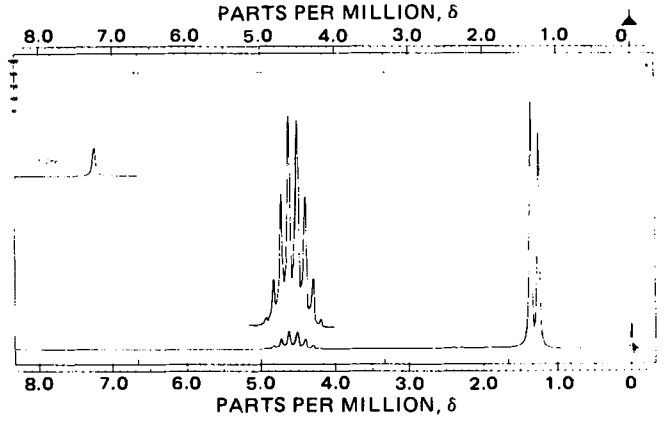

Figure 1—*PMR spectrum of diisopropylphosphate (I).*

[1] Lot 50989X, ICN, K & K Labs.
[2] Lot WCML, Mallinckrodt.
[3] Lot 030-127-1, Aldrich.
[4] Micro Tek MT-220.
[5] Varian A-60D.
[6] LKB model 9000S.
[7] Perkin-Elmer PE-521.
[8] Concentration of the petroleum ether was performed in open beakers. An isolable oil (mostly monoisopropyl ester) separated and was easily removed by decantation of the more mobile hydrocarbon phase into a clean beaker. The evaporation was continued.

0022-3549/79/0900-1194$01.00/0
© 1979, American Pharmaceutical Association

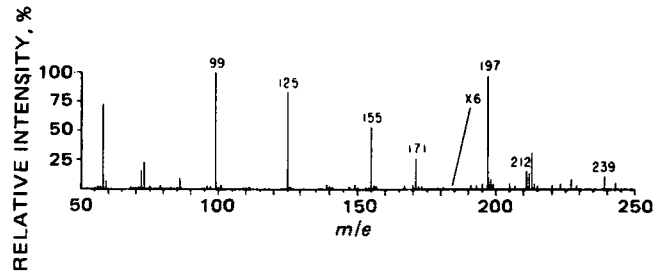

Figure 2—*Mass spectrum of diisopropylphosphate (I) as the trimethyl silyl derivative.*

The petroleum ether was warmed to ~30°. Caution was exercised to prevent sample loss through ebullition. Evaporation was continued using an air stream. The top phase was decanted[8] when the 150-, 125-, 100-, and 85-ml volumes had been reached. In this series of decantations[8], the insoluble oil phases were eluted in the same order that they were obtained with a single 35-ml portion of fresh petroleum. This eluate was combined with the 85 ml remaining from the evaporation step, placed in a separator, and extracted with 8 and then with 4 ml of absolute methanol. The petroleum ether phase was separated and evaporated using an air stream, with the last traces of solvents being removed at room temperature under vacuum. The product was dried over sulfuric acid. The yield was 6 g or 24% based on the claimed 1:1 mixed ester weight ratio.

RESULTS AND DISCUSSION

Although the starting mixture used to identify the isolated decomposition product was marketed as containing II, supportive analytical data were obtained to confirm this structure because previously reported IR spectral frequencies (6) of a II sample gave questionable agreement with the spectrum shown in Fig. 3. Close IR spectral checks, however, were obtained between the decomposition product isolate and the authentic II. The IR spectrum of II was sufficiently complex to provide a positive identification.

As indicated in Fig. 2, no molecular ion was observed in the mass spectrum of the trimethylsilyl derivative of authentic II; however, an M − 15 ion was observed at *m/e* 239 (characteristic methyl loss in trimethyl silyl derivative). Other characteristic ions were detected at the following *m/e* values: 212 (M − 42, loss of propylene due to McLafferty rearrangement), 211 (M − 43, homolytic cleavage of isopropyl group), 197 (loss of methyl and propylene), 171 (loss of two propylene moieties *via* McLafferty rearrangement mechanism), 155 [from $(HO)_2P(=O)\text{-}O{=}Si(CH_3)_2^+$ ion], and 99 [base peak, $^+HO{=}P(OH)_3$ ion]. The extremely low intensity ion at *m/e* 243 resulted from the ditetramethylsilyl phosphoric acid derivative.

Elemental analysis was obtained on "authentic" II.

Anal.—Calc. for $C_6H_{15}PO_4$: C, 39.56; H, 8.30. Found: C, 39.57; H, 8.32.

The PMR spectrum of authentic II (Fig. 1) was in accord with the structure both qualitatively and quantitatively within experimental error. Assignments are: 1.30-ppm methyl hydrogens on isopropyl groups, 4.58-ppm multiplet due to methine hydrogens on two isopropyl groups;

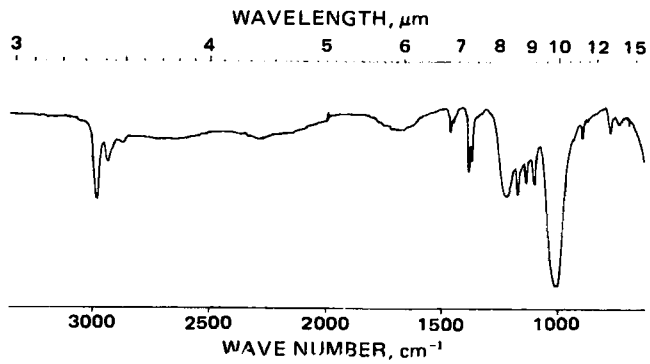

Figure 3—*Diisopropylphosphate IR spectrum.*

J = 7 Hz, with coupling of about the same J value to ^{31}P; and 12.35-ppm acidic exchangeable proton on P–O–H.

Assignments for the IR spectrum from Fig. 3 were reported in a study of band origins on analogous phosphoric acid derivatives (6).

GLC retention time data[9] were obtained for the decomposition product from mineral oil and authentic II. These retention times were matched by peaks obtained for decomposition caused by the action of water and by the action of 0.1 *N* NaOH (aqueous) on I. An old lot of a product formulation of 0.1% I in peanut oil chromatographed in the same system also showed the peak.

The GLC retention time of authentic II (225 sec) showed excellent agreement with the times for the following samples: (*a*) major product formed on reaction of I and water, 227 sec; (*b*) major product formed on reaction of I and aqueous 0.1 *N* NaOH, 227 sec; (*c*) 1:1 I–monoester mixture (starting material), 227 sec; and (*d*) aged 0.1% I in peanut oil, 226 sec.

REFERENCES

(1) "Remington's Pharmaceutical Sciences", 15th ed., Mack Publishing Co., Easton, Pa., 1975, p. 830.

(2) C. R. Szalkowski, W. J. Mader, and H. A. Frediani, *J. Am. Pharm. Assoc., Sci. Ed.*, **38**, 337 (1949).

(3) W. A. Waters and C. G. M. de Worms, *J. Chem. Soc.*, **1949**, 926.

(4) M. Kilpatrick and M. L. Kilpatrick, *J. Phys. Colloid Chem.*, **53**, 1371 (1949).

(5) "The United States Pharmacopeia", 19th rev., 1st suppl., Mack Publishing Co., Easton, Pa., 1975, p. 28.

(6) J. W. Maarsen, N. C. Smit, and J. Matze, *Rec. Trav. Chim.*, **76**, 713, 728 (1957).

ACKNOWLEDGMENTS

The authors thank Dr. Wayne M. Grim, Dr. Edward M. Cohen, and Mr. Warren B. Hagerman of the Pharmaceutical Research and Development Department for their encouragement and critical review.

[9] All retention time data refer to the methylated products.

Nasal Absorption of Propranolol in Rats

Keyphrases □ Propranolol—nasal absorption, rats, compared to oral and intravenous dosage forms, bioavailability □ β-Adrenergic blocking agents—propranolol, nasal absorption, compared to oral and intravenous dosage forms, rats, bioavailability □ Dosage forms, nasal—propranolol, absorption, compared to oral and intravenous dosage forms, rats, bioavailability

To the Editor:

Propranolol, the adrenergic β-receptor blocking drug, is widely used for hypertension management and angina pectoris treatment. The drug, however, is inefficiently and variably absorbed from oral dosage forms. A study in humans showed that the oral administration of propranolol results in considerable variation in plasma drug levels. Peak plasma levels in five subjects given 80-mg oral doses varied by sevenfold, while 10-mg iv doses in the same subjects varied by only twofold (1). Furthermore, drug bioavailability of an 80-mg oral dose in some subjects, as calculated from the ratio of the area under the curve, was as low as 16% of the bioavailability of a 10-mg iv dose. The variations in the blood levels as well as the low bioavailability for oral doses have been attributed to the extensive drug metabolism in the GI tract during absorption and/or to the first-pass effect (2, 3).

To enhance drug bioavailability and to minimize blood level variations from the nonparenteral route, drug availability from a nasal solution was investigated. Previous studies in rats, dogs, and humans showed that insulin is efficiently absorbed from the nasal mucosa (4–6).

Sprague–Dawley male rats, ~270 g, were used. For nasal administration, the rats were anesthetized with pentobarbital sodium (50 mg/kg). Drug administration to the nasal cavity with a micropipet, using two doses of 1 and 2 mg/rat in 0.1 ml of pH 7.2 isotonic buffer, was carried out according to the procedure described by Hirai *et al* (4). For intravenous administration, the rats were anesthetized and 1-mg doses of the drug in 0.2 ml of pH 7.2 isotonic buffer were injected through the femoral vein. After the intravenous and nasal administrations, blood was sampled from the femoral aorta periodically.

For oral administration, the rats were not anesthetized and 1-mg doses in 1 ml of pH 7.2 isotonic buffer were administered by a stomach tube. After oral administration, blood was sampled from the tail vein periodically. The blood drug levels were determined spectrophotofluorometrically by a minor modification of the method of Suzuki *et al.* (3).

Figure 1 shows the mean blood propranolol levels for the three administration routes. The blood drug levels after intravenous and nasal administrations of 1-mg doses were identical, whereas the oral administration resulted in considerably lower blood levels. The oral bioavailability calculated from the ratio of the area under the curve, (oral/intravenous) × 100 and (oral/nasal) × 100, within 4 hr was ~15%.

Furthermore, the area under the blood drug level curve was directly proportional to the dose administered nasally (Fig. 1). The results also indicate that propranolol is rapidly absorbed from the nasal mucosa. The peak plasma level was attained within 5 min of nose drop instillation.

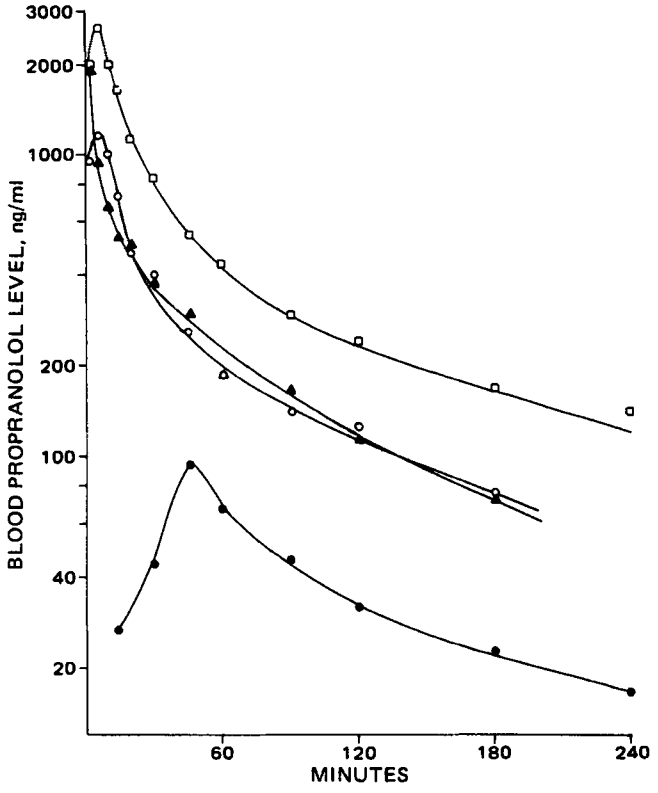

Figure 1—*Time course of the average blood propranolol levels in three rats after nasal administration of 1 mg/rat (○), intravenous administration of 1 mg/rat (▲), oral administration of 1 mg/rat (●), and nasal administration of 2 mg/rat (□).*

The nasal route for propranolol administration appears to be superior to the oral route and as effective as the intravenous route. A study is underway to examine propranolol bioavailability from nasal solutions in dogs.

(1) D. G. Shand, E. M. Nuckolls, and J. A. Oates, *Clin. Pharmacol. Ther.*, **11**, 112 (1970).

(2) C. T. Dollery and D. S. Davies, *Ann. N.Y. Acad. Sci.*, **179**, 109 (1971).

(3) T. Suzuki, Y. Saitoh, S. Isozaki, and R. Ishida, *Chem. Pharm. Bull.*, **20**, 2731 (1972).

(4) S. Hirai, T. Yashiki, and T. Matsuzawa, presented at the 98th Annual Meeting of the Pharmaceutical Society of Japan, Okayama, Japan, Apr. 1978.

(5) S. Hirai, T. Ikenaga, and T. Matsuzawa, *Diabetes*, **27**, 296 (1978).

(6) T. Yokosuka, Y. Omori, Y. Hirata, and S. Hirai, *J. Jpn. Diabetic Soc.*, **20**, 146 (1977).

Anwar A. Hussain ˣ
Shinichiro Hirai
Rima Bawarshi
College of Pharmacy
University of Kentucky
Lexington, KY 40506

Received March 16, 1979.
Accepted for publication June 1, 1979.

0022-3549/79/0900-1196$01.00/0
© 1979, American Pharmaceutical Association

Specificity of Nitroglycerin Assays

Keyphrases □ Nitroglycerin—analysis, stability, various procedures compared □ Vasodilators, coronary—nitroglycerin, stability analysis, various procedures compared □ Stability—nitroglycerin, analysis, various procedures compared

To the Editor:

Recently, intravenous nitroglycerin was shown to be beneficial in the management of acute myocardial infarction and of left ventricular failure (1, 2). This therapeutic use has sparked renewed interest in the determination of nitroglycerin stability in solutions. Several studies (3–5) demonstrated that while nitroglycerin infusion is stable when stored in glass containers, significant drug adsorption onto plastic intravenous bags does occur.

Suphajettra *et al.* (6) examined nitroglycerin stability at elevated temperatures in various nonaqueous solvents and found appreciable drug degradation only in polyethylene glycol 400. These investigators employed the Bell (7) and kinetic (8, 9) assays for their stability study and found that the former method gave an apparently slower degradation rate. They proposed that a reaction complex sequestered nitroglycerin from detection when using the kinetic assay but that this reaction complex was broken down during the workup in the Bell method. If this hypothesis is correct, then the Bell procedure is not stability indicating. Since neither of these assays involved a separation step, it is also possible that the difference in the observed rates was due to a difference in the extent of interference produced by nitroglycerin degradation products such as glyceryl dinitrates, glyceryl mononitrates, inorganic nitrate, and nitrite ions. Thus, the assay that is subject to interference from degradation products will produce an artifactually slower degradation rate.

Since comparative information on the specificity of nitroglycerin assays is not available, we examined the three most used methods—*viz.*, the Bell (7), the kinetic (8, 9), and the USP (10) procedures, for potential interference by nitroglycerin degradation products. Aqueous nitroglycerin solutions (~300 μg/ml), standardized by the USP procedure, were assayed in duplicate in the separate presence of approximately equimolar concentrations of the glyceryl dinitrates[1] and mononitrates[1]. Inorganic nitrate[2] and nitrite[2] ions were present at three times this concentration. Since the USP procedure requires a rather tedious column separation for each sample, some workers (6) have omitted it. This modified USP method was examined also for potential interference by nitroglycerin degradation products.

The degree of interference is expressed as an apparent molar interference factor, defined as the fractional change in spectrophotometric absorbance seen in the presence of an equimolar concentration of the potentially interfering substance. For example, an apparent molar interference factor of +0.50 indicates that when the interfering substance is present at equimolar concentration, the nitroglycerin absorbance would be artifactually increased by 50%. Ideally then, a stability-indicating assay should have an apparent molar interference factor close to zero for all possible degradation products.

Table I—Interference with Nitroglycerin Determination by Different Nitroglycerin Degradation Products

	Apparent Molar Interference Factor[a]			
	Kinetic[b] Assay	Bell[c] Assay	USP[d] Procedure	Modified USP Procedure
1,2-Glyceryl dinitrate	+0.01	+0.01	+0.02	+0.70
	+0.01	0.00	−0.05	+0.46
1,3-Glyceryl dinitrate	+0.02	+0.03	−0.02	+0.60
	+0.03	+0.02	−0.07	+0.50
1-Glyceryl mononitrate	−0.03	−0.01	−0.07	+0.25
	−0.03	−0.05	−0.04	+0.28
2-Glyceryl mononitrate	−0.02	−0.03	−0.09	+0.22
	−0.02	+0.01	−0.07	+0.19
Nitrite ion	0.00	+0.36	+0.01	+0.39
	0.00	+0.36	0.00	+0.40
Nitrate ion	0.00	−0.02	−0.01	+0.38
	0.00	−0.01	+0.01	+0.40

[a] By duplicate determinations. [b] References 8 and 9. [c] Reference 7. [d] Reference 10.

Table I shows the apparent molar interference factors produced by each nitroglycerin degradation product as measured by duplicate determinations in each assay. Within the limits of assay variation, the kinetic and USP assays were stability indicating. The Bell assay, which is effected *via* hydrolysis and subsequent reaction of the nitrite ion produced, showed predictable interference from inorganic nitrite. This finding is relevant if nitroglycerin degradation in solution produces nitrite ion. Ayres *et al.* (11) studied base-catalyzed nitroglycerin hydrolysis and found ~2 moles of nitrite ion formed for each mole reacted. Under the hydrolysis and reaction conditions of the Bell assay, the glyceryl dinitrates, mononitrates, and inorganic nitrate did not interfere. The modified USP method was nonspecific for nitroglycerin, and all substances tested gave positive interference in this procedure. This finding emphasizes the necessity of the column separation step in the USP procedure when specificity for nitroglycerin is desired, particularly when assaying a primary standard upon which all subsequent determinations are based.

The numerical values of the apparent molar interference factors were in general accord with stoichiometric considerations. Thus, when interference occurred, the glyceryl dinitrates gave about two-thirds of the absorbance value generated by an equimolar amount of nitroglycerin while the glyceryl mononitrates, inorganic nitrite, and nitrate ions gave approximately one-third of this value. Comparison of the kinetic and USP procedures showed that there was more apparent assay variability with the latter. This result was reflected by the larger coefficient of variation found for the USP procedure (CV = 4.6%, n = 14) compared with that for the kinetic method (CV = 1.6%, n = 14).

Since the kinetic and USP assays were shown to be free from interference from potential degradation products of nitroglycerin, stability studies may be conducted with either procedure.

[1] Supplied by Arnar-Stone Laboratories, McGaw Park, IL 60085.
[2] As potassium nitrate and sodium nitrite, respectively, both Baker analyzed reagents, J. T. Baker Chemical Co., Phillipsburg, NJ 08865.

(1) J. T. Flaherty, P. R. Reid, D. T. Kelly, D. R. Taylor, M. L. Weisfeldt, and B. Pitt, *Circulation*, **51**, 132 (1975).
(2) J. T. Flaherty, P. C. Come, M. G. Baird, J. Rouleau, D. R. Taylor,

0022-3549/79/0900-1197$01.00/0
© 1979, American Pharmaceutical Association

M. L. Weisfeldt, H. L. Greene, L. C. Becker, and B. Pitt, *Br. Heart J.*, **38**, 612 (1976).

(3) B. L. McNiff, E. F. McNiff, and H.-L. Fung, *Am. J. Hosp. Pharm.*, **32**, 173 (1979).

(4) J. K. Sturek, T. D. Sokoloski, W. T. Winsley, and P. E. Stach, *ibid.*, **35**, 537 (1978).

(5) D. J. Ludwig and C. T. Ueda, *ibid.*, **35**, 541 (1978).

(6) P. Suphajettra, J. H. Strohl, and J. K. Lim, *J. Pharm. Sci.*, **67**, 1394 (1978).

(7) F. K. Bell, *ibid.*, **53**, 752 (1964).

(8) H.-L. Fung, P. Dalecki, E. Tse, and C. T. Rhodes, *ibid.*, **62**, 696 (1973).

(9) S. K. Yap, C. T. Rhodes, and H.-L. Fung, *Am. J. Hosp. Pharm.*, **32**, 1039 (1975).

(10) "The United States Pharmacopeia," 19th rev., Mack Publishing Co., Easton, Pa., 1975.

(11) W. M. Ayres, G. C. Whitnack, and R. T. Merrow, Navweps Report 7608, NOTS TP 2604, 1961.

Richard A. Morrison
Ho-Leung Fung ˣ
Department of Pharmaceutics
School of Pharmacy
State University of New York
at Buffalo
Amherst, NY 14260

Received December 1, 1978.
Accepted for publication June 28, 1979.
Supported in part by National Institutes of Health Grant HL22273 from the National Heart, Lung, and Blood Institute.

Specificity of Nitroglycerin Assays: A Response

Keyphrases □ Nitroglycerin—analysis, stability, various procedures compared □ Vasodilators, coronary—nitroglycerin, stability analysis, various procedures compared □ Stability—nitroglycerin, analysis, various procedures compared

To the Editor:

This response will attempt to clarify several points raised by Morrison and Fung (1) concerning a report by Suphajettra *et al.* (2), which had discussed the possible formation of an interaction compound or complex between nitroglycerin in solution and polyethylene glycol 400. It was then suggested (2) that a loss of nitroglycerin "stability" had occurred due to the sequestering effect on it, which prevented its analysis by both UV (3) and colorimetric (4) techniques. As a result, the different apparent nitroglycerin degradation rates due to polyethylene glycol 400 (Fig. 1) as determined by these two methods simply reflected the relative recoveries of intact nitroglycerin or the "assayable" compound, attributable on one hand to "the more drastic hydrolysis procedure employed in the Bell method, which resulted in a relatively greater breakdown of the reaction compound . . ." (2). It was not our intention to imply that a basic deficiency existed with the UV–kinetic assay for determining free nitroglycerin molecules.

Furthermore, the term stability was used generically in the context of the report to describe not only degraded molecules but also those firmly bound or sequestered and, consequently, not available for analysis. Inasmuch as colorimetric nitroglycerin determination depends on the successful breakdown, in some stoichiometric fashion, of the molecule to a decomposition product, *i.e.*, nitrites, this method obviously cannot be regarded as stability indicating. It is precisely because of such a premise that the formation of an interaction compound, which effectively sequestered nitroglycerin from analysis by these two methods, was proposed. Furthermore, had no nitroglycerin "complex" been formed, the presence of nitrite ions, regardless of source (*i.e.*, as a chemical contaminant or as a nitroglycerin decomposition product), would produce linear curves closely parallel to the abscissa (Fig. 1) following the Bell colorimetric assay.

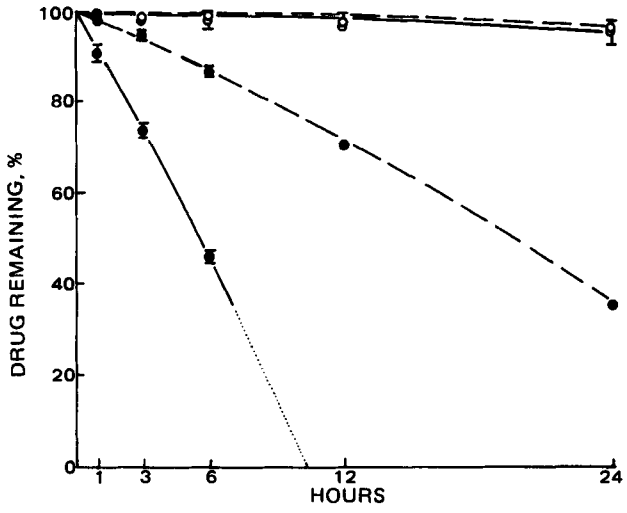

Figure 1—*Percentage of nitroglycerin remaining in povidone* (○) *and polyethylene glycol 400* (●) *solutions as a function of time at 80 ± 0.5° compared using the spectrophotometric* (—) *and colorimetric* (– –) *methods.*

(1) R. A. Morrison and H.-L. Fung, *J. Pharm. Sci.*, **68**, 1197 (1979).

(2) P. Suphajettra, J. H. Strohl, and J. K. Lim, *ibid.*, **67**, 1394 (1978).

(3) H.-L. Fung, P. Dalecki, E. Tse, and C. T. Rhodes, *ibid.*, **62**, 696 (1973).

(4) F. K. Bell, *ibid.*, **53**, 752 (1964).

J. K. Lim
School of Pharmacy
West Virginia University
Morgantown, WV 26506

Received December 27, 1978.
Accepted for publication June 19, 1979.

Percutaneous Butyrolactone Absorption in Rats

Keyphrases □ Butyrolactone—percutaneous absorption, with and without depilation, rats □ Hypnotics—butyrolactone, percutaneous absorption, with and without depilation, rats

To the Editor:

Butyrolactone (I) is a relatively nontoxic hypnotic agent when administered intravenously and orally to rats (1, 2). When I is introduced into the systemic circulation, it is instantaneously and completely converted to γ-hydroxybutyric acid (II). The latter is an endogenous substance in

0022-3549/79/0900-1198$01.00/0
© 1979, American Pharmaceutical Association

M. L. Weisfeldt, H. L. Greene, L. C. Becker, and B. Pitt, *Br. Heart J.*, **38**, 612 (1976).

(3) B. L. McNiff, E. F. McNiff, and H.-L. Fung, *Am. J. Hosp. Pharm.*, **32**, 173 (1979).

(4) J. K. Sturek, T. D. Sokoloski, W. T. Winsley, and P. E. Stach, *ibid.*, **35**, 537 (1978).

(5) D. J. Ludwig and C. T. Ueda, *ibid.*, **35**, 541 (1978).

(6) P. Suphajettra, J. H. Strohl, and J. K. Lim, *J. Pharm. Sci.*, **67**, 1394 (1978).

(7) F. K. Bell, *ibid.*, **53**, 752 (1964).

(8) H.-L. Fung, P. Dalecki, E. Tse, and C. T. Rhodes, *ibid.*, **62**, 696 (1973).

(9) S. K. Yap, C. T. Rhodes, and H.-L. Fung, *Am. J. Hosp. Pharm.*, **32**, 1039 (1975).

(10) "The United States Pharmacopeia," 19th rev., Mack Publishing Co., Easton, Pa., 1975.

(11) W. M. Ayres, G. C. Whitnack, and R. T. Merrow, Navweps Report 7608, NOTS TP 2604, 1961.

Richard A. Morrison
Ho-Leung Fung ˣ
Department of Pharmaceutics
School of Pharmacy
State University of New York
at Buffalo
Amherst, NY 14260

Received December 1, 1978.
Accepted for publication June 28, 1979.
Supported in part by National Institutes of Health Grant HL22273 from the National Heart, Lung, and Blood Institute.

Specificity of Nitroglycerin Assays: A Response

Keyphrases □ Nitroglycerin—analysis, stability, various procedures compared □ Vasodilators, coronary—nitroglycerin, stability analysis, various procedures compared □ Stability—nitroglycerin, analysis, various procedures compared

To the Editor:

This response will attempt to clarify several points raised by Morrison and Fung (1) concerning a report by Suphajettra *et al.* (2), which had discussed the possible formation of an interaction compound or complex between nitroglycerin in solution and polyethylene glycol 400. It was then suggested (2) that a loss of nitroglycerin "stability" had occurred due to the sequestering effect on it, which prevented its analysis by both UV (3) and colorimetric (4) techniques. As a result, the different apparent nitroglycerin degradation rates due to polyethylene glycol 400 (Fig. 1) as determined by these two methods simply reflected the relative recoveries of intact nitroglycerin or the "assayable" compound, attributable on one hand to "the more drastic hydrolysis procedure employed in the Bell method, which resulted in a relatively greater breakdown of the reaction compound . . ." (2). It was not our intention to imply that a basic deficiency existed with the UV–kinetic assay for determining free nitroglycerin molecules.

Furthermore, the term stability was used generically in the context of the report to describe not only degraded molecules but also those firmly bound or sequestered and, consequently, not available for analysis. Inasmuch as colorimetric nitroglycerin determination depends on the successful breakdown, in some stoichiometric fashion, of the molecule to a decomposition product, *i.e.*, nitrites, this method obviously cannot be regarded as stability indicating. It is precisely because of such a premise that the formation of an interaction compound, which effectively sequestered nitroglycerin from analysis by these two methods, was proposed. Furthermore, had no nitroglycerin "complex" been formed, the presence of nitrite ions, regardless of source (*i.e.*, as a chemical contaminant or as a nitroglycerin decomposition product), would produce linear curves closely parallel to the abscissa (Fig. 1) following the Bell colorimetric assay.

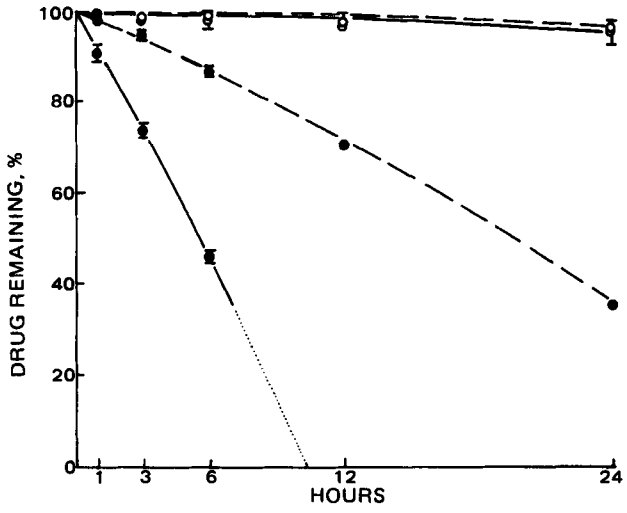

Figure 1—*Percentage of nitroglycerin remaining in povidone* (○) *and polyethylene glycol 400* (●) *solutions as a function of time at 80 ± 0.5° compared using the spectrophotometric* (—) *and colorimetric* (– –) *methods.*

(1) R. A. Morrison and H.-L. Fung, *J. Pharm. Sci.*, **68**, 1197 (1979).

(2) P. Suphajettra, J. H. Strohl, and J. K. Lim, *ibid.*, **67**, 1394 (1978).

(3) H.-L. Fung, P. Dalecki, E. Tse, and C. T. Rhodes, *ibid.*, **62**, 696 (1973).

(4) F. K. Bell, *ibid.*, **53**, 752 (1964).

J. K. Lim
School of Pharmacy
West Virginia University
Morgantown, WV 26506

Received December 27, 1978.
Accepted for publication June 19, 1979.

Percutaneous Butyrolactone Absorption in Rats

Keyphrases □ Butyrolactone—percutaneous absorption, with and without depilation, rats □ Hypnotics—butyrolactone, percutaneous absorption, with and without depilation, rats

To the Editor:

Butyrolactone (I) is a relatively nontoxic hypnotic agent when administered intravenously and orally to rats (1, 2). When I is introduced into the systemic circulation, it is instantaneously and completely converted to γ-hydroxybutyric acid (II). The latter is an endogenous substance in

0022-3549/79/0900-1198$01.00/0
© 1979, American Pharmaceutical Association

M. L. Weisfeldt, H. L. Greene, L. C. Becker, and B. Pitt, *Br. Heart J.*, **38**, 612 (1976).

(3) B. L. McNiff, E. F. McNiff, and H.-L. Fung, *Am. J. Hosp. Pharm.*, **32**, 173 (1979).

(4) J. K. Sturek, T. D. Sokoloski, W. T. Winsley, and P. E. Stach, *ibid.*, **35**, 537 (1978).

(5) D. J. Ludwig and C. T. Ueda, *ibid.*, **35**, 541 (1978).

(6) P. Suphajettra, J. H. Strohl, and J. K. Lim, *J. Pharm. Sci.*, **67**, 1394 (1978).

(7) F. K. Bell, *ibid.*, **53**, 752 (1964).

(8) H.-L. Fung, P. Dalecki, E. Tse, and C. T. Rhodes, *ibid.*, **62**, 696 (1973).

(9) S. K. Yap, C. T. Rhodes, and H.-L. Fung, *Am. J. Hosp. Pharm.*, **32**, 1039 (1975).

(10) "The United States Pharmacopeia," 19th rev., Mack Publishing Co., Easton, Pa., 1975.

(11) W. M. Ayres, G. C. Whitnack, and R. T. Merrow, Navweps Report 7608, NOTS TP 2604, 1961.

Richard A. Morrison
Ho-Leung Fung ˣ
Department of Pharmaceutics
School of Pharmacy
State University of New York
at Buffalo
Amherst, NY 14260

Received December 1, 1978.
Accepted for publication June 28, 1979.
Supported in part by National Institutes of Health Grant HL22273 from the National Heart, Lung, and Blood Institute.

Specificity of Nitroglycerin Assays: A Response

Keyphrases □ Nitroglycerin—analysis, stability, various procedures compared □ Vasodilators, coronary—nitroglycerin, stability analysis, various procedures compared □ Stability—nitroglycerin, analysis, various procedures compared

To the Editor:

This response will attempt to clarify several points raised by Morrison and Fung (1) concerning a report by Suphajettra *et al.* (2), which had discussed the possible formation of an interaction compound or complex between nitroglycerin in solution and polyethylene glycol 400. It was then suggested (2) that a loss of nitroglycerin "stability" had occurred due to the sequestering effect on it, which prevented its analysis by both UV (3) and colorimetric (4) techniques. As a result, the different apparent nitroglycerin degradation rates due to polyethylene glycol 400 (Fig. 1) as determined by these two methods simply reflected the relative recoveries of intact nitroglycerin or the "assayable" compound, attributable on one hand to "the more drastic hydrolysis procedure employed in the Bell method, which resulted in a relatively greater breakdown of the reaction compound . . ." (2). It was not our intention to imply that a basic deficiency existed with the UV–kinetic assay for determining free nitroglycerin molecules.

Furthermore, the term stability was used generically in the context of the report to describe not only degraded molecules but also those firmly bound or sequestered and, consequently, not available for analysis. Inasmuch as colorimetric nitroglycerin determination depends on the successful breakdown, in some stoichiometric fashion, of the molecule to a decomposition product, *i.e.*, nitrites, this method obviously cannot be regarded as stability indicating. It is precisely because of such a premise that the formation of an interaction compound, which effectively sequestered nitroglycerin from analysis by these two methods, was proposed. Furthermore, had no nitroglycerin "complex" been formed, the presence of nitrite ions, regardless of source (*i.e.*, as a chemical contaminant or as a nitroglycerin decomposition product), would produce linear curves closely parallel to the abscissa (Fig. 1) following the Bell colorimetric assay.

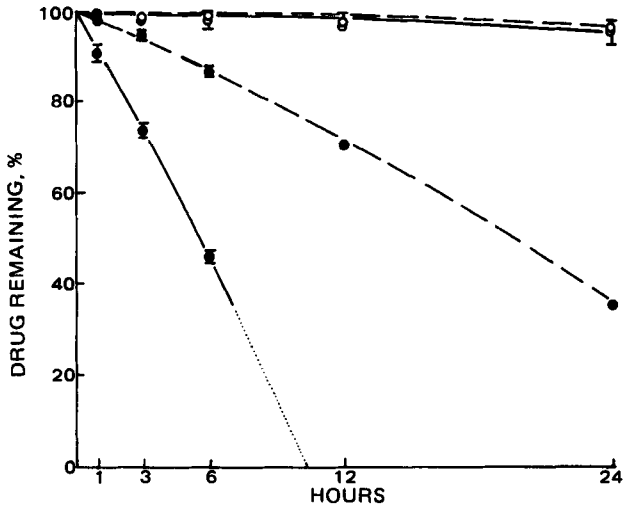

Figure 1—*Percentage of nitroglycerin remaining in povidone* (○) *and polyethylene glycol 400* (●) *solutions as a function of time at 80 ± 0.5° compared using the spectrophotometric* (—) *and colorimetric* (– –) *methods.*

(1) R. A. Morrison and H.-L. Fung, *J. Pharm. Sci.*, **68**, 1197 (1979).

(2) P. Suphajettra, J. H. Strohl, and J. K. Lim, *ibid.*, **67**, 1394 (1978).

(3) H.-L. Fung, P. Dalecki, E. Tse, and C. T. Rhodes, *ibid.*, **62**, 696 (1973).

(4) F. K. Bell, *ibid.*, **53**, 752 (1964).

J. K. Lim
School of Pharmacy
West Virginia University
Morgantown, WV 26506

Received December 27, 1978.
Accepted for publication June 19, 1979.

Percutaneous Butyrolactone Absorption in Rats

Keyphrases □ Butyrolactone—percutaneous absorption, with and without depilation, rats □ Hypnotics—butyrolactone, percutaneous absorption, with and without depilation, rats

To the Editor:

Butyrolactone (I) is a relatively nontoxic hypnotic agent when administered intravenously and orally to rats (1, 2). When I is introduced into the systemic circulation, it is instantaneously and completely converted to γ-hydroxybutyric acid (II). The latter is an endogenous substance in

0022-3549/79/0900-1198$01.00/0
© 1979, American Pharmaceutical Association

the brain (3) and has been used therapeutically as an intravenous anesthetic (4), particularly in pediatric and obstetric procedures.

Recently, DiVincenzo *et al.* (5) showed that a neurotoxic ketone, methyl butyl ketone, was absorbed through intact skin. Because II is subjected to extensive first-pass metabolism and has a short terminal biological half-life ($t_{1/2}$ $\simeq$0.5 hr in humans and rats), it is of interest to determine whether percutaneous I absorption is extensive and prolonged enough to provide sustained hypnosis. Furthermore, because I has physicochemical properties similar to other dipolar aprotic solvents such as dimethyl sulfoxide and thus might promote drug absorption through the skin, the absorption characteristics of I itself need to be determined.

The purpose of this study was to examine percutaneous I absorption. The rat was used as the experimental model because the pharmacokinetics of I were examined previously in this animal (1, 2) and because similar percutaneous absorption studies were carried out with another liquid (6, 7). Percutaneous I absorption was studied with and without a depilating agent since many percutaneous absorption studies in animals employ such an agent and the effect of depilating agents on skin permeability is not well documented.

Male Sprague–Dawley rats, 275–525 g, were prepared as previously described (6, 7). Absorption studies were conducted on the shaved abdomens of the animals over a 3 × 3-cm area. Compound I[1] was applied undiluted at a dose of 6.34 mmoles/kg (equivalent to 800 mg of II/kg) either over untreated skin (Topical Treatment A) or after treatment with 4 ml of thioglycolic acid-based depilating agent[2] (Topical Treatment B). The hair remover was left in contact with the shaved skin for 12 min and was then removed with wet gauze sponges; the skin was allowed to dry in air for 10 min before I application.

The animals were kept under light ether anesthesia, when required, throughout the experiments, and blood (~0.5 ml) was collected at selected intervals *via* the tail vein. Plasma II concentrations were determined according to a previously described procedure (8) and compared to those obtained from separate animals after intravenous and oral administration of the same dose (1, 2). When I is administered systemically, conversion to II is complete and no intact I can be measured.

Figure 1 shows the mean ($\pm SE$) plasma II concentrations obtained after the various routes of administration. Both intravenous and oral I doses gave relatively high plasma II concentrations, which were maintained above 2000 μg/ml for 2 hr after dosing. In contrast, when equimolar doses of I were applied topically, the mean plasma concentrations were <200 μg/ml during the whole 4-hr period. Comparison of the plasma concentrations after the two topical treatments showed that I absorption was more rapid and less variable after hair removal with a depilating agent. Statistical comparison using the two-tailed t-test showed that the concentrations obtained at the first two time points after dosing were significantly higher ($p < 0.02$) after pretreatment with the hair remover. Peak concentrations were observed within 0.5–1 hr after dosing

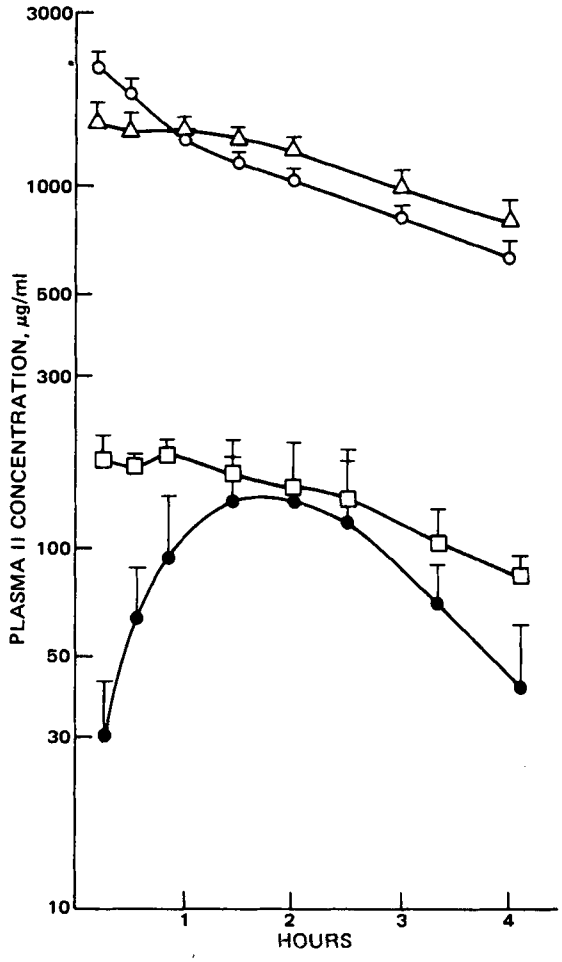

Figure 1—*Plasma II concentrations (mean ± SE) after 6.34 mmoles of I/kg administered through different routes. Key: ○, intravenous; △, oral; □, percutaneous, with hair remover; and ●, percutaneous, without hair remover.*

when a depilating agent was used and at about 1.5–2 hr in controls.

Table I gives the values of the area under the plasma concentration–time curve from 0–4 hr (AUC_{0-4}) for each treatment. Statistical comparison using the Tukey t-test (9) showed that $AUC_{0-4,iv}$ and $AUC_{0-4,po}$ were statistically different ($p < 0.01$) from those obtained after both percutaneous treatments, although $AUC_{0-4,iv}$ did not differ statistically from $AUC_{0-4,po}$ and the two values from the percutaneous treatments also did not differ from each other ($p > 0.05$).

A relative AUC_{0-4} value, defined as $AUC_{0-4,treatment}/AUC_{0-4,iv}$, also was determined for each treatment. In this case, the relative AUC_{0-4} values represent minimum estimates of the fraction of the dose absorbed, F, for the

Table I—Mean ± *SE* Values of the Area under the Plasma Concentration–Time Curve (0–4 hr) after Various I Treatments at 6.34 mmoles/kg

Treatment	$AUC_{0-4} \times 10^{-3}$, μg hr/ml	Relative AUC_{0-4}[a]
Intravenous	4.81 ± 0.37 (3)[b]	1.00
Oral	4.71 ± 0.38 (4)	0.98
Topical (A)	0.34 ± 0.18 (4)	0.07
Topical (B)	0.54 ± 0.08 (3)	0.11

[a] Relative to mean value obtained after intravenous administration. [b] Number in parentheses is the number of animals studied in each group.

[1] Eastman Organic Chemicals, Rochester, N.Y.
[2] Neet lotion hair remover, Whitehall Laboratories, New York, N.Y.

following reasons.

1. Capacity-limited elimination of II occurs at plasma concentrations above 400 μg/ml (2). Both intravenous and oral administrations at 6.34 mmoles/kg gave plasma concentrations well above this threshold, while percutaneous applications of I gave plasma concentrations below this concentration. When capacity-limited elimination occurs, the AUC increases disproportionally with respect to dose. The presence of capacity-limited elimination after the intravenous dose in the present case artifactually led to a larger $AUC_{0\text{-}4,iv}$ value for comparison with values obtained for the percutaneous treatments. Thus, the relative $AUC_{0\text{-}4}$ values for the percutaneous absorption experiments are likely to underestimate F.

2. Percutaneous drug absorption is sometimes fairly protracted. Some I absorption might still take place after the 4-hr period monitored in the percutaneous experiments. This factor would also lead to underestimation of F using the relative $AUC_{0\text{-}4}$ values. The present data could not be used for calculation of AUC from time zero to infinity because significant uncertainties in elimination $t_{1/2}$ estimates are produced by nonlinear elimination kinetics and possible incomplete absorption after the percutaneous doses.

The present results, however, suggested that at least ~10% of the percutaneous I dose was absorbed. Mean plasma II concentrations up to 200 μg/ml were obtained following a 6.34-mmoles/kg topical dose. These concentrations approach those levels (~400 μg/ml) required for complete hypnosis in the rat. In fact, some animals in the percutaneous experiments were sufficiently sedated that continued ether anesthesia was unnecessary. It is clear that the pharmacological effects of I can be elicited through skin absorption.

Hair removal by a commercial depilating agent apparently increased the rate of percutaneous I absorption in the rat. Although hair removal by shaving was done as close to the skin as possible, the remaining hair stubs probably still posed a significant barrier for drug absorption. On the other hand, the depilating agent might have caused some damage to the skin epidermis. This methodological uncertainty is encountered whenever haired animals are used for skin absorption experiments.

(1) J. T. Lettieri and H.-L. Fung, *Res. Commun. Chem. Pathol. Pharmacol.*, **22**, 107 (1978).

(2) J. T. Lettieri and H.-L. Fung, *J. Pharmacol. Exp. Ther.*, **208**, 7 (1979).

(3) S. P. Bessman and W. N. Fishbein, *Nature*, **200**, 1207 (1963).

(4) A. S. Hunter, W. J. Long, and C. G. Ryrie, *Br. J. Anaesth.*, **43**, 620 (1971).

(5) G. D. DiVincenzo, M. L. Hamilton, C. J. Kaplan, W. J. Krasavage, and J. L. O'Donoghue, *Toxicol. Appl. Pharmacol.*, **44**, 593 (1978).

(6) S. T. Horhota and H.-L. Fung, *J. Pharm. Sci.*, **67**, 1345 (1978).

(7) *Ibid.*, **68**, 608 (1979).

(8) J. T. Lettieri and H.-L. Fung, *Biochem. Med.*, **20**, 70 (1978).

(9) J. L. Bruning and B. L. Kintz, "Computational Handbook of Statistics," 2nd ed., Scott, Foresman, Glenview, Ill., 1977.

Ho-Leung Fung ˣ
John T. Lettieri
Robert Bochner

Department of Pharmaceutics
School of Pharmacy
State University of New York
at Buffalo
Amherst, NY 14260

Received May 31, 1979.
Accepted for publication June 18, 1979.
Supported in part by National Institutes of Health General Research Support Grant RR0545416.

Theophylline Analysis by Reversed-Phase High-Pressure Liquid Chromatography: Elimination of Interferences

Keyphrases ◻ Theophylline—analysis, reversed-phase high-pressure liquid chromatography, elimination of ampicillin and 1,7-dimethylxanthine interference ◻ Smooth muscle relaxants—theophylline, reversed-phase high-pressure liquid chromatographic analysis, elimination of ampicillin and 1,7-dimethylxanthine interference ◻ High-pressure liquid chromatography—analysis, theophylline, elimination of ampicillin and 1,7-dimethylxanthine interference

To the Editor:

High-pressure liquid chromatography (HPLC) has been applied to theophylline analysis in biological fluids (1–5). HPLC methods have distinct advantages over traditional UV spectrophotometric methods (6, 7) such as reduced sample requirement, greater specificity, and shorter analysis time. However, several drugs and drug metabolites interfere in the HPLC analysis of theophylline (8–11). Of particular concern are the interferences caused by ampicillin, a commonly used antibiotic, and by 1,7-dimethylxanthine, an important metabolite of caffeine. 1,7-Dimethylxanthine is difficult to detect using ratios of peak heights obtained at two different wavelengths because of the similarity of its UV spectrum to that of theophylline. We have found elevation of serum theophylline values caused by 1,7-dimethylxanthine to be as high as 2 μg/ml. Such a discrepancy could cause misleading interpretation of pharmacokinetic data and would lead to inaccurate dosage regimen calculations.

We modified the method of Orcutt *et al.* (2) to eliminate interferences caused by ampicillin and 1,7-dimethylxanthine by using either a reversed-phase column with a 5-μm support or a radial compression module with a reversed-phase cartridge. A mobile phase of methanol–tetrahydrofuran–sodium acetate buffer provided the desired resolution.

The HPLC system was composed of a single pump[1], a loop injector[2], and a dual-wavelength UV detector with absorbance capability at 254 and 280 nm[3]. A precolumn[4] helped prolong column life. Two types of prepacked columns were used. One consisted of a steel, 25 × 0.5-cm column packed with octadecylsilane bonded to a 5-μm irregular support[5]. The other, intended for use in a radial compression unit, was a polyethylene column packed with octadecylsilane bonded to a spherical 10-μm silica support[6].

[1] Model 6000A, Waters Associates, Milford, Mass.
[2] Model U6K, Waters Associates, Milford, Mass.
[3] Model 440, Waters Associates, Milford, Mass.
[4] Co:Pell ODS, Whatman, Clifton, N.J.
[5] Partisil PXS 5/25 ODS, Whatman, Clifton, N.J.
[6] RCM with radial pak A, Waters Associates, Milford, Mass.

0022-3549/79/0900-1200$01.00/0
© 1979, American Pharmaceutical Association

following reasons.

1. Capacity-limited elimination of II occurs at plasma concentrations above 400 μg/ml (2). Both intravenous and oral administrations at 6.34 mmoles/kg gave plasma concentrations well above this threshold, while percutaneous applications of I gave plasma concentrations below this concentration. When capacity-limited elimination occurs, the AUC increases disproportionally with respect to dose. The presence of capacity-limited elimination after the intravenous dose in the present case artifactually led to a larger $AUC_{0\text{-}4,iv}$ value for comparison with values obtained for the percutaneous treatments. Thus, the relative $AUC_{0\text{-}4}$ values for the percutaneous absorption experiments are likely to underestimate F.

2. Percutaneous drug absorption is sometimes fairly protracted. Some I absorption might still take place after the 4-hr period monitored in the percutaneous experiments. This factor would also lead to underestimation of F using the relative $AUC_{0\text{-}4}$ values. The present data could not be used for calculation of AUC from time zero to infinity because significant uncertainties in elimination $t_{1/2}$ estimates are produced by nonlinear elimination kinetics and possible incomplete absorption after the percutaneous doses.

The present results, however, suggested that at least ~10% of the percutaneous I dose was absorbed. Mean plasma II concentrations up to 200 μg/ml were obtained following a 6.34-mmoles/kg topical dose. These concentrations approach those levels (~400 μg/ml) required for complete hypnosis in the rat. In fact, some animals in the percutaneous experiments were sufficiently sedated that continued ether anesthesia was unnecessary. It is clear that the pharmacological effects of I can be elicited through skin absorption.

Hair removal by a commercial depilating agent apparently increased the rate of percutaneous I absorption in the rat. Although hair removal by shaving was done as close to the skin as possible, the remaining hair stubs probably still posed a significant barrier for drug absorption. On the other hand, the depilating agent might have caused some damage to the skin epidermis. This methodological uncertainty is encountered whenever haired animals are used for skin absorption experiments.

(1) J. T. Lettieri and H.-L. Fung, *Res. Commun. Chem. Pathol. Pharmacol.*, **22**, 107 (1978).

(2) J. T. Lettieri and H.-L. Fung, *J. Pharmacol. Exp. Ther.*, **208**, 7 (1979).

(3) S. P. Bessman and W. N. Fishbein, *Nature*, **200**, 1207 (1963).

(4) A. S. Hunter, W. J. Long, and C. G. Ryrie, *Br. J. Anaesth.*, **43**, 620 (1971).

(5) G. D. DiVincenzo, M. L. Hamilton, C. J. Kaplan, W. J. Krasavage, and J. L. O'Donoghue, *Toxicol. Appl. Pharmacol.*, **44**, 593 (1978).

(6) S. T. Horhota and H.-L. Fung, *J. Pharm. Sci.*, **67**, 1345 (1978).

(7) *Ibid.*, **68**, 608 (1979).

(8) J. T. Lettieri and H.-L. Fung, *Biochem. Med.*, **20**, 70 (1978).

(9) J. L. Bruning and B. L. Kintz, "Computational Handbook of Statistics," 2nd ed., Scott, Foresman, Glenview, Ill., 1977.

Ho-Leung Fung ˣ
John T. Lettieri
Robert Bochner

Department of Pharmaceutics
School of Pharmacy
State University of New York
at Buffalo
Amherst, NY 14260

Received May 31, 1979.
Accepted for publication June 18, 1979.
Supported in part by National Institutes of Health General Research Support Grant RR0545416.

Theophylline Analysis by Reversed-Phase High-Pressure Liquid Chromatography: Elimination of Interferences

Keyphrases ◻ Theophylline—analysis, reversed-phase high-pressure liquid chromatography, elimination of ampicillin and 1,7-dimethylxanthine interference ◻ Smooth muscle relaxants—theophylline, reversed-phase high-pressure liquid chromatographic analysis, elimination of ampicillin and 1,7-dimethylxanthine interference ◻ High-pressure liquid chromatography—analysis, theophylline, elimination of ampicillin and 1,7-dimethylxanthine interference

To the Editor:

High-pressure liquid chromatography (HPLC) has been applied to theophylline analysis in biological fluids (1–5). HPLC methods have distinct advantages over traditional UV spectrophotometric methods (6, 7) such as reduced sample requirement, greater specificity, and shorter analysis time. However, several drugs and drug metabolites interfere in the HPLC analysis of theophylline (8–11). Of particular concern are the interferences caused by ampicillin, a commonly used antibiotic, and by 1,7-dimethylxanthine, an important metabolite of caffeine. 1,7-Dimethylxanthine is difficult to detect using ratios of peak heights obtained at two different wavelengths because of the similarity of its UV spectrum to that of theophylline. We have found elevation of serum theophylline values caused by 1,7-dimethylxanthine to be as high as 2 μg/ml. Such a discrepancy could cause misleading interpretation of pharmacokinetic data and would lead to inaccurate dosage regimen calculations.

We modified the method of Orcutt *et al.* (2) to eliminate interferences caused by ampicillin and 1,7-dimethylxanthine by using either a reversed-phase column with a 5-μm support or a radial compression module with a reversed-phase cartridge. A mobile phase of methanol–tetrahydrofuran–sodium acetate buffer provided the desired resolution.

The HPLC system was composed of a single pump[1], a loop injector[2], and a dual-wavelength UV detector with absorbance capability at 254 and 280 nm[3]. A precolumn[4] helped prolong column life. Two types of prepacked columns were used. One consisted of a steel, 25 × 0.5-cm column packed with octadecylsilane bonded to a 5-μm irregular support[5]. The other, intended for use in a radial compression unit, was a polyethylene column packed with octadecylsilane bonded to a spherical 10-μm silica support[6].

[1] Model 6000A, Waters Associates, Milford, Mass.
[2] Model U6K, Waters Associates, Milford, Mass.
[3] Model 440, Waters Associates, Milford, Mass.
[4] Co:Pell ODS, Whatman, Clifton, N.J.
[5] Partisil PXS 5/25 ODS, Whatman, Clifton, N.J.
[6] RCM with radial pak A, Waters Associates, Milford, Mass.

0022-3549/79/0900-1200$01.00/0
© 1979, American Pharmaceutical Association

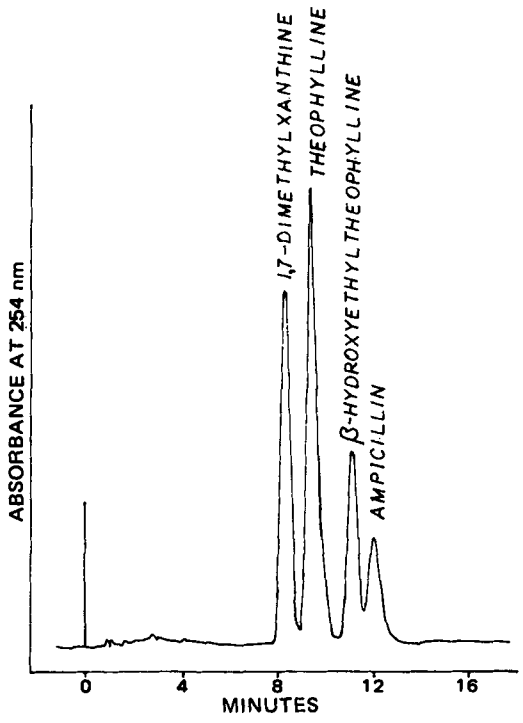

Figure 1—*Chromatogram of theophylline, ampicillin, 1,7-dimethylxanthine, and the internal standard, β-hydroxyethyltheophylline, on a radial compression, reversed-phase column. Conditions were: 6% methanol, 1.2% tetrahydrofuran in 0.01 mole of pH 5.0 sodium acetate/liter, flow rate of 3.0 ml/min, and detection at 280 nm, 0.01 aufs.*

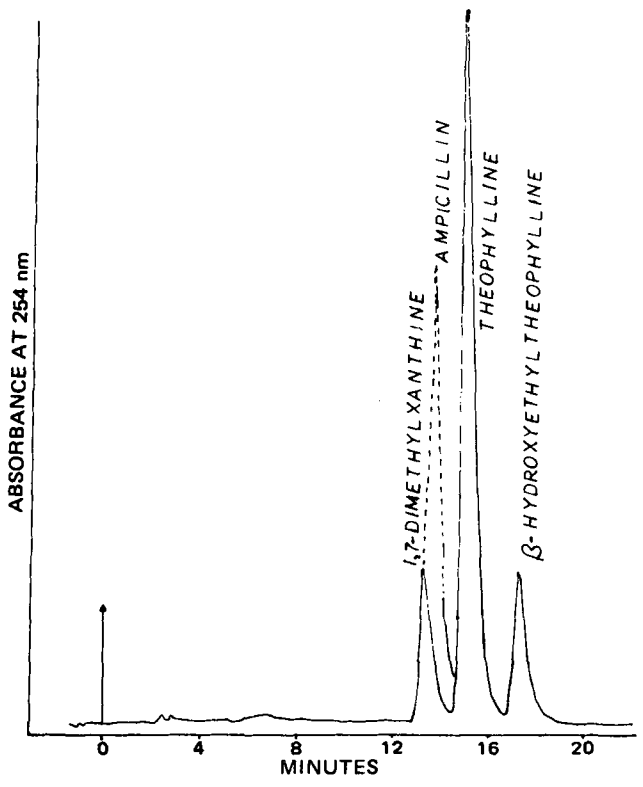

Figure 2—*Chromatogram of theophylline, ampicillin, 1,7-dimethylxanthine, and β-hydroxyethyltheophylline on a conventional column with a 5-μm support, reversed-phase column. Conditions were: 7% methanol, 1% tetrahydrofuran in 0.01 mole of pH 5.0 sodium acetate/liter, flow rate of 1.5 ml/min, and detection at 280 nm, 0.01 aufs.*

The mobile phase was made from 0.01 mole of sodium acetate/liter adjusted to pH 5.0 with acetic acid. This buffer was added to 60 ml of methanol and 12 ml of tetrahydrofuran to make 1 liter of eluent for use with the radial compression system. Eluents used with the 5-μm column were composed of 70 ml of methanol and 10 ml of tetrahydrofuran added to the sodium acetate buffer to make 1 liter. All chromatography solvents were filtered prior to use. Flow rates were 3.0 ml/min with the radial compression module and 1.5 ml/min with the 5-μm support column.

Blood and saliva samples were prepared by the method of Orcutt *et al.* (2) with the following modifications. The internal standard solution was 20–40 μg of β-hydroxyethyltheophylline/ml in 100% acetonitrile, and all samples were centrifuged at 11,500 rpm for 5 min after precipitation. Theophylline standards were prepared over the 2–50-μg/ml range in 0.01 mole of pH 5.0 sodium acetate/liter. These standards were diluted with an equal volume of internal standard solution and chromatographed. Peak height ratios (theophylline/β-hydroxyethyltheophylline) were used to define the standard curves.

The separation of theophylline, β-hydroxyethyltheophylline, ampicillin, and 1,7-dimethylxanthine obtained with the radial compression system is shown in Fig. 1. The chromatographic analysis time for theophylline was 12 min, and pressure did not exceed 1000 psi. Other substances that interfere with the analysis are acetazolamide, cephalexin, cefoxitin, and dyphylline. The major disadvantage of the radial compression module is the initial equipment cost. However, longer column life coupled with lower column cost when compared to conventional columns may counterbalance the initial expense. The system is easily interchangeable with most chromatographic equipment.

The separation of theophylline, β-hydroxyethyltheophylline, ampicillin, and 1,7-dimethylxanthine obtained with the 5-μm conventional column is shown in Fig. 2. The chromatographic analysis time for theophylline was 18 min. Pressures were ~3500 psi. Dyphylline caused interference, but acetazolamide did not. Although the high retention and resolution of the 5-μm support column provided excellent methylxanthine separation, analysis time was longer and pressures were much higher than in previously used 10-μm columns. The compatibility of pumping and injection systems with high pressures must be considered with these columns.

The two chromatographic systems provided excellent linearity with standard solutions over the concentration range examined ($R^2 = 0.9999$). No endogenous substances interfered in the analysis of the limited number of samples analyzed. The following methylxanthines and drugs were well resolved (resolution >2) from theophylline and the internal standard using either system: caffeine, theobromine, 1-methylxanthine, 1-methyluric acid, 1,3-dimethyluric acid, phenobarbital, cefamandole, cefazolin, cephalothin, and methicillin. The methods proposed for theophylline analysis offer the advantages of selectivity from two important interfering substances. In addition, the organic solvents used have less toxic properties and lower cost than acetonitrile. Care must be taken to prepare the mobile phase by a standardized method. Small fluc-

tuations in solvent strength can cause shifting of peaks and changes in peak height ratios. Resolution of theophylline and β-hydroxytheophylline can be optimized for each column by adjustments in the methanol concentration of ±2%.

(1) R. D. Thompson, H. T. Nagasawa, and J. W. Jenne, *J. Lab. Clin. Med.*, **84**, 584 (1974).
(2) J. J. Orcutt, P. P. Kozak, Jr., S. A. Gillman, and L. H. Cummins, *Clin. Chem.*, **23**, 599 (1977).
(3) R. F. Adams, F. L. Vandemark, and G. J. Schmidt, *ibid.*, **22**, 1903 (1976).
(4) L. C. Franconi, G. L. Hawk, B. J. Sandmann, and W. G. Haney, *Anal. Chem.*, **48**, 372 (1976).
(5) S. J. Soldin and J. G. Hill, *Clin. Biochem.*, **10**, 74 (1977).
(6) A. Schack and S. H. Waxler, *J. Pharmacol. Exp. Ther.*, **97**, 283 (1949).
(7) P. Jatlow, *Clin. Chem.*, **21**, 1518 (1975).
(8) C. A. Robinson, Jr., and J. Dobbs, *ibid.*, **24**, 2208 (1978).
(9) R. C. Kelly, D. E. Prentice, and G. M. Hearne, *ibid.*, **24**, 838 (1978).
(10) C. A. Robinson, Jr., B. Mitchell, J. Vasiliades, and A. Siegal, *ibid.*, **24**, 1847 (1978).
(11) J. W. Nelson, A. L. Cordry, C. G. Aron, and R. A. Bartell, *ibid.*, **23**, 124 (1977).

Joy R. Miksic
Benjamin Hodes ˣ
School of Pharmacy
Duquesne University
Pittsburgh, PA 15219

Received May 23, 1979.
Accepted for publication June 26, 1979.
Supported by the Pittsburgh Foundation, the Fisher Charitable Trust, the Hunkele Foundation, the James McCandles Charities, and the Brookes Educational Fund.
We acknowledge the assistance of E. Petzold, The Upjohn Co., Kalamazoo, Mich.

6,6′-Azopurine, a Potent *In Vitro* Inhibitor of Rabbit Liver Aldehyde Oxidase

Keyphrases □ 6,6′-Azopurine—inhibition of rabbit liver aldehyde oxidase, *in vitro*, prevention of azathioprine cytotoxicity □ Enzyme inhibitors—6,6′-azopurine, inhibition of rabbit liver aldehyde oxidase, *in vitro*, prevention of azathioprine cytotoxicity □ Azathioprine—prevention of cytotoxicity by 6,6′-azopurine

To the Editor:

Hepatic aldehyde oxidase (aldehyde:oxygen oxidoreductase, EC 1.2.3.1) oxidizes many purines at the C_8-position (1–3) and has been implicated in the metabolism of azathioprine (3), methotrexate and its dialkyl and dichloro derivatives (4), formycin B (5, 6), cyclophosphamide, and the *N*-alkylphenothiazines (7, 8). Inhibitors of aldehyde oxidase and xanthine oxidase, either endogenous or therapeutically administered, may change the conversion rate of azathioprine into active and inactive metabolites. This factor becomes significant for the development of treatment schedules for the most favorable balance between therapeutic effect and drug toxicity.

We wish to report the finding of such an inhibitor. During investigations of oxoazopurine pharmacology (9, 10), we observed that 6,6′-azopurine disodium salt (I) was a potent inhibitor of rabbit liver aldehyde oxidase and also acted as a substrate for this enzyme. The oxidation of I by the enzyme resulted in the formation of a known potent xanthine oxidase inhibitor, 8,8′-dioxo-6,6′-azopurine (II) (9).

Table I—Identification of the Product of Enzymic Oxidation of 6,6′-Azopurine Disodium Salt (I) by Rabbit Liver Aldehyde Oxidase

Solvent System	R_f Values[a] Chemically Synthesized II	Enzymatically Synthesized II	I
Ethanol–pyridine–water (67:20:13)	0.17	0.16	0.26
n-Propanol–ammonia (concentrated)–water (60:30:10)	0.36	0.37	0.59
Ethanol–0.5 *M* ammonium acetate (5:2)	0.09	0.09	0.4

[a] Chromatographic analyses were carried out using Whatman chromatography grade 1 paper. Results shown are averages of triplicate determinations.

A modified literature method (1) was used to obtain a partially purified aldehyde oxidase preparation from rabbit liver homogenates containing 5.04 mg of protein/ml. It was assayed using a spectrophotometric method based on measuring the rate of N^1-methylnicotinamide chloride oxidation at 300 nm (1, 6). The conversion of N^1-methylnicotinamide chloride to its 2-pyrone was measured by monitoring the increase in absorbance at 300 nm upon addition of the enzyme at ambient temperature to reaction mixtures containing, in 3 ml: substrate (0.5, 1, 2.5, 5, or 10 m*M*), desired concentration of I ranging from 2.6 to 13 μ*M* in 5 m*M* pH 7.8 potassium phosphate buffer, and 0.005% edetic acid. The double-reciprocal plot (Fig. 1) of the inhibition of rabbit liver aldehyde oxidase showed that I was a competitive inhibitor of this enzyme with a k_i of 3.3×10^{-6} *M*. The k_m for N^1-methylnicotinamide chloride was 318 μ*M*.

For the enzymatic synthesis of II from I, the following procedure was used. Compound I, 2.5 mg, was dissolved in 10 ml of water to obtain a clear yellow solution. To this solution were added 7.5 ml of 0.05 *M* potassium phosphate buffer containing 0.005% edetic acid at pH 7.8 and 2.5 ml of aldehyde oxidase suspension (5.04 mg of protein/ml). A control reaction was carried out using the same reactants except that 2.5 ml of the buffer was added in the last step instead of the aldehyde oxidase suspension. Both reaction mixtures were incubated at room temperature for 15 min.

At the end of 15 min, both solutions were brought to a 50% ammonium sulfate saturation by adding 313 g of solid

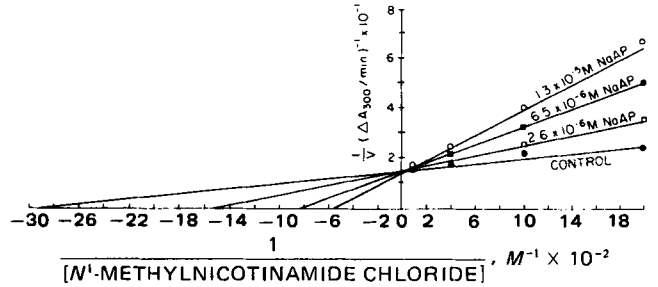

Figure 1—*Double-reciprocal plots of the* in vitro *inhibition of rabbit liver aldehyde oxidase by 6,6′-azopurine disodium salt (I, NaAP).*

0022-3549/79/0900-1202$01.00/0
© 1979, American Pharmaceutical Association

tuations in solvent strength can cause shifting of peaks and changes in peak height ratios. Resolution of theophylline and β-hydroxytheophylline can be optimized for each column by adjustments in the methanol concentration of ±2%.

(1) R. D. Thompson, H. T. Nagasawa, and J. W. Jenne, *J. Lab. Clin. Med.*, **84**, 584 (1974).
(2) J. J. Orcutt, P. P. Kozak, Jr., S. A. Gillman, and L. H. Cummins, *Clin. Chem.*, **23**, 599 (1977).
(3) R. F. Adams, F. L. Vandemark, and G. J. Schmidt, *ibid.*, **22**, 1903 (1976).
(4) L. C. Franconi, G. L. Hawk, B. J. Sandmann, and W. G. Haney, *Anal. Chem.*, **48**, 372 (1976).
(5) S. J. Soldin and J. G. Hill, *Clin. Biochem.*, **10**, 74 (1977).
(6) A. Schack and S. H. Waxler, *J. Pharmacol. Exp. Ther.*, **97**, 283 (1949).
(7) P. Jatlow, *Clin. Chem.*, **21**, 1518 (1975).
(8) C. A. Robinson, Jr., and J. Dobbs, *ibid.*, **24**, 2208 (1978).
(9) R. C. Kelly, D. E. Prentice, and G. M. Hearne, *ibid.*, **24**, 838 (1978).
(10) C. A. Robinson, Jr., B. Mitchell, J. Vasiliades, and A. Siegal, *ibid.*, **24**, 1847 (1978).
(11) J. W. Nelson, A. L. Cordry, C. G. Aron, and R. A. Bartell, *ibid.*, **23**, 124 (1977).

Joy R. Miksic
Benjamin Hodes ˣ
School of Pharmacy
Duquesne University
Pittsburgh, PA 15219

Received May 23, 1979.
Accepted for publication June 26, 1979.
Supported by the Pittsburgh Foundation, the Fisher Charitable Trust, the Hunkele Foundation, the James McCandles Charities, and the Brookes Educational Fund.
We acknowledge the assistance of E. Petzold, The Upjohn Co., Kalamazoo, Mich.

6,6′-Azopurine, a Potent *In Vitro* Inhibitor of Rabbit Liver Aldehyde Oxidase

Keyphrases □ 6,6′-Azopurine—inhibition of rabbit liver aldehyde oxidase, *in vitro*, prevention of azathioprine cytotoxicity □ Enzyme inhibitors—6,6′-azopurine, inhibition of rabbit liver aldehyde oxidase, *in vitro*, prevention of azathioprine cytotoxicity □ Azathioprine—prevention of cytotoxicity by 6,6′-azopurine

To the Editor:

Hepatic aldehyde oxidase (aldehyde:oxygen oxidoreductase, EC 1.2.3.1) oxidizes many purines at the C_8-position (1–3) and has been implicated in the metabolism of azathioprine (3), methotrexate and its dialkyl and dichloro derivatives (4), formycin B (5, 6), cyclophosphamide, and the *N*-alkylphenothiazines (7, 8). Inhibitors of aldehyde oxidase and xanthine oxidase, either endogenous or therapeutically administered, may change the conversion rate of azathioprine into active and inactive metabolites. This factor becomes significant for the development of treatment schedules for the most favorable balance between therapeutic effect and drug toxicity.

We wish to report the finding of such an inhibitor. During investigations of oxoazopurine pharmacology (9, 10), we observed that 6,6′-azopurine disodium salt (I) was a potent inhibitor of rabbit liver aldehyde oxidase and also acted as a substrate for this enzyme. The oxidation of I by the enzyme resulted in the formation of a known potent xanthine oxidase inhibitor, 8,8′-dioxo-6,6′-azopurine (II) (9).

Table I—Identification of the Product of Enzymic Oxidation of 6,6′-Azopurine Disodium Salt (I) by Rabbit Liver Aldehyde Oxidase

Solvent System	R_f Values[a] Chemically Synthesized II	Enzymatically Synthesized II	I
Ethanol–pyridine–water (67:20:13)	0.17	0.16	0.26
n-Propanol–ammonia (concentrated)–water (60:30:10)	0.36	0.37	0.59
Ethanol–0.5 *M* ammonium acetate (5:2)	0.09	0.09	0.4

[a] Chromatographic analyses were carried out using Whatman chromatography grade 1 paper. Results shown are averages of triplicate determinations.

A modified literature method (1) was used to obtain a partially purified aldehyde oxidase preparation from rabbit liver homogenates containing 5.04 mg of protein/ml. It was assayed using a spectrophotometric method based on measuring the rate of N^1-methylnicotinamide chloride oxidation at 300 nm (1, 6). The conversion of N^1-methylnicotinamide chloride to its 2-pyrone was measured by monitoring the increase in absorbance at 300 nm upon addition of the enzyme at ambient temperature to reaction mixtures containing, in 3 ml: substrate (0.5, 1, 2.5, 5, or 10 m*M*), desired concentration of I ranging from 2.6 to 13 μ*M* in 5 m*M* pH 7.8 potassium phosphate buffer, and 0.005% edetic acid. The double-reciprocal plot (Fig. 1) of the inhibition of rabbit liver aldehyde oxidase showed that I was a competitive inhibitor of this enzyme with a k_i of 3.3×10^{-6} *M*. The k_m for N^1-methylnicotinamide chloride was 318 μ*M*.

For the enzymatic synthesis of II from I, the following procedure was used. Compound I, 2.5 mg, was dissolved in 10 ml of water to obtain a clear yellow solution. To this solution were added 7.5 ml of 0.05 *M* potassium phosphate buffer containing 0.005% edetic acid at pH 7.8 and 2.5 ml of aldehyde oxidase suspension (5.04 mg of protein/ml). A control reaction was carried out using the same reactants except that 2.5 ml of the buffer was added in the last step instead of the aldehyde oxidase suspension. Both reaction mixtures were incubated at room temperature for 15 min.

At the end of 15 min, both solutions were brought to a 50% ammonium sulfate saturation by adding 313 g of solid

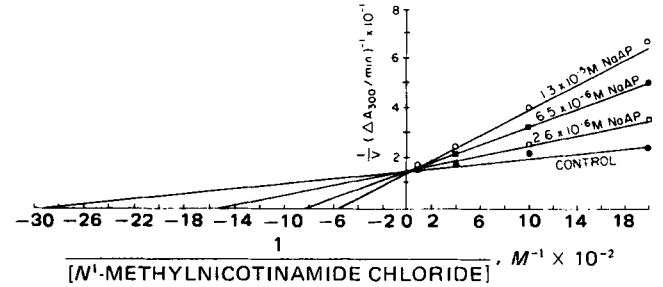

Figure 1—*Double-reciprocal plots of the* in vitro *inhibition of rabbit liver aldehyde oxidase by 6,6′-azopurine disodium salt (I, NaAP).*

0022-3549/79/0900-1202$01.00/0
© 1979, American Pharmaceutical Association

ammonium sulfate/liter of the reaction mixture. The solutions were centrifuged at 8000 rpm for 20 min at 4°. A brown precipitate was obtained from the reaction mixture with the enzyme suspension, while a yellow precipitate was obtained from the control reaction mixture. Both precipitates were dissolved in 25 ml of water separately, and 2.0 ml of 5 *N* HCl was added to each solution. These solutions were centrifuged at 8000 rpm for 20 min at 4°, and the precipitates were treated according to the same procedure again.

At the end, a bright-orange precipitate was obtained from the reaction mixture containing the enzyme suspension, while a yellow precipitate was obtained from the control reaction. The orange precipitate was identified as 8,8′-dioxo-6,6′-azopurine by comparing the R_f values in three different solvent systems (Table I) and the UV characteristics with authentic samples of II. The yellow precipitate was identified as I. Compound I was unchanged under the same conditions even after 6 hr in the absence of enzyme.

Compound I is the first example of a purine dimer that can react with rabbit liver aldehyde oxidase. This finding is significant because it has been suggested that controlled inhibition of aldehyde oxidase will reduce the cytotoxic effects of the immunosuppressive agent azathioprine and modify its chemotherapeutic effects in order to develop more effective treatment schedules (3). Compound I can be considered as a sequential inhibitor of two enzymes involved in azathioprine metabolism. It should inhibit aldehyde oxidase and be converted to II, which is a potent inhibitor of another enzyme in the metabolic pathway, xanthine oxidase. Thus, investigation of the inhibition of mammalian aldehyde oxidase by I may provide such an agent.

Because of the significance of aldehyde oxidase in the metabolism of various biologically active *N*-heterocyclic compounds, I can be used in the investigation of the mechanism of the action of these compounds.

(1) K. V. Rajagopalan and P. Handler, *J. Biol. Chem.*, **239**, 2027 (1964).

(2) T. L. Loo, C. Lim, and D. G. Johns, *Biochim. Biophys. Acta*, **134**, 467 (1967).

(3) A. H. Chalmers, P. R. Knight, and M. R. Atkins, *Aust. J. Exp. Biol. Med. Sci.*, **47**, 263 (1969).

(4) D. G. Johns, D. Farquhar, M. K. Wolpert, B. A. Chabner, and T. L. Loo, *Drug Metab. Dispos.*, **1**, 580 (1973).

(5) I. Tsukada, T. Kunimoto, M. Hori, and T. Komi, *J. Antibiot.*, **22**, 36 (1969).

(6) M. R. Sheen, H. R. Martin, and R. E. Parks, Jr., *Mol. Pharmacol.*, **6**, 225 (1970).

(7) D. L. Hill, W. R. Lester, Jr., and R. F. Struck, *Cancer Res.*, **32**, 658 (1972).

(8) D. L. Hill, W. R. Lester, Jr., M. C. Kirk, S. E. Dareer, and R. F. Struck, *ibid.*, **33**, 1016 (1973).

(9) J. R. Davis, A. L. Jadhav, and J. Fareed, *J. Med. Chem.*, **17**, 639 (1974).

(10) A. L. Jadhav, Ph.D. dissertation, Loyola University of Chicago, Maywood, Ill., 1976.

Arun L. Jadhav ˣ
Kanti G. Bhansali
School of Pharmacy
Texas Southern University
Houston, TX 77004
Joseph R. Davis
Department of Pharmacology
Loyola University of Chicago
Maywood, IL 60153

Received February 23, 1979.
Accepted for publication June 22, 1979.
The authors thank Dr. Alfred Giner-Sorolla for the gift of 6,6′-azopurine disodium salt.

Effect of Altered Plasma Protein Binding on Apparent Volume of Distribution

Keyphrases ◻ Volume of distribution—effect of altered plasma protein binding, pharmacokinetics ◻ Drug binding—plasma, volume of distribution, effect of altered plasma protein binding ◻ Plasma protein binding—effect of alterations on apparent drug volume of distribution ◻ Models, pharmacokinetic—apparent volume of distribution, effect of altered plasma protein binding

To the Editor:

Changes in the apparent volume of distribution occur with age, disease, and displacement (drug interaction) and in the presence of saturable binding. Relationships have been developed (1–6) to explain these changes based on alterations in plasma and/or tissue binding. Our discussion is restricted to measurement of drug concentrations in plasma. Gillette (1) showed that the volume of distribution, V, can be expressed by:

$$V = \alpha(V_f + XV_T) + (1 - \alpha)V_p \qquad \text{(Eq. 1)}$$

where α is the fraction unbound in plasma, V_f is the volume into which the unbound drug is distributed, X is the ratio of tissue drug concentration to unbound plasma drug concentration, V_T is the tissue volume, and V_p is the apparent volume of distribution of the plasma protein to which the drug binds. A simplified relationship, based on the physiological concepts of Gillette (1, 4–6), was proposed (2, 3) as follows:

$$V = V_P + (V_T)\left(\frac{\alpha}{\alpha_T}\right) \qquad \text{(Eq. 2)}$$

where V_P is the plasma volume, V_T is the volume outside plasma into which the drug distributes, and α and α_T are the fractions unbound in these two compartments.

The relationship of Eq. 2 does not take into account that plasma proteins are distributed throughout the extracellular fluids. When the binding to proteins in plasma is altered, similar changes are expected in the binding to these proteins located in other extracellular fluids. Furthermore, this relationship cannot distinguish between binding to these proteins and binding elsewhere in the body. This distinction is important for anticipating changes in the volume of distribution on altering drug binding and the converse.

The following derivation provides a method for making this distinction. From mass balance considerations:

$$A = A_P + A_E + A_R \qquad \text{(Eq. 3)}$$

where:

A = total amount of drug in the body
A_P = total amount of drug in plasma
A_E = total amount of drug in the extracellular fluid outside plasma

0022-3549/79/0900-1203$01.00/0
© 1979, American Pharmaceutical Association

ammonium sulfate/liter of the reaction mixture. The solutions were centrifuged at 8000 rpm for 20 min at 4°. A brown precipitate was obtained from the reaction mixture with the enzyme suspension, while a yellow precipitate was obtained from the control reaction mixture. Both precipitates were dissolved in 25 ml of water separately, and 2.0 ml of 5 *N* HCl was added to each solution. These solutions were centrifuged at 8000 rpm for 20 min at 4°, and the precipitates were treated according to the same procedure again.

At the end, a bright-orange precipitate was obtained from the reaction mixture containing the enzyme suspension, while a yellow precipitate was obtained from the control reaction. The orange precipitate was identified as 8,8′-dioxo-6,6′-azopurine by comparing the R_f values in three different solvent systems (Table I) and the UV characteristics with authentic samples of II. The yellow precipitate was identified as I. Compound I was unchanged under the same conditions even after 6 hr in the absence of enzyme.

Compound I is the first example of a purine dimer that can react with rabbit liver aldehyde oxidase. This finding is significant because it has been suggested that controlled inhibition of aldehyde oxidase will reduce the cytotoxic effects of the immunosuppressive agent azathioprine and modify its chemotherapeutic effects in order to develop more effective treatment schedules (3). Compound I can be considered as a sequential inhibitor of two enzymes involved in azathioprine metabolism. It should inhibit aldehyde oxidase and be converted to II, which is a potent inhibitor of another enzyme in the metabolic pathway, xanthine oxidase. Thus, investigation of the inhibition of mammalian aldehyde oxidase by I may provide such an agent.

Because of the significance of aldehyde oxidase in the metabolism of various biologically active *N*-heterocyclic compounds, I can be used in the investigation of the mechanism of the action of these compounds.

(1) K. V. Rajagopalan and P. Handler, *J. Biol. Chem.*, **239**, 2027 (1964).

(2) T. L. Loo, C. Lim, and D. G. Johns, *Biochim. Biophys. Acta*, **134**, 467 (1967).

(3) A. H. Chalmers, P. R. Knight, and M. R. Atkins, *Aust. J. Exp. Biol. Med. Sci.*, **47**, 263 (1969).

(4) D. G. Johns, D. Farquhar, M. K. Wolpert, B. A. Chabner, and T. L. Loo, *Drug Metab. Dispos.*, **1**, 580 (1973).

(5) I. Tsukada, T. Kunimoto, M. Hori, and T. Komi, *J. Antibiot.*, **22**, 36 (1969).

(6) M. R. Sheen, H. R. Martin, and R. E. Parks, Jr., *Mol. Pharmacol.*, **6**, 225 (1970).

(7) D. L. Hill, W. R. Lester, Jr., and R. F. Struck, *Cancer Res.*, **32**, 658 (1972).

(8) D. L. Hill, W. R. Lester, Jr., M. C. Kirk, S. E. Dareer, and R. F. Struck, *ibid.*, **33**, 1016 (1973).

(9) J. R. Davis, A. L. Jadhav, and J. Fareed, *J. Med. Chem.*, **17**, 639 (1974).

(10) A. L. Jadhav, Ph.D. dissertation, Loyola University of Chicago, Maywood, Ill., 1976.

Arun L. Jadhav ˣ
Kanti G. Bhansali
School of Pharmacy
Texas Southern University
Houston, TX 77004
Joseph R. Davis
Department of Pharmacology
Loyola University of Chicago
Maywood, IL 60153

Received February 23, 1979.
Accepted for publication June 22, 1979.
The authors thank Dr. Alfred Giner-Sorolla for the gift of 6,6′-azopurine disodium salt.

Effect of Altered Plasma Protein Binding on Apparent Volume of Distribution

Keyphrases ◻ Volume of distribution—effect of altered plasma protein binding, pharmacokinetics ◻ Drug binding—plasma, volume of distribution, effect of altered plasma protein binding ◻ Plasma protein binding—effect of alterations on apparent drug volume of distribution ◻ Models, pharmacokinetic—apparent volume of distribution, effect of altered plasma protein binding

To the Editor:

Changes in the apparent volume of distribution occur with age, disease, and displacement (drug interaction) and in the presence of saturable binding. Relationships have been developed (1–6) to explain these changes based on alterations in plasma and/or tissue binding. Our discussion is restricted to measurement of drug concentrations in plasma. Gillette (1) showed that the volume of distribution, V, can be expressed by:

$$V = \alpha(V_f + XV_T) + (1 - \alpha)V_p \qquad \text{(Eq. 1)}$$

where α is the fraction unbound in plasma, V_f is the volume into which the unbound drug is distributed, X is the ratio of tissue drug concentration to unbound plasma drug concentration, V_T is the tissue volume, and V_p is the apparent volume of distribution of the plasma protein to which the drug binds. A simplified relationship, based on the physiological concepts of Gillette (1, 4–6), was proposed (2, 3) as follows:

$$V = V_P + (V_T)\left(\frac{\alpha}{\alpha_T}\right) \qquad \text{(Eq. 2)}$$

where V_P is the plasma volume, V_T is the volume outside plasma into which the drug distributes, and α and α_T are the fractions unbound in these two compartments.

The relationship of Eq. 2 does not take into account that plasma proteins are distributed throughout the extracellular fluids. When the binding to proteins in plasma is altered, similar changes are expected in the binding to these proteins located in other extracellular fluids. Furthermore, this relationship cannot distinguish between binding to these proteins and binding elsewhere in the body. This distinction is important for anticipating changes in the volume of distribution on altering drug binding and the converse.

The following derivation provides a method for making this distinction. From mass balance considerations:

$$A = A_P + A_E + A_R \qquad \text{(Eq. 3)}$$

where:

A = total amount of drug in the body
A_P = total amount of drug in plasma
A_E = total amount of drug in the extracellular fluid outside plasma

0022-3549/79/0900-1203$01.00/0
© 1979, American Pharmaceutical Association

A_R = total amount of drug in the remainder of the body

The amount in plasma is equal to:

$$A_P = (V_P)(C) \quad \text{(Eq. 4)}$$

where V_P is the plasma volume and C is the total plasma concentration. The total amount of drug in the extracellular fluid outside the plasma is equal to:

$$A_E = (V_E)(C_E) \quad \text{(Eq. 5)}$$

where V_E is the extracellular space minus the plasma volume and C_E is the average total concentration in this fluid. The amount of drug in the remainder of the body is equal to:

$$A_R = (V_R)(C_R) \quad \text{(Eq. 6)}$$

where V_R is the physical volume into which the drug distributes minus the extracellular space and C_R is the average concentration in this space.

Substituting Eqs. 4–6 into Eq. 3, dividing by C, and knowing that A/C is, by definition, the apparent volume of distribution, we obtain:

$$V = V_P + (V_E)\left(\frac{C_E}{C}\right) + (V_R)\left(\frac{C_R}{C}\right) \quad \text{(Eq. 7)}$$

Unless active transport or other complications occur, at distribution equilibrium the unbound drug concentration, Cu, is the same in all tissues into which it distributes. Defining α_R as Cu/C_R, α as Cu/C, and Cb_E as the average concentration of bound drug in the extracellular space outside plasma, we obtain:

$$V = V_P + (V_E)(\alpha)\left(\frac{Cu + Cb_E}{Cu}\right) + (V_R)\left(\frac{\alpha}{\alpha_R}\right) \quad \text{(Eq. 8)}$$

For a given protein with one class of binding sites, the law of mass action gives:

$$K_a = \frac{Cb_P}{(Cu)(P)_P} = \frac{Cb_E}{(Cu)(P)_E} \quad \text{(Eq. 9)}$$

where Cb_P and Cb_E are the bound drug concentrations and $(P)_P$ and $(P)_E$ are the concentrations of unoccupied protein binding sites in the plasma and in the other extracellular fluids, respectively, and K_a is the association or affinity constant. Since the unbound drug concentration is identical in both fluids:

$$\frac{Cb_P}{(P)_P} = \frac{Cb_E}{(P)_E} \quad \text{(Eq. 10)}$$

Moreover, since:

$$(P)_P + Cb_P = (Pt)_P \quad \text{(Eq. 11)}$$

and:

$$(P)_E + Cb_E = (Pt)_E \quad \text{(Eq. 12)}$$

where $(Pt)_P$ and $(Pt)_E$ are the average total concentrations of binding sites in the plasma and in the other extracellular fluids, respectively, it follows that:

$$Cb_E = (Cb_P)\left[\frac{(Pt)_E}{(Pt)_P}\right] \quad \text{(Eq. 13)}$$

or:

$$Cb_E = (Cb_P)(R_{E/I})\left(\frac{V_P}{V_E}\right) \quad \text{(Eq. 14)}$$

where $R_{E/I}$ is the ratio of the total number of binding sites or the amount of protein in extracellular fluids outside the plasma to that in the plasma. Equation 14 can be shown to be valid also when there is more than one class of binding sites on a protein, when saturation is approached, and when several proteins are present, provided the ratio $R_{E/I}$ is the same for each protein. Substituting Eq. 14 into Eq. 8 gives:

$$V = V_P + \alpha\left[\frac{V_E Cu + Cb_P V_P R_{E/I}}{Cu}\right] + \frac{V_R \alpha}{\alpha_R} \quad \text{(Eq. 15)}$$

However, since:

$$Cb_P/Cu = (1 - \alpha)/\alpha \quad \text{(Eq. 16)}$$

then:

$$V = V_P(1 + R_{E/I}) + \alpha V_P(V_E/V_P - R_{E/I}) + \frac{V_R \alpha}{\alpha_R} \quad \text{(Eq. 17)}$$

This relationship is similar to that proposed by Gillette (1) (Eq. 1) but includes terms for the intravascular–extravascular distribution of the binding protein as well as the actual volumes of these extracellular fluids.

The extracellular fluid outside the plasma is usually considered to be 12 liters and the plasma volume to be 3 liters in a normal 70-kg man (7). Furthermore, 55–60% of the total extracellular albumin is usually found outside the plasma (8); with the assumption that the plasma proteins to which the drug binds are distributed like albumin, the extravascular to intravascular ratio, $R_{E/I}$, is ~1.4. With these normal values, Eq. 17 becomes:

$$V = 7.2 + \alpha(7.8) + (V_R)\left(\frac{\alpha}{\alpha_R}\right) \quad \text{(Eq. 18)}$$

or approximately:

$$V = 7 + 8(\alpha) + V_R\left(\frac{\alpha}{\alpha_R}\right) \quad \text{(Eq. 19)}$$

This equation states that when a drug is only distributed to the extracellular fluid and cannot enter the cells (V_R = 0), the smallest apparent volume of distribution a drug can have is:

$$V = 7 + 8(\alpha) \quad \text{(Eq. 20)}$$

Thus, at distribution equilibrium, the observed apparent volume of distribution of any drug cannot be less than 7 liters, no matter how tightly bound the drug is to albumin. For a drug restricted to the extracellular fluid only (V_R = 0) and not plasma protein bound (α = 1), the apparent volume of distribution is limited to the value of the total extravascular fluid volume, 15 liters.

Equations 17 and 19 are particularly useful for drugs with low apparent volumes of distribution (<15 liters or <0.2 liter/kg). For example, the volume of distribution of tolbutamide was shown to be essentially unchanged in hepatitis patients, even though the plasma albumin binding was altered in the acute phase of the disease (9). With Eq. 19 and the assumption of no change in α_R, the volume of distribution is calculated to increase from 0.15 to 0.164 liter/kg when the fraction unbound in plasma is increased from 0.068 to 0.087 in hepatitis (9). Thus, a 28% increase in α only results in a 9.5% increase in the apparent volume of distribution.

The observation of little or no change in the volume of distribution when α is increased is consistent with decreased binding to albumin throughout the extracellular fluids, and no alteration in α_R is indicated. However, if Eq. 2 is used, a change in α_T is necessary to explain this ob-

servation, as stated by Gibaldi and McNamara (3), even though only a change in albumin binding may have occurred. When the apparent drug volume of distribution is large (>50–100 liters), the sum $V_P(1 + R_{E/I}) + \alpha(V_P)(V_E/V_P - R_{E/I})$ in Eq. 17 can be neglected since its largest possible value is 15 liters. The apparent volume of distribution is then:

$$V \cong (V_R)\left(\frac{\alpha}{\alpha_R}\right) \qquad \text{(Eq. 21)}$$

which is also predicted by Eq. 2.

The relationship presented in Eq. 17 should be helpful in analyzing and predicting alterations in the apparent volume of distribution of any drug when there is an alteration in the unbound fraction in plasma, in the unbound fraction outside the extracellular fluids, in the volumes of the extracellular fluids, or in the extravascular to intravascular plasma protein ratio, as occurs, for example, in prolonged bed rest and in severe burns. It will also be useful to identify where the alteration occurs.

(1) J. R. Gillette, *Ann. N.Y. Acad. Sci.*, **281**, 136 (1976).

(2) G. R. Wilkinson and D. G. Shand, *Clin. Pharmacol. Ther.*, **18**, 377 (1975).

(3) M. Gibaldi and P. J. McNamara, *Eur. J. Clin. Pharmacol.*, **13**, 373 (1978).

(4) J. R. Gillette, in "Importance of Fundamental Principles in Drug Evaluation," D. H. Tedeschi and R. E. Tedeschi, Eds., Raven, New York, N.Y., 1968, p. 69.

(5) J. R. Gillette, *Ann. N.Y. Acad. Sci.*, **179**, 43 (1971).

(6) J. R. Gillette and K. S. Pang, *Clin. Pharmacol. Ther.*, **22**, 623 (1977).

(7) A. C. Guyton, "Textbook of Medical Physiology," Saunders, Philadelphia, Pa., 1976, p. 424.

(8) W. J. Jusko and M. Gretch, *Drug Metab. Rev.*, **5**, 43 (1976).

(9) R. L. Williams, T. F. Blaschke, P. J. Meffin, K. L. Melmon, and M. Rowland, *Clin. Pharmacol. Ther.*, **21**, 301 (1977).

Svein Øie ˣ
Thomas N. Tozer
School of Pharmacy
University of California
San Francisco, CA 94143

Received February 2, 1979.
Accepted for publication June 7, 1979.
Supported in part by Grant 1R01 GM 25807-01 from the National Institutes of Health.

BOOKS

REVIEWS

Pharmazeutische Technologie. Edited by HEINZ SUCKER, PETER FUCHS, and PETER SPEISER. George Thieme Verlag, Herdweg 63, Postfach 732, D-7000 Stuttgart 1, West Germany. 1978. 906 pp. 17 × 24 cm. Price DM 235.

Industrial pharmacy as a scientific and technological branch of the profession of pharmacy covers a wide spectrum of operations involving a multidisciplinary body of fundamental knowledge and a diversified technology constrained by a specific set of governmental regulations intended to serve as controls over the laboratory and manufacturing environment as well as the quality of the drug preparation itself. An area of such diversity and complexity remains dynamic, and advances in basic pharmaceutics and pharmaceutical technology have accelerated during the past three decades. These advances have come about as a consequence of the pharmaceutical industry's expanding research and development investment and through the acquisition of scientific knowledge and technology from external sources such as universities and other industries.

An early effort by the Pharmaceutical Institute (ETH) in Zurich to reduce the high level of empiricism in the teaching of pharmacy students through the introduction of "physical pharmacy" principles resulted in the publication of a textbook, "Galenisches Praktikum"[1], in which the authors attempted to relate theoretical concepts to practice by means of explanatory text, laboratory exercises, and pertinent literature references. A decade later, the publication of "The Theory and Practice of Industrial Pharmacy"[2] provided a text much closer to the reality of industrial operations and constraints in the development and production of drug preparations.

The latest textbook that endeavors to portray accurately industrial pharmacy is "Pharmazeutische Technologie," a collaborative effort involving 25 authors, most of whom are associated with Swiss or German pharmaceutical companies and each of whom has been selected as a working specialist in his field. By the judicious decision to organize the material as an applied science based on current theoretical concepts of unit operations, only seven chapters were needed. The book begins with a thorough and excellently organized chapter, which develops the mathematical concepts of practical importance to research and development pharmacists engaged in dosage form design. The statistical section is particularly noteworthy for the manner in which research design and optimization techniques and scale-up theory are presented. Along similar lines, the second chapter reviews the theoretical basis for most of the unit operations involved in pharmaceutical dosage form development and production. Among these are the flow properties of gases and liquids, heat transfer, dissolution, comminution, dispersion, mixing, granulating, compressing, and antimicrobial treatment.

In this period of high interest in biopharmaceutics, since a textbook on technology cannot overlook the biological aspects of pharmaceutical product development, a short third chapter covers pharmacokinetic modeling, methodology, and specific applications to bioavailability, sustained-release formulations, and new delivery systems. The fourth chapter treats the important and often neglected subject of pharmaceutical excipients in accordance with the functional role of the excipient in a dosage form. A series of tables listing most of the commonly used excipients conveniently provides incomplete but useful technical information, including average concentration range. Standards for excipients and other forms of regulatory control are described, but deficiencies in existing standards and variability in controls receive minimal attention.

In covering the key subject of dosage forms, the fifth chapter requires over 40% of the total number of pages in the book. The subdivision of topics is based on physical form, route of administration, and sequence of unit operations. This approach proves to be an effective means of organizing a large mass of technical material which, in general, is representative of the current state of pharmaceutics and process technology. The section on parenteral dosage forms and especially the discussions of production control methods and the organization and technological aspects of parenteral production operations are outstanding.

In the sixth chapter, attention is directed to the protective role of packaging, the types of packaging materials used in pharmaceutical containers, and the various chemical, physical, and microbiological tests used to control their quality. A second section includes a brief review of packaging line operations. The last chapter deals with quality control assurance and begins with a rarely seen section on quality of design as studied during preformulation. This discussion is followed by material covering the subsequent formulation studies, which involve drug release characteristics, bioavailability and tissue tolerance of various dosage

servation, as stated by Gibaldi and McNamara (3), even though only a change in albumin binding may have occurred. When the apparent drug volume of distribution is large (>50–100 liters), the sum $V_P(1 + R_{E/I}) + \alpha(V_P)(V_E/V_P - R_{E/I})$ in Eq. 17 can be neglected since its largest possible value is 15 liters. The apparent volume of distribution is then:

$$V \cong (V_R)\left(\frac{\alpha}{\alpha_R}\right) \qquad \text{(Eq. 21)}$$

which is also predicted by Eq. 2.

The relationship presented in Eq. 17 should be helpful in analyzing and predicting alterations in the apparent volume of distribution of any drug when there is an alteration in the unbound fraction in plasma, in the unbound fraction outside the extracellular fluids, in the volumes of the extracellular fluids, or in the extravascular to intravascular plasma protein ratio, as occurs, for example, in prolonged bed rest and in severe burns. It will also be useful to identify where the alteration occurs.

(1) J. R. Gillette, *Ann. N.Y. Acad. Sci.*, **281**, 136 (1976).

(2) G. R. Wilkinson and D. G. Shand, *Clin. Pharmacol. Ther.*, **18**, 377 (1975).

(3) M. Gibaldi and P. J. McNamara, *Eur. J. Clin. Pharmacol.*, **13**, 373 (1978).

(4) J. R. Gillette, in "Importance of Fundamental Principles in Drug Evaluation," D. H. Tedeschi and R. E. Tedeschi, Eds., Raven, New York, N.Y., 1968, p. 69.

(5) J. R. Gillette, *Ann. N.Y. Acad. Sci.*, **179**, 43 (1971).

(6) J. R. Gillette and K. S. Pang, *Clin. Pharmacol. Ther.*, **22**, 623 (1977).

(7) A. C. Guyton, "Textbook of Medical Physiology," Saunders, Philadelphia, Pa., 1976, p. 424.

(8) W. J. Jusko and M. Gretch, *Drug Metab. Rev.*, **5**, 43 (1976).

(9) R. L. Williams, T. F. Blaschke, P. J. Meffin, K. L. Melmon, and M. Rowland, *Clin. Pharmacol. Ther.*, **21**, 301 (1977).

Svein Øie ˣ
Thomas N. Tozer
School of Pharmacy
University of California
San Francisco, CA 94143

Received February 2, 1979.
Accepted for publication June 7, 1979.
Supported in part by Grant 1R01 GM 25807-01 from the National Institutes of Health.

BOOKS

REVIEWS

Pharmazeutische Technologie. Edited by HEINZ SUCKER, PETER FUCHS, and PETER SPEISER. George Thieme Verlag, Herdweg 63, Postfach 732, D-7000 Stuttgart 1, West Germany. 1978. 906 pp. 17 × 24 cm. Price DM 235.

Industrial pharmacy as a scientific and technological branch of the profession of pharmacy covers a wide spectrum of operations involving a multidisciplinary body of fundamental knowledge and a diversified technology constrained by a specific set of governmental regulations intended to serve as controls over the laboratory and manufacturing environment as well as the quality of the drug preparation itself. An area of such diversity and complexity remains dynamic, and advances in basic pharmaceutics and pharmaceutical technology have accelerated during the past three decades. These advances have come about as a consequence of the pharmaceutical industry's expanding research and development investment and through the acquisition of scientific knowledge and technology from external sources such as universities and other industries.

An early effort by the Pharmaceutical Institute (ETH) in Zurich to reduce the high level of empiricism in the teaching of pharmacy students through the introduction of "physical pharmacy" principles resulted in the publication of a textbook, "Galenisches Praktikum"[1], in which the authors attempted to relate theoretical concepts to practice by means of explanatory text, laboratory exercises, and pertinent literature references. A decade later, the publication of "The Theory and Practice of Industrial Pharmacy"[2] provided a text much closer to the reality of industrial operations and constraints in the development and production of drug preparations.

The latest textbook that endeavors to portray accurately industrial pharmacy is "Pharmazeutische Technologie," a collaborative effort involving 25 authors, most of whom are associated with Swiss or German pharmaceutical companies and each of whom has been selected as a working specialist in his field. By the judicious decision to organize the material as an applied science based on current theoretical concepts of unit operations, only seven chapters were needed. The book begins with a thorough and excellently organized chapter, which develops the mathematical concepts of practical importance to research and development pharmacists engaged in dosage form design. The statistical section is particularly noteworthy for the manner in which research design and optimization techniques and scale-up theory are presented. Along similar lines, the second chapter reviews the theoretical basis for most of the unit operations involved in pharmaceutical dosage form development and production. Among these are the flow properties of gases and liquids, heat transfer, dissolution, comminution, dispersion, mixing, granulating, compressing, and antimicrobial treatment.

In this period of high interest in biopharmaceutics, since a textbook on technology cannot overlook the biological aspects of pharmaceutical product development, a short third chapter covers pharmacokinetic modeling, methodology, and specific applications to bioavailability, sustained-release formulations, and new delivery systems. The fourth chapter treats the important and often neglected subject of pharmaceutical excipients in accordance with the functional role of the excipient in a dosage form. A series of tables listing most of the commonly used excipients conveniently provides incomplete but useful technical information, including average concentration range. Standards for excipients and other forms of regulatory control are described, but deficiencies in existing standards and variability in controls receive minimal attention.

In covering the key subject of dosage forms, the fifth chapter requires over 40% of the total number of pages in the book. The subdivision of topics is based on physical form, route of administration, and sequence of unit operations. This approach proves to be an effective means of organizing a large mass of technical material which, in general, is representative of the current state of pharmaceutics and process technology. The section on parenteral dosage forms and especially the discussions of production control methods and the organization and technological aspects of parenteral production operations are outstanding.

In the sixth chapter, attention is directed to the protective role of packaging, the types of packaging materials used in pharmaceutical containers, and the various chemical, physical, and microbiological tests used to control their quality. A second section includes a brief review of packaging line operations. The last chapter deals with quality control assurance and begins with a rarely seen section on quality of design as studied during preformulation. This discussion is followed by material covering the subsequent formulation studies, which involve drug release characteristics, bioavailability and tissue tolerance of various dosage

forms, scale-up effects, and in-process controls. The importance of the guidelines for good manufacturing practices as elaborated by the World Health Organization is reviewed in sections dealing with documentation, hygienic requirements, and clean room technology.

The subject matter covered by the text is of such great international interest to pharmaceutical scientists that at least a thousand articles or chapters in books appear annually. Therefore, it is of interest to check the bibliography of over 700 references used by the authors in the preparation of the text. Although the proportion does vary somewhat from chapter to chapter, the overall percentage cited from Swiss or German publications is about 60% of the total. This exceedingly high level may reflect the reading habits of the authors or their language preferences or limitations rather than the true proportion of scientific and technological activity taking place throughout the world.

The emphasis in this German-language book lies squarely in the domain of industrial pharmacy, and it can be highly recommended to pharmaceutical scientists active in the research, development, production, and control departments of the pharmaceutical industry; to teachers of pharmaceutics and pharmaceutical process technology and their graduate students in the universities; and to scientific members of regulatory agencies who wish to gain a valuable perspective of the complex nature of modern drug development and production.

The publisher deserves commendation for the high technical quality of the book itself. Format, typography, figures, and tables are numerous, clear, well-placed, and pertinent to the text. Perhaps that plus inflation explains the price of the book.

[1] "Galenisches Praktikum," K. Münzel, J. Büchi, and O.-E. Schultz, Eds., Wissenschaftliche Verlagsgesellschaft MBH, Stuttgart, West Germany, 1959.

[2] "The Theory and Practice of Industrial Pharmacy", L. Lachman, H. A. Lieberman, and J. L. Kanig, Eds., Lea & Febiger, Philadelphia, Pa., 1970.

Reviewed by Jack Cooper
School of Pharmacy
University of California
San Francisco, CA 94143

Diuretic Agents (ACS Symposium Series 83). Edited by EDWARD J. CRAGOE, Jr. American Chemical Society, Washington, D.C. 1978. IX + 238 pages. 15 × 23 cm. Price $21.50.

This book evolved primarily from an American Chemical Society Symposium on Diuretic Agents in 1977. However, as stated in the preface, since the symposium was brief and a more complete picture of research in this field was desired, four papers were added to the original seven.

The opening chapter (McGigg and Wong) contains an up-to-date review of the role of prostaglandins in renal function. It is followed by a chapter on the structure–activity relationships of the highly potent, high-ceiling aminobenzoic acid diuretics (Tvaermose, Nielsen, and Feit). The third chapter (Lang *et al.*) is on pharmacological effects of tizolemide (HOE 740) as an example of a novel class of sulfonamide compounds.

The fourth chapter (Werner *et al.*) reviews the structure–activity relationships of sulfonamide diuretics. The next two chapters (Bessin *et al.* and Maass *et al.*) are on pharmacology and structure–activity relationships of the newer diuretic uricosuric agent, tienilic acid (Ticrynafen). The seventh chapter (Smith *et al.*) is on 2-aminomethylphenols, a new class of saluretic agent characterized by the experimental compound MK-447. The following chapter (Horstmann *et al.*) reviews a new class of longer acting high-ceiling diuretics (1-aralkyl-2-pyrazolin-5-ones) characterized by muzolimine.

The ninth chapter (Boschman *et al.*) is a discussion of pharmacology and structural requirements of the quincarbates, a unique class of tricyclic diuretics. The following chapter (Saltzinger *et al.*) discusses the novel diuretic etozolin, which has mild choleretic properties. The last chapter (Woltersdorf *et al.*) discusses evolution of some (aryloxy)-acetic acid diuretics after more than a decade of research.

While this book is the result of the 1977 symposium, all chapters are dated as being received in August 1978 and many contain 1977 and a few 1978 references. Therefore, this book is a complete and current review of structure–activity relationships and pharmacology of various classes of diuretic agents. This book includes discussions on experimental agents undergoing testing for possible therapeutic use and would be useful for anyone seeking current information about the newer diuretic agents.

Reviewed by Gary L. Lage
Philadelphia College of
Pharmacy and Science
Philadelphia, PA 19104

NOTICES

Methods of Protein Separation. Vol. 2. Edited by NICHOLAS CATSIMPOOLAS. Plenum, 227 W. 17th St., New York, NY 10011, 1978. 326 pp. 15 × 23 cm. Price $35.00.

Neurotransmitter Systems and their Clinical Disorders. Edited by N. J. LEGG. Academic, 111 Fifth Ave., New York, NY 10003. 1978. 240 pp. 15 × 23 cm.

New Trends and Developments in Vaccines. Edited by A. VOLLER and H. FRIEDMAN. University Park Press, Chamber of Commerce Building, Baltimore, MD 21202. 1978. 323 pp. 15 × 23 cm. Price $29.50.

Pharmacy Technicians' Manual. 2nd Ed. Edited by JANE M. DURGIN, ZACHARY I. HANAN, and CHARLES O. WARD. C. V. Mosby St. Louis, Mo. 1978. 287 pp. 15 × 23 cm. Price $13.95

Psychopharmacology of Affective Disorders. A British Association for Psychopharmacology Monograph. Edited by E. S. PAYKEL and A. COPPEN. Oxford University Press, 200 Madison Ave , New York, NY 10016. 1979. 261 pp. 16 × 24 cm. Price $25.00.

Quality Control of Drugs. Certification Scheme on the Quality of Pharmaceuticals Products Moving in International Commerce. Reprint of the WHO Chronicle, Vol. 31, No. 12. World Health Organization, Geneva, Switzerland. 1977.

Research Design in Clinical Psychology and Psychiatry. 2nd Ed. Revised and enlarged by J. B. CHASSAN. Wiley, One Wiley Drive, Somerset, NJ 08873. 1979. 492 pp. 13 × 21 cm. Price $18.50.

Self-Administration of Abused Substances: Methods for Study. NIDA Research Monograph 20. By NORMAN A. KRASNEGOR. National Institute on Drug Abuse, Division of Research, 5600 Fishers Lane, Rockville, MD 20857. 1978. 246 pp. 15 × 23 cm.

Taxis and Behavior. Elementary Sensory Systems in Biology. Receptors and Recognition. Series B, Vol. 5. Edited by G. L. HAZELBAUER. Wiley, 605 Third Ave., New York, NY 10016, 1978. 341 pp. 15 × 23 cm. Price $45.00.

Topics in Antibiotic Chemistry. Vol. 2. Antibiotics from Marine Organisms, Oligosaccharides, Anthracyclines and their Biological Receptors. By P. G. SAMMES. Wiley, One Wiley Drive, Somerset, NJ 08873. 1979. 283 pp. 15 × 23 cm.

Webster's Medical Office Handbook. By ANNE H. SOUKHANOV and JOHN RHODES HAVERTY. G.& C. Merriam Co., 47 Federal St., Springfield, MA 01101. 1979. 596 pp. 17 × 25 cm. Price $10.95.

forms, scale-up effects, and in-process controls. The importance of the guidelines for good manufacturing practices as elaborated by the World Health Organization is reviewed in sections dealing with documentation, hygienic requirements, and clean room technology.

The subject matter covered by the text is of such great international interest to pharmaceutical scientists that at least a thousand articles or chapters in books appear annually. Therefore, it is of interest to check the bibliography of over 700 references used by the authors in the preparation of the text. Although the proportion does vary somewhat from chapter to chapter, the overall percentage cited from Swiss or German publications is about 60% of the total. This exceedingly high level may reflect the reading habits of the authors or their language preferences or limitations rather than the true proportion of scientific and technological activity taking place throughout the world.

The emphasis in this German-language book lies squarely in the domain of industrial pharmacy, and it can be highly recommended to pharmaceutical scientists active in the research, development, production, and control departments of the pharmaceutical industry; to teachers of pharmaceutics and pharmaceutical process technology and their graduate students in the universities; and to scientific members of regulatory agencies who wish to gain a valuable perspective of the complex nature of modern drug development and production.

The publisher deserves commendation for the high technical quality of the book itself. Format, typography, figures, and tables are numerous, clear, well-placed, and pertinent to the text. Perhaps that plus inflation explains the price of the book.

[1] "Galenisches Praktikum," K. Münzel, J. Büchi, and O.-E. Schultz, Eds., Wissenschaftliche Verlagsgesellschaft MBH, Stuttgart, West Germany, 1959.

[2] "The Theory and Practice of Industrial Pharmacy", L. Lachman, H. A. Lieberman, and J. L. Kanig, Eds., Lea & Febiger, Philadelphia, Pa., 1970.

Reviewed by Jack Cooper
School of Pharmacy
University of California
San Francisco, CA 94143

Diuretic Agents (ACS Symposium Series 83). Edited by EDWARD J. CRAGOE, Jr. American Chemical Society, Washington, D.C. 1978. IX + 238 pages. 15 × 23 cm. Price $21.50.

This book evolved primarily from an American Chemical Society Symposium on Diuretic Agents in 1977. However, as stated in the preface, since the symposium was brief and a more complete picture of research in this field was desired, four papers were added to the original seven.

The opening chapter (McGigg and Wong) contains an up-to-date review of the role of prostaglandins in renal function. It is followed by a chapter on the structure–activity relationships of the highly potent, high-ceiling aminobenzoic acid diuretics (Tvaermose, Nielsen, and Feit). The third chapter (Lang *et al.*) is on pharmacological effects of tizolemide (HOE 740) as an example of a novel class of sulfonamide compounds.

The fourth chapter (Werner *et al.*) reviews the structure–activity relationships of sulfonamide diuretics. The next two chapters (Bessin *et al.* and Maass *et al.*) are on pharmacology and structure–activity relationships of the newer diuretic uricosuric agent, tienilic acid (Ticrynafen). The seventh chapter (Smith *et al.*) is on 2-aminomethylphenols, a new class of saluretic agent characterized by the experimental compound MK-447. The following chapter (Horstmann *et al.*) reviews a new class of longer acting high-ceiling diuretics (1-aralkyl-2-pyrazolin-5-ones) characterized by muzolimine.

The ninth chapter (Boschman *et al.*) is a discussion of pharmacology and structural requirements of the quincarbates, a unique class of tricyclic diuretics. The following chapter (Saltzinger *et al.*) discusses the novel diuretic etozolin, which has mild choleretic properties. The last chapter (Woltersdorf *et al.*) discusses evolution of some (aryloxy)-acetic acid diuretics after more than a decade of research.

While this book is the result of the 1977 symposium, all chapters are dated as being received in August 1978 and many contain 1977 and a few 1978 references. Therefore, this book is a complete and current review of structure–activity relationships and pharmacology of various classes of diuretic agents. This book includes discussions on experimental agents undergoing testing for possible therapeutic use and would be useful for anyone seeking current information about the newer diuretic agents.

Reviewed by Gary L. Lage
Philadelphia College of
Pharmacy and Science
Philadelphia, PA 19104

NOTICES

Methods of Protein Separation. Vol. 2. Edited by NICHOLAS CATSIMPOOLAS. Plenum, 227 W. 17th St., New York, NY 10011, 1978. 326 pp. 15 × 23 cm. Price $35.00.

Neurotransmitter Systems and their Clinical Disorders. Edited by N. J. LEGG. Academic, 111 Fifth Ave., New York, NY 10003. 1978. 240 pp. 15 × 23 cm.

New Trends and Developments in Vaccines. Edited by A. VOLLER and H. FRIEDMAN. University Park Press, Chamber of Commerce Building, Baltimore, MD 21202. 1978. 323 pp. 15 × 23 cm. Price $29.50.

Pharmacy Technicians' Manual. 2nd Ed. Edited by JANE M. DURGIN, ZACHARY I. HANAN, and CHARLES O. WARD. C. V. Mosby St. Louis, Mo. 1978. 287 pp. 15 × 23 cm. Price $13.95

Psychopharmacology of Affective Disorders. A British Association for Psychopharmacology Monograph. Edited by E. S. PAYKEL and A. COPPEN. Oxford University Press, 200 Madison Ave , New York, NY 10016. 1979. 261 pp. 16 × 24 cm. Price $25.00.

Quality Control of Drugs. Certification Scheme on the Quality of Pharmaceuticals Products Moving in International Commerce. Reprint of the WHO Chronicle, Vol. 31, No. 12. World Health Organization, Geneva, Switzerland. 1977.

Research Design in Clinical Psychology and Psychiatry. 2nd Ed. Revised and enlarged by J. B. CHASSAN. Wiley, One Wiley Drive, Somerset, NJ 08873. 1979. 492 pp. 13 × 21 cm. Price $18.50.

Self-Administration of Abused Substances: Methods for Study. NIDA Research Monograph 20. By NORMAN A. KRASNEGOR. National Institute on Drug Abuse, Division of Research, 5600 Fishers Lane, Rockville, MD 20857. 1978. 246 pp. 15 × 23 cm.

Taxis and Behavior. Elementary Sensory Systems in Biology. Receptors and Recognition. Series B, Vol. 5. Edited by G. L. HAZELBAUER. Wiley, 605 Third Ave., New York, NY 10016, 1978. 341 pp. 15 × 23 cm. Price $45.00.

Topics in Antibiotic Chemistry. Vol. 2. Antibiotics from Marine Organisms, Oligosaccharides, Anthracyclines and their Biological Receptors. By P. G. SAMMES. Wiley, One Wiley Drive, Somerset, NJ 08873. 1979. 283 pp. 15 × 23 cm.

Webster's Medical Office Handbook. By ANNE H. SOUKHANOV and JOHN RHODES HAVERTY. G.& C. Merriam Co., 47 Federal St., Springfield, MA 01101. 1979. 596 pp. 17 × 25 cm. Price $10.95.

forms, scale-up effects, and in-process controls. The importance of the guidelines for good manufacturing practices as elaborated by the World Health Organization is reviewed in sections dealing with documentation, hygienic requirements, and clean room technology.

The subject matter covered by the text is of such great international interest to pharmaceutical scientists that at least a thousand articles or chapters in books appear annually. Therefore, it is of interest to check the bibliography of over 700 references used by the authors in the preparation of the text. Although the proportion does vary somewhat from chapter to chapter, the overall percentage cited from Swiss or German publications is about 60% of the total. This exceedingly high level may reflect the reading habits of the authors or their language preferences or limitations rather than the true proportion of scientific and technological activity taking place throughout the world.

The emphasis in this German-language book lies squarely in the domain of industrial pharmacy, and it can be highly recommended to pharmaceutical scientists active in the research, development, production, and control departments of the pharmaceutical industry; to teachers of pharmaceutics and pharmaceutical process technology and their graduate students in the universities; and to scientific members of regulatory agencies who wish to gain a valuable perspective of the complex nature of modern drug development and production.

The publisher deserves commendation for the high technical quality of the book itself. Format, typography, figures, and tables are numerous, clear, well-placed, and pertinent to the text. Perhaps that plus inflation explains the price of the book.

[1] "Galenisches Praktikum," K. Münzel, J. Büchi, and O.-E. Schultz, Eds., Wissenschaftliche Verlagsgesellschaft MBH, Stuttgart, West Germany, 1959.

[2] "The Theory and Practice of Industrial Pharmacy", L. Lachman, H. A. Lieberman, and J. L. Kanig, Eds., Lea & Febiger, Philadelphia, Pa., 1970.

Reviewed by Jack Cooper
School of Pharmacy
University of California
San Francisco, CA 94143

Diuretic Agents (ACS Symposium Series 83). Edited by EDWARD J. CRAGOE, Jr. American Chemical Society, Washington, D.C. 1978. IX + 238 pages. 15 × 23 cm. Price $21.50.

This book evolved primarily from an American Chemical Society Symposium on Diuretic Agents in 1977. However, as stated in the preface, since the symposium was brief and a more complete picture of research in this field was desired, four papers were added to the original seven.

The opening chapter (McGigg and Wong) contains an up-to-date review of the role of prostaglandins in renal function. It is followed by a chapter on the structure–activity relationships of the highly potent, high-ceiling aminobenzoic acid diuretics (Tvaermose, Nielsen, and Feit). The third chapter (Lang *et al.*) is on pharmacological effects of tizolemide (HOE 740) as an example of a novel class of sulfonamide compounds.

The fourth chapter (Werner *et al.*) reviews the structure–activity relationships of sulfonamide diuretics. The next two chapters (Bessin *et al.* and Maass *et al.*) are on pharmacology and structure–activity relationships of the newer diuretic uricosuric agent, tienilic acid (Ticrynafen). The seventh chapter (Smith *et al.*) is on 2-aminomethylphenols, a new class of saluretic agent characterized by the experimental compound MK-447. The following chapter (Horstmann *et al.*) reviews a new class of longer acting high-ceiling diuretics (1-aralkyl-2-pyrazolin-5-ones) characterized by muzolimine.

The ninth chapter (Boschman *et al.*) is a discussion of pharmacology and structural requirements of the quincarbates, a unique class of tricyclic diuretics. The following chapter (Saltzinger *et al.*) discusses the novel diuretic etozolin, which has mild choleretic properties. The last chapter (Woltersdorf *et al.*) discusses evolution of some (aryloxy)-acetic acid diuretics after more than a decade of research.

While this book is the result of the 1977 symposium, all chapters are dated as being received in August 1978 and many contain 1977 and a few 1978 references. Therefore, this book is a complete and current review of structure–activity relationships and pharmacology of various classes of diuretic agents. This book includes discussions on experimental agents undergoing testing for possible therapeutic use and would be useful for anyone seeking current information about the newer diuretic agents.

Reviewed by Gary L. Lage
Philadelphia College of
Pharmacy and Science
Philadelphia, PA 19104

NOTICES

Methods of Protein Separation. Vol. 2. Edited by NICHOLAS CATSIMPOOLAS. Plenum, 227 W. 17th St., New York, NY 10011, 1978. 326 pp. 15 × 23 cm. Price $35.00.

Neurotransmitter Systems and their Clinical Disorders. Edited by N. J. LEGG. Academic, 111 Fifth Ave., New York, NY 10003. 1978. 240 pp. 15 × 23 cm.

New Trends and Developments in Vaccines. Edited by A. VOLLER and H. FRIEDMAN. University Park Press, Chamber of Commerce Building, Baltimore, MD 21202. 1978. 323 pp. 15 × 23 cm. Price $29.50.

Pharmacy Technicians' Manual. 2nd Ed. Edited by JANE M. DURGIN, ZACHARY I. HANAN, and CHARLES O. WARD. C. V. Mosby St. Louis, Mo. 1978. 287 pp. 15 × 23 cm. Price $13.95

Psychopharmacology of Affective Disorders. A British Association for Psychopharmacology Monograph. Edited by E. S. PAYKEL and A. COPPEN. Oxford University Press, 200 Madison Ave , New York, NY 10016. 1979. 261 pp. 16 × 24 cm. Price $25.00.

Quality Control of Drugs. Certification Scheme on the Quality of Pharmaceuticals Products Moving in International Commerce. Reprint of the WHO Chronicle, Vol. 31, No. 12. World Health Organization, Geneva, Switzerland. 1977.

Research Design in Clinical Psychology and Psychiatry. 2nd Ed. Revised and enlarged by J. B. CHASSAN. Wiley, One Wiley Drive, Somerset, NJ 08873. 1979. 492 pp. 13 × 21 cm. Price $18.50.

Self-Administration of Abused Substances: Methods for Study. NIDA Research Monograph 20. By NORMAN A. KRASNEGOR. National Institute on Drug Abuse, Division of Research, 5600 Fishers Lane, Rockville, MD 20857. 1978. 246 pp. 15 × 23 cm.

Taxis and Behavior. Elementary Sensory Systems in Biology. Receptors and Recognition. Series B, Vol. 5. Edited by G. L. HAZELBAUER. Wiley, 605 Third Ave., New York, NY 10016, 1978. 341 pp. 15 × 23 cm. Price $45.00.

Topics in Antibiotic Chemistry. Vol. 2. Antibiotics from Marine Organisms, Oligosaccharides, Anthracyclines and their Biological Receptors. By P. G. SAMMES. Wiley, One Wiley Drive, Somerset, NJ 08873. 1979. 283 pp. 15 × 23 cm.

Webster's Medical Office Handbook. By ANNE H. SOUKHANOV and JOHN RHODES HAVERTY. G.& C. Merriam Co., 47 Federal St., Springfield, MA 01101. 1979. 596 pp. 17 × 25 cm. Price $10.95.

A publication of the
American Pharmaceutical Association—
the National Professional Society
of Pharmacists

JOURNAL OF PHARMACEUTICAL SCIENCES

INDEX TO AUTHORS
INDEX TO SUBJECTS

VOLUME 68
JANUARY TO DECEMBER, 1979

Published monthly under the supervision of the Board of Trustees

MARY H. FERGUSON
Editor

SHELLY ELLIOTT
Production Editor

MARCIA GARTRELL
Copy Editor

NICOLETTE TRIANTAFELLU
Copy Editor

EDWARD G. FELDMANN
Contributing Editor

SAMUEL W. GOLDSTEIN
Contributing Editor

BELLE R. BECK
Editorial Secretary

DAVID BOHARDT
Director of Publications

L. LUAN CORRIGAN
Assistant Director of Publications

EDITORIAL ADVISORY BOARD

John Autian
Norman R. Farnsworth
William O. Foye
William J. Jusko
Herbert A. Lieberman
David E. Mann, Jr.
Gerald J. Papariello
Edward G. Rippie

OCTOBER 1979
VOLUME 68 NUMBER 10

JOURNAL OF PHARMACEUTICAL SCIENCES

MARY H. FERGUSON
Editor

SHELLY ELLIOTT
Production Editor

MARCIA GARTRELL
Copy Editor

NICOLETTE TRIANTAFELLU
Copy Editor

EDWARD G. FELDMANN
Contributing Editor

SAMUEL W. GOLDSTEIN
Contributing Editor

BELLE R. BECK
Editorial Secretary

DAVID BOHARDT
Director of Publications

L. LUAN CORRIGAN
Assistant Director of Publications

EDITORIAL ADVISORY BOARD

JOHN AUTIAN
HERBERT A. LIEBERMAN
NORMAN R. FARNSWORTH
DAVID E. MANN, JR.
WILLIAM O. FOYE
GERALD J. PAPARIELLO
WILLIAM J. JUSKO
EDWARD G. RIPPIE

The *Journal of Pharmaceutical Sciences* (ISSN 0022-3549) is published monthly by the American Pharmaceutical Association (APhA) at 2215 Constitution Ave., N.W., Washington, DC 20037. Second-class postage paid at Washington, D.C., and at additional mailing office.

All expressions of opinion and statements of supposed fact appearing in articles or editorials carried in this journal are published on the authority of the writer over whose name they appear and are not to be regarded as necessarily expressing the policies or views of APhA.

Offices—Editorial, Advertising, and Subscription: 2215 Constitution Ave., N.W., Washington, DC 20037. Printing: 20th & Northampton Streets, Easton, PA 18042.

Annual Subscriptions—United States and foreign, industrial and government institutions $50, educational institutions $50, individuals *for personal use only* $30; single copies $5. All foreign subscriptions add $5 for postage. Subscription rates are subject to change without notice. Members of APhA may elect to receive the *Journal of Pharmaceutical Sciences* as a part of their annual $70 (foreign $75) APhA membership dues.

Claims—Missing numbers will not be supplied if dues or subscriptions are in arrears for more than 60 days or if claims are received more than 60 days after the date of the issue, or if loss was due to failure to give notice of change of address. APhA cannot accept responsibility for foreign delivery when its records indicate shipment was made.

Change of Address—Members and subscribers should notify at once both the Post Office and APhA of any change of address.

Photocopying—The code at the foot of the first page of an article indicates that APhA has granted permission for copying of the article beyond the limits permitted by Sections 107 and 108 of the U.S. Copyright Law provided that the copier sends the per copy fee stated in the code to the Copyright Clearance Center, Inc., P.O. Box 8891, Boston, MA 02114. Copies may be made for personal or internal use only and not for general distribution.

Microfilm—Available from University Microfilms International, 300 N. Zeeb Road, Ann Arbor, MI 48106.

© Copyright 1979, American Pharmaceutical Association, 2215 Constitution Ave., N.W., Washington, DC 20037; all rights reserved.

ON STAYING COMPETENT

As this editorial is being written, the teams in the "biggee" of American professional football—the National Football League—are in the process of making the final cuts in their rosters of players to meet the numerical limit permitted each team for the playing season. Consequently, the sports pages of the daily newspapers duly report the lists of names, many of whom were recent star players, who were given their termination notices in the cut-downs of the previous day.

As we read about the fate of one particular well-known place-kicker, we were reminded of the maxim that "staying is harder than getting there!" How true!

All of this has a very important lesson for pharmacy, pharmacists, and pharmaceutical scientists. As students, all of us worked hard to acquire the knowledge necessary to qualify for graduation and attain the academic degrees for which we were striving. Finally, one day we "arrived" and then joined the ranks of the professionally employed.

But rather than signaling the end of books, lectures, and learning, we found that this was just a transition to journals, short courses, and continuing education. Or, at least that is what we should have discovered if we did not want to become rapidly obsolete because our personal knowledge stood still while science and the world moved onward.

The American Pharmaceutical Association has long recognized this fact of life, and that explains why the Association has continually devoted so much of its efforts and resources to providing professional journals, technical book publications, and educational meeting programs. In recent years, this APhA activity has greatly expanded and become more specialized and sophisticated by offering various workshops, seminars, and short courses *via* its subdivisions, the Academy of Pharmacy Practice and the Academy of Pharmaceutical Sciences.

But, as in all other things in life, there must be some guidelines and directions as to what such programs should include or cover if they are to fulfill their objectives in a reasonably effective manner. In turn, this requires that we know the educational needs of those we seek to assist.

The American Association of Colleges of Pharmacy had similar concerns. Although the primary emphasis of the AACP and its member schools is the training of students to enter the profession, they shared with APhA the belief that there is an obligation to look after the ongoing educational needs of practitioners out in the field.

Out of this mutual recognition came the undertaking of a joint APhA/AACP Continuing Competency in Pharmacy Project. This project has been underway for over six years and a high point was reached during this past year with the release of a document entitled the *National Study of the Practice of Pharmacy* and the subsequent publication of "Standards of Practice" for the profession. These so-called "standards" simply reflect accepted, contemporary, high-level professionalism. They provide a reference point or bench mark for those out in the field to use as a basis to compare their own knowledge and performance, to identify any deficiencies, and then to move forward in filling any such gaps.

Both APhA and AACP have been pleased with the generally positive—indeed, enthusiastic—reception from educators, practitioners, and scientists that has been accorded the Continuing Competency Project. But recently, there has been a dissenting voice from one pharmacy organization. Its president said he "cannot understand the rush," and that competency is not "a burning issue."

But in his speech he went on to clarify that timing was neither his only nor his fundamental objection. Rather, he questioned the basic concept that there is a need for professional accountability. He stated that, "I dislike the idea of being accountable for my competency." The thrust of the speech was that each pharmacist has his or her own personal standards and that should be sufficient for the purpose.

There is no question but that the belief among either practitioners or scientists that "we are competent because we say we are competent" has appeal. Certainly, it is a very comfortable posture to take.

Correspondingly, most of those battle-scarred football veterans who got cut from their team rosters this fall also had the supreme confidence of self-made achievers. But that wasn't sufficient for a public that wants the best performance for its money. Professional competency, just like athletic skill, requires constant and continual attention to maintain it at peak performance. Staying is indeed harder than getting there! —EGF

Identical Bioequivalence?

It has been heard, with increasing frequency, from some professional pharmacists and academicians that decisions regarding bioequivalence between "identical" products will be impossible for a pharmacist to make until strict regulatory guidelines are developed. This "cookbook" approach to bioequivalency seems to me to be irrational at best and demeaning to the profession of pharmacy at worst.

Regulatory guidelines in terms of physical and biological effect characteristics of drug products, as base guidelines, could be misleading and confusing. For example, a high variation in established bioequivalency parameters might be acceptable for, for example, aspirin tablets. However, lifesaving and potentially dangerous drug forms such as digoxin tablets would require a narrower allowable variation. These variable limits would necessitate the stating of each acceptable level of variation for each stated bioequivalency parameter that would differ from drug to drug, dosage form to dosage form, and formulation to formulation.

I believe that a set of compendial or "quasicompendial" regulations or guidelines for bioequivalency determination would be needed only by the truly incompetent professional. The judgmental nature of the decision necessitates that it be made by a knowledgeable professional weighing appropriate negative and positive aspects.

For example, I can visualize several instances where valid differences in bioequivalency parameters could exist and would not preclude product selection of the "inferior" brand. What if there is a large monetary savings to the patient with little or no demonstrable compromise in therapeutic effect, as could conceivably occur with aspirin tablets USP? What if a pharmacist wants to prepare extemporaneously a potassium chloride elixir with a more palatable flavor for an individual patient rather than using a prescribed trade name product rejected by the patient on the basis of taste?

The major issue is whether compendial or regulatory agency guidelines dealing with bioequivalency remove a professional judgmental prerogative that the pharmacist only recently gained and leave in its place regulations that could confuse patients and needlessly restrict decisionmaking of highly trained professionals. I think that *informal* published guidelines (by APhA or other scientific/professional groups) would keep the pharmacist apprised of the status of bioequivalency and still maintain the prerogatives essential to a viable profession.

R. Saul Levinson
Arnold and Marie Schwartz College
of Pharmacy and Health Sciences
Long Island University
Brooklyn, NY 11201

Received July 27, 1979.

New Solubility Equation

We wish to report a new approach to extend the Hildebrand–Scatchard regular solution theory[1] to include strong solvent–solute interactions of hydrogen bonding and other types.

The modified Hildebrand approach provides results over the solvent range from nonpolar to polar. The activity coefficient of the solute, to be derived in a paper under preparation, takes the form:

$$\log \alpha_2 = A(\delta_1 - \delta_2)^2 + A(2\delta_1\delta_2 - 2W) \quad \text{(Eq. 1)}$$

$$\log \alpha_2 = A(\delta_1^2 + \delta_2^2 - 2W) \quad \text{(Eq. 2)}$$

where A is a quantity from regular solution theory that includes the solvent volume fraction and the solute molar volume, W is a term for the solute–solvent interaction to account for deviations from regular solution behavior, δ_1 is the total polar–nonpolar solvent solubility parameter, and δ_2 is the nonpolar solute parameter.

The value of W in any solvent may be back-calculated using a simple computer program to solve a polynomial equation. Once W is obtained, the approximate solubility of the compound in a solvent of known solubility parameter, ranging from nonpolar hydrocarbons to alcohols, glycols, and water, may be calculated.

Table I lists solubility results for naphthalene in several solvents. The experimental data are those of Gmehling *et al.*[2]. The method yields solubilities in good correspondence with experimental results, except where unusally strong solute–solvent interactions exist.

The following example for naphthalene in ethanol demonstrates the method. With experimental solubilities, a W is obtained for solvent–solute pairs of known solubility by employing Eq. 2. The W's are regressed against a polynomial (quartic) in δ_1 for as many experimental solubilities as are available. From the data in Table I, one obtains the expression:

$$W = -344.1932 + 144.0207\delta_1 - 18.8238\delta_1^2 + 1.1250\delta_1^3 - 0.0242\delta_1^4 \quad \text{(Eq. 3)}$$

To obtain the solubility in ethanol (assumed in this sample to be unknown), one back-calculates W using an ethanol δ_1 value of 12.79 (total solubility parameter of Hoy and Martin[3]). One then obtains X_2 by the application of Eq. 4:

$$-\log X_2 = \frac{\Delta H_m^f}{2.303RT}\frac{T_m - T}{T_m} + A(\delta_1^2 + \delta_2^2 - 2W) \quad \text{(Eq. 4)}$$

The negative logarithm of the ideal solubility of naphthalene at 40° (first right-hand term of Eq. 4) is 0.3565, and A is 0.06458.

The regression in δ_1 (Eq. 3) yields a value of 124.946 for W as compared with 124.659 obtained from experimental solubility results. The solubility of naphthalene in ethanol at 40° is then obtained using the modified Hildebrand expression (Eq. 4):

$$\log X_2 = -\{0.3565 + 0.06458[(12.79)^2 + (9.89)^2 - 2(124.946)]\} \quad \text{(Eq. 5)}$$

where X_2 (calc.) = 0.080 and X_2 (exp.) = 0.073. An equation relating $\log \alpha_2/A$ and δ_1 may also be written by substituting the expression for W from Eq. 3 into Eq. 4, and one may thus obtain predicted solubilities more directly.

As a means of estimating the solubility in individual and mixed solvents, the classical Hildebrand approach has frequently been criticized for its incapacity to deal with solute–solvent interactions any stronger than van der Waals dispersion forces. This new approach handles ill-behaved systems such as ethanol–naphthalene where the

Table I—Predicted Solubilities of Naphthalene (δ_2 = 9.89) in Various Solvents at 40°

Solvent	δ_1	A	W (Eq. 2)[a]	X_2 (obs.), Ref. 2	X_2 (calc.), Eq. 4
Hexane	7.27	0.05539	72.652 (72.634)	0.222	0.221
Chloroform	9.14	0.0523	89.645 (89.781)	0.473	0.413
Acetone	9.62	0.02124	93.625 (93.613)	0.378	0.378
Cyclohexanol	10.92	0.04847	105.527 (104.773)	0.225	0.190
Isopropanol	11.50	0.06867	109.476 (110.453)	0.076	0.103
n-Butanol	11.60	0.06353	111.629 (111.486)	0.116	0.111
n-Propanol	12.18	0.06417	117.862 (117.784)	0.094	0.092
Ethanol	12.79	0.06458	124.659 (124.946)	0.073	0.080
Acetic acid	12.94	0.05306	127.210 (126.780)	0.117	0.105
Methanol	14.50	0.06778	146.654 (146.689)	0.044	0.044

[a] Quantity in parentheses is the value of W back-calculated using Eq. 3.

Identical Bioequivalence?

It has been heard, with increasing frequency, from some professional pharmacists and academicians that decisions regarding bioequivalence between "identical" products will be impossible for a pharmacist to make until strict regulatory guidelines are developed. This "cookbook" approach to bioequivalency seems to me to be irrational at best and demeaning to the profession of pharmacy at worst.

Regulatory guidelines in terms of physical and biological effect characteristics of drug products, as base guidelines, could be misleading and confusing. For example, a high variation in established bioequivalency parameters might be acceptable for, for example, aspirin tablets. However, lifesaving and potentially dangerous drug forms such as digoxin tablets would require a narrower allowable variation. These variable limits would necessitate the stating of each acceptable level of variation for each stated bioequivalency parameter that would differ from drug to drug, dosage form to dosage form, and formulation to formulation.

I believe that a set of compendial or "quasicompendial" regulations or guidelines for bioequivalency determination would be needed only by the truly incompetent professional. The judgmental nature of the decision necessitates that it be made by a knowledgeable professional weighing appropriate negative and positive aspects.

For example, I can visualize several instances where valid differences in bioequivalency parameters could exist and would not preclude product selection of the "inferior" brand. What if there is a large monetary savings to the patient with little or no demonstrable compromise in therapeutic effect, as could conceivably occur with aspirin tablets USP? What if a pharmacist wants to prepare extemporaneously a potassium chloride elixir with a more palatable flavor for an individual patient rather than using a prescribed trade name product rejected by the patient on the basis of taste?

The major issue is whether compendial or regulatory agency guidelines dealing with bioequivalency remove a professional judgmental prerogative that the pharmacist only recently gained and leave in its place regulations that could confuse patients and needlessly restrict decisionmaking of highly trained professionals. I think that *informal* published guidelines (by APhA or other scientific/professional groups) would keep the pharmacist apprised of the status of bioequivalency and still maintain the prerogatives essential to a viable profession.

R. Saul Levinson
Arnold and Marie Schwartz College
of Pharmacy and Health Sciences
Long Island University
Brooklyn, NY 11201

Received July 27, 1979.

New Solubility Equation

We wish to report a new approach to extend the Hildebrand–Scatchard regular solution theory[1] to include strong solvent–solute interactions of hydrogen bonding and other types.

The modified Hildebrand approach provides results over the solvent range from nonpolar to polar. The activity coefficient of the solute, to be derived in a paper under preparation, takes the form:

$$\log \alpha_2 = A(\delta_1 - \delta_2)^2 + A(2\delta_1\delta_2 - 2W) \quad \text{(Eq. 1)}$$

$$\log \alpha_2 = A(\delta_1^2 + \delta_2^2 - 2W) \quad \text{(Eq. 2)}$$

where A is a quantity from regular solution theory that includes the solvent volume fraction and the solute molar volume, W is a term for the solute–solvent interaction to account for deviations from regular solution behavior, δ_1 is the total polar–nonpolar solvent solubility parameter, and δ_2 is the nonpolar solute parameter.

The value of W in any solvent may be back-calculated using a simple computer program to solve a polynomial equation. Once W is obtained, the approximate solubility of the compound in a solvent of known solubility parameter, ranging from nonpolar hydrocarbons to alcohols, glycols, and water, may be calculated.

Table I lists solubility results for naphthalene in several solvents. The experimental data are those of Gmehling *et al.*[2]. The method yields solubilities in good correspondence with experimental results, except where unusally strong solute–solvent interactions exist.

The following example for naphthalene in ethanol demonstrates the method. With experimental solubilities, a W is obtained for solvent–solute pairs of known solubility by employing Eq. 2. The W's are regressed against a polynomial (quartic) in δ_1 for as many experimental solubilities as are available. From the data in Table I, one obtains the expression:

$$W = -344.1932 + 144.0207\delta_1 - 18.8238\delta_1^2 + 1.1250\delta_1^3 - 0.0242\delta_1^4 \quad \text{(Eq. 3)}$$

To obtain the solubility in ethanol (assumed in this sample to be unknown), one back-calculates W using an ethanol δ_1 value of 12.79 (total solubility parameter of Hoy and Martin[3]). One then obtains X_2 by the application of Eq. 4:

$$-\log X_2 = \frac{\Delta H_m^f}{2.303RT}\frac{T_m - T}{T_m} + A(\delta_1^2 + \delta_2^2 - 2W) \quad \text{(Eq. 4)}$$

The negative logarithm of the ideal solubility of naphthalene at 40° (first right-hand term of Eq. 4) is 0.3565, and A is 0.06458.

The regression in δ_1 (Eq. 3) yields a value of 124.946 for W as compared with 124.659 obtained from experimental solubility results. The solubility of naphthalene in ethanol at 40° is then obtained using the modified Hildebrand expression (Eq. 4):

$$\log X_2 = -\{0.3565 + 0.06458[(12.79)^2 + (9.89)^2 - 2(124.946)]\} \quad \text{(Eq. 5)}$$

where X_2 (calc.) = 0.080 and X_2 (exp.) = 0.073. An equation relating $\log \alpha_2/A$ and δ_1 may also be written by substituting the expression for W from Eq. 3 into Eq. 4, and one may thus obtain predicted solubilities more directly.

As a means of estimating the solubility in individual and mixed solvents, the classical Hildebrand approach has frequently been criticized for its incapacity to deal with solute–solvent interactions any stronger than van der Waals dispersion forces. This new approach handles ill-behaved systems such as ethanol–naphthalene where the

Table I—Predicted Solubilities of Naphthalene (δ_2 = 9.89) in Various Solvents at 40°

Solvent	δ_1	A	W (Eq. 2)[a]	X_2 (obs.), Ref. 2	X_2 (calc.), Eq. 4
Hexane	7.27	0.05539	72.652 (72.634)	0.222	0.221
Chloroform	9.14	0.0523	89.645 (89.781)	0.473	0.413
Acetone	9.62	0.02124	93.625 (93.613)	0.378	0.378
Cyclohexanol	10.92	0.04847	105.527 (104.773)	0.225	0.190
Isopropanol	11.50	0.06867	109.476 (110.453)	0.076	0.103
n-Butanol	11.60	0.06353	111.629 (111.486)	0.116	0.111
n-Propanol	12.18	0.06417	117.862 (117.784)	0.094	0.092
Ethanol	12.79	0.06458	124.659 (124.946)	0.073	0.080
Acetic acid	12.94	0.05306	127.210 (126.780)	0.117	0.105
Methanol	14.50	0.06778	146.654 (146.689)	0.044	0.044

[a] Quantity in parentheses is the value of W back-calculated using Eq. 3.

JOURNAL OF PHARMACEUTICAL SCIENCES

OCTOBER 1979
VOLUME 68 NUMBER 10

RESEARCH ARTICLES

Degradation of Mecillinam in Aqueous Solution

B. BALTZER ˣ, F. LUND, and N. RASTRUP-ANDERSEN

Received September 25, 1978, from *Leo Pharmaceutical Products, DK-2750 Ballerup, Denmark.* Accepted for publication April 10, 1979.

Abstract □ The hydrolysis of mecillinam in aqueous solution (37°) was studied at pH 2–10. The degradation products observed by TLC and NMR were identified and quantified. Several of these compounds were synthesized. Mecillinam and the key degradation product, (6*R*)-6-formamidopenicillanic acid, underwent reversible 6-epimerization in basic solution. Some of the thiazolidine derivatives formed epimerized at position 2. In contrast to penicillins, the degradation pattern of mecillinam becomes more complex with increasing pH. Rate constants for some processes are given.

Keyphrases □ Mecillinam—degradation in aqueous solution, isolation of degradation products, degradation pathways, rate constants □ Hydrolysis—mecillinam in aqueous solution, degradation products □ Antibiotics—mecillinam, degradation in aqueous solution, isolation of degradation products, degradation pathways, rate constants

Degradation of penicillins in aqueous solution has been studied for more than 30 years, and many decomposition products have been identified. Different degradation pathways prevail in acidic and basic solutions. Although the side-chain amide group of penicillin is discernible in most primary degradation products, their fundamental structures apparently are not influenced by the nature of the acyl group, even if it contains substituents, *e.g.*, the ampicillin amino group, seemingly in an ideal position for further reaction with the strained β-lactam ring. Only the reactivity of the β-lactam ring is influenced by inductive and steric effects of the side chain (1, 2). A few degradation products are exclusively derived from the 6-aminopenicillanic acid nucleus common to all penicillins.

Mecillinam (FL 1060), (6*R*)-6-[(hexahydro-1*H*-azepin-1-yl)methyleneamino]penicillanic acid (I) (Table I), represents a new type of β-lactam antibiotic having the side chain linked to a 6-aminopenicillanic acid moiety through an amidine bond. These derivatives have predominant activity against Gram-negative bacilli and only weak activity against Gram-positive organisms (3). In accordance with this unusual antibacterial spectrum, Gram-negative bacteria are killed by I differently than by penicillins and cephalosporins (3, 4).

A substituted amidinopenicillanic acid may be expected to differ from the penicillins in its hydrolytic degradation, because amidines generally are hydrolyzed more easily than amides (5). Furthermore, the hydrolysis produces amine(s) capable of reaction with the β-lactam ring. Amidines show great variation in their hydrolysis rate (6), and the nature of the amidinopenicillanic acid substituents may also be expected to influence the rate of other degradation reactions.

In the present study, I was chosen as a representative amidinopenicillanic acid. TLC and NMR methods identified and semiquantified the major degradation products formed in aqueous I solutions as a function of time and pH. Previous investigations in these laboratories[1] showed that I is more stable in acidic than in basic solution. Optimum stability (half-life ~200 hr at 37°) was found at around pH 5, not far from the isoelectric point of I (5.8). Similar results were reported recently from other laboratories (7, 8).

EXPERIMENTAL

Materials—Mecillinam (I) and the reference compounds listed in Table I, except VI, VIII, X, and XII, were synthesized[2]. None of the yields quoted was optimized. TLC and NMR data of VI, VIII, X, and XII were obtained from aqueous solutions of their analogs with natural configuration after equilibration. Penicic acid was prepared according to a literature method (9). All other chemicals were analytical grade.

Melting points are uncorrected. NMR chemical shifts are given in parts per million (delta scale) with tetramethylsilane or sodium 3-trimethylsilylpropanoate as the internal reference. IR data are given in centimeters^{-1}.

Mecillinam (I)—This compound was prepared according to production methods (10) in better than 99% purity as determined by iodometric titration, spectrophotometric assay, and TLC; $[\alpha]_D^{20}$ +294° (H_2O, pH 2.5)[3]; PMR[4] (CD_3OD, tetramethylsilane): 1.66 (s, 2αCH_3), 1.73 (s, 2βCH_3), 4.28 (s, 3H), 5.37 (d, J = 4 Hz, 6H), 5.56 (d, J = 4 Hz, 5H), 1.5–2.1 [m, $(CH_2)_4$], 3.5–3.9 (m, CH_2NCH_2), and 8.10 (s, NCH=N); IR[5] (0.3% KBr): 1770, 1672, and 1590.

[1] E. Gundersen, Leo Laboratories, personal communication.
[2] Leo Laboratories.
[3] Perkin-Elmer PE 141.
[4] Varian A60A (cw), Jeol PMX 60 (cw), and Jeol FX 100 (ft, 24K).
[5] Perkin-Elmer PE 457 grating spectrophotometer.

0022-3549/79/1000-1207$01.00/0
© 1979, American Pharmaceutical Association

Table I—Structures of Mecillinam and Its Degradation Products

Compound[a]	R–[b]	Structure
I Mecillinam	(N—CH=N—	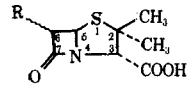
II (6*S*)-Mecillinam	(N—CH=N—	
III 6-Formamidopenicillanic acid	OCH—NH—	
IV (6*S*)-6-Formamidopenicillanic acid	OCH—NH—	
V Mecillinam penicilloic acid	(N—CH=N—CH(—COOH)—	
VI (6*S*)-Mecillinam penicilloic acid	(N—CH=N—CH(—COOH)—	
VII Mecillinam penilloic acid	(N—CH=N—CH_2—	
VIII (5*S*)-Mecillinam penilloic acid	(N—CH=N—CH_2—	
IX Penicilloic acid	OCH—NH—CH(—COOH)—	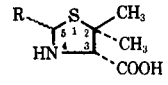
X (5*S*)-Penicilloic acid	OCH—NH—CH(—COOH)—	
XI Penilloic acid	OCH—NH—CH_2—	
XII (5*S*)-Penilloic acid	OCH—NH—CH_2—	
XIII Penicilloic amide	OCH—NH—CH(—CON)	

[a] Although not strictly correct, the nomenclature and numbering of penicillin are used for all degradation products including monocyclic compounds except in the *Experimental* part. When not otherwise indicated, the compounds have the natural penicillin configuration (3*S*, 5*R*, 6*R*). [b] (N stands for 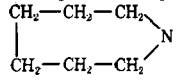

(6*S*)-6-[(Hexahydro-1*H*-azepin-1-yl)methyleneamino]penicillanic Acid (II)—*Isolation from Alkaline Degradation of I*—A I solution (60 g, 185 mmoles) in water (250 ml) was adjusted to pH 9.5 with 2 *N* NaOH and kept for 2.5 hr at 37° and pH 9.5, followed by treatment with 6,000,000 units of β-lactamase[6] (11) at constant pH 7 at room temperature. When no more 2 *N* NaOH was consumed (~1 hr), the pH was raised to 10 with hexamethyleneimine. The solution was extracted with ether (200 ml) and chloroform (2 × 800 ml), and the combined chloroform phases were dried and evaporated *in vacuo*.

The oily residue was dissolved in water (400 ml), the pH was adjusted to 5.5, and the solution was freeze dried. The product (12 g) was triturated with acetone (100 ml) for 0.5 hr. After filtration, the filtrate was evaporated *in vacuo* to leave a solid (11.2 g), which was dissolved in isopropanol (160 ml). Then 8 *N* hydrogen chloride in isopropanol (4.4 ml) and water (4 ml) was added, and the hydrochloride hydrate of II was precipitated (6.1 g) by the addition of isopropyl ether (300 ml).

Recrystallization from isopropanol–isopropyl ether yielded 3.8 g (5.5%) of the pure compound, mp 170–173°; $[\alpha]_D^{20}$ +248° (H_2O, pH 2.5); $[\alpha]_D^{20}$ +290° calculated as the anhydrous zwitterion; PMR (CD_3OD, tetramethylsilane): 1.53 (s, 2αCH_3), 1.62 (s, 2βCH_3), 1.5–2.1 [m, $(CH_2)_4$], 3.5–4.0 (m, CH_2NCH_2), 4.54 (s, 3H), 5.07 (d, J = 1.6 Hz, 6H), 5.43 (d, J = 1.6 Hz, 5H), and 8.23 (s, NCH=N); ^{13}C-NMR [$(CD_3)_2SO$, tetramethylsilane]: 32.7 (CH_3), 68.3 (C-3), 68.6 (C-5), 71.2 (C-6), 156.2 (NC=N), 166.8 (C-7), and 167.7 (COO); IR (0.3% KBr): 1774, 1723, and 1675.

Anal.—Calc. for $C_{15}H_{26}ClN_3O_4S$: C, 47.42; H, 6.90; N, 11.06; S, 8.44; H_2O, 4.73. Found: C, 47.69; H, 7.02; N, 11.00; S, 8.51; H_2O, 4.07.

Synthesis of Benzyl (6S)-6-[(Hexahydro-1H-azepin-1-yl)methyleneamino]penicillanate Nitrate—Benzyl (6*S*)-6-aminopenicillanate (12) (1.7 g, 5.5 mmoles) was stirred in hexamethyleneiminecarboxaldehyde dimethyl acetal (15 ml) for a few minutes. The resultant solution was kept at room temperature overnight, followed by stirring for 10 min at 0–5° with water (30 ml). The acidified reaction mixture (pH 2.5) was extracted with ether (30 ml) and subsequently with ether (2 × 30 ml) at pH 7.5.

The organic phase from the alkaline extraction was extracted with water (5 × 15 ml), dried, and evaporated *in vacuo* to leave an oil (2.5 g). To an isopropanolic solution (20 ml) of this oil was added a solution of concentrated nitric acid (0.3 ml) in isopropanol (3 ml), and the mixture was cooled to 0–5°. The precipitate (1.9 g) was recrystallized from methanol–ether to yield 1.4 g (53%) of the title compound, mp 172°; $[\alpha]_D^{20}$ +222° (96% C_2H_5OH); PMR [$(CD_3)_2SO$, tetramethylsilane]: 1.37 (s, 2αCH_3), 1.53 (s, 2βCH_3), 1.4–2.0 [m, $(CH_2)_4$], 4.71 (s, 3H), 5.11 (m, 6H), 5.22 (s, O$CH_2C_6H_5$), 5.33 (d, J = 2 Hz, 5H), 7.38 (s, C_6H_5), and 8.22 (bs, NCH=N); IR (0.3% KBr): 1775, 1748, 1682, 1382, 1202, 1180, 765, 752, 703, and 508.

[6] Cerius β-lactamase, Penase LEO, Leo Pharmaceutical Products.

Anal.—Calc. for $C_{22}H_{30}N_4O_6S$: C, 55.22; H, 6.32; N, 11.71. Found: C, 55.02; H, 6.27; N, 11.87.

Synthesis of (6S)-6-[(Hexahydro-1H-azepin-1-yl)methyleneamino]penicillanic Acid Hydrochloride Hydrate—A solution of the above-mentioned benzyl ester (1.4 g, 2.9 mmoles) in ethyl acetate (25 ml) was successively extracted with sodium hydrogen carbonate (0.85 g) in water (25 ml) and water (25 ml). After drying, the ethyl acetate was removed *in vacuo*; the residue (1.3 g), dissolved in water (25 ml) and 4 *N* HCl (0.73 ml, 2.9 mmoles), was extracted with ether (25 ml) and hydrogenated over 10% palladium-on-carbon (1 g) at slightly elevated pressure.

The catalyst was filtered off, and the filtrate was extracted with ether (15 ml) and freeze dried. The product (0.8 g) was crystallized from isopropanol–isopropyl ether and 96% ethanol–ether to yield 0.45 g (43%) of the title compound, mp 170–173°, shown to be identical with the substance isolated from alkaline degradation of I by TLC, PMR, and IR.

(6*R*)-6-Formamidopenicillanic Acid (III)—This compound was synthesized from acetic formic anhydride and trimethylsilyl 6-aminopenicillanate and isolated as the sodium salt (13). It was recrystallized from formamide–acetone, mp 235–240°; $[\alpha]_D^{20}$ +272° (H_2O); PMR (D_2O, sodium 3-trimethylsilylpropanoate): 1.58 (s, 2αCH_3), 1.67 (s, 2βCH_3), 4.32 (s, 3H), 5.67 (m, 5H and 6H), and 8.23 (s, OCH); IR (0.3% KBr): 1782, 1672, 1599, 1490, 1388, 1312, 1125, and 778.

(6*S*)-6-Formamidopenicillanic Acid (IV)—*Benzyl (6S)-6-Formamidopenicillanate*—A mixture of formic acid (1.1 ml, 28.9 mmoles), triethylamine (4.0 ml, 28.9 mmoles), and acetyl chloride (2.1 ml, 28.9 mmoles) in tetrahydrofuran (130 ml) was stirred for 15 min at −70° and subsequently added to a solution of benzyl (6*S*)-6-aminopenicillanate (12) (9.1 g, 29.7 mmoles) in tetrahydrofuran (165 ml) at −70°. The reaction mixture was stirred for 3 hr at room temperature and filtered. The filtrate was evaporated *in vacuo*; the oily residue (15.6 g) was taken up in a mixture of ether (130 ml) and ethyl acetate (25 ml) and successively extracted with water (35 ml), dilute hydrochloric acid (35 ml, pH 2.5), and water (2 × 35 ml).

The organic phase was dried and evaporated *in vacuo*. Crystallization of the residue (11.5 g) from ethyl acetate–petroleum ether yielded 7.0 g (71%) of the pure compound, mp 107–108°; $[\alpha]_D^{20}$ +209° (96% C_2H_5OH); PMR ($CDCl_3$, tetramethylsilane): 1.38 (s, 2αCH_3), 1.57 (s, 2βCH_3), 4.53 (s, 3H), 5.0–5.4 (m, 5H and 6H), 5.18 (m, O$CH_2C_6H_5$), 7.10 (d, J = 8 Hz, NH), 7.37 (s, C_6H_5), and 8.18 (s, CHO); IR (0.3% KBr): 1785, 1738, 1655, 1525, 1450, 1382, 1212, 1186, 1004, 992, 742, 735, 695, and 578.

Anal.—Calc. for $C_{16}H_{18}N_2O_4S$: C, 57.47; H, 5.43; N, 8.38. Found: C, 57.56; H, 5.61; N, 8.36.

Potassium (6S)-6-Formamidopenicillanate—A mixture of the above-mentioned benzyl ester (1.0 g, 3 mmoles) in ethyl acetate (15 ml) and potassium hydrogen carbonate (0.9 g, 3 mmoles) in water (25 ml) was hydrogenated over 10% palladium-on-carbon (2.5 g) at slightly elevated

pressure. After filtration, the aqueous phase was separated, extracted with ether (25 ml), and freeze dried. The greyish product (1.2 g) was extracted with ethanol (25 ml) and filtered. The filtrate was evaporated *in vacuo* to leave a solid residue (0.8 g), which was triturated with isopropanol (10 ml). A 0.7-g (83%) yield of potassium (6*S*)-6-formamidopenicillanate as an amorphous powder was obtained; PMR (D_2O, sodium 3-trimethylsilylpropanoate): 1.52 (s, $2\alpha CH_3$), 1.60 (s, $2\beta CH_3$), 4.33 (s, 3H), 4.93 (d, J = 1.8 Hz, 6H), 5.34 (d, J = 1.8 Hz, 5H), and 8.18 (s, CHO); IR (0.3% KBr): 1750, 1660, 1600, and 1525.

(1′*R*,2*R*,4*S*)-5,5-Dimethyl-2-[1′-((hexahydro- 1*H* -azepin-1-yl)-methyleneamino)methyl]thiazolidine-1′,4-dicarboxylic Acid[7] (V)—A mixture of I (5.0 g, 15.4 mmoles) and 1,500,000 units of β-lactamase[6] in water (50 ml) at room temperature was kept at a constant pH (7.0) by adding 1 *N* NaOH. When no more sodium hydroxide was consumed, the solution was freeze dried to yield 5.7 g (100%) of the crude sodium salt of V.

To a solution of this salt (3.7 g, 10 mmoles) in water (30 ml) was added 2-naphthalenesulfonic acid trihydrate (6.6 g, 25 mmoles) in water (70 ml) at room temperature. The precipitate (5.5 g) was recrystallized from acetone (25 ml) and water (5 ml) by addition of ether (50 ml) and from methanol–ether to yield the pure 2-naphthalenesulfonate hydrate of V (1.6 g, 28%), mp 132–133°; $[\alpha]_D^{20}$ +30° (CH_3OH); PMR (CD_3OD, tetramethylsilane): 1.28 (s, $5\alpha CH_3$), 1.60 (s, $5\beta CH_3$), 1.5–2.1 [m, $(CH_2)_4$], 3.72 (s, 4H), 3.3–3.8 (m, CH_2NCH_2), 4.27 (d, J = 7 Hz, 1′H), 5.14 (d, J = 7 Hz, 2H), 7.4–8.3 (m, $C_{10}H_7$), and 8.38 (bs, NCH=N); IR (0.3% KBr): 1730, 1682, and 1620.

Anal.—Calc. for $C_{25}H_{35}N_3O_8S_2$: C, 52.71; H, 6.19; N, 7.37; H_2O, 3.16. Found: C, 52.62; H, 6.24; N, 7.18; H_2O, 3.78.

(2*R*,4*S*)-5,5-Dimethyl-2-[(hexahydro- 1*H* -azepin-1-yl)methyleneaminomethyl]thiazolidine-4-carboxylic Acid[8] (VII)—A suspension of 2-aminomethyl-5,5-dimethylthiazolidine-4-carboxylic acid dihydrochloride dihydrate (16) (30 g, 100 mmoles) in chloroform (800 ml) was stirred for 0.5 hr at room temperature. Triethylamine (28 ml, 200 mmoles) was added. After stirring for 2.5 hr, the precipitate (21.5 g) was filtered off and washed with chloroform (4 × 100 ml) and ether (2 × 100 ml).

To a stirred suspension of this crude zwitterion (19 g, 100 mmoles) in methanol (1000 ml) was added hexamethyleneiminecarboxaldehyde dimethyl acetal (18.2 ml, 100 mmoles) at room temperature. After 2 hr, the solution was filtered and evaporated *in vacuo*. Addition of water (7 ml) followed by acetone (100 ml) to the solid residue yielded 17.6 g of crude VII, mp 153–155°. Treatment of this product in methanol (240 ml)–ether (240 ml) with hydrogen chloride in isopropanol afforded the hydrochloride of VII, mp 183–184°.

Recrystallization from methanol–ether yielded 7.1 g (24%) of the pure VII hydrochloride, mp 186.5–187°; $[\alpha]_D^{20}$ +150° (H_2O); PMR (D_2O, sodium 3-trimethylsilylpropanoate): 1.45 (s, $5\alpha CH_3$), 1.72 (s, $5\beta CH_3$), 1.4–2.1 [m, $(CH_2)_4$], 3.4–3.8 (m, CH_2NCH_2), 3.87 (m, 1′H), 4.07 (s, 4H), 5.12 (t, J = 6 Hz, 2H), and 8.03 (s, NCH=N); IR (0.3% KBr): 1685, 1600, 1460, 1128, and 787.

Anal.—Calc. for $C_{14}H_{26}ClN_3O_2S$: C, 50.05; H, 7.80; N, 12.51. Found: C, 50.12; H, 7.72; N, 12.70.

(1′*R*,2*R*,4*S*)-5,5-Dimethyl-2-(1′-formamidomethyl)thiazolidine-1′,4-dicarboxylic Acid[9] (IX)—A solution of the III sodium salt (2.6 g, 10 mmoles) in 50 ml of water was treated at room temperature with 500,000 units of β-lactamase[6]. The pH was kept at 7.0 by adding 1 *N* NaOH (10 ml). After freeze drying, the IX disodium salt was obtained in 100% yield (3.0 g); PMR: (D_2O, sodium 3-trimethylsilylpropanoate): 1.27 (s, $5\alpha CH_3$), 1.61 (s, $5\beta CH_3$), 3.42 (s, 4H), 5.03 (d, J = 7 Hz, 2H), 4.32 (m, 1H), and 8.13 (bs, OCH); IR (0.3% KBr): 1665, 1595, and 1398.

(2*R*,4*S*)-5,5-Dimethyl -2- formamidomethylthiazolidine-4-carboxylic Acid[10] (XI)—A mixture of 2-aminomethyl-5,5-dimethylthiazolidine-4-carboxylic acid dihydrochloride dihydrate (16) (9.0 g, 30 mmoles), triethylamine (8.4 ml, 60 mmoles), and tetrahydrofuran (300 ml) was stirred for 3 hr at room temperature and subsequently cooled to −70°.

In another flask, formic acid (1.16 ml, 30.6 mmoles), acetyl chloride (2.18 ml, 30.6 mmoles), and triethylamine (4.26 ml, 30.6 mmoles) were stirred in tetrahydrofuran (120 ml) at −70° for 10 min. While stirring, the resulting suspension was immediately added to the first mixture. The temperature was raised to 20–25° during 1.25 hr. After filtration and washing with tetrahydrofuran, the filtrate was evaporated *in vacuo*.

[7] Previously named BB 511 (14, 15).
[8] Previously named FL 1115 (14).
[9] Previously named BB 517 (14, 15).
[10] Previously named FL 1114 (14).

Table II—R_f Values of Mecillinam and Reference Compounds

Compound	R_f Values System A	System B	System C	System D	System E
I	0.05	0.25	0.60	0.05	0.45
II	0.05	0.30	0.65	0.05	0.45
III	0.50	0.70	0.75	0.50	0.55
IV	0.40	0.65	0.70	0.35	0.50
V	0.00	0.10	0.45	0.00	0.35
VI	0.00	0.15	0.25	0.00	—
VII	0.00	0.15	0.50	0.05	0.50
VIII	0.00	0.15	0.45	0.05	0.45
IX	0.05	0.10	0.20	0.00	0.15
X	0.05	0.10	0.15	0.00	0.15
XI	0.20	0.25	0.35	0.15	0.45
XII	0.20	0.25	0.35	0.15	0.45
XIII	0.45	0.50	0.65	0.45	0.65
⊂NH[a]	0.10	0.15	0.45	0.20	0.50
6-Aminopenicillanic acid	0.15	0.20	0.40	0.25	—
Penicic acid	0.05	0.05	0.20	0.05	0.15
Penicillamine	—	—	0.45	0.10	0.55

[a] Only visible with 4,4′-tetramethyldiaminodiphenylmethane spray reagent (11).

The oily residue (8.6 g) was crystallized from methanol (40 ml) to yield 2.6 g (40%) of XI, mp 160.5–161°; $[\alpha]_D^{20}$ +169° (H_2O); PMR [$(CD_3)_2SO$, tetramethylsilane]: 1.21 (s, $5\alpha CH_3$), 1.57 (s, $5\beta CH_3$), 3.17 (m, 1′H), 4.65 (m, 2H), 3.58 (s, 4H), 7.5 (bs, 3NH and COOH), and 8.02 (bs, OCH); IR (0.3% KBr): 1680, 1635, 1555, 1135, 1060, 1045, 780, and 595.

Anal.—Calc. for $C_8H_{14}N_2O_3S$: C, 44.02; H, 6.46; N, 12.83. Found: C, 44.27; H, 6.43; N, 12.71.

(1′*R*,2*R*,4*S*)-5,5-Dimethyl-2-(1′-formamido- 1′ -*N*,*N*-hexamethylenecarbamoylmethyl)thiazolidine-4-carboxylic Acid[11] (XIII) —*Isolation from Alkaline Degradation of I*—A I solution (10 g, 31 mmoles) in water (100 ml) was adjusted to pH 10 and kept for 4 hr at 37° and constant pH. After adjustment to pH 3, the solution was extracted with chloroform (3 × 100 ml). The combined organic phases were dried and evaporated *in vacuo*. For chromatography, 0.5 g of the residue (1.8 g) was dissolved in chloroform (2 ml), applied to a Sephadex LH 20 column (65 × 2.5 cm), and eluted with chloroform (2 ml/min). The separation was followed by TLC using System B (*Assay Methods* and Table II).

The combined fractions containing XIII were evaporated *in vacuo* to leave an oil (0.29 g); PMR ($CDCl_3$, tetramethylsilane): 1.30 (s, $5\alpha CH_3$), 1.67 (s, $5\beta CH_3$), 1.6–2.0 [s, $(CH_2)_4$], 3.4–3.8 (m, CH_2NCH_2), 3.78 (s, 4H), 4.8–5.5 (m, 2H and 1′H), 7.02 (bs, 3H and COOH), 7.81 (bs, J = 9 Hz, CONH), and 8.33 (d, J = 1.2 Hz, HCO); ^{13}C-NMR ($CDCl_3$, tetramethylsilane): 59.8 (C-5), 67.0 (C-2), 52.3 (C-1′), 72.5 (C-4), 163.5 (HCO), 169.5 (NCO), and 171.7 (COOH); IR (5% $CHCl_3$): 1722, 1675, and 1625.

Synthesis—A solution of the III sodium salt (6.4 g, 25 mmoles) in water (75 ml) was stirred for 1.5 hr at room temperature with hexamethyleneimine (2.8 ml, 25 mmoles). After extraction with ether (25 ml), the aqueous phase was cooled (0–5°) and acidified (pH 3), followed by extraction with chloroform (5 × 100 ml). After drying, the chloroform was removed *in vacuo*. To a filtered solution of the residue (4 g, 12 mmoles) in acetone (80 ml) was added 1.4 ml (12 mmoles) of cyclohexylamine. Without isolation, the precipitated salt was brought into solution by the addition of water (12 ml).

After filtration and addition of acetone (160 ml), 2.6 g (23% yield) of the XIII cyclohexylamine salt was obtained as a hemihydrate, mp 172–173°; $[\alpha]_D^{20}$ +96° (96% C_2H_5OH); PMR (D_2O, sodium 3-trimethylsilylpropanoate): 1.25 (s, $5\alpha CH_3$), 1.63 (s, $5\beta CH_3$), 1.2–2.3 [m, $(CH_2)_4$ and $(CH_2)_5$], 3.57 (s, 4H), 3.0–3.9 (m, CH_2NCH_2 and CH=N), 4.93 (m, 2H and 1′H), and 8.09 (s, CHO); IR (0.3% KBr): 1668, 1621, 1600, 1525, 1392, and 790.

Anal.—Calc. for $C_{21}H_{38}N_4O_4S \cdot 0.5H_2O$: C, 55.85; H, 8.71; N, 12.41; H_2O, 1.99. Found: C, 55.88; H, 8.67; N, 12.49; H_2O, 2.28.

Assay Methods—*Iodometric Method*—The residual concentration of intact β-lactam compound(s) was determined by an iodometric titration.

Spectrophotometric Method—The concentrations of mecillinam (I) and (6*S*)-mecillinam (II) were determined by a spectrophotometric measurement[12] at 330 nm of the imidazolone formed by reaction between I and glycine in aqueous solution (17).

[11] Previously named BB 514 (14).
[12] Beckman Acta C III.

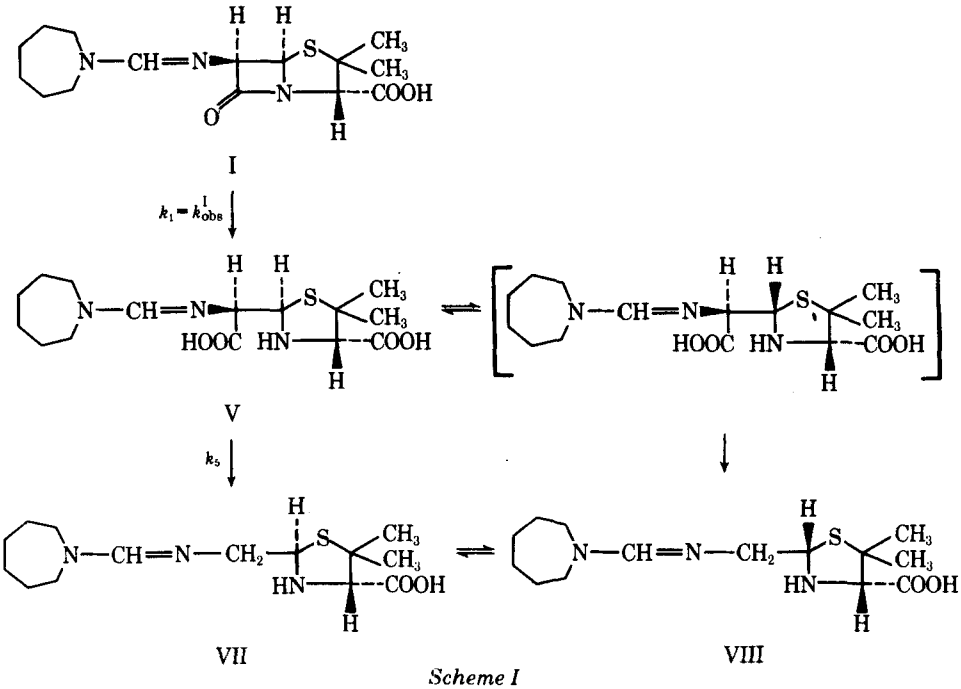

Scheme I

TLC—The degradation products were identified and semiquantified by comparing samples of appropriate reference compounds in different solvent systems. The R_f values of the reference compounds are given in Table II.

Solvent systems were: A, ethyl acetate–water–acetic acid (75:10:15); B, ethyl acetate–water–formic acid (80:10:10); C, chloroform–ethanol (96%)–formic acid (50:30:20); D, chloroform–ethanol (96%)–acetic acid (80:20:30); and E, chloroform–acetone–acetic acid–water (40:30:30:10).

For a semiquantitative estimation of degradation products in Systems A and B, 10-μl samples from the reaction solution as well as 10-μl samples from a 10-fold aqueous dilution of the reaction solution were linearly applied directly to the silica gel plate[13]. The aqueous standard blends were applied beside the test samples. With Systems C–E, samples (1.0 ml) of the reaction solution were freeze dried and dissolved in methanol (1.0 ml). Half of this solution was diluted to 5.0 ml with methanol, and 10 μl of each methanolic solution was applied linearly to the plate together with methanolic samples of the appropriate reference compounds.

The plates were developed in each solvent system until the mobile phase had ascended 12.5 cm. The chromatograms were visualized by exposing the plate to iodine vapor, followed by spraying with a starch indicator (1% in water). For chromatograms developed in System D, the visualization was performed with 4,4′-tetramethyldiaminodiphenylmethane reagent (18).

NMR Methods—The NMR data[4] of the pure compounds were obtained from 10% (w/v) solutions. Kinetic studies were performed either on freeze-dried samples redissolved in deuterium oxide or on samples taken directly from experiments performed in deuterium oxide or water. Deuterated acid or base was used for pD adjustment in deuterium oxide. The overall concentration of the kinetic experiments was ~1%, and hexamethyldisiloxane served as the internal reference.

In Fourier transform NMR, deuterium from the deuterated solvents was used as the internal lock. In water, a coaxial inner tube[14] with deuterium oxide served as the external lock. The digital resolution was kept better than the spectrometer resolution, and from 24–200 (proton) up to 60,000 (carbon 13) scans were accumulated. Usually, a carbon–proton 5-mm dual probe or, in special cases, a 10-mm carbon probe was used.

All spectra were obtained with 30 or 90° pulses, using a sufficient repetition time to allow full relaxation.

Homo and hetero decoupling experiments were performed with standard 8K software and standard hardware. The water band was mostly eliminated through homogated decoupling.

Overhauser enhancement was obtained from degassed samples. During data manipulation, a light positive exponential multiplication was performed. Whenever necessary and possible, reference compounds were added to the reaction mixtures in realistic concentrations to support individual compound identification and to facilitate proton spectrum interpretation.

Kinetic Procedures—An accurately weighed amount of I was dissolved in preheated water (37°) to produce an initial concentration of $\sim 3 \times 10^{-2}$ M (1% w/v). Hydrochloric acid or sodium hydroxide was added to give the reaction solution the desired pH (all integers of the pH interval from 2 to 10), and the pH was maintained by a pH-stat[15]. Before and after an experiment, the pH meter was standardized with a standard buffer at the same temperature. No significant pH change was observed. The reactions were carried out at constant temperature (37 ± 0.1°).

If the half-life of I was more than 1 day, a closed titration vessel was used. In some experiments (at pH 2, 5, and 8), the ionic strength was adjusted to 0.5 by addition of sodium chloride. Samples from the reaction solutions were taken at appropriate intervals and analyzed. Aqueous solutions of II, 6-formamidopenicillanic acid (III), and mecillinam penicilloic acid (V)[16] (1% w/v) were subjected to the same kinetic procedure.

Table III—Acidic Hydrolysis of Mecillinam (1% w/v) at pH 2 and 37°

Hours	Product Distribution, mole %			
	I	V	VII	VIII
0.25	99	2	—	—
3	90	5–10	2	—
6	80	5–10	10	5
24	35	5–10	35	25
50	15	5–10	45	35

RESULTS[16]

The degradation of mecillinam (I) was followed until most of the drug was destroyed. The results obtained at pH 2, 6, and 10 will suffice to outline the influence of pH on hydrolysis rate and product distribution.

The structures of the degradation products with unchanged stereochemistry were deduced by comparing their R_f values with those of synthetic specimens of likely candidates in several systems and were

[13] Silica gel 60 F_{254} (Merck 5715).

[14] Type WGS-5 BL, Wilmad Glass Co.

[15] Radiometer model TTT 1 b, SBR 2, and magnetic valve type MNVIC or Radiometer RTS 622.

[16] Although not strictly correct, the nomenclature and numbering of penicillin are used for all degradation products including monocyclic compounds except in the *Experimental* part. When not otherwise indicated, the compounds have the natural penicillin configuration (3*S*, 5*R*, 6*R*).

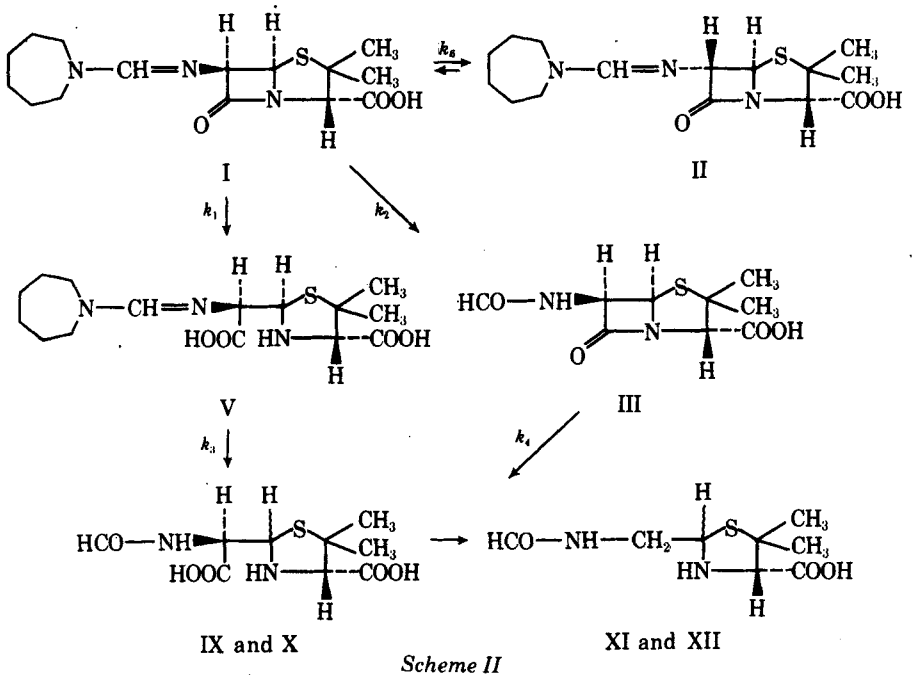

Scheme II

confirmed by NMR spectroscopy, except in the case of the penicilloic amide XIII (Table I). This compound, as well as (6*S*)-mecillinam (II), was initially isolated from reaction mixtures and identified. For the isolation of II, use was made of the resistanceof II toward β-lactamase (*cf.*, 11) to separate it from I.

The existence of other stereochemically abnormal degradation products, when suspected from NMR, was verified by equilibration experiments on the appropriate reference compounds with normal configuration. The structures of XIII, II, and (6*S*)-formamidopenicillanic acid (IV) were further confirmed by unambiguous syntheses. All were straightforward. The yields of degradation products were estimated by comparison with reference compounds by TLC and further supported by NMR.

In strong acid solution (pH 2, Table III and Scheme I), the β-lactam ring of I was opened rapidly to afford the penicilloic acid V in 5–10% yield. No further increase in the yield of this compound was noted during the next 50 hr. In the same period, an increasing amount of decarboxylated product (VII) was formed. After 50 hr, a 45% yield of VII was obtained. The other major product formed concurrently with VII, and in almost the same yield, was the (5*S*)-epimer VIII. The half-life of I at pH 2 was ~15 hr (k_{obs} = 0.039 hr^{-1}, Table IV). No compounds resulting from amidine bond hydrolysis were observed.

In weak acidic solution (pH 6) about its isoelectric point, I degraded more slowly, the half-life being ~100 hr (Tables IV and V and Scheme II). Amidine bond hydrolysis occurred during the formation of most of the observed products. In addition to hexamethyleneimine, the predominant products formed were 6-formamidopenicillanic acid (III) and compounds formally derived from it by hydrolysis of the β-lactam ring (IX and X) and subsequent decarboxylation (XI and XII). A 10% yield of II was noticed after 120 hr.

In strong basic solution (pH 10, Table VI and Scheme III), I was rapidly destroyed with a half-life of ~1 hr. Compounds undergoing amidine bond hydrolysis during the degradation formed a major part of the reaction mixture. Thus, the 6-epimeric formamidopenicillanic acids III and IV, the 5-epimeric penicilloic acids IX and X, and the penicilloic amide XIII were formed in a total yield of 50–60% during 2–3 hr, with XIII being of

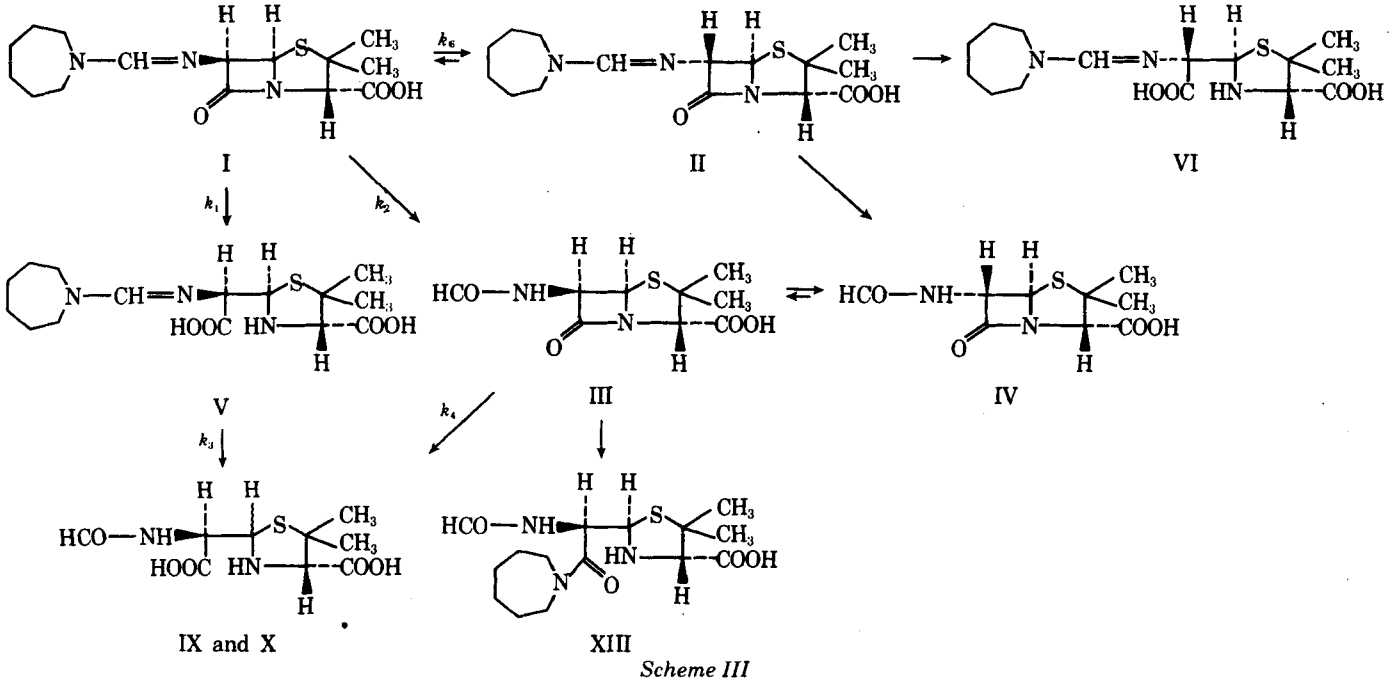

Scheme III

Table IV—Measured Rate Constants [a] at 37°

pH	k^{I}_{obs}, hr^{-1}	k^{II}_{obs}, hr^{-1}	k_3, hr^{-1}	k_4, hr^{-1}
2	0.039	0.0026	—	—
6	0.0076	0.0016	0.22	0.0022
10	0.79	0.29	0.32	0.32

[a] Estimated error <20%.

Table V—Weak Acidic Hydrolysis of Mecillinam (1% w/v) at pH 6 and 37°

Hours	Product Distribution, mole % I	II	III	IX + X [a]	XI + XII	⊂NH
0.25	99	—	—	—	—	—
2	99	—	—	0.5	—	—
5	95	0.5	0.5	2	—	3
24	85	1	3	10 (1:1)	—	15
50	70	5	7	20 (1:1.2)	2	25
120	40	10	15	30 (1:1.5)	10	50

[a] Figures in parentheses are the IX:X ratios estimated by NMR.

secondary importance. A 55–65% yield of hexamethyleneimine was obtained during the same period.

At the same time, compounds with the preserved amidine bond (the major component II, V, and VI) were produced in a 30% yield. 6-Aminopenicillanic acid, penicic acid, and penicillamine were not observed.

As seen from Tables VII and VIII, the yield of XIII was dependent on the I concentration. Increasing this concentration from 0.1 to 10% increased the yield of XIII.

In addition, experiments performed at pH 2, 5, and 8, either neat or with added sodium chloride to obtain an ionic strength of 0.5, showed no influence of ionic strength on the degradation rate and product distribution.

DISCUSSION

Methods—Although TLC has infrequently been applied to the study of penicillin degradation, several solvent systems have been developed for the separation of the penicillins and their major degradation products (19). In the present study, special solvent systems had to be developed in consequence of the strongly polar compounds formed from mecillinam (I). No single system was discovered that could separate all degradation products. Only with several systems did TLC on silica gel satisfactorily separate products formed in at least a 0.5% yield.

Many solvent systems were evaluated to ensure that no principal products were overlooked and that no artifacts were interpreted as degradation products. This procedure was supported by NMR and semiquantitative measurements. As seen from Tables III and V–VIII, the yields of degradation products accounted for nearly all lost I.

Generally, these results were estimated to be accurate with a relative uncertainty of 20%, although the determinations of hexamethyleneimine in basic reaction resolutions were more uncertain because of the unavoidable evaporation of some amine during the freeze-drying process involved in the TLC and NMR determinations.

PMR spectra in deuterium oxide or water could be used to separate and quantitate all products containing a formyl or an amidine proton (Fig. 1). As expected, large pD, pH shifts (up to 0.5 ppm) were observed in the formyl and amidine 8-ppm region. The amidine protons were more sensitive to pD, pH variations than were the formyl protons (Table IX).

The best separation of the hydrolysis compounds was obtained in basic solutions where all amidines could be detected separately to yield satisfactory integrals. In the absence of overlapping lines, integrals could be determined better than ±5%. With partly overlapping lines, the estimated error was <±25%. By changing the pD during observations, useful integrals of nearly all of the hydrolysis products could be obtained. Destruction products formed in yields of <5% could not be determined because of further degradation during the necessary accumulation time.

Outside the 8-ppm region, it was possible to identify all compounds through characteristic absorptions. However, quantitation of the hydrolysis mixture using these absorptions was often less profitable due to overlapping spin patterns.

The NMR results were in excellent agreement with the TLC observations. In some cases, products (V and VIII–XII) that could only be quantitated uncertainly, or as a sum from TLC, could be determined separately.

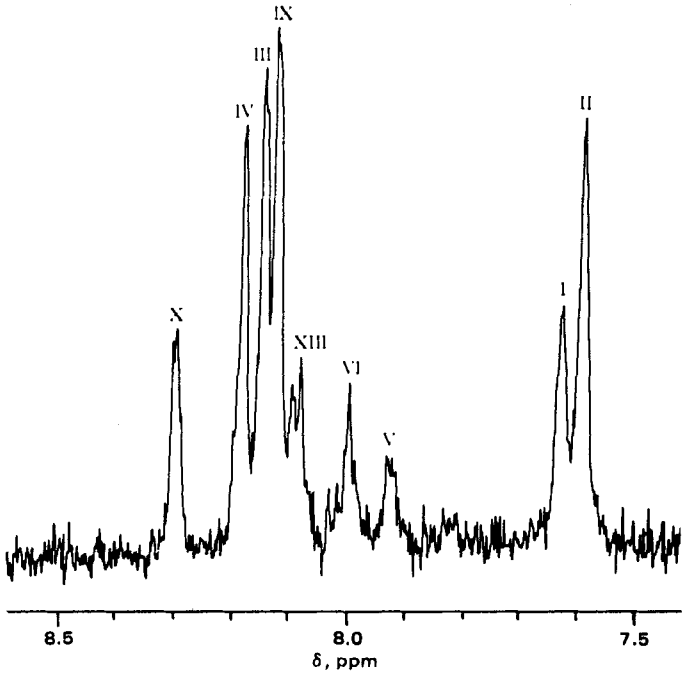

Figure 1—*PMR spectrum (99.6 MHz) of a freeze-dried sample from I hydrolysis (1% w/v, 3 hr, 37°, pH 10). Sample was redissolved in deuterium oxide and adjusted to a pH meter reading of 10.2; the 8-ppm region is shown. Conditions were: number of pulses, 64; flip angle, 30°; pulse repetition time, 15 sec; and digital resolution, 0.12 Hz.*

In addition to the TLC and NMR methods, intact I also has been determined by iodometric titration and a spectrophotometric method recently developed by Larsen and Bundgaard (17). Whereas the iodometric assay does not distinguish between different types of β-lactam-containing compounds, the spectrophotometric method is claimed to be highly specific for I and its pivaloyloxymethyl ester (pivmecillinam) since an intact β-lactam ring, as well as an amidine group at position 6, is necessary for the method. Under weak acidic to basic conditions, this method is invalidated due to the formation of II. The molar absorbance of II when subjected to this assay is only about 75% of the absorbance of I, presumably owing to slower reaction with the glycine reagent since the same 4-aminomethyleneimidazol-5(4*H*)-one derivative should be formed from both epimers. Therefore, this spectrophotometric assay cannot be used as a general specific method for quantitation of I under weak acidic to basic conditions.

Reaction Rate Constants—At constant pH and temperature, the observed rate for I degradation, obtained by measuring the remaining intact I, followed pseudo-first-order kinetics. The observed rate constants (k^{I}_{obs}) at pH 2, 6, and 10 are listed in Table IV. At pH 6, k^{I}_{obs} was the sum of three rate constants: k_1 (β-lactam opening), k_2 (hydrolysis of the amidine bond), and k_6 (6-epimerization). To calculate k_1, k_2, and k_6 at pH 6, the following differential equations were used:

$$\frac{d(\mathrm{I})}{dt} = -k^{I}_{obs}(\mathrm{I}) = (-k_1 - k_2 - k_6)(\mathrm{I}) \qquad \text{(Eq. 1)}$$

$$\frac{d(\mathrm{III})}{dt} = k_2(\mathrm{I}) - k_4(\mathrm{III}) \qquad \text{(Eq. 2)}$$

$$\frac{d(\mathrm{II})}{dt} = k_6(\mathrm{I}) - k^{II}_{obs}(\mathrm{II}) \qquad \text{(Eq. 3)}$$

where the observed rate constants for the degradation of II (k^{II}_{obs}) and III (k_4) were separately determined (Table IV).

The solutions of the differential equations are:

$$k_2 = \frac{[\mathrm{III}][k_4 - k^{I}_{obs}]}{[\mathrm{I}]_0[e^{-k^{I}_{obs}t} - e^{-k_4 t}]} \qquad \text{(Eq. 4)}$$

$$k_6 = \frac{[\mathrm{II}][k^{II}_{obs} - k^{I}_{obs}]}{[\mathrm{I}]_0[e^{-k^{I}_{obs}t} - e^{-k^{II}_{obs}t}]} \qquad \text{(Eq. 5)}$$

$$k_1 = k^{I}_{obs} - k_2 - k_6 \qquad \text{(Eq. 6)}$$

Comparison of Penicillin and Mecillinam Hydrolysis—In addition

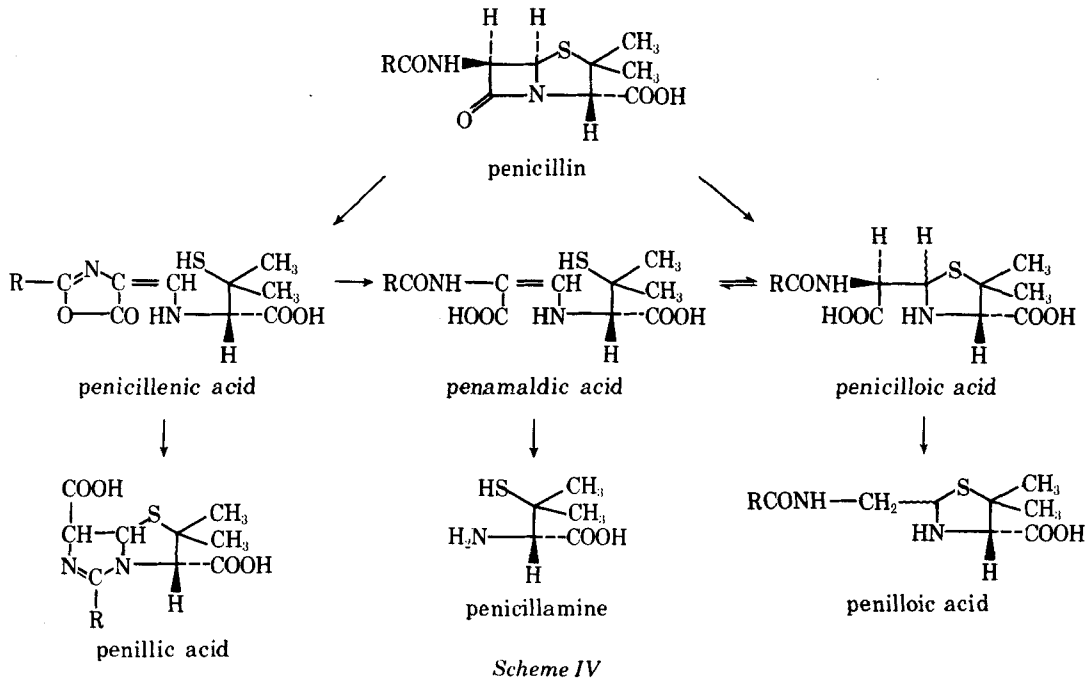

Scheme IV

to identifying the major hydrolytic degradation products of I, it was of interest to compare the influence of an amidine and an amide side chain on the hydrolytic patterns of their 6-aminopenicillanic acid derivatives. However, due to the complexity of penicillin transformations in aqueous solution (20), no completely satisfactory degradation schemes have been put forward for penicillin hydrolysis. Among the schemes found in the literature (2, 19, 21–29), only those of Blaha *et al.* (27) and Hartmann *et al.* (28) are exclusively based on accurate analyses. They followed the formation of a selection of known degradation products of penicillins G and V in aqueous solution as a function of pH, until most of the penicillins were destroyed, by high-pressure liquid chromatography (HPLC) and UV spectroscopy. Though slightly different, and despite the inherent incompleteness, their schemes with minor modifications are adopted in the discussion as representing the main features of penicillin degradation.

Acidic Solution—Scheme IV shows the degradation of penicillins in acidic solution. Nearly all of the primary degradation products of a penicillin retain the side chain either intact or in derived form (penicillenic and penillic acid). The only exception is penicillamine solely derived from the nucleus. The scheme differs from those of previous investigators (27, 28) mainly by the incorporation of the 5-epimerization of penicilloic acid. (5*S*)-Penicilloic acid was not included among their reference compounds. Depending on pH and temperature, at least some epimerization can be expected before decarboxylation to the 5-epimeric mixture of penilloic acids.

In I, the side chain is also preserved during acidic hydrolysis (Scheme I). Cleavage of the β-lactam ring initiates the formation of a series of 5-epimeric compounds closely corresponding to those found in the penicillin case with an intact side chain and a thiazolidine ring. No compounds of the penillic or penicillenic acid types are formed, as shown by the absence

Table VI—Basic Hydrolysis of Mecillinam (1% w/v) at pH 10 and 37°

Hours	Product Distribution, mole %								
	I	II	III	IV	V	VI	IX + X[a]	XIII	⊂NH
0.25	95	1	3	—	1	—	1	—	3
1	50	20	10	4	5	—	10	0.5	30
2	20	20	20	7	10	1	20 (5.5:1)	1	55
3	10	20	20	15	5	5	25 (4.5:1)	2	65
4	5	20	15	15	1	5	35 (2.5:1)	5	75

[a] Figures in parentheses are the IX:X ratios estimated by NMR.

Table VII—Basic Hydrolysis of Mecillinam (0.1% w/v) at pH 10 and 37°

Hours	Product Distribution, mole %								
	I	II	III	IV	V	VI	IX + X	XIII	⊂NH
0.25	95	1	3	—	1	—	1	—	3
1	50	20	10	4	5	0.5	10	0.5	30
2	20	20	20	7	10	1	20	1	55
3	10	20	20	15	10	2	25	2	65
4	5	20	15	15	5	2	35	5	75

Table VIII—Basic Hydrolysis of Mecillinam (10% w/v) at pH 10 and 37°

Hours	Product Distribution, mole %								
	I	II	III	IV	V	VI	IX + X	XIII	⊂NH
0.25	95	2	5	—	—	—	—	—	5
1	50	20	10	5	1	0.5	2	1	30
2	20	25	20	15	2	1	15	4	45
3	10	20	15	20	2	1	20	8	65
4	5	20	10	20	2	2	25	20	65

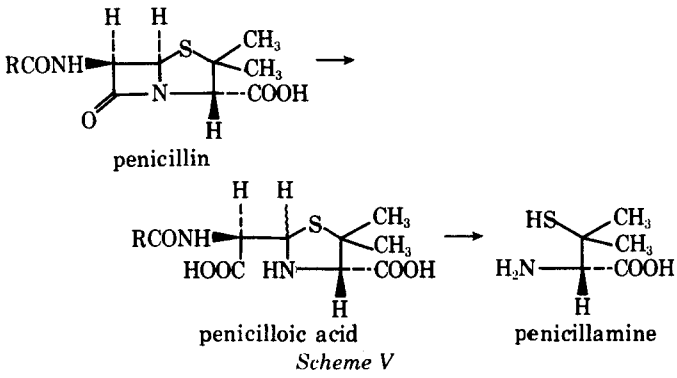

Scheme V

of hexamethyleneimine and a UV maximum higher than 260 nm when the hydrolysis was followed through 96 hr at pH 4 and 37°.

The observed (5*S*)-penilloic acid (VIII) is believed to result from 5-epimerization of the major degradation product (VII) rather than from a decarboxylation of the unobserved (5*S*)-penicilloic acid. This view was supported by epimerization experiments (NMR) of V and VII since V underwent rapid decarboxylation (k_5 = 0.4 hr^{-1}) and VII, under the same conditions (1 hr, pH 2, 37°), was converted to a 5-epimeric mixture of VII (60%) and VIII (40%).

During similar epimerization experiments in deuterium oxide, little, if any, deuterium incorporation at position 3, 5, or 6 took place. These findings indicate that 5-epimerization involving intermediates of the penamaldic acid type, as postulated for penicilloic acids of true penicillins, must be unimportant.

Weakly Acidic or Neutral Solution—Fewer degradation products, as well as an increased stability of penicillins, was observed under these conditions. The primary Scheme IV products still arose, but little, if any, penilloic acid or penicillamine was produced and penillic acid was not formed.

In contrast to penicillins, and in spite of the increased stability about the isoelectric point (5.8), additional degradation routes were observed for I (Scheme II). As in the acidic hydrolysis, the major part was degraded through the penicilloic acid V route (k_1 calculated to 0.005 hr^{-1}) with an intact side chain. The very low yield (<1%) of V underemphasized the importance of this route due to the subsequent rapid hydrolysis of the amidine bond of V (k_3 = 0.22 hr^{-1}, pH 6, 37°, Table IV) to yield IX, X, and hexamethyleneimine.

A second, less important degradation route leading to IX through III ("hydrogenpenicillin") involves the same hydrolytic reactions but in reversed order. The relatively low rate constant for the amidine bond hydrolysis (k_2 calculated to 0.002 hr^{-1}) as compared with the hundred times greater k_3 points to an intramolecularly assisted hydrolysis of the α-amidinocarboxylic acid V. A similar proposal was recently put forward by other investigators (30) who suggested the formation of a 4-(thiazolidin-2-yl)-oxazol-5-one intermediate with simultaneous expulsion of hexamethyleneimine.

The key degradation product (IX) was further transformed to its 5-epimeric product (X); in acidic solution, both compounds were decarboxylated to yield an epimeric mixture of the penilloic acids XI and XII. The mecillinam penicilloic acid V, on the other hand, was not decarboxylated because of the rapid competitive amidine bond hydrolysis to IX. This proposed degradation route for V was supported by the stability of the unobserved penilloic acid VII, which was stable for more than 24 hr at pH 6.

A third degradation route, unprecedented in the penicillin series, was a commencing epimerization at the 6-position. This epimerization was rather slow at pH 6 (k_6 calculated to 0.001 hr^{-1}), as was the further degradation of (6*S*)-mecillinam (II) when compared to I. No further 6-epimerized products were observed.

Basic Solution—At higher pH, the penicillin degradation (Scheme V) was even more simplified. The penicilloic acid was the only primary degradation product, presumably as a 5-epimeric mixture (31).

In basic solution, the primary steps of the I degradation (Scheme III) were identical to those in weakly acidic and neutral solutions (Scheme II). In contrast, the secondary steps showed increased complexity.

Because of the intricate degradation scheme, it was not possible from the results in Table VI to calculate k_1 (β-lactam opening), k_2 (amidine hydrolysis), and k_6 (6-epimerization) (Scheme III) with reasonable certainty. Nevertheless, some qualitative considerations can be given by combining the results in Tables IV and VI.

A drastic increase in k_1 as compared to k_3 occurred. This result follows from the observed degradation rate constant for I (Table IV) and the separately determined, almost unchanged, k_3 together with the detection of considerable amounts of V.

Furthermore, k_2 was the same order of magnitude or even greater than k_4 since the 150-fold increase in k_4 at pH 10 as compared to pH 6 was not reflected in a decrease in the III concentration, despite the two additional degradation routes for this compound. The increase of k_2 with increasing pH is a logical consequence of the lower stability of amidines in basic solutions (6). The small pH dependence of k_3 for the hydrolysis of the α-amidinocarboxylic acid (V) may reflect a special hydrolysis mechanism of this type of amidine compound.

As a third important degradation route, the 6-epimerization yielding II can be observed. It was not possible to determine the relative importance of the routes I → V, I → III, and I → II. However, the results in Tables IV and VI suggest that k_1, k_2, and k_6 are in the same order of magnitude.

In a secondary degradation step, the II hydrolysis afforded substantial amounts of (6*S*)-6-formamidopenicillanic acid (IV). This compound also can be produced from III, as proved in separate experiments. This is the first reported example of a 6-epimerization in aqueous solution of a true penicillin. Compound II can further degrade to a (6*S*)-penicilloic acid (VI), and small amounts of VI were observed. It could be expected that IV is degraded in a similar way as III to yield 6- and 6,5-epimeric products. No such compounds were observed. The only 5-epimeric compound detected was X.

A minor product from a secondary step is the penicilloic amide XIII, which has no counterpart in the penicillin degradation schemes. Compound XIII is not a primary degradation product of I, resulting from intramolecular nucleophilic attack of the amidine group on the β-lactam moiety. Although this mechanism is favored by Larsen and Bundgaard (7), the influence of the I concentration on the yield of XIII (Tables VII and VIII) clearly showed that XIII is formed by an intermolecular reaction, presumably between III and hexamethyleneimine or, alternatively, by an initial bimolecular reaction between two molecules of I, or between I and hexamethyleneimine, followed by hydrolysis of the amidine bond. The first mechanism is preferred since XIII does not appear until substantial amounts of III have been formed (Table VI). Besides, addition of 1 equivalent of hexamethyleneimine to a 1% aqueous solution of I at pH 10 and 37° was without influence on the I half-life, although the yield of XIII was increased at the expense of III. Furthermore, the half-life of III under similar conditions was decreased 50% when an equimolar amount of hexamethyleneimine was added.

6-Epimerization—At basic pH, the sum of residual I and produced III derived from TLC was smaller than the amount of β-lactam-containing compounds determined from iodometric titration. In the PMR spectra of the hydrolysis mixture at pH 10, a freeze-dried sample redissolved in deuterium oxide and adjusted to a pH reading of 10.4 showed two singlets (4.27 and 4.24 ppm) and two doublets [5.20 ppm (J = 1.1 Hz) and 5.32 ppm (J = 1.7 Hz)]. This finding suggests the existence of at least two more β-lactam-containing compounds. The small coupling constants indicate that in these compounds the 5- and 6-protons are *trans*. Further analysis of the PMR spectra supports this theory.

No epimerization at position 6 in intact penicillins subjected to base-catalyzed hydrolysis has been reported, whereas 6-epimerization has been described for other 6-aminopenicillanic acid derivatives [hetacillin (32) and 6-trimethylammonium penicillanic acid (33)] in aqueous solution.

Table IX—PMR Data of Mecillinam Degradation Products, δ-ppm Region, as a Function of pH [a]

Compound	pH Meter Reading		
	2	5.6	10.2
I	8.000	7.995	7.631
II	8.019	8.035	7.580
III	8.149	8.145	8.144
IV	8.159	8.137	8.177
V	8.035	7.943	7.930
VII	7.985	7.897	7.870
VIII	8.021	7.992	7.940
IX	8.188	8.137	8.122
X	8.243	8.291	8.298
XI	8.162	8.064	8.050
XII	—	8.139	8.137
XIII	8.189	8.090	8.078

[a] Spectra were taken in deuterium oxide. All data were obtained by using hexamethyldisiloxane as the reference but were converted to trimethylsilylpropanoate as the 0.000-ppm delta scale. First-order approximations were used. Uncertainty on the parts per million reading was ±0.005 ppm. Probe temperature was 28°.

In view of these findings, the two unknown compounds were expected to be II and IV, respectively. Spectroscopic analysis of II isolated from the hydrolysis mixture proved the expected structure. Finally, II and IV synthesized in an unambiguous way were identical to the two β-lactam-containing hydrolysis products. In agreement with this finding, basic hydrolysis of I performed in deuterium oxide showed deuterium incorporation at position 6 but no incorporation at position 5.

In hydrolysis experiments at pH 10 (37°), II equilibrated to a mixture of I and II. After 3 hr ($t^{II}_{1/2}$ = 2.4 hr), 2–5 mole % of I appeared. This result was in contrast to hetacillin, where no (6*R*)-hetacillin could be detected from (6*S*)-hetacillin (33, 34).

The formation of IV took place mainly from II and, unexpectedly, to a smaller degree from III (see the preceding section). Similarly to II, IV epimerized to III (pH 10, 37°), giving approximately 1 mole % of III after 4 hr ($t^{IV}_{1/2}$ = 9.5 hr). No epimerization of a (6*S*)- (or 6*R*-) penicillin was reported previously.

Among the β-lactam-opened thiazolidines, the only 6-epimeric compound observed was the penicilloic acid VI.

5-Epimerization—No 5-epimerization of penicillins has been reported in aqueous solution. In contrast, thiazolidines are known to be in equilibrium with their thiol precursors (35). 5-Epimerization of the β-lactam-opened compounds, *e.g.*, the penicilloic acids, is well documented (21, 31, 36, 37).

In the present work, only the β-lactam-opened compounds were found to undergo 5-epimerization in acidic (pH 2), neutral (pH 7), and basic (pH 10) solutions. Rate constants and equilibrium proportions for the different compounds were found to depend on the side chain at position 5[17].

In all observable cases[18], epimerization experiments performed in deuterium oxide yielded compounds that were not deuterated at positions 3, 5, and 6. These findings are consistent with observations for 6-aminopenicillanic acid (31) where no deuterium incorporation during base-catalyzed hydrolysis could be detected. Several mechanisms have been proposed for the 5-epimerization, either through different enamine- (21, 28, 37) or azomethine- (31) type intermediates. From these results, C-6 cannot be involved in the epimerization process, excluding an enamine-type intermediate. Therefore, it must be concluded that at least the thiazolidines derived from I 5-epimerize like 6-aminopenicillanic acid (31) through intermediates of the azomethine type.

3-Epimerization—No sign of 3-epimerization of penicillins (38) or of I or its degradation products was detected.

(5S,6S)-Compounds—In the present work, no β-lactam-containing compounds with both 5- and 6-epimerization were observed.

From the degradation of II and IV and from the work of Busson *et al.* (36), it would be expected that some (5*S*,6*S*)-compounds must be present at least in basic solutions. No such compounds were observed. Due to the relatively greater stability of II and IV, the amount of (5*S*,6*S*)-compounds is believed to be of minor importance and they accordingly are not included in Schemes II and III.

SUMMARY

Aqueous solutions of mecillinam (I), unlike the penicillins, showed an increased complexity of major degradation routes and compounds with increasing pH. Some degradation reactions are known from penicillin chemistry but others are not, resulting in new types of degradation products at pH ≥ 6. Conversely, several of the structures from acidic degradation of penicillins were not reproduced at pH < 6.

In acidic solution, only compounds closely corresponding to penicillin degradation products with an intact side chain and a thiazolidine ring were formed, *i.e.*, penicilloic acid V[16] (Table I) and 5-epimeric penilloic acids VII and VIII of I.

In weakly acidic or neutral solutions, hydrolysis of the I and V amidine bonds yielded the key degradation product (6*R*)-6-formamidopenicillanic acid (III) and its 5-epimeric penicilloic (IX and X) and penilloic (XI and XII) acids together with hexamethyleneimine. A reversible 6-epimerization of I to yield (6*S*)-mecillinam (II) constituted a third, less important degradation route of I.

In basic solution, the same products, except XI and XII, were formed. Further II degradation led to the penicilloic acid VI. In addition to β-lactam opening, III degraded *via* a reversible 6-epimerization to (6*S*)-6-formamidopenicillanic acid (IV) and by reaction with hexamethyleneimine to the penicilloic amide XIII.

[17] Unpublished data.

[18] In some experiments, the position-6 protons were partly or completely hidden by the water band, and quantitative observations could not be done even under homogated decoupling experiments.

REFERENCES

(1) J. M. Indelicato, T. T. Norvilas, R. R. Pfeiffer, W. J. Wheeler, and W. L. Wilham, *J. Med. Chem.*, **17**, 523 (1974).

(2) J. P. Hou and J. W. Poole, *J. Pharm. Sci.*, **58**, 447 (1969).

(3) F. Lund and L. Tybring, *Nature New Biol.*, **236**, 135 (1972).

(4) B. G. Spratt, *J. Antimicrob. Chemother.*, **3** (Suppl. B), 13 (1977).

(5) R. L. Schriner and F. W. Neumann, *Chem. Rev.*, **35**, 351 (1944).

(6) R. H. De Wolfe, in "The Chemistry of Amidines and Imidates," S. Patai, Ed., Wiley, London, England, 1975, pp. 349–384.

(7) C. Larsen and H. Bundgaard, *Arch. Pharm. Chem. Sci. Ed.*, **5**, 66 (1977); through *Chem. Abstr.*, **87**, 189363f (1977).

(8) G. A. Weinberg, E. M. Belevich, T. I. Krukle, and S. A. Giller, *Antibiotiki*, **21**, 688 (1976).

(9) D. W. Dennen, *J. Pharm. Sci.*, **56**, 1273 (1967).

(10) Løvens kemiske Fabrik Produktionsaktieselskab, Brit. pat. 1417099 (1975); through *Chem. Abstr.*, **81**, 136136d (1974).

(11) A. Vlietinck, E. Roests, P. Claes, G. Janssen, and H. Vanderhaeghe, *J. Chem. Soc. Perkin I*, **1973**, 937.

(12) R. A. Firestone, N. S. Maciejewicz, R. W. Ratcliffe, and B. G. Christensen, *J. Org. Chem.*, **39**, 437 (1974).

(13) Glaxo Laboratories Ltd., Ger. offen. 2337105 (1974); through *Chem. Abstr.*, **80**, 108550v (1974).

(14) I. Uemura, T. Tokiwa, H. Kadowaki, and M. Koike, *Chemotherapy (Jpn)*, **25**, 115 (1977).

(15) M. Hattori, K. Nishi, and T. Miyabayashi, ibid., **25**, 123 (1977).

(16) U. Eberhardt, J. Depner, and J. Schaumann, East German pat. 81111 (1971); through *Chem. Abstr.*, **76**, 99645t (1972).

(17) C. Larsen and H. Bundgaard, *Arch. Pharm. Chem. Sci. Ed.*, **5**, 1 (1977); through *Chem. Abstr.*, **87**, 58560v (1977).

(18) E. van Arx, M. Faupel, and M. Brugger, *J. Chromatogr.*, **120**, 224 (1976).

(19) D. W. Hughes, A. Vilim, and W. L. Wilson, *Can. J. Pharm. Sci.*, **11**, 97 (1976).

(20) "The Chemistry of Penicillin," H. T. Clarke, J. R. Johnson, and R. Robinson, Eds., Princeton University Press, Princeton, N.J., 1949.

(21) B. B. Levine, *Nature*, **187**, 939 (1960).

(22) M. A. Schwartz and F. H. Buckwalter, *J. Pharm. Sci.*, **51**, 1119 (1962).

(23) D. A. Johnson and C. A. Panetta, *J. Org. Chem.*, **29**, 1826 (1964).

(24) M. A. Schwartz, *J. Pharm. Sci.*, **54**, 472 (1965).

(25) M. A. Schwartz, *ibid.*, **58**, 643 (1969).

(26) J. P. Hou and J. W. Poole, *ibid.*, **60**, 503 (1971).

(27) J. M. Blaha, A. M. Knevel, D. P. Kessler, J. W. Mincy, and S. L. Hem, *ibid.*, **65**, 1165 (1976).

(28) V. Hartmann, M. Rödiger, and G. Schnabel, *Pharm. Ind.*, **38**, 991 (1976).

(29) T. Yamana, A. Tsuji, E. Kiya, and E. Miyamoto, *J. Pharm. Sci.*, **66**, 861 (1977).

(30) G. A. Weinberg and E. M. Belevich, *Antibiotiki*, **23**, 593 (1978).

(31) R. D. Carroll, S. Jung, and C. G. Sklavounos, *J. Heterocyclic Chem.*, **14**, 503 (1977).

(32) D. A. Johnson, D. Mania, C. A. Panetta, and H. H. Silvestri, *Tetrahedron Lett.*, **1968**, 1903.

(33) J. P. Clayton, J. H. C. Nayler, R. Southgate, and E. R. Stove, *J. Chem. Soc. Chem. Commun.*, **1969**, 129.

(34) T. Yamana, A. Tsuji, and Y. Itatani, *J. Antibiot.*, **28**, 242 (1975).

(35) A. H. Cook and I. M. Heilbron, in "The Chemistry of Penicillin," H. T. Clarke, J. R. Johnson, and R. Robinson, Eds., Princeton University Press, Princeton, N.J., 1949, pp. 921–972.

(36) R. Busson, P. J. Claes, and H. Vanderhaeghe, *J. Org. Chem.*, **41**, 2556 (1976).

(37) C. H. Schneider and A. L. de Weck, *Helv. Chim. Acta*, **50**, 2011 (1967).

(38) R. J. Stoodley, *Tetrahedron*, **31**, 2321 (1975).

ACKNOWLEDGMENTS

The authors gratefully acknowledge the skillful technical assistance of Mrs. Marie Pedersen, Mrs. Lis Finderup Johansen, and Mr. Gerhard Andersen and the helpful discussions about reaction kinetics with Dr. E. Ahlmann.

Syntheses and Bioactivities of 1-(Hydroxyphenyl)-1-nonen-3-ones and Related Ethers and Esters

J. R. DIMMOCK *x, C. B. NYATHI ‡, and P. J. SMITH ‡

Received January 24, 1979, from the *College of Pharmacy and the ‡Department of Chemistry and Chemical Engineering, University of Saskatchewan, Saskatoon, Saskatchewan, S7N 0W0, Canada. Accepted for publication March 30, 1979.

Abstract □ A number of nuclear hydroxy styryl ketones and related compounds were prepared and evaluated for antineoplastic and antimicrobial activities as well as for analgesic, anti-inflammatory, and antianaphylactic properties. The second-order rate constants for the reaction of several esters with hydroxide ion in aqueous dioxane (50% v/v) at 36.9° were determined. The screening results showed that activity against P-388 lymphocytic leukemia was found solely with the ethers and that antimicrobial properties were obtained virtually exclusively with the phenolic derivatives. All compounds showed analgesic properties, except for four that were algesic. While little anti-inflammatory activity was found, several compounds showed some antianaphylaxis.

Keyphrases □ Nuclear hydroxy styryl ketones—syntheses, antineoplastic activity, antimicrobial activity, analgesic activity, anti-inflammatory activity, antianaphylactic activity, structure–activity relationships □ Antineoplastic agents, potential—nuclear hydroxy styryl ketones, syntheses, structure–activity relationships □ Structure–activity relationships—nuclear hydroxy styryl ketones, antineoplastic activity, antimicrobial activity, analgesic activity, anti-inflammatory activity, antianaphylactic activity

A number of α,β-unsaturated ketones have antineoplastic and cytotoxic properties (1, 2). In particular, some nuclear hydroxy chalcones displayed activity against the Ehrlich ascites sarcoma in mice (3), while compounds with hydroxy groups in close proximity to the carbonylene function demonstrated activity against several neoplasms (4–8). Therefore, the preparation of certain nuclear hydroxy styryl ketones (Ia, Ic, Ie, and IIa) was suggested.

Since the hydroxy groups of phenols are susceptible to metabolic inactivation *in vivo* (9), the concept of latentiation (10) was applied in two ways. First, masking the hydroxy group by etherification would be expected to produce compounds (Ib, Id, If, IIb, IIIa, and IIIb) stable in alkali but capable of regeneration to phenols under acidic conditions (11). Since the claim has been made that the interstitial fluid pH of certain tumors is lower than the plasma of blood afferent to the tumor (12), selective regeneration of the precursor phenols in tumorous tissue might be possible. Second, the formation of benzoate esters (V and VI) of the phenols, which would be hydrolyzed *in vivo* to the phenol, might clarify the relationship between the hydrolysis rate and antineoplastic activity. In addition, since there appears to be a precarious balance between lipophilicity and hydrophilicity in relation to anticancer activity (13), formation of some water soluble Mannich bases (VIII) from nuclear hydroxy styryl ketones was contemplated.

To pursue the evaluation of styryl ketones and related Mannich bases for pharmacological (14, 15) and antimicrobial (16, 17) activities, the proposed compounds were tested in these screens. Since fungal diseases constitute a widespread problem with cancer patients (18), the emergence of an antifungal antineoplastic drug would be welcome.

DISCUSSION

Syntheses—The hydroxy and alkyloxymethoxy compounds I and II were prepared by reacting the appropriate hydroxybenzaldehyde with an alkyloxymethyl chloride followed by condensation with hexyl methyl ketone to give Ib, Id, If, and IIb, which were hydrolyzed with formic acid to give nuclear hydroxy styryl ketones Ia, Ic, Ie, and IIa. While the methoxy derivatives IIIa and IIIb were prepared by direct condensation of the dimethoxybenzaldehydes with hexyl methyl ketone, this conventional Claisen–Schmidt condition yielded only tars when nitrobenzaldehydes were employed in the attempted preparation of IIIc and IIId; similar problems were encountered in attempting the condensation of γ-butyrolactones with nitrobenzaldehydes (19). The failure of these reactions may be due to the high electrophilicity of the carbonyl carbon atom in nitrobenzaldehydes, which may lead to multiple side reactions, including formation of the corresponding phenols (20, 21).

In the present study, the Knoevenagel reaction was employed to give IIIc and IIId in yields of 52 and 30%, respectively. To increase the IIId yield, the heating time under reflux was increased from 4 to 36 hr, but the only product isolated was the bis-substituted compound IX in low yield. Attempted condensation of pentafluorobenzaldehyde with hexyl methyl ketone under Claisen–Schmidt conditions gave unreacted components plus resinous products; difficulties were encountered previously with pentafluorobenzaldehyde in the presence of aqueous alkali and other bases (22). Recourse to the methodology employed in the preparation of IIId afforded IV as well as piperidinyl tetrafluorobenzaldehyde.

The phenols Ia and Ie were acylated in the presence of pyridine to give the corresponding esters V–VII in yields of 59–85%. The Mannich bases VIIIb and VIIIc were obtained from the precursor ketones Id and If in crystalline form, while VIIIa could not be induced to crystallize.

Hydrolyses—The alkaline hydrolysis rate of esters V–VII was measured in an attempt to seek a correlation between the lability of the esters with antineoplastic activity. The second-order rate constants for reaction of the esters V and VI with hydroxide ion in aqueous dioxane (50% v/v) at 36.9° are given in Table I; as expected, the sulfonate VII as well as the ethers Ib, Id, and If were refractory to hydrolysis under the conditions employed. To ensure that no Michael addition reaction occurred, IIId was subjected to the same experimental procedures as the esters and was unaffected.

A Hammett plot for esters V and VI showed ρ values of 2.43 ± 0.08 and 1.84 ± 0.07, respectively. The positive ρ values indicate that the hydrolysis reaction is facilitated by electron-withdrawing substituents. In other words, there is a decrease in repulsive forces between the acyl ring and the carbonyl carbon atom in going from the initial state to the transition state for the formation of the tetrahedral intermediate XI (Scheme I). The higher value for the *ortho* esters indicates that the transition state leading to the intermediate XI occurs further along the reaction coordinate than the transition state leading to the corresponding *para* intermediate. This is in accord with the Hammond postulate (23) since the unsubstituted *ortho* ester Va is hydrolyzed at a slower rate than the *para*

Table I—Second-Order Rate Constants (k_2 M^{-1} min^{-1}) for the Hydrolysis of the Benzoate Esters V, VI, and X in Aqueous Dioxane (50% v/v) at 36.9°

Compound	Rate Constant	Compound	Rate Constant
Va	19.9 ± 0.10	VIe	72.0 ± 1.75
Vb	91.5 ± 2.41	VIf	11.1 ± 0.12
Vc	1646 ± 38.7	VIg	6.47 ± 0.14
VIa	25.3 ± 0.48	Xa	8.46 ± 0.35
VIb	77.1 ± 1.14	Xb	22.6 ± 0.13
VIc	542 ± 11.3	Xc	190 ± 1.08
VId	402 ± 8.54	Xd	5.49 ± 0.01

0022-3549/79/1000-1216$01.00/0
© 1979, American Pharmaceutical Association

unsubstituted ester VI*a* (Table I). Presumably, the *ortho* ester is less reactive than the *para* ester due to steric impediments to hydroxide-ion attack at the carbonyl function. The ρ value for X was 1.65 ± 0.05, consistent both with the fact that aryl substituents of phenylbenzoates have less effect on the reaction than acyl substituents and with the interpretation given to the different ρ values for V and VI.

Biological Activities—The antineoplastic evaluation of styryl ketones

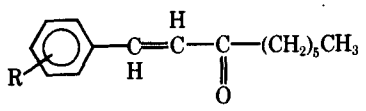

I*a*: R = 2-OH
I*b*: R = 2-OCH_2OCH_3
I*c*: R = 3-OH
I*d*: R = 3-$OCH_2OC_2H_5$
I*e*: R = 4-OH
I*f*: R = 4-OCH_2OCH_3

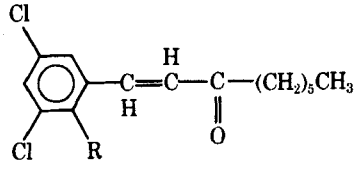

II*a*: R = OH
II*b*: R = OCH_2OCH_3

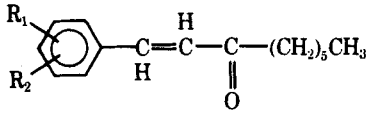

III*a*: R_1 = 2-OCH_3, R_2 = 5-OCH_3
III*b*: R_1 = 3-OCH_3, R_2 = 4-OCH_3
III*c*: R_1 = 3-NO_2, R_2 = H
III*d*: R_1 = 4-NO_2, R_2 = H

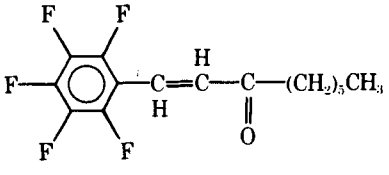

IV

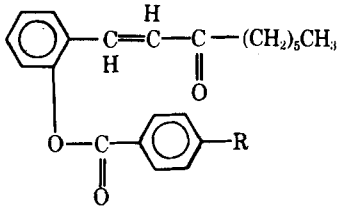

V*a*: R = H
V*b*: R = Cl
V*c*: R = NO_2

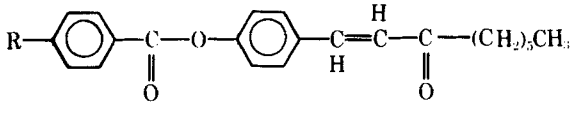

VI*a*: R = H
VI*b*: R = Cl
VI*c*: R = NO_2
VI*d*: R = CN
VI*e*: R = Br
VI*f*: R = CH_3
VI*g*: R = OCH_3

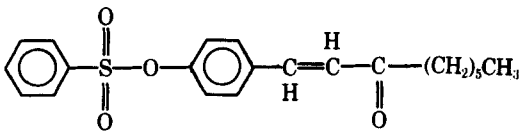

VII

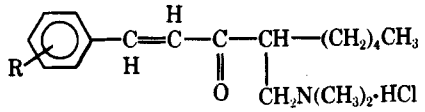

VIII*a*: R = 2-OH
VIII*b*: R = 3-OH
VIII*c*: R = 4-OH

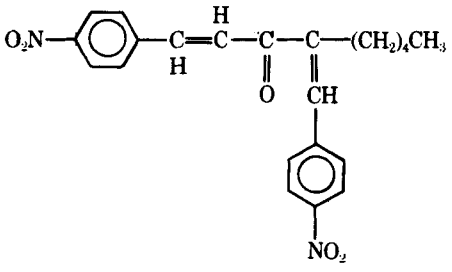

IX

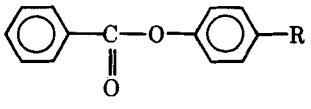

X*a*: R = H
X*b*: R = Cl
X*c*: R = NO_2
X*d*: R = CH_3

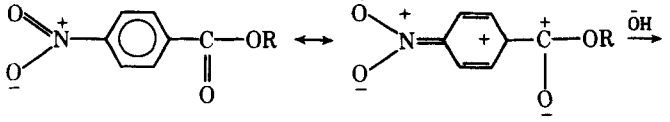

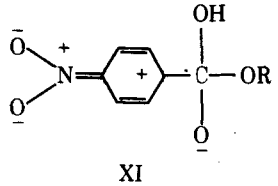

XI

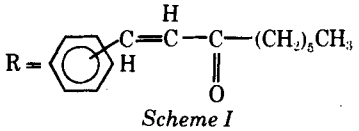

Scheme I

I–VIII is given in Table II. The parent compound, 1-phenyl-1-nonen-3-one, has a maximum T/C of 108%, which is similar to that of the nuclear hydroxy compounds I*a*, I*c*, I*e*, and II*a*, which have an average T/C of 107%. Masking the phenol to give the corresponding ethers I*b*, I*d*, I*f*, and II*b* produced compounds with a perceptible level of activity (an average 20% increase in the mean survival time in mice) unaccompanied by murine toxicity; this result is in contrast to earlier work in which styryl ketones with cytotoxic and antineoplastic properties had significant murine toxicity (16). While the ethers III*a* and III*b* had marginal activity, the nitro compounds III*c* and III*d* were inactive.

In contrast to the ether analogs of the phenols, esters V–VII were bereft

Table II—Evaluation of Styrenoid Ketones I–VIII for Antineoplastic, Analgesic, Anti-Inflammatory, and Antianaphylactic Activities

Compound	Maximum Increase in Mean Survival Time[a], dose in mg/kg	Analgesic Activity[b]		Anti-Inflammatory Activity[c]			Antianaphylactic Activity[d]	
		Dose, mg/kg	Percentage Protection	Dose mg/kg	Percentage Protection 3 hr	Percentage Protection 5 hr	Dose, mg/kg	Percentage Protection
I*a*	112 (200)	256	25	64	0	0	128	8
I*b*	116 (200)	—	—	—	—	—	—	—
I*c*	104 (100)	128	40	128	0	0	25	20
I*d*	125 (100)[e]	128	36	128	0	0	100	45
I*e*	105 (200)	256	12	64	0	−17	8	50
I*f*	121 (100)[f]	128	54	64	−17	0	128	67
II*a*	105 (50)	120	22	120	−34	−34	100	0
II*b*	116 (100)	120	48	120	−6	−17	100	0
III*a*	117 (50)	256	30	128	0	0	128	0
III*b*	115 (200)	128	Algesic[g]	128	17	0	100	20
III*c*	95 (100)	128	Algesic[g]	128	34	8	100	33
III*d*	99 (100)	256	36	128	0	0	128	78
V*b*	101 (25)	256	56	64	−50	0	—	—
V*c*	99 (100)	256	34	64	0	0	128	58
VI*a*	110 (200)	128	Algesic[g]	64	−17	0	128	36
VI*b*	97 (6.25)	128	44	64	0	0	4	0
VI*c*	105 (12.5)	128	59	64	−17	0	128	58
VI*d*	101 (100)	256	41	128	17	66	64	78
VI*e*	104 (12.5)	256	34	128	0	0	128	9
VI*f*	95 (50)	256	36	128	0	0	128	0
VI*g*	105 (12.5)	256	41	128	0	0	128	56
VII	105 (50)	128	Algesic[g]	128	0	0	100	59
VIII*b*	106 (50)[h]	64	90	128	64	100	16	0
VIII*c*	113 (100)[i]	64	96[j]	64	34	17	16	42

[a] The figures are the ratios of the survival time of treated animals to control animals expressed as a percentage. The figures for I*a*, I*b*, I*e*, I*f*, V*c*, VI*a*–VI*c*, and VIII*c* are taken from Ref. 25 and reproduced with permission of the copyright owner. [b] Analgesic activity was measured by the percentage protection in the phenylquinone writhing test. Under these conditions, aspirin gives 50% protection at 52 mg/kg. A compound displaying an effect greater than 50% is considered to be active. [c] The anti-inflammatory activity was measured by the percentage protection afforded by the compound to carrageenan-induced edema. The reference compound, indomethacin, gave 50% protection at 12 mg/kg under these conditions. Compounds showing greater than a 50% protection are considered active. Figures prefaced with a negative sign indicate the percentage increase in the size of edema volume. [d] The antianaphylactic screen measured the potential of a compound to inhibit passive cutaneous anaphylaxis in rats. The reference compound, disodium chromoglycate, reduced the wheal area by 90% at a dose of 100 mg/kg. A compound is considered active if the wheal area is reduced by 50%. [e] An increase of 30% in the lifespan of $B_6D_2F_1$ mice with B16 melanocarcinoma at 50 mg/kg was noted; one in 10 mice was cured. [f] There were 5/6 survivors on Day 5 at dose levels of 200 and 100 mg/kg. [g] The percentage increases in writhes for III*b*, III*c*, VI*a*, and VII were 15, 15, 2, and 10, respectively. [h] There were 2/6 and 5/6 survivors on Day 5 at dose levels of 200 and 100 mg/kg, respectively. [i] There was 1/6 survivors on Day 5 at a dose level of 200 mg/kg. [j] This compound elicited a Straub tail response (35).

Table III—Evaluation of the Nuclear Hydroxy Styryl Ketones and Related Ethers for Antimicrobial Activity[a,b]

Microorganism	I*a*	I*b*	I*c*	I*d*	I*e*	I*f*	II*a*	II*b*	VIII*b*	VIII*c*
Escherichia coli (ATCC 8739)	>500	>500	>500	>500	>500	>500	>500	>500	>500	>500
Pseudomonas aeruginosa (ATCC 10145)	>500	>500	>500	>500	>500	>500	>500	>500	>500	>500
Klebsiella pneumoniae (ATCC 4352)	>500	>500	<100	>500	>500	>500	>500	>500	>100	>500
Salmonella tymphimurium (G 46)	>100	>500	>500	>500	>500	>500	>500	>500	>500	>500
Bordetella bronchiseptica (ATCC 4617)	>500	>500	>500	>500	>500	>500	>500	>500	>500	>250
Staphylococcus aureus (ATCC 6538)	<100	>500	<100	>500	<100	>500	>250	>500	<100	>250
Streptococcus faecalis (ATCC 8030)	>500	>500	<100	>500	>500	>500	>500	>500	<100	>250
Bacillus subtilis (ATCC 6633)	<100	<100	<100	>500	<100	<100	>500	>500	>100	<100
Trichophyton mentagrophytes (ATCC 9533)	<10	>250	<100	>500	<10	<100	>500	>500	<10	<10
Microsporum gypseum (ATCC 14683)	<10	<100	<100	>500	<10	>100	>500	>500	<10	<100
Aspergillus niger (ATCC 10535)	>500	>500	>500	>500	>500	>500	>500	>500	>500	>500
Candida albicans (ATCC 10231)	<100	>250	<100	>500	>500	>500	>500	>500	>10	>100
Saccharomyces uvarum (ATCC 9080)	<10	>500	<100	>500	<10	>100	>500	>500	>10	<10
Average antimicrobial activity[c]	712	92	308	0	654	115	8	0	577	504

[a] The figures in the table are the minimum inhibitory concentrations of the compounds in micrograms per milliliter. [b] The data for I*a*, I*b*, I*e*, and I*f* and most of the results for VIII*c* are taken from Ref. 25 and reproduced with permission of the copyright owner. [c] Figures are calculated from the following expression: (combined antimicrobial activity × 100)/number of microorganisms in the screen. The combined antimicrobial activity was determined by giving the following scores at the highest potency of the compound against the microorganism: >250, 1; >100, 2.5; <100, 5; and <10, 25.

of bioactivity in this screen, with no correlation between the alkaline hydrolysis rate and antineoplastic activity. The Mannich bases VII*b* and VII*c*, while having greater water solubility than I*c* and I*e*, had similar activity against P-388 lymphocytic leukemia and displayed toxicity. Since several biological alkylating agents interfere with thymidylate synthetase and dihydrofolate reductase, which are key enzymes in DNA synthesis, a representative ether, II*b*, was examined and shown to have no effect on either enzyme.

Table II also lists some pharmacological screening data generated on I–VIII. These carbonylenes have either analgesic activity, ranging from 96% protection in the phenylquinone writhing test at a dose of 64 mg/kg in the case of VIII*c* to 12% protection at 256 mg/kg for I*e*, or algesic activity. The utility of an analgesic would be enhanced if anti-inflammatory properties were also present. Compounds V*b* and VIII*b* showed anti-inflammatory properties after 3 hr, and VIII*b* displayed potency at the end of 5 hr. In this series of compounds, antianaphylactic properties were

demonstrated in most compounds, and 36% of the compounds satisfied the criterion for activity; the *para*-cyano ester VI*d* showed the greatest potency.

The compounds listed in Table II were evaluated against 13 species of microorganisms, and the results of the nuclear hydroxy styryl ketones and related ethers are given in Table III. All of the phenolic compounds except II*a* displayed activity; the *ortho*- and *para*-hydroxy derivatives I*a* and I*e* exhibited the greatest potencies. The failure of nuclear halogenation of I*a* to II*a* to increase its antimicrobial activity was surprising since halogenation of phenols is often associated with an increase in antimicrobial activity (24). The most susceptible species to these compounds were *Trichophyton mentagrophytes* and *Microsporum gypseum*. The remaining compounds, III and V–VII, were either inactive at the highest concentration employed (500 μg/ml) or showed only weak activity against a few microorganisms.

EXPERIMENTAL[1]

Melting points and boiling points are uncorrected. Organic extracts were washed several times with water and dried over anhydrous magnesium sulfate. After filtration, the solvents were removed *in vacuo* with a water aspirator. The petroleum ether fraction with a boiling range of 100–120° was used unless otherwise stated. Mass spectra[2] were determined at 70 ev, and the 60-MHz NMR spectra[3] were carried out in deuterochloroform. TLC utilized 20 × 20 cm glass plates, which were pretreated with 0.5 mm silica gel G[4]. The solvent system was chloroform–ethyl acetate–diethylamine (92:5:3). The kinetic studies[5] were carried out with 1-cm quartz cells.

Synthesis of Compounds—Compounds I*a*, I*b*, I*e*, I*f*, V*b*, V*c*, VI*a*–VI*c*, and VIII*c* were prepared using the previously reported methodology (25). The remaining compounds were prepared as follows.

Nuclear Hydroxy and Alkyloxymethoxy Styryl Ketones (I, II, and VIII)—Reaction of *m*-hydroxybenzaldehyde and chloromethyloxyethyl ether produced *m*-ethoxymethyloxybenzaldehyde, bp 82°/0.14 mm, in a 71% yield; NMR spectroscopy was in accord with the proposed structure. The literature method (26) was used, except that the sodium hydride dispersion was added in one operation and the reaction mixture was stirred for 1 hr after the addition of sodium hydride.

3,5-Dichloro-2-methoxymethyloxybenzaldehyde was prepared from 3,5-dichlorosalicylaldehyde and chloromethyloxymethyl ether in a 61% yield in an analogous manner, except that the reaction time was quadrupled. The compound was recrystallized from petroleum ether, mp 90–92°. NMR spectroscopy was in accord with the proposed structure, and the mass spectrum gave peaks at *m/e* 234[6] (M^+, 5%) and 45 (100%).

Treatment of *m*-ethoxymethyloxybenzaldehyde with hexyl methyl ketone in the presence of aqueous sodium hydroxide solution, using the reported method for preparing I*b* and I*f*, gave (*E*)-1-(*m*-ethoxymethyloxyphenyl)-1-nonen-3-one (I*d*) as a yellow oil, bp 168°/0.13 mm, in a 67% yield. TLC indicated that the compound was homogeneous.

Anal.—Calc. for $C_{18}H_{26}O_3$: C, 74.45; H, 9.02. Found: C, 73.96; H, 8.91.

The analogous ketone II*b* was prepared in a similar manner as a yellow oil, bp 187°/0.25 mm, in a 37% yield; mass spectrum: *m/e* 344 (M^+, 0.7%) and 45 (100%). TLC indicated that the compound was chromatographically homogeneous.

Anal.—Calc. for $C_{17}H_{22}Cl_2O_3$: C, 59.14; H, 6.42. Found: C, 60.87; H, 6.31.

(*E*)-1-(*m*-Hydroxyphenyl)-1-nonen-3-one (I*c*) was prepared from I*d* by hydrolysis with aqueous formic acid using the procedure for the formation of I*e* (25). It was crystallized from petroleum ether as a colorless powder, mp 54–56°, in a 73% yield.

Anal.—Calc. for $C_{15}H_{20}O_2$: C, 77.54; H, 8.68. Found: C, 77.57; H, 8.93.

(*E*)-1-(3,5-Dichloro-2-hydroxyphenyl)-1-nonen-3-one (II*a*) was prepared similarly to I*a* (25) and recrystallized from petroleum ether, mp 104–105°, in a 74% yield; mass spectrum: *m/e* 302 (M^+, 6%) and 215 (100%).

Anal.—Calc. for $C_{15}H_{18}Cl_2O_2$: C, 59.81; H, 6.02. Found: C, 59.89; H, 6.23.

The Mannich base VIII*b*, prepared by the reported methodology for synthesizing VIII*c* (25), was recrystallized from acetone to give the desired ketone as a colorless powder, mp 154–156°, in a 38% yield; mass spectrum: *m/e* 238 (M^+ − HCl, 3%) and 58 (100%). TLC showed that the compound was homogeneous.

Anal.—Calc. for $C_{18}H_{28}ClNO_2$: C, 66.34; H, 8.66; N, 4.30. Found: C, 64.11; H, 8.56; N, 4.06.

An attempt to prepare VIII*a* by a similar method to that of VIII*b* (25) produced only a water-soluble blue-green oil; this oil could not be induced to crystallize either by prolonged storage in a vacuum desiccator or by trituration with ether, petroleum ether (bp 60–80°), and benzene. NMR spectroscopy was in accordance with the proposed structure.

Nuclear Methoxy, Nitro, and Fluoro Styryl Ketones (III and IV)—A mixture of 2,5-dimethoxybenzaldehyde (83.09 g, 0.50 mole), hexyl methyl ketone (76.90 g, 0.60 mole), and sodium hydroxide (10.0 g, 0.25 mole) in distilled water (300 ml) was heated under reflux for 12 hr and let stand at room temperature overnight. The two layers were separated, the aqueous layer was washed with benzene (3 × 100 ml), and the organic extracts were combined with the original organic layer and dried. Removal of the solvent and excess hexyl methyl ketone gave a crude product. This product was fractionally distilled to give 2,5-dimethoxybenzaldehyde (16.5 g, 20%), bp 105°/0.3 mm, and (*E*)-1-(2,5-dimethoxyphenyl)-1-nonen-3-one (III*a*) (79.0 g, 58%) as a yellow oil, bp 181°/0.4 mm, which solidified to a wax on standing. The residual tar in the distillation flask was not examined. The mass spectrum of III*a* showed *m/e* 276 (M^+, 44%) and 245 (100%).

Anal.—Calc. for $C_{17}H_{24}O_3$: C, 73.86; H, 8.76. Found: C, 74.00; H, 8.62.

Reaction of 3,4-dimethoxybenzaldehyde with hexyl methyl ketone proceeded in a similar fashion to produce a crude product. This product was fractionally distilled to give (*E*)-1-(3,4-dimethoxyphenyl)-1-nonen-3-one (III*b*) as a yellow oil (58%), bp 168°/0.14 mm, which solidified to a wax on standing, and an orange viscous oil (4 g), bp 183°/0.14 mm. The molecular weight of the orange oil was shown to be 552 by mass spectrometry. The mass spectrum of III*b* showed *m/e* 276 (M^+, 22%) and 191 (100%).

Anal.—Calc. for $C_{17}H_{24}O_3$: C, 73.86; H, 8.76. Found: C, 73.68; H, 8.73.

A solution of *m*-nitrobenzaldehyde (15.0 g, 0.10 mole), hexyl methyl ketone (14.1 g, 0.11 mole), piperidine (8.1 g, 0.10 mole), and acetic acid (6.6 g, 0.11 mole) in dry benzene (100 ml) was heated under reflux with mechanical stirring for 24 hr, cooled, and extracted with water (3 × 100 ml). The organic layer was separated and dried, and removal of the solvent gave a residual brown oil. This oil was fractionally distilled to give *m*-nitrobenzaldehyde (1.2 g, 8%), bp 97°/0.13 mm, mp 55°, and (*E*)-1-(*m*-nitrophenyl)-1-nonen-3-one (III*c*) (13.5 g, 52%), bp 215°/0.10 mm[7], which solidified on standing, yielding yellow flakes. Recrystallization of the flakes from petroleum ether gave III*c* as creamish flakes, mp 50–51°; mass spectrum: *m/e* 261 (M^+, 2%) and 176 (100%).

Anal.—Calc. for $C_{15}H_{19}NO_3$: C, 68.97; H, 7.28; N, 5.36. Found: C, 69.04; H, 7.31; N, 5.38.

The *p*-nitro analog III*d* was prepared as follows. To a vigorously stirred solution of *p*-nitrobenzaldehyde (20.0 g, 0.13 mole) and hexyl methyl ketone (19.0 g, 0.15 mole) in dry benzene (200 ml) were added acetic acid (7.8 g, 0.13 mole) and piperidine (11.1 g, 0.13 mole). The mixture was heated under reflux for 4 hr, using a condenser attached to a Dean–Stark trap, during which time water (3 ml) was collected. The benzene solution was cooled and extracted with water (3 × 100 ml). The organic solvent was removed *in vacuo* to give a black tar to which was added petroleum ether (500 ml); then the mixture was heated under reflux for 2 min.

On cooling, the mixture stood at room temperature for 20 min, and the yellow solution was decanted and evaporated to 200 ml. The solution was stored in a refrigerator overnight (0.05°), and the resultant yellow needles were collected (8.8 g). The original black tar was extracted again with petroleum ether (500 ml) and yielded a further quantity of material (1.7 g). The combined crude products were recrystallized from petroleum ether to give (*E*)-1-(*p*-nitrophenyl)-1-nonen-3-one (III*d*) (10.5 g, 30%) as yellow needles, mp 56–57.5°; mass spectrum: *m/e* 261 (M^+, 14%) and 191 (100%). TLC showed that the compound was homogeneous.

[1] Elemental analyses were carried out by Mr. R. G. Teed, Department of Chemistry and Chemical Engineering, University of Saskatchewan.

[2] AEI MS-12 mass spectrometer, Picker X-Ray Engineering Ltd. Mass spectra were determined by Mr. D. R. Bain, Department of Chemistry and Chemical Engineering, University of Saskatchewan.

[3] T60 spectrophotometer, Varian Associates of Canada Ltd., and WP 60 spectrophotometer, Brucker Spectrospin (Canada) Ltd.

[4] Silica gel N-HR/UV 254 polygram, Fisher Scientific Co. Ltd.

[5] Cary model 118 spectrophotometer.

[6] The molecular ions for compounds containing chlorine atoms refer to the ^{35}Cl-isotope.

[7] On one occasion, the residual black tar exploded violently during the distillation.

Anal.—Calc. for $C_{15}H_{19}NO_3$: C, 68.97; H, 7.28; N, 5.36. Found: C, 69.49; H, 7.43; N, 5.37.

When the time of heating the same quantities of reactants under reflux was extended to 36 hr, a crude product (7.1 g) was obtained. It was recrystallized from petroleum ether to give (*E*)-4-(*p*-nitrobenzylidene)-1-(*p*-nitrophenyl)-1-nonen-3-one (IX) (2.5 g, 5%) as yellow needles, mp 168–170°; mass spectrum: *m/e* 394 (M^+, 25%) and 176 (100%); NMR ($CDCl_3$): δ 8.37–7.26 (m, 11, aromatic H, olefinic H), 2.63–2.49 (m, 2, C_5H), and 1.55–0.79 [m, 9, $(CH_2)_3CH_3$]. TLC indicated a major component, R_f 0.46, with minute traces of three compounds with R_f values of 0.38, 0.51, and 0.58.

Anal.—Calc. for $C_{22}H_{22}N_2O_3$: C, 66.97; H, 5.63; N, 7.11. Found: C, 64.69; H, 5.77; N, 6.70.

The pentafluoro analog IV was prepared in the same manner as III*d*, except that the time of heating under reflux was 1 hr. Distillation of the crude reaction product afforded an oil, bp 108°/1.0 mm, which solidified to a wax and was tentatively identified as 4-piperidinyl-2,3,5,6-tetrafluorobenzaldehyde; mass spectrum: *m/e* 261 (M^+); NMR ($CDCl_3$): δ 10.60–10.30 (d, 1, CHO, J = 2), 3.66–3.00 (m, 6, piperidyl 3′H, 4′H, 5′H), and 2.10–1.54 (m, 4, piperidyl 2′H, 6′H). Continued distillation produced (*E*)-1-(pentafluorophenyl)-1-nonen-3-one (IV) in a 27% yield as a mobile yellow oil, bp 114°/1.0 mm; mass spectrum: *m/e* 306 (M^+, 7%) and 221 (100%); NMR ($CDCl_3$): δ 7.42 (d, 1, C_1H, $J_{1,2}$ = 16.0), 6.92 (d, 1, C_2H, $J_{2,1}$ = 16.0), 2.62 (t, 2, C_4H, $J_{4,5}$ = 7.0), and 2.18–0.63 [m, 11, $(CH_2)_4CH_3$].

Anal.—Calc. for $C_{15}H_{15}F_5O$: C, 58.82; H, 4.94. Found: C, 58.37; H, 4.76.

Esters of Nuclear Hydroxy Styryl Ketones (V–VII)—The method for preparing the esters V and VI was described previously (25). In the case of V*a*, the crude product was a yellow viscous oil, which gave an orange oil, bp 198–206°/0.2 mm, on distillation. TLC of the product indicated two components, R_f 0.64 and 0.18; the component with R_f 0.64 corresponded to the unreacted ketone I*a*. Attempted separation of the reaction components using silica gel column chromatography and the same solvent mixture as employed for TLC failed. The oil turned brown gradually on attempted redistillation, and the distillation was discontinued. NMR spectroscopy and mass spectrometry indicated that the desired ester had been formed.

The syntheses of VI*d*–VI*g* were undertaken successfully, and the esters were recrystallized from petroleum ether.

(*E*)-1-(*p*-Cyanobenzoyloxy)-phenyl-1-nonen-3-one (VI*d*) was prepared in a 72% yield as colorless crystals, mp 103–105°. TLC indicated that the compound was homogeneous.

Anal.—Calc. for $C_{23}H_{23}NO_3$: C, 76.43; H, 6.41; N, 3.88. Found: C, 75.92; H, 6.61; N, 3.59.

The corresponding *p*-bromo ester VI*e* was prepared in an 82% yield as colorless needles, mp 129–130.5°.

Anal.—Calc. for $C_{22}H_{23}BrO_3$: C, 63.62; H, 5.58. Found: C, 63.69; H, 5.55.

The corresponding *p*-methyl ester VI*f* was prepared in a 60% yield as colorless plates, mp 107–108°.

Anal.—Calc. for $C_{23}H_{26}O_3$: C, 78.83; H, 7.48. Found: C, 78.85; H, 7.46.

The corresponding *p*-methoxy ester VI*g* was prepared in a 67% yield as colorless plates, mp 100–101°.

Anal.—Calc. for $C_{23}H_{26}O_4$: C, 75.36; H, 7.15. Found: C, 75.19; H, 7.28.

The sulfonyl ester VII was prepared in a similar manner, except that the reactants were heated together under reflux for 1.5 hr and then stirred mechanically at room temperature for a further 1.5 hr. The crude product obtained by extraction was recrystallized from methanol to give (*E*)-1-(*p*-benzenesulfonyloxy)-phenyl-1-nonen-3-one (VII) as colorless flakes, mp 47–48.5°, in a 76% yield; mass spectrum: *m/e* 372 (M^+, 9%) and 77 (100%).

Anal.—Calc. for $C_{21}H_{24}O_3S$: C, 67.70; H, 6.50. Found: C, 68.03; H, 6.51.

Benzoate Esters (X)—Phenyl benzoate (X*a*) was obtained commercially[8], purified by recrystallization from ethanol, and melted at 69.5–70° [lit. (27) mp 71°]. The esters X*b*–X*d* were prepared by acylation of phenol with the appropriate acid chloride using the method applied to the synthesis of V and VI. The crude esters were recrystallized from petroleum ether to give: X*b*, mp 87–89° [lit. (28) mp 87–87.5°], in a 50% yield; X*c*, mp 142–143.5° [lit. (29) mp 142.5°], in a 64% yield; and X*d*, mp 70–72° [lit. (30) mp 71–72°], in a 39% yield. In addition, the structures of X*b*–X*d* were confirmed by elemental analysis.

[8] BDH Chemicals Ltd.

Kinetic Studies on V–VII and X—The hydrolysis rates of V, VI, and X were determined spectrophotometrically in aqueous 1,4-dioxane (50% v/v) by measuring the optical density (OD) of the appropriate phenoxide ion to completion of the reaction.

A mixture of analytical grade 1,4-dioxane (4 liters) and sodium hydroxide pellets (40 g) was heated under reflux for 18 hr and distilled *via* a 61-cm Vigreux column. The distilled 1,4-dioxane was reheated under reflux with sodium hydroxide pellets, distilled at atmospheric pressure, and stored unexposed to moisture. The wavelengths (max) of the phenoxide ions from I*a*, I*e*, phenol, *p*-chlorophenol, *p*-nitrophenol, and *p*-methylphenol were 406, 389, 299, 301, 405, and 289 nm, respectively. The Beer–Lambert law for the phenoxide ions in aqueous dioxane was confirmed by plotting the optical density *versus* phenoxide concentrations, using five different concentrations of the appropriate phenol to which was added a drop of aqueous sodium hydroxide solution (10 *M*).

The determinations proceeded as follows. Initially, a wavelength of the phenoxide ion was chosen that was least obstructed by absorptions of the corresponding ester. Then the ester was placed in a two-component kinetic flask and dissolved in aqueous 1,4-dioxane (50% v/v, 10 ml) while aqueous sodium hydroxide solution (10 ml) was placed in the side arm flask along with sufficient sodium chloride to maintain an ionic strength of 2.8×10^{-3} *M* of the resultant solution after mixing. The reaction flask was placed in a constant-temperature water bath at 36.9 ± 0.02° for 30 min. The side arm flask was then rotated upwards so that its contents were added to the solution of the ester in the main flask, and the resultant mixture was shaken to ensure thorough mixing and transferred immediately to the thermostated UV cells in the spectrophotometer.

The reaction was followed by recording continually the optical density of the phenoxide ion to infinity at the previously determined wavelength. The time lag between the mixing of the two solutions and the beginning of the recording of the optical density was ~22 sec and was incorporated into the subsequent calculations. The kinetic runs were carried out in duplicate under pseudo-first-order conditions at two different hydroxide concentrations (2.1×10^{-3} and 2.8×10^{-3} *M*), except for the *p*-nitro esters in which case the hydroxide concentrations were 2.1×10^{-3} and 7.0×10^{-4} *M*. The pseudo-first-order constants, k^1, were determined from the expression:

$$k^1 t = \frac{2.303 \log \mathrm{OD}\alpha - \mathrm{OD}_0}{\mathrm{OD}\alpha - \mathrm{OD}_t} \qquad \text{(Eq. 1)}$$

in which ODα is the optical density of the solution at infinity, *i.e.*, when 100% of the reaction had occurred, and it was found that the observed ODα = calculated ODα ± 3%. In addition, OD_0 represents the initial optical density and OD_t is the optical density at time t. The constant k^1 was calculated by plotting log ODα − OD_t *versus* time. The best fit of the line to the points was obtained by a least-squares treatment of the data using an HP 2000 computer. Table I indicates the second-order rate constants, k^2, which were obtained by dividing the values of k^1 by the sodium hydroxide concentration. For each ester series, log $(k^2R)/(k^2H)$ was plotted *versus* σ_p (31), and the rho values were obtained by computerization. The σ_p value of the 1-nonen-3-onyl group was obtained by plotting the k^2 values for VI*a* and X*a*–X*d* *versus* the Hammett σ_p values of the nuclear substituents (31) for X*a*–X*d*.

No hydrolysis of I*b*, I*d*, I*f*, or VII under these conditions was found using 2.0 *M* sodium hydroxide solutions, and attempted hydrolysis of VI*c* using imidazole (0.1 *M*) was unsuccessful.

Screening of Compounds—For the P-388 anticancer screen[9], the compounds were administered in saline with polysorbate 80[10], except for I*a*, VI*a*–VI*c*, and VIII*a*, which were administered in saline, I*b*, II*a*, and II*b*, which were administered in hydroxypropylcellulose, and I*f*, which was administered in saline with alcohol. The compounds were injected daily for 9 consecutive days by the intraperitoneal route into CD_2F_1 mice, except for I*c* and VIII*b* for which $B_6D_2F_1$ mice were used.

Literature procedures were used in the pharmacological evaluation[11] (33). The antimicrobial evaluation[11] was carried out by the reported methodology (25) using concentrations of 500, 250, 100, 50, and 10 μg/ml. Thus, a designation of >250 means that the compound inhibited growth of the microorganism at 250 μg/ml but not at 500 μg/ml. During the antimicrobial screening, the sample of *Salmonella typhimurium* (ATCC 13311) died and was replaced by a strain designated G46. All of the

[9] The anticancer screening was carried out by the Drug Research and Development Division, National Cancer Institute, Bethesda, Md., using their protocols (32).

[10] Tween 80, Atlas Chemical Industries.

[11] Pharmacological and antimicrobial evaluations were conducted by Bio-Research Laboratories, Montreal, Quebec, Canada.

compounds listed in Table II were screened *versus* the G46 strain of *S. typhimurium*, except for Ia, Ib, Ie, If, Vb, Vc, VIIa–VIIc, and VIIIc, which were assessed against the ATCC 13311 microorganism.

Evaluation of IIb against thymidylate synthetase and dihydrofolate reductase was done according to a literature method (34).

REFERENCES

(1) J. R. Dimmock and M. L. C. Wong, *Can. J. Pharm. Sci.*, **11**, 35 (1976).

(2) S. M. Kupchan, *Pure Appl. Chem.*, **21**, 227 (1970).

(3) O. K. Kabiev and S. M. Vermenichev, *Izv. Akad. Nauk Kaz. SSR Ser. Biol.*, **9**, 72 (1971); through *Chem. Abstr.*, **75**, 47091u (1971).

(4) M. Yamaguchi, M. Taniguchi, I. Kubo, and T. Kubola, *Agr. Biol. Chem.*, **41**, 2475 (1977).

(5) S. M. Kupchan and D. R. Streelman, *J. Org. Chem.*, **41**, 3481 (1976).

(6) P. W. Le Quesne, M. P. Pastore, and R. F. Raffauf, *Lloydia*, **39**, 391 (1976).

(7) S. M. Kupchan, J. A. Lacadie, G. A. Howie, and B. R. Sickles, *J. Med. Chem.*, **19**, 1130 (1976).

(8) S. M. Kupchan and G. Tsou, *J. Org. Chem.*, **38**, 1055 (1973).

(9) R. T. Williams, "Detoxication Mechanisms," 2nd ed., Wiley, New York, N.Y., 1959, p. 278.

(10) N. J. Harper, in "Progress in Drug Research," vol. 4, E. Jucker, Ed., Birkhauser Verlag, Basel, Switzerland, 1962, p. 221.

(11) H. J. E. Lowenthal, in "Protective Groups in Organic Chemistry," J. F. W. McOmie, Ed., Plenum, London, England, 1973, p. 330.

(12) P. M. Gullino, F. H. Crantham, S. H. Smith, and A. C. Haggerty, *J. Natl. Cancer Inst.*, **34**, 857 (1965).

(13) A. Burger, *J. Med. Chem.*, **21**, 2 (1978).

(14) A. F. Casy, N. J. Harper, and J. R. Dimmock, *J. Chem. Soc.*, **1964**, 3635.

(15) N. J. Harper, A. F. Casy, and J. R. Dimmock, *ibid.*, **1964**, 4280.

(16) J. R. Dimmock and W. G. Taylor, *J. Pharm. Sci.*, **64**, 241 (1975).

(17) J. R. Dimmock, A. M. Qureshi, L. M. Noble, P. J. Smith and H. A. Baker, *ibid.*, **65**, 38 (1976).

(18) H. Gershon and L. Shanks, *J. Med. Chem.*, **20**, 606 (1977).

(19) H. Zimmer and J. Rothe, *J. Org. Chem.*, **24**, 28 (1959).

(20) E. J. Forbes and M. J. Gregory, *J. Chem. Soc. B*, **1968**, 207.

(21) M. I. Vinnik and I. S. Kislina, *Kinet. Catal.*, **15**, 271 (1974).

(22) A. K. Barbour, M. W. Buxton, P. L. Coe, R. Stephens, and J. C. Tatlow, *J. Chem. Soc.*, **1961**, 808.

(23) G. S. Hammond, *J. Am. Chem. Soc.*, **77**, 334 (1955).

(24) J. W. Baker, I. Schumacher, and D. P. Roman, in "Medicinal Chemistry," 3rd ed., A. Burger, Ed., Wiley–Interscience, New York, N.Y., 1970, p. 631.

(25) J. R. Dimmock, C. B. Nyathi, and P. J. Smith, *J. Pharm. Sci.*, **67**, 1543 (1978).

(26) P. J. Nelson and A. F. A. Wallis, *Tappi*, **56**, 132 (1973).

(27) "Handbook of Chemistry and Physics," 49th ed., R. C. Weast, Ed., Chemical Rubber Co., Cleveland, Ohio, 1968, p. C-182.

(28) M. Hayashi, *J. Prakt. Chem.*, **123**, 289 (1929).

(29) "Dictionary of Organic Compounds," 4th ed., J. R. A. Pollock and R. Stevens, Eds., Eyre and Spottiswoode Publishers, London, England, 1965, p. 2477.

(30) *Ibid.*, p. 751.

(31) L. P. Hammett, "Physical Organic Chemistry," 2nd ed., McGraw-Hill, Toronto, Canada, 1970, p. 356.

(32) R. I. Geran, N. H. Greenberg, M. M. MacDonald, A. M. Schumacher, and B. J. Abbott, *Cancer Chemother. Rep. (Part 3)*, **3**(2), (Sept. 1972).

(33) J. R. Dimmock, P. J. Smith, and S. K. Tsui, *J. Pharm. Sci.*, in press.

(34) S. K. Srinivasan, V. S. Gupta, and R. E. Howarth, *Biochem. Pharmacol.*, **26**, 1027 (1977).

(35) T. Koppanyi and A. G. Karczmar, "Experimental Pharmacodynamics," 3rd ed., Burgess, Indianapolis, Ind., 1964, p. 67.

ACKNOWLEDGMENTS

The authors thank the Medical Research Council of Canada for the award of an operating grant (MA 5538) to J. R. Dimmock. Connlab Holdings Limited also provided financial assistance for the project. The United Nations Educational and Training Programme for Southern Africa provided a stipend to C. B. Nyathi which is gratefully acknowledged. The screening of certain compounds was provided by the National Cancer Institute, Bethesda, Md., and Bio-Research Laboratories, Montreal, Quebec, Canada, and is appreciated greatly.

New and Simple Methylene Blue Colorimetric Assay for Glycyrrhizin in Pharmaceuticals

A. A. M. HABIB *x, N. A. EL-SEBAKHY *, and H. A. KADRY ‡

Received December 8, 1978, from the **Department of Pharmacognosy, Faculty of Pharmacy, Alexandria University, Alexandria, Egypt*, and the ‡*Department of Pharmacognosy, Faculty of Pharmacy, Tanta University, Tanta, Egypt.* Accepted for publication April 10, 1979.

Abstract □ A new colorimetric method for glycyrrhizin in licorice and drug preparations is given. The method is based on coupling the acidic genin, glycyrrhetinic acid, with methylene blue and measuring the extinction of the coupled compound solution in chloroform–alcohol.

Keyphrases □ Glycyrrhizin—analysis, methylene blue colorimetry □ Antiulcerogenic agents—glycyrrhizin, methylene blue colorimetric analysis □ Colorimetry—analysis, glycyrrhizin, methylene blue □ Methylene blue—analysis, glycyrrhizin

Licorice, the root and subterranean stem of different varieties of *Glycyrrhiza glabra*, has long been used in medicine. The drug and some of its preparations are official in many pharmacopoeias. Besides being a valuable flavoring and sweetening agent, the drug has demulcent, expectorant, and antispasmodic action. Recently, it was shown to be effective in gastric ulcer treatment and to have a cortisone-like action in rheumatic arthritis and other inflammatory diseases (1–3). These activities are due to the active constituent glycyrrhizin, which is the calcium and potassium salt of glycyrrhizic acid; the latter is the diglucopyranosiduronic acid of the pentacyclic triterpenoid sapogenin, β-glycyrrhetinic acid. Simple derivatives of β-glycyrrhetinic acid such as the disodium salt of carbenoxolone have been used extensively in gastric ulcer treatment (4).

BACKGROUND

Glycyrrhizin has been estimated by gravimetric assays of variable weighing forms (5–7); volumetric assays such as direct titration of glycyrrhizic acid, glycyrrhetinic acid, or their salts (6, 8); colorimetric assays (6, 9–12); and colorimetric and spectrophotometric determination after chromatographic separation (13–18).

The reported glycyrrhizin content of licorice has varied greatly. Some investigators attributed this variation to the different analytical methods

0022-3549/79/1000-1221$01.00/0

© 1979, American Pharmaceutical Association

compounds listed in Table II were screened *versus* the G46 strain of *S. typhimurium*, except for Ia, Ib, Ie, If, Vb, Vc, VIIa–VIIc, and VIIIc, which were assessed against the ATCC 13311 microorganism.

Evaluation of IIb against thymidylate synthetase and dihydrofolate reductase was done according to a literature method (34).

REFERENCES

(1) J. R. Dimmock and M. L. C. Wong, *Can. J. Pharm. Sci.*, **11**, 35 (1976).

(2) S. M. Kupchan, *Pure Appl. Chem.*, **21**, 227 (1970).

(3) O. K. Kabiev and S. M. Vermenichev, *Izv. Akad. Nauk Kaz. SSR Ser. Biol.*, **9**, 72 (1971); through *Chem. Abstr.*, **75**, 47091u (1971).

(4) M. Yamaguchi, M. Taniguchi, I. Kubo, and T. Kubola, *Agr. Biol. Chem.*, **41**, 2475 (1977).

(5) S. M. Kupchan and D. R. Streelman, *J. Org. Chem.*, **41**, 3481 (1976).

(6) P. W. Le Quesne, M. P. Pastore, and R. F. Raffauf, *Lloydia*, **39**, 391 (1976).

(7) S. M. Kupchan, J. A. Lacadie, G. A. Howie, and B. R. Sickles, *J. Med. Chem.*, **19**, 1130 (1976).

(8) S. M. Kupchan and G. Tsou, *J. Org. Chem.*, **38**, 1055 (1973).

(9) R. T. Williams, "Detoxication Mechanisms," 2nd ed., Wiley, New York, N.Y., 1959, p. 278.

(10) N. J. Harper, in "Progress in Drug Research," vol. 4, E. Jucker, Ed., Birkhauser Verlag, Basel, Switzerland, 1962, p. 221.

(11) H. J. E. Lowenthal, in "Protective Groups in Organic Chemistry," J. F. W. McOmie, Ed., Plenum, London, England, 1973, p. 330.

(12) P. M. Gullino, F. H. Crantham, S. H. Smith, and A. C. Haggerty, *J. Natl. Cancer Inst.*, **34**, 857 (1965).

(13) A. Burger, *J. Med. Chem.*, **21**, 2 (1978).

(14) A. F. Casy, N. J. Harper, and J. R. Dimmock, *J. Chem. Soc.*, **1964**, 3635.

(15) N. J. Harper, A. F. Casy, and J. R. Dimmock, *ibid.*, **1964**, 4280.

(16) J. R. Dimmock and W. G. Taylor, *J. Pharm. Sci.*, **64**, 241 (1975).

(17) J. R. Dimmock, A. M. Qureshi, L. M. Noble, P. J. Smith and H. A. Baker, *ibid.*, **65**, 38 (1976).

(18) H. Gershon and L. Shanks, *J. Med. Chem.*, **20**, 606 (1977).

(19) H. Zimmer and J. Rothe, *J. Org. Chem.*, **24**, 28 (1959).

(20) E. J. Forbes and M. J. Gregory, *J. Chem. Soc. B*, **1968**, 207.

(21) M. I. Vinnik and I. S. Kislina, *Kinet. Catal.*, **15**, 271 (1974).

(22) A. K. Barbour, M. W. Buxton, P. L. Coe, R. Stephens, and J. C. Tatlow, *J. Chem. Soc.*, **1961**, 808.

(23) G. S. Hammond, *J. Am. Chem. Soc.*, **77**, 334 (1955).

(24) J. W. Baker, I. Schumacher, and D. P. Roman, in "Medicinal Chemistry," 3rd ed., A. Burger, Ed., Wiley–Interscience, New York, N.Y., 1970, p. 631.

(25) J. R. Dimmock, C. B. Nyathi, and P. J. Smith, *J. Pharm. Sci.*, **67**, 1543 (1978).

(26) P. J. Nelson and A. F. A. Wallis, *Tappi*, **56**, 132 (1973).

(27) "Handbook of Chemistry and Physics," 49th ed., R. C. Weast, Ed., Chemical Rubber Co., Cleveland, Ohio, 1968, p. C-182.

(28) M. Hayashi, *J. Prakt. Chem.*, **123**, 289 (1929).

(29) "Dictionary of Organic Compounds," 4th ed., J. R. A. Pollock and R. Stevens, Eds., Eyre and Spottiswoode Publishers, London, England, 1965, p. 2477.

(30) *Ibid.*, p. 751.

(31) L. P. Hammett, "Physical Organic Chemistry," 2nd ed., McGraw-Hill, Toronto, Canada, 1970, p. 356.

(32) R. I. Geran, N. H. Greenberg, M. M. MacDonald, A. M. Schumacher, and B. J. Abbott, *Cancer Chemother. Rep. (Part 3)*, **3**(2), (Sept. 1972).

(33) J. R. Dimmock, P. J. Smith, and S. K. Tsui, *J. Pharm. Sci.*, in press.

(34) S. K. Srinivasan, V. S. Gupta, and R. E. Howarth, *Biochem. Pharmacol.*, **26**, 1027 (1977).

(35) T. Koppanyi and A. G. Karczmar, "Experimental Pharmacodynamics," 3rd ed., Burgess, Indianapolis, Ind., 1964, p. 67.

ACKNOWLEDGMENTS

The authors thank the Medical Research Council of Canada for the award of an operating grant (MA 5538) to J. R. Dimmock. Connlab Holdings Limited also provided financial assistance for the project. The United Nations Educational and Training Programme for Southern Africa provided a stipend to C. B. Nyathi which is gratefully acknowledged. The screening of certain compounds was provided by the National Cancer Institute, Bethesda, Md., and Bio-Research Laboratories, Montreal, Quebec, Canada, and is appreciated greatly.

New and Simple Methylene Blue Colorimetric Assay for Glycyrrhizin in Pharmaceuticals

A. A. M. HABIB *x, N. A. EL-SEBAKHY *, and H. A. KADRY ‡

Received December 8, 1978, from the **Department of Pharmacognosy, Faculty of Pharmacy, Alexandria University, Alexandria, Egypt*, and the ‡*Department of Pharmacognosy, Faculty of Pharmacy, Tanta University, Tanta, Egypt.* Accepted for publication April 10, 1979.

Abstract □ A new colorimetric method for glycyrrhizin in licorice and drug preparations is given. The method is based on coupling the acidic genin, glycyrrhetinic acid, with methylene blue and measuring the extinction of the coupled compound solution in chloroform–alcohol.

Keyphrases □ Glycyrrhizin—analysis, methylene blue colorimetry □ Antiulcerogenic agents—glycyrrhizin, methylene blue colorimetric analysis □ Colorimetry—analysis, glycyrrhizin, methylene blue □ Methylene blue—analysis, glycyrrhizin

Licorice, the root and subterranean stem of different varieties of *Glycyrrhiza glabra*, has long been used in medicine. The drug and some of its preparations are official in many pharmacopoeias. Besides being a valuable flavoring and sweetening agent, the drug has demulcent, expectorant, and antispasmodic action. Recently, it was shown to be effective in gastric ulcer treatment and to have a cortisone-like action in rheumatic arthritis and other inflammatory diseases (1–3). These activities are due to the active constituent glycyrrhizin, which is the calcium and potassium salt of glycyrrhizic acid; the latter is the diglucopyranosiduronic acid of the pentacyclic triterpenoid sapogenin, β-glycyrrhetinic acid. Simple derivatives of β-glycyrrhetinic acid such as the disodium salt of carbenoxolone have been used extensively in gastric ulcer treatment (4).

BACKGROUND

Glycyrrhizin has been estimated by gravimetric assays of variable weighing forms (5–7); volumetric assays such as direct titration of glycyrrhizic acid, glycyrrhetinic acid, or their salts (6, 8); colorimetric assays (6, 9–12); and colorimetric and spectrophotometric determination after chromatographic separation (13–18).

The reported glycyrrhizin content of licorice has varied greatly. Some investigators attributed this variation to the different analytical methods

0022-3549/79/1000-1221$01.00/0

© 1979, American Pharmaceutical Association

utilized; they considered the figure given in the BPC 1963 (2%) to be low and favored the higher figure given in the later edition (7%) on the basis of good agreement with the 6–13% found by Houseman (5). However, recent reports criticized these high figures and showed most early gravimetric and colorimetric methods to be extremely nonspecific (4, 6), producing results that are appreciably higher than the true value.

Killacky *et al.* (4) criticized earlier colorimetric methods that rely on the reaction between β-glycyrrhetinic acid and vanillin–sulfuric acid as well as spectrophotometric methods that rely on UV absorption at 248 nm on the basis of the nonspecificity of the aromatic aldehyde–sulfuric acid color reaction. The numerous flavonoids, coumarins, and polyphenolic derivatives present in licorice extracts would absorb at 248 nm and are difficult to eliminate.

Some methods for the determination of glycyrrhizin and β-glycyrrhetinic acid were reported recently. These methods attempted chromatographic separation of the active principle by reversed-phase high-pressure liquid chromatography (HPLC) (4), ion-exchange HPLC (19), rod TLC (20), or GLC (21, 22).

A simple, specific method for glycyrrhizin estimation was developed through direct coupling of the acidic genin, β-glycyrrhetinic acid, with a basic dye, methylene blue.

EXPERIMENTAL

Instrument—A spectrocolorimeter[1] was used.

Material—One batch of powdered licorice[2], two batches of licorice[3] liquid extract, and one batch of glycyrrhizin flakes[4] were used.

Reagents—Aqueous methylene blue[5] (0.1%), chloroformic glycyrrhetinic acid reference[6] solution (5 mg/100 ml), and citrate–phosphate–borate–hydrochloride buffer[7] (Teorell and Stenhagen buffer) were prepared.

Determination of Optimum Coupling Conditions—Aliquots (20 ml) of reference glycyrrhetinic acid solution were shaken separately with 1 ml of dye solution and 20 ml of pH 6–12 buffer solution (Fig. 1). Solutions were shaken continuously for 1 min and set aside for 5 min. The chloroform layer was decanted into a 50-ml measuring flask.

The coupled compound was completely extracted by reshaking with an additional 10 and 5 ml of chloroform. The mixed chloroform extract was diluted to volume with ethanol, and the extinction of the chloroform–ethanol solution was measured at 640 nm (Fig. 1). The extractibility of the free dye was determined in a similar manner from blank experiments at the same pH values (Fig. 1).

Obedience to Beer's Law—Aliquots of glycyrrhetinic acid reference solution, corresponding to 0.05–1 mg of glycyrrhetinic acid, were coupled with methylene blue as described. Two series of experiments were attempted at pH 9.2 and 8.4. However, the extinction was measured in chloroform–ethanol (4:6). A linear relationship was maintained at both pH values (slopes of 0.21 and 0.14, respectively).

Molar Ratio of Coupled Compound—Eleven different coupling experiments were attempted with glycyrrhetinic acid aliquots ranging from 1 to 9 g-mole × 10^{-4}. They were coupled, at pH 9.2, with aliquots ranging from 9 to 1 g-mole × 10^{-4} of methylene blue, respectively (Fig. 2).

Assay—For powdered licorice, 1.0 g was refluxed four times for 15 min with four successive 15-ml portions of 70% ethanol. Each portion was decanted and filtered through the same filter paper. The alcohol was evaporated, 20 ml of warm water was added, and the procedure was completed as described for the liquid extract, starting with: "After cooling, 5 ml of ethanol . . . . "

For the liquid extract and flakes, 1.0 g, accurately weighed, of the liquid extract (or 0.25 g of flakes) was dissolved with 20 ml of boiling water. After complete dissolution, the mixture was transferred into a separator, the flask was washed with two 10-ml portions of boiling water, and the washings were added to the original mixture in the separator. After cooling, 5 ml of ethanol and 1 ml of 6 *N* H_2SO_4 were added; then the mixture was shaken very gently with successive portions of 20, 20, and 10 ml of chloroform. Each chloroform fraction was separated as completely as possible, taking care not to pass down any precipitated matter

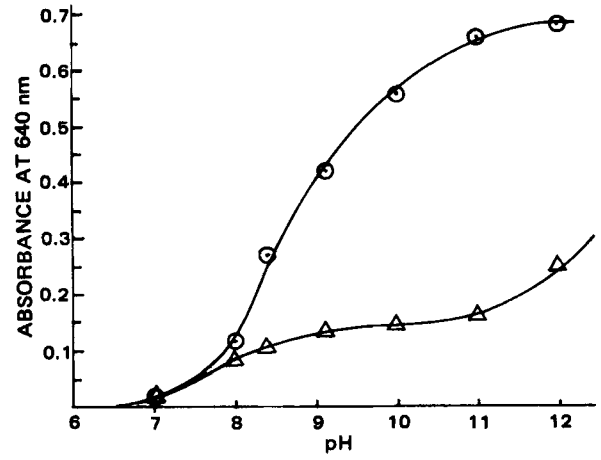

Figure 1—*Extractibility of methylene blue (△) and glycyrrhetinic acid–methylene blue coupled compound (○) at different pH values.*

or emulsion at the interphase. The chloroform extracts were discarded.

The aqueous phase with any suspended insoluble matter was quantitatively transferred into a boiling flask, using 5 ml of distilled water to wash off any clinging matter on the separator walls. Ten milliliters of 6 *N* H_2SO_4 was added, and the mixture was heated on a boiling water bath for 75 min.

The hydrolyzed mixture was transferred quantitatively, while hot, into a separator, and the flask was washed with 5 ml of distilled water. The aqueous acid solution was extracted with four 20-ml and one 10-ml portions of chloroform. Each chloroform fraction was filtered through a small piece of cotton surmounted by 2 g of anhydrous sodium sulfate. The chloroform filtrate was collected into a 100-ml measuring flask, and the volume was completed with chloroform.

Coupling Experiments—A 10-ml aliquot was transferred into a separator containing 20 ml of pH 9.2 buffer solution, 2 ml of dye solution, and 10 ml of chloroform. The mixture was shaken continuously for 1 min. (After separation of the two phases, the aqueous phase must be blue in color. If it has a greenish or yellow color, additional 1-ml aliquots of the dye solution must be added and the mixture must be reshaken.) The chloroform layer was separated into another separator containing 5 ml of pH 9.2 buffer. Then the mixture was shaken and, after complete separation, the chloroform layer was separated into a 100-ml measuring flask (without filtration or dehydration).

The contents of the first and second separators were reextracted with 10-, 5-, and 5-ml portions of chloroform in the same manner, and the combined chloroform extract in the measuring flask was completed to volume with ethanol.

A standard solution was prepared according to the same coupling procedure but with 10 ml of reference glycyrrhetinic acid solution instead of the 10-ml sample aliquot.

The extinctions of the test and standard solutions were measured at

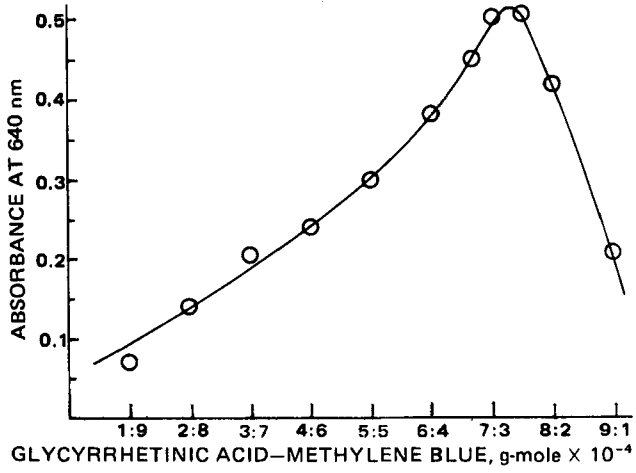

Figure 2—*Molar ratio curve of glycyrrhetinic acid–methylene blue coupled compound.*

[1] Spekol, Carl Zeiss, Jena, East Germany.
[2] Caesar and Loretz-Hilden.
[3] Lot 934, CID Laboratories, Cairo, Egypt, and batch 33, Memphis Chemical Co., Cairo, Egypt.
[4] CID Laboratories, Cairo, Egypt.
[5] Reidel-De Haen AG, Seelze-Hannover.
[6] Merck.
[7] According to "Scientific Tables," 7th ed., Ciba-Geigy, Basel, Switzerland, 1971, p. 280.

Table I—Glycyrrhizin Content of Certain Preparations

Sample	Original Preparation: Combined Glycyrrhetinic Acid, %	Original Preparation: Glycyrrhizin, %	Enriched Preparation: Added Glycyrrhetinic Acid, mg	Enriched Preparation: Found Glycyrrhetinic Acid, mg	Error, %
Liquid extract[a]	1.534	2.7	5.626	5.753	+2.26
Liquid extract[b]	0.649	1.14	5.138	5.227	+1.73
Powdered licorice	0.835	1.46	1.285	1.348	+4.9
Glycyrrhizin flakes[a]	8.21	14.37	6.779	6.901	+1.8

[a] CID Laboratories. [b] Memphis Chemical Co.

640 nm against a blank prepared at the same time by the same coupling procedure but with 10 ml of chloroform instead of the sample aliquot.

The glycyrrhizin percentage in the assayed preparation was calculated using:

$$\% \text{ glycyrrhizin} = \frac{E_t \times 0.5 \times 1.75}{E_s \times a} \qquad \text{(Eq. 1)}$$

where E_t is the extinction of the test, E_s is the extinction of the reference, a is the weight taken of the preparation, and 1.75 is the transformation factor of glycyrrhetinic acid to glycyrrhizin.

The reliability of the method was checked by assaying some pharmaceutical preparations before and after enrichment with authentic glycyrrhetinic acid (Table I).

DISCUSSION

Preliminary studies with methylene blue, safranin, brilliant cresyl blue, and basic fuchsin indicated that methylene blue was the best for coupling with glycyrrhetinic acid. The coupled compound was of comparably high extinction. The serious λ_{max} inconsistency of the methylene blue coupled compound in chloroform solutions was overcome by measuring the extinction in a chloroform–alcohol mixture in which the coupled compound showed a consistent λ_{max} at 640 nm.

The coupled compound was highly extractable with chloroform at all alkaline pH values; however, obedience to Beer's law was studied only at pH 9.2 and 8.4 rather than at higher pH values at which the free dye showed higher extractibility.

The specificity of the method was proved by resolution of the coupled compound (extraction with chloroform from acidic solution). Examination of the chloroform solution by TLC (23, 24) revealed one principal spot corresponding to glycyrrhetinic acid.

Molar ratio studies proved the coupled compound to be formed from three molecules of the acid and one molecule of the basic dye.

The proposed assay ensures complete glycyrrhizin extraction and complete elimination of free acidic constituents such as simple organic acids, sugar acids, free glycyrrhetinic acid, and other triterpene acids. The procedure also ensures complete glycyrrhizic acid hydrolysis and complete extraction of the liberated glycyrrhetinic acid.

The aliquot technique was followed in the coupling experiment to allow for possible repetition of that step.

The glycyrrhetinic acid recovery (Table I) was calculated to be 101.7–104.9%. This consistent positive error may be explained by a probable slight increase in solubility of the uncoupled dye in higher concentrations of the coupled compound (in the case of enriched samples).

The method is simple, rapid, and sensitive. The assay procedure, by ensuring complete initial elimination of free acids, renders the method specific for the acidic genins in the hydrolysate, which was proved chromatographically to consist principally of β-glycyrrhetinic acid.

REFERENCES

(1) F. E. Revers, *Ned. Tijdschr. Geneesh.*, **90,** 135 (1946). *Ibid.*, **92,** 2968, 3567 (1948); through Ref. 4.

(2) P. B. Hudson, A. M. Mittelman, and M. Podberezec, *N. Engl. J. Med.*, **251,** 641 (1954); through *Chem. Abstr.*, **49,** 3482 C (1955).

(3) National Research Development Corp., British pat. 713,651 (Aug. 18, 1954); through *Chem. Abstr.*, **49,** 3482 (1955).

(4) J. Killacky, M. S. F. Ross, and T. D. Turner, *Planta Med.*, **30,** 310 (1976).

(5) P. A. Houseman, *Am. J. Pharm.*, **84,** 351 (1912); through *Chem. Abstr.*, **84,** 558 (1913). P. A. Houseman, *J. Assoc. Offic. Org. Chem.*, **6,** 191 (1922).

(6) A. F. Selim, thesis, Cairo University, Cairo, Egypt, 1971, p. 199.

(7) I. A. Murawjew and N. A. Buska, *Aptechn. Delo,* **8,** 23 (1959); through *Chem. Abstr.*, **54,** 6033 (1960). *Ibid.*, **10,** 24 (1960); through *Chem. Abstr.*, **55,** 27778 (1961).

(8) I. A. Murawjew and W. D. Ponomarew, *Pharm. Zentralhalle,* **105,** 153 (1966); through *Chem. Abstr.*, **68,** 107868 (1968). I. A. Murawjew and W. D. Ponomarew, *Acta Pharm. Jugoslav.*, **16,** 3 (1966); through *Chem. Abstr.*, **69,** 44029 (1968). I. A. Murawjew and W. D. Ponomarew, *Med. Ind. USSR,* **16,** 43 (1962); through *Chem. Abstr.*, **57,** 3565 (1962).

(9) F. Wiest, dissertation, University of Zurich, Zurich, Switzerland, 1949.

(10) R. H. Cundiff, *Anal. Chem.*, **36,** 1871 (1964).

(11) C. H. Brieskorn and G. H. Mahran, *Arch. Pharm.*, **293,** 1075 (1960).

(12) C. H. Brieskorn and W. Wallenstaeter, *Arch. Pharm. (Weinheim),* **300,** 8, 717 (1967).

(13) J. Gootjes and W. T. Manta, *Rec. Trav. Chim. Pays Bas,* **73,** 886 (1954); through *Chem. Abstr.*, **49,** 9223c (1954).

(14) H. Hada and M. Inagaki, *J. Pharm. Soc. Jpn.*, **78,** 795 (1958); through *Chem. Abstr.*, **52,** 17357 (1958).

(15) G. Kurono and S. Sasaki, *Yakugaku Zasshi,* **90,** 497 (1970); through *Chem. Abstr.*, **73,** 28969d (1970).

(16) T. J. Coleman and D. V. Parke, *J. Pharm. Pharmacol.*, **15,** 84 (1963).

(17) K. S. H. Finny, G. F. Somers, and J. H. Wilkuison, *ibid.*, **10,** 687 (1958).

(18) B. Pasich, B. Adamezewski, and J. Wisniewski, *Farm. Pol.*, **22,** 35 (1966); through *Chem. Abstr.*, **61,** 15018 (1966).

(19) S. Ogawa, A. Yoshida, and Y. Mitani, *Yakugaku Zasshi,* **96,** 122 (1976); through Ref. 4.

(20) T. Namba, M. Yoshizaki, T. Tomimori, M. Tsuboi, and K. Kato, *ibid.*, **95,** 809 (1975); through *Chem. Abstr.*, **83,** 120949b (1975).

(21) D. Larry, J. M. Fuller, and P. G. Harrill, *J. Assoc. Off. Anal. Chem.*, **53,** 698 (1970). *Ibid.*, **55,** 570 (1972).

(22) T. Vondenhof, K. W. Glombitza, and M. Steiner, *Sci. Pharm.*, **41,** 155 (1973).

(23) "British Pharmacopoeia 1973," Her Majesty's Stationery Office, London, England, 1973.

(24) E. Stahl, "Thin-Layer Chromatography," 2nd ed., Springer-Verlag, Berlin, Germany, 1969.

Differential Thermal, Solubility, and Aging Studies on Various Sources of Digoxin and Digitoxin Powder: Biopharmaceutical Implications

WIN L. CHIOU ˣ and LESLIE E. KYLE

Received June 2, 1978, from the *Clinical Pharmacokinetics Laboratory and Department of Pharmacy, College of Pharmacy, University of Illinois at the Medical Center, Chicago, IL 60612.* Accepted for publication April 4, 1979.

Abstract □ Unlike most organic compounds, both digoxin and digitoxin melted over a wide temperature range, with the widest range being 88 and 33° for both compounds, respectively. Furthermore, the melting ranges varied markedly among several untriturated powders obtained from commercial sources and after recrystallization. Trituration produced dramatically sharper and generally lower melting temperatures. Apparent equilibrium solubility also varied considerably among different untriturated compounds. Correlation between solubility and final melting temperature was found. Results from dynamic solubility studies were used to explain the failure of trituration to enhance the apparent equilibrium solubility in certain samples. Storage at room temperature increased the melting points and decreased aqueous solubilities. Several reasons such as the presence of polymorphic and amorphous forms, crystal defects, impurities, and solvate formation were postulated to explain the findings. In a preliminary study, the *in vitro* dissolution rates of two commercial tablet products stored at elevated temperatures for 4–8 weeks progressively decreased. Biopharmaceutical implications and areas for further studies are discussed.

Keyphrases □ Digoxin—stability studies, temperature, solubility, aging, various commercial powders □ Digitoxin—stability studies, temperature, solubility, aging, various commercial powders □ Cardiotonic agents—digoxin and digitoxin, stability studies, various commercial powders □ Stability—digoxin, digitoxin, various commercial powders

Oral bioavailability of digoxin, a potent water-insoluble cardiac glycoside, has been the subject of intensive studies (1, 2). Each solid dosage form product must pass the oral absorption test in humans (2), and the *in vitro* dissolution study must be performed as a routine quality control procedure by manufacturers (3). However, studies on the underlying physicochemical factors that might contribute to poor dissolution and hence to poor absorption of digoxin from the dosage forms have been quite limited.

The particle size of digoxin within a tablet was a major dissolution rate determinant: the smaller the particle size, the better the absorption (1, 4–6). Effects of milling or grinding of digoxin powder on the enhancement of dissolution and solubility (7, 8) and oral bioavailability in dogs (9) were recently reported. Different results from X-ray diffraction studies on the effects of milling or grinding of digoxin powder on the crystallinity were obtained (7, 8). A complete transformation to an amorphous form (6) and the absence of any crystal–crystal transition (8) after extensive grinding and trituration were both proposed, although the latter study (7) did not rule out the partial transformation to the amorphous form.

Relatively little attention has been directed to the physicochemical properties of digitoxin, another less widely used cardiac glycoside. Since digitoxin is much less soluble in water than digoxin (9), similar poor bioavailability problems from various solid dosage forms may exist. In some preliminary studies, however, complete absorption from intramuscular and oral administration was reported (10, 11).

The purposes of this paper are to report studies on some physicochemical properties of digoxin and digitoxin from various sources using differential thermal, equilibrium, and dynamic solubility methods and to point out their potential biopharmaceutical implications.

EXPERIMENTAL

Digoxin Samples from Commercial Sources and after Recrystallization or Trituration—Two lots of digoxin powder, designated as digoxin L1 and L2, were obtained from a commercial source[1]. Additional samples from two other commercial sources were designated digoxin Z[2] and digoxin S[3].

Digoxin samples also were obtained after recrystallization of digoxin L1 from chloroform[4] and 95% ethanol[5]. For recrystallization, 200 and 100 mg of digoxin powder were dissolved in 800 ml of boiling chloroform and 100 ml of ethanol, respectively. These solutions were reduced with heat to about 50 and 3 ml, respectively. After filtration, the filtrates were cooled in an ethanol and dry ice bath. Recrystallized particles were obtained after filtration and placed in a vacuum for 2 hr.

Three hundred milligrams of digoxin L1, L2, and Z samples were triturated in a porcelain mortar for 30 sec. The powder was loosened from the side of the mortar with a spatula. This process was repeated until a total trituration time of 15 min had been achieved.

Digitoxin Samples from Commercial Sources and after Trituration—Digitoxin powder samples were obtained from three commercial sources and were identified as digitoxin L[6], Z[2], and S[3].

Triturated samples were prepared from digitoxin L and Z as described for the preparation of the triturated digoxin.

Thermal Analysis Studies—Thermal studies on all digoxin and digitoxin samples were conducted in a thermal analyzer attached to a differential scanning calorimetry cell[7]. The temperature was usually scanned from 50 to 300° at 20°/min. One to 2 mg of sample was used for each study. The thermal analyzer was calibrated with the standard ammonium nitrate supplied by the manufacturer[7].

Equilibrium Solubility Studies—A preliminary study conducted over 7 days indicated that 24 hr was sufficient to achieve the equilibrium solubility. Therefore, all subsequent studies were conducted in 24 hr.

Ten-milligram digoxin or digitoxin samples were placed in 16 × 125-mm culture tubes fitted with screw caps, and 10 ml of water was

Table I—Literature Melting Points of Digoxin and Digitoxin

Compound	Source (Reference)	Melting Point
Digoxin	A (12)	270°
	B (13)	235°
	C (14)	240°
	D (15)	265°
	E (7)	234° [a], 236° [a], 240° [a]
Digitoxin	F (16)	240°
	G (17)	256–257°
	A (12)	265°

[a] Based on three different sources of digoxin powder.

[1] Digoxin USP, lots 0609-J9623 and 0609-K7193, Lederle Laboratory, Pearl River, N.Y.
[2] Digoxin USP and digitoxin USP, Zenith Labortory, Northvale, N.J.
[3] Digoxin USP and digitoxin USP, Sandoz Co., East Hanover, N.J.
[4] Certified ACS grade, Fisher Scientific Co., Fair Lawn, N.J.
[5] Alcohol USP, Commercial Solvent Co., Terre Haute, Ind.
[6] Digitoxin USP, lot W11097, Eli Lilly & Co., Indianapolis, Ind.
[7] DuPont 990 thermal analyzer, E.I. du Pont de Nemours & Co., Wilmington, Del.

0022-3549/79/1000-1224$01.00/0
© 1979, American Pharmaceutical Association

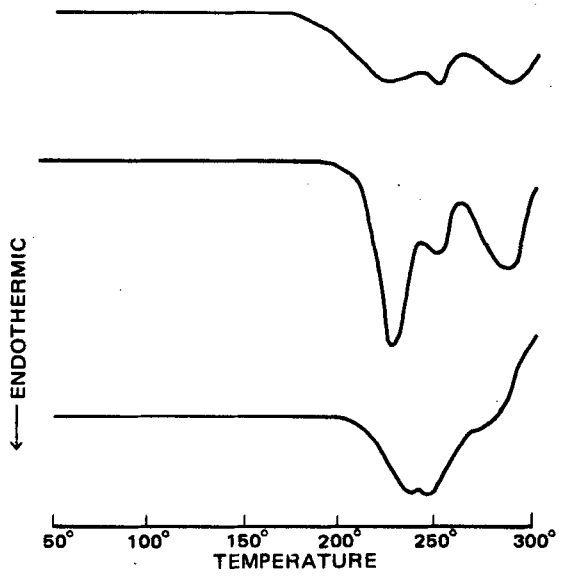

Figure 1—*Differential scanning calorimetric thermograms of three untriturated commercial digoxin samples. Key: top, S; middle, Z; and bottom, L1.*

added. The culture tubes were placed in an ultrasonic bath[8] for 30 min and then transferred to a shaker bath[9] maintained at 37° and shaking at 120 cpm. After 24 hr, the samples were filtered through 0.22-μm membrane filters[10], and the absorbance was read at 222 nm on a UV–visible spectrophotometer[11].

Concentrations were calculated according to a predetermined Beer's law plot. All studies were performed in triplicate. Excellent reproducibility was obtained; with some exceptions, only the average results are reported.

Dynamic Solubility Studies—Based on the results from the equilibrium solubility study, an excess amount (50 mg) of powder of digoxin L1, L2, and Z, digitoxin L and Z, and their triturated samples was added to 125 ml of water in a 250-ml beaker maintained at 37° in a water bath[12]. The medium was stirred at 200 rpm with a stirrer[13] centered in the beaker 2 cm from the bottom. The beaker was covered with parafilm to prevent water evaporation.

Three-milliliter samples were withdrawn at 5, 10, 20, 40, and 60 min and then periodically up to 24 hr. The samples were treated as in the equilibrium solubility studies, and the concentrations were determined. All studies were performed in duplicate, and only the average results are reported. The high agitation rate was necessary to overcome the effect of powder aggregation and agglomeration due to the hydrophobic nature of the cardiac glycosides and to enhance the dissolution rate.

Aging—Thermal studies were performed at various times on selected digoxin and digitoxin samples which were kept in sealed bottles at ambient temperature. The 24-hr equilibrium solubility study was conducted for digoxin L2 five times over a 1-year period.

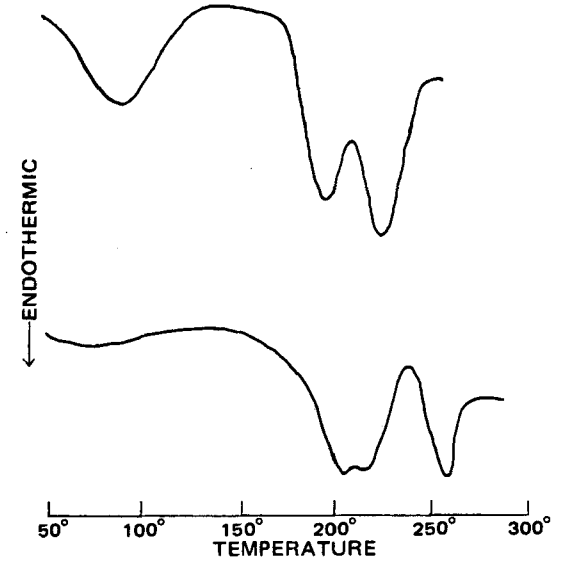

Figure 2—*Differential scanning calorimetric thermograms of digoxin recrystallized from chloroform (top) and 95% ethanol (bottom) from the L1 source.*

[8] Varian Aerograph, Walnut Creek, Calif.
[9] Eberbach Corp., Ann Arbor, Mich.
[10] Millipore filter (with Swinney filter device), Millipore Corp., Bedford, Mass.
[11] Beckman DBGT, Beckman Instruments, Fullerton, Calif.
[12] Fisher Versa-Bath, Fisher Scientific Co., Chicago, Ill.
[13] Nalgene stirrer, three blades, (1⅓ inch diameter), Fisher Scientific Co., Chicago, Ill.

Table II—Melting Ranges of Digoxin from Various Sources

Source	Date of Study	Beginning of Melting	End of Melting
L1	8/20/74	137°	225°
L1	10/22/74	146°	228°
L1	12/17/74	150°	230°
L1	10/14/75	182°	235°
L1 triturated	10/14/75	173°	176°
L2	10/28/74	150°	227°
L2	10/14/75	167°	233°
L2	3/5/76	167°	233°
L2 triturated	10/14/75	177°	184°
Z	10/28/74	192°	228°
S	10/22/74	180°	234°
L1 recrystallized from chloroform		175°	196°
L1 recrystallized from ethanol		150°	205°

RESULTS AND DISCUSSION

The melting test is often used for routine quality control of a drug or compound (3). The melting range is defined as those points of temperature within which the solid coalesces and is completely melted (3). Therefore, unless the melting of a compound takes place instantaneously, a melting temperature range should be reported. A literature survey on both glycosides found not only a large variation in the reported melting points but also an almost complete absence of any reported melting ranges. These literature data are summarized in Table I.

Differential thermal analyzers and differential scanning calorimeters are extremely sensitive instruments for studying the thermal behavior of compounds (18–22). They are particularly valuable in studying polymorphic transitions and the beginning of melting of a compound or a mixture. The temperature at which the suspected melting endothermic

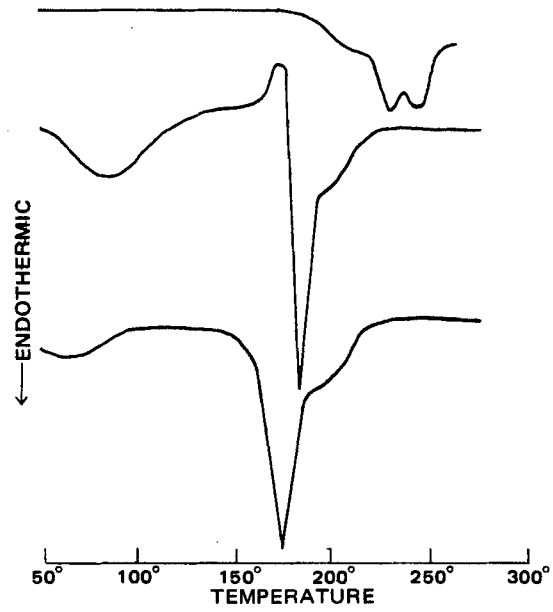

Figure 3—*Differential scanning calorimetric thermograms of digoxin from the L2 sample. Key: top, untreated; middle, triturated for 15 min; and bottom, triturated for 15 min, heated through exothermic transition, cooled, and reheated.*

Table III—Average Solubilities of Digoxin from Various Sources in Water at 37° after 24 hr of Equilibration

Source	Solubility, μg/ml
L1	41.8
L1 triturated	41.0
L2	68.2
L2 triturated	98.0
Z	40.1
Z triturated	39.5
S	28.9
L1 recrystallized from chloroform	64.7
L1 recrystallized from ethanol	52.1

peak begins (first deviation from the baseline in the thermogram) is considered to be the beginning of melting. When the conventional capillary tube method is used for the melting-point study, it is often difficult to determine the temperature at which the sample starts to melt, even when a small fraction of the sample has been melted already (20–22). On the other hand, when the sample melts slowly over a wide temperature range, the conventional capillary tube method is often superior in determining the final melting temperature.

In the present study, the differential scanning calorimeter was used to measure the beginning melting temperature, and both the differential scanning calorimetric and capillary tube methods were used to measure the final melting temperature. The final melting point of the sample generally corresponded to the first major endothermic peak in the differential scanning calorimetric study. Results on the melting ranges of digoxin are summarized in Table II, and some typical differential scanning calorimetric thermograms are shown in Figs. 1 and 2.

Consistent with the prior literature data, an extremely wide final melting-point range (176–235°) was found in the digoxin samples. The highest melting point reported previously was 270° (12). In contrast with previous reports, a wide melting-point range was found for each untreated digoxin sample obtained from the commercial sources or recrystallized from chloroform or ethanol. The largest range, 88°, was found in the L1 sample. Sample discoloration could be observed first at approximately the beginning of melting, and small droplets of melt could be observed with a hot-stage microscope well below the final melting temperature. Additional endothermic peaks above the melting point are believed to be due to decomposition.

Several possible reasons for such a marked variation in the melting range among all untreated digoxin samples studied can be postulated:

1. Polymorphic forms—The marked difference in melting ranges and thermograms might suggest that the phenomena are due to the existence of a different polymorphic (crystalline) form for each sample (19, 21). This possibility can be deemphasized, but not entirely ruled out, as a major cause because almost identical X-ray diffraction spectra were obtained previously (7, 8) from various digoxin sources, which also showed different dissolution, solubility, and melting properties.

The difference in the melting range possibly could result from various combinations of two or three polymorphic forms. Such a combination should produce the same X-ray diffraction peaks or lines with only different intensities from various samples. This hypothesis is not inconsistent with the reported X-ray diffraction data (7, 8). The possibility of varying fractions of an amorphous form with other crystalline digoxin seems unlikely because of the absence in the thermograms of an exothermic peak, which usually occurs when an amorphous form is converted to the crystalline form upon heating (21, 22). This point will be elaborated later.

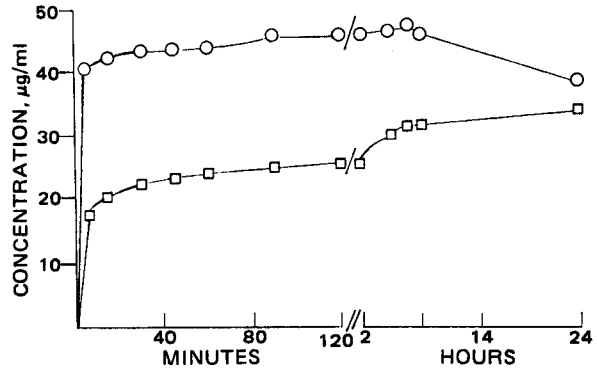

Figure 4—*Dynamic solubility study in water at 37° on the untriturated (bottom) and triturated (top) digoxin Z powder.*

Table IV—Effect of Aging on Solubility (Micrograms per Milliliter) of Digoxin in Water at 37°

Tube	Date of Study 3/16/75	7/11/75	9/15/75	12/3/75	3/2/76
1	67.5	63.7	61.0	55.2	53.5
2	68.5	62.2	61.0	56.2	53.8
3	68.5	62.7	61.5	56.7	52.5
Average	68.2	62.9	61.2	56.0	53.3

2. Crystal defects—Various degrees of extensive defects in the crystal lattice conceivably could produce various degrees of difference in the melting range, especially in light of the large molecular structure of digoxin (mol. wt. 780.92). Crystal defects might also be expected to alter the solubility and dissolution properties (19). Such a defect in the digoxin crystal might not be sufficient to produce any detectable shifts in diffraction peaks or lines.

3. Solvate formation—Various types of solvate possibly might be formed during the purification process with different solvents. The same digoxin sample (L1) recrystallized from chloroform and from ethanol yielded different thermal (Table II and Fig. 2) and solubility (discussed later) properties. Additional studies using the differential thermal gravimetric method should delineate this point.

4. Structurally related impurities—The possibility that the major cause of the wide melting range is the presence of impurities with chemical structures similar to digoxin is quite remote since the trituration of two digoxin samples resulted in sharper melting (Table II). This idea is an analogy to the common phenomenon of melting-point depression in the presence of impurities. The purity of digoxin samples seems to be supported by high-pressure liquid chromatographic (HPLC) analysis (23), which showed only one peak from both commercial and USP reference digoxin, and also by TLC analysis (24).

5. Any combination of the above four factors.

Digoxin samples recrystallized from chloroform and from ethanol had much lower final melting points than all of the untreated commercial samples in the present and previous studies (7). Their thermograms also were quite different from those obtained from the untreated commercial samples. A huge endothermic peak at about 80° was found in the sample recrystallized from chloroform, probably resulting from the chloroform desolvation. A quick and brief preheating of the sample to ~120° eliminated this endothermic peak upon rerun of the thermogram. This apparent desolvation endothermic peak was much weaker from the sample recrystallized from ethanol.

Trituration with a mortar and pestle dramatically affected the differential scanning calorimetric thermogram in both lots of digoxin powder (Fig. 3). A large endothermic peak at ~75° was followed by a relatively sharp exothermic peak at 175°, which was followed by a sharp endothermic peak. The reason for the first endothermic peak is unclear. It might be due to a phase transition in the amorphous or glassy state. The exothermic peak was probably due to the conversion of the amorphous form to the crystalline form, which subsequently melted with a sharp endothermic peak. The sharp melting of the triturated digoxin also was confirmed by the capillary tube method.

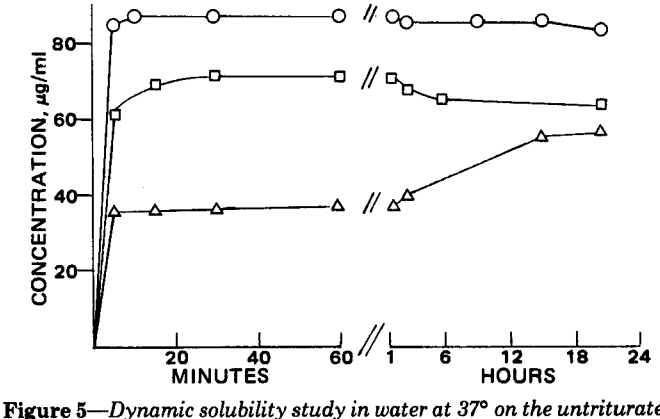

Figure 5—*Dynamic solubility study in water at 37° on the untriturated (bottom), freshly triturated (top), and triturated and stored (2–5 months; middle) digoxin L2 powder.*

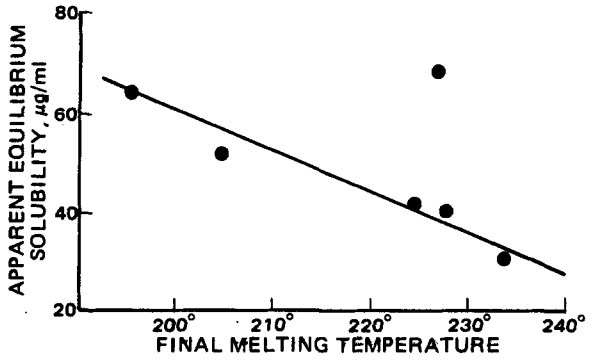

Figure 6—*Relationship between the apparent aqueous solubility and final melting temperature of various untriturated digoxin powders.*

This exothermic–endothermic thermogram was typical of the existence of an amorphous or glassy form, as found in melted and resolidified pure sulfisoxazole (21) and griseofulvin (22). Similar exothermic–endothermic thermograms obtained at temperatures above 140° also were reported for several ball-milled digoxin samples (7). As shown previously (7), the relative exothermic peak height varied with the source of the sample and the extent of trituration. This finding indicates that different degrees of conversion to the amorphous form might occur under various conditions. Furthermore, after rapidly heating the triturated sample in the differential scanning calorimetric cell through the exothermic transition, cooling to ambient temperature, and reheating, the exothermic peak disappeared and the final melting temperature decreased (Fig. 3).

Potential effects of storage on thermal, solubility, and dissolution properties of pure untreated digoxin powder apparently have not been reported. As shown in Table II, all three untreated commercial digoxin powders underwent some gradual changes in their thermal properties. An increase in the temperature for the beginning and/or final melting was generally observed. Two samples were studied for over 1 year, and these untreated samples were all in their metastable state during the study period. A very important question remaining to be answered is: "What is the final stable form?"

The results of the equilibrium solubility study conducted in water at 37° on digoxin powder from various sources are summarized in Table III. The solubilities ranged from 28.9 to 68.2 μg/ml among the untreated samples. A range of 24.3–63.6 μg/ml in water at 25° was reported from a study on four untreated commercial samples (7). Recrystallization from chloroform and from ethanol enhanced the solubility of the original L1 powder, and the two recrystallized samples differed in their solubility by 24.2%. Trituration significantly enhanced (43.7%) the solubility of the L2 sample and had a negligible effect on the L1 and Z samples. This finding is in contrast with the previous study (7) in which ball milling increased the solubilities of all four samples studied, with the highest increase being 118%.

The failure of trituration to enhance solubility can be explained by the results from the dynamic solubility study in which a large excess of digoxin powder was used and the concentrations were studied at very frequent intervals before the attainment of final equilibration. For digoxin Z, the triturated sample reached the highest concentration at 5 hr after study and started to decrease and approach the concentration obtained from the untreated sample (Fig. 4). A similar result was obtained with the L2 sample. Therefore, the failure of solubility enhancement by trituration clearly was due to the conversion of the higher energy amorphous form to the more stable, lower energy (crystalline) form during the 24-hr solubility study period. This effect, in turn, resulted in some precipitation of digoxin from the solution.

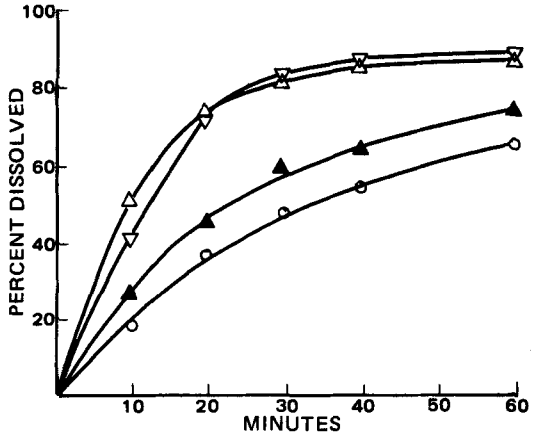

Figure 7—*Effect of temperature and length of storage time on the dissolution rate of digoxin from Tablet A. Key: △, fresh sample; ▽, sample stored at ambient temperature for 4 weeks; ▲, sample stored at 60–65° for 4 weeks; and ○, sample stored at 60–65° for 8 weeks.*

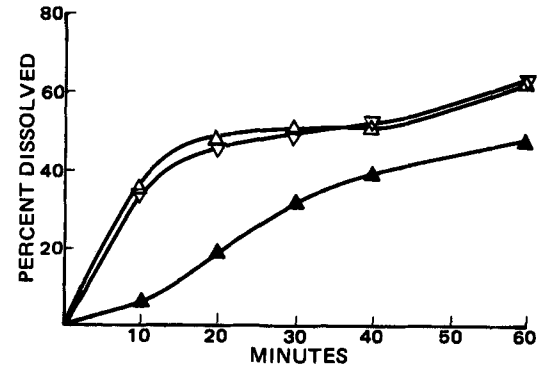

Figure 8—*Effect of storage on the dissolution rate of digoxin from Tablet B. Key: △, fresh sample; ▽, sample stored at ambient temperature for 4 weeks; and ▼, sample stored at 60–65° for 4 weeks.*

For digoxin L2, which had shown the solubility enhancement effect, the decrease in concentration during the dynamic solubility study was obvious also (Fig. 5). The same triturated sample after additional storage of about 2.5 months at ambient temperature showed a clear reduction in the digoxin concentration during the dynamic solubility study (Fig. 5). A further reduction in the dynamic solubility values will probably occur if the sample is studied again at a later date. Therefore, any gain in the apparent solubility and also the dissolution rate by the trituration or milling process appears to be temporary. These results demonstrate that the dynamic solubility method is superior to the equilibrium solubility method in detecting different thermodynamic states.

All solubility studies on the untreated digoxin samples reported in Table III were conducted on the same day. The different solubilities found in the two lots obtained from the same commercial source might be attributed to different aging or storage effects or to a different method of preparation.

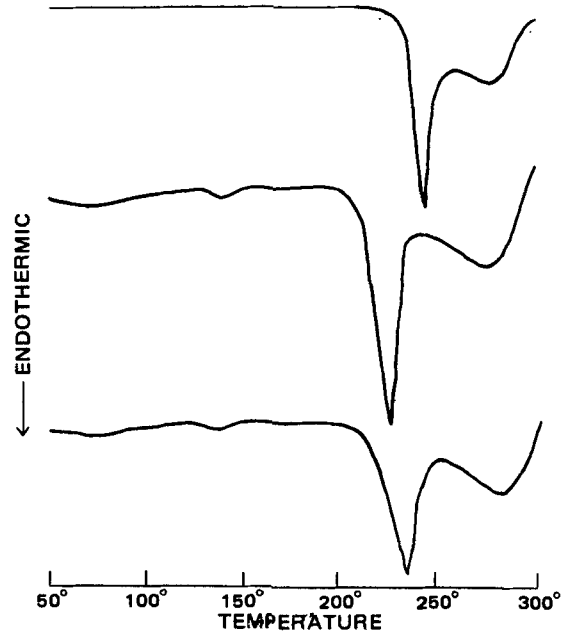

Figure 9—*Differential scanning calorimetric thermograms of three commercial untriturated sources of digitoxin. Key: top, Z; middle, L; and bottom, S.*

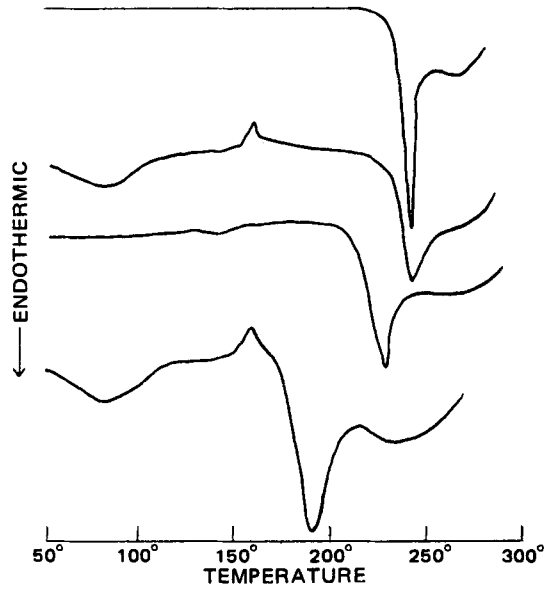

Figure 10—*Differential scanning calorimetric thermograms of digitoxin. Key: top, untriturated Z; upper middle, triturated Z; lower middle, untriturated L; and bottom, triturated L.*

The fact that essentially the same "apparent" equilibrium solubility was found over several days during the study for each untreated digoxin sample indicates a very slow phase transition in water. This transition is different from many drugs exhibiting polymorphism (19, 21).

Table IV summarizes the effects of aging at ambient temperature on the apparent equilibrium solubility of the untreated digoxin L2 sample. The decline in the solubility over the 1-year period was linearly related to time (coefficient of variation = 0.9913). This type of finding has not been reported to date. A slight increase in the melting range of this sample was found over the 1-year period (Table II).

The temperature at which the final melting of the sample takes place could be indicative of crystal intermolecular forces or thermodynamic stability, which both could be related to the dissolution rate or apparent equilibrium solubility. For all six untriturated digoxin samples studied, except L2, the apparent solubility, as expected, decreased almost linearly with the increase of the final melting temperature (Fig. 6). This result shows that the simple and fast differential thermal analysis method might be useful for routine quality control of digoxin powder.

In light of these findings on the effects of aging on the thermal and solubility properties of the untriturated digoxin powder, one could speculate that storage of commercial digoxin solid dosage forms at room temperature might also reduce the dissolution rate and oral absorption of digoxin from the products. A preliminary study on the effect of aging or storage at room temperature (22–26°) and at an elevated temperature on *in vitro* dissolution was conducted on two widely distributed 0.25-mg tablet products obtained from a local pharmacy. Three tablets were dropped gently to the bottom of a 600-ml beaker containing 500 ml of water maintained at 37 ± 0.5°. The stirrer[13], with a predetermined stirring rate of 60 rpm, was quickly lowered to the center of the dissolution medium. The dissolved digoxin concentration was measured by the official compendial method (11) at 10, 20, 30, 40, and 60 min.

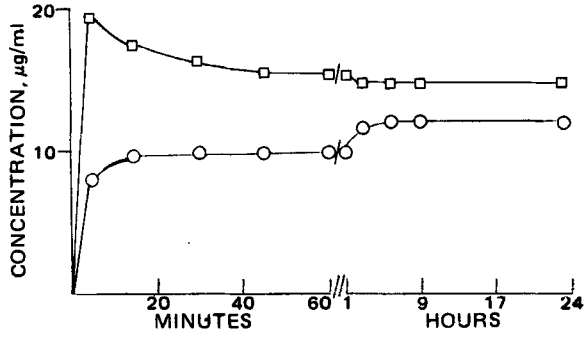

Figure 11—*Dynamic solubility study in water at 37° on the untriturated (bottom) and triturated (top) digitoxin Z powder.*

Table V—Melting Ranges of Digitoxin from Various Sources

Source	Date of Study	Beginning of Melting	End of Melting
L	11/11/74	195°	225°
L	9/20/75	195°	227°
L	10/15/75	201°	228°
L triturated	10/15/75	170°	192°
Z	10/15/75	230°	244°
Z triturated	10/15/75	220°	244°
S	11/11/74	200°	233°

Four duplicate studies were performed on each type of sample. For each tablet product, an initial control and samples stored at room temperature and at 60–65° in an oven for 4–8 (only one product) weeks were studied. All tablets were stored in air-tight glass vials. Very reproducible results were obtained from the duplicate studies. The average data on the percent dissolved as a function of time are shown in Figs. 7 and 8. Differences in dissolution rate from samples stored at room and elevated temperatures were highly statistically significant at all of the times ($p < 0.01$) for both products. Storage at room temperature for 4–8 weeks had a negligible effect on the dissolution rate. The reduction in the dissolution rate in the elevated temperature studies could not be attributed to digoxin chemical decomposition, as shown by the assay of both products. For the product studied for 8 weeks, the aging effect continued throughout this period (Fig. 7).

Based on the results from powder and tablet studies, it is obvious that serious consideration should be given to the possible aging effect of all solid digoxin products when evaluated by either the dissolution or the oral absorption method. A freshly manufactured product that has passed the dissolution and absorption tests might not pass these tests after storage. The potential clinical implications are obvious. These results should be regarded as preliminary since the experimental conditions were not very realistic.

The thermal analysis studies on digitoxin generally paralleled those of digoxin since digitoxin has only one hydroxyl group less than digoxin. Most of the discussion on digoxin can also be applied to digitoxin.

As shown in Fig. 9 and Table V, the melting ranges from the three untreated sources varied less than for digoxin. The widest range was 33°, found in digitoxin S. The final melting points for both digoxin and digitoxin in the present study were all much less than those reported in most of the literature (Table I). Although a very narrow melting range (256–257°) was reported for digitoxin from once source (17), it probably represents the final melting temperatures at which most of the sample was "observed" to melt.

The reason for the rough baseline below the beginning melting temperatures of digitoxins L and S is unknown. This phenomenon was not found in digitoxin Z or in the untreated commercial digoxin samples. The apparent endothermic peaks at ~135–140° found in the digitoxin L and S samples might be due to the eutectic melting caused by impurities (20, 22). This contention is supported by the fact that the official pharmacopeia only requires that digitoxin (powder) contain ≥90.0 and ≤101.0% (mean 95.5%) of pure digitoxin calculated on the dried basis (11), thereby allowing the presence of a significant amount of impurity. However, for official digoxin powder, a concentration range of 97–103% (mean 100%) is required (11).

The differential scanning calorimetric thermograms from two triturated digitoxin samples are shown in Fig. 10. Significant endothermic and exothermic properties prior to melting were observed in both samples, indicating the presence of an amorphous form after trituration. No reduction in the final melting temperature was found in the triturated Z sample.

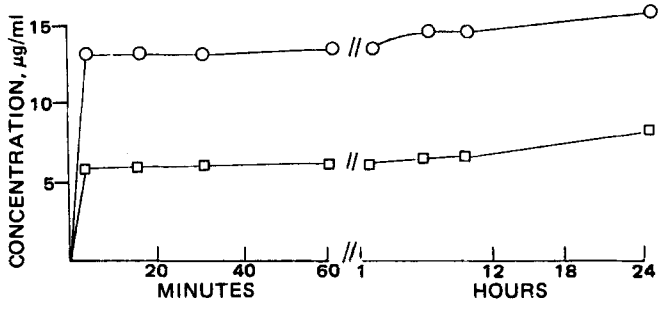

Figure 12—*Dynamic solubility study in water at 37° on the untriturated (bottom) and triturated (top) digitoxin L powder.*

Table VI—Average Solubilities of Digitoxin from Various Sources in Water at 37° after 24 hr of Equilibration

Source	Solubility, μg/ml
Z	15.2
Z triturated	15.8
L	8.0
L triturated	15.8
S	10.0

The results of the digitoxin solubility studies are summarized in Table VI. An almost twofold difference in the apparent equilibrium solubility was found between the Z and S samples. The highest solubility found in the Z sample (15.2 μg/ml) is 3.2 times that (4.8 μg/ml) reported in a previous study (25), indicating marked variations with the sources of material.

Trituration had a significant enhancement effect on the L sample but not on the Z sample. Such a discrepancy could be rationalized by the results from the dynamic solubility studies (Figs. 11 and 12).

Similar aging effects were also observed for the untriturated digitoxin stored at room temperature (for example, the thermal study of digitoxin L, Table IV). For the digitoxin Z sample, the solubility also decreased with time (Table VI and Fig. 11). The dynamic solubility study was conducted several months after the equilibrium solubility study.

The results of this preliminary study on digoxin and digitoxin raise many questions regarding the physicochemical properties and quality control of both cardiac glycosides. A more detailed and systematic investigation on the mechanisms behind the wide range and variation in melting, dissolution, and solubility is needed. The effect of particle size on these properties should be evaluated. All samples used in this study appeared to be very fine. For example, the particle size of digitoxin L1 ranged from 3.1 to 12.4 μm from the microscopic study and that of digitoxin L ranged from 12.4 to 86 μm.

Other questions remaining to be answered include:

1. Could a stable form with a sharp melting point be found for both drugs, and what is the most thermodynamically stable form?
2. How pure is the powder that meets all pharmacopeial requirements?
3. What are the effects of aging on dissolution and bioavailability, and are current regulatory requirements in these aspects adequate?
4. Could more water-soluble hydrates or solvates of both drugs be prepared?
5. Could a quantitative differential scanning calorimetric method be established for powder quality control? In this study, no attempts were made to evaluate thermal energy either quantitatively or qualitatively. This energy possibly might be directly related to dissolution and solubility.

REFERENCES

(1) D. J. Greenblatt, T. W. Smith, and J. Koch-Weser, *Clin. Pharmacokinet.*, 1, 36(1976).

(2) J. L. Colaizzi, *J. Am. Pharm. Assoc.*, **NS17**, 635 (1977).

(3) "The United States Pharmacopeia," 19th rev., Mack Publishing Co., Easton, Pa., 1975.

(4) T. R. D. Shaw and J. E. Carless, *Eur. J. Clin. Pharmacol.*, **7**, 269 (1974).

(5) A. J. Jounela, P. J. Pentikainen, and A. Sothmann, *ibid.*, **8**, 365 (1975).

(6) A. T. Florence, E. G. Salole, and J. B. Stenlake, *J. Pharm. Pharmacol.*, **26**, 479 (1974).

(7) A. T. Florence and E. G. Salole, *ibid.*, **28**, 637 (1976).

(8) E. G. Lovering, M. L. Rowe, and D. B. Black, *Can. J. Pharm. Sci.*, **12**, 77 (1977).

(9) W. L. Chiou and S. Riegelman, *J. Pharm. Sci.*, **59**, 937 (1970).

(10) D. Perrier, M. Mayersohn, and F. I. Marcus., *Clin. Pharmacokinet.*, **2**, 292 (1977).

(11) I. M. Jakovljevic, in "Analytical Profiles of Drug Substances," vol. 3, K. Florey, Ed., Academic, New York, N.Y., 1974, p. 149.

(12) "French Pharmacopeia," 10th rev., National Des Pharmaciens, Paris, France, 1965.

(13) "The United States Pharmacopeia," 15th rev., Mack Publishing Co., Easton, Pa., 1955.

(14) "British Pharmacopoeia," Pharmaceutical Press, London, England, 1958.

(15) "Dictionary of Organic Compounds," 4th ed., Oxford University Press, New York, N.Y., 1965.

(16) "Hackh's Chemical Dictionary," 4th ed., McGraw-Hill, New York, N.Y., 1969.

(17) "Merck Index," 9th ed., Merck and Co., Rahway, N.J., 1968.

(18) J. K. Guillory, S. L. Kwang, and J. L. Lach, *J. Pharm. Sci.*, **58**, 301 (1969).

(19) W. L. Chiou and S. Riegelman, *ibid.*, **60**, 1281 (1971).

(20) W. L. Chiou, *ibid.*, **60**, 1406 (1971).

(21) W. L. Chiou and S. Niazi, *ibid.*, **60**, 1333 (1971).

(22) *Ibid.*, **62**, 498 (1973).

(23) M. C. Castle, *J. Chromatogr.*, **115**, 437 (1975).

(24) R. Jelliffe, *ibid.*, **27**, 172 (1967).

(25) E. I. Stupak and T. R. Bates, *J. Pharm. Sci.*, **62**, 1806 (1973).

ACKNOWLEDGMENTS

Presented in part at the Basic Pharmaceutics Section, APhA Academy of Pharmaceutical Sciences, New Orleans meeting, 1976.

Abstracted from a thesis submitted by L. E. Kyle to the Graduate College, University of Illinois at the Medical Center, in partial fulfillment of the Master of Science degree requirements.

Percutaneous Toxicity of Thioglycolate Mixtures in Rabbits

LEON L. GERSHBEIN

Received October 12, 1978, from the *Biochemical Laboratories, Northwest Institute for Medical Research, Chicago, IL 60634.* Accepted for publication April 9, 1979.

Abstract □ The percutaneous absorption of pH 9.3, 0.60 *N* ammonium thioglycolate was ascertained in rabbits. Applications to a clipped skin site were made daily for 20 days, and the mortality rate was followed over 3 weeks. Surfactants, mainly anionic in nature, were incorporated into the mixtures at 0.5% activity, and the LD_{50} or the daily dosage causing 50% mortality was determined. The lowest toxicity was displayed by mixtures with sodium oleate, sodium stearate, and alkyl aryl sulfonate (VII) (LD_{50}: 4.1–4.4 ml/kg); intermediate activity was found with the sodium salt of alkyl aryl polyether sulfonate (III), a protein condensation product with oleyl chloride (IV), and sodium *N*-methyl-*N*-"coconut oil acid" taurate (VI) (LD_{50}: 3.4–3.7 ml/kg); and the highest activity was found with technical lauryl sulfate (V), the nonionic aromatic polyglycol ether condensate (I), and the cationic alkyldimethylbenzylammonium chloride (II) (LD_{50}: 2.3–2.8 ml/kg). The surfactant-free solution was relatively innocuous at 6.5 ml/kg/day. The LD_{50} fell with increased levels of wetting agents. The pH 9.3 sodium thioglycolate lotion with 4.0% III lowered the LD_{50} compared to the corresponding ammonium thioglycolate mixture. The percutaneous toxicity decreased when treatment was interrupted for several daily periods. Some insight into the penetration of 0.60 *N* thioglycolate through the skin was afforded by administration of the ^{35}S-compound at 1.0 ml/kg. The application of a pH 8.6 ammonium thioglycolate mixture with 4.0% III at 1.0 ml/kg over 20 days increased urinary ^{35}S-excretion; the activity fell during the last half of the tests. Although the tracer experiments showed some correlation with the general qualitative findings for several of the "cold" lotions, discrepancies were noted in relation to the LD_{50} values.

Keyphrases □ Thioglycolates—percutaneous toxicity, effect of surfactants, percutaneous penetration, rabbits □ Cosmetics—thioglycolates, percutaneous toxicity, effect of surfactants, percutaneous penetration, rabbits □ Burns, chemical—thioglycolates, percutaneous toxicity, effect of surfactants, percutaneous penetration, rabbits

The evaluation of the percutaneous irritancy of surfactants and other agents is a constant concern to workers in the cosmetic field. Extrapolation of animal skin patch tests to humans poses many problems. Among the earlier approaches toward surfactant screening (1) was an acute test involving the administration of large amounts of product to the clipped rabbit trunk over which a rubber sleeve was fitted. In subacute tests, lower dosages were applied to the clipped skin daily for 20 or 90 days. An occasional reversal in the results between humans and the animal species was noted. Since then, numerous reports have described patch testing procedures in humans and animals with cosmetic formulations and wetting agents and have presented pertinent statistical designs (2, 3) and physicochemical considerations in the absorption (4, 5) and anatomical changes (6). Middleton (7) noted that surfactants reduced the water binding with the stratum corneum in humid atmospheres. Good correlation between animal and human patch tests was found with highly active irritants and nonirritants, but poor agreement was found with materials of mild and moderate activity (8).

Although thioglycolates, especially the ammonium salt, have been used for many years in the permanent waving of hair, quantitative percutaneous toxicity data are sparse. Draize *et al.* (9) advanced preliminary subacute toxicity findings for rabbits administered a commercial 7% ammonium thioglycolate lotion daily at 0.5–4.0 ml/kg. In a later report (10), a 25% sodium thioglycolate solution containing a tracer amount of ^{35}S-thiol and without a wetting agent was applied once to the clipped skin of several rabbits at specified levels. Urinary specimens were withdrawn by catheter hourly over 4–5 hr, and the ^{35}S-activity was ascertained. Although significant penetration occurred, the amount absorbed per unit time showed little relation to the applied dosage. Other percutaneous tracer studies have been carried out *in vitro* with ^{14}C-labeled steroids (11), *in vitro* and *in vivo* with ^{35}S-dimethyl sulfoxide, (12), and *in vitro* with ^{3}H- and ^{14}C-labeled compounds employing human and hairless mouse skin (13).

In the current investigation, rabbits were subjected to 20-day percutaneous tests with pH 9.3, 0.60 *N* thioglycolate with ammonium hydroxide, among other formulations. Emphasis was on the changes in toxicity elicited by the type and level of wetting agent. The LD_{50}, expressed as the daily thioglycolate dosage, was deduced for these formulations by the usual statistical practice. For several mixtures, ^{35}S-thioglycolate was introduced and the urinary radioactivity was determined for single and repeated daily application to the skin site.

EXPERIMENTAL

Test Materials—Thioglycolic acid of high purity was distilled under vacuum. For the mixtures, ammonium hydroxide was added to the acid solution to yield 0.60 *N* ammonium thioglycolate with a final pH of 9.3, corresponding to 0.50–0.53 *N* free ammonia. The commercial wetting agents[1] were incorporated generally at 0.5% activity. With one product (L-7), the acid was treated with ammonium carbonate solution to a final concentration of 0.80 *M* and the pH was increased from 8.2 to 8.6 with ammonium hydroxide. Another mixture (L-19) was adjusted to pH 9.3 with sodium hydroxide.

For the product containing 0.5% active sodium oleate (L-3), the addition of the soap caused creaming on standing. With sodium stearate, the solution of the soap in hot water was cooled, and on addition to ammonium thioglycolate, some precipitation occurred in the resulting system (L-4). Preliminary tests also were instituted with a lotion (L-20) containing 0.20 *N*-oxidized salt, diammonium dithiodiglycolate of pH 9.30 with ammonium hydroxide (reducing agent concentration 0.050 *N*; detergent II at 4.0% activity).

Rabbits of either sex were purchased from one Illinois farm and housed individually. They were administered a stock pelleted feed and water *ad libitum*. The animals were observed for 2 weeks before use, at which time they weighed 2.3-3.0 kg. With few exceptions, the minimum number employed per dosage was 11.

General Animal Treatment Procedure—A right lateral site comprising about 15% of the body surface was clipped closely with electric clippers 3 days prior to treatment with the mixtures. Animals displaying nicks or cuts were excluded. A volume of mixture based on body weight was delivered to the skin site with a glass syringe with intermittent in-

[1] In the tables and text, the commercial wetting agents or surfactants are: I, Neutronyx 600 (aromatic polyglycol ether condensate; Onyx Oil & Chemical); II, BTC (alkyldimethylbenzylammonium chloride; Onyx Oil & Chemical); III, Triton X-200 (sodium salt of alkyl aryl polyether sulfonate; Rohm & Haas); IV, Maypon 4C (protein condensation product with oleyl chloride; Maywood Chemical Works); V, Duponal WA (technical lauryl sulfate; du Pont); VI, Igepon TC-42 (sodium *N*-methyl-*N*-"coconut oil acid" taurate; Antara Chemicals, Division of General Aniline); and VII, Nacconal NRSF (alkyl aryl sulfonate; National Aniline, Division of Allied Chemical & Dye). The respective thioglycolate lotions are designated L-1 *et seq.*

0022-3549/79/1000-1230$01.00/0
© 1979, American Pharmaceutical Association

Table I—Percutaneous Toxicity Data for Thioglycolate Mixtures [a] (20-day Tests)

Mixture	Ammonium Thioglycolate, *N* (pH)	Wetting Agent, Activity Percent, Type	Dosage Range Explored, mg/ml	Number of Animals	Mean Number of Applications prior to Death	Slope of Probit–Log Dose Curve	LD_{50}, ml/kg/day (mg of Thioglycolic Acid/kg/day) [b]
L-1	0.608 (9.32)	None	6.5	12	12[c]	—	>>6.5 (>>365)
L-2	0.613 (9.32)	I, 0.5, nonionic	2.0–2.75	36	8	4.24	2.61 ± 0.33 (147 ± 18.6)
L-3	0.593 (9.34)	Sodium oleate, 0.5, anionic	3.75–4.5	41	9	15.38	4.08 ± 0.10 (223 ± 5.5)
L-4	0.603 (9.34)	Sodium stearate, 0.5, anionic	3.75–4.5	42	13	26.02	4.24 ± 0.06 (236 ± 3.3)
L-5	0.610 (9.34)	II, 0.5, cationic	2.0–3.0	50	7	13.33	2.34 ± 0.06 (132 ± 3.4)
L-15	0.606 (9.34)	II, 4.0	0.95–1.5	32	8	7.21	1.43 ± 0.11 (79.7 ± 6.1)
L-21	0.600 (9.34)	II, 10.0	0.70–1.0	33	8	7.72	0.906 ± 0.066 (50.0 ± 3.6)
L-6	0.610 (9.34)	III, 0.5, anionic	3.0–4.0	37	11	5.22	3.50 ± 0.25 (197 ± 14.0)
L-7	0.600 (8.60)	III, 1.0	3.0–3.75	58	9	12.54	3.42 ± 0.12 (188 ± 5.5)
L-12	0.609 (9.29)	III, 1.0	3.0	11	12[d]	—	Four dead; 36.4% mortality
L-14	0.597 (9.32)	III, 4.0	1.75–2.5	33	10	4.81	2.11 ± 0.25 (116 ± 3.7)
L-19	0.600 (9.31 with sodium hydroxide)	III, 4.0	2.0–2.5	35	8	7.94	1.69 ± 0.11 (93.3 ± 6.1)
L-8	0.610 (9.35)	IV, 0.5, anionic	2.0–4.0	36	12	6.70	3.69 ± 0.21 (207 ± 11.8)
L-8A	0.600 (9.35)	IV, 0.15	4.0	20	19	—	Four dead; 20.0% mortality
L-9	0.610 (9.35)	V, 0.5, anionic	2.5–3.0	35	11	15.99	2.75 ± 0.07 (155 ± 3.9)
			3.0	11	9	—	Eight dead; 72.7% mortality
			4.0[e]	9	9	—	Three dead; 33.3% mortality
L-11	0.606 (9.32)	VI, 0.5, anionic	3.0–4.0	36	11	10.00	3.44 ± 0.14 (192 ± 8.9)
			3.0	11	13	—	Four dead; 36.4% mortality
L-11A	0.600 (9.35)	VI, 0.125	3.0	12	(20)	—	One dead; 8.3% mortality

[a] The pH of each mixture was brought to 9.3 with ammonium hydroxide except for L-7, which contained ammonium carbonate, and L-19, which contained sodium hydroxide. [b] The LD_{50} applies to the daily dosage causing death in 50% of the animals treated for 20 days and observed for 3 weeks. The dosage, in milligrams, is based on thioglycolic acid. The standard error of the mean appears after each ± sign. [c] The lone death occurred after 12 applications. [d] As with L-12, the mortality was 36.4% with L-6 at 3.0 ml/kg (11 animals). [e] Applied on 4 consecutive days followed by a rest period of 3 days (20 applications; duration of 32 days). Two rabbits died following application 12; the third one died after the fourth application.

unction with the side of the syringe. The procedure was well standardized and performed by one individual. Body weight was determined daily, and the dosage was adjusted accordingly.

The tests were conducted daily for 20 consecutive days, and the animals were observed for 3 weeks after the last application. Tissues from animals succumbing before the conclusion of the tests and from those sacrificed after the observation interval were examined grossly and microscopically. Except as otherwise stated, at least three dosages were investigated per mixture; the protocol allowed testing of up to three formulations at a given time. If necessary, the animals were restrained by hand.

The percutaneous LD_{50} was determined by converting the percentage mortalities to the probits and plotting the probits *versus* log dosages according to literature methods (14,15).

^{35}S-Thioglycolate Studies—^{35}S-Labeled thiol was introduced at a definite level into the test mixture and then inuncted into the skin site as described. Single and repeated daily applications were made; with one series, four skin sites were clipped and the mixture was applied to a different area each day over 4 days. The animals were housed in circular steel cages, with the floors covered with hardware cloth. The total sulfur content of each 24-hr urine sample was ascertained by oxidation to the sulfate with the Folin reagent, precipitation with barium chloride, and counting the tared barium sulfate (16).

RESULTS

Table I presents percutaneous toxicity data for 0.60 *N* thioglycolate brought to pH 9.3 with ammonium hydroxide and containing one nonionic wetting agent (I), the cationic agent (II), and the anionic detergents sodium oleate, sodium stearate, and III–VI, each at 0.5% activity, as well as II at 4.0 and 10.0% and III at 1.0, 2.0, and 4.0%. Agent III (4.0%) also was employed in the study of pH and sodium salt effects in 20-day skin tests. From at least three dosages per formulation, the LD_{50} values were ascertained. These values, together with the slope, *b*, of the probit–log dosage curves, are shown in the table. The effect of lower levels of IV (0.15%) and VI (0.125%) is also demonstrated for single dosages. A typical probit–log dosage curve appears in Fig. 1.

The LD_{50} refers to the daily level of a formulation killing 50% of the animals. The frequency of deaths varied over the 20-day testing period. The average number of applications preceding death is based on all dosages per mixture. The LD_{50} also is expressed in terms of milligrams of acid.

Mixtures Containing Surfactants at 0.5% Activity—Table I can be divided into three groups in order of increasing percutaneous toxicity.

Group A (LD_{50}: 4.1–4.4 ml/kg; L-3 and L-4)—With few exceptions, the respective sites treated daily with L-3 and L-4 were unirritated except for mild peripheral involvement which cleared before the last application. Several rabbits displayed prominent hair regrowth and "dry" skin conditions during the last half of the tests. Body weight losses were significant only in those animals that succumbed. The survivors recovered very rapidly over the 3-week observation period.

As with most of the test formulations, the mixtures were more easily absorbed following the first two or three applications, and some resistance was encountered during the last third of the tests. Death followed depression in two animals administered L-3 (3.75 and 4.0 ml/kg); convulsive activity ensued in two on L-4 (4.0 and 4.5 ml/kg), which also died. The average number of applications for all dosages employed prior to death was nine for L-3 and 13 for L-4.

Preliminary screening of percutaneous toxicity of a similar mixture containing the anionic agent, VII, at 0.5% activity indicated a 4.4-ml/kg LD_{50}, or 240 mg/kg in terms of the acid. Deaths occurred after an average of 12 applications. Extensive convulsive activity was noted in two animals, one receiving 3.0 ml/kg and the other receiving 4.0 ml/kg and succumbing 6 days after Treatment 20.

Group B (LD_{50}: 3.4–3.7 ml/kg; L-6, L-8, and L-11)—The mixtures containing III, IV, and VI produced similar LD_{50} values, and the skin sites

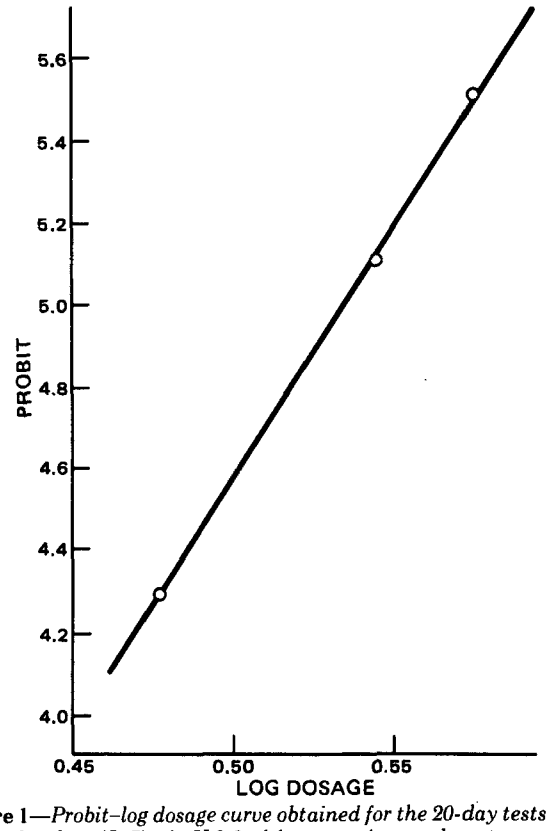

Figure 1—*Probit–log dosage curve obtained for the 20-day tests of 0.60* N *thioglycolate (L-7) of pH 8.6 with ammonium carbonate, ammonia, and 1.0% surfactant III.*

resembled those of Group A or were somewhat more irritated. Convulsive activity was displayed by four animals on L-6 (3.0 and 4.0 ml/kg; dead after four to nine applications), two on L-8 (3.0 ml/kg), and one on L-11 (3.5 ml/kg). One animal on L-8 at 3.0 ml/kg underwent severe convulsions after Treatment 20 but recovered during the 3-week observation period.

Group C (LD_{50}: 2.3–2.8 ml/kg; L-2, L-5, and L-9)—Greater toxicity was observed with the three mixtures containing I (L-2), III (L-5), and V(L-9). The skin sites with L-2 and L-9 were moderate in activity, especially at the peripheries. In marked contrast, L-5 provoked extreme skin alterations; intense inflammation arose after only one or two applications. This inflammation was followed by widespread irritation and necrosis so that inunction into the marginal sites was necessary with several rabbits due to the leathery consistency of the initially treated areas. Such animals screamed and struggled invariably during the first half of the tests, and body weight losses were excessive. A typical skin condition is illustrated in Fig. 2. Central nervous system involvement was apparent with two animals each on L-2 (3.0 and 3.5 ml/kg), L-5 (2.5 ml/kg), and L-9 (2.5 ml/kg).

Percutaneous Toxicity of Mixtures with Wetting Agents—Ammonium thioglycolate (L-1; detergent absent) was essentially without percutaneous effect (20-day tests) (Table I). Only one of 12 animals succumbed. Except for dry skin, involvement was minimal and hair regrowth was prominent during the second half of the tests. With the addition of a wetting agent, greater amounts of mixture were absorbed. Differences were apparent, depending on the detergent. Further studies were implemented to alter the levels of several wetting agents.

The LD_{50} of the thioglycolate formulation markedly decreased with increased II, the values being 2.34 ± 0.06, 1.43 ± 0.11, and 0.906 ± 0.066 ml/kg for mixtures containing 0.5, 4.0, and 10.0%, respectively (Fig. 3). Based on the testing of one group at a single dosage, III, the lotion with 1.0% (L-12), was similar in activity to the 0.5% mixture (L-6). The LD_{50} of L-7 with the wetting agent at 1.0% activity and pH 8.6 with ammonium carbonate at 0.80 *M* was similar to the L-6 LD_{50} (3.42 ± 0.11 ml/kg; for L-6, 3.50 ± 0.25 ml/kg). A much greater change was noted with the 0.60 *N* thioglycolate containing ammonium hydroxide at 0.60 *N* when the activity of III was raised to 4.0% (L-14; LD_{50}: 2.11 ± 0.25 ml/kg). A comparison of L-14 with the corresponding mixture of pH 9.31 with sodium hydroxide (L-19) showed the latter to be more toxic (LD_{50}: 1.69 ± 0.11 ml/kg or 93.3 ± 6.1 mg/kg based on the acid).

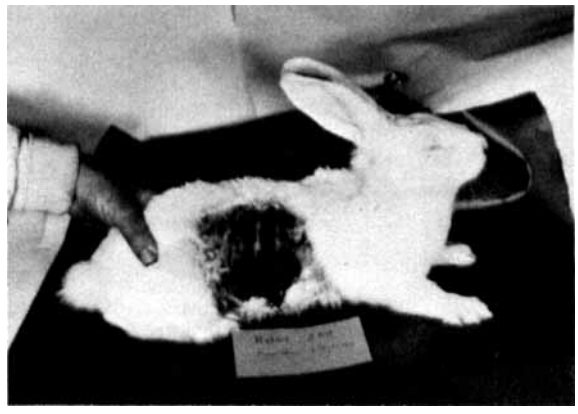

Figure 2—*Skin site of an animal after five daily applications of 0.60* N *ammonium thioglycolate containing 0.5% II (L-5) at 2.0 ml/kg/day.*

The effect of even lower detergent activities was screened with two of the anionic agents incorporated into pH 9.3, 0.60 *N* thioglycolate. With IV at 0.15% (L-8A), the mortality at 4.0 ml/kg was only 20% while the LD_{50} of L-8 was 3.7 ml/kg. The mean numbers of applications preceding death were 12 and 19 for L-8 and L-8A, respectively. Surfactant VI at 0.125% activity was responsible for one death of 12 animals at 3.0 ml/kg (L-11A) as compared to a mortality of 36.4% with L-11 at the same daily dosage.

Compound II at 4.0% activity also was incorporated into a mixture containing the oxidized salt, diammonium dithiodiglycolate at 2.0 *N* and adjusted to pH 9.30. The percutaneous application of L-20 at 3.5 ml/kg daily to five animals led to 100% mortality after an average of three treatments.

Relation of Percutaneous Treatment Frequency to Toxicity—Early runs with several mixtures showed that when 1 or more days, such as weekend periods, were missed in the percutaneous treatment schedule, toxicity decreased. The data are illustrated in Table I for L-9, which was applied for 4 days followed by a 3-day rest period. The se-

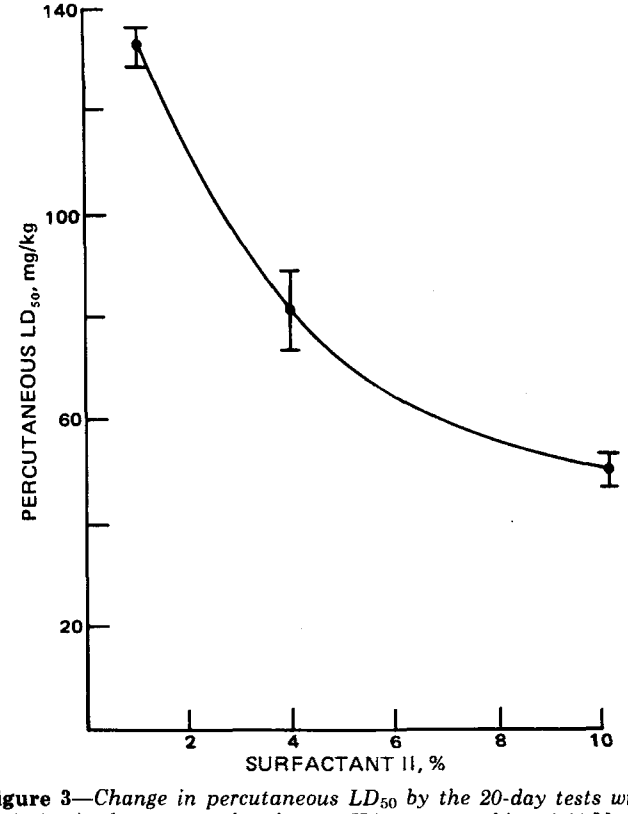

Figure 3—*Change in percutaneous LD_{50} by the 20-day tests with variation in the content of surfactant II incorporated into 0.60* N *ammonium thioglycolate (L-5, L-15, and L-21). The values are in milligrams of thioglycolic acid.*

Table II—Total Urinary ^{35}S Excreted over Periods up to 72 hr following a Single Percutaneous Application of Thioglycolate Mixtures at 1.0 ml/kg [a]

Product	Wetting Agent, Activity Percent	Percentage ^{35}S Excreted ± *SEM* at 24 hr	48 hr	72 hr
L-1	None	16.22 ± 0.55 (19)	4.29 ± 0.38 (14)	2.17 ± 0.30 (8)
L-1 [b]	—	17.23 ± 1.76 (3)	4.53 ± 1.11 (3)	1.73 ± 0.15 (3)
L-5	II, 0.5	20.85 ± 1.18 (8)	5.90 ± 1.12 (4)	1.98 ± 0.18 (4)
L-15	II, 4.0	22.10 ± 0.94 (7)	4.98 ± 0.34 (4)	2.00 ± 0.13 (4)
L-3	Sodium oleate, 0.5	7.72 ± 1.07 (5)	2.80 ± 0.34 (5)	1.07 ± 0.35 (5)
L-7 [c]	III, 1.0	18.12 ± 0.60 (17)	6.66 ± 0.82 (6)	1.90 ± 0.40 (4)
L-7 [b]	—	17.87 ± 1.09 (6)	5.28 ± 1.21 (4)	2.04 ± 0.45 (4)
L-14	III, 4.0	15.60 ± 1.45 (5)	4.40 ± 0.25 (4)	1.83 ± 0.10 (4)
L-19	III, 4.0 (with sodium hydroxide)	16.07 ± 0.71 (7)	4.50 ± 0.46 (5)	1.84 ± 0.22 (5)

[a] Composition of mixtures is given in Table I; pH was 9.3 with ammonium hydroxide except for L-7 (pH 8.6 with ammonium carbonate) and L-19 (pH 9.3 with sodium hydroxide). The decreases in 24-hr mean values for L-1, L-14, L-7, and L-19 compared to those for L-5 and L-15 were statistically significant at $p < 0.01$, except that for L-7 at 1.0 mg/kg *versus* L-5 (Fisher t value, 2.31; $p < 0.05$). The L-3 24-hr mean was markedly lower than any of the other averages, and the difference in L-5 and L-15 values was not significant. Number of animals is given in parentheses. [b] Dosage of 2.0 ml/kg. [c] For one animal, the ^{35}S of the treated skin site at 72 hr was 0.22%.

quence was repeated until 20 applications had been made. Three of the nine animals (33.3%) treated at 4.0 ml/kg succumbed, compared to a 72.7% mortality with a lower dose (3.0 ml/kg) applied daily on 20 consecutive days. The respective skin conditions were much milder in the series administered 4.0 ml/kg.

Anatomical Findings for Tissues from Thioglycolate-Treated Rabbits—Aside from the skin conditions, the gross and microscopic examination of tissues revealed little extreme alteration except for occasional lung congestion and, in a few cases, possible kidney cortical hemorrhage.

^{35}S-Thioglycolate Studies—Thioglycolate mixtures containing up to 0.40 μCi ^{35}S (most commonly 0.10–0.20 μCi) were applied to the skin site as in the "cold" series, and urine was collected over 24 hr following treatment and analyzed in duplicate.

Single Application—Urinary ^{35}S-levels 24, 48, and 72 hr following a single percutaneous thioglycolate mixture application at 1.0 ml/kg are shown in Table II. Based on the mean 24-hr values, the II-containing lotions L-5 and L-15 were responsible for percentages (20.85 ± 1.18 and 22.10 ± 0.94, respectively) that exceeded those for L-1, L-3, L-7, L-14, and L-19 as well as for L-1 or L-7 at 2.0 ml/kg. Mixture L-3 was responsible for the lowest excretion of ^{35}S at 24 hr (7.72 ± 1.07); at 48 and 72 hr, the values were 2.8 and 1.1%, compared to the respective means of 5.0 and 2.0% for the other mixtures. The residual ^{35}S-level was generally far below 1% at the 96th hr.

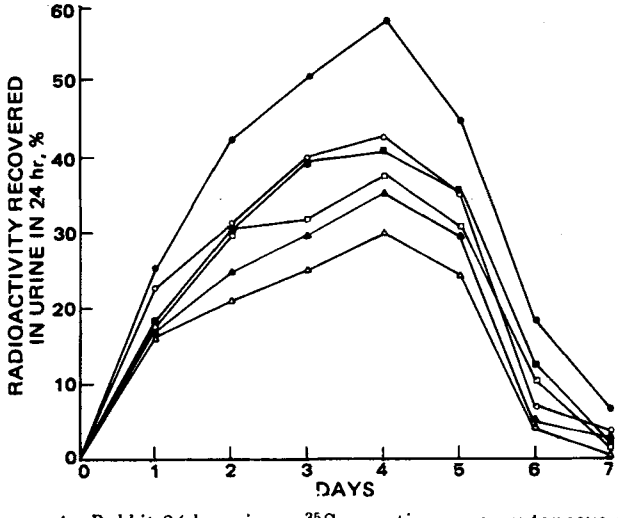

Figure 4—*Rabbit 24-hr urinary ^{35}S-excretion on percutaneous administration of the following mixtures concurrently in one series, each at 1.0 ml/kg/day and containing 0.1–0.2 μCi of labeled thioglycolate per dose for 4 days. Key: △, L-1, without wetting agent; ▲, L-19, with 4.0% III; □, L-7, with 1.0% III; ■, L-14, with 4.0% III; ○, L-5, with 0.5% II; and ●, L-15, with 4.0% II. The products comprised 0.60 N ammonium thioglycolate of pH 9.3 except for the sodium salt of the same pH (L-19) and the ammonium carbonate-containing system (L-7; pH 8.6). The additional points depict the residual ^{35}S-activity.*

Repeated Daily Applications—With more than one application of an agent at 1.0 ml/kg, further ^{35}S-distribution patterns could be discerned. Figure 4 presents graphical data for one series of rabbits inuncted daily for 4 days, the residual activity being included for 3 additional days. Mixture L-15 elicited the highest excretion of ^{35}S; L-5 and L-14 showed progressively lower activity, followed by L-7, L-19, and L-1. Both L-15 and L-1 present extremes in percutaneous efficacy with the remaining products being intermediate. This general pattern was observed with several other rabbits. Variations also were apparent in residual activity and were not dependent strictly on the applied isotope level.

A further illustration of the multiple-treatment schedule and of variations in ^{35}S-activity is presented in Fig. 5, where L-1 and L-7 were employed daily at 1.0 ml/kg for 5 days at levels of 0.203 and 0.043 μCi, respectively. The residual output of tracer was ascertained for an additional 4–5 days. With L-1, the overall urinary specific activity was 1.36×10^5 cpm and accounted for 37.6% of the isotopic dosage. With L-7, the corresponding figures were 3.65×10^4 cpm and 47.7%. The action of L-1 is shown in Fig. 6 for nine consecutive daily applications at 1.0 ml/kg. Treatment was not continued due to the development of anuria. Concurrently, a second animal was administered L-7 at the same dosage over 20 days. With this animal, the ^{35}S increased from the start but fell after the ninth application, reaching a low by the 13th day and then rising to a small plateau that persisted to almost the end of the tests. The residual activity thereafter was rather small.

Although many of the tests were conducted with thioglycolate systems at 1.0 ml/kg, much higher daily volumes of agent with incorporated ^{35}S also were investigated. No clear correlation could be drawn between dosage and absorption based on isotopic excretion. A few rabbits were anuric. With L-7 at 3.0 ml/kg applied daily for 5 days, the urinary ^{35}S-excretion amounted to 14.9, 30.7, 30.1, 28.7, and 27.1%, respectively, for Days 1–5. With two additional animals under the same conditions, the peak values at the 5th day were 18.0 and 16.4%. With a rabbit receiving L-19 at 2.0 ml/kg/day, the initial 24-hr value was 18.5%; the excretion levels fell progressively to 4.7% at the seventh application, and the animal succumbed 1 day later.

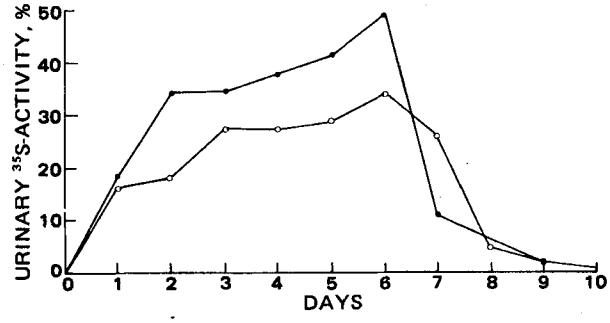

Figure 5—*Urinary ^{35}S-activity following percutaneous application of 0.60 N ammonium thioglycolate mixtures without wetting agent (L-1) (○) and with 1.0% III (L-7) (●) daily for 5 days. The ^{35}S-levels were 0.203 and 0.043 μCi/day with L-1 and L-7, respectively. The residual ^{35}S up to Days 9–10 was 13.8 and 13.7% of the total dosages applied based on urinary specific activities of 5.00×10^4 and 1.05×10^4 cpm for L-1 and L-7, respectively.*

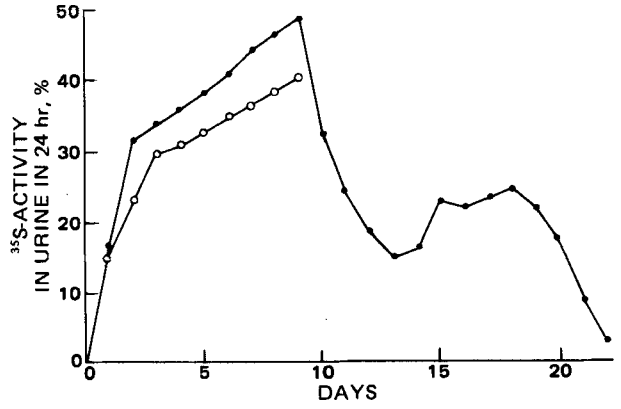

Figure 6—*Urinary ^{35}S-elimination with nine daily applications of the surfactant-free L-1 (○) and with 20 applications of L-7, containing 1.0% III (●). Since the rabbit treated with L-1 became anuric after the ninth treatment, further work was discontinued. The daily ^{35}S-dosage was 0.20 μCi.*

Repeated Application at Multiple Skin Sites—Percutaneous tests were instituted with L-5 and L-15 applied to rabbits with four clipped skin sites, a fresh one being inuncted with 1.0 ml/kg/day for 4 days. Histograms presenting the ^{35}S-excretion in such animals as well as in those with the single clipped skin site are shown in Fig. 7. Aside from little difference in each pair after the first treatment, animals with the multiple skin sites displayed higher isotopic elimination and the skin areas were less irritated. In another experiment employing L-15 (1.0 ml/kg) and multiple skin sites, the values were 18.2, 35.1, 38.3, and 41.3% at Days 1–4. With L-1 under comparable conditions, the urinary ^{35}S-levels were 12.4, 13.8, 17.1 and 15.8%, respectively, and were lower than the values from rabbits with a single clipped skin site.

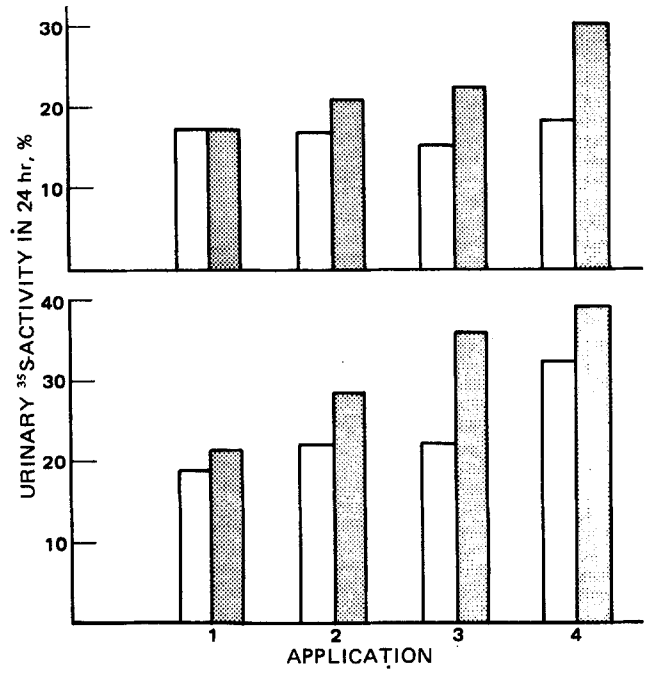

Figure 7—*Urinary ^{35}S-changes accompanying percutaneous 0.60 N ammonium thioglycolate containing II at 0.5% (L-5) (top) and at 4.0% (L-15) (bottom series) daily for 4 consecutive days. The solution was delivered either to the same clipped skin site (open areas) or to a different one of four sites each day (shaded areas). The daily ^{35}S-dosage was 0.20 μCi.*

DISCUSSION

The wetting agents were anionic except for the nonionic I and the cationic II. Wide differences in toxicity could be observed between the anionic agents compared on the basis of 0.5% activity by the 20-day tests. Thus, sodium oleate and stearate and, possibly, VII were responsible for the lowest toxicity of 0.60 *N* ammonium thioglycolate; III, IV, and VI were intermediate; V shared the highest toxicity with the nonionic and cationic surfactants. The solution without wetting agent, L-1, produced minimal skin alterations, and the LD_{50} was far in excess of 6.5 ml/kg.

The toxicity of thioglycolate with increasing surfactant percentage also was studied with II and III. The former was responsible for more extreme skin conditions, and the increase in percutaneous toxicity plateaued at ~10.0% (Fig. 3). Surfactant III caused little change in percutaneous activity at 0.5 and 1.0%. With 4.0%, the toxicity mounted but was below that elicited by the lotion with 4.0% II. The percutaneous toxicity of the pH 9.3 sodium salt solution exceeded that of the ammonium salt with 4.0% III as the wetting agent in each. As expected, a decrease in surfactant content, as illustrated by 0.15% IV (L-8A; Table I), led to a lowered percutaneous toxicity. Hair regrowth in the respective skin sites with several lotions was indicative of lower product irritancy; the hair growth cycle was minimally affected.

The derivation of percutaneous LD_{50} values in the present experiments is novel and in contrast to the usual parenteral toxicity. Repeated applications as in the 20-day testing schedule are mandatory for such data. A 2.0-ml/kg dose is the consumer level in hair waving as referred to the volume of product used and the consumer body weight. In addition, this method can shed light on percutaneous toxicity in regard to operators who are in almost daily contact with such lotions. In this report, the LD_{50} deduced for the various mixtures refers to mortality over 20 days of treatment followed by an observation interval of 3 weeks. Since the deaths resulted after an average of seven to 11 applications, an overall lethal dosage might be approximated. However, as noted from the ^{35}S-experiments, the percutaneous absorption was greatly reduced during the second half of the tests, at which time the respective skin sites underwent clearing and became more resistant to further inunctions.

An LD_{50} of 4.0 ml/kg would imply an overall dosage of 80 ml/kg or in excess of 4.4 g/kg based on thioglycolic acid for the survivors. Considering the large amount of mixture that is not absorbed due to poor wetting qualities coupled with losses as a result of evaporation, oxidation, and mechanical reasons, most of this dosage is not realized in the percutaneous testing. The large losses notwithstanding, many variables were controlled, so the resulting LD_{50} values do reflect the outstanding differences among the surfactants selected.

In another thioglycolate study, investigators (9) applied a 7% commercial ammonium thioglycolate lotion of undisclosed brand and wetting agent to rabbits for 90 days. The mortality at daily levels of 2.0 and 4.0 ml/kg was 11.8 and 61.1%, respectively. Such values might be in the range deduced for mixtures of similar thiol content in the current experiments and with VII or the sodium soaps at 0.5% activity.

^{35}S-Thioglycolate was incorporated into the test fluids to follow percutaneous absorption, emphasis being directed to levels of 1.0 ml/kg applied once or on repeated days. At single dosage, the ^{35}S-elimination by the II-containing mixtures L-5 and L-15 was in the same range but was significantly higher than the fluids containing III and sodium oleate as well as L-1 (Table II). In fact, the surfactant-free solution was as effective as the mixtures containing III and even exceeded the effectiveness of L-3 with sodium oleate in activity by the single-dosage criterion. At 2.0 ml/kg, L-1 and L-7 caused ^{35}S-excretion similar to that of the lower dosage, about one-fifth of the applied activity being eliminated over 72 hr.

In a previous study (10), single applications of a surfactant-free sodium thioglycolate solution to rabbits produced an average 29% excretion for five animals at 330 mg/kg as determined hourly for 4–5 hr after treatment and 7, 11, and 24% for three animals at 660 mg/kg. The last group succumbed in 24 hr. The extent of thiol absorbed was not closely related to the total applied. Compared to the current findings, the ^{35}S-activity with 330 mg/kg was somewhat higher than the 24-hr value for the sodium salt system containing 4.0% III (L-19), and the amount of salt inuncted was less (68 mg/kg).

The single-application series employing ^{35}S-labels presents discrepancies as already discussed in relation to the data of Table I. Inconsistencies persisted when repeated application of ^{35}S-thiol mixtures was instituted for 4 or 5 days, a period when skin irritation was usually prominent. As expected, tracer excretion was highest with L-15 and lowest with L-1, with the remaining products being intermediate (Fig. 4). The relative position of the latter may bear some qualitative relationship to the respective LD_{50} values, but the number of animals was too small for statistical testing. The sodium thioglycolate lotion (L-19) appeared to elicit a lower tracer excretion than the ammonium salt (L-14), both based on 4.0% III, but L-19 displayed a greater percutaneous toxicity (Table I). In contrast to the single-treatment series, ^{35}S-cumulation occurred, and it was difficult to correct for the prior residual activity with

each ensuing treatment. With either L-1 or L-7, each applied at 1.0 ml/kg daily for 5 days, the activity determined over 4–5 days after the final treatment was ~14%; the overall ^{35}S-excretion was 38 and 48% for L-1 and L-7, respectively (Fig. 5). A correlation might exist with the LD_{50} findings, a difference of 10% in isotopic elimination possibly being significant. At any rate, these discrepancies as well as those cited by others (10) bear out that percutaneous toxicological studies are fraught with difficulties.

^{35}S-Activity in one rabbit receiving L-7 at 1.0 ml/kg/day for 20 days reached a maximum at the 9th day and then fell rapidly. Based on cumulative activity, the peak may have been reached before the ninth treatment in this instance as well as with L-1 (Fig. 6). The question might be raised as to whether such tests should be continued daily for ≥20 days. Although the percutaneous penetration was apparently less during the last half of the tests, the absorption rallied over the final five to six inunctions, and a new peak or plateau was established. In addition, the seven to 11 applications preceding death were an average. Several animals malingered and succumbed toward the end of the treatment period and even into the 1st week of the observation interval.

To circumvent the extreme inflammation and necrosis at the skin sites with such products as L-5 and L-15, multiple areas were treated. A new site was involved for 4 days at 1.0 ml/kg/day. Greater absorption based on ^{35}S-excretion was noted for the second treatment compared to the single-site series. The present approach is well suited for extreme skin irritants and can yield further quantitative data in addition to those involving a single area that is repeatedly insulted. With L-1, the multiple-site method led to lower tracer excretion. Presumably, only after several applications at a given site with its ensuing irritancy, as small as it might be, was the percutaneous penetration heightened. This behavior also was apparent with L-3, a mixture that exceeded L-1 in toxicity (Table I) but that ranged lower than the latter in ^{35}S-activity elimination after a single application.

The most prominent form of sulfur excreted by the rabbit on tracer administration is neutral sulfur, followed by inorganic sulfur and ethereal sulfate (10, 16). Since oxidation is often cited as a source of thioglycolate activity loss, the disulfide, a prominent metabolite, also was screened. A diammonium dithiodiglycolate at 2.0 *N* of pH 9.3 with 4.0% II caused death after a few daily applications at 3.5 ml/kg or at 1150 mg/kg based on the acid. The thiol content as determined by titration was low (0.050 *N*). These exploratory runs justify further study of the disulfide as such and with ^{35}S-labeling.

The relative classification of the mixtures according to LD_{50} values and as spot-checked by ^{35}S-thioglycolate may have application to the human experience, but care must be taken in extrapolating such data. Along with the subacute methods, additional tests for cosmeceuticals should include acute toxicity coupled with primary irritancy evaluation employing mucous membranes and instillation of agents into the animal eye (1, 17). Thioglycolate is a potent chemical agent, which is readily metabolized on parenteral and percutaneous administration. It affects the nervous system and blood sugar (9, 18), *in vitro* tissue metabolism (19, 20), and sulfhydryl-dependent enzyme systems (21, 22).

Another approach may be useful in studying percutaneous thioglycolate absorption. Several vehicles might be suggested that are rapidly absorbed through the skin such as dimethyl sulfoxide, which also facilitates the penetration of other agents (23). Stoughton (12) demonstrated the rapid percutaneous absorption of the ^{35}S-agent *in vivo* and *in vitro*. However, by the *in vivo* approach, much sulfoxide is metabolized in other areas of the body; little, if any, is excreted in the urine. In percutaneous experiments with thioglycolate–dimethyl sulfoxide mixtures employing such species as the rabbit, the overall urinary sulfur output might reflect primarily the activity or metabolism of the thioglycolate.

REFERENCES

(1) J. H. Draize, G. Woodard, and H. O. Calvery, *J. Pharmacol. Exp. Ther.*, **82,** 377 (1944).

(2) A. M. Kligman and W. M. Wooding, *J. Invest. Dermatol.*, **49,** 78 (1967).

(3) W. M. Wooding and D. L. Opdyke, *J. Soc. Cosmet. Chem.*, **18,** 809 (1967).

(4) E. J. Lien and G. L. Tong, *ibid.*, **24,** 371 (1973).

(5) H. Schaeffer, *ibid.*, **25,** 93 (1974).

(6) R. K. Winkelmann, *Br. J. Dermatol.*, **81,** 11 (1969).

(7) J. D. Middleton, *J. Soc. Cosmet. Chem.*, **20,** 399 (1969).

(8) L. Phillips, M. Steinberg, H. I. Maibach, and W. A. Akers, *Toxicol. Appl. Pharmacol.*, **21,** 369 (1972).

(9) J. H. Draize, E. Alvarez, and M. F. Whitesell, *Proc. Sci. Sect. Toilet Goods Assoc.*, **7,** 29 (1947).

(10) M. V. Freeman, J. H. Draize, and P. K. Smith, *J. Pharmacol. Exp. Ther.*, **118,** 304 (1956).

(11) F. D. Malkinson, *J. Invest. Dermatol.*, **31,** 19 (1958).

(12) R. B. Stoughton, *Toxicol. Appl. Pharmacol.*, **7,** 1 (1965).

(13) R. B. Stoughton, *J. Invest. Dermatol.*, **63,** 305 (1974).

(14) J. T. Lichtfield, Jr., and J. W. Fertig, *Bull. Johns Hopkins Hosp.*, **69,** 276 (1941).

(15) J. T. Lichtfield, Jr., and F. Wilcoxon, *J. Pharmacol. Exp. Ther.*, **96,** 99 (1949).

(16) S. Bakshy and L. L. Gershbein, *Arch. Int. Pharmacodyn. Ther.*, **196,** 148 (1972).

(17) L. L. Gershbein and J. E. McDonald, *Food Cosmet. Toxicol.*, **14,** 131 (1977).

(18) M. V. Freeman, J. H. Draize, and P. K. Smith, *J. Pharmacol. Exp. Ther.*, **118,** 296 (1956).

(19) K. L. Spencer and L. L. Gershbein, *J. Cell. Comp. Physiol.*, **63,** 203 (1964).

(20) K. L. Spencer, L. L. Gershbein, and B. K. Krotoszynski, *Trans. Ill. St. Acad. Sci.*, **57,** 129 (1964).

(21) S. Bakshy and L. L. Gershbein, *Biochem. Biophys. Res. Commun.*, **42,** 765 (1971).

(22) S. Bakshy and L. L. Gershbein, *Arch. Int. Pharmacodyn. Ther.*, **201,** 77 (1973).

(23) R. B. Stoughton and W. Fritsch, *Arch. Dermatol. Syphilol.*, **90,** 512 (1964).

ACKNOWLEDGMENTS

The author is indebted to Dr. S. Bakshy for his aid in the ^{35}S-urinary analyses.

Synthesis and Pharmacology of Potential β-Blockers

JOHN P. O'DONNELL *x, SHIRISH PAREKH *, ROBERT J. BORGMAN ‡, and RICHARD J. GORCZYNSKI ‡

Received February 22, 1979, from the *School of Pharmacy, West Virginia University Medical Center, Morgantown, WV 26506, and the ‡Departments of Medicinal Chemistry and Pharmacology, Arnar-Stone Laboratories, McGaw Park, IL. Accepted for publication April 10, 1979.

Abstract □ Several 1-(4-substituted phenoxy)-2-hydroxy-3-isopropylaminopropanes and 1-(4-substituted phenoxy)-2-hydroxy-3-[3,4-dimethoxyphenethyl]aminopropanes were synthesized for possible β-adrenergic receptor blockade. The compounds were synthesized by reaction of the 4-substituted phenol with epichlorohydrin and subsequent opening of the resulting epoxide with either *N*-isopropylamine or *N*-3,4-dimethoxyphenethylamine. Preliminary biological testing indicated a decrease in the β-blocking potency and the duration of action.

Keyphrases □ β-Adrenergic blockers—synthesis and pharmacology, substituted aminopropanes, structure–activity relationships □ Aminopropanes, substituted—synthesis and pharmacology as potential β-adrenergic blockers, structure–activity relationships □ Structure–activity relationships—substituted aminopropanes as potential β-adrenergic blockers, synthesis and pharmacology

Several β-adrenergic receptor blocking drugs currently under clinical investigation differ pharmacologically on the basis of potency, selectivity, intrinsic sympathomimetic activity, membrane-stabilizing activity, and duration of action. Previous reports (1–3) indicated that polar substitution on the ring of aryloxypropanolamines increases intrinsic molecular activity while increased molecule lipophilicity enhances membrane-stabilizing activity. Furthermore, *para* substitution of phenoxypropanolamines enhances cardioselectivity (1, 2, 4, 5). Clearly defined structural requirements for modification of the duration of β-blocking activity have not been identified. The present study examined the effects of polar substitution in the *para* position of phenoxypropanolamines on several characteristics of β-receptor blockade.

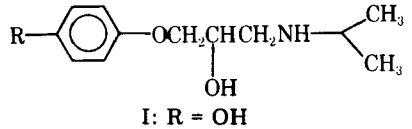

I: R = OH
II: R = CH_2OH
III: R = CO_2CH_3
IV: R = CO_2H

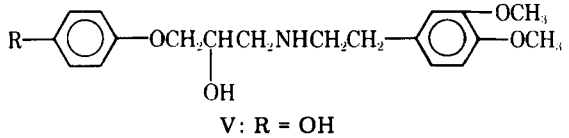

V: R = OH
VI: R = CH_2OH
VII: R = CO_2CH_3
VIII: R = CO_2H

Two series of compounds were synthesized and evaluated. The first series consisted of 1-(4-substituted phenoxy)-2-hydroxy-3-isopropylaminopropanes having structural properties similar to previously synthesized β-blockers. In the second series, the structural importance of the *N*-isopropyl group for β_1 *versus* β_2 adrenergic receptor blocking activity was explored by replacing it with a *N*-3,4-dimethoxyphenethyl group. As in the first series, polar substitutents were incorporated into the phenoxy ring system.

RESULTS AND DISCUSSION

Chemistry—Compounds I–IV were synthesized using a modification of established literature procedures (6). The synthetic route to VII utilized the approach developed by Hoefle *et al.* (7), wherein the methyl 4-hydroxybenzoate (IX) served as the starting material. Thus, condensation of IX with epichlorohydrin gave the requisite epoxide X (Scheme I) which, due to its instability, was rapidly opened with *N*-3,4-dimethoxyphenethylamine to give VII. Reduction of the ester VII provided the benzyl alcohol VI, while hydrolysis of VII with 2.0 *N* NaOH gave the acid VIII. 4-(Benzyloxy)phenol was converted to XIII (Scheme II) using the standard two-step procedure. Subsequent hydrogenolysis of the benzyl protecting group provided V.

Biology—Chronotropic ID_{25} and ID_{50} values for each compound and for propranolol are contained in Table I. All compounds except IV and VII appeared to have blocking activity but were considerably less potent than propranolol in blocking the heart rate effects of isoproterenol. A comparison of the relative potencies revealed that the compounds were five to 52 times less potent than propranolol on the heart. The methylene hydroxy derivatives of both series of compounds had potencies that approached those of propranolol. Propranolol produced 51, 61, and 59% inhibition of the diastolic pressure response to isoproterenol infusions at 0.008, 0.024, and 0.072 mg/kg, respectively. All compounds except I were, in general, much less effective than propranolol in blocking diastolic pressure, producing <26% inhibition at any dose. Compound I produced 68.8% inhibition at 10.0 mg/kg.

Table II summarizes the data on the duration of chronotropic block induced by the active compounds and propranolol. Duration of action has been normalized to equivalent pharmacological effect as described

Table I—Chronotropic Blocking Potency [a]

Compound	*n*	ID_{25} moles/kg × 10^{-8}	ID_{25} Relative Potency	ID_{50} moles/kg × 10^{-7}	ID_{50} Relative Potency
Propranol	10	3.3 ± 0.03 [b]	1	1.1 ± 0.2 [b]	1
I	3	28.0 ± 7.6	0.12	— [c]	— [c]
II	3	172.0 ± 54.9	0.019	166.0 ± 90.2	0.006
III	5	59.3 ± 9.9	0.056	15.7 ± 2.9	0.067
IV	3		Not active		
V	4	36.6 ± 6.6	0.093	8.6 ± 1.3	0.122
VI	3	15.1 ± 4.5	0.22	4.8 ± 1.8	0.22
VII	3	51.7 ± 11.8	0.064	11.1 ± 3.3	0.095
VIII	3		Not active		

[a] ID_{25} and ID_{50} refer to 25 and 50% inhibition of the chronotropic response to isoproterenol hydrochloride infusion at 1.0 μg/kg/min. [b] Values are means ± *SEM*. [c] Fifty-percent inhibition was not attained with this agent.

0022-3549/79/1000-1236$01.00/0
© 1979, American Pharmaceutical Association

Table II—Duration of Chronotropic Block (Minutes) [a]

Inhibition	Propranolol	I	II	III	V	VI	VII
ID_{25} [b]	14.8 ± 2.4	14.4 ± 1.2	6.0 ± 1.2	4.4 ± 1.4	3.5 ± 0.4	3.5 ± 1.1	4.5 ± 0.5
ID_{50} [b]	20.4 ± 2.4	—[c]	31.1 ± 10.2	9.5 ± 2.8	7.8 ± 0.7	6.7 ± 2.4	7.7 ± 1.4

[a] Duration was measured as the time associated with 50% recovery of the heart rate after dosing with the blocking agent. [b] Duration was normalized to doses producing 25 and 50% inhibition of the heart rate response to isoproterenol infusion. [c] Fifty-percent inhibition was not attained with this agent.

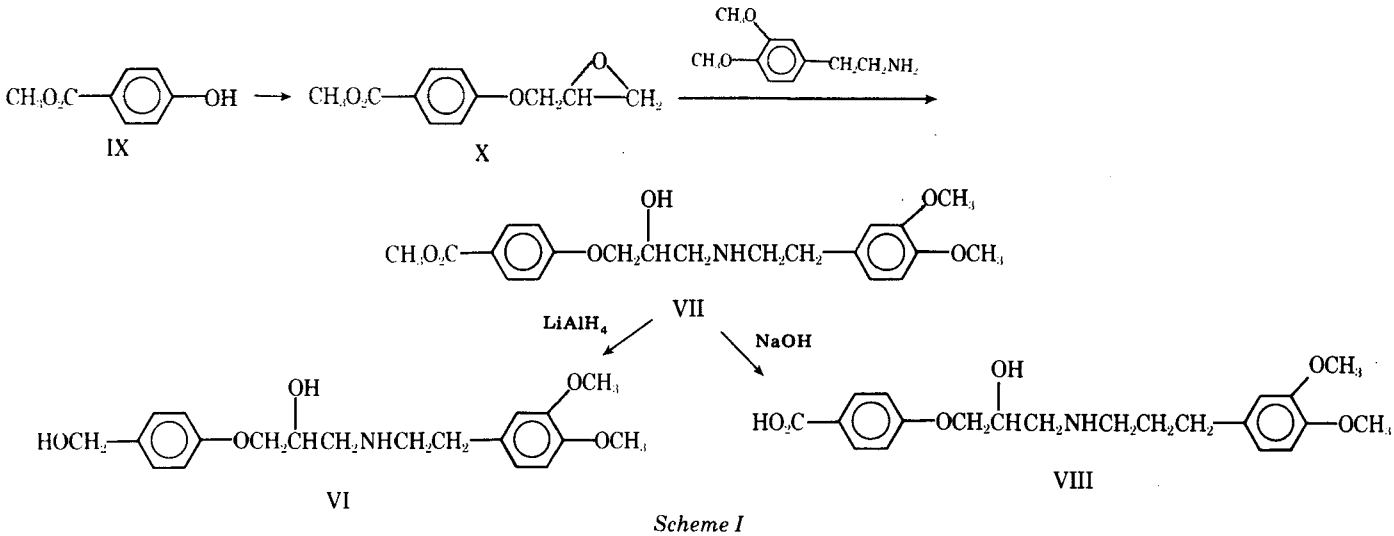

Scheme I

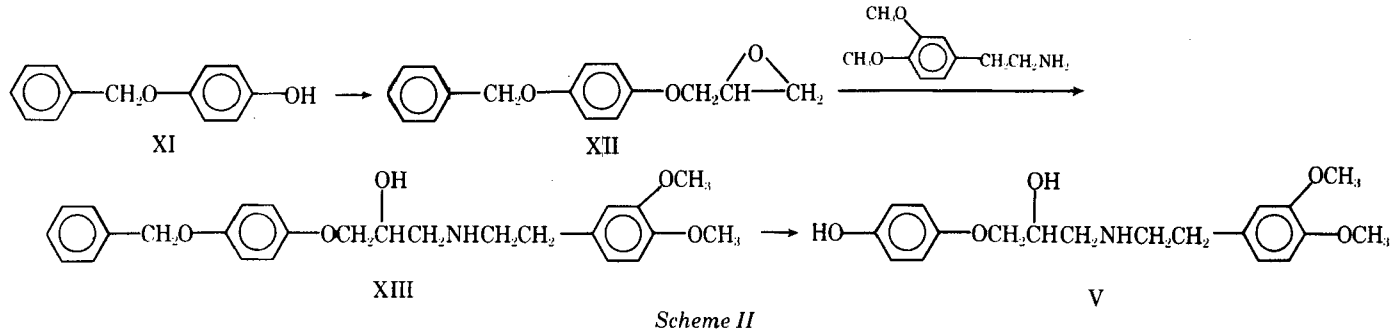

Scheme II

under *Experimental* to facilitate comparison. With two exceptions, the duration of block was considerably shorter with the polar-substituted compounds than with propranolol. Compound I, which has a hydroxy group in the *para* position of the ring, had a duration of action at the I_{25} level that approached that of propranolol. Compound II was peculiar. At low doses (I_{25}), it produced a significantly shorter blocking effect than propranolol; but at higher doses (I_{50}), its duration of action was equivalent to that of propranolol.

The isoproterenol infusion model used for compound evaluation is not appropriate for quantitative analysis of cardioselective properties. Nevertheless, the fact that all compounds except I caused considerably less diastolic pressure inhibition than did propranolol suggests that these agents are somewhat cardioselective. Indeed, *para* substitution (1, 2, 4, 5), especially with hydrogen bond acceptor groups (1), is thought to be favorable to the development of cardioselective properties. *N*-Substitution with the 3,4-dimethoxyphenethyl system also has been shown to impact on cardioselectivity (8); as shown by Hoefle *et al.* (7), combination of this end group with *para* substitution in the ring results in remarkable cardioselectivity.

The present findings indicate that *para* substitution of phenoxypropanolamines with polar substituents appears, in general, to produce β-receptor antagonists with a shorter duration of action than that of propranolol. The potency of these compounds, however, is considerably less than that of propranolol. This latter finding supports previous reports (1, 2), which indicated that *para* substitution almost universally lowers potency relative to both propranolol and to *ortho*-substituted derivatives. However, the potency was somewhat improved when *para* substitution was coupled with the *N*-3,4-dimethoxyphenethyl substituent. This effect was obvious with *p*-hydroxy and *p*-methylene hydroxy substitution but was less clear with the methyl esters. A similar phenomenon was reported by Hoefle *et al.* (7) for nonring-substituted and *para*-substituted amide compounds.

EXPERIMENTAL[1]

Methyl 4-(2,3-Epoxypropoxy)benzoate (X)—To 75 ml of methanol containing 2.4 g (0.06 mole) of NaOH were added 7.6 g (0.05 mole) of methyl 4-hydroxybenzoate and 30 ml (0.4 mole) of epichlorohydrin. The reaction mixture was stirred at room temperature for 20 hr and then was concentrated to a residual oil partitioned between 50 ml of chloroform and 25 ml of 1 *N* NaOH. The organic phase was separated, washed twice with 25-ml portions of water and once with 25 ml of saturated sodium chloride, and dried over magnesium sulfate. The chloroform was evaporated, and the product was obtained as a colorless oil in 99% yield; NMR (CDCl): δ 7.2 (m, 4H, Ar*H*) and 3.45 (s, 3H, $-OCH_3$).

1-(4-Methoxycarbonylphenoxy)-2-hydroxy -3- (3,4-dimethoxyphenethylamino)propane (VII)—A reaction mixture containing 6.24 (0.03 mole) of X and 5.5 g (0.03 mole) of 3,4-dimethoxyphenethylamine in 50 ml of methanol was refluxed for 2.0 hr. After the volatiles were removed, a viscous oil resulted and then solidified upon standing to yield 81% of theory. Recrystallization from ethyl acetate afforded an analytical sample, mp 117–118°.

[1] Melting points were determined in open glass capillaries using a Thomas-Hoover Uni-Melt apparatus and are uncorrected. IR absorption spectra were recorded on a Beckman model 18A spectrophotometer on either liquid films or potassium bromide pellets. NMR spectra were recorded on a Varian T-60 spectrometer with tetramethylsilane as the internal standard. Elemental analyses were performed by Galbraith Laboratories, Knoxville, Tenn.

The hydrochloride salt was obtained by acidifying an ethanolic solution of the base with anhydrous hydrochloric acid (93% yield). Recrystallization from 2-propanol afforded an analytical sample, mp 166–167°; IR (KBr): 1695 (C=O) cm^{-1}; NMR ($CDCl_3$): δ 6.7–8.0 (m, 7H, Ar*H*), 3.80 (s, 9H, $-OCH_3$), and 2.9–4.0 (m, 9H, $-CH_2$ and –CH).

Anal.—Calc. for $C_{21}H_{28}ClNO_6$: C, 59.19; H, 6.63; N, 3.29. Found: C, 59.10; H, 6.58; N, 3.24.

1-(4-Hydroxymethylphenoxy)-2-hydroxy -3- (3,4-dimethoxyphenethylamino)propane Hydrochloride (VI)—To a suspension of 5.3 g (0.015 mole) of VII in 150 ml of dry tetrahydrofuran was added 4.0 g of lithium tetrahydroaluminate in small portions. The resulting reaction mixture was refluxed overnight. After cooling, the excess lithium tetrahydroaluminate was decomposed by careful addition of 5 ml of 2 *N* NaOH. The white precipitate which formed was removed by filtration and discarded. The filtrate was dried over anhydrous magnesium sulfate and acidified with anhydrous hydrochloride. The volatiles were removed, and the residue was recrystallized twice from 2-propanol, yielding 4.0 g (66% yield) of product, mp 110° dec.; NMR (CF_3COOH): δ 6.9 (m, 7H, Ar*H*) and 3.9 (s, 6H, $-OCH_3$).

Anal.—Calc. for $C_{20}H_{28}ClNO_5$: C, 60.37; H, 7.10; N, 3.52. Found: C, 60.44; H, 7.14; N, 3.54.

1-(4-Hydroxycarbonylphenoxy)-2-hydroxy -3- (3,4-dimethoxyphenethylamino)propane (VIII)—A suspension of VII (1.95 g, 0.005 mole) in 15 ml of 2 *N* NaOH was refluxed for 1.5 hr. After the reaction mixture was cooled and acidified with concentrated hydrochloric acid (2 ml), the desired product precipitated as the hydrochloride salt. Recrystallization of the salt from methanol afforded an analytical sample (78% yield), mp 224–225°; IR (KBr): 3370 (–OH) and 1670 (CO_2H) cm^{-1}; NMR (CF_3COOH): δ 6.9–8.0 (m, 7H, Ar*H*), 3.8 (s, 6H, $-OCH_3$), 4.3, and 3.0–3.5 (m, 9H, $-CH_2$).

Anal.—Calc. for $C_{20}H_{26}ClNO_6$: C, 58.36; H, 6.36; N, 3.51. Found: C, 58.46; H, 6.40; N, 3.40.

3-(4-Benzyloxy)phenoxy-1,2-epoxypropane (XII)—A methanolic solution (250 ml) containing *p*-(benzyloxy)phenol (20.0 g, 0.1 mole), sodium hydroxide (4.0 g, 0.1 mole), and epichlorohydrin (0.5 mole) was stirred at room temperature for 18 hr. The reaction mixture was filtered, and the filtrate was concentrated under vacuum. The resulting residue was partitioned between 100 ml of chloroform and 40 ml of 0.1 *N* NaOH. The organic phase was dried over magnesium sulfate. Solvent removal under a vacuum afforded the product as a semisolid, which was recrystallized from methanol (21.3-g yield, 82%), mp 69–71°; NMR ($CDCl_3$): δ 6.9–7.4 (m, 9H, Ar*H*), 5.0 (s, 2H, ArCH_2), and 2.8–4.2 (m, 5H, $-CH_2$ and –CH).

1-(4-Benzyloxy)phenoxy-2-hydroxy -3- (3,4-dimethoxyphenethylamino)propane (XIII)—A solution of XII (6.45 g, 0.025 mole) and 3,4-dimethoxyphenethylamine (4.65 g, 0.025 mole) in 40 ml of methanol was refluxed for 2.0 hr, followed by evaporation of the solvent under reduced pressure. The residue was made basic with 3 *N* NaOH, and the basic solution was extracted with two 50-ml portions of chloroform. The organic phase was dried over magnesium sulfate, and the volatiles were removed under reduced pressure. The residue was recrystallized from ethyl acetate (8.2-g yield, 73%), mp 103–106°; NMR ($CDCl_3$): δ 6.8–7.4 (m, 9H, Ar*H*), 5.0 (s, 2H, ArCH_2), 3.8 (s, 6H, $-OCH_3$), and 2.7 (m, 9H, $-CH_2$ and –CH).

Anal.—Calc. for $C_{26}H_{32}NO_5$: C, 71.23; H, 7.30; N, 3.19. Found: C, 71.41; H, 7.23; N, 3.01.

1-(4-Hydroxyphenoxy)-2-hydroxy -3- (3,4-dimethoxyphenethylamino)propane Hydrochloride (V)—A methanolic solution (250 ml) containing 9.5 g (0.022 mole) of XIII was hydrogenated over 200 mg of 10% palladium-on-charcoal on a Parr hydrogenator until hydrogen uptake ceased. The catalyst was removed by filtration, and the filtrate was evaporated to give an oily residue. An ethanolic solution of the residue was acidified with anhydrous hydrochloric acid. The resulting white precipitate was recrystallized from ethanol (6.2-g yield, 74%), mp 180–182°; NMR (CF_3COOH): δ 6.9 (n, 7H, Ar*H*) and 3.9 (s, 6H, $-OCH_3$).

Anal.—Calc. for $C_{19}H_{26}ClNO_5$: C, 59.44; H, 6.82; N, 3.67. Found: C, 59.59; H, 6.97; N, 3.70.

Biology—The β-blocking activity of the eight experimental compounds and propranolol was assessed in vagotomized, pentobarbital-anesthetized dogs (30 mg/kg), prepared for measurement of pulsatile aortic blood pressure (carotid cannula) and heart rate[2]. β-Blocking activity was measured as the percent inhibition of the heart rate and diastolic blood pressure response produced by continuous isoproterenol hydrochloride infusion at 1.0 μg/kg/min. A continuous isoproterenol infusion was chosen to measure the duration of β-blockade associated with each compound studied. Preliminary studies indicated that the heart rate and diastolic pressure response to continuous isoproterenol infusion were stable for 4 hr.

Each experimental compound was tested at four dose levels: 0.01, 0.1, 1.0, and 10.0 mg/kg; propranolol was tested at 0.008, 0.024, and 0.072 mg/kg. All blockers were administered intravenously over a 15-sec period. Blocker administration commenced with the lowest dose first, and subsequent doses were administered 15 min after the effects of the previous dose had disappeared. Each animal received only one blocking drug.

Compound potency was compared with that of propranolol on the basis of doses (moles per kilogram) required to produce 25 and 50% inhibition (ID_{25} and ID_{50}, respectively) of the isoproterenol-induced heart rate change. These values were obtained from log dose–response curves for each agent. The duration of β-blockade was measured as the time associated with 50% recovery of the heart rate after dosing with blocking agents. Plots were then constructed of duration of action *versus* percent inhibition. An approximately linear relation existed between the two variables over the linear portion of the dose–response curve. Estimation of the 50% recovery times associated with 20 and 50% inhibition allowed normalization of the duration of action to the pharmacological effect.

REFERENCES

(1) R. Clarkson, in "Antihypertensive Agents," E. J. Englehardt, Ed., American Chemical Society, Washington, D.C., 1976.

(2) A. M. Barrett, in "Drug Design," vol. 3, E. J. Ariens, Ed., Academic, New York, N.Y., 1972.

(3) C. Kaiser, T. Jen, E. Garvey, W. D. Bowen, D. F. Colella, and J. R. Wardell, *J. Med. Chem.*, **20**, 687 (1977).

(4) E. J. Ariens and A. M. Sinonis, in "Beta Adrenergic Blocking Agents," P. R. Sarena and R. P. Forsyth, Eds., North-Holland, Amsterdam, The Netherlands, 1976.

(5) E. M. Vaughan Williams, E. E. Bagwell, and B. M. Singh, *Cardiovasc. Res.*, **7**, 226 (1973).

(6) Bochringer Lohn, French pat. 1,566,349 (Mar. 31, 1969).

(7) M. L. Hoefle, S. G. Hastings, R. F. Meyer, R. M. Corey, A. Holmes, and D. Stratton, *J. Med. Chem.*, **18**, 148 (1975).

(8) S. G. Hastings, R. D. Smith, R. M. Corey, A. D. Essenburg, C. E. Pettney, and D. K. Tessman, *Arch. Int. Pharmacodyn. Ther.*, **228**, 81 (1977).

[2] Beckman cardiotachometer, Beckman Instruments, Westbury, N.Y.

Microbial Transformations and ^{13}C-NMR Analysis of Colchicine

CHARLES D. HUFFORD ˣ, CATHY C. COLLINS, and ALICE M. CLARK

Received January 8, 1979, from the *Department of Pharmacognosy, School of Pharmacy, University of Mississippi, University, MS 38677.* Accepted for publication April 3, 1979.

Abstract □ Several microorganisms were screened for their ability to biotransform colchicine, and two were selected for preparative scale fermentations. *Streptomyces spectabilis* and *Streptomyces griseus* both produced O^2-demethylcolchicine and O^3-demethylcolchicine but in different amounts. The ^{13}C-NMR assignments of colchicine, O^{10}-demethylcolchicine, and trimethylcolchicinic acid are reported and were used to help identify the structures of the metabolites.

Keyphrases □ Colchicine—microbial transformations, ^{13}C-NMR spectra, metabolites □ Suppressant (gout)—colchicine, microbial transformations, NMR spectra, metabolites □ *Streptomyces spectabilis*—colchicine metabolism □ *Streptomyces griseus*—colchicine metabolism

Colchicine (I) is one of the oldest drugs used in the treatment of gout. It has no equal for the relief of pain from acute gouty arthritis (1). In spite of the large amount of information available concerning the pharmacology of I, its metabolism and mechanism of action in humans are still unknown.

Several reports (1–3) suggested that a metabolite(s) is (are) the biologically active form of the drug. The only report of a study of human metabolism of I in gout patients suggested that a major portion of I is deacetylated, but whether deacetylcolchicine is a human metabolite has not been established (4). With the modified Undenfriend system, a redox system similar in many respects to liver microsomes, I was converted to O^2-demethylcolchicine (II), O^3-demethylcolchicine (III), O^{10}-demethylcolchicine (colchiceine, IV), and a rearranged tropolone ring derivative given the trivial name colchinal (5). The O^2-, O^3-, and O^{10}-demethylcolchicines also were reported as metabolic products of I using mammalian liver microsomes (6).

While the production and isolation of quantities of drug metabolites from animals or animal tissue homogenates or from conventional synthesis or modification may be extremely difficult, microorganisms possess adaptive enzymes which often can be raised to high levels under suitable culture conditions to produce desired metabolic products. The application of this technique in the biotransformation of numerous classes of compounds has been successful, as shown by the appearance of three major "compendia" (7–9). Three reviews (10–12) indicated that microbial systems also can be used to study mammalian metabolism. This paper reports on the ^{13}C-NMR assignments for I and on the isolation and identification, using ^{13}C-NMR spectroscopy, of two microbial metabolites of I.

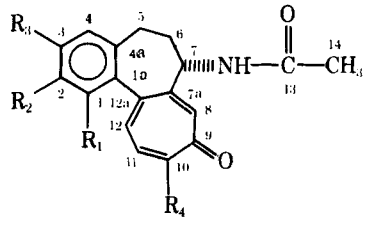

I: $R_1 = R_2 = R_3 = R_4 = OCH_3$
II: $R_1 = R_3 = R_4 = OCH_3$, $R_2 = OH$
III: $R_1 = R_2 = R_4 = OCH_3$, $R_3 = OH$
IV: $R_1 = R_2 = R_3 = OCH_3$, $R_4 = OH$
VI: $R_2 = R_3 = R_4 = OCH_3$, $R_1 = OH$

RESULTS AND DISCUSSION

The use of ^{13}C-NMR spectroscopy has become almost routine in structural elucidation studies of natural products as well as of other drugs. ^{13}C-NMR spectroscopy also is particularly well suited for microbial transformation studies since the starting materials are usually available in large quantities, thus allowing detailed studies of ^{13}C-NMR properties. A comparison of the ^{13}C-NMR data of metabolites and starting material will allow ready formulation of the structures of the metabolites.

There are two published ^{13}C-NMR spectra of colchicine (I). The biosynthesis of I was studied using ^{13}C-NMR data, but complete assignments were not made (13). In another report (14), the complete assignments for I were made using model compounds. Close examination of some of these spectral assignments (14) suggested that some assignments may be in error, and this situation prompted a more detailed study of the carbon assignments.

The assignments of C-1a, C-4, C-7, C-8, C-9, C-10, C-11, C-12, C-13, and C-14 (Table I) were made from known chemical shift theory, additivity principles, and model compounds (15–17) as well as from single-frequency off-resonance decoupling (SFORD) experiments and are in agreement with those reported (14). The signals for C-4, C-8, C-11, and C-12 were confirmed by selective single-frequency proton-decoupling experiments[1]. The other carbon assignments listed in Table I for I differ from those reported previously (14), and evidence is presented here to establish their correctness.

There are four methoxyl carbon signals at 61.5, 61.3, 56.6, and 56.3 ppm[2]. When methoxyl groups have di-*ortho* substituents, the chemical shift of these carbon signals appears at a lower field (60–63 ppm) than methoxyl groups that have none or only one *ortho* substituent (55–57 ppm) (19–23). Thus, the methoxyl groups at C-10 and C-3 can be assigned to the signals at 56.3 and/or 56.5 ppm, and those at C-1 and C-2 can be assigned to the signals at 61.3 and/or 61.5 ppm.

The two signals at 30.1 (t) and 36.6 (t) ppm are readily assigned to either C-5 or C-6. The most downfield signal was previously assigned to C-5 (13, 14). The assignments for C-5 and C-6 were made by using indan as a model (14). However, a better model for comparison would be 1-aminoindan whose ^{13}C-NMR data (17) show that C-2 is much farther downfield than the benzylic carbon (C-3), illustrating the deshielding effect of an amino group at C-2 (β effect) and shielding at C-3 (γ effect). A similar relationship as exists in 1-aminoindan exists in I, and thus the amide would be expected to deshield C-6 relative to C-5. Thus, the as-

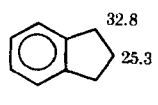

indan

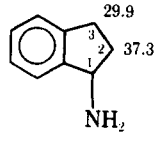

1-aminoindan

[1] The protons H-4, H-8, H-11, and H-12 were assigned in the ^1H-NMR spectrum of I (18).

[2] The authors of Ref. 14 reported only one signal at 61.3 and three signals at 56.1, 56.4, and 56.4. The authors of Ref. 13 reported two at 61.2 and 61.0 and two at 55.8 and 56.1, which are in close agreement with the signals listed in Table I.

0022-3549/79/1000-1239$01.00/0
© 1979, American Pharmaceutical Association

Table I—^{13}C-NMR Data for I–V [a]

Assignment [b]	I	II	III	IV [c]	V [d]	V·HCl [e]
C-1	153.8 s^1	147.8 s^1	150.3 s^1	153.9 s^1	153.7 s^1	155.2 s^1
C-2	142.2 s	138.1 s	139.3 s	141.8 s	141.6 s	141.6 s^2
C-3	151.4 s^1	145.0 s^1	149.9 s^1	151.1 s^1	153.3 s^1	150.7 s^1
C-4	107.9 d	107.0 d	110.3 d	107.7 d	107.3 d	108.2 d
C-5	30.1 t	29.8 t	29.7 t	29.9 t	30.6 t	29.6 t
C-6	36.6 t	36.9 t	36.6 t	37.6 t	41.8 t	37.0 t
C-7	52.8 d	52.8 d	52.8 d	52.9 d	53.7 d	54.7 d
C-8	130.7 d	130.7 d	130.7 d	119.5 d	118.6 d	124.8 d^3
C-9	179.6 s	179.7 s	179.7 s	170.1 s^2	172.2 s^2	168.9 s^4
C-10	164.3 s	164.3 s	164.2 s	170.2 s^2	168.7 s^2	168.3 s^4
C-11	113.1 d	112.8 d	112.9 d	122.5 d	123.8 d	126.7 d^3
C-12	134.5 d	135.1 d	135.3 d	141.6 d	141.6 d	144.7 d^3
C-13	170.0 s	170.0 s	170.2 s	170.5 s^2	—	—
C-14	22.7 q	22.9 q	22.8 q	22.8 q	—	—
C-1a	126.0 s	125.1 s	125.1 s	126.1 s	126.0 s	124.0 s
C-4a	134.4 s	129.9 s	134.2 s	134.6 s	135.7 s^3	134.3 s
C-7a	152.6 s	152.2 s	152.5 s	151.7 s	150.6 s^1	148.7 s^1
C-12a	137.2 s	136.9 s	137.1 s	136.5 s	135.6 s^3	141.5 s^2
C-1OCH_3	61.3 q^2	61.3 q	61.3 q^2	61.3 q^3	61.1 q^4	61.7 q^5
C-2OCH_3	61.5 q^2	—	61.5 q^2	61.5 q^3	60.9 q^4	61.2 q^5
C-3OCH_3	56.3 q^3	56.3 q^2	—	56.3 q	56.2 q	56.3 q
C-10OCH_3	56.5 q^3	56.5 q^2	56.4 q	—	—	—

[a] Run in deuterochloroform. [b] Assignments are based on predicted chemical shifts, comparisons with literature data, single-frequency off-resonance decoupling, selective proton-decoupling, and proton-coupled data. Assignments bearing the same numerical superscript in any one spectrum may be reversed. [c] Selective single-frequency proton-decoupling was done to confirm C-8, C-11, and C-12. However, since the H-11 and H-12 proton assignments are not unambiguously known (Ref. 18, p. 421), the C-11 and C-12 signals could be reversed, but the ones listed are preferred since it is unlikely that C-11 would change 28.5 ppm downfield (I → IV) and C-12 would change 12.9 ppm upfield (I → IV), as would be the case if the signals were reversed. The assignments of the 151.7-ppm signal to C-7a and the 141.8-ppm signal to C-2 followed from selective single-frequency proton-decoupling experiments at low decoupling power (irradiation at δ_H3.9). The proton-coupled spectrum was also recorded, and the multiplicities of the signals for C-4a and C-12a were the same as in I. [d] The assignments listed for V are based on analogy to IV and off-resonance experiments only. [e] A few drops of methanol-d_4 were added to increase solubility. Significant shifts have occurred between the amine (V) and its hydrochloride, making assignments somewhat ambiguous without selective single-frequency proton-decoupling and proton-coupled data, which were not obtained.

signments of the signal at 36.6 ppm to C-6 and at 30.1 ppm to C-5 in I would seem more appropriate.

The correctness of these assignments was established by several additional observations. To evaluate the effect of an amine *versus* an amide, the ^{13}C-NMR spectrum of trimethylcolchicinic acid (V) was obtained. It showed the triplet signals (off resonance) at 30.6 (C-5) and 41.8 (C-6) ppm. This downfield shift of about 5 ppm for C-6 is comparable to that observed in cyclohexylamine[3] *versus* *N*-acetylcyclohexylamine. It also has been reported that the C-2 carbon in cyclohexylamine shifts to a higher field (7.1 ppm) in the hydrochloride salt while the C-3 carbon shifts upfield by only 1.5 ppm[4]. Similarly, the hydrochloride salt of trimethylcolchicinic acid (V·HCl) was prepared and showed upfield shifts of 1.0 ppm for C-5 (29.6 ppm) and 4.8 ppm for C-6 (37.0 ppm).

The remaining unassigned signals in I (C-1, C-2, C-3, C-4a, C-7a, and C-12a) were assigned by interpretation of the proton-coupled ^{13}C-NMR spectral data and selective single-frequency proton-decoupling experiments. The use of long-range ^{13}C–H coupling is becoming increasingly important in making unambiguous carbon assignments, particularly for quaternary carbons in aromatic compounds; a number of empirical observations have become evident. Three-bond coupling constants ($^3J_{C\text{-}H}$) are always larger (4–10 Hz) than two- or four-bond coupling constants (usually <4 Hz) (24–26).

The proton-coupled spectrum of I showed the signal at 137.2 ppm as a broad triplet ($^3J_{C\text{-}H}$ = 8 Hz) and was assigned to C-12a since there are apparently two equal three-bond couplings (H-8 and H-11). The signal at 142.2 ppm was complex and was assigned to C-2 on the basis that C-2 would be expected to be either a pentet (equal coupling constants to H-4 and OCH_3) or an overlapping doublet of quartets (unequal coupling constants to H-4 and OCH_3). The 134.4-ppm signal was a broad singlet and was assigned to C-4a.

The correctness of these assignments, as well as the assignments for C-1, C-3, and C-7a, was confirmed by carrying out a selective single-frequency proton-decoupling experiment[5]. Irradiation at δ_H3.9 (OCH_3) showed the 142.2-ppm signal (C-2) as a doublet (three-bond coupling to H-4) and the 153.8- and 151.4-ppm signals (C-1 and/or C-3) as sharp singlets. The signal at 152.6 ppm appeared as a doublet and was assigned to C-7a[6] (three-bond coupling to H-12). The other signals (134.5 and 137.2) were unchanged. Irradiation at δ_H7.6 (C=CH) showed the signal at 137.2 ppm as a singlet, clearly identifying it as C-12a; the signals at 142.2 (C-2) and 134.4 (C-4a) were essentially the same as in the proton-coupled spectrum.

Finally, irradiation at δ_H2.5 (—CH_2—CH_2—) showed a sharp singlet for the 134.4-ppm signal while the 142.2 and 137.2 signals remained the same as in the proton-coupled spectrum. This sharpening results from eliminating the two-bond coupling of C-4a to the protons at C-5. Also, in this last experiment, the C-1a (126.0) signal appeared as a double doublet[7] (unequal three-bond coupling to H-4 and H-12). These experiments provided evidence that the assignments listed in Table I for C-1, C-2, C-3, C-4a, C-7a, and C-12a are correct. Thus, the complete assignments of the carbon signals in the ^{13}C-NMR spectrum of I have been made.

After preliminary screening of I for biotransformation products using several microorganisms in different media (Table II), only *Streptomyces spectabilis* (ATCC 27465) and *Streptomyces griseus* (ATCC 13968) (both grown in medium θ) were capable of metabolizing I as indicated by TLC. The other microorganisms did not show any ability to metabolize I. Incubation of I with stirred cultures of *S. spectabilis* showed that two more polar metabolites were being produced. These metabolites were very difficult to separate. The separation was accomplished by preparative TLC using 4% ethanol in chloroform on alumina impregnated with sodium hydroxide. With this procedure, both metabolites were obtained in pure form.

The ^{13}C-NMR spectra of the two metabolites (A and B) showed only three methoxyl carbon signals, immediately suggesting mono-*O*-de-

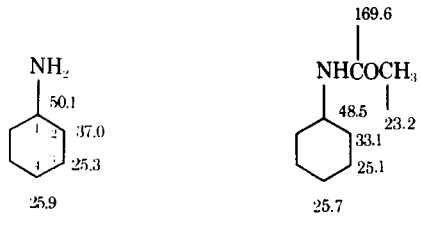

cyclohexylamine *N*-acetylcyclohexylamine

[3] The assignments for cyclohexylamine were reported on p. 153 of Ref. 16. The chemical shift values reported (on the structure) are those obtained on the instrument used in the present study.

[4] See p. 153 of Ref. 16.

[5] This experiment was conducted at low decoupling power such that in addition to one-bond coupling, long-range ^{13}C-H is also evident, although the splittings are no longer the true coupling constants (27).

[6] C-7a would be expected to be the most deshielded nonoxygenated carbon signal in colchicine since it is the β-carbon of an α,β-unsaturated carbonyl system and also experiences the β effect of the amide group. The 152.6-ppm signal was masked in the proton-coupled spectrum by the 153.8- and 151.4-ppm signals.

[7] The 126.0-ppm signal was obscured in the proton-coupled spectra (C-8 doublet) and appeared as a broad unresolved signal upon irradiation at δ_H3.9 and δ_H7.6.

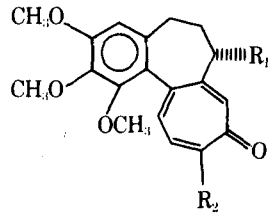

V: $R_1 = NH_2$, $R_2 = OH$
VII: $R_1 = NH_2$, $R_2 = OCH_3$
VIII: $R_1 = =O$, $R_2 = OCH_3$

methylated derivatives of I. O^{10}-Demethylcolchicine (colchiceine, IV), readily prepared by hydrolysis (0.1 *N* HCl) of I (28, 29), was not one of the metabolites (TLC), which left three possibilities: O^3-demethylcolchicine (III), O^2-demethylcolchicine (II), and O^1-demethylcolchicine[8]. The ^{13}C-NMR data for Metabolite A showed one methoxyl signal at 56.4 ppm and two at 61.5 and 61.3 ppm. Since the methoxyl carbon signals resonating near 56 ppm in I have been assigned to C-3 and/or C-10 and since Metabolite A does not correspond to O^{10}-demethylcolchicine (IV), it must be III. The other signals in the ^{13}C-NMR spectrum of Metabolite A are also in agreement (Table I). The ^{1}H-NMR spectrum of Metabolite A also was in agreement with that reported for III (5), and a direct comparison with an authentic sample confirmed the identity of Metabolite A as III.

The ^{13}C-NMR data for Metabolite B showed two methoxyl signals at 56.5 and 56.3 ppm (OCH_3 at C-3 and/or C-10) and one at 61.3 ppm, indicating that Metabolite B is either VI or II. The ^{1}H-NMR spectrum of Metabolite B showed a methoxyl group at δ_H3.64. Since a methoxyl group appearing near δ 3.6 in I derivatives has been assigned to C-1 (18), this would eliminate VI. The ^{1}H-NMR data were in agreement with those reported for II (5), and a direct comparison with an authentic sample confirmed the identity of Metabolite B as II.

The soil bacterium, *Arthobacter colchovorum*, metabolizes I to 7-deacetylcolchicine (VII) and 7-deacetamino-7-oxocolchicine (VIII) (30). One other report of the microbial metabolism of I using *S. griseus* has appeared, but the metabolite's structure was established only as a monodemethylated colchicine derivative (31, 32). However, it has been reported that this metabolite is VI (30). On the other hand, another report (9) suggested that this metabolite is probably IV.

When I was added to shaken cultures of *S. griseus* (ATCC 13968) using the fermentation conditions reported previously (32), two metabolites were observed. Subsequent preparative scale fermentations resulted in the isolation of mostly II and a small amount of III. The overall yields using *S. griseus* were lower than with *S. spectabilis*. Furthermore, II was the major product with *S. griseus* whereas III was the major product with *S. spectabilis*.

EXPERIMENTAL[9]

Fermentation Procedures—Stock cultures of microorganisms were maintained on mycophil (BBL) agar (fungi) or Eugonagar (bacteria). Preliminary biotransformation studies were carried out on gyrotory shakers operating at 200 rpm (room temperature) in erlenmeyer flasks holding one-fifth their volume of medium. A two-stage fermentation procedure was utilized in which a sterile liquid culture medium was inoculated with the surface growth from agar slants. These stage I cultures were incubated for 24 hr (200 rpm, room temperature). Two milliliters of the stage I culture broth was used as inoculum for stage II cultures. The substrate was added to 24-hr stage II cultures as a 10% ethanolic solution at a concentration of 0.1 mg/ml of stage II medium.

Fermentation Medium α consisted of: dextrose, 20 g; yeast extract, 5 g; peptone, 5 g; NaCl, 5 g; K_2HPO_4, 5 g; and H_2O, 1000 ml.

Fermentation Medium β consisted of: NH_4NO_3, 4 g; KH_2PO_4, 1.5 g; Na_2HPO_4, 1.5 g; $MgSO_4$, 0.2 g; $FeSO_4 \cdot 7H_2O$, 0.05 g; $MnSO_4 \cdot H_2O$, 0.002 g; $CaCl_2 \cdot H_2O$, 0.01 g; yeast extract, 0.5 g; and H_2O, 1000 ml.

Fermentation Medium γ consisted of: KH_2PO_4, 0.7 g; K_2HPO_4, 0.7 g; $MgSO_4$, 0.7 g; NH_4NO_3, 1.0 g; NaCl, 0.005 g; $FeSO_4 \cdot 7H_2O$, 0.002 g; $ZnSO_4$, 0.002 g; $MnSO_4 \cdot H_2O$, 0.001 g; glucose, 2 g; and H_2O, 1000 ml.

Table II—Microorganisms and Media Used for Screening of Colchicine

Organism	Medium			
Alternaria solani (11078)	α	δ	ϵ	θ
Arthrobacter simplex (6946)	β	δ		θ
Arthrobacter sp. (19140)	β	δ		θ
Arthrobacter sp. (21237)	β	δ		θ
Aspergillus flavipes (1030)	α	δ	ϵ	θ
Aspergillus flavipes (11013)	α	δ	ϵ	θ
Aspergillus flavipes (16795)	α	δ	ϵ	θ
Aspergillus flavus (9170)	α	δ	ϵ	θ
Aspergillus flavus (24741)	α	δ	ϵ	θ
Aspergillus niger (10548)	α	δ	ϵ	θ
Aspergillus niger (11394)	α	δ	ϵ	θ
Aspergillus niger (16888)		δ	ϵ	
Aspergillus ochraceus (18500)	α	δ	ϵ	θ
Aspergillus ochraceus (22947)	α	δ	ϵ	θ
Aspergillus parasiticus (15517)	α	δ	ϵ	θ
Beauvaria bussiana (13144)	α	δ	ϵ	θ
Botrytis allii (9435)	α	δ	ϵ	θ
Calonectria decora (14767)	α	δ	ϵ	θ
Chaetomium cochloides (10195)	α	δ	ϵ	θ
Cladosporium resinae (22712)	α	δ	ϵ	θ
Cladosporium resinae f. *avelleneum* (22711)	α	δ	ϵ	θ
Cunninghamella blakesleeana (8688a)	α	δ	ϵ	θ
Cunninghamella echinulata (NRRL 3655)	α	δ	ϵ	θ
Cunninghamella echinulata (9244)	α	δ	ϵ	θ
Cunninghamella echinulata (11585a)	α	δ	ϵ	θ
Cunninghamella echinulata (11585b)	α	δ	ϵ	θ
Cunninghamella elegans (9245)	α	δ	ϵ	θ
Curvularia lunata (13633)	α	δ	ϵ	θ
Curvularia lunata (12017)	α	δ	ϵ	θ
Cylindrocarpon radicicola (11011)	α	δ		θ
Fomes pinicola (15341)	α	δ	ϵ	θ
Fusarium javanicum (12575)	α	δ	ϵ	θ
Fusarium oxysporum (7601)	α	δ	ϵ	θ
Fusarium oxysporum (26297)	α	δ	ϵ	θ
Fusarium oxysporum f. sp. *cepue* (11711)	α	δ	ϵ	θ
Fusarium oxysporum f. sp. *gladioli* (11137)	α	δ	ϵ	θ
Fusarium oxysporum f. sp. *tulipae* (15652)	α	δ	ϵ	θ
Fusarium solani var. *coeruleum* (24389)	α	δ	ϵ	θ
Mucor griseo-cyanus (1207)	α	δ	ϵ	θ
Nocardia corallinia (19070)				θ
Nocardia corallinia (19071)				θ
Nocardia corallinia (19148)				θ
Nocardia minima (19050)				θ
Penicillium adametzi (10407)	α	δ		θ
Penicillium chrysogenum (9480)	α	δ		θ
Penicillium chrysogenum (10002)	α	δ		θ
Penicillium frequentans (10444)	α	δ		θ
Penicillium oxalicum (24784)	α	δ		θ
Penicillium spinulosum (16348)	α	δ		θ
Rhizopus arrhizus (11145)	α	δ		θ
Rhizopus stolonifer (6227b)	α	δ		θ
Rhizopus stolonifer (15441)	α	δ		θ
Septomyxa affinis (6737)	α	δ		θ
Streptomyces griseus (10137)	α	δ		θ
Streptomyces griseus (13968)	α	δ	β	θ
Streptomyces griseus (23337)		δ	β	θ
Streptomyces purpurascens (21326)		δ	β	θ
Streptomyces roseochromogenus (13400)		δ	β	θ
Streptomyces sp. (15077)		δ	β	θ
Streptomyces spectabilis (27465)		δ	β	θ
Syncephalastrum racemosum (18192)	α	δ		θ
Whetzelinia sclerotiorum (18015)	α	δ		θ
Whetzelinia sclerotiorum (24156)	α	δ		θ

[8] The ^{13}C-NMR data for IV are also recorded in Table I and show marked differences to I–III, particularly for those signals located in the tropolone ring (C-8, C-9, C-10, C-11, and C-12).

[9] Melting points were determined on a Thomas-Hoover apparatus and are uncorrected. IR spectra were run in potassium bromide using a Beckman IR-33 spectrophotometer. ^{1}H-NMR and ^{13}C-NMR spectra were recorded in deuterochloroform on a Jeol-FX60 Fourier-transform NMR spectrometer with tetramethylsilane as the internal standard. *N*-Acetylcyclohexylamine was prepared by acetylation of cyclohexylamine. Colchicine USP was purchased from Inverni & Della Beffa, Milan, Italy. Trimethylcolchicinic acid (V) was obtained commercially (K & K Laboratories-ICN) or was prepared by hydrolysis of I according to the published procedure (28), mp 156–158° [lit. (28, 29) mp 160–162°]. The hydrochloride salt was prepared, mp 202–204° [lit. (29) mp 191°]. O^{10}-Demethylcolchicine (IV) (colchiceine) was prepared by hydrolysis (0.1 *N* HCl) according to published procedures (29, 30), mp 175–177° [lit. (29) mp 178–179°].

^{13}C-NMR (15.03 MHz) data were recorded using a 4000-Hz spectral width, a 45° pulse, 8K data points, and a repetition rate of 10 sec. All proton resonances were decoupled by a broad band (1 kHz) irradiation for proton noise-decoupled spectra. The single-frequency off-resonance experiments were conducted by centering the decoupling frequency 1100 Hz downfield from tetramethylsilane. The selective single-frequency proton-decoupled experiments were carried out by centering the decoupling frequency on the appropriate proton resonance and recording the spectra at several power settings. The proton-coupled spectra were recorded using the gated decoupling mode (decoupler off during data acquisition) and 16K data points.

Fermentation Medium δ consisted of: dextrose, 20 g; yeast extract, 5 g; soytone, 5 g; NaCl, 5 g; K_2HPO_4, 5 g; and H_2O, 1000 ml.

Fermentation Medium ϵ consisted of: dextrose, 30 g; KH_2PO_4, 1.0 g; K_2HPO_4, 2.0 g; soytone, 10.0 g; $MgSO_4$, 0.5 g; $NaNO_3$, 2.0 g; $FeSO_4$, 0.02 g; KCl, 0.5 g; and H_2O, 1000 ml.

Fermentation Medium θ consisted of: dextrose, 10 g; cornsteep liquor, 10 g; soya flour, 10 g; dry malt extract, 5 g; $CaCO_3$, 1 g; NaCl, 5 g; and H_2O, 1000 ml.

Fermentation Sampling—The fermentations were sampled by withdrawing 5 ml of culture broth, adjusting to pH 7, and extracting with 3 × 5 ml of chloroform. The chloroform layers were evaporated to dryness, and the residues obtained were redissolved in chloroform and spotted on precoated silica gel G TLC plates. The plates were developed in 8% methanol in benzene–ethyl acetate–diethylamine (5:4:1) and were visualized with UV light and by spraying with 10% HCl, heating for 1–2 min, and spraying with 5% $FeCl_3$ in 0.5 *N* HCl.

Preparative Scale Biotransformation of Colchicine (I) Using *S. spectabilis*—*S. spectabilis*** was grown in 5 liters of Medium θ contained in a 7.5-liter fermentor jar[10]. After a 24-hr incubation, I (500 mg/5 ml of absolute ethanol) was added to the culture; the incubation (200-rpm stir rate, 2-liters/min air flow rate, room temperature) was continued for 14 days. The culture was filtered through a buchner funnel, and the aqueous culture broth was adjusted to pH >12 with potassium hydroxide and extracted with 12 × 500 ml of chloroform. The combined chloroform layers were dried over sodium sulfate and evaporated *in vacuo* (40°) to leave 632 mg of a yellow residue, shown by TLC [8% methanol in benzene–ethyl acetate–diethylamine (5:4:1), silica gel G] to consist mostly of I.

The aqueous basic layer was adjusted to pH 4–5 with acetic acid and extracted with 12 × 500 ml of chloroform. The combined chloroform layers were dried over sodium sulfate and evaporated *in vacuo* (40°) to leave 104 mg of a yellow-brown oily residue. This residue was applied to two precoated alumina plates (1 mm), which had been sprayed with 5% aqueous NaOH and dried for 10 min at 100°. Multiple development of the plate in 4% ethanol–chloroform (six times) separated the metabolites into two distinct bands (R_f 0.65 and 0.58).

The lower R_f band was located under UV light, scraped, and eluted with 20% methanol–chloroform to yield 39 mg of Metabolite A after solvent removal. This metabolite could not be induced to crystallize. The material (amorphous powder) was pure by TLC; IR: ν_{max} ($CHCl_3$) 3260 (broad), 3525, 3445, 2950, 1683, 1620, 1594, and 1555 cm^{-1}; ^{1}H-NMR ($CDCl_3$): δ 1.98 (3H, s, $NHCOCH_3$), 2.4 (4H, m, H-5,6), 3.64 (3H, s, C-1 OCH_3), 4.00 (6H, s, C-2, 10 OCH_3), 4.58 (1H, m, H-7), 6.58 (1H, s, H-4), 6.87 (1H, d, J = 11 Hz, H-11), 7.36 (1H, d, J = 11 Hz, H-12), 7.62 (1H, s, H-8), and 8.05 (1H, m, $NHCOCH_3$) ppm. A direct comparison of Metabolite A with an authentic sample of O^3-demethylcolchicine (III) showed that they had the same behavior on TLC (co-TLC), superimposable IR spectra, and the same ^{1}H-NMR spectra. The ^{13}C-NMR data for Metabolite A (III) are listed in Table I.

Extraction of the higher R_f band (0.65) in the same manner gave 20 mg of Metabolite B. Crystallization from chloroform–hexane afforded 4 mg of B as yellow needles, mp 184–186°; IR: ν_{max} (KBr) 3290 (broad), 2950, 1664, 1618, 1590, and 1550 cm^{-1}; ^{1}H-NMR ($CDCl_3$): δ 1.97 (3H, s, $NHCOCH_3$), 2.4 (4H, m, H-5,6), 3.64 (3H, s, C-1 OCH_3), 3.93 (3H, s, OCH_3), 4.02 (3H, s, OCH_3), 4.16 (1H, m, H-7), 6.53 (1H, s, H-4), 6.85 (1H, d, J = 11 Hz, H-11), 7.37 (1H, d, J = 11 Hz, H-12), 7.59 (1H, s, H-8), and 7.82 (1H, m, $NHCOCH_3$) ppm. A direct comparison of Metabolite B with an authentic sample of O^2-demethylcolchicine (II) showed no mixed melting-point depression, the same behavior on TLC (co-TLC), superimposable IR spectra (KBr), and the same ^{1}H-NMR spectra. The ^{13}C-NMR data for Metabolite B (II) are listed in Table I.

Preparative Scale Biotransformation of I Using *S. griseus*—*S. griseus*** (ATCC 13968) was grown in 5.0 liter of Medium θ contained in 50 500-ml erlenmeyer flasks. After a 24-hr incubation, 500 mg of I was evenly distributed among the cultures; incubation was continued for 12 days (300 rpm, 26°). The aqueous culture broth was adjusted to pH >12 with 1.0 *M* NaOH and then extracted with chloroform. The chloroform extract was dried over sodium sulfate and then evaporated to leave a brown oily residue (750 mg), which was shown by TLC to consist of starting material but not of metabolites.

The aqueous basic layer was adjusted to pH 5 with acetic acid and extracted with chloroform. The chloroform extract was dried over sodium sulfate and evaporated to give a yellow oily residue (85 mg), which was applied to an alumina plate (1.0 mm) impregnated with 5% NaOH and dried at 100° for 10 min. The plate was developed (four times) in 4% ethanol–chloroform, and the higher R_f band was located under UV light, scraped, and eluted with acetone to give a yellow crystalline residue (38 mg). Crystallization from chloroform–hexane afforded 26 mg of II, mp 185–187°, identical in all respects with authentic II [melting point, mixed melting point, TLC, co-TLC, ^{1}H-NMR, and superimposable IR spectra (KBr)].

Extraction of the lower R_f band in the same manner yielded 4 mg of III, which had the same mobility on TLC (co-TLC) as authentic III. The ^{1}H-NMR data clearly revealed two methoxyl signals at δ 4.00 and one at δ 3.64 and were essentially identical to those of authentic III.

[10] New Brunswick model FS307.

REFERENCES

(1) S. L. Wallace, *Am. J. Med.*, **30**, 439 (1961).

(2) Y.-H. Chang, *J. Pharmacol. Exp. Ther.*, **194**, 154 (1975).

(3) A. L. Hunter and C. D. Klassen, *ibid.*, **192**, 605 (1975).

(4) E. J. Walaszek, J. J. Koesis, G. V. Leroy, and E. M. K. Geiling, *Arch. Int. Pharmacodyn. Ther.*, **125**, 371 (1960).

(5) M. Schonharting, P. Pfaender, A. Rieker, and G. Siebert, *Hoppe-Seyler's Z. Physiol. Chem.*, **354**, 421 (1973).

(6) M. Schonharting, G. Mende, and G. Siebert, *ibid.*, **355**, 1391 (1974).

(7) W. Charney and H. L. Gerzog, "Microbial Transformations of Steroids, A Handbook," Academic, New York, N.Y., 1967.

(8) H. Iizuka and A. Naito, "Microbial Transformations of Steroids and Alkaloids," University Park Press, State College, Pa., 1967.

(9) K. Kieslich, "Microbial Transformations of Non-Steroid Cyclic Compounds," George Thieme, Stuttgart, West Germany, 1976.

(10) R. V. Smith and J. P. Rosazza, *J. Pharm. Sci.*, **64**, 1737 (1975).

(11) R. V. Smith and J. P. Rosazza, *Biotechnol. Bioeng.*, **17**, 785 (1975).

(12) R. V. Smith, D. Acosta, and J. P. Rosazza, in "Advances in Biochemical Engineering," vol. 5, A. Riechter, Ed., Springer-Verlag, New York, N.Y., 1977, pp. 69–100.

(13) A. R. Battersby, P. W. Sheldrake, and J. A. Midner, *Tetrahedron Lett.*, **37**, 3315 (1974).

(14) S. P. Singh, S. S. Parmar, V. I. Stenberg, and S. A. Farnum, *Spectroscopy Lett.*, **10**, 1001 (1977).

(15) G. C. Levy and G. L. Nelson, "Carbon-13 NMR for Organic Chemists," Wiley-Interscience, New York, N.Y., 1972.

(16) J. B. Sothers, "Carbon-13 NMR Spectroscopy," Academic, New York, N.Y., 1972.

(17) L. F. Johnson and W. C. Jankowski, "Carbon-13 NMR Spectra." Wiley-Interscience, New York, N.Y., 1972.

(18) W. C. Wildman and B. A. Pursey, in "The Alkaloids," vol. XI, P. H. Manske, Ed., Academic, New York, N.Y., 1968, chap. 11.

(19) K. S. Dhami and J. B. Sothers, *Can. J. Chem.*, **44**, 2855 (1966).

(20) G. W. Buchanan, G. Montaudo, and P. Finocchiaro, *ibid.*, **52**, 767 (1974).

(21) A. F. Erasmuson, R. J. Ferrier, N. C. Franca, H. E. Gottlieb, and E. Wenkert, *J. Chem. Soc. Perkin Trans. I*, 492 (1977).

(22) J. F. Castelao, Jr., O. R. Gottlieb, R. A. DeLima, A. A. L. Mesquita, H. E. Gottlieb, and E. Wenkert, *Phytochemistry*, **16**, 735 (1977).

(23) K. Panickpol and P. G. Waterman, *ibid.*, **17**, 1363 (1978).

(24) C.-J. Chang and G. E. Peck, *J. Pharm. Sci.*, **65**, 1019 (1976).

(25) C.-J. Chang, *Lloydia*, **41**, 17 (1978).

(26) H. E. Gottlieb, *Isr. J. Chem.*, **16**, 57 (1977).

(27) C.-J. Chang, H. G. Floss, and G. E. Peck, *J. Med. Chem.*, **18**, 505 (1975).

(28) E. Boyland and E. H. Mawson, *Biochem. J.*, **32**, 1204 (1938).

(29) J. W. Cook and J. D. London, in "The Alkaloids," vol. II, R. H. Manske, Ed., Academic, New York, N.Y., 1952, chap. X, pp. 269–271.

(30) H.-J. Zeitler and H. Niemer, *Hoppe-Seyler's Z. Physiol. Chem.*, **350**, 366 (1969).

(31) L. Velluz and P. Bellet, *C. R. Hebd. Seances Acad. Sci.*, **248**, 3453 (1959).

(32) P. Bellet and L. Velluz (Roussel-Uclaf), Brit. pat. 923 421 (1959).

ACKNOWLEDGMENTS

Supported in part by the Committee on Faculty Research, University of Mississippi, and the Research Institute of Pharmaceutical Sciences, School of Pharmacy, University of Mississippi.

The authors are grateful for the generous samples of O^2- and O^3-demethylcolchicine provided by Professor M. Schonharting and Professor G. Siebert and for technical assistance by Ms. Susan Price in conducting some of the screening experiments. A. M. Clark acknowledges a fellowship from the American Foundation for Pharmaceutical Education. The authors also acknowledge Dr. Ching-Jer Chang, Purdue University, for suggesting the selective single-frequency proton-decoupling experiments at very low decoupling power.

Urinary Excretion of Chlorpheniramine and Pseudoephedrine in Humans

C. M. LAI, R. G. STOLL, Z. M. LOOK, and A. YACOBI ˣ

Received January 29, 1979, from the *Pharmaceutical Development Department, Research and Medical Affairs, Arnar-Stone Laboratories, Inc., McGaw Park, IL 60085.* Accepted for publication April 10, 1979.

Abstract □ A specific high-pressure liquid chromatographic method for the determination of chlorpheniramine and pseudoephedrine in urine was developed and applied in a urinary excretion study of normal healthy subjects who received a sustained-release dosage form containing 8 mg of chlorpheniramine maleate and 120 mg of pseudoephedrine hydrochloride. Five subjects received one dose on Day 1, followed by multiple dosing every 12 hr for 7 days without ammonium chloride administration. Four subjects received one dose of the sustained-release dosage form together with ammonium chloride. Urine samples were collected during the 1st day and at steady state. The method is specific and simultaneously determines chlorpheniramine, two metabolites (mono- and didesmethylchlorpheniramine), pseudoephedrine, and norpseudoephedrine. The assay recovery was >97% (0.06–3 μg/ml) for chlorpheniramine maleate and >98% (1.5–75 μg/ml) for pseudoephedrine hydrochloride. Excretion of chlorpheniramine and its two metabolites in urine was enhanced after ammonium chloride administration. At steady state, a change in urine pH from 5.69 to 6.46 resulted in more than a 25% decrease in chlorpheniramine and monodesmethylchlorpheniramine excretion. In spite of expected changes in its biological half-life, the overall amount of unchanged pseudoephedrine excreted in urine was not affected by urine pH, presumably because it is primarily excreted in urine as intact drug.

Keyphrases □ Chlorpheniramine—urinary excretion, humans, high-pressure liquid chromatographic analysis □ Chlorpheniramine metabolites—urinary excretion, humans, high-pressure liquid chromatographic analysis □ Pseudoephedrine—urinary excretion, humans, high-pressure liquid chromatographic analysis □ Nasal decongestants—chlorpheniramine and pseudoephedrine, urinary excretion, humans □ High-pressure liquid chromatography—analysis, chlorpheniramine and pseudoephedrine in human urine

Chlorpheniramine and pseudoephedrine, two weak basic drugs, are often used together for treatment of nasal congestion. The extent and rate of urinary excretion of the unchanged drugs are pH and urine flow dependent (1–3). Chlorpheniramine is extensively metabolized *via* *N*-dealkylation and excreted as both mono- and didesmethyl compounds (1, 4–6), and it is expected that the excretion of these metabolites in urine is also urine pH dependent. Pseudoephedrine is primarily excreted unchanged in urine (7).

A GLC method was reported for the determination of chlorpheniramine in urine (2). Similarly, methods utilizing GLC (8, 9) or a radiolabeled technique (3) were reported for the determination of pseudoephedrine in urine. The purposes of this investigation were: (*a*) to develop a simple, specific, high-pressure liquid chromatographic (HPLC) method for the simultaneous determination of chlorpheniramine, its demethylated metabolites, and pseudoephedrine and (*b*) to apply this method in studying the urinary excretion of these drugs and their metabolites in humans.

EXPERIMENTAL

Protocol—Nine healthy, nonobese, male subjects participated. They did not receive any drugs, including enzyme-inducing agents and monoamine oxidase inhibitors, 1 month before and during the study. Caffeine-containing and alcoholic beverages also were withheld during the entire study.

Five of the subjects received one sustained-release capsule[1] containing 8 mg of chlorpheniramine maleate and 120 mg of pseudoephedrine hydrochloride on Day 1, after an overnight fast, followed by an additional 4-hr fasting period. Thereafter, the subjects received one capsule every 12 hr for 6 days (Days 2–7) and then one capsule on Day 8. Cumulative urine samples were collected during the 0–24-hr period and at the steady state during the 156–168- and 168–180-hr periods.

The other four subjects received one single capsule with and without ammonium chloride treatment according to a double crossover design. A washout period of 1 week was allowed between treatments. The capsule was always taken after an overnight fast and followed by 4 hr of fasting. One day before and throughout the study period (~68 hr), two enteric coated ammonium chloride tablets[2] (500 mg each) were administered every 2 hr. The first dose taken before retiring and that given on arising always consisted of four tablets (2 g). When a subject's urinary pH was >5.3, one additional ammonium chloride tablet was administered after the urinary pH measurement. If the urinary pH was <4.9, the next scheduled dose was omitted. An attempt was made to control the urine flow by frequent oral administration of liquids throughout the study periods. Urine samples were collected from −1 to 0 hr, *i.e.*, just before the drug was administered, and at frequent intervals up to 48 hr.

During the entire investigation, standard meals were given to all subjects. Urine pH was determined at room temperature, and the volume of each urine sample was measured in a graduated cylinder. An aliquot of 30 ml of the thoroughly mixed sample was withdrawn and stored at −15° until assayed.

Assay—Chlorpheniramine and pseudoephedrine concentrations were determined according to the following methods.

Method I—Two-milliliter samples of urine or standard solution containing 0.06–3 μg of chlorpheniramine maleate[3]/ml and 1.5–75 μg of pseudoephedrine hydrochloride[4]/ml were taken for assay. To the samples were added 0.5 ml of 5% KOH solution and 5 ml of an extraction solvent consisting of hexane–methylene chloride (60:40). The samples were shaken for 30 min and centrifuged. Four milliliters of the solvent was pipetted into a vial containing 0.5 ml of chlorpromazine hydrochloride[5], 1 μg/ml in methanol. The mixture was evaporated under nitrogen. The residue was dissolved in 50 μl of methanol from which 20 μl was removed for injection.

Method II—Two-milliliter samples of urine or standard solution

[1] Arnar-Stone Laboratories, McGaw Park, Ill.
[2] Eli Lilly & Co., Indianapolis, Ind.
[3] E. M. Labs, Elmsford, N.Y.
[4] A. G. Knoll, Whippany, N.J.
[5] H. Reisman Corp., Orange, N.J.

0022-3549/79/1000-1243$01.00/0
© 1979, American Pharmaceutical Association

The authors are grateful for the generous samples of O^2- and O^3-demethylcolchicine provided by Professor M. Schonharting and Professor G. Siebert and for technical assistance by Ms. Susan Price in conducting some of the screening experiments. A. M. Clark acknowledges a fellowship from the American Foundation for Pharmaceutical Education. The authors also acknowledge Dr. Ching-Jer Chang, Purdue University, for suggesting the selective single-frequency proton-decoupling experiments at very low decoupling power.

Urinary Excretion of Chlorpheniramine and Pseudoephedrine in Humans

C. M. LAI, R. G. STOLL, Z. M. LOOK, and A. YACOBI ˣ

Received January 29, 1979, from the *Pharmaceutical Development Department, Research and Medical Affairs, Arnar-Stone Laboratories, Inc., McGaw Park, IL 60085.* Accepted for publication April 10, 1979.

Abstract □ A specific high-pressure liquid chromatographic method for the determination of chlorpheniramine and pseudoephedrine in urine was developed and applied in a urinary excretion study of normal healthy subjects who received a sustained-release dosage form containing 8 mg of chlorpheniramine maleate and 120 mg of pseudoephedrine hydrochloride. Five subjects received one dose on Day 1, followed by multiple dosing every 12 hr for 7 days without ammonium chloride administration. Four subjects received one dose of the sustained-release dosage form together with ammonium chloride. Urine samples were collected during the 1st day and at steady state. The method is specific and simultaneously determines chlorpheniramine, two metabolites (mono- and didesmethylchlorpheniramine), pseudoephedrine, and norpseudoephedrine. The assay recovery was >97% (0.06–3 μg/ml) for chlorpheniramine maleate and >98% (1.5–75 μg/ml) for pseudoephedrine hydrochloride. Excretion of chlorpheniramine and its two metabolites in urine was enhanced after ammonium chloride administration. At steady state, a change in urine pH from 5.69 to 6.46 resulted in more than a 25% decrease in chlorpheniramine and monodesmethylchlorpheniramine excretion. In spite of expected changes in its biological half-life, the overall amount of unchanged pseudoephedrine excreted in urine was not affected by urine pH, presumably because it is primarily excreted in urine as intact drug.

Keyphrases □ Chlorpheniramine—urinary excretion, humans, high-pressure liquid chromatographic analysis □ Chlorpheniramine metabolites—urinary excretion, humans, high-pressure liquid chromatographic analysis □ Pseudoephedrine—urinary excretion, humans, high-pressure liquid chromatographic analysis □ Nasal decongestants—chlorpheniramine and pseudoephedrine, urinary excretion, humans □ High-pressure liquid chromatography—analysis, chlorpheniramine and pseudoephedrine in human urine

Chlorpheniramine and pseudoephedrine, two weak basic drugs, are often used together for treatment of nasal congestion. The extent and rate of urinary excretion of the unchanged drugs are pH and urine flow dependent (1–3). Chlorpheniramine is extensively metabolized *via* *N*-dealkylation and excreted as both mono- and didesmethyl compounds (1, 4–6), and it is expected that the excretion of these metabolites in urine is also urine pH dependent. Pseudoephedrine is primarily excreted unchanged in urine (7).

A GLC method was reported for the determination of chlorpheniramine in urine (2). Similarly, methods utilizing GLC (8, 9) or a radiolabeled technique (3) were reported for the determination of pseudoephedrine in urine. The purposes of this investigation were: (*a*) to develop a simple, specific, high-pressure liquid chromatographic (HPLC) method for the simultaneous determination of chlorpheniramine, its demethylated metabolites, and pseudoephedrine and (*b*) to apply this method in studying the urinary excretion of these drugs and their metabolites in humans.

EXPERIMENTAL

Protocol—Nine healthy, nonobese, male subjects participated. They did not receive any drugs, including enzyme-inducing agents and monoamine oxidase inhibitors, 1 month before and during the study. Caffeine-containing and alcoholic beverages also were withheld during the entire study.

Five of the subjects received one sustained-release capsule[1] containing 8 mg of chlorpheniramine maleate and 120 mg of pseudoephedrine hydrochloride on Day 1, after an overnight fast, followed by an additional 4-hr fasting period. Thereafter, the subjects received one capsule every 12 hr for 6 days (Days 2–7) and then one capsule on Day 8. Cumulative urine samples were collected during the 0–24-hr period and at the steady state during the 156–168- and 168–180-hr periods.

The other four subjects received one single capsule with and without ammonium chloride treatment according to a double crossover design. A washout period of 1 week was allowed between treatments. The capsule was always taken after an overnight fast and followed by 4 hr of fasting. One day before and throughout the study period (~68 hr), two enteric coated ammonium chloride tablets[2] (500 mg each) were administered every 2 hr. The first dose taken before retiring and that given on arising always consisted of four tablets (2 g). When a subject's urinary pH was >5.3, one additional ammonium chloride tablet was administered after the urinary pH measurement. If the urinary pH was <4.9, the next scheduled dose was omitted. An attempt was made to control the urine flow by frequent oral administration of liquids throughout the study periods. Urine samples were collected from −1 to 0 hr, *i.e.*, just before the drug was administered, and at frequent intervals up to 48 hr.

During the entire investigation, standard meals were given to all subjects. Urine pH was determined at room temperature, and the volume of each urine sample was measured in a graduated cylinder. An aliquot of 30 ml of the thoroughly mixed sample was withdrawn and stored at −15° until assayed.

Assay—Chlorpheniramine and pseudoephedrine concentrations were determined according to the following methods.

Method I—Two-milliliter samples of urine or standard solution containing 0.06–3 μg of chlorpheniramine maleate[3]/ml and 1.5–75 μg of pseudoephedrine hydrochloride[4]/ml were taken for assay. To the samples were added 0.5 ml of 5% KOH solution and 5 ml of an extraction solvent consisting of hexane–methylene chloride (60:40). The samples were shaken for 30 min and centrifuged. Four milliliters of the solvent was pipetted into a vial containing 0.5 ml of chlorpromazine hydrochloride[5], 1 μg/ml in methanol. The mixture was evaporated under nitrogen. The residue was dissolved in 50 μl of methanol from which 20 μl was removed for injection.

Method II—Two-milliliter samples of urine or standard solution

[1] Arnar-Stone Laboratories, McGaw Park, Ill.
[2] Eli Lilly & Co., Indianapolis, Ind.
[3] E. M. Labs, Elmsford, N.Y.
[4] A. G. Knoll, Whippany, N.J.
[5] H. Reisman Corp., Orange, N.J.

0022-3549/79/1000-1243$01.00/0
© 1979, American Pharmaceutical Association

Table I—Recovery and Day-to-Day Variation of the Simultaneous HPLC Determination of Chlorpheniramine and Pseudoephedrine in Urine

Concentration Range, μg/ml	Mean Percent Recovery ± SD		
		Method II[a]	
	Method I	First Determination	Second Determination
Chlorpheniramine			
0.06–3	97.3 ± 4.47	102.8 ± 1.61	97.9 ± 3.84
n	30	23	8
Pseudoephedrine			
1.5–75	89.7 ± 11.2	98.1 ± 4.78	98.4 ± 7.16
n	30	23	8

[a] There were 3 days between the first and second determinations.

containing 0.06–3 μg of chlorpheniramine maleate/ml and 1.5–75 μg of pseudoephedrine hydrochloride/ml were taken for the assay. To the samples were added 0.5 ml of 5% KOH solution and 4 ml of an extraction solvent consisting of ether–methylene chloride (70:30). The samples were shaken for 30 min, centrifuged, and then immersed in a dry ice–isopropanol bath.

After the aqueous layer was frozen, the organic layer was transferred to a clean tube containing 100 μl of imipramine hydrochloride[6] solution (8 μg/ml in 0.5% phosphoric acid). The mixture was vortexed, centrifuged,

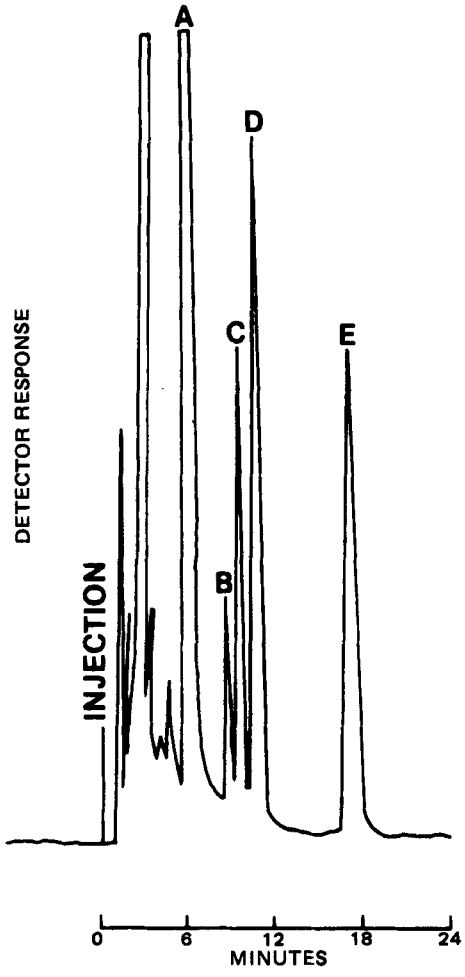

Figure 1—*Typical chromatogram of a urine sample from a subject after multiple-dose administration (for 8 days every 12 hr) of the sustained-release capsule containing 8 mg of chlorpheniramine maleate and 120 mg of pseudoephedrine hydrochloride. This sample was assayed according to Method I. Key: A, pseudoephedrine at 6 min; B, didesmethylchlorpheniramine at 8.5 min; C, monodesmethylchlorpheniramine at 9.0 min; D, chlorpheniramine at 10 min; and E, internal standard (chlorpromazine) at 16.0 min.*

[6] Sigma Chemical Co., St. Louis, Mo.

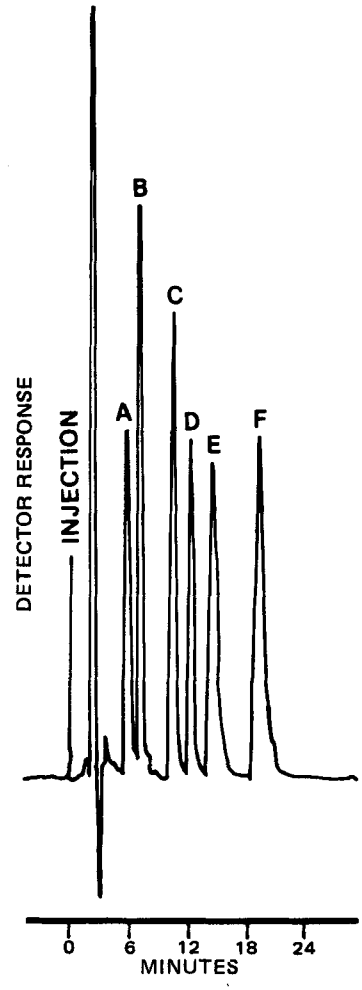

Figure 2—*Typical chromatogram of a blank urine sample spiked with the mixture of chlorpheniramine, pseudoephedrine, and their metabolites. This sample was assayed according to Method II. Key: A, norpseudoephedrine at 6.30 min; B, pseudoephedrine at 7.20 min; C, didesmethylchlorpheniramine at 10.6 min; D, monodesmethylchlorpheniramine at 12.3 min; E, chlorpheniramine at 14.6 min; and F, internal standard (imipramine) at 19.5 min.*

and frozen again. The organic layer was discarded and the aqueous layer was purified of residual organic solvents under vacuum. Twenty microliters of the remaining solution was injected.

For both methods, all glassware was washed first with 4 *N* nitric acid followed by a methanol wash. The specificity of each method was tested for two chlorpheniramine metabolites, mono- and didesmethylchlorpheniramine[7]. Method II also was tested for norpseudoephedrine[8].

All urine and the standard solution samples were assayed with a high-pressure liquid chromatograph[9] fitted with one[10] (Method I) or two[11] (Method II) 30-cm × 4-mm i.d. columns. The columns were packed with microparticulate silica permanently coated with a propylcyano layer. The mercury source UV absorbance detector was equipped with a 254-nm filter[12]. The flow rate of the mobile phase, acetonitrile–methanol–phosphate buffer (0.005 *M* Na_2HPO_4 and 0.01 *M* NaH_2PO_4, pH 6.6) (25:25:50), was 2 ml/min. The final pH of the mobile phase was 7.6.

RESULTS

Figure 1 depicts a typical chromatogram of a urine sample from a subject who received multiple dosing of the capsule containing 8 mg of

[7] Courtesy of Smith Kline & French Laboratories, Philadelphia, Pa.
[8] Aldrich Chemical Co., Milwaukee, Wis.
[9] Model ALC/GPC 204, Waters Associates, Milford, Mass.
[10] μBondapak CN column, packed in hexane, manufactured in 1977 and marketed until August 1977; Waters Associates, Milford, Mass.
[11] μBondapak CN column, packed in methanol–water (70:30), introduced in the market in December 1977; Waters Associates, Milford, Mass.
[12] Model 440 detector, Waters Associates, Milford, Mass.

Table II—Effect of pH on Excretion of Unchanged Chlorpheniramine and Pseudoephedrine in Urine

Urinary Excretion Time, hr	Urine pH	Total Amount Excreted[a], Mean ± *SD*, mg			
		Chlorpheniramine	Monodesmethyl-chlorpheniramine	Didesmethyl-chlorpheniramine	Pseudoephedrine
0–24 (single dose)[b]	5.31 ± 0.315	1.19 ± 0.267	0.835 ± 0.242	0.284 ± 0.158	116 ± 6.78
0–24 (single dose)[b]	5.95 ± 0.407	0.438 ± 0.071	0.537 ± 0.173	0.161 ± 0.163	104 ± 8.52
0–24 (multiple dose)	6.16 ± 0.470	0.557 ± 0.595	0.767 ± 0.517	0.265 ± 0.124	104 ± 10.3
156–168 (steady state)	5.69 ± 0.434	1.44 ± 1.19	1.80 ± 0.558	0.373 ± 0.086	109 ± 22.5
168–180 (steady state)[c]	6.46 ± 0.507	1.07 ± 1.26	1.32 ± 0.428	0.366 ± 0.119	104 ± 21.5

[a] These values are expressed in equivalents of chlorpheniramine maleate (for chlorpheniramine and its metabolites) and pseudoephredrine hydrochloride. [b] Mean of four subjects; all others are means of five subjects. These subjects received the drugs with and without ammonium chloride in a two-way crossover fashion. [c] Statistically significant difference (paired *t*-test) from 156–168-hr period with respect to urine pH ($p < 0.005$), chlorpheniramine ($p < 0.02$), and monodesmethylchlorpheniramine ($p < 0.025$).

chlorpheniramine maleate and 120 mg of pseudoephedrine hydrochloride. Figure 2 shows a typical chromatogram of a blank urine sample spiked with chlorpheniramine, mono- and didesmethylchlorpheniramine, pseudoephedrine, and norpseudoephedrine. The chromatograms shown in Figs. 1 and 2 were determined by assay Methods I and II, respectively.

Table I summarizes the results of the recovery and reproducibility study for chlorpheniramine and pseudoephedrine by both methods. The recovery with Method I was 97.3 ± 4.47% (mean ± *SD*, $n = 8$) for chlorpheniramine and 89.7 ± 11.2% for pseudoephedrine. The recovery with Method II, using the same urine samples 3 days later, was 97.9 ± 3.84% for chlorpheniramine and 98.4 ± 7.16% ($n = 8$) for pseudoephedrine. There was no correlation between the recovery and the urine concentration for either drug.

Figure 3 depicts the day-to-day reproducibility of Method II. A plot of the determined concentrations on the 1st day (x) *versus* the corresponding concentrations of the same urine samples determined 3 days later (y) gave regression lines of $y = 0.079 \pm 0.980x$ ($r = 0.999$) for 0.06–3 μg of chlorpheniramine maleate/ml of urine and $y = 0.0637 \pm 0.961x$ ($r = 0.997$) for 1.5–75 μg of pseudoephedrine hydrochloride/ml of urine.

Figure 4 shows the average time course of cumulative urinary excretion of chlorpheniramine and its metabolites in three subjects after ingestion of a single capsule containing 8 mg of chlorpheniramine maleate and 120 mg of pseudoephedrine hydrochloride. Table II summarizes the amounts of chlorpheniramine, its two metabolites, and pseudoephedrine excreted unchanged in urine after a single dose and at steady state after administration of the same dose every 12 hr for 8 days. Of the chlorpheniramine dose, 18.0% was excreted intact, 22.5% was excreted as monodesmethylchlorpheniramine, and 4.7% was excreted as didesmethylchlorpheniramine. During the same period, 91% of the pseudoephedrine dose was excreted intact in this group of subjects.

Table II also shows that a significant elevation in urine pH from an average of 5.69 to 6.46 apparently caused a significant decrease, about 25%, in the amount of chlorpheniramine and monodesmethylchlorpheniramine excreted in urine. There was no such effect on the excretion of pseudoephedrine in urine at steady state. Ammonium chloride enhanced excretion of chlorpheniramine and its metabolites but had relatively little effect on the total unchanged pseudoephedrine excreted in urine (Table II). The amount of norpseudoephedrine excreted in urine of these subjects was negligible with or without ammonium chloride treatment.

DISCUSSION

Method I was originally developed for a simultaneous determination of chlorpheniramine and pseudoephedrine in urine using a propylcyano HPLC column. It was successfully utilized to assay the urine samples from the multiple-dose study as well as some samples from the single-dose study. During an interim period, the HPLC column was improved by the manufacturer. Because of this change, certain adjustments had to be made in the extraction procedure, resulting in the development of Method II. Additionally, the internal standard from Method I, *i.e.*, chlorpromazine, was replaced by imipramine, which showed better stability under the acidic conditions of Method II and had a shorter retention time.

The assay is specific for the simultaneous determination of unchanged chlorpheniramine and pseudoephedrine. It also separates two metabolites of chlorpheniramine, mono- and didesmethylchlorpheniramine, and the pseudoephedrine metabolite, norpseudoephedrine. In spite of the similarity in the HPLC mobile phases, the retention times of the individual compounds determined by Method II were relatively longer than those determined by Method I. Method II also provided better resolution than did Method I. This finding was expected since the new assay utilized two columns and, therefore, the number of the theoretical chromatographic plates was larger, which consequently resulted in improved resolutions of the compounds by HPLC.

Both chlorpheniramine and pseudoephedrine are stable in aqueous solution under drastic temperature conditions (10). There was no indication of any instability in urine. The reproducibility and precision of the assay are very high for both compounds, as evidenced by relatively small coefficients of variation, 1.6 and 4.8% for chlorpheniramine and pseudoephedrine, respectively, and very little day-to-day variation (Table I and Fig. 3).

Chlorpheniramine is extensively metabolized to mono- and didesmethylchlorpheniramine and other nonextractable metabolites (4). In this study, under steady-state conditions, only about one-half of the dose was excreted in urine as chlorpheniramine and its two metabolites within one dosing interval. This result suggests that chlorpheniramine is excreted as unextractable metabolites in urine since there was no evidence of other measurable compounds by HPLC. Consistent with theory and the published literature (2), excretion of unchanged chlorpheniramine was urine pH dependent. The excretion of the two demethylated chlorpheniramine metabolites was also pH dependent after a single dose and at steady state. A small fluctuation in the urine pH at steady state

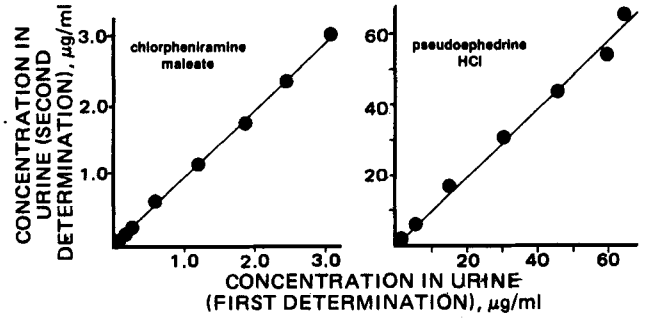

Figure 3—*Day-to-day variation of the simultaneous HPLC determination of chlorpheniramine and pseudoephedrine in urine by Method II. There were 3 days between the first and second determinations.*

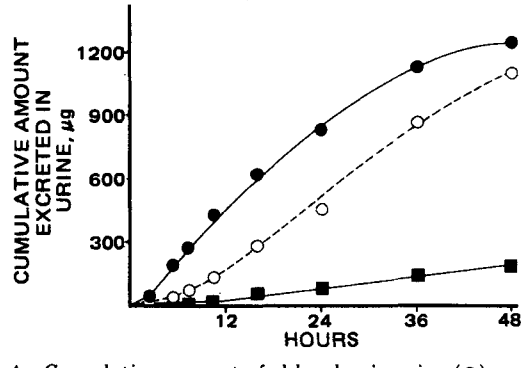

Figure 4—*Cumulative amount of chlorpheniramine (●) and its metabolites, monodesmethylchlorpheniramine (○) and didesmethylchlorpheniramine (■), expressed as chlorpheniramine equivalents following administration of a single dose of 8 mg of chlorpheniramine maleate and 120 mg of pseudoephedrine hydrochloride in a capsule to three normal subjects who also received ammonium chloride throughout the study.*

caused substantial changes in excretion of chlorpheniramine and the monodesmethyl metabolite. In this study, the change in urine pH during two different urine collection intervals was expected and was presumably due to variations in diet.

The urinary pseudoephedrine excretion rate was enhanced under controlled acidic urine pH (3). However, the overall amount excreted unchanged was not dependent on urine pH. The excretion of negligible norpseudoephedrine, the principal metabolite, with and without pH control also supports this observation.

REFERENCES

(1) G. R. Wilkinson and A. H. Beckett, *J. Pharmacol. Exp. Ther.*, **162**, 139 (1968).

(2) A. H. Beckett and G. R. Wilkinson, *J. Pharm. Pharmacol.*, **17**, 256 (1968).

(3) R. G. Kuntzman, I. Tsai, L. Brand, and L. C. Mark, *Clin. Pharmacol. Ther.*, **2**, 62 (1971).

(4) P. Kabasakalian, M. Taggart, and E. Townley, *J. Pharm. Sci.*, **57**, 856 (1968).

(5) J. J. Kamm, C. R. Fernllo, D. Miller, and E. J. Vanloon, *Biochem. Pharmacol.*, **18**, 659 (1969).

(6) E. A. Peets, M. Jackson, and S. Symchowicz, *J. Pharmacol. Exp. Ther.*, **180**, 464 (1972).

(7) C. Bye, H. M. Hill, D. T. D. Hughes, and A. W. Peck, *Eur. J. Clin. Pharmacol.*, **8**, 47 (1975).

(8) L. M. Cummins and M. J. Fourier, *Anal. Lett.*, **2**, 203 (1969).

(9) E. T. Lin, D. C. Brater, and L. Z. Benet, *J. Chromatogr.*, **140**, 275 (1977).

(10) A. Yacobi, Z. M. Look, and C. M. Lai, *J. Pharm. Sci.*, **67**, 1668 (1978).

Surface Properties of Membrane Systems: Interaction of Ketamine with Monomolecular Films of Gangliosides and Mitochondrial Lipids

GIUSEPPE COLACICCO *[x], JEANNE M. BURNELL, and MUKUL K. BASU

Received May 30, 1978, from the *Albert Einstein College of Medicine, Bronx, NY 10461.* Accepted for publication April 9, 1979.

*Present address: Bioelectrochemistry Laboratory, College of Physicians & Surgeons of Columbia University, New York, NY 10032.

Abstract □ Ketamine solutions did not form a film ($\pi = 0$) but had an appreciable surface potential (ΔV = 500 mv), indicating a significant array of ± oriented charge dipoles at the air–water interface, as opposed to calcium chloride solutions whose ΔV was zero. The ΔV values of ganglioside films spread on the aqueous phase varied in the order water < sodium chloride < calcium chloride < ketamine hydrochloride. At equivalent concentrations, calcium chloride was 500 times as effective as sodium chloride, and ketamine at the clinical concentrations of 10–20 μg/ml (36–72 μ*M*) was 6000 times as effective as calcium chloride in raising the surface potential of gangliosides; the ΔV effect with mitochondrial lipid was in the reverse order: water < sodium chloride = ketamine hydrochloride < calcium chloride. This calcium–ketamine inversion indicates a unique specificity of ketamine for gangliosides. Since ketamine acts on the brain and did not affect mitochondrial respiration, the surface potential data suggest that part of the mechanism of action of ketamine could be its interaction with synaptic surfaces and, specifically, with the sialic acid of gangliosides and/or glycoproteins present on the synaptic membrane surface.

Keyphrases □ Membranes—surface properties, ketamine interaction with ganglioside and mitochondrial lipid monomolecular films □ Ketamine—effect on monomolecular films of gangliosides and mitochondrial lipids □ Gangliosides—monomolecular films, effect of ketamine □ Mitochondrial lipids—monomolecular films, effect of ketamine □ Analgesics—ketamine, effect on monomolecular films of gangliosides and mitochondrial lipids

Ketamine, a potent analgesic, acts on the cerebral cortex (1–5). Although the pharmacological effects of ketamine on the cardiovascular and respiratory systems have been defined clinically and experimentally (1–4), little is known about its mechanism of action at the molecular level. A relatively small molecule, which is prepared synthetically as the 2-(*o*-chlorophenyl)-2-(methylamine)cyclohexanone hydrochloride (mol. wt. 275), ketamine has been widely used and discussed as an analgesic, a dissociative anesthetic, and a preanesthetic in experimental and clinical surgery (1–4).

Although rapid induction of analgesia and cardiovascular stimulation with little effect on respiration and respiratory resistance are recognized effects of ketamine (1–4), it is believed that the major effects are a consequence of the direct action of ketamine on the central nervous system (1–4), specifically, the cerebral cortex (5). As a working hypothesis, it was assumed that the negatively charged surfaces of the synaptic membranes in the cerebral cortex are the target of this positively charged molecule.

The surface potential of the monomolecular film at the air–water interface is a suitable model in which to study the ionic properties of both the ketamine and the acidic synaptic components. Interaction of positively charged ketamine with negatively charged lipid films was expected to increase the surface potential (6, 7), which could then be related to film pressure and ion concentrations in the aqueous phase. Because of the role that Ca^{2+} plays in bioelectric phenomena and in the release of acetylcholine from synapses (5), the effects of Ca^{2+} and Na^{+} ions in the subphase were studied also.

The acidic lipid of choice was ganglioside; it is abundant in the synapses in the gray matter forming the cerebral cortex (8). For a comparison, a neutral phospholipid, dipalmitoyl phosphatidylcholine (dipalmitoyl lecithin), was used since the phosphatidylcholines (lecithins) are important constituents of cell membranes. The total lipid extract of mitochondria and isolated cardiolipin were studied for two reasons: (*a*) the mitochondrion is an important intracellular organelle, which controls vital biochemical processes; and (*b*) besides lecithin, the mitochondrial lipid contains about 10% cardiolipin (diphosphatidylglycerol), which is also acidic but is quite different from the ganglioside.

EXPERIMENTAL

Highly purified ketamine[1] and reagent grade electrolytes were used.

[1] Gift of Dr. A. M. Moore, Parke-Davis and Co., Ann Arbor, Mich.

0022-3549/79/1000-1246$01.00/0

© 1979, American Pharmaceutical Association

caused substantial changes in excretion of chlorpheniramine and the monodesmethyl metabolite. In this study, the change in urine pH during two different urine collection intervals was expected and was presumably due to variations in diet.

The urinary pseudoephedrine excretion rate was enhanced under controlled acidic urine pH (3). However, the overall amount excreted unchanged was not dependent on urine pH. The excretion of negligible norpseudoephedrine, the principal metabolite, with and without pH control also supports this observation.

REFERENCES

(1) G. R. Wilkinson and A. H. Beckett, *J. Pharmacol. Exp. Ther.*, **162**, 139 (1968).

(2) A. H. Beckett and G. R. Wilkinson, *J. Pharm. Pharmacol.*, **17**, 256 (1968).

(3) R. G. Kuntzman, I. Tsai, L. Brand, and L. C. Mark, *Clin. Pharmacol. Ther.*, **2**, 62 (1971).

(4) P. Kabasakalian, M. Taggart, and E. Townley, *J. Pharm. Sci.*, **57**, 856 (1968).

(5) J. J. Kamm, C. R. Fernllo, D. Miller, and E. J. Vanloon, *Biochem. Pharmacol.*, **18**, 659 (1969).

(6) E. A. Peets, M. Jackson, and S. Symchowicz, *J. Pharmacol. Exp. Ther.*, **180**, 464 (1972).

(7) C. Bye, H. M. Hill, D. T. D. Hughes, and A. W. Peck, *Eur. J. Clin. Pharmacol.*, **8**, 47 (1975).

(8) L. M. Cummins and M. J. Fourier, *Anal. Lett.*, **2**, 203 (1969).

(9) E. T. Lin, D. C. Brater, and L. Z. Benet, *J. Chromatogr.*, **140**, 275 (1977).

(10) A. Yacobi, Z. M. Look, and C. M. Lai, *J. Pharm. Sci.*, **67**, 1668 (1978).

Surface Properties of Membrane Systems: Interaction of Ketamine with Monomolecular Films of Gangliosides and Mitochondrial Lipids

GIUSEPPE COLACICCO *[x], JEANNE M. BURNELL, and MUKUL K. BASU

Received May 30, 1978, from the *Albert Einstein College of Medicine, Bronx, NY 10461.* Accepted for publication April 9, 1979.

*Present address: Bioelectrochemistry Laboratory, College of Physicians & Surgeons of Columbia University, New York, NY 10032.

Abstract □ Ketamine solutions did not form a film ($\pi = 0$) but had an appreciable surface potential (ΔV = 500 mv), indicating a significant array of ± oriented charge dipoles at the air–water interface, as opposed to calcium chloride solutions whose ΔV was zero. The ΔV values of ganglioside films spread on the aqueous phase varied in the order water < sodium chloride < calcium chloride < ketamine hydrochloride. At equivalent concentrations, calcium chloride was 500 times as effective as sodium chloride, and ketamine at the clinical concentrations of 10–20 μg/ml (36–72 μ*M*) was 6000 times as effective as calcium chloride in raising the surface potential of gangliosides; the ΔV effect with mitochondrial lipid was in the reverse order: water < sodium chloride = ketamine hydrochloride < calcium chloride. This calcium–ketamine inversion indicates a unique specificity of ketamine for gangliosides. Since ketamine acts on the brain and did not affect mitochondrial respiration, the surface potential data suggest that part of the mechanism of action of ketamine could be its interaction with synaptic surfaces and, specifically, with the sialic acid of gangliosides and/or glycoproteins present on the synaptic membrane surface.

Keyphrases □ Membranes—surface properties, ketamine interaction with ganglioside and mitochondrial lipid monomolecular films □ Ketamine—effect on monomolecular films of gangliosides and mitochondrial lipids □ Gangliosides—monomolecular films, effect of ketamine □ Mitochondrial lipids—monomolecular films, effect of ketamine □ Analgesics—ketamine, effect on monomolecular films of gangliosides and mitochondrial lipids

Ketamine, a potent analgesic, acts on the cerebral cortex (1–5). Although the pharmacological effects of ketamine on the cardiovascular and respiratory systems have been defined clinically and experimentally (1–4), little is known about its mechanism of action at the molecular level. A relatively small molecule, which is prepared synthetically as the 2-(*o*-chlorophenyl)-2-(methylamine)cyclohexanone hydrochloride (mol. wt. 275), ketamine has been widely used and discussed as an analgesic, a dissociative anesthetic, and a preanesthetic in experimental and clinical surgery (1–4).

Although rapid induction of analgesia and cardiovascular stimulation with little effect on respiration and respiratory resistance are recognized effects of ketamine (1–4), it is believed that the major effects are a consequence of the direct action of ketamine on the central nervous system (1–4), specifically, the cerebral cortex (5). As a working hypothesis, it was assumed that the negatively charged surfaces of the synaptic membranes in the cerebral cortex are the target of this positively charged molecule.

The surface potential of the monomolecular film at the air–water interface is a suitable model in which to study the ionic properties of both the ketamine and the acidic synaptic components. Interaction of positively charged ketamine with negatively charged lipid films was expected to increase the surface potential (6, 7), which could then be related to film pressure and ion concentrations in the aqueous phase. Because of the role that Ca^{2+} plays in bioelectric phenomena and in the release of acetylcholine from synapses (5), the effects of Ca^{2+} and Na^{+} ions in the subphase were studied also.

The acidic lipid of choice was ganglioside; it is abundant in the synapses in the gray matter forming the cerebral cortex (8). For a comparison, a neutral phospholipid, dipalmitoyl phosphatidylcholine (dipalmitoyl lecithin), was used since the phosphatidylcholines (lecithins) are important constituents of cell membranes. The total lipid extract of mitochondria and isolated cardiolipin were studied for two reasons: (*a*) the mitochondrion is an important intracellular organelle, which controls vital biochemical processes; and (*b*) besides lecithin, the mitochondrial lipid contains about 10% cardiolipin (diphosphatidylglycerol), which is also acidic but is quite different from the ganglioside.

EXPERIMENTAL

Highly purified ketamine[1] and reagent grade electrolytes were used.

[1] Gift of Dr. A. M. Moore, Parke-Davis and Co., Ann Arbor, Mich.

0022-3549/79/1000-1246$01.00/0

© 1979, American Pharmaceutical Association

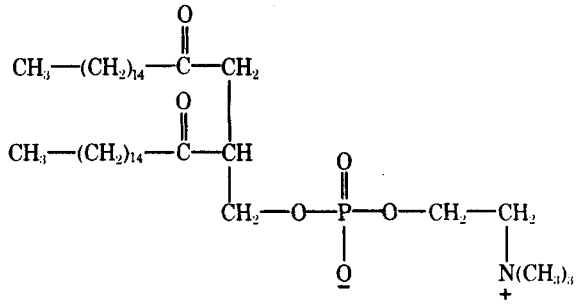

dipalmitoyl lecithin

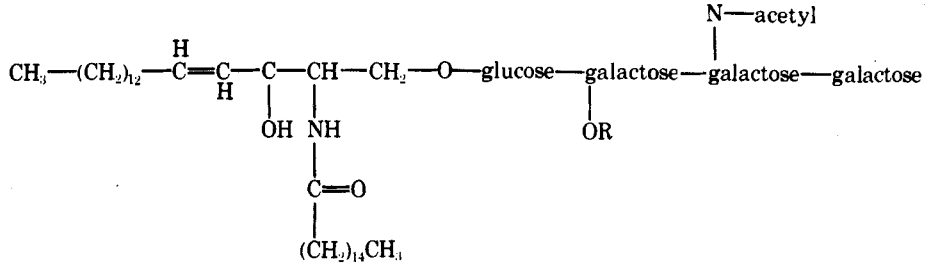

ganglioside (monosialo) (R = *N*-acetyl neuraminic acid)

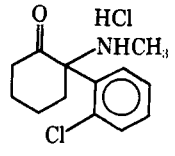

ketamine hydrochloride

Dipalmitoyl lecithin and beef heart cardiolipin (diphosphatidylglycerol) were chromatographically homogeneous[2]. Beef brain mixed ganglioside (9) and rat liver mitochondria (10) were prepared according to known methods[3]. Liver mitochondria were used, because they are more readily available than brain mitochondria and, for all practical purposes, the relative lipid composition is the same in various species and organs (11). The mitochondria exhibited a normal increase in respiratory rate upon addition of adenosine diphosphate[4].

The total lipid extract of the mitochondria was obtained by shaking the aqueous mitochondrial dispersion with four volumes of chloroform–methanol (2:1) and a second time with four volumes of chloroform. The mitochondrial lipids were identified by TLC on plates precoated with silica gel G, using chloroform–methanol–ammonia (65:35:5), the appropriate lipid standards, the work of Fleischer and Rouser (11), and various group reaction stains such as iodine vapors, the molybdenum trioxide spray for phosphorus, and the ninhydrin spray for the primary amino groups of phosphatidylethanolamine and phosphatidylserine (7).

The lipid solutions for the monolayer experiments were prepared in chloroform–methanol–hexane (50:40:20) and stored at −20°, but they were kept in ice during the experiments. Under these conditions, the lipids were stable for >2 weeks, as compared to 2 days when their solutions were stored at 0° (7). Since at −20° the ganglioside tended to precipitate out from the organic solvent, the solution was first warmed to complete clearness for 1 min at ~40° before it was put on ice for the duration of the experiment.

The procedures for the determination of surface pressure (π) and surface potential (ΔV) at the air–water interface have been described (12), except for minor modifications. Surface tension (γ) was measured by the Wilhelmy plate method, using a platinum blade suspended from a Cahn electrobalance; the film pressure (π) was calculated as the difference between γ_0 (without film) and γ (with film). The electrical potentials without film (V_0) and with film (V) were measured by a radioactive ^{226}Ra air electrode and a saturated calomel electrode connected with a high impedance electrometer; the surface potential (ΔV) was calculated as the difference $V - V_0$.

The lipid films were spread from organic solvent (1 mg/ml) on distilled water, ketamine hydrochloride, or electrolyte solutions in a circular glass trough whose useful area was 20 cm^2; ketamine films and other films were made by either spreading from organic solvent or adsorbing from aqueous solutions (13).

The electrolyte solutions were prepared with reagent grade salts and foamed to remove surface-active contaminants (12). The water was distilled twice, the second time from alkaline permanganate. A large long-neck flask and a tall fractionating Vigreux column were used upright in the distillation to avoid contamination of the distillate with permanganate sprays (14).

RESULTS AND DISCUSSION

Relation of Surface Activity to Molecular Structure—The structures of three molecules, dipalmitoyl phosphatidylcholine, a monosialoganglioside, and ketamine hydrochloride, are depicted. Although natural gangliosides are mixtures of molecules containing C_{18} and C_{20} sphingosine chains (8), only the C_{18} chain is specified for simplicity; similarly, details of the bonds between the sugar moieties were beyond the scope of the present article.

Unlike the molecules of dipalmitoyl phosphatidylcholine and monosialogangliosides, whose long hydrophobic chains confer the molecule asymmetry and amphiphilic or bimodal character and surface activity, the ketamine molecule is short and nearly spherical in its rotational volume and has a relatively symmetrical distribution of polar groups. Thus, ketamine hydrochloride is not expected to form stable films but, like Ca^{2+} and Na^+, should interact with water and anionic surfaces.

Spread Films—*Ketamine*—Upon application from organic solvent onto the surface of distilled water, ketamine did not spread as a film. The surface pressure was zero, but the surface potential oscillated erratically between 10 and 30 mv (Fig. 1). Similar results were obtained when ketamine was spread from aqueous solutions. The small fluctuating ΔV values may be ascribed to small local surface concentrations of ketamine,

[2] Applied Science Laboratories, State College, Pa.

[3] The ganglioside and mitochondria were kindly provided by Dr. R. Ledeen and Dr. D. Rezek, Departments of Neurology and Biochemistry, Albert Einstein College of Medicine, Bronx, NY 10461.

[4] D. Rezek, Department of Neurology, Albert Einstein College of Medicine, Bronx, NY 10461, personal communication.

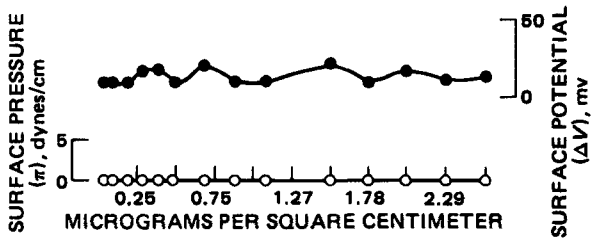

Figure 1—*Surface pressure and surface potential values on the distilled water surface after application of ketamine hydrochloride (micrograms per square centimeter).*

which diffused into the aqueous subphase until the surface potential became nearly zero.

Lipids—In marked contrast are the corresponding properties of spread films of dipalmitoyl lecithin and ganglioside. In Fig. 2, surface pressure (in dynes per centimeter) and surface potential (in millivolts) are related to the quantities of phospholipid and ganglioside (in micrograms per square centimeter) applied onto the distilled water surface. As with many known lipids, both the pressure and the surface potential curves of dipalmitoyl lecithin show the typical continuous rise to saturation. However, the ganglioside surface potential had an unusual maximum at ~25 dynes/cm, after which it decreased gradually from 220 to 200 mv, whereas the pressure rose regularly to a saturation value of 42 dynes/cm. Since the pressure continued to rise, the film was not collapsing.

Since the molecular correlates of the surface potential are not clearly established (7, 14–19), the cause for the unusual fall in the surface potential of the ganglioside is unclear. In accordance with the general meaning of the Helmoltz equation for the voltage of the parallel plate capacitor (17), possible reasons for lower potential are: (*a*) formation of hydrophilic interfacial structures having a high dielectric constant and (*b*) appearance of an excess of ∓ dipoles. The π–*A* curve of mitochondrial lipid on 0.15 *M* NaCl (not shown) resembled that of dipalmitoyl phosphatidylcholine, but the surface potential was lower (<500 mv), due probably to the anionic cardiolipin. Except for being more expanded because of the greater cross section of this lipid, the force–area curves of the latter and of mitochondrial lipid were very similar to those of dipalmitoyl lecithin and ganglioside. The ΔV–area curve of cardiolipin, however, differed markedly from those of ganglioside and mitochondrial lipid (20).

Adsorbed Ketamine Films—Since most of the experiments described later dealt with lipid films spread on either electrolyte or ketamine solutions, it was pertinent to determine the surface pressure and the surface potential of the aqueous hypophase. At concentrations of 10, 20, and 200 μg/ml, neither sodium chloride, calcium chloride, nor ketamine hydrochloride affected the surface tension; for all practical purposes, the film pressure was zero, as was that of distilled water. One concludes that the surface activity of ketamine was nil or <0.1 dyne/cm (the accuracy of the surface tension measurements). The surface potential, however, increased with the ketamine concentration (Fig. 3).

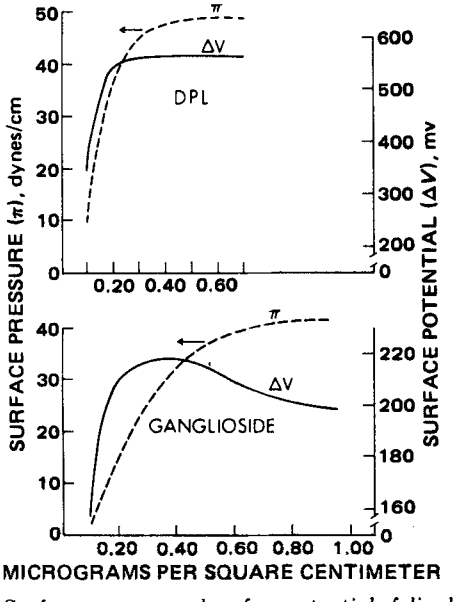

Figure 2—*Surface pressure and surface potential of dipalmitoyl lecithin (DPL) and beef brain mixed ganglioside films spread on distilled water. The lipid quantity applied on the aqueous phase surface is expressed in micrograms per square centimeter.*

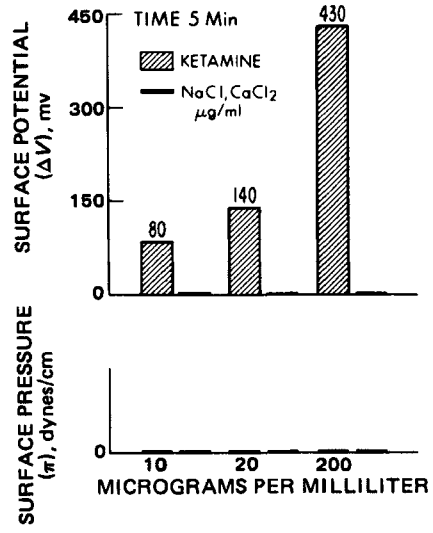

Figure 3—*Surface pressure and surface potential values of various sodium chloride, calcium chloride, and ketamine hydrochloride concentrations in distilled water 5 min after putting the solution in the trough.*

The zero pressure and large positive potential are consistent with a more marked effect of the ± ketamine hydrochloride dipole as compared to calcium chloride and sodium chloride, both of which had zero surface potential in the first 5 min. At 20 min, however, the ΔV values rose to 2, 5, and 530 mv with 200 μg of sodium chloride, calcium chloride, and ketamine hydrochloride/ml, respectively, in the subphase. With ketamine, a film pressure of 2 dynes/cm built up gradually between 10 and 20 min, whereas the pressure of the sodium chloride and calcium chloride solutions remained at zero. Similar results were observed with clinical preparations of ketamine hydrochloride[5].

Ketamine Interaction with Spread Lipid Films—The trough was filled with distilled water, the surface was cleaned (12), and measured volumes of concentrated aqueous ketamine solution were injected into the water with continuous magnetic stirring. After 2 min, the lipid was spread onto the aqueous subphase, and surface pressures and surface potentials were determined.

Gangliosides—In Fig. 4, the π and ΔV values are related to the quantity of ganglioside applied (in micrograms per square centimeter)

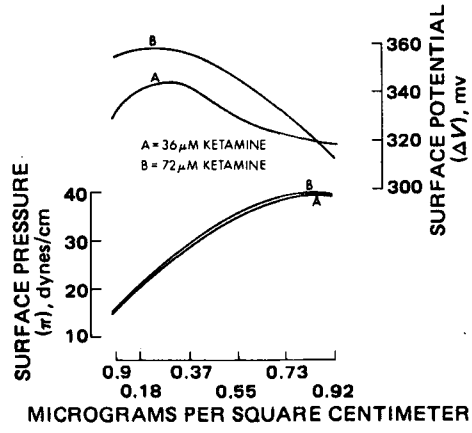

Figure 4—*Surface pressure and surface potential of ganglioside films spread on the aqueous subphase containing two different concentrations of ketamine hydrochloride The ganglioside quantity applied is expressed in micrograms per square centimeter.*

[5] G. Colacicco, A. Selis, and E. V. Cosmi, unpublished data.

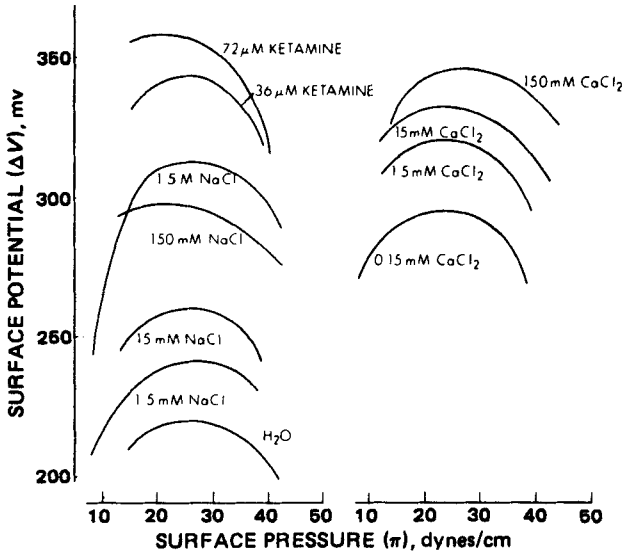

Figure 5—*Surface potential of ganglioside films spread on various sodium chloride, calcium chloride, or ketamine hydrochloride concentrations. The surface potential values are related to the values of the pressure of the ganglioside film.*

onto the surface of two different ketamine hydrochloride concentrations, 10 and 20 μg/ml, or 36 and 72 μ*M*, respectively. The ganglioside film pressure was practically the same for the two ketamine concentrations. The surface potential values, however, were greater for the greater ketamine concentration (curve B) and much greater than the values on distilled water (Fig. 2). Although the greater surface potential of the ganglioside on ketamine was probably due to interaction of the ketaminium cation with the anionic fixed charge of the ganglioside (6, 7), a contribution may come from ketamine penetration into the ganglioside film, as was recently suggested for the interaction of Ca^{2+} with dipalmitoyl lecithin films (14). As expected, the effect of ketamine on the dipalmitoyl lecithin surface potential was only a few millivolts, suggesting little interaction or penetration.

A comparison of ketamine with Na^+ and Ca^{2+} is shown in Fig. 5, which summarizes experiments where the ganglioside was spread on various concentrations of sodium chloride, calcium chloride, and ketamine hydrochloride. The surface potential values were related to the pressure of the ganglioside film on each electrolyte. In all cases, the ΔV values had a maximum at film pressure slightly above 25 dynes/cm, a maximum that appears to be a characteristic of the ganglioside.

The effectiveness of the electrolyte's cation was clearly in the order water < sodium chloride < calcium chloride < ketamine hydrochloride. The ΔV–π curve on distilled water was much lower than on 150 m*M* NaCl, which was near that on 150 μ*M* $CaCl_2$; this result indicates that the cation is important in causing a rise of the ganglioside surface potential. On an equivalents basis, Ca^{2+} was about 500 times as effective as Na^+. Since the surface potential on 150 m*M* $CaCl_2$ was about the same as on 50 μ*M* ketamine, on an equivalents basis, ketamine appears to be about 6000 times as effective as Ca^{2+}; *i.e.*, 6000 times the equivalent concentration of calcium chloride must be used to obtain the effect produced by 50 μ*M* ketamine.

Mitochondrial Lipids—Unlike the mixed gangliosides, the surface potential effect of ketamine on mitochondrial lipid was in the order water < ketamine = sodium chloride < calcium chloride (Fig. 6). Although it can distinguish between Ca^{2+} and Na^+ with a difference in ΔV that is customary with acidic phospholipids, namely $Ca^{2+} > Na^+ > H_2O$ (7), the anionic mitochondrial lipid apparently not only had no preference for ketamine, but the latter's effect was the same as that of Na^+, well below that of Ca^{2+}. This finding suggests a marked specificity and selectivity of the ketamine for the ganglioside.

This conclusion is supported by the fact that, in the interaction with cardiolipin, ketamine was markedly less effective than Ca^{2+} in raising the surface potential. Therefore, the diminished effect of ketamine with mitochondrial lipid is not caused just by a dilution of cardiolipin by lecithin and other nonionic lipids and is consistent with the fact that, in mixed films of dipalmitoyl lecithin and either dipalmitoyl phosphatidic acid or sodium dipalmitoyl phosphate, saturation of specific charge effects by Ca^{2+} occurred with 10–20 mole % of acidic lipid (14, 16), with ≥80 mole

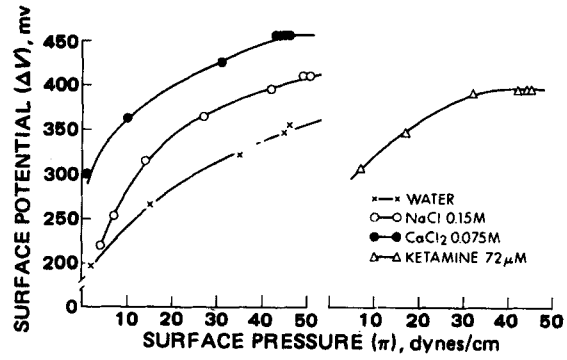

Figure 6—*Ketamine interactions with spread mitochondrial lipid films. The surface potential is related to the sodium chloride, calcium chloride, and ketamine hydrochloride concentrations in the aqueous phase.*

% of lecithin still in the film. Similarly, the large ΔV effect of the ganglioside–ketamine system was markedly reduced as the lecithin content was gradually increased.

This ionic behavior of cardiolipin, a mitochondrial lipid, and ganglioside could suggest that specificity of either interaction or penetration of ketamine requires homogeneous ganglioside rather than a mixed ganglioside–lecithin surface. To what extent this condition is realized in the biological system is still unknown; however, the biological significance of the experimental ganglioside–ketamine system is indicated by the fact that the ganglioside content is unusually high in gray matter, where ketamine is supposed to act (1–5).

Ketamine Effect on Rat Liver Mitochondrial Respiration—At a concentration of 10 μg/ml (37 μ*M*), at which it interacted strongly with the ganglioside, ketamine did not affect the oxidative phosphorylation coupling, measured by the rate of oxygen uptake[4].

This finding may indicate that unlike Ca^{2+}, which is known to affect the mitochrondrial respiration (21), ketamine did not interfere with either the surface potential of the mitochondrial lipid or intact mitochondrial respiration. Such results are consistent with the belief that mitochondria are probably not the site of action of ketamine.

Molecular Perspectives and Biological Significance—Two important properties of ketamine were shown: (*a*) a large surface potential (at zero pressure), which is relatable either to a unique orientation of ketamine's positive charge at the air–water interface or to a ± orientation of the dipoles of especially ionized surface water (18, 19), since ketamine pressure is zero or near zero and (*b*) the ability of micromolar ketamine concentrations to increase markedly the surface potential of ganglioside films, suggesting a unique ketamine interaction with ganglioside, indeed at concentrations at which Ca^{2+} and monovalent ions such as choline and acetylcholine hydrochloride had no comparable effect.

Although the large surface potential of ketamine solutions, about 500 mv in the absence of a film pressure, could be attributed to a large ketaminium$^+Cl^-$ dipole moment in the absence of film pressure, another contribution to the surface potential could derive from a ± orientation of ionized interfacial water on the ketamine solution surface (19).

Since ketamine was 6000 times more effective than Ca^{2+} in raising the surface potential of ganglioside, whereas the effect was comparably nil with dipalmitoyl lecithin films, and since Ca^{2+} plays a central role in acetylcholine discharge from the synapses during nerve function (5), invasion of the synaptic surfaces by ketamine may perhaps reversibly eliminate Ca^{2+} action. The experiments also suggest that the action of ketamine may be preferentially on synaptic surfaces and not on mitochondria.

REFERENCES

(1) R. W. Virtue, J. J. Alanis, M. Mori, R. T. Lafargue, J. H. K. Vogel, and D. R. Metcalf, *Anesthesiology*, **28**, 823 (1967).

(2) G. Corssen, M. Miyasaka, and E. F. Domino, *Anesth. Analg.*, **47**, 746 (1968).

(3) A. D. Ivankovich, D. J. Miletich, C. Reimann, R. F. Albrecht, and B. Zahed, *ibid.*, **53**, 924 (1974).

(4) D. L. Sparks, G. Corssen, B. Aizenman, and J. Black, *ibid.*, **54**, 184 (1975).

(5) "The Pharmacological Basis of Therapeutics," L. S. Goodman and A. Gilman, Eds., Macmillan, New York, N.Y., 1975.

(6) J. T. Davies, *Proc. R. Soc.*, **A208**, 224 (1951).

(7) G. Colacicco, *Chem. Phys. Lipids*, **10**, 66 (1973).
(8) R. W. Ledeen, J. L. Skrivanek, L. J. Tirri, R. K. Margolis, and R. U. Margolis, in "Ganglioside Function: Biochemical and Pharmacological Implications," G. Porcellati, B. Ceccarelli, and G. Tettamanti, Eds., Plenum, New York, N.Y., 1976, pp. 83–103.
(9) R. W. Ledeen, R. K. Yu, and L. F. Eng, *J. Neurochem.*, **21**, 928 (1973).
(10) D. Holtzman and C. L. Moore, *Biol. Neonate*, **22**, 230 (1973).
(11) S. Fleischer and G. Rouser, *J. Am. Oil Chem. Soc.*, **42**, 588 (1965).
(12) G. Colacicco and M. M. Rapport, *J. Lipid Res.*, **6**, 258 (1966).
(13) G. Colacicco, *J. Colloid Interface Sci.*, **29**, 345 (1969).
(14) G. Colacicco and M. K. Basu, *Biochim. Biophys. Acta*, **509**, 230 (1978).
(15) G. Colacicco, in "Biological Horizons of Surface Science," L. M. Prince and D. F. Sears, Eds., Academic, New York, N.Y., 1973, p. 247.
(16) A. Colacicco, M. K. Basu, and F. A. Tansey, *Adv. Chem. Ser.* (Am. Chem. Soc.), in press.
(17) G. Gaines, "Insoluble Monolayers at Liquid Gas Interfaces," Wiley, New York, N.Y., 1966.
(18) G. Colacicco, *Biochim. Biophys. Acta*, **266**, 213 (1972).
(19) G. Colacicco, *Biophys. J.*, **21**, 48a (1978).
(20) G. Colacicco and M. K. Basu, *J. Pharm. Sci.*, in press.
(21) A. L. Lehninger, "The Mitochondrion," Benjamin, New York, N.Y., 1965.

ACKNOWLEDGMENTS

Supported by a National Institutes of Health grant and a training grant (J. M. Burnell) from the Heart, Lung and Blood Institute

Long-Range Substituent Effects in Morphine-Type Agonists and Antagonists: A Possible Explanation for Some Opiate Anomalies

VERA M. KOLB

Received December 27, 1978, from the *Department of Chemistry and Biochemistry and the School of Medicine, Southern Illinois University, Carbondale, IL 62901.* Accepted for publication April 11, 1979.

Abstract □ Anomalous variations in the pKa values of variously substituted morphine-type agonists and antagonists are interpreted as a reflection of long-range substituent effects operating in these molecules. Based on the operation of long-range effects, a mechanism is proposed by which substitution into the *N*-normorphine portion of morphine-type agonists and antagonists changes the activity of the parent molecule. Thus, a remote substituent would distort the whole molecule *via* a conformational transmission effect and thereby (*a*) change the fit between the opiate and its receptor; (*b*) change the electron density distribution throughout the molecule and, therefore, at the nitrogen; (*c*) modify the directionality of the lone-electron pair on the nitrogen; and (*d*) affect the pKa of the drug. The operation of long-range effects as proposed here could account for some of the anomalous changes in opiate activity effected by substitution into the parent molecule.

Keyphrases □ Morphine-type agonists and antagonists—substituents, long-range effects, structure–activity relationships □ Opiates—substituents, long-range effects, structure–activity relationships □ Opiate receptors—effect of opiate substituents, structure–activity relationships □ Structure–activity relationships—substituted morphine-type agonists and antagonists

The analgesic activity of morphine-type opiate agonists as well as the antimorphine activity of morphine-type opiate antagonists is influenced by substitution into the *N*-normorphine portion of these molecules (1). In that study (1), the activities of several series of closely related compounds were obtained by means of standard whole animal testing[1].

The data (1) did not lead, however, to an understanding of the process by which a substituent changes the opiate activity of the parent molecule. Often, the direction of the change was unexpected, in which cases the observed behavior of the substituted opiate seemed to be "anomalous."

Table I—Substitution Effect on the Antimorphine Activity of a Series of *N*-Allylnormorphines and *N*-Propylnormorphines [a]

Normorphine Moiety	Relative Antimorphine Activity of *N*-Allyl-normorphines	Relative Antimorphine Activity of *N*-Propyl-normorphines
Unsubstituted	1.0	1.0
3,6-Diacetyl	0.5	0.9
7,8-Dihydro	0.7	1.9
6-Desoxy	2.2	1.9
7,8-Dihydro-6-desoxy	1.8	0.2
7,8-Dihydro-6-keto	1.3	2.3
7,8-Dihydro-3,6-diacetyl	0.1	0.1
3-Methoxy-7,8-dihydro-6-desoxy	1.4	0.4

[a] Taken from Ref. 1.

BACKGROUND

Winter *et al.* (1) measured the antimorphine activities of two series of substituted opiate antagonists: *N*-propylnormorphines and *N*-allylnormorphines. Identical substituents were introduced into the same positions of the *N*-normorphine moiety of these two parent antagonists so that the observed differences in activity between these two series did not reflect differences in the transport rate caused by the substituent *per se*. An examination of the data (Table I) reveals no apparent correlation between the structure (or position) of the substituent and the direction of antimorphine activity change caused by the substituent.

These investigators (1) also found that the introduction of a common substituent into the *N*-normorphine moiety of morphine agonists and the corresponding antagonists (*N*-allylnormorphines) changed respective agonist and antagonist activities which were, as often as not, unrelated (Table II). These data are difficult to rationalize, especially if one accepts the hypothesis that the same cavity of the opiate receptor accommodates morphine-type agonists and antagonists, as suggested in the opiate receptor models of Goldstein (3) and Kolb (4) and as implied in some other opiate receptor models (5).

Within the category of the compounds covered in Table II, the following example is intriguing: 3,6-diacetylmorphine (heroin) exhibits 2.4 (6) or 2.5 (7) times the *in vivo* analgesic activity of morphine[2], and 1.45

[1] Analgesic and antimorphine activities were tested by the tail flick response in rats by the method of D'Amour and Smith (2). Drugs were injected subcutaneously.

[2] Ratio of ED_{50} (milligrams per kilogram) relative to morphine from mouse hot-plate experiments.

0022-3549/79/1000-1250$01.00/0
© 1979, American Pharmaceutical Association

(7) G. Colacicco, *Chem. Phys. Lipids*, **10**, 66 (1973).
(8) R. W. Ledeen, J. L. Skrivanek, L. J. Tirri, R. K. Margolis, and R. U. Margolis, in "Ganglioside Function: Biochemical and Pharmacological Implications," G. Porcellati, B. Ceccarelli, and G. Tettamanti, Eds., Plenum, New York, N.Y., 1976, pp. 83–103.
(9) R. W. Ledeen, R. K. Yu, and L. F. Eng, *J. Neurochem.*, **21**, 928 (1973).
(10) D. Holtzman and C. L. Moore, *Biol. Neonate*, **22**, 230 (1973).
(11) S. Fleischer and G. Rouser, *J. Am. Oil Chem. Soc.*, **42**, 588 (1965).
(12) G. Colacicco and M. M. Rapport, *J. Lipid Res.*, **6**, 258 (1966).
(13) G. Colacicco, *J. Colloid Interface Sci.*, **29**, 345 (1969).
(14) G. Colacicco and M. K. Basu, *Biochim. Biophys. Acta*, **509**, 230 (1978).
(15) G. Colacicco, in "Biological Horizons of Surface Science," L. M. Prince and D. F. Sears, Eds., Academic, New York, N.Y., 1973, p. 247.
(16) A. Colacicco, M. K. Basu, and F. A. Tansey, *Adv. Chem. Ser.* (Am. Chem. Soc.), in press.
(17) G. Gaines, "Insoluble Monolayers at Liquid Gas Interfaces," Wiley, New York, N.Y., 1966.
(18) G. Colacicco, *Biochim. Biophys. Acta*, **266**, 213 (1972).
(19) G. Colacicco, *Biophys. J.*, **21**, 48a (1978).
(20) G. Colacicco and M. K. Basu, *J. Pharm. Sci.*, in press.
(21) A. L. Lehninger, "The Mitochondrion," Benjamin, New York, N.Y., 1965.

ACKNOWLEDGMENTS

Supported by a National Institutes of Health grant and a training grant (J. M. Burnell) from the Heart, Lung and Blood Institute

Long-Range Substituent Effects in Morphine-Type Agonists and Antagonists: A Possible Explanation for Some Opiate Anomalies

VERA M. KOLB

Received December 27, 1978, from the *Department of Chemistry and Biochemistry and the School of Medicine, Southern Illinois University, Carbondale, IL 62901.* Accepted for publication April 11, 1979.

Abstract □ Anomalous variations in the pKa values of variously substituted morphine-type agonists and antagonists are interpreted as a reflection of long-range substituent effects operating in these molecules. Based on the operation of long-range effects, a mechanism is proposed by which substitution into the *N*-normorphine portion of morphine-type agonists and antagonists changes the activity of the parent molecule. Thus, a remote substituent would distort the whole molecule *via* a conformational transmission effect and thereby (*a*) change the fit between the opiate and its receptor; (*b*) change the electron density distribution throughout the molecule and, therefore, at the nitrogen; (*c*) modify the directionality of the lone-electron pair on the nitrogen; and (*d*) affect the pKa of the drug. The operation of long-range effects as proposed here could account for some of the anomalous changes in opiate activity effected by substitution into the parent molecule.

Keyphrases □ Morphine-type agonists and antagonists—substituents, long-range effects, structure–activity relationships □ Opiates—substituents, long-range effects, structure–activity relationships □ Opiate receptors—effect of opiate substituents, structure–activity relationships □ Structure–activity relationships—substituted morphine-type agonists and antagonists

The analgesic activity of morphine-type opiate agonists as well as the antimorphine activity of morphine-type opiate antagonists is influenced by substitution into the *N*-normorphine portion of these molecules (1). In that study (1), the activities of several series of closely related compounds were obtained by means of standard whole animal testing[1].

The data (1) did not lead, however, to an understanding of the process by which a substituent changes the opiate activity of the parent molecule. Often, the direction of the change was unexpected, in which cases the observed behavior of the substituted opiate seemed to be "anomalous."

Table I—Substitution Effect on the Antimorphine Activity of a Series of *N*-Allylnormorphines and *N*-Propylnormorphines [a]

Normorphine Moiety	Relative Antimorphine Activity of *N*-Allyl-normorphines	Relative Antimorphine Activity of *N*-Propyl-normorphines
Unsubstituted	1.0	1.0
3,6-Diacetyl	0.5	0.9
7,8-Dihydro	0.7	1.9
6-Desoxy	2.2	1.9
7,8-Dihydro-6-desoxy	1.8	0.2
7,8-Dihydro-6-keto	1.3	2.3
7,8-Dihydro-3,6-diacetyl	0.1	0.1
3-Methoxy-7,8-dihydro-6-desoxy	1.4	0.4

[a] Taken from Ref. 1.

BACKGROUND

Winter *et al.* (1) measured the antimorphine activities of two series of substituted opiate antagonists: *N*-propylnormorphines and *N*-allylnormorphines. Identical substituents were introduced into the same positions of the *N*-normorphine moiety of these two parent antagonists so that the observed differences in activity between these two series did not reflect differences in the transport rate caused by the substituent *per se*. An examination of the data (Table I) reveals no apparent correlation between the structure (or position) of the substituent and the direction of antimorphine activity change caused by the substituent.

These investigators (1) also found that the introduction of a common substituent into the *N*-normorphine moiety of morphine agonists and the corresponding antagonists (*N*-allylnormorphines) changed respective agonist and antagonist activities which were, as often as not, unrelated (Table II). These data are difficult to rationalize, especially if one accepts the hypothesis that the same cavity of the opiate receptor accommodates morphine-type agonists and antagonists, as suggested in the opiate receptor models of Goldstein (3) and Kolb (4) and as implied in some other opiate receptor models (5).

Within the category of the compounds covered in Table II, the following example is intriguing: 3,6-diacetylmorphine (heroin) exhibits 2.4 (6) or 2.5 (7) times the *in vivo* analgesic activity of morphine[2], and 1.45

[1] Analgesic and antimorphine activities were tested by the tail flick response in rats by the method of D'Amour and Smith (2). Drugs were injected subcutaneously.

[2] Ratio of ED_{50} (milligrams per kilogram) relative to morphine from mouse hot-plate experiments.

0022-3549/79/1000-1250$01.00/0
© 1979, American Pharmaceutical Association

Table II—Typical Change of Analgesic Activity of Morphine Agonists or Antimorphine Activity of the Corresponding Morphine Antagonists as Caused by the Change in the *N*-Normorphine Moiety of These Molecules [a]

Change in *N*-Normorphine Moiety of Morphine or *N*-Allylnormorphine	Analgesic Activity of Morphines		Antimorphine Activity of *N*-Allylnormorphines	
	Increased	Decreased	Increased	Decreased
Muzzling the 3-hydroxyl		++[b]		+[c]
Muzzling the 6-hydroxyl	++			+
Saturation of 7,8-double bond	+			
Removal of 6-hydroxyl	++		+	
Replacement of 6-hydroxyl by ketone	++		+	

[a] Based on quantitative data from Ref. 1. [b] A ++ indicates a large increase or decrease in activity. [c] A + indicates a moderate increase or decrease in activity.

times the *in vitro* receptor binding activity of morphine[3,4] (8). 6-Acetylmorphine is 4.2 times as potent an analgesic as morphine *in vivo*[2] (6). However, the corresponding acetylated antagonists, namely, *N*-allyl-3,6-diacetylnormorphine and *N*-allyl-6-acetylnormorphine, both show a *lower* antimorphine activity than their nonacetylated precursor, as illustrated quantitatively in Table III (1).

The change in the activity[5] of morphine agonists and antagonists by the introduction of a substituent may be associated with the *direct participation* of the substituent in binding to the receptor (9). The data from Table I, however, indicate that this possibility alone cannot account for the differences in activity observed with the same substituents.

The conclusions put forth here about the structure–activity relationships based on the *in vivo* study of Winter *et al.* (1) are meaningful if it is assumed that the concentrations of all of the structurally similar analogs compared are identical at the opiate receptor; the differences in potencies of these analogs, therefore, would be directly related to the respective differences in structure. While this assumption is usually implicit (9), exceptions have been reported. Sometimes even minor structural changes among the analogs significantly affect distribution, metabolism, or the ability of the compound to pass the blood–brain barrier (11), causing considerable differences in the analog concentrations in the brain. Qualification of the above assumption becomes irrelevant if the *in vitro* binding affinities[5] of these analogs to the opiate receptor are compared directly.

Tables IV and V present the binding affinities of a series of opiates to opiate receptors prepared from rat brain homogenate without added sodium chloride. Under these binding conditions, agonists as well as antagonists compete for the same population of identical binding sites (12) at the receptor, and the binding affinities of agonists and antagonists are approximately the same (10). This testing mode provides a meaningful method of observing the substitution effect on the binding affinities of agonists and antagonists and, therefore, of mixed agonist–antagonists[6].

Data from Tables IV and V reveal that the direction of change in the binding affinity resulting from the substitution into the parent molecule is not consistent and, therefore, is unpredictable. Thus, Table IV demonstrates that the binding affinity of oxymorphone exceeds that of morphine while the relationship is *reversed* for their 3-methyl ethers, *i.e.*, oxycodone and codeine. Therefore, the introduction of the same substituent in the same position of oxymorphone and morphine causes opposite effects on their binding affinities.

The inconsistency of this pattern is further illustrated by the examples in Table V. Thus, substitution of the *N*-methyl group with the *N*-allyl group may not change the binding affinity (levorphanol *versus* levallorphan), may improve the binding affinity (morphine *versus* nalorphine), or may lower the binding affinity (oxymorphone *versus* naloxone). As a consequence of this inconsistent pattern, the binding affinities of an *N*-methyl series (*e.g.*, levorphanol, morphine, and oxymorphone equal 1.0, 3.0, and 1.0, respectively) do not necessarily follow the same order as the binding affinities of the corresponding *N*-allyl series (levallorphan, nalorphine, and naloxone equal 1.0, 1.5, and 1.5, respectively).

To rationalize these anomalies exhibited by the *in vivo* as well as *in vitro* systems, one has to gain more insight into the mechanism(s) by which a substituent in the opiate molecule influences its activity. One such mechanism is proposed here.

EVIDENCE FOR LONG-RANGE SUBSTITUENT EFFECTS

While trying to find an explanation for these opiate anomalies, the following question was posed: Might a substituent introduced in an opiate molecule impart long-range effects[7]? That is, might the presence of this substituent distort the *whole* molecule and thereby change the fit between the opiate and its receptor, and might it also change the electron density distribution throughout the molecule and, therefore, at the nitrogen[8]?

This question is valid since such long-range substituent effects have been reported for other large and rigid molecules: steroids (*e.g.*, 17, 23, 24, 31–34), triterpenes (24, 25), spiranes (35), and sparteines (36). Although long-range effects in morphines have not been reported, it is not unreasonable to predict that these effects should operate within the rigid morphine frame also. Long-range inductive effects are transmitted[9] by all available bonds between the substituent and remote sites. The net effect is believed to be the sum of the individual effects (19–22). Electrostatic field effects should be prominent in morphines due to their T-shape, which enables a relatively close steric relation of "T-arms" with "T-body." Conformational transmission effects are to be expected on the basis of the work of Barton and coworkers (23–25) who showed that in large, rigid, polycyclic structures, a local conformational distortion caused by a local strain is transmitted through the entire molecule by a slight flexing of bond angles and torsional angles. In this way, the strain is

Table III—Relative Antimorphine Activities of *N*-Allylnormorphine and Its Acetyl Derivatives [a]

Compound	Relative Antimorphine Activity
N-Allylnormorphine (hydrochloride)	1.0
N-Allyl-3,6-diacetylnormorphine (tartrate)	0.5
N-Allyl-6-acetylnormorphine (sulfate)	0.3

[a] Taken from Ref. 1.

Table IV—Receptor Binding Affinity (EC_{50} of Stereospecific ^{3}H-Naloxone Binding to Rat Brain Homogenates; No Sodium Chloride)

Compound	EC_{50}, nm	Reference
Morphine	3.0	12
Oxymorphone	1.0	12
Codeine	20,000	13
Oxycodone	30,000	13

[3] Value of K_e (morphine)/K_e (heroin) from data in Ref. 8, where K_e = equilibrium dissociation constant (9).

[4] Tested in guinea pig ileum.

[5] The activity is directly related to the binding affinity with the opiate receptor (10).

[6] In contrast, when binding studies are conducted with receptors prepared from rat brain homogenate to which sodium chloride is added, the binding of antagonists is enhanced while that of agonists is dramatically diminished (12). Sodium has been reported to alter: (*a*) the number of binding sites for an agonist and antagonist, increasing the number for the latter but decreasing the number for the former (12; however, *cf.* 14); (*b*) the binding affinities of an agonist and an antagonist, enhancing that of the latter but decreasing that of the former (15, 16); and (*c*) the rates of dissociation and association of opiate agonists and antagonists, accelerating the dissociation rate of the former while accelerating the association rate of the latter (*e.g.*, 15, 16).

[7] Long-range effects are the effects of remote structural features on reactions in organic molecules (17). A substituent in a rigid molecule can influence reactivity at remote centers in three distinct ways: inductive effects (17–22), electrostatic field effects (17), and conformational transmission effects (17, 23–25).

[8] It is generally agreed that an absolutely necessary feature of an opiate molecule is its basic nitrogen (26). It is believed that the opiate nitrogen interacts with the opiate receptor either *via* its lone electron pair (4, 27) or in its protonated form (*e.g.*, 28–30). In either case, the electron density on the nitrogen would appear to be relevant to the opiate activity.

[9] Subject to the normal exponential decrease of the effect with distance (18).

Table V—Receptor Binding Affinity [a] (EC_{50} of Stereospecific ^{3}H-Naloxone Binding to Rat Brain Homogenates; No Sodium Chloride)

Compound	EC_{50}, nm
Levorphanol	1.0
Levallorphan	1.0
Morphine	3.0
Nalorphine	1.5
Oxymorphone	1.0
Naloxone	1.5

[a] Taken from Ref. 12.

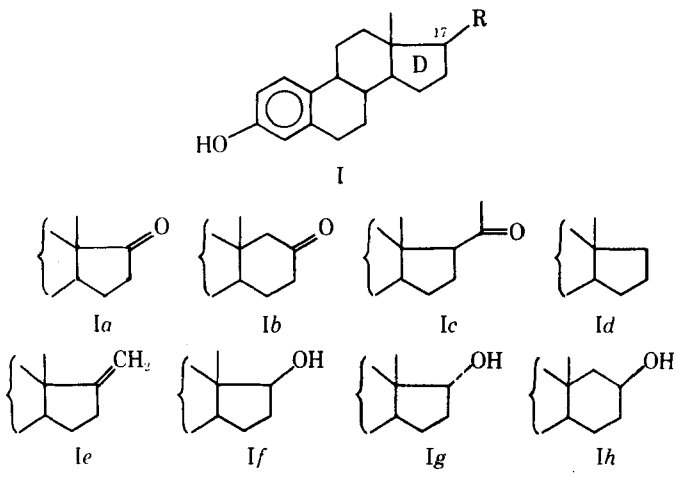

shared by the *whole structure*, and the effect of the resulting distortions is transmitted to a remote site, thereby influencing the reaction rate. The mechanism of conformational distortion transmission within a polycyclic framework also was studied (35, 37).

In this context, the following example of the operation of the long-range effects in steroidal phenols (estrone derivatives) is striking. Legrand *et al.* (32) observed that the pKa values of steroidal phenols (I*a*–I*h*) changed with the nature of the substituent in the 17-position, which is *nine* carbons away from the phenolic OH. They attributed these results to the operation of long-range effects (Table VI).

It is reasonable to believe, therefore, that similar long-range effects in morphine systems (II–VII) would be manifested by changes in pKa values with alteration of remote substituents. Indeed, the anomalous variations in the pKa values of a series of substituted morphines (38) provide convincing support for the operation of long-range effects here too. Thus, data in Table VII show that the substituent on nitrogen influences not only the acidity of the amino nitrogen but also that of the phenolic hydroxyl seven atoms away (*cf.*, II and III and V–VII). Conversely, the substituent on the phenolic oxygen influences the pKa of the amino nitrogen (*cf.*, II and IV).

DISCUSSION

Extrapolation of these data suggests the generalization that the introduction of a substituent in a morphine molecule is likely to affect its pKa. The pKa of a morphine influences its transport rate (38) which, in turn, influences the *in vivo* activity. The *in vitro* binding affinity, being a thermodynamic value (39), also is influenced by the pKa value of the compound in question[10]. It is quite possible, however, that the actual binding of the morphines to the receptor in the process that elicits the biological response is kinetically controlled[11]; if so, the intrinsic drug activity is not necessarily influenced by pKa (thermodynamic) values.

Introduction of a substituent in a rigid molecule like morphine is likely to cause distortions of bond angles and torsional angles locally as well as throughout the molecule. For example, X-ray studies of morphine (41) and codeine (42) revealed a difference of about 3° in their T-angles. These distortions could cause a change in the fit between the opiate and its receptor that may be large enough to influence the opiate activity. These distortions may also cause a change in the directionality of the lone-electron pair on the nitrogen, and such a change would influence the

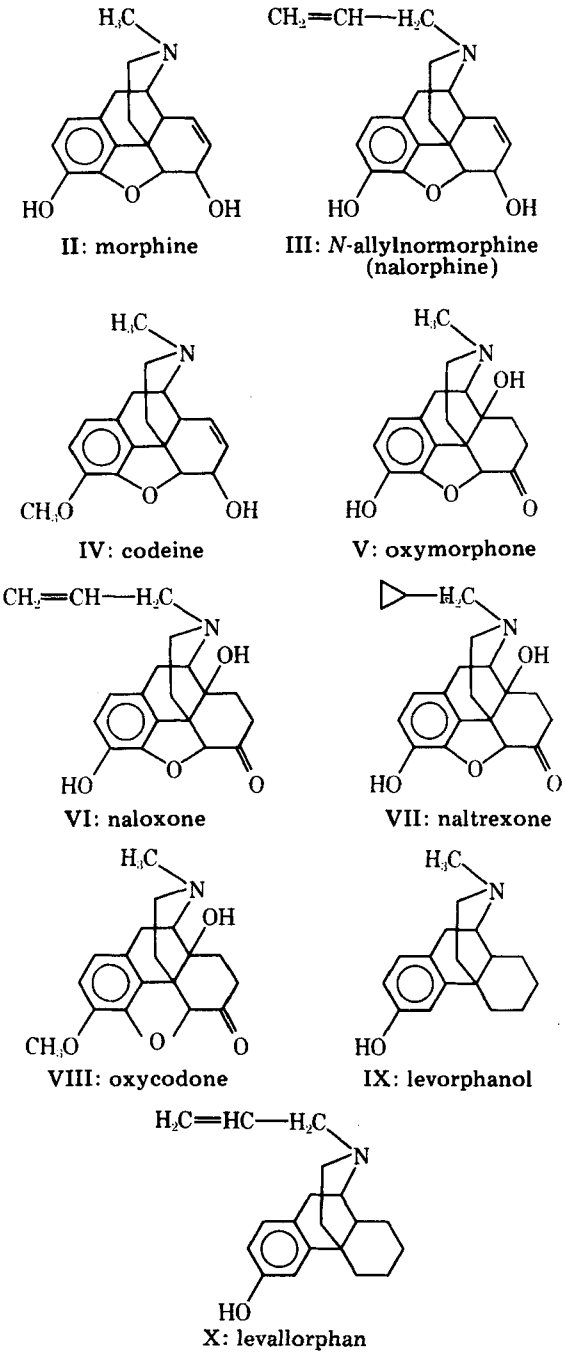

Table VI—Dependence of pKa Values of Steroidal Phenols on the Substituent in the 17-Position [a]

Compound	ΔpKa (in CH_3OH–CH_3ONa) [b]
Estrone (I*a*)	0.10
D-Homoestrone (I*b*)	0.09
Progesterone (I*c*)	0.07
3-Hydroxy-1,3,5(10)-estratriene (I*d*)	0.01
3-Hydroxy-17-methylene-1,3,5(10)estratriene (I*e*)	0.02
17β-Estradiol (standard) (I*f*)	0.00
17α-Estradiol (I*g*)	0.02
D-Homoestradiol (I*h*)	0.00

[a] Taken from Ref. 32. [b] These pKa values (pKa 17β-estradiol − pKa compound) were obtained by statistical interpretation of the results from several pKa measurements.

[10] This reasoning is valid whether the free (4, 27) *or* protonated (*e.g.*, 28–30) amine function is the *active species* at the receptor.

[11] For example, one could easily visualize "clastic binding" (40), which involves an electron-transfer reaction, as kinetically controlled.

Table VII—pKa Values of Some Morphine-Type Opiate Agonists and Antagonists [a]

Compound	Temperature	pKa[b] (in Water) pKa1 (Proton on Nitrogen)	pKa2 (Phenolic Hydrogen)
Morphine[c]	20°	8.02	9.76
	37°	7.93	9.63
N-Allylnormorphine[d]	20°	7.73	9.36
	37°	7.59	9.28
Codeine[e]	20°	8.18	—
	37°	8.10	—
Oxymorphone[d]	20°	8.25	9.71
	37°	8.17	9.54
Naloxone[d]	20°	7.94	9.44
	37°	7.82	9.25
Naltrexone[d]	20°	8.38	9.93
	37°	8.13	9.51

[a] Taken from Ref. 38. [b] The pKa values were measured by a microelectrometric titration method. Each pKa value represents the average of at least five determinations, and the maximum deviation from the given value is ±0.02. [c] Sulfate. [d] Hydrochloride. [e] Phosphate.

opiate activity according to Belleau *et al.* (27) and Kolb (4). Belleau *et al.* (27) pointed out that (referring to the activities of *N*-methylmorphinans *versus* *N*-methyl-D-normorphinans): "It appears probable then that conformational transmission of subtle distortions effects in the lone pair *orientation* of morphinans and related analogs may account at least in part for structurally induced variations in their pharmacological properties."

A substituent introduced in the morphine molecule also would influence the electron density distribution throughout the molecule; the nitrogen atom would certainly be affected. The electron density on the nitrogen seems to be relevant to opiate activity (see footnote 8), especially if one accepts the elastic binding hypothesis proposed by Belleau and Morgan (40), which invokes a stereospecific electron transfer from the lone electron pair on the opiate nitrogen to the receptor. Electron transfer processes are known to depend greatly on the electron density of the electron donors (43).

Evaluation of long-range effects of substituents is complicated by the fact that these effects are not necessarily additive[12]. Net substituent effects within steroids were studied quantitatively by Barton *et al.* (24) who actually measured the "group-rate factors" for a series of substituents[12]. Unfortunately, such quantitative data are not yet available for morphines.

All of these possible processes by which a substituent in the morphines influences the opiate activity *via* long-range effects are variations of the proposed general "long-range effect" mechanism.

Finally, the following comparison between the morphines and the estrones (and some other steroidal hormones) can be made: both classes of compounds are large, rigid, biologically active molecules that interact with their respective receptors by a lock-and-key mechanism (44, 45), and both classes of compounds exhibit long-range effects. The importance of these effects to the biological activity of steroids is already recognized (34). An intriguing question arises: Is the long-range effect mechanism a general mechanism by which a fine tuning of the biological activity is achieved in all rigid molecules that act at the receptor? An answer may be forthcoming.

REFERENCES

(1) C. A. Winter, P. Orahovats, and E. G. Lehman, *Arch. Int. Pharmacodyn. Ther.*, **11**, 186 (1957).

(2) F. E. D'Amour and D. M. Smith, *J. Pharmacol. Exp. Ther.*, **72**, 74 (1941).

(3) A. Goldstein, in "Narcotic Antagonists," M. C. Braude, L. S. Harris, E. L. May, J. P. Smith, and J. E. Villareal, Eds., Raven, New York, N.Y., 1973, p. 471.

(4) V. M. Kolb, *J. Pharm. Sci.*, **67**, 999 (1978).

(5) S. Archer and W. F. Michne, in "Progress in Research," vol. 20, E. Jucker, Ed., Birkhäuser Verlag, Basel, Switzerland, 1976, pp. 82–88.

(6) O. J. Braenden, N. B. Eddy, and H. Halbach, *Bull. WHO*, **13**, 937 (1955).

(7) B. M. Cox and M. Weinstock, *Br. J. Pharmacol. Chemother.*, **27**, 81 (1966).

(8) A. Kosterlitz and A. J. Watt, *ibid.*, **33**, 266 (1966).

(9) G. H. Loew, D. Berkowitz, H. Weinstein, and S. Srebrenik, in "Molecular and Quantum Pharmacology," E. Bergmann and B. Pullman, Eds., D. Reidel Publ., Dordrecht, The Netherlands, 1974, pp. 355–389.

(10) S. H. Snyder, *Sci. Am.*, **236**, 44 (1977).

(11) A. F. Casy, in "A Guide to Molecular Pharmacology-Toxicology," part I, R. M. Featherstone, Ed., Dekker, New York, N.Y., 1973, pp. 222, 223.

(12) C. B. Pert and S. H. Snyder, *Mol. Pharmacol.*, **10**, 868 (1974).

(13) C. B. Pert and S. H. Snyder, *Proc. Natl. Acad. Sci. USA*, **70**, 2243 (1973).

(14) V. Höllt and M. Wüster, in "Developments in Opiate Research," A. Herz, Ed. (vol. 14 in Modern Pharmacology-Toxicology series), Dekker, New York, N.Y., 1978, pp. 11–13.

(15) E. J. Simon, J. M. Hiller, J. Groth, and J. Edelman, *J. Pharmacol. Exp. Ther.*, **192**, 531 (1975).

(16) E. J. Simon, J. M. Hiller, J. Edelman, J. Groth, and K. D. Stahl, *Life Sci.*, **16**, 1795 (1975).

(17) D. N. Kirk and M. P. Hartshorn, in "Steroid Reaction Mechanisms," C. Eaborn, Ed. (monograph 7 in Reaction Mechanisms in Organic Chemistry series), Elsevier, New York, N.Y., 1968, pp. 17–23, 99–181.

(18) R. W. Taft, in "Steric Effects in Organic Chemistry," M. S. Newman, Ed., Wiley, New York, N.Y., 1956, p. 592.

(19) K. Takeda, H. Tanida, and K. Horiki, *J. Org. Chem.*, **31**, 734 (1966).

(20) V. Schwarz, S. Heřmánek, and J. Trojánek, *Chem. Ind.*, **1960**, 1212.

(21) V. Schwarz and S. Heřmánek, *Tetrahedron Lett.*, **1962**, 809.

(22) P. E. Peterson, *ibid.*, **1963**, 181.

(23) D. H. R. Barton and A. J. Head, *J. Chem. Soc.*, **1956**, 932.

(24) D. H. R. Barton, F. McCapra, P. J. May, and F. Thudium, *ibid.*, **1960**, 1297.

(25) D. H. R. Barton, A. J. Head, and P. J. May, *ibid.*, **1957**, 935.

(26) A. F. Casy, *Progr. Med. Chem.*, **7**, 229 (1970).

(27) B. Belleau, T. Conway, F. R. Ahmed, and A. D. Hardy, *J. Med. Chem.*, **17**, 907 (1974).

(28) A. P. Feinberg, I. Creese, and S. H. Snyder, *Proc. Natl. Acad. Sci. USA*, **73**, 4215 (1976).

(29) P. S. Portoghese, *J. Pharm. Sci.*, **55**, 865 (1966).

(30) A. H. Beckett and A. F. Casy, *J. Pharm. Pharmacol.*, **6**, 986 (1954).

(31) P. E. Peterson and D. M. Chevli, *J. Org. Chem.*, **39**, 3684 (1974).

(32) M. Legrand, V. Delaroff, and J. Mathieu, *Bull. Soc. Chim. Fr.*, **1961**, 1346.

(33) J. C. Orr, P. Carter, and L. L. Engel, *Biochemistry*, **6**, 1065 (1967).

(34) R. Turner, in "Mechanism of Action of Steroid Hormones," C. A. Villee and L. L. Engel, Eds., Pergamon, New York, N.Y., 1961, pp. 188–199.

(35) S. Smoliński, J. Nowicka, J. Mokrocz, M. Jamrozik, M. Jaworski, and E. Wiekiera, *Tetrahedron*, **33**, 1219 (1977), and references cited therein.

(36) M. Wiewiórowski, "Abstracts," Sixth Symposium on Chemistry of Heterocyclic Compounds, Brno, Czechoslovakia, July 1978, PL 7.

(37) M. J. T. Robinson and W. B. Whalley, *Tetrahedron*, **19**, 2123 (1963).

(38) J. J. Kaufman, N. M. Semo, and W. S. Koski, *J. Med. Chem.*, **18**, 647 (1975).

(39) W. B. Dandliker, R. J. Brawn, M.-L. Hsu, P. N. Brawn, J. Levin, C. Y. Meyers, and V. M. Kolb, *Cancer Res.*, **38**, 4212 (1978).

(40) B. Belleau and P. Morgan, *J. Med. Chem.*, **17**, 908 (1974).

(41) L. Gylbert, *Acta Crystallogr.*, **B 29**, 1630 (1973).

(42) G. Kartha, F. R. Ahmed, and W. H. Barnes, *ibid.*, **15**, 326 (1962).

(43) C. Y. Meyers, W. S. Matthews, L. L. Ho, V. M. Kolb, and T. E. Parady, in "Catalysis in Organic Synthesis," G. V. Smith, Ed., Academic, New York, N.Y., 1978, pp. 217, 260–278, and references cited therein.

(44) A. Korolkovas, "Essentials of Molecular Pharmacology," Wiley-Interscience, New York, N.Y., 1970, pp. 254–256.

(45) R. J. B. King and W. I. P. Mainwaring, "Steroid-Cell Interactions," University Park Press, Baltimore, Md., 1974, pp. 221–223.

[12] Barton *et al.* (24) showed that the observed rate of condensation of 5α-steroidal 3-ketones with benzaldehyde is: $R_s = R_0(f_1)(f_2)(f_3)\ldots(f_n)$, where R_s is the rate of the substituted steroid, R_0 is the rate of the parent (unsubstituted) steroid, and f_n is the group rate factor for the substituent concerned.

ACKNOWLEDGMENTS

Presented at the joint meeting of the American Chemical Society and the Chemical Society of Japan, Honolulu, Hawaii, April 1979 (Abstract 96, Medicinal Chemistry).

Supported in part by a grant from the University Research Foundation, La Jolla, Calif.

The author thanks Professor Cal Y. Meyers and Dr. Augusta R. Auerbach for editorial help and Professor Meyers and his research group for a helpful discussion.

Modification of Metoclopramide GLC Assay: Application to Human Biological Specimens

Y. K. TAM *, J. E. AXELSON *x, and R. ONGLEY ‡

Received January 4, 1979, from the **Faculty of Pharmaceutical Sciences and the* ‡*Faculty of Medicine, University of British Columbia, Vancouver, British Columbia, Canada V6T 1W5.* Accepted for publication April 11, 1979.

Abstract □ A modified electron-capture GLC assay for metoclopramide in human biological specimens is reported. This assay involves the incorporation of a back-extraction method to remove endogenous contaminants. Its applicability was demonstrated by studying the time course of metoclopramide in plasma and urine from a human subject. The lowest quantifiable metoclopramide concentration in plasma was 7 ng/ml, provided 0.5 ml of plasma was used.

Keyphrases □ Metoclopramide—analysis, electron-capture GLC, human plasma and urine □ Antiemetic agents—metoclopramide, electron-capture GLC analysis, human plasma and urine □ GLC, electron capture—analysis, metoclopramide, human plasma and urine

A highly sensitive electron-capture GLC assay was developed recently for the determination of metoclopramide (I), mol. wt. 299.81, in biological specimens from the rat (1). However, when the same procedures were used to analyze human plasma, quantitation of I was impossible due to interferences from endogenous substances (Fig. 1*a*). A slight modification of this method, involving a "cleanup step," successfully removed endogenous substances from the human plasma samples. The purpose of this report is to describe this improved assay.

EXPERIMENTAL

Materials—Metoclopramide monohydrochloride monohydrate[1] (II) (mol. wt. 336.31), benzene[2], 4% ammonium hydroxide[3], 1 *N* NaOH[4], 5 *N* NaOH[4], 1 *N* HCl[5], heptafluorobutyric anhydride[6] (III), and diazepam[7] were used.

GLC—A reporting gas–liquid chromatograph[8] equipped with a ^{63}Ni-electron-capture detector (^{63}Ni-15 mCi) and a 1.2-m × 2-mm i.d. glass column, containing 3% OV-225 coated onto 80–100-mesh Chromosorb W, was used to analyze plasma samples. The operating temperatures for routine analysis were: injection port, 250°; oven, 245°; and detector, 350°. The carrier gas (95% argon–5% methane) flow rate was 40 ml/min. For urine analyses, all GLC conditions were identical except that a 0.6-m × 2 mm-i.d. 3% OV-225 column was used and the oven temperature was 230°.

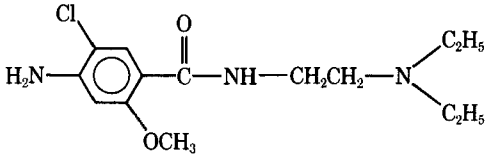

I

Extraction Procedure—*Plasma*—A 0.5-ml sample of human plasma (blank) was spiked with serial concentrations of II (concentration equivalent to 7–93 ng of I/ml of water) (Table I). To each spiked sample, 0.5 ml of 1 *N* NaOH was added. The final volume was made up to 2 ml with water (pH ≃ 12). The aqueous phase was extracted with 8 ml of benzene by shaking with a wrist-action shaker[9] for 15 min. After centrifugation at 3000×*g* for 10 min, 7 ml of the organic phase was removed and back-extracted (extraction time, 15 min) with 2 ml of 1 *N* HCl.

The benzene layer was aspirated, and the sample was washed two times with benzene (4 ml each). The remaining aqueous layer was alkalinized with 0.5 ml of 5 *N* NaOH (pH ≃ 12). Finally, this layer was extracted with 6 ml of benzene (extraction time, 15 min). A 5-ml aliquot of the organic phase was removed and dried under a gentle nitrogen stream at ambient temperature. The residues were reconstituted with 0.5 ml of internal standard solution (50 ng of diazepam/ml of benzene).

Urine—A 0.1–0.5-ml volume of urine containing I was extracted in the same manner as described by Tam and Axelson (1).

Derivative Formation and Quantitative Analysis—A 20-μl volume of III was added to the reconstituted solution. The reaction mixtures were incubated at 55° for 10 min. Excess III was removed by hydrolysis with 0.5 ml of water and neutralization with 0.5 ml of 4% NH_4OH (1). A 5-μl volume of the derivative solution was injected into the reporting gas–liquid chromatograph by an automatic sampler. Quantitative estimation of I in human plasma and urine samples was accomplished by plotting the area ratios of the derivative and the internal standard against a range of solutions of known I concentration.

Human Study—A 20-mg metoclopramide monohydrochloride[10] (IV) dose was administered orally to a fasted normal healthy volunteer during a drug interaction study with griseofulvin. Five-milliliter blood samples were withdrawn at 0, 0.25, 0.5, 0.75, 1.0, 1.5, 2.0, 3.0, 4.0, 5.0, 6.0, 8.0, and 24 hr after drug administration. The blood samples were immediately centrifuged, and the plasma was separated. Cumulative urine samples were collected up to 96 hr after drug consumption. Both the plasma and urine samples were stored at −20° until analysis.

Table I—Quantitative Metoclopramide Estimation in Human Plasma

Metoclopramide Concentration, ng/ml	n^a	Area Ratio	*SD*
7	3	0.409	±0.03
15	3	0.812	±0.05
37	3	2.140	±0.25
56	3	2.935	±0.20
93	3	4.768	±0.36

[a] Each *n* is the average of three injections.

[1] Analysis No. 9207, A. H. Robins, Montreal, Canada.
[2] Distilled in glass, Caledon, Georgetown, Ontario, Canada.
[3] Reagent ACS code 1293, Allied Chemical Canada Ltd., Pointe Claire, Quebec, Canada.
[4] Mallinckrodt Chemical Works, St. Louis, Mo.
[5] Reagent ACS, Allied Chemical Canada Ltd., Pointe Claire, Quebec, Canada.
[6] Pierce Chemical Co., Rockford, Ill.
[7] Lot R-6685, Hoffmann-La Roche, Montreal, Canada.
[8] Hewlett-Packard model 5840.
[9] Patent pending, Burrell Corp., Pittsburgh, Pa.
[10] Maxeran tablets (10 mg), Nordic, Laval, Quebec, Canada.

0022-3549/79/1000-1254$01.00/0
© 1979, American Pharmaceutical Association

ACKNOWLEDGMENTS

Presented at the joint meeting of the American Chemical Society and the Chemical Society of Japan, Honolulu, Hawaii, April 1979 (Abstract 96, Medicinal Chemistry).

Supported in part by a grant from the University Research Foundation, La Jolla, Calif.

The author thanks Professor Cal Y. Meyers and Dr. Augusta R. Auerbach for editorial help and Professor Meyers and his research group for a helpful discussion.

Modification of Metoclopramide GLC Assay: Application to Human Biological Specimens

Y. K. TAM *, J. E. AXELSON *x, and R. ONGLEY ‡

Received January 4, 1979, from the **Faculty of Pharmaceutical Sciences and the* ‡*Faculty of Medicine, University of British Columbia, Vancouver, British Columbia, Canada V6T 1W5.* Accepted for publication April 11, 1979.

Abstract □ A modified electron-capture GLC assay for metoclopramide in human biological specimens is reported. This assay involves the incorporation of a back-extraction method to remove endogenous contaminants. Its applicability was demonstrated by studying the time course of metoclopramide in plasma and urine from a human subject. The lowest quantifiable metoclopramide concentration in plasma was 7 ng/ml, provided 0.5 ml of plasma was used.

Keyphrases □ Metoclopramide—analysis, electron-capture GLC, human plasma and urine □ Antiemetic agents—metoclopramide, electron-capture GLC analysis, human plasma and urine □ GLC, electron capture—analysis, metoclopramide, human plasma and urine

A highly sensitive electron-capture GLC assay was developed recently for the determination of metoclopramide (I), mol. wt. 299.81, in biological specimens from the rat (1). However, when the same procedures were used to analyze human plasma, quantitation of I was impossible due to interferences from endogenous substances (Fig. 1*a*). A slight modification of this method, involving a "cleanup step," successfully removed endogenous substances from the human plasma samples. The purpose of this report is to describe this improved assay.

EXPERIMENTAL

Materials—Metoclopramide monohydrochloride monohydrate[1] (II) (mol. wt. 336.31), benzene[2], 4% ammonium hydroxide[3], 1 *N* NaOH[4], 5 *N* NaOH[4], 1 *N* HCl[5], heptafluorobutyric anhydride[6] (III), and diazepam[7] were used.

GLC—A reporting gas–liquid chromatograph[8] equipped with a ^{63}Ni-electron-capture detector (^{63}Ni-15 mCi) and a 1.2-m × 2-mm i.d. glass column, containing 3% OV-225 coated onto 80–100-mesh Chromosorb W, was used to analyze plasma samples. The operating temperatures for routine analysis were: injection port, 250°; oven, 245°; and detector, 350°. The carrier gas (95% argon–5% methane) flow rate was 40 ml/min. For urine analyses, all GLC conditions were identical except that a 0.6-m × 2 mm-i.d. 3% OV-225 column was used and the oven temperature was 230°.

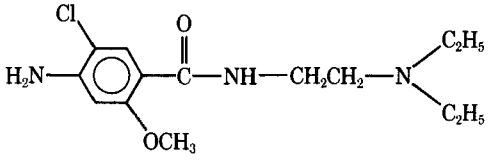

I

Extraction Procedure—*Plasma*—A 0.5-ml sample of human plasma (blank) was spiked with serial concentrations of II (concentration equivalent to 7–93 ng of I/ml of water) (Table I). To each spiked sample, 0.5 ml of 1 *N* NaOH was added. The final volume was made up to 2 ml with water (pH ≃ 12). The aqueous phase was extracted with 8 ml of benzene by shaking with a wrist-action shaker[9] for 15 min. After centrifugation at 3000×*g* for 10 min, 7 ml of the organic phase was removed and back-extracted (extraction time, 15 min) with 2 ml of 1 *N* HCl.

The benzene layer was aspirated, and the sample was washed two times with benzene (4 ml each). The remaining aqueous layer was alkalinized with 0.5 ml of 5 *N* NaOH (pH ≃ 12). Finally, this layer was extracted with 6 ml of benzene (extraction time, 15 min). A 5-ml aliquot of the organic phase was removed and dried under a gentle nitrogen stream at ambient temperature. The residues were reconstituted with 0.5 ml of internal standard solution (50 ng of diazepam/ml of benzene).

Urine—A 0.1–0.5-ml volume of urine containing I was extracted in the same manner as described by Tam and Axelson (1).

Derivative Formation and Quantitative Analysis—A 20-μl volume of III was added to the reconstituted solution. The reaction mixtures were incubated at 55° for 10 min. Excess III was removed by hydrolysis with 0.5 ml of water and neutralization with 0.5 ml of 4% NH_4OH (1). A 5-μl volume of the derivative solution was injected into the reporting gas–liquid chromatograph by an automatic sampler. Quantitative estimation of I in human plasma and urine samples was accomplished by plotting the area ratios of the derivative and the internal standard against a range of solutions of known I concentration.

Human Study—A 20-mg metoclopramide monohydrochloride[10] (IV) dose was administered orally to a fasted normal healthy volunteer during a drug interaction study with griseofulvin. Five-milliliter blood samples were withdrawn at 0, 0.25, 0.5, 0.75, 1.0, 1.5, 2.0, 3.0, 4.0, 5.0, 6.0, 8.0, and 24 hr after drug administration. The blood samples were immediately centrifuged, and the plasma was separated. Cumulative urine samples were collected up to 96 hr after drug consumption. Both the plasma and urine samples were stored at −20° until analysis.

Table I—Quantitative Metoclopramide Estimation in Human Plasma

Metoclopramide Concentration, ng/ml	n^a	Area Ratio	*SD*
7	3	0.409	±0.03
15	3	0.812	±0.05
37	3	2.140	±0.25
56	3	2.935	±0.20
93	3	4.768	±0.36

[a] Each *n* is the average of three injections.

[1] Analysis No. 9207, A. H. Robins, Montreal, Canada.
[2] Distilled in glass, Caledon, Georgetown, Ontario, Canada.
[3] Reagent ACS code 1293, Allied Chemical Canada Ltd., Pointe Claire, Quebec, Canada.
[4] Mallinckrodt Chemical Works, St. Louis, Mo.
[5] Reagent ACS, Allied Chemical Canada Ltd., Pointe Claire, Quebec, Canada.
[6] Pierce Chemical Co., Rockford, Ill.
[7] Lot R-6685, Hoffmann-La Roche, Montreal, Canada.
[8] Hewlett-Packard model 5840.
[9] Patent pending, Burrell Corp., Pittsburgh, Pa.
[10] Maxeran tablets (10 mg), Nordic, Laval, Quebec, Canada.

0022-3549/79/1000-1254$01.00/0
© 1979, American Pharmaceutical Association

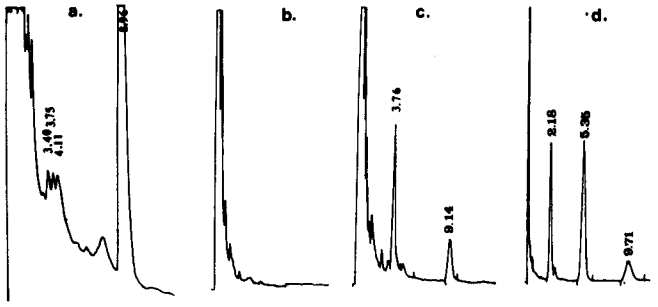

Figure 1—*Representative chromatograms of: (a) a blank plasma extract after a single extraction; (b) blank plasma after back-extraction; (c) a plasma sample containing 60 ng of metoclopramide/ml (3.76 min) and 50 ng of diazepam/ml (9.1 min); and (d) a urine sample using a 0.6-m 3% OV-225 column instead of a 1.2-m 3% OV-225 column. Peaks at 2.18, 5.35, and 9.71 min are the derivative of metoclopramide, diazepam, and an unidentified metabolite, respectively. Chart speed was 0.5 cm/min.*

RESULTS AND DISCUSSION

Extraction and GLC—With the single-extraction method (1), it was observed that not only I but also other endogenous substances that contributed to the extraneous peaks were effectively removed from human plasma samples (Fig. 1*a*). These interfering peaks prevented the quantitation of I in human plasma. Those contaminants responsible for the interfering peaks were successfully removed by back-extracting I into an acidic medium (Fig. 1*b*). A representative chromatogram of the plasma extract after the plasma was spiked with II is shown in Fig. 1*c*. The retention times of the derivatives of I and diazepam were 3.75 and 9.14 min, respectively. Back-extraction of human urine samples was unnecessary since no interference was observed in the chromatogram (Fig. 1*d*).

The peaks at 2.18, 5.35, and 9.71 min were the derivatives of I, diazepam, and an unidentified metabolite, respectively. The identification of this metabolite by mass spectrometry is planned. Since simultaneous quantitation of this metabolite and I is desirable, and the elution time of the peaks would be relatively long if a 1.2-m column (Fig. 1*c*) were used, a shorter column might be preferable in the urine sample analyses. A 0.6-m column provided baseline separation between the peaks, and a short elution time for all three compounds also was observed (Fig. 1*d*). Alternatively, a 1.2-m column was required to separate the derivative peak from the solvent front in plasma analyses due to interfering substances not observed in urine.

Chromatographic response was linear in the range studied (concentration equivalent to 7–93 ng of I/ml of plasma and 0.04–2.2 μg of I/ml of urine). The calibration curves were obtained by analyzing blank urine or plasma samples spiked with various drug concentrations (Tables I and II). From the linear regression analyses, the best-fit line through the data points was described by $y = 0.051x - 0.062$ for plasma and $y = 1.345x - 0.446$ for urine, with $r^2 = 0.99$ in both cases. The recovery of I after

Table II—Quantitative Metoclopramide Estimation in Human Urine

Metoclopramide Concentration, μg/ml	n^a	Area Ratio	*SD*
0.04	3	0.075	±0.001
0.37	3	0.569	±0.002
0.7	3	1.058	±0.017
1.1	3	1.531	±0.024
1.5	3	2.030	±0.054
1.9	3	2.562	±0.113
2.2	3	3.044	±0.053

[a] Each *n* is the average of three injections.

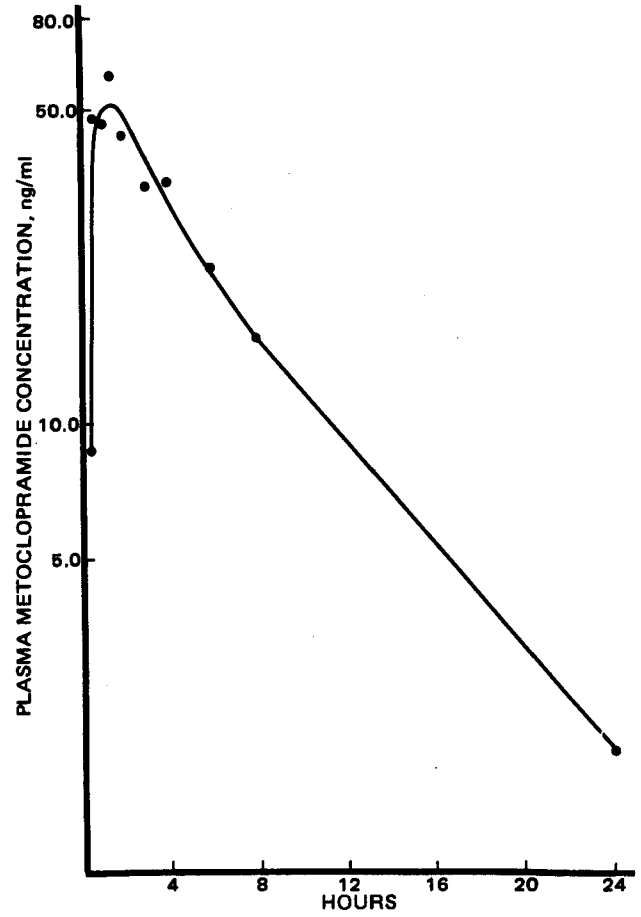

Figure 2—*Plasma metoclopramide profile after a dose of 20 mg of metoclopramide monohydrochloride po to a normal healthy volunteer.*

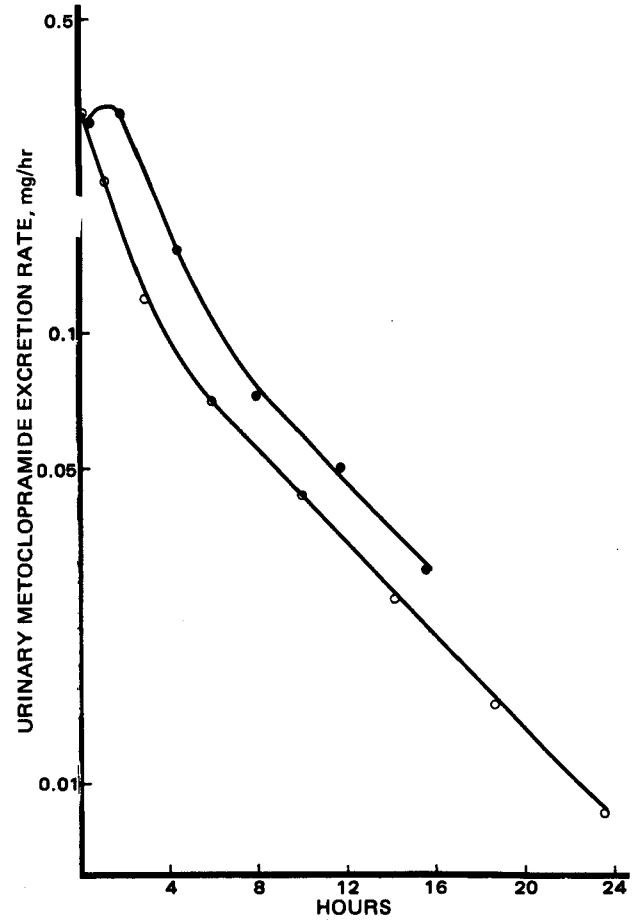

Figure 3—*Midpoint urinary excretion rate plots. Key: ●, urine samples collected along with blood samples; and ○, urine samples collected in a separate study using the same dose (20 mg of metoclopramide monohydrochloride) and subject.*

extraction from the plasma samples was 84 ± 9%. The minimum quantifiable amount of I was ~25 pg/injection.

Human Data—To demonstrate the application of the assay modification, urine and plasma I concentrations were measured in a human subject receiving IV[10] during a drug interaction study.

The peak plasma I concentration was achieved at ~1.5 hr after an oral dose of IV. Despite the somewhat scattered plasma data, the elimination half-life could be estimated using truncated plasma data, as reported previously (2, 3). When the truncated 8-hr plasma data were evaluated, an apparent half-life of 3.9 hr was noted; other investigators noted a half-life of 2.8 hr (3) and 4.0 hr (2) using similar data. However, when a 24-hr plasma sample was taken into account (Fig. 2), the elimination half-life was 5.4 hr. It becomes apparent that the use of 8-hr plasma data results in an underestimation of the terminal elimination half-life. Since no blood samples were taken between 8 and 24 hr after drug administration, an accurate estimation of the true elimination half-life was hampered using plasma data.

It was possible, however, to assess accurately the I elimination half-life using the urinary excretion rate data. When the urinary excretion rate of I was determined, the peak excretion rate was at 1.5 hr, in agreement with the time required for peak plasma concentrations to occur in this subject (Fig. 3), and the elimination half-life was 6 hr. In the postabsorptive phase of the plasma concentration and urinary excretion rate data, a biexponential decline was observed (Figs. 2 and 3), suggesting that I may follow multicompartment kinetics in humans. Following intravenous administration, Bateman *et al.* (3) reported biexponential kinetics for I, but these investigators may have missed the true terminal elimination phase noted in this subject (Fig. 3). This finding was confirmed by the fact that measurement of the half-life for I using truncated urinary excretion data (0–8 hr only, Fig. 3) yielded a half-life of 3 hr, in agreement with the reported value (3).

When the urinary excretion rate for I was determined in another experiment, the time for the maximal excretion rate was attained more rapidly. Slopes observed in the postabsorptive phase in both experiments (Fig. 3) were virtually identical, yielding a half-life of 6 hr. Thirteen percent of the dose was recovered as the intact drug after 96-hr cumulative urinary excretion. Acid hydrolysis of urine samples yielded a threefold increase in intact drug recovered.

Although urinary excretion rate data strongly suggest a longer half-life for I, the precise determination of the I elimination half-life in human plasma requires more blood samples. Additional studies are planned to confirm this observation.

REFERENCES

(1) Y. K. Tam and J. E. Axelson, *J. Pharm. Sci.*, **67**, 1073 (1978).

(2) T. Teng, R. B. Bruce, and L. K. Dunning, *ibid.*, **66**, 1615 (1977).

(3) D. N. Bateman, C. Kahn, K. Mashiter, and D. S. Davis, *Br. J. Clin. Pharmacol.*, **6**, 401 (1978).

ACKNOWLEDGMENTS

Supported by University of British Columbia Grant 32-9400, B.C. Heart Foundation Grant 65-0566, and M.R.C. Grant MA-5358.

Kinetic Studies of Hydralazine Reaction with Acetaldehyde

JOHN P. O'DONNELL, WOODROW J. PROVEAUX, and JOSEPH K. H. MA ˣ

Received February 21, 1979, from the *School of Pharmacy, West Virginia University, Morgantown, WV 26506.* Accepted for publication April 12, 1979.

Abstract □ *In vitro* kinetic studies of the reaction of hydralazine with acetaldehyde at physiological concentrations and pH were conducted. This reaction, which leads to the formation of 3-methyl-*S*-triazolo[3,4-*a*]phthalazine, may occur in the plasma and may represent an alternative pathway for hydralazine metabolism. The reaction of hydralazine with acetaldehyde followed second-order kinetics with an activation energy of 16.9 kcal/mole. At 37°, the half-life of the reaction for a solution containing 2.3 μg of acetaldehyde/ml and 1 μg of hydralazine/ml was 4.5 hr. The rate increased with increasing acetaldehyde concentrations.

Keyphrases □ Hydralazine—reaction with acetaldehyde, kinetics, half-life, therapeutic implications □ Antihypertensive agents—hydralazine, reaction with acetaldehyde, kinetics, half-life, therapeutic implications □ Kinetics—hydralazine reaction with acetaldehyde □ Acetaldehyde—reaction with hydralazine, kinetics, half-life, therapeutic implications

Since the early 1950's, hydralazine has been used to treat hypertension by direct peripheral vasodilation. More recently, the drug has been used in the treatment of severe congestive heart failure (1, 2). Its use, however, has been limited due to inadequate pharmacokinetic data on the drug and its metabolites.

BACKGROUND

The complete metabolism of hydralazine remains undefined. Studies (3, 4) showed that hydralazine undergoes polymorphic *N*-acetylation to form 3-methyl-*S*-triazolo[3,4-*a*]phthalazine as the major metabolic pathway, with phenotypically slow acetylators having higher steady-state plasma concentrations than fast acetylators. However, it was pointed out that the thermal half-life of hydralazine among slow acetylators is only slightly longer than or is not significantly different from that of fast acetylators (5). Thus, it seems doubtful that the enzymatic *N*-acetylation can represent the major metabolic pathway of hydralazine in humans.

Hydralazine metabolism is also more complicated because hydralazine is chemically reactive. It undergoes condensation with biogenic aldehydes and ketones to form hydrazones. Studies (6) in this laboratory showed that the reaction of hydralazine with formaldehyde and acetaldehyde forms *S*-triazolo[3,4-*a*]phthalazine and 3-methyl-*S*-triazolo[3,4-*a*]-phthalazine, respectively. Both products are known hydralazine metabolites (3, 4).

The formation of 3-methyl-*S*-triazolo[3,4-*a*]phthalazine from acetaldehyde and hydralazine was mentioned previously (7). These findings suggest that the formation of the hydralazine metabolites in humans may be at least partially due to the reaction of hydralazine with acetaldehyde. The acetaldehyde concentration in biological fluids is subject to significant increase by alcohol consumption and certain disease states (8). Thus, metabolite formation *via* this chemical reaction is significant with respect to proper drug use, especially in alcoholism, diabetes, and fasting states and on prolonged hydralazine administration.

To examine the effect of this chemical reaction on hydralazine metabolism and pharmacokinetics, the *in vitro* kinetics of 3-methyl-*S*-triazolo[3,4-*a*]phthalazine formation from hydralazine and acetaldehyde were studied. The importance of this reaction is discussed.

EXPERIMENTAL

Materials—Hydralazine (I), hydrochloride salt[1], and acetaldehyde[2] (II) were used as obtained. 3-Methyl-*S*-triazolo[3,4-*a*]phthalazine (III)

[1] Courtesy of Dr. M. Wilhem, Ciba-Geigy, Summit, N.J.
[2] Aldrich Chemical Co., Milwaukee, Wis.

0022-3549/79/1000-1256$01.00/0

© 1979, American Pharmaceutical Association

extraction from the plasma samples was 84 ± 9%. The minimum quantifiable amount of I was ~25 pg/injection.

Human Data—To demonstrate the application of the assay modification, urine and plasma I concentrations were measured in a human subject receiving IV[10] during a drug interaction study.

The peak plasma I concentration was achieved at ~1.5 hr after an oral dose of IV. Despite the somewhat scattered plasma data, the elimination half-life could be estimated using truncated plasma data, as reported previously (2, 3). When the truncated 8-hr plasma data were evaluated, an apparent half-life of 3.9 hr was noted; other investigators noted a half-life of 2.8 hr (3) and 4.0 hr (2) using similar data. However, when a 24-hr plasma sample was taken into account (Fig. 2), the elimination half-life was 5.4 hr. It becomes apparent that the use of 8-hr plasma data results in an underestimation of the terminal elimination half-life. Since no blood samples were taken between 8 and 24 hr after drug administration, an accurate estimation of the true elimination half-life was hampered using plasma data.

It was possible, however, to assess accurately the I elimination half-life using the urinary excretion rate data. When the urinary excretion rate of I was determined, the peak excretion rate was at 1.5 hr, in agreement with the time required for peak plasma concentrations to occur in this subject (Fig. 3), and the elimination half-life was 6 hr. In the postabsorptive phase of the plasma concentration and urinary excretion rate data, a biexponential decline was observed (Figs. 2 and 3), suggesting that I may follow multicompartment kinetics in humans. Following intravenous administration, Bateman *et al.* (3) reported biexponential kinetics for I, but these investigators may have missed the true terminal elimination phase noted in this subject (Fig. 3). This finding was confirmed by the fact that measurement of the half-life for I using truncated urinary excretion data (0–8 hr only, Fig. 3) yielded a half-life of 3 hr, in agreement with the reported value (3).

When the urinary excretion rate for I was determined in another experiment, the time for the maximal excretion rate was attained more rapidly. Slopes observed in the postabsorptive phase in both experiments (Fig. 3) were virtually identical, yielding a half-life of 6 hr. Thirteen percent of the dose was recovered as the intact drug after 96-hr cumulative urinary excretion. Acid hydrolysis of urine samples yielded a threefold increase in intact drug recovered.

Although urinary excretion rate data strongly suggest a longer half-life for I, the precise determination of the I elimination half-life in human plasma requires more blood samples. Additional studies are planned to confirm this observation.

REFERENCES

(1) Y. K. Tam and J. E. Axelson, *J. Pharm. Sci.*, **67**, 1073 (1978).

(2) T. Teng, R. B. Bruce, and L. K. Dunning, *ibid.*, **66**, 1615 (1977).

(3) D. N. Bateman, C. Kahn, K. Mashiter, and D. S. Davis, *Br. J. Clin. Pharmacol.*, **6**, 401 (1978).

ACKNOWLEDGMENTS

Supported by University of British Columbia Grant 32-9400, B.C. Heart Foundation Grant 65-0566, and M.R.C. Grant MA-5358.

Kinetic Studies of Hydralazine Reaction with Acetaldehyde

JOHN P. O'DONNELL, WOODROW J. PROVEAUX, and JOSEPH K. H. MA ˣ

Received February 21, 1979, from the *School of Pharmacy, West Virginia University, Morgantown, WV 26506.* Accepted for publication April 12, 1979.

Abstract □ *In vitro* kinetic studies of the reaction of hydralazine with acetaldehyde at physiological concentrations and pH were conducted. This reaction, which leads to the formation of 3-methyl-*S*-triazolo[3,4-*a*]phthalazine, may occur in the plasma and may represent an alternative pathway for hydralazine metabolism. The reaction of hydralazine with acetaldehyde followed second-order kinetics with an activation energy of 16.9 kcal/mole. At 37°, the half-life of the reaction for a solution containing 2.3 μg of acetaldehyde/ml and 1 μg of hydralazine/ml was 4.5 hr. The rate increased with increasing acetaldehyde concentrations.

Keyphrases □ Hydralazine—reaction with acetaldehyde, kinetics, half-life, therapeutic implications □ Antihypertensive agents—hydralazine, reaction with acetaldehyde, kinetics, half-life, therapeutic implications □ Kinetics—hydralazine reaction with acetaldehyde □ Acetaldehyde—reaction with hydralazine, kinetics, half-life, therapeutic implications

Since the early 1950's, hydralazine has been used to treat hypertension by direct peripheral vasodilation. More recently, the drug has been used in the treatment of severe congestive heart failure (1, 2). Its use, however, has been limited due to inadequate pharmacokinetic data on the drug and its metabolites.

BACKGROUND

The complete metabolism of hydralazine remains undefined. Studies (3, 4) showed that hydralazine undergoes polymorphic *N*-acetylation to form 3-methyl-*S*-triazolo[3,4-*a*]phthalazine as the major metabolic pathway, with phenotypically slow acetylators having higher steady-state plasma concentrations than fast acetylators. However, it was pointed out that the thermal half-life of hydralazine among slow acetylators is only slightly longer than or is not significantly different from that of fast acetylators (5). Thus, it seems doubtful that the enzymatic *N*-acetylation can represent the major metabolic pathway of hydralazine in humans.

Hydralazine metabolism is also more complicated because hydralazine is chemically reactive. It undergoes condensation with biogenic aldehydes and ketones to form hydrazones. Studies (6) in this laboratory showed that the reaction of hydralazine with formaldehyde and acetaldehyde forms *S*-triazolo[3,4-*a*]phthalazine and 3-methyl-*S*-triazolo[3,4-*a*]-phthalazine, respectively. Both products are known hydralazine metabolites (3, 4).

The formation of 3-methyl-*S*-triazolo[3,4-*a*]phthalazine from acetaldehyde and hydralazine was mentioned previously (7). These findings suggest that the formation of the hydralazine metabolites in humans may be at least partially due to the reaction of hydralazine with acetaldehyde. The acetaldehyde concentration in biological fluids is subject to significant increase by alcohol consumption and certain disease states (8). Thus, metabolite formation *via* this chemical reaction is significant with respect to proper drug use, especially in alcoholism, diabetes, and fasting states and on prolonged hydralazine administration.

To examine the effect of this chemical reaction on hydralazine metabolism and pharmacokinetics, the *in vitro* kinetics of 3-methyl-*S*-triazolo[3,4-*a*]phthalazine formation from hydralazine and acetaldehyde were studied. The importance of this reaction is discussed.

EXPERIMENTAL

Materials—Hydralazine (I), hydrochloride salt[1], and acetaldehyde[2] (II) were used as obtained. 3-Methyl-*S*-triazolo[3,4-*a*]phthalazine (III)

[1] Courtesy of Dr. M. Wilhem, Ciba-Geigy, Summit, N.J.
[2] Aldrich Chemical Co., Milwaukee, Wis.

0022-3549/79/1000-1256$01.00/0

© 1979, American Pharmaceutical Association

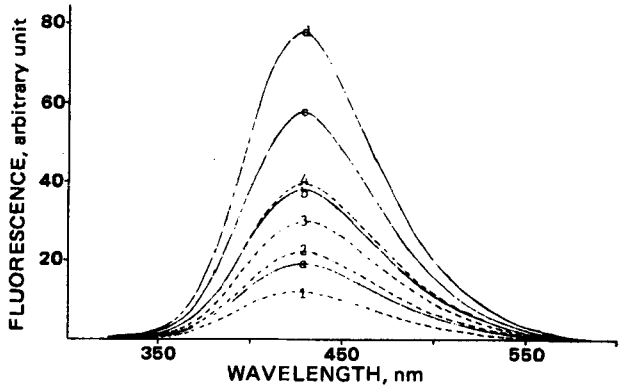

Figure 1—*Fluorescence spectrum of 3-methyl-S-triazolo[3,4-a]-phthalazine (III) in pH 7.4 phosphate buffer. The solid lines represent standard solutions of III: a, 1.36 × 10⁻⁶ M; b, 2.72 × 10⁻⁶ M; c, 4.07 × 10⁻⁶ M; and d, 5.43 × 10⁻⁶ M. The broken lines represent formation of III from solutions containing 2.036 × 10⁻⁵ M hydralazine (I) and 5.227 × 10⁻⁵ M acetaldehyde (II) at 25° at the end of 45 (1), 75 (2), 120 (3), and 180 (4) min.*

was prepared and purified according to a literature procedure (9). All other chemicals were analytical or chromatographic grade.

Methods—The kinetics of the reaction of I with II were studied by measuring the formation of III using a fluorometric technique. The experiments were carried out in pH 7.4 phosphate buffer with physiological concentrations of I (1–4 μg/ml) and II (2.3 μg/ml) at 25, 30, 35, 37, and 40°. Stock solutions of I and II were prepared daily using chromatographic grade methanol. Sufficient stock solution of I was diluted to 100 ml with the buffer, and the solution was equilibrated at a desired temperature using a temperature-controlled water bath. After the addition of the desired amount of II, samples were taken at selected time intervals and analyzed immediately for III.

The fluorescence measurements were made with a spectrophotofluorometer[3] equipped with a 150-w xenon lamp and a 1P21 photomultiplier tube. The cell compartment of the spectrophotofluorometer also was equilibrated at the desired temperature by a circulatory temperature-controlled water bath. In pH 7.4 buffer, I and II are nonfluorescent, but III exhibits strong fluorescence at 430 nm when excited at 240 nm. The formation of III in solutions containing I and II was monitored by fluorescence measurement, and the concentration of III was determined using a fluorescence calibration curve of known III concentrations in the 5 × 10^{-7}–1 × 10^{-5} *M* range.

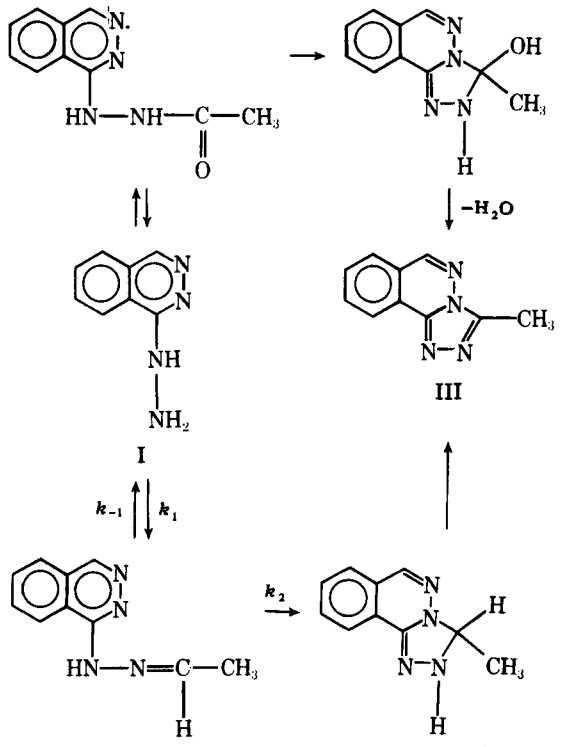

Scheme I—Mechanisms of the formation of III by acetylation and hydrazone pathways

[3] Aminco-Bowman, American Instruments Co., Silver Spring, Md.

Table I—Kinetic Results for the Reaction of Hydralazine (I) with Acetaldehyde (II) at Physiological pH and Concentrations

Temperature	*k*, liters/mole/min	$t_{1/2}$, hr[a]
25°	18.8	12.01
30°	26.3	8.59
35°	39.2	5.77
37°	50.0	4.50
40°	62.6	3.61

[a] Calculated for solutions containing 5.09 × 10^{-6} *M* I and 52.27 × 10^{-6} *M* II as initial concentrations.

The formation of III from I and II followed second-order kinetics. The overall rate constants of the reaction were determined using:

$$\left(\frac{1}{C_I - C_{II}}\right)\left(\log\frac{C_{II}(C_I - X)}{C_I(C_{II} - X)}\right) = \left(\frac{k}{2.303}\right)(t) \qquad \text{(Eq. 1)}$$

where k is the overall rate constant; C_I and C_{II} are the initial concentrations of I and II, respectively; and X is the concentration of III at time t. The relationship between the rate constant and temperature was examined using the Arrhenius equation, from which the activation energy of the reaction also was calculated.

RESULTS AND DISCUSSION

The fluorescence spectra of 3-methyl-*S*-triazolo[3,4-*a*]phthalazine (III) in pH 7.4 phosphate buffer are shown in Fig. 1. Spectra a, b, c, and d were obtained from solutions prepared with standard Compound III, whereas spectra 1, 2, 3, and 4 represent the formation of III in solutions containing hydralazine (I) and acetaldehyde (II). The formation of III in these solutions was confirmed also by a high-pressure liquid chromatographic study at conditions reported previously (6).

Figure 2 shows the plots of the percentage of I remaining as a function of time for solutions containing 5.227 × 10^{-5} *M* (2.3 μg/ml) of II and varying concentrations of I measured at 25°. The reaction half-life was dependent on the concentration of I, indicating that the reaction followed second- or higher order kinetics. When these data were treated with Eq. 1, it was found that the reaction was second order. The plot of Eq. 1 for the data of Fig. 2 is shown in Fig. 3. A straight line was obtained for solutions containing different concentrations of I. Similar results also were obtained for the reaction carried out at other temperatures.

A possible mechanism of the condensation of I with II and comparison of this reaction with the acetylation process in the formation of III are shown in Scheme I. Hydralazine condensation with II forms an intermediate hydrazone, which is subsequently cyclized and oxidized to form

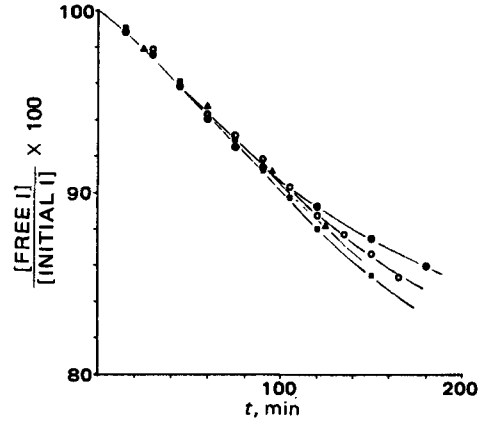

Figure 2—*Plot of the ratio of free and initial concentrations of hydralazine (I) as a function of time for solutions containing 52.27 × 10^{-6} M acetaldehyde (II) and 5.09 × 10^{-6} M I (■), 10.18 × 10^{-6} M I (▲), 15.27 × 10^{-6} M I (○), and 20.36 × 10^{-6} M I (●). The reaction temperature was 25°.*

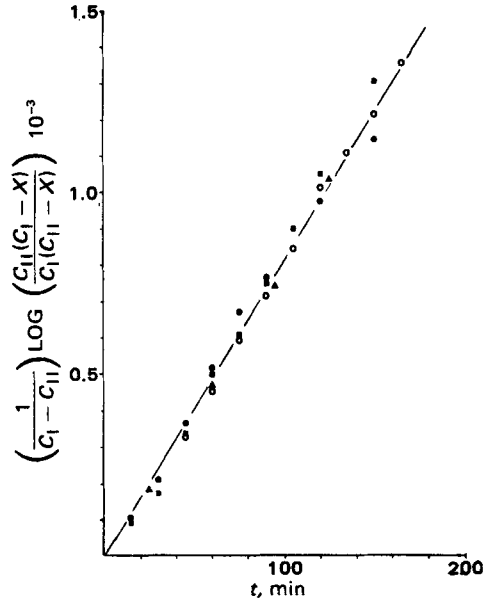

Figure 3—*Plot of Eq. 1 for the data shown in Fig. 2.*

III *via* the driving force of the formation of a completely aromatic system. Such oxidation reactions also were reported in analogous heterocyclic systems (7, 10). The acetylation process is enzyme dependent and occurs primarily in the intestine and liver (11), whereas the condensation reaction may occur primarily in the plasma. From the mechanism shown in Scheme I, the kinetics of the reaction of I with II may be approximated by the steady-state approach (Schemes II and III).

$$\text{I} + \text{II} \underset{k_1}{\overset{k_1}{\rightleftarrows}} \text{intermediate}$$

Scheme II

$$\text{intermediate} \xrightarrow{k_2} \text{III}$$

Scheme III

This approach will also give second-order kinetics with $k_1k_2/(k_1 + k_2)$ equal to the overall rate constant of Eq. 1.

The overall rate constants determined at various temperatures are shown in Table I. When the log values of the rate constants were plotted *versus* $1/T$, where T is the absolute temperature, a straight line was obtained, indicating that the reaction obeys the Arrhenius principle. From the slope of the plot, the activation energy of the reaction is found to be 16.9 kcal/mole.

The half-lives listed in Table I were calculated for solutions containing 5.09×10^{-6} *M* (1 μg/ml) I and 5.227×10^{-5} *M* (2.3 μg/ml) II, typical physiological concentrations (12). At 37°, the reaction has a half-life of 4.5 hr. The physiological half-life of I in humans was reported to be in the 4–8-hr range (13). Although the half-life measured for the chemical reaction of I is not to be mistaken for the biological half-life, it does indicate that the reaction of I with II may significantly affect drug metabolism and pharmacokinetics. This result is especially true in conditions such as chronic or acute alcohol ingestion, fasting states, and diabetes, which result in elevated levels of II. Since the reaction is second order, an increase of the blood level of II will result in an increase of the formation rate of III. On the other hand, with low levels of I, as in the case of noncompliant patients who take less than the prescribed dose and patients with poor absorption, the reaction also becomes more significant. The effect of II levels on the elimination of I and on the formation of III is being studied in this laboratory.

REFERENCES

(1) K. Chaterjee, W. W. Parmley, and W. Ganz, *Circulation*, **48**, 1183 (1973).

(2) P. A. Majid, B. Sharma, and S. H. Taylor, *Lancet*, **2**, 719 (1971).

(3) M. M. Reidenberg, D. Drayer, A. L. Demarco, and C. T. Bell, *Clin. Pharmacol. Ther.*, **14**, 970 (1973).

(4) J. Wagner, J. W. Faile, P. Imhof, and G. Licher, *Arzneim.-Forsch.*, **27**, 2388 (1977).

(5) T. Talseth, *Clin. Pharmacol. Ther.*, **21**, 715 (1977).

(6) J. P. O'Donnell, W. J. Proveaux, and J. K. H. Ma, *J. Pharm. Sci.*, in press.

(7) J. Druey and B. H. Ringier, *Helv. Chim. Acta*, **34**, 195 (1951).

(8) M. A. Korsten, S. Matsuzki, L. Feinman, and C. S. Lieber, *N. Engl. J. Med.*, **292**, 386 (1975).

(9) K. D. Haegele, H. B. Skrdlant, N. W. Robie, D. Lalka, and J. L. McNay, *J. Chromatogr.*, **126**, 517 (1976).

(10) R. A. Coburn and J. P. O'Donnell, *J. Org. Chem.*, **37**, 17011 (1972).

(11) T. Talseth, *Clin. Pharmacokinet.*, **2**, 317 (1977).

(12) G. A. Goldsmith, in "Nutrition," vol. 2, G. H. Beaton and E. W. McHenry, Eds., Academic, New York, N.Y., 1964, p. 109.

(13) J. M. Lesser, Z. H. Israili, D. C. Davis, and P. G. Dayton, *Drug Metab. Dispos.*, **2**, 351 (1974).

Carbenicillin Prodrugs: Stability Kinetics of α-Phenyl and α-Indanyl Esters in Aqueous Solution

AKIRA TSUJI, ETSUKO MIYAMOTO, TETSUYA TERASAKI, and TSUKINAKA YAMANA ˣ

Received September 6, 1978, from the *Faculty of Pharmaceutical Sciences, Kanazawa University, Takara-machi, Kanazawa 920, Japan.* Accepted for publication April 13, 1979.

Abstract □ Both ester and β-lactam degradations of α-esters of carbenicillin disodium, carbenicillin indanyl sodium, and carbenicillin phenyl sodium in aqueous solution at 35° and at 0.5 ionic strength were investigated. The reactions were followed by spectrophotometric assay, reversed-phase high-pressure liquid chromatography, and colorimetric assay. The degradation pathways were established, and the rate–pH profiles for ester and β-lactam cleavage reactions are given for pH 1–11. Below pH 3, the β-lactam degradation of the prodrugs proceeded exclusively. Above pH 7, the degradation was superseded by the ester hydrolysis to carbenicillin. β-Lactams of both prodrugs are around three times more stable than carbenicillin disodium at pH 1, six times at pH 2, and 17 times at pH 3. The half-lives for carbenicillin production were predicted to be 17 hr for carbenicillin indanyl sodium and 8.5 hr for carbenicillin phenyl sodium at pH 7.0 and 37°.

Keyphrases □ Carbenicillin—prodrugs, stability in aqueous solutions, pH effects, degradation kinetics □ Carbenicillin indanyl sodium—prodrug, stability in aqueous solutions, pH, degradation kinetics □ Carbenicillin phenyl sodium—prodrug, stability in aqueous solutions, pH, degradation kinetics □ Antibiotics—carbenicillin, prodrugs, stability in aqueous solutions, pH effects, degradation kinetics

Intravenous or intramuscular carbenicillin is effective against serious infections caused by *Pseudomonas aeruginosa* and other Gram-negative bacteria (1). This antibiotic is unstable in acidic solutions (2, 3) and gastric juice (4, 5) and is poorly absorbed from the GI tract after oral administration (1).

Several α-carboxyl esters of carbenicillin were synthesized to increase its oral bioavailability (5, 6). Carbenicillin indanyl sodium (carindacillin) and carbenicillin phenyl sodium (carfecillin) have been marketed as oral carbenicillin prodrugs.

This paper describes the kinetics of carbenicillin indanyl sodium and carbenicillin phenyl sodium in aqueous solution at various pH values. Their good stability at pH 2 in gastric juice has been well known, but complete kinetics for β-lactam cleavage and hydrolysis of the ester moiety to produce carbenicillin have not been reported.

EXPERIMENTAL

Materials—Carbenicillin disodium[1] (799 μg/mg), carbenicillin indanyl sodium[1] (704 μg/mg as carbenicillin free acid), and carbenicillin phenyl sodium[2] (979 μg/mg) were used as received.

All other chemicals were analytical grade and were used without further purification except imidazole, which was purified as described in the literature (7).

Reagents—The imidazole reagent was prepared according to the literature (7). The acidic reagent was 0.2 *M* acetate buffer solution adjusted to pH 4.

Prodrug Hydrolysis—Kinetic studies were carried out, unless otherwise stated, at 35° and an ionic strength of 0.5. Each antibiotic was dissolved in the buffer or in 0.5 *M* KCl, maintained at the desired pH by a pH-stat[3], to the final concentration of 5×10^{-5}–5×10^{-3} *M*, depending on the solubility. At appropriate intervals, aliquots were withdrawn, cooled, and analyzed. The pseudo-first-order rate constants, k_{obs}, were calculated by the least-squares analysis of the slopes of starting antibiotic concentration logarithm *versus* time plots.

Analytical Procedure—*Simultaneous Determination of Carbenicillin and Its Prodrug*—Carbenicillin and its prodrug were determined simultaneously by a spectrophotometric assay. This analytical method, utilizing the difference in the acid stability between carbenicillin and the prodrug, is based on the imidazole method (7).

If necessary, the sample was diluted with distilled water. Four equal samples of 1 ml each, A_1, A_2, B_1, and B_2, of the test solution were pipetted into separate test tubes. Five milliliters of imidazole reagent was added to A_1 and 5 ml of distilled water was added to B_1, followed by incubation at 60° for 25 min. After cooling, absorbances, E_{A1} and E_{B1}, were measured[4] at 325 nm. To samples of A_2 and B_2, 1 ml of acidic reagent was added, and the samples were incubated in a water bath at 60° for exactly 25 min and cooled. After addition of 5 ml of the imidazole reagent to A_2 and 5 ml of distilled water to B_2, these samples were incubated in a water bath at 60° for 25 min and cooled; their absorbances, E_{A2} and E_{B2}, were measured at the same wavelength.

The concentrations of each compound can be calculated from Eqs. 1 and 2 using the difference in absorbance between A and B; *i.e.*, E_1 ($= E_{A1} - E_{B1}$) and E_2 ($= E_{A2} - E_{B2}$):

$$E_1 = S_{p1}C_p + S_{c1}C_c \qquad \text{(Eq. 1)}$$

$$E_2 = S_{p2}C_p + S_{c2}C_c \qquad \text{(Eq. 2)}$$

where subscripts *c* and *p* refer to carbenicillin and its prodrug, respectively; *C* is the concentration of the antibiotic in sample solution, and *S* is the slope of the calibration curve of the antibiotics for respective reaction periods of 0 and 25 min with the acidic reagent.

A good straight-line relation between the absorbance and the concentration of each antibiotic was obtained within 0–3×10^{-4} *M* of the antibiotic in a sample solution. Both S_{c1} and S_{p1} were 3.95×10^3, and S_{p2} was 3.19×10^3 and 1.83×10^3 for two prodrugs and carbenicillin, respectively. The carbenicillin molar absorptivity, which could be calculated from S_{c1} and the final concentration in the analytical solution, was 2.37×10^4, comparable to the 2.67×10^4 reported previously (7). Synthetic mixtures of carbenicillin and its prodrug were analyzed in this way, and entirely satisfactory results were obtained (Table I).

High-Pressure Liquid Chromatography (HPLC)—To ensure the accuracy of the spectrophotometric method, the same samples in some reactions were determined also by reversed-phase HPLC. The liquid

Table I—Recovery of Carbenicillin Phenyl Sodium (I) and Carbenicillin Disodium (II) from a Synthetic Mixture in 0.1 *M* Phosphate Buffer at pH 6.54 and Ionic Strength 0.5 [a]

Added (10^3 *M*)		Found (10^3 *M*)		Recovery, %	
I	II	I	II	I	II
1.00	0.00	1.01	0.00	101.1	100.0
0.80	0.20	0.78	0.21	97.5	105.0
0.40	0.60	0.38	0.59	95.0	98.3
0.20	0.80	0.20	0.78	100.0	97.5
0.00	1.00	0.00	0.99	100.0	99.0

[a] The mixture was diluted fivefold with distilled water and analyzed according to the described procedure.

[1] Taito Pfizer Co., Tokyo, Japan.
[2] Beecham Yakuhin Co., Tokyo, Japan.
[3] pH-Stat titrator assembly consisting of TTT2 titrator and ABU12b autoburet, Radiometer, Copenhagen, Denmark.
[4] Double-beam spectrophotometer, UV-200S, Shimadzu, Kyoto, Japan.

0022-3549/79/1000-1259$01.00/0
© 1979, American Pharmaceutical Association

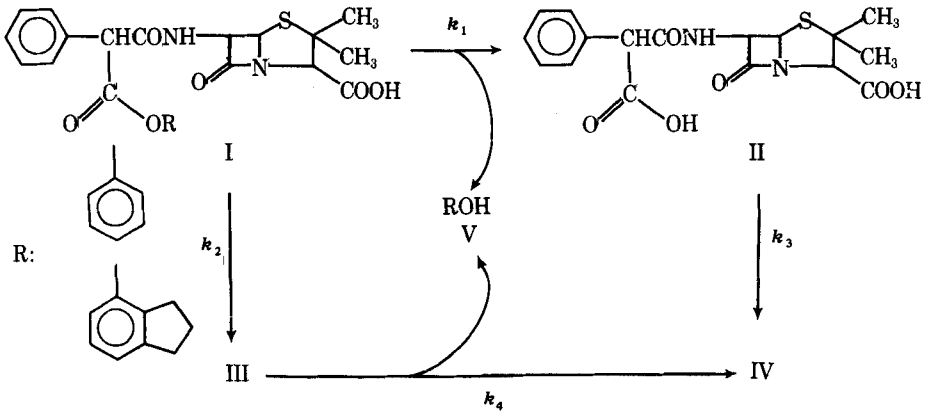

Scheme I—Prodrug degradation pathway in aqueous solution

chromatograph[5] was equipped with a UV detector[6] set at 254 nm. The stationary phase was octadecylsilane chemically bonded on totally porous silica gel, prepacked into a 300-mm stainless steel column[7] (4-mm i.d.). The mobile phase was 20% acetonitrile–0.01 *M* ammonium acetate. The instrument was operated at ambient temperature at a flow rate of 2 ml/min to produce the pressure of 110 kg/cm^2. Samples were injected through a 100-μl loop injector on flow. Peak heights were used for quantification.

Colorimetric Determination of Phenol—Phenol liberated from carbenicillin phenyl sodium was measured by the colorimetric method (8). The sample was diluted with distilled water, if necessary, and placed in a 20-ml volumetric flask. Then 1 ml of 0.3% 4-aminoantipyrine, 2 ml of 1% ferricyanide, and 5 ml of 0.2 *M* borate buffer (pH 9.2) were added consecutively, and the absorbance of the solution, adjusted to 20 ml with distilled water, was measured at 510 nm. The calibration curve was prepared with the standard phenol solution, and the concentration of phenol liberated was calculated.

RESULTS

Prodrug Degradation Pathway—Degradation of carbenicillin esters may proceed as depicted in Scheme I. In this scheme, I represents carbenicillin indanyl sodium and carbenicillin phenyl sodium, II represents carbenicillin, III represents β-lactam-cleaved products of I, IV represents the sum of products resulting from β-lactam cleavage of II and from ester hydrolysis of III, and V represents indanol or phenol.

Figures 1–3 show time courses of molar fractions of I–V during I degradation. Compounds I and II were determined by the UV spectrometric method developed in this study. As seen in Fig. 1, these concentrations were in good agreement with those determined by HPLC. Phenol (V) liberated from carbenicillin phenyl sodium (I) and III was determined by colorimetry. Concentrations of III and IV, therefore, were calculated from Eqs. 3 and 4 for carbenicillin phenyl sodium degradation:

$$[III] = [I]_0 - [I] - [V] \quad \text{(Eq. 3)}$$

$$[IV] = [V] - [II] \quad \text{(Eq. 4)}$$

where the molar concentration of all species is expressed with brackets and $[I]_0$ is the initial I concentration.

By solving the differential equation for Scheme I, the rate expression for the molar fraction of each species may be written as:

$$[I]/[I]_0 = e^{-(k_1+k_2)t} \quad \text{(Eq. 5)}$$

$$[II]/[I]_0 = \frac{k_1}{k_1+k_2-k_3}(e^{-k_3t} - e^{-(k_1+k_2)t}) \quad \text{(Eq. 6)}$$

$$[III]/[I]_0 = \frac{k_2}{k_1+k_2-k_4}(e^{-k_4t} - e^{-(k_1+k_2)t}) \quad \text{(Eq. 7)}$$

$$[IV]/[I]_0 = 1 - \frac{k_3k_4 - k_1k_3 - k_2k_4}{(k_1+k_2-k_3)(k_1+k_2-k_4)}e^{-(k_1+k_2)t} - \frac{k_2}{k_1+k_2-k_4}e^{-k_4t} - \frac{k_1}{k_1+k_2-k_3}e^{-k_3t} \quad \text{(Eq. 8)}$$

$$[V]/[I]_0 = 1 - \frac{k_1-k_4}{k_1+k_2-k_4}e^{-(k_1+k_2)t} - \frac{k_2}{k_1+k_2-k_4}e^{-k_4t} \quad \text{(Eq. 9)}$$

To evaluate k_3, degradation of II was performed under similar conditions (Fig. 3). The rate constants k_1, k_2, k_3, and k_4 to best fit all experimental points were obtained by the nonlinear least-squares regression analysis according to Eqs. 5–9. The resulting rate constants are listed in Table II, providing calculated curves fitting the observed values (Figs. 1–3).

In most cases, rate constants k_1 and k_4 for the ester hydrolysis of both I and III were almost identical, suggesting that β-lactam cleavage had no effect on the rate for α-ester hydrolysis.

Kinetics of Apparent First-Order Rate Constants—By plotting the logarithm of $[I]/[I]_0$ against time, the apparent first-order rate con-

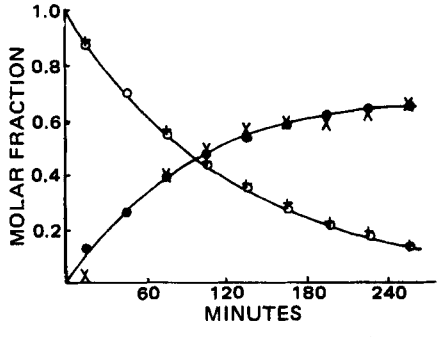

Figure 1—*Time course for carbenicillin phenyl sodium (○, separation assay; +, HPLC) and carbenicillin (●, separation assay; ×, HPLC) during degradation at pH 6.35 (0.2 M phosphate buffer), 60°, and ionic strength 0.5. The lines are the least-squares fits of the experimental points consistent with Scheme I on the assumption of* $k_1 = k_4$ ($k_1 = k_4 = 42.8 \times 10^{-2}\ hr^{-1}$, $k_2 = 5.58 \times 10^{-2}\ hr^{-1}$, *and* $k_3 = 6.38 \times 10^{-2}\ hr^{-1}$).

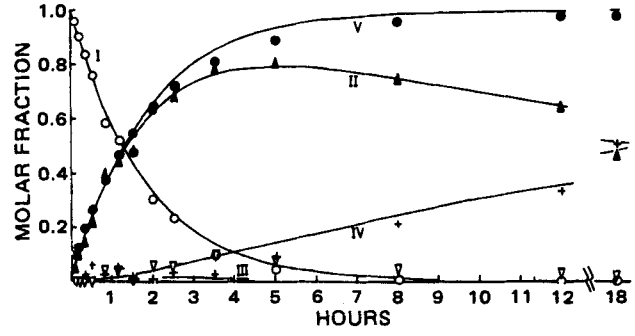

Figure 2—*Time course for carbenicillin phenyl sodium (I) (○), II (▲), III (▽), IV (+), and V (●) during degradation at pH 6.60 (0.1 M phosphate buffer), 60°, and ionic strength 0.5. The lines are the least-squares best fits to the experimental points consistent with Scheme I on the assumption of* $k_1 = k_4$ ($k_1 = k_4 = 53.9 \times 10^{-2}\ hr^{-1}$, $k_2 = 2.05 \times 10^{-2}\ hr^{-1}$, *and* $k_3 = 3.88 \times 10^{-2}\ hr^{-1}$). *The compound numbers are defined in the text.*

[5] Model FLC-A700, Japan Spectroscopic Co., Tokyo, Japan.
[6] Model UVIDEC-100, Japan Spectroscopic Co., Tokyo, Japan.
[7] μBondapak C_{18}, Waters Associates, Milford, Mass.

Table II—Rate Constants [a] for Carbenicillin Phenyl Sodium Degradation at pH 6.60 (60°, 0.1 *M* Phosphate Buffer), pH 6.35 (60°, 0.2 *M* Phosphate Buffer), and pH 4.60 (35°, 0.2 *M* Acetate Buffer) and Ionic Strength 0.5

pH	$k_1 \pm SD$, $10^2\ hr^{-1}$	$k_2 \pm SD$, $10^2\ hr^{-1}$	$k_3 \pm SD$, $10^2\ hr^{-1}$	$k_4 \pm SD$, $10^2\ hr^{-1}$
6.60	53.9 ± 1.27	2.05 ± 1.16	3.88 ± 0.31	53.9 ± 1.27 [b]
6.35	42.8 ± 0.78	5.58 ± 0.89	6.38 ± 0.96	42.8 ± 0.78 [b]
4.60	0.84 ± 0.05	0.50 ± 0.05	5.12 ± 0.20	0.66 ± 0.17

[a] The values were evaluated by the nonlinear least-squares analysis of experimental points in Figs. 1–3. [b] The calculation was carried out on the assumption of $k_1 = k_4$.

Table III—Various Rate Constants [a] for the Degradation of Prodrugs at 35° and Ionic Strength 0.5

Antibiotic	$(k_2)_H$, $M^{-1}\ hr^{-1}$	$10^2(k_2)_0$, hr^{-1}	$10^2(k_1)_H$, $M^{-1}\ hr^{-1}$	$10^3(k_1)_0$, hr^{-1}	$10^{-5}(k_1)_{OH}$, $M^{-1}\ hr^{-1}$
Carbenicillin disodium	52.2 [b]	183 [b]	—	—	—
Carbenicillin phenyl sodium	17.9 ± 1.1	9.79 ± 1.12	4.98 ± 1.40	3.72 ± 0.48	3.09 ± 0.35
Carbenicillin indanyl sodium	24.4 ± 0.3	8.22 ± 0.22	—	3.53 ± 0.49	1.46 ± 0.08

[a] Rate constants are defined in Eqs. 15 and 16, and they were calculated using the nonlinear regression analysis of the experimental points in Fig. 7. [b] Reference 15.

stants k_{obs} for overall degradation of I was obtained from the slopes, *i.e.*:

$$k_{obs} = k_1 + k_2 \qquad \text{(Eq. 10)}$$

The typical first-order plots obtained from the UV spectrophotometric separation assay are given in Fig. 4 for both prodrugs.

On the assumption that $k_1 = k_4$, as verified for carbenicillin phenyl sodium, Eq. 9 may be simplified to:

$$[V]/[I]_0 = 1 - e^{-k_1 t} \qquad \text{(Eq. 11)}$$

Good first-order plots were obtained for carbenicillin phenyl sodium, consistent with the prediction of Eq. 11 when $\log (1 - [V]/[I]_0)$ was plotted against time (Fig. 4).

During the kinetic runs above pH 7, the degradation of both prodrugs resulted in a gradual increase of the characteristic UV absorbance at 270–290 nm. Plots of $\log (E_\infty - E_t)$ at λ_{max} (268 nm for carbenicillin phenyl sodium and 280 nm for carbenicillin indanyl sodium) *versus* t become reasonably linear according to the first-order expression:

$$\log (E_\infty - E_t) = \log (E_\infty - E_0) - \frac{k_{obs}}{2.303} t \qquad \text{(Eq. 12)}$$

where E_t, E_0, and E_∞ are the absorbances at times t, zero, and infinity, respectively. All reactions were followed for one to three half-lives, and values for the pseudo-first-order rate constant k_{obs} were obtained by plots of Eq. 12 or by the method of Guggenheim (9). Figure 4 shows typical plots of the logarithm of $(E_\infty - E_t)/(E_\infty - E_0)$. The k_{obs} values obtained by UV spectrophotometry were equal to $(k_1 + k_2)$ determined by the separation assay. For carbenicillin phenyl sodium, the rate constants above pH 7 were almost in agreement with the k_1 values determined by the colorimetric method.

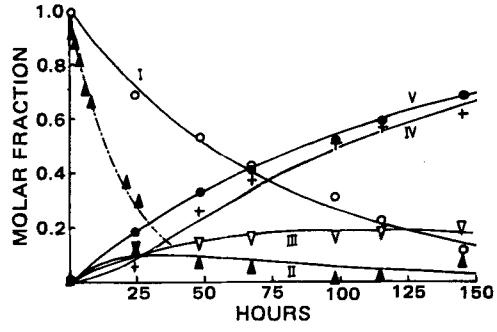

Figure 3—*Time course for carbenicillin phenyl sodium (I) (○), II (▲), III (▽), IV (+), and V (●) during degradation at pH 4.60 (0.2 M acetate buffer), 35°, and ionic strength 0.5. The lines are the least-squares best fits to the experimental points consistent with Scheme I ($k_1 = 0.84 \times 10^{-2}\ hr^{-1}$, $k_2 = 0.50 \times 10^{-2}\ hr^{-1}$, $k_3 = 5.12 \times 10^{-2}\ hr^{-1}$, and $k_4 = 0.66 \times 10^{-2}\ hr^{-1}$). Carbenicillin (▲) on the broken line was determined by degradation of II under the same conditions. The compound numbers are defined in the text.*

Buffer Concentration Effect on Degradation Rates—At constant pH and in the presence of excess buffer, the rate constants k_{obs} for the total loss of I and k_1 for the ester hydrolysis were affected by general acid–base catalysis by buffer components. Typical plots for the catalytic effect of various buffers on k_{obs} and k_1 are shown in Figs. 5 and 6, respectively, giving a reasonably straight line at constant pH in all cases. Extrapolation of such plots to zero buffer concentration provides, as intercepts, the values of the pseudo-first-order rate constants $(k_{obs})_{pH}$ and $(k_1)_{pH}$, corresponding to the non-buffer-catalyzed degradation of the β-lactam and of the ester bond of the prodrug nucleus. For ester linkage hydrolysis, the rate constant may be defined in the phosphate buffer system as:

$$k_1 = (k_1)_{pH} + k_{H_2PO_4^-}[H_2PO_4^-] + k_{HPO_4^{2-}}[HPO_4^{2-}] \qquad \text{(Eq. 13)}$$

Equation 13 can be written in terms of the total buffer concentration, $[B]_T$:

$$k_1 = (k_1)_{pH} + [k_{H_2PO_4^-} + (k_{HPO_4^{2-}} - k_{H_2PO_4^-}) f_{HPO_4^{2-}}][B]_T \qquad \text{(Eq. 14)}$$

where $f_{HPO_4^{2-}}$ is the fraction of monohydrogen phosphate ion. By employing pKa = 6.59 at 35° and ionic strength 0.5 for phosphate (10), plots of the slopes at pH 6.93, 6.38, and 5.87 against $f_{HPO_4^{2-}}$ provided the catalytic constant of $k_{HPO_4^{2-}} = 0.240\ M^{-1}\ hr^{-1}$ for the HPO_4^{2-} buffer component. No significant catalytic effect could be assigned to the $H_2PO_4^-$ buffer component.

Log k_{pH}–pH Profiles—The k_{pH} values were obtained by extrapolation of k_{obs} to zero buffer concentration. These values also were determined by the pH-stat.

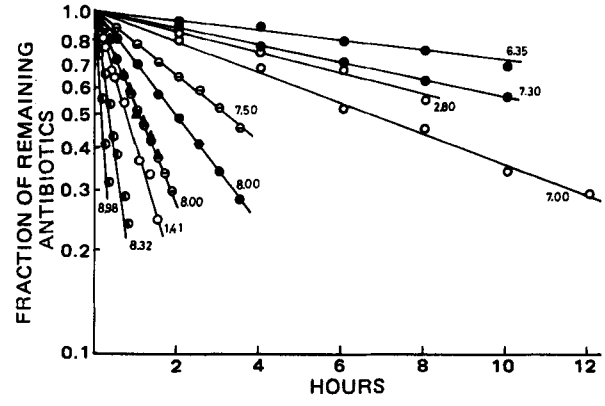

Figure 4—*Apparent first-order plots followed by spectrophotometric assay for degradation of carbenicillin indanyl sodium (●, separation assay; ◐, UV method) and carbenicillin phenyl sodium (○, separation assay; ⊖, colorimetric method; ▲, UV method) at various pH values, 35°, and ionic strength 0.5. The 0.5 M KCl solution was maintained at each pH (8.98, 8.00, 7.50, 7.30, 7.00, 2.80, and 1.41) by means of a pH-stat; the 0.2 M borate buffer was at pH 8.32, and the 0.2 M phosphate buffer was at pH 6.35.*

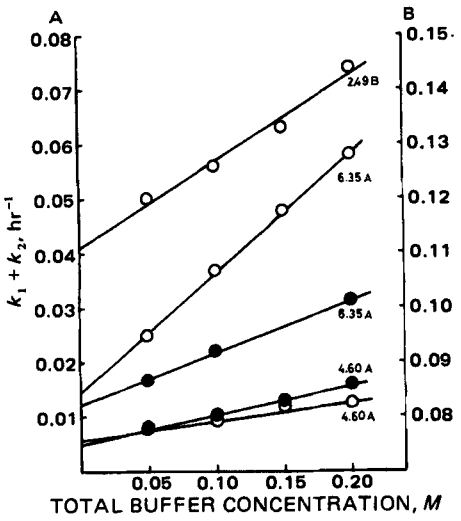

Figure 5—*Pseudo-first-order rate constants,* $k_1 + k_2$, *versus total buffer concentration for degradation of carbenicillin indanyl sodium* (●) *and carbenicillin phenyl sodium* (○) *in various buffer systems at 35° and ionic strength 0.5. The rate constants were determined from the spectrophotometric assay. The phosphate buffer was at pH 2.49 and 6.35; the acetate buffer was at pH 4.60.*

In Fig. 7 is plotted log $(k_{obs})_{pH}$ and log $(k_1)_{pH}$ *versus* pH for carbenicillin phenyl sodium degradation at 35° and ionic strength 0.5. The pH dependency of the ester hydrolysis indicated a simple and U-shaped curve fitted by:

$$(k_1)_{pH} = (k_1)_H a_{H^+} + (k_1)_0 + (k_1)_{OH} K_w / a_{H^+} \qquad \text{(Eq. 15)}$$

where a_{H^+} is the hydrogen-ion activity as determined by glass electrodes; K_w is the autoprotolytic constant for water; $(k_1)_H$ and $(k_1)_{OH}$ are the second-order rate constants for the hydrogen-ion catalyzed- and hydroxide-ion-catalyzed ester hydrolysis, respectively; and $(k_1)_0$ is the first-order rate constant for spontaneous or water-catalyzed hydrolysis.

At pH >6, $(k_{obs})_{pH}$ was almost identical with $(k_1)_{pH}$, indicating that ester hydrolysis to produce carbenicillin proceeds exclusively in this pH region. Below pH 3, $(k_{obs})_{pH}$ was 10–100 times larger than $(k_1)_{pH}$. This finding suggests that β-lactam degradation rather than ester hydrolysis proceeds predominantly in carbenicillin phenyl sodium. It is obvious, therefore, that the rate constant $(k_{obs})_{pH}$ below pH 3 is approximately equal to $(k_2)_{pH}$.

For the acid degradation of the β-lactam of penicillin, $(k_2)_{pH}$ obeys the general rate law (10):

$$(k_2)_{pH} = [(k_2)_H a_{H^+} + (k_2)_0] \frac{a_{H^+}}{K_a + a_{H^+}} \qquad \text{(Eq. 16)}$$

where K_a is the dissociation constant of I, and $(k_2)_{pH}$ and $(k_2)_0$ represent hydrogen-ion-catalyzed and spontaneous or water-catalyzed degradation rates, respectively, of undissociated I.

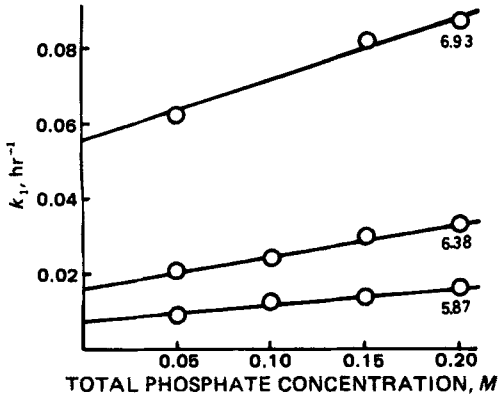

Figure 6—*Pseudo-first-order rate constants* k_1 *for the liberation of phenol from carbenicillin phenyl sodium* versus *total phosphate concentration at 35° and ionic strength 0.5. The rate constants were determined by colorimetry.*

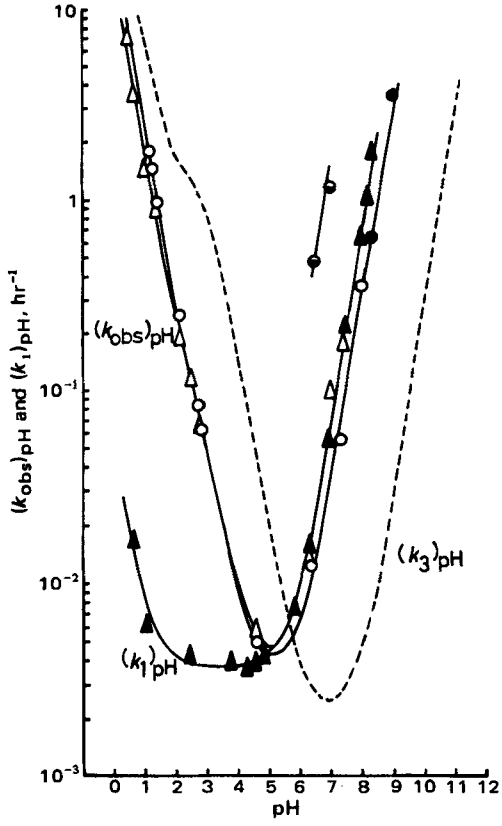

Figure 7—*Log* $(k_{obs})_{pH}$–*pH profiles for the degradation and log* $(k_1)_{pH}$–*pH profiles for the ester hydrolysis of carbenicillin indanyl sodium* (○) *and carbenicillin phenyl sodium* (△) *at 35° and ionic strength 0.5. The lines represent the curves calculated from Eqs. 15–17 and the constants in Table III; the points are experimental values. Open symbols are data determined by the separation assay, and closed ones are data determined by the colorimetric and/or UV method. The degradation of carbenicillin phenyl sodium* (●) *was determined at 60° in 0.2 M phosphate buffer. The broken line represents the log* $(k_3)_{pH}$–*pH profile of carbenicillin* (2).

Log $(k_{obs})_{pH}$–pH profiles for carbenicillin indanyl sodium degradation are shown in Fig. 7, providing a similar shape to those for carbenicillin phenyl sodium. Therefore, Eqs. 15 and 16 apply to both compounds.

By employing the pKa values (11) of 2.94 for carbenicillin indanyl sodium and 2.91 for carbenicillin phenyl sodium and $K_w = 2.09 \times 10^{-14}$ (12), these specific rate constants that produced the best fits of the observed points above pH 7 and below pH 3 are listed in Table III. The calculated curves for $(k_{obs})_{pH}$ were generated from Eq. 17, corresponding to the sum of Eqs. 15 and 16 by the use of appropriate parameters, and were in reasonable agreement with all experimental values:

$$(k_{obs})_{pH} = (k_1)_H a_{H^+} + (k_1)_0 + [(k_2)_H a_{H^+} + (k_2)_0] \frac{a_{H^+}}{K_a + a_{H^+}} + (k_1)_{OH} K_w / a_{H^+} \qquad \text{(Eq. 17)}$$

To compare the β-lactam stability between the prodrugs and carbenicillin, the log $(k_3)_{pH}$–pH profiles for carbenicillin degradation under the same conditions are redrawn in Fig. 7 from the literature (2). It can be seen that the β-lactam of both carbenicillin indanyl sodium and carbenicillin phenyl sodium is more stable than that in carbenicillin by about three times at pH 1, six times at pH 2, and 17 times at pH 3. The half-lives at 35° and ionic strength of 0.5 were ~20 min, 2.6 hr, and 13 hr at pH 1, 2, and 3, respectively.

Temperature Effect on Degradation Rate—Arrhenius plots of the observed first-order rate constants k_{obs} for I degradation in buffer solutions of two different pH values are illustrated in Fig. 8. The enthalpies of activation, $\Delta H^{\neq}$, calculated from the slope of the line at pH 3.87 (in 0.2 *M* acetate buffer), were 17.7 and 18.1 kcal/mole for carbenicillin indanyl sodium and carbenicillin phenyl sodium, respectively; the enthalpy of activation at pH 6.98 (in 0.2 *M* phosphate buffer) was 16.6 kcal/mole for carbenicillin phenyl sodium. Because of the small catalytic effect of acetate buffer, activation enthalpy at pH 3.87 may be regarded

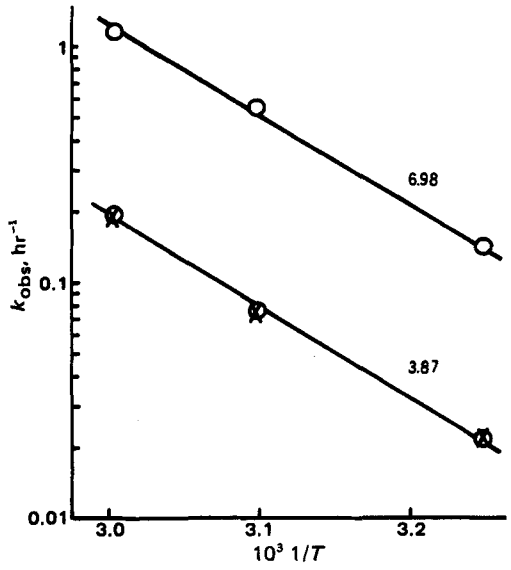

Figure 8—*Arrhenius plots for the apparent first-order rate constants k_{obs} for carbenicillin indanyl sodium (×) and carbenicillin phenyl sodium (○) at pH 6.98 (0.2 M phosphate buffer) and pH 3.87 (0.2 M acetate buffer) and ionic strength 0.5.*

as that of spontaneous degradation of the β-lactam of undissociated I, comparable with enthalpies in the 18–21-kcal/mole range for other penicillin antibiotics (2).

The apparent activation energy of 17.2 kcal/mole at pH 6.98 may include the energies for hydroxide-ion-catalyzed and diphosphate-ion-catalyzed hydrolysis and also for heat of ionization of water. If this energy were to be employed to predict the hydrolysis rate of the I ester linkage at constant pH in nonbuffered solution, half-lives at 37° for production of H from carbenicillin indanyl sodium and carbenicillin phenyl sodium would be 17 and 8.5 hr, respectively, at the small intestinal pH of 7.0 and 7 and 3.5 hr, respectively, at the body fluid pH of 7.4.

DISCUSSION

The degradation of the two prodrugs of II proceeds through a total cleavage of the β-lactam ring and of the ester bond. In acidic media below pH 3, the β-lactam degradation pathway contributes >92%, and ester hydrolysis contributes <8%. Susceptibility of the β-lactam of penicillins to acid-catalyzed degradation is attributed not only to the strained ring (13) but also to the intramolecular attack of the side-chain amide on the β-lactam carbonyl (14). The intramolecular reaction results in the acceleration of the rates by electron-donating substituents, while electron-withdrawing substituents reduce the β-lactam cleavage rate. Enhanced stability of I compared to II may be due to the increased inductive effect of indanyl and phenyl esters compared to the carboxylate anion. The magnitude of the corresponding reaction rate constants $(k_2)_H$ and $(k_2)_0$ for both prodrugs was similar to those of phenoxy and isoxazolyl derivatives of orally effective penicillins (2, 15).

Previous studies (16) clarified that, in an environment below pH 5, GI absorption of penicillins, excluding amphoteric derivatives such as ampicillin, follows the common lipoidal membrane transport mechanism of the undissociated species permeating through the aqueous diffusion layer barrier. This mechanism predicts that the increased lipophilicity of the undissociated penicillin molecules enhances the GI absorption rate according the quantitative relationship described previously (17). The partition coefficient of the undissociated species, P_u, of orally effective penicillins in an octanol–water system as the lipophilic index is above 90 (11, 18). The corresponding values of carbenicillin indanyl sodium and carbenicillin phenyl sodium are 5900 and 910, respectively (11), suggesting that these prodrugs would be absorbed well from the GI membrane. In fact, this possibility was substantiated previously; intestinal absorption of carbenicillin indanyl sodium at pH 4.0 is 4.7 and 2.2 times faster than absorption of penicillin V and propicillin, respectively (19).

Above pH 7, on the other hand, I degradation is superseded in importance by ester hydrolysis to produce II. The second-order rate constant of the β-lactam hydrolysis by nucleophilic hydroxide-ion attack is $\sim 10^3$ M^{-1} hr^{-1} at 35° and $\mu = 0.5$, independent of the electronic nature of the side chain at position 6 (2, 10, 20, 21). The present kinetic data indicate that the ester hydrolysis of I by the nucleophilic hydroxide-ion attack is ~100 times faster than the β-lactam hydrolysis. However, such chemical degradation of I ester bonds is almost negligible, as predicted, under intestinal pH conditions between pH 5 and 7.

A nonspecific esterase present on the GI lumen surface and/or in solution may facilitate ester hydrolysis producing II, as verified previously in recirculating intestinal perfusion experiments in rats (19). Intestinal absorption of ionized penicillins follows the transport mechanism almost independently of the lipoidal nature of penicillin molecules above pH 6 and is very slow (17). These results suggest that a slow prodrug release above pH 5–6 from oral tablets may result in the significant bioavailability reduction because of the decreased concentration of well-absorbed undissociated prodrug species and the rapid yield of poorly absorbed II by the possible action of intestinal esterase rather than by the chemical hydrolysis before I absorption.

In summary, the two prodrugs investigated have appropriate acid stability and lipoidal solubility to serve as oral dosage forms. The two prodrugs are well designed, from the pharmaceutical viewpoint, to improve II absorption and acid lability, to exhibit sufficient ester bond chemical stability before absorption, and to yield II rapidly by the action of tissue and serum esterase after absorption (6). If the two prodrugs were to be controlled for sufficient dissolution below pH 4 by a suitable pharmaceutical technique, the dissolved prodrugs might be absorbed rapidly both in the stomach, to a small extent, and in the upper small intestine, which has relatively low pH values and a large surface area, to a larger extent.

REFERENCES

(1) L. Weinstein, in "The Pharmacological Basis of Therapeutics," 5th ed., L. S. Goodman and A. Gilman, Eds., Macmillan, New York, N.Y., 1975, chap. 57.

(2) T. Yamana, A. Tsuji, and Y. Mizukami, *Chem. Pharm. Bull.*, **22**, 1186 (1974).

(3) H. Zia, M. Tehrani, and R. Zargarbashi, *Can. J. Pharm. Sci.*, **9**, 112 (1974).

(4) A. R. English, J. A. Retsema, V. A. Ray, and J. E. Lynch, *Antimicrob. Agents Chemother.*, **1**, 185 (1972).

(5) K. Butler, A. R. English, B. Briggs, E. Gralla, R. B. Stebbins, and D. C. Hobbs, *J. Infect. Dis., Suppl.*, **127**, S97 (1973).

(6) J. P. Clayton, M. Cole, S. W. Elson, K. D. Hardy, L. W. Mizen, and R. Surtherland, *J. Med. Chem.*, **18**, 172 (1975).

(7) H. Bundgaard and K. Ilver, *J. Pharm. Pharmacol.*, **24**, 790 (1972).

(8) R. J. Lacoste, S. H. Venable, and J. C. Stone, *Anal. Chem.*, **31**, 1246 (1959).

(9) E. A. Guggenheim, *Phil. Mag.*, **2**, 538 (1926).

(10) T. Yamana, A. Tsuji, E. Kiya, and E. Miyamoto, *J. Pharm. Sci.*, **66**, 861 (1977).

(11) A. Tsuji, O. Kubo, E. Miyamoto, and T. Yamana, *ibid.*, **66**, 1675 (1977).

(12) H. S. Harned and W. J. Hamer, *J. Am. Chem. Soc.*, **55**, 2194 (1933).

(13) M. S. Manhas and A. K. Bose, "beta-Lactams: Natural and Synthetic," part I, Wiley, New York, N.Y., 1971, chap. 2.

(14) J. P. Hou and J. W. Poole, *J. Pharm. Sci.*, **60**, 503 (1971).

(15) T. Yamana and A. Tsuji, *ibid.*, **65**, 1563 (1976).

(16) A. Tsuji, E. Miyamoto, N. Hashimoto, and T. Yamana, *ibid.*, **67**, 1705 (1978).

(17) A. Tsuji, E. Miyamoto, O. Kubo, and T. Yamana, *ibid.*, **68**, 812 (1979).

(18) A. E. Bird and A. C. Marshall, *J. Chromatogr.*, **63**, 313 (1971).

(19) A. Tsuji, E. Miyamoto, I. Kagami, H. Sakaguchi, and T. Yamana, *J. Pharm. Sci.*, **67**, 1701 (1978).

(20) M. A. Schwartz and G.-M. Wu, *ibid.*, **55**, 550 (1966).

(21) H. Bundgaard, *Dan. Tidsskr. Farm.*, **46**, 85 (1972).

ACKNOWLEDGMENTS

The authors thank Taito Pfizer Co. and Beecham Yakuhin Co. for their gifts of carbenicillin indanyl sodium, carbenicillin phenyl sodium, and carbenicillin disodium. They also acknowledge the excellent technical assistance of Miss N. Honjo and Miss S. Nishikawa. The computer analysis was carried out with a FACOM M-160 digital computer at the Data Processing Center, Kanazawa University.

High-Performance Liquid Chromatography of Two Peripheral Vasodilators, Nylidrin Hydrochloride and Isoxsuprine Hydrochloride, in Pharmaceutical Dosage Forms

FRANK VOLPE ×, JAMES ZINTEL *, and DONALD SPIEGEL

Received November 27, 1978, from the *Quality Services Department, R & D Division, USV Pharmaceutical Corporation, Tuckahoe, NY 10707.* Accepted for publication April 13, 1979. *Formerly of Arlington Laboratories, Montreal, Canada. Present address: Barnes-Hind Pharmaceuticals, Sunnyvale, CA 94086.

Abstract □ A reliable and selective high-pressure liquid chromatographic (HPLC) procedure for the quantitative determination of nylidrin hydrochloride or isoxsuprine hydrochloride in pharmaceutical dosage forms is described. The specificity of the stability-indicating HPLC procedure is presented for nylidrin hydrochloride.

Keyphrases □ Nylidrin hydrochloride—analysis, high-performance liquid chromatography, tablets, stability indicating □ Isoxsuprine hydrochloride—analysis, high-performance liquid chromatography, tablets, stability indicating □ Vasodilators, peripheral—nylidrin hydrochloride and isoxsuprine hydrochloride, high-performance liquid chromatographic analysis □ High-performance liquid chromatography—analysis, isoxsuprine hydrochloride, nylidrin hydrochloride, tablets, stability indicating

Nylidrin hydrochloride (I, *p*-hydroxy-α-[1-[(1-methyl-3-phenylpropyl)amino]ethyl]benzyl alcohol hydrochloride) and isoxsuprine hydrochloride (II, *p*-hydroxy-α-[1-[(1-methyl-2-phenoxyethyl)amino]ethyl]benzyl alcohol hydrochloride) are sympathomimetic agents that presumably act predominantly by β-adrenergic receptor stimulation (1). Analytical methods currently available include UV spectrophotometry (2), nonaqueous titration of the basic amine (2), colorimetry (3, 4), and GLC after derivatization by silylation (5). All of these methods except GLC lack analytical specificity or selectivity for the active drug substances and are, therefore, not suitable stability-indicating assays.

Application of GLC for the derivatization of I was only partially successful because the derivatives formed were sometimes unstable. This result was demonstrated by precipitate formation accompanied by a decrease in peak area. The high-presssure liquid chromatographic (HPLC) method described in this paper is specific and provides direct and accurate determinations of I or II, which could be used to evaluate pharmaceutical product stability.

EXPERIMENTAL

Apparatus—The high-pressure liquid chromatograph[1] was equipped with a microliter loop injector[2], a reversed-phase column[3], and a variable wavelength spectrophotometric detector[4] interfaced to an electronic integrator[5].

Reagents—Nylidrin hydrochloride[6], isoxsuprine hydrochloride[7], UV grade methanol[8], fluorene[9], reagent grade dibasic ammonium phosphate, and phosphoric acid[10] were used.

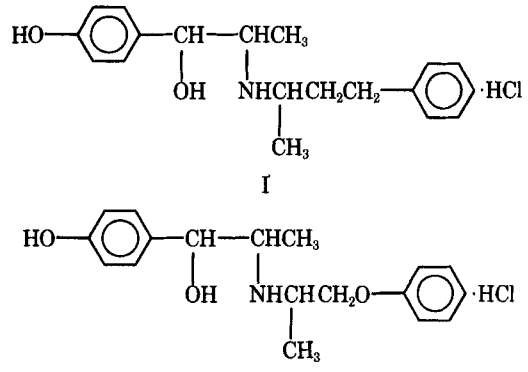

I

II

Chromatographic Conditions—The mobile phase consisted of methanol–aqueous buffer (75:25 v/v). The buffer was prepared by weighing 1.32 g of dibasic ammonium phosphate into a 1000-ml volumetric flask and dissolving with distilled water. The final volume was adjusted to pH 7.5 with 85% phosphoric acid. The methanol and buffer were filtered separately through membrane filters[11] before mixing. The mobile phase flow rate was set at 1.5 ml/min. The column effluent was monitered by UV absorption at 276 nm (maximum for both active ingredients).

Procedure—The internal standard stock solution was prepared by dissolving fluorene in the mobile phase at 0.5 mg/ml. A standard pair

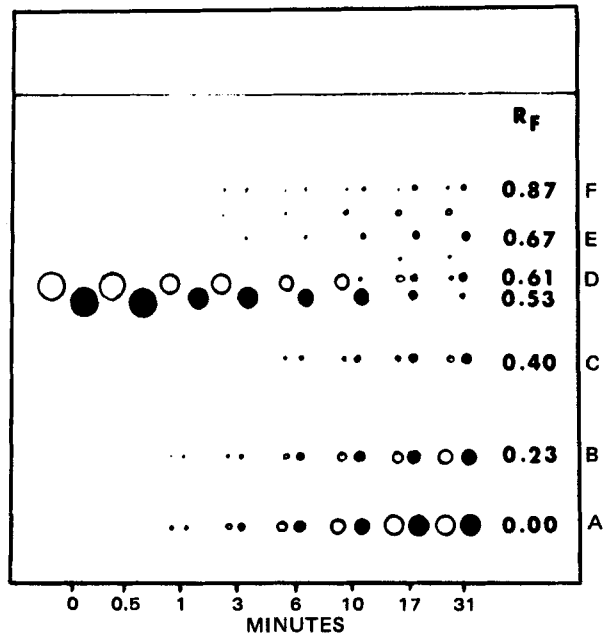

Figure 1—*TLC of partially photothermal-degraded nylidrin and isoxsuprine as a function of exposure time. The intensity of the spots is indicated by size. Key: A–F, degradation products;* ●, *nylidrin; and* ○, *isoxsuprine.*

[1] Model 601, Perkin-Elmer Corp., Norwalk, Conn.
[2] Model 7120, Rheodyne Inc., Berkeley, Calif.
[3] μBondapak C_{18}, 3.9 mm i.d. × 30 cm, Waters Associates, Milford, Mass.
[4] Model LC-55, Perkin-Elmer Corp., Norwalk, Conn.
[5] Model 3385 A, Hewlett-Packard, Paramus, N.J.
[6] USV Pharmaceutical Corp., Tuckahoe, N.Y.
[7] Mead Johnson and Co., Evansville, Ind.
[8] Burdick & Jackson Laboratories, Muskegon, Mich.
[9] Aldrich Chemical Co., Metuchen, N.J.
[10] Fisher Scientific Co., Fair Lawn, N.J.
[11] Type BD, Millipore Corp., Bedford, Mass.

0022-3549/79/1000-1264$01.00/0
© 1979, American Pharmaceutical Association

Table I—Location of the Photothermal Degradation Products (A–F) and Postulated Degradation Products of Nylidrin Hydrochloride as a Function of Retention Time

Compound	Structure	Retention Time, min
A	—	1.6
p-Hydroxybenzoic acid	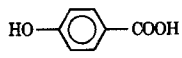	1.6
B	—	2.1
4-Hydroxybenzaldehyde	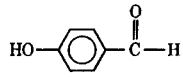	2.1
4-Hydroxybenzyl alcohol	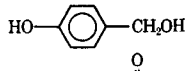	2.2
p-Hydroxyacetophenone	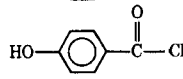	2.2
p-Hydroxyephedrine hydrochloride	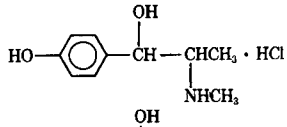	3.4
α-(1-Aminoethyl)-*p*-hydroxybenzyl alcohol hydrochloride	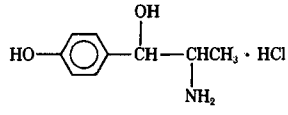	3.4
C	—	3.6
Isoxsuprine hydrochloride	II	4.0
Nylidrin hydrochloride	I	5.2
1-Methyl-3-phenylpropylamine	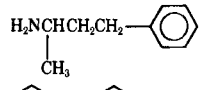	6.5[a]
Fluorene (internal standard)	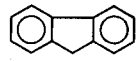	7.0
D	—	9–10
E	—	—[b]
F	—	—[b]

[a] Detected at 254 nm. [b] Not detected.

solution of I (1.2 mg/ml) and fluorene (0.1 mg/ml) was made by accurately weighing ~30 mg of previously dried I and quantitatively transferring it into a 25-ml volumetric flask. Five milliliters of the internal standard stock solution was pipetted into the volumetric flask and diluted to volume with mobile phase. In a similar manner, a standard pair solution of II (1.0 mg/ml) and fluorene (0.1 mg/ml) was prepared.

The respective active ingredients were extracted from tablet preparations by finely powdering 20 tablets and weighing a portion of powder equivalent to ~30 mg of I or ~25 mg of II into 50-ml centrifuge tubes. Five milliliters of the internal standard stock solution was pipetted into each tube, and 20 ml of mobile phase was added. The tubes were sonicated for ~2 min, shaken mechanically for 30 min, and centrifuged. Clear filtrates were obtained by filtering a portion of each supernate through membrane filters[11].

RESULTS AND DISCUSSION

Assay Selectivity—This HPLC assay was intended for stability testing in addition to finished product release testing. To be stability indicating, the method must discriminate between degradation products and the active ingredient. Preferably, a stability-indicating procedure should also quantitatively demonstrate the inverse relationship between the decrease in the active ingredient and the increase in degradation products.

To show that a method is stability indicating, degradation routes and the resulting products may be postulated and tested in the assay system for interference. Alternatively, the active ingredient may be subjected to severe conditions that simulate most modes of expected degradation, and the reaction products, if any, may be tested for interference in the method. Base hydrolysis, acid hydrolysis, and photothermal oxidation were chosen as the most likely modes of degradation. Proof of specificity was obtained only for I. The specificity for II and the structural elucidation of degradation products will be the subjects of a future publication.

Base Hydrolysis—A sample of I was dissolved in 1 *N* NaOH (2 g in 100 ml), and 2-ml aliquots of this solution were placed in 10-ml tubes sealed with polytef-lined screw caps. The tubes were stored at 23 and 70° for 96 hr. The contents were neutralized with acid and evaporated to dryness. HPLC showed there was no significant change in the amount of I since no measurable degradation was detected. A sample was then incubated in 1 *N* NaOH for 36 days at 70°. The chromatograms revealed that the I peak remained unchanged; however, additional unknown peaks appeared with retention times of ~2 min.

Acid Hydrolysis—Two hundred milligrams of I was dissolved in 100

Table II—Linearity of I

Concentration, mg/ml	Peak Area Ratio (I/Fluorene)	Response Factor Ratio[a]
0.90	0.70	0.078
1.01	0.80	0.079
1.10	0.88	0.080
1.23	0.98	0.080
1.33	1.07	0.080
1.42	1.14	0.080

[a] Slope = 0.84, *RSD* = 1.65%, and *y* intercept = 0.05.

Table III—Linearity of II

Concentration, mg/ml	Peak Area Ratio (II/Fluorene)	Response Factor Ratio[a]
0.31	0.36	0.116
0.59	0.69	0.117
0.92	1.06	0.115
1.21	1.44	0.119
1.52	1.80	0.118
1.86	2.20	0.118

[a] Slope = 1.19, *RSD* = 0.84%, and *y* intercept = −0.01.

Table IV—HPLC and NF Analyses of Commercial Tablets

Compound[a]	Sample	Dosage Claimed, mg/ tablet	HPLC, mg/ tablet	NF, mg/ tablet
I	1	6.0	6.16	5.98
I	2	6.0	5.87	5.66
I	3	6.0	6.16	6.06
I	4	12.0	11.9	12.2
I	5	12.0	12.1	11.5
I	6	12.0	12.5	11.9
II	7	10.0	9.81	9.98
II	8	10.0	9.94	9.98
II	9	10.0	9.76	9.99
II	10	20.0	19.6	19.7
II	11	20.0	19.5	19.5
II	12	20.0	19.4	19.7

[a] Compounds I and II were obtained from different manufacturers.

ml of 1 *N* HCl and refluxed for 2 hr. Aliquots were drawn after 1 and 2 hr, neutralized with sodium hydroxide, evaporated to dryness, dissolved in mobile phase, and chromatographed. There was little difference in the number and size of peaks between the two time intervals; three, possibly four, small peaks had retention times of ~1.5 min. The apparent lack of any dependency on reaction times probably meant that the degradation products did not arise from acid treatment alone but from pyrolysis during the drying step.

Photothermal Decomposition—An alternative approach degraded I in a few minutes. Compounds I (320 μg/spot) and II (160 μg/spot) were applied to a 250-μm silica gel GF plate[12] and irradiated with intense UV light[13] (heat also was emitted from this UV source). The plate was developed using chloroform–methanol–concentrated ammonium hydroxide (90:15:15).

Figure 1 clearly shows the decrease in I and II as well as the concomitant increase in degradation products in both numbers and intensity as a function of exposure time. Since the formation of degradation products (A–F) under the same stress conditions was nearly the same for both compounds, the presence of an ether linkage in II compared to I does not confer additional degradation paths on the former compared to the latter. However, one degradation product (R_f 0.75) originated from II only. The retention times of the degradation products isolated from TLC, known compounds, I, and II are listed in Table I.

To test the selectivity of this method, I was assayed to establish potency (Fig. 2). A portion of this powder was spread thinly on a glass plate and

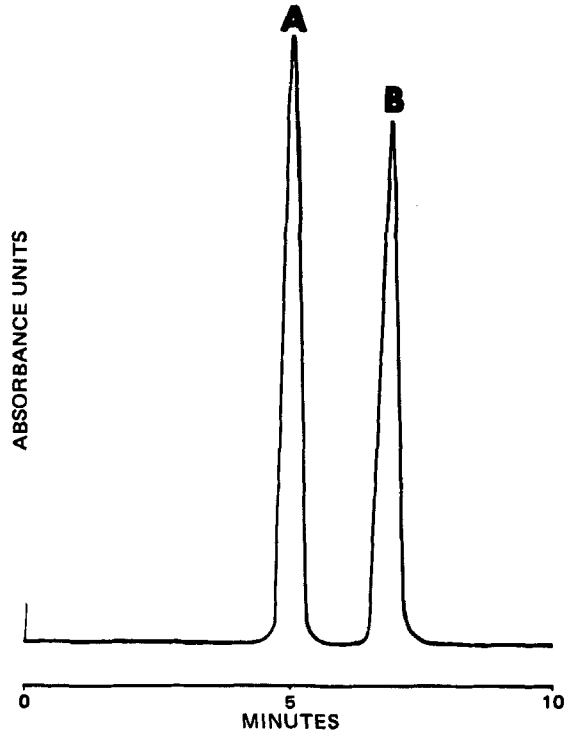

Figure 2—*High-pressure liquid chromatogram of nylidrin hydrochloride. Key: A, nylidrin hydrochloride; and B, fluorene (internal standard).*

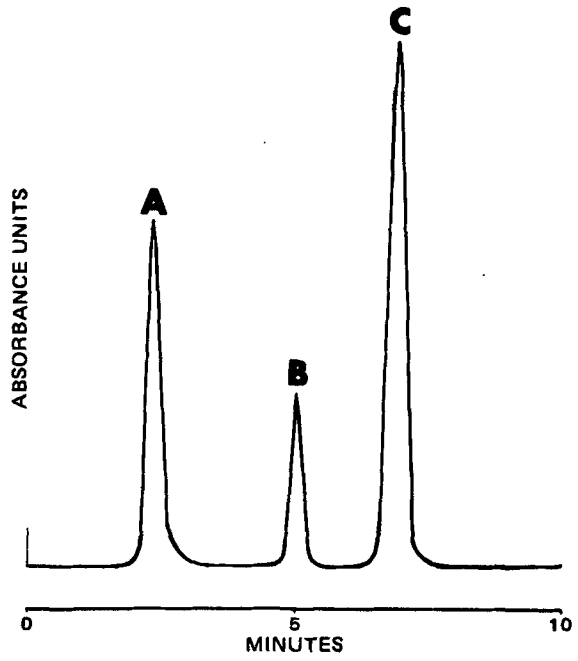

Figure 3—*High-pressure liquid chromatogram of partially degraded nylidrin hydrochloride. Key: A, major degradation product (labeled previously as Product B); B, nylidrin hydrochloride; and C, fluorene (internal standard).*

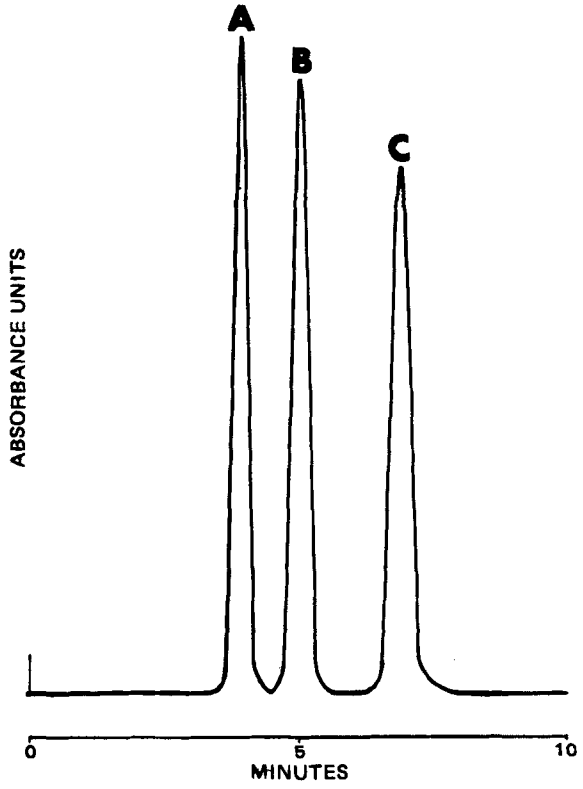

Figure 4—*High-pressure liquid chromatogram. Key: A, isoxsuprine hydrochloride; B, nylidrin hydrochloride; and C, fluorene (internal standard).*

[12] Analtech, Newark, Del.
[13] Model 420-U11, George W. Gates & Co., Long Island, N.Y.

photothermally degraded by irradiating with intense UV light[13] for 30 min. A 100-mg sample of partially degraded I was accurately weighed, quantitatively transferred into a 50-ml volumetric flask, and dissolved in methanol. Then 20.0- and 15.0-ml aliquots were removed, the solvent was evaporated, and the sample was reassayed (Fig. 3). The recovery was 101% by the official NF XIV assay but only 33% by HPLC. The system selectivity is demonstrated further in Fig. 4, where I is resolved from II. These compounds are very similar in structure, size, and polarity.

Statistical Evaluation—The linearity of typical standard curves is summarized in Tables II and III. The response factor ratios, defined as the area ratio (active ingredient/fluorene) times the concentration ratio (fluorene/active ingredient), were quite constant for all concentrations. Precision was demonstrated by a relative standard deviation of 0.4% for nine replicate injections. Analysis of active–placebo mixtures demonstrated the accuracy of the proposed method with an average 99.1% recovery.

The experimental data shown in Table IV were obtained on randomly selected commercial tablet samples. Each sample was analyzed by the HPLC method and by the official NF XIV procedures. The results from both methods are comparable, but since the HPLC method has been shown to be a stability-indicating assay, it is more selective than the NF method and more accurately reflects true tablet potency.

REFERENCES

(1) S. J. Manley and J. W. Lawson, *Arch. Int. Pharmacodyn. Ther.*, **175**, 239 (1968).

(2) "The National Formulary," 14th ed., Mack Publishing Co., Easton, Pa., 1975.

(3) Troponwerke Köln, Biochem. Bericht., No. 32, *Biochem. Forsch.* (Dec. 1968).

(4) J. H. Weikel, Jr., A. G. Wheeler, and P. D. Joiner, *Toxicol. Appl. Pharmacol.*, **1**, 579 (1959).

(5) H. Li and P. Cervoni, *J. Pharm. Sci.*, **65**, 1352 (1976).

ACKNOWLEDGMENTS

The authors thank Dr. D. Lamontanaro and Mr. R. Kirsch for help in the development of this method and Mr. N. Gaddipati and Mr. J. Shastri for assistance in obtaining and isolating degradation products.

Solubility Determination of Barely Aqueous-Soluble Organic Solids

TAKERU HIGUCHI, FONG-MEI L. SHIH, TOSHIKIRO KIMURA, and J. HOWARD RYTTING ×

Received September 15, 1978, from the *Departments of Pharmaceutical Chemistry and Chemistry, University of Kansas, Lawrence, KS 66045.* Accepted for publication April 18, 1979.

Abstract □ Solubility determination of organic molecules having very low solubilities is hampered by such problems as slow equilibration during measurement, influence of impurities, and inherent heterogeneity in the energetic content of the crystalline solid. Three approaches to meeting these problems are presented. The first approach involves enhancing the dissolution rate by the addition of a water-immiscible solvent in which the organic solute is more soluble, thereby increasing the surface area available for dissolution. The second method is a combination of experimental data with a group contribution approach that allows the estimation of extremely insoluble solids. This approach involves measurement of the solubility in an organic solvent and calculation of the aqueous solubility from the estimated partition coefficient and the organic solvent data. The third approach is based on using a large excess of the solid and a highly specific analytical determination of the main component. The first two approaches were explored in detail and tested using norethindrone, norethindrone acetate, methyltestosterone, and methyltestosterone acetate.

Keyphrases □ Solubility determinations—organic solids, barely aqueous soluble, group contribution, partition coefficient □ Organic solids—solubility determinations, barely aqueous soluble, group contribution, partition coefficient □ Aqueous solubility—organic solids, barely soluble, solubility determination

The solubilities of solids are very useful parameters in the daily practice of chemistry and pharmacy. Solubility information is particularly vital in formulating products, developing analytical methods, chemical processing, predicting ecological impact, and assessing drug transport and distribution problems.

Solubility determination of solids that are moderately soluble, *i.e.*, ≥ 0.2%, normally poses no serious problem. Direct solubility measurement of solids having very low solubilities involves special difficulties, which can lead to large discrepancies in reported values. For example, the reported solubility of cholesterol in water ranges from 0.025 to 2600 μg/ml (1). This paper is concerned with an analysis of these problems and offers several approaches for overcoming them, particularly for determinations carried out in water.

BACKGROUND

Equilibration Kinetics—The low equilibration rate during solubility measurement of slightly soluble species presents a serious problem which has not been adequately addressed from an experimental standpoint. The solubility of a solid in a given solvent is the amount that goes into solution at equilibrium at some selected temperature. Since it is impossible to attain a true equilibrium state in real life, in practice, results are reported for systems that are reasonably close to equilibrium. Such situations are not particularly difficult to attain for moderately soluble substances. An aqueous suspension of benzoic acid crystals, for example, probably reaches a near equilibrium state with moderate stirring at 25° within a few hours. The exact rate depends on the fineness of the crystals, the amount of solid added, and the degree of agitation.

According to various studies on dissolution kinetics, the classical equation (Noyes–Whitney) (2, 3) appears to be an empirically useful relationship. A simplified form of the equation for situations where the various geometric factors are essentially held constant can be written as:

$$\frac{dc}{dt} = k(C_s - C) \qquad \text{(Eq. 1)}$$

where dc/dt is the rate of increase in the solute concentration, k is a constant, C_s is the solubility, and C is the solute concentration in solution. Upon integrating, one obtains:

$$\ln \frac{C_s - C}{C_s} = -kt \qquad \text{(Eq. 2)}$$

Under these conditions, the kinetics suggest an approximately first-order approach to saturation, with a given degree of saturation being achieved somewhat independently of the solid being studied. Under experimental conditions, however, unless a substantial excess of the solid is used, the effective surface area will decrease significantly during the dissolution process, with a corresponding delay in the attainment of equilibrium.

0022-3549/79/1000-1267$01.00/0

© 1979, American Pharmaceutical Association

photothermally degraded by irradiating with intense UV light[13] for 30 min. A 100-mg sample of partially degraded I was accurately weighed, quantitatively transferred into a 50-ml volumetric flask, and dissolved in methanol. Then 20.0- and 15.0-ml aliquots were removed, the solvent was evaporated, and the sample was reassayed (Fig. 3). The recovery was 101% by the official NF XIV assay but only 33% by HPLC. The system selectivity is demonstrated further in Fig. 4, where I is resolved from II. These compounds are very similar in structure, size, and polarity.

Statistical Evaluation—The linearity of typical standard curves is summarized in Tables II and III. The response factor ratios, defined as the area ratio (active ingredient/fluorene) times the concentration ratio (fluorene/active ingredient), were quite constant for all concentrations. Precision was demonstrated by a relative standard deviation of 0.4% for nine replicate injections. Analysis of active–placebo mixtures demonstrated the accuracy of the proposed method with an average 99.1% recovery.

The experimental data shown in Table IV were obtained on randomly selected commercial tablet samples. Each sample was analyzed by the HPLC method and by the official NF XIV procedures. The results from both methods are comparable, but since the HPLC method has been shown to be a stability-indicating assay, it is more selective than the NF method and more accurately reflects true tablet potency.

REFERENCES

(1) S. J. Manley and J. W. Lawson, *Arch. Int. Pharmacodyn. Ther.*, **175**, 239 (1968).

(2) "The National Formulary," 14th ed., Mack Publishing Co., Easton, Pa., 1975.

(3) Troponwerke Köln, Biochem. Bericht., No. 32, *Biochem. Forsch.* (Dec. 1968).

(4) J. H. Weikel, Jr., A. G. Wheeler, and P. D. Joiner, *Toxicol. Appl. Pharmacol.*, **1**, 579 (1959).

(5) H. Li and P. Cervoni, *J. Pharm. Sci.*, **65**, 1352 (1976).

ACKNOWLEDGMENTS

The authors thank Dr. D. Lamontanaro and Mr. R. Kirsch for help in the development of this method and Mr. N. Gaddipati and Mr. J. Shastri for assistance in obtaining and isolating degradation products.

Solubility Determination of Barely Aqueous-Soluble Organic Solids

TAKERU HIGUCHI, FONG-MEI L. SHIH, TOSHIKIRO KIMURA, and J. HOWARD RYTTING ×

Received September 15, 1978, from the *Departments of Pharmaceutical Chemistry and Chemistry, University of Kansas, Lawrence, KS 66045.* Accepted for publication April 18, 1979.

Abstract □ Solubility determination of organic molecules having very low solubilities is hampered by such problems as slow equilibration during measurement, influence of impurities, and inherent heterogeneity in the energetic content of the crystalline solid. Three approaches to meeting these problems are presented. The first approach involves enhancing the dissolution rate by the addition of a water-immiscible solvent in which the organic solute is more soluble, thereby increasing the surface area available for dissolution. The second method is a combination of experimental data with a group contribution approach that allows the estimation of extremely insoluble solids. This approach involves measurement of the solubility in an organic solvent and calculation of the aqueous solubility from the estimated partition coefficient and the organic solvent data. The third approach is based on using a large excess of the solid and a highly specific analytical determination of the main component. The first two approaches were explored in detail and tested using norethindrone, norethindrone acetate, methyltestosterone, and methyltestosterone acetate.

Keyphrases □ Solubility determinations—organic solids, barely aqueous soluble, group contribution, partition coefficient □ Organic solids—solubility determinations, barely aqueous soluble, group contribution, partition coefficient □ Aqueous solubility—organic solids, barely soluble, solubility determination

The solubilities of solids are very useful parameters in the daily practice of chemistry and pharmacy. Solubility information is particularly vital in formulating products, developing analytical methods, chemical processing, predicting ecological impact, and assessing drug transport and distribution problems.

Solubility determination of solids that are moderately soluble, *i.e.*, ≥ 0.2%, normally poses no serious problem. Direct solubility measurement of solids having very low solubilities involves special difficulties, which can lead to large discrepancies in reported values. For example, the reported solubility of cholesterol in water ranges from 0.025 to 2600 μg/ml (1). This paper is concerned with an analysis of these problems and offers several approaches for overcoming them, particularly for determinations carried out in water.

BACKGROUND

Equilibration Kinetics—The low equilibration rate during solubility measurement of slightly soluble species presents a serious problem which has not been adequately addressed from an experimental standpoint. The solubility of a solid in a given solvent is the amount that goes into solution at equilibrium at some selected temperature. Since it is impossible to attain a true equilibrium state in real life, in practice, results are reported for systems that are reasonably close to equilibrium. Such situations are not particularly difficult to attain for moderately soluble substances. An aqueous suspension of benzoic acid crystals, for example, probably reaches a near equilibrium state with moderate stirring at 25° within a few hours. The exact rate depends on the fineness of the crystals, the amount of solid added, and the degree of agitation.

According to various studies on dissolution kinetics, the classical equation (Noyes–Whitney) (2, 3) appears to be an empirically useful relationship. A simplified form of the equation for situations where the various geometric factors are essentially held constant can be written as:

$$\frac{dc}{dt} = k(C_s - C) \qquad \text{(Eq. 1)}$$

where dc/dt is the rate of increase in the solute concentration, k is a constant, C_s is the solubility, and C is the solute concentration in solution. Upon integrating, one obtains:

$$\ln \frac{C_s - C}{C_s} = -kt \qquad \text{(Eq. 2)}$$

Under these conditions, the kinetics suggest an approximately first-order approach to saturation, with a given degree of saturation being achieved somewhat independently of the solid being studied. Under experimental conditions, however, unless a substantial excess of the solid is used, the effective surface area will decrease significantly during the dissolution process, with a corresponding delay in the attainment of equilibrium.

0022-3549/79/1000-1267$01.00/0

© 1979, American Pharmaceutical Association

Table I—Measured Molar Solubilities and Isooctane–Water Distribution Coefficients for Steroids [a]

Substance	Molar Solubility in Isooctane[b]	Molar Solubility in Water[b]	Molar Solubility in Water in Contact with Isooctane	Isooctane–Water Partition Coefficient
Norethindrone	$6.90 \pm 0.13 \times 10^{-5}$ (5.85×10^{-5})[c]	$2.36 \pm 0.06 \times 10^{-5}$	$2.13 \pm 0.05 \times 10^{-5}$ (1.67×10^{-5})[c]	3.9 ± 0.17 (4.4)[b]
Norethindrone acetate	$2.52 \pm 0.04 \times 10^{-3}$ (2.53×10^{-3})[c]	$1.57 \pm 0.01 \times 10^{-5}$	$1.76 \pm 0.01 \times 10^{-5}$ (1.65×10^{-5})[c]	210 ± 5 (183)[c]
Norethindrone enanthate	0.0232[b]		($7 \pm 3 \times 10^{-8}$)[c]	(3.3×10^{5})[c]
Methyltestosterone	$1.3 \pm 0.03 \times 10^{-3}$	$1.12 \pm 0.02 \times 10^{-4}$ (7.47×10^{-5})[d]	$1.11 \pm 0.01 \times 10^{-4}$	16.0 ± 0.5
Methyltestosterone acetate	$5.3 \pm 0.05 \times 10^{-3}$	$1.43 \pm 0.03 \times 10^{-5}$ (5.20×10^{-6})[d]	$8.16 \pm 0.06 \times 10^{-7}$	3300 ± 173

[a] Uncertainties are expressed as standard errors of the mean. [b] Obtained by conventional method. [c] R. E. Enever, University of London, London, England, personal communication. [d] Literature value from D. B. Bowen, K. C. James, and M. Roberts, *J. Pharm. Pharmacol.*, **22**, 518 (1970).

The final rate of approach to saturation is approximately directly proportional to the excess of solid present—the larger the excess, the faster the saturation rate. A slightly soluble solid of equivalent surface area would require many times greater excess for saturation than would be needed for a moderately soluble solid. Thus, the terminal rate of attainment of equilibrium in water for benzoic acid (solubility in water = 3.4 mg/ml) (4) containing initially twice the amount necessary to saturate the solution will be equal to that of norethindrone (solubility in water $\cong$ 6 μg/ml) only if approximately the same amount (the same surface area) is left undissolved at the end. In this situation, the initial amount necessary to leave the same surface area undissolved as a onefold excess for benzoic acid would be an ~500-fold excess for norethindrone.

Although a relatively rapid equilibration even for a rather insoluble system would seem possible with a very large excess of the test solid, this process is not feasible for many real situations because the effects of impurities and energetic heterogeneity of crystals are magnified greatly when solute is present in a large excess.

The influence of impurities on the apparent solubility of crystalline solids is well known and can be visualized from a typical phase solubility diagram (Fig. 1) for a solid containing 10% of a soluble impurity. Typically, the apparent solubility increases with the amount of sample used until the system becomes saturated with respect to the impurity. Although in this example the indicated true solubility corresponds to 4.5 mg, the apparent solubility continues to increase with an increase in sample size. The increase corresponds to onefold for each 10-fold increase in the amount added for the situation shown. In the case of norethindrone with a 500-fold excess, each 1% of total soluble impurities in the sample will produce a fivefold increase in the apparent solubility of the material, that going into solution being largely the impurities present rather than the main compound.

Thus, direct solubility determinations on relatively insoluble species are difficult. If a large sample is used to obtain a fairly short equilibration time (hours to weeks), the impurities may pose a problem. On the other hand, if a small excess of sample is used to minimize the impurity effect, the equilibration time may extend to months or years. Use of only a onefold excess of norethindrone, for example, will require an ~500-fold greater equilibration time than for the described benzoic acid system, the corresponding time being on the order of months.

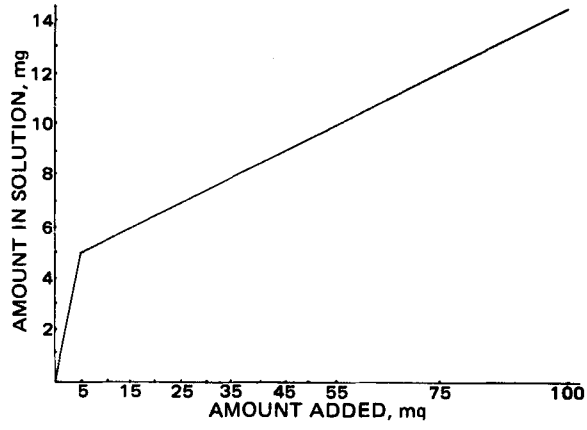

Figure 1—*Phase solubility diagram of a crystalline solid containing 10% soluble impurity.*

A possible solution to this dilemma is to eliminate the complication introduced by any impurity by utilizing a highly specific method for determining the amount of principal component in solution. If only the principal component is measured, the concentration in solution in Fig. 1, for example, would become independent of the amount. Since, however, the minor components present in the solid sample are usually not eliminated during typical purification procedures, they would probably be similar to the main component and lead to analytical complications. In solubility ranges below 1 ng/ml, highly exquisite and specific analytical methods would be required since at these solubilities the main component concentration may be one-millionth of the concentrations of the main impurities to obtain a reasonable equilibration time. Nevertheless, this approach can probably be used effectively in many situations.

Another factor that affects the solubility is the energetic heterogeneity that results from the spectrum of particle sizes and individual crystals with cracks and other energetic defects in a real sample. This factor would be self-correcting under normal conditions. When large excesses are permitted, however, the observed solubility will correspond to the thermodynamic activity of the most energetic component and may be supersaturated with respect to the most stable crystal form. Because of the very low solute concentration in solution, the recrystallization rate, which brings the supersaturated solution back to normal, will be extremely slow.

Proposed Approaches—There are several possible ways to approach this dilemma. One is a direct, experimental approach in which a minimal amount of solid sample is used to minimize the effect of impurities yet allow a near equilibrium state to be attained in a reasonable time. A combination of an experimental procedure with a group contribution approach allows solubility estimation of extremely insoluble solids with some accuracy. Another possibility is that suggested earlier based on a very large excess of the solid and highly specific determination of the main component. The first two approaches will be discussed in some detail.

Dissolution Facilitation by Immiscible Solvent Addition—As already discussed, the saturation rate of a solution by a relatively insoluble solid becomes extremely slow if only a small excess of the solid is used due to the limited surface area of the solid exposed to the dissolutive process. Generally, one would expect the available area to parallel the amount of solid used. Thus, for the benzoic acid system cited earlier, a onefold excess

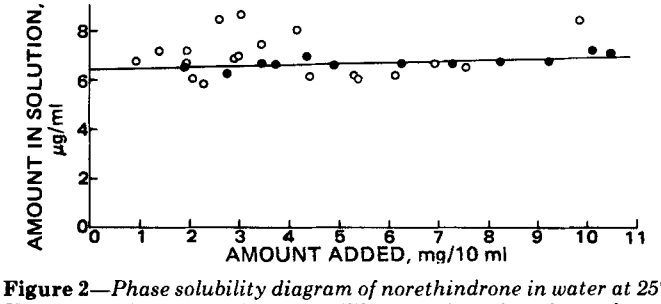

Figure 2—*Phase solubility diagram of norethindrone in water at 25°. Key: ○, 10 ml of water with an equilibration time of 120 hr; and ●, 10 ml of water plus 0.5 ml of isooctane with an equilibration time of 12 hr.*

Table II—Isooctane–Water Partition Coefficients and Standard Free Energy of Transfer for Organic Molecules [a]

Compound	Partition Coefficient	$\Delta G°$, cal/mole
2-Cyclohexen-1-one	0.46 ± 0.01	460
1-Ethynylcyclopentanol	0.36 ± 0.01	580
1-Ethynylcyclopentyl acetate	36.5 ± 1.4	−2100
1-Methylcyclopentanol	0.46 ± 0.01	460
1-Methylcyclopentyl acetate	227 ± 11	−3200

[a] Uncertainties are expressed as standard deviations.

corresponds to 6.8 mg/ml or a surface area of ~4 cm^2/ml of water at the beginning and a little more than 2 cm^2/ml at saturation if the initial average diameter of the benzoic acid is ~100 μm. Similar calculations for norethindrone acetate would be 6×10^{-3} and 4×10^{-3} cm^2/ml, much smaller values.

One way of increasing the interfacial area across which the solute is allowed to diffuse is to add a limited amount of a second immiscible solvent to the system in which the solute is significantly more soluble. The solubility of norethindrone acetate in isooctane at 25° is 860 μg/ml, 200 times that in water. If the solvent phase consists of 100 ml of water and 2 ml of isooctane with 5 mg of norethindrone acetate added to it, ~40% of the initial solid will go into solution. The isooctane phase will contain at near equilibrium ~1.8 mg and the aqueous phase will contain 0.5 mg.

If all of the hydrophobic steroid remains with the organic solvent, there will be 3 mg of the solid in contact with 2 ml of the isooctane solution or 1.0 cm^2/ml of solution. This surface area–solution volume ratio can be expected to yield a reasonable equilibration rate in the organic phase. The equilibration rate from isooctane to water will be determined effectively by the interfacial area between the two and will be independent of the amount of solid present. Since any reasonable configuration will correspond to a fairly high interfacial area–water volume ratio, a relatively rapid equilibration rate would be expected under even mild agitation. The equilibration rate in the organic phase will depend, of course, on the surface area of the solid available per milliliter of solvent used.

The suggested approach presupposes that: (*a*) the solid phase effectively stays with the organic phase, (*b*) the solubility in water is sufficient for measurement after equilibration, and (*c*) the organic solvent is sufficiently immiscible in water not to affect the solubility significantly. Although some of these conditions may not be met in all instances, the method offers a solution to many situations where equilibration may be a problem. This approach would be contraindicated for solids containing impurities that are significantly more soluble in water than in the organic phase as compared to the main component.

Estimation of Aqueous Solubility of Extremely Insoluble Hydrophobic Solids—For systems that are significantly less soluble than a few nanograms per milliliter, the equilibration rate as well as the measurement of the solute concentration presents serious experimental problems, requiring methods other than direct measurement.

One possible approach is based on the fact that hydrophobic compound solubilities are generally sufficient in a water-immiscible organic solvent to allow direct measurement. Once the solubility in some selected organic solvent is known, the solubility in water can be calculated from the directly measured or, more usually, the estimated partition coefficients.

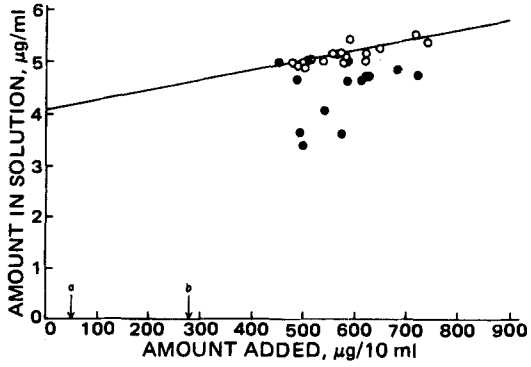

Figure 3—*Phase solubility diagram of norethindrone acetate in water at 25° with an equilibration time of 51 hr. Key: ○, 10 ml of water and 0.25 ml of isooctane; ●, 10 ml of water; a, amount of drug that saturated 10 ml of water; and b, amount of drug that saturated 10 ml of water and 0.25 ml of isooctane.*

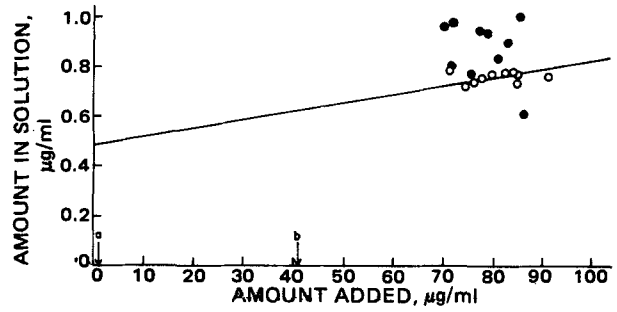

Figure 4—*Phase solubility diagram of methyltestosterone acetate in water at 25° with an equilibration time of 34 hr. Key: ○, 10 ml of water and 0.2 ml of isooctane; ●, 10 ml of water; a, amount of drug that saturated 10 ml of water; and b, amount of drug that saturated 10 ml of water and 0.2 ml of isooctane.*

At present, prediction of solubility is difficult because it depends on cooperative interactions within the crystal structure of the molecular components. However, changes in partition coefficients with alterations in molecular structure can be predicted with reasonable confidence since partitioning is, from a practical standpoint, a noncooperative operation (Scheme I).

The solubility of a crystalline solid in the organic solvent is measured accurately by the phase solubility technique. Its partition coefficient between water and the organic phase is estimated by the usual group contribution approach based on experimental results obtained on the nearest appropriate analog. Aqueous solubility is calculated from these two numbers.

Data are presented and analyzed to illustrate the utility of the two proposed approaches.

EXPERIMENTAL

Materials—Norethindrone[1] (I), norethindrone acetate[1] (II), methyltestosterone[1] (III), 2-cyclohexen-1-one[2], 1-ethynylcyclopentanol[2], and 1-methylcyclopentanol[2] were used without further purification.

The acetylation of 1-ethynylcyclopentanol was accomplished by combining the alcohol with acetic anhydride and stirring for 2 hr at 55°, using pyridine as the solvent. 1-Methylcyclopentanol and methyltestosterone were acetylated by the method of Steglich and Höfle (5) with 4-*N*,*N*-dimethylaminopyridine as a catalyst. Product purity was checked by IR and NMR spectra. The melting point of methyltestosterone acetate (IV) was 167.5°.

Distilled water was obtained by distilling previously deionized water[3]. Isooctane[4] was distilled from potassium permanganate and filtered through neutral alumina. Methanol[5] and isopropyl alcohol[6] were used without further purification.

Procedure—Solubilities in each solvent were determined by the phase solubility technique (6). Seven to 15 15-ml glass, polytef-lined, screw-capped tubes were scrupulously cleaned. To each tube, increasingly larger amounts of the test substance were added. A constant volume (10 ml) of solvent (water or isooctane) was added to each tube. If the approximate

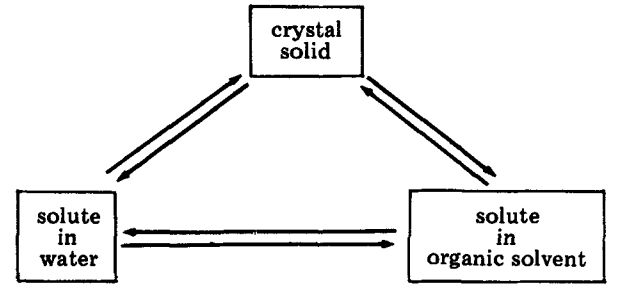

Scheme I—Determination of solubility of extremely water-insoluble hydrophobic solids.

[1] Sigma Chemical Co.
[2] Aldrich Chemical Co.
[3] Model AG-1a distillation apparatus, Corning Glass Works.
[4] Analytical grade, Fisher Scientific Co.
[5] Spectral grade, Fisher Scientific Co.
[6] Analytical grade, Mallinckrodt Chemical Works.

Table III—Calculation of the Free Energy of Transfer and Partition Coefficients for Norethindrone, Methyltestosterone, and Their Acetates

Functional Group	Structure	$\Delta(\Delta G°)$, cal/mole	Added or Subtracted I	II	III	IV
17-Androstyl	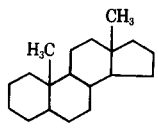	−10,700[a]	+	+	+	+
Methyl		−900[a]	−	−		
Cyclohexyl		−4400[a]	−	−	−	−
2-Cyclohexen-1-one		460[b]	+	+	+	+
Cyclopentyl		−3700[a]	−	−	−	−
1-Ethynylcyclopentanol	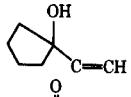	580[b]	+			
1-Ethynylcyclopentyl acetate	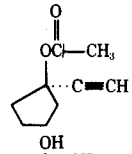	−2100[b]		+		
1-Methylcyclopentanol	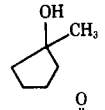	460[b]			+	
1-Methylcyclopentyl acetate	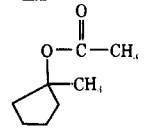	−3200[b]				+

	I	II	III	IV
$\Delta G_t°$	−660	−3340	−1680	−5340
Partition coefficient (calculated)	3.05	281	17.0	8200
Partition coefficient (measured)	3.9	230	9.4	3300

[a] Reference 7. The relative surface area used for the 17-androstyl group was 2.91; for the methyl group, it was 0.51 where the *tert*-butyl group has a value of 1. [b] Table II.

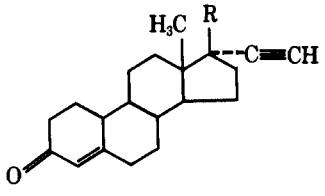

I: R = OH
II: R = $OCOCH_3$

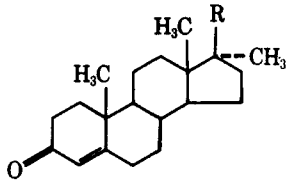

III: R = OH
IV: R = $OCOCH_3$

solubility was reasonably large, the tubes were prepared so that the contents would be completely dissolved in at least one tube.

The tubes were sealed with parafilm and fixed on a rotating shaft in the constant-temperature bath. They were equilibrated at 25° for ≥7 days, depending on the system.

After equilibration, the tubes were taken out of the bath and centrifuged. The sample was filtered immediately under pressure through a sintered-glass filter, which was presaturated with the tested compound. A desired volume of filtrate was diluted with the solvent, which was used to construct the calibration curve. The diluted solutions were analyzed spectrophotometrically[7].

In cases of facilitated dissolution, an additional isooctane aliquot was added to the top of the aqueous layer. The solutions were allowed to equilibrate in the same manner as before. The isooctane layer was removed and discarded before filtration under pressure. The filtrate was measured spectrophotometrically either directly or after dilution.

Partition coefficients from water to isooctane were measured using a standard procedure, which involved preparing a stock solution in isooctane (or water). Stock solution aliquots were diluted quantitatively to several concentrations, and at least two or three samples for each concentration were prepared. A suitable amount of water (or isooctane) was added to each flask, and these flasks were capped and sealed with parafilm. Each sample was shaken by hand for 2 min and allowed to stand in a water bath at 25 ± 0.5° for 8 min. The process was repeated six times, and the samples were allowed to stand in a thermostated water bath for 24 hr. The solute concentrations in each layer were measured by UV spectroscopy or GLC.

The relative surface areas needed were estimated by the method of Harris *et al.* (7) or were taken from Ref. 7.

Analytical Methods—Norethindrone, norethindrone acetate, methyltestosterone, methyltestosterone acetate, and 2-cyclohexen-1-one were determined spectrophotometrically[7]. 1-Ethynylcyclopentanol, 1-methylcyclopentanol, and their acetates were determined by GLC[8]. The column temperature was 115° for 1-ethynylcyclopentanol and 1-ethynylcyclopentyl acetate, yielding a retention time of 11.2 min for each; 1-heptanol, the internal standard, had a retention time of 7.2 min. A column temperature of 75° was used for 1-methylcyclopentanol and 1-methylcyclopentyl acetate, resulting in retention times of 9.5 and 9.6 min, respectively, compared with 10.7 min for the internal standard, 1-pentanol.

RESULTS AND DISCUSSION

Facilitated Dissolution Approach—The solubilities and isooctane–water partition coefficients at 25° for norethindrone, norethindrone

[7] Cary model 15, 16, or 118.

[8] Varian aerograph series 2100 with flame-ionization detectors using a glass column packed with 10% Carbowax 20M on Gas Chrom Q (80–100 mesh). Injection port and detector temperatures were both 145°, and the carrier gas (nitrogen) flow rate was 50 ml/min.

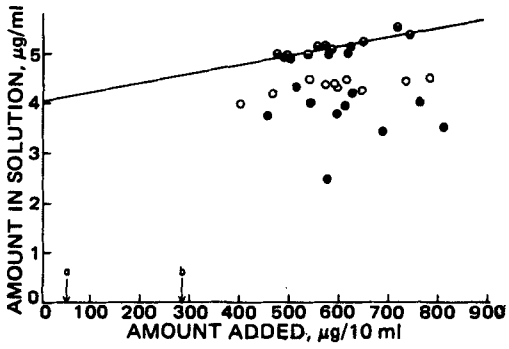

Figure 5—*Comparison of concentrations of norethindrone acetate obtained by the facilitated dissolution method and by the conventional method at the preequilibration state of 6 hr at 25°. Key: ○, 10 ml of water and 0.25 ml of isooctane; ●, 10 ml of water; and ⊖, 10 ml of water and 0.25 ml of isooctane at 51 hr (Fig. 3).*

acetate, methyltestosterone, and methyltestosterone acetate are given in Table I. Phase solubility diagrams (Figs. 2–5) for norethindrone, norethindrone acetate, and methyltestosterone acetate show equilibration both in pure water and in water to which a small amount (<5% of total volume) of isooctane had been added.

There was considerably greater scatter among the experimental points for the solubility determinations in pure water, particularly at the shorter equilibration times. The addition of an immiscible solvent definitely enhanced the equilibrium rate and yielded more precise results with at least comparable, and usually improved, accuracy.

The scatter observed in the data obtained with small excesses of solute in pure water may have resulted from particle-size heterogeneity as well as from crystalline differences. Particle-size heterogeneity is magnified greatly when small amounts are used. The facilitiated dissolution method prevented this problem even at an early stage of equilibration (Fig. 5). This procedure also reduced the effect of impurities on the apparent solubility if these impurities were more soluble in isooctane than in water. Methyltestosterone acetate, for example, was prepared containing 14% soluble impurities as calculated from the phase solubility diagram in isooctane. Attempts to extrapolate its aqueous solubility directly from its phase solubility diagram in water were not successful. The addition of 5% isooctane to the system greatly reduced the difficulty (Fig. 4).

The facilitated dissolution method offers an attractive alternative for aqueous solubility measurements where equilibration may be a problem. With radioactive labeling techniques, it should be feasible to apply this approach to solubilities at the nanogram per milliliter level.

Group Contribution Approach—As already described, substances that are extremely insoluble in water present great difficulties in direct solubility measurements. An approach suggested here consists of calculating the solubility in water from the measured solubility in an organic solvent combined with either a measured or estimated partition coefficient. This approach was tested with norethindrone, methyltestosterone, and their acetates.

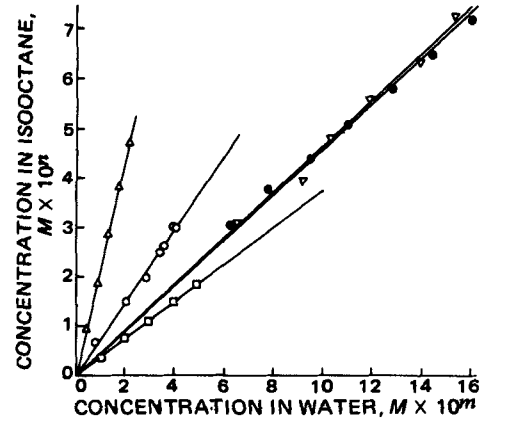

Figure 6—*Data used for the determination of isooctane–water distribution coefficients for several organic compounds at 25°. Key: ●, cyclohexen-1-one, m = 5, n = 5; △, 1-methylcyclopentanol, m = 4, n = 4; □, 1-methylcyclopentyl acetate, m = 4, n = 3; ▽, 1-ethynylcyclopentanol, m = 4, n = 4; and ○, 1-ethynylcyclopentyl acetate, m = 4, n = 3.*

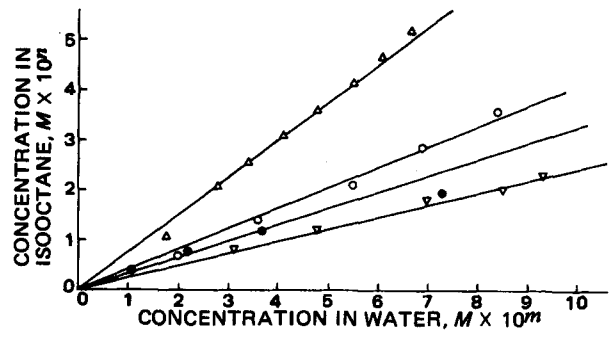

Figure 7—*Distribution of several steroidal compounds between isooctane and water at 25°. Key: ○, norethindrone, m = 6, n = 5; ▽, norethindrone acetate, m = 7, n = 4; △, methyltestosterone, m = 6, n = 5; and ●, methyltestosterone acetate, m = 7, n = 3.*

The measured solubilities and partition coefficients are given in Table I. The predicted partition coefficients were determined using a group contribution approach, which assumes that certain thermodynamic or other physical properties of a molecule can be found from the sum of the values for the different groups comprising the molecule (7, 8). Isooctane was the organic solvent, and the group contribution for transfer between water and isooctane for the saturated hydrocarbon moieties was taken from the data of Harris *et al.* (7) or determined as described by them using the relationship:

$$\Delta(\Delta G) = -4070 \text{ (relative surface area)} + 1156 \qquad \text{(Eq. 3)}$$

where $\Delta(\Delta G)$ is in calories per mole and the correlation coefficient is 0.992.

The partition coefficients for moieties having polar groups were measured (Fig. 6) and are reported in Table II along with the corresponding free energy of transfer from the relationship:

$$\Delta G^\circ = -RT \ln K \qquad \text{(Eq. 4)}$$

where K is the partition coefficient.

Prediction of Partition Coefficients—Based on the assumptions of the group contribution approach (8), one should be able to predict partition coefficients for a molecule when the partition characteristics of its constituent parts are known, assuming that they are additive. This approach should be helpful for highly hydrophobic compounds for which

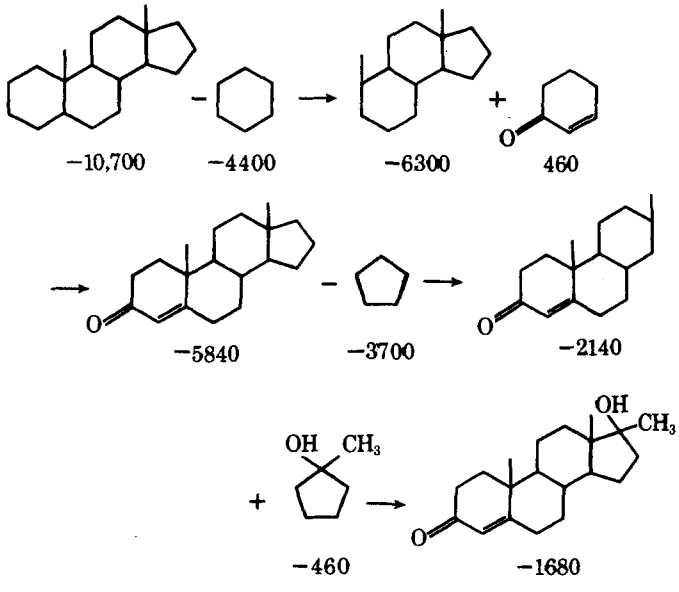

Scheme II—Schematic diagram for calculating the free energy of transfer for methyltestosterone using the 17-androstyl group as the beginning group. The numbers represent the values for each group and intermediate used in the calculations.

actual measurement is difficult. Scheme II illustrates such a calculation for methyltestosterone starting from the 17-androstyl group.

Table III summarizes similar calculations of the free energy of transfer of the compounds studied along with the measured partition coefficients taken from the data shown in Fig. 7.

Agreement (within a factor of 2) was obtained between the calculated partition coefficients and the measured values with the exception of methyltestosterone acetate. The measured value for methyltestosterone added to the acetyl group contribution determined from the data for 1-methylcyclopentanol and 1-methylcyclopentyl acetate gave a value of ~5000 for the partition coefficient, which is in much better agreement with the experimental value.

This study shows that in cases where experimental values are difficult to obtain, estimates based on the group contribution approach are reasonably accurate.

If one takes the measured solubility in isooctane and divides by the partition coefficient as an approximation to the solubility in water, reasonable agreement with the measured solubility values is obtained. Thus, in the special case of extremely low solubility in water, estimating the partition coefficient by the group contribution approach and combining it with the known solubility in an organic solvent provide a good estimate of the aqueous solubility. In such cases, this approach may be the only feasible method of obtaining an accurate solubility estimate.

REFERENCES

(1) D. K. Madan and D. E. Cadwallader, *J. Pharm. Sci.*, **62**, 1567 (1973).

(2) A. A. Noyes and W. R. Whitney, *J. Am. Chem. Soc.*, **19**, 930 (1897).

(3) W. Nernst and E. Brunner, *Z. Phys. Chem.*, **47**, 56 (1904).

(4) "The Merck Index," M. Windholz, Ed., Merck & Co., Rahway, N.J., 1976, p. 142.

(5) W. Steglich and G. Höfle, *Angew. Chem. Int. Ed.*, **8**, 981 (1969).

(6) T. Higuchi and K. Connors, in "Advances in Analytical Chemistry and Instrumentation," vol. 4, C. N. Reilley, Ed., Interscience, New York, N.Y., 1965, p. 117.

(7) M. J. Harris, T. Higuchi, and J. H. Rytting, *J. Phys. Chem.*, **77**, 2694 (1973).

(8) S. S. Davis, T. Higuchi, and J. H. Rytting, in "Advances in Pharmaceutical Sciences," vol. 4, H. S. Bean, A. H. Beckett, and J. E. Carless, Eds., Academic, London, England, 1974, pp. 73–261.

ACKNOWLEDGMENTS

Supported in part by National Institutes of Health Grant GM22357.

Determination of Phenylmercuric Nitrate by Potentiometric Titration

RAY W. WOOD and HARRY L. WELLES ˣ

Received March 20, 1979, from the *College of Pharmacy, Faculty of Health Professions, Dalhousie University, Halifax, Nova Scotia, Canada B3H 3J5.* Accepted for publication April 13, 1979.

Abstract □ A procedure was developed for measuring small amounts of phenylmercuric nitrate in aqueous solutions. The method depends on the formation of insoluble phenylmercuric iodide upon titration of phenylmercuric nitrate with potassium iodide. The end-point can be detected using an iodide-sensitive electrode. The method is able to measure down to 0.000125% aqueous solution of phenylmercuric nitrate with a 1% accuracy. Procedural details and descriptions of excipient effects on the assay are presented. Naphazoline hydrochloride, phenylephrine hydrochloride, fluorescein sodium, and antipyrine interfered with the method, while the common buffer systems, polyvinyl alcohol, sodium thiosulfate, edetate sodium, and chloramphenicol had no effect.

Keyphrases □ Phenylmercuric nitrate—analysis, potentiometric titration, dilute aqueous solutions, excipients □ Ophthalmic dosage forms—phenylmercuric nitrate, potentiometric titration analysis, dilute aqueous solutions, excipients □ Potentiometric titration—analysis, phenylmercuric nitrate, dilute aqueous solutions

Phenylmercuric nitrate is frequently used as a preservative for ophthalmic and other preparations. To carry out routine determinations of small amounts of phenylmercuric nitrate in aqueous solution, a simple, rapid, and sensitive assay is necessary. Published methods for determining phenylmercuric nitrate have been numerous, but many of these are tedious or lack sensitivity.

BACKGROUND

Microbiological methods (1) are time consuming and are only semiquantitative. Spectrophotometric methods take advantage of the UV absorption at 257 nm by phenylmercuric nitrate (2). Although this assay is rapid, its sensitivity is limited. Many procedures involve conversion of organomercury to mercuric ion, followed by classical thiocyanate titrimetry (3). Again, this method lacks the sensitivity required for very dilute solutions.

The British Pharmacopoeia lists the dithizone extraction method (4), which involves extraction of the mercury from an acidic solution with a solution of dithizone in chloroform. The dithizonate is then measured spectrophotometrically. Because of the extractions involved, this method is tedious for routine determinations.

Ordinary polarographic methods have been used for higher phenylmercuric nitrate concentrations (5); cathode ray polarography of phenylmercuric nitrate has been investigated (6) and is a simple, rapid, and sensitive assay for routine determinations. Furthermore, phenylmercuric nitrate has been detected satisfactorily by atomic absorption spectroscopy (7). This procedure is based on "protodemercuration" of the mercurial compound with hydrochloric acid under various heating conditions, followed by reduction of the resulting mercuric ion to elemental mercury with subsequent detection and quantitation by vapor phase atomic absorption spectroscopy. Since these procedures require instruments that may not be readily available, the technique described in this paper was developed. This relatively rapid, simple, and sensitive assay is based on the precipitation of the phenylmercuric moiety with iodide ion.

Insoluble phenylmercuric iodide, $K_{sp} = 9.7 \times 10^{-16}$ (8), is formed when an aqueous solution containing phenylmercuric ions is titrated with iodide according to Scheme I.

$$C_6H_5—Hg^+ + I^- \rightleftharpoons C_6H_5—HgI$$

Scheme I

In the developed procedure, the end-point for this reaction is detected potentiometrically using an electrode sensitive to iodide ions.

EXPERIMENTAL

Five milliliters of an aqueous phenylmercuric nitrate[1] solution was transferred to a 50-ml beaker equipped with a magnetic stirring bar. The amount of phenylmercuric nitrate in solution ranged from ~0.05 to 2.5

[1] Lot 0900030, British Drug Houses Chemicals Ltd., Poole, England.

0022-3549/79/1000-1272$01.00/0

© 1979, American Pharmaceutical Association

actual measurement is difficult. Scheme II illustrates such a calculation for methyltestosterone starting from the 17-androstyl group.

Table III summarizes similar calculations of the free energy of transfer of the compounds studied along with the measured partition coefficients taken from the data shown in Fig. 7.

Agreement (within a factor of 2) was obtained between the calculated partition coefficients and the measured values with the exception of methyltestosterone acetate. The measured value for methyltestosterone added to the acetyl group contribution determined from the data for 1-methylcyclopentanol and 1-methylcyclopentyl acetate gave a value of ~5000 for the partition coefficient, which is in much better agreement with the experimental value.

This study shows that in cases where experimental values are difficult to obtain, estimates based on the group contribution approach are reasonably accurate.

If one takes the measured solubility in isooctane and divides by the partition coefficient as an approximation to the solubility in water, reasonable agreement with the measured solubility values is obtained. Thus, in the special case of extremely low solubility in water, estimating the partition coefficient by the group contribution approach and combining it with the known solubility in an organic solvent provide a good estimate of the aqueous solubility. In such cases, this approach may be the only feasible method of obtaining an accurate solubility estimate.

REFERENCES

(1) D. K. Madan and D. E. Cadwallader, *J. Pharm. Sci.*, **62**, 1567 (1973).

(2) A. A. Noyes and W. R. Whitney, *J. Am. Chem. Soc.*, **19**, 930 (1897).

(3) W. Nernst and E. Brunner, *Z. Phys. Chem.*, **47**, 56 (1904).

(4) "The Merck Index," M. Windholz, Ed., Merck & Co., Rahway, N.J., 1976, p. 142.

(5) W. Steglich and G. Höfle, *Angew. Chem. Int. Ed.*, **8**, 981 (1969).

(6) T. Higuchi and K. Connors, in "Advances in Analytical Chemistry and Instrumentation," vol. 4, C. N. Reilley, Ed., Interscience, New York, N.Y., 1965, p. 117.

(7) M. J. Harris, T. Higuchi, and J. H. Rytting, *J. Phys. Chem.*, **77**, 2694 (1973).

(8) S. S. Davis, T. Higuchi, and J. H. Rytting, in "Advances in Pharmaceutical Sciences," vol. 4, H. S. Bean, A. H. Beckett, and J. E. Carless, Eds., Academic, London, England, 1974, pp. 73–261.

ACKNOWLEDGMENTS

Supported in part by National Institutes of Health Grant GM22357.

Determination of Phenylmercuric Nitrate by Potentiometric Titration

RAY W. WOOD and HARRY L. WELLES ˣ

Received March 20, 1979, from the *College of Pharmacy, Faculty of Health Professions, Dalhousie University, Halifax, Nova Scotia, Canada B3H 3J5.* Accepted for publication April 13, 1979.

Abstract □ A procedure was developed for measuring small amounts of phenylmercuric nitrate in aqueous solutions. The method depends on the formation of insoluble phenylmercuric iodide upon titration of phenylmercuric nitrate with potassium iodide. The end-point can be detected using an iodide-sensitive electrode. The method is able to measure down to 0.000125% aqueous solution of phenylmercuric nitrate with a 1% accuracy. Procedural details and descriptions of excipient effects on the assay are presented. Naphazoline hydrochloride, phenylephrine hydrochloride, fluorescein sodium, and antipyrine interfered with the method, while the common buffer systems, polyvinyl alcohol, sodium thiosulfate, edetate sodium, and chloramphenicol had no effect.

Keyphrases □ Phenylmercuric nitrate—analysis, potentiometric titration, dilute aqueous solutions, excipients □ Ophthalmic dosage forms—phenylmercuric nitrate, potentiometric titration analysis, dilute aqueous solutions, excipients □ Potentiometric titration—analysis, phenylmercuric nitrate, dilute aqueous solutions

Phenylmercuric nitrate is frequently used as a preservative for ophthalmic and other preparations. To carry out routine determinations of small amounts of phenylmercuric nitrate in aqueous solution, a simple, rapid, and sensitive assay is necessary. Published methods for determining phenylmercuric nitrate have been numerous, but many of these are tedious or lack sensitivity.

BACKGROUND

Microbiological methods (1) are time consuming and are only semiquantitative. Spectrophotometric methods take advantage of the UV absorption at 257 nm by phenylmercuric nitrate (2). Although this assay is rapid, its sensitivity is limited. Many procedures involve conversion of organomercury to mercuric ion, followed by classical thiocyanate titrimetry (3). Again, this method lacks the sensitivity required for very dilute solutions.

The British Pharmacopoeia lists the dithizone extraction method (4), which involves extraction of the mercury from an acidic solution with a solution of dithizone in chloroform. The dithizonate is then measured spectrophotometrically. Because of the extractions involved, this method is tedious for routine determinations.

Ordinary polarographic methods have been used for higher phenylmercuric nitrate concentrations (5); cathode ray polarography of phenylmercuric nitrate has been investigated (6) and is a simple, rapid, and sensitive assay for routine determinations. Furthermore, phenylmercuric nitrate has been detected satisfactorily by atomic absorption spectroscopy (7). This procedure is based on "protodemercuration" of the mercurial compound with hydrochloric acid under various heating conditions, followed by reduction of the resulting mercuric ion to elemental mercury with subsequent detection and quantitation by vapor phase atomic absorption spectroscopy. Since these procedures require instruments that may not be readily available, the technique described in this paper was developed. This relatively rapid, simple, and sensitive assay is based on the precipitation of the phenylmercuric moiety with iodide ion.

Insoluble phenylmercuric iodide, $K_{sp} = 9.7 \times 10^{-16}$ (8), is formed when an aqueous solution containing phenylmercuric ions is titrated with iodide according to Scheme I.

$$C_6H_5—Hg^+ + I^- \rightleftharpoons C_6H_5—HgI$$

Scheme I

In the developed procedure, the end-point for this reaction is detected potentiometrically using an electrode sensitive to iodide ions.

EXPERIMENTAL

Five milliliters of an aqueous phenylmercuric nitrate[1] solution was transferred to a 50-ml beaker equipped with a magnetic stirring bar. The amount of phenylmercuric nitrate in solution ranged from ~0.05 to 2.5

[1] Lot 0900030, British Drug Houses Chemicals Ltd., Poole, England.

0022-3549/79/1000-1272$01.00/0

© 1979, American Pharmaceutical Association

Table I—Comparison of Known and Measured Phenylmercuric Nitrate Concentrations

Known Phenylmercuric Nitrate Concentration, % w/v	Measured Concentration, % of known[a]
0.0100	99.4 ± 0.06
0.00500	98.4 ± 0.00
0.00200	99.5 ± 0.00
0.00100	101.7 ± 1.15
0.000500	100.6 ± 2.06
0.000250	100.0 ± 1.13
0.000125[b]	98.9 ± 0.92

[a] Average of three determinations ± *SD*. [b] The lowest concentration that the assay could detect with confidence.

mg. Twenty milliliters of distilled water was added to make a workable volume, and the solution was acidified with concentrated sulfuric acid[2]. This solution was titrated, using a potentiograph[3], with a solution of known concentration of potassium iodide[4] saturated with iodine[5]. The potassium iodide concentration was approximately equal to the concentration of phenylmercuric nitrate being assayed. The solution was stirred continuously *via* a magnetic stirrer.

A platinum electrode[6] was used to detect the iodide concentration, and a calomel electrode[7] equipped with a potassium nitrate[8] salt bridge was used as the reference electrode. The end-point of each titration was read directly from the recording chart of the potentiograph.

The iodine-saturated potassium iodide solution was standardized by titrating a known amount of analytical standard phenylmercuric acetate[9] with the potassium iodide solution.

RESULTS AND DISCUSSION

The potentiometric method is based on the ability of the electrode to detect the sudden increase of iodide ions once the phenylmercuric cation in the solution has precipitated as phenylmercuric iodide. Platinum in contact with iodine is sensitive to iodide (9) and was used as the indicating electrode. The iodine necessary for detecting the iodide ions was present in the potassium iodide solution. In a solution that contains iodide ion and molecular iodine, a reaction between the two species occurs as in Scheme II.

$$I_2 + I^- \rightleftharpoons I_3^-$$

Scheme II

Then, according to the law of mass action:

$$K = \frac{[I_3^-]}{[I_2][I^-]} \qquad \text{(Eq. 1)}$$

At 18°, K is equal to 8.70×10^2 (9). Therefore, in fact, the phenylmercuric nitrate is being titrated by the I_3^- species, which consequently generates the I^- species. Kolthoff and Furman (9) suggested that, for the titration of mercuric ions with iodide, I_2 be introduced as an alcohol solution into the solution being titrated. However, when this was done, end-point reproducibility became a problem. This result was probably due to competition for the iodide ion by the phenylmercuric cation and the molecular iodine or to the formation of small amounts of iodide from the iodine (9). When the iodine is in the potassium iodide solution, the competition is prevented and the added iodide is accounted for during the standardization.

As an alternative to platinum in contact with iodine to detect the iodide ions, one may use an iodide-specific electrode[10]. Several determinations made with such an electrode gave results similar to those obtained with the platinum electrode.

Figure 1 shows a plot of potential *versus* titrant volume. Equilibrium apparently was established rapidly between the species involved in the titration. Therefore, no drift was observed, and the end-point was sharp. The sulfuric acid, which was added to the phenylmercuric nitrate solution before the titration began, was crucial to the sharpness of the end-point. This observation may be similar to that seen in the titration of iodide with silver nitrate (9). When the titration was carried out in acidic solution, the phenylmercuric iodide flocculated from the start of the titration, whereas in a neutral medium the iodide remained in colloidal solution and flocculated just before the equivalence point was reached. Owing to the high degree of dispersion, the adsorbing capacity of the iodide was much greater in the latter case than in an acidic medium. However, too much sulfuric acid caused reproducibility problems. About 5 drops of concentrated sulfuric acid sufficed.

Table II—Effect of Excipients on Assay of 0.002% Phenylmercuric Nitrate Solution

Excipient	Percent, w/v	Percent of Original Concentration[a]
Boric acid	1.00	98.3 ± 1.04
Sodium borate	0.05	98.6 ± 1.26
Acetic acid	0.005	99.7 ± 1.04
Sodium acetate	1.0	99.5 ± 0.87
Dibasic sodium phosphate	1.0	99.8 ± 0.58
Monobasic sodium phosphate	1.0	100.3 ± 0.76
Polyvinyl alcohol	1.4	100.5 ± 0.58
Sodium thiosulfate	0.1	100.4 ± 0.58
Edetate sodium	0.1	99.5 ± 1.15
Chloramphenicol	0.5	89.3 ± 0.29[b]
Naphazoline hydrochloride	0.1	0[b]
Phenylephrine hydrochloride	0.12	0[b]
Fluorescein sodium	0.1	0[b]
Antipyrine	0.1	0[b]

[a] Average of three determinations ± *SD*. [b] Significantly different from original phenylmercuric nitrate concentration.

To check the sensitivity, precision, and accuracy of the analytical procedure followed for phenylmercuric nitrate, measurements were made with known amounts of phenylmercuric nitrate (Table I). The accuracy throughout the concentration range was ~1%. The lowest measurable concentration was 0.000125%. Below this concentration, the end-points were not sharp enough. A t-test performed on these data showed that the

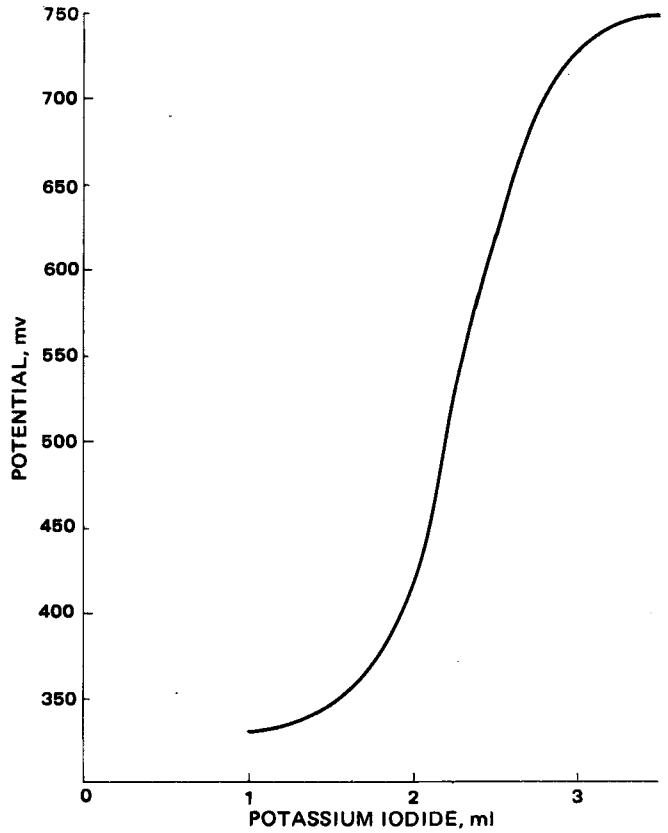

Figure 1—*Potential change for the titration of 0.002% phenylmercuric nitrate with 0.002% potassium iodide.*

[2] ACS approved, J. T. Baker Chemical Co., Phillipsburg, NJ 08865.
[3] Model E 336 A, Metrohm, Herisau, Switzerland.
[4] Lot 83176, British Drug Houses Chemicals Ltd., Poole, England.
[5] Lot 710919, laboratory grade, Fisher Scientific Co., Fair Lawn, NJ 07410.
[6] Model EA201, Metrohm, Herisau, Switzerland.
[7] Model EA436, Metrohm, Herisau, Switzerland.
[8] Lot 723124, laboratory grade, Fisher Scientific Co., Fair Lawn, NJ 07410.
[9] Lot 12028, analytical standard, British Drug Houses Chemicals Ltd., Poole, England.
[10] Model 94-53A, Orion Research Inc., Cambridge, MA 02139.

average of the results is not significantly different from 100%, so the method does not appear to have any bias.

Ophthalmic products that contain phenylmercuric nitrate have other substances in the solution such as the active drug, reducing agents, buffer systems, and surfactants. To assess the effectiveness of the assay for phenylmercuric nitrate in ophthalmic products, the effect of these other substances on the assay was determined. Table II shows the approximate concentration of the excipient used to determine its effect on the assay. Concentrations of buffer pairs were such that the solutions were isotonic and at pH 7.

Table II shows four excipients that interfered completely with the phenylmercuric nitrate assay; *i.e.*, no end-point could be obtained. Although they are used in commercial products (10) with phenylmercuric nitrate, the drugs naphazoline hydrochloride and phenylephrine hydrochloride probably cause precipitation of insoluble phenylmercuric chloride even before the titrating begins, as shown in Scheme III.

$$C_6H_5—Hg^+ + Cl^- \rightleftharpoons C_6H_5HgCl$$

Scheme III

The K_{sp} for this reaction is 5.0×10^{-10} (8); therefore, the solubility limit of phenylmercuric chloride is exceeded in the phenylmercuric nitrate solutions containing naphazoline hydrochloride and phenylephrine hydrochloride. This would no doubt also happen in solutions of other halide salts. It was reported that antipyrine complexes with mercury compounds (11). If this complexation occurs with phenylmercuric nitrate, it might prevent the formation of the insoluble phenylmercuric salt, which is crucial to the titration. In contrast to the other systems, the effect of fluorescein sodium on the assay and the significant decrease of phenylmercuric nitrate in the presence of chloramphenicol remain unexplained.

In summary, this method of analysis for phenylmercuric salts should prove useful in applications requiring phenylmercuric nitrate determination in dilute solution.

REFERENCES

(1) A. K. Klein, *J. Assoc. Off. Agr. Chem.*, **35**, 537 (1952).

(2) F. Neuwald and G. Schmitzek, *J. Mond. Pharm.*, **11**, 5 (1968).

(3) E. E. Theimer and P. Arnow, *J. Am. Pharm. Assoc., Sci. Ed.*, **44**, 381 (1955).

(4) Analytical Methods Committee, *Analyst*, **90**, 515 (1965).

(5) R. Benesch and R. E. Benesch, *J. Am. Chem. Soc.*, **73**, 3391 (1951).

(6) G. S. Porter, *J. Pharm. Pharmacol., Suppl.*, **20**, 435 (1968).

(7) R. D. Thompson and T. J. Hoffman, *J. Pharm. Sci.*, **64**, 1863 (1975).

(8) T. D. Waugh, H. F. Walton, and J. A. Laswick, *J. Phys. Chem.*, **59**, 395 (1955).

(9) I. M. Kolthoff and N. H. Furman, "Potentiometric Titrations," Wiley, London, England, 1931, pp. 191–194.

(10) "Compendium of Pharmaceuticals and Specialties," 13th ed., Canadian Pharmaceutical Association, Toronto, Ontario, Canada, 1978.

(11) V. K. Akimov, A. I. Busev, B. E. Zaitsev, and L. S. Khintibidze, *Zh. Obshch. Khim.*, **37**, 2462 (1967); through *Chem. Abstr.*, **68**, 84083u (1968).

ACKNOWLEDGMENTS

Supported in part by Grant Ma-6420 from the Medical Research Council, Ottawa, Canada.

Stereospecific Assay and Stereospecific Disposition of Racemic Carprofen in Rats

J. M. KEMMERER *, F. A. RUBIO *, R. M. McCLAIN ‡, and B. A. KOECHLIN *x

Received January 11, 1979, from the **Department of Biochemistry and Drug Metabolism and the* ‡*Department of Toxicology, Hoffmann-La Roche Inc., Nutley, NJ 07110.* Accepted for publication April 18, 1979.

Abstract □ A procedure was developed for the separation and selective quantitative determination of the (*S*)(+)- and (*R*)(−)-enantiomers of the racemic anti-inflammatory drug carprofen as their diastereomeric *l*-(−)-α-methylbenzylamides. These derivatives are obtained in equivalent yields by reacting purified ^{14}C-carprofen from biological specimens with *l*-(−)-α-methylbenzylamine *via* the 1,1′-carbonyldiimidazole intermediate, followed by extraction and differential radiometric quantitation of the TLC-separated diastereomers. In the rat, the (*R*)(−)-carprofen enantiomer was eliminated from blood and secreted in the bile as the ester glucuronide at a rate approximately twice that of the (*S*)-(+)-enantiomer, resulting in the accumulation of the pharmacologically more active (*S*)(+)-enantiomer in the rat blood. Evidence for an additional process favoring the elimination of the (*R*)(−)-enantiomer in the rat was derived from pharmacokinetic data evaluation.

Keyphrases □ Carprofen—racemic mixtures, stereospecific assay, stereospecific metabolism, rats □ Enantiomers—carprofen, stereospecific assay, stereospecific metabolism, rats □ Anti-inflammatory agents—carprofen, racemic mixtures, stereospecific assay, stereospecific metabolism, rats

The anti-inflammatory agent carprofen (1), (D,L)-6-chloro-α-methylcarbazole-2-acetic acid (I), is a racemic compound with a chiral center at the α-carbon. The optically active carprofen enantiomers have been resolved, and their confirmations have been identified by X-ray analysis[1].

The properties of the dextrorotatory (*S*)(+)-enantiomer (II) and the levorotatory (*R*)(−)-enantiomer (III) have been compared in biological *in vivo* and *in vitro* tests (1). In the acute adjuvant arthritis test in the rat, the (*R*)-(−)-enantiomer was less than one-tenth as active (ID_{30}) as the (*S*)(+)-enantiomer. In contrast to the latter, the former was virtually inactive as an inhibitor of platelet aggregation, prostaglandin synthetase, and arachidonic acid-induced diarrhea; it produced no ulcerogenesis nor any other *in vivo* manifestation of toxicity in the rat.

Therefore, a stereoselective disposition of the two carprofen enantiomers could result in a different pharmacokinetic profile of the biologically active enantiomer from that previously determined by nonstereospecific procedures following administration of the racemate (2, 3). Possible stereoselective drug disposition processes include selective biotransformation reactions, tissue uptake,

[1] The identification by X-ray crystallography of the chiral configuration of the carprofen enantiomers was performed by Dr. J. F. Blout of the Roche Department of Physical Chemistry.

0022-3549/79/1000-1274$01.00/0

© 1979, American Pharmaceutical Association

average of the results is not significantly different from 100%, so the method does not appear to have any bias.

Ophthalmic products that contain phenylmercuric nitrate have other substances in the solution such as the active drug, reducing agents, buffer systems, and surfactants. To assess the effectiveness of the assay for phenylmercuric nitrate in ophthalmic products, the effect of these other substances on the assay was determined. Table II shows the approximate concentration of the excipient used to determine its effect on the assay. Concentrations of buffer pairs were such that the solutions were isotonic and at pH 7.

Table II shows four excipients that interfered completely with the phenylmercuric nitrate assay; *i.e.*, no end-point could be obtained. Although they are used in commercial products (10) with phenylmercuric nitrate, the drugs naphazoline hydrochloride and phenylephrine hydrochloride probably cause precipitation of insoluble phenylmercuric chloride even before the titrating begins, as shown in Scheme III.

$$C_6H_5—Hg^+ + Cl^- \rightleftharpoons C_6H_5HgCl$$

Scheme III

The K_{sp} for this reaction is 5.0×10^{-10} (8); therefore, the solubility limit of phenylmercuric chloride is exceeded in the phenylmercuric nitrate solutions containing naphazoline hydrochloride and phenylephrine hydrochloride. This would no doubt also happen in solutions of other halide salts. It was reported that antipyrine complexes with mercury compounds (11). If this complexation occurs with phenylmercuric nitrate, it might prevent the formation of the insoluble phenylmercuric salt, which is crucial to the titration. In contrast to the other systems, the effect of fluorescein sodium on the assay and the significant decrease of phenylmercuric nitrate in the presence of chloramphenicol remain unexplained.

In summary, this method of analysis for phenylmercuric salts should prove useful in applications requiring phenylmercuric nitrate determination in dilute solution.

REFERENCES

(1) A. K. Klein, *J. Assoc. Off. Agr. Chem.*, **35**, 537 (1952).

(2) F. Neuwald and G. Schmitzek, *J. Mond. Pharm.*, **11**, 5 (1968).

(3) E. E. Theimer and P. Arnow, *J. Am. Pharm. Assoc., Sci. Ed.*, **44**, 381 (1955).

(4) Analytical Methods Committee, *Analyst*, **90**, 515 (1965).

(5) R. Benesch and R. E. Benesch, *J. Am. Chem. Soc.*, **73**, 3391 (1951).

(6) G. S. Porter, *J. Pharm. Pharmacol., Suppl.*, **20**, 435 (1968).

(7) R. D. Thompson and T. J. Hoffman, *J. Pharm. Sci.*, **64**, 1863 (1975).

(8) T. D. Waugh, H. F. Walton, and J. A. Laswick, *J. Phys. Chem.*, **59**, 395 (1955).

(9) I. M. Kolthoff and N. H. Furman, "Potentiometric Titrations," Wiley, London, England, 1931, pp. 191–194.

(10) "Compendium of Pharmaceuticals and Specialties," 13th ed., Canadian Pharmaceutical Association, Toronto, Ontario, Canada, 1978.

(11) V. K. Akimov, A. I. Busev, B. E. Zaitsev, and L. S. Khintibidze, *Zh. Obshch. Khim.*, **37**, 2462 (1967); through *Chem. Abstr.*, **68**, 84083u (1968).

ACKNOWLEDGMENTS

Supported in part by Grant Ma-6420 from the Medical Research Council, Ottawa, Canada.

Stereospecific Assay and Stereospecific Disposition of Racemic Carprofen in Rats

J. M. KEMMERER *, F. A. RUBIO *, R. M. McCLAIN ‡, and B. A. KOECHLIN *x

Received January 11, 1979, from the **Department of Biochemistry and Drug Metabolism and the* ‡*Department of Toxicology, Hoffmann-La Roche Inc., Nutley, NJ 07110.* Accepted for publication April 18, 1979.

Abstract □ A procedure was developed for the separation and selective quantitative determination of the (*S*)(+)- and (*R*)(−)-enantiomers of the racemic anti-inflammatory drug carprofen as their diastereomeric *l*-(−)-α-methylbenzylamides. These derivatives are obtained in equivalent yields by reacting purified ^{14}C-carprofen from biological specimens with *l*-(−)-α-methylbenzylamine *via* the 1,1′-carbonyldiimidazole intermediate, followed by extraction and differential radiometric quantitation of the TLC-separated diastereomers. In the rat, the (*R*)(−)-carprofen enantiomer was eliminated from blood and secreted in the bile as the ester glucuronide at a rate approximately twice that of the (*S*)-(+)-enantiomer, resulting in the accumulation of the pharmacologically more active (*S*)(+)-enantiomer in the rat blood. Evidence for an additional process favoring the elimination of the (*R*)(−)-enantiomer in the rat was derived from pharmacokinetic data evaluation.

Keyphrases □ Carprofen—racemic mixtures, stereospecific assay, stereospecific metabolism, rats □ Enantiomers—carprofen, stereospecific assay, stereospecific metabolism, rats □ Anti-inflammatory agents—carprofen, racemic mixtures, stereospecific assay, stereospecific metabolism, rats

The anti-inflammatory agent carprofen (1), (D,L)-6-chloro-α-methylcarbazole-2-acetic acid (I), is a racemic compound with a chiral center at the α-carbon. The optically active carprofen enantiomers have been resolved, and their confirmations have been identified by X-ray analysis[1].

The properties of the dextrorotatory (*S*)(+)-enantiomer (II) and the levorotatory (*R*)(−)-enantiomer (III) have been compared in biological *in vivo* and *in vitro* tests (1). In the acute adjuvant arthritis test in the rat, the (*R*)-(−)-enantiomer was less than one-tenth as active (ID_{30}) as the (*S*)(+)-enantiomer. In contrast to the latter, the former was virtually inactive as an inhibitor of platelet aggregation, prostaglandin synthetase, and arachidonic acid-induced diarrhea; it produced no ulcerogenesis nor any other *in vivo* manifestation of toxicity in the rat.

Therefore, a stereoselective disposition of the two carprofen enantiomers could result in a different pharmacokinetic profile of the biologically active enantiomer from that previously determined by nonstereospecific procedures following administration of the racemate (2, 3). Possible stereoselective drug disposition processes include selective biotransformation reactions, tissue uptake,

[1] The identification by X-ray crystallography of the chiral configuration of the carprofen enantiomers was performed by Dr. J. F. Blout of the Roche Department of Physical Chemistry.

0022-3549/79/1000-1274$01.00/0

© 1979, American Pharmaceutical Association

Table I—Optical Enantiomer Ratio of ^{14}C-Carprofen

Amount of ^{14}C-D,L-Carprofen Reacted, μg	Reacted ^{14}C Extracted, %	Microgram Equivalents per TLC[a]	(S)(+), %	(R)(−), %	(S)(+)/(R)(−) Ratio	(S)(+)/(R)(−) Average
2.43	89.2	0.542	32.4	32.6	0.994	1.022
	90.2	0.548	37.7	35.8	1.050	
4.86	89.8	1.091	35.0	34.0	1.029	1.015
	90.0	1.093	39.5	39.5	1.000	
9.73	98.8	2.40	35.0	36.1	0.970	0.981
	96.3	2.34	34.7	34.4	1.009	
19.46	92.6	4.50	34.8	35.5	0.980	0.986
	95.2	4.63	33.6	33.9	0.991	

[a] Chromatographing one-fourth of the total reaction product (a larger aliquot may be chromatographed).

Table II—^{14}C-Carprofen Enantiomer Ratio in Rat Bile

Concentration of ^{14}C-D,L-Carprofen, μg/ml	Bile Volume, ml	Carprofen Recovered from Bile, %	Microgram Equivalents ^{14}C per TLC[a]	(S)(+), %	(R)(−), %	(S)(+)/(R)(−) Ratio	(S)(+)/(R)(−) Average
22.6	0.5	87.1	1.44	43.2	43.1	1.002	1.014
22.6	0.5	90.8	1.62	39.6	38.6	1.026	
45.2	0.5	92.3	3.13	32.5	32.9	0.988	1.034
45.2	0.5	94.8	3.45	38.2	35.4	1.079	
14.1	—	—	3.08	32.8	32.7	1.000	1.026
14.1	—	—	3.25	34.9	34.2	1.052	

[a] Indicates the total microgram equivalents of the diastereoisomers applied to the TLC plate in each experiment using a 50–200-μl aliquot. One microgram equivalent represents 1086 dpm and is detectable on the plate.

protein binding, and elimination of the two enantiomeric forms (4).

Closely related carprofen analogs, having in common an asymmetric α-phenyl propionic acid grouping, have been reported to undergo an enzymatic inversion at the chiral center at the α-carbon whereby the (R)(−)-enantiomer is converted to the (S)(+)-enantiomer. Lan *et al.* (5) demonstrated, in the rat and in the monkey, a conversion of the (R)(−)-form of cicloprofen (α-methylfluorene-2-acetic acid), to the (S)(+)-form accompanied by a stereoselective elimination process. Furthermore, the (R)(−)-enantiomer of the anti-inflammatory agent ibuprofen [2-(4-isopropylphenyl)propionic acid] underwent inversion to the (S)(+)-isomer in humans and, at the same time, was subjected to stereospecific oxidations at the isopropyl side chain leading to the formation of a second chiral center (6–9).

A procedure has been reported for the separate quantitation by GLC (7, 10) of the diastereomeric amides of ibuprofen obtained by reaction with *l*-(−)-α-methylbenzylamine. A similar, highly sensitive, selective procedure (4) involves the TLC separation and radiometric quantitation of the diastereomeric amides (peptides) obtained when reacting *d,l*-cicloprofen with ^{14}C-*l*-leucine.

This report describes a microprocedure that permits the selective determination of ^{14}C-carprofen diastereomers in biological fluids (11). Experiments applying this procedure to stereospecific pathways of carprofen metabolism in the rat (2) are described. In these studies, the chiral composition changes of free carprofen, the main drug component in the blood, and of carprofen ester glucuronide, a main biliary secretion product, were measured in carprofen-treated rats.

EXPERIMENTAL

Selective Determination of (S)(+)- and (R)(−)-Carprofen Enantiomers—The procedure relies on the: (*a*) reaction of racemic ^{14}C-carprofen (I) with *l*-(−)-α-methylbenzylamine (IV) to form the two diastereomeric *l*-methylbenzylamides (V) *via* the 1,1′-carbonyldiimidazole intermediate (7, 8) (Scheme I), (*b*) separation of the diastereomers by TLC, and (*c*) quantitation of radioactivity in the isolated TLC bands. From biological materials, I was extracted directly or after cleavage of its ester glucuronide and was purified by TLC prior to derivatization, as described previously (2).

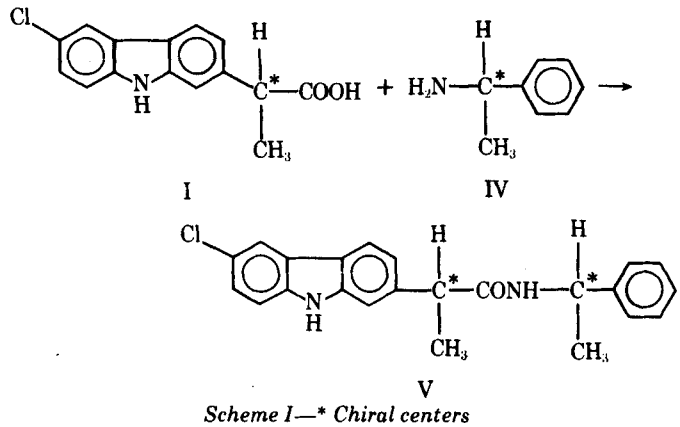

Scheme I— Chiral centers*

Materials—*^{14}C-Carprofen* (*I*)—$C_{15}H_{12}ClNO_2$, mol. wt. 273.72. A stock solution of 1 mg/ml of ethanol was prepared. The original specific activity of the ^{14}C-labeled compound[2] of 9.91 μCi/mg was diluted in solution with appropriate amounts of unlabeled compound.

Table III—^{14}C-Carprofen Enantiomer Ratio in Pooled Rat Bile Specimen

^{14}C-Carprofen Specimen	^{14}C-Carprofen Reacted, μg	(S)(+), μg	(R)(−), μg	S(+)/R(−) Ratio
Standard added to rat bile	23.2	4.52	4.55	0.99
		6.04	5.72	1.06
Rat bile extract (see text)	14.52	2.26	4.48	0.510
		2.43	4.70	0.517
	29.04	4.84	8.89	0.540
		4.65	8.30	0.560
Mean ± *SD*				0.532 ± 0.023

[2] The labeled carprofen was synthesized by Dr. A. Liebman and Dr. R. Muccino of the Roche Department of Chemical Research.

Table IV—Secretion in the Bile of Total ^{14}C-Carprofen Ester Glucuronide and of Its (*S*)(+)- and (*R*)(−)-Enantiomers in Four Male Rats (Pooled Hourly Bile Fractions)

Biliary Fraction	0–1 hr		1–2 hr		2–3 hr		3–4 hr	
	Per Hour[a]	Cumulative[b]	Per Hour[a]	Cumulative[b]	Per Hour[a]	Cumulative[b]	Per Hour[a]	Cumulative[b]
Total ^{14}C	14.40	14.40	12.30	26.7	9.45	36.15	7.55	43.70
Total ^{14}C-carprofen glucuronide	5.76	5.76	4.37	10.13	3.07	13.2	2.34	15.54
Hydroxy metabolites, conjugates plus polar components[c]	8.64	8.64	7.93	16.57	6.38	22.95	5.21	28.16
Ratio of carprofen (*S*)(+)/(*R*)(−)	0.46	—	0.56	—	0.69	—	0.81	0.58[d]
(*R*)(−)-Enantiomer	3.94	3.94	2.80	6.74	1.82	8.56	1.29	9.84
(*S*)(+)-Enantiomer	1.81	1.81	1.57	3.37	1.25	4.62	1.05	5.70
Excess (*R*)(−) [(*R*)(−) minus (*S*)(+)]	2.13	2.13	1.23	3.37	0.57	3.92	0.24	4.14

[a] Percent of dose per hour. [b] Cumulative percent of dose. [c] Unidentified polar component (after conjugate cleavage) represents ~20% of this fraction. [d] Calculated (*S*)(+)/(*R*)(−) ratio for 0–4-hr bile pool.

(S)(+)-*Enantiomer*—$C_{15}H_{12}ClNO_2$, mol. wt. 273.72, specific rotation in methanol $[\alpha]_D^{23}$ +53.7°.

(R)(−)-*Enantiomer*—$C_{15}H_{12}ClNO_2$, mol. wt. 273.72, specific rotation in methanol $[\alpha]_D^{23}$ −54.2°.

l-(−)-α-*Methylbenzylamine* (*IV*)—$C_8H_{11}N$, mol. wt. 121.18, bp 187°.

1,1′-Carbonyldiimidazole—$C_7H_6N_4O$, mol. wt. 162.15, mp 118–120°.

Solvent—A solution of 65 mg/ml of chloroform (stabilized with 0.75% ethanol) was prepared daily and was stable for 24–48 hr.

Reagents—The following reagent grade compounds were used: 6 *N* NaOH; 4 *N* HCl; pH 5 acetate buffer, 1 and 0.2 *M*; acetic acid; formic acid; methanol; ethanol (anhydrous); chloroform (stabilized); benzene; and ether (anhydrous).

TLC—TLC plates were precoated with silica gel 60 F-254[3]. Filter paper[4] was used for lining the TLC tanks. A shortwave UV lamp was used for visualization of spots on the TLC plates.

Derivatization—^{14}C-Carprofen standards (specific activity 0.5 μCi/mg) were processed with each series of unknowns in duplicate at 5 and 10 μg. The reaction was performed in 15-ml conical glass-stoppered centrifuge tubes. To the dried residues of the standards and the unknowns, 0.1 ml of the 1,1′-carbonyldiimidazole solution was added. Each tube was rotated to permit the reactant to contact the residue completely. The mixture was allowed to react at room temperature for 5 min; then 10 μl of acetic acid was added, and the solution was mixed. *l*-(−)-α-Methylbenzylamine, 50 μl, was added; then the solution was mixed well in the supermixer, centrifuged briefly to concentrate it at the tip of the tube, and allowed to react at room temperature for 20 min.

After completion of the reaction, 5 ml of ether and 3 ml of 0.2 *M* acetate buffer (pH 5) were added. The tubes were stoppered tightly, shaken for 10 min in a reciprocating shaker, and centrifuged for 5 min. As much ether as possible was transferred to a 15-ml conical centrifuge tube. The extraction was repeated with 5 ml of ether, which was combined with the previous extract and evaporated to dryness under nitrogen in a 30–40° water bath. The walls were rinsed, and the derivative was brought to the tip of the tube with 200 μl of ethanol. The solvent was evaporated, and the residue was dried thoroughly for 5 min in a desiccator under vacuum. The residue was redissolved in exactly 200 μl of ethanol, and duplicate 10-μl aliquots were counted.

Diastereomeric Derivative Quantitation—An aliquot of 50 or 100 μl was applied as a streak, 2–2.5 cm wide, on a precoated silica gel 60 F-254 plate (10 × 20 cm; two samples per plate). The solvent system was benzene–ether–methanol (60:35:5). The TLC tank was lined with solvent-soaked filter paper to achieve solvent saturation of the atmosphere. The solvent was allowed to ascend a distance of 14 cm from the origin to the front. The plate was examined under a shortwave UV lamp, and the absorbing bands corresponding to the diastereomeric methylbenzylamide derivatives (III) of the dextrorotatory (*S*)(+)-enantiomer at $R_f \simeq 0.36$ and the levorotatory (*R*)(−)-enantiomer at $R_f \simeq 0.41$ (carprofen R_f is

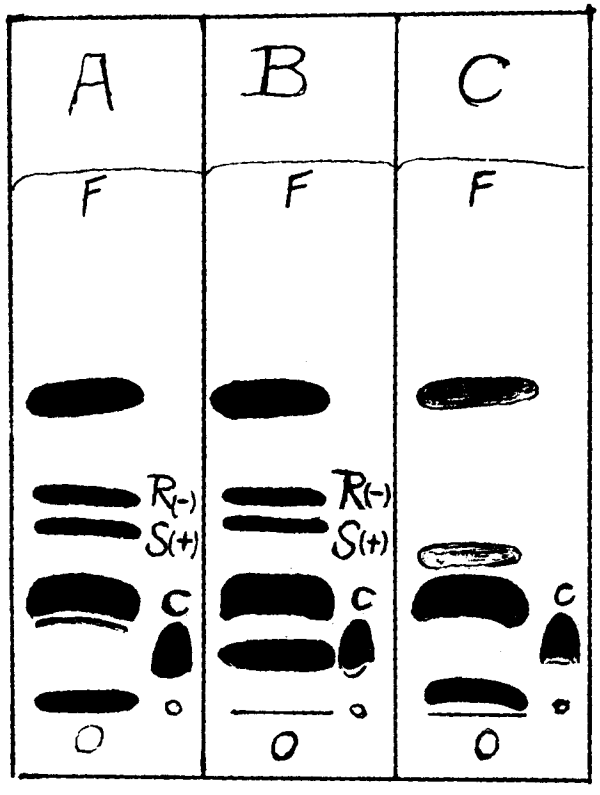

Figure 1—*TLC separation of the* (S)(+)- (R_f *0.47*) *and* (R)(−)- (R_f *0.55*) *diastereomeric* l-(−)-α-*methylbenzylamides of carprofen excreted in human urine. Key: A and B, duplicate aliquot of reaction mixture extract; C, control product; F, solvent front; O, origin; and c, carprofen standard.*

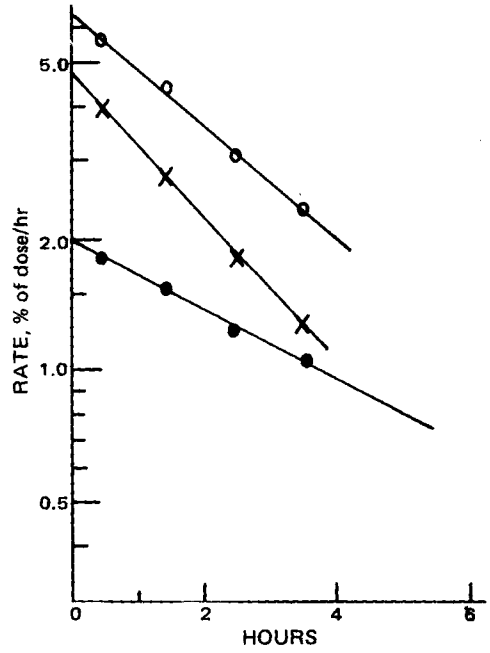

Figure 2—*Secretion of* ^{14}C-*DL-carprofen ester glucuronide* (O) *and of its individual* (S)(+)- (●) *and* (R)(−)- (×) *enantiomers. The dose was 3 mg/kg iv, measured in pooled bile from four male rats.*

[3] Brinkmann Instruments.
[4] Whatman No. 1.

Table V—Secretion in the Bile of Total ^{14}C, of ^{14}C-Carprofen Ester Glucuronide, and of Its (*S*)(+)- and (*R*)(−)-Enantiomers in Rat 1

Biliary Fraction	0–1 hr		1–2 hr		2–3 hr		3–4 hr		4–5 hr		5–6 hr	
	Per Hour[a]	Cumulative[b]	Per Hour[a]	Cumulative[b]	Per Hour[a]	Cumulative[b]	Per Hour[a]	Cumulative[b]	Per Hour[a]	Cumulative[b]	Per Hour[a]	Cumulative[b]
Total ^{14}C	11.3	11.3	12.1	23.4	8.6	32.0	7.6	39.6	6.1	45.7	4.80	50.5
Total ^{14}C-carprofen glucuronide	4.56	4.56	3.98	8.54	2.68	11.22	1.95	13.17	1.39	14.56	1.09	15.65
Hydroxy metabolites, conjugates plus polar component[c]	6.74	6.74	8.12	14.86	5.92	20.78	5.65	26.43	4.71	31.14	3.71	34.85
Ratio of carprofen (*S*)(+)/(*R*)(−)	0.430		0.517		0.618		0.723		0.842		0.854	0.575[d]
(*R*)(−)-Enantiomer	3.19	3.19	2.62	5.81	1.66	7.47	1.13	8.60	0.755	9.35	0.588	9.93
(*S*)(+)-Enantiomer	1.37	1.37	1.36	2.73	1.02	3.75	0.82	4.57	0.635	5.21	0.502	5.71
Excess (*R*)(−) [(*R*)(−) minus (*S*)(+)]		1.79		3.06		3.69		4.02		4.14		4.22

[a] Percent of dose per hour. [b] Cumulative percent of dose. [c] Unidentified polar component (after conjugate cleavage) represents ~20% of this fraction. [d] Calculated (*S*)(+)/(*R*)(−) ratio for 0–6-hr bile pool.

0.18) were traced. Each band was scraped, and the scrapings were transferred to a counting vial; 2 ml of water plus 10 ml of counting cocktail solution[5] was added. Quantitation was by scintillation counting.

RESULTS AND DISCUSSION

Stereospecific Carprofen Assay—The linearity of the reaction and the relative reactivity of the two enantiomers were determined by directly reacting standard amounts of ^{14}C-carprofen, ranging from 2.43 to 19.46 μg of a specific activity of 1000 dpm/μg. The data presented in Table I indicate that the combined yield of the two disastereomeric derivatives was reproducible and ranged from 64 to 80%. When these standards of racemic ^{14}C-carprofen were reacted, the (*S*)(+)/(*R*)(−) ratio had a mean value of 1.009 (± 0.05 *SD*) for $n = 50$. For a 95% confidence level, the confidence limits for the (*S*)(+)/(*R*)(−) value were 0.91 and 1.11. This finding suggests equal reactivity of the two enantiomers. Doubling the *l*-(−)-α-methylbenzylamine concentration and the reaction time did not significantly increase the yield, indicating that the low yields were probably due to side-product formation rather than to incompleteness of the reaction.

Identical results were obtained with internal ^{14}C-carprofen standards added to control bile in the range 22–45 μg/0.5 ml and subjected to the alkaline condition for conjugate cleavage prior to extraction (Table II).

The separated diastereomers on the chromatogram were identified by separately derivatizing the unlabeled (*S*)(+)-enantiomer and the (*R*)(−)-enantiomer, along with the labeled racemate, and by cochromatographing the three products. The (*S*)(+)-derivative moved with the R_f 0.35 component, and the (*R*)(−)-derivative moved with the R_f 0.41 component.

Of a number of TLC solvent systems, benzene–ether–methanol (60:35:5), producing sharp and minimally trailing bands, appeared to give the best separation and the enantiomer ratios closest to unity (Fig. 1).

By extraction from the reaction mixtures with ether at pH 5, the methylbenzylamide derivatives (III) were quantitatively separated in sufficient purity for good TLC separation. Coextracted labeled side products did not interfere because of their much lower R_f value in this system. Attempts to remove putative remaining acidic material by an alkaline backwash of the ether extract proved not to be advantageous.

Good reaction yields and products could be achieved directly with carprofen extracted from bile after alkaline ester cleavage without further TLC purification. In the present study, however, all carprofen samples obtained from biological materials were purified routinely by preparative TLC prior to reacting to avoid unpredictable interference by coextracted material with the reaction and with the TLC diastereomer separation. Contamination by moisture and buffer salts accidentally transferred during the carprofen extraction into the ether interfered with the chemical reaction and led to the formation of polar reaction products.

In the described TLC assay, the sensitivity can be improved by increasing the specific activity of the labeled carprofen. By adding and coprocessing 10 μg of unlabeled carprofen as a carrier, the diastereomer detection on the TLC plate was facilitated without affecting the original enantiomer ratio that was measured radiometrically. For a specific activity of 1000 dpm/μg (0.5 μCi/mg) of ^{14}C-carprofen, the minimum amount of the compound that could be analyzed with accuracy was 0.6–1.0 μg, depending on the prevailing enantiomer ratio. To see clearly the diastereomer bands on the plate, at least 1.5 μg of total carprofen had to be reacted.

[5] Aquasol counting cocktail, New England Nuclear Corp., Boston, Mass.

Stereoselective Disposition of ^{14}C-D,L-Carprofen in Rats—In the rat, 80% of an intravenous carprofen dose (2) was eliminated by biliary secretion; the ester glucuronide of carprofen and the ethereal glucuronides of two phenolic metabolites represented the main biliary secretion products.

In an exploratory experiment, a specimen of ^{14}C-carprofen obtained by alkaline cleavage of the ester glucuronide and extraction from pooled 0–4-hr rat bile was analyzed. This bile originated from an experiment in which 5 mg of radioactive compound/kg (specific activity of 0.5 μCi/mg) had been injected into a group of male rats. The (*S*)(+)/(*R*)(−) ratio of this pooled bile specimen was 0.53 [35% (*S*)(+) and 65% (*R*)(−)], indicating a strong stereoselective effect (Table III).

To study this relative increase of the (*R*)(−)-enantiomer in bile as a function of time, consecutive hourly bile specimens that had been collected for 4 hr after dosing and pooled from four rats were examined. These young male rats (Charles River, 300–320 g) had received 3 mg of ^{14}C-carprofen/kg iv (specific activity of 0.5 μCi/mg). The relative amount of carprofen ester glucuronide secreted and the distribution of its enantiomers in the consecutive biliary fractions are listed in Table IV.

Calculating from these data the percentages of each enantiomer se-

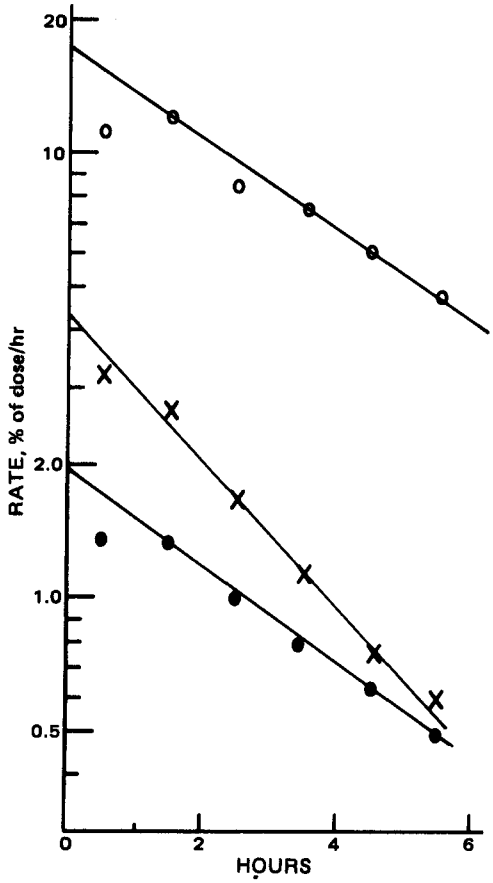

Figure 3—*Biliary secretion in Rat 1 of ^{14}C-DL-carprofen ester glucuronide* (O) *and of its individual* (S)(+)- (●) *and* (R)(−)- (×) *enantiomers. The dose was 3 mg/kg iv.*

Table VI—Secretion in the Bile of Total ^{14}C, of ^{14}C-Carprofen Ester Glucuronide, and of Its (*S*)(+)- and (*R*)(−)-Enantiomers in Rat 2

Biliary Fraction	0–1 hr		1–2 hr		2–3 hr		3–4 hr		4–5 hr		5–6 hr	
	Per Hour[a]	Cumulative[b]	Per Hour[a]	Cumulative[b]	Per Hour[a]	Cumulative[b]	Per Hour[a]	Cumulative[b]	Per Hour[a]	Cumulative[b]	Per Hour[a]	Cumulative[b]
Total ^{14}C	12.8	12.8	12.7	25.5	9.4	34.9	7.3	42.2	5.7	47.9	4.4	52.3
Total ^{14}C-carprofen glucuronide	8.46	8.46	7.53	15.99	4.88	20.87	3.3	24.20	2.24	26.44	1.55	27.99
Hydroxy metabolites, conjugates plus polar component[c]	4.34	4.34	5.17	9.51	4.52	14.03	3.97	18.0	3.46	21.46	2.85	24.31
Ratio of carprofen (*S*)(+)/(*R*)(−)	0.494		0.612		0.718		0.858		0.994		1.083	0.66[d]
(*R*)(−)-Enantiomer	5.67	5.67	4.67	10.34	2.84	13.18	1.80	14.98	1.11	16.09	0.75	15.84
(*S*)(+)-Enantiomer	2.79	2.79	2.86	5.65	2.04	7.69	1.56	9.25	1.10	10.35	0.80	11.15
Excess (*R*)(−) [(*R*)(−) minus (*S*)(+)]		2.88		4.69		5.49		5.75		5.74		5.69

[a] Percent of dose per hour. [b] Cumulative percent of dose. [c] Unidentified polar component (after conjugate cleavage) represents ~20% of this fraction. [d] Calculated (*S*)(+)/(*R*)(−) ratio for 0–6-hr bile pool.

Table VII—Blood Levels and Elimination Rates of ^{14}C-D,L-Carprofen and Its Enantiomers in Rats

Rat	Hours	D,L-, μg/ml	Calc.[a]	(*S*)(+)/(*R*)(−) Ratio	(*S*)(+) Found, μg/ml	Calc.[a]	Percent Dose[b] Eliminated per Hour	(*R*)(−) Found, μg/ml	Calc.[a]	Percent Dose[b] Eliminated per Hour
1	0	—	11.40			5.83			5.74	
	1	9.81	9.53	1.143	5.23	5.11	6.17	4.58	4.45	11.24
	2	7.48	7.97	1.29	4.21	4.48	5.42	3.27	3.46	8.62
	3		6.69			3.94	4.62		2.721	6.45
	4	5.88	5.57	1.70	3.70	3.45	4.21	2.18	2.10	5.48
	5		4.72			3.04	3.52		1.643	3.92
	6	3.82	3.90	2.09	2.58	2.66	3.26	1.24	1.26	3.31
	k		0.179			0.131	0.131		0.253	0.247
	r^{2} [c]		0.992			0.980	0.996		0.997	
2	0		11.18			5.98			5.36	
	1	8.66	8.70	1.21	4.74	4.88	9.20	3.92	3.84	14.18
	2	6.67	6.67	1.52	4.02	3.99	7.44	2.65	2.75	10.17
	3		5.31			3.27	6.02		2.00	6.99
	4	4.27	4.10	1.95	2.82	2.66	5.10	1.45	1.41	5.51
	5		3.22			2.18	4.01		1.03	3.54
	6	2.42	2.48	2.39	1.71	1.77	3.43	0.72	0.73	2.84
	k		0.251	0.248		0.200	0.199		0.330	0.327
	r^{2} [c]		0.999			0.985	0.999		0.999	0.997

[a] $c = c_0e^{-kt}$, where c = blood level at time t, and c_0 = blood level at zero time. [b] Rate (percent dose per hour) = $(c_{n-1} - c_n)/c_0 \times 50$, where n = 1, 2, 3, 4, 5, and 6 hr, and c_n = blood level (micrograms per milliliter) at time n. [c] r^2 = multiple correlation coefficient.

Table VIII—Pharmacokinetic Parameters of Optically Selective Elimination of ^{14}C-D,L-Carprofen in Rats

Parameter	Rat 1				Rat 2			
	Total Carprofen	(*S*)(+)	(*R*)(−)	(*R*)(−)/(*S*)(+) Ratio	Total Carprofen	(*S*)(+)	(*R*)(−)	(*R*)(−)/(*S*)(+) Ratio
Biliary secretion								
k[a]	0.304	0.246	0.376	1.53	0.394	0.314	0.460	1.46
$t_{1/2}$	2.28	2.81	1.84	0.655	1.76	2.21	1.51	0.683
c_0	6.63	1.92	4.34	2.26	16.19	4.75	9.14	1.92
r^{2} [b]	0.995	0.994	0.994		0.996	0.999	0.999	
Blood elimination								
k[c]	0.174	0.131	0.248	1.89	0.247	0.199	0.327	1.64
$t_{1/2}$	3.98	5.29	2.81	0.53	2.78	3.48	2.12	0.61
c_0	17.67	6.55	12.50	1.91	24.8	10.1	17.0	1.68
r^2	0.991	0.996	0.997		0.992	0.999	0.997	
k bile/k blood elimination	1.75	1.88	1.52		1.60	1.58	1.41	

[a] Expressed as percent per hour. [b] Multiple correlation coefficient. [c] Blood level fall-off or elimination rate (percent per hour).

creted per hour and plotting the logarithms of these rates against time produced a linear fall-off curve (Fig. 2). The initially higher secretion rate of (*R*)(−)-ester glucuronide declined faster and approached the initially lower but more slowly declining secretion rate of the (*S*)(+)-enantiomer by the end of 4 hr. Furthermore, the data (Table IV) indicate that a 4.12% excess of the (*R*)(−)-enantiomer over the (*S*)(+)-enantiomer had been excreted during the 4-hr period.

This finding suggested the accumulation (retention) of a complementary amount of the (*S*)(+)-enantiomer during the same period and the development of an (*S*)(+)/(*R*)(−) ratio greater than unity in some other compartments, possibly in the plasma. Analysis of the carprofen fraction of a 4-hr plasma pool from the same four rats verified this conclusion, showing an (*S*)(+)/(*R*)(−)-enantiomer ratio of 2.24.

This change of the blood level ratio of the two carprofen enantiomers with time, together with the concurrent secretion rate of the enantiomeric ester glucuronides in the bile, was studied in two individual rats. Following bile duct cannulation, two male rats (200–300 g) were injected with 3 mg of D,L-^{14}C-carprofen/kg iv (specific activity of 2.5 μCi/mg) and were kept under continuous anesthesia (40 mg of pentobarbital sodium/kg) at controlled body temperature for 6 hr. Blood specimens of 0.4–0.6 ml were obtained at 1, 2, and 4 hr by tail clipping, in addition to a large terminal 6-hr specimen; bile was collected in six hourly fractions.

The biliary secretion data from both rats (Tables V and VI) and the semilogarithmic plots of the biliary secretion rates *versus* time (Figs. 3 and 5) were consistent with the results from the pooled rat specimens (Table IV and Fig. 2). In both rats, practically the same percentages of the dose were recovered as total biliary carbon 14. The fractions secreted as ^{14}C-carprofen glucuronide differed, being much higher in Rat 2 than in Rat 1. With it, a larger excess of (*R*)(−)-enantiomer was secreted by Rat 2.

The blood levels of (*S*)(+)- and (*R*)(−)-enantiomers (Table VII) of intact carprofen, when plotted semilogarithmically *versus* time (Figs.

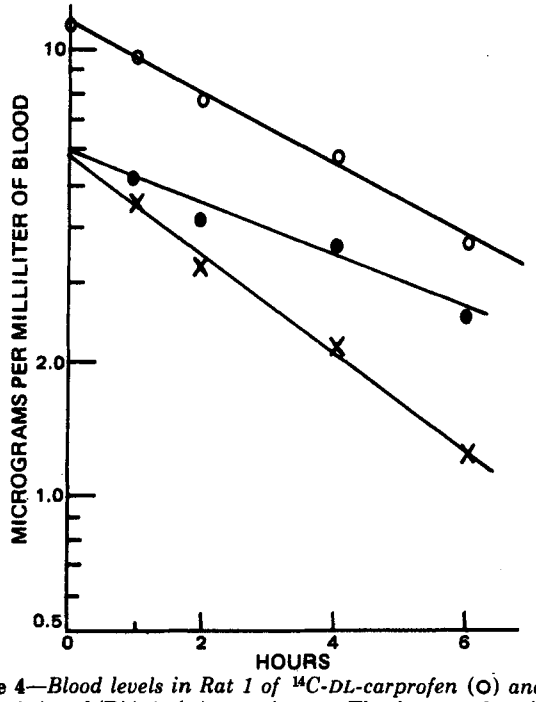

Figure 4—*Blood levels in Rat 1 of ^{14}C-DL-carprofen* (○) *and of its* (S)(+)- (●) *and* (R)(−)- (×) *enantiomers. The dose was 3 mg/kg iv.*

4 and 6), declined linearly. The elimination rate constants estimated for Rats 1 and 2 were higher for the (*R*)(−)-enantiomer than for the (*S*)-(+)-enantiomer by factors of 1.93 and 1.64, respectively.

If it is assumed that the distribution volume of intact free carprofen enantiomers remained constant over the experimental period, the blood level data can be characterized as elimination (disappearance) rates for each enantiomer, expressed as percent dose per hour (Table VII).

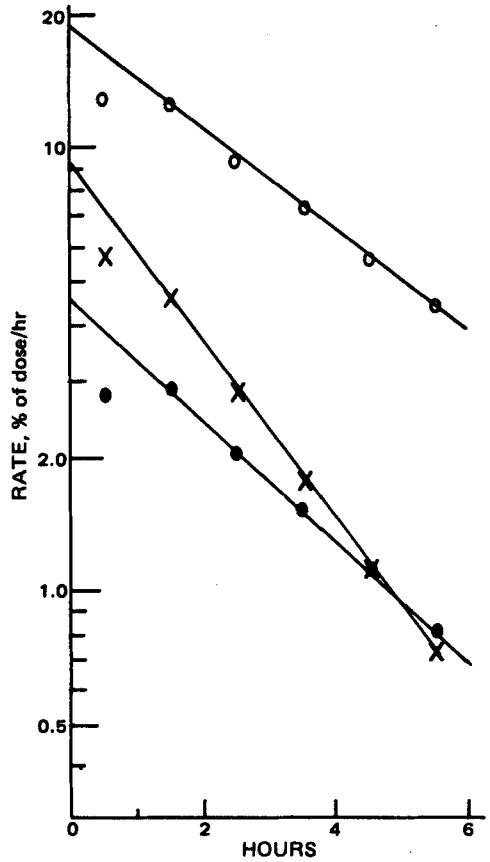

Figure 5—*Biliary secretion in Rat 2 of ^{14}C-carprofen ester glucuronide* (○) *and of its individual* (S)(+)- (●) *and* (R)(−)- (×) *enantiomers. The dose was 3 mg/kg iv.*

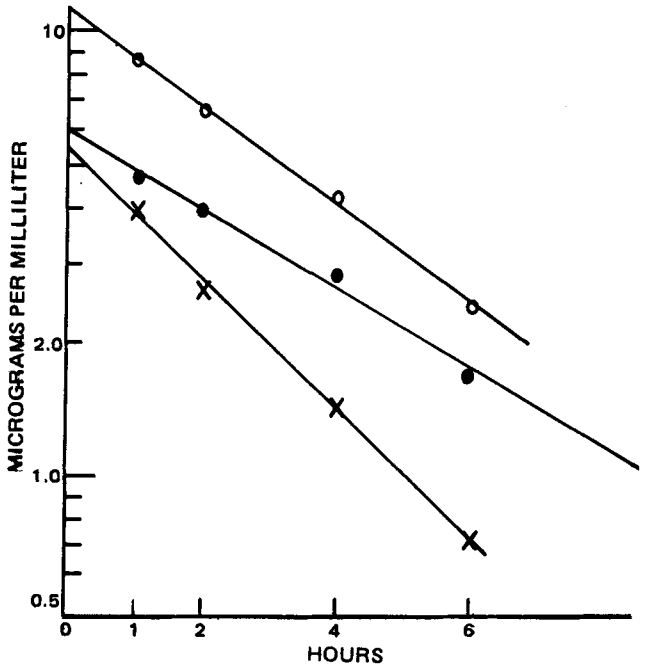

Figure 6—*Blood levels in Rat 2 of ^{14}C-DL-carprofen* (○) *and of its* (S)(+)- (●) *and* (R)(−)- (×) *enantiomers. The dose was 3 mg/kg iv.*

These elimination rate values for the (*R*)(−)- and (*S*)(+)-enantiomers in blood, when compared with the corresponding rates of biliary secretion of each enantiomer as the ester glucuronides (Tables V and VI), indicate that the excess (*R*)(−)-enantiomer secreted in the bile can account for only a fraction of the (*R*)(−)-excess eliminated from the blood during the same period. Based on an overall balance of both enantiomers, it can be estimated that ~64% of the (*R*)(−)-excess eliminated from the blood in Rat 1 was removed by an additional stereospecific process compared to ~37% in Rat 2, a difference that is related to the lower percentage secreted as the ester glucuronide of carprofen by Rat 1 as compared to Rat 2 (Tables V and VI). Evidence for an additional selective process is of interest in view of the reports of a metabolic chiral inversion of the (*R*)(−)- to the (*S*)(+)-enantiomer occurring in certain analogous compounds (3–6). While the data leave several possibilities open for such an additional process, including selective biotransformation, tissue uptake, and excretion, a chiral inversion process in which the (*R*)(−) is transformed to (*S*)(+)-enantiomer remains as a possibility equally compatible with the present data.

The pharmacokinetic constants derived from the data of the two rat experiments are presented in Table VIII. In both rats, the ratios of the (*R*)(−) to the (*S*)(+) rate constants for the elimination from blood and for the secretion into the bile are similar, ranging from 1.5 to 1.9. In both rats, however, the blood elimination constants for both enantiomers are significantly and consistently lower than the corresponding constants for biliary ester glucuronide secretion. This finding suggests that carprofen elimination from the blood into the bile as the ester glucuronide is a complex nonlinear process. The data at hand, therefore, do not permit a quantitative analysis of the elimination kinetics, nor do they allow quantitative predictions concerning other processes not directly measured but postulated from the data.

The main pharmacological conclusion from these stereoselective metabolic studies in the rat is that the biologically active (*S*)(+)-enantiomer is eliminated more slowly than the inactive (*R*)(−)-enantiomer and that, therefore, the half-life of the entity that counts pharmacologically is longer than that obtained when measuring total carprofen by a nonselective standard assay procedure.

The validity of this observation in respect to the disposition of this drug in humans and the possible effect of other stereoselective pathways on overall carprofen disposition in the rat and other species will be studied.

REFERENCES

(1) Z. N. Gaut, H. Baruth, L. O. Randall, C. Ashley, and J. R. Paulsrud, *Prostaglandins*, **10**, 59 (1975).

(2) F. Rubio, S. Seawall, B. Koechlin, and R. Pocelinko, *Fed. Proc.*,

37, 605 (1978).
(3) C. V. Puglisi, J. C. Meyer, and J. A. F. de Silva, *J. Chromatogr.*, **136**, 391 (1977).
(4) P. Jenner and B. Testa, *Drug Metab. Rev.*, **2**, 117 (1973).
(5) S. J. Lan, K. J. Kripalani, A. V. Dean, P. Egli, L. T. Difazio, and E. C. Schreiber, *Drug Metab. Dispos.*, **4**, 330 (1976).
(6) W. J. Wechter, R. J. Reischer, D. G. Loughhead, G. J. Van Giessen, and D. Kaiser, *Natl. Med. Chem. Symp.*, **14**, 91 (1974).
(7) G. J. Van Giessen and D. G. Kaiser, *J. Pharm. Sci.*, **64**, 798 (1975).
(8) W. J. Wechter, D. G. Loughhead, R. J. Reischer, G. J. Van Giessen, and D. G. Kaiser, *Biochem. Biophys. Res. Commun.*, **61**, 833 (1974).
(9) D. G. Kaiser, G. J. Van Giessen, R. J. Reischer, and W. J. Wechter, *J. Pharm. Sci.*, **65**, 269 (1976).
(10) D. G. Kaiser and G. J. Van Giessen, *ibid.*, **63**, 219 (1974).
(11) J. M. Kemmerer, B. A. Koechlin, and F. A. Rubio, *Fed. Proc.*, **37**, 605 (1978).

ADS-12: An Automated Programmable 12-Tablet Dissolution Testing System

F. J. CIOFFI ˣ, S. MARTYNOVYCH, and H. BENDROT *

Received June 30, 1978, from *E. R. Squibb & Sons, Inc., New Brunswick, NJ 08903.* Accepted for publication April 17, 1979. *Present address: Computer Mart, Iselin, N.J.

Abstract □ A novel computerized automated system is described which conforms to the basic requirements set forth in the compendia for testing the dissolution characteristics of solid dosage forms. This modular system can test 12 tablets simultaneously. It can maintain sink conditions at all times and can handle any chemistry amenable to an automatic analyzer. Dissolution, sampling, chemistry, and readout are all accomplished simultaneously, reducing the complete test time for 12 tablets to the dissolution time itself.

Keyphrases □ Dissolution testing systems—automated programmable 12-tablet system □ Automated testing—dissolution testing system, automated, programmable, 12 tablet

In recent years, investigation of dissolution rates of solid dosage forms has become of prime importance to the pharmaceutical industry, due in part to the commitment by the Food and Drug Administration (FDA) to assure the bioavailability of active drugs from their various dosage forms. In a few cases, the FDA has already shown a correlation between *in vitro* dissolution results and *in vivo* bioavailability.

Dissolution testing can serve also as an important criterion of the effects of different constituents in drug formulations. In manufacturing, it can be useful for determining uniformity within and between different production batches. The USP considers this latter use to be so important that its 1980 revision will require a dissolution test for all tablet and capsule dosage forms. Guidelines for establishing dissolution requirements for oral solid dosage forms have been established already and are available from the USP.

BACKGROUND

Due to the increased testing workload that will result from this new USP requirement, many pharmaceutical companies have begun automating dissolution testing. Multiple automated dissolution testing apparatus have also been developed (1–3) and were reviewed critically in a previous paper (4), which pointed out that none of them met the requirements of a truly versatile, completely automated multiple dissolution testing system. The ADS-6 (4) (computerized six-tablet automatic dissolution testing system), which was developed in this laboratory in 1972, incorporates the USP-recommended dissolution apparatus (either the basket or paddle) and can test six tablets simultaneously. Unlike other systems, it is completely automated from tablet introduction to final readout of the raw data on punched paper tape. In addition, this system maintains sink conditions[1] at all times and performs any type of chemistry amenable to the automated analyzer. The raw data are computer analyzed in minutes, and final results are presented as a complete tabular report, a graphical dissolution profile, or both.

The ADS-12 has all of the features of the ADS-6, but it can test 12 tablets from one lot simultaneously, which is important in view of the latest USP requirement, or two different lots of six tablets each.

EXPERIMENTAL

Description of ADS-12—The ADS-12 is modular with seven functional components (Fig. 1).

Dual Six-Spindle Dissolution–Water Bath Assemblies[2] (*a*)—These assemblies contain the sample tablets in wire mesh baskets immersed in the dissolution flasks (USP Method I) or directly in the dissolution flasks (USP Method II). Basket rotation speeds are variable from 25 to 250 rpm. The bath temperature is maintained at 37°.

12-Channel Peristaltic Pump[3] (*b*)—The peristaltic pump has a pumping range of 0–50 ml/min. Each channel services a single dissolution kettle in the bath assembly. Silicone tubing is used to circulate liquid from the kettle continuously past the solenoid sampling valve assembly and to return it to the original kettle. In effect, a continuous sampling loop is formed.

If "induced" sink conditions are necessary due to very low solubility of the drug in the solvent used, then a second 12-channel pump is incorporated into the system. In this case, one pump continuously removes solution from the dissolution kettles at the proper rate while the second pump pumps fresh solvent back into the dissolution kettles at the same rate, thereby maintaining constant volume and sink conditions in the kettles.

Solenoid Sampling Valve Assembly[4] (*c*)—The valve assembly consists of 16 solenoid valves arranged in four blocks of four valves each. Three of the four valves per valve block are used in sampling the liquid from the dissolution kettles; the fourth valve is used for inserting an air segment between each liquid sample. The solenoid valves are of a single-channel design whereby the liquid sample passes from the sample loop *via* the T-connections, flows through the valve block into a five-pronged cross fitting, and finally flows to the sample pump tube of the automated chemistry system. The solenoid valves are operated automatically by an electrical signal put out by the system controller.

Figure 2 is a schematic view of two of the four solenoid valve blocks, showing the T-connections and the electrical hookup of the solenoid valves to the terminal bar. The solenoid valves are connected *via* this terminal bar to a circuit-indicating light box, which presents a visual

[1] Defined as never allowing the drug concentration in the dissolution flask to exceed 10–20% of saturation.
[2] Model QC-72R, Hanson Research Corp., Northridge, Calif.
[3] Model 7555-20 standard Ultramasterflex drive system, Cole-Parmer Co., Chicago, Ill.
[4] Catalog No. 18-4, General Valve Corp., East Hanover, N.J.

0022-3549/79/1000-1280$01.00/0
© 1979, American Pharmaceutical Association

37, 605 (1978).
(3) C. V. Puglisi, J. C. Meyer, and J. A. F. de Silva, *J. Chromatogr.*, **136**, 391 (1977).
(4) P. Jenner and B. Testa, *Drug Metab. Rev.*, **2**, 117 (1973).
(5) S. J. Lan, K. J. Kripalani, A. V. Dean, P. Egli, L. T. Difazio, and E. C. Schreiber, *Drug Metab. Dispos.*, **4**, 330 (1976).
(6) W. J. Wechter, R. J. Reischer, D. G. Loughhead, G. J. Van Giessen, and D. Kaiser, *Natl. Med. Chem. Symp.*, **14**, 91 (1974).
(7) G. J. Van Giessen and D. G. Kaiser, *J. Pharm. Sci.*, **64**, 798 (1975).
(8) W. J. Wechter, D. G. Loughhead, R. J. Reischer, G. J. Van Giessen, and D. G. Kaiser, *Biochem. Biophys. Res. Commun.*, **61**, 833 (1974).
(9) D. G. Kaiser, G. J. Van Giessen, R. J. Reischer, and W. J. Wechter, *J. Pharm. Sci.*, **65**, 269 (1976).
(10) D. G. Kaiser and G. J. Van Giessen, *ibid.*, **63**, 219 (1974).
(11) J. M. Kemmerer, B. A. Koechlin, and F. A. Rubio, *Fed. Proc.*, **37**, 605 (1978).

ADS-12: An Automated Programmable 12-Tablet Dissolution Testing System

F. J. CIOFFI ˣ, S. MARTYNOVYCH, and H. BENDROT *

Received June 30, 1978, from *E. R. Squibb & Sons, Inc., New Brunswick, NJ 08903.* Accepted for publication April 17, 1979. *Present address: Computer Mart, Iselin, N.J.

Abstract □ A novel computerized automated system is described which conforms to the basic requirements set forth in the compendia for testing the dissolution characteristics of solid dosage forms. This modular system can test 12 tablets simultaneously. It can maintain sink conditions at all times and can handle any chemistry amenable to an automatic analyzer. Dissolution, sampling, chemistry, and readout are all accomplished simultaneously, reducing the complete test time for 12 tablets to the dissolution time itself.

Keyphrases □ Dissolution testing systems—automated programmable 12-tablet system □ Automated testing—dissolution testing system, automated, programmable, 12 tablet

In recent years, investigation of dissolution rates of solid dosage forms has become of prime importance to the pharmaceutical industry, due in part to the commitment by the Food and Drug Administration (FDA) to assure the bioavailability of active drugs from their various dosage forms. In a few cases, the FDA has already shown a correlation between *in vitro* dissolution results and *in vivo* bioavailability.

Dissolution testing can serve also as an important criterion of the effects of different constituents in drug formulations. In manufacturing, it can be useful for determining uniformity within and between different production batches. The USP considers this latter use to be so important that its 1980 revision will require a dissolution test for all tablet and capsule dosage forms. Guidelines for establishing dissolution requirements for oral solid dosage forms have been established already and are available from the USP.

BACKGROUND

Due to the increased testing workload that will result from this new USP requirement, many pharmaceutical companies have begun automating dissolution testing. Multiple automated dissolution testing apparatus have also been developed (1–3) and were reviewed critically in a previous paper (4), which pointed out that none of them met the requirements of a truly versatile, completely automated multiple dissolution testing system. The ADS-6 (4) (computerized six-tablet automatic dissolution testing system), which was developed in this laboratory in 1972, incorporates the USP-recommended dissolution apparatus (either the basket or paddle) and can test six tablets simultaneously. Unlike other systems, it is completely automated from tablet introduction to final readout of the raw data on punched paper tape. In addition, this system maintains sink conditions[1] at all times and performs any type of chemistry amenable to the automated analyzer. The raw data are computer analyzed in minutes, and final results are presented as a complete tabular report, a graphical dissolution profile, or both.

The ADS-12 has all of the features of the ADS-6, but it can test 12 tablets from one lot simultaneously, which is important in view of the latest USP requirement, or two different lots of six tablets each.

EXPERIMENTAL

Description of ADS-12—The ADS-12 is modular with seven functional components (Fig. 1).

Dual Six-Spindle Dissolution–Water Bath Assemblies[2] (*a*)—These assemblies contain the sample tablets in wire mesh baskets immersed in the dissolution flasks (USP Method I) or directly in the dissolution flasks (USP Method II). Basket rotation speeds are variable from 25 to 250 rpm. The bath temperature is maintained at 37°.

12-Channel Peristaltic Pump[3] (*b*)—The peristaltic pump has a pumping range of 0–50 ml/min. Each channel services a single dissolution kettle in the bath assembly. Silicone tubing is used to circulate liquid from the kettle continuously past the solenoid sampling valve assembly and to return it to the original kettle. In effect, a continuous sampling loop is formed.

If "induced" sink conditions are necessary due to very low solubility of the drug in the solvent used, then a second 12-channel pump is incorporated into the system. In this case, one pump continuously removes solution from the dissolution kettles at the proper rate while the second pump pumps fresh solvent back into the dissolution kettles at the same rate, thereby maintaining constant volume and sink conditions in the kettles.

Solenoid Sampling Valve Assembly[4] (*c*)—The valve assembly consists of 16 solenoid valves arranged in four blocks of four valves each. Three of the four valves per valve block are used in sampling the liquid from the dissolution kettles; the fourth valve is used for inserting an air segment between each liquid sample. The solenoid valves are of a single-channel design whereby the liquid sample passes from the sample loop *via* the T-connections, flows through the valve block into a five-pronged cross fitting, and finally flows to the sample pump tube of the automated chemistry system. The solenoid valves are operated automatically by an electrical signal put out by the system controller.

Figure 2 is a schematic view of two of the four solenoid valve blocks, showing the T-connections and the electrical hookup of the solenoid valves to the terminal bar. The solenoid valves are connected *via* this terminal bar to a circuit-indicating light box, which presents a visual

[1] Defined as never allowing the drug concentration in the dissolution flask to exceed 10–20% of saturation.
[2] Model QC-72R, Hanson Research Corp., Northridge, Calif.
[3] Model 7555-20 standard Ultramasterflex drive system, Cole-Parmer Co., Chicago, Ill.
[4] Catalog No. 18-4, General Valve Corp., East Hanover, N.J.

0022-3549/79/1000-1280$01.00/0
© 1979, American Pharmaceutical Association

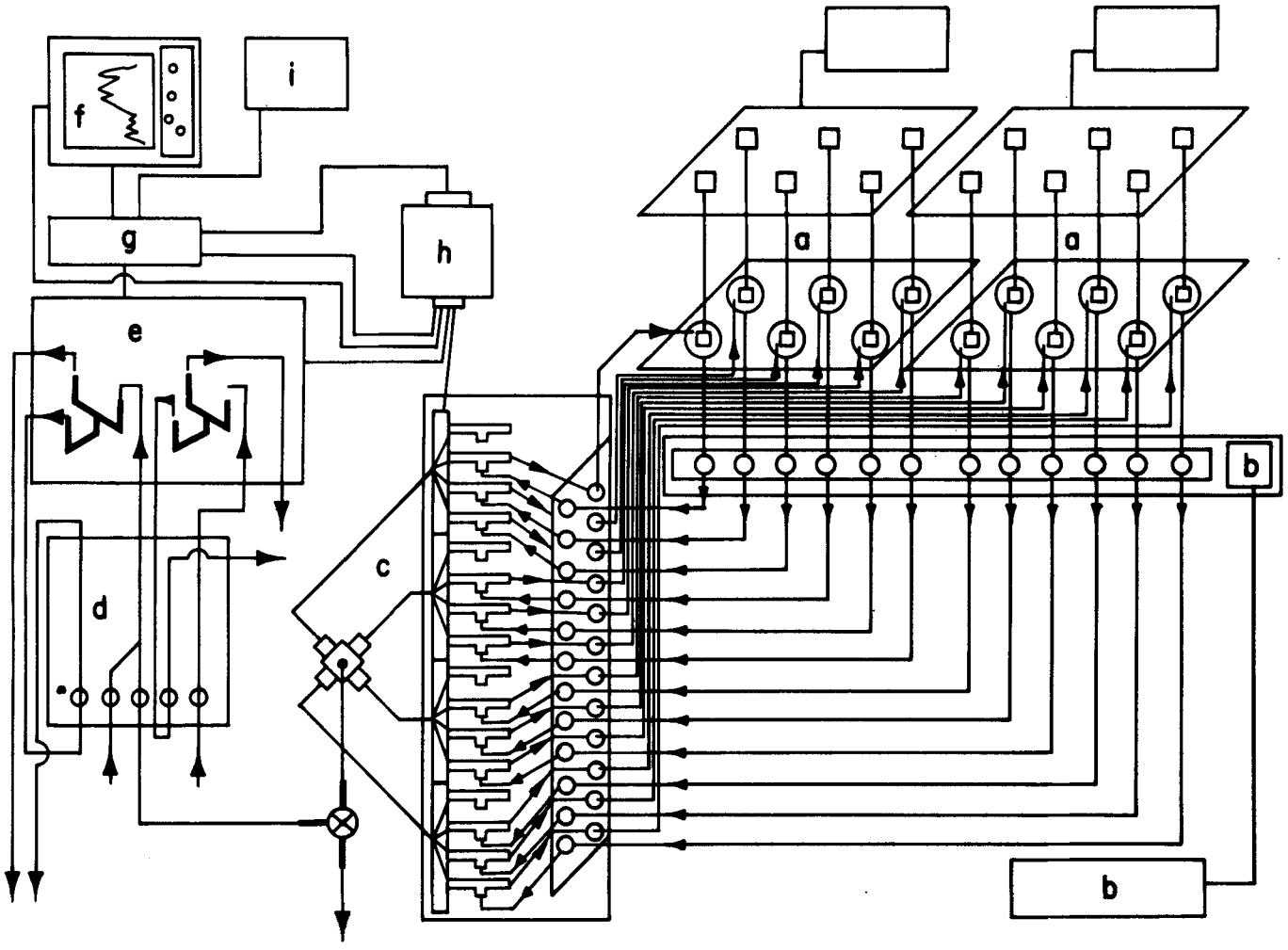

Figure 1—*Schematic diagram of ADS-12 system. Key: a, dissolution/water bath assemblies; b, 12-channel peristaltic pump; c, solenoid valve block assembly; d, proportioning pump/automated chemistry; e, double-beam UV–visible spectrophotometer; f, dual-pen recorder; g, controller; h, function indicating light box; and i, teletype.*

indication of what functions are being engaged at any time, *e.g.*, recorder pen activation or solenoid valve activation.

The center port of the five-port cross to which the four solenoid valve banks are attached leads to a three-way stopcock mounted on the module cover. A second port of the three-way stopcock is connected to a solvent container, and the third port is connected to the automatic chemistry platter. Thus, the automatic chemistry platter may be rapidly flushed with solvent by properly positioning this stopcock.

Automated Chemistry Platter (*d*)—The automated chemistry is performed using a continuous flow proportioning pump[5] with an appropriate chemistry platter, the liquid sample being pumped through the single flowcell of the UV–visible spectrophotometer.

Spectrophotometer[6] (*e*)—The double-beamed instrument has a diffraction grating monochromator with a wavelength range of 200–900 nm. It has twin high-precision quartz flowcells with built-in debubblers and identical optical characteristics for accurate, simultaneous blanking. The path length of the flowcells is 15 mm, and the volume is 45 μl.

Dual-Pen Recorder[7] (*f*)—Any dual-pen recorder that has 100-mv full-scale deflection may be used. The recorder is connected to the automatic system controller, and each pen provides a bar graph for each of six samples so that a full recorder run has 12 sample bars shown for each sampling period. Thus, pen 1 shows the dissolution profile for the six tablets for lot 1, and pen 2 does the same for lot 2. Usually, different colored pens are used for the two lots. A typical recorder chart showing standards and sample bar graphs is shown in Fig. 3.

Digital Data Acquisition and Controller (*g*)—The data acquisition and control system (DDAC) consists of a modified digital integrator (MDI) (system controller)[8] and teletypewriter[9]. The MDI receives the electrical analog absorbance signal from the spectrophotometer and converts it to digital form for input to the teletype while retaining the analog form for the recorder. The system controller receives its instructions from a continuous preprogrammed punched Mylar tape put into the teletype tape reader.

The "master program tape" contains the complete set of instructions for the dissolution test. This tape gives specific instructions to the MDI which, in turn, controls the entire system. The tape is made manually using the teletype tape punch and Mylar "paper" for strength and durability. Each linear series of perforations in the tape constitutes a seven-digit numerical command which regulates the operation of a single function or a group of functions and the operation time sequence.

During the dissolution test, the coded program tape, in conjunction with the MDI, controls the proper sequential implementation of the following system operations: sample and air solenoid valve sequence, time from zero for valve operation, digitization of sample peak absorbance, pen activation (either 1 or 2), recorder run (length of time recorder chart will run), sample number advance (SNA), sample number reset (SNR), and time reset. Thus, complete system control versatility is provided with respect to tablet number, sampling interval, recorder dissolution profile depiction, *etc.*, depending on the manner in which the system operations are preprogrammed onto the master control tape.

The teletypewriter gives absorbance data in digital form both on a printout and on punched paper tape. The punched tape is used for calculating the dissolution profile of the product *via* a timeshare computer program.

[5] Technicon Corp., Tarrytown, N.Y.
[6] Catalog No. 00-951000-00 Varichrom detector, Varian Instrument Corp., Florham Park, N.J.
[7] Model 412, Pharmacia Fine Chemicals, Piscataway, N.J.
[8] Modified model CSI-208, Columbia Scientific Industries, Austin, Tex.
[9] Model ASR-33.

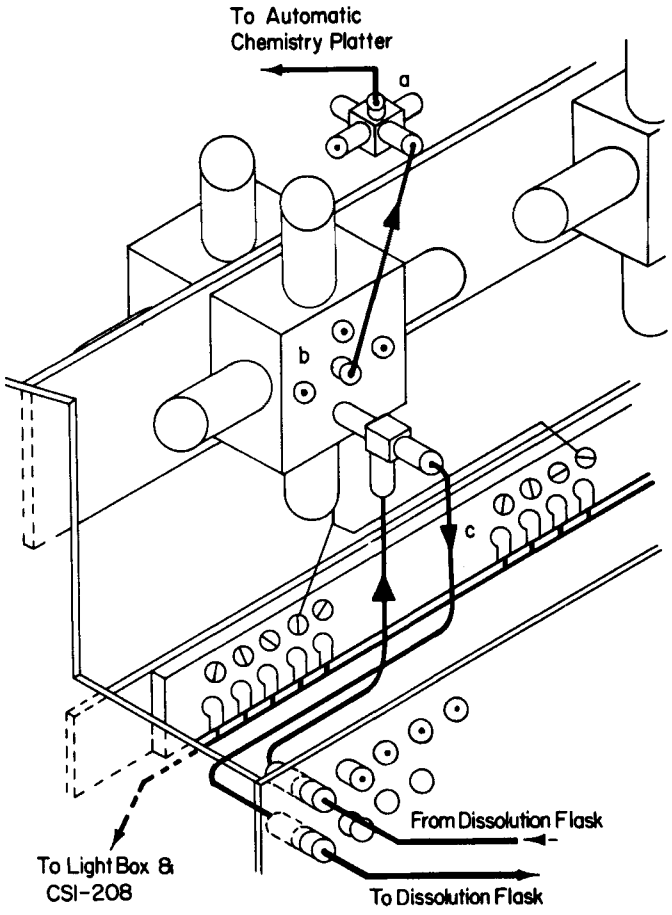

Figure 2—*Valve blocks and terminal bar legend. Key: a, five-prong cross fitting; b, valve block 1; and c, terminal bar.*

The raw data obtained on the teletype printout and on punched paper tape appear as a single column of absorbance data repetitively numbered from 1 to 12 to correspond to each tablet. Each tablet solution passes through the spectrophotometer sample flowcell for 22 sec and is separated from the next tablet solution by an 8-sec air segment. Thus, each of the 12 tablet solutions is sampled for 22 sec at 6-min intervals. The steady-state absorbance of each tablet solution is averaged over a 5-sec interval and digitized.

Operation—*Modified Digital Integrator (MDI)*—The following controls and/or indicator lights on the MDI are not required and have been rendered *inoperative* in the ADS-12 dissolution testing system: track rate/UV-minimum, minimum peak width-seconds, maximum peak width-seconds, peak sensor gain, and positive/negative slope light.

The following controls on the MDI are *preset* as follows: (*a*) mark—"off"; (*b*) recorder—"linear"; and (*c*) recorder attenuator—"1" (when using a 100-mv full-scale recorder).

The recorder attenuator may be changed if the absorbance peak of the sample goes off scale. Increased attenuation brings the visual recorder bar graph into the full-scale range but does not affect the numerical printout of the teletypewriter. For example, if the spectrophotometer reading is 1500 counts on the MDI and the recorder attenuator is set at 2, then the recorder pen would show a deflection of 750 divisions on the chart but the teletypewriter would print 1500 counts on the data printout.

When the recorder pen zero is to be set, the MDI attenuator is changed to infinity. The zero is then set by using the appropriate pen control on the dual-pen recorder.

The following *operational controls* are functional and are used routinely:

1. Power switch. This switch, located on the rear panel, is normally left on constantly so that the MDI is warm, stable, and ready for use.
2. "Reset" button. When the Reset button is lit, it indicates that the MDI is in the standby mode. This button should be depressed whenever the MDI is not in use.
3. "Manual" button. The Manual button is depressed at the beginning of a test run. This step activates the teletypewriter, control tape reader, all electronic circuits, and the program. However, automatic data digitization commands contained in the program tape remain inoperative until the number of seconds entered in the time delay control are exceeded.

Thus, the first several digitize commands are inhibited during the first circuit of the control tape to allow Sample 1 to move from the solenoid valve to the flowcell before its absorbance is digitized on the teletypewriter printout and data tape.

4. "Auto" button. Hitting the Auto button allows all functions to perform. This is the normal operational mode and may be entered manually by pushing the Auto button or automatically by expiration of the time (in seconds) entered in the time delay window by the thumbwheel switches.
5. "Time delay" thumbwheel switches. These switches are used to set the time delay before which no data digitization will occur. For example, if a time delay of 200 sec is entered, the MDI would wait 200 sec before a command would be given to the teletypewriter to print anything. During this 200 sec, there could be up to six or seven digitized commands written in the program, but they would not be carried through until the time delay sequence had been completed. The time delay sequence is necessary

Table I—Dissolution Data for 250-mg Erythromycin Stearate Tablets in 0.1 *N* HCl

	Percent Dissolved (Basis Label)			
	Lot A		Lot B	
Minutes	ADS-12	Manual	ADS-12	Manual
0	0	0	0	0
6	6		1	
12	27		14	
15		61		78
18	47		33	
24	65		56	
30	82	89	83	85
36	88		93	
42	90		94	
45		97		93
48	91		95	
54	91			
60	92	99		96
66	92			

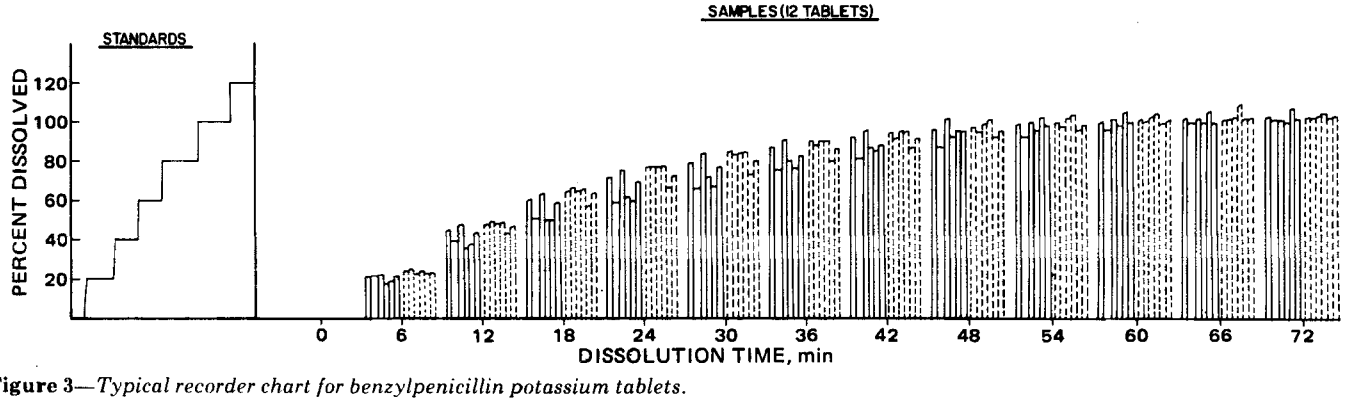

Figure 3—*Typical recorder chart for benzylpenicillin potassium tablets.*

Table II—Collaborative Study Data for 50-mg Prednisone Tablets [a]

Speed, rpm	Minutes	$\bar{x}$	Variance: Between Laboratories	Variance: Within Laboratories	Variance: ADS-12	Acceptance Limits: Range	Acceptance Limits: $\bar{x}$	Acceptance Limits: σ	ADS-12: $\bar{x}$	ADS-12: σ
				Rotating Basket (USP Method I)						
50	15	22.0	41.06	10.56	1.80	10.0–33.7	8.9–35.1	6.4	18.3	3.3
	30	34.8	44.74	11.64	6.99	21.4–48.5	21.1–48.5	6.7	37.2	3.4
	45	43.0	48.25	10.49	6.19	28.6–57.5	28.9–57.1	6.4	46.2	2.5
	60	48.9	52.55	12.61	5.56	33.7–63.9	34.1–63.7	7.0	53.4	2.4
100	15	45.8	52.46	14.56	2.85	33.7–56.7	31.0–60.6	7.5	39.9	1.3
	30	64.1	61.94	14.10	5.51	50.5–76.3	48.0–80.1	7.4	60.1	5.1
	45	74.0	59.98	14.54	7.83	59.2–85.6	58.2–89.8	7.5	70.2	7.3
	60	80.0	51.01	14.64	7.98	65.5–89.2	65.4–94.7	7.5	75.7	8.5
				Rotating Paddle (USP Method II)						
50	15	44.0	34.61	21.83	9.58	30.3–57.2	31.6–56.4	9.2	38.7	3.1
	30	62.3	35.73	22.09	1.00	46.3–75.7	49.7–74.8	9.3	58.8	1.0
	45	73.1	31.97	23.54	12.53	56.0–83.6	61.1–85.1	9.6	70.8	3.5
	60	79.8	25.09	25.63	14.98	64.2–86.4	69.0–90.7	10.0	77.4	3.9
100	15	57.7	20.80	4.77	2.03	48.1–66.1	48.4–67.0	4.3	48.1	1.4
	30	74.6	14.61	3.00	2.77	67.6–81.2	66.8–82.4	3.4	67.6	1.7
	45	83.6	11.06	1.74	1.11	78.9–89.6	76.8–90.2	2.6	79.8	1.0
	60	87.9	10.23	1.48	0.57	82.3–93.6	81.5–94.4	2.4	87.5	0.8

[a] This study was conducted by 17 participating laboratories in August 1978. Six tablets were used in all cases. The dissolution medium was distilled water, 900 ml. Measurement was at 242 nm.

because it takes a fixed amount of time for Sample 1 to reach the flowcell from the sampling valve. This time depends on the particular automated chemistry platter being used. During this time, only reagents and solvents are passing through the flowcell. Since the program tape is a loop, initial digitization commands on the tape are suppressed until the first sample has entered the flowcell. Thus, the time delay is set so that Sample 1 is the first data point recorded on the teletypewriter.

6. "Integrate" button. Depressing this button initiates a readout in either the Manual or Auto mode. The program command tape initiates a readout only in the Auto mode. The readout lamp lights whenever a readout is initiated.

7. "Fast/Zero" button. Pushing the Fast button illuminates the yellow Fast light and causes the MDI to track the detector output at zero reference (baseline). Upon completion of this function, the yellow light goes out and the white Zero light blinks slowly. The "Fast/Zero" is used to set the integrator zero baseline. Normally, it is set as close to recorder zero as possible but may be set to within ±10% of actual recorder zero. When setting the integrator zero baseline, the Fast/Zero button is depressed only once. This button must never be depressed after the dissolution test run has begun, because it will cause the integrator to reset its zero baseline to whatever level the recorder pen is at that particular time.

8. "Multiplier factor" thumbwheel switches. These switches are normally set at 5000, in which case full scale on the strip chart will read 1000 counts on the teletype printout. During calibration, this setting may be adjusted to any desired full-scale reading.

Samples—After the appropriate automated chemistry platter has been

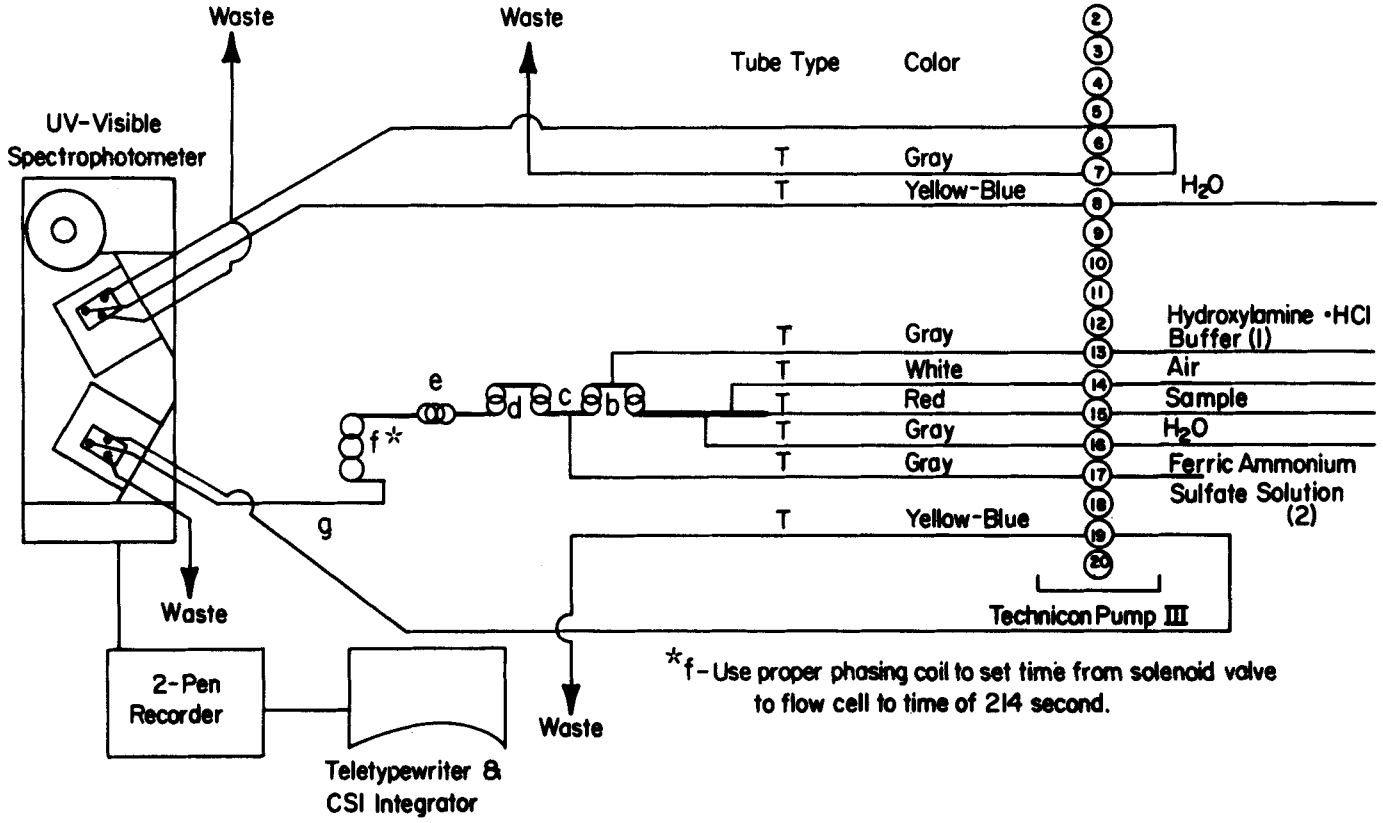

Figure 4—*Automated chemistry platter for penicillin dissolution testing. Key: (1), 5 M hydroxylamine hydrochloride brought to pH 7.0 with sodium hydroxide–sodium acetate buffer and then diluted 10 to 1 with 20% ethanol; and (2), 200 g of ferric ammonium sulfate dissolved in 1 liter of 1 N* H_2SO_4.

AUTOMATED DISSOLUTION TEST

PRODUCT: 500MG CT PENTIDS — DATE TESTED:1/12/77
CODE: PLATTER C-1 — ANALYST:FJC
LOT NUMBER: LOT-1
CONTROL:5G545(1)

SOLVENT:DISTILLED WATER
VOLUME: 1000ML. — F=0 ML/MINUTE
BASKET ROTATION RATE:100RPM — T=37 DEG.C

PERCENT DISSOLVED (CORRECTED TO SINK CONDITIONS)
(BASIS-LABEL)

TIME (MIN)	TABLET NUMBER 1	2	3	4	5	6	MIN	MAX	AVG
0	.6	.7	.8	.6	.7	.7	.6	.8	.7
6	22.9	22.6	23.3	18.8	20.5	22.3	18.8	23.3	21.7
12	47.2	40.7	50.2	37.9	39.5	45.4	37.9	50.2	43.5
18	63.2	52.9	66.5	52.2	52.1	61.5	52.1	66.5	58.1
24	75.3	62.2	79.2	64.7	62.3	73.4	62.2	79.2	69.5
30	83.9	69.6	88.4	76.5	71.5	82.2	69.6	88.4	78.7
36	92.6	80.0	95.9	85.8	81.1	87.5	80.0	95.9	87.2
42	97.3	86.4	101.9	91.5	89.3	92.9	86.4	101.9	93.2
48	101.4	91.7	106.0	96.7	99.9	98.7	91.7	106.0	99.1
54	103.9	96.5	104.2	99.7	106.7	102.8	96.5	106.7	102.3
60	105.1	100.5	106.0	103.9	110.5	104.7	100.5	110.5	105.1
66	106.9	104.1	106.7	104.3	110.3	104.0	104.0	110.3	106.0
72	108.4	106.3	107.1	105.9	113.9	107.0	105.9	113.9	108.1

	ACROSS AVG.	VAR.	DOWN
DT(50)=13.1 16.6 12.0 17.1 17.0 13.7	14.9	5.1	14.7Minutes
DT(85)=30.8 40.7 27.8 35.5 38.9 33.2	34.5	23.8	34.4Minutes

AUTOMATED DISSOLUTION TEST

PRODUCT:500MG CT PENTIDS — DATE TESTED:1/12/77
CODE:PLATTER C-1 — ANALYST:FJC
LOT NUMBER:LOT-2
CONTROL:5G545(2)

SOLVENT:DISTILLED WATER
VOLUME:1000ML. — F=0 ML/MINUTE
BASKET ROTATION RATE:100RPM — T=37 DEG.C

PERCENT DISSOLVED(CORRECTED TO SINK CONDITIONS)
(BASIS-LABEL)

TIME (MIN)	TABLET NUMBER 1	2	3	4	5	6	MIN	MAX	AVG
0	.7	.6	.6	.5	.7	.7	.5	.7	.6
6	24.8	25.6	23.5	24.7	24.0	23.9	23.5	25.6	24.4
12	49.9	52.2	50.2	51.4	44.7	49.2	44.7	52.2	49.6
18	67.9	69.6	68.7	69.2	59.7	66.9	59.7	69.6	67.0
24	81.4	81.3	80.5	82.1	69.9	77.1	69.9	82.1	78.7
30	91.0	89.1	89.0	89.9	77.7	84.5	77.7	91.0	86.9
36	94.9	92.8	94.7	95.2	83.9	90.5	83.9	95.2	92.0
42	100.0	97.7	101.6	100.3	91.5	95.5	91.5	101.6	97.8
48	102.2	99.3	103.7	106.7	96.7	100.3	96.7	106.7	101.5
54	104.5	102.5	107.2	108.5	100.0	103.1	100.0	108.5	104.3
60	105.8	104.8	107.1	109.3	104.6	105.7	104.6	109.3	106.2
66	106.6	106.9	107.9	115.7	107.4	107.5	106.6	115.7	108.6
72	108.8	106.0	109.3	111.1	110.4	110.4	106.0	111.1	109.0

	ACROSS AVG.	VAR.	DOWN
DT(50)= 12.0 11.5 12.0 11.7 14.1 12.3	12.3	.9	12.1Minutes
DT(85)= 26.3 26.8 27.2 26.2 36.9 30.5	29.0	17.5	28.6Minutes

Figure 5—*Dissolution test report printouts.*

set in place and the correct wavelength has been set on the spectrophotometer, the general procedure for a run is that a tablet or capsule is placed into each of the 12 wire mesh baskets in the respective dissolution kettles and rotated at a prescribed revolutions per minute. As the tablet dissolves, the dissolution fluid is drawn up continuously through a sintered-glass filter by the 12-channel peristaltic pump. Each sample is circulated past a solenoid sampling valve assembly and back to its respective dissolution kettle. A continuous sampling loop is thus formed.

At the solenoid sampling valves, a liquid sample is periodically drawn off from the loop for analysis in the automated chemistry system. As the individual tablet solution samples pass through the spectrophotometer flowcell, their absorbances and sample number are printed on the teletype and also are recorded on punched paper tape. In addition, the absorbances are recorded as bar graphs on the dual-pen recorder. The raw data tape is then used *via* a timesharing computer system to obtain a dissolution test report for each six-tablet lot tested.

The system is set into automatic operation as follows:

1. The desired master control tape is placed onto the teletype tape reader, and the proper time delay is set using the thumbwheel switch on the MDI.

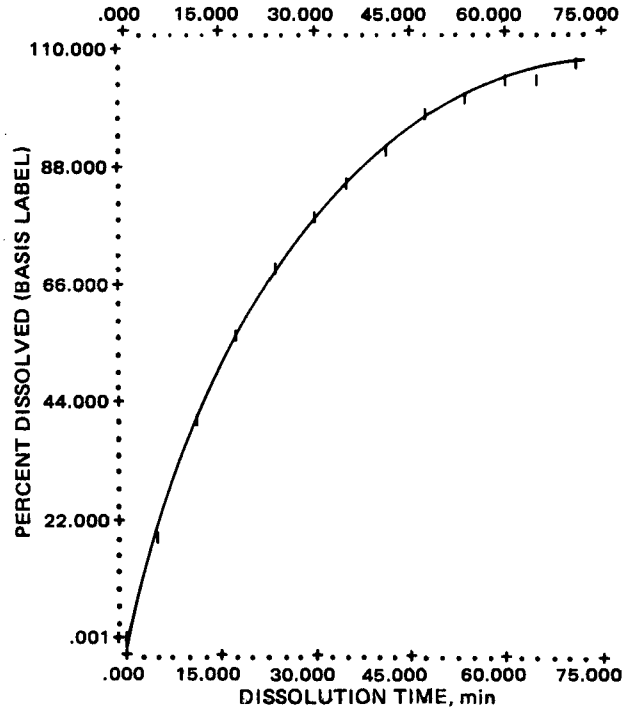

Figure 6—*Computer-drawn dissolution profile curve for 500-mg penicillin G potassium tablets, lot 1.*

2. Pure solvent is pumped through the system, while both recorder pens are set at Zero and the Zero absorbance reading is set to ~5000 on the MDI digital readout.

3. The 12 tablet-containing baskets are positioned on their spindles over their respective dissolution flasks, and rotation is begun.

4. At time zero, a stopwatch is started and the first basket is lowered into its dissolution flask. The remaining 11 baskets are individually lowered at consecutive 30-sec intervals.

5. At x[10] sec from time zero, the "On" switch for the master control program tape is pressed to start the automatic operation of the system; the "On" switch for the sample data tape punch is pressed 20 sec later. The system will now run automatically until it is shut off at the end of the run.

Standards—Standards may be run either before or after the samples. The procedure for running the standards is similar to that for the samples. Normally, six standard concentration levels are run, representing 20, 40, 60, 80, 100, and 120% of the labeled amount of drug in the dosage form.

The glass tubes containing the standard solutions are placed into the water bath prior to the run and maintained at 37°. The peristaltic pump is then turned on, and each of the six standard solutions is circulated continuously past its respective solenoid valve. During the time it takes to ensure homogeneous concentrations of each standard level in the lines, pure solvent is pumped through the system to obtain a baseline. The appropriate control tape is then inserted onto the teletype tape reader, and the proper time delay is set by the thumbwheel switch. The standard run is then begun by depressing the Auto switch on the MDI.

The data analysis computer program will accept and average standard data in either of two formats: (*a*) each standard level run once with several absorbance readings digitized for each level, or (*b*) several circuits of Standards 1–6 with the absorbance readings of each level digitized only once per circuit.

Data Handling—Data handling is automatically accomplished by feeding the data tape into a timeshare computer system, and all calculations are done *via* software developed in this laboratory. The standard data are fit to six possible equations, and the equation that best fits the data is chosen by the computer for further calculations on the sample data. The percent dissolved is then calculated for each tablet at 6-min intervals up to complete dissolution. In addition, the high, low, and av-

[10] The x is the time required for the sample solutions to be pumped from the dissolution kettles to the solenoid valves, and it depends on the peristaltic pump rate. Since the length of the tubing from each kettle to the solenoid valves is the same, x is also the same for each sample solution.

Table III—Collaborative Study Data for 300-mg Salicylic Acid Tablets [a]

Speed, rpm	Minutes	$\bar{x}$	Variance: Between Laboratories	Variance: Within Laboratories	Variance: ADS-12	Acceptance Limits: Range	Acceptance Limits: $\bar{x}$	Acceptance Limits: σ	ADS-12: $\bar{x}$	ADS-12: σ
				Rotating Basket (USP Method I)						
50	15	8.3	1.18	0.59	0.08	5.8–10.5	6.0–10.6	1.5	5.8	0.4
	30	16.2	1.80	1.48	0.08	13.6–18.8	13.3–19.0	2.4	13.9	0.5
	45	24.0	3.05	2.06	0.24	20.7–27.1	20.3–27.7	2.8	21.8	0.7
	60	31.6	4.20	3.33	0.33	27.2–34.9	27.2–35.9	3.6	29.3	1.1
100	15	13.4	2.34	1.30	0.25	8.4–15.4	10.2–16.6	2.2	11.1	0.6
	30	26.1	3.37	2.94	1.64	21.0–29.1	22.1–30.0	3.4	24.7	1.3
	45	37.8	3.89	7.33	3.72	33.0–40.8	33.3–42.3	5.3	36.5	1.8
	60	49.2	4.25	12.40	5.87	44.2–52.8	44.1–54.2	6.9	46.7	1.6
				Rotating Paddle (USP Method II)						
50	15	9.9	0.99	1.35	0.55	8.3–11.6	7.7–12.1	2.3	9.1	0.9
	30	19.1	2.95	3.44	1.83	16.5–22.2	15.4–22.9	3.7	20.3	1.4
	45	28.1	6.42	6.98	4.27	24.5–32.8	22.6–33.6	5.2	30.6	2.1
	60	36.5	12.20	11.30	5.85	31.3–43.0	29.0–44.0	6.6	40.4	2.7

[a] This study was conducted by 17 participating laboratories in August 1978. Six tablets were used in all cases. The dissolution medium was 0.05 *M* phosphate buffer, pH 7.40, 900 ml. Measurement was at 296 nm.

erage results of the 12 tablets (or six tablets from each lot) are calculated for each time interval. If necessary, the results are corrected for dilution at this point based on a literature method (4, 5).

RESULTS AND DISCUSSION

A typical dissolution test run on a penicillin tablet formulation is shown in Figs. 3–7. The dissolution rate was followed *via* the hydroxamic acid method (6) whereby the β-lactam ring of the penicillin is split by reaction with hydroxylamine, forming a hydroxamic acid (I).

The addition of ferric ion to the hydroxamic acid solution produces a colored chelate (Scheme I), which is measured at 480 nm (7). This reaction has been automated for routine penicillin assays and dissolution testing *via* the automated chemistry platter shown in Fig. 4. Several other penicillin tablet and capsule formulations are also run *via* the same automated chemistry system.

The raw data are also obtained on punched paper tape for calculation *via* a timeshare computer system. After the paper tape data have been input, a brief dialog ensues with the computer during which both descriptive parameters and those required for calculations are input. The computer then fits the standard data to six possible equations, chooses

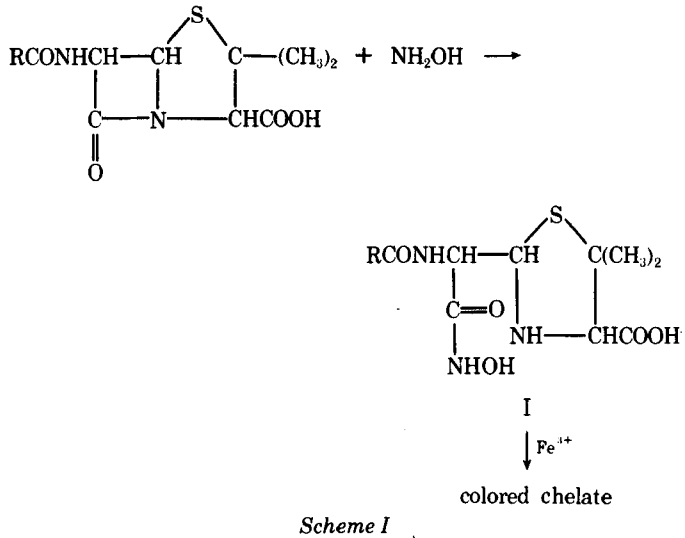

Scheme I

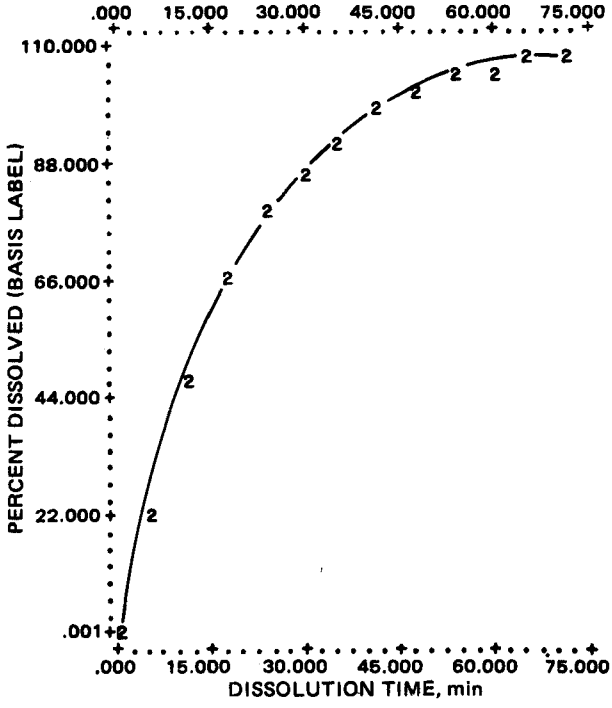

Figure 7—*Computer-drawn dissolution profile curve for 500-mg penicillin G potassium tablets, lot 2.*

the equation that best fits the standard data, prints out the index of determination and coefficients, and finally prints out the standard curve.

The percent dissolved is then calculated for each tablet at each sampling interval using the chosen equation for the standard data, and dissolution profile reports are printed out for each lot. In addition, the time required for a designated amount of sample to dissolve (50 and 85% were chosen for penicillin G potassium) is printed for each tablet below the dissolution test report (Fig. 5).

If requested during the input dialog, profile curves for each lot are also printed out as shown in Figs. 6 and 7. The numerical points on the curves indicate the lot being graphed.

Table I compares the results of a dissolution test for an erythromycin stearate tablet formulation run both on the ADS-12 and manually. This test involved acid hydrolysis of the drug with absorbance measurement at 482 nm. The dissolution medium was 0.1 *N* HCl. The ADS-12 data are the average of six tablets, while the manual data are the average of three tablets.

This ADS-12 automated system was used in a collaborative study[11] of dissolution calibration, which involved 17 different pharmaceutical laboratories using both manual and automated test methods. Some data from this study for 300-mg salicylic acid tablets and 50-mg prednisone tablets are given in Tables II and III to show the precision and accuracy of the ADS-12 system. Both USP Method I (rotating basket) and Method II (rotating paddle) were used; six tablets were used in all cases. Details of this study will be published. As can be seen from these tables, the ADS-12 results were within the Pharmaceutical Manufacturers Association recommended acceptance limits for both calibrators, with standard deviations well below the listed acceptable values. Furthermore, the

[11] Initiated by the Pharmaceutical Manufacturers Association.

within-laboratory variance for the ADS-12 data was significantly lower than the average for the 17 participating laboratories.

CONCLUSION

The described computerized automated dissolution testing system conforms to the basic requirements of the USP dissolution test. The system, which can be adapted to almost any type of tablet agitation technique, can test 12 solid dosage forms simultaneously under either sink or nonsink conditions and can test products requiring any type of chemistry amenable to an automatic analyzer. Total run time is reduced essentially to sample dissolution time since sampling and analysis are performed simultaneously with sample dissolution. A complete dissolution profile report, with or without graphs, is obtained within minutes after the required sample dissolution time.

REFERENCES

(1) R. A. Castello, G. Jellinek, J. Konieczny, K. C. Kwan, and R. O. Toberman, *J. Pharm. Sci.*, **57**, 485 (1968).

(2) A. Ferrari and A. Khoury, *Ann. N.Y. Acad. Sci.*, **153**, 660 (1968).

(3) W. F. Beyer and E. W. Smith, *J. Pharm. Sci.*, **60**, 1556 (1971).

(4) F. J. Cioffi, H. M. Abdou, and A. T. Warren, *ibid.*, **65**, 1234 (1976).

(5) A. Richter, B. Myhre, and S. C. Khanna, *J. Pharm. Pharmacol.*, **21**, 409 (1969).

(6) T. Higuchi and E. Brochmann-Hanssen, "Pharmaceutical Analysis," Interscience, New York, N.Y., 1961.

(7) G. Boxer and P. Everett, *Anal. Chem.*, **21**, 670 (1949).

Use of Rabbits for GI Drug Absorption Studies: Relationship between Dissolution Rate and Bioavailability of Griseofulvin Tablets

TADAO MAEDA ˣ, HIROSHI TAKENAKA, YOSHIYA YAMAHIRA, and TAKESHI NOGUCHI

Received October 30, 1978, from the *Formulation Research Department, Pharmaceuticals Division, Sumitomo Chemical Co., Ltd., Kurakakiuchi 1-3-45, Ibaraki-City, Osaka 567, Japan.* Accepted for publication April 17, 1979.

Abstract □ The correlation between the dissolution rate and bioavailability of griseofulvin tablets was studied in stomach-emptying-controlled rabbits and in humans. Three different test tablets, each consisting of two dose levels (62.5 or 125 mg) of griseofulvin, were used. The dissolution rates in 0.5 hr were ~75, 40, and 12%. With oral administration at 62.5 mg/rabbit, the ratio of peak plasma level, C_{max}, was 1.00:0.66:0.40 and that of the area under the curve (AUC) was 1.00:0.73:0.46 for the three tablets. The corresponding C_{max} ratio was 1.00:0.74:0.34 and the AUC ratio was 1.00:0.72:0.33 in humans at the dose level of 500 mg. A good correlation was observed for the rank order of C_{max} and AUC between rabbits and humans, but such a correlation was not seen between *in vivo* data and *in vitro* data at a larger dose of 125 mg/rabbit. This finding was attributable to the dose, which exceeded the GI drug dissolution or absorption capacities. These results suggest that the stomach-emptying-controlled rabbit is useful for evaluating oral dosage forms for human use and that dose level selection is important in the bioavailability study of a barely water-soluble drug.

Keyphrases □ Models, animals—rabbits, use in GI drug absorption studies, griseofulvin tablet dissolution rate and bioavailability, compared to humans □ Griseofulvin—dissolution rate and bioavailability, rabbits compared to humans □ GI tract—drug absorption, griseofulvin, rabbits compared to humans □ Antifungal agents—griseofulvin, dissolution rate and bioavailability, rabbits compared to humans

Use of human subjects in bioavailability studies for dosage forms provides the most appropriate results; but in new drug development and preformulation studies, such use presents economic, ethical, analytical, and statistical difficulties.

The availability of adequate animal models has been desired for estimating the bioavailability of dosage forms in humans. The beagle dog has been used as a model animal in some studies (1–3). Although rabbits are easy to breed, have a mild temper, and are a low-cost laboratory animal, they have not been considered useful for drug absorption studies because of the difficulty in obtaining an empty stomach (4). However, control of the stomach emptying rate increased the usefulness of rabbits in GI drug absorption studies and produced a good correlation in GI drug absorption between rabbits and humans (5). Since the earlier work was performed on powdered drugs using griseofulvin, indomethacin, and nalidixic acid, further investigation on oral dosage forms was desired. This paper describes the usefulness of rabbits in dosage form bioavailability studies.

While the dissolution test has been widely used as an *in vitro* test for solid dosage forms, efforts have been made to obtain good correlations between *in vitro* data and *in vivo* data (6–8). In this study, three groups of griseofulvin tablets were prepared using three grades of polyvinyl alcohol as binders for granulation so that the dissolution rate of each group was different. With these tablets, bioavailability tests were performed in stomach-emptying-controlled rabbits, and the correlation between *in vitro* dissolution tendency and *in vivo* absorption characteristics was examined. Bioavailability studies were also conducted in humans, and the suitability of the stomach-emptying-controlled rabbit as an animal model for dosage form evaluation was reviewed.

EXPERIMENTAL

Materials—Griseofulvin USP was micronized to <5 μm using a fluid energy mill. The granule was prepared by the conventional wet granulation method. The granule contained, by weight, 83.3 parts of micronized griseofulvin, 6.7 parts of calcium carboxymethylcellulose JP, 8.0 parts of lactose USP, and 1.5 parts of polyvinyl alcohol as the binder.

To control drug release from the tablet, three grades of polyvinyl alcohol[1], prepared by partial or full saponification of polyvinyl acetate, were used as the binders for granulation: grade L for Formula L, grade H for Formula N, and grades M and H (2:1) for Formula M (Table I). After 99.5 parts of the granules was mixed with 0.5 part of magnesium stearate USP

[1] Gohsenol, Nippon Gohsei Kagaku Kogyo Co., Tokyo, Japan.

0022-3549/79/1000-1286$01.00/0

© 1979, American Pharmaceutical Association

within-laboratory variance for the ADS-12 data was significantly lower than the average for the 17 participating laboratories.

CONCLUSION

The described computerized automated dissolution testing system conforms to the basic requirements of the USP dissolution test. The system, which can be adapted to almost any type of tablet agitation technique, can test 12 solid dosage forms simultaneously under either sink or nonsink conditions and can test products requiring any type of chemistry amenable to an automatic analyzer. Total run time is reduced essentially to sample dissolution time since sampling and analysis are performed simultaneously with sample dissolution. A complete dissolution profile report, with or without graphs, is obtained within minutes after the required sample dissolution time.

REFERENCES

(1) R. A. Castello, G. Jellinek, J. Konieczny, K. C. Kwan, and R. O. Toberman, *J. Pharm. Sci.*, **57**, 485 (1968).

(2) A. Ferrari and A. Khoury, *Ann. N.Y. Acad. Sci.*, **153**, 660 (1968).

(3) W. F. Beyer and E. W. Smith, *J. Pharm. Sci.*, **60**, 1556 (1971).

(4) F. J. Cioffi, H. M. Abdou, and A. T. Warren, *ibid.*, **65**, 1234 (1976).

(5) A. Richter, B. Myhre, and S. C. Khanna, *J. Pharm. Pharmacol.*, **21**, 409 (1969).

(6) T. Higuchi and E. Brochmann-Hanssen, "Pharmaceutical Analysis," Interscience, New York, N.Y., 1961.

(7) G. Boxer and P. Everett, *Anal. Chem.*, **21**, 670 (1949).

Use of Rabbits for GI Drug Absorption Studies: Relationship between Dissolution Rate and Bioavailability of Griseofulvin Tablets

TADAO MAEDA ˣ, HIROSHI TAKENAKA, YOSHIYA YAMAHIRA, and TAKESHI NOGUCHI

Received October 30, 1978, from the *Formulation Research Department, Pharmaceuticals Division, Sumitomo Chemical Co., Ltd., Kurakakiuchi 1-3-45, Ibaraki-City, Osaka 567, Japan.* Accepted for publication April 17, 1979.

Abstract □ The correlation between the dissolution rate and bioavailability of griseofulvin tablets was studied in stomach-emptying-controlled rabbits and in humans. Three different test tablets, each consisting of two dose levels (62.5 or 125 mg) of griseofulvin, were used. The dissolution rates in 0.5 hr were ~75, 40, and 12%. With oral administration at 62.5 mg/rabbit, the ratio of peak plasma level, C_{max}, was 1.00:0.66:0.40 and that of the area under the curve (AUC) was 1.00:0.73:0.46 for the three tablets. The corresponding C_{max} ratio was 1.00:0.74:0.34 and the AUC ratio was 1.00:0.72:0.33 in humans at the dose level of 500 mg. A good correlation was observed for the rank order of C_{max} and AUC between rabbits and humans, but such a correlation was not seen between *in vivo* data and *in vitro* data at a larger dose of 125 mg/rabbit. This finding was attributable to the dose, which exceeded the GI drug dissolution or absorption capacities. These results suggest that the stomach-emptying-controlled rabbit is useful for evaluating oral dosage forms for human use and that dose level selection is important in the bioavailability study of a barely water-soluble drug.

Keyphrases □ Models, animals—rabbits, use in GI drug absorption studies, griseofulvin tablet dissolution rate and bioavailability, compared to humans □ Griseofulvin—dissolution rate and bioavailability, rabbits compared to humans □ GI tract—drug absorption, griseofulvin, rabbits compared to humans □ Antifungal agents—griseofulvin, dissolution rate and bioavailability, rabbits compared to humans

Use of human subjects in bioavailability studies for dosage forms provides the most appropriate results; but in new drug development and preformulation studies, such use presents economic, ethical, analytical, and statistical difficulties.

The availability of adequate animal models has been desired for estimating the bioavailability of dosage forms in humans. The beagle dog has been used as a model animal in some studies (1–3). Although rabbits are easy to breed, have a mild temper, and are a low-cost laboratory animal, they have not been considered useful for drug absorption studies because of the difficulty in obtaining an empty stomach (4). However, control of the stomach emptying rate increased the usefulness of rabbits in GI drug absorption studies and produced a good correlation in GI drug absorption between rabbits and humans (5). Since the earlier work was performed on powdered drugs using griseofulvin, indomethacin, and nalidixic acid, further investigation on oral dosage forms was desired. This paper describes the usefulness of rabbits in dosage form bioavailability studies.

While the dissolution test has been widely used as an *in vitro* test for solid dosage forms, efforts have been made to obtain good correlations between *in vitro* data and *in vivo* data (6–8). In this study, three groups of griseofulvin tablets were prepared using three grades of polyvinyl alcohol as binders for granulation so that the dissolution rate of each group was different. With these tablets, bioavailability tests were performed in stomach-emptying-controlled rabbits, and the correlation between *in vitro* dissolution tendency and *in vivo* absorption characteristics was examined. Bioavailability studies were also conducted in humans, and the suitability of the stomach-emptying-controlled rabbit as an animal model for dosage form evaluation was reviewed.

EXPERIMENTAL

Materials—Griseofulvin USP was micronized to <5 μm using a fluid energy mill. The granule was prepared by the conventional wet granulation method. The granule contained, by weight, 83.3 parts of micronized griseofulvin, 6.7 parts of calcium carboxymethylcellulose JP, 8.0 parts of lactose USP, and 1.5 parts of polyvinyl alcohol as the binder.

To control drug release from the tablet, three grades of polyvinyl alcohol[1], prepared by partial or full saponification of polyvinyl acetate, were used as the binders for granulation: grade L for Formula L, grade H for Formula N, and grades M and H (2:1) for Formula M (Table I). After 99.5 parts of the granules was mixed with 0.5 part of magnesium stearate USP

[1] Gohsenol, Nippon Gohsei Kagaku Kogyo Co., Tokyo, Japan.

0022-3549/79/1000-1286$01.00/0

© 1979, American Pharmaceutical Association

Table I—Properties of Polyvinyl Alcohol [a]

Grade	Degree of Polymerization	Degree of Saponification, mole %	Viscosity[b], cps
L	1000	86.5–89	5.3 ± 0.5
M	1000–1500	86.5–89	18 ± 2
H	1500	99.4–100	39 ± 4

[a] Polyvinyl alcohol manufactured by partial or full saponification of polyvinyl acetate. [b] A 40% aqueous solution at 20°.

as a lubricant, the mixture was compressed with a single-punch machine into 6.3- and 8-mm diameter flat tablets, containing 62.5 and 125 mg of griseofulvin, respectively.

Dissolution Rate Study—A slightly modified literature method (9) was used. Ten liters of distilled water was poured into a glass bath (30 cm in length, 23 cm in width, and 30 cm in depth) and maintained at 37 ± 2°. The test tablet was placed in a plastic cylinder (22 × 77.5 mm) covered at each end with a 42-mesh screen. The cylinder was moved up and down in the water at 30 ± 2 strokes/min. The test fluid was stirred continuously with a six-blade turbine-type propeller rotating at 200 ± 3 rpm. At a predetermined time, an aliquot was removed using a 0.45-μm pore membrane filter; the dissolved drug was assayed spectrophotometrically[2].

***In Vivo* Studies in Rabbits**—The stomach emptying rate of white male rabbits, 2.5–3.2 kg, was controlled by the method reported previously (5). Six rabbits were employed first. The rabbits were given one of the three kinds of tablets (Formula L, M, or N) containing 125 mg of griseofulvin. Administration of the other two kinds of tablets followed in a strict crossover manner after 2-week washout periods. Similarly, six other rabbits were given tablets of Formulas L, M, and N containing 62.5 mg of griseofulvin in turn in a strict crossover manner. Blood samples were collected by cardiac puncture periodically up to 10 hr.

***In Vivo* Studies in Humans**—The four male volunteers, 29–46 years of age and 55–67 kg in weight, were all in good health. Each subject took a standard breakfast at 7:00 am and received 500 mg of griseofulvin (four 125-mg tablets) with a glass of water at 9:00 am. At 1-week intervals, three different tablets of griseofulvin (Formulas L, M, and N) were given to these four subjects in a crossover manner. Blood samples were taken from the cubital vein at the predetermined time for analysis.

Analytical Method and Equipment—Griseofulvin was extracted with ether from aqueous or plasma samples and was determined by a gas chromatograph equipped with a ^{63}Ni-electron capture detector[3]. Diazepam was used as an internal standard, and the procedure of Shah *et al.* (10) was followed. The column was a 1.5-m × 3-mm glass tube packed with 10% SE-30 on Chromosorb W. The column temperature was 270°, the injection port temperature was 300°, and the detector block temperature was 310°. The carrier gas (99.999% nitrogen) flow rate was 60 ml/min.

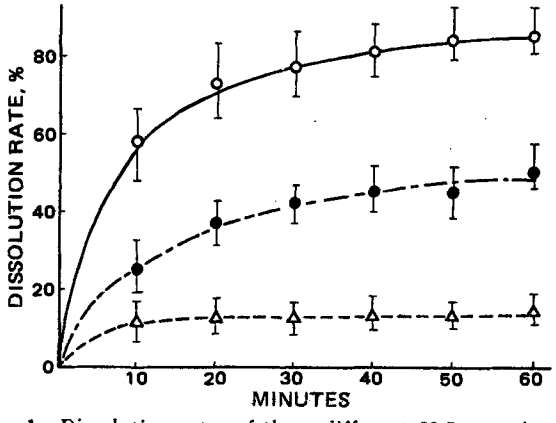

Figure 1—*Dissolution rates of three different 62.5-mg griseofulvin tablets in distilled water at 37°. Each point represents the average and range of triplicate experiments. Key: ○, Formula L; ●, Formula M; and △, Formula N.*

[2] Shimadzu spectrophotometer UV-200.
[3] Shimadzu GC-5APTFE.

Table II—Plasma Level–Time Parameters following Oral Administration of 62.5-mg Griseofulvin Tablets in Stomach-Emptying-Controlled Rabbits

Parameter	Formula L	Formula M	Formula N
C_{max}[a], μg/ml	1.12[b,c]	0.55	0.40
	(1.00)[d]	(0.49)	(0.36)
C'_{max}[e], μg/ml	1.21[b,c]	0.80[c]	0.48
	(1.00)	(0.66)	(0.40)
T_{max}[f], hr	2	2	3
	(1.00)	(1.00)	(1.50)
T'_{max}[g], hr	2.2	2.5	3.0
	(1.00)	(1.14)	(1.36)
AUC[h], hr μg/ml	5.64[c]	4.14[c]	2.57
	(1.00)	(0.73)	(0.46)

[a] Average plasma level peak. [b] Significantly different from Formula M at $p < 0.05$. [c] Significantly different from Formula N at $p < 0.05$. [d] Each value in parentheses means relative ratio of parameters among Formulas L, M, and N. [e] Average of individual peak plasma levels. [f] Time of the average plasma level peak. [g] Average of individual peak times. [h] Area under the plasma level–time curve to 10 hr calculated by the trapezoidal rule.

RESULTS AND DISCUSSION

To conduct dissolution rate studies on a dosage form containing a barely water-soluble drug, it is important to select an appropriate experimental method. In a preliminary study, the dissolution rates of three tablet types (Formulas L, M, and N), each containing 125 mg of griseofulvin, were estimated according to Dissolution Test Method II of NF XIV, using 1 liter of distilled water as the medium. As a result, the dissolution rate was very low, only ~12% in 1 hr for Formula L and M tablets with no significant difference between the two. Since griseofulvin solubility is very limited (11, 12), only ~10% of 125 mg of griseofulvin present in the tablet could be dissolved in 1 liter of water at 37°. In fact, the drug concentration seemed to have reached saturation for Formula L and M tablets in ~20 min, and no difference was observed thereafter between the two.

In a subsequent dissolution test, the method of Katchen (9) was employed with 10 liters of water as the medium. The dissolution rate–time curves for tablets of Formulas L, M, and N containing 62.5 mg of griseofulvin are shown in Fig. 1. The average dissolution rates at 0.5 hr after initiation of the experiment were 77.4, 41.5, and 13.2%, respectively, and a difference of ~30% was observed between L–M and M–N. Similarly, the average dissolution rates at 0.5 hr after initiation of the experiment for the 125-mg tablets, which were prepared using the same granules as the 62.5-mg tablets, were 73.1, 38.2, and 10.7% for L, M, and N, respectively. There was no significant difference in dissolution rates between the 62.5- and 125-mg tablets. Furthermore, good reproducibility was seen in the dissolution rates obtained with this method (Fig. 1). To examine the relationship between *in vitro* and *in vivo* data, tablet dissolution properties must be estimated adequately; these results demonstrated that the selected method was satisfactory.

Bioavailability studies were carried out on the tablets of Formulas L, M, and N to determine how the described *in vitro* dissolution charac-

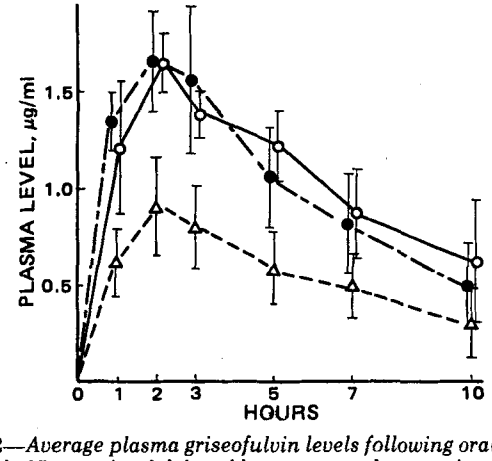

Figure 2—*Average plasma griseofulvin levels following oral administration of 125-mg griseofulvin tablets to stomach-emptying-controlled rabbits. Each point represents the average ± SE in six animals. Key: see Fig. 1.*

Table III—Plasma Level–Time Parameters following Oral Administration of 500 mg of Griseofulvin (125-mg Tablet × 4) in Humans

Parameter	Formula L	Formula M	Formula N
C_{max}[a], μg/ml	1.61[b,c] (1.00)[d]	1.13[c] (0.70)	0.55 (0.34)
C'_{max}[e], μg/ml	1.61[b,c] (1.00)	1.19[c] (0.74)	0.55 (0.34)
T_{max}[f], hr	3 (1.00)	3 (1.00)	5 (1.67)
T'_{max}[g], hr	3 (1.00)	4 (1.33)	5 (1.67)
AUC[h], hr μg/ml	11.70[c] (1.00)	8.40[c] (0.72)	3.91 (0.33)

[a] Average plasma level peak. [b] Significantly different from Formula M at $p < 0.05$. [c] Significantly different from Formula N at $p < 0.05$. [d] Each value in parentheses means relative ratio of parameters among Formulas L, M, and N. [e] Average of individual peak plasma levels. [f] Time of the average plasma level peak. [g] Average of individual peak times. [h] Area under the plasma level–time curve to 10 hr calculated by the trapezoidal rule.

teristics were reflected in the stomach-emptying-controlled rabbits. Since the minimum active ingredient content of ordinary griseofulvin tablets for clinical use is 125 mg/tablet (NF XIV and USP XIX), the 125-mg tablets of Formulas L, M, and N first were administered to six rabbits in a strictly crossover manner; the results obtained are shown in Fig. 2. Both the peak of the average plasma level, C_{max}, and the area under the average plasma level–time curve up to 10 hr, AUC, showed an order of L ≃ M > N. The plasma level after administration of the 125-mg Formula L tablet did not increase in parallel with its dissolution rate as expected.

Among the Formula L, M, and N tablets, no evident correlation was found between the dissolution rate and C_{max} or AUC. These results were attributable to griseofulvin overdose. As already mentioned, the water solubility of griseofulvin is extremely low (11, 12); its limited solubility has been the rate-limiting factor in drug absorption (13–15). These facts suggested that *in vitro* and *in vivo* correlation studies should be conducted under the dose level where a dose–response should be seen in the drug absorption.

To avoid the overdose problem, the griseofulvin dose level was reduced by one-half in subsequent studies in rabbits. The 62.5-mg tablets of Formulas L, M, and N were administered to six rabbits in a strictly crossover manner, and the plasma level–time curves and relevant data are shown in Fig. 3 and Table II. For 62.5-mg tablets, a good correlation was found between dissolution rate and bioavailability indexes such as the rate and extent of drug absorption. The C_{max} values for Formulas L, M, and N were 1.12, 0.55, and 0.40 μg/ml, respectively, in a ratio of 1.00:0.49:0.36. The AUC values were 5.64, 4.14, and 2.57 hr μg/ml, and the ratio was 1.00:0.73:0.46. Thus, both the C_{max} and AUC values were consistent with the dissolution rate order.

Although the times of peak average plasma level, T_{max}, for Formulas L, M, and N were 2, 2, and 3 hr, respectively, showing no difference between L and M, the averages of the individual peak times, T'_{max}, were 2.2, 2.5, and 3.0 hr, which were consistent with the dissolution rate order. Not only the average data but also the area under the individual rabbit plasma level–time curves showed the order L > M > N. These results were in contrast with the report of Fischer and Riegelman (16), who pointed out large individual variations when griseofulvin was given orally to rabbits fasted by the conventional method.

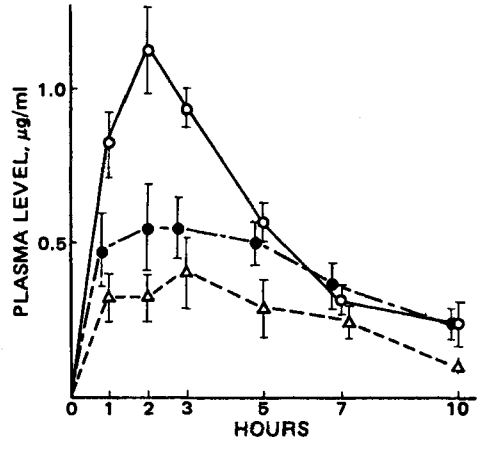

Figure 3—*Average plasma griseofulvin levels following oral administration of 62.5-mg griseofulvin tablets to stomach-emptying-controlled rabbits. Each point represents the average ± SE in six animals. Key: see Fig. 1.*

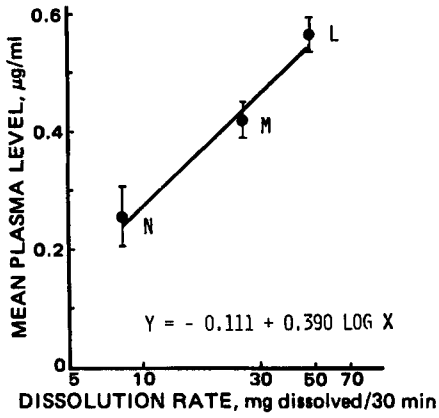

Figure 4—*Correlation of dissolution rates and mean plasma griseofulvin levels in stomach-emptying-controlled rabbits for Formulas L, M, and N. Correlation coefficient = 0.988 (p < 0.10).*

The average plasma level after administration of Formulas L, M, and N was examined statistically by the Student t test. The plasma level of Formula L differed significantly from that of Formula M at 2 and 3 hr ($p < 0.05$) and from that of Formula N at 1, 2, 3, and 5 hr ($p < 0.05$). There was no significant difference between the plasma levels of Formulas M and N. According to the method of Katchen (9), the mean plasma level, C_m, was the value of one-tenth of the AUC up to 10 hr, and this C_m was plotted against the logarithm of griseofulvin dissolved in 0.5 hr in the *in vitro* study (log $D_{0.5}$). A very close correlation was obtained between C_m and log $D_{0.5}$, with a correlation coefficient of 0.988 ($p < 0.10$) (Fig. 4). All of these data show that the best correlation was obtained between the dissolution rates and bioavailability of griseofulvin tablets by using stomach-emptying-controlled rabbits and selecting an adequate dose level.

Further studies were undertaken to examine the relationship between the stomach-emptying-controlled rabbits and human subjects. Four 125-mg tablets, corresponding to 500 mg of griseofulvin, of Formulas L, M, and N were given orally to four human volunteers in a crossover manner. The plasma level–time curves and relevant data are shown in Fig. 5 and Table III. The correlation between tablet dissolution rates and bioavailability was very high. The C_{max} values for Formulas L, M, and N were 1.61, 1.13, and 0.55 μg/ml, respectively, and their ratio was 1.00:0.70:0.34. The AUC values for Formulas L, M, and N were 11.70, 8.40, and 3.91 hr μg/ml, respectively, and the ratio was 1.00:0.72:0.33. This AUC ratio was in good agreement with that of rabbits administered 62.5 mg of the drug. Although the T_{max} for Formulas L, M, and N were 3, 3, and 5 hr, showing no difference between L and M, the individual peak time averages, T'_{max}, were 3, 4, and 5 hr for L, M, and N, which suggested a faster absorption of the tablet with superior dissolution (Table III).

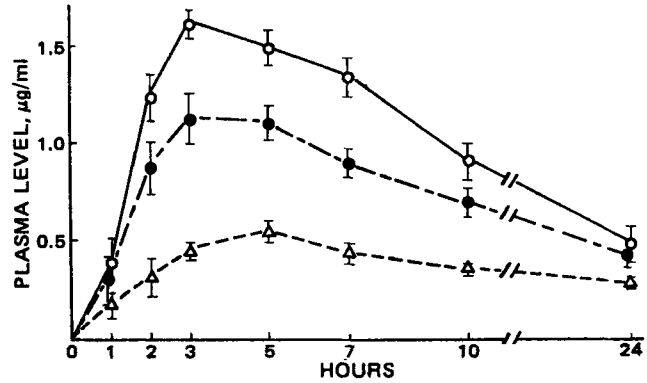

Figure 5—*Average plasma griseofulvin levels following oral administration of 500 mg of griseofulvin (125-mg tablet × 4) in humans. Each point represents the average ± SE in four men. Key: see Fig. 1.*

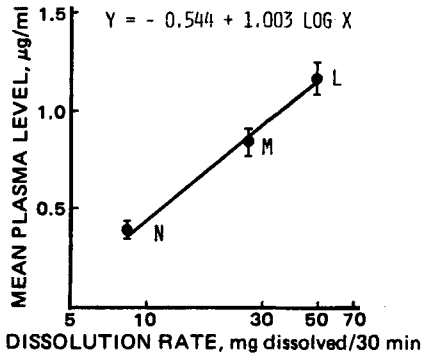

Figure 6—*Correlation of dissolution rates and mean plasma griseofulvin levels in humans for Formulas L, M, and N. Correlation coefficient = 0.995 (p < 0.10).*

While individual data are not shown, both the area under the plasma level–time curve and the peak plasma level were in the order L > M > N in all four subjects. The average plasma level of Formula L was significantly higher than that of Formula M at 3, 5, and 7 hr and than that of Formula N at 2, 3, 5, and 7 hr ($p < 0.05$). Similarly, the average plasma level of Formula M was significantly higher than that of Formula N at 2, 3, 5, 7, and 10 hr ($p < 0.05$).

The relationship between the mean plasma level, C_m, and the logarithm of griseofulvin dissolved in 0.5 hr ($\log D_{0.5}$) is shown in Fig. 6. As in the rabbit study, high correlation between C_m and $\log D_{0.5}$ was confirmed in humans, with a correlation coefficient of 0.995 ($p < 0.10$). These results support the view of previous investigators (13–15) that the dissolution process is the rate-determining step in griseofulvin absorption.

To examine the relationship between the stomach-emptying-controlled rabbit and humans, the C_m values after administering the tablets of Formulas L, M, and N to humans were plotted on the ordinate and those of the rabbit were plotted on the abscissa (Fig. 7). While the straight-line gradient suggested that the C_m of human subjects was a little more sensitive to the dissolution rate than that of the rabbit, a high correlation existed between rabbits and humans, with a correlation coefficient of 0.997 ($p < 0.05$). Although the absolute values of T_{max} and T'_{max} seemed slightly smaller in the rabbit, the ratio for Formulas L, M, and N was fairly compatible between rabbits and humans for both T_{max} and T'_{max} (Tables II and III).

Although the dose levels of 500 mg/human and 62.5 mg/rabbit corresponded to ~10 mg/kg for humans and 20 mg/kg for rabbits, being twice as large in the rabbit, both the C_{max} and the AUC were larger in humans than in rabbits. This result probably comes from the difference in the drug absorption capacity of the GI tract or in the metabolism in the two species. This difference makes it difficult to compare the absolute values of bioavailability indexes. However, these findings suggest that the stomach-emptying-controlled rabbit is a useful animal model for examining comparative bioavailability properties for oral dosage forms.

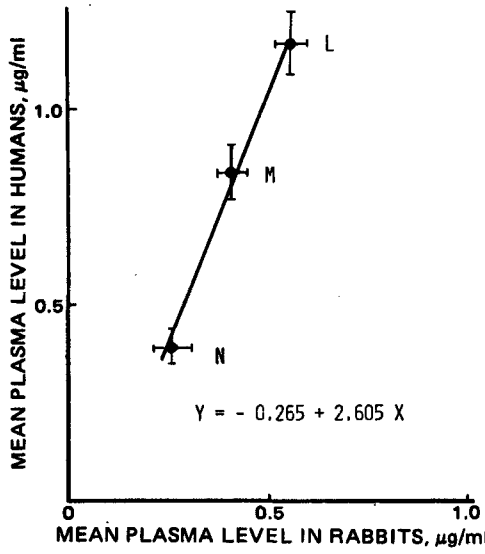

Figure 7—*Correlation of mean plasma griseofulvin levels in humans and in stomach-emptying-controlled rabbits for Formulas L, M, and N. Correlation coefficient = 0.997 (p < 0.05).*

REFERENCES

(1) H. L. Newmark, J. Berger, and J. T. Carstensen, *J. Pharm. Sci.*, **59**, 1249 (1970).

(2) W. A. Cressman and D. Sumner, *ibid.*, **60**, 132 (1971).

(3) J. W. Poole, *Rev. Can. Biol. Suppl.*, **32**, 43 (1973).

(4) W. L. Chiou, S. Riegelman, and J. R. Amberg, *Chem. Pharm. Bull.*, **17**, 2170 (1969).

(5) T. Maeda, H. Takenaka, Y. Yamahira, and T. Noguchi, *J. Pharm. Sci.*, **66**, 69 (1977).

(6) T. R. Bates, D. A. Lambert, and W. H. Johns, *ibid.*, **58**, 1468 (1969).

(7) T. J. Sullivan, R. G. Stoll, E. Sakmar, D. C. Blair, and J. G. Wagner, *J. Pharmacokinet. Biopharm.*, **2**, 29 (1974).

(8) A. Polbrant, P. Glenne, A. Sundwall, J. Vessman, and M. Wrestlind, *Acta Pharmacol. Toxicol. Suppl. 1*, **40**, 7 (1977).

(9) B. Katchen, *Acta Pharmacol. Toxicol. Suppl. 3*, **29**, 88 (1971).

(10) V. P. Shah, S. Riegelman, and W. L. Epstein, *J. Pharm. Sci.*, **61**, 634 (1972).

(11) S. H. Crowdy, J. F. Grove, and P. McCloskey, *Biochem. J.*, **72**, 241 (1959).

(12) P. H. Elworthy and J. Lipscomb, *J. Pharm. Pharmacol.*, **20**, 790 (1968).

(13) R. M. Atkinson, C. Bedford, K. J. Child, and E. G. Tomich, *Antibiot. Chemother.*, **12**, 232 (1962).

(14) M. Rowland, S. Riegelman, and W. L. Epstein, *J. Pharm. Sci.*, **57**, 984 (1968).

(15) S. Symchowicz and B. Katchen, *ibid.*, **57**, 1383 (1968).

(16) L. J. Fischer and S. Riegelman, *ibid.*, **54**, 1571 (1965).

ACKNOWLEDGMENTS

The authors thank Mr. Takeshi Yoshida for technical assistance.

Dissolution Behavior of Commercial Enteric-Coated Aspirin Tablets

KORAL EMBIL and GEORGE TOROSIAN ˣ

Received September 18, 1978, from the *College of Pharmacy, University of Florida, Gainesville, FL 32610.* Accepted for publication April 17, 1979.

Abstract □ Dissolution behavior was studied for four commercial batches of enteric-coated aspirin tablets from two companies. The USP XIX dissolution procedure was modified by including pretreatment in simulated gastric juice. The effects of five pretreatment times were studied. Pretreated tablets yielded higher dissolution profiles and fewer undissolved fractions than nonpretreated tablets. Among pretreatments, 15 min was adequate and 60 min produced the highest dissolution profiles. None of the pretreatments differed significantly from each other. An F test conducted on the data indicated that Product X was significantly better than Product Y at the $p = 0.05$ level. Batch C was ranked as the best batch irrespective of pretreatment time, followed by Batch D. Batches A and B were equal, although Batch A appeared to be better than B for the 60-min pretreatment, as indicated by the lower $t_{80\%}$ value.

Keyphrases □ Aspirin—tablets, commercial, enteric coated, dissolution procedures, dissolution times, pretreatment with simulated gastric juice □ Dissolution studies—aspirin tablets, commercial, enteric coated, dissolution times, pretreatment with simulated gastric juice □ Dosage forms, solid—tablets, aspirin, enteric coated, commercial, dissolution procedures, dissolution times, pretreatment with simulated gastric juice

Historically, enteric-coated tablets have not enjoyed the same success as other dosage forms. From time to time, new enteric coatings have been presented, but they have not been entirely successful. In 1964, Levy and Hollister (1) pointed out the failure of the USP disintegration test to assess the physiological availability of enteric-coated tablets. Subsequently, the product evaluated by these investigators was reformulated to yield a new tablet, which was said to be physiologically available (2).

In 1973, Wagner *et al.* (3) demonstrated the failure of the USP disintegration test to assess the *in vivo* availability of commercial enteric-coated aminosalicylic acid tablets. They showed that a tablet could pass the dissolution test at a high rotation speed (200 rpm) but failed to do so at the slower speed of 50 rpm. Hence, the failure of the dissolution test provided an explanation for the lack of *in vivo* availability.

Since the official compendia do not provide a method or criteria by which to judge the dissolution performance of this dosage form *in vitro,* baseline dissolution data on commercial enteric-coated aspirin tablets were needed to use as a comparison for future development of enteric coatings. In so doing, the *in vitro* dissolution profiles of two commercially available enteric-coated aspirin tablets were evaluated after varying pretreatment periods. The usual USP procedure for uncoated tablets was adapted for this purpose. Additionally, the product-to-product and batch-to-batch variations were observed.

EXPERIMENTAL

Reagents—Purified resin powder[1] (pepsin) and pancreatin[2] obtained from porcine pancreas (Grade II) stored below 0° were used without further treatment. All other materials, sodium chloride, sodium hydroxide, monobasic potassium phosphate, and hydrochloric acid, were reagent grade and were used as obtained. The commercial enteric-coated aspirin tablets were purchased over the counter from various pharmacies, and the batches were selected at random. Two brands were involved; Brand X consisted of Batches C and D, and Brand Y consisted of Batches A and B.

Equipment—The dissolution equipment[3] was manufactured to USP XIX (4) standards, which included the dissolution motor and variable-speed controller with a stainless steel basket assembly. The dissolution vessel was a 900-ml round-bottom resin flask fitted with an appropriate glass cup. Two dissolution apparatus, designated left (L) and right (R), were matched in their performance using a single batch of tablets and modified to reduce unwanted vibrations by the incorporation of a 1000-μF capacitor in the speed control circuit (5).

The rotation speed of the basket assembly was fixed at 50 ± 1.5 rpm throughout the experiment. The dissolution assembly was immersed in a water bath at 37 ± 0.1°. The UV absorbance was measured with a spectrophotometer[4]. All absorbance data were processed using a desktop computer[5]. The final statistical analysis was conducted by the statistical analysis system[6] (SAS) program package.

Method—The USP XIX (4) dissolution procedure for uncoated tablets was used with the modification noted later. The dissolution study involved a pretreated and a nonpretreated regimen. A total of 200 tablets was tested.

Two experiments were conducted. The first involved the direct introduction of the enteric-coated tablets into the simulated intestinal juice for 10 hr. The second involved the pretreatment of the enteric-coated tablet in simulated gastric juice for variable intervals of 15, 30, 60, and 120 min, followed by immersion in simulated intestinal juice for 10 hr. A single gastric juice sample was analyzed for salicylate content after pretreatment. This test was followed by the analysis of the simulated intestinal juice samples collected every 2 hr.

Aspirin was assayed by hydrolysis of acetylsalicylic acid (aspirin) to

Table I—Analysis of Variance for Overall Data Collected (1000 Observations)

Source of Variation	Degrees of Freedom	F Value[a]	Probability, $>F$
Batch	3	39.83+	0.0001
Pretreat	4	70.99+	0.0001
Time	4	1450.98	0.0001
Machine	1	43.77+	0.0001
Batch–pretreat	12	7.93+	0.0001
Batch–time	12	4.22	0.0001
Pretreat–time	16	6.14	0.0001
Batch–pretreat–time	48	3.09	0.0001
Pretreat–machine	4	1.35+	0.2531
Time–machine	4	7.15	0.0001
Batch–machine	3	1.72+	0.1641
Pretreat–time–machine	16	0.12+	1.0000
Batch–pretreat–machine	12	12.31	0.0001
Batch–time–machine	12	1.64	0.0755
Batch–pretreat–time–machine	48	1.41	0.0393
Tablet (batch–pretreat–machine)	160	15.39	0.0001
Error	640		
Corrected total	999		

[a] The plus sign indicates test of hypotheses using analysis of variance sum of squares for the tablet (batch–pretreat–machine) as the error term.

[1] Fisher Scientific Co., Orlando, Fla.
[2] Sigma Chemical Co., St. Louis, Mo.
[3] Hanson Research Corp., Northridge, Calif.
[4] Beckman DB-GT connected to a 25.4-cm Beckman recorder.
[5] Hewlett-Packard 9815A attached to a model 9862 desktop calculator plotter.
[6] Amdahl 470 computer.

0022-3549/79/1000-1290$01.00/0
© 1979, American Pharmaceutical Association

Table II—Effect of Pretreatment on Dissolution ($t_{80\%}$)

Batch	Pretreatment Time			
	15 min	30 min	60 min	120 min
A	448	374	232	330
B	322	206	264	370
C	224	188	153	176
D	252	212	208	218

salicylate ion and subsequent UV spectrophotometry. A dissolution medium aliquot was filtered into a 25-ml volumetric flask to which, just prior to UV analysis, 10 ml of 2 *N* NaOH was added to achieve the pH 14 necessary for rapid and complete hydrolysis. The UV absorbance of this solution was measured at 302 nm. Constant dissolution volume was maintained by the addition of fresh dissolution fluid. Simulated gastric and intestinal juices were prepared fresh and were brought to temperature just prior to the actual dissolution experiment.

Statistical Analysis—The analysis of variance (ANOVA) study was conducted using a mixed model to analyze statistically the dissolution experiment data. To stabilize the variances, the data were transformed by taking the arc sine of the square root of 1/100 of each observation. The overall analysis of variance was conducted for all 1000 observations. The *F* statistic for the mixed model was calculated by dividing the sum of squares for the effect by the sum of squares for the tablet (batch–pretreatment–time) nested triple interaction term for the values indicated by the plus sign in Table I. All other values were calculated in the usual fashion by dividing the sum of squares for the effect by the sum of squares for the error term (6).

The overall analysis of variance was designed to determine the independent variable that caused the most interactions. All observations could be sorted by that variable, enabling inferences to be drawn with more accuracy. A point-by-point analysis for significance was conducted for percent dissolved at each time interval using Duncan's multiple-range test (7). Finally, an *F* test was conducted to determine if the two brands were significantly different in performance based on the four batches tested.

RESULTS AND DISCUSSION

The overall analysis of variance indicated that batch, pretreatment time, dissolution time, and apparatus all significantly affected the dissolution profiles of commercial enteric-coated aspirin tablets (Table I). Because most interactions were caused by batch-to-batch variations, the data were sorted by batches, and an analysis of variance was conducted for each batch. Pretreatment significantly altered the dissolution profiles from all batches except D.

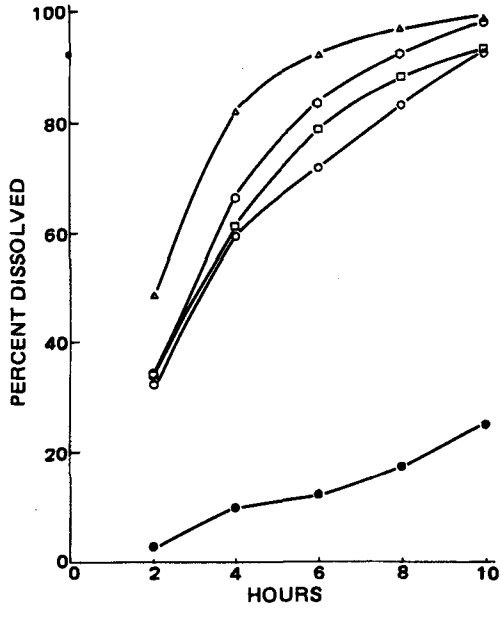

Figure 1—*Dissolution profile of Batch A in simulated intestinal juice after different gastric juice pretreatment times. Key: ●, no pretreatment; ○, 15-min pretreatment; □, 30-min pretreatment; △, 60-min pretreatment; and ○, 120-min pretreatment.*

Table III—Number out of 10 Tablets Remaining Partially Undissolved after 10 hr of Dissolution [a]

Pretreatment	Brand Y		Brand X	
	Batch A	Batch B	Batch C	Batch D
None	0	5	3	0
	10	5	1	0
15 min	2	2	0	0
	0	0	0	0
30 min	0	2	0	0
	0	0	0	0
60 min	1	1	0	0
	0	0	0	0
120 min	2	2	1	0
	0	0	0	0

[a] First row of numbers represents <50% and the second row represents >50% of the tablets that remained undissolved after 10 hr.

Figure 1 demonstrates the typical effect of simulated gastric juice pretreatment on tablet dissolution in simulated intestinal juice. Figure 2 presents the percent dissolved at each pretreatment time after 2 hr of dissolution in simulated intestinal juice and is typical of the results obtained for 4-, 6-, 8-, and 10-hr intervals. Duncan's multiple-range test for significance indicated no significant difference among 15-, 30-, and 60-min pretreatments for Batches A, C, and D. The 60-min pretreatment yielded higher values for percent dissolved, but they were not statistically significant.

The data suggests (Figs. 1 and 2) that a 15-min pretreatment would be adequate for three of the four batches. The 60-min pretreatment was consistently higher than other pretreatment times within a given batch. The 60-min pretreatment was not significantly different from the 15-min pretreatment except for Batch B. However, there was a trend for the dissolution values to peak following the 60-min pretreatment. The percent dissolved value diminished slightly after 120 min of pretreatment. This slight reduction for three of the four batches was not statistically significant from that observed for the 60-min pretreatment. Batch D, on the other hand, did have a significant reduction in the percent dissolved after 120 min of pretreatment and 2 hr of dissolution. This apparently anomalous behavior was not consistent in magnitude or in order with the data obtained at later dissolution intervals up to and including 10 hr. Similar plots of percent dissolved *versus* pretreatment time for the data at 4-, 6-, 8-, and 10-hr dissolution intervals showed the same rank order and confirmed the conclusions drawn from the data presented in Fig. 2.

Percent dissolved *versus* pretreatment time plots were made for all four batches after 15, 30, 60, and 120 min of pretreatment. Figure 3 presents the typical results of the 60-min pretreatment. Batch C gave the highest value at all pretreatment times. Table II summarizes the dissolution profile with respect to $t_{80\%}$, the time for 80% of the tablet to be dissolved for each batch. These values appear to be smallest after 60 min of pretreatment for Batches A, C, and D; Batch B had a minimum $t_{80\%}$ after 30 min of pretreatment. Overall, the $t_{80\%}$ values range from 2 hr and 33 min for Batch C to 4 hr and 24 min for Batch B after 60 min of pretreatment. The tablets pretreated for 15 min had higher $t_{80\%}$ values than the 60-min pretreatment results, suggesting a relationship between pretreatment time and the minimum $t_{80\%}$ values; *i.e.*, increased pretreatment time appeared to reduce the $t_{80\%}$ values.

A similar relationship may exist for the *in vivo* dissolution process.

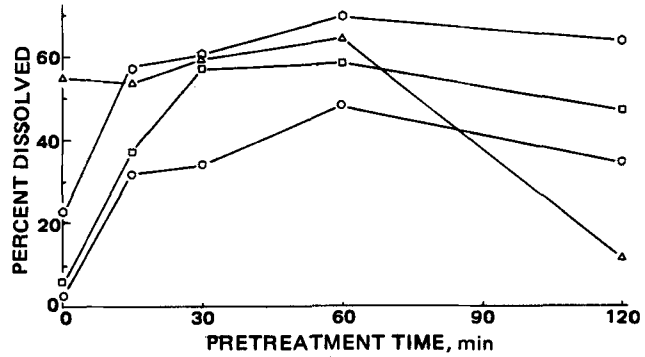

Figure 2—*Percent dissolved* versus *pretreatment time for all four batches after 2 hr of dissolution in simulated intestinal fluid. Key: ○, Batch A; □, Batch B; ○, Batch C; and △, Batch D.*

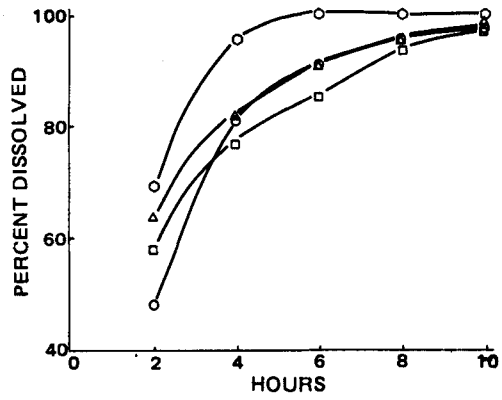

Figure 3—*Dissolution plots of all four batches after 60-min pretreatment. Key:* ○, *Batch A;* □, *Batch B;* ○, *Batch C; and* △, *Batch D.*

Table III shows that the number of tablets undissolved after 10 hr of dissolution with no pretreatment was greater for Product Y than for Product X. For Batches A and B with no pretreatment, all tablets tested were partially undissolved after 10 hr. Batch C similarly yielded four out of 10 undissolved, whereas the tablets in Batch D were totally dissolved. Pretreatment decreased both the number and size of undissolved tablet residues after 10 hr of dissolution. Overall, the 60-min pretreatment resulted in the fewest undissolved residues for all batches tested, suggesting it as the optimum pretreatment time. Furthermore, Product X appeared to perform *in vitro* better than Product Y with respect to the number of undissolved tablet fractions at all pretreatment times. This finding supports the F test result, which indicated that Brand X performed significantly better *in vitro* than Brand Y ($p = 0.05$).

SUMMARY

Pretreated tablets yielded higher dissolution profiles than nonpretreated tablets. The analysis of variance showed that pretreatment significantly increased the tablet dissolution profiles from all batches except Batch D at the $p = 0.0001$ level. Furthermore, Table III indicates that pretreatment in simulated gastric juice reduced both the number and the size of undissolved fractions. The 15-min pretreatment was adequate and was not statistically different from the other pretreatment periods. However, the 60-min pretreatment yielded higher dissolution profiles for all batches and fewer tablet residues. While the tendency for higher dissolution profiles cannot be supported statistically, this trend is consistent with the reduction in tablet residues after 10 hr of dissolution.

A relationship between the pretreatment time and the $t_{80\%}$ reduction appeared to exist, suggesting that a similar relationship may exist *in vivo* and should be studied. Product X performed better than Y, as indicated by higher dissolution profiles. The smaller $t_{80\%}$ values for Product X (Table II) support this argument. The F test using averages obtained after each time interval indicates that Product X was significantly better than Y at the $p = 0.05$ level. Furthermore, Table III shows that there were fewer undissolved tablet residues for Product X than for Product Y after 10 hr of dissolution in simulated intestinal fluid.

The batch ranking indicated that Batch C was the best batch irrespective of the pretreatment times, and it was followed by Batch D. Batches A and B were interchangeable, although Batch A appeared to be better than B for the 60-min pretreatment, as indicated by the lower $t_{80\%}$ value. Since the conclusions are based on *in vitro* data, any extrapolations to the biological system should be confirmed *in vivo*.

REFERENCES

(1) G. Levy and L. E. Hollister, *N.Y. State J. Med.*, **15**, 3002 (1964).

(2) J. G. Wagner, "Biopharmaceutics and Relevant Pharmacokinetics," Drug Intelligence Publications, Hamilton, Ill., 1971, p. 77.

(3) J. G. Wagner, P. K. Wilkinson, A. J. Sedman, and R. G. Stoll, *J. Pharm. Sci.*, **62**, 859 (1973).

(4) "The United States Pharmacopeia," 19th rev., Mack Publishing Co., Easton, Pa., 1975, p. 650.

(5) K. Embil and G. Torosian, *J. Pharm. Sci.*, **68**, 1336 (1979).

(6) G. W. Snedecor and W. G. Cochran, "Statistical Methods," 6th ed., Iowa University Press, Ames, Iowa, 1967, p. 258.

(7) R. G. D. Steel and J. H. Torrie, "Principles and Procedures of Statistics," McGraw-Hill, New York, N.Y., 1960, p. 107.

ACKNOWLEDGMENTS

Abstracted in part from a thesis submitted by K. Emil to the University of Florida in partial fulfillment of the Master of Science in Pharmacy degree requirements.

The authors thank Mr. J. A. Ondrasik for help in the statistical analysis and computer programs.

Anomalous Solution Behavior of 2-Palmitate Esters of Lincomycin and Clindamycin

E. L. ROWE

Received June 22, 1978, from *Pharmacy Research, The Upjohn Company, Kalamazoo, MI 49001.* Accepted for publication April 18, 1979.

Abstract □ The aqueous solubilities of lincomycin and clindamycin 2-palmitate esters are compared. Clindamycin 2-palmitate hydrochloride has an unusually high solubility at 25°, which is due to micelle formation. Both compounds are surface active with relatively low critical micelle concentrations. However, since the Krafft point of lincomycin palmitate is ~43°, it does not form micelles below that temperature and appears to be quite insoluble until heated above 43°. The experimental monomeric solubilities of the two compounds agree with calculations based on group contributions to lipophilicity. Clindamycin 2-palmitate hydrochloride solutions are quite sensitive to ions, being salted out as unprotonated base in the form of oily droplets. Salting out correlates well with anionic strength, which is quite constant for the various salts studied. A viscosity maximum occurs with increasing salt addition, with the peaks of the different salts occurring at the same anionic strengths.

Keyphrases □ Lincomycin—palmitate ester, aqueous solubility, pH, temperature, micelle formation □ Clindamycin—palmitate ester, aqueous solubility, pH, temperature, micelle formation □ Antibacterial agents—lincomycin, palmitate ester, aqueous solubility, pH, temperature, micelle formation □ Antibacterial agents—clindamycin, palmitate ester, aqueous solubility, pH, temperature, micelle formation □ Aqueous solubility—lincomycin and clindamycin palmitate esters

Lincomycin and clindamycin are medium spectrum antibiotics whose hydrochloride salts are quite soluble in water. Both compounds have a bitter taste which is difficult to mask. Since clindamycin hydrochloride is considerably more bitter than lincomycin hydrochloride, chemical modification was required to make an acceptable liquid dosage form. A variety of prodrug esters were synthesized to reduce or eliminate the bitter taste of these anti-

0022-3549/79/1000-1292$01.00/0
© 1979, American Pharmaceutical Association

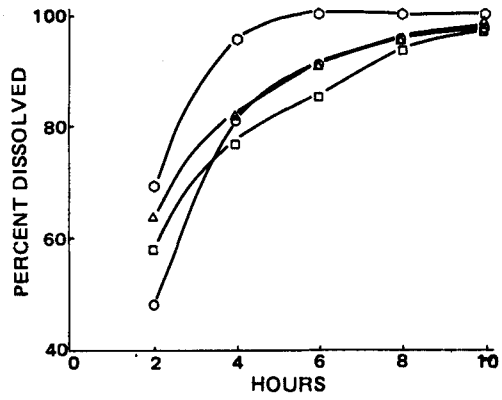

Figure 3—*Dissolution plots of all four batches after 60-min pretreatment. Key:* ○, *Batch A;* □, *Batch B;* ○, *Batch C; and* △, *Batch D.*

Table III shows that the number of tablets undissolved after 10 hr of dissolution with no pretreatment was greater for Product Y than for Product X. For Batches A and B with no pretreatment, all tablets tested were partially undissolved after 10 hr. Batch C similarly yielded four out of 10 undissolved, whereas the tablets in Batch D were totally dissolved. Pretreatment decreased both the number and size of undissolved tablet residues after 10 hr of dissolution. Overall, the 60-min pretreatment resulted in the fewest undissolved residues for all batches tested, suggesting it as the optimum pretreatment time. Furthermore, Product X appeared to perform *in vitro* better than Product Y with respect to the number of undissolved tablet fractions at all pretreatment times. This finding supports the F test result, which indicated that Brand X performed significantly better *in vitro* than Brand Y ($p = 0.05$).

SUMMARY

Pretreated tablets yielded higher dissolution profiles than nonpretreated tablets. The analysis of variance showed that pretreatment significantly increased the tablet dissolution profiles from all batches except Batch D at the $p = 0.0001$ level. Furthermore, Table III indicates that pretreatment in simulated gastric juice reduced both the number and the size of undissolved fractions. The 15-min pretreatment was adequate and was not statistically different from the other pretreatment periods. However, the 60-min pretreatment yielded higher dissolution profiles for all batches and fewer tablet residues. While the tendency for higher dissolution profiles cannot be supported statistically, this trend is consistent with the reduction in tablet residues after 10 hr of dissolution.

A relationship between the pretreatment time and the $t_{80\%}$ reduction appeared to exist, suggesting that a similar relationship may exist *in vivo* and should be studied. Product X performed better than Y, as indicated by higher dissolution profiles. The smaller $t_{80\%}$ values for Product X (Table II) support this argument. The F test using averages obtained after each time interval indicates that Product X was significantly better than Y at the $p = 0.05$ level. Furthermore, Table III shows that there were fewer undissolved tablet residues for Product X than for Product Y after 10 hr of dissolution in simulated intestinal fluid.

The batch ranking indicated that Batch C was the best batch irrespective of the pretreatment times, and it was followed by Batch D. Batches A and B were interchangeable, although Batch A appeared to be better than B for the 60-min pretreatment, as indicated by the lower $t_{80\%}$ value. Since the conclusions are based on *in vitro* data, any extrapolations to the biological system should be confirmed *in vivo*.

REFERENCES

(1) G. Levy and L. E. Hollister, *N.Y. State J. Med.*, **15**, 3002 (1964).

(2) J. G. Wagner, "Biopharmaceutics and Relevant Pharmacokinetics," Drug Intelligence Publications, Hamilton, Ill., 1971, p. 77.

(3) J. G. Wagner, P. K. Wilkinson, A. J. Sedman, and R. G. Stoll, *J. Pharm. Sci.*, **62**, 859 (1973).

(4) "The United States Pharmacopeia," 19th rev., Mack Publishing Co., Easton, Pa., 1975, p. 650.

(5) K. Embil and G. Torosian, *J. Pharm. Sci.*, **68**, 1336 (1979).

(6) G. W. Snedecor and W. G. Cochran, "Statistical Methods," 6th ed., Iowa University Press, Ames, Iowa, 1967, p. 258.

(7) R. G. D. Steel and J. H. Torrie, "Principles and Procedures of Statistics," McGraw-Hill, New York, N.Y., 1960, p. 107.

ACKNOWLEDGMENTS

Abstracted in part from a thesis submitted by K. Emil to the University of Florida in partial fulfillment of the Master of Science in Pharmacy degree requirements.

The authors thank Mr. J. A. Ondrasik for help in the statistical analysis and computer programs.

Anomalous Solution Behavior of 2-Palmitate Esters of Lincomycin and Clindamycin

E. L. ROWE

Received June 22, 1978, from *Pharmacy Research, The Upjohn Company, Kalamazoo, MI 49001.* Accepted for publication April 18, 1979.

Abstract □ The aqueous solubilities of lincomycin and clindamycin 2-palmitate esters are compared. Clindamycin 2-palmitate hydrochloride has an unusually high solubility at 25°, which is due to micelle formation. Both compounds are surface active with relatively low critical micelle concentrations. However, since the Krafft point of lincomycin palmitate is ~43°, it does not form micelles below that temperature and appears to be quite insoluble until heated above 43°. The experimental monomeric solubilities of the two compounds agree with calculations based on group contributions to lipophilicity. Clindamycin 2-palmitate hydrochloride solutions are quite sensitive to ions, being salted out as unprotonated base in the form of oily droplets. Salting out correlates well with anionic strength, which is quite constant for the various salts studied. A viscosity maximum occurs with increasing salt addition, with the peaks of the different salts occurring at the same anionic strengths.

Keyphrases □ Lincomycin—palmitate ester, aqueous solubility, pH, temperature, micelle formation □ Clindamycin—palmitate ester, aqueous solubility, pH, temperature, micelle formation □ Antibacterial agents—lincomycin, palmitate ester, aqueous solubility, pH, temperature, micelle formation □ Antibacterial agents—clindamycin, palmitate ester, aqueous solubility, pH, temperature, micelle formation □ Aqueous solubility—lincomycin and clindamycin palmitate esters

Lincomycin and clindamycin are medium spectrum antibiotics whose hydrochloride salts are quite soluble in water. Both compounds have a bitter taste which is difficult to mask. Since clindamycin hydrochloride is considerably more bitter than lincomycin hydrochloride, chemical modification was required to make an acceptable liquid dosage form. A variety of prodrug esters were synthesized to reduce or eliminate the bitter taste of these anti-

0022-3549/79/1000-1292$01.00/0
© 1979, American Pharmaceutical Association

Table I—Aqueous Solubility of Lincomycin and Clindamycin 2-Palmitate Hydrochloride at 24.3°

I		II	
pH[a]	Solubility, mg/ml	pH[a]	Solubility, mg/ml
2.3	0.124	3.7	53.2
—	—	5.8	<0.001
7.4	0.0249	7.4	<0.0002

[a] Saturated solution pH at the end of the equilibration period.

biotics (1, 2). The esters are inactive until enzymatically hydrolyzed, which occurs readily *in vivo*, providing reasonably good blood levels of the parent compounds.

With respect to taste, stability, and bioavailability, lincomycin 2-palmitate hydrochloride (I) and clindamycin 2-palmitate hydrochloride (II) are the most useful of the prodrugs synthesized. This study explores some of the unusual solution properties of these esters, including surface activity, pH–solubility relationships, and sensitivity to ions.

EXPERIMENTAL

Materials—Compounds I and II were obtained from research stock and were used as received for the solubility studies. For surface activity measurement, II was purified by column chromatography. A concentrated aqueous II solution was eluted through a silica gel column with a solvent system of hexane–2-pentanone–pyridine (49:49:5). The filtrate was monitored by TLC, and a narrow fraction containing the main component was collected. The hydrochloride salt was formed by addition of chloroform saturated with hydrogen chloride gas. The product was precipitated by slow acetonitrile addition, filtered, washed with additional acetonitrile, and dried under vacuum at ambient temperatures.

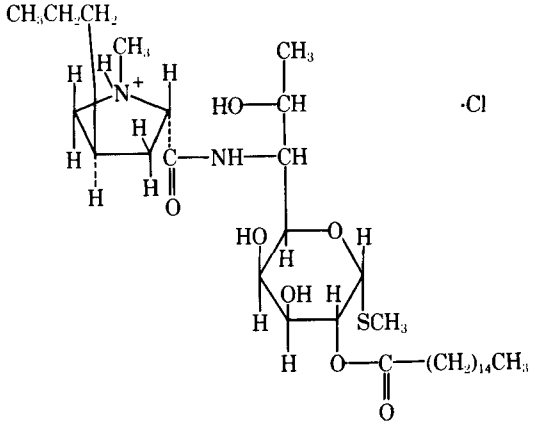

I

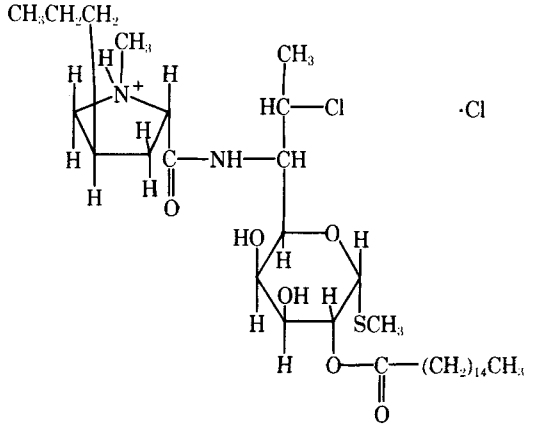

II

Anal.—Calc. (when corrected for water): C, 58.35; H, 9.22; N, 4.00; Cl, 10.13; S, 4.58. Found: C, 57.92; H, 9.17; N, 3.91; Cl, 10.46; S, 4.42; H_2O, 2.25.

Flavored II granules were obtained from regular production stock. All electrolytes, solvents, and other chemicals were reagent grade.

Solubility Determination—An excess of the compounds was added to double-distilled water in tightly capped tubes and equilibrated for 2 or more days at 24.3 ± 0.3° using an oscillating shaker at 18 cpm.

A portion of the samples was filtered through medium glass frit funnels and again through 0.22-μm membrane filters[1]. The natural pH of the filtrates was measured with a pH meter[2]. The remaining unfiltered suspensions were each titrated with 1.0 *N* NaOH to ~pH 10, equilibrated for 2 or more days at 24.3°, and then filtered as before.

The solubility–temperature study on I was conducted in a constant-temperature bath[3] equipped with a sample holder that rotated at 6 rpm. The solutions were filtered through a preheated glass filtering apparatus[4]. Portions of the filtrate were transferred to vials with a preheated pipet. The solutions were either freeze dried and then redissolved in internal standard solution or extracted with chloroform after the aqueous solutions were made basic with sodium bicarbonate. The chloroform solutions were assayed by GLC using the conditions described previously (3, 4).

Surface Tension Measurement—A stock purified II solution was prepared in double-distilled water at ~10^{-2} *M*. Serial dilutions were made so that each successive solution had a concentration one-half that of the previous solution. The surface tension of each solution was measured at 25° in an automated drop-volume apparatus described earlier (5). The surface tension of the same solutions also was measured with a Wilhelmy plate apparatus[5].

Viscosity Measurement—Twenty-four grams of flavored granules containing II at a concentration of 37.5 mg of clindamycin activity per gram was added to 60-ml clear flint bottles. Stock electrolyte solutions were made from reagent grade salts and deionized water to give final concentrations of 6000 mg/liter.

These stock solutions were diluted to give a series of solutions with salt concentrations ranging from 100 to 6000 mg/liter. Forty-five milliliters of each salt solution was added to the bottled granules and shaken to obtain complete dissolution. Observations and measurements were made after standing at room temperature. Viscosity was measured using a viscometer[6] with a No. 2 spindle at 12 rpm.

RESULTS AND DISCUSSION

Comparative Solubilities of I and II—The solubilities obtained for I and II are shown in Table I. The solubility of II in the acid range was abnormally high (400-fold greater than I). It should actually be lower than I since the substitution of a chlorine group for a hydroxyl is expected to lower the aqueous solubility. At the very least, the solubilities should be about equal if the solvated protonated amine group dominates over lipophilic differences at C_7. This apparent anomaly was due to micelle formation by II, which occurs only in the protonated state. This phenomenon will be discussed more fully in the following section.

At pH 7.4 in the nonmicellar region, the solubilities of the two compounds differed in the "right" direction, *i.e.*, I was more soluble than II. The relative solubilities of I and II at this pH can be calculated from group contributions to lipophilicity (6). On this basis, one would expect I to be more water soluble (less lipophilic) than II. With the Hansch equation:

$$\log \frac{1}{S} = a \log P + b \qquad \text{(Eq. 1)}$$

where S is the molal solubility of the compound in water, P is the partition coefficient between 1-octanol and water, and a and b are constants, the solubility ratio of I and II can be obtained by combining their respective equations:

$$\log \frac{S_I}{S_{II}} = a(\log P_{II} - \log P_I) \qquad \text{(Eq. 2)}$$

The effect of group substitution on the partition coefficient can be evaluated using substituent constants:

$$\pi_x = \log P_x - \log P_H \qquad \text{(Eq. 3)}$$

[1] Type GS11, Millipore Corp., Bedford, Mass.
[2] Model NX, Sargent-Welch Scientific Co., Skokie, Ill.
[3] Constructed at The Upjohn Co., Kalamazoo, Mich.
[4] Medium glass frit funnel fitted with ground glass joints to a suction flask with an upward extended sidearm.
[5] Rosano surface tensiometer, Federal Pacific Electric Co., Newark, N.J.
[6] Model LVF, Brookfield Engineering Laboratories, Stoughton, Mass.

Table II—Critical Salting-Out Concentrations of Electrolytes for Clindamycin 2-Palmitate Hydrochloride

Salt	Molar Concentration	Ionic Strength	Anionic Strength
Na_2SO_4	0.014	0.042	0.056
$FeSO_4$	0.013	0.052	0.052
$MgSO_4$	0.017	0.068	0.068
$MgCl_2$	0.032	0.096	0.064
$CaCl_2$	0.027	0.081	0.054
NaCl	0.052	0.052	0.052
KCl	0.054	0.054	0.054
$NaHCO_3$	0.024	0.024	0.024

where P_x is the partition coefficient of a derivative and P_H is that of the parent molecule. When the appropriate constants are substituted into Eq. 2:

$$\log \frac{S_I}{S_{II}} = a(\pi_{Cl} - \pi_{OH}) \qquad \text{(Eq. 4)}$$

Taking established values for the constants (6) gives:

$$\log \frac{S_I}{S_{II}} = 1.339\ (0.39 + 1.16) = 2.075 \qquad \text{(Eq. 5)}$$

and:

$$\frac{S_I}{S_{II}} = 119 \qquad \text{(Eq. 6)}$$

Thus, I should be 119 times more soluble than II. The experimental solubility ratio in Table I at pH 7.4 is (0.0249/<0.0002) ≥ 125, which is a close approximation of the calculated value. The same semiquantitative solubility relationship holds true for the parent compounds, lincomycin and clindamycin. Their solubility ratio should also be 119. The respective experimental solubilities were determined previously (7) to be >400 and 4 mg/ml, giving a ratio of ≥100, again in close agreement with theory.

Surface Activity and Solubility—Clindamycin 2-palmitate hydrochloride (II) has an amphiphilic structure conducive to surface activity and micellar aggregation. The combination of a lipophilic palmitate side chain and a protonated head group is responsible for the enhanced solubility through association into micelles.

The compound is highly surface active, reducing the water surface tension from 72 to 30 dynes/cm. The data obtained from drop-volume measurements on the automated drop-volume apparatus (5) showed a distinct critical micelle concentration (CMC) at 3.40×10^{-4} mole/liter (Fig. 1). This finding was confirmed by Wilhelmy plate data, which gave a CMC of $\sim 3.5 \times 10^{-4}$ mole/liter. This value is about one order of magnitude lower than an estimate published earlier (8).

Above the CMC, the monomer concentration stays essentially constant, with the excess molecules forming micelles (9). Therefore, the monomer concentration in equilibrium with micelles is $\sim 3.4 \times 10^{-4}$ *M* or ~0.238 mg/ml.

As a first approximation, this value can be considered the monomer solubility of II. It is close to the experimental solubility of I (0.124 mg/ml, Table I). Apparently, lipophilicity differences due to the substitution at C_7 are overshadowed by the highly hydrophilic, protonated amine function.

Compound I has the same amphiphilic structure as II but does not appear to have sufficient surface activity to provide micellar solubilization

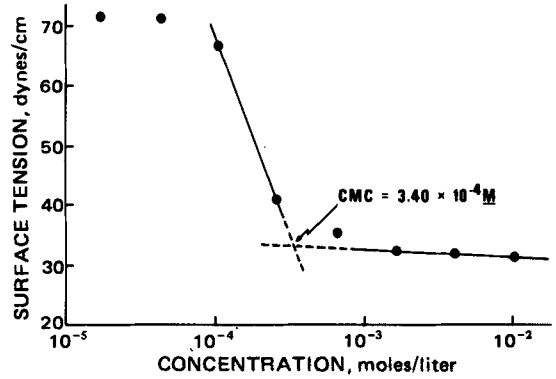

Figure 1—*Surface tension* versus *log concentration of aqueous clindamycin 2-palmitate hydrochloride solutions at 25°.*

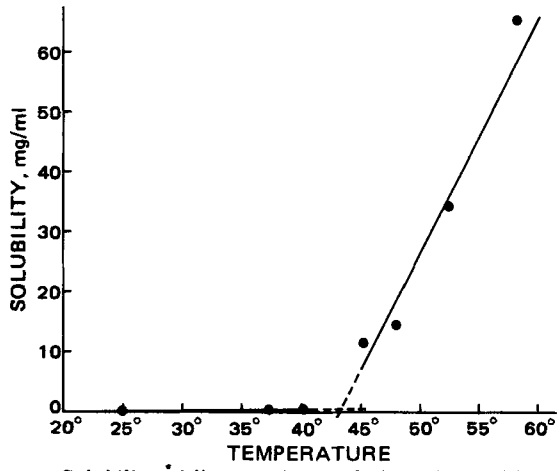

Figure 2—*Solubility of lincomycin 2-palmitate hydrochloride as a function of temperature.*

at 25°. However, at higher temperatures, the solubility increased sharply (Fig. 2). The solubility increased slowly with increasing temperature until ~43°, when a sudden change in slope occurred. Many surfactants exhibit similar solubility changes at a critical temperature known as the Krafft point (10). At this temperature, the monomer solubility has increased sufficiently to make micelle formation possible. Above the Krafft point, of course, the apparent solubility is due to micellar aggregation. The CMC at the Krafft point is $\sim 3.62 \times 10^{-4}$ *M* or ~0.247 mg/ml, which is a fair estimate of the monomer solubility at 43°. At 25°, the monomer solubility would be less and much closer to the experimental value of 0.124 mg/ml.

pH Dependence of Clindamycin Palmitate Hydrochloride Solubility—The solubility of II varied greatly with pH. In the free base form, II was extremely insoluble and difficult to measure quantitatively. Even at pH 7.4, which is slightly below the estimated pKa of 7.6[7], the observed solubility was below the detection limit (<0.0002 mg/ml). Below pH 4, the protonated drug had a monomeric solubility over 1000 times greater than the base solubility. Thus, the solubility–pH curve had a steep slope, and acidic II solutions appeared to precipitate out quantitatively as the pH increased. For example, if an acidic solution (pH 3) containing 15 mg of II/ml is titrated with base to pH 5.8 where the solubility of II is <0.001 mg/ml, >99.9% of the initial concentration would precipitate out. The pH–solubility profile shown in Fig. 3 was calculated from:

$$S_t = [CPH^+] + [CP] \qquad \text{(Eq. 7)}$$

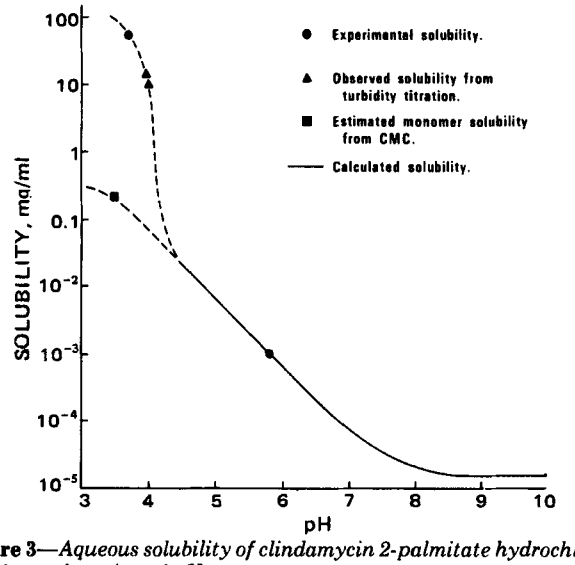

Figure 3—*Aqueous solubility of clindamycin 2-palmitate hydrochloride at 25° as a function of pH.*

[7] The pKa of II is difficult to determine because of the low solubility at high pH. However, the palmitate ester is too remote (both conformationally and along the chain) from the protonated amine function to have any noticeable effect on the pKa. Therefore, it is reasonable to assume that the pKa of the parent molecule, clindamycin, is unchanged by esterification at the 2-hydroxy position.

Table III—Effect of 2:1 Salt Mixtures on Salting Out of Clindamycin 2-Palmitate Hydrochloride from Syrup Solution

Mixture Number	Salt	Salt Concentration, mg/liter	Anionic Strength	Critical[a] Anionic Strength	Appearance of Reconstituted Solution
1a	$MgCl_2$	1333	0.028		Very slight turbidity
	Na_2SO_4	667	0.019		
	Total	2000	0.047		
				0.061	
1b	$MgCl_2$	2000	0.042		Very turbid with thick oil layer
	Na_2SO_4	1000	0.028		
	Total	3000	0.070		
2a	$CaCl_2$	1333	0.024		Very slight turbidity
	$NaHCO_3$	667	0.008		
	Total	2000	0.032		
				0.044	
2b	$CaCl_2$	2000	0.036		Turbid with oil layer
	$NaHCO_3$	1000	0.012		
	Total	3000	0.048		

[a] Calculated for the salt mixtures from the data in Table II, assuming that the individual values are additive.

where S_t is the total solubility, $[CPH^+]$ is the II concentration, and [CP] is the concentration of the unprotonated base form of II. The $[CPH^+]$ values at various pH's were obtained from the Henderson–Hasselbach equation:

$$\log [CPH^+] = pKa + \log [CP] - pH \qquad \text{(Eq. 8)}$$

where [CP] is assumed to be constant at pH 4–10 and was calculated to be $<1.56 \times 10^{-5}$ mg/ml using the experimental solubility value at pH 5.8 and the estimated pKa of 7.6. The solid line in Fig. 3, constructed from Eqs. 7 and 8, is a reasonably good estimate of the maximum solubility of II in the pH region shown.

As the pH decreases below the pKa, the concentration of protonated II molecules increases until the CMC is reached, at which time micelles form, causing a large jump in apparent solubility at ~pH 4. The experimentally observed CMC, which is a good estimate of the monomer concentration of II, was at 0.238 mg/ml. Without micelle formation, presumably the solubility would plateau at about this level. The triangular points (Fig. 3) are semiquantitative solubility values obtained from observations of the first appearance of turbidity when 1 *M* NaOH was added to syrup solutions of II.

The solubility curve in Fig. 3, while qualitative, does characterize the unusual pH–solubility relationship of II. The extremely low solubility of the base form kept the total solubility very low throughout most of the pH range. Only when the pH was 3 or 4 units below the pKa did it become significant. At pH 3.6, four units below the pKa, the protonated monomer concentration was 10^4 times the base solubility, which was at most 0.0001 mg/ml. Therefore, the monomer solubility at pH 3.6 was only ≤1 mg/ml. Of course, this result does not take into account the solubility due to micelle formation, which can amount to >50 mg/ml (Fig. 3).

Effect of Salts on Solubility—The solubility of II was greatly reduced by inorganic salts. When the salt concentration exceeded a certain critical value, the drug precipitated in the form of microscopic oil droplets, making the solution turbid. As the electrolyte concentration increased, the precipitation became more pronounced, leading to visible oil droplets and, finally, coalescence to an oily layer.

In a series of experiments, the reconstitution water for formulated flavored II[8] granules was spiked with salts normally found in drinking water. Observations were made on the first appearance of visible oil drops as the salt concentration was systematically increased. The critical oiling-out concentration of the different salts varied considerably (Table II), as did the ionic strength.

The individual contributions of cations and anions to ionic strength were calculated by:

$$\mu_\pm = mn_\pm Z_\pm^2 \qquad \text{(Eq. 9)}$$

where μ is the cationic or anionic strength, m is the salt molarity, n is the number of cations or anions per molecule, and Z is the charge on the ion. The cationic strength for oiling-out varied even more than ionic strength, but *anionic* strength proved to be fairly constant (Table II). The one exception, sodium bicarbonate, raised the pH as well as the ionic strength and thus had the additional effect of reducing solubility by pH change (Fig. 3). The pH effect of the other salts was minimal until the concentration approached 0.060 *M*, which was above the critical oiling-out concentration for all salts listed (Fig. 4). Thus, the pH of the sulfate and chloride solutions was not a significant factor in the "salting-out" phenomenon. The sharp increase in pH that occurred when sodium bicarbonate was added predominated over the ionic effect in reducing solubility.

The anion effect is additive, as shown by several qualitative experiments. Syrup solutions of II at ~25 mg/ml were made using water containing various salt concentrations (Table II). The pairs of solutions were made up so that one member of the pair had an additive anionic strength below the calculated critical value while the other member had an additive ionic strength above the critical value. Thus, the critical anionic strength of 2:1 magnesium chloride–sodium sulfate mixtures was calculated (assuming additivity) from the values in Table II to be 0.061. For 2:1 calcium chloride–sodium bicarbonate mixtures, the critical value was 0.044. Addition of the lower salt concentrations to clindamycin palmitate

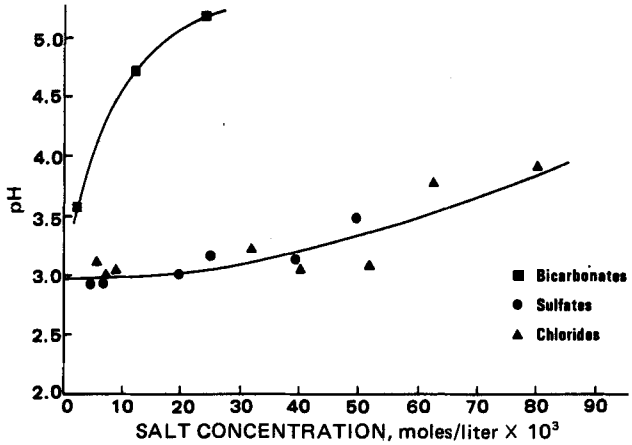

Figure 4—*Final pH of clindamycin 2-palmitate hydrochloride syrups reconstituted with various salt solutions.*

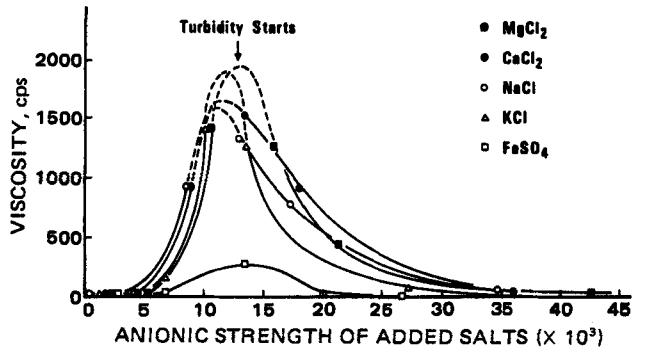

Figure 5—*Viscosity of clindamycin 2-palmitate hydrochloride solutions containing inorganic salts.*

[8] Cleocin Pediatric, 75 mg of clindamycin/5 ml.

syrup had very little effect while the higher salt concentrations caused II to "oil out" extensively (Table III). The oily precipitation was a salting-out phenomenon in which the monomeric solubility of II was reduced (11). Demicellization also may have occurred due to electrostatic suppression of the charge on the micelles by the increased ionic environment.

Effect of Salts on Viscosity—Inorganic salts also affect the viscosity of clindamycin palmitate hydrochloride solutions. Salt concentrations of ~400–800 mg/liter in syrup solutions of II caused the viscosity to increase with a fairly sharp peak. When concentrations were converted to anionic strength, as was done for the critical oiling-out point, a very close grouping of the peaks was obtained (Fig. 5). The anionic strengths of the peaks ranged from 0.011 to 0.013, the same range in which haziness or turbidity started in II solutions. At concentrations above this critical range, the viscosity was back to baseline levels well below the oiling-out point.

The chlorides were particularly effective in raising viscosity. Their peaks exceeded 1600 cps whereas the carbonate and sulfates produced more modest maxima. The common ion effect may have been dominant here, suppressing the dissociation of the II hydrochloride salt and thereby reducing the electrostatic repulsion forces between micelles (and also molecules). This can lead to increased intermicellar and intermolecular association forming flow-resistant aggregates or structures.

Following this hypothesis, as the salt concentrations increased, structure formation by II molecules increased until precipitation began, as evidenced by turbidity. The viscosity then peaked out and declined as the drug precipitated out in oily microdroplet form. Well beyond the peak viscosity, the oil droplets coalesced to form visible oil particles, at which point the precipitation was nearly complete.

REFERENCES

(1) W. Morozowich, A. A. Sinkula, F. A. MacKellar, and C. Lewis, *J. Pharm. Sci.*, **62**, 1102 (1973).

(2) A. A. Sinkula, W. Morozowich, and E. L. Rowe, *ibid.*, **62**, 1106 (1973).

(3) L. W. Brown, *ibid.*, **63**, 1597 (1974).

(4) E. L. Rowe and S. M. Machkovech, *ibid.*, **66**, 273 (1977).

(5) E. L. Rowe, *ibid.*, **61**, 781 (1972).

(6) C. Hansch, J. E. Quinlan, and G. L. Lawrence, *J. Org. Chem.*, **33**, 347 (1968).

(7) W. Morozowich, presented at the 13th Annual National Industrial Pharmaceutical Research Conference, Land O' Lakes, Wis., June 1971.

(8) T. I. Abbott, D. P. Benton, and C. A. Hampson, *J. Pharm. Pharmacol.*, **29**, 529 (1977).

(9) P. Mukerjee and K. J. Mysels, "Critical Micelle Concentrations of Aqueous Surfactant Systems," National Standard Reference Data Service NBS36, 1970, p. 4.

(10) K. Shinoda, T. Nakagawa, B. Tamamushi, and T. Isemura, "Colloidal Surfactants," Academic, New York, N.Y., 1963, p. 7.

(11) J. T. Edsall and J. Wyman, "Biophysical Chemistry," vol. I, Academic, New York, N.Y., 1958, pp. 263 ff.

ACKNOWLEDGMENTS

The authors thank Ms. K. A. Fitch and Mr. R. W. Smith for assistance in the solubility determinations and Dr. W. Morozowich for helpful discussions.

Reversed-Phase High-Performance Liquid Chromatographic Investigation of Levodopa Preparations I: Amino Acid Impurities

GARY W. SCHIEFFER

Received March 23, 1979, from the *Pharmaceutical Research Division, Norwich-Eaton Pharmaceuticals, Division of Morton-Norwich Products, Inc., Norwich, NY 13815.* Accepted for publication April 19, 1979.

Abstract □ A reversed-phase high-performance liquid chromatographic procedure with UV detection at 280 nm is presented for the determination of 6-hydroxydopa, tyrosine, 3-*O*-methyldopa, and other trace amino acid impurities in levodopa preparations. The method is fast and sufficiently sensitive to determine trace impurities at 0.1% of the levodopa concentration with a relative standard deviation of 4–6%. The trace impurities can be estimated at ≤0.01%.

Keyphrases □ Levodopa—analysis, high-performance liquid chromatography, amino acid impurities, commercial preparations □ Antiparkinsonian agents—levodopa, high-performance liquid chromatographic analysis, amino acid impurities, commercial preparations □ High-performance liquid chromatography—analysis, levodopa, amino acid impurities, commercial preparations

Current USP requirements (1) limit the impurities in levodopa [L-3-(3,4-dihydroxyphenyl)alanine] preparations to 0.1% of the levodopa concentration for 6-hydroxydopa [3-(2,4,5-trihydroxyphenyl)alanine] and to 0.5% for 3-*O*-methyldopa [3-methoxytyrosine or 3-(4-hydroxy-3-methoxyphenyl)alanine]. The designated USP method (1) for the estimation of these impurities is a TLC technique with a cellulose stationary phase and an acetic acid–butanol–methanol–water mobile phase. However, this laboratory found that the USP method suffers from a rather lengthy analysis time (>5 hr) and from the fact that the 6-hydroxydopa spot is not easily visualized. In addition, tyrosine, a frequently observed levodopa impurity, yields a spot with nearly the same R_f as 3-*O*-methyldopa. For these reasons, a quicker, simpler, and more universal method would be preferred.

BACKGROUND

A GLC procedure for the determination of levodopa purity was developed (2). However, this technique requires derivatization and was developed for impurities at a level of 1% with a stated detection limit for each component of ~0.1%. Thus, a more sensitive method is needed.

The standard amino acid analyzer procedure of separation on an ion-exchange column followed by detection of the ninhydrin color-forming reaction (3) was attempted but had long elution times (>80 min) and resulted in incomplete resolution of 3-*O*-methyldopa from tyrosine with the pH 3.4 citrate buffer employed[1]. Because of the greater speed and efficiency associated with microparticulate reversed-phase materials as opposed to ion-exchange materials (4) and because of the need to derivatize the amino acids (5) or to deposit a liquid phase on the solid support (6) when normal phase materials are used, a technique involving reversed-phase high-performance liquid chromatography (HPLC) was sought.

Knox and Jurand (7) resolved tyrosine from levodopa with reversed-phase HPLC by employing "soap" or ion-pair chromatography; the re-

[1] G. S. Denning, Jr., and G. Ginther, Norwich-Eaton Pharmaceuticals, Norwich, N.Y., unpublished results, 1970.

0022-3549/79/1000-1296$01.00/0

© 1979, American Pharmaceutical Association

syrup had very little effect while the higher salt concentrations caused II to "oil out" extensively (Table III). The oily precipitation was a salting-out phenomenon in which the monomeric solubility of II was reduced (11). Demicellization also may have occurred due to electrostatic suppression of the charge on the micelles by the increased ionic environment.

Effect of Salts on Viscosity—Inorganic salts also affect the viscosity of clindamycin palmitate hydrochloride solutions. Salt concentrations of ~400–800 mg/liter in syrup solutions of II caused the viscosity to increase with a fairly sharp peak. When concentrations were converted to anionic strength, as was done for the critical oiling-out point, a very close grouping of the peaks was obtained (Fig. 5). The anionic strengths of the peaks ranged from 0.011 to 0.013, the same range in which haziness or turbidity started in II solutions. At concentrations above this critical range, the viscosity was back to baseline levels well below the oiling-out point.

The chlorides were particularly effective in raising viscosity. Their peaks exceeded 1600 cps whereas the carbonate and sulfates produced more modest maxima. The common ion effect may have been dominant here, suppressing the dissociation of the II hydrochloride salt and thereby reducing the electrostatic repulsion forces between micelles (and also molecules). This can lead to increased intermicellar and intermolecular association forming flow-resistant aggregates or structures.

Following this hypothesis, as the salt concentrations increased, structure formation by II molecules increased until precipitation began, as evidenced by turbidity. The viscosity then peaked out and declined as the drug precipitated out in oily microdroplet form. Well beyond the peak viscosity, the oil droplets coalesced to form visible oil particles, at which point the precipitation was nearly complete.

REFERENCES

(1) W. Morozowich, A. A. Sinkula, F. A. MacKellar, and C. Lewis, *J. Pharm. Sci.*, **62**, 1102 (1973).

(2) A. A. Sinkula, W. Morozowich, and E. L. Rowe, *ibid.*, **62**, 1106 (1973).

(3) L. W. Brown, *ibid.*, **63**, 1597 (1974).

(4) E. L. Rowe and S. M. Machkovech, *ibid.*, **66**, 273 (1977).

(5) E. L. Rowe, *ibid.*, **61**, 781 (1972).

(6) C. Hansch, J. E. Quinlan, and G. L. Lawrence, *J. Org. Chem.*, **33**, 347 (1968).

(7) W. Morozowich, presented at the 13th Annual National Industrial Pharmaceutical Research Conference, Land O' Lakes, Wis., June 1971.

(8) T. I. Abbott, D. P. Benton, and C. A. Hampson, *J. Pharm. Pharmacol.*, **29**, 529 (1977).

(9) P. Mukerjee and K. J. Mysels, "Critical Micelle Concentrations of Aqueous Surfactant Systems," National Standard Reference Data Service NBS36, 1970, p. 4.

(10) K. Shinoda, T. Nakagawa, B. Tamamushi, and T. Isemura, "Colloidal Surfactants," Academic, New York, N.Y., 1963, p. 7.

(11) J. T. Edsall and J. Wyman, "Biophysical Chemistry," vol. I, Academic, New York, N.Y., 1958, pp. 263 ff.

ACKNOWLEDGMENTS

The authors thank Ms. K. A. Fitch and Mr. R. W. Smith for assistance in the solubility determinations and Dr. W. Morozowich for helpful discussions.

Reversed-Phase High-Performance Liquid Chromatographic Investigation of Levodopa Preparations I: Amino Acid Impurities

GARY W. SCHIEFFER

Received March 23, 1979, from the *Pharmaceutical Research Division, Norwich-Eaton Pharmaceuticals, Division of Morton-Norwich Products, Inc., Norwich, NY 13815.* Accepted for publication April 19, 1979.

Abstract □ A reversed-phase high-performance liquid chromatographic procedure with UV detection at 280 nm is presented for the determination of 6-hydroxydopa, tyrosine, 3-*O*-methyldopa, and other trace amino acid impurities in levodopa preparations. The method is fast and sufficiently sensitive to determine trace impurities at 0.1% of the levodopa concentration with a relative standard deviation of 4–6%. The trace impurities can be estimated at ≤0.01%.

Keyphrases □ Levodopa—analysis, high-performance liquid chromatography, amino acid impurities, commercial preparations □ Antiparkinsonian agents—levodopa, high-performance liquid chromatographic analysis, amino acid impurities, commercial preparations □ High-performance liquid chromatography—analysis, levodopa, amino acid impurities, commercial preparations

Current USP requirements (1) limit the impurities in levodopa [L-3-(3,4-dihydroxyphenyl)alanine] preparations to 0.1% of the levodopa concentration for 6-hydroxydopa [3-(2,4,5-trihydroxyphenyl)alanine] and to 0.5% for 3-*O*-methyldopa [3-methoxytyrosine or 3-(4-hydroxy-3-methoxyphenyl)alanine]. The designated USP method (1) for the estimation of these impurities is a TLC technique with a cellulose stationary phase and an acetic acid–butanol–methanol–water mobile phase. However, this laboratory found that the USP method suffers from a rather lengthy analysis time (>5 hr) and from the fact that the 6-hydroxydopa spot is not easily visualized. In addition, tyrosine, a frequently observed levodopa impurity, yields a spot with nearly the same R_f as 3-*O*-methyldopa. For these reasons, a quicker, simpler, and more universal method would be preferred.

BACKGROUND

A GLC procedure for the determination of levodopa purity was developed (2). However, this technique requires derivatization and was developed for impurities at a level of 1% with a stated detection limit for each component of ~0.1%. Thus, a more sensitive method is needed.

The standard amino acid analyzer procedure of separation on an ion-exchange column followed by detection of the ninhydrin color-forming reaction (3) was attempted but had long elution times (>80 min) and resulted in incomplete resolution of 3-*O*-methyldopa from tyrosine with the pH 3.4 citrate buffer employed[1]. Because of the greater speed and efficiency associated with microparticulate reversed-phase materials as opposed to ion-exchange materials (4) and because of the need to derivatize the amino acids (5) or to deposit a liquid phase on the solid support (6) when normal phase materials are used, a technique involving reversed-phase high-performance liquid chromatography (HPLC) was sought.

Knox and Jurand (7) resolved tyrosine from levodopa with reversed-phase HPLC by employing "soap" or ion-pair chromatography; the re-

[1] G. S. Denning, Jr., and G. Ginther, Norwich-Eaton Pharmaceuticals, Norwich, N.Y., unpublished results, 1970.

0022-3549/79/1000-1296$01.00/0

© 1979, American Pharmaceutical Association

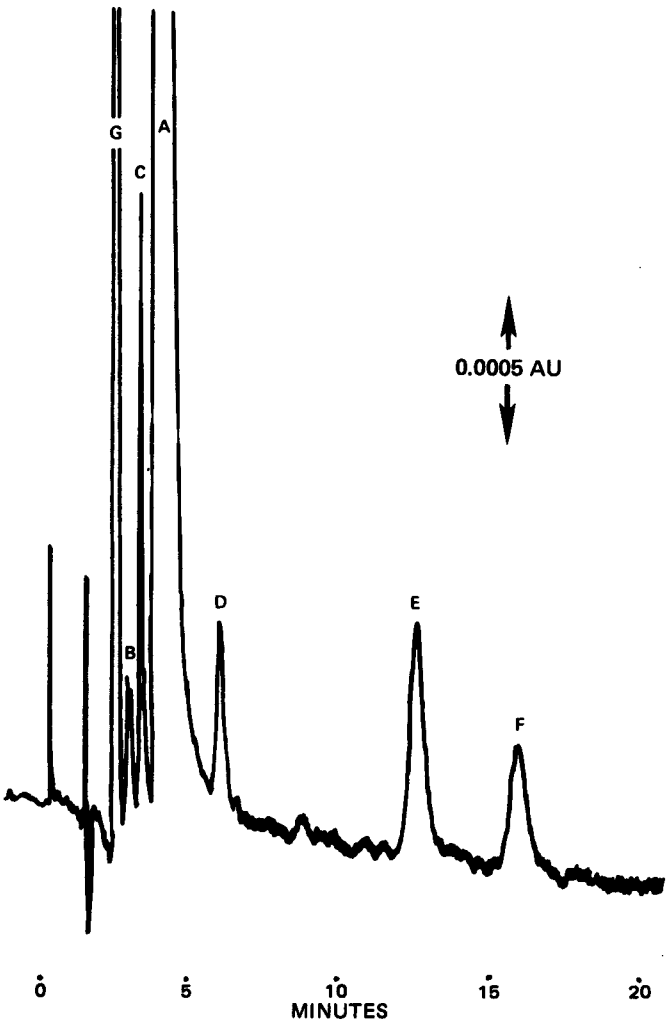

Figure 1—*Chromatographic trace of a standard solution containing 1 mg of levodopa/ml (A), 0.146% 5-hydroxydopa (B), 0.099% 6-hydroxydopa (C), 0.105% tyrosine (D), 0.150% 3-O-methyldopa (E), 0.118% 3-(3-hydroxy-4-methoxyphenyl)alanine (F), and ~0.1 mg of ascorbic acid/ml (G).*

tention arises from either the modification of the hydrophobicity of the hydrocarbon-bonded phase by the adsorption of ion-pairing molecules (8) or the formation of neutral ion-pairs in the eluent (9). However, to obtain reasonably short retention times and sharp peaks, an acid concentration of $>10^{-2}$ *M* (pH ~1.8) was employed, a requirement that can lead to slow hydrolysis of the bonded alkyl groups and eventual column deterioration (7) (pH 2 is the lower limit specified by column manufacturers). Raising the pH to ~2.4 greatly increased the retention times (from ~15 to ~25 min for tyrosine), indicating long analysis times (7).

Recently, Molnar and Horvath (10, 11) reported the reversed-phase HPLC separation of catecholamines and metabolites (including tyrosine and levodopa) utilizing a purely aqueous phosphate buffer mobile phase without ion-pairing reagents. The retention mechanism is apparently the association of the hydrophobic moiety of the molecule with the hydrocarbon-bonded phase, the driving force being the decrease in the nonpolar surface area exposed to the aqueous eluent (12). This paper evaluates a similar technique for determining 6-hydroxydopa, 3-*O*-methyldopa, tyrosine, and other related trace amino acid impurities in levodopa.

EXPERIMENTAL

Apparatus—A high-performance liquid chromatograph[2] with an injection valve and a 280-nm UV detector was used. A commercial[3] 30-cm × 3.9-mm i.d. stainless steel column was obtained prepacked with totally porous 10-μm average diameter silica particles containing an octadecyl monolayer chemically bonded to the silica. The flow rate was 2.0 ml/min.

Reagents and Materials—Levodopa, 6-hydroxydopa, tyrosine, and 3-*O*-methyldopa equivalent to USP specifications were used. In addition, an azalactone amino acid synthesis was used to prepare 5-hydroxydopa [3-(3,4,5-trihydroxyphenyl)alanine] (13) and 3-(3-hydroxy-4-methoxyphenyl)alanine (14). All other reagents and chemicals were ACS reagent grade or equivalent.

Mobile Phase—A 0.01 *M* NaH_2PO_4 solution was adjusted to pH 2.5 with phosphoric acid. This solution was filtered daily through a 0.5-μm membrane filter[4] and degassed prior to use.

Levodopa Standard Solution—A standard trace amino acid solution was prepared by accurately weighing (using an electrobalance[5]) 1–5-mg quantities of the amino acids to be determined, transferring them to a 100-ml volumetric flask, dissolving them with 10 ml of 0.1 *M* phosphoric acid, and diluting the solutions to volume with distilled water. About 50 mg of reference standard levodopa was accurately weighed and transferred to a 50-ml volumetric flask and dissolved with 5 ml of 0.1 *M* phosphoric acid. Exactly 5.0 ml of the standard trace amino acid solution and ~5 mg of ascorbic acid were added to the flask, and the contents were diluted to volume with distilled water. (The ascorbic acid was added to inhibit 6-hydroxydopa oxidation.)

Sample Solution—A quantity of the typical commercial levodopa preparation sufficient to yield 50 mg of levodopa was weighed and transferred to a 50-ml volumetric flask. Five milliliters of 0.1 *M* phosphoric acid and 5 mg of ascorbic acid were added. The flask was shaken mechanically for 15 min to effect levodopa dissolution, and the solution was diluted to volume with distilled water. A portion of the sample was centrifuged and filtered through the 0.5-μm filter.

Synthetic samples containing known quantities of trace amino acid impurities were prepared by adding 1-mg quantities of the accurately weighed trace amino acids to a 1-liter volumetric flask containing a quantity of the levodopa preparation sufficient to yield 1 g of levodopa. About 100 mg of ascorbic acid was added, and the dry mixture was shaken mechanically for 15 min. Prior to analysis, 100 ml of 0.1 *M* phosphoric acid was added to the flask, and the flask was shaken mechanically for 15 min to effect dissolution. The contents were diluted to volume, and a portion was centrifuged and filtered as before.

Sample Analysis and Linearity—Fifty microliters of the standard and sample solutions were injected. The amount of each trace amino acid present in the sample, expressed as percent of levodopa concentration, was calculated from:

$$\%\ \text{levodopa} = 0.1 W_s (h_u/h_s) \qquad \text{(Eq. 1)}$$

where W_s is the weight, in milligrams, of the trace amino acid used to prepare the standard trace amino acid solution, and h_u and h_s are the peak heights observed for the sample and standard solutions, respectively.

A linearity study was performed by analyzing actual sample solutions containing known quantities of amino acid impurities.

Table I—Linearity

Parameter	5-Hydroxydopa	6-Hydroxydopa	Tyrosine	3-*O*-Methyldopa	3-Hydroxy-4-methoxyphenylalanine
Correlation coefficient	0.9968	0.9997	0.9997	0.9997	0.9997
Standard error of estimate ($S_{y/x}$)	1.29	1.95	0.453	1.35	0.565
Intercept[a], %	−3.7	−3.6	13.4[b]	13.3[b]	0.72
Variation[c], %	6.9	2.4	1.8	1.7	2.0

[a] The (*y* intercept/$\bar{y}$) × 100, where $\bar{y}$ is the average *y*. [b] The significant positive intercepts observed for these compounds are due to the presence of these amino acids as trace impurities in the levodopa. [c] ($S_{y/x}/\bar{y}$) × 100.

RESULTS AND DISCUSSION

A sample chromatogram obtained with a new column is shown in Fig.

[2] ALC/GPC 202 equipped with an M6000 pump and a U6K injector, Waters Associates, Milford, Mass.
[3] μBondapak C_{18}, Waters Associates, Milford, Mass.
[4] Millipore.
[5] Cahn Instrument Co., Paramount, Calif.

Table II—Analysis of Spiked Samples

Compound	Sample 1		Sample 2		Sample 3		Sample 4		Sample 5		Sample 6		Average Recovered[a], %
	Added, %	Found, %	Added, %	Found, %	Added, %	Found, %	Added, %	Found, %	Added, %	Found, %	Added, %	Found, %	
6-Hydroxydopa	0.099	0.098	0.112	0.110	0.142	0.145	0.104	0.095	0.096	0.095	0.060	0.059	98 (4)
Tyrosine	0.106	0.088	0.100	0.085	0.115	0.108	0.161	0.134	0.141	0.130	0.080	0.069	87 (5)
3-*O*-Methyldopa	0.110	0.104	0.100	0.105	0.150	0.157	0.128	0.123	0.135	0.123	0.178	0.166	97 (6)
5-Hydroxydopa											0.139	0.160	115
3-Hydroxy-4-methoxyphenylalanine											0.084	0.092	110

[a] Values in parentheses are relative standard deviations (1σ) for the data.

Table III—Analysis of Commercial Samples for Trace Amino Acid Impurities

Sample	Levodopa Dosage, mg	6-Hydroxydopa, %	Tyrosine, %	3-*O*-Methyldopa, %
1	250	0	0.013 (0.003)[a]	0.02 (0.01)[a]
2	100	0.005	0.010	0.202
3	100	0	0.012	0.010
4	100	0.007	0.022	—
5	250	0.003	0.017	0
6	500	0	0.012	0.010

[a] Values in parentheses are standard deviations (1σ); $n = 4$. Data were obtained on 4 separate days with two different columns.

1. The two USP-monitored compounds, 6-hydroxydopa and 3-*O*-methyldopa, as well as the frequently observed impurity tyrosine and the related compounds 5-hydroxydopa and 3-(3-hydroxy-4-methoxyphenyl)alanine, all were resolved. A much older column, which had shown loss of resolution through long usage with other reversed-phase separations, still yielded acceptable resolution of all amino acids in the present study, although the retention times of the slower eluting components were ~30% less with this column. Increasing the eluent pH from 2.5 to ≥3 further reduced the retention times observed with both columns and resulted in a significant loss of resolution between the 6-hydroxydopa and levodopa peaks.

Linearity data for the trace amino acids are presented in Table I. Linearity was observed over the concentration ranges studied: 0.02–0.2% for 6-hydroxydopa and tyrosine, 0.04–0.2% for 5-hydroxydopa and 3-(3-hydroxy-4-methoxyphenyl)alanine, and 0.06–0.6% for 3-*O*-methyldopa (0.1% represents 50 ng of injected sample).

Samples spiked with known quantities of trace amino acids yielded the recovery values listed in Table II after correction for any trace quantities of amino acids initially present (usually <0.02%). The results indicate sufficient precision and accuracy for trace analysis at the 0.1% level.

The results of an analysis of several commercial levodopa preparations from four different manufacturers are listed in Table III. Except for Sample 2, the trace impurities were ≤0.02%. [Sample 4 contained 10 mg of carbidopa as an active ingredient, which interfered with both the HPLC and the TLC determinations of 3-*O*-methyldopa, although the two compounds could be resolved by increasing the HPLC eluent pH to 3.5 (15).]

The method employed is relatively fast. Prior derivatization, the addition of a liquid stationary phase, or the addition of an organic solvent or ion-pairing reagent to the mobile phase is not required. Less than 1.5 hr is required for the preparation of the eluent, standard, and sample solutions, and <15 min is required for elution of the major amino acids.

The method also is sufficiently precise without an internal standard and sufficiently sensitive to determine accurately trace contaminants at the 0.1% level and to estimate them at levels of <0.01%. The resolution problems associated with the amino acid analyzer and TLC approaches are avoided, and the chromatogram is a documented record that yields an objective evaluation of the impurity content as opposed to subjective evaluation of the intensities of TLC spots.

REFERENCES

(1) "The United States Pharmacopeia," 19th rev., Mack Publishing Co., Easton, Pa., 1975, p. 280.

(2) J. R. Watson, *J. Pharm. Sci.*, **63,** 96 (1974).

(3) D. H. Spackman, W. H. Stein, and S. Moore, *Anal. Chem.*, **30,** 1190 (1958).

(4) R. M. Riggin and P. T. Kissinger, *ibid.*, **49,** 2109 (1977).

(5) E. Bayer, E. Grom, B. Kaltenegger, and R. Uhmann, *ibid.*, **48,** 1106 (1976).

(6) B.-A. Persson and B. L. Karger, *J. Chromatogr. Sci.*, **12,** 521 (1974).

(7) J. H. Knox and J. Jurand, *J. Chromatogr.*, **125,** 89 (1976).

(8) P. T. Kissinger, C. S. Bruntlett, G. C. Davis, L. J. Felice, R. M. Riggin, and R. E. Shoup, *Clin. Chem.*, **23,** 1449 (1977).

(9) C. Horvath, W. Melander, I. Molnar, and P. Molnar, *Anal. Chem.*, **49,** 2295 (1977).

(10) I. Molnar and C. Horvath, *Clin. Chem.*, **22,** 1497 (1976).

(11) I. Molnar and C. Horvath, *J. Chromatogr.*, **145,** 371 (1978).

(12) C. Horvath, W. Melander, and I. Molnar, *ibid.*, **125,** 129 (1976).

(13) von Fr. Schaaf and A. Labouchere, *Helv. Chim. Acta*, **7,** 357 (1924).

(14) V. Deulofeu and O. Reppetto, *Anales Soc. Espan. Fis. Quim.*, **32,** 149 (1934); through *Chem. Abstr.*, **28,** 3396.

(15) G. W. Schieffer, *J. Pharm. Sci.*, **68,** 1299 (1979).

ACKNOWLEDGMENTS

The author is grateful to T. Schwan and J. Michels for the synthesis of 5-hydroxydopa and 3-(3-hydroxy-4-methoxyphenyl)alanine and to S. Casamento for the TLC work.

Reversed-Phase High-Performance Liquid Chromatographic Investigation of Levodopa Preparations II: Levodopa Determination

GARY W. SCHIEFFER

Received March 23, 1979, from the *Pharmaceutical Research Division, Norwich-Eaton Pharmaceuticals, Division of Morton-Norwich Products, Inc., Norwich, NY 13815.* Accepted for publication April 19, 1979.

Abstract □ A reversed-phase high-performance liquid chromatographic procedure with UV detection at 280 nm is presented for levodopa determination in pharmaceutical preparations. The method is fast and specific for levodopa in the presence of its most likely impurities and degradation products.

Keyphrases □ Levodopa—analysis, high-performance liquid chromatography, commercial preparations, impurities, degradation products □ Antiparkinsonian agents—levodopa, high-performance liquid chromatographic analysis, commercial preparations, impurities, degradation products □ High-performance liquid chromatography—analysis, levodopa, commercial preparations, impurities, degradation products

Fluorometric (1), electrochemical (2), GLC (3), and high-performance liquid chromatographic (HPLC) (4, 5) techniques have been presented for levodopa (I). Although some techniques are specific with respect to postulated impurities (3) or levodopa decomposition products formed in alkaline solution (5), a complete study of the specificity of a method with respect to a wide range of possible degradation products has not been reported. Such a specificity study for a proposed levodopa stability-indicating method should include the examination of dopamine (3-hydroxytyramine) (II) [decarboxylated levodopa (6)] and intermediates in the aminochrome formation reaction (7). The latter include the initial oxidation product levodopa-*o*-quinone (III) as well as the cyclization product dopachrome (IV) and the final internal oxidation–reduction products 5,6-dihydroxyindole-2-carboxylic acid (V) and 5,6-dihydroxyindole (VI).

An HPLC method was presented (8) for determining trace amino acid impurities in levodopa preparations. This report discusses extending this technique to include a stability-indicating assay specific for levodopa with respect to the postulated degradation products.

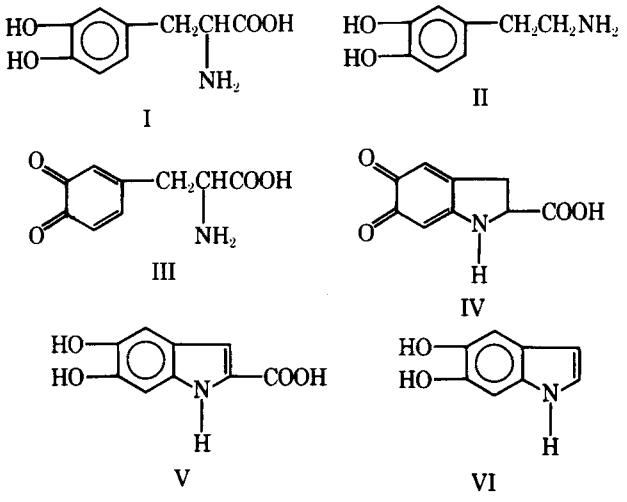

EXPERIMENTAL

Apparatus—The liquid chromatographic apparatus described previously (8) was used. A variable-wavelength absorbance detector[1] adjusted to 485 nm was used for some studies in addition to the 280-nm UV detector used for the assay. Peak areas were determined with a computerized laboratory data acquisition system. The flow rate was 2.0 ml/min.

Reagents and Materials—The levodopa, 6-hydroxydopa, tyrosine, 3-*O*-methyldopa (3-methoxytyrosine), 5-hydroxydopa, and 3-(3-hydroxy-4-methoxyphenyl)alanine described previously (8) were used. 5,6-Dihydroxyindole and 5,6-dihydroxyindole-2-carboxylic acid were synthesized according to the procedure of Benigni and Minnis (9).

Dopachrome was prepared by adding a few drops of a ferricyanide solution [13 g of potassium ferricyanide and 4.2 g of sodium bicarbonate diluted to 50 ml with water (10)] to 10 ml of a 0.01 *M* phosphoric acid solution containing 2 mg/ml of levodopa, tyrosine, 3-*O*-methyldopa, and hypoxanthine. (The latter three compounds did not react with ferricyanide but were added to demonstrate chromatographic specificity.) The resulting dark-red solution was injected directly.

Levodopa-*o*-quinone was generated electrochemically (11, 12) with a specially designed precolumn tubular electrode cell (13). Hypoxanthine[2] and dopamine hydrochloride[3] were obtained commercially. All other reagents and chemicals were ACS reagent grade or the equivalent.

Mobile Phase—A 0.01 *M* NaH_2PO_4 solution was adjusted to pH 3.5 with phosphoric acid. This solution was filtered daily through a 0.5-μm membrane filter[4] and degassed prior to use.

Internal Standard Solution—About 150 mg of hypoxanthine was weighed into a 100-ml volumetric flask, dissolved on a steam bath with 40 ml of 0.1 *M* phosphoric acid, and diluted to volume with water.

Levodopa Standard Solution—About 50 mg of reference standard levodopa was accurately weighed into a 50-ml volumetric flask, dissolved with 5 ml of 0.1 *M* phosphoric acid, and diluted to volume with water. Exactly 10.0 ml of this solution was added to a 100-ml volumetric flask containing 20.0 ml of the internal standard solution, and the contents were diluted to volume with water.

Sample Solution—Twenty levodopa capsules or tablets were ground and mixed well, and a quantity sufficient to yield 250 mg of levodopa was accurately weighed into a 250-ml volumetric flask. Fifty milliliters of 0.1 *M* phosphoric acid was added, and the flask was shaken mechanically for 30 min. The contents were diluted to volume with water, and a portion of the solution was centrifuged. Exactly 10.0 ml of the centrifugate and 20.0 ml of the internal standard solution were added to a 100-ml volumetric flask, the contents of which were diluted to volume with water and further clarified by filtration through the 0.5-μm filter.

Table I—Linearity

Parameter	Area Ratios		Height Ratios	
	Levodopa	Hypoxanthine	Levodopa	Hypoxanthine
Correlation coefficient	0.9999	0.9999	0.9995	0.9999
Standard error of estimate ($S_{y/x}$)	0.004	0.004	0.02	0.007
Intercept[a], %	0.2	3.0	−0.5	3.8
Variation[b], %	0.6	0.3	2.0	0.4

[a] The (y intercept/$\bar{y}$) × 100, where $\bar{y}$ is the average y. [b] ($S_{y/x}/\bar{y}$) × 100.

[1] Model 770, Schoeffel Instrument Corp., Westwood, N.J.
[2] Heterocyclic Chemical Corp., Harrisonville, Mo.
[3] Aldrich Chemical Co., Milwaukee, Wis.
[4] Millipore.

0022-3549/79/1000-1299$01.00/0
© 1979, American Pharmaceutical Association

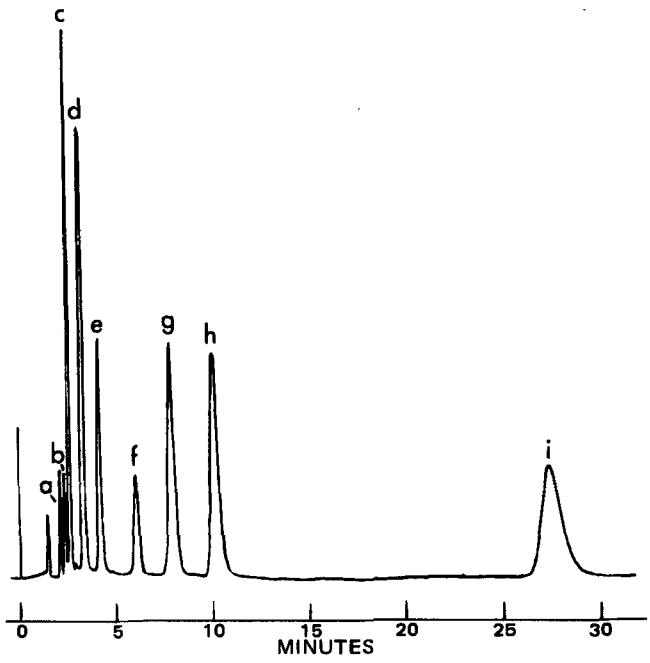

Figure 1—*Chromatogram of levodopa, hypoxanthine internal standard, and possible interferences: (a) 5-hydroxydopa, (b) 6-hydroxydopa, (c) levodopa, (d) dopamine and tyrosine, (e) hypoxanthine, (f) 3-O-methyldopa, (g) 3-(3-hydroxy-4-methoxyphenyl)alanine, (h) 5,6-dihydroxyindole, and (i) 5,6-dihydroxyindole-2-carboxylic acid.*

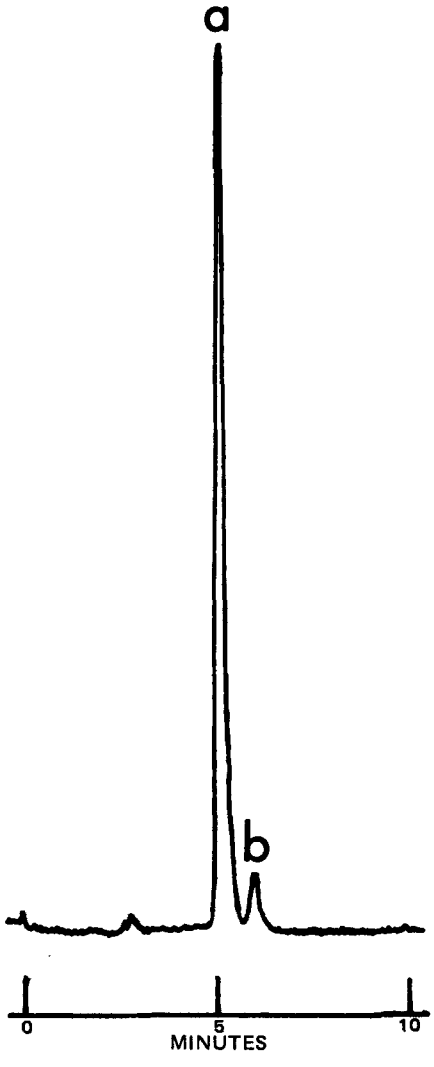

Figure 2—*Chromatogram of levodopa (a) and electrochemically generated levodopa-o-quinone (b). Electrode generation potential was 0.8* versus *Ag–AgCl reference electrode. Flow rate was 1.0 ml/min.*

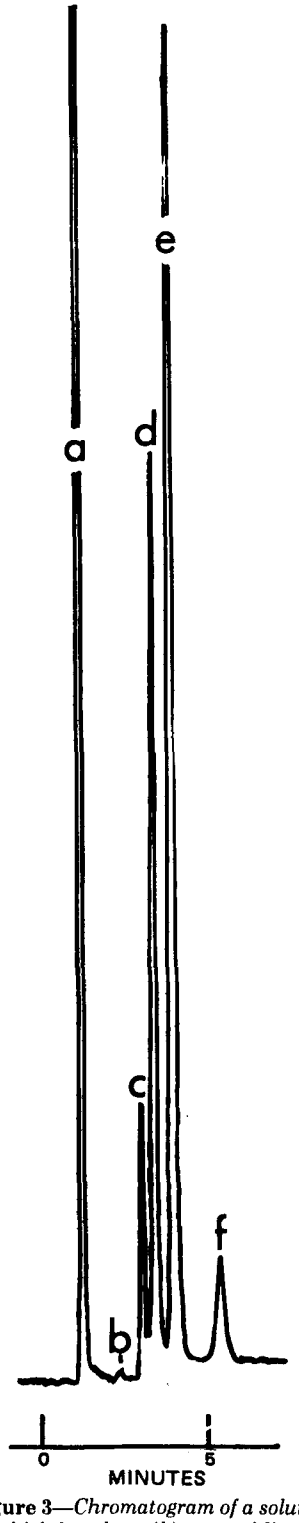

Figure 3—*Chromatogram of a solution in which levodopa (b) was oxidized to dopachrome (d) with ferricyanide (a). Tyrosine (c), hypoxanthine (e), and 3-O-methyldopa (f) remained unoxidized.*

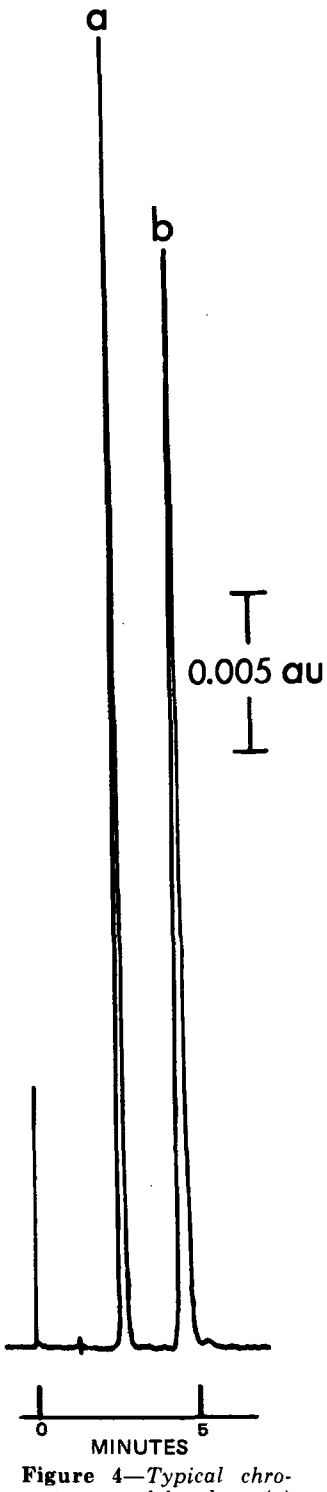

Figure 4—*Typical chromatogram of levodopa (a) and hypoxanthine (b) (1 μg of levodopa and 3 μg of hypoxanthine were injected).*

Synthetic samples were made by mixing known quantities of reference standard levodopa and excipients in the dry state and treating the mixture according to the procedure for the actual samples.

Sample Analysis and Linearity—Ten microliters each of the standard and sample solutions were injected. The amount of levodopa present in the sample, expressed as milligrams of levodopa per gram of sample weight, was calculated from:

$$\text{levodopa} = 5(R_x/R_s)(W_s/W_x) \qquad \text{(Eq. 1)}$$

Table II—Assay of Levodopa in Actual Commercial Samples by HPLC, USP Spectrophotometric, and Amino Acid Analyzer (AAA) Techniques

Sample	Levodopa per Dosage Unit, mg	n	Amount Found[a] HPLC[b]	USP[c]	AAA[c]
1	100	14	100.4 (0.7)	—	100.7
2	100	5	105.9 (0.7)	—	—
3	100	5	104.4 (0.8)	—	—
4	250	4	99.4 (0.8)	99.9	99.7
5	250	5	99.3 (1.1)	—	—
6	500	4	91.3 (2.0)	91.6	92.3

[a] Expressed as percent label for the ungrouped data (ranging from 50 to 150% of the nominal sample size). [b] Values in parentheses represent relative standard deviations. [c] Average of two or three assay values.

where R_x and R_s are the peak height or area ratios (levodopa to hypoxanthine) of the sample and standard solution, respectively; W_s is the weight of the levodopa standard in milligrams, and W_x is the weight of the sample in grams.

Linearity studies were performed by (*a*) varying the levodopa concentration over 0.02–0.2 mg/ml and holding the internal standard concentration constant, and (*b*) varying the internal standard concentration over 0.075–0.6 mg/ml and holding the levodopa concentration constant.

RESULTS AND DISCUSSION

The initial attempt was to combine the HPLC assay of levodopa impurities described previously (8) with a stability-indicating levodopa assay. However, the pH 2.5 phosphate buffer eluent did not resolve the decarboxylated degradation product, dopamine, from levodopa, although the four other postulated degradation products were resolved from levodopa and the impurities (8). The pH had to be increased to 3.5 to achieve a separation.

With the pH 3.5 phosphate buffer eluent, adequate resolution was obtained among levodopa, the hypoxanthine internal standard, and the impurities (8). (The pH 3.5 buffer could not be used for the impurities assay because the resolution of 6-hydroxydopa and tyrosine from levodopa was not sufficient to determine these impurities accurately at the 0.1% level.) In addition, dopamine as well as 5,6-dihydroxyindole and 5,6-dihydroxyindole-2-carboxylic acid, the final products in the levodopa aminochrome reaction (7), were all resolved. A chromatogram containing all of these postulated interferences is shown in Fig. 1.

The initial oxidation product in the aminochrome reaction, levodopa-*o*-quinone, eluted immediately following the levodopa peak and did not interfere (Fig. 2). Dopachrome eluted just before the hypoxanthine internal standard peak and did not interfere (Fig. 3). [The dopachrome peak in Fig. 3 also was observed when the absorbance detector was set at 485 nm, a characteristic absorption maximum for aminochromes (7).]

Linearity data of levodopa and hypoxanthine, obtained by plotting peak area or peak height ratios *versus* weight ratios, are presented in Table I. Linearity was observed over the ranges studied: 0.2–2.0 μg for levodopa and 0.8–6.0 μg for the hypoxanthine internal standard. A typical chromatogram is shown in Fig. 4.

Fifteen synthetic samples prepared with levodopa weights ranging from 50 to 150% of theory (100% representing 100 mg of levodopa/dosage unit or 515 mg/g) yielded an average recovery and relative standard deviation of 99.0 ± 0.9% for the ungrouped data. A linear regression analysis of milligrams of levodopa found *versus* milligrams added yielded a straight line with a slope of 0.98 ± 0.02 and an intercept of 0.5 ± 1.4 (appended values are 99% confidence limits), indicating a slope and intercept not significantly different from 1 and 0, respectively, and no bias in the method.

The results of an analysis of actual commercial samples obtained from four different manufacturers are presented in Table II. Some of the HPLC assays were checked with the USP UV spectrophotometric technique (14) and with an amino acid analyzer technique utilizing an ion-exchange column and a pH 4.05 citrate buffer eluent[5]. Excellent agreement was found among the techniques. Furthermore, a six-point standard addition of a portion of Sample 1 using the HPLC technique yielded an assay value of 100.8% of label, in excellent agreement with the sample assay. [Sample 3 contained 10 mg of carbidopa/dosage unit as an active ingredient, which eluted between the hypoxanthine and 3-*O*-methyldopa peaks (Fig. 1) and did not interfere.]

In summary, an HPLC stability-indicating assay was developed that is specific for levodopa in pharmaceutical preparations with respect to at least five postulated degradation products and five impurities. The method is fast, allowing injections every 5 min and the assay of ~25 samples/8-hr day. The stability-indicating assay may be applied in conjunction with the impurities assay (8) merely by adjusting the eluent pH from 2.5 to 3.5.

REFERENCES

(1) J. C. Johnson, G. J. Gold, and D. H. Clouet, *Anal. Biochem.*, **54**, 129 (1973).

(2) W. D. Mason, *J. Pharm. Sci.*, **62**, 999 (1973).

(3) J. R. Watson, *ibid.*, **63**, 96 (1974).

(4) R. M. Riggin, R. L. Alcorn, and P. T. Kissinger, *Clin. Chem.*, **22**, 782 (1976).

(5) A. G. Ghanekar and V. D. Gupta, *J. Pharm. Sci.*, **67**, 1247 (1978).

(6) W. H. Vogel, *Naturwissenschaften*, **56**, 462 (1969).

(7) R. A. Heacock, *Chem. Rev.*, **59**, 181 (1959).

(8) G. W. Schieffer, *J. Pharm. Sci.*, **68**, 1296 (1979).

(9) J. D. Benigni and R. L. Minnis, *J. Heterocycl. Chem.*, **2**, 387 (1965).

(10) G. L. Mattok and R. A. Heacock, *Can. J. Chem.*, **42**, 481 (1964).

(11) M. D. Hawley, S. V. Tatawawadi, S. Piekarski, and R. N. Adams, *J. Am. Chem. Soc.*, **89**, 447 (1967).

(12) A. W. Sternson, R. McCreery, B. Feinberg, and R. N. Adams, *J. Electroanal. Chem. Interfacial Electrochem.*, **46**, 313 (1973).

(13) G. W. Schieffer, *Anal. Chem.*, in press.

(14) "The United States Pharmacopeia," 19th rev., Mack Publishing Co., Easton, Pa., 1975, p. 281.

ACKNOWLEDGMENTS

The author is grateful to B. Stevenson and C. Finch for the synthesis of 5,6-dihydroxyindole and 5,6-dihydroxyindole-2-carboxylic acid, to S. Casamento for the sample assay, and to P. J. Palermo for helpful discussions.

[5] G. S. Denning, Jr., Norwich-Eaton Pharmaceuticals, Norwich, N.Y., unpublished results, 1975.

Biosynthesis of Prostaglandin D_2, 15-Ketoprostaglandin E_2, and Hydroxy Fatty Acids by Ram Seminal Vesicle Microsomes

P. R. RAVIKUMAR, J. K. PAI, M. J. ZMIJEWSKI, and C. J. SIH ˣ

Received February 21, 1979, from the *School of Pharmacy, University of Wisconsin, Madison, WI 53706.* Accepted for publication April 18, 1979.

Abstract □ At high arachidonic acid concentrations (164 μM) and without exogenous cofactors, ram seminal vesicle microsomes produced prostaglandin E_2 and two less polar products, identified as prostaglandin D_2 and 15-ketoprostaglandin E_2. The ratio of the biosynthetic products formed depended on the exogenous cofactor and on the arachidonic acid concentration. At high arachidonic acid concentrations (>150 μM), tryptophan, phenol, and glutathione stimulated prostaglandin E_2 formation, but each affected the formation of the other prostaglandins differently. Ascorbic acid markedly stimulated hydroxy fatty acid formation. GLC–mass spectral analysis of the hydroxy fatty acid fraction indicated the presence of 11-hydroxy-5,8,12,14-eicosatetraenoic acid, 15-hydroxy-5,8,11,13-eicosatetraenoic acid, and 12-hydroxy-5,8,10-heptadecatrienoic acid. At low arachidonic acid concentrations (30 μM), glutathione still stimulated prostaglandin E_2 biosynthesis, but the other cofactors stimulated 6-ketoprostaglandin $F_{1\alpha}$ and hydroxy fatty acid formation.

Keyphrases □ Prostaglandin D_2—biosynthesis, ram seminal vesicle microsomes, dependence on arachidonic acid, cofactors □ 15-Ketoprostaglandin E_2—biosynthesis, ram seminal vesicles, dependence on arachidonic acid, cofactors □ Seminal vesicles—microsomes, prostaglandin synthesis, arachidonic acid metabolism □ Microsomes—seminal vesicles, prostaglandin synthesis, arachidonic acid metabolism

Ram seminal vesicle microsomes convert arachidonic and eicosatrienoic acids into prostaglandins of the D, E, and F series (1–5). Recently, it was reported (6) that, at low substrate to enzyme ratios and in the absence of reduced glutathione, the major prostaglandin synthesized by the ram seminal vesicle cyclo-oxygenase from arachidonic acid was 6-ketoprostaglandin $F_{1\alpha}$. When the substrate concentration was increased to 50 μM, only traces of 6-ketoprostaglandin $F_{1\alpha}$ were formed, the major products being prostaglandin E_2, prostaglandin $F_{2\alpha}$, and two unidentified less polar products.

This paper reports experimental data that characterize these unknowns as prostaglandin D_2 and 15-ketoprostaglandin E_2. The effect of exogenous cofactors on the ratio of biosynthetic products was also examined.

EXPERIMENTAL

Materials—Radioactive 1-^{14}C-arachidonic acid[1] (60 mCi/mmole), unlabeled arachidonic acid[2] (Grade 1), reduced glutathione[2], L-epinephrine[2], serotonin[2], methemoglobin[2], prostaglandin E_2[3], prostaglandin D_2[4], 15-ketoprostaglandin E_2[4], and frozen ram seminal vesicles[5] were used. All solvents were reagent grade and were redistilled.

Silicic acid[6] was used for column chromatography. Precoated analytical silica gel plates[7] were used for TLC separation. Radioactivity was assayed in a scintillation spectrometer[8] after the addition of 10 ml of Bray's solution. The radiochromatogram was assayed on an autoscanner[9].

Mass spectra were recorded on a mass spectrometer[10] with an ion source temperature of 220° and an electron potential of 70 ev. GLC–mass spectral analyses were carried out in a gas chromatograph–mass spectrometer[11] equipped with a data system[12]. The column, 1.83 m, was 3% SE-30 with temperature programming from 200 to 250° at 6°/min; the electronic energy was kept at 70 ev. UV spectra were recorded on a recording spectrophotometer[13].

PMR spectra (δ value) were recorded on a spectrometer[14] in deuterochloroform. All chemical shifts were recorded relative to internal tetramethylsilane. 15-Hydroperoxyarachidonic acid was prepared according to the method of Hamberg and Samuelsson (7) and purified by column chromatography, using hexane–ether as the solvent.

Enzymatic Transformation of 1-^{14}C-Arachidonic Acid—Ram seminal vesicle microsomes were prepared as described elsewhere (8) and were freeze dried and stored at −78° until used. Enzymatic incubations

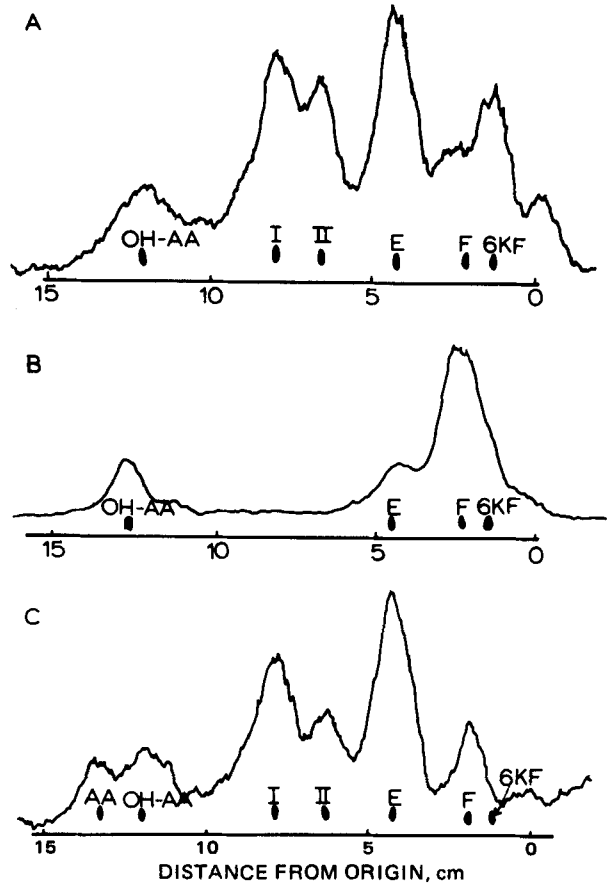

Figure 1—*Radiochromatographic profiles of 0.2 μCi of 1-^{14}C-arachidonic acid (164 μM) metabolism by ram seminal vesicle microsomes. Key: A, ethyl acetate extract; B, ethyl acetate extract plus sodium borohydride; and C, incubation mixture consisting of 15-hydroperoxyeicosa-5,8,11,13-tetraenoic acid (100 μM) and 0.2 μCi of 1-^{14}C-arachidonic acid (164 μM).*

[1] Amersham/Searle Co., Arlington Heights, Ill.
[2] Sigma Chemical Co., St. Louis, Mo.
[3] G. D. Searle Co., Chicago, Ill.
[4] Miles Laboratories, Madison, Wis.
[5] Roth Products, Gwynedd, Pa.
[6] Mallinckrodt 2847, 100 mesh.
[7] Brinkmann 0.25 F0254 (EM).
[8] Packard model 2002.
[9] Vangard model 930.
[10] AEI MS-9.
[11] Varian MAT 112.
[12] SS 100C.
[13] Cary model 14.
[14] Varian EM 390.

0022-3549/79/1000-1302$01.00/0
© 1979, American Pharmaceutical Association

Table I—Effect of Cofactors on Product Distribution at High Arachidonic Acid Concentration [a] (164 μM)

Cofactor	Concentration	Percent of Products Formed						Radioactivity in Products, %
			Prostaglandin					
		Hydroxy-Fatty Acids	15-Keto-E_2	D_2	E_2	$F_{2\alpha}$	6-Keto-$F_{1\alpha}$	
None	—	10.0	21.4	13.9	26.5	10.2	10.6	93
Glutathione	20 μM	0	22.1	0	48.1	0	0	70
Ascorbic acid	1 mM	35.1	0	8.4	16.8	21.0	18.5	99.8
Phenol	1 mM	13.7	0	15.0	42.7	3.6	22.2	97
L-Tryptophan	1 mM	14.4	0	13.4	38.3	7.1	23.4	96.6
L-Epinephrine	1 mM	19.6	4.1	9.4	23.8	17.2	22.6	96.7
Serotonin	1 mM	19.7	0	17.1	37.8	5.2	2.6	82.4
Methemoglobin	8 μM	8.8	19.8	13.9	30.3	7.2	20.0	99

[a] The reaction mixture contained ram seminal vesicle microsomes (10 mg) dissolved in 1.0 ml of 0.1 M tromethamine buffer. The cofactors were added at the concentrations indicated, and the reaction was initiated by the addition of 0.2 μCi of 1-^{14}C-arachidonic acid containing 50 μg of unlabeled arachidonic acid. Products were extracted and analyzed as described.

were carried out at 25° in 1.0 ml of pH 7.5 tromethamine buffer containing 10 mg of lyophilized enzyme powder (3.85 mg of protein by biuret), 50 μg of arachidonic acid, 0.2 μCi of 1-^{14}C-arachidonic acid, and cofactors when necessary. The reaction was initiated by the addition of arachidonic acid and was terminated after 20 min by the addition of 25 μl of 1.0 N HCl (final pH 3.0).

The reaction mixture was extracted with 2.0 ml of ethyl acetate; the organic layer was dried over sodium sulfate and evaporated with a nitrogen stream. The total recovery of radioactivity was generally 60%. The residue was redissolved in ethyl acetate, and a portion of this solution was spotted on TLC plates. They were developed twice in the organic phase of ethyl acetate–isooctane–acetic acid–water (11:5:2:10) and scanned for radioactivity.

The percent incorporation of radioactivity into each product was determined by the cut and weigh method. Radioactive peaks on the chromatogram corresponding to the products were traced with tracing paper, cut out, and weighed. The total weight of all peaks represented 100% of the sample. The weight of each peak was divided by the total weight and multiplied by 100 to obtain the percentage of that product present.

Isolation of Compounds I and II—Ram seminal vesicle microsomes (11–3.94 g of protein) were suspended in 1.1 liters of 0.1 M, pH 7.5 tromethamine buffer. The enzymatic reaction was initiated by the addition of 55 mg of arachidonic acid containing 47 μCi of 1-^{14}C-arachidonic acid. After 20 min at 25°, the incubation mixture was acidified with hydrochloric acid to pH 3.0 and extracted with ethyl acetate (4 × 250 ml). The combined ethyl acetate extracts were washed with water (3 × 250 ml) and dried over sodium sulfate. Approximately 44% of the radioactivity was recovered.

The residue was chromatographed over 10 g of silicic acid–diatomaceous earth (85:15); the column (1 × 23 cm) was eluted with benzene–ethyl acetate (8:2), with gradually increasing ethyl acetate concentrations. Fractions (8 ml) were collected. Fractions 2–14 contained arachidonic acid and hydroxy fatty acids (20.7% of radioactivity), fractions 15–22 consisted of I (14.7%), fractions 56–60 consisted of II (5.5%), fractions 64–74 afforded prostaglandin E_2 (24.8%), fractions 74–82 gave prostaglandin $F_{2\alpha}$ (7.56%), and fractions 104–107 yielded 6-ketoprostaglandin $F_{1\alpha}$ (4.4%).

Fractions 15–22 were combined and further purified by chromatography over an LH-20 column (1 × 36 cm). The column was eluted with methylene chloride–benzene–methanol (10:10:1), and 6-ml fractions were collected. Fractions 9–13 (82% radioactivity) were pooled and evaporated to dryness. The residue was methylated with diazomethane and further purified over a silica gel (10 g) column (1 × 23.5 cm). The column was eluted successively with benzene–ethyl acetate (100 ml of 95:5, 200 ml of 7:3, and 200 ml of 1:1), and 6-ml fractions were collected. Fraction 28, consisting of the pure methyl ester of I (23% of the added radioactivity), was used for NMR and mass spectrometric analyses.

Fractions 56–60, consisting of II, were similarly purified.

Hydroxy Fatty Acid Isolation—Ram seminal vesicle microsomes (24 g) were suspended in 2.4 liters of 0.1 M, pH 7.5 tromethamine buffer. Ascorbic acid (1 mM) was added. The enzyme reaction was initiated by the addition of 120 mg of arachidonic acid containing 32 μCi of 1-^{14}C-arachidonic acid. After incubation at 25° for 20 min with gentle shaking on a Dubnoff shaker, the reaction mixture was extracted in the same manner as that for 15-ketoprostaglandin E_2 and prostaglandin D_2. The total recovery of radioactivity was 47.3%.

This material was chromatographed over 30 g of silicic acid–diatomaceous earth (85:15), and the column was eluted with the following solvent systems: 50 ml of benzene–ethyl acetate (8:2), 250 ml of benzene–ethyl acetate (7:3), and a gradient system consisting of 300 ml of benzene–ethyl acetate (7:3) in the mixing chamber and 300 ml of ethyl acetate in the reservoir chamber. Fractions (6.5 ml) were collected.

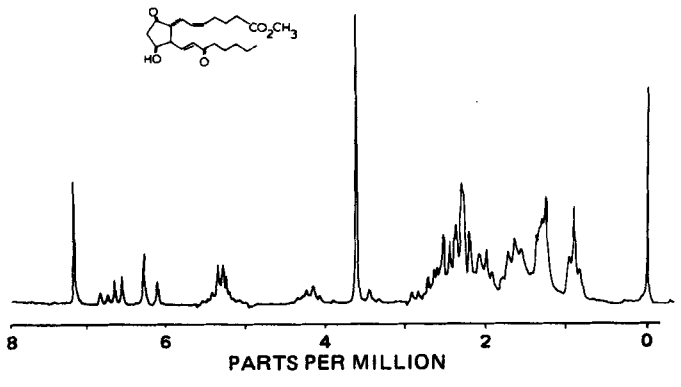

Figure 2—^1H-*NMR spectrum of I methyl ester.*

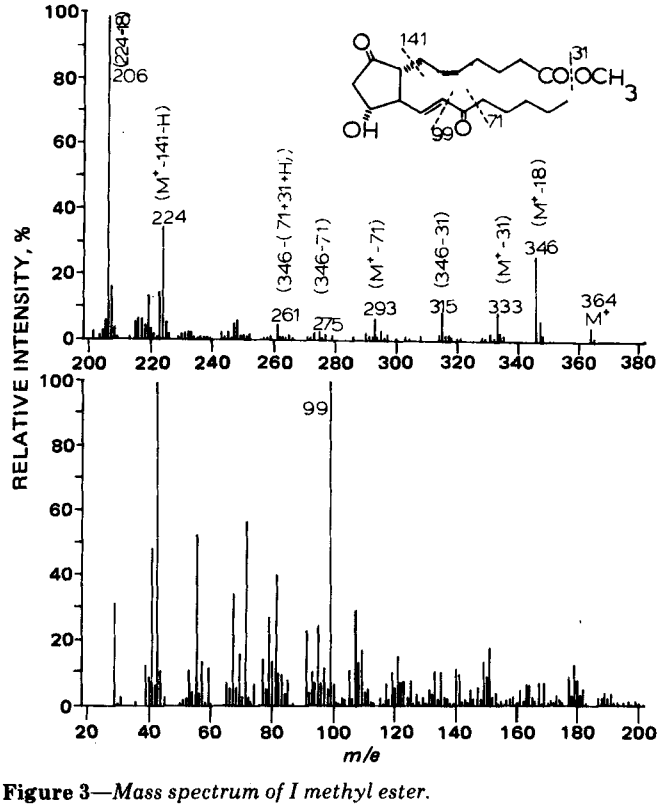

Figure 3—*Mass spectrum of I methyl ester.*

Table II—Effect of Cofactors on Product Distribution at Low Arachidonic Acid Concentration [a] (30 μM)

Cofactor	Concentration	Percent of Products Formed						Radioactivity in Products, %
			Prostaglandin					
		Hydroxy Fatty Acids	15-Keto-E_2	D_2	E_2	$F_{2\alpha}$	6-Keto-$F_{1\alpha}$	
None	—	17.7	14.9	19.9	28.1	8.9	7.8	97.3
Glutathione	20 μM	4.8	0	3.4	91.8	0	0	100
Ascorbic acid	1 mM	34.2	4.7	6.4	8.7	19.8	26.2	100
Phenol	1 mM	18.5	0	24.3	31.7	7.7	7.1	89.3
L-Tryptophan	1 mM	17.6	6.5	14.2	19.0	10.3	30.8	98.4
L-Epinephrine	1 mM	23.4	0	20.5	25.0	20.3	10.8	100
Serotonin	1 mM	21.6	0	24.4	30.4	11.5	7.8	95.7
Methemoglobin	8 μM	15.7	13.6	21.9	32.2	7.2	6.0	96.7

[a] The reaction mixture was the same as that described in Table I except that 10 μg of unlabeled arachidonic acid was used.

Fractions 6–20, containing 25.75% of radioactivity, were pooled and rechromatographed over an LH-20 column (1.8 × 24.5 cm). The column was eluted with benzene–methylene chloride (6:4), and 4-ml fractions were collected. Fractions 45–95 (28% of radioactivity), containing 11-hydroxy- and 15-hydroxyeicosatetraenoic acids and 12-hydroxy-5,8,10-heptadecatrienoic acid, were methylated with diazomethane and used for GLC–mass spectral analysis.

RESULTS

When 1-^{14}C-arachidonic acid at a concentration greater than 150 μM was exposed to ram seminal vesicle microsomes, several radioactive products were formed (Fig. 1A). Besides those products corresponding in mobilities to prostaglandin E_2, prostaglandin $F_{2\alpha}$, and 6-ketoprostaglandin $F_{1\alpha}$, two compounds (I and II) less polar than prostaglandin E_2 were produced. When a portion of the organic extract of this reaction mixture was treated with sodium borohydride, the radioactive chromatographic profile of the products was markedly changed (Fig. 1B). The radioactive peaks corresponding to I and II disappeared, the prostaglandin E_2 peak was considerably reduced, and there was a radioactivity increase in the prostaglandin $F_{2\alpha}$ region. These observations suggested that both I and II possessed ketonic functions, which, upon reduction with sodium borohydride, afforded compounds similar in polarity to prostaglandin $F_{2\alpha}$.

It was previously reported (6) that addition of 15-hydroperoxyarachidonic acid (100 μM) to the incubation medium inhibited the formation of 6-ketoprostaglandin $F_{1\alpha}$ but did not affect the formation of prostaglandin E_2, I, and II. This observation suggests that I and II were not derived from the prostacyclin pathway. This observation was confirmed by evidence that 15-hydroperoxyarachidonic acid did not significantly inhibit the formation of I and II (Fig. 1C).

To establish conclusively the chemical structures of I and II, the arachidonic acid-derived products were resolved by silicic acid column chromatography. The PMR spectrum of the I methyl ester (Fig. 2) showed characteristic prostaglandin signals: a pair of doublets centered at δ 6.76 (1H, $J_{12,13}$ = 7.8 Hz, C-13H), a doublet at δ 6.3 (1H, $J_{13,14}$ = 16 Hz, C-14H), a multiplet at δ 5.39 (2H, vinylic protons at C-5 and C-6), and a multiplet at δ 4.25 (1H, C-11H). The mass spectrum of the I methyl ester (Fig. 3) gave prominent ions at *m/e* 364 (M^+), 346 (M − 18), 333 (M − 31), 315 (346 − 31), 293 (M − 71), 275 (346 − 71), 261 [346 − (71 + 31 + H)], 224 [M − (141 − H)], and 206 (224 − 18). The UV spectrum of the I methyl ester (Fig. 4) exhibited a maximum at 228 nm (ε 11,000) characteristic of an α,β-unsaturated ketone.

These spectral data are consistent with the supposition that the chemical structure of I is either 15-ketoprostaglandin E_2 or its regioisomer, 15-ketoprostaglandin D_2. However, when the I methyl ester was treated with 0.1 *N* NaOH, a compound with a chromophore at 500 nm (ε 22,400) was formed. This experiment clearly established that I is 15-ketoprostaglandin E_2 (9), because the presence of 15-ketoprostaglandin D_2 would have resulted in the formation of a stable chromophore at 415 nm (10).

In a similar fashion, II was identified as prostaglandin D_2 (11, 12). The NMR (Fig. 5) and mass (Fig. 6) spectra as well as the chromatographic behavior of the II methyl ester were identical to those of the authentic sample of prostaglandin D_2 methyl ester.

The ratio of the products formed by ram seminal vesicle microsomes had been shown to be dependent on the arachidonic acid concentration (6). Thus, it appeared of interest to examine the effect of cofactors on biosynthesis at high (Table I) and low (Table II) substrate concentrations. At high arachidonic acid concentrations (164 μM), the addition of tryptophan and phenol reduced the formation of 15-ketoprostaglandin E_2 and prostaglandin $F_{2\alpha}$ whereas synthesis of prostaglandin E_2 and 6-ketoprostaglandin $F_{1\alpha}$ was enhanced. On the other hand, reduced glutathione favored the biosynthesis of prostaglandin E_2 and 15-ketoprostaglandin E_2, but the overall conversion of arachidonic acid to these products was reduced (70%) compared to control (93%).

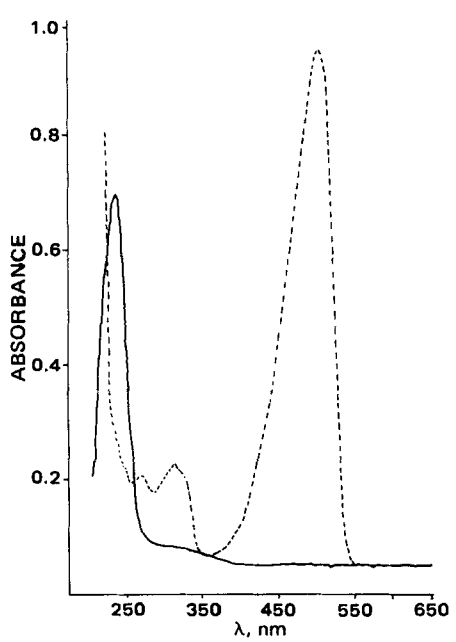

Figure 4—*Alkali effect of I absorption properties. Key: —, 0.01 mg of I/ml of methanol; and ---, after 5 min in 0.1* N *NaOH.*

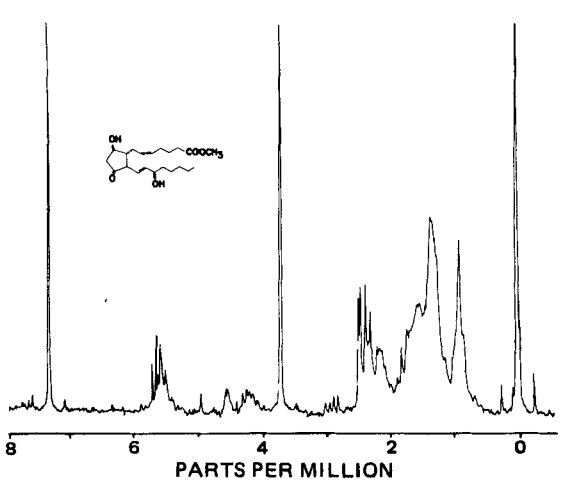

Figure 5—^{1}*H-NMR spectrum of II methyl ester.*

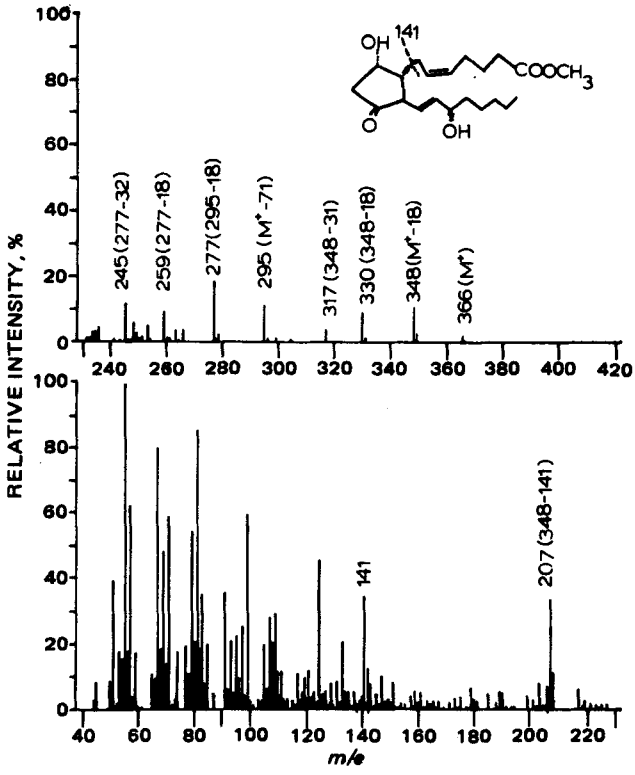

Figure 6—*Mass spectrum of II methyl ester.*

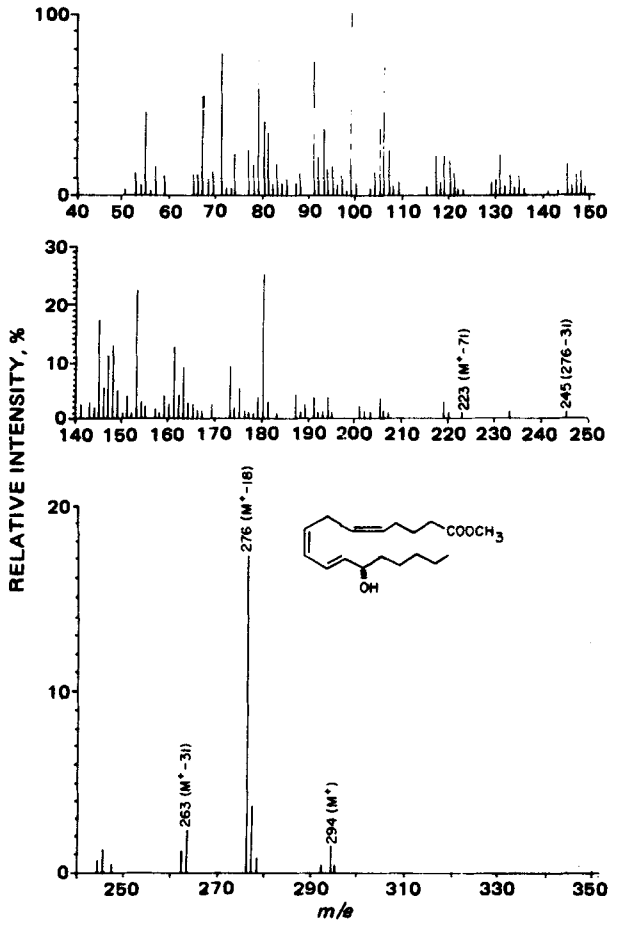

Figure 7—*Mass spectrum of 12-hydroxy-5,8,10-heptadecatrienoic acid methyl ester.*

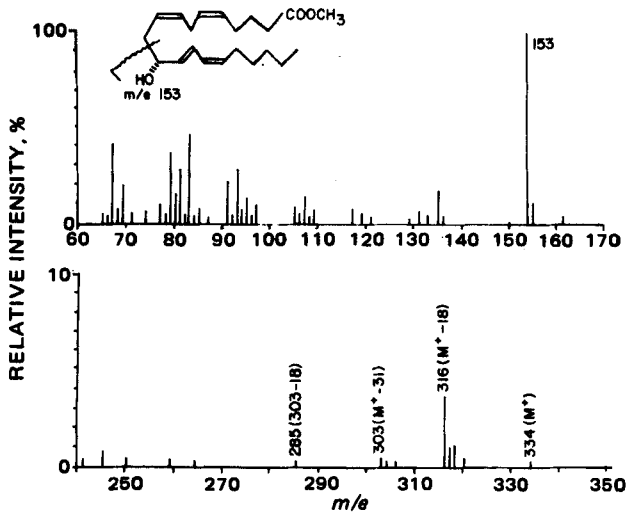

Figure 8—*Mass spectrum of 11-hydroxy-5,8,12,14-eicosatetraenoic acid methyl ester.*

Ascorbic acid markedly stimulated the formation of hydroxy fatty acids. GLC–mass spectrometric analysis of the methyl esters of this mixture revealed two major and one minor hydroxy fatty acids. They were characterized on the basis of the mass spectral data as 12-hydroxy-5,8,10-heptadecatrienoic acid methyl ester, which showed a molecular ion at *m/e* 294 (M^+) with principal fragments at 276 (M − 18), 263 (M − 31), 245 (M − 31 − 18), 223 (M − C_5H_{11}), and 207 (M − 87) (Fig. 7); 11-hydroxy-5,8,12,14-eicosatetraenoic acid methyl ester, showing prominent ions at *m/e* 334 (M^+), 316 (M − 18), 303 (M − 31), 285 (M − 31 − 18), 275 (M − 59), 153 (M − 181) [$CH_2CH{=}CHCH_2CH{=}CH(CH_3)_3CO_2CH_3$], and 135 (153 − 18) (Fig. 8); and 15-hydroxy-5,8,11,13-eicosatetraenoic acid methyl ester as the minor component, showing a molecular ion at *m/e* 334 (M^+) with fragments appearing at 316 (M − 18), 303 (M − 31), 285 (303 − 18), 263 (M − 71), and 245 (263 − 18).

At a low arachidonic concentration (30 μM), reduced glutathione greatly favored prostaglandin E_2 biosynthesis, but no 15-ketoprostaglandin E_2 was detectable. Ascorbic acid again dramatically enhanced hydroxy fatty acid synthesis but also stimulated the formation of 6-ketoprostaglandin $F_{1\alpha}$. L-Tryptophan again caused a significant increase in 6-ketoprostaglandin $F_{1\alpha}$ (Table II).

DISCUSSION

By comparing the spectral data to those of authentic samples, the two known products formed after exposure of relatively high arachidonic acid concentrations (164 μM) to ram seminal vesicle microsomes were identified as 15-ketoprostaglandin E_2 and prostaglandin D_2. The formation of these two products was not inhibited significantly by the exogenous addition of 15-hydroperoxyeicosa-5,8,11,13-tetraenoic acid to the incubation mixture, confirming the report of Cottee *et al.* (6). However, the compound originally designated by them in their thin-layer chromatograms as prostaglandin D_2 was probably 8-isoprostaglandin E_2.

Although a small quantity of 15-ketoprostaglandin E_1 had been detected in previous ram seminal vesicle microsomal incubations with eicosatrienoic acid (13), the formation of a substantial quantity of 15-ketoprostaglandin E_2 in these incubations deserves comment. Perhaps 15-ketoprostaglandin E_2 may be derived from the oxidation of the 15(S)-hydroxyl group in prostaglandin E_2 or prostaglandin H_2 by a hydroxyprostaglandin dehydrogenase. However, exposure of 1-^{14}C-prostaglandin E_2 to ram seminal vesicle microsomes under these conditions did not produce detectable 15-ketoprostaglandin E_2. Thus, the 15-keto functionality probably originated from the nonenzymatic decomposition of the 15-hydroperoxy group either at the prostaglandin G_2 or at the 15-hydroperoxyprostaglandin E_2 stage. The corresponding regioisomer, 15-ketoprostaglandin D_2, was not formed in any detectable quantities.

REFERENCES

(1) D. A. Van Dorp, R. K. Beerthuis, D. H. Nugteren, and H. Von Keman, *Nature*, **203**, 839 (1964).

(2) S. Bergstrom, H. Danielsson, and B. Samuelsson, *Biochim. Biophys. Acta*, **90**, 207 (1964).

(3) E. Granstrom, W. E. M. Lands, and B. Samuelsson, *J. Biol. Chem.*, **243**, 4104 (1968).
(4) D. A. Van Dorp, R. K. Beerthuis, D. H. Nugteren, and H. Von Keman, *Biochim. Biophys. Acta*, **90**, 204 (1964).
(5) S. Bergstrom, H. Danielsson, D. Klenberg, and B. Samuelsson, *J. Biol. Chem.*, **239**, 4006 (1964).
(6) F. Cottee, R. J. Flower, S. Moncada, J. A. Salmon, and J. R. Vane, *Prostaglandins*, **14**, 413 (1977).
(7) M. Hamberg and B. Samuelsson, *J. Biol. Chem.*, **242**, 5329 (1967).
(8) R. J. Flower, H. S. Cheung, and D. W. Cushman, *Prostaglandins*, **4**, 325 (1973).
(9) E. Anggard and B. Samuelsson, *Ark. Kemi.*, **25**, 293 (1966).
(10) R. L. Jones and N. H. Wilson, *J. Chem. Soc. (Perkin I)*, **1978**, 209.
(11) E. F. Jenny, P. Schaublin, H. Fritz, and H. Fuhrer, *Tetrahedron Lett.*, **1974**, 2235.
(12) M. Hayaishi and T. Tanouchi, *J. Org. Chem.*, **38**, 2115 (1973).
(13) D. H. Nugteren, R. K. Beerthuis, and D. A. Van Dorp, *Rec. Trav. Chim. Pays-Bas*, **85**, 405 (1966).

ACKNOWLEDGMENTS

Supported in part by National Institutes of Health Grant AM-9688.

p-Aminophenol Fluorescence and Determination in the Presence of Acetaminophen

KENNETH W. STREET, Jr.*, and GEORGE H. SCHENK ‡x

Received February 15, 1978, from the **Department of Chemistry, University of Cincinnati, Cincinnati, OH 45221*, and the ‡*Department of Chemistry, Wayne State University, Detroit, MI 48202.* Accepted for publication April 30, 1979.

Abstract □ The spectrophotometric and fluorometric properties of the aminophenols and of several compounds related to *p*-aminophenol were examined. A direct spectrofluorometric method for *p*-aminophenol determination at trace levels in methanol was developed and evaluated for the effect of inner filtering by acetaminophen. The method was applied to the determination of *p*-aminophenol as an impurity in acetaminophen and acetaminophen-containing tablets.

Keyphrases □ *p*-Aminophenol—analysis, spectrofluorometry, as impurity in acetaminophen tablets □ Acetaminophen—tablets, spectrofluorometric analysis of *p*-aminophenol as impurity □ Spectrofluorometry—analysis, *p*-aminophenol as impurity in acetaminophen tablets

Most methods for determining *p*-aminophenol (I) as an impurity in acetaminophen (II) involve spectrophotometric measurement of a chromophore developed *via* reaction with an appropriate reagent, either before or after chromatographic separation from II (1–10). In many of these methods, the chromophore has not been identified (4–10). Other methods involve nonaqueous titrations with perchloric acid (11) or polarographic analysis (12, 13).

To date, only an indirect fluorometric procedure for the determination of I in the presence of II has been reported (14). The fluorometric method involves a lengthy prior derivatization with benzylamine in alkaline solution. The fluorophore has not been identified.

This paper introduces a direct spectrofluorometric method for the determination of I either alone or as an impurity in II or tablets containing II. Due to overlapping UV absorption bands of these compounds, a critical evaluation of the inner filter effect was necessary. The effect of other aminophenols on the determination of I is less critical, but the possibility of positive interference in mixtures exists.

EXPERIMENTAL[1]

Solvents—Since most "spectro" quality solvents are not of suitable purity, all fluorescence work was done with purified alcohols, except where indicated. Purified alcohols were easily prepared from analytical reagent grade anhydrous alcohols by percolating each through a column packed with 30–40 cm of 40–80-mesh activated coconut charcoal[2]. The first portion (~50 ml) of the eluate from each column was highly contaminated with fluorescent impurities and was discarded. After the initial 50 ml, each column produced 5–10 liters of purified solvent before the packing was replaced.

n-Propanol did not purify as well as ethanol or methanol. Spectroquality chloroform always was used except where the chloroform fluorescence blank exceeded 3 in 100 units of full scale. To prepare fluorescent grade solvent from spectro or analytical reagent grade reagent, the chloroform was first vigorously extracted with a small volume (~10:1 v/v) of 0.45 *M* NaOH. The chloroform was recovered, washed twice with small volumes (~10:1 v/v) of water, and filtered through chloroform-wet filter paper. The resulting chloroform was suitable for spectrophotometry or spectrofluorometry.

Solutions of I—Crystals of I[3] decompose on standing and were available as black granules. Compound I was easily sublimed to gray crystals under ~4 torr at 180°; a second sublimation under similar conditions yielded white crystals with a 186–188° melting-point range (15). Alcohol or chloroform solutions, 0.01–0.001 *M*, were prepared fresh daily prior to use.

***o*-Aminophenol**—The *o*-aminophenol[3] deteriorated to black granules on standing. It was easily sublimed to pale-red crystals under ~4 torr at ~150°; a second sublimation under similar conditions yielded pale-yellow needles with a 170–174° melting-point range (16). Standard solutions were prepared fresh daily prior to use.

***m*-Aminophenol**—The *m*-aminophenol[4] was used without further purification. Although the *m*-aminophenol is somewhat more stable in alcoholic solution than the other aminophenols, standard solutions had to be prepared fresh daily.

Acetaminophen[5], Phenacetin[6], Aniline[7], Acetanilid[8], and Phenol[9]—These chemicals were used to prepare solutions without further purification.

Working Standards for Solvent Studies—All standard solutions of drugs (and related compounds) were prepared by dissolving an appropriate amount of the drug in the desired solvent and volumetrically diluting to the correct molarity. Compound I was sparingly soluble in chloroform. Standards of I in chloroform were prepared by volumetric dilutions of a concentrated methanolic I standard to the correct molarity

[1] Absorption spectra were taken on a Beckman DK-2A spectrophotometer. All fluorescence spectra were taken on a Perkin–Elmer MPF-2A spectrofluorometer.

[2] Fisher 50–200 mesh.
[3] Eastman practical grade.
[4] NF sample courtesy of Parke, Davis.
[5] NF sample courtesy of Wyeth Laboratories.
[6] American Pharmaceutical Co. USP grade.
[7] Mallinckrodt practical grade.
[8] Matheson, Coleman and Bell practical grade.
[9] Baker Chemical Co. practical grade.

0022-3549/79/1000-1306$01.00/0
© 1979, American Pharmaceutical Association

(3) E. Granstrom, W. E. M. Lands, and B. Samuelsson, *J. Biol. Chem.*, **243**, 4104 (1968).
(4) D. A. Van Dorp, R. K. Beerthuis, D. H. Nugteren, and H. Von Keman, *Biochim. Biophys. Acta*, **90**, 204 (1964).
(5) S. Bergstrom, H. Danielsson, D. Klenberg, and B. Samuelsson, *J. Biol. Chem.*, **239**, 4006 (1964).
(6) F. Cottee, R. J. Flower, S. Moncada, J. A. Salmon, and J. R. Vane, *Prostaglandins*, **14**, 413 (1977).
(7) M. Hamberg and B. Samuelsson, *J. Biol. Chem.*, **242**, 5329 (1967).
(8) R. J. Flower, H. S. Cheung, and D. W. Cushman, *Prostaglandins*, **4**, 325 (1973).
(9) E. Anggard and B. Samuelsson, *Ark. Kemi.*, **25**, 293 (1966).
(10) R. L. Jones and N. H. Wilson, *J. Chem. Soc. (Perkin I)*, **1978**, 209.
(11) E. F. Jenny, P. Schaublin, H. Fritz, and H. Fuhrer, *Tetrahedron Lett.*, **1974**, 2235.
(12) M. Hayaishi and T. Tanouchi, *J. Org. Chem.*, **38**, 2115 (1973).
(13) D. H. Nugteren, R. K. Beerthuis, and D. A. Van Dorp, *Rec. Trav. Chim. Pays-Bas*, **85**, 405 (1966).

ACKNOWLEDGMENTS

Supported in part by National Institutes of Health Grant AM-9688.

p-Aminophenol Fluorescence and Determination in the Presence of Acetaminophen

KENNETH W. STREET, Jr.*, and GEORGE H. SCHENK ‡x

Received February 15, 1978, from the **Department of Chemistry, University of Cincinnati, Cincinnati, OH 45221*, and the ‡*Department of Chemistry, Wayne State University, Detroit, MI 48202.* Accepted for publication April 30, 1979.

Abstract □ The spectrophotometric and fluorometric properties of the aminophenols and of several compounds related to *p*-aminophenol were examined. A direct spectrofluorometric method for *p*-aminophenol determination at trace levels in methanol was developed and evaluated for the effect of inner filtering by acetaminophen. The method was applied to the determination of *p*-aminophenol as an impurity in acetaminophen and acetaminophen-containing tablets.

Keyphrases □ *p*-Aminophenol—analysis, spectrofluorometry, as impurity in acetaminophen tablets □ Acetaminophen—tablets, spectrofluorometric analysis of *p*-aminophenol as impurity □ Spectrofluorometry—analysis, *p*-aminophenol as impurity in acetaminophen tablets

Most methods for determining *p*-aminophenol (I) as an impurity in acetaminophen (II) involve spectrophotometric measurement of a chromophore developed *via* reaction with an appropriate reagent, either before or after chromatographic separation from II (1–10). In many of these methods, the chromophore has not been identified (4–10). Other methods involve nonaqueous titrations with perchloric acid (11) or polarographic analysis (12, 13).

To date, only an indirect fluorometric procedure for the determination of I in the presence of II has been reported (14). The fluorometric method involves a lengthy prior derivatization with benzylamine in alkaline solution. The fluorophore has not been identified.

This paper introduces a direct spectrofluorometric method for the determination of I either alone or as an impurity in II or tablets containing II. Due to overlapping UV absorption bands of these compounds, a critical evaluation of the inner filter effect was necessary. The effect of other aminophenols on the determination of I is less critical, but the possibility of positive interference in mixtures exists.

EXPERIMENTAL[1]

Solvents—Since most "spectro" quality solvents are not of suitable purity, all fluorescence work was done with purified alcohols, except where indicated. Purified alcohols were easily prepared from analytical reagent grade anhydrous alcohols by percolating each through a column packed with 30–40 cm of 40–80-mesh activated coconut charcoal[2]. The first portion (~50 ml) of the eluate from each column was highly contaminated with fluorescent impurities and was discarded. After the initial 50 ml, each column produced 5–10 liters of purified solvent before the packing was replaced.

n-Propanol did not purify as well as ethanol or methanol. Spectroquality chloroform always was used except where the chloroform fluorescence blank exceeded 3 in 100 units of full scale. To prepare fluorescent grade solvent from spectro or analytical reagent grade reagent, the chloroform was first vigorously extracted with a small volume (~10:1 v/v) of 0.45 *M* NaOH. The chloroform was recovered, washed twice with small volumes (~10:1 v/v) of water, and filtered through chloroform-wet filter paper. The resulting chloroform was suitable for spectrophotometry or spectrofluorometry.

Solutions of I—Crystals of I[3] decompose on standing and were available as black granules. Compound I was easily sublimed to gray crystals under ~4 torr at 180°; a second sublimation under similar conditions yielded white crystals with a 186–188° melting-point range (15). Alcohol or chloroform solutions, 0.01–0.001 *M*, were prepared fresh daily prior to use.

***o*-Aminophenol**—The *o*-aminophenol[3] deteriorated to black granules on standing. It was easily sublimed to pale-red crystals under ~4 torr at ~150°; a second sublimation under similar conditions yielded pale-yellow needles with a 170–174° melting-point range (16). Standard solutions were prepared fresh daily prior to use.

***m*-Aminophenol**—The *m*-aminophenol[4] was used without further purification. Although the *m*-aminophenol is somewhat more stable in alcoholic solution than the other aminophenols, standard solutions had to be prepared fresh daily.

Acetaminophen[5], Phenacetin[6], Aniline[7], Acetanilid[8], and Phenol[9]—These chemicals were used to prepare solutions without further purification.

Working Standards for Solvent Studies—All standard solutions of drugs (and related compounds) were prepared by dissolving an appropriate amount of the drug in the desired solvent and volumetrically diluting to the correct molarity. Compound I was sparingly soluble in chloroform. Standards of I in chloroform were prepared by volumetric dilutions of a concentrated methanolic I standard to the correct molarity

[1] Absorption spectra were taken on a Beckman DK-2A spectrophotometer. All fluorescence spectra were taken on a Perkin–Elmer MPF-2A spectrofluorometer.

[2] Fisher 50–200 mesh.
[3] Eastman practical grade.
[4] NF sample courtesy of Parke, Davis.
[5] NF sample courtesy of Wyeth Laboratories.
[6] American Pharmaceutical Co. USP grade.
[7] Mallinckrodt practical grade.
[8] Matheson, Coleman and Bell practical grade.
[9] Baker Chemical Co. practical grade.

0022-3549/79/1000-1306$01.00/0
© 1979, American Pharmaceutical Association

Table I—Absorption and Emission Characteristics of Pharmaceuticals in Methanol

Compound	λ_A, nm	ϵ_{max}	λ_F, nm	F^a
	Fluorescent Compounds			
p-Aminophenol	235	7.9×10^3		
	300	3.7×10^3	365	100
m-Aminophenol	233	5.9×10^3		
	285	2.1×10^3	330	29
o-Aminophenol	233	6.2×10^3		
	287	3.1×10^3	330	27
Aniline	234	9.8×10^3		
	285	1.3×10^3	335	50
Phenol	230	—		
	273	1.7×10^3	297	32
Compounds Whose Fluorescence Could Not Be Characterized[b]				
Acetanilid	228	1.3×10^4	—	—
Acetaminophen	248	1.6×10^4	—	—
Phenacetin	250	1.5×10^4	—	—

[a] Based on a reading of 100 for *p*-aminophenol as an arbitrary standard. [b] In methanol, no characteristic fluorescence bands were observable.

with chloroform (the final solution was always less than 1% methanol). All synthetic samples were homogenized in a micro mill[10].

Determination of I in II—A 300-mg sample of II was accurately weighed, transferred to a 100-ml volumetric flask, and diluted to volume with methanol. A 1:100 dilution with methanol produced a solution that was retained for UV measurement of II.

The solution was inserted into the spectrofluorometer and excited at 300 nm (10-nm slit width); emission was measured at 365 nm (20-nm slit width). To minimize error from inner filtering, standards of pure (containing less than the detection limit of the method) I in the $0–12 \times 10^{-7}$ *M* range in methanol containing 3.0 mg of pure II/100 ml were prepared. To zero the instrument, a blank containing 3.0 mg of pure II/100 ml of methanol was used. A calibration plot of emission at 365 nm *versus* concentration of pure I (typically $0–12 \times 10^{-7}$ *M*) was prepared.

Determination of I in Tablets of II—For a "lot" analysis, 10 tablets of II (or the entire contents of 10 capsules of II) were weighed accurately and ground in a mortar to homogeneity. A portion of the homogeneous powder containing 300 ± 3 mg of II was weighed and transferred to a 100-ml volumetric flask, and ~75 ml of methanol was added. The solution was agitated gently for 10 min and diluted to volume with methanol. The solution was filtered through medium-speed filter paper, diluted 1:100 with methanol, and retained for fluorometric determination of I as already described. An additional 1:10 dilution of the latter solution was retained for UV measurement of II.

The UV absorbance of the solution prepared for this purpose was measured at 248 nm, and a scan of the UV spectrum from 350 to 230 nm of a representative sample for each brand of tablets or capsules was examined. If the UV scan showed additional peaks in the 300-nm region (from other drugs or additives), the sample was analyzed by another method. If the absorbance of the 1:10 dilution at 248 nm did not fall within ±0.05 unit (preferably within ±0.03 unit) of that of a 1:10 dilution of a 6×10^{-7} *M* standard containing 3.0 mg of II/100 ml, the fluorescence solution concentration was adjusted by redilution of the original sample so that its absorbance was within the desired range after a 1:10 dilution. Then the fluorescence emission was measured again as described.

RESULTS AND DISCUSSION

All aminophenols and compounds related to I contain a benzene ring; therefore, these compounds were expected to absorb intensely in the UV region (Table I). Qualitatively, the order of the molar absorptivities (ϵ_{max}) was: *p*-aminophenol > *o*-aminophenol > *m*-aminophenol > phenol > aniline.

Because the fluorescence emission process is dependent on the ability of the molecule to absorb radiant energy, it might be expected that the fluorescence emission intensity in this group of compounds would exhibit an order similar to that of the molar absorptivities. On the uncorrected spectrofluorometer, this did not appear to be the case. On that instrument, 10^{-5} *M* solutions of these compounds in methanol yielded the following order for fluorescence emission intensity: *p*-aminophenol > aniline > phenol ≅ *m*-aminophenol ≅ *o*-aminophenol.

With the assumption of a constant intensity of the xenon arc source over the small excitation wavelength range (17) and a linear photomultiplier response over the narrow emission range (18), the actual fluorescence intensity for these compounds was approximated more closely by the ratio (19) of the relative fluorescence divided by ϵ_{max}. Relative fluorescence was the emission reading for 10^{-5} *M* solutions. Reevaluation of the fluorescence emission sequence in terms of this ratio gave the following sequence: aniline > *p*-aminophenol > phenol ≅ *m*-aminophenol ≅ *o*-aminophenol.

The direct determination of any one of the fluorescent compounds in Table I would, therefore, be subject to positive interference by the presence of any of the remaining fluorescent compounds listed. The presence of large amounts of any of the last three compounds listed in Table I would cause a negative interference due to inner filtering. No error due to the possible fluorescence of the last three compounds was observed in pure methanol.

Child *et al.* (20) reported that II fluoresced at 400 nm in 1% ethanol–water but at about twice the maximum concentration used in the present study (30 μg/ml) and at 40 nm away from the 360-nm measurement using much higher signal amplification. This apparent fluorescence was not a source of error. Nang and Pitet (21) also reported fluorescence of 3×10^{-3} *M* II at 430 nm in an acidic 100% aqueous solvent, but their concentrations were much higher than those used in the present study (1.5×10^{-4} *M*) and required much higher signal amplification. Apparently, the use of methanol as a solvent reduces II fluorescence to negligible levels.

Solvent—Several other solvents were tested. Compound I did not fluoresce significantly in either water or chloroform. The small amounts of methanol did not affect the UV absorptive properties of I; and since methanol promotes fluorescence, it is more likely that the high degree of fluorescence quenching observed in chloroform was an effect of the chloroform itself rather than interference from methanol or a mixed solvent. However, I fluoresced in most common alcohols intensely enough to permit its determination in any of them (Table II). Methanol was selected because it is easily obtained and easily purified for analytical purposes. For the determination of I in II, fluorescence grade methanol must be used for all solution preparation.

Experimental Parameters—The spectrofluorometer was used because its xenon arc source provided excitation in the 300-nm region. With this spectrofluorometer, plots of the fluorescence of I *versus* concentration were linear but did not pass through the origin, indicating that a reagent blank (Fig. 1) correction was necessary. This blank effect could be seen with pure I or II in methanol. As a result, the choices of slit width, instrumental sensitivity, and excitation wavelength were critical.

With slit widths of 10 nm for excitation and 20 nm for emission, it was possible to measure 0.25% I in samples containing II with excellent sensitivity; at wider slit widths, the blank spectrum became severely distorted, making it difficult to obtain reliable blank values. At a sensitivity setting of three, the readings were more reliable than at a sensitivity setting of four, although the detection limit was lower at the latter setting. A 300-nm excitation wavelength was chosen even though the excitation maximum on the spectrofluorometer occurred at 304 nm. Excitation at wavelengths appreciably greater than 300 nm caused large variations in

Table II—Absorption and Emission Characteristics of I in Various Solvents

Solvent	λ_A, nm	ϵ_{max}	F
Water	226	5.8×10^3	
	296	1.6×10^3	4[a]
Methanol	232	7.3×10^3	
	300	2.3×10^3	48
Ethanol	301	2.5×10^3	54
n-Propanol	299	2.3×10^3	47
Chloroform	303	2.3×10^3	None

[a] Fluorescence at 375-nm emission maximum.

Table III—Evaluation of the Inner Filter Effect of II on the Determination of I in Methanol

II in Sample, mg	*A* at 300 nm[a]	Percent *IF*[b]
100	0.09	4.3
150	0.13	16
300 ± 30	0.26	18 (±3)[c]
450	0.39	33

[a] Calculated. [b] Percent $IF = (F_I + F_{I+II}/F_I) \times 100\%$, where the blank for each study contains the same milligrams of II as each sample. [c] Standard deviation = 3.3% for eight determinations on different days.

[10] Obtainable through Chemical Rubber Co., Cleveland, Ohio.

Table IV—Detection Limits of I in Pure Solution or in the Presence of II

Sample	Instrument Sensitivity Setting	Detection Limits			
		By Inspection		By Graph	
		I, %	I, *M*	I, %	I, *M*
Pure I	4	—	0.6×10^{-7}	—	0.2×10^{-7}
I in 3.0 mg % II	3	0.063	1.7×10^{-7}	0.038	1.0×10^{-7}

the blank reading while excitation below 300 nm drastically lowered the fluorescence emission intensity because of inner filtering by II and decreased excitation efficiency.

Reagent Purity and Inner Filtering—The I crystals should be white with no traces of gray. Freshly sublimed I should be stored in a tightly capped container out of the light. Moisture, air, and light tend to decompose I crystals rapidly to gray and then to black. Stock I solutions darken within several hours of preparation (~14% deterioration/day); for this reason, it is recommended that standards and samples be prepared immediately before use. Storing solutions under refrigeration in the dark slows decomposition only slightly. The filtering of solutions through medium-speed filter paper did not alter the concentration of any of the components in the samples.

If I is to be determined in the presence of II, it is important to examine the effect of the latter on the UV spectrum of the former. At II–I ratios >1000:1 (the working ratio for the analyses), the UV spectrum of the mixture actually approximated that of II alone. Thus, II should absorb an extremely large fraction of the 300-nm excitation radiation striking a typical mixture of these two compounds. Consequently, a large inner filter effect from II was observed in the direct fluorometric determination of I (Table III). Although calibration curves at various II concentrations were linear, a large variation in the magnitude of the inner filter effect was observed from day to day (Table III).

To check a sample's absorbance at 300 nm, a 1:10 dilution was made and the UV absorbance was determined at the 248-nm maximum rather than reading absorbance directly at 300 nm on the highly sloping portion

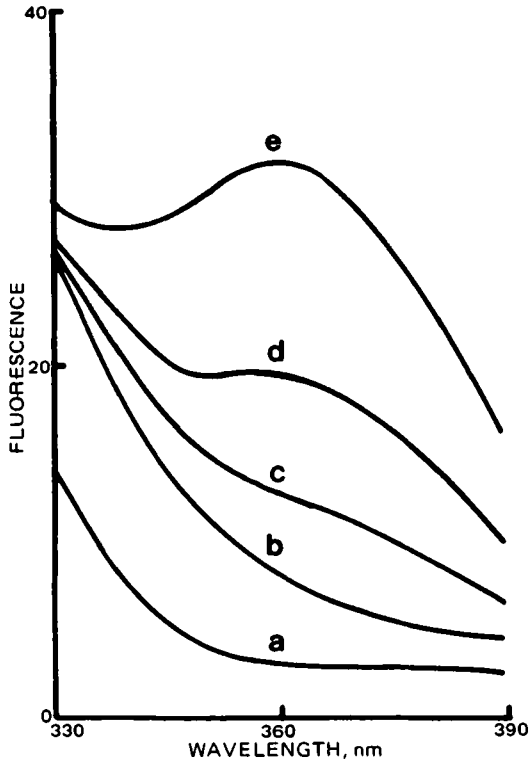

Figure 1—*Fluorescence spectra of various I concentrations in the presence of II in methanol. Key: a, methanol; b, 3.0 mg % II in methanol (blank for the determination of I in II); c, 3.0 mg % II containing 0.027 % I as an impurity in methanol; d, 3.0 mg % II containing 0.067% I as an impurity in methanol; and e, 3.0 mg % II containing 0.133% I as an impurity in methanol.*

Table V—Determination of I in Pharmaceuticals

Acetaminophen Preparation[a]	I Added[b], %	I Determined, %	Instrumental Sensitivity
Tablets 1	0.000	0.014	3
Tablets 1	0.000	0.021	4
Tablets 1	0.000	0.029	4
Tablets 2[c]	0.040	0.035[d]	3
Tablets 2	0.040	0.028	4
Tablets 3[c]	0.073	0.074	3
Tablets 3	0.073	0.067	4

[a] Tylenol tablets 2 and 3 were synthetic samples. [b] Calculated. [c] Tablet excipients had no apparent effect on the determination of I. [d] Since the amount of I is at the detection limit of I, the agreement with the expected value is not expected to be extremely good.

of the UV absorption band of II. This procedure ensured the proper content of II in the fluorescence test solution. As long as the UV absorbance of the sample solution fell within ±0.03 unit of any standard containing II (0.33 absorbance unit for 2×10^{-5} *M* II), the change in inner filter effect was negligible.

Determination of I—Compound I could be determined at low concentrations (<0.1%) in II either by inspection of the fluorescence emission spectrum (Fig. 1) or by graphical analysis. Determination by inspection only involved visual comparison of the sample fluorescence emission spectrum to those of standards and was only an estimation of one significant figure.

The detection limit of the method may not be obvious from Fig. 1. For the determination of I by inspection of spectra (Table IV), the spectrum should be scanned at medium chart speed with the scanning device at high speed to make the fluorescence band more apparent. For graphical analysis (Table IV), the fluorescence emission can be read either directly from the meter scale at the 365-nm emission peak or from the recorded spectrum using medium chart and scanning speeds (Fig. 1).

Quantitative results are shown in Table V. All commercially available II[11] tablets analyzed (Table V) contained <0.038% I in II, the detection limit of the method (Table IV). A duplicate analysis of commercially available II tablets (Tablet 1) at an instrumental sensitivity setting of four gave higher results than analysis using the same sample solutions at an instrumental sensitivity setting of three due to large variations in sample and blank readings at the former instrumental sensitivity setting (Table V).

Synthetic samples (Tablets 2 and 3) were prepared by combining known amounts of pure I with known amounts of previously analyzed tablets (Tablet 1) and then rehomogenizing in the micro mill. The results of analysis of synthetic samples were thus dependent on a "blank" correction due to II and possibly to the suspected I content of Tablet 1. For analysis at instrumental sensitivity setting four, the unspiked tablets (Tablet 1) gave higher apparent concentrations of I with large variation between replicate samples (Table V) and, therefore, much lower recoveries for the synthetic samples.

The results of the synthetic sample analyses at an instrumental sensitivity setting of three depended on a lower correction for the actual tablet content of I, and experimentally determined values compared more favorably to calculated values for the amount of I used to spike the samples. Apparent deviations from the calculated values at a lower I content (0.040%) were probably due to lower precision in both the determination of low percent of I and in the actual tablet content that falls below the detection limit for the method rather than other possible sources of interference (*e.g.*, insoluble excipients). This speculation is supported by the small positive error in the analytical results where the content of I was higher (Tablet 3).

CONCLUSION

Since no TLC or column chromatography was used, there was no loss of I during the analysis as is possible in methods involving separations (22). Also, there was no possibility of an incomplete or competing chromophore- or fluorophore-forming reaction. This fact decreased the possibility of formation of interfering species or of the decomposition of I. Most methods for the determination of I are quite sensitive, but many specify no detection limit for I alone or in combination with II (1, 3, 10, 16, 23, 24). Many methods that do specify detection limits, expressed as percent I in II, possess sensitivities that are not lower than the direct

[11] Tylenol preparation containing 500 mg/tablet, McNeil Laboratories.

fluorometric method (1, 10, 14, 22, 24). Other methods were specifically designed for the determination of I in biological specimens (1, 10) or for the determination of II and related compounds after conversion to I (1, 10, 14).

REFERENCES

(1) B. B. Brodie and J. Axelrod, *J. Pharmacol. Exp. Ther.*, **94**, 22 (1948).

(2) "The United States Pharmacopeia," 19th ed., Mack Publishing Co., Easton, Pa., 1974, p. 11.

(3) E. Kalatzis, *J. Pharm. Sci.*, **59**, 193 (1970).

(4) E. Klug, *Aerztl. Lab.*, **16(a)**, 295 (1970).

(5) M. Kuzolova, V. Kunor, and J. Merhaut, *Pract. Lek.*, **22**, 126 (1970).

(6) M. Geldmacher-von Mallinckrodt and A. Herrmann, *Z. Klin. Chem. Klin. Biochem.*, **7**, 34 (1969).

(7) G. Ropa, E. Radulescu-Jercan, and F. M. Albert, *Rev. Roum. Chim.*, **11**, 1449 (1966).

(8) T. Yaichiro, S. Shigeru, K. Akemi, and S. Satomi, *Tokushima Daigaku Yakugaku Kenkyu Nempo*, **15**, 23 (1966).

(9) H. Thielmann, *Sci. Pharm.*, **40**, 206 (1972).

(10) H. L. Gurtoo and B. M. Phillips, *J. Pharm. Sci.*, **62**, 383 (1973).

(11) W. Jedrzejewsky and J. Badecka-Jedrzejewska, *Chem. Anal. (Warsaw)*, **14**, 73 (1969).

(12) Y. I. Beilis, *Khim. Prom.*, **43**, 767 (1967).

(13) R. D. Tiwari, J. P. Sharma, and I. C. Shukla, *Talanta*, **14**, 853 (1967).

(14) T. Kaito and K. Sagara, *Yakugaku Zasshi*, **94**, 639 (1974).

(15) "The Merck Index," 8th ed., Merck & Co., Rahway, N.J., 1968, p. 59.

(16) "The National Formulary," 13th ed., Mack Publishing Co., Easton, Pa., 1970, p. 17.

(17) G. H. Schenk, "Absorption of Light and Ultraviolet Radiation: Fluorescence and Phosphorescence Emission," Allyn and Bacon, Boston, Mass., 1973, p. 114.

(18) "Photomultiplier Tubes," RCA, PIT-700B, Somerville, N.J., 1971.

(19) S. Udenfriend, "Fluorescence Assay in Biology and Medicine," Academic, New York, N.Y., 1962.

(20) K. J. Child, C. Bedford, and E. G. Tomich, *J. Pharm. Pharmacol.*, **14**, 374 (1962).

(21) L. S. Nang and G. Pitet, *Ann. Pharm. Fr.*, **23**, 45 (1965).

(22) E. Kalatzis and I. Zarbi, *J. Pharm. Sci.*, **65**, 71 (1976).

(23) "British Pharmacopoeia," Pharmaceutical Press, London, England, 1968, p. 707.

(24) I. K. Shih, *J. Pharm. Sci.*, **60**, 1853 (1971).

ACKNOWLEDGMENTS

The authors thank Wayne State University and the Wayne County Medical Examiners Office for the use of their facilities.

Comparative Pharmacokinetics of Coumarin Anticoagulants XLII: Effect of Phenobarbital on Systemic Availability of Orally Administered Dicumarol in Rats with Ligated Bile Ducts

JAMES W. CROW, MILO GIBALDI, and GERHARD LEVY ˣ

Received February 22, 1979, from the *Department of Pharmaceutics, School of Pharmacy, State University of New York at Buffalo, Amherst, NY 14260.* Accepted for publication April 19, 1979.

Abstract □ The purpose of this investigation was to determine if the previously demonstrated inhibitory effect of phenobarbital treatment on the systemic availability of orally administered dicumarol in rats is related to the known effect of phenobarbital on bile output. It was found that phenobarbital had no apparent effect on the systemic availability of an aqueous dicumarol suspension in rats with ligated bile ducts. Compared to results obtained previously on normal rats, bile duct-ligated rats absorbed and eliminated dicumarol much more slowly and absorbed much less of the anticoagulant. On the other hand, the relative inductive effect of phenobarbital treatment on dicumarol elimination was similar in normal and in bile duct-ligated animals. The latter exhibited substantial serum transaminase elevations, indicative of liver damage presumably secondary to cholestasis. These results demonstrate that a drug–drug interaction can depend markedly on the pathophysiological status of the animals.

Keyphrases □ Phenobarbital—effect on dicumarol systemic availability in bile duct-ligated rats □ Dicumarol—phenobarbital effect on systemic availability in bile duct-ligated rats □ Anticoagulants—dicumarol, systemic availability, effect of phenobarbital in bile duct-ligated rats □ Bile duct—ligation, effect on rats, dicumarol systemic availability, phenobarbital □ Drug interactions—phenobarbital effect on dicumarol systemic availability in bile duct-ligated rats

The systemic availability of orally administered dicumarol in humans (1) and rats (2) is reduced by pretreatment of the subjects with a barbiturate. Oral phenobarbital sodium administration, 75 mg/kg, for 5 days before and 2 days after oral administration of dicumarol suspension to rats reduced the systemic availability of the anticoagulant from 84 ± 8 to 48.7 ± 10% (mean ± *SD*). Similar effects were observed when phenobarbital was administered intravenously (2).

Since phenobarbital treatment increased bile output (3), the inhibitory effect of phenobarbital on dicumarol absorption possibly is mediated by complexation of the anticoagulant with bile salts or by altered GI motility caused by increased bile flow. A study was initiated to determine if phenobarbital treatment affects systemic dicumarol availability in rats with ligated bile ducts.

EXPERIMENTAL

The experimental procedures were described previously (2). Briefly, adult male Sprague–Dawley rats weighing ~300 g received daily oral doses of phenobarbital sodium, 75 mg/kg, or the same volume of saline solution for 5 days. Their right jugular vein was cannulated on the 5th day to facilitate frequent blood withdrawal. In the morning of the 6th day, the rats received an intravenous tracer dose of ^{14}C-dicumarol by rapid injection and 50 mg of dicumarol/kg in aqueous suspension by gastric tube.

Blood samples were collected periodically, and daily phenobarbital treatment was continued until the end of the experiment. Food, but not water, was withdrawn for 24 hr, starting 12 hr before dicumarol administration. Plasma was assayed for ^{14}C-dicumarol and unlabeled dicumarol. The ratio of areas under the concentration–time curves for the labeled and unlabeled drug, normalized for dose, was used to calculate systemic

0022-3549/79/1000-1309$01.00/0

© 1979, American Pharmaceutical Association

fluorometric method (1, 10, 14, 22, 24). Other methods were specifically designed for the determination of I in biological specimens (1, 10) or for the determination of II and related compounds after conversion to I (1, 10, 14).

REFERENCES

(1) B. B. Brodie and J. Axelrod, *J. Pharmacol. Exp. Ther.*, **94**, 22 (1948).

(2) "The United States Pharmacopeia," 19th ed., Mack Publishing Co., Easton, Pa., 1974, p. 11.

(3) E. Kalatzis, *J. Pharm. Sci.*, **59**, 193 (1970).

(4) E. Klug, *Aerztl. Lab.*, **16(a)**, 295 (1970).

(5) M. Kuzolova, V. Kunor, and J. Merhaut, *Pract. Lek.*, **22**, 126 (1970).

(6) M. Geldmacher-von Mallinckrodt and A. Herrmann, *Z. Klin. Chem. Klin. Biochem.*, **7**, 34 (1969).

(7) G. Ropa, E. Radulescu-Jercan, and F. M. Albert, *Rev. Roum. Chim.*, **11**, 1449 (1966).

(8) T. Yaichiro, S. Shigeru, K. Akemi, and S. Satomi, *Tokushima Daigaku Yakugaku Kenkyu Nempo*, **15**, 23 (1966).

(9) H. Thielmann, *Sci. Pharm.*, **40**, 206 (1972).

(10) H. L. Gurtoo and B. M. Phillips, *J. Pharm. Sci.*, **62**, 383 (1973).

(11) W. Jedrzejewsky and J. Badecka-Jedrzejewska, *Chem. Anal. (Warsaw)*, **14**, 73 (1969).

(12) Y. I. Beilis, *Khim. Prom.*, **43**, 767 (1967).

(13) R. D. Tiwari, J. P. Sharma, and I. C. Shukla, *Talanta*, **14**, 853 (1967).

(14) T. Kaito and K. Sagara, *Yakugaku Zasshi*, **94**, 639 (1974).

(15) "The Merck Index," 8th ed., Merck & Co., Rahway, N.J., 1968, p. 59.

(16) "The National Formulary," 13th ed., Mack Publishing Co., Easton, Pa., 1970, p. 17.

(17) G. H. Schenk, "Absorption of Light and Ultraviolet Radiation: Fluorescence and Phosphorescence Emission," Allyn and Bacon, Boston, Mass., 1973, p. 114.

(18) "Photomultiplier Tubes," RCA, PIT-700B, Somerville, N.J., 1971.

(19) S. Udenfriend, "Fluorescence Assay in Biology and Medicine," Academic, New York, N.Y., 1962.

(20) K. J. Child, C. Bedford, and E. G. Tomich, *J. Pharm. Pharmacol.*, **14**, 374 (1962).

(21) L. S. Nang and G. Pitet, *Ann. Pharm. Fr.*, **23**, 45 (1965).

(22) E. Kalatzis and I. Zarbi, *J. Pharm. Sci.*, **65**, 71 (1976).

(23) "British Pharmacopoeia," Pharmaceutical Press, London, England, 1968, p. 707.

(24) I. K. Shih, *J. Pharm. Sci.*, **60**, 1853 (1971).

ACKNOWLEDGMENTS

The authors thank Wayne State University and the Wayne County Medical Examiners Office for the use of their facilities.

Comparative Pharmacokinetics of Coumarin Anticoagulants XLII: Effect of Phenobarbital on Systemic Availability of Orally Administered Dicumarol in Rats with Ligated Bile Ducts

JAMES W. CROW, MILO GIBALDI, and GERHARD LEVY ˣ

Received February 22, 1979, from the *Department of Pharmaceutics, School of Pharmacy, State University of New York at Buffalo, Amherst, NY 14260.* Accepted for publication April 19, 1979.

Abstract □ The purpose of this investigation was to determine if the previously demonstrated inhibitory effect of phenobarbital treatment on the systemic availability of orally administered dicumarol in rats is related to the known effect of phenobarbital on bile output. It was found that phenobarbital had no apparent effect on the systemic availability of an aqueous dicumarol suspension in rats with ligated bile ducts. Compared to results obtained previously on normal rats, bile duct-ligated rats absorbed and eliminated dicumarol much more slowly and absorbed much less of the anticoagulant. On the other hand, the relative inductive effect of phenobarbital treatment on dicumarol elimination was similar in normal and in bile duct-ligated animals. The latter exhibited substantial serum transaminase elevations, indicative of liver damage presumably secondary to cholestasis. These results demonstrate that a drug–drug interaction can depend markedly on the pathophysiological status of the animals.

Keyphrases □ Phenobarbital—effect on dicumarol systemic availability in bile duct-ligated rats □ Dicumarol—phenobarbital effect on systemic availability in bile duct-ligated rats □ Anticoagulants—dicumarol, systemic availability, effect of phenobarbital in bile duct-ligated rats □ Bile duct—ligation, effect on rats, dicumarol systemic availability, phenobarbital □ Drug interactions—phenobarbital effect on dicumarol systemic availability in bile duct-ligated rats

The systemic availability of orally administered dicumarol in humans (1) and rats (2) is reduced by pretreatment of the subjects with a barbiturate. Oral phenobarbital sodium administration, 75 mg/kg, for 5 days before and 2 days after oral administration of dicumarol suspension to rats reduced the systemic availability of the anticoagulant from 84 ± 8 to 48.7 ± 10% (mean ± *SD*). Similar effects were observed when phenobarbital was administered intravenously (2).

Since phenobarbital treatment increased bile output (3), the inhibitory effect of phenobarbital on dicumarol absorption possibly is mediated by complexation of the anticoagulant with bile salts or by altered GI motility caused by increased bile flow. A study was initiated to determine if phenobarbital treatment affects systemic dicumarol availability in rats with ligated bile ducts.

EXPERIMENTAL

The experimental procedures were described previously (2). Briefly, adult male Sprague–Dawley rats weighing ~300 g received daily oral doses of phenobarbital sodium, 75 mg/kg, or the same volume of saline solution for 5 days. Their right jugular vein was cannulated on the 5th day to facilitate frequent blood withdrawal. In the morning of the 6th day, the rats received an intravenous tracer dose of ^{14}C-dicumarol by rapid injection and 50 mg of dicumarol/kg in aqueous suspension by gastric tube.

Blood samples were collected periodically, and daily phenobarbital treatment was continued until the end of the experiment. Food, but not water, was withdrawn for 24 hr, starting 12 hr before dicumarol administration. Plasma was assayed for ^{14}C-dicumarol and unlabeled dicumarol. The ratio of areas under the concentration–time curves for the labeled and unlabeled drug, normalized for dose, was used to calculate systemic

0022-3549/79/1000-1309$01.00/0

© 1979, American Pharmaceutical Association

Table I—Effect of Phenobarbital Treatment on Dicumarol Pharmacokinetics in Adult Male Sprague–Dawley Rats with Ligated Bile Ducts (32-hr Study)

Pharmacokinetic Constant[a]	Control Animals	Phenobarbital-Treated Animals	Statistical Significance of Difference (p)[b]
Total clearance, ml/hr/kg	4.7 ± 1.5[c]	10.0 ± 3.1	<0.005
Apparent volume of distribution, ml/kg	93 ± 7	80 ± 20	N.S.
β, hr^{-1}	0.0512 ± 0.0185	0.129 ± 0.039	<0.001

[a] Based on ^{14}C-dicumarol injected intravenously. [b] Two-sample t-test. [c] All data are mean ± SD, n = 7.

availability. Drug absorption and elimination kinetics were characterized by conventional methods (2).

In the present study, bile duct ligation was performed on the 5th day, *i.e.*, 1 day before dicumarol administration. The bile duct was exposed by a midline abdominal incision under ether anesthesia, ligatures were placed near the liver and near the intestine, and the duct was severed between the two ligatures. The incision was closed with wound clips.

Blood sampling in the first group of animals was carried out for 32 hr. When this period proved to be insufficient to determine systemic availability, a second group of animals was studied for 60 hr. At the end of the experiment, as much blood as possible was removed from the aorta of the rats under ether anesthesia and the hematocrit was measured. Serum was separated and used to determine the free fraction of dicumarol, total protein and albumin concentration (4, 5), glutamate–oxaloacetate transaminase[1] (SGOT), and glutamate–pyruvate transaminase[2,3] (SGPT). The liver was excised, excess blood was removed by mild compression between tissue paper, and the organ was weighed. The animals were weighed daily during the pretreatment period, immediately before bile duct ligation, before dicumarol administration, and at the end of the 60-hr experiment prior to sacrifice.

RESULTS

The results obtained from the first (32-hr blood sampling) study showed that dicumarol was absorbed and eliminated much more slowly than anticipated from a previous study on rats with intact bile ducts (2). Consequently, systemic availability could not be determined from the data. The drug concentration data derived from the intravenous injection of ^{14}C-dicumarol were used to characterize the drug elimination kinetics. Treatment with phenobarbital increased the total dicumarol clearance about twofold, increased the disposition rate constant (β), and had no statistically significant effect on the apparent volume of distribution (Table I). The animals appeared ill; they were inactive, they ate little, their fur became rough, and their skin acquired a yellow color.

Table II—Effect of Phenobarbital Treatment on Dicumarol Pharmacokinetics in Adult Male Sprague–Dawley Rats with Ligated Bile Ducts (60-hr Study)

Pharmacokinetic Constant[a]	Control Animals	Phenobarbital-Treated Animals	Statistical Significance of Difference (p)[b]
Total clearance, ml/hr/kg	4.4 ± 1.5[c]	8.1 ± 2.4	<0.05
Apparent volume of distribution, ml/kg	90 ± 7	76 ± 10	N.S.
β, hr^{-1}	0.0492 ± 0.020	0.105 ± 0.020	<0.01
Intrinsic clearance of free drug, ml/hr/kg × 10^{-4}	0.769 ± 0.344	1.42 ± 0.73	N.S.
Serum free fraction[d] × 10^4	7.08 ± 4.67	7.23 ± 4.36	N.S.

[a] Based on ^{14}C-dicumarol injected intravenously. [b] Two-sample t-test. [c] All data are mean ± SD, n = 4. [d] Determined at the end of the experiment.

[1] Determined with Calbiochem GOT reagent kit, Calbiochem, La Jolla, Calif.
[2] Determined with Calbiochem GPT reagent kit, Calbiochem, La Jolla, Calif.
[3] The transaminase determinations were carried out by Dr. Kenneth L. Hintze in this laboratory.

Table III—Pathophysiological Characteristics of Rats with Ligated Bile Ducts (60-hr Study)

Parameter[a]	Control Animals	Phenobarbital-Treated Animals	Statistical Significance of Difference (p)[b]
Weight loss[c], %	12.5 ± 0.6[d]	10.8 ± 3.9	N.S.
Liver weight, g/kg	42.4 ± 2.3	53.3 ± 6.7	<0.025
SGOT[e], mU/ml	627 ± 64	521 ± 76	N.S.
SGPT[e], mU/ml	263 ± 81	229 ± 9	N.S.
Total serum protein, g/100 ml	7.30 ± 0.99	6.95 ± 0.40	N.S.
Serum albumin, g/100 ml	3.18 ± 0.76	2.82 ± 0.27	N.S.
Hematocrit, %	29 ± 7	40 ± 2	<0.05

[a] All reported measurements were made at the end of the experiment. [b] Two-sample t-test. [c] Relative to body weight before bile duct ligation. [d] All data are mean ± SD, n = 4. [e] Normal value <40 mU/ml.

The dicumarol elimination kinetics observed in the second (60-hr blood sampling) study are presented in Table II. The results were almost identical to those in the first study; total clearance and β were significantly increased by phenobarbital. The average intrinsic clearance of free drug increased about twofold, but the difference was not statistically significant due to large interanimal variations. The average free fraction of dicumarol in serum of the two groups of animals was almost identical. Despite the poor physical state of the rats, the postintravenous drug concentration–time curves were "clean" in that drug concentrations declined exponentially without significant perturbations or time-dependent changes in slope (Figs. 1 and 2).

All animals exhibited appreciable weight loss and elevation of serum transaminases (Table III). There were no significant differences in these and other clinical chemical parameters between control and phenobarbital-treated rats, except that the latter had larger livers (a characteristic consequence of treatment with an enzyme inducer such as phenobarbital; Refs. 5 and 6) while the control animals, for unknown reasons, had a lower hematocrit at the end of the study (Table III).

Absorption of orally administered dicumarol was slow (Fig. 1) and in some cases persisted for the duration of the experiment (Fig. 2). Therefore, extrapolation of drug concentrations in plasma beyond the last data point was carried out by two methods representing the limiting cases of continuing absorption beyond ~60 hr (Method I) and no further absorption after ~60 hr (Method II) (Ref. 2; footnotes *b* and *c*, Table IV). The two methods yielded essentially identical systemic availability estimates for control animals but somewhat different estimates for phenobarbital-treated rats (Table IV). The latter difference was due primarily to one rat that absorbed dicumarol particularly slowly (Fig. 2). Comparing the systemic availability estimates by either Method I or II

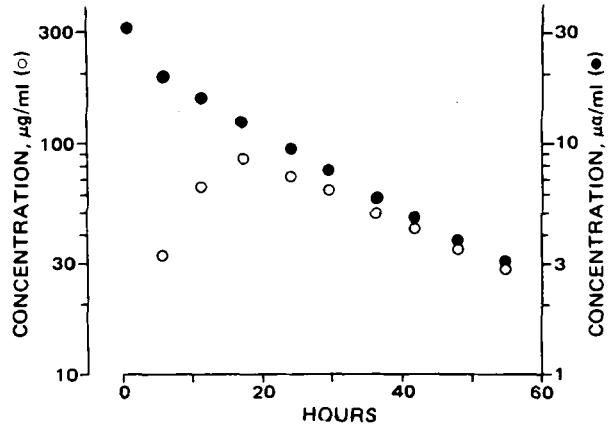

Figure 1—*Plasma dicumarol concentrations as a function of time after simultaneous administration of 50 mg/kg po (○) and 2 mg/kg iv (●) to a control rat with ligated bile duct. ^{14}C-Labeled drug was used for the intravenous injection.*

Table IV—Effect of Phenobarbital Treatment on the Systemic Availability[a] of Orally Administered Dicumarol in Rats (60-hr Study)

Control Animals				Phenobarbital-Treated Animals			
Rat	Method I[b]	Method II[c]	I/II Ratio	Rat	Method I[b]	Method II[c]	I/II Ratio
1C	46	43	1.07	1P	42	41	1.02
2C	29	27	1.07	2P	30	28	1.07
3C	49	47	1.04	3P	34	21	1.68
4C	19	17	1.12	4P	54	41	1.32
Mean	36	34	1.08		40[d]	33[d]	1.27
SD	14	14	0.03		11	10	0.30

[a] Expressed as percent of oral dose. [b] Method I: Area under plasma concentration–time curve of orally administered drug (AUC_{oral}) determined by extrapolation of apparently exponential concentration decay phase from last data point to zero concentration. [c] Method II: AUC_{oral} determined by assuming that concentrations after the last data point decline at the same relative rate as the postdistribution concentrations of ^{14}C-dicumarol administered by intravenous injection. [d] Not significantly different from the appropriate control value by two-sample *t*-test.

leads to the conclusion that phenobarbital treatment had no apparent effect on the extent of dicumarol absorption.

Figure 3 is a plot of the cumulative fraction of the dicumarol dose absorbed as a function of time after administration of the anticoagulant. Absorption kinetics are presented in Fig. 4. These data show that phenobarbital had no apparent effect on the rate or extent of dicumarol absorption by bile duct-ligated rats; the average time required to absorb 50% of the amount of drug eventually absorbed (not the administered dose) was ~11 hr, and the average amount absorbed was 33–40% of the dose.

DISCUSSION

The original intent of this investigation was to determine the effect of phenobarbital treatment on the systemic availability of orally administered dicumarol when bile was not present in the intestinal tract, *i.e.*, under conditions where an effect of phenobarbital on bile output would not influence the results. All else being equal, a lack of phenobarbital effect on dicumarol absorption in the absence of bile together with the previously demonstrated pronounced absorption inhibitory effect of phenobarbital on dicumarol in normal animals (2) would suggest strongly that the phenobarbital effect in normal animals is mediated by an altered bile output. The results of this study show, however, that bile duct ligation causes a profound change in the pathophysiological status of the animals.

The total dicumarol clearance in bile duct-ligated control rats was much lower than in previously studied normal control rats (2, 7). This finding is particularly significant since the serum free fraction of dicumarol was higher in the bile duct-ligated animals (5, 8), presumably due to accumulation of endogenous displacing agents. All else being equal, an increase in the serum free fraction should increase the total anticoagulant clearance (8). Serum transaminase elevation in the bile duct-ligated rats is indicative of hepatotoxicity, apparently caused by cholestasis. The latter condition may also account for the somewhat larger liver of the bile duct-ligated control rats as compared to the liver of normal animals (5, 6). Liver damage, in turn, is probably at least partly responsible for the decreased dicumarol clearance since the drug is eliminated by hepatic biotransformation (9). Bile acids are known to be hepatotoxic; they also block the type I binding site on cytochrome P-450 (10). Impairment of microsomal drug metabolism in cholestasis has been observed by other investigators (10).

The relative magnitude of enzyme induction caused by phenobarbital was similar in bile duct-ligated and normal animals; total dicumarol clearance was approximately doubled by phenobarbital in both types of animals (Tables I and II and Ref. 2). Therefore, phenobarbital may be potentially useful as a therapeutic tool to compensate for some biotransformation deficiencies in certain types of impaired liver function.

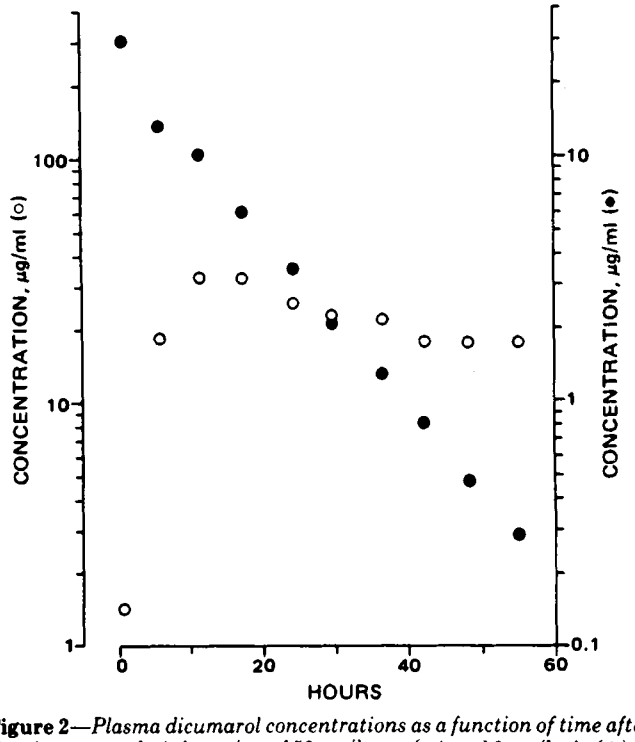

Figure 2—*Plasma dicumarol concentrations as a function of time after simultaneous administration of 50 mg/kg po (○) and 2 mg/kg iv (●) to a bile duct-ligated rat treated with oral phenobarbital sodium, 75 mg/kg/day, beginning 5 days before dicumarol administration. ^{14}C-Labeled dicumarol was used for the intravenous injection.*

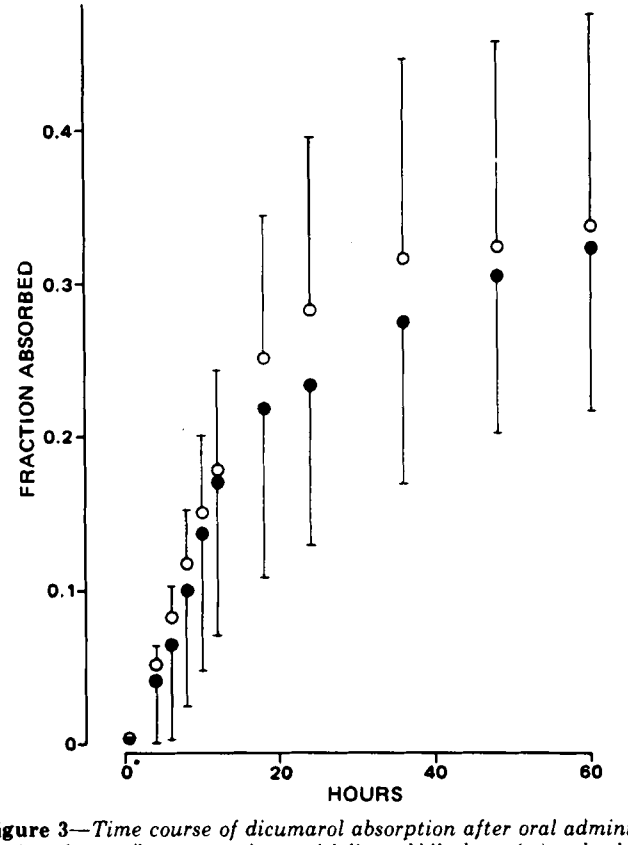

Figure 3—*Time course of dicumarol absorption after oral administration of 50 mg/kg to control rats with ligated bile ducts (○) and to bile duct-ligated rats treated orally with phenobarbital sodium, 75 mg/kg/day, beginning 5 days before dicumarol administration (●). Points are mean + or − SD of four control and four phenobarbital-treated animals.*

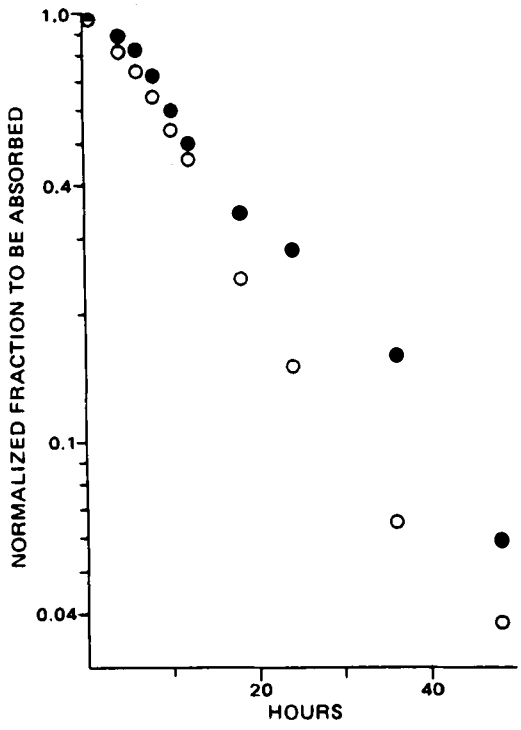

Figure 4—*Dicumarol absorption kinetics in four control (○) and four oral phenobarbital-treated (●) rats, all with ligated bile ducts. Plotted on the ordinate is the fraction of total absorbed dicumarol that was remaining to be absorbed at various times after oral administration of a 50-mg/kg dose.*

Dicumarol was absorbed much more slowly by bile duct-ligated animals ($t_{50\%} \simeq 11$ hr) than by normal rats ($t_{1/2} \simeq 3$ hr; Ref. 2). The reason for this difference is not evident from the available data. Bile duct-ligated control rats absorbed ≤40% of the oral dose while normal control rats absorbed >80% under the same experimental conditions (2). Perhaps bile enhances absorption by increasing the dissolution rate of the almost water-insoluble dicumarol. It will be of interest to determine systemic dicumarol availability in rats with exteriorized bile ducts who are receiving a concomitant intravenous bile infusion, *i.e.*, animals that are not cholestatic or bile salt deficient and presumably have normal liver function but no bile in the intestine.

Systemic dicumarol availability in normal rats was reduced from >80 to <50% by phenobarbital treatment (2). No such absorption inhibitory effect was observed in bile duct-ligated rats. Dicumarol availability is likely to be affected by many factors such as the solubilizing effect of intestinal fluids, GI motility, and gut wall metabolism. (Significant first-pass hepatic biotransformation can be excluded on theoretical grounds; Ref. 6.) Since bile duct ligation changed the pathophysiological status of the animals (rather than only preventing bile entry into the intestine), the lack of a significant phenobarbital effect on systemic dicumarol availability in bile duct-ligated rats cannot be ascribed to any one factor. However, the results of this investigation demonstrate that a drug–drug interaction such as the one between dicumarol and phenobarbital may be pronounced in normal animals and either absent or less pronounced in animals with altered pathophysiological status.

REFERENCES

(1) P. M. Aggeler and R. A. O'Reilly, *J. Lab. Clin. Med.*, **74**, 229 (1969).

(2) J. W. Crow, M. Gibaldi, and G. Levy, *J. Pharm. Sci.*, **68**, 958 (1979).

(3) C. D. Klaassen, *J. Pharmacol. Exp. Ther.*, **176**, 743 (1971).

(4) A. G. Gornall, C. J. Bardawill, and M. M. David, *J. Biol. Chem.*, **177**, 751 (1949).

(5) A. Yacobi, J. T. Slattery, and G. Levy, *J. Pharm. Sci.*, **66**, 941 (1977).

(6) C.-M. Lai, A. Yacobi, and G. Levy, *J. Pharmacol. Exp. Ther.*, **199**, 74 (1976).

(7) C.-M. Lai and G. Levy, *J. Pharm. Sci.*, **67**, 337 (1978).

(8) *Ibid.*, **66**, 1739 (1977).

(9) R. Nagashima, G. Levy, and E. J. Sarcione, *J. Pharm. Sci.*, **57**, 1881 (1968).

(10) F. Hutterer, H. Greim, D. Trülzsch, P. Czygan, and J. B. Schenkman, in "Progress in Liver Diseases," vol. IV, H. Popper and F. Schaffner, Eds., Grune and Stratton, New York, N.Y., 1972, chap. 9.

ACKNOWLEDGMENTS

Supported in part by Grant GM 20852 and by postdoctoral fellowship 5 F32 GM05653 (J. W. Crow) from the National Institute of General Medical Sciences, National Institutes of Health.

Double Latin Square Study to Determine Variability and Relative Bioavailability of Methylprednisolone

K. S. ALBERT[x], S. W. BROWN, Jr., K. A. DeSANTE, A. R. DiSANTO, R. D. STEWART, and T. T. CHEN

Received December 15, 1978, from *The Upjohn Company, Kalamazoo, MI 49001.* Accepted for publication May 4, 1979.

Abstract □ The variability and relative bioavailability of methylprednisolone tablets were evaluated utilizing a double Latin square crossover design in which each of 20 subjects was given four of five treatments. Three different lots of methylprednisolone tablets exhibited virtually identical absorption, with similar ranges and coefficients of variation of some selected bioavailability parameters indicative of lot-to-lot uniformity in bioavailability. Within-lot and between-lot uniformities in bioavailability also were similar, suggesting that the observed variability in serum methylprednisolone levels was not due to manufacturing process variables. With respect to intra- *versus* intersubject variability, no differences were found for the absorption rate or terminal half-life. In contrast, between-subject variability associated with extent of absorption was greater than that within subjects. Relative to an aqueous suspension, methylprednisolone tablets were fully bioavailable.

Keyphrases □ Methylprednisolone—bioavailability, tablet variability, commercial preparations, Latin square study □ Glucocorticoids—methylprednisolone, bioavailability, tablet variability, commercial preparations, Latin square study □ Bioavailability—commercial methylprednisolone preparations

On January 7, 1977, the Food and Drug Administration published a list of rules and regulations for conducting bioequivalency studies in humans (1). Their intent was to assure product interchangeability by demonstrating that, on the average, two or more products would exhibit similar bioavailabilities. However, the rules and regulations appear to have ignored the variability in the bioavailability of a given product; and this variability might result in thera-

0022-3549/79/1000-1312$01.00/0
© 1979, American Pharmaceutical Association

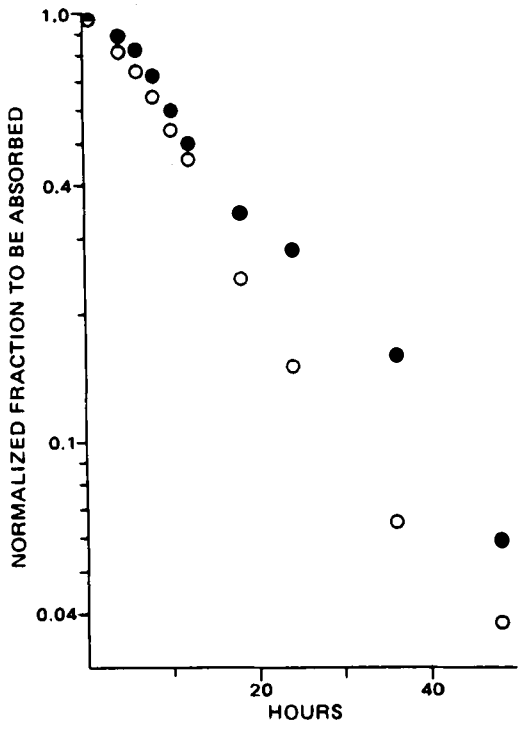

Figure 4—*Dicumarol absorption kinetics in four control (○) and four oral phenobarbital-treated (●) rats, all with ligated bile ducts. Plotted on the ordinate is the fraction of total absorbed dicumarol that was remaining to be absorbed at various times after oral administration of a 50-mg/kg dose.*

Dicumarol was absorbed much more slowly by bile duct-ligated animals ($t_{50\%} \simeq 11$ hr) than by normal rats ($t_{1/2} \simeq 3$ hr; Ref. 2). The reason for this difference is not evident from the available data. Bile duct-ligated control rats absorbed ≤40% of the oral dose while normal control rats absorbed >80% under the same experimental conditions (2). Perhaps bile enhances absorption by increasing the dissolution rate of the almost water-insoluble dicumarol. It will be of interest to determine systemic dicumarol availability in rats with exteriorized bile ducts who are receiving a concomitant intravenous bile infusion, *i.e.*, animals that are not cholestatic or bile salt deficient and presumably have normal liver function but no bile in the intestine.

Systemic dicumarol availability in normal rats was reduced from >80 to <50% by phenobarbital treatment (2). No such absorption inhibitory effect was observed in bile duct-ligated rats. Dicumarol availability is likely to be affected by many factors such as the solubilizing effect of intestinal fluids, GI motility, and gut wall metabolism. (Significant first-pass hepatic biotransformation can be excluded on theoretical grounds; Ref. 6.) Since bile duct ligation changed the pathophysiological status of the animals (rather than only preventing bile entry into the intestine), the lack of a significant phenobarbital effect on systemic dicumarol availability in bile duct-ligated rats cannot be ascribed to any one factor. However, the results of this investigation demonstrate that a drug–drug interaction such as the one between dicumarol and phenobarbital may be pronounced in normal animals and either absent or less pronounced in animals with altered pathophysiological status.

REFERENCES

(1) P. M. Aggeler and R. A. O'Reilly, *J. Lab. Clin. Med.*, **74**, 229 (1969).

(2) J. W. Crow, M. Gibaldi, and G. Levy, *J. Pharm. Sci.*, **68**, 958 (1979).

(3) C. D. Klaassen, *J. Pharmacol. Exp. Ther.*, **176**, 743 (1971).

(4) A. G. Gornall, C. J. Bardawill, and M. M. David, *J. Biol. Chem.*, **177**, 751 (1949).

(5) A. Yacobi, J. T. Slattery, and G. Levy, *J. Pharm. Sci.*, **66**, 941 (1977).

(6) C.-M. Lai, A. Yacobi, and G. Levy, *J. Pharmacol. Exp. Ther.*, **199**, 74 (1976).

(7) C.-M. Lai and G. Levy, *J. Pharm. Sci.*, **67**, 337 (1978).

(8) *Ibid.*, **66**, 1739 (1977).

(9) R. Nagashima, G. Levy, and E. J. Sarcione, *J. Pharm. Sci.*, **57**, 1881 (1968).

(10) F. Hutterer, H. Greim, D. Trülzsch, P. Czygan, and J. B. Schenkman, in "Progress in Liver Diseases," vol. IV, H. Popper and F. Schaffner, Eds., Grune and Stratton, New York, N.Y., 1972, chap. 9.

ACKNOWLEDGMENTS

Supported in part by Grant GM 20852 and by postdoctoral fellowship 5 F32 GM05653 (J. W. Crow) from the National Institute of General Medical Sciences, National Institutes of Health.

Double Latin Square Study to Determine Variability and Relative Bioavailability of Methylprednisolone

K. S. ALBERT[x], S. W. BROWN, Jr., K. A. DeSANTE, A. R. DiSANTO, R. D. STEWART, and T. T. CHEN

Received December 15, 1978, from *The Upjohn Company, Kalamazoo, MI 49001.* Accepted for publication May 4, 1979.

Abstract □ The variability and relative bioavailability of methylprednisolone tablets were evaluated utilizing a double Latin square crossover design in which each of 20 subjects was given four of five treatments. Three different lots of methylprednisolone tablets exhibited virtually identical absorption, with similar ranges and coefficients of variation of some selected bioavailability parameters indicative of lot-to-lot uniformity in bioavailability. Within-lot and between-lot uniformities in bioavailability also were similar, suggesting that the observed variability in serum methylprednisolone levels was not due to manufacturing process variables. With respect to intra- *versus* intersubject variability, no differences were found for the absorption rate or terminal half-life. In contrast, between-subject variability associated with extent of absorption was greater than that within subjects. Relative to an aqueous suspension, methylprednisolone tablets were fully bioavailable.

Keyphrases □ Methylprednisolone—bioavailability, tablet variability, commercial preparations, Latin square study □ Glucocorticoids—methylprednisolone, bioavailability, tablet variability, commercial preparations, Latin square study □ Bioavailability—commercial methylprednisolone preparations

On January 7, 1977, the Food and Drug Administration published a list of rules and regulations for conducting bioequivalency studies in humans (1). Their intent was to assure product interchangeability by demonstrating that, on the average, two or more products would exhibit similar bioavailabilities. However, the rules and regulations appear to have ignored the variability in the bioavailability of a given product; and this variability might result in thera-

0022-3549/79/1000-1312$01.00/0
© 1979, American Pharmaceutical Association

Table I—Dosage Schedule

Group	Subjects per Group	Subjects in Group[a]	Treatment Assignments Phase I	Phase II	Phase III	Phase IV
I	2	2, 17	A	B	D	C
II	2	1, 20	B	C	A	D
III	2	4, 5	C	D	B	A
IV	2	8, 19	D	A	C	B
V	3	9, 11, 13	A	B	E	C
VI	3	6, 14, 18	B	C	A	E
VII	3	7, 12, 16	C	E	B	A
VIII	3	3, 10, 15	E	A	C	B

[a] Subjects were randomly assigned to each group.

peutic failure or untoward drug reactions in a given segment of the patient population.

Variability for a product may be documented by evaluating its lot-to-lot uniformity in bioavailability. By administering at least one of the lots on two separate occasions, information on variability within a given lot as well as between lots can be obtained.

This paper describes results of a bioavailability study designed to document the lot-to-lot variability and relative bioavailability of methylprednisolone tablets. With respect to the rate and extent of absorption, within-lot and between-lot uniformities in bioavailability were similar, suggesting that the observed variability in serum methylprednisolone levels was free from manufacturing influences.

EXPERIMENTAL

The 20 normal, nonobese male volunteers, whose average age was 22 years (19–27 years) and whose average weight was 74.8 kg (63–97 kg), exhibited normal vital signs and selected laboratory parameters and were without any evidence of cardiac, renal, or GI abnormalities. Subjects did not receive any repository steroid preparation for 60 days prior to the study or any other steroid or nonsteroid product, including topical preparations, for 14 days before the protocol was initiated. During the study, volunteers received only the medication prescribed, with 5 days separating each treatment.

Subjects were fasted (food and beverage) from 10:00 pm the night before their allocated treatment until 4 hr after their medication. Except for 180 ml of water taken with their medication at zero time, no water was permitted for 1 hr before or for 2 hr after dosing; at all other times, it was taken *ad libitum*. Smoking was permitted if it was the usual custom of a subject. Volunteers remained ambulatory during each sampling day, not engaging in strenuous or athletic activities.

Each volunteer received four of the following five 12-mg oral doses of methylprednisolone in crossover fashion, utilizing a double Latin square design (details are summarized in Table I):

Treatment A—Three 4-mg methylprednisolone tablets at zero time, lot 1[1].

Treatment B—Three 4-mg methylprednisolone tablets at zero time, lot 2[2].

Treatment C—Three 4-mg methylprednisolone tablets at zero time, lot 3[3].

Treatment D—Fifteen milliliters of an aqueous suspension of 4 mg of methylprednisolone/5 ml at zero time.

Treatment E—Three 4-mg methylprednisolone tablets at zero time, lot 1[1].

Lots of tablets tested were manufactured from different lots of bulk drug and were of typical production size. Tablets used in the study were randomly selected from one bottle for each lot. Whereas Treatments A–C represented different lots of methylprednisolone tablets, Treatments A and E were the same lot. Table I shows that Treatments A–C were each administered to 20 subjects. Treatment D was given to eight subjects, while Treatment E was given to 12 subjects.

[1] C. T. Medrol, 4 mg, lot 278ER, The Upjohn Co., Kalamazoo, MI 49001.
[2] C. T. Medrol, 4 mg, lot 778ER, The Upjohn Co., Kalamazoo, MI 49001.
[3] C. T. Medrol, 4 mg, lot 423ES, The Upjohn Co., Kalamazoo, MI 49001.

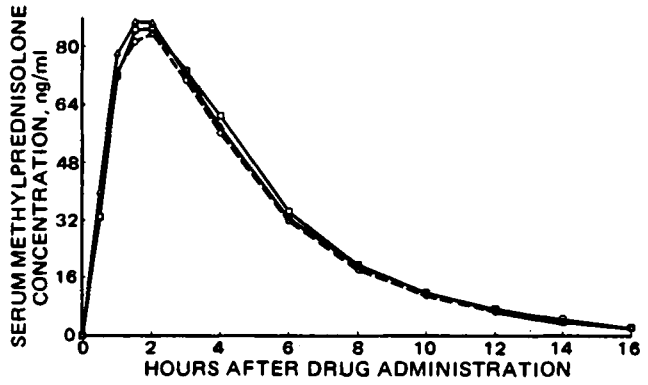

Figure 1—*Average serum methylprednisolone levels after oral administration of a 12-mg dose of three different lots of 4-mg tablets. Key:* □—□, *Treatment A;* O- - -O, *Treatment B; and* △—△, *Treatment C.*

During each phase of the study, all subjects were given two tablets of dexamethasone, 0.75 mg[4]. One tablet was taken 9 hr before and the second tablet was taken 9 hr after methylprednisolone administration. Dexamethasone was given to reduce the level of endogenous cortisol to preclude its interference in the radioimmunoassay for methylprednisolone. Dexamethasone itself does not cross-react with the radioimmunoassay antibody for methylprednisolone (2).

Blood samples were drawn at 0, 0.5, 1.0, 1.5, 2.0, 3.0, 4.0, 6.0, 8.0, 12.0, 14.0, and 16.0 hr after each methylprednisolone treatment. Serum was harvested from each specimen, frozen, and kept in a frozen state until assayed for methylprednisolone by the radioimmunoassay (2).

RESULTS

Average serum methylprednisolone concentrations and related bioavailability parameters obtained from the 20 subjects, each having received three different lots of methylprednisolone as 12-mg oral doses, are shown in Table II. A summary of the statistical evaluation of the data (see *Appendix*) is given in Table II. No significant differences among treatment average values were found at any sampling time.

Figure 1 clearly shows that the average time courses in serum of methylprednisolone from the three lots tested were superimposable, suggesting identical rates and extents of drug absorption. The correspondence among the averages of individual peak serum concentrations and the times of their occurrence, average areas under the individual serum concentration–time curves through 16 hr and through infinity, and the averages of individual half-lives support this premise. These results indicate lot-to-lot uniformity in methylprednisolone bioavailability. Further evidence for this conclusion comes from Table III, which shows that the ranges and coefficients of variation among the bioavailability parameters listed in Table II were similar.

Methylprednisolone variability can also be evaluated by comparing between-lot variability in bioavailability to the variability within a given lot. This evaluation was accomplished using serum methylprednisolone levels from the 12 subjects who each received Treatments A–C and E and simultaneously verifying the equivalency of variances within lots and the equivalency of covariances between lots. Results of the statistical analysis for the area under the curve, peak maximum, time to peak, and half-life are summarized in Table IV; details are given in the *Appendix*. All of the statistics were not significant at the 5% level. Therefore, within-lot and between-lot uniformities in methylprednisolone bioavailability apparently were similar, suggesting that the manufacturing process had little to do with the observed variability associated with the temporal change of methylprednisolone in serum.

On the assumption that Treatments A and E were identical, a comparison can be made of the inter- *versus* intrasubject variability in methylprednisolone bioavailability. This comparison was accomplished for the parameters peak maximum, time to peak, area under the curve through infinity, and half-life utilizing statistical methodology that permitted an estimate and confidence interval for the ratio of between-subject to within-subject variability. According to the method (see *Appendix*), if the left end-point of the confidence interval exceeds unity, then intersubject variability is greater than intrasubject variability, the

[4] Decadron, Merck Sharp and Dohme, West Point, Pa.

Table II—Average Methylprednisolone Serum Concentrations and Related Bioavailability Parameters for the 20 Subjects Who Each Received Three Lots of Methylprednisolone [a]

Parameter	Treatment A	Treatment B	Treatment C
Average serum levels of methylprednisolone, ng/ml, at:			
0.5 hr	33.9	32.8	40.7
1.0 hr	73.1	72.8	77.8
1.5 hr	85.4	81.4	86.7
2.0 hr	85.2	82.4	86.1
3.0 hr	73.1	69.9	71.9
4.0 hr	60.4	55.4	57.4
6.0 hr	34.1	31.5	32.3
8.0 hr	19.2	17.9	18.7
10.0 hr	11.8	11.0	11.7
12.0 hr	7.13	6.62	6.76
14.0 hr	4.33	3.40	3.57
16.0 hr	2.02	1.81	1.85
Average of individual peak serum concentrations, ng/ml	91.2	91.7	94.2
Average time of individual peak serum concentrations, hr	1.84	1.66	1.54
Average area under individual serum concentration–time curve[b], ng/ml × hr			
Through 16 hr	479	451	473
Through infinity	489	462	480
Half-life, hr[b]	2.63	2.61	2.59

[a] Comparisons were made using an approximation to the *t* test by adjusting for unequal variances between Latin squares (see *Appendix*). The mean differences between Treatments A *versus* B, A *versus* C, and B *versus* C were not significant for any parameter at any time. [b] See *Appendix* for calculation method.

Table III—Ranges and Coefficients of Variation among Selected Bioavailability Parameters

	Range						Percent *SD*		
	Treatment A		Treatment B		Treatment C		Treatment	Treatment	Treatment
Parameter	Low	High	Low	High	Low	High	A	B	C
Peak plasma level, ng/ml	58.5	124	64.1	129	61.9	123	18.9	21.1	20.1
Time to peak, hr	1.0	4.0	1.0	3.0	1.0	3.0	48.1	36.6	32.9
Area under curve[a] through 16 hr, ng/ml × hr	247	643	243	662	271	818	22.1	26.3	28.3
Area under curve[a] through infinity, ng/ml × hr	255	655	251	691	278	854	22.0	26.5	28.7
Half-life, hr[a]	2.16	3.14	2.10	3.28	2.21	3.32	10.7	12.8	11.5

[a] See *Appendix* for calculation method.

magnitude of which is given by the value of the ratio. In contrast, if the left end-point of the constructed interval is less than unity, between- and within-subject variabilities are probably similar because between-subject variability is small.

Table V shows that the left end-point of the confidence interval exceeded unity only for the area under the curve through infinity. Therefore, it can be concluded that with respect to the extent of absorption, intersubject variability was about sixfold greater than intrasubject variability. For the absorption rate (as measured by peak maximum and time to peak) and the half-life (an indicator of disposition), inter- and intrasubject variabilities were similar.

Bioavailability estimates relative to an aqueous methylprednisolone suspension were determined for the eight subjects who received this treatment in addition to the three lots of methylprednisolone. Table VI summarizes the individual bioavailability estimates, which were calculated as ratios of the area under the curve through infinity. The only significant differences were between the means $F^A/F^D = 1.04$ *versus* $F^B/F^D = 0.931$. However, since the three lots were already judged bioequivalent based on data from 20 subjects (Table II and Fig. 1), it was possible to conclude that this observed difference based on eight subjects was biopharmaceutically meaningless. A grand bioavailability ratio (based on 24 observations) was calculated. The overall value of 0.990, which was not significantly different from unity, illustrates that methylprednisolone tablets were fully bioavailable relative to an aqueous suspension given orally.

DISCUSSION

A limited number of studies have been published addressing lot-to-lot uniformity in bioavailability. In 1973, Butler (3) compared two lots of a chemically equivalent oxytetracycline product against a recognized standard and found that one lot was clearly bioinequivalent. Subsequently, DiSanto *et al.* (4) demonstrated a pronounced lot-to-lot variability in nitrofurantoin bioavailability; four lots that were tested against an appropriate reference standard exhibited relative bioavailabilities of 6, 27, 80, and 96%. More recently, Stoll *et al.* (5) compared the within-lot uniformities of two digoxin preparations and found one brand to be significantly more variable than the other. Until now, however, no study has addressed both within-lot and between-lot uniformities in bioavailability.

The selection of a five-treatment study design to document the intra- and interlot uniformity in absorption and the relative bioavailability of methylprednisolone tablets was based on a set of rated objectives and a desire to limit the number of phases to four. Therefore, a five-way Latin square study was precluded. Since the most important objective was the demonstration of between-lot uniformity, a decision was made to administer each of three different lots of drug to all 20 subjects (Treatments A–C). More weight was also placed on the intra- to interlot comparisons than on the bioavailability estimate relative to the aqueous suspension. Accordingly, 12 subjects each received one lot of tablets on a second occasion (Treatment E) while eight subjects each received the aqueous suspension (Treatment D). The overall design was, in essence, a combination of two Latin squares, referred to herein as a double Latin square. As shown in Table I, the eight-subject square was used to estimate bioavailability relative to the aqueous suspension, the 12-subject square was used to estimate intra/inter effects, and the two squares were combined to estimate between-lot uniformity in bioavailability.

The assessment of intrasubject *versus* intersubject variability required the assumption that Treatments A and E were identical. Since they represented tablets from the same lot of drug and since *in vitro* physicochemical tests (such as dissolution rate, disintegration time, and content uniformity) indicated that the lots were homogeneous, these assumptions appeared to be valid. In addition, the statistical methodology requires that period effects normally tested for during individual Latin square analyses of variance be absent or ignored if present. No such effects were observed in the 12-subject A, B, C, E square[5], facilitating the statistical evaluation. A future publication will deal with a design that can accommodate order effects without biasing the statistical conclusions.

In evaluating the statistical results of a comparison of intersubject *versus* intrasubject variability, the magnitude of the variance and resulting coefficient of variation for the tested bioavailability parameter should be considered since they are measures of the sum of the two variations. Where within-subject and between-subject variabilities are

[5] Data available from the authors upon request.

Table IV—Comparison of Between-Lot and Within-Lot Variabilities in the Bioavailability of Methylprednisolone for 12 Subjects Receiving Treatments A–C and E[a]

Parameter	Square Root of Common Variability: Within-Lot Variance	Square Root of Common Variability: Between-Lot Covariance	χ-Square Statistic (8 *df*)
Area under curve[b] through infinity	117	97.5	11.3
Peak maximum	19.4	13.7	3.40
Time to peak	0.75	−0.3[c]	8.76
Half-life[b]	0.26	0.20	9.09

[a] No significant differences were found. [b] See *Appendix* for calculation method. [c] Negative value probably due to sampling variation.

similar and the coefficient of variation is sizable (*e.g.*, ~50%), large intrasubject variations would be anticipated, suggesting that clinical failure may occur for a given segment of the patient population. Both disposition and absorption parameters should be evaluated since the former is drug related while the latter is product related. Accordingly, a less variable drug or less variable product might be dictated.

For the case of a large coefficient of variation where intersubject variability is significantly different than intrasubject variability, an unbiased estimate of the variance ratio of between-subject to within-subject data should be calculated so that the magnitude of the intrasubject contribution can be determined. Its therapeutic effect can, therefore, be evaluated to permit a more rational decision of product substitution. In contrast, when the coefficient of variation is small (25%, as observed here for the area under the curve), loss of therapy or untoward reactions due to the variability of a particular product would not be anticipated regardless of whether intersubject and intrasubject variabilities were significantly different[6]. A future report will address the influence of variability of bioavailability assessment as it relates to product interchangeability.

In summary, the lot-to-lot uniformity and relative bioavailability of methylprednisolone tablets along with an estimate of intrasubject and intersubject variations have been documented in humans. Based on the uniformity between lots and within lots, the small intersubject and intrasubject variations in absorption, and the fact that, on the average, tablets were fully bioavailable relative to an aqueous drug suspension, it can be concluded that the dosage form tested was optimal with respect to bioavailability.

APPENDIX

Comparisons among Treatments A–C—Data from two Latin squares were combined with equal weight to yield comparisons of A *versus* B, B *versus* C, and A *versus* C. Since the residual variations differed, for the most part, between the two squares[5], an approximation to the t statistic was employed:

$$t' = \frac{\bar{d}}{S_{\bar{d}}} \qquad \text{(Eq. A1)}$$

where:

$$\bar{d} = \frac{\bar{d}_1 + \bar{d}_2}{2} \qquad \text{(Eq. A2)}$$

$$\bar{d}_i = \bar{x}_i^A - \bar{x}_i^B; \bar{x}_i^A - \bar{x}_i^C; \bar{x}_i^B - \bar{x}_i^C \quad (i = 1, 2) \qquad \text{(Eq. A3)}$$

and:

$$S_{\bar{d}} = \left(\frac{S_1^2}{2n_1} + \frac{S_2^2}{2n_2}\right)^{1/2} \qquad \text{(Eq. A4)}$$

where $\bar{x}_i$ represents a given average of individual observations from either square 1 ($i = 1$) or square 2 ($i = 2$), with the superscripts referring to a specified treatment within each square; S_i^2 refers to the residual mean square from the analysis of variance; n_i is the number of subjects; and the subscripts refer to either square 1 or square 2.

The value of t_c' such that larger observed values are judged significant is calculated using Eq. A5:

$$t_c' = \frac{w_1 t_1 + w_2 t_2}{w_1 + w_2} \qquad \text{(Eq. A5)}$$

[6] Care should be exercised in interpreting data having a small coefficient of variation resulting from data with a large variance.

Table V—Intersubject *versus* Intrasubject Variability in Methylprednisolone Bioavailability for 12 Subjects Receiving Treatments A–C and E

Parameter	95% Confidence Interval for B/W[a]	B/W[b]
Area under curve[c] through infinity	$1.76 \le B/W \le 20.1$	5.9
Peak maximum	$0.328 \le B/W \le 3.74$	—
Time to peak	$0.033 \le B/W \le 0.379$	—
Half-life[c]	$0.216 \le B/W \le 2.46$	—

[a] Calculated according to Eq. A13. [b] Calculated according to Eq. A12 only where left end-point of 95% confidence interval exceeded unity. [c] See *Appendix* for calculation method.

where t_i is the critical values for the ith square with $(n_i - 2)(k - 1)$ degrees of freedom, $w_i = S_i^2/2n_i$, and k is the number of treatments (6).

For purposes of testing, t_c' need not be calculated if $t' < \min(t_1, t_2)$ or $t' > \max(t_1, t_2)$.

Comparison of Between-Lot and Within-Lot Variabilities—To compare between-lot and within-lot variabilities, the equality of within-lot total variance and between-lot covariance must be simultaneously tested.

The covariance matrix, S, for the 12 subjects who each received Treatments A–C and E is first computed, permitting the overall average variance and the overall average covariance to be estimated. The average covariance matrix, S_0, is then obtained by setting all treatment variances equal to the overall average variance and all treatment covariances equal to the overall average covariance.

Then, according to Box (7):

$$M = -(n - 1) \ln(\det S / \det S_0) \qquad \text{(Eq. A6)}$$

$$C = \frac{k(k+1)^2(2k-3)}{6(n-1)(k-1)(k^2+k-4)} \qquad \text{(Eq. A7)}$$

$$f = \frac{k^2 + k - 4}{2} \qquad \text{(Eq. A8)}$$

where n is the total number of subjects, k is the number of treatments, $\det S$ is the determinant of the matrix S, $\det S_0$ is the determinant of the matrix S_0, and f is the computed degrees of freedom.

Under the null hypothesis of simultaneous equalities of variances and covariances, the following X^2 statistic can be computed whose sampling distribution is approximated by a χ-square with degrees of freedom f:

$$X^2 = (1 - C)M \qquad \text{(Eq. A9)}$$

Comparison of Inter- *versus* Intrasubject Variability—Between-subject variability was estimated under the assumption that Treatments A and E were identical. Period effects were not present.

Table VI—Individual Bioavailability Estimates for Methylprednisolone Tablets Relative to an Aqueous Methylprednisolone Suspension for Eight Subjects Receiving Treatments A–D

Subject	Bioavailability Ratios[a] F^A/F^D	F^B/F^D	F^C/F^D
1	0.775	0.762	0.954
2	0.955	0.849	0.894
4	0.991	0.806	0.844
5	1.11	0.988	0.932
8	1.06	0.966	1.04
17	1.11	0.969	1.16
19	1.28	1.16	1.04
20	1.04	0.946	1.04
Mean	1.04	0.931	1.00
SD, %	14.0	13.4	11.4
Level of significance between pairs[b]			
F^A/F^D *versus* F^B/F^D	$p = 0.001$		
F^A/F^D *versus* F^C/F^D	NS		
F^B/F^D *versus* F^C/F^D	NS		
Grand mean = 0.990[c]			
Grand percent *SD* = 13.3			

[a] Individual ratios of areas under the curve through infinity for tablet lots (Treatments A–C) divided by aqueous suspension (Treatment D). See *Appendix* for calculation method. [b] Comparison was made using a paired t test. [c] Not statistically significantly different from unity using t test.

Then:

$$\text{between-subject sum of squares} = \sum_{i=1}^{12} \frac{S_i^2}{2} - \frac{\left(\sum_{i=1}^{12} S_i\right)^2}{24} \quad \text{(Eq. A10)}$$

with 11 degrees of freedom, $S_i = X_{iA} + X_{iE}$, and:

$$\text{within-subject sum of squares} = \sum_{i=1}^{12} \frac{(X_{iA} - X_{iE})^2}{2} \quad \text{(Eq. A11)}$$

with 12 degrees of freedom.

In Eqs. A10 and A11, X_{iA} and X_{iE} refer to individual subject data following Treatments A and E, respectively.

An estimate of the ratio of between-subject variability to within-subject variability is given by Eq. A12:

$$B/W = \frac{MS_{\text{between}}}{MS_{\text{within}}} \times \frac{1}{k} - \frac{1}{k} \quad \text{(Eq. A12)}$$

when MS_{between} and MS_{within} represent the between-subject mean square and within-subject mean square, respectively, obtained by dividing the appropriate sum of squares by the corresponding number of degrees of freedom; and k is the number of treatments.

The 95% confidence interval for B/W is given by:

$$\text{prob}\left[\frac{MS_{\text{between}}}{kMS_{\text{within}}} \times \frac{1}{F_{0.975}(11,12)} - \frac{1}{k} \le B/W \le \frac{MS_{\text{between}}}{kMS_{\text{within}}} \times \frac{1}{F_{0.025}(11,12)} - \frac{1}{k}\right] = 0.95 \quad \text{(Eq. A13)}$$

If the left end-point of the constructed interval exceeds unity, between-subject variability is considered greater than within-subject variability, the magnitude of which is given by Eq. A12.

Area under Curve and Half-Life Estimation—The area under the curve (AUC) was calculated for each subject following each treatment by the following equation:

$$AUC_\infty = AUC_T + \hat{C}_{T/\beta} \quad \text{(Eq. A14)}$$

where AUC_∞ is the area under the curve through infinity, AUC_T is the area estimated by the trapezoidal rule up to time T, T is the last sampling time (usually 16 hr) when the observed concentration was above the sensitivity limit of the radioimmunoassay, β is the apparent elimination rate constant obtained by the method of least squares in the terminal log-linear phase, and $\hat{C}_T$ is the estimated serum concentration at time T observed by use of the exponential equation that defines the log-linear region.

The half-life ($t_{1/2}$) was estimated by the equation:

$$t_{1/2} = 0.693/\beta \quad \text{(Eq. A15)}$$

REFERENCES

(1) *Fed. Regist.*, 1624 (Jan. 7, 1977).

(2) W. A. Colburn and R. H. Buller, *Steroids*, **22**, 687 (1973).

(3) K. Butler, *Rev. Can. Biol.*, **32**, 53 (1973).

(4) A. R. DiSanto, D. J. Chodos, J. P. Phillips, K. A. DeSante, and R. G. Stroll, *Int. J. Chem. Pharmacol.*, **13**, 220 (1976).

(5) R. G. Stroll, R. R. Schwartz, G. C. Chao, A. Yacobi, D. J. Weidler, J. W. Ayres, E. Sakmar, M. R. Hallmark, and J. G. Wagner, *Clin. Pharmacol. Ther.*, **23**, 131 (1978).

(6) W. G. Cochran, *Biometrics*, **20**, 191 (1964).

(7) G. E. P. Box, *ibid.*, **6**, 362 (1950).

ACKNOWLEDGMENTS

Presented in part at the APhA Academy of Pharmaceutical Sciences, Montreal meeting, May 1978.

NOTES

Separation of Penicillin G Potassium and Its Degradation Products Using High-Pressure Liquid Chromatography

W. A. VADINO *x, E. T. SUGITA, R. L. SCHNAARE, H. Y. ANDO, and P. J. NIEBERGALL ‡

Received November 20, 1978, from the *Department of Pharmacy, Philadelphia College of Pharmacy and Science, Philadelphia, PA 19104.* Accepted for publication March 8, 1979.

*Present address: Pharmaceutical Division, Ciba-Geigy Corp., Summit, NJ 07901. ‡Marion Laboratories, Kansas City, MO 64141.

Abstract □ A high-pressure liquid chromatographic technique was developed for the separation of penicillin G potassium and several of its decomposition products. The method utilized a buffered acetonitrile–phosphate mobile phase on a reversed-phase C_{18} column. Separation of penicillin G potassium and six degradation products was attained within 25 min.

Keyphrases □ Penicillin G potassium—analysis, high-pressure liquid chromatography, separation from degradation products □ High-pressure liquid chromatography—analysis, penicillin G potassium, separation from degradation products □ Antibacterial agents—penicillin G potassium, high-pressure liquid chromatographic analysis, separation from degradation products

The separation of penicillin G from mixtures of penicillin or related decomposition products was reported previously (1–7). Separation methods include TLC (1–3), GLC (4, 5), and high-pressure liquid chromatography (HPLC) (6, 7). Continuing interest in this area is due in part to ongoing efforts to identify the causative agents in penicillin allergy. Most degradation products formed during penicillin G hydrolysis can elicit an allergic response (8).

This report describes an HPLC technique which separates penicillin G potassium and six decomposition products within 25 min.

EXPERIMENTAL

Materials—Penicillin G potassium[1] and D,L-penicillamine[2] were obtained commercially and used as received. Benzylpenicilloic acid, benzylpenillic acid, benzylpenilloic acid, and benzylpenamaldic acid were prepared using standard procedures (9–11). Acetonitrile[3] was spectral

[1] Lot W732511, Wyeth Laboratories, West Chester, Pa.
[2] Sigma Chemical Co., St. Louis, Mo.
[3] Matheson, Coleman and Bell, Norwood, Ohio.

0022-3549/79/1000-1316$01.00/0

© 1979, American Pharmaceutical Association

Then:

$$\text{between-subject sum of squares} = \sum_{i=1}^{12} \frac{S_i^2}{2} - \frac{\left(\sum_{i=1}^{12} S_i\right)^2}{24} \quad \text{(Eq. A10)}$$

with 11 degrees of freedom, $S_i = X_{iA} + X_{iE}$, and:

$$\text{within-subject sum of squares} = \sum_{i=1}^{12} \frac{(X_{iA} - X_{iE})^2}{2} \quad \text{(Eq. A11)}$$

with 12 degrees of freedom.

In Eqs. A10 and A11, X_{iA} and X_{iE} refer to individual subject data following Treatments A and E, respectively.

An estimate of the ratio of between-subject variability to within-subject variability is given by Eq. A12:

$$B/W = \frac{MS_{\text{between}}}{MS_{\text{within}}} \times \frac{1}{k} - \frac{1}{k} \quad \text{(Eq. A12)}$$

when MS_{between} and MS_{within} represent the between-subject mean square and within-subject mean square, respectively, obtained by dividing the appropriate sum of squares by the corresponding number of degrees of freedom; and k is the number of treatments.

The 95% confidence interval for B/W is given by:

$$\text{prob}\left[\frac{MS_{\text{between}}}{kMS_{\text{within}}} \times \frac{1}{F_{0.975}(11,12)} - \frac{1}{k} \le B/W \le \frac{MS_{\text{between}}}{kMS_{\text{within}}} \times \frac{1}{F_{0.025}(11,12)} - \frac{1}{k}\right] = 0.95 \quad \text{(Eq. A13)}$$

If the left end-point of the constructed interval exceeds unity, between-subject variability is considered greater than within-subject variability, the magnitude of which is given by Eq. A12.

Area under Curve and Half-Life Estimation—The area under the curve (AUC) was calculated for each subject following each treatment by the following equation:

$$AUC_\infty = AUC_T + \hat{C}_{T/\beta} \quad \text{(Eq. A14)}$$

where AUC_∞ is the area under the curve through infinity, AUC_T is the area estimated by the trapezoidal rule up to time T, T is the last sampling time (usually 16 hr) when the observed concentration was above the sensitivity limit of the radioimmunoassay, β is the apparent elimination rate constant obtained by the method of least squares in the terminal log-linear phase, and $\hat{C}_T$ is the estimated serum concentration at time T observed by use of the exponential equation that defines the log-linear region.

The half-life ($t_{1/2}$) was estimated by the equation:

$$t_{1/2} = 0.693/\beta \quad \text{(Eq. A15)}$$

REFERENCES

(1) *Fed. Regist.*, 1624 (Jan. 7, 1977).

(2) W. A. Colburn and R. H. Buller, *Steroids*, **22**, 687 (1973).

(3) K. Butler, *Rev. Can. Biol.*, **32**, 53 (1973).

(4) A. R. DiSanto, D. J. Chodos, J. P. Phillips, K. A. DeSante, and R. G. Stroll, *Int. J. Chem. Pharmacol.*, **13**, 220 (1976).

(5) R. G. Stroll, R. R. Schwartz, G. C. Chao, A. Yacobi, D. J. Weidler, J. W. Ayres, E. Sakmar, M. R. Hallmark, and J. G. Wagner, *Clin. Pharmacol. Ther.*, **23**, 131 (1978).

(6) W. G. Cochran, *Biometrics*, **20**, 191 (1964).

(7) G. E. P. Box, *ibid.*, **6**, 362 (1950).

ACKNOWLEDGMENTS

Presented in part at the APhA Academy of Pharmaceutical Sciences, Montreal meeting, May 1978.

NOTES

Separation of Penicillin G Potassium and Its Degradation Products Using High-Pressure Liquid Chromatography

W. A. VADINO *x, E. T. SUGITA, R. L. SCHNAARE, H. Y. ANDO, and P. J. NIEBERGALL ‡

Received November 20, 1978, from the *Department of Pharmacy, Philadelphia College of Pharmacy and Science, Philadelphia, PA 19104.* Accepted for publication March 8, 1979.

*Present address: Pharmaceutical Division, Ciba-Geigy Corp., Summit, NJ 07901. ‡Marion Laboratories, Kansas City, MO 64141.

Abstract □ A high-pressure liquid chromatographic technique was developed for the separation of penicillin G potassium and several of its decomposition products. The method utilized a buffered acetonitrile–phosphate mobile phase on a reversed-phase C_{18} column. Separation of penicillin G potassium and six degradation products was attained within 25 min.

Keyphrases □ Penicillin G potassium—analysis, high-pressure liquid chromatography, separation from degradation products □ High-pressure liquid chromatography—analysis, penicillin G potassium, separation from degradation products □ Antibacterial agents—penicillin G potassium, high-pressure liquid chromatographic analysis, separation from degradation products

The separation of penicillin G from mixtures of penicillin or related decomposition products was reported previously (1–7). Separation methods include TLC (1–3), GLC (4, 5), and high-pressure liquid chromatography (HPLC) (6, 7). Continuing interest in this area is due in part to ongoing efforts to identify the causative agents in penicillin allergy. Most degradation products formed during penicillin G hydrolysis can elicit an allergic response (8).

This report describes an HPLC technique which separates penicillin G potassium and six decomposition products within 25 min.

EXPERIMENTAL

Materials—Penicillin G potassium[1] and D,L-penicillamine[2] were obtained commercially and used as received. Benzylpenicilloic acid, benzylpenillic acid, benzylpenilloic acid, and benzylpenamaldic acid were prepared using standard procedures (9–11). Acetonitrile[3] was spectral

[1] Lot W732511, Wyeth Laboratories, West Chester, Pa.
[2] Sigma Chemical Co., St. Louis, Mo.
[3] Matheson, Coleman and Bell, Norwood, Ohio.

0022-3549/79/1000-1316$01.00/0

© 1979, American Pharmaceutical Association

Table I—Retention Time of Penicillin G Potassium and Various Degradation Products Separated by HPLC [a]

Compound	Retention Time, min
Buffer salts	3.6
Penicillamine	3.9
Compound F	4.9
Benzylpenillic acid	6.7
Benzylpenicilloic acid	12.7
Benzylpenilloic acid	14.5
Benzylpenamaldic acid	18.0
Penicillin G potassium	25.0

[a] μBondapak C_{18}; conditions as described.

quality; all other chemicals were reagent grade. Distilled, deionized, degassed water was used to prepare all solutions.

Apparatus—A liquid chromatograph[4] equipped with a 254-nm UV detector and a reciprocating pump[5] to deliver the mobile phase were used. A stainless steel column (4 mm i.d. × 30 cm), prepacked with a small diameter silica having a monomolecular layer of octadecyltrichlorosilane[6] chemically bonded to its surface, was obtained commercially. A precolumn (3 mm i.d. × 10.16 cm) filled with a high-capacity reversed-phase packing[7] was used to protect the microparticular packing from disturbance and contamination.

Mobile Phase—The mobile phase was prepared by dissolving 4.24 g of monobasic potassium phosphate in sufficient water to make 400 ml. One hundred milliliters of acetonitrile was added to this solution, and the pH of the final solution was adjusted to 4.15 with 1.00 *N* HCl.

Chromatographic Conditions—The chromatographic column was operated at ambient temperature, and injections were made into a stopped-flow injection port[8] using a 10-μl syringe[9]. The UV detector was set at 0.08 absorbance unit full scale (aufs) for penicillin G potassium, benzylpenicilloic acid, benzylpenamaldic acid, benzylpenilloic acid, and penicillamine. The detector range was varied for benzylpenillic acid. Chromatograms were recorded on a single-pen strip-chart recorder[10]. The flow rate and chart speed were maintained at 0.75 ml/min and 1.27 mm/min, respectively. Fifty milliliters of mobile phase was passed through the column prior to use each day.

Individual samples of penicillin G potassium and possible acid degradation products were prepared by dissolving an appropriate amount of material in sufficient water to make 50.0 ml. Samples of penicillin G potassium degraded in acidic media were prepared by dissolving penicillin G potassium in sufficient preheated pH 2.83 phosphate buffer to make 50.0 ml.

RESULTS AND DISCUSSION

In the past, the separation of penicillin G in mixtures of penicillins or related degradation products has been accomplished using TLC and GLC. However, these methods have several shortcomings. The long development time required for TLC separation does not lend itself to kinetic studies; and, while GLC provides shorter analysis time, the separations require derivatization and are limited by the labile nature of the compounds.

Several recent reports noted the use of HPLC with anionic (6) and cationic (7) exchange resins to effect separation. The reported retention times of benzylpenicilloic acid and benzylpenilloic acid using cation exchange were 156 and 768 min, respectively, making this procedure unsuitable for kinetic studies. Another criticism of ion exchange is the inherent potential of the system to serve as a possible source of degradation catalysis.

Liquid–liquid reversed-phase chromatography, with its less severe operating conditions, provides an advantage over previously reported methods.

Initial separations were obtained using a pellicular C_{18} packing[11] with various aqueous buffer solutions mixed with methanol or acetonitrile. However, a tailing problem could not be eliminated.

A reversed-phase packing with a heavier coating of stationary liquid phase[11] was used with some success. Initial separations were accomplished using a prepacked column (2 mm i.d. × 61 cm) and also a hand-packed (12) column (3.18 mm i.d. × 1 m). Improvement in the technique resulted when two of the latter columns were butted end to end.

Vastly improved separation was obtained with a microparticular reversed-phase packing[6]. The packing has a monomolecular layer of octa-

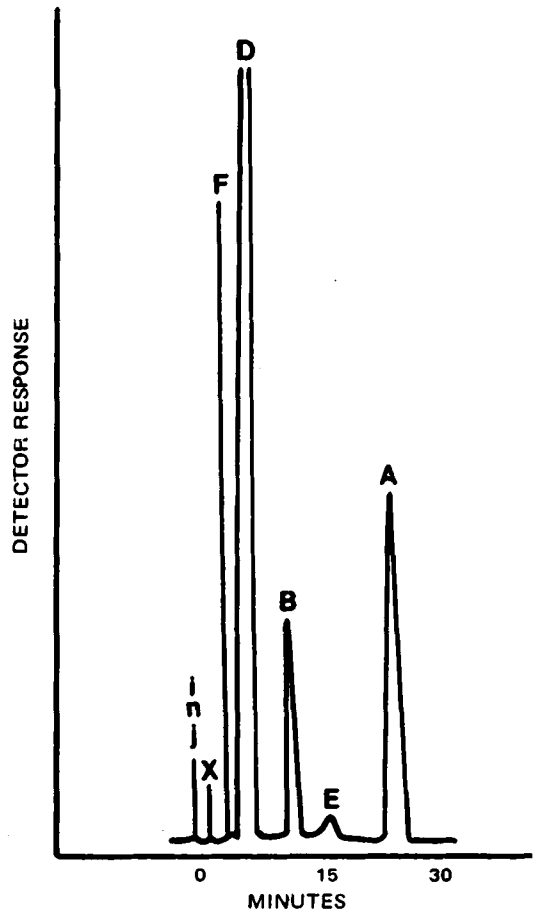

Figure 1—*Representative high-pressure liquid chromatogram of an aged penicillin potassium G sample in 0.100* M *phosphate buffer. Key: A, penicillin G potassium; B, benzylpenicilloic acid; D, benzylpenillic acid; E, benzylpenilloic acid; F, Compound F; and X, buffer salts.*

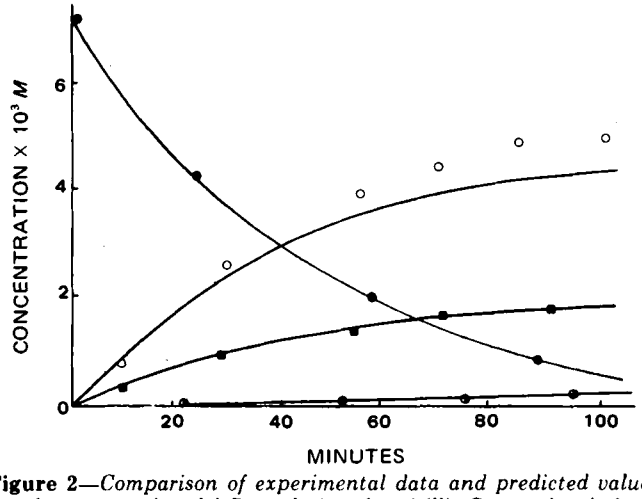

Figure 2—*Comparison of experimental data and predicted values based on proposed model. Degradation of penicillin G potassium in 0.100* M *phosphate buffer at pH 2.83, μ = 0.500, and 30.5°. Key: solid lines, predicted value; ●, penicillin G potassium; ■, benzylpenillic acid; ○, benzylpenicilloic acid, and ◑, benzylpenilloic acid.*

[4] Model 1205, Laboratory Data Control, Riviera Beach, Fla.
[5] Mini-Pump, Milton Roy Co., St. Petersburg, Fla.
[6] μBondapak C_{18}, Waters Associates, Milford, Mass.
[7] C_{18} Porasil B, Waters Associates, Milford, Mass.
[8] Model LIB, Reeve Angel, Clifton, N.J.
[9] Model LC-210, Precision Sampling Corp., Baton Rouge, La.
[10] Model 3301, Laboratory Data Control, Riviera Beach, Fla.
[11] VYDAC RP, The Separations Group, Hesperia, Calif.

decyltrichlorosilane chemically bonded to a small diameter (<10 μm) silica particle. The smaller particle size results in faster analysis time with improved resolution.

The retention times of penicillin G potassium and several degradation products formed during acid hydrolysis of penicillin G potassium at pH 2.83 are given in Table I. Identification of penicillin G potassium and related compounds was accomplished by comparing the retention time of the unknown with that of known standards. An unidentified compound with a retention time of 4.9 min was detected and designated as Compound F. A representative chromatogram for pH 2.83 is shown in Fig. 1. No penicillamine and penamaldic acid were detected at this pH.

The stability of penicillin G potassium and its degradation products in the HPLC mobile phase also was determined. Samples of penicillin G potassium and its degradation products were aged in the acetonitrile–phosphate mobile phase for a period at least equal to the retention for the particular compound. Samples were injected onto the HPLC column to observe any change in peak height or any increase in the number of peaks. Additionally, solutions containing mixtures of penicillin G potassium and its degradation products were aged in the mobile phase and subjected to the same test. No change in the number of peaks or peak height was noted.

Figure 2 illustrates the results obtained for penicillin G potassium degradation at pH 2.83 using the described HPLC process. The studies are continuing, and the complete kinetic scheme will be reported in a subsequent article.

REFERENCES

(1) R. R. Goodall and A. A. Levi, *Analyst*, **72**, 277 (1947).

(2) I. J. McGilveray and R. D. Strickland, *J. Pharm. Sci.*, **56**, 77 (1967).

(3) J. R. Fooks and G. L. Mattock, *ibid.*, **58**, 1357 (1969).

(4) E. Evrard, M. Claesen, and H. Vanderhaeghe, *Nature*, **201**, 124 (1964).

(5) C. Hishta, D. L. Mays, and M. Garofalo, *Anal. Chem.*, **43**, 1530 (1971).

(6) J. M. Blaha, A. M. Knevel, and S. L. Hem, *J. Pharm. Sci.*, **64**, 1384 (1975).

(7) P. Adriens, B. Meesschaert, H. Eyssen, E. Roets, and H. Vanderhaeghe, *J. Chromatogr.*, **144**, 93 (1977).

(8) M. Schwartz, *J. Pharm. Sci.*, **58**, 643 (1969).

(9) M. Cole, M. D. Kenig, and V. A. Hewitt, *Antimicrob. Agents Chemother.*, **1973**, 463.

(10) J. V. Vasani, Ph.D. thesis, Philadelphia College of Pharmacy and Science, Philadelphia, Pa., 1977.

(11) J. L. Longridge and D. Timms, *J. Chem. Soc., B*, **1971**, 852.

(12) L. R. Snyder and J. J. Kirkland, "Introduction to Modern Liquid Chromatography," Wiley, New York, N.Y., 1974, p. 89.

ACKNOWLEDGMENTS

Abstracted in part from a dissertation submitted by W. A. Vadino to the Graduate School, Philadelphia College of Pharmacy and Science, in partial fulfillment of the Doctor of Philosophy degree requirements.

Supported in part by Research Grant AI 11399 from the National Institutes of Health, Bethesda, Md.

The authors thank Dr. J. Vasani for the preparation of penicillin G degradation products.

Sensitive High-Pressure Liquid Chromatographic Determination of Disopyramide and Mono-*N*-dealkyldisopyramide

GLORIA NYGARD, WILLIAM H. SHELVER, and S. K. WAHBA KHALIL ˣ

Received March 19, 1979, from the *College of Pharmacy, North Dakota State University, Fargo, ND 58105.* Accepted for publication April 5, 1979.

Abstract □ A high-pressure liquid chromatographic procedure for the accurate determination of disopyramide and its chief metabolite in plasma is presented. The method is suitable for monitoring patients receiving disopyramide therapy. A reversed-phase cyanopropylsilane column is utilized with a mobile phase of 50% acetonitrile and 50% 0.01 *M* sodium acetate buffer at pH 4.0. Absorption was monitored at 254 nm with a detection limit of 0.2 μg/ml of plasma. The reproducibility and precision of the procedure were demonstrated on samples containing 0.50–12 μg/ml of plasma.

Keyphrases □ Disopyramide—analysis, high-pressure liquid chromatography, plasma, metabolites, humans □ Disopyramide—metabolites, analysis, high-pressure liquid chromatography, humans □ Mono-*N*-dealkyldisopyramide—analysis, high-pressure liquid chromatography, plasma, humans □ Antiarrhythmic agents—disopyramide, high-pressure liquid chromatographic analysis, plasma, humans

Disopyramide phosphate[1] is a relatively new antiarrhythmic drug with electrophysiological properties similar to quinidine, but it is reported to be better tolerated (1). The wide range of plasma half-lives (2) of disopyramide phosphate in humans (4–18 hr) indicates that patients may require individualized dosage regimens. The side effects of the drug (3, 4) and the antiarrhythmic effects of disopyramide phosphate have been related to concentration (5, 6). Consequently, measurement of the concentration may provide a method to maximize therapeutic effect while minimizing potential side effects.

Direct spectrophotometric (7) and spectrofluorometric (8) determinations have been reported. Both these techniques are nonspecific because the major metabolite (mono-*N*-dealkyldisopyramide) has similar spectral characteristics to the parent compound (7, 8). GLC procedures also have been reported, but they either require derivatization of the compound (9) or a selective (nitrogen) detector (10). Quantitation of disopyramide and its metabolite has also been performed by high-pressure liquid chromatography (HPLC). The reported methods require the ion-pair modification of octadecylsilane reversed-phase chromatography (11) or the use of a multiwavelength detector (12, 13).

This paper describes a rapid, specific method for the determination of disopyramide and its major metabolite by HPLC using a reversed-phase cyanopropylsilane column and a 254-nm detector. The method is applicable to the direct determination of plasma levels, even in the

[1] Norpace.

0022-3549/79/1000-1318$01.00/0

© 1979, American Pharmaceutical Association

decyltrichlorosilane chemically bonded to a small diameter (<10 μm) silica particle. The smaller particle size results in faster analysis time with improved resolution.

The retention times of penicillin G potassium and several degradation products formed during acid hydrolysis of penicillin G potassium at pH 2.83 are given in Table I. Identification of penicillin G potassium and related compounds was accomplished by comparing the retention time of the unknown with that of known standards. An unidentified compound with a retention time of 4.9 min was detected and designated as Compound F. A representative chromatogram for pH 2.83 is shown in Fig. 1. No penicillamine and penamaldic acid were detected at this pH.

The stability of penicillin G potassium and its degradation products in the HPLC mobile phase also was determined. Samples of penicillin G potassium and its degradation products were aged in the acetonitrile–phosphate mobile phase for a period at least equal to the retention for the particular compound. Samples were injected onto the HPLC column to observe any change in peak height or any increase in the number of peaks. Additionally, solutions containing mixtures of penicillin G potassium and its degradation products were aged in the mobile phase and subjected to the same test. No change in the number of peaks or peak height was noted.

Figure 2 illustrates the results obtained for penicillin G potassium degradation at pH 2.83 using the described HPLC process. The studies are continuing, and the complete kinetic scheme will be reported in a subsequent article.

REFERENCES

(1) R. R. Goodall and A. A. Levi, *Analyst*, **72**, 277 (1947).

(2) I. J. McGilveray and R. D. Strickland, *J. Pharm. Sci.*, **56**, 77 (1967).

(3) J. R. Fooks and G. L. Mattock, *ibid.*, **58**, 1357 (1969).

(4) E. Evrard, M. Claesen, and H. Vanderhaeghe, *Nature*, **201**, 124 (1964).

(5) C. Hishta, D. L. Mays, and M. Garofalo, *Anal. Chem.*, **43**, 1530 (1971).

(6) J. M. Blaha, A. M. Knevel, and S. L. Hem, *J. Pharm. Sci.*, **64**, 1384 (1975).

(7) P. Adriens, B. Meesschaert, H. Eyssen, E. Roets, and H. Vanderhaeghe, *J. Chromatogr.*, **144**, 93 (1977).

(8) M. Schwartz, *J. Pharm. Sci.*, **58**, 643 (1969).

(9) M. Cole, M. D. Kenig, and V. A. Hewitt, *Antimicrob. Agents Chemother.*, **1973**, 463.

(10) J. V. Vasani, Ph.D. thesis, Philadelphia College of Pharmacy and Science, Philadelphia, Pa., 1977.

(11) J. L. Longridge and D. Timms, *J. Chem. Soc., B*, **1971**, 852.

(12) L. R. Snyder and J. J. Kirkland, "Introduction to Modern Liquid Chromatography," Wiley, New York, N.Y., 1974, p. 89.

ACKNOWLEDGMENTS

Abstracted in part from a dissertation submitted by W. A. Vadino to the Graduate School, Philadelphia College of Pharmacy and Science, in partial fulfillment of the Doctor of Philosophy degree requirements.

Supported in part by Research Grant AI 11399 from the National Institutes of Health, Bethesda, Md.

The authors thank Dr. J. Vasani for the preparation of penicillin G degradation products.

Sensitive High-Pressure Liquid Chromatographic Determination of Disopyramide and Mono-*N*-dealkyldisopyramide

GLORIA NYGARD, WILLIAM H. SHELVER, and S. K. WAHBA KHALIL ˣ

Received March 19, 1979, from the *College of Pharmacy, North Dakota State University, Fargo, ND 58105.* Accepted for publication April 5, 1979.

Abstract □ A high-pressure liquid chromatographic procedure for the accurate determination of disopyramide and its chief metabolite in plasma is presented. The method is suitable for monitoring patients receiving disopyramide therapy. A reversed-phase cyanopropylsilane column is utilized with a mobile phase of 50% acetonitrile and 50% 0.01 *M* sodium acetate buffer at pH 4.0. Absorption was monitored at 254 nm with a detection limit of 0.2 μg/ml of plasma. The reproducibility and precision of the procedure were demonstrated on samples containing 0.50–12 μg/ml of plasma.

Keyphrases □ Disopyramide—analysis, high-pressure liquid chromatography, plasma, metabolites, humans □ Disopyramide—metabolites, analysis, high-pressure liquid chromatography, humans □ Mono-*N*-dealkyldisopyramide—analysis, high-pressure liquid chromatography, plasma, humans □ Antiarrhythmic agents—disopyramide, high-pressure liquid chromatographic analysis, plasma, humans

Disopyramide phosphate[1] is a relatively new antiarrhythmic drug with electrophysiological properties similar to quinidine, but it is reported to be better tolerated (1). The wide range of plasma half-lives (2) of disopyramide phosphate in humans (4–18 hr) indicates that patients may require individualized dosage regimens. The side effects of the drug (3, 4) and the antiarrhythmic effects of disopyramide phosphate have been related to concentration (5, 6). Consequently, measurement of the concentration may provide a method to maximize therapeutic effect while minimizing potential side effects.

Direct spectrophotometric (7) and spectrofluorometric (8) determinations have been reported. Both these techniques are nonspecific because the major metabolite (mono-*N*-dealkyldisopyramide) has similar spectral characteristics to the parent compound (7, 8). GLC procedures also have been reported, but they either require derivatization of the compound (9) or a selective (nitrogen) detector (10). Quantitation of disopyramide and its metabolite has also been performed by high-pressure liquid chromatography (HPLC). The reported methods require the ion-pair modification of octadecylsilane reversed-phase chromatography (11) or the use of a multiwavelength detector (12, 13).

This paper describes a rapid, specific method for the determination of disopyramide and its major metabolite by HPLC using a reversed-phase cyanopropylsilane column and a 254-nm detector. The method is applicable to the direct determination of plasma levels, even in the

[1] Norpace.

0022-3549/79/1000-1318$01.00/0

© 1979, American Pharmaceutical Association

Table I—Precision and Percent Recovery of Disopyramide Phosphate and Mono-*N*-dealkyldisopyramide

Level, μg/ml	*n*	Recovery, %	*CV*
	Disopyramide Phosphate		
0.5	4	90.8	12.0
1.5	5	101.5	6.4
4.0	5	103.3	2.9
6.0	4	104.7	1.7
9.0	4	101.7	1.4
12.0	5	99.5	2.0
	Mono-*N*-dealkyldisopyramide		
0.5	4	111.1	12.5
1.5	5	96.0	12.8
4.0	5	91.5	4.1
6.0	5	99.1	5.2
9.0	5	96.8	3.5
12.0	4	100.9	6.9

presence of other antiarrhythmic drugs. The applicability was demonstrated by the analysis of plasma from patients taking disopyramide.

EXPERIMENTAL

Instrumentation—A high-pressure liquid chromatograph[2] was equipped with a cyanopropylsilane[3] column, 300 mm long × 4 mm i.d. The degassed mobile phase was pumped through the column at 1.2 ml/min (1800–2000 psi) at ambient temperature until a stable baseline was obtained.

Chemicals and Reagents—Sodium acetate, sodium hydrogen phosphate, acetic acid, and phosphoric acid were ACS certified grade. HPLC grade methanol, methylene chloride, and acetonitrile were used. Disopyramide phosphate[4], mono-*N*-dealkyldisopyramide[4], and cyclomethycaine sulfate[5] were supplied by the manufacturers.

Mobile Phase—Sodium acetate solution, 0.01 *M*, was prepared in distilled water, and the pH was adjusted to 4 by the gradual addition of acetic acid. An equal volume of acetonitrile was added to the buffer, and the mixture was degassed under vacuum.

Stock Solutions—*Disopyramide Phosphate and Mono-*N*-dealkyldisopyramide*—A solution containing 4 mg of the drug and 4 mg of its metabolite in 100 ml of methanol was prepared. The solution was stored in a refrigerator and made fresh each month.

Cyclomethycaine Sulfate (Internal Standard)—A solution was prepared by dissolving 8 mg in 5 ml of methanol and diluting to 100 ml with methylene chloride. This solution was prepared fresh daily.

Working Internal Standard Solution—With a volumetric pipet, 1.0 ml of the stock cyclomethycaine solution was transferred to a 500-ml volumetric flask and diluted with methylene chloride to volume (0.16 μg/ml).

Sample Preparation—To 0.5 ml of heparinized plasma in a 15-ml screw-capped centrifuge tube, an aliquot of the methanolic solution of disopyramide phosphate and dealkyldisopyramide containing 0.25–6.0 μg of each drug, 0.5 ml of phosphate buffer (pH 7.4, 0.1 *M*), and 5.0 ml of methylene chloride containing 0.16 μg of cyclomethycaine sulfate/ml were added. The tubes were vortexed for 10 sec and centrifuged for 5 min at 900×*g*. A 4.0-ml volume of the organic phase was transferred to special concentration tubes[6] and evaporated to dryness at ambient temperature under a gentle nitrogen stream.

HPLC Separation and Quantitation—The residue was dissolved in 200 μl of acetonitrile, and 50–100-μl injections were made using a 50-μl syringe[7]. A standard curve was constructed utilizing a minimum of four replicate plasma extractions simulating concentrations of disopyramide phosphate and mono-*N*-dealkyldisopyramide from 0.5 to 12 μg/ml. The chromatograms were recorded[8] at a chart speed of 5 mm/min.

Disopyramide and its metabolite were identified on the basis of retention time. The peak heights were measured, and the disopyramide phosphate/cyclomethycaine and mono-*N*-dealkyldisopyramide/cyclomethycaine ratios were calculated and plotted *versus* concentration, expressed as micrograms per milliliter of plasma.

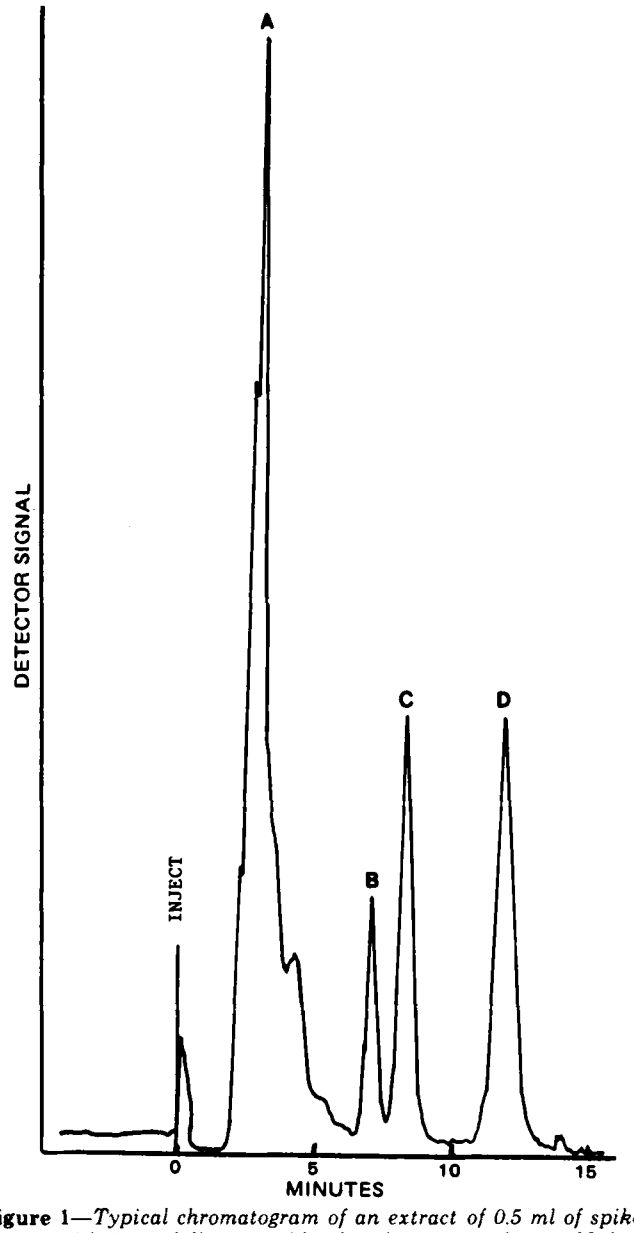

Figure 1—*Typical chromatogram of an extract of 0.5 ml of spiked plasma with 2 μg of disopyramide phosphate, 2 μg of mono-*N*-dealkyldisopyramide, and 8 μg of the internal standard. Key: A, plasma extractable; B, mono-*N*-dealkyldisopyramide; C, disopyramide; and D, internal standard.*

Interferences—Possible interferences from normal plasma constituents and other antiarrhythmic drugs were studied by adding therapeutic amounts to plasma containing disopyramide phosphate, its metabolite, and the internal standard and performing the analysis.

Sample Preparation and Assay—Heparinized plasma samples from patients on oral disopyramide phosphate therapy were processed in duplicate as described. The amounts of disopyramide and its metabolite were calculated by comparison with the standard curve prepared daily.

RESULTS AND DISCUSSION

Methylene chloride was used as the organic solvent in the extraction procedure because it exhibits good extractibility for disopyramide, propranolol, and other antiarrhythmic amines (14). Moreover, it extracts a minimum of interfering constituents from plasma and evaporates easily. The extraction at pH 7.4 gave excellent recoveries of disopyramide and the internal standard (90–95%). The recovery of the metabolite was only 32%.

[2] Model 202 chromatograph, M 600 pump, and U6K universal injector, Waters Associates, Milford, Mass.
[3] μBondapak CN, Waters Associates, Milford, Mass.
[4] Searle Laboratories, Chicago, Ill.
[5] Eli Lilly, Indianapolis, Ind.
[6] Concentratubes, Laboratory Research Co., Los Angeles, Calif.
[7] Hamilton Co., Reno, Nev.
[8] Model 56, Perkin-Elmer, Norwalk, Conn.

The ratios of the peak heights of disopyramide and its metabolite to the peak height of the internal standard were calculated. Statistical analysis of the data (Table I) by linear regression indicated excellent linearity and reproducibility with correlation coefficients of 0.9991 and 0.9955, slopes of 0.3655 and 0.3100, and intercepts of 0.0030 and −0.0038 in the range of 0.5–12.0 μg/ml of plasma for disopyramide and its metabolite, respectively. This range includes the therapeutic range of the drug.

The use of reversed-phase chromatography on a cyanopropylsilane column and a mobile phase of 50% acetonitrile and 50% acetate buffer (pH 4, 0.01 *M*) afforded excellent separation with sharp peaks for disopyramide, mono-*N*-dealkyldisopyramide, and cyclomethycaine (Fig. 1).

The method was applied for the determination of disopyramide and its metabolite in patient plasma before and after administration of disopyramide phosphate. No interference was noted from commonly utilized cardiac drugs. Quinidine, lidocaine, procainamide, and the more recent β-blockers metoprolol and timolol were eluted at different retention times. Although propranolol and its 4-hydroxy metabolite have the same retention times as disopyramide and its mono-*N*-dealkylated metabolite, respectively, the accurate determination of the two drugs is still possible since disopyramide and its metabolite do not fluoresce while propranolol and its metabolite fluoresce but have no appreciable absorption at 254 nm. Cyclomethycaine is an ideal internal standard since it absorbs at 254 nm and fluoresces at 276-nm excitation with a 340-nm cutoff filter (14).

Major advantages of the proposed method are its simplicity and rapidity. Both disopyramide and its metabolite are determined in a single procedure using a standard single wavelength UV detector. Moreover, propranolol can be determined using the same extraction and chromatographic conditions by the incorporation of a spectrofluorometric detector. Other chromatographic methods require separate conditions for the determination of each drug or even for the determination of metabolites. In addition, the method gave excellent separation without the ion-pair technique, which results in limited use of the column and a decrease in the capacity factor (15).

REFERENCES

(1) M. E. Josephson, A. R. Caracta, and S. H. Lau, *Am. Heart J.*, **86**, 771 (1973).

(2) "Facts and Comparisons," E. K. Kastrup and J. R. Boyd, Eds., Facts and Comparisons, Inc., St. Louis, Mo., 1977, p. 146c.

(3) F. A. Peters and R. A. Winkle, *Hosp. Form.*, **13**, 989 (1978).

(4) P. P. Mathur, *Am. Heart J.*, **84**, 764 (1972).

(5) L. A. Vismara, D. T. Mason, and E. A. Amsterdam, *Clin. Pharmacol. Ther.*, **16**, 330 (1974).

(6) L. A. Vismara, Z. Vera, and R. R. Miller, *Am. J. Cardiol.*, **39**, 1027 (1977).

(7) D. Martin, L. Burke, W. Nordin, and S. Ehen, *Clin. Chem.*, **24**, 991 (1978).

(8) R. E. Ranney, R. R. Dean, A. Karim, and F. M. Radzialowski, *Arch. Int. Pharmacodyn. Ther.*, **191**, 162 (1971).

(9) T. C. Hutsell and S. J. Stachelski, *J. Chromatogr.*, **106**, 151 (1975).

(10) A. M. J. A. Duchateau, F. W. H. M. Merkus, and F. Schobben, *ibid.*, **109**, 432 (1975).

(11) P. J. Meffin, S. R. Harapat, and D. C. Harrison, *ibid.*, **132**, 503 (1977).

(12) P.-O. Lagerstrom and B.-A. Persson, *ibid.*, **149**, 331 (1978).

(13) L. A. Broussard and C. S. Frings, *Clin. Chem.*, **24**, 1007 (1978).

(14) G. Nygard, W. H. Shelver, and S. K. W. Khalil, *J. Pharm. Sci.*, **68**, 379 (1979).

(15) G. Schill, K. O. Borg, R. Modin, and B.-A. Persson, in "Progress in Drug Metabolism," vol. 2, L. F. Chasseaud and J. Bridges, Eds., Wiley, New York, N.Y., 1977, chap. 5.

ACKNOWLEDGMENTS

Supported in part by the Pharmacokinetic Drug Analysis Laboratory, Veterans Administration Center, Fargo, N.D.

Plasma Binding of Benzodiazepines in Humans

R. F. JOHNSON, S. SCHENKER, R. K. ROBERTS, P. V. DESMOND, and G. R. WILKINSON ˣ

Received December 29, 1978, from the *Departments of Medicine and Pharmacology, Vanderbilt University School of Medicine and Veterans Administration Hospital, Nashville, TN 37203.* Accepted for publication April 5, 1979.

Abstract □ Plasma binding of chlordiazepoxide, diazepam, lorazepam, and oxazepam was determined by equilibrium dialysis in 20 male, healthy volunteers, 25–86 years old. A wide range of binding was observed, with the free fraction varying twofold for lorazepam, fourfold for chlordiazepoxide and diazepam, and over 20-fold for oxazepam. Statistically significant linear relationships were not observed between the degree of binding and age, serum albumin, or total protein for any of the drugs. There was, however, a correlation between the extent of binding for the four drugs. Because of the importance of unbound benzodiazepine levels in eliciting any pharmacological response and also in disposition, consideration of the wide interindividual variability in plasma binding must be made in interpreting pharmacodynamic and pharmacokinetic data.

Keyphrases □ Benzodiazepines—plasma binding, equilibrium dialysis, humans, individual variation, age □ Sedatives—benzodiazepines, plasma binding, equilibrium dialysis, humans, individual variation, age □ Plasma binding—benzodiazepines, humans, individual variation, age

During a study of the effects of age on lorazepam disposition in humans, the results obtained from 11 apparently healthy subjects, 15–73 years old, suggested that the extent of plasma binding of this drug decreased with age (1). This result was in contrast to previous findings with the related 1,4-benzodiazepines, diazepam (2), chlordiazepoxide (3), and oxazepam (4). Accordingly, studies of lorazepam binding were performed with plasma from a larger group of subjects to determine whether the observed trend was real or had occurred by chance. The investigation also provided an opportunity to compare directly the relative plasma binding behavior of the various benzodiazepines.

EXPERIMENTAL

^{14}C-Chlordiazepoxide[1] (59.95 mCi/mmole), ^{14}C-diazepam[1] (13.01 mCi/mmole), ^{14}C-lorazepam[2] (10.79 mCi/mmole), and ^{14}C-oxazepam[2] (5.91 mCi/mmole) were examined for radiopurity by TLC. All except lorazepam were >98% pure. Purification of the latter to this level was achieved by preparative TLC using silica GF plates[3] and a mobile phase of ethyl acetate[4]–ethanol[5]–ammonium hydroxide[4] (5:5:1 v/v). Separate drug standard solutions were prepared in pH 7.4 buffer as follows:

[1] Hoffmann-La Roche, Nutley, NJ 07110.
[2] Wyeth Laboratories, Radnor, PA 19087.
[3] I.C.N. Pharmaceuticals, Cleveland, OH 44128.
[4] ACS grade, Fisher Scientific Co., Pittsburgh, PA 15219.
[5] USI absolute ethyl alcohol, USP-NF reagent.

0022-3549/79/1000-1320$01.00/0

© 1979, American Pharmaceutical Association

The ratios of the peak heights of disopyramide and its metabolite to the peak height of the internal standard were calculated. Statistical analysis of the data (Table I) by linear regression indicated excellent linearity and reproducibility with correlation coefficients of 0.9991 and 0.9955, slopes of 0.3655 and 0.3100, and intercepts of 0.0030 and −0.0038 in the range of 0.5–12.0 μg/ml of plasma for disopyramide and its metabolite, respectively. This range includes the therapeutic range of the drug.

The use of reversed-phase chromatography on a cyanopropylsilane column and a mobile phase of 50% acetonitrile and 50% acetate buffer (pH 4, 0.01 *M*) afforded excellent separation with sharp peaks for disopyramide, mono-*N*-dealkyldisopyramide, and cyclomethycaine (Fig. 1).

The method was applied for the determination of disopyramide and its metabolite in patient plasma before and after administration of disopyramide phosphate. No interference was noted from commonly utilized cardiac drugs. Quinidine, lidocaine, procainamide, and the more recent β-blockers metoprolol and timolol were eluted at different retention times. Although propranolol and its 4-hydroxy metabolite have the same retention times as disopyramide and its mono-*N*-dealkylated metabolite, respectively, the accurate determination of the two drugs is still possible since disopyramide and its metabolite do not fluoresce while propranolol and its metabolite fluoresce but have no appreciable absorption at 254 nm. Cyclomethycaine is an ideal internal standard since it absorbs at 254 nm and fluoresces at 276-nm excitation with a 340-nm cutoff filter (14).

Major advantages of the proposed method are its simplicity and rapidity. Both disopyramide and its metabolite are determined in a single procedure using a standard single wavelength UV detector. Moreover, propranolol can be determined using the same extraction and chromatographic conditions by the incorporation of a spectrofluorometric detector. Other chromatographic methods require separate conditions for the determination of each drug or even for the determination of metabolites. In addition, the method gave excellent separation without the ion-pair technique, which results in limited use of the column and a decrease in the capacity factor (15).

REFERENCES

(1) M. E. Josephson, A. R. Caracta, and S. H. Lau, *Am. Heart J.*, **86**, 771 (1973).

(2) "Facts and Comparisons," E. K. Kastrup and J. R. Boyd, Eds., Facts and Comparisons, Inc., St. Louis, Mo., 1977, p. 146c.

(3) F. A. Peters and R. A. Winkle, *Hosp. Form.*, **13**, 989 (1978).

(4) P. P. Mathur, *Am. Heart J.*, **84**, 764 (1972).

(5) L. A. Vismara, D. T. Mason, and E. A. Amsterdam, *Clin. Pharmacol. Ther.*, **16**, 330 (1974).

(6) L. A. Vismara, Z. Vera, and R. R. Miller, *Am. J. Cardiol.*, **39**, 1027 (1977).

(7) D. Martin, L. Burke, W. Nordin, and S. Ehen, *Clin. Chem.*, **24**, 991 (1978).

(8) R. E. Ranney, R. R. Dean, A. Karim, and F. M. Radzialowski, *Arch. Int. Pharmacodyn. Ther.*, **191**, 162 (1971).

(9) T. C. Hutsell and S. J. Stachelski, *J. Chromatogr.*, **106**, 151 (1975).

(10) A. M. J. A. Duchateau, F. W. H. M. Merkus, and F. Schobben, *ibid.*, **109**, 432 (1975).

(11) P. J. Meffin, S. R. Harapat, and D. C. Harrison, *ibid.*, **132**, 503 (1977).

(12) P.-O. Lagerstrom and B.-A. Persson, *ibid.*, **149**, 331 (1978).

(13) L. A. Broussard and C. S. Frings, *Clin. Chem.*, **24**, 1007 (1978).

(14) G. Nygard, W. H. Shelver, and S. K. W. Khalil, *J. Pharm. Sci.*, **68**, 379 (1979).

(15) G. Schill, K. O. Borg, R. Modin, and B.-A. Persson, in "Progress in Drug Metabolism," vol. 2, L. F. Chasseaud and J. Bridges, Eds., Wiley, New York, N.Y., 1977, chap. 5.

ACKNOWLEDGMENTS

Supported in part by the Pharmacokinetic Drug Analysis Laboratory, Veterans Administration Center, Fargo, N.D.

Plasma Binding of Benzodiazepines in Humans

R. F. JOHNSON, S. SCHENKER, R. K. ROBERTS, P. V. DESMOND, and G. R. WILKINSON ˣ

Received December 29, 1978, from the *Departments of Medicine and Pharmacology, Vanderbilt University School of Medicine and Veterans Administration Hospital, Nashville, TN 37203.* Accepted for publication April 5, 1979.

Abstract □ Plasma binding of chlordiazepoxide, diazepam, lorazepam, and oxazepam was determined by equilibrium dialysis in 20 male, healthy volunteers, 25–86 years old. A wide range of binding was observed, with the free fraction varying twofold for lorazepam, fourfold for chlordiazepoxide and diazepam, and over 20-fold for oxazepam. Statistically significant linear relationships were not observed between the degree of binding and age, serum albumin, or total protein for any of the drugs. There was, however, a correlation between the extent of binding for the four drugs. Because of the importance of unbound benzodiazepine levels in eliciting any pharmacological response and also in disposition, consideration of the wide interindividual variability in plasma binding must be made in interpreting pharmacodynamic and pharmacokinetic data.

Keyphrases □ Benzodiazepines—plasma binding, equilibrium dialysis, humans, individual variation, age □ Sedatives—benzodiazepines, plasma binding, equilibrium dialysis, humans, individual variation, age □ Plasma binding—benzodiazepines, humans, individual variation, age

During a study of the effects of age on lorazepam disposition in humans, the results obtained from 11 apparently healthy subjects, 15–73 years old, suggested that the extent of plasma binding of this drug decreased with age (1). This result was in contrast to previous findings with the related 1,4-benzodiazepines, diazepam (2), chlordiazepoxide (3), and oxazepam (4). Accordingly, studies of lorazepam binding were performed with plasma from a larger group of subjects to determine whether the observed trend was real or had occurred by chance. The investigation also provided an opportunity to compare directly the relative plasma binding behavior of the various benzodiazepines.

EXPERIMENTAL

^{14}C-Chlordiazepoxide[1] (59.95 mCi/mmole), ^{14}C-diazepam[1] (13.01 mCi/mmole), ^{14}C-lorazepam[2] (10.79 mCi/mmole), and ^{14}C-oxazepam[2] (5.91 mCi/mmole) were examined for radiopurity by TLC. All except lorazepam were >98% pure. Purification of the latter to this level was achieved by preparative TLC using silica GF plates[3] and a mobile phase of ethyl acetate[4]–ethanol[5]–ammonium hydroxide[4] (5:5:1 v/v). Separate drug standard solutions were prepared in pH 7.4 buffer as follows:

[1] Hoffmann-La Roche, Nutley, NJ 07110.
[2] Wyeth Laboratories, Radnor, PA 19087.
[3] I.C.N. Pharmaceuticals, Cleveland, OH 44128.
[4] ACS grade, Fisher Scientific Co., Pittsburgh, PA 15219.
[5] USI absolute ethyl alcohol, USP-NF reagent.

0022-3549/79/1000-1320$01.00/0

© 1979, American Pharmaceutical Association

Table I—Plasma Binding (Percent) of Benzodiazepines

Subject	Age, years	Diazepam	Oxazepam	Lorazepam	Chlordiazepoxide	Serum Albumin	Total Protein
1	25	91.21	96.13	86.30	92.70	5.00	6.90
2	29	96.94	99.23	92.26	96.26	5.60	7.40
3	29	95.85	98.69	91.52	96.45	—	—
4	29	93.39	98.87	91.45	95.09	5.00	7.20
5	29	95.36	98.84	92.47	96.98	5.70	7.60
6	30	97.32	99.31	92.47	96.88	5.40	7.30
7	31	97.39	97.45	93.35	97.13	5.10	7.80
8	34	96.17	93.33	88.00	91.43	5.50	7.10
9	35	97.57	98.62	92.00	93.08	5.20	6.70
10	35	97.58	98.63	91.04	93.08	—	—
11	35	91.04	90.67	86.30	89.07	4.60	7.40
12	35	97.64	99.29	93.33	96.64	—	—
13	42	94.01	98.00	90.49	94.98	5.00	7.60
14	48	95.57	98.80	87.78	95.79	4.60	6.70
15	68	97.27	99.28	91.65	95.53	—	—
16	68	91.73	95.01	93.36	—	4.40	7.60
17	69	97.21	99.43	91.45	95.47	4.10	6.80
18	83	96.52	98.98	91.03	92.21	4.70	6.70
19	83	93.83	98.33	92.79	92.62	—	—
20	86	97.17	99.56	89.92	96.26	4.80	6.90
Mean	46.15	95.54	97.82	90.95	94.66	4.98	7.18
±*SD*	21.23	2.23	2.33	2.21	2.23	0.46	0.38

Table II—Cross-Correlations of Binding Parameters

	Age	Chlordiazepoxide	Diazepam	Lorazepam	Oxazepam	Serum Albumin	Total Protein
Age		0.063[a]	0.248	0.082	0.065	0.656	0.392
		(0.79)[b]	(0.31)	(0.74)	(0.79)	(0.004)	(0.15)
Chlordiazepoxide			0.634	0.636	0.518	0.308	0.243
			(0.004)	(0.003)	(0.023)	(0.23)	(0.382)
Diazepam				0.743	0.810	0.144	0.169
				(<0.001)	(<0.001)	(0.58)	(0.547)
Lorazepam					0.653	0.328	0.326
					(0.002)	(0.25)	(0.25)
Oxazepam						0.237	0.293
						(0.42)	(0.31)
Serum albumin							0.489
							(0.076)

[a] Correlation coefficient. [b] Level of significance.

chlordiazepoxide, 10 μg/ml in 0.05 *M* tromethamine buffer; diazepam, 2.5 μg/ml, and oxazepam, 10 μg/ml, in 0.067 *M* phosphate buffer; and lorazepam, 1 μg/ml in ethanol.

Blood (25 ml) was collected by venipuncture into heparinized glass-stoppered tubes from 20 normal and apparently healthy male subjects, 25–86 years old, who were not receiving any medication. After separation, appropriate drug standards were added to the plasma to produce concentrations typical of those observed in clinical studies: chlordiazepoxide, 0.1, 0.5, and 1.0 μg/ml; diazepam, 25, 50, and 100 ng/ml; lorazepam, 10, 25, and 50 ng/ml; and oxazepam, 50, 100, and 200 ng/ml.

Plasma binding was determined at room temperature by equilibrium dialysis (5) using semimicrocells[6] and a semipermeable membrane with a molecular cutoff of 12,000–14,000[7]. Plasma (1 ml) was dialyzed against an equal volume of 0.067 *M* phosphate buffer, pH 7.4, for 2 hr (chlordiazepoxide and diazepam) and 4 hr (lorazepam and oxazepam). These times had been shown to be adequate for the attainment of equilibrium. After dialysis was completed, 0.5-ml aliquots of plasma and buffer were analyzed for radioactivity by adding 10 ml of scintillant solution[8] and 20 μl of acetic acid[4] and counting in a liquid scintillation counter[9], using the automatic external standardization procedure to correct for quenching. The extent of plasma binding was then calculated from:

$$\% \text{ bound} = \frac{\text{plasma dpm} - \text{buffer dpm}}{\text{plasma dpm}} \times 100 \qquad \text{(Eq. 1)}$$

RESULTS AND DISCUSSION

As previously noted (1, 3, 6), plasma binding of the drugs was apparently not affected by drug concentration over the dose and age ranges studied. Accordingly, the three binding values for each subject were averaged. With all four drugs, considerable interindividual variability in the extent of binding was present (Table I). When expressed in terms of free drug, lorazepam exhibited an almost twofold, chlordiazepoxide and diazepam a fourfold, and oxazepam a 20-fold range between the highest and lowest values. Preliminary studies indicated that the coefficient of variation for binding was <0.7% for all of the drugs, and, therefore, the observed variability did not represent a methodological artifact.

No statistically significant linear correlations were seen betweeen the extent of drug binding with serum albumin, total protein, or subject age. However, there were significant relationships between the binding of the four drugs (Table II). Previous binding studies with human serum albumin indicated that the benzodiazepines are mainly bound to a single class of binding sites (7). Thus, it is not surprising that the latter correlation was observed, although the coefficients of determination are quite small. This result, plus the lack of correlation of binding with serum albumin, suggests that other factors probably are involved in the overall binding phenomenon. The absence of any age-related changes in binding, despite the decrease in serum albumin with aging as noted previously (8) and observed in the present study, is consistent with this hypothesis. Therefore, the earlier observation with regard to lorazepam binding and age (1) was fortuitous.

The unbound benzodiazepine concentration is probably more important than the total drug level with regard to pharmacological response. Moreover, for the investigated drugs, clearance from the circulation and extravascular distribution are determined by the unbound fraction (1–4, 9). Therefore, the wide variability in observed binding suggests that this factor must be considered in the interpretation of pharmacodynamic and pharmacokinetic studies with the benzodiazepines, as exemplified by recent studies on sex differences in chlordiazepoxide disposition (10).

[6] Dianorm equilibrium dialyzing system, Spectrum Medical Industries, Los Angeles, CA 90054.

[7] Spectrapore membrane No. 2, Spectrum Medical Industries, Los Angeles, CA 90054.

[8] Aqueous counting scintillant, Amersham Corp., Arlington Heights, IL 60005.

[9] ISOCAP 300, Searle Analytic Inc., Des Plaines, IL 60018.

REFERENCES

(1) J. W. Kraus, J. P. Marshall, R. A. Branch, G. R. Wilkinson, and S. Schenker, *Clin. Pharmacol. Ther.*, **24**, 411 (1978).

(2) U. Klotz, G. R. Avant, A. M. Hoyumpa, S. Schenker, and G. R. Wilkinson, *J. Clin. Invest.*, **55**, 347 (1975).

(3) R. K. Roberts, R. A. Branch, G. R. Wilkinson, and S. Schenker, *Gastroenterology*, **75**, 479 (1978).

(4) H. J. Shull, Jr., G. R. Wilkinson, R. F. Johnson, and S. Schenker, *Ann. Intern. Med.*, **84**, 420 (1976).

(5) H. C. Weder, J. Schildknecht, and A. Kesselring, *Am. Lab.*, **10**, 15 (1971).

(6) E. van der Klein, *Arch. Int. Pharmacodyn. Ther.*, **179**, 15 (1969).

(7) W. Muller and U. Wollert, *Naunyn-Schmiedebergs Arch. Pharmacol.*, **280**, 229 (1973).

(8) E. Woodford-Williams, A. S. Alvares, D. Webster, B. Landless, and M. P. Dixon, *Gerontologia*, **10**, 86 (1964).

(9) G. R. Wilkinson and D. G. Shand, *Clin. Pharmacol. Ther.*, **18**, 377 (1975).

(10) R. K. Roberts, P. V. Desmond, G. R. Wilkinson, and S. Schenker, *ibid.*, **25**, 826 (1979).

ACKNOWLEDGMENTS

Supported by the Medical Research Service of the Veterans Administration and National Institutes of Health Grants AA00267, GM15341, and 5 M01 RR0095.

Identification of an Imidazolinium Salt, the Major Product from Reaction of Benzathine with Iodine

W. L. WILSON and M. J. LeBELLE ˣ

Received February 9, 1979, from the *Drug Research Laboratories, Health Protection Branch, Health and Welfare Canada, Tunney's Pasture, Ottawa, Canada K1A 0L2.* Accepted for publication April 4, 1979.

Abstract □ The isolation and identification of an imidazolinium salt are described. Unambiguous determination of structure was accomplished by independent synthesis. The isolated product interferes in the iodometric assay of the benzathine salts of penicillin.

Keyphrases □ Imidazolinium salts—analysis, product from reaction of benzathine with iodine □ Penicillin V benzathine—analysis, iodometric assay, interference by imidazolinium salt reaction product □ Iodometric assays—penicillin V benzathine, interference by imidazolinium salt

A recent report (1) described the interference of benzathine (I) in the official iodometric assay of penicillin V benzathine as presently described in the "Code of Federal Regulations" (CFR) (2). A high-performance liquid chromatographic (HPLC) method (3) of analysis for formulations containing this drug was suggested subsequently.

The present article describes the isolation and identification of an imidazolinium salt (II) as the product from the reaction of iodine with benzathine.

EXPERIMENTAL[1]

1,3-Dibenzyl-2-phenylimidazolinium Triiodide (II)—To 4.0 g of I in 5 ml of methanol at room temperature were added 5-ml aliquots of a methanolic iodine solution (2.5 g in 125 ml); the color was allowed to discharge after each addition. When a reddish color persisted, addition of methanolic iodine was continued until the precipitation of a red product was complete. The red solid was removed by filtration, and recrystallization from methanol–acetone yielded 2.1 g of II as deep-red needles, mp 163.5–165° [lit. (4) mp 165–166°]; NMR (acetone-d_6): δ 4.22 (s, 4, H_2C-4, H_2C-5), 4.68 (s, 4, H_2C-phenyl), 7.42 (s, 10, C-phenyl), and 7.85 (s, 5, phenyl-C-2).

Anal.—Calc. for $C_{23}H_{23}I_3N_2$ (mol. wt. 708.15): C, 39.01; H, 3.27; I, 53.76; N, 3.96. Found: C, 39.18; H, 3.36; I, 53.69; N, 4.05.

Conversion of II to *N*-Benzoyl-*N,N*-dibenzylethylenediamine (IV)—To a slurry of 1.303 g of II in 20 ml of methanol was added a saturated methanolic solution of sodium thiosulfate until a colorless solution was obtained. The solution was evaporated to dryness, and the residue was dissolved in chloroform and evaporated to dryness to give 934 mg of III as a pale-yellow foam; IR (film): 3030, 2915 (C–H), 1590 (C=N⁺<), 1250 (C–N), 1580, 1450, 750, and 700 (aromatic) cm^{-1}; NMR ($CDCl_3$): δ 4.17 (s, 4, H_2C-4, H_2C-5), 4.62 (s, 4, H_2C-phenyl), 7.37 (s, 10, C-phenyl), and 7.60–8.13 (m, 5, phenyl-C-2).

To 200 mg of III in 3 ml of methanol was added 3 ml of 3 *N* NaOH, and the solution was heated at 40° for 1.5 hr. Extraction with chloroform

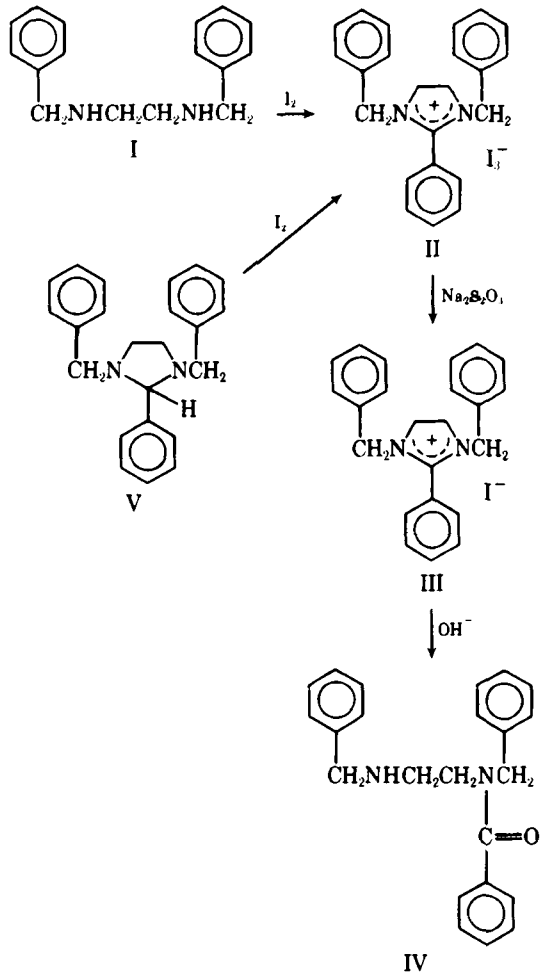

Scheme I

[1] NMR spectra were obtained using Bruker WP-80 and Varian A-60A instruments. IR spectra were obtained on a Beckman IR-20 spectrophotometer. All melting points are uncorrected.

0022-3549/79/1000-1322$01.00/0
© 1979, American Pharmaceutical Association

(2) U. Klotz, G. R. Avant, A. M. Hoyumpa, S. Schenker, and G. R. Wilkinson, *J. Clin. Invest.*, **55**, 347 (1975).

(3) R. K. Roberts, R. A. Branch, G. R. Wilkinson, and S. Schenker, *Gastroenterology*, **75**, 479 (1978).

(4) H. J. Shull, Jr., G. R. Wilkinson, R. F. Johnson, and S. Schenker, *Ann. Intern. Med.*, **84**, 420 (1976).

(5) H. C. Weder, J. Schildknecht, and A. Kesselring, *Am. Lab.*, **10**, 15 (1971).

(6) E. van der Klein, *Arch. Int. Pharmacodyn. Ther.*, **179**, 15 (1969).

(7) W. Muller and U. Wollert, *Naunyn-Schmiedebergs Arch. Pharmacol.*, **280**, 229 (1973).

(8) E. Woodford-Williams, A. S. Alvares, D. Webster, B. Landless, and M. P. Dixon, *Gerontologia*, **10**, 86 (1964).

(9) G. R. Wilkinson and D. G. Shand, *Clin. Pharmacol. Ther.*, **18**, 377 (1975).

(10) R. K. Roberts, P. V. Desmond, G. R. Wilkinson, and S. Schenker, *ibid.*, **25**, 826 (1979).

ACKNOWLEDGMENTS

Supported by the Medical Research Service of the Veterans Administration and National Institutes of Health Grants AA00267, GM15341, and 5 M01 RR0095.

Identification of an Imidazolinium Salt, the Major Product from Reaction of Benzathine with Iodine

W. L. WILSON and M. J. LeBELLE ˣ

Received February 9, 1979, from the *Drug Research Laboratories, Health Protection Branch, Health and Welfare Canada, Tunney's Pasture, Ottawa, Canada K1A 0L2.* Accepted for publication April 4, 1979.

Abstract □ The isolation and identification of an imidazolinium salt are described. Unambiguous determination of structure was accomplished by independent synthesis. The isolated product interferes in the iodometric assay of the benzathine salts of penicillin.

Keyphrases □ Imidazolinium salts—analysis, product from reaction of benzathine with iodine □ Penicillin V benzathine—analysis, iodometric assay, interference by imidazolinium salt reaction product □ Iodometric assays—penicillin V benzathine, interference by imidazolinium salt

A recent report (1) described the interference of benzathine (I) in the official iodometric assay of penicillin V benzathine as presently described in the "Code of Federal Regulations" (CFR) (2). A high-performance liquid chromatographic (HPLC) method (3) of analysis for formulations containing this drug was suggested subsequently.

The present article describes the isolation and identification of an imidazolinium salt (II) as the product from the reaction of iodine with benzathine.

EXPERIMENTAL[1]

1,3-Dibenzyl-2-phenylimidazolinium Triiodide (II)—To 4.0 g of I in 5 ml of methanol at room temperature were added 5-ml aliquots of a methanolic iodine solution (2.5 g in 125 ml); the color was allowed to discharge after each addition. When a reddish color persisted, addition of methanolic iodine was continued until the precipitation of a red product was complete. The red solid was removed by filtration, and recrystallization from methanol–acetone yielded 2.1 g of II as deep-red needles, mp 163.5–165° [lit. (4) mp 165–166°]; NMR (acetone-d_6): δ 4.22 (s, 4, H_2C-4, H_2C-5), 4.68 (s, 4, H_2C-phenyl), 7.42 (s, 10, C-phenyl), and 7.85 (s, 5, phenyl-C-2).

Anal.—Calc. for $C_{23}H_{23}I_3N_2$ (mol. wt. 708.15): C, 39.01; H, 3.27; I, 53.76; N, 3.96. Found: C, 39.18; H, 3.36; I, 53.69; N, 4.05.

Conversion of II to *N*-Benzoyl-*N,N*-dibenzylethylenediamine (IV)—To a slurry of 1.303 g of II in 20 ml of methanol was added a saturated methanolic solution of sodium thiosulfate until a colorless solution was obtained. The solution was evaporated to dryness, and the residue was dissolved in chloroform and evaporated to dryness to give 934 mg of III as a pale-yellow foam; IR (film): 3030, 2915 (C–H), 1590 (C=N⁺<), 1250 (C–N), 1580, 1450, 750, and 700 (aromatic) cm^{-1}; NMR ($CDCl_3$): δ 4.17 (s, 4, H_2C-4, H_2C-5), 4.62 (s, 4, H_2C-phenyl), 7.37 (s, 10, C-phenyl), and 7.60–8.13 (m, 5, phenyl-C-2).

To 200 mg of III in 3 ml of methanol was added 3 ml of 3 *N* NaOH, and the solution was heated at 40° for 1.5 hr. Extraction with chloroform

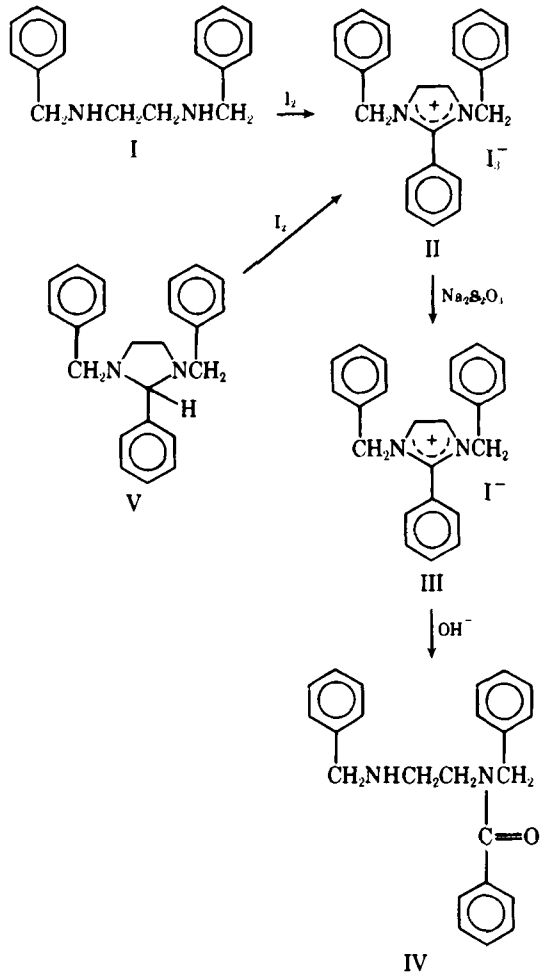

Scheme I

[1] NMR spectra were obtained using Bruker WP-80 and Varian A-60A instruments. IR spectra were obtained on a Beckman IR-20 spectrophotometer. All melting points are uncorrected.

0022-3549/79/1000-1322$01.00/0
© 1979, American Pharmaceutical Association

yielded 137 mg of IV as a colorless oil; IR (film): 3310 (N–H), 3050, 3020, 1600, 750, 700 (aromatic), 2910, 2810 (C–H), and 1635 (C=O) cm^{-1}; NMR ($CDCl_3$): δ 1.34 (s, 1, N–H, exchangeable), 2.66–2.94 (m, 2, C–CH_2–NH), 3.25–3.78 [m, 4, C–CH_2–N–C(–)=O and NH–CH_2-phenyl], 4.66 (s, 2, phenyl-CH_2–N–C=O), and 7.13–7.50 (m, 15, aromatic).

Benzoylation of Benzathine to Give IV—To 960 mg of I in 3 ml of chloroform and 0.5 ml of triethylamine was added dropwise 550 mg of benzoyl chloride in 1 ml of chloroform. After 1.5 hr at room temperature, the solution was added to 20 ml of water, brought to pH 11 with sodium hydroxide, and extracted with chloroform. Workup afforded 1.5 g of white solid. A portion of the crude product was chromatographed by preparative TLC to yield 65 mg of IV.

1,3-Dibenzyl-2-phenyltetrahydroimidazole (V)—Equimolar (0.02 *M*) amounts of I and benzaldehyde with 150 mg of *p*-toluenesulfonic acid in 100 ml of benzene were condensed over 3 hr to yield a white solid, 4.1 g, mp 99–99.5° (hexane) [lit. (5) mp 99°].

Oxidation of V to II—To 1.235 g (3.76 mmoles) of V in 10 ml of benzene was added dropwise 956 mg (3.76 mmoles) of iodine in 100 ml of benzene. To the resulting solution was added, all at once, an equal aliquot of iodine in benzene. The solution was cooled, and the red solid, 2.8 g (90%), was collected. Recrystallization from methanol–acetone gave deep-red needles of II, mp 163.5–166°.

RESULTS AND DISCUSSION

The reaction of benzathine with iodine in methanol resulted in the isolation of one product; the NMR spectrum was consistent with Structure II. Further confirmation of Structure II was derived from the partial reduction of II to the iodide III, which, under basic conditions, yielded the ring-opened benzoylbenzathine (IV), analogous to other imidazolinium salts (6).

Unambiguous confirmation of Structure II resulted from the iodine oxidation of the tetrahydroimidazole (V) to II.

Product II probably results from a reaction sequence beginning with oxidation of benzathine to give an imine, which then hydrolyzes to give the benzaldehyde (Scheme I). The benzaldehyde is free to condense with intact benzathine to give V, which oxidizes with excess iodine to II.

Therefore, this reaction sequence leads to erroneously low results in the CFR iodometric assay as presently described for penicillin V benzathine. It also accounts for the fact that interference by benzathine in the iodometric assay is dependent on pH since the initial oxidation requires a free amino function.

REFERENCES

(1) M. J. LeBelle and W. L. Wilson, *J. Pharm. Sci.*; **67**, 1495 (1978).

(2) "Code of Federal Regulations," part 440, title 21, 1977.

(3) M. LeBelle, K. Graham, and W. L. Wilson, *J. Pharm. Sci.*, **68**, 555 (1979).

(4) G. Lob, *Rec. Trav. Chim. Pays-Bas*, **55**, 859 (1936).

(5) A. W. Archer, *J. Pharm. Pharmacol.*, **17**, 376 (1965).

(6) D. R. Robinson, *J. Am. Chem. Soc.*, **92**, 3138 (1970).

ACKNOWLEDGMENTS

Presented in part at the APhA Academy of Pharmaceutical Sciences, Hollywood, Fla., meeting, November 1978.

Capacity-Limited Gut Wall Metabolism of 5-Aminosalicylic Acid, a Therapeutically Active Metabolite of Sulfasalazine, in Rats

HENRY J. PIENIASZEK, Jr. *, and THEODORE R. BATES ‡x

Received January 18, 1979, from the *Department of Pharmaceutics, School of Pharmacy, State University of New York at Buffalo, Amherst, NY 14260.* Accepted for publication April 6, 1979.

*Present address: College of Pharmacy, University of Arizona, Tucson, AZ 87521. ‡Present address: Department of Pharmaceutics, School of Pharmacy, University of Pittsburgh, Pittsburgh, PA 15261.

Abstract □ The metabolic fate of 5-aminosalicylic acid (reported to be the active therapeutic moiety of sulfasalazine) was assessed in fasting rats as a function of dose (25–200 mg/kg) and administration route (oral, intraperitoneal, and intravenous). 5-Aminosalicylic acid is subject to both capacity-limited presystemic (apparently during first passage through the intestinal epithelium) and systemic acetylation. The possibility exists that 5-aminosalicylic acid also is acetylated presystemically after oral sulfasalazine administration to patients with inflammatory bowel disease. Any alteration in the absorption rate of this active metabolite from the colon could affect the time course of local anti-inflammatory activity if *N*-acetyl-5-aminosalicylic acid is inactive or less active than 5-aminosalicylic acid.

Keyphrases □ 5-Aminosalicylic acid—metabolism, gut wall, effect of dose and administration route □ Sulfasalazine metabolites—5-aminosalicylic acid, metabolism, gut wall, effect of dose and administration route □ Antibacterial agents—sulfasalazine, 5-aminosalicylic acid metabolite, metabolism, gut wall, effect of dose and administration route □ Intestinal epithelium—metabolism, 5-aminosalicylic acid, effect of dose and administration route

Sulfasalazine (salicylazosulfapyridine) is widely used for the treatment of ulcerative colitis and Crohn's disease (1). After oral administration to rats and humans, the drug is almost completely metabolized in the colon and cecum by bacterial azo reductases. The metabolic products sulfapyridine and 5-aminosalicylic acid are absorbed from the colon and are further metabolized to N^4-acetylsulfapyridine, to the *O*-glucuronide and *O*-sulfate conjugates of 5′-hydroxysulfapyridine and N^4-acetyl-5′-hydroxysulfapyridine, and to *N*-acetyl-5-aminosalicylic acid (2–6).

Several investigators (3, 5–8) suggested that sulfasalazine itself may not be an active therapeutic agent but may serve only as a means of delivering its metabolic products, 5-aminosalicylic acid (a possible anti-inflammatory agent) and sulfapyridine (an antibacterial agent), to the inflammation site in the colon where either or both of these agents exert the desired pharmacological effects. Recent studies in which sulfasalazine, 5-aminosalicylic acid, and sulfapyridine were administered rectally to patients with ulcerative colitis (9) and idiopathic proctitis (10) suggest that 5-aminosalicylic acid is the active therapeutic moiety of sulfasalazine and acts topically on the inflammed mucosa. Although this finding requires confirmation in a larger patient population and does not explain the mode of action of 5-aminosalicylic acid, it may be relevant that sulfasalazine and 5-aminosalicylic acid are inhibitors of prostaglandin synthesis (10–13) and that patients with active ulcerative colitis have increased fecal levels and colonic venous blood levels of prostaglandins (13). Prostaglandins are known to be involved in inflammation

0022-3549/79/1000-1323$01.00/0

© 1979, American Pharmaceutical Association

yielded 137 mg of IV as a colorless oil; IR (film): 3310 (N–H), 3050, 3020, 1600, 750, 700 (aromatic), 2910, 2810 (C–H), and 1635 (C=O) cm^{-1}; NMR ($CDCl_3$): δ 1.34 (s, 1, N–H, exchangeable), 2.66–2.94 (m, 2, C–CH_2–NH), 3.25–3.78 [m, 4, C–CH_2–N–C(–)=O and NH–CH_2-phenyl], 4.66 (s, 2, phenyl-CH_2–N–C=O), and 7.13–7.50 (m, 15, aromatic).

Benzoylation of Benzathine to Give IV—To 960 mg of I in 3 ml of chloroform and 0.5 ml of triethylamine was added dropwise 550 mg of benzoyl chloride in 1 ml of chloroform. After 1.5 hr at room temperature, the solution was added to 20 ml of water, brought to pH 11 with sodium hydroxide, and extracted with chloroform. Workup afforded 1.5 g of white solid. A portion of the crude product was chromatographed by preparative TLC to yield 65 mg of IV.

1,3-Dibenzyl-2-phenyltetrahydroimidazole (V)—Equimolar (0.02 *M*) amounts of I and benzaldehyde with 150 mg of *p*-toluenesulfonic acid in 100 ml of benzene were condensed over 3 hr to yield a white solid, 4.1 g, mp 99–99.5° (hexane) [lit. (5) mp 99°].

Oxidation of V to II—To 1.235 g (3.76 mmoles) of V in 10 ml of benzene was added dropwise 956 mg (3.76 mmoles) of iodine in 100 ml of benzene. To the resulting solution was added, all at once, an equal aliquot of iodine in benzene. The solution was cooled, and the red solid, 2.8 g (90%), was collected. Recrystallization from methanol–acetone gave deep-red needles of II, mp 163.5–166°.

RESULTS AND DISCUSSION

The reaction of benzathine with iodine in methanol resulted in the isolation of one product; the NMR spectrum was consistent with Structure II. Further confirmation of Structure II was derived from the partial reduction of II to the iodide III, which, under basic conditions, yielded the ring-opened benzoylbenzathine (IV), analogous to other imidazolinium salts (6).

Unambiguous confirmation of Structure II resulted from the iodine oxidation of the tetrahydroimidazole (V) to II.

Product II probably results from a reaction sequence beginning with oxidation of benzathine to give an imine, which then hydrolyzes to give the benzaldehyde (Scheme I). The benzaldehyde is free to condense with intact benzathine to give V, which oxidizes with excess iodine to II.

Therefore, this reaction sequence leads to erroneously low results in the CFR iodometric assay as presently described for penicillin V benzathine. It also accounts for the fact that interference by benzathine in the iodometric assay is dependent on pH since the initial oxidation requires a free amino function.

REFERENCES

(1) M. J. LeBelle and W. L. Wilson, *J. Pharm. Sci.*; **67**, 1495 (1978).

(2) "Code of Federal Regulations," part 440, title 21, 1977.

(3) M. LeBelle, K. Graham, and W. L. Wilson, *J. Pharm. Sci.*, **68**, 555 (1979).

(4) G. Lob, *Rec. Trav. Chim. Pays-Bas*, **55**, 859 (1936).

(5) A. W. Archer, *J. Pharm. Pharmacol.*, **17**, 376 (1965).

(6) D. R. Robinson, *J. Am. Chem. Soc.*, **92**, 3138 (1970).

ACKNOWLEDGMENTS

Presented in part at the APhA Academy of Pharmaceutical Sciences, Hollywood, Fla., meeting, November 1978.

Capacity-Limited Gut Wall Metabolism of 5-Aminosalicylic Acid, a Therapeutically Active Metabolite of Sulfasalazine, in Rats

HENRY J. PIENIASZEK, Jr. *, and THEODORE R. BATES ‡x

Received January 18, 1979, from the *Department of Pharmaceutics, School of Pharmacy, State University of New York at Buffalo, Amherst, NY 14260.* Accepted for publication April 6, 1979.

*Present address: College of Pharmacy, University of Arizona, Tucson, AZ 87521. ‡Present address: Department of Pharmaceutics, School of Pharmacy, University of Pittsburgh, Pittsburgh, PA 15261.

Abstract □ The metabolic fate of 5-aminosalicylic acid (reported to be the active therapeutic moiety of sulfasalazine) was assessed in fasting rats as a function of dose (25–200 mg/kg) and administration route (oral, intraperitoneal, and intravenous). 5-Aminosalicylic acid is subject to both capacity-limited presystemic (apparently during first passage through the intestinal epithelium) and systemic acetylation. The possibility exists that 5-aminosalicylic acid also is acetylated presystemically after oral sulfasalazine administration to patients with inflammatory bowel disease. Any alteration in the absorption rate of this active metabolite from the colon could affect the time course of local anti-inflammatory activity if *N*-acetyl-5-aminosalicylic acid is inactive or less active than 5-aminosalicylic acid.

Keyphrases □ 5-Aminosalicylic acid—metabolism, gut wall, effect of dose and administration route □ Sulfasalazine metabolites—5-aminosalicylic acid, metabolism, gut wall, effect of dose and administration route □ Antibacterial agents—sulfasalazine, 5-aminosalicylic acid metabolite, metabolism, gut wall, effect of dose and administration route □ Intestinal epithelium—metabolism, 5-aminosalicylic acid, effect of dose and administration route

Sulfasalazine (salicylazosulfapyridine) is widely used for the treatment of ulcerative colitis and Crohn's disease (1). After oral administration to rats and humans, the drug is almost completely metabolized in the colon and cecum by bacterial azo reductases. The metabolic products sulfapyridine and 5-aminosalicylic acid are absorbed from the colon and are further metabolized to N^4-acetylsulfapyridine, to the *O*-glucuronide and *O*-sulfate conjugates of 5′-hydroxysulfapyridine and N^4-acetyl-5′-hydroxysulfapyridine, and to *N*-acetyl-5-aminosalicylic acid (2–6).

Several investigators (3, 5–8) suggested that sulfasalazine itself may not be an active therapeutic agent but may serve only as a means of delivering its metabolic products, 5-aminosalicylic acid (a possible anti-inflammatory agent) and sulfapyridine (an antibacterial agent), to the inflammation site in the colon where either or both of these agents exert the desired pharmacological effects. Recent studies in which sulfasalazine, 5-aminosalicylic acid, and sulfapyridine were administered rectally to patients with ulcerative colitis (9) and idiopathic proctitis (10) suggest that 5-aminosalicylic acid is the active therapeutic moiety of sulfasalazine and acts topically on the inflammed mucosa. Although this finding requires confirmation in a larger patient population and does not explain the mode of action of 5-aminosalicylic acid, it may be relevant that sulfasalazine and 5-aminosalicylic acid are inhibitors of prostaglandin synthesis (10–13) and that patients with active ulcerative colitis have increased fecal levels and colonic venous blood levels of prostaglandins (13). Prostaglandins are known to be involved in inflammation

0022-3549/79/1000-1323$01.00/0

© 1979, American Pharmaceutical Association

Table I—Effect of Dose and Administration Route on 5-Aminosalicylic Acid Biotransformation in Fasting Rats

Administration Route	Dose of 5-Aminosalicylic Acid[a], mg/kg	Mean Urinary Excretion in 48 hr ($n = 4$) ± SE		
		Total Recovery, % of dose	N-Acetyl-5-aminosalicylic Acid, % of total[b]	Free 5-Aminosalicylic Acid, % of total[b]
Oral	25	90.5 ± 3.8	82.0 ± 2.8	18.0 ± 2.8
	50	91.0 ± 5.7	69.8 ± 4.3	30.2 ± 4.3
	100	95.2 ± 7.1	50.1 ± 5.5	49.9 ± 5.5
	200	101 ± 3.3	33.2 ± 2.4	66.8 ± 2.4
Intraperitoneal	25	101 ± 2.4	54.2 ± 4.3	45.8 ± 4.3
	50	104 ± 1.7	41.3 ± 3.0	58.7 ± 3.0
	200	104 ± 3.3	29.8 ± 5.9	70.2 ± 5.9
Intravenous	25	102 ± 2.1	55.8 ± 6.4	44.2 ± 6.4
	50	92.3 ± 1.9	44.8 ± 4.8	55.2 ± 4.8
	200	103 ± 2.4	25.9 ± 5.2	74.1 ± 5.2

[a] Administered as an aqueous solution (pH 7). [b] Free and acetylated 5-aminosalicylic acid.

(10–13). No information exists in the literature related to factors affecting the biotransformation of 5-aminosalicylic acid.

The present study used the rat as an animal model to assess whether 5-aminosalicylic acid is acetylated presystemically after oral administration and to explore the possible dose-dependent characteristics of this metabolic process.

EXPERIMENTAL

Reagents—5-Aminosalicylic acid[1] was purified prior to use (14). Reagent grade sodium nitrite[2], ammonium sulfamate[2], N-(1-naphthyl)-ethylenediamine dihydrochloride[2], acetic anhydride[2], and isopropylacetone[2] (methyl isobutylketone) were used as received.

Animals—Adult male Sprague–Dawley rats[3], 250–350 g, were fasted for 16 hr prior to the studies but had access to water at all times. Food[4] was supplied 24 hr after drug administration. All biotransformation studies were initiated between 9:00 and 10:00 am to eliminate possible circadian variation.

Effect of Dose and Administration Route on 5-Aminosalicylic Acid Metabolism—The same four fasting rats received single doses of 5-aminosalicylic acid (in aqueous solution at pH 7), 25–200 mg/kg po, ip, or iv, in two four-way and one two-way crossover studies. In a subsequent study, 8.33 mg of 5-aminosalicylic acid/kg was administered intraperitoneally to the fasting animals every 20 min for three doses. Dosing volumes of 5.0 and 2.5 ml/kg were used for oral and parenteral drug administrations, respectively.

Quantitative urine collections were made daily for 2 days, and the specimens were stored at −20° pending assay for free and N-acetylated 5-aminosalicylic acid. A 4-day washout period was allowed between drug administrations.

Assay of Free and Acetylated 5-Aminosalicylic Acid in Urine—A specific colorimetric method (15) was employed. Accordingly, 1 ml of urine (previously centrifuged and diluted with distilled water when necessary) was acidified with 1.0 ml of 1.0 M HCl, and N-acetyl-5-aminosalicylic acid was first extracted directly into 5.0 ml of isopropylacetone and then reextracted from a 4.0-ml aliquot of the organic (upper) phase into 3.0 ml of pH 6.0 phosphate buffer. After centrifugation, a 0.5-ml aliquot of the buffered aqueous phase was withdrawn, mixed with 0.5 ml of 8.0 M HCl in a polytef-lined screw-capped culture tube, and heated at 100° for 45 min to effect metabolite deacetylation.

The acidic solution was cooled to room temperature, and the free 5-aminosalicylic acid was subjected to a modified Bratton–Marshall reaction (16) by adding, at 3-min intervals, 1.0-ml quantities of aqueous solutions of sodium nitrite (0.12%), ammonium sulfamate (0.8%), and N-(1-naphthyl)ethylenediamine dihydrochloride (0.8%). The reaction mixture was stored in the dark for 4 hr to allow for maximum color development, and the absorbance of the violet-colored solution was measured on a double-beam spectrophotometer[5] at 560 nm using 1.0-cm cells.

Total 5-aminosalicylic acid (free and acetylated) was analyzed by the same procedure after quantitative acetylation of the free 5-aminosalicylic acid content of a second biological sample with 20 μl of acetic anhydride. The amount of free 5-aminosalicylic acid present in the urine specimen was determined from the difference between the total and acetylated 5-aminosalicylic acid assay results. A linear Beer's law calibration plot was constructed by subjecting standard samples containing 0–70 μg of 5-aminosalicylic acid/ml to the procedure for total 5-aminosalicylic acid.

Twenty-four-hour urine blank values were small but were used to correct all free and acetylated 5-aminosalicylic acid excretion data.

Statistical Analysis—Differences among more than two mean values were evaluated by analysis of variance, and differences between any two means were compared using Tukey's multiple comparison test (at $p = 0.05$) or the Student paired t test (17, 18).

RESULTS AND DISCUSSION

The results of the study of 5-aminosalicylic acid biotransformation after intraperitoneal, intravenous, and oral administration of 25–200-mg/kg doses to the same group of four fasting rats are presented in Table I. Analyses of variance indicated that the urinary recovery of total 5-aminosalicylic acid (sum of free and acetylated drug) was independent of dose and administration route ($F_{9,30} = 2.17$, $p > 0.05$). Recovery ranged from 91 to 104% of the dose, with 90–95% of the total recovery being achieved within 24 hr after drug administration.

The mean fraction of total 5-aminosalicylic acid excreted in the urine as the N-acetylated metabolite significantly decreased as the intraperitoneal and intravenous doses of 5-aminosalicylic acid were increased from 25 to 200 mg/kg ($F_{2,9} = 7.24$ for the intraperitoneal route and $F_{2,9} = 7.58$ for the intravenous route, $p < 0.025$; Table I). Lukas *et al.* (19) demonstrated that drugs administered intraperitoneally are absorbed primarily into the portal circulation and, therefore, must pass through the liver before reaching the systemic circulation. After intravenous administration, only 28% of the cardiac output reaches the liver (19). Thus, the fact that no significant difference in the degree of acetylation existed between the two routes after each dose ($p > 0.05$; Table I) suggests that 5-aminosalicylic acid is not subject to first-pass liver metabolism and that its systemic elimination is capacity limited. The lack of an effect of the intraperitoneal administration rate on drug biotransformation after the 25-mg/kg dose (Table II) suggests that systemic 5-aminosalicylic acid elimination is linear at or below this dosage level.

Dose-dependent decreases in the extent of 5-aminosalicylic acid metabolism were also observed after oral administration ($F_{3,12} = 10.8$, $p < 0.001$; Table I). The drug fraction converted to the acetylated metabolite after the 25- and 50-mg/kg po doses were greater than those observed after comparable intraperitoneal and intravenous doses ($p < 0.05$, Tukey's multiple range tests; Table I). These findings suggest that 5-aminosalicylic acid is subject to capacity-limited presystemic (gut wall) and systemic acetylation after oral administration. Based on the average metabolic data presented in Table I, the extent of acetylation by the intestinal epithelium was estimated to be ~25–28% of a 25- or 50-mg/kg po dose. The N-acetyltransferase enzyme systems at the presystemic site appear to be nearly saturated after a 200-mg 5-aminosalicylic acid/kg dose ($F_{2,9} = 0.579$, $p > 0.1$; Table I).

The ability of enzyme systems present in the intestinal epithelium to acetylate the structurally related drugs p-aminobenzoic acid and p-aminosalicylic acid *in vitro* is well documented (20, 21). p-Aminobenzoic acid (22) and p-aminosalicylic acid (23, 24) are also subject to capacity-

[1] Aldrich Chemical Co., Milwaukee, Wis.
[2] Fisher Scientific Co., Rochester, N.Y.
[3] Blue Spruce Farms, Altamont, N.Y.
[4] Charles River rat chow.
[5] Beckman DB-G, Beckman Instruments, Fullerton, Calif.

Table II—Effect of Administration Rate on 5-Aminosalicylic Acid Biotransformation in Fasting Rats

Rat	Urinary Excretion in 48 hr: Total Recovery, % of dose		*N*-Acetyl-5-aminosalicylic Acid, % of total[a]	
	Regimen A[b]	Regimen B[c]	Regimen A[b]	Regimen B[c]
1	99.3	104	58.2	53.8
2	104	103	63.4	57.4
3	105	98.2	43.7	42.8
4	94.4	99.0	51.6	51.1
Mean	101	101	54.2	51.3
SE	2.4	1.4	4.3	3.1
Paired *t* test	N.S. ($p > 0.8$)		N.S. ($p > 0.1$)	

[a] Free and acetylated 5-aminosalicylic acid. [b] Regimen A = single 25 mg/kg ip dose. [c] Regimen B = 8.33 mg/kg ip every 20 min for three doses.

limited acetylation during their intestinal absorption in humans. Studies are currently in progress to determine whether a food-induced decrease in the gastric emptying rate can, by decreasing the rate of 5-aminosalicylic acid absorption, further increase the extent of gut wall metabolism.

These results demonstrate that orally administered 5-aminosalicylic acid is subject to both capacity-limited gut wall and systemic metabolism. A similar capacity-limited presystemic metabolic profile for 5-aminosalicylic acid may exist after oral administration of sulfasalazine to patients with ulcerative colitis and Crohn's disease. If *N*-acetyl-5-aminosalicylic acid is inactive or less active than 5-aminosalicylic acid (a possibility remaining to be explored), then the time course of local anti-inflammatory activity may be affected.

REFERENCES

(1) G. H. Smith and T. G. Tong, *J. Am. Pharm. Assoc.*, **NS15**, 202 (1975).

(2) M. A. Peppercorn and P. Goldman, *J. Pharmacol. Exp. Ther.*, **181**, 555 (1972).

(3) M. A. Peppercorn and P. Goldman, *Gastroenterology*, **64**, 240 (1973).

(4) H. Schroder and B. E. Gustafsson, *Xenobiotica*, **3**, 225 (1973).

(5) H. Schroder and D. E. S. Campbell, *Clin. Pharmacol. Ther.*, **13**, 539 (1972).

(6) H. Schroder, R. M. Lewkonia, and D. A. Price Evans, *Clin. Pharmacol. Ther.*, **14**, 802 (1973).

(7) P. Goldman, M. A. Peppercorn, and B. R. Goldin, *Am. J. Clin. Nutr.*, **27**, 1348 (1974).

(8) P. Goldman and M. A. Peppercorn, *N. Engl. J. Med.*, **293**, 20 (1975).

(9) A. K. Azad Khan, J. Piris, and S. C. Truelove, *Lancet*, **2**, 892 (1977).

(10) P. A. M. vanHees, J. H. M. vanTongeren, J. H. Bakker, and H. J. J. vanLier, *Lancet*, **2**, 277 (1978).

(11) S. R. Gould, *Lancet*, **2**, 988 (1975).

(12) S. R. Gould, *Prostaglandins*, **2**, 489 (1976).

(13) S. R. Gould and J. E. Lennard-Jones, *Gut*, **17**, 828 (1976).

(14) K.-A. Hansson, *Acta Pharm. Suec.*, **10**, 153 (1973).

(15) H. J. Pieniaszek, Jr. and T. R. Bates, *Res. Commun. Chem. Pathol. Pharmacol.*, **12**, 571 (1975).

(16) K.-A. Hansson and M. Sandberg, *Acta Pharm. Suec.*, **10**, 87 (1973).

(17) G. W. Snedecor and W. G. Cochran, "Statistical Methods," 6th ed., Iowa State University Press, Ames, Iowa, 1967, pp. 258–298.

(18) W. C. Guenther, "Analysis of Variance," Prentice-Hall, Englewood Cliffs, N.J., 1964, pp. 54–57.

(19) G. Lukas, S. D. Bundle, and P. Greengard, *J. Pharmacol. Exp. Ther.*, **178**, 562 (1971).

(20) K. Hartiala, *Physiol. Rev.*, **53**, 496 (1973).

(21) D. J. Hearse and W. W. Weber, *Biochem. J.*, **132**, 519 (1973).

(22) M. M. Drucker, S. H. Blondheim, and L. Wislicki, *Clin. Sci.*, **27**, 133 (1964).

(23) J. G. Wagner, P. D. Holmes, P. K. Wilkinson, D. C. Blair, and R. G. Stoll, *Am. Rev. Respir. Dis.*, **108**, 536 (1973).

(24) P. Pentikainen, S. H. Wan, and D. L. Azarnoff, *ibid.*, **108**, 1340 (1973).

ACKNOWLEDGMENTS

Supported in part by Grants GM 20852 and GRS-RR0545415 from the National Institutes of Health, Bethesda, MD 20014.

4-Acetoxy-1,2,3,4-tetrahydro-2,2-dimethyl-6,7-methylenedioxyisoquinolinium Iodide, an Acetylcholine Analog

THOMAS J. SCHWAN ˣ, MARVIN M. GOLDENBERG, and NELSON J. MILES

Received December 26, 1978, from the *Scientific Affairs Department, Norwich-Eaton Pharmaceuticals, Division of Morton-Norwich Products, Inc., Norwich, NY 13815.* Accepted for publication April 2, 1979.

Abstract □ 4-Acetoxy - 1,2,3,4 - tetrahydro - 2,2-dimethyl-6,7-methylenedioxyisoquinolinium iodide, an analog of acetylcholine, was synthesized and a pharmacological profile of its GI effects was compiled. The agent inhibited dog colonic contraction in response to pelvic nerve stimulation and to acetylcholine. In rats, the compound markedly reduced gastric acid output and the volume of gastric secretions. The lack of inhibition of chromodacryorrhea production in response to carbachol indicates a lack of anticholinergic action. The agent failed to affect the acute inflammatory response of the rat hindpaw in response to carrageenan. The precursor of the compound was ineffective in the pharmacological tests.

Keyphrases □ Acetylcholine analogs—synthesis, pharmacodynamics, structure–activity relationships □ Cholinergic agents—acetylcholine analogs, synthesis, pharmacodynamics, structure–activity relationships □ Structure–activity relationships—acetylcholine analogs

As part of a program directed toward the synthesis of novel GI agents, an acetylcholine analog was desired in which the tetraalkylammonium function of the molecule was incorporated as part of a rigid annular system. Accordingly, a route to 4-acetoxy-1,2,3,4-tetrahydro-2,2-dimethyl-6,7-methylenedioxyisoquinolinium iodide (I) was devised.

DISCUSSION

Reaction of the previously reported (1) 4-hydroxy-6,7-methylenedioxy-1,2,3,4-tetrahydroisoquinoline (II) with methyl iodide gave the quaternary Compound III which, upon treatment with acetic anhydride, afforded the racemic acetylcholine analog I.

Compound I, 10 mg/kg iv in three dogs, caused marked, but brief (20 min), antagonism of colonic contractions in response to intermittent pelvic nerve stimulation (2). In addition, acetylcholine-induced con-

0022-3549/79/1000-1325$01.00/0

© 1979, American Pharmaceutical Association

Table II—Effect of Administration Rate on 5-Aminosalicylic Acid Biotransformation in Fasting Rats

Rat	Urinary Excretion in 48 hr: Total Recovery, % of dose		*N*-Acetyl-5-aminosalicylic Acid, % of total[a]	
	Regimen A[b]	Regimen B[c]	Regimen A[b]	Regimen B[c]
1	99.3	104	58.2	53.8
2	104	103	63.4	57.4
3	105	98.2	43.7	42.8
4	94.4	99.0	51.6	51.1
Mean	101	101	54.2	51.3
SE	2.4	1.4	4.3	3.1
Paired *t* test	N.S. ($p > 0.8$)		N.S. ($p > 0.1$)	

[a] Free and acetylated 5-aminosalicylic acid. [b] Regimen A = single 25 mg/kg ip dose. [c] Regimen B = 8.33 mg/kg ip every 20 min for three doses.

limited acetylation during their intestinal absorption in humans. Studies are currently in progress to determine whether a food-induced decrease in the gastric emptying rate can, by decreasing the rate of 5-aminosalicylic acid absorption, further increase the extent of gut wall metabolism.

These results demonstrate that orally administered 5-aminosalicylic acid is subject to both capacity-limited gut wall and systemic metabolism. A similar capacity-limited presystemic metabolic profile for 5-aminosalicylic acid may exist after oral administration of sulfasalazine to patients with ulcerative colitis and Crohn's disease. If *N*-acetyl-5-aminosalicylic acid is inactive or less active than 5-aminosalicylic acid (a possibility remaining to be explored), then the time course of local anti-inflammatory activity may be affected.

REFERENCES

(1) G. H. Smith and T. G. Tong, *J. Am. Pharm. Assoc.*, **NS15**, 202 (1975).

(2) M. A. Peppercorn and P. Goldman, *J. Pharmacol. Exp. Ther.*, **181**, 555 (1972).

(3) M. A. Peppercorn and P. Goldman, *Gastroenterology*, **64**, 240 (1973).

(4) H. Schroder and B. E. Gustafsson, *Xenobiotica*, **3**, 225 (1973).

(5) H. Schroder and D. E. S. Campbell, *Clin. Pharmacol. Ther.*, **13**, 539 (1972).

(6) H. Schroder, R. M. Lewkonia, and D. A. Price Evans, *Clin. Pharmacol. Ther.*, **14**, 802 (1973).

(7) P. Goldman, M. A. Peppercorn, and B. R. Goldin, *Am. J. Clin. Nutr.*, **27**, 1348 (1974).

(8) P. Goldman and M. A. Peppercorn, *N. Engl. J. Med.*, **293**, 20 (1975).

(9) A. K. Azad Khan, J. Piris, and S. C. Truelove, *Lancet*, **2**, 892 (1977).

(10) P. A. M. vanHees, J. H. M. vanTongeren, J. H. Bakker, and H. J. J. vanLier, *Lancet*, **2**, 277 (1978).

(11) S. R. Gould, *Lancet*, **2**, 988 (1975).

(12) S. R. Gould, *Prostaglandins*, **2**, 489 (1976).

(13) S. R. Gould and J. E. Lennard-Jones, *Gut*, **17**, 828 (1976).

(14) K.-A. Hansson, *Acta Pharm. Suec.*, **10**, 153 (1973).

(15) H. J. Pieniaszek, Jr. and T. R. Bates, *Res. Commun. Chem. Pathol. Pharmacol.*, **12**, 571 (1975).

(16) K.-A. Hansson and M. Sandberg, *Acta Pharm. Suec.*, **10**, 87 (1973).

(17) G. W. Snedecor and W. G. Cochran, "Statistical Methods," 6th ed., Iowa State University Press, Ames, Iowa, 1967, pp. 258–298.

(18) W. C. Guenther, "Analysis of Variance," Prentice-Hall, Englewood Cliffs, N.J., 1964, pp. 54–57.

(19) G. Lukas, S. D. Bundle, and P. Greengard, *J. Pharmacol. Exp. Ther.*, **178**, 562 (1971).

(20) K. Hartiala, *Physiol. Rev.*, **53**, 496 (1973).

(21) D. J. Hearse and W. W. Weber, *Biochem. J.*, **132**, 519 (1973).

(22) M. M. Drucker, S. H. Blondheim, and L. Wislicki, *Clin. Sci.*, **27**, 133 (1964).

(23) J. G. Wagner, P. D. Holmes, P. K. Wilkinson, D. C. Blair, and R. G. Stoll, *Am. Rev. Respir. Dis.*, **108**, 536 (1973).

(24) P. Pentikainen, S. H. Wan, and D. L. Azarnoff, *ibid.*, **108**, 1340 (1973).

ACKNOWLEDGMENTS

Supported in part by Grants GM 20852 and GRS-RR0545415 from the National Institutes of Health, Bethesda, MD 20014.

4-Acetoxy-1,2,3,4-tetrahydro-2,2-dimethyl-6,7-methylenedioxyisoquinolinium Iodide, an Acetylcholine Analog

THOMAS J. SCHWAN ˣ, MARVIN M. GOLDENBERG, and NELSON J. MILES

Received December 26, 1978, from the *Scientific Affairs Department, Norwich-Eaton Pharmaceuticals, Division of Morton-Norwich Products, Inc., Norwich, NY 13815.* Accepted for publication April 2, 1979.

Abstract □ 4-Acetoxy - 1,2,3,4 - tetrahydro - 2,2-dimethyl-6,7-methylenedioxyisoquinolinium iodide, an analog of acetylcholine, was synthesized and a pharmacological profile of its GI effects was compiled. The agent inhibited dog colonic contraction in response to pelvic nerve stimulation and to acetylcholine. In rats, the compound markedly reduced gastric acid output and the volume of gastric secretions. The lack of inhibition of chromodacryorrhea production in response to carbachol indicates a lack of anticholinergic action. The agent failed to affect the acute inflammatory response of the rat hindpaw in response to carrageenan. The precursor of the compound was ineffective in the pharmacological tests.

Keyphrases □ Acetylcholine analogs—synthesis, pharmacodynamics, structure–activity relationships □ Cholinergic agents—acetylcholine analogs, synthesis, pharmacodynamics, structure–activity relationships □ Structure–activity relationships—acetylcholine analogs

As part of a program directed toward the synthesis of novel GI agents, an acetylcholine analog was desired in which the tetraalkylammonium function of the molecule was incorporated as part of a rigid annular system. Accordingly, a route to 4-acetoxy-1,2,3,4-tetrahydro-2,2-dimethyl-6,7-methylenedioxyisoquinolinium iodide (I) was devised.

DISCUSSION

Reaction of the previously reported (1) 4-hydroxy-6,7-methylenedioxy-1,2,3,4-tetrahydroisoquinoline (II) with methyl iodide gave the quaternary Compound III which, upon treatment with acetic anhydride, afforded the racemic acetylcholine analog I.

Compound I, 10 mg/kg iv in three dogs, caused marked, but brief (20 min), antagonism of colonic contractions in response to intermittent pelvic nerve stimulation (2). In addition, acetylcholine-induced con-

0022-3549/79/1000-1325$01.00/0

© 1979, American Pharmaceutical Association

traction of the dog colon was markedly reduced (2). In the modified Shay technique in rats (3), I (100 or 300 mg/kg po, 1 hr before stomach pylorus ligation) evoked a dose-related inhibition of gastric acid output and reduced the gastric secretion volume. The gastric acid inhibitory activity of I at 100 mg/kg po was very weak (12.5%) compared to that at the 300-mg/kg po (78.6%) dose.

When I was given orally to six rats at a dose of 300 mg/kg po and challenged 1 hr later by 0.25 mg of carbachol/kg ip (4), the signs of chromodacryorrhea (bloody tears) were not prevented, indicating that I is not an anticholinergic drug. Compound I failed to reduce the inflammatory response evoked by an injection of carrageenan into the rat hindpaw (5).

Compound III, 10 mg/kg iv, slightly inhibited dog colonic contractions in response to intermittent pelvic nerve stimulation. The contractile response of the colon to acetylcholine was reduced slightly. A dose of 300 mg/kg po in rats failed to affect the gastric secretion volume or gastric acid output in the modified Shay technique. Compound III did not inhibit the chromodacryorrhea evoked by a carbachol injection, thereby indicating no anticholinergic effect. Finally, III was totally ineffective in preventing the inflammatory response of the rat hindpaw induced by a subplantar carrageenan injection.

Inhibition of acetylcholine-induced contraction of the dog colon by I and lack of inhibition of carbachol-induced chromodacryorrhea following I indicate a nonspecific antagonism of smooth muscle activity by I. Therefore, the action of I could be attributed to smooth muscle depression or relaxation which would inhibit any smooth muscle stimulant (*i.e.*, acetylcholine and histamine) or excitation of intrinsic cholinergic nerves. The chromodacryorrhea response to carbachol is a specific cholinergic response and can be blocked only by specific anticholinergic drugs such as atropine (4) and not by nonspecific smooth muscle relaxants.

The pharmacological profile of I and III suggests that the former possesses greater GI inhibitory activity than the latter. Such a difference in activity may be attributed to the acetyl substitution on the isoquinolinium structure. The acetyl moiety converts a relatively inactive choline into the powerful agent acetylcholine, a quaternary ammonium compound. The carbonyl atom of the acetate portion of I may possibly increase the drug–receptor affinity and cause a greater pharmacological antagonism in comparison to that of III.

EXPERIMENTAL

Melting points were determined on a melting-point apparatus[1] and are uncorrected. IR spectra[2] were determined as mineral oil mulls. NMR spectra[3] were compared with tetramethylsilane as an internal standard.

1,2,3,4-Tetrahydro-4-hydroxy-2,2-dimethyl-6,7-methylenedioxyisoquinolinium Iodide (III)—A mixture of 84 g (0.37 mole) of 4-hydroxy-6,7-methylenedioxy-1,2,3,4-tetrahydroisoquinoline hydrochloride (II) (1), 102 g (0.74 mole) of potassium carbonate, 78.8 g (0.56 mole) of methyl iodide, and 1000 ml of methanol was refluxed for 27 hr (Scheme I). The slurry was filtered while hot. The filtrate was refrigerated overnight and filtered. A light-tan solid was washed with methanol and ether and dried to give 55 g (43%) of the desired product, mp 223–226°.

An analytical sample, mp 224–226°, was obtained by recrystallization from methanol; IR: 3.03 (O–H), 9.40, and 9.70 (C–OH) μm; NMR (dimethyl sulfoxide-d_6): δ 3.25 [s, 6, $(CH_3)_2N^+$], 3.63–3.85 (m, 2, 3-CH_2), 4.56 (s, 2, 1-CH_2), 4.75–5.03 (m, 1, 4-CH), 6.05, 6.13 (d, J = 5 Hz, 1, exchangeable in D_2O, O–H), 6.08 (s, 2, –O–CH_2–O–), 6.80, and 7.08 (2 s, 2, aromatic C–H).

Anal.—Calc. for $C_{12}H_{16}INO_3$: C, 41.28; H, 4.62; I, 36.35; N, 4.01. Found: C, 41.33; H, 4.68; I, 36.10; N, 3.92.

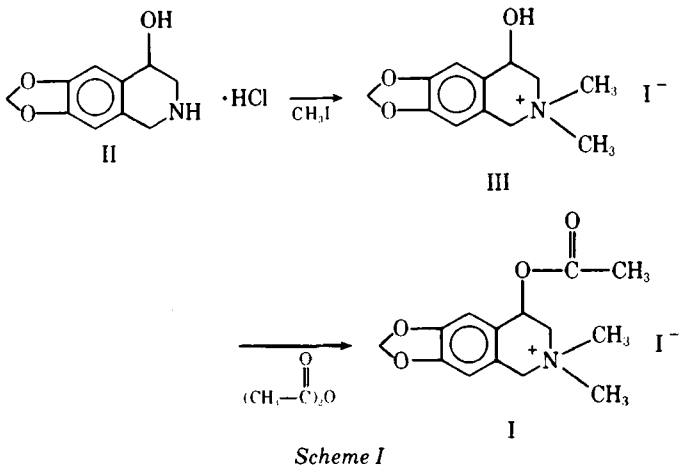

Scheme I

4-Acetoxy-1,2,3,4-tetrahydro-2,2-dimethyl-6,7-methylenedioxyisoquinolinium Iodide (I)—A 26-g (0.075 mole) portion of III was added to 200 ml of acetic anhydride, and the reaction mixture was refluxed for 1.7 hr, cooled to room temperature, and filtered. The off-white solid was washed with 400 ml of ether and air dried, mp 249–250° dec. The yield was 28 g (97%).

An analytical sample, mp 246–248° dec., was obtained by recrystallization from 95% ethanol; IR: 5.70 (CO, ester) and 8.01 (C–O–C ester) μm; NMR (dimethyl sulfoxide-d_6): δ 2.11 (s, 3, CH_3–C=O), 3.20, 3.33 [2 s, 6, $(CH_3)_2N^+$], 4.00, 4.06 (d, J = 4 Hz, 2, 3-CH_2), 4.63 (s, 2, 1-CH_2), 5.91–6.16 (m, 1, 4-CH), 6.10 (s, 2, –O–CH_2–O–), 6.70, and 6.86 (2 s, 2, aromatic C–H).

Anal.—Calc. for $C_{14}H_{18}INO_4$: C, 42.98; H, 4.64; I, 32.44; N, 3.58. Found: C, 43.14; H, 4.54; I, 32.60; N, 3.51.

REFERENCES

(1) J. M. Bobbitt and J. C. Sih, *J. Org. Chem.*, **33**, 856 (1968).

(2) M. M. Goldenberg, *Arzneim.-Forsch.*, **26**, 341 (1976).

(3) S. A. Shay, S. A. Komarov, S. S. Fels, D. Meranzi, M. Gruenstein, and A. Siplet, *Gastroenterology*, **5**, 43 (1945).

(4) M. M. Winbury, D. M. Schmalgemeier, and W. E. Hambourger, *J. Pharm. Exp. Ther.*, **95**, 53 (1949).

(5) M. M. Goldenberg and A. C. Ilse, *Arch. Int. Pharmacodyn. Ther.*, **228**, 153 (1977).

ACKNOWLEDGMENTS

The authors are indebted to Mr. Grant M. Gustin for the microanalysis and to Mrs. Patricia Curtis for the NMR spectra. The technical assistance of Mr. M. Phelps, Mrs. P. Dowell, and Mr. K. Boise is appreciated.

[1] Mel-Temp.
[2] Model 137B, Perkin-Elmer.
[3] Model A-60A, Varian.

Urinary Excretion of Dyphylline in Humans

KEITH J. SIMONS *x **and F. ESTELLE R. SIMONS** ‡

Received March 15, 1979, from the *Faculty of Pharmacy, University of Manitoba, Winnipeg, Canada, R3T 2N2, and the ‡Section of Allergy and Clinical Immunology, Department of Pediatrics, Faculty of Medicine, University of Manitoba, Winnipeg, Canada, R3E 0W1. Accepted for publication April 9, 1979.

Abstract □ The pharmacokinetics and urinary excretion of a single dyphylline dose were studied in five normal volunteers. The mean dyphylline half-life was 1.8 ± 0.2 hr; the mean total body clearance rate and mean renal clearance rate were 333 ± 62 and 276 ± 52 ml/min, respectively; and the mean volume of distribution was 0.8 ± 0.2 liter/kg. In the urine, 83 ± 5% of the dose was excreted as unchanged drug, and theophylline was not detected. Dyphylline doses of 19–27 mg/kg, resulting in peak serum dyphylline concentrations of 19.3–23.5 μg/ml, were tolerated well by four subjects. One subject had a severe headache following a 28-mg/kg dose, associated with a peak serum dyphylline concentration of 36.4 μg/ml. This study confirms speculation that dyphylline is not metabolized to theophylline *in vivo*.

Keyphrases □ Dyphylline—urinary excretion, pharmacokinetics, humans □ Muscle relaxants, smooth—dyphylline, urinary excretion, pharmacokinetics, humans □ Pharmacokinetics—dyphylline, urinary excretion, humans

Dyphylline (dihydroxypropyltheophylline) is 70% theophylline by molecular weight ratio (1) and is said to be stable *in vitro* and *in vivo* (2). Whether it is eliminated by metabolism, excretion, or both is unknown.

Dyphylline has a mean half-life of 2.1 hr in humans (3) and, therefore, might be expected to be clinically useful only if given very frequently or in very high doses. Although doses of 15 mg/kg (4) and 1000 mg (5), resulting in mean peak serum dyphylline concentrations of 12 and 16 μg/ml, respectively, have some bronchodilator effects, *in vitro* studies indicated that much higher doses may be required for optimal bronchodilation (6).

The tolerance to high single dyphylline doses in normal volunteers was assessed, and an attempt was made to determine whether the drug is metabolized *in vivo* or is excreted unchanged.

EXPERIMENTAL

Materials—All solvents and reagents were analytical grade[1].

Dyphylline Assay—Dyphylline concentrations in aqueous solution, serum, urine, and feces were measured by reversed-phase, high-performance liquid chromatography (HPLC) using a modified method of Orcutt *et al.* (7).

To 50 μl of water or serum in a 10 × 75-mm test tube was added 100 μl of aqueous β-hydroxyethyltheophylline[2] (7.5 μg/ml) as the internal standard. A 25-μl aliquot of 20% trichloroacetic acid was added, and the solution was mixed and centrifuged. The supernate was transferred to a clean 13 × 100-mm test tube. After buffering with 300 μl of 2.5 *M*, pH 6.4 acetate buffer, the solution was extracted with 2 ml of 20% isopropanol in chloroform by mixing and centrifugation. The aqueous supernate was aspirated, and the organic layer was evaporated to dryness using low heat and a dry nitrogen stream. The sample was redissolved in 50–100 μl of mobile phase, and 25 μl was injected directly into the chromatograph.

To 50 μl of urine or fecal slurry were added 50 μl of aqueous β-hydroxyethyltheophylline (15 μg/ml) and 300 μl of 2.5 *M*, pH 6.4 acetate buffer. This sample was extracted directly with 2 ml of 20% isopropanol in chloroform and then treated similarly to the serum samples.

Instrument—A component-system high-performance liquid chromatograph[3] was used with a 30-cm × 3.9-mm i.d. stainless steel column[4] containing reversed-phase packing. The solvent was 6.5% acetonitrile in 0.01 *M*, pH 4.0 sodium acetate buffer. The flow rate was 2 ml/min at an operating pressure of 1500–2000 psi. Absorbance was measured at 280 nm. Under these conditions, dyphylline and the internal standard eluted at 9.0 and 10.5 min, respectively.

Dyphylline Conjugation in Urine—Pooled 24-hr urine samples from four subjects were analyzed for dyphylline conjugates. To 0.5-ml aliquots of urine were added 100 μl of water, 100 μl of concentrated hydrochloric acid, or 100 μl of β-glucuronidase[5] solution, 250 U/100 μl in 0.15 *M*, pH 6.9 phosphate buffer. Samples were incubated at 37° for 24 hr and analyzed for dyphylline.

Dosage Form—The dyphylline content in five tablets[6] was determined by crushing the tablets and dissolving the dyphylline in water.

Kinetic Study—Dyphylline pharmacokinetics were studied in five volunteers, ages 20–35 years, after informed consent was obtained. All were healthy, nonobese, nonsmokers who were not taking any medication. They abstained from methylxanthine-containing foods and beverages for 15 hr before and during the study.

Each fasting subject received a single dose of 1400 or 1600 mg of dyphylline[6] by mouth (range 19–28 mg/kg) with 180 ml of water. A light lunch was permitted 3 hr later. Venipuncture was performed before drug ingestions and then every 15 min until 1.5 hr and hourly from 2 to 8 hr. Urine samples were collected before and for 24 hr after drug ingestion. For four volunteers, the urine collected after drug ingestion was pooled and measured, and an aliquot was analyzed for dyphylline. For the fifth volunteer, timed urine specimens and fecal samples were collected for 24 hr, and the dyphylline content of each was analyzed.

Data Analysis (8)—The log serum dyphylline concentration *versus* time data were plotted, and the terminal linear portion of the graph was fitted to Eq. 1 by linear regression using a programmable pocket calculator[7]:

$$\ln C_p = \ln C_p^0 - Kt \qquad \text{(Eq. 1)}$$

where C_p is the serum dyphylline concentration at any time (t), C_p^0 is the serum dyphylline concentration extrapolated to zero time, and K is the first-order elimination rate constant.

Table I—Serum Dyphylline Concentrations (Micrograms per Milliliter) and Amount of Dyphylline Excreted in Urine

Hours	Subject 1	2	3	4	5
0.25	6.7	8.3	1.4	0	0
0.5	12.5	34.7	10.9	1.0	16.3
0.75	19.3	33.9	22.2	6.2	23.3
1.0	18.1	36.4	23.5	13.7	21.0
1.25	17.4	33.7	22.1	19.3	20.0
1.5	16.6	29.7	21.5	14.4	19.7
1.75	—	—	20.2	14.0	16.6
2.0	14.2	23.2	18.1	12.0	16.0
3.0	9.8	17.7	11.8	9.9	10.4
4.0	7.4	9.4	7.9	7.0	7.8
5.0	4.7	6.3	4.7	4.5	5.3
6.0	3.8	4.0	3.0	2.6	3.3
7.0	2.3	2.9	1.9	2.4	2.0
8.0	1.4	1.9	1.2	1.9	1.8
AUC, μg/ml/hr	67.68	110.97	74.31	57.29	74.57
A_e^∞, mg	1227	1301	1230	1150	1222

[1] Fisher Scientific Co., Fair Lawn, NJ 07410.
[2] Pierce Chemical Co., Rockford, IL 61105.
[3] Model UK injector, model 6000A high-pressure pump, and model 440 absorbance detector, Waters Associates, Milford, MA 01757.
[4] μBondapak C_{18}, Waters Associates, Milford, MA 01757.
[5] β-Glucuronidase type I crude bacterial powder, Sigma Chemical Co., St. Louis, MO 63178.
[6] Airet 400-mg tablets, Baylor Laboratories, Hurst, TX 76053.
[7] H-P 67, Hewlett-Packard, Corvallis, OR 97330.

0022-3549/79/1000-1327$01.00/0
© 1979, American Pharmaceutical Association

Table II—Dyphylline Pharmacokinetic Constants

Parameter	Subject 1	2	3	4	5	Mean ± *SD*
Weight, kg	73	57	60	68	68	65 ± 7
Dose, mg/kg	19	28	27	21	21	23 ± 4
K, hr^{-1}	0.38	0.43	0.45	0.32	0.38	0.39 ± 0.05
$t_{1/2}$, hr	1.8	1.6	1.5	2.1	1.8	1.8 ± 0.2
$C_{p_{max}}$, μg/ml	19.3	36.4	23.5	19.3	23.3	24.4 ± 7.0
t_{max}, hr	0.75	1.0	1.0	1.25	0.75	1.0 ± 0.2
V_d, liters/kg	0.75	0.59	0.80	1.11	0.73	0.80 ± 0.19
Cl, ml/min	345	240	360	407	313	333 ± 62
f, %	88	81	77	82	87	83 ± 5
Cl_R, ml/min	303	195	276	334	272	276 ± 52

Total body clearance (Cl) was calculated using:

$$Cl = \frac{AUC}{D} \qquad \text{(Eq. 2)}$$

where AUC is the area under the serum dyphylline concentration–time curve calculated using the trapezoid rule. The apparent volume of distribution (V_d) was determined using:

$$V_d = \frac{Cl}{K} \qquad \text{(Eq. 3)}$$

In one subject from whom timed urine samples were collected, renal clearance (Cl_R) was calculated using:

$$Cl_R = \frac{\left(\frac{dA_e}{dt}\right)}{C_p} \qquad \text{(Eq. 4)}$$

where dA_e/dt is the excretion rate calculated at the same time that C_p was determined. In this study, dA_e/dt was calculated as $\Delta A_e/\Delta t$ at 2-hr intervals. In the other four subjects in which pooled 24-hr urine was collected, renal clearance was calculated using:

$$Cl_R = (f)(Cl) \qquad \text{(Eq. 5)}$$

where f is the dose fraction excreted in the urine as unchanged drug.

RESULTS AND DISCUSSION

Dyphylline content in five tablets of 400-mg label strength was 393.8 ± 11.2 mg. Although the range of tablet content was ±3%, within the usual USP range of ±7% of label strength, the doses used in this study were probably less than calculated.

Serum dyphylline concentrations in the five subjects following 19–28-mg/kg doses are shown in Table I, and the pharmacokinetic parameters are listed in Table II. A typical log serum dyphylline concentration *versus* time plot is shown in Fig. 1.

In the five subjects, peak serum dyphylline concentrations occurred within 1 hr (Table II), confirming a previous report (3). The maximum dyphylline concentration in the present study was 36.4 μg/ml in a subject who received 28 mg/kg. The mean dyphylline half-life was 1.8 ± 0.2 hr, similar to the previously reported value of 2.1 ± 0.4 hr (3). The mean dyphylline clearance rate was 333 ± 62 ml/min, while the mean apparent volume of distribution was 0.8 ± 0.2 liter/kg.

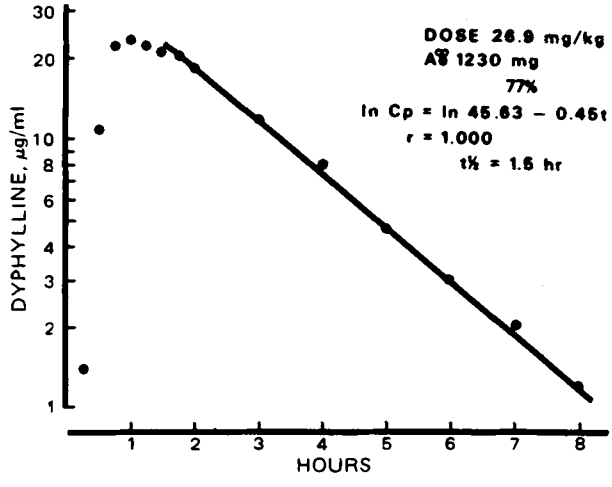

Figure 1—*Log serum dyphylline concentration* versus *time for Subject 3.*

It has been speculated that dyphylline is not metabolized *in vivo*, although unchanged dyphylline has not been detected in the urine by GLC (9). The dyphylline elimination mechanism has not been reported previously. In these five subjects, 83 ± 5% of the dyphylline dose was excreted in the urine in the unchanged form. Theophylline was not identified in serum or urine. There was no evidence of glucuronide or other types of conjugation; pooled urine samples treated with acid or β-glucuronidase showed no change in the dyphylline concentration (10).

In Subject 1, the renal clearance of dyphylline calculated using Eq. 4 was 311 ml/min, consistent with 303 ml/min calculated from Eq. 5. The mean renal clearance in the five subjects was 276 ± 52 ml/min. These results suggest that dyphylline is actively secreted as well as filtered by the glomerulus.

Dyphylline bioavailability from oral tablets is ~100% of availability from intramuscular administration (3). Analysis of feces collected at 12 and 23 hr in Subject 1 accounted for only a further 9.4 mg (0.7%) of the dose in addition to the 88% found in urine. The small amount of drug in feces may have been secreted by the bile or may not have been absorbed.

Presently, the recommended dyphylline dose in adults is 400 mg tid, although effective single doses are at least 15 mg/kg (4) or 1000 mg (5). The range of serum levels associated with optimal bronchodilation without toxicity is unknown, although dyphylline is said to have a wider therapeutic–toxic range than theophylline and to cause fewer adverse effects in the GI and central nervous systems (11, 12). In the present study, only one subject experienced adverse effects, namely severe headache, after a single 28-mg/kg dyphylline dose, associated with a peak serum dyphylline concentration of 36.4 μg/ml. The other four subjects tolerated doses of 19–27 mg/kg and peak serum dyphylline concentrations of 19.3–23.5 μg/ml without symptoms.

The adverse effects following a single high dyphylline dose in one subject and the short drug half-life remain major obstacles to its effective use in clinical practice, even with sustained-release formulations (9).

REFERENCES

(1) E. F. Ellis and E. D. Eddy, *J. Allergy Clin. Immunol.*, **53**, 116 (1974).

(2) L. Hendeles and M. Weinberger, *Drug Intell. Clin. Pharm.*, **11**, 424 (1977).

(3) F. E. R. Simons, K. J. Simons, and C. W. Bierman, *J. Allergy Clin. Immunol.*, **56**, 347 (1975).

(4) F. E. R. Simons, C. W. Bierman, A. C. Sprenkle, and K. J. Simons, *Pediatrics*, **56**, 916 (1975).

(5) L. D. Hudson, M. L. Tyler, and T. L. Petty, *Curr. Ther. Res.*, **15**, 367 (1973).

(6) N. Svedmyr, *Scand. J. Resp. Dis. Suppl.*, **101**, 125 (1977).

(7) J. J. Orcutt, P. P. Kozak, S. A. Gillman, and L. H. Cummins, *Clin. Chem.*, **23**, 599 (1977).

(8) M. Gibaldi and D. Perrier, "Pharmacokinetics," Dekker, New York, N.Y., 1975, pp. 1–17.

(9) K. J. Simons, F. E. R. Simons, and C. W. Bierman, *J. Clin. Pharmacol.*, **17**, 237 (1977).

(10) L. P. Amsel and G. Levy, *J. Pharm. Sci.*, **58**, 321 (1969).

(11) P. V. Maney, J. W. Jones, E. G. Gross, and H. M. Korns, *J. Am. Pharm. Assoc., Sci. Ed.*, **35**, 266 (1946).

(12) K. Svedmyr, T. Mellstrand, and N. Svedmyr, *Scand. J. Resp. Dis. Suppl.*, **101**, 139 (1977).

ACKNOWLEDGMENTS

Supported by the Children's Hospital of Winnipeg Research Foundation Inc.

F. E. R. Simons is the recipient of a Queen Elizabeth II Scientist Award.

The authors are grateful to Mrs. Evelyn Frith for technical assistance.

Stability of Amitriptyline Hydrochloride in a Commercial Aqueous Solution

R. ROMAN ˣ, E. M. COHEN, M. E. CHRISTY, and W. B. HAGERMAN

Received March 12, 1979, from the *Pharmacy Research and Development Department, Merck Sharp & Dohme Research Laboratories, West Point, PA 19486.* Accepted for publication April 19, 1979.

Abstract □ A commercial amitriptyline hydrochloride solution was stored at 80° for up to 3 months. High-performance liquid chromatography showed no evidence of amitriptyline hydrochloride degradation. The method also indicated that two reported degradates, 3-(propa-1,3-dienyl)-1,2:4,5-dibenzocyclohepta-1,4-diene and dibenzosuberone, were present at levels less than 0.1% (the detection limit of the method) under the storage conditions. The stability of the commercial solutions is attributed to their relatively low ratio of headspace oxygen to amitriptyline hydrochloride.

Keyphrases □ Amitriptyline hydrochloride—stability, commercial aqueous solutions, high-performance liquid chromatography □ Antidepressants—amitriptyline hydrochloride, stability, commercial aqueous solutions, high-performance liquid chromatography □ High-performance liquid chromatography—analysis, amitriptyline hydrochloride in commercial aqueous solutions, stability

Amitriptyline hydrochloride decomposition products in aqueous solution were identified by Enever *et al.* (1). More recently, the same investigators reported a number of factors that influence the drug's decomposition rate (2). The latter study indicated that aqueous amitriptyline hydrochloride solutions could undergo appreciable decomposition after even a few days of storage at 80°.

Neither study reported data for amitriptyline hydrochloride stability in marketed parenteral solutions. The purpose of this investigation was to assess the stability of an aqueous amitriptyline hydrochloride solution in one such formulation[1].

EXPERIMENTAL

Materials—Amitriptyline hydrochloride[2], dibenzosuberone[3], and methanesulfonic acid[4] were used without further purification. All other chemicals were reagent grade.

High-Performance Liquid Chromatography (HPLC)—*Apparatus*—The liquid chromatograph[5] was equipped with a fixed-wavelength detector (254 nm), an oven, and an integrator.

Column—A 30 × 0.39-cm (i.d.) column containing a nitrile-bonded phase packing[6] was used at 30° with a mobile phase flow of 2 ml/min.

Mobile Phase—For amitriptyline hydrochloride analysis, acetonitrile–0.02 *M* ammonium acetate plus 0.01 *M* methanesulfonic acid in distilled water (90:10) was used. For degradate detection, the ratio was 50:50.

Sample Preparation—The sample was prepared by diluting a 2.0-ml aliquot to 25.0 ml with distilled water. The sample was filtered prior to analysis, and 10 μl was injected onto the column (attenuation 0.0256 absorbance unit/cm). Samples containing degradates were prepared in the same manner and injected at an attenuation of 0.0032 absorbance unit/cm.

Quantitation—Quantitation was achieved using the ratio of the sample peak area to that of an amitriptyline hydrochloride reference standard[2].

Storage of Amitriptyline Hydrochloride Solutions—Multiple-dose vials[1] (10 ml) were stored in a forced-air oven[7] maintained at 80°. Vials were withdrawn at predetermined times and stored at 5° prior to analysis at the completion of the study (3 months).

Synthesis of 3-(Propa-1,3-dienyl)-1,2:4,5-dibenzocyclohepta-1,4-diene (I)—An authentic sample of I was prepared from amitriptyline *N*-oxide dihydrate (3) by Cope elimination (125°/2 hr). The product was isolated by ether extraction and purified by column chromatography on silica gel with carbon tetrachloride elution. The purified sample was characterized by TLC and spectra (UV, NMR, and mass) and was stored at 5°.

Table I—Amitriptyline Hydrochloride in Aqueous Solution Stored at 80°

Days	Found, mg/ml	Percent of Initial
Initial	10.21	
4	10.32	101
8	10.25	100.4
11	10.24	100.3
16	10.20	99.9
20	10.10	98.9
24	10.15	99.4
28	10.16	99.5
35	10.19	99.8
90	10.08	98.7

RESULTS AND DISCUSSION

The results (Table I) showed no detectable amitriptyline hydrochloride loss in aqueous solutions stored at 80° for up to 90 days. The results are unusual only in that the solutions studied by Enever *et al.* (2) showed amitriptyline hydrochloride losses from 5 to 90% after storage at 80° for 30 days. The solutions used in the earlier study contained 2 mg of amitriptyline hydrochloride/ml buffered at pH 3.0 or 5.0 and were sealed in ampuls with a 4:1 ratio of headspace to solution (2). The commercial formulation contained 10 mg of amitriptyline hydrochloride/ml in an unbuffered solution that also included 44 mg of dextrose/ml, 1.5 mg of

[1] Elavil, 10 mg/ml in a 10-ml multidose vial, Merck Sharp & Dohme, West Point, Pa.
[2] Merck Sharp & Dohme, West Point, Pa.
[3] Aldrich Chemical Co., Milwaukee, Wis.
[4] Eastman Kodak Co., Rochester, N.Y.
[5] Hewlett-Packard model 1084, Avondale, Pa.
[6] μBondapak CN, Waters Associates, Milford, Mass.
[7] Model OV-490A-2, Blue M Electric Co., Blue Island, Ill.

0022-3549/79/1000-1329$01.00/0
© 1979, American Pharmaceutical Association

ACKNOWLEDGMENTS

Supported by the Children's Hospital of Winnipeg Research Foundation Inc.

F. E. R. Simons is the recipient of a Queen Elizabeth II Scientist Award.

The authors are grateful to Mrs. Evelyn Frith for technical assistance.

Stability of Amitriptyline Hydrochloride in a Commercial Aqueous Solution

R. ROMAN ˣ, E. M. COHEN, M. E. CHRISTY, and W. B. HAGERMAN

Received March 12, 1979, from the *Pharmacy Research and Development Department, Merck Sharp & Dohme Research Laboratories, West Point, PA 19486.* Accepted for publication April 19, 1979.

Abstract □ A commercial amitriptyline hydrochloride solution was stored at 80° for up to 3 months. High-performance liquid chromatography showed no evidence of amitriptyline hydrochloride degradation. The method also indicated that two reported degradates, 3-(propa-1,3-dienyl)-1,2:4,5-dibenzocyclohepta-1,4-diene and dibenzosuberone, were present at levels less than 0.1% (the detection limit of the method) under the storage conditions. The stability of the commercial solutions is attributed to their relatively low ratio of headspace oxygen to amitriptyline hydrochloride.

Keyphrases □ Amitriptyline hydrochloride—stability, commercial aqueous solutions, high-performance liquid chromatography □ Antidepressants—amitriptyline hydrochloride, stability, commercial aqueous solutions, high-performance liquid chromatography □ High-performance liquid chromatography—analysis, amitriptyline hydrochloride in commercial aqueous solutions, stability

Amitriptyline hydrochloride decomposition products in aqueous solution were identified by Enever *et al.* (1). More recently, the same investigators reported a number of factors that influence the drug's decomposition rate (2). The latter study indicated that aqueous amitriptyline hydrochloride solutions could undergo appreciable decomposition after even a few days of storage at 80°.

Neither study reported data for amitriptyline hydrochloride stability in marketed parenteral solutions. The purpose of this investigation was to assess the stability of an aqueous amitriptyline hydrochloride solution in one such formulation[1].

EXPERIMENTAL

Materials—Amitriptyline hydrochloride[2], dibenzosuberone[3], and methanesulfonic acid[4] were used without further purification. All other chemicals were reagent grade.

High-Performance Liquid Chromatography (HPLC)—*Apparatus*—The liquid chromatograph[5] was equipped with a fixed-wavelength detector (254 nm), an oven, and an integrator.

Column—A 30 × 0.39-cm (i.d.) column containing a nitrile-bonded phase packing[6] was used at 30° with a mobile phase flow of 2 ml/min.

Mobile Phase—For amitriptyline hydrochloride analysis, acetonitrile–0.02 *M* ammonium acetate plus 0.01 *M* methanesulfonic acid in distilled water (90:10) was used. For degradate detection, the ratio was 50:50.

Sample Preparation—The sample was prepared by diluting a 2.0-ml aliquot to 25.0 ml with distilled water. The sample was filtered prior to analysis, and 10 μl was injected onto the column (attenuation 0.0256 absorbance unit/cm). Samples containing degradates were prepared in the same manner and injected at an attenuation of 0.0032 absorbance unit/cm.

Quantitation—Quantitation was achieved using the ratio of the sample peak area to that of an amitriptyline hydrochloride reference standard[2].

Storage of Amitriptyline Hydrochloride Solutions—Multiple-dose vials[1] (10 ml) were stored in a forced-air oven[7] maintained at 80°. Vials were withdrawn at predetermined times and stored at 5° prior to analysis at the completion of the study (3 months).

Synthesis of 3-(Propa-1,3-dienyl)-1,2:4,5-dibenzocyclohepta-1,4-diene (I)—An authentic sample of I was prepared from amitriptyline *N*-oxide dihydrate (3) by Cope elimination (125°/2 hr). The product was isolated by ether extraction and purified by column chromatography on silica gel with carbon tetrachloride elution. The purified sample was characterized by TLC and spectra (UV, NMR, and mass) and was stored at 5°.

Table I—Amitriptyline Hydrochloride in Aqueous Solution Stored at 80°

Days	Found, mg/ml	Percent of Initial
Initial	10.21	
4	10.32	101
8	10.25	100.4
11	10.24	100.3
16	10.20	99.9
20	10.10	98.9
24	10.15	99.4
28	10.16	99.5
35	10.19	99.8
90	10.08	98.7

RESULTS AND DISCUSSION

The results (Table I) showed no detectable amitriptyline hydrochloride loss in aqueous solutions stored at 80° for up to 90 days. The results are unusual only in that the solutions studied by Enever *et al.* (2) showed amitriptyline hydrochloride losses from 5 to 90% after storage at 80° for 30 days. The solutions used in the earlier study contained 2 mg of amitriptyline hydrochloride/ml buffered at pH 3.0 or 5.0 and were sealed in ampuls with a 4:1 ratio of headspace to solution (2). The commercial formulation contained 10 mg of amitriptyline hydrochloride/ml in an unbuffered solution that also included 44 mg of dextrose/ml, 1.5 mg of

[1] Elavil, 10 mg/ml in a 10-ml multidose vial, Merck Sharp & Dohme, West Point, Pa.
[2] Merck Sharp & Dohme, West Point, Pa.
[3] Aldrich Chemical Co., Milwaukee, Wis.
[4] Eastman Kodak Co., Rochester, N.Y.
[5] Hewlett-Packard model 1084, Avondale, Pa.
[6] μBondapak CN, Waters Associates, Milford, Mass.
[7] Model OV-490A-2, Blue M Electric Co., Blue Island, Ill.

0022-3549/79/1000-1329$01.00/0
© 1979, American Pharmaceutical Association

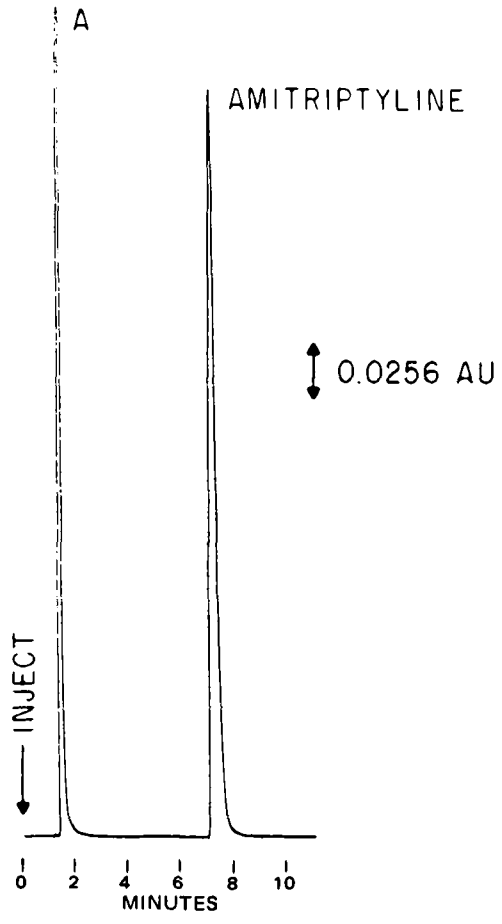

Figure 1—*Chromatogram of diluted amitriptyline hydrochloride formulation. Peak A represents methylparaben, propylparaben, and I and II, if present. The mobile phase was acetonitrile–0.02* M *ammonium acetate and 0.01* M *methanesulfonic acid (90:10).*

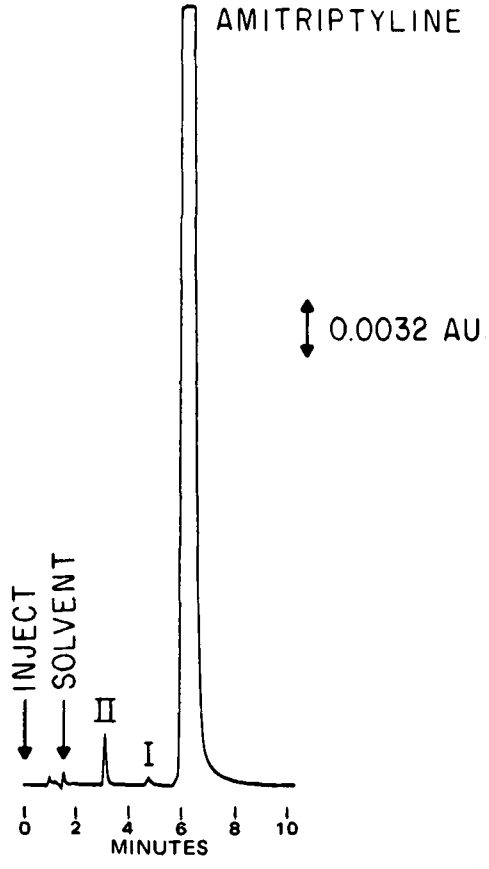

Figure 2—*Chromatogram of amitriptyline hydrochloride standard (0.64 mg/ml) spiked with I (0.00065 mg/ml) and II (0.0016 mg/ml). The mobile phase was acetonitrile–0.02* M *ammonium acetate and 0.01* M *methanesulfonic acid (50:50).*

methylparaben/ml, and 0.2 mg of propylparaben/ml. The ratio of headspace to liquid in the multiple-dose vial was 1:6, and the pH was 4.0–6.0 (4).

Enever *et al.* (2) demonstrated the involvement of oxygen in amitriptyline hydrochloride degradation with an experiment showing no decomposition of drug sealed in ampuls under nitrogen. An accurate prediction of the headspace oxygen effect on amitriptyline hydrochloride decomposition would require detailed knowledge of the reaction kinetics. However, the fact that the headspace to amitriptyline ratio in the marketed formulation was less than 1/100th of that for the solutions studied previously (2) is a likely explanation for the different extents of degradation.

Assay—Enever *et al.* (2) used ether extraction followed by GLC to assay the intact amitriptyline. In the present study, an HPLC procedure using a dilute solution of the formulation was more convenient. In this method, which was modified from one reported for amitriptyline hydrochloride–perphenazine tablets (5), the neutral compounds, methyl- and propylparaben, as well as the degradates, 3-(propa-1,3-dienyl)-1,2:4,5-dibenzocyclohepta-1,4-diene (I) and dibenzosuberone (II), were unretained and eluted well before the basic amitriptyline (Fig. 1). A third degradate reported by Enever *et al.* (1), 3-(2-oxoethylidene)-1,2:4,5-dibenzocyclohepta-1,4-diene (III), was not available for testing. Since III is a neutral compound, it should exhibit polarity similar to II and should almost certainly be separated from amitriptyline under the conditions used.

Detection of Degradates—The k' values for I and II could be increased by decreasing the acetonitrile percentage in the mobile phase while maintaining a relatively constant k' value for amitriptyline by increasing the methanesulfonic acid level. Thus, it was possible to separate and detect I, II, and amitriptyline in the same chromatogram (Fig. 2). This chromatogram of amitriptyline spiked with I and II illustrates potential degradate detection at levels as low as 0.1%. Even under these conditions, it was not possible to detect either I or II in amitriptyline hydrochloride solutions at 80° for up to 3 months. To test whether storage for longer periods at lower temperatures might induce degradation, three lots of commercial material that had been stored at room temperature for longer than 5 years (the expiration date for the product) were analyzed, but neither I nor II could be detected.

Although the commercial formulation is clearly more stable than the aqueous amitriptyline hydrochloride solutions studied by Enever *et al.* (2), the absence of detectable degradates in the former solutions even after 3 months of storage at 80° is surprising. One explanation for the absence of I and II might be the formation of other transformation products. Compound I polymerized readily. Both the formulation and solutions containing all ingredients except amitriptyline hydrochloride discolored during storage at 80° and eventually formed a brown oil, presumably due to dextrose decomposition, thus obscuring the visual detection of insoluble amitriptyline degradates.

REFERENCES

(1) R. P. Enever, A. Li Wan Po, B. J. Millard, and E. Shotton, *J. Pharm. Sci.*, **64**, 1497 (1975).

(2) R. P. Enever, A. Li Wan Po, and E. Shotton, *ibid.*, **66**, 1087 (1977).

(3) Merck & Co., Netherlands pat. 6,511,947 (1966); through *Chem. Abstr.*, **65**, 7122c (1966).

(4) "The United States Pharmacopeia," 19th rev., Mack Publishing Co., Easton, Pa., 1975, p. 28.

(5) A. G. Butterfield and R. W. Sears, *J. Pharm. Sci.*, **66**, 1117 (1977).

ACKNOWLEDGMENTS

The authors thank Mr. Frederick Bacher and Dr. Gerald Brenner for reviewing the manuscript.

1,2-Dialkyl-4-pyrazolidinethiols as Potential Antiradiation Agents

MILTON J. KORNET *x and **RALPH DANIELS** ‡

Received March 16, 1979, from the *College of Pharmacy, University of Kentucky, Lexington, KY 40506, and the ‡Health Sciences Center, University of Oklahoma, Oklahoma City, OK 73190. Accepted for publication April 17, 1979.

Abstract □ The reaction between 3-chloropropylene sulfide and the 1,2-dialkylhydrazines was employed to prepare a series of 1,2-dialkyl-4-pyrazolidinethiols. Evidence is presented to support the structure proposed for the product. These mercaptoheterocycles are related to the β-mercaptoethylamines and were prepared as potential radiation protective agents. No significant activity was observed.

Keyphrases □ Dialkyl pyrazolidinethiols—synthesis, potential antiradiation agents, structure-activity relationships □ Antiradiation agents, potential—dialkyl pyrazolidinethiols, synthesis, structure-activity relationships □ Structure-activity relationships—dialkyl pyrazolidinethiols, as potential antiradiation agents

It has been firmly established that an important pharmacophoric grouping among radiation protective compounds is the 2-aminoethylmercaptan group or a closely related derivative (1, 2). In a program designed to synthesize molecular modifications of this grouping or a chemically similar group, a series of 4-pyrazolidinethiols (I) was investigated.

Examination of the parent structure (I) reveals the fundamental 2-aminoethylmercaptan moiety with the following modifications: (*a*) two such moieties are present owing to the presence of two nitrogen atoms, (*b*) these basic nitrogen atoms are present as a hydrazino group, and (*c*) the entire pharmacophore is contained in a rigid cyclic system. Conceivably, such a rigid system will show enhanced protective activity but lowered toxicity when compared with analogous open chain compounds. This report describes the preparation and antiradiation effects of a series of I compounds.

DISCUSSION

Chemistry—The preparation of an oxygen analog of I (II) was discovered by Gerhardt (3) in 1891. In that early work, treatment of epichlorohydrin with phenylhydrazine in ether afforded a very small yield of 1-phenyl-4-pyrazolidinol (II). A pathway to I was envisaged based on the anticipation that 3-chloropropylene sulfide would behave in a manner analogous to epichlorohydrin. Accordingly, the sulfur analog was treated with 1,2-diethylhydrazine in a 1:1.5 molar ratio in ether. The product isolated gave an elemental analysis consistent with either the desired

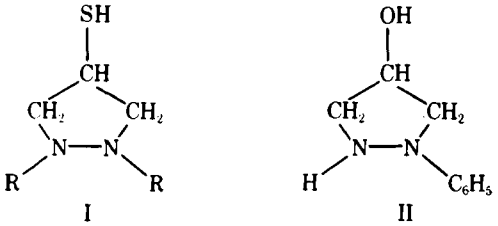

I

II

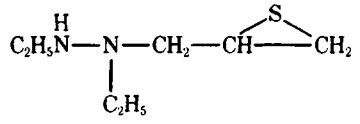

III

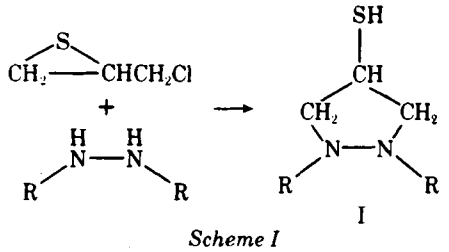

Scheme I

1,2-diethyl-4-pyrazolidinethiol (I*b*, R = C_2H_5) or the isomeric substance 1,2-epithio-4-ethyl-4,5-diazaheptane (III) (Scheme I).

Structure III was ruled out because there was no absorption in the N–H region of the IR spectrum of the product. Further support for the cyclic Structure I*b* was obtained by desulfurizing the product with Raney nickel and isolating 1,2-diethylpyrazolidine (IV). The structure of the desulfurized product was established by its unequivocal synthesis from 1,2-diethylhydrazine and trimethylene bromide (Scheme II). The IR spectrum of the picrate of the product was superimposable upon that of the picrate of the desulfurized product. Furthermore, no depression was obtained when a mixed melting point was determined.

In a similar manner, four other 1,2-dialkyl-4-pyrazolidinethiols were prepared in 12–32% yields. Because N–H absorption bands were absent in the IR spectra of all products, they were assigned the 4-pyrazolidinethiol structure (I). All of the compounds were oils and possessed the distinctive disagreeable mercaptan odor. They were characterized as their hydrochloride salts or as their 3,5-dinitrothiolbenzoates.

Attempts were made to prepare 4-pyrazolidinethiol (I, R = H) through hydrazine addition to 3-chloropropylenesulfide. However, this reaction produced polymeric material only. Table I records relevant data for the 1,2-dialkyl-4-pyrazolidinethiols.

Antiradiation Activity—The 4-pyrazolidinethiols were tested[1] for antiradiation activity as reported previously (4). The compounds were administered to mice intraperitoneally 15–30 min before whole body lethal radiation. Compounds I*a*, I*c*, and I*e* at doses of 48, 200, and 500 mg/kg, respectively, all produced 0% 30-day survivors. Compounds I*b* and I*d* were not tested. An explanation for the observed lack of activity

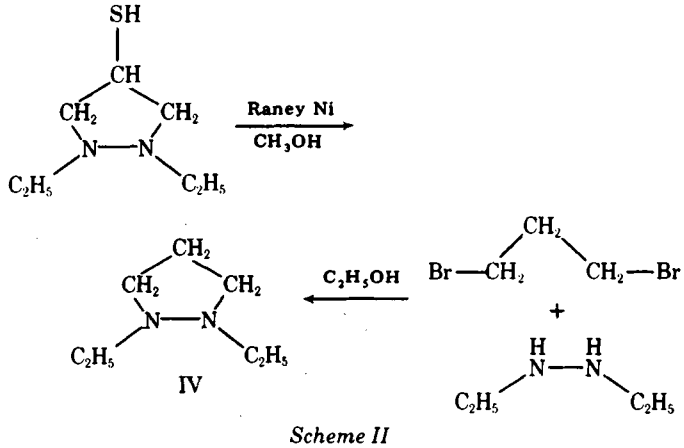

Scheme II

[1] At the Walter Reed Army Institute of Research.

0022-3549/79/1000-1331$01.00/0
© 1979, American Pharmaceutical Association

Table I—Physical Properties of 1,2-Dialkyl-4-pyrazolidinethiols

Compound	R	Reaction Time, days	Boiling Point (torr) or Melting Point	n_D	Yield, %	Recrystallization Solvent[a]	Formula	Analysis, %	Calc.	Found
Ia	CH_3	11[b]	69.5° (33)	1.5031 (24.5°)	12	—	$C_5H_{12}N_2S$	C	45.42	45.57
								H	9.15	9.38
								N	21.19	20.81
								S	24.25	23.80
Ia HCl	—	—	88–90°	—	—	A	$C_5H_{12}N_2S$·HCl	C	35.60	35.19
								H	7.77	8.18
								Cl	21.02	20.59
								N	16.61	16.39
								S	19.01	18.79
Ib	CH_3CH_2	7	82° (9)	1.4911 (22.5°)	31	—	$C_7H_{16}N_2S$	C	52.45	52.60
								H	10.06	9.96
								N	17.48	17.41
								S	20.01	19.80
Ib HCl	—	—	82–84°	—	—	A	$C_7H_{16}N_2S$·HCl	C	42.73	42.52
								H	8.71	8.97
								Cl	18.02	18.00
								N	14.24	14.20
								S	16.30	16.28
Ic	$CH_3(CH_2)_2$	4	108° (10)	1.4835 (24.5°)	29	—	$C_9H_{20}N_2S$	C	57.39	57.00
								H	10.70	10.67
								N	14.88	15.28
								S	17.03	17.05
Ic HCl	—	—	91.5–92.5°	—	—	A	$C_9H_{20}N_2S$·HCl	C	48.08	48.36
								H	9.42	9.83
								Cl	15.77	15.38
								N	12.46	12.25
								S	14.26	14.20
Id	$(CH_3)_2CH$	27	34° (0.03)	1.4845 (22°)	26	—	$C_9H_{20}N_2S$[c]		—	—
Id HCl	—	—	105.5–107.5°	—	—	B	$C_9H_{20}N_2S$·HCl	C	48.08	47.98
								H	9.42	9.02
								Cl	15.77	15.98
								N	12.46	12.60
								S	14.26	14.58
Ie	$(CH_3)_2CHCH_2$	20	64° (0.12)	1.4740 (31°)	32	—	$C_{11}H_{24}N_2S$	C	61.05	61.06
								H	11.18	11.23
								N	12.95	13.15
								S	14.82	14.85
Ie[d]	—	—	104.5–105°	—	—	C	$C_{18}H_{26}N_4SO_5$	C	52.66	52.52
								H	6.38	6.52
								N	13.65	13.44
								S	7.81	7.90

[a] A = ethanol–diethyl ether, B = ethyl acetate, and C = 95% ethanol. [b] 4°. [c] Not analyzed. [d] 3,5-Dinitrothiolbenzoate.

is not readily apparent; however, nitrogen alkylation has generally resulted in diminished activity (5).

EXPERIMENTAL[2]

Hydrazines—1,2-Dimethylhydrazine (6), 1,2-diethylhydrazine (7), 1,2-dipropylhydrazine (7), and 1,2-diisopropylhydrazine (7) were prepared by literature methods. 1,2-Diisobutylhydrazine was obtained by the lithium aluminum hydride reduction of isobutylideneazine (8) following the method of Renaud and Leitch (7). A 71% yield of a colorless product was obtained, bp 64° (11 torr), n_D^{24} 1.4312 [lit. (9) bp 169.5–170°, 70.5° (16 torr) and 63.5° (10 torr)].

1,2-Dialkyl-4-pyrazolidinethiols (Ia–Ie)—A typical reaction is described, that for the preparation of 1,2-diethyl-4-pyrazolidinethiol (Ib). Table I lists the physical and analytical data.

To a solution of 20.0 g (0.227 mole) of 1,2-diethylhydrazine in 100 ml of anhydrous ether was added 16.4 g (0.152 mole) of 3-chloropropylene sulfide (10, 11). The stoppered flask was kept at room temperature for 1 week. The precipitated hydrochloride salt was filtered, and the ether was evaporated under reduced pressure. The residue was distilled and gave 7.2 g (31%) of a colorless liquid, bp 82° (9 torr), $n_D^{22.5}$ 1.4911. A substantial amount of residue, which was undoubtedly a polymerization product of 3-chloropropylene sulfide, always remained in the distillation flask.

A hydrochloride was prepared and recrystallized from alcohol–ether, mp 82–84°.

[2] Melting points and boiling points are uncorrected. Analyses were performed by Dr. Kurt Eder, Geneva, Switzerland, and Drs. Weiler and Strauss, Oxford, England. IR spectra were determined on a Beckman IR-4 spectrophotometer using sodium chloride optics.

1,2-Diethylpyrazolidine (IV)—*By Desulfurization of 1,2-Diethyl-4-pyrazolidinethiol (Ib)*—To a stirred suspension of 2 spoons of W-2 Raney nickel in 250 ml of methanol was added a solution of 7.30 g (0.0456 mole) of Ib in 50 ml of methanol over 45 min. After 2.5 hr, another spoonful of W-2 Raney nickel was added. One hour later, an additional 2 spoonfuls were added. A total of 5 spoonfuls (~15 g) was added.

After an additional hour (total stirring time of 5.25 hr), the mixture was filtered. The dark-brown filtrate was distilled at atmospheric pressure through a 20-cm column packed with glass helixes to remove the methanol. The residue was distilled and yielded 0.3 g (5.1%) of a liquid, bp 62° (46 torr), n_D^{24} 1.4382 [lit. (12) bp 138°, $n_D^{27.8}$ 1.4409].

A picrate was prepared and recrystallized from absolute ethanol, mp 149.5–150°.

Anal.—Calc. for $C_{13}H_{19}N_5O_7$: C, 43.69; H, 5.36; N, 19.60. Found: C, 44.20; H, 5.31; N, 19.70.

By Alkylation of 1,2-Diethylhydrazine with Trimethylene Bromide—A solution of 34.5 g (0.392 mole) of 1,2-diethylhydrazine and 45.9 g (0.227 mole) of trimethylene bromide in 250 ml of 95% ethanol was added dropwise over 5 hr to 750 ml of refluxing 95% ethanol. The mixture was refluxed for an additional 10 hr, cooled, and neutralized with 28 g (0.50 mole) of solid potassium hydroxide.

The precipitated salts were removed by filtration, and the filtrate was concentrated at atmospheric pressure through a 20-cm column packed with glass helixes. After distillation of the ethanol, the fraction boiling at 132–150° (760 torr) was collected. It was redistilled through the same column to yield 1.7 g (5.8%) of product, bp 140–144°, n_D^{22} 1.4409 [lit. (12) bp 138°, $n_D^{27.8}$ 1.4409].

A picrate was prepared and recrystallized from absolute ethanol, mp 149.5–150.5°.

Anal.—Calc. for $C_{13}H_{19}N_5O_7$: C, 43.69; H, 5.36; N, 19.60. Found: C, 44.15; H, 5.65; N, 19.50.

A mixed melting point taken with the picrate obtained by desulfuri-

zation of 1,2-diethyl-4-pyrazolidinethiol was not depressed. The IR spectra of the two picrates were superimposable.

REFERENCES

(1) M. J. Kornet and R. Daniels, presented in part at the 144th National Meeting of the American Chemical Society, Los Angeles, Calif., Apr. 1963, Abstract MEDI 14.

(2) J. F. Thomson, "Radiation Protection in Mammals," Reinhold, New York, N.Y., 1962.

(3) Gerhardt, *Ber.*, **24**, 352 (1891).

(4) L. Field, A. Ferretti, R. R. Crenshaw, and T. C. Owen, *J. Med. Chem.*, **7**, 39 (1964).

(5) W. O. Foye, in "Medicinal Chemistry," part II, 3rd ed., A. Burger, Ed., Wiley-Interscience, New York, N.Y., 1970, p. 1670.

(6) R. L. Hinman, *J. Am. Chem. Soc.*, **78**, 1645 (1956).

(7) R. Renaud and L. C. Leitch, *Can. J. Chem.*, **32**, 545 (1954).

(8) A. Franke, *Monatsh.*, **19**, 531 (1898).

(9) K. A. Taipale, *J. Russ. Phys. Chem. Soc.*, **56**, 81 (1925).

(10) C. C. J. Culvenor, W. Davies, and K. H. Pausacher, *J. Chem. Soc.*, **1946**, 1050.

(11) K. Furukawa, M. Nomura, and R. Oda, *J. Chem. Soc. Jpn, Chem. Ind. Sect.*, **56**, 184 (1953); through *Chem. Abstr.*, **49**, 4581 (1955).

(12) M. J. Kornet and S. I. Tan, *J. Heterocycl. Chem.*, **6**, 325 (1969).

ACKNOWLEDGMENTS

Abstracted in part from a dissertation submitted by M. J. Kornet to the Graduate College, University of Illinois at the Medical Center, in partial fulfillment of the Doctor of Philosophy degree requirements.

Supported by the U.S. Army Medical Research and Development Command under Contract DA-49-193-MD-2212.

The authors are grateful to Dr. T. R. Sweeney for the antiradiation test results.

Colorimetric Determination of Penicillins and Related Compounds in Intravenous Solutions by Nickel(II)-Catalyzed Hydroxamic Acid Formation

J. W. MUNSON *, D. PAPADIMITRIOU, and P. P. DeLUCA ˣ

Received February 9, 1979, from the *College of Pharmacy, University of Kentucky, Lexington, KY 40506.* Accepted for publication April 30, 1979. *Present address: The Upjohn Co., Kalamazoo, MI 49001.

Abstract □ Solutions of ampicillin, carbenicillin, methicillin, oxacillin, penicillin G, and cephalothin in 5% dextrose were analyzed by nickel(II)-catalyzed hydroxylaminolysis. The reactions of these antibiotics were complete within 20 min at room temperature. Under the analytical conditions, molar absorptivities of the ferric–hydroxamate complexes ranged from 830 to 1005 liters/mole/cm. Coefficients of variation for the analysis of these antibiotics in 5% dextrose were typically <3% at concentrations of 1 mg/ml. Oxacillin was analyzed by the same method in normal saline and/or lactated Ringer solutions. The method also was applied to the analysis of chloramphenicol in aqueous solutions. Only ampicillin showed a significant decrease in concentration in 48 hr.

Keyphrases □ Penicillins—analysis, colorimetry, intravenous solutions, dextrose, nickel(II)-catalyzed hydroxamic acid formation □ Antibiotics—analysis, colorimetry, ampicillin, carbenicillin, methicillin, oxacillin, penicillin G, cephalothin, intravenous solutions, dextrose □ Colorimetry—analysis, penicillins in intravenous solutions, dextrose, nickel(II)-catalyzed hydroxamic acid formation

Hydroxamic acid formation has been employed in the analysis of various carboxylic acid derivatives. Typically, the substrate is reacted with an alkaline hydroxylamine solution, acidified, and then complexed with ferric iron to form a reddish-violet complex. This complex absorbs in the 515–545-nm range with molar absorptivities near 10^3 liters/mole/cm. Esters (1–3), amides (4–6), acid chlorides (7), acid anhydrides (8), lactones (9), and imides (10) have been determined by the alkaline hydroxylaminolysis reaction.

Compounds containing the β-lactam moiety, *e.g.*, penicillins, also have been analyzed by the alkaline reaction (11). However, these compounds also react satisfactorily with hydroxylamine at neutral pH (12, 13). Nickel(II)-catalyzed hydroxylaminolysis has been applied to the analysis of carboxylic acids and acid hydrazides (14, 15). This method also has been applied to cephalosporins that contain the β-lactam group (16).

Table I—Stability of the Ferric–Hydroxamate Complex in Methicillin–Dextrose 5% Solutions

	Neutral Hydroxylamine Method (12)		Nickel(II)-Hydroxylamine Method	
Time[a]	In Water, absorbance[b]	In 5% Dextrose, absorbance[b]	In Water, absorbance[c]	In 5% Dextrose, absorbance[c]
2	0.465	0.455	0.485	0.475
5	0.450	0.400	0.480	0.475
10	0.440	0.330	0.477	0.475
15	0.425	0.165	0.470	0.455
30	—	—	0.463	0.455

[a] Time after mixing ferric iron reagent with the reaction mixture. [b] Absorbance at 490 nm in 1-cm cell. [c] Absorbance at 520 nm in 1-cm cell.

In this study, the stability of some penicillins and cephalothin was examined in solutions for intravenous administration. In the presence of relatively high dextrose concentrations (5% w/v), the neutral hydroxylamine method produced low color yields and color instability. Since the drugs were present in low concentrations, it was not feasible to dilute the samples to reduce the dextrose concentration. Consequently, the nickel(II)-catalyzed hydroxylaminolysis method was applied to these systems.

This paper reports the results on the application of the nickel(II)-catalyzed method to the analysis of ampicillin, carbenicillin, methicillin, oxacillin, penicillin G, and

0022-3549/79/1000-1333$01.00/0

© 1979, American Pharmaceutical Association

zation of 1,2-diethyl-4-pyrazolidinethiol was not depressed. The IR spectra of the two picrates were superimposable.

REFERENCES

(1) M. J. Kornet and R. Daniels, presented in part at the 144th National Meeting of the American Chemical Society, Los Angeles, Calif., Apr. 1963, Abstract MEDI 14.

(2) J. F. Thomson, "Radiation Protection in Mammals," Reinhold, New York, N.Y., 1962.

(3) Gerhardt, *Ber.*, **24**, 352 (1891).

(4) L. Field, A. Ferretti, R. R. Crenshaw, and T. C. Owen, *J. Med. Chem.*, **7**, 39 (1964).

(5) W. O. Foye, in "Medicinal Chemistry," part II, 3rd ed., A. Burger, Ed., Wiley-Interscience, New York, N.Y., 1970, p. 1670.

(6) R. L. Hinman, *J. Am. Chem. Soc.*, **78**, 1645 (1956).

(7) R. Renaud and L. C. Leitch, *Can. J. Chem.*, **32**, 545 (1954).

(8) A. Franke, *Monatsh.*, **19**, 531 (1898).

(9) K. A. Taipale, *J. Russ. Phys. Chem. Soc.*, **56**, 81 (1925).

(10) C. C. J. Culvenor, W. Davies, and K. H. Pausacher, *J. Chem. Soc.*, **1946**, 1050.

(11) K. Furukawa, M. Nomura, and R. Oda, *J. Chem. Soc. Jpn, Chem. Ind. Sect.*, **56**, 184 (1953); through *Chem. Abstr.*, **49**, 4581 (1955).

(12) M. J. Kornet and S. I. Tan, *J. Heterocycl. Chem.*, **6**, 325 (1969).

ACKNOWLEDGMENTS

Abstracted in part from a dissertation submitted by M. J. Kornet to the Graduate College, University of Illinois at the Medical Center, in partial fulfillment of the Doctor of Philosophy degree requirements.

Supported by the U.S. Army Medical Research and Development Command under Contract DA-49-193-MD-2212.

The authors are grateful to Dr. T. R. Sweeney for the antiradiation test results.

Colorimetric Determination of Penicillins and Related Compounds in Intravenous Solutions by Nickel(II)-Catalyzed Hydroxamic Acid Formation

J. W. MUNSON *, D. PAPADIMITRIOU, and P. P. DeLUCA ˣ

Received February 9, 1979, from the *College of Pharmacy, University of Kentucky, Lexington, KY 40506.* Accepted for publication April 30, 1979. *Present address: The Upjohn Co., Kalamazoo, MI 49001.

Abstract □ Solutions of ampicillin, carbenicillin, methicillin, oxacillin, penicillin G, and cephalothin in 5% dextrose were analyzed by nickel(II)-catalyzed hydroxylaminolysis. The reactions of these antibiotics were complete within 20 min at room temperature. Under the analytical conditions, molar absorptivities of the ferric–hydroxamate complexes ranged from 830 to 1005 liters/mole/cm. Coefficients of variation for the analysis of these antibiotics in 5% dextrose were typically <3% at concentrations of 1 mg/ml. Oxacillin was analyzed by the same method in normal saline and/or lactated Ringer solutions. The method also was applied to the analysis of chloramphenicol in aqueous solutions. Only ampicillin showed a significant decrease in concentration in 48 hr.

Keyphrases □ Penicillins—analysis, colorimetry, intravenous solutions, dextrose, nickel(II)-catalyzed hydroxamic acid formation □ Antibiotics—analysis, colorimetry, ampicillin, carbenicillin, methicillin, oxacillin, penicillin G, cephalothin, intravenous solutions, dextrose □ Colorimetry—analysis, penicillins in intravenous solutions, dextrose, nickel(II)-catalyzed hydroxamic acid formation

Hydroxamic acid formation has been employed in the analysis of various carboxylic acid derivatives. Typically, the substrate is reacted with an alkaline hydroxylamine solution, acidified, and then complexed with ferric iron to form a reddish-violet complex. This complex absorbs in the 515–545-nm range with molar absorptivities near 10^3 liters/mole/cm. Esters (1–3), amides (4–6), acid chlorides (7), acid anhydrides (8), lactones (9), and imides (10) have been determined by the alkaline hydroxylaminolysis reaction.

Compounds containing the β-lactam moiety, *e.g.*, penicillins, also have been analyzed by the alkaline reaction (11). However, these compounds also react satisfactorily with hydroxylamine at neutral pH (12, 13). Nickel(II)-catalyzed hydroxylaminolysis has been applied to the analysis of carboxylic acids and acid hydrazides (14, 15). This method also has been applied to cephalosporins that contain the β-lactam group (16).

Table I—Stability of the Ferric–Hydroxamate Complex in Methicillin–Dextrose 5% Solutions

	Neutral Hydroxylamine Method (12)		Nickel(II)-Hydroxylamine Method	
Time[a]	In Water, absorbance[b]	In 5% Dextrose, absorbance[b]	In Water, absorbance[c]	In 5% Dextrose, absorbance[c]
2	0.465	0.455	0.485	0.475
5	0.450	0.400	0.480	0.475
10	0.440	0.330	0.477	0.475
15	0.425	0.165	0.470	0.455
30	—	—	0.463	0.455

[a] Time after mixing ferric iron reagent with the reaction mixture. [b] Absorbance at 490 nm in 1-cm cell. [c] Absorbance at 520 nm in 1-cm cell.

In this study, the stability of some penicillins and cephalothin was examined in solutions for intravenous administration. In the presence of relatively high dextrose concentrations (5% w/v), the neutral hydroxylamine method produced low color yields and color instability. Since the drugs were present in low concentrations, it was not feasible to dilute the samples to reduce the dextrose concentration. Consequently, the nickel(II)-catalyzed hydroxylaminolysis method was applied to these systems.

This paper reports the results on the application of the nickel(II)-catalyzed method to the analysis of ampicillin, carbenicillin, methicillin, oxacillin, penicillin G, and

0022-3549/79/1000-1333$01.00/0

© 1979, American Pharmaceutical Association

Table II—Analysis of Penicillins in 5% Dextrose Solutions (n = 4)

Drug	Molar Absorptivity		Concentration Added, mg/ml	Concentration Found, mg/ml	CV, %
	In Water[a]	In 5% Dextrose[a]			
Methicillin sodium	860	831	1.00	1.05	2.3
Carbenicillin disodium	798	791	1.00	1.01	1.1
Oxacillin sodium	1005	911	0.84	0.87	2.9
Penicillin G potassium	934	894	0.60	0.59	1.4
Ampicillin trihydrate	916	849	1.28	1.32	1.9

[a] Calculated on the basis of the concentration of the sample in the final solution. Units are liters per mole per centimeter at 520 nm.

Table III—Analysis of Oxacillin Sodium in Other Intravenous Fluids by Nickel(II)-Catalyzed Hydroxylaminolysis

Intravenous Fluid	Apparent Molar Absorptivity[a], M^{-1} cm^{-1}	Concentration Added, mg/ml	Concentration Found, mg/ml	CV, %	n
Normal saline	837	1.00	0.95	1.6	3
5% Dextrose in normal saline	770	0.998	1.00	2.4	4
Lactated Ringer	778	0.998	0.98	2.2	4
5% Dextrose in lactated Ringer	801	0.998	0.94	3.6	3

[a] At 520 nm.

cephalothin in 5% dextrose solutions. Data also are presented on oxacillin analysis in normal saline solution, lactated Ringer solution, and mixtures of these solutions with 5% dextrose. Finally, data are presented on the application of this method to chloramphenicol analysis.

EXPERIMENTAL

Materials—Ampicillin trihydrate[1], carbenicillin disodium[2], methicillin sodium[3], oxacillin sodium[4], penicillin G potassium[4], cephalothin sodium[5], and chloramphenicol[6] were used as received. Hydroxylamine hydrochloride, nickel(II) chloride, sodium hydroxide, hydrochloric acid, and ferric chloride hexahydrate were reagent grade. Dextrose solutions (5% w/v) were obtained commercially[7]. All water was double distilled in an all-glass system.

The nickel–hydroxylamine reagent was prepared by dissolving 6.95 g of hydroxylamine hydrochloride and 2.38 g of nickel chloride in 30 ml of distilled water. Sodium hydroxide, 10 N, was added (~7.5 ml) to adjust the solution to pH 6.2 using a silver–silver chloride reference electrode. This solution was then quantitatively diluted with water to 50.0 ml.

The ferric chloride reagent (0.35 M) was prepared by dissolving 94.6 g of ferric chloride hexahydrate in 400 ml of 0.1 N HCl. This solution was quantitatively transferred to a 1-liter volumetric flask with the aid of 0.1 N HCl and was diluted to exactly 1 liter with 0.1 N HCl. The final solution was stored in the dark to prevent photoreduction of the ferric ion.

Assay—Samples from the intravenous solutions containing the drug (2.0 or 3.0 ml) were transferred to a test tube, and sufficient water was added to make exactly 4.0 ml. Exactly 2.0 ml of the nickel–hydroxylamine reagent was added to the samples, which were allowed to stand for 20 min at room temperature. Exactly 1.0 ml of 4 N HCl and 5.0 ml of the ferric chloride solution were then added. After 5 min, the absorbance was measured in 1-cm cells on a recording spectrophotometer at the appropriate wavelength. An appropriate blank was prepared for all analyses. Concentrations were determined from calibration curves obtained from the analysis of standard solutions prepared in 5% dextrose solutions.

RESULTS AND DISCUSSION

The effect of dextrose on the stability of the ferric–hydroxamate complex generated by the neutral hydroxylaminolysis reaction (12, 13) and the nickel(II)-catalyzed method on methicillin is shown in Table I. With the neutral reaction, absorbance decreased with time even without dextrose, but the decrease was far more dramatic in the presence of 5% dextrose. A spectral shift toward higher wavelengths also was observed with time in the dextrose-containing samples.

As shown in Table I, the color instability was less with the nickel(II)-catalyzed method. Minimal absorbance changes occurred within the first 15 min after mixing. The 520-nm wavelength was chosen to minimize the blank absorbance values while maximizing the analytical sample absorbance. In some cases, a gradual increase in absorbance by the blank was observed with time. The use of freshly prepared blanks avoided this problem. No shifts in wavelength maxima were observed with this method. The greater stability in the nickel(II)-catalyzed method was probably due to nickel complexation with hydroxylamine, which lessened its tendency to reduce ferric iron to ferrous iron.

The nickel(II)-catalyzed method was applied to the analysis of methicillin, carbenicillin, oxacillin, penicillin G, and ampicillin in intravenous solutions containing 5% dextrose. In all cases, the absorbance of the resultant ferric–hydroxamate complex was linearly related to the drug concentration in the reaction mixture. A typical calibration curve for methicillin sodium can be described by:

$$\text{absorbance (520 nm)} = 0.00194\ \text{concentration (mg/ml)} + 0.015 \quad \text{(Eq. 1)}$$

In the 80–400-μg/ml range, the correlation coefficient for this line was 0.9993.

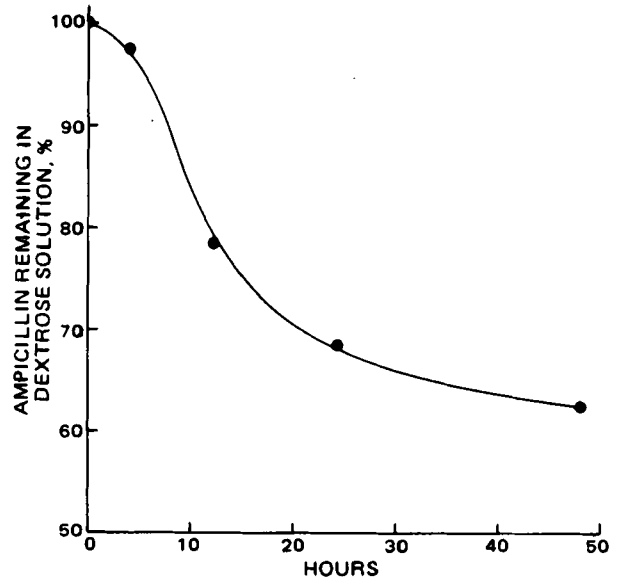

Figure 1—*Ampicillin in 5% dextrose as a function of time as determined by the nickel(II)-catalyzed hydroxylamine method.*

[1] Bristol Laboratories, Syracuse, N.Y.
[2] Pfizer Laboratories, New York, N.Y.
[3] Beecham Laboratories, Piscataway, N.J.
[4] E. R. Squibb, Princeton, N.J.
[5] USP reference standard, Rockville, Md.
[6] Parke-Davis, Detroit, Mich.
[7] McGaw Laboratories, Irvine, Calif.

The analyses of the penicillins in 5% dextrose solutions are summarized in Table II.

In most cases, the apparent molar absorptivities of the ferric–hydroxamate complexes were slightly lower in the 5% dextrose samples. Replicate determinations of 1-mg of methicillin sodium/ml samples gave good precision and accuracy.

Only ampicillin in 5% dextrose showed any appreciable change in concentration over 48 hr at room temperature (Fig. 1). Samples were obtained at zero time and at 48 hr and were analyzed by TLC. A large spot at R_f 0.65, indicative of ampicillin degradation, appeared in the 48-hr sample.

Although cephalothin was previously determined by this method (16), a study was undertaken to determine if the method is applicable to cephalothin analysis in dextrose solutions. Replicate analyses of a solution containing cephalothin sodium (1.00 mg/ml) gave an average value of 1.04 mg/ml with a coefficient of variation of 2.7%. In this study, the absorbance was measured at 490 nm and the complex was stable for at least 15 min.

Oxacillin was analyzed in several other intravenous fluids with good precision and accuracy (Table III).

The nickel-catalyzed method also was applied to a chloramphenicol succinate sodium solution. In this case, it was necessary to heat the reaction for 2 hr at 80° to obtain an adequate color yield. Under these conditions, as little as 25 μg/ml could be detected. A typical calibration curve can be described by:

$$\text{absorbance} = 0.00273 \text{ concentration } (\mu g/ml) + 0.00 \quad \text{(Eq. 2)}$$

In the 25–250-μg/ml range, correlation coefficients for this equation were typically 0.999.

Considering the extensive use of β-lactam antibiotics in intravenous admixtures, the nickel(II)-catalyzed hydroxylaminolysis method offers a rapid and reliable means of assessing antibiotic stability in numerous intravenous fluids.

REFERENCES

(1) V. Goldenberg and P. E. Spoerri, *Anal. Chem.*, **31**, 1735 (1959).

(2) J. A. Feldman and B. J. Robb, *J. Pharm. Sci.*, **59**, 1648 (1970).

(3) L. Dryanovska and I. Iovchev, *Farmatsiya*, **25**, 10 (1975); through *Chem. Abstr.*, **84**, 79751m.

(4) F. Bergman, *Anal. Chem.*, **24**, 1367 (1952).

(5) E. Schleider, D. M. Eno, J. A. Feldman, and A. M. Galinsky, *J. Pharm. Sci.*, **58**, 1258 (1969).

(6) J. A. Feldman and V. U. Patel, *ibid.*, **60**, 1696 (1971).

(7) R. F. Goddu, N. F. LeBlank, and C. M. Wright, *Anal. Chem.*, **27**, 1252 (1955).

(8) W. M. Diggle and J. C. Gage, *Analyst*, **78**, 473 (1953).

(9) I. S. Gibbs and M. N. Tuckerman, *J. Pharm. Sci.*, **59**, 395 (1970).

(10) R. E. Notari, *ibid.*, **58**, 1064 (1969).

(11) J. H. Ford, *Anal. Chem.*, **19**, 1004 (1947).

(12) J. F. Gallelli, *Am. J. Hosp. Pharm.*, **24**, 425 (1967).

(13) W. W. Holl, M. O'Brien, J. Filian, T. Mazeika, A. Post, D. Pitkin, and P. Actor, *J. Pharm. Sci.*, **64**, 1232 (1975).

(14) K. A. Connors and J. W. Munson, *Anal. Chem.*, **44**, 336 (1972).

(15) J. W. Munson and K. A. Connors, *J. Pharm. Sci.*, **61**, 211 (1972).

(16) D. L. Mays, F. K. Bangert, W. C. Cantrell, and W. G. Evans, *Anal. Chem.*, **47**, 2229 (1975).

ACKNOWLEDGMENTS

Presented in part at the APhA Academy of Pharmaceutical Sciences, Hollywood, Fla., meeting, November 1978.

Supported in part by a grant from McGaw Laboratories, Irvine, Calif.

COMMUNICATIONS

Identification of Griseofulvic Acid as a Urine Metabolite of Griseofulvin in Humans

Keyphrases □ Griseofulvin—human urinary metabolite, identification, griseofulvic acid □ Antifungal agents—griseofulvin, human urinary metabolite, identification, griseofulvic acid □ Metabolite—of griseofulvin, human urine, identification, griseofulvic acid □ Griseofulvic acid—metabolite of griseofulvin, human urine, identification

To the Editor:

Griseofulvin was introduced in 1959 as an effective oral antifungal agent for humans and animals. Many studies of griseofulvin metabolism have been reported since then. Investigators of griseofulvin metabolism in humans reported that almost all of a daily griseofulvin dose was excreted as 6-desmethylgriseofulvin in the urine in 24 hr (1). Studies using ^{14}C-griseofulvin and GLC showed that the major metabolite was 6-desmethylgriseofulvin but that the drug also was excreted partially as 4-desmethylgriseofulvin and as several other unidentified metabolites (2). Although these unidentified compounds represent only a small portion of the total drug, their identities are important in understanding griseofulvin metabolism.

A simple and rapid determination of griseofulvin and its derivatives using reversed-phase high-pressure liquid chromatography was developed in this laboratory. Analysis of human urine samples by this method revealed that, in addition to 6-desmethylgriseofulvin, griseofulvic acid (7-chloro-4,6-dimethoxy-6′-methylgrisan-3,2′,4′-trione) also is a urinary griseofulvin metabolite. However, the reported 4-desmethylgriseofulvin was not observed in this study. The urinary concentration ratio of griseofulvic acid to 6-desmethylgriseofulvin was ~1:15.

Figure 1 shows chromatograms of urine samples obtained from a normal subject 6 hr after a 250-mg oral griseofulvin dose. The griseofulvin metabolites in the urine sample were extracted into cyclohexane–ethylene dichloride (1:1) (3), and the mixture then was evaporated to dryness and reconstituted with the chromatographic mobile phase solvent. Figure 1A represents the direct extraction of the urine sample. Figure 1B represents the same sample after incubation overnight at 37° with β-glucuronidase to hydrolyze the glucuronide conjugate prior to the extraction.

The chromatograms were obtained with a reversed-phase column[1] at a 1.0-ml/min flow rate. The mobile phase was 45% acetonitrile in water (v/v), with the pH adjusted to 3.4 using acetic acid. The upper chromatograms represent the response of a fluorescence detector excited at 280 nm. The lower chromatograms represent the response of a UV detector at 290 nm. The advantage of using both

[1] μBondapak C_{18}, Waters Associates, Milford, Mass.

0022-3549/79/1000-1335$01.00/0

© 1979, American Pharmaceutical Association

The analyses of the penicillins in 5% dextrose solutions are summarized in Table II.

In most cases, the apparent molar absorptivities of the ferric–hydroxamate complexes were slightly lower in the 5% dextrose samples. Replicate determinations of 1-mg of methicillin sodium/ml samples gave good precision and accuracy.

Only ampicillin in 5% dextrose showed any appreciable change in concentration over 48 hr at room temperature (Fig. 1). Samples were obtained at zero time and at 48 hr and were analyzed by TLC. A large spot at R_f 0.65, indicative of ampicillin degradation, appeared in the 48-hr sample.

Although cephalothin was previously determined by this method (16), a study was undertaken to determine if the method is applicable to cephalothin analysis in dextrose solutions. Replicate analyses of a solution containing cephalothin sodium (1.00 mg/ml) gave an average value of 1.04 mg/ml with a coefficient of variation of 2.7%. In this study, the absorbance was measured at 490 nm and the complex was stable for at least 15 min.

Oxacillin was analyzed in several other intravenous fluids with good precision and accuracy (Table III).

The nickel-catalyzed method also was applied to a chloramphenicol succinate sodium solution. In this case, it was necessary to heat the reaction for 2 hr at 80° to obtain an adequate color yield. Under these conditions, as little as 25 μg/ml could be detected. A typical calibration curve can be described by:

$$\text{absorbance} = 0.00273 \text{ concentration } (\mu g/ml) + 0.00 \quad \text{(Eq. 2)}$$

In the 25–250-μg/ml range, correlation coefficients for this equation were typically 0.999.

Considering the extensive use of β-lactam antibiotics in intravenous admixtures, the nickel(II)-catalyzed hydroxylaminolysis method offers a rapid and reliable means of assessing antibiotic stability in numerous intravenous fluids.

REFERENCES

(1) V. Goldenberg and P. E. Spoerri, *Anal. Chem.*, **31**, 1735 (1959).

(2) J. A. Feldman and B. J. Robb, *J. Pharm. Sci.*, **59**, 1648 (1970).

(3) L. Dryanovska and I. Iovchev, *Farmatsiya*, **25**, 10 (1975); through *Chem. Abstr.*, **84**, 79751m.

(4) F. Bergman, *Anal. Chem.*, **24**, 1367 (1952).

(5) E. Schleider, D. M. Eno, J. A. Feldman, and A. M. Galinsky, *J. Pharm. Sci.*, **58**, 1258 (1969).

(6) J. A. Feldman and V. U. Patel, *ibid.*, **60**, 1696 (1971).

(7) R. F. Goddu, N. F. LeBlank, and C. M. Wright, *Anal. Chem.*, **27**, 1252 (1955).

(8) W. M. Diggle and J. C. Gage, *Analyst*, **78**, 473 (1953).

(9) I. S. Gibbs and M. N. Tuckerman, *J. Pharm. Sci.*, **59**, 395 (1970).

(10) R. E. Notari, *ibid.*, **58**, 1064 (1969).

(11) J. H. Ford, *Anal. Chem.*, **19**, 1004 (1947).

(12) J. F. Gallelli, *Am. J. Hosp. Pharm.*, **24**, 425 (1967).

(13) W. W. Holl, M. O'Brien, J. Filian, T. Mazeika, A. Post, D. Pitkin, and P. Actor, *J. Pharm. Sci.*, **64**, 1232 (1975).

(14) K. A. Connors and J. W. Munson, *Anal. Chem.*, **44**, 336 (1972).

(15) J. W. Munson and K. A. Connors, *J. Pharm. Sci.*, **61**, 211 (1972).

(16) D. L. Mays, F. K. Bangert, W. C. Cantrell, and W. G. Evans, *Anal. Chem.*, **47**, 2229 (1975).

ACKNOWLEDGMENTS

Presented in part at the APhA Academy of Pharmaceutical Sciences, Hollywood, Fla., meeting, November 1978.

Supported in part by a grant from McGaw Laboratories, Irvine, Calif.

COMMUNICATIONS

Identification of Griseofulvic Acid as a Urine Metabolite of Griseofulvin in Humans

Keyphrases □ Griseofulvin—human urinary metabolite, identification, griseofulvic acid □ Antifungal agents—griseofulvin, human urinary metabolite, identification, griseofulvic acid □ Metabolite—of griseofulvin, human urine, identification, griseofulvic acid □ Griseofulvic acid—metabolite of griseofulvin, human urine, identification

To the Editor:

Griseofulvin was introduced in 1959 as an effective oral antifungal agent for humans and animals. Many studies of griseofulvin metabolism have been reported since then. Investigators of griseofulvin metabolism in humans reported that almost all of a daily griseofulvin dose was excreted as 6-desmethylgriseofulvin in the urine in 24 hr (1). Studies using ^{14}C-griseofulvin and GLC showed that the major metabolite was 6-desmethylgriseofulvin but that the drug also was excreted partially as 4-desmethylgriseofulvin and as several other unidentified metabolites (2). Although these unidentified compounds represent only a small portion of the total drug, their identities are important in understanding griseofulvin metabolism.

A simple and rapid determination of griseofulvin and its derivatives using reversed-phase high-pressure liquid chromatography was developed in this laboratory. Analysis of human urine samples by this method revealed that, in addition to 6-desmethylgriseofulvin, griseofulvic acid (7-chloro-4,6-dimethoxy-6′-methylgrisan-3,2′,4′-trione) also is a urinary griseofulvin metabolite. However, the reported 4-desmethylgriseofulvin was not observed in this study. The urinary concentration ratio of griseofulvic acid to 6-desmethylgriseofulvin was ~1:15.

Figure 1 shows chromatograms of urine samples obtained from a normal subject 6 hr after a 250-mg oral griseofulvin dose. The griseofulvin metabolites in the urine sample were extracted into cyclohexane–ethylene dichloride (1:1) (3), and the mixture then was evaporated to dryness and reconstituted with the chromatographic mobile phase solvent. Figure 1A represents the direct extraction of the urine sample. Figure 1B represents the same sample after incubation overnight at 37° with β-glucuronidase to hydrolyze the glucuronide conjugate prior to the extraction.

The chromatograms were obtained with a reversed-phase column[1] at a 1.0-ml/min flow rate. The mobile phase was 45% acetonitrile in water (v/v), with the pH adjusted to 3.4 using acetic acid. The upper chromatograms represent the response of a fluorescence detector excited at 280 nm. The lower chromatograms represent the response of a UV detector at 290 nm. The advantage of using both

[1] μBondapak C_{18}, Waters Associates, Milford, Mass.

0022-3549/79/1000-1335$01.00/0

© 1979, American Pharmaceutical Association

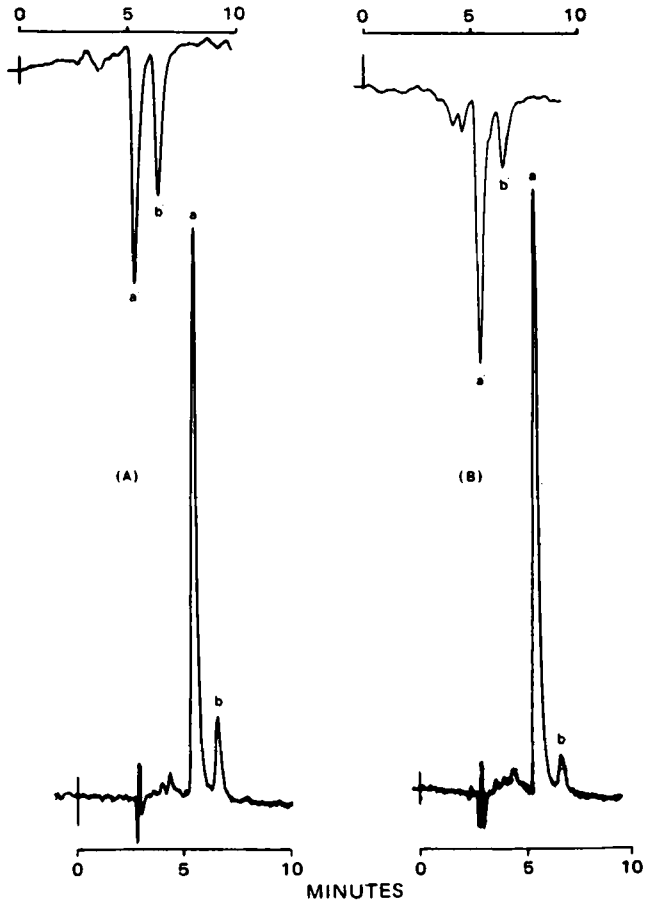

Figure 1—*Chromatograms of human urinary griseofulvin metabolites. Key: A, untreated sample; and B, the same sample after incubation overnight with β-glucuronidase at 37°. Peak response in A represents the original urine concentration; in B, the urine concentration was diluted to one-half. The top and bottom chromatograms were obtained with fluorescence and UV detection, respectively.*

detectors is that the purity of a separated component in a chromatogram may be evaluated with the peak response ratio of the two detections; if the peak response ratio of a component is different from that of the standard, then either the peak response represents a different species or some impurities may have eluted with the same retention time.

Peaks a and b, which were not observed in the blank urine sample, had retention times identical to those of standards of 6-desmethylgriseofulvin and griseofulvic acid, respectively. Furthermore, the UV–fluorescence peak response ratios of peaks a and b also were the same with respect to their standards. It is concluded that peak a represents 6-desmethylgriseofulvin and that peak b represents griseofulvic acid. The presence of griseofulvic acid in urine samples was evidenced further in TLC studies. With a silica gel plate[2] and chloroform–methanol (10:1 v/v), two urinary metabolites were observed and identified by comparison with 6-desmethylgriseofulvin (R_f 0.18) and griseofulvic acid (R_f 0.05) standards. 4-Desmethylgriseofulvin (R_f 0.36) was not found in the urine samples.

The 6-desmethylgriseofulvin standard was isolated from dog urine according to a literature method (3). The purified product was positively identified as 6-desmethylgriseofulvin by a melting-point measurement (4) and by its mass spectrum, which was identical with that reported previously (5). The griseofulvic acid standard was synthesized by reacting griseofulvin with boron tribromide at −60°. The purified product showed a melting point and a mass spectrum identical to those reported for griseofulvic acid (4, 5). The 4-desmethylgriseofulvin standard was prepared according to a literature method (4), and it also was identified by its melting point and its mass spectrum.

The griseofulvic acid formation is speculated to occur *via* microsomal demethylation at the 2′-position and subsequent tautomerization of the 2′-enol to the 2′,4′-dione. The pharmacokinetics of this metabolite and its toxicological effect are under investigation.

(1) M. J. Barnes and B. Boothroyd, *Biochem. J.*, **78**, 41 (1961).
(2) C. C. Lin, J. Magat, R. Chang, J. McGlotten, and S. Synchowicz, *J. Pharmacol. Exp. Ther.*, **187**, 415 (1973).
(3) P. A. Harris and S. Riegelman, *J. Pharm. Sci.*, **58**, 93 (1969).
(4) V. Arkley, J. Attenburrow, G. I. Gregory, and T. Walder, *J. Chem. Soc.*, **1962**, 1260.
(5) J. A. Ballantine and R. G. Fenwick, *Org. Mass Spectrom.*, **2**, 1145 (1969).

Hossein Zia
School of Pharmacy
University of Isfahan
Isfahan, Iran
John P. O'Donnell
Joseph K. H. Ma ˣ
School of Pharmacy
West Virginia University
Morgantown, WV 26506

Received April 19, 1979.
Accepted for publication July 26, 1979.

Effect of Instrumental Vibration Levels on Dissolution

Keyphrases □ Dissolution tests—effects of instrumental vibration, tablets □ Vibration—effect on dissolution tests, tablets

To the Editor:

In the process of investigating the dissolution of two commercial enteric-coated aspirin tablets, large variations in dissolution profiles were observed between two dissolution apparatus (1). The dissolution profiles were followed in simulated intestinal juice for 10 hr using the dissolution procedure described in USP XIX (2). The apparatus[1], designated left (L) and right (R), were operated at a stirring speed of 50 ± 1.5 rpm throughout the study. The tablets in the L apparatus dissolved more slowly, leaving partial tablet residues after 10 hr of dissolution. Additionally, the dissolution profiles were low, indicating poor dissolution characteristics. However, in the R apparatus, tablets from the same batch dissolved completely in the same time period, and dissolution profiles were substan-

[2] Silica gel 60F, 0.05 mm thick, E. Merck, Darmstadt, West Germany.

[1] Hanson Research Corp., Northridge, Calif.

0022-3549/79/1000-1336$01.00/0
© 1979, American Pharmaceutical Association

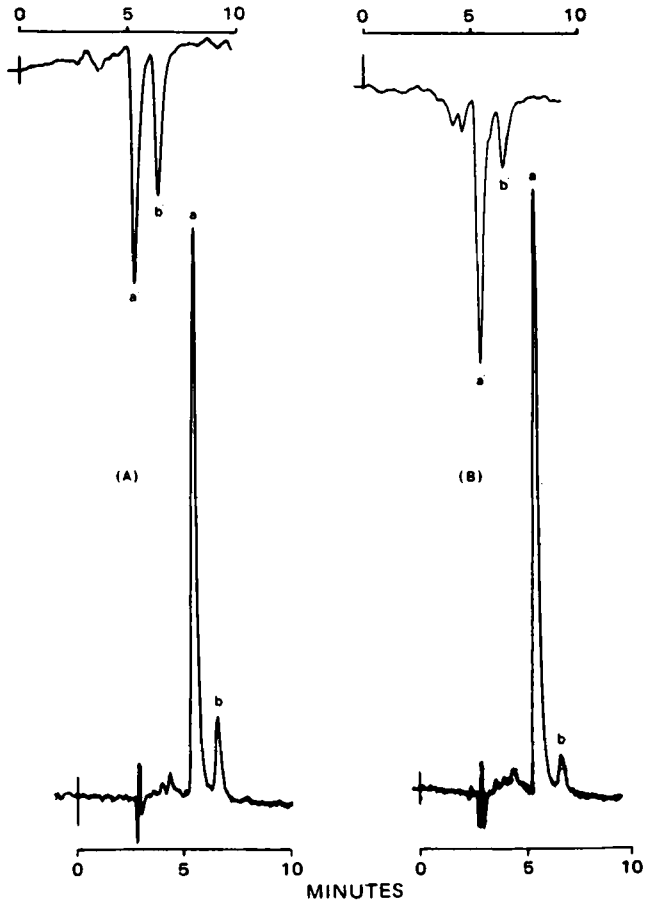

Figure 1—*Chromatograms of human urinary griseofulvin metabolites. Key: A, untreated sample; and B, the same sample after incubation overnight with β-glucuronidase at 37°. Peak response in A represents the original urine concentration; in B, the urine concentration was diluted to one-half. The top and bottom chromatograms were obtained with fluorescence and UV detection, respectively.*

detectors is that the purity of a separated component in a chromatogram may be evaluated with the peak response ratio of the two detections; if the peak response ratio of a component is different from that of the standard, then either the peak response represents a different species or some impurities may have eluted with the same retention time.

Peaks a and b, which were not observed in the blank urine sample, had retention times identical to those of standards of 6-desmethylgriseofulvin and griseofulvic acid, respectively. Furthermore, the UV–fluorescence peak response ratios of peaks a and b also were the same with respect to their standards. It is concluded that peak a represents 6-desmethylgriseofulvin and that peak b represents griseofulvic acid. The presence of griseofulvic acid in urine samples was evidenced further in TLC studies. With a silica gel plate[2] and chloroform–methanol (10:1 v/v), two urinary metabolites were observed and identified by comparison with 6-desmethylgriseofulvin (R_f 0.18) and griseofulvic acid (R_f 0.05) standards. 4-Desmethylgriseofulvin (R_f 0.36) was not found in the urine samples.

The 6-desmethylgriseofulvin standard was isolated from dog urine according to a literature method (3). The purified product was positively identified as 6-desmethylgriseofulvin by a melting-point measurement (4) and by its mass spectrum, which was identical with that reported previously (5). The griseofulvic acid standard was synthesized by reacting griseofulvin with boron tribromide at −60°. The purified product showed a melting point and a mass spectrum identical to those reported for griseofulvic acid (4, 5). The 4-desmethylgriseofulvin standard was prepared according to a literature method (4), and it also was identified by its melting point and its mass spectrum.

The griseofulvic acid formation is speculated to occur *via* microsomal demethylation at the 2′-position and subsequent tautomerization of the 2′-enol to the 2′,4′-dione. The pharmacokinetics of this metabolite and its toxicological effect are under investigation.

(1) M. J. Barnes and B. Boothroyd, *Biochem. J.*, **78**, 41 (1961).
(2) C. C. Lin, J. Magat, R. Chang, J. McGlotten, and S. Synchowicz, *J. Pharmacol. Exp. Ther.*, **187**, 415 (1973).
(3) P. A. Harris and S. Riegelman, *J. Pharm. Sci.*, **58**, 93 (1969).
(4) V. Arkley, J. Attenburrow, G. I. Gregory, and T. Walder, *J. Chem. Soc.*, **1962**, 1260.
(5) J. A. Ballantine and R. G. Fenwick, *Org. Mass Spectrom.*, **2**, 1145 (1969).

Hossein Zia
School of Pharmacy
University of Isfahan
Isfahan, Iran
John P. O'Donnell
Joseph K. H. Ma ˣ
School of Pharmacy
West Virginia University
Morgantown, WV 26506

Received April 19, 1979.
Accepted for publication July 26, 1979.

Effect of Instrumental Vibration Levels on Dissolution

Keyphrases □ Dissolution tests—effects of instrumental vibration, tablets □ Vibration—effect on dissolution tests, tablets

To the Editor:

In the process of investigating the dissolution of two commercial enteric-coated aspirin tablets, large variations in dissolution profiles were observed between two dissolution apparatus (1). The dissolution profiles were followed in simulated intestinal juice for 10 hr using the dissolution procedure described in USP XIX (2). The apparatus[1], designated left (L) and right (R), were operated at a stirring speed of 50 ± 1.5 rpm throughout the study. The tablets in the L apparatus dissolved more slowly, leaving partial tablet residues after 10 hr of dissolution. Additionally, the dissolution profiles were low, indicating poor dissolution characteristics. However, in the R apparatus, tablets from the same batch dissolved completely in the same time period, and dissolution profiles were substan-

[2] Silica gel 60F, 0.05 mm thick, E. Merck, Darmstadt, West Germany.

[1] Hanson Research Corp., Northridge, Calif.

0022-3549/79/1000-1336$01.00/0
© 1979, American Pharmaceutical Association

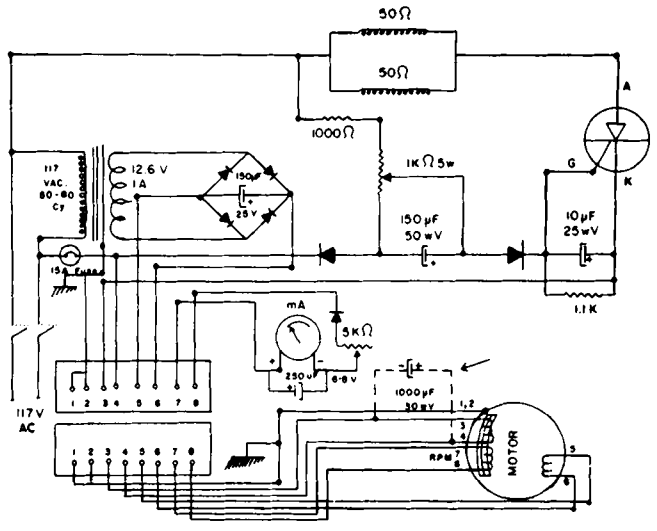

Figure 1—*Dissolution motor control circuit. Modification is indicated by arrow.*

tially higher at all times.

Upon observation, the L motor was noticed to sound and feel rough. Vibrations appeared to be the cause of the performance differences. Since both dissolution vessels were immersed in the same water bath and shared stands with the dissolution and stirring motors, vibrations could be transmitted by the motors *via* the shared stands. These vibrations might increase the extent of dissolution. To test this hypothesis, the mixers[2] and the dissolution motors were isolated from each other and from other components of the apparatus; supporting stands were sandbagged to reduce vibrations. Additionally, the shafts connecting the baskets to the dissolution motors were shortened to reduce shaft whip.

After these measures were taken, the dissolution profiles improved in likeness but continued to be high for the R apparatus. This difference in dissolution profiles could not be explained by random error for a given batch of tablets. When the dissolution motors were switched, the results interchanged. An analysis of variance (ANOVA) showed

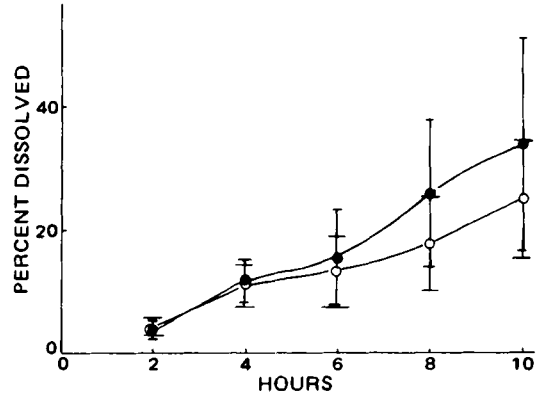

Figure 2—*Dissolution profiles of L apparatus. Key: ●, average of three observations before modification to rectifying circuit; and ○, average of five observations after modification to rectifying circuit. Vertical bars indicate ±1 SE around the mean.*

[2] Lightnin mixers, Mixing Equipment Co., Rochester, N.Y.

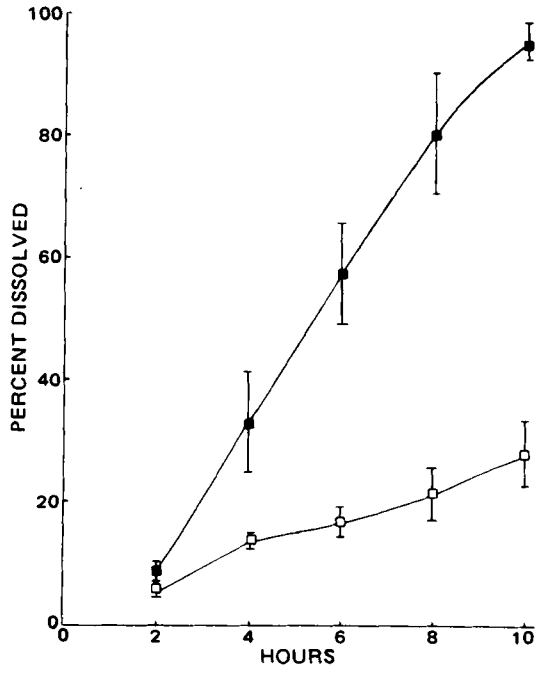

Figure 3—*Dissolution profiles of R apparatus. Key: ■, average of three observations before modification to rectifying circuit; and □, average of five observations after modification to rectifying circuit. Vertical bars indicate ±1 SE around the mean.*

that dissolution profiles for a given batch were still significantly different at the $p = 0.03$ level, indicating that the dissolution apparatus were not operating in a matched fashion. Further reduction of vibration levels was necessary. These observations are in agreement with those of Beyer and Smith (3), but differ in that Beyer and Smith indicated their sources of vibration to be external in nature, such as the circulating pump and activities in the surrounding environment, originating from various benchtop sources.

The speed control circuit appeared to require a 1000-μF capacitor to absorb the high-frequency component of the applied pulses and to smooth out the jerky movement of the motor. This modification can be observed in Fig. 1; connections of the capacitor are designated as dotted lines. Subsequently, the dissolution profiles from the same batch appeared to be more evenly matched. Hence, unlike earlier reports (3), the vibrations we observed seem to have their origins within the motor. An analysis of variance after the electrical modification determined that the adjustment to the circuit decreased vibration levels for each apparatus such that the difference between the two was no longer statistically significant. While the L apparatus dissolution profile did not change very much (Fig. 2), the R apparatus had a large reduction in vibration levels, resulting in a significant reduction in the dissolution profile at all times. By making the modification to the speed control circuit, we were able to reduce the dissolution profile of the R apparatus by 20–70% in 2–10 hr (Fig. 3).

Because the capacitor used in the modification did not affect both instruments equally, there may be an inherent difference between the two dissolution motors. The addition of the capacitor treated the symptom but did not cure the problem. Even though a better speed control circuit may have resulted in even lower vibration levels,

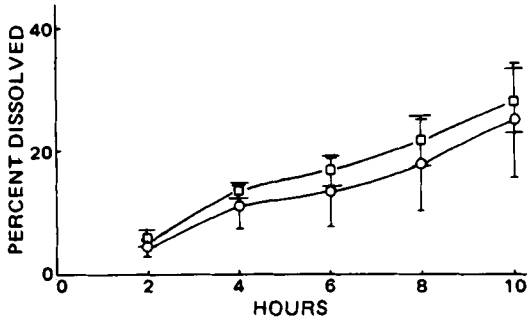

Figure 4—*Dissolution profiles of both dissolution apparatus after modification, indicating matched behavior. Key:* ○, *average of five observations for L apparatus; and* □, *average of five observations for R apparatus. Vertical bars indicate* ±*1* SE *around the mean.*

the problem appears to lie within the motor. Such factors as the number of poles on the motor, the quality of the brushes and the bearings, and the internal lubrication play an important role. While the performances of the two apparatus appeared to be matched statistically, the profiles obtained from the R apparatus were consistently higher than the L apparatus. This trend was observed throughout 200 dissolutions. The two dissolution apparatus now appeared to be matched, as seen by the similarity between the dissolution profiles obtained. The overall effect on the reduction in vibrations is summarized in Fig. 4.

Wagner *et al.* (4) indicated that high stirring speeds, such as the 200 rpm used for aminosalicylic acid tablets, tended to cause the tablets to disintegrate and dissolve with ease, masking the individual differences between tablets. At stirring speeds approximating 50 rpm, these individual characteristics were discernible in the differing tablet dissolution profiles. At these lower speeds, vibration levels begin to play a more important role and may cause a decrease in the dissolution time, suggesting good performance for poorly dissolving tablets. The apparatus differences due to vibration levels may not be detected in tablets that dissolve rapidly because the time for vibrations to have a significant effect may not exist and the vibrational component of the motor also may be reduced at higher speeds.

If we assume that vibrations are at a constant level and cause an increase in the true revolutions per minute, at high speeds the percent change will be small and may be unnoticed. However, with dosage forms that dissolve slowly due to design or to poor solubility of the active ingredient, the effect of these vibrations may be more obvious. Standardization in vibration levels should be achieved to operate dissolution equipment in a matched fashion. To determine whether dissolution equipment are mismatched, dissolutions using the same "standard" batch of tablets should be run on both apparatus and the results compared statistically. Vibrational levels in the dissolution apparatus may be partly responsible for differences in dissolution data observed between laboratories.

We suggest that the USP indicate the source and quality of the dissolution motor and the electronic equipment necessary for its control. Other parameters such as the distance from the dissolution motor to the stand supporting it and the distance from the rotating basket to the point connecting the shaft to the dissolution motor should be specified; all of these factors yield potentially different results with different levels of vibration dampening resulting in different stirring speeds.

(1) K. Embil and G. Torosian, *J. Pharm. Sci.*, **68**, 1290 (1979).

(2) "The United States Pharmacopeia," 19th rev., Mack Publishing Co., Easton, Pa., 1975, p. 650.

(3) W. F. Beyer and D. L. Smith, *J. Pharm. Sci.*, **60**, 496 (1971).

(4) J. G. Wagner, P. K. Wilkinson, A. J. Sedman, and R. G. Stoll, *J. Pharm. Sci.*, **62**, 859 (1973).

Koral Embil
George Torosian ˣ
College of Pharmacy
University of Florida
Gainesville, FL 32610

Received September 18, 1978.

Accepted for publication May 10, 1979.

Abstracted in part from a thesis submitted by K. Embil to the University of Florida in partial fulfillment of the Master of Science in Pharmacy degree requirements.

We thank Mr. J. A. Ondrasik for help in the statistical analysis and computer programs.

REVIEWS

Index Nominum 1978. 9th Ed. The Swiss Pharmaceutical Society. 1977. xiv + 814 pp. 21 × 30 cm. Price $88.00. Available from Drug Intelligence Publications, 1241 Broadway, Hamilton, IL 62341. (*Introduction in French, German, and English; text in French.*)

This edition of *Index Nominum* introduces a two-column format, allowing the incorporation of additional information while maintaining this reference as a single volume. As in the preceding edition, this volume uses a single alphabet to list International Nonproprietary Names (INN) and other generic names, trade names and manufacturers, chemical names and structures, pharmacopeial monographs on each drug, and main therapeutic uses. More than 3645 compounds and derivatives, including 270 new entries, are listed in this edition, along with more than 24,000 references. Several listings of derivatives were transferred to the entry of the parent substance, and numerous entries concerning obsolete or poorly defined substances were deleted.

Features retained from previous editions include the listing of monograph titles from internationally important pharmacopeias under "Monographie," the distinction of new listings by a point preceding the name or synonym, and the English translation of expressions used in the designations (which remain in French). The convenience of consulting only one cross-reference to find the main entry is continued in this edition. Cross-references to the main entry now include a dash instead of "voir." Several new signs and abbreviations were added.

Staff Review

Pharmacy in Health Care and Institutional Systems. Edited by PEDRO J. LECCA and C. PATRICK THARP. C. V. Mosby, 11830 Westline Industrial Drive, St. Louis, MO 63141. 1978. 275 pp. 18 × 25 cm. Price $13.95

The purposes of this book are "to identify and examine the more important concerns being raised by the interaction between pharmacy practice and the health establishment, to provide an interdisciplinary base of understanding of health care and institutional systems, to anticipate the difficulties that lie ahead and to indicate the probable direction of future developments." These are broad and grandiose objectives for a book of readings, and the reader closes this book with the feeling that none of them has been achieved.

For example, there is no reference to or mention of physicians, nurses, dentists, podiatrists, or any other health professional. It is difficult to understand how the authors can "provide an interdisciplinary base of understanding of health care and institutional systems" when the roles and attitudes of other health professionals are not discussed. Moreover, there is little discussion of "future developments." In fact, the last section is titled, "Current Trends."

The book has four basic sections: Part One, "Considerations in Health Care and Institutional Systems"; Part Two, "The Health Care System"; Part Three, "Health Care Institutions"; and Part Four, "Current Trends." Each section is composed of three chapters; all chapters present extensive bibliographies for the interested reader. Dr. Lecca is the author of Chapter 1, "The Introduction," and Chapter 5, "Pharmacy in Community Health Planning." Dr. Tharp is the author of Chapter 9, "Pharmacy in Group Practice and Pharmacy Foundations."

The brief biographical sketches on the title page do not adequately indicate the extent of the authors' experience with health care and institutional systems. Dr. Lecca is presently the Assistant Commissioner of Interagency Affairs, New York City Department of Mental Health & Mental Retardation. Dr. Tharp is the Director of Technical Services, Applied Technology Division of K. V. Pharmaceutical Co. A description of the authors' backgrounds in health care services is necessary for readers unacquainted with their work.

There are a number of basic flaws in the book. One is an overall lack of editorial supervision; pharmacy manpower is adequately addressed in Chapter 3, yet Chapters 2 and 4 contain information on this topic. The same problem occurs for skilled nursing facilities. They are discussed thoroughly in Chapter 7, yet Chapter 8 also discusses this area. Another problem is that information in many chapters is now outdated, such as the extensive undiscussed tables on national health insurance proposals for 1974 in Chapter 2 and Pharmacy Foundations in Chapter 9. Furthermore, the connection between the content in Chapters 10 and 11 and institutional systems is unclear. The sequencing of chapters is also inappropriate: Chapter 4, "The Health Care System—An Overview," should be Chapter 1. Some chapters cover their intended objective in depth, others are incomplete; for example, Chapter 8 fails to discuss long-term care facilities, and Chapter 5 does not present a discussion on Area Health Educational Centers.

A few chapters stand on their own for providing good information and data on their respective subjects such as Chapter 2, "Cost Control"; Chapter 3, "Institutional Pharmacy Manpower"; Chapter 4, "An Overview of the Health Care System"; Chapter 7, "Institutional Service in Hospitals"; Chapter 10, "The Impact of Sociological Research"; and Chapter 11, "Planning Development and Evaluation of Continuing Education." Other chapters are incomplete such as Chapter 6, "Clinical Pharmacy in the Health Care System"; Chapter 8, "Nursing Home Pharmacy Services"; and Chapter 9, "Pharmacy in Group Practice and Pharmacy Foundations."

Because much of the information in this book is already outdated, it has little value other than as a historical reference. For someone interested in reviewing early national health insurance legislation and community health planning prior to 1977, Chapters 2 and 5 might be of interest. The value of this book to the experienced teacher and researcher in the social and administrative sciences is only temporary and may have passed. For anyone who scans *Current Contents* for social and behavioral sciences and *International Pharmacy Abstracts* and maintains a respectable reprint file, this book is not worth its price. It may have limited value as a reference source in an undergraduate pharmacy course on pharmacy and health care.

Reviewed by Jean Paul Gagnon
School of Pharmacy
University of North Carolina
Chapel Hill, NC 27514

Annual Reports in Medicinal Chemistry, Vol. 13. Edited by F. H. CLARKE. Academic Press, New York, N.Y. 1978. 337 pp.

Volume 13 of "Annual Reports in Medicinal Chemistry" continues the series tradition of updating various major research areas in medicinal chemistry. Also, several brief chapters highlight research trends in new areas of interest or in areas with which most medicinal chemists are less familiar.

Like previous volumes in this series, Volume 13 is divided into six sections: Central Nervous System Agents, Pharmacodynamic Agents, Chemotherapeutic Agents, Metabolic Diseases and Endocrine Function, Topics in Biology, and Topics in Chemistry. Each section is subdivided into five or six chapters of approximately 10 pages each. The section on Central Nervous System Agents contains the standard chapters on antidepressants, antipsychotic agents, narcotic analgesics, and antianxiety agents, the latter chapter being further subdivided into benzodiazepines and nonbenzodiazepines. In addition, these and other chapters deal with the most recent work on dopamine agonists, agents affecting GABA, and opiate receptors, reflecting current research interests in these important areas.

Pharmacodynamic Agents covers topics including antiallergy drugs, diuretics, and antihypertensive agents. Unlike recent volumes which have covered specific cardiovascular areas in detail, Volume 13 contains a chapter entitled Agents for the Treatment of Heart Failure. This chapter outlines advances in areas such as the cardiac glycosides, vasodilators, β-adrenoreceptor stimulants, phosphodiesterase inhibitors, and cardiac stimulant peptides. Included also in this section is an interesting chapter on a rarely reviewed topic: Inhibitors of the Renin–Angiotensin System.

The section on Chemotherapeutic Agents contains a wealth of the most recent research findings on antibiotic, antifungal, antineoplastic, antiparasitic, and antiviral agents. In addition, there is an impressive review of the structure–activity relationships of "non-classical" β-lactam antibiotics, *i.e.*, β-lactam antibiotics in which the bicyclic nucleus has been altered. Metabolic Diseases and Endocrine Function covers chronic

REVIEWS

Index Nominum 1978. 9th Ed. The Swiss Pharmaceutical Society. 1977. xiv + 814 pp. 21 × 30 cm. Price $88.00. Available from Drug Intelligence Publications, 1241 Broadway, Hamilton, IL 62341. (*Introduction in French, German, and English; text in French.*)

This edition of *Index Nominum* introduces a two-column format, allowing the incorporation of additional information while maintaining this reference as a single volume. As in the preceding edition, this volume uses a single alphabet to list International Nonproprietary Names (INN) and other generic names, trade names and manufacturers, chemical names and structures, pharmacopeial monographs on each drug, and main therapeutic uses. More than 3645 compounds and derivatives, including 270 new entries, are listed in this edition, along with more than 24,000 references. Several listings of derivatives were transferred to the entry of the parent substance, and numerous entries concerning obsolete or poorly defined substances were deleted.

Features retained from previous editions include the listing of monograph titles from internationally important pharmacopeias under "Monographie," the distinction of new listings by a point preceding the name or synonym, and the English translation of expressions used in the designations (which remain in French). The convenience of consulting only one cross-reference to find the main entry is continued in this edition. Cross-references to the main entry now include a dash instead of "voir." Several new signs and abbreviations were added.

Staff Review

Pharmacy in Health Care and Institutional Systems. Edited by PEDRO J. LECCA and C. PATRICK THARP. C. V. Mosby, 11830 Westline Industrial Drive, St. Louis, MO 63141. 1978. 275 pp. 18 × 25 cm. Price $13.95

The purposes of this book are "to identify and examine the more important concerns being raised by the interaction between pharmacy practice and the health establishment, to provide an interdisciplinary base of understanding of health care and institutional systems, to anticipate the difficulties that lie ahead and to indicate the probable direction of future developments." These are broad and grandiose objectives for a book of readings, and the reader closes this book with the feeling that none of them has been achieved.

For example, there is no reference to or mention of physicians, nurses, dentists, podiatrists, or any other health professional. It is difficult to understand how the authors can "provide an interdisciplinary base of understanding of health care and institutional systems" when the roles and attitudes of other health professionals are not discussed. Moreover, there is little discussion of "future developments." In fact, the last section is titled, "Current Trends."

The book has four basic sections: Part One, "Considerations in Health Care and Institutional Systems"; Part Two, "The Health Care System"; Part Three, "Health Care Institutions"; and Part Four, "Current Trends." Each section is composed of three chapters; all chapters present extensive bibliographies for the interested reader. Dr. Lecca is the author of Chapter 1, "The Introduction," and Chapter 5, "Pharmacy in Community Health Planning." Dr. Tharp is the author of Chapter 9, "Pharmacy in Group Practice and Pharmacy Foundations."

The brief biographical sketches on the title page do not adequately indicate the extent of the authors' experience with health care and institutional systems. Dr. Lecca is presently the Assistant Commissioner of Interagency Affairs, New York City Department of Mental Health & Mental Retardation. Dr. Tharp is the Director of Technical Services, Applied Technology Division of K. V. Pharmaceutical Co. A description of the authors' backgrounds in health care services is necessary for readers unacquainted with their work.

There are a number of basic flaws in the book. One is an overall lack of editorial supervision; pharmacy manpower is adequately addressed in Chapter 3, yet Chapters 2 and 4 contain information on this topic. The same problem occurs for skilled nursing facilities. They are discussed thoroughly in Chapter 7, yet Chapter 8 also discusses this area. Another problem is that information in many chapters is now outdated, such as the extensive undiscussed tables on national health insurance proposals for 1974 in Chapter 2 and Pharmacy Foundations in Chapter 9. Furthermore, the connection between the content in Chapters 10 and 11 and institutional systems is unclear. The sequencing of chapters is also inappropriate: Chapter 4, "The Health Care System—An Overview," should be Chapter 1. Some chapters cover their intended objective in depth, others are incomplete; for example, Chapter 8 fails to discuss long-term care facilities, and Chapter 5 does not present a discussion on Area Health Educational Centers.

A few chapters stand on their own for providing good information and data on their respective subjects such as Chapter 2, "Cost Control"; Chapter 3, "Institutional Pharmacy Manpower"; Chapter 4, "An Overview of the Health Care System"; Chapter 7, "Institutional Service in Hospitals"; Chapter 10, "The Impact of Sociological Research"; and Chapter 11, "Planning Development and Evaluation of Continuing Education." Other chapters are incomplete such as Chapter 6, "Clinical Pharmacy in the Health Care System"; Chapter 8, "Nursing Home Pharmacy Services"; and Chapter 9, "Pharmacy in Group Practice and Pharmacy Foundations."

Because much of the information in this book is already outdated, it has little value other than as a historical reference. For someone interested in reviewing early national health insurance legislation and community health planning prior to 1977, Chapters 2 and 5 might be of interest. The value of this book to the experienced teacher and researcher in the social and administrative sciences is only temporary and may have passed. For anyone who scans *Current Contents* for social and behavioral sciences and *International Pharmacy Abstracts* and maintains a respectable reprint file, this book is not worth its price. It may have limited value as a reference source in an undergraduate pharmacy course on pharmacy and health care.

Reviewed by Jean Paul Gagnon
School of Pharmacy
University of North Carolina
Chapel Hill, NC 27514

Annual Reports in Medicinal Chemistry, Vol. 13. Edited by F. H. CLARKE. Academic Press, New York, N.Y. 1978. 337 pp.

Volume 13 of "Annual Reports in Medicinal Chemistry" continues the series tradition of updating various major research areas in medicinal chemistry. Also, several brief chapters highlight research trends in new areas of interest or in areas with which most medicinal chemists are less familiar.

Like previous volumes in this series, Volume 13 is divided into six sections: Central Nervous System Agents, Pharmacodynamic Agents, Chemotherapeutic Agents, Metabolic Diseases and Endocrine Function, Topics in Biology, and Topics in Chemistry. Each section is subdivided into five or six chapters of approximately 10 pages each. The section on Central Nervous System Agents contains the standard chapters on antidepressants, antipsychotic agents, narcotic analgesics, and antianxiety agents, the latter chapter being further subdivided into benzodiazepines and nonbenzodiazepines. In addition, these and other chapters deal with the most recent work on dopamine agonists, agents affecting GABA, and opiate receptors, reflecting current research interests in these important areas.

Pharmacodynamic Agents covers topics including antiallergy drugs, diuretics, and antihypertensive agents. Unlike recent volumes which have covered specific cardiovascular areas in detail, Volume 13 contains a chapter entitled Agents for the Treatment of Heart Failure. This chapter outlines advances in areas such as the cardiac glycosides, vasodilators, β-adrenoreceptor stimulants, phosphodiesterase inhibitors, and cardiac stimulant peptides. Included also in this section is an interesting chapter on a rarely reviewed topic: Inhibitors of the Renin–Angiotensin System.

The section on Chemotherapeutic Agents contains a wealth of the most recent research findings on antibiotic, antifungal, antineoplastic, antiparasitic, and antiviral agents. In addition, there is an impressive review of the structure–activity relationships of "non-classical" β-lactam antibiotics, *i.e.*, β-lactam antibiotics in which the bicyclic nucleus has been altered. Metabolic Diseases and Endocrine Function covers chronic

REVIEWS

Index Nominum 1978. 9th Ed. The Swiss Pharmaceutical Society. 1977. xiv + 814 pp. 21 × 30 cm. Price $88.00. Available from Drug Intelligence Publications, 1241 Broadway, Hamilton, IL 62341. (*Introduction in French, German, and English; text in French.*)

This edition of *Index Nominum* introduces a two-column format, allowing the incorporation of additional information while maintaining this reference as a single volume. As in the preceding edition, this volume uses a single alphabet to list International Nonproprietary Names (INN) and other generic names, trade names and manufacturers, chemical names and structures, pharmacopeial monographs on each drug, and main therapeutic uses. More than 3645 compounds and derivatives, including 270 new entries, are listed in this edition, along with more than 24,000 references. Several listings of derivatives were transferred to the entry of the parent substance, and numerous entries concerning obsolete or poorly defined substances were deleted.

Features retained from previous editions include the listing of monograph titles from internationally important pharmacopeias under "Monographie," the distinction of new listings by a point preceding the name or synonym, and the English translation of expressions used in the designations (which remain in French). The convenience of consulting only one cross-reference to find the main entry is continued in this edition. Cross-references to the main entry now include a dash instead of "voir." Several new signs and abbreviations were added.

Staff Review

Pharmacy in Health Care and Institutional Systems. Edited by PEDRO J. LECCA and C. PATRICK THARP. C. V. Mosby, 11830 Westline Industrial Drive, St. Louis, MO 63141. 1978. 275 pp. 18 × 25 cm. Price $13.95

The purposes of this book are "to identify and examine the more important concerns being raised by the interaction between pharmacy practice and the health establishment, to provide an interdisciplinary base of understanding of health care and institutional systems, to anticipate the difficulties that lie ahead and to indicate the probable direction of future developments." These are broad and grandiose objectives for a book of readings, and the reader closes this book with the feeling that none of them has been achieved.

For example, there is no reference to or mention of physicians, nurses, dentists, podiatrists, or any other health professional. It is difficult to understand how the authors can "provide an interdisciplinary base of understanding of health care and institutional systems" when the roles and attitudes of other health professionals are not discussed. Moreover, there is little discussion of "future developments." In fact, the last section is titled, "Current Trends."

The book has four basic sections: Part One, "Considerations in Health Care and Institutional Systems"; Part Two, "The Health Care System"; Part Three, "Health Care Institutions"; and Part Four, "Current Trends." Each section is composed of three chapters; all chapters present extensive bibliographies for the interested reader. Dr. Lecca is the author of Chapter 1, "The Introduction," and Chapter 5, "Pharmacy in Community Health Planning." Dr. Tharp is the author of Chapter 9, "Pharmacy in Group Practice and Pharmacy Foundations."

The brief biographical sketches on the title page do not adequately indicate the extent of the authors' experience with health care and institutional systems. Dr. Lecca is presently the Assistant Commissioner of Interagency Affairs, New York City Department of Mental Health & Mental Retardation. Dr. Tharp is the Director of Technical Services, Applied Technology Division of K. V. Pharmaceutical Co. A description of the authors' backgrounds in health care services is necessary for readers unacquainted with their work.

There are a number of basic flaws in the book. One is an overall lack of editorial supervision; pharmacy manpower is adequately addressed in Chapter 3, yet Chapters 2 and 4 contain information on this topic. The same problem occurs for skilled nursing facilities. They are discussed thoroughly in Chapter 7, yet Chapter 8 also discusses this area. Another problem is that information in many chapters is now outdated, such as the extensive undiscussed tables on national health insurance proposals for 1974 in Chapter 2 and Pharmacy Foundations in Chapter 9. Furthermore, the connection between the content in Chapters 10 and 11 and institutional systems is unclear. The sequencing of chapters is also inappropriate: Chapter 4, "The Health Care System—An Overview," should be Chapter 1. Some chapters cover their intended objective in depth, others are incomplete; for example, Chapter 8 fails to discuss long-term care facilities, and Chapter 5 does not present a discussion on Area Health Educational Centers.

A few chapters stand on their own for providing good information and data on their respective subjects such as Chapter 2, "Cost Control"; Chapter 3, "Institutional Pharmacy Manpower"; Chapter 4, "An Overview of the Health Care System"; Chapter 7, "Institutional Service in Hospitals"; Chapter 10, "The Impact of Sociological Research"; and Chapter 11, "Planning Development and Evaluation of Continuing Education." Other chapters are incomplete such as Chapter 6, "Clinical Pharmacy in the Health Care System"; Chapter 8, "Nursing Home Pharmacy Services"; and Chapter 9, "Pharmacy in Group Practice and Pharmacy Foundations."

Because much of the information in this book is already outdated, it has little value other than as a historical reference. For someone interested in reviewing early national health insurance legislation and community health planning prior to 1977, Chapters 2 and 5 might be of interest. The value of this book to the experienced teacher and researcher in the social and administrative sciences is only temporary and may have passed. For anyone who scans *Current Contents* for social and behavioral sciences and *International Pharmacy Abstracts* and maintains a respectable reprint file, this book is not worth its price. It may have limited value as a reference source in an undergraduate pharmacy course on pharmacy and health care.

Reviewed by Jean Paul Gagnon
School of Pharmacy
University of North Carolina
Chapel Hill, NC 27514

Annual Reports in Medicinal Chemistry, Vol. 13. Edited by F. H. CLARKE. Academic Press, New York, N.Y. 1978. 337 pp.

Volume 13 of "Annual Reports in Medicinal Chemistry" continues the series tradition of updating various major research areas in medicinal chemistry. Also, several brief chapters highlight research trends in new areas of interest or in areas with which most medicinal chemists are less familiar.

Like previous volumes in this series, Volume 13 is divided into six sections: Central Nervous System Agents, Pharmacodynamic Agents, Chemotherapeutic Agents, Metabolic Diseases and Endocrine Function, Topics in Biology, and Topics in Chemistry. Each section is subdivided into five or six chapters of approximately 10 pages each. The section on Central Nervous System Agents contains the standard chapters on antidepressants, antipsychotic agents, narcotic analgesics, and antianxiety agents, the latter chapter being further subdivided into benzodiazepines and nonbenzodiazepines. In addition, these and other chapters deal with the most recent work on dopamine agonists, agents affecting GABA, and opiate receptors, reflecting current research interests in these important areas.

Pharmacodynamic Agents covers topics including antiallergy drugs, diuretics, and antihypertensive agents. Unlike recent volumes which have covered specific cardiovascular areas in detail, Volume 13 contains a chapter entitled Agents for the Treatment of Heart Failure. This chapter outlines advances in areas such as the cardiac glycosides, vasodilators, β-adrenoreceptor stimulants, phosphodiesterase inhibitors, and cardiac stimulant peptides. Included also in this section is an interesting chapter on a rarely reviewed topic: Inhibitors of the Renin–Angiotensin System.

The section on Chemotherapeutic Agents contains a wealth of the most recent research findings on antibiotic, antifungal, antineoplastic, antiparasitic, and antiviral agents. In addition, there is an impressive review of the structure–activity relationships of "non-classical" β-lactam antibiotics, *i.e.*, β-lactam antibiotics in which the bicyclic nucleus has been altered. Metabolic Diseases and Endocrine Function covers chronic

complications of diabetes, newer agents for the treatment of arthritis, mechanisms of action of glucocorticosteroids, and pharmacological regulation of serum lipoproteins.

Topics in Biology has a general review of various enzyme classes and selected examples of enzyme inhibitors. This is followed by a more detailed look at two classes of enzymes: β-lactamases and proteolytic enzymes. The section is rounded off by timely reviews of iron chelation therapy and peptide conformation. In addition to the usual review on Reactions of Interest, the final section, Topics in Chemistry, contains a useful and interesting chapter on asymmetric synthesis. There is a chapter that deals with newer methods and applications of quantitative structure–activity relationships in drug design and another on the stereochemistry of drug–nucleic acid interactions. Scattered throughout this volume are chapters on drug metabolism and a general review followed by reviews on the molecular aspects of, and enantioselectivity in, drug metabolism.

The more than 50 contributors to this issue of Annual Reports have put together an excellent volume which is certain to be of value to medicinal chemists, pharmacologists, and researchers in related fields.

Reviewed by Richard A. Glennon
Department of Pharmaceutical Chemistry
Medical College of Virginia
Virginia Commonwealth University
Richmond, VA 23298

Genetics of Industrial Microorganisms: Proceedings of the Third International Symposium. Edited by O. K. SEBEK and A. I. LASKIN. American Society of Microbiology, 1913 I St., N.W., Washington, DC 20006. 1979. 283 pp. 15 × 23 cm. Price $12.00.

A symposium on the genetics of industrial microorganisms held June 4–9, 1978, at the University of Wisconsin, Madison, was attended by approximately 500 university and industrial scientists interested in the genetics and biochemistry of existing and potential fermentation products such as antibiotics, amino acids, enzymes, alcohol, and hormones. University scientists recognized for excellent studies in processes basic to fermentation product development—mutation, selection, recombination, regulation, gene cloning—presented lectures, as did industrial scientists recognized for applications of these processes. Those lectures have been condensed into the articles appearing in this book.

In general, the papers reflect recent trends in applied microbiology. Most articles emphasize previously unpublished work, work not yet published at the time of the symposium, or work published just prior to the symposium. A few are well-referenced reviews of recent findings. For example, genetic crosses to improve processes and to find new antibiotics were illustrated by a striking example of the protoplast fusion technique applied to the breeding of fungi for cephalosporin production, presented by C. Ball and P. F. Hamlyn. An equally noteworthy example was the use of interspecific recombination *via* natural conjugation in *Streptomyces* to produce new "hybrid" anthracycline antibiotics, written by W. F. Fleck.

An emphasis on nitrosoguanidine as a mutagen in many strain programs is reflected in a paper by E. Cerdá-Olmedo and P. Ruis-Vásquez. That article succinctly outlines how the peculiarities of nitrosoguanidine action on DNA *in vivo* can be employed to obtain more efficient use of this mutagen. A paper on yeast protoplast transformation with hybrid yeast plasmids is representative of significant academic and industrial efforts to develop useful cloning systems in organisms other than *Escherichia coli*. This paper and other sections of the book illustrate the extent to which basic and applied research in microbiology have meshed. A paper by H. J. Treichler *et al.* on the role of sulfur metabolism in cephalosporin and penicillin biosynthesis illustrates how knowledge of a biosynthetic pathway and analyses of mutants altered in that pathway and its regulation are leading to more directed and more effective means of improving fermentation processes.

The papers by K. F. Chater and M. Okanishi provide an excellent review of plasmid genetics in *Streptomycetes* and of plasmid roles in antibiotic production. This active research area has become more important now that *Streptomycete* protoplasts have been transformed with plasmid DNA, bringing a cloning system in these industrial bacteria closer to reality. This and other key developments were emphasized in the symposium's keynote address by D. A. Hopwood. The Hopwood paper presents an excellent overview of trends to be expected in the application of genetics to industrial fermentations. The articles by N. D. Lomovskaya *et al.* and by K. F. Chater demonstrate an increasing interest in developing transduction in industrial bacteria and their possible use as cloning vectors. Articles by Y. Aharonowitz, B. M. Pogell, and J. F. Martin *et al.* on metabolic regulations in industrial microorganisms likewise show an expanding interest in the basic mechanisms that regulate antibiotic synthesis. Recombinant DNA experiments for the production of mammalian hormones, which have been repeated recently, are not included in this book, but there is a useful discussion of government regulation of recombinant DNA experiments.

The book should be read by all industrial scientists looking for new fermentation products and/or improved strains for producing existing products. Genetic engineering has increased the interest of industrial managers in basic genetic studies. The quest for new challenging problems has led more university microbiologists, biochemists, and geneticists to look with keener interest at organisms traditionally used only in industry. These individuals also will benefit by adding *Genetics of Industrial Microorganisms* to their personal library. The editors, O. K. Sebek and A. I. Laskin, are to be commended for expediting an early publication of this volume, thereby increasing its value as a current reference work in this rapidly progressing field. The American Society for Microbiology is to be commended for offering the volume at a price that makes it available to the interested graduate student.

Reviewed by Stephen W. Queener
Department of Antibiotic Culture Development
Eli Lilly and Company
Indianapolis, IN 46206

Microbiology—1979. Edited by DAVID SCHLESSINGER. American Society for Microbiology, Washington, D.C. 365 pp. Price $22.00.

This volume contains an introductory note by the editor and then is divided into seven topical sections, with each section written by one or more authors. The sectional divisions are as follows:

I Microbial Membranes with an introduction followed by subsections of articles on Lipids (four articles)
Membranes and Membrane Proteins (five articles)
Transport and Energetics (seven articles)
II Mechanisms of Microbial Virulence (Introduction and 30 articles)
III Biochemical Genetics of Pathogenicity (six articles)
IV Antibiotic-Associated Colitis (Introduction and five articles)
V Resistant Gram-Positive Cocci (five articles)
VI Mutasynthesis of Antibiotics (five articles)
VII Ontogeny of the Immune System (five articles)

These articles were written by 134 authors, and each article in the various section divisions is complete with literature citations. The volume contains an author index and a complete subject index for easy reference.

This volume, containing many well-written articles under the topical divisions, would make a worthy addition to the reference library of any scientist in microbiological research.

Reviewed by Dale H. Cronk
College of Pharmacy and Health Sciences
Northeast Louisiana University
Monroe, LA 71209

complications of diabetes, newer agents for the treatment of arthritis, mechanisms of action of glucocorticosteroids, and pharmacological regulation of serum lipoproteins.

Topics in Biology has a general review of various enzyme classes and selected examples of enzyme inhibitors. This is followed by a more detailed look at two classes of enzymes: β-lactamases and proteolytic enzymes. The section is rounded off by timely reviews of iron chelation therapy and peptide conformation. In addition to the usual review on Reactions of Interest, the final section, Topics in Chemistry, contains a useful and interesting chapter on asymmetric synthesis. There is a chapter that deals with newer methods and applications of quantitative structure–activity relationships in drug design and another on the stereochemistry of drug–nucleic acid interactions. Scattered throughout this volume are chapters on drug metabolism and a general review followed by reviews on the molecular aspects of, and enantioselectivity in, drug metabolism.

The more than 50 contributors to this issue of Annual Reports have put together an excellent volume which is certain to be of value to medicinal chemists, pharmacologists, and researchers in related fields.

Reviewed by Richard A. Glennon
Department of Pharmaceutical Chemistry
Medical College of Virginia
Virginia Commonwealth University
Richmond, VA 23298

Genetics of Industrial Microorganisms: Proceedings of the Third International Symposium. Edited by O. K. SEBEK and A. I. LASKIN. American Society of Microbiology, 1913 I St., N.W., Washington, DC 20006. 1979. 283 pp. 15 × 23 cm. Price $12.00.

A symposium on the genetics of industrial microorganisms held June 4–9, 1978, at the University of Wisconsin, Madison, was attended by approximately 500 university and industrial scientists interested in the genetics and biochemistry of existing and potential fermentation products such as antibiotics, amino acids, enzymes, alcohol, and hormones. University scientists recognized for excellent studies in processes basic to fermentation product development—mutation, selection, recombination, regulation, gene cloning—presented lectures, as did industrial scientists recognized for applications of these processes. Those lectures have been condensed into the articles appearing in this book.

In general, the papers reflect recent trends in applied microbiology. Most articles emphasize previously unpublished work, work not yet published at the time of the symposium, or work published just prior to the symposium. A few are well-referenced reviews of recent findings. For example, genetic crosses to improve processes and to find new antibiotics were illustrated by a striking example of the protoplast fusion technique applied to the breeding of fungi for cephalosporin production, presented by C. Ball and P. F. Hamlyn. An equally noteworthy example was the use of interspecific recombination *via* natural conjugation in *Streptomyces* to produce new "hybrid" anthracycline antibiotics, written by W. F. Fleck.

An emphasis on nitrosoguanidine as a mutagen in many strain programs is reflected in a paper by E. Cerdá-Olmedo and P. Ruis-Vásquez. That article succinctly outlines how the peculiarities of nitrosoguanidine action on DNA *in vivo* can be employed to obtain more efficient use of this mutagen. A paper on yeast protoplast transformation with hybrid yeast plasmids is representative of significant academic and industrial efforts to develop useful cloning systems in organisms other than *Escherichia coli*. This paper and other sections of the book illustrate the extent to which basic and applied research in microbiology have meshed. A paper by H. J. Treichler *et al.* on the role of sulfur metabolism in cephalosporin and penicillin biosynthesis illustrates how knowledge of a biosynthetic pathway and analyses of mutants altered in that pathway and its regulation are leading to more directed and more effective means of improving fermentation processes.

The papers by K. F. Chater and M. Okanishi provide an excellent review of plasmid genetics in *Streptomycetes* and of plasmid roles in antibiotic production. This active research area has become more important now that *Streptomycete* protoplasts have been transformed with plasmid DNA, bringing a cloning system in these industrial bacteria closer to reality. This and other key developments were emphasized in the symposium's keynote address by D. A. Hopwood. The Hopwood paper presents an excellent overview of trends to be expected in the application of genetics to industrial fermentations. The articles by N. D. Lomovskaya *et al.* and by K. F. Chater demonstrate an increasing interest in developing transduction in industrial bacteria and their possible use as cloning vectors. Articles by Y. Aharonowitz, B. M. Pogell, and J. F. Martin *et al.* on metabolic regulations in industrial microorganisms likewise show an expanding interest in the basic mechanisms that regulate antibiotic synthesis. Recombinant DNA experiments for the production of mammalian hormones, which have been repeated recently, are not included in this book, but there is a useful discussion of government regulation of recombinant DNA experiments.

The book should be read by all industrial scientists looking for new fermentation products and/or improved strains for producing existing products. Genetic engineering has increased the interest of industrial managers in basic genetic studies. The quest for new challenging problems has led more university microbiologists, biochemists, and geneticists to look with keener interest at organisms traditionally used only in industry. These individuals also will benefit by adding *Genetics of Industrial Microorganisms* to their personal library. The editors, O. K. Sebek and A. I. Laskin, are to be commended for expediting an early publication of this volume, thereby increasing its value as a current reference work in this rapidly progressing field. The American Society for Microbiology is to be commended for offering the volume at a price that makes it available to the interested graduate student.

Reviewed by Stephen W. Queener
Department of Antibiotic Culture Development
Eli Lilly and Company
Indianapolis, IN 46206

Microbiology—1979. Edited by DAVID SCHLESSINGER. American Society for Microbiology, Washington, D.C. 365 pp. Price $22.00.

This volume contains an introductory note by the editor and then is divided into seven topical sections, with each section written by one or more authors. The sectional divisions are as follows:

I Microbial Membranes with an introduction followed by subsections of articles on Lipids (four articles)
Membranes and Membrane Proteins (five articles)
Transport and Energetics (seven articles)
II Mechanisms of Microbial Virulence (Introduction and 30 articles)
III Biochemical Genetics of Pathogenicity (six articles)
IV Antibiotic-Associated Colitis (Introduction and five articles)
V Resistant Gram-Positive Cocci (five articles)
VI Mutasynthesis of Antibiotics (five articles)
VII Ontogeny of the Immune System (five articles)

These articles were written by 134 authors, and each article in the various section divisions is complete with literature citations. The volume contains an author index and a complete subject index for easy reference.

This volume, containing many well-written articles under the topical divisions, would make a worthy addition to the reference library of any scientist in microbiological research.

Reviewed by Dale H. Cronk
College of Pharmacy and Health Sciences
Northeast Louisiana University
Monroe, LA 71209

complications of diabetes, newer agents for the treatment of arthritis, mechanisms of action of glucocorticosteroids, and pharmacological regulation of serum lipoproteins.

Topics in Biology has a general review of various enzyme classes and selected examples of enzyme inhibitors. This is followed by a more detailed look at two classes of enzymes: β-lactamases and proteolytic enzymes. The section is rounded off by timely reviews of iron chelation therapy and peptide conformation. In addition to the usual review on Reactions of Interest, the final section, Topics in Chemistry, contains a useful and interesting chapter on asymmetric synthesis. There is a chapter that deals with newer methods and applications of quantitative structure–activity relationships in drug design and another on the stereochemistry of drug–nucleic acid interactions. Scattered throughout this volume are chapters on drug metabolism and a general review followed by reviews on the molecular aspects of, and enantioselectivity in, drug metabolism.

The more than 50 contributors to this issue of Annual Reports have put together an excellent volume which is certain to be of value to medicinal chemists, pharmacologists, and researchers in related fields.

Reviewed by Richard A. Glennon
Department of Pharmaceutical Chemistry
Medical College of Virginia
Virginia Commonwealth University
Richmond, VA 23298

Genetics of Industrial Microorganisms: Proceedings of the Third International Symposium. Edited by O. K. SEBEK and A. I. LASKIN. American Society of Microbiology, 1913 I St., N.W., Washington, DC 20006. 1979. 283 pp. 15 × 23 cm. Price $12.00.

A symposium on the genetics of industrial microorganisms held June 4–9, 1978, at the University of Wisconsin, Madison, was attended by approximately 500 university and industrial scientists interested in the genetics and biochemistry of existing and potential fermentation products such as antibiotics, amino acids, enzymes, alcohol, and hormones. University scientists recognized for excellent studies in processes basic to fermentation product development—mutation, selection, recombination, regulation, gene cloning—presented lectures, as did industrial scientists recognized for applications of these processes. Those lectures have been condensed into the articles appearing in this book.

In general, the papers reflect recent trends in applied microbiology. Most articles emphasize previously unpublished work, work not yet published at the time of the symposium, or work published just prior to the symposium. A few are well-referenced reviews of recent findings. For example, genetic crosses to improve processes and to find new antibiotics were illustrated by a striking example of the protoplast fusion technique applied to the breeding of fungi for cephalosporin production, presented by C. Ball and P. F. Hamlyn. An equally noteworthy example was the use of interspecific recombination *via* natural conjugation in *Streptomyces* to produce new "hybrid" anthracycline antibiotics, written by W. F. Fleck.

An emphasis on nitrosoguanidine as a mutagen in many strain programs is reflected in a paper by E. Cerdá-Olmedo and P. Ruis-Vásquez. That article succinctly outlines how the peculiarities of nitrosoguanidine action on DNA *in vivo* can be employed to obtain more efficient use of this mutagen. A paper on yeast protoplast transformation with hybrid yeast plasmids is representative of significant academic and industrial efforts to develop useful cloning systems in organisms other than *Escherichia coli*. This paper and other sections of the book illustrate the extent to which basic and applied research in microbiology have meshed. A paper by H. J. Treichler *et al.* on the role of sulfur metabolism in cephalosporin and penicillin biosynthesis illustrates how knowledge of a biosynthetic pathway and analyses of mutants altered in that pathway and its regulation are leading to more directed and more effective means of improving fermentation processes.

The papers by K. F. Chater and M. Okanishi provide an excellent review of plasmid genetics in *Streptomycetes* and of plasmid roles in antibiotic production. This active research area has become more important now that *Streptomycete* protoplasts have been transformed with plasmid DNA, bringing a cloning system in these industrial bacteria closer to reality. This and other key developments were emphasized in the symposium's keynote address by D. A. Hopwood. The Hopwood paper presents an excellent overview of trends to be expected in the application of genetics to industrial fermentations. The articles by N. D. Lomovskaya *et al.* and by K. F. Chater demonstrate an increasing interest in developing transduction in industrial bacteria and their possible use as cloning vectors. Articles by Y. Aharonowitz, B. M. Pogell, and J. F. Martin *et al.* on metabolic regulations in industrial microorganisms likewise show an expanding interest in the basic mechanisms that regulate antibiotic synthesis. Recombinant DNA experiments for the production of mammalian hormones, which have been repeated recently, are not included in this book, but there is a useful discussion of government regulation of recombinant DNA experiments.

The book should be read by all industrial scientists looking for new fermentation products and/or improved strains for producing existing products. Genetic engineering has increased the interest of industrial managers in basic genetic studies. The quest for new challenging problems has led more university microbiologists, biochemists, and geneticists to look with keener interest at organisms traditionally used only in industry. These individuals also will benefit by adding *Genetics of Industrial Microorganisms* to their personal library. The editors, O. K. Sebek and A. I. Laskin, are to be commended for expediting an early publication of this volume, thereby increasing its value as a current reference work in this rapidly progressing field. The American Society for Microbiology is to be commended for offering the volume at a price that makes it available to the interested graduate student.

Reviewed by Stephen W. Queener
Department of Antibiotic Culture Development
Eli Lilly and Company
Indianapolis, IN 46206

Microbiology—1979. Edited by DAVID SCHLESSINGER. American Society for Microbiology, Washington, D.C. 365 pp. Price $22.00.

This volume contains an introductory note by the editor and then is divided into seven topical sections, with each section written by one or more authors. The sectional divisions are as follows:

I Microbial Membranes with an introduction followed by subsections of articles on Lipids (four articles)
Membranes and Membrane Proteins (five articles)
Transport and Energetics (seven articles)
II Mechanisms of Microbial Virulence (Introduction and 30 articles)
III Biochemical Genetics of Pathogenicity (six articles)
IV Antibiotic-Associated Colitis (Introduction and five articles)
V Resistant Gram-Positive Cocci (five articles)
VI Mutasynthesis of Antibiotics (five articles)
VII Ontogeny of the Immune System (five articles)

These articles were written by 134 authors, and each article in the various section divisions is complete with literature citations. The volume contains an author index and a complete subject index for easy reference.

This volume, containing many well-written articles under the topical divisions, would make a worthy addition to the reference library of any scientist in microbiological research.

Reviewed by Dale H. Cronk
College of Pharmacy and Health Sciences
Northeast Louisiana University
Monroe, LA 71209

A publication of the
American Pharmaceutical Association—
the National Professional Society
of Pharmacists

JOURNAL OF PHARMACEUTICAL SCIENCES

INDEX TO AUTHORS
INDEX TO SUBJECTS

VOLUME 68
JANUARY TO DECEMBER, 1979

Published monthly under the supervision of the Board of Trustees

MARY H. FERGUSON
Editor

SHELLY ELLIOTT
Production Editor

MARCIA GARTRELL
Copy Editor

NICOLETTE TRIANTAFELLU
Copy Editor

EDWARD G. FELDMANN
Contributing Editor

SAMUEL W. GOLDSTEIN
Contributing Editor

BELLE R. BECK
Editorial Secretary

DAVID BOHARDT
Director of Publications

L. LUAN CORRIGAN
Assistant Director of Publications

EDITORIAL ADVISORY BOARD

John Autian
Norman R. Farnsworth
William O. Foye
William J. Jusko
Herbert A. Lieberman
David E. Mann, Jr.
Gerald J. Papariello
Edward G. Rippie

NOVEMBER 1979
VOLUME 68 NUMBER 11

JOURNAL OF PHARMACEUTICAL SCIENCES

MARY H. FERGUSON
Editor

SHELLY ELLIOTT
Production Editor

MARCIA GARTRELL
Copy Editor

NICOLETTE TRIANTAFELLU
Copy Editor

EDWARD G. FELDMANN
Contributing Editor

SAMUEL W. GOLDSTEIN
Contributing Editor

BELLE R. BECK
Editorial Secretary

DAVID BOHARDT
Director of Publications

L. LUAN CORRIGAN
Assistant Director of Publications

EDITORIAL ADVISORY BOARD

JOHN AUTIAN
HERBERT A. LIEBERMAN
NORMAN R. FARNSWORTH
DAVID E. MANN, JR.
WILLIAM O. FOYE
GERALD J. PAPARIELLO
WILLIAM J. JUSKO
EDWARD G. RIPPIE

The *Journal of Pharmaceutical Sciences* (ISSN 0022-3549) is published monthly by the American Pharmaceutical Association (APhA) at 2215 Constitution Ave., N.W., Washington, DC 20037. Second-class postage paid at Washington, D.C., and at additional mailing office.

All expressions of opinion and statements of supposed fact appearing in articles or editorials carried in this journal are published on the authority of the writer over whose name they appear and are not to be regarded as necessarily expressing the policies or views of APhA.

Offices—Editorial, Advertising, and Subscription: 2215 Constitution Ave., N.W., Washington, DC 20037. Printing: 20th & Northampton Streets, Easton, PA 18042.

Annual Subscriptions—United States and foreign, industrial and government institutions $50, educational institutions $50, individuals *for personal use only* $30; single copies $5. All foreign subscriptions add $5 for postage. Subscription rates are subject to change without notice. Members of APhA may elect to receive the *Journal of Pharmaceutical Sciences* as a part of their annual $70 (foreign $75) APhA membership dues.

Claims—Missing numbers will not be supplied if dues or subscriptions are in arrears for more than 60 days or if claims are received more than 60 days after the date of the issue, or if loss was due to failure to give notice of change of address. APhA cannot accept responsibility for foreign delivery when its records indicate shipment was made.

Change of Address—Members and subscribers should notify at once both the Post Office and APhA of any change of address.

Photocopying—The code at the foot of the first page of an article indicates that APhA has granted permission for copying of the article beyond the limits permitted by Sections 107 and 108 of the U.S. Copyright Law provided that the copier sends the per copy fee stated in the code to the Copyright Clearance Center, Inc., P.O. Box 8891, Boston, MA 02114. Copies may be made for personal or internal use only and not for general distribution.

Microfilm—Available from University Microfilms International, 300 N. Zeeb Road, Ann Arbor, MI 48106.

© Copyright 1979, American Pharmaceutical Association, 2215 Constitution Ave., N.W., Washington, DC 20037; all rights reserved.

INSTILLING SCIENCE IN THE REGULATORY PROCESS

When mention is made of the U.S. Food and Drug Administration among pharmacists or pharmaceutical scientists, the image that apparently comes to mind for most of them is that of police officers—the "cops who watch over drugs."

Such an image is not at all inappropriate because the monitoring and surveillance of drug product quality is one of the most important responsibilities of the FDA. But FDA has often gotten undeservedly low marks as a science-based agency. Overall, the FDA staff has not enjoyed a strong reputation within the scientific community.

This is unfortunate, because the agency has long benefitted from the presence of some truly outstanding individuals among its cadre of staff scientists, and in recent years the number and general quality of its scientific component have grown greatly. A similar conclusion may also be found in the various critical studies or commissioned reviews of the FDA operation that have been conducted over the past few years.

However, as in the case with most federal regulatory agencies, the FDA is often constrained by laws, regulations, and judicial processes which necessitate that it go about its business in certain legalistic or regulatory-oriented manners. This is in contrast to the freedom enjoyed in the private sector by academic-based scientists or even by scientists employed by industry. Indeed, scientists within other government agencies, such as the National Institutes of Health and the National Bureau of Standards, suffer none of the operating constraints that are commonplace for their FDA colleagues.

But observers of the Washington scene have also felt that FDA could do more than it has in the past to institute procedures that would effectively draw upon and utilize science resources both within and outside of the agency.

Recently, however, the agency announced an action that we would classify as a major step in this direction. Specifically, early this summer FDA announced that sometime this year it would be convening *"a scientific Board of Inquiry to recommend to the Commissioner whether to approve the artificial sweetener aspartame."*

To the calorie-conscious, the big news here was the prospect of an artificial sweetener to replace their lost cyclamate and the threatened loss of saccharin. As to those not calorie-conscious, probably little, if any, attention was paid to this announcement.

To us, however, this represented a significant development. FDA's own news release states it quite well in the following excerpt: *"This will be the first Board of Inquiry ever convened by the Agency. The Board of Inquiry system was established as a means for helping the Commissioner resolve scientific issues; it is an alternative to a formal evidentiary hearing before an administrative law judge. It is designed to provide a forum in which scientific issues can be considered by scientists without the legal formalities of an evidentiary hearing. The procedure is experimental and FDA will evaluate its success after the aspartame hearing has been completed."*

The board will consist of three members selected from respective lists of nominees submitted by interested private parties, by the manufacturer of aspartame (G. D. Searle Company), and by FDA staff.

The procedure for the board's operation was also spelled out in the FDA announcement: *"It is expected that the board will be selected and begin its deliberations by late summer or early fall. The board will hear oral presentations from anyone it believes can contribute valuable information. After evaluating the information, the board will render an 'initial decision.' The participants will be given time to file 'exceptions' or objections to the Commissioner, after which time he will decide whether to approve or permanently withdraw approval for aspartame."*

Chemically, aspartame is a simple dipeptide, L-α-aspartyl-L-phenylalanine methyl ester. Its manufacturer received news of the FDA action with apparent mixed emotions. Although "encouraged" and "pleased" that FDA is moving forward with its evaluation of aspartame, the firm felt that existing data were sufficient for the agency to take action to approve the agent without the need for further assessment.

Despite this difference of opinion on the adequacy of the proof of safety of aspartame—or perhaps *because* of it—the effectiveness, usefulness, and credibility of the Board of Inquiry as a mechanism for considering scientific issues by this regulatory agency will be subjected to the acid test. We are hopeful and optimistic that this trial will prove to be successful in fulfilling its objectives.

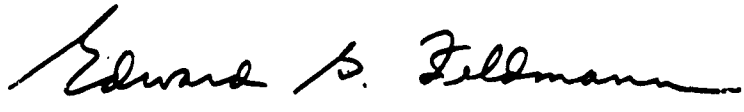

Hospital Pharmacy and the CGMP: Additional Comments

In their response[1] to Dr. Feldmann's editorial[2], Dr. Belson and Dr. Loftus claimed that, in FDA's view, the guidelines issued by the American Society of Hospital Pharmacists in the December 1977 issue of the *American Journal of Hospital Pharmacy* are suitable equivalents to the CGMP's for normal hospital pharmacy practice and that Dr. Kennedy has endorsed those guidelines. What is a normal hospital pharmacy practice? Furthermore, one of these guidelines is: "In the absence of valid stability data, an arbitrary expiration date of not more than 60 days from the date of repacking, or as defined by the FDA or USP, should be used."

In an earlier response[3] to Dr. Feldmann's editorial, I reported that some drugs that are being repackaged in hospital pharmacies are not stable even for 30 days. How could one go by an arbitrary expiration date of 60 days? Incidentally, the above guidelines do state that if stability data are available, the data should be used to determine the expiration date. The data on the products that were not stable even for 30 days were not available to justify an expiration date of less than 60 days, that is, less than 60 days of the arbitrary date as suggested by the above quoted guideline.

In the February 1979 issue of the *American Journal of Hospital Pharmacy,* the Society revised this guideline and deleted the arbitrary expiration date of 60 days. The new guideline is: "It is the responsibility of the pharmacist, taking into account the nature of the drug repackaged, the characteristics of the package and the storage conditions to which the drug may be subjected, to determine the expiration date to be placed on the package. This date must not be beyond that of the original package."

This guideline is far better than the original one. However, how many hospital pharmacists are determining the expiration dates by actual data! Perhaps less than 1% of those who are engaged in repackaging drugs.

V. Das Gupta
College of Pharmacy
University of Houston
Houston, TX 77004

Received August 27, 1979.

[1] J. J. Belson and B. T. Loftus, *J. Pharm. Sci.,* 68 (8), IV (1979).
[2] E. G. Feldmann, *ibid.,* 68 (5), I (1979).
[3] V. D. Gupta, *ibid.,* 68 (7), IV (1979).

Faculty Position in Clinical Pharmacy at the Assistant Professor Level

Applications are invited for a full-time appointment, effective January 1, 1980.
The position requires the Pharm.D. degree and recent clinical experience. Responsibilities include didactic and clerkship instruction within the Clinical Pharmacy component of the curriculum; and participation in the laboratory component of the course in Professional Pharmacy Practice.
A strong commitment to participation in the College's Continuing Education efforts is vital.
Interested candidates should send a letter of application, curriculum vitae and the names of three references to: **Abraham J. Haddad, Ph.D., Dean, Hampden Campus, Massachusetts College of Pharmacy & Allied Health Sciences, 24 Bellamy Road, Springfield, MA 01119.**
The Massachusetts College of Pharmacy & Allied Health Sciences is an equal opportunity employer.

RESEARCHERS' TRANSLATION SERVICE

HIGHLY TRAINED–EXPERIENCED
ACCURATE TRANSLATING
TECHNICAL INTERPRETATIONS
Chinese—Arabic—Russian
Japanese—German—Italian—English
Spanish—French—Polish
Special team of Medical & Pharmaceutical translators
(2779 McGuffey Rd) P.O. Box 5794
Columbus, Ohio 43221
Phone (614)-261-6610
or: (614)-267-1736

PHARMACOKINETICS-BIOPHARMACEUTICS

A full-time faculty position is available at the University of Kentucky College of Pharmacy in the area of pharmacokinetics-biopharmaceutics. Applications are sought from either established scientists or recent Ph.D. recipients who have demonstrated exceptional scholarship and commitment to research. Responsibilities include teaching in the area of interest at the professional and graduate level, and the development of a strong research program. The position is a tenure track 12-month appointment. Academic rank and salary are open and commensurate with experience and qualifications. The University of Kentucky College of Pharmacy offers well equipped and staffed laboratory and clinical facilities and an academic environment conducive to excellence in teaching and research.
Please direct resumes and inquiries to **Dr. Harry B. Kostenbauder, Associate Dean, College of Pharmacy, University of Kentucky, Lexington, Ky 40506.**
The University of Kentucky is an Equal Opportunity Employer.

Faculty Positions: Pharmaceutics and Industrial Sciences

The Arnold & Marie Schwartz College of Pharmacy and Health Sciences (formerly Brooklyn College of Pharmacy) in New York City is expanding its faculty in the Division of Pharmaceutics and Industrial Sciences. Only those individuals with a proven record of research leading to publication in recognized scientific and professional journals should apply.
Applicants are invited to apply for a full-time (12 months) faculty position at the Assistant Professor or Associate Professor level in the Division of Pharmaceutics and Industrial Sciences of the Arnold & Marie Schwartz College of Pharmacy and Health Sciences. Applicants must possess an undergraduate degree in Pharmacy from an accredited U.S. College of Pharmacy, a Ph.D. in Pharmaceutics or Industrial Pharmacy, and must be qualified to teach undergraduate and graduate courses in pharmaceutical analysis. A strong background in the Industrial Sciences is highly desirable. The successful applicant is expected to participate in the graduate program and to pursue research programs leading to recognized scientific publications and grant acquisitions. The salary and rank are negotiable, and are based on past experiences and activities of the candidates.
Applicants are invited to submit their credentials, including references to: **Dr. Anthony J. Cutie, Director of the Division of Pharmaceutics and Industrial Sciences, Arnold & Marie Schwartz College of Pharmacy and Health Sciences of Long Island University, 75 DeKalb Avenue at University Plaza, Brooklyn, New York 11201.**
The Arnold & Marie Schwartz College of Pharmacy and Health Sciences is an Equal Opportunity-Affirmative Action Employer.

FACULTY POSITION IN PHARMACOKINETICS
College of Pharmacy
University of Arizona

Applications are invited for a new twelve month tenure track position in Pharmacokinetics at the Assistant or Associate Professor level. Candidates should have a Ph.D. in Pharmaceutical Sciences with an emphasis in pharmacokinetics. The position involves undergraduate and graduate teaching and the candidate must be able to develop a strong research program.
The position is available immediately. Qualified applicants should submit a current curriculum vitae along with the names of three references by January 1, 1980 to:

Michael Mayersohn, Ph.D.—College of Pharmacy
University of Arizona, Tucson, Arizona 85721
Equal Opportunity/Affirmative Action Employer

JOURNAL OF PHARMACEUTICAL SCIENCES

NOVEMBER 1979
VOLUME 68 NUMBER 11

RESEARCH ARTICLES

Physical Model Evaluation of Topical Prodrug Delivery—Simultaneous Transport and Bioconversion of Vidarabine-5′-valerate I: Physical Model Development

CHENG DER YU *, JEFFREY L. FOX, NORMAN F. H. HO, and WILLIAM I. HIGUCHI ˣ

Received January 17, 1979, from the *College of Pharmacy, University of Michigan, Ann Arbor, MI 48109.* Accepted for publication April 18, 1979. *Present address: Syntex Research, Stanford Industrial Park, Palo Alto, CA 94304.

Abstract □ A physical model approach to the topical delivery of a vidarabine ester prodrug was investigated. It involved modeling, theoretical simulations, experimental method development for factoring and quantifying parameters, and, finally, employment of the deduced parameters to determine the steady-state species fluxes and concentration profiles in the target tissue. The present report describes the physical modeling and theoretical simulation aspects. The physical model for the simultaneous transport and bioconversion of a topically delivered prodrug was formulated assuming homogeneous enzyme distributions and constant diffusivities in the membrane. The mathematical problem was solved, and the solution yielded concentration profiles and fluxes of all species in the biomembrane. These results provided the prevailing levels of the prodrug, the drug, and the metabolite at the target site and the transport rates of all species into the bloodstream. Computations of concentration profiles and fluxes were carried out for a reasonable range of the parameters. The relative activities of the esterase and the deaminase enzymes, as well as the stratum corneum permeabilities, were important in influencing the concentration profiles and fluxes of all species.

Keyphrases □ Vidarabine valerate prodrug—topical dosage forms, physical models, pharmacokinetics □ Antiviral agents—vidarabine valerate prodrug, topical dosage forms, physical models, pharmacokinetics □ Prodrugs—vidarabine valerate, topical dosage forms, physical models, pharmacokinetics □ Models, physical—vidarabine valerate prodrug, topical dosage forms, mouse skin □ Pharmacokinetics—vidarabine valerate prodrug, topical dosage forms, physical models

A physical model that described simultaneous drug transport and bioconversion across the skin was reported recently (1). The model treated the skin as a two-ply laminate composed of the stratum corneum and the viable epidermis. Only the epidermis was assumed to contain enzymes responsible for metabolism; for mathematical simplicity, the enzyme distribution was assumed to be homogeneous. Two theoretical situations were investigated. In one, the stratum corneum was considered impermeable to the drug and the drug was allowed to penetrate from the dermis side of the epidermal membrane. In the other, the stratum corneum was assumed to be permeable and the drug penetrated the stratum corneum from the stratum corneum side of the tissue and then permeated the metabolizing epidermis. Preliminary experimental transport studies (2) on vidarabine (9-β-D-arabinofuranosyladenine, I) were conducted using full thickness hairless mouse skin. The metabolic rate constant was calculated for the first case from the rate of change in the drug concentration on the dermis side.

The present report describes the results of a more comprehensive investigation dealing with the physical model approach for the delivery of therapeutically active drugs in the skin, with emphasis on the simultaneous transport and bioconversion for the system: prodrug → drug → metabolite.

BACKGROUND

Compound I has broad-spectrum activity against DNA viruses (3–6) including the herpes simplex virus type I, which is the cause of recurrent herpes labialis ("cold sores"). When applied topically for the treatment of herpetic skin infection in the hairless mouse, the drug was ineffective, which was attributed to poor transepidermal penetration (7). When injected intradermally, I improved the course of the infection (8). Recent *in vitro* studies (2) of hairless mouse skin mounted in a diffusion cell found the stratum corneum to be relatively impermeable to I, in support of earlier observations by Fondak *et al.* (7).

Compound I has many suboptimal properties (9) including low aqueous solubility [0.5 mg/ml at 25° and 1.8 mg/ml at 37° (5)], low lipophilicity (log partition coefficient in *n*-pentanol–water of −0.48)[1], and rapid

[1] Dr. David C. Baker, Department of Chemistry, University of Alabama, University, AL 35486, personal communication.

0022-3549/79/1100-1341$01.00/0
© 1979, American Pharmaceutical Association

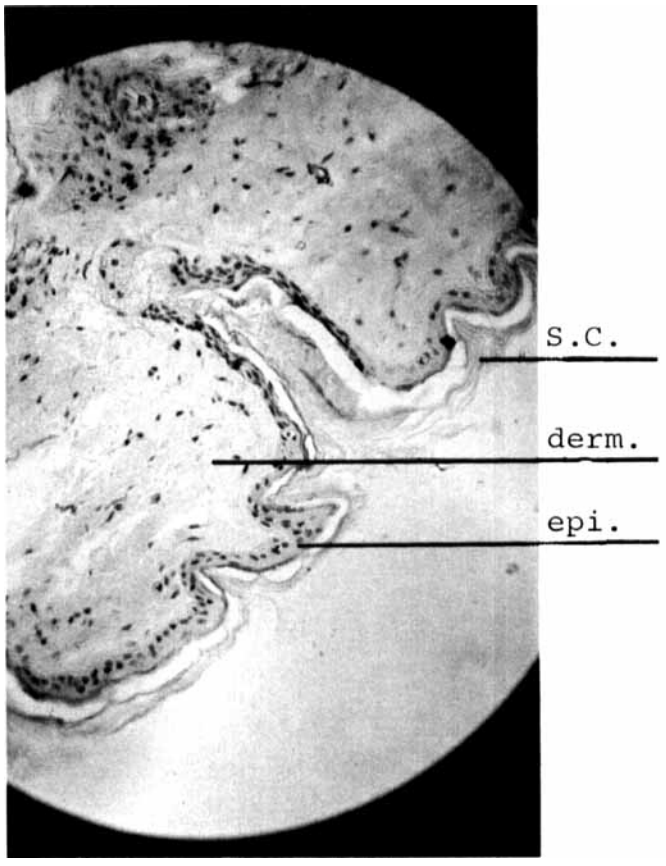

Figure 1—*Cross-section of hairless mouse skin (1040× magnification). Key: S.C., stratum corneum; derm., dermis; and epi., epidermis.*

conversion to 9-β-D-arabinofuranosylhypoxanthine (II) by adenosine deaminase (10–17). While the metabolite possesses antiviral activity, it is about one-thirtieth as potent as I (18–20). Because of these shortcomings, I appeared to be a good candidate for the prodrug approach.

Vidarabine-5′-valerate (III) is an example of a model prodrug of I. Although preliminary experiments (2) indicated that the stratum corneum is almost impermeable to I, this barrier might be overcome by the 5′-ester prodrug. Because of its increased lipophilicity, this prodrug might penetrate the lipoidal stratum corneum more readily. After passing through the stratum corneum, the prodrug may be converted by esterase into the parent drug, which subsequently may be degraded by deaminases located in the viable cutaneous tissue. Since back-diffusion of I and II across the stratum may be negligible, a relatively high buildup of these species may result in the cutaneous tissue, depending on the ratio of the activities of the two enzymes.

In the case of topical I therapy for herpes simplex virus infection, it is believed that the higher the concentration of I in the target tissue, the more effective is the therapy. An appropriately designed prodrug may be able to achieve both a high stratum corneum permeability and good access to esterase activity, both of which lead to an enhanced bioavailability[2] compared to the parent drug.

For quantitative assessment of the efficacy and possible consequences of side effects, however, the mathematical problem of the simultaneous diffusion and enzyme reactions must be solved. The solution to this problem yields directly the concentration profiles of all species in the skin as well as the fluxes for all species. The former provides the prevailing levels of the prodrug, drug, and metabolite in the target sites; the latter yields a direct measure of the rate of prodrug, drug, and metabolite transport into the bloodstream.

THEORY

Considerations in General Model Development—A cross section of the hairless mouse skin used as the model is shown in Fig. 1. It consists

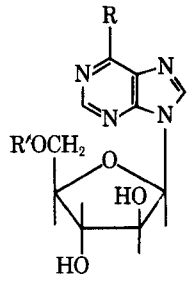

I: R = NH_2, R′ = H
II: R = OH, R′ = H
III: R = NH_2, R′ = $CH_3(CH_2)_3CO$

of the stratum corneum (~50 μm thick); the epidermis, which is approximately a layer or two of cells; and the dermis, which contributes most of the skin thickness. Accordingly, a model treating the skin as a two-ply laminate composed of a metabolically inactive stratum corneum and a metabolically active cutaneous tissue (epidermis and dermis) was formulated.

Homogeneous enzyme distribution will be assumed here for mathematical simplicity, while the more general case of nonhomogeneous enzyme distribution will be discussed in another report (21).

General Model Description—The physical model for the simultaneous diffusion transport and bioconversion of the prodrug, III, in the skin is shown in Fig. 2. It consists of a two-ply biomembrane composed of the stratum corneum of thickness s and the cutaneous tissue (epidermis and dermis) of thickness m followed by a blood sink. The following assumptions were made:

1. The relevant enzymes are homogeneously distributed in the cutaneous tissue and are not present in the dead stratum corneum tissue.
2. The stratum corneum is essentially permeable to the highly lipophilic prodrug and serves as a relatively natural barrier preventing the backflow of the more hydrophilic parent drug and its metabolite.
3. The enzyme reactions in the cutaneous tissue are simple, sequential first-order and irreversible reactions of prodrug → drug → metabolite (Scheme I):

$$\text{III} \xrightarrow{k_1} \text{I} \xrightarrow{k_2} \text{II}$$

Scheme I

4. Diffusivities of all species are independent of distance within the viable cutaneous tissue.
5. Steady-state conditions prevail.

Steady-State Flux and Concentration–Distance Expressions—The flux of the prodrug in the stratum corneum is:

$$F_V = P_{sc}[V(-s) - V(0)] \qquad \text{(Eq. 1)}$$

where F_V is the flux across the stratum corneum per unit area, P_{sc} is the permeability coefficient of the stratum corneum, and $V(-s)$ and $V(0)$ are the prodrug concentrations at $x = -s$ and 0, respectively.

The changes in concentrations of the prodrug, drug, and metabolite with distance x for $0 \le x \le m$ in the cutaneous tissue are described by:

$$D_V \frac{d^2V}{dx^2} - k_1 V = 0 \qquad \text{(Eq. 2)}$$

$$D_A \frac{d^2A}{dx^2} - k_2 A + k_1 V = 0 \qquad \text{(Eq. 3)}$$

$$D_H \frac{d^2H}{dx^2} + k_2 A = 0 \qquad \text{(Eq. 4)}$$

where V, A, and H are the concentrations of the prodrug, drug, and metabolite, respectively; D_V, D_A, and D_H are the diffusion coefficients in the cutaneous tissue; and k_1 and k_2 are the apparent first-order rate constants for the III → I and I → II reactions, respectively.

These expressions can be rewritten as follows:

$$\frac{d^2V}{dx^2} = K_1^2 V \qquad \text{(Eq. 5)}$$

$$\frac{d^2A}{dx^2} - K_2^2 A = \left(-\frac{k_1}{D_A}\right) V \qquad \text{(Eq. 6)}$$

$$\frac{d^2H}{dx^2} = \left(-\frac{k_2}{D_H}\right) A \qquad \text{(Eq. 7)}$$

[2] In this study, prodrug bioavailability was defined as the topically available concentration of the parent drug in the cutaneous tissue.

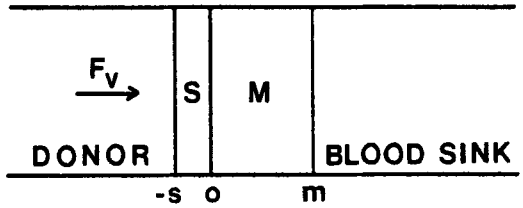

Figure 2—*Physical model for topical prodrug delivery in skin. Key:* M, *viable epidermis and dermis;* S, *stratum corneum;* F_V, *prodrug flux; and* s *and* m, *thickness of stratum corneum and epidermis–dermis layers.*

where:

$$K_1 = \sqrt{k_1/D_V} \qquad \text{(Eq. 8)}$$

$$K_2 = \sqrt{k_2/D_A} \qquad \text{(Eq. 9)}$$

The boundary conditions are:

$$P_{sc}[V(-s) - V(0)] = -D_V \left.\frac{dV}{dx}\right|_{x=0} \qquad \text{(Eq. 10)}$$

$$D_A \left.\frac{dA}{dx}\right|_{x=0} = 0 \qquad \text{(Eq. 11)}$$

$$D_H \left.\frac{dH}{dx}\right|_{x=0} = 0 \qquad \text{(Eq. 12)}$$

The last two conditions account for the absence of back-diffusion of species A and H across the stratum corneum. Because sink conditions are assumed, it follows that:

$$V = A = H = 0 \qquad \text{(Eq. 13)}$$

at $x = m$.

The details of the solutions to Eqs. 5–7 are given in the *Appendix*. However, the results are:

$$V(x) = -\beta \sinh K_1(m - x) \qquad \text{(Eq. 14)}$$

$$A(x) = \omega \sinh K_2(m - x) + \left(\frac{\beta}{(K_1^2 - K_2^2)}\right)\left(\frac{k_1}{D_A}\right)[\sinh K_1(m - x)] \qquad \text{(Eq. 15)}$$

$$H(x) = \left(\frac{k_2}{D_H}\right)\left[\frac{\omega}{K_2}(\cosh K_2 m) + \left(\frac{\beta}{(K_1^2 - K_2^2)K_1}\right)\left(\frac{k_1}{D_A}\right)(\cosh K_1 m)\right](m - x) - \frac{k_2}{D_H}\left[\frac{\omega}{K_2^2}[\sinh K_2(m - x)] + \left(\frac{\beta}{(K_1^2 - K_2^2)K_1^2}\right)\left(\frac{k_1}{D_A}\right)[\sinh K_1(m - x)]\right] \qquad \text{(Eq. 16)}$$

where $(0 \leq x \leq m)$, $(K_1 \neq K_2)$, and:

$$\beta = \frac{[-V(-s)](P_{sc})}{D_V K_1 \cosh K_1 m + P_{sc} \sinh K_1 m} \qquad \text{(Eq. 17)}$$

$$\omega = \left(\frac{-\beta K_1}{(K_1^2 - K_2^2)K_2}\right)\left(\frac{k_1}{D_A}\right)\left(\frac{\cosh K_1 m}{\cosh K_2 m}\right) \qquad \text{(Eq. 18)}$$

Since $A(x)$ and $H(x)$ in Eqs. 15 and 16 must be bounded for physical reasons, it is required that $K_1 \neq K_2$; otherwise, $A(x)$ and $H(x)$ will go to infinity.

In the case of $K_1 = K_2 = K$:

$$A(x) = \left(-\frac{\beta}{2}\right)\left(\frac{D_V}{D_A}\right)\left[\begin{matrix}\sinh K(m - x) + (Kx)[\cosh K(m - x)] \\ -(Km)(\operatorname{sech} Km)(\cosh Kx)\end{matrix}\right] \qquad \text{(Eq. 19)}$$

$$H(x) = \left(\frac{-\beta}{2}\right)\left(\frac{D_V}{D_A}\right)\left[\begin{matrix}-3 \sinh K(m - x) + (Km)(\operatorname{sech} Km)(\cosh Kx) \\ -(Kx)[\cosh K(m - x)] + 2K(m - x)(\cosh Km)\end{matrix}\right] \qquad \text{(Eq. 20)}$$

The fluxes of all species per unit area across the membrane system (Fig. 2) are readily found by evaluating the derivatives of Eqs. 14–16, 19, and 20 at $x = m$. Thus (see *Appendix*):

$$F_V = -\beta D_V K_1 \qquad \text{(Eq. 21)}$$

$$F_A = \omega D_A K_2 + \left(\frac{\beta D_A K_1}{(K_1^2 - K_2^2)}\right)\left(\frac{k_1}{D_A}\right) \qquad (K_1 \neq K_2) \qquad \text{(Eq. 22)}$$

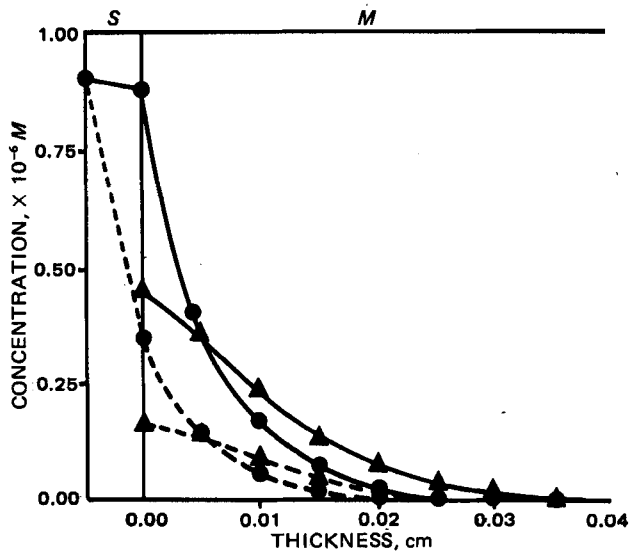

Figure 3—*Effect of III permeability across the stratum corneum on the concentration–distance profiles of III and I. Key:* ●, *prodrug; and* ▲, *drug* ($K_1 = K_2 = 163\ cm^{-1}$). *Solid lines denote the case of* $P_{sc} = 1 \times 10^{-2}$ *cm/sec; dotted lines denote the case of* $P_{sc} = 1 \times 10^{-4}$ *cm/sec.*

$$F_A = -\frac{\beta K^2 m D_V}{2} \tanh Km \qquad (K_1 = K_2 = K) \qquad \text{(Eq. 23)}$$

$$F_H = \frac{\omega k_2}{K_2}(\cosh K_2 m - 1) + \left(\frac{\beta k_2}{(K_1^2 - K_2^2)K_1}\right)\left(\frac{k_1}{D_A}\right)(\cosh K_1 m - 1) \qquad (K_1 \neq K_2) \qquad \text{(Eq. 24)}$$

$$F_H = \left(-\frac{\beta K D_H}{2}\right)\left(\frac{D_V}{D_A}\right)[2 \cosh Km - (Km) \tanh Km - 2] \qquad (K_1 = K_2 = K) \qquad \text{(Eq. 25)}$$

As can be seen in these equations, the concentration–distance expressions and fluxes are functions of membrane thickness, enzyme rate constants, prodrug donor concentration, species diffusivities in the cutaneous tissue, and the prodrug permeability coefficient in the stratum corneum.

THEORETICAL SIMULATIONS AND DISCUSSION

Computations were carried out for a reasonable range of parameter values (Table I). The stratum corneum permeabilities for III were arbitrarily chosen. The thickness of hairless mouse skin, used as the model skin, was determined previously to be 0.04 cm. The epidermis–dermis diffusivities of the prodrug, drug, and metabolite species were equated to 1.0×10^{-6} cm²/sec, which seems reasonable for drugs in tissues.

The apparent rate constant[3], k_2, for the I metabolism by deaminases was taken to be 2.66×10^{-2} sec^{-1}. The values of the k_1 rate constant for the cleavage of III by esterases were varied arbitrarily to demonstrate the effect of esterase activity on bioavailability. Equations 14–20 were used to obtain the concentration–distance profiles, and Eqs. 21–25 were used to estimate the fluxes. Computations centered about the stratum corneum permeability, P_{sc}, and the K_1 parameter, which is indicative of the esterase activity on the prodrug, since these phenomenological constants are considered to be the principal determinants in bringing about effective prodrug delivery in the dermis and concomitant high concentrations of the active species.

Figure 3 shows the effect of the P_{sc} of III on the concentration–distance curves of III and I. A higher P_{sc} leads to a higher I concentration in the dermis. Beyond the first 50-μm depth in the dermis, the I concentration buildup is higher than its precursor for both high and low stratum corneum permeability cases. Since the stratum corneum is relatively impermeable to topically applied I and since the I that enters the dermis is metabolized by deaminases, the prodrug approach allows for the advantageous buildup of I in the cutaneous tissue.

[3] This value of 2.66×10^{-2} sec^{-1} was obtained from preliminary *in vitro* kinetic studies of I in homogenates of hairless mouse skin.

Table I—Constants Used in Theoretical Computations Including the Calculated Fluxes of the Prodrug, Drug, and Metabolites [a]

K_1, cm^{-1}	K_2, cm^{-1}	P_{sc}, cm/sec	Flux, moles/sec III	Flux, moles/sec I	Flux, moles/sec II	All Species	Concentration–Distance Profile
163	163	1×10^{-2}	4.2×10^{-13}	1.4×10^{-12}	1.4×10^{-10}	1.42×10^{-10}	Fig. 3
163	163	1×10^{-4}	1.6×10^{-13}	0.53×10^{-12}	0.55×10^{-10}	0.56×10^{-10}	Fig. 3
54.5	163	1×10^{-4}	7.2×10^{-12}	0.89×10^{-12}	0.24×10^{-10}	0.32×10^{-10}	Fig. 4
490.5	163	1×10^{-4}	4.5×10^{-19}	0.25×10^{-12}	0.75×10^{-10}	0.75×20^{-10}	Fig. 4

[a] $V(-s) = 9 \times 10^{-7}$ M; $D_V = D_A = D_H = 1 \times 10^{-6}$ cm^2/sec; $m = 0.04$ cm; $k_1 = 2.66 \times 10^{-2}$ sec^{-1} when $K_1 = 163$ cm^{-1}; $k_1 = 0.3 \times 10^{-2}$ sec^{-1} when $K_1 = 54.5$; $k_1 = 24.1 \times 10^{-2}$ sec^{-1} when $K_1 = 490.5$; and $k_2 = 2.66 \times 10^{-2}$ sec^{-1} when $K_2 = 163$ cm^{-1}.

The relative influence of esterase and deaminase activities on the tissue concentrations is shown in Fig. 4. When the esterase activity ($k_1 = 24.1 \times 10^{-2}$ sec^{-1}) is nine times higher than the deaminase activity ($k_2 = 2.66 \times 10^{-2}$ sec^{-1}), the overall tissue concentration of the active parent drug is markedly enhanced. Despite the unfavorable situation where the esterase activity is nine times smaller than the deaminase activity, the prodrug delivery system is still better than the parent drug itself since the stratum corneum is almost impermeable to I.

In all of the cases shown in Figs. 3 and 4, the stratum corneum permeability is the dominant factor affecting the prodrug and parent drug levels in the dermis. From the standpoint of overall prodrug design for I, ester prodrug lipophilicity should be optimized to improve stratum corneum permeability, but lability to cleavage by esterases and enzymatic deamination of the parent drug are also important. Thus, methods for assessing relevant enzymic activities in the skin become an important issue in evaluating prodrug bioavailability for topical delivery. Theoretical and experimental studies to assess quantitatively the *in situ* activities of esterases and deaminases in skin are in progress.

The fluxes of all three species that enter the bloodstream are direct measurements of potential toxicity. Table I shows that the total flux of all three species is a function of both stratum corneum permeability and enzyme activity. At constant enzyme activities, an increase in stratum corneum permeability results in an increase in the total flux. With the same stratum corneum permeability, an increase in esterase activity is accompanied by an increase in the total flux. Although a higher stratum corneum permeability and a greater esterase activity are favorable factors for a higher active species level in the skin, the accompanied elevation of total flux could mean higher systemic toxicity. From the therapeutic viewpoint, bioavailability and toxicity are both important. The compromise between the bioavailability factors (stratum corneum permeability and esterase activity) and toxicity factor (total flux) becomes one criterion for designing a successful prodrug.

Bioavailability of topically applied III can be assessed readily on a quantitative basis when the concentration–distance profiles (Fig. 3 or 4) are known. For example, the theoretical results in Fig. 4 focus attention on the concentration of the therapeutically active vidarabine species within the first 10 μm of the tissue (epidermis) where the herpes simplex virus is believed to proliferate in cold sores. The I concentration is ~40% of the topically applied prodrug concentration. In contrast, the available I level is only 6% of the applied prodrug level when the esterase activity is less than the deaminase activity. As indicated in Fig. 3, the bioavailability of I is 50% in the high stratum corneum permeability case and 20% in the lower permeability situation.

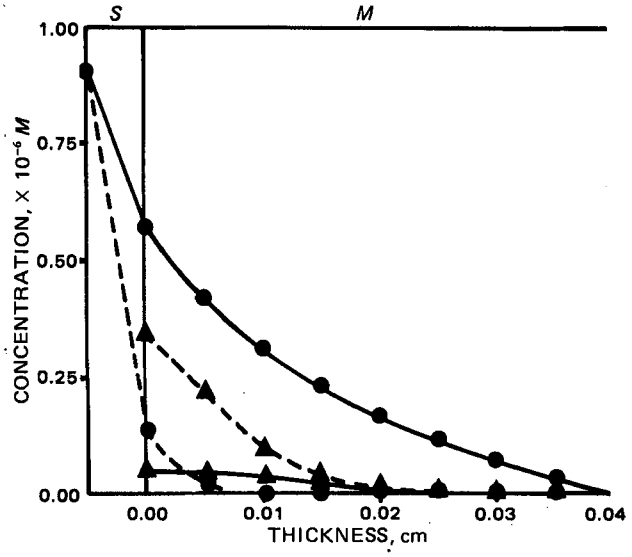

Figure 4—*Effect of esterase and deaminase activities on the concentration–distance profiles of III and I. Key:* ●, *prodrug; and* ▲, *drug* ($P_{sc} = 1 \times 10^{-4}$ *cm/sec*). *Solid lines denote the case when* $K_1 = 54.5$ cm^{-1} *and* $K_2 = 163$ cm^{-1}; *dotted lines denote the case when* $K_1 = 490.5$ cm^{-1} *and* $K_2 = 163$ cm^{-1}.

APPENDIX: MATHEMATICAL SOLUTIONS TO SKIN TRANSPORT MODEL (Fig. 2)

Flux of Prodrug across Stratum Corneum—The steady-state flux per unit area, F_V, of the prodrug within the stratum corneum is given by Fick's law:

$$F_V = \frac{D_{sc}}{h_{sc}}[V_{sc}(-s) - V_{sc}(0)] \qquad \text{(Eq. A1)}$$

where the subscript *sc* refers to the stratum corneum region. The other terms are self-explanatory. If it is assumed that the partition coefficients of the prodrug for stratum corneum–water and stratum corneum–cutaneous tissue are the same:

$$K_p = \frac{V_{sc}(-s)}{V(-s)} = \frac{V_{sc}(0)}{V(0)} \qquad \text{(Eq. A2)}$$

then the flux becomes:

$$F_V = P_{sc}[V(-s) - V(0)] \qquad \text{(Eq. A3)}$$

where the permeability coefficient is:

$$P_{sc} = \frac{D_{sc}K_p}{h_{sc}} \qquad \text{(Eq. A4)}$$

Cutaneous Concentration–Distance Expressions for Prodrug—To begin, Eq. 5 is employed:

$$\frac{d^2V}{dx^2} = K_1^2V \qquad \text{(Eq. A5)}$$

with $K_1 = \sqrt{k_1/D_V}$. The general solution is:

$$V(x) = C_1 \sinh K_1x + C_2 \cosh K_1x \qquad (0 \le x \le m) \quad \text{(Eq. A6)}$$

where C_1 and C_2 are the integration constants. By applying the stratum corneum–cutaneous interphase transfer and sink boundary conditions, *i.e.*:

$$P_{sc}[V(-s) - V(0)] = -D_V\frac{dV}{dx}\bigg|_{x=0} \qquad \text{(Eq. A7)}$$

and:

$$V = 0 \qquad \text{at } x = m \qquad \text{(Eq. A8)}$$

to Eq. A5, the integration constants are:

$$C_1 = \frac{-[V(-s)](P_{sc}\cosh K_1m)}{D_VK_1\cosh K_1m + P_{sc}\sinh K_1m} \qquad \text{(Eq. A9)}$$

and:

$$C_2 = \frac{[V(-s)](P_{sc}\sinh K_1m)}{D_VK_1\cosh K_1m + P_{sc}\sinh K_1m} \qquad \text{(Eq. A10)}$$

Thus, the particular solution is:

$$V(x) = -\beta \sinh K_1(m - x) \qquad \text{(Eq. A11)}$$

where:

$$\beta = \frac{[-V(-s)](P_{sc})}{D_VK_1\cosh K_1m + P_{sc}\sinh K_1m} \qquad \text{(Eq. A12)}$$

Cutaneous Concentration–Distance Expressions for Drug: Case

of $K_1 \neq K_2$—The solution to Eq. 6 is sought. With Eq. 14 (or A12), the equation becomes:

$$\frac{d^2A}{dx^2} - K_2^2A = (\beta)\left(\frac{k_1}{D_A}\right)[\sinh K_1(m-x)] \qquad \text{(Eq. A13)}$$

with $K_2 = \sqrt{k_2/D_A}$. This nonhomogeneous equation is conveniently solved by the method of undetermined coefficients. The homogeneous solution is:

$$A(x)_h = C_1 \sinh K_2x + C_2 \cosh K_2x \qquad (0 \leq x \leq m) \qquad \text{(Eq. A14)}$$

whereas the particular solution is:

$$A(x)_p = (C_3\beta)\left(\frac{k_1}{D_A}\right)[\sinh K_1(m-x)] \qquad \text{(Eq. A15)}$$

where C_1, C_2, and C_3 are arbitrary constants. In finding C_3, the first and second derivatives of Eq. A15 are taken and applied to Eq. A13, whereupon:

$$C_3 = \frac{1}{K_1^2 - K_2^2} \qquad \text{(Eq. A16)}$$

The general solution, which is the sum of $A(x)_h$ and $A(x)_p$, becomes:

$$A(x) = C_1 \sinh K_2x + C_2 \cosh K_2x + \left(\frac{\beta}{(K_1^2 - K_2^2)}\right)\left(\frac{k_1}{D_A}\right)[\sinh K_1(m-x)] \qquad \text{(Eq. A17)}$$

With the boundary conditions accounting for the impermeability of the stratum corneum with respect to the drug and the sink conditions:

$$D_A \left.\frac{dA}{dx}\right|_{x=0} = 0 \qquad \text{(Eq. A18)}$$

and:

$$A = 0 \qquad \text{at } x = m \qquad \text{(Eq. A19)}$$

the integration constants are:

$$C_1 = \frac{\beta K_1}{(K_1^2 - K_2^2)K_2}\left(\frac{k_1}{D_A}\right)(\cosh K_1m) \qquad \text{(Eq. A20)}$$

and:

$$C_2 = -\frac{C_1 \sinh K_2m}{\cosh K_2m} \qquad \text{(Eq. A21)}$$

After substitution of C_1 and C_2 into Eq. A17 and algebraic rearrangement, the concentration–distance expression for the drug is:

$$A(x) = \omega \sinh K_2(m-x) + \frac{\beta}{(K_1^2 - K_2^2)}\left(\frac{k_1}{D_A}\right)[\sinh K_1(m-x)] \qquad \text{(Eq. A22)}$$

where:

$$\omega = \frac{-\beta K_1}{(K_1^2 - K_2^2)K_2}\left(\frac{k_1}{D_A}\right)\left(\frac{\cosh K_1m}{\cosh K_2m}\right) \qquad \text{(Eq. A23)}$$

and $K_1 \neq K_2$.

Cutaneous Concentration–Distance Expression for Drug: Case of $K_1 = K_2$—As shown in the previous section, a necessary criterion for the existence of Eq. A22 is that $K_1 \neq K_2$. To obtain an expression for $A(x)$ for the case of $K_1 = K_2$, a different approach is used, *e.g.*, the variation of parameters method.

In pursuing the case of $K_1 = K_2 = K$, it follows that the enzyme rate constants are $k_1 = D_VK^2$ and $k_2 = D_AK^2$ such that Eq. A13 can be rewritten as:

$$\frac{d^2A}{dx^2} - K^2A = \left(\frac{\beta K^2 D_V}{D_A}\right)[\sinh K(m-x)] \qquad \text{(Eq. A24)}$$

By the method of the variation of parameters, the homogeneous solution is:

$$A(x)_h = C_1 \sinh Kx + C_2 \cosh Kx \qquad \text{(Eq. A25)}$$

and the particular solution is:

$$A(x)_p = u_1 \sinh Kx + u_2 \cosh Kx \qquad \text{(Eq. A26)}$$

In determining the parameters u_1 and u_2, which are variables in x, the following set of auxiliary equations is identified:

$$u_1' \sinh Kx + u_2' \cosh Kx = 0 \qquad \text{(Eq. A27)}$$

and:

$$u_1'K \cosh Kx + u_2'K \sinh Kx = \left(\frac{\beta K^2 D_V}{D_A}\right)[\sinh K(m-x)] \qquad \text{(Eq. A28)}$$

where u_1' and u_2' are derivatives of u_1 and u_2. After solving for u_1' and u_2' by determinants and then integrating, one gets:

$$u_1 = \frac{\beta D_V}{D_A}\left[\sinh Km\left(\frac{\sinh 2Kx}{4} - \frac{Kx}{2}\right) - \frac{(\cosh Km)(\cosh^2 Kx)}{2}\right] \qquad \text{(Eq. A29)}$$

and:

$$u_2 = \frac{\beta D_V}{D_A}\left[\cosh Km\left(\frac{\sinh 2Kx}{4} - \frac{Kx}{2}\right) - \frac{(\sinh Km)(\sinh^2 Kx)}{2}\right] \qquad \text{(Eq. A30)}$$

The substitution of Eqs. A29 and A30 into A26 and subsequent algebraic manipulation give rise to a simple expression for $A(x)_p$:

$$A(x)_p = -\frac{\beta D_V}{2D_A}(Kx)\cosh K(m-x) \qquad \text{(Eq. A31)}$$

The general solution is:

$$A(x) = A(x)_h + A(x)_p \qquad \text{(Eq. A32)}$$

or:

$$A(x) = C_1 \sinh Kx + C_2 \cosh Kx - \frac{\beta D_V}{2D_A}(Kx)\cosh K(m-x) \qquad \text{(Eq. A33)}$$

After applying the boundary conditions found in Eqs. A18 and A19, the integration constants are:

$$C_1 = \left(\frac{\beta D_V}{2D_A}\right)(\cosh Km) \qquad \text{(Eq. A34)}$$

and:

$$C_2 = \frac{\beta D_V}{2D_A}[(Km)\,\text{sech}\,Km - \sinh Km] \qquad \text{(Eq. A35)}$$

Finally, the drug concentration as a function of distance in the cutaneous tissue for the case of $K_1 = K_2 = K$ is expressed by:

$$A(x) = -\frac{\beta D_V}{2D_A}[\sinh K(m-x) + (Kx)\cosh K(m-x) - (Km)\,\text{sech}\,Km \cosh Kx] \qquad \text{(Eq. A36)}$$

Cutaneous Concentration–Distance Expressions for Metabolite—For the case of $K_1 \neq K_2$, utilization of Eqs. 7 and 15 provides the start in the derivation of $H(x)$. Thus:

$$\frac{d^2H}{dx^2} = -\frac{k_2}{D_H}\left[\omega \sinh K_2(m-x) + \left(\frac{\beta}{K_1^2 - K_2^2}\right)\left(\frac{k_1}{D_A}\right)[\sinh K_1(m-x)]\right] \qquad \text{(Eq. A37)}$$

Upon integrating twice, one obtains:

$$H(x) = -\frac{k_2}{D_H}\left[\left(\frac{\omega}{K_2^2}\right)[\sinh K_2(m-x)] + \left(\frac{\beta}{(K_1^2 - K_2^2)K_1^2}\right)[\sinh K_1(m-x)]\right] + C_1x + C_2 \qquad \text{(Eq. A38)}$$

whereby the integration constants C_1 and C_2 are evaluated from the following boundary conditions:

$$D_H \left.\frac{dH}{dx}\right|_{x=0} = 0 \qquad \text{(Eq. A39)}$$

and:

$$H = 0 \qquad \text{at } x = m \qquad \text{(Eq. A40)}$$

Accordingly:

$$C_1 = -\frac{k_2}{D_H}\left[\frac{\omega}{K_2}(\cosh K_2m) + \left(\frac{\beta}{(K_1^2 - K_2^2)K_1}\right)\left(\frac{k_1}{D_A}\right)(\cosh K_1m)\right] \qquad \text{(Eq. A41)}$$

$$C_2 = -C_1m \qquad \text{(Eq. A42)}$$

The final solution becomes:

$$H(x) = \frac{k_2}{D_H}\left[\left(\frac{\omega}{K_2}\right)(\cosh K_2 m) + \left(\frac{\beta}{(K_1^2 - K_2^2)K_1}\right)\left(\frac{k_1}{D_A}\right)(\cosh K_1 m)\right](m - x) - \frac{k_2}{D_H}\left[\left(\frac{\omega}{K_2^2}\right)[\sinh K_2(m - x)] + \left(\frac{\beta}{(K_1^2 - K_2^2)K_1^2}\right)\left(\frac{k_1}{D_A}\right)[\sinh K_1(m - x)]\right] \quad \text{(Eq. A43)}$$

where $K_1 \neq K_2$.

In the case of $K_1 = K_2 = K$, Eqs. 7 and 19 are combined to give the following homogeneous differential equation:

$$\frac{d^2H}{dx^2} = \frac{\beta K^2 D_V}{2D_A}\left[\begin{matrix}\sinh K(m - x) + (Kx)\cosh K(m - x)\\ -(Km)\,\text{sech}\,Km\cosh Kx\end{matrix}\right] \quad \text{(Eq. A44)}$$

The solution to Eq. A44 is given by:

$$H(x) = \frac{\beta D_V}{2D_A}\left[\begin{matrix}2\sinh K(m - x) - (Km)\,\text{sech}\,Km\cosh Kx\\ -\sinh Km[(Kx)\sinh Kx - \cosh Kx]\\ +\cosh Km[(Kx)\cosh Kx - \sinh Kx]\end{matrix}\right] + C_3 x + C_4 \quad \text{(Eq. A45)}$$

where, with the boundary conditions given by Eqs. A39 and A40:

$$C_3 = \left(\frac{\beta K D_V}{D_A}\right)(\cosh Km) \quad \text{(Eq. A46)}$$

and:

$$C_4 = \left(-\frac{\beta D_V}{D_A}\right)[(Km)\cosh Km] \quad \text{(Eq. A47)}$$

After substitution of the evaluated constants C_3 and C_4 back into Eq. A45 and simplification of the algebra, the final expression is:

$$H(x) = -\frac{\beta D_V}{2D_A}\left[\begin{matrix}-3\sinh K(m - x) + (Km)\,\text{sech}\,Km\cosh Kx\\ -(Kx)\cosh K(m - x) + 2K(m - x)\cosh Km\end{matrix}\right] \quad \text{(Eq. A48)}$$

Total Flux of All Species across Membrane System—The total fluxes of the prodrug V, parent drug A, and metabolite H are readily found by applying the following relationships:

$$F_V = -D_V\left.\frac{dV(x)}{dx}\right|_{x=m} \quad \text{(Eq. A49)}$$

$$F_A = -D_A\left.\frac{dA(x)}{dx}\right|_{x=m} \quad \text{(Eq. A50)}$$

$$F_H = -D_H\left.\frac{dH(x)}{dx}\right|_{x=m} \quad \text{(Eq. A51)}$$

Without going into the details of the mathematics, the final flux expressions are given in Eqs. 21–25.

REFERENCES

(1) H. Y. Ando, N. F. H. Ho, and W. I. Higuchi, *J. Pharm. Sci.*, **66,** 1525 (1977).

(2) *Ibid.*, **66,** 755 (1977).

(3) F. M. Schabel, Jr., *Chemotherapy (Basel)*, **13,** 321 (1968).

(4) R. J. Suhadolnik, "Nucleoside Antibiotics" Wiley–Interscience, New York, N.Y., 1970, pp. 123–169.

(5) W. M. Shannon, in "Adenine Arabinoside: An Antiviral Agent," D. Pavan-Langston, R. A. Buchanan, and C. A. Alford, Jr., Eds., Raven, New York, N.Y., 1975, pp. 1–44.

(6) B. J. Sloan, in *ibid.*, pp. 45–94.

(7) A. A. Fondak, A. E. Friedman, and R. J. Klein, in "Antivirals with Clinical Potential," abstracts from a symposium at Stanford University, Stanford, Calif., Aug. 26–29, 1975.

(8) M. Lieberman, T. W. Schafer, and P. E. Came, *J. Invest. Dermatol.*, **60,** 203 (1973).

(9) D. C. Baker, T. H. Haskell, and S. R. Putt, presented at the American Chemical Society, Chicago meeting, Aug. 28–Sept. 2, 1977.

(10) J. J. Brink and G. A. LePage, *Cancer Res.*, **24,** 312 (1964).

(11) *Ibid.*, **24,** 1042 (1964).

(12) M. Hubert-Habart and S. S. Cohen, *Biochim. Biophys. Acta*, **59,** 468 (1962).

(13) G. A. LePage and I. G. Junga, *Cancer Res.*, **25,** 46 (1965).

(14) R. Koshiura and G. A. LePage, *ibid.*, **28,** 1014 (1968).

(15) J. G. Cory and R. J. Suhadolnik, *Biochemistry*, **4,** 1729 (1965).

(16) S. Frederiksen, *Arch. Biochem. Biophys.*, **113,** 383 (1966).

(17) A. Block, M. J. Robins, and J. R. McCarthy, *J. Med. Chem.*, **10,** 908 (1967).

(18) B. J. Sloan, J. K. Kielty, and F. A. Miller, *Ann. N.Y. Acad. Sci.*, **284,** 60 (1977).

(19) P. M. Schwartz, C. Shipman, Jr., and J. C. Drach, *Antimicrob. Agents Chemother.*, **10,** 64 (1976).

(20) J. D. Connor, L. Sweetman, S. Carey, M. A. Stuckey, and R. Buchanan, *ibid.*, **6,** 630 (1974).

(21) J. L. Fox, C. D. Yu, W. I. Higuchi, and N. F. H. Ho, *Int. J. Pharm.*, in press.

ACKNOWLEDGMENTS

Abstracted in part from a thesis submitted by C. D. Yu to the University of Michigan in partial fulfillment of the Doctor of Philosophy degree requirements.

Supported by National Institutes of Health Research Grant AI14987 and Training Grant DE00204.

The authors thank Dr. D. C. Baker, University of Alabama, and Dr. A. J. Glazko and Dr. T. H. Haskell, Warner-Lambert/Parke-Davis, for supplying ^{3}H-labeled and nonlabeled vidarabine-5′-valerate ester.

Physical Model Evaluation of Topical Prodrug Delivery—Simultaneous Transport and Bioconversion of Vidarabine-5′-valerate II: Parameter Determinations

CHENG DER YU *, JEFFREY L. FOX, NORMAN F. H. HO, and WILLIAM I. HIGUCHI ×

Received January 17, 1979, from the *College of Pharmacy, University of Michigan, Ann Arbor, MI 48109.* Accepted for publication April 18, 1979. *Present address: Syntex Research, Stanford Industrial Park, Palo Alto, CA 94304.

Abstract □ Results of initial studies on methods for determining various model parameters are reported. By employing excised hairless mouse skin in a diffusion cell system, numerous model parameter values were deduced. The stratum corneum permeability was estimated from steady-state fluxes with preparations of heat-separated epidermal membranes. Determinations of dermis diffusivities and enzyme rate constants *in situ* involved considering the simultaneous transport and the enzyme processes and factoring the diffusivities and enzyme rate constants from the overall kinetics. Dermal diffusivities were on the order of 10^{-6} cm²/sec for vidarabine and its 5′-valerate ester. The enzyme rate constants were 1.70×10^{-3} sec^{-1} for the esterase and 8.68×10^{-3} sec^{-1} for the deaminase.

Keyphrases □ Vidarabine valerate—topical dosage forms, prodrugs, physical models, pharmacokinetics □ Antiviral agents—vidarabine valerate prodrugs, topical dosage forms, physical models, pharmacokinetics □ Prodrugs—vidarabine valerate, topical dosage forms, physical models, pharmacokinetics □ Models, physical—vidarabine valerate prodrugs, topical dosage forms, mouse skin □ Pharmacokinetics—vidarabine valerate prodrugs, topical dosage forms, physical models

A physical model for the topical delivery of an ester prodrug of vidarabine (9-β-D-arabinofuranosyladenine) (I) was presented previously (1). The model treats the skin as a two-ply membrane composed of a stratum corneum and a viable cutaneous tissue. When the I prodrug is applied on the skin surface, the prodrug is transported across the stratum corneum and reaches the viable cutaneous tissue where the esterase converts some of the prodrug to I and the deaminase metabolizes a portion of the latter to its metabolite, 9-β-D-arabinofuranosylhypoxanthine (II). Concurrently, all three species diffuse toward the blood sink.

The mathematical problem of the simultaneous diffusion and bioconversion was solved, and the solution provided expressions for the concentration–distance profiles in the cutaneous tissue as well as for the transport rates of the three species into the bloodstream. Simulation calculations (Figs. 3 and 4 in Ref. 1) showed the influences of the stratum corneum permeability and the esterase activity on prodrug bioavailability[1]. Since knowledge of the actual parameters would make the proposed physical model useful for quantitative predictions and mechanism evaluations in topical bioavailability, it was desirable to develop methods for parameter determinations. These parameters include the stratum corneum permeability coefficients and the dermis diffusivities for the prodrug, the drug, and the metabolite; the enzyme rate constants for the esterase and the deaminase reactions; and the skin thickness.

The present paper reports the results of an initial investigation on methods for determining these parameters. Vidarabine-5′-*n*-valerate (III) was selected as the prodrug because preliminary experiments showed that III is significantly deacylated by the hairless mouse skin.

By employing excised hairless mouse skin in a well-designed *in vitro* experimental system, all parameters could be determined. The skin thickness could be measured with a micrometer by sandwiching the specimen between two glass slides. The stratum corneum permeability coefficients could be determined in a diffusion cell with preparations of the heat-separated epidermal membrane[2]. The evaluations of dermis diffusivities and the enzyme reaction rate constants, however, presented certain difficulties because of the simultaneous transport and the enzyme processes and because of the need to factor out the diffusivities and the enzyme reaction rate constants from the overall kinetics. The proposed procedures combined experiments and theory in a novel way and provided the means for determining the transport and enzyme activity parameters in the tissues.

THEORY

Aqueous Permeability Coefficient (P_{aq}) Determinations—Although the transport resistances arising from the aqueous diffusion layers generally do not greatly influence the overall transport and metabolism, estimations of them are desirable. The following procedures provide the means for approximating P_{aq}.

The aqueous diffusion layer thickness, h, may be determined by conducting a dissolution rate experiment with a reference solute (such as benzoic acid) for which both the solubility and the diffusivity are known. The data are plotted as $\ln [C_s/(C_s - C_t)]$ *versus* t, which gives a slope equal to (D/h) (area/volume) according to the dissolution rate equation:

$$\ln\left(\frac{C_s}{C_s - C_t}\right) = \left(\frac{D}{h}\right)\left[\frac{\text{area}}{\text{volume}}(t - t_l)\right] \qquad \text{(Eq. 1)}$$

where C_s is the solubility of benzoic acid, C_t is the concentration of benzoic acid at time t, t_l is the extrapolated lag time at which the first benzoic acid molecule theoretically appeared in the bulk solution, area is the dissolutional area of the benzoic acid pellet, volume is the bulk solution volume, and D is the aqueous diffusivity of benzoic acid (2). Therefore, h may be calculated from the slope.

The aqueous diffusivities of I, II, or III may be estimated using:

$$D_i = \left(\frac{M}{M_i}\right)^{1/3} D \qquad \text{(Eq. 2)}$$

where i = I, II, or III; M is the molecular weight of benzoic acid; M_i is the molecular weight of species i; D is the aqueous diffusivity of benzoic acid; and D_i is the aqueous diffusivity of species i.

[1] Prodrug bioavailability is defined as the topically available concentration of the parent drug in the cutaneous tissue.

[2] Scotch-tape stripped skin was also employed. Data from these preparations and those obtained from full-thickness skin may be used to calculate the stratum corneum permeability coefficients.

0022-3549/79/1100-1347$01.00/0
© 1979, American Pharmaceutical Association

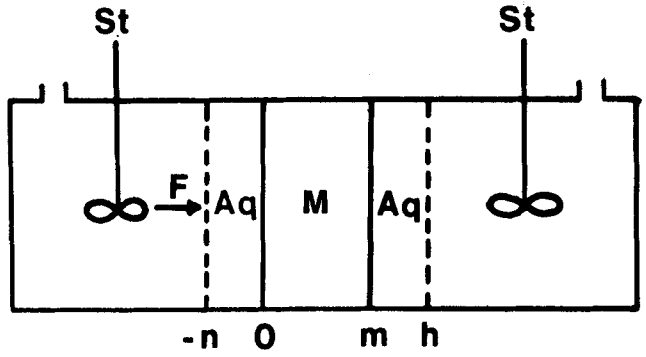

Figure 1—*Go-through experiment. Key: M, viable epidermis and dermis; Aq, aqueous diffusion layer; F, flux of diffusant; and St, stirrer.*

The P_{aq} of I, II, or III in the aqueous diffusion layer is simply:

$$(P_{aq})_i = \frac{D_i}{h} \qquad \text{(Eq. 3)}$$

Membrane–Water Partition Coefficient ($K_{m/w}$)—By the definition of partition coefficient, the following relationship exists:

$$(K_{m/w})_i = \frac{[C_m]_i}{[C_w]_i} = \frac{(M_m)_i/V_m}{(M_w)_i/V_w} \qquad \text{(Eq. 4)}$$

where, for species i, $[C_m]_i$ is the equilibrium concentration of i in the membrane, $[C_w]_i$ is the equilibrium concentration of i in the aqueous solution, $(M_m)_i$ is the mass of i in the membrane at equilibrium, $(M_w)_i$ is the mass of i in the aqueous solution at equilibrium, V_m is the membrane volume, and V_w is the aqueous solution volume.

The $(M_m)_i$ may be expressed in terms of $(M_w)_i$ and $(M_w^0)_i$, the total mass of i initially present in the aqueous solution:

$$(M_m)_i = (M_w^0)_i - (M_w)_i \qquad \text{(Eq. 5)}$$

Therefore, Eq. 4 may be rearranged to give:

$$(K_{m/w})_i = \left(\frac{[C_w^0]_i - [C_w]_i}{[C_w]_i}\right)\left(\frac{V_w}{V_m}\right) \qquad \text{(Eq. 6)}$$

where $[C_w^0]_i$ is the initial concentration of i in the aqueous phase. By assaying $[C_w^0]_i$ and $[C_w]_i$, $(K_{m/w})_i$ may be determined by Eq. 6.

Diffusivity and Permeability Coefficient Determinations—With a diffusion cell, the steady-state flux method may be used for the determinations of permeability coefficients of I, II, or III in different skin preparations (epidermal membrane or dermis) according to:

$$F_i = \frac{1}{\frac{1}{P_i} + \frac{2}{P_{aq}}} \Delta C_i \qquad \text{(Eq. 7)}$$

where F_i is the steady-state flux of diffusant i, P_i is the permeability coefficient of i, and ΔC_i is the concentration gradient of i across the membrane.

The diffusivity, D_i, may be related to P_i, $(K_{m/w})_i$, and m, the thickness of the membrane, by:

$$D_i = \frac{(P_i)(M)}{(K_{m/w})_i} \qquad \text{(Eq. 8)}$$

Simultaneous Determinations of Diffusivity and Enzyme Reaction Rate Constant in "Go-Through" Experiments—In the present studies, an inhibitor of the esterase activity was not employed. Therefore, a direct measurement of the prodrug diffusivity in the dermis was not possible. However, the diffusivity may be determined indirectly in the following manner. Figure 1 illustrates the go-through experiment that provides a situation for determining simultaneously the diffusivity of a prodrug and its esterase activity. The system consists of two identical aqueous diffusion layers and a membrane in between. The membrane is assumed to have a homogeneous enzyme distribution[3]. The diffusivity is assumed to be constant[3] through the membrane.

The enzymatic reactions involved are taken as simple first-order reactions for mathematical simplicity. Sink conditions on the receiver side and steady-state conditions are assumed to prevail throughout the experimental period. Based on these assumptions, the mathematical problem for the simultaneous diffusion and bioconversion may be set up and the differential equations describing the steady-state simultaneous diffusion and bioconversion of a prodrug may be written as:

$$D_V \frac{d^2V}{dx^2} - k_1 V = 0 \qquad \text{(Eq. 9)}$$

$$D_A \frac{d^2A}{dx^2} + k_1 V - k_2 A = 0 \qquad \text{(Eq. 10)}$$

$$D_H \frac{d^2H}{dx^2} + k_2 A = 0 \qquad \text{(Eq. 11)}$$

where V, A, and H are concentrations of the prodrug, drug, and metabolite, respectively; D_V, D_A, and D_H are diffusivities of the prodrug, drug, and metabolite in the membrane, respectively; and k_1 and k_2 are first-order rate constants for the bioconversion shown in Scheme I:

$$\text{prodrug} \xrightarrow[\text{esterase}]{k_1} \text{drug} \xrightarrow[\text{deaminase}]{k_2} \text{metabolite}$$

Scheme I

When an inhibitor[4] is used to block the deaminase activity, the situation is simplified and involves only the first step of the bioconversion. Then the differential equations become:

$$D_V \frac{d^2V}{dx^2} - k_1 V = 0 \qquad \text{(Eq. 12)}$$

$$D_A \frac{d^2A}{dx^2} + k_1 V = 0 \qquad \text{(Eq. 13)}$$

For the steady-state situation and sink conditions, the boundary conditions at $x = 0$ are:

$$-D_V \left.\frac{dV}{dx}\right|_{x=0} = P_{aq}[V(-n) - V(0)] \qquad \text{(Eq. 14)}$$

$$-D_A \left.\frac{dA}{dx}\right|_{x=0} = P_{aq}[0 - A(0)] \qquad \text{(Eq. 15)}$$

At $x = m$, they are:

$$-D_V \left.\frac{dV}{dx}\right|_{x=m} = P_{aq}[V(m) - 0] \qquad \text{(Eq. 16)}$$

$$-D_A \left.\frac{dA}{dx}\right|_{x=m} = P_{aq}[A(m) - 0] \qquad \text{(Eq. 17)}$$

With these boundary conditions, analytical solutions (*Appendix I*) for Eqs. 12 and 13 may be obtained. These solutions give concentration–distance profiles of the prodrug and drug in the domain of $0 \le x \le m$. The species flow into the receiver chamber is, by definition, the product of the diffusivity and the derivative of the concentration with respect to x at $x = m$. Therefore, the fluxes, F_{hV} and F_{hA}, are related to D_V and k_1 by:

$$F_{hV} = \frac{-\gamma P_{aq}}{(K_{m/w})_V} \qquad \text{(Eq. 18)}$$

$$F_{hA} = \frac{\gamma P_{aq}}{(K_{m/w})_V} + \psi \qquad \text{(Eq. 19)}$$

where:

$$K_1 = \sqrt{k_1/D_V}$$

$$\gamma = \frac{-\frac{P_{aq}V(-n)}{D_V K_1}}{\left(1 + \frac{P_{aq}^2}{D_V^2 K_1^2 (K_{m/w})_V^2}\right)\sinh K_1 m + \frac{2P_{aq}}{D_V K_1 (K_{m/w})_V}\cosh K_1 m}$$

$$\psi = \frac{-D_A}{\frac{P_{aq} m}{(K_{m/w})_A} + 2D_A}\left[\frac{\gamma k_1}{K_1}\left(1 + \frac{P_{aq}^2}{K_1^2 D_A D_V (K_{m/w})_A (K_{m/w})_V}\right)\sinh K_1 m + \frac{\gamma k_1 P_{aq}}{K_1^2}\left(\frac{1}{D_V (K_{m/w})_V} + \frac{1}{D_A (K_{m/w})_A}\right)\cosh K_1 m - \frac{\gamma k_1 P_{aq}}{K_1^2}\left(\frac{1}{D_V (K_{m/w})_V} - \frac{1}{D_A (K_{m/w})_A}\right)\right]$$

[3] A more general case with variations in diffusivity and enzyme reaction rate constants with respect to position in the membrane will be considered later.

[4] An inhibitor of deaminase activity, covidarabine, was provided by Dr. T. H. Haskell, Warner-Lambert/Parke-Davis, Ann Arbor, MI 48106.

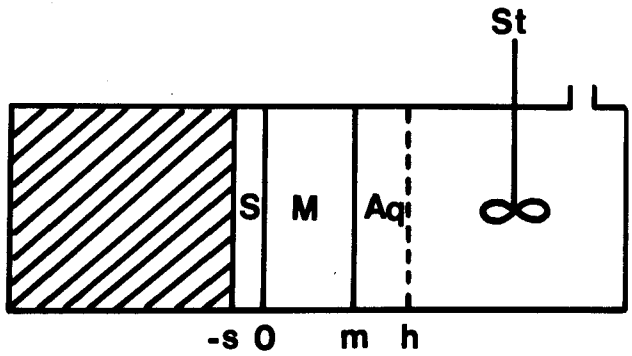

Figure 2—*In-and-out experiment. Key: M, viable epidermis and dermis; S, stratum corneum; Aq, aqueous diffusion layer; and St, stirrer.*

Similarly, species flow at $x = -n$ may be expressed by:

$$F_{-nV} = -\gamma\left[D_V K_1 \sinh K_1 m + \frac{P_{aq}}{(K_{m/w})_V}\cosh K_1 m\right] \quad \text{(Eq. 20)}$$

$$F_{-nA} = \gamma\left[D_V K_1 \sinh K_1 m + \frac{P_{aq}}{(K_{m/w})_V}\cosh K_1 m\right] + \psi \quad \text{(Eq. 21)}$$

where F_{-nV} is the prodrug transport rate from the donor chamber into the membrane and F_{-nA} is the back-diffusion rate of the drug out of the membrane and into the donor side.

Examination of Eqs. 18–21 demonstrates that:

$$F_{-nV} + F_{-nA} = F_{hV} + F_{hA} \quad \text{(Eq. 22)}$$

Equation 22 is a mathematical statement of the prevailing steady-state condition at which the net flux into the membrane at $x = -n$ is equal to the total flux out of the membrane at $x = h$.

Equations 18–21 may be used to determine simultaneously k_1 and D_V from the measured fluxes and the predetermined D_A. These equations are more than adequate since there are four equations and only two unknowns. In the conversion of the parent drug to its metabolite, the unknown reduces to k_2 only since D_A and D_H are predetermined. The equations involved in the k_2 determination are:

$$F_{hA} = -\frac{\delta P_{aq}}{(K_{m/w})_A} \quad \text{(Eq. 23)}$$

$$F_{hH} = \frac{\delta k_2 P_{aq}}{K_2^2 D_A (K_{m/w})_A} + \phi \quad \text{(Eq. 24)}$$

$$F_{-nA} = -\delta\left[D_A K_2 \sinh K_2 m + \frac{P_{aq}}{(K_{m/w})_A}\cosh K_2 m\right] \quad \text{(Eq. 25)}$$

$$F_{-nH} = \delta\left[D_A K_2 \sinh K_2 m + \frac{P_{aq}}{(K_{m/w})_A}\cosh K_2 m\right] + \phi \quad \text{(Eq. 26)}$$

where:

$$K_2 = \sqrt{k_2/D_A}$$

$$\delta = \frac{-\dfrac{P_{aq} A(-n)}{D_A K_2}}{\left(\dfrac{P_{aq}^2}{D_A^2 K_2^2 (K_{m/w})_A^2} + 1\right)(\sinh K_2 M) + \dfrac{2P_{aq}}{D_A K_2 (K_{m/w})_A}(\cosh K_2 m)}$$

$$\phi = \frac{-D_H}{\dfrac{P_{aq} m}{(K_{m/w})_H} + 2D_H}\left[\frac{\delta k_2}{K_2}\left(1 + \frac{P_{aq}^2}{K_2^2 D_H D_A (K_{m/w})_H (K_{m/w})_A}\right)\sinh K_2 m + \frac{\delta k_2 P_{aq}}{K_2^2}\left(\frac{1}{D_A (K_{m/w})_A} + \frac{1}{D_H (K_{m/w})_H}\right)\cosh K_2 m - \frac{\delta k_2 P_{aq}}{K_2^2}\left(\frac{1}{D_A (K_{m/w})_A} - \frac{1}{D_H (K_{m/w})_H}\right)\right]$$

Enzyme Reaction Rate Constants in "In-and-Out" Experiments—A modification of the go-through design (Fig. 2) involves substituting one side of the diffusion cell with an impermeable glass plate. In this case, the prodrug (or drug) in the bulk solution is allowed to penetrate from the dermis side and is metabolized by the cutaneous enzymes. The products then back-diffuse into the bulk phase.

The solution to the mathematical problem for such an in-and-out system provides equations for the determination of the enzyme reaction rate constants from the observed fluxes. The mathematics are similar to those for the go-through case but with different boundary conditions. For the determination of k_1 in the presence of covidarabine, the relevant differential equation is:

$$D_V \frac{d^2V}{dx^2} - k_1 V = 0 \quad \text{(Eq. 27)}$$

and the boundary conditions at $x = 0$ are:

$$-D_V \left.\frac{dV}{dx}\right|_{x=0} = 0 \quad \text{(Eq. 28)}$$

At $x = m$, they are:

$$-D_V \left.\frac{dV}{dx}\right|_{x=0} = P_{aq}[V(m) - V(h)] \quad \text{(Eq. 29)}$$

The solution (*Appendix II*) to Eq. 27 gives the concentration–distance profiles of the prodrug in the domain $0 \le x \le m$. Taking the derivative at $x = m$ and relating the derivative to the flux by Fick's law give:

$$\frac{1}{(K_{m/w})_V K_1 \tanh K_1 m} = D_V\left[\frac{V(h)}{-F_{hV}} - \frac{1}{P_{aq}}\right] \quad \text{(Eq. 30)}$$

where F_{hV} is the flux of the prodrug transporting into the dermis from the bulk solution and $(K_{m/w})_V$ is the partition coefficient of the prodrug between the dermis and the aqueous phase. Therefore, k_1 may be determined from the observed flux using Eq. 30. A similar expression may be obtained for k_2:

$$\frac{1}{(K_{m/w})_A K_2 \tanh K_2 m} = D_A\left[\frac{A(h)}{-F_{hA}} - \frac{1}{P_{aq}}\right] \quad \text{(Eq. 31)}$$

where F_{hA} is the flux of the drug transporting into the dermis from the bulk solution and $(K_{m/w})_A$ is the drug partition coefficient between the dermis and the aqueous phase.

EXPERIMENTAL

Materials—^{3}H-2-I[5] and ^{3}H-2-III[6] were used as received after the purity was checked by TLC. ^{3}H-2-II was made from the enzyme conversion of ^{3}H-2-I by a commercial adenosine deaminase[7] followed by TLC examination of purity. Compounds I[8], II[8], and III[9] were used to make a 1-μg/μl aqueous solution for UV visualization of the respective TLC spots. Covidarabine was dissolved in distilled water to make a 5-μg/ml solution before use.

The liquid scintillation counter cocktail[10] was stored in a dark place, and 5 ml was transferred by a repipet into each vial for the scintillation counting. Male hairless mice[11], ~8–12 weeks old, were employed. Normal saline[12] was used for all experiments as a bulk phase solution. A dermatome[13] was employed for slicing the skin.

Diffusion Cells—A modified Karush-type diffusion cell[14] was further modified by a local glass shop; a 3-cm stirring shaft was attached for each half-cell. The stirrer, made of stainless steel and equipped with a small polytef propeller ~8 mm in length, was driven by a 150-rpm constant-speed motor[15]. The sampling ports, one for each half-cell, were 1 cm in length. The volume of each half-cell was ~3 ml. The effective diffusion area was 1.767 cm^2.

With the membrane in between, the two cell halves were assembled as shown in Fig. 3 using a No. 18 spring clamp. The assembled cell was then immersed in a 37° water bath so that the stirring and sampling ports were the only cell components above the water bath surface. A cell was then ready for a go-through experiment. A smaller cell, 1.5-ml half-cell volume and 0.7126 cm^2 diffusion area, also was used in permeability experiments.

A specially designed glass cell (Fig. 4) was employed for the in-and-out experiments. The cell consisted of a glass plate and a modified half-cell of a regular diffusion cell. The glass plate was for blocking the stratum

[5] New England Nuclear, Boston, MA 02118.
[6] Courtesy of Dr. A. J. Glazko, Warner-Lambert/Parke-Davis, Ann Arbor, MI 48106.
[7] Boehringer Mannheim GmbH, 15069 EAAT, Germany.
[8] Calbiochem, Los Angeles, CA 90054.
[9] Courtesy of Dr. D. C. Baker, Warner-Lambert/Parke-Davis, Ann Arbor, MI 48106.
[10] Aquasol, New England Nuclear, Boston, MA 02118.
[11] HRS/J mice, Jackson Laboratory, Bar Harbor, ME 04609.
[12] Sodium chloride irrigation (0.9%), Abbott Laboratories, North Chicago, IL 60064.
[13] Castroviejo, a small electrical dermatome, Storz Instrument Co., St. Louis, MO 63110.
[14] Bellco, Vineland, N.J.
[15] Hurst, Princeton, Ind.

Table I—Permeability Coefficients of I–III in Full-Thickness, Hairless Mouse Skin

Mouse	Permeability Coefficients[a], $\times 10^8$ cm/sec I	II	III
801034[b]	2.96	1.82	—
611031	2.33	—	5.43
611031 after 6 hr of soaking in saline	1.87	—	—

[a] Calculated from steady-state fluxes using Eq. 7, where P_{aq} was 1.05×10^{-3} cm/sec. [b] Raw data are shown in Fig. 12.

corneum side of the skin so that no drug could escape from that side. The half-cell opening was 0.635 cm in diameter, providing a 0.317-cm^2 effective contact area between the skin and the bulk solution, which was 1 ml in volume. The cell was equipped with two ports, one for the stirrer and the other for sampling. The two parts of the cell were held together by a No. 12 spring clamp. The assembled cell was immersed in a 37° constant-temperature water bath in the same way as was the go-through cell, and the cell contents were stirred continuously at 150 rpm.

Procedure for Skin Preparations—A male hairless mouse, ~6–12 weeks of age, was sacrificed by snapping the spinal cord at the neck. A square section of the abdominal skin, ~3 cm in each dimension, was excised from the animal with surgical scissors. After the incision was made, the skin was lifted and the adhering fat and other visceral debris were removed carefully from the under surface. Prior to removing the skin, a uniform circle was made on the abdomen with a marker pen, using the diffusion opening of a half-cell as the template. This circle marked the precise skin section to be positioned between the half-cells. After the skin was mounted between half-cells and clamped, the excess skin was trimmed.

For a dermis preparation, the top 50–150 μm of the abdominal skin was removed with a dermatome before any incision was made. Although the dermatome was preset at 100 μm, the thickness of the removed layer

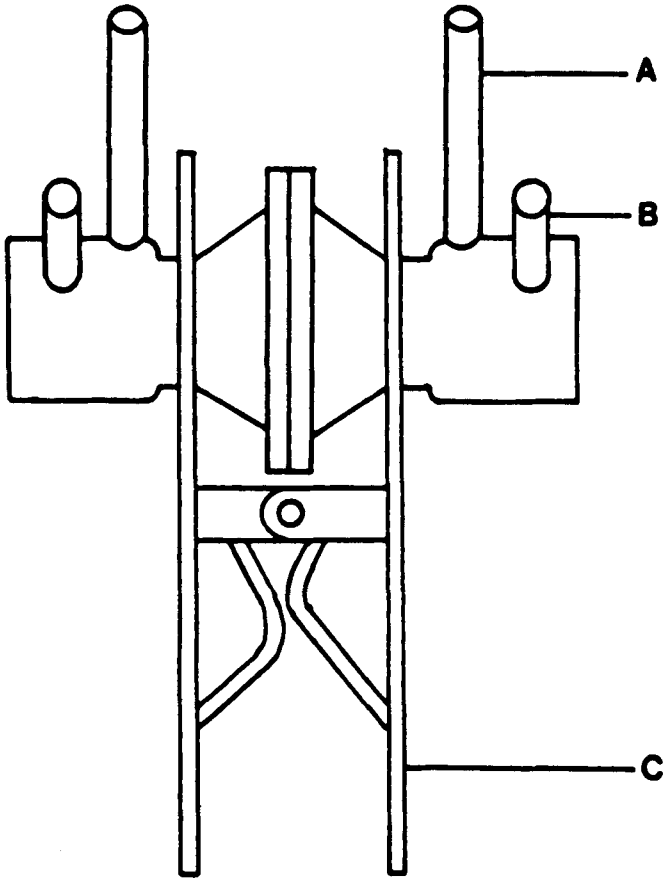

Figure 3—*Diffusion cell for the go-through experiment. Key: A, stirrer port; B, sampling port; and C, spring clamp.*

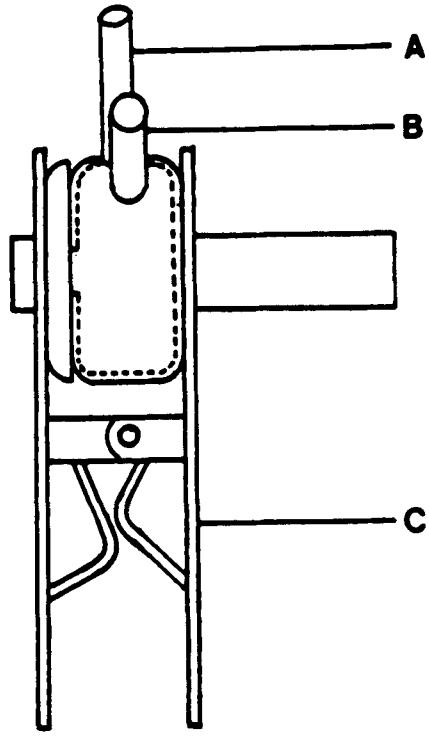

Figure 4—*Diffusion cell for the in-and-out experiment. Key: A, stirrer port; B, sampling port; and C, spring clamp.*

varied from 50 to 150 μm due to the different pressures applied by hand from one preparation to another. After planing, the remaining dermis was excised from the animal and mounted between half-cells as before. The dermis thickness was measured with a micrometer before and after the experiment by sandwiching the membrane between two glass slides.

An epidermal membrane was prepared by a heat separation method (3). A sacrificed mouse was water bathed at 60° for 30 sec, and the body was dried with cleaning tissue. The abdominal skin was marked as usual. The edge of a square, 3 cm in each dimension, was cut to the required depth by a surgical scalpel. A disposable tip of an Eppendorf pipet was employed to separate the epidermal membrane. Due to the thinness of the membrane, the procedure was carried out with care to prevent holes. The separated membrane was spread out on the surface of a saline solution and examined for holes. The membrane was then mounted between half-cells for an experimental run.

Stripped skin was obtained by stripping the stratum corneum off with tape[16] 25 times. The stripped skin was then excised from the animal and was ready for an experimental run.

Preparations of full-thickness skin were used for the in-and-out experiment to determine the enzyme reaction rate constants. The dermis was employed in the go-through experiment for both the determination of the enzyme reaction rate constants and the diffusivity calculation. For the permeability studies, all kinds of skin preparations were used.

TLC—Precoated silica gel TLC plates[17] were used to isolate I–III. The eluent was the lower layer of a mixture of 3% acetic acid–methanol–chloroform (1:2:3). With a disposable micropipet[18], a 3-μl aliquot of the bulk solution (or the receiver chamber solution in a go-through experiment) was spotted on a TLC plate, followed by an equal volume of the nonradiolabeled compound solution for visualization. The plates were developed in a closed chamber for 2–3 hr until the solvent front reached 15 cm from the origin.

After residual solvent evaporation, the spots were localized by UV light. A square, ~2.5 cm in each dimension with the spot in the center, was scraped off and collected in a scintillation vial. To each vial, 5 ml of the scintillation counter cocktail was added. After overnight equilibration in the dark, the samples were counted in a liquid scintillation counter[19].

[16] Scotch.
[17] Silica gel 60 F-254, Brinkmann Instruments, Westbury, NY 11590.
[18] Unopette, A. H. Thomas Co., Philadelphia, PA 19105.
[19] Beckman LS-200, Beckman Instruments, Fullerton, Calif.

Table II—Permeability Coefficients and Diffusivities of I–III in the Dermis Membrane Preparations

Mouse	Thickness of Dermis, μm	Permeability Coefficients[a], × 10^5 cm/sec			Diffusivities[b], × 10^6 cm^2/sec		
		I	II	III	I	II	III
703153[c]	320	4.43	4.48	4.06	1.79	1.77	—
703153 after 30 hr of soaking in saline	320	4.76	—	—	1.93	—	—
611032	400	1.87	—	1.30	0.95	—	—
703154	400	2.59	1.96	—	1.31	0.98	—
706081	400	—	—	—	—	—	0.97[d]
Average					1.50	1.38	0.97

[a] Calculated from steady-state fluxes using Eq. 7, where P_{aq} was 1.05×10^{-3} cm/sec. [b] Determined by using Eq. 8, where $(K_{m/w})_i$ values were the average values shown in Table IX. [c] Raw data shown in Fig. 10. [d] From a rigorous determination (Table XIII) as discussed in the text.

Liquid Scintillation Counting—Samples from a given experiment always were counted along with a blank control. For samples from TLC plates, the control was prepared from a blank plate that had been eluted along with the sample plates. For solution samples, the blank was prepared from a saline solution.

Vials containing silica gel were counted on the 2nd day after the addition of the cocktail, while those containing no silica gel were counted on the same day. The quenching effect of the silica gel was a function of time for the first 3 hr after the cocktail addition and then reached a stable state corresponding to ~50% quenching. Accordingly, the TLC samples were counted on the 2nd day after the cocktail addition. The counts per minute value was converted into percentage concentration on the basis of the prevailing mass balance in an in-and-out experiment.

Leaching of Enzymes from Dermis Side—A full-thickness skin preparation was mounted in the in-and-out cell as described. A 1.0-ml aliquot of saline was introduced into the chamber and stirred. A 100-μl aliquot of the bulk solution was withdrawn and transferred into a small vial at predetermined times, and 100 μl of fresh saline was added to the bulk solution immediately after each withdrawal to keep a constant volume. Necessary corrections for the dilution were made accordingly.

Except when a sample was taken, the sampling port was covered to avoid evaporation. The aliquots withdrawn were incubated with 1 μCi each of ^{3}H-I or ^{3}H-III to determine the enzyme activity. The initial enzyme reaction rate was taken as a measure of the enzyme concentration.

Aqueous Permeability Coefficients—For dissolution rate determinations, benzoic acid[20] pellets were prepared by directly compressing 100 mg of the material in a die, 1.3 cm (0.5 in.) i.d., under a force of 1362 kg (3000 lb) using a laboratory press[21]. The pellet was mounted on the opening of the in-and-out cell and secured firmly by coating the "pellet and cell" setup with melted paraffin. One milliliter of 0.01 *N* HCl, equilibrated at 37°, was introduced into the chamber at zero time. The stirring speed was maintained at 150 rpm during dissolution. To measure the dissolution rate, the amount of benzoic acid dissolved in the solvent was analyzed against time.

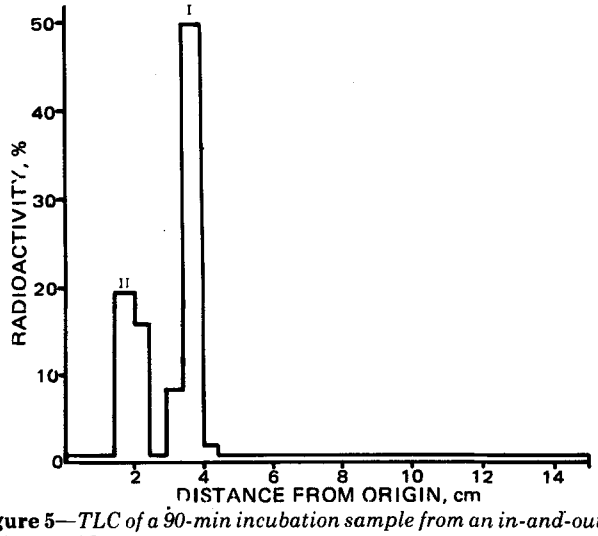

Figure 5—*TLC of a 90-min incubation sample from an in-and-out experiment of I.*

Membrane–Water Partition Coefficient Determinations—Dermis preparations of ~100–200 mg were equilibrated with solutions of ^{3}H-I or ^{3}H-II in vials for 12 hr at 37°. Covidarabine, 5 μg/ml, was included in the solutions to inhibit ^{3}H-I deamination. The initial and equilibrium concentrations of the bulk ^{3}H-I or ^{3}H-II solutions were assayed by scintillation counting. The dermis preparations were weighed before equilibration, and their volumes were calculated from the weights and average density of the skin.

The average skin density was obtained in the following manner. A full-thickness skin of ~400–600 mg was weighed before being transferred into a finely calibrated 10-ml graduated cylinder, which contained 8 ml of a detergent[22] solution. The skin was carefully unfolded with a needle after being submerged in the solution. The detergent helped remove bubbles from the skin surface. To obtain the density, the weight was divided by the volume increment of the detergent solution.

Diffusivity and Permeability Coefficients—The membrane was mounted between the two half-cells immediately after preparation, and appropriate volumes (as specified in a given experiment) of saline solution and covidarabine were introduced into each chamber. Five minutes was allowed for the cell wall, the membrane, and the bulk solution to reach thermal equilibrium with the water bath. Compound ^{3}H-I, ^{3}H-II, or ^{3}H-III was introduced into the chamber, which faced the epidermal side of the membrane (the donor chamber). A 50- or 100-μl sample from the receiver solution was withdrawn at predetermined times and was transferred immediately into a scintillation vial containing 5 ml of the scintillation counter cocktail. The donor solution concentrations were determined in the same way during the 1st min of the run and at the end of the run. All samples were counted together on the liquid scintillation counter.

Go-Through Experiment—The procedure was the same as that for the diffusivity experiment except that instead of obtaining the total counts per minute for each sample, the 3-μl sample solution was subjected to TLC separation before counting to determine the individual fluxes for I, II, or III.

In-and-Out Experiment—A full-thickness skin sample was mounted between the glass plate and the half-cell of the in-and-out cell in such a

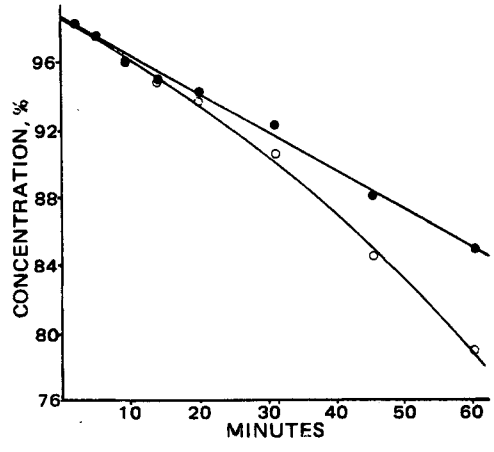

Figure 6—*Correction for the bulk phase metabolism in the in-and-out experiment of I. The slope of the corrected line is −0.222%/min. Numerical data are shown in Table VI. Key: ○, observed; and ●, corrected.*

[20] J. T. Baker Chemical Co., Phillipsburg, N.J.
[21] Model B, Fred Carver Inc., Summit, N.J.
[22] Alconon, Alconox, Inc., New York, N.Y.

Table III—Determinations of k_1 and k_2 from the In-and-Out Experiments

Mouse	Deaminase Slope[a]	Deaminase $k_2 \times 10^2$, sec^{-1}	Esterase Slope[a]	Esterase $k_1 \times 10^2$, sec^{-1}	Correlation Coefficients
702245	—	—	−0.0562	0.104	0.9814
611033[b]	—	—	−0.0558	0.103	0.9626
703011	—	—	−0.0641	0.124	0.9817
608261[c]	−0.222	1.154	—	—	0.9538
611032	−0.224	1.178	—	—	0.9924
611031[d] preleached for 7 hr	−0.203	0.948	—	—	0.9954
Average		1.093		0.110	

[a] Slopes of linear regression lines from concentration–time plots. Steady-state fluxes were obtained from slopes according to flux = (slope)(volume/area), where volume = 1.0 ml and area = 0.317 cm^2. Then k_1 and k_2 were calculated from these fluxes using Eqs. 30 and 31, respectively. [b] Raw data are shown in Fig. 16. [c] Raw data are shown in Fig. 6. [d] Raw data are shown in Fig. 8.

way that the dermis side faced the bulk solution and the stratum corneum side was covered by the glass plate. A 1.0-ml aliquot of saline was introduced into the chamber. For the K_1 determination, 50 μl of the saline solution was replaced by an equal volume of the covidarabine solution.

At zero time, 10 μCi of ^{3}H-I (for the k_2 determination) or ^{3}H-III (for the k_1 determination) was introduced, and 3-μl aliquots were withdrawn at predetermined times. Samples were spotted on TLC plates and localized under UV light. The separated spots were scraped into scintillation vials and counted.

RESULTS AND DISCUSSION

Reproducibility and Sources of Error—The primary purpose of the present studies was to investigate methods for determining parameters of the physical model describing the transport and metabolism of a prodrug in hairless mouse skin. Consequently, some results were obtained for illustrative purposes, and only single determinations were made. In many situations, however, repeat experiments were conducted and the reproducibility of the techniques was investigated.

The reproducibility of the transport experiments was generally good when full-thickness skin preparations (Table I) or when dermis membrane preparations (Table II) were involved. In the permeation experiment, repeat experiments with the same membranes were generally within 20% of each other (Tables I and II). The variations were greater than when membranes from different animals were compared but typically were within a factor of two (Tables I and II).

The repeat experiment studies involving the same membrane indicated that the permeability properties of the full-thickness skin and of the dermis preparation generally remained constant up to 30 hr, and the deaminase and the esterase activities were stable up to at least 7 hr (Table III). Thus, the "viability" of these membrane preparations was good in experiments up to several hours.

The heat-treated epidermal membrane showed greater preparation-to-preparation and stability with time variabilities (Table IV). Table V shows the results of thickness measurements. These data illustrate the degree of uncertainty in the measurements and variations encountered with typical membrane preparations.

Table IV—Permeability Coefficients of I–III in the Heat-Separated Epidermal Membrane

Mouse	Permeability Coefficients[a], $\times 10^8$ cm/sec I	II	III
801031[b]	98.0	173.0	135.0
801034	342.0	480.0	—
610202	—	—	9.9
705103 after 18 hr of soaking in saline	—	—	5.8
708021 after 48 hr of soaking in saline	40.2	—	—
801035 after 48 hr of soaking in saline	46.8	—	—

[a] Calculated from steady-state fluxes using Eq. 7, where P_{aq} was 1.05×10^{-3} cm/sec. [b] Raw data are shown in Fig. 11.

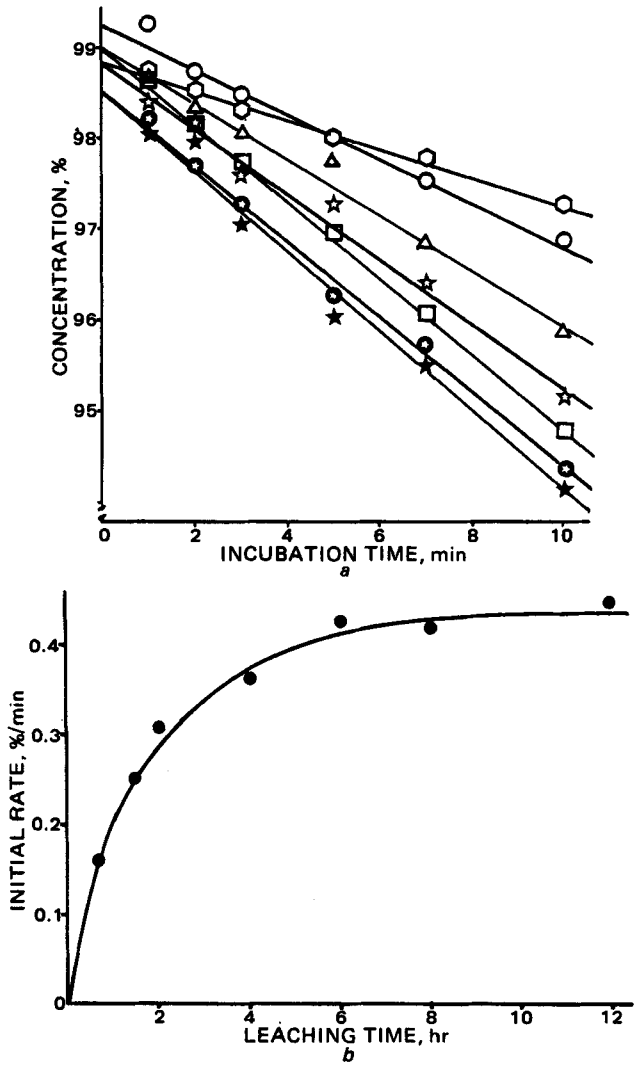

Figure 7—*Deaminase leaching. (a) A 0.01-ml aliquot of the bulk solution, into which the deaminase had leached for the time indicated, was incubated with I at 37°. The initial rates are proportional to the enzyme concentrations at the given times. Key (leaching times): ○, 40 min; ○, 80 min; △, 2 hr; ☆, 4 hr; □, 6 hr; ●, 8 hr; and ★, 12 hr. (b) The initial rates from Fig. 7a were plotted* versus *leaching time. The enzyme leaching rate of the 1st hr, from a linear estimation of the curve, is equal to 3.33 × 10^{-3}%/min^2.*

Metabolites Other than II—The TLC system used was able to isolate many nucleotides and nucleosides (4). Possible metabolites other than II, such as 9-β-D-arabinofuranosylxanthine (IV), which could be the next metabolite after II in the metabolism sequence of purine nucleosides, and the phosphorylation products of I and II were considered; the TLC system was employed for the detection of their presence. The TLC plate on which the 90-min sample of an in-and-out experiment was developed was examined by differential scraping (Fig. 5). No major metabolites other than II were found.

Enzyme Leaching Problem—The deaminase was reported (5) to leach out from the dermis side of the whole skin into the bulk solution, and the bulk solution deaminase activity was found to increase linearly with time over a 2-hr period. Thus, the rate of species concentration change in the bulk solution during an in-and-out experiment reflected not only the cutaneous phase metabolism but also a bulk phase enzyme reaction. Such a combined disappearance rate of I that is not properly corrected for the bulk phase reaction will give an overestimation of k_2.

The correction procedure for this bulk phase metabolism was proposed by Ando *et al.* (5) based on the linear increase of the deaminase activity in the bulk solution with respect to time. The bulk phase kinetics are described by:

$$-\frac{dA_b}{dt} = (k_b t)A_b \qquad \text{(Eq. 32)}$$

Table V—Measurements of Thickness (Micrometers) of Hairless Mouse Skin [a]

	Mouse 801034		Mouse 802141,	Mouse 705103, Abdomen	
	Abdomen, Full-Thickness Skin	Back, Full-Thickness Skin	Back, Full-Thickness Skin	Heat-Separated Epidermal Membrane	Remaining Dermis
Skin preparation plus two glass slides	2328	2405	2405	1914	2396
	2326	2409	2393	1910	2380
	2318	2397	2385	1904	2380
	2314	2393	2380	1900	2382
	2314	2386	2378	1911	2400
	2308	2377	2375	1906	2396
	2305	2374	2360	1904	2386
Mean	2316	2392	2398	1907	2388
Glass slides alone	1938	1938	1941	1864	2048
	1937	1937	1940	1860	2052
	1937	1937	1941	1869	2043
Mean	1937	1937	1941	1864	2047
Net thickness, μm	379	455	457	43	342

[a] Mouse 801034 was 16 weeks old, Mouse 802141 was 11 weeks old, and Mouse 705103 was 18 weeks old.

Table VI—Corrections for the Bulk Phase Metabolism

Parameter	Minutes							
	2	5	9	14	20	31	45.5	60
$\%A_{obs}$	97.99	97.36	95.78	94.64	93.64	90.63	84.53	79.04
$\%A_{bulk}$ [a]	0.01	0.05	0.13	0.33	0.66	1.59	3.39	5.82
$\%A_{corr}$ [b]	97.98	97.31	95.65	94.31	92.98	89.04	81.14	73.22

[a] $\%A_{bulk} = 100 - 100 \exp(-0.5K_b t^2)$, where $K_b = 3.33 \times 10^{-3}\%/min^2$. [b] $\%A_{corr} = \%A_{obs} - \%A_{bulk}$.

where k_b is the increment of the bulk phase enzyme activity per unit time and A_b is the bulk concentration of I. Integration gives:

$$\frac{A_b}{A_b^0} = e^{-k_b t^2/2} \quad \text{(Eq. 33)}$$

or:

$$\frac{A_b}{A_2^0}(\%) = 100e^{-k_b t^2/2} \quad \text{(Eq. 34)}$$

On a percentage scale, the remaining I at a given time is A_b/A_b^0 (percent). Therefore, the percentage disappearance of I caused by the bulk phase metabolism at a given time is $100 - (A_b/A_b^0)$ (percent). Subtraction of this value from the observed percentage of I remaining gives the net level of I corresponding to the skin metabolism only. The entire procedure is summarized in Table VI. The observed concentration–time curve for I bent downwards before correction but appeared to be linear with time up to 60 min after the correction (Fig. 6).

The data in Fig. 7*b*, which is a plot of the initial rates from Fig. 7*a* *versus* the leaching times, reveal that Eq. 32 with a constant k_b of 3.33×10^{-3} % *A*/min (*i.e.*, a linear approximation) is actually good only for the first 1 or 2 hr; the enzyme activity in the bulk solution levels off rapidly after this early time period. The plateau value, 0.425% *A*/min/ml, corresponds to about one-third of the total deaminase in the skin before leaching.

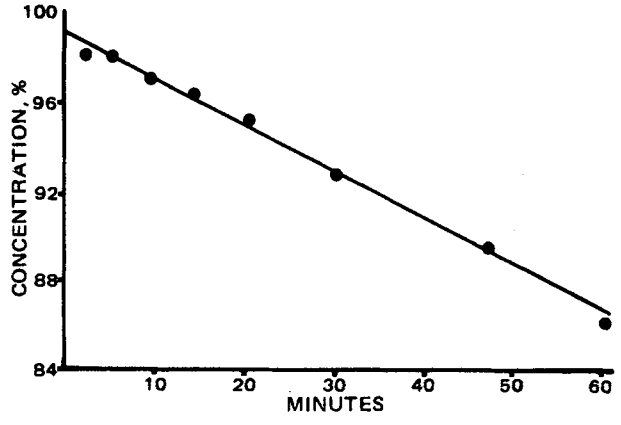

Figure 8—*In-and-out experiment of I with a skin preparation that had been preleached for 7 hr to remove the free enzyme. The slope of the regression line is −0.203%/min.*

An in-and-out experiment conducted with a 7-hr leached skin preparation is shown in Fig. 8. The result of this experiment is in good agreement with the corrected curve of Fig. 6. This finding indicates two things: the stability of the bound enzyme and the reliability of the correction procedure.

Other tests showed that the leached enzyme solution remained stable when stored in a refrigerator (4°). For up to 1 week, no changes in activity were observed.

To see if the esterase also leaches out, two identical aliquots of the bulk phase from a 2-hr leaching experiment were tested for esterase and deaminase activities. The results show a <2% conversion of III to I, in contrast with a 10% conversion of I to II in a 30-min incubation at 37° (Table VII).

Stratum Corneum Permeabilities and Dermal Diffusivities—*Aqueous Permeability Coefficients of I–III*—The thickness of the aqueous diffusion layer for a 150-rpm hydrodynamic system was found to be ~0.010 cm from the benzoic acid dissolution rate experiment (Fig. 9) using Eq. 1. The aqueous permeability coefficients of I–III for this diffusion layer were estimated according to Eqs. 2 and 3 (Table VIII).

Membrane–Water Partition Coefficients—Results of $K_{m/w}$ determinations for I and II are summarized in Table IX. Equation 4 was used in the calculations. The V_m values were obtained by dividing the dermis

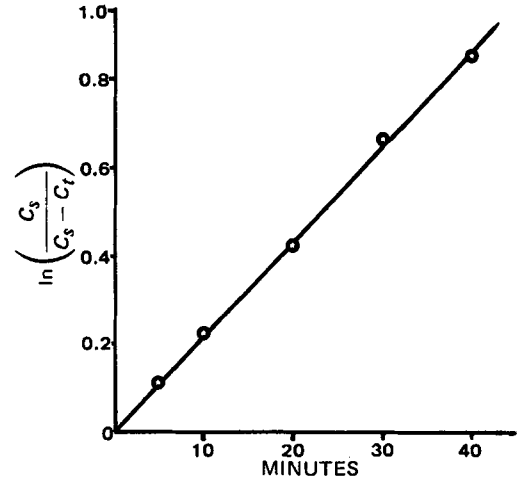

Figure 9—*Benzoic acid dissolution in the in-and-out experimental setup.*

Table VII—Leaching Out of the Enzymes, Deaminase and Esterase

Activity[a]	Percent I	Percent II	Percent III
Esterase	1.82	0.12	98.08
Deaminase	90.01	9.99	—

[a] Identical aliquots of the bulk solution from an in-and-out experimental setup were incubated separately with ^{3}H-I (for deaminase activity) and ^{3}H-III (for esterase activity) at 37° for 30 min.

mass by the average dermis density obtained as shown in Table X. The $K_{m/w}$ of III was undeterminable because an esterase inhibitor was not employed. However, it may not be unreasonable to assume that III has a $K_{m/w}$ value similar to that of I and II.

Dermis Diffusivities of I–III—Figure 10 shows the raw data of permeation of I–III across a dermis membrane. The accumulation of I, II, or III in the receiver chamber increased linearly after a short lag time. The slopes give fluxes of the respective species according to:

$$F_i = [(\text{slopes})_i]\left(\frac{\text{volume}}{\text{area}}\right) \qquad \text{(Eq. 35)}$$

where volume is the volume of the receiver and area is the effective diffusion area. The permeability coefficients were calculated from the resultant fluxes and values of ΔC_i according to Eq. 7. According to Eq. 8, the diffusivities of I and II were calculated from P_i, m, and $(K_{m/w})_i$. Table II summarizes these determinations. The diffusivity of III was undeterminable due to the lack of $K_{m/w}$ data.

Because of the uncertainty in the thickness measurement, a meaningful comparison of magnitudes in permeability or diffusivity of the three species must be done with the same piece of skin preparation. Data shown in Table II are based on such an experimental design.

Diffusivity of II was obtained from a direct flux measurement since the species was inert to the enzymes involved. Diffusivity of I also was obtained directly from the flux because the deaminase was inhibited with covidarabine. For III in the presence of covidarabine, however, the flux gave a measure of mixed diffusivity because an esterase inhibitor was not employed. The receiver solution consisted of 15% of I and 85% of III after 25 min of permeation. The mixed permeability coefficient was not significantly different from the permeability coefficient of I (Table II). Therefore, the permeability coefficient of III is probably of the same magnitude as that of I. A rigorous determination of the diffusivity of III was made possible through the use of Eqs. 18–21, which simultaneously calculate k_1 and D_V.

The diffusivities for the three species were of the same order of magnitude (Table II). From their molecular sizes and configurations, the similar diffusivities were not unexpected for I–III.

The possible diffusivity variations with respect to position in the membrane are currently under investigation and will be reported later.

Stratum Corneum Permeability Coefficients of I–III—Figure 11 gives the permeation data of I–III across a heat-separated epidermal membrane. The permeability coefficients calculated with Eq. 7 are given in Table IV.

Permeation of I and II (Fig. 12) and III across full-thickness skin was much slower than across the heat-separated epidermal membrane. Permeability coefficients of I–III for full-thickness skin are shown in Table I. These findings contradict the conclusion obtained from studies involving the low carbon number n-alkanols (6, 7) where the heat-separated epidermal membrane retained the major diffusion resistance of the intact full-thickness skin. Apparently, heat treatment has a profound effect on the barrier nature for the transport of I–III.

Valeryl esterification of the 5′-OH gave only a small increase in the permeability across the epidermal membrane and the whole skin. To obtain a substantial increase in the permeability, a longer chain substitution or di- or triester derivatization may be necessary. The effect of the di- or triester derivatization and the chain length effect of the substituting group will be reported later.

Table VIII—Aqueous Permeability Coefficients[a] of I–III

i	$(P_{aq})_2 \times 10^3$, cm/sec	$D_i \times 10^5$, cm^2/sec	M_i
I	1.08	1.08	267.3
II	1.08	1.08	268.3
III	0.98	0.98	351.3
Average	1.05	—	—

[a] An h value of 0.01 cm was determined from the line given in Fig. 9 using Eq. 1, where $D = 1.4 \times 10^{-5}$ cm^2/sec, area = 0.317 cm^2, and volume = 1.2 ml. Then $(P_{aq})_i$ and D_i were calculated from h, D, M, and M_i using Eqs. 2 and 3.

Table IX—Determinations[a] of $(K_{m/w})_i$

i	$(M_m)_i$, g	$(V_m)_i$, ml	$(V_w)_i$, ml	$[C_w^0]_i$, cpm/50 µl	$[C_w]_i$, cpm/50 µl	$(K_{m/w})_i$
I	0.215	0.207	1.000	3489	2899	0.98
	0.147	0.141	0.500	3489	2898	0.60
Average	—	—	—	—	—	0.79
II	0.207	0.199	1.000	6733	5519	0.91
	0.113	0.109	0.500	6733	5655	0.73
	0.207	0.199	2.000	6507	6063	0.74
	0.113	0.199	2.000	6507	6210	0.84
Average	—	—	—	—	—	0.81

[a] Using Eq. 4.

Enzyme Reaction Rate Constants—*Go-Through Experiments with Dermis Membrane and Simultaneous Determination of Enzyme Reaction Rate Constant and Diffusivity*—The go-through experiment together with Eqs. 18–21 provides a novel method for simultaneously determining the diffusivity and the enzyme constant. Figure 13 shows the measurements of the four fluxes that are used with Eqs. 18–21 for the determination of D_V and k_1. According to Eq. 22, the sum (or the difference in absolute values) of the observed fluxes in the donor chamber should be equal to the sum of the observed fluxes in the receiver chamber. For k_1 and D_V determinations, the receiver chamber data were used because the flux calculations based on the donor chamber data always were subject to large errors (Figs. 13–15).

The computer iterations of the fluxes from Eqs. 18 and 19 were done with the predetermined D_A value (Table VIII) by varying k_1 and D_V. The best fit of the calculated fluxes to the measured fluxes then determined a pair of D_V and k_1 values (Table XI). Simultaneous determinations of D_A and k_2 also were carried out similarly with flux data from Figs. 14 and 15 (Tables XII and XIII). The D_A value obtained by this method is consistent with that from the direct measurement (Table VIII).

In-and-Out Experiments with Full-Thickness Skin and Enzyme Reaction Rate Constant Determination—Figures 6, 8, and 16 show the measurements of fluxes in the in-and-out experiments. Since the fluxes are in terms of percentage of total radioactivities, the $V(h)$ and $A(h)$ terms in Eqs. 30 and 31, respectively, take the value of 100%. With Eqs. 30 and 31, k_1 and k_2 were calculated from the respective fluxes, F_V and F_A (Table III).

As a comparison, k_1 and k_2 values obtained from the go-through and in-and-out experiments are listed in Table XIII. The in-and-out method gave lower values for k_1 than did the go-through method. The discrepancy raises the question of validity of the various assumptions made in the models for the system. One assumption is that first-order kinetics obtain for the enzyme reaction. The steady-state approximation and the sink conditions were demonstrated to be valid for the present system, but the constant diffusivity and the homogeneous enzyme distribution assumptions have not been verified.

Studies on the possible variations in the diffusivity and the enzyme rate constants (both the deaminase and the esterase) with respect to position in the viable cutaneous tissue will be reported later.

APPENDIX I: MATHEMATICAL SOLUTIONS TO PERMEATION EXPERIMENT (Fig. 1)

Case I: Go-Through Experiment with III in the Presence of Covidarabine—*Flux of Prodrug across Aqueous Diffusion Layer*—The steady-state flux per unit area of the prodrug, F_V, within the aqueous diffusion layer is given by Fick's law:

$$F_V = \frac{D_{aq}}{h_{aq}}[V(-n) - V_{aq}(0)] \qquad \text{(Eq. A1)}$$

Table X—Density of the Hairless Mouse Skin

Mouse	Weight, g	Volume[a], ml	Density
705101	0.609	0.59	1.03
704264	0.398	0.38	1.05
704263	0.396	0.38	1.04
Average	—	—	1.04

[a] The method for skin volume measurements is described in the text.

Table XI—Simultaneous Determination of D_V and k_1

	Iteration Parameters[a]		(Flux/Initial Donor Concentration) × 10^5, cm/sec			
			Donor		Receiver	
	$D_V \times 10^6$, cm^2/sec	$k_1 \times 10^3$, sec^{-1}	III	I	III	I
Observed[b]	—	—	—	—	1.33	0.89
Best fit	0.97	1.70	—	—	1.33	0.89

[a] Other parameters used were $m = 420\ \mu m$, $D_A = 1.50 \times 10^{-6}\ cm^2/sec$, and $P_{aq} = 1.08 \times 10^{-3}$ cm/sec. [b] A dermatome-planed dermis (Mouse 706081) was used, and the permeation direction was dermis → epidermis. Raw data are shown in Fig. 13.

Table XII—Simultaneous Determination of D_A and k_2 with Dermatome-Planed Dermis

	Iteration Parameters[a]		(Flux/Initial Donor Concentration) × 10^5, cm/sec			
			Donor		Receiver	
Mouse	$D_A \times 10^6$, cm^2/sec	$k_2 \times 10^3$, sec^{-1}	I	II	I	II
703154						
Observed[b]	—	—	—	8.24	1.19	2.18
Best fit	1.46	9.46	—	6.79	1.15	2.72
705245						
Observed[c]	—	—	—	—	1.49	2.75
Best fit	1.62	8.68	—	—	1.49	2.75

[a] Other parameters used were $m = 350\ \mu m$, $D_H = 1.38 \times 10^{-6}\ cm^2/sec$, and $P_{aq} = 1.08 \times 10^{-3}$ cm/sec. [b] The permeation direction was dermis → epidermis. Raw data are shown in Fig. 14. [c] The permeation direction was epidermis → dermis. Raw data are shown in Fig. 15.

or:

$$F_V = \frac{D_{aq}}{h_{aq}}[V_{aq}(m) - V(h)] \qquad \text{(Eq. A2)}$$

for the donor side or the receiver side aqueous diffusion layer as shown in Fig. 1, where the subscript aq refers to the aqueous diffusion region. The other terms are self-explanatory. The membrane–water partition coefficient of the prodrug is:

$$(K_{m/w})_V = \frac{V(0)}{V_{aq}(0)} = \frac{V(m)}{V_{aq}(m)} \qquad \text{(Eq. A3)}$$

Therefore, the fluxes become:

$$F_V = P_{aq}\left[V(-n) - \frac{V(0)}{(K_{m/w})_V}\right] \qquad \text{(Eq. A4)}$$

and:

$$F_V = P_{aq}\left[\frac{V(m)}{(K_{m/w})_V} - V(h)\right] \qquad \text{(Eq. A5)}$$

where the aqueous permeability coefficient is:

$$P_{aq} = \frac{D_{aq}}{h_{aq}} \qquad \text{(Eq. A6)}$$

Concentration–Distance Expressions for Prodrug in Membrane—Equation 12 can be rearranged to give:

$$\frac{d^2V}{dx^2} = (K_1^2)V \qquad \text{(Eq. A7)}$$

with:

$$K_1 = \sqrt{k_1/D_V} \qquad \text{(Eq. A8)}$$

The general solution is:

$$V(x) = C_1 \sinh K_1 x + C_2 \cosh K_1 x \qquad \text{(Eq. A9)}$$

where $0 \le x \le m$ and C_1 and C_2 are the integration constants. By applying the aqueous layer–membrane interphase transfer and sink boundary conditions, *i.e.*:

$$P_{aq}\left[V(-n) - \frac{V(0)}{(K_{m/w})_V}\right] = -D_V \left.\frac{dV}{dx}\right|_{x=0} \qquad \text{(Eq. A10)}$$

and:

$$-D_V \left.\frac{dV}{dx}\right|_{x=m} = P_{aq}\left[\frac{V(m)}{(K_{m/w})_V} - 0\right] \qquad \text{(Eq. A11)}$$

to Eq. A9, the integration constants are found to be:

$$C_1 = \gamma\left[\sinh K_1 m + \frac{P_{aq}}{D_V K_1 (K_{m/w})_V}\cosh K_1 m\right] \qquad \text{(Eq. A12)}$$

$$C_2 = \gamma\left[\cosh K_1 m + \frac{P_{aq}}{D_V K_1 (K_{m/w})_V}\sinh K_1 m\right] \qquad \text{(Eq. A13)}$$

where:

$$\gamma = \frac{-\dfrac{P_{aq}V(-n)}{D_V K_1}}{\left(1 + \dfrac{P_{aq}^2}{D_V^2 K_1^2 (K_{m/w})_V^2}\right)\sinh K_1 m + \dfrac{2P_{aq}}{D_V K_1 (K_{m/w})_V}\cosh K_1 m} \qquad \text{(Eq. A14)}$$

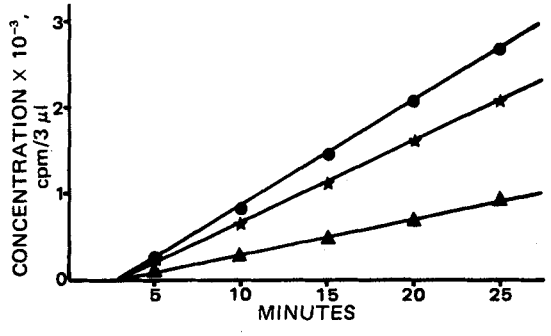

Figure 10—*Permeation of I (●), II (★), and III (▲) across a dermis membrane (320 μm). The three experiments were run concurrently, and the ΔC values were 5.60 × 10⁶ cpm/3 μl for I, 4.95 × 10⁴ cpm/3 μl for II, and 2.38 × 10⁴ cpm/3 μl for III. The fluxes may be calculated from the slopes according to flux = (slope)(volume/area), where volume = 2.5 ml and area = 1.767 cm².*

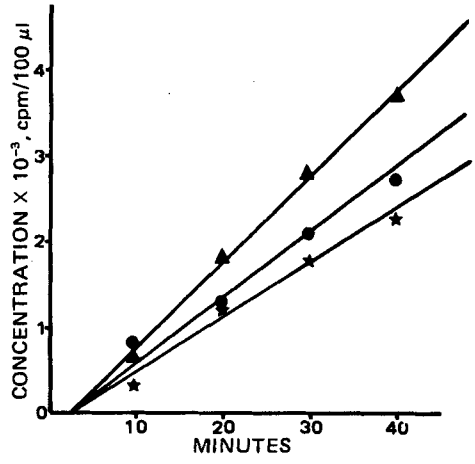

Figure 11—*Permeation of I (●), II (★), and III (▲) across a heat-separated epidermal membrane (57 μm). The three experiments were run concurrently, and the ΔC values were 2.59 × 10⁶ cpm/100 μl for I, 1.15 × 10⁶ cpm/100 μl for II, and 2.61 × 10⁶ cpm/100 μl for III. The fluxes may be calculated from the slopes according to flux = (slope)(volume/area), where volume = 1.5 ml and area = 0.713 cm².*

Table XIII—Comparison of the Enzyme Rate Constants Obtained from the Reflection Boundary and the Permeation Methods

Method	Esterase, $k_1 \times 10^2$, sec^{-1}	Deaminase, $k_2 \times 10^2$, sec^{-1}
In-and-out	0.11[a]	1.09[a]
Go-through	0.17[b]	0.91[c]

[a] From Table III. [b] From Table XI. [c] From Table XII.

Thus, the particular solution is:

$$V(x) = -\gamma\left[\cosh K_1(m-x) + \frac{P_{aq}\sinh K_1(m-x)}{D_V K_1 (K_{m/w})_V}\right] \quad \text{(Eq. A15)}$$

Concentration-Distance Expressions for Drug in Membrane—Equation 13 can be arranged to give:

$$\frac{d^2A}{dx^2} = \left(-\frac{k_1}{D_A}\right)V \quad \text{(Eq. A16)}$$

Substitution of Eq. A15 into Eq. A16 gives:

$$\frac{d^2A}{dx^2} = \left(-\frac{k_1}{D_A}\right)(\gamma)\left[\cosh K_1(m-x) + \frac{P_{aq}\sinh K_1(m-x)}{D_V K_1 (K_{m/w})_V}\right] \quad \text{(Eq. A17)}$$

Upon integrating twice, one obtains:

$$A(x) = \frac{\gamma k_1}{D_A K_1^2}\left[\cosh K_1(m-x) + \frac{P_{aq}\sinh K_1(m-x)}{D_V K_1 (K_{m/w})_V}\right] + C_3 x + C_4 \quad \text{(Eq. A18)}$$

whereby the integration constants C_3 and C_4 are evaluated from the following boundary conditions:

$$D_A \left.\frac{dA}{dx}\right|_{x=0} = P_{aq}\left[\frac{A(0)}{(K_{m/w})_A} - 0\right] \quad \text{(Eq. A19)}$$

$$-D_A \left.\frac{dA}{dx}\right|_{x=m} = P_{aq}\left[\frac{A(m)}{(K_{m/w})_A} - 0\right] \quad \text{(Eq. A20)}$$

Accordingly:

$$C_3 = \frac{1}{\dfrac{P_{aq}m}{(K_{m/w})_A} + 2D_A}\left[\frac{\gamma k_1}{K_1}\left(1 + \frac{P_{aq}^2}{K_1^2 D_A D_V (K_{m/w})_A (K_{m/w})_V}\right)\sinh K_1 m + \frac{\gamma k_1 P_{aq}}{K_1^2}\left(\frac{1}{D_V (K_{m/w})_V} + \frac{1}{D_A (K_{m/w})_A}\right)\cosh K_1 m - \frac{\gamma k_1 P_{aq}}{K_1^2}\left(\frac{1}{D_V (K_{m/w})_V} - \frac{1}{D_A (K_{m/w})_A}\right)\right] \quad \text{(Eq. A21)}$$

$$C_4 = \frac{1}{\dfrac{P_{aq}}{(K_{m/w})_A}\left(\dfrac{P_{aq}m}{(K_{m/w})_A} + 2D_A\right)}\left\{\frac{\gamma k_1 D_A P_{aq}}{K_1^2}\left(\frac{1}{D_V (K_{m/w})_V} - \frac{1}{D_A (K_{m/w})_A}\right) - \left(D_A + \frac{P_{aq}m}{(K_{m/w})_A}\right)\left[\frac{\gamma k_1}{K_1}\left(1 + \frac{P_{aq}^2}{K_1^2 D_A D_V (K_{m/w})_A (K_{m/w})_V}\right)\sinh K_1 m + \frac{\gamma k_1 P_{aq}}{K_1^2}\left(\frac{1}{D_V (K_{m/w})_V} + \frac{1}{D_A (K_{m/w})_A}\right)\cosh K_1 m\right]\right\} \quad \text{(Eq. A22)}$$

Finally, the substitution of C_3 and C_4 into Eq. A18 completes the concentration-distance expression for $A(x)$.

Fluxes of Species V *and* A—The fluxes of V and A in both the donor chamber and the receiver chamber are readily found by applying the following relationships:

$$F_{hV} = F_{mV} = -D_V \left.\frac{dV}{dx}\right|_{x=m} \quad \text{(Eq. A23)}$$

$$F_{hA} = F_{mA} = -D_A \left.\frac{dA}{dx}\right|_{x=m} \quad \text{(Eq. A24)}$$

$$F_{-nV} = F_{mV} = -D_V \left.\frac{dV}{dx}\right|_{x=0} \quad \text{(Eq. A25)}$$

$$F_{-nA} = F_{mA} = -D_A \left.\frac{dA}{dx}\right|_{x=0} \quad \text{(Eq. A26)}$$

Without going into the details of the mathematics, the final flux expressions are given in Eqs. 18–21.

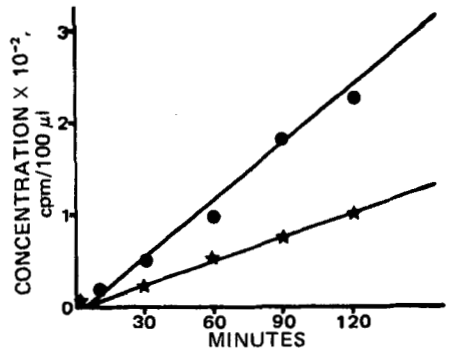

Figure 12—*Permeation of I (●) and II (★) across a full-thickness skin. The two experiments were run concurrently, and the ΔC values were 2.35 × 10⁶ cpm/100 µl for I and 1.82 × 10⁶ cpm/100 µl for II. The fluxes may be calculated from the slopes according to flux = (slope)(volume/area), where volume = 1.5 ml and area = 0.713 cm².*

Case II: Go-Through Experiment with I—In the permeation experiment with I, the mathematics are the same as in the previous case, with species H replacing species A, species A replacing species V, and k_2 replacing k_1. The final flux expressions are given in Eqs. 23–26.

APPENDIX II: MATHEMATICAL SOLUTIONS TO REFLECTION BOUNDARY EXPERIMENT (Fig. 2)

Case I: In-and-Out Experiment with III in the Presence of Covidarabine—*Flux of Prodrug across Aqueous Diffusion Layer*—The steady-state flux per unit area of the prodrug, F_V, within the aqueous diffusion layer is given by Fick's law:

$$F_V = \frac{D_{aq}}{h_{aq}}[V(h) - V_{aq}(m)] \quad \text{(Eq. A27)}$$

where the subscript aq refers to the aqueous diffusion region. The other terms are self-explanatory. The membrane–water partition coefficient of the prodrug is:

$$(K_{m/w})_V = \frac{V(m)}{V_{aq}(m)} \quad \text{(Eq. A28)}$$

Therefore:

$$F_V = P_{aq}\left[V(h) - \frac{V(m)}{(K_{m/w})_V}\right] \quad \text{(Eq. A29)}$$

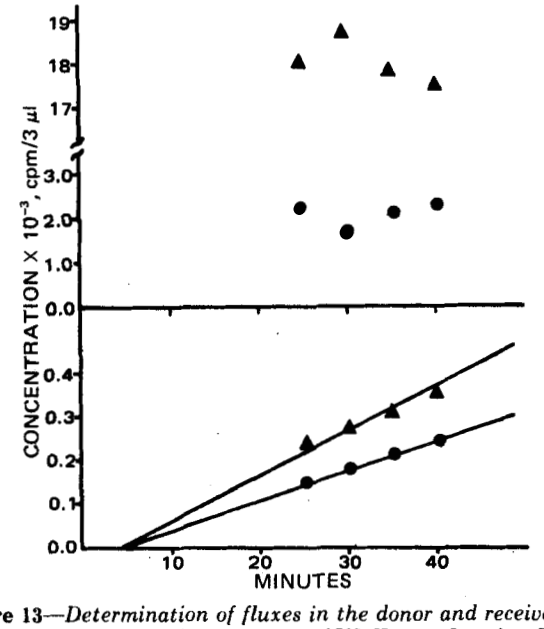

Figure 13—*Determination of fluxes in the donor and receiver compartments of a go-through experiment of III. Key: ●, I; and ▲, III. Flux = (slope)(volume/area), where volume = 3.0 ml and area = 1.767 cm². Covidarabine was employed to inhibit deaminase activity.*

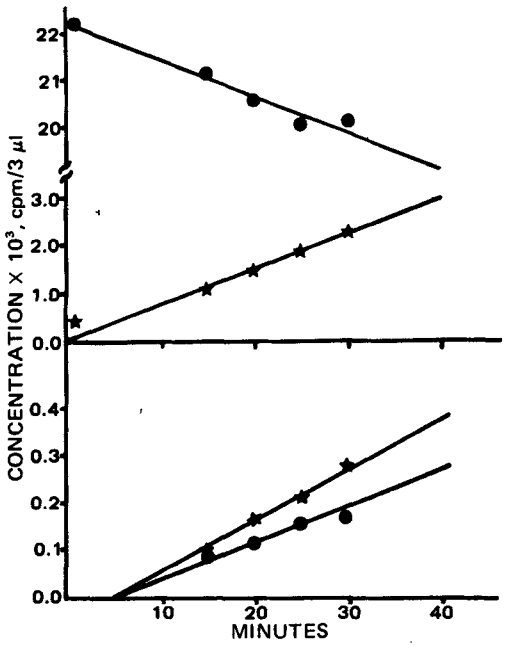

Figure 14—*Determination of fluxes in the donor and receiver compartments of a go-through experiment of I. Key: ●, I; and ★, II. The dermis was preleached for 3 hr. Flux = (slope)(volume/area), where volume = 3.0 ml and area = 1.767 cm².*

where the aqueous permeability coefficient is as given by Eq. A6.

Concentration–Distance Expressions for Prodrug in Membrane—Equation 27 can be rearranged to give Eq. A7 with Eq. A8. The general solution is given by Eq. A9, where $0 \leq x \leq m$ and C_1 and C_2 are the integration constants. By applying the aqueous layer–membrane interphase transfer condition (at $x=m$) and an impermeable boundary condition (at $x=0$), *i.e.*:

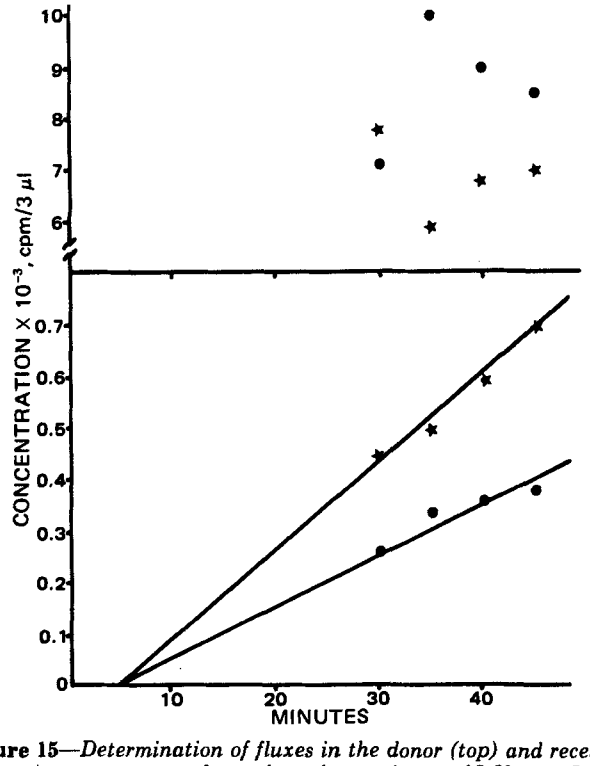

Figure 15—*Determination of fluxes in the donor (top) and receiver (bottom) compartments of a go-through experiment of I. Key: ●, I; and ★, II. The dermis membrane was preleached for 3 hr. Flux = (slope)(volume/area), where volume = 3.0 ml and area = 1.767 cm².*

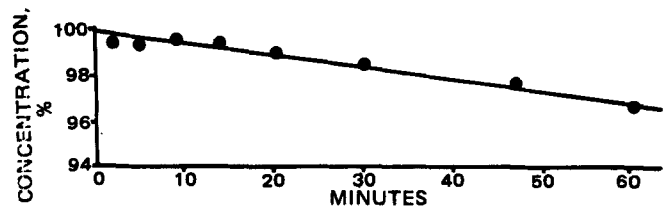

Figure 16—*In-and-out experiment of III. Slope = −0.0558%/min.*

$$P_{aq}\left[V(h) - \frac{V(m)}{(K_{m/w})_V}\right] = D_V \left.\frac{dV}{dx}\right|_{x=m} \quad \text{(Eq. A30)}$$

and:

$$D_V \left.\frac{dV}{dx}\right|_{x=0} = 0 \quad \text{(Eq. A31)}$$

to Eq. A7, the integration constants are found to be:

$$C_1 = 0 \quad \text{(Eq. A32)}$$

$$C_2 = \frac{P_{aq} V(h)}{\frac{P_{aq}}{(K_{m/w})_V}\cosh K_1 m + D_V K_1 \sinh K_1 m} \quad \text{(Eq. A33)}$$

Thus, the particular solution is:

$$V(x) = \frac{P_{aq} V(h) \cosh K_1 x}{\frac{P_{aq}}{(K_{m/w})_V}\cosh K_1 m + D_V K_1 \sinh K_1 m} \quad \text{(Eq. A34)}$$

Flux of Prodrug Entering Membrane—The flux expression for the prodrug entering the membrane is readily obtained by applying:

$$F_{hV} = F_{mV} = -D \left.\frac{dV}{dx}\right|_{x=m} \quad \text{(Eq. A35)}$$

After rearrangement, the final flux equation gives Eq. 30.

Case II: In-and-Out Experiment with I—In the reflection boundary experiment with I, the mathematics are the same as the previous case, with species H replacing species A, species A replacing species V, and k_2 replacing k_1. The final flux expression is given in Eq. 31.

REFERENCES

(1) C. D. Yu, J. L. Fox, N. F. H. Ho, and W. I. Higuchi, *J. Pharm. Sci.*, **68**, 1341 (1979).

(2) W. I. Higuchi, S. Prakongpan, and F. Young, *ibid.*, **62**, 945 (1973).

(3) O. D. Laerum, *J. Invest. Dermatol.*, **52**, 204 (1969).

(4) J. C. Drach and J. M. Novack, *Anal. Biochem.*, **52**, 633 (1973).

(5) H. Y. Ando, N. F. H. Ho, and W. I. Higuchi, *J. Pharm. Sci.*, **66**, 755 (1977).

(6) R. J. Scheuplein, *J. Invest. Dermatol.*, **45**, 334 (1965).

(7) G. L. Flynn, H. Durrheim, and W. I. Higuchi, presented at the APhA Academy of Pharmaceutical Sciences, New York meeting, May 1977, Abstract 11.

ACKNOWLEDGMENTS

Abstracted in part from a thesis submitted by C. D. Yu to the University of Michigan in partial fulfillment of the Doctor of Philosophy degree requirements.

Supported by National Institutes of Health Research Grant AI14987 and Training Grant DE00204.

The authors thank Dr. D. C. Baker, University of Alabama, and Dr. A. J. Glazko and Dr. T. H. Haskell, Warner-Lambert/Parke-Davis, for supplying ^{3}H-labeled and nonlabeled vidarabine-5′-valerate ester.

Factors Affecting Theophylline Clearances: Age, Tobacco, Marijuana, Cirrhosis, Congestive Heart Failure, Obesity, Oral Contraceptives, Benzodiazepines, Barbiturates, and Ethanol

WILLIAM J. JUSKO ˣ, MARK J. GARDNER, ANTOINETTE MANGIONE, JEROME J. SCHENTAG, JEFFREY R. KOUP, and JOHN W. VANCE

Received December 6, 1978, from the *Clinical Pharmacokinetics Laboratory, Departments of Pharmaceutics and Medicine, Schools of Pharmacy and Medicine, State University of New York at Buffalo and Millard Fillmore Hospital, Buffalo, NY 14209.* Accepted for publication May 7, 1979.

Abstract □ Pharmacokinetic, pathophysiologic, and historic data were systematically collected while monitoring theophylline therapy in adult pulmonary patients and from special studies in pediatric patients, normal volunteers, and patients with other diseases. Total body clearances (Cl_T) were estimated by nonlinear computer analysis after infusion dosage or from area under the curve data following single oral or intravenous theophylline doses. The Cl_T values, primarily reflecting the theophylline biotransformation rate, averaged 58 (±30) ml/hr/kg and ranged from 4 to 143 ml/hr/kg. Factors examined for their effect on theophylline Cl_T included age; sex; liver disease; congestive heart failure; obesity; renal function; history of drug, tobacco, marijuana, caffeine, or alcohol use; and pregnancy. The NYBAID (automatic interaction detector) computer program for analysis of variance was employed to determine the order, priority, and combinations of independent variables correlating with Cl_T. The major factors that affected theophylline Cl_T in this population included age, liver disease, smoking status, and congestive heart failure. Age showed strong correlation ($r = -0.49$) with Cl_T. Much additional variability was accounted for in specific subgroups. For example, young adult (20–40 years) marijuana users exhibited highest Cl_T values (83 ± 29 ml/hr/kg) while older patients (>40 years) with liver disease had the lowest metabolism rates (22 ± 10 ml/hr/kg). In particular subject types, sex (in teenagers), oral contraceptives (in smokers), obesity (in young nonsmokers), and barbiturates also affected theophylline disposition. In contrast, several common factors such as chronic theophylline, chronic corticosteroids, caffeine, sex (in adults), and pregnancy did not alter theophylline Cl_T. This unique clinical pharmacokinetic monitoring and statistical approach to drug clearance characterization in patients permits identification of criteria in a format that may be useful for the prediction of drug disposition rates and dosage regimens.

Keyphrases □ Theophylline—metabolism, effect of age, tobacco, marijuana, cirrhosis, congestive heart failure, obesity, oral contraceptives, benzodiazepines, barbiturates, ethanol, pulmonary patients □ Smooth muscle relaxants—theophylline, metabolism, effect of age, tobacco, marijuana, cirrhosis, congestive heart failure, obesity, oral contraceptives, benzodiazepines, barbiturates, ethanol, pulmonary patients □ Dosage regimen—theophylline, predictive scheme, effect of various patient variables on metabolism

The drug elimination rate as reflected by the total body clearance (Cl_T) and the plasma–tissue distribution as represented by the apparent volume of distribution (V_D) are the primary clinical pharmacokinetic requirements for devising dosage regimens in patients. Reasonable success has been achieved in predicting dosage requirements for drugs whose body clearance is determined largely by renal function where the serum creatinine concentration or creatinine clearance can be used to estimate drug clearance (1, 2). In contrast, numerous genetic, environmental, pathophysiologic, and pharmacokinetic factors that affect biotransformation rates make dosages highly unpredictable for extensively metabolized drugs. Serum concentration monitoring has assisted in the clinical use of many such drugs (3, 4).

Theophylline, an extensively metabolized drug, poses clinical pharmacokinetic difficulties. This xanthine derivative is ~90% biotransformed by microsomal oxidative enzymes with the remaining 10% of the dose excreted unchanged in the urine (5). Numerous studies have demonstrated highly variable half-life and body clearance values in typical adult and pediatric patients (6–9). Many reports indicated that dosage requirements of patients are highly unpredictable and illustrated the need for serum level monitoring (6, 10, 11). The 8–20-mg/liter "window" of serum theophylline concentrations usually produces optimum bronchodilation (6, 12).

Rapid and specific theophylline assays in biological fluids using methods such as high-pressure liquid chromatography (HPLC) (13) have been helpful in patient therapy (10, 11). Serum theophylline concentration measurements are not always possible, however, and the blood collection, analytical, and interpretive procedures take time. It is important, therefore, to develop dosage guidelines for different types of patients to be used before or in the absence of the feedback information from theophylline assays (3).

This report describes common factors that determine theophylline clearance. Pharmacokinetic, pathophysiologic, and historic data were systematically collected while monitoring theophylline therapy in adult pulmonary patients and from special studies in pediatric patients, normal adult volunteers, and subjects with unique characteristics such as obesity or cirrhosis. Pharmacokinetic and statistical methods were utilized to characterize the variability in body theophylline clearances in 200 such persons.

EXPERIMENTAL

Subjects—Body theophylline clearances were determined prospectively in 100 adult inpatients at the Millard Fillmore Hospital. These patients were studied during routine medical management with theophylline administered by intravenous infusion for at least 24 hr. The dosage guidelines (nomogram) and other aspects of the clinical pharmacokinetic monitoring system were described previously (9).

Additional clinical and pharmacokinetic data were obtained from the literature for single-dose aminophylline administration to 15 pediatric patients (7), for normal late-teen or adult subjects (14–17), for 14 obese adults (18), for eight cirrhotic patients (19), and for pregnant women (20). All patients and volunteer subjects were residents of western New York state at the time of the study.

Survey Design—The body clearance, or more precisely the total serum theophylline clearance (Cl_T), was taken as the dependent variable for correlation with various factors likely to affect the drug disposition rate. This parameter was chosen because it could be generated from all

0022-3549/79/1100-1358$01.00/0
© 1979, American Pharmaceutical Association

Table I—Statistical Categories Describing Theophylline Body Clearances

Parameter (Abbreviation)	Division	Group Code	Number of Subjects	Body Clearance, ml/hr/kg IBW, mean (*SD*)
Body clearance	—	All	200	57.9 (29.8)
Age, years	<20	1	23	91.9 (28.1)
	20–39.9	2	79	64.2 (27.2)
	40–59.9	3	37	47.8 (24.8)
	>60	4	61	43.1 (23.2)
Sex	F	2	105	57.0 (24.5)
	M	1	95	58.9 (34.8)
Congestive heart failure (CHF)[a]	None	0	149	64.1 (30.1)
	Mild	1	27	46.5 (21.2)
	Moderate	2	15	34.8 (16.6)
	Severe	3	9	28.0 (13.5)
Obesity[b]	None	0	133	55.5 (28.3)
	Moderate	1	62	62.9 (33.1)
	Severe	2	5	59.7 (21.2)
Creatinine clearance (*CrCl*), ml/min/1.73 m^2	≥100	1	62	60.6 (23.8)
	50–99	2	116	60.4 (32.3)
	20–49	3	20	37.1 (24.3)
	<20	4	2	34.8
Theophylline history	None	0	117	54.3 (28.0)
	User	1	83	62.9 (31.5)
Steroid history	None	0	139	57.0 (29.6)
	User	1	61	59.9 (30.3)
Oral contraceptives (OC)	None	0	186	58.5 (30.4)
	User	1	14	49.8 (18.6)
Barbiturate history (BARBS)	None	0	175	57.9 (29.1)
	User	1	25	57.6 (34.5)
Benzodiazepine history (BENZ)	None	0	175	59.3 (29.7)
	User	1	25	48.2 (29.1)
Phenothiazine history	None	0	196	57.9 (29.7)
	User	1	4	56.2 (36.3)
Tricyclic antidepressant history	None	0	195	58.2 (29.8)
	User	1	5	44.1 (29.6)
Smoking[c] (CIG)	None	0	107	57.0 (30.4)
	Light	1	54	61.1 (29.0)
	Heavy	2	39	55.9 (29.3)
Caffeine use[d]	Slight	0	42	74.0 (30.3)
	Moderate	1	82	49.7 (29.4)
	Heavy	2	76	57.8 (26.4)
Ethanol (EtOH) and cirrhosis	None	0	66	65.1 (30.5)
	Social drinker	1	119	58.3 (27.9)
	Heavy drinker or cirrhotic	2	15	22.4 (10.5)
Marijuana use[e] (MJ)	None	0	177	56.1 (29.5)
	Light	1	9	54.1 (17.5)
	Heavy	2	14	82.9 (28.8)
Pregnancy	No	0	190	57.7 (30.3)
	Yes	1	10	61.5 (17.5)

[a] Based on criteria of Peck *et al.* (27). [b] Moderate obesity = 15–55% overweight; severe obesity = >55% overweight. [c] Light = <1 and heavy = ≥1 pack/day. [d] Slight = ≤2, moderate = 3–5, and heavy = >5 cups of coffee or tea/day; caffeine equivalents from cola were typically "slight." [e] Light = <1 and heavy = ≥2 joints/week.

serum concentration *versus* time data collected and because it is needed to determine maintenance doses (D/T) for achieving a desired steady-state serum concentration (C_p^{ss}):

$$D/T = (Cl_T)(C_p^{ss}) \quad \text{(Eq. 1)}$$

where D is the dose given at time intervals, T. To correct for body size, the Cl_T value was adjusted for lean body weight (18). The lean body weight (IBW) was estimated as the "ideal" weight based on height and bone structure (21). Weight, rather than surface area, was chosen for normalizing the data because of the limited body size range of the subjects, because theophylline clearances are conventionally expressed as milliliters per hour per kilogram (12, 15, 18), and because such Cl_T values are converted easily into a dosage regimen using Eq. 1.

Patient Surveillance—Clinical descriptive data regarding the patients were collected over a 4-year period. The survey approach was described previously (9). Similar information from the normal volunteers was usually obtained in confidence.

The factors gathered as independent variables for this analysis are listed in Table I. Each patient parameter was chosen on the basis of its generally known influence on drug metabolism or because of its potential for affecting theophylline disposition. Only factors capable of being obtained by examination (physical and history) of a patient upon hospital admission or by rapid automated analyzer analysis (serum biochemistry profile) were included. This approach was chosen to yield useful information for designing future dosage regimens for typical patients.

The relationship of age to theophylline clearance was examined because previous studies revealed differences in theophylline disposition between adolescents and adults (7) and because elimination of various drugs is slower in older patients (22–24). Sex was included because of known differences between genders in metabolism of drugs such as antipyrine (23, 25). Congestive heart failure was examined because of the reduction in hepatic clearance that accompanies this disease (26). The severity of congestive heart failure was ranked as absent (0) or graded 1–3, using criteria described by Peck *et al.* (27).

Obesity was examined because physiological changes occur in obese subjects, including increased cardiac output and hepatic blood flow (28). Also, considerable uncertainty has existed regarding use of lean rather than total body weight as a basis for drug dosage regimens (18). Creatinine clearance was included because ~10% of a theophylline dose usually is excreted by the kidneys (5). The creatinine clearance was estimated from the serum creatinine concentration, lean body weight, sex, and age of each patient using the nomogram of Siersbaek-Nielsen *et al.* (29). Creatinine data were not available for the 15 pediatric patients. Normal age-related values were used for these subjects, none of whom had kidney disease.

The patient history was completed by questioning the patient (or guardian) or by consulting the patient's chart or physician. Previous theophylline use was examined because the drug induces its own metabolism in animals (30). Steroid history was included because corticosteroids accelerate the biotransformation of many drugs (31, 32) and have been posed as an interaction factor with theophylline (33). In contrast, oral contraceptives may decrease drug metabolism rates (34) and were noted as a separate variable.

Four other drug history categories were included: barbiturates, because of their well-known enzyme inductive effects (35, 36) and their possible effect on theophylline disposition (37); benzodiazepines, because of their common use in patients and their potential for altering drug biotransformation (38); and phenothiazines and tricyclic antidepressants for similar reasons (39, 40). Other potentially interacting drugs such as erythromycin (41) and troleandomycin (42) were not observed.

Social drug habits studied including smoking because of its well-established effect on drug disposition in general (43) and on theophylline in particular (14, 44, 45). Marijuana use was included for identical reasons (17). Caffeine consumption (number of cups of coffee or tea per day) was quantitated in recognition of the weak inductive effect of caffeine (46) and catechin (47) on drug metabolism in animals and because of the recent observation of an effect of dietary methylxanthine intake on theobromine disposition (48).

Ethanol consumption was included because small quantities of alcohol can stimulate oxidative drug biotransformation pathways, while large amounts may either diminish drug metabolism acutely or cause liver disease (49, 50). In fact, patients with cirrhosis and those consuming large quantities of ethanol were grouped together because of the latter likelihood and the earlier finding of markedly impaired theophylline disposition in cirrhotics (19, 51).

Pregnancy was of interest because the biotransformation of some drugs is enhanced during pregnancy (52) and because asthmatic, pregnant women often experience difficulties in breathing.

Other patient characteristics also were recorded but were not included in this analysis because they either occurred infrequently or not at all. Also, many facts were not recorded because they were not recognized as interaction factors at the time of this study. Acute pulmonary edema (53), thyroid dysfunction (54), low arterial PO_2 (55), acute steroid administration (31), marked dietary changes (56), recent ingestion of charcoaled foods (57), and respiratory viral illness (58) may alter the microsomal oxidation of drugs such as theophylline. Subjects were Caucasian except for two persons from India and Iran and six Negroes. Genetic differences related to race were not examined. Surveillance data included a serum biochemistry profile (SMAC P7), which was largely used to confirm certain disease categories (*e.g.*, liver dysfunction).

Drug Assay—Theophylline concentrations in serum were measured by HPLC (13) in most patients and volunteers and by spectrophotometric assay (59) in the pediatric patients (7) and in some normal adult subjects (15). Good agreement has been found between the two assay methods (13).

Pharmacokinetics—For subjects who received a single oral solution or intravenous dose of theophylline, the body clearance was calculated from:

$$Cl_T = \text{dose/area} \qquad \text{(Eq. 2)}$$

where area represents the area under the serum concentration *versus* time curve extrapolated to time infinity. Because theophylline poses no known GI absorption problems, especially when given in solution (60), and because its low Cl_T should cause little "first-pass" hepatic metabolism, complete systemic bioavailability of oral drug doses was assumed.

Most pulmonary patients received theophylline by continuous intravenous infusion, usually with administration of a loading dose or following previous therapy with the drug. The time course (t) of serum theophylline concentrations (C_p) was characterized by:

$$C_p = (C_p^0)\, e^{(-Cl_T)(t)/V_D} + \frac{k_0}{Cl_T}\left[1 - e^{(-Cl_T)(t)/V_D}\right] \qquad \text{(Eq. 3)}$$

where C_p^0 is the initial serum concentration, V_D is the apparent volume of distribution, and k_0 is the drug infusion rate. Blood samples were generally collected at 1, 12, and 24 hr and often at later times. It was assumed that V_D = 0.45 liter/kg of ideal body weight for each patient, and the 1-hr C_p value was used as C_p^0. The NONLIN computer program (61) generated the least-squares fitted Cl_T value. The suitability of this method for calculating theophylline Cl_T was demonstrated previously (9).

Equation 3 reduces to $C_p^{ss} = k_0/Cl_T$ as the steady state (C_p^{ss}) is approached or attained. This equation is model, volume, and time independent, which accounts for the extremely good Cl_T estimates for most patients who were close to steady state after 24 hr of loading and infusion therapy.

Statistics—Statistical procedures used to assess the relationship of theophylline Cl_T to the selected patient parameters included linear regression analysis (62, 63) and the NYBAID computer program (64). This program quantitates the variance associated with the dependent variable by assessing the order, priority, and combinations of independent variables that allow maximum statistical discrimination between groups. Information fed to the program involved the Cl_T value as a continuous, dependent variable along with 17 independent variables. As shown in Table I, it was necessary to partition each independent variable into coded integers. Selection of the number of subgroups for each variable was based either on obvious discriminating factors (*e.g.*, sex and user/nonuser) or on the ability to quantitate differences based on conventional criteria (*e.g.*, congestive heart failure and smoking).

The largely noncontinuous, nominal, and nonlinear nature of the patient characteristics precluded effective use of multiple linear regression analysis but allowed advantageous employment of the NYBAID program. The program subdivides the Cl_T sample through a series of binary splits into a mutually exclusive series of subgroups with the branching process based on variance analysis techniques. The possibility of interaction between variables at different stages is handled by reintroducing factors whose simple effects already have been reviewed but which may also mediate the effects of factors at a later stage. The linearity and additivity assumptions inherent in conventional multiple regression techniques are not required.

Program control includes reducibility criteria for splitting groups ($p < 0.01$), minimum size of groups before and after splitting (no minima used), and weights (all data were weighted = 1). Subgroups are produced based on a primary test of reduction of the unexplained sums of squares rather than on differences between subgroups as assessed by conventional t tests. Several patients were studied on more than one occasion, and their data were included each time to self-weight such multiple observations and to account for clinical changes occurring between these times.

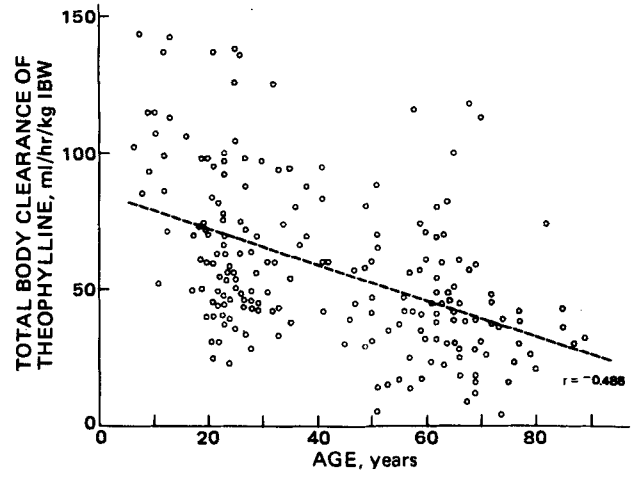

Figure 1—*Total body clearances of theophylline in relation to age of 200 patients and normal volunteers who received oral or intravenous theophylline. The regression line depicts age dependence of theophylline biotransformation in spite of the great variability in clearances.*

RESULTS AND DISCUSSION

Body Clearances—Half of the pharmacokinetic data for this survey were obtained while monitoring theophylline therapy in hospital patients. Dosing guidelines (65) provided an intravenous loading dose (short-term infusion) based on body weight with a dosage reduction if recent theophylline administration had occurred. The maintenance infusion rate was based on body weight and on three levels of anticipated biotransformation capability. An initial serum concentration (C_p^0) was achieved at 1 hr after the loading dose. Serum concentrations thereafter attained or progressed toward a steady state. Least-squares fitting using Eq. 3 generated the designated Cl_T values and their standard deviations (SD). In most cases, the SD was relatively small, indicative of a close fit of the equation to the experimental data (9).

The Cl_T values in relation to the age of 200 subjects are summarized in Fig. 1. The major characteristic of theophylline disposition is the pronounced variability in Cl_T values over all age groups. The Cl_T averaged 58 (SD = 30) ml/hr/kg and ranged from 4 to 143 ml/hr/kg. However, the trend ($r = -0.488$) for Cl_T to decrease with age was apparent and statistically significant ($p < 0.01$). The figure also shows the wide age range of subjects, with a generous distribution of persons within each

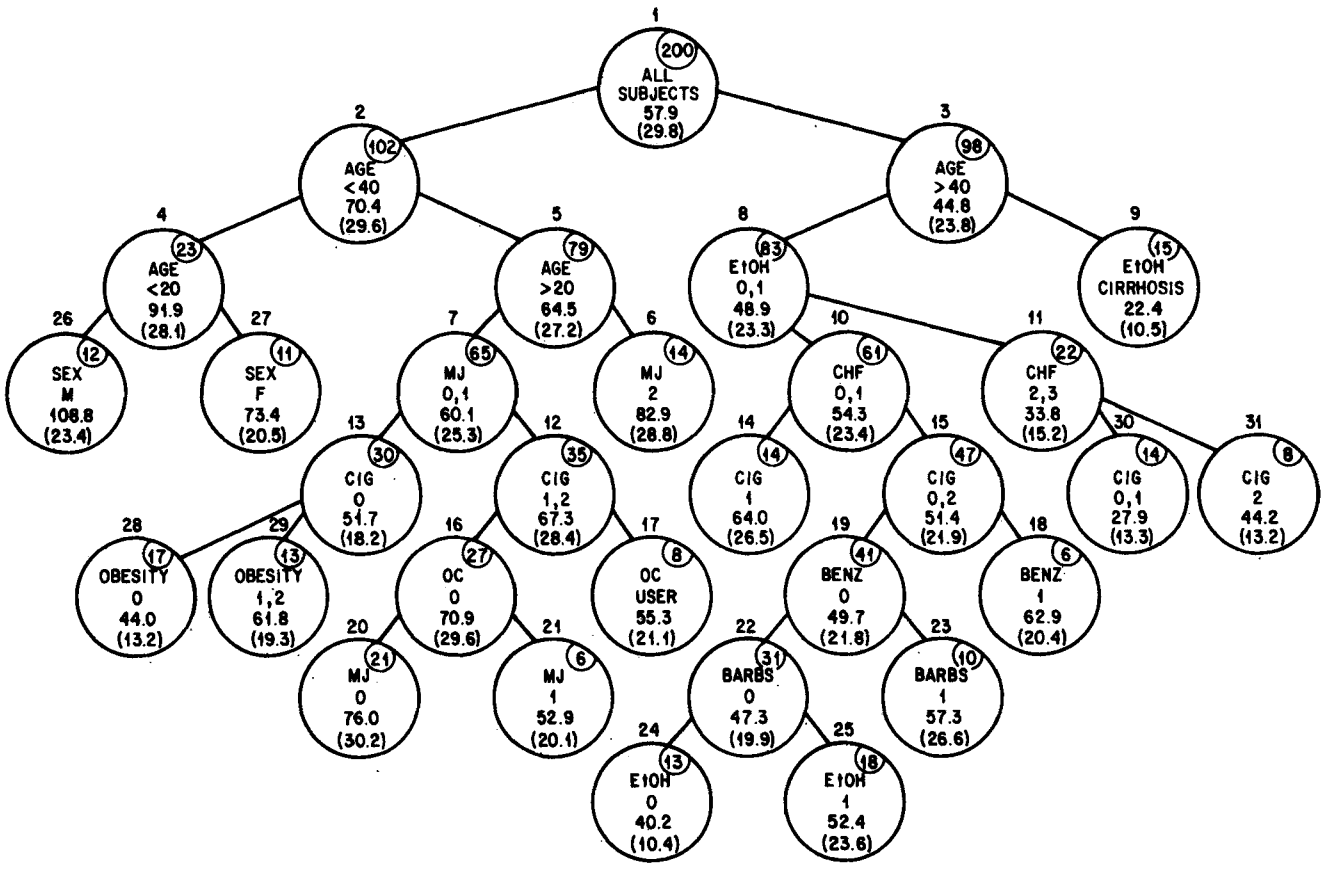

Figure 2—*Cascade of factors determining theophylline total body clearances. The NYBAID statistical computer program was used to seek the order, priority, and combinations of independent variables (Table I) that correlate with theophylline clearances. Each partition represents a statistical difference of* $p < 0.01$, *and the circles list the number of subjects (circled), descriptive factor, group mean, and standard deviation (in parentheses).*

decade past childhood. Because of this finding and the extraction of data from patients actually undergoing therapy, the information is reasonably representative of the typical cross-section of persons requiring theophylline.

Two additional patients with extraordinarily high Cl_T values (195 and 217 ml/hr/kg) were identified and excluded from this and all other statistical analyses. These patients were outside the general characteristics of this population (*i.e.*, were outliers), and inclusion of their variances distorted the analysis. Acute high-dose steroid therapy (rather than chronic steroid use), a factor that accelerates antipyrine metabolism (31), may account for the high Cl_T value in one female patient. The other patient was a male heavy smoker with severe renal impairment and hypertension who had been receiving a variety of drugs including phenobarbital, diazepam, propranolol, reserpine, and methyldopa.

Patient Variables—The NYBAID computer program was employed to examine the patient variables listed in Table I. This table provides the division of variables into subgroups with the number of patients, mean Cl_T, and *SD* for each subgroup. The study population characteristics can be best appreciated from this summary. For example, many patients were over 60 years old, which is typical of an adult hospital patient population. There were nearly equal numbers of male and female subjects. Fifty-one patients had some degree of congestive heart failure, and 15 patients had liver disease (cirrhosis). Only two patients had very poor renal function.

Obesity was a frequent occurrence, although only five patients were grossly overweight (>55%). Many persons were chronically receiving theophylline, corticosteroids, oral contraceptives, and various tranquilizers. Ninety-three subjects were smokers including 45 of the 100 adult patients with pulmonary disease. All marijuana smokers were young, normal adults. Many persons consumed moderate to appreciable quantities of caffeinated drinks and ethanol.

The mean values in Table I are of interest in examining the patient subgroups representing each factor. Parameters that had the strongest influence on theophylline disposition can be identified by inspection. For example, young age, congestive heart failure, liver disease, and marijuana use stand out. On the other hand, because of drug–disease interactions and diverse patient characteristics, the role of many important factors determining theophylline Cl_T can be discerned only after further patient data become available.

Analysis of Variance—*Age*—The cascade of patient variables associated with differences in theophylline Cl_T values among 200 persons is shown in Fig. 2. Complementing the regression analysis, the data were initially partitioned according to age with 40 years as the demarcating age. As will be demonstrated by the types of patients found further down the cascade (a lower Cl_T in cell 10 than in cell 5), this age difference may be a dual effect of aging and of a greater incidence of hepatic dysfunction, cirrhosis, and congestive heart failure among the older group. In the under 40-year group, a second split based on age separated the adolescent/teenage subjects from the young adults.

These data, while partly derived from the prospective study by Ellis *et al.* (7), further confirm the observation that children metabolize theophylline more rapidly than do adults. This enhanced theophylline biotransformation extends down to the 1–4-year range as well. Loughnan *et al.* (66) found a mean Cl_T of 100 (±36) ml/hr/kg in such younger children.

Gender—A new finding in the young subjects, 6–19 years old, is an apparent gender difference in Cl_T. These data (Fig. 3) indicate that young males metabolize theophylline more rapidly than do females. Reexamination of the data of Leung *et al.* (67) for children 6–16 years old lends support to this observation. They listed Cl_T values averaging 89.8 (34.3) ml/hr/kg in 19 males and 58.8 (17.8) ml/hr/kg in 11 females. On the other hand, the original data of Ellis *et al.* (7) and of Loughnan *et al.* (66) suggest no gender differences in theophylline Cl_T. This possible sex effect on theophylline biotransformation does not extend into adults; Powell

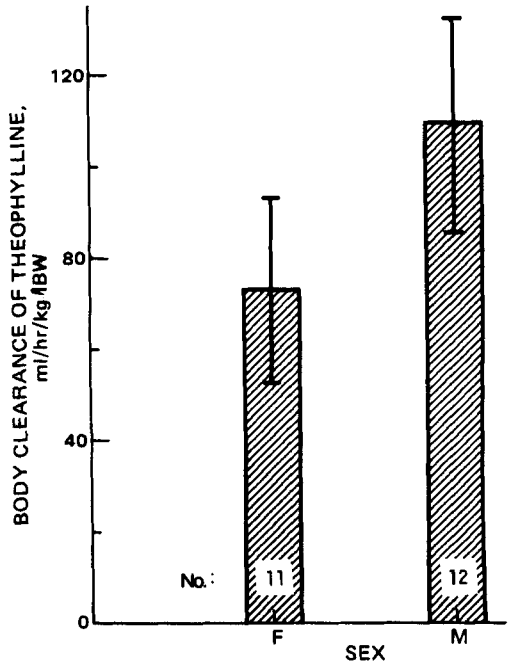

Figure 3—*Effect of sex on total body clearances of theophylline in adolescents and teenagers. This and subsequent graphs show mean values as bars, standard deviations as vertical lines, and numbers of subjects within bars. Subject groups correspond to cells 26 and 27 in Fig. 2.*

et al. (45) previously observed no differences in Cl_T in young adults, and our remaining cascade data (Fig. 2) provided no further gender discrimination.

Smoking—The major factors affecting theophylline disposition in young adults are tobacco and marijuana smoking. This factor emerges largely because an appreciable number of the subjects in the 20–39.9 year class were relatively healthy persons with no overt hepatic or cardiac diseases (17). Use of social drugs (tobacco, alcohol, marijuana, and caffeine), tranquilizers (benzodiazepines), and oral contraceptives was common in this group and provided the only unique characteristics for examination by the NYBAID program. Many asthmatic patients were included in the 79 persons in this age range, and the data probably are highly representative of young adults who need theophylline therapy.

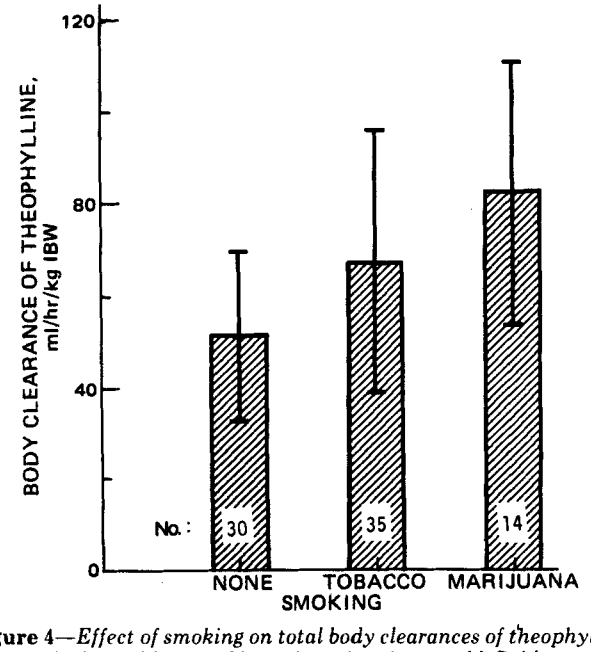

Figure 4—*Effect of smoking on total body clearances of theophylline in normal adult subjects and in patients 20–40 years old. Subject groups correspond to cells 13, 12, and 6, respectively, in Fig. 2.*

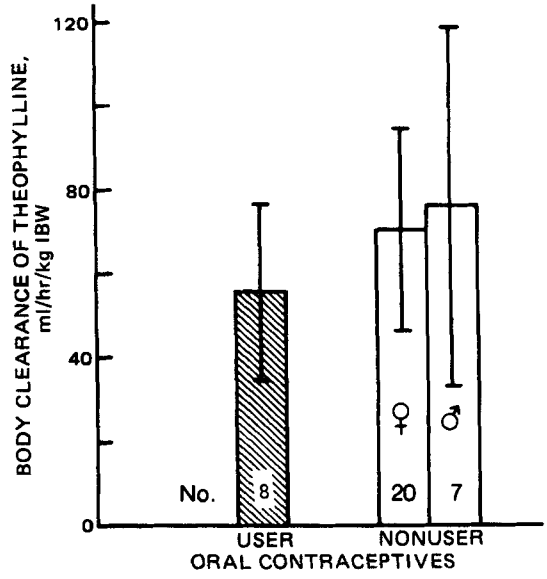

Figure 5—*Effect of oral contraceptives on total body clearances of theophylline in adult smokers. Subject groups correspond to cells 17 and 16, respectively, with the latter partitioned further according to sex.*

Figure 4 shows the differences in Cl_T among young adults in relation to smoking habits. The enhanced theophylline Cl_T in both marijuana and tobacco smokers extends and confirms previous findings (14, 17). This phenomenon is probably due to induction by polycyclic aromatic hydrocarbons present in smoking materials (43) as well as in charcoaled foods (57). The use of marijuana or a combination of marijuana and tobacco produced the largest clearances observed in young adults (83 ± 29 ml/hr/kg). Other effects of smoking on theophylline Cl_T will be described in subsequent sections.

Oral Contraceptives—An interesting finding (Fig. 2) is that the effect of oral contraceptives on theophylline Cl_T was obtained only in smokers. The use of oral contraceptives was associated with a diminished Cl_T (55 ± 21 ml/hr/kg in users *versus* 71 ± 30 ml/hr/kg in nonusers). This result is, in part, consistent with data of Homeida *et al.* (34) who found a lower antipyrine clearance in young women during prolonged oral contraceptive therapy. Since the oral contraceptive nonusers included both males and females, the data were further examined by splitting Group 16 (Fig. 2) according to sex (Fig. 5). This approach confirmed the lack of gender difference in Cl_T at this branch of the cascade. The metabolic interaction of smoking and oral contraceptives is intriguing in view of mounting evidence for other associations of these two factors, such as an increased incidence of circulatory disorders and mortality risk (68, 69).

Liver Disease—The most profound determinant of theophylline Cl_T in persons >40 years of age is the presence of liver impairment, expressed as either clinically diagnosed cirrhosis or inferred from heavy use of ethanol and abnormal serum biochemistry. Patients with the latter two factors (Fig. 6) exhibited a mean Cl_T of only 22.4 (10.5) ml/hr/kg, the smallest grouped value in the entire cascade. This result includes and extends the previous study of eight cirrhotics (19) and further confirms the findings of Piafsky *et al.* (51) who also found extremely low Cl_T values in most patients with cirrhosis. There was an additional difference in Cl_T lower in the cascade between persons who used ethanol socially and those who abstained, as will be described.

Congestive Heart Failure—The presence of congestive heart failure was the second major factor accounting for decreased theophylline clearance in older adults (Figs. 2 and 7). Mild congestive heart failure apparently was without effect, since these patients were grouped with noncongestive heart failure subjects with a mean Cl_T of 54 (23) ml/hr/kg. Patients with moderate and severe congestive heart failure were combined and exhibited a Cl_T of 34 (15) ml/hr/kg, a substantial difference from the remaining patients.

Congestive heart failure may induce hepatic congestion with structural and functional derangements. In addition, the clearance of drugs that are highly dependent on liver blood flow is usually diminished (26). Decreased theophylline clearance was found in nine of the 10 reported patients with left-sided heart failure (53, 70), but the effects of right heart failure are less clear. Fourteen of our patients with congestive heart failure

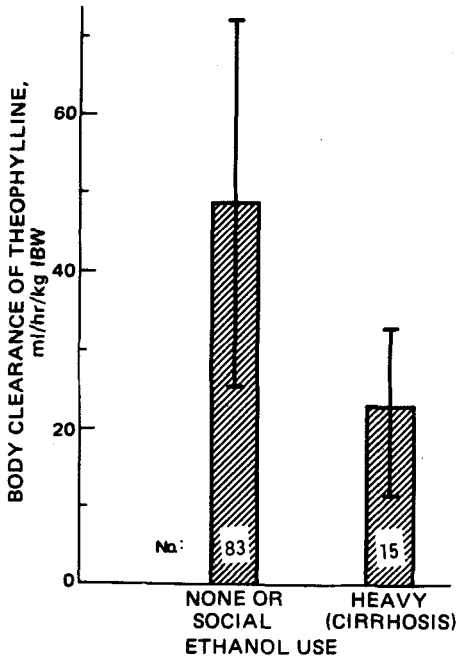

Figure 6—*Effect of heavy ethanol use and/or hepatic cirrhosis on body clearances of theophylline in adult subjects >40 years of age. Subject groups correspond to cells 8 and 9 in Fig. 2.*

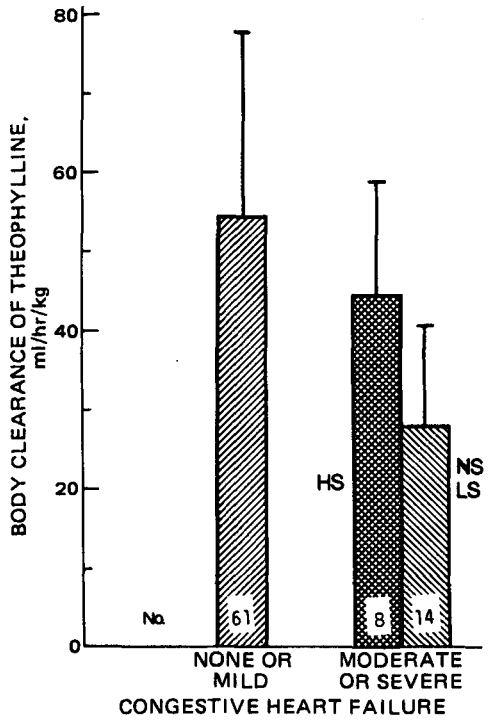

Figure 7—*Effect of congestive heart failure (CHF) and smoking on body clearances of theophylline in older adult patients (>40 years) without liver impairment. Congestive heart failure diminishes theophylline clearance, but heavy smokers (HS) with congestive heart failure exhibit larger clearances than nonsmokers (NS) or light smokers (LS). Subject groups correspond to cells 10, 30, and 31, respectively, in Fig. 2.*

(including two with liver disease) were previously found to exhibit a mean Cl_T of 31.8 (14.8) ml/hr/kg (65). In the overall surveillance, the presence of congestive heart failure was usually indicated by history and physical findings including edema and elevated central venous pressure. The gradation of the disease was characterized according to the criteria of Peck *et al.* (27). However, these groups should be accepted only as approximate since the criteria were applied by the clinical pharmacokineticist in concert with the house staff or consulting physician and were not unbiased scores solicited from a "blinded" cardiologist. Nevertheless, the congestive heart failure diagnosis was obtained without knowledge of the patient's theophylline Cl_T.

An interesting finding was the interaction between congestive heart failure and smoking (Fig. 7). Heavy smoking appeared to offset the diminished Cl_T found in moderate to severe congestive heart failure. This is the first observation of an effect of smoking superimposed on major organ dysfunction. The ability to discern this type of drug–disease interaction is a unique advantage of the NYBAID approach.

Obesity—An effect of obesity on theophylline disposition is seen in the younger subjects (<40 years) on the cascade (Fig. 2). The overweight subjects tended to have larger clearances than the lean persons. Since this finding disagrees somewhat with previous results (18), the data were assessed more rigorously using a continuous regression analysis. Figure 8 depicts the Cl_T values (normalized for ideal body weight in relation to the ratio of total to ideal body weight. Both the correlation coefficient ($r = 0.476$) and the regression slope (0.168) were statistically significant ($p < 0.025$). Thus, a trend for increased Cl_T with obesity occurs in a select group of young adults who are nonsmokers.

In contrast, previous investigation of theophylline disposition in 57 normal and 14 obese subjects yielded essentially identical Cl_T values when normalized for ideal body weight in this way (18). The disparity between the two studies may be explained in noting that the data were previously assessed without separating possible confounding factors. A similar gross evaluation of mean data (Table I) reveals no differences among lean, moderately obese, and severely obese persons. The small increase in Cl_T in uncomplicated obesity is consistent with physiological expectations, because severely obese persons have been shown to have increased cardiac output, resulting in a small increase in hepatic blood flow (28). Moreover, it was previously found (18) that the apparent volume of distribution of theophylline corresponds to total body weight rather than to ideal weight, suggesting that theophylline readily distributes into body fat.

Benzodiazepine, Barbiturate, and Ethanol Use—A splitting of subgroups that is awkward to explain is shown as Groups 14 and 15 in Fig. 2. Older adults without significant liver or cardiac impairment were split on the basis of smoking, but the non- and heavy smokers were merged. This result may be a statistical artifact or suggest a lack of a dose–effect relationship for the role of smoking in older subjects, or unclassified secondary factors such as disease or drug use may overwhelm the primary effect in one subgroup. This anomaly would cast some suspicion on the remaining elements of the cascade, except that they are comprised of expected drug interaction effects.

An observation that emerges in older subjects once the effects of liver disease and congestive heart failure are separated is an effect of chronic benzodiazepine, barbiturate, and ethanol use on theophylline Cl_T. As shown in Figs. 2 and 9, users of these compounds exhibited larger Cl_T values than nonusers. These groups were comprised almost entirely of pulmonary patients (most of the normal volunteers were <40 years old), and these data thus provide the first indication that these enzyme inducers may alter theophylline disposition under conventional clinical conditions.

The barbiturate effect is consistent with recent observations of Landay

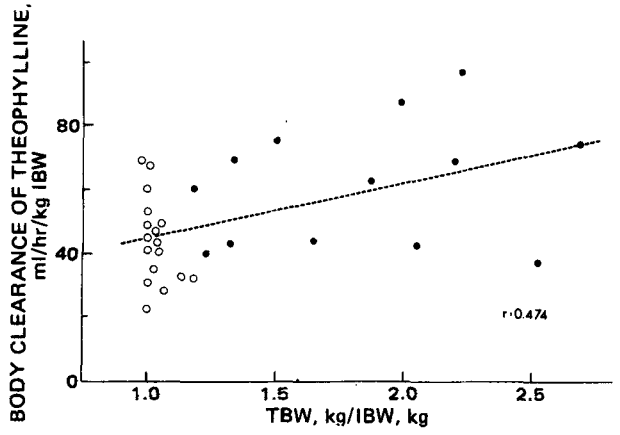

Figure 8—*Effect of obesity on body clearances of theophylline in adult nonsmoking subjects 20–40 years of age. Key: ○, cell 28 in Fig. 2; and ●, cell 29 in Fig. 2.*

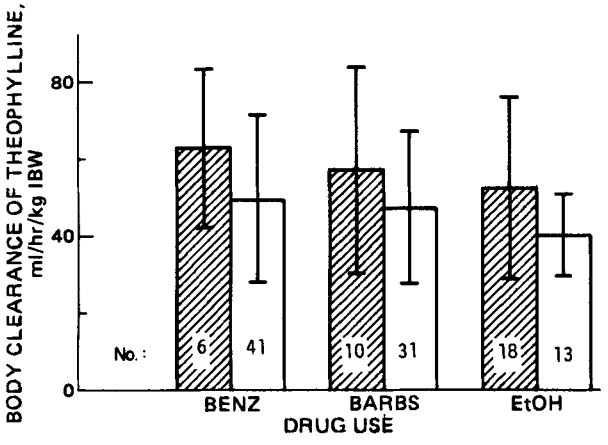

Figure 9—*Effect of use of benzodiazepines (BENZ), barbiturates (BARBS), and social ethanol (EtOH) on body clearances of theophylline in patients >40 years of age without liver or cardiac disease.*

et al. (37) who found a mean increase in theophylline Cl_T of 34% in six healthy subjects following 4 weeks of phenobarbital administration. In contrast, Piafsky *et al.* (71) found no such effect after briefer phenobarbital treatment in healthy adults. Microsomal enzymes for theophylline metabolism in the rat also are weakly susceptible to barbiturate induction, but, as in humans, are more strongly affected by polycyclic aromatic hydrocarbons (30). While theophylline is largely a substrate for the P-448 microsomal enzymes, phenobarbital is capable also of altering liver size and hepatic blood flow and may thereby indirectly affect the apparent theophylline clearance by a nonenzymatic mechanism (36).

The effects of the benzodiazepines and ethanol (social use) are similar to those of the barbiturates. These effects are consistent with known drug interaction mechanisms (38, 50). However, the small number of benzodiazepine users diminishes the credibility of this finding; an additional study is needed to substantiate both effects.

Other Factors—The NYBAID program provided a further breakdown of patient characteristics into many additional groups. However, the analysis was terminated with 31 cells (Fig. 2) because the number of subjects per group was becoming small and statistically less reliable. In fact, the authors of the NYBAID program advise against splitting cells containing fewer than 25 observations unless there is an *a priori* hypothesis to be tested (64). However, these subsequent splittings provided the opportunity to analyze the final groupings with regard to the major parameters listed in Table I. This approach ruled out any underlying effects of the dominating factors affecting theophylline Cl_T in a portion of the subgroup. In addition, a histogram of the residuals in the NYBAID analysis was constructed to assess whether the unaccounted variance may have a nonnormal distribution. The residuals clearly showed a Gaussian distribution, suggesting that a random array of factors (rather than a pharmacogenetic source, for instance) produce the remaining variability in the data.

Several factors existed in numerous patients but failed to emerge as important determinants of theophylline disposition. These factors include sex in adults and chronic use of theophylline, corticosteroids, and caffeine (Table I). Also, no effects of pregnancy were found. It is not appropriate to rule out any effects of phenothiazines, tricyclic antidepressants, severe renal impairment, or oral contraceptives in nonsmokers at this time because too few patients were encountered for these categories.

COMMENTARY

The clinical pharmacokinetic surveillance of patients provides the opportunity to collect data for evaluating basic assumptions about pharmacokinetics and for identifying useful criteria for the dosage regimen design (3, 72). One rationale underlying such an approach to digoxin pharmacokinetics was described by Sheiner *et al.* (73). These investigators included factors such as serum digoxin concentration, digoxin dosage history, body weight, sex, serum creatinine concentration, and thyroid function in developing a computerized system for interpreting serum digoxin concentrations in patients and predicting digoxin dosages. Digoxin is primarily eliminated by renal excretion, which simplifies optimum dosage prediction (2). The characterization of biotransformation rate determinants has remained a more formidable task because of the myriad factors affecting liver function and the lack of a good marker for the hepatic metabolism rate.

Surveillance Limitations—There are several limitations to this analysis. Not all factors that may modify theophylline disposition were included. For example, marked dietary changes (56, 57), respiratory viral infections (58), and immaturity (74, 75) have been identified as affecting theophylline biotransformation and were not included. The Cl_T may change with clinical status (67), possibly increasing with resolution of acute bronchial obstruction; our data usually represented only one to three 24-hr periods (typically at the onset of therapy).

Some diseases that may affect theophylline biotransformation such as thyroid disorders, which were sought, were not encountered frequently enough to be included in the current analysis. Genetic determinants of theophylline disposition (race, twin, or family data) were neither obtained nor considered, partly because of the predominance of Caucasian subjects and partly because genetic data are not likely to be available in newly admitted patients in a manner useful for drug metabolism rate estimation. Finally, the possibility of dose dependence or nonlinearity in theophylline pharmacokinetics could not be tested (76–78). This aspect of theophylline disposition requires administration of at least two dosage levels in a subset of patients. These inaccuracies, coupled with the analytical and curve-fitting errors associated with estimating the Cl_T values and the qualitative nature of most of the factor or disease categories, contribute to the large variances remaining in the metabolic cascade.

If a correlation is made between the 16 peripheral group mean values (using the outer cells as "predicted" clearances) and the individual clearances for the 200 subjects, the resulting correlation coefficient is 0.720. Thus, 51.8% ($r^2 \times 100$) of the variance in the data is accounted for. An enlargement of the number of factors, subgroups, and patients, more precise Cl_T values, and better linear quantitation of the factor subgroups would be required to improve this analysis. However, even this degree of predictability should be helpful for clinical purposes where dosage regimens must be devised to fit a wide therapeutic range (8–20 mg/liter) rather than to attain a specific serum concentration (65).

The factors identified as important in theophylline body clearances are associations found by retrospective statistical analysis which need not imply a cause-and-effect relationship, especially where a pathophysiologic or drug interaction rationale does not exist. Often these factors need further confirmation by prospective examination of cohorts of subjects with the disease or history in question. This approach may be almost impossible for many uncommon factors under the restrictions that the subjects also be patients with pulmonary dysfunction undergoing therapy with theophylline. However, several of the isolated determinants of theophylline disposition—youth (7), tobacco use (14), marijuana (17), cirrhosis (19), congestive heart failure (65), and barbiturate use (36)—have already evolved, and the NYBAID program recovered these factors in a realistic configuration in spite of the confounding effect of being merged with an array of additional data and variables. This analysis confirmed the role of these effects in actual patients, and this observation lends greater credibility to the new associations that emerged on evaluation of theophylline clearances.

Dosage Guidelines—The NYBAID computer program is generally available as a library program. This facilitates its use by other investigators, although it has had little use in the biomedical sciences to date. The grouping of patient variables affecting theophylline Cl_T by the NYBAID analysis is both attractive and practical. The results of the statistical analysis are provided in a format (Fig. 2) directly useful to any practicing clinician since it does not require access to a computer. We only included factors known or presumed to affect the biotransformation of theophylline or other durgs and that could be assessed easily and rapidly from most patients.

Figure 2 can be greatly simplified and adapted for use as a dosing nomogram by clinicians who need only to assign patients to the proper Cl_T categories and aim for an appropriate steady-state serum concentration. The theophylline maintenance dose can be obtained using Eq. 1 with a target serum concentration of 14 mg/liter (6, 12):

$$D/\mathrm{T}\ (\mathrm{mg/hr}) = [Cl_T\ (\mathrm{ml/hr/kg})][\mathrm{IBW}\ (\mathrm{kg})][0.014\ (\mathrm{mg/ml})] \quad \text{(Eq. 4)}$$

where IBW is the lean body weight. If a loading dose is desired, it should be the commonly recommended dose of 5.6 mg of aminophylline/kg (or 4.8 mg of theophylline/kg) administered orally or intravenously over a 20-min interval (78).

Employment of Fig. 2 in construction of a dosing nomogram should be with the reservations that most cells contain appreciable variance, that

many of the drug/disease/history/physiologic associations remain to be proven in a prospective clinical trial, and that many potential factors affecting theophylline disposition remain to be added to the metabolic cascade as described in the previous section.

Pharmacokinetic Monitoring—The advantage of the NYBAID analysis in clinical pharmacokinetics is the ability to examine the interrelationships between patient variables commonly expected to affect the drug biotransformation rate in patients undergoing medical therapy. Pharmacokinetic guidelines for drug therapy are often based on studies in reasonably normal subjects which may only approximate the dosage needs of distressed patients. Most studies of factors altering drug metabolism take place under ideal conditions in groups of subjects who are preselected on the basis of having a specific disease. Medical patients, on the other hand, are encountered with a variety of pathophysiologic problems, their drug and environmental histories are highly diversified, and any expectations of biotransformation rates have been fraught with considerable uncertainty.

This study demonstrates one approach to resolving several clinical pharmacokinetic problems simultaneously. Serum concentration monitoring aids in managing the immediate therapeutic needs of the patient, the appropriate timing in blood specimen collection assists in anticipating the pharmacokinetic behavior of the drug, and the retrospective correlation of a reasonable array of patient variables with the pharmacokinetics confirms or enlarges the knowledge of factors determining drug disposition rates while providing guidelines for future clinical drug use.

REFERENCES

(1) "The Effect of Disease States on Drug Pharmacokinetics," L. Benet, Ed., Academy of Pharmaceutical Sciences, American Pharmaceutical Association, Washington, D.C., 1976.

(2) J. R. Koup, W. J. Jusko, C. M. Elwood, and R. K. Kohli, *Clin. Pharmacol. Ther.*, **18**, 9 (1975).

(3) "Clinical Pharmacokinetics: A Symposium," G. Levy, Ed., Academy of Pharmaceutical Sciences, American Pharmaceutical Association, Washington, D.C., 1974.

(4) J. Koch-Weser, *N. Engl. J. Med.*, **287**, 227 (1972).

(5) J. W. Jenne, H. T. Nagasawa, and R. D. Thompson, *Clin. Pharmacol. Ther.*, **19**, 375 (1976).

(6) J. W. Jenne, E. Wyze, F. S. Rood, and F. M. MacDonald, *ibid.*, **13**, 349 (1972).

(7) E. F. Ellis, R. Koysooko, and G. Levy, *Pediatrics*, **58**, 542 (1976).

(8) P. A. Mitenko and R. I. Ogilvie, *Clin. Pharmacol. Ther.*, **14**, 509 (1973).

(9) J. R. Koup, J. J. Schentag, J. W. Vance, P. M. Kuritzky, D. R. Pyszczynski, and W. J. Jusko, *Am. J. Hosp. Pharm.*, **33**, 949 (1976).

(10) M. H. Jacobs, R. M. Senior, and G. Kessler, *J. Am. Med. Assoc.*, **235**, 1983 (1976).

(11) M. W. Weinberger, R. A. Matthay, E. J. Ginchansky, C. A. Chidsey, and T. L. Petty, *ibid.*, **235**, 2110 (1976).

(12) P. A. Mitenko and R. I. Ogilvie, *N. Engl. J. Med.*, **289**, 600 (1973).

(13) W. J. Jusko and A. Poliszczuk, *Am. J. Hosp. Pharm.*, **33**, 1193 (1976).

(14) S. N. Hunt, W. J. Jusko, and A. M. Yurchak, *Clin. Pharmacol. Ther.*, **19**, 546 (1976).

(15) R. Koysooko, E. F. Ellis, and G. Levy, *ibid.*, **15**, 454 (1974).

(16) A. M. Yurchak and W. J. Jusko, *Pediatrics*, **57**, 518 (1976).

(17) W. J. Jusko, J. J. Schentag, J. H. Clark, M. Gardner, and A. M. Yurchak, *Clin. Pharmacol. Ther.*, **24**, 406 (1978).

(18) P. Gal, W. J. Jusko, A. M. Yurchak, and B. A. Franklin, *ibid.*, **23**, 438 (1978).

(19) A. Mangione, T. E. Imhoff, R. V. Lee, L.-Y. Shum, and W. J. Jusko, *Chest*, **73**, 616 (1978).

(20) P. L. Sutton, J. R. Koup, J. Q. Rose, and E. Middleton, *J. Allergy Clin. Immunol.*, **61**, 174 (1978).

(21) "Documenta Geigy Scientific Tables," 7th ed., K. Diem and C. Lentner, Eds., Geigy Pharmaceuticals, Basel, Switzerland, 1970, p. 712.

(22) U. Klotz, G. R. Avant, A. Hoyumpa, S. Schenker, and G. R. Wilkinson, *J. Clin. Invest.*, **55**, 347 (1975).

(23) K. O'Malley, J. Crooks, E. Duke, and I. H. Stevenson, *Br. Med. J.*, **3**, 607 (1971).

(24) E. J. Triggs and R. L. Nation, *J. Pharmacokinet. Biopharm.*, **6**, 387 (1975).

(25) F. C. Gable, *Adv. Pharmacol. Chemother.*, **13**, 173 (1975).

(26) G. D. Dunn, P. Hayes, K. J. Breen, and S. Schenker, *Am. J. Med. Sci.*, **265**, 174 (1973).

(27) C. C. Peck, L. B. Sheiner, C. M. Martin, D. T. Combs, and K. L. Melmon, *N. Engl. J. Med.*, **289**, 441 (1973).

(28) J. K. Alexander, E. W. Dennis, W. G. Smith, K. H. Amod, W. C. Duncan, and R. C. Austin, *Cardiovasc. Res. Center Bull.*, **1**, 39 (1962).

(29) K. Siersbaek-Nielsen, J. M. Hansen, J. Kampman, and M. Kristensen, *Lancet*, **1**, 1133 (1971).

(30) S. M. Lohman and R. P. Miech, *J. Pharmacol. Exp. Ther.*, **196**, 213 (1976).

(31) A. Breckenridge, M. L. E. Orme, H. Wesseling, M. Berding, and R. J. Lewis, in "Drug Interactions," P. L. Morselli, S. Garrattini, and S. N. Cohen, Eds., Raven, New York, N.Y., 1974, pp. 223–230.

(32) C. A. Dujovne and D. L. Azarnoff, in "Steroid Therapy," D. L. Azarnoff, Ed., Saunders, Philadelphia, Pa., 1975, pp. 27–41.

(33) J. W. Ayres, M. Freundlich, S. Makker, J. Easton, M. Hallmark, T. Sudds, J. J. MacKichan, and J. G. Wagner, in press.

(34) M. Homeida, M. Halliwell, and R. A. Branch, *Clin. Pharmacol. Ther.*, **24**, 228 (1978).

(35) A. H. Conney, *Pharmacol. Rev.*, **19**, 317 (1967).

(36) A. S. Nies, G. R. Wilkinson, B. D. Rush, J. T. Strother, and D. G. McDevitt, *Biochem. Pharmacol.*, **25**, 1991 (1976).

(37) R. A. Landay, M. A. Gonzalez, and J. C. Taylor, *J. Allergy Clin. Immunol.*, **62**, 27 (1978).

(38) "Evaluations of Drug Interactions," 2nd ed., American Pharmaceutical Association, Washington, D.C., 1976.

(39) K. O'Malley, M. Browning, I. Stevenson, and M. J. Turnbull, *Eur. J. Clin. Pharmacol.*, **6**, 102 (1973).

(40) "Drug Interactions," P. L. Morselli, S. Garattini, and S. N. Cohen, Raven, New York, N.Y., 1974.

(41) M. Weinberger, D. Hudgel, S. Spector, and C. Chidsey, *J. Allergy Clin. Immunol.*, **59**, 228 (1977).

(42) P. P. Kozak, L. H. Cummins, and S. A. Gillman, *ibid.*, **60**, 149 (1977).

(43) W. J. Jusko, *J. Pharmacokinet. Biopharm.*, **6**, 7 (1978).

(44) J. Jenne, H. Nagasawa, R. McHugh, F. MacDonald, and E. Wyse, *Life Sci.*, **17**, 195 (1975).

(45) J. R. Powell, J.-F. Thiercelin, S. Vozeh, L. Sansom, and S. Riegelman, *Am. Rev. Resp. Dis.*, **116**, 17 (1977).

(46) C. Mitoma, T. J. Sorich, and S. E. Neubauer, *Life Sci.*, **7**, 145 (1968).

(47) J. G. Babish and G. S. Stoewsand, *Nutr. Rep. Int.*, **12**, 109 (1975).

(48) D. D. Drouillard, E. S. Vesell, and B. H. Dvorchik, *Clin. Pharmacol. Ther.*, **23**, 296 (1978).

(49) C. S. Lieber, *Gastroenterology*, **65**, 821 (1973).

(50) E. Mezey, *Biochem. Pharmacol.*, **25**, 869 (1976).

(51) K. M. Piafsky, D. S. Sitar, R. E. Rangno, and R. I. Ogilvie, *N. Engl. J. Med.*, **296**, 1495 (1977).

(52) K. I. Mygind, M. Dam, and J. Christiansen, *Acta Neurol. Scand.*, **54**, 160 (1976).

(53) K. M. Piafsky, D. S. Sitar, R. E. Rangno, and R. I. Ogilvie, *Clin. Pharmacol. Ther.*, **21**, 310 (1977).

(54) E. S. Vesell, J. R. Shapiro, G. T. Passananti, H. Jorgensen, and C. A. Shively, *ibid.*, **17**, 48 (1975).

(55) J. F. Cumming, *ibid.*, **19**, 468 (1976).

(56) A. Kappas, K. E. Anderson, A. H. Conney, and A. P. Alvares, *ibid.*, **20**, 643 (1976).

(57) A. Kappas, A. P. Alvares, K. E. Anderson, E. J. Pantuck, C. B. Pantuck, R. Chang, and A. H. Conney, *ibid.*, **23**, 445 (1978).

(58) K. C. Chang, T. D. Bell, B. A. Lauer, and H. Choi, *Lancet*, **1**, 1132 (1978).

(59) J. A. Schack and S. H. Waxler, *J. Pharmacol. Exp. Ther.*, **97**, 283 (1949).

(60) L. Hendeles, M. Weinberger, and L. Bighley, *Am. J. Hosp. Pharm.*, **34**, 525 (1977).

(61) C. M. Metzler, "NONLIN: A Computer Program for Parameter Estimation in Nonlinear Situations," The Upjohn Co., Kalamazoo, Mich., 1969.

(62) N. R. Draper and H. Smith, "Applied Regression Analysis," Wiley, New York, N.Y., 1966, pp. 234–242.

(63) "BMD03R: Multiple Regression with Case Combinations, Biomedical Computer Programs," W. J. Dixon, Ed., University of California, Los Angeles, Calif., 1972.

(64) J. A. Sonquist and J. N. Morgan, "The Detection of Interaction Effects," Monograph 35, Survey Reserach Center, Institute for Social Research, University of Michigan, 1964 (as program "NYBAID" by the

Computing Center of the State University of New York) and *J. Am. Stat. Assoc.*, **58**, 415 (1963).
(65) W. J. Jusko, J. R. Koup, J. W. Vance, J. J. Schentag, and P. M. Kuritzky, *Ann. Intern. Med.*, **86**, 400 (1977).
(66) P. M. Loughnan, D. S. Sitar, R. I. Ogilvie, A. Eisen, Z. Fox, and A. H. Neims, *J. Pediatr.*, **88**, 874 (1976).
(67) P. Leung, A. Kalisker, and T. D. Bell, *J. Allergy Clin. Immunol.*, **59**, 440 (1977).
(68) A. K. Jain, *Am. J. Obstet. Gynecol.*, **126**, 301 (1976).
(69) Royal College of General Practitioners' Oral Contraception Study, *Lancet*, **2**, 727 (1977).
(70) J. W. Jenne, T. W. Chick, B. A. Miller, and R. D. Strickland, *Am. J. Hosp. Pharm.*, **34**, 408 (1977).
(71) K. M. Piafsky, D. S. Sitar, and R. I. Ogilvie, *Clin. Pharmacol. Ther.*, **22**, 336 (1977).
(72) L. B. Sheiner, B. Rosenberg, and V. V. Marathe, *J. Pharmacokinet. Biopharm.*, **5**, 445 (1977).
(73) L. B. Sheiner, B. Rosenberg, and K. L. Melmon, *Comp. Biomed. Res.*, **5**, 441 (1972).
(74) J. V. Aranda, D. S. Sitar, W. D. Parsons, P. M. Loughnan, and A. H. Neims, *N. Engl. J. Med.*, **295**, 413 (1976).
(75) G. Giacoia, W. J. Jusko, J. Menke, and J. R. Koup, *J. Pediatr.*, **89**, 829 (1976).
(76) M. Weinberger and E. Ginchansky, *ibid.*, **91**, 820 (1977).
(77) S. Sved, I. J. McGilveray, and D. L. Wilson, presented at the APhA Academy of Pharmaceutical Sciences, Montreal meeting, 1978.
(78) R. I. Ogilvie, *Clin. Pharmacokinet.*, **3**, 267 (1978).

ACKNOWLEDGMENTS

Presented in part at the APhA Academy of Pharmaceutical Sciences, New Orleans meeting, April 1976.

Supported in part by Grant 20852 from the National Institutes of General Medical Sciences, by Grant 1079 from the Council for Tobacco Research–U.S.A., Inc., and by a grant-in-aid from Breon Laboratories.

The authors appreciate the technical assistance of Mrs. Anna Poliszczuk and Ms. Kathy Vance, the clinical help of the nurses and staff of the Millard Fillmore Hospital, the computer and statistical services of Mr. Harry Piniarski of the Computer Center at the State University of New York at Buffalo, the secretarial assistance of Ms. Sherlyn Sion, and the provision of theophylline data by Dr. Gerhard Levy and Dr. Elliot F. Ellis.

N-Benzoyl Derivatives of Amino Acids and Amino Acid Analogs as Growth Inhibitors in Microbial Antitumor Screen

THEODORE T. OTANI ˣ and MARY R. BRILEY

Received November 16, 1978, from the *Laboratory of Pathophysiology, National Cancer Institute, Bethesda, MD 20205.* Accepted for publication May 4, 1979.

Abstract □ Twenty-seven *N*-benzoyl derivatives of amino acids and amino acid analogs were prepared and tested for growth-inhibitory activity in a microbial antitumor screen. Of these, 19 showed some inhibitory capacity, from a modest 13% to a potent 96% at 1 mg/ml. The activities of the "modest" inhibitors were comparable to those of most inhibitory chloroacetyl and trifluoroacetyl derivatives reported earlier. The intermediate inhibitors were as active as *N*-chloroacetyl-β-hydroxy-D-norleucine isomer B, the most active acyl derivative noted previously. The most active compounds in this study were *N*-benzoyl-*p*-chloro-DL-phenylalanine and *N*-benzoyl-*m*-fluoro-DL-phenylalanine, which inhibited the test organism almost completely under the assay conditions.

Keyphrases □ *N*-Benzoyl amino acid derivatives—antineoplastic activity, potential, inhibition of microbial antitumor screen, structure–activity relationships □ Amino acid derivatives—*N*-benzoyl, potential antineoplastic activity, inhibition of microbial antitumor screen, structure–activity relationships □ Antineoplastic agents, potential—*N*-benzoyl amino acid derivatives, inhibition of microbial antitumor screen, structure–activity relationships □ Structure–activity relationships—*N*-benzoyl amino acid derivatives, inhibition of microbial antitumor screen

Studies of possible antimetabolic effects of novel β-hydroxyamino acids produced evidence that an otherwise inert amino acid could, upon *N*-chloroacetylation, actively inhibit growth of a microbial antitumor screen (1). This study was extended to include the *N*-chloroacetyl (2) as well as the *N*-acetyl (2), *N*-propionyl (2), and *N*-trifluoroacetyl (3) derivatives of other amino acids, both natural and unnatural. Both the amino acid and the *N*-acyl moieties of the acyl amino acid were important in imparting the growth-inhibitory characteristic to the compound, since only certain amino acids and certain acyl groups were capable of doing so (2).

One deterrent to using amino acid analogs as antimetabolites in mammalian systems is their high toxicity (4–7). In view of the finding that there is an alteration in biological properties, especially cytotoxicity, upon *N*-acylation (2), more potent inhibitors might be prepared by attachment of acyl groups other than those studied previously. Since a more lipophilic acyl group might increase the mobility of these compounds in a lipoid milieu such as the cellular membranes in mammalian systems, a benzoyl derivative series was prepared. These compounds were tested for growth inhibition in a microbial system selected specifically as an antitumor screen. Although the ultimate objective of these studies is to find compounds for cancer therapy, the immediate aim has been to improve the growth-inhibitory properties of the compounds in the screen described earlier.

The present paper reports the results of these studies.

EXPERIMENTAL

The free amino acids except the β-hydroxynorleucines, which were prepared in this laboratory (8, 9), were obtained commercially and were recrystallized from water–ethanol before use. Some *N*-benzoyl derivatives were obtained commercially and were recrystallized from ethanol–water before use. Others, especially those of amino acid analogs, were prepared by the Schotten–Baumann procedure (10) and were recrystallized from ethanol or ethanol–water. The sources of the amino acids and of the benzoyl derivatives are shown in Table I.

The purity of the amino acids and of the benzoyl derivatives was ascertained by: (*a*) Van Slyke nitrous acid determination of primary amino nitrogen (11), (*b*) optical rotation measurement, where applicable, and (*c*) elemental analysis. In addition, the purity of the free amino acids was checked by paper chromatography in at least four different solvent systems (8), and that of the benzoyl derivatives was checked by melting-point determination (Table I).

0022-3549/79/1100-1366$01.00/0
© 1979, American Pharmaceutical Association

Computing Center of the State University of New York) and *J. Am. Stat. Assoc.*, **58**, 415 (1963).
(65) W. J. Jusko, J. R. Koup, J. W. Vance, J. J. Schentag, and P. M. Kuritzky, *Ann. Intern. Med.*, **86**, 400 (1977).
(66) P. M. Loughnan, D. S. Sitar, R. I. Ogilvie, A. Eisen, Z. Fox, and A. H. Neims, *J. Pediatr.*, **88**, 874 (1976).
(67) P. Leung, A. Kalisker, and T. D. Bell, *J. Allergy Clin. Immunol.*, **59**, 440 (1977).
(68) A. K. Jain, *Am. J. Obstet. Gynecol.*, **126**, 301 (1976).
(69) Royal College of General Practitioners' Oral Contraception Study, *Lancet*, **2**, 727 (1977).
(70) J. W. Jenne, T. W. Chick, B. A. Miller, and R. D. Strickland, *Am. J. Hosp. Pharm.*, **34**, 408 (1977).
(71) K. M. Piafsky, D. S. Sitar, and R. I. Ogilvie, *Clin. Pharmacol. Ther.*, **22**, 336 (1977).
(72) L. B. Sheiner, B. Rosenberg, and V. V. Marathe, *J. Pharmacokinet. Biopharm.*, **5**, 445 (1977).
(73) L. B. Sheiner, B. Rosenberg, and K. L. Melmon, *Comp. Biomed. Res.*, **5**, 441 (1972).
(74) J. V. Aranda, D. S. Sitar, W. D. Parsons, P. M. Loughnan, and A. H. Neims, *N. Engl. J. Med.*, **295**, 413 (1976).
(75) G. Giacoia, W. J. Jusko, J. Menke, and J. R. Koup, *J. Pediatr.*, **89**, 829 (1976).
(76) M. Weinberger and E. Ginchansky, *ibid.*, **91**, 820 (1977).
(77) S. Sved, I. J. McGilveray, and D. L. Wilson, presented at the APhA Academy of Pharmaceutical Sciences, Montreal meeting, 1978.
(78) R. I. Ogilvie, *Clin. Pharmacokinet.*, **3**, 267 (1978).

ACKNOWLEDGMENTS

Presented in part at the APhA Academy of Pharmaceutical Sciences, New Orleans meeting, April 1976.

Supported in part by Grant 20852 from the National Institutes of General Medical Sciences, by Grant 1079 from the Council for Tobacco Research–U.S.A., Inc., and by a grant-in-aid from Breon Laboratories.

The authors appreciate the technical assistance of Mrs. Anna Poliszczuk and Ms. Kathy Vance, the clinical help of the nurses and staff of the Millard Fillmore Hospital, the computer and statistical services of Mr. Harry Piniarski of the Computer Center at the State University of New York at Buffalo, the secretarial assistance of Ms. Sherlyn Sion, and the provision of theophylline data by Dr. Gerhard Levy and Dr. Elliot F. Ellis.

N-Benzoyl Derivatives of Amino Acids and Amino Acid Analogs as Growth Inhibitors in Microbial Antitumor Screen

THEODORE T. OTANI ˣ and MARY R. BRILEY

Received November 16, 1978, from the *Laboratory of Pathophysiology, National Cancer Institute, Bethesda, MD 20205.* Accepted for publication May 4, 1979.

Abstract □ Twenty-seven *N*-benzoyl derivatives of amino acids and amino acid analogs were prepared and tested for growth-inhibitory activity in a microbial antitumor screen. Of these, 19 showed some inhibitory capacity, from a modest 13% to a potent 96% at 1 mg/ml. The activities of the "modest" inhibitors were comparable to those of most inhibitory chloroacetyl and trifluoroacetyl derivatives reported earlier. The intermediate inhibitors were as active as *N*-chloroacetyl-β-hydroxy-D-norleucine isomer B, the most active acyl derivative noted previously. The most active compounds in this study were *N*-benzoyl-*p*-chloro-DL-phenylalanine and *N*-benzoyl-*m*-fluoro-DL-phenylalanine, which inhibited the test organism almost completely under the assay conditions.

Keyphrases □ *N*-Benzoyl amino acid derivatives—antineoplastic activity, potential, inhibition of microbial antitumor screen, structure–activity relationships □ Amino acid derivatives—*N*-benzoyl, potential antineoplastic activity, inhibition of microbial antitumor screen, structure–activity relationships □ Antineoplastic agents, potential—*N*-benzoyl amino acid derivatives, inhibition of microbial antitumor screen, structure–activity relationships □ Structure–activity relationships—*N*-benzoyl amino acid derivatives, inhibition of microbial antitumor screen

Studies of possible antimetabolic effects of novel β-hydroxyamino acids produced evidence that an otherwise inert amino acid could, upon *N*-chloroacetylation, actively inhibit growth of a microbial antitumor screen (1). This study was extended to include the *N*-chloroacetyl (2) as well as the *N*-acetyl (2), *N*-propionyl (2), and *N*-trifluoroacetyl (3) derivatives of other amino acids, both natural and unnatural. Both the amino acid and the *N*-acyl moieties of the acyl amino acid were important in imparting the growth-inhibitory characteristic to the compound, since only certain amino acids and certain acyl groups were capable of doing so (2).

One deterrent to using amino acid analogs as antimetabolites in mammalian systems is their high toxicity (4–7). In view of the finding that there is an alteration in biological properties, especially cytotoxicity, upon *N*-acylation (2), more potent inhibitors might be prepared by attachment of acyl groups other than those studied previously. Since a more lipophilic acyl group might increase the mobility of these compounds in a lipoid milieu such as the cellular membranes in mammalian systems, a benzoyl derivative series was prepared. These compounds were tested for growth inhibition in a microbial system selected specifically as an antitumor screen. Although the ultimate objective of these studies is to find compounds for cancer therapy, the immediate aim has been to improve the growth-inhibitory properties of the compounds in the screen described earlier.

The present paper reports the results of these studies.

EXPERIMENTAL

The free amino acids except the β-hydroxynorleucines, which were prepared in this laboratory (8, 9), were obtained commercially and were recrystallized from water–ethanol before use. Some *N*-benzoyl derivatives were obtained commercially and were recrystallized from ethanol–water before use. Others, especially those of amino acid analogs, were prepared by the Schotten–Baumann procedure (10) and were recrystallized from ethanol or ethanol–water. The sources of the amino acids and of the benzoyl derivatives are shown in Table I.

The purity of the amino acids and of the benzoyl derivatives was ascertained by: (*a*) Van Slyke nitrous acid determination of primary amino nitrogen (11), (*b*) optical rotation measurement, where applicable, and (*c*) elemental analysis. In addition, the purity of the free amino acids was checked by paper chromatography in at least four different solvent systems (8), and that of the benzoyl derivatives was checked by melting-point determination (Table I).

0022-3549/79/1100-1366$01.00/0
© 1979, American Pharmaceutical Association

Table I—Purity of *N*-Benzoyl Derivatives [a]

N-Benzoyl Derivative	Source [b]	Melting Point		Optical Rotation [d] $[\alpha]_D^{21-24}$		Concentration and Solvent	Empirical Formula	Analysis [e], %		
		Reported	Observed [c]	Reported	Observed				Calc.	Obs.
L-Alanine	1	150–151° [f]	150–151°	+37.1° [f]	+36.1°	9.3%, water + 1 eq of potassium hydroxide	$C_{10}H_{11}NO_3$	C	62.17	61.93
								H	5.74	6.03
								N	7.25	7.24
DL-Allylglycine	1	—	112–114°	—	0	2% ethanol	$C_{12}H_{13}NO_3$	C	65.74	65.98
								H	5.98	6.24
								N	6.39	6.44
L-Arginine (α-mono), hemihydrate	2	298° dec. [f]	290°	−8.1° [f]	−8.5°	1.2%, water + 1 eq of hydrochloric acid	$C_{13}H_{19}N_4O_{3\frac{1}{2}}$	C	54.34	54.15
								H	6.67	6.65
								N	19.50	19.48
L-Aspartic acid, monohydrate	3	184–185° [f]	182°	+37.4° [f]	+38.0° [g]	9%, water + 2 eq of potassium hydroxide	$C_{11}H_{13}NO_6$	C	51.76	51.85
								H	5.13	4.81
								N	5.90	5.67
p-Chloro-DL-phenylalanine	1	—	178–180°	—	0	2%, ethanol	$C_{16}H_{14}ClNO_3$	C	63.27	62.98
								H	4.64	4.77
								N	4.61	4.58
o-Fluoro-DL-phenylalanine	1	—	189–190°	—	0	2%, ethanol	$C_{16}H_{14}FNO_3$	C	66.89	67.06
								H	4.91	5.07
								N	4.88	5.14
m-Fluoro-DL-phenylalanine	1	—	188–189°	—	0	2%, water + 1 eq of sodium hydroxide	$C_{16}H_{14}FNO_3$	C	66.89	66.80
								H	4.91	4.91
								N	4.88	4.82
p-Fluoro-DL-phenylalanine	1	—	166–168°	—	0	2%, ethanol	$C_{16}H_{14}FNO_3$	C	66.89	67.21
								H	4.91	4.91
								N	4.88	5.16
L-Glutamic acid, hemihydrate	4	137–139° [f]	137–138°	+17.2° [f]	+16.8° [g]	10%, water + 2 eq of potassium hydroxide	$C_{12}H_{14}NO_{5\frac{1}{2}}$	C	55.38	55.56
								H	5.42	5.24
								N	5.38	5.20
Glycine	4	187.5° [f]	192°	—	—	—	$C_9H_9NO_3$	C	60.33	60.60
								H	5.06	4.93
								N	7.82	7.86
L-Histidine, monohydrate	5	249° [f]	243° dec.	−47.4° [f]	−46.9°	6.8%, 0.5 *M* hydrochloric acid	$C_{13}H_{15}N_3O_4$	C	56.31	56.12
								H	5.45	5.59
								N	15.15	14.85
β-Hydroxy-DL-norleucine A	1	—	153–154°	—	—	—	$C_{13}H_{17}NO_4$	C	62.14	62.09
								H	6.82	6.98
								N	5.58	5.64
β-Hydroxy-DL-norleucine B [h]	1	—	189–190°	—	—	—	$C_{13}H_{17}NO_4$	C	62.14	61.55
								H	6.82	7.02
								N	5.58	6.10
L-Leucine	3	105–107° [f]	105–107°	+6.6° [f]	+6.5°	9.5%, 0.5 *M* potassium hydroxide	$C_{13}H_{17}NO_3$	C	66.36	66.55
								H	7.28	7.39
								N	5.95	6.01
L-Lysine (α-mono)	3	250° dec. [f]	258° dec.	+21.6° [f]	+20.4°	2%, water + 1 eq of sodium hydroxide	$C_{13}H_{18}N_2O_3$	C	62.38	62.21
								H	7.24	7.40
								N	11.19	11.31
DL-Methionine	1	151° [f]	150–151°	—	—	—	$C_{12}H_{16}NO_3S$	C	56.67	56.42
								H	6.34	6.19
								N	5.51	5.51
L-Methionine	1	—	98°	—	−14.6°	2%, ethanol	$C_{12}H_{16}NO_3S$	C	56.67	56.42
								H	6.34	6.18
								N	5.51	5.46
p-Nitro-L-phenylalanine	1	—	205–208°	—	−72.6°	2%, ethanol	$C_{16}H_{14}N_2O_5$	C	61.14	60.50
								H	4.49	4.69
								N	8.91	8.62
DL-Norleucine	1	—	137°	—	0	2%, ethanol	$C_{13}H_{17}NO_3$	C	66.36	66.55
								H	7.28	7.26
								N	5.95	5.85
DL-Norvaline	1	—	152–154°	—	—	—	$C_{12}H_{15}NO_3$	C	65.14	64.98
								H	6.83	6.94
								N	6.33	6.40
L-Phenylalanine, hemihydrate	3	—	141–143°	—	+10.0°	2%, 1 *M* potassium hydroxide	$C_{16}H_{16}NO_{3\frac{1}{2}}$	C	69.05	69.09
								H	5.80	5.82
								N	5.03	4.94
β-2-Thienyl-DL-alanine	1	—	184°	—	0	2%, water	$C_{14}H_{13}NO_3S$	C	61.07	61.12
								H	4.76	4.92
								N	5.09	4.79
β-3-Thienyl-DL-alanine, hemihydrate	1	—	167–168°	—	—	—	$C_{14}H_{14}NO_{3\frac{1}{2}}S$	C	59.14	59.46
								H	4.96	4.68
								N	4.93	5.21
L-Threonine	1	143–144° [f]	141–143°	+27.1°	+26.1°	0.8%, water	$C_{11}H_{13}NO_4$	C	59.19	58.99
								H	5.87	5.86
								N	6.28	6.11
L-Tryptophan, hemihydrate	3	104–105° [f]	105–107°	—	−7.4°	6%, ethanol	$C_{18}H_{17}N_2O_{3\frac{1}{2}}$	C	68.13	68.06
								H	5.40	5.57
								N	8.83	8.87
L-Tyrosine ethyl ester	5	—	207–208°	—	+24.3°	2%, ethanol	$C_{18}H_{19}NO_4$	C	68.99	68.72
								H	6.11	6.11
								N	4.47	4.49
L-Valine	3	131–132° [f]	132–134°	+21.8°	+21.2°	4.9%, ethanol	$C_{12}H_{15}NO_3$	C	65.14	64.91
								H	6.83	6.95
								N	6.33	6.32

[a] Van Slyke nitrous acid determination of primary amino nitrogen (11) made on a 1-ml sample containing an equivalent of 0.3 mg of amino nitrogen (when hydrolyzed) yielded no detectable quantity of nitrogen. [b] Source of compounds: 1, prepared in this laboratory; 2, ICN Pharmaceuticals, Cleveland, Ohio; 3, Vega-Fox Biochemicals, Tucson, Ariz.; 4, Nutritional Biochemicals Corp., Cleveland, Ohio; and 5, Sigma Chemical Co., St. Louis, Mo. Data on commercial products were obtained from recrystallized materials. [c] Melting points (uncorrected) were determined on a Fisher–Johns melting-point block. [d] Optical rotation was determined on a Rudolph polarimeter (Rudolph Research, Fairfield, N.J.), model 80, sodium lamp, using 100-mm tubes (bore size of 3 mm) and a sample capacity of 0.7 ml, except where noted. [e] Elemental analyses were performed by the Microanalytical Laboratory, National Institute of Arthritis, Metabolism, and Digestive Diseases, National Institutes of Health, Bethesda, Md. [f] *Cf.*, Ref. 10. [g] Optical rotation was measured in 50-mm tubes. [h] Crude.

The test solutions were prepared by adding an equivalent amount of 0.1 *N* NaOH to a prescribed amount of the test compound and diluting to volume, and they were sterilized by filtration through an all-glass system[1]. The pH of the assay system containing the maximum amount of test compound was checked on a duplicate set of tubes containing equivalent amounts of the ingredients and was within ±0.05 pH unit of the control tube containing all components except the test compound.

Inhibition studies were made initially in a system containing graded amounts of the test compound, *i.e.*, 0.1-, 0.5-, and 1.0-mg/ml final concentration; the highest concentration was the level specified in the microbiological antitumor screening protocol (12). When inhibition was noted in this system, the active compounds were compared on an equimolar basis at a final concentration of 4.47 μmoles/ml, which was equivalent to 1 mg of *N*-chloroacetyl-β-hydroxy-D-norleucine B[2]/ml, the compound found previously to be the most active in this system.

The organism used was *Lactobacillus casei* 7469[3], which was carried on agar[4], subcultured at least bimonthly, and transferred to a broth[4] for the preparation of the inoculum. The inoculum was a 1:20 suspension of the washed organism in normal saline. The riboflavin assay medium[4] was supplemented with the minimal amount of riboflavin[5] (0.03 μg/ml in the final system) required for optimal organism growth. The assay was incubated at 37° for 19 hr, after which growth was terminated by immersion of the assay tubes in boiling water for 10 min. The extent of growth was determined turbidimetrically on a Klett–Summerson colorimeter equipped with a red filter (660 nm). The details of the assay were described previously (1).

RESULTS AND DISCUSSION

The results of the inhibition studies of 27 benzoyl derivatives of amino acids and amino acid analogs containing graded amounts of the test compounds (up to 1 mg/ml final concentration) are shown in Table II. Of these, 19 showed some growth inhibition. The degree of inhibition ranged from a modest 13–33% for *N*-benzoyl derivatives of DL-allylglycine, β-hydroxy-DL-norleucine A and B, L-leucine, L- and DL-methionines, DL-norleucine, DL-norvaline, L-phenylalanine, L-tyrosine ethyl ester, and L-valine to a potent 89–96% inhibition for the benzoyl derivatives of *p*-chloro-DL-phenylalanine and *m*-fluoro-DL-phenylalanine. Intermediate inhibition was observed with other benzoyl derivatives, such as those of *o*-fluoro-DL-phenylalanine, *p*-fluoro-DL-phenylalanine, *p*-nitro-L-phenylalanine, β-2-thienyl-DL-alanine, β-3-thienyl-DL-alanine, and L-tryptophan.

The activity of the "modest" inhibitor observed in these experiments was comparable to that observed for most of the active chloroacetyl and trifluoroacetyl derivatives (2, 3). The "appreciable" inhibitory activity was considerably better than for most of the "active"compounds reported previously, being as active as *N*-chloroacetyl-β-hydroxy-D-norleucine B, the most active compound reported previously in this series (9). The activities of benzoyl-*p*-chloro-DL-phenylalanine and benzoyl-*m*-fluoro-DL-phenylalanine were the most pronounced yet observed based on the activity at 1 mg/ml, the concentration limit set in the protocol (12) to determine the positivity of the test compounds. Hence, five benzoyl compounds reported here (the benzoyl derivatives of *p*-chloro-DL-phenylalanine, *o*-fluoro-DL-phenylalanine, *m*-fluoro-DL-phenylalanine, *p*-nitro-L-phenylalanine, and L-tryptophan) meet the criterion of positivity. Further tests of these compounds in mammalian tumor systems are indicated.

The compounds showing little or no activity were not restricted to the benzoyl derivatives of nonessential amino acids since, in addition to the benzoyl derivatives of L-alanine, L-aspartic acid, L-glutamic acid, and glycine, those of L-arginine, L-histidine, L-lysine, and L-threonine also were inactive. With the exception of benzoyl-L-tyrosine ethyl ester, however, the active compounds were benzoyl derivatives of essential amino acids or of essential amino acid analogs.

When the 19 active compounds were compared on an equimolar basis (Table III), the more active ones were the benzoyl derivatives of phenylalanine analogs and the less active ones were derivatives of the alicyclic essential amino acid analogs. Benzoyl-L-phenylalanine and benzoyl-DL-norleucine were exceptions in that the former was somewhat less active and the latter was somewhat more active than other compounds of their respective groups. The degree of inhibition by the benzoyl alicyclic amino acids and analogs was approximately that noted for the chloroacetyl and trifluoroacetyl amino acids (2, 3). However, the degree of inhibition exhibited by the benzoyl derivatives of phenylalanine analogs was much greater than any inhibition noted previously with the *N*-acylated compounds. These results suggest that a number of other ring-substituted benzoyl derivatives should be tested, and such studies are now in progress.

Table II—Effect of N^{α}-Benzoyl Derivatives of Amino Acids and Amino Acid Analogs on Growth of *L. casei* 7469 [a]

N^{α}-Benzoyl Derivative	Concentration at 1 mg/ml, m*M*	Inhibition[b], % 0.1 mg/ml[c]	0.5 mg/ml[c]	1.0 mg/ml[c]
L-Alanine	5.12	0	2	8
DL-Allylglycine	4.56	2	8	15
L-Arginine (α-mono)	4.60	+3	+1	6
L-Aspartic acid	3.92	1	2	1
p-Chloro-DL-phenylalanine	3.29	6	60	89
o-Fluoro-DL-phenylalanine	3.48	5	21	50
m-Fluoro-DL-phenylalanine	3.48	7	84	96
p-Fluoro-DL-phenylalanine	3.48	5	23	46
L-Glutamic acid	3.84	+2	1	+5
Glycine	5.58	1	4	8
L-Histidine	3.61	+3	3	8
β-Hydroxy-DL-norleucine A	3.98	3	7	23
β-Hydroxy-DL-norleucine B	3.98	6	9	17
L-Leucine	4.25	2	13	26
L-Lysine (α-mono)	4.00	1	2	1
DL-Methionine	3.93	2	8	23
L-Methionine	3.93	2	10	16
p-Nitro-L-phenylalanine	3.18	4	28	56
DL-Norleucine	4.25	4	14	33
DL-Norvaline	4.52	2	7	14
L-Phenylalanine	3.59	2	14	29
β-2-Thienyl-DL-alanine	3.63	8	23	44
β-3-Thienyl-DL-alanine	3.52	6	22	41
L-Threonine	4.48	2	0	6
L-Tryptophan	3.15	5	28	53
L-Tyrosine ethyl ester	3.19	0	5	16
L-Valine	4.52	0	8	13
Benzoic acid[d]	8.19	3	6	9

[a] For details of assay, see Ref. 1. [b] Turbidity readings of the inoculated control tubes (containing no test compound) were 168–188 Klett units. At least three duplicate determinations were made for each compound. The duplicate values in each determination agreed within ±5 Klett units. The standard deviation of a compound showing a mean value of ~20% inhibition, for example, was 2.7 and the standard error was 0.95. The + indicates stimulation of growth but was considered insignificant. [c] Final concentration in assay system. [d] Free acid.

It is difficult to propose a mechanism of inhibitory action from these experiments. However, hydrolytic release of the constituent benzoic acid and the parent amino acid appears unlikely as a cause of inhibition in view of the findings that: (*a*) benzoic acid itself was innocuous in this system (Table II), (*b*) a mole equivalent of the free parent amino acid in this system under identical conditions exhibited less inhibition than the benzoyl compounds (2), (*c*) no free amino nitrogen was detectable in the test solution, indicating that no hydrolysis occurred during preparation of the solution, and (*d*) there was no detectable increase in the amount of amino nitrogen after the assay (2). Nevertheless, the possibility that the inhibition could be due to the membrane permeability of the benzoylated derivatives and an intracellular hydrolysis of the derivatives to free benzoic acid and the amino acid moiety is not excluded. Since not all benzoyl derivatives tested were inhibitory, intracellular hydrolysis seems an unlikely explanation unless the acylases involved exhibited specificity only to certain benzoyl amino acids.

Although the initial design of the test compounds was directed to an increase in lipophilic character, the present experiment, which was conducted solely to note inhibitory capacities, did not investigate the mechanism of action, and no attempt was made to correlate the lipophilic character with the inhibitory activity. A study of the mechanism of action requires a more sophisticated system and should include an investigation of such properties as relative lipid solubility, partition coefficients, and coacervation distribution values.

The similarity of inhibition shown by the *N*-benzoylated alicyclic amino acids with the *N*-chloroacetyl and *N*-trifluoroacetyl amino acids, which showed ~25% inhibition (2, 3), and the marked inhibition shown by the *N*-benzoylated phenylalanine analogs indicate that the mecha-

[1] Morton bacteriological filters, ultrafine porosity, Arthur H. Thomas Co., Philadelphia, Pa.

[2] The diastereomeric forms are arbitrarily referred to as Isomers A and B, the former moving faster and the latter slower when chromatographed on paper using methyl ethyl ketone–*n*-butanol–ammonia–water (3:5:1:1), ascending.

[3] American Type Culture Collection, Rockville, Md.

[4] Micro assay culture agar (Difco B319), micro inoculum broth (Difco B320), and riboflavin assay medium (Difco B325), Difco Laboratories, Detroit, Mich.

[5] Calbiochem, La Jolla, Calif.

Table III—Comparison of Effect of Equimolar Concentrations of *N*-Benzoyl Amino Acids and Amino Acid Analogs on Growth of *L. casei* 7469 [a]

N-Benzoyl Derivative	Inhibition [b], %
DL-Allylglycine	17
p-Chloro-DL-phenylalanine	94
o-Fluoro-DL-phenylalanine	82
m-Fluoro-DL-phenylalanine	97
p-Fluoro-DL-phenylalanine	72
β-Hydroxy-DL-norleucine A	14
β-Hydroxy-DL-norleucine B	22
L-Leucine	23
DL-Methionine	20
L-Methionine	18
p-Nitro-L-phenylalanine	78
DL-Norleucine	47
DL-Norvaline	13
L-Phenylalanine	39
β-2-Thienyl-DL-alanine	76
β-3-Thienyl-DL-alanine	56
L-Tryptophan	74
L-Tyrosine ethyl ester	26
L-Valine	16

[a] Maximum growth in inoculated control tube (containing no test compound) was 166–173 Klett units. For explanation of extent of variation of values, see footnote to Table II. [b] Concentration was 4.47 μmoles/ml and was the final concentration in the assay system. For details of assay, see Ref. 1.

nisms of inhibition of these compounds could be dissimilar. Certain tumor systems, as well as bacterial and mammalian asparaginase and glutamine synthetase, are inhibited by carbobenzoxy, phenacetyl, and phenylpropionyl amino acids (13–15).

Most compounds exhibiting notable inhibitory activity in the present studies were benzoyl derivatives of phenylalanine analogs. Therefore, it will be interesting to test the activity of these compounds against melanomas, wherein the phenylalanine metabolism is believed to be intimately involved. In view of the effect of similar compounds on mammalian tumor systems and certain isolated enzyme systems (13–15), the study of the activity of the compounds in asparaginase-sensitive tumors is also indicated.

REFERENCES

(1) T. T. Otani, *Cancer Chemother. Rep.*, **38**, 25 (1964).

(2) T. T. Otani and M. R. Briley, *J. Pharm. Sci.*, **67**, 520 (1978).

(3) *Ibid.*, **68**, 496 (1979).

(4) M. D. Armstrong and J. D. Lewis, *J. Biol. Chem.* **188**, 91 (1951).

(5) V. du Vigneaud, H. McKennish, Jr., S. Simmonds, K. Dittmer, and G. B. Brown, *ibid.*, **159**, 385 (1945).

(6) R. G. Garst, E. Campaigne, and H. G. Day, *ibid.*, **180**, 1013 (1949).

(7) M. F. Ferger and V. du Vigneaud, *ibid.*, **179**, 61 (1949).

(8) T. T. Otani and M. Winitz, *Arch. Biochem. Biophys.*, **102**, 464 (1963).

(9) T. T. Otani and M. R. Briley, *J. Pharm. Sci.*, **65**, 534 (1976).

(10) J. P. Greenstein and M. Winitz, in "Chemistry of the Amino Acids," Wiley, New York, N.Y., 1961.

(11) D. D. Van Slyke, *J. Biol. Chem.*, **83**, 425 (1929).

(12) G. E. Foley, R. E. McCarthy, V. M. Binns, E. E. Snell, B. M. Guirard, G. W. Kidder, V. C. Dewey, and P. S. Thayer, *Ann. N. Y. Acad. Sci.*, **76**, 413 (1958).

(13) N. Lustig, H. Spiegelstein-Klarfeld, E. Schneider, and N. Lichenstein, *Isr. J. Chem.*, **12**, 757 (1974).

(14) H. Spiegelstein-Klarfeld, N. Lustig, and N. Lichenstein, *Experientia*, **30**, 1233 (1974).

(15) N. Lichenstein, N. Grossowicz, and M. Schlesinger, *Isr. J. Med. Sci.*, **13**, 316 (1977).

Degradation Kinetics of a New Cephalosporin Derivative in Aqueous Solution

ELISABETH S. RATTIE *, JAMES J. ZIMMERMAN ‡, and LOUIS J. RAVIN *x

Received December 8, 1978, from the **Research and Development Division, Smith Kline and French Laboratories, Philadelphia, PA 19101,* and the ‡*Department of Pharmaceutics, School of Pharmacy, Temple University, Philadelphia, PA 19140.* Accepted for publication May 8, 1979.

Abstract □ The degradation kinetics of a new cephalosporin derivative (I) in aqueous solution were investigated at 60°, $\mu = 0.5$, at pH 2.0–10.0. The observed degradation rates followed pseudo-first-order kinetics and were influenced significantly by H_2O and OH^- catalysis. No primary salt effect was observed in the acid region, but a positive salt effect was observed at pH 9.4. A general base catalytic effect by a phosphate buffer species was observed at pH 7–8. The pH–rate profile for I exhibited a degradation minimum at pH 6.05. The Arrhenius activation energies determined at pH 4.0 and 9.4 were 27.2 and 24.5 kcal/mole, respectively. Excellent agreement between the theoretical pH–rate profile and the experimental data supported the hypothesized degradation process. A comparison of I and cefazolin revealed close structural and stability analogies.

Keyphrases □ Cephalosporins—derivatives, degradation kinetics, aqueous solution, compared to cefazolin □ Antibacterial agents—cephalosporin derivatives, degradation kinetics, aqueous solution, compared to cefazolin □ Pharmacokinetics—cephalosporin derivatives, degradation, aqueous solutions, compared to cefazolin

Yamana and Tsuji (1) reported the comparative stability of several commercially available cephalosporin derivatives including those with an α-amino group in their side chain (*e.g.*, cephalexin, cephradine, and cephaloglycin) and those lacking the side-chain α-amino group (*e.g.*, cephalothin, cephaloridine, and cefazolin). Cephalosporins possessing the α-amino group may be administered orally, and cephalexin and cephradine have the highest stability of the derivatives investigated. Cephalosporins lacking the α-amino group are not administered orally, and cefazolin in particular is very unstable in the acid pH region.

This report describes the stability kinetics of a new cephalosporin derivative, 3-[2-(5-methyl-1,3,4-thiadiazyl)mercaptomethyl]-7-[D-(−)-mandelamido]-3-cephem-4-carboxylic acid sodium salt (I) (Table I). Of the cephalosporin derivatives previously investigated (1), I most closely resembles cefazolin. These two compounds have the same R_2 group but different R_1 groups. The continued investigation of cefazolin-like derivatives appears to be warranted in view of the clinical advantages of cefazolin over other cephalosporins (2).

BACKGROUND

As a result of previous studies (1, 3), the following conclusions may be

0022-3549/79/1100-1369$01.00/0

© 1979, American Pharmaceutical Association

Table III—Comparison of Effect of Equimolar Concentrations of *N*-Benzoyl Amino Acids and Amino Acid Analogs on Growth of *L. casei* 7469 [a]

N-Benzoyl Derivative	Inhibition [b], %
DL-Allylglycine	17
p-Chloro-DL-phenylalanine	94
o-Fluoro-DL-phenylalanine	82
m-Fluoro-DL-phenylalanine	97
p-Fluoro-DL-phenylalanine	72
β-Hydroxy-DL-norleucine A	14
β-Hydroxy-DL-norleucine B	22
L-Leucine	23
DL-Methionine	20
L-Methionine	18
p-Nitro-L-phenylalanine	78
DL-Norleucine	47
DL-Norvaline	13
L-Phenylalanine	39
β-2-Thienyl-DL-alanine	76
β-3-Thienyl-DL-alanine	56
L-Tryptophan	74
L-Tyrosine ethyl ester	26
L-Valine	16

[a] Maximum growth in inoculated control tube (containing no test compound) was 166–173 Klett units. For explanation of extent of variation of values, see footnote to Table II. [b] Concentration was 4.47 μmoles/ml and was the final concentration in the assay system. For details of assay, see Ref. 1.

nisms of inhibition of these compounds could be dissimilar. Certain tumor systems, as well as bacterial and mammalian asparaginase and glutamine synthetase, are inhibited by carbobenzoxy, phenacetyl, and phenylpropionyl amino acids (13–15).

Most compounds exhibiting notable inhibitory activity in the present studies were benzoyl derivatives of phenylalanine analogs. Therefore, it will be interesting to test the activity of these compounds against melanomas, wherein the phenylalanine metabolism is believed to be intimately involved. In view of the effect of similar compounds on mammalian tumor systems and certain isolated enzyme systems (13–15), the study of the activity of the compounds in asparaginase-sensitive tumors is also indicated.

REFERENCES

(1) T. T. Otani, *Cancer Chemother. Rep.*, **38**, 25 (1964).

(2) T. T. Otani and M. R. Briley, *J. Pharm. Sci.*, **67**, 520 (1978).

(3) *Ibid.*, **68**, 496 (1979).

(4) M. D. Armstrong and J. D. Lewis, *J. Biol. Chem.* **188**, 91 (1951).

(5) V. du Vigneaud, H. McKennish, Jr., S. Simmonds, K. Dittmer, and G. B. Brown, *ibid.*, **159**, 385 (1945).

(6) R. G. Garst, E. Campaigne, and H. G. Day, *ibid.*, **180**, 1013 (1949).

(7) M. F. Ferger and V. du Vigneaud, *ibid.*, **179**, 61 (1949).

(8) T. T. Otani and M. Winitz, *Arch. Biochem. Biophys.*, **102**, 464 (1963).

(9) T. T. Otani and M. R. Briley, *J. Pharm. Sci.*, **65**, 534 (1976).

(10) J. P. Greenstein and M. Winitz, in "Chemistry of the Amino Acids," Wiley, New York, N.Y., 1961.

(11) D. D. Van Slyke, *J. Biol. Chem.*, **83**, 425 (1929).

(12) G. E. Foley, R. E. McCarthy, V. M. Binns, E. E. Snell, B. M. Guirard, G. W. Kidder, V. C. Dewey, and P. S. Thayer, *Ann. N. Y. Acad. Sci.*, **76**, 413 (1958).

(13) N. Lustig, H. Spiegelstein-Klarfeld, E. Schneider, and N. Lichenstein, *Isr. J. Chem.*, **12**, 757 (1974).

(14) H. Spiegelstein-Klarfeld, N. Lustig, and N. Lichenstein, *Experientia*, **30**, 1233 (1974).

(15) N. Lichenstein, N. Grossowicz, and M. Schlesinger, *Isr. J. Med. Sci.*, **13**, 316 (1977).

Degradation Kinetics of a New Cephalosporin Derivative in Aqueous Solution

ELISABETH S. RATTIE *, JAMES J. ZIMMERMAN ‡, and LOUIS J. RAVIN *x

Received December 8, 1978, from the **Research and Development Division, Smith Kline and French Laboratories, Philadelphia, PA 19101,* and the ‡*Department of Pharmaceutics, School of Pharmacy, Temple University, Philadelphia, PA 19140.* Accepted for publication May 8, 1979.

Abstract □ The degradation kinetics of a new cephalosporin derivative (I) in aqueous solution were investigated at 60°, $\mu = 0.5$, at pH 2.0–10.0. The observed degradation rates followed pseudo-first-order kinetics and were influenced significantly by H_2O and OH^- catalysis. No primary salt effect was observed in the acid region, but a positive salt effect was observed at pH 9.4. A general base catalytic effect by a phosphate buffer species was observed at pH 7–8. The pH–rate profile for I exhibited a degradation minimum at pH 6.05. The Arrhenius activation energies determined at pH 4.0 and 9.4 were 27.2 and 24.5 kcal/mole, respectively. Excellent agreement between the theoretical pH–rate profile and the experimental data supported the hypothesized degradation process. A comparison of I and cefazolin revealed close structural and stability analogies.

Keyphrases □ Cephalosporins—derivatives, degradation kinetics, aqueous solution, compared to cefazolin □ Antibacterial agents—cephalosporin derivatives, degradation kinetics, aqueous solution, compared to cefazolin □ Pharmacokinetics—cephalosporin derivatives, degradation, aqueous solutions, compared to cefazolin

Yamana and Tsuji (1) reported the comparative stability of several commercially available cephalosporin derivatives including those with an α-amino group in their side chain (*e.g.*, cephalexin, cephradine, and cephaloglycin) and those lacking the side-chain α-amino group (*e.g.*, cephalothin, cephaloridine, and cefazolin). Cephalosporins possessing the α-amino group may be administered orally, and cephalexin and cephradine have the highest stability of the derivatives investigated. Cephalosporins lacking the α-amino group are not administered orally, and cefazolin in particular is very unstable in the acid pH region.

This report describes the stability kinetics of a new cephalosporin derivative, 3-[2-(5-methyl-1,3,4-thiadiazyl)mercaptomethyl]-7-[D-(−)-mandelamido]-3-cephem-4-carboxylic acid sodium salt (I) (Table I). Of the cephalosporin derivatives previously investigated (1), I most closely resembles cefazolin. These two compounds have the same R_2 group but different R_1 groups. The continued investigation of cefazolin-like derivatives appears to be warranted in view of the clinical advantages of cefazolin over other cephalosporins (2).

BACKGROUND

As a result of previous studies (1, 3), the following conclusions may be

0022-3549/79/1100-1369$01.00/0

© 1979, American Pharmaceutical Association

Table I—Structural Comparisons between I and Cefazolin

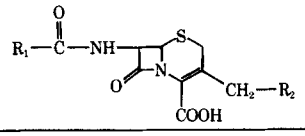

Cephalosporin	Substituents R_1	Substituents R_2	pKa
I	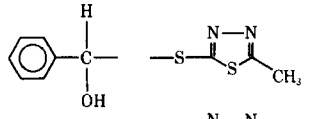		2.50[a]
Cefazolin	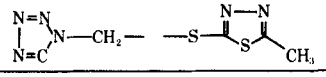		1.70, 2.54[b], 2.38[c]

[a] The pKa was determined spectrophotometrically and apparently refers to the carboxylic acid group (present study). [b] The pKa of 1.70 was determined kinetically and apparently refers to the thiadiazole moiety; pKa 2.54 was determined potentiometrically and refers to the carboxylic acid group (Ref. 1). [c] The pKa of 2.38 was determined potentiometrically at 60° (Ref. 10).

offered concerning the effect of substituent changes at R_1 on degradation rates of cephalosporin derivatives at various pH values:

1. Substituent changes at R_1 appear to have little effect on the rate constants for H^+- and OH^--catalyzed hydrolysis. Cephalothin and cephaloglycin with identical R_2 groups but different R_1 groups have nearly identical rate constants for H^+ and OH^- catalysis (1).

2. Substituent changes at R_1 may affect the shape of the pH profile in the neutral pH region. Thus, cephalosporins with an α-amino group at R_1 show a sharp rise in their pH profiles at pH 6.0–8.0, and they also show an inflection point at pH ~8.0 (1).

Furthermore, a comparison of the rate constants for substituted phenylcephalosporins reveals a 3.2-fold range in the rate constants for spontaneous hydrolysis. A similar comparison for the two phenyldeacetylcephalosporin derivatives shows no such change. In view of these structure–activity relationships, the effect, if any, of structural change at R_1 in I would be expected to appear in the neutral pH region.

EXPERIMENTAL

Materials—Compound I[1] was purified from acetic acid–water. All other chemicals were reagent grade. The water used for buffers was freshly distilled from a stainless steel still[2].

Buffer Solutions—The following buffers were used in the kinetic studies: hydrochloric acid–potassium chloride[3] (pH 2.0), citrate buffer (pH 3.0, 4.0, 5.0, and 5.5), phosphate buffer (pH 6.0, 6.5, 7.0, 7.5, and 8.0), and carbonate buffer (pH 9.4 and 10.0). They were freshly prepared by dissolving hydrochloric acid, citric acid, monobasic sodium phosphate, or sodium bicarbonate together with potassium chloride in distilled water and adjusting the pH with drops of concentrated sodium hydroxide. The pH readings were made using a research pH meter[4] equipped with a combination electrode[5].

The buffers were 0.1 *M* with respect to hydrochloric acid and citrate, phosphate, and carbonate ions (except when a buffer effect was investigated) and were adjusted to an ionic strength of 0.5 with potassium chloride except when primary salt effects were investigated.

Kinetic Procedure—Approximately 200 mg of I was accurately weighed and dissolved in 200 ml of appropriate buffer, which had been heated to 60° to produce a 1.99×10^{-3} *M* concentration. At this temperature, degradation proceeded at a rate convenient for analysis. The flasks were kept at 60° in a constant-temperature oil bath with a precision of ±0.1°[6].

Two 10-ml samples were withdrawn at appropriate intervals, which had been determined after preliminary studies. The samples were cooled in an ice bath and analyzed.

Analytical Procedure—Residual intact I was determined iodometrically using a procedure similar to that of Finholt *et al.* (4) for penicillin G. From the reaction solutions, two 10-ml samples, A and B, were pipetted into separate 125-ml erlenmeyer flasks. To A, 5 ml of 1 *N* NaOH was added. After the sample stood 15 min at room temperature, 5 ml of 1 *N* HCl, 20 ml of acetate buffer [35% (w/v) sodium acetate; 42.4% (v/v) acetic acid], and 25 ml of 0.02 *N* iodine[7] were added. To B, 20 ml of acetate buffer and 25 ml of 0.02 *N* iodine were added.

The flasks were stoppered and kept in darkness for 3.5 hr at room temperature. The excess iodine in both samples was then titrated with 0.025 *N* sodium thiosulfate using Thyodene as an indicator[8]. The difference between the two titration values gave the amount of iodine equivalent to the amount of I present. The iodine equivalence for I was calculated to be 12, and each milliliter of 0.02 *N* iodine was equivalent to 5.2 mg of I.

pKa Determination at 60°—The pKa of I was determined spectrophotometrically (5) using a spectrophotometer[9] with a thermostatically controlled cell compartment. Compound I was dissolved sequentially in a series of buffer solutions to a concentration of 0.08 mg/ml, and spectra were obtained between 240 and 400 nm. The buffers were: 0.1 *N* HCl; 0.1 *M* chloroacetic acid adjusted to pH 2.2, 2.4, 2.8, and 3.2; 0.1 *M* formic acid adjusted to pH 4.4; and 0.1 *M* phosphoric acid adjusted to pH 6.0. The adjustments were made with 0.1 *N* KOH at 60° on a research pH meter. Each solution of I yielded λ_{max} = 268 nm with an isosbestic point at 292 nm. Equation 1 was used to estimate a pKa = 2.50 for I at 268 nm:

$$\text{pKa} = \text{pH} + \log [(d_I - d)/(d - d_M)] \qquad \text{(Eq. 1)}$$

where d_I is the ionized species absorbance at pH 6.0, d_M is the nonionized species absorbance at pH 1.0, and d is the absorbance at intermediate pH.

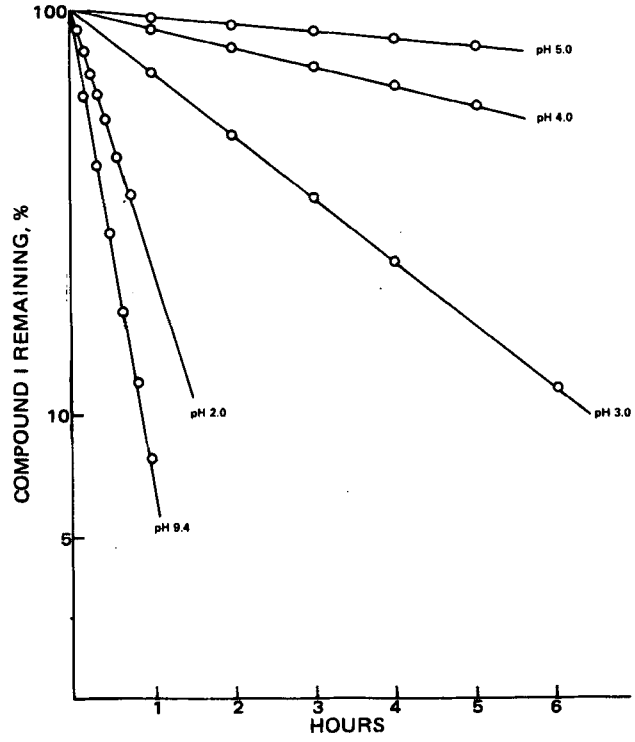

Figure 1—*Pseudo-first-order plots for the degradation of I at various pH values, 60°, and* $\mu \doteq 0.5$.

RESULTS AND DISCUSSION

Reaction Order and Observed Rate Constants—The degradation of I followed pseudo-first-order kinetics at constant pH, temperature, and ionic strength at pH 2.0–10.0. This result is shown by the linear log concentration *versus* time plots at 60° in Fig. 1. The pseudo-first-order rate constants, k_{obs}, for each pH value are given in Table II together with associated buffer species fractions, f. The number of half-lives over which the data were collected was 1–5 × $t_{1/2}$, depending on the pH.

[1] SK&F Laboratories, Philadelphia, Pa.
[2] Barnstead.
[3] The hydrochloric acid–potassium chloride buffer contained 5% *N,N*-dimethylacetamide to solubilize I below pH 3.0.
[4] Beckman Instruments.
[5] Fisher Scientific Co.
[6] Philadelphia Roto-Stat.
[7] Iodine, 0.1 *N*, Harleco.
[8] Standards were freshly prepared by appropriate dilution before each study.
[9] Cary model 15.

Table II—Observed Rate Constants for Degradation of I and Buffer Species Fractions, *f*, at 60° and $\mu = 0.5$

pH	Buffer System[a,b]	Species Fractions						k_{obs}, $min^{-1} \times 10^3$
		f_{H_3A}	$f_{H_2A^-}$	$f_{HA^{2-}}$	$f_{A^{3-}}$	f_{HA^-}	$f_{A^{2-}}$	
2.0	HCl/KCl	—	—	—	—	—	—	24.01
3.0	Citrate	0.333	0.635	0.032	—	—	—	5.96
4.0	Citrate	0.033	0.637	0.319	0.011	—	—	1.77
5.0	Citrate	—	0.130	0.650	0.220	—	—	0.647
5.5	Citrate	—	0.030	0.468	0.502	—	—	0.623
6.0	Phosphate	—	0.776	0.224	—	—	—	0.606
6.5	Phosphate	—	0.523	0.477	—	—	—	0.626
7.0	Phosphate	—	0.257	0.743	—	—	—	0.749
7.5	Phosphate	—	0.099	0.901	—	—	—	1.43
8.0	Phosphate	—	0.034	0.966	—	—	—	2.22
9.4	Carbonate	—	—	—	—	0.876	0.124	35.5
10.0	Carbonate	—	—	—	—	0.640	0.360	114.2

[a] The ionization constants for the citrate and phosphate buffers at 60° and $\mu = 0.5$ are from Ref. 4. For citric acid and citrate ions, $pK_1 = 2.72$, $pK_2 = 4.30$, and $pK_3 = 5.47$. For dihydrogen phosphate ion, $pK_2 = 6.54$. The ionization constant for bicarbonate ion at 60° and $\mu = 0.5$ is $pK_2 = 10.25$ from Ref. 11. [b] Buffer species fractions were calculated according to Ref. 12.

General Acid–Base Catalysis—The catalytic effects of buffer species for the citrate, phosphate, and carbonate buffers were investigated at constant pH, temperature, and ionic strength in solutions containing 1 mg of I/ml. For each buffer system, the rate constant, k_{obs}, was determined experimentally as a function of buffer concentrations of 0.05–0.2 *M*. The observed rate constants and corresponding buffer concentrations are given in Table III.

The results in Table III indicate that k_{obs} is independent of citrate buffer concentration at pH 3 and 4. Since the dominant citrate species in solution at these pH values are H_3A, H_2A^-, and HA^{2-} (Table I), these species may be disregarded as general acid–base catalysts. The citrate buffer effect was not investigated at pH 5.5, where the dominant species are HA^{2-} and A^{3-}, but A^{3-} also may be disregarded as a catalyst because of the close fit obtained for the pH–rate profile without it.

Figure 2 illustrates the variable effect of phosphate buffers on the degradation of I at pH 6.0–8.0. Based on Tables II and III, it is apparent that $H_2PO_4^-$ is the dominant species in solution at pH 6, where the rate constant is independent of buffer concentration, while HPO_4^{2-} is the dominant species in solution at pH 7.0 and 7.5, where the rate constant is increasingly dependent on buffer concentrations. These trends suggest that HPO_4^{2-} is a general base catalyst within the phosphate buffer region. An attempt to estimate the rate constant, $k_{HPO_4^{2-}}$, for the catalytic effect was based on:

$$k_{obs} = k_0 + k''[P] \qquad \text{(Eq. 2)}$$

where k_0 is the rate constant at zero buffer concentration, $[P]$ is the total buffer concentration, and:

$$k'' = (k_{HPO_4^{2-}})(f_{HPO_4^{2-}}) \qquad \text{(Eq. 3)}$$

where $f_{HPO_4^{2-}} = K_2/(a_{H^+} + K_2)$.

Table III—Effect of Buffer Concentration on the Pseudo-First-Order Rate Constants for I Degradation at 60° and $\mu = 0.5$

pH (Buffer)	k_{obs}, $min^{-1} \times 10^3$			
	0.05 *M*	0.10 *M*	0.15 *M*	0.20 *M*
3.0 (citrate)	6.43	5.96	—	6.00
4.0 (citrate)	1.80	1.77	1.73	—
6.0 (phosphate)	0.594	0.606	—	0.598
6.5 (phosphate)	0.686	0.626	—	0.643
7.0 (phosphate)	0.724	0.749	—	0.790
7.5 (phosphate)	1.18	1.43	—	1.92
8.0 (phosphate)	1.68	2.22	2.61	—
9.4 (carbonate)	—	35.5	35.7	37.8

Table IV—Values of k_0 and k'' Estimated from Eq. 3

pH	k_0, $min^{-1} \times 10^{3a}$	k'', $M^{-1}\ min^{-1} \times 10^{3b}$
6.0	0.599	—
6.5	0.626	—
7.0	0.703	0.437
7.5	0.932	4.97
8.0	1.48	9.28

[a] $k_0 = k_{obs}$ independent of buffer effects. [b] k'' = second-order rate constant for buffer effects.

Equation 3 predicts a zero intercept when k'' (Table IV) is plotted against $f_{HPO_4^{2-}}$ (Table II), but a plot of the appropriate values for these constants yielded a relatively large negative intercept ($-2.783 \times 10^{-2}\ M^{-1}\ min^{-1}$), which was significantly different from zero at the 80% confidence level. Furthermore, k'' should vary to the same extent as $f_{HPO_4^{2-}}$ when the pH is varied. This was not the case since the relative k'' values were 1, 11.4, and 21.2 at pH 7.0, 7.5, and 8.0, respectively, while the relative $f_{HPO_4^{2-}}$ values were 1.0, 1.2, and 1.3. Either HPO_4^{2-} is not the sole contributing catalytic species or its activity is far greater than predicted from its pKa.

Table III further indicates that k_{obs} is independent of the carbonate buffer concentration at pH 9.4. At this pH, HCO_3^- is the dominant species in solution (Table II) and may, therefore, be excluded as a general base catalyst.

Primary Salt Effect—The primary salt effect on the hydrolysis of I was studied at constant pH and temperature, but the ionic strength was varied with potassium chloride addition. Studies were conducted at pH 4.0 and 9.4 where general base catalysis was absent and secondary salt effects would be unimportant. The data at these pH values for ionic strength, μ, 0.3–1.0 are given in Table V.

Within restricted ranges of μ, plots of log k_{obs} *versus* $\sqrt{\mu}$ *or* $\sqrt{\mu}/(1 + \sqrt{\mu})$ should yield theoretical slopes equal to $2AZ_AZ_B$, where A is a constant for the solvent at a given temperature and Z_A and Z_B are the charges on reaction species A and B, respectively (6). While such plots would be expected to be linear only within limits of the Debye–Huckel expressions, Carstensen (7) recently reviewed kinetic salt effects in the pharmaceutical literature to show that plots utilizing $\sqrt{\mu}$ or $\sqrt{\mu}/(1 + \sqrt{\mu})$ may be linear with ionic strength ≥ 1.0. This author pointed out that the use of $\sqrt{\mu}/(1 + \sqrt{\mu})$ instead of $\sqrt{\mu}$ at higher ionic strengths more fre-

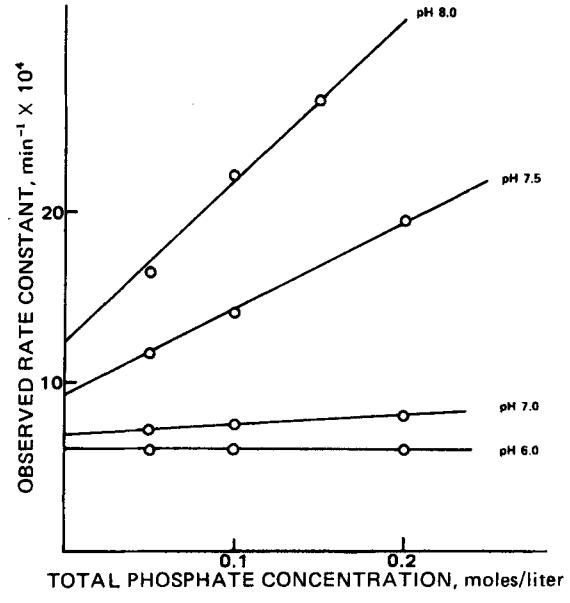

Figure 2—*Plots of* k_{obs} versus *the total phosphate buffer concentration for the degradation of I at various pH values, 60°, and* $\mu = 0.5$.

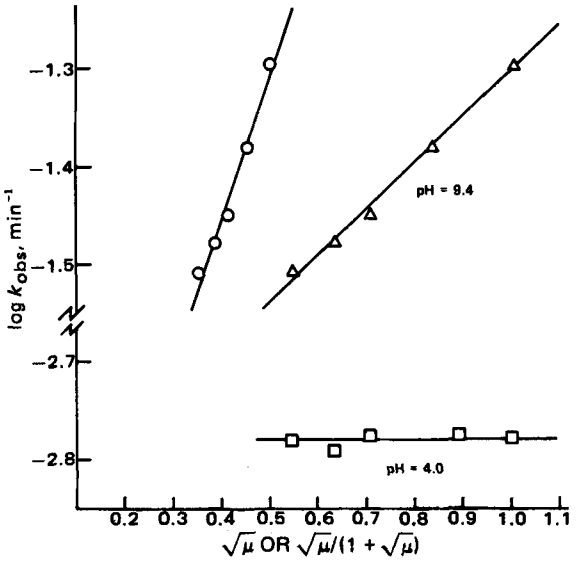

Figure 3—*Plots of log* k_{obs} versus $\sqrt{\mu}$ (△ *and* □) *or* $\sqrt{\mu}/(1+\sqrt{\mu})$ (○) *for the degradation of I at 60° and pH 4.0 and 9.4.*

quently produces values of $2AZ_AZ_B$ that are in agreement with theoretical values.

The data from Table V were used in preparing plots of log k_{obs} *versus* $\sqrt{\mu}$ and $\sqrt{\mu}/(1+\sqrt{\mu})$ in Fig. 3. A larger positive kinetic salt effect was obtained at pH 9.4 when the data were plotted with $\sqrt{\mu}/(1+\sqrt{\mu})$ than with $\sqrt{\mu}$, for which the slopes were 1.47 and 0.48, respectively. This result can be used as evidence for the reaction between two negatively charged species. By contrast, a kinetic salt effect was not observed at pH 4.0 (Fig. 3), and this result requires that at least one reactant be noncharged.

pH–Rate Profile—Values of log k_0 (*i.e.*, log k_{obs} independent of buffer effects) were plotted *versus* pH to yield the pH–rate profile for I (Fig. 4). In the absence of general base and intramolecular catalyses, the following specific acid–base reactions can be written for the hydrolysis of I, where HC stands for the nonionized form and C^- represents the ionized form:

$$HC + H^+ \xrightarrow{k_1} \text{products}$$
Scheme I

$$HC + H_2O \xrightarrow{k_2} \text{products}$$
Scheme II

$$HC + OH^- \xrightarrow{k_3} \text{products}$$
Scheme III

$$C^- + H^+ \xrightarrow{k_4} \text{products}$$
Scheme IV

$$C^- + H_2O \xrightarrow{k_5} \text{products}$$
Scheme V

$$C^- + OH^- \xrightarrow{k_6} \text{products}$$
Scheme VI

Of these reactions, Schemes II, V, and VI are sufficient to yield an excellent fit to the data as shown by the theoretical solid line in Fig. 4. The rate expressions associated with these reactions, expressed in terms of the total I concentration, [*a*], are:

$$-d[HC]/dt = k'_2 f_{HC}[a] \quad \text{(Eq. 4)}$$

$$-d[C^-]/dt = k'_5 f_{C^-}[a] \quad \text{(Eq. 5)}$$

$$d[C^-]/dt = k_6[OH^-]f_{C^-}[a] \quad \text{(Eq. 6)}$$

where $f_{HC} = a_{H^+}/(a_{H^+} + K_a)$, $f_{C^-} = K_a/(a_{H^+} + K_a)$, $k'_2 = k_2[H_2O]$, and $k'_5 = k_5[H_2O]$.

The overall rate is given as a sum of these reactions as expressed by:

$$-d[a]/dt = k_0[a] \quad \text{(Eq. 7)}$$

where:

$$k_0 = k'_2 f_{HC} + k'_5 f_{C^-} + k_6[OH^-]f_{C^-} \quad \text{(Eq. 8)}$$

Table V—Effect of Ionic Strength (μ) on Pseudo-First-Order Rate Constants for I Degradation at pH 4.0 and 9.4

μ	k_{obs}, min^{-1} × 10^3 pH 4.0	pH 9.4
0.3	1.66	31.1
0.4	1.62	33.3
0.5	1.79	35.5
0.7	—	41.6
0.8	1.80	—
1.0	1.71	50.7

Schemes II, V, and VI are compatible with the results of the ionic strength analysis. Thus, Scheme VI requires a positive kinetic salt effect (Fig. 3, pH 9.4) while Schemes II and V require a zero kinetic salt effect (Fig. 3, pH 4.0). The experimental slope of 1.47 at pH 9.4, however, is not in exact agreement with the theoretical value of 1.092 (7), and this disparity is not explained. These schemes also are compatible with the experimental slope values in the various regions of the pH–rate profile. Based on the data points at pH 8.0, 9.4, and 10.0, a slope of 0.95 is obtained compared with the theoretical value of 1.0 for Scheme VI. Within the plateau region, the zero slope is in agreement with that expected theoretically for Scheme V. From the data points at pH 2.0, 3.0, and 4.0, a slope value of −0.57 is obtained, which is intermediate to the theoretical extremes of −1.0 and 0 for Scheme II alone. This result is reasonable because of the variations in f_{HC} within this pH region (Eq. 4).

The exclusion of Schemes I, III, and IV from the analysis may be rationalized as follows. Scheme I would probably contribute a much greater negative component to pH 2.5–4.5 than the actual value of −0.57 since the theoretical slope = −2.0 when $K_a > a_{H^+}$ and provided that $k_1(a_{H^+})^2 > k_2 a_{H^+}$. Scheme I also predicts a slope of −1.0 when $a_{H^+} > K_a$ (pH < 2.5), but this low pH region was not investigated because of the low solubility of I below pH 2. Scheme III is potentially compatible with the plateau effect when $K_a > a_{H^+}$, but this reaction would require the unlikely value of $k_3 \approx 10^7$ ($K_3 = k_{obs} K_a/K_{w(exp)}$). Scheme IV was rejected on the basis of the ionic strength data since this reaction would require a negative kinetic salt effect at pH 4.0.

Estimates of k'_2, k'_5, and k_6 were obtained from a simultaneous solution of k_0 (Eq. 8) at pH 2.0, 6.0, and 10. The terms f_{HC} and f_{C^-} were calculated as described with $K_a = 3.162 \times 10^{-3}$ and $[OH^-]$ calculated according to:

$$[OH^-] = a_{OH^-}/\gamma_{\pm} \quad \text{(Eq. 9a)}$$

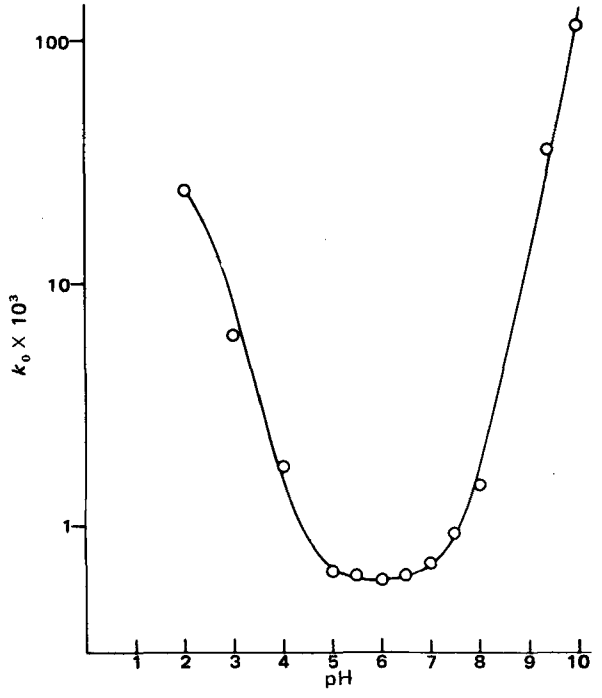

Figure 4—*Log* k_0*–pH profile for the degradation of I in aqueous solution at 60° and* $\mu = 0.5$. *The points are experimental values, and the solid line is the theoretical curve calculated from Eq. 8.*

Table VI—Rate Constants and Arrhenius Activation Parameters for I Degradation in Buffer Solutions at $\mu = 0.5$

pH	T	k_{obs}, $min^{-1} \times 10^3$	E_a, kcal/mole	log A, min^{-1}	$\Delta H^{\ddagger}$, kcal/mole	$\Delta S^{\ddagger}$, cal/deg/mole
4.0	35°	0.0624	27.2	15.1	—	—
	45°	0.277	—	—	—	—
	60°	1.77	—	—	—	—
9.4[a,b]	35°	1.77	24.5	14.6	23.8	−1.98
	45°	5.91	—	—	(11.9)	(13.9)
	60°	32.5	—	—	—	—

[a] Activation parameters calculated for 60° using the following equations: $k_{obs} = [(ekT/h)e^{\Delta S^{\ddagger}/R}e^{-E_a/RT}$, where $ek/h = 5.664 \times 10^{10}$ deg^{-1} sec^{-1} and $\Delta H^{\ddagger} = E_a - RT$ (13). [b] Values in parentheses are corrected values discussed in the text.

Table VII—Stability Comparisons between I and Cefazolin: $k_0 = k'_2 f_{HC} + k'_5 f_{C^-} + k_6[OH^-]f_{C^-}$ [a]

Parameter	I	Cefazolin	
k_0, min^{-1} (35° and $\mu = 0.5$)			
pH 4	6.24×10^{-5}	6.66×10^{-5} [b]	
pH 9.4	1.77×10^{-3}	1.03×10^{-3} [b]	
pH_{min}	6.05 (60°)	5.95 (35°)	5.51 (60°)[c]
E_a, kcal/mole	24.5 (pH 9.4)	28.5 (pH 10)	24.3 (pH 5.5)
$\Delta H^{\ddagger}$, kcal/mole[d]	11.9	14.8	11.7

[a] In Ref. 1, $k'_2 = k_a$, $k'_5 = k_0$, and $k_0 = k_{pH}$. [b] Values for cefazolin were computed from rate constants given in Table III of Ref. 1. [c] Data for cefazolin are from Ref. 10. [d] Values for the enthalpy of activation are corrected for the heat of ionization of water.

$$[OH^-] = K_{w(exp)}/a_{H^+}\gamma_{\pm} \quad \text{(Eq. 9b)}$$

where $K_{w(exp)} = a_{H^+}a_{OH^-} = 9.614 \times 10^{-14}$ and $\gamma_{\pm}$ = mean ionic activity coefficient product of water = 0.70, both at 60° and $\mu = 0.5$ (8). The resulting rate constants were: $k'_2 = 3.14 \times 10^{-2}$ min^{-1}, $k'_5 = 5.78 \times 10^{-4}$ min^{-1}, and $k_6 = 82.7$ M^{-1} min^{-1}. These constants, together with the K_a, $[OH^-]$, and a_{H^+} values, were used in the expression for k_0 to generate the theoretical profile in Fig. 4.

A theoretical pH minimum for the degradation of I was obtained by taking the derivative of Eq. 10 with respect to a_{H^+}, equating it to zero, and making appropriate substitutions:

$$k_0 = k'_2 f_{HC} + k_6 f_{C^-} \quad \text{(Eq. 10)}$$

The contribution from $k'_5 f_{C^-}$ was omitted from Eq. 10 since $dk_0/da_{H^+} = 0$ within the plateau region. The derivative equation is given by:

$$a_{H^+(min)} = [k_6 K_{w(exp)}/k'_2][1 + \sqrt{(1 + k'_2 K_a)/k_6 K_{w(exp)}}] \quad \text{(Eq. 11)}$$

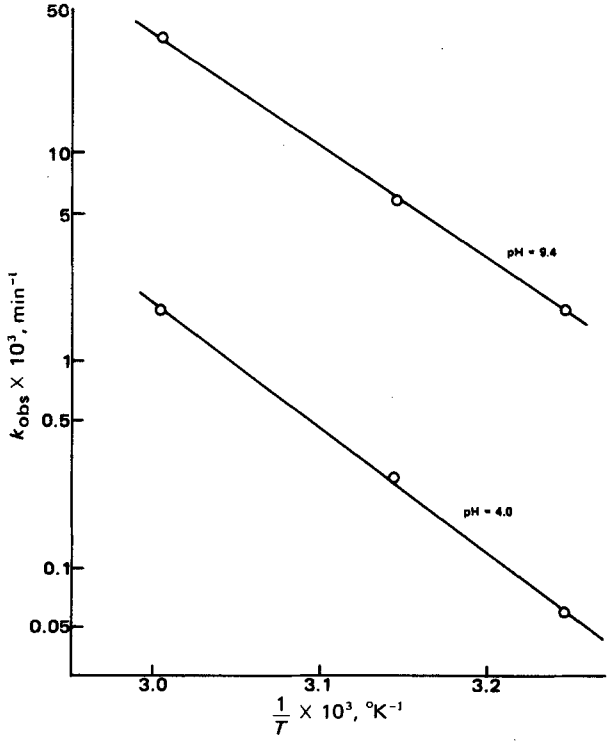

Figure 5—*Arrhenius plots for the degradation of I at $\mu = 0.5$ and pH 4.0 and 9.4.*

from which $a_{H^+(min)} = 8.948 \times 10^{-1}$ and $pH_{min} = 6.05$ may be calculated.

Micelle Formation—Since penicillin G forms micelles (9), which affect the kinetic data, I was investigated also for its ability to form micelles. High-resolution NMR was used to determine the possibility of micelle formation in 1, 10, and 30% aqueous I solutions (D_2O) at 60°. Spectra before and after the addition of deuterated methanol were identical. No micelle formation could be demonstrated.

Temperature Effect—The effect of temperature on the degradation of I was determined by measuring the degradation rates at 35, 45, and 60° in buffered solutions and $\mu = 0.5$. These measurements were made at pH 4.0 and 9.4. The values of k_{obs}, E_a, log A, and the enthalpies and entropies of activation are given in Table VI. The corresponding Arrhenius plots are shown in Fig. 5.

The Arrhenius parameters at pH 4.0 and 9.4 were very similar. Activation parameters were not computed at pH 4.0, where more than one reaction (Schemes II and V) apparently contributes significantly. However, activation parameters were calculated at pH 9.4 where Scheme VI is probably the dominant reaction. At this pH value, $k_{obs} = k_6[OH^-]$ and $\Delta S^{\ddagger}$ is given by:

$$\Delta S^{\ddagger}_{obs} = 1.9872\{\ln k_6 + \ln [OH^-] - \ln (ekT/h) + E_a/RT\} \quad \text{(Eq. 12)}$$

To obtain the entropy of activation independent of pH effects, the quantity 1.9872 ln $[OH^-]$ must be subtracted from the value of $\Delta S^{\ddagger}_{obs}$. Similarly, the calculated value of $\Delta H^{\ddagger}_{obs}$ includes the heat of ionization of water, which equals 11.9 kcal at 60° (8). This value must be subtracted from the overall enthalpy of activation to obtain the net value for the specific degradation reaction (Scheme VI). These corrected values of the entropy and enthalpy activations are given in parentheses in Table VI.

Comparative Stability—Based on Tables I and VI, there are close structural and stability analogies between I and cefazolin (Table VII). The structural difference at R_1 apparently is sufficient to alter the solubility such that cefazolin degradation can be followed kinetically below pH 1 at 5×10^{-3} M while I has a lower pH limit of 2.0 at 1.99×10^{-3} M. Consequently, a pKa of 1.70, probably associated with the thiadiazole moiety, was determined kinetically for cefazolin, but an analogous constant could not be determined for I (Table I).

It is apparent from Table VI that the data for both compounds fit the same kinetic expression for k_0. Indeed, the pH profile for cefazolin (1) is similar to that for I. The values of k_0 (35° and $\mu = 0.5$) for these two compounds were nearly identical at pH 4 and were similar at pH 9.4. The primary kinetic difference between cefazolin and I lies in the ionizable group affecting the degradation in the acid pH region. For cefazolin, a group with pKa 1.70 is required to fit the experimental data; for I, a group with pKa 2.50 is required. In attempting to fit the experimental data for I using pKa 1.70, the theoretical profile deviated excessively from k_0 at pH 3 and 4.

Further closeness in the degradation kinetics of the two compounds was manifested in pH_{min} similarities. Finally, their energies and enthalpies of activation are similar. Nevertheless, the enthalpy of acti-

vation for I was ~3 kcal/mole less than that of cefazolin. This difference was manifested in the larger k_0 value at pH 9.4 for I. The results of this study are in agreement with expected effects of structural changes at R_1 on the pH–rate profiles of cephalosporin derivatives.

REFERENCES

(1) T. Yamana and A. Tsuji, *J. Pharm. Sci.*, **65**, 1563 (1976).

(2) C. H. Nightingale, D. S. Greene, and R. Quintiliani, *ibid.*, **64**, 1899 (1975).

(3) J. M. Indelicato, T. T. Norvilas, W. J. Wheeler, and W. L. Wilham, *J. Med. Chem.*, **17**, 523 (1974).

(4) P. Finholt, G. Jurgensen, and H. Kristiansen, *J. Pharm. Sci.*, **54**, 387 (1965).

(5) A. Albert and E. P. Serjeant, "The Determination of Ionization Constants," 2nd ed., Barnes and Noble, New York, N.Y., 1971, chap. 4.

(6) A. Frost and R. Pearson, "Kinetics and Mechanisms," 2nd ed., Wiley, New York, N.Y., 1971, chap. 7.

(7) J. T. Carstensen, *J. Pharm. Sci.*, **59**, 1140 (1970).

(8) H. S. Harned and W. J. Hamer, *J. Am. Chem. Soc.*, **55**, 2194 (1933).

(9) J. T. Ong and H. B. Kostenbauder, *J. Pharm. Sci.*, **64**, 1379 (1975).

(10) E. S. Rattie, D. E. Guttman, and L. J. Ravin, *Arzneim.-Forsch. Drug Res.*, **28**, 6, 944 (1978).

(11) Landholt-Bornstein, *Physikalisch-Chemische Tabellen*, 5. Auflage, 2. Ergänzungsband.

(12) P. J. Niebergall, *Am. J. Pharm.*, **138**, 232 (1966).

(13) K. J. Laidler, "Chemical Kinetics," 2nd ed., McGraw-Hill, New York, N.Y., 1965, p. 88.

ACKNOWLEDGMENTS

Abstracted in part from a dissertation submitted by E. S. Rattie to the Graduate School, Temple University, in partial fulfillment of the Master of Science degree requirements.

Fluorometric High-Pressure Liquid Chromatographic Determination of Hydrocortisone in Human Plasma

THOMAS J. GOEHL ˣ, GLORIA M. SUNDARESAN, and VADLAMANI K. PRASAD

Received February 28, 1979, from the *Division of Biopharmaceutics, Food and Drug Administration, Washington, DC 20204.* Accepted for publication May 8, 1979.

Abstract □ A highly sensitive and specific method for hydrocortisone determination in plasma is described. In this method, an internal standard (Δ^4-pregnen-17α,20α,21-triol-3,11-dione) was added to plasma, which was then extracted with a mixture of methylene chloride–ether (60:40). After separation and evaporation of the organic phase, derivatization was carried out with dansylhydrazine. Upon completion of the reaction, the excess dansylhydrazine was reacted with pyruvic acid and a second extraction and evaporation step was performed. The residue was taken up in 100 μl of the high-pressure liquid chromatographic mobile phase, and 5 μl was injected onto a microparticulate silica column. Elution was carried out with an ethylene dichloride–butanol–water (91:8.5:0.5) mobile phase. The effluent was monitored with a fluorescence detector (excitation 240 nm; emission 470-nm cutoff filter). A linear calibration curve was found from 5 to 150 ng/ml with the precision estimated to be ±7% (*CV*).

Keyphrases □ Hydrocortisone—analysis, high-pressure liquid chromatography, fluorometry, plasma, humans □ Glucocorticoids—hydrocortisone, high-pressure liquid chromatographic and fluorometric analysis, plasma, humans □ High-pressure liquid chromatography—analysis, hydrocortisone, human plasma, fluorometry

Hydrocortisone is a potent anti-inflammatory, immunosuppressive, and antiallergenic drug (1). Since the discovery of hydrocortisone, numerous synthetic glucocorticoids have been prepared. However, hydrocortisone remains an important agent in modern adrenocorticoid steroid therapy.

Various analytical methods have been used to assay hydrocortisone in plasma including fluorescence (2, 3), competitive protein binding (4), enzyme immunoassay (5), and radioimmunoassay (6). All of these methods have problems with specificity. More recently, high-pressure liquid chromatographic (HPLC) methods for hydrocortisone assay in plasma have appeared (7–10). Most HPLC methods exhibit the required specificity but do not provide the low nanogram per milliliter sensitivity needed for bioequivalence studies. This paper describes a highly sensitive and specific HPLC assay for plasma hydrocortisone that can be used in bioequivalence studies.

EXPERIMENTAL

Apparatus—The modular high-performance liquid chromatograph consisted of a constant-flow pump[1], a valve-type injector[2], a fluorescence detector[3] (excitation 240 nm; emission 470-nm cutoff filter), and a strip-chart recorder[4] (0.5 cm/min). A stainless steel column (4.6 mm i.d. × 250 mm) packed with fully porous, irregularly shaped 5-μm silica[5] was obtained commercially.

Chromatographic Conditions—The mobile phase was ethylene dichloride–butanol–water (91:8.5:0.5). A flow rate of 1.5 ml/min was established (2200 psig), and the column was equilibrated for 16 hr. The column was maintained at 19.5° by inserting it into a glass sleeve, which was immersed in a constant-temperature water bath[6].

Reagents and Materials—Hydrocortisone[7], Δ^4-pregnen-17α,-20α,21-triol-3,11-dione[7] (internal standard), pyruvic acid[8], and dansylhydrazine[9] were obtained from commercial sources. All were used as received except dansylhydrazine, which was recrystallized from chloroform prior to use. Solvents used were spectroanalyzed ethylene dichloride[8], HPLC-grade butanol, methylene chloride, and ether[10]. All other materials were reagent grade.

[1] Chromatography pump, model M6000A, Waters Associates, Milford, Mass.
[2] Sample injection valve, model U6K, Waters Associates, Milford, Mass.
[3] Model FS970, Schoeffel Instruments, Westwood, N.J.
[4] Model 9176, Varian Instruments, Palo Alto, Calif.
[5] Prepacked Hibar II column with Lichrosorb SI-60 5-μm silica, Applied Science Laboratories, State College, Pa.
[6] Model 3080, Lab-Line Instruments, Melrose Park, Ill.
[7] Sigma Chemical Co., St. Louis, Mo.
[8] Fisher Scientific Co., Pittsburgh, Pa.
[9] Regis Chemical Co., Morton Grove, Ill.
[10] Burdick & Jackson Laboratories, Muskegon, Mich.

0022-3549/79/1100-1374$01.00/0

© 1979, American Pharmaceutical Association

vation for I was ~3 kcal/mole less than that of cefazolin. This difference was manifested in the larger k_0 value at pH 9.4 for I. The results of this study are in agreement with expected effects of structural changes at R_1 on the pH–rate profiles of cephalosporin derivatives.

REFERENCES

(1) T. Yamana and A. Tsuji, *J. Pharm. Sci.*, **65**, 1563 (1976).

(2) C. H. Nightingale, D. S. Greene, and R. Quintiliani, *ibid.*, **64**, 1899 (1975).

(3) J. M. Indelicato, T. T. Norvilas, W. J. Wheeler, and W. L. Wilham, *J. Med. Chem.*, **17**, 523 (1974).

(4) P. Finholt, G. Jurgensen, and H. Kristiansen, *J. Pharm. Sci.*, **54**, 387 (1965).

(5) A. Albert and E. P. Serjeant, "The Determination of Ionization Constants," 2nd ed., Barnes and Noble, New York, N.Y., 1971, chap. 4.

(6) A. Frost and R. Pearson, "Kinetics and Mechanisms," 2nd ed., Wiley, New York, N.Y., 1971, chap. 7.

(7) J. T. Carstensen, *J. Pharm. Sci.*, **59**, 1140 (1970).

(8) H. S. Harned and W. J. Hamer, *J. Am. Chem. Soc.*, **55**, 2194 (1933).

(9) J. T. Ong and H. B. Kostenbauder, *J. Pharm. Sci.*, **64**, 1379 (1975).

(10) E. S. Rattie, D. E. Guttman, and L. J. Ravin, *Arzneim.-Forsch. Drug Res.*, **28**, 6, 944 (1978).

(11) Landholt-Bornstein, *Physikalisch-Chemische Tabellen*, 5. Auflage, 2. Ergänzungsband.

(12) P. J. Niebergall, *Am. J. Pharm.*, **138**, 232 (1966).

(13) K. J. Laidler, "Chemical Kinetics," 2nd ed., McGraw-Hill, New York, N.Y., 1965, p. 88.

ACKNOWLEDGMENTS

Abstracted in part from a dissertation submitted by E. S. Rattie to the Graduate School, Temple University, in partial fulfillment of the Master of Science degree requirements.

Fluorometric High-Pressure Liquid Chromatographic Determination of Hydrocortisone in Human Plasma

THOMAS J. GOEHL ˣ, GLORIA M. SUNDARESAN, and VADLAMANI K. PRASAD

Received February 28, 1979, from the *Division of Biopharmaceutics, Food and Drug Administration, Washington, DC 20204.* Accepted for publication May 8, 1979.

Abstract □ A highly sensitive and specific method for hydrocortisone determination in plasma is described. In this method, an internal standard (Δ^4-pregnen-17α,20α,21-triol-3,11-dione) was added to plasma, which was then extracted with a mixture of methylene chloride–ether (60:40). After separation and evaporation of the organic phase, derivatization was carried out with dansylhydrazine. Upon completion of the reaction, the excess dansylhydrazine was reacted with pyruvic acid and a second extraction and evaporation step was performed. The residue was taken up in 100 μl of the high-pressure liquid chromatographic mobile phase, and 5 μl was injected onto a microparticulate silica column. Elution was carried out with an ethylene dichloride–butanol–water (91:8.5:0.5) mobile phase. The effluent was monitored with a fluorescence detector (excitation 240 nm; emission 470-nm cutoff filter). A linear calibration curve was found from 5 to 150 ng/ml with the precision estimated to be ±7% (*CV*).

Keyphrases □ Hydrocortisone—analysis, high-pressure liquid chromatography, fluorometry, plasma, humans □ Glucocorticoids—hydrocortisone, high-pressure liquid chromatographic and fluorometric analysis, plasma, humans □ High-pressure liquid chromatography—analysis, hydrocortisone, human plasma, fluorometry

Hydrocortisone is a potent anti-inflammatory, immunosuppressive, and antiallergenic drug (1). Since the discovery of hydrocortisone, numerous synthetic glucocorticoids have been prepared. However, hydrocortisone remains an important agent in modern adrenocorticoid steroid therapy.

Various analytical methods have been used to assay hydrocortisone in plasma including fluorescence (2, 3), competitive protein binding (4), enzyme immunoassay (5), and radioimmunoassay (6). All of these methods have problems with specificity. More recently, high-pressure liquid chromatographic (HPLC) methods for hydrocortisone assay in plasma have appeared (7–10). Most HPLC methods exhibit the required specificity but do not provide the low nanogram per milliliter sensitivity needed for bioequivalence studies. This paper describes a highly sensitive and specific HPLC assay for plasma hydrocortisone that can be used in bioequivalence studies.

EXPERIMENTAL

Apparatus—The modular high-performance liquid chromatograph consisted of a constant-flow pump[1], a valve-type injector[2], a fluorescence detector[3] (excitation 240 nm; emission 470-nm cutoff filter), and a strip-chart recorder[4] (0.5 cm/min). A stainless steel column (4.6 mm i.d. × 250 mm) packed with fully porous, irregularly shaped 5-μm silica[5] was obtained commercially.

Chromatographic Conditions—The mobile phase was ethylene dichloride–butanol–water (91:8.5:0.5). A flow rate of 1.5 ml/min was established (2200 psig), and the column was equilibrated for 16 hr. The column was maintained at 19.5° by inserting it into a glass sleeve, which was immersed in a constant-temperature water bath[6].

Reagents and Materials—Hydrocortisone[7], Δ^4-pregnen-17α,-20α,21-triol-3,11-dione[7] (internal standard), pyruvic acid[8], and dansylhydrazine[9] were obtained from commercial sources. All were used as received except dansylhydrazine, which was recrystallized from chloroform prior to use. Solvents used were spectroanalyzed ethylene dichloride[8], HPLC-grade butanol, methylene chloride, and ether[10]. All other materials were reagent grade.

[1] Chromatography pump, model M6000A, Waters Associates, Milford, Mass.
[2] Sample injection valve, model U6K, Waters Associates, Milford, Mass.
[3] Model FS970, Schoeffel Instruments, Westwood, N.J.
[4] Model 9176, Varian Instruments, Palo Alto, Calif.
[5] Prepacked Hibar II column with Lichrosorb SI-60 5-μm silica, Applied Science Laboratories, State College, Pa.
[6] Model 3080, Lab-Line Instruments, Melrose Park, Ill.
[7] Sigma Chemical Co., St. Louis, Mo.
[8] Fisher Scientific Co., Pittsburgh, Pa.
[9] Regis Chemical Co., Morton Grove, Ill.
[10] Burdick & Jackson Laboratories, Muskegon, Mich.

0022-3549/79/1100-1374$01.00/0

© 1979, American Pharmaceutical Association

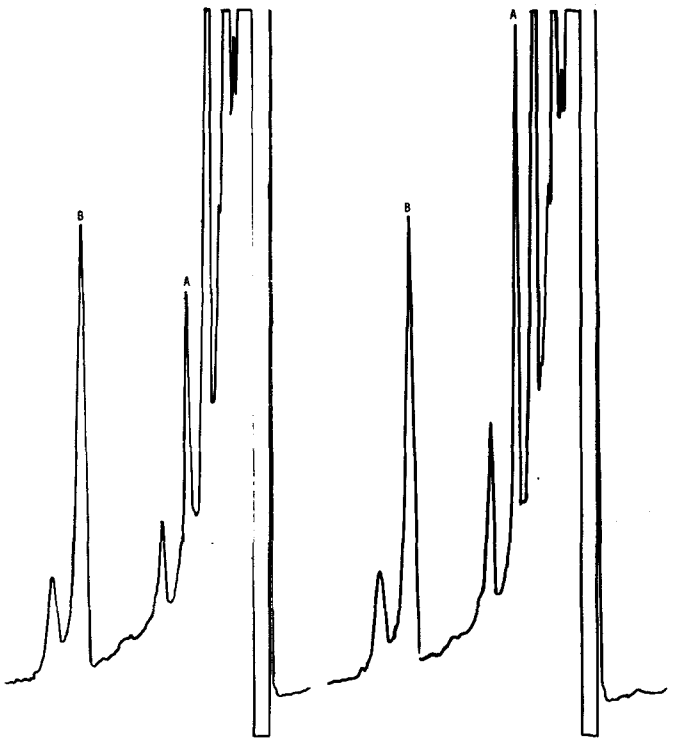

Figure 1—*Chromatogram obtained from HPLC assay of control human plasma (left) and control plasma spiked with an additional 50 ng of hydrocortisone/ml (A) (right). Both were spiked with 200 ng of internal standard/ml (B).*

Stock solutions of hydrocortisone and the internal standard were prepared individually by dissolving 10 mg of each in 100 ml of methanol and making appropriate dilutions. Plasma standards were prepared by taking small volumes of the stock hydrocortisone solutions and adding them to control plasma. The dansylhydrazine solution was prepared by dissolving 20 mg of reagent in 10 ml of absolute ethanol.

The ethanolic hydrochloric acid solution was prepared by adding 0.65 ml of concentrated hydrochloric acid to 1 liter of absolute ethanol. For the pyruvic acid solution, 40 mg of pyruvic acid was added to 10 ml of absolute ethanol. The phosphate buffer was prepared by titrating a 1.0 *M* solution of dibasic potassium phosphate to pH 8.8 with a 1.0 *M* solution of monobasic potassium phosphate.

Assay—To 1 ml of plasma in a 12-ml glass-stoppered conical centrifuge tube was added 200 ng of the internal standard (20 μl of a 10-ng/μl methanolic solution). The tubes were mixed[11], and then 6 ml of methylene chloride–ether (60:40) was added. After mixing for 30 sec, the samples were centrifuged and the organic phase was transferred to a second tube. The solvent was evaporated[12] under a gentle nitrogen stream. To the residue were added 100 μl of ethanolic hydrochloric acid and 100 μl of ethanolic dansylhydrazine.

After the solution reacted for 1 hr at room temperature, 100 μl of the pyruvic acid solution was added. After 15 min at room temperature, 2 ml of phosphate buffer and 6 ml of methylene chloride–ether (60:40) were added. The samples were mixed for 30 sec and centrifuged, and the organic phase was transferred to a third test tube. After solvent evaporation, the residue was dissolved in 100 μl of the HPLC mobile phase and 5 μl was injected.

The hydrocortisone concentrations were determined from standard curves prepared by plotting peak height ratios of the dansylhydrazones of hydrocortisone and internal standard *versus* the spiked concentrations. To correct the standard curve for endogenous hydrocortisone in control plasma, the corresponding peak height ratio was subtracted from all data points used in the standard curve.

Recovery—Plasma aliquots (1 ml) were spiked with known serial hydrocortisone quantities. After the samples were treated as described, the peak heights for the hydrocortisone dansylhydrazones (corrected for endogenous hydrocortisone) were compared to the peak heights obtained from the same amount of drug that was derivatized but not extracted. The ratio of the slopes was used to estimate percent recovery.

Precision—Normal human plasma aliquots were spiked with known amounts of hydrocortisone to give several concentrations. The samples were assayed in quadruplicate as described.

RESULTS AND DISCUSSION

Before bioequivalence requirements are proposed for a drug, adequate methodology should be available. Although numerous methods exist for assaying hydrocortisone, no one method has the required specificity or sensitivity.

In initial studies with the existing HPLC methods, sensitivity seemed to be the major obstacle for bioequivalence studies. Levels of 25 ng/ml or lower were difficult to measure. One approach to increase the sensitivity of these HPLC assays would be to introduce a fluorophore into the molecule. This fluorophore would allow the use of a fluorescence detector with its inherent greater sensitivity.

Derivatization of steroid keto groups has been extensively studied (12–15). In reactions with 2,4-dinitrophenylhydrazines, Reich *et al.* (12) reported that the 3-keto group reacted faster than the 17- or 20-keto group. Van Den Heuvel and Horning (15) also found that the reaction between 1,1-dimethylhydrazine and the steroid keto groups was position dependent, with the 3-keto group reacting more easily than the 20-keto group and with no reaction for the 11-keto group.

With the introduction of dansylhydrazine (11), a valuable reagent was added to the armory of derivatization reagents that could enhance chromatographic sensitivity. Dansylhydrazine was found to follow the same position dependency as the other hydrazines (13).

When the hydrocortisone dansylhydrazone (I) was prepared and subjected to HPLC analysis, two peaks were observed. These peaks were collected and analyzed by NMR. Both peaks had similar properties, pointing to the formation of *syn-* and *anti*-isomers at the 3-keto position, although no definitive conclusion could be drawn. Similar geometric isomers of the *syn-* and *anti*-types have been found for the 3-keto steroids when reacted with pentafluorobenzylhydroxylamine (14). Further evidence that the two peaks were indeed the *syn-* and *anti*-forms of the 3-keto dansylhydrazones was obtained by reacting the internal standard with dansylhydrazine.

The internal standard used in these studies is a particularly good one, since the functionality is identical, differing from hydrocortisone only in the position of the second keto group. Even though the internal standard has only one reactive keto group in the 3-position, again two peaks with similar chromatographic properties were found. These results indicate that at least with hydrocortisone and the internal standard, the 3-keto group is most reactive with dansylhydrazine and the two derivatives formed are the *syn-* and *anti*-isomers.

Attempts were made to vary the reaction conditions to change the ratio of the two peaks. No change was observed when temperature or reaction time was varied. Similar results were observed with the internal standard. The ratio was independent also of the hydrocortisone concentration. Therefore, the use of this derivatization for quantitative purposes seemed possible.

Both reversed-phase partition chromatography on a C-18 column and normal-phase adsorption chromatography on a microparticulate silica column were studied. The adsorption mode was chosen because a cleaner chromatogram was found after analysis of control plasma. The initial column stability problem was overcome by incorporating a small percentage of water in the mobile phase (16). In addition, room temperature variations affected column performance, resulting in peak shape changes

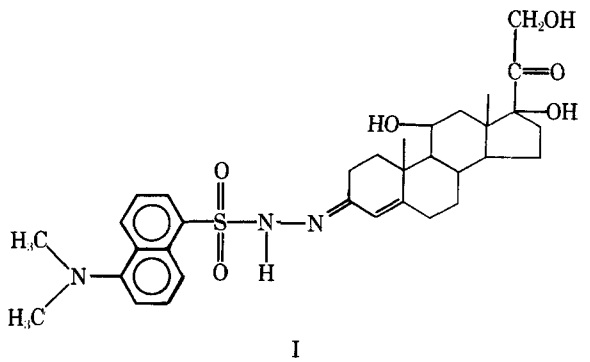

I

[11] Vortex-Genie, Fisher Scientific Co., Pittsburgh, Pa.
[12] N-Evap, Organomation Associates, Shrewsbury, Mass.

Table I—HPLC Method Precision

Theoretical Concentration, ng/ml	Experimental Concentration, ng/ml, Mean[a] (Range)	*CV*, %
10	9.8 (8.1–11)	12.3
20	19 (17–21)	8.6
40	38 (38–40)	2.3
60	60 (53–65)	8.3
80	80 (78–84)	3.0

[a] $n = 4$.

that adversely affected assay precision. Instituting column temperature control resolved this issue.

After plasma was analyzed for endogenous hydrocortisone, the resulting peaks had the same retention times and peak widths as the standard. For further confirmation that hydrocortisone was present and that no interfering peaks were hidden under the dansylhydrazone peaks, the standard addition technique was used. The peak heights were additive, and the peak widths at half-height were constant.

Chromatograms obtained in the analysis of human plasma containing only endogenous hydrocortisone and 200 ng of internal standard/ml and the same plasma spiked with an additional 50 ng of hydrocortisone/ml and 200 ng of internal standard/ml are shown in Fig. 1. Two peaks were found for each of the two compounds, as discussed previously. The peaks associated with the hydrocortisone derivatization had retention times of 8.4 and 10.0 min. The peaks associated with the internal standard derivatization had retention times of 16.8 and 18.6 min. The first of these two peaks for each compound was used in calculating peak ratios.

A standard linear plasma calibration curve was obtained in the 5–150-ng/ml range. Sensitivity studies with the hydrocortisone dansylhydrazone showed that as little as 0.25 ng can be detected. The recovery of hydrocortisone added to control plasma was studied by comparing the ratio of slopes obtained for the plasma extraction standard curve and for the direct standard curve. The recovery was calculated to be 83%.

To study method precision, known drug amounts were added to control plasma. These samples were assayed in quadruplicate as described. The coefficients of variation (*CV*) for the assay of hydrocortisone over the range of 10–80 ng/ml are reported in Table I.

This method was developed for planned bioequivalence studies with hydrocortisone tablets in which dexamethasone was to be used to suppress endogenous hydrocortisone. Therefore, the possibility of dexamethasone interference in the assay had to be explored. In these studies, dexamethasone was added to plasma to give a final concentration of 200 ng/ml. This concentration was well above the dexamethasone concentration expected in the study. These samples and the same control plasma were assayed for endogenous hydrocortisone. The hydrocortisone concentration in the control plasma was determined to be the same as that in the control plasma to which dexamethasone had been added. Thus, it can be concluded that dexamethasone had no effect on the HPLC assay for hydrocortisone.

Table II—Plasma Endogenous Hydrocortisone from Three Human Volunteers

Subject	Concentration, ng/ml	*CV*[a], %
A	83.2	5.1
B	79.6	1.2
C	80.8	4.0

[a] $n = 3$.

To demonstrate the utility of this method as a routine procedure for hydrocortisone determination, plasma from normal volunteers was assayed (Table II). Results were in the accepted concentration range for endogenous hydrocortisone (17).

REFERENCES

(1) "The Pharmacological Basis of Therapeutics," 5th ed., L. Goodman and A. Gilman, Eds., Macmillan, New York, N.Y., 1975, p. 1496.

(2) G. Dower and F. Stahl, *Ger. Med. Monthly*, **10**, 443 (1965).

(3) D. Mattingly, *J. Clin. Pathol.*, **15**, 374 (1962).

(4) B. Murphy and C. Poltee, *J. Clin. Endocrinol.*, **24**, 919 (1964).

(5) Y. Kobayashi, T. Ogihara, K. Amitani, F. Watanabe, T. Kiguchi, I. Ninomiya, and Y. Kumahara, *Steroids*, **32**, 137 (1978).

(6) J. Seth and L. M. Brown, *Clin. Chim. Acta*, **86**, 109 (1978).

(7) F. Trefz, D. Byrd, and W. Kochen, *J. Chromatogr.*, **107**, 181 (1975).

(8) W. Wortmann, C. Schnabel, and J. Touchstone, *ibid.*, **84**, 396 (1973).

(9) J. Van Den Berg, C. R. Mol, R. S. Deelder, and J. H. H. Thijssen, *Clin. Chim. Acta*, **78**, 165 (1977).

(10) D. Gorg, J. Ayres, and J. Wagner, *Res. Commun. Chem. Pathol. Pharmacol.*, **18**, 137 (1977).

(11) R. Chayen, R. Dvir, S. Gould, and A. Harell, *Isr. J. Chem.*, **8**, 157p (1970).

(12) H. Reich, K. Crane, and S. Sanfilippo, *J. Org. Chem.*, **18**, 822 (1953).

(13) R. Chayen, R. Dvir, S. Gould, and A. Harell, *Anal. Biochem.*, **42**, 283 (1971).

(14) K. T. Koshy, D. G. Kaiser, and A. L. Van Der Slik, *J. Chromatogr. Sci.*, **13**, 97 (1975).

(15) W. Van Den Heuvel and E. Horning, *Biochim. Biophys. Acta*, **74**, 560 (1963).

(16) S. E. Tsuei and J. J. Ashley, *J. Chromatogr.*, **145**, 213 (1978).

(17) R. W. Farmer and C. E. Pierce, *Clin. Chem.*, **20**, 411 (1974).

ACKNOWLEDGMENTS

The authors thank M. A. Tischler and E. B. Sheinin of the Division of Drug Chemistry, Food and Drug Administration, for the NMR analyses.

Synthesis of New Mercaptotriazoles with Potential Antibilharzial Activity

RAAFAT SOLIMAN *x **and NIBAL A. HAMMOUDA** ‡

Received February 12, 1979, from the *Department of Pharmaceutical Chemistry, Faculty of Pharmacy, and the ‡Department of Parasitology, Faculty of Medicine, University of Alexandria, Alexandria, Egypt. Accepted for publication May 9, 1979.

Abstract □ Several 3-mercaptotriazoles with the 8-hydroxyquinoline moiety in the 5-position were prepared and tested for antiparasitic activity. Preliminary biological tests on experimentally infected mice with *Schistosoma mansoni* worms revealed that the new compounds possess potent schistosomicidal activity.

Keyphrases □ Antibilharzial agents—mercaptotriazoles, synthesis, screening, *Schistosoma mansoni*, structure–activity relationships □ Mercaptotriazoles—antibilharzial activity, synthesis, screening, *Schistosoma mansoni*, structure–activity relationships □ Structure–activity relationships—mercaptotriazoles, antibilharzial activity, synthesis, screening, *Schistosoma mansoni* □ *Schistosoma mansoni*—treatment with mercaptotriazoles, synthesis, screening in mice, structure–activity relationships

The fact that lucanthone (1) and its active metabolite hycanthone (2) were the first metal-free compounds to show clinical activity against bilharziasis initiated the synthesis of a distantly related compound, 6-chloro-5-(2-diethylaminoethylamino)-8-methylquinoline. The latter exhibited outstanding activity against experimental schistosomiasis (3, 4). Unfortunately, preclinical toxicity studies indicated wide differences among various species of laboratory animals, precluding early clinical trials of this compound (3).

BACKGROUND

A novel schistosomicide of apparent clinical utility is 1-(5-nitro-2-thiazolyl)-2-imidazolidinone (niridazole). This compound showed considerable efficacy against *Schistosoma mansoni* and *S. haematobium via* oral administration (5), but three types of side effects were encountered: frequent ECG changes; neuropsychic effects, and transitory spermatogenesis impairment (6).

A new entry in bilharzial chemotherapy is 1,2,3,4-tetrahydro-2-[[(1-methylethyl)amino]methyl]-7-nitro-6-quinoline methanol (oxamniquine). It has potent schistosomicidal activity against *S. mansoni* by causing worms to shift from the mesenteric veins to the liver where they are destroyed (7).

Recently, interest has been focused on the pharmacology of 1-phenyl-1,2,4-triazoles and 4-phenyl-1,2,4-triazoles (8), which showed diverse biological activities. Furthermore, 1,4-disubstituted thiosemicarbazides (the precursors for cyclized triazole synthesis) possess a broad spectrum of biological activities (9, 10).

These observations prompted the synthesis of several 3-mercaptotriazoles having the substituted 8-hydroxyquinoline moiety in the 5-position. Incorporation of the potent antiparasitic drug iodochlorhydroxyquin or diiodohydroxyquin in the 3-mercaptotriazole ring produced compounds with potential schistosomicidal activity and no undesirable or toxic effects.

CHEMISTRY

The various substituted 1,2,4(4*H*)-triazoles were synthesized by reactions outlined in Scheme I. Conversion of the 8-hydroxyquinoline derivative (I) to the corresponding ethyl 8-quinolinoxyacetate (II) was carried out to synthesize 8-quinolinoxyacetic acid hydrazide (III) through refluxing in ethanol with 99–100% hydrazine hydrate.

Substituted thiosemicarbazides (IV, Table I), prepared by the reaction of III with the appropriate isothiocyanate, were cyclized to the corresponding mercaptotriazoles (V, Table II) in 2 *N* NaOH. Condensation

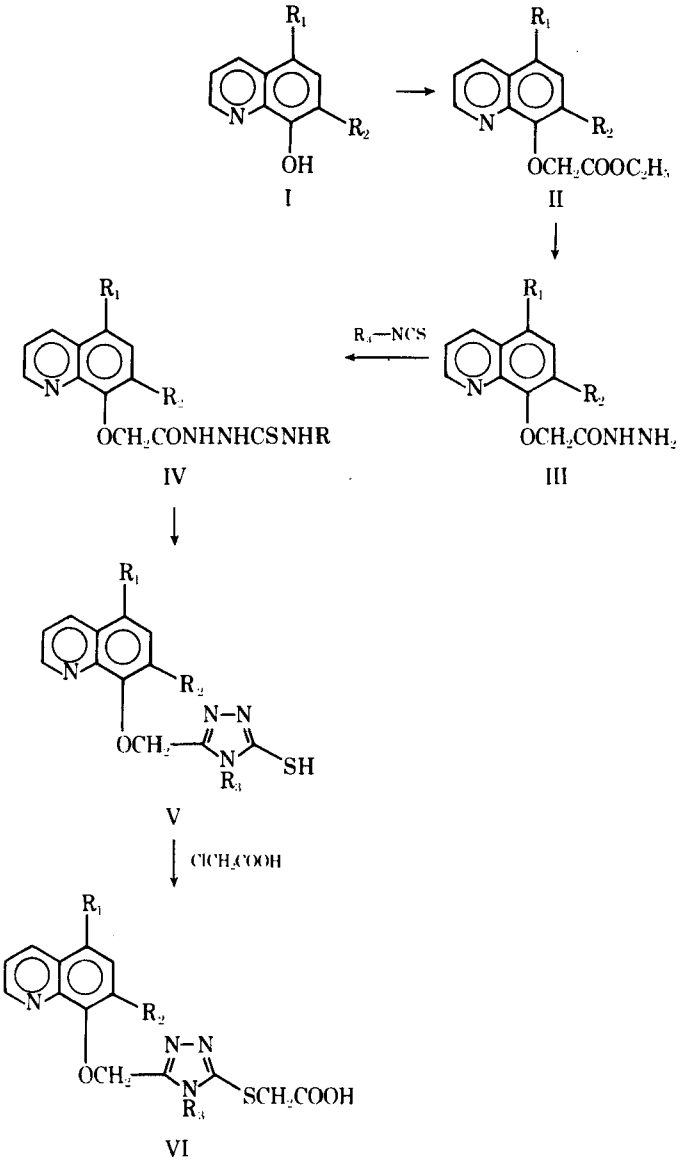

Scheme I

of the substituted triazoles with chloroacetic acid produced substituted triazole-3-mercaptoacetic acids (VI, Table III). All compounds were characterized by their sharp melting points, elemental analyses, and IR spectra.

EXPERIMENTAL[1]

Ethyl 8-Quinolinoxyacetate (IIa): Method A—To a solution of 8-hydroxyquinoline (0.1 mole) in absolute ethanol (60 ml) was added

[1] Melting points were determined in open glass capillaries and are uncorrected. IR spectra were determined as Nujol mulls with a Beckman IR-4210. Microanalyses were performed by the Microanalytical Unit, Faculty of Science, University of Cairo, Cairo, Egypt.

0022-3549/79/1100-1377$01.00/0
© 1979, American Pharmaceutical Association

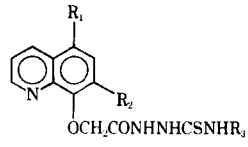

Table I—1-(8-Quinolinoxyacetyl)-4-Substituted Thiosemicarbazides

Compound	R_3	R_1	R_2	Yield, %	Melting Point	Formula	Analysis, %	Calc.	Found
IV*a*	C_2H_5	H	H	65	198°	$C_{14}H_{16}N_4O_2S$	C	55.3	55.4
							H	5.3	5.5
							N	18.4	18.6
IV*b*	$CH_2{=}CHCH_2$	H	H	68	129°	$C_{15}H_{16}N_4O_2S$	C	57.0	57.0
							H	5.1	5.1
							N	17.7	17.9
IV*c*	$CH_3(CH_2)_3$	H	H	66	194°	$C_{16}H_{20}N_4O_2S$	C	58.2	58.0
							H	6.1	6.0
							N	17.0	17.1
IV*d*	C_6H_{11}	H	H	70	150°	$C_{18}H_{22}N_4O_2S$	C	60.3	60.5
							H	6.1	6.1
							N	15.6	15.8
IV*e*	C_6H_5	H	H	75	234°	$C_{18}H_{16}N_4O_2S$	C	61.4	61.6
							H	4.5	4.5
							N	15.9	15.9
IV*f*	$C_6H_5CH_2$	H	H	78	169°	$C_{19}H_{18}N_4O_2S$	C	62.3	62.6
							H	4.9	5.0
							N	15.3	15.0
IV*g*	$CH_2{=}CHCH_2$	Cl	I	70	177°	$C_{15}H_{14}ClIN_4O_2S$	C	37.8	38.0
							H	2.9	3.1
							N	11.8	11.5
IV*h*	$CH_3(CH_2)_3$	Cl	I	68	172°	$C_{16}H_{18}ClIN_4O_2S$	C	39.0	39.4
							H	3.7	4.0
							N	11.4	11.5
IV*i*	C_6H_{11}	Cl	I	62	169°	$C_{18}H_{20}ClIN_4O_2S$	C	41.7	41.9
							H	3.9	4.1
							N	10.8	11.1
IV*j*	C_6H_5	Cl	I	70	165°	$C_{18}H_{14}ClIN_4O_2S$	C	42.1	42.4
							H	2.7	3.0
							N	10.9	11.0
IV*k*	$C_6H_5CH_2$	Cl	I	75	106°	$C_{19}H_{16}ClIN_4O_2S$	C	43.3	43.5
							H	3.0	3.3
							N	10.6	11.0
IV*l*	*m*-$CH_3C_6H_4$	Cl	I	66	160°	$C_{19}H_{16}ClIN_4O_2S$	C	43.3	43.4
							H	3.0	3.1
							N	10.6	10.9
IV*m*	C_2H_5	I	I	64	196°	$C_{14}H_{14}I_2N_4O_2S$	C	30.2	30.6
							H	2.5	2.8
							I	45.7	46.0
IV*n*	$CH_2{=}CHCH_2$	I	I	68	183°	$C_{15}H_{14}I_2N_4O_2S$	C	31.7	31.9
							H	2.5	2.7
							I	44.7	44.9
IV*o*	$CH_3(CH_2)_3$	I	I	60	194°	$C_{16}H_{18}I_2N_4O_2S$	C	32.9	33.1
							H	3.1	3.3
							I	43.5	43.6
IV*p*	C_6H_{11}	I	I	72	190°	$C_{18}H_{20}I_2N_4O_2S$	C	35.4	35.8
							H	3.3	3.5
							I	41.6	42.0
IV*q*	C_6H_5	I	I	75	185°	$C_{18}H_{14}I_2N_4O_2S$	C	35.8	36.1
							H	2.3	2.6
							I	42.1	42.2
IV*r*	$C_6H_5CH_2$	I	I	78	180°	$C_{19}H_{16}I_2N_4O_2S$	C	36.9	37.2
							H	2.6	3.0
							I	41.1	41.5

sodium ethoxide (0.1 mole of sodium in 20 ml of absolute ethanol) followed by ethyl chloroacetate (0.1 mole). The reaction mixture was refluxed under anhydrous conditions for 3 hr and filtered. The filtrate was poured over 100 ml of ice-cold water. The separated ester was extracted with ether and dried over anhydrous magnesium sulfate. Excess ether was removed by distillation, and the remaining crude ester was used to prepare the corresponding hydrazide.

Ethyl 8-(5-Chloro-7-iodo)-quinolinoxyacetate (II*b*): Method B—Equimolar quantities of iodochlorhydroxyquin (I*b*, R_1 = Cl, R_2 = I) (0.1 mole), ethyl chloroacetate (0.1 mole), and potassium carbonate (0.12 mole) in absolute ethanol (100 ml) were refluxed for 3 hr. The reaction mixture was filtered, and the filtrate was concentrated and allowed to cool. The crude ester was collected and recrystallized from ethanol as yellow needles, mp 168°, in an 80% yield.

Anal.—Calc. for $C_{13}H_{11}ClINO_3$: C, 39.8; H, 2.8; N, 3.6. Found: C, 39.6; H, 2.7; N, 3.9.

Ethyl 8-(5,7-Diiodo)-quinolinoxyacetate (II*c*)—Method B produced yellow needles, mp 195°, in an 84% yield.

Anal.—Calc. for $C_{13}H_{11}I_2NO_3$: C, 32.3; H, 2.3; I, 52.6. Found: C, 32.0; H, 2.3; I, 52.4.

8-Quinolinoxyacetic Acid Hydrazides (III*a*–III*c*)—To a solution of 0.1 mole of II*a*–II*c* in absolute ethanol (50 ml) was added 7 g of 99–100% hydrazine hydrate, and the mixture was refluxed for 2 hr. The crude hydrazide, which separated on cooling, was collected by filtration and recrystallized from ethanol. Compound III*a* was obtained as white needles, mp 71°, in a 60% yield.

Anal.—Calc. for $C_{11}H_{11}N_3O_2$: C, 60.8; H, 5.1; N, 19.4. Found: C, 60.6; H, 5.2; N, 19.4.

Compound III*b* was obtained as yellow needles, mp 178°, in a 65% yield.

Anal.—Calc. for $C_{11}H_9ClIN_3O_2$: C, 35.0; H, 2.4; N, 11.1. Found: C, 34.8; H, 2.5; N, 11.0.

Compound III*c* was obtained as yellow needles, mp 186°, in a 68% yield.

Anal.—Calc. for $C_{11}H_9I_2N_3O_2$: C, 28.1; H, 1.9; I, 54.2. Found: C, 28.0; H, 2.0; I, 54.5.

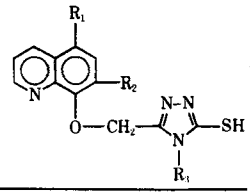

Table II—5-(8-Quinolinoxymethyl)-4-Substituted-3-mercapto-1,2,4(4*H*)-triazoles

Compound	R_3	R_1	R_2	Yield, %	Melting Point	Formula	Analysis, %	Calc.	Found
V*a*	C_2H_5	H	H	68	180°	$C_{14}H_{14}N_4OS$	C	58.7	58.8
							H	4.9	5.2
							N	19.6	20.0
V*b*	$CH_2{=}CHCH_2$	H	H	66	208°	$C_{15}H_{14}N_4OS$	C	60.4	60.8
							H	4.7	5.0
							N	18.8	18.6
V*c*	$CH_3(CH_2)_3$	H	H	71	162°	$C_{16}H_{18}N_4OS$	C	61.1	61.3
							H	5.7	5.7
							N	17.8	17.8
V*d*	C_6H_{11}	H	H	75	175°	$C_{18}H_{20}N_4OS$	C	63.5	63.5
							H	5.9	6.0
							N	16.5	16.5
V*e*	C_6H_5	H	H	78	182°	$C_{18}H_{14}N_4OS$	C	64.7	64.9
							H	4.2	4.4
							N	16.8	17.1
V*f*	$C_6H_5CH_2$	H	H	73	145°	$C_{19}H_{16}N_4OS$	C	65.5	65.6
							H	4.6	4.5
							N	16.1	15.8
V*g*	$CH_2{=}CHCH_2$	Cl	I	65	185°	$C_{15}H_{12}ClIN_4OS$	C	39.3	39.5
							H	2.6	2.7
							N	12.2	12.5
V*h*	$CH_3(CH_2)_3$	Cl	I	67	168°	$C_{16}H_{16}ClIN_4OS$	C	40.5	40.8
							H	3.4	3.3
							N	11.8	12.1
V*i*	C_6H_{11}	Cl	I	72	138°	$C_{18}H_{18}ClIN_4OS$	C	43.2	43.3
							H	3.6	3.4
							N	11.2	11.1
V*j*	C_6H_5	Cl	I	78	182°	$C_{18}H_{12}ClIN_4OS$	C	43.7	44.1
							H	2.4	2.6
							N	11.3	11.0
V*k*	$C_6H_5CH_2$	Cl	I	70	120°	$C_{19}H_{14}ClIN_4OS$	C	44.8	45.1
							H	2.8	2.4
							N	11.0	11.0
V*l*	*m*-$CH_3C_6H_4$	Cl	I	66	170°	$C_{19}H_{14}ClIN_4OS$	C	44.8	44.7
							H	2.8	3.1
							N	11.0	11.2
V*m*	C_2H_5	I	I	60	172°	$C_{14}H_{12}I_2N_4OS$	C	31.2	31.0
							H	2.2	2.5
							I	47.2	47.5
V*n*	$CH_2{=}CHCH_2$	I	I	64	142°	$C_{15}H_{12}I_2N_4OS$	C	32.7	32.9
							H	2.2	2.4
							I	46.2	46.4
V*o*	$CH_3(CH_2)_3$	I	I	72	150°	$C_{16}H_{16}I_2N_4OS$	C	33.9	34.1
							H	2.8	3.0
							I	44.9	45.3
V*p*	C_6H_{11}	I	I	77	154°	$C_{18}H_{18}I_2N_4OS$	C	36.5	36.7
							H	3.0	3.2
							I	42.9	43.1
V*q*	C_6H_5	I	I	68	168°	$C_{18}H_{14}I_2N_4OS$	C	36.7	36.8
							H	2.4	2.4
							I	43.2	43.2
V*r*	$C_6H_5CH_2$	I	I	70	134°	$C_{19}H_{14}I_2N_4OS$	C	38.0	38.1
							H	2.3	2.5
							I	42.3	42.0

1-(8-Quinolinoxyacetyl)-4-Substituted Thiosemicarbazides (IV)—Equimolar quantities of III*a*–III*c* (0.02 mole) and the appropriate isothiocyanate (0.02 mole) were mixed in dry benzene, and the mixture was refluxed on a steam bath for 2 hr. Excess benzene was removed by distillation. The separated solid was collected by filtration, washed with cold ethanol–water, dried, and recrystallized from ethanol. The various substituted thiosemicarbazides (Table I) were characterized by their sharp melting points and elemental analyses.

5-(8-Quinolinoxymethyl)-4-Substituted-3-mercapto-1,2,4(4*H*)-triazoles (V)—A solution of 1-(8-quinolinoxyacetyl)-4-substituted thiosemicarbazide (0.01 mole) in 2 *N* NaOH (20 ml) was refluxed for 2–3 hr. After cooling, the mixture was filtered; the filtrate was acidified with dilute hydrochloric acid until complete precipitation occurred (11, 12). The separated solid was collected by filtration, washed with water, dried, and recrystallized from ethanol. Various substituted mercaptotriazoles were characterized by their sharp melting points and elemental analyses (Table II).

5-(8-Quinolinoxymethyl) -4- Substituted-1,2,4(4*H*)-triazole-3-mercaptoacetic Acids (VI)—A mixture of the appropriate substituted mercaptotriazole (0.005 mole), chloroacetic acid (0.005 mole), and sodium hydroxide (0.01 mole) in ethanol (20 ml) was refluxed for 3 hr. The mixture was cooled and acidified with dilute hydrochloric acid. The solid mass, which separated, was collected and recrystallized from ethanol (Table III).

Antibilharzial Activity—Swiss albino mice were infected with 100 cercariae of *S. mansoni* by the tail immersion technique (13). Eight weeks after infection, the animals were divided into six groups: a control group and a group for each of the new drugs to be tested (V*b*, V*d*, V*g*, V*i*, and hycanthone as a standard).

The drugs were given orally as a single 100-mg/kg dose. Hycanthone was given as a single injection, 70 mg/kg im in 0.1 ml of distilled water. Oogram studies of the liver and intestine were made every 3rd day on five

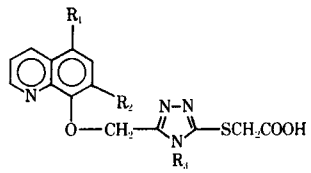

Table III—5-(8-Quinolinoxymethyl)-4-Substituted-1,2,4(4*H*)-triazole-3-mercaptoacetic Acids

Compound	R_3	R_1	R_2	Yield, %	Melting Point	Formula	Analysis, %	Calc.	Found
VI*d*	C_6H_{11}	H	H	70	226°	$C_{20}H_{22}N_4O_3S$	C	60.3	60.3
							H	5.5	5.6
							N	14.1	14.1
VI*e*	C_6H_5	H	H	80	196°	$C_{20}H_{16}N_4O_3S$	C	61.2	61.4
							H	4.1	4.1
							N	14.3	14.5
VI*f*	$C_6H_5CH_2$	H	H	78	145°	$C_{21}H_{18}N_4O_3S$	C	62.1	62.1
							H	4.4	4.4
							N	13.8	14.1
VI*g*	$CH_2{=}CHCH_2$	Cl	I	75	180°	$C_{17}H_{14}ClIN_4O_3S$	C	39.5	39.1
							H	2.7	3.0
							N	10.8	11.0
VI*h*	$CH_3(CH_2)_3$	Cl	I	72	164°	$C_{18}H_{18}ClIN_4O_3S$	C	40.6	41.0
							H	3.4	3.5
							N	10.5	10.5
VI*i*	C_6H_{11}	Cl	I	68	168°	$C_{20}H_{20}ClIN_4O_3S$	C	43.0	43.2
							H	3.6	3.8
							N	10.0	9.8
VI*j*	C_6H_5	Cl	I	85	172°	$C_{20}H_{14}ClIN_4O_3S$	C	43.4	43.6
							H	2.5	3.0
							N	10.1	10.5
VI*k*	$C_6H_5CH_2$	Cl	I	82	166°	$C_{21}H_{16}ClIN_4O_3S$	C	44.5	44.7
							H	2.9	3.3
							N	10.0	10.2
VI*m*	C_2H_5	I	I	75	168°	$C_{16}H_{14}I_2N_4O_3S$	C	32.2	32.5
							H	2.3	2.6
							I	44.6	45.0
VI*o*	$CH_3(CH_2)_3$	I	I	77	175°	$C_{18}H_{18}I_2N_4O_3S$	C	34.6	34.9
							H	2.9	3.2
							I	40.7	41.1
VI*p*	C_6H_{11}	I	I	73	180°	$C_{20}H_{20}I_2N_4O_3S$	C	36.9	37.2
							H	3.1	3.5
							I	39.1	38.8
VI*q*	C_6H_5	I	I	78	200°	$C_{20}H_{14}I_2N_4O_3S$	C	37.3	37.6
							H	2.2	2.5
							I	39.4	39.0
VI*r*	$C_6H_5CH_2$	I	I	70	190°	$C_{21}H_{16}I_2N_4O_3S$	C	38.3	38.1
							H	2.4	2.8
							I	38.6	39.0

Table IV—Oogram Findings in the Liver and Small Intestine of Infected Mice Treated with Experimental Compounds

Compound	Liver: Total Immature Eggs, %	Liver: Mature Eggs, %	Liver: Dead Eggs, %	Intestine: Total Immature Eggs, %	Intestine: Mature Eggs, %	Intestine: Dead Eggs, %
Control	76	18	6	70	28	2
Hycanthone	—	—	—	0	48	52
V*b*	0	70	30	0	68	32
V*d*	0	86	14	18	74	8
V*g*	10	70	12	20	60	20
V*i*	15	70	15	20	56	24

animals from each group.

Table IV shows the average oogram pattern in the liver and intestine during the period of maximum drug effect, which was usually at the end of the 1st week, compared with hycanthone (14).

Effect on *Toxocara canis* Larvae—Swiss albino mice were infected with 1000 larvated *T. canis* eggs by intragastric tube. Compound V*g* was given as a single 100-mg/kg po dose to a group of the infected animals and a second group served as controls. Table V shows the larval counts in the brain of the treated group compared with the control group.

Table V—Average Larval Counts in the Brain of Mice Infected with *T. canis* Larvae

Duration of Autopsy, days	Average Larval Count: Control Mice	Average Larval Count: Treated Mice
7	33	20
15	41	27

RESULTS AND DISCUSSION

The efficiency of a new antischistosomal drug was assessed in experimental infection by the oogram changes, which were said to be caused by loss of schistosoma worm muscle tone, drug action on the parasite reproductive organs, and death of the worms (15).

Deviation of the oogram picture from normal was considered when there was an absence of any immature stages or when the number of mature ova exceeded 50% (15).

Results obtained with V*b*, V*d*, V*g*, and V*i* showed marked deviation of the oogram picture from normal, indicating their potent antibilharzial effect. Furthermore, V*b* and V*d* eliminated all immature stages, demonstrating a powerful effect on the worm reproductive organs.

Compound Vg reduced the number of *T. canis* larvae in the brains of mice experimentally infected with visceral larva migrans.

REFERENCES

(1) W. Kikuth and R. Gonnert, *Ann. Trop. Med. Parasitol.*, **42**, 256 (1948).

(2) D. Rosi, G. Peruzzotti, E. W. Dennis, D. A. Berberian, H. Freele, and S. Archer, *Nature (London)*, **208**, 1005 (1965).

(3) N. W. Bristow, B. Lessel, H. C. Richards, and G. A. Williams, *ibid.*, **216**, 282 (1967).

(4) J. Pellegrino, N. Katz, and J. F. Scherrer, *J. Parasitol.*, **53**, 1225 (1967).

(5) P. Schmidt and M. Wilhelm, *Angew. Chem. Int. Ed.*, **5**, 857 (1966).

(6) L. C. Brumt, A. Degremont, M. Barbier, A. Coumbaras, and V. Lavarde, *Presse Med.*, **76**, 797 (1968).

(7) A. L. C. Domingues and A. Coutinho, *Rev. Inst. Med. Trop. S. Paulo*, **17**, 164 (1975); through *Trop. Dis. Bull.*, **73**, 66 (1976).

(8) S. S. Parmar, M. Chaudhary, S. K. Chaudhary, S. Kumar, and H. R. Spiro, *J. Pharm. Sci.*, **66**, 971 (1977).

(9) A. K. Bhat, R. P. Bhamaria, R. A. Bellare, and C. V. Deliwala, *Indian J. Chem.*, **5**, 397 (1967).

(10) T. Zsolnai, *Biochem. Pharmacol.*, **11**, 271 (1962).

(11) J. S. Shukla, H. H. Singh, and S. S. Parmar, *J. Prakt. Chem.*, **311**, 523 (1969).

(12) M. H. Shah, M. Y. Mhasalkar, M. N. Varaya, R. A. Bellare, and C. V. Deliwala, *Indian J. Chem.*, **5**, 391 (1967).

(13) J. M. Watson and M. Abdel-Azim, *Ann. Trop. Med. Parasitol.*, **43**, 41 (1949).

(14) H. F. Farag, M. Youssef, N. A. Hammouda, and H. N. Awadalla, *Egypt. J. Soc. Parasitol.*, **8**, 1 (1978).

(15) J. Pellegrino, C. A. Oliveira, J. Faria, and A. Cunha, *Am. J. Trop. Med. Hyg.*, **11**, 201 (1962).

Kinetics of Digestive Enzyme Stability in Solid State I: Application of Weibull Distribution Function to Solid-State Enzyme Inactivation

MAMORU SUGIURA ˣ, MASAYUKI KUROBE, SUMIHIRO TAMURA, and SHINICHI IKEDA

Received August 28, 1978, from the *Gifu College of Pharmacy, Mitahora-higashi, Gifu 502, Japan.* Accepted for publication February 9, 1979.

Abstract □ The Weibull distribution function was applied to solid-state enzyme inactivation. On Weibull probability paper (within a narrow range), the plots of the accumulated inactivation ratio of each enzyme *versus* time regressed to a straight line. The parameters m and k, which correspond to the type and rate of the inactivation, were characteristic of each enzyme. The effect of temperature and parameter reproducibility are discussed.

Keyphrases □ Weibull distribution function—application to solid-state enzyme inactivation studies □ Enzyme kinetics—application of Weibull distribution to inactivation studies □ Enzyme inactivation—kinetics, application of Weibull distribution to solid-state studies

Stability is important for drug quality assurance, and reports on drug stability in solid dosage forms have been published (1, 2). The essential requirement in stability studies is the selection of rate equations, which have been determined in practical systems by trial and error.

Some investigations using enzymes in the solid state failed because there was an inherent difficulty in fitting common rate equations to experimental data. Enzyme stability is complicated and is readily affected by factors such as temperature, humidity, and coexisting substances.

This paper[1] describes application of the Weibull distribution function to solid-state enzyme inactivation. The Weibull distribution originally was applied to stability predictions of other solid drugs (3, 4).

THEORETICAL

Efforts have been made to interpret the shelflife of enzymes in solids and solutions and to describe mathematically the inactivation profile with meaningful parameters. Although equations possibly could be derived from empirical treatment of the process, *e.g.*, pseudo-first-order kinetics, no suitable function has been found. Therefore, shelflives rarely have been mentioned in solid-state enzyme inactivation studies.

A general function, applicable to all inactivation curves, was derived by Weibull (5) and discussed in detail (6–8). A concise survey also was reported (9). When applied to enzyme inactivation rate data in the solid state, the Weibull distribution expresses the accumulated inactivation ratio, α, of the enzyme activity at time, t, by:

$$\alpha = 1 - \exp[-(t)^{m/k}] \qquad \text{(Eq. 1)}$$

where the scale parameter, k, defines the time scale of the process and the shape parameter, m, characterizes the curve as an exponential function. The relationship between m and curve shape was discussed previously (8, 9).

Graphical representation of the data according to the Weibull distribution and the practical aspects of linearizing experimental data were reported (6, 7). Equation 1 may be rearranged:

$$\ln \ln (1/1 - \alpha) = \ln k + m \ln t \qquad \text{(Eq. 2)}$$

From Eq. 2, a linear relation is obtained from a ln ln plot of $\ln (1/1 - \alpha)$ *versus* t. The shape parameter, m, is obtained from the slope, and k is obtained from the ordinate value at $t = 1$.

The theoretical correlation between Eq. 2 and chemical kinetics was discussed in detail (4). The equation expressing chemical kinetics varies according to the inactivation mechanism. However, within a narrow range, it is possible to express them by:

$$\frac{d\alpha}{dt} = Kg(a, \alpha, P_i) \qquad \text{(Eq. 3)}$$

where K is the rate constant, a is the initial enzyme activity, and P_i is the parameter independent of time, t. The integrated form of Eq. 3 is:

$$f(a, \alpha, P_i) = Kt \qquad \text{(Eq. 4)}$$

Equations 2 and 4 can be correlated by assuming that logarithms of Eq. 4 are expressed approximately as a linear function of Eq. 2:

$$\ln f(a, \alpha, P_i) = \ln K + \ln t \fallingdotseq A_0 + A_1 \ln \ln (1/1 - \alpha) \qquad \text{(Eq. 5)}$$

$$\ln \ln (1/1 - \alpha) \fallingdotseq 1/A_1 (\ln K - A_0) + 1/A_1 \ln t \qquad \text{(Eq. 6)}$$

[1] This paper is Part CLVII of "Studies on Enzymes" by M. Sugiura.

0022-3549/79/1100-1381$01.00/0

© 1979, American Pharmaceutical Association

Compound Vg reduced the number of *T. canis* larvae in the brains of mice experimentally infected with visceral larva migrans.

REFERENCES

(1) W. Kikuth and R. Gonnert, *Ann. Trop. Med. Parasitol.*, **42**, 256 (1948).

(2) D. Rosi, G. Peruzzotti, E. W. Dennis, D. A. Berberian, H. Freele, and S. Archer, *Nature (London)*, **208**, 1005 (1965).

(3) N. W. Bristow, B. Lessel, H. C. Richards, and G. A. Williams, *ibid.*, **216**, 282 (1967).

(4) J. Pellegrino, N. Katz, and J. F. Scherrer, *J. Parasitol.*, **53**, 1225 (1967).

(5) P. Schmidt and M. Wilhelm, *Angew. Chem. Int. Ed.*, **5**, 857 (1966).

(6) L. C. Brumt, A. Degremont, M. Barbier, A. Coumbaras, and V. Lavarde, *Presse Med.*, **76**, 797 (1968).

(7) A. L. C. Domingues and A. Coutinho, *Rev. Inst. Med. Trop. S. Paulo*, **17**, 164 (1975); through *Trop. Dis. Bull.*, **73**, 66 (1976).

(8) S. S. Parmar, M. Chaudhary, S. K. Chaudhary, S. Kumar, and H. R. Spiro, *J. Pharm. Sci.*, **66**, 971 (1977).

(9) A. K. Bhat, R. P. Bhamaria, R. A. Bellare, and C. V. Deliwala, *Indian J. Chem.*, **5**, 397 (1967).

(10) T. Zsolnai, *Biochem. Pharmacol.*, **11**, 271 (1962).

(11) J. S. Shukla, H. H. Singh, and S. S. Parmar, *J. Prakt. Chem.*, **311**, 523 (1969).

(12) M. H. Shah, M. Y. Mhasalkar, M. N. Varaya, R. A. Bellare, and C. V. Deliwala, *Indian J. Chem.*, **5**, 391 (1967).

(13) J. M. Watson and M. Abdel-Azim, *Ann. Trop. Med. Parasitol.*, **43**, 41 (1949).

(14) H. F. Farag, M. Youssef, N. A. Hammouda, and H. N. Awadalla, *Egypt. J. Soc. Parasitol.*, **8**, 1 (1978).

(15) J. Pellegrino, C. A. Oliveira, J. Faria, and A. Cunha, *Am. J. Trop. Med. Hyg.*, **11**, 201 (1962).

Kinetics of Digestive Enzyme Stability in Solid State I: Application of Weibull Distribution Function to Solid-State Enzyme Inactivation

MAMORU SUGIURA ˣ, MASAYUKI KUROBE, SUMIHIRO TAMURA, and SHINICHI IKEDA

Received August 28, 1978, from the *Gifu College of Pharmacy, Mitahora-higashi, Gifu 502, Japan.* Accepted for publication February 9, 1979.

Abstract □ The Weibull distribution function was applied to solid-state enzyme inactivation. On Weibull probability paper (within a narrow range), the plots of the accumulated inactivation ratio of each enzyme *versus* time regressed to a straight line. The parameters m and k, which correspond to the type and rate of the inactivation, were characteristic of each enzyme. The effect of temperature and parameter reproducibility are discussed.

Keyphrases □ Weibull distribution function—application to solid-state enzyme inactivation studies □ Enzyme kinetics—application of Weibull distribution to inactivation studies □ Enzyme inactivation—kinetics, application of Weibull distribution to solid-state studies

Stability is important for drug quality assurance, and reports on drug stability in solid dosage forms have been published (1, 2). The essential requirement in stability studies is the selection of rate equations, which have been determined in practical systems by trial and error.

Some investigations using enzymes in the solid state failed because there was an inherent difficulty in fitting common rate equations to experimental data. Enzyme stability is complicated and is readily affected by factors such as temperature, humidity, and coexisting substances.

This paper[1] describes application of the Weibull distribution function to solid-state enzyme inactivation. The Weibull distribution originally was applied to stability predictions of other solid drugs (3, 4).

THEORETICAL

Efforts have been made to interpret the shelflife of enzymes in solids and solutions and to describe mathematically the inactivation profile with meaningful parameters. Although equations possibly could be derived from empirical treatment of the process, *e.g.*, pseudo-first-order kinetics, no suitable function has been found. Therefore, shelflives rarely have been mentioned in solid-state enzyme inactivation studies.

A general function, applicable to all inactivation curves, was derived by Weibull (5) and discussed in detail (6–8). A concise survey also was reported (9). When applied to enzyme inactivation rate data in the solid state, the Weibull distribution expresses the accumulated inactivation ratio, α, of the enzyme activity at time, t, by:

$$\alpha = 1 - \exp[-(t)^{m/k}] \qquad \text{(Eq. 1)}$$

where the scale parameter, k, defines the time scale of the process and the shape parameter, m, characterizes the curve as an exponential function. The relationship between m and curve shape was discussed previously (8, 9).

Graphical representation of the data according to the Weibull distribution and the practical aspects of linearizing experimental data were reported (6, 7). Equation 1 may be rearranged:

$$\ln \ln (1/1 - \alpha) = \ln k + m \ln t \qquad \text{(Eq. 2)}$$

From Eq. 2, a linear relation is obtained from a ln ln plot of $\ln (1/1 - \alpha)$ *versus* t. The shape parameter, m, is obtained from the slope, and k is obtained from the ordinate value at $t = 1$.

The theoretical correlation between Eq. 2 and chemical kinetics was discussed in detail (4). The equation expressing chemical kinetics varies according to the inactivation mechanism. However, within a narrow range, it is possible to express them by:

$$\frac{d\alpha}{dt} = Kg(a, \alpha, P_i) \qquad \text{(Eq. 3)}$$

where K is the rate constant, a is the initial enzyme activity, and P_i is the parameter independent of time, t. The integrated form of Eq. 3 is:

$$f(a, \alpha, P_i) = Kt \qquad \text{(Eq. 4)}$$

Equations 2 and 4 can be correlated by assuming that logarithms of Eq. 4 are expressed approximately as a linear function of Eq. 2:

$$\ln f(a, \alpha, P_i) = \ln K + \ln t \fallingdotseq A_0 + A_1 \ln \ln (1/1 - \alpha) \qquad \text{(Eq. 5)}$$

$$\ln \ln (1/1 - \alpha) \fallingdotseq 1/A_1 (\ln K - A_0) + 1/A_1 \ln t \qquad \text{(Eq. 6)}$$

[1] This paper is Part CLVII of "Studies on Enzymes" by M. Sugiura.

0022-3549/79/1100-1381$01.00/0

© 1979, American Pharmaceutical Association

Table I—Regression Line Parameters on Weibull Probability Paper for Lipase and Amylase Inactivation at Various Temperatures

Enzyme	Water, %	Parameter	Temperature 60°	55°	50°	45°	40°
Lipase							
Aspergillus	7.8	m	—	0.82	0.90	0.91	0.93
		$\ln k$	—	−2.74	−3.53	−4.28	−5.13
Rhizopus	8.5	m	4.55	4.73	4.20	4.52	—
		$\ln k$	−10.74	−13.28	−15.56	−20.15	—
Candida	7.3	m	—	2.12	1.40	1.43	1.44
		$\ln k$	—	−5.60	−4.97	−6.00	−6.60
Pancreatic	7.9	m	—	0.68	0.50	0.52	0.52
		$\ln k$	—	−1.69	−2.12	−2.78	−3.47
Amylase							
Aspergillus	8.6	m	—	1.45	1.49	1.57	1.55
		$\ln k$	—	−3.90	−5.20	−6.67	−7.67
Diastase	7.8	m	—	1.69	2.18	2.17	2.21
		$\ln k$	—	−4.90	−7.96	−8.93	−10.68
Pancreatic	7.6	m	—	0.90	0.79	0.83	1.30
		$\ln k$	—	−0.96	−2.50	−4.21	−8.70

Table II—Reproducibility of the Parameters k and m

Enzyme	Water, %	Temperature	Number of Experiments	Parameter m	$\ln k$	$(1/m) \times \ln k$
Aspergillus lipase	4.9	50°	1	0.79	−3.90	−4.91
			2	0.85	−4.09	−4.81
			3	0.68	−3.53	−5.10
			4	0.85	−4.10	−4.82
Aspergillus lipase	11.2	40°	1	1.03	−4.52	−4.39
			2	1.05	−4.60	−4.38
			3	1.08	−4.48	−4.15
Pancreatic lipase	10.1	50°	1	0.50	−2.25	−4.50
			2	0.50	−2.05	−4.10
			3	0.50	−2.12	−4.24

From Eqs. 2 and 6, the relationship between the constants determined on Weibull probability paper and the relationship determined by chemical kinetics are:

$$\ln k = 1/A_1 (\ln K - A_0) \quad \text{(Eq. 7a)}$$

$$m = 1/A_1 \quad \text{(Eq. 7b)}$$

Therefore, from Eq. 7b, m corresponds to the shape of $f(a, \alpha, P_i)$, *i.e.*, the reaction mechanism, and $k^{1/m}$ is proportional to the reaction rate constant. Therefore, the selection of rate equations becomes unnecessary.

EXPERIMENTAL

Enzymes—The enzymes were microbial lipases from *Aspergillus genus*[2], *Rhizopus* sp. NR 400[3], and *Candida cylindracea* nov. sp.[4]; microbial α-amylase from *Aspergillus oryzae*[5]; pancreatin from porcine pancreas[6]; and diastase from malt[7].

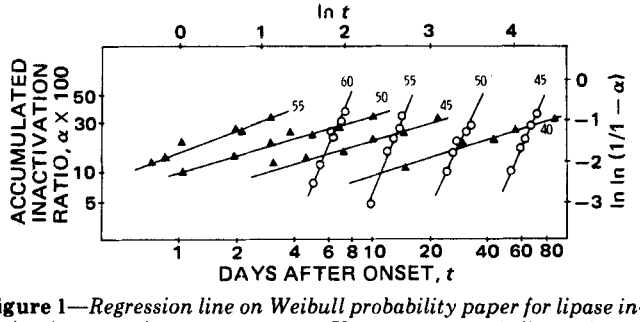

Figure 1—*Regression line on Weibull probability paper for lipase inactivation at various temperatures. Key:* ▲, *pancreatic lipase (water content 7.9%); and* O, Rhizopus *lipase (water content 8.5%).*

[2] Lipase AP, Amano Pharmaceutical Co., Nagoya, Japan.
[3] Lipase Saiken, Osaka Saiken Co., Osaka, Japan.
[4] Lipase MY, Meito Sangyo Co., Nagoya, Japan.
[5] Biodiastase 1000, Amano Pharmaceutical Co., Nagoya, Japan.
[6] Pancreatin, Amano Pharmaceutical Co., Nagoya, Japan.
[7] Diastase, Toyo Jozo Co., Shizuoka, Japan.

Stability Test—All enzymes were tested initially by placing the accurately weighed lyophilizates in open ampuls in a humidity chamber for 1 week. At the end of the equilibrium period, the samples were weighed, and the weight gain was noted. Moisture pickup was expressed as the percent weight gain. The humidity chambers, which were glass desiccators, were kept at ~25°. Constant humidities were obtained by placing appropriate saturated salt solutions in the bottoms of the desiccators.

After the ampuls were sealed, each enzyme was placed in thermostated water baths at 40, 45, 50, 55, and 60°. Samples were removed at appropriate periods, and the remaining activity was determined.

Enzyme Activity Assay—The activities of lipases and α-amylases were determined according to a reported procedure (10, 11). The remaining activity was expressed as a ratio relative to that of the enzyme stored in a refrigerator.

RESULTS AND DISCUSSION

The inactivation behavior of pancreatic lipase and *Rhizopus* lipase at various temperatures is shown in Fig. 1; the accumulated inactivation ratios were plotted *versus* time according to the linearized form of Eq. 2. Within a narrow range (inactivation ratio 5–30%), the inactivation data plots yielded a straight regression line. The Weibull distribution function distorted the original scale of the observation greatly; in particular, deviations occurring in the lower and the upper tail were overemphasized compared to those in the middle of the plot.

The same stress test was carried out with lipase and α-amylase samples. The inactivation ratio plot of each enzyme also regressed to a straight line, which confirmed that enzyme inactivation could be followed by the Weibull distribution function. The parameters m and k were determined by a graphic calculation (Table I). Table I shows the specific parameters that characterize the inactivation profile for each enzyme. Temperatures of <55–60° had no influence on the parameters, which indicated that the stress test could be applied to solid enzyme inactivation studies during preservation.

The finding that most of the m values for each enzyme differed from those of common rate equations, estimated at ~1.0 (4), confirmed an inherent difficulty in fitting other common rate equations to experimental data and thereby interpreting enzyme stabilities.

Table II shows the reproducibility of the parameters with pancreatic lipase and *Rhizopus* lipase as a model. Table II shows that the resultant parameter variation was satisfactorily small. Therefore, the Weibull distribution is applicable to solid-state enzyme inactivation studies in practical fields.

Enzyme inactivation in aqueous systems has been studied extensively with regard to protein structures and biochemical functions (12–14). The present study was confined to application of the Weibull distribution function to solid-state enzyme inactivation. Enzyme inactivation in the solid state could be described by a straight regression line in terms of meaningful parameters. The excellent parameter reproducibility and the absence of temperature influence ensure that this function will be useful in further work involving the quantitative prediction of solid-state enzyme stabilities.

REFERENCES

(1) R. Tardif, *J. Pharm. Sci.*, **54**, 281 (1965).

(2) J. T. Carstensen, E. S. Aron, D. C. Spera, and J. J. Vance, *ibid.*, **55**, 561 (1966).
(3) N. Okusa and K. Kinuno, *Yakuzaigaku*, **28**, 23 (1968).
(4) N. Okusa, *Chem. Pharm. Bull.*, **23**, 794 (1975).
(5) W. Weibull, *J. Appl. Mech.*, **18**, 293 (1951).
(6) J. H. K. Kao, *Technometrics*, **1**, 389 (1959).
(7) R. K. Ruzicka, *J. Electronics Div. (American Society for Quality Control)*, **1**, 38 (1962).
(8) F. Langenbucher, *J. Pharm. Pharmacol.*, **24**, 979 (1972).
(9) E. L. Grant, "Statistical Quality Control," 3rd ed., McGraw-Hill, New York, N.Y., 1964, p. 505.
(10) T. Ogiso and M. Sugiura, *Chem. Pharm. Bull.*, **17**, 1025 (1969).
(11) M. Sugiura, *Yakuzaigaku*, **28**, 48 (1968).
(12) S. Nakayama and Y. Kano, *J. Biochem. (Tokyo)*, **44**, 25 (1957).
(13) C. Tanford, *J. Am. Chem. Soc.*, **86**, 2050 (1964).
(14) C. Tanford, K. C. Anue, and A. Ikai, *J. Mol. Biol.*, **73**, 185 (1973).

Evaluation of 1-(3,4-Dichlorophenyl)-4-dimethylaminomethyl-1-nonen-3-one Hydrochloride Effect on Nucleic Acid and Protein Syntheses Using Murine Leukemia L-1210 Cells

C. B. NYATHI *, V. S. GUPTA *, and J. R. DIMMOCK ‡x

Received March 2, 1979, from the **Department of Physiological Sciences, Western College of Veterinary Medicine, and the* ‡*College of Pharmacy, University of Saskatchewan, Saskatoon, Saskatchewan, Canada, S7N 0W0.* Accepted for publication May 11, 1979.

Abstract □ Several Mannich bases derived from conjugated styryl ketones were shown to have potent cytotoxicity toward murine leukemia L-1210 cells and Walker 256 carcinosarcoma cells in culture. The most cytotoxic derivative, (*E*)-1-(3,4-dichlorophenyl)-4-dimethylaminomethyl-1-nonen-3-one hydrochloride, profoundly inhibited the incorporation of tritiated leucine into protein(s) and tritiated deoxythymidine into DNA at concentrations of 0.79–1.32 μM in L-1210 cells. At higher concentrations, incorporation of tritiated uridine into RNA and tritiated deoxyuridine into DNA was inhibited to a lesser degree. This compound failed to inhibit the enzymes thymidylate synthetase or dihydrofolate reductase up to a concentration of 10^{-4} M and was ineffective in retarding the growth of the Walker 256 carcinosarcoma in rats.

Keyphrases □ Mannich bases—derived from conjugated styryl ketones, cytotoxicity, murine leukemia L-1210 and Walker 256 carcinosarcoma cells, *in vitro* and *in vivo* □ Antineoplastic agents, potential—Mannich bases derived from conjugated styryl ketones, cytotoxicity, murine leukemia L-1210 and Walker 256 carcinosarcoma cells, *in vitro* and *in vivo* □ 1-(3,4-Dichlorophenyl)-4-dimethylaminomethyl-1-nonen-3-one hydrochloride—cytotoxicity against murine leukemia L-1210 and Walker 256 carcinosarcoma cells, *in vitro* and *in vivo*

Several Mannich bases derived from acyclic α,β-unsaturated ketones (I) have shown antitumor and cytotoxic activities (1–3). Previous studies showed a correlation between cytotoxicity and murine toxicity with mitochondrial function disturbance (4). With the representative Mannich bases II*b*–II*e*, competition with coenzyme Q_{10} occurred (5). The purpose of this study was to discover whether these Mannich bases act at sites other than mitochondria or whether the biological activity observed is due solely to the effect on mitochondria.

Since series I compounds may be regarded as biological alkylating agents, a class of compounds known to interfere with the syntheses of DNA and RNA (6–8) as well as protein (9, 10), the effect on the syntheses of these biological macromolecules is reported.

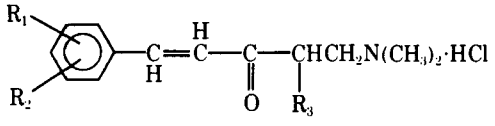

I

$R_1 = R_2 = H, Cl$
$R_3 = H, CH_3, (CH_2)_4CH_3$

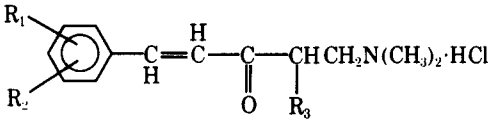

II

II*a*: $R_1 = R_2 = R_3 = H$
II*b*: $R_1 = R_2 = H, R_3 = (CH_2)_4CH_3$
II*c*: $R_1 = 2\text{-Cl}, R_2 = 4\text{-Cl}, R_3 = (CH_2)_4CH_3$
II*d*: $R_1 = 2\text{-Cl}, R_2 = 6\text{-Cl}, R_3 = (CH_2)_4CH_3$
II*e*: $R_1 = 3\text{-Cl}, R_2 = 4\text{-Cl}, R_3 = (CH_2)_4CH_3$

RESULTS AND DISCUSSION

Earlier work from these laboratories, which showed that the established biological alkylating agents chlorambucil and cyclophosphamide inhibited DNA synthesis, employed murine leukemia L-1210 and Walker ascites carcinoma 256 cells (11, 12). The first consideration in the present study was to establish whether representative compounds in Series I were cytotoxic to these two cell lines. Since II*a*–II*e* had previously demonstrated activity in the KB screen (4, 5), an *in vitro* screen using human epidermoid carcinoma of the nasopharynx in Eagle's medium, these compounds were examined for cytotoxicity against the L-1210 and Walker 256 cells. Both tumors showed essentially the same sensitivity to II*a*–II*e* with ID_{50} values (inhibitory doses for 50% reduction in cell numbers) in the range of 3.44–3.96 μM. The most potent compound against L-1210 cells was II*e*, with an ID_{50} of 3.46 μM (Fig. 1). This compound was used in subsequent studies.

Some reactions involved in the DNA, RNA, and protein syntheses are summarized in Scheme I. During the exponential growth phase, cells preferentially utilize deoxyuridine for the *de novo* synthesis of deoxythymidine monophosphate (13). This reaction is catalyzed by thymidylate synthetase. An alternative route for deoxythymidine monophosphate synthesis is by direct phosphorylation of deoxythymidine. Deoxythymidine monophosphate, after conversion to its corresponding triphosphate, is utilized for DNA synthesis (13). Thus, the effect of compounds on DNA synthesis can be monitored by studying the incorporation of either tritiated deoxythymidine or tritiated deoxyuridine.

Similarly, the effects of biologically active compounds on RNA synthesis can be investigated by studying their effects on the incorporation

0022-3549/79/1100-1383$01.00/0
© 1979, American Pharmaceutical Association

(2) J. T. Carstensen, E. S. Aron, D. C. Spera, and J. J. Vance, *ibid.*, **55**, 561 (1966).
(3) N. Okusa and K. Kinuno, *Yakuzaigaku*, **28**, 23 (1968).
(4) N. Okusa, *Chem. Pharm. Bull.*, **23**, 794 (1975).
(5) W. Weibull, *J. Appl. Mech.*, **18**, 293 (1951).
(6) J. H. K. Kao, *Technometrics*, **1**, 389 (1959).
(7) R. K. Ruzicka, *J. Electronics Div. (American Society for Quality Control)*, **1**, 38 (1962).
(8) F. Langenbucher, *J. Pharm. Pharmacol.*, **24**, 979 (1972).
(9) E. L. Grant, "Statistical Quality Control," 3rd ed., McGraw-Hill, New York, N.Y., 1964, p. 505.
(10) T. Ogiso and M. Sugiura, *Chem. Pharm. Bull.*, **17**, 1025 (1969).
(11) M. Sugiura, *Yakuzaigaku*, **28**, 48 (1968).
(12) S. Nakayama and Y. Kano, *J. Biochem. (Tokyo)*, **44**, 25 (1957).
(13) C. Tanford, *J. Am. Chem. Soc.*, **86**, 2050 (1964).
(14) C. Tanford, K. C. Anue, and A. Ikai, *J. Mol. Biol.*, **73**, 185 (1973).

Evaluation of 1-(3,4-Dichlorophenyl)-4-dimethylaminomethyl-1-nonen-3-one Hydrochloride Effect on Nucleic Acid and Protein Syntheses Using Murine Leukemia L-1210 Cells

C. B. NYATHI *, V. S. GUPTA *, and J. R. DIMMOCK ‡x

Received March 2, 1979, from the **Department of Physiological Sciences, Western College of Veterinary Medicine, and the* ‡*College of Pharmacy, University of Saskatchewan, Saskatoon, Saskatchewan, Canada, S7N 0W0.* Accepted for publication May 11, 1979.

Abstract □ Several Mannich bases derived from conjugated styryl ketones were shown to have potent cytotoxicity toward murine leukemia L-1210 cells and Walker 256 carcinosarcoma cells in culture. The most cytotoxic derivative, (*E*)-1-(3,4-dichlorophenyl)-4-dimethylaminomethyl-1-nonen-3-one hydrochloride, profoundly inhibited the incorporation of tritiated leucine into protein(s) and tritiated deoxythymidine into DNA at concentrations of 0.79–1.32 μM in L-1210 cells. At higher concentrations, incorporation of tritiated uridine into RNA and tritiated deoxyuridine into DNA was inhibited to a lesser degree. This compound failed to inhibit the enzymes thymidylate synthetase or dihydrofolate reductase up to a concentration of 10^{-4} M and was ineffective in retarding the growth of the Walker 256 carcinosarcoma in rats.

Keyphrases □ Mannich bases—derived from conjugated styryl ketones, cytotoxicity, murine leukemia L-1210 and Walker 256 carcinosarcoma cells, *in vitro* and *in vivo* □ Antineoplastic agents, potential—Mannich bases derived from conjugated styryl ketones, cytotoxicity, murine leukemia L-1210 and Walker 256 carcinosarcoma cells, *in vitro* and *in vivo* □ 1-(3,4-Dichlorophenyl)-4-dimethylaminomethyl-1-nonen-3-one hydrochloride—cytotoxicity against murine leukemia L-1210 and Walker 256 carcinosarcoma cells, *in vitro* and *in vivo*

Several Mannich bases derived from acyclic α,β-unsaturated ketones (I) have shown antitumor and cytotoxic activities (1–3). Previous studies showed a correlation between cytotoxicity and murine toxicity with mitochondrial function disturbance (4). With the representative Mannich bases II*b*–II*e*, competition with coenzyme Q_{10} occurred (5). The purpose of this study was to discover whether these Mannich bases act at sites other than mitochondria or whether the biological activity observed is due solely to the effect on mitochondria.

Since series I compounds may be regarded as biological alkylating agents, a class of compounds known to interfere with the syntheses of DNA and RNA (6–8) as well as protein (9, 10), the effect on the syntheses of these biological macromolecules is reported.

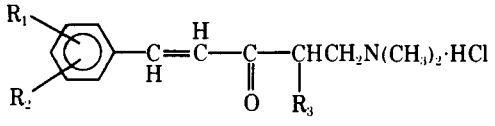

I

$R_1 = R_2 = H, Cl$
$R_3 = H, CH_3, (CH_2)_4CH_3$

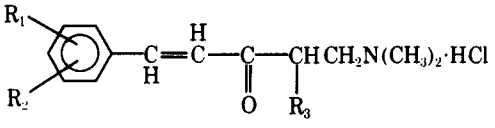

II

II*a*: $R_1 = R_2 = R_3 = H$
II*b*: $R_1 = R_2 = H, R_3 = (CH_2)_4CH_3$
II*c*: $R_1 = 2\text{-Cl}, R_2 = 4\text{-Cl}, R_3 = (CH_2)_4CH_3$
II*d*: $R_1 = 2\text{-Cl}, R_2 = 6\text{-Cl}, R_3 = (CH_2)_4CH_3$
II*e*: $R_1 = 3\text{-Cl}, R_2 = 4\text{-Cl}, R_3 = (CH_2)_4CH_3$

RESULTS AND DISCUSSION

Earlier work from these laboratories, which showed that the established biological alkylating agents chlorambucil and cyclophosphamide inhibited DNA synthesis, employed murine leukemia L-1210 and Walker ascites carcinoma 256 cells (11, 12). The first consideration in the present study was to establish whether representative compounds in Series I were cytotoxic to these two cell lines. Since II*a*–II*e* had previously demonstrated activity in the KB screen (4, 5), an *in vitro* screen using human epidermoid carcinoma of the nasopharynx in Eagle's medium, these compounds were examined for cytotoxicity against the L-1210 and Walker 256 cells. Both tumors showed essentially the same sensitivity to II*a*–II*e* with ID_{50} values (inhibitory doses for 50% reduction in cell numbers) in the range of 3.44–3.96 μM. The most potent compound against L-1210 cells was II*e*, with an ID_{50} of 3.46 μM (Fig. 1). This compound was used in subsequent studies.

Some reactions involved in the DNA, RNA, and protein syntheses are summarized in Scheme I. During the exponential growth phase, cells preferentially utilize deoxyuridine for the *de novo* synthesis of deoxythymidine monophosphate (13). This reaction is catalyzed by thymidylate synthetase. An alternative route for deoxythymidine monophosphate synthesis is by direct phosphorylation of deoxythymidine. Deoxythymidine monophosphate, after conversion to its corresponding triphosphate, is utilized for DNA synthesis (13). Thus, the effect of compounds on DNA synthesis can be monitored by studying the incorporation of either tritiated deoxythymidine or tritiated deoxyuridine.

Similarly, the effects of biologically active compounds on RNA synthesis can be investigated by studying their effects on the incorporation

0022-3549/79/1100-1383$01.00/0
© 1979, American Pharmaceutical Association

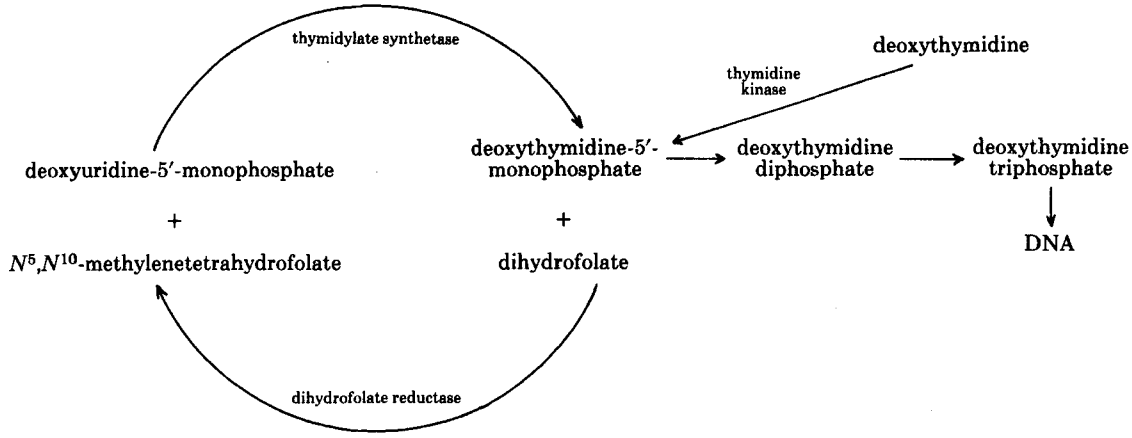

A. Metabolic pathways leading to the incorporation of deoxyuridine and deoxythymidine into DNA

$$\text{uridine} \rightarrow \text{ribonucleotides} \xrightarrow[\text{RNA polymerases}]{\text{DNA dependent}} \text{RNA}$$

B. Some reactions involved in RNA synthesis

$$\text{amino acids (}e.g.\text{, leucine)} \rightarrow \text{amino acids–}t\text{-RNA} \rightarrow\!\rightarrow \text{protein}$$

C. Some reactions involved in protein synthesis

Scheme I—Simplified schematic representation of reactions involved in the syntheses of DNA, RNA, and protein

of an appropriate labeled ribonucleoside precursor such as tritiated uridine. The ribonucleic acids are synthesized *in vivo* from four ribonucleosides, one of which is uridine. These ribonucleosides, after conversion to their corresponding triphosphates, are incorporated into RNA under the direction of a DNA template. This latter transcription process is mediated by DNA-dependent RNA polymerases (14).

Protein synthesis from amino acids is carried out by a series of complex reactions in which RNA, in its different forms, plays a major role in peptide bond formation. The present investigation studied the effect of 1-(3,4-dichlorophenyl)-4-dimethylaminomethyl-1-nonen-3-one hydrochloride (IIe) on the incorporation of tritiated leucine into protein.

The effect of IIe on the uptake of the tritiated precursors into the corresponding biological macromolecules (deoxyuridine and deoxythymidine into DNA, uridine into RNA, and leucine into protein) is summarized in Table I. Incorporation of tritiated deoxythymidine and tritiated leucine was markedly reduced, followed by tritiated uridine and tritiated deoxyuridine. Since incorporation of tritiated leucine and tritiated deoxythymidine was profoundly reduced at the dose levels of 2.64 μM (Table I), the effect of lower IIe concentrations (1.32, 0.79, and 0.26 μM) on the uptake of these precursors was investigated (Figs. 2A and 2C).

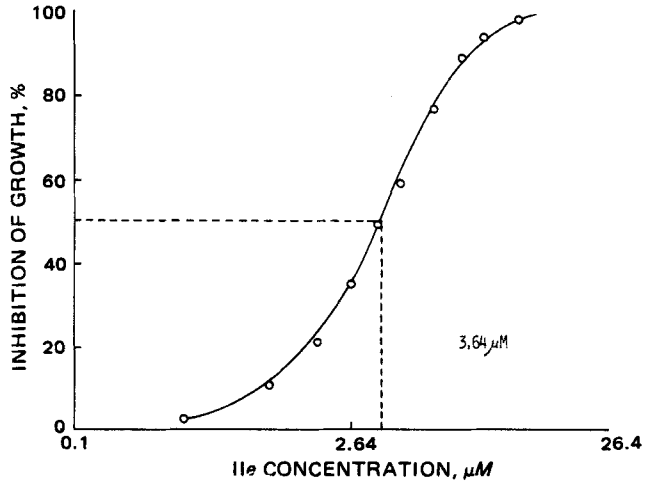

Figure 1—*Dose–response curve for IIe against L-1210 cells in tissue culture.*

The results for the IIe inhibition of tritiated uridine and tritiated deoxyuridine incorporation are shown in Figs. 2B and 2D.

After 30 min of preincubation with IIe (2.64 μM), tritiated uridine incorporation was inhibited by ~60% (Fig. 2B). Increasing either the IIe concentrations up to 13.2 μM or the incubation time up to 4 hr did not further decrease tritiated uridine incorporation into RNA. Incorporation of tritiated deoxyuridine into the DNA of drug-treated cells was inhibited only slightly (~30%) even after preincubation for 4 hr with 13.2 μM of IIe (Fig. 2D and Table I). In marked contrast, the rate of tritiated deoxythymidine incorporation into the DNA of L-1210 cells was reduced significantly (~90%) at 1.32 μM (Fig. 2C). Interestingly, the loss of tritiated deoxythymidine uptake was dependent on the IIe concentration in the medium (up to 1.32 μM) and on the incubation time. Similarly, tritiated leucine incorporation was depressed by ~60% within 10 min of preincubation in the presence of 1.32 μM of IIe (Fig. 2A).

In the presence of IIe, decreased incorporation of tritiated nucleosides into the nucleic acids could have been due to: (*a*) inactivation of the enzymes involved in DNA and RNA syntheses, (*b*) interference with the transport of nucleosides into cells, and (*c*) direct binding with the DNA template and destruction of its priming ability. Enzyme inactivation was possibly not a major factor because the inhibitory effects on the incorporation of tritiated deoxyuridine and tritiated uridine were not proportional to the IIe concentration. In addition, IIe failed to inhibit thymidylate synthetase or dihydrofolate reductase up to a concentration of 10^{-4} M (a concentration ~70-fold higher than the amount required to inhibit tritiated deoxyuridine incorporation into DNA).

Decreased incorporation of these nucleosides probably was due to interference of IIe with the nucleoside transport mechanisms. On the other hand, markedly reduced deoxythymidine incorporation obviously was due to a combination of IIe effects on tritiated deoxythymidine transport and on inactivation of enzymes (such as thymidine kinase or the thymidylate kinases) involved in the utilization of thymidine for DNA synthesis. Another possible active site of IIe may be direct binding with the DNA template, thus destroying its priming ability. The leucine incorporation rate was inhibited significantly and quickly at very low IIe concentrations. The site of action of IIe was probably interaction with some enzymes involved in protein synthesis.

These results indicate that a new biological alkylating agent, IIe, markedly inhibits DNA and protein syntheses at low concentrations, while RNA synthesis is also retarded, although to a lesser degree. Since α,β-unsaturated ketones are known to react with thiols (9, 15–18), IIe may be a general sulfhydryl alkylator which accounts, in part at least, for the observed inhibition of DNA, RNA, and protein syntheses. The effect of IIe is, however, in contrast to the established biological alkylating

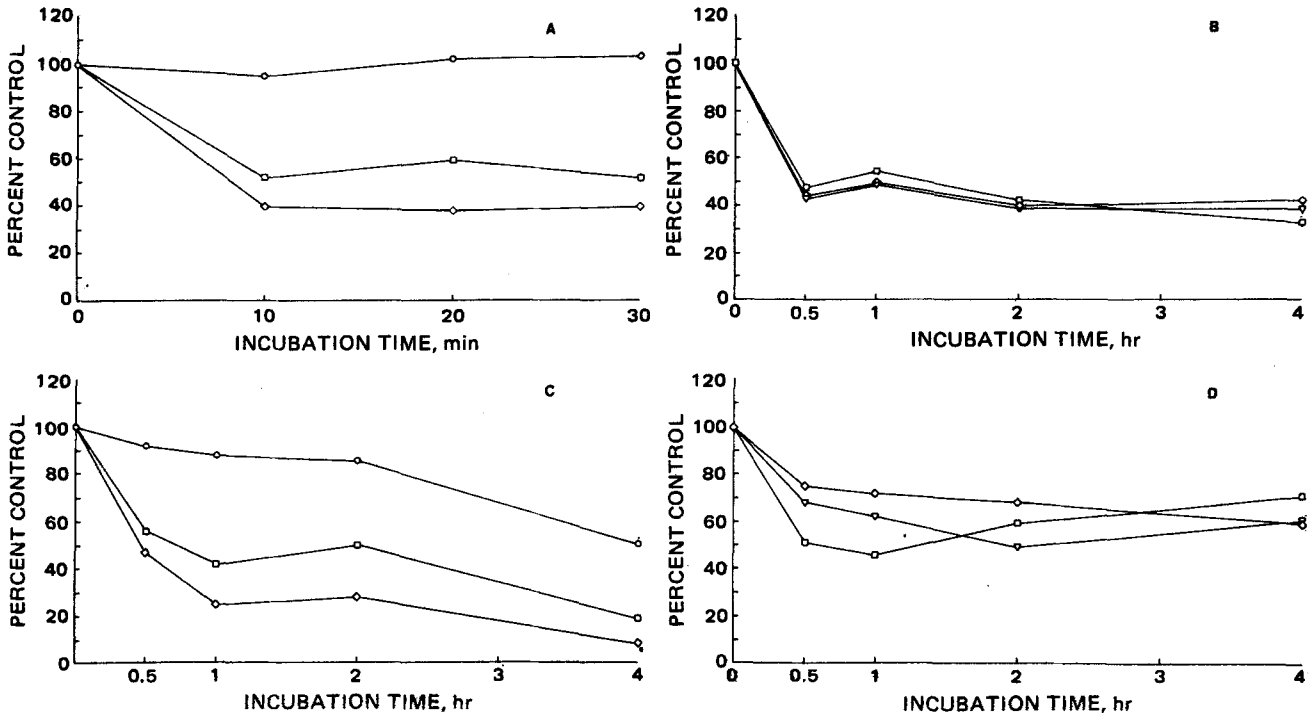

Figure 2—*Effects of IIe treatment on the incorporation of labeled precursors into macromolecules. Dose–response curves in the presence of IIe for: tritiated leucine (A) at 0.26 μM (○), 0.79 μM (□), and 1.32 μM (◇); tritiated uridine (B) at 2.64 μM (□), 7.93 μM (△), and 13.2 μM (▽); tritiated deoxythymidine (C) at 0.26 μM (○), 0.79 μM (□), and 1.32 μM (◇); and tritiated deoxyuridine (D) at 2.64 μM (◇), 7.93 μM (▽), and 13.2 μM (□).*

agents chlorambucil and cyclophosphamide, which affect DNA synthesis only at low concentrations (11, 12).

Finally, the *in vitro* studies showed that IIe along with other Mannich bases IIa–IId were cytotoxic to both L-1210 and Walker 256 cells *in vitro*. A previous report revealed that intraperitoneal administration of IIb–IIe did not produce perceptible increases in the mean survival time of mice inoculated with L-1210 leukemia (1). Therefore, it was of interest to see whether IIe would display *in vivo* activity against the Walker 256 tumors in rats, a tumor susceptible to a number of biological alkylating agents (19). Prolongation of the lifespan of animals bearing the Walker tumor did not occur at the maximum tolerated dose (25 mg/kg). At this dose, there was some evidence of toxicity, as manifested by loss of weight and diarrhea.

EXPERIMENTAL

Syntheses—The II compounds were prepared by literature procedures (1, 20).

Cell Cultures—The stock cultures of Walker ascites carcinosarcoma 256[1] and L-1210[2] cell lines were cultured in Fischers medium containing 10% horse serum[3] and were incubated at 37° in a humid carbon dioxide (5%) atmosphere. The mean generation time of the cells was determined by diluting the actively growing cells with growth medium to 1.84×10^5 cells/ml in 100-mm petri dishes. Cell counts[4] were made at 24, 48, and 72 hr. Under these conditions, the mean generation time was 16 ± 1 hr for both cell lines. Determinations were undertaken in duplicate.

Table I—Percentage Inhibition by IIe of the Incorporation of Tritiated Deoxyuridine and Tritiated Deoxythymidine into DNA, Tritiated Uridine into RNA, and Tritiated Leucine into Protein by Cultured L-1210 Cells

Dose, μM	Tritiated Deoxyuridine	Tritiated Deoxythymidine	Tritiated Uridine	Tritiated Leucine
2.64	20	84	49	71
7.93	29	90	66	78
13.2	27	86	59	79

Cell Growth Inhibition—The cytotoxicity of the II compounds toward L-1210 and Walker 256 cells was investigated as follows. Solutions of the compounds at twice the concentrations required were prepared by dissolving in water immediately prior to use, and each solution was sterilized by passage through a 45-μm filter[5]. The actively growing cells were diluted to 3.68×10^5 cells/ml with growth medium (10 ml), and the test compound solution (10 ml) was added to the cells.

The petri dishes were incubated at 37° in a 5% carbon dioxide atmosphere. The cell count[4] after 48 hr, expressed as a percentage of the control cell count, was plotted against drug concentration for 10 different concentrations of each compound. From the graph, the drug concentration giving 50% of the control cell count (ID_{50}) was obtained. All determinations were carried out in duplicate.

Effect of IIe on Incorporation of Tritiated Deoxythymidine, Tritiated Deoxyuridine, Tritiated Uridine, and Tritiated Leucine—Incorporation of the appropriate labeled precursor[6] into macromolecules was studied by a modification of the published procedure (21, 22) using L-1210 cells. A cell suspension (0.8 ml) containing $2.0–2.3 \times 10^6$ cells was placed in sterile plastic tubes, and a IIe solution was added to give the desired final concentrations. The cell suspensions were incubated at 37° in a 5% carbon dioxide atmosphere.

At regular intervals of 0.5, 1.0, 2.0, and 4.0 hr after contact with IIe, 0.1 ml of tritiated deoxythymidine (3.0 μCi, 6.52×10^{-6} *M*), tritiated deoxyuridine (3.0 μCi, 8.33×10^{-6} *M*), tritiated uridine (3.0 μCi, 5.7×10^{-6} *M*), or tritiated leucine (3.0 μCi, 2.8×10^{-6} *M*) was added to the tubes, and the samples were reincubated at 37°. In another set of experiments involving leucine incorporation, the cells were left in contact with IIe for only 10, 20, and 30 min before the tritiated leucine addition (3.0 μCi, 2.8×10^{-6} *M*). An aliquot of the cell suspension (0.2 ml from each sample) was removed at intervals of 5, 10, 15, and 20 min and added to ice-cold trichloroacetic acid (10%, 5 ml). The resultant suspension was mixed[7], left overnight at 4°, and centrifuged for 20 min at 4° at 3000 rpm.

The supernatant liquid was discarded, and the precipitate was washed three more times with cold trichloroacetic acid (10%, 5 ml) to remove unadsorbed radioactivity. The precipitate was dissolved in a solubilizer[8]

[1] Obtained from Professor J. R. Bertino, Department of Pharmacology, School of Medicine, Yale University, New Haven, Conn.
[2] Obtained from Dr. A. R. Paterson, Cancer Research Unit, University of Alberta, Edmonton, Canada.
[3] Grand Island Biological Co., New York, N.Y.
[4] Model FN Coulter counter, Coulter Electronics, Hialeah, Fla.
[5] Millipore.
[6] Amersham/Searle, Oakville, Ontario, Canada.
[7] Vortex mixer, Fisher Scientific Co., Edmonton, Alberta, Canada.
[8] NSC, Amersham/Searle, Oakville, Ontario, Canada.

(0.5 ml) and diluted with scintillation fluid[9] (12 ml), and the amount of radioactivity incorporated into DNA, RNA, or protein was counted using a liquid scintillation counter[10]. The results were expressed as the percentage of labeled precursor incorporated by treated cells divided by that of control cells. All determinations were carried out in duplicate.

Enzyme Studies—*Enzyme Isolation*—Frozen Walker 256 tumors (200 g) were cut into small cubes (1–2 cm), suspended in 500 ml of TKEM buffer (pH 7.0, 50 m*M* tromethamine hydrochloride[11] containing 100 m*M* of potassium chloride, 1 m*M* of edetate disodium, and 10 m*M* of mercaptoethanol) and homogenized for 90 sec in a blender[12]. The resulting homogenate was centrifuged at 22,000×*g*, and streptomycin sulfate solution (20%) was added dropwise with constant stirring at the ratio of 1 ml/100 ml of extract. After 30 min, the mixture was centrifuged, and the precipitate was discarded.

Solid ammonium sulfate was added to the supernatant liquid gradually with constant stirring to 35% of saturation, and the precipitate was removed by centrifugation. The ammonium sulfate concentration was raised to 55% of saturation and stirred for 30 min, and the precipitate was collected by centrifugation (Fraction I). Additional ammonium sulfate was added slowly to 95% of saturation, and the precipitate was removed by centrifugation (Fraction II). Both fractions were stored frozen at −65°. Approximately 80–90% of the total thymidylate synthetase and dihydrofolate reductase activity was recovered in Fractions I and II.

Enzyme activities were stable in the frozen state up to 3 months. A small quantity of the precipitate of Fraction I or II was dissolved in the minimum quantity of TKEM buffer, dialyzed against the same buffer for 4 hr, and centrifuged, and the supernatant liquid was used for enzyme assays.

Enzyme Activities—Thymidylate synthetase activity was assayed by a modified procedure (11) of Wahba and Friedkin (23), and dihydrofolate reductase activity was measured by the method of Perkins *et al.* (24). Reactions were initiated by the addition of substrates. Corrections were made for blanks, and all assays were carried out in duplicate.

Thymidylate Synthetase and Dihydrofolate Reductase Inhibition by IIe—An enzyme sample of Fraction I or II was incubated with varying IIe concentrations along with the assay components (except substrate) for 30 min at 22 or 37°. The reaction involving thymidylate synthetase was initiated by deoxyuridine monophosphate[10] addition, and the dihydrofolate reductase reaction was initiated with dihydrofolic acid prepared from folic acid by a literature method (25).

Effect of IIe on Growth of Walker Ascites Carcinosarcoma 256—*Tumor Transplantation*—Six-week-old male Wistar rats[13], 140–160 g, were used for all experiments. The tumor was propagated by regular transplantation every 10 days as described previously (11). The tumor size was measured on alternate days, and the tumor weight was calculated as described earlier (11).

Treatment Schedule—Fresh solutions of IIe in saline were sterilized by passage through a 45-μm filter[5] and used immediately. The concentrations were adjusted so that 0.2–0.3 ml of solution was administered at each dose. Treatment commenced on Day 8 after tumor transplantation, when the size of the tumor was 16–18 mm. Compound IIe was administered at doses of 5, 10, 15, and 25 mg/kg ip while control animals were given the same volume of solvent. Six to eight rats were used for each dose.

[9] The scintillation fluid consisted of 2,5-diphenyloxazole (5.0 g), 4-(methyl-5-phenyloxazolyl)benzene (75 mg) (obtained from Amersham/Searle, Oakville, Ontario, Canada), and scintillation grade toluene (1 liter) (obtained from Fisher Scientific Co., Edmonton, Alberta, Canada).

[10] Model 300, Isocap, Searle Analytical Inc., Chicago, Ill.

[11] Sigma Chemical Co., St. Louis, Mo.

[12] Osteriser, Oster Corp., Milwaukee, Wis.

[13] Canadian Breeding Farm and Laboratories Ltd., Quebec, Canada.

REFERENCES

(1) J. R. Dimmock and W. G. Taylor, *J. Pharm. Sci.*, **64**, 241 (1975).

(2) W. von Werner, W. Jungstand, and W. Gutsche, *Arzneim.-Forsch.*, **20**, 246 (1970).

(3) H. Schoenenberger, T. Bastug, L. Bindl, A. Adam, D. Adam, A. Petter, and W. Zwez, *Pharm. Acta Helv.*, **44**, 691 (1969).

(4) J. R. Dimmock, N. W. Hamon, K. W. Hindmarsh, D. G. Mills, L. E. Negrave, G. H. Rank, and A. J. Robertson, *J. Pharm. Sci.*, **65**, 482 (1976).

(5) N. W. Hamon, D. L. Bassendowski, D. E. Wright, J. R. Dimmock, and L. M. Noble, *ibid.*, **67**, 1539 (1978).

(6) K. Folkers, T. H. Porter, E. Acton, D. L. Taylor, and D. Henry, *Biochem. Biophys. Res. Commun.*, **83**, 353 (1978).

(7) A. J. Lin, L. A. Cosby, C. W. Shansky, and A. C. Sartorelli, *J. Med. Chem.*, **15**, 1247 (1972).

(8) A. J. Lin, R. S. Pardini, L. A. Cosby, B. J. Lillis, C. W. Shansky, and A. C. Sartorelli, *ibid.*, **16**, 1268 (1973).

(9) I. H. Hall, K.-H. Lee, E. C. Mar, C. O. Starnes, and T. G. Waddell, *ibid.*, **20**, 333 (1977).

(10) I. H. Hall, K.-H. Lee, and S. A. ElGebaly, *J. Pharm. Sci.*, **67**, 1232 (1978).

(11) S. K. Srinivasan, V. S. Gupta, and R. E. Howarth, *Biochem. Pharmacol.*, **26**, 1027 (1977).

(12) S. K. Srinivasan, Ph.D. thesis, University of Saskatchewan, Saskatoon, Canada, 1977.

(13) M. Friedkin, *Adv. Enzymol.*, **38**, 235 (1973).

(14) L. Stryer, "Biochemistry," W. H. Freeman, San Francisco, Calif., 1975, p. 603.

(15) T. Posner, *Chem. Ber.*, **35**, 799 (1902).

(16) *Ibid.*, **37**, 502 (1904).

(17) S. M. Kupchan, D. C. Fessler, M. A. Eakin, and T. J. Giacobbe, *Science*, **168**, 376 (1970).

(18) A. Rosowsky, N. Papathanasopoulos, H. Lazarus, G. E. Foley, and E. J. Modest, *J. Med. Chem.*, **17**, 672 (1974).

(19) A. Goldin, S. Carter, and N. Mantel, in "Antineoplastic and Immunosuppressive Agents," part I, A. C. Sartorelli and D. G. Johns, Eds., Springer-Verlag, Berlin, Germany, 1974, p. 12.

(20) J. R. Dimmock and W. G. Taylor, *J. Pharm. Sci.*, **63**, 69 (1974).

(21) W. M. Hryniuk and J. R. Bertino, *J. Clin. Invest.*, **48**, 2140 (1969).

(22) B. A. Chabner, P. L. Chello and J. R. Bertino, *Cancer Res.*, **32**, 2114 (1972).

(23) A. J. Wahba and M. Friedkin, *J. Biol. Chem.*, **237**, 3794 (1962).

(24) J. P. Perkins, B. L. Hillcoat, and J. R. Bertino, *ibid.*, **242**, 4771 (1967).

(25) R. L. Blakley, *Nature (London)*, **188**, 231 (1960).

ACKNOWLEDGMENTS

Supported by grants from the National Cancer Institute of Canada (V. S. Gupta) and the Medical Research Council of Canada (J. R. Dimmock). Financial assistance to C. B. Nyathi was provided by the University of Saskatchewan, Connlab Holdings, Montreal, Quebec, Canada, and by the United Nations.

The authors are grateful to Walter Tsoi for technical assistance.

Simultaneous Automated Determination of Free and Total Sulfisoxazole and Sulfamethoxazole in Plasma and Urine

ROBERT E. WEINFELD ˣ **and TEH LO LEE**

Received February 22, 1979, from the *Department of Pharmacokinetics and Biopharmaceutics, Hoffmann-La Roche Inc., Nutley, NJ 07110.* Accepted for publication May 11, 1979.

Abstract □ A fully automated method for the determination of sulfisoxazole, N_4-acetylsulfisoxazole, sulfamethoxazole, and N_4-acetylsulfamethoxazole in human plasma and urine was developed. Untreated plasma is analyzed by automation of dialysis, hydrolysis, color development, and quantitation. The method has a sensitivity limit of 2 μg/ml of plasma and has been used successfully to determine sulfonamide levels following administration of sulfisoxazole and a combination drug product containing sulfamethoxazole and trimethoprim in humans. Samples are processed at the rate of 40 per hour, with a minimum of sample handling, data reduction, and materials.

Keyphrases □ Sulfisoxazole—automated analysis, human plasma and urine, with sulfamethoxazole □ Sulfamethoxazole—automated analysis, human plasma and urine, with sulfisoxazole □ Automated analysis—sulfisoxazole and sulfamethoxazole, human plasma and urine □ Antibacterial agents—sulfisoxazole, sulfamethoxazole, automated analysis, human plasma and urine

The ability to analyze numerous biological specimens rapidly has been the goal of many laboratories responsible for the routine application of analytical procedures. Samples resulting from bioequivalency and pharmacokinetic studies have placed increased demands on laboratories in recent years, in part due to increased drug regulatory requirements and drug development programs.

The sulfonamides have been determined in biological fluids by modifications of the Bratton–Marshall manual procedure since its publication in 1939 (1). All of these manual methods involve time-consuming sample preparations and sequential additions of reagents to form the chromophore, which is then measured spectrophotometrically. Other analytical methods for sulfonamide determination in various media including biological fluids, are fluorometry (2), TLC (3), GLC (4–6), and high-pressure liquid chromatography (HPLC) (7, 8). Although these methods often provided improved sensitivity and specificity when compared to the nonspecific, although sensitive, colorimetric assay, they also involved additional sample preparatory steps, including solvent extractions, derivatization, evaporation, sample injection, and quantitation.

The need to process numerous samples in a single workday led to the development of the automated method described here. The procedure allows for the simultaneous determination of "free" [1] sulfisoxazole (I) and "total" [2] sulfisoxazole [predominantly N_4-acetylsulfisoxazole (II)] or sulfamethoxazole (III) and its major plasma metabolite, N_4-acetylsulfamethoxazole (IV), in plasma and urine by employing the principles of continuous-flow analysis, with emphasis on reliability. Although use of continuous-flow systems is not unique, this procedure permits direct plasma analysis with no prior sample manipulation and utilizes automated dialysis, sample hydrolysis, and direct concentration readout.

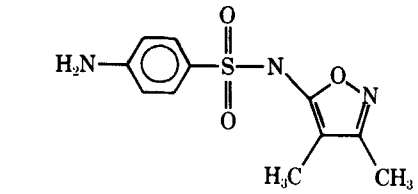

I

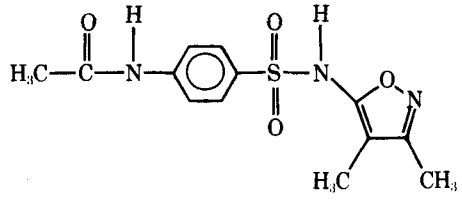

II

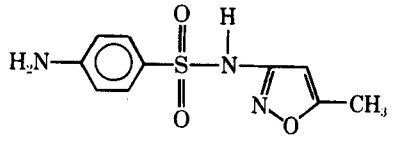

III

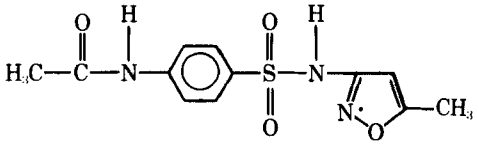

IV

BACKGROUND

The introduction of automated analytical equipment based on continuous-flow principles and techniques in 1957 by Skeggs (9) and subsequent application of such techniques to sulfonamides made possible the rapid processing of numerous samples. Falk and Kelly (10) described a procedure for measuring free sulfisoxazole levels in dog plasma following drug administration. The automated procedure is adequate for dog plasma sulfonamide levels since that species does not acetylate sulfonamides. It would be applicable to human plasma provided only free sulfonamide levels were required. In pharmacokinetic and bioavailability studies in humans, however, both free and total sulfonamide levels are needed. The plasma levels of both intact sulfonamide and its N_4-acetylated metabolite must be measured in renal insufficiency patients so that changes in the biotransformation and elimination of these compounds can be detected.

A previously reported semiautomated procedure (11) for determining free and total sulfisoxazole levels in human plasma required manual hydrolysis of protein-free filtrates of whole blood or plasma prior to automated colorimetry. A more recent procedure (12) for determining

[1] "Free" sulfonamide levels reflect those sulfonamides that react with the Bratton–Marshall reagents without hydrolysis. They reflect not only intact sulfonamide but any sulfonamide metabolite that still possesses a free primary aromatic amine group, *e.g.*, N_1- or ring N-glucuronides and possibly sulfanilamide.

[2] "Total" sulfonamide levels include all free components plus all metabolites that, upon acid hydrolysis, yield a substance capable of producing the Bratton–Marshall chromophore. The N_4-acetyl sulfonamide derivative is usually the major metabolite in humans. Generally, the sum of all of these components is expressed in equivalents of the intact drug.

0022-3549/79/1100-1387$01.00/0
© 1979, American Pharmaceutical Association

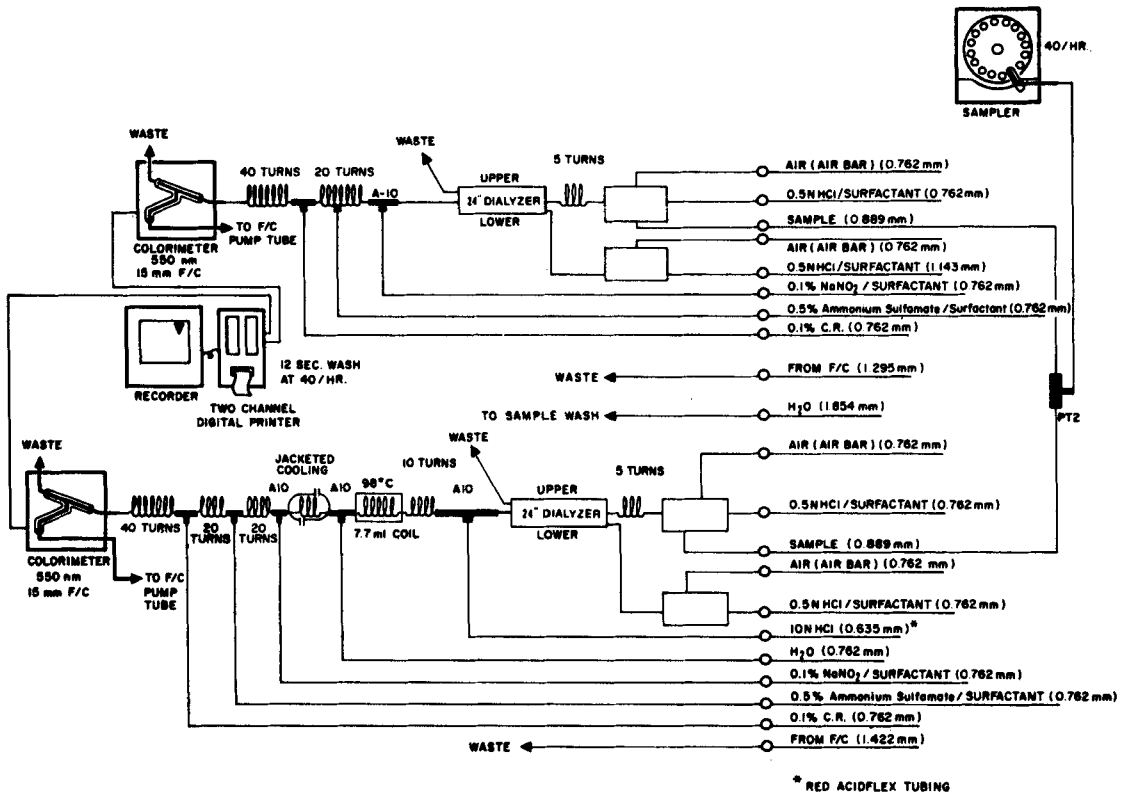

Figure 1—*Manifold for simultaneous automated determination of free and total sulfonamides in plasma and urine. Pump tubing, with size indicated, was all Tygon, except where noted.*

sulfamethoxazole still required manual sample preparation and hydrolysis prior to automation to quantitate the N_4-acetylated component.

The fully automated system described here is capable of simultaneously measuring free and total sulfisoxazole[3] or sulfamethoxazole[4] in undiluted plasma and in diluted urine. The sensitivity requirements for the determination of I and III in human plasma depend on the dose administered and typically range from 2 to 200 μg/ml of plasma during 24 hr following a single oral 2.0-g dose in normal subjects (13, 14). The automated system has a sensitivity limit of ~2 μg of I or III/ml of plasma, is precise, and can accelerate analysis greatly with a minimum of sample handling.

EXPERIMENTAL[5]

Reagents—All chemicals were reagent grade: hydrochloric acid, 0.5 *N* containing 1 ml of surfactant[6]/liter; hydrochloric acid, 10 *N*; sodium nitrite, 0.1% aqueous[7], containing 0.5 ml of surfactant[6]/liter; ammonium sulfamate, 0.5% aqueous[7], containing 0.5 ml of surfactant[6]/liter; *N*-(1-naphthyl)ethylenediamine dihydrochloride, 0.1% aqueous[7]; methanol; and concentrated ammonium hydroxide.

Standards—Compounds of pharmaceutical grade purity (>99%) were used to prepare the analytical standards: sulfisoxazole (I) [N_1-(3,4-dimethyl-5-isoxazolyl)sulfanilamide], mol. wt. 267.31; N_4-acetylsulfisoxaole (II), mol. wt. 309.35; sulfamethoxazole (III) [N_1-(5-methyl-3-isoxazolyl)sulfanilamide], mol. wt. 253.28; and N_4-acetylsulfamethoxazole (IV), mol. wt. 295.32.

Standard Solutions for Plasma Analysis—Solutions of I–IV were prepared as follows. Ten mg of I and III and 11.6 mg of II and IV were weighed into separate 10-ml volumetric flasks. The compounds were dissolved in absolute methanol to yield 1 mg of I and III/ml and solutions of II and IV equivalent to 1 mg of I and III/ml. These solutions were used to prepare internal standards of I–IV in plasma.

Standard Solutions for Urine Analysis and Aqueous Standard Curves—Aqueous stock solutions of I–IV were prepared as follows. One hundred milligrams of I and III and 116.6 mg of II and IV were weighed into four separate 100-ml volumetric flasks. About 10 ml of distilled water was added to suspend the compounds, and a sufficient amount of concentrated ammonium hydroxide was added (dropwise) to dissolve them. Solutions were brought to volume with distilled water to yield 1 mg of I and III/ml and solutions of II and IV equivalent to 1 mg of I and III/ml.

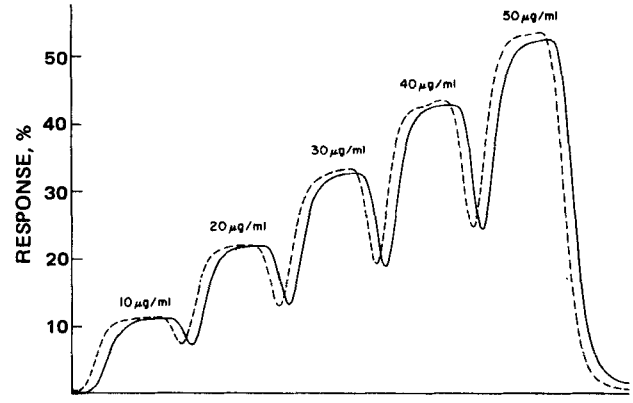

Figure 2—*Chart recordings of aqueous standard solutions of III analyzed on the automated manifold. Key: —, free channel; and - - -, total channel.*

[3] Sulfisoxazole is the active drug substance in Gantrisin, Roche Laboratories Division, Hoffmann–La Roche Inc.

[4] Sulfamethoxazole is the active drug substance in Gantanol and one active component in the combination drug Bactrim (combination of sulfamethoxazole and trimethoprim), both products of Roche Laboratories Division, Hoffmann–La Roche Inc.

[5] The equipment and instruments used were one Technicon sampler IV (Technicon Instruments Corp., Tarrytown, N.Y.); one Technicon proportioning pump, model III; two Technicon colorimeters equipped with 15-mm flowcells and 550-nm interference filters; two Technicon voltage stabilizers; two Technicon analytical cartridges containing 24-in. dialyzers with type "C" premount dialysis membranes and Auto Analyzer II glassware; and one Technicon two-pen recorder (chart speed: 60 in./hr) for use with Technicon digital printer, one Technicon modular digital printer (two channel), and one Techne heating module, modified Dri-block model DB-3 (Techne, Inc., Princeton, N.J.), machined to accept a 7.7-ml capacity Technicon coil (Fig. 1).

[6] Brij-35 (Technicon).

[7] Stored refrigerated in an amberized or light-protected container; stable for several weeks.

Table I—Standard Curve Preparation

Concentration, μg/ml	I–IV, ml
10	1.0
20	2.0
30	3.0
40	4.0
50	5.0
75	7.5
100	10.0

With the aqueous stock solutions of each standard I–IV, the aliquots shown in Table I were pipetted into four separate 100-ml volumetric flasks and diluted to volume with distilled water.

For convenience, these solutions were stored in 125-ml plastic drop-dispensing bottles[8] under refrigeration. The squeeze-type bottles provided a quick means of transferring the standards to sample cups for analysis. The dilutions were used to establish standard curves and to determine percent recovery, dialysis, and hydrolysis.

Sample Preparation—*Plasma*—An internal standard of 50 μg of sulfonamide/ml of plasma was prepared by evaporating 500 μl of the methanolic standards of I and II or III and IV to dryness in a 15-ml glass-stoppered centrifuge tube, adding 10 ml of plasma (control, drug free), and mixing well[9] to dissolve the compounds in the plasma. Unknown plasma specimens were run without dilution by transfer of ~1.5 ml into sample cups[10] and placement on the sampler.

Aqueous sulfonamide standards were run by transferring ~1.5 ml into sample cups along with the unknowns at concentrations of 10, 20, 30, 40, 50, 75, and 100 μg/ml. These standards were used to establish a curve and to determine the percent recovery of dialysis, percent hydrolysis of the 50-μg/ml internal standards, and linearity of response.

Urine—One milliliter of urine was diluted to 20 ml with distilled water, and ~1.5 ml was transferred to sample cups for analysis.

An internal standard of 50 μg of sulfonamide/ml of diluted urine was prepared by adding 1 mg (1.0 ml) of the aqueous stock standard solutions of I and II or III and IV separately to 1.0-ml urine samples (control, drug free) in a 25-ml graduated cylinder and diluting to 20 ml with distilled water.

External aqueous standards, ranging in concentration from 10 to 100 μg of sulfonamide/ml, were run along with the samples to determine percent recovery of dialysis and hydrolysis.

Unknowns that were off scale were diluted further and then were reanalyzed.

Automated Analytical Procedure—The complete automated system is diagrammed in Fig. 1. The sampler was operated at a rate of 40 samples/hr using a 12-sec wash[11]. All pump tubing lines were placed in distilled water containing 0.5 ml of surfactant[6]/liter and allowed to pump through the entire system for 5 min. Then the lines were transferred to appropriate reagent containers and pumped for at least 15 min to establish reagent baselines for each channel on the recorder.

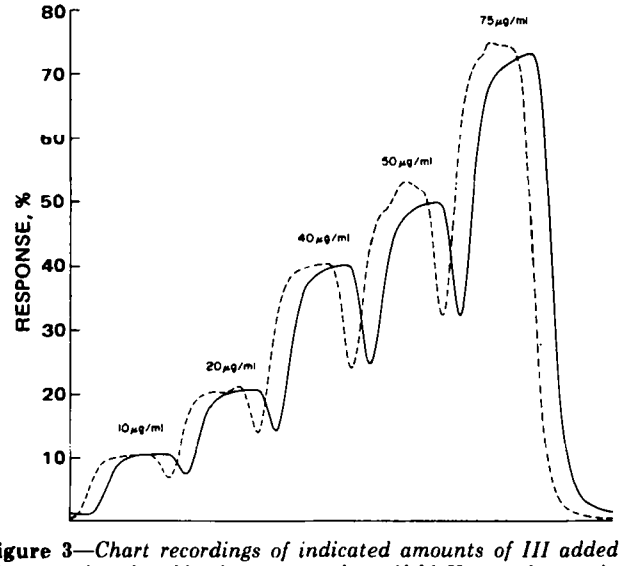

Figure 3—*Chart recordings of indicated amounts of III added to plasma and analyzed by the automated manifold. Key: —, free; and ---, total.*

Table II—Percent Dialysis, Hydrolysis, and Recovery of Compounds I–IV

Sample and Concentration Range	Percent Dialysis	Percent Hydrolysis	Percent Recovery (Overall)
10–100 μg of I/ml, aqueous	—	—	100
10–100 μg of I/ml of plasma	96.1	—	96.1
10–100 μg of II/ml, aqueous	87.3	84.8	74.0
10–100 μg of II/ml of plasma	47.2	84.8	40.0
10–75 μg of III/ml, aqueous	—	—	100
10–75 μg of III/ml of plasma	93.5	—	93.5
10–75 μg of IV/ml, aqueous	79.6	79.6	63.4
10–75 μg of IV/ml of plasma	50	79.6	39.8

Approximately 3.0 ml of the internal standard (50 μg/ml of plasma or 50 μg/ml of diluted urine) was transferred to a 3.5-ml conical base sample cup and placed on the sampler. The sampler probe was placed into the cup and allowed to sample for 2–2.5 min, introducing a continuous sample stream to permit adjustment of the "steady-state" plateau generated on the recorder for the internal standard. Day-to-day instrumental fluctuations were eliminated by adjustment of the colorimeter sensitivities for each module (free and total) to give a set recorder deflection (50% of full scale).

Once this parameter was established, the identical internal standard was placed in two or three sample cups (2.0 ml) and run with the sampler operating at a rate of 40 per hour to adjust the digital printer[11], which provided a concentration readout based on peak height of the recorder response and preset calibration of the digital printer range.

The internal standards containing 50 μg of I or 50 μg of III/ml of plasma or diluted urine served to adjust both the free and total channel (digital printer and recorder) results. In this manner, a more precise estimation of the total concentration could be attained (see *Calculations*).

The manifold was designed for the simultaneous determination of free and total sulfonamide by use of an initial sample stream splitter and parallel analytical manifolds, one for free sulfonamide (without hydrolysis) and the other for total sulfonamide (with hydrolysis) (Fig. 1). The free sample stream was adjusted so that its chart recording did not coincide with that of the total peak recording. This was accomplished by introduction of time delay coils (10 or more turns, as required) after the addition of *N*-(1-naphthyl)ethylenediamine dihydrochloride and before the colorimeter in the hydrolysis cartridge. In this manner, the free and total results associated with a particular sample were not confused. A two-pen recorder with different colored inks for each channel was used.

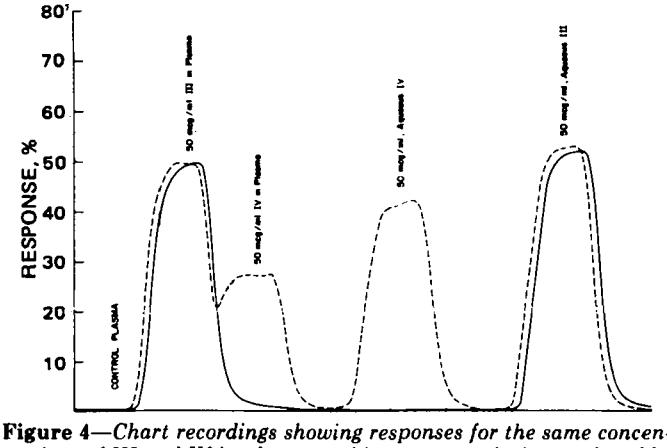

Figure 4—*Chart recordings showing responses for the same concentrations of III and IV in plasma and in aqueous solution analyzed by the automated manifold. Key: —, free; and ---, total.*

[8] Nalgene Labware, Rochester, N.Y.
[9] Vortex mixer.
[10] Technicon, polystyrene, 2-ml size, conical base or equivalent.
[11] Digital printer controlling samples and wash cycles. For digital printer operation, refer to Technicon Operations Manual TA1-170-10.

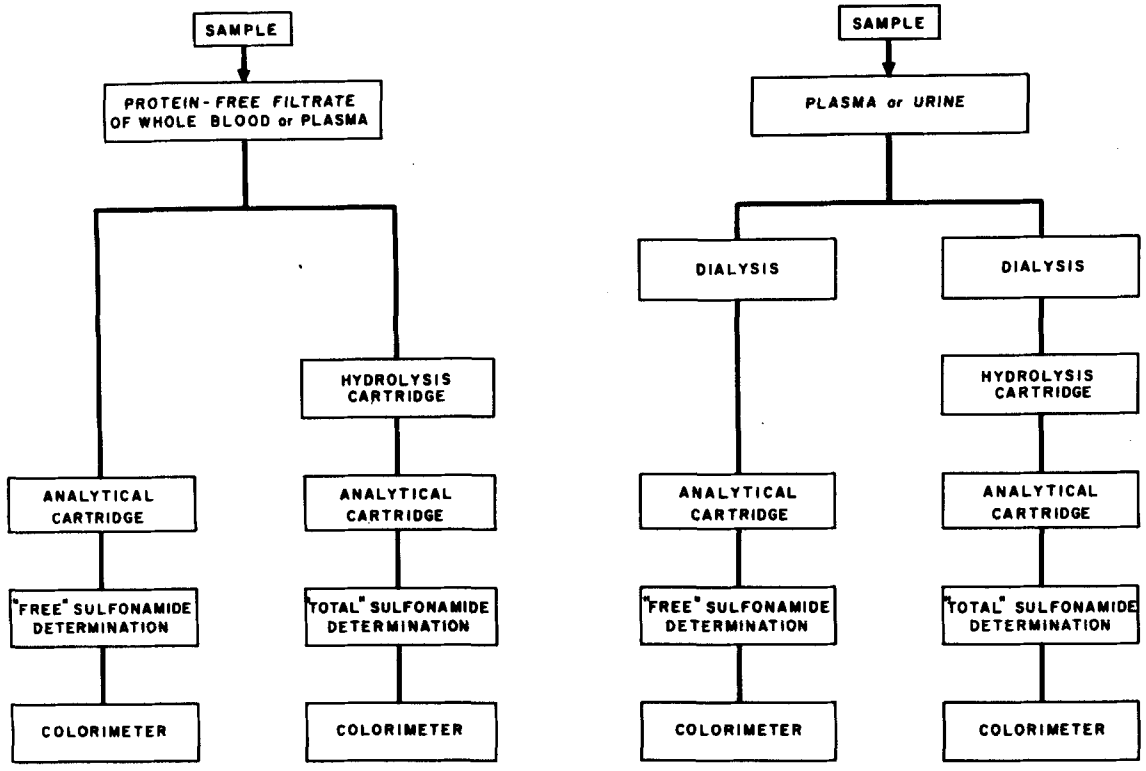

Figure 5—*Sample preparation schemes and analytical modules for automated analysis. Left: protein-free filtrates requiring a manual sample preparation step prior to automation (no dialysis). Right: untreated plasma directly analyzed (with dialysis).*

RESULTS

Standard Curves—The aqueous standards were added to individual sample cups, and their responses were used to establish a calibration curve for 10–100 μg/ml. Typical responses are illustrated in Fig. 2 for aqueous III standards in the range of 10–50 μg/ml. Typical responses of III added to plasma (10–75 μg/ml) and analyzed by the automated procedure are shown in Fig. 3. For the analysis of urine samples, the identical standards were used to establish a calibration curve.

Calculations and Determination of Percent Recovery—Calculation of plasma and urine concentrations required determination of the degree of metabolite hydrolysis to intact compound and the extent of metabolite dialysis (or recovery) from the plasma and urine matrix. These factors were determined for I–IV separately in plasma and in urine by running standards, added to plasma through the dialysis system and following them with aqueous standards of the same concentrations (Fig. 4). The percent recovery values of I–IV from plasma and the percent hydrolysis values of II to I and of IV to III are summarized in Table II.

In calculating the results from unknown specimens following dialysis and hydrolysis, it was unnecessary to introduce any correction for the free analysis since the colorimeter and digital printer were adjusted using the I or III internal standard. The total analysis represents an amount of I or III equal to the already determined free plus the amount of II or IV dialyzed, converted to free by acid hydrolysis, and measured colorimetrically following reaction. Thus, to determine the amount of N_4-acetyl metabolite in the sample, these equations are used:

$$\text{total } \mu\text{g/ml} - \text{free } \mu\text{g/ml} = \mu\text{g of II or IV/ml} \quad \text{(Eq. 1)}$$

$$(\mu\text{g of II or IV/ml})\,(\text{dialysis factor}) \times (\text{hydrolysis factor}) = \text{corrected } \mu\text{g of II or IV/ml} \quad \text{(Eq. 2)}$$

Assay Specificity—Interferences from drugs with primary aromatic amine groups other than the sulfonamides or their metabolites can produce false-positive values. In controlled studies, *e.g.*, bioequivalency or pharmacokinetic studies, this interference can be held to a minimum or eliminated entirely by screening of individuals. In such studies, the classical free and total sulfonamide measurements in plasma represent primarily intact parent drug (free) and N_4-acetyl metabolite (total − free), as demonstrated by Rieder (15, 16) using a procedure developed to quantitate the intact, active sulfonamide component in plasma.

In another study, comparison of results by TLC densitometric and colorimetric assays demonstrated essentially no differences in the plasma sulfonamide levels (17). Therefore, the colorimetric assay is specific for plasma sulfonamide determinations. Interferences from other drug substances, which can occur in clinical situations, are generally not a major problem in plasma since the sulfonamide levels following the relatively high doses used therapeutically far exceed levels of other classes of compounds (*e.g.*, benzodiazepines). In addition, no interferences in the colorimetric assay were reported due to trimethoprim, chloramphenicol, tetracycline, colistin, and ampicillin, all of which are often administered in situations requiring sulfonamide therapy (12, 18, 19).

Standards of the following benzodiazepines were introduced into the automated system: bromazepam (V), demoxepam (VI), and *N*-desmethyldiazepam (VII) (Scheme I). Each of these compounds, in addition to chlordiazepoxide, oxazepam, lorazepam, and other 1,4-benzodiazepines, is capable of being acid hydrolyzed to the corresponding benzophenone, which contains a primary aromatic amine and will, therefore, give a positive Bratton–Marshall diazotization reaction under the conditions used in the automated sulfonamide assay. However, only concentrations greater than 2 μg of benzodiazepine/ml could be detected, so plasma samples containing benzodiazepines would have to be present in much higher than usual therapeutic concentrations to cause errors in the sulfonamide quantitation. In addition, the extent of dialysis of these compounds from a biological matrix has not been established and could further reduce potential interferences.

In urine, free and total sulfonamides were measured. However, metabolites other than the N_4-acetyl metabolite, *e.g.*, the N_1- and the ring *N*-glucuronides, represent a significant percentage of the urinary excretion products in humans (20). Therefore, free and total measurements in urine by the automated assay yield results only in terms of equivalents of intact drug and the N_4-acetyl derivative. The urinary data are useful, however, in determining the percent recovery of the administered dose and for monitoring purposes.

Application to Biological Specimens—Plasma samples collected following the intravenous administration of 2 g of I to one subject in a study to determine the pharmacokinetic profile of the drug in anephric patients were analyzed by the manual sulfonamide procedure (1) and by the described automated procedure. Plasma I concentrations ranged from 11 to 134 μg/ml and metabolite levels (total − free) were from 16 to 117 μg/ml in a set of 18 specimens collected over 4 days. The coefficients of correlation between the two methods were 0.999 and 0.970, respectively, for the two data sets.

Study designs that involved oral administration of the combination product containing III and trimethoprim to humans provided for whole

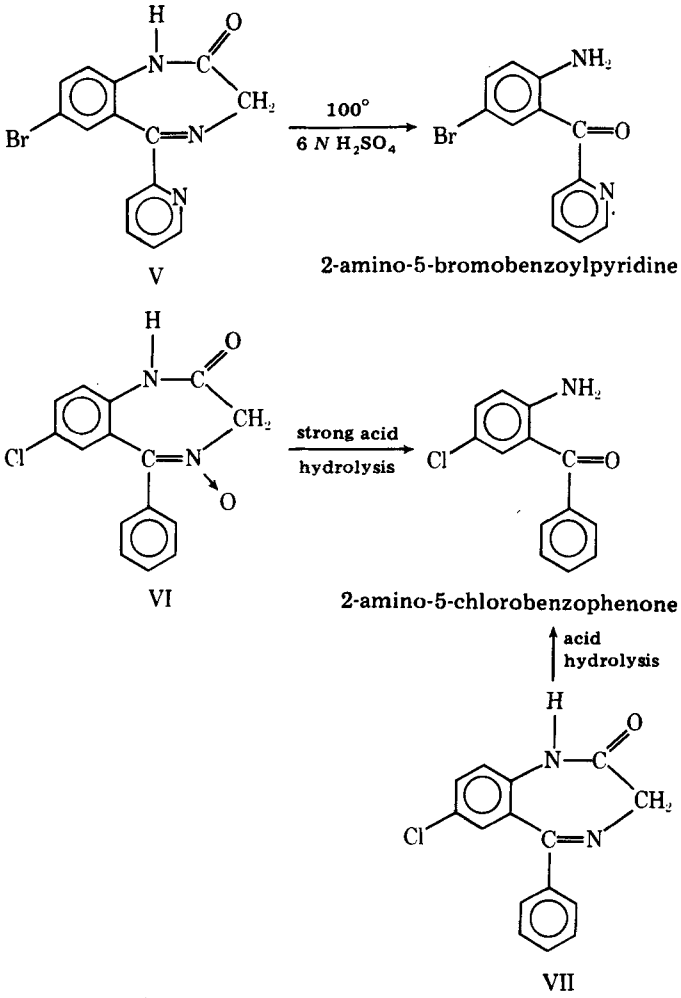

V

2-amino-5-bromobenzoylpyridine

VI

2-amino-5-chlorobenzophenone

VII

Scheme I—Structures of three benzodiazepines (V–VII) and the hydrolysis conditions under which a benzophenone containing a primary aromatic amine function is produced.

blood specimens rather than plasma. In these studies, a minor modification of the automated method involved preparation of protein-free filtrates of whole blood[12] (11) and used the same automated manifold (Fig. 1) with dialyzers removed from both channels (Fig. 5). There was no increase in sensitivity by using whole blood or a protein-free filtrate for analysis, and the results were analytically similar to those obtained using direct untreated plasma (Fig. 6) for standards of III added to blood. In a series of blood samples collected from subjects who had received a combination of 2 g of sulfamethoxazole plus 400 mg of trimethoprim orally, the blood levels ranged from 11 to 65 μg of free sulfamethoxazole/ml of blood and from 9 to 94 μg of total sulfamethoxazole/ml. Comparison of 25 data sets analyzed by the manual and automated methods showed a coefficient of correlation of 0.996 for the free. For 51 sets of data for the total analyses, the coefficient of correlation was 0.990.

DISCUSSION

During the development of this automated methodology, certain inconsistencies were discovered when the N_4-acetyl metabolites of I and III were analyzed. Compounds II and IV were not as extensively dialyzed from the plasma matrix as I and III (Table II); only by running standards of those compounds alone, with and without plasma, could a suitable correction factor be introduced into the calculations. The alternative was to prepare and hydrolyze manually the protein-free filtrates as previously reported (11, 12). The automated method successfully overcomes these problems; by coupling the system to a suitable peak height detection system[11], direct concentration readout was accomplished. It is still necessary to prepare internal standards for the automated system and to tool-up the system prior to sample introduction. However, once this is accomplished, the system is capable of operating an entire workday and beyond if new samples are placed in the sampler tray as the samples are processed.

[12] Attempts to dialyze whole blood directly in this automated system were unsuccessful due to clogging of tubing and dialyzers.

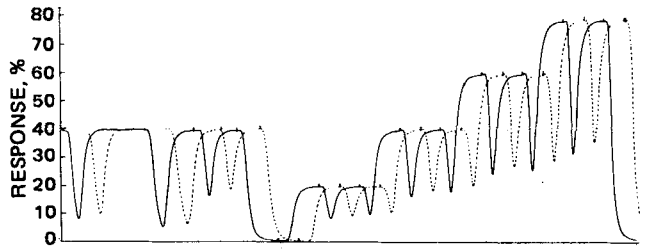

Figure 6—*Chart recording showing, from left to right: steady-state plateau of a continuously sampled 5 μg of III/ml of protein-free filtrate (equivalent to 50 μg of III added to 0.5 ml of blood) (11); duplicate determinations of the same sample analyzed at 40 per hour rate; and duplicate determinations of a series of aqueous standards of increasing concentrations (2, 4, 6, and 8 μg of III/ml). Key: —, free; and ---, total; using the automated manifolds without dialyzers (Figs. 1 and 5).*

The rate of automated analysis is 40 samples per hour, which allows for 200–240 samples per workday, leaving sufficient time for startup and washout periods after all analyses are completed. It is unlikely that any other available analytical method could provide results at the same rate and with as little sample manipulation, glassware, and time as the automated plasma method. Although the recently published HPLC procedure for sulfisoxazole in plasma (8) is fairly rapid, sample manipulation is still extensive. The procedure requires centrifugation and transfer of the supernate followed by injection into the liquid chromatograph, so the number of samples and standards that could be processed in a single day would be ~30.

In addition, the automated system is flexible in that it is easily converted to a colorimetric reaction system (without dialyzers) when sample preparation must be performed manually (Fig. 5). The reaction system also is useful for processing compounds other than sulfonamides if they yield a primary aromatic amine following acid hydrolysis (Scheme I). Although no immediate application was found for the benzodiazepines other than to demonstrate this feasibility, automated acid hydrolysis can be an interface with other automated analytical procedures when required. This application would be useful only when the reactant concentrations were in microgram quantities or where other more sensitive techniques (*e.g.*, fluorometry) were employed following hydrolysis.

In conclusion, although more sensitive instrumentation and specific methodologies have been developed in recent years, the classical Bratton–Marshall method for sulfonamide quantitation in biological fluids remains useful in certain analytical situations, such as in bioequivalency studies involving *in vivo* comparison of formulations containing sulfisoxazole and sulfamethoxazole. In such situations, the administered dose is sufficiently high to permit the use of the colorimetric assay (Bratton–Marshall) to define a plasma level–time profile for at least 24 and possibly 48 hr. By totally automating the analysis following the introduction of untreated plasma into the system, the analyst is freed of manual sample preparation steps.

REFERENCES

(1) A. C. Bratton and E. K. Marshall, Jr., *J. Biol. Chem.*, **128**, 537 (1939).

(2) Y. Ogawa and T. Matsuo, *Ann. Rep. Shiongi Res. Lab.*, **13**, 23 (1963).

(3) C. W. Sigel, J. L. Wooley, Jr., and C. A. Nichol, *J. Pharm. Sci.*, **64**, 973 (1975).

(4) R. J. Daun, *J. Assoc. Off. Anal. Chem.*, **54**, 1277 (1971).

(5) E. Roder and W. Stuthe, *Anal. Chem.*, **266**, 358 (1973).

(6) N. Nose, S. Kobayashi, A. Hirose, and A. Watanabe, *J. Chromatogr.*, **123**, 167 (1976).

(7) S. C. Su, A. V. Hartkopk, and B. L. Karger, *ibid.*, **119**, 523 (1976).

(8) G. W. Peng, M. A. F. Gadalla, and W. L. Chiou, *Res. Commun. Chem. Pathol Pharmacol.*, **18**, 233 (1977).

(9) L. T. Skeggs, *Am. J. Clin. Pathol.*, **28**, 311 (1957).

(10) H. B. Falk and R. G. Kelly, *Clin. Chem.*, **11**, 1045 (1965).

(11) S. A. Kaplan, R. E. Weinfeld, and C. W. Abruzzo, *Adv. Automated Anal.*, **2**, 405 (1971).
(12) A. Bye and A. F. J. Fox, *Clin. Chem.*, **20**, 288 (1974).
(13) S. A. Kaplan, R. E. Weinfeld, C. W. Abruzzo, and M. Lewis, *J. Pharm. Sci.*, **61**, 773 (1972).
(14) S. A. Kaplan, R. E. Weinfeld, C. W. Abruzzo, K. McFaden, M. L. Jack, and L. Weissman, *J. Infect. Dis., Suppl.*, **128**, S547 (1973).
(15) J. Rieder, *Chemotherapy*, **17**, 1 (1972).
(16) *Ibid.*, **22**, 84 (1976).
(17) C. W. Sigel, M. E. Grace, C. A. Nichol, and G. H. Hitchings, *J. Pharm. Sci.*, **63**, 1202 (1974).
(18) D. E. Schwartz, B. A. Koechlin, and R. E. Weinfeld, *Chemotherapy, Suppl.*, **14**, 22 (1969).
(19) S. A. Kaplan, R. E. Weinfeld, and T. L. Lee, *J. Pharm. Sci.*, **62**, 1865 (1973).
(20) J. Rieder, *J. Infect. Dis., Suppl.*, **128**, S567 (1973).

ACKNOWLEDGMENTS

The authors thank the Special Treatment Unit of Newark Beth Israel Medical Center for conducting the human studies, Mr. R. McGlynn for the drawings of the figures, and Mrs. V. Waddell for the preparation of this manuscript.

Pharmacokinetics and Relative Bioavailability of Oral Theophylline Capsules

L. J. LESKO *¶x, A. T. CANADA ‡, G. EASTWOOD ‡, D. WALKER *, and D. R. BROUSSEAU §

Received January 12, 1979, from the **Pfeiffer Clinical Pharmacokinetics Laboratory, Massachusetts College of Pharmacy, Boston, MA 02115,* the ‡*University of Massachusetts Medical Center, Worcester, MA 01605,* and §*Fisons Corporation, Bedford, MA 01730.* Accepted for publication April 20, 1979. ¶Present address: Drug Concentration Laboratory, University of Massachusetts Medical Center, Worcester, MA 01605.

Abstract □ The oral bioavailability of liquid-filled theophylline capsules relative to a nonalcoholic aminophylline solution was determined in normal volunteers. In addition, theophylline absorption and elimination kinetics were reexamined. There were no statistically significant differences between the bioavailability of capsules and liquid as measured by the area under the curve (AUC) from time $0 \rightarrow \infty$ ($p > 0.05$). The bioavailability parameters of C_{max}, t_{max}, and AUC were determined from actual serum theophylline concentration–time data and from a nonlinear least-squares fit of the serum concentration–time data. Theophylline absorption from the capsules was noticeably faster than from the liquid in most subjects, although the differences in absorption rates were not significantly different ($p > 0.05$). The determined apparent volume of distribution, elimination half-life, and plasma clearance of theophylline were similar to values reported by other investigators. Marked inter- and intraindividual variations in the elimination half-life were noted.

Keyphrases □ Theophylline—oral dosage forms, pharmacokinetics, bioavailability, capsule compared to liquid □ Muscle relaxants (smooth muscle)—theophylline, oral dosage forms, pharmacokinetics, bioavailability, capsule compared to liquid □ Bioavailability—theophylline, various oral dosage forms

The clinical importance of satisfactory oral theophylline bioavailability is well recognized in the scientific and medical communities. Bioavailability problems, particularly with tablets and capsules, are thought to be related primarily to the dosage form formulation and not to physiological factors that influence absorption (1).

Although reported bioavailability studies of various theophylline oral dosage forms have demonstrated satisfactory bioavailability, all commercial oral theophylline dosage forms may not have equally satisfactory bioavailability (2, 3). It is important to evaluate the bioavailability of each theophylline formulation to confirm that formulation factors do not affect *in vivo* absorption.

One major goal of this investigation was to evaluate the relative bioavailability of liquid-filled oral theophylline capsules[1] in a random, crossover study. The rationale was to determine if any formulation factors associated with liquid-filled capsules might affect theophylline bioavailability when compared to the bioavailability from a nonalcoholic, rapidly absorbed aminophylline oral liquid[2]. Another major goal was to examine the absorption and elimination kinetics of theophylline when administered as a liquid-filled capsule or as a liquid.

EXPERIMENTAL

Subjects—Seven male and seven female subjects, 21–40 years old, were selected with the approval of the Institutional Human Subjects Review Committee. Valid written informed consent was obtained from each subject prior to entrance into the study. The body weight (mean ± *SD*, 67 ± 12 kg) of the volunteers was within 10% of normal limits for their height and build (4).

All subjects were determined to be in good physical health, with no history of alcoholism or cardiovascular disease. They were judged to be medically sound based on a medical history, physical examination, vital signs, ECG, and the usual battery of blood and urine clinical chemistry tests. All subjects were nonsmokers and had not smoked regularly at any time within the last 3 years.

All subjects were instructed to refrain from any medication for at least 7 days prior to the study and to abstain from alcohol and xanthine-containing foods or beverages for 24 hr prior to dosing. All volunteers were fasted, with the exception of water, for 12 hr prior to dosing, and the fasting was continued for 4 hr after dosing. A modest meal, low in carbohydrates and fat, was served at 4 hr, and a light dinner, likewise low in fat and carbohydrates, was served at 8 hr after dosing.

Drug Administration and Blood Sampling—On each study day, an oral dose equivalent to 300 mg of anhydrous theophylline was randomly administered either as liquid-filled capsules or as a nonalcoholic aminophylline solution. Previous analysis for potency showed the capsules to contain 98% of the label claim. The study days were separated by a washout period of 7 days, after which the subjects took the alternate formulation. On each study day, the subjects were administered the medication with 240 ml of water at approximately 8:00 am.

Predose blood samples (1 ml) were obtained immediately before dosing *via* an indwelling catheter in the forearm vein. After dosing with the capsules, blood samples were collected at 0.25, 0.5, 0.75, 1, 1.5, 2, 3, 4, 5, 6, 7, 8, 10, 12, 16, and 24 hr. After dosing with the liquid, blood samples

[1] Somophyllin capsules, lots 02977 and 07677, Fisons Corp., Bedford, Mass.

[2] Somophyllin oral liquid, lot 02287, Fisons Corp., Bedford, Mass.

0022-3549/79/1100-1392$01.00/0
© 1979, American Pharmaceutical Association

(11) S. A. Kaplan, R. E. Weinfeld, and C. W. Abruzzo, *Adv. Automated Anal.*, **2**, 405 (1971).
(12) A. Bye and A. F. J. Fox, *Clin. Chem.*, **20**, 288 (1974).
(13) S. A. Kaplan, R. E. Weinfeld, C. W. Abruzzo, and M. Lewis, *J. Pharm. Sci.*, **61**, 773 (1972).
(14) S. A. Kaplan, R. E. Weinfeld, C. W. Abruzzo, K. McFaden, M. L. Jack, and L. Weissman, *J. Infect. Dis., Suppl.*, **128**, S547 (1973).
(15) J. Rieder, *Chemotherapy*, **17**, 1 (1972).
(16) *Ibid.*, **22**, 84 (1976).
(17) C. W. Sigel, M. E. Grace, C. A. Nichol, and G. H. Hitchings, *J. Pharm. Sci.*, **63**, 1202 (1974).
(18) D. E. Schwartz, B. A. Koechlin, and R. E. Weinfeld, *Chemotherapy, Suppl.*, **14**, 22 (1969).
(19) S. A. Kaplan, R. E. Weinfeld, and T. L. Lee, *J. Pharm. Sci.*, **62**, 1865 (1973).
(20) J. Rieder, *J. Infect. Dis., Suppl.*, **128**, S567 (1973).

ACKNOWLEDGMENTS

The authors thank the Special Treatment Unit of Newark Beth Israel Medical Center for conducting the human studies, Mr. R. McGlynn for the drawings of the figures, and Mrs. V. Waddell for the preparation of this manuscript.

Pharmacokinetics and Relative Bioavailability of Oral Theophylline Capsules

L. J. LESKO *¶x, A. T. CANADA ‡, G. EASTWOOD ‡, D. WALKER *, and D. R. BROUSSEAU §

Received January 12, 1979, from the **Pfeiffer Clinical Pharmacokinetics Laboratory, Massachusetts College of Pharmacy, Boston, MA 02115,* the ‡*University of Massachusetts Medical Center, Worcester, MA 01605,* and §*Fisons Corporation, Bedford, MA 01730.* Accepted for publication April 20, 1979. ¶Present address: Drug Concentration Laboratory, University of Massachusetts Medical Center, Worcester, MA 01605.

Abstract □ The oral bioavailability of liquid-filled theophylline capsules relative to a nonalcoholic aminophylline solution was determined in normal volunteers. In addition, theophylline absorption and elimination kinetics were reexamined. There were no statistically significant differences between the bioavailability of capsules and liquid as measured by the area under the curve (AUC) from time $0 \rightarrow \infty$ ($p > 0.05$). The bioavailability parameters of C_{max}, t_{max}, and AUC were determined from actual serum theophylline concentration–time data and from a nonlinear least-squares fit of the serum concentration–time data. Theophylline absorption from the capsules was noticeably faster than from the liquid in most subjects, although the differences in absorption rates were not significantly different ($p > 0.05$). The determined apparent volume of distribution, elimination half-life, and plasma clearance of theophylline were similar to values reported by other investigators. Marked inter- and intraindividual variations in the elimination half-life were noted.

Keyphrases □ Theophylline—oral dosage forms, pharmacokinetics, bioavailability, capsule compared to liquid □ Muscle relaxants (smooth muscle)—theophylline, oral dosage forms, pharmacokinetics, bioavailability, capsule compared to liquid □ Bioavailability—theophylline, various oral dosage forms

The clinical importance of satisfactory oral theophylline bioavailability is well recognized in the scientific and medical communities. Bioavailability problems, particularly with tablets and capsules, are thought to be related primarily to the dosage form formulation and not to physiological factors that influence absorption (1).

Although reported bioavailability studies of various theophylline oral dosage forms have demonstrated satisfactory bioavailability, all commercial oral theophylline dosage forms may not have equally satisfactory bioavailability (2, 3). It is important to evaluate the bioavailability of each theophylline formulation to confirm that formulation factors do not affect *in vivo* absorption.

One major goal of this investigation was to evaluate the relative bioavailability of liquid-filled oral theophylline capsules[1] in a random, crossover study. The rationale was to determine if any formulation factors associated with liquid-filled capsules might affect theophylline bioavailability when compared to the bioavailability from a nonalcoholic, rapidly absorbed aminophylline oral liquid[2]. Another major goal was to examine the absorption and elimination kinetics of theophylline when administered as a liquid-filled capsule or as a liquid.

EXPERIMENTAL

Subjects—Seven male and seven female subjects, 21–40 years old, were selected with the approval of the Institutional Human Subjects Review Committee. Valid written informed consent was obtained from each subject prior to entrance into the study. The body weight (mean ± *SD*, 67 ± 12 kg) of the volunteers was within 10% of normal limits for their height and build (4).

All subjects were determined to be in good physical health, with no history of alcoholism or cardiovascular disease. They were judged to be medically sound based on a medical history, physical examination, vital signs, ECG, and the usual battery of blood and urine clinical chemistry tests. All subjects were nonsmokers and had not smoked regularly at any time within the last 3 years.

All subjects were instructed to refrain from any medication for at least 7 days prior to the study and to abstain from alcohol and xanthine-containing foods or beverages for 24 hr prior to dosing. All volunteers were fasted, with the exception of water, for 12 hr prior to dosing, and the fasting was continued for 4 hr after dosing. A modest meal, low in carbohydrates and fat, was served at 4 hr, and a light dinner, likewise low in fat and carbohydrates, was served at 8 hr after dosing.

Drug Administration and Blood Sampling—On each study day, an oral dose equivalent to 300 mg of anhydrous theophylline was randomly administered either as liquid-filled capsules or as a nonalcoholic aminophylline solution. Previous analysis for potency showed the capsules to contain 98% of the label claim. The study days were separated by a washout period of 7 days, after which the subjects took the alternate formulation. On each study day, the subjects were administered the medication with 240 ml of water at approximately 8:00 am.

Predose blood samples (1 ml) were obtained immediately before dosing *via* an indwelling catheter in the forearm vein. After dosing with the capsules, blood samples were collected at 0.25, 0.5, 0.75, 1, 1.5, 2, 3, 4, 5, 6, 7, 8, 10, 12, 16, and 24 hr. After dosing with the liquid, blood samples

[1] Somophyllin capsules, lots 02977 and 07677, Fisons Corp., Bedford, Mass.

[2] Somophyllin oral liquid, lot 02287, Fisons Corp., Bedford, Mass.

0022-3549/79/1100-1392$01.00/0
© 1979, American Pharmaceutical Association

were collected at 5, 10, 15, 20, 25, 30, 40, and 50 min and at 1, 1.5, 2, 3, 4, 5, 6, 7, 8, 10, 12, 16, and 24 hr. Some of the later blood samples were drawn by venipuncture after removal of the indwelling catheter. Serums were separated from coagulated blood samples and frozen at −20° until assayed for theophylline. During each study period, blood pressure and pulse and respiratory rates were recorded at regular intervals. Any side effects were noted.

Theophylline Assay—Serum theophylline determinations were made by high-pressure liquid chromatography (HPLC) as follows. Serum, 200 μl, was treated with an equal volume of acetonitrile containing the internal standard, β-hydroxyethyltheophylline, to precipitate serum proteins. After centrifugation, a 20-μl sample of the supernate was injected immediately on a microparticulate reversed-phase column[3]. The column was used with a septumless injector[4], a solvent delivery system consisting of a dual-piston pump[5], and a fixed-wavelength UV absorbance detector[6] equipped with a 280-nm filter. The eluting solvent was 7% acetonitrile in a 0.01 *M* acetate buffer adjusted to pH 4. The flow rate through the column was 2 ml/min. The sensitivity for 0.005 aufs was 0.5 μg/ml of serum.

The coefficient of variation for intra- and interday analyses of duplicate serum theophylline controls was negligible (<2%). This method is specific for theophylline. Theophylline recovery was virtually 100% from spiked serum samples, and a plot of peak height ratio (theophylline/internal standard) as a function of theophylline concentration was linear up to 40 μg/ml. During the study, the analyst was unaware of the treatment regimen.

Pharmacokinetic Analysis—Serum theophylline concentrations (mean ± *SE*) were tabulated at each sampling time and plotted as a function of time on Cartesian coordinates. Individual serum data for each subject after each dose were fitted graphically to obtain initial estimates and by nonlinear least-squares regression analysis to a one-compartment pharmacokinetic model defined by:

$$C = \frac{FD}{V_d}\left(\frac{K_a}{K_a - K_E}\right)(e^{-K_E t} - e^{-K_a t}) \qquad \text{(Eq. 1)}$$

where C is the theophylline concentration at any time, t, after dosing; F is the fraction of dose, D, absorbed; V_d is the apparent volume of distribution; and K_a and K_E are the apparent first-order rate constants of absorption and elimination, respectively. In some cases, a lag time, t_0, had to be introduced into Eq. 1 to obtain an optimal fit.

Nonlinear regression analysis was performed on a digital computer[7] using the NONLIN program (5). From computer analysis, values for K_a, absorption half-life ($t_{1/2\text{-abs}}$), K_E, and elimination half-life ($t_{1/2\text{-elim}}$) were obtained. Additional pharmacokinetic parameters were calculated as:

$$Cl = \frac{FD}{AUC_{0\to\infty}BW} \qquad \text{(Eq. 2)}$$

where Cl is plasma clearance, $AUC_{0\to\infty}$ is the area under the actual serum theophylline concentration–time curve from zero to infinity, BW is the individual body weight in kilograms, and F is assumed to be 1, and:

$$V_d = \frac{Cl}{K_E} \qquad \text{(Eq. 3)}$$

where V_d and K_E are as defined for Eq. 1.

The area under the individual serum concentration–time curve from zero to infinity was determined by the trapezoidal rule. When the last data point was >0.5 μg/ml, the area from the last data point to infinity was calculated as the quotient of the last data point and the overall elimination rate constant, K_E. The $AUC_{0\to\infty}$ also was calculated from computer-fit parameters as described in:

$$AUC_{0\to\infty} = \frac{FD}{V_d}\left(\frac{K_a}{K_a - K_E}\right)\left(\frac{1}{K_E} - \frac{1}{K_a}\right) \qquad \text{(Eq. 4)}$$

where $(FD/V_d)[K_a/(K_a - K_E)]$ was the intercept of the best computer fit of the individual data.

The other bioavailability parameters, time of maximum serum theophylline concentration (t_{max}) and maximum serum theophylline concentration (C_{max}), were obtained directly from the actual serum assay values and from the nonlinear least-squares fit.

The relative bioavailability, F_{rel}, of the liquid-filled theophylline capsules was calculated using the $AUC_{0\to\infty}$ values corrected for intraindividual variation in the elimination rate:

$$F_{rel} = \frac{(AUC_{0\to\infty}, \text{capsule})(K_E, \text{capsule})}{(AUC_{0\to\infty}, \text{liquid})(K_E, \text{liquid})} \qquad \text{(Eq. 5)}$$

Statistical Analysis—A two-way analysis of variance for a randomized complete block experimental design was performed on the bioavailability parameters calculated from the actual assay values ($AUC_{0\to\infty}$, t_{max}, and C_{max}) obtained for each dosage form to determine the significance of differences between the capsules and liquid. A paired t-test of the other pharmacokinetic parameters determined if there were any significant differences in the mean values after administration of a capsule or liquid.

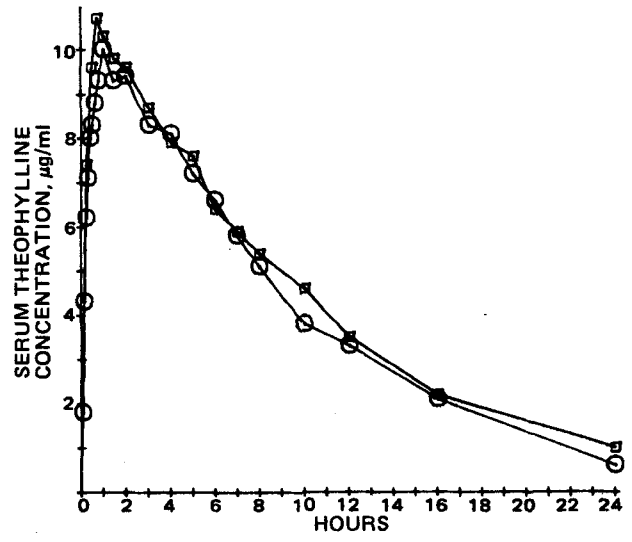

Figure 1—*Mean serum theophylline levels in 14 subjects after a 300-mg oral theophylline dose. Key: □, capsules; and ○, liquid.*

RESULTS AND DISCUSSION

The mean (±*SE*) serum theophylline levels in 14 subjects as a function of time after administration of 300 mg of theophylline either as a liquid-filled oral capsule or as an oral liquid are illustrated in Fig. 1. As expected, individual serum theophylline concentrations at each sampling time varied, but the curves of mean serum theophylline levels in Fig. 1 show that the two dosage forms produced serum levels over time that were essentially the same. Semilogarithmic plots of mean serum theophylline concentrations *versus* time revealed a monoexponential decrease in observed serum levels after the peak with no significant distribution phase, indicating that a one-compartment open model is appropriate for evaluating the pharmacokinetics of these data. The correlation coefficients observed for individual serum level data fitted to the one-compartment open model were ≥0.95 in all cases.

The bioavailability parameters, *i.e.*, the area under the serum level–time curve ($AUC_{0\to\infty}$), the maximum serum level (C_{max}), and the time to maximum serum level (t_{max}), are listed in Table I. The parameters were obtained from both the experimentally observed serum theophylline levels and the computer-generated, one-compartment fits of the individual data. The AUC values for both the capsules and the liquid, when corrected for intraindividual variation in elimination, were not significantly different ($p > 0.05$). The mean (±*SE*) relative bioavailability (F_{rel}) of the oral theophylline capsules was 1.01 ± 0.06 (Table I) with a range of 0.70–1.56. With paired individual data, the F_{rel} was larger for the capsules in six of the 14 subjects. The difference in bioavailability between the formulations was not significant ($p > 0.05$). A previous study showed that the absolute bioavailability of the oral aminophylline liquid used as a reference dosage form in this study was 100%[8]. Thus, the absolute bioavailability of the oral theophylline capsules probably approximates 100%.

The oral liquid was absorbed rapidly, as noted from the mean (±*SE*) t_{max} value of 1.24 ± 0.3 hr (range of 0.25–4.0 hr). The oral capsules appeared to have rapid and complete dissolution *in vivo*, as indicated from the mean (±*SE*) t_{max} value of 0.98 ± 0.3 hr (range of 0.25–5.0 hr). Al-

[3] μBondapak C_{18}, Waters Associates, Milford, Mass.
[4] Model U6K, Waters Associates, Milford, Mass.
[5] Model 6000A, Waters Associates, Milford, Mass.
[6] Model 440, Waters Associates, Milford, Mass.
[7] Prime Computer Co., Framingham, Mass.

[8] Data on file, Fisons Corp., Bedford, Mass.

Table I—Bioavailability Parameter Values (Mean ± *SE*) for Theophylline after Oral Administration of a 300-mg Dose to 14 Subjects

Parameter	Formulation		Statistical Significance
	Liquid	Capsule	
AUC^a, μg hr/ml			
Observed[b]	98.0 ± 6.4	104 ± 8.3	NS ($p > 0.05$)
Calculated[c]	95.0 ± 6.4	118 ± 11.0	
C_{max}, μg/ml			
Observed	11.5 ± 0.7	15.1 ± 1.2	Significant
Calculated	10.3 ± 0.6	11.5 ± 0.7	($p < 0.05$)
t_{max}, hr			
Observed	1.24 ± 0.3	0.98 ± 0.30	NS ($p > 0.05$)
Calculated	1.20 ± 0.2	0.92 ± 0.20	
F_{rel}[d]			
Observed	—	1.01 ± 0.06	NS ($p > 0.05$)
Calculated	—	1.09 ± 0.04	

[a] From zero to infinity. [b] Based on actual assay values in serum. [c] Based on computer fit of data to one-compartment model. [d] Corrected for intraindividual variation in elimination.

though the t_{max} observed after capsule administration occurred earlier in time, the differences were not significant ($p > 0.05$). Intersubject variability in theophylline absorption was estimated using the coefficients of variation (standard deviation × 100/mean) of the bioavailability parameters of both dosage forms, and the t_{max} values showed the greatest variation.

The mean t_{max} observed in this study for the oral liquid was similar to the mean t_{max} reported (1) for a hydroalcoholic theophylline solution (1.4 hr, $SE = 0.03$) administered to 10 patients and similar to the mean t_{max} reported (3) for a similar solution administered to 12 subjects (1.208, $SD = 0.620$). The ranges and variability of t_{max} in the earlier studies were essentially the same as those observed in the present investigation. By contrast, the mean t_{max} observed in the oral capsule study (0.98 ± 0.3 hr) was earlier than the mean t_{max} reported (1, 3) for oral, compressed tablets (2.0 ± 0.9 and 1.458 ± 0.542, respectively), although greater intrapatient variability was observed in this study. The rapid absorption from the oral capsules may be related to the absence of the disintegration step characteristic of oral tablets or to the suspending medium within the oral capsule. Indeed, Lindenbaum (6) reported that digoxin bioavailability from a liquid concentrate contained in a soft gelatin capsule was better than the bioavailability of a nonalcoholic digoxin solution or tablet, although this result has not been found consistently (7).

The measured mean C_{max} after capsule administration was 15.1 ± 1.2 μg/ml. This C_{max} was significantly different ($p < 0.05$) from the measured mean C_{max} of 11.5 ± 0.7 μg/ml for the oral liquid. The higher C_{max} of the capsules is consistent with the shorter t_{max} and faster K_a (Table II) observed for this formulation.

The values for theophylline absorption, distribution, and elimination calculated for the capsules and liquid are listed in Table II. The mean (±*SE*) K_a for the capsule (13.98 ± 3.1) was significantly different ($p < 0.05$) from the mean (±*SE*) K_a (5.22 ± 1.18) for the liquid, although the corresponding mean $t_{abs\text{-}1/2}$ (±*SE*) values for the capsules (0.18 ± 0.06) and liquid (0.27 ± 0.07) were not significantly different ($p > 0.05$). The absorption lag times (t_0) were averaged for the capsule and liquid formulations. The difference between the mean lag times was significant ($p < 0.05$), with the capsule t_0 equal to 0.143 ± 0.038 (±*SE*) and the liquid equal to 0.047 ± 0.017. The faster K_a after the capsule accounted for the higher C_{max} and shorter t_{max} observed for the formulation.

Theophylline elimination kinetics after capsule and liquid administration were essentially the same. The K_E for the capsule was 0.11 ± 0.01 (±*SE*), and the corresponding $t_{1/2}$ was 6.98 ± 0.61 (±*SE*). The K_E and the $t_{1/2}$ for the liquid were 0.12 ± 0.01 (±*SE*) and 6.19 ± 0.31, respectively, and there were no significant differences ($p > 0.05$) between the formulations in either K_E or $t_{1/2}$. These elimination parameters are in agreement with those reported for theophylline by other investigators (8). Some researchers have reported significant intrapatient variability in K_E and $t_{1/2}$ after single doses, with both short and long time intervals separating the individual doses. In this study, intrapatient variability in K_E and $t_{1/2}$ also was noted. For example, nine subjects exhibited an increase in $t_{1/2}$ and five subjects had a decrease in $t_{1/2}$ from one study period to the next. The mean percentage difference in $t_{1/2}$ was 26% (range of −30–+54%).

By contrast, there was very little intrapatient variability in V_d. After the capsule, the mean V_d was 0.38 ± 0.01 (±*SE*); after the liquid, the mean V_d was 0.42 ± 0.02 (±*SE*). These values are within the range of

Table II—Pharmacokinetic Parameters (Mean ± *SE*) for Theophylline after Oral Administration of a 300-mg Dose to 14 Subjects

Parameter	Formulation		Statistical Significance
	Liquid	Capsule	
K_a, hr^{-1}	5.22 ± 1.18	13.98 ± 3.10	Significant ($p < 0.05$)
$t_{1/2\text{-}abs}$, hr	0.27 ± 0.07	0.18 ± 0.16	NS ($p > 0.05$)
t_0, hr[a]	0.047 ± 0.017	0.143 ± 0.038	Significant ($p < 0.05$)
K_E, hr^{-1}	0.12 ± 0.01	0.11 ± 0.01	NS ($p > 0.05$)
$t_{1/2\text{-}elim}$, hr	6.19 ± 0.31	6.98 ± 0.61	NS ($p > 0.05$)
V_d, liters/kg	0.42 ± 0.02	0.38 ± 0.01	NS ($p > 0.05$)
Cl_B, ml/min/kg	0.84 ± 0.06	0.70 ± 0.07	NS ($p > 0.05$)

[a] Where t_0 is equal to absorption lag time.

mean values expected for the subject population in this study (9). The difference in V_d between formulations was not significant ($p > 0.05$).

Theophylline clearance was not significantly different after the capsule or liquid ($p > 0.05$). However, the mean clearance after the liquid was 0.84 ± 0.06 ml/min/kg (±*SE*), slightly faster than, but not significantly different from, the mean clearance of 0.70 ± 0.07 ml/min/kg (±*SE*) found for the capsule. The difference between the mean clearance values was not unexpected and was primarily related to the intrapatient variability in K_E and/or $t_{1/2}$ and not in V_d. The mean clearance values were similar to and within the range of values reported elsewhere (10, 11).

No significant side effects were reported during the study. Palpitations and mild headaches occurred in two subjects and coincided with peak serum theophylline concentrations. Vital signs were not altered during the study.

SUMMARY

Liquid-filled, soft gelatin theophylline capsules are unique among the large number of theophylline dosage forms. Solid oral theophylline dosage forms are thought to have many practical advantages over theophylline solutions. For example, the capsules evaluated in this study effectively masked the bitter theophylline taste. In addition, liquid-filled capsules may improve GI tract tolerance of the sometimes irritating theophylline.

The capsules evaluated appear to be a solid dosage form with rapid dissolution *in vivo*. They produce serum theophylline concentrations comparable to an oral theophylline liquid, and the relative bioavailability is the same as the oral liquid. Thus, in practice, these capsules would act as a reliable dosage form for oral theophylline administration.

REFERENCES

(1) L. Hendeles, M. Weinberger, and L. Bighley, *Am. J. Hosp. Pharm.*, **34**, 525 (1977).

(2) P. A. Mitenko and R. I. Ogilvie, *Clin. Pharmacol. Ther.*, **16**, 720 (1974).

(3) R. A. Holley, C. A. Mildon, and I. W. French, *Curr. Ther. Res.*, **23**, 330 (1978).

(4) "Desirable Weights of Adults," Statistical Bull. 40, Metropolitan Life Insurance, New York, N.Y., 1959.

(5) C. M. Metzler, Technical Report 7292-69-7293-005, Upjohn Co., Kalamazoo, Mich., 1969.

(6) J. Lindenbaum, *Curr. Ther. Res.*, **21**, 278 (1977).

(7) L. Padeletti and A. Brat, *Int. J. Clin. Pharmacol.*, **16**, 320 (1978).

(8) P. D. Walson, R. C. Strong, and L. M. Taussig, *J. Pediatr.*, **91**, 321 (1977).

(9) J. W. Kern and A. G. Lipman, *Drug Intell. Clin. Pharm.*, **11**, 152 (1977).

(10) P. A. Mitenko and R. I. Ogilvie, *Clin. Pharmacol. Ther.*, **14**, 509 (1972).

(11) M. W. Weinberger, R. A. Matthay, E. J. Ginchansky, C. A. Chidsey, and T. L. Petty, *J. Am. Med. Assoc.*, **235**, 2110 (1976).

ACKNOWLEDGMENTS

Presented at the Basic Pharmaceutics Section, APhA Academy of Pharmaceutical Sciences, Hollywood, Fla., meeting, November 1978.

Supported by a grant from Fisons Corp., Bedford, Mass.

The technical assistance of Julie Palmeri is gratefully acknowledged.

Discontinuous Absorption Processes in Pharmacokinetic Models

RICHARD SÜVERKRÜP

Received January 4, 1979, from the *Pharmazeutische Technologie, Pharmazeutisches Institut der Universität Bonn, An der Immenburg, 5300 Bonn-Endenich, West Germany.* Accepted for publication May 22, 1979.

Abstract □ The limited contact time of absorbable drug with absorbing surfaces is, in some cases, a significant factor determining the fraction of the dose absorbed. A simple modification of customary linear compartmental models is presented to account for this situation, and a general input function in the Laplace domain for truncated first-order absorption is derived. An extension to series of truncated absorption processes is discussed.

Keyphrases □ Bioavailability—pharmacokinetic models, limited absorption time, fraction of dose absorbed □ Models, pharmacokinetic—bioavailability, limited absorption time, fraction of dose absorbed □ Drug absorption—pharmacokinetic models, limited absorption time

For clinical purposes, a detailed knowledge of intestinal and rectal drug absorption times from dosage forms is not essential. Information about the fraction of the dose entering the general circulation or available at the site of action, peak plasma levels and the times at which they occur, and the time range during which the minimum effective concentration is exceeded is all that is necessary for treating patients. However, in bioavailability assessment for dosage form development and some diagnostic purposes, details of absorption kinetics are important and approximation by an infinite first-order process is not always sufficient. A simple but flexible way to handle this problem in linear models is presented.

BACKGROUND

Kübler (1–3) worked out an intestinal absorption theory on the basic assumption that drug is absorbed from a columnar volume of chymus traveling down the gut, which is considered as a tube of finite length. His results on ascorbic acid absorption indicate that there may be several intestinal segments with different absorption efficiencies.

In the simplest case (one homogeneous absorption segment and a one-compartment open body model without drug degradation in the intestinal lumen, gut wall metabolism, and first-pass effect), four rather unhandy equations describe the plasma concentration–time course (*b*).

Let t_1 be the time when the column has completely entered the absorbing segment and let t_2 be the time when its front first reaches the end of this segment. With the assumptions that entry starts at $t = 0$, the column does not increase in length during passage, the transport rate is equal at entry and exit, and the column can be regarded as a well-stirred compartment, for the time interval $0 < t < t_1$:

$$b = \frac{D_0}{V_c k_1 t_1 (k_1 - k_2)} [k_1(1 - e^{-k_2 t}) - k_2(1 - e^{-k_1 t})] \quad \text{(Eq. 1)}$$

where V_c is the volume of the body compartment and k_1 and k_2 are the first-order rate constants of absorption and overall elimination, respectively. When $t_1 < t < t_2$, the whole length of the column is in contact with the absorbing surface and the plasma level function reads:

$$b = \frac{D_0}{V_c k_2 t_1 (k_1 - k_2)} [k_1 e^{-k_2 t}(e^{k_2 t_1} - 1) - k_2 e^{-k_1 t}(e^{k_1 t_1} - 1)] \quad \text{(Eq. 2)}$$

During exit, for $t_2 < t < t_1 + t_2$:

$$b = \frac{D_0}{V_c k_2 t_1 (k_1 - k_2)} \{k_1 e^{-k_2 t}[e^{k_2 t_1} + e^{-(k_1 - k_2)t_2} - 1] - k_2 e^{-k_1(t - t_1)} - (k_1 - k_2) e^{-k_1 t_2}\} \quad \text{(Eq. 3)}$$

Finally, when there is no more absorption going on at $t > t_1 + t_2$, the terminal phase is described by:

$$b = \frac{D_0}{V_c k_2 t_1 (k_1 - k_2)} k_1 e^{-k_2 t}(e^{k_2 t_1} - 1)[1 - e^{-(k_1 - k_2)t_2}] \quad \text{(Eq. 4)}$$

Although this approach is evidently better suited to describing the kinetics of first-order absorption than any model based on the assumption that the intestine behaves like a well-stirred compartment in which unabsorbed drug potentially resides indefinitely, there can be no doubt that the situation is really more complex.

Dilution occurs during intestinal passage, and there may be losses due to microbial or enzymatic degradation in the gut lumen as well as to intestinal wall metabolism. If the latter processes are linear, they are easily accounted for by introducing into Eqs. 1–4 a factor, f, defined as the quotient of the absorption rate constant for unchanged drug over the sum of all rate constants of parallel first-order processes removing drug from the absorption site. It is this sum that appears as k_1 in Eqs. 1–4.

Dilution may be worth more consideration. During intestinal transport, the remaining unchanged drug is distributed in a steadily increasing volume of intestinal contents; the amount of drug immediately available for absorption per unit area of absorbing surface is decreased while the total area of contact between the absorbing gut wall and the drug-containing chymus is increased. If the drug were not distributed in a solid column but in an infinitely thin layer covering the gut wall, these effects would cancel out so that absorption would proceed as a first-order process independent of the area of intestinal surface actually participating in drug absorption. Even if the assumption of an infinitely thin layer is not valid, a first-order process frequently approximates the time course of absorption if absorption is fast.

In Kübler's equations (1–3), the length of the drug-containing chymus column and its transport rate are implicit parameters. They contribute significantly to the complexity without, however, giving much additional information since their influence on plasma concentrations is significant only during the relatively short intervals of entry and exit. These problems do not exist if absorption is treated as if it occurred from a small volume of chymus traveling down the intestinal tract at an arbitrary and even variable rate. This condition is true if a rapidly absorbed drug is released in a first-order process from a nondisintegrating preparation and may be a reasonable approximation in other cases.

PROCEDURE[1]

Consider a drug-containing volume of chymus that is so small that it passes through the absorbing length of intestine in a time interval shorter than the reciprocal of the corresponding sampling frequencies. With the assumption that absorption can be approximated reasonably well by a first-order process as discussed earlier, three equations are sufficient to describe the time course of plasma concentrations in a one-compartment open body model.

Let t_1 and t_2 be the points in time at which the drug enters and leaves the absorbing segment of intestine and let k_a and k_e be the apparent rate constants of absorption and elimination, respectively. Then, for $t < t_1$:

$$b = 0 \quad \text{(Eq. 5)}$$

For $t_1 < t < t_2$:

$$b = \frac{f D_0 k_a}{V_c (k_e - k_a)} [e^{-k_a(t - t_1)} - e^{-k_e(t - t_1)}] \quad \text{(Eq. 6)}$$

And for $t > t_2$:

$$b = \frac{f D_0 k_a}{V_c (k_e - k_a)} [e^{-k_a(t_2 - t_1)} - e^{-k_e(t_2 - t_1)}] e^{-k_e(t - t_2)} \quad \text{(Eq. 7)}$$

[1] Fitting programs are written in FORTRAN IV and were run on a PDP 11/10 computer with 24 K memory and RK 11/05 disk drive. They are available upon request to the author as listings and/or on cassettes.

0022-3549/79/1100-1395$01.00/0
© 1979, American Pharmaceutical Association

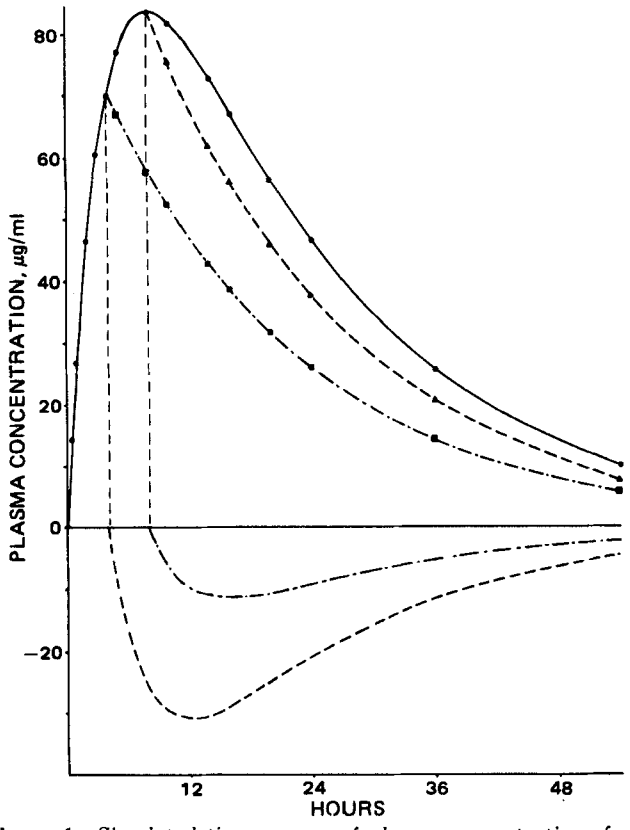

Figure 1—*Simulated time courses of plasma concentrations for a one-compartment model with truncated first-order absorption:*

Equation 18 Parameter Values	——	– – –	–·–·
k_e, hr^{-1}	*0.4*	*0.4*	*0.4*
k_e, hr^{-1}	*0.05*	*0.05*	*0.05*
V_c, *ml*	*8000.0*	*8000.0*	*8000.0*
f	*1*	*1*	*1*
t_1, *hr*	*0*	*0*	*0*
t_2, *hr*	*48.0*	*8.0*	*4.0*
D_0, *g*	*1.0*	*1.0*	*1.0*

There is a simpler and more generally applicable way to look at the problem. At $t = t_2$, the amount of drug not yet absorbed is:

$$D_1 = D_0 e^{-k_a(t_2-t_1)} \qquad \text{(Eq. 8)}$$

At all times $t > t_2$, plasma concentrations are lower by:

$$\Delta b = \frac{fD_0 e^{-k_a(t_2-t_1)}k_a}{V_c(k_e-k_a)}\left[e^{-k_a(t-t_2)} - e^{-k_e(t-t_2)}\right] \qquad \text{(Eq. 9)}$$

if absorption stops at $t = t_2$ than if absorption continues. This situation is illustrated in Fig. 1.

By extending the range of definition, Eqs. 5 and 6 can be combined to:

$$b = \frac{fD_0}{V_c}\zeta_0\frac{k_a}{(k_e-k_a)}\left[e^{-k_a(t-t_1)} - e^{-k_e(t-t_1)}\right] \qquad \text{(Eq. 10)}$$

where ζ_0 is:

$$\zeta_0 = \begin{cases} 0 & t < t_1 \\ 1 & t > t_1 \end{cases} \qquad \text{(Eq. 11)}$$

Similarly, an alternative to Eq. 9 is:

$$\Delta b = \frac{fD_0}{V_c}\zeta_1\frac{k_a}{(k_e-k_a)}\left[e^{-k_a(t-t_2)} - e^{-k_e(t-t_2)}\right] \qquad \text{(Eq. 12)}$$

with:

$$\zeta_1 = \begin{cases} 0 & t < t_2 \\ e^{-k_a(t_2-t_1)} & t > t_2 \end{cases} \qquad \text{(Eq. 13)}$$

According to the theorem, if $\mathcal{L}[F(t)] = f(s)$ and:

$$G(t) = \begin{cases} 0 & t < a \\ F(t-a) & t > a \end{cases} \qquad \text{(Eq. 14)}$$

then $\mathcal{L}[G(t)] = f(s)e^{-as}$, and one has the transforms:

$$\bar{b}(s) = \left(\frac{fD_0}{V_c}\right)(e^{-st_1})\left[\frac{k_a}{(k_e-k_a)(s+k_a)} + \frac{k_a}{(k_a-k_e)(s+k_e)}\right]$$
$$= \left(\frac{fD_0}{V_c}\right)(e^{-st_1})\left[\frac{k_a}{(s+k_a)(s+k_e)}\right] \qquad \text{(Eq. 15)}$$

and:

$$\bar{\Delta b}(s) = \left(\frac{fD_0}{V_c}\right)[e^{-k_a(t_2-t_1)}](e^{-st_2})\left[\frac{k_a}{(k_e-k_a)(s+k_a)} + \frac{k_a}{(k_a-k_e)(s+k_e)}\right]$$
$$= \left(\frac{fD_0}{V_c}\right)[e^{-k_a(t_2-t_1)}](e^{-st_2})\left[\frac{k_a}{(s+k_a)(s+k_e)}\right] \qquad \text{(Eq. 16)}$$

Subtracting Eq. 16 from Eq. 15 gives the transform of the function for concentrations in the body for a one-compartment model with first-order absorption starting at $t = t_1$ and stopping at $t = t_2$:

$$b(s) = \bar{b}(s) - \bar{\Delta b}(s) = \left(\frac{fD_0}{V_c}e^{-st_1}\right)\left[\frac{k_a}{(s+k_a)(s+k_e)}\right] - \left[\frac{fD_0}{V_c}e^{-k_a(t_2-t_1)}\right](e^{-st_2})\left[\frac{k_a}{(s+k_a)(s+k_e)}\right]$$
$$= \left(\frac{fD_0}{V_c}\right)\left[\frac{k_a}{(s+k_a)(s+k_e)}\right]\{e^{-st_1} - [e^{-k_a(t_2-t_1)}(e^{-st_2})]\} \qquad \text{(Eq. 17)}$$

This equation can be transformed back into the time domain:

$$b(t) = \frac{fD_0k_a}{V_c(k_e-k_a)}\{\zeta_0[e^{-k_a(t-t_1)} - e^{-k_e(t-t_1)}] - \zeta_1[e^{-k_a(t-t_2)} - e^{-k_e(t-t_2)}]\} \qquad \text{(Eq. 18)}$$

Thus, the input function for unlimited first-order absorption starting at zero time:

$$\text{in}_s = \frac{fD_0k_a}{(s+k_a)} \qquad \text{(Eq. 19)}$$

is replaced by:

$$\text{in}_s = \frac{fD_0k_a}{(s+k_a)}\{e^{-st_1} - [e^{-k_a(t_2-t_1)}(e^{-st_2})]\} \qquad \text{(Eq. 20)}$$

if the absorption rate is proportional to the amount of drug not yet absorbed during the time interval $t_1 < t < t_2$ but is zero otherwise.

A general equation for disposition from the central compartment of a linear mammillary model with n driving force compartments, where elimination may occur from any compartment, was given by Benet (4). Division by the volume of the central compartment changes the reference to concentrations rather than amounts:

$$d_{s,1} = \frac{1}{V_c}\frac{\prod_{i=2}^{n}(s+E_i)}{\prod_{i=1}^{n}(s+E_i) - \sum_{j=2}^{n}k_{1j}k_{j1}\prod_{\substack{m=2\\m\neq j}}^{n}(s+E_m)} = \frac{P(s)}{Q(s)} \qquad \text{(Eq. 21)}$$

where k_{1j} and k_{j1} are first-order rate constants for transfer from the central to the jth compartment and back, E_i is the sum of the exit rate constants from the ith compartment, and n is the number of driving force compartments. Both $P(s)$ and $Q(s)$ are polynomials in s, with Q being of higher degree than P so that partial fraction expansion is possible.

Alternatively, $Q(s)$ may be written as the product of its roots:

$$d_{s,1} = \frac{1}{V_c}\frac{P(s)}{\prod_{i=1}^{n}(s+\lambda_i)} \qquad \text{(Eq. 22)}$$

The convolution of the input function (Eq. 20) and the general disposition function (Eq. 22) is obtained by inverse transformation of their product formed in the Laplace domain:

$$c_{s,1} = \frac{fD_0}{V_c}\left[\frac{k_aP(s)}{\prod_{i=1}^{n}(s+\lambda_i)(s+k_a)}\right]\{e^{-st_1} - [e^{-k_a(t_2-t_1)}(e^{-st_2})]\} \qquad \text{(Eq. 23)}$$

Partial fraction expansion of the expression in the left brackets and introduction of shift-and-scale factors from the right brackets give, in the

time domain:

$$b(t) = \mathcal{L}^{-1}\{c_{s.1}\} = \frac{fD_0}{V_c}\left\{\zeta_0\left[\sum_{i=1}^{n} C_i e^{-\lambda_i(t-t_1)} + C_{n+1}e^{-k_a(t-t_1)}\right] - \zeta_1\left[\sum_{i=1}^{n} C_i e^{-\lambda_i(t-t_2)} + C_{n+1}e^{-k_a(t-t_2)}\right]\right\} \quad \text{(Eq. 24)}$$

Absorption from Several Segments—Where absorption does not drop to zero at t_2 but assumes a different finite value, there are two sequential absorption processes with first-order rate constants k_{a1} and k_{a2}. Although such a change may be due to transition into an intestinal segment with different absorption efficiency, alternative explanations can be a change in the release characteristics of the formulation or a change in the concentration of the absorbable drug species at the membrane caused by pH variations.

In this case, the situation is handled adequately by recursive application of Eq. 24 since all functions are linear and, therefore, additive. The system behaves as if absorption stopped completely at $t = t_2$ and as if a second dose of $D_0e^{-k_{a1}(t_1-t_2)}$ started to be absorbed simultaneously with a different rate constant k_{a2}. If absorption from the second segment approaches completion, the end of absorption due to drug removal from absorptive sites cannot be observed and just one more term is added to Eq. 24:

$$b(t) = \frac{fD_0}{V_c}\left\{\zeta_0\left[\sum_{i=1}^{n} C_{1i}e^{-\lambda_i(t-t_1)} + C_{1(n+1)}e^{-k_{a1}(t-t_1)}\right] - \zeta_1\left[\sum_{i=1}^{n} C_{1i}e^{-\lambda_i(t-t_2)} + C_{1(n+1)}e^{-k_{a1}(t-t_2)}\right] + \zeta_2\left[\sum_{i=1}^{n} C_{2i}e^{-\lambda_i(t-t_2)} + C_{2(n+1)}e^{-k_{a2}(t-t_2)}\right]\right\} \quad \text{(Eq. 25)}$$

which is readily extended to absorption from m segments in an n-compartment mammillary model, extending the definition given in Eq. 13:

$$\zeta_m = \begin{cases} 0 & t < t_{m+1} \\ \prod_{j=1}^{m} e^{-k_{aj}(t_{j+1}-t_j)} & t > t_{m+1} \end{cases} \quad \text{(Eq. 26)}$$

where k_{aj} is the absorption rate in the jth segment. In this notation, lag times are represented by an initial segment with index zero and absorption rate constant k_{a0} equal to zero. The generalized equation for this type of model is then:

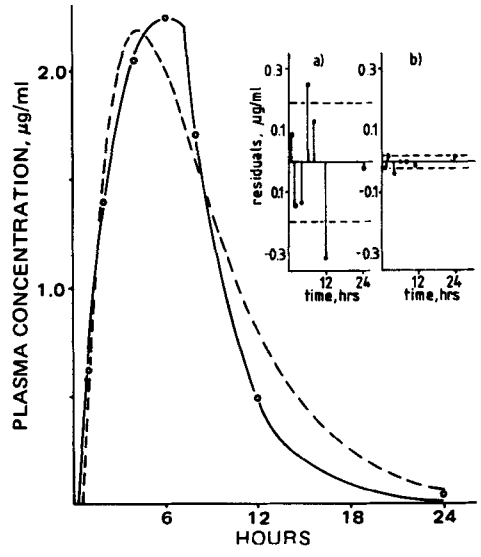

Figure 2—*Plasma griseofulvin concentrations in rats (5):*

Equation 18 Parameter Values	———	- - -
k_a, hr^{-1}	*0.09066*	*0.2602*
k_e, hr^{-1}	*0.3090*	*0.2944*
V_c/f, *ml/k*	*3939.3*	*7952.0*
t_1, *hr*	*0.3612*	*0.6387*
t_2, *hr*	*7.168*	*>24.0*
D_0, *mg/k*	*50.0*	*50.0*

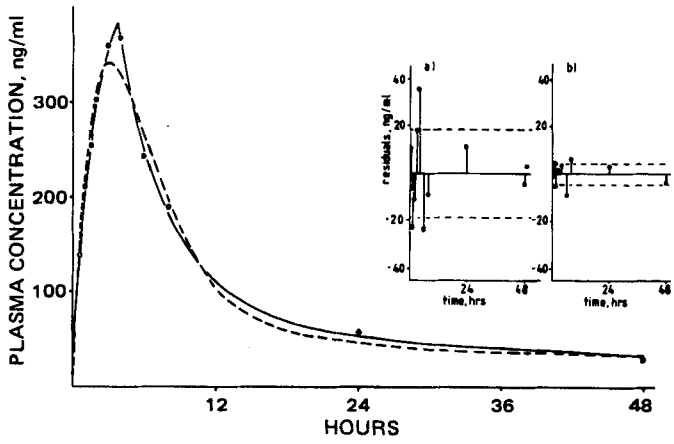

Figure 3—*Plasma buformin levels in humans (sustained-released preparation) (7):*

$$C_1 = \frac{k_a(k_{21}-\alpha)}{(k_a-\alpha)(\beta-\alpha)} \quad C_2 = \frac{k_a(k_{21}-\beta)}{(k_a-\beta)(\alpha-\beta)} \quad C_3 = \frac{k_a(k_{21}-k_a)}{(\alpha-k_a)(\beta-k_a)}$$

$$\lambda_1 = \alpha \qquad \lambda_2 = \beta$$

Equation 24 Parameter Values	———	- - -
k_a, hr^{-1}	*0.1836*	*0.3422*
k_{21}, hr^{-1}	*0.05106*	*0.03523*
α, hr^{-1}	*0.2362*	*0.3420*
β, hr^{-1}	*0.0202*	*0.01314*
t_1, *hr*	*−0.3016*	*0.0*
t_2, *hr*	*3.722*	*>60.0*
V_c/f, *liters*	*3203.4*	*90.04*
D_0, *mg*	*100*	*100*

$$b(t) = \frac{fD_0}{V_c}\left\{\sum_{j=1}^{m}\left[\zeta_{j-1}\left(\sum_{i=1}^{n} C_{ji}e^{-\lambda_i(t-t_j)} + C_{(j)(n+1)}e^{-k_{aj}(t-t_j)}\right) - \zeta_j\left(\sum_{i=1}^{n} C_{ji}e^{-\lambda_i(t-t_{j+1})} + C_{(j)(n+1)}e^{-k_{aj}(t-t_{j+1})}\right)\right]\right\} \quad \text{(Eq. 27)}$$

Each segment is thus represented by two terms, both zero before the segment becomes involved in absorption. At this time, the first term assumes positive values whereas the second term changes to smaller negative values as soon as the segment is no longer active in absorption.

The solution is very general and of little use in any practical situation. Nevertheless, it indicates that any time course of absorption, however irregular, can be approximated by a sequence of first-order absorption processes, provided that the set of measurements is accurate and large enough. In fact the same effect can be achieved by a sequence of any well-defined input processes. An example is the simulation of first-order absorption by a sequence of zero-order infusions with decreasing rates, which Loo and Riegelman (5) used to demonstrate the applicability of their method of calculating intrinsic absorption rates. In this context, repeated administration of identical doses at equal time intervals may be viewed as an imperfect realization of a zero-order input function; the approximation becomes more and more perfect as the time intervals between administrations decrease.

Zero-Order Absorption—Since the liberation of rapidly absorbed drugs from sustained-release preparations ideally should be close to a zero-order process, this case will be touched on briefly. With ζ_1 and ζ_2 defined as:

$$\zeta_1 = \begin{cases} 0 & t < t_1 \\ 1 & t > t_1 \end{cases} \quad \text{(Eq. 28a)}$$

$$\zeta_2 = \begin{cases} 0 & t < t_2 \\ 1 & t > t_2 \end{cases} \quad \text{(Eq. 28b)}$$

the time course of plasma concentrations during and after zero-order infusion of a drug, conferring the properties of a two-compartment model upon the body, is given by:

$$b(t) = \frac{k_0}{V_c}\left\{\zeta_1\left[\frac{k_{21}}{\alpha\beta} + \frac{k_{21}-\alpha}{\alpha(\alpha-\beta)}e^{-\alpha(t-t_1)} + \frac{\beta-k_{21}}{\beta(\alpha-\beta)}e^{-\beta(t-t_1)}\right] - \zeta_2\left[\frac{k_{21}}{\alpha\beta} + \frac{k_{21}-\alpha}{\alpha(\alpha-\beta)}e^{-\alpha(t-t_2)} + \frac{\beta-k_{21}}{\beta(\alpha-\beta)}e^{-\beta(t-t_2)}\right]\right\} \quad \text{(Eq. 29)}$$

and, after rearrangement:

$$b(t) = \frac{k_0}{V_c}\left\{\frac{k_{21}}{\alpha\beta}(\zeta_1 - \zeta_2) + \frac{k_{21} - \alpha}{\alpha(\alpha - \beta)}[\zeta_1 e^{-\alpha(t-t_1)} - \zeta_2 e^{-\alpha(t-t_2)}] + \frac{\beta - k_{21}}{\beta(\alpha - \beta)}[\zeta_1 e^{-\beta(t-t_1)} - \zeta_2 e^{-\beta(t-t_2)}]\right\} \quad \text{(Eq. 30)}$$

where t_1 is the time when infusion starts and t_2 is the time when it stops.

The zero-order rate constant can be expressed as $k_0 = [D_0/(t_2 - t_1)]$.

In zero-order intestinal absorption, t_1 is the time of onset of release and t_2 is the time when the formulation is exhausted. Linear losses by gut wall metabolism and nonsaturable first-pass metabolism may be considered by multiplying Eq. 29 by a factor, f, which is smaller than or equal to unity. In this case, f is not a quotient of the rate constants but still reflects the fraction of absorbed drug that reaches the general circulation.

Let t_3 be the time when the formulation leaves the absorbing segment of the intestine, which may be earlier or later than t_2. For $t_2 < t_3$:

$$b = \frac{fD_0}{V_c(t_2 - t_1)}\left\{\frac{k_{21}}{\alpha\beta}(\zeta_1 - \zeta_2) + \frac{k_{21} - \alpha}{\alpha(\alpha - \beta)}[\zeta_1 e^{-\alpha(t-t_1)} - \zeta_2 e^{-\alpha(t-t_2)}] + \frac{\beta - k_{21}}{\beta(\alpha - \beta)}[\zeta_1 e^{-\beta(t-t_1)} - \zeta_2 e^{-\beta(t-t_2)}]\right\} \quad \text{(Eq. 31)}$$

For $t_2 > t_3$:

$$b = \frac{fD_0}{V_c(t_2 - t_1)}\left\{\frac{k_{21}}{\alpha\beta}(\zeta_1 - \zeta_3) + \frac{k_{21} - \alpha}{\alpha(\alpha - \beta)}[\zeta_1 e^{-\alpha(t-t_1)} - \zeta_3 e^{-\alpha(t-t_3)}] + \frac{\beta - k_{21}}{\beta(\alpha - \beta)}[\zeta_1 e^{-\beta(t-t_1)} - \zeta_3 e^{-\beta(t-t_3)}]\right\} \quad \text{(Eq. 32)}$$

where:

$$\zeta_3 = \begin{cases} 0 & t < t_3 \\ 1 & t > t_3 \end{cases} \quad \text{(Eq. 33)}$$

The difference between this case and an intravenous infusion is that complete bioavailability is no longer assured and that the input rate and duration are no longer experimental variables with known values but are model parameters to which values have to be assigned.

Examples—Three examples from the literature (6–9) are given in which time-limited absorption explained experimental data better than models with continuing absorption. In the papers quoted, observations on individuals are reported. Time courses of the best-fitting continuous absorption models are indicated by broken lines; corresponding functions with truncated absorption are solid.

Griseofulvin—Carrigan and Bates (6) administered doses of 50 mg of micronized griseofulvin/kg to rats. The drug was given in an aqueous suspension, in a corn oil suspension, and in a triphasic system with griseofulvin suspended in a corn oil-in-water emulsion. Polysorbate 60

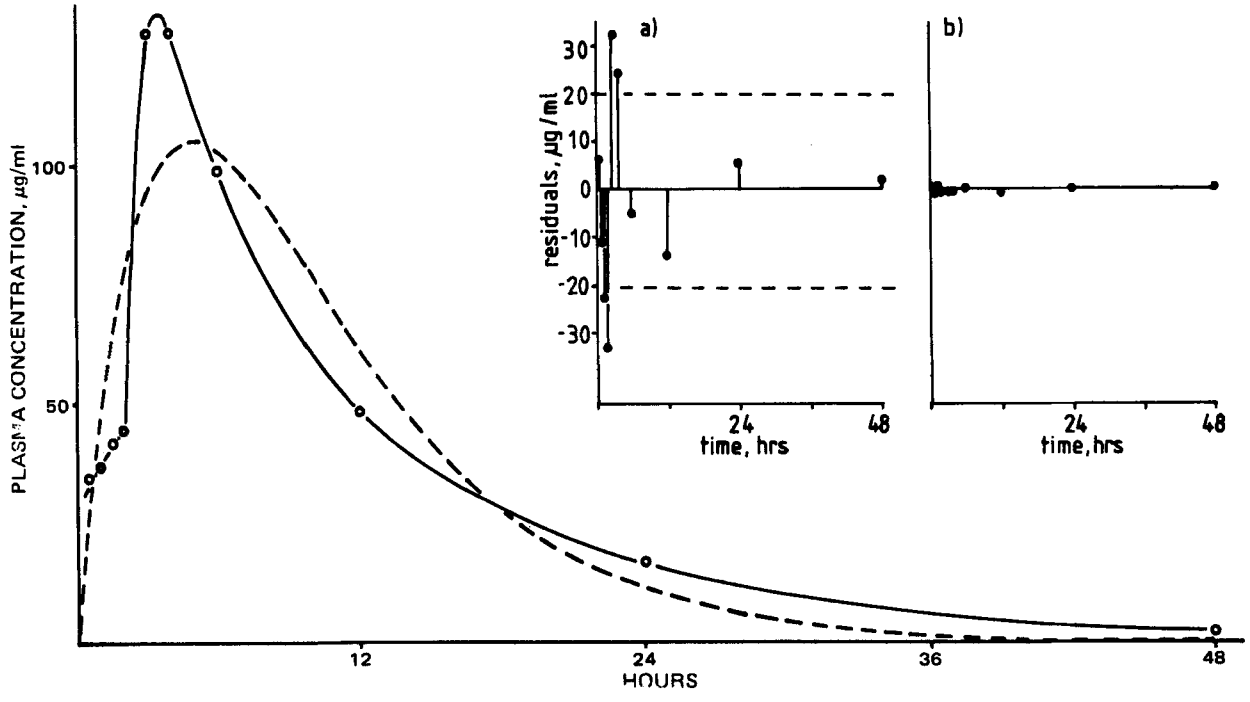

Figure 4—*Plasma sulfisoxazole concentrations in humans after oral administration (8):*

$$C_{11} = \frac{k_{a1}(k_{21} - \alpha)}{(k_{a1} - \alpha)(\beta - \alpha)} \quad C_{12} = \frac{k_{a1}(k_{21} - \beta)}{(k_{a1} - \beta)(\alpha - \beta)} \quad C_{13} = \frac{k_{a1}(k_{21} - k_{a1})}{(\alpha - k_{a1})(\beta - k_{a1})}$$

$$C_{21} = \frac{k_{a2}(k_{21} - \alpha)}{(k_{a2} - \alpha)(\beta - \alpha)} \quad C_{22} = \frac{k_{a2}(k_{21} - \beta)}{(k_{a2} - \beta)(\alpha - \beta)} \quad C_{23} = \frac{k_{a2}(k_{21} - k_{a2})}{(\alpha - k_{a2})(\beta - k_{a2})}$$

$$\lambda_1 = \alpha \quad \lambda_2 = \beta \quad \zeta_0 = \begin{cases} 0 & t < t_1 \\ 1 & t > t_1 \end{cases} \quad \zeta_1 = \begin{cases} 0 & t < t_2 \\ e^{-k_{a1}(t_2 - t_1)} & t > t_2 \end{cases}$$

Equation 27 Parameter Values	
k_{a1}, hr^{-1}	*0.1080*
k_{a2}, hr^{-1}	*1.6788*
k_{21}, hr^{-1}	*0.1941*
α, hr^{-1}	*0.2938*
β, hr^{-1}	*0.08086*
t_1, *hr*	*−1.6656*
t_2, *hr*	*2.0807*
V_c, *ml*	*10749.0*
fD_0, *g*	*2.0*

Equation 6 Parameter Values	
k_a, hr^{-1}	*0.2013*
k_e, hr^{-1}	*0.2010*
V_c/f, *ml*	*6978.0*
t_1, *hr*	*0.0*
t_2, *hr*	*>48.0*
D_0, *g*	*2.0*

was added to all preparations. Seven samples were obtained between 1 and 24 hr after administration. Significant differences in peak plasma levels attributable to the liquid phases were observed with mean values of 0.892, 1.30, and 2.07 μg/ml, respectively. There were no corresponding shifts in the times when peak concentrations occurred.

Figure 2 shows data from an animal that received the drug suspended in corn oil. The peak plasma level was the highest in its group and occurred late. The better fit of the discontinuous model, although conspicuous, is statistically not significant because of the small number of degrees of freedom for the truncated absorption model (five parameters are estimated from seven observations).

Buformin—A two-compartment model is adequate to describe the plasma concentration–time course after injection of buformin (7). The drug is not metabolized. A sustained-release formulation containing 100 mg of ^{14}C-buformin hydrochloride in a wax matrix was administered to six diabetic patients (8). Ten plasma samples were taken during 48 hr after ingestion. Both urinary and fecal excretion were followed.

Figure 3 gives the plasma data for one subject. As predicted on the basis of *in vitro* liberation studies, release and absorption appear to be first order, although truncated. (Zero order was tested and gave a reasonable but inferior fit.) Fecal recovery was 44.8% of the dose, and 38.4% was excreted during the first 24 hr by this route. This finding is consistent with a fecal excretion of 48% predicted by the truncated absorption model. The negative lag time obtained in the fit is indicative of a short phase of rapid absorption, which cannot be resolved on the basis of the sampling schedule used. The variances of the residuals are 355.8 and 20.09 $(ng/ml)^2$ for the continuous and truncated absorption models with five and three degrees of freedom. Therefore, the latter model is significantly better on the 95% confidence level.

Sulfisoxazole—Kaplan *et al.* (9) compared sulfisoxazole pharmacokinetic profiles after intravenous, intramuscular, and oral administrations to six volunteers. After intravenous injection, the plasma concentration–time course corresponded to a two-compartment model. The data given in Fig. 4 were observed in the third subject after oral administration of a 2.0-g dose. It stands out among the experiments reported in this paper because of its apparent absence of scatter. Although a two-compartment, two-segment absorption model gives an excellent fit, there remains some doubt about its general applicability for the drug and the formulation used. Again, a negative lag time indicates that there is an initial phase of rapid absorption.

Attempts to fit these data by a two-compartment model with continuing first-order kinetics failed because the model degenerated when k_a, α, and β became identical within the first three significant digits. Therefore, a one-compartment model with unlimited absorption was used for comparison. With residual variances of 404.38 and 0.1337 $(\mu g/ml)^2$ for seven and two degrees of freedom, the biphasic absorption model is superior on the 99% confidence level.

DISCUSSION

The type of models presented is not really new except for the notation, which was in part adapted from electronics (10). Time-limited intestinal absorption was demonstrated for lincomycin and clindamycin (11) and applied to the rectal absorption of lincomycin and aspirin as well, where the fraction of dose absorbed increased with retention time (12, 13).

Hybrids of flow models for absorption and compartmental models for distribution, metabolism, and elimination have advantages over a purely compartmental approach, which is included as a limiting case. Even in the simplest single-segment version, they provide a logical link between the rate and amount aspects of bioavailability and eliminate the flip-flop phenomenon if absorption is incomplete. Multisegment models are flexible tools to obtain more information about the time course of absorption. The models are parsimonious since a minimum of new parameters (one rate constant and an exit time) is introduced for each absorption segment and good exit time estimates can be found by simple inspection of the data. They appear to be superior over models approximating the intestine by a chain of compartments, as recently proposed by Hradil *et al.* (14), since they avoid the physiologically doubtful assumption of first-order transport between gut sections, which gives rise to poorly defined transition rate constants.

If absorption stops abruptly, the graphical method of residuals fails as shown in Fig. 5, in which simulated data from Fig. 1 were redrawn semilogarithmically. As discussed by Perrier and Gibaldi (15), apparent absorption rates increase when only the absorption time interval is shortened. Other procedures to set up fraction absorbed *versus* time plots (5, 16) are still operative, but, like all sequential data analysis methods,

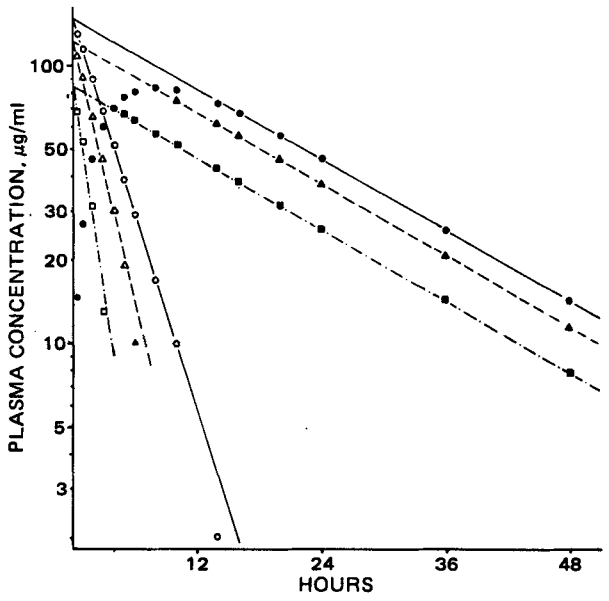

Figure 5—*Failure of the method of residuals if applied to data from Fig. 1.*

they suffer from error propagation problems and are ineffective if few samples are taken during the absorption phase.

Some problems are associated with the type of models proposed here. Obviously, spline functions cannot be used for interpolation in the neighborhood of discontinuities. Less obviously, commonly used fitting algorithms, such as the Gauss–Newton method, require that derivatives of model equations with respect to their parameters are continuous. This condition is not true for transition times and reduces both the computation efficiency and the precision of the final estimates. This problem does not occur if inherently less efficient direct search strategies, such as the Nelder–Mead method (17), are applied.

The increase in adaptability to measurements makes truncated absorption models more vulnerable to influences of experimental error than more rigid alternatives, and the ease of improving a fit by just throwing in another absorption segment adds to this problem. The risk can be controlled by careful analysis of the residuals and, possibly, by inspection of confidence contours of the parameter estimates. In test calculations, a typical error, indicating improper use of limited absorption models, was a significant underestimation of the central compartment volume.

Time-limited absorption models are implemented easily on both analog and digital computers and can be valuable tools in further studies of intestinal drug absorption. They can also provide diagnostic help if absorption kinetics are pathologically altered, as in mucoviscidosis[2].

REFERENCES

(1) W. Kübler, *Gastroenterologia (Suppl.)*, **104**, 231 (1965).

(2) W. Kübler, *Verh. Wiss. Kongr. Dtsch. Ges. Ernährung*, Munchen, West Germany, 1968.

(3) W. Kübler, *Z. Kinderheilkd.*, **108**, 187 (1970).

(4) L. Z. Benet, *J. Pharm. Sci.*, **61**, 536 (1972).

(5) J. C. K. Loo and S. Riegelman, *ibid.*, **57**, 918 (1968).

(6) D. J. Carrigan and T. R. Bates, *ibid.*, **62**, 1476 (1973).

(7) P. Botterman, A. Sovatzoglou, and U. Schweigart, in "Proceedings of the Second International Biguanid Symposium," K. Oberdisse, H. Daweke, and G. Michael, Eds., Thieme, Stuttgart, West Germany, 1968.

(8) H. Gutsche, L. Blumenbach, W. Losert, and H. Wiemann, *Arzneim.-Forsch.*, **26**, 1227 (1976).

(9) S. A. Kaplan, R. E. Weinfeld, C. W. Abruzzo, and M. Lewis, *J. Pharm. Sci.*, **61**, 773 (1972).

(10) A. Ameling, "Laplace Transformation," Bertelsmann Universitätsverlag, Düsseldorf, West Germany, 1975.

(11) H. M. v. Hattingberg, *Infection (Suppl. 1)*, **5**, S29 (1977).

[2] H. M. v. Hattingberg, Zentrum für Kinderheilkunde, Universität Giessen, 6300 Giessen, West Germany, personal communication.

(12) J. G. Wagner, C. H. Carter, and I. J. Martens, *J. Clin. Pharmacol.*, **8**, 154 (1968).
(13) M. M. Nowak, B. Grundhofer, and M. Gibaldi, *Pediatrics*, **5**, 23 (1974).
(14) J. Hradil, Z. Fendrich, K. E. O. Senius, and J. Kvetina, *Arzneim.-Forsch.*, **25**, 2127 (1978).
(15) D. Perrier and M. Gibaldi, *J. Pharm. Sci.*, **62**, 225 (1973).
(16) J. G. Wagner and E. Nelson, *ibid.*, **53**, 1392 (1964).
(17) J. A. Nelder and R. Mead, *Comput. J.*, **7**, 308 (1964).

ACKNOWLEDGMENTS

The author is indebted to Professor Müller and Dipl. Phys. Kaul for support and stimulating discussions, to Dipl. Math. Dr. Witsch for reviewing the manuscript, and to the Federal Ministry of Research and Technology for funding under Grant BAM 08.

NMR Spectroscopic Determination of Preferred Conformations of Quinidine and Hydroquinidine

YEHUDA YANUKA, SHIMONA YOSSELSON SUPERSTINE, and EDWARD SUPERSTINE ˣ

Received January 23, 1978, from the *Department of Pharmaceutics, School of Pharmacy, Faculty of Medicine, Hadassah-Hebrew University Medical Center, Jerusalem, Israel.* Accepted for publication May 9, 1979.

Abstract □ NMR spectra of quinidine (I), hydroquinidine (II), and their respective acetyl derivatives (III and IV) were compared. The chemical shifts of some protons in I differed from those of their counterparts in II. These values were concentration dependent in I and II; they were similar in III and IV but not concentration dependent. The implications of these findings and the correlation of the NMR data with the preferred conformations are discussed.

Keyphrases □ Quinidine—conformation, NMR spectroscopic analysis, concentration dependence □ Hydroquinidine—conformation, NMR spectroscopic analysis, concentration dependence □ NMR spectroscopy—quinidine and hydroquinidine, conformations, concentration dependence

Of all of the cinchona alkaloids, quinidine (I) remains the most important because of its extensive use as an antiarrhythmic agent. Hydroquinidine (II) is an impurity found in commercial I and also has antiarrhythmic activity. The absolute configuration of all asymmetric carbon atoms in these molecules has been assigned by different methods including NMR spectroscopy (1–4). The evidence of these studies is considered conclusive.

No comprehensive studies have been carried out concerning the conformation of the different fragments of I and II. Knowledge concerning the preferred stable conformation of these compounds facilitates structural elucidation of the metabolic products. The objectives of this work were to analyze the NMR spectra of I and II and their 9-acetyl derivatives III and IV, stressing the importance of acetylation, and to discover new information related to their structure and conformation.

EXPERIMENTAL

Spectra were obtained at 100 MHz using an analytical NMR spectrometer[1] equipped with an automatic recorder. Tetramethylsilane in deuterochloroform was used as the internal standard; the chemical shift of its protons does not appear in the spectra. Pure I and II were obtained from commercial quinidine sulfate[2]. TLC and preparative TLC were carried out on aluminum oxide[3] plates. The developing solvent was ethyl acetate.

Purification of Commercial Quinidine—Commercial quinidine sulfate (500 mg) was dissolved in water (20 ml). A slight excess of sodium bicarbonate was added, and the free base was extracted in a separator by three 30-ml portions of chloroform. The chloroform solution was filtered through anhydrous sodium sulfate and evaporated.

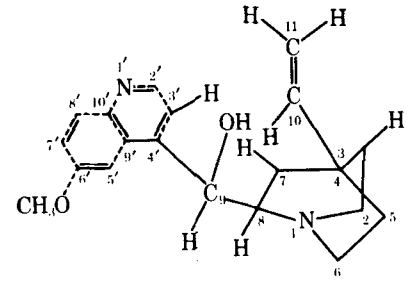

I

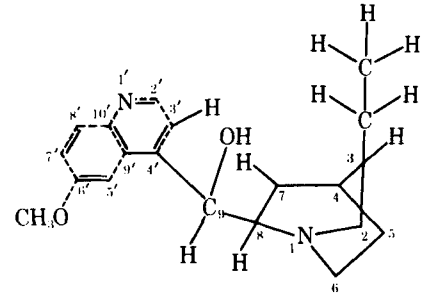

II

Portions of the free base (30 mg) were chromatographed on aluminum oxide plates. The fluorescing material was viewed under UV light and divided into three fractions. The upper strip was scraped and dispersed in 20 ml of 0.1 *N* H_2SO_4. Sodium bicarbonate (240 mg) was added, and pure quinidine was extracted with chloroform. The mixture was transferred to a separator, and the chloroform solution was filtered through anhydrous sodium sulfate and evaporated. A readily crystallized pure quinidine was obtained after solvent removal, mp 170–171°, R_f 0.135 (chloroform–ethyl acetate, 2:1). The NMR spectrum is shown in Fig. 1.

The lower strip, containing II contaminated by small quantities of I, was scraped and extracted as described. Pure II was obtained by a repetition of the chromatographic procedure. Recrystallization from methanol yielded crystals, mp 169° [lit. (5) mp 169 and 174°]; R_f 0.1 (chloroform–ethyl acetate, 2:1). The NMR spectral data are given in Table I.

Acetylation—Pure quinidine (40 mg) was dissolved in pyridine (1 ml), and acetic anhydride (1 ml) was added. The reaction mixture was allowed to stand at room temperature for 24 hr. Solvents were removed with an air stream, and the solid residue was dissolved in 30 ml of chloroform. The

[1] Varian A-100 D.
[2] Quinidine sulfate USP, Sigma Chemical Co., St. Louis, Mo.
[3] Aluminum oxide GF 254, Stahl, Merck.

0022-3549/79/1100-1400$01.00/0
© 1979, American Pharmaceutical Association

(12) J. G. Wagner, C. H. Carter, and I. J. Martens, *J. Clin. Pharmacol.*, **8**, 154 (1968).
(13) M. M. Nowak, B. Grundhofer, and M. Gibaldi, *Pediatrics*, **5**, 23 (1974).
(14) J. Hradil, Z. Fendrich, K. E. O. Senius, and J. Kvetina, *Arzneim.-Forsch.*, **25**, 2127 (1978).
(15) D. Perrier and M. Gibaldi, *J. Pharm. Sci.*, **62**, 225 (1973).
(16) J. G. Wagner and E. Nelson, *ibid.*, **53**, 1392 (1964).
(17) J. A. Nelder and R. Mead, *Comput. J.*, **7**, 308 (1964).

ACKNOWLEDGMENTS

The author is indebted to Professor Müller and Dipl. Phys. Kaul for support and stimulating discussions, to Dipl. Math. Dr. Witsch for reviewing the manuscript, and to the Federal Ministry of Research and Technology for funding under Grant BAM 08.

NMR Spectroscopic Determination of Preferred Conformations of Quinidine and Hydroquinidine

YEHUDA YANUKA, SHIMONA YOSSELSON SUPERSTINE, and EDWARD SUPERSTINE ˣ

Received January 23, 1978, from the *Department of Pharmaceutics, School of Pharmacy, Faculty of Medicine, Hadassah-Hebrew University Medical Center, Jerusalem, Israel.* Accepted for publication May 9, 1979.

Abstract □ NMR spectra of quinidine (I), hydroquinidine (II), and their respective acetyl derivatives (III and IV) were compared. The chemical shifts of some protons in I differed from those of their counterparts in II. These values were concentration dependent in I and II; they were similar in III and IV but not concentration dependent. The implications of these findings and the correlation of the NMR data with the preferred conformations are discussed.

Keyphrases □ Quinidine—conformation, NMR spectroscopic analysis, concentration dependence □ Hydroquinidine—conformation, NMR spectroscopic analysis, concentration dependence □ NMR spectroscopy—quinidine and hydroquinidine, conformations, concentration dependence

Of all of the cinchona alkaloids, quinidine (I) remains the most important because of its extensive use as an antiarrhythmic agent. Hydroquinidine (II) is an impurity found in commercial I and also has antiarrhythmic activity. The absolute configuration of all asymmetric carbon atoms in these molecules has been assigned by different methods including NMR spectroscopy (1–4). The evidence of these studies is considered conclusive.

No comprehensive studies have been carried out concerning the conformation of the different fragments of I and II. Knowledge concerning the preferred stable conformation of these compounds facilitates structural elucidation of the metabolic products. The objectives of this work were to analyze the NMR spectra of I and II and their 9-acetyl derivatives III and IV, stressing the importance of acetylation, and to discover new information related to their structure and conformation.

EXPERIMENTAL

Spectra were obtained at 100 MHz using an analytical NMR spectrometer[1] equipped with an automatic recorder. Tetramethylsilane in deuterochloroform was used as the internal standard; the chemical shift of its protons does not appear in the spectra. Pure I and II were obtained from commercial quinidine sulfate[2]. TLC and preparative TLC were carried out on aluminum oxide[3] plates. The developing solvent was ethyl acetate.

Purification of Commercial Quinidine—Commercial quinidine sulfate (500 mg) was dissolved in water (20 ml). A slight excess of sodium bicarbonate was added, and the free base was extracted in a separator by three 30-ml portions of chloroform. The chloroform solution was filtered through anhydrous sodium sulfate and evaporated.

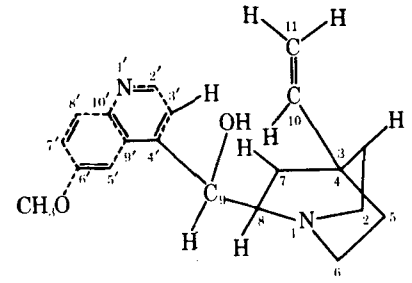

I

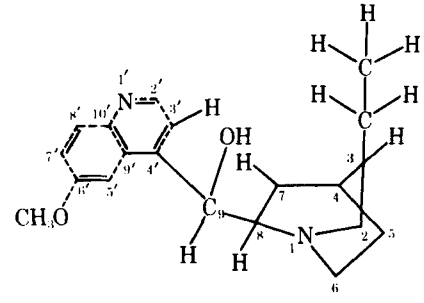

II

Portions of the free base (30 mg) were chromatographed on aluminum oxide plates. The fluorescing material was viewed under UV light and divided into three fractions. The upper strip was scraped and dispersed in 20 ml of 0.1 *N* H_2SO_4. Sodium bicarbonate (240 mg) was added, and pure quinidine was extracted with chloroform. The mixture was transferred to a separator, and the chloroform solution was filtered through anhydrous sodium sulfate and evaporated. A readily crystallized pure quinidine was obtained after solvent removal, mp 170–171°, R_f 0.135 (chloroform–ethyl acetate, 2:1). The NMR spectrum is shown in Fig. 1.

The lower strip, containing II contaminated by small quantities of I, was scraped and extracted as described. Pure II was obtained by a repetition of the chromatographic procedure. Recrystallization from methanol yielded crystals, mp 169° [lit. (5) mp 169 and 174°]; R_f 0.1 (chloroform–ethyl acetate, 2:1). The NMR spectral data are given in Table I.

Acetylation—Pure quinidine (40 mg) was dissolved in pyridine (1 ml), and acetic anhydride (1 ml) was added. The reaction mixture was allowed to stand at room temperature for 24 hr. Solvents were removed with an air stream, and the solid residue was dissolved in 30 ml of chloroform. The

[1] Varian A-100 D.
[2] Quinidine sulfate USP, Sigma Chemical Co., St. Louis, Mo.
[3] Aluminum oxide GF 254, Stahl, Merck.

0022-3549/79/1100-1400$01.00/0
© 1979, American Pharmaceutical Association

Table I—Chemical Shift Values [a] (in Parts per Million) of the Protons of Quinidine (I) and Hydroquinidine (II) at Various Concentrations (Milligrams per 0.5 ml)

Proton	I				II			
	15 mg	30 mg	60 mg	100 mg	13 mg	30 mg	60 mg	100 mg
H-2′	8.59 (d) (J = 4 Hz)	8.52 (d) (J = 4 Hz)	8.45 (d) (J = 4 Hz)	8.38 (d) (J = 4 Hz)	8.63 (d) (J = 4 Hz)	8.59 (d) (J = 4 Hz)	8.47 (d) (J = 4 Hz)	8.44 (d) (J = 4 Hz)
H-8′	7.94 (d) (J = 9 Hz)	7.90 (d) (J = 9 Hz)	7.86 (d) (J = 9 Hz)	7.83 (d) (J = 10 Hz)	7.95 (d) (J = 10 Hz)	7.93 (d) (J = 10 Hz)	7.88 (d) (J = 9 Hz)	7.87 (d) (J = 9 Hz)
H-3′	7.49 (d) (J = 4 Hz)	7.47 (d) (J = 4 Hz)	7.46 (d) (J = 4 Hz)	7.46 (d) (J = 4 Hz)	7.52 (d) (J = 4 Hz)	7.51 (d) (J = 4 Hz)	7.47 (d) (J = 4 Hz)	7.46 (d) (J = 4 Hz)
H-10	6.00 (m)	6.03 (m)	6.03 (m)	6.06 (m)	—	—	—	—
H–C-9–OH	5.57 (d) (J = 4 Hz)	5.57 (d) (J = 4 Hz)	5.57 (a)	5.58 (a)	5.62 (d) (J = 4 Hz)	5.59 (a)	5.55 (m)	5.54 (m)
H-11	5.09	5.09	5.09 (d) (J = 3 Hz)	5.08 (d) (J = 3 Hz)	—	—	—	—
H-11	4.95 (d) (J = 3 Hz)	4.96	4.94	4.93	—	—	—	—
CH_3O–	3.84	3.81	3.79	3.79	3.81	3.80	3.80	3.79

[a] d = doublet; m = multiplet; and a = ill-defined doublet.

chloroform solution was transferred to a separator, washed with 20 ml of water, and filtered without delay through anhydrous sodium sulfate since it was prone to hydrolysis; R_f 0.315 (chloroform–ethyl acetate, 2:1). The NMR spectrum is given in Fig. 1.

Acetylation of II was carried out under the same conditions described for acetylation of I; R_f 0.315 (chloroform–ethyl acetate, 2:1).

RESULTS AND DISCUSSION

The protons of I–IV may be classified on the basis of their chemical shifts by comparison with literature data (6, 7).

NMR Spectral Analysis of I and III—The spectra of I and III (Fig. 1) were determined at a concentration of 30 mg/0.5 ml.

Aromatic Protons—In I, H-2′ appeared as a doublet at δ 8.52 (J = 4 Hz) and was split by H-3′; therefore, the doublet with the same splitting constant at δ 7.47 was assigned to H-3′. After acetylation, H-2′ appeared at δ 8.70. The H-3′ shifted to a higher field at δ 7.27, indicating the H-2′ and H-3′ were in the vicinity of the acetoxy group. The H-3′ was within the shielding zone and H-2′ was within the deshielding zone of the carbonyl cone (Fig. 2).

The H-8′ proton resonated at δ 7.90 (J = 9 Hz) in I and at δ 7.99 in III and was split by H-7′. The splitting of H-8′ by H-5′ was negligible.

Vinylic Protons—These protons in I appeared as two separate groups: the methine proton at C-10 and the two methylene protons at C-11:

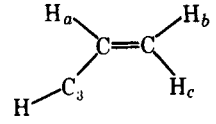

These findings and those of others (6) with regard to the chemical shifts and J values are not in accord with the theoretical data (8). Thus, the H_a proton resonated at δ 6.03 as a multiplet instead of at δ 5.30, a field 0.73 ppm lower than the theoretical value. The H_b and H_c protons absorbed at δ 5.09 and 4.96 (0.44 and 0.33 ppm downfield). Furthermore, the splitting constants between H_a and H_c (*trans* coupling) and between H_a and H_b (*cis* coupling) were barely discernible. The theoretical values for the *trans* coupling are 11–20 Hz, and those for the *cis* coupling are 6–14 Hz. No doubt these differences in the chemical shifts may be associated with the spatial orientation of the vinylic group under the influence of the aromatic ring in the quinoline moiety.

Replacement of the hydrogen in the OH group at C-9 by $COCH_3$ affected the chemical shifts of the methylene vinylic protons. The *cis* proton H_b resonated at δ 5.16, and the *trans* proton H_c appeared as a double doublet at δ 5.02 [$J(H_c - H_a)$ = 6 Hz, and J (H_c – $H_{c\text{-}3}$) = 2 Hz].

A proton alpha to the OH group at C-9, appearing as a doublet, resonated at δ 5.57 (J = 4 Hz) in the vicinity of the vinylic methine proton. After acetylation, the chemical shift and the coupling constant were altered, and the proton at C-9 absorbed at δ 6.55 (J = 7 Hz). The vicinal coupling between the protons of C-8 and C-9 corresponded to a three single-bond system, H–C–C–H, in which the J value depended on both the dihedral angle and the electronegativity of the substituents (9). In I, this system was disubstituted by both a hydroxyl and nitrogen. Therefore, it is not surprising that both the chemical shift and the J value were altered after acetylation. The bulk of the $OCOCH_3$ and its electronegativity differed from that of the OH group. The actual dihedral angle is determined from the steric interactions experienced by the quinoline molecule in this vicinity and from the mutual interactions of the π-systems.

Assignment of Preferred Stable Conformation of Quinidine Molecule: Rotamer Populations—NMR data of I and II showed that the preferred stable conformation of I around the C-4′–C-9 and the C-8–C-9 bonds occurred when the quinoline ring was arranged spatially so that its nitrogen atom was on the same side as the vinylic group and opposite the nitrogen atom in the quinuclidine ring. The proton at C-3′ was in the neighborhood of the O–R group at C-9 (R = H, $COCH_3$). In III, this proton was within the shielding zone of the anisotropic acetoxy group and the proton at C-2′ was within the deshielding zone of this group.

The vinylic group plane was almost perpendicular to the quinoline ring and extended upwards to the deshielding zone of the aromatic ring. Since the methine proton H_a was more exposed to the aromatic magnetic field, it was deshielded to a greater extent than the vinylic protons at H_b and H_c.

This preferred stable conformation establishes the dihedral angle between the C-8 and C-9 protons and places the OH group at C-9 between the vinylic proton at C-10 and the C-2 proton alpha to the nitrogen in the quinuclidine ring. In addition, the hydrogen at C-3′ is positioned between the two vinylic protons at C-10 and C-11, minimizing nonbonded interactions. These observations appear to indicate the predominance of one rotamer.

NMR Spectra of I and III in Mixtures—Two mixtures were prepared, one rich in I and the other rich in III. The most striking change in the NMR analysis of these mixtures was the appearance of two separate

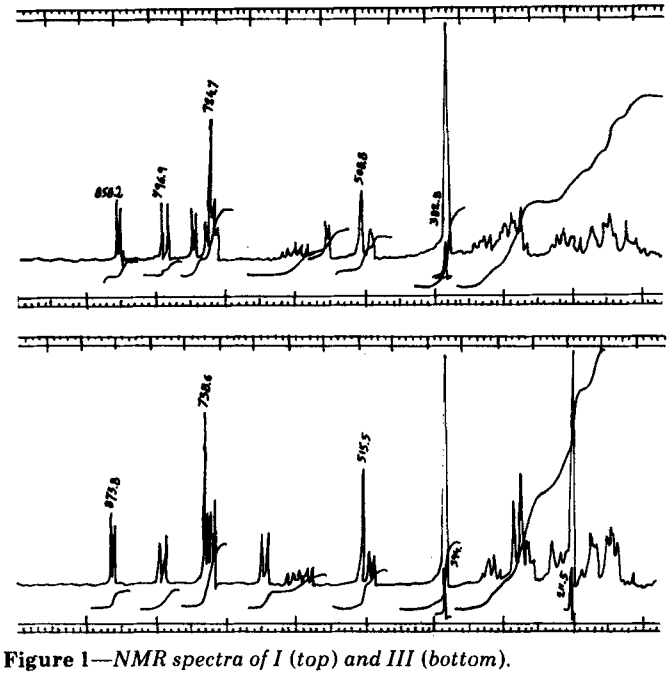

Figure 1—*NMR spectra of I (top) and III (bottom).*

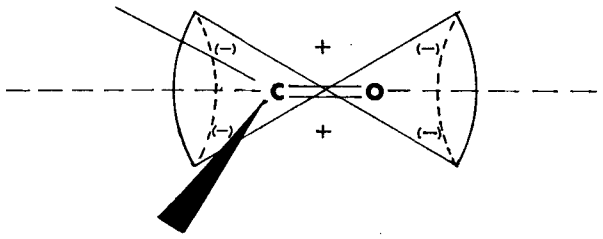

Figure 2—*Carbonyl cone.*

peaks for the methoxy protons (Figs. 3 and 4). Integration makes it possible to estimate with great accuracy the relative amounts of each component. Another pronounced deviation was found in the chemical shifts of the aromatic and vinylic protons of both I and III, which were different from those found in the NMR spectra of the pure substances, apparently as a result of slight intermolecular interactions.

Comparison of NMR Spectra of I and II and Concentration Dependence of Their Chemical Shifts—A comparison of the NMR spectra of I and II shows that the chemical shift values of certain protons were concentration dependent. When these NMR spectra were recorded at various concentrations (Table I), the data indicated that the chemical shifts of some protons of I and II differed at the same concentration and that they were concentration dependent in both alkaloids. Therefore, the comparison of the NMR spectra of I and II was made with dilute solutions to minimize the concentration effect on the chemical shift values and to produce a clear contrast.

The aromatic protons H-2′, H-3′, and H-8′ in II appeared at lower fields in comparison to the corresponding protons in I, demonstrating the shielding effect of the vinylic group which was absent in II. This finding is in keeping with the preferred stable conformation assigned to I. The proton alpha to the OH group at C-9 in II appeared at a lower field when compared to its counterpart in I, suggesting that the shielding effect of the vinylic group also extends to this proton in I.

At higher concentrations, the influence of intermolecular forces due to molecular association becomes more pronounced and may blur the mentioned mutual intermolecular effects of the various groups. This association is apparently initiated through hydrogen bonding between the C-9 OH groups in the same molecules of both alkaloids. Blocking these OH groups by acetylation prevents molecular association, as reflected by the appearance of identical chemical shifts in all concentrations of III and IV.

Additional proof that molecular association is brought about by hydrogen bonding between C-9 OH groups is shown by the change in the peaks of the proton alpha to the OH group at C-9. In dilute solution, this peak in both I and II appeared as a clear doublet, but it became ill defined at higher concentrations. This result implies a change in the dihedral angle between the protons of C-8 and C-9 during association. In contrast, the proton alpha to the acetoxy group in both III and IV appeared as a clear doublet in all concentrations, suggesting that no association takes place in these molecules where the OH groups are blocked by the bulky acetyl groups. The rotations about the C-8–C-9 bonds are now more difficult; thus, the chemical shifts of III and IV are similar.

The diamagnetic shift of H-2′, H-3′, and H-8′ observed in I was related to the vinylic group. The enhancement of this effect as the concentration was increased suggests that, as the association initiated by the hydrogen bonding proceeds, the molecules approach each other so that the aromatic rings and the quinuclidine rings of the same molecules tend to overlap. In other words, the association may be seen as being head to head and tail to tail. Additional evidence supporting this mode of association can be found in the change of the multiplicity and the chemical shift values

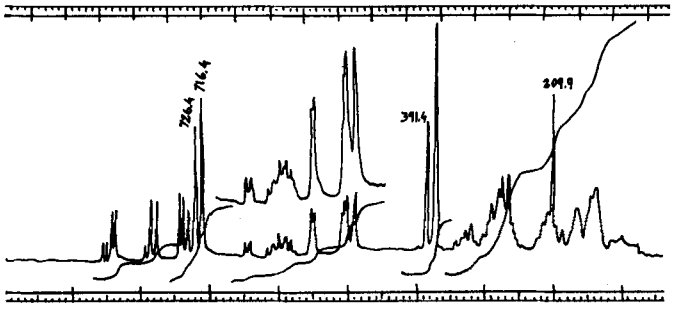

Figure 3—*NMR spectrum of mixture rich in I.*

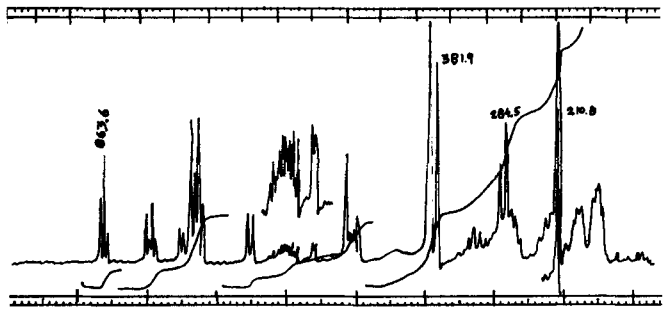

Figure 4—*NMR spectrum of mixture rich in III.*

of the vinylic protons (Table I). These pronounced alterations may be explained on the basis of the overlapping of the two systems of the vinylic groups as well. It is not surprising, therefore, that published NMR spectra show the methylene proton of the vinylic group at a lower field both as a singlet (6) and a doublet (10). This alteration in the methylene proton signal shapes encountered in I was absent in III, which provides further evidence that in I the association extends up to the vinylic group. No sign of association was observed in III and IV.

In II, the aromatic protons resonated at lower fields when compared to their counterparts in I, and this finding was related to the absence of the shielding effect of the vinylic group. However, a diamagnetic effect on some protons in II was observed when the concentration was increased. This effect indicates that one π-system is sufficient to affect the chemical shift values of the pertinent protons. Thus, the intermolecular association in II probably takes place in a similar fashion to that of the molecules of I, that is, head to head and tail to tail.

Commercial I containing II exhibits a similar NMR spectrum to that of pure I. On the basis of the data presented in Table I, II present in commercial I as a contaminant in small quantities should have appeared as a separate entity in the NMR spectrum of the mixture. The fact that this was not the case gives further evidence that the two molecules have similar steric structures and that pronounced association takes place between I and II, compared to the lesser association occurring between I and III. This phenomenon emphasizes the importance of hydrogen bonding in the association process.

The similarity in the NMR spectra of III and IV suggests that the conformations of both molecules are similar. The variations in the chemical shifts for I and II when passing from dilute to more concentrated solutions were more striking than the variations found in the two molecules at the same concentration. This finding suggests that the preferred stable conformations in I and II are similar. The small changes that were observed may be attributed to minor rotations about the C-8–C-9 bond causing movement of the quinoline ring toward the quinuclidine nitrogen and away from the ethyl group at C-3. This minimizes the steric interaction between the quinoline moiety and the ethyl group protons.

Acetylation Advantages—Since the chemical shift of the OH proton is highly dependent on the solvent, temperature, and concentration, its absorption may occur almost anywhere in the NMR spectrum. Therefore, it is not surprising that different investigators have reported varying data concerning the chemical shift of this OH proton (5). Thus, the diagnostic value of this proton is very limited. Acetylation of the OH groups at C-9 proved to be of great advantage for the following reasons:

1. The protons of the $OCOCH_3$ group have definite chemical shift values (δ 2.12 in III).
2. The proton alpha to the $OCOCH_3$ group at C-9 departs from the vinylic proton zone and appears separately downfield; it is more discernible and any changes in the vicinity of this proton can be more easily analyzed by NMR spectroscopy.
3. The NMR spectral data of III and IV are not concentration dependent, so these derivatives are more reliable in determining molecular structures and in quantitative analysis.

REFERENCES

(1) R. B. Turner and R. B. Woodward, in "The Alkaloids," vol. 3, R. H. F. Manske and H. L. Holmes, Eds., Academic, New York, N.Y., 1953, pp. 1–63.

(2) T. A. Henry, "The Plant Alkaloids," 3rd ed., Blakiston's, Philadelphia, Pa., 1939, pp. 394–446.

(3) K. W. Bemtley, "The Alkaloids," Interscience, New York, N.Y., 1957, pp. 132–142.

(4) G. G. Lyle and L. K. Keefer, *Tetrahedron*, **23**, 3253 (1967).
(5) E. Smith, S. Barkan, B. Ross, M. Maienthal, and J. Levine, *J. Pharm. Sci.*, **62**, 1151 (1973).
(6) T. Huynh-Ngoc and G. Sirois, *ibid.*, **62**, 1334 (1973).
(7) L. M. Jackman and S. Sternhell, "Applications of Nuclear Magnetic Resonance Spectroscopy in Organic Chemistry," 2nd ed., Pergamon, Oxford, England, 1972.
(8) *Ibid.*, pp. 184–192.
(9) *Ibid.*, p. 283.
(10) Sadtler NMR Spectrum (No. 8025M) Quinidine Monohydrate, Aldrich Chemical Co., Milwaukee, Wis.

ACKNOWLEDGMENTS

Supported in part by a grant from the Joint Research Fund of the Hebrew University and the Hadassah Medical Organization.

The authors are indebted to Mr. Nashif Afif, Mr. Dow Fareed, and Mr. Allen Rosen for technical assistance and dedication.

Cytotoxicity of Modified Indole Alkaloids

DAVID G. I. KINGSTON[x] and S. M. SAMI

Received January 29, 1979, from the *Department of Chemistry, Virginia Polytechnic Institute and State University, Blacksburg, VA 24061.* Accepted for publication May 14, 1979.

Abstract □ Indole alkaloids of the iboga series were structurally modified by incorporation of a 3,4-dimethoxybenzyl or -benzoyl unit so that they contained the N–O–O triangle required for antileukemic activity according to the triangulation hypothesis. The cytotoxicities of the modified alkaloids in the *in vitro* P-388 system were not significantly increased over the unmodified alkaloids, suggesting that the triangulation hypothesis does not apply in this series at least.

Keyphrases □ Indole alkaloids—semisynthetic, cytotoxicity, structure–activity relationships □ Antineoplastic agents, potential—modified indole alkaloids, cytotoxicity, structure–activity relationships □ Structure–activity relationships—modified indole alkaloids, antineoplastic activity □ Voacangine—derivatives, cytotoxicity, structure–activity relationships □ Catharanthine—derivatives, cytotoxicity, structure–activity relationships

In an earlier paper (1), the cytotoxicity of various bisindole alkaloids of the voacamine type was shown to be strikingly dependent on the detailed structure of the alkaloid and, in particular, on the position of the vobasane unit attachment to the iboga unit of the bisalkaloid. The antileukemic activity of various compounds, including the bisindole alkaloids vincristine and vinblastine, can be correlated with the structural feature of an N–O–O triangle of defined dimensions in these molecules (2). It was possible that indole alkaloids of modest antileukemic activity could be modified to contain the N–O–O triangle and might then show an increased antileukemic activity. This paper presents the results of some studies directed toward this question.

RESULTS AND DISCUSSION

The iboga alkaloids voacangine (I) and catharanthine were selected as the parent alkaloids for structural modification. Voacangine, which was available from previous isolation studies on *Tabernaemontana arborea* (3), shows a weak cytotoxicity in the P-388 cell culture system. This system, using a leukemia-derived cell line, was selected for the initial bioassay, with *in vivo* testing available at a later stage for promising candidates.

Reaction of I with 3,4-dimethoxybenzyl alcohol yielded the dimethoxybenzyl derivatives II and III, together with unreacted I and more highly substituted products. Assignment of Structures II and III to the two major substitution products was done primarily on the basis of PMR and mass spectra. Compound II showed singlets in its PMR spectrum at δ 6.89 and 6.84 ppm, assignable to H-14 and H-11, respectively. In III, the relevant signals appeared as doublets at δ 7.14 and 6.90 ppm, corresponding to H-14 and H-13, respectively. The mass spectra of both

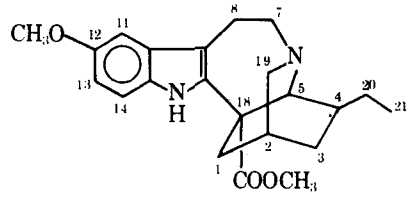

I

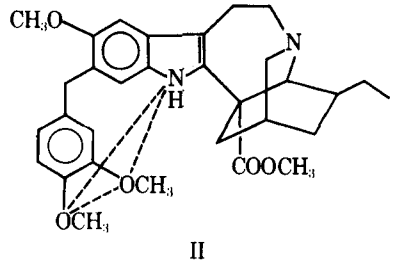

II

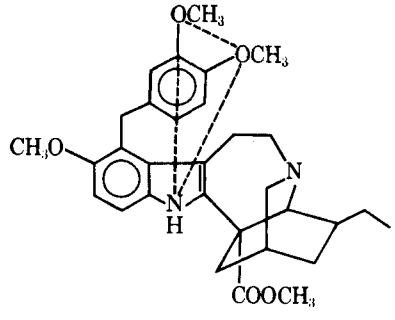

III

compounds showed molecular ion peaks at *m/e* 518 and typical peaks for iboga alkaloids at *m/e* 136 and 124 (4).

Reduction of I with lithium aluminum hydride yielded the known compound voacanginol (5). Esterification of voacanginol with 3,4-dimethoxybenzoyl chloride yielded the ester IV, which had NMR and mass spectra consistent with its assigned structure. Coupling of IV with vobasinol yielded the bisalkaloid V; its PMR spectrum was essentially a superimposition of the vobasane spectrum on that of IV. Coupling of the vobasine molecule to the 13′-position of IV (rather than the 11′-position) was indicated by the singlet resonances assignable to the 11′- and 14′-protons and by the broadening of the resonance of the I methoxyl group at δ 3.93 ppm due to hydrogen bonding (6).

Conversion of catharanthine to its epoxy lactam (VIII) was effected by published procedures (7, 8). Coupling of the intermediate iodolactone (VII) with 3,4-dimethoxybenzyl alcohol yielded the 3,4-dimethoxybenzyl derivative (IX). The assignment of Structure IX to the coupled product

© 1979, American Pharmaceutical Association

(4) G. G. Lyle and L. K. Keefer, *Tetrahedron*, **23**, 3253 (1967).
(5) E. Smith, S. Barkan, B. Ross, M. Maienthal, and J. Levine, *J. Pharm. Sci.*, **62**, 1151 (1973).
(6) T. Huynh-Ngoc and G. Sirois, *ibid.*, **62**, 1334 (1973).
(7) L. M. Jackman and S. Sternhell, "Applications of Nuclear Magnetic Resonance Spectroscopy in Organic Chemistry," 2nd ed., Pergamon, Oxford, England, 1972.
(8) *Ibid.*, pp. 184–192.
(9) *Ibid.*, p. 283.
(10) Sadtler NMR Spectrum (No. 8025M) Quinidine Monohydrate, Aldrich Chemical Co., Milwaukee, Wis.

ACKNOWLEDGMENTS

Supported in part by a grant from the Joint Research Fund of the Hebrew University and the Hadassah Medical Organization.

The authors are indebted to Mr. Nashif Afif, Mr. Dow Fareed, and Mr. Allen Rosen for technical assistance and dedication.

Cytotoxicity of Modified Indole Alkaloids

DAVID G. I. KINGSTON[x] and S. M. SAMI

Received January 29, 1979, from the *Department of Chemistry, Virginia Polytechnic Institute and State University, Blacksburg, VA 24061.* Accepted for publication May 14, 1979.

Abstract □ Indole alkaloids of the iboga series were structurally modified by incorporation of a 3,4-dimethoxybenzyl or -benzoyl unit so that they contained the N–O–O triangle required for antileukemic activity according to the triangulation hypothesis. The cytotoxicities of the modified alkaloids in the *in vitro* P-388 system were not significantly increased over the unmodified alkaloids, suggesting that the triangulation hypothesis does not apply in this series at least.

Keyphrases □ Indole alkaloids—semisynthetic, cytotoxicity, structure–activity relationships □ Antineoplastic agents, potential—modified indole alkaloids, cytotoxicity, structure–activity relationships □ Structure–activity relationships—modified indole alkaloids, antineoplastic activity □ Voacangine—derivatives, cytotoxicity, structure–activity relationships □ Catharanthine—derivatives, cytotoxicity, structure–activity relationships

In an earlier paper (1), the cytotoxicity of various bisindole alkaloids of the voacamine type was shown to be strikingly dependent on the detailed structure of the alkaloid and, in particular, on the position of the vobasane unit attachment to the iboga unit of the bisalkaloid. The antileukemic activity of various compounds, including the bisindole alkaloids vincristine and vinblastine, can be correlated with the structural feature of an N–O–O triangle of defined dimensions in these molecules (2). It was possible that indole alkaloids of modest antileukemic activity could be modified to contain the N–O–O triangle and might then show an increased antileukemic activity. This paper presents the results of some studies directed toward this question.

RESULTS AND DISCUSSION

The iboga alkaloids voacangine (I) and catharanthine were selected as the parent alkaloids for structural modification. Voacangine, which was available from previous isolation studies on *Tabernaemontana arborea* (3), shows a weak cytotoxicity in the P-388 cell culture system. This system, using a leukemia-derived cell line, was selected for the initial bioassay, with *in vivo* testing available at a later stage for promising candidates.

Reaction of I with 3,4-dimethoxybenzyl alcohol yielded the dimethoxybenzyl derivatives II and III, together with unreacted I and more highly substituted products. Assignment of Structures II and III to the two major substitution products was done primarily on the basis of PMR and mass spectra. Compound II showed singlets in its PMR spectrum at δ 6.89 and 6.84 ppm, assignable to H-14 and H-11, respectively. In III, the relevant signals appeared as doublets at δ 7.14 and 6.90 ppm, corresponding to H-14 and H-13, respectively. The mass spectra of both

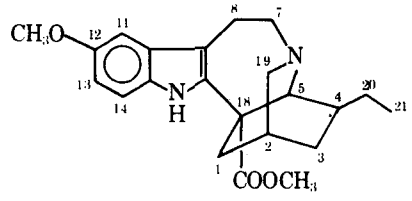

I

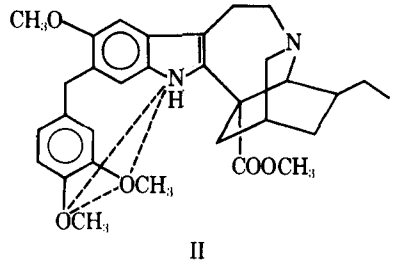

II

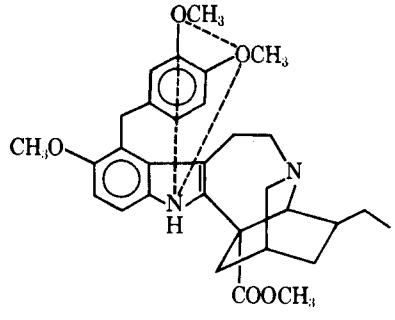

III

compounds showed molecular ion peaks at *m/e* 518 and typical peaks for iboga alkaloids at *m/e* 136 and 124 (4).

Reduction of I with lithium aluminum hydride yielded the known compound voacanginol (5). Esterification of voacanginol with 3,4-dimethoxybenzoyl chloride yielded the ester IV, which had NMR and mass spectra consistent with its assigned structure. Coupling of IV with vobasinol yielded the bisalkaloid V; its PMR spectrum was essentially a superimposition of the vobasane spectrum on that of IV. Coupling of the vobasine molecule to the 13′-position of IV (rather than the 11′-position) was indicated by the singlet resonances assignable to the 11′- and 14′-protons and by the broadening of the resonance of the I methoxyl group at δ 3.93 ppm due to hydrogen bonding (6).

Conversion of catharanthine to its epoxy lactam (VIII) was effected by published procedures (7, 8). Coupling of the intermediate iodolactone (VII) with 3,4-dimethoxybenzyl alcohol yielded the 3,4-dimethoxybenzyl derivative (IX). The assignment of Structure IX to the coupled product

© 1979, American Pharmaceutical Association

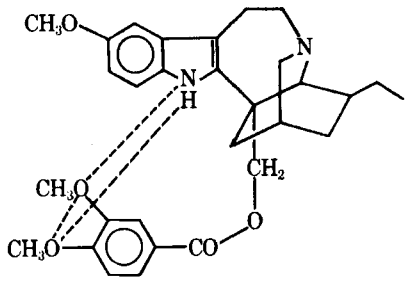

IV

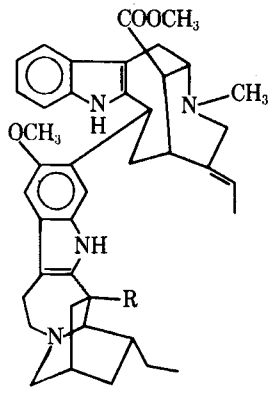

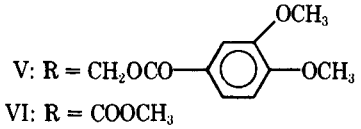

V: R = CH_2OCO—

VI: R = $COOCH_3$

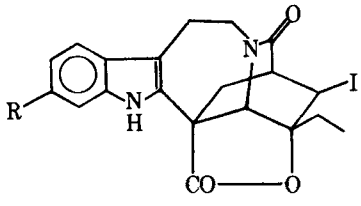

VII: R = H

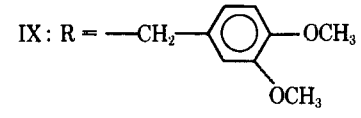

IX: R = $-CH_2-$

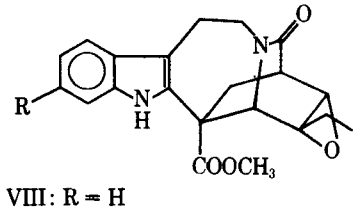

VIII: R = H

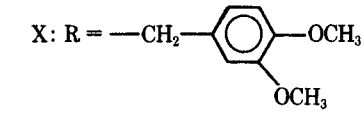

X: R = $-CH_2-$

was based on an analysis of its PMR spectrum, which showed a doublet at δ 7.30 ppm assignable to the 11-proton, and by analogy to the synthesis of tabernamine, in which coupling also took place at the 13-position of an unsubstituted iboga alkaloid (9). Conversion of the iodolactone IX to the epoxide X was effected with base and gave a product with spectral data in accord with the assigned structure.

According to the triangulation hypothesis (2), antileukemic activity can be correlated with the presence of an N–O–O triangle in the molecule with the following dimensions: N–O_1, 652–764 pm; N–O_2, 804–920 pm; and O_1–O_2, 270–400 pm. The crucial triangle does not have to be rigidly fixed since the activity of molecules such as daunorubicin, streptovitacin, and vinblastine, which contain the triangle in one particular conformation, is explained by the hypothesis. An examination of Dreiding models

Table I—Interatomic Distance Measurements (Picometers) of Some Semisynthetic Indole Alkaloids in Their Optimum Conformations

Alkaloid	N–O_1	N–O_2	O_1–O_2
II	740	860	303
III	760	840	303
IV, V	708	840	303
X	740	860	303

of the modified alkaloids II–V and X showed that each contained an N–O–O triangle of appropriate dimensions in at least one conformation; the dimensions of the conformation that gave the best fit in each case are given in Table I.

The P-388 *in vitro* cytotoxicities of synthetic II–V and X are given in Table II, together with the corresponding data for the natural alkaloids voacangine (I) and voacamine (VI). Inspection of these data indicates that the synthesized compounds appear not to have any additional activity due to the triangulation effect. Thus, although II and III both have N–O–O triangles of comparable size, one is slightly more active than the parent alkaloid and one is slightly less active. The modified bisindole alkaloid V, which contains the N–O–O triangle, is considerably less active than VI, which does not. Neither modified alkaloid VIII nor X shows any significant activity, although both contain an alkylating (epoxy) function, and one contains the N–O–O triangle.

The four compounds II–V also were tested for activity in the P-388 *in vivo* test system. None showed significant activity at dose levels in the 0.5–25-mg/kg range.

In interpreting the results, it must be remembered that the N–O–O triangular arrangement was never envisioned as a necessary and sufficient criterion for antileukemic activity (2). Clearly, it cannot be applied in any simple way to improving the activity of marginally active compounds such as the iboga alkaloids. Further experiments are required to test its applicability in other systems.

EXPERIMENTAL

Materials, methods, and procedures were identical to those described previously (9).

13-(3,4-Dimethoxybenzyl)voacangine (II) and 11-(3,4-Dimethoxybenzyl)voacangine (III)—A mixture of voacangine (I) (1.22 g) and 3,4-dimethoxybenzyl alcohol (0.57 g) was heated under reflux in 1.5% methanolic hydrochloric acid for 10 days. Usual workup yielded a crude product, which gave six major spots on TLC. Purification of the crude product by preparative TLC (hexane–ether–methanol, 5:4:1) yielded unreacted I (0.23 g), II (0.22 g), and III (0.31 g) from the first, second, and third bands, respectively. The remaining bands consisted of mixtures of oxidized and *N*-benzylated products and were not investigated further.

Compound II showed major ions in its mass spectrum at *m/e* 518 (M^+, 100), 503 (12), 433 (20), 394 (14), 323 (12), 311 (17), 310 (43), 260 (11), 259 (20), 208 (16), 151 (39), 148 (24), 137 (18), 136 (99), 135 (43), 124 (38), 123 (12), and 122 (43). Its PMR spectrum showed peaks at δ 7.66 (1H, s, NH), 6.89 (1H, s, H-14), 6.84 (1H, s, H-11), 6.80–6.75 (3H, m, H-2′,5′,6′), 3.96 (2H, s, $ArCH_2Ar'$), 3.86, 3.82, 3.80 (3H each, s, $-OCH_3$), and 3.66 (3H, s, $COOCH_3$) ppm, together with signals for 18 protons in the 3.5–0.9-ppm region, which closely matched signals in the corresponding region in the spectrum of I. Its IR spectrum showed ν_{max} 3350 (NH) and 1710 ($COOCH_3$) cm^{-1}, and it had λ_{max} (ethanol) 296 (sh) (log ε 4.00), 283 (4.09), and 224 (4.49) nm.

Anal.—Calc. for $C_{31}H_{38}N_2O_5$: *m/e* 518.2778. Found: *m/e* 518.2785.

Compound III had a similar mass spectrum to II, showing major peaks of *m/e* 518 (M^+, 100), 503 (10), 433 (11), 384 (10), 367 (15), 311 (11), 151 (21), 136 (87), 135 (37), 124 (15), and 122 (26). Its PMR spectrum ($CDCl_3$) showed peaks at δ 7.84 (1H, s, NH), 7.14 (1H, d, J = 8 Hz, H-14), 6.90 (1H, d, J = 8 Hz, H-13), 6.8–6.6 (3H, m, H-2′,5′,6′), 4.42 (2H, s, $ArCH_2Ar'$), 3.80, 3.78, 3.76 (3H each, s, $-OCH_3$), and 3.68 (3H, s, $COOCH_3$) ppm, together with signals for 18 protons in the 3.5–0.9-ppm region. In this case, the signals for the eight protons in the 3.5–2.5-ppm region did not match the corresponding signals in the spectrum of I, indicating some shielding of the seven, eight, and, possibly, 19 protons by the dimethoxybenzyl ring system. Signals in the 2.2–0.9-ppm region matched the corresponding signals in I quite well. Its IR spectrum showed ν_{max} 3370 (NH) and 1725 ($COOCH_3$) cm^{-1}.

Anal.—Calc. for $C_{31}H_{38}N_2O_5 \cdot H_2O$: C, 69.36; H, 7.51; N, 5.27. Found: C, 68.96; H, 7.13; N, 5.13.

Table II—Cytotoxicity of Various Semisynthetic Indole Alkaloids

	Alkaloid	Cytotoxicity (ED_{50} in P-388 Cell Culture), μg/ml
I	Voacangine	6.8
II	13-(3,4-Dimethoxybenzyl)voacangine	10
III	11-(3,4-Dimethoxybenzyl)voacangine	3.8
IV	*O*-(3,4-Dimethoxybenzoyl)voacanginol	16
V	13′-Vobasi-*O*-(3,4-dimethoxybenzoyl)voacanginol	16
VI	Voacamine	2.6
VIII	3α,4α-Epoxy-19-oxodihydrocatharanthine	>100
X	13-(3,4-Dimethoxybenzyl)-3α,4α-epoxy-19-oxodihydrocatharanthine	31

***O*-(3,4-Dimethoxybenzoyl)voacanginol (IV)**—A mixture of voacanginol (5) (0.28 g), 3,4-dimethoxybenzoyl chloride (0.22 g), and pyridine (2 ml) was allowed to stand for 2 days at room temperature. The reaction mixture was poured into water, and the crude product was recovered by filtration. Purification by preparative TLC in hexane–ether–methanol (6:3:1) yielded IV as an amorphous white powder. The compound showed major mass spectral peaks at *m/e* 504 (M^+, 74), 489 (6), 323 (100), 322 (53), 307 (23), 239 (13), 237 (23), 215 (98), 200 (24), 198 (15), 182 (9), 174 (12), 165 (50), 162 (18), 136 (76), 135 (99), 124 (8), and 122 (56).

Its PMR spectrum ($CDCl_3$) showed peaks at δ 8.35 (1H, s, NH), 7.45 (1H, dd, J = 8 Hz, H-6′), 7.25 (1H, d, J = 2 Hz, H-2′), 7.13 (1H, d, J = 8 Hz, H-14), 6.89 (1H, d, J = 2 Hz, H-11), 6.71 (1H, d, J = 8 Hz, H-5′), 6.71 (1H, dd, J = 8 and 2 Hz, H-13), 4.71 (1H, d, J = 12 Hz, H-22a), 4.33 (1H, d, J = 12 Hz, H-22b), and 3.83, 3.83, 3.65 (3H each, s, 3 × $-OCH_3$) ppm, together with signals for 18 protons in the region 3.5–0.9 ppm corresponding to the signals in this region in the spectrum of voacanginol. Its IR spectrum showed ν_{max} 3370 (NH) and 1700 (ArCOOR′) cm^{-1}, and it had λ_{max} (ethanol) 288 (log ε 4.21), 262 (4.32), and 217 (4.73) nm.

Anal.—Calc. for $C_{30}H_{36}N_3O_5 \cdot H_2O$: C, 68.94; H, 7.24; N, 5.44. Found: C, 69.43; H, 7.67; N, 5.44.

13′-Vobasi-*O*-(3,4-dimethoxybenzoyl)voacanginol (V)—A solution of vobasinol (0.177 g) and IV (0.252 g) in 1.5% methanolic hydrogen chloride (10 ml) was heated under reflux for 48 hr. Usual workup yielded a crude product (0.40 g), which was purified by preparative TLC in hexane–ether–methanol (4:5:1) to yield unreacted IV (0.055 g) and V (0.172 g). After a second preparative TLC, V was obtained as a white solid, homogeneous on TLC in two systems (0.110 g).

The isolated material had a PMR spectrum ($CDCl_3$) with peaks at δ 7.88 (1H, s, NH), 7.70 (1H, s, NH), 7.5 (2H, C, H-12 and H-6″), 7.24 (1H, d, J = 2 Hz, H-2″), 7.0 (3H, c, H-9,10,11), 6.89 (1H, s, H-14′), 6.77 (1H, s, H-11′), 6.72 (1H, d, J = 8 Hz, H-5″), 5.2 (2H, c, H-3 and H-19), 4.54 (1H, d, J = 12 Hz, H-22′), 4.28 (1H, d, J = 12 Hz, H-22′), 3.93 (3H, bd s, $-OCH_3$), 3.85 (3H, s, $-OCH_3$), 3.69 (3H, s, $-OCH_3$), 3.52 (3H, s, $-COOCH_3$), 2.43 (3H, s, $-NCH_3$), 1.64 (3H, d, J = 7 Hz, $-CHCH_3$), and 0.88 (3H, t, J = 7 Hz, CH_2CH_3), together with peaks in the 3.5–1.0-ppm region assignable to the voacangine or vobasine portions of the molecule. Its IR spectrum showed ν_{max} 3380 (NH) and 1710 (broad peak, $-COOCH_3$ and ArCOOR′) cm^{-1}, and it had λ_{max} (ethanol) 288 (log ε 4.29), 263 (4.31), and 218 (4.77) nm.

Anal.—Calc. for $C_{51}H_{60}N_4O_7$: N, 6.66. Found: N, 6.65.

3α,4α-Epoxy-19-oxodihydrocatharanthine (VIII)—Compound VIII was prepared by treatment of 4α-hydroxy-3β-iodo-19-oxodihydrocatharanthinic acid lactone (VII) with base as previously described (7, 8). The material had identical properties to those described.

13-(3,4-Dimethoxybenzyl)-4α-hydroxy-3β-iodo-19-oxodihydrocatharanthinic Acid Lactone (IX)—Treatment of VII (200 mg) with 3,4-dimethoxybenzyl alcohol (85 mg) in 1.5% methanolic hydrogen chloride under reflux for 48 hr yielded a mixture of six major components after the usual workup. Separation of the mixture by preparative TLC (acetone–hexane, 1:2) yielded the benzyl iodolactone IX (63 mg); IR: ν_{max} (KBr) 1770 and 1690 cm^{-1}; PMR ($CDCl_3$): δ 9.32 (1H, bd s, NH), 7.30 (1H, d, J = 8 Hz, 11-H), 7.2–6.9 (2H, complex), 6.68 (3H, bd s), 4.65–4.36 (2H, m, 2-H and 3-H), 4.30 (1H, s, 5-H), 3.96 (2H, s, $ArCH_2Ar'$), 3.79 (3H, s, OCH_3), 3.76 (3H, s, OCH_3), and 1.00 (3H, t, 21-CH_3); mass spectrum: *m/e* 612 (M^+, 3), 384 (4), 319 (11), 253 (100), 169 (8), 168 (11), 167 (6), 151 (20), 142 (25), and 127 (90).

13-(3,4-Dimethoxybenzyl) -3α,4α- epoxy-19-oxodihydrocatharanthine (X)—The benzyl iodolactone IX (40 mg) was added to sodium methoxide (4 mg) in methanol (2 ml), and the mixture was allowed to stand at room temperature for 2 hr. The resulting solution was poured into dilute acid; the aqueous layer was extracted with chloroform to yield a crude product, which was purified by preparative TLC on silica gel (acetone–hexane, 1:2). Elution of the major band yielded X as a homogeneous powder, R_f 0.44; PMR ($CDCl_3$): δ 8.16 (1H, bd s, NH), 7.4–6.8 (3H, complex), 6.64 (3H, bd s), 4.74 (1H, s), 3.92 (2H, s, $ArCH_2Ar'$), 3.76 (3H, s, OCH_3), 3.74 (3H, s, OCH_3), 3.68 (3H, s, OCH_3), and 1.00 (3H, t, 21-CH_3); mass spectrum: *m/e* 516 (M^+, 65), 457 (10), 413 (9), 377 (11), 345 (15), 320 (17), 294 (23), 164 (80), 151 (100), 137 (25), and 136 (31).

Anal.—Calc. for $C_{30}H_{32}N_2O_6$: *m/e* 516.2259. Found: *m/e* 516.2267.

REFERENCES

(1) D. G. I. Kingston, *J. Pharm. Sci.*, **67**, 272 (1978).

(2) K. Y. Zee-Cheng and C. C. Cheng, *ibid.*, **59**, 1630 (1970).

(3) D. G. I. Kingston, *ibid.*, **67**, 271 (1978).

(4) M. Hesse, in "Progress in Mass Spectrometry," vol. 1, Verlag Chemie, Weinheim, West Germany, 1974.

(5) Y. Morita, M. Hesse, U. Renner, and M. Schmid, *Helv. Chim. Acta*, **59**, 532 (1976).

(6) J. R. Knox and J. Slobbe, *Aust. J. Chem.*, **28**, 1813 (1975).

(7) J. P. Kutney, G. H. Bokelman, M. Ichikawa, E. Jahngen, A. V. Joshua, P. Liao, and B. R. Worth, *Heterocycles*, **4**, 1267 (1976).

(8) Y. Honma and Y. Ban, *ibid.*, **6**, 285 (1977).

(9) D. G. I. Kingston, B. B. Gerhart, F. Ionescu, M. M. Mangino, and S. M. Sami, *J. Pharm. Sci.*, **67**, 249 (1978).

ACKNOWLEDGMENTS

Supported by Research Grant CA-12831 from the National Cancer Institute, U.S. Department of Health, Education, and Welfare, Bethesda, MD 20014.

The authors thank Dr. Gordon H. Svoboda and Dr. Koert Gerzon of the Lilly Research Laboratories for generous gifts of perivine and catharanthine.

Sarin Transport across Excised Human Skin I: Permeability and Adsorption Characteristics

DALE E. WURSTER, JAMES A. OSTRENGA *, and LLOYD E. MATHESON, Jr.[x]

Received February 5, 1979, from the *College of Pharmacy, University of Iowa, Iowa City, IA 52242.* Accepted for publication May 21, 1979. *Present address: Pharm Chem, Palo Alto, CA 94301.

Abstract □ The transport rates and permeability coefficients for the transport of sarin in solution across both hydrous and anhydrous excised human skin were determined quantitatively. An activation energy was determined from study of the temperature influence on the transport of sarin in solution across anhydrous callus membranes. The transport of pure sarin and of sarin as a water-soluble and water-insoluble gel was studied also. The adsorption characteristics of sarin on powdered keratin were studied to determine their role in permeation. Both equilibrium and nonequilibrium measurements were made, which allowed calculation of the heat of adsorption, the heat of activation for adsorption, and the heat of activation for desorption. The results show that interaction between the membrane and penetrant plays a significant role in sarin transport across human skin.

Keyphrases □ Sarin—transport across excised human skin, hydrous, anhydrous, temperature influence, activation energy, adsorption and desorption, powdered keratin, permeability □ Cholinesterase inhibitors—sarin, transport across excised human skin, permeability, adsorption □ Transepidermal transport—sarin, excised human skin, permeability, adsorption

Diffusion of various penetrants through the stratum corneum has been studied for years; however, few investigators have considered the effects of adsorption and desorption of the penetrant by the membrane on transport.

The purpose of this study was to elucidate some factors involved in the diffusion of the nerve gas, sarin[1], across excised human skin membranes. The role of physical adsorption in transport also was studied for both equilibrium and nonequilibrium conditions.

THEORETICAL

For the permeability studies, it was assumed that a diffusion process occurs and that the entire exposed area of the membrane participates. For the solution phase studies, diffusion can be represented by:

$$\log (C_0 - 2C_2) = (-2k/2.303)t + \log C_0 \qquad \text{(Eq. 1)}$$

where C_0 is the initial solute concentration to which the barrier is exposed; C_2 is the concentration at time, t, on the opposite side of the barrier in the permeability cell (1); and k is the permeability coefficient. The permeability cell shown in Fig. 1*a* was used.

In studying the transport rate of pure sarin and of sarin in the gelled state, it was not experimentally practical to have the same volume of diffusing medium on each side of the barrier. Therefore, the permeability cells shown in Figs. 1*b* and 1*c* were used.

To examine the effect of sarin adsorption by keratin on diffusion, both adsorption and desorption were studied. It was assumed that the solvent and adsorbate do not compete for the same adsorption sites. Since adsorption may be considered to be a reversible equilibrium process:

$$K = \frac{k_a}{k_d} = \frac{C_{\text{powder}}}{C_{\text{bulk}}} \qquad \text{(Eq. 2)}$$

where K is the equilibrium constant; k_a and k_d are the specific rate constants for adsorption and desorption, respectively; C_{powder} is the milligrams adsorbed per milliliter; and C_{bulk} is the milligrams per milliliter remaining in the bulk solution after equilibration. At temperatures T_1 and T_2, for equal adsorbent weights and equal bulk solution volumes:

$$\frac{K_2}{K_1} = \frac{X_2}{X_1} \qquad \text{(Eq. 3)}$$

where K_1 and K_2 are the equilibrium constants, and X_1 and X_2 are the amounts adsorbed at temperatures T_1 and T_2. From the integrated form of the van't Hoff equation:

$$\log \frac{X_2}{X_1} = \frac{\Delta H^\circ}{2.303R}\left[\frac{(T_2 - T_1)}{(T_1 T_2)}\right] \qquad \text{(Eq. 4)}$$

and the difference in the amount of adsorbate adsorbed at two temperatures, it is possible to calculate the heat of adsorption for a relatively small temperature range. In addition:

$$k_a = Ae^{-H_a^\ddagger/RT} \qquad \text{(Eq. 5)}$$

$$k_d = Ae^{-H_d^\ddagger/RT} \qquad \text{(Eq. 6)}$$

where $H_a^\ddagger$ is the heat of activation for adsorption, $H_d^\ddagger$ is the heat of activation for desorption, A is the frequency factor, and the remaining terms are as defined earlier. Then:

$$K = \frac{k_a}{k_d} = \frac{e^{-(H_a^\ddagger - H_d^\ddagger)}}{RT} = e^{-\Delta H/RT} \qquad \text{(Eq. 7)}$$

Thus:

$$\Delta H_a = H_a^\ddagger - H_d^\ddagger \qquad \text{(Eq. 8)}$$

When desorption is first order and with the assumptions that, upon desorption, the adsorbate does not return to the adsorbent surface and

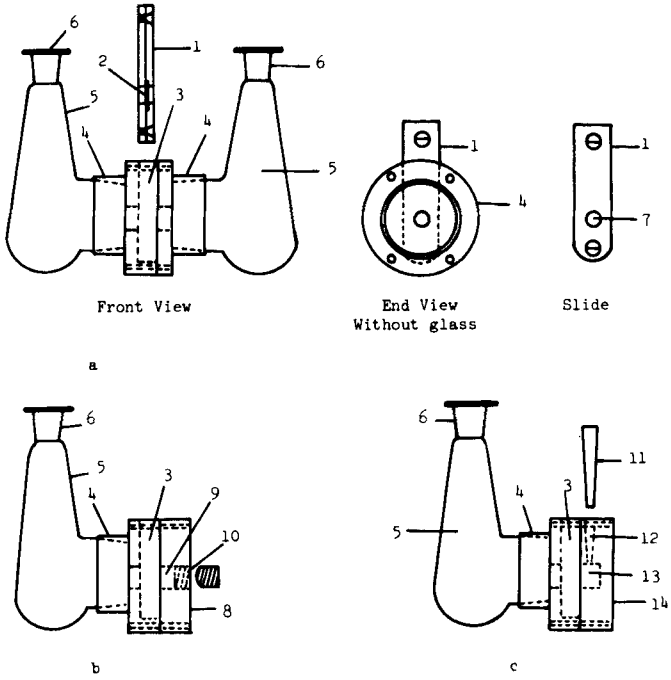

Figure 1—*Permeability cell for solution phase* (a), *for gel phase* (b), *and for pure penetrant* (c). *Key: 1, slide device; 2, membrane; 3, slide slot; 4, aluminum chassis; 5, glass chamber; 6, glass stopper; 7, slide orifice; 8, aluminum disk; 9, cavity for gel; 10, threaded port; 11, tapered pin; 12, tapered port; 13, cavity for pure penetrant; and 14, stainless steel disk.*

[1] Isopropoxymethylphosphoryl fluoridate.

0022-3549/79/1100-1406$01.00/0
© 1979, American Pharmaceutical Association

Table I—Average Transport Rates and Average Permeability Coefficients for Solution Phase Experiments

Experiment	Transport Rate, mg/cm²/hr	Permeability Coefficient, $k \times 10^4$/hr
Callus, anhydrous	0.05	2.81
Callus, hydrous	0.21	13.10
Stratum corneum conjunctum, anhydrous	0.21	19.45
Stratum corneum conjunctum, hydrous	0.49	28.77

the volume of desorbing solvent remains constant, it can be shown that (2):

$$\log \frac{X_e}{X_e - X} = \frac{k_d T}{2.303} \qquad \text{(Eq. 9)}$$

where X_e is the equilibrium amount of adsorbate in solution and X is the amount in solution at time t. The determination of k_d at various temperatures then permits calculation of $H_d^{\ddagger}$.

EXPERIMENTAL

Permeability Apparatus—The design of the permeability cell depended on whether the donor chamber contained a dilute solution, a concentrated gel, or pure sarin (Fig. 1).

Membrane Preparation—Callus membranes were sectioned from excised human callus to a 100-μm thickness. The stratum corneum conjunctum membranes were obtained by the well-known technique of stripping the human forearm[2]. The thickness of these membranes was 10–15 μm. Both the callus and the stratum corneum conjunctum membranes were stored first in ether followed by n-heptane, each for 24 hr. In the hydrous studies, the membranes were stored in a 100% relative humidity chamber for 24 hr prior to use.

The membranes were fixed in the slide of the permeability cell, and a small amount of silicone grease was employed to ensure a good seal. The areas exposed for the callus and the stratum corneum conjunctum membranes were 0.28 and 0.07 cm², respectively (6- and 3-mm orifices).

Gel Preparation—A water-insoluble sarin gel was prepared by making an 8% (w/v) solution of polymethyl methacrylate (mol. wt. 1.776 $\times 10^6$) in a 20-ml glass hypodermic syringe. The metal tip was threaded and sealed with a screw. The syringe was placed in a suitable container, sealed, immersed in a water bath at 25°, and shaken vigorously for 24 hr or until a uniform gel was produced.

A water-soluble gel was prepared similarly by making a 3% (w/v) solution of carboxypolymethylene[3].

Permeability Studies—For the solution phase studies, the permeability cell and slide were completely assembled. Then 50 ml of an n-heptane solution containing 7.8×10^{-3} M sarin, at the appropriate temperature, was placed in the donor chamber with the simultaneous addition of an equal volume of pure n-heptane in the receiver chamber. n-Heptane was dried by storage over anhydrous sodium sulfate. For the hydrous studies, the n-heptane was saturated with water at the appropriate temperature before the sarin solution in n-heptane was made. Water-saturated n-heptane also was used in the receiver chamber.

The permeability cells were maintained in a constant-temperature water bath with gentle shaking in the plane of the membrane. The transport rate was followed by withdrawing 1-ml samples from the receiver chamber at suitable times and analyzing for sarin. In the activation energy determination for the transport through anhydrous callus membranes, the rate was followed beginning with the lowest temperature (25°) and ending with the highest temperature (45°). The same set of membranes was used at all temperatures.

For the gel phase studies, 0.6 ml of the gel was placed on the membrane with a syringe through the threaded port on the side of the aluminum disk in cell-type 1*b*. The cavity was sealed with the set screw. Fifty milliliters of n-heptane was added immediately to the receiver chamber. An identical procedure for the pure penetrant studies was utilized, except that

Table II—Average Transport Rates of Sarin across Callus Tissue Membranes for Various Systems

Experimental Condition	Transport Rate, mg/cm²/hr
Sarin in n-heptane, anhydrous membrane	0.03
Pure sarin, anhydrous membrane	0.60
8% Polymethyl methacrylate gel, anhydrous membrane	0.49
3% Carboxypolymethylene gel, anhydrous membrane	0.55
8% Polymethyl methacrylate gel, hydrous membrane	1.1
3% Carboxypolymethylene gel, hydrous membrane	2.76

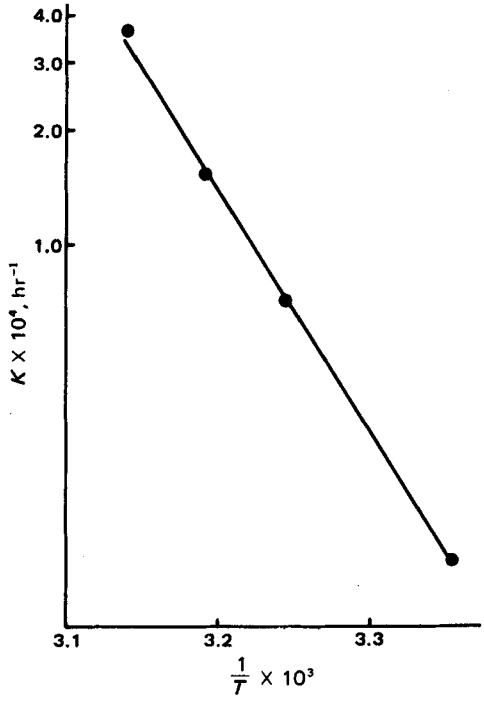

Figure 2—*Arrhenius plot for transport of sarin through callus membranes at 25, 35, 40, and 45°.*

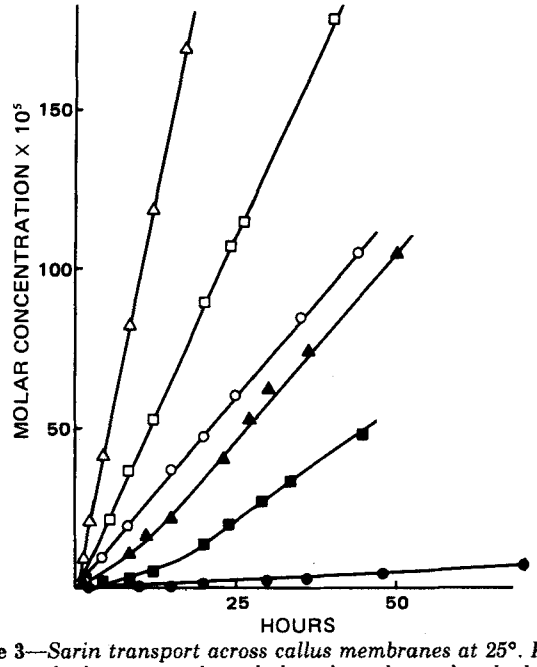

Figure 3—*Sarin transport across callus membranes at 25°. Key: ●, solution, anhydrous; □, polymethyl methacrylate gel, anhydrous; ▲, carboxypolymethylene gel, anhydrous; ○, pure anhydrous; □, polymethyl methacrylate gel, hydrous; and △, carboxypolymethylene gel, hydrous.*

[2] Scotch Brand No. 600 tape, 3M Corp., St. Paul, MN 55100.

[3] Carbopol 934, B. F. Goodrich Chemical Co., Cleveland, OH 44115.

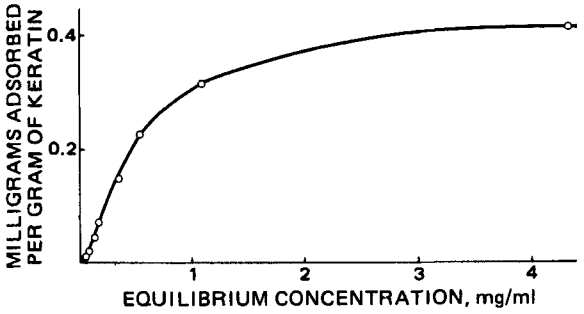

Figure 4—*Isotherm for sarin adsorption by powdered callus at 25°.*

sarin was injected from a syringe through the tapered part at the top of the aluminum disk in cell-type 1c. All gel and pure penetrant experiments were performed on the same set of membranes. Solution phase transport rates were then redetermined using a 7.74×10^{-3} *M* sarin solution in anhydrous *n*-heptane.

Assay—The analytical procedure (3) employed to determine the sarin concentration in *n*-heptane was as follows. One-milliliter samples were placed in a separator and the following solutions were added at the indicated time intervals: first, 2 ml of 0.625% (w/v) *o*-dianisidine in acetone; after 30 sec, 1 ml of 3% (w/v) hydrogen peroxide; after 1 min, 3 ml of 0.1 *M* tribasic sodium phosphate in redistilled water; and after 30 sec, 10 ml of xylene was added.

The mixture was shaken for 30 sec, and the xylene layer became yellow. After separation of the layers, the aqueous layer was removed, and the xylene layer was analyzed at 425 nm. The absorbance was directly proportional to the sarin concentration. The *o*-dianisidine was purified before use (4).

Adsorbent—Anhydrous excised callus tissue was pulverized in a blender[4] with the aid of dry ice. The dried powder that passed through a No. 170 standard sieve but was retained on a No. 200 sieve was used. The average particle size also was determined[5]. The powdered callus was extracted with anhydrous ether for 48 hr and then dried before use.

Adsorption Isotherm—A weighed quantity of the adsorbent was placed in a 50-ml volumetric flask, and 25 ml of a known sarin concentration in anhydrous *n*-heptane was added. The suspension was shaken in a constant-temperature bath at 25° for 3 hr. Under the conditions of these experiments, it was established previously that equilibrium was attained within this period. After equilibration, three 1-ml samples were withdrawn from the flask and filtered through glass wool in tubing[6] attached to the tip of the pipet.

The sarin concentration was determined by the analytical procedure

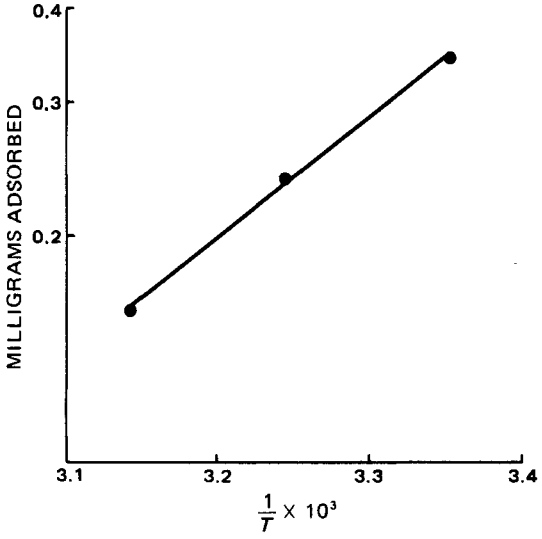

Figure 5—*Arrhenius plot of sarin adsorbed at 25, 35, and 45° by powdered callus. Initial sarin concentration was 44 mg/liter.*

[4] Waring Products Corp., Winsted, CT 06098.
[5] Subsieve sizer, Fisher Scientific Co., Pittsburgh, PA 15219.
[6] Tygon, Norton Plastics and Synthetics Division, Akron, OH 44309.

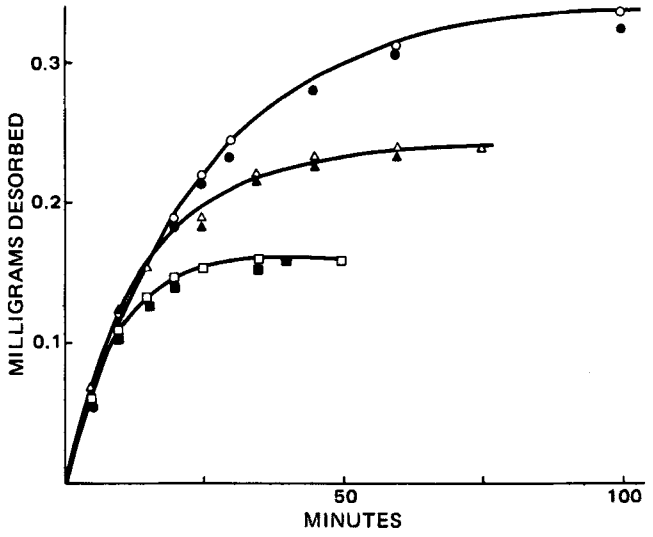

Figure 6—*Corrected desorption isotherms for sarin desorption from powdered callus at 25, 35, and 45°. Key: ○, ●, 25°; △, ▲, 35°; and □, ■, 45°.*

described earlier, and the average value for three samples was used in the calculations. The amount of sarin adsorbed per gram of powdered callus was calculated from the change in the bulk solution concentration. This procedure was repeated using weighed quantities of adsorbent and various concentrations of sarin in *n*-heptane.

Adsorption and Desorption Kinetics—To determine the heat of adsorption, equilibrium measurements of the amount of sarin adsorbed per gram of adsorbent were made at 25, 35, and 45°. After equilibration, the desorption rate was followed at each temperature. A known weight

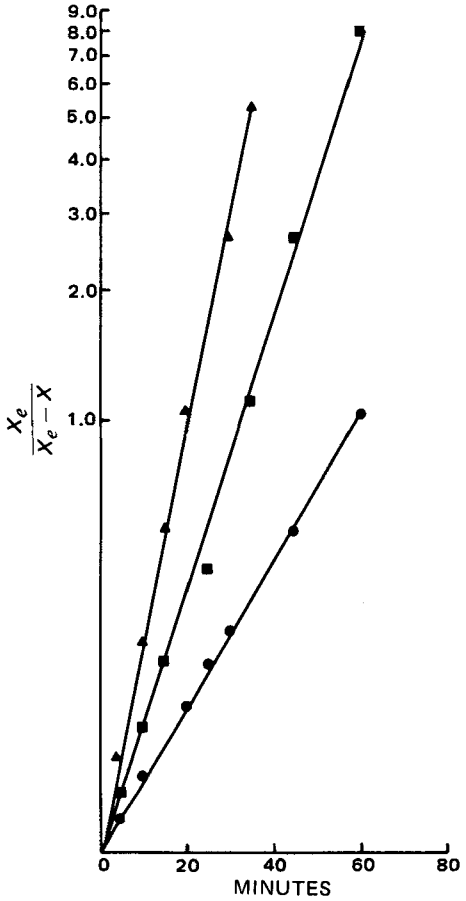

Figure 7—*First-order plots for sarin desorption from powdered callus at 25, 35, and 45°. Key: ●, 25°; ■, 35°; and ▲, 45°.*

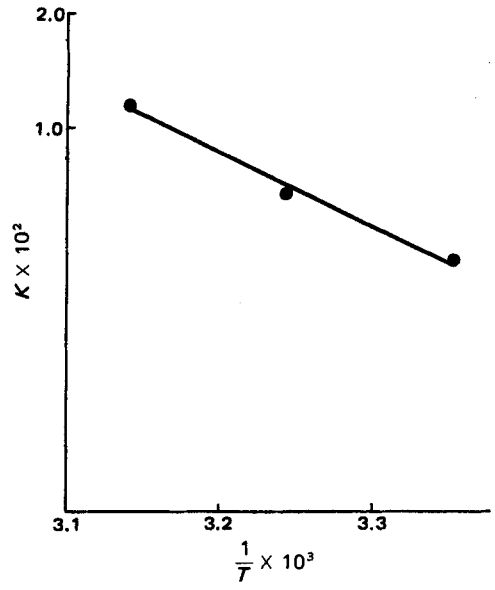

Figure 8—*Arrhenius plot for sarin desorption from powdered callus at 25, 35, and 45°.*

(~20 g) of ether-extracted powdered callus was placed in a 100-ml round-bottom glass-stoppered flask. Fifty milliliters of a known concentration (~44 mg/liter) of sarin in *n*-heptane was added. The flask was maintained at the appropriate temperature in a water bath and was shaken vigorously. Equilibrium measurements were made as described previously.

After adsorption was complete, the insoluble powdered callus was filtered out with a sintered-glass filter and washed on the filter with 50 ml of *n*-heptane using minimum vacuum. The powder was placed in 50 ml of *n*-heptane and maintained at the appropriate temperature during shaking. The desorption process was followed by withdrawing 1-ml samples periodically and assaying them for sarin. This procedure was repeated for each temperature.

RESULTS

Solution Phase Permeability—Average permeability constants and transport rates are shown in Table I. Each is the mean of 18–35 membranes for each solution system.

Activation Energy—Sarin transport through the same callus membranes was followed at temperatures of 25, 35, 40, and 45°. The activation energy calculated from the slope of the Arrhenius plot shown in Fig. 2 is 29.1 kcal/mol.

Gel Phase and Pure Sarin Permeability—The average sarin transport rates through callus membranes for each experimental series are given in Table II. Representative, but not averaged, plots of concentration *versus* time are shown in Fig. 3 on common coordinates.

Adsorption Studies—The isotherm for sarin adsorption by powdered callus at 25° is shown in Fig. 4. An Arrhenius-type plot of the sarin adsorbed at different temperatures from a solution with an initial sarin concentration of 44 mg/liter is given in Fig. 5. The heat of adsorption (ΔH_a) calculated from the slope was −7.2 kcal/mole. The average particle size at a porosity of 0.50 was 14 μm.

Desorption Studies—The corrected desorption isotherms are shown in Fig. 6. Data obtained from the desorption isotherm curves in Fig. 6 were utilized to obtain plots of log $[X_e/(X_e - X)]$ *versus* time (Fig. 7). The rate constants for desorption calculated from the slopes were 4.5×10^{-2} (25°), 6.75×10^{-2} (35°), and 11.5×10^{-2} (45°) min^{-1}. The heat of activation for desorption ($H_d^{\ddagger}$) calculated from the Arrhenius plot (Fig. 8) is 9.6 kcal/mole. Thus, according to Eq. 9, the heat of activation for adsorption is 2.4 kcal/mole.

DISCUSSION

Hydration increased the sarin transport rate in solution for both stratum corneum conjunctum and callus membranes. With the callus membranes, a four- to fivefold increase was found; with the stratum corneum conjunctum membranes, the rate increased ~1.5 times. The fact that hydration enhanced the transport rate agrees with previous studies (5–10). From Table I, it can be seen that the transport rate of sarin across stratum corneum conjunctum membranes was faster than that across callus membranes, and the difference in rate was in accordance with the difference in thickness of the two membranes. This result suggests that the two types of membranes have similar barrier properties.

Since sarin transport in solution followed the discussed mathematical models for diffusion, the results suggest that a diffusion process is largely responsible for sarin penetration through these membranes. This result, along with the high activation energy for transport, strongly supports the theory of transepidermal penetration. If the permeability mechanism were largely the transport of the penetrant *via* diffusional pores, a much lower value for the activation energy would be characteristic of such a process. The high value for the transport activation energy also suggests that the penetrant and the membrane may interact strongly.

REFERENCES

(1) L. M. Lueck, D. E. Wurster, T. Higuchi, A. P. Lemberger, and L. W. Busse, *J. Am. Pharm. Assoc., Sci. Ed.*, **46**, 694 (1957).

(2) R. L. Patrick and G. O. Payne, Jr., *J. Colloid Sci.*, **16**, 93 (1961).

(3) B. Gehauf, J. Epstein, G. B. Wilson, B. Witten, S. Sass, V. E. Bauer, and W. H. C. Rueggeberg, *Anal. Chem.*, **29**, 278 (1957).

(4) R. Proper and R. W. Rosenthal, *Chemist-Analyst*, **45**, 79 (1956).

(5) D. E. Wurster and S. F. Kramer, *J. Pharm. Sci.*, **50**, 288 (1961).

(6) T. Higuchi, *J. Soc. Cosmet. Chem.*, **11**, 85 (1960).

(7) J. B. Shelmire, *Arch. Dermatol.*, **82**, 24 (1960).

(8) E. P. Laug, E. A. Vos, F. M. Kunze, and E. J. Umberger, *J. Pharmacol. Exp. Ther.*, **89**, 52 (1947).

(9) H. Leslie-Roberts, *Br. J. Dermatol.*, **40**, 325 (1928).

(10) W. B. Shelley and F. M. Melton, *J. Invest. Dermatol.*, **13**, 61 (1949).

ACKNOWLEDGMENTS

Abstracted in part from a dissertation submitted by J. A. Ostrenga to the University of Wisconsin in partial fulfillment of the Doctor of Philosophy degree requirements.

Supported by U.S. Naval Ordinance Test Station Contract N123-(60530)51696A., China Lake, Calif.

Sarin Transport across Excised Human Skin II: Effect of Solvent Pretreatment on Permeability

LLOYD E. MATHESON, Jr.[x], DALE E. WURSTER, and JAMES A. OSTRENGA *

Received February 5, 1979, from the *College of Pharmacy, University of Iowa, Iowa City, IA 52242.* Accepted for publication May 21, 1979. *Present address: Pharm Chem, Palo Alto, CA 94301.

Abstract □ The effect of pretreating callus membranes with dimethyl sulfoxide, dimethylacetamide, dimethylformamide, formamide, dioxane, or methyl orthoformate on sarin permeability was studied at three temperatures to determine the activation energy for transport. In addition, the effect of membrane pretreatment on permeability through callus membranes from either a sarin–carboxypolymethylene gel or a sarin–polymethyl methacrylate gel was studied.

Keyphrases □ Sarin—transport across excised human skin, effect of pretreating callus membranes with dimethyl sulfoxide, dimethylacetamide, dimethylformamide, formamide, dioxane, methyl orthoformate □ Cholinesterase inhibitors—sarin, transport across excised human skin, effect of pretreatment on permeability □ Transepidermal transport—sarin, excised human skin, effect of pretreatment

The presence of water in the skin or diffusing media increases percutaneous absorption (1–7). Much work also has been done on the effects of solvents other than water; dimethyl sulfoxide (8–20), dimethylacetamide (17, 21), and dimethylformamide (17, 21) influence the penetration rate of various chemicals. Some of this work was reviewed recently (22).

Penetration rates of sarin through excised human callus tissue from dilute solution and concentrated gels under both anhydrous and hydrous conditions were reported previously (23). The purpose of this study was to determine the effect of solvent pretreatment of callus membranes with dimethyl sulfoxide, dimethylacetamide, dimethylformamide, formamide, dioxane, and methyl orthoformate on sarin transport rates and on the transport activation energy.

Table I—Influence of Membrane Conditioning in Solution Phase Sarin Transport Systems

Membrane Conditioning Solvent	Average Transport Rate, mg/cm²/hr		Rate[a] Ratio	Temperature
	Unconditioned	Conditioned		
Dimethyl sulfoxide[b]	0.032	0.553	17.3	25°
Dimethylformamide[b]	0.017	0.218	12.8	30°
Dimethylacetamide[b]	0.019	0.192	10.1	25°
Formamide[b]	0.008	0.810	101.3	25°
Dioxane[c]	0.010	0.034	3.4	25°
Methyl orthoformate[c]	0.017	0.003	0.18	25°

[a] Rate ratio = [rate (conditioned)/rate (unconditioned)]. [b] Membrane conditioned and *n*-heptane saturated with given solvent. [c] Membrane conditioned but no solvent in *n*-heptane.

EXPERIMENTAL

Permeability Cell—The design of the permeability cell depended on whether the study involved diffusion from a dilute sarin solution or from a concentrated sarin gel. Both cells were described previously (23).

Membrane Preparation—Callus membranes were microtomed to a thickness of 100 μm and delipidized in anhydrous ether for 24 hr as reported earlier (23).

The membranes were placed in the diffusion cell membrane holder, using a small amount of silicone grease as an edge sealer. All membranes were examined microscopically after positioning in the membrane holder, which was immersed in the particular membrane conditioning solvent for 24 hr.

Permeability Cell Preparation for Solution Phase Studies—The slide containing the membrane was positioned between the two chambers of the permeability cell. Then 50 ml of $\sim 7.8 \times 10^{-3}$ *M* sarin in *n*-heptane,

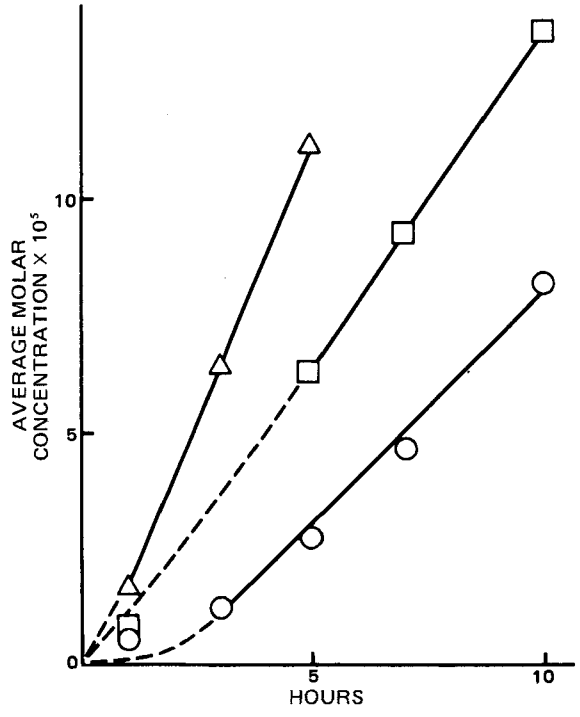

Figure 1—*Average sarin transport across dimethyl sulfoxide-conditioned callus membranes. Key:* ○, *25°;* □, *35°; and* △, *45°.*

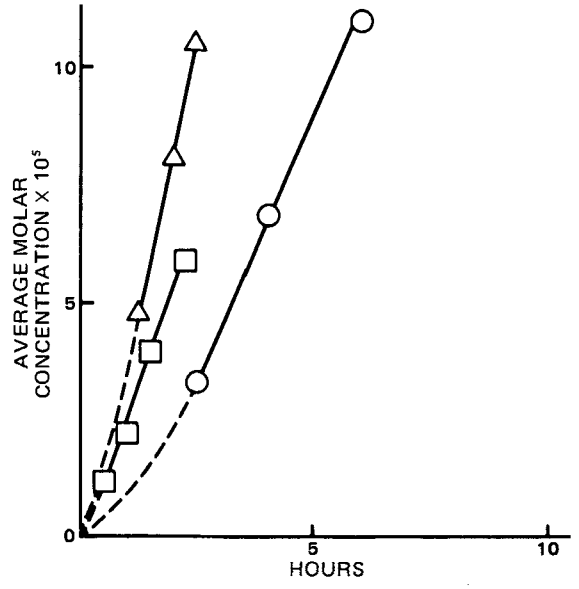

Figure 2—*Average sarin transport across formamide-conditioned callus membranes. Key:* ○, *25°;* □, *35°; and* △, *45°.*

0022-3549/79/1100-1410$01.00/0
© 1979, American Pharmaceutical Association

Table II—Influence of Membrane Conditioning and Gel Formation on Sarin Transport

Membrane Conditioning Solvent	Average Transport Rate, mg/cm²/hr: Polymethyl Methacrylate Gel, Unconditioned Solution Phase	Polymethyl Methacrylate Gel, Conditioned Gel Phase	Rate[a] Ratio	Carboxypolymethylene Gel, Unconditioned Solution Phase	Carboxypolymethylene Gel, Conditioned Gel Phase	Rate[a] Ratio
Dimethyl sulfoxide	0.005	5.47	911	0.008	18.2	2223
Dimethylformamide	0.085	24.0	282	0.004	6.64	1660
Dimethylacetamide	0.002	2.6	1300	0.008	8.60	1075
Formamide	0.003	3.34	1113	0.021	2.72	129.5
Dioxane	0.014	0.287	20.5	0.023	0.132	5.7
Methyl orthoformate	0.025	0.148	5.9	0.106	0.114	1.1

[a] Rate ratio = [rate (conditioned, gel)/rate (unconditioned, solution)].

Table III—Influence of Membrane Conditioning on Sarin Transport in Gel System

Membrane Conditioning Solvent	Solvent Dielectric Constant	Transport Rate, Polymethyl Methacrylate, mg/cm²/hr	Rate[a] Ratio	Transport Rate, Carboxypolymethylene, mg/cm²/hr	Rate[a] Ratio
None	—	0.407[b]	—	0.547[b]	—
Dimethyl sulfoxide	45	5.47	13	18.23	33
Dimethylformamide	27	24.0	59	6.64	12
Dimethylacetamide	38	2.6	6	8.60	15
Formamide	109	3.34	8	2.72	5
Dioxane	2.2	0.287	0.71	0.132	0.24
Methyl orthoformate	3	0.148	0.36	0.114	0.21

[a] Rate ratio = [rate (conditioned, gel)/rate (unconditioned, gel)]. [b] Reference 23.

at the appropriate temperature, was placed in the donor chamber with the simultaneous addition of an equal volume of *n*-heptane at the same temperature in the receiver chamber. The *n*-heptane in each chamber was saturated with the appropriate immiscible polar solvent at the temperature of the experiment but did not contain any dioxane or methyl orthoformate in the permeability comparison experiments. In the activation energy studies, the solvent composition was the same, except that 50 ml of dioxane or methyl orthoformate was added to 950 ml of *n*-heptane.

The permeability cells were maintained in a constant-temperature bath with gentle shaking in the plane of the membrane. The transport rate was followed by withdrawing 1-ml samples from the receiver chamber at suitable times and analyzing them colorimetrically for sarin.

Permeability Cell Preparation for Sarin Gel Studies—The preparation of the carboxypolymethylene[1] and polymethyl methacrylate gels and cell were described earlier (23). Fifty milliliters of *n*-heptane saturated with dimethyl sulfoxide, dimethylformamide, dimethylacetamide, or formamide was added immediately to the receiver chamber to start the experiment. No dioxane or methyl orthoformate was placed in the *n*-heptane. The permeability cell was maintained at 30° in a water bath with gentle shaking in the plane of the membrane. The transport rate was followed as in the solution phase studies.

Colorimetric Assay—The analytical procedure employed was a modification of the Schoenmann method (24) and was described earlier (23).

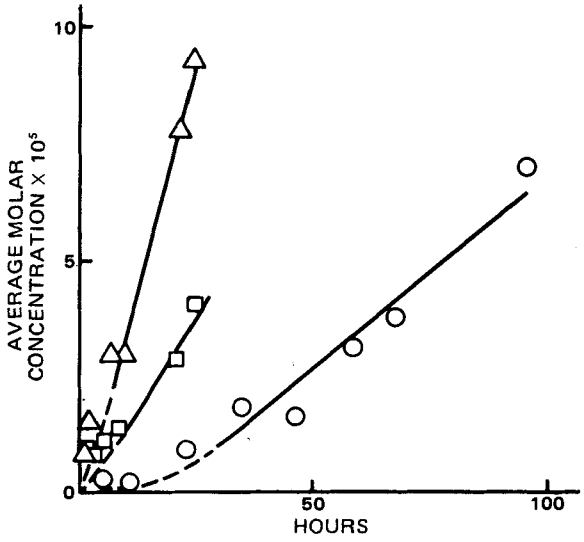

Figure 3—*Average sarin transport across dimethylformamide-conditioned callus membranes. Key:* ○, *25°;* □, *35°; and* △, *45°.*

RESULTS AND DISCUSSION

Solution Phase Permeability Comparison Studies—The initial sarin concentration in all experiments was $\sim 8 \times 10^{-3}$ *M*. Average sarin transport rates, in milligrams per square centimeter per hour, during the quasi-steady state through untreated membranes and the same solvent-conditioned membranes, along with a calculated membrane conditioning ratio, [rate (conditioned)/rate (unconditioned)] are shown in

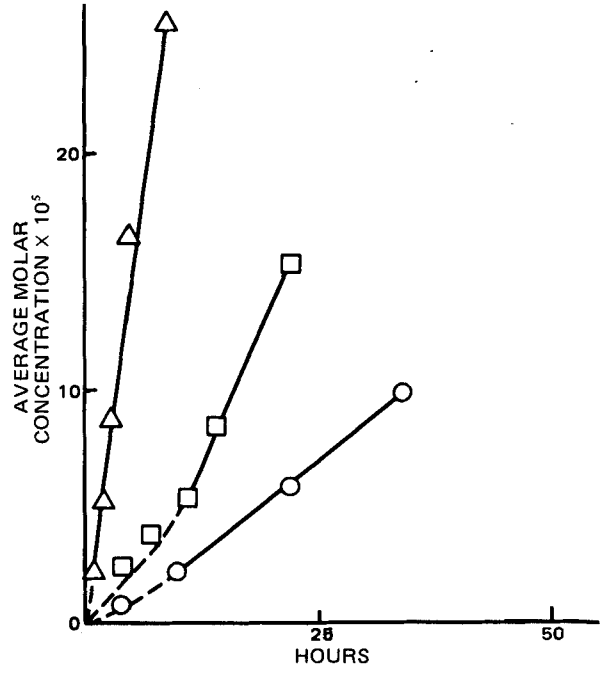

Figure 4—*Average sarin transport across dioxane-conditioned callus membranes. Key:* ○, *25°;* □, *35°; and* △, *45°.*

[1] Carbopol 934, B. F. Goodrich Chemical Co., Cleveland, OH 44100.

Table IV—Permeability Coefficients and Activation Energies for Solvent-Treated Membranes

Membrane Conditioning Solvent	Temperature	Permeability Coefficient, $k \times 10^4$/hr	Activation Energy, kcal/mole
Dimethyl sulfoxide	24.9°	13.00	8.2
	35.0°	18.65	
	44.9°	31.09	
Dioxane	25.0°	4.13	21.2
	34.9°	11.72	
	44.9°	39.00	
Methyl orthoformate	25.0°	2.75	22.3
	34.9°	10.05	
	44.8°	28.79	
Dimethylformamide	26.0°	1.07	14.4
	35.1°	1.83	
	45.0°	4.54	
Formamide	25.0°	28.29	6.2
	35.0°	37.51	
	44.5°	54.16	

Table I. Pretreating the membrane with dimethyl sulfoxide, dimethylformamide, dimethylacetamide, or formamide markedly increased the transport rate; dioxane caused only a slight increase, and methyl orthoformate actually decreased the rate.

Gel Phase Permeability Comparison Studies—The sarin transport rate through the solvent-treated membranes used in the gel study was determined first using the anhydrous solution phase conditions described previously. The combined influence of membrane conditioning and increased sarin concentration on sarin transport is shown in Table II, along with a calculated ratio defined as [rate (conditioned, gel)/rate (unconditioned, solution)].

The influence of membrane conditioning can to some degree be separated from the concentration effects by comparing these sarin transport rates from the gels through solvent-conditioned membranes [rate (conditioned, gel)] to some previously reported transport rates (23) from the gels through unconditioned membranes [rate (unconditioned, gel)]. These data, along with a calculated rate ratio defined as [rate (conditioned, gel)/rate (unconditioned, gel)] are shown in Table III. This approach was necessary since it was not possible to study the rates through untreated membranes in the gel system followed by their determination through the same membranes after solvent treatment. Polymeric material, especially the polymethyl methacrylate, collected on the membranes and could not be removed, making their reuse impossible.

The transport rate change in the gel system was due not only to the effect of solvent conditioning of the membrane but also to the effect of the conditioning solvent on the polymer in the gel, which may affect the release rate from the gel. There appeared to be an optimum range for the dielectric constant for the conditioning solvent in each gel system. The best conditioner for the more oil-soluble polymethyl methacrylate gel was dimethylformamide with a dielectric constant of 27, whereas the best conditioner for the more hydrophilic carbomer gel was dimethyl sulfoxide with a dielectric constant of 45. In both cases, as the dielectric constant of the conditioning solvent shifted away in either direction from the optimum range, a decrease in the ratio [rate (conditioned, gel)/rate (unconditioned, gel)] was observed (Table III).

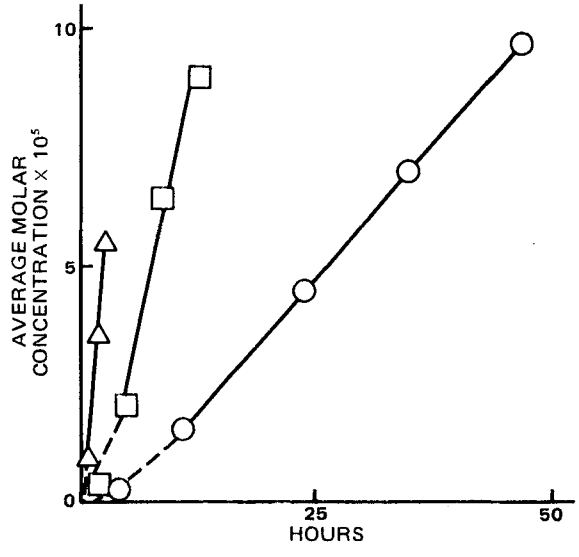

Figure 5—*Average sarin transport across methyl orthoformate-conditioned callus membranes. Key:* ○, *25°;* □, *35°; and* △, *45°.*

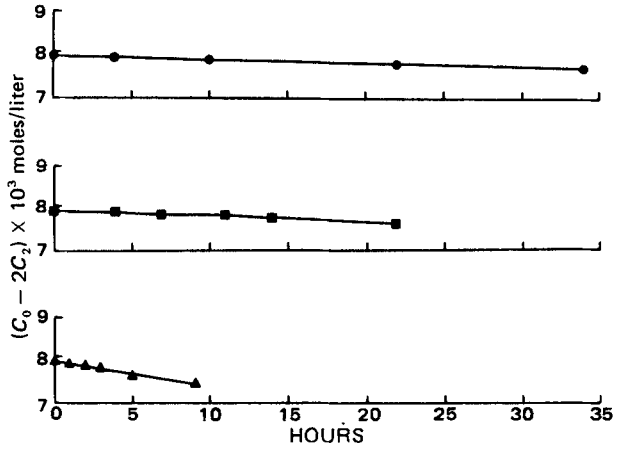

Figure 6—*First-order plots for sarin transport across dioxane-conditioned callus membranes. Key:* ●, *25°;* ■, *35°; and* ▲, *45°.*

Effect of Solvent Pretreatment on Transport Process Activation Energy—Different membranes were used at each temperature for each solvent treatment since repeated conditioning with dimethyl sulfoxide increased the subsequent permeability constants of the membranes.

Plots of the average molar concentration on the receiver side *versus* time at the three temperatures studied are shown in Figs. 1–5. The slope in the quasi-steady states allows calculation of the transport rate. A plot of log $(C_0 - 2C_2)$ *versus* time is shown in Fig. 6 for the dioxane solvent system at the three temperatures. The permeability coefficient at each

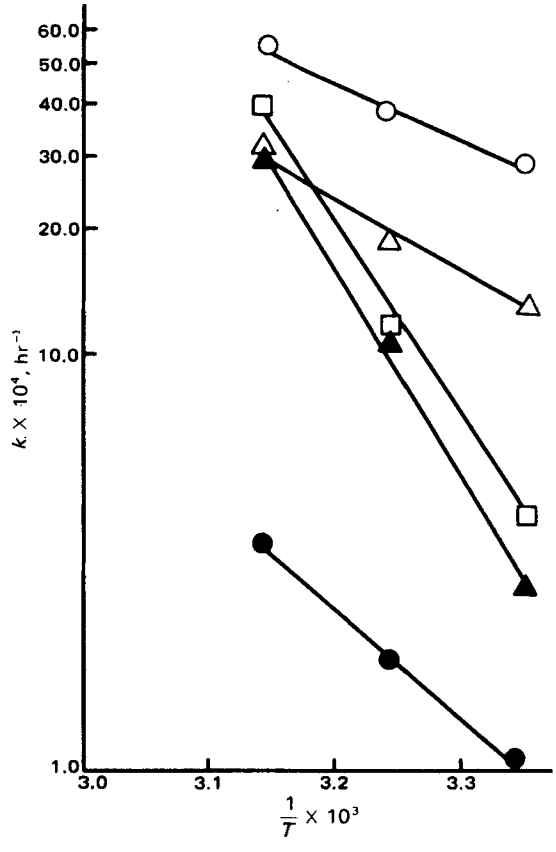

Figure 7—*Arrhenius plot of average permeability coefficients for sarin penetration through conditioned callus membranes at 25, 35, and 45°. Key:* ○, *formamide;* □, *dioxane;* △, *dimethyl sulfoxide;* ▲, *methyl orthoformate; and* ●, *dimethylformamide.*

temperature is calculated from the slope as described previously (23). The activation energy for the transport process for each solvent system is obtained from the slope of an Arrhenius plot of log permeability constant *versus* the reciprocal of the absolute temperature (Fig. 7). The permeability coefficients at each temperature and the activation energy for each system are shown in Table IV, with the expected inverse order between the rate ratio and the activation energy being observed.

REFERENCES

(1) T. Higuchi, *J. Soc. Cosmet. Chem.*, **11**, 85 (1960).

(2) J. E. Treherne, *J. Physiol.*, **133**, 171 (1956).

(3) W. B. Shelly and F. M. Melton, *J. Invest. Dermatol.*, **13**, 61 (1949).

(4) J. B. Shelmire, Jr., *Arch. Dermatol.*, **82**, 24 (1960).

(5) E. P. Laug, E. A. Vos, F. M. Kunze, and E. J. Umberger, *J. Pharmacol. Exp. Ther.*, **89**, 52 (1947).

(6) H. Leslie-Roberts, *Br. J. Dermatol.*, **40**, 325 (1928).

(7) D. E. Wurster and S. F. Kramer, *J. Pharm. Sci.*, **50**, 288 (1961).

(8) A. Horita and L. J. Weber, *Life Sci.*, **3**, 1389 (1964).

(9) S. W. Jacob, M. Bischel, and R. J. Herschler, *Curr. Ther. Res.*, **6**, 193 (1964).

(10) R. B. Stoughton and W. Fritsch, *Arch. Dermatol.*, **90**, 512 (1964).

(11) A. M. Kligman, *J. Am. Med. Assoc.*, **193**, 796 (1965).

(12) R. J. Feldmann and H. I. Maibach, *Arch. Dermatol.*, **94**, 649 (1966).

(13) H. L. McDermot, G. W. Murray, and R. M. Heggie, *Can. J. Physiol. Pharmacol.*, **43**, 845 (1965).

(14) J. M. Stelzer, J. L. Colaizzi, and P. J. Wurdock, *J. Pharm. Sci.*, **57**, 1732 (1968).

(15) H. L. McDermot, A. J. Finkbeiner, W. J. Willis, and R. M. Heggie, *Can. J. Physiol. Pharmacol.*, **45**, 299 (1967).

(16) J. E. Wahlberg and E. Skog, *Acta Dermatol.*, **47**, 209 (1967).

(17) D. D. Munro and R. B. Stoughton, *Arch. Dermatol.*, **92**, 585 (1965).

(18) W.-W. Shen, A. G. Danti, and F. N. Bruscato, *J. Pharm. Sci.*, **65**, 1780 (1976).

(19) J. P. Astley and M. Levine, *ibid.*, **65**, 210 (1976).

(20) F. Marcus, J. L. Colaizzi, and H. Barry, *ibid.*, **59**, 1616 (1970).

(21) R. J. Scheuplein, Final Report (1965) to U.S. Army Chemical Research and Development Laboratories, Md., Contact DA 18-108-AMC-148 (A).

(22) B. Idson, *J. Pharm. Sci.*, **64**, 901 (1975).

(23) D. E. Wurster, J. A. Ostrenga, and L. E. Matheson, Jr., *ibid.*, **68**, 1406 (1979).

(24) B. Gehauf, J. Epstein, G. B. Wilson, B. Witten, S. Sass, V. E. Bauer, and W. H. C. Rueggeberg, *Anal. Chem.*, **29**, 278 (1957).

ACKNOWLEDGMENTS

Abstracted in part from a dissertation submitted by L. E. Matheson, Jr., to the University of Wisconsin in partial fulfillment of the Doctor of Philosophy degree requirements.

Supported by U.S. Naval Ordinance Test Station Contract N123-(60530)51696A., China Lake, Calif.

High-Performance Liquid Chromatographic Determination of Azosemide in Commercial Animal Feed

HENRY S. I. TAN *x, NICHOLAS W. BRAKE, HUBERT J. KEILY, KAMALKISHORE J. DALAL, and HAROLD G. HIGSON

Received December 12, 1978, from *Merrell Research Center, Merrell-National Laboratories, Division of Richardson-Merrell Inc., Cincinnati, OH 45215.* Accepted for publication May 24, 1979.

*College of Pharmacy, University of Cincinnati–Medical Center, Cincinnati, OH 45267.

Abstract □ A high-performance liquid chromatographic (HPLC) method was developed for the assay of 2-chloro-5-(1*H*-tetrazol-5-yl)-4-[(2-thienylmethyl)amino]benzenesulfonamide (I) in animal feed diet mixtures. The sample is extracted with acetone, an aliquot of the extract is evaporated to dryness, and the residue is dissolved in chloroform. This solution can be subjected to either of two cleanup procedures. The first traps I on a sodium hydroxide–diatomaceous earth column. Compound I is then recovered using an acetic acid–ethyl acetate–chloroform eluent, which is removed by evaporation, followed by dissolution of the residue in aqueous sodium hydroxide. The second procedure involves the direct extraction of I from the chloroform solution. A linear relationship exists between the HPLC UV detector response at 254 nm and concentration up to 170 μg/ml. The sodium hydroxide extraction procedure resulted in an overall recovery (±*SD*) of 92.9 ± 1.6 and 97.4 ± 1.8% ($n = 5$) at levels of 200 and 6000 ppm, respectively. Overall recoveries (±*SD*) obtained by the diatomaceous earth column procedure for the 200- and 6000-ppm levels were 90.0 ± 2.0 and 95.9 ± 1.6% ($n = 5$), respectively.

Keyphrases □ Azosemide—analysis, high-performance liquid chromatography, commercial animal feed □ Diuretic agents—azosemide, high-performance liquid chromatographic analysis, commercial animal feed □ High-performance liquid chromatography—analysis, azosemide, commercial animal feed

Azosemide, 2-chloro-5-(1*H*-tetrazol-5-yl)-4-[(2-thienylmethyl)amino]benzenesulfonamide (I), is a new diuretic and saluretic agent (1). The drug has been formulated into tablets, injectable solutions, and lyophilizates in combination with other diuretics for the treatment of hydropic conditions (2, 3).

In long-term toxicological studies, drug administration to laboratory animals is usually done by incorporation into feed because of the inconvenience of individual manual dosing and the time involved in preparing individual dosages. Analytical methodology is required to determine that appropriate dosages are administered and that the drug is uniformly distributed and stable in the feed mix under the storage conditions used. Recent papers dealt with the determination of cyclobenzaprine, sulindac, halofenate, estradiol, and phenobarbital in animal feed mixtures for use in toxicity and/or carcinogenesis studies (4–6).

Reported quantitative analyses of sulfonamides in animal feed include spectrophotometric measurement of the diazotized sulfonamide after alumina column cleanup (7), GLC assay after purification by conventional extraction methods (8, 9), quantitative TLC (10), and spectrophotofluorometry and GLC after successive percolation through silica and alumina columns or successive base–acid extractions (11).

This paper presents a method for the assay of I in animal feed mix at 200- and 6000-ppm levels using high-perfor-

0022-3549/79/1100-1413$01.00/0

© 1979, American Pharmaceutical Association

temperature is calculated from the slope as described previously (23). The activation energy for the transport process for each solvent system is obtained from the slope of an Arrhenius plot of log permeability constant *versus* the reciprocal of the absolute temperature (Fig. 7). The permeability coefficients at each temperature and the activation energy for each system are shown in Table IV, with the expected inverse order between the rate ratio and the activation energy being observed.

REFERENCES

(1) T. Higuchi, *J. Soc. Cosmet. Chem.*, **11**, 85 (1960).

(2) J. E. Treherne, *J. Physiol.*, **133**, 171 (1956).

(3) W. B. Shelly and F. M. Melton, *J. Invest. Dermatol.*, **13**, 61 (1949).

(4) J. B. Shelmire, Jr., *Arch. Dermatol.*, **82**, 24 (1960).

(5) E. P. Laug, E. A. Vos, F. M. Kunze, and E. J. Umberger, *J. Pharmacol. Exp. Ther.*, **89**, 52 (1947).

(6) H. Leslie-Roberts, *Br. J. Dermatol.*, **40**, 325 (1928).

(7) D. E. Wurster and S. F. Kramer, *J. Pharm. Sci.*, **50**, 288 (1961).

(8) A. Horita and L. J. Weber, *Life Sci.*, **3**, 1389 (1964).

(9) S. W. Jacob, M. Bischel, and R. J. Herschler, *Curr. Ther. Res.*, **6**, 193 (1964).

(10) R. B. Stoughton and W. Fritsch, *Arch. Dermatol.*, **90**, 512 (1964).

(11) A. M. Kligman, *J. Am. Med. Assoc.*, **193**, 796 (1965).

(12) R. J. Feldmann and H. I. Maibach, *Arch. Dermatol.*, **94**, 649 (1966).

(13) H. L. McDermot, G. W. Murray, and R. M. Heggie, *Can. J. Physiol. Pharmacol.*, **43**, 845 (1965).

(14) J. M. Stelzer, J. L. Colaizzi, and P. J. Wurdock, *J. Pharm. Sci.*, **57**, 1732 (1968).

(15) H. L. McDermot, A. J. Finkbeiner, W. J. Willis, and R. M. Heggie, *Can. J. Physiol. Pharmacol.*, **45**, 299 (1967).

(16) J. E. Wahlberg and E. Skog, *Acta Dermatol.*, **47**, 209 (1967).

(17) D. D. Munro and R. B. Stoughton, *Arch. Dermatol.*, **92**, 585 (1965).

(18) W.-W. Shen, A. G. Danti, and F. N. Bruscato, *J. Pharm. Sci.*, **65**, 1780 (1976).

(19) J. P. Astley and M. Levine, *ibid.*, **65**, 210 (1976).

(20) F. Marcus, J. L. Colaizzi, and H. Barry, *ibid.*, **59**, 1616 (1970).

(21) R. J. Scheuplein, Final Report (1965) to U.S. Army Chemical Research and Development Laboratories, Md., Contact DA 18-108-AMC-148 (A).

(22) B. Idson, *J. Pharm. Sci.*, **64**, 901 (1975).

(23) D. E. Wurster, J. A. Ostrenga, and L. E. Matheson, Jr., *ibid.*, **68**, 1406 (1979).

(24) B. Gehauf, J. Epstein, G. B. Wilson, B. Witten, S. Sass, V. E. Bauer, and W. H. C. Rueggeberg, *Anal. Chem.*, **29**, 278 (1957).

ACKNOWLEDGMENTS

Abstracted in part from a dissertation submitted by L. E. Matheson, Jr., to the University of Wisconsin in partial fulfillment of the Doctor of Philosophy degree requirements.

Supported by U.S. Naval Ordinance Test Station Contract N123-(60530)51696A., China Lake, Calif.

High-Performance Liquid Chromatographic Determination of Azosemide in Commercial Animal Feed

HENRY S. I. TAN *x, NICHOLAS W. BRAKE, HUBERT J. KEILY, KAMALKISHORE J. DALAL, and HAROLD G. HIGSON

Received December 12, 1978, from *Merrell Research Center, Merrell-National Laboratories, Division of Richardson-Merrell Inc., Cincinnati, OH 45215.* Accepted for publication May 24, 1979.

*College of Pharmacy, University of Cincinnati–Medical Center, Cincinnati, OH 45267.

Abstract □ A high-performance liquid chromatographic (HPLC) method was developed for the assay of 2-chloro-5-(1*H*-tetrazol-5-yl)-4-[(2-thienylmethyl)amino]benzenesulfonamide (I) in animal feed diet mixtures. The sample is extracted with acetone, an aliquot of the extract is evaporated to dryness, and the residue is dissolved in chloroform. This solution can be subjected to either of two cleanup procedures. The first traps I on a sodium hydroxide–diatomaceous earth column. Compound I is then recovered using an acetic acid–ethyl acetate–chloroform eluent, which is removed by evaporation, followed by dissolution of the residue in aqueous sodium hydroxide. The second procedure involves the direct extraction of I from the chloroform solution. A linear relationship exists between the HPLC UV detector response at 254 nm and concentration up to 170 μg/ml. The sodium hydroxide extraction procedure resulted in an overall recovery (±*SD*) of 92.9 ± 1.6 and 97.4 ± 1.8% ($n = 5$) at levels of 200 and 6000 ppm, respectively. Overall recoveries (±*SD*) obtained by the diatomaceous earth column procedure for the 200- and 6000-ppm levels were 90.0 ± 2.0 and 95.9 ± 1.6% ($n = 5$), respectively.

Keyphrases □ Azosemide—analysis, high-performance liquid chromatography, commercial animal feed □ Diuretic agents—azosemide, high-performance liquid chromatographic analysis, commercial animal feed □ High-performance liquid chromatography—analysis, azosemide, commercial animal feed

Azosemide, 2-chloro-5-(1*H*-tetrazol-5-yl)-4-[(2-thienylmethyl)amino]benzenesulfonamide (I), is a new diuretic and saluretic agent (1). The drug has been formulated into tablets, injectable solutions, and lyophilizates in combination with other diuretics for the treatment of hydropic conditions (2, 3).

In long-term toxicological studies, drug administration to laboratory animals is usually done by incorporation into feed because of the inconvenience of individual manual dosing and the time involved in preparing individual dosages. Analytical methodology is required to determine that appropriate dosages are administered and that the drug is uniformly distributed and stable in the feed mix under the storage conditions used. Recent papers dealt with the determination of cyclobenzaprine, sulindac, halofenate, estradiol, and phenobarbital in animal feed mixtures for use in toxicity and/or carcinogenesis studies (4–6).

Reported quantitative analyses of sulfonamides in animal feed include spectrophotometric measurement of the diazotized sulfonamide after alumina column cleanup (7), GLC assay after purification by conventional extraction methods (8, 9), quantitative TLC (10), and spectrophotofluorometry and GLC after successive percolation through silica and alumina columns or successive base–acid extractions (11).

This paper presents a method for the assay of I in animal feed mix at 200- and 6000-ppm levels using high-perfor-

0022-3549/79/1100-1413$01.00/0

© 1979, American Pharmaceutical Association

Table I—Comparative Study of Cleanup Procedures with and without Soxhlet or Manual Acetone Extraction

Cleanup Procedure	Recovery of I, %: Dry Feed Mix[a] Soxhlet	Dry Feed Mix[a] Manual	Feed Extract[a]
Procedure a	—	87.1–92.2[b]	87.4–91.7[b]
Procedure b	81.4–86.0[b]	91.0–94.5[b]	94.6–15.6[c]
Successive base–acid–base	79.9–86.2[c]	91.4–93.1[b]	94.1–95.7[c]

[a] Using 0.2 mg of I/g of dry feed or 0.02 mg of I/ml of feed extract. [b] Range of three determinations. [c] Range of two determinations.

mance liquid chromatography (HPLC) after cleanup of the feed extract by two different procedures.

EXPERIMENTAL

Apparatus—The following were used: a high-performance liquid chromatograph[1] fitted with a sample injection valve with a 20-μl sample loop[2], a fixed-wavelength UV detector (254 nm), and an electronic computing integrator[3] provided with a teletypewriter[4]; a glass chromatography tube, 15 mm (i.d.) × 350 mm, with a polytef stopcock; a mechanical shaker; a centrifuge; and 50-ml centrifuge tubes fitted with polytef-lined screw caps.

Reagents and Materials—The following were used: I, mp 210° dec.[5]; diatomaceous earth[6]; animal feed[7]; 25% (v/v) acetonitrile[8] in 0.1 *M* pH 3.2 phosphate buffer; and acetic acid–ethyl acetate–chloroform (0.15:5:25). All chemicals were analytical grade.

HPLC Conditions—A 100-cm × 2.1-mm (i.d.) column packed with 37–50-μm Bondapak phenyl/Corasil[9] was used at ambient temperature. An isocratic mobile phase system of acetonitrile–0.1 *M* pH 3.2 phosphate buffer (25:75) was delivered at the rate of 1 ml/min (~600 psi). The detector was attenuated to 0.08 and 0.16 aufs for the 200- and 6000-ppm samples, respectively.

Standard Solution Preparation—About 25 mg of I was weighed accurately into a 100-ml volumetric flask. About 80 ml of 0.01 *M* NaOH was added and shaken for 15 min to dissolve the solid. The solution was diluted to volume with 0.01 *M* NaOH and mixed well. Twenty milliliters (for use with purification Procedure a) or 10.0 ml (for use with Procedure b) of this solution was pipetted into a 100-ml volumetric flask, diluted to volume with 0.01 *M* NaOH, and mixed well.

Diatomaceous Earth Column Preparation—A small glass wool plug was placed at the base of the glass chromatographic tube. Two grams of diatomaceous earth AW was transferred to the tube and tamped lightly. Three grams of diatomaceous earth and 1.5 ml of 0.1 *M* NaOH were mixed gently and transferred to the tube. The tube was tapped on a padded bench to settle the packing and then tamped very lightly but evenly.

Sample Preparation—About 10 or 5 g of sample for concentrations of 200 or 6000 ppm, respectively, was weighed accurately into a glass-stoppered, 250-ml boiling flask. About 25 ml of acetone was added, and the flask was stoppered and shaken for 20 min. The extract was filtered through a glass wool pledget into a 100-ml volumetric flask. The extraction was repeated three more times with 20-ml portions of acetone. The flask and filter were washed with acetone, and the washings were used to dilute the combined extract to volume.

About 40 ml of the solution was transferred to a centrifuge tube, and the tube was capped and centrifuged at ~2000 rpm for 2 min. Then 25.0 or 30.0 ml of the clear supernatant liquid for purification Procedure a or b, respectively, for the 200-ppm sample or 2.0 ml for both purification procedures for the 6000-ppm sample was pipetted into a glass-stoppered, 100-ml boiling flask and evaporated to dryness on the rotary evaporator at ~45°. Acetone traces were removed under a nitrogen stream, and the residue was subjected to one of the following cleanup procedures.

Procedure a: Diatomaceous Earth Column Cleanup—About 10 ml of water-saturated chloroform was added and shaken to dissolve the residue. The solution was transferred, using a Pasteur pipet, to the diatomaceous earth column, and the flow rate was adjusted to 1–1.5 ml/min. The flask was rinsed twice with 10-ml portions of water-saturated chloroform, and the rinsings were transferred to the column. The eluate was discarded.

The adsorbed I was eluted with 40 ml of acetic acid–ethyl acetate–chloroform, and the eluate was collected in a 100-ml boiling flask. The eluate was evaporated to dryness on the rotary evaporator at ~45°. Acetic acid traces were removed under a nitrogen stream. Ten milliliters of 0.01 *M* NaOH was pipetted into the flask, and the flask was stoppered and shaken vigorously for 15 min. The solution was filtered through a 5-μm filter[10].

Procedure b: Sodium Hydroxide Extraction Cleanup—The residue

Table II—Recovery of I from Spiked Feed Mix at 200 and 6000 ppm

Amount of I Added, ppm	Amount of I Found, ppm: Procedure a	Amount of I Found, ppm: Procedure b	Recovery, %: Procedure a	Recovery, %: Procedure b
		200 ppm		
199.6	174	—	87.2	—
199.3	—	188	—	94.3
200.2	185	—	92.4	—
202.0	184	190	91.1	94.1
198.2	178	186	89.8	93.8
194.7	—	177	—	90.9
201.6	—	184	—	91.3
203.7	182	—	89.3	—
Overall recovery, %			90.0	92.9
SD			2.0	1.6
		6000 ppm		
5994	—	5870	—	97.9
6034	5920	6060	98.1	100.4
5948	5570	5740	93.6	96.5
6036	5770	5800	95.6	96.1
6044	5780	5820	95.6	96.3
6030	5820	—	96.5	—
Overall recovery, %			95.9	97.4
SD			1.6	1.8

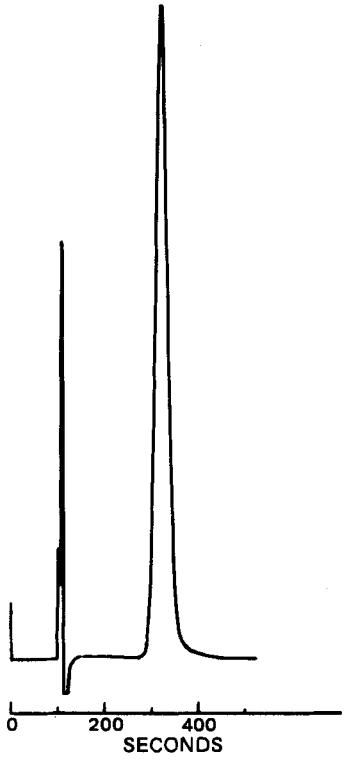

Figure 1—*Liquid chromatogram of pure I in 0.01* M *NaOH.*

[1] Model 8500, Varian Associates, Palo Alto, Calif.
[2] Model 70-10, Rheodyne, Berkeley, Calif.
[3] Model 3370 A, Hewlett-Packard, Avondale, Pa.
[4] Model ASR 33, Hewlett-Packard, Avondale, Pa.
[5] Boehringer, Mannheim G.M.b.H., West Germany.
[6] Celite 545 AW, Supelco Inc., Bellefonte, Pa.
[7] Purina Laboratory Chow, Ralston Purina Co., St. Louis, Mo.
[8] Burdick & Jackson, Muskegon, Mich.
[9] Waters Associates, Milford, Mass.
[10] Type HA, Millipore Corp., Bedford, Mass.

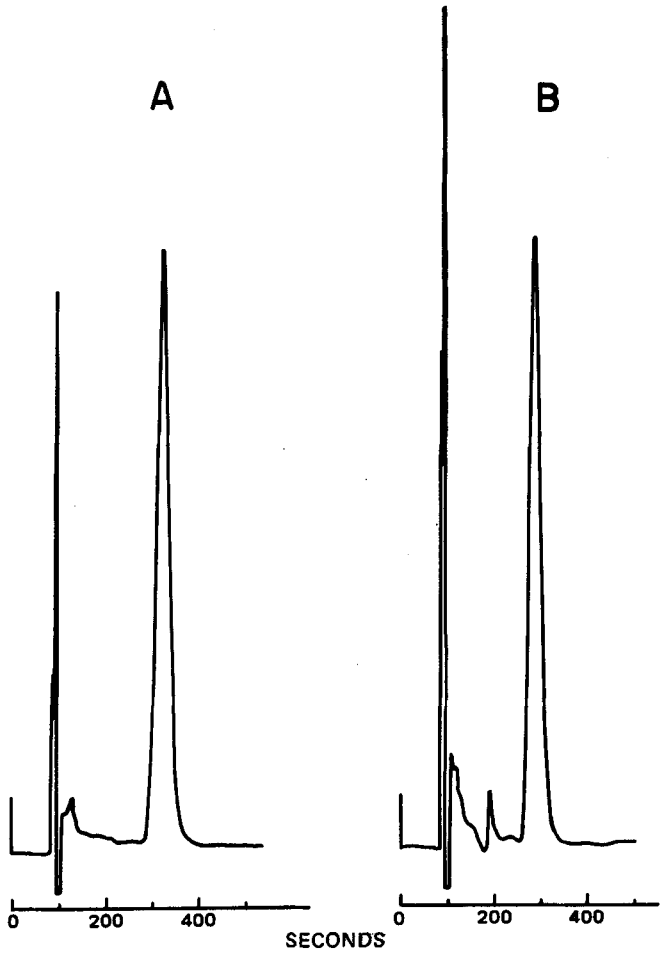

Figure 2—*Liquid chromatograms of I from 200-ppm feed sample. Key: A, Procedure a; and B, Procedure b.*

was dissolved in 10 ml of chloroform and transferred quantitatively into a centrifuge tube. The flask was rinsed twice with 10-ml portions of chloroform, and the rinsings were added to the centrifuge tube. The solution was extracted four times with 6-ml portions of 0.01 *M* NaOH. Each time, the mixture was shaken gently and centrifuged at 2000 rpm for 5 min. With a Pasteur pipet, the clear supernate was transferred carefully into a 25-ml volumetric flask. It was diluted to volume with 0.01 *M* NaOH and filtered through a 5-μm filter[10].

Chromatographic Procedure—By using the sample injection valve, 20 μl of the standard solution and 20 μl of the prepared feed sample solution were chromatographed under the described HPLC conditions. The chromatogram was quantitated by relating the peak area of I from the sample to that of I from the standard solution.

RESULTS AND DISCUSSION

Toxicological studies with I employed concentrations levels of 200 and 6000 ppm in the feed mix. Since the low level samples were expected to be more difficult to assay, the developmental work was undertaken with the 200-ppm samples. The assay of I and the cleanup procedures are based on its acidic nature.

Preliminary tests to determine the solvent for extracting I from the feed mix indicated that acetone was the solvent of choice. Attempts to extract I from the feed mix using a soxhlet extractor resulted in recoveries that were consistently lower than those obtained by manual extractions with acetone and the same sample cleanup procedure (Table I). Presumably, a fraction of I was adsorbed on the extraction thimble and/or decomposed on heating. Bowman and Rushing (6) also reported that soxhlet extractions of phenobarbital from animal feed yielded low recoveries. Soxhlet extractions were also performed with mixed solvents such as chloroform–acetone and chloroform–methanol, but the recoveries were very low.

In addition to the two sample cleanup procedures (Procedures a and b described under *Sample Preparation*), several purification procedures were attempted. A successive base–acid–base extraction was investigated whereby a methanol-containing chloroform solution of feed extract was extracted with aqueous base, followed by extraction into chloroform after acidification of the aqueous phase and reextraction into 0.01 *M* NaOH. This procedure resulted in sharp separations of the phases in each extraction, in contrast to the direct sodium hydroxide extraction cleanup procedure (Procedure b). In the latter procedure, emulsions were formed during the extraction, and the two phases could not be sharply separated even by centrifugation. Although the successive base–acid–base extraction gave cleaner liquid chromatograms than Procedure b, the recoveries using the two procedures were similar (Table I). Because of the longer analysis time required, the successive base–acid–base extraction procedure was not investigated further.

Attempts to clean up I-containing feed extracts on neutral or acid silica gel or on acid alumina columns were not successful. Trapping of I on these columns was only successful when pure I solutions were employed. In these cases, quantitative recoveries were obtained. When acetone-extractable feed constituents were present, the recoveries were always <85%. With anion-exchange columns, complete recovery of I could not be achieved even from pure solutions with various eluting solutions.

In the sodium hydroxide–diatomaceous earth column procedure (Procedure a), the sodium hydroxide strength for adsorption on diatomaceous earth and the total amount needed were determined. Various eluants and mixtures were investigated for optimum recovery of the trapped I. The addition of a bottom layer of plain diatomaceous earth in the column helped to break emulsions when they formed in the column.

Under the described HPLC conditions, I eluted as a symmetrical peak with a retention time of ~5 min (Fig. 1). The average height equivalent to a theoretical plate of the column was 1.79 ± 0.19 (*SD*) mm (n = 10). The linearity of the detector response at 254 nm was established previously. The response was linear up to 170 μg/ml.

Both cleanup procedures gave liquid chromatograms that resolved the I peak from any feed constituents present (Figs. 2 and 3). Procedure b

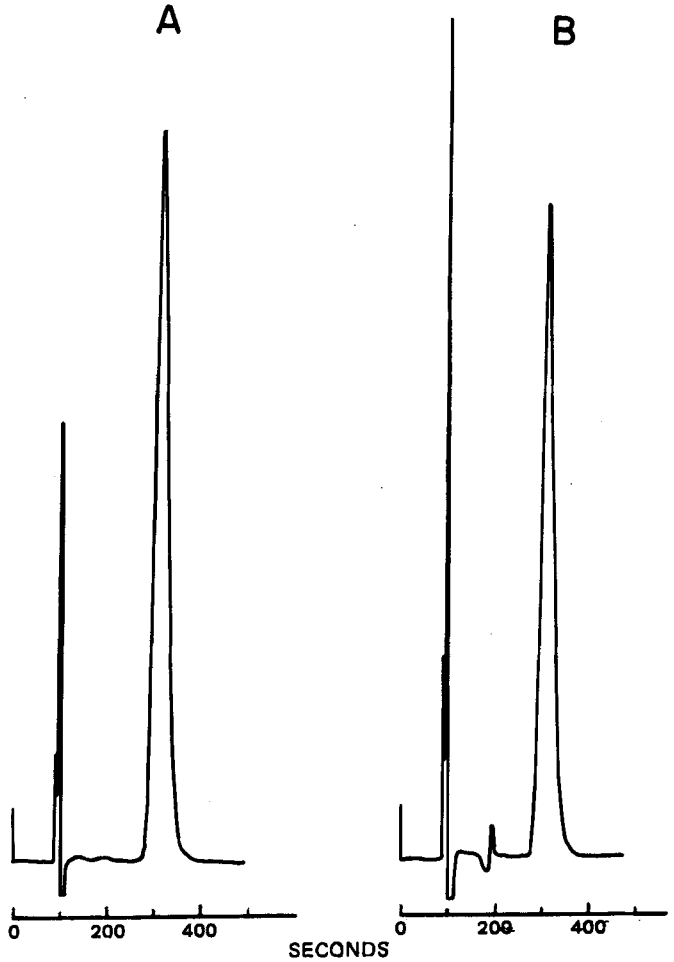

Figure 3—*Liquid chromatograms of I from 6000-ppm feed sample. Key: A, Procedure a; and B, Procedure b.*

gave a chromatogram that showed many extraneous peaks for the 200-ppm sample, but the chromatogram of the 6000-ppm sample was relatively clean. The difference on the baseline between I and the nearest extraneous peak on the 6000-ppm chromatogram was >1 min (Fig. 3). Procedure a gave very few additional peaks for the 200-ppm sample (Fig. 2). In the liquid chromatogram of the 6000-ppm sample, only two small peaks were observed.

Essentially complete recoveries were obtained when known amounts of I were analyzed in the absence of feed using both cleanup procedures. When a solution of I in acetone was added to a placebo feed, however, the overall percent recoveries ($\pm SD$) obtained by Procedure a were 90.0 ± 2.0 (n = 5) and 95.9 ± 1.6% (n = 5) for the 200- and 6000-ppm samples, respectively (Table II). Similarly, Procedure b gave overall percent recoveries ($\pm SD$) of 92.9 ± 1.6 (n = 5) and 97.4 ± 1.8% (n = 5) for the 200- and 6000-ppm samples, respectively (Table II). To provide better representation of the analytical potency, a concomitant standard may be used; *i.e.*, the standard can be subjected to the same analytical steps in the cleanup procedures.

The cleanup procedures were evaluated by spiking acetone extracts of a placebo feed with a solution of I in acetone. The recoveries, again <100%, were in close agreement with those obtained when the drug was added directly to the dry feed followed by manual extraction (Table I). Attempts to improve the recoveries by doubling the analytical sample size were not successful. Apparently, an interaction occurs between the drug and one or more of the extractable feed components, which affects the analytical recovery.

This hypothesis was supported by subsequent recovery studies using cleanup Procedure a and placebo feed samples spiked with I at the 6000-ppm level. Duplicate results of 90.9 and 92.1% were obtained when the synthetic samples were mixed using a mortar and pestle. When two similar samples were assayed 7 days after mixing, recoveries of only 82.8 and 82.5% were achieved. No peaks that could be attributed to decomposition products of I were seen in the chromatograms.

The HPLC method is stability indicating; various degradation studies showed that the I peak decreased upon decomposition with or without the appearance of new peaks.

REFERENCES

(1) A. Popelak, A. Lerch, K. Stach, E. Roesch, and K. Hardebeck, U.S. pat. 3,665,002 (Cl. 260/239.9) (1972).

(2) R. Kuhn, K. Hardebeck, H. Heinemann, and K. Osmers, U.S. pat. 3,963,834 (Cl. 424/240) (1976).

(3) R. Kuhn, K. Hardebeck, and H. Heinemann, U.S. pat. 4,031,213 (Cl. 424/229) (1977).

(4) H. B. Hucker and S. C. Stauffer, *J. Chromatogr.*, **131**, 357 (1977).

(5) M. C. Bowman and C. R. Nony, *J. Chromatogr. Sci.*, **15**, 160 (1977).

(6) M. C. Bowman and L. G. Rushing, *ibid.*, **16**, 23 (1978).

(7) C. R. Szalkowski, *J. Assoc. Off. Anal. Chem.*, **56**, 758 (1973).

(8) R. J. Daun, *ibid.*, **54**, 1277 (1971).

(9) A. Fravolini and A. Begliomini, *ibid.*, **52**, 767 (1969).

(10) U. R. Cieri, *ibid.*, **56**, 1475 (1973).

(11) J. R. King and M. C. Bowman, *Biochem. Med.*, **12**, 313 (1975).

ACKNOWLEDGMENTS

Presented at the Pharmaceutical Analysis and Control Section, APhA Academy of Pharmaceutical Sciences, Anaheim meeting, April 1979.

Potentiometric Determination of Iodine in Pharmaceutical Preparations

M. VANDEPUTTE, L. DRYON, L. DE HERTOGH, and D. L. MASSART ˣ

Received March 20, 1978, from the *Farmaceutisch Instituut, Vrije Universiteit Brussel, Bosstraat, 1090 Brussels, Belgium.* Accepted for publication June 1, 1979.

Abstract □ Methods for the determination of organically bound iodine were compared. A preliminary destruction of the sample was preferable. The sample was mineralized using the Schöniger combustion. Since direct potentiometry of the iodide ion was used, further reduction of the sample was necessary. Several reductors were compared, and the best results were obtained with Devarda alloy. The proposed method was employed for the determination of iodine in X-ray contrast products. Pure compounds and pharmaceutical preparations were investigated. The coefficient of variation of the method was 0.9%.

Keyphrases □ Iodine—analysis, potentiometric, various pharmaceuticals, ion-selective electrodes □ Potentiometry—analysis, iodine in various pharmaceuticals

The increased number of commercially available ion-selective electrodes has stimulated their use in pharmaceutical analysis. The potentiometric determination of halide salts of pharmaceutical compounds such as alkaloids and phenothiazines was described (1–3). Halogen-containing organic compounds also can be determined by ion-selective electrodes. Since halide ion-specific electrodes measure only the inorganic ionic halogen in solution, preliminary liberation of the covalently bound halogen from the organic product is necessary and usually is achieved by destruction of organic matter (3–11). Methods for halogen liberation from organic compounds (hydrolysis, decomposition by acids or oxidizing acids, melting of solids, combustion in a gas stream, and oxygen flask combustion) were discussed previously (12).

Some investigators reported the liberation of organically bound iodine by a metallic reductor. Catalytic dehalogenation with sodium borohydride in the presence of palladium was described for the analysis of X-ray contrasting media (13). The use of an aluminum foil in alkaline solution was proposed for the iodine determination in liothyronine (triiodo-L-thyronine, T_3) and thyroxine (tetraiodo-L-thyronine, T_4) (14).

If a combustion method such as the Schöniger combustion (15, 16) is used to mineralize the organic matter, the halogen content can be determined by measuring the iodate or iodide content. After combustion, the iodine is present as iodine and iodate. The iodine and iodate can be reduced to iodide ions, which can be measured potentiometrically with an iodide-ion-selective electrode. In this case, a reduction step is necessary. Reduction of iodate has already been described.

Stannous chloride was used for iodate determination in iodized cooking salt with an iodide-selective electrode (17), and use of an aluminum foil in alkaline solution was reported for the iodate reduction (18). The purpose of this

0022-3549/79/1100-1416$01.00/0

© 1979, American Pharmaceutical Association

gave a chromatogram that showed many extraneous peaks for the 200-ppm sample, but the chromatogram of the 6000-ppm sample was relatively clean. The difference on the baseline between I and the nearest extraneous peak on the 6000-ppm chromatogram was >1 min (Fig. 3). Procedure a gave very few additional peaks for the 200-ppm sample (Fig. 2). In the liquid chromatogram of the 6000-ppm sample, only two small peaks were observed.

Essentially complete recoveries were obtained when known amounts of I were analyzed in the absence of feed using both cleanup procedures. When a solution of I in acetone was added to a placebo feed, however, the overall percent recoveries ($\pm SD$) obtained by Procedure a were 90.0 ± 2.0 (n = 5) and 95.9 ± 1.6% (n = 5) for the 200- and 6000-ppm samples, respectively (Table II). Similarly, Procedure b gave overall percent recoveries ($\pm SD$) of 92.9 ± 1.6 (n = 5) and 97.4 ± 1.8% (n = 5) for the 200- and 6000-ppm samples, respectively (Table II). To provide better representation of the analytical potency, a concomitant standard may be used; *i.e.*, the standard can be subjected to the same analytical steps in the cleanup procedures.

The cleanup procedures were evaluated by spiking acetone extracts of a placebo feed with a solution of I in acetone. The recoveries, again <100%, were in close agreement with those obtained when the drug was added directly to the dry feed followed by manual extraction (Table I). Attempts to improve the recoveries by doubling the analytical sample size were not successful. Apparently, an interaction occurs between the drug and one or more of the extractable feed components, which affects the analytical recovery.

This hypothesis was supported by subsequent recovery studies using cleanup Procedure a and placebo feed samples spiked with I at the 6000-ppm level. Duplicate results of 90.9 and 92.1% were obtained when the synthetic samples were mixed using a mortar and pestle. When two similar samples were assayed 7 days after mixing, recoveries of only 82.8 and 82.5% were achieved. No peaks that could be attributed to decomposition products of I were seen in the chromatograms.

The HPLC method is stability indicating; various degradation studies showed that the I peak decreased upon decomposition with or without the appearance of new peaks.

REFERENCES

(1) A. Popelak, A. Lerch, K. Stach, E. Roesch, and K. Hardebeck, U.S. pat. 3,665,002 (Cl. 260/239.9) (1972).

(2) R. Kuhn, K. Hardebeck, H. Heinemann, and K. Osmers, U.S. pat. 3,963,834 (Cl. 424/240) (1976).

(3) R. Kuhn, K. Hardebeck, and H. Heinemann, U.S. pat. 4,031,213 (Cl. 424/229) (1977).

(4) H. B. Hucker and S. C. Stauffer, *J. Chromatogr.*, **131**, 357 (1977).

(5) M. C. Bowman and C. R. Nony, *J. Chromatogr. Sci.*, **15**, 160 (1977).

(6) M. C. Bowman and L. G. Rushing, *ibid.*, **16**, 23 (1978).

(7) C. R. Szalkowski, *J. Assoc. Off. Anal. Chem.*, **56**, 758 (1973).

(8) R. J. Daun, *ibid.*, **54**, 1277 (1971).

(9) A. Fravolini and A. Begliomini, *ibid.*, **52**, 767 (1969).

(10) U. R. Cieri, *ibid.*, **56**, 1475 (1973).

(11) J. R. King and M. C. Bowman, *Biochem. Med.*, **12**, 313 (1975).

ACKNOWLEDGMENTS

Presented at the Pharmaceutical Analysis and Control Section, APhA Academy of Pharmaceutical Sciences, Anaheim meeting, April 1979.

Potentiometric Determination of Iodine in Pharmaceutical Preparations

M. VANDEPUTTE, L. DRYON, L. DE HERTOGH, and D. L. MASSART ˣ

Received March 20, 1978, from the *Farmaceutisch Instituut, Vrije Universiteit Brussel, Bosstraat, 1090 Brussels, Belgium.* Accepted for publication June 1, 1979.

Abstract □ Methods for the determination of organically bound iodine were compared. A preliminary destruction of the sample was preferable. The sample was mineralized using the Schöniger combustion. Since direct potentiometry of the iodide ion was used, further reduction of the sample was necessary. Several reductors were compared, and the best results were obtained with Devarda alloy. The proposed method was employed for the determination of iodine in X-ray contrast products. Pure compounds and pharmaceutical preparations were investigated. The coefficient of variation of the method was 0.9%.

Keyphrases □ Iodine—analysis, potentiometric, various pharmaceuticals, ion-selective electrodes □ Potentiometry—analysis, iodine in various pharmaceuticals

The increased number of commercially available ion-selective electrodes has stimulated their use in pharmaceutical analysis. The potentiometric determination of halide salts of pharmaceutical compounds such as alkaloids and phenothiazines was described (1–3). Halogen-containing organic compounds also can be determined by ion-selective electrodes. Since halide ion-specific electrodes measure only the inorganic ionic halogen in solution, preliminary liberation of the covalently bound halogen from the organic product is necessary and usually is achieved by destruction of organic matter (3–11). Methods for halogen liberation from organic compounds (hydrolysis, decomposition by acids or oxidizing acids, melting of solids, combustion in a gas stream, and oxygen flask combustion) were discussed previously (12).

Some investigators reported the liberation of organically bound iodine by a metallic reductor. Catalytic dehalogenation with sodium borohydride in the presence of palladium was described for the analysis of X-ray contrasting media (13). The use of an aluminum foil in alkaline solution was proposed for the iodine determination in liothyronine (triiodo-L-thyronine, T_3) and thyroxine (tetraiodo-L-thyronine, T_4) (14).

If a combustion method such as the Schöniger combustion (15, 16) is used to mineralize the organic matter, the halogen content can be determined by measuring the iodate or iodide content. After combustion, the iodine is present as iodine and iodate. The iodine and iodate can be reduced to iodide ions, which can be measured potentiometrically with an iodide-ion-selective electrode. In this case, a reduction step is necessary. Reduction of iodate has already been described.

Stannous chloride was used for iodate determination in iodized cooking salt with an iodide-selective electrode (17), and use of an aluminum foil in alkaline solution was reported for the iodate reduction (18). The purpose of this

0022-3549/79/1100-1416$01.00/0

© 1979, American Pharmaceutical Association

Table I—Performance of Metallic Reductors for the Reduction of a Sodium Iodate Solution Equivalent to 1.000 ppm of I^-

Metallic Reductor	Yield, %	Mean Yield, %	s
Raney nickel	90.2, 97.5, 102.0, 103.0 93.6, 95.5	97.0	4.9
Devarda alloy	95.5, 96.4, 101.1, 95.5, 99.2, 100.2	98.0	2.5
Aluminum wire	62.7, 45.3, 85.2, 84.0, 85.0	72.4	14.8

work was to develop a suitable method for potentiometric determination of iodine in organic compounds. Two methods for the liberation of organically bound iodine were compared: dehalogenation without complete destruction and mineralization. Furthermore, several metallic reductors for iodine and iodate reduction were tested. Finally, the preferred method was employed for iodine determination in pharmaceutical preparations.

EXPERIMENTAL

Apparatus—Potential readings were taken on a high-input-impedance digital pH/mv meter[1]. Potentiometric measurements were carried out using an iodide-specific electrode[2] in conjunction with a single-junction reference electrode[3] in a thermostated (25.0 ± 0.1°) polyethylene vessel.

Reagents—All reagents were analytical grade. Reductors were Devarda alloy[4], nickel–aluminum alloy (50:50)[5], and aluminum wire[6]. Raney nickel was prepared from the nickel–aluminum alloy according to a literature procedure (19).

A stock solution of 1000 ppm of I^- was prepared with dried sodium iodide. The solution was standardized by potentiometric titration using a silver nitrate solution. A stock potassium iodate solution (equivalent to 1000 ppm of I^-) was prepared by dissolving 1.6864 g of potassium iodate in 1 liter of water.

Iodine Determination in Pharmaceutical Compounds without Preliminary Destruction—The method proposed by Paletta and Pazenbeck (14) was followed except that an aluminum spiral, 30 cm in length, was used instead of aluminum foil. The wire was activated before use by boiling for 20 min in 1 *N* NaOH. The iodide determination was performed with and without neutralization of the solution with 1 *N* HCl.

Reductor Testing—The following reductors were tested: Devarda alloy powder at room temperature, Raney nickel at 55°, and aluminum wire at 60°. A 5-ml volume of iodate solution was mixed with 20 ml of 5 *M* NaOH. After shaking for 30 min at the respective temperatures, the solution was cooled, filtered, and made up to 100 ml with water. This solution was diluted 1:1 with 2 *M* KNO_3, and the iodide content was determined by direct potentiometry. Appropriate standards prepared from the iodide stock solution were treated in the same manner.

Potentiometric Determination of Iodine in Pharmaceutical Compounds after Schöniger Combustion[7] (Preferred Method)—An amount of sample[8] containing ~5 mg of iodine was weighed accurately on ashless paper[9]. A 20-ml volume of 5 *M* NaOH was used as the absorption liquid. The combustion was carried out in a Schöniger flask filled with oxygen.

After combustion, the content of the combustion flask was transferred quantitatively to a conical flask. After 1 g of Devarda alloy powder was added, the mixture was shaken for 30 min at room temperature, filtered into a 100-ml volumetric flask, and made up to volume with water.

This solution was diluted 1:1 with 2 *M* KNO_3. The iodide content was determined by direct potentiometry, using a calibration curve obtained by standards treated in the same manner.

[1] Model 801, Orion Research, Cambridge, Mass.
[2] Model 94-53, Orion Research, Cambridge, Mass.
[3] Model 90-01, Orion Research, Cambridge, Msss.
[4] U.C.B., Brussels, Belgium.
[5] Catalytic quality, B.D.H. Chemicals, Poole, England.
[6] Carlo Erba, Milan, Italy.
[7] Model mikro K, Heraeus, Hanau, Germany.
[8] Tablets are ground first; solutions are spotted directly or after dilution on ashless paper.
[9] Whatman.

Table II—Iodine Determination in Pharmaceutical Compounds

Compound Analyzed	Iodine Calculated, %	Iodine Measured, %	Mean Yield, %
		Preferred Method	
Ipodate sodium	61.4	61.6, 61.6, 60.9, 61.2, 61.1, 61.5, 60.5, 61.8, 62.5, 61.5	100.0 ± 0.9
Ipodate calcium	61.7	61.5, 61.1, 62.2	99.8
Ioglycamic acid	67.5	63.4, 63.3, 64.1, 64.9	94.7
Iodomethamate sodium	51.5	47.5, 47.5	92.3
Iothalamic acid	62.0	63.1, 64.1, 64.1, 62.1	102.2
Amidotrizoic acid	62.0	59.3, 59.4, 59.1	95.6
Iopydol	60.3	57.7, 57.8, 58.0	95.9
Iodipamide	66.8	68.4, 66.3, 67.3, 67.0	100.7
Iobenzamic acid	57.5	57.0, 58.2, 57.0	99.8
Liothyronine sodium	56.6	53.5, 54.0, 54.6	95.5
		BP Method	
Ipodate sodium	61.4	60.3, 60.5, 60.6, 60.5, 264.3, 61.3	99.7 ± 2.5

RESULTS AND DISCUSSION

The quantitative liberation of organically bound iodine by reductive dehalogenation (14) was used for the determination of iodomethamate sodium, an X-ray contrast product: iodine calculated (%), 51.4; iodine found after neutralization (%), 10.6, 17.1, 19.9, 18.1, 20.2, and 13.8; yield (% of given content), 32.3; iodine found without neutralization (%), 38.2, 35.7, and 38.2; and yield (% of given content), 72.6. The recovery was very poor with neutralization. The aluminum hydroxide precipitate, which is formed at a neutral pH, might have adsorbed iodide ions so that the latter could not be detected by the electrode. To avoid precipitation, the determination was also performed without neutralizing the solution with hydrochloric acid after reduction; the recovery was better but not satisfactory.

These findings suggest that this procedure was not able to liberate quantitatively the organically bound iodine and that a mineralization of the organic product is required. The Schöniger combustion was chosen over other mineralization methods because it is the least time consuming. However, with this method, the liberated halogen will be present as iodate and iodine, which cannot be detected potentiometrically by the iodide electrode. Hence, a reduction step is necessary to convert the iodate and iodine to iodide. Metallic reductors that can be removed from the solution after the reduction step are indicated for this purpose; otherwise, reductors can damage the electrode surface (20).

The performance of several iodate reductors was tested (Table I). Comparable yields were obtained with Raney nickel and Devarda alloy, but the latter was preferred because the dispersion on the results was smaller. The recovery with the aluminum wire was much lower.

The quantitative liberation of organically bound iodine with Devarda alloy, but without combustion, was tested on ipodate sodium. Since the mean recovery was only 43.6%, preliminary destruction was necessary.

The iodine contents of the pharmaceutical compounds were determined after Schöniger combustion (Table II). The iodine recovery was at least 95% except for one compound. The lower yield obtained for the iodomethamate sodium sample can be explained by its possible obsolescence. Unfortunately, a new sample could not be obtained from the manufacturer.

The precision of the method was 0.9%. These results were compared with those obtained with the method proposed by the British Pharmacopoeia (21) for the determination of organically bound iodine in ipodate sodium. The method involves volumetric titration with sodium thiosulfate after quantitative oxidation of iodine to iodate (Table II). A comparison of these values with those obtained with the developed method for ipodate sodium shows that the recovery was nearly the same. The potentiometric method precision was slightly better. The latter method is preferable for routine analysis because it is less cumbersome.

Table III—Iodine Determination in Pharmaceutical Preparations

Active Compound	Iodine Calculated, %	Iodine Measured, %	Mean Yield, %
		Tablets	
Iodochlorhydroxyquin, 200 mg	41.5	31.0[a], 40.8[b], 27.4[a], 39.9[b]	70.3[a], 97.2[b]
Iobenzamic acid, 750 mg	57.5	53.2[a], 57.6[b], 54.0[a], 58.7[b]	93.2[a], 101.2[b]
		Suspensions/Solutions	
Ipodate calcium, 3 g/8 g	61.7	61.5, 61.6	99.8
Iodomethylhexamethylenetetramine, 250 mg/ml	45.0	44.9, 44.9	99.7
		Ampuls	
Iodazine, 5 mg/ml	63 8	61.1, 59.9	94.8
Meglumine amidotrizoate, 650 mg/ml	47.1	46.4, 48.6	100.0
Meglumine iodipamide, 300 mg/ml	49.8	50.7, 50.3	101.5
Ioglycamic acid, 260 mg/ml	67.5	66.4, 66.4	98.3
Meglumine iothalamate, 600 mg/ml	47.0	47.4, 48.5, 47.4	101.5
Meglumine iocarmate, 604 mg/ml	46.4	45.2, 46.6, 47.0	99.8

[a] The active compound was extracted with a suitable solvent from the ground sample. [b] Direct determination on the ground sample without the extraction step.

The developed method also was applied to check the active compound content of pharmaceutical preparations. Tablets, suspensions, and solutions were analyzed. For tablets, the determination was performed on the ground tablet and for two preparations after extraction with a suitable solvent. Pyridine was used for iodochlorhydroxyquin, and dioxane was used for iobenzamic acid. A known volume of the obtained solution was then spotted on ashless paper.

All recovery values obtained for the pharmaceutical preparations were between 94.8 and 101.5% (Table III). For the tablets, however, the yield was better when the determination was performed directly on the ground tablet instead of on the extract, which shows that the extraction of the active compound was incomplete.

The proposed method yields accurate and reproducible results for the determination of organically bound iodine in pharmaceutical compounds. It is useful for routine analysis and is sensitive enough to determine the active compound in unit doses.

REFERENCES

(1) E. Papp and E. Pungor, *Z. Anal. Chem.*, **250,** 31 (1970).

(2) J. Kálmán, K. Tóth, and D. Küttel, *Acta Pharm. Hung.*, **42,** 152 (1972).

(3) E. Pungor, K. Tóth, and M. K. Pápay, *Chem. Anal.*, **17,** 947 (1972).

(4) L. Mázor, M. K. Pápay, and P. Klatsmányi, *Talanta*, **10,** 557 (1963).

(5) R. Willemart and J. Robin, *Ann. Pharm. Fr.*, **21,** 423 (1963).

(6) F. Pellerin, *ibid.*, **28,** 685 (1970).

(7) Y. M. Dessouky, K. Tóth, and E. Pungor, *Analyst*, **95,** 1027 (1970).

(8) W. Potman and E. A. M. F. Dahmen, *Mikrochim. Acta*, **1972,** 303.

(9) S. S. M. Hassan, *Z. Anal. Chem.*, **266,** 272 (1973).

(10) R. C. Rittner and T. S. Ma, *Mikrochim. Acta*, **1976,** 243.

(11) F. Friedrich and K. Kottke, *Zentralbl. Pharm.*, **115,** 235 (1976).

(12) L. Mázor, "Analytical Chemistry of Organic Halogen Compounds," Akadémiai Kiadó, Budapest, Hungary, 1975.

(13) R. A. Egli, *Z. Anal. Chem.*, **247,** 39 (1969).

(14) B. Paletta and K. Pazenbeck, *Clin. Chim. Acta*, **26,** 11 (1969).

(15) W. Schöniger, *Mikrochim. Acta*, **1955,** 123.

(16) *Ibid.*, **1956,** 869.

(17) I. C. Popescu and M. Halalau, *Rev. Chim.*, **27,** 161 (1976).

(18) B. Paletta, *Mikrochim. Acta*, **1969,** 1210.

(19) J. Mertens and D. L. Massart, *Bull. Soc. Chim. Belg.*, **80,** 151 (1971).

(20) "Instruction Manual for Halide Electrodes," Orion Research, Cambridge, Mass., 1974.

(21) "British Pharmacopoeia 1973", Pharmaceutical Press, London, England, 1973, p. A93.

ACKNOWLEDGMENTS

The authors thank A. Schoonjans and J. Lambrecht for technical assistance and F.G.W.O. for financial assistance.

Development of Radioimmunoassay for Guanethidine

L. J. LOEFFLER *x and A. W. PITTMAN ‡

Received January 19, 1979, from the *Divisions of *Medicinal Chemistry and ‡Pharmacy Practice, School of Pharmacy, University of North Carolina at Chapel Hill, Chapel Hill, NC 27514.* Accepted for publication May 23, 1979.

Abstract □ A radioimmunoassay was developed for measuring plasma concentrations of the antihypertensive agent guanethidine at the nanogram level. Guanethidine was conjugated covalently to human serum albumin by two procedures, and the degree of conjugation was determined using tracer amounts of ^{3}H-guanethidine. Immunization of sheep with various conjugates afforded antiserums with specificity for guanethidine, as determined in competitive binding studies using ^{3}H-guanethidine and a dextran-coated charcoal technique for the separation of free and antibody-bound drug. The major human metabolites, an *N*-oxide and a ring-opened derivative, were not cross-reactive in antibody binding studies. Constituents of human plasma or serum do not appear to interfere with the assay. Preliminary results from immunoassay of plasma samples from patients receiving guanethidine indicate potential use for assessing dosage regimens and studying pharmacokinetics.

Keyphrases □ Guanethidine—radioimmunoassay, human plasma, nanogram level □ Antihypertensive agents—guanethidine, radioimmunoassay, human plasma, nanogram level □ Radioimmunoassay—guanethidine, human plasma, nanogram level

A need exists for an improved quantitative assay for the antihypertensive guanethidine[1] (I). Such a method should be simple, inexpensive, and clinically applicable with high sensitivity (nanogram or picogram level) and specificity. A radioimmunoassay could fill this need, making possible improved clinical monitoring of patient dosage regimens and the acquisition of pharmacokinetic data, the analysis of which could lead to more effective therapy.

BACKGROUND

A literature review (1–8) indicated that pharmacokinetic information concerning the absorption, distribution, and elimination of orally administered guanethidine sulfate is conflicting and has limited clinical applicability. Difficulties in applying this research to patient care may stem from insufficient assay sensitivity (and, in some cases, specificity), which has precluded the evaluation of samples containing very low guanethidine concentrations. Conflicting data may have arisen because plasma levels were not sampled over an adequate period.

Bioavailability studies comparing the usual oral dosage form with drug administered intravenously or as an aqueous oral solution have not been completed. Loading dose regimens for guanethidine have been developed (8–11). These efforts were in patients who did not demonstrate remarkable renal insufficiency. This previous research did not consider the influence of renal function on the drug disposition, and the pharmacokinetic parameters used in those dosage regimens may have been derived empirically.

In assessing the relationship between the guanethidine dose and the hypotensive response, Walter *et al.* (12) utilized the most definitive analytical technique for guanethidine (13); it determines guanethidine in biological fluids by GLC with flame-ionization detection or multiple-ion detection (mass spectrometry). Although this assay is specific and sensitive to concentrations as low as 1 ng/ml, the complexity of the manipulations (extractions and hydrolyses) and the limited availability and expense of the assay equipment (GLC–mass spectrometry and its operation) reduce its applicability in clinical studies.

Other methods for guanethidine appear to lack the desired sensitivity (and, in some cases, the specificity) for clinical studies. Briefly, these methods involve preliminary extraction and/or chromatographic procedures followed by quantitation *via* colorimetry (14–18) or fluorometry (19–21) and are not useful below microgram or milligram levels. The use of radiolabeled drug affords sensitivity to nanogram or picogram quantities (22); however, specificity for the drug and metabolites is not achieved.

Any analytical procedure for guanethidine must enable its determination in the presence of known metabolites and other interfering substances. The literature on guanethidine metabolism was reviewed recently (23), particularly the work of four research groups (19, 23–25). In two of the studies, direct metabolites were identified, the first involving ring *N*-oxide formation and the second involving ring α-hydroxylation followed by hydrolysis to a ring-opened amino acid (Scheme I, Structures II and III).

This paper describes the development of a sensitive and specific radioimmunoassay for guanethidine and some initial results on its clinical application.

EXPERIMENTAL

Materials—The following were used: human serum albumin[2] (crystalline, B grade); bovine serum albumin[2] (crystalline, A grade); guanethidine sulfate[3]; Freund's complete adjuvant[4]; dextran[5]; charcoal[5]; formalin solution[6]; commercial liquid scintillation fluid[7]; guanethidine metabolites 2-(octahydro-1-azocinyl-1-oxido)ethylguanidine[8] ("guanethidine-*N*-oxide"), 2-(6-carboxyhexylamine)ethylguanidine[8] ("ring-opened metabolite"), and 1-(6-carboxyhexyl)-2-iminoimidazolidine (a possible artifact arising from ring closure of the ring-opened metabolite)[8]; and ^{3}H-guanethidine[8] of low specific activity (62 mCi/mmole) (labeled on the C-2 of the ethyl group) (26).

Tritiated material of high specific activity (~300 mCi/mmole) was prepared commercially[9] and purified as described later. Liquid scintillation counting was accomplished using a spectrometer[10] with internal standardization to compute efficiency and disintegrations per minute in individual samples.

Coupling of Guanethidine to Human Serum Albumin (Scheme II)—Two methods involving formaldehyde as a coupling reagent were employed, one in glacial acetic acid and the other with sodium acetate in an aqueous medium (27). To 2.0 g of guanethidine sulfate in 20 ml of water was added 4 ml of ethanol containing approximately 2×10^6 cpm of ^{3}H-guanethidine[8]. The solution was evaporated *in vacuo* to dryness. After addition of 6 ml of cold 30% KOH, the free base was extracted into 5 × 50 ml of chloroform. The combined extracts were dried over magnesium sulfate and evaporated, affording 0.40 g of free base, which was stored under nitrogen.

Coupling Method A—To 82 mg of free base in 3.6 ml of glacial acetic acid was added 400 mg of human serum albumin in 4 ml of distilled water. Formaldehyde solution (38%), 2.4 ml, was added to this clear mixture. The mixture was heated and stirred at 50° under nitrogen for 1 hr and then stirred overnight at room temperature. The resulting clear solution was dialyzed *versus* several portions of distilled water until negligible radioactivity was detected in the dialysates. Scintillation counting of both dialysates and bag contents indicated 5.8 moles of guanethidine bound/mole of serum albumin based on a molecular weight of 70,000. The product was lyophilized to a white powder and stored in the cold.

Coupling Method B (28)—To 200 mg of human serum albumin in 2 ml of distilled water was added 2.0 ml of 3 *M* sodium acetate. Formaldehyde solution (38%), 4.0 ml, was added, and the mixture was stirred for 5 min at room temperature. A solution of 28 mg of guanethidine (free base) in 1 ml of water was added. The mixture was stirred under nitrogen

[1] Guanethidine sulfate (Ismelin), Ciba-Geigy Corp., Summit, NJ 07901.

[2] Calbiochem Corp.
[3] Ciba-Geigy Corp., Summit, NJ 07901.
[4] Difco Laboratories.
[5] Radioimmunoassay grade materials, Schwarz/Mann.
[6] J. T. Baker Chemical Co.
[7] Scintaverse, Fisher Chemical Co.
[8] Gift of Dr. D. F. Elliott, Ciba Laboratories, Horsham, England.
[9] New England Nuclear.
[10] Model 3255, Packard Instrument Co., Downers Grove, Ill.

0022-3549/79/1100-1419$01.00/0
© 1979, American Pharmaceutical Association

Table I—Data for Typical Guanethidine Standard Radioimmunoassay Curve

Tube	Buffer[a], ml	Bovine Serum Albumin[b], ml	Antiserum[c], ml	Guanethidine (Cold)[d] Milliliters	Guanethidine (Cold)[d] Nanograms	^{3}H-Guanethidine[e], ml	Dextran-Coated Charcoal[f], ml
1	1.30	0.10	—	—	—	0.10	—
2	0.80	0.10	—	—	—	0.10	0.50
3	0.70	0.10	0.10	0	0	0.10	0.50
4	0.68	0.10	0.10	0.02	2.0	0.10	0.50
5	0.66	0.10	0.10	0.04	4.0	0.10	0.50
6	0.62	0.10	0.10	0.08	8.0	0.10	0.50
7	0.50	0.10	0.10	0.20	20.0	0.10	0.50
8	0.60	0.10	0.10	0.10[g]	100.0	0.10	0.50

[a] Buffer was 0.15 *M* NaCl and 0.01 *M* sodium phosphate, pH 7.4. [b] Crystalline bovine serum albumin 2× (Armour). [c] Guanethidine antiserum was diluted 1:60 with buffer (final dilution 1:600 in tube). [d] Guanethidine (cold) was 0.10 ng/μl in buffer (used 2–100 ng in curve). [e] ^{3}H-Guanethidine was 0.1 ng/μl in buffer (12 ng/tube, ~1500 dpm). [f] Dextran-coated charcoal suspension contained 0.01 g of immunoassay grade charcoal per milliliter and 0.25 mg of dextran (immunoassay grade) per milliliter. [g] Concentration was 1.0 ng/ml in buffer.

at room temperature, dialyzed, and lyophilized as in Method A. Counting of tracer ^{3}H-guanethidine indicated 33 moles of guanethidine bound/mole of serum albumin.

Immunization Procedure and Schedule—Each guanethidine–albumin conjugate was injected intramuscularly (two sheep per conjugate) at several injection sites (shoulders and flanks) at monthly intervals. Initial and subsequent injections consisted of 3 mg of conjugate in 1.5 ml of physiological saline emulsified with 1.5 ml of Freund's complete adjuvant. Bleedings were made from the neck vein approximately 7–10 days after each monthly booster injection. To date, three of the four sheep have been boosted and bled for 18 months. Serum was frozen after the addition of thimerosal (final concentration, 0.01%) as an antibacterial.

Titer Determination—Individual serum samples were evaluated by serial dilution for their ability to bind 12 ng of ^{3}H-guanethidine in the absence of added nonradioactive guanethidine. For this evaluation, 100-μl samples of antiserum dilutions were used as described later. In routine work, the antiserum dilution giving 40–60% binding was optimum.

Standard Radioimmunoassay Curve for Guanethidine—Table I indicates the order of reagent addition and the contents of various triplicate assay tubes utilized in the construction of a typical standard radioimmunoassay curve. Polystyrene test tubes (5 ml, 12 × 75 mm) were used. Bovine serum albumin (0.5%) was added to the buffer to minimize adsorption of ^{3}H-guanethidine[8] (62 mCi/mmole) and cold guanethidine onto the vessel walls, although no evidence for such adsorption had been observed. Antiserum was freshly diluted from stock on the day of use.

Following the antiserum addition, various quantities of cold guanethidine and 12 ng of ^{3}H-guanethidine (~1500 dpm) were added to each tube. The tubes were incubated at 37° for 2 hr and chilled in ice for 30 min. Then 0.5 ml of dextran-coated charcoal suspension was added to the desired tubes (Table I, footnote *f*). After vortexing, suspensions were left at 0° for exactly 15 min and then centrifuged at 2° for 10 min.

Exactly 1.0 ml of the supernate was removed carefully by automatic pipet and counted in 10 ml of scintillation cocktail in a counting vial. Percent binding figures were calculated. Nonspecific binding (~3%) was obtained from Tube 2 figures and subtracted from the total percentage figures observed for all tubes. In specificity (cross-reactivity) studies, cold guanethidine was replaced with desired quantities of the test compound. In the assay of clinical samples, up to 0.1 ml of unknown plasma or serum was employed, with pooled control plasma in all tubes.

Synthesis of Randomly Labeled ^{3}H-Guanethidine of Increased Specific Activity—Guanethidine sulfate, 50 mg, was dissolved in 0.3 ml of dry dimethylformamide and heated overnight at 80° with 100 mg of 5% rhodium-on-aluminum oxide catalyst and 25 Ci of tritiated water[9]. After removal of excess tritiated water, purification was accomplished as follows. Approximately 45 μCi (100 × 10^6 dpm) of crude material was dissolved in 200 μl of water and placed on a column of 1.0 g of Dowex 50× (acid form, 100–200 mesh, 4% cross-linked), packed in a Pasteur pipet. Upon elution with water in 1-ml fractions, 25% of the radioactivity was recovered in the first five fractions. The remainder of the material was eluted in one peak with 5 *N* HCl, collected in approximately 10 fractions. The peak fractions were checked for purity by TLC and paper chromatographic radioscan [solvent systems: 2-butanol–3% (v/v) ammonia (3:1), R_f 0.8; and *n*-butanol–acetic acid–water (40:10:50), R_f 0.3 (20)]. The product was estimated by isotope dilution to have a specific activity of 300 mCi/mmole, or five times that of material obtained previously[8].

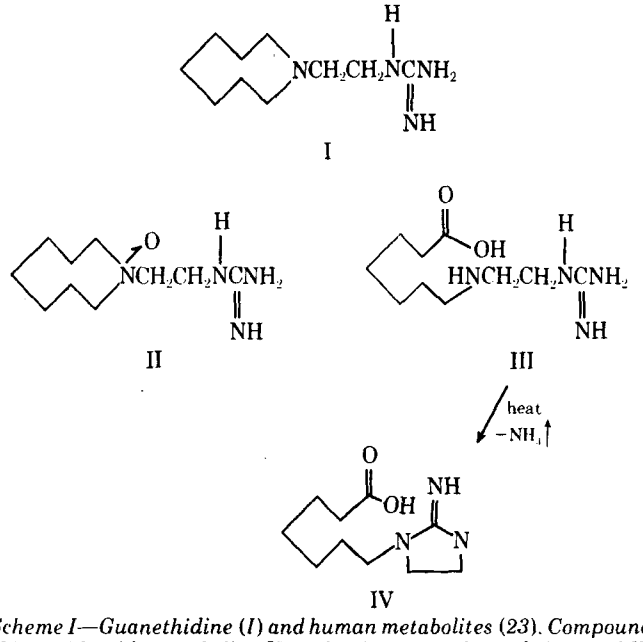

Scheme I—Guanethidine (I) and human metabolites (23). Compound II is the N-oxide metabolite, III is the ring-opened metabolite, and IV is a probable artifact of the isolation workup, involving cyclization of III.

RESULTS AND DISCUSSION

Antigen and Antiserum Preparation—It appeared desirable in antigen preparation to utilize the terminal guanidino group of the hapten guanethidine for attachment to a protein carrier. This approach would leave unaltered immunodeterminant features near the metabolism sites, favoring the formation of antibody specific for guanethidine (I) and not the major metabolites, the *N*-oxide (II) and the ring-opened product (III) (Scheme I). Three coupling methods were employed successfully; how-

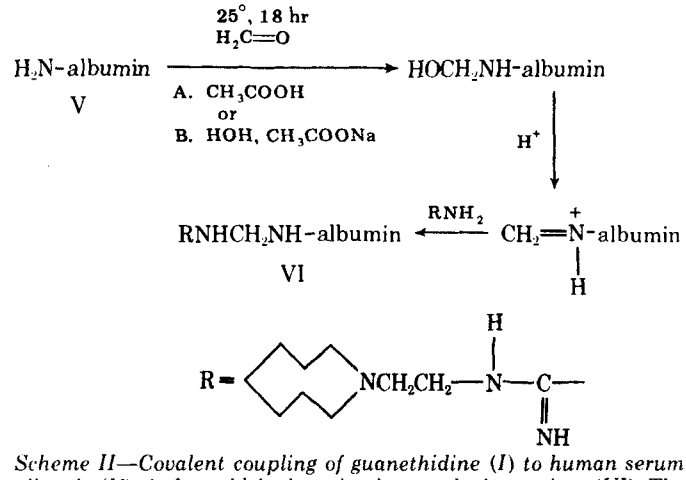

Scheme II—Covalent coupling of guanethidine (I) to human serum albumin (V) via formaldehyde activation, producing antigen (VI). The guanethidine–albumin ratio in Method A was 5.8; in Method B, it was 33.

Table II—Reproducibility in the Assay of Known Quantities of Guanethidine

Sample	Guanethidine Added, ng/ml	Guanethidine Found, ng/ml[a] Mean (n = 3)	CV, %
1	2.00	2.07	±6.4
2	5.00	4.68	±3.8
3	10.0	9.77	±7.8
4	20.0	19.8	±8.9
5	50.0	48.1	±3.3

[a] Each value is the mean of three individual samples and the coefficient of variation of individual samples from this mean ($SD \times 100$/mean). The guanethidine content of each sample was calculated from a percentage binding figure, and a standard curve was constructed from the means of samples run in triplicate.

ever, only the formaldehyde method produced antiserum of useful titer (Scheme II). Tracer quantities of ^{3}H-guanethidine were added to the reaction media to enable ready calculation of the ratio of drug to albumin in the conjugate. With formaldehyde in glacial acetic acid (Method A), this ratio was 5.8 moles of guanethidine/mole of albumin. With formaldehyde in water containing sodium acetate (Method B) (28), this figure increased to 33 moles of guanethidine/mole of albumin.

With a mechanism of coupling involving only lysine amino groups (tryptophan and imidazole also might be involved), the maximum ratio for albumin would be about 60. Two other coupling procedures were employed to move the hapten guanethidine moiety further away from the protein, perhaps improving titer and specificity. The first procedure, involving the reaction of guanethidine with succinic anhydride followed by water-soluble carbodiimide coupling of the newly generated terminal carboxyl group to albumin, resulted in a hapten to protein ratio of 4–5:1. The second procedure involved initial selective coupling of toluene-2,5-diisocyanate (29) to albumin at pH 7.4 (at the 5-position) and coupling of the more hindered 2-isocyanate group to guanethidine at pH 9.0. In this case, a hapten to protein ratio of 13 was obtained. Unfortunately, however, neither the succinic anhydride nor the diisocyanate conjugates elicited antiserum of useful titer with the animals and conditions employed.

Immunization of four sheep with the two formaldehyde conjugates (two sheep per conjugate) was accomplished as discussed under *Experimental.* All four sheep produced antibodies after 2–3 months, two of titer approximately 1:600. The highest titer serum was taken from the two sheep immunized with the conjugate of the lower hapten to protein ratio of 5.8. All sheep have now been bled monthly for 18 months, with the titer remaining essentially constant, dropping off slightly only in one animal. This relatively low titer probably could be increased considerably with radiolabeled guanethidine of higher specific activity, either a tritiated or an iodinated derivative (^{125}I). Antiserum stored frozen in small portions has shown no evidence of loss of guanethidine binding ability.

Standard Immunoassay Curve—Because of interest in radiolabeled material of higher specific activity (enabling increased sensitivity), exhaustive work has not been carried out to determine optimum assay conditions with available tritiated material. Nevertheless, the assay appears to be reproducible and directly clinically applicable for guanethidine concentrations above 4–5 ng/ml of plasma or serum.

The order of reagent addition and the contents of various triplicate assay tubes utilized in the preparation of a typical standard curve are indicated in Table I. Antiserum was freshly diluted from frozen stock serum on the day of use. Fresh solutions of ^{3}H-guanethidine and cold standard guanethidine also were prepared daily by dilution of more concentrated frozen stock solutions. The entire process, including the incubation and subsequent charcoal adsorption, was completed in ~4 hr.

Data for a typical standard immunoassay sigmoid curve are plotted in Fig. 1. Each medium of different composition was run in triplicate. The data in Fig. 1 include typical results for standard deviations of triplicate samples. Curves could be linearized *via* logit transformation procedures to extend the useful range of application and enable curve fitting and computer interpolation. However, this was not done routinely because the errors found by utilizing points at the logit curve ends were much larger than those encountered by diluting samples so that they fall within the central portion of the sigmoid curve. If assay conditions were controlled, the standard curve varied only slightly; however, at least five points on the curve were always incorporated into each day's work. No significant differences were observed by altering the incubation times between 1 and 4 hr at 37° or varying the time of incubation with dextran-coated charcoal between 15 and 30 min at 0°.

Table III—Recovery of Guanethidine Added (50 ng/ml) to Patient Serum Samples in Various Concentrations

Sample	Guanethidine, ng/ml Found in Original Sample[a]	Guanethidine, ng/ml Total Found	Recovery of Added Guanethidine[d], %
GC	57	106	98
ML	76	120	88
PL	16	62	92
PL	26	74	96
CM	14	61	94
CM	28	73	90
CM	29	80	102
CM	43	101	116

[a] Values are the averages of two separate assays done in triplicate. Percentage recovery figures, therefore, reflect errors in the original assay, errors in the addition step, and errors in the assay of the "spiked" sample. Whole serum samples were used, and all necessary dilutions were repeated after spiking. [b] Average deviation of recovery from 100% was −3%.

Nonspecific binding in the absence of antiserum amounted to about 3%, and this figure was subtracted from samples containing antiserum. The addition of up to 10% (0.1 ml/ml) pooled normal human serum or plasma to the assay tubes did not appear to alter the shape or position of the curve, nor did heparin, disodium ethylenediaminetetraacetic acid, or citrate in normal concentrations utilized for anticoagulation. Preliminary experiments also indicate that the assay is applicable to urine analysis.

Sensitivity—For blood guanethidine levels observed during patient loading protocols, conditions giving the curve shown in Fig. 1 were most convenient. The reliable concentration range with the ^{3}H-guanethidine (64 mCi/mmole) employed was about 2–20 ng in the assay. Since 0.10-ml plasma aliquots were used, this level corresponds to a direct measurement in the range of 20–200 ng/ml of plasma. Use of ^{3}H-guanethidine of specific activity 300 mCi/mmole (2.5 ng/assay tube) enabled an increase in sensitivity to about 4–5 ng/ml of plasma (lower limit of 0.4–0.5 ng in the assay). This curve is not shown but affords a useful range of 4–~50 ng/ml of plasma.

Walter *et al.* (12) reported therapeutic levels of guanethidine as assayed by the method of Hengstmann *et al.* (13) to be 8–17 ng/ml. Therefore, as it stands, the immunoassay sensitivity, while adequate for the measurement of levels observed during loading or during "normal" therapeutic control, is not adequate for detailed pharmacokinetic studies. Consideration of the literature and practical experience at North Carolina Memorial Hospital indicate that such a procedure could contribute significantly to pharmacokinetic studies if it were sensitive to levels below 1 ng/ml, perhaps 0.1 ng/ml. It is plausible that accurate mathematical (pharmacokinetic) statements describing guanethidine elimination from plasma of normal volunteers or hypertensive patients can be made, providing the terminal elimination phase can be evaluated until guanethidine concentrations decline to such levels (27). Efforts to increase assay sensitivity through synthesis of hotter tritiated material or a suitably iodinated (^{125}I) derivative are in progress.

Specificity—Studies of cross-reactivity and antibody specificity were carried out on major metabolites II and III and the isolation artifact IV (23); the concentrations at which these compounds reduced binding of ^{3}H-guanethidine (12 ng) were compared to the concentration of guanethidine (cold) that had the same effect. Approximately 1% cross-reactivity was observed with the *N*-oxide (II); less than 0.1% was observed with the ring-opened metabolite (III) and IV. Antihypertensive agents diazoxide, methyldopa, hydralazine, and furosemide showed less than 0.1% cross-reactivity. To date, all of these specificity studies have been performed on bleedings from one sheep, with three bleedings appearing to be essentially identical.

Assay Reproducibility and Recovery Studies (30, 31)—Table II indicates the reproducibility of the assay as measured in prepared standards (10% pooled human plasma), giving means and coefficients of variation for amounts found *versus* amounts actually added. Results are based on triplicate tubes for each unknown concentration. These results were derived by using a standard curve similar to Fig. 1.

Recovery studies were conducted using actual plasma samples. Sample guanethidine content was measured on several patients (Table III). Selected samples encompassing a wide concentration range were "spiked" with 50-ng amounts of standard guanethidine and reassayed for total guanethidine. Recovery, expressed as percent, indicates that drug added to each original plasma sample over a range of concentrations is recovered in quantities between 88 and 116% (mean = 97%).

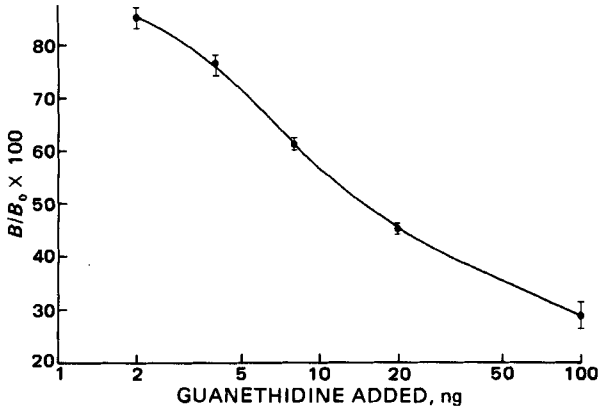

Figure 1—*Typical radioimmunoassay curve for guanethidine [serum dilution 1:600 (Sheep 37, 3-month bleeding), 12 ng of ^{3}H-guanethidine (62 mCi/mmole)]. Key: B_0, percent binding minus nonspecific binding in absence of cold guanethidine (maximum binding); and B, percent binding minus nonspecific binding in presence of cold guanethidine.*

Clinical Application during Patient Loading—Plasma concentrations have been monitored in several hypertensive patients receiving guanethidine as part of their antihypertensive regimen. Data on one patient are presented in Fig. 2. Patient CM was a 30-year-old male undergoing guanethidine loading. Guanethidine was given orally every 8 hr during the loading period as 50 mg of the sulfate. The therapeutic end-point was considered to be a standing diastolic (phase V) blood pressure in the 90–100-mm Hg range 8 hr after a 50-mg dose. In this patient, loading was reinstituted when concomitant hydralazine doses were halved and clinical effectiveness of the total therapeutic regimen diminished.

In Fig. 2, plasma guanethidine concentrations are shown superimposed on the total guanethidine dose administered during a single day. All determinations were made on plasma collected immediately prior to the administration of loading doses. Samples associated with maintenance doses were obtained approximately 26 hr following previous doses or, on two occasions, at 3 hr after the daily dose. Preliminary assessment of the utility of the analysis of plasma guanethidine concentrations suggests that monitoring during the administration of loading doses has limited interpretability. Variation in absorption from available tablets and, more importantly, the effects of the time necessary for complete tissue distribution may explain the observed fluctuations in plasma concentrations. Nevertheless, plasma level monitoring when steady state is approached represents a rational mechanism to assist in the evaluation of the clinical effectiveness of guanethidine. More complete data on patients over an extended time will be of interest.

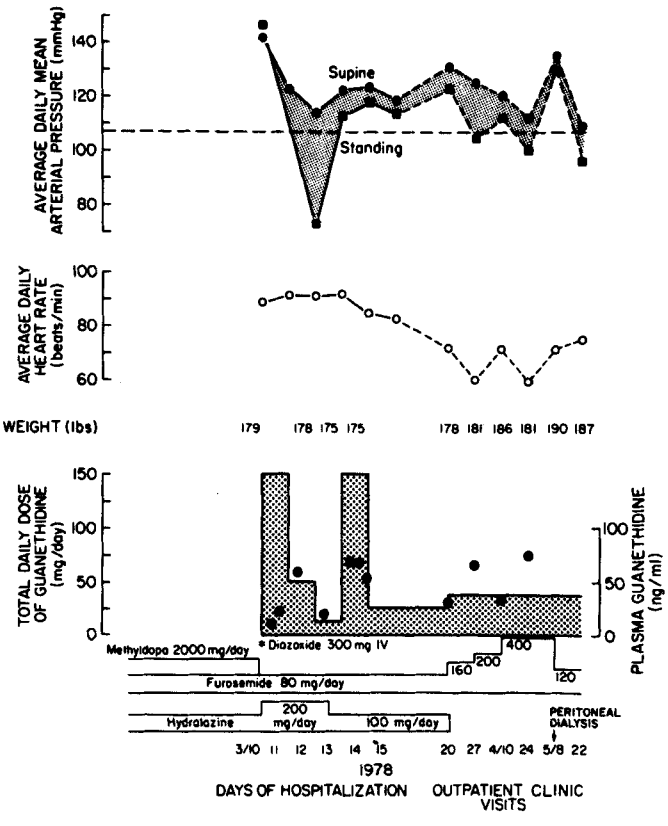

Figure 2—*Clinical application: response to guanethidine loading in a 30-year-old male with severe hypertension and renal insufficiency (Patient CM). Guanethidine levels in nanograms per milliliters are shown superimposed on lower bar graph (solid circles).*

Evaluation and Potential of Immunoassay Technique—In its present state, the assay described represents a rapid and direct method for the determination of plasma or serum guanethidine levels at concentrations encountered clinically without interference from major metabolites [which are inactive (23)], other antihypertensive agents, or common anticoagulants employed in blood collection tubes. Extractions or chromatographic purification procedures are avoided, and the determination is accurate to 4–5 ng/ml with an error of less than ±10%. Access to expensive equipment (*e.g.*, a mass spectrometer) with a skilled operator is obviated, with only scintillation counting instruments required.

Further work in progress using tritiated material of higher specific activity or a suitably labeled guanethidine analog containing iodine 125 should increase the titer, sensitivity, and convenience so that levels as low as 100 pg/ml might be measured directly. Such a convenient method should facilitate greatly the acquisition of accurate clinical data for research with the following goals: description of the relationship of plasma concentration to clinical effect (as measured by blood pressure), evaluation of bioequivalence and bioavailability of the drug from various dosage forms, description of the drug's pharmacokinetics, confirmation of the influence of renal function on guanethidine elimination from plasma, development and evaluation of loading dose regimens based on pharmacokinetic parameters, and overall provision of more rational methods for the selection of guanethidine dosages.

REFERENCES

(1) K. H. Rahn and L. T. Goldberg, *Clin. Pharmacol. Ther.*, **10**, 858 (1969).

(2) D. McMartin and P. Simpson, *ibid.*, **12**, 73 (1970).

(3) C. McMartin, R. K. Rondel, J. Vinter, B. R. Allan, P. M. Humberstone, A. W. D. Leishman, G. Sandler, and J. L. Thirkettle, *ibid.*, **11**, 423 (1970).

(4) K. H. Rahn, *Clin. Nephrol.*, **1**, 14 (1973).

(5) K. H. Rahn and W. Rupp, *Prog. Nephrol. Proc. Symp., Ges. Nephrol., 7th*, **23–25**, 55 (1971).

(6) C. T. Dollery, D. Emslie-Smith, and M. D. Milne, *Lancet*, **2**, 381 (1976).

(7) J. A. Oates, J. R. Mitchell, O. T. Feagin, J. S. Kaufman, and D. G. Shand, *Ann. N.Y. Acad. Sci.*, **179**, 302 (1971).

(8) D. G. Shand, A. S. Nies, R. G. McAllister, and J. A. Oates, *Clin. Pharmacol. Ther.*, **18**, 139 (1975).

(9) A. W. D. Leishman and G. Sandler, *Lancet*, **1**, 668 (1975).

(10) D. G. Shand, A. S. Nies, R. G. McAllister, and J. A. Oates, *Clin. Res.*, **20**, 413 (Abstr.) (1972).

(11) R. G. McAllister, *J. Clin. Pharmacol.*, **15**, 771 (1975).

(12) I. E. Walter, J. Khandelwal, F. Faulkner, and A. S. Nies, *Clin. Pharmacol. Ther.*, **18**, 571 (1975).

(13) J. H. Hengstmann, F. C. Faulkner, J. T. Watson, and J. Oates, *Anal. Chem.*, **46**, 34 (1974).

(14) S. L. Tompsett, W. Forshall, and D. C. Smith, *Acta Pharmacol. Toxicol.*, **18**, 75 (1961).

(15) S. L. Tompsett, *ibid.*, **19**, 365 (1962).

(16) B. C. Bose and R. Bigayvargiya, *J. Pharm. Pharmacol.*, **16**, 561 (1964).

(17) H. Tomankov, *Cesk. Farm.*, **19**, 96 (1970).

(18) C. N. Corder, T. Klaniecki, and R. H. McDonald, Jr., *Pharmacologist*, **15**, 194 (Abstr.) (1973).

(19) H. J. Rahn and P. G. Dayton, *Biochem. Pharmacol.*, **18**, 1809 (1969).

(20) G. M. Bisson and E. Muscholl, *Naunyn-Schmiedeberg's Arch. Exp. Pathol. Pharmakol.*, **244**, 185 (1962).

(21) R. B. Conn, Jr., and R. B. Davis, *Nature*, **183**, 1053 (1959).

(22) C. McMartin, P. Simpson, and N. Thorpe, *J. Chromatogr.*, **43**, 72 (1969).

(23) B. Lukas, *Drug Metab. Rev.*, **2**, 101 (1973).

(24) C. M. McMartin, *Biochem. Pharmacol.*, **18**, 238 (1969).
(25) C. M. McMartin and J. Vinter, *J. Chromatogr.*, **41**, 188 (1962).
(26) F. B. Abramson, C. I. Furst, C. McMartin, and R. Wade, *Biochem. J.*, **113**, 143 (1969).
(27) J. G. Wagner, "Fundamentals of Clinical Pharmacokinetics," 1st ed., Drug Intelligence Publications, Hamilton, Ill., 1975, p. 142.
(28) A. Levy, K. Kawishima, and S. Spector, *Life Sci.*, **19**, 1421 (1976).
(29) J. Haimovich, E. Hurwitz, N. Novik, and M. Sela, *Biochim. Biophys. Acta*, **207**, 115 (1970).
(30) L. J. Loeffler, M. R. Blum, and M. A. Nelsen, *Cancer Res.*, **36**, 3306 (1976).
(31) L. J. Loeffler and J. V. Pierce, *J. Pharm. Sci.*, **62**, 1817 (1973).

ACKNOWLEDGMENTS

Presented in part at the Medicinal Chemistry Section, APhA Academy of Pharmaceutical Sciences, Phoenix meeting, November 1977.

Supported in part by a grant from the University of North Carolina Research Council.

High-Pressure Liquid Chromatographic Assay for Hydralazine in Human Plasma

T. M. LUDDEN *‡x, L. K. GOGGIN *, J. L. McNAY, Jr. *, K. D. HAEGELE *, and A. M. M. SHEPHERD *

Received March 12, 1979, from the **Division of Clinical Pharmacology, Departments of Pharmacology and Medicine, University of Texas Health Science Center, San Antonio, TX 78284,* and the ‡*College of Pharmacy, University of Texas, Austin, TX 78712.* Accepted for publication June 4, 1979.

Abstract □ A specific high-performance liquid chromatographic assay for hydralazine in human plasma was developed. Plasma hydralazine is reacted with 10 μl of *p*-anisaldehyde for 7 min at room temperature to form hydralazine *p*-anisaldehyde hydrazone. This derivative is extracted into ethyl acetate, and the solvent is removed by evaporation. The residue is reconstituted in 100 μl of methanol, and 90 μl is injected onto a reversed-phase column. The mobile phase is 32% acetonitrile in 0.75 *M* acetate buffer, pH 3.4, at a flow rate of 2 ml/min. The retention time of hydralazine *p*-anisaldehyde hydrazone is 6.5 min. The average coefficient of variation over 10–200 ng/ml is 5.5%, and the sensitivity limit is 5 ng/ml. Under the assay conditions, hydralazine pyruvic acid hydrazone, a known plasma metabolite of hydralazine, yields <0.1% hydralazine. Detectable plasma hydralazine levels of 5–20 ng/ml were found 10–30 min after a 0.5-mg/kg oral dose of hydralazine hydrochloride was given to a male volunteer.

Keyphrases □ Hydralazine—extraction, high-pressure liquid chromatographic assay, human plasma □ High-pressure liquid chromatographic assay—hydralazine, human plasma □ Vasodilators—hydralazine, extraction, high-pressure liquid chromatographic assay

Hydralazine (1-hydrazinophthalazine, I) is a vasodilator used for treating hypertension (1). It undergoes extensive metabolism in humans, with detectable amounts of 3-methyl-*s*-triazolo[3,4-*a*]phthalazine, phthalazine, phthalazinone, 1-hydrazinophthalazine pyruvic acid hydrazone, 1-hydrazinophthalazine acetone hydrazone, 4-hydroxy-1-hydrazinophthalazine, and glucuronides (2–6) appearing in urine.

Previous attempts to assay I included derivatization with *p*-hydroxybenzaldehyde (7) or *p*-anisaldehyde (*p*-methoxybenzaldehyde) (8), followed by spectrophotometric determination or the conversion of I to tetrazolo[1,5-*a*]phthalazine followed by electron-capture GLC analysis (9, 10). All of these techniques are nonspecific in that acid-labile hydralazine hydrazones present in plasma, such as hydralazine pyruvic acid hydrazone, are hydrolyzed to some extent and detected as I (11).

This report describes a specific high-pressure liquid chromatographic (HPLC) assay for I in human plasma.

EXPERIMENTAL

Reagents and Chemicals—Ethyl acetate, acetonitrile, and methanol were purchased as glass-distilled solvents. No further processing was necessary. Hydralazine hydrochloride[1] and *p*-anisaldehyde[2] also were used as purchased. Hydralazine pyruvic acid hydrazone and hydralazine *p*-anisaldehyde hydrazone (II) were prepared as described previously (5) with the reaction mixture pH maintained at 7.4. The identity and purity of the synthesized products were verified by combined GLC–mass spectrometry. No by-products or starting materials were detected.

The absence of I was confirmed first by derivatizing samples of each synthetic product with bis(trimethylsilyl)trifluoroacetamide to form the *N,N'*-di-trimethylsilyl derivative of any I that might be present and then subjecting them to GLC–mass spectrometry. To demonstrate that I could be detected by this procedure, known amounts of I were added to samples of each synthetic product and assayed similarly. By this technique, it was demonstrated that the synthetic samples of hydralazine hydrazones contained <0.03% I.

Standard Curve Samples—Fresh human plasma, 1 ml, with ethylenediaminetetraacetic acid as the anticoagulant and 10 μl of *p*-anisaldehyde were placed in a 15-ml culture tube fitted with a polytef-lined screw cap. An appropriate volume, 0.5–20 μl (5–200 ng), of a fresh solution of 10 ng of I/μl of 0.1 *M* potassium phosphate buffer, pH 7.4, was added; the contents were mixed by vortexing.

After standing at room temperature (23°) for 7 min to allow formation of II, 1 ml of 0.1 *M* potassium phosphate buffer, pH 7.4, and 7 ml of ethyl acetate were added. The samples were mixed for 10 min on a reciprocal shaker, and the phases were separated by centrifugation at 1000×*g* for 2 min. The ethyl acetate was transferred to a conical tube, and the solvent was removed in a gentle nitrogen stream.

Chromatography—Each extraction residue was mixed with 100 μl of methanol, and 90 μl was injected into a high-pressure liquid chromatograph[3] equipped with a reversed-phase column[4] (3.9 mm i.d. × 30 cm) and a variable-wavelength detector[5] set at 365 nm. The mobile phase was 32% acetonitrile in 0.75 *M* acetate buffer, pH 3.4, at a flow rate of 2 ml/min.

Derivatization and Extraction—The efficiency of derivatization was determined during three analyses by comparing the II recovery from 100-ng/ml standard hydralazine samples to the II recovery from blank plasma samples to which an equimolar concentration (173 ng/ml) of II had been added prior to extraction. Extraction efficiency was evaluated during three analyses by comparing the II peak height for plasma samples to which 173 ng of II was added before extraction to the II peak height for extracts of blank plasma samples to which 173 ng had been added just before injection into the liquid chromatograph.

Specificity—To assure that I does not react with an endogenous

[1] Sigma Chemical Co., St. Louis, Mo.
[2] Eastman Kodak Co., Rochester, N.Y.
[3] Model 995, Tracor, Austin, Tex.
[4] μBondapak C_{18}, Waters Associates, Milford, Mass.
[5] Model 970, Tracor, Austin, Tex.

0022-3549/79/1100-1423$01.00/0
© 1979, American Pharmaceutical Association

(24) C. M. McMartin, *Biochem. Pharmacol.*, **18**, 238 (1969).
(25) C. M. McMartin and J. Vinter, *J. Chromatogr.*, **41**, 188 (1962).
(26) F. B. Abramson, C. I. Furst, C. McMartin, and R. Wade, *Biochem. J.*, **113**, 143 (1969).
(27) J. G. Wagner, "Fundamentals of Clinical Pharmacokinetics," 1st ed., Drug Intelligence Publications, Hamilton, Ill., 1975, p. 142.
(28) A. Levy, K. Kawishima, and S. Spector, *Life Sci.*, **19**, 1421 (1976).
(29) J. Haimovich, E. Hurwitz, N. Novik, and M. Sela, *Biochim. Biophys. Acta*, **207**, 115 (1970).
(30) L. J. Loeffler, M. R. Blum, and M. A. Nelsen, *Cancer Res.*, **36**, 3306 (1976).
(31) L. J. Loeffler and J. V. Pierce, *J. Pharm. Sci.*, **62**, 1817 (1973).

ACKNOWLEDGMENTS

Presented in part at the Medicinal Chemistry Section, APhA Academy of Pharmaceutical Sciences, Phoenix meeting, November 1977.

Supported in part by a grant from the University of North Carolina Research Council.

High-Pressure Liquid Chromatographic Assay for Hydralazine in Human Plasma

T. M. LUDDEN *‡x, L. K. GOGGIN *, J. L. McNAY, Jr. *, K. D. HAEGELE *, and A. M. M. SHEPHERD *

Received March 12, 1979, from the **Division of Clinical Pharmacology, Departments of Pharmacology and Medicine, University of Texas Health Science Center, San Antonio, TX 78284,* and the ‡*College of Pharmacy, University of Texas, Austin, TX 78712.* Accepted for publication June 4, 1979.

Abstract □ A specific high-performance liquid chromatographic assay for hydralazine in human plasma was developed. Plasma hydralazine is reacted with 10 μl of *p*-anisaldehyde for 7 min at room temperature to form hydralazine *p*-anisaldehyde hydrazone. This derivative is extracted into ethyl acetate, and the solvent is removed by evaporation. The residue is reconstituted in 100 μl of methanol, and 90 μl is injected onto a reversed-phase column. The mobile phase is 32% acetonitrile in 0.75 *M* acetate buffer, pH 3.4, at a flow rate of 2 ml/min. The retention time of hydralazine *p*-anisaldehyde hydrazone is 6.5 min. The average coefficient of variation over 10–200 ng/ml is 5.5%, and the sensitivity limit is 5 ng/ml. Under the assay conditions, hydralazine pyruvic acid hydrazone, a known plasma metabolite of hydralazine, yields <0.1% hydralazine. Detectable plasma hydralazine levels of 5–20 ng/ml were found 10–30 min after a 0.5-mg/kg oral dose of hydralazine hydrochloride was given to a male volunteer.

Keyphrases □ Hydralazine—extraction, high-pressure liquid chromatographic assay, human plasma □ High-pressure liquid chromatographic assay—hydralazine, human plasma □ Vasodilators—hydralazine, extraction, high-pressure liquid chromatographic assay

Hydralazine (1-hydrazinophthalazine, I) is a vasodilator used for treating hypertension (1). It undergoes extensive metabolism in humans, with detectable amounts of 3-methyl-*s*-triazolo[3,4-*a*]phthalazine, phthalazine, phthalazinone, 1-hydrazinophthalazine pyruvic acid hydrazone, 1-hydrazinophthalazine acetone hydrazone, 4-hydroxy-1-hydrazinophthalazine, and glucuronides (2–6) appearing in urine.

Previous attempts to assay I included derivatization with *p*-hydroxybenzaldehyde (7) or *p*-anisaldehyde (*p*-methoxybenzaldehyde) (8), followed by spectrophotometric determination or the conversion of I to tetrazolo[1,5-*a*]phthalazine followed by electron-capture GLC analysis (9, 10). All of these techniques are nonspecific in that acid-labile hydralazine hydrazones present in plasma, such as hydralazine pyruvic acid hydrazone, are hydrolyzed to some extent and detected as I (11).

This report describes a specific high-pressure liquid chromatographic (HPLC) assay for I in human plasma.

EXPERIMENTAL

Reagents and Chemicals—Ethyl acetate, acetonitrile, and methanol were purchased as glass-distilled solvents. No further processing was necessary. Hydralazine hydrochloride[1] and *p*-anisaldehyde[2] also were used as purchased. Hydralazine pyruvic acid hydrazone and hydralazine *p*-anisaldehyde hydrazone (II) were prepared as described previously (5) with the reaction mixture pH maintained at 7.4. The identity and purity of the synthesized products were verified by combined GLC–mass spectrometry. No by-products or starting materials were detected.

The absence of I was confirmed first by derivatizing samples of each synthetic product with bis(trimethylsilyl)trifluoroacetamide to form the *N,N'*-di-trimethylsilyl derivative of any I that might be present and then subjecting them to GLC–mass spectrometry. To demonstrate that I could be detected by this procedure, known amounts of I were added to samples of each synthetic product and assayed similarly. By this technique, it was demonstrated that the synthetic samples of hydralazine hydrazones contained <0.03% I.

Standard Curve Samples—Fresh human plasma, 1 ml, with ethylenediaminetetraacetic acid as the anticoagulant and 10 μl of *p*-anisaldehyde were placed in a 15-ml culture tube fitted with a polytef-lined screw cap. An appropriate volume, 0.5–20 μl (5–200 ng), of a fresh solution of 10 ng of I/μl of 0.1 *M* potassium phosphate buffer, pH 7.4, was added; the contents were mixed by vortexing.

After standing at room temperature (23°) for 7 min to allow formation of II, 1 ml of 0.1 *M* potassium phosphate buffer, pH 7.4, and 7 ml of ethyl acetate were added. The samples were mixed for 10 min on a reciprocal shaker, and the phases were separated by centrifugation at 1000×*g* for 2 min. The ethyl acetate was transferred to a conical tube, and the solvent was removed in a gentle nitrogen stream.

Chromatography—Each extraction residue was mixed with 100 μl of methanol, and 90 μl was injected into a high-pressure liquid chromatograph[3] equipped with a reversed-phase column[4] (3.9 mm i.d. × 30 cm) and a variable-wavelength detector[5] set at 365 nm. The mobile phase was 32% acetonitrile in 0.75 *M* acetate buffer, pH 3.4, at a flow rate of 2 ml/min.

Derivatization and Extraction—The efficiency of derivatization was determined during three analyses by comparing the II recovery from 100-ng/ml standard hydralazine samples to the II recovery from blank plasma samples to which an equimolar concentration (173 ng/ml) of II had been added prior to extraction. Extraction efficiency was evaluated during three analyses by comparing the II peak height for plasma samples to which 173 ng of II was added before extraction to the II peak height for extracts of blank plasma samples to which 173 ng had been added just before injection into the liquid chromatograph.

Specificity—To assure that I does not react with an endogenous

[1] Sigma Chemical Co., St. Louis, Mo.
[2] Eastman Kodak Co., Rochester, N.Y.
[3] Model 995, Tracor, Austin, Tex.
[4] μBondapak C_{18}, Waters Associates, Milford, Mass.
[5] Model 970, Tracor, Austin, Tex.

0022-3549/79/1100-1423$01.00/0
© 1979, American Pharmaceutical Association

Table I—Intraassay Precision of Hydralazine Assay

Hydralazine Added, ng/ml	n	Relative Peak Height[a]	Hydralazine Found, ng/ml
10	3	15.3 ± 1.53	9.1
50	4	79.8 ● 2.22	52.7
100	4	146 ± 5.69	97.8
200	4	298 ± 15.5	200

[a] Mean ± *SD*.

plasma component to yield a substance with a retention time identical to that of II, 5 μg of I/ml was added to plasma without *p*-anisaldehyde and taken through the procedure.

Hydralazine pyruvic acid hydrazone, a metabolite of I found in plasma, was added at 20 μg/ml to blank serum containing 10 μl of *p*-anisaldehyde and immediately taken through the assay.

Precision—Intraassay precision was evaluated by preparing and assaying multiple standard samples at 10, 50, 100, and 200 ng/ml. Intersubject differences on a given day were evaluated by preparing 10-, 50-, and 100-ng/ml standard samples using plasma from three human volunteers. Interassay precision was evaluated by comparing the slopes and intercepts of standard curves for different days.

Human Volunteer—A 29-year-old, 66-kg, male volunteer, known to be a slow acetylator, was given 33 mg of hydralazine hydrochloride orally. Blood samples were obtained at 0, 5, 10, 20, 25, 30, 40, 50, and 60 min. Blood was drawn into evacuated tubes containing ethylenediaminetetraacetic acid as an anticoagulant. The red cells were separated by centrifugation for 5 min at 1000×*g*.

Plasma, 1 ml, was then added to a culture tube containing 10 μl of *p*-anisaldehyde and vortexed. The interval between the midpoint of blood drawing and the mixing of plasma with *p*-anisaldehyde was kept between 6.5 and 8.0 min. Unknown samples were then treated exactly like the standard curve samples described earlier. Apparent plasma hydralazine levels also were determined by a modified (11) GLC procedure, similar to that reported by Jack *et al.* (9).

RESULTS

The retention time for II was about 6.5 min with the chromatographic conditions used. Occasional adjustment of the acetonitrile concentration between 31 and 33% was necessary to obtain optimal separation of the II peak from an extraneous peak (Fig. 1). Maximum sensitivity was 3–5 ng/ml, depending on column age.

Derivatization efficiency was 91.2 ± 7.8% (n = 3), while extraction recovery was 80.4 ± 9.3% (n = 3). These determinations were performed on 3 days.

After addition of hydralazine pyruvic acid hydrazone, 20 μg/ml, to blank plasma standards, there was only 8 ng of I/ml (0.06 mole %). Addition of I, 5 μg/ml, to plasma without *p*-anisaldehyde did not yield chromatographic peaks under the described conditions.

The results of the intraassay precision study are shown in Table I. The mean coefficient of variation was 5.5%. There were no differences in the coefficients of variation of 10-, 50-, and 100-ng/ml standards prepared in plasma from three volunteers. However, the slope and intercept of the standard curve varied somewhat from day to day: slope, 1.28 ± 0.135; and intercept, 0.15 ± 3.97 (mean ± *SD*). A daily standard curve was assayed with each set of unknowns.

Unchanged I could be detected transiently in the plasma of the human volunteer after an oral hydralazine hydrochloride dose of 0.5 mg/kg (Table II). The values obtained for apparent hydralazine using the GLC

Table II—Plasma Hydralazine Levels in a Human Volunteer after Oral Administration of 0.5 mg/kg

Minutes	Unchanged Hydralazine Concentration, ng/ml[a]	Apparent Hydralazine Concentration, ng/ml[b]
5	<5.0	50
10	14.4	210
20	19.6	250
25	11.5	240
30	11.2	227
40	<5.0	195
50	<5.0	172
60	<5.0	150

[a] Determined by described HPLC procedure. Concentration was at 6.5–8 min after blood drawing. Sensitivity limit was 5.0 ng/ml. [b] Determined by a modification (11) of a commonly used GLC procedure (9).

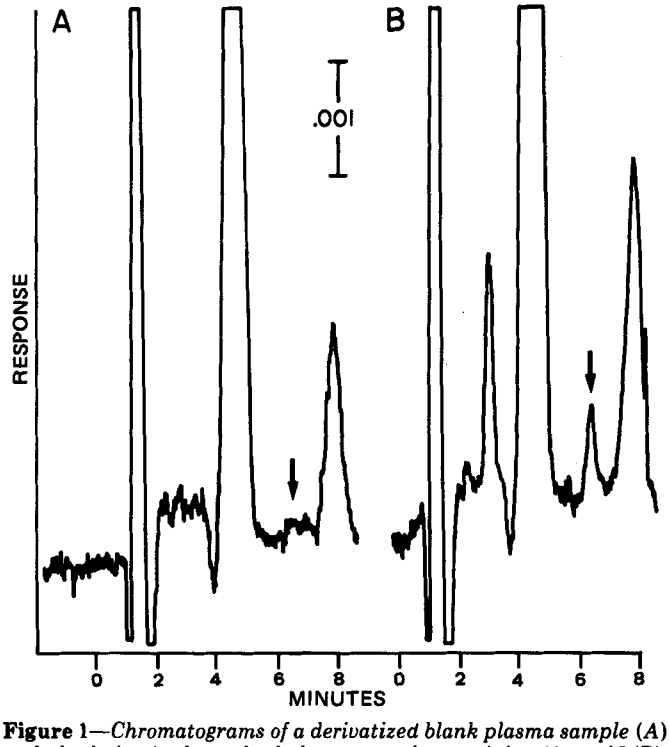

Figure 1—*Chromatograms of a derivatized blank plasma sample (A) and of a derivatized standard plasma sample containing 10 ng of I (B). The arrows indicate the retention time of II. The peak at 3.5 min in B appeared sporadically and was not related to the presence of I.*

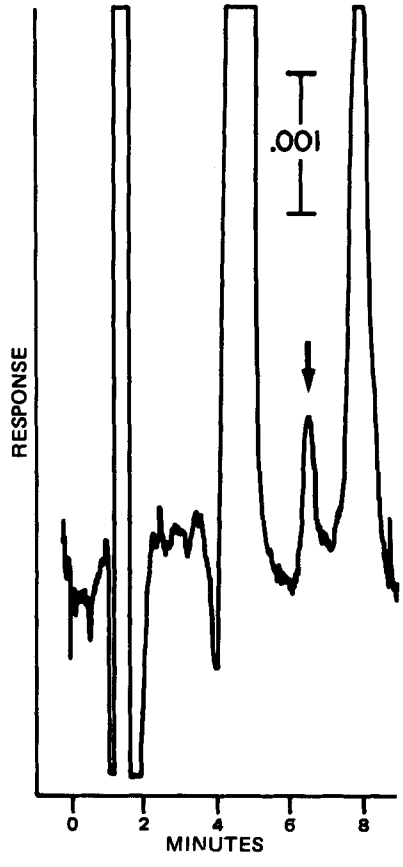

Figure 2—*Chromatogram of a derivatized plasma sample obtained 10 min after an oral dose of hydralazine hydrochloride, 0.5 mg/kg, to a human volunteer. The arrow indicates the retention time of II.*

procedure were considerably higher (Table II). The high-pressure liquid chromatogram of the 10-min sample is shown in Fig. 2.

DISCUSSION

The spectrophotometric assays that were used previously to measure the *p*-hydroxybenzaldehyde (7) or *p*-anisaldehyde (8) derivatives of I are nonspecific. These procedures used heat and acid catalysis to form the hydrazone derivatives of I in plasma. Under these conditions, acid-labile hydrazones of I, such as hydralazine pyruvic acid hydrazone, break down to I (10). Likewise, the GLC procedure of Jack *et al.* (9), which requires the formation of tetrazolo[1,5-a]phthalazine from I using nitrous acid (pH < 1), converts acid-labile hydrazones to free I.

Zak *et al.* (10) modified the GLC procedure so that the pH for tetrazolophthalazine formation was about 2.85 instead of <1. These investigators found considerably lower values for the concentration of "apparent" hydralazine in plasma than were reported previously. However, stability studies of hydralazine pyruvic acid hydrazone (11) indicated that this hydrazone is unstable at acid pH values. The plasma I levels found following a 0.5-mg/kg oral dose of hydralazine hydrochloride to a human volunteer using the described HPLC procedure are considerably lower than would be expected from previous studies, which used less specific analytical techniques (7–10, 12–14).

The described procedure avoids the use of acid or heat for formation of II in plasma. Authentic hydralazine pyruvic acid hydrazone, a major circulating metabolite of I in humans (15), yields <0.1 mole % of I when taken through the assay. Additional information about the circulating levels of other labile hydrazones is needed to assess method specificity.

Studies of the *in vitro* disappearance of I in plasma at 23° indicated a first-order process with a mean half-life of 16.1 min (16). Additional stability studies, carried out *in vitro* using whole blood and plasma, indicated that the disappearance of I is quite rapid at 37° (half-life ~6–10 min) but that loss during sample processing can be retarded by cooling in an ice water bath and centrifuging at 4°[6] (half-life ~1–2 hr). In the current study, blood samples from the volunteer were processed at room temperature, with the time between blood drawing and the addition of *p*-anisaldehyde to plasma held at 6.5–8.0 min. As much as 50% of I in plasma at the time blood was drawn could have been lost during processing. Even if the losses of I during processing were this high, apparent hydralazine levels (Table II) would still be fivefold or more higher than the concentration of unchanged hydralazine.

Although not sensitive enough for detailed pharmacokinetic studies following usual oral doses, the current assay can be applied to stability studies of I and its hydrazones in biological fluids and to pharmacokinetic studies following intravenous I administration to animals and humans (15). In addition, it can be used to monitor peak plasma levels of I in patients receiving chronic therapy.

[6] Unpublished data.

REFERENCES

(1) M. Nickerson and J. Reudy, in "The Pharmacological Basis of Therapeutics," 5th ed., L. S. Goodman and A. Gilman, Eds., Macmillan, New York, N.Y., 1975, p. 705.

(2) Z. H. Israili and P. G. Dayton, *Drug Metab. Rev.*, **6**, 293 (1977).

(3) J. Wagner, J. W. Faigle, P. Imhof, and G. Liehr, *Arzneim.-Forsch.*, **27**, 2388 (1977).

(4) T. Talseth, *Clin. Pharmacokinet.*, **2**, 317 (1977).

(5) K. D. Haegele, H. B. Skrdlant, N. W. Robie, D. Lalka, and J. L. McNay, Jr., *J. Chromatogr.*, **126**, 517 (1976).

(6) K. D. Haegele, A. J. McLean, P. duSouich, K. Barron, J. Laquer, J. L. McNay, and O. Carrier, *Br. J. Clin. Pharmacol.*, **5**, 489 (1978).

(7) R. Zacest and J. Koch-Weser, *Clin. Pharmacol. Ther.*, **13**, 420 (1972).

(8) S. B. Zak, M. F. Barlett, W. E. Wagner, T. G. Gilleran, and G. Lukas, *J. Pharm. Sci.*, **63**, 225 (1974).

(9) D. B. Jack, S. Brechbühler, P. H. Degen, P. Zbinden, and W. Riess, *J. Chromatogr.*, **115**, 87 (1975).

(10) S. B. Zak, G. Lukas, and T. G. Gilleran, *Drug Metab. Dispos.*, **5**, 115 (1977).

(11) P. A. Reece, P. E. Stanley, and R. Zacest, *J. Pharm. Sci.*, **67**, 1150 (1978).

(12) T. Talseth, *Eur. J. Clin. Pharmacol.*, **10**, 183 (1976).

(13) *Ibid.*, **10**, 395 (1976).

(14) T. Talseth, *Clin. Pharmacol. Ther.*, **21**, 715 (1977).

(15) A. M. M. Shepherd, K. D. Haegele, T. M. Ludden, T. Talseth, W. A. Clementi, and J. L. McNay, *Clin. Res.*, **27**, 318A (1979).

(16) T. M. Ludden, L. K. Goggin, K. D. Haegele, A. M. M. Shepherd, and J. L. McNay, *Fed. Proc.*, **38**, 268 (1979).

ACKNOWLEDGMENTS

Presented as a poster session at the 63rd Annual Meeting of the Federation of American Societies for Experimental Biology, Dallas, Tex., April 1979.

Supported in part by U.S. Public Health Service NIH Grant GM24092.

The authors thank Ms. Diana Resendez and Ms. Barbara Boyle for their help in preparing this manuscript.

Occurrence of Short-Duration Hypotensive Phospholipid from Dog Peritoneal Dialysate

HIROAKI TSUKATANI ˣ, SADAJI YAMADA, AKIRA TOKUMURA, TAKAFUMI ITAMI, and KENKICHI TAKAUCHI

Received December 5, 1978, from the *Faculty of Pharmaceutical Science, University of Tokushima, Schomachi, Tokushima 770, Japan.* Accepted for publication June 1, 1979.

Abstract □ From the total lipid fraction of dog peritoneal dialysate after freeze drying and extraction, a hypotensive phospholipid was isolated through silicic acid, cellulose, and Sephadex LH-20 column chromatography in a pure grade; it showed a single spot on TLC. The purified hypotensive factor, designated as Peritoneal Dialysate Depressor-I, elicited potent depressor responses in anesthetized rats, and its threshold dose was ~35 μg/kg. The material resisted proteases and 15-hydroxyprostanoate oxidoreductase. In mobility on TLC, the hypotensive factor was distinguishable from water-soluble hypotensive substances and also from depressor lipids. Judging from its behavior on TLC and column chromatography during the purification procedure, the hypotensive factor seems to be a choline-containing phospholipid and shows the general characteristics of lysolecithin, except for its potent hypotensive activity, instability, and positive reactions against 2,4-dinitrophenylhydrazine and 2′,7′-dichlorofluorescein on TLC. The molar ratio of phosphorus–glycerol–choline–ester was ~1:1:1:0.8. Most of the fatty acids were saturated ones such as stearic and palmitic acids.

Keyphrases □ Antihypertensive agents—endogenous lipids, phospholipid from dog peritoneal dialysate, TLC, IR, NMR analysis □ Phospholipids—antihypertensive activity, endogenous phospholipid from dog peritoneal dialysate, TLC, IR, NMR analysis

Reports concerning the cardiovascular activity of endogenous lipids other than prostaglandins, especially phospholipids, have presented only limited information. Certain papers reported the renin inhibitory activity of lysophosphatidylethanolamines (1-acyl-*sn*-glycero-3-phosphoethanolamine) (1–4). Martini and coworkers (5–12) extracted vasoactive lipids from various sources, but the compounds remain unpurified. Previous papers reported purification of the vasoactive lipids in the tissues and fluids and isolation of "Depressor-I" (13) and 2,2,6,6-tetramethylpiperidone-(4) (14) from normal and protease-treated bovine brains, respectively.

The hypotensive activity of synthetic L-α-lysolecithins (1-acyl-*sn*-glycero-3-phosphocholine), carrying various fatty acid moieties on anesthetized rats also was reported (15). Moreover, a strong and unique vasoactivity was observed in L-α-lysophosphatidic acid (1-acyl-*sn*-glycero-3-phosphate) obtained from crude soybean lecithin (16–18).

The present paper reports the chromatographic purification of a potent hypotensive factor from dog peritoneal dialysate. The substance is considered to be a phospholipid and tentatively designated as Peritoneal Dialysate Depressor-I.

EXPERIMENTAL

Chemicals—Prostaglandins were used as received[1]. L-α-Lysolecithin (palmitoyl), DL-α-lecithin (dipalmitoyl) (1,2-dipalmitoylglycero-3-phosphocholine), and sphingomyelin[2] (from bovine brain) were used without further purification. Also used as received were urethan[3] and pentobarbital sodium[4]. Chloroform, methanol[5], and other solvents were redistilled before use.

Bioassay—For routine assay, male Wistar rats, 240–260 g, were used under urethan anesthesia (1.8 g/kg ip) or pentobarbital anesthesia (50 mg/kg ip). The trachea and left carotid artery or left femoral artery were cannulated, and the latter was connected to a direct-writing mercury manometer. The arterial blood pressure response was recorded on a slow-moving smoked drum. The pressure response also was recorded by a pressure transducer[6] connected to a multipurpose polygraph[7].

The right femoral vein was cannulated and connected to a polyethylene tube for sample application. Samples were dissolved in 0.15 ml of saline (0.9% w/v NaCl), injected, and flushed with 0.1 ml of saline.

Purification of Peritoneal Dialysate Depressor-I—Conscious adult dogs were injected with 50–100 ml of 5.5% glucose solution/kg ip, and peritoneal dialysate was withdrawn after 3 hr according to a literature method (9). The dialysate was frozen immediately, lyophilized, extracted with chloroform–methanol (2:1 v/v), and washed with one-fifth of its volume of 0.7% NaCl solution (19). The chloroform-rich layer was separated and dried *in vacuo*. Approximately 300 mg of the total lipid fraction/liter of peritoneal dialysate was obtained. Because the crude extract (I) thus obtained was soluble in ethanol and partially soluble in acetone, it appeared that the lipid fraction consisted of simple lipids and lecithin.

For the purification of the crude extract (I), columns were prepared as follows:

1. Silicic acid[8] was activated at 110° overnight and partially deactivated (activity II B) before use. Silicic acid (50 g) and magnesium trisilicate[9] (25 g) were washed twice with 500 ml of chloroform and hexane and poured into a 2.8 × 60-cm glass column.
2. Fourteen grams of cellulose[10] was suspended in 40 ml of 95% methanol and poured into a 1.8 × 35-cm glass column. The column was washed with methanol and chloroform.
3. One hundred grams of Sephadex LH-20[11] was washed with 500 ml each of methanol, chloroform, and chloroform–methanol (1:1 v/v) or acetone–ethanol (1:1 v/v). The mixture was poured into a 2.7 × 90-cm glass column.

The crude extract (I) was applied to the top of the silicic acid column. Discontinuous gradient elution was carried out with hexane, hexane–chloroform (1:1 v/v), chloroform, and chloroform–methanol (98:2, 95:5, 90:10, 80:20, 70:30, 60:40, 50:50, and 40:60 v/v). Finally, methanol was applied. Five hundred-milliliter portions of the eluates were collected. An aliquot of each fraction was used for assay or phosphorus determination. The depressor activity was located in the chloroform–methanol 60:40, 50:50, and 40:60 (v/v) eluates.

From 1.29 g of I equivalent to 4200 ml of peritoneal dialysate, 596 mg of the active fraction (II) was obtained. Fraction II was applied to a cellulose column, and III was obtained. Fraction III was further subjected to a Sephadex LH-20 column, eluting with chloroform–methanol (1:1 v/v). The depressor activity (IV) was eluted in the fractions of the first 150–180 ml.

Finally, IV was chromatographed on another Sephadex LH-20 column with acetone–ethanol (1:1 v/v). The depressor factor was eluted in the first 190–210 ml and purified to an almost pure grade chromatographically (active fraction V).

TLC—In the routine work, the lipids in the chromatographed fractions

[1] Gift from Ono Pharmaceutical Industries Co. Ltd., Japan.
[2] Sigma.
[3] Wako, Japan.
[4] Dainippon, Japan.
[5] Nakarai, Japan.
[6] Nihon Kohden MPU-0.5.
[7] Nihon Kohden RM-45.
[8] Mallinckrodt AR 100 mesh.
[9] Hyflosuper-cel.
[10] Toyoroshi 300 mesh.
[11] Pharmacia.

0022-3549/79/1100-1426$01.00/0
© 1979, American Pharmaceutical Association

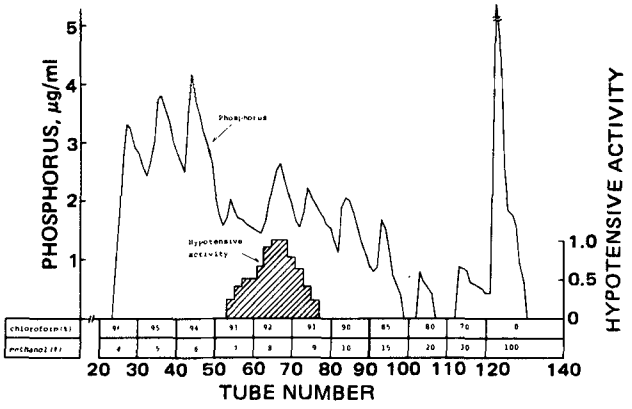

Figure 1—*Elution profile of Peritoneal Dialysate Depressor-I on a cellulose column. Active fraction II obtained through silicic acid chromatography (284 mg) of 2000 ml of original peritoneal dialysate was subjected to a cellulose column and developed with chloroform–methanol with stepwise polarity increases. Ten milliliters of eluate was collected. An aliquot of each tube was taken, dried, dissolved in saline, and bioassayed on an anesthetized rat. Phosphorus was determined according to the method described by Chalvardjian and Rudnicki (21).*

were monitored by TLC on a silica gel plate[12] with acidic, neutral, and basic solvent systems. The lipids were detected by charring with ethanolic sulfuric acid reagent or exposure in iodine vapor. Antimony trichloride, ethanolic phosphoric acid, phosphomolybdate, potassium permanganate, and 2′,7′-dichlorofluorescein spray reagents were used. The following specific spray reagents were used also: Dittmer's for phospholipids, Dragendorff's for choline bases, ferrous hydroxamate for ester groups, osmic acid for unsaturated bonds, ninhydrin for amino groups, ammoniacal silver nitrate and diphenylamine (acid free) for sugar moieties, benzidine for amide groups, mercuric chloride–Schiff's for plasmal, ferrous rhodanide for peroxide groups, periodate–Schiff's for α-glycol groups, and blue tetrazolium for corticoid moieties.

To identify the active material, preparative TLC was performed on a silica gel plate[12]. The active fraction (V) was spotted as a streak in the central part of a plate, and the plate was developed with chloroform–methanol–water (70:30:5 v/v) at −20° in the dark. Each desired zone of the central plate was scraped off horizontally and extracted with chloroform–methanol (1:1 v/v) and with methanol containing acetic acid (0.2 ml in 100 ml). The extracts were decanted off, filtered through a glass filter packed with a small amount of magnesium trisilicate[9], combined, and evaporated to dryness for bioassay. Most extraction procedures were carried out at 4° and completed within 6 hr.

For the partition experiment, aliquots of fraction V, dissolved in *n*-butanol, were added with equal volumes of distilled water, which were first adjusted to the desired pH. After vigorous shaking for 10 min at room temperature, *n*-butanol layers were separated from aqueous layers by centrifugation.

Both layers were neutralized and evaporated *in vacuo* for bioassay. The stability of the active material (V) was examined. Aliquots of V were dissolved in distilled water, adjusted to the desired pH, and incubated at 37° for 8 hr. The aqueous solutions were dried *in vacuo* after neutralization for bioassay. Fraction V was incubated with subtilisin or trypsin in phosphate buffer at pH 7.0 at 37° for 30 min.

Each reaction mixture was extracted with chloroform–methanol (2:1 v/v) three times and washed (19). The combined organic layers were dried over anhydrous sodium sulfate and evaporated *in vacuo*. Fraction V was tested with 15-hydroxyprostanoate oxidoreductase (20). To estimate the functional groups in V (194 μg containing 9.2 μg of phosphorus), various chemical reactions were tested and the recoveries of depressor activity were examined as follows:

1. With 5 ml of 0.1% hydrogen peroxide solution, the sample was kept at 25° for 30 min. An aliquot was assayed after drying *in vacuo*.

2. In 2 ml of chloroform sample solution, 10 ml of diluted bromine solution in chloroform was added, and the mixture stood at room temperature overnight.

3. To the sample dissolved in 5 ml of chloroform, diazomethane was added; the solution was kept at 0° for 12 hr in the dark.

[12] Merck silica gel plate 60, 9.25-mm thickness.

Table I—Mobilities of a Peritoneal Dialysate Depressor-I on TLC [a]

Substance	Solvent 1[b]	Solvent 2[c]	Solvent 3[d]
Peritoneal Dialysate Depressor-I	0.18	0.29	0.13
Prostaglandin A_2	0.89	0.97	0.83
Dinoprostone	0.82	0.93	0.73
DL-Lecithin	0.52	0.86	0.53
L-α-Lysolecithin	0.16	0.28	0.11
Sphingomyelin (from bovine brain)	0.29	0.61	0.35

[a] Silica gel 60 TLC plate and iodine vapor detection. [b] Chloroform–methanol–acetic acid–water (260:100:4:14 v/v). [c] Chloroform–methanol–water (70:30:5 v/v). [d] Chloroform–methanol–0.3 *N* ammonia (230:90:15 v/v).

4. A chloroform solution of the sample and triphenylphosphine (500 μg) was allowed to stand for 5 hr.

5. A mixture of the sample dissolved in chloroform and phenyl isocyanate (5 mg) dissolved in dry benzene (2 ml) was left for 24 hr, treated with ethanol, dried, extracted with chloroform, and centrifuged. Both extract and sediment were bioassayed suspended in saline containing 2% polysorbate 80[13].

Analytical Procedure—Phosphorus was determined by the Chalvardjian–Rudnicki method (21). The glycerol (22) and choline (23, 24) contents were also determined. Fatty acid methyl esters prepared by methanolysis (25) were determined by GLC[14] and confirmed by combined GLC–mass spectrometry[15]. The inlet system was equipped with a glass column (3 mm i.d. × 2 m) packed with 1.5% SE-30 on 60–80-mesh Gas Chrom Q[3].

The column temperature was increased from 150 to 260° at a rate of 5°/min; the injection temperature was 260°; the carrier gas was helium at 40 ml/min. The molecular separator was maintained at 260°, and the mass spectrometer ion source was at 270°. Accelerating voltage was 3.2 kv. Spectra were recorded at ionizing energies of 20 and 70 ev. The IR spectrum[16] was recorded by liquid film. NMR[17] was measured by dissolving V (15 mg) in 0.35 ml of deuterochloroform.

RESULTS

Purification of Peritoneal Dialysate Depressor-I—By the described extraction procedure, the hypotensive factor in dog peritoneal dialysate was extracted with high efficiency, and the procedure was more advantageous than previously reported methods. Previous investigators (7–9, 11) reported that the crude extract obtained by their methods elicited hyper- or hypotensive responses, depending on the oxidation–reduction state of the extract. However, the total lipid fraction of dog peritoneal dialysate obtained in the present investigation elicited only depressor responses by intraperitoneal injections into anesthesized rats.

The behavior of the lipid fraction toward solvent fractionation suggests that the crude lipid contains no cephalins or mucolipids and that the hypotensive factor possibly belongs to the lecithin fraction. On silicic acid chromatography, a depressor factor was located on the eluates obtained at the near chloroform–methanol (50:50 v/v) mixture; no detectable hyper- or hypotensive activity was observed in other fractions. In subsequent cellulose chromatography, the depressor activity was located in the chloroform–methanol eluates (93:7, 92:8, and 91:9 v/v) (active fraction III) (Fig. 1). This cellulose chromatography was followed by gel filtration.

The elution pattern on a Sephadex LH-20 column eluting with chloroform–methanol (1:1 v/v) is depicted in Fig. 2. The chemical analysis showed the association of detectable organophosphorus with the hypotensive activity, suggesting that the active factor was a phospholipid resembling lysolecithin and apparently distinguishable from primary prostaglandin family compounds (active fraction IV). In the last chromatography on the second Sephadex LH-20 column, eluting with acetone–ethanol (1:1 v/v), the remaining minor contaminants such as sphingomyelin and lecithin were eliminated (active fraction V). The active depressor factor showed a single spot on TLC with three different solvent systems (Table I). Through purification procedures, the depressor

[13] Tween 80, Nakarai, Japan.
[14] Shimadzu gas chromatograph GC-5A.
[15] Hitachi GC–mass spectrometer RMU-6M equipped with datalyzer system.
[16] Hitachi grating IR spectrophotometer EPI-GII.
[17] Jeol NMR spectrometer JNM-PS-100.

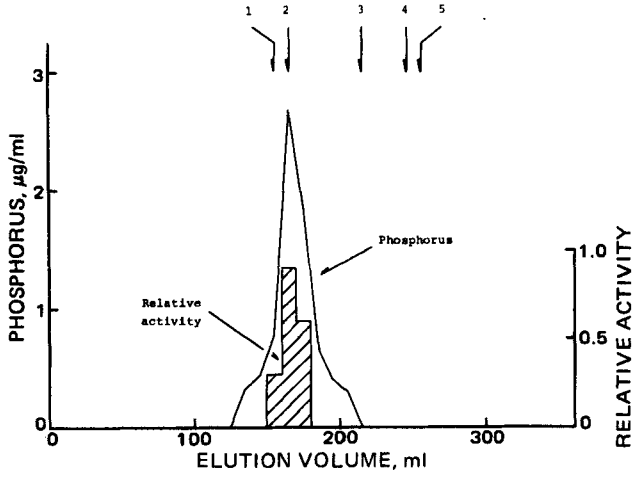

Figure 2—*Elution profile of Peritoneal Dialysate Depressor-I on a Sephadex LH-20 column. Active fraction (III) obtained through silicic acid and cellulose chromatography (3.50 mg), equivalent to 400 ml of original peritoneal dialysate, was subjected to a Sephadex LH-20 column and eluted with chloroform–methanol (1:1 v/v). Ten milliliters of the eluate was collected. Bioassay or phosphorus determination was carried out in the same manner as in Fig. 1. Arrows show locations of reference compounds: 1, tripalmitin; 2, L-α-palmitoyl-lysolecithin (1-palmitoyl-sn-glycero-3-phosphocholine); 3, palmitic acid; 4, prostaglandin A_2; and 5, cholesterol.*

activity was recovered almost quantitatively at each stage and the hypotensive factor Peritoneal Dialysate Depressor-I was purified ~150-fold over the crude extract (I). Per liter of original peritoneal dialysate, 1.94 mg of purified hypotensive factor (V) was obtained, which corresponded to ~0.65% of the total dog peritoneal dialysate lipid and contained ~92 µg of phosphorus.

The blood pressure responses of an anesthetized rat to the intravenous injections of the purified Peritoneal Dialysate Depressor-I preparation and to acetylcholine are shown in Fig. 3. A dose of 117.3 µg of the preparation/kg (4 U/kg) evoked a brief hypotensive response (~25 mm Hg) similar to that from acetylcholine. The purified preparation depressor activity was represented with a unit (U) value utilizing acetylcholine as a standard agent. The threshold dose was ~35.2 µg/kg (1.2 U/kg).

Chemical Properties of Peritoneal Dialysate Depressor-I—Although the purified preparation of Peritoneal Dialysate Depressor-I shows a single spot on TLC, whether the spot was responsible for the hypotensive activity was not certain. To solve that question, preparative TLC was carried out at −20°. The zone where the depressor activity was

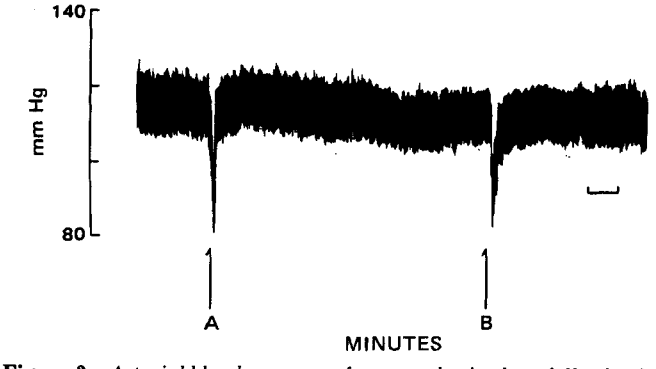

Figure 3—*Arterial blood pressure of an anesthetized rat following intravenous injections of acetylcholine and purified Peritoneal Dialysate Depressor-I. A male Wistar rat, 250 g, was anesthetized with pentobarbital (50 mg/kg ip). Arrows show intravenous sample injections: A, acetylcholine, 5 × 10^{-8} g/kg; and B, purified Peritoneal Dialysate Depressor-I, 4 U/kg (117.3 µg/kg containing 5.57 µg of phosphorus/kg or 0.18 µmole of phosphate/kg). The hypotensive activity of the purified factor was represented with a unit value. One unit (U) equals the response produced by injection of 5 × 10^{-8} g of acetylcholine/kg into the femoral vein of an anesthetized rat weighing 250 g; horizontal scale = 2 min.*

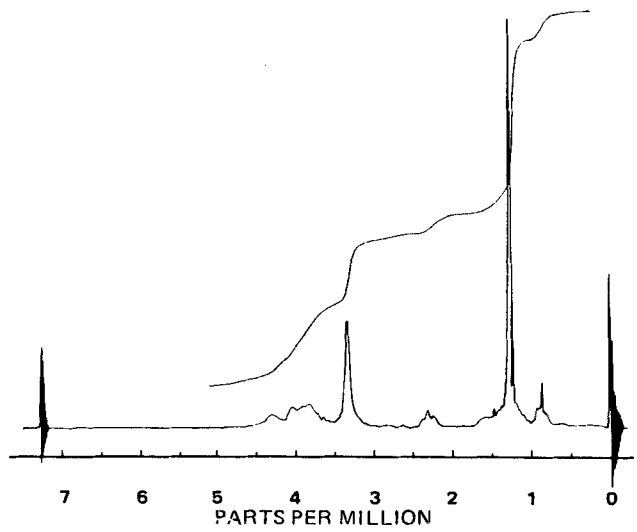

Figure 4—*NMR spectrum of Peritoneal Dialysate Depressor-I.*

recovered corresponded to the spot identified by exposure in iodine vapor; the recovery of the hypotensive activity was excellent (~90%).

The spot also was detectable by charring with ethanolic sulfuric acid reagent or by staining with antimony trichloride, ethanolic phosphoric acid, phosphomolybdate, 2′,7′-dichlorofluorescein, or potassium permanganate reagent. It gave positive tests against the sprays of Dittmer's, Dragendorff's, ferrous hydroxamate, and osmic acid reagents but negative tests against the sprays of ninhydrin, ammoniacal silver nitrate, diphenylamine (acid free), benzidine, mercuric chloride–Schiff's, ferrous rhodanide, periodate–Schiff's, and blue tetrazolium reagents.

A comparison of R_f values of Peritoneal Dialysate Depressor-I with other compounds is shown in Table I. In three different solvent systems, the depressor factor was distinguishable from water-soluble known hypotensive substances such as acetylcholine, histamine, serotonin, and adenosine derivatives and from known depressor active lipids such as prostaglandins and arachidonic acid, although all data were not listed. In a comparison with polar lipids, Peritoneal Dialysate Depressor-I strongly resembled lysolecithin. A purified preparation of the depressor active factor was readily soluble in polar solvents (methanol, ethanol, and *n*-butanol) but sparingly soluble in nonpolar solvents (*n*-hexane, benzene, ether, and ethyl acetate). In partitioning behavior between *n*-butanol and aqueous media at pH 3.0, 7.0, and 10.0, most depressor activity (~95%) was recovered from the organic layer regardless of the pH.

The preparation was relatively unstable and tended to lose activity when exposed to room temperature for a long time, especially when alkaline. The material in a syrup form, however, could be stored for months below −20° under a nitrogen atmosphere without loss of activity. When the preparation stood in aqueous media at 37° for 8 hr at pH 3.0 and 7.0, the depressor activity recoveries were ~80 and 100%, respectively, whereas the recovery was only ~40% at pH 11.0. Since the depressor activity of Peritoneal Dialysate Depressor-I was unaffected by incubations with proteolytic enzymes such as subtilisin and trypsin, it is not a peptide like substance P or bradykinin.

Neither prostaglandin E nor F was found in the purified preparation by a fluorometric determination based on an enzymic cycling system utilizing resazurin, nicotinamide adenine dinucleotide (nadide), and 15-hydroxyprostanoate oxidoreductase. No prostaglandins A, B, E, nor F were detected by GLC in the preparation.

For assessment of functional groups, examinations were performed for estimating the depressor activity recovery after treatment with various chemical reagents. After oxidation with 0.1% hydrogen peroxide, the hypotensive activity disappeared completely. The activity was substantially (~50%) damaged by bromine absorption; after treatment with cold diazomethane or triphenylphosphine, the depressor activity was recovered. Phenyl isocyanate destroyed the hypotensive activity.

No special IR or NMR absorption or signal was observable in the biologically active substance; only those corresponding to common lysolecithin were found, suggesting that the active factor may be a minor component in the lysolecithin fraction. The following absorptions were observed in the IR spectrum of the hypotensive factor: 3400, 2920, 2840, 1730, 1470, 1380, 1230, 1085, 1050, and 970 cm^{-1}. The NMR spectrum (Fig. 4) showed the following signals (δ): 0.88, 1.3, 2.26, 3.30, and 3.6–4.6 ppm.

In the chemical analysis of the purified Peritoneal Dialysate Depres-

sor-I preparation, the molar ratio of phosphorus–glycerol–choline was 1.00:0.99:0.97. The ratio of phosphorus–ester was 1.00:0.81 for the sample obtained by methanolysis of the active fraction. In the fatty acid analysis with GLC–mass spectrometry, stearic (54.0%) and palmitic (39.4%) acids were found most abundantly, similar to lysolecithins in mammalian organs and fluids. Oleic (3.1%) and myristic (1.8%) acids were the next most abundant. No other acids were detectable. No methylal of long chain aldehyde due to plasmal was detected.

DISCUSSION

In the present investigation, the hypotensive factor Peritoneal Dialysate Depressor-I was highly purified to show a single spot on TLC by extraction and repeated column chromatography. This active factor showed brief, potent hypotensive effects in anesthetized animals in dosages of some 10 μg/kg. Peritoneal Dialysate Depressor-I was a principal vasoactive factor in the total lipid fraction of the dog peritoneal dialysate, but its content was very minor.

Judging from the mobilities and findings obtained by TLC, the depressor factor resembles lysolecithin, and its effect was not due to known water-soluble compounds such as acetylcholine, histamine, serotonin, adenosine derivatives, lactic acid, or 2,2,6,6-tetramethylpiperidone-(4). The active peptides may be eliminated by the study with proteolysis. The possibility that the depressor effect is ascribable to prostaglandin compounds may be eliminated because Peritoneal Dialysate Depressor-I was more polar than the primary prostaglandin family compounds on column chromatography and TLC. On gel filtrations, the depressor active factor also was distinguished from prostaglandins. No report with phospholipid derivative of prostaglandins has been published. Lands and Samuelsson (26) were unsuccessful in isolating a phospholipid prostaglandin derivative from 1-palmitoyl-2-([2′-^{14}C]eicosatrienoyl)-glycero-3-phosphorylcholine by incubation with the seminal vesicle microsomal fraction.

No primary prostaglandin was detected in the hypotensive preparation by GLC. The presence of prostaglandins E or F was not detected enzymatically by assaying with 15-hydroxyprostanoate oxidoreductase. The hypotensive factor does not belong to a peroxide compound such as the prostaglandin endoperoxide intermediate since no detectable color was developed by the ferrous rhodanide reagent on TLC. Furthermore, its activity was recovered after treatment with triphenylphosphine.

Other known hypotensive lipids can be eliminated also. Peritoneal Dialysate Depressor-I resembles lysolecithin, but apparent differences were observed between two. The depressor active factor was detectable with 2,4-dinitrophenylhydrazine and by 2′,7′-dichlorofluorescein on TLC. In a comparison of hypotensive potency, the depressor factor showed a much stronger effect than the usual lysolecithin occurring in mammalian tissues. On the basis of phosphorus content, the hypotensive factor is ~60 times more potent than L-α-stearoyl-lysolecithin (15). The hypotensive factor was more unstable than lysolecithin, especially in alkaline conditions. In the active factor, the molar ratio of phosphorus–glycerol–choline was ~1:1:1; its fatty acid composition was mostly stearic and palmitic acids, like ordinary lysolecithin.

However, the molar ratio of phosphorus–ester was ~1.0:0.8, and this molar ratio gap differentiates the active factor from lysolecithin. The possibility remains that the active factor is new and different from the usual known lysolecithin, although its concentration may be very minor.

Several reports have been published on the hypotensive effects of lysophosphatidylethanolamines extracted from various animal kidneys (1–4). The effects of lysophosphatidylethanolamines were only observed in rats under physiologically abnormal conditions (acute or chronic renal hypertension) and were considered to be due to inhibition of the renin–angiotensin–aldosterone system. On the other hand, L-α-lysophosphatidic acid had strong hypertensive effects in rats and strong hypotensive effects in cats (18), although L-α-lysophosphatidic acid was first obtained from crude soybean lecithin (16, 17). The lyso-type phospholipid structure appears to have a close relation to the cardiovascular effect. Peritoneal Dialysate Depressor-I is considered to be a phospholipid closely resembling lysolecithin and possibly an analog, although its chemical structure remains undefined. Further pharmacological properties of the hypotensive factor will be reported.

REFERENCES

(1) S. Rakhit, *Can. J. Biochem.*, **49**, 1012 (1971).

(2) D. O. Tinker, H.-J. Schwartz, D. H. Osmond, and L. J. Ross, *ibid.*, **51**, 863 (1973).

(3) A. Antonello, B. Baggio, S. Favaro, A. Corsini, S. Todesco, and A. Borsatti, *Pfluegers Arch.*, **341**, 113 (1973).

(4) J. G. Turcotte, R. E. Boyd, J. G. Quinn, and R. R. Smeby, *J. Med. Chem.*, **16**, 166 (1973).

(5) E. Martini, A. Marzorati, and E. Morpurgo, *Experientia*, **8**, 225 (1952).

(6) F. Chiesa, *Ist. Lomb. (Rend. Sci.)*, **93**, 26 (1959).

(7) E. Martini, F. Chiesa, A. Spiga, and R. Oberosler, *Enzymologia*, **29**, 1 (1965).

(8) F. Chiesa, E. Martini, R. Oberosler, and A. Spiga, *ibid.*, **29**, 38 (1965).

(9) E. Martini, F. Chiesa, R. Oberosler, G. Maffeo, and C. Secchi, *ibid.*, **33**, 100 (1967).

(10) F. Chiesa, R. Oberosler, C. Secchi, G. Maffeo, E. Seren, and E. Martini, *ibid.*, **34**, 369 (1968).

(11) E. Martini, F. Chiesa, R. Oberosler, E. Seren, and V. Beghelli, *ibid.*, **38**, 189 (1970).

(12) C. Secchi and E. Martini, *Ital. J. Biochem.*, **20**, 98 (1971).

(13) H. Tsukatani, S. Yamada, A. Tokumura, T. Miyamoto, and K. Takauchi, *Chem. Pharm. Bull.*, **24**, 2294 (1976).

(14) H. Tsukatani, T. Itami, T. Awaji, and K. Takauchi, *ibid.*, **19**, 2201 (1971).

(15) H. Tsukatani, S. Yamada, K. Fukuzawa, and C. Hamaguchi, *J. Pharm. Pharmacol.*, **31**, 110 (1979).

(16) A. Tokumura, Y. Akamatsu, S. Yamada, and H. Tsukatani, *Agr. Biol. Chem.*, **42**, 515 (1978).

(17) A. Tokumura, K. Fukuzawa, Y. Akamatsu, S. Yamada, T. Suzuki, and H. Tsukatani, *Lipids*, **13**, 468 (1978).

(18) A. Tokumura, K. Fukuzawa, and H. Tsukatani, *ibid.*, **13**, 572 (1978).

(19) J. Folch, M. Lees, and G. H. S. Stanley, *J. Biol. Chem.*, **226**, 497 (1957).

(20) T. Itami, K. Fukuzawa, M. Takahashi, and H. Tsukatani, *Chem. Pharm. Bull.*, **23**, 1152 (1975).

(21) A. Chalvardjian and E. Rudnicki, *Anal. Biochem.*, **36**, 225 (1970).

(22) O. Renkonen, *Biochim. Biophys. Acta*, **56**, 367 (1962).

(23) D. Glick, *J. Biol. Chem.*, **156**, 643 (1944).

(24) C. J. Argoudelis and J. Tobias, *Anal. Biochem.*, **64**, 276 (1975).

(25) Y. Kishimoto and N. S. Radin, *J. Lipid Res.*, **6**, 435 (1965).

(26) W. E. M. Lands and B. Samuelsson, *Biochim. Biophys. Acta*, **164**, 426 (1968).

ACKNOWLEDGMENTS

The authors thank Dr. M. Nishida for his stimulating discussion and exacting criticism and also Ono Pharmaceutical Industries Co. Ltd. for the prostaglandins.

Kinetics of Drug–Drug Interactions: Biliary Excretion of Iodoxamic Acid and Iopanoic Acid in Rhesus Monkeys

SHENG K. LIN *§, ALBERT A. MOSS ‡x, and SIDNEY RIEGELMAN *‡

Received December 26, 1978, from the *Department of Pharmacy, School of Pharmacy, and the ‡Department of Radiology, School of Medicine, University of California, San Francisco, CA 94143. Accepted for publication June 5, 1979. §Present address: A314, 5115 N. Mesa, El Paso, TX 79912.

Abstract □ The dynamic method originally developed for studying the capacity-limited kinetics of the cholecystographic agents iodoxamic acid and iopanoic acid was applied to study the *in vivo* interactions of these two compounds following coadministration in the monkey. Results indicate that these interactions are complex. The compounds appear to compete for plasma protein binding sites as well as for binding sites on intrahepatic proteins. The biliary excretion data apparently fit the "ligand exclusion" model in which iopanoic acid acts as an inhibitor and competes with iodoxamic acid for binding to either of two identical sites within the liver. This competition probably is the rate-limiting step in the liver's overall elimination of these radiographic contrast agents.

Keyphrases □ Drug–drug interactions—pharmacokinetics, iodoxamic acid, iopanoic acid, biliary excretion, rhesus monkeys □ Pharmacokinetics—drug–drug interactions, iodoxamic acid, iopanoic acid, biliary excretion, rhesus monkeys □ Cholecystographic agents—iodoxamic acid, iopanoic acid, interactions, biliary excretion, pharmacokinetics, rhesus monkeys

In cholecystography, the degree of biliary system opacification depends directly on the concentration and the amount of iodine excreted in the bile (1). Therefore, a reasonable approach to increasing the degree of opacification would be to increase the cholecystographic agent dose. This approach, however, is limited by the fact that most cholecystographic compounds are handled in the liver by saturable processes, *e.g.*, by binding to the intrahepatic binding proteins—the so-called Y- and Z-proteins (2, 3); above a certain dose level, these processes become saturated and the excretion rate does not increase. High doses would also produce excessively high blood levels of the compound and add stress to eliminating organs, such as the kidney, which could lead to systemic toxicity (4, 5).

An alternative approach to increasing the biliary iodine concentration would be to coadminister more than one compound. If, however, the compounds share hepatic elimination mechanisms, coadministration might result in competition for the binding sites of the intrahepatic (Y and Z) proteins or for other carrier systems responsible for hepatic uptake, biotransformation, and biliary excretion of the compounds. Therefore, biliary excretion of two or more compounds may be no greater than that for a single agent.

Reported here is an *in vivo* study of the interaction of two cholecystographic agents, iodoxamic acid and iopanoic acid, coadministered to rhesus monkeys. The capacity-limited biliary excretion of these two compounds in dogs was reported previously (6, 7). During these studies, TLC confirmed that iodoxamic was excreted in the bile unchanged, while iopanoic acid was 98% metabolized to the glucuronide. At the same time, the blood concentrations contained only intact drugs with both agents. They, therefore, represent an interesting combination of cholecystographic agents with which to study drug interactions.

THEORETICAL

One or two identical binding sites may exist on the enzyme or the carrier for a substrate. This condition produces a competitive situation if the binding of an inhibitor to one of the sites prevents the substrate from binding to the site(s). This competition may also distort the substrate binding sites by the binding of the inhibitor or from mutual steric hindrance. Alternatively, the inhibitor may have a binding site that overlaps or utilizes part of each substrate binding site. The equation of the ligand exclusion model (8) can be applied to describe this latter system:

$$v = \frac{\overline{V}_m(S/K_m + S^2/K_m^2)}{1 + 2S/K_m + S^2/K_m^2 + I/K_i} \quad \text{(Eq. 1)}$$

where v is the enzymatic reaction rate, $\overline{V}_m$ is the maximum reaction rate when all binding sites are saturated, K_m is the Michaelis–Menten constant for the substrate, S is the substrate concentration, K_i is the Michaelis–Menten constant for the inhibitor, and I is the inhibitor concentration.

In the absence of the inhibitor ($I = 0$), Eq. 1 can be simplified by multiplying the numerator and the denominator by K_m^2:

$$v = \frac{\overline{V}_m[(K_m)(S + S^2)]}{K_m^2 + 2[(K_m)(S + S^2)]} \quad \text{(Eq. 2)}$$

$$v = \frac{(\overline{V}_m)(S)(K_m + S)}{(K_m + S)^2} \quad \text{(Eq. 3)}$$

$$v = \frac{\overline{V}_m S}{K_m + S} \quad \text{(Eq. 4)}$$

Therefore, in the absence of the inhibitor, Eq. 1 reduces to the Michaelis–Menten equation (Eq. 4), and the v *versus* S plot is the usual hyperbola. In the presence of the inhibitor, the v *versus* S plot becomes sigmoidal.

EXPERIMENTAL

Materials—Studies were performed on one male (Monkey A) and one female (Monkey B) rhesus monkey, 9.1 and 4.5 kg, respectively. Both monkeys had been used previously for exp ents (6, 7) in which iodoxamic acid or iopanoic acid alone had been infused. Thus, each monkey served as its own control. The monkeys were restrained in plastic chairs and had, as previously described (9), a T-tube in the common bile duct for bile collection and another T-tube in the duodenum for bile salts recycling. Both monkeys had been cholecystectomized.

^{125}I-Labeled iodoxamic acid[1] was used. Its radiopurity was >99% by TLC. For infusion, the ^{125}I-iodoxamic acid was diluted with normal saline to 26.5 and 28.4 m*M*, as determined according to its iodine content by fluorescent excitation analysis (10).

The iopanoic acid infusion solution was prepared by dissolving 913 mg of iopanoate sodium[2] in 10 ml of water. The resultant solution was filtered through a membrane filter[3] and diluted to 100 ml with normal saline.

Piston-type infusion pumps[4] were used for infusing the solutions. An automatic γ-counter[5] was used for determining ^{125}I-radioactivity. A multiple equilibrium dialysis system[6] was used for plasma protein binding studies.

[1] Iodine-125 meglumine iodoxamate, E. R. Squibb and Sons, Princeton, N.J.
[2] Sterling-Winthrop Research Institute, Division of Sterling Drug, Rensselaer, N.Y.
[3] Millex disposable filter unit, Millipore Corp., Bedford, Mass.
[4] Lamda pump and driver, serial 1300 and 1301, Harvard Apparatus Co., Millis, Mass.
[5] Auto-gamma-scintillation spectrometer, model 1185, Searle Analytical, Des Plaines, Ill.
[6] Dianorm, Innorativ-Medizin AG, CH-Esslingen, Switzerland.

0022-3549/79/1100-1430$01.00/0
© 1979, American Pharmaceutical Association

Table I—Protein Binding of Iodoxamic Acid and Iopanoic Acid in Monkey A [a]

Minutes	$C_{b_{IDX}}$, μM	$C_{f_{IDX}}$, μM	$C_{f'_{IDX}}$, μM	$C_{b_{IPA}}$, μM	$C_{f_{IPA}}$, μM	$C_{f'_{IPA}}$, μM
90	217	29.8	76.2	160	1.27	1.13
106	97	9.6	34.2	92	0.27	0.80
121	43	3.1	14.1	39	0.02	0.51
151	17	0.84	5.5	16	0.002	0.11
181	13	0.56	3.6	8.7	—[b]	—[b]
211	11	0.46	3.3	2.6	—[b]	—[b]
241	10	0.40	3.0	0.5	—[b]	—[b]
286	8.7	0.33	2.7	0.3	—[b]	—[b]

[a] $C_{b_{IDX}}$ and $C_{f_{IDX}}$ are the blood and unbound plasma concentrations, respectively, of iodoxamic acid in the absence of iopanoic acid; $C_{f'_{IDX}}$ is the unbound concentration of iodoxamic acid in the presence of iopanoic acid; $C_{b_{IPA}}$ and $C_{f_{IPA}}$ are the blood and unbound iopanoic acid concentrations in the absence of iodoxamic acid, respectively; and $C_{f'_{IPA}}$ is the unbound iopanoic acid concentration in the presence of iodoxamic acid. The samples were collected in the presence of heparin, which was not evaluated for its effect on the protein binding. [b] Below HPLC assay sensitivity.

Procedure—The dynamic infusion method used for studying the capacity-limited kinetics of iodoxamic acid and iopanoic acid (6, 7) was used. One infusion study was performed in Monkey A. Iopanoic acid was infused at the rate of 1.09 μmoles/kg/min. After 30 min, ^{125}I-iodoxamic acid was infused at the rate of 1.60 μmoles/kg/min. Ninety minutes after the first infusion, both infusions were terminated.

Another infusion study was performed in Monkey B. Iopanoic acid was infused at the rate of 0.73 μmole/kg/min for 150 min; 90 min after the initiation of the iopanoic acid infusion, ^{125}I-iodoxamic acid was infused at the rate of 1.20 μmoles/kg/min for 60 min.

Generally, except for ascertaining lag times, bile samples were collected for both monkeys every 5–15 min for 285 min. Sodium taurocholate[7] (1% in water) was infused into the duodenum at the rate of 5.56 μmoles/kg/min 1 hr before and throughout both experiments to replace the bile salts lost due to bile collection and to maintain as much as possible a constant bile flow (11, 12).

To determine the lag time between the presence of contrast material in the biliary canaliculi and that at the biliary sampling site, bile samples were also collected every 2–4 min during the first 30 min of each experiment. The lag time was estimated by plotting the cumulative amount of iopanoic acid excreted in the bile during the first 30 min against time and extrapolating the initial linear portion to the abscissa (Fig. 1). The lag time varied from 2 to 7 min. After correcting for the lag time, the biliary excretion rates were plotted for the midpoint of each collection period.

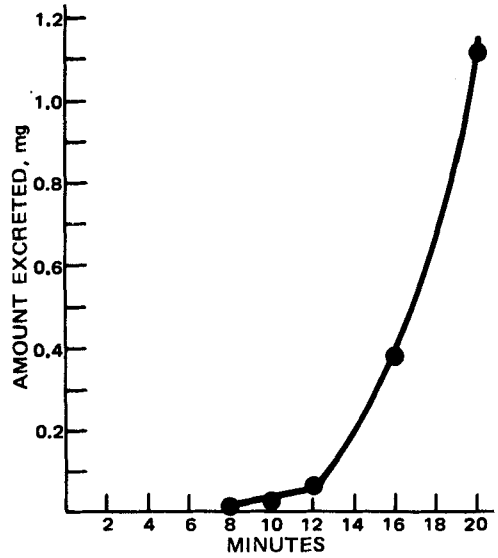

Figure 1—*Cumulative iopanoic acid excreted in the bile* versus *time during the first 30 min of infusion at 1.09 μmoles/kg/min into Monkey A.*

[7] ICN Pharmaceuticals, Cleveland, Ohio.

Table II—Protein Binding of Iodoxamic Acid and Iopanoic Acid in Monkey B [a]

Minutes	$C_{b_{IDX}}$, μM	$C_{f_{IDX}}$, μM	$C_{f'_{IDX}}$, μM	$C_{b_{IPA}}$, μM	$C_{f_{IPA}}$, μM	$C_{f'_{IPA}}$, μM
151	187.9	25.0	85.40	136.48	0.52	1.46
171	52.6	3.82	23.65	49.87	0.14	0.90
191	25.0	1.27	10.51	15.75	0.03	0.45
226	14.5	0.57	5.25	5.25	0.008	0.34
250	12.0	0.43	4.73	4.20	0.005	0.24
280	9.6	0.31	3.81	5.79	—[b]	—[b]
310	8.3	0.25	3.68	4.20	—[b]	—[b]
353	7.6	0.22	3.02	7.35	—[b]	—[b]

[a,b] See Table I.

Blood samples were collected at appropriate time intervals such that the total amount of blood taken did not exceed 20 ml/study.

For each blood and bile sample, the total iodine concentration was determined by fluorescent excitation analysis (10). The iodoxamic acid concentration in each sample was determined by counting the ^{125}I-radioactivity. The ^{125}I-iodoxamic acid iodine concentration was subtracted from the total iodine concentration to obtain the iopanoic acid concentration in each bile and blood sample.

For each animal, whole blood samples were used for equilibrium dialysis studies of each drug alone (6, 7) and in the presence of the other compound. The samples were taken from whole blood obtained during the interaction studies. The proportion of unbound iodoxamic acid was determined by counting ^{125}I-radioactivity in the protein-free buffer; the proportion of unbound iopanoic acid was determined using the high-pressure liquid chromatographic (HPLC) method described previously (7). The resultant unbound concentrations are plotted on the same graphs as those for biliary excretion rates of the two acids (Fig. 2).

RESULTS AND DISCUSSION

Goergen *et al.* (13) coadministered iodipamide, a compound chemically similar to iodoxamic acid (4, 5), and iopanoic acid in dogs and found that iodipamide biliary concentration decreased to ~12% of the control level.

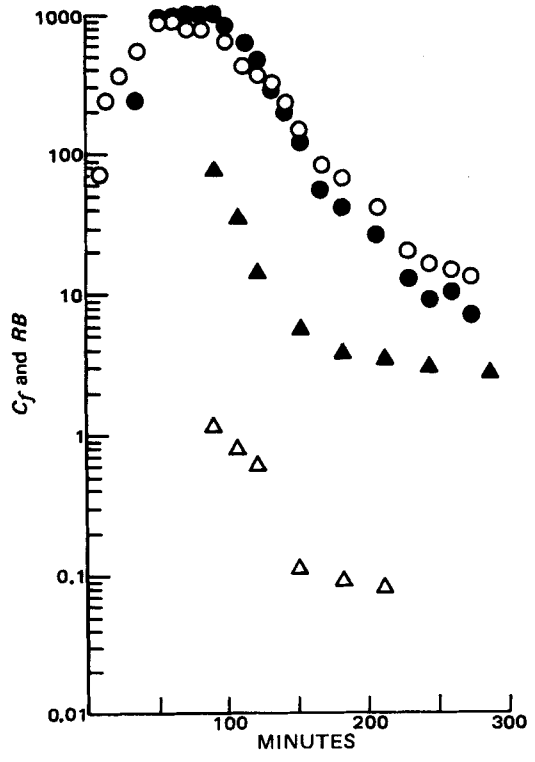

Figure 2—*Semilog plot of the time course of biliary excretion rate* (RB, *in nanomoles per kilogram per minute*) *of iodoxamic acid* (●) *and iopanoic acid* (○) *and the unbound plasma concentration* (C_f, *micromolar*) *of iodoxamic acid* (▲) *and iopanoic acid* (△) *in Monkey A. The same results were found for Monkey B.*

Table III—Results of the Coadministration Experiment in Monkey B [a]

$C_{f'IDX}$, μM	$C_{f'IPA}$, μM	RB, μmole/kg/min	RB', μmole/kg/min	Residual, μmole/kg/min
5.05	0.32	0.056	0.087	0.031
6.40	0.38	0.082	0.108	0.026
8.62	0.41	0.123	0.155	0.032
10.62	0.44	0.196	0.193	−0.003
14.10	0.58	0.293	0.234	−0.059
26.19	0.95	0.459	0.369	−0.090
66.47	1.33	0.618	0.707	0.089

[a] $C_{f'IDX}$ and $C_{f'IPA}$ are the unbound plasma concentrations of iodoxamic and iopanoic acids, respectively; RB is the biliary excretion of iodoxamic acid; and RB' is the computer-fitted biliary excretion rate of iodoxamic acid according to Eq. 1. Residual is the difference between RB and RB'.

These results were confirmed when Moss *et al.* (14) administered a bolus dose of iopanoic acid to dogs being infused with iodipamide and showed that the total biliary iodine concentration was reduced, although the blood iodine concentration was increased. In this latter study, however, biliary excretion of each agent was not measured.

In a recent study (15), iopanoic acid was administered into the duodenum of dogs either simultaneously or 1 hr after an intravenous iodipamide infusion. Biliary iodipamide excretion was diminished concomitantly with an increased urinary iodipamide output.

Both iodoxamic acid and iopanoic acid bind readily to plasma proteins and have low blood clearances (6, 7, 16). Therefore, a displacement of plasma protein binding by one of these compounds may alter the elimination of the other. The coadministration studies described earlier did not assess this factor. Neither has the site nor the type of the interactions been evaluated.

The present investigation of protein binding (Tables I and II) shows that unbound concentrations of either iodoxamic acid or iopanoic acid, when infused in the presence of the other (the "competitor"), were greater than that when either acid was infused alone (6, 7) (11 of 12 instances for Monkey A and in all instances for Monkey B). These results suggest that the two compounds compete for binding sites in the proteins. Because of insufficient data, no attempts were made to determine the type of competition.

Furthermore, in both monkeys, the biliary excretion rate of each drug was lower when coadministered than when administered alone (6, 7); this finding confirms previous reports (13–15) that the biliary excretion of

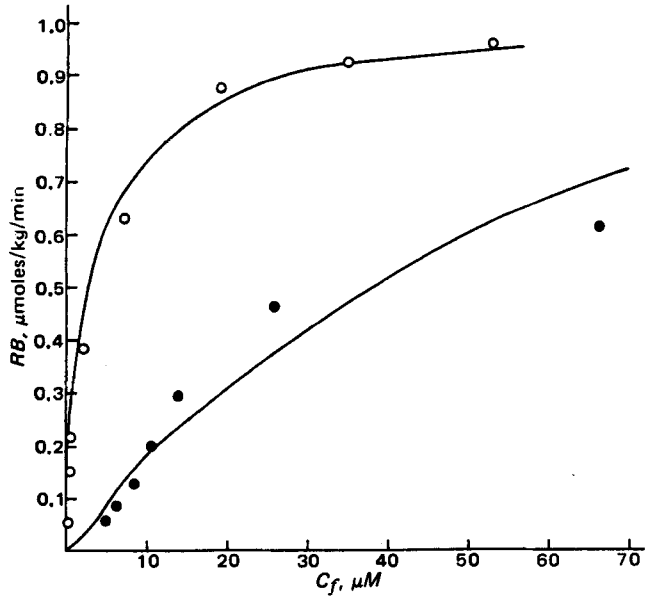

Figure 3—*Relationship between the biliary excretion rate* (RB) *and the unbound plasma concentration* (C_f) *of iodoxamic acid in the absence* (○) *and in the presence* (●) *of iopanoic acid in Monkey B. The upper solid line represents the computer-fitted values according to Eq. 4. The lower solid line represents the computer-fitted values according to Eq. 1.*

Table IV—Michaelis-Menten Parameter for Biliary Excretion of Iodoxamic and Iopanoic Acids in Monkey B

Parameter	Iodoxamic Acid	Iopanoic Acid	Combination Experiment [a]
$\overline{V}_m$, μmoles/kg/min	1.01 (0.07) [b]	1.1 (0.04)	1.01 (0.08)
K_m μM	3.5 (1.0)	0.22 (0.02)	3.5 (13.0)
K_i, μM	—	—	0.08 (0.49)

[a] $\overline{V}_m$ and K_m are fixed at iodoxamic values, and K_i is allowed to float. [b] Numbers in parentheses represent standard error of the mean.

one cholecystographic agent is reduced when coadministered with the other. In addition, the lower rate of iodoxamic acid was comparable to that of iopanoic acid (Fig. 2).

Finally, in both experiments, when the compounds were coadministered, even though the biliary excretion rates for both compounds were comparable, unbound concentrations of iopanoic acid were much lower than those of iodoxamic acid (Fig. 2 and Tables I and II). These findings suggest that iopanoic acid has a higher affinity than iodoxamic acid for the intrahepatic binding proteins (*e.g.*, Y- and Z-proteins) responsible for hepatic uptake or biliary excretion. Furthermore, relative to control values, when the compounds were administered concomitantly, competition for the intrahepatic uptake or biliary excretion between these two compounds led to lower overall excretion of both acids, with a greater reduction of iodoxamic acid excretion, despite the increased unbound plasma concentration.

In the present investigation, the "inhibitor" (iopanoic acid) was infused virtually to steady state. However, when the substrate (iodoxamic acid) infusion was started, protein binding equilibria were disturbed and the binding of both drugs was shifted. This displacement also affected the uptake or biliary excretion of both drugs, which is dependent on the free drug. After a period, the infusion of one or both compounds was discontinued. Safety considerations prevented a steady-state experiment relative to both drugs. Because the potential for drug accumulation was not known, it was feared that the animal might be killed if the infusion was continued.

After correction for the lag time, the midpoints of biliary excretion no longer coincided with the blood sampling times. Therefore, an INTERPOLATE program of the PROPHET computer system[8] was used to determine the unbound concentrations of iodoxamic acid present in the blood at the midpoints of biliary excretion. A graph (Fig. 3) of these data for Monkey B shows that the relationship between the biliary excretion rates of iodoxamic acid and its unbound concentrations during the coadministration reveals a curve that appears sigmoidal rather than hyperbolic, as was the case in the control study of the compound infused alone (6). A sigmoid curve was also demonstrated in the experiment for Monkey A. At the lowest biliary excretion rate (almost zero value), considerable unbound iodoxamic acid was still in the plasma.

Because the relationship between the biliary excretion rate (RB) and unbound concentration of iodoxamic acid (C_f) is sigmoidal rather than hyperbolic in the presence of the inhibitor, iopanoic acid, one of the following types of enzyme inhibition probably takes place: (*a*) ligand exclusion, (*b*) a two-substrate system forming a ternary complex, or (*c*) an activator of an allosteric enzyme mimicing the substrate and excluding the inhibitor (8). Only the ligand exclusion model does not require a sigmoidal relationship between the rate of enzymic reaction (v) and the substrate concentration (S) *in the absence* of the inhibitor (8). According to this model, in the absence of an inhibitor, a hyperbolic v *versus* S relationship exists (see *Theoretical*), which was the case for iodoxamic acid.

In both monkeys, a hyperbolic curve was obtained for iodoxamic acid in the absence of an inhibitor and a sigmoidal curve was obtained in the presence of iopanoic acid serving as the inhibitor. The relationships between the biliary excretion rate and the plasma unbound iodoxamic acid concentration in the absence and in the presence of the inhibitor in Monkey B are shown in Fig. 3 (Table III). The PROPHET computer system program "Hyperbolic" was used with the data weighted using the reciprocal of the variances. Both $\overline{V}_m$ and K_m were fixed at the values listed for iodoxamic acid, and K_i was at the $\overline{V}_m$ value of iopanoic acid (Table IV). Under such constraints, the data could not be fitted to Eq. 1. However, when K_i was allowed to float, results were obtained (column

[8] PROPHET system is a specialized computer resource developed by the Chemical/Biological Information Handling Program of the National Institutes of Health. A detailed description of the system's features appeared in *Proc. Natl. Compt. Conf. Exposition*, **43**, 457 (1974).

4 in Table IV). With the parameter estimates, the computer-fitted excretion rate values (RB') and residual values listed in columns 4 and 5 of Table III were obtained. These values indicate that the interaction between iodoxamic acid and iopanoic acid in the liver can be described by the ligand exclusion model. In such a model, iopanoic acid acts as an inhibitor and competes with iodoxamic acid for binding to either of two identical sites within the liver, which presumably is the rate-limiting step in the liver's overall elimination of these radiographic contrast agents. However, because of the large standard error of the mean of the estimated values of K_m and K_i, the fit may be fortuitous. Further studies will be required to investigate this tentative conclusion.

Presumably, the experimental method and the data analysis used in the present investigation can be applied to the study of the interactions between other compounds (*e.g.*, indocyanine green, sulfobromophthalein, propranolol, lidocaine, and propoxyphene) that have high hepatic excretion. To apply this approach, one must have assay procedures for each compound independently and be able to measure the unbound concentrations in plasma water.

REFERENCES

(1) R. E. Wise and F. J. Scholz, *Gastroenterology*, **65**, 967 (1973).

(2) H. Reyes, A. J. Levi, Z. Gatmaitan, and I. M. Arias, *J. Clin. Invest.*, **50**, 2242 (1971).

(3) J. Sokoloff, R. N. Berk, J. H. Lang, and E. C. Lasser, *Radiology*, **106**, 519 (1973).

(4) S. K. Lin, A. A. Moss, and S. Riegelman, *Invest. Radiol.*, **12**, 175 (1977).

(5) S. K. Lin, A. A. Moss, and S. Riegelman, *J. Pharm. Sci.*, **66**, 1670 (1977).

(6) S. K. Lin, A. A. Moss, R. Motson, and S. Riegelman, *ibid.*, **67**, 930 (1978).

(7) A. A. Moss, S. K. Lin, E. Margules, R. W. Motson, and S. Riegelman, *Invest. Radiol.*, **14**, 54 (1979).

(8) I. H. Segel, "Enzyme Kinetics," Wiley, New York, N.Y., 1975, pp. 385, 395, 460.

(9) R. H. Dowling, E. Mack, J. Picott, J. Berger, and D. M. Small, *J. Lab. Clin. Med.*, **72**, 169 (1968).

(10) A. A. Moss, L. Kaufman, and J. A. Nelson, *Invest. Radiol.*, **7**, 335 (1972).

(11) A. A. Moss, J. R. Amberg, and R. S. Jones, *ibid.*, **7**, 11 (1972).

(12) S. M. Strasberg, K. A. Siminovitch, and R. G. Ilson, *Ann. Surg.*, **180**, 356 (1974).

(13) T. Goergen, L. E. Goldberger, and R. N. Berk, *Radiology*, **111**, 543 (1974).

(14) A. A. Moss, J. A. Nelson, and J. Amberg, *Am. J. Roentgenol., Radium Ther. Nucl. Med.*, **117**, 406 (1973).

(15) W. M. Thompson, R. S. Jones, J. H. Lang, and J. R. Amberg, *Invest. Radiol.*, **13**, 79 (1978).

(16) J. H. Lang and E. C. Lasser, *ibid.*, **2**, 396 (1967).

ACKNOWLEDGMENTS

Supported in part by U.S. Public Health Service Grants NIGMS 16-496 and GM 00728 and in part by the University of California Patent Fund.

Antibody Specificity Studies for Reserpine, Its Metabolites, and Synthetic Reserpine Congeners: Radioimmunoassay

LARRY J. LOEFFLER ˣ and HORST F. SCHRAN *

Received February 6, 1979, from the *Division of Medicinal Chemistry, School of Pharmacy, University of North Carolina at Chapel Hill, Chapel Hill, NC 27514.* Accepted for publication May 24, 1979.

*Present address: Drug Metabolism Section, Pharmaceutical Research and Development, Sandoz, Inc., East Hanover, NJ 07936.

Abstract □ Progress in the development of radioimmunoassay techniques for reserpine and related compounds is reported. A conjugate of reserpine with human serum albumin was prepared, involving linkage at the indole nitrogen atom of reserpine. Injection of the purified conjugate into sheep elicited antibodies of high titer, which bound reserpine selectively. Tritiated reserpine was employed in the procedure, and dextran-coated charcoal was utilized to separate free and bound forms of the drug. Antibodies exhibited a selectivity for reserpine and did not cross-react significantly with major human metabolites. Cross-reactivity of antibodies with other reserpine derivatives (*i.e.*, syrosingopine, deserpidine, and rescinnamine) also was investigated. A stable tritiated or radioiodinated reserpine derivative of high specific activity is being sought to improve assay sensitivity for use in bioequivalence and bioavailability studies. In the absence of any extraction or concentration procedures, at least a 10-fold increase in immunoassay sensitivity would be required to follow reserpine levels in humans given normal doses of the drug. The methods show promise also for the assay of reserpine derivatives such as deserpidine, which exhibits cross-reactivity to reserpine antibodies.

Keyphrases □ Reserpine—antibody specificity studies, metabolites, synthetic congeners, radioimmunoassay □ Radioimmunoassay—analysis, reserpine, metabolites, synthetic congeners □ Antihypertensive agents—reserpine, radioimmunoassay, antibody specificity studies, metabolites, synthetic congeners

Levy *et al.* (1) reported the development of a sensitive and specific radioimmunoassay for the antihypertensive agent reserpine, with a sensitivity of 15 ng/ml in rat plasma and no interference from major metabolites. Application of the method in human bioavailability and bioequivalence studies, without preliminary extraction procedures, has been limited by sensitivity. This limitation results from the instability of tritiated reserpine of high specific activity. Experience in this laboratory with reserpine immunoassay development has been entirely analogous, but the method holds promise if a suitable tritiated or iodinated reserpine analog can be prepared.

Earlier reserpine assays, which were reviewed recently (2, 3), are useful for certain applications but involve time-consuming separations and extractions and have inadequate sensitivity and specificity for reserpine determinations in plasma or urine. A recent method (4) is reportedly sensitive to 200 pg/ml and, perhaps, to 50 pg/ml with less confidence. However, this procedure is indirect, involving extraction followed by TLC and a fluorometric densitometer scan. Recovery during extraction may be variable and must be established.

The purposes of this report are to compare specificities of antiserums produced in these laboratories during immunoassay development with the work of Levy *et al.* (1) and to discuss the potential utility of reserpine antiserums in the immunoassay of commercially available reserpine analogs such as deserpidine and rescinnamine.

0022-3549/79/1100-1433$01.00/0

© 1979, American Pharmaceutical Association

4 in Table IV). With the parameter estimates, the computer-fitted excretion rate values (RB') and residual values listed in columns 4 and 5 of Table III were obtained. These values indicate that the interaction between iodoxamic acid and iopanoic acid in the liver can be described by the ligand exclusion model. In such a model, iopanoic acid acts as an inhibitor and competes with iodoxamic acid for binding to either of two identical sites within the liver, which presumably is the rate-limiting step in the liver's overall elimination of these radiographic contrast agents. However, because of the large standard error of the mean of the estimated values of K_m and K_i, the fit may be fortuitous. Further studies will be required to investigate this tentative conclusion.

Presumably, the experimental method and the data analysis used in the present investigation can be applied to the study of the interactions between other compounds (*e.g.*, indocyanine green, sulfobromophthalein, propranolol, lidocaine, and propoxyphene) that have high hepatic excretion. To apply this approach, one must have assay procedures for each compound independently and be able to measure the unbound concentrations in plasma water.

REFERENCES

(1) R. E. Wise and F. J. Scholz, *Gastroenterology*, **65**, 967 (1973).

(2) H. Reyes, A. J. Levi, Z. Gatmaitan, and I. M. Arias, *J. Clin. Invest.*, **50**, 2242 (1971).

(3) J. Sokoloff, R. N. Berk, J. H. Lang, and E. C. Lasser, *Radiology*, **106**, 519 (1973).

(4) S. K. Lin, A. A. Moss, and S. Riegelman, *Invest. Radiol.*, **12**, 175 (1977).

(5) S. K. Lin, A. A. Moss, and S. Riegelman, *J. Pharm. Sci.*, **66**, 1670 (1977).

(6) S. K. Lin, A. A. Moss, R. Motson, and S. Riegelman, *ibid.*, **67**, 930 (1978).

(7) A. A. Moss, S. K. Lin, E. Margules, R. W. Motson, and S. Riegelman, *Invest. Radiol.*, **14**, 54 (1979).

(8) I. H. Segel, "Enzyme Kinetics," Wiley, New York, N.Y., 1975, pp. 385, 395, 460.

(9) R. H. Dowling, E. Mack, J. Picott, J. Berger, and D. M. Small, *J. Lab. Clin. Med.*, **72**, 169 (1968).

(10) A. A. Moss, L. Kaufman, and J. A. Nelson, *Invest. Radiol.*, **7**, 335 (1972).

(11) A. A. Moss, J. R. Amberg, and R. S. Jones, *ibid.*, **7**, 11 (1972).

(12) S. M. Strasberg, K. A. Siminovitch, and R. G. Ilson, *Ann. Surg.*, **180**, 356 (1974).

(13) T. Goergen, L. E. Goldberger, and R. N. Berk, *Radiology*, **111**, 543 (1974).

(14) A. A. Moss, J. A. Nelson, and J. Amberg, *Am. J. Roentgenol., Radium Ther. Nucl. Med.*, **117**, 406 (1973).

(15) W. M. Thompson, R. S. Jones, J. H. Lang, and J. R. Amberg, *Invest. Radiol.*, **13**, 79 (1978).

(16) J. H. Lang and E. C. Lasser, *ibid.*, **2**, 396 (1967).

ACKNOWLEDGMENTS

Supported in part by U.S. Public Health Service Grants NIGMS 16-496 and GM 00728 and in part by the University of California Patent Fund.

Antibody Specificity Studies for Reserpine, Its Metabolites, and Synthetic Reserpine Congeners: Radioimmunoassay

LARRY J. LOEFFLER ˣ and HORST F. SCHRAN *

Received February 6, 1979, from the *Division of Medicinal Chemistry, School of Pharmacy, University of North Carolina at Chapel Hill, Chapel Hill, NC 27514.* Accepted for publication May 24, 1979.

*Present address: Drug Metabolism Section, Pharmaceutical Research and Development, Sandoz, Inc., East Hanover, NJ 07936.

Abstract □ Progress in the development of radioimmunoassay techniques for reserpine and related compounds is reported. A conjugate of reserpine with human serum albumin was prepared, involving linkage at the indole nitrogen atom of reserpine. Injection of the purified conjugate into sheep elicited antibodies of high titer, which bound reserpine selectively. Tritiated reserpine was employed in the procedure, and dextran-coated charcoal was utilized to separate free and bound forms of the drug. Antibodies exhibited a selectivity for reserpine and did not cross-react significantly with major human metabolites. Cross-reactivity of antibodies with other reserpine derivatives (*i.e.*, syrosingopine, deserpidine, and rescinnamine) also was investigated. A stable tritiated or radioiodinated reserpine derivative of high specific activity is being sought to improve assay sensitivity for use in bioequivalence and bioavailability studies. In the absence of any extraction or concentration procedures, at least a 10-fold increase in immunoassay sensitivity would be required to follow reserpine levels in humans given normal doses of the drug. The methods show promise also for the assay of reserpine derivatives such as deserpidine, which exhibits cross-reactivity to reserpine antibodies.

Keyphrases □ Reserpine—antibody specificity studies, metabolites, synthetic congeners, radioimmunoassay □ Radioimmunoassay—analysis, reserpine, metabolites, synthetic congeners □ Antihypertensive agents—reserpine, radioimmunoassay, antibody specificity studies, metabolites, synthetic congeners

Levy *et al.* (1) reported the development of a sensitive and specific radioimmunoassay for the antihypertensive agent reserpine, with a sensitivity of 15 ng/ml in rat plasma and no interference from major metabolites. Application of the method in human bioavailability and bioequivalence studies, without preliminary extraction procedures, has been limited by sensitivity. This limitation results from the instability of tritiated reserpine of high specific activity. Experience in this laboratory with reserpine immunoassay development has been entirely analogous, but the method holds promise if a suitable tritiated or iodinated reserpine analog can be prepared.

Earlier reserpine assays, which were reviewed recently (2, 3), are useful for certain applications but involve time-consuming separations and extractions and have inadequate sensitivity and specificity for reserpine determinations in plasma or urine. A recent method (4) is reportedly sensitive to 200 pg/ml and, perhaps, to 50 pg/ml with less confidence. However, this procedure is indirect, involving extraction followed by TLC and a fluorometric densitometer scan. Recovery during extraction may be variable and must be established.

The purposes of this report are to compare specificities of antiserums produced in these laboratories during immunoassay development with the work of Levy *et al.* (1) and to discuss the potential utility of reserpine antiserums in the immunoassay of commercially available reserpine analogs such as deserpidine and rescinnamine.

0022-3549/79/1100-1433$01.00/0

© 1979, American Pharmaceutical Association

Table I—Data for Standard Radioimmunoassay Curve

Tube	Buffer[a], ml	Bovine Serum Albumin[b], ml	Reserpine Antiserum[c], ml	Reserpine (Cold)[d] Milliliters	Reserpine (Cold)[d] Nanograms	^{3}H-Reserpine[e], ml	Dextran-Coated Charcoal[f], ml
1	1.30	0.10	—	—	—	0.10	—
2	0.80	0.10	—	—	—	0.10	0.50
3	0.70	0.10	0.10	0	0	0.10	0.50
4	0.69	0.10	0.10	0.010	1.0	0.10	0.50
5	0.68	0.10	0.10	0.025	2.5	0.10	0.50
6	0.65	0.10	0.10	0.050	5.0	0.10	0.50
7	0.63	0.10	0.10	0.075	7.5	0.10	0.50
8	0.60	0.10	0.10	0.100	10.0	0.10	0.50
9	0.55	0.10	0.10	0.150	15.0	0.10	0.50
10	0.50	0.10	0.10	0.200	20.0	0.10	0.50

[a] Buffer was 0.15 *M* NaCl and 0.01 *M* sodium phosphate, pH 7.4. [b] Bovine serum albumin was 5 g of 2X crystalline bovine serum albumin (Armour)/100 ml. [c] Reserpine antiserum was diluted 1:50 with buffer; final dilution was 1:500 in tube. [d] Reserpine (cold) was 0.10 ng/μl in 10% ethanol in buffer. [e] ^{3}H-Reserpine was 0.10 ng/μl in 10% ethanol in buffer (10 ng/tube, ~5000 dpm). [f] Dextran-coated charcoal suspension contained 0.01 g of radioimmunoassay grade charcoal/ml and 0.25 mg of dextran (radioimmunoassay grade)/ml.

EXPERIMENTAL

Materials—The following were used: human serum albumin[1] (crystalline, B grade), bovine serum albumin[1] (crystalline, A grade), reserpine[2], Freund's complete adjuvant[3], formalin solution[4], dextran[5], charcoal[5], a commercial liquid scintillation fluid[6], deserpidine[7], rescinnamine[2], syrosingopine[8], methylreserpate[8], reserpic acid[8], and ^{3}H-reserpine[9]. Tritium counting was performed using a liquid scintillation spectrometer with automatic external standardization to enable computation of efficiency and disintegrations per minute of individual samples[10].

Reserpine Conjugation with Human Serum Albumin (Antigen Preparation)—To 5 μCi of ^{3}H-reserpine in 2 ml of ethanol was added 150 mg of reserpine. After solvent removal *in vacuo*, the solid was dissolved in 3.6 ml of acetic acid and added to 400 mg of human serum albumin in 4 ml of distilled water. To the resulting clear solution was added 2.4 ml of 38% formaldehyde, and the mixture was warmed at 50° under nitrogen for 1 hr. Solvents were removed *in vacuo* at room temperature (10 hr), and the residue was slurried in 10 ml of 5% sodium bicarbonate, collected by centrifugation, washed several times with 50% ethanol, and dried.

The solid product was thoroughly washed with chloroform–methanol (1:1) until no further reserpine appeared in the washings as determined by counting tracer radioactivity. Digestion of 2-mg samples of the 350 mg of conjugate obtained was carried out on a steam bath in a mixture of 10 drops of 30% hydrogen peroxide and 30 drops of 70% perchloric acid, and the digest was counted in a scintillation cocktail. Two separate determinations indicated 4.1 and 4.0 moles of reserpine/mole of human serum albumin (based on mol. wt. 70,000).

Immunization and Titer Determination—Two sheep were injected intramuscularly at several sites at monthly intervals with a solution of 3 mg of conjugate in 1.5 ml of physiological saline emulsified with 1.5 ml of Freund's complete adjuvant. Bleedings were made from the neck vein ~7–10 days after each booster injection. Serum, prepared by the usual procedures, was tested for reserpine-binding ability using 10 or 2 ng of ^{3}H-reserpine, according to the procedure described later.

Both sheep responded similarly to the conjugate, producing antiserum of usable titer (*i.e.*, 1:500–700 with 10 ng of ^{3}H-reserpine and 1:3000 with 2 ng of ^{3}H-reserpine) after 2–3 months. Bleedings taken subsequently up to 18 months maintained approximately equivalent titers and specificity. In experiments described later, serum from one sheep (LT 7-8-76) was employed.

Standard Immunoassay Curve and Specificity Studies—Table I indicates the contents of the assay tubes utilized for the standard immunoassay curve. Bovine serum albumin (0.5%) was added to the buffer (physiological saline–phosphate buffer, pH 7.4) to minimize adsorption of ^{3}H-reserpine and cold reserpine onto vessel walls. Antiserum was freshly diluted from stock on the day of use. Following antiserum addition, varying quantities of the cold reserpine, metabolite, or other reserpine analog were added. Finally, 10 ng of ^{3}H-reserpine (~5000 dpm) was added to each tube.

Tubes were incubated at 37° for 2 hr and chilled in ice for 30 min, and 0.5 ml of dextran-coated charcoal suspension (Table I, footnote *f*) was added to desired tubes. After vortexing, suspensions were left at 0° for exactly 15 min and then centrifuged at 2° for 10 min. Exactly 1.0 ml of the supernate was removed carefully by automatic pipet and counted in 10 ml of scintillation cocktail in a counting vial. Percent binding figures were calculated. Nonspecific binding (~5%) was subtracted from the total percentage figures observed. The entire procedure was essentially identical to that described previously for methotrexate (5).

Typical standard curves obtained for two different antiserum dilutions are shown in Fig. 1. Curves apparently were reproducible in initial studies and were not shifted significantly by the addition of up to 0.1 ml (10% of the total tube contents) of human serum, plasma, cerebrospinal fluid, or urine to the assay medium. Curve fitting (linearization) was also carried out using logit transformation procedures (6), particularly for cross-reactivity (specificity) studies.

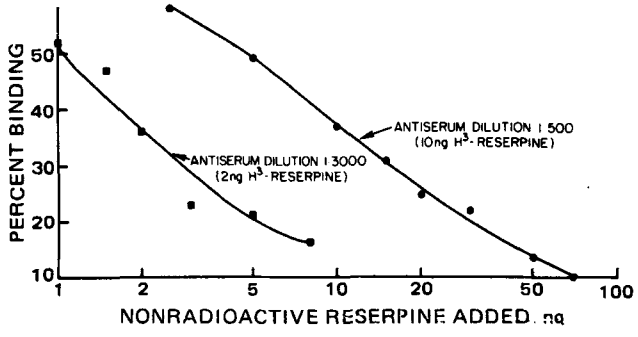

Figure 1—*Standard reserpine radioimmunoassay curve.*

RESULTS AND DISCUSSION

Immunogen and Antiserum Preparation—By employing a modification of a literature procedure (7), reserpine was coupled through the indole nitrogen *via* formaldehyde treatment in acetic acid to lysine groupings of human serum albumin. The inclusion of tracer quantities of ^{3}H-reserpine enabled estimation of the conjugate reserpine content at 4 moles/mole of human serum albumin. This level compares closely to the "Mannich-type" conjugation carried out in dimethyl sulfoxide (using bovine serum albumin) by Levy *et al.* (1), which gave a hapten–carrier ratio of about 5. The coupling site at the indole nitrogen of reserpine appears to be ideal since major metabolic (hydrolytic) transformation sites, the trimethoxybenzoyl group at position 18 and the methyl ester at position 16 (Table II), remain unmasked as potential immunodeterminant groups, and the resultant antibodies should be able to distinguish reserpine from its major metabolic products reserpic acid, methylreserpate, and trimethoxybenzoic acid (8).

Each of two sheep responded similarly to initial antigen injections and monthly boosters. After 3 months, antiserum of usable titer (1:500–700 as determined using 10 ng of ^{3}H-reserpine and 1:3000 using 2 ng of ^{3}H-reserpine) resulted; these titers remained essentially constant over the 15 additional months during which the boosters were maintained. In

[1] Calbiochem Corp., La Jolla, Calif.
[2] Sigma Chemical Co., St. Louis, Mo.
[3] Difco Laboratories, Detroit, Mich.
[4] J. T. Baker Chemical Co., Phillipsburg, N.J.
[5] Radioimmunoassay grade materials, Schwarz/Mann, Orangeburg, N.Y.
[6] Scintaverse, Fisher Chemical Co., Raleigh, N.C.
[7] Gift of Abbott Laboratories, North Chicago, Ill.
[8] Gift of Ciba-Geigy Corp., Summit, N.J.
[9] New England Nuclear Corp., Boston, Mass. (specific activity 157 mCi/mmole, ^{3}H-trimethoxybenzoyl ring).
[10] Model 3255, Packard Instrument Co., Downers Grove, Ill.

Table II—Structures of Reserpine and Related Compounds

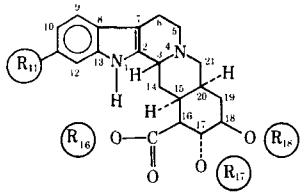

Compound	R_{11}	R_{16}	R_{17}	R_{18}
Reserpine	CH_3O	CH_3	CH_3	3′,4′,5′-Trimethoxybenzoyl
Deserpidine	H	CH_3	CH_3	3′,4′,5′-Trimethoxybenzoyl
Rescinnamine	CH_3O	CH_3	CH_3	3′,4′,5′-Trimethoxycinnamoyl
Syrosingopine	CH_3O	CH_3	CH_3	3′,5′-Dimethoxy-4′-ethylcarbonatobenzoyl
Methylreserpate	CH_3O	CH_3	CH_3	H
Reserpic acid	CH_3O	H	CH_3	H

comparison with these results, Levy *et al.* (1) reported a maximal titer of only 1:100 (1 ng of ^{3}H-reserpine) with their Mannich-type immunogen and eventually based their immunoassay on higher titer antiserum that originated from a "diazo-type" conjugate coupled in the indole benzene ring.

Standard Immunoassay Curve—With the components described in Table I and the conditions discussed under *Experimental*, typical standard immunoassay curves (Fig. 1) were obtained. Points were usually determined in triplicate, with a coefficient of variation of <8% in all cases when 10 ng of ^{3}H-reserpine was used. The position and shape of the curve were not influenced appreciably by the addition of up to 10% (0.1 ml) of human plasma, serum, or cerebrospinal fluid. With 2 ng of ^{3}H-reserpine, increased error was observed (Fig. 1).

Because of interest in obtaining radiolabeled material of higher specific activity (producing increased sensitivity), exhaustive work has not been carried out to determine optimum conditions for the assay with the available tritiated reserpine of low specific activity. The obvious deficiency of the system employing commercially available ^{3}H-reserpine is sensitivity insufficient to reach levels normally found (estimated by gross radioactivity measurements) in human subjects. These levels are 0.2–2.0 ng/ml according to one study after a single oral 0.25-mg dose (9). Levy *et al.* (1), using ^{3}H-reserpine of specific activity 1.7 Ci/mmole (of limited stability but ~10 times that available commercially), apparently encountered similar difficulties, with sensitivity limited to ~15 ng/ml of plasma, unless Tripp's extraction procedure was employed for primary reserpine concentration in the sample. In this laboratory, iodination procedures with iodine 125 have been unsuccessful, and similar difficulties were reported by Levy *et al.* (1).

Cross-Reactivity Studies (Specificity Determinations)—The major reserpine metabolites as well as several semisynthetic analogs were studied for their ability to displace ^{3}H-reserpine from antibody binding sites under the conditions outlined earlier. Metabolites were reserpic acid, methylreserpate, and 3,4,5-trimethoxybenzoic acid; commercially available synthetic analogs were rescinnamine, syrosingopine, and deserpidine (Table II). Results (Table III) are expressed as the ratio of the amount of compound to the amount of reserpine producing 50% binding inhibition (also expressed as percent cross-reactivity, derived from the reciprocal of the ratio in question). These figures were obtained *via* logit transformation linearization of sigmoid curves such as those shown in Fig. 1 (6).

The results in Table III indicate that major reserpine metabolites in humans, specifically reserpic acid, methylreserpate, and 3,4,5-trimethoxybenzoic acid, do not cross-react to any significant extent (<0.6%) with reserpine antibodies. Similar results were obtained by Levy *et al.* (1) using both their Mannich-type immunogen and a preferable "higher titer" antiserum involving coupling of bovine serum albumin through an azobenzoyl linkage adjacent to the 11-methoxy substituent of reserpine. Such results with all three conjugates are expected, because coupling sites are remote from the metabolism sites at the 16- and 18-positions; *i.e.*, these groups are left free as immunodeterminants in the hapten.

Table III—Cross-Reactivity of Reserpine Analogs and Metabolites in Reserpine Radioimmunoassay

Compound	Ratio of Amount of Compound to Amount of Reserpine Producing 50% Binding Inhibition: This Study	"Mannich" Immunogen (Ref. 1)	"Diazo-Coupled" Immunogen (Ref. 1)
Reserpine	1.0 (100)[a]	1.0 (100)	1.0 (100)
Reserpic acid	167 (0.6)	>2200 (<0.1)	>2000 (<0.1)
Methylreserpate	167 (0.6)	85 (1.2)	90 (1.1)
Serotonin	—	>2500 (<0.1)	>2500 (<0.1)
3,4,5-Trimethoxybenzoic acid	≫670 (<0.2)	>2300 (<0.1)	>2000 (<0.1)
Rescinnamine	38 (2.6)	5 (20)	130 (0.8)
Syrosingopine	≫670 (<0.2)	—	—
Deserpidine	1.33 (75)	—	—

[a] Figures in parentheses express percent cross-reactivity.

Of particular interest is the observation that deserpidine, which differs from reserpine only in the absence of an 11-methoxy grouping, was bound to antibody prepared in this work nearly as well as reserpine (75% cross-reactivity), indicating that the 11-position on the aromatic ring, which is rather close to the N-1 indole nitrogen atom, the point of coupling, is thus hindered as an immunodeterminant group in antibody formation. This observed cross-reactivity is of special interest as a potential basis for a deserpidine immunoassay. Little cross-reactivity was observed between antiserum and the two additional synthetic reserpine analogs, syrosingopine (0.2%) and rescinnamine (2.6%), although the latter was bound significantly to the Roche antibody ("Mannich immunogen," 20% cross-reactivity).

Such specificity studies, especially if combined with a stable tritiated or iodinated reserpine derivative (or one of the other drugs mentioned), could contribute valuable methodology for bioavailability, bioequivalence, and metabolism studies of reserpine or its analogs.

REFERENCES

(1) A. Levy, K. Kawashima, and S. Spector, *Life Sci.*, **19**, 1421 (1976).

(2) R. E. Stitzel, *Pharm. Rev.*, **28**, 179 (1976).

(3) R. E. Schirmer, in "Analytical Profiles of Drug Substances," vol. 4, K. Florey, Ed., Academic, New York, N.Y., 1975, pp. 385–430.

(4) S. L. Tripp, E. Williams, W. E. Wagner, Jr., and G. Lucas, *Life Sci.*, **16**, 1167 (1975).

(5) L. J. Loeffler, M. R. Blum, and M. A. Nelsen, *Cancer Res.*, **26**, 3306 (1976).

(6) D. Rodbard, R. H. Lenox, H. L. Wray, and D. Ramseth, *Clin. Chem.*, **22**, 350 (1976).

(7) A. Taunton-Rigby, S. E. Sher, and P. R. Kelley, *Science*, **181**, 165 (1973).

(8) A. J. Glazko, W. A. Dill, L. M. Wolf, and A. Kazenko, *J. Pharmacol. Exp. Ther.*, **118**, 377 (1956).

(9) A. R. Maass, B. Jenkins, Y. Shen, and P. Tannenbaum, *Clin. Pharmacol. Ther.*, **10**, 366 (1969).

ACKNOWLEDGMENTS

Presented in part at the Medicinal Chemistry Section, APhA Academy of Pharmaceutical Sciences, Phoenix meeting, November 1977.

Supported in part through a grant from the University of North Carolina Research Council.

The authors acknowledge the valuable technical assistance of Mr. Mark H. Holshouser.

Pseudomonas cepacia Resistance to Antibacterials

R. M. E. RICHARDS [x] **and JOAN M. RICHARDS**

Received April 16, 1979, from the *Department of Pharmaceutics, University of Strathclyde, Glasgow G1 1XW, Scotland.* Accepted for publication June 4, 1979.

Abstract □ Reproducible growth rates of *Pseudomonas cepacia* were obtained. *P. cepacia* had a markedly different resistance pattern to single and combined antibacterials from that characteristic of *Pseudomonas aeruginosa*. Benzalkonium and chlorhexidine were more active against log phase *P. cepacia* than against log phase *P. aeruginosa*, but polymyxin B sulfate was inactive against log phase *P. cepacia* at all concentrations tested (≤16 units/ml). Antagonism of antibacterial activity between edetate disodium–benzalkonium and edetate disodium–chlorhexidine combinations was marked with 16-hr *P. cepacia* and with 16-hr *Staphylococcus aureus*. Phenylethanol–benzalkonium and phenylethanol–chlorhexidine combinations had no more than additive activity against log phase *P. cepacia*. These results have relevance to hospital disinfection and preservation of pharmaceutical solutions.

Keyphrases □ *Pseudomonas cepacia*—resistance to antibacterial agents, benzalkonium chloride, chlorhexidine, phenylethanol □ Antibacterial agents—*Pseudomonas cepacia*, resistance to benzalkonium chloride, chlorhexidine, phenylethanol

Pseudomonas cepacia is one of a number of unusual *Pseudomonas* species that have increased in clinical significance since the 1960's (1).

In 1950 (2), Burkholder described *P. cepacia*. Subsequently, other workers described the same species but did not recognize it as *P. cepacia* (3–6). The designations "eugonic oxidisers group 1" (EO-1) (4), *Pseudomonas kingii* (5), and *Pseudomonas multivorans* (6) were given before it was established that all were *P. cepacia* (7, 8).

Soil, vegetation, and water are natural environmental sources (2, 3, 6, 9), but the hospital environment also has proved to be a source of *P. cepacia;* several clinical infections have occurred (10–14). The infecting organism has been shown to survive common concentrations of chlorhexidine (11, 15), a cetrimide–chlorhexidine combination (12), benzalkonium chloride (13), and a dimethylbenzylammonium chloride–phenoxypolyethoxyethanol combination (14, 16).

P. cepacia is resistant also to a wide range of antibiotics, and its antibiotic-resistance spectrum is different from that of *Pseudomonas aeruginosa* (1, 17).

Table I—Doubling Times of Replicate Log Phase *P. cepacia* Cultures

Culture	Mean Doubling Time, min	95% Confidence Limits
A	34.5	33.6–35.6
B	34.3	33.0–35.7
C	34.7	33.3–36.1
D	34.3	33.1–35.6
E	34.4	33.1–35.8
F	35.4	34.3–36.5

Table II—Effect of Benzalkonium Chloride on the Doubling Times of Log Phase *P. cepacia* Cultures

Benzalkonium, μg/ml	Mean Doubling Time, min	95% Confidence Limits
None	35.2	34.1–36.4
1	41.1	39.6–42.7
2	45.8	44.5–47.3
4	70.0	62.5–79.5

Table III—Effect of Chlorhexidine Gluconate on the Doubling Times of Log Phase *P. cepacia* Cultures

Chlorhexidine, μg/ml	Mean Doubling Time, min	95% Confidence Limits
None	36.4	35.3–37.6
1	54.8	47.2–65.4
2	81.5	62.2–103.6

Table IV—Effect of Polymyxin B Sulfate on the Doubling Time of Log Phase *P. cepacia* Cultures

Polymyxin, units/ml	Mean Doubling Time, min	95% Confidence Limits
None	34.3	33.4–35.3
1	33.8	32.3–35.4
2	34.4	33.2–35.9
4	34.5	33.3–35.7
8	34.8	33.8–35.9
16	35.6	34.2–37.2

The present investigation was undertaken to evaluate the resistance of *P. cepacia* to chemical antibacterials including combinations previously shown to be active against *P. aeruginosa* (18–23).

EXPERIMENTAL

Materials—*P. cepacia*[1] and *Staphylococcus aureus*[2] were the test organisms. Nutrient broth No. 2[3] and nutrient agar[3] were the liquid and solid culture media, respectively. Chlorhexidine gluconate[4], benzalkonium chloride[5] (alkyldimethylbenzylammonium chloride: C_{14}, 50%; C_{12}, 40%; and C_{16}, 10%), polymyxin B sulfate[6], phenylethanol[7], and edetate disodium[7] were used as supplied.

Methods—Growth rate determinations and estimates of killing times of one or two chemical antibacterial systems were carried out. Viable counts were determined by the pour plate method, and cultures were maintained as described previously (24). Incubation was at 37°.

Estimation of Growth Rates—Log phase cultures were prepared as follows. A separate *P. cepacia* agar stab culture was used as the source of inoculum for each determination to prepare 10 ml of 24-hr broth culture. A loopful of this culture was used to inoculate 25 ml of broth in a 250-ml conical flask shaking at 100 throws/min. After 16 hr, this culture was diluted 1:50 with prewarmed broth and shaken at 150 throws/min for 10 min to disperse clumps. Aliquots, 5 ml, were added separately to 95-ml quantities of prewarmed broth in 250-ml conical flasks shaking at 100 throws/min. Growth was followed for each culture as was already described for *P. aeruginosa* (19). Typical growth rates (Table I) were calculated as described previously (25).

The effect of chemicals on the growth rate was determined for single chemicals and for combinations as for *P. aeruginosa* (19, 25). Tables II–IV give the growth rates of *P. cepacia* grown in broth and in broth plus varying concentrations of benzalkonium chloride, chlorhexidine gluconate, or polymyxin B sulfate. Tables V and VI show the effect of a combination of benzalkonium chloride and phenylethanol and a combination of chlorhexidine gluconate and phenylethanol, respectively.

[1] NCTC 10661, National Collection of Type Cultures, Colindale, London, England.
[2] NCTC 6751, National Collection of Type Cultures, Colindale, London, England.
[3] Oxoid, Oxo Ltd., London, England.
[4] I.C.I., Alderly Park, Macclesfield, Cheshire, England.
[5] Rohm & Haas (UK) Ltd., Croydon, England.
[6] Burroughs and Wellcome Ltd., Dartford, England.
[7] B. D. H., Poole, Dorset, England.

0022-3549/79/1100-1436$01.00/0
© 1979, American Pharmaceutical Association

Table V—Effect of a Combination of Benzalkonium Chloride and Phenylethanol against Log Phase *P. cepacia* Cultures

Chemical	Mean Doubling Time, min	95% Confidence Limits
None	34.5	33.2–35.9
Phenylethanol, 0.05%	57.6	54.1–61.4
Phenylethanol, 0.1%	107.8	96.8–121.6
Phenylethanol, 0.05%, + benzalkonium chloride, 1 μg/ml	66.5	61.2–72.9
Benzalkonium chloride, 1 μg/ml	48.4	45.6–51.5
Benzalkonium chloride, 2 μg/ml	62.4	59.1–66.1

Table VI—Effect of a Combination of Chlorhexidine Gluconate and Phenylethanol against Log Phase *P. cepacia* Cultures

Chemical	Mean Doubling Time, min	95% Confidence Limits
None	35.6	34.6–36.8
Phenylethanol, 0.05%	52.6	51.1–54.3
Phenylethanol, 0.1%	112.6	102.3–125.2
Phenylethanol, 0.05%, + chlorhexidine gluconate, 0.5 μg/ml	72.7	70.5–75.1
Chlorhexidine gluconate, 0.5 μg/ml	44.9	43.0–46.9
Chlorhexidine gluconate, 1.0 μg/ml	59.0	55.5–63.0

Estimation of Killing Times—Determinations for *P. cepacia* and *S. aureus* were carried out separately as described previously (26) (Tables VII and VIII).

RESULTS AND DISCUSSION

Table I shows that the growth rates of replicate log phase cultures prepared as described gave reproducible results. Benzalkonium and chlorhexidine showed greater activity against exponentially growing cultures of *P. cepacia* than against log phase *P. aeruginosa* cultures (27).

Phenylethanol plus either benzalkonium or chlorhexidine had an additive effect against log phase *P. cepacia* cultures (Tables V and VI), but a synergistic effect was demonstrated with these combinations against *P. aeruginosa* under similar conditions (18, 20, 25).

Polymyxin B sulfate, ≤16 units/ml, showed no activity against *P. cepacia*. This finding is in marked contrast to results obtained with *P. aeruginosa*, where 1 unit/ml reduced the growth rate (21). The growth rates of five *P. cepacia* cultures plus five graded concentrations of polymyxin were indistinguishable from the growth rates in broth containing no added chemical (Table IV compared with Table I).

Study of polysorbate 80 on the activity of benzalkonium and chlorhexidine against log phase *P. cepacia* indicated that polysorbate 80 antagonized their antibacterial action[8]. This result also differs from that seen with *P. aeruginosa*, where synergism was observed (27).

The killing time results (Tables VII and VIII) show a difference, with respect to edetate disodium resistance, between *P. cepacia* and *P. aeruginosa*. In fact, *P. cepacia* had similar resistance to *S. aureus* toward the edetate disodium combinations with benzalkonium or chlorhexidine. This finding has considerable application to the formulation of ophthalmic solutions and contact lens solutions, which often contain edetate disodium–antibacterial agent combinations as the preservative system. Edetate disodium plus benzalkonium in ophthalmic solutions had increased activity against *P. aeruginosa* (28), but edetate disodium with either benzalkonium or chlorhexidine had less activity against *P. cepacia* and *S. aureus* than either benzalkonium or chlorhexidine solutions used singly. That is, edetate disodium antagonized the action of both chemicals against these two organisms.

Phenylethanol plus benzalkonium or chlorhexidine had shorter killing times against 16-hr *P. cepacia* cultures at the concentrations tested than any of the chemicals alone. These results in conjunction with the *P. cepacia* growth rate results indicate that the kill of *P. cepacia* cells obtained with the phenylethanol plus either benzalkonium or chlorhexidine is likely the result of each chemical exerting its individual action independently of the second member of the combination. The overall effect appears to be additive.

[8] R. M. E. Richards and J. M. Richards, unpublished results.

Table VII—Killing Times at 22° for the Test Chemicals Singly and in Combination against ~2 × 10^6 Organisms (16-hr *P. cepacia*)/ml

Chemical	Concentration, %	Killing Time, min
Benzalkonium chloride	0.01	120–150
Phenylethanol	0.4	>360
Edetate disodium	0.1	>360
Benzalkonium + phenylethanol	0.01 0.4	60–90
Benzalkonium + edetate disodium	0.01 0.1	>360
Chlorhexidine gluconate	0.01	60–90
Chlorhexidine gluconate + phenylethanol	0.01 0.4	<15
Chlorhexidine gluconate + edetate disodium	0.01 0.1	>360

Table VIII—Killing Times at 22° for the Test Chemicals Singly and in Combination against ~2 × 10^6 Organisms (16-hr *S. aureus*)/ml

Chemical	Concentration, %	Killing Time, min
Benzalkonium chloride	0.004	45–60
Phenylethanol	0.4	>360
Edetate disodium	0.1	>360
Benzalkonium + phenylethanol	0.004 0.4	45–60
Benzalkonium chloride + edetate disodium	0.004 0.1	180–240
Chlorhexidine gluconate	0.004	120–150
Chlorhexidine gluconate + phenylethanol	0.004 0.4	45–60
Chlorhexidine gluconate + edetate disodium	0.004 0.1	>360

The different resistance pattern of *P. cepacia* to *P. aeruginosa* is important in the hospital situation where a breakdown in disinfectant procedure can have serious consequences for the compromised patient.

The antagonism of benzalkonium and chlorhexidine by edetate disodium against *S. aureus* is probably most significant for chlorhexidine, which is less active against *S. aureus* than benzalkonium.

Significant differences in the structure of the cell envelope of the two pseudomonads are implicated by the marked difference in sensitivity to polymyxin alone or to edetate disodium–benzalkonium, edetate disodium–chlorhexidine, phenylethanol–benzalkonium, or phenylethanol–chlorhexidine as combinations (29).

REFERENCES

(1) A. von Graevenitz, *Prog. Clin. Pathol.*, **5**, 185 (1973).

(2) W. H. Burkholder, *Phytopathology*, **40**, 115 (1950).

(3) M. B. Morris and J. B. Roberts, *Nature (London)*, **183**, 1538 (1959).

(4) E. O. King, National Communicable Disease Center, Atlanta, Ga., 1964, rev. 1967; through Ref. 1.

(5) V. Jonsson, *Int. J. Syst. Bacteriol.*, **20**, 255 (1970).

(6) R. Y. Stanier, N. J. Palleroni, and M. Doudoroff, *J. Gen. Microbiol.*, **43**, 159 (1966).

(7) R. W. Ballard, M. J. Palleroni, M. Doudoroff, and M. Mandel, *ibid.*, **60**, 199 (1970).

(8) D. C. Sands, M. N. Schroth, and D. C. Hildebrand, *J. Bacteriol.*, **101**, 9 (1970).

(9) D. Taplin, D. C. J. Bassett, and P. M. Mertz, *Lancet*, **2**, 568 (1971).

(10) R. G. Mitchell and A. C. Hayward, *ibid.*, **1**, 793 (1966).

(11) D. W. Burdon and J. L. Whitby, *Br. Med. J.*, **2**, 153 (1967).

(12) D. C. J. Bassett, J. J. Stokes, and W. R. G. Thomas, *Lancet*, **1**, 1188 (1970).

(13) G. L. Gilardi, *Appl. Microbiol.*, **20**, 521 (1970).

(14) I. Phillips, S. Eykyn, M. A. Curtis, and J. J. S. Snell, *Lancet*, **1**, 375 (1971).

(15) D. C. E. Speller, M. E. Stephens, and A. C. Viant, *ibid.*, **1**, 798 (1971).

(16) P. C. Hardy, G. M. Ederer, and J. M. Matsen, *N. Engl. J. Med.*,

282, 33 (1970).
(17) J. J. Rahal, M. S. Simberkoff, and P. J. Hyams, *J. Infect. Dis., Suppl.*, 128, 762 (1973).
(18) R. M. E. Richards and R. J. McBride, *J. Pharm. Sci.*, 61, 1075 (1972).
(19) *Ibid.*, 62, 585 (1973).
(20) *Ibid.*, 62, 2035 (1973).
(21) *Ibid.*, 63, 54 (1974).
(22) R. M. E. Richards and R. H. Cavill, *J. Pharm. Sci.*, 65, 76 (1976).
(23) R. M. E. Richards and R. H. Cavill, *J. Pharm. Pharmacol.*, 28, 935 (1976).
(24) M. R. W. Brown and R. M. E. Richards, *ibid.*, 16, 41T (1964).
(25) R. M. E. Richards and R. J. McBride, *ibid.*, 23, 141S (1971).
(26) R. M. E. Richards and L. M. Mizrahi, *J. Pharm. Sci.*, 67, 380 (1978).
(27) M. R. W. Brown and R. M. E. Richards, *J. Pharm. Pharmacol.*, 16, 51T (1964).
(28) R. M. E. Richards, *ibid.*, 23, 136S (1971).
(29) *Ibid.*, 30, 14P (1978).

Urinary Iodine Excretion Rates following Intrathecal Injections of Iodinated Organic Carbonates

A. E. STAUBUS *x, B. N. NEWTON ‡, L. C. KLEIN ‡, A. B. WEINRIB *, and A. L. KUNZ ‡

Received May 17, 1978, from the **College of Pharmacy, Ohio State University, Columbus, OH 43210,* and the ‡*Research and Development Department, Lafayette Pharmacal, Division of Alcon Laboratories, Inc., Lafayette, IN 47902.* Accepted for publication June 4, 1979.

Abstract □ Oily iodinated organic carbonates were investigated for use as myelographic media. The urinary excretion of total iodine was used to monitor the apparent elimination rate of these compounds from the subarachnoid space. Within the chain length series of C_2–C_6, the decrease of elimination rates and disposition rate constants with increasing chain length was demonstrated. This observation is consistent with a dissolution rate-limited elimination model. Such a model was derived and successfully NONLIN computer fitted to the observed elimination data. The model-derived parameter of clearance from the cerebrospinal fluid through the lipid "blood–brain barrier" correlated well with the compound's water solubilities and projected octanol–water partition coefficients. Additional compounds need to be tested to evaluate the postulated model system.

Keyphrases □ Myelographic agents—oily iodinated organic carbonates, biological elimination □ Pharmacokinetics—myelographic agents, oily iodinated organic carbonates, biological elimination □ Contrast media—oily iodinated organic carbonates, biological elimination

Positive-contrast myelography is the X-ray visualization of the subarachnoid space using a radiopaque substance. It is used to evaluate trauma to the spinal column and to delineate tumors and other canal obstructions. The only approved myelographic agent in the United States is iophendylate [ethyl 10-(*p*-iodophenyl)undecylate[1]] (I).

Iophendylate has been used in the United States in several million examinations since the early 1940's. It is considered to be very safe; however, it is removed at the conclusion of the examination because its biological elimination has been reported to be 1 ml/year (1). Water-soluble contrast agents have been used in Europe for over 30 years, but they have not been approved for use in the United States due to their higher incidence of adverse reactions.

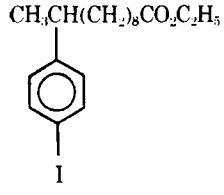

I

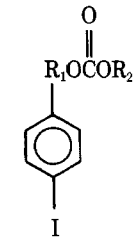

II

$R_1 = -(CH_2)-_n$, n = 0–4
$R_2 = -C_nH_{2n+1}$, n = 1–10

Drawbacks with the current agents necessitated a search for a readily absorbable, nontoxic, oily myelographic medium. Oily iodinated organic carbonates of the general Structure II (2) were investigated. To understand quantitatively the biological elimination of these compounds, four representative carbonates were selected for study.

EXPERIMENTAL

The urinary excretion of total iodine was used to monitor the apparent elimination rate of the four carbonates from the subarachnoid space. In preliminary studies, the rate-limiting step for the overall elimination of compounds from the body appeared to be absorption from the subarachnoid space.

In an additional study, a series of rats was sacrificed at 24, 48, and 72 hr and on Day 5 following suboccipital injection. Other than expected high brain tissue levels, the only detectable iodine concentrations were in trace amounts (~0.3 μmole/g) found in skin samples at 24, 48, and 72 hr. Heart, kidney, liver, leg muscle, lung, and intestine samples on any of the 4 days and Day 5 skin samples all showed no detectable iodine. Consequently, the urinary excretion of the iodinated metabolites should reflect the relative absorption rates. For statistical purposes, each of the four compounds was tested in six rats. This method quantitatively confirmed the radiographic disappearance observed in these animals.

Thirty-six adult Sprague–Dawley female rats, 197–225 g, were divided into six equal groups. Each group was dosed with a different test compound. The purity of each test compound (Table I) was determined by GLC and NMR and agreed with analytically pure samples (~99% pure).

[1] Pantopaque.

0022-3549/79/1100-1438$01.00/0
© 1979, American Pharmaceutical Association

282, 33 (1970).
(17) J. J. Rahal, M. S. Simberkoff, and P. J. Hyams, *J. Infect. Dis., Suppl.*, 128, 762 (1973).
(18) R. M. E. Richards and R. J. McBride, *J. Pharm. Sci.*, 61, 1075 (1972).
(19) *Ibid.*, 62, 585 (1973).
(20) *Ibid.*, 62, 2035 (1973).
(21) *Ibid.*, 63, 54 (1974).
(22) R. M. E. Richards and R. H. Cavill, *J. Pharm. Sci.*, 65, 76 (1976).
(23) R. M. E. Richards and R. H. Cavill, *J. Pharm. Pharmacol.*, 28, 935 (1976).
(24) M. R. W. Brown and R. M. E. Richards, *ibid.*, 16, 41T (1964).
(25) R. M. E. Richards and R. J. McBride, *ibid.*, 23, 141S (1971).
(26) R. M. E. Richards and L. M. Mizrahi, *J. Pharm. Sci.*, 67, 380 (1978).
(27) M. R. W. Brown and R. M. E. Richards, *J. Pharm. Pharmacol.*, 16, 51T (1964).
(28) R. M. E. Richards, *ibid.*, 23, 136S (1971).
(29) *Ibid.*, 30, 14P (1978).

Urinary Iodine Excretion Rates following Intrathecal Injections of Iodinated Organic Carbonates

A. E. STAUBUS *x, B. N. NEWTON ‡, L. C. KLEIN ‡, A. B. WEINRIB *, and A. L. KUNZ ‡

Received May 17, 1978, from the **College of Pharmacy, Ohio State University, Columbus, OH 43210,* and the ‡*Research and Development Department, Lafayette Pharmacal, Division of Alcon Laboratories, Inc., Lafayette, IN 47902.* Accepted for publication June 4, 1979.

Abstract □ Oily iodinated organic carbonates were investigated for use as myelographic media. The urinary excretion of total iodine was used to monitor the apparent elimination rate of these compounds from the subarachnoid space. Within the chain length series of C_2–C_6, the decrease of elimination rates and disposition rate constants with increasing chain length was demonstrated. This observation is consistent with a dissolution rate-limited elimination model. Such a model was derived and successfully NONLIN computer fitted to the observed elimination data. The model-derived parameter of clearance from the cerebrospinal fluid through the lipid "blood–brain barrier" correlated well with the compound's water solubilities and projected octanol–water partition coefficients. Additional compounds need to be tested to evaluate the postulated model system.

Keyphrases □ Myelographic agents—oily iodinated organic carbonates, biological elimination □ Pharmacokinetics—myelographic agents, oily iodinated organic carbonates, biological elimination □ Contrast media—oily iodinated organic carbonates, biological elimination

Positive-contrast myelography is the X-ray visualization of the subarachnoid space using a radiopaque substance. It is used to evaluate trauma to the spinal column and to delineate tumors and other canal obstructions. The only approved myelographic agent in the United States is iophendylate [ethyl 10-(*p*-iodophenyl)undecylate[1]] (I).

Iophendylate has been used in the United States in several million examinations since the early 1940's. It is considered to be very safe; however, it is removed at the conclusion of the examination because its biological elimination has been reported to be 1 ml/year (1). Water-soluble contrast agents have been used in Europe for over 30 years, but they have not been approved for use in the United States due to their higher incidence of adverse reactions.

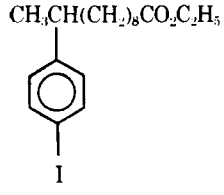

I

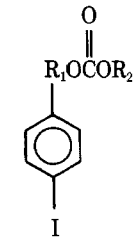

II

$R_1 = -(CH_2)-_n$, n = 0–4
$R_2 = -C_nH_{2n+1}$, n = 1–10

Drawbacks with the current agents necessitated a search for a readily absorbable, nontoxic, oily myelographic medium. Oily iodinated organic carbonates of the general Structure II (2) were investigated. To understand quantitatively the biological elimination of these compounds, four representative carbonates were selected for study.

EXPERIMENTAL

The urinary excretion of total iodine was used to monitor the apparent elimination rate of the four carbonates from the subarachnoid space. In preliminary studies, the rate-limiting step for the overall elimination of compounds from the body appeared to be absorption from the subarachnoid space.

In an additional study, a series of rats was sacrificed at 24, 48, and 72 hr and on Day 5 following suboccipital injection. Other than expected high brain tissue levels, the only detectable iodine concentrations were in trace amounts (~0.3 μmole/g) found in skin samples at 24, 48, and 72 hr. Heart, kidney, liver, leg muscle, lung, and intestine samples on any of the 4 days and Day 5 skin samples all showed no detectable iodine. Consequently, the urinary excretion of the iodinated metabolites should reflect the relative absorption rates. For statistical purposes, each of the four compounds was tested in six rats. This method quantitatively confirmed the radiographic disappearance observed in these animals.

Thirty-six adult Sprague–Dawley female rats, 197–225 g, were divided into six equal groups. Each group was dosed with a different test compound. The purity of each test compound (Table I) was determined by GLC and NMR and agreed with analytically pure samples (~99% pure).

[1] Pantopaque.

0022-3549/79/1100-1438$01.00/0
© 1979, American Pharmaceutical Association

Table I—Physical Properties of *p*-Iodobenzyl Carbonates

Compound	R_1	R_2	Viscosity[a] at 25°, cps	Density	n_D^{25}	Water Solubility, mole/liter	Molecular Formula	Analysis, % Calc.	Found
II*a*	$-CH_2-$	$-C_2H_5$	11.76	1.6108	1.5587	6×10^{-5}	$C_{10}H_{11}IO_3$	C 39.22	39.24
								H 3.62	3.77
								I 41.48	41.49
II*b*	$-CH_2-$	$-C_4H_9$	14.37	1.4959	1.5431	1.3×10^{-5}	$C_{12}H_{15}IO_3$	C 43.11	42.87
								H 4.53	4.40
								I —[b]	—[b]
II*c*	$-CH_2-$	$-C_5H_{11}$	16.68	1.4584	1.5439	2.8×10^{-6}	$C_{13}H_{17}IO_3$	C 44.82	44.50
								H 4.92	4.84
								I 36.46	37.51
II*d*	$-CH_2-$	$-C_6H_{13}$	18.58	1.4100	1.5368	1.9×10^{-6}	$C_{14}H_{19}IO_3$	C 46.40	46.25
								H 5.29	5.36
								I 35.05	34.77

[a] Ostwald viscosity technique. [b] Not available.

Table II—Reproducibility of Urinary Iodine Concentrations

Standard, μmole/ml	Mean Concentration, μmoles/ml	*CV*, %
0.15	0.149	12.0
0.25	0.218	10.2
0.50	0.553	5.5
1.00	1.019	3.0

Table III—Daily Means and Standard Deviations for Cumulative Urinary Excretion of II*a* (Micromoles per Kilogram)

Day	Mean	*SD*
1	354.7	105.4
2	935.1	114.9
3	1237.4	119.8
4	1306.1	143.2
5	1345.9	155.6
6	1358.9	161.7
7	1367.5	166.7
8→∞	1372.7	170.1

The animals were removed from feed 18 hr before dosing. After anesthetization with ether, the back of the neck was clipped closely. The animal was then placed on a grooved board that allowed the head to be declined at 45°. With a 27-gauge needle, a puncture was made at the base of the atlas and 2.5 mmoles/kg of the test material was injected uniformly over 15 sec. Suboccipital injection was confirmed radiographically. The animals were then placed in individual metabolism cages, and the urine was collected at 24-hr intervals until the urine concentrations dropped below the assay reliability.

Individual rat urine volumes were measured in 50-ml graduated cylinders, and representative 1.5-ml aliquots were removed and transferred to disposable plastic analyzer cups[2]. The daily urinary iodine concentration of each rat was determined using k-shell fluorescent activation analysis (3). The reproducibility of eight replicates of four representative concentrations is shown in Table II.

RESULTS AND DISCUSSION

Daily Urinary Excretion Rate Variability—Figures 1A and 1B illustrate the urinary excretion rate variability for individual rats. The correlation coefficient (r) of the terminal log-linear disposition phases ranged from $r > 0.99$ (Fig. 1A) to $r > 0.88$ (Fig. 1B). In general, correlation coefficients were >0.96.

Mean Urinary Excretion Rate Data—As can be seen from the mean urinary excretion rate plots (Figs. 2–5), peak iodine excretion rates occurred within 1–2 days following intrathecal administration. With increasing chain length of the R_2 group (II), the terminal log-linear half-life ($t_{1/2}$) progressively increased. The terminal $t_{1/2}$ values ranged from 0.78 day for II*a* to 11.3 days for II*d*.

Cumulative Urinary Excretion Data—The same relative correlation with chain length can be seen in both the mean cumulative urinary excretion plot (Fig. 6) and the plot of the percent remaining to be eliminated (Fig. 7). Intersubject variability can be evaluated from the means and standard deviations provided in Tables III–VI for the cumulative urinary excretion of these compounds. Compound II*c* had the least intersubject variability.

For all four compounds, the percent of the dose excreted into the urine was essentially identical (54.9 ± 0.9%). Since no radiopaque residues were observed at the end of each study, the remaining dose was presumed to be eliminated *via* the biliary fecal route. Spot checking of fecal samples for iodine content confirmed the biliary excretion component of elimination.

Terminal Disposition Rate Constants—The mean, standard deviation, and corresponding $t_{1/2}$ values for the terminal disposition rate constants are shown in Table VII. Again, the influence of increasing the chain length of the alkyl portion of the molecule was reflected in dramatic changes in the magnitude of the terminal disposition rate constants and in the harmonic means of their corresponding $t_{1/2}$ values.

Table IV—Daily Means and Standard Deviations for Cumulative Urinary Excretion of II*b* (Micromoles per Kilogram)

Day	Mean	*SD*	Day	Mean	*SD*
1	283.5	32.6	12	1242.4	148.8
2	538.0	43.0	13	1266.4	153.1
3	712.3	78.0	14	1285.2	156.5
4	815.0	97.0	15	1303.3	158.5
5	905.1	113.9	16	1316.1	160.9
6	991.7	119.1	17	1328.6	162.5
7	1053.4	127.3	18	1337.9	165.9
8	1104.7	129.7	19	1347.1	169.7
9	1149.9	134.6	20	1354.3	171.5
10	1187.7	140.3	21	1360.5	172.9
11	1215.6	145.5	22→∞	1398.0	187.2

Table V—Daily Means and Standard Deviations[a] for Cumulative Urinary Excretion of II*c* (Micromoles per Kilogram)

Day	Mean	*SD*	Day	Mean	*SD*
1	280.9	69.3	19	1284.3	93.5
2	505.1	108.5	20	1294.0	93.9
3	656.8	113.7	21	1303.9	93.3
4	755.9	95.4	22	1311.8	93.2
5	842.5	95.1	23	1318.8	93.5
6	930.6	85.9	24	1324.9	93.6
7	989.3	94.5	25	1330.2	93.5
8	1037.2	103.1	26	1335.4	93.2
9	1079.1	100.8	27	1340.1	93.0
10	1121.2	97.1	28	1343.7	92.4
11	1153.2	96.9	29	1346.3	91.6
12	1173.4	97.9	30	1349.6	90.8
13	1196.2	97.5	31	1352.3	90.2
14	1215.6	95.9	32	1354.8	90.2
15	1233.3	95.0	33	1357.4	90.1
16	1247.1	94.1	34	1360.2	89.1
17	1262.0	93.4	35	1362.0	88.8
18	1274.6	93.3	36→∞	1377.0	84.1

[a] The reported values for II*c* pertain to the mean and standard deviation of only five of the six administered rats. One rat had to be rejected based on radiographic evidence of subcutaneous injection instead of intrathecal injection and its grossly dissimilar elimination behavior.

[2] Sherwood Medical Industries, St. Louis, Mo.

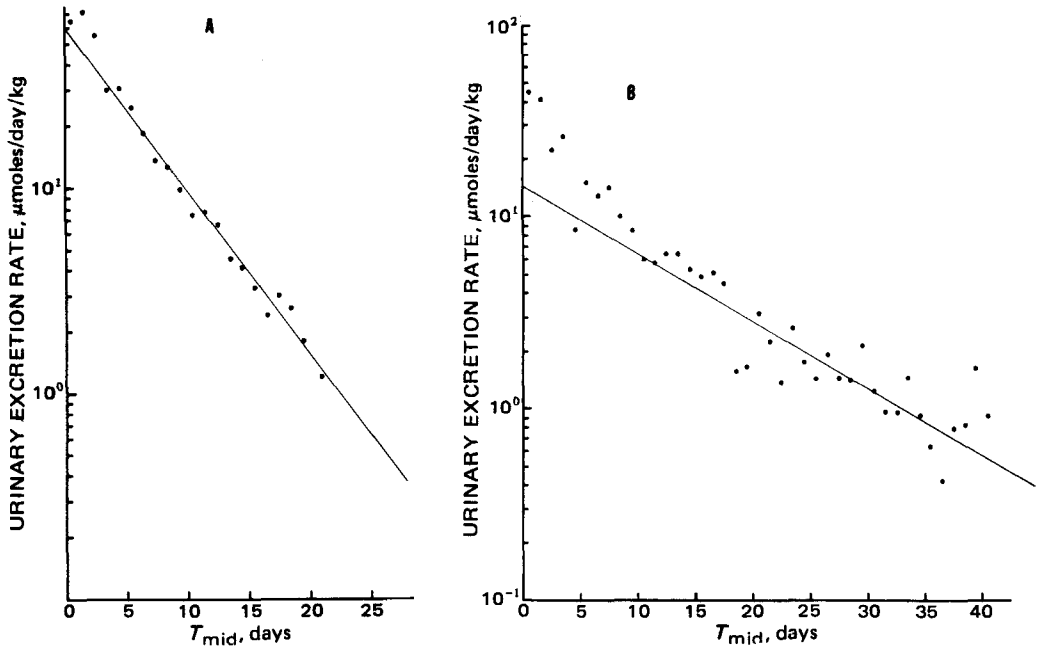

Figure 1—*A. Example of the best individual rat's urinary excretion rate plot. Compound IIb was administered. Straight line and corresponding half-life value were derived from log-linear regression of terminal data points. B. Example of the worst individual rat's urinary excretion rate plot. Compound IId was administered. Straight line and corresponding half-life value were derived from log-linear regression of terminal data points.*

Pharmacokinetic Model Fitting—Based on the extremely low water solubilities of the compounds and the apparent correlation of the amounts remaining to be eliminated with X-ray evidence of the oil droplets adhering to the spinal cord, an attempt was made to computer fit the excretion data with a dissolution rate-limited elimination mode. The model chosen incorporated the following assumptions:

1. The rate-limiting step for the overall elimination from the body was the oil dissolution into the aqueous environment of the cerebrospinal fluid (CSF).
2. Following oil dissolution into the cerebrospinal fluid, diffusion and cerebrospinal fluid circulation carried the dissolved compound to an absorption surface ("blood–brain barrier"), where the dissolved drug was cleared rapidly by a passive first-order mechanism into the venous circulation system.
3. The subsequent metabolism and excretion of the compounds were rapid and nonrate limited, permitting the daily elimination rate to approximate the daily flux of the compound from the cerebrospinal fluid.

Passage through the blood–brain barrier can be represented pharmacokinetically by:

$$\frac{dA_e}{dt} = (Cl_{CSF})(C) \qquad \text{(Eq. 1)}$$

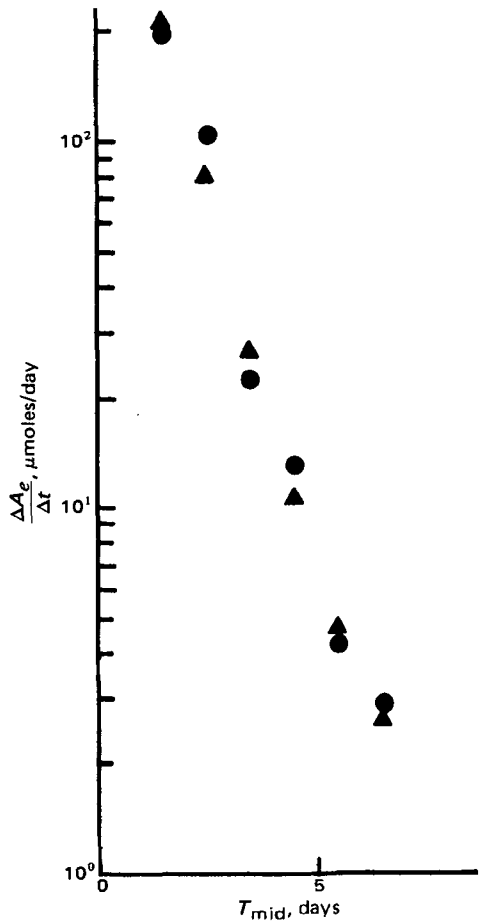

Figure 2—*Predicted (▲) and observed (●) elimination rates* versus *midpoint times for IIa.*

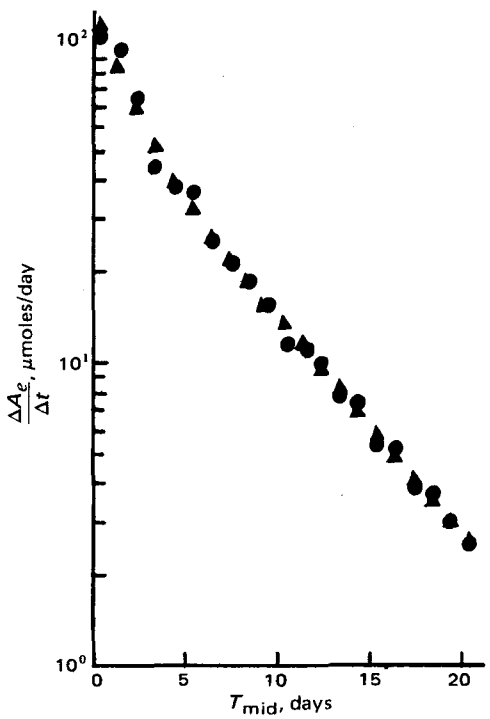

Figure 3—*Predicted (▲) and observed (●) elimination rates* versus *midpoint times for IIb.*

Table VI—Daily Means and Standard Deviations for Cumulative Urinary Excretion of II*d* (Micromoles per Kilogram)

Day	Mean	*SD*	Day	Mean	*SD*
1	270.3	93.2	22	1148.5	251.7
2	436.8	95.0	23	1159.0	251.3
3	537.5	84.8	24	1169.7	251.1
4	629.1	163.6	25	1181.9	252.0
5	687.9	163.6	26	1190.3	251.3
6	755.0	191.0	27	1198.7	252.0
7	814.5	203.4	28	1207.1	251.9
8	863.9	217.3	29	1215.3	252.2
9	903.5	227.5	30	1223.0	252.1
10	937.6	227.7	31	1230.5	251.6
11	962.9	230.0	32	1237.8	251.2
12	987.1	232.8	33	1243.0	251.4
13	1008.5	235.5	34	1248.8	250.6
14	1029.9	238.7	35	1254.3	249.7
15	1049.8	241.5	36	1259.2	248.8
16	1068.7	245.5	37	1263.3	249.2
17	1085.1	245.7	38	1267.7	249.2
18	1099.9	247.0	39	1271.7	249.2
19	1110.8	247.2	40	1276.7	248.4
20	1122.5	247.6	41	1280.9	247.9
21	1137.5	250.7	42→∞	1343.2	236.5

where:

$\frac{dA_e}{dt}$ = average total daily elimination rate (calculated from fraction excreted) or average daily flux from the cerebrospinal fluid (grams per day)

Cl_{CSF} = cerebrospinal fluid clearance through the blood–brain barrier (liters per day)

C = concentration of the compound at the absorption surface of the blood–brain barrier (grams per cubic centimeter)

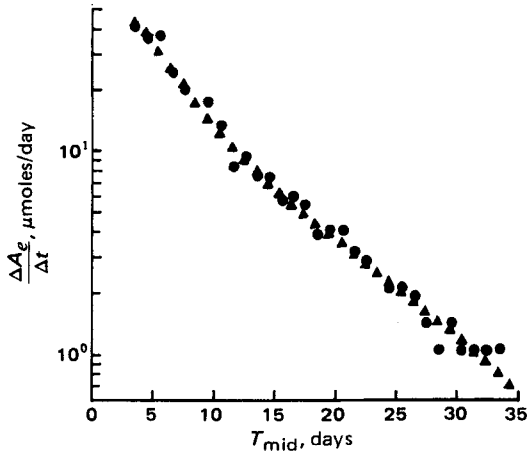

Figure 4—*Predicted (▲) and observed (●) elimination rates* versus *midpoint times for II*c.

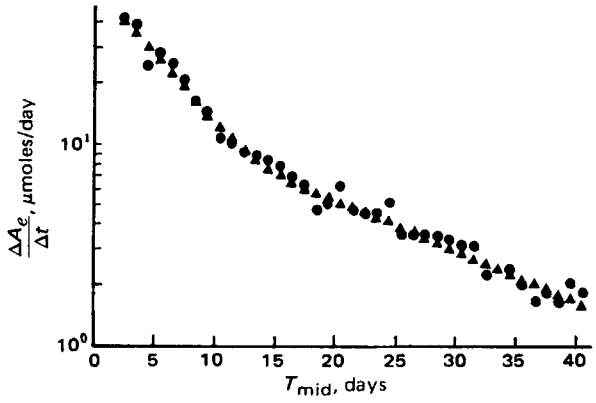

Figure 5—*Predicted (▲) and observed (●) elimination rates* versus *midpoint times for II*d.

Table VII—Mean, Standard Deviation, and Corresponding $t_{1/2}$ Values for the Terminal Disposition Rate Constants

Compound	Disposition Rate Constant, day^{-1} Mean	*SD*	$t^*_{1/2}$[a], days (Range of Individual $t_{1/2}$ Values)
II*a*	0.9273	0.1605	0.75 (0.63–0.95)
II*b*	0.1755	0.0385	3.95 (3.02–5.24)
II*c*	0.1147	0.0143	6.04 (5.47–7.58)
II*d*	0.0630	0.0144	10.99 (8.26–14.59)

[a] $t^*_{1/2}$ = (0.693/mean terminal disposition rate constant).

Selection of the dissolution rate-limited model allows use of the Noyes–Whitney equation (4):

$$\frac{dA_e}{dt} = \frac{AD}{h}(C_s - C) \qquad \text{(Eq. 2)}$$

where dA_e/dt and C are the same as already given, A is the average daily surface area of oil droplets (square centimeters), D is the diffusion coefficient of the compound through the cerebrospinal fluid (square centimeters per day), h is the average effective diffusion layer thickness (centimeters), and C_s is the water solubility of the compound (grams per cubic centimeter).

Since both Eqs. 1 and 2 share the term C, they can be rearranged into the following equation for the average daily elimination rate:

$$\frac{dA_e}{dt} = \left(\frac{C_s}{\frac{1}{Cl_{CSF}} + \frac{1}{(AD/h)}}\right) \qquad \text{(Eq. 3)}$$

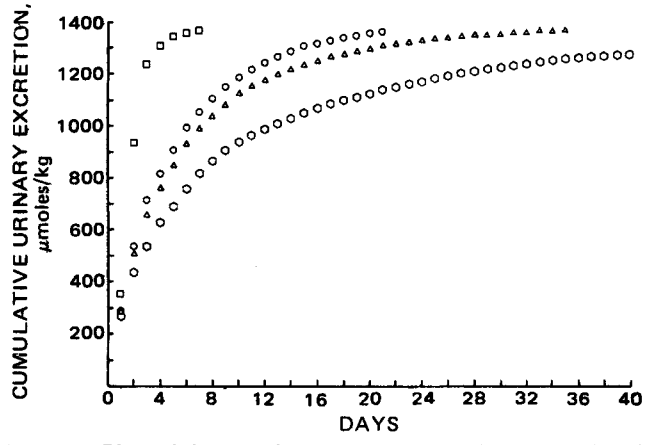

Figure 6—*Plots of the cumulative urinary excretion* versus *time for each of the four compounds.*

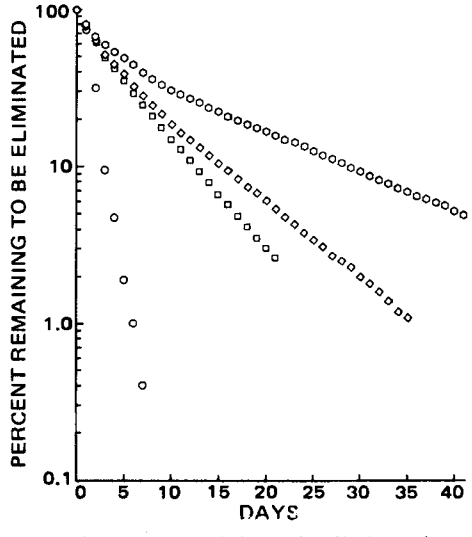

Figure 7—*Plots of percent remaining to be eliminated* versus *time for each of the four compounds.*

Table VIII—Estimates for the Dissolution Rate-Limited Model

Compound	$A \times 10^{-12}$, cm³/day³	$B \times 10^{-12}$, cm³/day³	α, days^{-1}	β, days^{-1}	$Cl \times 10^{-4}$, ml/day
II*a*	4.723	1.997×10^{-3}	1.629	3.497×10^{-2}	1.121
II*b*	3.954	2.142×10^{-1}	0.9686	1.819×10^{-1}	2.417
II*c*	250.0	3.136	0.5387	1.143×10^{-1}	3.562
II*d*	326.0	1.393	0.5357	6.619×10^{-2}	3.908

Table IX—Comparison of Weighted Sum of Squares Deviations

Compound	Dissolution Rate-Limited Model	Model-Independent Biexponential
II*a*	0.1236	0.1654
II*b*	0.1148	0.1280
II*c*	0.4566	0.4604
II*d*	0.4678	0.4978

Equation 3 accurately predicts the expected elimination rate for two possible extreme conditions: (*a*) if the amount of oil injected into the cerebrospinal fluid is extremely large, then with a large surface area, $[1/(AD/h)]$ will be overshadowed by $[1/(Cl_{CSF})]$, resulting in a pseudo-zero-order elimination rate of $(Cl_{CSF})(C_s)$; and (*b*) if the amount of oil remaining within the cerebrospinal fluid approaches zero, $[1/(AD/h)]$ will approach infinity and will overshadow $[1/(Cl_{CSF})]$, resulting in an elimination rate of nearly zero.

To utilize Eq. 3, it is necessary to approximate the average daily surface area. It can be calculated based on the average daily amount remaining to be eliminated $[(ARE_i + ARE_{i-1})/2]$, the oil density, the apparent average daily number of oil droplets (n), and the assumption of spherical oil drops. The resulting surface area equation is:

$$A = \left(\frac{9\pi n}{\text{density}^2}\right)^{1/3} (ARE_{i-1} + ARE_i)^{2/3} \qquad \text{(Eq. 4)}$$

By substitution of Eq. 4 into Eq. 3, Eq. 5 results:

$$\frac{dA_e}{dt} = \frac{C_s}{\dfrac{1}{Cl_{CSF}} + \dfrac{1}{\left[\left(\dfrac{D}{h}\right)^3 n\right]^{1/3} \left(\dfrac{9\pi}{\text{density}^2}\right)^{1/3} (ARE_{i-1} + ARE_i)^{2/3}}} \qquad \text{(Eq. 5)}$$

Knowing *in vitro* determinations of C_s and density (Table I) and *in vivo* determinations of dA_e/dt and ARE values, Eq. 5 can be NONLIN (5) fitted to solve for Cl_{CSF} and $(D/h)^3n$. Initial NONLIN fitting of Eq. 5 using 5-day segments of II*d* revealed that the Cl_{CSF} parameter remained essentially constant throughout the 41-day study while $[(D/h)^3n]$ decreased with increasing time. The decrease in $[(D/h)^3n]$ was found to fit empirically a simple biexponential equation. Consequently, the standard biexponential equation $[(D/h)^3n] = (A_e^{-\alpha t} + B_e^{-\beta t})$ was substituted into Eq. 5. The elimination data were then NONLIN fitted to Eq. 5, iterating five parameters: Cl_{CSF}, A, B, α, and β.

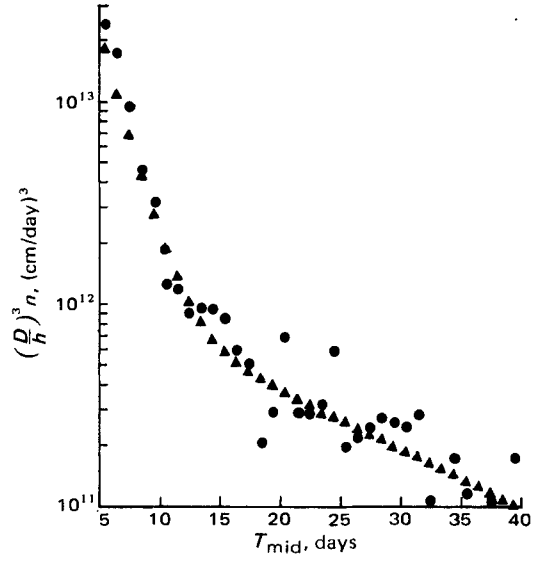

Figure 8—*Predicted (▲) and observed (●) particle number factor [(D/h)³n] versus midpoint times for II*d*. The predicted values were derived from the NONLIN biexponential equation of the particle number factor. The observed values were derived from Eq. 6, which utilizes the daily elimination rate data and the NONLIN-calculated apparent cerebrospinal fluid clearance.*

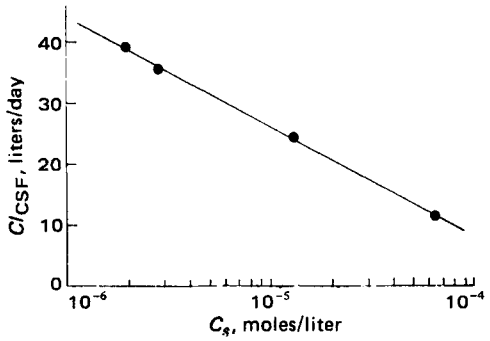

Figure 9—*Plot of the water solubilities of the four compounds versus their apparent cerebrospinal fluid clearance.*

With the NONLIN-derived value for Cl_{CSF}, $[(D/h)^3n]$ can be generated by rearranging Eq. 5:

$$\left[\left(\frac{D}{h}\right)^3 n\right] = \frac{\text{density}^2}{9\pi} \left[\frac{Cl_{CSF}\left(\dfrac{dA_e}{dt}\right)}{\left(C_s Cl_{CSF} - \dfrac{dA_e}{dt}\right)(ARE_{i-1} + ARE_i)^{2/3}}\right] \qquad \text{(Eq. 6)}$$

The plot of $[(D/h)^3n]$ *versus* T_{mid} of II*d* (calculated from Eq. 6) can be compared (Fig. 8) to the NONLIN-parameter-derived values of the biexponential equation. The biexponential equation gives a reasonable empirical approximation for this parameter.

All four compounds were then NONLIN fitted to Eq. 5; data fits can be seen in Figs. 2–5. Parameter values are summarized in Table VIII. The fits are applied to the mean elimination rate data of each of the four compounds.

For comparison purposes, the elimination rate data also were NONLIN computer fitted to a series of model-independent polyexponential equations. A simple model-independent biexponential expression was found to describe accurately the observed data. Table IX illustrates the comparison between the sets of NONLIN fitting with respect to the weighted sum of squares deviations. The dissolution rate-limited model gave equal or only slightly better fits to the data. However, the dissolution rate-limited model has at least one advantage in that it predicts decreasing elimination rates with decreasing water solubilities.

In addition, an interesting correlation exists between the nonrate-limiting Cl_{CSF} parameter and the compound's water solubilities (Fig. 9) and projected octanol–water partition coefficients (Fig. 10). These correlations ($r^2 > 0.999$) predict that the water solubilities of other oils possibly could be large enough for the rate-limiting elimination step to become the passage through the lipid blood–brain barrier rather than dissolution into the cerebrospinal fluid. This behavior is consistent with the Hansch postulates pertaining to drug transport and distribution for biological activity within a series of analog compounds (6–8).

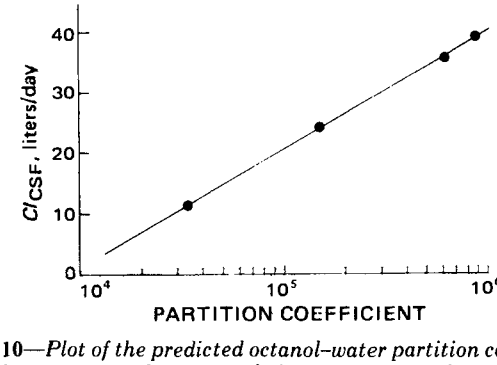

Figure 10—*Plot of the predicted octanol–water partition coefficients of the four compounds versus their apparent cerebrospinal fluid clearance.*

No other correlation was found between water solubilities and other observed or derived parameter values.

CONCLUSIONS

Within the chain length series of C_2–C_6, the decrease of elimination rates and disposition rate constants with increasing chain length was demonstrated. This observation is consistent with a dissolution rate-limited elimination model. Such a model was derived and successfully NONLIN computer fitted to the observed elimination data. The model-derived parameter of clearance from the cerebrospinal fluid through the lipid blood–brain barrier correlated well with the compound's water solubilities and projected octanol–water partition coefficients. Additional compounds need to be tested to evaluate the postulated model system.

REFERENCES

(1) B. W. McKee, R. Ethier, J. L. Vezina, and D. Melacon, *Am. J. Roentgenol.*, **107**, 612 (1969).

(2) B. N. Newton, *J. Med. Chem.*, **19**, 1362 (1976).

(3) A. A. Moss, L. Kaufman, and J. A. Nelson, *Invest. Radiol.*, **7**, 335 (1972).

(4) A. Noyes and J. Whitney, *J. Am. Chem. Soc.*, **19**, 930 (1897).

(5) C. M. Metzler, "NONLIN, A Computer Program for Parameter Estimation in Nonlinear Situations," Upjohn Co., Kalamazoo, Mich., 1969.

(6) C. Hansch and T. Fujita, *J. Am. Chem. Soc.*, **86**, 1616 (1964).

(7) C. Hansch and W. J. Dunn, III, *J. Pharm. Sci.*, **61**, 1 (1972).

(8) C. Hansch and J. M. Clayton, *ibid.*, **62**, 1 (1973).

Distribution and Elimination of Poly(methyl-2-^{14}C-methacrylate) Nanoparticle Radioactivity after Injection in Rats and Mice

JÖRG KREUTER *x, ULRICH TÄUBER ‡, and VOLKER ILLI ‡

Received December 22, 1978, from the **School of Pharmacy, Swiss Federal Institute of Technology, CH-8092 Zürich, Clausiusstr. 25, Switzerland,* and the ‡*Research Laboratories of Schering AG, Berlin/Bergkamen, Germany.* Accepted for publication June 5, 1979.

Abstract □ The organ distribution of poly(methyl-2-^{14}C-methacrylate) nanoparticles after 0.5, 1, 2, 6, and 24 hr and after 7 days, as well as the elimination of degradation products in urine, feces, and breath, was measured for 7 days after intravenous administration to rats. The radioactivity was determined quantitatively after preparation of the organs and qualitatively by macroautoradiography. In addition, nanoparticle distribution after intramuscular administration to mice was determined by macroautoradiography after 7, 35, and 70 days. Thirty minutes after intravenous administration, the nanoparticles were found in the lungs in high concentrations (758 μg/g fresh weight ≅ 22% of the administered dose); 60% (261 μg/g) of the dose was found in the liver. During the first 7 days, the concentration in the lungs decreased from 758 to 284 μg/g while the concentration in the liver increased from 261 to 372 μg/g (≅ 68% of the administered dose), the concentration in the spleen increased from 33 to 131 μg/g (≅ 4%), and the concentration in the bones increased from 3 to 6 μg/g. In all other organs and tissues, the radioactivity decreased significantly. During the first 7 days after intravenous administration, 1% of the administered dose was eliminated in the urine, 3.5% in the feces, and 1% in the breath. After intramuscular administration, all of the ^{14}C-radioactivity still present in the body persisted at the injection site for 70 days.

Keyphrases □ Poly(methyl methacrylate) nanoparticles—distribution and elimination, intravenous and intramuscular administration, radioactive tracer study, rats, mice □ Nanoparticles—poly(methyl methacrylate), elimination and distribution, intravenous and intramuscular administration, rats, mice □ Methyl methacrylate—polymers, distribution and elimination, intravenous and intramuscular administration, rats, mice

During the past few years, nanoparticles and nanocapsules were introduced as new drug delivery systems (1–4). Poly(methyl methacrylate) nanoparticles with incorporated or adsorbed antigens seem to be especially promising as adjuvants for immunology (1, 2, 5, 6). Incorporation into, as well as adsorption onto, these particles yielded much higher antibody titers than aluminum hydroxide and fluid vaccines and gave better protection (1, 5, 6).

Poly(methyl methacrylate) has been used in surgery for over 30 years as a material for artificial bones (7). Implanted poly(methyl methacrylate) seemed to be well tolerated if the implants were monomer-free and under a certain threshold size (8–11).

However, little is known about the biodegradability and the elimination of poly(methyl methacrylate) from the body. Oppenheimer *et al.* (12) implanted small pieces of poly(^{14}C-methyl methacrylate) films [—$CH_2C(CH_3)$-$COO^{14}CH_3$], having 3.6×10^4 cpm/mg, into rats. The rats began to excrete radioactive material after 54 weeks. When the film was removed, the urinary radioactivity disappeared. These investigators concluded that the radioactivity could not be due to any residual monomer in the films since no radioactive material appeared in the urine immediately upon embedding but only after an extended interval. Tomatis (13) implanted poly(methyl methacrylate) films, with a diameter of 15 mm^2, subcutaneously in mice. The urinary excretion of the label was initially low but slowly increased between 2 and 6 weeks after implantation. It fell suddenly to a minimal amount during the 9th week.

Particles in the nanometer range [nanoparticles and nanocapsules (2, 4)] exhibit a much larger surface area than the implants used by previous investigators. In addition, due to the minute size of the nanoparticles, transport from the site of application might occur even after intramuscular injection or implantation. This study was aimed at gaining information about the fate of these nanoparticles after intravenous and intramuscular administrations.

EXPERIMENTAL

Synthesis of Methyl-2-^{14}C-methacrylate [$CH_2{}^{14}C(CH_3)COOCH_3$] (I)—Compound I was synthesized from 2-^{14}C-acetone[1] by the cyanohydrin procedure (14).

[1] 2-^{14}C-Acetone was prepared by conventional methods starting from barium ^{14}C-carbonate *via* Grignard carboxylation and pyrolysis of lithium 1-^{14}C-acetate (20).

0022-3549/79/1100-1443$01.00/0

© 1979, American Pharmaceutical Association

No other correlation was found between water solubilities and other observed or derived parameter values.

CONCLUSIONS

Within the chain length series of C_2–C_6, the decrease of elimination rates and disposition rate constants with increasing chain length was demonstrated. This observation is consistent with a dissolution rate-limited elimination model. Such a model was derived and successfully NONLIN computer fitted to the observed elimination data. The model-derived parameter of clearance from the cerebrospinal fluid through the lipid blood–brain barrier correlated well with the compound's water solubilities and projected octanol–water partition coefficients. Additional compounds need to be tested to evaluate the postulated model system.

REFERENCES

(1) B. W. McKee, R. Ethier, J. L. Vezina, and D. Melacon, *Am. J. Roentgenol.*, **107**, 612 (1969).

(2) B. N. Newton, *J. Med. Chem.*, **19**, 1362 (1976).

(3) A. A. Moss, L. Kaufman, and J. A. Nelson, *Invest. Radiol.*, **7**, 335 (1972).

(4) A. Noyes and J. Whitney, *J. Am. Chem. Soc.*, **19**, 930 (1897).

(5) C. M. Metzler, "NONLIN, A Computer Program for Parameter Estimation in Nonlinear Situations," Upjohn Co., Kalamazoo, Mich., 1969.

(6) C. Hansch and T. Fujita, *J. Am. Chem. Soc.*, **86**, 1616 (1964).

(7) C. Hansch and W. J. Dunn, III, *J. Pharm. Sci.*, **61**, 1 (1972).

(8) C. Hansch and J. M. Clayton, *ibid.*, **62**, 1 (1973).

Distribution and Elimination of Poly(methyl-2-^{14}C-methacrylate) Nanoparticle Radioactivity after Injection in Rats and Mice

JÖRG KREUTER *x, ULRICH TÄUBER ‡, and VOLKER ILLI ‡

Received December 22, 1978, from the **School of Pharmacy, Swiss Federal Institute of Technology, CH-8092 Zürich, Clausiusstr. 25, Switzerland,* and the ‡*Research Laboratories of Schering AG, Berlin/Bergkamen, Germany.* Accepted for publication June 5, 1979.

Abstract □ The organ distribution of poly(methyl-2-^{14}C-methacrylate) nanoparticles after 0.5, 1, 2, 6, and 24 hr and after 7 days, as well as the elimination of degradation products in urine, feces, and breath, was measured for 7 days after intravenous administration to rats. The radioactivity was determined quantitatively after preparation of the organs and qualitatively by macroautoradiography. In addition, nanoparticle distribution after intramuscular administration to mice was determined by macroautoradiography after 7, 35, and 70 days. Thirty minutes after intravenous administration, the nanoparticles were found in the lungs in high concentrations (758 μg/g fresh weight ≅ 22% of the administered dose); 60% (261 μg/g) of the dose was found in the liver. During the first 7 days, the concentration in the lungs decreased from 758 to 284 μg/g while the concentration in the liver increased from 261 to 372 μg/g (≅ 68% of the administered dose), the concentration in the spleen increased from 33 to 131 μg/g (≅ 4%), and the concentration in the bones increased from 3 to 6 μg/g. In all other organs and tissues, the radioactivity decreased significantly. During the first 7 days after intravenous administration, 1% of the administered dose was eliminated in the urine, 3.5% in the feces, and 1% in the breath. After intramuscular administration, all of the ^{14}C-radioactivity still present in the body persisted at the injection site for 70 days.

Keyphrases □ Poly(methyl methacrylate) nanoparticles—distribution and elimination, intravenous and intramuscular administration, radioactive tracer study, rats, mice □ Nanoparticles—poly(methyl methacrylate), elimination and distribution, intravenous and intramuscular administration, rats, mice □ Methyl methacrylate—polymers, distribution and elimination, intravenous and intramuscular administration, rats, mice

During the past few years, nanoparticles and nanocapsules were introduced as new drug delivery systems (1–4). Poly(methyl methacrylate) nanoparticles with incorporated or adsorbed antigens seem to be especially promising as adjuvants for immunology (1, 2, 5, 6). Incorporation into, as well as adsorption onto, these particles yielded much higher antibody titers than aluminum hydroxide and fluid vaccines and gave better protection (1, 5, 6).

Poly(methyl methacrylate) has been used in surgery for over 30 years as a material for artificial bones (7). Implanted poly(methyl methacrylate) seemed to be well tolerated if the implants were monomer-free and under a certain threshold size (8–11).

However, little is known about the biodegradability and the elimination of poly(methyl methacrylate) from the body. Oppenheimer *et al.* (12) implanted small pieces of poly(^{14}C-methyl methacrylate) films [—$CH_2C(CH_3)$-$COO^{14}CH_3$], having 3.6×10^4 cpm/mg, into rats. The rats began to excrete radioactive material after 54 weeks. When the film was removed, the urinary radioactivity disappeared. These investigators concluded that the radioactivity could not be due to any residual monomer in the films since no radioactive material appeared in the urine immediately upon embedding but only after an extended interval. Tomatis (13) implanted poly(methyl methacrylate) films, with a diameter of 15 mm^2, subcutaneously in mice. The urinary excretion of the label was initially low but slowly increased between 2 and 6 weeks after implantation. It fell suddenly to a minimal amount during the 9th week.

Particles in the nanometer range [nanoparticles and nanocapsules (2, 4)] exhibit a much larger surface area than the implants used by previous investigators. In addition, due to the minute size of the nanoparticles, transport from the site of application might occur even after intramuscular injection or implantation. This study was aimed at gaining information about the fate of these nanoparticles after intravenous and intramuscular administrations.

EXPERIMENTAL

Synthesis of Methyl-2-^{14}C-methacrylate [$CH_2{}^{14}C(CH_3)COOCH_3$] (I)—Compound I was synthesized from 2-^{14}C-acetone[1] by the cyanohydrin procedure (14).

[1] 2-^{14}C-Acetone was prepared by conventional methods starting from barium ^{14}C-carbonate *via* Grignard carboxylation and pyrolysis of lithium 1-^{14}C-acetate (20).

0022-3549/79/1100-1443$01.00/0

© 1979, American Pharmaceutical Association

Table I—Distribution of ^{14}C-Radioactivity after Intravenous Administration of Poly(methyl-2-^{14}C-methacrylate) Nanoparticles to Rats (n = 4; Two Males and Two Females)[a]

Sample	30 min		1 hr		2 hr		6 hr		24 hr		7 days	
	Percent Dose	Micrograms per Gram	Percent Dose	Micrograms per Gram	Percent Dose	Micrograms per Gram	Percent Dose	Micrograms per Gram	Percent Dose	Micrograms per Gram	Percent Dose	Micrograms per Gram
Blood (1 ml)	0.253 ± 0.102	20.2 ± 8.1	0.134 ± 0.059	10.7 ± 4.7	0.077 ± 0.024	6.16 ± 1.89	0.117 ± 0.069	7.77 ± 4.17	0.127 ± 0.093	10.1 ± 7.4	0.020 ± 0.000	1.60 ± 0.00
Fatty tissue abdominal[b]	0.032 ± 0.011	1.29 ± 0.42	0.020 ± 0.006	0.817 ± 0.225	0.019 ± 0.006	0.771 ± 0.259	0.032 ± 0.012	1.28 ± 0.46	0.014 ± 0.005	0.563 ± 0.189	0.006 ± 0.003	0.237 ± 0.103
Fatty tissue subcutaneous[b]	0.023 ± 0.006	0.904 ± 0.240	0.018 ± 0.004	0.700 ± 0.152	0.014 ± 0.003	0.549 ± 0.107	0.025 ± 0.011	1.00 ± 0.43	0.016 ± 0.006	0.648 ± 0.221	0.007 ± 0.001	0.289 ± 0.044
Skin[b]	0.026 ± 0.001	1.03 ± 0.04	0.030 ± 0.012	1.20 ± 0.49	0.023 ± 0.003	0.922 ± 0.121	0.104 ± 0.079	4.17 ± 3.18	0.046 ± 0.026	1.82 ± 1.05	0.005 ± 0.001	0.190 ± 0.037
Bones[b]	0.079 ± 0.026	3.17 ± 1.05	0.071 ± 0.024	2.85 ± 0.96	—	—	0.072 ± 0.029	2.87 ± 1.15	0.097 ± 0.043	3.89 ± 1.71	0.158 ± 0.061	6.34 ± 2.45
Spinal cord[b]	0.029 ± 0.010	1.14 ± 0.39	0.030 ± 0.010	1.21 ± 0.42	—	—	0.023 ± 0.007	0.908 ± 0.299	0.028 ± 0.022	1.11 ± 0.89	0.003 ± 0.001	0.133 ± 0.051
Skeleton muscles[b]	0.225 ± 0.177	8.99 ± 7.08	0.045 ± 0.028	1.81 ± 1.13	0.092 ± 0.038	3.66 ± 1.54	0.072 ± 0.037	2.90 ± 1.47	0.021 ± 0.004	0.855 ± 0.172	0.009 ± 0.002	0.353 ± 0.061
Cerebrum	0.048 ± 0.019	2.48 ± 1.10	0.058 ± 0.014	2.76 ± 0.71	—	—	0.042 ± 0.010	1.94 ± 0.48	0.009 ± 0.001	0.465 ± 0.029	0.008 ± 0.000	0.324 ± 0.050
Cerebellum	0.027 ± 0.003	1.86 ± 0.23	0.023 ± 0.010	1.81 ± 0.73	—	—	0.016 ± 0.008	1.17 ± 0.42	0.004 ± 0.002	0.754 ± 0.392	0.003 ± 0.000	0.258 ± 0.067
Heart	0.101 ± 0.034	7.22 ± 2.31	0.083 ± 0.029	5.64 ± 2.54	0.062 ± 0.015	4.12 ± 1.02	0.045 ± 0.008	3.06 ± 0.79	0.023 ± 0.004	1.75 ± 0.31	0.018 ± 0.002	1.27 ± 0.01
Liver	59.1 ± 1.7	261.2 ± 10.6	57.2 ± 1.7	276.5 ± 28.4	52.4 ± 3.9	268.1 ± 33.1	52.3 ± 2.5	281.9 ± 52.6	63.0 ± 2.5	304.7 ± 28.5	67.7 ± 5.4	371.8 ± 55.2
Lungs	21.8 ± 2.5	758.1 ± 50.5	19.1 ± 2.2	660.2 ± 79.1	19.2 ± 2.2	758.2 ± 149.0	17.4 ± 0.8	483.5 ± 155.9	16.3 ± 1.6	568.9 ± 158.3	13.2 ± 2.8	284.3 ± 89.3
Lymph nodes[b]	0.065 ± 0.029	2.62 ± 1.15	0.064 ± 0.015	2.58 ± 0.61	—	—	0.138 ± 0.131	5.51 ± 5.22	0.024 ± 0.018	0.947 ± 0.715	0.013 ± 0.002	0.538 ± 0.074
Spleen	1.23 ± 0.44	33.2 ± 11.8	1.17 ± 0.38	42.1 ± 13.4	1.01 ± 0.41	39.7 ± 5.3	1.33 ± 0.35	54.8 ± 24.3	2.98 ± 0.25	89.6 ± 12.5	3.92 ± 1.60	131.0 ± 66.4
Suprarenal gland	0.007 ± 0.001	8.06 ± 2.80	0.010 ± 0.007	8.82 ± 7.11	—	—	0.009 ± 0.003	6.85 ± 2.17	0.004 ± 0.001	5.20 ± 1.05	0.002 ± 0.000	1.52 ± 0.42
Kidneys	0.439 ± 0.054	13.3 ± 2.3	0.374 ± 0.026	10.6 ± 1.3	0.333 ± 0.065	10.3 ± 1.8	0.286 ± 0.079	8.42 ± 2.52	0.156 ± 0.024	4.69 ± 0.75	0.104 ± 0.002	2.82 ± 0.08
Thyroid gland	0.009 ± 0.003	4.28 ± 1.32	0.006 ± 0.002	2.48 ± 0.64	—	—	0.006 ± 0.004	2.40 ± 1.08	0.003 ± 0.001	1.30 ± 0.54	0.004 ± 0.001	1.35 ± 0.24
Eyes	0.005 ± 0.001	0.858 ± 0.143	0.003 ± 0.000	0.533 ± 0.085	—	—	0.006 ± 0.002	0.892 ± 0.354	0.002 ± 0.000	0.347 ± 0.126	0.001 ± 0.000	0.151 ± 0.012
Testicles	0.609 ± 0.369	11.4 ± 8.4	0.035 ± 0.001	0.595 ± 0.000	0.009 ± 0.002	0.171 ± 0.046	0.020 ± 0.004	0.348 ± 0.052	0.008 ± 0.001	0.164 ± 0.047	0.003 ± 0.002	0.030 ± 0.022
Ovary	0.023 ± 0.004	8.88 ± 0.60	0.010 ± 0.002	3.44 ± 0.55	—	—	0.008 ± 0.000	3.54 ± 0.19	0.005 ± 0.001	1.68 ± 0.11	—	—
Uterus	0.004 ± 0.003	0.596 ± 0.578	0.004 ± 0.000	0.471 ± 0.160	—	—	0.005 ± 0.001	0.622 ± 0.137	0.002 ± 0.000	0.343 ± 0.118	—	—
Pancreas	0.040 ± 0.009	2.83 ± 0.33	0.033 ± 0.003	2.37 ± 0.35	—	—	0.027 ± 0.002	1.94 ± 0.41	0.011 ± 0.006	1.50 ± 0.44	0.023 ± 0.003	1.85 ± 0.46
GI tract	1.74 ± 0.46	9.45 ± 2.02	1.84 ± 0.44	10.4 ± 1.8	1.07 ± 0.38	6.10 ± 1.31	0.631 ± 0.040	3.57 ± 0.20	0.203 ± 0.033	1.27 ± 0.27	0.173 ± 0.023	0.867 ± 0.126
Gastric wall	0.162 ± 0.050	7.33 ± 0.95	0.157 ± 0.032	5.88 ± 1.28	0.058 ± 0.011	2.33 ± 0.43	0.063 ± 0.017	2.44 ± 0.66	0.156 ± 0.124	6.56 ± 4.47	0.138 ± 0.125	5.77 ± 5.01
Residual body	6.18 ± 1.52	2.27 ± 0.58	10.5 ± 8.2	3.73 ± 2.77	5.41 ± 1.91	1.95 ± 0.66	5.60 ± 2.07	2.03 ± 0.75	5.23 ± 0.92	1.91 ± 0.46	3.81 ± 0.37	1.35 ± 0.02
GI tract contents	1.48 ± 0.76	—	1.40 ± 0.49	—	2.81 ± 0.53	—	3.07 ± 0.35	—	0.159 ± 0.036	—	0.030 ± 0.005	—
Percent of applied dose in rat body	93.7 ± 2.4	—	92.4 ± 6.9	—	82.6 ± 2.1	—	81.4 ± 5.1	—	88.6 ± 3.5	—	89.4 ± 6.9	—
Percent of applied dose in urine	0.076 ± 0.086	—	0.031 ± 0.001	—	0.593 ± 0.212	—	1.05 ± 0.02	—	1.03 ± 0.35	—	0.950 ± 0.980	—
Percent of applied dose in feces	—	—	—	—	—	—	—	—	—	—	3.53 ± 0.88	—
Total, %	93.8 ± 2.4	—	92.4 ± 6.9	—	83.2 ± 2.4	—	82.4 ± 5.1	—	89.6 ± 3.6	—	93.9 ± 7.4	—

[a] All values are given in percent of the administered dose (mean ± SD) and in micrograms of nanoparticles per gram of organ fresh weight (mean ± SD). [b] Refers to 1 g of organ fresh weight.

Table II—Elimination of ^{14}C-Radioactivity after Intravenous Administration of Poly(methyl-2-^{14}C-methacrylate) Nanoparticles to Rats (n = 4; Two Males and Two Females)[a]

Time	Feces	Urine	Breath
2 hr			0.0394 ± 0.0071
1st day	2.59 ± 0.73	0.850 ± 0.981	0.0186 ± 0.0064
2nd day	0.397 ± 0.096	0.042 ± 0.022	0.0114 ± 0.0076
3rd day	0.192 ± 0.075	0.017 ± 0.005	—[b]
4th day	0.103 ± 0.010	0.012 ± 0.005	—[b]
5th day	0.099 ± 0.022	0.010 ± 0.000	—[b]
6th day	0.066 ± 0.028	0.010[b] ± 0.000	—[b]
7th day	0.076 ± 0.015	0.008[b] ± 0.005	—[b]
Total	3.53 ± 0.88	0.949 ± 0.980	0.0694 ± 0.0157[c] 0.8328 ± 0.188[d]

[a] All values are in percent of the administered dose (mean ± SD). [b] Not significantly different from blank value. [c] Refers to 2-hr daily determination time. [d] Extrapolated to 24 hr.

2-^{14}C-Acetone Cyanohydrin (II)—Sulfuric acid (40%, 7.35 ml) was added to a well-stirred solution of potassium cyanide (2.2 g, 33.8 mmoles) and 2-^{14}C-acetone (2.5 ml, 34 mmoles, 34 mCi[1]) in 3.2 ml of water at 15° for 15 min. After another 15 min, the solution was filtered, extracted with ether, and dried over anhydrous sodium sulfate. Chloroacetic acid (5 mg) was added for stabilization, and the solvent was removed *in vacuo*. Distillation of the residue yielded 1.8 g (26 mCi) of II, bp 74–76°/15 mm.

Methyl-2-^{14}C-methacrylate (I)—The yield of cyanohydrin was added drop by drop to a stirred mixture of 98% H_2SO_4 (2.25 ml) and copper powder (20 mg) at 70–80°. After 15 min at 160° (bath temperature), the solution was cooled in ice water. Hydrochinone (20 mg), water (0.3 ml), and methanol (2.4 ml) were added and refluxed for 4.5 hr at 120°. The product was distilled using a copper spire in the distillation head. The distillate was extracted with 3 × 3 ml of water and dried over molecular sieves (4 Å). Distillation yielded 458 mg (5.2 mCi) of I, bp 100°.

The sample was analyzed using a gas chromatograph[2] equipped with a flame detector and a column (2 m, 10% SE 30, 80–100 mesh) at 80–210°, 10°/min, with helium as the carrier gas.

TLC was carried out on silica gel plates[3] in chloroform–acetone (9:1) and chloroform–methanol (9:1) with radioactivity[4] scanning.

Phosphate-Buffered Saline—To prepare the buffered saline, 7.60 g of $Na_2HPO_4 \cdot 2H_2O$, 1.45 g of KH_2PO_4, and 4.80 g of NaCl were dissolved in double-distilled water to give 1000.0 ml of phosphate-buffered saline.

Production of Nanoparticles—Methyl-2-^{14}C-methacrylate, 0.95 ml, was dissolved in phosphate-buffered saline to give 95 ml of a 1% solution. This solution was irradiated with 500 krad at a rate of 2.2 krad/min in a ^{60}Co-source (15). The resulting polymer was freeze dried. A powder consisting of 40% poly(methyl-2-^{14}C-methacrylate) nanoparticles and 60% salt (dibasic sodium phosphate dihydrate–monobasic potassium phosphate–sodium chloride, 7.6:1.45:4.8 w/w) was obtained. The specific radioactivity of this nanoparticle powder mixture was 1.74 μCi/mg of mixture.

Macroautoradiography—Four Wistar rats[5], ~100 g, received 0.5 ml of nanoparticle suspension intravenously. One-half milliliter of suspension contained 10 mg of nanoparticle powder mixture corresponding to 4 mg of polymer with a radioactivity of 17.4 μCi. The rats were sacrificed after 0.5, 6, and 24 hr and after 7 days.

Three male mice, ~35 g, received 50 μl of nanoparticle suspension intramuscularly. Fifty microliters of suspension contained 5.7 mg of the nanoparticle powder mixture corresponding to 2.28 mg of polymer with a radioactivity of 10 μCi. The mice were sacrificed after 7, 35, and 70 days.

Rats and mice were sacrificed with ether, sheared, and frozen for 2 min in an acetone–dry ice mixture. After 1 day in the freezer, the animals were imbedded in ground meat and cut into 40-μm sections with a cryomicrotome[6]. The slices were applied to adhesive tape, dried in a freezer for 2 days, and placed on an X-ray film for 10–40 days.

Organ Distribution and Elimination of Radioactivity—Ten milligrams of the nanoparticle powder mixture was suspended in water to give 0.5 ml of suspension containing 4 mg of polymer with a radioactivity of 17.4 μCi. Twenty Wistar rats[5], ~170 g, received 0.5 ml of suspension/rat iv. After 0.5, 1, 2, 6, and 24 hr and after 7 days, four animals (two males and two females) were sacrificed, and the organs were examined for radioactivity.

Radioactivity elimination in feces and urine was followed for 7 days in the four rats that were sacrificed after this time.

Organs—The organ fresh weight was determined, the organs were homogenized, and an aliquot (50 mg) was combusted in an oxidizer[7]. Smaller organs were combusted whole. The resulting $^{14}CO_2$ was absorbed in 5 ml of absorption medium[8] and analyzed after being mixed with 15 ml of scintillation cocktail[9] in the scintillation counter[10].

Urine—Urine, 0.5 ml, was mixed with 15 ml of scintillation cocktail A and analyzed in the scintillation counter[9].

Feces—The feces were freeze dried, homogenized, and weighed, and a 50-mg aliquot was combusted in the oxidizer[7]. The resulting $^{14}CO_2$ was absorbed in 5 ml of absorption medium[8], mixed with 15 ml of scintillation cocktail[9], and analyzed in the scintillation counter[10].

Breath—The animals were placed in special metabolism cages for 2 hr/day for 7 days to determine the $^{14}CO_2$ eliminated by exhalation. The air in the cages was pumped in succession through three wash bottles. The wash bottles were filled with a mixture of 50 ml of ethanolamine and 50 ml of methanol. The ^{14}C-activity was determined daily in a scintillation counter[10] after mixing with 15 ml of scintillation cocktail B–methanol (3:1).

Standardization—One-half milliliter of the nanoparticle suspension (≅4 mg of polymer) was dissolved in 5 ml of acetone. Methanol, 45 ml, was added; 0.5 ml of this standard solution was mixed with 0.5 ml of inactive urine or 50 mg of inactive, freeze-dried feces. The urine–standard solution mixture was analyzed in the scintillation counter[10] after addition of 15 ml of scintillation cocktail A. The feces–standard solution mixture was combusted in the oxidizer[7]. The resulting $^{14}CO_2$ was absorbed in 5 ml of absorption medium[8] and analyzed after mixing with 15 ml of scintillation cocktail[9].

The calculation, in percent of the dose (Tables I and II), was based on these standard values.

The values listed in Table I, given in percent of the administered dose, were calculated for the whole organ; for the skin, bones, fatty tissue, lymph nodes, and spinal cord, these values refer to 1 g.

Scintillation Cocktail A—2,5-Diphenyloxazole[11] (10 g), 2,2′-p-phenylene-bis-5-phenyloxazole[11] (0.25 g), and naphthalene (100 g) were dissolved in 1 liter of dioxane.

Scintillation Cocktail B—2,5-Diphenyloxazole[11] (55 g) and 2,2′-p-phenylene-bis-5-phenyloxazole[11] (4 g) were dissolved in 5 liters of toluene.

RESULTS

Macroautoradiography after Intravenous Administration of Nanoparticles to Rats—The distribution of the ^{14}C-activity in the rat bodies after 0.5, 6, and 24 hr and after 7 days is shown in Figs. 1–4. One-half hour after intravenous administration, most activity was found in the lungs and in the liver; minor activity was found in the spleen, kidneys, and bone marrow. After 6 hr, activity also was observed in parts of the intestines, which points to biliary excretion (Fig. 2). All radioactivity had disappeared from the kidneys and intestines 24 hr after administration (Fig. 3). Strong radioactivity still could be found in the liver, lungs, and spleen 7 days after administration. The radioactivity in the bone marrow did not change significantly.

Macroautoradiography after Intramuscular Adminstration of Nanoparticles to Mice—Figures 5–7 show the distribution of ^{14}C-radioactivity in mice 7, 35, and 70 days after intramuscular administration of labeled nanoparticles. All radioactivity was found at the injection site.

Elimination Kinetics in Urine, Feces, and Breath—The kinetics of the ^{14}C-elimination in urine, feces, and breath after intravenous administration were followed for 7 days (Table II). The exhaled ^{14}C-activity (Table II) corresponded to a daily determination period of 2 hr. One percent of the administered dose was excreted in the urine, 3.5% in the

[2] Varian 3700, Varian AG, Zug, Switzerland.
[3] 60 F 254, E. Merck, Darmstadt, West Germany.
[4] Berthold LB 2722, Berthold, Wildbad, West Germany.
[5] Brünger, 4801 Bokel, West Germany.
[6] Jung/Dittes, Heidelberg, West Germany.
[7] Tritium carbon oxidizer type 306, Packard Instrument Co., Downers Grove, Ill.
[8] Chromosorb, Packard Instrument Co., Downers Grove, Ill.
[9] Permafluor, Packard Instrument Co., Downers Grove, Ill.
[10] Liquid scintillation spectrometer type 3380, Packard Instrument Co., Downers Grove, Ill.
[11] Fa. Zinsser, Frankfurt, West Germany.

Figure 1—*Macroautoradiography of a rat 30 min after intravenous administration of poly(methyl-2-^{14}C-methacrylate) nanoparticles.*

Figure 2—*Macroautoradiography of a rat 6 hr after intravenous administration of poly(methyl-2-^{14}C-methacrylate) nanoparticles.*

Figure 3—*Macroautoradiography of a rat 24 hr after intravenous administration of poly(methyl-2-^{14}C-methacrylate) nanoparticles.*

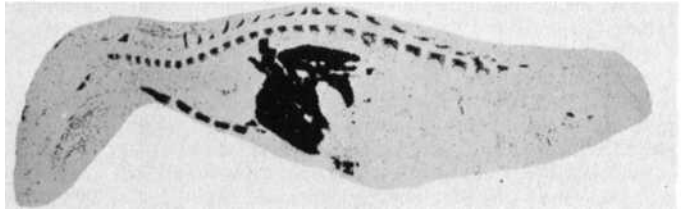

Figure 4—*Macroautoradiography of a rat 7 days after intravenous administration of poly(methyl-2-^{14}C-methacrylate) nanoparticles.*

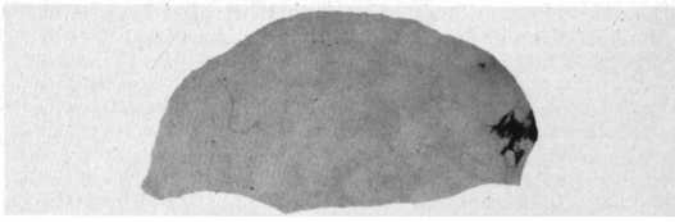

Figure 5—*Macroautoradiography of a mouse 7 days after intramuscular administration of poly(methyl-2-^{14}C-methacrylate) nanoparticles.*

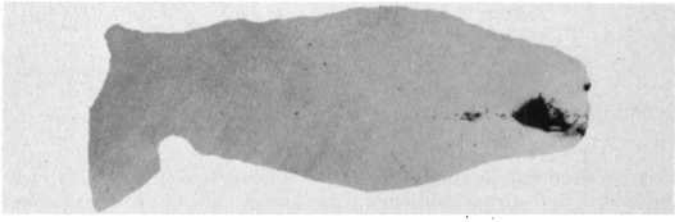

Figure 6—*Macroautoradiography of a mouse 35 days after intramuscular administration of poly(methyl-2-^{14}C-methacrylate) nanoparticles.*

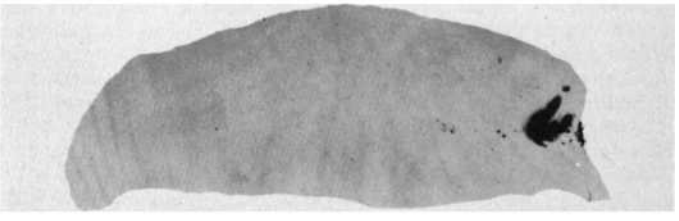

Figure 7—*Macroautoradiography of a mouse 70 days after intramuscular administration of poly(methyl-2-^{14}C-methacrylate) nanoparticles.*

feces, and 1% in the breath within 7 days. The ^{14}C-activity in the breath was significantly higher than the blank for only 2 days. The excretion in urine and feces reached a maximum at 0.9 and 2.6%, respectively, on the 1st day and decreased rapidly until Day 7.

Organ Distribution of Radioactivity—Table I shows the distribution of ^{14}C-radioactivity in the organs and tissue after intravenous administration of the nanoparticles. The values are given in percent of the administered dose and in micrograms of nanoparticles per gram of fresh weight. After 30 min, the most activity (~60%) was found in the liver, 22% in the lungs, 1.2% in the spleen, 1.7% in the GI tract, 1.5% in the GI tract contents, 0.4% in the kidneys, and 0.6% in the testicles. All other tissue and organs had an activity significantly lower than 1%.

The radioactivity distribution changed with increasing time. The portion of radioactivity in the lungs was reduced to 13.2% after 7 days, while the portion of activity in the liver increased to 67.6%. The portion of activity was also reduced in the GI tract, kidneys, and testicles but increased slightly in the spleen and bones.

This change in distribution of activity in the organism was demonstrated clearly by the nanoparticle concentrations, given in micrograms per gram of fresh weight. In the lungs, the concentration dropped from 758 μg/g after administration to 284 μg/g after 7 days. The nanoparticle concentration in the liver increased from 261 to 372 μg/g; in the spleen, it increased from 33 to 131 μg/g; and in the bones, it increased from 3 to 6 μg/g. In all other organs, the concentration of nanoparticles or their degradation products decreased markedly.

DISCUSSION

The distribution and elimination of radioactivity after intravenous administration of ^{14}C-labeled nanometer-sized poly(methyl methacrylate) particles (nanoparticles) was followed in rats for 7 days. The results obtained by quantitative determination of radioactivity in organs, tissue, and excreta correlate well with the findings obtained by macroautoradiography. At first, possibly during the first pass through the lungs, the nanoparticles were filtered out by the lung capillaries. After 30 min, the concentration of nanoparticle radioactivity reached a maximum of 758 μg/g, the highest concentration of radioactivity in any organ during the whole observation period. The concentration in the liver after 30 min was 261 μg/g, which still represented ~60% of the administered dose.

^{14}C-Radioactivity in the kidneys and GI tract was detected by using quantitative distribution measurements as well as macroautoradiography. The ^{14}C-activity in the intestine points to certain biliary excretion.

Seven days after administration, the ^{14}C-activity in most organs and tissue had decreased markedly while the greatest amount was found in the liver (~68% ≅ 372 μg/g). Furthermore, the concentration of the nanoparticles or their degradation products had increased in the spleen and the bone marrow. Liver, spleen, and bone marrow belong to the immune system. The accumulation of the nanoparticles in these immunocompetent organs may be related to the adjuvant effect and the protection yielded by these particles (1, 4).

The elimination of radioactivity in urine, in feces, and by exhalation was maximal shortly after application. With increasing time, the ^{14}C-activity in the excreta decreased. This decrease was accompanied by an activity decrease in the GI tract as well as in the kidneys and may have been due to an elimination of lower molecular weight contents of the nanoparticles. Approximately 5.3% of the administered dose was excreted within 7 days. It is unlikely that all of this material was monomeric since it was shown previously with nanoparticles (15) that no more than 1% of fugitive material such as methacrylate monomers is present in the final product.

After intramuscular administration of the labeled nanoparticles, all residual ^{14}C-activity was found at the injection site. No transportation and distribution of particles occurred during 70 days.

The results after intravenous and intramuscular administrations show that poly(methyl methacrylate) nanoparticles are not rapidly biodegradable. Although macroautoradiographies give mainly qualitative information about ^{14}C-radioactivity, the strong blackening of the autora-

diographs shows that a considerable amount of carbon-14 persisted in the body. In addition, as shown previously (12), a lag period might exist before the elimination of the polymer.

The long period of nanoparticle accumulation at the injection site after intramuscular administration correlates well with the previously observed prolonged adjuvant activity of these particles (1, 6). This prolonged activity was especially pronounced after incorporation into larger amounts of polymer and in comparison to other adjuvants (1).

The attraction of the nanoparticles to the immune system has already been mentioned. However, transporation of the adjuvant from the administration site is not necessary for a good immune response. This is also the case with other adjuvants (16, 17). In contrast to these other adjuvants (16–18), poly(methyl methacrylate) nanoparticles did not induce granulomas in guinea pigs within 1 year (6). Histological reactions were the same as with the fluid control. In spite of the long-term persistence at the injection site, poly(methyl methacrylate) nanoparticles might be an improvement over the presently used adjuvants from a toxicity standpoint; the other adjuvants also persist at the site of injection, but they exhibit much stronger adverse histological reactions (16–19).

REFERENCES

(1) J. Kreuter and P. P. Speiser, *Infect. Immun.*, **13**, 204 (1976).

(2) G. Birrenbach and P. P. Speiser, *J. Pharm. Sci.*, **65**, 1763 (1976).

(3) J. J. Marty, R. C. Oppenheim, and P. Speiser, *Pharm. Acta Helv.*, **53**, 17 (1978).

(4) J. Kreuter, *ibid.*, **53**, 33 (1978).

(5) J. Kreuter and E. Liehl, *Med. Microbiol. Immunol.*, **165**, 111 (1978).

(6) J. Kreuter, R. Mauler, H. Gruschkau, and P. P. Speiser, *Exp. Cell Biol.*, **44**, 12 (1976).

(7) J. Charnley, "Acrylic Cement in Orthopaedic Surgery," Livingstone, Edinburgh, Scotland, 1970.

(8) H. Nothdurft, *Naturwissenschaften*, **42**, 106 (1955).

(9) F. Bischoff and G. Brynson, *Progr. Exp. Tumor Res.*, **5**, 85 (1964).

(10) N. E. Stinson, *Br. J. Exp. Pathol.*, **45**, 21 (1964).

(11) *Ibid.*, **46**, 135 (1965).

(12) B. S. Oppenheimer, E. T. Oppenheimer, I. Danishefsky, A. P. Stout, and F. R. Eirich, *Cancer Res.*, **15**, 333 (1955).

(13) L. Tomatis, *Tumori*, **52**, 165 (1966).

(14) J. Urban, *Collect. Czech. Chem. Commun.*, **24**, 4050 (1959).

(15) J. Kreuter and H.-J. Zehnder, *Radiat. Eff.*, **35**, 161 (1978).

(16) W. J. Herbert, *Immunology*, **14**, 301 (1968).

(17) R. Haas and R. Thommssen, *Ergebn. Bakteriol. Immunitätsforsch. Exp. Ther.*, **34**, 27 (1961).

(18) F. M. Davenport, *Ann. Allergy*, **26**, 288 (1968).

(19) H. Raskova and K. Masek, in "International Symposium on Adjuvants on Immunity, Utrecht 1966," Symposia Series Immunobiological Standardization, vol. 6, R. H. Regamey, W. Hennessen, D. Ikic, and J. Ungar, Eds., Karger, Basel, Switzerland, 1967, p. 115.

(20) A. Roe and J. B. Finlay, *J. Am. Chem. Soc.*, **74**, 2442 (1952).

Analysis of Cyclazocine in Plasma

J. E. PETERSON ˣ, C. T. BARNICK, D. BENZIGER, M. P. KULLBERG, R. BROWN, P. O'MELIA, S. CLEMANS, and J. EDELSON

Received April 2, 1979, from the *Department of Drug Metabolism and Disposition, Sterling-Winthrop Research Institute, Rensselaer, NY 12144.* Accepted for publication June 5, 1979.

Abstract □ The analysis of plasma cyclazocine by two methods is described. The radioimmunoassay employed a ^{125}I-labeled radioligand, rabbit antiserum, and separation of bound from free cyclazocine with a second antibody. The radioimmunoassay was specific for cyclazocine and had a detection limit of ~20 pg/ml. The GLC method employed a mass spectrometer as the detector and had a detection limit of ~109 pg/ml. Both techniques had acceptable accuracy and precision when used to quantitate cyclazocine in dog and human plasma. The methods were used successfully to quantitate cyclazocine from beagle hounds receiving 0.5 mg of ^{3}H-cyclazocine/kg iv. The decline in plasma cyclazocine fitted a two-compartment body model with a mean plasma clearance rate of 39.2 liters/hr.

Keyphrases □ Cyclazocine—analysis, GLC–mass spectrometry, radioimmunoassay, human and dog plasma, pharmacokinetics □ Analgesics—cyclazocine, GLC–mass spectrometric analysis, radioimmunoassay, human and dog plasma, pharmacokinetics □ GLC–mass spectrometry—analysis, cyclazocine, human and dog plasma □ Radioimmunoassay—analysis, cyclazocine, human and dog plasma

Cyclazocine, (2α,6α,11R*) - (±) - 3 - (cyclopropylmethyl)-1,2,3,4,5,6-hexahydro -6,11- dimethyl-2,6-methano-3-benzazocin-8-ol (I), is a member of the benzomorphan series (1). It is a relatively long-acting, orally effective narcotic antagonist (2) and may find clinical usefulness in the treatment of opiate dependence (3). Doses as low as 0.1–0.25 mg po have provided effective pain relief in humans (4).

Previously reported analytical methods for cyclazocine include TLC (5) and GLC (6). These methods have a detection limit of ~10 ng/ml. From these laboratories, a radioimmunoassay using ^{3}H-cyclazocine was previously reported (7) with a sensitivity of ~3 ng/ml. The antibody dilution was 1:50, and the antiserum for this assay was soon exhausted.

To estimate accurately the cyclazocine concentration in plasma following low oral doses, a sensitive measurement method is needed. This article reports the development of two new analytical methods: a radioimmunoassay using a ^{125}I-labeled cyclazocine derivative and a a GLC method using a mass spectrometer as the detector. Both techniques demonstrate sensitivity in the picogram range. These assays have been used to measure cyclazocine added to human and dog plasma. The techniques successfully measured cyclazocine in the plasma of dogs receiving 0.5 mg/kg iv. The pharmacokinetic parameters were determined from the radioimmunoassay data.

EXPERIMENTAL

Radioimmunoassay—*Solutions*—Phosphate-buffered saline was prepared by dissolving 8.17 g of NaCl, 0.50 g of $NaH_2PO_4 \cdot H_2O$, 1.07 g of Na_2HPO_4, and 0.095 g of thimerosal[1] in 1 liter of distilled water and adjusting to pH 7.0. The assay buffer contained 0.1% (w/v) gelatin dissolved in phosphate-buffered saline. Nonimmune normal rabbit serum was diluted 1:500 in phosphate-buffered saline containing 0.05 *M* edetate

[1] Sigma Chemical Co., St. Louis, Mo.

0022-3549/79/1100-1447$01.00/0

© 1979, American Pharmaceutical Association

diographs shows that a considerable amount of carbon-14 persisted in the body. In addition, as shown previously (12), a lag period might exist before the elimination of the polymer.

The long period of nanoparticle accumulation at the injection site after intramuscular administration correlates well with the previously observed prolonged adjuvant activity of these particles (1, 6). This prolonged activity was especially pronounced after incorporation into larger amounts of polymer and in comparison to other adjuvants (1).

The attraction of the nanoparticles to the immune system has already been mentioned. However, transporation of the adjuvant from the administration site is not necessary for a good immune response. This is also the case with other adjuvants (16, 17). In contrast to these other adjuvants (16–18), poly(methyl methacrylate) nanoparticles did not induce granulomas in guinea pigs within 1 year (6). Histological reactions were the same as with the fluid control. In spite of the long-term persistence at the injection site, poly(methyl methacrylate) nanoparticles might be an improvement over the presently used adjuvants from a toxicity standpoint; the other adjuvants also persist at the site of injection, but they exhibit much stronger adverse histological reactions (16–19).

REFERENCES

(1) J. Kreuter and P. P. Speiser, *Infect. Immun.*, **13**, 204 (1976).

(2) G. Birrenbach and P. P. Speiser, *J. Pharm. Sci.*, **65**, 1763 (1976).

(3) J. J. Marty, R. C. Oppenheim, and P. Speiser, *Pharm. Acta Helv.*, **53**, 17 (1978).

(4) J. Kreuter, *ibid.*, **53**, 33 (1978).

(5) J. Kreuter and E. Liehl, *Med. Microbiol. Immunol.*, **165**, 111 (1978).

(6) J. Kreuter, R. Mauler, H. Gruschkau, and P. P. Speiser, *Exp. Cell Biol.*, **44**, 12 (1976).

(7) J. Charnley, "Acrylic Cement in Orthopaedic Surgery," Livingstone, Edinburgh, Scotland, 1970.

(8) H. Nothdurft, *Naturwissenschaften*, **42**, 106 (1955).

(9) F. Bischoff and G. Brynson, *Progr. Exp. Tumor Res.*, **5**, 85 (1964).

(10) N. E. Stinson, *Br. J. Exp. Pathol.*, **45**, 21 (1964).

(11) *Ibid.*, **46**, 135 (1965).

(12) B. S. Oppenheimer, E. T. Oppenheimer, I. Danishefsky, A. P. Stout, and F. R. Eirich, *Cancer Res.*, **15**, 333 (1955).

(13) L. Tomatis, *Tumori*, **52**, 165 (1966).

(14) J. Urban, *Collect. Czech. Chem. Commun.*, **24**, 4050 (1959).

(15) J. Kreuter and H.-J. Zehnder, *Radiat. Eff.*, **35**, 161 (1978).

(16) W. J. Herbert, *Immunology*, **14**, 301 (1968).

(17) R. Haas and R. Thommssen, *Ergebn. Bakteriol. Immunitätsforsch. Exp. Ther.*, **34**, 27 (1961).

(18) F. M. Davenport, *Ann. Allergy*, **26**, 288 (1968).

(19) H. Raskova and K. Masek, in "International Symposium on Adjuvants on Immunity, Utrecht 1966," Symposia Series Immunobiological Standardization, vol. 6, R. H. Regamey, W. Hennessen, D. Ikic, and J. Ungar, Eds., Karger, Basel, Switzerland, 1967, p. 115.

(20) A. Roe and J. B. Finlay, *J. Am. Chem. Soc.*, **74**, 2442 (1952).

Analysis of Cyclazocine in Plasma

J. E. PETERSON ˣ, C. T. BARNICK, D. BENZIGER, M. P. KULLBERG, R. BROWN, P. O'MELIA, S. CLEMANS, and J. EDELSON

Received April 2, 1979, from the *Department of Drug Metabolism and Disposition, Sterling-Winthrop Research Institute, Rensselaer, NY 12144.* Accepted for publication June 5, 1979.

Abstract □ The analysis of plasma cyclazocine by two methods is described. The radioimmunoassay employed a ^{125}I-labeled radioligand, rabbit antiserum, and separation of bound from free cyclazocine with a second antibody. The radioimmunoassay was specific for cyclazocine and had a detection limit of ~20 pg/ml. The GLC method employed a mass spectrometer as the detector and had a detection limit of ~109 pg/ml. Both techniques had acceptable accuracy and precision when used to quantitate cyclazocine in dog and human plasma. The methods were used successfully to quantitate cyclazocine from beagle hounds receiving 0.5 mg of ^{3}H-cyclazocine/kg iv. The decline in plasma cyclazocine fitted a two-compartment body model with a mean plasma clearance rate of 39.2 liters/hr.

Keyphrases □ Cyclazocine—analysis, GLC–mass spectrometry, radioimmunoassay, human and dog plasma, pharmacokinetics □ Analgesics—cyclazocine, GLC–mass spectrometric analysis, radioimmunoassay, human and dog plasma, pharmacokinetics □ GLC–mass spectrometry—analysis, cyclazocine, human and dog plasma □ Radioimmunoassay—analysis, cyclazocine, human and dog plasma

Cyclazocine, (2α,6α,11R*) - (±) - 3 - (cyclopropylmethyl)-1,2,3,4,5,6-hexahydro -6,11- dimethyl-2,6-methano-3-benzazocin-8-ol (I), is a member of the benzomorphan series (1). It is a relatively long-acting, orally effective narcotic antagonist (2) and may find clinical usefulness in the treatment of opiate dependence (3). Doses as low as 0.1–0.25 mg po have provided effective pain relief in humans (4).

Previously reported analytical methods for cyclazocine include TLC (5) and GLC (6). These methods have a detection limit of ~10 ng/ml. From these laboratories, a radioimmunoassay using ^{3}H-cyclazocine was previously reported (7) with a sensitivity of ~3 ng/ml. The antibody dilution was 1:50, and the antiserum for this assay was soon exhausted.

To estimate accurately the cyclazocine concentration in plasma following low oral doses, a sensitive measurement method is needed. This article reports the development of two new analytical methods: a radioimmunoassay using a ^{125}I-labeled cyclazocine derivative and a a GLC method using a mass spectrometer as the detector. Both techniques demonstrate sensitivity in the picogram range. These assays have been used to measure cyclazocine added to human and dog plasma. The techniques successfully measured cyclazocine in the plasma of dogs receiving 0.5 mg/kg iv. The pharmacokinetic parameters were determined from the radioimmunoassay data.

EXPERIMENTAL

Radioimmunoassay—*Solutions*—Phosphate-buffered saline was prepared by dissolving 8.17 g of NaCl, 0.50 g of $NaH_2PO_4 \cdot H_2O$, 1.07 g of Na_2HPO_4, and 0.095 g of thimerosal[1] in 1 liter of distilled water and adjusting to pH 7.0. The assay buffer contained 0.1% (w/v) gelatin dissolved in phosphate-buffered saline. Nonimmune normal rabbit serum was diluted 1:500 in phosphate-buffered saline containing 0.05 *M* edetate

[1] Sigma Chemical Co., St. Louis, Mo.

0022-3549/79/1100-1447$01.00/0

© 1979, American Pharmaceutical Association

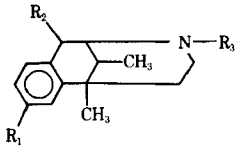

Table I—Relative Affinities of Cyclazocine and Related Compounds to the Antiserum

Compound (Trivial Name)	R_1	R_2	R_3	Relative Affinity
I (cyclazocine)	—OH	—H	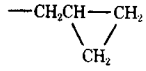	1.000
IV (volazocine)	—H	—H	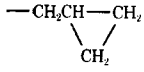	0.4500
V	—OH	—H	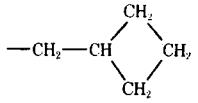	0.2000
VI	—OH	—H	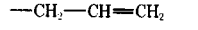	0.2000
VII (ketazocine)	—OH	=O	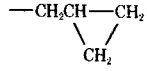	0.0200
VIII (pentazocine)	—OH	—H	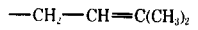	0.0080
IX	—OH	—OH	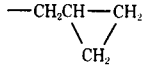	0.0020
X (norcyclazocine)	—OH	—H	—H	0.0008
XI	—H	—H	—H	0.0006
XII	—OCH_3	—H	—H	0.0004

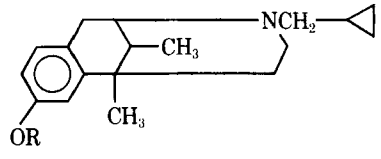

I: R = —H
II: R = —$(CH_2)_3COOH$
III: R = —$(CH_2)_3CONHCH(p\text{-hydroxyphenyl})CO_2CH_3$

disodium[2]. Iodination buffer contained 0.5 *M* Na_2HPO_4–0.5 *M* NaH_2PO_4 (4:1) adjusted to pH 7.5. Dilute iodination buffer was the same buffer diluted 1:10 with distilled water.

Preparation of Cyclazocine Antiserum—A carbodiimide condensation (8) was performed to conjugate a cyclazocine hapten[3] (II) with bovine serum albumin. A trinitrobenzenesulfonic acid determination of free amine groups (9) indicated that approximately 14 hapten molecules were attached to each albumin molecule. The hapten–protein conjugate (1.0–2.0 mg) was emulsified in complete Freund's adjuvant[4] and injected intradermally at multiple sites on the backs of Dutch belted rabbits. Conjugate (1.0 mg/rabbit) in incomplete Freund's adjuvant was administered as a booster immunization at ~3-week intervals. The rabbits were bled periodically *via* the marginal ear vein, and serum was obtained.

Preparation of Second Antibody—Anti-rabbit γ-globulin was raised in two castrated rams. Rabbit γ-globulin[5] (0.5 mg) emulsified in complete Freund's adjuvant was injected intradermally at multiple sites in the rump. Booster immunizations in incomplete adjuvant were administered at monthly intervals. The sheep were bled at 2-week intervals, and serum was obtained. Serum from numerous bleedings was pooled, and the titer of the second antibody (1:16) was determined by a danazol assay (10).

Radioiodination—A modification of the Greenwood and Hunter (11) method was used to radioiodinate a methyltyrosinate derivative (III) of cyclazocine at room temperature. A methanol solution of III (10 μg) was mixed with 50 μl of iodination buffer. Sodium ^{125}I-iodide[6] (1.0 mCi) was added, the vial was stoppered, and the contents were mixed gently. Dilute iodination buffer, 15 μl, containing 30 μg of chloramine-T[7] was added, and the mixture was allowed to react for 2 min. The reaction was stopped by 60 μg of sodium metabisulfite in 30 μl of dilute iodination buffer.

Table II—Estimated Cyclazocine Concentration by Radioimmunoassay in Human Plasma Samples Supplemented with Cyclazocine

Cyclazocine Added, pg/ml	Assayed Mean[a], pg/ml	
	Day 1	Day 2
50	50.2 (6.0, +0.3)[b]	51.2 (8.2, +2.5)
100	98.4 (5.3, −1.6)	99.8 (6.6, −0.3)
200	209 (4.3, +4.5)	198 (7.0, −0.8)
500	520 (2.9, +3.9)	517 (2.0, +3.4)
800	799 (2.7, −0.1)	867 (2.4, +8.3)
1000	931 (1.7, −6.9)	1010 (2.7, +0.8)

[a] $n = 12$. [b] Numbers in parentheses are the percent standard error and the percent difference from expected, respectively.

One hundred microliters of a solution containing sucrose (16% w/v) dissolved in assay buffer was added, and the contents of the vial were transferred to a gel filtration[8] column previously equilibrated with assay buffer. A solution containing 8% (w/v) sucrose dissolved in assay buffer (70 μl) was used to rinse the vial, and the wash solution was added to the column. The column eluate was collected in 1.0-ml fractions, which were counted to locate the radioiodinated derivative.

Assay—Duplicate unknown or standard plasma samples (2.0 ml) were measured into extraction tubes (15 × 85 mm). The standards contained 50–1000 pg of cyclazocine/ml. Extraction buffer (0.2 ml), consisting of a solution saturated with both sodium bicarbonate and sodium carbonate, was added to each tube. A solution containing 5% (v/v) of ethanol in toluene (7 ml) was added, and the tubes were shaken mechanically for 15 min. The tubes were centrifuged, and aliquots of the organic phase were transferred to assay tubes (12 × 75 mm). The solvent was evaporated under a nitrogen stream, and the residue was suspended in 0.5 ml of assay buffer. The tubes were mixed, covered, and allowed to remain overnight at 4°.

The cyclazocine antiserum (200 μl) at a 1:12,000 dilution in normal rabbit serum was added to each tube. Radioiodinated III (100 μl) was added, and the tubes were incubated for 4–6 hr at 4°. Appropriately diluted second antibody (200 μl) was added, and the incubation was continued for an additional 12–18 hr. After incubation, 2.5 ml of cold phos-

[2] Edetate disodium, Sigma Chemical Co., St. Louis, Mo.
[3] 4-[3-(Cyclopropylmethyl)-1,2,3,4,5,6-hexahydro-*cis*-6,11-dimethyl-2,6-methano-3-benzazocin-8-yloxy]butanoic acid methanesulfonate.
[4] Difco Laboratories, Detroit, Mich.
[5] Fraction II, Miles Laboratories, Kankakee, Ill.
[6] New England Nuclear, Boston, Mass.
[7] Eastman Kodak, Rochester, N.Y.
[8] Sephadex G-25-150, Sigma Chemical Co., St. Louis, Mo.

Table III—Estimated Cyclazocine Concentration by GLC–Mass Spectrometry in Human Plasma Samples Supplemented with Cyclazocine

Cyclazocine Added, pg/ml	Assayed Mean[a], pg/ml	
	Day 1	Day 2
300	342 (2.0, +13.9)[b]	307 (9.1, +2.2)
450	449 (1.7, −0.3)	506 (0.8, +12.5)
600	530 (4.7, −11.7)	609 (5.4, +1.5)
800	760 (0.2, −5.0)	844 (15.7, +5.5)
1500	1320 (1.0, −12.2)	1560 (2.0, +4.2)

[a] $n = 3$. [b] Numbers in parentheses are the percent standard error and the percent difference from expected, respectively.

phate-buffered saline was added, and the tubes were centrifuged at 2200×*g* for 30 min; the supernates were decanted, and the precipitates were counted. The computer program, based on a weighted least-squares regression analysis (12), used the reciprocal of the variance as the weight for the individual points on the standard curve.

GLC–Mass Spectrometry—*Glassware and Solutions*—All test tubes were thoroughly cleaned with concentrated chromic acid; rinsed several times with water, 5% aqueous ammonia, deionized water, and methanol[9]; and oven dried. All tubes were silanized using 5% dichlorodimethylsilane in toluene. Saturated potassium carbonate–potassium bicarbonate buffer was extracted twice with an equal volume of toluene prior to use.

Assay—Cyclazocine (100 ng/ml of methanol) was added to plasma to produce duplicate 300–3000-pg/ml standards. Plasma (1.0 ml) was added to a tube, followed by 3 ng of internal standard[10] and 0.3 ml of buffer. The sample was extracted twice with 5 ml of benzene[11], and the combined extracts were evaporated to dryness. Trimethylamine, 100 μl of a 0.002 *M* solution in benzene, and pentafluorobenzoyl chloride, 20 μl of 1:100 (v/v) in benzene, were added to the tube. The tube was mixed and allowed to stand at room temperature for 15 min. Benzene (0.3 ml) was added, the tube was mixed, and the benzene was evaporated as described.

The residue was dissolved in 20 μl of toluene, and a 5-μl aliquot was analyzed on a GLC–mass spectrometer[12] operated in the chemical-ionization mode, employing a selected ion monitor program. The conditions were as follows: 91.44-cm glass column[13]; column temperature, 260°; injection port temperature, 300°; source temperature, 200°; methane carrier/reactant gas, 10 ml/min at 0.8 torr; 230-ev electron energy; and 50-mamp emission. The two programs were: (*a*) *m/e* 466, MH^+, pentafluorobenzoyl derivative of cyclazocine, 50-msec dwell time; and (*b*) *m/e* 482, MH^+, pentafluorobenzoyl derivative of internal standard, 50-msec dwell time.

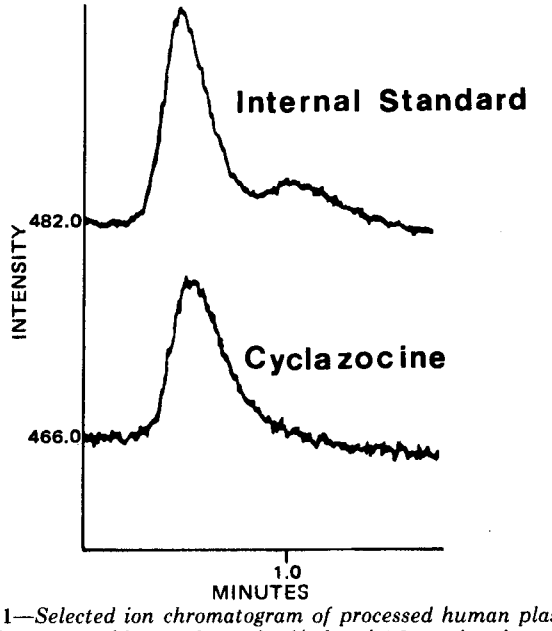

Figure 1—*Selected ion chromatogram of processed human plasma containing 3.0 ng of internal standard/ml and 1.2 ng of cyclazocine/ml.*

[9] Analytical reagent, Mallinckrodt, St. Louis, Mo.
[10] 1,2,3,4,5,6-Hexahydro-6(*eq*),11(*ax*)-dimethyl-3-(3-methylbutyl)-2,6-methano-3-benzazocin-8-ol.
[11] Nanograde, Mallinckrodt, St. Louis, Mo.
[12] Model 5982, Hewlett-Packard.
[13] Three percent SP-2100 on 100–200-mesh Gas Chrom Q, Supelco, Bellfonte, Pa.

Table IV—Mean[a] Cyclazocine Concentration in Dog Plasma after 0.5 mg of ^{3}H-Cyclazocine/kg iv

Hours	Values Obtained by Radioimmunoassay, ng/ml	Values Obtained by GLC–Mass Spectrometry, ng/ml	Values Obtained by Extractable Radioactivity, ng/ml
0.016	171 ± 26	164 ± 37	130 ± 19
0.050	126 ± 21	119 ± 23	107 ± 14
0.083	94 ± 6.1	73 ± 13	95 ± 6.8
0.166	99 ± 7.3	85 ± 14	78 ± 5.2
0.250	93 ± 4.8	87 ± 2.0	65 ± 4.4
0.500	56 ± 10	60 ± 21	36 ± 3.5
0.750	35 ± 3.4	49 ± 5.0	23 ± 1.8
1.00	21 ± 1.5	22 ± 2.0	16 ± 1.9
1.50	11 ± 2.8	9.5 ± 1.6	8.0 ± 0.9
2.00	9.6 ± 0.6	9.0 ± 0.96	4.9 ± 0.7
4.00	1.5 ± 0.03	—[b]	—[c]
6.00	0.8 ± 0.05	0.89 ± 0.05	—[c]
24.0	0.22 ± 0.09	—[c]	—[c]

[a] Mean ± *SE* of three animals. [b] Not analyzed. [c] Below detection limits.

Pharmacokinetic Study in Dogs—Three female beagle hounds were medicated intravenously with 0.5 mg of ^{3}H-cyclazocine/kg[14]. The dose was prepared as a 1-mg/ml solution of cyclazocine in physiological saline containing 1% lactic acid. The specific activity of the dose was 1.12×10^9 dpm/mg.

Blood samples were collected from an indwelling venous catheter at appropriate intervals, using potassium oxalate as the anticoagulant. The samples were centrifuged to separate the plasma. An aliquot was counted, and the remainder was frozen until analyzed. When necessary, plasma samples were diluted with control dog plasma prior to analysis.

Another plasma sample (0.2–0.5 ml) was extracted as described for the radioimmunoassay procedure. Cyclazocine (5 μg) and norcyclazocine (5 μg) were added to each extract, which was evaporated to dryness. The residue was dissolved in 100 μl of toluene–methanol (1:1 v/v). A 10-μl aliquot was counted in Biofluor[6]; radioactivity was measured, and the counting efficiency was determined by the channels-ratio method. The remaining extract was analyzed by TLC[15] with a solvent system of toluene–methanol–isopropylamine (80:20:3 v/v/v).

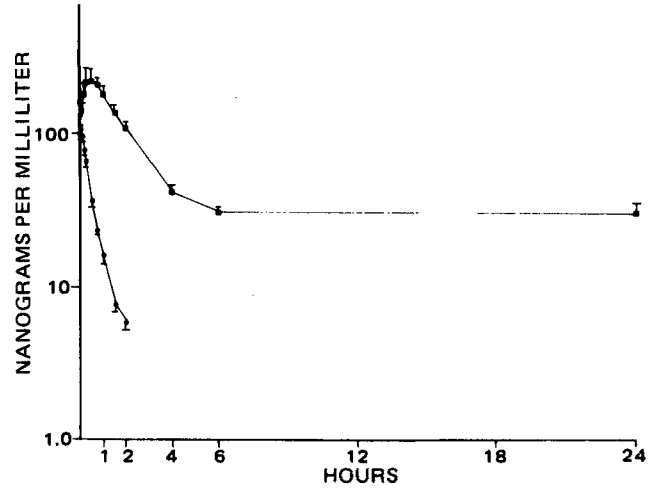

Figure 2—*Plasma levels of total (■) and extractable (●) radioactivity after intravenous administration of 0.5 mg of ^{3}H-cyclazocine/kg to beagle hounds* (n = 3, *mean* ± SE).

[14] Amersham, Arlington Heights, Ill.
[15] Silica gel, E. M. Laboratories, Elmsford, N.Y.

Table V—Pharmacokinetic Parameters for Cyclazocine Disappearance from Plasma of Beagle Hounds following an Intravenous Dose of ^{3}H-Cyclazocine (0.5 mg/kg)

Animal Weight, kg	Rate Constants, hr^{-1} k_{12}	k_{21}	k_{10}	Plasma Clearance Rate, liters/hr	Apparent Volume of Distribution at Steady State, liters	Terminal $t_{1/2}$[a], min	Area under Curve, ng hr^{-1} ml
7.0	0.46	0.08	1.50	33.2	152	702	99.8
7.4	0.37	0.11	1.52	43.6	122	460	86.5
8.2	0.13	0.13	1.22	41.0	67.5	349	108
Mean	0.32	0.11	1.41	39.2	114	504	98.0
$\pm SE$	±0.09	±0.01	±0.09	±3.13	±24.8	±104	±6.21

[a] Calculated from $\frac{0.693}{1/2\,|(k_{12}+k_{21}+k_{10}) - [(k_{12}+k_{21}+k_{10})^2 - 4k_{12}k_{21}]^{1/2}|}$.

RESULTS AND DISCUSSION

The rabbits produced antiserum within 5 months, and the antiserum titer ranged from 1:1000 to 1:15,000. The antiserum dilution that was chosen as the most sensitive and specific was 1:12,000, equivalent to a 1:60,000 final dilution in the assay tube; this dilution resulted in 45–50% radioligand binding.

The antiserum specificity was assessed by determining the ability of related compounds to compete with the radioiodinated III for binding to the antibody. The amounts of each compound required for 50% displacement of radioactivity were determined by comparison with cyclazocine standard curves to arrive at a relative affinity (13). The antiserum exhibiting the least cross-reactivity was selected for all subsequent work. The relative affinities of the related compounds for this antiserum are shown in Table I. Three compounds (IV–VI) demonstrated affinity for the cyclazocine antibody. However, these compounds are not metabolites and, therefore, pose no problem. The known metabolite (norcyclazocine, X) (14, 15) showed little affinity for the cyclazocine antiserum.

The sensitivity or detection limit of the assay is defined as the smallest amount of compound that is significantly different from zero at the 95% confidence limits (16). Thus, the detection limit in human plasma was ~20 pg/ml; it was ~25 pg/ml in dog plasma.

Exogenous cyclazocine was quantitated accurately when varying amounts were added to human plasma, extracted, and assayed in the cyclazocine radioimmunoassay system (Table II). One set of samples was analyzed immediately after preparation (Day 1), and a second set was analyzed after storage in the frozen state for several days (Day 2). No statistical difference was found between standards prepared in dog and human plasma. The assay accuracy ranged from 6.9 to 8.3% over 50–1000 pg/ml. The assay had acceptable precision with a maximum within-concentration standard error of 8.2%.

The GLC–mass spectrometric analysis of plasma standards indicated that the relationship between peak area ratio and cyclazocine concentration fitted a linear model over the 300–3000-pg/ml range. The retention times for cyclazocine and the internal standard, as their pentafluorobenzoyl derivatives, were both ~0.9 min; separation was dependent on the selective ion monitoring capability of the instrument (Fig. 1).

Exogenous cyclazocine was quantitated accurately (Table III) when varying amounts were added to human plasma. The accuracy ranged from 12.2 to 13.9%, and the method had acceptable precision with a maximum within-concentration standard error of 15.7%. The detection limit as determined from a "robust" statistical analysis (17) of the plasma standards were 110 and 146 pg/ml in human and dog plasma, respectively. The average cyclazocine recovery from plasma was 96%, as determined by comparison of direct and extracted standards.

Total and extractable radioactivities from the pharmacokinetic study are presented in Fig. 2. In contrast to the anticipated decline in plasma tritium, the amount of tritium in the systemic circulation increased, reaching a maximum after 30 min. After a moderate decline, total radioactivity was similar after 6 and 24 hr. The pattern with extractable tritium was different; there was a rapid decline during the first 2 hr. TLC of plasma extracts collected during the first 45 min revealed a single radioactive zone with migration characteristics identical to authentic cyclazocine. Later samples lacked sufficient radioactivity for TLC.

The higher levels of total radioactivity as compared to extractable cyclazocine radioactivity imply that the difference is the result of polar conjugated drug or metabolite. It was reported that dogs excrete ~30–38% of cyclazocine as a glucuronide conjugate in the urine (15). The initial rise in total radioactivity, which is accompanied by a concomitant decline in free cyclazocine, suggests rapid formation of a slowly cleared metabolite.

The mean cyclazocine concentrations in dog plasma after ^{3}H-cyclazocine are shown in Table IV. There was good agreement between the analytical methods. The radioimmunoassay values were used to generate pharmacokinetic parameters (Table V) by a modified computer program (18) using a two-compartment body model. The high plasma clearance rate, 39.2 liters/hr, supports the hypothesis of fast elimination of free cyclazocine from the plasma.

Cyclazocine disappearance from dog plasma during the first 2 hr followed apparent first-order kinetics. The half-lives were determined by linear regression from the logarithm of the concentration data; the half-life values were 25, 28, and 20 min for the radiotracer, radioimmunoassay, and GLC–mass spectrometry techniques, respectively.

REFERENCES

(1) S. Archer, N. F. Albertson, L. S. Harris, A. K. Pierson, J. G. Bird, A. S. Keats, J. Telford, and C. N. Papadopoulous, *Science*, **137**, 541 (1962).

(2) L. S. Harris and A. K. Pierson, *J. Pharmacol. Exp. Ther.*, **143**, 141 (1964).

(3) R. B. Resnick, M. Fink, and A. M. Freedman, *Compr. Psychiatry*, **12**, 491 (1971).

(4) L. Lasagna, T. J. DeKornfeld, and J. W. Pearson, *J. Pharmacol. Exp. Ther.*, **144**, 12 (1964).

(5) S. J. Mule, *Anal. Chem.*, **36**, 1907 (1964).

(6) R. F. Kaiko and C. E. Inturrisi, *J. Chromatogr.*, **100**, 63 (1974).

(7) K. A. Pittman and T. A. Williams, *Pharmacologist*, **15**, 167 (1973).

(8) B. F. Erlanger, *Pharmacol. Rev.*, **25**, 271 (1973).

(9) A. F. S. A. Habeeb, *Anal. Biochem.*, **14**, 328 (1966).

(10) J. E. Peterson, M. E. King, W. F. Banks, J. F. Baker, A. F. Jensen, R. W. Ross, Jr., S. Clemans, and J. Edelson, *J. Pharm. Sci.*, **67**, 1425 (1978).

(11) F. C. Greenwood and W. M. Hunter, *Biochem. J.*, **89**, 114 (1963).

(12) D. Rodbard and J. E. Lewald, *Acta Endocrinol., Suppl. 147*, **64**, 79 (1970).

(13) G. E. Abraham, *ibid., Suppl. 183*, **75**, 1 (1974).

(14) S. J. Mule and C. W. Gorodetzky, *J. Pharmacol. Exp. Ther.*, **154**, 632 (1966).

(15) S. J. Mule, T. H. Clements, and C. W. Gorodetzky, *ibid.*, **160**, 387 (1968).

(16) A. R. Midgley, Jr., G. D. Niswender, and R. W. Rebar, *Acta Endocrinol. Suppl. 142*, **63**, 163 (1969).

(17) M. Hollander and D. H. Wolfe, "Nonparametric Statistical Methods," Wiley, New York, N.Y., 1973, p. 200.

(18) M. Pfeffer, *J. Pharmacokinet. Biopharm.*, **1**, 137 (1973).

ACKNOWLEDGMENTS

The authors thank W. Banks, M. Graham, S. Thorpe, M. Brown, S. O'Neil, D. Soto, and K. Parise for technical assistance and K. O. Gelotte and A. G. Hlavac for syntheses of the compounds required to develop the radioimmunoassay.

High-Pressure Liquid Chromatographic Analysis of Ticrynafen and One of Its Metabolites in Urine and Serum

W. C. RANDOLPH ˣ, V. L. OSBORNE, and A. P. INTOCCIA

Received February 27, 1979, from *Smith Kline and French Laboratories, Philadelphia, PA 19101.* Accepted for publication June 4, 1979.

Abstract □ A method is described for the extraction of ticrynafen, a new hypotensive agent, and its reduced metabolite from serum and urine. Drug-related material is extracted from biological fluids with ether under strongly acidic conditions and then back-extracted into an alkaline aqueous phase, which is subjected to high-pressure liquid chromatographic analysis. Separations are performed on a reversed-phase column with a mobile phase consisting of phosphate buffer–acetonitrile. This accurate and reproducible method measures serum concentrations of ticrynafen and its reduced metabolite as low as 1.0 and 0.4 μg/ml, respectively.

Keyphrases □ Ticrynafen—analysis, extraction, high-pressure liquid chromatography, reduced metabolite, urine and serum □ Hypotensive agents—ticrynafen, reduced metabolite, extraction, high-pressure liquid chromatography, urine and serum □ High-pressure liquid chromatography—ticrynafen, reduced metabolite

Ticrynafen, [2,3-dichloro-4-(2-thienylcarbonyl)phenoxy]acetic acid (I), is a new hypotensive agent which combines thiazide-like diuretic activity with uricosuric properties (1, 2). The drug is metabolized by reduction to the alcohol (II) or by oxidative cleavage to the dicarboxylic acid (III) (3). Maurer *et al.* (4) described a spectrophotometric analysis of I and II in which plasma and urine samples were extracted and purified by TLC. The material eluted from the scrapings was measured by UV absorption at 290 nm. GLC also has been described for measurement of I (5) and I–III (6) in plasma and urine following extraction and derivatization of the drug and its metabolites.

This paper describes a high-pressure liquid chromatographic (HPLC) procedure for measuring I and II in serum and urine. The method is more rapid than either the spectrophotometric or GLC procedure, and its usefulness in providing bioavailability and clearance data has been proven in studies in dogs and humans. Although III is not measured by the HPLC analysis, this component constitutes a very small portion of drug-related material, both in dogs (3) and humans (6).

EXPERIMENTAL

Instrumentation—A constant-flow pumping system[1] was coupled with a variable-wavelength detector[2] set at 210 nm. The column, 2.6-mm i.d. × 25 cm, was obtained prepacked with reversed-phase material[3]; a rotary injection valve[4] equipped with a 15-μl loop was used to introduce samples into the system at the column inlet.

Reagents—Analytical reagent grade ether[5] was used for the extraction of I and II from biological fluids. The HPLC mobile phase was 0.05 *M* phosphate buffer (pH 7.0)–glass-distilled acetonitrile[6] (78:22).

Standard Solutions—Appropriate concentration ranges of I and II[7] were prepared in serum or urine for each set of experimental samples, and these standards were extracted and analyzed concurrently with the unknowns. Following a 250-mg oral dose in humans, suitable concentration ranges were: serum, 1.0–25 μg of I/ml and 0.4–2.5 μg of II/ml; and urine, 20–125 μg of I/ml and 8–50 μg of II/ml. The internal standard in the assay was prepared by dissolving 40 mg of ethacrynic acid in 100 ml of methanol.

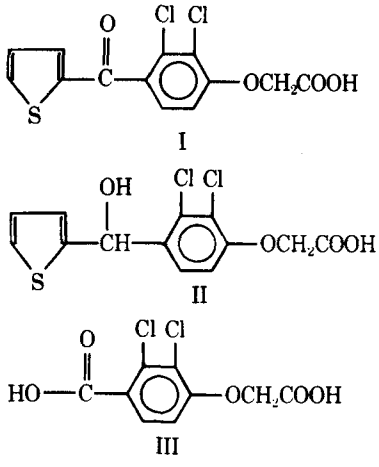

Extraction—*Serum*—Serum aliquots, 0.5 ml, were pipetted into 12-ml conical centrifuge tubes, and 10 μl of the internal standard solution, 0.5 ml of 3 *N* HCl, and 1.5 ml of water were added sequentially with vortexing after each addition. Diethyl ether, 5 ml, was added. The tubes were tightly stoppered, placed horizontally in a reciprocating shaker, and shaken slowly (about 60 oscillations/min) for 30 min.

After shaking, samples were centrifuged to separate the layers sharply, and 4.0 ml of the organic layer was transferred to a second 12-ml centrifuge tube containing 0.3 ml of 0.035 *M* Na_2HPO_4. The tubes were shaken

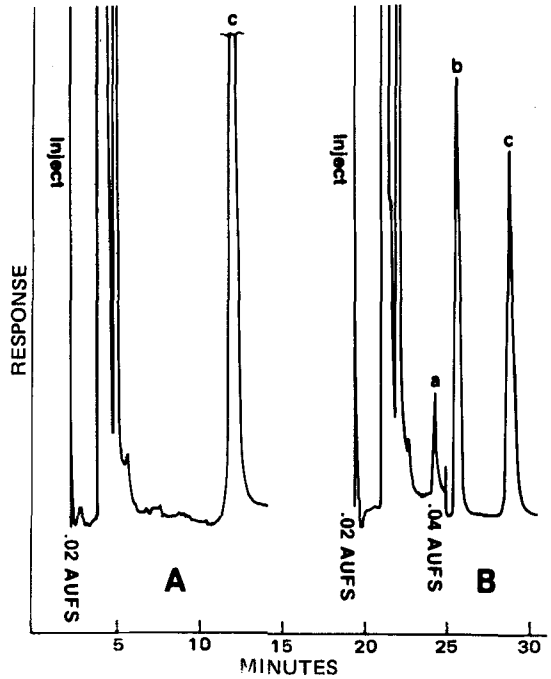

Figure 1—*Chromatograms of extracts from control human serum (A) and serum containing 5 μg of I/ml plus 0.5 μg of II/ml (B). Key: a, II; b, I; and c, ethacrynic acid (internal standard).*

[1] Perkin-Elmer 601.
[2] Perkin-Elmer LC-55.
[3] Perkin-Elmer ODS-HC SIL-X-1.
[4] Valco Instruments Co., Houston, Tex.
[5] Mallinckrodt.
[6] Burdick & Jackson.
[7] Smith Kline & French Laboratories.

0022-3549/79/1100-1451$01.00/0
© 1979, American Pharmaceutical Association

Table I—Recovery from Serum Based on Peak Height Ratios

Sample	Extracted I, 20 μg/ml	Extracted II, 2 μg/ml	Unextracted[a] I, 33.4 μg/ml	Unextracted[a] II, 3.34 μg/ml
1	1.84	1.16	1.98	1.25
2	1.78	1.18	1.98	1.27
3	1.84	1.20	2.02	1.28
4	1.80	1.16	2.02	1.25
5	1.78	1.13	1.97	1.25
$\bar{x}$	1.81	1.17	1.99	1.26
$SD_{\bar{x}}$	±0.03	±0.03	±0.02	±0.01
Recovery[b], %	104	107		

[a] Concentration that would represent 100% recovery, 0.5 ml of serum → 0.3-ml final volume. [b] Recovery = $\bar{x}$ extracted/$\bar{x}$ unextracted, corrected for volume loss in which 4.0 ml was taken from a total 4.6-ml organic layer.

Table II—Recovery from Urine Based on Peak Height Ratios

Sample	Extracted I, 80 μg/ml	Extracted II, 32 μg/ml	Unextracted[a] I, 6.67 μg/ml	Unextracted[a] II, 2.67 μg/ml
1	0.63	0.28	0.78	0.39
2	0.64	0.29	0.80	0.39
3	0.64	0.29	0.80	0.38
4	0.61	0.27	0.78	0.39
5	0.62	0.27	0.77	0.39
$\bar{x}$	0.63	0.28	0.79	0.39
$SD_{\bar{x}}$	±0.01	±0.01	±0.01	±0.004
Recovery[b], %	98	88		

[a] Concentration that would represent 100% recovery, 0.025 ml of urine → 0.3-ml final volume. [b] Recovery = $\bar{x}$ extracted/$\bar{x}$ unextracted, corrected for volume loss in which 4.0 ml was taken from a total 4.9-ml organic layer.

horizontally at high speed (about 120 oscillations/min) for 15 min. The phases were separated by centrifugation, and the organic layer was aspirated and discarded. The unstoppered tubes were placed in a warm water bath for 10 min to remove traces of ether, and the remaining aqueous portion was retained for HPLC analysis.

Urine—Urine samples were diluted (1:10) with distilled water. Aliquots of diluted urine samples, 0.25 ml, were pipetted into 12-ml conical centrifuge tubes and 10 μl of the internal standard solution, 0.25 ml of 3 *N* HCl, and 1.75 ml of water were added with vortexing after each addition. Diethyl ether, 5 ml, was added and the procedure was completed as with serum.

Chromatography—New columns were conditioned with the mobile phase at a flow rate of 0.75 ml/min for several hours. This same flow rate was then used for sample analysis. Column life may be extended by the use of a precolumn packed with pellicular reversed-phase material. Retention times in this system were 4.7 min for the reduced metabolite (II), 6.3 min for ticrynafen (I), and 9.7 min for the internal standard. Because of large differences between the concentrations of I and II in the same sample, it is often necessary to attenuate between peaks and, therefore, to employ a detector that provides linear response at different attenuations.

Quantitation—The ratios of the I and II peak heights to the internal standard peak height were calculated for each standard. Each of these ratios was plotted *versus* concentration, and the resulting curves were used to convert peak height ratios of experimental samples to concentrations.

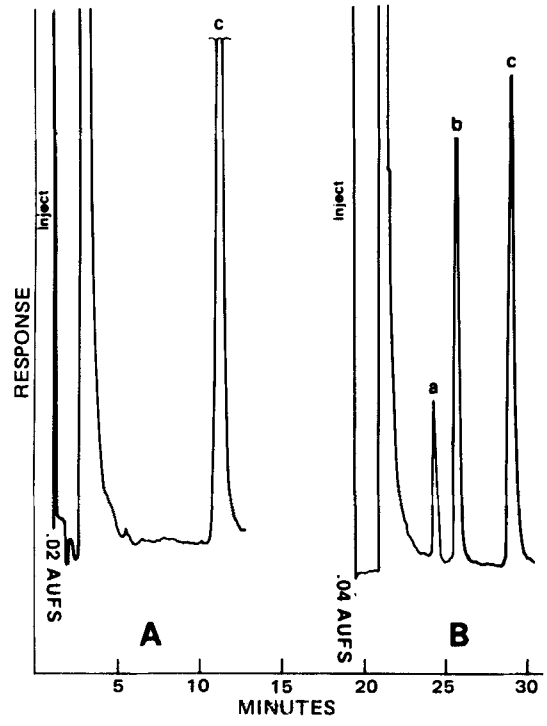

Figure 2—*Chromatograms of extracts from control human urine (A) and urine containing 40 μg of I/ml plus 16 μg of II/ml (B). Key: a, II; b, I; and c, ethacrynic acid (internal standard).*

RESULTS AND DISCUSSION

Recoveries of I and II were determined by adding known amounts of each to blank human serum and urine and extracting as described under *Experimental*. However, for recovery purposes only, the internal standard was not added initially to the samples but was contained in the 0.035 *M* Na_2HPO_4 used for back-extraction. The apparent recoveries of I and II would then not be influenced if the ethacrynic acid extraction was less than 100%. Corresponding unextracted samples were prepared in 0.035 *M* Na_2HPO_4 (also containing internal standard) so that their concentrations would be equal to 100% recovery from the extracted group. Peak height ratios obtained with extracted serum samples and corresponding unextracted standards are shown in Table I; the same information for urine is shown in Table II. These results show good reproducibility and complete recovery of I and II from both serum and urine.

The relationship between peak height ratio and concentration was linear in serum over the ranges of 1.0–50 μg of I/ml and 0.4–5.0 μg of II/ml. Likewise, linear relationships were obtained in urine for concentration ranges of 20–125 μg of I/ml and 8–50 μg of II/ml. The lower detection limits for the described method were 1.0 μg of I/ml and 0.4 μg of II/ml in serum and 20 μg of I/ml and 8 μg of II/ml in urine. Lower levels could be measured by increasing the injection volume for serum samples and using a smaller dilution factor with urine. The 1:10 dilution of urine containing high concentrations of drug prevented unnecessary loading of columns.

Typical chromatograms obtained with blank human serum and serum to which I and II had been added are shown in Fig. 1; chromatograms from control urine and urine with added I and II are shown in Fig. 2. The method is specific for ticrynafen and its reduced metabolite since no endogenous materials interfering with the analysis of either component have been seen in the analysis of numerous control serum and urine samples from dogs and humans. Although UV absorption maxima for both I and II have been reported to be about 290 nm (3), the response was increased threefold for I and 25-fold for II when the column effluents were monitored at 210 nm compared to the response at 290 nm.

Two groups of samples, 18 replicates each, were prepared in blank human serum to test the accuracy of the method. One group contained 4.0 μg of I/ml and 0.5 μg of II/ml; the other contained 12.0 μg of I/ml and 1.2 μg of II/ml. Six samples from each group were analyzed on each of 3 days as described under *Experimental*. For the 36 serum samples analyzed, the averages of actual content measured were: ticrynafen (I), 100.2 ± 4.2%; and reduced metabolite (II), 102.9 ± 8.0%. Similar sets of replicates in blank human urine, containing 40 and 125 μg of I/ml and 16 and

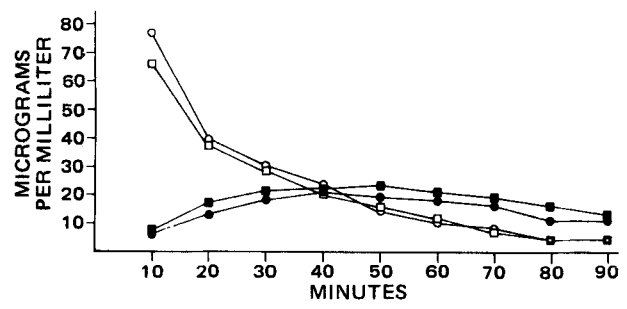

Figure 3—*Serum levels of I and II in a dog following intravenous administration of 10 mg of I/kg, as measured by HPLC and GLC. Key: ○, I (HPLC); □, I (GLC); ●, II (HPLC); and ■, II (GLC).*

50 μg of II/ml, showed averages of actual content measured in 36 samples to be 98.7 ± 4.2% (I) and 97.1 ± 4.1% (II).

Following intravenous administration of 10 mg of I/kg to a dog, serum levels of I and II, measured by this HPLC method and a GLC method (6), were compared (Fig. 3). The two methods differed by an average of 9% in the measurement of total drug-related material (I plus II) in the nine serum samples compared.

REFERENCES

(1) M. Nemati, M. C. Kyle, and E. D. Freis, *J. Am. Med. Assoc.*, **237**, 652 (1977).

(2) J. G. R. de Carvalho, F. G. Dunn, S. G. Chrysant, and E. D. Frohlich, *Arch. Intern. Med.*, **138**, 53 (1978).

(3) J. C. Levron, J. M. LeFur, P. Adnot, and Y. Dormard, *Eur. J. Drug Metab. Pharmacokinet.*, **2**, 107 (1977).

(4) G. Maurer, M. Roche, P. Darmenton, and H. Pacheco, *ibid.*, **1**, 202 (1976).

(5) J. P. Desager, M. Vanderbist, B. Hwang, and P. Levandoski, *J. Chromatogr.*, **123**, 379 (1976).

(6) B. Hwang, G. Konicki, R. Dewey, and C. Miao, *J. Pharm. Sci.*, **67**, 1095 (1978).

ACKNOWLEDGMENTS

The authors thank Dr. Bruce Hwang and Mr. George Konicki for performing GLC analyses with which the HPLC method was compared and Ms. Janice Christie for typing the manuscript.

NOTES

Frozen Conformers of Clotrimazole: Reaction of Imidazole with 1-Chloro-9-hydroxy-9-phenylxanthene

PAUL L. WARNER, Jr.ˣ, EDWARD LUBER, Jr., and F. CHRISTOPHER ZUSI

Received March 1, 1979, from the *Department of Medicinal Chemistry, Westwood Pharmaceuticals Inc., Buffalo, NY 14213.* Accepted for publication May 3, 1979.

Abstract □ 1-Chloro-9-hydroxy-9-phenylxanthene reacts with imidazole at 180° to form a 5:1 mixture of the 9-(imidazo-1-yl)- and 9-(imidazo-2-yl)-1-chloro-9-phenylxanthenes. These products lack significant antifungal activity.

Keyphrases □ Clotrimazole—analogs, frozen conformers, imidazole substitution, antifungal activity □ Antifungal agents—clotrimazole analogs, frozen conformers, imidazole substitution, antifungal activity

The advent of clotrimazole (I) (1, 2) as a clinically useful, broad spectrum antifungal agent has elicited considerable research on the synthesis and testing of analogs of this molecule including the preparation of "frozen conformers." The fluorene analogs II and III were prepared and exhibited good antifungal activity (3).

DISCUSSION

Various other compounds in which the covalent bridge between two phenyl rings (as in II and III) is replaced by sulfur, oxygen, ethylene, or polymethylene have been reported (4–7). The usual synthetic method for these compounds has been displacement of the appropriate tertiary carbinol with thionyl bis-*N,N'*-imidazole (4, 5) or displacement of the appropriate tertiary chloride with imidazole by refluxing in benzene (3) or acetonitrile (6, 7). In all cases, the expected N_1-imidazole derivative was obtained with no mention of other isomers.

To elucidate the pharmacophoric conformation of clotrimazole, 1-chloro-9-(imidazo-1-yl)-9-phenylxanthene (V) was prepared. When 1-chloro-9-hydroxy-9-phenylxanthene (IV) was fused with imidazole at 180°, the expected V was isolated in a 46% yield along with a 9% yield of the unexpected 1-chloro-9-(imidazo-2-yl)-9-phenylxanthene (VI) (Scheme I).

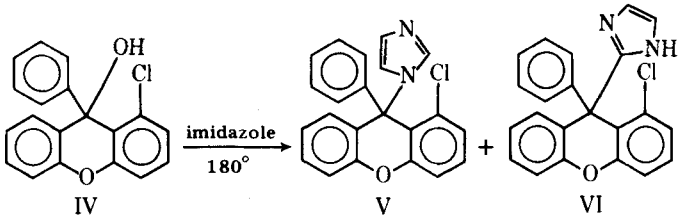

Scheme I

Structures V and VI were assigned to the two reaction products based on their identical elemental analysis and their physical and spectral properties. Compound V displayed considerably greater mobility on silica gel in accord with its expected lower basicity. The IR spectrum of VI contained an absorption at 2850 cm^{-1} corresponding to the imidazole NH bond, which was absent from V. In the 100-MHz NMR spectrum, both V and VI showed a complex aromatic splitting pattern from δ 6.8 to 7.4. Compound V displayed a pair of overlapping triplets at δ 7.5 and 7.6 corresponding to two imidazole ring CH protons, each individually coupled to the two ring protons (the third proton apparently was concealed under the major aromatic peaks). Compound VI showed two distorted doublets at δ 6.4 and 7.55, each a single proton. These doublets sharpened on deuterium oxide exchange, indicating that a free NH was present but also concealed under the main aromatic peak.

Neither V nor VI displayed significant antifungal activity compared to clotrimazole (Table I).

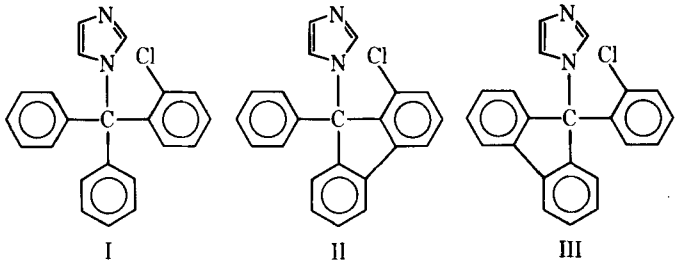

EXPERIMENTAL[1]

Chemistry—*1-Chloro-9-hydroxy-9-phenylxanthene (IV)*—To a stirred suspension of 4.4 g (0.019 mole) of 1-chloroxanthone (8) in 100 ml of anhydrous ether was added dropwise, over 10 min, 22 ml (0.039

[1] NMR spectra were obtained on a Varian XL-100. IR spectra were taken on a Perkin-Elmer model 281 spectrophotometer. UV spectra were taken in absolute ethanol on a Beckman DB-G grating spectrophotometer. Elemental analyses were obtained from Galbraith Laboratories, Knoxville, Tenn. Melting points were taken on a Mel-Temp melting-point apparatus and are uncorrected.

0022-3549/79/1100-1453$01.00/0

© 1979, American Pharmaceutical Association

50 μg of II/ml, showed averages of actual content measured in 36 samples to be 98.7 ± 4.2% (I) and 97.1 ± 4.1% (II).

Following intravenous administration of 10 mg of I/kg to a dog, serum levels of I and II, measured by this HPLC method and a GLC method (6), were compared (Fig. 3). The two methods differed by an average of 9% in the measurement of total drug-related material (I plus II) in the nine serum samples compared.

REFERENCES

(1) M. Nemati, M. C. Kyle, and E. D. Freis, *J. Am. Med. Assoc.*, **237**, 652 (1977).

(2) J. G. R. de Carvalho, F. G. Dunn, S. G. Chrysant, and E. D. Frohlich, *Arch. Intern. Med.*, **138**, 53 (1978).

(3) J. C. Levron, J. M. LeFur, P. Adnot, and Y. Dormard, *Eur. J. Drug Metab. Pharmacokinet.*, **2**, 107 (1977).

(4) G. Maurer, M. Roche, P. Darmenton, and H. Pacheco, *ibid.*, **1**, 202 (1976).

(5) J. P. Desager, M. Vanderbist, B. Hwang, and P. Levandoski, *J. Chromatogr.*, **123**, 379 (1976).

(6) B. Hwang, G. Konicki, R. Dewey, and C. Miao, *J. Pharm. Sci.*, **67**, 1095 (1978).

ACKNOWLEDGMENTS

The authors thank Dr. Bruce Hwang and Mr. George Konicki for performing GLC analyses with which the HPLC method was compared and Ms. Janice Christie for typing the manuscript.

NOTES

Frozen Conformers of Clotrimazole: Reaction of Imidazole with 1-Chloro-9-hydroxy-9-phenylxanthene

PAUL L. WARNER, Jr.ˣ, EDWARD LUBER, Jr., and F. CHRISTOPHER ZUSI

Received March 1, 1979, from the *Department of Medicinal Chemistry, Westwood Pharmaceuticals Inc., Buffalo, NY 14213.* Accepted for publication May 3, 1979.

Abstract □ 1-Chloro-9-hydroxy-9-phenylxanthene reacts with imidazole at 180° to form a 5:1 mixture of the 9-(imidazo-1-yl)- and 9-(imidazo-2-yl)-1-chloro-9-phenylxanthenes. These products lack significant antifungal activity.

Keyphrases □ Clotrimazole—analogs, frozen conformers, imidazole substitution, antifungal activity □ Antifungal agents—clotrimazole analogs, frozen conformers, imidazole substitution, antifungal activity

The advent of clotrimazole (I) (1, 2) as a clinically useful, broad spectrum antifungal agent has elicited considerable research on the synthesis and testing of analogs of this molecule including the preparation of "frozen conformers." The fluorene analogs II and III were prepared and exhibited good antifungal activity (3).

DISCUSSION

Various other compounds in which the covalent bridge between two phenyl rings (as in II and III) is replaced by sulfur, oxygen, ethylene, or polymethylene have been reported (4–7). The usual synthetic method for these compounds has been displacement of the appropriate tertiary carbinol with thionyl bis-*N,N'*-imidazole (4, 5) or displacement of the appropriate tertiary chloride with imidazole by refluxing in benzene (3) or acetonitrile (6, 7). In all cases, the expected N_1-imidazole derivative was obtained with no mention of other isomers.

To elucidate the pharmacophoric conformation of clotrimazole, 1-chloro-9-(imidazo-1-yl)-9-phenylxanthene (V) was prepared. When 1-chloro-9-hydroxy-9-phenylxanthene (IV) was fused with imidazole at 180°, the expected V was isolated in a 46% yield along with a 9% yield of the unexpected 1-chloro-9-(imidazo-2-yl)-9-phenylxanthene (VI) (Scheme I).

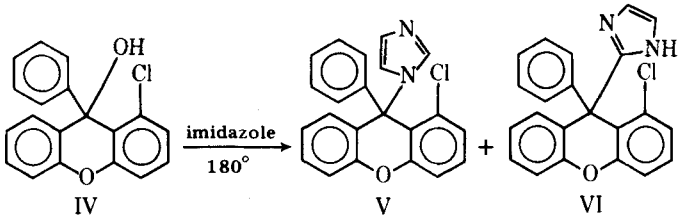

Scheme I

Structures V and VI were assigned to the two reaction products based on their identical elemental analysis and their physical and spectral properties. Compound V displayed considerably greater mobility on silica gel in accord with its expected lower basicity. The IR spectrum of VI contained an absorption at 2850 cm^{-1} corresponding to the imidazole NH bond, which was absent from V. In the 100-MHz NMR spectrum, both V and VI showed a complex aromatic splitting pattern from δ 6.8 to 7.4. Compound V displayed a pair of overlapping triplets at δ 7.5 and 7.6 corresponding to two imidazole ring CH protons, each individually coupled to the two ring protons (the third proton apparently was concealed under the major aromatic peaks). Compound VI showed two distorted doublets at δ 6.4 and 7.55, each a single proton. These doublets sharpened on deuterium oxide exchange, indicating that a free NH was present but also concealed under the main aromatic peak.

Neither V nor VI displayed significant antifungal activity compared to clotrimazole (Table I).

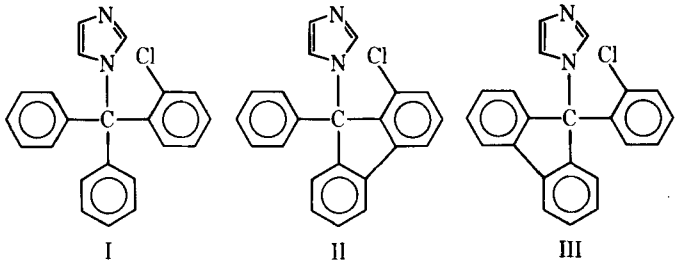

EXPERIMENTAL[1]

Chemistry—*1-Chloro-9-hydroxy-9-phenylxanthene (IV)*—To a stirred suspension of 4.4 g (0.019 mole) of 1-chloroxanthone (8) in 100 ml of anhydrous ether was added dropwise, over 10 min, 22 ml (0.039

[1] NMR spectra were obtained on a Varian XL-100. IR spectra were taken on a Perkin-Elmer model 281 spectrophotometer. UV spectra were taken in absolute ethanol on a Beckman DB-G grating spectrophotometer. Elemental analyses were obtained from Galbraith Laboratories, Knoxville, Tenn. Melting points were taken on a Mel-Temp melting-point apparatus and are uncorrected.

0022-3549/79/1100-1453$01.00/0

© 1979, American Pharmaceutical Association

Table I—Minimum Inhibitory Concentration [a] by Agar Dilution Method in Sabouraud's Dextrose Agar

Test Organism	V[b]	VI[c]	Clotrimazole
Candida albicans (two strains)	>256	>512	1
Candida tropicalis	>256	>512	1
Rhodotorula sp.	>256	>512	8
Aspergillus niger	>256	>512	8
Trichophyton mentagrophytes	>256	>512	0.5

[a] Micrograms per milliliter of medium. [b] Target concentration was 256 μg/ml. [c] Target concentration was 512 μg/ml.

mole) of 1.76 *M* phenyllithium in benzene–ether[2]. After stirring at room temperature for 15 min, the reaction was gently refluxed with stirring for 1 hr. The cooled mixture was treated carefully dropwise with 10 ml of saturated aqueous ammonium chloride followed by 20 ml of water. The organic layer was separated, washed with water, dried with anhydrous magnesium sulfate, and evaporated.

The residual oil was then triturated with petroleum ether and filtered, and the solid was crystallized from an ethanol–hexane mixture to provide 4.3 g (73.4%) of white crystals, mp 131–134.5°; UV: λ_{max} 236 (A_m = 13,100), 281 (3000), and 290 (4400) nm; IR (KBr): 3540, 3450, 3065, 1595, 1570, 1445, 1115, and 755 cm^{-1}.

Anal.—Calc. for $C_{19}H_{13}ClO_2$: C, 73.91; H, 4.24; Cl, 11.48. Found: C, 74.45; H, 4.27; Cl, 11.54.

1-Chloro-9-(imidazo-1-yl)-9-phenylxanthene (V) and 1-Chloro-9-(imidazo-2-yl)-9-phenylxanthene (VI)—A mixture of 0.9 g (0.003 mole) of IV and 3.0 g (0.44 mole) of imidazole was heated under a nitrogen atmosphere at 180° for 5 hr. After cooling, the reaction mixture was digested with 30 ml of water, and the insoluble solid was separated by filtration. The solid was dissolved in chloroform, chromatographed on 75 g of a 2-cm silica gel (40–140 mesh) column[3], eluted with ether–chloroform (1:1), and collected in 100-ml fractions. Compound V eluted first followed by VI. Following evaporation of the appropriate fractions, both V and VI were crystallized from ethanol–water.

For V, the yield was 0.5 g (46%), mp 235–237°; R_f 0.7 [silica gel GF, ether–chloroform (1:1 v/v)]; UV: λ_{max} 285 (A_m = 3280) nm; IR (KBr): 3065, 1590, 1570, 1440, 1368 (CN), 1110, 1100, and 755 cm^{-1}; NMR ($CDCl_3$–dimethyl sulfoxide-d_6): δ 6.8–7.4 (m, 13H, aromatic) and 7.5 and 7.6 (overlapping triplet, 1H each, imidazole ring H).

Anal.—Calc. for $C_{22}H_{15}ClN_2O$: C, 73.64; H, 4.21; Cl, 9.88; N, 7.81. Found: C, 73.89; H, 4.31; Cl, 10.00; N, 7.76.

[2] Aldrich Chemical Co.
[3] Baker.

For VI, the yield was 0.1 g (9%), mp 223–225°; R_f 0.3 (same system as for V); UV: λ_{max} 285 (A_m = 3140) nm; IR (KBr): 3070, 2860 (imidazole NH), 1590, 1570, 1440, 1100, 1090, and 755 cm^{-1}; NMR ($CDCl_3$–dimethyl sulfoxide-d_6): δ 6.48 (distorted doublet, 1H, imidazole CH), 6.8–7.4 (m, 13H, aromatic H), and 7.55 (distorted doublet, 1H, imidazole CH); NMR (dimethyl sulfoxide-d_6–D_2O): δ 6.33 (d, imidazole CH), 6.8–7.4 (m, aromatic H), and 7.54 (d, imidazole CH).

Anal.—Calc. for $C_{22}H_{15}ClN_2O$: C, 73.64; H, 4.21; Cl, 9.88; N, 7.81. Found: C, 73.61; H, 4.40; Cl, 9.91; N, 7.66.

Mycology—The antifungal activity of V and VI, using clotrimazole as a reference, was determined by using a Steer's replicator (9) to inoculate plates of Sabouraud's dextrose agar containing twofold serial dilutions of the compounds. The replicator wells contained fungal suspensions at concentrations greater than 6×10^5 colony-forming units/ml. The minimum inhibitory concentration was determined as the lowest concentration that prevented substantial growth of the test organisms. The data summarized in Table I show that neither V nor VI was active against fungi at the concentrations tested.

REFERENCES

(1) K. H. Buchel, E. Regel, and M. Plempel, U.S. pat. 3,660,577 (1972).

(2) P. R. Sawyer, R. N. Brogden, R. M. Pinder, T. M. Speight, and G. S. Avery, *Drugs*, **9**, 424 (1975).

(3) S. Casadio, A. Donetti, and G. Coppi, *J. Pharm. Sci.*, **62**, 773 (1973).

(4) W. Draber, H. Timmler, K. H. Buchel, and M. Plempel, U.S. pat. 3,814,802 (1974).

(5) *Ibid.*, U.S. pat. 3,778,447 (1973).

(6) W. Draber, K. H. Buchel, and M. Plempel, U.S. pat. 3,737,548 (1973).

(7) *Ibid.*, U.S. pat. 3,647,816 (1972).

(8) A. A. Goldberg and A. H. Wragge, *J. Chem. Soc.*, **1958**, 4234.

(9) E. Steers, E. L. Foltz, and B. S. Graves, *Antibiot. Chemother.*, **9**, 307 (1959).

ACKNOWLEDGMENTS

The authors thank the Analytical Chemistry Research Department, Bristol Laboratories, Syracuse, N.Y., for the NMR spectra and the Westwood Microbiology Department for the antifungal testing data. They also thank Delbay Pharmaceuticals, Inc., Bloomfield, N.J., for a clotrimazole sample and Dr. A. J. Solo, State University of New York at Buffalo, for reviewing the manuscript.

High-Performance Liquid Chromatographic Determination of (*Z*)- and (*E*)-Doxepin Hydrochloride Isomers

T. J. WHALL ˣ and J. DOKLADALOVA

Received February 15, 1979, from the *Special Testing and Analytical Development Laboratories, Quality Control Division, Pfizer Inc., Groton, CT 06340.* Accepted for publication May 8, 1979.

Abstract □ A high-performance liquid chromatographic method for the determination of (*Z*)- and (*E*)-doxepin hydrochloride isomers was developed. The analysis employs a column packed with spherical silica microparticles (5–6 μm), and a mobile phase of acetonitrile–chloroform–diethylamine (750:250:0.2) permits baseline resolution and simultaneous determination of the (*Z*)- and (*E*)-doxepin isomers. Process-related substances do not interfere. The method is accurate and precise (the relative standard deviation was 0.3% for both isomers). The simple procedure is highly suitable for routine doxepin hydrochloride analysis.

Keyphrases □ Doxepin hydrochloride—isomers, high-performance liquid chromatographic analysis □ Antidepressants—doxepin hydrochloride, isomers, high-performance liquid chromatographic analysis □ High-performance liquid chromatography—analysis, doxepin hydrochloride isomers

Doxepin hydrochloride, 3-dibenz[*b,e*]oxepin-11(6*H*)-ylidene-*N,N*-dimethyl-1-propanamine hydrochloride, is a dual-action antianxiety and antidepression psychotherapeutic agent (1). Chemically, it is a mixture of (*Z*)- and (*E*)-isomers (I*a* and I*b*, respectively) in an ~15:85% ratio. Recently, a GLC procedure (2), which requires an extraction step to convert the hydrochloride to free base, was recommended for doxepin hydrochloride analysis.

0022-3549/79/1100-1454$01.00/0

© 1979, American Pharmaceutical Association

Table I—Minimum Inhibitory Concentration [a] by Agar Dilution Method in Sabouraud's Dextrose Agar

Test Organism	V[b]	VI[c]	Clotrimazole
Candida albicans (two strains)	>256	>512	1
Candida tropicalis	>256	>512	1
Rhodotorula sp.	>256	>512	8
Aspergillus niger	>256	>512	8
Trichophyton mentagrophytes	>256	>512	0.5

[a] Micrograms per milliliter of medium. [b] Target concentration was 256 μg/ml. [c] Target concentration was 512 μg/ml.

mole) of 1.76 *M* phenyllithium in benzene–ether[2]. After stirring at room temperature for 15 min, the reaction was gently refluxed with stirring for 1 hr. The cooled mixture was treated carefully dropwise with 10 ml of saturated aqueous ammonium chloride followed by 20 ml of water. The organic layer was separated, washed with water, dried with anhydrous magnesium sulfate, and evaporated.

The residual oil was then triturated with petroleum ether and filtered, and the solid was crystallized from an ethanol–hexane mixture to provide 4.3 g (73.4%) of white crystals, mp 131–134.5°; UV: λ_{max} 236 (A_m = 13,100), 281 (3000), and 290 (4400) nm; IR (KBr): 3540, 3450, 3065, 1595, 1570, 1445, 1115, and 755 cm^{-1}.

Anal.—Calc. for $C_{19}H_{13}ClO_2$: C, 73.91; H, 4.24; Cl, 11.48. Found: C, 74.45; H, 4.27; Cl, 11.54.

1-Chloro-9-(imidazo-1-yl)-9-phenylxanthene (V) and 1-Chloro-9-(imidazo-2-yl)-9-phenylxanthene (VI)—A mixture of 0.9 g (0.003 mole) of IV and 3.0 g (0.44 mole) of imidazole was heated under a nitrogen atmosphere at 180° for 5 hr. After cooling, the reaction mixture was digested with 30 ml of water, and the insoluble solid was separated by filtration. The solid was dissolved in chloroform, chromatographed on 75 g of a 2-cm silica gel (40–140 mesh) column[3], eluted with ether–chloroform (1:1), and collected in 100-ml fractions. Compound V eluted first followed by VI. Following evaporation of the appropriate fractions, both V and VI were crystallized from ethanol–water.

For V, the yield was 0.5 g (46%), mp 235–237°; R_f 0.7 [silica gel GF, ether–chloroform (1:1 v/v)]; UV: λ_{max} 285 (A_m = 3280) nm; IR (KBr): 3065, 1590, 1570, 1440, 1368 (CN), 1110, 1100, and 755 cm^{-1}; NMR ($CDCl_3$–dimethyl sulfoxide-d_6): δ 6.8–7.4 (m, 13H, aromatic) and 7.5 and 7.6 (overlapping triplet, 1H each, imidazole ring H).

Anal.—Calc. for $C_{22}H_{15}ClN_2O$: C, 73.64; H, 4.21; Cl, 9.88; N, 7.81. Found: C, 73.89; H, 4.31; Cl, 10.00; N, 7.76.

[2] Aldrich Chemical Co.
[3] Baker.

For VI, the yield was 0.1 g (9%), mp 223–225°; R_f 0.3 (same system as for V); UV: λ_{max} 285 (A_m = 3140) nm; IR (KBr): 3070, 2860 (imidazole NH), 1590, 1570, 1440, 1100, 1090, and 755 cm^{-1}; NMR ($CDCl_3$–dimethyl sulfoxide-d_6): δ 6.48 (distorted doublet, 1H, imidazole CH), 6.8–7.4 (m, 13H, aromatic H), and 7.55 (distorted doublet, 1H, imidazole CH); NMR (dimethyl sulfoxide-d_6–D_2O): δ 6.33 (d, imidazole CH), 6.8–7.4 (m, aromatic H), and 7.54 (d, imidazole CH).

Anal.—Calc. for $C_{22}H_{15}ClN_2O$: C, 73.64; H, 4.21; Cl, 9.88; N, 7.81. Found: C, 73.61; H, 4.40; Cl, 9.91; N, 7.66.

Mycology—The antifungal activity of V and VI, using clotrimazole as a reference, was determined by using a Steer's replicator (9) to inoculate plates of Sabouraud's dextrose agar containing twofold serial dilutions of the compounds. The replicator wells contained fungal suspensions at concentrations greater than 6×10^5 colony-forming units/ml. The minimum inhibitory concentration was determined as the lowest concentration that prevented substantial growth of the test organisms. The data summarized in Table I show that neither V nor VI was active against fungi at the concentrations tested.

REFERENCES

(1) K. H. Buchel, E. Regel, and M. Plempel, U.S. pat. 3,660,577 (1972).

(2) P. R. Sawyer, R. N. Brogden, R. M. Pinder, T. M. Speight, and G. S. Avery, *Drugs*, **9**, 424 (1975).

(3) S. Casadio, A. Donetti, and G. Coppi, *J. Pharm. Sci.*, **62**, 773 (1973).

(4) W. Draber, H. Timmler, K. H. Buchel, and M. Plempel, U.S. pat. 3,814,802 (1974).

(5) *Ibid.*, U.S. pat. 3,778,447 (1973).

(6) W. Draber, K. H. Buchel, and M. Plempel, U.S. pat. 3,737,548 (1973).

(7) *Ibid.*, U.S. pat. 3,647,816 (1972).

(8) A. A. Goldberg and A. H. Wragge, *J. Chem. Soc.*, **1958**, 4234.

(9) E. Steers, E. L. Foltz, and B. S. Graves, *Antibiot. Chemother.*, **9**, 307 (1959).

ACKNOWLEDGMENTS

The authors thank the Analytical Chemistry Research Department, Bristol Laboratories, Syracuse, N.Y., for the NMR spectra and the Westwood Microbiology Department for the antifungal testing data. They also thank Delbay Pharmaceuticals, Inc., Bloomfield, N.J., for a clotrimazole sample and Dr. A. J. Solo, State University of New York at Buffalo, for reviewing the manuscript.

High-Performance Liquid Chromatographic Determination of (*Z*)- and (*E*)-Doxepin Hydrochloride Isomers

T. J. WHALL ˣ and J. DOKLADALOVA

Received February 15, 1979, from the *Special Testing and Analytical Development Laboratories, Quality Control Division, Pfizer Inc., Groton, CT 06340.* Accepted for publication May 8, 1979.

Abstract □ A high-performance liquid chromatographic method for the determination of (*Z*)- and (*E*)-doxepin hydrochloride isomers was developed. The analysis employs a column packed with spherical silica microparticles (5–6 μm), and a mobile phase of acetonitrile–chloroform–diethylamine (750:250:0.2) permits baseline resolution and simultaneous determination of the (*Z*)- and (*E*)-doxepin isomers. Process-related substances do not interfere. The method is accurate and precise (the relative standard deviation was 0.3% for both isomers). The simple procedure is highly suitable for routine doxepin hydrochloride analysis.

Keyphrases □ Doxepin hydrochloride—isomers, high-performance liquid chromatographic analysis □ Antidepressants—doxepin hydrochloride, isomers, high-performance liquid chromatographic analysis □ High-performance liquid chromatography—analysis, doxepin hydrochloride isomers

Doxepin hydrochloride, 3-dibenz[*b,e*]oxepin-11(6*H*)-ylidene-*N,N*-dimethyl-1-propanamine hydrochloride, is a dual-action antianxiety and antidepression psychotherapeutic agent (1). Chemically, it is a mixture of (*Z*)- and (*E*)-isomers (I*a* and I*b*, respectively) in an ~15:85% ratio. Recently, a GLC procedure (2), which requires an extraction step to convert the hydrochloride to free base, was recommended for doxepin hydrochloride analysis.

0022-3549/79/1100-1454$01.00/0

© 1979, American Pharmaceutical Association

Table I—Recovery of (*Z*)- and (*E*)-Doxepin Hydrochloride from Known Mixtures

Mixture	Doxepin Isomer Concentration, mg/ml		Total Isomer Concentration, mg/ml	(*Z*)-Isomer, %		(*E*)-Isomer, %	
	(*Z*)-Isomer	(*E*)-Isomer		Theory	Determined	Theory	Determined
I	0.0077	0.0638	0.0715	10.8	10.8	88.3	88.8
II	0.0149	0.0568	0.0717	20.8	20.7	78.5	79.0
III	0.0185	0.0532	0.0717	25.8	25.9	74.1	74.6
IV	0.0221	0.0496	0.0717	30.8	30.7	69.0	69.3
V	0.0367	0.0355	0.0722	50.8	50.7	49.3	49.6

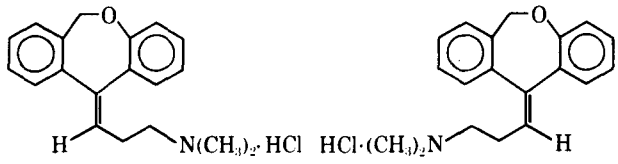

Ia *Ib*

Earlier, a high-performance liquid chromatographic (HPLC) procedure[1] was considered (3) but suffered from insufficient resolution of the two isomers, resulting in poor reproducibility. In the current work, modification of the HPLC column system produced a rapid, simple procedure that consistently afforded reproducible baseline resolution and quantification of the isomers.

EXPERIMENTAL

Chemicals and Reagents—(*Z*)-Doxepin hydrochloride [specified as 100% (*Z*)] and (*E*)-doxepin hydrochloride [specified as 99.4% (*E*) and 0.6% (*Z*)] were obtained as crystalline substances[2]. The following solvents were used: ACS grade diethylamine[3], acetonitrile[4] (distilled in glass, UV), and chloroform[4] (distilled in glass, without ethanol preservative).

Apparatus—A high-pressure pump[5] equipped with a 25-μl sample loop injection valve[6] and a multiple-wavelength detector[7] set at 254 nm and attached to a recorder[8] were used.

Column—The column[9] (4.6 mm i.d. × 25 cm) was purchased and used as received. It consisted of porous spherical silica microparticles (5–6 μm).

Mobile Phase Preparation—The mobile phase was prepared by mixing 750 ml of acetonitrile, 250 ml of chloroform, and 0.2 ml of diethylamine. The mobile phase was vacuum filtered through a polytef filter[10] and degassed prior to use.

Conditions for Chromatographic Analysis—The column was conditioned for 16 hr with the mobile phase at a flow rate of 0.2 ml/min. The approximate chromatographic conditions used were a flow rate of 0.7 ml/min (inlet pressure of 400 psig), a chart speed of 0.5 cm/min, and a detector sensitivity of 0.2 absorbance unit full scale (aufs). The column temperature was maintained at 28° by a water jacket controlled by a thermostat.

Standard Solutions of Doxepin Hydrochloride Isomers—Standard solutions of (*Z*)-doxepin hydrochloride in mobile phase contained 0.007–0.040 mg/ml. (*E*)-Doxepin hydrochloride standard solutions contained 0.035–0.070 mg/ml. With these (*Z*)- and (*E*)-doxepin hydrochloride standard solutions, five (*Z*)/(*E*)-doxepin hydrochloride mixtures of known concentrations (Table I) were prepared.

Calibration Curves and Mixture Analysis—Calibration curves were prepared by injecting aliquots (25 μl) of the individual (*Z*)- and (*E*)-doxepin hydrochloride standard solutions into the chromatographic system. The peak heights (centimeters) were plotted against the isomer concentrations (milligrams per milliliter), and the slopes of the curves were calculated.

The (*Z*)- and (*E*)- content of the five *cis/trans*-mixtures was determined by injecting 25-μl aliquots and measuring the resulting isomer peak heights. The following formulas were used to calculate the percentage of (*Z*) and (*E*)-doxepin hydrochloride in each mixture:

$$\%\ (Z)\text{-isomer} = \frac{H_r}{C} \times \frac{100}{S_Z} \qquad \text{(Eq. 1)}$$

$$\%\ (E)\text{-isomer} = \frac{H_e}{C} \times \frac{100}{S_E} \qquad \text{(Eq. 2)}$$

where H_r and H_e are the heights of the (*Z*)- and (*E*)-isomer peaks, respectively; C is the concentration (milligrams per milliliter) of both isomers in the mixture, and S_Z and S_E are the slopes of the (*Z*)- and (*E*)-isomer calibration curves, respectively. Once the linearity was proven, one (*Z*)- and (*E*)-doxepin standard solution was sufficient to determine accurately the isomeric content of doxepin hydrochloride samples.

RESULTS AND DISCUSSION

A typical chromatogram of a (*Z*)- and (*E*)-doxepin hydrochloride sample is shown in Fig. 1. Figure 2 illustrates that baseline resolution is easily attainable for (*Z*)- and (*E*)-doxepin hydrochloride mixtures of widely varying compositions.

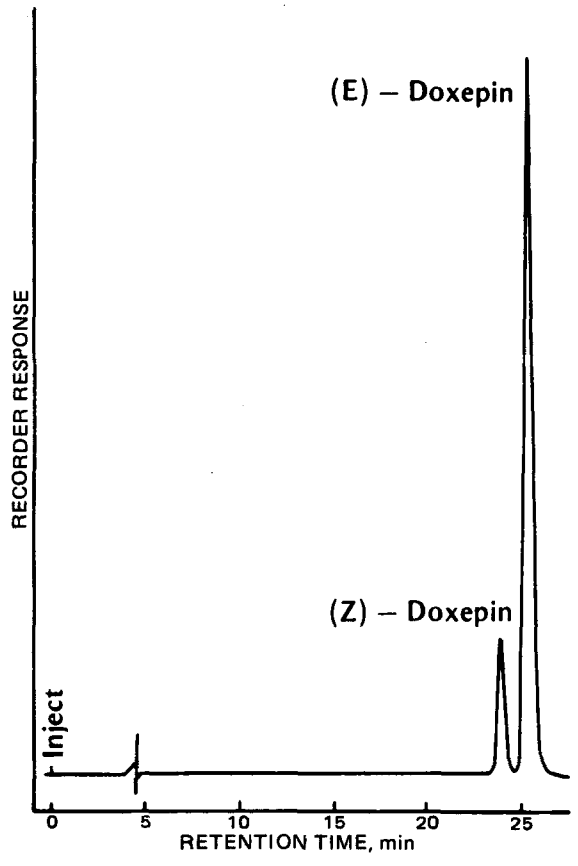

Figure 1—*Typical HPLC chromatogram of doxepin hydrochloride.*

[1] The published HPLC method was originally developed in the Laboratories of Central Research and Quality Control, Pfizer Inc., Groton, Conn., by Mr. T. J. Toolan and Dr. W. P. Zeronsa.
[2] Pfizer, Inc.
[3] Matheson, Coleman and Bell, Norwood, Ohio.
[4] Burdick & Jackson Laboratories, Muskegon, Mich.
[5] Model M6000A, Waters Associates, Milford, Mass.
[6] Valco model CV-UHPa-C-20, 7000-psi pressure rating, distributed by Alltech Associates, Arlington Heights, Ill.
[7] Spectroflow monitor 770, Schoeffel Instrument Corp., Westwood, N.J.
[8] A-25, Varian Instrument Division, Palo Alto, Calif.
[9] Zorbax SIL, Catalog No. 850952702, Du Pont Instruments, Wilmington, Del.
[10] Millipore type LS, 5.0 μm pore, Catalog No. LS (WP) 04700, Millipore Corp., Bedford, Mass.

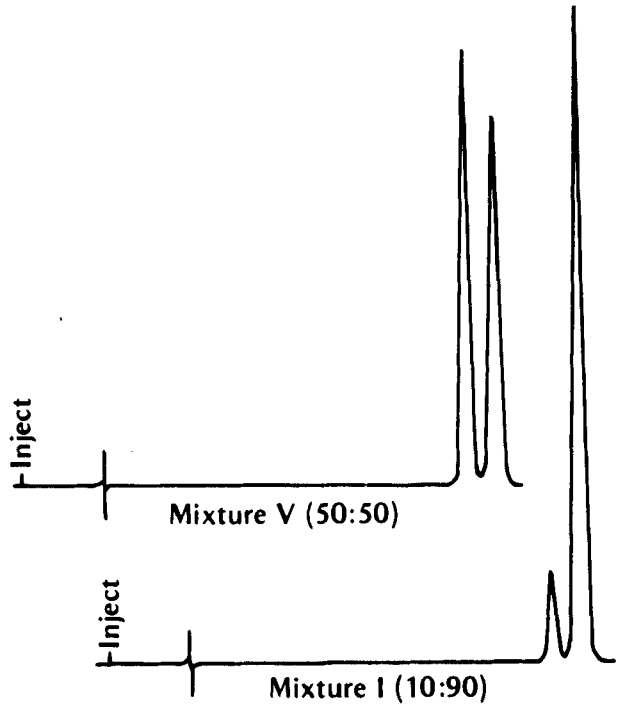

Figure 2—*HPLC chromatograms of mixtures of* (Z)- *and* (E)-*doxepin hydrochloride standards (Table I).*

The precision of the HPLC method was tested by injecting five aliquots of a 15% (*Z*)- and 85% (*E*)-doxepin hydrochloride isomer standard solution. The relative standard deviation was 0.3% for each isomer. The method was calibrated using separate solutions of individual isomers. Excellent linearity of the HPLC response–concentration relationship was demonstrated.

Assay accuracy was investigated by analyzing the five different (*Z*)- and (*E*)-doxepin hydrochloride mixtures of known composition (Fig. 2). The (*Z*)- and (*E*)-isomer content was calculated *via* Eqs. 1 and 2, respectively. The accuracy of the HPLC method is shown by the data presented in Table I. Assay selectivity was challenged by analysis of process-related substances. The results summarized in Table II illustrate the selectivity of the procedure. Long-term reproducibility and adaptability for routine analysis were verified by analyzing doxepin hydrochloride on columns of widely differing assay usage. (For instance, a new column was tested *versus* a 2-year-old column employed in assay work other than doxepin hydrochloride analysis and subjected to methanol deactivation). Equivalent assay data and comparable doxepin isomer resolution were observed in all cases.

The modified HPLC assay for the (*Z*)- and (*E*)-doxepin hydrochloride isomers has been established to be precise, accurate, and selective. The method is amenable to routine laboratory usage, and interlaboratory adoption of the methodology should present no procedural difficulties.

Table II—Retention Times of Process-Related Substances

Compound	Relative Retention Time
6,11-Dihydrodibenz[*b,e*]oxepin-11-one	0.18
Phthalide	0.20
Phenol	0.43
11-(3-Dimethylamino-1-propyl)-6*H*-dibenz[*b,e*]oxepin-11-ol	0.81
(*Z*)-Doxepin	1.00
(*E*)-Doxepin	1.06
2-(Phenoxymethyl)benzoic acid	>1.60

REFERENCES

(1) R. M. Pinder, R. N. Brogden, T. M. Speight, and G. S. Avery, *Drugs*, **13**, 161 (1977).

(2) *Pharmacopeial Forum*, Sept.–Oct. 1978, p. 514.

(3) *Ibid.*, July–Aug. 1978, p. 434.

Sensitive Assay for Determination of Hydroxyzine in Plasma and Its Human Pharmacokinetics

HASSAN G. FOUDA, DONALD C. HOBBS ˣ, and JOHN E. STAMBAUGH *

Received February 21, 1979, from the *Drug Metabolism Department, Pfizer Inc., Groton, CT 06340.* Accepted for publication May 8, 1979. *Department of Pharmacology, Thomas Jefferson University, Philadelphia, PA 19107.

Abstract □ An assay suitable for hydroxyzine determination in human plasma following therapeutic doses was developed. The method involves GLC and chemical-ionization mass spectrometry of the acetate derivatives of hydroxyzine and of a pentadeuterated analog internal standard. Following administration of 100-mg single oral doses to normal male volunteers, peak plasma concentrations of ~80 ng/ml were observed; the half-life of drug removal was ~3 hr.

Keyphrases □ Hydroxyzine—analysis, GLC–mass spectrometry, human plasma, following therapeutic doses □ Tranquilizers (minor)—hydroxyzine, GLC–mass spectrometric analysis, human plasma, following therapeutic doses □ GLC–mass spectrometry—analysis, hydroxyzine, human plasma

Hydroxyzine, 2-[2-[4-[(4-chlorophenyl)phenylmethyl]-1-piperazinyl]ethoxy]ethanol (I), is an antihistamine compound with antianxiety and antiemetic properties used in the treatment of nervous and emotional disturbances (1), for controlling nausea and vomiting (2), and for preoperative and postoperative sedation and analgesia (3). Procedures for hydroxyzine detection by TLC (4) and electrophoresis (5) do not have the sensitivity necessary for analysis of biological samples. GLC methods have been described (6–8) but the flame-ionization detection was inadequate for plasma samples; use of mass spectrometric detection was suggested (7, 8).

Preliminary studies in this laboratory indicated that the direct analysis of hydroxyzine was complicated by peak tailing with common stationary phases. The oxidation of hydroxyzine to a benzophenone, a product with improved GLC properties, has been examined (9, 10). However, several hydroxyzine metabolites can be expected to form the same benzophenone, rendering such a method nonspecific. Hydroxyzine is metabolized in the rat to *p*-chloro-*p'*-hydroxybenzophenone, *p*-chlorobenzhydrol, [2-(1-piperazinyl)ethoxy]ethanol (norchlorcyclizine), *p*-

0022-3549/79/1100-1456$01.00/0
© 1979, American Pharmaceutical Association

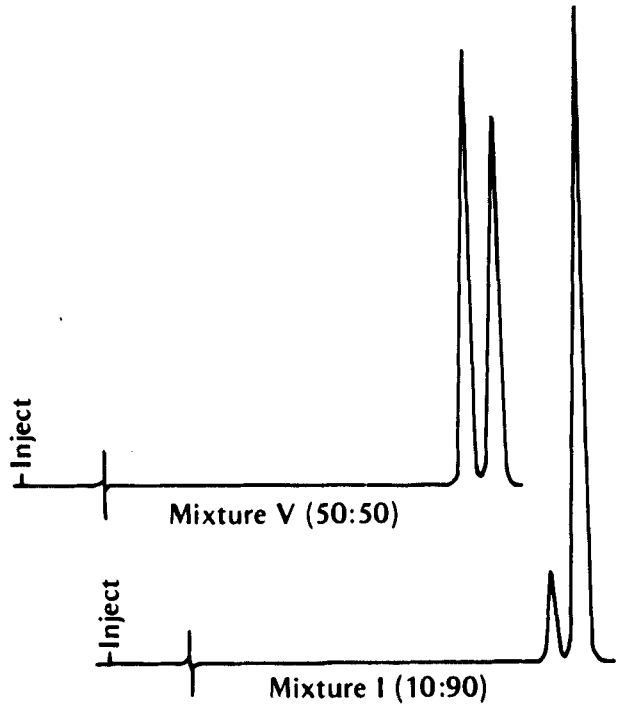

Figure 2—*HPLC chromatograms of mixtures of* (Z)- *and* (E)-*doxepin hydrochloride standards (Table I).*

The precision of the HPLC method was tested by injecting five aliquots of a 15% (*Z*)- and 85% (*E*)-doxepin hydrochloride isomer standard solution. The relative standard deviation was 0.3% for each isomer. The method was calibrated using separate solutions of individual isomers. Excellent linearity of the HPLC response–concentration relationship was demonstrated.

Assay accuracy was investigated by analyzing the five different (*Z*)- and (*E*)-doxepin hydrochloride mixtures of known composition (Fig. 2). The (*Z*)- and (*E*)-isomer content was calculated *via* Eqs. 1 and 2, respectively. The accuracy of the HPLC method is shown by the data presented in Table I. Assay selectivity was challenged by analysis of process-related substances. The results summarized in Table II illustrate the selectivity of the procedure. Long-term reproducibility and adaptability for routine analysis were verified by analyzing doxepin hydrochloride on columns of widely differing assay usage. (For instance, a new column was tested *versus* a 2-year-old column employed in assay work other than doxepin hydrochloride analysis and subjected to methanol deactivation). Equivalent assay data and comparable doxepin isomer resolution were observed in all cases.

The modified HPLC assay for the (*Z*)- and (*E*)-doxepin hydrochloride isomers has been established to be precise, accurate, and selective. The method is amenable to routine laboratory usage, and interlaboratory adoption of the methodology should present no procedural difficulties.

Table II—Retention Times of Process-Related Substances

Compound	Relative Retention Time
6,11-Dihydrodibenz[*b,e*]oxepin-11-one	0.18
Phthalide	0.20
Phenol	0.43
11-(3-Dimethylamino-1-propyl)-6*H*-dibenz[*b,e*]oxepin-11-ol	0.81
(*Z*)-Doxepin	1.00
(*E*)-Doxepin	1.06
2-(Phenoxymethyl)benzoic acid	>1.60

REFERENCES

(1) R. M. Pinder, R. N. Brogden, T. M. Speight, and G. S. Avery, *Drugs*, **13**, 161 (1977).

(2) *Pharmacopeial Forum*, Sept.–Oct. 1978, p. 514.

(3) *Ibid.*, July–Aug. 1978, p. 434.

Sensitive Assay for Determination of Hydroxyzine in Plasma and Its Human Pharmacokinetics

HASSAN G. FOUDA, DONALD C. HOBBS ˣ, and JOHN E. STAMBAUGH *

Received February 21, 1979, from the *Drug Metabolism Department, Pfizer Inc., Groton, CT 06340.* Accepted for publication May 8, 1979. *Department of Pharmacology, Thomas Jefferson University, Philadelphia, PA 19107.

Abstract □ An assay suitable for hydroxyzine determination in human plasma following therapeutic doses was developed. The method involves GLC and chemical-ionization mass spectrometry of the acetate derivatives of hydroxyzine and of a pentadeuterated analog internal standard. Following administration of 100-mg single oral doses to normal male volunteers, peak plasma concentrations of ~80 ng/ml were observed; the half-life of drug removal was ~3 hr.

Keyphrases □ Hydroxyzine—analysis, GLC–mass spectrometry, human plasma, following therapeutic doses □ Tranquilizers (minor)—hydroxyzine, GLC–mass spectrometric analysis, human plasma, following therapeutic doses □ GLC–mass spectrometry—analysis, hydroxyzine, human plasma

Hydroxyzine, 2-[2-[4-[(4-chlorophenyl)phenylmethyl]-1-piperazinyl]ethoxy]ethanol (I), is an antihistamine compound with antianxiety and antiemetic properties used in the treatment of nervous and emotional disturbances (1), for controlling nausea and vomiting (2), and for preoperative and postoperative sedation and analgesia (3). Procedures for hydroxyzine detection by TLC (4) and electrophoresis (5) do not have the sensitivity necessary for analysis of biological samples. GLC methods have been described (6–8) but the flame-ionization detection was inadequate for plasma samples; use of mass spectrometric detection was suggested (7, 8).

Preliminary studies in this laboratory indicated that the direct analysis of hydroxyzine was complicated by peak tailing with common stationary phases. The oxidation of hydroxyzine to a benzophenone, a product with improved GLC properties, has been examined (9, 10). However, several hydroxyzine metabolites can be expected to form the same benzophenone, rendering such a method nonspecific. Hydroxyzine is metabolized in the rat to *p*-chloro-*p'*-hydroxybenzophenone, *p*-chlorobenzhydrol, [2-(1-piperazinyl)ethoxy]ethanol (norchlorcyclizine), *p*-

0022-3549/79/1100-1456$01.00/0
© 1979, American Pharmaceutical Association

Table I—Analysis of Human Plasma Samples Containing Known Amounts of Hydroxyzine [a]

Amount Added, ng/ml	Amount Found, ng/ml	*RSD*, %
2	2.7	29.6
5	5.0	10.0
25	24.0	7.9
50	49.0	3.7
75	77.3	6.6
100	98.9	5.6

[a] Five samples were examined at each concentration.

chlorobenzophenone, and piperazine (11). Glucuronides of the first two also were identified. The formation of hydroxyzine-*N*-oxide by the rat was reported (12). Metabolism studies have not been conducted in humans.

This report describes a specific and sensitive assay for hydroxyzine determination in human plasma; pharmacokinetic properties were assessed following the administration of a single oral 100-mg dose.

EXPERIMENTAL

Materials—All solvents were glass distilled[1], and all reagents were ACS grade and used as received. The centrifuge and culture tubes were silylated with 10% dichlorodimethylsilane[2] in toluene. The tubes were rinsed in succession with toluene, methanol, and acetone and were dried at room temperature. Standard hydroxyzine hydrochloride[3] solutions were prepared weekly in methanol at concentrations of 1 mg/ml (free base) and were kept at 4°.

Pentadeuterated Hydroxyzine (II) Synthesis—*p*-Chlorobenzhydryl-d_5 diethyldiamine (1.45 g, 5 mmoles) (13), chloroethoxyethanol (0.62 g, 5 mmoles), and triethylamine (0.5 ml, 6 mmoles) were stirred with toluene (25 ml) and heated at reflux for 48 hr. The reaction mixture was allowed to cool to room temperature. Water (20 ml) was added, and stirring was continued for 20 min. The mixture was filtered, and the aqueous layer was adjusted to pH 8. After phase separation, the aqueous layer was extracted with three 25-ml portions of toluene. The combined toluene phases were washed with two 5-ml portions of dilute hydrochloric acid (pH 6.8) and then reextracted with three 25-ml portions of dilute hydrochloric acid (pH 1).

The aqueous layers were treated with 40% aqueous NaOH to adjust the pH to 11–12 and were extracted four times with 25-ml portions of benzene. The combined benzene extracts were filtered through anhydrous sodium sulfate and then evaporated, leaving the crude product, parts of which were purified by preparative TLC (methanol–water, 67:33). The material having the R_f of hydroxyzine was dissolved in 5 ml of ethyl acetate. Several drops of dry hydrogen chloride gas in isopropanol (6.8%) were added to form the hydrochloride salt, which was separated by centrifugation and washed three times with 10 ml of hexane.

The final product was left under vacuum overnight to remove excess solvent. The identity and the isotopic purity of the hydroxyzine-d_5 thus obtained were established by high-resolution mass spectrometry. The parent ion (M^+) was within 2 millimass units of the theoretical value. The relative abundance of the ion at M − 5 (d_0) was <0.1% of the parent ion, indicating an isotopic purity of >99.9%. The hydroxyzine-d_5 was chemically pure by GLC and by TLC (chloroform–methanol, 9:1).

Assay—Plasma samples (2 ml) in 15-ml centrifuge tubes were mixed with 200 ng of hydroxyzine-d_5 and with 0.25 ml of aqueous 10 *N* NaOH.

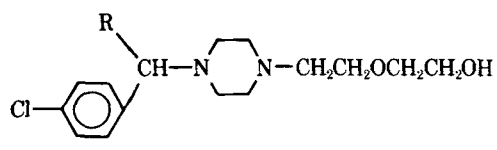

I: R = C_6H_5
II: R = C_6D_5

[1] Burdick & Jackson, Muskegon, Mich.
[2] Aldrich, Milwaukee, Wis.
[3] Vistaril, Pfizer, New York, N.Y.

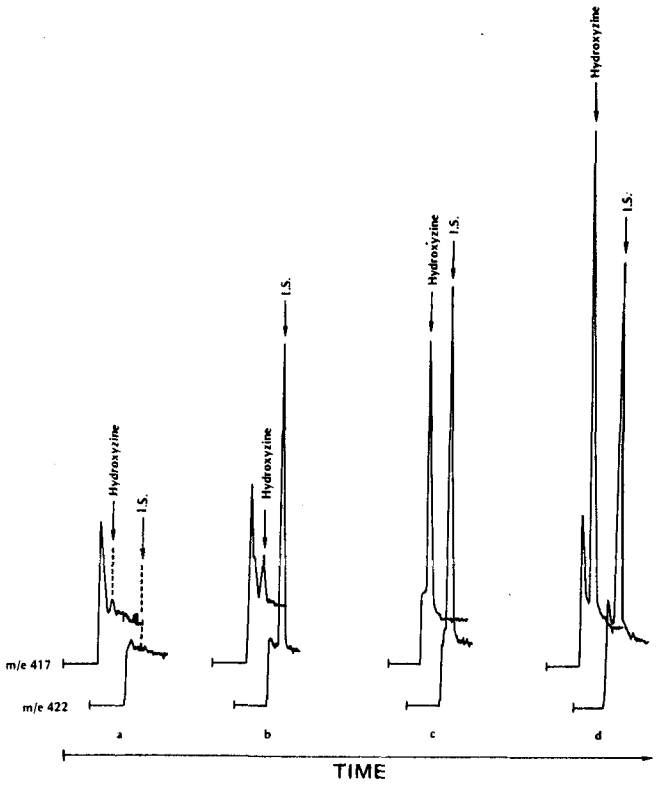

Figure 1—*Selected ion current profiles of control plasma* (a); *control plasma fortified at 2 ng of hydroxyzine/ml* (b), *control plasma fortified at 50 ng of hydroxyzine/ml* (c), *and Subject 1, 2 hr post dose* (d).

The mixture was extracted with hexane (3 × 10 ml), and the hexane extracts were discarded. The aqueous phase was diluted with water (3 ml) and extracted with ether (8 ml). After centrifugation, each tube was dipped in a dry ice–acetone bath to freeze the aqueous phase, and the organic phase was transferred to a 10-ml culture tube and evaporated to dryness by a dry nitrogen stream.

The residues were treated with acetyl chloride (0.1 ml) and vortexed[4] for 30 sec, and the excess acetyl chloride was removed with a dry nitrogen stream. Immediately before analysis, the residues were dissolved in 50 μl of methanol, and aliquots (3–5 μl) were injected into the chromatograph.

Instrumentation—Analyses were carried out on a mass spectrometer equipped for chemical ionization[5]. Samples were introduced by GLC on a 0.8-m × 2-mm i.d. glass column packed with 3% OV-17 on Chromosorb W (80–100 mesh). The column, the injection port, and the transfer lines were kept at 290°. Methane was used as a carrier gas. The ion source temperature was maintained at 165° with a temperature controller[6]. The reagent gas, a mixture of methane and ammonia, was made up by bleeding ammonia directly into the ion source to give a pressure of 0.35–0.40 torr; methane flow through the column was adjusted to give a final pressure of 0.95–1.0 torr in the ion source.

Voltage switching to monitor the ion currents at *m/e* 417 and 422 was controlled by PROMIM units. The signals from the mass spectrometer were recorded on a four-pen recorder[7]. Parameters were adjusted to give maximum sample intensities while unit resolution was maintained.

Calculations—Plasma hydroxyzine concentrations were calculated from the peak height at *m/e* 417 relative to the internal standard peak at *m/e* 422 with reference to a standard curve constructed from plasma samples fortified with known amounts of hydroxyzine.

Human Studies—Hydroxyzine hydrochloride was administered to four healthy male volunteers in the form of commercial 100-mg tablets following an overnight fast. Food was withheld for an additional 2 hr. Blood samples were drawn into heparinized tubes at 0, 0.5, 1, 2, 4, 6, 8, and 24 hr. Plasma was obtained by centrifugation and frozen until assay.

[4] Vortex Genie, Scientific Industries.
[5] Finnigan model 3200.
[6] LFE Corp., Waltham, Mass.
[7] Model HR-4, Houston Instruments, Austin, Tex.

Table II—Human Plasma Concentrations following Oral Administration of 100 mg of Hydroxyzine

Subject[a]	Weight, kg	Nanograms per Milliliter						
		0.5 hr	1 hr	2 hr	4 hr	6 hr	8 hr	24 hr
1	91	<2	<2	74	65	57	38	<2
2	84	<2	23	39	89	65	34	<2
3	77	<2	4	65	82	58	31	<2
4	82	<2	51	86	75	58	38	<2
Mean		<2	20	66	78	59	35	<2

[a] All subjects were male, ages 24–26 years.

Table III—Pharmacokinetic Parameters

Subject	A	α	Absorption Half-Life, hr	B	β	Elimination Half-Life, hr	Lag Time, hr	t_{max}	C_{max}
1	439	1.043	0.66	192	0.203	3.42	1.0	2.9	85
2	467	0.443	1.56	418	0.258	2.68	0.6	3.5	70
3	526	0.670	1.03	362	0.281	2.46	1.0	3.2	85
4	270	0.844	0.82	206	0.208	3.33	0.4	2.6	90
Mean			1.02			2.97	0.7	3.0	82

RESULTS AND DISCUSSION

Hydroxyzine could not be analyzed directly by GLC–mass spectrometry because of poor GLC characteristics at low concentrations due to the polar hydroxy side chain. Attempts to prepare the hexafluoroacetate or the heptafluorobutyrate ester were not successful because hydroxyzine was unstable under the reaction conditions. Acetate ester formation using acetyl chloride proved to be simple and rapid, requiring only a few seconds at room temperature. The excess derivatizing agent was conveniently removed by evaporation. Although hydroxyzine acetate was less volatile than hydroxyzine, it exhibited excellent GLC properties, giving sharp and symmetric peaks at low concentrations (Fig. 1).

Initial studies showed that the use of ammonia as a reagent gas for chemical ionization favored the formation of the hydroxyzine acetate adduct ion (M + H). This has been the case also for the structurally related meclizine (13) and for some amines (14). Chemical ionization and detection of the pseudomolecular ion obviated difficulties in specificity arising from the known animal (11) hydroxyzine metabolites.

Calibration curves for hydroxyzine in plasma were linear from 2 to 100 ng/ml. One factor limiting the assay sensitivity was the presence of a small peak at *m/e* 417 and at the hydroxyzine acetate retention time in plasma of untreated human volunteers. With 2 ml of plasma, this peak was equivalent to 0.59 ± 0.01 ng of hydroxyzine/ml (Fig. 1). The relative standard deviation of the assay was high at the lowest detectable hydroxyzine level but was 10% or less at concentrations of ≥5 ng/ml (Table I). Hydroxyzine recovery from human plasma samples containing 50 ng/ml was 82%.

Plasma concentrations in four subjects receiving single oral 100-mg hydroxyzine doses are given in Table II. The drug appears to be consistently absorbed, giving peak concentrations of ~80 ng/ml 2–4 hr following administration. The data from each subject were applied to an iterative computer program by which the data were fitted to a one-compartment open model represented by:

$$C_t = -Ae^{-\alpha t} + Be^{-\beta t} \qquad \text{(Eq. 1)}$$

Excellent fits were obtained; the kinetic parameters are indicated in Table III. The absorption and elimination half-lives were obtained directly from the rate constants, α and β. Lag time, t_0, was estimated (15) from:

$$t_0 = \frac{\ln A - \ln B}{\alpha - \beta} \qquad \text{(Eq. 2)}$$

This lag time presumably corresponds to the time required for formulation disintegration and drug dissolution and for transport to the absorption site. The time of maximum plasma concentration, t_{max}, was calculated from:

$$t_{max} = \frac{2.303}{\alpha - \beta} \log \frac{\alpha}{\beta} + t_0 \qquad \text{(Eq. 3)}$$

and was applied to Eq. 1 to calculate the maximum plasma concentration.

The mean absorption half-life of 1.02 hr indicates that hydroxyzine is absorbed by humans at a rate typical of many drugs. The mean elimination half-life, 3 hr, is similar to that of the chemically related drug meclizine (13).

REFERENCES

(1) H. L. Goldbert and R. J. Finnerty, *Psychosomatics*, **14**, 38 (1973).

(2) J. C. Snow, *Anesth. Analg.*, **44**, 487 (1965).

(3) A. Matsuki and E. K. Zsigmund, *Agressologie*, **14**, 67 (1973).

(4) S. J. Mule, *J. Chromatogr.*, **55**, 255 (1971).

(5) S. N. Tewari, *Z. Anal. Chem.*, **275**, 31 (1975).

(6) C. Cardini, V. Quercia, and A. Calo, *J. Chromatogr.*, **37**, 190 (1968).

(7) H. Brandenberger, *Pharm. Acta Helv.*, **45**, 394 (1970).

(8) E. van der Kleijn, G. C. Beelen, and M. A. Frederick, *Clin. Chim. Acta*, **34**, 345 (1971).

(9) B. Caddy, F. Fish, and J. Tranter, *Analyst*, **99**, 555 (1974).

(10) P. Hartvig and W. Handl, *Acta Pharm. Suec.*, **12**, 349 (1975).

(11) S. F. Pong and C. L. Huang, *J. Pharm. Sci.*, **63**, 1527 (1974).

(12) J. A. Close, J. G. Gobert, and L. A. M. Rodriguez, *Proc. Eur. Soc. Study Drug Toxic.*, **9**, 144 (1968).

(13) H. G. Fouda, F. C. Falkner, D. C. Hobbs, and E. W. Luther, *Biomed. Mass Spectrom.*, **5**, 491 (1978).

(14) I. Dzidic, *J. Am. Chem. Soc.*, **94**, 8333 (1972).

(15) J. G. Wagner, "Fundamentals of Clinical Pharmacokinetics," Drug Intelligence Publications, Hamilton, Ill., 1975, p. 81.

ACKNOWLEDGMENTS

The authors thank D. Cristina and S. Plucker for technical assistance.

High-Performance Liquid Chromatographic Determination of Plasma Propylthiouracil

H. G. GILES ˣ, R. MILLER, and E. M. SELLERS

Received February 26, 1979, from the *Clinical Institute, Addiction Research Foundation, Toronto, Ontario, M5S 2S1, Canada,* and the *Departments of Pharmacology and Medicine, University of Toronto, Toronto, Ontario, Canada.* Accepted for publication May 3, 1979.

Abstract □ A reversed-phase high-performance liquid chromatographic analysis was developed for propylthiouracil in plasma (1 ml). After protein precipitation with acetonitrile, the solution was diluted with water and injected into a liquid chromatograph equipped with C-18 and C-8 columns in series. The peak area was linear over the 0.25–10-mg/liter range, and the recovery was 101 ± 4.5%. This assay has the advantages of specificity, simplicity, and speed over previously published methods and requires smaller sample volumes. None of 19 drugs tested interfered with the assay.

Keyphrases □ Propylthiouracil—analysis, high-performance liquid chromatography in plasma, alcoholic liver disease □ Thyroid inhibitors—propylthiouracil, high-performance liquid chromatographic analysis in plasma, alcoholic liver disease □ High-performance liquid chromatography—analysis, propylthiouracil in plasma, alcoholic liver disease

Propylthiouracil has been used in the management of hyperthyroidism for many years. Attention has been given to its analysis in plasma and to its pharmacokinetics in normal subjects and in patients with thyroid dysfunction (1–11). The drug is presently being evaluated in the treatment of alcoholic liver disease (12) where its clearance and apparent distribution volume may be altered (13).

BACKGROUND

For pharmacokinetic studies, plasma propylthiouracil concentrations have been determined. Because of normal and disease-related interindividual variations in kinetics, a rapid, specific, and sensitive method for plasma analysis would help in determining dosage adjustments for the individual patient. Previously published analysis methods lack either specificity or simplicity and are not suitable for routine determinations in a heterogeneous patient population.

One hour after a single propylthiouracil dose (200–400 mg po), the peak plasma concentration is often 10 mg/liter. After distribution equilibrium has been achieved, the plasma concentration declines exponentially, with a half-life commonly in the range of 60 min (3, 5–11), although other apparent elimination rates have been reported (1, 4). First-order kinetics have been demonstrated over a wide range of doses (10). Five hours after drug administration, the plasma concentration is commonly 1 mg/liter. During chronic propylthiouracil administration (100 mg every 8 hr) to patients with usual propylthiouracil kinetics, the mean steady-state concentration may be calculated to be ~1 mg/liter (14). Therefore, the sensitivity limit of any propylthiouracil assay should be at or below 1 mg/liter as in the previously published methods (2, 6, 7).

Although the sensitivity of the other methods seems adequate to determine pharmacokinetics, the specificity of the total radioactivity method (1) and the colorimetric method (2) has been questioned (6, 7). In particular, the lack of analytical specificity may have been responsible, in part, for some of the unusually prolonged half-lives reported (4). A further small disadvantage of the colorimetric method is that 2 ml of serum is required.

Two specific methods for plasma propylthiouracil determination have been reported. A time-consuming and technically difficult GLC method (7) employs tetrapropylammonium hydroxide as an alkylating agent for propylthiouracil after an ether extraction. One milliliter of plasma is required for this method. An ion-exchange high-performance liquid chromatographic (HPLC) analysis measures propylthiouracil after a chloroform extraction (6). The serious disadvantages of this method are the excessive volume of plasma required (5 ml), the long propylthiouracil retention time (20 min), and the column temperature control required. Neither method is suitable for routine use.

The present paper reports a sensitive and specific HPLC assay for the rapid determination of propylthiouracil in plasma.

EXPERIMENTAL

Reagents—Propylthiouracil was obtained from propylthiouracil tablets[1] after recrystallization from ethanol. The purity was checked by melting point [221–222°, lit. (15) 219–221°] and by comparison of the HPLC retention time with that of propylthiouracil obtained from another source[2]. The chromatographic peak was identified by determination of its maximum UV absorption [275 nm, lit. (16) 275 nm in methanol]. Water was triple distilled in glass. Acetonitrile was HPLC grade[3]. Phosphoric acid and monobasic sodium phosphate were ACS grade[4].

Instrumentation—The high-performance liquid chromatograph[5] was equipped with a universal injector[6], a column inlet filter[7], a column guard[8], C-18[9] and C-8[10] reversed-phase columns in series, a variable-wavelength UV detector set at 275 nm (0–0.04 absorbance unit)[11], and a recording integrator (attenuation ×8)[12]. The mobile phase flow rate was 2.1 ml/min, and the pressure was 232 bar. Overnight, the UV detector was left on and the flow rate was reduced to 0.2 ml/min.

Solutions—The stock propylthiouracil solution was made in methanol. The mobile phase was made by dissolving 1.4 g of monobasic sodium phosphate in 1 liter of water (0.01 *M*), lowering the pH to 3.0 with 5 *N* phosphoric acid, and adding 450 ml of acetonitrile.

Sample Preparation—For standards, appropriate volumes of the propylthiouracil stock solution were added to glass tubes (13 × 100 mm), and the solvent was evaporated under a nitrogen stream. Patient plasma samples were frozen at −20° until analyzed. Plasma (1 ml) was added, and the tubes were vortexed for 1 min. Acetonitrile (2.5 ml) was added to precipitate proteins, and the mixture was vortexed for 1 min and centrifuged for 5 min at 2000 rpm[13]. To 1 ml of the supernate was added 2 ml of water, and 0.25 ml of this solution was analyzed on the chromatograph.

RESULTS AND DISCUSSION

HPLC has proven to be fast, accurate, and precise for determining drugs in biological fluids. This particular analytical system uses a variable-wavelength UV detector for increased sensitivity and specificity. Detection at 254 nm resulted in a 60% loss of sensitivity.

The standard curves obtained from measurement of the propylthiouracil peak area in spiked plasma samples were linear ($r = 0.99$) over 0.25–10 mg of propylthiouracil/liter. The minimum detectable concentration was ~0.1 mg/liter. The assay reproducibility is shown in Table I. Recovery was calculated in two ways: by reference to the linear regression equation (Table I) and by comparison with results obtained from 1-ml water samples ($n = 8$) containing 4 mg of propylthiouracil/liter. The latter method gave the recovery as 101 ± 4.5%. The daily variation in the standard curve slope was 5.2% ($n = 6$).

Although 1-ml plasma volumes were used for convenience, smaller sample sizes are clearly possible. In the sample preparation, a 10.5-fold dilution occurs and only 8% of the final volume is injected into the liquid chromatograph. Therefore, a simple scaledown would permit the analysis

[1] Propyl-thyracil, Charles E. Frosst and Co., Dorval, Quebec, Canada.
[2] Aldrich Chemical Co., Milwaukee, Wis.
[3] J. T. Baker Chemical Co., Phillipsburg, N.J.
[4] Fisher Scientific Co., Fair Lawn, N.J.
[5] HP 1081A, Hewlett-Packard, Boblingen, West Germany.
[6] CV-6-UHPa-N60, Valco Instruments Co., Houston, Tex.
[7] 7302, Rheodyne, Berkeley, Calif.
[8] μBondapak C_{18}, 400 mg, Waters Associates, Mississauga, Ontario, Canada.
[9] μBondapak C_{18}, 3.9 mm i.d. × 30 cm, Waters Associates.
[10] RP-8, Brownlee, 4.6 mm i.d. × 25 cm, Santa Clara, Calif.
[11] SF 700, Schoeffel, Westwood, N.J.
[12] HP 3380A, Hewlett-Packard, Avondale, Pa.
[13] Sorvall, GLC-2B, Du Pont Instruments, Newton, Conn.

0022-3549/79/1100-1459$01.00/0
© 1979, American Pharmaceutical Association

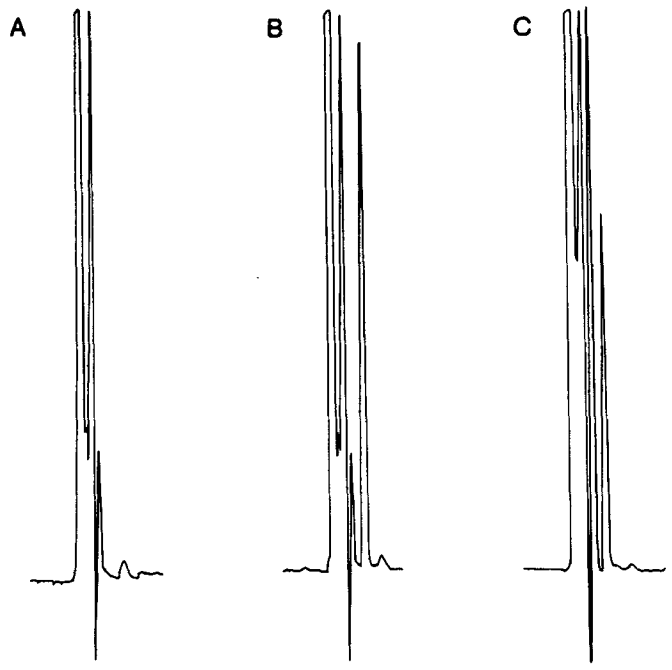

Figure 1—*Chromatograms of normal blank plasma (A), spiked normal plasma containing propylthiouracil (4 mg/liter) (B), and plasma from a patient with alcoholic liver disease, taking propylthiouracil, 150 mg twice a day, 3.67 hr after the last dose (C). The propylthiouracil retention time was 4.5 min.*

of 0.1-ml plasma samples. In addition, the good peak shape, peak separation, and noise level may allow a further reduction in sample size, which may be useful in pediatrics and in studies with small animals.

Propylthiouracil metabolism in humans is virtually unknown, although Kampmann (10) reported that most propylthiouracil in the urine is present as the glucuronide. The parent compound and this conjugate would not be expected to have similar retention times under the present chromatographic conditions. Interference tests with 19 commonly used drugs at concentrations often encountered during therapy (17) were negative. The drugs tested and the concentrations (milligrams per liter) were: amphetamine, 0.1; acetaminophen, 10.0; amitriptyline, 0.05; amobarbital, 0.1; chlordiazepoxide, 1.0; codeine, 0.1; *N*-desmethyldiazepam, 0.3; diazepam, 0.2; phenytoin, 10.0; flurazepam, 0.05; meperidine, 0.5; methadone, 0.3; methamphetamine, 0.1; morphine, 0.1; phenobarbital, 0.1; propranolol, 0.05; quinine, 0.1; sodium salicylate, 200.0; and warfarin, 1.0.

To test the method, two plasma samples (3 ml) were obtained from each of two patients with alcoholic liver disease who had been taking propylthiouracil, 150 mg twice a day, for >3 weeks. The sampling times, relative to the last dose, and the plasma concentrations were: Patient 1, 3.67 hr, 2.66 mg/liter, and 5.1 hr, 0.79 mg/liter; and Patient 2, 3.08 hr, 1.56 mg/liter, and 5.17 hr, 0.76 mg/liter. Two-point estimates of the apparent elimination half-lives are: Patient 1, 0.80 hr; and Patient 2, 2.0 hr.

The analysis of propylthiouracil in plasma from patients with alcoholic liver disease showed no serious interference from other compounds in plasma, although the peak separation was not as good as with plasma from normal subjects (Fig. 1). This finding shows the advantage of a two-column system for studies in a heterogeneous patient population. The estimated propylthiouracil apparent elimination half-lives of both patients were in the normal range. This result was supported by the fact that there was no unusual propylthiouracil accumulation in these patients during therapy. A more complete description of propylthiouracil kinetics in patients with alcoholic liver disease has not been reported but would be useful.

Table I—Propylthiouracil Assay Reproducibility Using Spiked Human Plasma (1 ml)

Amount Added, mg/liter[a]	Amount Recovered, mg/liter	Percent Recovered	CV, %
0	0.00		
0.25	0.26	103	5.4
0.5	0.47	94	3.7
1	0.99	99	4.7
2	2.02	101	2.7
4	3.89	97	4.5
6	6.17	103	5.7
8	7.70	96	3.3
10	10.2	102	3.6

[a] Eight samples were determined in each case.

REFERENCES

(1) W. D. Alexander, V. Evans, A. MacAulay, T. F. Gallagher, Jr., and J. Londono, *Br. Med. J.*, **2**, 290 (1969).

(2) C. R. Ratliff, P. F. Gilliland, and F. F. Hall, *Clin. Chem.*, **18**, 1373 (1972).

(3) J. Kampmann and L. Skovsted, *Acta Pharmacol. Toxicol.*, **35**, 361 (1974).

(4) E. S. Vessell, J. R. Shapiro, G. T. Passananti, H. Jorgensen, and C. A. Shively, *Clin. Pharmacol. Ther.*, **17**, 48 (1975).

(5) J. F. McMurry, Jr., P. F. Gilliland, C. R. Ratliff, and P. D. Bourland, *J. Clin. Endocrinol. Metab.*, **41**, 362 (1975).

(6) D. S. Sitar and D. B. Hunninghake, *ibid.*, **40**, 26 (1975).

(7) D. Schuppan, S. Riegelman, B. v. Lehmann, A. Pilbrant, and C. Becker, *J. Pharmacokinet. Biopharm.*, **1**, 307 (1973).

(8) M. Eichelbaum, *Clin. Pharmacokinet.*, **1**, 339 (1976).

(9) J. Kampmann and L. Skovsted, *Acta Pharmacol. Toxicol.*, **37**, 201 (1975).

(10) J. P. Kampmann, *J. Pharmacokinet. Biopharm.*, **5**, 435 (1977).

(11) H. G. Giles, R. Miller, E. M. Sellers, E. A. Roberts, and H. Orrego, *Fed. Proc.*, **38**, 528 (1979).

(12) H. Orrego, H. Kalant, Y. Israel, J. Blake, A. Medline, J. G. Rankin, A. Armstrong, and B. Kapur, *Gastroenterology*, **76**, 105 (1979).

(13) T. F. Blashke, *Clin. Pharmacokinet.*, **2**, 32 (1977).

(14) M. Gibaldi and D. Perrier, "Pharmacokinetics," Dekker, New York, N.Y., 1975, p. 119.

(15) G. W. Anderson, I. F. Halverstadt, W. H. Miller, and R. O. Roblin, Jr., *J. Am. Chem. Soc.*, **67**, 2197 (1945).

(16) "Atlas of Spectral Data and Physical Constants for Organic Compounds," J. G. Grasselli and W. M. Ritchey, Eds., CRC Press, Cleveland, Ohio, 1975, p. 735.

(17) C. L. Winek, *Clin. Chem.*, **22**, 832 (1976).

ACKNOWLEDGMENTS

The authors thank Dr. H. Orrego for access to patients under his care.

High-Pressure Liquid Chromatographic Determination of Propylthiouracil in Human Plasma

H. PAUL RINGHAND *x and WOLFGANG A. RITSCHEL ‡

Received September 11, 1978, from the **Food and Drug Administration, Cincinnati, OH 45202,* and the ‡*College of Pharmacy, University of Cincinnati Medical Center, Cincinnati, OH 45267.* Accepted for publication May 9, 1979.

Abstract □ A high-pressure liquid chromatographic procedure was developed for the determination of propylthiouracil in plasma. The method utilizes a reversed-phase C_{18} chromatographic column and UV detection at 280 nm. The method is sufficiently sensitive for most bioavailability and pharmacokinetic studies. Concentrations between 0.1 and 5.0 μg/ml were measured with a coefficient of variation of 0.6–5.3% for a given day. Methylthiouracil was employed as an internal standard.

Keyphrases □ Propylthiouracil—analysis, high-pressure liquid chromatography, human plasma □ Thyroid inhibitors—propylthiouracil, high-pressure liquid chromatographic analysis, human plasma □ High-pressure liquid chromatography—analysis, propylthiouracil, human plasma

Several methods have been reported for the analysis of the thyrostatic drug propylthiouracil in biological fluids. Each method has some disadvantage with respect to sensitivity, selectivity, reproducibility, and/or adaptability for use in a large-scale bioavailability study. The use of radioactive isotopes (1, 2) is generally unsuitable in bioavailability studies because some modification has to be made in the normal production of the propylthiouracil dosage forms. Existing colorimetric procedures (3, 4) either are relatively insensitive or lack the necessary selectivity to distinguish between the parent drug and metabolites formed by the side-chain oxidation of propylthiouracil (2).

A GLC method (5) was employed in two separate studies in humans (5, 6). The major disadvantages of this procedure are the inherent problems associated with the formulation of derivatives by flash alkylation (7) and the necessity of elevating the column temperature after every two or three injections to remove slowly eluting compounds.

A high-pressure liquid chromatographic (HPLC) procedure using an ion-exchange column was described by Sitar and Hunninghake (8). The procedure was reported to have a lower detection limit of 0.2 μg/ml, comparable to the sensitivity claimed for the GLC procedure (5). Neither the GLC nor HPLC method was considered to be sufficiently sensitive to determine plasma propylthiouracil levels over an 8-hr period following ingestion of a single 150-mg dose.

A specific HPLC method employing an internal standard is presented here. It is both reproducible and sensitive.

EXPERIMENTAL

Reagents and Materials—Propylthiouracil[1] (assayed 101.0%), methylthiouracil[2], reagent grade or equivalent acetic acid, chloroform, methanol, and ammonium sulfate were used as supplied. A stock propylthiouracil solution (60 μg/ml), which also served as a working standard, was prepared in distilled water and stored in the dark at room temperature. Appropriate dilutions were made with water each week to produce additional working standards of 1.2–60 μg/ml. A working standard of the internal standard, methylthiouracil (1.75 μg/ml), was prepared in chloroform and stored in amber glass bottles at room temperature.

Table I—Precision of HPLC Assay of Propylthiouracil for a Given Day [a]

Propylthiouracil, μg/ml	Reproducibility at a Given Concentration: Mean ± *SD*[b], μg/ml	*CV*, %
0.1	0.708 ± 0.037	5.23
0.25	0.676 ± 0.026	3.85
0.5	0.708 ± 0.017	2.40
1.0	0.714 ± 0.011	1.54
2.5	0.724 ± 0.012	1.66
5.0	0.730 ± 0.004	0.55

[a] Six samples were measured at each concentration. [b] Area under the propylthiouracil peak divided by area under the internal standard peak.

Apparatus—A modular high-pressure liquid chromatograph was outfitted with a constant-flow pump[3], a valve-type injector[4], a fixed-wavelength detector[5] employing a 280-nm detector conversion kit[6], an electronic integrator[7], and a stainless steel column, 25 cm long × 3.1 mm i.d., packed with an octadecylsilane reversed-phase support[8]. Absorbance was measured at 280 nm, using a sensitivity of 0.02 absorbance unit full scale (aufs).

Chromatographic Conditions—The mobile phase consisted of deaerated acetic acid–methanol–water (10:75:915). The flow rate was 2.3 ml/min (1500 psi). All determinations were performed at room temperature.

Sample Preparation—Plasma, 3.0 ml, was placed in a suitable silylated (9) glass-stoppered centrifuge tube containing 0.5 g of ammonium sulfate and was mixed vigorously for 1 min. The samples were extracted by mixing for 10 min with 15.0 ml of chloroform, using gentle mechanical agitation. The mixture was centrifuged at 500×*g* for 10 min, and 10.0 ml of the lower layer was transferred to a 15-ml silicon-coated vacuum tube[9] containing 1.0 ml of the internal standard.

The chloroform was evaporated with the aid of a water bath maintained at 60–65° and a gentle air stream. The residue was dissolved in 250 μl of the mobile solvent; the walls of the tube were rinsed with a microsyringe, and the contents were mixed with a vortex mixer. Samples (25 μl) were injected into the chromatograph.

Calibration—Calibration curves were constructed in duplicate for each batch of unknown samples by adding known amounts of propylthiouracil to control plasma. The internal standard was added after the chloroform extraction because preliminary experiments indicated that the methylthiouracil extraction was not reproducible. The propylthiouracil in unknown samples was determined from the calibration curve prepared daily by plotting the average ratio of the area under the peak (*AUPR*) of propylthiouracil to that of the internal standard against the plasma propylthiouracil concentration (micrograms per milliliter). The correlation coefficients exceeded 0.99 for each daily calibration curve. Normalized *AUPR* values were determined by dividing the *AUPR* for each standard by the plasma propylthiouracil concentration (micrograms per milliliter).

[1] Lot 86328, ICN-K&K Laboratories, Irvine, Calif.
[2] ICN Pharmaceuticals, Plainview, N.J.
[3] Model 6000, Waters Associates, Milford, Mass.
[4] Universal injector model, Waters Associates, Milford, Mass.
[5] Model 202/401, Waters Associates, Milford, Mass.
[6] Waters Associates, Milford, Mass.
[7] Model 3380A, Hewlett-Packard, Avondale, Pa.
[8] Spherisorb 10 μ, Spectra-Physics, Santa Clara, Calif.
[9] Red stopper vacuum tube, Becton-Dickinson, Rutherford, N.J.

0022-3549/79/1100-1461$01.00/0
© 1979, American Pharmaceutical Association

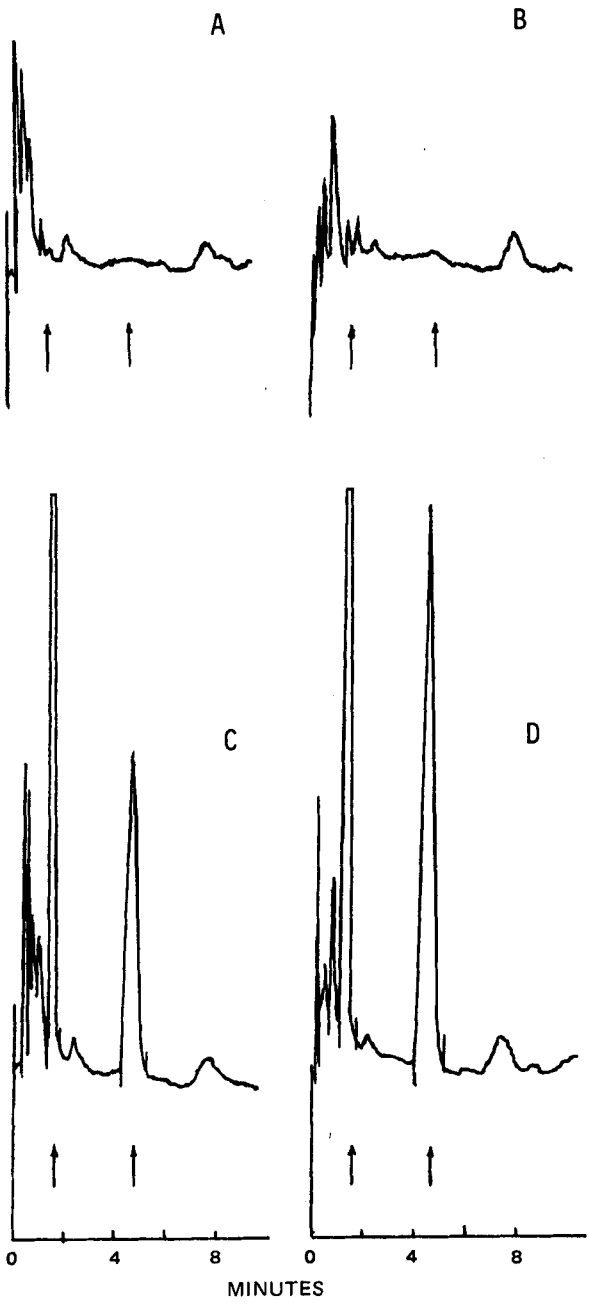

Figure 1—*HPLC determination of propylthiouracil in human plasma. Key: A, chromatogram obtained when 3 ml of control plasma was extracted and the absorbance was measured at 254 nm; B, chromatogram of the same control plasma with the absorbance measured at 280 nm; C, representative chromatogram of plasma containing propylthiouracil and the internal standard with the absorbance measured at 254 nm; and D, chromatogram of the same plasma sample containing propylthiouracil and the internal standard with the absorbance measured at 280 nm. The arrows refer to the retention times of propylthiouracil (4.8 min) and the internal standard (1.5 min).*

RESULTS AND DISCUSSION

A selective method for measuring propylthiouracil in plasma at suitably low concentrations was desired. Because of the large numbers of plasma samples expected in a planned bioavailability study (10), the time required for each analysis was critical. Because of its relative ease of operation and sensitivity, HPLC appeared to represent the best approach. A reversed-phase microparticulate column was found to be superior to the ion-exchange column used by Sitar and Hunninghake (8) because of reduced analytical times, greater peak sharpness, and less baseline noise.

The chloroform extraction of propylthiouracil is similar to that described by Sitar and Hunninghake (8). In an effort to improve the extraction efficiency, the pH of the plasma was lowered before the chloroform extraction. Results were negative and were attributed to the coagulation of protein material, which hindered extraction of propylthiouracil that may have been occluded. The addition of ammonium sulfate has been demonstrated to have a positive effect on the propylthiouracil extraction efficiency (5).

Irreversible propylthiouracil adsorption to the surface of laboratory glassware was encountered in preliminary recovery studies, particularly during the evaporation of the chloroform extract. As a result, silylated or silicon-treated glassware was used.

Chromatograms obtained in the analysis of control human plasma and human plasma from a volunteer who had received a single propylthiouracil dose are shown in Fig. 1. The chromatogram of control human plasma demonstrated no interfering peaks. Sensitivity was increased approximately twofold when propylthiouracil was measured at 280 nm instead of 254 nm, with no significant increase in the area of the extraneous peaks or background noise.

While the chromatographic methods (5, 8) probably measure only unchanged propylthiouracil, their selectivity was not specifically investigated. The effect of known propylthiouracil metabolites on the assay was evaluated by adding propyluracil (11), *S*-methylpropylthiouracil (11), propylthiouracil glucuronide (11–14), the sulfinic and sulfonic acid derivatives of propylthiouracil (15), and sulfate (11) to plasma samples, which were then analyzed.

Propyluracil exhibited a retention time that did not interfere with the measurement of propylthiouracil or the internal standard peaks. *S*-Methylpropylthiouracil was extracted but failed to elute from the column under the described conditions. The sulfinic and sulfonic acid derivatives, propylthiouracil glucuronide, and sulfate were not extracted from the aqueous layer by chloroform. Since none of the known metabolites interfered with methylthiouracil or propylthiouracil, the method is probably specific for propylthiouracil.

The precision or reproducibility of the method for a given day is shown in Table I using normalized data. Propylthiouracil stability in plasma was assessed also. Control plasma was spiked with standard propylthiouracil solutions, and the samples were frozen. On Days 1–4 and 8, duplicates of each standard concentration were thawed and analyzed. No significant differences were observed.

REFERENCES

(1) W. D. Alexander, V. Evans, A. MacAuley, T. F. Gallagher, Jr., and J. Londono, *Br. Med. J.*, **2**, 290 (1969).

(2) D. S. Sitar and D. P. Thornhill, *J. Pharmacol. Exp. Ther.*, **183**, 440 (1972).

(3) D. A. McGinty, E. A. Sharp, W. A. Dill, and R. W. Rawson, *J. Clin. Endocrinol.*, **8**, 1043 (1950).

(4) C. R. Ratliff, P. F. Gilliland, and F. F. Hall, *Clin. Chem.*, **18**, 1373 (1972).

(5) D. Schuppan, S. Riegelman, B. v. Lehmann, A. Pilbrant, and C. Becker, *J. Pharmacokinet. Biopharm.*, **1**, 307 (1973).

(6) A. Melander, E. Wahlin, K. Danielson, and A. Hanson, *Acta Med. Scand.*, **201**, 41 (1977).

(7) J. MacGee, in "Methods of Analysis of Anti-epileptic Drugs," Proceedings of the Workshop on Determination of Anti-epileptic Drugs in Body Fluids, Int. Congr. Ser. 286, Excerpta Medica, Amsterdam, The Netherlands, 1972.

(8) D. S. Sitar and D. B. Hunninghake, *J. Clin. Endocrinol. Metab.*, **40**, 26 (1975).

(9) D. C. Fenimore, C. M. Davis, J. H. Whitford, and C. A. Harrington, *Anal. Chem.*, **48**, 2289 (1976).

(10) M. C. Meyer and A. B. Straughn, "Final Report, Propylthiouracil Bioavailability Study," DHEW/PHS/FDA, Contract No. FDA 223-77-3011, Feb. 27, 1978.

(11) R. H. Lindsay, J. B. Hill, K. Kelly, and A. Vaughn, *Endocrinology*, **94**, 1689 (1974).

(12) B. Marchant, W. D. Alexander, J. W. K. Robertson, and J. H. Lazarus, *Metabolism*, **20**, 989 (1971).

(13) P. D. Papapetrou, B. Marchant, H. Gavias, and W. D. Alexander, *Biochem. Pharmacol.*, **21**, 363 (1972).

(14) M. L. Desbarats-Schonbaum, L. Endrenyi, E. Koves, E. Schonbaum, and E. A. Sellers, *Eur. J. Pharmacol.*, **19**, 104 (1972).

(15) R. H. Lindsay, K. Kelly, and J. B. Hill, *Ala. J. Med. Sci.*, **15**, 149 (1978).

ACKNOWLEDGMENTS

Supported by the Food and Drug Administration under the SARAP Program.

The authors thank Dr. Raymond H. Lindsay, Director of Pharmaceutical Research, Veterans Administration Hospital, Birmingham, Ala., for generously supplying propylthiouracil glucuronide, propylthiouracil sulfinic acid, and propylthiouracil sulfonic acid.

Ion-Pair Reversed-Phase High-Pressure Liquid Chromatography of Cough–Cold Syrups I: Pseudoephedrine Hydrochloride, Brompheniramine Maleate, and Dextromethorphan Hydrobromide

MARCUS K. CHAO ˣ, IRA J. HOLCOMB, and SALVATORE A. FUSARI

Received March 23, 1979, from *Parke-Davis, Division of Warner-Lambert Company, Morris Plains, NJ 07950.* Accepted for publication May 14, 1979.

Abstract □ Pseudoephedrine hydrochloride (I), brompheniramine maleate (II), and dextromethorphan hydrobromide (III) in a cough–cold syrup were separated and determined by ion-pair reversed-phase high-pressure liquid chromatography. The separation was carried out using a μBondapak C_{18} column (30 cm × 3.9 mm i.d.) and a mobile phase of acetonitrile–water–acetic acid (40:60:1) with 0.01 *N* 1-octanesulfonic acid sodium salt and 0.05 *N* potassium nitrate. Detection was accomplished using a UV detector at 265 nm for I and II; III was monitored at 280 nm. Concentration *versus* peak height plots in the ranges of 0.37–1.9 mg/ml for I, 0.025–0.126 mg/ml for II, and 0.125–0.625 mg/ml for III were linear. Ten consecutive injections of a mixture gave a percent relative standard deviation of <1% for all three components. Average recoveries from laboratory-prepared samples were 100.5% for I, 100.9% for II, and 100.1% for III. No precolumn cleanup was necessary, and the chromatogram was complete in 16 min.

Keyphrases □ Cough–cold syrup—analysis, ion-pair reversed-phase high-pressure liquid chromatography, pseudoephedrine hydrochloride, brompheniramine maleate, dextromethorphan hydrobromide □ Pseudoephedrine hydrochloride—analysis, ion-pair reversed-phase high-pressure liquid chromatography, cough–cold syrups □ Brompheniramine maleate—analysis, ion-pair reversed-phase high-pressure liquid chromatography, cough–cold syrups □ Dextromethorphan hydrobromide—analysis, ion-pair reversed-phase high-pressure liquid chromatography, cough–cold syrups

Antihistamines, antitussives, and decongestants are used extensively in cough–cold syrups. Often, two or more of these compounds are combined in a preparation, and an isolation of the desired analyte from the other components is necessary prior to measurement.

Reversed-phase high-pressure liquid chromatography (HPLC) was used to investigate 21 antihistaminic, antitussive, and analgesic drugs in cough–cold mixtures (1), and the separation of four antihistamines was examined by reversed-phase HPLC (2). Ion-pair reversed-phase HPLC is a relatively new and extremely useful technique. General discussions of the method were published (3, 4).

The present study investigated the feasibility of applying ion-pair reversed-phase HPLC to the separation and assay of a mixture of antihistaminic, antitussive, and decongestant drugs in a cough–cold syrup.

EXPERIMENTAL

Apparatus—A piston pump[1], an automatic sampler[2], and two detectors (one set at 280 nm[3] and the other at 265 nm[4]) were used. The chromatograms were recorded on a two-pen recorder[5].

Column—A bonded reversed-phase C_{18} column[6] was used.

Samples—A cough–cold syrup was prepared so that each 5 ml contained 30 mg of pseudoephedrine hydrochloride (I), 2 mg of brompheniramine maleate (II), 10 mg of dextromethorphan hydrobromide (III), and 5% alcohol. The standard solution was prepared by dissolving 120 mg of I[7], 8 mg of II[8], and 40 mg of III[7] in water and diluting to 100.0 ml. The sample solution was prepared by transferring 5 ml of the cough–cold syrup quantitatively to a 25-ml volumetric flask and diluting to volume with water.

Analysis—The chromatographic conditions were: flow rate, 0.8 ml/min (700 psi); mobile phase, acetonitrile[9]–water–acetic acid (40:60:1) with 0.01 *N* 1-octanesulfonic acid sodium salt[10] and 0.05 *N* potassium nitrate[11]; temperature, 25°; and detector scale, 0.064 aufs for 280 nm and 0.1 aufs for 265 nm.

Ten-microliter aliquots of standard and sample solutions were injected in duplicate onto the column using the chromatographic conditions.

Table I—Accuracy Study for HPLC Assay of Pseudoephedrine Hydrochloride (I), Brompheniramine Maleate (II), and Dextromethorphan Hydrobromide (III) from Aqueous Solutions

Percent of Target	Recovery, % I	II	III
85.0	100.6	99.9	102.0
90.0	98.4	97.2	100.3
95.0	102.0	101.8	100.9
97.0	101.4	102.1	99.2
99.0	100.6	98.8	99.8
101.0	100.0	98.8	99.8
103.0	100.0	100.0	100.0
105.0	98.9	98.4	99.1
110.0	100.7	100.9	100.0
115.0	98.3	101.3	100.1
Average	100.1	99.9	100.1
Range	98.3–102.0	97.2–102.1	99.1–102.0
RSD	±1.2	±1.6	±0.84

DISCUSSION

Mobile Phase Selection—Methanol and water or acetonitrile and water mixtures in various proportions were tested with no satisfactory separation of I–III. Sulfonic acid sodium salts of 1-butane, 1-pentane, 1-hexane, and 1-octane and dioctylsulfosuccinate sodium salt[7] (IV) were

[1] Milton Roy.
[2] DuPont 834.
[3] Laboratory Data Control model 1203.
[4] Perkin-Elmer LC 55.
[5] Linear recorder 385.
[6] μBondapak C_{18} column, Waters Associates.
[7] NF reference standard.
[8] USP reference standard.
[9] Burdick & Jackson.
[10] Eastman Organic Chemicals.
[11] Baker Analyzed Reagent.

0022-3549/79/1100-1463$01.00/0
© 1979, American Pharmaceutical Association

ACKNOWLEDGMENTS

Supported by the Food and Drug Administration under the SARAP Program.

The authors thank Dr. Raymond H. Lindsay, Director of Pharmaceutical Research, Veterans Administration Hospital, Birmingham, Ala., for generously supplying propylthiouracil glucuronide, propylthiouracil sulfinic acid, and propylthiouracil sulfonic acid.

Ion-Pair Reversed-Phase High-Pressure Liquid Chromatography of Cough–Cold Syrups I: Pseudoephedrine Hydrochloride, Brompheniramine Maleate, and Dextromethorphan Hydrobromide

MARCUS K. CHAO ˣ, IRA J. HOLCOMB, and SALVATORE A. FUSARI

Received March 23, 1979, from *Parke-Davis, Division of Warner-Lambert Company, Morris Plains, NJ 07950.* Accepted for publication May 14, 1979.

Abstract □ Pseudoephedrine hydrochloride (I), brompheniramine maleate (II), and dextromethorphan hydrobromide (III) in a cough–cold syrup were separated and determined by ion-pair reversed-phase high-pressure liquid chromatography. The separation was carried out using a μBondapak C_{18} column (30 cm × 3.9 mm i.d.) and a mobile phase of acetonitrile–water–acetic acid (40:60:1) with 0.01 *N* 1-octanesulfonic acid sodium salt and 0.05 *N* potassium nitrate. Detection was accomplished using a UV detector at 265 nm for I and II; III was monitored at 280 nm. Concentration *versus* peak height plots in the ranges of 0.37–1.9 mg/ml for I, 0.025–0.126 mg/ml for II, and 0.125–0.625 mg/ml for III were linear. Ten consecutive injections of a mixture gave a percent relative standard deviation of <1% for all three components. Average recoveries from laboratory-prepared samples were 100.5% for I, 100.9% for II, and 100.1% for III. No precolumn cleanup was necessary, and the chromatogram was complete in 16 min.

Keyphrases □ Cough–cold syrup—analysis, ion-pair reversed-phase high-pressure liquid chromatography, pseudoephedrine hydrochloride, brompheniramine maleate, dextromethorphan hydrobromide □ Pseudoephedrine hydrochloride—analysis, ion-pair reversed-phase high-pressure liquid chromatography, cough–cold syrups □ Brompheniramine maleate—analysis, ion-pair reversed-phase high-pressure liquid chromatography, cough–cold syrups □ Dextromethorphan hydrobromide—analysis, ion-pair reversed-phase high-pressure liquid chromatography, cough–cold syrups

Antihistamines, antitussives, and decongestants are used extensively in cough–cold syrups. Often, two or more of these compounds are combined in a preparation, and an isolation of the desired analyte from the other components is necessary prior to measurement.

Reversed-phase high-pressure liquid chromatography (HPLC) was used to investigate 21 antihistaminic, antitussive, and analgesic drugs in cough–cold mixtures (1), and the separation of four antihistamines was examined by reversed-phase HPLC (2). Ion-pair reversed-phase HPLC is a relatively new and extremely useful technique. General discussions of the method were published (3, 4).

The present study investigated the feasibility of applying ion-pair reversed-phase HPLC to the separation and assay of a mixture of antihistaminic, antitussive, and decongestant drugs in a cough–cold syrup.

EXPERIMENTAL

Apparatus—A piston pump[1], an automatic sampler[2], and two detectors (one set at 280 nm[3] and the other at 265 nm[4]) were used. The chromatograms were recorded on a two-pen recorder[5].

Column—A bonded reversed-phase C_{18} column[6] was used.

Samples—A cough–cold syrup was prepared so that each 5 ml contained 30 mg of pseudoephedrine hydrochloride (I), 2 mg of brompheniramine maleate (II), 10 mg of dextromethorphan hydrobromide (III), and 5% alcohol. The standard solution was prepared by dissolving 120 mg of I[7], 8 mg of II[8], and 40 mg of III[7] in water and diluting to 100.0 ml. The sample solution was prepared by transferring 5 ml of the cough–cold syrup quantitatively to a 25-ml volumetric flask and diluting to volume with water.

Analysis—The chromatographic conditions were: flow rate, 0.8 ml/min (700 psi); mobile phase, acetonitrile[9]–water–acetic acid (40:60:1) with 0.01 *N* 1-octanesulfonic acid sodium salt[10] and 0.05 *N* potassium nitrate[11]; temperature, 25°; and detector scale, 0.064 aufs for 280 nm and 0.1 aufs for 265 nm.

Ten-microliter aliquots of standard and sample solutions were injected in duplicate onto the column using the chromatographic conditions.

Table I—Accuracy Study for HPLC Assay of Pseudoephedrine Hydrochloride (I), Brompheniramine Maleate (II), and Dextromethorphan Hydrobromide (III) from Aqueous Solutions

Percent of Target	Recovery, % I	II	III
85.0	100.6	99.9	102.0
90.0	98.4	97.2	100.3
95.0	102.0	101.8	100.9
97.0	101.4	102.1	99.2
99.0	100.6	98.8	99.8
101.0	100.0	98.8	99.8
103.0	100.0	100.0	100.0
105.0	98.9	98.4	99.1
110.0	100.7	100.9	100.0
115.0	98.3	101.3	100.1
Average	100.1	99.9	100.1
Range	98.3–102.0	97.2–102.1	99.1–102.0
RSD	±1.2	±1.6	±0.84

DISCUSSION

Mobile Phase Selection—Methanol and water or acetonitrile and water mixtures in various proportions were tested with no satisfactory separation of I–III. Sulfonic acid sodium salts of 1-butane, 1-pentane, 1-hexane, and 1-octane and dioctylsulfosuccinate sodium salt[7] (IV) were

[1] Milton Roy.
[2] DuPont 834.
[3] Laboratory Data Control model 1203.
[4] Perkin-Elmer LC 55.
[5] Linear recorder 385.
[6] μBondapak C_{18} column, Waters Associates.
[7] NF reference standard.
[8] USP reference standard.
[9] Burdick & Jackson.
[10] Eastman Organic Chemicals.
[11] Baker Analyzed Reagent.

0022-3549/79/1100-1463$01.00/0
© 1979, American Pharmaceutical Association

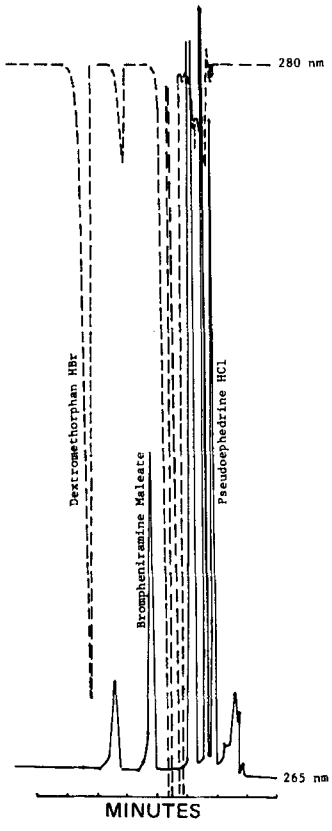

Figure 1—*High-pressure liquid chromatogram for a commercial sample containing pseudoephedrine hydrochloride, brompheniramine maleate, and dextromethorphan hydrobromide.*

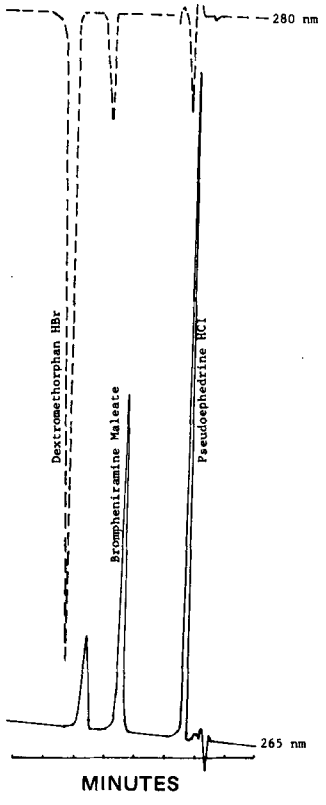

Figure 2—*High-pressure liquid chromatogram for the standard mixture of pseudoephedrine hydrochloride, brompheniramine maleate, and dextromethorphan hydrobromide.*

used as ion-pair reagents. With the reagents having a carbon chain fewer than eight, I was eluted with the solvent front; with IV, III was retained on the column too long. 1-Octanesulfonic acid sodium salt gave an optimum separation of all three analytes.

Potassium nitrate was used to reduce peak tailing. A 0.05 *N* concentration was selected on the basis of the chromatogram and the reproducibility of injections. Excess potassium nitrate (>0.1 *N*) resulted in poor reproducibility of injections.

Stationary Phase Selection—Several microparticle reversed-phase columns including μBondapak CN, μBondapak phenyl, μBondapak C_{18}[6], and Zorbax C_{18}[12] were tested. With μBondapak CN and μBondapak phenyl columns, the separation of II and III was acceptable, but I was eluted with the solvent front. With Zorbax C_{18}, II and III were retained on the column too long. The use of μBondapak C_{18} resulted in a satisfactory separation for I–III. The greater retention with Zorbax C_{18} was probably due to the higher loading of the organic material on the column.

[12] DuPont Instruments.

Table II—Assay of Pseudoephedrine Hydrochloride (I), Brompheniramine Maleate (II), and Dextromethorphan Hydrobromide (III) in Commercial Cough–Cold Syrup Samples

Sample	Recovery, %		
	I	II	III
1	98.8	98.1	99.9
2	99.6	99.5	99.9
3	98.8	99.7	98.1

Detector Wavelength Selection—The most selective analytical absorption wavelengths for I, II, and III were at 257, 265, and 278 nm, respectively. Since II was present in a small amount, 265 nm was selected to obtain the maximum sensitivity for II, and I was also run at this wavelength. Compound III was determined at 280 nm. If desired, I–III can be monitored using one variable-wavelength detector[13] at 265 nm.

RESULTS

With the selected mobile and stationary phases and specified detector wavelengths, the active ingredients (I–III) in the cough–cold syrup could be separated and assayed quantitatively using ion-pair reversed-phase HPLC.

A linearity study showed that the peak height of each ingredient was directly related to the concentration (0.377–1.885 mg of I/ml, 0.025–0.126 mg of II/ml, and 0.125–0.625 mg of III/ml).

No chromatographic interference was encountered with the pharmaceutical ingredients used for the syrup base. The average recoveries of weighed amounts of I–III (85–115% of target) added to the laboratory-prepared syrup vehicle were 100.5% for I, 100.9% for II, and 101.1% for III.

Ten consecutive injections of a standard preparation mixture gave a relative standard deviation of <1% for all three components.

The accuracy of the method was studied based on percent recovery of 10 solutions containing I–III in amounts equivalent to 85, 90, 95, 97, 99, 101, 103, 105, 110, and 115% of target relative to a standard solution at 100% target (Table I). The assay bias for all three components was ±0.1%.

The HPLC method was used to assay I–III in commercial samples, and results are presented in Table II.

The analytical results demonstrate the ability of the ion-pair reversed-phase HPLC procedure to assay the complex drug mixtures in a cough–cold syrup. Typical chromatograms of the sample and standard preparations are shown in Figs. 1 and 2. The drugs can be analyzed in their salt forms, and the sample pretreatment is simple and rapid. The complete separation only requires 16 min.

REFERENCES

(1) I. L. Honigberg, J. T. Stewart, and A. P. Smith, *J. Pharm. Sci.*, **63**, 766 (1974).

(2) A. G. Ghanekar and V. D. Gupta, *Am. J. Hosp. Pharm.*, **34**, 651 (1977).

(3) R. Gloor and E. L. Johnson, *J. Chromatogr. Sci.*, **15**, 413 (1977).

(4) C. Horvath, W. Melander, I. Mulnar, and P. Mulnar, *Anal. Chem.*, **49**, 2295 (1977).

[13] Laboratory Data Control model 1204.

Stability-Indicating Assay of Acetaminophen in an Effervescent Tablet by Ion-Pair High-Performance Liquid Chromatography

F. J. SENA ˣ, J. T. PIECHOCKI *, and K. L. LI

Received June 26, 1978, from the *Research and Development Laboratories, Block Drug Co., Inc., Jersey City, NJ 07302.* Accepted for publication May 21, 1979. *Present address: Pitman Moore, Washington Crossing, NJ 08560.

Abstract □ A stability-indicating analytical method is described for determining acetaminophen and its degradation product, *p*-aminophenol, in an effervescent tablet. Tablets assayed by ion-pair high-performance reversed-phase liquid partition chromatography required no sample cleanup. The method applied to tablets containing 325 mg of acetaminophen yielded an average recovery of 99.6% with a relative standard deviation of 0.70% (n = 10). As little as 0.005% *p*-aminophenol could be detected.

Keyphrases □ Acetaminophen—analysis, ion-pair high-performance liquid chromatography, effervescent tablets, with *p*-aminophenol, stability indicating □ *p*-Aminophenol—analysis, ion-pair high-performance liquid chromatography, effervescent tablets, with acetaminophen, stability □ Analgesics—acetaminophen, ion-pair high-performance liquid chromatographic analysis, effervescent tablets, with *p*-aminophenol, stability □ High-performance liquid chromatography—analysis, acetaminophen, *p*-aminophenol, effervescent tablets

Acetaminophen is used extensively in nonprescription analgesic preparations. The current USP assay (1) for acetaminophen and its degradation product, *p*-aminophenol, in tablets, while selective and sensitive, is time consuming and tedious. Additionally, the novel matrix of an effervescent tablet presents interferences not commonly encountered in the assay for *p*-aminophenol, rendering it nonapplicable as a stability-indicating assay. Other rapid methods for acetaminophen involve either the formation of *O*-heptyl-*N*-methyl derivatives followed by GLC (2) or hydrolysis to *p*-aminophenol, followed by oxidation to *p*-quinonechlorimide and reaction with phenol to form indophenol, which is then determined colorimetrically (3). These methods assay the total drug content and are not suitable for simple one-step differentiation between intact acetaminophen and its degradation products. Other

Table I—Recovery Percentage for Spiked Samples Containing 325 mg of Acetaminophen

Sample	Recovery of Acetaminophen, %
1	102.6
2	102.4
3	100.9
4	99.9
5	100.1
6	99.7
7	101.6
8	99.3
Average	100.8
RSD, %	1.28

Table II—Assay Results for Effervescent Tablets Containing 325 mg of Acetaminophen

Sample	Acetaminophen Found, mg	Percent of Label
A	322.7	99.3
B	323.4	99.5
C	322.1	99.1
D	322.7	99.5
E	322.4	99.2
F	328.0	100.9
G	326.7	100.5
H	322.7	99.5
I	321.4	98.9
J	326.0	100.3
Average	323.8	99.6
RSD, %	0.70	0.70

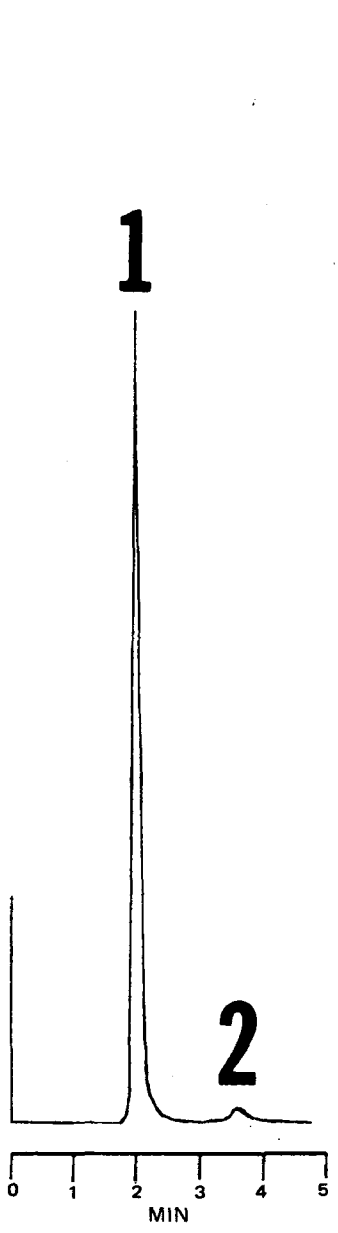

Figure 1—*Representative chromatograms. Key: 1, acetaminophen; and 2, tablet excipient.*

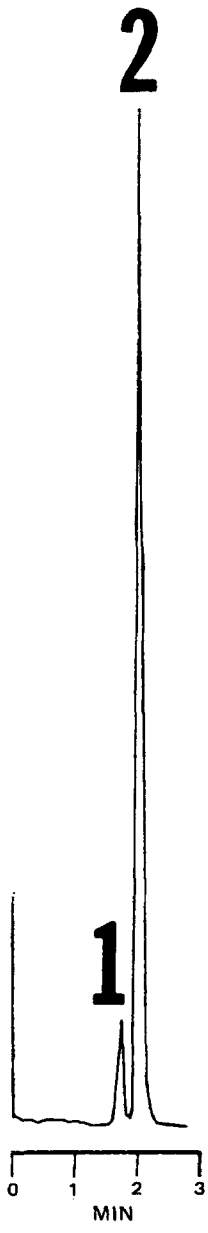

Figure 2—*Separation of mixture containing acetaminophen and* p*-aminophenol. Key: 1,* p*-aminophenol; and 2, acetaminophen.*

0022-3549/79/1100-1465$01.00/0
© 1979, American Pharmaceutical Association

chromatographic methods for intact acetaminophen and *p*-aminophenol are too lengthy for large numbers of samples (4, 5) or require unusual apparatus for measuring trace amounts of *p*-aminophenol (6).

To overcome these problems, ion-pair high-pressure partition liquid chromatography was investigated. This method was simple, rapid, precise, and selective for determining the acetaminophen concentration in an effervescent tablet matrix while providing a measurement of the *p*-aminophenol present.

EXPERIMENTAL

Chemicals and Reagents—Acetaminophen USP[1] was assayed spectrophotometrically by comparison to the USP reference standard and was used without further purification. *p*-Aminophenol[1] (98+%), acetonitrile[2] (UV, distilled in glass), and tetrabutylammonium phosphate solution[3] were used as received.

Apparatus—The liquid chromatograph[4] was fitted with a septumless injector[5], a fixed-wavelength UV detector[6] (254 nm), and a strip-chart recorder.

Column—A 30-cm × 4-mm i.d. column containing 10-μm phenyl bonded phase packing[7] was used.

Chromatographic Conditions—The chromatographic solvent was 0.005 *M* tetrabutylammonium phosphate in distilled water containing 15% (v/v) acetonitrile, adjusted to pH 7.5 with phosphoric acid or sodium hydroxide. The solvent was vacuum filtered through a 0.45-μm filter[8] and vacuum degassed for 2 min with stirring before use. The temperature was ambient, the solvent flow rate was 3.0 ml/min, and the inlet pressure was 2000 psig. Sensitivities used were 0.2 aufs for acetaminophen and 0.005 aufs for *p*-aminophenol.

Standard Solutions—Standard solutions containing 1.0, 1.4, 1.8, and 3.0 mg of acetaminophen/100 ml were prepared in distilled water containing 15% (v/v) acetonitrile and filtered as described prior to injection.

Assay for Pharmaceuticals—Each tablet containing 325 mg of acetaminophen was dissolved in 100.0 ml of distilled water containing 15% (v/v) acetonitrile. One milliliter of this solution was pipetted into a 200-ml volumetric flask, diluted to volume with the same solvent, and filtered as described before injection.

Spiked Samples—Accurately weighed quantities of acetaminophen were admixed with a placebo granulation of the effervescent tablet. These mixes, formulated to contain 325 mg/tablet weight (the same percentage of acetaminophen as found in the tablets), were assayed as described.

Quantitation—Since peak heights of acetaminophen were directly proportional to concentration, all results were calculated using peak heights.

RESULTS AND DISCUSSION

The recovery data for acetaminophen from spiked samples presented in Table I illustrate the validity of the method for effervescent tablets. Average recovery for spiked samples was 100.8%. Linearity between peak height and concentration was excellent over the range of 1.0–3.0 mg of acetaminophen/100 ml and had a correlation coefficient of 0.9998. This method has been used routinely in a stability program and found to be accurate and precise with a relative standard deviation of 0.70% ($n = 10$). These data are summarized in Table II. A chromatogram obtained from a typical tablet assay is presented in Fig. 1. Since no sample cleanup is required, the assay time is only 20 min compared to 3–4 hr by the official USP procedure.

To demonstrate the selectivity of the method for acetaminophen in the presence of *p*-aminophenol, samples of acetaminophen containing 10, 1, 0.1, and 0.005% *p*-aminophenol were prepared and assayed. A chromatogram of acetaminophen containing 10% *p*-aminophenol is given in Fig. 2. Excellent resolution of *p*-aminophenol from its parent compound, an essential requirement for a stability-indicating assay, was obtained. Quantification of 0.005% *p*-aminophenol required the optimization of assay conditions, namely, maximization of both the acetaminophen sample size and the UV detector sensitivity. Average recovery at the 0.005% *p*-aminophenol level was 96.9% with a standard deviation of ±4.55 ($n = 4$). This separation could not be achieved with a reversed-phase C_{18} column using the same chromatographic conditions. Presumably, the π-bond to π-bond interaction between the phenyl stationary phase and the phenyl backbone of the solute molecules provides the necessary selectivity for the separation of acetaminophen and *p*-aminophenol.

REFERENCES

(1) "The United States Pharmacopeia," 19th rev., Mack Publishing Co., Easton, Pa., 1975, p. 60.

(2) W. A. Dechtiaruk, G. F. Johnson, and H. M. Solomon, *Clin. Chem.* **22,** 879 (1976).

(3) C. T. H. Ellcock and A. G. Fogg, *Analyst,* **100,** 16 (1975).

(4) J. H. Knox and J. Jurand, *J. Chromatogr.,* **82,** 398 (1973).

(5) E. Kalatzis and I. Zarbi, *J. Pharm. Sci.,* **65,** 71 (1976).

(6) R. M. Riggen, A. L. Schmidt, and P. T. Kissenger, *ibid.,* **64,** 680 (1975).

[1] Mallinckrodt Chemical Co.
[2] Burdick & Jackson Laboratories.
[3] PIC reagent A, Waters Associates.
[4] Model 6000A pump, Waters Associates.
[5] Valco model CV-6-UHPa-N60, 7000-psig sample injection valve equipped with a 10-μl sampling loop.
[6] Model 440, Waters Associates.
[7] μBondapak Phenyl, Waters Associates.
[8] HA filters, Millipore Corp.

High-Pressure Liquid Chromatographic Determination of Chlordiazepoxide and Its Major Metabolites in Biological Fluids

MICHAEL A. PEAT *‡ˣ, BRYAN S. FINKLE *‡, and MARY E. DEYMAN *

Received November 14, 1978, from the *Center for Human Toxicology, University of Utah, and the ‡Department of Pathology, University of Utah Medical Center, Salt Lake City, UT 84112. Accepted for publication May 22, 1979.

Abstract □ A simple, isocratic, reversed-phase, high-pressure liquid chromatographic procedure was developed for the determination of chlordiazepoxide and its major metabolites in plasma and urine. The within-run coefficient of variation was 3.4–8.0%, and the day-to-day variation was 4.0–8.0%. Recoveries of 80–91% with sensitivity limits of 50 ng/ml were obtained for the parent drug and its metabolites. Plasma and urine samples collected after single intravenous and single oral doses were analyzed using this procedure.

Keyphrases □ Chlordiazepoxide—analysis, high-pressure liquid chromatography, biological fluids, metabolites □ Sedatives—chlordiazepoxide, high-pressure liquid chromatographic analysis, biological fluids, metabolites □ High-pressure liquid chromatography—analysis, chlordiazepoxide and metabolites, biological fluids

Chlordiazepoxide hydrochloride (7-chloro-2-methylamino-5-phenyl-3*H*-1,4-benzodiazepin-4-oxide hydrochloride) (I) was synthesized by Sternbach in 1957 (1) and found to possess pronounced central nervous system activity coupled with low toxicity. At present, I is recommended for the relief of anxiety and tension, withdrawal symptoms associated with acute alcoholism, and preoperative apprehension and anxiety and as an adjunct in the treatment of various disease states in which anxiety and tension are manifest (2).

BACKGROUND

Compound I is metabolized to a number of biotransformation products in humans (3, 4). Of these, *N*-desmethylchlordiazepoxide (II), demoxepam (III), and *N*-desmethyldiazepam (IV) are measurable in plasma after chronic administration. All three compounds exhibit muscle relaxant and anticonvulsant properties in animal species (5, 6) and, therefore, presumably have pharmacological activity in humans.

Various methods have been used for the determination of chlordiazepoxide in blood and other biological fluids, including spectrophotometry (7), colorimetry (8), fluorometry (9, 10), GLC (11–13), and differential pulse polarography (14). All of these procedures have various disadvantages when applied to the analysis of the parent drug and its metabolites.

High-pressure liquid chromatography (HPLC) has been applied to the analysis of the benzodiazepines (15) and also to the quantitation of specific benzodiazepines and their metabolites (16, 17). Recently, the technique was used to quantitate I and its metabolites (18, 19). A gradient elution procedure was described for I and II with chlorpromazine as the internal standard (18), and a reversed-phase column was used to determine I and its metabolites in plasma after oral doses (19).

This report describes a new, simple, isocratic, reversed-phase HPLC procedure that has been used for the analysis of I–III in plasma and urine samples collected after the controlled administration of I to human volunteers.

EXPERIMENTAL

Reagents—Sodium borate[1] (analytical reagent), dibasic sodium phosphate[2] (analytical reagent), methanol[3] (UV grade), and chloroform[3] were used without further purification.

Chlordiazepoxide hydrochloride[4], *N*-desmethylchlordiazepoxide[4], demoxepam[4], and diazepam[4] were used as received.

Apparatus—The modular high-pressure liquid chromatograph consisted of a constant-flow pump[5], a 10-μl loop injector[6], a fixed-wavelength (254 nm) UV detector[7], and a strip-chart recorder[8]. A stainless steel column (4.6 mm × 25 cm) packed with 10-μm silica particles with chemically bonded octadecylsilane[9] was obtained commercially.

Chromatographic Conditions—The mobile phase of methanol–0.025 *M* dibasic sodium phosphate (pH 7.5) (56:44) was used at a flow rate of 1.6 ml/min.

Analytical Procedure—Methanolic solutions (A) corresponding to 1 μg of I, II, or III (free base)/ml were prepared. Solutions of 100 (B) and 10 (C) ng/μl were prepared by serial dilutions of A. All solutions were stored at 0° in the dark. For the quantitation of the drug and its metabolites, standards were prepared by evaporating appropriate amounts of these methanolic solutions to dryness under an air stream at room temperature. Ten milliliters of drug-free plasma or urine was added, and the solutions were shaken for 30 min.

Solutions B and C were prepared every 4 weeks; however, A was stable for a longer period if kept in the dark at 0°. The stability was checked by injecting 1 μg of the drug or metabolite under the described HPLC conditions and comparing the peak height with that obtained initially.

The extraction procedure for plasma consisted of adding 1 μg of diazepam (as the internal standard) and 1 ml of saturated sodium borate (pH 9.0) to 1 ml of plasma. Seven milliliters of chloroform was added, and the mixture was shaken for 10 min. It was centrifuged at 2500 rpm to separate the layers, and the chloroform was transferred to a 15-ml conical tube, where it was evaporated to dryness under an air stream at 60°. The residue was dissolved in 20 μl of the HPLC eluent, and 10 μl was injected. Both the extraction and evaporation tubes had been silanized previously with 10% dimethylchlorosilane[10] in toluene[1].

A similar method was used for the urine samples, except that a 3-ml aliquot was taken and 0.5 μg of the internal standard was used.

Diazepam was chosen as the internal standard because of its similarity in structure and in retention time. Quantitation was achieved by plotting peak height ratio of the drug (or metabolite) to the internal standard against concentration. If the described method is to be used for toxicological screening, a more suitable internal standard would be prazepam, which is not encountered as frequently in toxicology cases.

Table I—Calibration Curve Data ($y = c + mx$)

Sample	Compound	Range, μg/ml	Slope (m)	Intercept (c)	r^a
Plasma	I	0.05–1.0	0.0033	−0.07	0.998
	II	0.05–0.75	0.0044	−0.08	0.996
	III	0.05–0.50	0.005	0.14	0.998
Urine	I	0.025–0.20	0.013	−0.12	0.991
	II	0.025–0.20	0.014	−0.04	0.999
	III	0.025–0.20	0.014	0.072	0.999

[a] Regression coefficient

[1] Mallinckrodt, St. Louis, Mo.

[2] J. T. Baker Chemical Co., Phillipsburg, N.J.
[3] Burdick & Jackson Laboratories, Muskegon, Mich.
[4] Hoffmann-La Roche, Nutley, N.J.
[5] Model 3200, Spectra-Physics, Santa Clara, Calif.
[6] Valco, Spectra-Physics, Santa Clara, Calif.
[7] Model SP 8200, Spectra-Physics, Santa Clara, Calif.
[8] Model 300, Linear Instruments Corp., Irvine, Calif.
[9] Prepacked Spherisorb ODS, Spectra-Physics, Santa Clara, Calif.
[10] Applied Science Laboratories, State College, Pa.

0022-3549/79/1100-1467$01.00/0
© 1979, American Pharmaceutical Association

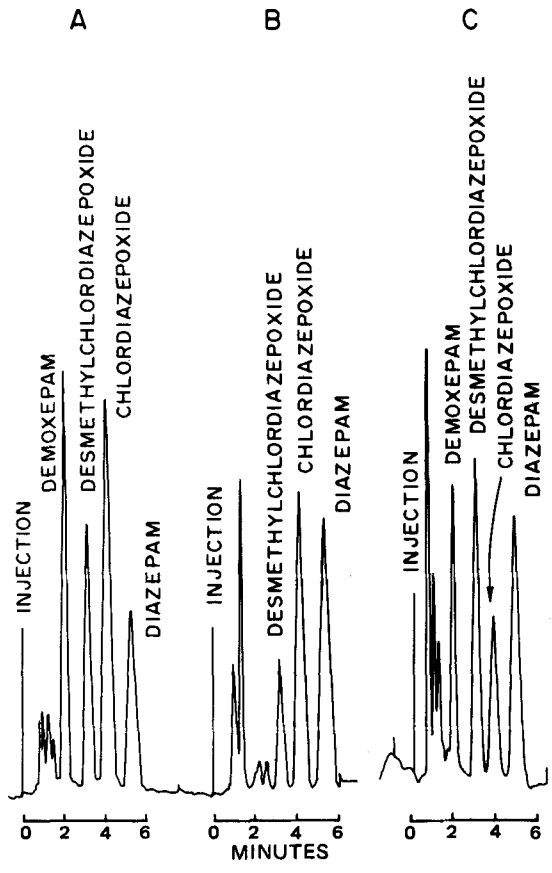

Figure 1—*High-pressure liquid chromatograms of an extracted standard (A), a plasma extract from a patient given 0.12 mg of chlordiazepoxide hydrochloride/kg iv (B), and a plasma extract from a patient on long-term therapy (C).*

RESULTS AND DISCUSSION

The results were linear over the following ranges: I, 50–1000 ng/ml; II, 50–750 ng/ml; and III, 50–600 ng/ml. If the method is to be used at appreciably higher concentrations, two- or fourfold dilution of the sample would be necessary. The equations for the calibration curves and the regression coefficients are listed in Table I. The results of precision studies, both within run and day to day, are shown in Table II.

Recovery studies were performed on I–III using the described conditions. Recoveries were 81 ± 6% of I, 88 ± 5% of II, and 91 ± 4% of III. Sensitivity limits were ~50 ng/ml for each compound using a 1-ml plasma sample per assay. These sensitivity limits possibly could be improved with a detector wavelength of 240 nm.

No interfering peaks were observed on analysis of blank plasma and urine samples. Chromatograms from an extracted standard, a plasma extract from a patient who was given 0.12 mg of I/kg iv, and a plasma extract from a patient on long-term therapy with the drug are shown in Fig. 1.

The described procedure has been used successfully for measuring the drug and its desmethyl metabolite in plasma after oral and intravenous administrations of the parent drug. The plasma concentration–time course curves obtained from four patients were similar to those described by Boxenbaum *et al.* (20).

N-Desmethyldiazepam (IV), a reported metabolite of I, would elute between the parent compound and the internal standard under the described HPLC conditions and have a sensitivity limit of 75 ng/ml. No measurable amounts of IV were seen in plasma samples collected in a 24-hr period following single oral and intravenous doses. This finding is in agreement with that of Dixon *et al.* (4), who found low concentrations (10–60 ng/ml) of IV in plasma samples collected 24–72 hr after a single intravenous dose.

Table II—Statistics for Chlordiazepoxide and Its Metabolites

Compound	Concentration when First Analyzed	Mean	*SD*	*CV*, %
	Within Run (n = 10)			
I	384	383	13	3.4
	220	221	15	6.8
II	271	273	12	4.4
	133	132	9.7	7.4
III	303	307	19	6.3
	117	118	9.4	8.0
	Day to Day (n = 5)			
I	805	750	54.3	7.2
	198	184	7.3	4.0
II	692	666	51.7	7.8
	110	103	5.4	5.2
III	431	424	33.8	8.0
	84	78	3.5	4.5

Urine samples also were analyzed using this method. Demoxepam was the most common metabolite detected, although the percentage of the total dose recovered in the urine as I–III was extremely small (~1% in the first 24 hr after administration).

REFERENCES

(1) L. H. Sternbach, *Agents Actions*, **2**, 193 (1972).

(2) "Physicians' Desk Reference," 29th ed., Medical Economics, Oradell, N.J., 1975, p. 245.

(3) M. A. Schwartz, in "The Benzodiazepines," S. Garattini, E. Mussini, and L. O. Randall, Eds., Raven, New York, N.Y., 1973, p. 53.

(4) R. Dixon, M. A. Brooks, E. Postma, M. R. Hackman, S. Spector, J. D. Moore, and M. A. Schwartz, *Clin. Pharmacol. Ther.*, **20**, 450 (1976).

(5) L. O. Randall, C. L. Scheckel, and R. F. Banziger, *Curr. Ther. Res.*, **7**, 590 (1965).

(6) L. O. Randall and B. Kappell, in "The Benzodiazepines," S. Garattini, E. Mussini, and L. O. Randall, Eds., Raven, New York, N.Y., 1973, p. 27.

(7) P. Jatlow, *Clin. Chem.*, **18**, 516 (1972).

(8) C. S. Frings and P. S. Cohen, *Am. J. Clin. Pathol.*, **56**, 216 (1971).

(9) B. A. Koechlin and L. D'Arconte, *Anal. Biochem.*, **5**, 195 (1963).

(10) M. A. Schwartz and E. Postma, *J. Pharm. Sci.*, **61**, 123 (1972).

(11) F. Marcucci, R. Fanelli, and E. Mussini, *J. Chromatogr.*, **37**, 318 (1968).

(12) H. F. Proelss and H. J. Lohmann, *Clin. Chem.*, **17**, 222 (1971).

(13) I. A. Zingales, *J. Chromatogr.*, **61**, 237 (1971).

(14) M. R. Hackman, M. A. Brooks, J. A. F. deSilva, and T. S. Ma, *Anal. Chem.*, **46**, 1075 (1974).

(15) D. M. Osselton, M. D. Hammond, and P. J. Twitchett, *J. Pharm. Pharmacol.*, **29**, 460 (1977).

(16) T. B. Vree, B. Lenselink, and E. Van der Kleijn, *J. Chromatogr.*, **143**, 530 (1977).

(17) P. M. Kabra, G. L. Stevens, and L. J. Marton, *ibid.*, **150**, 335 (1978).

(18) H. B. Greizerstein and C. Woitowicz, *Anal. Chem.*, **49**, 2235 (1977).

(19) N. Stronjy, C. V. Puglisi, and J. A. F. deSilva, *Anal. Lett.*, **B11**, 135 (1978).

(20) H. G. Boxenbaum, K. A. Geitner, M. L. Jack, W. R. Dixon, and S. A. Kaplan, *J. Pharmacokinet. Biopharm.*, **5**, 3 (1977).

ACKNOWLEDGMENTS

Supported by National Institute on Drug Abuse Contract 271-76-3323.

Effect of Diffusional Lag Time on Multicompartmental Pharmacokinetics for Transepidermal Infusion

E. R. COOPER

Received March 6, 1979, from the *Miami Valley Laboratories, Procter & Gamble Company, Cincinnati, OH 45247.* Accepted for publication June 7, 1979.

Abstract □ A simple proof is given to demonstrate that the lag time to reach steady state from transepidermal infusion is the sum of the diffusional and pharmacokinetic lag times.

Keyphrases □ Diffusion—effect of lag time on multicompartmental pharmacokinetics for transepidermal infusion □ Transepidermal infusion—effect of diffusional lag time on multicompartmental pharmacokinetics □ Models, pharmacokinetic—transepidermal infusion, effect of diffusional lag time

When a compound is administered to an animal *via* constant intravenous infusion, a lag time exists before steady-state values of elimination, blood levels, *etc.*, are obtained (1). If the total amount of compound eliminated is plotted *versus* time, a linear asymptotic form obtains. The lag time is defined as the intercept of this linear asymptote. If, however, a compound is infused transepidermally, there is a lag time to reach cutaneous steady-state transport in addition to the lag time required to distribute and eliminate the compound in the body (2, 3).

Even though the nonsteady-state behavior of the blood levels and other parameters is coupled with the nonsteady-state flux of the skin transport, the total lag time is uncoupled; *i.e.*, the lag time is the sum of the diffusional and the pharmacokinetic lag times. The purpose of this report is to show that this result can be proven rather simply for multicompartmental pharmacokinetics.

MATHEMATICAL MODEL

The kinetics for absorption into a central compartment and distribution between the central compartment and other compartments can be described by:

$$\frac{dC_0}{dt} = -k_{e0}C_0 + \sum_{i=1}^{n} k_{i0}C_i - \left(\sum_{i=1}^{n} k_{0i}\right)C_0 + \frac{AJ}{V_0} \qquad \text{(Eq. 1)}$$

and:

$$\frac{dC_i}{dt} = -k_{ei}C_i - k_{i0}C_i + k_{0i}C_0 \quad i = 1, 2, \ldots, n \qquad \text{(Eq. 2)}$$

where C_j is the concentration in the jth compartment ($j = 0$ is the central compartment), k_{ej} is the elimination rate constant for the jth compartment, and k_{0j} and k_{j0} are the distribution rate constants from and into the central compartment, respectively. Here, V_0 is the central compartment volume, J is the flux of material into the central compartment, and A is the area of tissue from which transport occurs. The kinetic scheme for absorption, distribution, and elimination is given in Scheme I.

At steady state, Eqs. 1 and 2 become:

$$0 = -k_{e0}C_0^s + \sum_{i=1}^{n} k_{i0}C_i^s - \left(\sum_{i=1}^{n} k_{0i}\right)C_0^s + \frac{AJ^s}{V_0} \qquad \text{(Eq. 3)}$$

and:

$$0 = -k_{ei}C_i^s - k_{i0}C_i^s + k_{0i}C_0^s \quad i = 1, 2, \ldots, n \qquad \text{(Eq. 4)}$$

where the superscript s denotes the steady-state value of the quantity.

The long time integral (4) of Eqs. 1 and 2 gives:

$$C_0^s = -k_{e0}M_0 + \sum_{i=1}^{n} k_{i0}M_i - \left(\sum_{i=1}^{n} k_{0i}\right)M_0 + \frac{AJ^s}{V_0}(t - t_D) \qquad \text{(Eq. 5)}$$

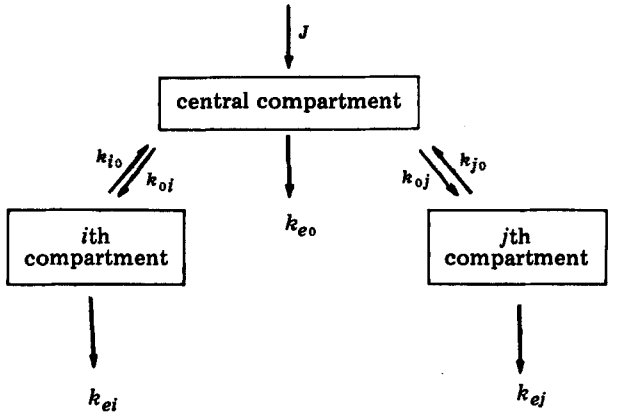

Scheme I—Absorption, distribution, and elimination for topical infusion.

and:

$$C_i^s = -k_{ei}M_i - k_{i0}M_i + k_{0i}M_0 \quad i = 1, 2, \ldots, n \qquad \text{(Eq. 6)}$$

where t_D is the diffusional or transport lag time and:

$$M_i = \int_0^t C_i\, dt' \qquad \text{(Eq. 7)}$$

Here the integral is for t much greater than the time to reach steady state. The addition of Eq. 6 to Eq. 5 gives:

$$Q_e(t) \equiv \sum_{i=0}^{n} k_{ei}M_i = \frac{AJ^s}{V_0}(t - t_D - t_\alpha) \qquad \text{(Eq. 8)}$$

where $Q_e(t)$ is the amount eliminated as a function of time and:

$$t_\alpha = \frac{V_0 \sum_{i=0}^{n} C_i^s}{AJ^s} \qquad \text{(Eq. 9)}$$

The expression for t_α can be written as a function of the rate constants by using Eqs. 3 and 4 to obtain:

$$t_\alpha = \frac{1 + \sum_{i=1}^{n} \frac{k_{0i}}{k_{ei} + k_{i0}}}{k_{e0} + \sum_{i=1}^{n} \frac{k_{ei}k_{0i}}{k_{ei} + k_{i0}}} \qquad \text{(Eq. 10)}$$

The quantity t_α is just the pharmacokinetic lag time. Thus, the total lag time is simply the sum of the transport lag time and the pharmacokinetic lag time.

DISCUSSION

Another way to determine the lag time for transepidermal infusion is to solve Eqs. 1 and 2 *via* a LaPlace transform technique. A quick look for just two compartments reveals that some unwieldly infinite sums must be evaluated and that the lag time could contain cross-terms. However, all of these sums cancel appropriately to give the results of Eq. 8, which demonstrates that the lag times are additive. That is, the time to reach steady state does not contain cross-terms as it does in transport across more than one membrane (5), and one does not have to be concerned with any unexpected delays in the establishment of steady state.

REFERENCES

(1) J. G. Wagner, "Fundamentals of Clinical Pharmacokinetics," Drug

0022-3549/79/1100-1469$01.00/0
© 1979, American Pharmaceutical Association

Intelligence Publications, Hamilton, Ill., 1975.
(2) E. R. Cooper, *J. Pharm. Sci.*, **65**, 1396 (1976).
(3) S. K. Chandrasekaran, W. Bayne, and J. E. Shaw, *ibid.*, **67**, 1370 (1978).
(4) J. Crank, "The Mathematics of Diffusion," Oxford University Press, Oxford, England, 1970.
(5) J. Crank and G. S. Park, "Diffusion in Polymers," Academic, New York, N.Y., 1968.

COMMUNICATIONS

Micellar Catalysis of an Analytical Reaction: Spectrophotometric Determination of Amino Acids and Peptides after Cetrimonium Bromide-Catalyzed Reaction with 1-Fluoro-2,4-dinitrobenzene

Keyphrases □ Surfactants—cetrimonium bromide, micelle formation, catalysis of amino acid and peptide derivatization, spectrophotometry of derivatives □ Amino acids—spectrophotometric determination following derivatization, catalysis by surfactant micelles □ Peptides—spectrophotometric determination following derivatization, catalysis by surfactant micelles

To the Editor:

Surfactants can alter chemical reaction rates through their micelle-forming capabilities. During the past decade, intensive study of this phenomenon has been stimulated by the hope that micellar catalysis of organic reactions might be a useful model of enzyme catalysis. Although the dynamic and fluid structure of micelles limits their utility as enzyme models, micelle-induced alterations in reaction rates are worth studying on their own account (1, 2). It was suggested (3, 4) that micellar catalysis might be exploited for organic analytical purposes, but no such experimental studies have been reported. We describe the use of micellar catalysis to increase the derivative formation rate prior to spectrophotometric measurement of a product.

1-Fluoro-2,4-dinitrobenzene undergoes aromatic nucleophilic substitution by amines to give arylated amines. This reaction was employed to study the amino acid sequence of insulin (5), and it has since been adapted to the analysis of other amines and polyamines (6–8). The reaction is carried out in an alkaline medium, and the product is measured spectrophotometrically. For the determination of many amines and amino acids, the reaction was essentially complete (within 5% of its maximum) for most samples in 10 min at 65°; some compounds required ≥20 min at this temperature (8).

Several surfactants, notably the cation cetrimonium bromide (cetyltrimethylammonium bromide), catalyze substitution reactions between fluorodinitrobenzene and amine nucleophiles (9); rate enhancements of ~five- to 30-fold were found. Therefore, this reaction appeared to provide an appropriate system for testing the proposal (3, 4) that micellar catalysis may be analytically useful.

Rates were measured for the substitution reaction between fluorodinitrobenzene and some amino compounds in the presence and absence of cetrimonium bromide. In these reactions, the fluorodinitrobenzene was in excess, as it would be in an analytical system; samples were withdrawn and examined spectrophotometrically by a literature method (8). The kinetics were apparent first order over at least two half-lives. Table I gives the half-lives and conditions for these reactions. (Tyrosine showed a slow secondary reaction, resulting in a small absorbance decrease.) All compounds gave slightly higher absorbances (~10%) in the presence of the surfactant compared with the final absorbance in its absence.

Table I—Micellar Catalysis of Amine–Fluorodinitrobenzene Reactions by Cetrimonium Bromide

Amine	Half-Life, min[a]	
	No Surfactant	0.035 *M* Surfactant[b]
Glycine	37.2	2.0
Alanine	85.0	4.7
Phenylalanine	32.0	0.5
Tyrosine	22.0	<0.5
Glycylglycine	63.5	5.4
Glycylglycylglycine	94	7.5

[a] Using 5×10^{-4} *M* amine, 3.5×10^{-3} *M* fluorodinitrobenzene, pH 9.2, 23°. [b] About twice the concentration recommended in the analytical procedure.

The following analytical procedure was developed. To a 25-ml volumetric flask were added 0.12 g of cetrimonium bromide, 1.0 ml of 1.3% (v/v) 1-fluoro-2,4-dinitrobenzene in acetone, 9.0 ml of 2.5% sodium borate in water, and 10.0 ml of an aqueous amine solution (1×10^{-4}–1×10^{-3} *M*). After about five half-lives (Table I) at room temperature, 1.0 ml of the solution was pipetted into 9.0 ml of a 1:100 dilution of concentrated hydrochloric acid in dioxane. The absorbance was read in a 1-cm cell at the absorption maximum against a reagent blank carried through the same procedure.

The absorption maximum was at 340 nm for the tyrosine derivative and at 350 nm for the other samples in Table I. Calibration plots were linear over the sample concentration range.

According to Table I, the more hydrophobic reactants (the aromatic amino acids) gave much larger relative rate enhancements, as expected for micellar catalysis. All rate enhancements are analytically useful, and this method can be applied with the reaction carried out at room temperature. This work provides the scope for further study of this analytical system and of the potential applications of micellar catalysis to other analytical reactions.

(1) J. H. Fendler and E. J. Fendler, "Catalysis in Micellar and Macromolecular Systems," Academic, New York, N.Y., 1975.
(2) C. A. Bunton, in "Applications of Biochemical Systems in Organic Chemistry," vol. X, Part 2 of "Techniques of Chemistry," J. B. Jones, C. J. Sih, and D. Perlman, Eds., Wiley–Interscience, New York, N.Y., 1976, chap. 4.
(3) K. A. Connors, "Reaction Mechanisms in Organic Analytical

0022-3549/79/1100-1470$01.00/0
© 1979, American Pharmaceutical Association

Intelligence Publications, Hamilton, Ill., 1975.
(2) E. R. Cooper, *J. Pharm. Sci.*, **65**, 1396 (1976).
(3) S. K. Chandrasekaran, W. Bayne, and J. E. Shaw, *ibid.*, **67**, 1370 (1978).
(4) J. Crank, "The Mathematics of Diffusion," Oxford University Press, Oxford, England, 1970.
(5) J. Crank and G. S. Park, "Diffusion in Polymers," Academic, New York, N.Y., 1968.

COMMUNICATIONS

Micellar Catalysis of an Analytical Reaction: Spectrophotometric Determination of Amino Acids and Peptides after Cetrimonium Bromide-Catalyzed Reaction with 1-Fluoro-2,4-dinitrobenzene

Keyphrases □ Surfactants—cetrimonium bromide, micelle formation, catalysis of amino acid and peptide derivatization, spectrophotometry of derivatives □ Amino acids—spectrophotometric determination following derivatization, catalysis by surfactant micelles □ Peptides—spectrophotometric determination following derivatization, catalysis by surfactant micelles

To the Editor:

Surfactants can alter chemical reaction rates through their micelle-forming capabilities. During the past decade, intensive study of this phenomenon has been stimulated by the hope that micellar catalysis of organic reactions might be a useful model of enzyme catalysis. Although the dynamic and fluid structure of micelles limits their utility as enzyme models, micelle-induced alterations in reaction rates are worth studying on their own account (1, 2). It was suggested (3, 4) that micellar catalysis might be exploited for organic analytical purposes, but no such experimental studies have been reported. We describe the use of micellar catalysis to increase the derivative formation rate prior to spectrophotometric measurement of a product.

1-Fluoro-2,4-dinitrobenzene undergoes aromatic nucleophilic substitution by amines to give arylated amines. This reaction was employed to study the amino acid sequence of insulin (5), and it has since been adapted to the analysis of other amines and polyamines (6–8). The reaction is carried out in an alkaline medium, and the product is measured spectrophotometrically. For the determination of many amines and amino acids, the reaction was essentially complete (within 5% of its maximum) for most samples in 10 min at 65°; some compounds required ≥20 min at this temperature (8).

Several surfactants, notably the cation cetrimonium bromide (cetyltrimethylammonium bromide), catalyze substitution reactions between fluorodinitrobenzene and amine nucleophiles (9); rate enhancements of ~five- to 30-fold were found. Therefore, this reaction appeared to provide an appropriate system for testing the proposal (3, 4) that micellar catalysis may be analytically useful.

Rates were measured for the substitution reaction between fluorodinitrobenzene and some amino compounds in the presence and absence of cetrimonium bromide. In these reactions, the fluorodinitrobenzene was in excess, as it would be in an analytical system; samples were withdrawn and examined spectrophotometrically by a literature method (8). The kinetics were apparent first order over at least two half-lives. Table I gives the half-lives and conditions for these reactions. (Tyrosine showed a slow secondary reaction, resulting in a small absorbance decrease.) All compounds gave slightly higher absorbances (~10%) in the presence of the surfactant compared with the final absorbance in its absence.

Table I—Micellar Catalysis of Amine–Fluorodinitrobenzene Reactions by Cetrimonium Bromide

Amine	Half-Life, min[a]	
	No Surfactant	0.035 *M* Surfactant[b]
Glycine	37.2	2.0
Alanine	85.0	4.7
Phenylalanine	32.0	0.5
Tyrosine	22.0	<0.5
Glycylglycine	63.5	5.4
Glycylglycylglycine	94	7.5

[a] Using 5×10^{-4} *M* amine, 3.5×10^{-3} *M* fluorodinitrobenzene, pH 9.2, 23°. [b] About twice the concentration recommended in the analytical procedure.

The following analytical procedure was developed. To a 25-ml volumetric flask were added 0.12 g of cetrimonium bromide, 1.0 ml of 1.3% (v/v) 1-fluoro-2,4-dinitrobenzene in acetone, 9.0 ml of 2.5% sodium borate in water, and 10.0 ml of an aqueous amine solution (1×10^{-4}–1×10^{-3} *M*). After about five half-lives (Table I) at room temperature, 1.0 ml of the solution was pipetted into 9.0 ml of a 1:100 dilution of concentrated hydrochloric acid in dioxane. The absorbance was read in a 1-cm cell at the absorption maximum against a reagent blank carried through the same procedure.

The absorption maximum was at 340 nm for the tyrosine derivative and at 350 nm for the other samples in Table I. Calibration plots were linear over the sample concentration range.

According to Table I, the more hydrophobic reactants (the aromatic amino acids) gave much larger relative rate enhancements, as expected for micellar catalysis. All rate enhancements are analytically useful, and this method can be applied with the reaction carried out at room temperature. This work provides the scope for further study of this analytical system and of the potential applications of micellar catalysis to other analytical reactions.

(1) J. H. Fendler and E. J. Fendler, "Catalysis in Micellar and Macromolecular Systems," Academic, New York, N.Y., 1975.
(2) C. A. Bunton, in "Applications of Biochemical Systems in Organic Chemistry," vol. X, Part 2 of "Techniques of Chemistry," J. B. Jones, C. J. Sih, and D. Perlman, Eds., Wiley–Interscience, New York, N.Y., 1976, chap. 4.
(3) K. A. Connors, "Reaction Mechanisms in Organic Analytical

0022-3549/79/1100-1470$01.00/0
© 1979, American Pharmaceutical Association

Chemistry," Wiley–Interscience, New York, N.Y., 1973, p. 284.
(4) C. A. Bunton, in "Applications of Biochemical Systems in Organic Chemistry," vol. X, Part 2 of "Techniques of Chemistry," J. B. Jones, C. J. Sih, and D. Perlman, Eds., Wiley–Interscience, New York, N.Y., 1976, p. 806.
(5) F. Sanger, *Biochem. J.*, **39**, 507 (1945).
(6) F. C. McIntire, L. W. Clements, and M. Sproull, *Anal. Chem.*, **25**, 1757 (1953).
(7) S. M. Rosenthal and C. W. Tabor, *J. Pharmacol. Exp. Ther.*, **116**, 131 (1956).
(8) D. T. Dubin, *J. Biol. Chem.*, **235**, 783 (1960).
(9) C. A. Bunton and L. Robinson, *J. Am. Chem. Soc.*, **92**, 356 (1970).

Kenneth A. Connors ˣ
Michelle P. Wong
School of Pharmacy
University of Wisconsin
Madison, WI 53706

Received May 10, 1979.
Accepted for publication August 21, 1979.
Supported in part by a grant from The Upjohn Co.

Desmethyldiazepam: A Specific Radioimmunoassay

Keyphrases □ Desmethyldiazepam—radioimmunoassay □ Radioimmunoassay—desmethyldiazepam □ Diazepam, desmethyl metabolite—radioimmunoassay □ Benzodiazepines—desmethyldiazepam, radioimmunoassay

To the Editor:

Desmethyldiazepam, a 1,4-benzodiazepine, has particular clinical significance because it is a pharmacologically active metabolite of diazepam and several other benzodiazepines (1). Thus, blood levels of desmethyldiazepam and the parent compounds are important parameters in the pharmacokinetic understanding of anxiolytic drug therapy and in the biopharmaceutical evaluation of different drug formulations.

Although many analytical procedures, primarily employing electron-capture GLC and high-performance liquid chromatography, have been reported for the quantitation of desmethyldiazepam in blood or plasma, none achieves the high sample throughput attainable with radioimmunoassay in which the compound may be measured directly in microsamples. Radioimmunoassay is particularly advantageous in bioequivalency studies, where numerous samples may be generated, and in pharmacokinetic studies in the neonate, where a limited sample volume is available for analysis. We now report the development of a specific radioimmunoassay for desmethyldiazepam which satisfies the requirements for both high throughput and small samples.

The hapten 7-chloro-1,3-dihydro-5-(4-hydrazinocarbonylmethoxyphenyl)-2*H*-1,4-benzodiazepin-2-one was converted to its reactive acyl azide with nitrous acid and was coupled covalently to bovine serum albumin as described previously (2). The immunogen consisted of 15 moles of hapten covalently coupled to 1 mole of albumin. Rabbits were immunized intradermally, and the antiserum with the highest titer (1:7500 dilution) of antibodies to desmethyldiazepam was used for all studies.

The radioligand 9-^{3}H-desmethyldiazepam was prepared by catalytic exchange of 9-iododesmethyldiazepam with tritium gas. The reaction was carried out in tetrahydrofuran containing 0.5% triethylamine with a 10% palladium-on-charcoal catalyst. After removal of the labile tritium by repeated freeze drying from methanol, the reaction product was chromatographed on a silica gel column packed in ethyl acetate. The appropriate fractions were combined to yield 9-^{3}H-desmethyldiazepam with a specific activity of 26.5 Ci/mmole.

The radioimmunoassay was identical to that described recently for diazepam (3). A logit-log calibration curve for desmethyldiazepam was linear from 30 to 2000 pg/tube; thus a working sensitivity limit of 3 ng/ml was achieved using a 10-μl plasma sample. This sensitivity is comparable to that achieved by electron-capture GLC with a 1-ml sample. The intra- and interassay coefficients of variation did not exceed 6 and 11%, respectively.

The specificity of the antiserum was evaluated by cross-reactivity studies with those drugs and/or their metabolites of which desmethyldiazepam is a known metabolite. Diazepam, chlordiazepoxide, desmethylchlordiazepoxide, demoxepam, prazepam, and medazepam all cross-reacted less than 1% relative to desmethyldiazepam (100% cross-reactivity). Clorazepate exhibited an apparent cross-reactivity of >50%, which undoubtedly was due in part to its decomposition to desmethyldiazepam during the assay incubation period. Tricyclic antidepressants, commonly prescribed in conjunction with benzodiazepines, did not cross-react with the antiserum.

Further evidence for the specificity of the radioimmunoassay was obtained by comparison with an established electron-capture GLC method for the determination of desmethyldiazepam (4). The joint determinations of desmethyldiazepam in 30 plasma samples from subjects who had received various doses of clorazepate or diazepam were subjected to linear regression analysis by a method (5) using a 95% confidence ellipse. Over a nearly 300-fold desmethyldiazepam concentration range (24–6400 ng/ml), the correlation coefficient, regression line slope, and y-intercept were 0.998, 1.07, and −5.8, respectively. Thus, the radioimmunoassay measures desmethyldiazepam as precisely and specifically as the electron-capture GLC method.

(1) D. J. Greenblatt and R. I. Shader, *South. Med. J.*, 71, 2 (1978).
(2) R. Dixon, J. Earley, and E. Postma, *J. Pharm. Sci.*, **64**, 937 (1975).
(3) R. Dixon and T. Crews, *J. Anal. Toxicol.*, **2**, 210 (1978).
(4) R. E. Weinfeld, H. N. Postmanter, K. C. Khoo, and C. V. Puglisi, *J. Chromatogr.*, **143**, 581 (1977).
(5) M. Kendall and S. Stuart, "The Advanced Theory of Statistics," vol. 2, Hafner, New York, N.Y., 1961, pp. 397–405.

Ross Dixon ˣ
William Glover
James Earley
Michael Delaney
Research Division
Hoffmann–La Roche Inc.
Nutley, NJ 07110

Received July 16, 1979.
Accepted for publication August 13, 1979.

0022-3549/79/1100-1471$01.00/0
© 1979, American Pharmaceutical Association

Chemistry," Wiley–Interscience, New York, N.Y., 1973, p. 284.
(4) C. A. Bunton, in "Applications of Biochemical Systems in Organic Chemistry," vol. X, Part 2 of "Techniques of Chemistry," J. B. Jones, C. J. Sih, and D. Perlman, Eds., Wiley–Interscience, New York, N.Y., 1976, p. 806.
(5) F. Sanger, *Biochem. J.*, **39**, 507 (1945).
(6) F. C. McIntire, L. W. Clements, and M. Sproull, *Anal. Chem.*, **25**, 1757 (1953).
(7) S. M. Rosenthal and C. W. Tabor, *J. Pharmacol. Exp. Ther.*, **116**, 131 (1956).
(8) D. T. Dubin, *J. Biol. Chem.*, **235**, 783 (1960).
(9) C. A. Bunton and L. Robinson, *J. Am. Chem. Soc.*, **92**, 356 (1970).

Kenneth A. Connors ˣ
Michelle P. Wong
School of Pharmacy
University of Wisconsin
Madison, WI 53706

Received May 10, 1979.
Accepted for publication August 21, 1979.
Supported in part by a grant from The Upjohn Co.

Desmethyldiazepam: A Specific Radioimmunoassay

Keyphrases □ Desmethyldiazepam—radioimmunoassay □ Radioimmunoassay—desmethyldiazepam □ Diazepam, desmethyl metabolite—radioimmunoassay □ Benzodiazepines—desmethyldiazepam, radioimmunoassay

To the Editor:

Desmethyldiazepam, a 1,4-benzodiazepine, has particular clinical significance because it is a pharmacologically active metabolite of diazepam and several other benzodiazepines (1). Thus, blood levels of desmethyldiazepam and the parent compounds are important parameters in the pharmacokinetic understanding of anxiolytic drug therapy and in the biopharmaceutical evaluation of different drug formulations.

Although many analytical procedures, primarily employing electron-capture GLC and high-performance liquid chromatography, have been reported for the quantitation of desmethyldiazepam in blood or plasma, none achieves the high sample throughput attainable with radioimmunoassay in which the compound may be measured directly in microsamples. Radioimmunoassay is particularly advantageous in bioequivalency studies, where numerous samples may be generated, and in pharmacokinetic studies in the neonate, where a limited sample volume is available for analysis. We now report the development of a specific radioimmunoassay for desmethyldiazepam which satisfies the requirements for both high throughput and small samples.

The hapten 7-chloro-1,3-dihydro-5-(4-hydrazinocarbonylmethoxyphenyl)-2*H*-1,4-benzodiazepin-2-one was converted to its reactive acyl azide with nitrous acid and was coupled covalently to bovine serum albumin as described previously (2). The immunogen consisted of 15 moles of hapten covalently coupled to 1 mole of albumin. Rabbits were immunized intradermally, and the antiserum with the highest titer (1:7500 dilution) of antibodies to desmethyldiazepam was used for all studies.

The radioligand 9-^{3}H-desmethyldiazepam was prepared by catalytic exchange of 9-iododesmethyldiazepam with tritium gas. The reaction was carried out in tetrahydrofuran containing 0.5% triethylamine with a 10% palladium-on-charcoal catalyst. After removal of the labile tritium by repeated freeze drying from methanol, the reaction product was chromatographed on a silica gel column packed in ethyl acetate. The appropriate fractions were combined to yield 9-^{3}H-desmethyldiazepam with a specific activity of 26.5 Ci/mmole.

The radioimmunoassay was identical to that described recently for diazepam (3). A logit-log calibration curve for desmethyldiazepam was linear from 30 to 2000 pg/tube; thus a working sensitivity limit of 3 ng/ml was achieved using a 10-μl plasma sample. This sensitivity is comparable to that achieved by electron-capture GLC with a 1-ml sample. The intra- and interassay coefficients of variation did not exceed 6 and 11%, respectively.

The specificity of the antiserum was evaluated by cross-reactivity studies with those drugs and/or their metabolites of which desmethyldiazepam is a known metabolite. Diazepam, chlordiazepoxide, desmethylchlordiazepoxide, demoxepam, prazepam, and medazepam all cross-reacted less than 1% relative to desmethyldiazepam (100% cross-reactivity). Clorazepate exhibited an apparent cross-reactivity of >50%, which undoubtedly was due in part to its decomposition to desmethyldiazepam during the assay incubation period. Tricyclic antidepressants, commonly prescribed in conjunction with benzodiazepines, did not cross-react with the antiserum.

Further evidence for the specificity of the radioimmunoassay was obtained by comparison with an established electron-capture GLC method for the determination of desmethyldiazepam (4). The joint determinations of desmethyldiazepam in 30 plasma samples from subjects who had received various doses of clorazepate or diazepam were subjected to linear regression analysis by a method (5) using a 95% confidence ellipse. Over a nearly 300-fold desmethyldiazepam concentration range (24–6400 ng/ml), the correlation coefficient, regression line slope, and y-intercept were 0.998, 1.07, and −5.8, respectively. Thus, the radioimmunoassay measures desmethyldiazepam as precisely and specifically as the electron-capture GLC method.

(1) D. J. Greenblatt and R. I. Shader, *South. Med. J.*, 71, 2 (1978).
(2) R. Dixon, J. Earley, and E. Postma, *J. Pharm. Sci.*, **64**, 937 (1975).
(3) R. Dixon and T. Crews, *J. Anal. Toxicol.*, **2**, 210 (1978).
(4) R. E. Weinfeld, H. N. Postmanter, K. C. Khoo, and C. V. Puglisi, *J. Chromatogr.*, **143**, 581 (1977).
(5) M. Kendall and S. Stuart, "The Advanced Theory of Statistics," vol. 2, Hafner, New York, N.Y., 1961, pp. 397–405.

Ross Dixon ˣ
William Glover
James Earley
Michael Delaney
Research Division
Hoffmann–La Roche Inc.
Nutley, NJ 07110

Received July 16, 1979.
Accepted for publication August 13, 1979.

0022-3549/79/1100-1471$01.00/0
© 1979, American Pharmaceutical Association

Comparison of GLC and High-Pressure Liquid Chromatographic Methods for Analysis of Urinary Pseudoephedrine

Keyphrases □ Pseudoephedrine—analysis, comparison of GLC and high-pressure liquid chromatographic methods, urine □ GLC—analysis, pseudoephedrine, comparison with high-pressure liquid chromatographic method, urine □ Adrenergics (vasoconstrictors)—pseudoephedrine, analysis, comparison of GLC and high-pressure liquid chromatographic methods, urine

To the Editor:

We recently reported a simple high-pressure liquid chromatographic (HPLC) method for the simultaneous determination of pseudoephedrine, chlorpheniramine, and their metabolites in urine (1). This method is specific and sensitive, has 98% recovery, and has been used successfully to study pseudoephedrine pharmacokinetics in humans. In this communication, the specificity of the HPLC method for pseudoephedrine is compared with that of a reported GLC method (2).

Standards were prepared by spiking blank human urine samples with pseudoephedrine[1] and its metabolite, norpseudoephedrine[2]. Urine samples from three normal subjects were collected at intervals of −2–0, 0–12, 12–24, and 24–48 hr after they received a capsule[3] containing 120 mg of pseudoephedrine hydrochloride and 8 mg of chlorpheniramine maleate. These samples and the standard urine samples were assayed (blinded study) independently in duplicate for pseudoephedrine and norpseudoephedrine by the HPLC (1) and GLC (2) methods.

The GLC method (2) involved extraction of urine samples containing pseudoephedrine, norpseudoephedrine, and ephedrine[4] (internal standard) into benzene. To a portion of the benzene were added pyridine and heptafluorobutyric[2] acid for derivatization. The solvent then was acid washed to remove the excess reagent before GLC analysis.

The HPLC method (1) involved extraction of urine containing pseudoephedrine and norpseudoephedrine into ether–methylene chloride (70:30), followed by back-extraction into 0.5% phosphoric acid containing the internal standard (imipramine[5]). A portion of the acidic layer was injected for analysis.

The GLC and HPLC methods produced essentially identical results (Table I) for pseudoephedrine; the correlation between their results was highly statistically significant ($r = 0.996$, $p < 0.001$). Both methods showed minute norpseudoephedrine concentrations in these subjects. On the average, these subjects excreted 91% of the dose as intact pseudoephedrine, which is consistent with the data reported previously (1). The HPLC method does not resolve pseudoephedrine from ephedrine; ephedrine is used as the internal standard for the GLC method and it does not present a specificity problem in either method. The results indicate that the methods are equally specific for pseudoephedrine, with the HPLC method being less time consuming.

Table I—Comparison of the GLC and HPLC Methods for the Determination of Urinary Pseudoephedrine

Urinary Excretion Time, hr	Pseudoephedrine Hydrochloride[a], μg/ml					
	Subject 1		Subject 2		Subject 3	
	GLC	HPLC	GLC	HPLC	GLC	HPLC
−2–0	0.00	0.00	0.00	0.00	0.00	0.35
0–12	41.9	41.3	46.3	43.7	43.5	42.3
12–24	32.6	34.1	47.9	50.2	44.2	42.3
24–48	7.24	8.43	8.29	9.65	3.19	3.87

[a] Determined in duplicate. Each value represents pseudoephedrine hydrochloride equivalents.

(1) C. M. Lai, R. G. Stoll, Z. M. Look, and A. Yacobi, *J. Pharm. Sci.*, **68**, 1243 (1979).

(2) E. T. Lin, D. C. Brater, and L. Z. Benet, *J. Chromatogr.*, **140**, 275 (1977).

David M. Baaske
Chii-Ming Lai
Lawrence Klein
Zee M. Look
Avraham Yacobi [x]
Pharmaceutical Development Department
Research and Medical Affairs
Arnar-Stone Laboratories
McGaw Park, IL 60085

Received July 2, 1979.
Accepted for publication July 26, 1979.

[1] A. G. Knoll, Whippany, N.J.
[2] Aldrich Chemical Co., Milwaukee, Wis.
[3] Arnar-Stone Laboratories, McGaw Park, Ill.
[4] Henley and Co., New York, N.Y.
[5] Sigma Chemical Co., St. Louis, Mo.

0022-3549/79/1100-1472$01.00/0
© 1979, American Pharmaceutical Association

REVIEWS

Instrumental Applications in Forensic Drug Chemistry: Proceedings of the International Symposium, May 29–30, 1978. Edited by MICHAEL KLEIN, ALICE V. KRUEGEL, and STANLEY P. SOBOL. U.S. Government Printing Office (stock number 027-000-00770-8), Washington, D.C. Soft cover, 20 × 26 cm.

This volume records the papers presented at an international symposium hosted by the Drug Enforcement Administration in Arlington, Va. on May 29 and 30, 1978. This symposium brought together international forensic scientists to highlight recent advances in instrumentation and methodology that have been applied to forensic drug analysis. The volume contains topics of interest to forensic scientists and clinical analysts. Twenty-three papers are included in four areas: spectroscopy, computer applications, chromatographic advances, and special topics. Contributors include recognized experts in their respective fields.

In the spectroscopy section, a review (72 references) of mass spectrometry is presented, and specific papers address the use of stable isotopes for quantitation and the development of negative-ion mass spectrometry for forensic applications. Papers on Fourier transform IR and NMR applications complete this section. The computer applications section includes several papers on drug identification which emphasize spectra retrieval systems. Numerous general laboratory information systems used by various national and state government agencies also are described.

Chromatographic instrumentation, methodology, and specific drug analyses are discussed. One paper describes a direct liquid inlet interface for coupling a high-performance liquid chromatograph with a quadrapole mass spectrometer. An extensive review (73 references) is given on the application of derivatization techniques in forensic drug analysis. In addition, GLC profiling of drug seizures using selective detectors is described. Chromatographic techniques used by the forensic toxicologist also are discussed. The final section of the volume includes papers on drug reference standards, a review of immunoassay with a detailed bibliography (445 references), and papers on light microscopy and the scanning electron microscope.

This volume assimilates much useful information pertaining to drug analysis and captures the forensic perspective. An additional benefit is the list of symposium attendees, which provides many contacts for people working in this discipline.

Reviewed by Lyal Hood
U.S. Customs Service
Department of the Treasury
Washington, DC 20229

Body Temperature: Regulation, Drug Effects, and Therapeutic Implications (Modern Pharmacology–Toxicology Series, Vol. 16). Edited by PETER LOMAX and EDWARD SCHONBAUM. Dekker, 270 Madison Ave., New York, NY 10016. 1979. 680 pp. 16 × 24.5 cm. Price $59.75.

This reference is the outcome of an awareness that the time was right for thorough consideration of the current understanding of the physiological mechanisms that affect body temperature and their modification by certain neuroregulators and several specific drug classes. It is the collective work of 40 contributors and contains 25 chapters with an added section on recent developments.

The introductory chapters lead the reader through an extensive historical development of thermoregulation from the first article published in 1797 up to 1940 when the hypothalamus was generally acknowledged as the center for thermoregulation in mammals including humans. This introduction is followed by six chapters concerning postulated neural models for neuroregulation, hypothalamic and extrathalamic thermoregulatory centers, heat production, heat transfer and loss, the effect of ions on body temperature, and the effect of drugs on thermoregulatory behavior. These chapters are followed by 12 chapters on specific body chemicals and drug classes and one chapter each on pyrexia, thermoregulation in the newborn, malignant hyperthermia, accidental hypothermia, body temperature during general anesthesia, and clinical hypothermia.

Convincing evidence published during the last 20 years is cited for the existence of extrahypothalamic thermosensitive neurons throughout the central nervous system. In addition, the data presented show clearly that there is an interaction of certain nodal points in the spinal cord, medulla oblongata, midbrain-pons, and the hypothalamus in the very complex physiological maintenance of thermoregulation.

The material concerning the neurotransmitters serotonin, dopamine, norepinephrine, histamine, and acetylcholine is exhaustive and points out the varied hypothermic and hyperthermic responses observed among different species as well as in the same species and the variations observed when these agents are used *via* different administration routes and at different ambient temperatures. Specific sites and/or cells that appear to respond to these chemicals are well documented. The reader should be aware that the reference material is filled with not only the most recent research articles but also contains enough of the past literature to use as a guide for future research.

This book should be of value to anyone involved in thermoregulation, including clinicians and researchers in the pathophysiology or pharmacotherapeutics of fever.

Reviewed by Ronald F. Gautieri
Department of Pharmacology
School of Pharmacy
Temple University
Philadelphia, PA 19140

The Alkaloids. Chemistry and Physiology. Vol. XVII. Edited by R. H. F. MANSKE and R. G. A. RODRIGO. Academic, 111 Fifth Ave., New York, NY 10003. 1979. xx + 611 pp. 14 × 23 cm. Price $55.00.

R. G. A. Rodrigo became coeditor of this classic series on alkaloids upon the death of the series' founder, Dr. R. M. F. Manske, who commissioned the reviews found in this volume. The high standards required by Dr. Manske are maintained in this excellent book.

S. W. Pelletier and N. V. Mody wrote the first chapter which covers work published since July 1968 dealing with the structure and synthesis of C_{19}-diterpenoid alkaloids. One section gives references to the ^{13}CMR spectra of these alkaloids, and another section discusses some mass spectral fragmentation schemes since these two methods are invaluable in structural elucidation. Of particular interest is a catalog of 73 known C_{19}-diterpenoid alkaloids with their correct structures, physical properties, plant sources, and key references.

Chapter 2, by M. F. Grundon, deals with quinoline alkaloids related to anthranilic acid (*o*-aminobenzoic acid) which were reviewed in Vol. IX. Since then, more than 70 new quinoline alkaloids have been isolated, and this review brings the alkaloid chemist up to date on their occurrence and structural determination. Syntheses for new quinolines and improvements in existing syntheses are presented. The quinolines covered include 4-methoxy-2-quinolones, 3-prenyl-2-quinolones and related tricyclics, furoquinolines, 1,1- and 1,2-dimethylallyl alkaloids, and 2-alkyl- and 2-aryl-4-quinolones.

In Chapter 3, G. A. Cordell reviews the monomeric *Aspidosperma* alkaloids. This chapter is organized especially well considering the vast quantity of material generated since Vol. IX. The isolation and structural elucidation of new alkaloids are presented in detail. Particularly helpful are two tables that summarize the isolation of new and previously known *Aspidosperma* alkaloids, giving their plant sources, physical data, and references. Cordell devotes a section to the chemistry of these alkaloids and then discusses the syntheses developed by various authors. The use of ^{13}CMR and X-ray crystallography for structural determination is covered, including a table of ^{13}CMR chemical shifts for selected *Aspidosperma* alkaloids. The chapter format facilitates access to selected information, which should make this review a favorite for those interested in *Aspidosperma* alkaloids.

The Papaveraceae alkaloids are reviewed in Chapter 4 by F. Santavy, who reviewed this group in Vol. XII. Alkaloids in this family are grouped by structure for the discussion of their structures, syntheses, biosyntheses,

REVIEWS

Instrumental Applications in Forensic Drug Chemistry: Proceedings of the International Symposium, May 29–30, 1978. Edited by MICHAEL KLEIN, ALICE V. KRUEGEL, and STANLEY P. SOBOL. U.S. Government Printing Office (stock number 027-000-00770-8), Washington, D.C. Soft cover, 20 × 26 cm.

This volume records the papers presented at an international symposium hosted by the Drug Enforcement Administration in Arlington, Va. on May 29 and 30, 1978. This symposium brought together international forensic scientists to highlight recent advances in instrumentation and methodology that have been applied to forensic drug analysis. The volume contains topics of interest to forensic scientists and clinical analysts. Twenty-three papers are included in four areas: spectroscopy, computer applications, chromatographic advances, and special topics. Contributors include recognized experts in their respective fields.

In the spectroscopy section, a review (72 references) of mass spectrometry is presented, and specific papers address the use of stable isotopes for quantitation and the development of negative-ion mass spectrometry for forensic applications. Papers on Fourier transform IR and NMR applications complete this section. The computer applications section includes several papers on drug identification which emphasize spectra retrieval systems. Numerous general laboratory information systems used by various national and state government agencies also are described.

Chromatographic instrumentation, methodology, and specific drug analyses are discussed. One paper describes a direct liquid inlet interface for coupling a high-performance liquid chromatograph with a quadrapole mass spectrometer. An extensive review (73 references) is given on the application of derivatization techniques in forensic drug analysis. In addition, GLC profiling of drug seizures using selective detectors is described. Chromatographic techniques used by the forensic toxicologist also are discussed. The final section of the volume includes papers on drug reference standards, a review of immunoassay with a detailed bibliography (445 references), and papers on light microscopy and the scanning electron microscope.

This volume assimilates much useful information pertaining to drug analysis and captures the forensic perspective. An additional benefit is the list of symposium attendees, which provides many contacts for people working in this discipline.

Reviewed by Lyal Hood
U.S. Customs Service
Department of the Treasury
Washington, DC 20229

Body Temperature: Regulation, Drug Effects, and Therapeutic Implications (Modern Pharmacology–Toxicology Series, Vol. 16). Edited by PETER LOMAX and EDWARD SCHONBAUM. Dekker, 270 Madison Ave., New York, NY 10016. 1979. 680 pp. 16 × 24.5 cm. Price $59.75.

This reference is the outcome of an awareness that the time was right for thorough consideration of the current understanding of the physiological mechanisms that affect body temperature and their modification by certain neuroregulators and several specific drug classes. It is the collective work of 40 contributors and contains 25 chapters with an added section on recent developments.

The introductory chapters lead the reader through an extensive historical development of thermoregulation from the first article published in 1797 up to 1940 when the hypothalamus was generally acknowledged as the center for thermoregulation in mammals including humans. This introduction is followed by six chapters concerning postulated neural models for neuroregulation, hypothalamic and extrathalamic thermoregulatory centers, heat production, heat transfer and loss, the effect of ions on body temperature, and the effect of drugs on thermoregulatory behavior. These chapters are followed by 12 chapters on specific body chemicals and drug classes and one chapter each on pyrexia, thermoregulation in the newborn, malignant hyperthermia, accidental hypothermia, body temperature during general anesthesia, and clinical hypothermia.

Convincing evidence published during the last 20 years is cited for the existence of extrahypothalamic thermosensitive neurons throughout the central nervous system. In addition, the data presented show clearly that there is an interaction of certain nodal points in the spinal cord, medulla oblongata, midbrain-pons, and the hypothalamus in the very complex physiological maintenance of thermoregulation.

The material concerning the neurotransmitters serotonin, dopamine, norepinephrine, histamine, and acetylcholine is exhaustive and points out the varied hypothermic and hyperthermic responses observed among different species as well as in the same species and the variations observed when these agents are used *via* different administration routes and at different ambient temperatures. Specific sites and/or cells that appear to respond to these chemicals are well documented. The reader should be aware that the reference material is filled with not only the most recent research articles but also contains enough of the past literature to use as a guide for future research.

This book should be of value to anyone involved in thermoregulation, including clinicians and researchers in the pathophysiology or pharmacotherapeutics of fever.

Reviewed by Ronald F. Gautieri
Department of Pharmacology
School of Pharmacy
Temple University
Philadelphia, PA 19140

The Alkaloids. Chemistry and Physiology. Vol. XVII. Edited by R. H. F. MANSKE and R. G. A. RODRIGO. Academic, 111 Fifth Ave., New York, NY 10003. 1979. xx + 611 pp. 14 × 23 cm. Price $55.00.

R. G. A. Rodrigo became coeditor of this classic series on alkaloids upon the death of the series' founder, Dr. R. M. F. Manske, who commissioned the reviews found in this volume. The high standards required by Dr. Manske are maintained in this excellent book.

S. W. Pelletier and N. V. Mody wrote the first chapter which covers work published since July 1968 dealing with the structure and synthesis of C_{19}-diterpenoid alkaloids. One section gives references to the ^{13}CMR spectra of these alkaloids, and another section discusses some mass spectral fragmentation schemes since these two methods are invaluable in structural elucidation. Of particular interest is a catalog of 73 known C_{19}-diterpenoid alkaloids with their correct structures, physical properties, plant sources, and key references.

Chapter 2, by M. F. Grundon, deals with quinoline alkaloids related to anthranilic acid (*o*-aminobenzoic acid) which were reviewed in Vol. IX. Since then, more than 70 new quinoline alkaloids have been isolated, and this review brings the alkaloid chemist up to date on their occurrence and structural determination. Syntheses for new quinolines and improvements in existing syntheses are presented. The quinolines covered include 4-methoxy-2-quinolones, 3-prenyl-2-quinolones and related tricyclics, furoquinolines, 1,1- and 1,2-dimethylallyl alkaloids, and 2-alkyl- and 2-aryl-4-quinolones.

In Chapter 3, G. A. Cordell reviews the monomeric *Aspidosperma* alkaloids. This chapter is organized especially well considering the vast quantity of material generated since Vol. IX. The isolation and structural elucidation of new alkaloids are presented in detail. Particularly helpful are two tables that summarize the isolation of new and previously known *Aspidosperma* alkaloids, giving their plant sources, physical data, and references. Cordell devotes a section to the chemistry of these alkaloids and then discusses the syntheses developed by various authors. The use of ^{13}CMR and X-ray crystallography for structural determination is covered, including a table of ^{13}CMR chemical shifts for selected *Aspidosperma* alkaloids. The chapter format facilitates access to selected information, which should make this review a favorite for those interested in *Aspidosperma* alkaloids.

The Papaveraceae alkaloids are reviewed in Chapter 4 by F. Santavy, who reviewed this group in Vol. XII. Alkaloids in this family are grouped by structure for the discussion of their structures, syntheses, biosyntheses,

REVIEWS

Instrumental Applications in Forensic Drug Chemistry: Proceedings of the International Symposium, May 29–30, 1978. Edited by MICHAEL KLEIN, ALICE V. KRUEGEL, and STANLEY P. SOBOL. U.S. Government Printing Office (stock number 027-000-00770-8), Washington, D.C. Soft cover, 20 × 26 cm.

This volume records the papers presented at an international symposium hosted by the Drug Enforcement Administration in Arlington, Va. on May 29 and 30, 1978. This symposium brought together international forensic scientists to highlight recent advances in instrumentation and methodology that have been applied to forensic drug analysis. The volume contains topics of interest to forensic scientists and clinical analysts. Twenty-three papers are included in four areas: spectroscopy, computer applications, chromatographic advances, and special topics. Contributors include recognized experts in their respective fields.

In the spectroscopy section, a review (72 references) of mass spectrometry is presented, and specific papers address the use of stable isotopes for quantitation and the development of negative-ion mass spectrometry for forensic applications. Papers on Fourier transform IR and NMR applications complete this section. The computer applications section includes several papers on drug identification which emphasize spectra retrieval systems. Numerous general laboratory information systems used by various national and state government agencies also are described.

Chromatographic instrumentation, methodology, and specific drug analyses are discussed. One paper describes a direct liquid inlet interface for coupling a high-performance liquid chromatograph with a quadrapole mass spectrometer. An extensive review (73 references) is given on the application of derivatization techniques in forensic drug analysis. In addition, GLC profiling of drug seizures using selective detectors is described. Chromatographic techniques used by the forensic toxicologist also are discussed. The final section of the volume includes papers on drug reference standards, a review of immunoassay with a detailed bibliography (445 references), and papers on light microscopy and the scanning electron microscope.

This volume assimilates much useful information pertaining to drug analysis and captures the forensic perspective. An additional benefit is the list of symposium attendees, which provides many contacts for people working in this discipline.

Reviewed by Lyal Hood
U.S. Customs Service
Department of the Treasury
Washington, DC 20229

Body Temperature: Regulation, Drug Effects, and Therapeutic Implications (Modern Pharmacology–Toxicology Series, Vol. 16). Edited by PETER LOMAX and EDWARD SCHONBAUM. Dekker, 270 Madison Ave., New York, NY 10016. 1979. 680 pp. 16 × 24.5 cm. Price $59.75.

This reference is the outcome of an awareness that the time was right for thorough consideration of the current understanding of the physiological mechanisms that affect body temperature and their modification by certain neuroregulators and several specific drug classes. It is the collective work of 40 contributors and contains 25 chapters with an added section on recent developments.

The introductory chapters lead the reader through an extensive historical development of thermoregulation from the first article published in 1797 up to 1940 when the hypothalamus was generally acknowledged as the center for thermoregulation in mammals including humans. This introduction is followed by six chapters concerning postulated neural models for neuroregulation, hypothalamic and extrathalamic thermoregulatory centers, heat production, heat transfer and loss, the effect of ions on body temperature, and the effect of drugs on thermoregulatory behavior. These chapters are followed by 12 chapters on specific body chemicals and drug classes and one chapter each on pyrexia, thermoregulation in the newborn, malignant hyperthermia, accidental hypothermia, body temperature during general anesthesia, and clinical hypothermia.

Convincing evidence published during the last 20 years is cited for the existence of extrahypothalamic thermosensitive neurons throughout the central nervous system. In addition, the data presented show clearly that there is an interaction of certain nodal points in the spinal cord, medulla oblongata, midbrain-pons, and the hypothalamus in the very complex physiological maintenance of thermoregulation.

The material concerning the neurotransmitters serotonin, dopamine, norepinephrine, histamine, and acetylcholine is exhaustive and points out the varied hypothermic and hyperthermic responses observed among different species as well as in the same species and the variations observed when these agents are used *via* different administration routes and at different ambient temperatures. Specific sites and/or cells that appear to respond to these chemicals are well documented. The reader should be aware that the reference material is filled with not only the most recent research articles but also contains enough of the past literature to use as a guide for future research.

This book should be of value to anyone involved in thermoregulation, including clinicians and researchers in the pathophysiology or pharmacotherapeutics of fever.

Reviewed by Ronald F. Gautieri
Department of Pharmacology
School of Pharmacy
Temple University
Philadelphia, PA 19140

The Alkaloids. Chemistry and Physiology. Vol. XVII. Edited by R. H. F. MANSKE and R. G. A. RODRIGO. Academic, 111 Fifth Ave., New York, NY 10003. 1979. xx + 611 pp. 14 × 23 cm. Price $55.00.

R. G. A. Rodrigo became coeditor of this classic series on alkaloids upon the death of the series' founder, Dr. R. M. F. Manske, who commissioned the reviews found in this volume. The high standards required by Dr. Manske are maintained in this excellent book.

S. W. Pelletier and N. V. Mody wrote the first chapter which covers work published since July 1968 dealing with the structure and synthesis of C_{19}-diterpenoid alkaloids. One section gives references to the ^{13}CMR spectra of these alkaloids, and another section discusses some mass spectral fragmentation schemes since these two methods are invaluable in structural elucidation. Of particular interest is a catalog of 73 known C_{19}-diterpenoid alkaloids with their correct structures, physical properties, plant sources, and key references.

Chapter 2, by M. F. Grundon, deals with quinoline alkaloids related to anthranilic acid (*o*-aminobenzoic acid) which were reviewed in Vol. IX. Since then, more than 70 new quinoline alkaloids have been isolated, and this review brings the alkaloid chemist up to date on their occurrence and structural determination. Syntheses for new quinolines and improvements in existing syntheses are presented. The quinolines covered include 4-methoxy-2-quinolones, 3-prenyl-2-quinolones and related tricyclics, furoquinolines, 1,1- and 1,2-dimethylallyl alkaloids, and 2-alkyl- and 2-aryl-4-quinolones.

In Chapter 3, G. A. Cordell reviews the monomeric *Aspidosperma* alkaloids. This chapter is organized especially well considering the vast quantity of material generated since Vol. IX. The isolation and structural elucidation of new alkaloids are presented in detail. Particularly helpful are two tables that summarize the isolation of new and previously known *Aspidosperma* alkaloids, giving their plant sources, physical data, and references. Cordell devotes a section to the chemistry of these alkaloids and then discusses the syntheses developed by various authors. The use of ^{13}CMR and X-ray crystallography for structural determination is covered, including a table of ^{13}CMR chemical shifts for selected *Aspidosperma* alkaloids. The chapter format facilitates access to selected information, which should make this review a favorite for those interested in *Aspidosperma* alkaloids.

The Papaveraceae alkaloids are reviewed in Chapter 4 by F. Santavy, who reviewed this group in Vol. XII. Alkaloids in this family are grouped by structure for the discussion of their structures, syntheses, biosyntheses,

and physical properties. An interesting table lists all known alkaloids isolated from each Papaveraceae species. A short section deals with the confusing chemotaxonomy of the family. This chapter involves a complex group of alkaloids, and Santavy has been quite thorough, as evidenced by the citation of 853 references.

The final chapter, by R. S. Kapil and R. T. Brown, covers monoterpene alkaloid glycosides. Many alkaloids of this novel class were discovered after biosynthetic studies that predicted their existence. They are condensation products of secologanin with dopamine, tryptamine, and tryptophan derivatives and are considered biosynthetic precursors of the *Ipecacuanha*, terpenoid indole, and *Camptotheca* alkaloids. This class of alkaloids is expected to expand as isolation methods become more sophisticated and different biosynthetic schemes are investigated.

This volume, like its predecessors, should prove invaluable to alkaloid chemists.

Reviewed by Susan Tafur
Philip Morris Research Center
Richmond, VA 23261

Pharmacological and Biochemical Properties of Drug Substances, Vol. 2. Edited by MORTON E. GOLDBERG. American Pharmaceutical Association, 2215 Constitution Ave., N.W., Washington, DC 20037. 1979. 557 pp. 16 × 23 cm. Price $29.00 ($20.00 member rate).

Volume 2 of this series reviews 20 new drug entities in various therapeutic classes. The monographs discuss the chemistry, animal pharmacology, metabolism and pharmacokinetics, toxicology, and clinical pharmacology of agents that represent prototypes for major therapeutic drug classes. The drug substances considered are amoxapine, butorphanol, valproic acid, atenolol, bretylium tosylate, disopyramide, metoprolol, labetalol, sulfinpyrazone, cephradine, doxycycline, miconazole, tamoxifen, auranofin, levamisole, penicillamine, acetylcysteine, ipratropium bromide, sincalide, and endorphins. The information conveniently presented in this series concerning the biological properties of agents may be difficult to locate in other sources. In most instances, the monograph authors are associated with the company responsible for developing the drug and as such offer a unique perspective of the various stages of discovery and testing.

Staff Review

NOTICES

The Action of Drugs on Calcium Metabolism. Progress in Pharmacology. Vol. 2, No. 1. Edited by P. A. van ZWIETEN and E. SCHONBAUM. Gustav Fisher Verlag, D-7000 Stuttgart 72 Postfach 720 143, West Germany. 1978. 83 pp. 16 × 24 cm.

Botanical Dermatology. Plants and Plant Products Injurous to the Skin. By JOHN MITCHELL and ARTHUR ROCK. Lea & Febiger, 600 South Washington Square, Philadelphia, PA 19106. 1979. 786 pp. 13 × 22 cm. Price $39.50.

Evaluation and Optimization of Laboratory Methods and Analytical Procedures. A Survey of Statistical and Mathematical Techniques. By DESIRE L. MASSART, AUKE DIJKSTRA, and LEONARD KAUFMAN. Elsevier Scientific Publishing, 52 Vanderbilt Ave., New York, NY 10017. 1978. 596 pp. 16 × 24 cm. Price $57.75.

Glycoproteins and Glycolipids in Disease Processes. ACS Symposium Series 80. By EARL F. WALBORG, Jr. American Chemical Society, 1155 16th St., N.W., Washington, DC 20036. 1978. 479 pp. 15 × 23 cm. Price $33.50.

Hospital-Associated Infections in The Compromised Host. (Handbook on Hospital-Associated Infections, Vol. 2.) Edited by GERALD P. BODEY and VICTORIO RODRIQUEZ. Dekker, 270 Madison Ave., New York, NY 10016. 1979. 263 pp. 15 × 23 cm. Price $32.75.

Hospital-Associated Infections in the General Hospital Population and Specific Measures of Control. (Handbook on Hospital-Associated Infections, Vol. 3.) Edited by DIETER GROSCHEL. Dekker, 270 Madison Ave., New York, NY 10016. 1979. 188 pp. 14 × 23 cm. Price $25.00.

Molecular Interactions and Activity in Proteins. Ciba Foundation Symposium 60 (new series). Elsevier/North-Holland, 52 Vanderbilt Ave., New York, NY 10017. 1978. 279 pp. 16 × 24 cm.

Pharmacy Management for Students and Practitioners. 2nd Ed. By C. PATRICK THARP and PEDRO J. LECCA. C. V. Mosby, 11830 Westline Industrial Drive, St. Louis, MO 63141. 1979. 226 pp. 17 × 25 cm. Price $15.95.

Sex Hormones and Behavior. CIBA Foundation Symposium 62 (new series). Elsevier/North-Holland, 52 Vanderbilt Ave., New York, NY 10017. 1979. 382 pp. 16 × 24 cm.

Sleeping Pills, Insomnia, and Medical Practice. Report of a Study from the Institute of Medicine. National Academy of Sciences, Washington, D.C. 1979. 127 pp. 21 × 28 cm. Price $6.00.

Recent Developments in Chromatography and Electrophoresis. Proceedings of the 9th International Symposium on Chromatography and Electrophoresis, Riva del Gara, 15–17 May 1978. Edited by ALBERTO FRIGERIO and LEIKA RENOZ. Elsevier/North-Holland, 52 Vanderbilt Ave., New York, NY 10017. 1979. 357 pp. 19 × 24 cm. Price $58.50.

Legemiddel-forbruket i Norge. En statistik fremstilling av legemiddel-forbruket i Norge for arena 1975–77 basert pa omsetnig av legemidler fra Norsk Medisinaldepot til apotek og sykehus. Redaktor: Sjefsanalytiker Kare ydvin Norsk Medisinaldepot. 185 pp. 21 × 30 cm.

Reviews of Physiology, Biochemistry and Pharmacology. Vol. 82. Catecholamine Receptors, Synthesis and Secretion of Albumin, Gating Currents in Excitable Membranes. By R. H. ADRIAN *et al.* Springer-Verlag, 175 Fifth Ave., New York, NY 10010. 1978. 213 pp. 16 × 24 cm. Price $39.80.

Reviews of Physiology, Biochemistry and Pharmacology. Vol. 83. Transport Processes in Formation of Cerebrospinal Fluid, Optical Measurement of Membrane Potential, Cell-Cell Adhesion, Pharmacogenetics, Biochemistry and Pharmacology. By R. H. ADRIAN *et al.* Springer-Verlag, 175 Fifth Ave., New York, NY 10010. 1978. 196 pp. 16 × 24 cm. Price $39.00.

Serotonin in Health and Disease Vol. III: The Central Nervous System. Edited by WALTER B. ESSMAN. Spectrum, 175-20 Wexford Terrace, Jamaica, NY 11432. 1978. 460 pp. 15 × 24 cm. Price $37.50.

and physical properties. An interesting table lists all known alkaloids isolated from each Papaveraceae species. A short section deals with the confusing chemotaxonomy of the family. This chapter involves a complex group of alkaloids, and Santavy has been quite thorough, as evidenced by the citation of 853 references.

The final chapter, by R. S. Kapil and R. T. Brown, covers monoterpene alkaloid glycosides. Many alkaloids of this novel class were discovered after biosynthetic studies that predicted their existence. They are condensation products of secologanin with dopamine, tryptamine, and tryptophan derivatives and are considered biosynthetic precursors of the *Ipecacuanha*, terpenoid indole, and *Camptotheca* alkaloids. This class of alkaloids is expected to expand as isolation methods become more sophisticated and different biosynthetic schemes are investigated.

This volume, like its predecessors, should prove invaluable to alkaloid chemists.

Reviewed by Susan Tafur
Philip Morris Research Center
Richmond, VA 23261

Pharmacological and Biochemical Properties of Drug Substances, Vol. 2. Edited by MORTON E. GOLDBERG. American Pharmaceutical Association, 2215 Constitution Ave., N.W., Washington, DC 20037. 1979. 557 pp. 16 × 23 cm. Price $29.00 ($20.00 member rate).

Volume 2 of this series reviews 20 new drug entities in various therapeutic classes. The monographs discuss the chemistry, animal pharmacology, metabolism and pharmacokinetics, toxicology, and clinical pharmacology of agents that represent prototypes for major therapeutic drug classes. The drug substances considered are amoxapine, butorphanol, valproic acid, atenolol, bretylium tosylate, disopyramide, metoprolol, labetalol, sulfinpyrazone, cephradine, doxycycline, miconazole, tamoxifen, auranofin, levamisole, penicillamine, acetylcysteine, ipratropium bromide, sincalide, and endorphins. The information conveniently presented in this series concerning the biological properties of agents may be difficult to locate in other sources. In most instances, the monograph authors are associated with the company responsible for developing the drug and as such offer a unique perspective of the various stages of discovery and testing.

Staff Review

NOTICES

The Action of Drugs on Calcium Metabolism. Progress in Pharmacology. Vol. 2, No. 1. Edited by P. A. van ZWIETEN and E. SCHONBAUM. Gustav Fisher Verlag, D-7000 Stuttgart 72 Postfach 720 143, West Germany. 1978. 83 pp. 16 × 24 cm.

Botanical Dermatology. Plants and Plant Products Injurous to the Skin. By JOHN MITCHELL and ARTHUR ROCK. Lea & Febiger, 600 South Washington Square, Philadelphia, PA 19106. 1979. 786 pp. 13 × 22 cm. Price $39.50.

Evaluation and Optimization of Laboratory Methods and Analytical Procedures. A Survey of Statistical and Mathematical Techniques. By DESIRE L. MASSART, AUKE DIJKSTRA, and LEONARD KAUFMAN. Elsevier Scientific Publishing, 52 Vanderbilt Ave., New York, NY 10017. 1978. 596 pp. 16 × 24 cm. Price $57.75.

Glycoproteins and Glycolipids in Disease Processes. ACS Symposium Series 80. By EARL F. WALBORG, Jr. American Chemical Society, 1155 16th St., N.W., Washington, DC 20036. 1978. 479 pp. 15 × 23 cm. Price $33.50.

Hospital-Associated Infections in The Compromised Host. (Handbook on Hospital-Associated Infections, Vol. 2.) Edited by GERALD P. BODEY and VICTORIO RODRIQUEZ. Dekker, 270 Madison Ave., New York, NY 10016. 1979. 263 pp. 15 × 23 cm. Price $32.75.

Hospital-Associated Infections in the General Hospital Population and Specific Measures of Control. (Handbook on Hospital-Associated Infections, Vol. 3.) Edited by DIETER GROSCHEL. Dekker, 270 Madison Ave., New York, NY 10016. 1979. 188 pp. 14 × 23 cm. Price $25.00.

Molecular Interactions and Activity in Proteins. Ciba Foundation Symposium 60 (new series). Elsevier/North-Holland, 52 Vanderbilt Ave., New York, NY 10017. 1978. 279 pp. 16 × 24 cm.

Pharmacy Management for Students and Practitioners. 2nd Ed. By C. PATRICK THARP and PEDRO J. LECCA. C. V. Mosby, 11830 Westline Industrial Drive, St. Louis, MO 63141. 1979. 226 pp. 17 × 25 cm. Price $15.95.

Sex Hormones and Behavior. CIBA Foundation Symposium 62 (new series). Elsevier/North-Holland, 52 Vanderbilt Ave., New York, NY 10017. 1979. 382 pp. 16 × 24 cm.

Sleeping Pills, Insomnia, and Medical Practice. Report of a Study from the Institute of Medicine. National Academy of Sciences, Washington, D.C. 1979. 127 pp. 21 × 28 cm. Price $6.00.

Recent Developments in Chromatography and Electrophoresis. Proceedings of the 9th International Symposium on Chromatography and Electrophoresis, Riva del Gara, 15–17 May 1978. Edited by ALBERTO FRIGERIO and LEIKA RENOZ. Elsevier/North-Holland, 52 Vanderbilt Ave., New York, NY 10017. 1979. 357 pp. 19 × 24 cm. Price $58.50.

Legemiddel-forbruket i Norge. En statistik fremstilling av legemiddel-forbruket i Norge for arena 1975–77 basert pa omsetnig av legemidler fra Norsk Medisinaldepot til apotek og sykehus. Redaktor: Sjefsanalytiker Kare ydvin Norsk Medisinaldepot. 185 pp. 21 × 30 cm.

Reviews of Physiology, Biochemistry and Pharmacology. Vol. 82. Catecholamine Receptors, Synthesis and Secretion of Albumin, Gating Currents in Excitable Membranes. By R. H. ADRIAN *et al.* Springer-Verlag, 175 Fifth Ave., New York, NY 10010. 1978. 213 pp. 16 × 24 cm. Price $39.80.

Reviews of Physiology, Biochemistry and Pharmacology. Vol. 83. Transport Processes in Formation of Cerebrospinal Fluid, Optical Measurement of Membrane Potential, Cell-Cell Adhesion, Pharmacogenetics, Biochemistry and Pharmacology. By R. H. ADRIAN *et al.* Springer-Verlag, 175 Fifth Ave., New York, NY 10010. 1978. 196 pp. 16 × 24 cm. Price $39.00.

Serotonin in Health and Disease Vol. III: The Central Nervous System. Edited by WALTER B. ESSMAN. Spectrum, 175-20 Wexford Terrace, Jamaica, NY 11432. 1978. 460 pp. 15 × 24 cm. Price $37.50.

A publication of the
American Pharmaceutical Association—
the National Professional Society
of Pharmacists

JOURNAL OF PHARMACEUTICAL SCIENCES

INDEX TO AUTHORS
INDEX TO SUBJECTS

VOLUME 68
JANUARY TO DECEMBER, 1979

Published monthly under the supervision of the Board of Trustees

MARY H. FERGUSON
Editor

SHELLY ELLIOTT
Production Editor

MARCIA GARTRELL
Copy Editor

NICOLETTE TRIANTAFELLU
Copy Editor

EDWARD G. FELDMANN
Contributing Editor

SAMUEL W. GOLDSTEIN
Contributing Editor

BELLE R. BECK
Editorial Secretary

DAVID BOHARDT
Director of Publications

L. LUAN CORRIGAN
Assistant Director of Publications

EDITORIAL ADVISORY BOARD

John Autian
Norman R. Farnsworth
William O. Foye
William J. Jusko
Herbert A. Lieberman
David E. Mann, Jr.
Gerald J. Papariello
Edward G. Rippie

DECEMBER 1979
VOLUME 68 NUMBER 12

JOURNAL OF PHARMACEUTICAL SCIENCES

MARY H. FERGUSON
Editor

SHELLY ELLIOTT
Production Editor

MARCIA GARTRELL
Copy Editor

NICOLETTE TRIANTAFELLU
Copy Editor

EDWARD G. FELDMANN
Contributing Editor

SAMUEL W. GOLDSTEIN
Contributing Editor

BELLE R. BECK
Editorial Secretary

DAVID BOHARDT
Director of Publications

L. LUAN CORRIGAN
Assistant Director of Publications

EDITORIAL ADVISORY BOARD

JOHN AUTIAN
HERBERT A. LIEBERMAN
NORMAN R. FARNSWORTH
DAVID E. MANN, JR.
WILLIAM O. FOYE
GERALD J. PAPARIELLO
WILLIAM J. JUSKO
EDWARD G. RIPPIE

The *Journal of Pharmaceutical Sciences* (ISSN 0022-3549) is published monthly by the American Pharmaceutical Association (APhA) at 2215 Constitution Ave., N.W., Washington, DC 20037. Second-class postage paid at Washington, D.C., and at additional mailing office.

All expressions of opinion and statements of supposed fact appearing in articles or editorials carried in this journal are published on the authority of the writer over whose name they appear and are not to be regarded as necessarily expressing the policies or views of APhA.

Offices—Editorial, Advertising, and Subscription: 2215 Constitution Ave., N.W., Washington, DC 20037. Printing: 20th & Northampton Streets, Easton, PA 18042.

Annual Subscriptions—United States and foreign, industrial and government institutions $50, educational institutions $50, individuals *for personal use only* $30; single copies $5. All foreign subscriptions add $5 for postage. Subscription rates are subject to change without notice. Members of APhA may elect to receive the *Journal of Pharmaceutical Sciences* as a part of their annual $70 (foreign $75) APhA membership dues.

Claims—Missing numbers will not be supplied if dues or subscriptions are in arrears for more than 60 days or if claims are received more than 60 days after the date of the issue, or if loss was due to failure to give notice of change of address. APhA cannot accept responsibility for foreign delivery when its records indicate shipment was made.

Change of Address—Members and subscribers should notify at once both the Post Office and APhA of any change of address.

Photocopying—The code at the foot of the first page of an article indicates that APhA has granted permission for copying of the article beyond the limits permitted by Sections 107 and 108 of the U.S. Copyright Law provided that the copier sends the per copy fee stated in the code to the Copyright Clearance Center, Inc., P.O. Box 8891, Boston, MA 02114. Copies may be made for personal or internal use only and not for general distribution.

Microfilm—Available from University Microfilms International, 300 N. Zeeb Road, Ann Arbor, MI 48106.

© Copyright 1979, American Pharmaceutical Association, 2215 Constitution Ave., N.W., Washington, DC 20037; all rights reserved.

POSTMARKETING DRUG SURVEILLANCE

After being approved for marketing, any number of useful drugs have subsequently been found to have serious side effects associated with their use. This situation occurs because clinical testing during investigational trials involves relatively small numbers of test subjects—usually a few hundred at most—and the principal objective is to determine the effectiveness of the new agent.

Consequently, side effects which are relatively rare, or which may show up only in certain patient populations, or which might be so unusual or bizarre that they are not associated with the therapy being administered, often will not be detected until the drug goes into general marketing and has been in wide scale distribution for some time.

Recognition of this problem has long troubled many people and groups with an interest in improved health care. Hence, various approaches to providing a solution have been tried and even more have been offered. Most observers have concluded that the only possible means of getting a handle on this problem is through some program of postmarketing drug surveillance.

Efforts made in the past have proven unsatisfactory, however, because they relied on voluntary reporting *via* poorly coordinated and inadequately publicized systems. Although both individuals and groups may have been well intended, this problem and the resulting programs hardly were "top priority" in terms of either resources or commitment. Understandably, therefore, the problem continued to grow as more drugs and more potent drugs were approved for marketing.

Finally, in early 1976, Senator Edward M. Kennedy laid down a challenge to the drug industry in a speech at the Annual Meeting of the Pharmaceutical Manufacturers Association.

The PMA responded to this challenge and invited half-a-dozen professional health societies to join with it in funding an expert commission to study and analyze the problem and to develop and propose a solution.

To the credit of the respective organizations, there was quick general support for the PMA proposal. In late November 1976 the Joint Commission on Prescription Drug Use was officially launched with due pomp and ceremony under the bright lights of television cameras in a major chamber of the U.S. Capitol building, with Senator Kennedy personally presiding.

It is fair to say that the Joint Commission has not enjoyed either a speedy or tranquil voyage during the three-year period that has ensued.

At the time of its establishment, the message was made loud and clear that the Commission was to complete its work within a maximum of three years and preferably less. Moreover, it was anticipated that progress would be such that the framework for a postmarketing system could begin to take shape in tandem during the latter half of this same three-year period. In this manner, the system could be operative shortly after the Commission completed its work.

But such was not to be, and for the purposes of this column it is unnecessary to delve into the reasons causing these delays. Similarly, it is unnecessary here to recount what has been a rather bumpy road for the Joint Commission to travel or the reasons for that bumpy ride.

Rather, our purpose is to call attention to the expected imminent release of the final report of findings, conclusions, and recommendations of the Joint Commission.

Reports from study commissions very often have a way of rapidly slipping into oblivion. This fate seems to be especially common in Washington because the commissions themselves are often created out of political expediency. It is a convenient and simple way to temporarily dispose of a controversial, emotionally charged issue. Then, by the time a few years have passed, and the commission issues its report, public interest has greatly diminished—if it has not disappeared altogether. When the issue is forgotten, it should hardly be surprising, then, that the report pertaining to that issue gets little and fleeting attention.

We hope, however, that this will not be the fate of whatever comes by way of a report from the Joint Commission on Prescription Drug Use. The need for an answer to postmarketing drug surveillance is as great, if not greater, today than it was in 1976. Moreover, much in the way of time, effort, and money has been spent during this three-year project.

As one of the sponsoring organizations, APhA has a special interest in seeing that the Joint Commission's report is given the careful examination and thoughtful scrutiny that it deserves. And, in particular, the fact that it is expected to deal with substantial scientific issues ought to make it of specific interest to the readers of this journal.

We urge that they, as well as all health care scientists and practitioners, give the report their close attention, and that they actively participate in whatever forums develop for discussion and debate regarding its proposals. —EGF

JOURNAL OF PHARMACEUTICAL SCIENCES

DECEMBER 1979
VOLUME 68 NUMBER 12

RESEARCH ARTICLES

Suspending Agent Effects on Steroid Suspension Dissolution Profiles

STEPHEN A. HOWARD ˣ, JOHN MAUGER, JENG WU HSIEH, and KIRIT AMIN

Received April 23, 1979, from the *School of Pharmacy, West Virginia University, Morgantown, WV 26506.* Accepted for publication July 25, 1979.

Abstract □ Dissolution profiles and particle-size analyses were determined for two lots of prednisolone acetate. The effects of common suspending agents on dissolution and particle-size distributions of these suspensions also were investigated. Lot-to-lot variation in the prednisolone acetate dissolution rate was observed and was apparently related to the percentage of fine particles within the distribution. Carboxymethylcellulose sodium inhibition of prednisolone acetate dissolution occurred with only one lot of raw material and seemed to be related to aggregation of the fine particles. Hydroxypropyl methylcellulose inhibited both prednisolone acetate lots and was observed with or without small particle aggregation. The dissolution variations observed have important implications in suspension formulation.

Keyphrases □ Dissolution—suspending agent effects on steroid suspensions □ Steroids—prednisolone acetate suspensions, effects of suspending agents on dissolution □ Suspensions—steroids, effects of suspending agents on dissolution

Suspensions, capsules, and tablets share dissolution as a rate-limiting step for absorption and bioavailability. *In vitro* suspension dissolution has been related to the absorption rate (1, 2). Several investigators showed that the relationship between the dissolution rate and the formulation is most important (3–9). In particular, suspending agents are important in suspension dissolution (6–9).

The dissolution of handmade and commercial prednisolone acetate suspensions has been investigated (6). Hydroxypropyl methylcellulose inhibits prednisolone acetate dissolution, and this inhibition might be reflected in dissolution differences among commercial suspensions. Similar inhibition of sulfa drug dissolution was found with increasing carboxymethylcellulose sodium concentrations (7).

The purpose of the present study was to investigate systematically the dissolution-retarding effects of common agents on steroid suspensions (*e.g.*, prednisolone acetate). Information regarding the retardation mechanism as well as concentration dependence and viscosity effects was desired. By testing a number of agents, compounds with minimal retarding effects could be recognized. Such information should help to improve steroid suspension formulation.

EXPERIMENTAL

Dissolution data were obtained using a device reported by Shah *et al.* (10) with the sample basket removed. This apparatus featured a large-volume fluid container, a rotating filter assembly, and an external variable-speed magnetic stirrer. The rotating filter assembly provided variable mild laminar liquid agitation, and it also functioned as an *in situ* nonclogging filter to permit efficient intermittent or continuous sample filtration during dissolution. A 0.5-μm stainless steel filter was used.

One liter of distilled water was the dissolution medium. The temperature was maintained at 37°, and the filter assembly stirring speed was 300 rpm. A strobe lamp was employed to standardize the stirring speed.

Filtered fluid samples were withdrawn continuously at a 100-ml/min rate and were circulated through a spectrophotometer[1] for assay and then back into the dissolution flask. Air bubbles were released periodically with an air trap. The system was allowed to equilibrate at least 15 min before the sample was added.

Dissolution experiments were initiated by injecting 0.5 ml of a 0.25% prednisolone acetate suspension at a fixed position in the beaker with a syringe fitted with an extra-long needle. This concentration is below 10% saturation for prednisolone acetate. The chart paper was marked at the exact time the suspension was introduced. The absorbance of dissolved prednisolone acetate was recorded from the digital display of the spectrophotometer at 5-sec intervals for 1500 sec and then periodically for ~2 hr. Usually, a final 24-hr reading was taken.

[1] Cary model 118, Varian Instrument Division, Palo Alto, Calif.

0022-3549/79/1200-1475$01.00/0
© 1979, American Pharmaceutical Association

Table I—Composition of Lot A Suspensions [a]

Suspension	Active Ingredient, %	Suspending Agent, %
Prednisolone acetate	0.25	—
Prednisolone acetate containing carboxymethylcellulose sodium	0.25	0.5
Prednisolone acetate containing hydroxypropyl methylcellulose 4000 cps	0.25	0.5
Prednisolone acetate containing hydroxypropyl methylcellulose 4000 cps	0.25	0.1
Prednisolone acetate containing hydroxypropyl methylcellulose 50 cps	0.25	0.5

[a] The amount used of each suspension in the dissolution tests was 0.5 mg/liter.

The prednisolone acetate was assayed at 246 nm. The absorbance of the suspending agents was accounted for by assaying similar dilutions of suspending agents as found in the dissolution flask but without prednisolone acetate.

The described suspensions were prepared with a glass mortar and pestle. This method provided reproducible results and was easier to use than any other small-scale suspension methods attempted. The composition of the suspensions is listed in Table I.

The particle-size distribution data were obtained using an electronic flow counter[2] with a population accessory. A convenient aspect of this apparatus is that the volume distribution is obtained automatically with no calculation by the operator. The population accessory also allows for a direct determination of a numbers distribution. A meter is used to maintain sufficient dilution to prevent multiple counts.

A commercially available balanced electrolyte[3] was saturated with prednisolone acetate. Particulate contamination of the electrolyte was avoided by filtering the saturated solutions twice through a 0.22-μm filter.

RESULTS AND DISCUSSION

Dissolution profiles and particle-size analyses were determined for two lots of prednisolone acetate (Lots A and B[4]). Lot A was studied initially.

The dissolution profiles for suspensions of Lot A prednisolone acetate and Lot A prednisolone acetate containing 0.5% carboxymethylcellulose sodium are shown in Fig. 1. Carboxymethylcellulose sodium retarded

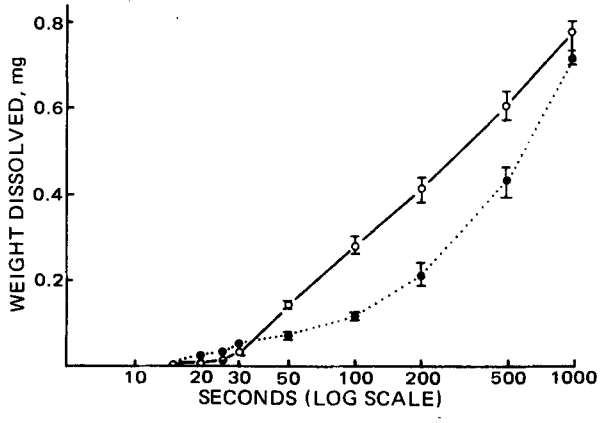

Figure 1—*Dissolution profiles for suspensions of Lot A prednisolone acetate (○) and Lot A prednisolone acetate containing 0.5% carboxymethylcellulose sodium (●) (n = 3; bars show extremes).*

[2] Coulter counter model TA II with a 200-μm aperture tube, Coulter Electronics, Hialeah, Fla.

[3] Isoton, Coulter Diagnostics, Miami Springs, Fla.

[4] Lot A was code 66010 MI 19636 and Lot B was code 66010 MI 70425, Schering Corp., Kenilworth, N.J.

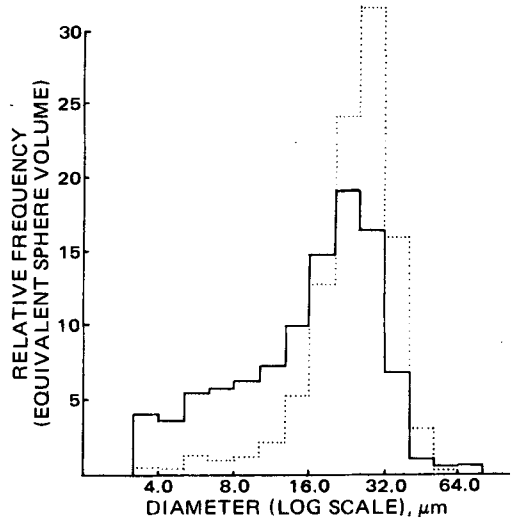

Figure 2—*Particle-size distributions of suspensions of Lot A prednisolone acetate (—) and Lot A prednisolone acetate containing 0.5% carboxymethylcellulose sodium (·····) (n = 3).*

prednisolone acetate dissolution. Dissolution of 0.4 mg required 500 sec when carboxymethylcellulose sodium was present, whereas an equal amount with no suspending agent dissolved in 200 sec.

Since dissolution characteristics are highly dependent on particle size, the particle-size distributions for the two suspensions were compared (Fig. 2). The distribution with the plain prednisolone acetate suspension showed an approximate mean diameter of 23 μm, and the suspensions containing 0.5% carboxymethylcellulose sodium had slightly larger particles with an approximate mean diameter of 29 μm. The major difference between the two distributions was the volume of fine particles found in each sample. The prednisolone acetate suspension without carboxymethylcellulose sodium had a considerably higher volume percent of fine particles when compared with the steroid suspension containing the suspending agent.

Dissolution experiments were run using 0.5 and 0.1% hydroxypropyl methylcellulose 4000 cps and 0.5% hydroxypropyl methylcellulose 50 cps as suspending agents (Fig. 3). The dissolution curves show that each of these suspending agents inhibited prednisolone acetate dissolution. The particle-size distributions were essentially identical to those in Fig. 2, where the suspensions containing suspending agents had somewhat larger mean particle diameters than the suspension without a suspending agent. The suspensions containing a suspending agent again contained fewer fine particles than the suspensions without one.

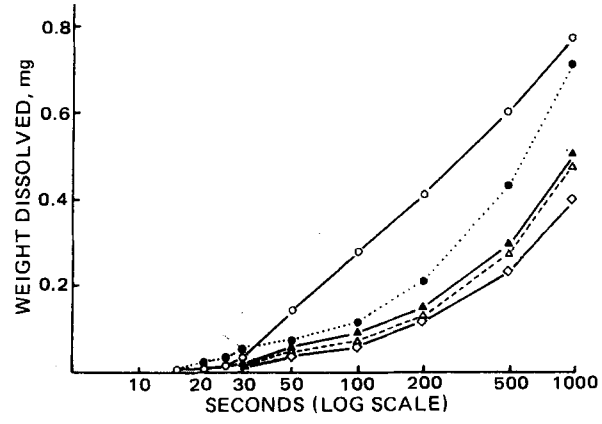

Figure 3—*Suspension dissolution profiles. Key: ○, Lot A prednisolone acetate; ●, Lot A prednisolone acetate containing 0.5% carboxymethylcellulose sodium; ▲, Lot A prednisolone acetate containing 0.5% hydroxypropyl methylcellulose 4000 cps; △, Lot A prednisolone acetate containing 0.1% hydroxypropyl methylcellulose 4000 cps; and ◇, Lot A prednisolone acetate containing 0.5% hydroxypropyl methylcellulose 50 cps.*

Table II—Particle-Size Analyses of Hydroxypropyl Methylcellulose Solutions and Lot A Prednisolone Acetate Suspensions (n = 3)

Hydroxypropyl Methylcellulose, 0.5%		Plain Prednisolone Acetate Suspension, 0.25%		Suspension of 0.25% Prednisolone Acetate Containing 0.5% Hydroxypropyl Methylcellulose		Particle-Size Diameter, μm
Percent Total Volume	Counts/ Channel	Percent Total Volume	Counts/ Channel	Percent Total Volume	Counts/ Channel	
Too few	1474	1.8	17,219	0.4	9,825	3.17
counts to	590	2.5	11,172	0.4	5,009	4.00
normalize data	269	4.2	7,879	1.1	3,309	5.04
	114	4.1	4,530	0.9	2,069	6.35
	59	4.5	4,530	0.9	2,069	6.35
	32	6.1	1,723	2.6	1,499	10.08
	20	10.1	1,388	6.1	1,695	12.70
	16	15.9	1,087	13.8	1,911	16.00
	9	22.5	769	24.6	1,693	20.20
	5	19.2	344	30.1	1,077	25.40
	2	7.3	70	15.1	297	32.00
	1	0.9	5	2.1	23	40.30
	1	0.1	0	0.8	4	50.80
	0	0.7	1	0.5	1	64.00
Total	2592	(99.9)	48,806	(99.9)	29,966	

The dissolution curves in Fig. 3 for Lot A show that all of the suspending agents retarded prednisolone acetate dissolution, with carboxymethylcellulose sodium having a lesser effect than hydroxypropyl methylcellulose.

Due to dilution with the large volume of the dissolution medium, the high viscosity of the suspension medium seemed to exert little or no effect on dissolution. Carboxymethylcellulose sodium was the most viscous suspension medium, and it showed the least dissolution retardation. The 0.5% carboxymethylcellulose sodium solutions showed a viscosity of 140 cps. Hydroxypropyl methylcellulose 50 cps, which showed the greatest dissolution retardation effect, was the least viscous suspending medium, with a 0.5% solution having a viscosity of 2.7 cps. Hydroxypropyl methylcellulose 4000 cps had a viscosity of 19.2 cps in a 0.5% solution. Figure 3 shows that the 0.1 and 0.5% solutions of hydroxypropyl methylcellulose 4000 cps had approximately the same retarding effects on prednisolone acetate; at least in this original concentration range, retardation was concentration independent.

The addition of a suspending agent was thought to contribute to particle-size increases, resulting in the dissolution inhibition. To determine the contribution of the suspending agents to the particle-size increase, a 0.5% hydroxypropyl methylcellulose 4000 cps solution was sized utilizing the electronic counter[2] population accessory. Prednisolone acetate suspensions with and without 0.5% hydroxypropyl methylcellulose 4000 cps and 0.5% solutions of hydroxypropyl methylcellulose 4000 cps were tested in the same manner. Exactly one-third of a milliliter of each solution or suspension was added to 170 ml of presaturated and filtered electrolyte solution in a 250-ml conical beaker. The percentages of relative volume and particle count for each channel were recorded (Table II).

As can be seen from Table II, the total and overall counts for the simple 0.5% hydroxypropyl methylcellulose solution after dilution were insignificant when compared to the counts for the prednisolone acetate suspension containing the same amount of suspending agent. Total counts for the 0.5% hydroxypropyl methylcellulose solution were approximately 2600, compared to 30,000 total counts for the prednisolone acetate suspension containing 0.5% hydroxypropyl methylcellulose. There were too few particles in the hydroxypropyl methylcellulose solution to calculate the percent total volume. Therefore, the presence of 0.5% hydroxypropyl methylcellulose does not in itself add counts or size to the suspension.

A comparison of the suspension containing no suspending agent and the suspension containing 0.5% hydroxypropyl methylcellulose 4000 cps was interesting. The total counts for the plain prednisolone acetate suspension (~48,000 counts) were much greater. Nevertheless, the number of counts in the larger channels (≥16 μm) was greater for the hydroxypropyl methylcellulose-containing suspension, especially in the 25.4- and 32-μm channels. The increased counts in the large channels account for the shift in the particle means for the relative volume distributions.

For particles less than 10.08 μm, the pure prednisolone acetate suspension had approximately twice the counts when compared with the suspension containing a suspending agent. This finding also was reflected in the relative volume percentage. The suspension without a suspending agent had ~17% of its total volume with particle sizes less than 10.08 μm, whereas the suspension containing a suspending agent had only 4% of its volume below 10.08 μm in particle size. These data substantiate the

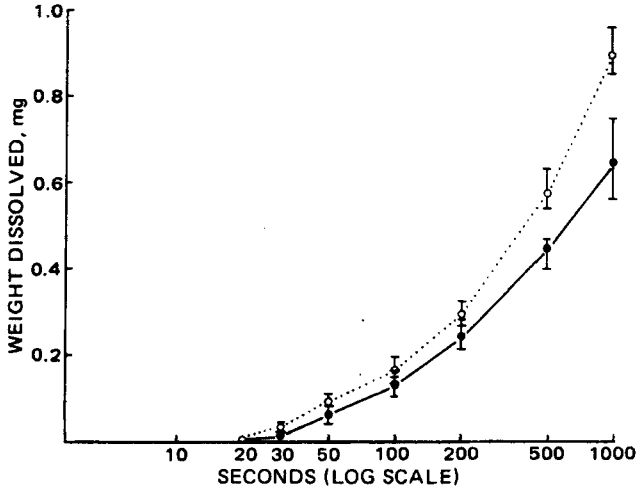

Figure 4—*Dissolution profiles for suspensions of Lot B prednisolone acetate (●) and Lot B prednisolone acetate containing 0.5% carboxymethylcellulose sodium (○).*

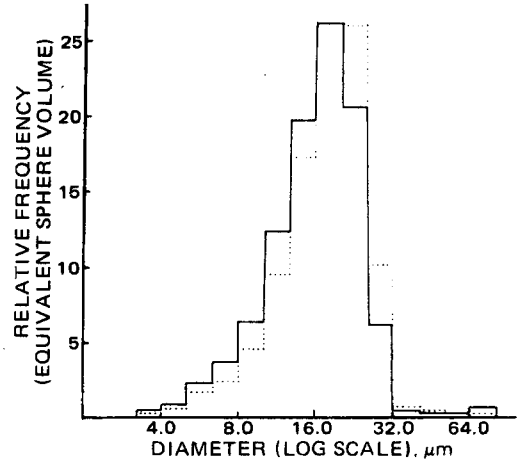

Figure 5—*Particle-size distribution of suspensions of Lot B prednisolone acetate (—) and Lot B prednisolone acetate containing 0.5% carboxymethylcellulose sodium (·····).*

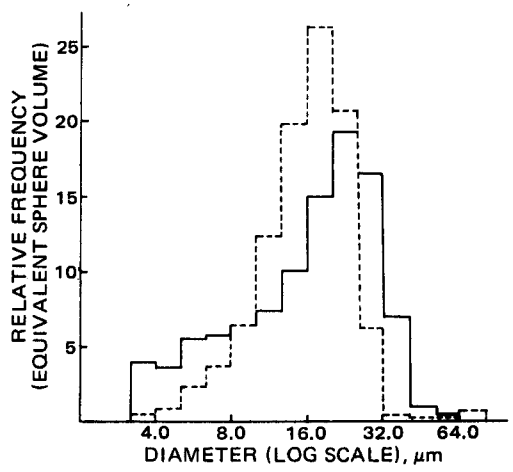

Figure 6—*Particle-size distributions of suspensions of Lot A (—) and Lot B (- - -) prednisolone acetate.*

idea that the suspending agent contributes to a particle distribution shift which, as will be demonstrated further, results in longer dissolution times for the steroid suspensions.

Lot A prednisolone acetate was exhausted at the end of these experiments. A new lot, Lot B, was obtained from the same supplier, and several experiments were repeated. The experimental conditions for Lot B were identical with those for Lot A.

The dissolution profiles for Lot B prednisolone acetate with and without 0.5% carboxymethylcellulose sodium are shown in Fig. 4. The 0.5% carboxymethylcellulose sodium did not inhibit dissolution. This finding is not consistent with previous dissolution data for Lot A prednisolone acetate, where carboxymethylcellulose sodium significantly inhibited steroid dissolution (Fig. 1). In view of this inconsistency, both lots were investigated further by differential scanning calorimetry, zeta-potential measurement, and particle-size distribution based on volume.

Pure prednisolone acetate from each lot (A and B) was studied with a differential scanning calorimeter at a heating rate of 40°/min. The thermograms showed no significant differences. Thus, the crystalline forms of each lot apparently were the same and polymorphic forms were not the cause of the dissolution differences.

The electromobilities of Lots A and B as determined with a zeta-meter were identical, indicating that the surface nature of the two lots was the same.

The size distributions based on volume for Lot B prednisolone acetate with and without 0.5% carboxymethylcellulose sodium are shown in Fig. 5. The presence of carboxymethylcellulose sodium caused a shift to the right on the volume distribution curve. The magnitude of the shift was much less pronounced, particularly in the area of fine particles, when compared with similar data for Lot A (Fig. 2). A further comparison of particle-size characteristics is shown in Fig. 6 where the particle-size distribution for Lots A and B prednisolone acetate are presented. These

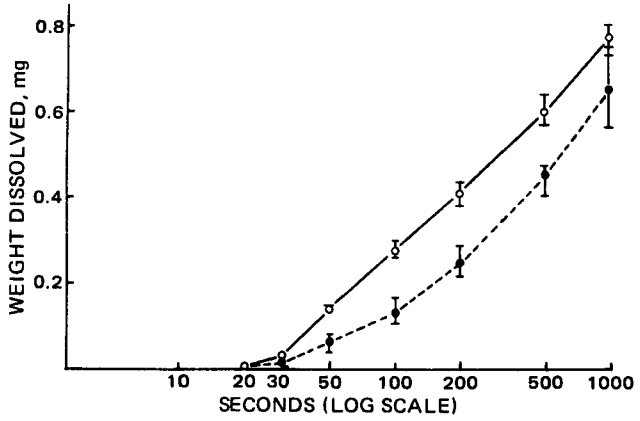

Figure 7—*Dissolution profiles for suspensions of Lot A (○) and Lot B (●) prednisolone acetate.*

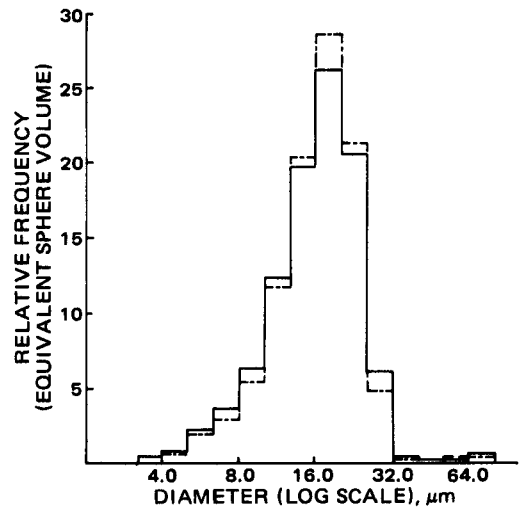

Figure 8—*Particle-size distributions of suspensions of Lot B prednisolone acetate (—) and Lot B prednisolone acetate containing 0.5% hydroxypropyl methylcellulose 4000 cps (- · -).*

data show that Lot A contained considerably more fine particles than did Lot B. In fact, 20% of the population for Lot A based on volume was ≤10 μm, whereas only 10% by volume of Lot B was in the same size range. Thus, the dissolution rate for Lot A was expected to exceed that for Lot B because of increased surface area. This rationalization was substantiated by comparing the dissolution profiles for Lots A and B. The dissolution data are shown in Fig. 7 where the initial dissolution rate for Lot A exceeded that for Lot B.

It is apparent that Lot A prednisolone acetate dissolved at a more rapid rate than Lot B (Fig. 7) because of particle-size differences (Fig. 6). Therefore, it is believed that carboxymethylcellulose sodium interacts with prednisolone acetate in some manner and that this interaction may have a twofold effect: (*a*) it might reduce the number of fine particles (≤10 μm) in suspension (dominant in Lot A), and (*b*) it might enhance the dissolution of larger prednisolone acetate particles (dominant in Lot B). With Lot A, where many fine particles exist, the removal of fine particles predominates and an apparent dissolution reduction occurs. With Lot B, there are fewer fine particles initially and an apparent prednisolone acetate dissolution increase occurs (Fig. 4) when carboxymethylcellulose sodium is present.

Unlike carboxymethylcellulose sodium, hydroxypropyl methylcellulose inhibited the dissolution of Lot B prednisolone acetate. This inhibition

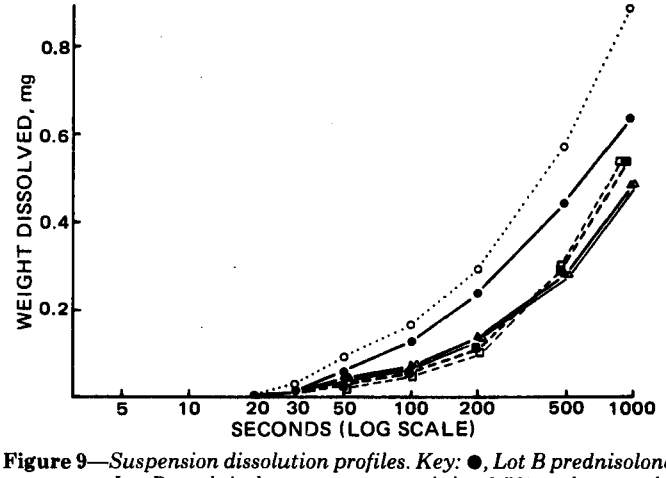

Figure 9—*Suspension dissolution profiles. Key: ●, Lot B prednisolone acetate; ○, Lot B prednisolone acetate containing 0.5% carboxymethylcellulose sodium; ▲, Lot B prednisolone acetate containing 0.5% hydroxypropyl methylcellulose 4000 cps; △, Lot B prednisolone acetate containing 0.5% hydroxypropyl methylcellulose 50 cps; ■, Lot B prednisolone acetate containing 0.1% hydroxypropyl methylcellulose 4000 cps; and □, Lot B prednisolone acetate containing 0.1% hydroxypropyl methylcellulose 50 cps; n = 3.*

was unrelated to the particle size. The size distributions for suspensions of Lot B prednisolone acetate with and without the presence of hydroxypropyl methylcellulose were almost identical (Fig. 8).

The dissolution profiles for Lot B prednisolone acetate suspensions are summarized in Fig. 9. The presence of hydroxypropyl methylcellulose in all concentrations and at all viscosities seemed to inhibit the dissolution of Lot B. This finding is similar to the results found in experiments with Lot A. As with Lot A, the degree of inhibition did not appear to depend on the original viscosity or concentration of hydroxypropyl methylcellulose used. The 0.1 and 0.5% hydroxypropyl methylcellulose 4000 cps and the 0.1 and 0.5% hydroxypropyl methylcellulose 50 cps all inhibited Lot B prednisolone acetate to approximately the same degree.

The agents studied are common suspending agents, and brand-to-brand variations in the dissolution of commercial prednisolone acetate products exist (5). Particle-size differences are not the only factors to consider when studying the variation of drug dissolution profiles. Other factors such as the method of manufacture (milling and order of milling and mixing) and aging may alter these results.

In conclusion, the common ionic suspending agent carboxymethylcellulose sodium acted in two ways. It seemed to alter the particle-size distribution by reducing the percentage of fine prednisolone acetate particles in suspension, and it enhanced prednisolone acetate dissolution. With Lot A prednisolone acetate, which contained a larger percentage of fine particles, the reduction of these fine particles was sufficient to exceed the concurrent dissolution rate increase. Therefore, the net result was decreased prednisolone acetate dissolution. But with Lot B, where the proportion of fine particles was small and there was no significant change in particle-size distribution, the dissolution enhancement properties of carboxymethylcellulose sodium predominated. Thus, the effects of carboxymethylcellulose sodium on prednisolone acetate dissolution were lot-to-lot dependent, with the main variable being the particle distribution of the powder.

Dissolution inhibition of the two lots by nonionic hydroxypropyl methylcellulose, which also can alter particle-size distribution, was independent of lot-to-lot variation. This inhibition might be due to the formation of a viscous diffusion layer similar to that described for methylcellulose (4). Since hydroxypropyl methylcellulose is used in many commercial prednisolone acetate suspensions, this finding should be considered by formulation scientists.

REFERENCES

(1) T. Bates, H. Rosenberg, and A. Tembo, *J. Pharm. Sci.* **62,** 2057 (1973).

(2) T. R. Bates, D. A. Lambert, and W. H. Johns, *ibid.*, **58,** 1468 (1969).

(3) M. Short, *ibid.*, **61,** 1732 (1972).

(4) I. Ullah and D. E. Cadwallader, *ibid.*, **60,** 1496 (1971).

(5) P. Finholt and S. Solvang, *ibid.*, **57,** 1322 (1968).

(6) S. Howard, J. Mauger, and L. Phusanti, *ibid.*, **66,** 557 (1977).

(7) V. A. Davydova; through *Chem. Abstr.*, **78,** 1283–99 (1973).

(8) S. Motola, "Abstracts, 17th National Meeting of the APhA Academy of Pharmaceutical Sciences," vol. 4, no. 2, Washington, D.C., 1974, p. 8.

(9) N. Shah and B. Sheth, *J. Pharm. Sci.*, **65,** 1618 (1976).

(10) A. C. Shah, C. B. Peot, and J. F. Ochs, *ibid.*, **62,** 671 (1973).

ACKNOWLEDGMENTS

The authors thank Schering Laboratories, Kenilworth, N.J., and Allergan Pharmaceuticals, Irvine, Calif., for donating chemicals and The Upjohn Co., Kalamazoo, Mich., for the use of their diffusion apparatus.

Corticosteroid Determination in Skin Preparations by a Reaction Rate Method

MICHAEL A. KOUPPARIS *, KEN M. WALCZAK ‡, and HOWARD V. MALMSTADT ‡x

Received March 19, 1979, from the **Laboratory of Analytical Chemistry, University of Athens, Athens, Greece,* and the ‡*School of Chemical Sciences, University of Illinois at Urbana-Champaign, Urbana, IL 61801.* Accepted for publication June 5, 1979.

Abstract □ A reaction rate method for the determination of betamethasone, betamethasone valerate, triamcinolone acetonide, and fluocinolone acetonide is described. The method is based on a modification of the widely accepted blue tetrazolium reaction. Analysis times of 30–70 sec are required. Relative standard deviations of 0.3–1.9% are obtained, and the analytical working curves are linear. Analysis of pharmaceutical skin preparations by the new method gave results that correlated well with the time-consuming standard equilibrium method. Analysis of betamethasone and betamethasone valerate mixtures by measuring absorbance values at two different times was performed also.

Keyphrases □ Corticosteroids—analysis, skin preparations, reaction rate method □ Betamethasone—analysis, skin preparations, reaction rate method □ Betamethasone valerate—analysis, skin preparations, reaction rate method □ Triamcinolone acetonide—analysis, skin preparations, reaction rate method □ Fluocinolone acetonide—analysis, skin preparations, reaction rate method □ Skin preparations—analysis, corticosteroids, reaction rate method

A widely used spectrophotometric method for the determination of corticosteroid purity and the potency of dosage forms containing such steroids is based on the blue tetrazolium reaction (1). Blue tetrazolium (I), 3,3′-(3,3′-dimethoxy[1,1′-biphenyl]-4,4′-diyl)bis[2,5-diphenyl-2*H*-tetrazolium] dichloride, in an alcoholic solution of a strong base oxidizes the α-ketol group on the C_{17} side chain and is reduced quantitatively to red formazan, which is measured spectrophotometrically at 525 nm. This absorbance, measured a specified time after mixing of the sample with I and the base, is compared to the absorbances of a blank and of a standard solution to quantitate the steroid concentration in the sample. This procedure is the basis for the official NF (2) and USP (3) method.

BACKGROUND

Extensive investigations (4–13) of the reaction conditions established that the analytical procedure is subject to many variables such as temperature; solvent; concentrations of base, water, and tetrazolium; steric configuration of the corticosteroid molecule; light; and air oxygen. The effect of these variables is minimized by analyzing reagent blanks, standards, and samples concurrently. In addition to these problems, which decrease the precision and the accuracy of the official equilibrium method, long measurement times of 30–470 min are necessary for maximum absorbance (10).

Under the conditions usually employed in the assay, where the steroid

0022-3549/79/1200-1479$01.00/0

© 1979, American Pharmaceutical Association

was unrelated to the particle size. The size distributions for suspensions of Lot B prednisolone acetate with and without the presence of hydroxypropyl methylcellulose were almost identical (Fig. 8).

The dissolution profiles for Lot B prednisolone acetate suspensions are summarized in Fig. 9. The presence of hydroxypropyl methylcellulose in all concentrations and at all viscosities seemed to inhibit the dissolution of Lot B. This finding is similar to the results found in experiments with Lot A. As with Lot A, the degree of inhibition did not appear to depend on the original viscosity or concentration of hydroxypropyl methylcellulose used. The 0.1 and 0.5% hydroxypropyl methylcellulose 4000 cps and the 0.1 and 0.5% hydroxypropyl methylcellulose 50 cps all inhibited Lot B prednisolone acetate to approximately the same degree.

The agents studied are common suspending agents, and brand-to-brand variations in the dissolution of commercial prednisolone acetate products exist (5). Particle-size differences are not the only factors to consider when studying the variation of drug dissolution profiles. Other factors such as the method of manufacture (milling and order of milling and mixing) and aging may alter these results.

In conclusion, the common ionic suspending agent carboxymethylcellulose sodium acted in two ways. It seemed to alter the particle-size distribution by reducing the percentage of fine prednisolone acetate particles in suspension, and it enhanced prednisolone acetate dissolution. With Lot A prednisolone acetate, which contained a larger percentage of fine particles, the reduction of these fine particles was sufficient to exceed the concurrent dissolution rate increase. Therefore, the net result was decreased prednisolone acetate dissolution. But with Lot B, where the proportion of fine particles was small and there was no significant change in particle-size distribution, the dissolution enhancement properties of carboxymethylcellulose sodium predominated. Thus, the effects of carboxymethylcellulose sodium on prednisolone acetate dissolution were lot-to-lot dependent, with the main variable being the particle distribution of the powder.

Dissolution inhibition of the two lots by nonionic hydroxypropyl methylcellulose, which also can alter particle-size distribution, was independent of lot-to-lot variation. This inhibition might be due to the formation of a viscous diffusion layer similar to that described for methylcellulose (4). Since hydroxypropyl methylcellulose is used in many commercial prednisolone acetate suspensions, this finding should be considered by formulation scientists.

REFERENCES

(1) T. Bates, H. Rosenberg, and A. Tembo, *J. Pharm. Sci.* **62,** 2057 (1973).

(2) T. R. Bates, D. A. Lambert, and W. H. Johns, *ibid.*, **58,** 1468 (1969).

(3) M. Short, *ibid.*, **61,** 1732 (1972).

(4) I. Ullah and D. E. Cadwallader, *ibid.*, **60,** 1496 (1971).

(5) P. Finholt and S. Solvang, *ibid.*, **57,** 1322 (1968).

(6) S. Howard, J. Mauger, and L. Phusanti, *ibid.*, **66,** 557 (1977).

(7) V. A. Davydova; through *Chem. Abstr.*, **78,** 1283–99 (1973).

(8) S. Motola, "Abstracts, 17th National Meeting of the APhA Academy of Pharmaceutical Sciences," vol. 4, no. 2, Washington, D.C., 1974, p. 8.

(9) N. Shah and B. Sheth, *J. Pharm. Sci.*, **65,** 1618 (1976).

(10) A. C. Shah, C. B. Peot, and J. F. Ochs, *ibid.*, **62,** 671 (1973).

ACKNOWLEDGMENTS

The authors thank Schering Laboratories, Kenilworth, N.J., and Allergan Pharmaceuticals, Irvine, Calif., for donating chemicals and The Upjohn Co., Kalamazoo, Mich., for the use of their diffusion apparatus.

Corticosteroid Determination in Skin Preparations by a Reaction Rate Method

MICHAEL A. KOUPPARIS *, KEN M. WALCZAK ‡, and HOWARD V. MALMSTADT ‡x

Received March 19, 1979, from the **Laboratory of Analytical Chemistry, University of Athens, Athens, Greece,* and the ‡*School of Chemical Sciences, University of Illinois at Urbana-Champaign, Urbana, IL 61801.* Accepted for publication June 5, 1979.

Abstract □ A reaction rate method for the determination of betamethasone, betamethasone valerate, triamcinolone acetonide, and fluocinolone acetonide is described. The method is based on a modification of the widely accepted blue tetrazolium reaction. Analysis times of 30–70 sec are required. Relative standard deviations of 0.3–1.9% are obtained, and the analytical working curves are linear. Analysis of pharmaceutical skin preparations by the new method gave results that correlated well with the time-consuming standard equilibrium method. Analysis of betamethasone and betamethasone valerate mixtures by measuring absorbance values at two different times was performed also.

Keyphrases □ Corticosteroids—analysis, skin preparations, reaction rate method □ Betamethasone—analysis, skin preparations, reaction rate method □ Betamethasone valerate—analysis, skin preparations, reaction rate method □ Triamcinolone acetonide—analysis, skin preparations, reaction rate method □ Fluocinolone acetonide—analysis, skin preparations, reaction rate method □ Skin preparations—analysis, corticosteroids, reaction rate method

A widely used spectrophotometric method for the determination of corticosteroid purity and the potency of dosage forms containing such steroids is based on the blue tetrazolium reaction (1). Blue tetrazolium (I), 3,3′-(3,3′-dimethoxy[1,1′-biphenyl]-4,4′-diyl)bis[2,5-diphenyl-2*H*-tetrazolium] dichloride, in an alcoholic solution of a strong base oxidizes the α-ketol group on the C_{17} side chain and is reduced quantitatively to red formazan, which is measured spectrophotometrically at 525 nm. This absorbance, measured a specified time after mixing of the sample with I and the base, is compared to the absorbances of a blank and of a standard solution to quantitate the steroid concentration in the sample. This procedure is the basis for the official NF (2) and USP (3) method.

BACKGROUND

Extensive investigations (4–13) of the reaction conditions established that the analytical procedure is subject to many variables such as temperature; solvent; concentrations of base, water, and tetrazolium; steric configuration of the corticosteroid molecule; light; and air oxygen. The effect of these variables is minimized by analyzing reagent blanks, standards, and samples concurrently. In addition to these problems, which decrease the precision and the accuracy of the official equilibrium method, long measurement times of 30–470 min are necessary for maximum absorbance (10).

Under the conditions usually employed in the assay, where the steroid

0022-3549/79/1200-1479$01.00/0

© 1979, American Pharmaceutical Association

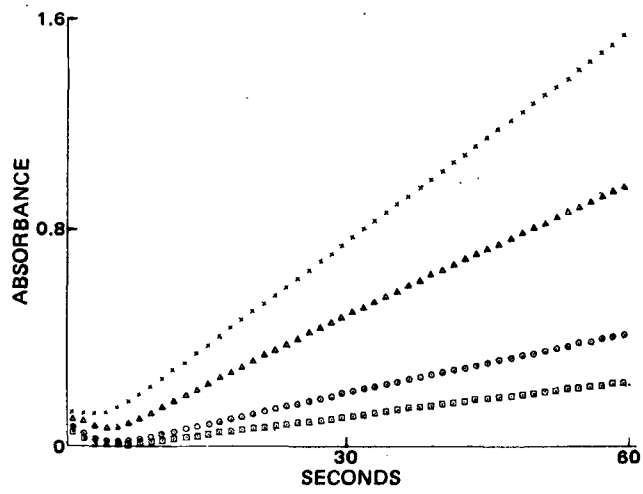

Figure 1—*Effect of tetramethylammonium hydroxide concentration (□, 0.5%; ○, 1%; △, 3%; and ×, 5%) on the reaction rate for 14 mg of betamethasone/100 ml.*

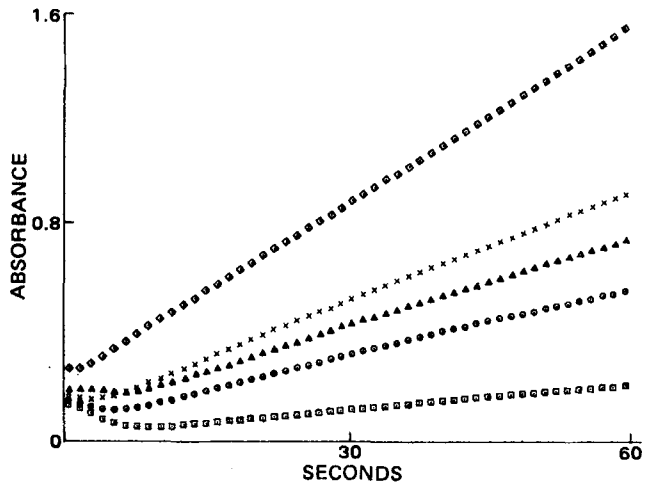

Figure 3—*Reaction rate curves for betamethasone concentrations of 2.00 (□), 6.00 (○), 8.00 (△), 10.0 (×), and 14.0 (◇) mg/100 ml using 5% tetramethylammonium hydroxide.*

is present at a much lower concentration than that of the base and the I reagent, the formazan appearance rate exhibits a first-order dependency on the steroid concentration (6). This behavior is of potential analytical utility because the reaction rate methods (14) are time saving and less sensitive to the reaction variables. Oteiza *et al.* (15), using the stopped-flow technique, developed a new reaction rate procedure for hydrocortisone determination which decreases the analysis time and increases the precision and accuracy considerably.

In this paper, the application of the reaction rate procedure is extended to betamethasone, betamethasone valerate, triamcinolone acetonide, and fluocinolone acetonide. Results obtained by the reaction rate method are compared with the USP–NF method for pharmaceutical skin preparations. The same technique was used to analyze betamethasone and betamethasone valerate mixtures.

EXPERIMENTAL

Apparatus—The apparatus used for the reaction rate method was the automated system described previously (16, 17). This system provided for automatic aliquoting and mixing of the sample and reagent and for delivery of the mixed solution into the measurement cell (2-cm path length, 60-μl volume) by a stopped-flow unit incorporated in a modular spectrophotometer. Automation was achieved by a minicomputer[1] with a 16 K memory. Associated peripheral devices were a teletype, a dual magnetic tape I/O, a linear printer, and an oscilloscope display.

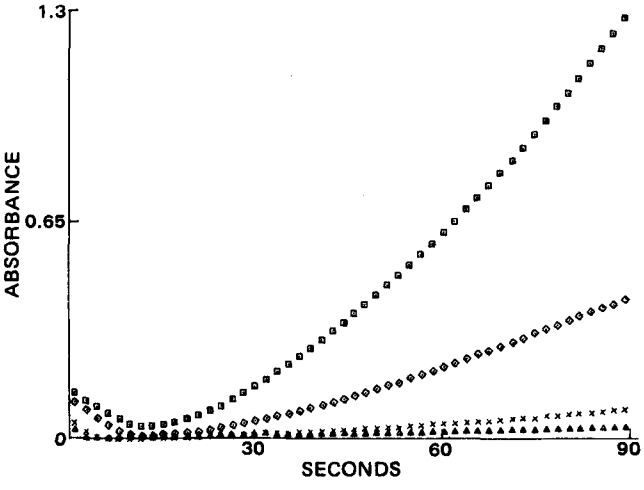

Figure 2—*Effect of tetramethylammonium hydroxide concentration (△, 0.5%; ×, 1%; ◇, 3%; and □, 5%) on the reaction rate for 30.0 mg of betamethasone valerate/100 ml.*

Several programs have been developed for the investigative or the routine operation mode. The investigative mode provides flexible data-taking options, oscilloscope display, data printing, and extraction of rate or equilibrium information from various portions of the absorbance–time curve. It generally is used for initial characterization or fundamental studies. The routine mode provides sequential analyses of standards and samples placed on a turntable and printing of a working curve and sample values. Either rate or equilibrium methods may be selected. An automated computer-controlled solution-handling system utilizing weights of solution can be used in conjunction with this system for the preparation of standards and samples (18). A ratio-recording spectrophotometer[2] was used for the equilibrium measurements.

Reagents—Corticosteroid stock solutions, 20 mg/100 ml, were prepared weekly by dissolving 20 mg of betamethasone[3], betamethasone valerate[3], triamcinolone acetonide[4], or fluocinolone acetonide[5] in 100 ml of 95% ethanol. A 0.5% blue tetrazolium[6] solution was prepared by dissolving 0.5 g of blue tetrazolium in 100 ml of absolute methanol. This solution was protected from light. A 5% solution of tetramethylammonium hydroxide was prepared by dissolving 2.5 g of tetramethylammonium hydroxide pentahydrate[6] in 50 ml of USP reagent quality absolute ethanol[7]. Different base concentrations were prepared from the 5% solution by appropriate dilution with absolute ethanol.

The standard corticosteroid solutions were prepared daily by adding 2 ml of the blue tetrazolium solution to an appropriate volume of the stock corticosteroid solution and diluting to 10 ml with 95% ethanol. Standard betamethasone and betamethasone valerate solutions were prepared similarly.

Sample Preparation—Samples were prepared from the pharmaceutical preparations—lotions, creams, and ointments—by the column chromatographic procedure of Graham *et al.* (19), in which the corticosteroid is held on the acetonitrile–diatomaceous earth column while decomposition products and interfering substances are removed by *n*-heptane. The corticosteroid was eluted from the column with chloroform. The eluate was evaporated carefully to dryness, and the residue was dissolved in 95% ethanol and diluted to 25 ml. A 5-ml aliquot was added to 2 ml of blue tetrazolium solution and diluted to 10 ml with 95% ethanol. This 10-ml solution is referred to here as the sample. The column could be readily modified to include acidic, basic, or neutral aqueous trap layers when necessary. Approximately 30 min was routinely required to prepare an interference-free sample for analysis.

Equilibrium Procedure—The equilibrium procedures were the official procedures given in USP XIX and NF XIV. The absorbance was measured at a specified time (45–90 min) after the standards and samples

[1] PDP 8/f, Digital Equipment Corp.

[2] Model 721, GCA/McPherson, Acton, MA 01720.
[3] Schering Co.
[4] Squibb Inc.
[5] Syntex Lab.
[6] Sigma Chemical Co., St. Louis, MO 63178.
[7] U.S. Industrial Chemicals Co., Tuscola, IL 61953.

Table I—Reaction Rates for Different Measurement Times for Triamcinolone Acetonide [a]

Measurement Time, sec	Rate, Δmamp/sec[b]	*RSD*, %
5.0	12.1	1.7
10.0	12.0	1.0
15.0	12.0	0.6
20.0	11.8	0.4
25.0	11.8	0.8

[a] Analysis of 5 mg/100-ml standard with 10-sec delay time. [b] Average of five determinations on a single sample.

Table II—Results Used for Corticosteroid Reaction Rate Working Curves

Corticosteroid	Concentration, mg/100 ml	Rate, Δmamp/sec[a]	*RSD*, %
Betamethasone[b]	2.00	7.7	1.5
	5.00	11.1	1.1
	10.0	16.3	1.6
	15.0	22.3	0.7
Betamethasone valerate[c]	10.0	6.9	1.2
	15.0	10.5	0.6
	20.0	14.5	0.9
	30.0	22.0	0.9
Triamcinolone acetonide[d]	1.00	2.3	1.4
	3.00	6.8	0.4
	5.00	11.4	0.7
	7.00	16.2	0.3
	10.0	23.6	0.7
Fluocinolone acetonide[e]	0.50	3.1	1.9
	1.00	6.2	1.7
	2.50	15.6	0.8
	3.50	22.5	0.8

[a] Average of five determinations on a single sample. [b] Working curve: slope = 1.11, intercept = 5.4, and r = 0.9991. [c] Working curve: slope = 0.758, intercept = −0.7, and r = 0.9998. [d] Working curve: slope = 2.37, intercept = −0.2, and r = 0.9996. [e] Working curve: slope = 6.44, intercept = −0.2, and r = 0.9995.

were mixed with the two reagents, and the mixtures were allowed to stand in the dark.

Reaction Rate Procedure—One hundred microliters each of the tetramethylammonium hydroxide solution and the appropriate standard or sample were sampled by the automatic syringes of the stopped-flow module (17). The syringes in the module then drove the solutions through the mixer and transferred the mixed solution to the observation cell. The change in absorbance was automatically monitored at 525 nm during the selected measurement time and used to construct a rate curve and a working curve or to provide quantitative concentration information for the pharmaceutical skin preparations.

The solutions and spectrophotometer were at ambient temperature in a temperature-controlled laboratory maintained at a nominal temperature of 25°.

RESULTS AND DISCUSSION

As shown in Fig. 1, the reaction rate was strongly dependent on the base concentration. The appropriate base strength could be chosen to provide the sensitivity needed at a minimum cost per analysis. Good sensitivities and precisions could be obtained in relatively short measurement times with the 5% base. The effect of base concentration was more critical for corticosteroid-17 ester reactions where the ester hydrolysis was a prerequisite. As shown in Fig. 2, in the betamethasone valerate reaction, the hydrolysis step appeared prior to the reaction process. Attempts to provide ester hydrolysis before the reaction with blue tetrazolium showed that both the corticosteroid and its esters were partially decomposed after contact with tetramethylammonium hydroxide.

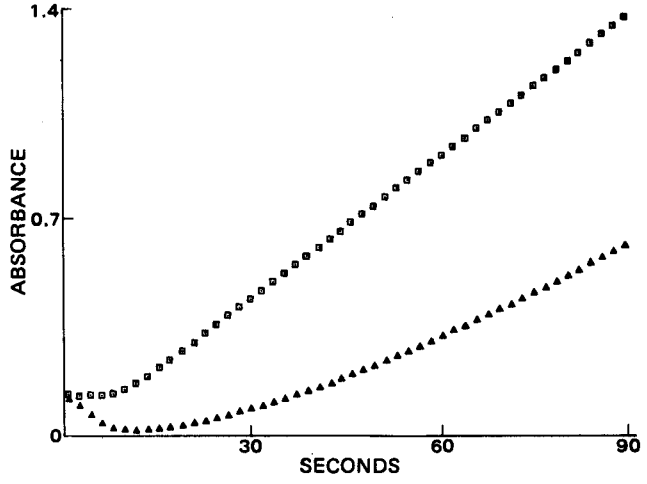

Figure 4—*Reaction rate curves for 10 mg of betamethasone/100 ml (□) and for 15 mg of betamethasone valerate/100 ml (△).*

The reaction rate curves for the four standards of betamethasone with 5% base over 60 sec are shown in Fig. 3. The reaction curves are sufficiently straight lines, as a result of the first-order conditions. A 10-sec delay after mixing was employed before the measurement period for betamethasone, triamcinolone acetonide, and fluocinolone acetonide. This time allowed for any nonreproducible behavior near the beginning of the reaction to terminate. For betamethasone valerate, a 40-sec delay was needed for completion of hydrolysis. The optimum measurement times were determined by using these delay times and varying the rate measurement over various periods. The results for triamcinolone acetonide are shown in Table I. The best reproducibility, ~0.4%, was obtained with a 20-sec measurement time. Similar results were obtained for betamethasone and fluocinolone acetonide. For betamethasone valerate, a 30-sec measurement time was optimum.

The results obtained for the working curves are shown in Table II. Good linearity was obtained for concentrations of 2–15 mg/100 ml for betamethasone, 10–30 mg/100 ml for betamethasone valerate, 1–10 mg/100 ml for triamcinolone acetonide, and 0.5–3.5 mg/100 ml for fluocinolone acetonide. The relative standard deviations varied from 0.3 to 1.9%. The working curves could be generated in ~8 min for triplicate analyses on each standard. This period is more than a factor of 10 less than the time required to prepare a working curve for the equilibrium method where single determinations on a standard, sample, and blank are generally performed (2, 3). Thus, the total analysis time, including sample prepa-

Table III—Corticosteroid Assay Results from Commercial Skin Preparations

Preparation		Concentration, %	Product Type	Assay, % of declared		
				Reaction Rate[a]	Equilibrium[b]	Difference[c]
Betamethasone valerate	1	0.1	Lotion	76.0	75.2	+0.8
	2	0.1	Lotion	74.8	75.5	−0.7
	3	0.01	Cream	94.2	95.0	−0.8
	4	0.01	Cream	90.8	90.0	+0.8
Triamcinolone acetonide	5	0.1	Ointment	90.9	91.8	−0.9
	6	0.5	Ointment	94.2	96.2	−2.0
	7	0.5	Cream	91.5	90.0	+1.5
	8	0.1	Cream	79.9	82.1	−2.2
Fluocinolone acetonide	9	0.025	Cream	97.4	98.9	−1.5
	10	0.025	Cream	95.2	95.0	+0.2
	11	0.025	Cream	95.1	94.6	+0.5
	12	0.01	Cream	97.8	98.5	−0.7

[a] Average of three determinations on a single sample. [b] Average of two determinations on a single sample. [c] Percent of reaction rate minus percent by equilibrium.

Table IV—Analysis of Betamethasone and Betamethasone Valerate Mixtures

Steroid Taken, mg/100 ml		Steroid Found[a], mg/100 ml	
Betamethasone	Betamethasone Valerate	Betamethasone	Betamethasone Valerate
4.00	30.0	4.41	27.5
6.00	25.0	6.13	24.4
8.00	20.0	7.61	21.8
10.0	15.0	9.30	17.5
12.0	5.0	12.5	4.3

[a] Average of three determinations on a single sample where $K_B = 4.494$ (intercept = −0.006 and $r = 0.9994$), $K_{BV} = 1.078$ (intercept = +0.02 and $r = 0.9998$), $K'_B = 8.443$ (intercept = −0.07 and $r = 0.9994$), and $K'_{BV} = 3.379$ (intercept = −0.04 and $r = 0.998$).

ration, can be reduced from over 2 hr using the equilibrium procedure to slightly over 30 min with the reaction rate procedure. The addition of acid to stop the very slow reaction, used in equilibrium procedures for betamethasone valerate and triamcinolone acetonide, is also unnecessary. Table III shows results obtained on a series of commercial lotions, creams, and ointments by the new reaction rate method and by the official method for steroid analysis. Good agreement exists between the two methods (differences of 0.2–2.2%).

The difference in the betamethasone and betamethasone valerate reaction rates can be used for analyzing mixtures of these closely related steroids. Betamethasone valerate, being an ester, has a relatively slow reaction rate due to the hydrolysis step. Figure 4 shows reaction curves for equivalent quantities of the two steroids. For the analysis of mixtures, the method of proportional equations (20) was employed. In a reacting mixture containing both steroids, a common product, the formazan, was produced by the two simultaneous processes. Although the kinetics of formazan generation in ester reaction are complex and not first order, absorbance at a constant reaction time is directly proportional to the initial ester concentration. Therefore, the method of proportional equations can be used to analyze mixtures of betamethasone and betamethasone valerate. The absorbance, which is specific for the product, is thus established at any time by:

$$A = K_B B + K_{BV} BV \qquad \text{(Eq. 1)}$$

where A is the absorbance at 525 nm; B and BV are the initial concentrations of betamethasone and betamethasone valerate, respectively; and K_B and K_{BV} are the experimental slopes of absorbance *versus* betamethasone and betamethasone valerate concentrations, respectively.

Measurement of absorbance values at a shorter time, t, and at a longer time, t', allows the formulation of two equations, which can be solved simultaneously to yield values for B and BV. The experimental factors K_B and K_{BV} for time t and K'_B and K'_{BV} for time t' were calculated by measuring absorbance values for standard steroid solutions. For this system, 30- and 50-sec times were appropriate. Analysis of binary mixtures containing 4–12 mg/100 ml of betamethasone and 30–5 mg/100 ml of betamethasone valerate were carried out (Table IV).

The method was also applied to an aged 0.1% betamethasone valerate lotion (a year after the expiration date). Only 67.5% of betamethasone valerate was present, and 8.3% was hydrolyzed to betamethasone. Decomposition of the rest must be assumed.

These results were obtained on an automatic stopped-flow spectrophotometric system with several features to ensure high reliability in its measurements. A beam splitter and a reference detector were employed to correct for light source fluctuations (16). The stopped-flow module provided precisions better than 0.1% *RSD* for the aliquoting, mixing, and transferring of solutions to the 2-cm observation cell. The entire system was controlled by a minicomputer, eliminating most manual steps required for investigative or routine use. Finally, the rapid analysis time and excellent results recommended this system for routine analytical applications.

REFERENCES

(1) W. J. Mader and R. R. Buck, *Anal. Chem.*, **24**, 666 (1952).

(2) "The National Formulary," 14th ed., Mack Publishing Co., Easton, Pa., 1975, p. 976.

(3) "The United States Pharmacopeia," 19th rev., Mack Publishing Co., Easton, Pa., 1975, p. 622.

(4) W. Nowaczynski, M. Goldner, and J. Genest, *J. Lab. Clin. Med.*, **45**, 818 (1955).

(5) R. O. Rechnagel and M. Litteria, *ibid.*, **48**, 463 (1956).

(6) D. E. Guttman, *J. Pharm. Sci.*, **55**, 919 (1966).

(7) C. A. Johnson, R. King, and C. Vickers, *Analyst*, **85**, 714 (1960).

(8) P. Ascione and C. Fogelin, *J. Pharm. Sci.*, **52**, 709 (1963).

(9) J. J. Callahan, F. Litterio, E. Britt, B. D. Rosen, and J. Owens, *ibid.*, **51**, 333 (1962).

(10) R. E. Graham, E. R. Biehl, C. T. Kenner, G. H. Luttrell, and D. L. Middleton, *ibid.*, **64**, 226 (1975).

(11) F. M. Kunze and J. S. Davis, *ibid.*, **53**, 1259 (1964).

(12) R. E. Graham, P. A. Williams, and C. T. Kenner, *ibid.*, **59**, 1152 (1970).

(13) R. E. Graham, E. R. Biehl, and C. T. Kenner, *ibid.*, **66**, 966 (1977).

(14) H. V. Malmstadt, E. A. Cordos, and C. J. Delaney, *Anal. Chem.*, **44**, 26A (1972).

(15) R. M. Oteiza, D. L. Krottinger, M. S. McCracken, and H. V. Malmstadt, *ibid.*, **49**, 1586 (1977).

(16) K. R. O'Keefe and H. V. Malmstadt, *ibid.*, **47**, 707 (1975).

(17) D. L. Krottinger, M. S. McCracken, and H. V. Malmstadt, *Am. Lab.*, **9**, 51 (1977).

(18) B. W. Renoe, K. R. O'Keefe, and H. V. Malmstadt, *Anal. Chem.*, **48**, 661 (1976).

(19) R. E. Graham, P. A. Williams, and C. T. Kenner, *J. Pharm. Sci.*, **59**, 1472 (1970).

(20) R. G. Garmon and C. N. Reilley, *Anal. Chem.*, **34**, 600 (1962).

ACKNOWLEDGMENTS

Supported in part by Grant NIGMS 21984-04 from the Department of Health, Education, and Welfare.

The authors thank Schering, Squibb, and Syntex Corporations for the standards and pharmaceutical skin preparations used.

Effect of Heparin Injection on Plasma Protein Binding of Bilirubin and Salicylate in Rats

ULF W. WIEGAND and GERHARD LEVY ˣ

Received March 12, 1979, from the *Department of Pharmaceutics, School of Pharmacy, State University of New York at Buffalo, Amherst, NY 14260.* Accepted for publication June 7, 1979.

Abstract □ Intravenous heparin injection significantly increased the free bilirubin and salicylate fractions in the plasma of rats. This effect occurred within 2 min after injection of 500 U of heparin/kg and lasted for 15–45 min (bilirubin) or for >45 min (salicylate). *In vitro* addition of heparin to plasma had no quantitatively significant effect on the protein binding of bilirubin and salicylate. The *in vivo* effect of heparin on protein binding was reversible by treating the plasma with activated charcoal, a procedure known to remove fatty acids from albumin. Since protein binding affects the pharmacokinetic characteristics and the pharmacological activity of drugs, the heparin–drug interaction may have significant clinical implications. Use of heparinized plasma for exchange transfusion in the treatment of neonatal jaundice may be hazardous.

Keyphrases □ Heparin—effect on plasma protein binding of bilirubin and salicylate, rats □ Anticoagulants—heparin, effect on plasma protein binding of bilirubin and salicylate, rats □ Bilirubin—plasma protein binding, effect of heparin, rats □ Salicylate—plasma protein binding, effect of heparin, rats

Heparin is a widely used injectable anticoagulant. It is not only administered for direct therapeutic purposes but also as a concomitant of blood exchange transfusions and to facilitate hemodialysis. There have been reports that heparin injection or infusion decreases the plasma or serum protein binding of endogenous substances such as triiodothyronine (1), of the neutral drugs digoxin and digitoxin (2), and of the basic drug propranolol (3). On the other hand, the plasma protein binding of warfarin, a weak acid, has been reported to increase greatly after heparin injection (4).

Plasma protein binding can have a pronounced effect on the pharmacokinetic characteristics and pharmacological activity of drugs that are normally extensively bound (5). Sudden displacement of such drugs or of a potentially toxic endogenous substance from plasma protein binding sites could have serious consequences (6, 7). Heparin effects on plasma protein binding, if not recognized and accounted for, may also influence pharmacokinetic and toxicological findings in animals. It is desirable, therefore, to assess the magnitude, time course, dose dependence, and mechanism of the heparin effect on the plasma protein binding of important drugs and endogenous substances.

In this investigation, the effect of heparin injection on the plasma protein binding of bilirubin and salicylate was determined as a function of time in rats. Bilirubin was selected because its total (sum of free and bound) concentration in plasma is often used as a diagnostic index of liver function; a decrease in the protein binding of this heme pigment causes a decrease of total concentration (6, 7) and may lead to erroneous clinical interpretations.

Unconjugated hyperbilirubinemia in neonates is often treated with exchange transfusions of heparinized blood (8, 9); a displacement of protein-bound bilirubin during this procedure may be hazardous. Salicylic acid was employed in this study as a representative and widely used weakly acidic drug. Its binding to plasma proteins is affected by age and disease (10, 11), and there are indications that its pharmacological effect is a function of the free drug concentration (12).

Previous investigations of the effect of heparin injection on plasma protein binding of drugs revealed a strong correlation between the change in protein binding and the concentration of free fatty acids (2, 3). It has been suggested, therefore, that the heparin effect is the result of drug displacement from plasma protein binding sites by free fatty acids whose concentration in plasma has been elevated due to the increased lipoprotein lipase activity caused by heparin administration (2, 3). Fatty acids adsorbed on serum albumin can be removed by treatment with activated charcoal (13). This treatment was employed to determine if heparin-induced changes in the plasma protein binding of bilirubin and salicylate are reversible upon removal of fatty acids (and possibly other bound substances) from plasma proteins.

EXPERIMENTAL

The effect of heparin injection on the plasma protein binding of bilirubin as a function of time was determined by administering 200 or 500 U of heparin/kg[1] or an equal volume of saline solution by rapid intravenous injection to male Sprague–Dawley rats[2] weighing 300–325 g and maintained on a standard diet[3]. The solutions were injected into the right jugular vein through a cannula implanted 1 day earlier (14). Crossover experiments were carried out 2 weeks later.

Mainstream blood samples (0.7–0.8 ml) were withdrawn into a plastic syringe[4] through one outlet of a three-way stopcock as described previously (14), except that the cannulas were filled with saline solution rather than with heparin between blood withdrawals. The blood samples were immediately transferred to heparinized glass capillary tubes[5], which were centrifuged for plasma separation. These blood withdrawals were made before injection and 5, 10, 15, and 45 min after injection.

In a subsequent study on other rats, blood was collected before and 2, 3, and 4 min after injection. The jugular cannulas of some rats did not remain patent for 2 weeks. These animals were recannulated on the left side 1 day before the crossover study.

An aqueous bilirubin[6] solution was prepared by dissolving the pigment in a small volume of distilled water with the aid of a few drops of 2.5 *N* NaOH and adding sufficient distilled water and 0.5 *N* HCl to yield a pH 7.8–8.0 solution containing 6 mg of bilirubin/ml. The solution was always freshly prepared and protected from light. Five microliters of this solution was added to 300 μl of plasma to produce a plasma bilirubin concentration of 10 mg/100 ml. The free bilirubin fraction in plasma was determined in triplicate by the peroxidase-catalyzed reaction rate method (6, 15). The reaction time was always 2 min.

The effect of heparin injection on the plasma protein binding of salicylate was studied in another group of rats, using the same *in vivo* tech-

[1] Heparin sodium injection USP, 1000 U/ml, from beef lung, The Upjohn Co., Kalamazoo, Mich.
[2] Blue Spruce Farms, Altamont, N.Y.
[3] Charles River formula 4RF.
[4] Plastipak, 1 cc TB, Becton Dickinson Co., Rutherford, N.J.
[5] Red Tip Caraway, HR1 8889-306000, Sherwood Medical Industries, St. Louis, Mo.
[6] Crystalline bilirubin from bovine gallstones, Sigma Chemical Co., St. Louis, Mo.

0022-3549/79/1200-1483$01.00/0
© 1979, American Pharmaceutical Association

Table I—Effect of Heparin Injection, 500 U/kg, on Plasma Protein Binding of Bilirubin in Rats

Minutes	Free Fraction × 10^4, mean ± *SD*, *n* = 7		Statistical Significance of Difference[a]
	Heparin	Saline	
0	5.8 ± 1.8	5.6 ± 1.6	NS
5	23.1 ± 12.1	6.9 ± 1.5	$p < 0.0025$
10	11.2 ± 3.5	6.2 ± 1.2	$p < 0.025$
15	9.5 ± 4.0	6.4 ± 2.1	$p < 0.05$
45	6.6 ± 1.9	5.6 ± 1.5	NS

[a] Paired *t* test.

Table II—Effect of Heparin Injection, 200 U/kg, on Plasma Protein Binding of Bilirubin in Rats

Minutes	Number of Animals	Free Fraction × 10^4, mean ± *SD*		Statistical Significance of Difference[a]
		Heparin	Saline	
0	5	5.1 ± 1.7	5.3 ± 1.2	NS
5	3	7.9 ± 0.9	5.4 ± 1.2	
10	5	7.5 ± 2.4	4.7 ± 0.6	$p < 0.025$
15	3	6.4 ± 0.5	5.3 ± 0.8	
45	5	5.0 ± 2.0	4.8 ± 1.1	NS

[a] Paired *t* test. Done only for groups with $n = 5$.

niques as those employed in the bilirubin experiment. The free salicylate fraction was determined by equilibrium dialysis of 400 μl of plasma against an equal volume of 0.134 *M* phosphate buffer, pH 7.4, containing 30 mg of sodium salicylate/100 ml. Dialysis was carried out for 4 hr at 37° with Plexiglas cells rotated in a water bath. The cell chambers were separated by a membrane made from natural cellulose with a molecular weight cutoff between 12,000 and 14,000[7]. Salicylate was assayed by the method of Brodie *et al.* (16), using carbon tetrachloride for extraction.

Plasma for experiments to determine the effect of treatment with activated charcoal on the protein binding of bilirubin and salicylate was obtained by withdrawing ~10 ml of blood from the abdominal aorta of ether-anesthetized rats into a plastic syringe[8] containing ~250 U of heparin. Plasma was separated by centrifugation in polypropylene tubes. Such blood withdrawals were made from rats that had not received heparin or saline injections (representative of conditions before injection) and from other rats 5 min after intravenous injection of heparin, 500 U/kg, or of an equal volume of saline solution.

Treatment of plasma with activated charcoal was carried out by a literature procedure (13), which consisted of acidifying the plasma to pH 3 after charcoal addition, separation of charcoal by centrifugation (20,000×*g* for 20 min at 2°) after 1 hr of stirring in an ice bath, and readjustment of the plasma pH to 7.4. To minimize plasma dilution, 1 *N* rather than 0.2 *N* HCl and NaOH (as specified in Ref. 13) were used for pH adjustment. The charcoal[9] was prewashed by preparing a slurry in 2 *N* HCl. The acid was removed by decanting, and the procedure was repeated several times with distilled water until the decanted water pH was nearly neutral. This process also removed very fine charcoal particles, which would have been difficult to separate from plasma. The charcoal was dried at room temperature. Another group of plasma samples was acidified, stirred, centrifuged, and readjusted to pH 7.4 without addition of charcoal to determine the effect of pH manipulation on binding characteristics. Total plasma protein concentrations were determined by the biuret method (17) with crystalline rat serum albumin as the standard. The albumin fraction was determined by electrophoresis[10].

Protein binding of bilirubin and salicylate in the charcoal-treated plasma samples and in the appropriate control plasma was determined as described in a preceding paragraph.

To determine the possible effect of ether anesthesia on protein binding, rats were anesthetized with ether, and a cannula was implanted in the right jugular vein (14). Blood was withdrawn immediately after implantation (after ~25 min of anesthesia) and 45 min and 24 hr after recovery. Plasma was separated and used for bilirubin binding determinations as described previously.

[7] Spectrapor 2, Spectrum Medical Industries, Los Angeles, Calif.
[8] Plastipak, 10 ml, Becton Dickinson Co., Rutherford, N.J.
[9] DARCO activated carbon, grade G 60, Atlas Chemical Ind., Wilmington, Del.
[10] Sepratek system, Gelman Instrument Co., Ann Arbor, Mich.

Table III—Effect of Heparin Injection, 500 U/kg, on Plasma Protein Binding of Salicylate in Rats

Minutes	Number of Animals	Free Fraction × 100, mean ± *SD*		Statistical Significance of Difference[a]
		Heparin	Saline	
0	6	53.6 ± 8.9	58.4 ± 7.2	NS
5	5	92.2 ± 7.4	60.1 ± 6.3	$p < 0.0005$
10	6	85.5 ± 6.7	59.8 ± 7.2	$p < 0.0005$
15	6	80.3 ± 6.7	59.2 ± 1.6	$p < 0.0005$
45	5	78.0 ± 7.2	58.4 ± 2.4	$p < 0.0005$

[a] Paired *t* test.

Table IV—*In Vitro* Effect of Heparin, 25,000 U/liter, on the Protein Binding of Bilirubin and Salicylate in Rat Plasma

	Bilirubin Free Fraction × 10^4		Salicylate Free Fraction × 100	
	Heparin	Control	Heparin	Control
	6.22	5.07	66.6	68.2
	5.93	5.32	65.2	65.8
	6.30	5.53	67.3	63.9
	6.13	5.67	65.4	65.6
Mean	6.15	5.40	66.1	65.9
	$p < 0.01$		NS	

RESULTS

Heparin, 500 U/kg iv, caused a pronounced increase in the free bilirubin fraction for at least 15 min after injection. At 45 min after injection, the free bilirubin fraction value had returned to near normal (Table I). A considerably less pronounced effect was obtained when only 200 U of heparin/kg was injected (Table II). Since the largest effect of heparin was observed at the first postinjection blood withdrawal (*i.e.*, at 5 min), additional studies were carried out on another group of rats at 2, 3, and 4 min after heparin injection. The most pronounced effect on bilirubin binding was observed at 2 min after injection of 500 U of heparin/kg. The average free bilirubin fraction at that time was 32×10^{-4} in three rats.

Heparin, 500 U/kg iv, also significantly increased the free salicylate fraction in plasma. This effect was still quite pronounced at the end of the experiment, *i.e.*, at 45 min after injection (Table III). Additional studies on three other rats revealed that the maximum heparin effect was already evident 2 min after injection. The average salicylate free fraction at that time was 0.922.

To determine if the heparin effect on the plasma protein binding of bilirubin was direct or indirect, a large amount of heparin was added to plasma *in vitro*. An equal volume of saline solution (25 ml/liter) was added to control plasma from the same animals. Heparin had no apparent effect on the plasma protein binding of salicylate (Table IV). *In vitro* addition of heparin had a statistically significant effect on bilirubin binding, but the increase in the free bilirubin fraction was only 14% on the average and, therefore, quantitatively insignificant compared to the effects observed *in vivo* (Table IV).

Activated charcoal treatment of plasma obtained 5 min after heparin injection completely reversed the heparin-induced bilirubin binding decrease (Table V). Even the process of plasma acidification and subsequent neutralization caused a partial reversal of the heparin effect but not as much as that produced by activated charcoal. Similar effects were obtained with respect to the protein binding of salicylate (Table VI).

Table V—Effect of Activated Charcoal Treatment on Heparin-Induced Changes in Plasma Protein Binding of Bilirubin in Rats

Type of Plasma[a]	Bilirubin Free Fraction × 10^4	
	Heparin	Saline
No injection, untreated	5.7 ± 1.3 (9)[b]	4.6 ± 0.6 (5)
After injection, untreated	16.4 ± 9.3 (9)[c]	5.8 ± 1.1 (7)
After injection, treated with activated charcoal	5.4 ± 1.2 (9)	6.2 ± 0.6 (6)
After injection, acidified and neutralized	9.5 ± 2.6 (9)	7.6 ± 1.3 (6)

[a] Blood to yield plasma was drawn from uninjected animals and from injected animals after intravenous injection of heparin, 500 U/kg, or of an equal volume of saline solution. [b] Mean ± *SD*; number of animals in parentheses. [c] Significantly different from plasma obtained from uninjected animals and from activated charcoal-treated plasma obtained after injection ($p < 0.01$).

Table VI—Effect of Activated Charcoal Treatment on Heparin-Induced Changes in Plasma Protein Binding of Salicylate in Rats

Type of Plasma[a]	Salicylate Free Fraction × 100	
	Heparin	Saline
No injection, untreated	46.9 ± 4.6 (8)[b]	43.0 ± 3.1 (5)
After injection, untreated	87.8 ± 6.1 (8)[c]	50.9 ± 3.8 (5)
After injection, treated with activated charcoal	54.7 ± 6.1 (8)	46.6 ± 3.7 (5)
After injection, acidified and neutralized	64.8 ± 10.4 (8)	48.2 ± 1.7 (5)

[a,b] See Table V. [c] Significantly different from plasma obtained from uninjected animals and from activated charcoal-treated plasma obtained after injection ($p < 0.001$).

The dilution of plasma caused by acidification and neutralization and the additional effect of some albumin adsorption on activated charcoal reduced the albumin concentration of the treated plasma samples (Table VII). This obviously will have affected the results presented in Tables V and VI and makes the observed charcoal treatment effects even more significant. To permit an assessment of the charcoal treatment effect on the protein binding of salicylate from a different perspective, the results are also presented as the ratio of the amount of bound salicylic acid to the amount of albumin in plasma (Table VIII). Treatment with activated charcoal actually increased this ratio to a value greater than that of plasma from rats that did not receive heparin. A similar tabulation for bilirubin is not informative, because the latter is >99% bound under all of the experimental conditions.

Since blood for the charcoal treatment experiments was obtained from ether-anesthetized rats, it was desirable to determine the effect of ether anesthesia on the plasma protein binding of bilirubin. Plasma samples obtained through a jugular catheter after 25 min of ether anesthesia yielded essentially the same free bilirubin fraction values as did plasma samples collected from the same animals 45 min and 24 hr after anesthesia (Table IX).

DISCUSSION

The results of this investigation show that an intravenous heparin injection can significantly decrease the plasma protein binding of bilirubin and salicylate. This effect occurred within 2 min after injection. It was relatively brief in the case of bilirubin, a compound with very high affinity to albumin, and of appreciably longer duration in the case of salicylate, a drug with much less affinity to albumin.

Heparin, even at a very high concentration, had no quantitatively significant direct *in vitro* effect on the plasma protein binding of bilirubin and salicylate. Thus, an *in vivo* competition by heparin or by the preservative contained in the heparin solution (9 mg of benzyl alcohol/ml) with bilirubin or salicylate for plasma protein binding sites can be ruled out. Benzyl alcohol in relatively high concentration can displace bilirubin from albumin binding sites (18, 19) and is possibly responsible for the small displacing effect observed *in vitro* (Table IV). However, the plasma concentrations of benzyl alcohol produced by heparin injections are so low that apparently no significant bilirubin displacement by benzyl alcohol will occur *in vivo*.

The heparin-induced reduction of bilirubin and salicylate binding to plasma proteins can be reversed by treating the plasma with activated charcoal. Such treatment is known to remove fatty acids from albumin binding sites but may also remove other endogenous inhibitors. Some reversal of the heparin effect can be produced simply by acidification and subsequent neutralization of the plasma. Acidification to pH 3 causes a conformational change (*i.e.*, N-F transformation and acid expansion) of albumin (20), which can facilitate the dissociation of a bound substance from the protein (21). Thus, the results of this investigation are consistent with a mechanism involving the formation or release into the blood of competitive inhibitor(s) of plasma protein binding as a consequence of heparin administration. These competitors may be free fatty acids in view of the temporal relationship between plasma protein binding changes and free fatty acid concentrations in plasma demonstrated by previous investigators (2–4).

It appears that a rapidly injected intravenous dose of 200 U/kg is approximately the minimum dose of heparin required to decrease the binding of bilirubin in rat plasma since this dose barely affected the protein binding of the pigment (Table II). On that basis, and assuming the heparin effect to be rapidly reversible, the duration of the effect of a 500-U/kg dose should be equal to one to two times the biological half-life of heparin. A recent study (22) showed that the biological half-life of 500 U of heparin/kg in rats is 69 ± 13 min (mean ± *SD*, $n = 12$). The duration of the effect of 500 U of heparin/kg on the plasma protein binding of bilirubin, as observed in this investigation (Table I), appears to be somewhat less than the 69-min average biological half-life of the anticoagulant. This finding suggests that there may be a limited amount of precursor of the endogenous displacing agent(s) or a limited depot of releasable endogenous displacing agent accessible or responsive to injected heparin. Once this amount of displacer has been discharged into the circulation, further discharge may be controlled by another rate-limiting step and may proceed at a much lower rate than that occurring immediately after heparin injection. It is also quite evident that the displacing agent itself must have a very short half-life in plasma. These characteristics are not inconsistent with previous suggestions that heparin affects plasma protein binding by causing a transient elevation of free fatty acid concentration in plasma (2–4).

The drug displacement from plasma protein binding sites caused by heparin administration can have significant pharmacokinetic and toxicological implications, as pointed out previously (3). In the case of bilirubin, such a displacing effect is of particular concern because heparinized blood in large quantities is administered to severely jaundiced infants in exchange transfusions. The heparin effect on salicylate binding is also striking since a 500-U/kg dose almost abolishes the plasma protein binding of salicylate during the first 5 min after rapid injection. The effect of the heparin injection on the plasma protein binding of salicylate lasts much longer than on the binding of bilirubin, probably because of the greater affinity of the latter to binding sites on albumin. It will be important to determine if the salicylate binding in tissues is reduced also by heparin administration.

Ongoing clinical studies indicate that significant alterations in the plasma protein binding of bilirubin are produced by considerably lower heparin doses than those required to decrease the plasma protein binding of this compound in rats.

Table VII—Effect of Activated Charcoal Treatment on Albumin Concentration in Rat Plasma

Treatment of Plasma[a]	Albumin Concentration, g/100 ml	
	Heparin ($n = 8$)	Saline ($n = 5$)
None	3.1 ± 0.2	3.1 ± 0.3
Acidification and neutralization	2.3 ± 0.2	2.4 ± 0.1
Activated charcoal	1.9 ± 0.2	2.1 ± 0.1

[a] Blood to yield plasma was drawn 5 min after intravenous injection of heparin, 500 U/kg, or of an equal volume of saline solution.

Table VIII—Effect of Activated Charcoal Treatment on the Amount of Salicylate Bound per Gram of Albumin in Plasma of Rats after Heparin Injection

Type of Plasma[a]	Bound Salicylic Acid/Albumin			
	Heparin ($n = 8$)		Saline ($n = 5$)	
	Milligrams per Gram	Molar Ratio	Milligrams per Gram	Molar Ratio
No injection, untreated	3.1 ± 0.8[b]	1.5	3.2 ± 0.2	1.5
After injection, untreated	0.8 ± 0.3	0.4	3.2 ± 0.4	1.5
After injection, treated with activated charcoal	4.8 ± 1.3	2.3	5.2 ± 0.9	2.5
After injection, acidified and neutralized	3.1 ± 1.2	.1.5	4.2 ± 0.6	2.0

[a] Blood to yield plasma was drawn from uninjected animals and from injected animals 5 min after intravenous injection of heparin, 500 U/kg, or of an equal volume of saline solution. [b] Mean ± *SD*.

Table IX—Plasma Protein Binding of Bilirubin in Rats during and after Ether Anesthesia

Time	Bilirubin Free Fraction × 10^4
During anesthesia[a]	5.1 ± 0.7[b]
45 min after anesthesia	4.5 ± 1.3
24 hr after anesthesia	4.6 ± 0.7

[a] Ether anesthesia for ~25 min. Blood was collected just before withdrawal of ether. [b] Mean ± *SD*, $n = 3$.

REFERENCES

(1) J. E. Thomson, S. G. Baird, and J. A. Thomson, *Br. J. Clin. Pharmacol.*, **4**, 701 (1977).

(2) L. Storstein and H. Janssen, *Clin. Pharmacol. Ther.*, **20**, 15 (1976).

(3) M. Wood, D. G. Shand, and A. J. J. Wood, *ibid.*, **25**, 103 (1979).

(4) O. G. Nilsen, L. Storstein, and S. Jacobsen, *Biochem. Pharmacol.*, **26**, 229 (1977).

(5) G. Levy, in "The Effect of Disease States on Drug Pharmacokinetics," L. Z. Benet, Ed., American Pharmaceutical Association, Washington, D.C., 1976, chap. 9.

(6) S. Øie and G. Levy, *J. Pharm. Sci.*, **68**, 1 (1979).

(7) *Ibid.*, **68**, 6 (1979).

(8) P. A. Davies, R. J. Robinson, J. W. Scopes, J. P. M. Tizard, and J. S. Wigglesworth, "Medical Care of Newborn Babies," Lippincott, Philadelphia, Pa., 1972, pp. 152–155, 272–278.

(9) F. A. Oski and J. L. Naiman, "Hematological Problems in the Newborn," 2nd ed., Saunders, Philadelphia, Pa., 1972, pp. 212–216.

(10) G. Levy, J. A. Procknal, and L. K. Garrettson, *Clin. Pharmacol. Ther.*, **18**, 210 (1975).

(11) G. Levy, T. Baliah, and J. A. Procknal, *ibid.*, **20**, 512 (1976).

(12) R. C. Reynolds and L. E. Cluff, *Bull. Johns Hopkins Hosp.*, **107**, 278 (1960).

(13) R. F. Chen, *J. Biol. Chem.*, **242**, 173 (1967).

(14) J. J. Ashley and G. Levy, *Res. Commun. Chem. Pathol. Pharmacol.*, **4**, 297 (1972).

(15) J. Jacobsen and O. Fedders, *Scand. J. Clin. Lab. Invest.*, **26**, 237 (1970).

(16) B. B. Brodie, S. Udenfriend, and A. F. Coburn, *J. Pharmacol. Exp. Ther.*, **80**, 144 (1944).

(17) A. C. Gornall, C. J. Bardawill, and M. M. David, *J. Biol. Chem.*, **177**, 751 (1949).

(18) L. Ballowitz, F. Hanefeld, and H. Schmid, *J. Perinat. Med.*, **4**, 168 (1976).

(19) L. Ballowitz, *J. Pediatr.*, **92**, 166 (1978).

(20) J. J. Foster, in "Albumin Structure, Function and Uses," V. M. Rosenoer, M. Oratz, and M. A. Rothschild, Eds., Pergamon, Oxford, England, 1977, pp. 53–84.

(21) R. Nagashima, G. Levy, and E. Nelson, *J. Pharm. Sci.*, **57**, 58 (1968).

(22) T. D. Bjornsson and G. Levy, *J. Pharmacol. Exp. Ther.*, in press.

ACKNOWLEDGMENTS

Supported in part by Grant GM 19568 from the National Institute of General Medical Sciences, National Institutes of Health, by an unrestricted grant from an anonymous donor, and by a fellowship from the Deutsche Forschungsgemeinschaft for U. W. Wiegand.

Correlation of Urinary Excretion with *In Vitro* Dissolution Using Several Dissolution Methods for Hydrochlorothiazide Formulations

KIRIT A. SHAH *x and THOMAS E. NEEDHAM ‡

Received May 22, 1978, from the **School of Pharmacy, Texas Southern University, Houston, TX 77004,* and the ‡*School of Pharmacy, University of Georgia, Athens, GA 30602.* Accepted for publication June 5, 1979.

Abstract □ Four different hydrochlorothiazide formulations were prepared, and cumulative urinary hydrochlorothiazide excretion was determined in a crossover study using six volunteers. A comparison of *in vivo* results showed that one formulation (Formulation D) was significantly different from the others at 2, 3, 4, 5, 8, and 14 hr. A dissolution study was conducted on each formulation using the flask, USP basket, and magnetic basket methods at agitation speeds of 50, 100, and 150 rpm. Formulation D was significantly different from other formulations when determined using the USP basket method at 150 rpm and a sampling time of 10 min; the USP basket method at 100 rpm and a sampling time of 100 min; the flask method at 100 rpm and sampling times of 30, 40, 60, and 120 min; and the flask method at 150 rpm and sampling times of 30 and 40 min. Significant *in vitro* and *in vivo* correlations were found using a regression analysis and *F* test. With a correlation coefficient and 95% confidence intervals, it was established that the USP basket method at 150 rpm was the best predictor of urinary hydrochlorothiazide excretion among the dissolution methods tested.

Keyphrases □ Hydrochlorothiazide—urinary excretion correlated with *in vitro* dissolution, various methods, bioavailability □ Diuretic agents—hydrochlorothiazide, urinary excretion correlated with *in vitro* dissolution, various methods, bioavailability □ Dissolution testing—hydrochlorothiazide, urinary excretion correlated with *in vitro* dissolution

Hydrochlorothiazide is a widely used diuretic and antihypertensive agent. Due to its limited aqueous solubility, this drug has a potential for poor absorption from the GI tract. In January 1977, the Food and Drug Administration (FDA) issued final regulations on bioequivalency and bioavailability (1). Hydrochlorothiazide was included in a list of drug entities described as having "known or potential bioequivalency or bioavailability problems."

In this publication, FDA also reported that: "A bioequivalence requirement for the majority of products should be an *in vitro* test in which the drug product is compared to a reference material. Preferably, the *in vitro* test should be an *in vitro* bioequivalence standard, *i.e.*, a test that has been correlated with human *in vivo* data. In most instances, the *in vitro* test should be a dissolution test" (1). FDA further stated that since *in vivo* testing requires an enormous number of human subjects and clinical investigators, the *in vitro* test as a valid predictor of bioequivalency can greatly reduce human subject risk and cost involved with *in vivo* testing. With these regulations, correlation between *in vitro* dissolution and bioavailability for drugs having bioavailability problems becomes more important.

McGilveray *et al.* (2) studied hydrochlorothiazide tablets manufactured by 39 Canadian companies. *In vitro* dissolution times using the USP method and bioavailability using urinary excretion were measured. Very poor correlation was found between these two parameters.

Meyer *et al.* (3) studied 14 different commercial hydrochlorothiazide formulations marketed in the United States. This work also did not reveal any apparent rela-

0022-3549/79/1200-1486$01.00/0

© 1979, American Pharmaceutical Association

REFERENCES

(1) J. E. Thomson, S. G. Baird, and J. A. Thomson, *Br. J. Clin. Pharmacol.*, **4**, 701 (1977).

(2) L. Storstein and H. Janssen, *Clin. Pharmacol. Ther.*, **20**, 15 (1976).

(3) M. Wood, D. G. Shand, and A. J. J. Wood, *ibid.*, **25**, 103 (1979).

(4) O. G. Nilsen, L. Storstein, and S. Jacobsen, *Biochem. Pharmacol.*, **26**, 229 (1977).

(5) G. Levy, in "The Effect of Disease States on Drug Pharmacokinetics," L. Z. Benet, Ed., American Pharmaceutical Association, Washington, D.C., 1976, chap. 9.

(6) S. Øie and G. Levy, *J. Pharm. Sci.*, **68**, 1 (1979).

(7) *Ibid.*, **68**, 6 (1979).

(8) P. A. Davies, R. J. Robinson, J. W. Scopes, J. P. M. Tizard, and J. S. Wigglesworth, "Medical Care of Newborn Babies," Lippincott, Philadelphia, Pa., 1972, pp. 152–155, 272–278.

(9) F. A. Oski and J. L. Naiman, "Hematological Problems in the Newborn," 2nd ed., Saunders, Philadelphia, Pa., 1972, pp. 212–216.

(10) G. Levy, J. A. Procknal, and L. K. Garrettson, *Clin. Pharmacol. Ther.*, **18**, 210 (1975).

(11) G. Levy, T. Baliah, and J. A. Procknal, *ibid.*, **20**, 512 (1976).

(12) R. C. Reynolds and L. E. Cluff, *Bull. Johns Hopkins Hosp.*, **107**, 278 (1960).

(13) R. F. Chen, *J. Biol. Chem.*, **242**, 173 (1967).

(14) J. J. Ashley and G. Levy, *Res. Commun. Chem. Pathol. Pharmacol.*, **4**, 297 (1972).

(15) J. Jacobsen and O. Fedders, *Scand. J. Clin. Lab. Invest.*, **26**, 237 (1970).

(16) B. B. Brodie, S. Udenfriend, and A. F. Coburn, *J. Pharmacol. Exp. Ther.*, **80**, 144 (1944).

(17) A. C. Gornall, C. J. Bardawill, and M. M. David, *J. Biol. Chem.*, **177**, 751 (1949).

(18) L. Ballowitz, F. Hanefeld, and H. Schmid, *J. Perinat. Med.*, **4**, 168 (1976).

(19) L. Ballowitz, *J. Pediatr.*, **92**, 166 (1978).

(20) J. J. Foster, in "Albumin Structure, Function and Uses," V. M. Rosenoer, M. Oratz, and M. A. Rothschild, Eds., Pergamon, Oxford, England, 1977, pp. 53–84.

(21) R. Nagashima, G. Levy, and E. Nelson, *J. Pharm. Sci.*, **57**, 58 (1968).

(22) T. D. Bjornsson and G. Levy, *J. Pharmacol. Exp. Ther.*, in press.

ACKNOWLEDGMENTS

Supported in part by Grant GM 19568 from the National Institute of General Medical Sciences, National Institutes of Health, by an unrestricted grant from an anonymous donor, and by a fellowship from the Deutsche Forschungsgemeinschaft for U. W. Wiegand.

Correlation of Urinary Excretion with *In Vitro* Dissolution Using Several Dissolution Methods for Hydrochlorothiazide Formulations

KIRIT A. SHAH *x and THOMAS E. NEEDHAM ‡

Received May 22, 1978, from the **School of Pharmacy, Texas Southern University, Houston, TX 77004,* and the ‡*School of Pharmacy, University of Georgia, Athens, GA 30602.* Accepted for publication June 5, 1979.

Abstract □ Four different hydrochlorothiazide formulations were prepared, and cumulative urinary hydrochlorothiazide excretion was determined in a crossover study using six volunteers. A comparison of *in vivo* results showed that one formulation (Formulation D) was significantly different from the others at 2, 3, 4, 5, 8, and 14 hr. A dissolution study was conducted on each formulation using the flask, USP basket, and magnetic basket methods at agitation speeds of 50, 100, and 150 rpm. Formulation D was significantly different from other formulations when determined using the USP basket method at 150 rpm and a sampling time of 10 min; the USP basket method at 100 rpm and a sampling time of 100 min; the flask method at 100 rpm and sampling times of 30, 40, 60, and 120 min; and the flask method at 150 rpm and sampling times of 30 and 40 min. Significant *in vitro* and *in vivo* correlations were found using a regression analysis and *F* test. With a correlation coefficient and 95% confidence intervals, it was established that the USP basket method at 150 rpm was the best predictor of urinary hydrochlorothiazide excretion among the dissolution methods tested.

Keyphrases □ Hydrochlorothiazide—urinary excretion correlated with *in vitro* dissolution, various methods, bioavailability □ Diuretic agents—hydrochlorothiazide, urinary excretion correlated with *in vitro* dissolution, various methods, bioavailability □ Dissolution testing—hydrochlorothiazide, urinary excretion correlated with *in vitro* dissolution

Hydrochlorothiazide is a widely used diuretic and antihypertensive agent. Due to its limited aqueous solubility, this drug has a potential for poor absorption from the GI tract. In January 1977, the Food and Drug Administration (FDA) issued final regulations on bioequivalency and bioavailability (1). Hydrochlorothiazide was included in a list of drug entities described as having "known or potential bioequivalency or bioavailability problems."

In this publication, FDA also reported that: "A bioequivalence requirement for the majority of products should be an *in vitro* test in which the drug product is compared to a reference material. Preferably, the *in vitro* test should be an *in vitro* bioequivalence standard, *i.e.*, a test that has been correlated with human *in vivo* data. In most instances, the *in vitro* test should be a dissolution test" (1). FDA further stated that since *in vivo* testing requires an enormous number of human subjects and clinical investigators, the *in vitro* test as a valid predictor of bioequivalency can greatly reduce human subject risk and cost involved with *in vivo* testing. With these regulations, correlation between *in vitro* dissolution and bioavailability for drugs having bioavailability problems becomes more important.

McGilveray *et al.* (2) studied hydrochlorothiazide tablets manufactured by 39 Canadian companies. *In vitro* dissolution times using the USP method and bioavailability using urinary excretion were measured. Very poor correlation was found between these two parameters.

Meyer *et al.* (3) studied 14 different commercial hydrochlorothiazide formulations marketed in the United States. This work also did not reveal any apparent rela-

0022-3549/79/1200-1486$01.00/0

© 1979, American Pharmaceutical Association

tionship between bioavailability and *in vitro* dissolution. These workers measured dissolution times using the USP apparatus and bioavailability using urinary excretion data.

A literature review revealed that only the USP dissolution method had been used in the search for a correlation between *in vitro* dissolution and *in vivo* bioavailability for hydrochlorothiazide formulations. The purposes of this study were to investigate several different dissolution methods and to determine conditions and parameters for predicting the bioavailability of hydrochlorothiazide formulations.

EXPERIMENTAL

Materials—Hydrochlorothiazide powder was obtained from a commercial source[1]. Microcrystalline cellulose pH 101[2], magnesium stearate[3], lactose[4], corn starch[5], and gelatin[3] were purchased.

Tablet Formulations—Two basic formulations were designed for this investigation. Formula I (direct compression) contained (in milligrams per 150-mg tablet): hydrochlorothiazide, 25.0; microcrystalline cellulose, 124.0; and magnesium stearate, 1.0. Formula II (wet granulation) contained (in milligrams per 142.5-mg tablet): hydrochlorothiazide, 25.0; lactose, 95.5; corn starch, 20.0; gelatin (as 5% solution), 1.5; and magnesium stearate, 0.5.

Tablets were compressed on a single-punch tablet machine[6] using a 0.64-cm (0.25-in.) flat face punch and die set. Tablets were compressed to produce two different hardnesses from each formula and were tested using a motor-driven hardness tester[7]. Formulations A and C were produced from the wet granulation at hardnesses of 2.15 ± 0.98 and 7.85 ± 0.80, respectively. Formulations B and D were produced by direct compression at hardnesses of 5.35 ± 0.34 and 10.85 ± 0.63, respectively. The formulations also were subjected to weight variation and content uniformity testing, and they conformed to the USP requirements.

***In Vitro* Studies**—The three dissolution methods were the USP method (4), the flask method (5), and the magnetic basket method (6). All dissolution studies were carried out at 37 ± 0.5° in 500 ml of 0.1 *N* HCl. At various times, 1.0-ml samples were pipetted through a glass wool plug; an equal amount of 0.1 *N* HCl was added to the dissolution medium to replace each sample. The rotational agitation speeds used were 50, 100, and 150 rpm. An electronically controlled stirring motor[8] was used in each experiment, and an appropriate propeller or basket was mounted on the stirrer.

***In Vivo* Studies**—Six male volunteers, 21–30 years old and within 90–110% of their ideal body weight, were within normal limits after undergoing a chest X-ray, an ECG, and a normal blood profile. Each subject gave written informed consent before participation. All volunteers were asked to refrain from any drugs or alcohol for 72 hr prior to and during the experiment. A 25-mg dose of hydrochlorothiazide tablet or powder was taken with 200 ml of water in the morning following overnight fasting. The powder was suspended in water before administration. No food or liquid other than water was permitted until 4 hr after drug ingestion.

Cumulative urine samples were collected at 0, 1, 2, 3, 4, 5, 8, 11, 14, and 24 hr. The various formulations were administered to six volunteers at weekly intervals according to a 5 (formulations) × 6 (subjects) × 9 (sampling times) repeated measures design. Urine samples were immediately refrigerated until analysis.

Analytical Methods—In Vitro *Assay*—Hydrochlorothiazide concentration was determined using a spectrophotometer[9] at 273 nm against a blank of 0.1 *N* HCl.

In Vivo *Assay*—The method of Rehm and Smith (7) was used with some modifications. Four milliliters of urine was pipetted into a 50-ml separator and extracted with 10 ml of ethyl acetate. The ethyl acetate portion was separated, and the urine portion was reextracted with an additional 3 ml of ethyl acetate. Both ethyl acetate portions were combined and washed with 10 ml of 0.2 *N* NaOH on a mechanical shaker[10] for at least 6 hr. The ethyl acetate portion was separated from the alkali.

Two 5-ml portions of the ethyl acetate solution were transferred into separate 50-ml volumetric flasks. The volumetric flasks were transferred to a boiling water bath, and solutions were evaporated. The residue was hydrolyzed by addition of 1 ml of 0.7% hydroxylamine hydrochloride and immersion in a boiling water bath for 30 min. Both flasks were cooled, and 2 ml of 1% $NaNO_3$ and 5 ml of 1 *N* HCl were added to each. Both flasks were allowed to stand for 2 min, and 4 ml of 2% ammonium sulfate was added.

To one flask, 1 ml of 0.5% chromotropic acid was added. Finally, 10 ml of 1 *N* sodium acetate was added to both flasks and the volume was adjusted to 50 ml with distilled water. The absorbance was determined at 500 nm. The absorbance of the solution without chromotropic acid was subtracted from the value of the solution with chromotropic acid. The concentration of each sample was determined by comparison of absorbance values with those obtained from a standard curve. The color produced by hydrochlorothiazide in amounts of 12.5–62.5 μg when carried through the procedure was reproducible and followed Beer's law (r = 0.9979).

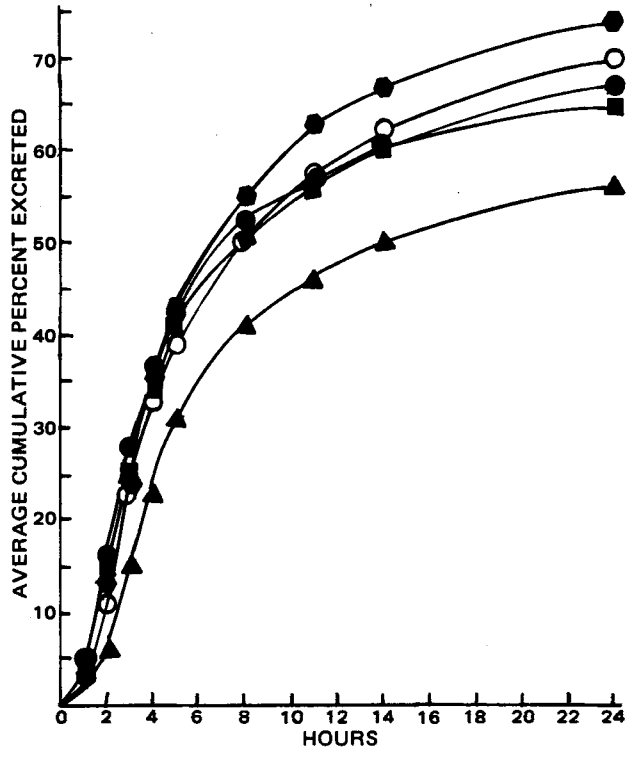

Figure 1—*Average cumulative percent of hydrochlorothiazide excreted following the administration of five formulations to each of six subjects. Key: ■, Formulation A; ●, Formulation B; ●, Formulation C; ▲, Formulation D; and ○, powder.*

RESULTS AND DISCUSSION

***In Vivo* Data**—The mean cumulative percentages of hydrochlorothiazide excreted by six subjects receiving each of the four tablet formulations (A–D) and powder (E) are shown in Fig. 1. The powder was included so that results could be compared with the other dosage forms as well as with a previously reported study (3). The average cumulative percent excretion of the powdered drug in 24 hr was 69.0 ± 10.5 (*SD*). The calculated excretion half-lives for the powdered drug administered in this study and of that reported previously (3) were 6.8 and 7.4 hr, respectively.

All data as percent excreted were transformed using an arc sine transformation to conform to the assumption of normal distribution and

[1] MSD, Division of Merck and Co., West Point, Pa.
[2] FMC Corp., Newark, Del.
[3] Fisher Chemicals, Fair Lawn, N.J.
[4] Mallinckrodt Chemical Works, St. Louis, Mo.
[5] Roger Chemical Co., Irving, N.J.
[6] Model F, F. J. Stokes Machine Co., Philadelphia, Pa.
[7] Erweka Chemical and Pharmaceutical Industry Co., New York, N.Y.
[8] GT21 laboratory stirrer, Gerald K. Heller Co., Long Island, N.Y.
[9] Cary model 118, Varian Instruments, Monrovia, Calif.
[10] Ernest D. Menold, Lester, Calif.

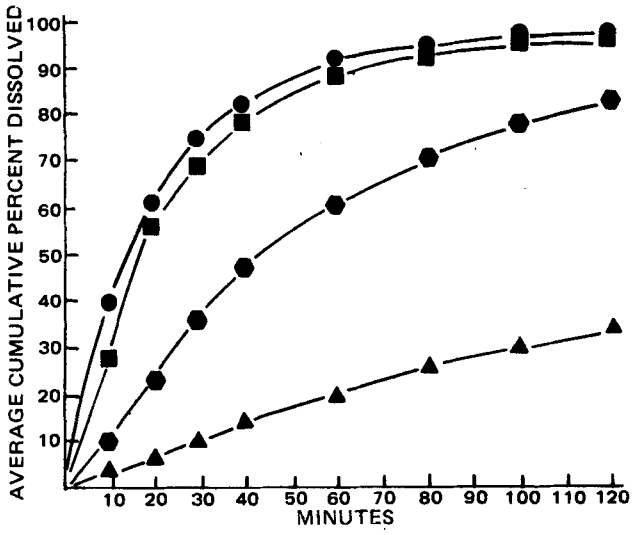

Figure 2—*Comparison of the dissolution profiles of hydrochlorothiazide formulations found using the USP basket method at 50 rpm. Each data point is the mean of five determinations. Key:* ■, *Formulation A;* ●, *Formulation B;* ●, *Formulation C; and* ▲, *Formulation D.*

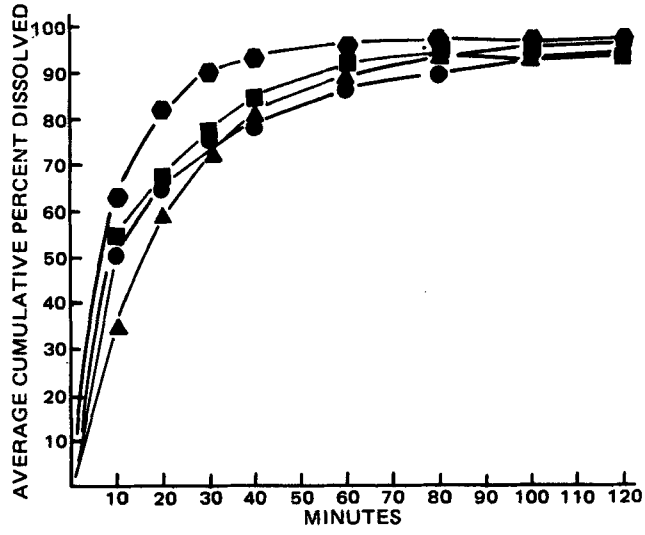

Figure 4—*Comparison of the dissolution profiles of hydrochlorothiazide formulations found using the USP basket method at 150 rpm. Each data point is the mean of five determinations. Key:* ■, *Formulation A;* ●, *Formulation B;* ●, *Formulation C; and* ▲, *Formulation D.*

equal variance (8). A two-way classification of an analysis of variance was used to compare the urinary hydrochlorothiazide excretion from the four tablet formulations and the powder at selected sampling times. The calculated F value of 4.72 was significantly higher than the tabulated $F_{0.95}$ value of 2.7, suggesting that there were significant differences ($p = 0.05$) among the formulations.

The calculated F value of 908.49 for the time factor was significantly higher than the tabulated $F_{0.95}$ value of 2.25, because cumulative data were used for this factor. Significant interactions between sampling times and formulations were found also. Thus, a one-way analysis of variance at each sampling time was used to determine the times at which significant differences between formulations existed. At all sample times studied except 1 hr, the calculated F exceeded the tabular $F_{0.95}$ value of 2.76 and confirmed that significant differences in excretion existed at each sample time. A Newman–Keuls multiple-range test (8) was performed to determine which formulations were significantly different. Only Formulation D was significantly different from all other formulations at 2, 3, 4, 5, 8, and 14 hr.

***In Vitro* Data**—Each formulation administered *in vivo* was dissolved using the USP basket method (4), the flask method (5), and the magnetic basket method (6) to determine any significant differences in drug release as a function of the dissolution method. In all cases, the percent of drug dissolved was transformed using an arc sine transformation to conform to the assumption of normal distribution and equal variance (8).

Comparison of the individual dissolution methods at agitation speeds of 50, 100, and 150 rpm showed that Formulation D dissolved slower at all agitation speeds. For each method, the gradual grouping of dissolution profiles was observed as the agitation speed was increased. This finding illustrates the difficulty in distinguishing the difference between formulations at higher agitation speeds. Examples of this behavior are shown in Figs. 2–4 for the USP method. The other two methods showed similar behavior.

Statistically significant differences ($p = 0.05$) between and within formulations were found using a repeated measures, two-way analysis of variance to compare hydrochlorothiazide formulations over time for the USP basket, flask, and magnetic basket methods at each agitation speed. Again, as with the *in vivo* analysis, the interactions between the sampling times and formulations were significant at all agitation speeds for each dissolution method. Therefore, a one-way analysis of variance was performed at each sampling time to determine if any significant differences between formulations could be detected. The calculated F value for the different formulations exceeded the tabular F value of 3.24 at the 0.95 level. To find which formulations were significantly different, a Newman–Keuls multiple-range test (8) was performed (Table I).

Correlation of *In Vitro* with *In Vivo* Results—Hydrochlorothiazide is a potential candidate for bioavailability problems because of its limited aqueous solubility. Previous studies (2, 3) showed very poor correlation between *in vivo* urinary excretion and the *in vitro* dissolution procedure for various formulations of this drug. It was postulated that comparison of the dissolution profiles from several methods using different agitation rates with urinary excretion data in which a significant difference in formulations had been found could help determine the correlation between these two parameters. Therefore, rank-order correlations were determined using cumulative excretion sample times of 1, 2, 3, 4, 5, 8, 11, 14, and 24 hr and dissolution times of 10, 20, 30, 40, 60, 80, 100, and 120 min for the USP basket, flask, and magnetic basket methods at 50-, 100-, and 150-rpm agitation speeds.

The sequential order correlation of the *in vivo* and *in vitro* results produced very few simple correlations between these two parameters. Most of these correlations were present between urinary excretion of 1 hr and only a few *in vitro* dissolution sample times. The magnetic basket method at 50 rpm failed to produce any rank-order correlation; the USP basket method at 150 rpm produced a greater number of correlations than any other combination of method and agitation speed.

To determine if a quantitative correlation existed between the transformed data of percent cumulative excretion and the cumulative percent of drug dissolved for each of the four formulations, a regression analysis was performed at each *in vivo* and *in vitro* sampling times. The F ratio was used to determine significance ($\alpha = 0.99$) (Table II). The correlation

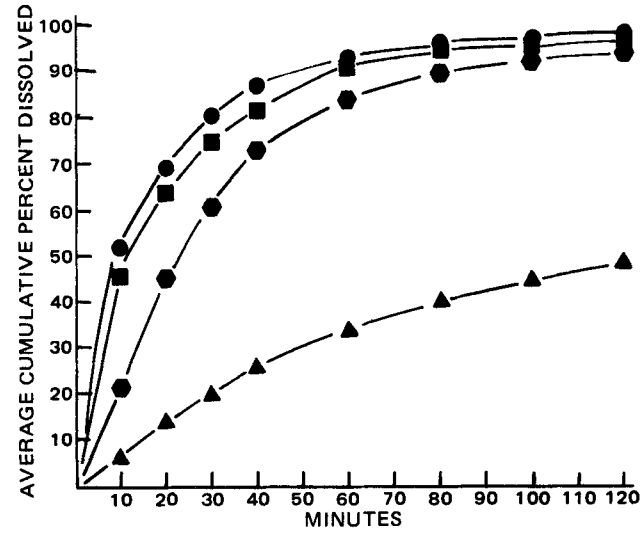

Figure 3—*Comparison of the dissolution profiles of hydrochlorothiazide formulations found using the USP basket method at 100 rpm. Each data point is the mean of five determinations. Key:* ■, *Formulation A;* ●, *Formulation B;* ●, *Formulation C; and* ▲, *Formulation D.*

Table I—Newman–Keuls Multiple-Range Test Comparing *In Vitro* Dissolution of Hydrochlorothiazide Formulations Using USP Basket, Flask, and Magnetic Basket Methods at Different Agitation Speeds and Sampling Times

Dissolution Method	Agitation Speed, rpm	Sampling Time, min 10	20	30	40	60	80	100	120
USP basket	50	CABD[a]	CABD	CABD	CABD	CABD	CABD	CABD	CABD
	100	CABD	ACBD	CABD	CABD	CABD	CABD	CABD	BADC
	150	BACD	BACD	BACD	BADC	BADC	BADC	BADC	ABCD
Flask	50	CABD	CABD	CABD	DBAD	CBAD	CBAD	BCAD	CBAD
	100	CABD	CABD	CBAD	CABD	ABCD	ACBD	ACBD	ACBD
	150	CABD	CBAD	CBAD	BCAD	ABCD	ABDC	ABCD	ACBD
Magnetic basket	50	ACBD	ACBD	ACBD	ACBD	ACBD	ACBD	ACBD	ACBD
	100	CABD	CABD	CABD	CABD	CABD	CABD	CABD	CABD
	150	CABD	CABD	CABD	CABD	CABD	CABD	CABD	CABD

[a] Products underlined by a common line indicate statistical similarity. Product rankings are from highest to lowest.

Table II—Correlation[a] of *In Vivo* Excretion and *In Vitro* Dissolution Found Using Different Dissolution Methods[b] for Four Hydrochlorothiazide Formulations

In Vivo Excretion Time, hr	50-rpm Agitation Speed 10 min	20 min	30 min	40 min	60 min	80 min	100 min	120 min	100-rpm Agitation Speed 10 min	20 min	30 min	40 min	60 min	80 min	100 min	120 min	150-rpm Agitation Speed 10 min	20 min	30 min	40 min	60 min	80 min	100 min	120 min
1	—	—	—	—	—	—	—	—	—	—	—	—	—	—	—	—	—	—	—	—	—	—	—	—
2	—	—	—	—	M	—	—	—	—	F	U F	M F	M U F	M U	M U	M U	—	—	—	—	M F	—	—	—
3	—	—	—	—	—	—	—	—	—	—	—	F	U	U	U	U	—	—	—	—	F	—	—	—
4	—	—	—	—	F	F	F	F	—	F	F	F	U	M U	U	U	U	—	—	M	M	—	—	—
5	—	—	—	—	—	—	F	F	—	F	—	F	—	—	—	—	U	—	—	—	—	—	—	—
8	—	—	F	F	F	F	F	F	—	F	F	F	U F	U	M U	U	U	U F	U F	U F	M	M	M	—
11	—	—	F	F	F	F	F	F	—	F	F	—	—	U	M U	U	U	U F	U F	U F	—	M	—	—
14	—	—	F	F	F	F	F	F	F	F	F	F	M U F	M U	M U	U	U	U F	U F	M F	M	M	M	—
24	—	—	F	F	F	F	F	F	—	F	F	M F	M U F	M U	M U	U	U F	U F	F	M F	M	M	—	M

[a] Correlation was determined using regression analysis and *F* test. [b] U, F, and M indicates significant correlation ($\alpha = 0.99$) found using USP basket, flask, and magnetic basket methods, respectively.

coefficients were computed for each *in vivo* and *in vitro* sampling time for four hydrochlorothiazide formulations for each dissolution procedure. The correlation coefficient between the excretion at the sample time of 14 hr and the *in vitro* dissolution at the sample time of 80 min for the flask method at 50 rpm was the highest correlation coefficient ($r = 0.748$). When the same apparatus was used with an agitation speed of 100 rpm, the highest correlation was obtained between the urinary excretion at the sample time of 14 hr and an *in vitro* sample time of 30 min ($r = 0.698$). For the same method with an agitation speed of 150 rpm, the highest correlation was present between the *in vivo* sample time of 14 hr and the *in vitro* sample time of 20 min ($r = 0.644$). All of these correlation coefficient values were statistically significant ($p = 0.01$).

With the magnetic basket method, the highest significant correlations ($p = 0.01$) were found between the *in vivo* sample time of 2 hr and the *in vitro* sample time of 60 min for each agitation speed ($r = 0.630$, 50 rpm; $r = 0.672$, 100 rpm; and $r = 0.604$, 150 rpm).

For the USP basket method, the highest correlation was found between the urinary excretion at the sample time of 2 hr and the *in vitro* sample time of 60 min at 50- and 100-rpm agitation speeds ($r = 0.656$, 100 rpm; and $r = 0.609$, 50 rpm). With an agitation speed of 150 rpm, the highest correlation was between the excretion data obtained at the sample time of 8 hr and the *in vitro* data obtained at the sample time of 10 min ($r = 0.649$). All of these correlation coefficient values were statistically significant ($p = 0.01$).

The urinary hydrochlorothiazide excretion at the sample time of 14 hr and the dissolution data at the sample time of 80 min using the flask method at 50 rpm produced the highest correlation when compared with all other *in vivo–in vitro* correlation coefficients. However, the use of these

Table III—Regression Analysis of *In Vitro* Dissolution and *In Vivo* Excretion for *In Vitro–In Vivo* Times Where Highest Significant Correlation Was Found

Method	Agitation Speed, rpm	*In Vivo* Time, hr	*In Vitro* Time, min	Slope	Intercept	Correlation Coefficient[a]
Flask	50	14	80	2.29	−1.90	0.748
Flask	100	14	30	2.07	−1.54	0.698
Flask	150	14	20	1.33	−0.21	0.644
Magnetic basket	50	2	60	1.88	−1.09	0.630
Magnetic basket	100	2	60	2.02	−0.48	0.672
Magnetic basket	150	2	60	2.13	−0.17	0.604
USP basket	50	2	60	2.36	−0.33	0.609
USP basket	100	2	60	2.18	−0.69	0.656
USP basket	150	8	10	1.18	−0.25	0.649

[a] Significant at 0.99 level.

Table IV—Prediction of Average Percent Hydrochlorothiazide Excretion at Sample Time Where Highest Significant Correlation Was Found

Method	Agitation Speed, rpm	*In Vivo* Time, hr	*In Vitro* Time, min	Mean *In Vitro* Dissolution[a], %	Mean *In Vivo* Prediction[a], %
Flask	50	14	80	77	60 ± 0.8
Flask	100	14	30	77	60 ± 0.9
Flask	150	14	20	77	60 ± 0.5
Magnetic basket	50	2	60	52	2 ± 0.6
Magnetic basket	100	2	60	64	11 ± 0.1
Magnetic basket	150	2	60	86	25 ± 0.1
USP basket	50	2	60	68	11 ± 1.0
USP basket	100	2	60	79	11 ± 0.4
USP basket	150	8	10	50	49 ± 0.3

[a] Values were converted to percent from arc sine transformation.

two parameters for prediction seems to be limited since the *in vitro* time was not found on the rate-limiting portion of the curve and the analysis of variance and Newman–Keuls multiple-range test for this particular *in vitro* time could not differentiate among Formulations A–D (Table I). Thus, selection of the best dissolution procedure probably should be based on something more than a correlation coefficient and should include considerations of the: (*a*) use of a correlation coefficient that is statistically significant, (*b*) use of an *in vitro* time that is on the rate-limiting portion of the dissolution–time curve, and (*c*) use of analysis of variance and Newman–Keuls multiple-range data that show significant differences between formulations within the experimental design.

Table III shows the slope, intercept, and *in vitro–in vivo* parameters where the highest correlation coefficients were obtained for each dissolution method. The regression equation that produced a significant correlation for each method can be used for urinary excretion prediction. The following equation was used:

$$UE = \frac{(\textit{in vitro}\text{ dissolution at time } T) - \text{intercept}}{\text{slope}} \quad \text{(Eq. 1)}$$

where UE is the prediction of *in vivo* urinary hydrochlorothiazide excretion at the sample time where the highest significant correlation was obtained. *In vitro* dissolution data as percent dissolved should be transformed using an arc sine transformation before insertion into Eq. 1.

Table IV shows the prediction of mean hydrochlorothiazide excretion along with confidence intervals. The confidence limits can be calculated using this formula (9):

$$\text{prediction of urinary hydrochlorothiazide excretion at time } T \pm t_{0.95} = (\text{residual mean square})\left(\frac{1}{n}\right) \quad \text{(Eq. 2)}$$

where n is the sample size used for regression and the residual mean square was calculated from analysis of variance for regression.

The percent of *in vitro* dissolution for each dissolution procedure that produced the highest significant correlation with urinary excretion is shown in Table IV. Comparison of these values with those from the previous dissolution profiles (Figs. 2–4) showed that all predicted values for percent of *in vitro* dissolution that were used for prediction of *in vivo* excretion lay on the plateau region of the curve, except the values obtained for the USP basket method and for the flask method at 150 rpm. These values fell within that portion of the profile that could be considered to be rate limited. Thus, it seems logical to select either the USP basket or the flask method at an agitation speed of 150 rpm for the prediction of urinary hydrochlorothiazide excretion.

Formulations A–C were statistically similar and significantly different from Formulation D when *in vivo* data at 8 hr and *in vitro* data at 10 min were compared after using the USP basket. However, the urinary hydrochlorothiazide excretion at 14 hr and *in vitro* dissolution at 20 min using the flask method at 150 rpm produced different results when Formulations A–D were compared (Table I).

This approach has good utility for establishing a standard for *in vitro* dissolution. Once correlation is established between *in vitro* and *in vivo* parameters and it is found that the regression equation can be utilized for predicting *in vivo* activity, interlot or intralot variations can be determined for hydrochlorothiazide formulations. In this case, the standard to produce an acceptable formulation should be that at least 50% hydrochlorothiazide is dissolved in 10 min using the USP basket method at the 150-rpm agitation speed. As shown in Fig. 4, Formulation D had only 35% dissolution at the 10-min sample time. Formulations A, B, and C had 54, 63, and 50% dissolution, respectively. Thus, Formulation D will have urinary excretion less than 49% at a sample time of 8 hr when administered orally. Moreover, a statistical comparison using a Newman–Keuls multiple-range test (8) for the USP basket method showed that Formulations A–C were statistically the same and that Formulation D was statistically different from the other three formulations.

REFERENCES

(1) *Fed. Regist.*, **42**, 1621 (1977).

(2) I. J. McGilveray, R. D. Hossie, and A. L. Mattok, *Can. J. Pharm. Sci.*, **8**, 13, (1973).

(3) M. C. Meyer, A. P. Milikian, P. L. Whyatt, and G. A. Slywka, *Curr. Ther. Res.*, **17**, 570 (1975).

(4) "The United States Pharmacopeia," 19th rev., Mack Publishing Co., Easton, Pa., 1975, p. 651.

(5) T. W. Underwood and D. E. Cadwallader, *J. Pharm. Sci.*, **61**, 239 (1972).

(6) R. E. Shepherd, J. C. Price, and L. A. Luzzi, *ibid.*, **61**, 1152 (1972).

(7) C. R. Rehm and J. B. Smith, *J. Am. Pharm. Assoc., Sci. Ed.*, **49**, 386 (1960).

(8) V. L. Anderson and R. A. Mclean, "Design of Experiments," Dekker, New York, N.Y., 1974, p. 10.

(9) F. Freese, "Elementary Statistical Methods for Foresters," U. S. Department of Agriculture Forest Service, Washington, D.C., 1967, pp. 55, 56.

ACKNOWLEDGMENTS

Abstracted in part from a dissertation submitted by K. A. Shah to the University of Georgia in partial fulfillment of the Doctor of Philosophy degree requirements.

Flocculation of Sulfamerazine Suspensions by a Cationic Polymer

JOEL L. ZATZ ˣ, LARRY SCHNITZER, and PRAMOD SARPOTDAR

Received April 9, 1979, from the *College of Pharmacy, Rutgers—the State University of New Jersey, Piscataway, NJ 08854.* Accepted for publication June 11, 1979.

Abstract □ Flocculation by a cationic polymer of sulfamerazine suspensions containing a wetting agent was evaluated. Suspensions with sufficient surfactant concentrations to ensure complete wetting were deflocculated. When the anionic surfactant, dioctyl sodium sulfosuccinate, was used as a wetting agent, the suspensions were flocculated over a limited polymer concentration range. Flocculation was attributed to simultaneous interaction of a polymer molecule with more than one particle. At higher polymer concentrations, the particles were covered completely with polymer, leading to repulsion between the particles and deflocculation of the suspensions. The polymer concentration required for flocculation provided evidence for interaction between the anionic surfactant and the cationic polymer. Suspensions containing a nonionic surfactant also were flocculated using various polymer concentrations. When a surfactant mixture was employed in the suspensions, the peak sedimentation volume of flocculated systems and the concentration of polymer at the peak depended on the surfactant mixture composition.

Keyphrases □ Sulfamerazine—suspensions, flocculation, cationic polymer, anionic and nonionic surfactants □ Flocculation—sulfamerazine suspensions, cationic polymer, anionic and nonionic surfactants □ Cationic polymer—sulfamerazine suspensions, flocculation, anionic and nonionic surfactants

Resistance to caking is a principal objective in pharmaceutical suspension formulation (1). Suspensions that form a voluminous, porous sediment upon standing may be shaken by hand to reconstitute a uniform product and to allow correct dose transfer. Suspensions that sediment in this manner are referred to as flocculated systems.

Deflocculated suspensions, in which the internal phase has been dispersed into individual particles, usually appear more elegant when first prepared. They sediment more slowly than flocculated suspensions but produce a dense, compact layer of solid material at the container bottom. Such suspensions are difficult to redisperse and, consequently, are not suitable as pharmaceutical dosage forms.

BACKGROUND

Two possible formulation avenues were suggested (2). One uses a structured vehicle to avoid settling altogether. The other (the more usual approach) involves a flocculation process, resulting in a system that sediments and is then readily redispersed prior to use.

Salts may function as flocculating agents. Previous work on flocculation mainly concerned the valence and concentration effects of simple salts. Little study has been made of the flocculation of pharmaceutical suspensions by polymers. Although polymers commonly are included in suspensions as thickening or structuring agents, they also may function by adsorbing onto suspended particles and altering the attraction or repulsion between particles.

Smellie and LaMer (3) used polymers to clarify turbid water containing low dispersed phosphate concentrations. The polymer actions were ascribed to a bridging mechanism in which the long polymer molecules joined two or more particles together. Polymer adsorption is a key requirement for bridging. However, since complete coverage of the dispersed particles by polymer molecules makes it unlikely that the same polymer molecule will attach to more than one particle, too high a polymer concentration may reduce the flocculation efficiency or inhibit it altogether. These mechanisms are similar to the "sensitization" and "protection" of hydrophobic sols by polymers (4).

Subsequent investigations confirmed the validity of a bridging mechanism in polymer flocculation (5–8). Charge neutralization may be involved in the attachment of the polymer to the particle surface (5), although a nonionic mechanism also may be operative (6). The first study of polymer flocculation in pharmaceutical systems (7) concerned the effect of xanthan gum in several suspensions. Flocculation of some antacids by xanthan gum also was investigated (8).

Surfactants often are employed as wetting and dispersing agents in suspensions. However, surfactants were not included in any of the polymeric flocculation studies reported. Since flocculation is basically an interfacial phenomenon and surfactants accumulate at interfaces, they may influence the action of polymers. The present investigation concerned the effect of a cationic polymer on the flocculation state of sulfamerazine suspensions containing surfactants.

EXPERIMENTAL

Sulfamerazine was USP grade. Dioctyl sodium sulfosuccinate[1] and polysorbate 40[2] were employed as wetting agents. The polymer preparation (I) was a commercial cationic flocculant[3], supplied as an aqueous solution containing 30% active material (9). All other chemicals were reagent grade and were used as supplied.

To prepare 100 ml of sulfamerazine suspension, 10 g of the drug was placed in a glass mortar. Twenty milliliters of an aqueous solution containing the wetting agent was added to the powder, and the concentrated suspension was mixed thoroughly. The polymer preparation (when present) then was added as a concentrated aqueous solution by pipet, and the suspension was mixed for <1 min and transferred into a 100-ml graduated mixing cylinder. The mortar was rinsed several times with distilled water. The rinsings were added to the graduated cylinder, and sufficient distilled water was used to make up to volume. The suspension was shaken thoroughly and then permitted to settle.

The suspensions were allowed to stand until no further changes were observed in the sediment height. The sediment volume then was recorded.

Surface tension was measured by the Wilhelmy plate method.

RESULTS AND DISCUSSION

Sedimentation volume, F, was used as an indication of flocculation in the suspensions. The value of F is determined by:

$$F = \frac{V_u}{V_0} \qquad \text{(Eq. 1)}$$

where V_u is the ultimate sediment volume and V_0 is the total suspension volume.

The deflocculated suspension sedimentation volume is relatively small. Flocculated systems exhibit higher F values. In the suspensions studied, no changes in the sediment volume were observed after about 5 days.

Figure 1 shows the effect of the I concentration on the sedimentation volume of sulfamerazine suspensions in the absence of any surfactant. The F value decreased when the I concentration in the suspension reached 0.1%. However, even at 1%, a small amount of sulfamerazine powder floated at the top of the suspension. The F decrease corresponded to lowering of the surface tension, γ, of the medium by the polymer (Fig. 2). The critical sulfamerazine surface tension is 32 dynes/cm (10). Apparently, γ is not lowered sufficiently by the polymer to allow complete wetting.

The relationship between surfactant concentration in the absence of I and sedimentation volume is shown in Fig. 3. There were slight differ-

[1] Aerosol OT, American Cyanamid.
[2] Tween 40, ICI America.
[3] Primafloc C-3, Rohm & Haas.

0022-3549/79/1200-1491$01.00/0
© 1979, American Pharmaceutical Association

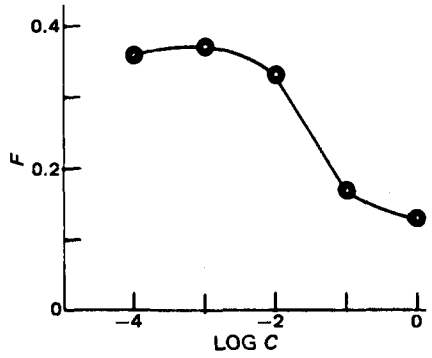

Figure 1—*Sedimentation volume of sulfamerazine suspensions in the presence of various I concentrations.*

ences in F values between the surfactants at low concentrations, but the experimental points were close enough for a single curve to describe all of the data. At low surfactant concentrations, F was comparatively high but powder wetting was incomplete. Wetting improved with an increase in surfactant concentration, becoming essentially complete at about 0.1%. At this concentration, F reached its minimum value. The sedimentation volume at higher surfactant concentrations was the same. The same F also was observed in suspensions containing 1% of the polymer and no surfactant (Fig. 1). The members of this group of suspensions behaved similarly and exhibited the characteristics of the deflocculated state, evident from the turbidity observed during sedimentation and the slow settling rate. After standing for about 1 week, a cake formed in the bottom of the cylinders.

In systems containing a surfactant, the polymer effect on flocculation depended on the surfactant. Figure 4 contains plots of sedimentation volume as a function of I concentration in suspensions wetted with dioctyl sodium sulfosuccinate. At low I concentrations, there was no effect on the flocculation state of the suspensions. A sedimentation volume increase occurred in suspensions containing 0.2% of the anionic surfactant (curve 1, Fig. 4) when the I concentration approached 0.1%. This sedimentation volume change indicates that the suspensions became flocculated, as confirmed by their appearance. Large particles were visible, and they settled quickly, leaving behind a clear supernate. The flocculated suspensions could be resuspended with little effort, even after standing for about 6 weeks, in contrast to the deflocculated systems. A higher I concentration (1%) caused a reduction in sediment volume to 0.15, indicating that the suspensions were deflocculated.

The experiments were repeated using a higher dioctyl sodium sulfosuccinate concentration (1.0%) in the suspensions. The same pattern was

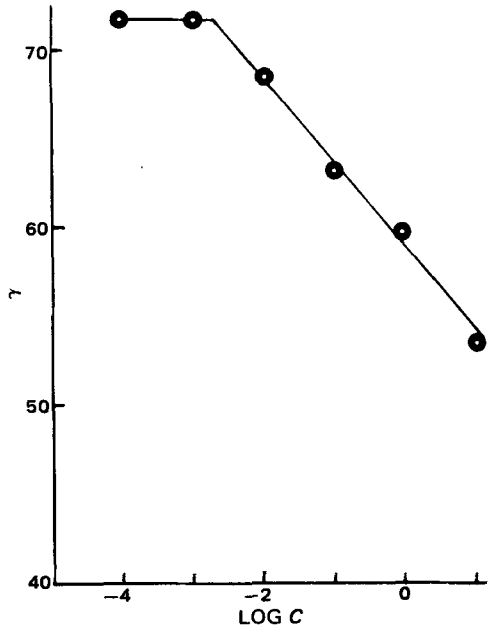

Figure 2—*Surface tension of aqueous I solutions as a function of concentration.*

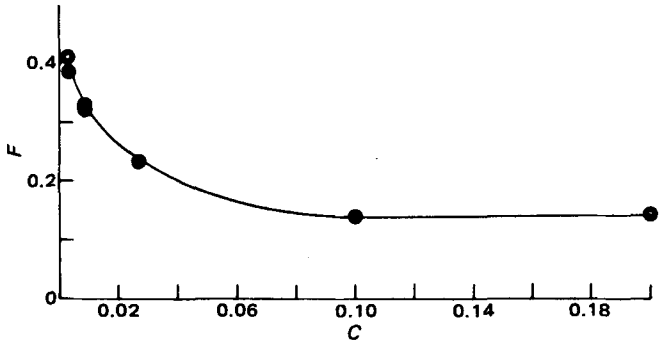

Figure 3—*Sedimentation volume of sulfamerazine suspensions in the presence of various concentrations of surfactants in the absence of I. Key: ○, polysorbate 40; and ●, dioctyl sodium sulfosuccinate.*

found as with the lower surfactant concentration (curve 2, Fig. 4), but the amount of I required to induce flocculation was higher. This result does not rule out an adsorption-dependent flocculation mechanism, but it does implicate a polymer–surfactant interaction as one important factor controlling the suspension properties.

The polymer action does not apparently involve disruption of the adsorbed dioctyl sodium sulfosuccinate film on the particle surface, although the evidence for this conclusion is indirect. It may be assumed that the air–water and particle–water interfaces are similar in that the kinds of forces responsible for adsorption are similar and surfactant orientation is the same (*i.e.*, the charged end of the surfactant molecules faces the bulk water phase). Removal of surfactant from the air–water surface by the polymer should be accompanied by a surface tension increase since the surface tension of the polymer solutions (Fig. 2) is higher than that of dioctyl sodium sulfosuccinate at the concentrations used. Instead, the changes in surface tension were quite small. The surface tension of 0.2% aqueous dioctyl sodium sulfosuccinate was 26.9 dynes/cm.

In surfactant solutions containing 0.1 and 1.0% of I, the surface tension was 26.0 dynes/cm, implying that the surfactant remains adsorbed at the air–water surface and, by inference, at the particle–water interface in the presence of added polymer.

A suggested explanation for the flocculating effect of the polymer is outlined in Fig. 5. Adsorbed surfactant carries a negative charge to the surface of the sulfamerazine particles. The particles repel each other (Fig. 5*a*) and, in the absence of I, the suspensions are deflocculated. Added polymer interacts with the excess surfactant in solution and also with the adsorbed molecules. At relatively low polymer concentrations, a limited number of polymer segments are available and the free surfactant molecules and micelles in solution compete effectively with the negatively charged particles for polymer. Increasing the polymer concentration makes more segments available, so a polymer molecule can interact simultaneously with two particles (Fig. 5*b*). The joining of adjacent particles probably is due to bridging resulting from simultaneous adsorption to more than one particle, although it is difficult to exclude an electro-

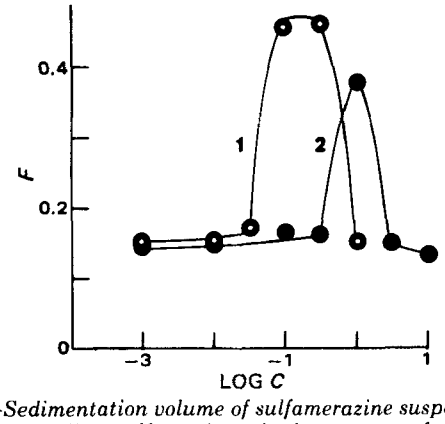

Figure 4—*Sedimentation volume of sulfamerazine suspensions containing dioctyl sodium sulfosuccinate in the presence of various I concentrations. Key: curve 1, 0.2% dioctyl sodium sulfosuccinate; and curve 2, 1.0% dioctyl sodium sulfosuccinate.*

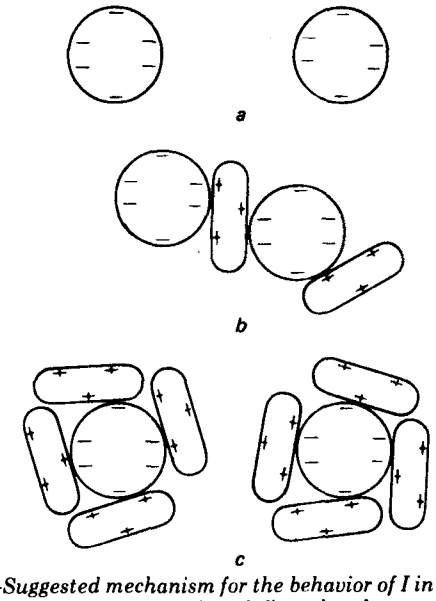

Figure 5—*Suggested mechanism for the behavior of I in suspensions. Key: a, low polymer concentration, deflocculated suspension; b, flocculation by bridging; and c, deflocculation at high polymer concentrations.*

static component (11). At much higher polymer concentrations, polymer molecules can still attach to particle surfaces but the chance of joining two particles together is greatly reduced because many other polymer molecules are readily available for adsorption. As a result, the particles become surrounded with a polymer sheath (Fig. 5c) whose charge again causes particle separation and suspension deflocculation.

The effect of raising the surfactant concentration according to this model would be to reduce the number of free polymer segments available for adsorption. Particle–polymer interaction cannot occur until higher polymer concentrations are reached. This pattern was actually observed (Fig. 4).

The influence of the polymer on suspensions containing the nonionic surfactant, polysorbate 40, is shown in Fig. 6. Deflocculated suspensions were obtained at very low and very high I concentrations. An increase in sedimentation volume was observed when the I concentration was between 0.001 and 0.01%. These suspensions were judged to be partly flocculated. The supernatant suspension medium was considerably clearer, and the sedimentation rate was more rapid than with the deflocculated systems. These suspensions did not cake. In comparison to flocculated suspensions containing the anionic surfactant, dioctyl sodium sulfosuccinate, the suspensions with the nonionic agent appeared less coarse.

As shown by a comparison of Figs. 4 and 6, the suspensions containing the nonionic surfactant had significantly smaller sedimentation volumes. The amount of polymer required to induce flocculation in these systems was about 1% of that needed in suspensions containing the anionic surfactant. The flocculation pattern as a function of the I concentration is consistent with a bridging mechanism. As with the suspensions in which dioctyl sodium sulfosuccinate was used, an excess of polymer molecules reduced the probability of polymer adsorption on more than a single particle, resulting in deflocculation.

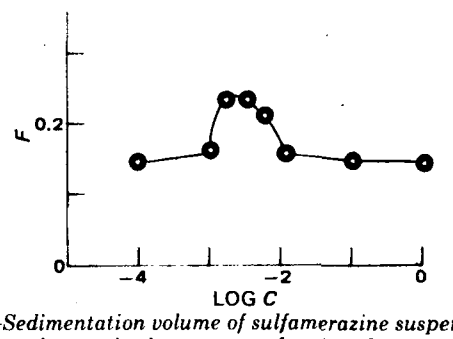

Figure 6—*Sedimentation volume of sulfamerazine suspensions containing polysorbate 40 in the presence of various I concentrations.*

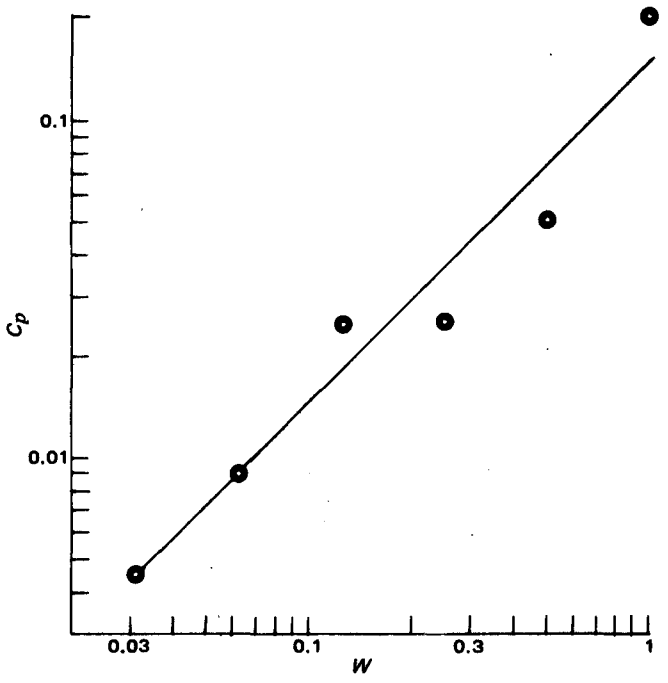

Figure 7—*Relationship between the I concentration at peak flocculation as a function of the weight fraction of dioctyl sodium sulfosuccinate in the surfactant mixture.*

Because the choice of wetting agent influenced the sedimentation volume of flocculated suspensions and the polymer concentration needed for flocculation, additional experiments were performed to determine whether these characteristics could be manipulated by using a surfactant mixture in the suspensions. The total surfactant concentration was maintained at 0.2%, but the relative concentrations of dioctyl sodium sulfosuccinate and polysorbate 40 were varied. For each surfactant combination, a series of sulfamerazine suspensions containing a range of I concentrations was prepared.

Plots of sedimentation volume as a function of the concentration of I had the same shape as the curves in Figs. 4 and 6. From these plots, the peak sedimentation volume and C_p, the concentration of I at the peak, were determined. The relationship between the I concentration required for maximum flocculation and the weight fraction of dioctyl sodium sulfosuccinate in the surfactant mixture is shown in Fig. 7. A log–log plot was used because of the large concentration range. The slope is unity, indicating a linear dependence of C_p on the content of dioctyl sodium sulfosuccinate. This relationship was anticipated because of the interaction between the polymer and dioctyl sodium sulfosuccinate discussed earlier.

The suspensions in which the weight fraction of dioctyl sodium sulfosuccinate in the surfactant mixture was less than 0.25 had peak sedimentation volumes of 0.23–0.26, which were quite close to those for suspensions containing only the nonionic surfactant. When the weight fraction of dioctyl sodium sulfosuccinate was 0.25 or greater, the sedimentation volume increased as the proportion of the anionic surfactant was increased, reaching its highest value in suspensions containing only dioctyl sodium sulfosuccinate.

These experiments demonstrated the feasibility of adjusting the surfactant combination to manipulate suspension properties. Thus, it was possible to produce adequately flocculated suspensions using a smaller amount of I than was necessary with dioctyl sodium sulfosuccinate alone as a wetting agent.

REFERENCES

(1) B. A. Haines and A. N. Martin, *J. Pharm. Sci.*, **50**, 228 (1961).

(2) E. N. Hiestand, *ibid.*, **53**, 1 (1964).

(3) R. H. Smellie, Jr., and V. K. LaMer, *J. Colloid Sci.*, **13**, 589 (1958).

(4) J. T. G. Overbeek, in "Colloid Science," vol. 1, 1st ed., Elsevier, New York, N.Y., 1952, pp. 317, 318.

(5) H. E. Ries and B. L. Meyers, *Science*, **160**, 1449 (1968).

(6) R. W. Slater and J. A. Kitchener, *Discuss. Faraday Soc.*, **42**, 267 (1966).
(7) A. Felmeister, G. M. Kuchtyak, S. Koziol, and C. J. Felmeister, *J. Pharm. Sci.*, **62**, 2026 (1973).
(8) J. Tempio, Ph.D. thesis, Rutgers University, Piscataway, N.J., 1978.
(9) Primafloc C-3 Technical Notes, Rohm & Haas, Philadelphia, Pa., 1975.
(10) W.-C. Liao and J. L. Zatz, *J. Pharm. Sci.*, **68**, 488 (1979).
(11) W. D. Corry, *J. Colloid Interface Sci.*, **63**, 151 (1978).

Solid-State Acetylation of Codeine Phosphate by Aspirin

ROBERT N. GALANTE ˣ, ANTHONY J. VISALLI, and DAHYABHAI M. PATEL

Received December 14, 1978, from the *Analytical and Physical Chemistry Department, Research and Development, William R. Rorer, Inc., Fort Washington, PA 19034.* Accepted for publication June 6, 1979.

Abstract □ A nonsolvolytic (solid-state) acetylation of codeine phosphate in the presence of aspirin to yield acetylcodeine phosphate is reported. GLC assays for the simultaneous determination of aspirin and salicylic acid and codeine and acetylcodeine are described. The apparent heat of activation for codeine phosphate is estimated, and the possible reaction mechanisms are discussed.

Keyphrases □ Codeine phosphate—acetylation by aspirin, solid dosage forms, GLC analysis of aspirin and salicylic acid, and codeine and acetylcodeine, pharmacokinetics □ Aspirin—acetylation of codeine phosphate in solid dosage forms, GLC analysis of aspirin and salicylic acid, and codeine and acetylcodeine, pharmacokinetics □ Antitussive agents—codeine phosphate, acetylation by aspirin in solid dosage forms, pharmacokinetics □ Analgesics—aspirin, acetylation of codeine phosphate in solid dosage forms, pharmacokinetics

Solid-state acetylation of codeine (I) by aspirin to yield acetylcodeine (II) has been reported (1). Other workers investigated solid-state acetylation by aspirin on homatropine (2), acetaminophen (3), and phenylephrine hydrochloride (4). Capsule and tablet formulations containing aspirin and codeine phosphate have yielded detectable amounts of acetylcodeine on aging. GLC analyses of aspirin and salicylic acid have been reported (5–13). Various silylation and methylation reagents have been employed in aspirin and salicylic acid determinations in biological fluids and pharmaceutical solid dosage forms. Although the GLC analysis of codeine and related alkaloids has been reported (14–16), there has been no report concerning the simultaneous detection and quantitation of acetylcodeine by GLC in formulations containing aspirin and codeine. This study describes the kinetics and possible mechanisms of the nonsolvolytic reactions and quantitation by GLC.

EXPERIMENTAL

Materials—Aspirin USP, a crystalline powder, was used as received (USP XIX assay: aspirin, 100.2%; salicylic acid, <0.1%. GLC purity: aspirin, 99.90%; salicylic acid, 0.1%). Codeine phosphate USP, a crystalline powder, also was used as received (USP XIX assay: 100.1%. GLC purity: 100.0% with no detectable acetylcodeine). The two drugs were mixed (aspirin–codeine phosphate, 9:1 w/w) gently by hand in a glass mortar, transferred into a twin-shell dry blender, and mixed for 2 hr. The mixture was initially assayed by GLC with the following results: aspirin, 89.40%; codeine phosphate, 10.0%; and salicylic acid, 0.1%. The water content was 0.36%, as determined by the Karl Fischer titrimetric method.

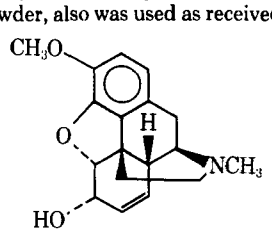

I

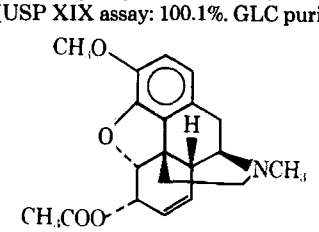

II

Kinetic Studies—About 300 mg of the mixture was transferred into preweighed glass ampuls, and the ampuls were then weighed again. The ampuls were flame sealed and stored at 60, 70, 80, and 90° in constant-temperature water baths (±0.2°). Water baths were kept covered from light, and samples were periodically removed and assayed. Samples that were removed and not assayed the same day were stored at 5°. Because a eutectic forms after a period of time, the entire contents of the ampul were used for analysis to ensure no loss of material.

Acetylcodeine Synthesis—About 400–500 mg of codeine phosphate, accurately weighed, was transferred into a 50-ml screw-capped test tube. Two milliliters of acetic anhydride and 0.5 ml of pyridine were added. The test tube was tightly capped and placed in a water bath maintained at 80° for 2 hr. Then it was placed in an ice bath for 10 min, following which 2 ml of water was added. Cautiously, stronger ammonia water was added dropwise until the mixture was distinctly alkaline.

The test tube was replaced into the ice bath for ~15 min with occasional shaking to complete acetylcodeine precipitation. About 10 ml of chloroform was added to the test tube, and the mixture was shaken vigorously for 2 min. The upper aqueous layer was removed by vacuum, the chloroform was washed with 2 × 5-ml portions of water, and the water was removed by vacuum. About 500 mg of anhydrous sodium sulfate was added to the test tube, which was shaken to remove residual water.

The chloroform was decanted carefully through glass wool into a suitable evaporating dish. The test tube was rinsed with two additional 10-ml portions of chloroform and passed through the glass wool into the same dish. Then the chloroform was evaporated carefully to near dryness on a steam bath under a nitrogen stream. The residue was air dried at room temperature for 2 hr and then dried in a vacuum oven at 60° for 4 hr. The dry residue weight corresponded to a 96% yield of acetylcodeine.

Anal.—Calc. for $C_{20}H_{23}NO_4$: C, 70.40; H, 6.80; N, 4.10. Found: C, 70.42; H, 6.78; N, 4.02.

GLC Purity—The purity was 99.14% calculated by area percent.

TLC Purity—One spot was observed at R_f 0.67 when the sample was chromatographed on precoated silica gel G plates[1] in chloroform–methanol (10:1) and sprayed with Dragendorff's reagent.

NMR and IR—NMR and IR were used to confirm the identity of acetylcodeine.

High-Pressure Liquid Chromatography (HPLC)—Acetylcodeine phosphate and codeine phosphate were separated by isocratic reversed-phase HPLC using a literature method (17). The mobile phase was 0.1 *M* NaH_2PO_4 in 25% acetonitrile–water. The retention times for codeine phosphate and acetylcodeine phosphate were 6 and 16 min, respectively. Codeine was not detected in the synthesized acetylcodeine.

Isolation and Identification of Reaction Product—Acetylcodeine was characterized in the degraded samples of codeine phosphate and aspirin by fractionating the mixture using preparative TLC. The sepa-

[1] Analtech, Newark, Del.

0022-3549/79/1200-1494$01.00/0
© 1979, American Pharmaceutical Association

(6) R. W. Slater and J. A. Kitchener, *Discuss. Faraday Soc.*, **42**, 267 (1966).
(7) A. Felmeister, G. M. Kuchtyak, S. Koziol, and C. J. Felmeister, *J. Pharm. Sci.*, **62**, 2026 (1973).
(8) J. Tempio, Ph.D. thesis, Rutgers University, Piscataway, N.J., 1978.
(9) Primafloc C-3 Technical Notes, Rohm & Haas, Philadelphia, Pa., 1975.
(10) W.-C. Liao and J. L. Zatz, *J. Pharm. Sci.*, **68**, 488 (1979).
(11) W. D. Corry, *J. Colloid Interface Sci.*, **63**, 151 (1978).

Solid-State Acetylation of Codeine Phosphate by Aspirin

ROBERT N. GALANTE ˣ, ANTHONY J. VISALLI, and DAHYABHAI M. PATEL

Received December 14, 1978, from the *Analytical and Physical Chemistry Department, Research and Development, William R. Rorer, Inc., Fort Washington, PA 19034.* Accepted for publication June 6, 1979.

Abstract □ A nonsolvolytic (solid-state) acetylation of codeine phosphate in the presence of aspirin to yield acetylcodeine phosphate is reported. GLC assays for the simultaneous determination of aspirin and salicylic acid and codeine and acetylcodeine are described. The apparent heat of activation for codeine phosphate is estimated, and the possible reaction mechanisms are discussed.

Keyphrases □ Codeine phosphate—acetylation by aspirin, solid dosage forms, GLC analysis of aspirin and salicylic acid, and codeine and acetylcodeine, pharmacokinetics □ Aspirin—acetylation of codeine phosphate in solid dosage forms, GLC analysis of aspirin and salicylic acid, and codeine and acetylcodeine, pharmacokinetics □ Antitussive agents—codeine phosphate, acetylation by aspirin in solid dosage forms, pharmacokinetics □ Analgesics—aspirin, acetylation of codeine phosphate in solid dosage forms, pharmacokinetics

Solid-state acetylation of codeine (I) by aspirin to yield acetylcodeine (II) has been reported (1). Other workers investigated solid-state acetylation by aspirin on homatropine (2), acetaminophen (3), and phenylephrine hydrochloride (4). Capsule and tablet formulations containing aspirin and codeine phosphate have yielded detectable amounts of acetylcodeine on aging. GLC analyses of aspirin and salicylic acid have been reported (5–13). Various silylation and methylation reagents have been employed in aspirin and salicylic acid determinations in biological fluids and pharmaceutical solid dosage forms. Although the GLC analysis of codeine and related alkaloids has been reported (14–16), there has been no report concerning the simultaneous detection and quantitation of acetylcodeine by GLC in formulations containing aspirin and codeine. This study describes the kinetics and possible mechanisms of the nonsolvolytic reactions and quantitation by GLC.

EXPERIMENTAL

Materials—Aspirin USP, a crystalline powder, was used as received (USP XIX assay: aspirin, 100.2%; salicylic acid, <0.1%. GLC purity: aspirin, 99.90%; salicylic acid, 0.1%). Codeine phosphate USP, a crystalline powder, also was used as received (USP XIX assay: 100.1%. GLC purity: 100.0% with no detectable acetylcodeine). The two drugs were mixed (aspirin–codeine phosphate, 9:1 w/w) gently by hand in a glass mortar, transferred into a twin-shell dry blender, and mixed for 2 hr. The mixture was initially assayed by GLC with the following results: aspirin, 89.40%; codeine phosphate, 10.0%; and salicylic acid, 0.1%. The water content was 0.36%, as determined by the Karl Fischer titrimetric method.

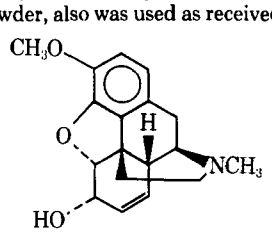

I

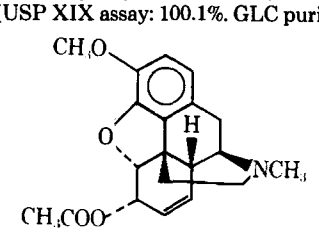

II

Kinetic Studies—About 300 mg of the mixture was transferred into preweighed glass ampuls, and the ampuls were then weighed again. The ampuls were flame sealed and stored at 60, 70, 80, and 90° in constant-temperature water baths (±0.2°). Water baths were kept covered from light, and samples were periodically removed and assayed. Samples that were removed and not assayed the same day were stored at 5°. Because a eutectic forms after a period of time, the entire contents of the ampul were used for analysis to ensure no loss of material.

Acetylcodeine Synthesis—About 400–500 mg of codeine phosphate, accurately weighed, was transferred into a 50-ml screw-capped test tube. Two milliliters of acetic anhydride and 0.5 ml of pyridine were added. The test tube was tightly capped and placed in a water bath maintained at 80° for 2 hr. Then it was placed in an ice bath for 10 min, following which 2 ml of water was added. Cautiously, stronger ammonia water was added dropwise until the mixture was distinctly alkaline.

The test tube was replaced into the ice bath for ~15 min with occasional shaking to complete acetylcodeine precipitation. About 10 ml of chloroform was added to the test tube, and the mixture was shaken vigorously for 2 min. The upper aqueous layer was removed by vacuum, the chloroform was washed with 2 × 5-ml portions of water, and the water was removed by vacuum. About 500 mg of anhydrous sodium sulfate was added to the test tube, which was shaken to remove residual water.

The chloroform was decanted carefully through glass wool into a suitable evaporating dish. The test tube was rinsed with two additional 10-ml portions of chloroform and passed through the glass wool into the same dish. Then the chloroform was evaporated carefully to near dryness on a steam bath under a nitrogen stream. The residue was air dried at room temperature for 2 hr and then dried in a vacuum oven at 60° for 4 hr. The dry residue weight corresponded to a 96% yield of acetylcodeine.

Anal.—Calc. for $C_{20}H_{23}NO_4$: C, 70.40; H, 6.80; N, 4.10. Found: C, 70.42; H, 6.78; N, 4.02.

GLC Purity—The purity was 99.14% calculated by area percent.

TLC Purity—One spot was observed at R_f 0.67 when the sample was chromatographed on precoated silica gel G plates[1] in chloroform–methanol (10:1) and sprayed with Dragendorff's reagent.

NMR and IR—NMR and IR were used to confirm the identity of acetylcodeine.

High-Pressure Liquid Chromatography (HPLC)—Acetylcodeine phosphate and codeine phosphate were separated by isocratic reversed-phase HPLC using a literature method (17). The mobile phase was 0.1 *M* NaH_2PO_4 in 25% acetonitrile–water. The retention times for codeine phosphate and acetylcodeine phosphate were 6 and 16 min, respectively. Codeine was not detected in the synthesized acetylcodeine.

Isolation and Identification of Reaction Product—Acetylcodeine was characterized in the degraded samples of codeine phosphate and aspirin by fractionating the mixture using preparative TLC. The sepa-

[1] Analtech, Newark, Del.

0022-3549/79/1200-1494$01.00/0
© 1979, American Pharmaceutical Association

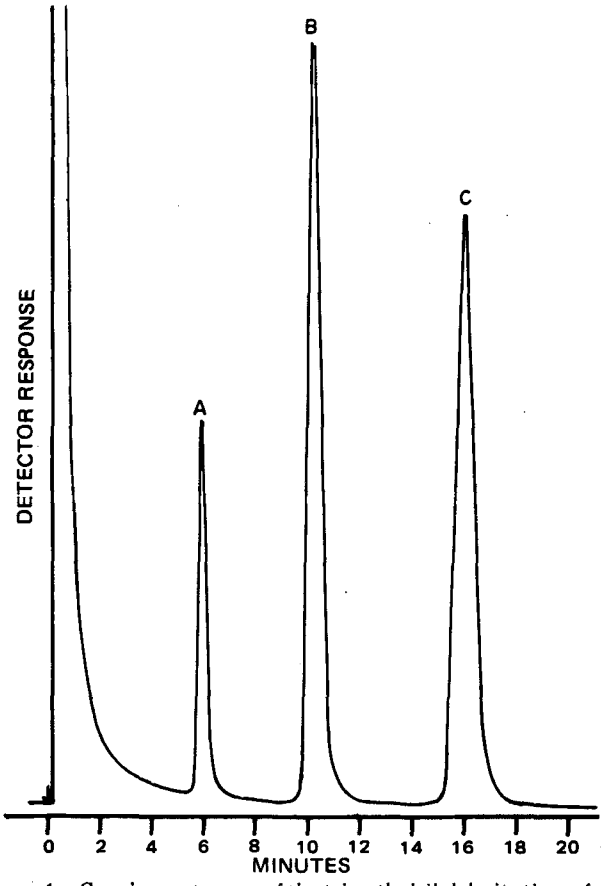

Figure 1—*Gas chromatogram of the trimethylsilyl derivatives of salicylic acid (A), aspirin (B), and the internal standard propylparaben (C).*

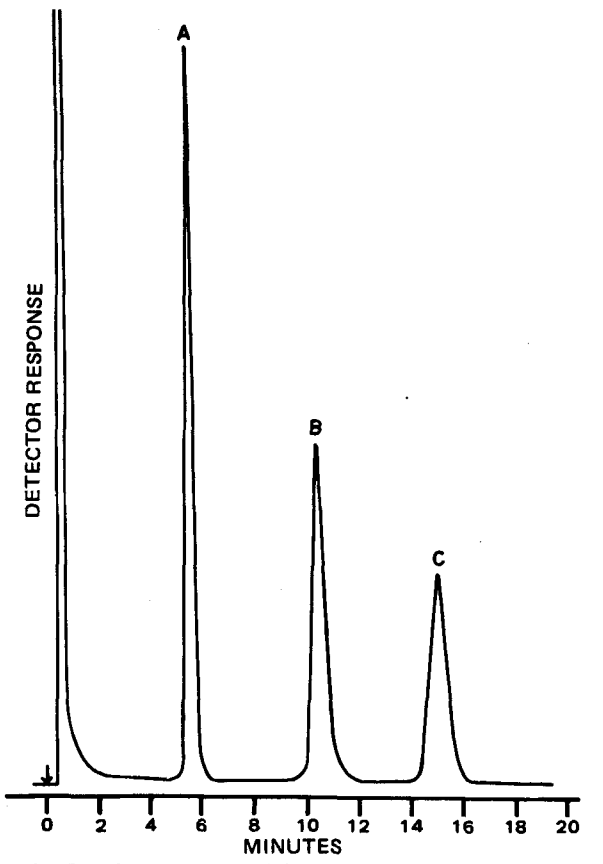

Figure 2—*Gas chromatogram of the internal standard methaqualone (A), codeine (B), and acetylcodeine (C).*

rated degradation spot was scraped from the plate and extracted with chloroform. The chloroform was evaporated to dryness, and the residue was subjected to a comparative IR analysis with synthesized acetylcodeine. The spectra were identical. This finding confirmed the presence of acetylcodeine in the degraded mixture of codeine phosphate and aspirin as reported previously (1).

Simultaneous GLC Analysis of Aspirin and Salicylic Acid—*Instrumentation*—A gas chromatograph[2] and an electronic integrator[3] equipped with a flame-ionization detector and a glass column [1.8 m (6 ft) × 2 mm i.d., packed with 3% phenyl methyl silicone[4] on 100–120-mesh silanized diatomaceous earth[5]] were used. The operating temperatures were: column, 120°; detector, 225°; and injection port, 225°. Nitrogen, with a flow rate of 35 ml/min, was the carrier gas. The injection volume was 2.0 μl.

Internal Standard Preparation—About 500 mg of propylparaben USP was diluted to 100 ml with chloroform and mixed.

Aspirin Standard Preparation—About 60–65 mg of aspirin USP reference standard, accurately weighed, was transferred into a 25-ml volumetric flask, diluted to volume with chloroform, and mixed. Once prepared, the aspirin standard was derivatized within 2 hr. The trimethylsilyl derivative was stable for 48 hr in an airtight container.

Salicylic Acid Standard Preparation—About 35 mg of salicylic acid USP reference standard, accurately weighed, was transferred into a 25-ml volumetric flask, diluted to volume with chloroform, and mixed.

Sample Preparation—The entire contents of the ampul were quantitatively transferred into a 100-ml volumetric flask, diluted to volume with chloroform, and mixed. Aged samples that were slightly turbid in chloroform were not filtered prior to derivatization. Sample preparations were derivatized within 2 hr.

Procedure—A 2.0-ml aliquot of the sample preparation was transferred into a suitable reaction vial. A 2.0-ml aliquot of the aspirin standard preparation and a 1.0-ml aliquot of the salicylic acid standard preparation were combined in a second reaction vial. A 1.0-ml aliquot of the internal standard preparation was transferred into each of the sample and standard vials. All vials were derivatized with 200 μl of *N,O*-bis(trimethylsilyl)acetamide[6].

The vials were capped and shaken for 1 min and then were allowed to stand at room temperature for at least 1 hr for complete derivatization. The peak area ratios of the trimethylsilyl derivatives were determined, and the percentages of aspirin and salicylic acid were calculated in the samples. The retention times for salicylic acid, aspirin, and the propylparaben trimethylsilyl derivatives were 6.0, 10.2, and 16 min, respectively (Fig. 1). At the end of each day's run, the column temperature was raised to 250° to elute codeine and acetylcodeine, which do not elute under the conditions for analysis of salicylic acid and aspirin.

Simultaneous GLC Analysis of Codeine Phosphate and Acetylcodeine Phosphate—*Instrumentation*—The instrumentation was the same as described earlier, except that a glass column [1.2 m (4 ft) × 4 mm i.d., packed with 3.8% methyl vinyl silicone gum rubber[7] on 80–100-mesh silanized diatomaceous earth[8]] was used. The operating temperatures were: column, 230°; detector, 250°; and injection port, 250°. Nitrogen, with a flow rate of 45 ml/min, was the carrier gas. The injection volume was 2.0 μl.

Internal Standard Preparation—About 80 mg of methaqualone NF was diluted to 100 ml with chloroform and mixed.

Codeine Phosphate Standard Preparation—About 30 mg of codeine phosphate, accurately weighed, was transferred into a 125-ml separator containing 30 ml of chloroform, 20 ml of water, and 2 ml of stronger ammonia solution. The separator was shaken for 1 min, and the lower chloroform layer containing the codeine base was transferred through glass wool into a 100-ml volumetric flask. The extraction was repeated with two additional 30-ml portions of chloroform, and the contents were diluted to volume and mixed.

[2] Hewlett-Packard 7620A.
[3] Hewlett-Packard 3370A.
[4] OV-17, Analabs, Northhaven, Conn.
[5] Gas Chrom Q, Applied Science Laboratories, State College, Pa.
[6] Pierce Chemical Co., Rockford, Ill.
[7] UC-W98, Analabs, Northhaven, Conn.
[8] Chromosorb W-H.P., Celite Division, Johns Manville.

Table I—Assay Data for Kinetic Mixtures[a]

Temperature	Hours	Codeine Phosphate, %	Codeine Phosphate[b] Degraded, %	Aspirin, %	Aspirin[c] Degraded, %
90°	504	<0.5	58.2	67.2	6.4
80°	747	<0.5	51.7	80.0	6.3
70°	842	<0.5	50.1	87.0	6.8
60°	4000	<0.5	50.5	82.5	6.9

[a] All percentages are expressed as a percent of the theoretical amount of aspirin and codeine phosphate in the initial mixture. [b] Percent codeine phosphate degraded to acetylcodeine phosphate. [c] Percent aspirin degraded to salicylic acid.

Acetylcodeine Standard Preparation—About 20 mg of acetylcodeine, accurately weighed, was transferred into a 100-ml volumetric flask, diluted to volume with chloroform, and mixed.

Sample Preparation—The contents of each ampul were quantitatively transferred into a 100-ml volumetric flask with chloroform, diluted to volume, and mixed.

Procedure—A 10.0-ml aliquot of the sample preparation was transferred into a 125-ml separator containing 20 ml of water and 2 ml of stronger ammonia solution. The separator was shaken for 1 min, and the lower chloroform layer was filtered through glass wool and collected in a beaker containing 3.0 ml of the internal standard preparation. The extraction was repeated with two additional 15-ml portions of chloroform.

The standard was prepared by transferring and combining 10.0-ml aliquots each of the codeine and acetylcodeine standard preparations into a beaker containing 3.0 ml of the internal standard preparation. Both the sample and standard beakers were placed on a steam bath, and the volume was reduced to 2–3 ml with a nitrogen stream. The peak area ratios were determined, and the percentages of codeine phosphate and acetylcodeine phosphate were calculated in the samples. The retention times for methaqualone, codeine, and acetylcodeine were 5.8, 10.4, and 15.0 min, respectively (Fig. 2).

RESULTS AND DISCUSSION

Linearity and Precision—The response linearity of the described GLC methods was suitable for the entire assay range. The precision, on multiple injections, was ±0.42% for the codeine–acetylcodeine procedure and ±0.50% for the aspirin–salicylic acid procedure.

Codeine Phosphate Disappearance—The evaluation of such a complex system did not lend itself to a detailed kinetic analysis. Table I shows the percentages of codeine phosphate degraded to acetylcodeine phosphate and of aspirin degraded to salicylic acid when the codeine phosphate remaining was <0.5% at various temperatures. From the kinetic plots shown in Figs. 3 and 4, the correlation coefficients at 60, 70, 80, and 90° were 0.998, 0.998, 0.998, and 0.998, respectively.

The kinetics of codeine phosphate disappearance were pseudo-first order after an initial lag time. The lag time was attributed to a delay in aspirin hydrolysis to salicylic acid. This delay was more evident at 60 than at 90°. The reaction rate constants and half-lives for codeine phosphate disappearance are given in Table II. An Arrhenius plot (Fig. 5) yielded an activation energy of 35.8 kcal/mole. A composite representation of codeine phosphate degradation to acetylcodeine phosphate at various temperatures is given in Fig. 6. Since ~50–58% of the original codeine phosphate degraded to acetylcodeine phosphate, other degradation pathways were apparent.

TLC examination of the degraded samples, after spraying with Dragendorff's reagent, showed two or three other distinct spots of nitrogen-containing compounds. This finding indicated possible thermal decomposition of the codeine phosphate, Hoffman degradation, or acid-catalyzed rearrangements of the side chain and cleavage of the oxide bridge. The complex chemistry and mechanisms of these reactions were discussed by Manske and Holmes (18).

Acetylcodeine Appearance—Since acetic acid is necessary for acetylcodeine formation, aspirin hydrolysis must occur before any

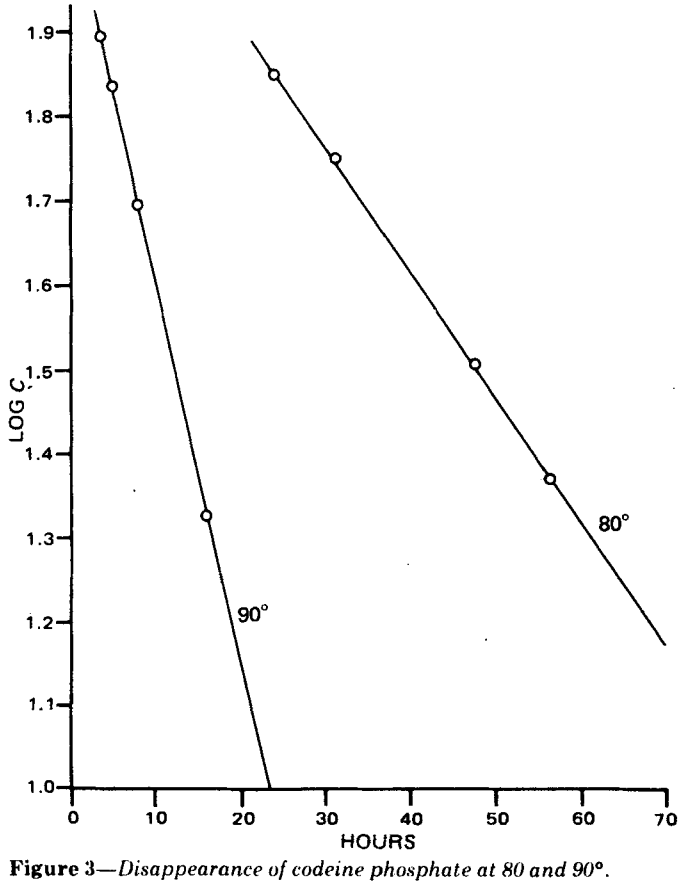

Figure 3—*Disappearance of codeine phosphate at 80 and 90°.*

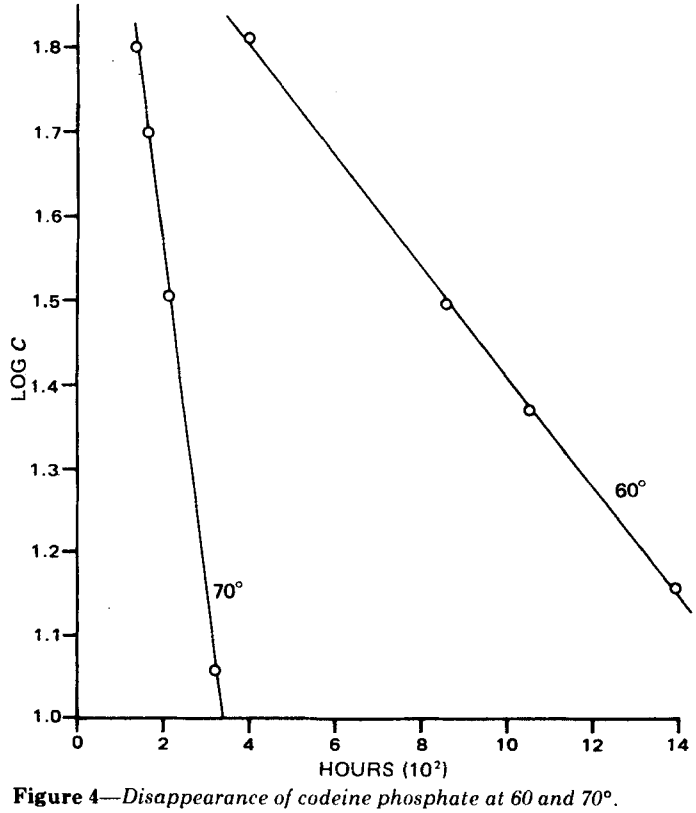

Figure 4—*Disappearance of codeine phosphate at 60 and 70°.*

Table II—Reaction Rate Constants and Half-Lives for Codeine Phosphate Disappearance

Temperature	Reaction Rate Constant, hr^{-1}	Half-Life, hr
90°	0.090040	7.7
80°	0.019810	35
70°	0.003962	175
60°	0.001020	680

acetylcodeine is detected. The rate of acetylcodeine phosphate formation followed no specific order, and the kinetics were of some complex order not directly related to codeine phosphate disappearance.

Salicylic Acid Appearance—Aspirin degradation to salicylic acid levels off to 6–7% at all temperatures. However, the theoretical amount of salicylic acid formation should be 4.0%, calculated from the 0.36% water content in the mixture. Additional water is generated from the following reactions:

1. One molecule of water is generated from each molecule of codeine phosphate acetylated by aspirin.
2. Acid-catalyzed rearrangement of the side chain of the codeine phosphate produces one molecule of water for each molecule of codeine phosphate undergoing decomposition.
3. Cleavage of the oxide bridge in the codeine phosphate degradation produces additional water.
4. One molecule of water is generated in the reaction of two molecules of aspirin to form acetylsalicylic acid anhydride.
5. Acetic anhydride may be generated from acetic acid, resulting in one molecule of water for each molecule of acetic anhydride formed.

The calculated amount of additional water required to produce the 6–7% level of salicylic acid formation is 0.81 mg/300 mg of mixture. From the acetylation reaction, 0.66 mg of water was generated at all temperatures based on the average of 50% degradation of codeine phosphate to acetylcodeine phosphate. This amount accounts for ~80% of the additional water required. The other reactions listed, occurring concomitantly, would easily account for the additional water required to justify the 6–7% salicylic acid formation. The rate of salicylic acid formation in this study did not follow any specific kinetic order because of the complex reactions involved.

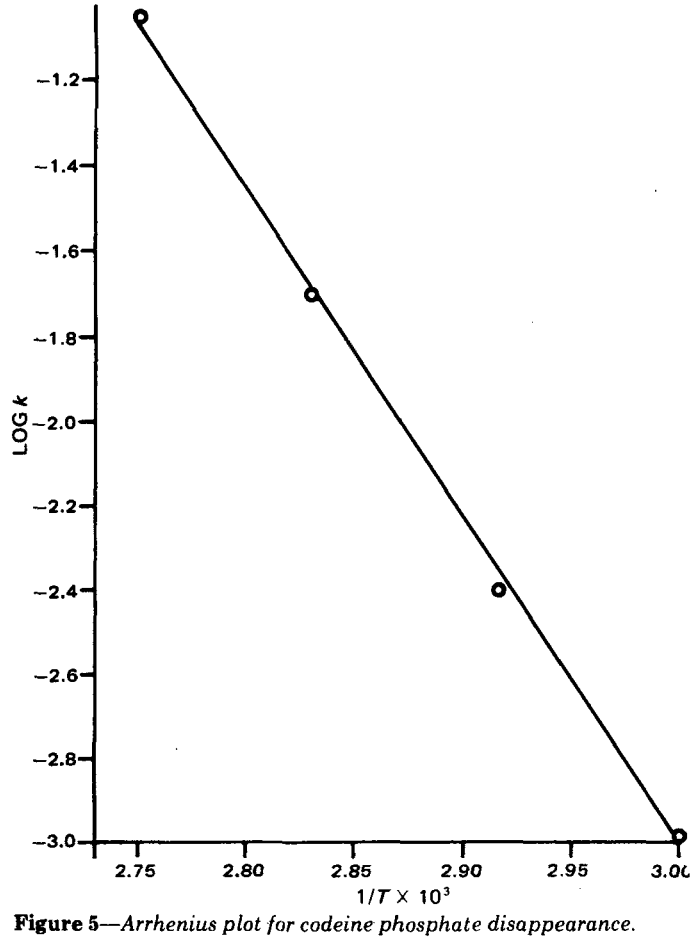

Figure 5—*Arrhenius plot for codeine phosphate disappearance.*

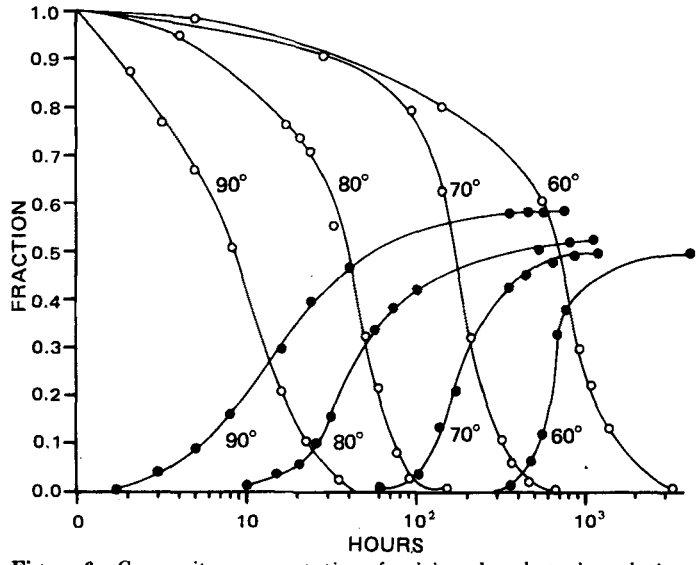

Figure 6—*Composite representation of codeine phosphate degradation to acetylcodeine phosphate under varying temperature conditions. Key:* ○, *codeine phosphate remaining; and* ●, *codeine phosphate degraded to acetylcodeine phosphate.*

Aspirin Disappearance—Aspirin continued to degrade slowly even after salicylic acid formation leveled off. Aspirin degradation may also include the formation of acetylsalicylsalicylic acid and acetylsalicylic anhydride (19, 20). Positive identification of these species was not made, but their formation cannot be excluded since the limited amount of water in the mixture prevents total hydrolysis of aspirin to salicylic acid.

SUMMARY

Pharmaceutical solid dosage forms containing aspirin in combination with codeine phosphate and other drug species are subject to nonsolvolytic acetylation by aspirin even at a low moisture level. Acid–base titrimetric methods for the analysis of codeine in combination with aspirin in pharmaceutical dosage forms cannot detect acetylcodeine formation. This study demonstrates the reactivity of aspirin; the drug acetylated 50–58% of the codeine phosphate in the experimental mixture.

Acetylation of a drug substance by aspirin may alter a drug's physiological activity or toxicity. However, for acetylcodeine, the physiological activity is reported to be about the same as codeine (21). The extensive use of aspirin in pharmaceutical solid dosage forms in combination with alkaloids, antihistamines, and other analgesics requires stability-specific methods of analysis to ascertain the molecular transformations of nonsolvolytic reactions.

REFERENCES

(1) A. L. Jacobs, A. E. Dilatush, S. Weinstein, and J. J. Windheuser, *J. Pharm. Sci.*, **55**, 893 (1966).

(2) E. Shami, J. Dudzinski, L. Lachman, and J. Tingstad, *ibid.*, **62**, 1283 (1973).

(3) K. T. Koshy, A. E. Troup, R. N. Duvall, R. C. Conwell, and L. L. Shankle, *ibid.*, **56**, 1117 (1967).

(4) A. E. Troup and H. Mitchner, *ibid.*, **53**, 375 (1964).

(5) P. P. Ascione and G. P. Chrekian, *ibid.*, **64**, 1029 (1975).

(6) R. C. Crippen and H. C. Freimuth, *Anal. Chem.*, **36**, 273 (1964).

(7) J. R. Watson, F. Matsui, P. M. J. McConnell, and R. C. Lawrence, *J. Pharm. Sci.*, **61**, 929 (1972).

(8) E. B. Dechene, L. H. Booth, and J. J. Caughey, *J. Pharm. Pharmacol.*, **21**, 678 (1969).

(9) M. J. Rance, B. J. Jordan, and J. D. Nichols, *ibid.*, **27**, 425 (1975).

(10) B. H. Thomas, G. Solomonraj, and B. B. Coldwell, *ibid.*, **25**, 201 (1973).

(11) P. H. Ko, *J. Pharm. Sci.*, **66**, 731 (1977).

(12) M. Rowland and S. Riegelman, *ibid.*, **56**, 717 (1967).

(13) W. E. Lange and S. A. Bell, *ibid.*, **55**, 386 (1966).
(14) W. O. R. Ebbighausen, J. H. Mowat, P. Vestergaard, and N. S. Kline, *Adv. Biochem. Psychopharmacol.*, **7**, 135 (1973).
(15) M. K. Brunson and J. F. Nash, *Clin. Chem.*, **21**, 1956 (1975).
(16) N. C. Jain, T. C. Sneath, R. D. Budd, and W. J. Leung, *ibid.*, **21**, 1486 (1975).
(17) C. Y. Wu and J. J. Wittick, *Anal. Chem.*, **49**, 359 (1977).
(18) R. H. F. Manske and H. L. Holmes, "The Alkaloids—Chemistry and Physiology," vol. 2, Academic, New York, N.Y., 1952.
(19) S. Patel, J. H. Perrin, and J. J. Windheuser, *J. Pharm. Sci.*, **61**, 1795 (1972).
(20) S. L. Ali, *J. Chromatogr.*, **126**, 651 (1976).
(21) W. R. Buckett, M. E. Farquharson, and G. G. Haining, *J. Pharm. Pharmacol.*, **16**, 174 (1963).

Effect of Interaction of Aluminum Hydroxycarbonate Gel and Magnesium Hydroxide Gel on Acid Neutralization

ROGER K. VANDERLAAN *, JOE L. WHITE ‡, and STANLEY L. HEM *x

Received March 19, 1979, from the **Industrial and Physical Pharmacy Department and the* ‡*Department of Agronomy, Purdue University, West Lafayette, IN 47907.* Accepted for publication June 7, 1979.

Abstract □ Acid neutralization by mixtures of aluminum hydroxycarbonate gel and magnesium hydroxide gel differs from the sum of the acid neutralization of each gel. Acid neutralization by magnesium hydroxide gel in the mixture is not observed until after a substantial portion of the aluminum hydroxycarbonate gel has reacted with acid, even though magnesium hydroxide gel is the faster reacting of the two gels. It is hypothesized that amorphous aluminum hydroxycarbonate forms a coating on the crystalline magnesium hydroxide particles due to electrostatic attraction. This coating prevents protons from reaching the highly reactive magnesium hydroxide until the coating is dissolved by the acid neutralization of aluminum hydroxycarbonate.

Keyphrases □ Aluminum hydroxycarbonate gel—acid neutralization, effect of interaction with magnesium hydroxide gel □ Magnesium hydroxide gel—acid neutralization, effect of interaction with aluminum hydroxycarbonate gel □ Antacids—aluminum hydroxycarbonate, magnesium hydroxide, effect of interaction on acid neutralization

Aluminum hydroxycarbonate gel (1) and magnesium hydroxide gel are formulated in combination in many antacid products. Aluminum hydroxycarbonate gel exhibits antacid activity only when amorphous. With aging, order develops in the amorphous structure, which reduces the acid reactivity and ultimately leads to the formation of an inactive crystalline state (2, 3).

A chemical property of aluminum hydroxycarbonate gel that makes it useful as an antacid is its ability to maintain pH 3.5–4.0 while reacting with acid (4). Aluminum hydroxycarbonate is not systemically absorbed and, aside from causing constipation, is free of side effects (5).

BACKGROUND

The solid phase of magnesium hydroxide gel has a crystalline structure known mineralogically as brucite. However, in contrast to the behavior of crystalline aluminum hydroxide, the crystalline magnesium hydroxide gel rapidly reacts with acid (6). Due to its well-ordered crystal structure, it exhibits excellent stability.

Magnesium hydroxide gel reacts with acid at a constant pH of 8.0–8.5. This pH is not as desirable as the one maintained during acid neutralization by aluminum hydroxycarbonate gel and, therefore, magnesium hydroxide gel is not frequently used as an antacid. In addition, magnesium ion produced during acid neutralization may be systemically absorbed, so a warning to patients with kidney disease is required (5). Magnesium ion also causes a cathartic effect, which balances the action of aluminum hydroxide gel on the intestine and provides the rationale for combining aluminum hydroxycarbonate gel and magnesium hydroxide gel in antacid products.

The addition of less than stoichiometric amounts of acid does not lower the pH of magnesium hydroxide gel below 8. However, a mixture of aluminum hydroxycarbonate gel–magnesium hydroxide gel drops to ~pH 4 after the addition of a relatively small amount of acid. Furthermore, it remains at ~pH 4 even when more acid is added (7). This behavior suggests an interaction between the amorphous aluminum hydroxycarbonate and the crystalline magnesium hydroxide gels. The investigation was undertaken to study this interaction, with emphasis on its effect on acid neutralization.

EXPERIMENTAL

Materials—Aluminum hydroxycarbonate gel containing the equivalent of 4% Al_2O_3 was prepared by the reaction of aluminum chloride, sodium bicarbonate, and sodium carbonate to a final pH of 6.5 (8).

Magnesium hydroxide gel[1] was obtained commercially, and a gel containing the equivalent of 7% MgO was prepared by dilution.

All chemicals were either official or reagent grade.

Preparation of Gel Mixtures—Mixtures of aluminum hydroxycarbonate gel and magnesium hydroxide gel containing 0.6 mmole of metal ion/g were prepared on a weight basis. For example, a 200-g mixture with a 5:1 molar ratio of magnesium to aluminum was prepared by weighing magnesium hydroxide gel and aluminum hydroxycarbonate gel containing 100 mmoles of magnesium and 20 mmoles of aluminum, respectively. The final weight of the mixture was adjusted to 200 g with double-distilled water, and the mixture was stirred mechanically until uniform.

Analytical Procedures—The aluminum and magnesium contents of the mixtures were determined by chelatometric titration (9).

The acid-neutralization reaction was monitored by an automated[2] pH-stat titration (10). For a typical pH-stat titration, 20 ml of double-distilled water was added to the reaction flask and brought to pH 3.0. An accurately weighed gel mixture sample, which would theoretically neutralize 2.25 meq of acid, was added; the recorder was started simultaneously. The cumulative amount of acid needed to maintain pH 3.0 was recorded as a function of time.

Atomic absorption spectrophotometry was employed to determine the concentrations of aluminum and magnesium ions in solution during acid neutralization. The pH-stat titration was halted at various times, the reaction medium was filtered quickly through a 0.22-μm filter, and the filtrate was analyzed for aluminum and magnesium.

RESULTS

Characteristic pH-stat titrigrams of aluminum hydroxycarbonate gel and magnesium hydroxide gel are shown in Fig. 1.

Kerkhof *et al.* (10) characterized the pH-stat titrigram of an aluminum

[1] HydroMagma, Merck & Co., Rahway, N.J.
[2] PHM 26, TTT II, ABU 12 (2.5 ml), TTA 3, SBR 2, Radiometer, Copenhagen, Denmark.

0022-3549/79/1200-1498$01.00/0
© 1979, American Pharmaceutical Association

(13) W. E. Lange and S. A. Bell, *ibid.*, **55**, 386 (1966).
(14) W. O. R. Ebbighausen, J. H. Mowat, P. Vestergaard, and N. S. Kline, *Adv. Biochem. Psychopharmacol.*, **7**, 135 (1973).
(15) M. K. Brunson and J. F. Nash, *Clin. Chem.*, **21**, 1956 (1975).
(16) N. C. Jain, T. C. Sneath, R. D. Budd, and W. J. Leung, *ibid.*, **21**, 1486 (1975).
(17) C. Y. Wu and J. J. Wittick, *Anal. Chem.*, **49**, 359 (1977).
(18) R. H. F. Manske and H. L. Holmes, "The Alkaloids—Chemistry and Physiology," vol. 2, Academic, New York, N.Y., 1952.
(19) S. Patel, J. H. Perrin, and J. J. Windheuser, *J. Pharm. Sci.*, **61**, 1795 (1972).
(20) S. L. Ali, *J. Chromatogr.*, **126**, 651 (1976).
(21) W. R. Buckett, M. E. Farquharson, and G. G. Haining, *J. Pharm. Pharmacol.*, **16**, 174 (1963).

Effect of Interaction of Aluminum Hydroxycarbonate Gel and Magnesium Hydroxide Gel on Acid Neutralization

ROGER K. VANDERLAAN *, JOE L. WHITE ‡, and STANLEY L. HEM *x

Received March 19, 1979, from the **Industrial and Physical Pharmacy Department and the* ‡*Department of Agronomy, Purdue University, West Lafayette, IN 47907.* Accepted for publication June 7, 1979.

Abstract □ Acid neutralization by mixtures of aluminum hydroxycarbonate gel and magnesium hydroxide gel differs from the sum of the acid neutralization of each gel. Acid neutralization by magnesium hydroxide gel in the mixture is not observed until after a substantial portion of the aluminum hydroxycarbonate gel has reacted with acid, even though magnesium hydroxide gel is the faster reacting of the two gels. It is hypothesized that amorphous aluminum hydroxycarbonate forms a coating on the crystalline magnesium hydroxide particles due to electrostatic attraction. This coating prevents protons from reaching the highly reactive magnesium hydroxide until the coating is dissolved by the acid neutralization of aluminum hydroxycarbonate.

Keyphrases □ Aluminum hydroxycarbonate gel—acid neutralization, effect of interaction with magnesium hydroxide gel □ Magnesium hydroxide gel—acid neutralization, effect of interaction with aluminum hydroxycarbonate gel □ Antacids—aluminum hydroxycarbonate, magnesium hydroxide, effect of interaction on acid neutralization

Aluminum hydroxycarbonate gel (1) and magnesium hydroxide gel are formulated in combination in many antacid products. Aluminum hydroxycarbonate gel exhibits antacid activity only when amorphous. With aging, order develops in the amorphous structure, which reduces the acid reactivity and ultimately leads to the formation of an inactive crystalline state (2, 3).

A chemical property of aluminum hydroxycarbonate gel that makes it useful as an antacid is its ability to maintain pH 3.5–4.0 while reacting with acid (4). Aluminum hydroxycarbonate is not systemically absorbed and, aside from causing constipation, is free of side effects (5).

BACKGROUND

The solid phase of magnesium hydroxide gel has a crystalline structure known mineralogically as brucite. However, in contrast to the behavior of crystalline aluminum hydroxide, the crystalline magnesium hydroxide gel rapidly reacts with acid (6). Due to its well-ordered crystal structure, it exhibits excellent stability.

Magnesium hydroxide gel reacts with acid at a constant pH of 8.0–8.5. This pH is not as desirable as the one maintained during acid neutralization by aluminum hydroxycarbonate gel and, therefore, magnesium hydroxide gel is not frequently used as an antacid. In addition, magnesium ion produced during acid neutralization may be systemically absorbed, so a warning to patients with kidney disease is required (5). Magnesium ion also causes a cathartic effect, which balances the action of aluminum hydroxide gel on the intestine and provides the rationale for combining aluminum hydroxycarbonate gel and magnesium hydroxide gel in antacid products.

The addition of less than stoichiometric amounts of acid does not lower the pH of magnesium hydroxide gel below 8. However, a mixture of aluminum hydroxycarbonate gel–magnesium hydroxide gel drops to ~pH 4 after the addition of a relatively small amount of acid. Furthermore, it remains at ~pH 4 even when more acid is added (7). This behavior suggests an interaction between the amorphous aluminum hydroxycarbonate and the crystalline magnesium hydroxide gels. The investigation was undertaken to study this interaction, with emphasis on its effect on acid neutralization.

EXPERIMENTAL

Materials—Aluminum hydroxycarbonate gel containing the equivalent of 4% Al_2O_3 was prepared by the reaction of aluminum chloride, sodium bicarbonate, and sodium carbonate to a final pH of 6.5 (8).

Magnesium hydroxide gel[1] was obtained commercially, and a gel containing the equivalent of 7% MgO was prepared by dilution.

All chemicals were either official or reagent grade.

Preparation of Gel Mixtures—Mixtures of aluminum hydroxycarbonate gel and magnesium hydroxide gel containing 0.6 mmole of metal ion/g were prepared on a weight basis. For example, a 200-g mixture with a 5:1 molar ratio of magnesium to aluminum was prepared by weighing magnesium hydroxide gel and aluminum hydroxycarbonate gel containing 100 mmoles of magnesium and 20 mmoles of aluminum, respectively. The final weight of the mixture was adjusted to 200 g with double-distilled water, and the mixture was stirred mechanically until uniform.

Analytical Procedures—The aluminum and magnesium contents of the mixtures were determined by chelatometric titration (9).

The acid-neutralization reaction was monitored by an automated[2] pH-stat titration (10). For a typical pH-stat titration, 20 ml of double-distilled water was added to the reaction flask and brought to pH 3.0. An accurately weighed gel mixture sample, which would theoretically neutralize 2.25 meq of acid, was added; the recorder was started simultaneously. The cumulative amount of acid needed to maintain pH 3.0 was recorded as a function of time.

Atomic absorption spectrophotometry was employed to determine the concentrations of aluminum and magnesium ions in solution during acid neutralization. The pH-stat titration was halted at various times, the reaction medium was filtered quickly through a 0.22-μm filter, and the filtrate was analyzed for aluminum and magnesium.

RESULTS

Characteristic pH-stat titrigrams of aluminum hydroxycarbonate gel and magnesium hydroxide gel are shown in Fig. 1.

Kerkhof *et al.* (10) characterized the pH-stat titrigram of an aluminum

[1] HydroMagma, Merck & Co., Rahway, N.J.
[2] PHM 26, TTT II, ABU 12 (2.5 ml), TTA 3, SBR 2, Radiometer, Copenhagen, Denmark.

0022-3549/79/1200-1498$01.00/0
© 1979, American Pharmaceutical Association

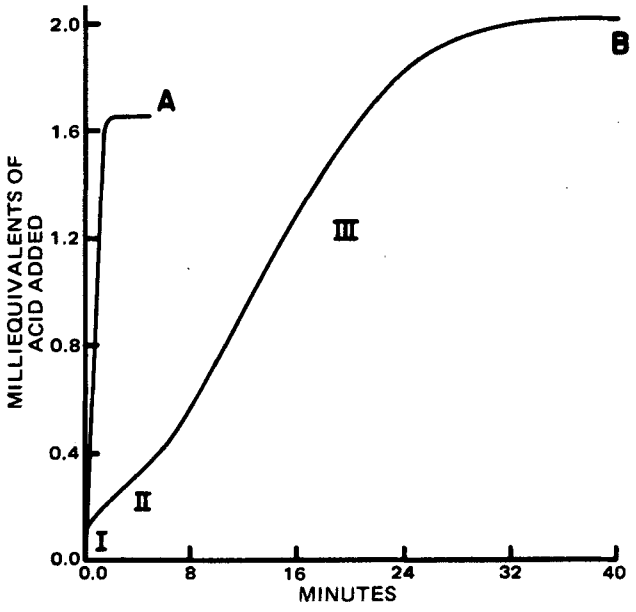

Figure 1—*The pH-stat titrigrams at pH 3.0 of magnesium hydroxide gel (A) and aluminum hydroxycarbonate gel with the three phases of the neutralization reaction indicated as described by Kerkhof* et al. *(10) (B).*

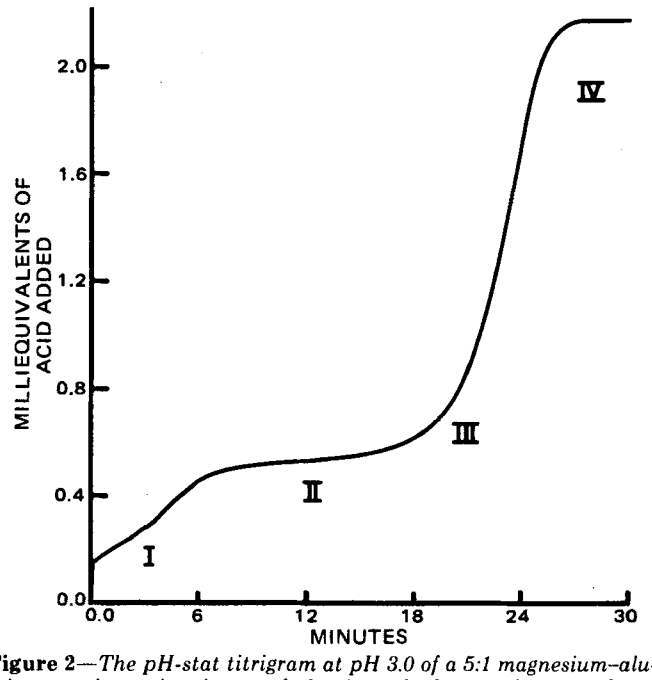

Figure 2—*The pH-stat titrigram at pH 3.0 of a 5:1 magnesium–aluminum molar ratio mixture of aluminum hydroxycarbonate gel and magnesium hydroxide gel with the four phases of the neutralization reaction indicated.*

hydroxycarbonate gel as consisting of three phases. The first phase represents a rapid reaction, which exceeds the maximum rate of acid addition and is attributed to the neutralization of free hydroxyl and carbonate as well as to small aluminum hydroxycarbonate polymers. Additional carbonate reacts in the second phase, which disrupts the polymeric structure and permits the rapid neutralization observed in the third phase.

The pH-stat titrigram of magnesium hydroxide gel exhibits a single high reactivity phase.

The pH-stat titrigram of a mixture of aluminum hydroxycarbonate gel and magnesium hydroxide gel shows four phases (Fig. 2). The first phase is a period of relatively rapid acid neutralization. Close examination of Phase I reveals three phases similar to those observed for aluminum hydroxycarbonate gel. Phase II, a lag phase, is a period of minimal acid reactivity. Phase III is characterized by a very rapid rate of acid neutralization, as is seen in the magnesium hydroxide gel titrigram. Phase IV represents the termination of the reaction and may be characterized either by an immediate cessation in acid neutralization or by a prolonged period of slow neutralization.

The pH-stat titrigram obtained when an aluminum hydroxycarbonate gel and a magnesium hydroxide gel were injected simultaneously into the pH-stat reaction vessel so that the gels were not mixed prior to the neutralization reaction is shown in Fig. 3A. The titrigram shows a phase of very rapid acid reactivity followed by slower neutralization during the termination phase. The aluminum hydroxycarbonate gel and the magnesium hydroxide gel appear to react simultaneously, with the neutralization reactions being additive.

A quite different neutralization reaction occurred if the aluminum hydroxycarbonate gel and magnesium hydroxide gel were mixed prior to being introduced into the pH-stat reaction vessel. A contact time of only 15 min prior to testing resulted in a four-phase titrigram (Fig. 3B) similar to the titrigram seen for mixtures of aluminum hydroxycarbonate gel and magnesium hydroxide gel (Fig. 2).

Clearly, an immediate interaction takes place between the aluminum hydroxycarbonate gel and the magnesium hydroxide gel, which yields a pH-stat titrigram that cannot be interpreted in terms of the simple sum of the acid reactivities of the two gels.

The acid reactivity of a 5:1 magnesium–aluminum molar ratio mixture of magnesium hydroxide gel and aluminum hydroxycarbonate gel was examined at different pH values along with the acid reactivity of each gel. Figure 4 compares the effect of pH on the acid-neutralization reactions of aluminum hydroxycarbonate and magnesium hydroxide gels.

Magnesium hydroxide gel reacts very rapidly at pH 3.0 and 4.5. Since magnesium hydroxide is not precipitated by base below pH 9.5 (11), the difference in the driving force for dissolution between neutralization reactions at pH 3.0 and 4.5 would be expected to be relatively small.

The pH-stat titrigram for aluminum hydroxycarbonate gel at pH 3.0 shows that the theoretical amount of acid is neutralized. However, negligible acid is neutralized by aluminum hydroxycarbonate gel at pH 4.5. Since aluminum hydroxycarbonate gel may be precipitated at a pH as low as 4 (12), the relative difference in the forces causing the aluminum hydroxycarbonate gel dissolution are great between pH 3.0 and 4.5. Rapid aluminum hydroxycarbonate dissolution would not be expected at a pH where precipitation of aluminum hydroxycarbonate may occur.

Titrigrams of the aluminum hydroxycarbonate gel–magnesium hy-

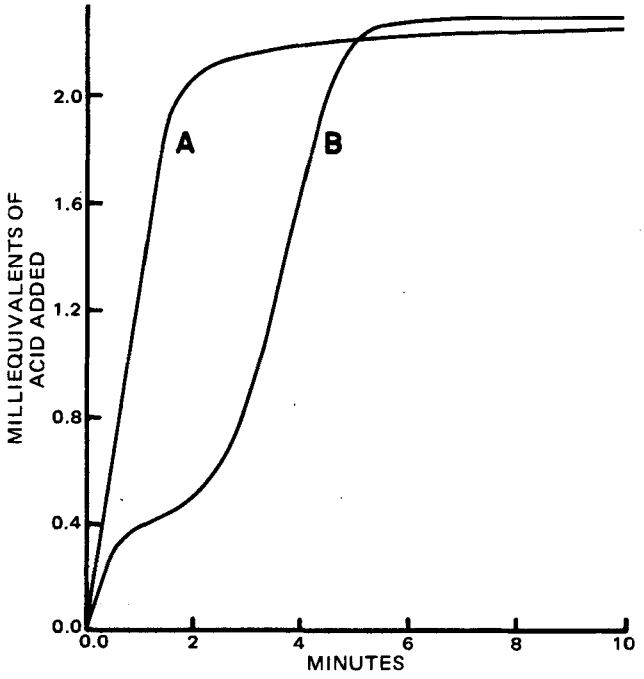

Figure 3—*The pH-stat titrigrams at pH 3.0 of a 5:1 molar ratio magnesium hydroxide gel and aluminum hydroxycarbonate gel mixture. Key: A, gels injected simultaneously into the reaction vessel without premixing; and B, gels mixed for 15 min before injection of the mixture into the reaction vessel.*

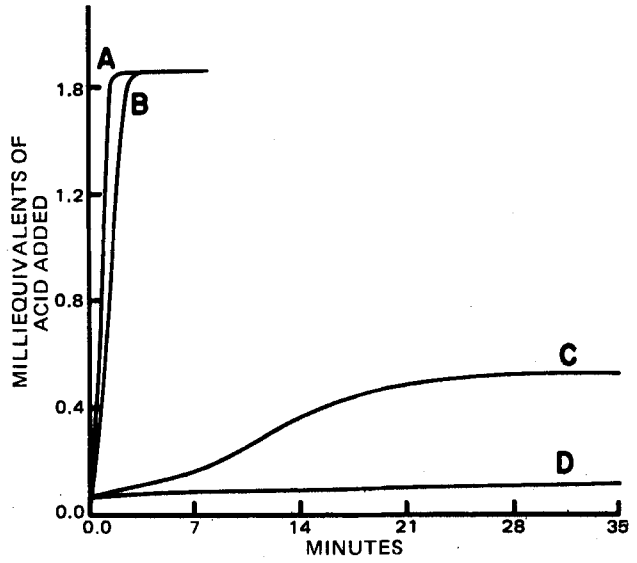

Figure 4—*The pH-stat titrigrams of magnesium hydroxide gel at pH 3.0 (A) and 4.5 (B) and of aluminum hydroxycarbonate gel at pH 3.0 (C) and 4.5 (D).*

droxide gel mixture were obtained at pH 1.5–4.5. Figure 5 shows that the titrigram retains its four-phase profile between pH 1.5 and 4.25 and that the time required for neutralization increases substantially as the pH approaches 4.5.

However, the neutralization reaction of the mixture at pH 4.5 showed no increase in acid neutralization, even after 6 hr. Although aluminum hydroxycarbonate gel was expected to be unreactive at pH 4.5, the magnesium hydroxide gel exhibited rapid reactivity at pH 3.0 and 4.5 (Fig. 4).

The total amount of acid neutralized by the mixtures was the sum of the acid neutralized by each component for pH 1.5–4.0. The aluminum hydroxycarbonate became unreactive at pH 4.5, as did the mixture of aluminum hydroxycarbonate gel and magnesium hydroxide gel, even though individually the magnesium hydroxide reacted completely with acid at this pH (Fig. 4).

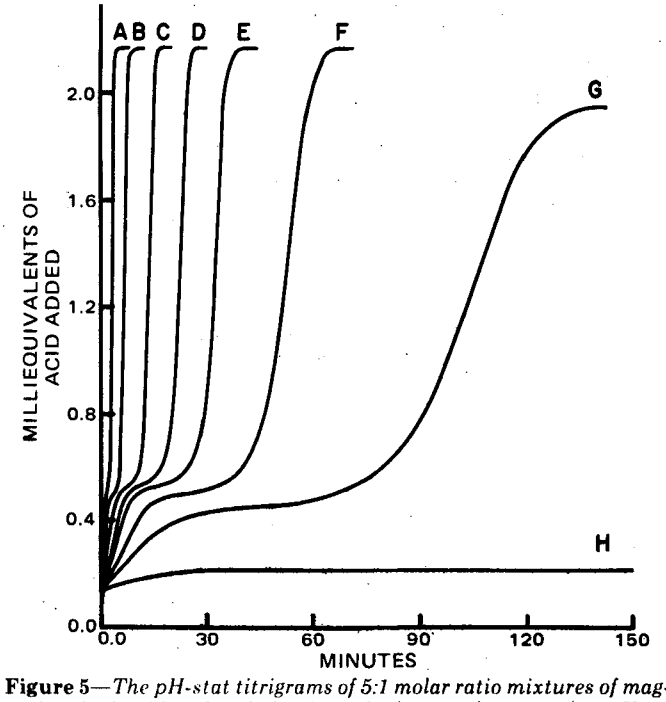

Figure 5—*The pH-stat titrigrams of 5:1 molar ratio mixtures of magnesium hydroxide gel and aluminum hydroxycarbonate gel at pH 1.5 (A), 2.0 (B), 2.5 (C), 3.0 (D), 3.5 (E), 4.0 (F), 4.25 (G), and 4.5 (H).*

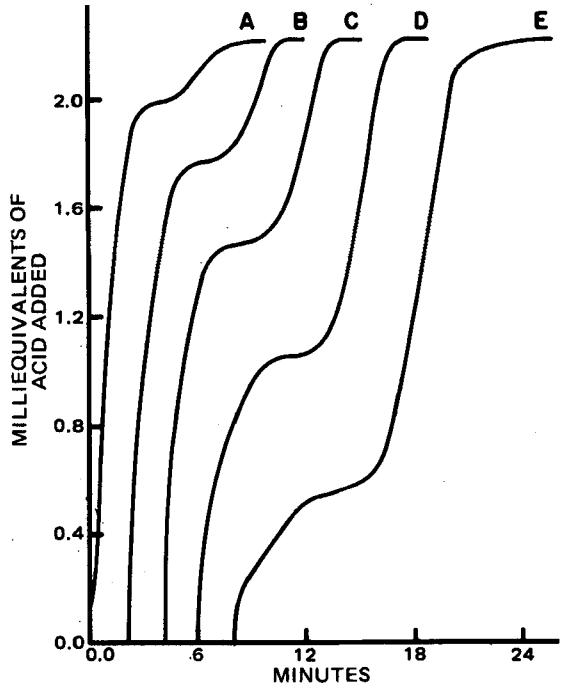

Figure 6—*The pH-stat titrigrams at pH 3.0 of mixtures of aluminum hydroxycarbonate gel and magnesium hydroxide gel of various molar ratios of magnesium to aluminum. Key: A, 1:5; B, 1:2; C, 1:1; D, 2:1; and E, 5:1.*

The pH-stat titrigrams of five aluminum hydroxycarbonate gel and magnesium hydroxide gel mixtures containing 0.6 mmole of metal/g at various magnesium to aluminum molar ratios are compared in Fig. 6. A direct relationship is seen between the magnesium to aluminum ratio of the gel mixture and the ratio of the amounts of acid neutralized during Phases III and I. In each case, the aluminum hydroxycarbonate gel appears to react with acid before the magnesium hydroxide gel reacts.

The liberation of aluminum and magnesium ions during the pH-stat neutralization at pH 3.0 of an aluminum hydroxycarbonate gel–magnesium hydroxide gel mixture was monitored by atomic absorption spectrophotometry. The milliequivalents of each metal ion in solution were compared to the milliequivalents of acid neutralized (Fig. 7). The magnesium-ion concentration did not begin to increase until virtually all of the aluminum was in solution. The total milliequivalents of metal ion in solution showed the expected 1:1 relationship to the milliequivalents of acid neutralized.

DISCUSSION

The pH of the aluminum hydroxycarbonate gel and magnesium hydroxide gel mixtures ranged from 8.0 for the 1:5 magnesium–aluminum molar ratio mixture to 8.6 for the 5:1 magnesium–aluminum molar ratio mixture. The magnesium hydroxide gel pH was 10.3, while the aluminum hydroxycarbonate gel was precipitated to pH 6.5.

The apparent surface charge of a particle in suspension is determined by the isoelectric point or zero point charge. The apparent surface charge is negative when the pH is above the zero point charge and positive if the pH is below the zero point charge (13).

The isoelectric point of magnesium hydroxide gel was reported as pH 12 (14). At the pH of the gel mixtures, the magnesium hydroxide surface would be expected to have a net positive charge.

Isoelectric points from pH 6.3 to 9.1 were reported for aluminum hydroxide (15–18) as a result of the diverse nature of the substance commonly termed aluminum hydroxide. Schott (17) recently reported an isoelectric point of 8.5 for aluminum hydroxide but was very careful to exclude coordinating anions from the aluminum hydroxide. According to Parks (13), anions such as those found in aluminum hydroxide gels with desirable acid reactivity for use as antacids substantially lower the isoelectric point. Thus, at the pH of the gel mixtures, the aluminum hydroxycarbonate surface would be expected to be negative.

It is hypothesized that the electrostatic attraction between the aluminum hydrocarbonate gel and the magnesium hydroxide gel causes

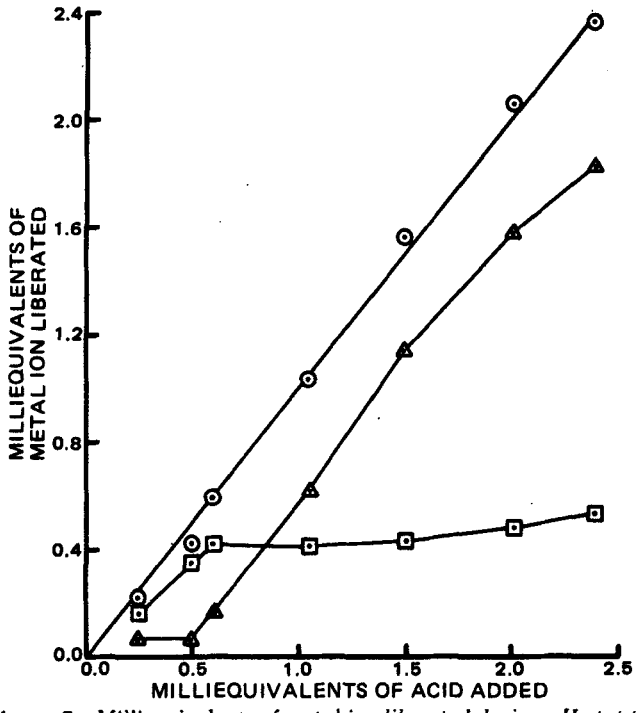

Figure 7—*Milliequivalents of metal ion liberated during pH-stat titration at pH 3.0 of a 5:1 magnesium–aluminum molar ratio mixture of aluminum hydroxycarbonate gel and magnesium hydroxide gel. Key: △, milliequivalents of magnesium ion in solution; □, milliequivalents of aluminum ion in solution; and ○, total milliequivalents of magnesium and aluminum ions in solution.*

agglomeration in the gel mixtures. Treadwell and Bernasconi (19) proposed an adsorption bonding of this type. Thus, the amorphous aluminum hydroxycarbonate would form a coating on the crystalline brucite magnesium hydroxide gel. The aluminum hydroxycarbonate coating would prevent protons from reaching the highly reactive brucite until the coating dissolves due to acid neutralization of the aluminum hydroxycarbonate. As was observed in the pH-stat titrigrams of mixed aluminum hydroxycarbonate–magnesium hydroxide gels, the acid neutralization will occur more slowly than expected due to the coating of the faster reacting magnesium hydroxide gel by the slower reacting aluminum hydroxycarbonate gel.

REFERENCES

(1) C. J. Serna, J. L. White, and S. L. Hem, *J. Pharm. Sci.*, **67**, 1144 (1978).
(2) S. L. Nail, J. L. White, and S. L. Hem, *ibid.*, **65**, 231 (1976).
(3) *Ibid.*, **65**, 1192 (1976).
(4) S. L. Hem, *J. Chem. Educ.*, **52**, 383 (1975).
(5) *Fed. Regist.*, **39** (108), 19875 (June 4, 1974).
(6) C. J. Serna, J. L. White, and S. L. Hem, *J. Pharm. Sci.*, **67**, 324 (1978).
(7) J. F. Morrissey and R. F. Barreras, *N. Engl. J. Med.*, **290**, 550 (1974).
(8) S. L. Hem, E. J. Russo, S. M. Bahal, and R. S. Levi, *J. Pharm. Sci.*, **59**, 317 (1970).
(9) "The United States Pharmacopeia," 19th rev., Mack Publishing Co., Easton, Pa., 1975, p. 290.
(10) N. J. Kerkhof, R. K. Vanderlaan, J. L. White, and S. L. Hem, *J. Pharm. Sci.*, **66**, 1528 (1977).
(11) R. C. Turner and J. E. Brydon, *Science*, **136**, 1052 (1962).
(12) G. J. Ross and H. Kodama, *Am. Mineral.*, **52**, 1036 (1967).
(13) G. A. Parks, *Chem. Rev.*, **65**, 177 (1965).
(14) S. Mattson and A. J. Pugh, *Soil Sci.*, **38**, 229 (1934).
(15) R. Fricke and H. Keefer, *Naturforschung*, **4A**, 76 (1949).
(16) S. Mattson, *Soil Sci.*, **30**, 459 (1930).
(17) H. Schott, *J. Pharm. Sci.*, **66**, 1548 (1977).
(18) N. Tewari and S. Ghosh, *Kolloid-Z.*, **138**, 93 (1954).
(19) W. D. Treadwell and E. Bernasconi, *Helv. Chim. Acta*, **13**, 500 (1930).

ACKNOWLEDGMENTS

Supported in part by an American Foundation for Pharmaceutical Education Fellowship to R. K. Vanderlaan.
This report is Journal Paper 7558, Purdue University Agricultural Experiment Station, West Lafayette, IN 47907.

Simple Epoxide Analogs of Trichothecans

NEAL C. CORBIN, PHILLIP FRAHER, and JAMES D. McCHESNEY *x

Received January 15, 1979, from the *Department of Medicinal Chemistry, School of Pharmacy, University of Kansas, Lawrence, KS 66045.* Accepted for publication June 21, 1979. *Present address: Department of Pharmacognosy, School of Pharmacy, University of Mississippi, University, MS 38677.

Abstract □ To define clearly the epoxide grouping role in trichothecan biological activity, a series of hindered epoxides was prepared. They possessed α,α′-substitution reminiscent of the epoxide environment of the natural products. None of these analogs demonstrated biological activities similar to the natural toxins.

Keyphrases □ Trichothecans—epoxide analogs, structure–activity relationships, toxicity □ Fungistatic agents—trichothecans, epoxide analogs, structure–activity relationships, toxicity

In 1946, as part of a program to discover new antibiotics, a highly fungistatic principle was isolated from a culture filtrate of *Metarrhizium glutinosum* S. Pope (1). This principle was highly irritating to human skin. Similar agents were produced by various microorganisms, including *Trichothecium roseum* and species of *Fusaria* and *Trichoderma* (2). Continued work with these materials led to the isolation in pure form of one of these principles; it was named trichothecin (3). Since that time, many related compounds have been isolated and characterized and are collectively known as the trichothecans (I), a name coined for the ring system possessed by all of these materials (4).

BACKGROUND

All trichothecans contain a 12,13-epoxy group, a 9,10-double bond, and the 4-β-hydroxyl. The simplest of the group, trichodermin (II), contains an acetate ester and only functionalities characteristic of all trichothecans. The most complex materials contain a fifth, macrocyclic ring, which is formed *via* esterification of hydroxyls at positions 4 and 15 by a long chain diacid.

0022-3549/79/1200-1501$01.00/0
© 1979, American Pharmaceutical Association

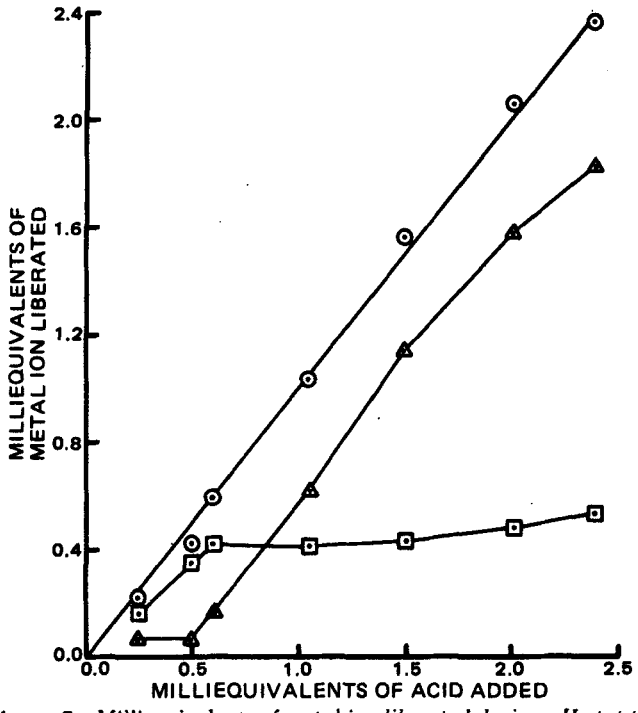

Figure 7—*Milliequivalents of metal ion liberated during pH-stat titration at pH 3.0 of a 5:1 magnesium–aluminum molar ratio mixture of aluminum hydroxycarbonate gel and magnesium hydroxide gel. Key: △, milliequivalents of magnesium ion in solution; □, milliequivalents of aluminum ion in solution; and ○, total milliequivalents of magnesium and aluminum ions in solution.*

agglomeration in the gel mixtures. Treadwell and Bernasconi (19) proposed an adsorption bonding of this type. Thus, the amorphous aluminum hydroxycarbonate would form a coating on the crystalline brucite magnesium hydroxide gel. The aluminum hydroxycarbonate coating would prevent protons from reaching the highly reactive brucite until the coating dissolves due to acid neutralization of the aluminum hydroxycarbonate. As was observed in the pH-stat titrigrams of mixed aluminum hydroxycarbonate–magnesium hydroxide gels, the acid neutralization will occur more slowly than expected due to the coating of the faster reacting magnesium hydroxide gel by the slower reacting aluminum hydroxycarbonate gel.

REFERENCES

(1) C. J. Serna, J. L. White, and S. L. Hem, *J. Pharm. Sci.*, **67**, 1144 (1978).
(2) S. L. Nail, J. L. White, and S. L. Hem, *ibid.*, **65**, 231 (1976).
(3) *Ibid.*, **65**, 1192 (1976).
(4) S. L. Hem, *J. Chem. Educ.*, **52**, 383 (1975).
(5) *Fed. Regist.*, **39** (108), 19875 (June 4, 1974).
(6) C. J. Serna, J. L. White, and S. L. Hem, *J. Pharm. Sci.*, **67**, 324 (1978).
(7) J. F. Morrissey and R. F. Barreras, *N. Engl. J. Med.*, **290**, 550 (1974).
(8) S. L. Hem, E. J. Russo, S. M. Bahal, and R. S. Levi, *J. Pharm. Sci.*, **59**, 317 (1970).
(9) "The United States Pharmacopeia," 19th rev., Mack Publishing Co., Easton, Pa., 1975, p. 290.
(10) N. J. Kerkhof, R. K. Vanderlaan, J. L. White, and S. L. Hem, *J. Pharm. Sci.*, **66**, 1528 (1977).
(11) R. C. Turner and J. E. Brydon, *Science*, **136**, 1052 (1962).
(12) G. J. Ross and H. Kodama, *Am. Mineral.*, **52**, 1036 (1967).
(13) G. A. Parks, *Chem. Rev.*, **65**, 177 (1965).
(14) S. Mattson and A. J. Pugh, *Soil Sci.*, **38**, 229 (1934).
(15) R. Fricke and H. Keefer, *Naturforschung*, **4A**, 76 (1949).
(16) S. Mattson, *Soil Sci.*, **30**, 459 (1930).
(17) H. Schott, *J. Pharm. Sci.*, **66**, 1548 (1977).
(18) N. Tewari and S. Ghosh, *Kolloid-Z.*, **138**, 93 (1954).
(19) W. D. Treadwell and E. Bernasconi, *Helv. Chim. Acta*, **13**, 500 (1930).

ACKNOWLEDGMENTS

Supported in part by an American Foundation for Pharmaceutical Education Fellowship to R. K. Vanderlaan.
This report is Journal Paper 7558, Purdue University Agricultural Experiment Station, West Lafayette, IN 47907.

Simple Epoxide Analogs of Trichothecans

NEAL C. CORBIN, PHILLIP FRAHER, and JAMES D. McCHESNEY *x

Received January 15, 1979, from the *Department of Medicinal Chemistry, School of Pharmacy, University of Kansas, Lawrence, KS 66045.* Accepted for publication June 21, 1979. *Present address: Department of Pharmacognosy, School of Pharmacy, University of Mississippi, University, MS 38677.

Abstract □ To define clearly the epoxide grouping role in trichothecan biological activity, a series of hindered epoxides was prepared. They possessed α,α′-substitution reminiscent of the epoxide environment of the natural products. None of these analogs demonstrated biological activities similar to the natural toxins.

Keyphrases □ Trichothecans—epoxide analogs, structure–activity relationships, toxicity □ Fungistatic agents—trichothecans, epoxide analogs, structure–activity relationships, toxicity

In 1946, as part of a program to discover new antibiotics, a highly fungistatic principle was isolated from a culture filtrate of *Metarrhizium glutinosum* S. Pope (1). This principle was highly irritating to human skin. Similar agents were produced by various microorganisms, including *Trichothecium roseum* and species of *Fusaria* and *Trichoderma* (2). Continued work with these materials led to the isolation in pure form of one of these principles; it was named trichothecin (3). Since that time, many related compounds have been isolated and characterized and are collectively known as the trichothecans (I), a name coined for the ring system possessed by all of these materials (4).

BACKGROUND

All trichothecans contain a 12,13-epoxy group, a 9,10-double bond, and the 4-β-hydroxyl. The simplest of the group, trichodermin (II), contains an acetate ester and only functionalities characteristic of all trichothecans. The most complex materials contain a fifth, macrocyclic ring, which is formed *via* esterification of hydroxyls at positions 4 and 15 by a long chain diacid.

0022-3549/79/1200-1501$01.00/0
© 1979, American Pharmaceutical Association

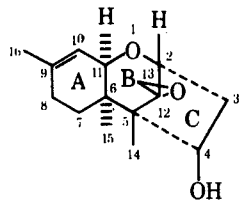

I

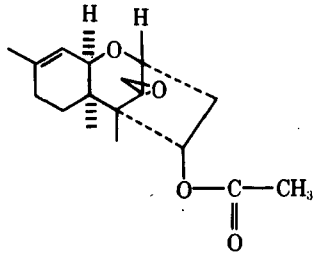

II

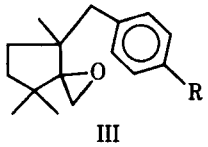

III

All trichothecans possess a high degree of biological activity. They also are very toxic to mammals and cause severe skin irritation on contact.

The chemistry and biology of this group of sesquiterpenoids were reviewed (5).

The trichothecans are interesting from several viewpoints. They seem to have great potential medicinal utility, particularly as antifungal, antibiotic, and antitumor agents. Although their toxicity has precluded extensive clinical use, their high activity warrants a search for active analogs that are less toxic. Since trichodermin is a potent antifungal agent and yet much less toxic than other trichothecans, high toxicity is not necessarily inherent in their basic structural features.

The trichothecans are also of likely agricultural significance. Elucidation of the features responsible for their toxicity to livestock could be useful in determining which trichothecans cause the various types of toxicity and could aid in the design of inhibitors or antidotes for their effects.

To elucidate the mechanism of action and the structural features necessary for the various types of activity possessed by the trichothecans, a series of compounds was proposed (III). This series is a model of the C ring of the trichothecan nucleus. It contains the epoxide, which is probably necessary for activity, plus heavy substitution on the adjacent carbon atoms. It has been proposed that lipophilicity is important for trichothecan activity (6); therefore, a benzyl group was attached to the cyclopentane ring, and the hydroxyl present at C-4 in the natural products was deleted.

The compounds in the series are identical except for a varying substituent on the phenyl group *para*-position. Eventually, correlations may be attempted between activity, the Hammet σ value, and the partition coefficient; if such correlations exist, they would either lend support to or refute the hypothesis that lipophilicity is important. Also, making the epoxide even more hindered than it is in the natural product might produce a more selective agent.

DISCUSSION

The intermediates for the synthesis of the compounds were a series of 2-benzylcyclopentanones containing a variety of substituents in the phenyl ring *para*-position. Several 2-benzylcyclopentanones were synthesized using the appropriate benzyl halide and the pyrrolidine or morpholine enamine of cyclopentanone (7) (Scheme I).

The enamine alkylation was acceptable, except when a strong electron-withdrawing substituent was present on the phenyl ring. This effect is not easily rationalized; however, while many enamine alkylations proceed in yields of 45–55%, strong electron-withdrawing substituents decrease the yields. This alkylation has been used when the substituent is H, CH_3, OCH_3, OBz, Cl, NO_2, CN, or CO_2CH_3. In the *p*-nitrobenzyl halides, the yields are so low that the enamine alkylation is not synthetically useful[1].

The benzylic halides were commercially available, except for the methoxy derivative. This derivative was prepared from anise alcohol by

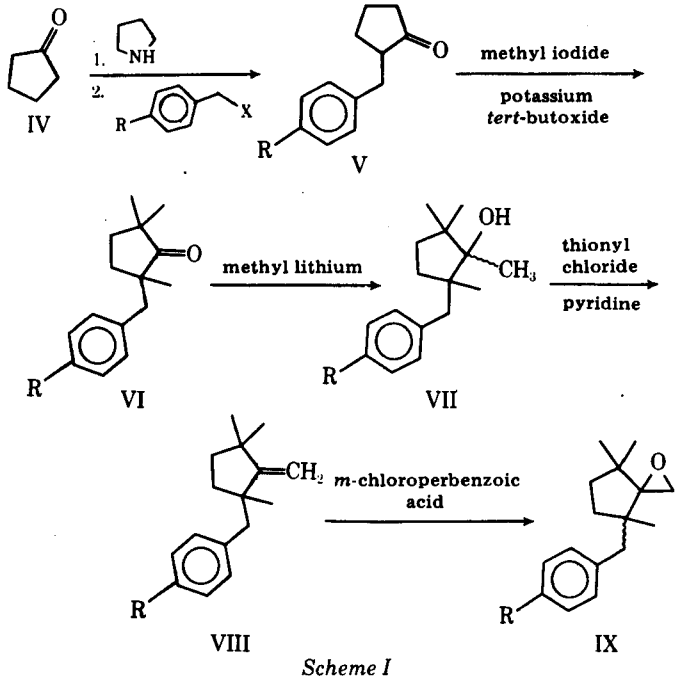

Scheme I

treatment with hydrobromic acid (8). Since this benzylic bromide is reported to be unstable, it was used immediately without purification.

The next step in the synthetic sequence was the conversion of the benzylcyclopentanones to the tetrasubstituted ketones. The reaction of all of the various 2-benzylcyclopentanones with potassium *tert*-butoxide in *tert*-butanol and excess methyl iodide resulted in the desired ketones in 72–81% yields.

It was anticipated that the tetrasubstituted ketones could be converted directly to the desired epoxides by treatment with either dimethylsulfonium methylide or dimethylsulfoxonium methylide (9). In no case would the highly hindered ketones react. An attempt also was made to effect a Wittig reaction with the ketones (10). As with the sulfur ylides, no reaction occurred and only starting material was recovered. This finding again shows the lack of reactivity of these tetrasubstituted ketones, a property that may best be explained by steric hindrance.

After direct conversion to the epoxide or olefin failed, the longer route of addition to the carbonyl, dehydration, and epoxidation was followed. Addition of the ketone, in ether, to an ethereal solution of excess methyl lithium followed by a reflux period led to a high alcohol yield (11). The use of less vigorous conditions, such as stirring at room temperature for 24 hr or refluxing for 6 hr, led to mixtures of starting material and the desired alcohol. No effort was made to separate the isomeric mixture of alcohols. The dehydration of the tertiary alcohols proceeded smoothly in yields of ~75%.

The final step in the synthesis was the epoxidation of the exocyclic olefins, which was performed both by peracid oxidation and by formation and base-catalyzed closure of an intermediate bromohydrin. The yield of epoxide was comparable in both procedures, and both procedures gave a mixture of isomers (~2:1 by GLC and NMR analysis). No attempt was made to separate the isomers. The peracid product was chromatographed on activated magnesium silicate[2] to yield the pure epoxide fraction.

The epoxides were assayed for antibiotic (12) and antimitotic (13) activity. None showed activity of ≥1% in the antimitotic screen of T-2 toxin, a naturally occurring trichothecan X. In the antibiotic screen of *Staphylococcus aureus, Escherichia coli, Salmonella gallinarum, Klebsiella, Pneumoniae, Mycobacterium smegmatis,* and *Candida albicans,* only *M. smegmatis* was inhibited by the simple epoxides prepared in this study (Table I). However, the activities were not sufficient to encourage further work.

Care was taken that all test media were near neutrality so that the epoxides would not be degraded by the medium. Apparently, the epoxide moiety of the model compounds does not meet the steric and/or electronic characteristics necessary for high activity if the epoxide group is the major pharmacophore of the trichothecans as proposed. It may well be that the

[1] Three explosions occurred while using *p*-nitrobenzyl bromide: twice while trying to distill the crude product mixture when the bath temperature reached 190° and once while stirring and refluxing a combination of *p*-nitrobenzyl bromide, 1-pyrrolidinocyclopentene, and dioxane. Since the dioxane was used immediately after distillation from lithium aluminum hydride, it is unlikely that peroxide formation was responsible.

[2] Florisil.

Table I—Minimum Inhibitory Concentration (MIC) against *Mycobacterium smegmatis* (ATCC 607)

Epoxide IX	MIC, μg/ml
R = H	100
R = Cl	50
R = CH_3	50
R = OCH_3	25

complete substitution of the α-carbons creates too high a steric hindrance for reactivity of the materials as alkylating agents of essential cellular components. These materials were not tested for skin irritation.

EXPERIMENTAL

Melting points[3] are uncorrected. All compounds gave satisfactory elemental analyses[4]. IR spectra[5] are reported in reciprocal centimeters. NMR spectra[6] were recorded with tetramethylsilane as an internal standard. NMR data are reported in parts per million (δ). Mass spectra[7] and GLC[8] data were obtained also. TLC employed aluminum oxide[9] and silica gel with fluorescent indicators. Column chromatography was done on silica gel[9] (70–325 mesh) and neutral alumina[10].

Benzylcyclopentanone Preparation—The procedure of Stork *et al.* was used (7). To a stirred solution of 1-pyrrolidinocyclopentene (1 mole equivalent) in dry dioxane, under nitrogen, was added benzyl halide (1.25 mole equivalent). The mixture was stirred and refluxed for 12 hr and cooled. Water was added, and the mixture was refluxed for an additional 3 hr. The solvent was removed *in vacuo*, and the residue was extracted three times with ether. The combined ethereal extracts were washed with 10% HCl, saturated sodium bicarbonate, water, and saturated brine and dried over sodium sulfate. Solvent removal and residue distillation yielded the benzylcyclopentanone.

2-Benzylcyclopentanone (*V, R = H*)—A 58% yield was obtained; bp 70–73°/0.2 mm [lit. (14) bp 108–110°/0.75 mm]; IR (neat): 1740; NMR ($CDCl_3$): 1.3–3.2 (9H, m, methylene and benzyl) and 7.23 (5H, s, ar); mass spectrum: *m/e* 174 (M^+) and 91 (base peak).

2-(p-Chlorobenzyl)cyclopentanone (*V, R = Cl*)—A 31% yield was obtained; bp 112–113°/0.1 mm; semicarbazone, mp 206–207° dec.; IR (neat): 1740; NMR ($CDCl_3$): 1.2–3.2 (9H, m, methylene and benzyl) and 7.1–7.25 (4H, m, ar); mass spectrum: *m/e* 208, 210 (M^+), and 126 (base peak).

Anal. (semicarbazone)—Calc. for $C_{13}H_{16}ClN_3O$: C, 58.87; H, 6.04; N, 15.85. Found: C, 58.69; H, 5.79; N, 15.63.

2-(p-Methoxybenzyl)cyclopentanone (*V, R = OCH_3*)—A 55% yield was obtained; bp 96–100°/0.05 mm; semicarbazone, mp 194–195° dec.; IR (neat): 1740 (CO), 1615, and 1585 (ar); NMR ($CDCl_3$): 1.4–3.2 (9H, m, methylene and benzyl), 3.8 (3H, s, OCH_3), and 6.5–7.0 (4H, m, ar); mass spectrum: *m/e* 204 (M^+) and 121 (base peak).

Anal. (semicarbazone)—Calc. for $C_{14}H_{19}N_3O_2$: C, 64.39; H, 7.28; N, 16.09. Found: C, 64.79; H, 7.41; N, 16.30.

2-(p-Methylbenzyl)cyclopentanone (*V, R = CH_3*)—A 52% yield was obtained; bp 68–70°/0.1 mm; semicarbazone, mp 211.5–212.5° dec.; IR (neat): 1740; NMR ($CDCl_3$): 2.3 (3H, s, ar CH_3), 1.5–3.2 (9H, m, methylene and benzyl), and 7.0 (4H, s, ar); mass spectrum: *m/e* 188 (M^+) and 105 (base peak).

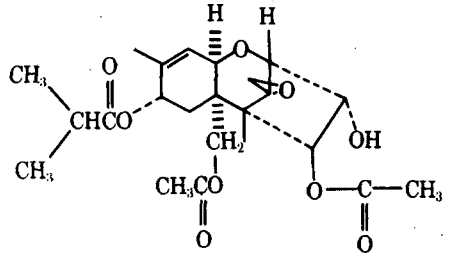

X

Anal. (semicarbazone)—Calc. for $C_{14}H_{19}N_3O$: C, 68.57; H, 7.76; N, 17.14. Found: C, 68.84; H, 7.92; N, 17.31.

2,2,5-Trimethyl-5-benzylcyclopentanone Preparation—The McMurray procedure was used (11). A solution of potassium *tert*-butoxide was prepared by refluxing potassium metal in dry *tert*-butanol until the potassium had dissolved. About 1 mole equivalent of this solution was added slowly to a solution of the ketone in *tert*-butanol under nitrogen. The mixture was stirred for 10 min, and additional equivalents of potassium *tert*-butoxide and methyl iodide (sixfold excess) were added simultaneously at equal rates with cooling.

The mixture was stirred and heated at 40° for 48 hr. Filtration of the cooled mixture and subsequent removal of most of the *tert*-butanol *in vacuo* were followed by dilution with water and extraction three times with ether. The ethereal extracts were combined, washed with water and saturated brine, and dried with magnesium sulfate. Solvent removal and residue distillation afforded the respective fully methylated benzylcyclopentanones.

2,2,5-Trimethyl-5-benzylcyclopentanone (*VI, R = H*)—A 78% yield was obtained; bp 71–73°/0.05 mm; IR (neat): 1740 (CO); NMR ($CDCl_3$): 0.7 (3H, s, CH_3), 1.1 (6H, s, 2 CH_3), 1.3–2.0 (4H, m, methylene), 2.8 (2H, *AB* quartet, *J* = 14 Hz, benzylic), and 7.2 (5H, m, ar).

Anal.—Calc. for $C_{15}H_{20}O$: C, 83.33; H, 9.26. Found: C, 83.08; H, 9.24.

2,2,5-Trimethyl-5-(p-chlorobenzyl)cyclopentanone (*VI, R = Cl*)—A 72% yield was obtained; bp 83–85°/0.02 mm; IR: 1740 (CO); NMR ($CDCl_3$): 0.7 (3H, s, CH_3), 1.05 (6H, s, 2 CH_3), 1.2–2.0 (4H, m, methylene), 2.4 (2H, *AB* quartet, *J* = 14 Hz, benzylic), and 7.2 (4H, m, ar).

Anal.—Calc. for $C_{15}H_{19}ClO$: C, 72.00; H, 7.60; Cl, 14.00. Found: C, 71.75; H, 7.61; Cl, 13.78.

2,2,5-Trimethyl-5-(p-methoxybenzyl)cyclopentanone (*VI, R = OCH_3*)—An 81% yield was obtained; bp 95–99°/0.03 mm; IR (neat): 1740 (CO); NMR ($CDCl_3$): 0.72 (3H, s, CH_3), 1.08 (6H, s, 2 CH_3), 3.74 (3H, s, OCH_3), and 6.7–7.1 (4H, m, ar).

Anal.—Calc. for $C_{16}H_{22}O_2$: C, 78.05; H, 8.94. Found: C, 77.75; H, 8.82.

2,2,5-Trimethyl-5-(p-methylbenzyl)cyclopentanone (*VI, R = CH_3*)—A 75% yield was obtained; bp 72–76°/0.03 mm; IR (neat): 1740 (CO); NMR ($CDCl_3$): 0.72 (3H, s, CH_3), 1.05 (6H, s, 2 CH_3), 1.3–2.0 (4H, methylene), 2.3 (3H, aromatic CH_3), 2.7 (2H, *AB* quartet, *J* = 14 Hz, benzylic), and 7.0 (4H, s, ar).

Anal.—Calc. for $C_{16}H_{22}O$: C, 83.48; H, 9.57. Found: C, 83.25; H, 9.39.

1,2,2,5-Tetramethyl-5-benzylcyclopentanol Preparation—The McMurray procedure was used (11). The ketone in ether was added dropwise, with stirring, to an ethereal methyl lithium solution. The mixture was stirred and refluxed under nitrogen for 24 hr. Then the reaction mixture was cooled, water was added slowly to destroy the excess methyl lithium (cessation of gas evolution), and the reaction mixture was diluted with more water so that the volumes of water and ether were approximately equal. The layers were separated, and the aqueous layer was extracted with ether. The combined ethereal extracts were washed with water and saturated brine and dried over sodium sulfate. The alcohols were isolated by solvent removal *in vacuo* and subsequent distillation of the residue.

1,2,2,5-Tetramethyl-5-benzylcyclopentanol (*VII, R = H*)—A 98% yield was obtained; bp 85–87°/0.02 mm; IR (neat): 3500 (broad, OH) and 1603 (ar).

Anal.—Calc. for $C_{16}H_{24}O$: C, 82.74; H, 10.34. Found: C, 82.44; H, 10.35.

1,2,2,5-Tetramethyl-5-(p-chlorobenzyl)cyclopentanol (*VII, R = Cl*)—A 97% yield was obtained; bp 90–92°/0.02 mm; IR (neat): 3550 (broad, OH) and 1600 (ar).

Anal.—Calc. for $C_{16}H_{23}ClO$: C, 72.18; H, 8.65; Cl, 13.16. Found: C, 71.90; H, 8.68; Cl, 12.90.

1,2,2,5-Tetramethyl-5-(p-methoxybenzyl)cyclopentanol (*VII, R = OCH_3*)—A 95% yield was obtained; bp 120–122°/0.02 mm; IR (neat): 3600 (broad, OH), 1620, and 1590 (ar).

Anal.—Calc. for $C_{17}H_{26}O_2$: C, 77.86; H, 9.92. Found: C, 78.13; H, 9.69.

1,2,2,5-Tetramethyl-5-(p-methylbenzyl)cyclopentanol (*VII, R = CH_3*)—A 92% yield was obtained; bp 86–89°/0.02 mm; IR (neat): 3540 (broad, OH).

Anal.—Calc. for $C_{17}H_{26}O$: C, 82.83; H, 10.57. Found: C, 82.98; H, 10.29.

Tertiary Cyclopentanol Dehydration—The McMurray procedure

[3] Thomas-Hoover Unimelt.
[4] Analyses were performed by Midwest Microlab, Indianapolis, Ind., or on a 185B CHN analyzer, University of Kansas.
[5] Beckman IR 10 or IR 33 spectrometer.
[6] Varian Associates A-60-A or T-60 spectrometer.
[7] Varian Atlas CH5.
[8] Hewlett-Packard 5750 B gas chromatograph.
[9] E. Merck.
[10] Woelm.

was employed (11). The alcohol was dissolved in dry pyridine (15 ml/mmole of alcohol) and cooled to −5° under nitrogen. To the stirring solution was added thionyl chloride (0.34 ml/mmole of alcohol) at such a rate that the temperature did not rise above 5°. The mixture was stirred at 0° for 30 min; then water was added, with cooling, to destroy excess thionyl chloride.

After the exothermic destruction of thionyl chloride had ceased, the mixture was diluted with excess water, and the resulting aqueous mixture was extracted three times with ether. The combined ethereal extracts were washed with 6 *N* HCl (cold), saturated sodium bicarbonate, water, and saturated brine and dried over sodium sulfate. After solvent removal *in vacuo*, olefins were isolated by distillation.

2,2,5-Trimethyl-5-benzyl-1-methylenecyclopentane (*VIII*, *R* = *H*)—An 87% yield was obtained; bp 50–52°/0.01 mm; IR (neat): 3040, 3080 (vinyl), 1650 (vinyl), and 1605 (ar); NMR ($CDCl_3$): 0.69 (3H, s, CH_3), 1.07 (3H, s, CH_3), 1.10 (3H, s, CH_3), 1.2–1.9 (4H, m, methylene), 2.6 (2H, broad s, benzylic), 4.74 (1H, broad s, vinyl), 4.85 (1H, broad s, vinyl), and 7.2 (5H, broad s, ar).

Anal.—Calc. for $C_{16}H_{22}$: C, 89.72; H, 10.28. Found: C, 89.90; H, 10.19.

2,2,5-Trimethyl-5-(p-*chlorobenzyl*)*-1-methylenecyclopentane* (*VIII*, *R* = *Cl*)—A 79% yield was obtained; bp 63–66°/0.03 mm; IR (neat): 3070, 3100 (vinyl), 1660 (vinyl), and 1610 (ar); NMR ($CDCl_3$): 0.95 (3H, s, CH_3), 1.05 (3H, s, CH_3), 1.08 (3H, s, CH_3), 1.2–1.9 (4H, m, methylene), 2.63 (2H, broad s, benzylic), 4.7 (1H, broad s, vinyl), 4.90 (1H, broad s, vinyl), and 7.0–7.15 (4H, m, ar).

Anal.—Calc. for $C_{16}H_{21}Cl$: C, 77.42; H, 8.48; Cl, 14.10. Found: C, 77.22; H, 8.34; Cl, 13.93.

2,2,5-Trimethyl-5- (p-*methoxybenzyl*)*-1-methylenecyclopentane* (*VIII*, *R* = OCH_3)—A 76% yield was obtained; bp 83–86°/0.03 mm; IR (neat): 3050, 3090 (vinyl), 1645 (vinyl), and 1575 (ar); NMR ($CDCl_3$): 0.97 (3H, s, CH_3), 1.05 (3H, s, CH_3), 1.08 (3H, s, CH_3), 1.2–1.8 (4H, m, methylene), 2.59 (2H, broad s, benzylic), 3.72 (3H, s, OCH_3), 4.73 (1H, broad s, vinyl), 4.87 (1H, broad s, vinyl), and 6.8–7.05 (4H, m, ar).

Anal.—Calc. for $C_{17}H_{24}O$: C, 83.61; H, 9.84. Found: C, 83.87; H, 9.72.

2,2,5-Trimethyl-5-(p-*methylbenzyl*)*-1-methylenecyclopentane* (*VII*, *R* = CH_3)—A 62% yield was obtained; bp 71–72°/0.03 mm; IR (neat): 3040, 3090 (vinyl), and 1645 (vinyl); NMR ($CDCl_3$): 0.99 (3H, s, CH_3), 1.06 (3H, s, CH_3), 1.08 (3H, s, CH_3), 1.2–1.9 (4H, m, methylene), 2.31 (3H, s, ar CH_3), 2.61 (2H, broad s, benzylic), 4.68 (1H, s, vinyl), 4.82 (1H, s, vinyl), and 6.95 (4H, s, ar).

Anal.—Calc. for $C_{17}H_{24}$: C, 89.47; H, 10.53. Found: C, 89.22; H, 10.81.

Epoxidation and Purification of Epoxides—The olefin was dissolved in dry, acid-free methylene chloride. An equivalent of *m*-chloroperbenzoic acid (calculated as 85%) was dissolved in dry, acid-free methylene chloride and added slowly, with stirring, at room temperature. When TLC showed the disappearance of the starting olefin, freshly prepared 5% sodium hydrosulfite solution was added just to the disappearance of excess peracid (starch–potassium iodide paper).

The organic phase was separated and washed with water, 10% sodium bicarbonate, water, and saturated brine and dried over potassium carbonate. The solvent was removed *in vacuo*, and the residual oil was adsorbed onto an activated magnesium silicate column prepared in hexane (100:1) from a small volume of hexane. The column was eluted with hexane to remove unreacted olefin and then with 1% ether–hexane to elute the desired epoxide. This procedure gave products of sufficient purity for bioassay. Analytical samples were prepared by distillation.

1-Epoxymethylene-2,2,5-trimethyl-5-benzylcyclopentane (*IX*, *R* = *H*)—A 68% yield was obtained; bp 62–64°/0.02 mm; IR (neat): 3040 (CH, epoxide), 1600 (ar), and 830 (epoxide); NMR ($CDCl_3$); 2.4–3.0 (4H, m, benzylic and epoxide methylene); mass spectrum: *m/e* 230 (M^+) and 91 (base peak).

Anal.—Calc. for $C_{17}H_{24}O$: C, 83.48; H, 9.57. Found: C, 83.14; H, 9.94.

1-Epoxymethylene-2,2,5-trimethyl-5-(p-*chlorobenzyl*)*cyclopentane* (*IX*, *R* = *Cl*)—A 65% yield was obtained; IR (neat): 3040 (CH, epoxide), 1600 (ar), and 820 (epoxide); NMR ($CDCl_3$); 2.1–2.8 (4H, m, benzylic and epoxide methylene); mass spectrum: *m/e* 264, 266 (M^+), and 69 (base peak).

Anal. (by peak-matching mass spectrometry)—Calc. for $C_{16}H_{21}ClO$: 264.12795. Found: 264.12539.

1-Epoxymethylene-2,2,5-trimethyl-5-(p-*methoxybenzyl*)*cyclopentane* (*IX*, *R* = OCH_3)—A 73% yield was obtained; IR (neat): 3040 (CH, epoxide), 1610, 1580 (ar), and 820 (epoxide); NMR ($CDCl_3$): 2.1–2.8 (4H, m, benzylic and epoxide methylene); mass spectrum: *m/e* 260 (M^+) and 121 (base peak).

Anal.—Calc. for $C_{17}H_{24}O_2$: C, 78.46; H, 9.23. Found: C, 78.67; H, 8.95.

1-Epoxymethylene -2,2,5-trimethyl-5- (p-*methylbenzyl*)*cyclopentane* (*IX*, *R* = CH_3)—A 61% yield was obtained; IR (neat): 3050 (CH, epoxide) and 890 (epoxide); NMR ($CDCl_3$): 2.2–2.7 (4H, m, benzylic and epoxide methylene); mass spectrum: *m/e* 244 (M^+) and 105 (base peak).

Anal.—Calc. for $C_{17}H_{24}O$: C, 83.61; H, 9.84. Found: C, 83.46; H, 9.94.

REFERENCES

(1) P. W. Brian and J. C. McGowan, *Nature*, **157**, 334 (1946).

(2) P. W. Brian and H. G. Hemming, *J. Gen. Microbiol.*, **1**, 158 (1947).

(3) G. G. Freeman and R. I. Morrison, *Nature*, **162**, 30 (1948).

(4) W. O. Godtfredsen, J. F. Grove, and C. Tamm, *Helv. Chim. Acta*, **50**, 1666 (1967).

(5) J. R. Bamberg and F. M. Strong, in "Microbial Toxins," vol. 7, S. Kadis, A. Ciegler, and S. J. Ajl, Eds., Academic, New York, N.Y., 1971.

(6) J. F. Grove and P. H. Mortimer, *Biochem. Pharmacol.*, **18**, 1473 (1969).

(7) G. Stork, A. Brizzolara, H. Lendesman, J. Szmuszkovicz, and T. Terrell, *J. Am. Chem. Soc.*, **85**, 207 (1963).

(8) K. Rorig, J. D. Johnson, R. W. Hamilton, and T. Telinski, *Org. Syn. Coll. Vol.*, **4**, 576 (1963).

(9) E. J. Corey and M. Chaykovsky, *J. Am. Chem. Soc.*, **87**, 1353 (1965).

(10) R. Greenwald, M. Chaykovsky, and E. J. Corey, *J. Org. Chem.*, **28**, 1128 (1963).

(11) J. E. McMurray, *J. Am. Chem. Soc.*, **98**, 6821 (1968).

(12) L. A. Mitscher, R. R. Leu, M. S. Bathala, W.-N. Wu, J. L. Beal, and R. White, *Lloydia*, **35**, 157 (1972).

(13) E. E. Smissman, R. J. Murray, J. D. McChesney, L. L. Houston, and T. L. Pazdernik, *J. Med. Chem.*, **19**, 148 (1976).

(14) R. Elsinger, *Org. Synth.*, **45**, 7 (1965).

ACKNOWLEDGMENTS

Adapted in part from a dissertation submitted by N. C. Corbin to the University of Kansas in partial fulfillment of the Doctor of Philosophy degree requirements.

The financial assistance of the National Institutes of Health and the General Research Fund of the University of Kansas is gratefully acknowledged.

Structure of Polyvinylpyrrolidone-Iodine (Povidone-Iodine)

HANS-UWE SCHENCK ˣ, PETR SIMAK, and ERICH HAEDICKE

Received April 2, 1979, from the *Plastics Laboratory, BASF Aktiengesellschaft, D 6700 Ludwigshafen, Federal Republic of Germany.* Accepted for publication June 7, 1979.

Abstract □ Hydrogen triiodide adducts were prepared from *N,N*-dimethylacetamide, *N*-alkylpyrrolidone derivatives, and polyvinylpyrrolidone, and their structures were investigated by IR spectra and X-ray structure analyses and compared with the structure of povidone-iodine USP. The results suggest that the iodine in povidone-iodine USP is complexed by the polymer such that a proton is fixed *via* a short hydrogen bond between two carbonyl groups of two pyrrolidone rings and that a triiodide anion is bound ionically to this cation.

Keyphrases □ Povidone-iodine—structure, hydrogen triiodide adducts, IR spectra, X-ray structure analysis □ Anti-infectives, topical—povidone-iodine, structure, hydrogen triiodide adducts, IR spectra, X-ray structure analysis □ Models, molecular—povidone-iodine

Povidone-iodine has been used as a multivalent, local, broad-spectrum antiseptic having bactericidal, fungicidal, sporicidal, protocidal, and virucidal properties. Based on the observation that combining iodine with polyvinylpyrrolidone (PVP) reduces iodine vapor pressure and increases iodine solubility in water (1), methods were patented that provide a polyvinylpyrrolidone-iodine adduct (povidone-iodine USP). Its aqueous solution has a higher stability in storage (smaller loss of available thiosulfate-titratable iodine) than an iodine solution in water containing polyvinylpyrrolidone.

BACKGROUND

A conventional method of preparing powdered povidone-iodine involves efficient mixing of elemental iodine with powdered polyvinylpyrrolidone[1]. The mixture is heated at an elevated temperature until the ratio of thiosulfate-titratable iodine to iodide ions is ~2:1 (2, 3). Only this ratio of iodine to iodide ions ensures adequate povidone-iodine stability. Stability is defined as: (*a*) a low iodine loss as determined in a 10% aqueous povidone-iodine solution, and (*b*) a high iodine distribution coefficient, c_{iodine} in water/c_{iodine} in *n*-heptane, between an aqueous phase and an *n*-heptane phase.

The distribution coefficient is the quotient of the iodine concentrations in water and in *n*-heptane as obtained according to a literature method (4) on extracting iodine from an aqueous povidone-iodine solution with *n*-heptane. Povidone-iodine also may be obtained without heating by mixing iodine with polyvinylpyrrolidone[1] and an iodide-containing substance at room temperature or by drying an iodide-containing polyvinylpyrrolidone[1] solution and mixing the polyvinylpyrrolidone-iodide with iodine (5).

In addition to the patent literature, numerous publications have dealt with the polyvinylpyrrolidone-iodine structure. The term polyvinylpyrrolidone-iodine has been used both for the product obtained by annealing iodine with polyvinylpyrrolidone at an elevated temperature and for the adduct formed on dissolving iodine in water containing this polymer. The papers discussed investigations into the structure of iodine adducts of natural and other synthetic polymers.

A comprehensive review article, published in 1953, dealt with numerous polyvinylpyrrolidone complexes and mentioned the adsorptivity of polyvinylpyrrolidone for iodine (6). The IR spectra were interpreted as suggesting that iodine molecules, triiodide ions, and adducts of polyvinylpyrrolidone and iodine coexist. Furthermore, strong polarization of the iodine molecules in the adduct was inferred from the direction of dissociation of the iodine molecule as discussed recently (Scheme I) (7). Disproportionation of the iodine into hypoiodite and iodide also was postulated (8–10).

$$\text{PVP}\ (i-1)\ I_2 + I_2 \rightleftarrows \text{PVP}\ (i\cdot I_2)\ \text{(outer complex)} \rightleftarrows (\text{PVP}\cdot I_{i/2})^{i/2+} \cdot (I_{3i/2})^{i/2-}\ \text{(inner complex)}$$

Scheme I

The influence of the iodide ion on iodine bonding to polyvinylpyrrolidone in chloroform and water was investigated (11–17). Molecular iodine was bonded to polyvinylpyrrolidone in chloroform (18). In aqueous solution in the presence of potassium iodide, the polymer-bonded species was triiodide, with the potassium ion complexed directly so that an insoluble product was precipitated from solution.

The literature provides few details of the solid polyvinylpyrrolidone-iodine structure. The only existing reference (19) concerns the structure of polyvinylpyrrolidone-iodine obtained by heating polyvinylpyrrolidone containing 10% water with iodine at 60° for 24 hr. According to the ratio of polyvinylpyrrolidone to iodine, some of the iodine was no longer titratable with thiosulfate. The greater the ratio, the higher was the molar polyvinylpyrrolidone excess. On extrapolation to an infinitely large polymer excess, 38.3% of the iodine was calculated to be present after complexation in a form that was not titratable with thiosulfate.

Moreover, water was involved in the reaction of iodine and polyvinylpyrrolidone; 7.4 ± 3.8 moles of water was lost per mole of nontitratable iodine and 2.33 ± 0.16 moles of acid was liberated per mole of nontitratable iodine. The UV–visible spectra revealed that triiodide ions were present.

To explain the amount of triiodide and protons formed, the decrease in the amount of water, and the residual iodine, previous investigators (19) assumed that the iodine hydrolysis reaction (Scheme II):

$$I_2 + H_2O \rightleftarrows IO^- + I^- + 2H^+$$

Scheme II

is favored greatly by the presence of polyvinylpyrrolidone so that an iodine complex, $PVP\text{-}(I_2)_x(IO^-, I^-)_y$, $y/x < 1.5$, results in which iodide and hypoiodite are present in addition to iodine. Similarly, Takikawa *et al.* (20, 21) postulated accelerated iodine hydrolysis in aqueous solution in the presence of polyvinylpyrrolidone and complexation to the polymer of the triiodide ion made up of iodide and nonhydrolyzed iodine.

The normal iodine hydrolysis equilibrium constant is $K_{25} = 5.4 \times 10^{-13}$ (22). Such an extreme shift of the iodine hydrolysis equilibrium by polyvinylpyrrolidone seems unlikely. Rather, it was assumed that heating a mixture containing ~8.3 mole % of iodine/mole (based on monomer) of polyvinylpyrrolidone containing 1–5% (w/w) water [the ratio typical of povidone-iodine containing 10% (w/w) active iodine] reduced iodine to iodide with hydrogen iodide formation until, after reduction of one-third of the iodine amount used, a stable hydrogen triiodide–polyvinylpyrrolidone complex was present. The formation of 2 moles of acid/mole of nontitratable iodine could be explained by hydrogen iodide formation with hydrolysis of an intermediate iodized compound (Scheme III):

$$RH + I_2 + H_2O \rightarrow ROH + 2I^- + 2H^+$$

Scheme III

The iodine could have oxidized impurities or end groups (RH) in the polyvinylpyrrolidone in small amounts [~0.028 equivalent/mole (based on monomer) of polymer in commercial povidone-iodine].

To confirm this hypothesis, some well-defined crystalline adducts of the $lig_2 \cdot HI_3$ type were prepared as models of povidone-iodine materials. The ligands (lig) included *N,N*-dimethylacetamide, *N*-alkylpyrrolidones, and 1,3-bis(2′-pyrrolidinon-1′-yl)butane (1), a section of a polyvinylpyrrolidone chain with the structure:

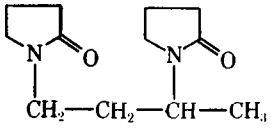

[1] According to the USP definition for povidone.

0022-3549/79/1200-1505$01.00/0
© 1979, American Pharmaceutical Association

The resultant complexes were identified structurally and compared by IR spectroscopy with the analogous hydrogen triiodide adduct of polyvinylpyrrolidone prepared from polyvinylpyrrolidone, hydrogen iodide, and iodine and with polyvinylpyrrolidone-iodine or povidone-iodine obtained by annealing polyvinylpyrrolidone or povidone with iodine. Both a low ($\overline{M}_n \sim 1000$) and a high ($\overline{M}_n \sim 10{,}000$) molecular weight product (povidone USP) were used to analyze bonding in compounds having one or two pyrrolidone rings, oligomers having about nine pyrrolidone rings (polyvinylpyrrolidone of $\overline{M}_n \sim 1000$), and polymers having ~90 pyrrolidone rings ($\overline{M}_n \sim 10{,}000$).

EXPERIMENTAL[2]

Preparation of (*N,N*-Dimethylacetamide)$_2$ · Hydrogen Triiodide (I)—To a solution of 33.84 g (133 mmoles) of iodine in 34.84 g (400 mmoles) of *N,N*-dimethylacetamide was added dropwise at room temperature 24.32 g (133 mmoles) of hydrogen iodide as a 70% aqueous solution. The mixture was well stirred and cooled throughout the addition. Then the solution was diluted with 200 ml of methylene chloride and was added to 6000 ml of *n*-hexane. A dark solid precipitated and was filtered. The residue was washed with *n*-hexane and dried *in vacuo* to give 69.7 g (94% yield) of I as a dark solid (mp 79°). Recrystallization from methanol gave 53.5 g (72% yield) of I as dark-brown crystals (mp 81°).

Anal.—Calc. for $C_8H_{19}I_3N_2O_3$: C, 17.3; H, 3.4; I^-, 22.9; I^0, 45.8; N, 5.04. Found: C, 17.4; H, 3.6; I^-, 22.6; I^0, 45.9; N, 5.1.

Other hydrogen triiodide adducts were prepared similarly.

(N-*Methylpyrrolidone*)$_2$ · *Hydrogen Triiodide* (*II*)—Compound II formed dark red-brown crystals, mp 72–74°, in a 72% yield. The IR spectrum is shown in Fig. 1. The structure was identified by X-ray structure analysis (25) (Figs. 2 and 3).

Anal.—Calc. for $C_{10}H_{19}I_3N_2O_3$:C, 20.7; H, 3.3; I_3^-, 65.6; I^0, 43.8; N, 4.8. Found: C, 20.9; H, 3.2; I_3^-, 65.7; I^0, 44.3; N, 4.8.

(N-*Isopropylpyrrolidone*)$_2$ · *Hydrogen Triiodide* (*III*)—Compound III formed dark-red-brown crystals, mp 108–110°, in a 23% yield.

Anal.—Calc. for $C_{14}H_{27}I_3N_2O_2$: C, 26.4; H, 4.3; I_3^-, 55.9; I^0, 39.9; N, 4.4. Found: C, 26.6; H, 4.1; I_3^-, 59.5; I^0, 39.8; N, 4.8.

(N-sec-*Butylpyrrolidone*)$_2$ · *Hydrogen Triiodide* (*IV*)—Compound IV formed a brown powder, mp 87–88°, in a 99% yield.

Anal.—Calc. for $C_{16}H_{31}I_3N_2O_2$: C, 28.9; H, 4.7; I_3^-, 57.3; I^0, 38.2; N, 4.2. Found: C, 29.2; H, 4.7; I_3^-, 56.8; I^0, 39.1; N, 4.2.

Preparation of [1,3-Bis(2′-pyrrolidinon-1′-yl)butane] · Hydrogen Triiodide (V)—To a cooled and well-stirred solution of 12.7 g (50 mmoles) of iodine and 11.2 g (50 mmoles) of 1,3-bis(2′-pyrrolidinon-1′-yl)butane in 45 ml of methylene chloride was added dropwise at room temperature 9.14 g (50 mmoles) of hydrogen iodide as a 70% aqueous solution. The solution was added to 1.5 liters of *n*-hexane, and 29.9 g of V precipitated as a red-violet powder (98.5% yield, mp 128°). Recrystallization afforded red-brown crystals (mp 136°). The IR spectrum is shown in Figs. 1 and 4.

Anal.—Calc. for $C_{12}H_{22}I_3N_2O_2$: C, 23.7; H, 3.5; I_3^-, 62.7; I^0, 41.8; N, 4.6. Found: C, 24.2; H, 3.6; I_3^-, 62.7; I^0, 42.2; N, 4.8.

Preparation of Polyvinylpyrrolidone Hydrogen Triiodide Adduct $[(C_6H_9NO)_2 \cdot HI_3]_{\sim 5}$ (VI)—The direct synthesis of VI was performed as follows. Polyvinylpyrrolidone[3] (calc. 100%), 11.1 g (0.1 mole based on monomer), was dissolved in 400 ml of analytical grade methanol, and 9.14 g of 70% aqueous hydrogen iodide solution (0.05 mole) was added. Iodine, 12.7 g (0.05 mole), dissolved in 250 ml of analytical grade methylene chloride, was dripped slowly into the solution; a homogeneous, slightly turbid solution was obtained. The solvents were distilled off *in vacuo* in a rotary evaporator (≤40°). The resultant solid was dried over phosphorus pentoxide to constant weight in a vacuum desiccator.

The product (VI), a black-brown powder, was sparingly soluble in water. Its IR spectrum is shown in Figs. 1 and 4.

Anal.—Calc. for $(C_{12}H_{19}I_3NO)_n$: C, 23.8; I_{total}, 63.0; I_3^-, 63.0; I^-, 42.0; N, 4.6. Found: C, 24.6; I_{total}, 59.5; I_3^-, 57.8; I^-, 40.7; N, 4.4.

Preparation of Polyvinylpyrrolidone Hydrogen Triiodide Adduct

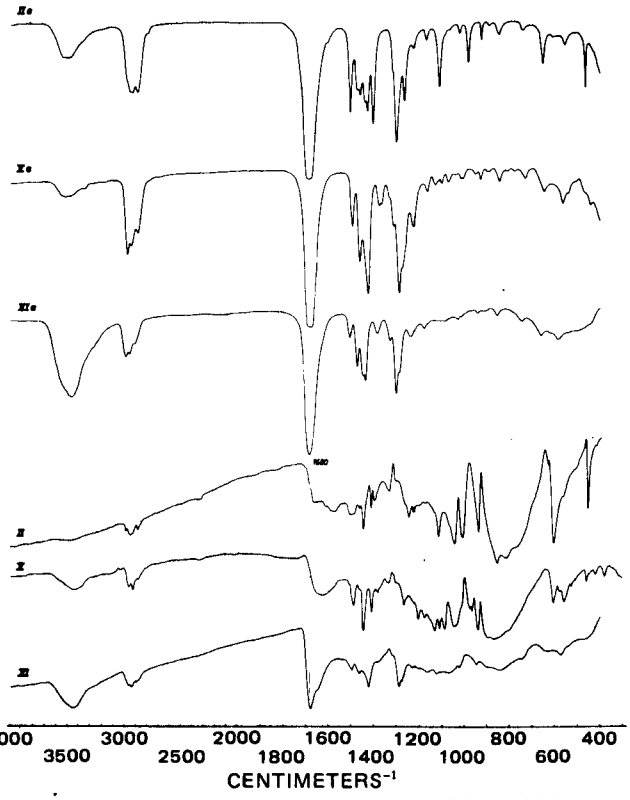

Figure 1—*IR spectra of* N-*methylpyrrolidone* (*II*a), *1,3-bis(2′-pyrrolidinon-1′-yl)butane* (*V*a), *polyvinylpyrrolidone with* $\overline{M}_n \sim 1000$ (*VI*a), (N-*methylpyrrolidone*)$_2$ · *hydrogen triiodide* (*II*), *[1,3-bis(2′-pyrrolidinon-1′-yl)butane] · hydrogen triiodide* (*V*), *and* $[(C_6H_9NO)_2 \cdot HI_3]_{\sim 5}$ (*VI*) *based on polyvinylpyrrolidone with* $\overline{M}_n \sim 1000$.

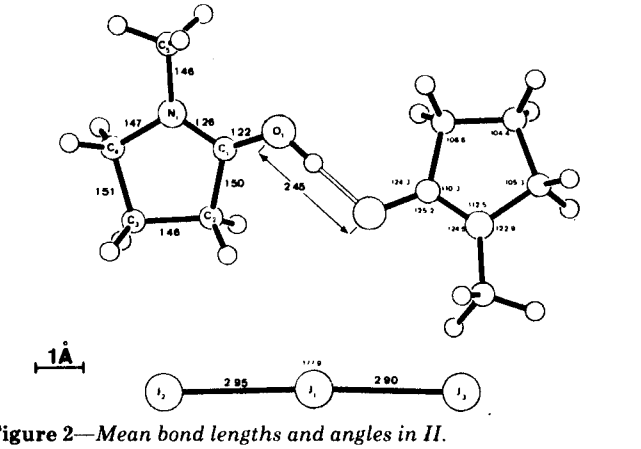

Figure 2—*Mean bond lengths and angles in II.*

[2] Melting points are uncorrected. IR spectra of the solid crystalline samples were recorded on potassium bromide pellets (1–2 mg of substance/300 mg of potassium bromide), while liquid samples were measured as thin films between potassium bromide disks or in thin cells. Spectra were taken with a Perkin-Elmer spectrometer, model 521 or 325, or a Digilab FTIR B/D-15. The absorptions discussed in the text and figures are in reciprocal centimeters. Microanalyses were run by the analytical laboratory of BASF Aktiengesellschaft.

Iodine (bisublimed), hydrogen iodide, and potassium iodide were obtained from E. Merck, Darmstadt, West Germany, and were reagent grade. *N,N*-Dimethylacetamide and the *N*-alkylpyrrolidones were obtained from BASF Aktiengesellschaft, Ludwigshafen, West Germany, and distilled before use (purity > 99.0% by GLC). Reagent grade methylene chloride, methanol, and *n*-hexane were used as solvents as supplied by E. Merck.

1,3-Bis(2′-pyrrolidinon-1′-yl)butane was obtained by a literature method (23) from *N*-vinylpyrrolidone by dimerization and hydrogenation. The product was pure both analytically and by GLC (>99.0%) on distillation in a spinning band column.

The low molecular weight polyvinylpyrrolidone was obtained by free radical polymerization [$\overline{M}_n \sim 1000$, $\overline{M}_w \sim 2500$, ~2% (w/w) water] and was used as supplied by BASF Aktiengesellschaft without further purification.

The high molecular weight polyvinylpyrrolidone was obtained by free-radical polymerization [$\overline{M}_n \sim 10{,}000$, $\overline{M}_w \sim 40{,}000$, ~2.1% (w/w) water] and was used as supplied by BASF Aktiengesellschaft without further purification. It met the USP requirements for povidone.

The povidone-iodine distribution coefficient was determined by a literature method (4). The decrease in available iodine on heat storage (15 hr, 80°) of a 10% aqueous povidone-iodine solution was determined according to USP XIX by a method similar to that described in the literature (24).

[3] $\overline{M}_n \sim 1000$, $\overline{M}_w \sim 2500$, ~2% water.

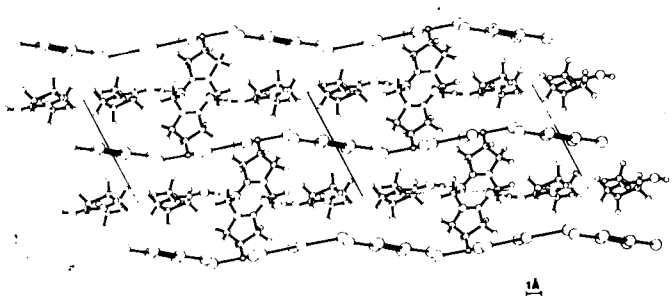

Figure 3—*Structure of II determined by X-ray structure analysis: a/b projection.*

$[(C_6H_9NO)_{19.4} \cdot HI_3]_n$ (Low Molecular Weight) (VII) According to Composition of Povidone-Iodine USP XIX—*Method A: Direct Synthesis*—Polyvinylpyrrolidone[3] (calc. 100%), 111.1 g (1 mole based on monomer), was dissolved in 105 ml of distilled water. Then 9.4 g (0.052 mole) of 70% aqueous hydrogen iodide and 13.07 g (0.052 mole) of powdered iodine were added and dissolved. The solution was freeze dried, ground, and dried over phosphorus pentoxide *in vacuo* in a desiccator. The product (VII*a*), a red-brown powder, was readily soluble in water.

The distribution coefficient was 163, and the iodine loss was 22.0%. The differential IR spectrum between VII*a* and the starting polyvinylpyrrolidone is shown in Fig. 5.

Anal.—Calc. for $[(C_6H_9NO)_{19.4} \cdot HI_3]_n$: C, 55.1; H^+, 0.38; I_{total}, 15.0; I_3^-, 15.0; I^-, 10.0; N, 10.7. Found: C, 52.5; H^+, 0.38; I_{total}, 15.0; I_3^-, 14.5; I^-, 9.7; N, 9.5.

Method B: Thermic Reaction—Polyvinylpyrrolidone[4], 121 g (1 mole based on monomer), was mixed intimately with 19.6 g (0.0772 mole) of iodine, and the mixture was heated at 90° until no further decrease in thiosulfate-titratable iodine occurred. The product (VII*b*), a red-brown powder, was readily soluble in water.

The distribution coefficient was 189, and the iodine loss was 18.2%. The differential IR spectrum between VII*b* and the starting polyvinylpyrrolidone is shown in Fig. 5.

Anal.—Calc. for $[(C_6H_9NO)_{19.4} \cdot HI_3]_n$: Found: C, 52.0; H^+, 0.40; I_{total}, 14.9; I_3^-, 14.0; I^-, 9.8; N, 9.6.

Preparation of Polyvinylpyrrolidone Hydrogen Triiodide Adduct $[(C_6H_9NO)_2 \cdot HI_3]_{\sim 45}$ (VIII)—The direct synthesis of VIII was accomplished as follows. Polyvinylpyrrolidone[5] (calc. 100%), 11.1 g (0.1 mole based on monomer), was dissolved in 800 ml of analytical grade methanol. Then 11.37 g of 55.9% (0.05 mole) aqueous hydrogen iodide solution was added with efficient stirring, and 12.7 g (0.05 mole) of iodine in 500 ml of analytical grade methanol was dripped slowly into the solution. The product was prepared as described for VI.

Compound VIII formed as a black-brown powder (30.2 g, 99.5% yield). Its IR spectrum is shown in Fig. 4.

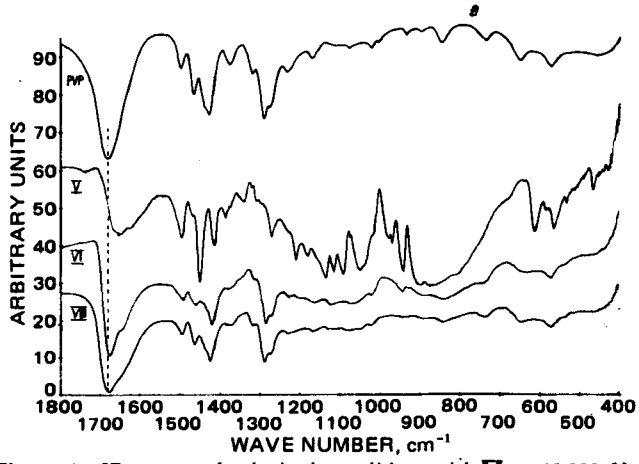

Figure 4—*IR spectra of polyvinylpyrrolidone with $\overline{M}_n \sim 10{,}000$, V, VI based on polyvinylpyrrolidone with $\overline{M}_n \sim 1000$, and $[(C_6H_9NO)_2 \cdot HI_3]_{\sim 45}$ (VIII) based on polyvinylpyrrolidone with $\overline{M}_n \sim 10{,}000$.*

[4] $\overline{M}_n \sim 1000$, $\overline{M}_w \sim 2500$, ~8% water.

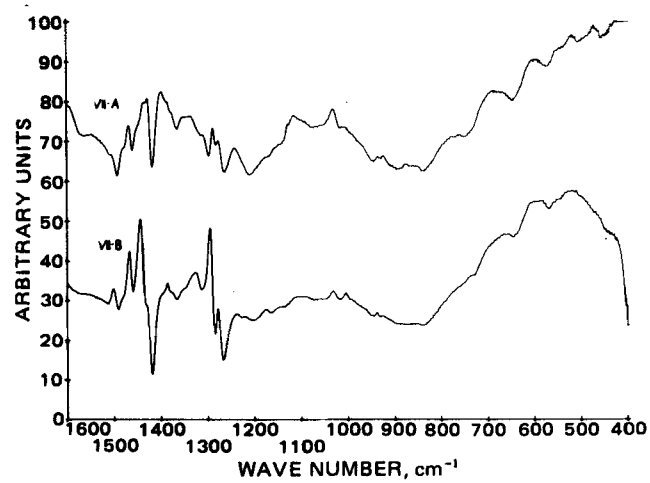

Figure 5—*Differential IR spectra between $[(C_6H_9NO)_{19.7} \cdot HI_3]_n$ based on polyvinylpyrrolidone with $\overline{M}_n \sim 1000$ (VII*a*, direct synthesis; VII*b*, heating with iodine) and the starting polyvinylpyrrolidone.*

Anal.—Calc. for $(C_{12}H_{19}I_3NO)_n$: C, 23.8; I_{total}, 63.0; I_3^-, 63.0; I^0, 42.0; N, 4.6; acid value (strongly acidic), 94.8. Found: C, 23.4; I_{total}, 62.2; I_3^-, 62.0; I^0, 45.2; N, 4.6; acid value (strongly acidic), 88.0.

Preparation of Povidone Hydrogen Triiodide Adduct $[(C_6H_9NO)_{19.4} \cdot HI_3]_n$ (High Molecular Weight) (IX) (Povidone-Iodine USP XIX)—*Method A: Direct Synthesis*—Polyvinylpyrrolidone[5] (calc. 100%), 11.1 g (0.1 mole based on monomer), was dissolved in 50 g of distilled water. Then 1.17 g of 55.9% (0.052 mole) aqueous hydrogen iodide and 1.31 g (0.052 mole) of iodine were added and dissolved by stirring for 10 hr at 50°. The solution was freeze dried, ground, and dried in a desiccator over phosphorus pentoxide. Compound IX*a* formed as a brown, water-soluble powder.

The distribution coefficient was 243, and the iodine loss was 2.4%. The differential IR spectrum between IX*a* and the starting polymer is shown in Fig. 6.

Anal.—Calc. for $[(C_6H_9NO)_{19.4} \cdot HI_3]_n$: C, 55.1; I_{total}, 15.0; I_3^-, 15.0; I^0, 10.0; I^-, 5.0; N, 10.7. Found: C, 55.0; I_{total}, 14.8; I_3^-, 13.5; I^-, 4.5; N, 11.1.

Method B: Thermic Reaction—Polyvinylpyrrolidone[5], 113.5 g (1 mole based on monomer), was mixed intimately with 21.14 g (0.0833 mole) of iodine. Then the mixture was heated at 80–100° until no further decrease in thiosulfate-titratable iodine occurred. Compound IX*b* formed as a red-brown powder and was readily soluble in water.

The distribution coefficient was 229, and the iodine loss was ~4.5%.

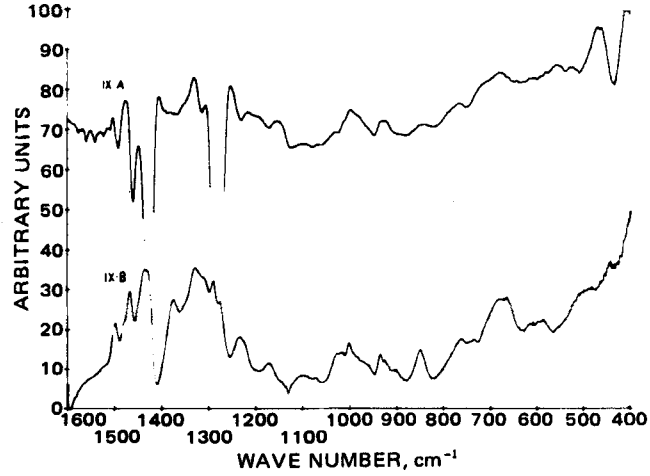

Figure 6—*Differential IR spectra between $[(C_6H_9NO)_{19.4\ (18)} \cdot HI_3]_n$ based on polyvinylpyrrolidone with $\overline{M}_n \sim 10{,}000$ (IX*a*, direct synthesis; IX*b*, heating with iodine) and the starting polyvinylpyrrolidone*

[5] $\overline{M}_n \sim 10{,}000$, $\overline{M}_w \sim 40{,}000$, ~2.1% water = povidone USP.

The differential IR spectrum between IX*b* and the starting polyvinylpyrrolidone is shown in Fig. 6.

Anal.—Calc. for $[(C_6H_9NO)_{18.0} \cdot HI_3]_n$: C, 54.4; I_{total}, 16.0; I_3^-, 16.0; I^0, 10.7; I^-, 5.3; N, 10.6; acid value (strongly acidic), 23.5. Found: C, 51.4; I_3^-, 15.9; I^-, 5.5; N, 10.2; acid value (strongly acidic), 30.

RESULTS AND DISCUSSION

Well-defined crystalline ligand$_2$ · hydrogen triiodide or ligand · hydrogen triiodide adducts were obtained by reaction of low molecular weight model substances for povidone-iodine [*N,N*-dimethylacetamide, *N*-alkylpyrrolidones, and 1,2-bis(2′-pyrrolidinon-1′-yl)butane, a section of a polyvinylpyrrolidone chain] with iodine and hydrogen iodide. The compounds had characteristic IR spectra different from those of the free ligands (Fig. 1). The elemental analyses were consistent with the indicated structures.

The hydrogen triiodide adducts prepared usually were soluble in strongly polar organic solvents such as methanol. They were only sparingly water soluble and hydrolyzed with the release of iodine (iodine flakes, heavy iodine odor). The aqueous solutions showed a strong mineral acid reaction due to the hydrogen iodide. The adducts may be regarded as ligand-stabilized forms of hydrogen triiodide acid, which does not exist in the free form.

As iodophores, the compounds had a high thiosulfate-titratable iodine content (45.6% in I). The adducts were stable for months at room temperature without iodine loss. Dark-red single crystals of II of ≤2 cm in edge length were grown.

On reaction with hydrogen iodide and iodine, 1,3-bis(2′-pyrrolidinon-1′-yl)butane yielded an adduct of the stoichiometry [1,3-bis(2′-pyrrolidinon-1′-yl)butane]·hydrogen triiodide and not a [1,3-bis(2′-pyrrolidinon-1′-yl)butane]$_2$ · hydrogen triiodide adduct. The same adduct was obtained when using excess ligand. The ligand$_2$ · hydrogen triiodide adduct was not obtained with this ligand in any experiment.

An attempt to prepare a $[(C_6H_9NO)_2 \cdot HI_3]_n$ adduct based on polyvinylpyrrolidone of different molecular weights ($\overline{M}_n \sim 1000$ or 10,000) by reacting 2 moles (based on monomer) of polymer with 1 mole of iodine and 1 mole of hydrogen iodide resulted in the loss of minor portions of the iodine and iodide and yielded products in which the pyrrolidone rings could not all have taken part in the complexation. Based on steric and statistical considerations, participation of all pyrrolidone rings had not been expected.

Polyvinylpyrrolidone-iodine or commercial povidone-iodine, which USP XIX requires to contain ≤6.6% iodide ions and 9.0–12.0% (w/w) thiosulfate-titratable iodine (I^0), can be prepared by reacting 1 mole (based on monomer) of polyvinylpyrrolidone[6] or povidone[7] with 0.052 mole of hydrogen iodide and 0.052 mole of iodine (VII or IX, Method A) or by heating 1 mole (monomer based) of polyvinylpyrrolidone[6] or povidone[7] with 0.083 mole of iodine (VII or IX, Method B). The two methods gave products with identical color, solubility, distribution coefficient, iodine loss, elemental analysis, and IR spectrum (Figs. 5 and 6).

The iodine loss of the aqueous solutions of the polyvinylpyrrolidone-iodines was ~18–20% (polymer of $\overline{M}_n \sim 1000$) or ~2–4% (polymer of $\overline{M}_n \sim 10{,}000$) and was independent of the preparation method. Apparently, every proton introduced (Method A) or formed during heating (Method B) readily found the pyrrolidone carbonyl groups needed for complexation due to the large molar excess of polyvinylpyrrolidone monomer units.

Unequivocal proof of the structure of the hydrogen triiodide adducts of the model substances was provided by the complete X-ray structure analysis of II (25). The compound crystallized in the triclinic space group $P\bar{1}$ with two triiodide units and four *N*-methylpyrrolidone molecules per asymmetric unit. The result is shown in Figs. 2 and 3. A proton was fixed *via* a short hydrogen bond between two carbonyl oxygen atoms of two pyrrolidone rings. The large triiodide anion was coordinated ionically to this large complex cation. Similar bonds were found (26) for adducts of *N,N*-dimethylacetamide and hexafluoroarsenic acid or hexafluorophosphoric acid. A short hydrogen bond (2.40–2.45 Å) links the two carbonyl oxygen atoms of two *N,N*-dimethylacetamide molecules (26).

The other hydrogen triiodide adducts of the model substances (I–V) and the corresponding complexes prepared using polyvinylpyrrolidone ($\overline{M}_n \sim 1000$, $\overline{M}_n \sim 10{,}000$) are believed to be analogous in structure, with

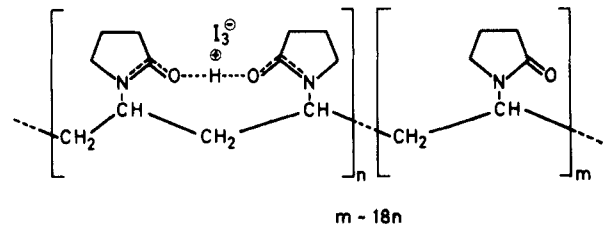

m - 18n

Figure 7—*Proposed structure of povidone-iodine.*

their IR spectra undergoing similar changes on transition from the free ligand to the hydrogen triiodide adduct. Reference is made to the IR spectra (Figs. 1 and 4) of the free model substances polyvinylpyrrolidone and the hydrogen triiodide adducts. The structural analogy is particularly evident in the complex based on polyvinylpyrrolidone of $\overline{M}_n \sim 1000$. It is less evident, although still detectable by differential spectroscopy, in the complex based on polyvinylpyrrolidone of $\overline{M}_n \sim 10{,}000$[7] due to the broad bands (Figs. 5 and 6).

Even without detailed knowledge of the origin of the absorptions, it is apparent that the IR spectra of the model substances agree with the polyvinylpyrrolidone spectrum. The differences between individual spectra are due almost exclusively to different alkyl groups (and methyl groups in particular). Therefore, the frequency and intensity of the vibrations of the CN–, NC=O, and carbonyl groups and the ring are largely independent of the *N*-alkyl side chain. The bonds in the complexes of the model substances and in the corresponding polyvinylpyrrolidone adducts must be at least very similar. This view may be confirmed by comparing IR spectra of model substances with those of the polyvinylpyrrolidone hydrogen triiodide adducts.

While there have been numerous IR spectroscopic investigations into polyamides and the corresponding low molecular weight compounds, few publications have dealt with the IR spectra of alkylpyrrolidones. Therefore, bands were assigned on the basis of the known spectra of *N,N*-dimethylacetamide (27), *N,N*-dimethylacetamide-d_9 (28), tetramethylurea (29), dialkylurea (30), monoalkylurea (31), δ-valerolactam (32), and cyclopentanol (33). Further comparisons made it possible to assign the bands of the hydrogen triiodide adducts.

Notable features in the IR spectra of the hydrogen triiodide adducts were a very broad and intense absorption at about 815 cm^{-1} and the high intensity of the band at about 560 cm^{-1}. Compared with the spectra of the starting compounds, which absorbed intensely due to the carbonyl groups at about 1685 cm^{-1}, the stretching vibration of the carbonyl groups of the adducts was hardly detectable. It appeared as a weak, very broad band at 1650–1600 cm^{-1}. Such a change in the IR spectra was attributed to the bonding changes in the region of the carbonyl and O=CN groups. The shift in position with a simultaneous intensity decrease can be explained easily by assuming a C=OH bond, including the hydrogen atom of hydrogen triiodide, as detected for II by X-ray structure analysis (25). The hydrogen bonds shift the position of the carbonyl band toward smaller wave numbers because the double bond of the group is weakened. Strong C–O···H···O–C bonds were found in other classes of compounds and were investigated spectroscopically. For example, the IR and Raman spectra of compounds of the metal-$H(CH_3COO)_2$ type were investigated and given the following assignments of the bands for $(CH_3COO\cdots H\cdots OOCCH_3)Na$ (34):

	vibration				
	$\overline{\nu_{as}O—H—O}$	$\overline{OH}$	$\overline{OH}$	$\overline{\nu_{sym}O—H—O}$	$\overline{C{=}O}$
frequency	720	1540	1285	IR inactive	1710
intensity	vs, b	m	s	—	s

The very broad and intense absorption at 850 cm^{-1} in the potassium hydrogen oxalate spectrum, obtained by IR measurements on single crystals using polarized light, was described as another hydroxyl stretching vibration (35). The IR spectra of the hydrogen triiodide adducts of polyvinylpyrrolidone (VI, VII*a*, VII*b*, VIII, IX*a*, and IX*b*) (Figs. 4–6) showed that the carbonyl groups did not all participate in the adduct formation (this was expected in view of the elemental analysis of VI and VIII and because of the large excess of pyrrolidone rings in the VII and IX mixture). The absorptions at ~800 and 1020 cm^{-1}, characteristic of the adduct structure, occurred.

In adducts VI and VIII, these characteristic absorptions were clearly visible. In VII*a*, IX*a*, VII*b*, and IX*b*, which have the composition of

[6] $\overline{M}_n \sim 1000$, $\overline{M}_w \sim 2500$.
[7] $\overline{M}_n \sim 10{,}000$, $\overline{M}_w \sim 40{,}000$ = povidone USP.

commercial povidone-iodine with an approximately 10-fold molar excess of pyrrolidone rings, these characteristic absorptions showed up in the differential spectra between the starting polyvinylpyrrolidone and the adducts.

Contrary to conventional assumptions on the structure of polyvinylpyrrolidone-iodine prepared by heating polyvinylpyrrolidone[8] with iodine, the compound probably is an adduct of the polymer and hydrogen triiodide in which a proton is fixed between two carbonyl groups of two pyrrolidone rings (*cf.*, Fig. 7) and the triiodide anion is bound ionically to this complex cation. Incidentally, the pyrrolidone rings participating in the complexation need not be vicinal in the polymer chain as shown in Fig. 7. Due to an appreciable excess of free pyrrolidone rings in povidone-iodine USP XIX, the product was readily soluble in water.

SUMMARY

N,N-Dimethylacetamide and *N*-alkylpyrrolidones are capable of forming stable ligand$_2$ · hydrogen triiodide adducts. This finding coincides neatly with the complex chemistry of these organic compounds discussed in the literature. The bonding is similar in all adducts of this type, where a proton is fixed between two carbonyl groups of two ligands *via* a short hydrogen bond. This bonding manifests itself in similar IR spectra of the complexes, which all show a strong shift of the carbonyl band toward lower wave numbers. For II, this structure could be unequivocally verified (25).

By analogy with the model compounds, polyvinylpyrrolidone[8] can be reacted with hydrogen iodide and iodine to form adducts whose spectroscopic properties are analogous to those of the low molecular weight complexes, which suggests identical bonding. However, for steric reasons, it seems impossible for all pyrrolidone rings to take part in adduct formation. If there is more halogen, halogen losses occur on drying. If there are ≤20 pyrrolidone rings for every hydrogen triiodide, as in commercial povidone-iodine, complexation is good and the excess pyrrolidone rings not taking part in the complexation provide the desired water solubility.

The structure of povidone-iodine USP XIX prepared by heating polyvinylpyrrolidone[7] with iodine agrees with that of a product obtained by the direct synthesis of polyvinylpyrrolidone[7], hydrogen iodide, and iodine. Previous assumptions regarding the structure of polyvinylpyrrolidone-iodine (18–20) are not consistent with the results discussed in this paper.

REFERENCES

(1) H. A. Shelanski, U.S. pat. 2,739,922 (1956); through *Chem. Abstr.*, **50**, 11623g (1956).

(2) H. Beller and W. A. Hosmer (General Aniline & Film Corp.), U.S. pat. 2,706,701 (1955); through *Chem. Abstr.*, **49**, 12788a (1955).

(3) S. Siggia (General Aniline & Film Corp.), U.S. pat. 2,900,305 (1956).

(4) A. Cantor and M. W. Winicov (West Laboratories Inc.), U.S. pat. 3,028,300 (1960).

(5) A. Cantor and M. W. Winicov (West Laboratories Inc.), German pat. 2,422,767 (1974); through *Chem. Abstr.*, **82**, 103138y (1975).

(6) W. Scholtan, *Makromol. Chem.*, **11**, 131 (1954).

(7) I. Moriguchi, Y. Araki, and N. Kaneniwa, *Chem. Pharm. Bull.*, **17**, 2088 (1969).

(8) V. O. Mokhnach and L. N. Propp, *Dokl. Akad. Nauk SSR*, **170**, 103 (1966); through *Chem. Abstr.*, **66**, 60485j (1967).

(9) V. O. Mokhnach and I. P. Zueva, *Zh. Neorgan. Khim.*, **8**, 668 (1963); through *Chem. Abstr.*, **58**, 13304h (1963).

(10) W. W. Korshak, L. B. Zubakova, L. Y. Nikiforova, and N. V. Kachurina, *Tr. Mosk. Khim.-Tekhnol. Inst.*, **1972**, No. 70, 201; through *Chem. Abstr.*, **79**, 23822q (1973).

(11) S. M. Barkin, H. P. Frank, and F. R. Eirich, *Ric. Sci.*, **25**, *Suppl. Simp. Int. Chim. Macromol., Milan-Turin*, **1954**, 844; through *Chem. Abstr.*, **54**, 11554a (1960).

(12) J. Neél and B. Sébille, *C. R. Hebd. Seances Acad. Sci. Ser. C*, **252**, 405 (1961).

(13) J. Neél and B. Sébille, *J. Chim. Phys.-Chim. Biol.*, **58**, 738 (1961).

(14) G. Oster and E. H. Immergut, *J. Am. Chem. Soc.*, **76**, 1393 (1954).

(15) N. Kaneniwa and A. Ikekawa, *Chem. Pharm. Bull.*, **22**, 2990 (1974).

(16) F. Eirich, *Chem. Eng. News*, **32**, 2768 (1954).

(17) J. Neél and B. Sébille, *C. R. Hebd. Seances Acad. Sci. Ser. C*, **252**, 867 (1961).

(18) J. Eliassaf, *Eur. Polym. J.*, **2**, 269 (1966).

(19) R. F. Cournoyer and S. Siggia, *J. Polym. Sci. Polym. Chem.*, **12**, 603 (1974).

(20) K. Takikawa, M. Nakano, and T. Arita, *Chem. Pharm. Bull.*, **26**, 874 (1978).

(21) *Ibid.*, **26**, 1370 (1978).

(22) T. L. Allen and R. M. Keefer, *J. Am. Chem. Soc.*, **77**, 2957 (1955).

(23) J. W. Breitenbach, F. Galinovsky, H. Nesvadba, and E. Wolf, *Monatsh. Chem.*, **87**, 580 (1956).

(24) Defense Medical Purchase Description No. 4, Jan. 4, 1972, p. 4, 6505-491-7557 and 6505-994-7224.

(25) H. U. Schenck, P. Simak, and E. Haedicke, *Makromol. Chem.*, in press.

(26) D. Cook, *Can. J. Chem.*, **42**, 2721 (1964).

(27) G. Durgaprasad, D. N. Sathyanarayana, C. C. Patel, H. S. Randhawa, A. Goel, and C. N. R. Rao, *Spectrochim. Acta, Part A*, **28**, 2311 (1972).

(28) K. L. Dorris, T. H. Sidall, W. E. Stewart, and M. L. Good, *ibid.*, **23**, 1657 (1967).

(29) H. Spell and J. Laane, *ibid.*, **28**, 295 (1972).

(30) Y. Mido, *ibid.*, **28**, 1503 (1972).

(31) C. I. Jose, *ibid.*, **25**, 111 (1969).

(32) M. Rey-Lafon and M. T. Forel, *ibid.*, **29**, 471 (1973).

(33) J. Durig, J. M. Karriker, and W. C. Harris, *ibid.*, **27**, 1955 (1971).

(34) D. Hadži, B. Orel, and A. Novak, *ibid.*, **29**, 1745 (1973).

(35) B. Orel, thesis, University of Ljubljana, Yugoslavia, 1972.

[8] $\overline{M}_n \sim 1000$, $\overline{M}_w \sim 2500$ or $\overline{M}_n \sim 10{,}000$, $\overline{M}_w \sim 40{,}000$.

Cryptolepine Hydrochloride Effect on *Staphylococcus aureus*

KWABENA BOAKYE-YIADOM * **and SAMUEL M. HEMAN-ACKAH** ˣ

Received September 5, 1978, from the *Department of Pharmacy, College of Pharmacy and Pharmacal Sciences, Howard University, Washington, DC 20001.* Accepted for publication June 22, 1979. *Present address: Faculty of Pharmacy, University of Science and Technology, Kumasi, Ghana, West Africa.

Abstract □ *Staphylococcus aureus* cultures treated with the hydrochloride salt of the indoquinoline alkaloid, cryptolepine, which was isolated from the roots of *Cryptolepis sanguinolenta*, showed biphasic steady-state generation curves at the same dose level. The apparent generation rate constant for the initial phase of action (phase I) was greater than that for phase II. The formal dependence of the apparent generation rate constant on drug concentration for the phase I action was linear at low drug concentrations but asymptotically approached zero at high concentrations, indicating saturation of the receptor sites engaged in microbial protein synthesis. The dependence for phase II action was linear in the entire concentration range and demonstrated a process that did not conform to a saturable receptor site model but resulted in a kill or lysis of the cells. Cryptolepine possesses bacteriostatic and bactericidal actions. Both phenomena occur in the initial stages of drug–bacteria reaction, but the bactericidal action predominates in subsequent stages. The effects of pH changes in broth media on generation inhibition of *S. aureus* by cryptolepine hydrochloride action indicated that the unprotonated drug fraction contributes to its activity, possibly because of its ready penetration through the cell membrane.

Keyphrases □ Cryptolepine hydrochloride—action on *Staphylococcus aureus*, microbial kinetics □ Antibacterial agents—cryptolepine hydrochloride, action on *Staphylococcus aureus*, microbial kinetics □ *Staphylococcus aureus*—effect of cryptolepine hydrochloride, microbial kinetics

Cryptolepine, an alkaloid, was first isolated in 1929 (1) from the roots of *Cryptolepis triangularis* N.E.Br. growing wild in the Belgian Congo. The alkaloid also has been isolated from another genus, *Cryptolepis sanguinolenta* (Lindl.) Schlecter, which is native to West Africa (2). It has the indoquinoline structure shown in Scheme I (3). Cryptolepis plants belong to the family *Asclepiadaceae* and grow as shrubs in tropical Africa. Extracts from these plants have been used in folk medicine and as a dye by the indigenous people (3). In Ghana[1], aqueous extracts from the roots of *C. sanguinolenta* have been used by herbalists to treat urinary tract infections and malaria.

Cryptolepine is reported to possess hypotensive properties and to produce a marked and prolonged fall in blood pressure as well as to lower body temperature (4, 5). Recent studies demonstrated that aqueous *C. sanguinolenta* extracts possess antimicrobial action against some urinary tract pathogens (6), while cryptolepine hydrochloride has a wide spectrum of activity against Gram-positive and Gram-negative bacteria as well as *Candida albicans* (7).

Microbial kinetic studies (8–11) were applied to evaluate the action of cryptolepine hydrochloride on *Staphylococcus aureus*, which is a susceptible organism. This paper discusses the functional dependency of kinetic parameters derived from growth inhibition of *S. aureus* cultures on cryptolepine hydrochloride concentrations, broth constituents, inoculum size, broth pH, and other conditions. A possible mechanism of cryptolepine action on *S. aureus* cells is postulated.

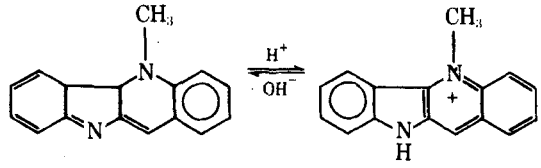

cryptolepine

Scheme I

EXPERIMENTAL

Materials and Methods—*Staphylococcus aureus* (ATCC 6538) was used in all experiments. It was cultivated in broth medium[2] and was used in determining cryptolepine–bacteria reactions as described previously (8–11). Cryptolepine hydrochloride solutions were made by dissolving cryptolepine hydrochloride crystals[3] (mp 263–265°), referred to as cryptolepine in this paper, in aqueous 1% (v/v) polysorbate 80.

A particle-size counter[4] and the poured plate method with sandwiched agar plates were employed in determining the total and viable counts, respectively, on drug-free and drug-affected *S. aureus* cultures as described previously (8–11). Culture samples were withdrawn at 30-min intervals for both counts.

Effect of 0.04% (v/v) Polysorbate 80 on Generation Rates—Aliquots (2.0 ml) of sterile aqueous 1% (v/v) polysorbate 80 were added aseptically to replicate 48-ml volumes of *S. aureus* cultures growing at 37.5°. At this time, growth was in the logarithmic phase and the cell population was 2.0×10^6 organisms/ml. Culture samples were withdrawn every 30 min, and the cell population was determined by the total count method. Fifty-milliliter volumes of *S. aureus* cultures containing 0.04% (v/v) polysorbate 80 were used as controls in all experiments.

Effect of Cryptolepine Hydrochloride Concentrations on Generation Rates—Two-milliliter aliquots of cryptolepine hydrochloride solutions were added to replicate 48-ml culture samples to yield the required drug concentrations. Drug was added when the cultures were in the exponential growth phase at 37.5° and the cell population was 2.0×10^6 cells/ml. Generation curves were obtained by the total count method for cultures affected by cryptolepine concentrations within the 0–30-μg/ml range. Generation curves of the cultures affected with 0, 5, 10, 20, and 30 μg of cryptolepine/ml also were obtained by the total and viable count methods.

Nutrient Concentration Effect on Drug-Affected Generation Rates—Antibiotic Medium 3 was prepared to contain half, single, and double the concentrations of ingredients specified by the manufacturer, with pH adjustment to 7.05 ± 0.05 where necessary. The three media were used in determining generation curves of cultures treated with 0, 2, 10, 18, and 26 μg of cryptolepine/ml at 37.5°. The cell population at the time of drug addition was 2.0×10^6 cells/ml. Total counts were obtained on culture samples withdrawn at 30-min intervals.

Organism Population Effect on Drug-Affected Generation Rates—Generation curves of replicate cultures treated with 0, 2, 10, 18, and 26 μg of cryptolepine/ml at three bacterial population levels (2.0×10^5, 2.0×10^6, and 1.0×10^7 cells/ml) were determined. Total counts were obtained on samples withdrawn every 30 min.

pH Effect on Drug-Affected Generation Rates—Broth media were adjusted with 2.0 *N* HCl and 2.0 *N* NaOH to pH 6.5, 7.0, and 7.5. Replicates of each broth were inoculated with the test organism and incubated at 37.5°. Aliquots (2.0 ml) of cryptolepine solutions were added to replicate cultures to yield 0 and 14 μg of cryptolepine/ml. The cell population

[1] Dr. Oku-Ampofo, Centre for Plant Medicine Research, Mampong-Akwapim, Ghana, personal communication.

[2] Antibiotic medium 3, Difco Laboratories, Detroit, Mich.

[3] Prepared in the Department of Pharmaceutical Chemistry, University of Science and Technology, Kumasi, Ghana.

[4] Coulter counter, model ZBI, Coulter Electronics Co., Hialeah, Fla.

0022-3549/79/1200-1510$01.00/0
© 1979, American Pharmaceutical Association

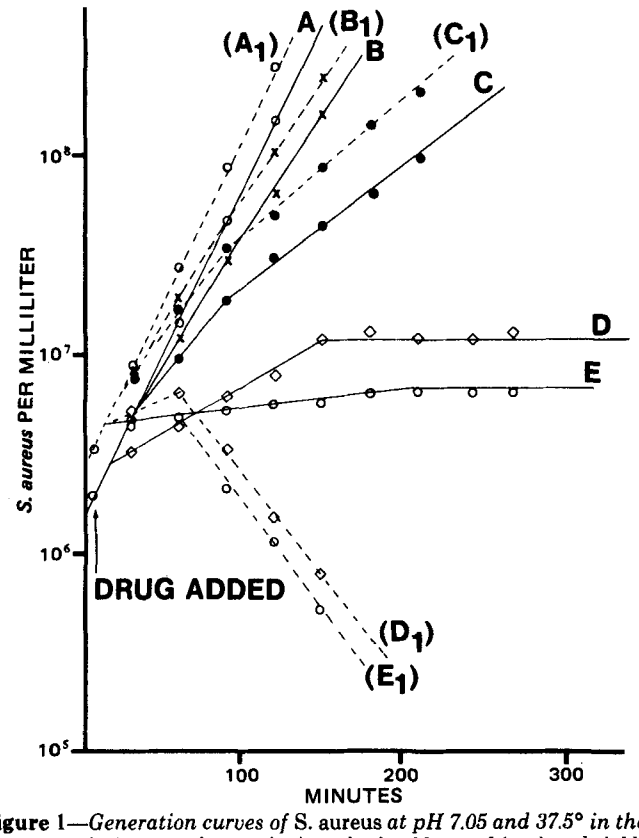

Figure 1—*Generation curves of* S. aureus *at pH 7.05 and 37.5° in the absence and presence of cryptolepine, obtained by total (—) and viable (---) counts. The curves and respective drug concentrations (micrograms per milliliter) were: A, A_1 = 0; B, B_1 = 5; C, C_1 = 10; D, D_1 = 20; and E, E_1 = 30.*

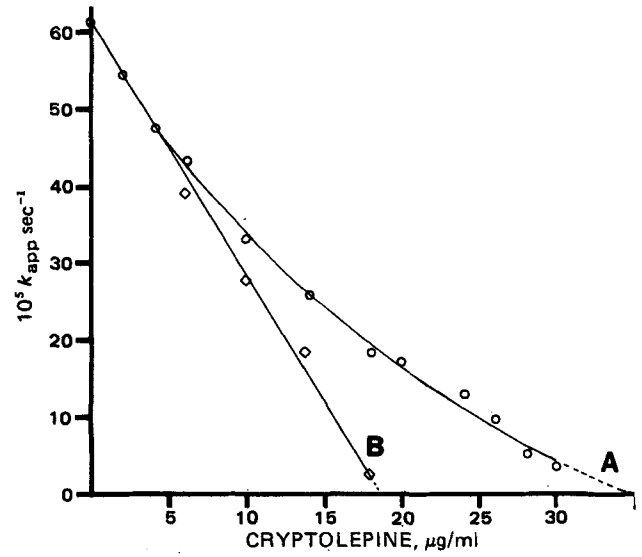

Figure 2—*Functional dependence of apparent generation rate constant,* k_{app} *in seconds*$^{-1}$*, for drug-affected* S. aureus *on cryptolepine concentrations (micrograms per milliliter) at pH 7.05 and 37.5°. Curve A (○) is for dependence in phase I, and curve B (□) is for dependence in phase II.*

at the time of drug addition was 2.0×10^6/ml, and total counts were determined on samples withdrawn every 30 min.

Size Frequency Distribution of Drug-Free and Drug-Treated Cultures—Size frequency distribution curves of a control drug-free culture and test culture treated with 14 μg of cryptolepine/ml were generated from a Channelyzer[5] calibrated with a threshold factor of 0.034, at base channel threshold 5 and window width 100. The curves were recorded with an *x–y* recorder II[5].

RESULTS

Effect of 0.04% (v/v) Polysorbate 80 on Generation of *S. aureus* Cultures—*S. aureus* growing in the absence or presence of 0.04% (v/v) polysorbate 80 showed an exponential generation phase:

$$\ln N = \ln N_0 + k_0 t \qquad \text{(Eq. 1)}$$

where N is the number of organisms per unit volume at a time t; N_0 is the number of organisms per unit volume at some initial time, 0; and k_0 is the apparent generation rate constant. The apparent generation rate constant, k_0 in seconds^{-1}, obtained from the slopes of ln N *versus* t plots, was 40.93×10^{-5} sec^{-1} in the absence of polysorbate 80 but was 61.17×10^{-5} sec^{-1} in the presence of 0.04% (v/v) polysorbate 80. The mean generation time (mgt) for *S. aureus* was calculated in accordance with:

$$\text{mgt} = 0.693/k_0 \qquad \text{(Eq. 2)}$$

The mgt of the test organism decreased by ~30% in the presence of 0.04% (v/v) polysorbate 80 to 18.88 min (8). The increased rate of cell growth and division of *S. aureus* in the presence of polysorbate 80 may be attributed to: (*a*) the surfactant effect of polysorbate 80 enhancing the nutrient material permeation and/or oxygen availability into the cells, or (*b*) the polysorbate 80 enriching the broth medium as a nutrient source (12–16).

[5] Coulter Electronics Co., Hialeah, Fla.

Generation Curves of Cryptolepine-Treated *S. aureus* Cultures—Semilogarithmic plots of the total count *versus* time are shown in Fig. 1. The addition of graded cryptolepine concentrations to balanced *S. aureus* cultures decreased the generation rate after a lag phase of ~10 min. The initial steady-state generation phase (phase I) was followed by another steady-state generation phase (phase II) after one to four successive generations of the cultures affected by high drug concentrations. Apparent generation rate constants (k_{app} in seconds^{-1}) of drug-affected cultures were obtained from linear portions of ln N *versus* t plots in accordance with:

$$\ln N = \ln N_0 + k_{app} t \qquad \text{(Eq. 3)}$$

The generation rate constants, k_{app_I}, for phase I generation were greater than those, $k_{app_{II}}$, for phase II generations. These observations suggest that cryptolepine has more than one mechanism of action on *S. aureus*.

Comparison of Generation Curves of Drug-Treated Cultures by Total and Viable Count Methods—Semilogarithmic plots of the total and viable counts *versus* time for *S. aureus* cultures treated with 0, 5, 10, 20, and 30 μg of cryptolepine/ml, also are shown in Fig. 1. Parallel curves were obtained for plots of the total and viable counts for cultures affected with low cryptolepine concentrations, 0–10 μg/ml, in all growth phases.

Cultures affected with higher drug concentrations, 20 and 30 μg/ml, yielded curves that were parallel and coincident, respectively, for 55 min in phase I growth. Thereafter, the viable count dropped rapidly with time, which may indicate a bactericidal or lytic action superimposed on generation inhibition at the higher concentration range. Where parallel curves were obtained, the total count was 50–60% of the viable count.

Generation Rate Dependency on Drug Concentrations—A plot of k_{app} *versus* concentration is shown in Fig. 2. The extent of generation inhibition was directly proportional to the cryptolepine concentration in the ranges of 0–4.25 μg/ml for phase I action and 0–18.55 μg/ml for phase II action. The k_{app} dependence on cryptolepine concentration (D) is expressed:

$$k_{app} = k_0 - k_d D \qquad \text{(Eq. 4)}$$

where k_d is the specific inhibitory rate constant. At a >4.25-μg/ml concentration in phase I, k_{app} was not a linear function of increasing drug concentration but asymptotically approached zero.

Applicability of Saturation Kinetics to Cryptolepine Action on *S. aureus*—Figure 3 shows a plot of $D/(k_0 - k_{app})$ *versus* D in accordance with a previously derived (12) saturable receptor site model:

$$D/(k_0 - k_{app}) = D(k_b/k_a) + 1/k_a \qquad \text{(Eq. 5)}$$

Table I—Derived [a] Kinetic Parameters from Generation Curves of Cryptolepine-Treated *S. aureus* Cultures

Kinetic Parameter	Phase I	Phase II
$10^5\ k_d$, ml/μg sec[b]	3.33	3.26
$10^5\ k_A$, ml/μg sec[c]	3.77	—
$10^5\ k_a^1$, ml/μg sec[d]	—	3.30
$10^5\ k_a$, ml/μg sec[e]	0.47	—
$10^5\ k_b$, ml/μg[c]	3460.00	—
$10^5\ k_a k_b^1$, sec^{-1}	13.58	—
$(k_a/k_b)/k_0$	0.22	—
MIC, μg/ml[f]	37.07	18.54

[a] Derived from Fig. 2 data. [b] Calculated from the slope of the plot of k_{app} *versus* concentration from 0–4.25 μg of cryptolepine/ml in phase I and from 0–18 μg of cryptolepine/ml in phase II. [c] The k_A and k_b values were estimated from the slope and intercept of the plot of $D/(k_0 - k_{app})$ *versus* D from Eq. 5 for cryptolepine concentrations greater than 4.25 μg/ml in phase I. [d] Derived from the slope of the plot of $1/(k_0 - k_{app})$ *versus* $1/D$ from Eq. 4. [e] The difference between the k_A and k_a^1 values from Eq. 17*a*. [f] Calculated from Eqs. 6 and 8 for phases I and II, respectively, when cryptolepine is at the minimal inhibitory concentration.

where k_a and k_b are proportionality constants related to drug availability in the biophase and drug affinity for receptor or binding sites. Adherence to Eq. 5 is observed for linear plots obtained for cryptolepine concentrations greater than 4.25 μg/ml in phase I. Deviation of the plot from linearity occurs at concentrations less than 4.25 μg/ml, indicating nonadherence to a saturable process at lower concentration ranges in phase I. There was no adherence to the model for phase II of cryptolepine action in the concentration range studied. These findings demonstrate a different mechanism of action for phases I and II. The k_a and k_b values are given in Table I. The minimum inhibitory concentration (MIC) of cryptolepine during phase I was calculated from the expression (8):

$$D_{m_I} = k_0/(k_a - k_0 k_b) \qquad \text{(Eq. 6)}$$

where D_{m_I} is the minimum inhibitory concentration of phase I. The minimum inhibitory concentration during phase II, $D_{m_{II}}$, is derived from:

$$k_{app_{II}} = k_0 - k_a^1 D \qquad \text{(Eq. 7)}$$

where $k_a^1 = k_d$ in Eq. 4 during phase II. At $D_{m_{II}}$, where $k_{app_{II}} = 0$, Eq. 4 simplifies to:

$$D_{m_{II}} = k_0/k_a^1 \qquad \text{(Eq. 8)}$$

The calculated D_{m_I} and $D_{m_{II}}$ values are given in Table I.

Medium Composition Effect on Drug-Affected Generation Rates—Apparent generation rate constants, k_{app}, of drug-free and drug-treated *S. aureus* in Antibiotic Medium 3 at three concentrations are given in Table II. The generation rate constants varied significantly when the medium concentration was varied, which may indicate interference with drug action by medium constituents.

Cell Population Effect at Time of Drug Addition on Generation Rates—Table II also gives apparent generation rate constants of drug-free and drug-affected *S. aureus* in single strength Antibiotic Medium 3 with three different organism populations at the time of drug addition. There were no significant variations of the generation rate constants with organism populations at any of the drug concentrations.

pH Effect on Generation Rates—The generation rate constants of drug-free and drug-affected *S. aureus* in broth adjusted to pH 6.5, 7.0, and 7.5 are given in Table III. The generation rate constant, k_0, of drug-free cultures was invariant with pH, and that of drug-treated cultures varied significantly with changes in pH. A pH increase reduced the generation rate constant, indicating an increase in drug action on *S. aureus* cultures.

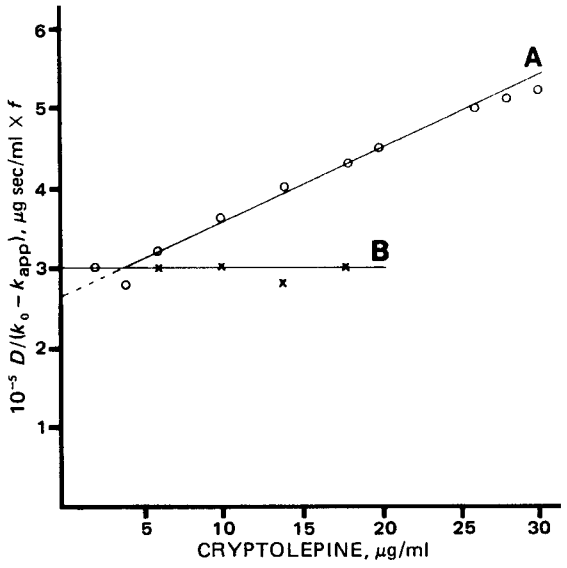

Figure 3—*Applicability of saturation kinetic model to the dependency of apparent growth rate constants,* k_{app}, *of drug-affected* S. aureus *on higher cryptolepine concentrations at pH 7.05 and 37.5°. Curve A is for* S. aureus*-affected culture in phase I generation, and curve B is for* S. aureus*-affected culture in phase II generation. The actual values of* $D/(k_0 - k_{app})$ *are multiplied by a factor,* f, *where* f = 0.001.

Cryptolepine Effect on Size Frequency Distribution Curves of *S. aureus*—The size frequency distributions of drug-free and drug-affected *S. aureus* cultures are given in Fig. 4. Table IV shows the predominance of two population types with mean cell diameters of 0.769 and 1.549 μm. The drug-free cultures demonstrated a relative percentage increase of cell diameter throughout the experiment. The drug-treated cultures showed an initial cell diameter increase in 20% of the population, but this increase was followed by cessation of growth.

DISCUSSION

S. aureus cultures treated with cryptolepine showed biphasic steady-state generation curves (Fig. 1). The generation rate constant in phase I was greater than that in phase II, indicating an enhanced generation inhibition in the latter phase. Figure 2 shows that the dependency of the generation rate constant on cryptolepine concentration for phase I was linear at low drug concentrations, 0–4.25 μg of cryptolepine/ml, but gave an asymptotic curve at concentrations greater than 4.25 μg/ml. The phase II dependency was linear in the entire concentration range.

The plot of $D/(k_0 - k_{app})$ *versus* D (Fig. 3) reveals that the phase I cryptolepine action in the high concentration range adhered to a saturable receptor site model, except that deviations occurred in the low concentration range (17). The phase II cryptolepine action in the entire concentration range did not follow saturation kinetics, which may imply that few receptors interacted with cryptolepine molecules to produce generation inhibition. The inference is that the mechanism of cryptolepine in phase II is different from phase I.

Organism population at the time of drug addition did not affect the generation rate (Table II), demonstrating that cryptolepine was not metabolized by *S. aureus*. Moreover, the drug was not depleted in the medium as a result of adsorption to cellular components, and the drug

Table II—Effect of Variation in Broth Composition and Inoculum Size on Phase I and II Generation Rates of Cryptolepine-Treated *S. aureus*

Cryptolepine, μg/ml	Phase I			Phase II			Phase I			Phase II		
	B_1[a]	B_2[b]	B_3[c]	B_1	B_2	B_3	I_1[d]	I_2[e]	I_3[f]	I_1	I_2	I_3
0	61.91	60.40	63.61	—	—	—	60.12	62.10	61.81	—	—	—
2	48.19	55.01	63.18	—	—	—	55.54	56.21	57.00	—	—	—
10	19.17	34.50	57.76	7.0	27.0	38.78	34.63	35.28	36.94	27.57	28.86	25.53
18	9.61	18.25	46.55	0	2.50	23.56	15.85	16.51	16.08	2.49	3.18	2.71
26	5.77	9.5	23.70	0	0	7.74	9.27	9.10	8.20	0	0	0

[a] Half-strength broth (B_1). [b] Normal-strength broth (B_2). [c] Double-strength broth (B_3). [d] Inoculum of 2.0×10^5 cells/ml (I_1). [e] Inoculum of 2.0×10^6 cells/ml (I_2). [f] Inoculum of 1.0×10^7 cells/ml (I_3).

Table III—Effect of Broth pH on Phase I and II Generation Rates of *S. aureus* Cultures Treated with 14 μg of Cryptolepine/ml

pH	$k_{app} \times 10^{-5}$ sec^{-1}				
	k_0	k_{appI}	k_{appII}	$k_0 - k_{appI}$	$k_0 - k_{appII}$
6.5	61.37	40.08	26.97	21.29	34.40
7.0	60.92	24.09	13.36	36.84	47.57
7.5	61.09	15.66	3.01	45.43	58.00

was not inactivated either by cellular excretions or by other interactions as a function of organism numbers.

Variation in the concentration of medium constituents significantly altered the generation rate constant (Table II). This variation is attributed to the fact that the drug either is bound to broth constituents or is inactivated by metabolites in the broth medium that competitively bind to the drug receptor site in the biophase. However, the curve for k_{app} dependency on cryptolepine concentration (Fig. 2) does not yield an initial lag phase that is typical of drug binding to broth constituents or of drug complexation with metal ions in the broth medium. Therefore, the latter assumption holds.

The viable count determinations (Fig. 1) showed that, during phase I action, there was a generation inhibition of *S. aureus* by low cryptolepine concentrations, 0–20 μg/ml, as demonstrated by parallelism of the curves for both total and viable counts. At 30 μg of cryptolepine/ml, dynamic bacteriostasis (18) is superimposed on generation inhibition, evidenced by coincident curves for both total and viable counts. During phase II, however, generation inhibition was observed only in cryptolepine concentrations of <20 μg/ml. At 20–30 μg of cryptolepine/ml, the viable count fell rapidly ~55 min after drug addition, which indicates cell death and/or lysis.

The size frequency analysis in Table IV reveals two predominant population types with mean cell diameters of 0.769 and 1.549 μm for the drug-free culture. The former diameter agrees with the reported (19) minimal cell diameter for *S. aureus*. The latter diameter is double the minimal diameter and is the maximum cell diameter attained by a majority of the cell population before cell division. About 20% of the cell population in the cultures treated with cryptolepine (14 μg/ml) showed a cell diameter increase equal to that of the drug-free culture at 5 min. This increase occurred during the first 30 min after drug addition, when the drug was being equilibrated in the biophase. Thereafter, the cells maintained the minimal cell diameter with a concomitant cell number decrease.

These observations support the hypothesis that cryptolepine possesses bactericidal action that is superimposed on normal generation inhibition. The bactericidal action predominates in the later stages of the drug–

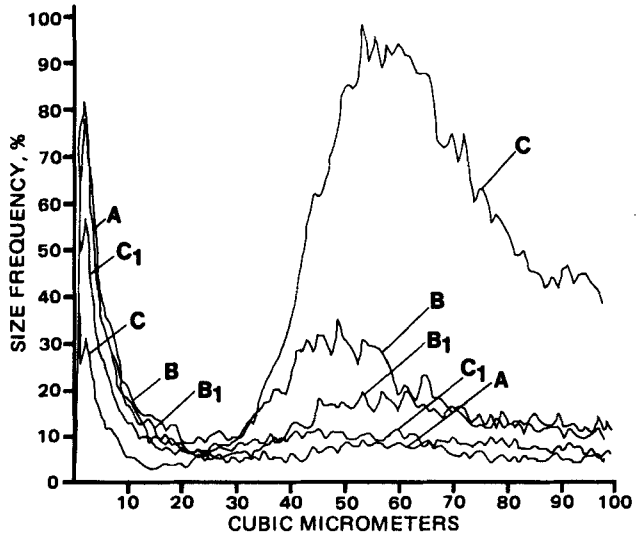

Figure 4—*Size frequency distribution curves of drug-free and drug-affected* S. aureus *cultures. Curve A is for the drug-free culture 5 min before cryptolepine addition (14 μg/ml); curves B and B_1 are for drug-free and drug-affected cultures, respectively, 30 min after drug addition; and curves C and C_1 are for drug-free and drug-affected cultures, respectively, 120 min after drug addition.*

Table IV—Size Frequency Distribution of *S. aureus* Cultures Treated with 0 and 14 μg of Cryptolepine/ml

Minutes	Drug-Free Cells		Drug-Treated Cells	
	Mean Cell Diameter, μm	Relative Frequency, %	Mean Cell Diameter, μm	Relative Frequency, %
5	0.769	78	—	—
30	0.769	69.3	0.769	80.40
	1.521	30.7	1.589	19.60
60	0.769	52	0.769	86.00
	1.537	48		
120	0.769	23.85	0.769	57.00
	1.555	76.15		
180	1.547	99.00	0.769	52.00

bacteria reaction. A kinetic model that may define the mechanism of cryptolepine action on *S. aureus* is shown in Scheme II:

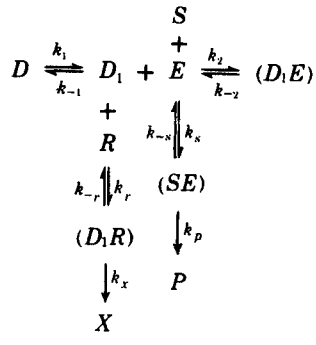

Scheme II

In this model, D is the cryptolepine concentration in the broth medium, which is equilibrated with cryptolepine concentration in the biophase D_1, which is reversibly bound with enzyme E to form a drug–enzyme complex D_1E; S is a metabolite in the broth medium that is used as a substrate by the enzyme E in the synthesis of protein product P from the substrate–enzyme complex, SE. Moreover, D_1 reacts with a receptor site, R, to form an injured site or toxic product, X, from a reaction complex, D_1X. The receptor site may be a vital target site that is a sensitive cell membrane component, a protoplasmic or nuclear material, or a transport agent essential for organism survival (20–23).

By assuming that the microbial generation rate is proportional to: (*a*) the difference between the protein synthesis rate, dP/dt, which causes a microbial number increase from cell growth and division, and the rate of injury or formation of toxic product, dX/dt, which causes a microbial number decrease from kill or lysis of the cells, and (*b*) the number of viable organisms, N, present, the following apply:

$$dN/dt = k(dP/dt - dX/dt)N = k_{app}N \quad \text{(Eq. 9)}$$

where k is a proportionality constant and k_{app} is the apparent generation rate constant of the drug-treated culture. Therefore:

$$k_{app} = k(dP/dt - dX/dt) \quad \text{(Eq. 10)}$$

$$k_{app} = k[\{[k_p k_s(S)(E)]/(k_p + k_{-s})\} - \{[k_x k_r(D_1)(R)]/(k_x + k_{-r})\}] \quad \text{(Eq. 11)}$$

$$k_{app} = k_p^1 S(1 - \theta)E_T - k^1(D_1)(R) \quad \text{(Eq. 12)}$$

where $\theta = (D_1E)/E_T$ is the fraction of total enzyme bound to drug, $k_p^1 = kk_pk_s/(k_p + k_{-s})$, and $k^1 = k_xk_r/(k_x + k_{-r})$.

Expansion of Eq. 12 yields:

$$k_{app} = k_p^1 SE_T - k_p^1 SE_T\theta - k^1(D_1)(R) \quad \text{(Eq. 13)}$$

In the absence of drug, $D_1 = 0$, $\theta = 0$, and Eq. 13 simplifies to:

$$k_{app} = k_p^1 SE_T = k_0 \quad \text{(Eq. 14)}$$

where S and E_T are assumed to be available in constant amounts during bacteria–drug reaction and k_0 is the generation rate constant for drug-free cultures. Substituting Eq. 14 in Eq. 13 gives:

$$k_{app} = k_0 - k_0\theta - k^1(D_1)(R) \quad \text{(Eq. 15)}$$

θ is expressed (17, 24) as $K_1K_2D/1 + K_1K_2D$, where K_1 is the drug par-

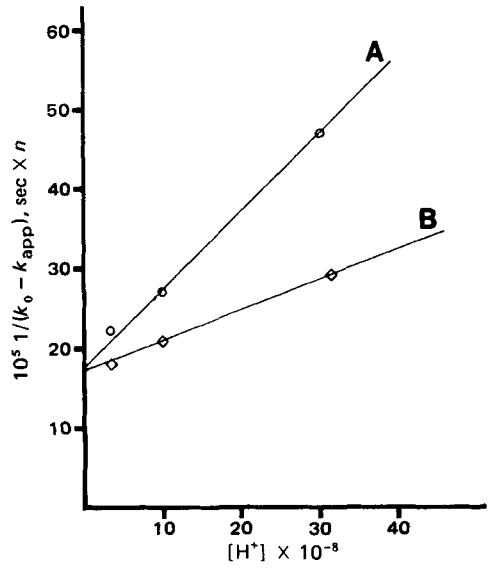

Figure 5—*Dependence of apparent generation rate constant,* k_{app}, *for* S. aureus *on broth medium pH. Curve A is for dependence of* k_{app} *on pH during phase I generation, and curve B is for dependence of* k_{app} *on pH during phase II generation. The actual values of* $1/(k_0 - k_{app})$ *are multiplied by a factor,* n, *where* n = 0.001.

tition constant through cell membranes and K_2 is the drug affinity constant for the enzyme E. Therefore:

$$k_{app} = k_0 - k_0(K_1K_2D/1 + K_1K_2D) - k^1(K_1D)(R) \quad \text{(Eq. 16)}$$

Equation 16 may be simplified to:

$$k_{app} = k_0 - [k_aD/(1 + k_bD) + k_a^1D] \quad \text{(Eq. 17}a\text{)}$$

where $k_a = k_0K_1K_2$, $k_b = K_1K_2$, $k_d = kK_1R$, and R is assumed to be present in an infinitely large amount relative to drug molecules.

At low cryptolepine concentrations when few receptors are interacted with drug, $k_bD \ll 1$ and Eq. 17a reduces to:

$$k_{app} = k_0 - (k_aD + k_a^1D) = k_0 - k_AD \quad \text{(Eq. 17}b\text{)}$$

where $k_A = k_a + k_a^1$. Equation 17b is Eq. 4, where $k_A = k_d$, and describes the functional dependency of k_{app} on drug concentrations of 0–42.5 μg/ml for cryptolepine-affected *S. aureus* in phase I (Fig. 2).

Equation 17a may be expanded to:

$$k_{app} = k_0 - \{(k_a + k_a^1)D + k_bk_a^1D^2\}/1 + k_bD \quad \text{(Eq. 18)}$$

At high drug concentrations in phase I, where the cryptolepine bactericidal action is negligible and $(k_a + k_a^1)D \gg k_bk_a^1D^2$, Eq. 18 simplifies to:

$$k_{app} = k_0 - (k_a + k_a^1)D/(1 + k_bD) = k_0 - k_AD/(1 + k_bD) \quad \text{(Eq. 19)}$$

Rearrangement of Eq. 19 yields Eq. 5, where $k_b/k_A = k_b/(k_a + k_a^1)(k_b/k_a)\,1/k_0$. At the minimal inhibitory concentration in phase I when $k_{app} = 0$, Eq. 19 simplifies to Eq. 6.

In phase II, where cryptolepine bactericidal action predominates over its growth inhibitory action, k_{app} becomes solely dependent on the rate of cell death or lysis. Therefore, Eq. 17a approaches the expression $k_{app} = k_0 - k_a^1D$, which is Eq. 4, where $k_a^1 = k_d$. At the minimal inhibitory concentration where $k_{app} = 0$, Eq. 4 simplifies to Eq. 8. The minimal inhibitory concentration values for phases I and II of cryptolepine on *S. aureus* calculated from derived kinetic parameters in Eqs. 6 and 8, respectively (Table I), agree with the experimental minimal inhibitory concentration values (Fig. 2).

Changes in broth medium pH influenced the cryptolepine effect on *S. aureus*. The extent of generation inhibition $(k_0 - k_{app})$ increased as some function of the broth medium pH (Table III).

If f is the fraction of the total cryptolepine salt concentration (D_T) that is unprotonated, then for a weak basic compound like cryptolepine:

$$f = K_a/[H^+] + K_a \quad \text{(Eq. 20)}$$

and, therefore:

$$D^1 = D_TK_a/[H^+] + K_a \quad \text{(Eq. 21)}$$

where K_a is the dissociation constant, $[H^+]$ is the hydrogen-ion concentration, and D^1 is the unprotonated drug concentration at a specified pH. By assuming that the unprotonated drug concentration contributes to cryptolepine activity and then substituting Eq. 21 in Eq. 19 and simplifying, the k_{app} dependency on pH in phase I may be expressed as:

$$1/(k_0 - k_{app}) = [H^+]/k_aK_aD_T + 1/k_aD_T(1 + k_bD_T) \quad \text{(Eq. 22)}$$

Equation 22 is an expression for the linear dependency of the plot of $1/(k_0 - k_{app})$ *versus* $[H^+]$ in Fig. 5. Likewise, the k_{app} dependency on pH during phase II cryptolepine action is described by an expression derived from Eqs. 21 and 4:

$$1/(k_0 - k_{app}) = [H^+]/k_a^1K_aD_T + 1/k_a^1D_T \quad \text{(Eq. 23)}$$

where K_a was calculated from the slope and intercept obtained from the linear plot of $1/(k_0 - k_{app})$ *versus* $[H^+]$ in phase II (Fig. 5). The pKa of cryptolepine was 6.34. The linear plots (Fig. 5) obtained from experimental data in accordance with Eqs. 22 and 23 confirm the assumption that the unprotonated cryptolepine molecules contribute to the activity because of their possible ready penetration through cell membranes.

REFERENCES

(1) E. Clinquart, *Bull. Acad. R. Med. Belg.*, **9**, 627 (1929).

(2) E. Gellert, Raymond-Hamet, and E. Schlittler, *Helv. Chim. Acta*, **34**, 642 (1951).

(3) J. E. Saxton, in "The Alkaloids, Chemistry and Physiology," vol. VIII, R. H. F. Manske, Ed., Academic, New York, N.Y., 1965, p. 19.

(4) Raymond-Hamet, *C.R. Soc. Biol.*, **126**, 768 (1937).

(5) Raymond-Hamet, *C.R. Acad. Sci.*, **207**, 1016 (1938).

(6) K. Boakye-Yiadom, *J. Crude Drug Res.*, in press.

(7) K. Boakye-Yiadom and D. Dwuma-Badu, "Proceedings of the 3rd Symposium on African Medicinal Plants," University of Ife, Ile-Ife, Nigeria, July 11–15, 1977, in press.

(8) S. M. Heman-Ackah, *J. Pharm. Sci.*, **63**, 1077 (1974).

(9) *Ibid.*, **64**, 1612 (1975).

(10) *Ibid.*, **64**, 1621 (1975).

(11) S. M. Heman-Ackah, *Antimicrob. Agents Chemother.*, **10**, 223 (1976).

(12) J. H. Baker, *J. Soc. Cosmet. Chem.*, **10**, 133 (1959).

(13) M. Barr and L. F. Tice, *J. Am. Pharm. Assoc., Sci. Ed.*, **46**, 442 (1957).

(14) O. Engler, These' de Doctorat. No. 1149, Geneva; cited by D. L. Wedderburn in "Handbook of Cosmetic Science—An Introduction to Principles and Applications," Pergamon, Oxford, England, 1963, p. 445.

(15) E. J. Ordal, J. L. Wilson, and A. F. Borg, *J. Bacteriol.*, **42**, 117 (1941).

(16) W. L. Williams, N. P. Broquist, and E. E. Snell, *J. Biol. Chem.*, **170**, 619 (1947).

(17) E. R. Garrett, *Progr. Drug Res.*, **15**, 27 (1971).

(18) Parkinson, Ph.D. thesis, London, England, 1954; cited by A. M. Cook, *J. Pharm. Pharmacol.*, **6**, 629 (1954).

(19) B. D. Davies, R. Dulbecco, H. N. Eisen, H. S. Ginsberg, and W. B. Wood, Jr., "Microbiology," 2nd ed., Harper and Row, Hagerstown, Md., 1973, p. 728.

(20) O. Rhan, *J. Gen. Physiol.*, **13**, 179 (1929).

(21) C. Hinshelwood, *Nature*, **167**, 666 (1951).

(22) O. Rhan, *Biodynamica*, **14**, 81 (1943).

(23) W. B. Hugo, in "Disinfection," M.A. Benard, Ed., Dekker, New York, N.Y., 1970, p. 31.

(24) S. M. Heman-Ackah and E. R. Garrett, *J. Med. Chem.*, **15**, 247 (1971).

ACKNOWLEDGMENTS

K. Boakye-Yiadom is grateful to the University of Science and Technology, Kumasi, Ghana, for a sabbatical leave; the Council for International Exchange of Scholars for a Fulbright–Hays Fellowship; the Cancer Research Center at Howard University for partial support; and the College of Pharmacy and Pharmacal Sciences in Howard University for facilities that enabled this research project to be completed.

Effects of Phenylbutazone, Tolbutamide, and Clofibric Acid on Binding of Racemic Warfarin and Its Enantiomers to Human Serum Albumin

K. VERONICH *, G. WHITE *, and A. KAPOOR ˣ

Received February 1, 1979, from the *Department of Pharmaceutical Sciences, College of Pharmacy and Allied Health Professions, St. John's University, Jamaica, NY 11439.* Accepted for publication June 15, 1979. *Present address: Endo Laboratories, Garden City, NY 11530.

Abstract □ The effect of phenylbutazone, tolbutamide, and clofibric acid on the binding of racemic warfarin and its enantiomers to human serum albumin was studied by equilibrium dialysis. Warfarin had one primary and two secondary binding sites on the albumin molecule. No difference in binding was detected at the primary binding site; the extent of *R*(+)-isomer binding at the secondary binding sites was 2.5 times greater than the corresponding *S*(−)-isomer binding. Phenylbutazone and warfarin appear to compete for the same primary binding site on the albumin molecule. Tolbutamide interferes with the binding of warfarin enantiomers at their secondary sites. Clofibric acid has a less pronounced effect on warfarin binding than does phenylbutazone or tolbutamide.

Keyphrases □ Phenylbutazone—effect on binding of racemic warfarin and its enantiomers to human serum albumin □ Tolbutamide—effect on binding of racemic warfarin and its enantiomers to human serum albumin □ Clofibric acid—effect on binding of racemic warfarin and its enantiomers to human serum albumin □ Warfarin—effect of phenylbutazone, tolbutamide, and clofibric acid on binding of racemate and enantiomers to human serum albumin

The pharmacokinetics of the warfarin isomers show similarities as well as dissimilarities. The two isomers exhibit similar absorption patterns (1) and do not differ significantly in their volumes of distribution (2–4). The *S*(−)-isomer is several times more potent in anticoagulant activity than the *R*(+)-form (1, 4), and it is eliminated primarily as its oxidation product, 7-hydroxywarfarin, while the *R*(+)-isomer is predominantly reduced and eliminated as warfarin alcohol (1, 3, 5). Although interindividual differences produce a wide range of plasma half-lives (6–8), the *S*(−)-isomer has a shorter half-life than the *R*(+)-isomer (1–4).

In the present investigation, the binding behavior of the isomers with human serum albumin was characterized by equilibrium dialysis to determine if there is a correlation between the free fraction of the isomers *in vitro* and clinically observed elimination kinetics. In two studies (9, 10), the *S*(−)-isomer had a significantly higher affinity for the primary site; in two other studies (11, 12), no significant differences in isomer binding were found.

Phenylbutazone (13–18), tolbutamide (19), and clofibrate (17, 20, 21) have been reported to potentiate the anticoagulant effects of warfarin. Extensive work has been done on the phenylbutazone–warfarin interaction, including several clinical studies with the isomers (1, 22). Analysis of the elimination products during warfarin–phenylbutazone treatment provided interesting results: the clearance of *R*(+)-warfarin was stimulated while that of the *S*(−)-isomer was retarded (1). The greater prothrombin time response observed in these cases can be attributed to a combination of two effects: increased free warfarin concentration and inhibition of the metabolism and elimination of the more potent *S*(−)-isomer.

In view of the stereoselective interaction suggested by these findings, the effects of phenylbutazone, tolbutamide, and clofibric acid on the binding of racemic warfarin and its isomers to human serum albumin *in vitro* were studied. Since clofibrate undergoes hydrolysis *in vivo* to its corresponding acid, which is presumed to be the active drug (23), clofibric acid was used. Although binding parameters have been reported for phenylbutazone (24, 25), tolbutamide (26–28), and clofibric acid (29) under various conditions, they were experimentally estimated under the same conditions used here for comparison.

Table I—Estimated Binding Parameters

Compound	n_1	$k_1 \times 10^{-5}\ M^{-1}$	n_2	$k_2 \times 10^{-4}\ M^{-1}$
Racemic warfarin	1	14	2	1.8
R(+)-Warfarin	1	14	2	2.5
S(−)-Warfarin	1	14	2	1.0
Phenylbutazone	1	7.0	1	1.0
Tolbutamide	1	1.3	2	0.25
Clofibric acid	1	0.17	2	0.43

EXPERIMENTAL

Materials—The warfarin isomers[1], tolbutamide[2], clofibric acid[3], and phenylbutazone[4] were obtained commercially. Human serum albumin, rechromatographed, was used without further purification[5]. Dialysis membranes[6] were rinsed with distilled water several times during the 2 hr prior to use. Chloroform and dimethylformamide were spectrophotometric quality[7]. All other chemicals were certified ACS grade. All solutions were prepared in 0.067 *M* mixed sodium and potassium phosphate buffer, pH 7.4 (30).

Dialysis Procedure—Dialysis experiments were carried out at 4° in cells constructed from 30- and 60-ml glass jars attached by Plexiglas flanges. Cells were rotated at 6 rpm for ~135 hr. One compartment contained the drug (or drugs) in 30.0 ml of buffered 0.4% human serum albumin, and the other compartment contained 60.0 ml of buffer. A larger volume was used in the albumin-free compartment to increase the amount of free drug available for extraction and analysis. Cells without drugs were used as spectrophotometric blanks in the assay and to check for albumin transfer across the membrane.

Analytical Methods—The purity of the warfarin isomers, phenylbutazone, and tolbutamide was determined by comparison to their corresponding USP–NF reference standards. Clofibric acid purity was verified by titration. Optical rotation[8] of the warfarin enantiomers was measured to prove their optical purity: $[\alpha]_D^{25}$ +149.4° (c 1.2, 0.5 *M* NaOH) for *R*(+)-warfarin, and $[\alpha]_D^{25}$ −148.4° (c 1.2, 0.5 *M* NaOH) for *S*(−)-warfarin. Fluorescence[9] intensity of warfarin at 410 nm, excited at 327 nm, was linear over the standard concentration range and was unaffected by phenylbutazone, tolbutamide, or clofibric acid.

The warfarin–albumin solutions for dialysis were used as calibration standards for warfarin determinations on the albumin side after dialysis.

[1] Gift of Endo Laboratories, Garden City, N.Y.
[2] Gift of The Upjohn Co., Kalamazoo, Mich.
[3] Gift of Ayerst Laboratories, New York, N.Y.
[4] Sigma Chemical Co., St. Louis, Mo.
[5] Worthington Biochemical Corp., Freehold, N.J.
[6] Spectra/Por 2, Spectrum Medical Industries, Los Angeles, Calif.
[7] Burdick & Jackson Laboratories, Muskegon, Mich.
[8] Model A polarimeter, Bellingham-Stanley Ltd., London, England.
[9] Model RRS 1000 spectrofluorometer, Schoeffel Instrument Corp., Westwood, N.J.

0022-3549/79/1200-1515$01.00/0
© 1979, American Pharmaceutical Association

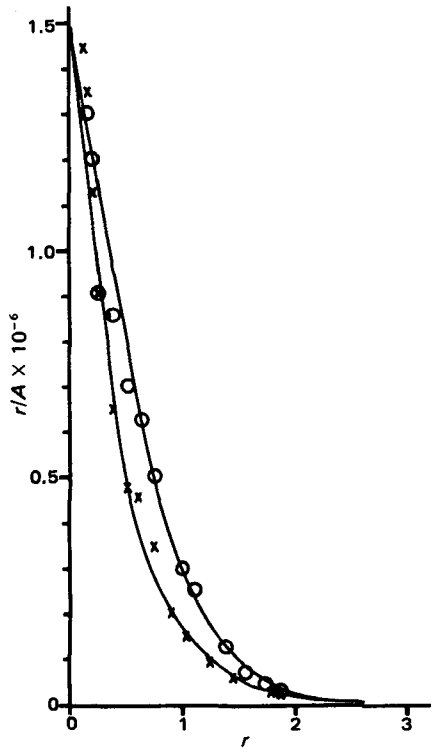

Figure 1—*Binding of warfarin enantiomers to albumin in 0.067* M *phosphate buffer, pH 7.4, at 4°. The smooth curve fitted to each set of points is based on the values in Table I. Key:* O, R(+)-*warfarin;* ×, S(−)-*warfarin;* r, *number of moles of warfarin bound per mole of human serum albumin; and* A, *molar concentration of free warfarin.*

Five milliliters of the standard and dialyzed solutions were diluted to 100 ml with dimethylformamide, and the resulting precipitate of buffer salts and albumin was allowed to settle overnight prior to fluorescence analysis of the clear supernate. The free warfarin side of the cell was treated similarly except for the lower levels, which were acidified, extracted with chloroform, converted to a residue, and dissolved in a minimum volume of dimethylformamide. Standard warfarin solutions were prepared to encompass the range of experimental free warfarin values.

The concentration of free phenylbutazone was determined from the absorbance of the dialysate at 264 nm[10], and the concentration of free tolbutamide was similarly determined at 227 nm. Clofibric acid levels were determined either from the solution absorbance at 228 nm or by GLC[11]. Clofibric acid estimation was not attempted in the presence of warfarin because of significant interference from warfarin.

For GLC, aliquots of the dialysate were acidified, extracted with chloroform, and converted to a residue. The residue was treated with 30 μl of bis(trimethylsilyl)trifluoroacetamide containing 1% trimethylchlorosilane[12] and then diluted with 5.00 ml of internal standard solution consisting of 6.5 μl of heptadecane/100 ml of carbon disulfide. The samples were stoppered and allowed to stand overnight at room temperature to ensure complete derivatization prior to injection onto a 1.2-m × 3.5-mm i.d. coiled glass column packed with 3.0% dimethyl silicone fluid[13] on flux-calcined diatomaceous earth[14], 100–120 mesh, at 170° with a nitrogen carrier. Injection and flame-ionization detector temperatures were 225°. Quantitation of clofibric acid was accomplished by comparison to standard solutions similarly treated.

Binding Constants—Three dialysis determinations, each consisting of seven concentrations of $R(+)$-, $S(-)$-, and racemic warfarin, were made over the range of 6×10^{-6}–1.0×10^{-4} M. Binding constants for the other drugs were estimated from dialysis solutions covering the following ranges: phenylbutazone, 1.5×10^{-5}–1.7×10^{-4} M; tolbutamide, 2.7×10^{-5}–1.8×10^{-4} M; and clofibric acid, 1.2×10^{-5}–2.1×10^{-4} M. Direct spectrophotometric methods were used for determination of phenylbutazone, tolbutamide, and clofibric acid concentrations.

Displacement Experiments—Duplicate runs for warfarin and each competing drug were performed. Fixed concentrations of the competing drug were studied with the warfarin concentration from 6×10^{-6} to 3×10^{-5} M (2.5–10 mg/liter). Final concentrations for the competing drugs were: phenylbutazone, 1.7×10^{-4} M (52 mg/liter); tolbutamide, 1.4×10^{-4} M (38 mg/liter); and clofibric acid, 1.1×10^{-4} M (24 mg/liter).

In all cases, the free competing drug concentration was measured in addition to both bound and free warfarin levels. Free phenylbutazone and free tolbutamide were determined spectrophotometrically; free clofibric acid was measured by GLC.

RESULTS AND DISCUSSION

Racemic warfarin was used as the control in all cases to relate the present work to prior investigations and as a check on results obtained for isomers and competing drugs.

Analytical methods were developed for accuracy and facility of determining small drug quantities. Dimethylformamide was chosen as the solvent for the fluorescence measurements of warfarin because of its ability to enhance the fluorescence intensity (31, 32). To ensure the accuracy of the warfarin data, the drug was measured on both sides of all dialysis membranes, and the recovery of total warfarin was verified. The overall mean recovery for 185 determinations of both free and bound warfarin, alone and in combination with other drugs, was 100 ± 2%.

Scatchard plots (33) are presented in Fig. 1 for the $R(+)$- and $S(-)$-isomers. Curvature is present in both cases, suggesting multiple binding sites. At low bound drug-to-total protein ratios ($r < 0.5$), there appears to be no significant difference in the binding of the two isomers; at higher binding levels ($r > 0.5$), a distinct difference is observed. This finding suggests either different secondary sites or stereoselectivity at identical sites. Estimates of binding constants made by computer-assisted successive approximations from the experimental curves are presented in Table I. The computer was used to generate r values for the Scatchard equations for two independent binding sites, using experimental free warfarin concentrations and varying values for the binding constants. Coincidence of fit was tested by visual comparison of the plotted experimental and computed values. The binding pattern observed for racemic warfarin and the constants determined reflect the average behavior of the isomers. Primary constants were the same for both isomers, but secondary binding constants were quite different, with the value for the $R(+)$-isomer (2.5×10^4) being significantly larger than the corresponding value for the $S(-)$-isomer (1.0×10^4).

Binding parameters for the competing drugs were experimentally estimated for comparison. Curvature is evident in Scatchard plots for all drugs, suggesting multiple sites with differing affinities. The estimated binding parameters for these drugs, obtained by computer-assisted successive approximations from the experimental curves, are presented in Table I.

Duplicate runs for warfarin and each competing drug were performed to evaluate the possible effect of addition order on the binding behavior. In the first case, the warfarin–albumin solutions were allowed to equilibrate overnight at 4°, the competing drug was added, and the solutions were dialyzed. In the second case, the competing drug–albumin solutions were allowed to equilibrate before warfarin addition. Equilibrium concentrations for all drugs were essentially the same in both runs. This finding suggests that, within the ranges studied, equilibrium concentrations of the drugs are a function of the concentrations and affinity constants of the particular drugs and are not related to the addition order.

The concentration of free competing drug was measured as well as bound and free warfarin to estimate the extent of competing drug binding and to correlate this information with the observed behavior for warfarin alone. The warfarin concentration was varied over the range where one binding site for warfarin would be primarily operative in the absence of competition. This range includes the therapeutic blood levels reported for warfarin (34). To minimize the drug-to-albumin ratio, the competing drug concentration added was adjusted so that the final total competing drug concentration at equilibrium would represent about half the average blood levels reported for these drugs (35–37).

Since the Klotz plot (38) is one of the best graphical representations of binding over a narrow concentration range, this treatment was chosen for data presentation (Figs. 2–5). Values for these figures are averages of two runs with reverse initial equilibration as previously described. Apparent primary binding constants for warfarin in the presence of the three competing drugs are presented in Table II. Since no curvature was

[10] Model 200 UV-visible spectrophotometer, Perkin-Elmer Corp., Norwalk, Conn.
[11] Model 5840 gas chromatograph, Hewlett-Packard, Paramus, N.J.
[12] Regisil, RC-2, Regis Chemical Co., Morton Grove, Ill.
[13] OV-101, Ohio Valley Specialty Chemical, Marietta, Ohio.
[14] Gas Chrom Q, Applied Science Laboratories, State College, Pa.

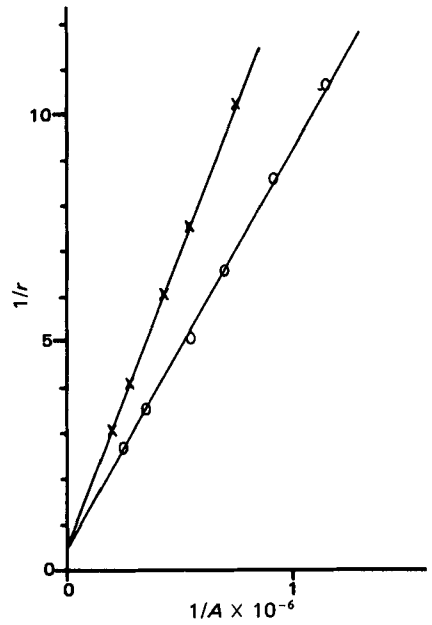

Figure 2—*Effect of phenylbutazone, 1.7 × 10⁻⁴ M, on binding of warfarin enantiomers to albumin. The warfarin concentration range was 6 × 10⁻⁶–3 × 10⁻⁵ M. Key:* O, R(+)-*warfarin;* ×, S(−)-*warfarin;* r, *number of moles of warfarin bound per mole of human serum albumin; and* A, *molar concentration of free warfarin.*

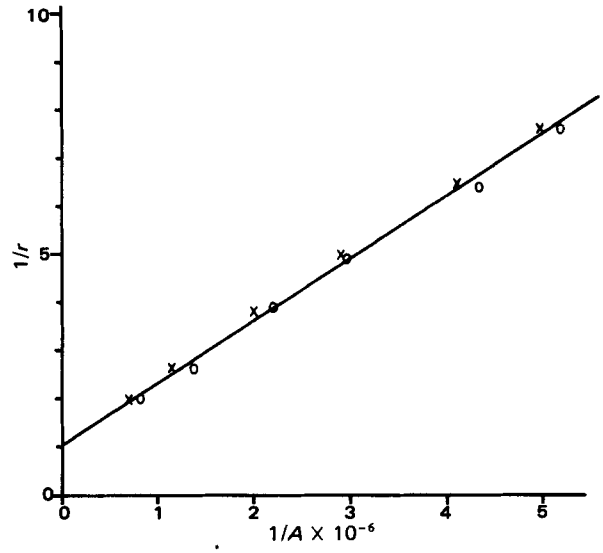

Figure 4—*Effect of clofibric acid, 1.1 × 10⁻⁴ M, on binding of warfarin enantiomers to albumin. The warfarin concentration range was 6 × 10⁻⁶–3 × 10⁻⁵ M. Key:* O, R(+)-*warfarin;* ×, S(−)-*warfarin;* r, *number of moles of warfarin bound per mole of human serum albumin; and* A, *molar concentration of free warfarin.*

evident in the Klotz plots, linear regression analysis was used to estimate the apparent binding parameters for warfarin in the presence of the competing drugs.

A marked increase in free warfarin was observed when phenylbutazone was present (14–20% *versus* 1–3% free warfarin without phenylbutazone). An r value of 1.57 was determined for phenylbutazone, indicating that it was occupying most of its primary sites as well as a significant number of its secondary sites. The apparent number of binding sites for warfarin, three, suggests substantial use of secondary binding sites. The apparent binding constant for the $R(+)$-isomer was significantly larger than the apparent binding constant for the $S(-)$-isomer, which is consistent with secondary site binding and with the significant differences observed in the free warfarin level between the two isomers [14–16% for the $R(+)$ *versus* 20–22% for the $S(-)$].

This difference in isomer behavior is clearly evident in the Klotz plot in Fig. 2. In view of the observed behavior, it appears that phenylbutazone and warfarin compete for the same primary binding site. With most primary sites occupied by phenylbutazone, warfarin binding is essentially limited to the secondary sites. This behavior is substantiated by the observed higher percentage of free $S(-)$-isomer. It is unlikely that phenylbutazone and warfarin also compete for the same secondary sites since, with r = 1.57 for phenylbutazone, the level of free warfarin would be higher than observed.

A significant increase in percent free warfarin was seen when tolbu-

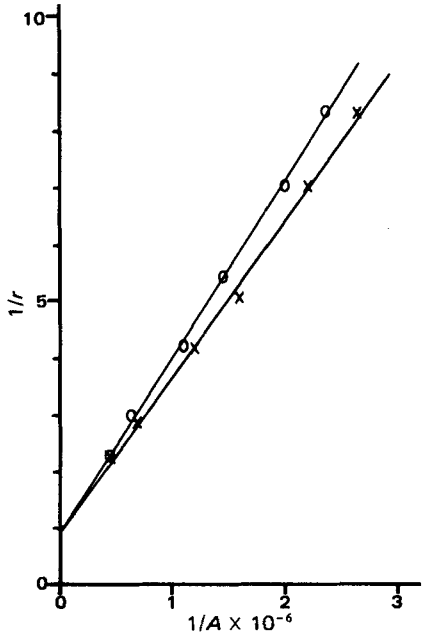

Figure 3—*Effect of tolbutamide, 1.4 × 10⁻⁴ M, on binding of warfarin enantiomers to albumin. The warfarin concentration range was 6 × 10⁻⁶–3 × 10⁻⁵ M. Key:* O, R(+)-*warfarin;* ×, S(−)-*warfarin;* r, *number of moles of warfarin bound per mole of human serum albumin; and* A, *molar concentration of free warfarin.*

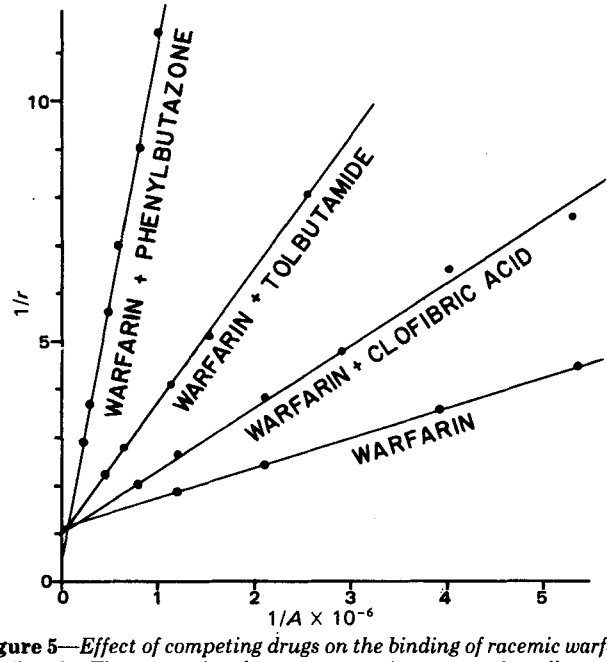

Figure 5—*Effect of competing drugs on the binding of racemic warfarin to albumin. The competing drug concentrations were: phenylbutazone, 1.7 × 10⁻⁴ M; tolbutamide, 1.4 × 10⁻⁴ M; and clofibric acid, 1.1 × 10⁻⁴ M. The warfarin concentration range was 6 × 10⁻⁶–3 × 10⁻⁵ M. Key:* r, *number of moles of warfarin bound per mole of human serum albumin; and* A, *molar concentration of free warfarin.*

Table II—Apparent Binding Parameters for Warfarin and Its Enantiomers in the Presence of Competing Drugs

Competing Drug	Racemic Warfarin		*R*(+)-Warfarin		*S*(−)-Warfarin	
	n	$k \times 10^{-5}$ M^{-1}	*n*	$k \times 10^{-5}$ M^{-1}	*n*	$k \times 10^{-5}$ M^{-1}
Phenylbutazone	2.9	0.32	2.8	0.40	3.4	0.22
Tolbutamide	1.1	3.1	1.3	2.4	1.1	3.5
Clofibric acid	0.85	9.5	0.89	9.2	0.89	8.6

tamide was added to the system (5–8% *versus* 1–3% free warfarin without tolbutamide). The *r* value was determined to be about one, indicating that tolbutamide was occupying a significant number of its primary sites. Therefore, it is unlikely that tolbutamide and warfarin compete for the same primary site since the increase in free warfarin would have been larger, similar to the case of phenylbutazone. Also, the apparent *n* for warfarin in the presence of tolbutamide was about one, indicating that it was binding predominantly at its primary site.

Tolbutamide binding probably affects the secondary sites for warfarin. The additional free warfarin observed was in the same range as the contribution of the secondary sites to warfarin binding (4–7%). Warfarin behavior, however, was anomalous (Fig. 3). The apparent primary affinity constant for the *S*(−)-isomer was significantly larger than that observed for the *R*(+)-isomer, resulting in a reversal of the relative amounts of free isomers. Tolbutamide binding may cause a conformational change in the albumin molecule, which results in a change in the affinities of the stereoselective secondary sites for the warfarin enantiomers.

The increase in free warfarin in the presence of clofibric acid was less than that found with either phenylbutazone or tolbutamide (3–5% *versus* 1–3% free warfarin without clofibric acid). Figure 4 shows essentially no difference in the binding behavior of the isomers. The *r* value of about one indicates that clofibric acid was occupying a significant number of its primary sites. Therefore, it is unlikely that clofibric acid and warfarin compete for the same primary site since the increase in free warfarin would have been larger. Also, the apparent *n* for warfarin in the presence of clofibric acid was about one, indicating that it was binding principally at its primary site. Some interaction at the secondary sites may be occurring.

In all cases, the behavior of free warfarin reflected the average behavior for the two isomers. To depict the relative effects of the three competing drugs, the data obtained for racemic warfarin alone and in combination with each competing drug were composited (Fig. 5). The relative magnitude of their effects was proportional to their relative affinity constants for human serum albumin. Significant effects were observed when phenylbutazone, with a similar primary affinity constant to that of warfarin, acted as the competing drug. Less pronounced but potentially significant effects were demonstrated with tolbutamide and clofibric acid. These findings indicate that interactions at the albumin binding sites may contribute to the reported potentiating effects of these drugs *in vivo*.

Significant correlations have been demonstrated between the free fraction and total body clearance of racemic warfarin (39, 40). This correlation has been predicted on theoretical grounds and indicates that serum protein binding is a major determinant of the elimination kinetics of warfarin and of interindividual variations in its body clearance. Since no difference in binding was detected at the primary site, the corresponding free fractions for the isomers at this site do not correlate with warfarin elimination kinetics. The greater free fraction of the *S*(−)-isomer resulting from differences in secondary site binding correlates with its clinically observed shorter plasma half-life. This finding suggests that binding at the secondary sites may be more significant *in vivo* due to endogenous substances (such as free fatty acids), which have been reported to compete with warfarin for its primary binding site (24, 41).

REFERENCES

(1) R. J. Lewis, W. F. Trager, K. K. Chan, A. Breckenridge, M. Orme, M. Roland, and W. Schary, *J. Clin. Invest.*, **53**, 1607 (1974).

(2) R. A. O'Reilly, *Clin. Pharamcol. Ther.*, **16**, 348 (1974).

(3) D. S. Hewick and J. McEwen, *J. Pharm. Pharmacol.*, **25**, 458 (1973).

(4) A. Breckenridge, M. Orme, H. Wesseling, R. J. Lewis, and R. Gibbons, *Clin. Pharmacol. Ther.*, **15**, 424 (1974).

(5) K. K. Chan, R. J. Lewis, and W. F. Trager, *J. Med. Chem.*, **15**, 1265 (1972).

(6) A. Yacobi, L. B. Wingard, and G. Levy, *J. Pharm. Sci.*, **63**, 868 (1974).

(7) R. A. O'Reilly, P. M. Aggeler, M. S. Hoag, and L. Leong, *Thromb. Diath. Haemorrh.*, **8**, 82 (1962).

(8) L. B. Wingard, Jr., R. A. O'Reilly, and G. Levy, *Clin. Pharmacol. Ther.*, **23**, 212 (1978).

(9) J. H. M. Miller and G. A. Smail, *J. Pharm. Pharmacol.*, **29**, 33P (1977).

(10) E. M. Sellers and J. Koch-Weser, *Pharmacol. Res. Commun.*, **7**, 331 (1975).

(11) N. A. Brown, E. Jähnchen, W. E. Müller, and U. Wollert, *Mol. Pharmacol.*, **13**, 70 (1977).

(12) R. A. O'Reilly, *ibid.*, **7**, 209 (1971).

(13) S. Chierichetti, G. Bianchi, and B. Cerri, *Curr. Ther. Res. Clin. Exp.*, **18**, 568 (1975).

(14) W. L. Schary, R. J. Lewis, and M. Rowland, *Res. Commun. Chem. Pathol. Pharmacol.*, **10**, 663 (1975).

(15) R. A. O'Reilly and P. M. Aggeler, *Proc. Soc. Exp. Biol. Med.*, **128**, 1081 (1968).

(16) P. M. Aggeler, R. A. O'Reilly, L. Leong, and P. E. Kowitz, *N. Engl. J. Med.*, **276**, 496 (1967).

(17) J. A. Udall, *Clin. Med.*, **77**, 20 (1970).

(18) R. A. O'Reilly, *Ann. N.Y. Acad. Sci.*, **226**, 293 (1973).

(19) E. W. Martin, "Hazards of Medication," Lippincott, Philadelphia, Pa., 1971, pp. 470–484.

(20) R. A. O'Reilly, M. A. Sahud, and A. J. Robinson, *Thromb. Diath. Haemorrh.*, **27**, 309 (1972).

(21) S. M. Pond, G. G. Graham, N. D. Wade, and G. Sudlow, *Aust. N.Z. J. Med.*, **5**, 324 (1975).

(22) R. A. O'Reilly, *J. Am. Med. Assoc.*, **238**, 574 (1977).

(23) J. M. Thorp, *Lancet*, **1**, 1323 (1962).

(24) M. H. Solomon, J. J. Schrogie, and D. Williams, *Biochem. Pharmacol.*, **17**, 143 (1968).

(25) C. F. Chignell, *Mol. Pharmacol.*, **5**, 224 (1969).

(26) M. J. Crooks and K. F. Brown, *J. Pharm. Sci.*, **62**, 1904 (1973).

(27) P. Hsu, J. K. H. Ma, and L. A. Luzzi, *ibid.*, **63**, 570 (1974).

(28) J. Judis, *ibid.*, **61**, 89 (1972).

(29) R. I. Nazareth, T. D. Sokoloski, D. T. Witiak, and A. T. Hopper, *ibid.*, **63**, 203 (1974).

(30) I. M. Kolthoff and C. Rosenblum, "Acid-Base Indicators," Macmillan, New York, N.Y., 1937, p. 249.

(31) C. F. Chignell, *Ann. N.Y. Acad. Sci.*, **226**, 44 (1973).

(32) K. A. Bachmann and A. M. Burkman, *J. Pharm. Pharmacol.*, **27**, 832 (1975).

(33) G. Scatchard, *Ann. N.Y. Acad. Sci.*, **51**, 660 (1949).

(34) P. B. Andreasen and E. S. Vesell, *Clin. Pharmacol. Ther.*, **16**, 1059 (1974).

(35) J. J. Burns, R. K. Rose, T. Chenkin, A. Goldman, A. Schulert, and B. B. Brodie, *J. Pharmacol. Exp. Ther.*, **109**, 346 (1953).

(36) S. B. Matin, S. H. Wan, and J. H. Karam, *Clin. Pharmacol. Ther.*, **16**, 1052 (1974).

(37) T. Taylor and L. F. Chasseaud, *J. Pharm. Sci.*, **66**, 1639 (1977).

(38) I. M. Klotz and F. M. Walker, *J. Am. Chem. Soc.*, **70**, 943 (1948).

(39) A. Yacobi, J. A. Udall, and G. Levy, *Clin. Pharmacol. Ther.*, **19**, 552 (1976).

(40) A. Yacobi, T. Lampman, and G. Levy, *ibid.*, **21**, 286 (1977).

(41) O. G. Nelson, L. Storstein, and S. Jacobsen, *Biochem. Pharmacol.*, **26**, 229 (1977).

ACKNOWLEDGMENTS

The authors thank Dr. P. Forrest Eisenhardt, Dr. S. Hanna, and Dr. L. Lachman for advice and support and Mrs. K. Diana for assistance in manuscript preparation. They also acknowledge Endo Laboratories for providing the use of their facilities and resources.

Catecholamine Analogs as Potential Antitumor Agents

JOHN S. DRISCOLL

Received March 22, 1979, from the *Drug Design and Chemistry Section, Laboratory of Medicinal Chemistry and Biology, Developmental Therapeutics Program, Division of Cancer Treatment, National Cancer Institute, National Institutes of Health, Bethesda, MD 20205.* Accepted for publication June 13, 1979.

Abstract □ The structural requirements for murine P-388 leukemia activity in the dopamine series were investigated. Eight of the 31 analogs evaluated possessed reproducible antitumor activity. The *ortho*-aromatic hydroxyl groups were required for activity, but the aminoethyl side chain was not crucial since this group could be replaced by methyl or aminomethyl groups with the retention of activity. The lack of activity of *O*-alkylated and monosubstituted analogs suggests that *o*-quinone formation may be important for activity, a possibility supported by the observed P-388 activity of 5-hydroxydopamine compared with the inactivity of the 6-hydroxy isomer.

Keyphrases □ Pyrocatecholamine—analogs, antitumor activity, structure–activity relationship □ Antitumor activity—pyrocatecholamine analogs, structure–activity relationship □ Structure–activity relationship—pyrocatecholamine analogs, antitumor activity

In a previous study of the antitumor properties of psychotropic drugs (1), dopamine (I) was found to possess reproducible activity against P-388 and L-1210 leukemia in mice. This compound had been shown earlier to be active against the sarcoma-180 tumor model (2), while conflicting reports exist on I activity against B16 melanoma (1, 3). Certain other catecholamine neurotransmitters and their precursors were reported to have cancer-related properties (2, 4–8). Even catechol (9) and simple *o*-aminophenols (10) were reported to be antitumor active. The objective of this study was the establishment of the structural features critical to *in vivo* catecholamine P-388 leukemia antitumor activity.

EXPERIMENTAL[1]

Antitumor activity was determined as percent T/C values[2], with T/C ≥125% defined as statistically significant (Table I). Dose–response studies were carried out for each compound according to published NCI protocols (11). Six mice per dose were treated intraperitoneally with 10^6 P-388 leukemia cells on Day 0. Control (untreated) mice usually died about Day 11. Mice receiving drug were treated on Days 1–9 with intraperitoneal doses of the compound under investigation. Physiological saline (0.9%) was the vehicle.

Duplicate tests were carried out on each compound. When the duplicate test results did not agree (one active and one inactive test), a third dose–response experiment was scheduled. The mice (average weight 20 g) were weighed on Day 5, and the weight difference between the treated and control mice (T − C) was taken as an indication of the dose toxicity. Weight losses greater than 4 g were considered excessive.

RESULTS

Dopamine hydrochloride activity against P-388 leukemia was reconfirmed (Table I). This compound was active in five of five experiments. L-Dopa (II), the physiological precursor to dopamine, was inactive. The initial part of the study focused on β-phenethylamine analogs (III–XIV) of dopamine (I). *N*-Methyldopamine (III) retained activity. Either mono- or dialkylation of the phenolic hydroxyl groups (IV and V) converted dopamine into inactive compounds. Removal of the hydroxyl group from position 3 (tyramine, VI) also abolished activity. Neither the monosubstituted analogs (VI–IX) nor unsubstituted β-phenethylamine (X) was active.

Table I—P-388 Lymphocytic Leukemia Antitumor Activity

Compound	Dose Range, mg/kg/day	Optimum Dose, mg/kg/day	T/C, %	T − C, g
I	600–37.5	600	168	−1.7
	1200–150	600	153	−1.6
II	600–100	400	102	−0.9
	600–100	600	109	−0.5
III	600–100	400	156	−0.5
	600–100	600	126	−2.8
IV	600–100	200	110	−2.5
	600–100	100	108	−0.7
V	600–100	600	114	+0.1
	600–100	400	107	−1.5
VI	600–100	200	102	−0.7
	600–100	200	101	−0.1
VII	600–50	50	106	−1.7
	600–50	50	101	−2.2
VIII	400–50	50	105	+0.9
	400–50	50	100	−1.9
IX	400–50	100	105	−3.0
	400–50	50	104	+0.1
X	600–50	50	104	−1.8
	600–50	50	104	−0.9
XI	200–1.56	1.56	106	0.0
	200–1.56	1.56	94	+0.4
XII	600–50	50	111	−1.2
	600–50	100	106	−0.6
XIII	50–6.25	12.5	101	−0.9
	50–6.25	25	100	−0.7
XIV	600–50	200	131	−3.7
	600–50	400	129	−2.7
XV	50–6.25	50	111	−3.1
	50–6.25	25	101	−3.9
XVI	400–50	400	168	−3.6
	600–50	400	153	−4.1
XVII	200–50	100	110	+1.5
	200–50	50	105	−1.2
XVIII	700–350	700	158	−2.9
	700–350	600	144	−2.6
XIX	600–100	100	116	+0.3
	600–100	100	104	−0.3
XX	600–100	200	109	−0.6
	600–100	200	105	−1.2
XXI	100–6.25	6.25	116	−0.7
	100–6.25	6.25	110	−0.8
XXII	600–50	100	109	−0.1
	600–50	50	103	+0.4
XXIII	50–3.12	6.25	113	0.0
	50–3.12	3.12	112	−0.5
XXIV	400–25	200	164	−2.7
	400–25	200	133	−2.2
XXV	600–50	200	131	−1.4
	600–50	100	129	+0.4
XXVI	600–50	50	111	−1.8
	600–50	50	104	−3.5
XXVII	600–50	100	107	0.0
	600–50	100	105	0.0
XXVIII	600–50	400	115	−1.3
	600–50	400	111	−3.8
XXIX	600–50	100	118	−0.9
	600–50	50	103	+0.5
XXX	600–50	400	132	−2.2
	600–50	600	126	−1.4
XXXI	600–50	200	118	−0.7
	600–50	600	111	−0.8

[1] The compounds studied were obtained from the Developmental Therapeutics Program of the National Cancer Institute (NCI) or from commercial sources (Aldrich and Sigma). The P-388 lymphocytic leukemia testing was carried out at Hazleton Laboratories, Vienna, Va., under NCI Contract N01-CM5-7007.

[2] Percent T/C = (treated survival/control survival) × 100.

0022-3549/79/1200-1519$01.00/0
© 1979, American Pharmaceutical Association

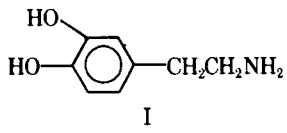

I

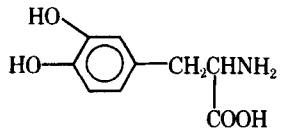

II

Among the four α-hydroxy compounds tested (XI–XIV), only isoproterenol (XIV) was reproducibly active. *dl*-Norepinephrine (XI) was inactive; *l*-epinephrine was P-388 inactive in earlier NCI testing. When a third hydroxyl group was added to dopamine in position 6 (XV), a P-388-inactive material resulted. When the extra hydroxyl group was added to position 5, however, the resulting 3,4,5-trihydroxy-β-phenethylamine (XVI) was as active as I.

The availability of benzylamine analogs of dopamine (XVIII–XXII) allowed evaluation of the importance of the aminoethyl side chain. Compound XVIII possessed good, reproducible P-388 activity. However, alkylation of one (XIX) or both (XX) hydroxyl groups again produced inactive materials. Halogens (XXI) could not be substituted for hydroxyl groups with retention of activity.

Since the dopamine aminoethyl group did not appear critical for activity, 4-substituted catechol (pyrocatechol) analogs with simple side chains (XXIII–XXX) were evaluated. Replacing the aminoethyl group in I with either a methyl (XXIV) or an aldehyde (XXV) function provided active compounds, but none of the four carboxyl-containing analogs (XXVI–XXIX) was active. Although catechol (XXIII) was inactive, *o*-aminophenol (XXX) possessed modest, but reproducible, activity. Gallic acid (XXXI), the carboxyl counterpart of active 5-hydroxydopamine (XVI), was inactive. The high optimal doses observed for most active compounds in this series were indicative of their relative nontoxicity.

DISCUSSION

Eight of the 31 compounds evaluated possessed reproducible activity against P-388 leukemia. These compounds (I, III, XIV, XVI, XVIII, XXIV, XXV, and XXX) are *o*-dihydroxybenzene (catechol) derivatives

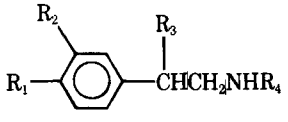

phenethylamine analogs	R_1	R_2	R_3	R_4	salt
I	OH	OH	H	H	HCl
III	OH	OH	H	CH_3	—
IV	OCH_3	OCH_3	H	H	—
V	OH	OCH_3	H	H	HCl
VI	OH	H	H	H	HCl
VII	OCH_3	H	H	H	—
VIII	NH_2	H	H	H	—
IX	NO_2	H	H	H	HCl
X	H	H	H	H	—
XI	OH	OH	OH	H	—
XII	OH	H	OH	H	HCl
XIII	H	OH	OH	H	HCl
XIV	OH	OH	OH	isopropyl	HCl

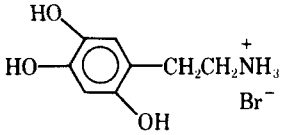

XV

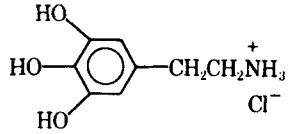

XVI

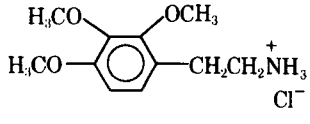

XVII

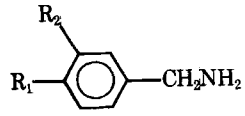

benzylamine analogs	R_1	R_2	salt
XVIII	OH	OH	HBr
XIX	OH	OCH_3	HCl
XX	OCH_3	OCH_3	—
XXI	Cl	Cl	—
XXII	H	H	—

and analogs. While the lead compound, dopamine, is a neurotransmitter, this physiological property may be related only coincidentally to P-388 activity since the analogous aminomethyl (XVIII) and methyl (XXIV) compounds also are active.

The fact that alkylation of one or both hydroxyl groups converts active compounds into inactive ones (I, IV, and V; XVIII, XIX, and XX) suggests that biological oxidation to *ortho*-quinones may be related to the observed antitumor activity. Studies of the oxidative pathways of brain catecholamines and the chemical reactivity of their oxidation products are consistent with this speculation. Tse *et al.* (12) showed that dopamine *o*-quinone was exceptionally reactive toward nucleophilic attack by cysteine or glutathione sulfhydryl groups. These reactions occurred 10^3 times faster than intramolecular cyclization by the aminoethyl side chain. Graham *et al.* (13, 14) studied the oxidation of dopamine, epinephrine, and norepinephrine and found dopamine to be the most easily autoxidized but the slowest to undergo intramolecular cyclization, thus giving it an opportunity to react with external nucleophiles.

Quinones as catechol oxidation products also have been suggested as biologically reactive intermediates (4, 8, 10, 15–20). Many of these studies were concerned with the elucidation of relationships existing between catecholamine oxidation products and malignant melanoma or neuroblastoma. While quinone–sulfhydryl interactions are studied most commonly, catecholamines also have been observed to cause DNA breaks (2), to inhibit prolactin secretion (4), and to be involved in the production of cytotoxic hydrogen peroxide and superoxide or hydroxyl radicals (14, 21, 22). A number of *o*-quinones tested by NCI were cytotoxic *in vitro* against KB cells (23). Several of these compounds possessed *in vivo* sarcoma 180 or Walker 256 activity. Furthermore, quinoid formation may possibly play a role in the P-388 activity of the polyhydroxypyridines (24).

The results indicate that within the series of compounds studied: (*a*) *o*-hydroxyl groups are required for activity; (*b*) *N*-methylation (III) of dopamine does not abolish activity but *O*-methylation (IV and V) does; (*c*) the aminoethyl side chain is not crucial for activity; (*d*) isoproterenol (XIV), but not epinephrine or norepinephrine, is active; (*e*) catechol is not active, but the 4-methyl analog (XXIV), a depigmenting agent which was used previously as a model compound in catechol oxidation (12) and

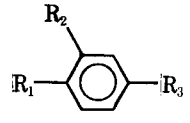

catechol analogs	R_1	R_2	R_3
XXIII	OH	OH	H
XXIV	OH	OH	CH_3
XXV	OH	OH	CHO
XXVI	OH	OH	COOH
XXVII	OH	OH	CH_2COOH
XXVIII	OH	OH	CH_2CH_2COOH
XXIX	OH	OH	CH=CHCOOH
XXX	OH	NH_2	H

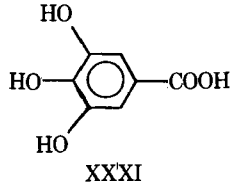

XXXI

antimelanoma studies (25, 26), possesses activity; and (*f*) no carboxyl-containing catechol is active.

The data from the testing of the trihydroxyphenethylamines (XV and XVI) indicate that it may be important to restrict potential quinone formation possibilities to only an *o*-quinoid structure. The P-388-inactive neurotoxin, 6-hydroxydopamine (XV), when oxidized, can form either an *o*- or a *p*-quinone. When given this choice, quinones in general and XV in particular (13) form hydroxy-*p*-quinones, which weakly react with sulfhydryl groups (17). The other trihydroxy compound studied, 5-hydroxydopamine (XVI), can form only an *o*-quinone. It has good P-388 activity. Therefore, one would expect that 2-hydroxydopamine, the perdemethyl analog of XVII, should have P-388 activity. Studies are in progress to determine further structure–activity relationships among polyhydroxy derivatives of benzene and pyridine.

REFERENCES

(1) J. S. Driscoll, N. R. Melnick, F. R. Quinn, N. Lomax, J. P. Davignon, R. Ing, B. J. Abbott, G. Congleton, and L. Dudeck, *Cancer Treat. Rep.*, **62**, 45 (1978).

(2) K. Yamafuji, H. Murakami, and M. Shinozuka, *Z. Krebsforsch.*, **73**, 195 (1970).

(3) M. M. Wick, *J. Invest. Dermatol.*, **71**, 163 (1978).

(4) S. Bang and K. M. Gautvik, *Acta Pharmacol. Toxicol.*, **41**, 317 (1977).

(5) E. Chelmicka-Szorc and B. Arnason, *Cancer Res.*, **36**, 2382 (1976).

(6) B. M. Boulos, C. Dajuvone, and D. L. Azarnoff, *Panminerva Med.*, **18**, 95 (1976).

(7) I. K. Cohen and C. G. Thomas, *Proc. Am. Assoc. Cancer Res.*, **4**, 11 (1963).

(8) M. M. Wick, *Science*, **199**, 775 (1978).

(9) K. Yamafuji and H. Murakami, *Enzymologia*, **35**, 139 (1968).

(10) L. R. Morgan and L. E. Posey, *Proc. Am. Assoc. Cancer Res.*, **19**, 51 (1978).

(11) R. I. Geran, N. H. Greenberg, M. M. MacDonald, A. M. Schumacher, and B. J. Abbott, *Cancer Chemother. Rep., Part 3*, **3**, 1 (1972).

(12) D. C. S. Tse, R. L. McCreery, and R. N. Adams, *J. Med. Chem.*, **19**, 37 (1976).

(13) D. G. Graham, *Mol. Pharmacol.*, **14**, 633 (1978).

(14) D. G. Graham, S. M. Tiffany, W. R. Bell, and W. F. Gutknecht, *ibid.*, **14**, 644 (1978).

(15) D. G. Graham, S. M. Tiffany, and F. S. Vogel, *J. Invest. Dermatol.*, **70**, 113 (1978).

(16) G. Agrup, C. Hansson, H. Rorsman, A. M. Rosengren, and E. Rosengren, *Acta Derm. Venereol. (Stockholm)*, **58**, 270 (1978).

(17) R. T. Borchardt, *Mol. Pharmacol.*, **11**, 436 (1975).

(18) M. E. Maguire, P. H. Goldman, and A. G. Gilman, *ibid.*, **10**, 563 (1974).

(19) F. S. Vogel, L. A. K. Kemper, P. W. Jeffs, M. W. Cass, and D. G. Graham, *Cancer Res.*, **37**, 1133 (1977).

(20) S. M. Tiffany, D. G. Graham, F. S. Vogel, M. W. Cass, and P. W. Jeffs, *ibid.*, **38**, 3230 (1978).

(21) N. R. Bachur, S. L. Gordon, and M. V. Gee, *ibid.*, **38**, 1745 (1978).

(22) R. T. Borchardt, S. K. Burgess, J. R. Reid, Y.-O. Liang, and R. N. Adams, *Mol. Pharmacol.*, **13**, 805 (1977).

(23) J. S. Driscoll, G. F. Hazard, H. B. Wood, and A. Goldin, *Cancer Chemother. Rep., Part 2*, **4**, 1 (1974).

(24) D. R. Hwang and J. S. Driscoll, *J. Pharm. Sci.*, **68**, 816 (1979).

(25) W. Wohlrab and R. P. Zaumseil, *Yale J. Biol. Med.*, **50**, 154 (1977).

(26) D. A. Paslin, *Acta Derm. Venereol. (Stockholm)*, **53**, 119 (1973).

Adsorption of Antineoplastic Drugs to Polyalkylcyanoacrylate Nanoparticles and Their Release in Calf Serum

P. COUVREUR *x, B. KANTE *, M. ROLAND *, and P. SPEISER ‡

Received February 6, 1979, from the **Laboratoire de Pharmacie Galénique, Université Catholique de Louvain, B-1200 Brussels, Belgium*, and the ‡*School of Pharmacy, Federal Institute of Technology, Zürich, Switzerland.* Accepted for publication June 25, 1979.

Abstract □ Conditions are described for attaching anticancer drugs to polyalkylcyanoacrylate nanoparticles, a new drug delivery system for cells that exhibit endocytic uptake. They are ultrafine, metabolizable, and able to associate with various drugs in a nonspecific manner. Data are given for the *in vitro* degradation and for drug release from this new drug carrier system.

Keyphrases □ Polyalkylcyanoacrylate nanoparticles—adsorption and release of dactinomycin and methotrexate, liberation kinetics, controlled release □ Dactinomycin—controlled-release dosage forms, polyalkylcyanoacrylate nanoparticles, adsorption and release kinetics □ Methotrexate—controlled-release dosage forms, polyalkylcyanoacrylate nanoparticles, adsorption and release kinetics □ Dosage forms, controlled release—polyalkylcyanoacrylate nanoparticles, adsorption and release of dactinomycin and methotrexate

Entrapment of cytotoxic drugs inside endocytizable carriers such as liposomes improves drug specificity and reduces toxicity toward nondiseased cells (1, 2). Work in this field has resulted in the development of polyacrylamide nanocapsules (3, 4). Polyacrylamide nanocapsules also may be useful in promoting cellular uptake *via* endocytosis for compounds that do not gain access to lysosomes (5).

Due to their polymeric nature, these small capsules (diameter of ~200 nm) may be more stable than liposomes in biological fluids and during storage (6–9). Furthermore, they can entrap various molecules in a stable and reproducible way (3, 5). However, this new lysosomotropic carrier is unlikely to be digested by lysosomal enzymes, which may restrict its clinical use. With these considerations, biodegradable nanoparticles made by polymerization of various alkylcyanoacrylate monomers were developed recently (10, 11). Similar polymers are used in surgery as sutures and adhesive agents (12, 13).

This paper describes techniques for attaching two cytostatic drugs to these polyalkylcyanoacrylate particles. Data concerning the degradability of these nanoparticles and drug liberation from this new intracellular formulation (14) are presented also.

0022-3549/79/1200-1521$01.00/0

© 1979, American Pharmaceutical Association

antimelanoma studies (25, 26), possesses activity; and (*f*) no carboxyl-containing catechol is active.

The data from the testing of the trihydroxyphenethylamines (XV and XVI) indicate that it may be important to restrict potential quinone formation possibilities to only an *o*-quinoid structure. The P-388-inactive neurotoxin, 6-hydroxydopamine (XV), when oxidized, can form either an *o*- or a *p*-quinone. When given this choice, quinones in general and XV in particular (13) form hydroxy-*p*-quinones, which weakly react with sulfhydryl groups (17). The other trihydroxy compound studied, 5-hydroxydopamine (XVI), can form only an *o*-quinone. It has good P-388 activity. Therefore, one would expect that 2-hydroxydopamine, the perdemethyl analog of XVII, should have P-388 activity. Studies are in progress to determine further structure–activity relationships among polyhydroxy derivatives of benzene and pyridine.

REFERENCES

(1) J. S. Driscoll, N. R. Melnick, F. R. Quinn, N. Lomax, J. P. Davignon, R. Ing, B. J. Abbott, G. Congleton, and L. Dudeck, *Cancer Treat. Rep.*, **62**, 45 (1978).

(2) K. Yamafuji, H. Murakami, and M. Shinozuka, *Z. Krebsforsch.*, **73**, 195 (1970).

(3) M. M. Wick, *J. Invest. Dermatol.*, **71**, 163 (1978).

(4) S. Bang and K. M. Gautvik, *Acta Pharmacol. Toxicol.*, **41**, 317 (1977).

(5) E. Chelmicka-Szorc and B. Arnason, *Cancer Res.*, **36**, 2382 (1976).

(6) B. M. Boulos, C. Dajuvone, and D. L. Azarnoff, *Panminerva Med.*, **18**, 95 (1976).

(7) I. K. Cohen and C. G. Thomas, *Proc. Am. Assoc. Cancer Res.*, **4**, 11 (1963).

(8) M. M. Wick, *Science*, **199**, 775 (1978).

(9) K. Yamafuji and H. Murakami, *Enzymologia*, **35**, 139 (1968).

(10) L. R. Morgan and L. E. Posey, *Proc. Am. Assoc. Cancer Res.*, **19**, 51 (1978).

(11) R. I. Geran, N. H. Greenberg, M. M. MacDonald, A. M. Schumacher, and B. J. Abbott, *Cancer Chemother. Rep., Part 3*, **3**, 1 (1972).

(12) D. C. S. Tse, R. L. McCreery, and R. N. Adams, *J. Med. Chem.*, **19**, 37 (1976).

(13) D. G. Graham, *Mol. Pharmacol.*, **14**, 633 (1978).

(14) D. G. Graham, S. M. Tiffany, W. R. Bell, and W. F. Gutknecht, *ibid.*, **14**, 644 (1978).

(15) D. G. Graham, S. M. Tiffany, and F. S. Vogel, *J. Invest. Dermatol.*, **70**, 113 (1978).

(16) G. Agrup, C. Hansson, H. Rorsman, A. M. Rosengren, and E. Rosengren, *Acta Derm. Venereol. (Stockholm)*, **58**, 270 (1978).

(17) R. T. Borchardt, *Mol. Pharmacol.*, **11**, 436 (1975).

(18) M. E. Maguire, P. H. Goldman, and A. G. Gilman, *ibid.*, **10**, 563 (1974).

(19) F. S. Vogel, L. A. K. Kemper, P. W. Jeffs, M. W. Cass, and D. G. Graham, *Cancer Res.*, **37**, 1133 (1977).

(20) S. M. Tiffany, D. G. Graham, F. S. Vogel, M. W. Cass, and P. W. Jeffs, *ibid.*, **38**, 3230 (1978).

(21) N. R. Bachur, S. L. Gordon, and M. V. Gee, *ibid.*, **38**, 1745 (1978).

(22) R. T. Borchardt, S. K. Burgess, J. R. Reid, Y.-O. Liang, and R. N. Adams, *Mol. Pharmacol.*, **13**, 805 (1977).

(23) J. S. Driscoll, G. F. Hazard, H. B. Wood, and A. Goldin, *Cancer Chemother. Rep., Part 2*, **4**, 1 (1974).

(24) D. R. Hwang and J. S. Driscoll, *J. Pharm. Sci.*, **68**, 816 (1979).

(25) W. Wohlrab and R. P. Zaumseil, *Yale J. Biol. Med.*, **50**, 154 (1977).

(26) D. A. Paslin, *Acta Derm. Venereol. (Stockholm)*, **53**, 119 (1973).

Adsorption of Antineoplastic Drugs to Polyalkylcyanoacrylate Nanoparticles and Their Release in Calf Serum

P. COUVREUR *x, B. KANTE *, M. ROLAND *, and P. SPEISER ‡

Received February 6, 1979, from the **Laboratoire de Pharmacie Galénique, Université Catholique de Louvain, B-1200 Brussels, Belgium*, and the ‡*School of Pharmacy, Federal Institute of Technology, Zürich, Switzerland.* Accepted for publication June 25, 1979.

Abstract □ Conditions are described for attaching anticancer drugs to polyalkylcyanoacrylate nanoparticles, a new drug delivery system for cells that exhibit endocytic uptake. They are ultrafine, metabolizable, and able to associate with various drugs in a nonspecific manner. Data are given for the *in vitro* degradation and for drug release from this new drug carrier system.

Keyphrases □ Polyalkylcyanoacrylate nanoparticles—adsorption and release of dactinomycin and methotrexate, liberation kinetics, controlled release □ Dactinomycin—controlled-release dosage forms, polyalkylcyanoacrylate nanoparticles, adsorption and release kinetics □ Methotrexate—controlled-release dosage forms, polyalkylcyanoacrylate nanoparticles, adsorption and release kinetics □ Dosage forms, controlled release—polyalkylcyanoacrylate nanoparticles, adsorption and release of dactinomycin and methotrexate

Entrapment of cytotoxic drugs inside endocytizable carriers such as liposomes improves drug specificity and reduces toxicity toward nondiseased cells (1, 2). Work in this field has resulted in the development of polyacrylamide nanocapsules (3, 4). Polyacrylamide nanocapsules also may be useful in promoting cellular uptake *via* endocytosis for compounds that do not gain access to lysosomes (5).

Due to their polymeric nature, these small capsules (diameter of ~200 nm) may be more stable than liposomes in biological fluids and during storage (6–9). Furthermore, they can entrap various molecules in a stable and reproducible way (3, 5). However, this new lysosomotropic carrier is unlikely to be digested by lysosomal enzymes, which may restrict its clinical use. With these considerations, biodegradable nanoparticles made by polymerization of various alkylcyanoacrylate monomers were developed recently (10, 11). Similar polymers are used in surgery as sutures and adhesive agents (12, 13).

This paper describes techniques for attaching two cytostatic drugs to these polyalkylcyanoacrylate particles. Data concerning the degradability of these nanoparticles and drug liberation from this new intracellular formulation (14) are presented also.

0022-3549/79/1200-1521$01.00/0

© 1979, American Pharmaceutical Association

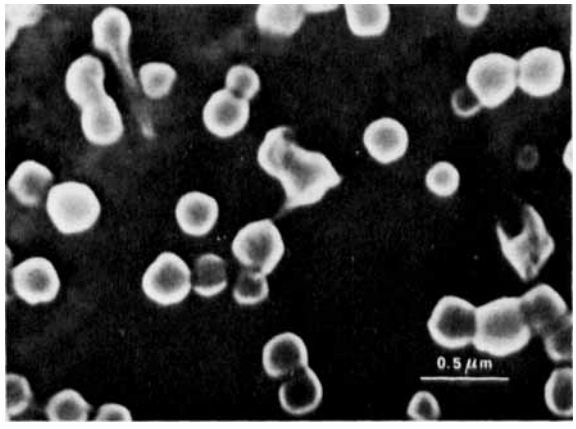

Figure 1—*Scanning electron micrograph of nanoparticles.*

EXPERIMENTAL

Polyalkylcyanoacrylate Nanoparticle Preparation—The nanoparticles were prepared by literature methods (10,11). After dissolution of the cytotoxic drug (methotrexate or ^{3}H-dactinomycin[1]) in 50 ml of water containing 0.25 g of polysorbate 20[2] and 5 ml of 0.1 *M* HCl, 0.83 ml of monomer (methylcyanoacrylate[3] or ethylcyanoacrylate[3]) or of various monomer mixtures was added with stirring. After 30 min, the nanoparticles appeared as a milky suspension displaying the Tyndall effect. They were buffered to pH 7 with 10 ml of a phosphate buffer (15). Scanning electron microscopy showed mostly spherical particles with a diameter of ~0.2 μm (Fig. 1).

Measurement of Dactinomycin Linked to Polymethyl- and Polyethylcyanoacrylate Nanoparticles—Dactinomycin, 1 mg, and ^{3}H-dactinomycin solution, 20 μl, were dissolved in 50 ml of the acid solution containing polysorbate 20. The nanoparticles were prepared as already described. The radioactive concentration of the tritiated dactinomycin solution was 0.5 mCi/ml with a specific activity of 16.5 Ci/mmole. The dactinomycin concentration of the radioactive solution was 90 μg/ml.

The nanoparticle suspensions (10 ml) were centrifuged at 20,000 rpm to separate dactinomycin bound to the particles from free dactinomycin. The sediment was dissolved in 10 ml of dimethylformamide. This solution was diluted to 20 ml with a mixture of calf serum and 0.45% polysorbate 20 in 0.009 *N* HCl (3:1). The supernate was diluted to 20 ml with dimethylformamide. The ^{3}H-dactinomycin in sediment and supernatant layers was measured by scintillation counting.

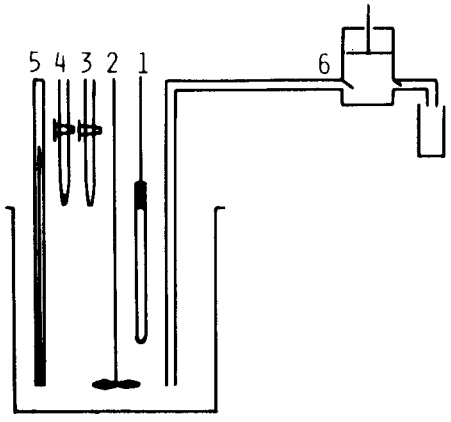

Figure 2—*System for nanoparticle incubation (17). Key: 1, pH measurement electrode; 2, stirrer; 3, automatic buret, hydrochloric acid solution; 4, automatic buret, sodium hydroxide solution; 5, thermometer; and 6, automatic sampler.*

[1] M.B.L.E., The Radiochemical Centre, Amersham, England.
[2] Tween 20, I.C.I., Atlas International Division, Everberg, Belgium.
[3] Loctite, Dublin, Ireland.

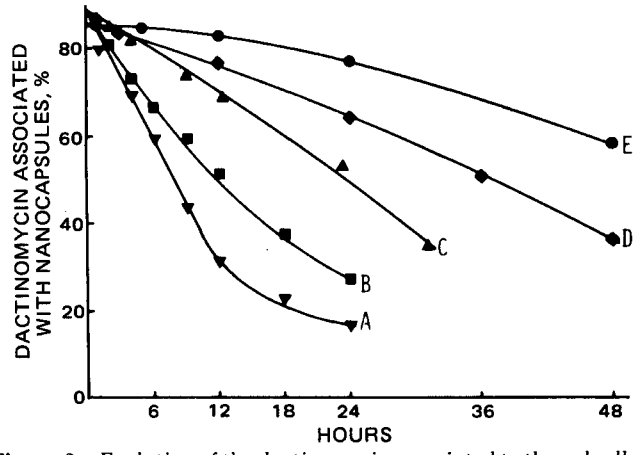

Figure 3—*Evolution of the dactinomycin associated to the polyalkylcyanoacrylate nanospherules as a function of the incubation time. Key: A, polymethylcyanoacrylate; B, mixture of polymethyl- and polyethylcyanoacrylate (2:1); C, mixture of polymethyl- and polyethylcyanoacrylate (1:1); D, mixture of polymethyl- and polyethylcyanoacrylate (1:2); and E, polyethylcyanoacrylate.*

Sample Preparation for Scintillation Counting—One-milliliter aliquots of the sediment and supernate were pretreated with 0.75 ml of 0.5 *N* quaternary ammonium hydroxide in toluene[4]. Isopropanol, 0.75 ml, and 0.5 ml of 30% H_2O_2 were then added to decolorize the samples. After 60 min, 15 ml of xylol[5]–0.5 *M* HCl (9:1) was added, and the samples were counted in a liquid scintillation counter[6]. Quench correction was obtained using a channels ratio method. The results were expressed as the percent of dactinomycin bound to the nanoparticles.

Test for Degradation of Polyalkylcyanoacrylate Nanoparticles—One hundred-milliliter portions of the various buffered polyalkylcyanoacrylate nanoparticle suspensions were incubated at 37° in 200-ml portions of calf serum–modified Eagle-Earle Dulbecco medium (1:9) (16).

The incubation took place in a thermostated cell. The cell was connected to a pH regulator by a glass electrode. The pH regulator was composed of two automatic burets and a pH meter. The burets maintained pH 7 ± 0.05 by delivery of 1.0 *N* HCl or NaOH. An automatic system permitted the uptake of nanocapsule samples at various times (Fig. 2).

Measurement of Methotrexate Linked to Both Polymethyl- and Polyethylcyanoacrylate Nanoparticles—Methotrexate nanoparticles were prepared with various amounts of drug (10–200 μg/ml) and monomers (1–16.7 μl/ml) to determine the influence of these two factors on the adsorptive capacity of polymethyl- and polyethylcyanoacrylate nanoparticles. The determination of the nanoparticle methotrexate content was made according to a fluorometric method (18).

After centrifugation of a 10-ml suspension of methotrexate nanoparticles at 20,000 rpm for 1 hr, the sediment was dissolved in 10 ml of acetone. This solution (40 μl) was added to distilled water (9 ml) and pH 5, 5 *M* acetate buffer[7] (200 μl). Distilled water was then added to exactly 10 ml. After addition of 4% potassium permanganate (100 μl) and a 5-min wait, the solution was decolorized with hydrogen peroxide (200 μl).

The supernate (40 μl) was treated in the same manner. The samples corresponding to the sediment and to the supernate were measured fluorometrically according to the method described previously.

RESULTS AND DISCUSSION

Degradation of Polymethyl- and Polyethylcyanoacrylate Nanoparticles Associated with ^{3}H-Dactinomycin—After dilution of the nanoparticle suspension (100 ml) in the calf serum (200 ml) and before incubation at 37°, 90.2% of the ^{3}H-dactinomycin was linked to the polymethylcyanoacrylate nanoparticles. With polyethylcyanoacrylate, 85.9% of the ^{3}H-dactinomycin was associated with the nanoparticles. The

[4] Soluène 350, Packard Instruments S.A., Brussels, Belgium.
[5] Instagel, Packard Instrument S.A., Brussels, Belgium.
[6] Philips PW 4510 computer, MBLE S.A., Brussels, Belgium.
[7] Prepared by adding 700 ml of 5.0 *M* sodium acetate to 300 ml of 5.0 *M* acetic acid.

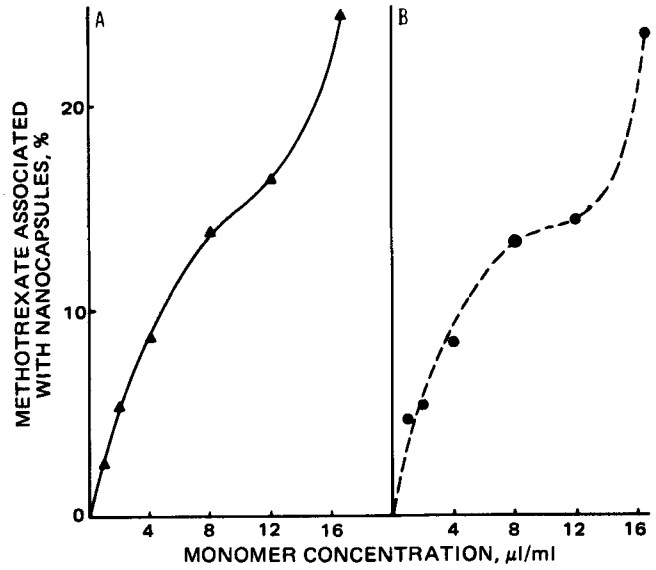

Figure 4—*Isothermic association of methotrexate with the nanoparticles at room temperature (20°). Methotrexate concentration = 100 µg/ml. Key: A, polymethylcyanoacrylate nanoparticles; and B, polyethylcyanoacrylate nanoparticles.*

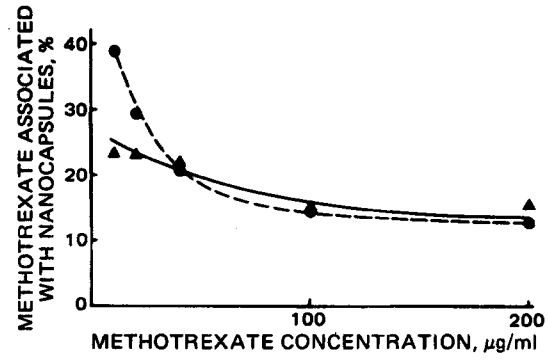

Figure 5—*Decrease of the methotrexate bound to the nanoparticles (percent) as a function of the drug amount in the initial solution. Monomer concentration = 12 µl/ml. Key: ▲—, polymethylcyanoacrylate; and ●—, polyethylcyanoacrylate.*

dactinomycin concentration was 20 µg/ml, and the monomer concentration was 16.6 µl/ml.

The measurement of dactinomycin disappearance from the sediment and its appearance in the supernate provided a good estimation of the nanoparticle degradation in the calf serum. The degradation velocity was related directly to the drug liberation. When the particles were degraded completely, no sediment was observed, and the whole dactinomycin activity was found in the supernate. When the nanoparticles were still intact, the sediment contained most of the dactinomycin activity, and only 10–15% of the drug was in the supernate.

The nanoparticle degradation kinetics, as indicated by dactinomycin release, seem to strongly depend on the alkyl chain length of the cyanoacrylate polymer product.

The polymethylcyanoacrylate nanoparticles (Fig. 3, curve A) were degraded almost entirely after 18 hr, whereas the polyethylcyanoacrylate nanoparticles (Fig. 3, curve E) retained practically 50% of the dactinomycin after 2 days of incubation at 37°. Nanoparticle preparation with various mixtures of methyl- and ethylcyanoacrylates (2:1, 1:1, and 1:2) provided intermediate degradation velocity values (Fig. 3, curves B, C, and D, respectively). These results show that polyalkylcyanoacrylate nanoparticles might represent a new drug delivery system which could degrade at various rates.

Methotrexate Adsorption on Polymethyl- and Polyethylcyanoacrylate Nanoparticles—Methotrexate was bound less extensively to the nanoparticles than was dactinomycin. In the better cases, an adsorption rate of ~25% was observed (Fig. 4). At the same monomer concentration (16 µl/ml), nanoparticles adsorbed about 90% of dactinomycin. Nanoparticles were prepared with various quantities of monomers and methotrexate to determine their influence on the associative tendency of the drug to optimize a nanoparticle formulation containing methotrexate.

The extent of methotrexate bound to the nanoparticles for polymethyl- (Fig. 4, curve A) and for polyethylcyanoacrylate (Fig. 4, curve B) increased sinusoidally with the monomer content in the initial solution. Monomer concentrations above 16.6 µl/ml were practically unusable due to the very high suspension viscosity. The percentage of methotrexate associated with the nanoparticles decreased with increasing drug in the initial solution (Fig. 5). This finding confirmed the poor methotrexate adsorption in comparison with dactinomycin. Indeed, only 38.5% methotrexate was adsorbed for the most dilute solution (10 µl/ml) with the ethyl product.

CONCLUSIONS

Many tumors cells exhibit a high endocytic capacity (19, 20). This knowledge was exploited by several investigators (21, 22) to entrap anticancer agents within phospholipid vesicles (liposomes) and albumin microspheres (23). Likewise, a DNA–daunorubicin complex was developed and was found to be endocytizable (24, 25). The therapeutic potential of nanocapsules-entrapped substances has stimulated numerous studies of their behavior *in vivo* (26, 27) and of their interactions with cells *in vitro* (5). The accumulation of polyacrylamide nanocapsules in cell lysosomes by endocytosis was demonstrated (5). However, since that polymer is unlikely to be degraded in the lysosomes, its use might be restricted because prolonged overloading of lysosomes could ensue.

This paper describes the design of digestible polyalkylcyanoacrylate nanocapsules, which can degrade at various speeds based on the monomer chosen. The drug liberation kinetics may be controlled also. The binding capacity of these nanoparticles to both dactinomycin (90%) and methotrexate (15–40%) exceeds that from the entrapment of these drugs in liposomes. Indeed, percentages of drug entrapment in liposomes are 4–18% for methotrexate (28, 19) and 2.3–11.6% for dactinomycin (30).

Polyalkylcyanoacrylate nanoparticles could be a new drug delivery system for cells that exhibit endocytic uptake since they are ultrafine, degradable, and able to associate with various drugs in a nonspecific manner. Furthermore, the morphology and drug adsorption of these particles are reproducible. Such nanoparticles are possible biodegradable lysosomotropic drug carriers. Future investigation with polyalkylcyanoacrylate nanoparticles will be carried out *in vivo*.

REFERENCES

(1) Y. E. Rahman, E. A. Cerny, S. L. Tollaksen, B. J. Wright, S. L. Nance, and J. F. Thompson, *Proc. Soc. Exp. Biol. Med.*, **146**, 1173 (1974).

(2) G. Gregoriadis, *Biochem. Soc. Trans.*, **3**, 613 (1975).

(3) P. Speiser, *Prog. Colloid Polym. Sci.*, **59**, 48 (1976).

(4) J. Marty, R. C. Oppenheim, and P. Speiser, *Pharm. Acta Helv.*, **53**, 17 (1978).

(5) P. Couvreur, P. Tulkens, M. Roland, A. Trouet, and P. Speiser, *FEBS Lett.*, **84**, 323 (1977).

(6) H. K. Kimelberg, E. Mayhew, and D. Papahadjopoulos, *Life Sci.*, **17**, 715 (1975).

(7) R. A. Klein, *Biochim. Biophys. Acta*, **210**, 486 (1970).

(8) P. Merry, *New Sci.*, **70**, 453 (1976).

(9) J. J. Marty, Ph.D. thesis, Victorian College of Pharmacy, Australia, 1977.

(10) P. Couvreur, B. Kante, M. Roland, P. Guiot, P. Baudhuin, and P. Speiser, *J. Pharm. Pharmacol.*, **31**, 331 (1979).

(11) P. Couvreur, M. Roland, and P. Speiser, Belgian pat. 189.366 (1978).

(12) J. A. Collins, K. C. Pani, M. Seidenstein, G. Brandes, and F. Leonard, *Surgery*, **65**, 256 (1969).

(13) C. H. Heisterkamp, R. L. Simmons, J. Vernick, and T. Matsumoto, *J. Trauma*, **9**, 587 (1969).

(14) P. Tulkens and A. Trouet, presented at the 4th National Congress of the Pharmaceutical Sciences Society of Belgium, Mar. 1979.

(15) "The United States Pharmacopeia," 19th rev., Mack Publishing Co., Easton, Pa., 1975, p. 654.

(16) P. Tulkens, H. Beaufay, and A. Trouet, *J. Cell Biol.*, **63**, 383 (1974).

(17) H. Vranckx, Ph.D. thesis, Université Catholique de Louvain, Louvain-en-Woluwe, Belgium, 1978.

(18) M. V. Freeman, *J. Pharmacol. Exp. Ther.*, **120**, 1 (1957).
(19) T. Ghose, R. C. Nairn, and J. E. Fothergill, *Nature (London)*, **196**, 1108 (1962).
(20) H. Busch, E. Fujiwara, and D. C. Firszt, *Cancer Res.*, **21**, 371 (1961).
(21) A. W. Segal, G. Gregoriadis, J. P. Lavender, D. Tarin, and T. J. Peters, *Clin. Sci. Mol. Med.*, **51**, 421 (1976).
(22) A. W. Segal, G. Gregoriadis, and C. D. V. Black, *Clin. Sci. Mol. Med.*, **49**, 99 (1975).
(23) P. A. Kramer, *J. Pharm. Sci.*, **63**, 1646 (1974).
(24) A. Trouet, D. Deprez-Decampeneere, and C. de Duve, *Nature (London)*, **239**, 110 (1972).
(25) A. Trouet, D. Deprez-Decampeneere, M. De Smedt-Malengraux, and G. Atassi, *Eur. J. Cancer*, **10**, 405 (1974).
(26) G. Birrenbach, Ph.D. thesis, No. 5071, Zürich, Switzerland, 1973.
(27) U. Berg and P. Speiser, "Immunologische Aspekte von ultrafeinen Latexteilchen," Handbook of the 24 Jahreskongress APV, Karlsruhe, Germany, 1978.
(28) H. K. Kimelberg, T. F. Tracy, J. S. Biddlecome, and R. S. Bourke, *Cancer Res.*, **36**, 2949 (1976).
(29) C. M. Colley and B. R. Ryman, *Biochem. Soc. Trans.*, **3**, 157 (1975).
(30) G. Gregoriadis, *FEBS Letters*, **36**, 292 (1973).

ACKNOWLEDGMENTS

Supported in part by the Belgian Fonds National de la Recherche Scientifique.
P. Couvreur is "Chargé de Recherches" to the Belgian Fonds National de la Rechereche Scientifique.
The authors thank Dr. Dunn (Loctite Co., Ireland) for the generous gift of the monomers.

High-Performance Liquid Chromatographic Studies of Reaction of Hydralazine with Biogenic Aldehydes and Ketones

JOHN P. O'DONNELL ˣ, WOODROW J. PROVEAUX, and JOSEPH K. H. MA

Received July 17, 1978, from the *School of Pharmacy, West Virginia University, Morgantown, WV 26506.* Accepted for publication July 2, 1979.

Abstract □ To understand hydrazone formation in hydralazine metabolism, the reaction of hydralazine with various biogenic aldehydes and ketones (acetone, pyruvic acid, acetoacetic acid, formaldehyde, and acetaldehyde) in pH 7.4 buffer was studied for potential alterations in hydralazine pharmacokinetics secondary to alcoholism and diabetes. The corresponding hydrazones were isolated, and their structures were characterized. High-performance liquid chromatography was used to monitor the reactions. An aqueous solvent reversed-phase liquid chromatographic system was used to separate hydralazine and its derivatives. Reaction of hydralazine with formaldehyde or acetaldehyde produced the corresponding hydrazones. Formation of an *s*-triazolo ring system yielded the known *s*-triazolo[3,4-α]phthalazine and 3-methyl-*s*-triazolo[3,4-α]phthalazine metabolites, which also were isolated and characterized and suggested nonenzymatic metabolism.

Keyphrases □ Hydralazine—reaction with biogenic aldehydes and ketones, hydrazone formation, high-performance liquid chromatographic analysis □ Antihypertensive agents—hydralazine, reaction with biogenic aldehydes and ketones, hydrazone formation, high-performance liquid chromatographic analysis □ High-performance liquid chromatography—analysis, hydralazine reaction with biogenic aldehydes and ketones, hydrazone formation

The mechanism of hydralazine condensation with biogenic aldehydes and ketones is significant. The reaction, involving hydrazone formation, may be enhanced in alcoholism, diabetes, and fasting states and during prolonged hydralazine administration. Hydrazone formation is important for investigating hydralazine toxicity and alterations in hydralazine metabolism and pharmacokinetics. While hydrazone formation has been evaluated *in vivo* (1–5), no supporting chemical studies have been reported.

A recently developed high-performance liquid chromatographic (HPLC) method (6) is sufficiently sensitive for clinical assay of derivatized hydralazine. The reaction of hydralazine with biogenic aldehydes and ketones apparently is nonenzymatic. The chemistry in an *in vitro* homogeneous solution at physiological conditions should be analogous to the *in vivo* process. Thorough study of this chemistry is complicated by the numerous biogenic ketones and aldehydes available to undergo this condensation *in vivo*.

This report describes the use of HPLC to determine the overall reaction of hydralazine with biogenic aldehydes and ketones to form hydrazones and the subsequent reaction of specific hydrazones to form *s*-triazolo[3,4-α]phthalazine and 3-methyl-*s*-triazolo[3,4-α]phthalazine. HPLC is well suited to this objective since the reversible reaction is usually sufficiently slow to permit discrete analysis of the reaction mixtures. This investigation was undertaken as a part of a long-term study of *in vivo* hydrazone formation from hydralazine in drug toxicity.

EXPERIMENTAL

Materials—Hydralazine[1], acetaldehyde[2], pyruvic acid[2], formaldehyde[2], 8-chlorotheophylline[3], acetone[4], and acetoacetic acid[4] were used as obtained. High purity samples of *s*-triazolo[3,4-α]phthalazine (III*a*) and 3-methyl-*s*-triazolo[3,4-α]phthalazine (III*b*) were prepared (5, 7) and used as standards.

Apparatus—A high-pressure liquid chromatograph[5] was equipped with a septumless injector port[6] and variable-wavelength UV absorption[7] and fluorescence detectors[8]. The column eluate was monitored by UV absorption at 240 nm and by fluorometry with excitation at 240 nm and

[1] Courtesy of Dr. M. Wilhem, Ciba-Geigy, Summit, N.J.
[2] Aldrich Chemical Co., Milwaukee, Wis.
[3] Sigma Chemical Co., St. Louis, Mo.
[4] Fisher Scientific Co., Pittsburgh, Pa.
[5] Model 6000A, Waters Associates, Milford, Mass.
[6] Model U6K, Waters Associates, Milford, Mass.
[7] Model SF-770, Schoeffel Instruments Corp., Westwood, N.J.
[8] Model FS-970, Schoeffel Instruments Corp., Westwood, N.J.

0022-3549/79/1200-1524$01.00/0
© 1979, American Pharmaceutical Association

(18) M. V. Freeman, *J. Pharmacol. Exp. Ther.*, **120**, 1 (1957).
(19) T. Ghose, R. C. Nairn, and J. E. Fothergill, *Nature (London)*, **196**, 1108 (1962).
(20) H. Busch, E. Fujiwara, and D. C. Firszt, *Cancer Res.*, **21**, 371 (1961).
(21) A. W. Segal, G. Gregoriadis, J. P. Lavender, D. Tarin, and T. J. Peters, *Clin. Sci. Mol. Med.*, **51**, 421 (1976).
(22) A. W. Segal, G. Gregoriadis, and C. D. V. Black, *Clin. Sci. Mol. Med.*, **49**, 99 (1975).
(23) P. A. Kramer, *J. Pharm. Sci.*, **63**, 1646 (1974).
(24) A. Trouet, D. Deprez-Decampeneere, and C. de Duve, *Nature (London)*, **239**, 110 (1972).
(25) A. Trouet, D. Deprez-Decampeneere, M. De Smedt-Malengraux, and G. Atassi, *Eur. J. Cancer*, **10**, 405 (1974).
(26) G. Birrenbach, Ph.D. thesis, No. 5071, Zürich, Switzerland, 1973.
(27) U. Berg and P. Speiser, "Immunologische Aspekte von ultrafeinen Latexteilchen," Handbook of the 24 Jahreskongress APV, Karlsruhe, Germany, 1978.
(28) H. K. Kimelberg, T. F. Tracy, J. S. Biddlecome, and R. S. Bourke, *Cancer Res.*, **36**, 2949 (1976).
(29) C. M. Colley and B. R. Ryman, *Biochem. Soc. Trans.*, **3**, 157 (1975).
(30) G. Gregoriadis, *FEBS Letters*, **36**, 292 (1973).

ACKNOWLEDGMENTS

Supported in part by the Belgian Fonds National de la Recherche Scientifique.
P. Couvreur is "Chargé de Recherches" to the Belgian Fonds National de la Rechereche Scientifique.
The authors thank Dr. Dunn (Loctite Co., Ireland) for the generous gift of the monomers.

High-Performance Liquid Chromatographic Studies of Reaction of Hydralazine with Biogenic Aldehydes and Ketones

JOHN P. O'DONNELL ˣ, WOODROW J. PROVEAUX, and JOSEPH K. H. MA

Received July 17, 1978, from the *School of Pharmacy, West Virginia University, Morgantown, WV 26506.* Accepted for publication July 2, 1979.

Abstract □ To understand hydrazone formation in hydralazine metabolism, the reaction of hydralazine with various biogenic aldehydes and ketones (acetone, pyruvic acid, acetoacetic acid, formaldehyde, and acetaldehyde) in pH 7.4 buffer was studied for potential alterations in hydralazine pharmacokinetics secondary to alcoholism and diabetes. The corresponding hydrazones were isolated, and their structures were characterized. High-performance liquid chromatography was used to monitor the reactions. An aqueous solvent reversed-phase liquid chromatographic system was used to separate hydralazine and its derivatives. Reaction of hydralazine with formaldehyde or acetaldehyde produced the corresponding hydrazones. Formation of an *s*-triazolo ring system yielded the known *s*-triazolo[3,4-α]phthalazine and 3-methyl-*s*-triazolo[3,4-α]phthalazine metabolites, which also were isolated and characterized and suggested nonenzymatic metabolism.

Keyphrases □ Hydralazine—reaction with biogenic aldehydes and ketones, hydrazone formation, high-performance liquid chromatographic analysis □ Antihypertensive agents—hydralazine, reaction with biogenic aldehydes and ketones, hydrazone formation, high-performance liquid chromatographic analysis □ High-performance liquid chromatography—analysis, hydralazine reaction with biogenic aldehydes and ketones, hydrazone formation

The mechanism of hydralazine condensation with biogenic aldehydes and ketones is significant. The reaction, involving hydrazone formation, may be enhanced in alcoholism, diabetes, and fasting states and during prolonged hydralazine administration. Hydrazone formation is important for investigating hydralazine toxicity and alterations in hydralazine metabolism and pharmacokinetics. While hydrazone formation has been evaluated *in vivo* (1–5), no supporting chemical studies have been reported.

A recently developed high-performance liquid chromatographic (HPLC) method (6) is sufficiently sensitive for clinical assay of derivatized hydralazine. The reaction of hydralazine with biogenic aldehydes and ketones apparently is nonenzymatic. The chemistry in an *in vitro* homogeneous solution at physiological conditions should be analogous to the *in vivo* process. Thorough study of this chemistry is complicated by the numerous biogenic ketones and aldehydes available to undergo this condensation *in vivo*.

This report describes the use of HPLC to determine the overall reaction of hydralazine with biogenic aldehydes and ketones to form hydrazones and the subsequent reaction of specific hydrazones to form *s*-triazolo[3,4-α]phthalazine and 3-methyl-*s*-triazolo[3,4-α]phthalazine. HPLC is well suited to this objective since the reversible reaction is usually sufficiently slow to permit discrete analysis of the reaction mixtures. This investigation was undertaken as a part of a long-term study of *in vivo* hydrazone formation from hydralazine in drug toxicity.

EXPERIMENTAL

Materials—Hydralazine[1], acetaldehyde[2], pyruvic acid[2], formaldehyde[2], 8-chlorotheophylline[3], acetone[4], and acetoacetic acid[4] were used as obtained. High purity samples of *s*-triazolo[3,4-α]phthalazine (III*a*) and 3-methyl-*s*-triazolo[3,4-α]phthalazine (III*b*) were prepared (5, 7) and used as standards.

Apparatus—A high-pressure liquid chromatograph[5] was equipped with a septumless injector port[6] and variable-wavelength UV absorption[7] and fluorescence detectors[8]. The column eluate was monitored by UV absorption at 240 nm and by fluorometry with excitation at 240 nm and

[1] Courtesy of Dr. M. Wilhem, Ciba-Geigy, Summit, N.J.
[2] Aldrich Chemical Co., Milwaukee, Wis.
[3] Sigma Chemical Co., St. Louis, Mo.
[4] Fisher Scientific Co., Pittsburgh, Pa.
[5] Model 6000A, Waters Associates, Milford, Mass.
[6] Model U6K, Waters Associates, Milford, Mass.
[7] Model SF-770, Schoeffel Instruments Corp., Westwood, N.J.
[8] Model FS-970, Schoeffel Instruments Corp., Westwood, N.J.

0022-3549/79/1200-1524$01.00/0
© 1979, American Pharmaceutical Association

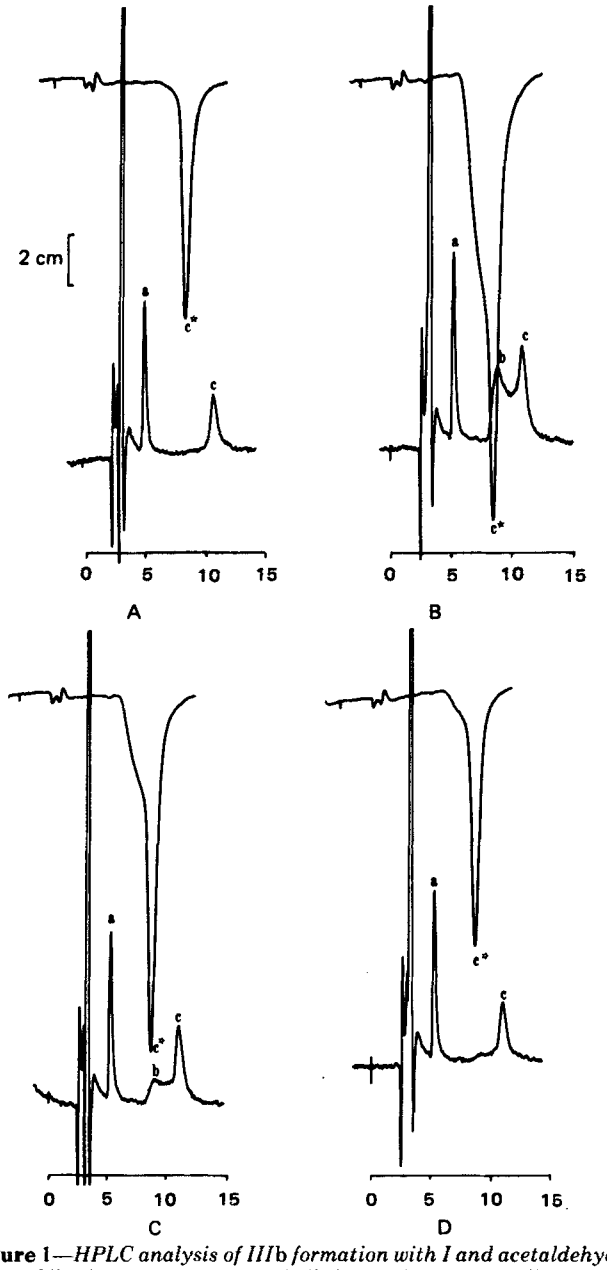

Figure 1—*HPLC analysis of IIIb formation with I and acetaldehyde. The mobile phase was 23% acetonitrile in 0.01* M *acetate buffer, pH 4.0, with a 1.0-ml/min flow rate. Key: A, standard IIIb, 1 μg/ml; B, mixture of 1 μg of I/ml with acetaldehyde after 5 min of mixing; C, Sample B after 30 min; and D, Sample B after 45 min. The chromatograms consist of both the UV (bottom) and fluorescence (top) detections. Peak a represents 8-chlorotheophylline (internal standard); peak b is the intermediate hydrazone IVb; and c and c* are the UV and fluorescence peaks of IIIb, respectively.*

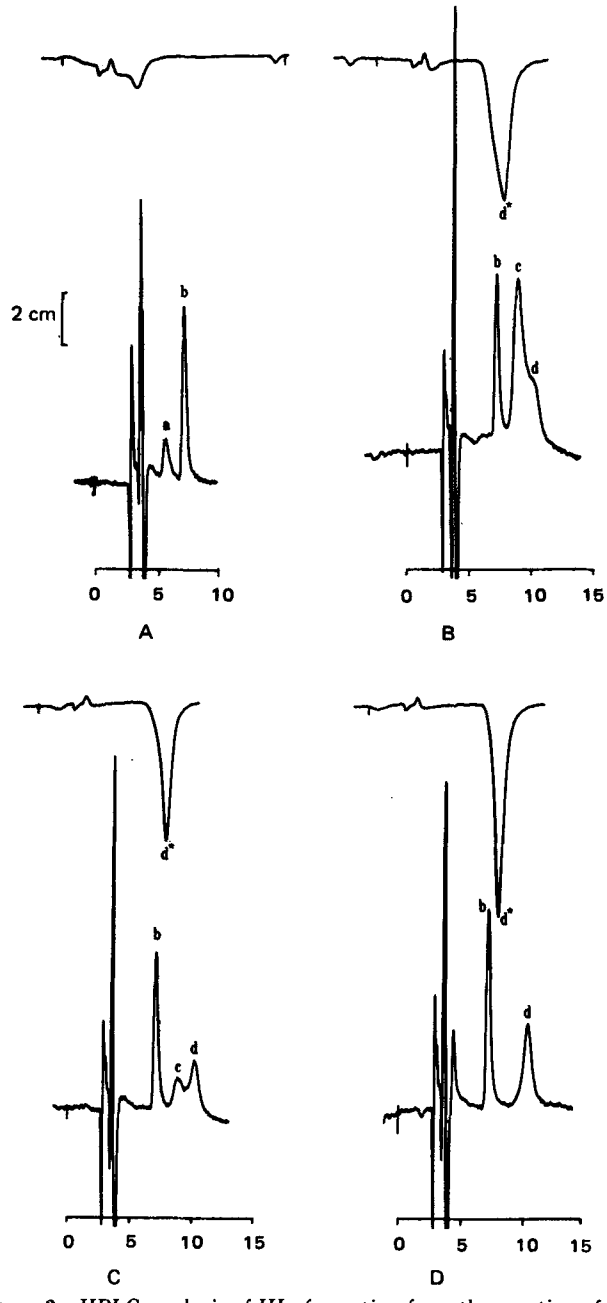

Figure 2—*HPLC analysis of IIIa formation from the reaction of hydralazine with formaldehyde. The mobile phase was 17% acetonitrile in 0.01* M *acetate buffer, pH 4.0, with a 1.0-ml/min flow rate. Key: A, standard I, 1 μg/ml; B, mixture of 1 μg of I/ml with formaldehyde after 5 min of mixing; C, Sample B after 30 min; and D, Sample B after 45 min. The chromatograms consist of both the UV (bottom) and fluorescence (top) detections. Peak a represents I; peak b is 8-chlorotheophylline (internal standard); peak c is the intermediate hydrazone IVa; and d and d* are the UV and fluorescence peaks of IIIa, respectively.*

emission above 389 nm. The UV detector was operated at 0.01 aufs with the fluorescence detector at 0.05 μamp full scale.

Chromatographic Parameters—Unless otherwise mentioned, the mobile phase was 17% acetonitrile[9] in 0.01 *M* sodium acetate, adjusted to pH 4.0 with acetic acid. It was pumped at 1.0 ml/min (1500 psi) through a stainless steel column (4 mm i.d. × 30 cm) with a high efficiency bonded-phase adsorption packing[10].

Procedure—The ketone or aldehyde was added to a 4-ml solution of hydralazine hydrochloride (1 μg/ml, 0.05 μ*M*) in 0.1 *M* phosphate buffer, pH 7.4, at 30°. The final concentration of the ketones or aldehydes was

[9] Nanograde, Mallinckrodt, St. Louis, Mo.
[10] μBondapak C_{18}, Waters Associates, Milford, Mass.

Table I—Retention Times of Hydralazine Derivatives with Aldehydes and Ketones Measured at a 1-ml/min Flow Rate with a Mobile Phase of 17% Acetonitrile in Acetate Buffer (pH 4)

Compound	Minutes
1-Hydrazinophthalazine (I)	5.7
1-Hydrazinophthalazine pyruvic acid hydrazone	4.8
1-Hydrazinophthalazine acetoacetic acid hydrazone	5.2
s-Triazolo[3,4-α]phthalazine (IIIa)	10.5
3-Methyl-*s*-triazolo[3,4-α]phthalazine (IIIb)	18.2
1-Hydrazinophthalazine acetone hydrazone	21.0

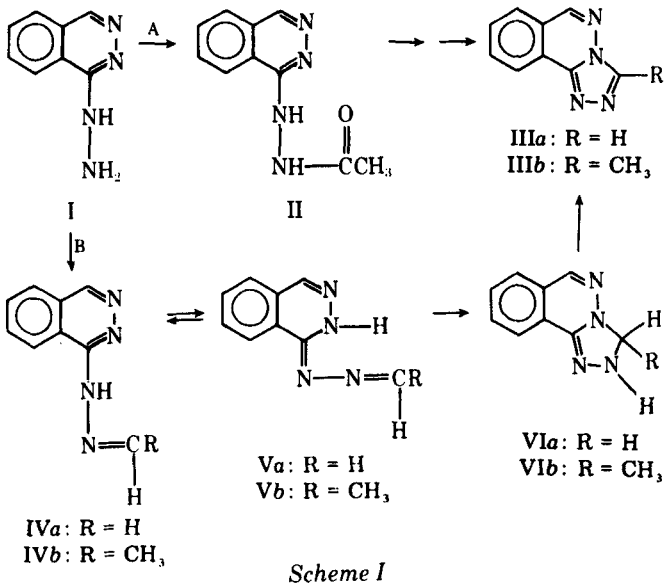

Scheme I

10 μg/ml. After 30 min, 6 μl of the reaction mixture was injected into the HPLC system. The hydrazones from hydralazine and other derived products were identified by comparison to standards of the acetone hydrazone, pyruvic acid hydrazone, and acetoacetic hydrazone of hydralazine prepared by literature procedures (5, 7) and to III*a* and III*b*.

Chemistry[11]—*1-Hydrazinophthalazine Acetaldehyde Hydrazone* (*IV*b)—Acetaldehyde (0.3 g, 6.82 mmoles) was added with stirring to 500 ml of 0.05 *M* phosphate buffer at pH 7.4 and 0.5 g (2.54 mmoles) of 1-hydrazinophthalazine (I) at 37°. The reaction mixture was stirred at 37° for 10 min and then filtered. The filtrate was dried *in vacuo* to yield a solid residue. Recrystallization from chloroform–ether gave 0.440 g (92%) of IV*b* as off-white crystals, mp 108–110° [lit. (7) mp 108–110°].

The 1-hydrazinophthalazine formaldehyde hydrazone (IV*a*) was prepared in the same manner as IV*b* using formaldehyde instead of acetaldehyde.

3-Methyl-s-triazolo[3,4-α]phthalazine (*III*b)—Acetaldehyde (0.3 g, 6.82 mmoles) was added with stirring to 500 ml of 0.05 *M* phosphate buffer at pH 7.4 and 0.5 g (2.54 mmoles) of I at 37°. The reaction mixture was stirred at 37° for 12 hr and then extracted with 3 × 100 ml of chloroform. The organic phase was dried over anhydrous magnesium sulfate, and the volatiles were removed under reduced pressure to give a solid residue. Recrystallization from chloroform–ether gave 0.388 g (85.3%) of III*b* as off-white crystals, mp 170–171° [lit. (7) mp 170–171°].

s-Triazolo[3,4-α]phthalazine (III*a*) was prepared in the same manner as III*b* using formaldehyde instead of acetaldehyde.

RESULTS AND DISCUSSION

Hydralazine was reported to condense *in vivo* with ketones to form hydrazones (2, 4, 5). While the details are not well understood, the first step was to assess the effect of the individual aldehydes and ketones on the overall formation of different hydrazones with hydralazine.

The formation of hydrazone derivatives with hydralazine and cyclized products was observed, and these compounds were separated using reversed-phase liquid chromatography. The retention times are listed in Table I. The linewidths of these peaks were within 1 min. The ketone hydrazones of hydralazine did not fluoresce under the conditions employed and were detected by UV. On elution, the more polar acetoacetic acid and pyruvic acid hydrazones preceded hydralazine. The less polar acetone hydrazone had a longer retention time. The chromatogram of the acetoacetic acid hydrazone also showed the acetone hydrazone, which occurs from the facile decarboxylation of acetoacetic acid.

The retention times listed in Table I may vary with changes in the percent of acetonitrile in the solvent, but the elution sequence remains the same. The reactions were supported by synthesis of the hydrazone derivatives at physiological conditions. In all instances, a reaction time of 30 min gave reactions with recrystallized yields of >80%.

The literature contains numerous examples of the *in vivo* formation of III*b*, a known major metabolite of hydralazine (8, 9), *via* enzymatic acetylation of hydralazine and subsequent dehydration (Scheme I, Pathway A) (3, 4). Hydralazine reaction with formaldehyde and acetaldehyde for 30 min at 37° resulted in the formation of III*a* and III*b*, respectively, which showed strong fluorescence and UV absorption. Figure 1 shows the chromatograms of the reaction mixture obtained during III*b* formation using a mobile phase of 23% acetonitrile and a 1.0-ml/min flow rate. The intermediate hydrazone product was observed prior to III*b* formation. Similar reaction intermediates also were found (Fig. 2) in the reaction of hydralazine with formaldehyde.

The results suggest an alternative competitive chemical pathway, B (Scheme I). This reaction occurs readily *in vitro* at 37° at pH 7.4 and involves the formation of the hydrazones IV*a* and IV*b*, which was supported by comparison of the retention times to the known hydrazone standards. The intermediate hydrazones IV*a* and IV*b* were observed (Figs. 1 and 2) and were isolated at simulated physiological conditions. Cyclization and subsequent oxidation of the 2,3-dihydro-3-methyl-*s*-triazolo[3,4-α]phthalazine (VI*b*) to III*b* occurs *via* the driving force of the ring system to become a completely aromatic system. Numerous analogous heterocyclic systems undergo similar oxidation (7, 10). Hydralazine reacts *in vitro* at 37°, pH 7.4, with formaldehyde to form III*a* *via* an analogous mechanism.

This HPLC approach is applicable to numerous related problems, in which hydrazines may react with biogenic aldehydes and ketones, because of its excellent selectivity and sensitivity (routine detection limits of 5 ng/ml). The pharmacokinetic importance of this reaction of hydralazine remains to be determined. *In vivo* experiments are planned.

[11] Melting points were taken on a Thomas–Hoover capillary apparatus and are uncorrected. The structures were confirmed by comparison of their IR (Beckman model 18A) and NMR (Varion T-60 spectrometer) spectra to those prepared from standards.

REFERENCES

(1) J. M. Lesser, Z. H. Israili, D. C. Davis, and P. G. Dayton, *Drug Metab. Dispos.*, **2**, 351 (1974).

(2) S. B. Zak, G. Lukas, and T. G. Gilleran, *ibid.*, **5**, 116 (1977).

(3) T. Talseth, *Clin. Pharmacokinet.*, **2**, 317 (1977).

(4) J. Wagner, J. W. Faile, P. Imhof, and G. Lieherm *Arzneim.-Forsch.*, **27**, 2388 (1977).

(5) K. D. Haegele, J. B. Skrdlant, N. W. Robie, D. Lalka, and J. L. McMay, *J. Chromatogr.*, **126**, 517 (1976).

(6) J. K. H. Ma, W. Proveaux, and J. P. O'Donnell, *J. Chromatogr.*, in press.

(7) J. Druey and B. H. Ringier, *Helv. Chim. Acta*, **34**, 195 (1951).

(8) S. B. Zak, T. G. Gilleran, J. Karliner, and G. Lukas, *J. Med. Chem.*, **17**, 381 (1974).

(9) H. Zimmer, R. Glaser, J. Kokosa, D. A. Garteiz, E. V. Hess, and A. Litwin, *ibid.*, **18**, 1031 (1975).

(10) R. A. Coburn and J. P. O'Donnell *J. Org. Chem.*, **37**, 17011 (1972).

Liquid Chromatographic Determination of Minocycline in Human Serum

A. P. De LEENHEER [x] **and H. J. C. F. NELIS**

Received March 26, 1979, from the *Laboratoria voor Medische Biochemie en voor Klinische Analyse, Rijksuniversiteit Gent, Fakulteit van de Farmaceutische Wetenschappen, 135 De Pintelaan, B-9000 Gent, Belgium.* Accepted for publication June 25, 1979.

Abstract □ A rapid, specific, and sensitive liquid chromatographic assay for minocycline in human serum is described. The drug and an internal standard (oxytetracycline) were extracted into ethyl acetate from 0.5 ml of buffered serum (pH 6.5). Chromatographic separation was achieved on a 10-μm Lichrospher 100 CH 8 column with acetonitrile–citric acid (0.1 *M*) as the eluent. The column effluent was monitored at 352 nm. The assay was linear up to 3 μg/ml with a mean coefficient of variation of 3.3% ($n = 6$). An extraction recovery of 89.4 ± 3.2% (mean ± *SD*, $n = 17$) was obtained over the 0.5–2.6-μg/ml range. The detection limit averaged 50 ng/ml. A serum concentration–time profile in humans after oral intake is presented.

Keyphrases □ Minocycline—analysis, liquid chromatography, human serum □ Antibiotics—minocycline, liquid chromatographic analysis, human serum □ Liquid chromatography—analysis, minocycline in human serum

A new generation of semisynthetic tetracyclines has almost completely replaced the older group members in antibiotic therapy. Removal of the hydroxyl group at C-6 of the molecule yields acid-stable 6-deoxytetracyclines (1), which now are amenable to substitution at C-7 (2). A new series of highly active, alkylated 7-amino-6-demethyl-6-deoxytetracyclines was developed (3), of which minocycline (I) showed the most favorable properties. The additional dimethylamino group at C-7 accounts for better lipid solubility (4) and, consequently, for improved pharmacokinetics in humans (5). This compound has the highest biological activity among the tetracyclines and still occupies a unique position in broad spectrum chemotherapy (6). In addition, because the uptake mechanism of minocycline in bacteria is different from that of other tetracyclines (7), it remains active against tetracycline-resistant pathogens, including staphylococci (3, 6, 8).

BACKGROUND

Long-term treatment of patients with minocycline requires monitoring of serum levels (9). Therefore, the possibility of metabolism *in vivo* was suggested (10, 11). Existing microbiological (12) and fluorometric (13–15) assays have limited use because they lack specificity.

A few TLC methods for various tetracyclines in pure solutions include the separation of minocycline from its analogs (16, 17) but lack the sensitivity required for application to biological materials. Liquid chromatography offers a valuable alternative; it allows separate quantitation of the parent drug and its metabolites (including those devoid of antimicrobial and/or fluorescent activity). Only two papers have dealt with liquid chromatography of minocycline. The first employed pellicular ion-exchange column systems (18) with poor efficiency and sensitivity. The other described a complex mobile phase and gradient elution (19).

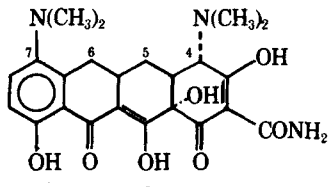

I

A major disadvantage is the considerable time (25–44 min) required to separate minocycline from its analogs.

Some high-pressure liquid chromatographic (HPLC) procedures for the determination of three classical tetracyclines in biological fluids were reported but were not applied to minocycline (20–23). A similar assay for doxycycline in serum and urine (24) undoubtedly could be adapted to tetracyclines other than minocycline.

This paper presents a new and efficient reversed-phase system for the specific and sensitive determination of minocycline in human serum.

EXPERIMENTAL

Reagents—All chemicals[1] were analytical grade and were used as received. Distilled water was used to prepare the solutions. A pH 6.5 phosphate–sulfite buffer consisted of 1.2 *M* monobasic sodium phosphate and 2.0 *M* sodium sulfite. Standard minocycline[2] solutions (10 and 30 μg/ml) were prepared in water adjusted to pH 4.2 with 0.1 *M* HCl. This optimal pH (4) provided stable solutions for at least 1 week when stored at 4° and protected from light.

Oxytetracycline[3] was dissolved in 0.03 *M* HCl (50 μg/ml) and was stable for several months (25). Methanolic solutions of ascorbic acid (0.2% w/v) and cysteine (0.1% w/v) were prepared. A 10% (v/v) solution of hexamethyldisilazane in toluene was used to silanize the glassware.

Apparatus and Operating Conditions—The liquid chromatograph was equipped with a constant-flow pump[4], a sampling valve[5] with a 20-μl loop, and a variable-wavelength detector[6]. A 15 × 0.32-cm i.d. column was packed with 10-μm Lichrospher 100 CH 8[1] under the following conditions: carbon tetrachloride slurry, 10% (w/v); packing pressure, 34.47 MPa; and pressurizing liquid, acetonitrile. Elution was performed with 9% (v/v) acetonitrile in 0.1 *m* citric acid at a flow rate of 1 ml/min (3.45 MPa). The column effluent was monitored at 352 nm.

Extraction—Serum, 0.5 ml, 50 μl of the internal standard solution, and 1 ml of phosphate–sulfite buffer were mixed[7] thoroughly and extracted with 6 ml of ethyl acetate on a rotating mixer[8]. After centrifugation at 3000 rpm, the organic layer was transferred to a conical tube containing 100 μl of ascorbic acid and cysteine in methanol. The mixture was evaporated to dryness at room temperature under vacuum[9]. The residue was dissolved immediately in 200 μl of 9:91 (v/v) acetonitrile–hydrochloric acid (0.1 *M*), and a 20-μl aliquot was injected on top of the liquid chromatographic column.

The same procedure was applied to urine samples (100–200 μl), using 0.4 ml of buffer solution and 2.5 ml of ethyl acetate.

Standard Curves—Standardization samples were prepared by adding 26–51 μl of the minocycline stock solutions to 0.5 ml of a blank serum pool. Calibration curves were constructed by plotting peak height ratios (minocycline to internal standard) *versus* the corresponding minocycline concentration.

Blood Concentrations—A human volunteer received two 100-mg capsules po just after a light breakfast. Venous blood samples were withdrawn at 0.5, 1, 1.5, 2, 3, 4, 8, 12, 25, 49, and 78 hr after dosage. Blood serum was isolated and stored at −20° until analyzed.

RESULTS AND DISCUSSION

Chromatography—A suitable chromatographic system for minocycline was critical in the development of a specific assay. During earlier

[1] E. Merck, Darmstadt, West Germany.
[2] Lederle Laboratories, Brussels, Belgium.
[3] Pfizer Inc., Brussels, Belgium.
[4] Model 8500, Varian Associates, Palo Alto, Calif.
[5] Model CV-6-UHPa-N60, Valco Instruments Co., Houston, Tex.
[6] Varichrom, Varian Associates, Palo Alto, Calif.
[7] Super mixer 1291, Lab-Line Instruments, Melrose Park, Ill.
[8] Cenco Instruments, Breda, The Netherlands.
[9] Rotary Evapo-Mix, Büchler Instruments, Fort Lee, N.J.

0022-3549/79/1200-1527$01.00/0
© 1979, American Pharmaceutical Association

Table I—Capacity Factors (k') of Tetracyclines on a 10-μm Lichrospher 100 CH 8 Column (15 × 0.32 cm i.d.) [a]

Compound	k'
Minocycline	2.2
Lymecycline by-product	3.2
Lymecycline	4.9
4-Epitetracycline (quatrimycin)	6.3
Oxytetracycline	6.6
Rolitetracycline	7.9
Tetracycline	10.0
4-Epidemeclocycline	10.6
Demeclocycline	16.6
Chlortetracycline	33.7
Methacycline	60.1
Doxycycline	76.2
Anhydrotetracycline	>80.0
4-Epianhydrotetracycline	>80.0

[a] The eluent was acetonitrile–0.1 *M* citric acid (9:91 v/v), and the temperature was ambient.

studies, efficient and reproducible reversed-phase systems were established for all tetracyclines except minocycline (24, 26). Minocycline always eluted as a severely tailing peak, useless for quantitation. This chromatographic behavior, atypical for tetracyclines, is associated with the presence of two dimethylamino groups, affording strongly different physicochemical properties.

Lichrospher 100 CH 8, a recently marketed reversed-phase packing material, consists of spherical particles with a large pore size, 100 Å instead of the usual 60 Å. The potential of larger pore particles for the chromatography of relatively large molecules was suggested previously[10]. Although its smaller surface area and carbon content predicted smaller capacity ratios, the material showed a unique selectivity for the different tetracyclines. With an acidic mobile phase, which is essential for the chromatography of other tetracyclines (26), good peak shape (asymmetry factor 1.3) and reasonable column efficiencies (h = 10 at a flow rate of 1 ml/min) were obtained.

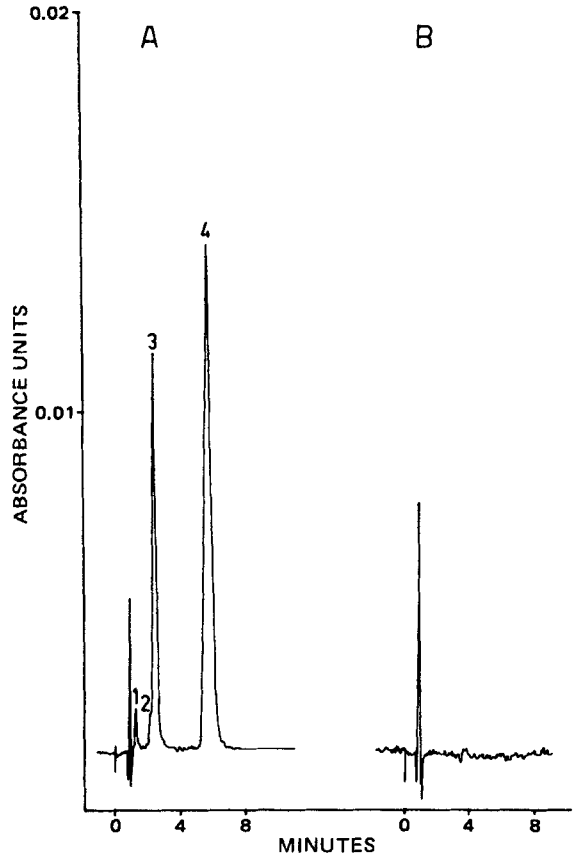

Figure 1—*Chromatograms of serum containing 1.5 μg of minocycline/ml (A) and of blank serum (B). Key: 1 and 2, possible minocycline metabolites; 3, minocycline; and 4, oxytetracycline (internal standard). The flow rate was 1 ml/min, the temperature was ambient, and the chart speed was 0.5 cm/min.*

[10] J. H. M. Van den Berg, Institute of Technology, Eindhoven, The Netherlands, personal communication.

Table II—Minocycline Extraction Recovery from Human Serum

Added, μg/ml	Measured, μg/ml	Recovery, %
0.51	0.45	87.4
0.51	0.43	84.8
0.91	0.81	89.3
0.91	0.81	89.3
1.44	1.27	88.5
1.44	1.26	87.8
1.44	1.32	91.7
1.44	1.31	91.1
1.44	1.23	85.7
1.44	1.33	92.5
2.00	1.83	91.5
2.00	1.67	83.6
2.55	2.27	89.1
2.55	2.38	93.6
2.55	2.19	86.0
2.55	2.39	93.8
2.55	2.38	93.6
	Mean ± *SD*	89.4 ± 3.2

Table I lists the k' values of different tetracyclines on the Lichrospher column. The elution sequence of tetracyclines on this packing material essentially could be related to their partition behavior at pH 2.1, *i.e.*, the mobile phase pH, in a two-phase *in vitro* model (27). High partition coefficients (octanol–aqueous buffer) correspond to strong retention. Although minocycline was the most lipophilic of the tetracyclines (at neutral pH), its low capacity ratio was not surprising. As a result of its two dimethylamino cationic groups, its apparent partition coefficient at pH 2.1 is zero (27). Consequently, no other commonly used tetracyclines will interfere in this system.

The described elution pattern also excluded several derivatives from use as an internal standard. Only three early eluting compounds were considered. Lymecycline was unsuitable because it is very unstable (three decomposition peaks in the chromatogram). Epitetracycline (quatrimycin) gave poor extraction yields, as expected from its stronger basic character (28). However, oxytetracycline fulfilled the conditions of stability and extraction yield and was chosen as the internal standard.

Extraction—Several general problems involved in tetracycline extraction were discussed elsewhere (24). The direct application of a doxycycline extraction procedure (24) to minocycline resulted in unsatisfactory extraction yields. The acid-base characteristics of minocycline differ markedly from those of other tetracyclines. A fourth pKa value (4), assigned to the dimethylamino group at C-7, accounts for a higher isoelectric point of 6.5. The partition into an organic solvent such as ethyl acetate is maximal around this pH. Thus, a pH 6.5 buffer system produced significantly higher extraction yields. A phosphate–sulfite buffer provided cleaner extracts than a previously described phosphate buffer (14). The advantages of concentrated sulfite-containing buffers for tetracycline extraction were noted previously (13, 24).

Minocycline is more susceptible to oxidation than the other tetracyclines (4). For example, thiol-containing substances were reported to possess tetracycline-stabilizing properties (29). Therefore, antioxidants

Table III—Calibration Curve Linearity and Precision for 0.56–2.83 μg/ml (n = 6)

Day	Mean Normalized PHR[a], $(\mu g/ml)^{-1}$	*SD*, $(\mu g/ml)^{-1}$	*CV*, %
1	0.539	0.008	1.5
2	0.513	0.014	2.7
3	0.503	0.024	4.7
4	0.545	0.016	2.9
5	0.512	0.032	6.2
6	0.508	0.008	1.6
Average	0.520	0.017	3.3

[a] Normalized PHR equals the peak height ratio of each minocycline standard divided by the corresponding concentration.

Table IV—Day-to-Day Precision Data over a Period of 6 Days (n = 6)

Concentration, μg/ml	Mean Normalized PHR[a], $(\mu g/ml)^{-1}$	SD, $(\mu g/ml)^{-1}$	CV, %
0.56	0.507	0.039	7.6
0.92	0.508	0.019	3.7
1.44	0.528	0.020	3.8
2.00	0.527	0.022	4.1
2.55	0.520	0.020	3.9
2.83	0.529	0.013	2.6

[a] See footnote to Table III.

such as cysteine and ascorbic acid were added routinely. In addition, ascorbic acid should have a protecting effect against epimerization at C-4 of certain tetracyclines (24). In general, slightly higher extraction yields were obtained by including these preservatives.

Considerable response loss occurred when the extraction residue was dissolved in a small volume of chromatographic solvent. The use of stronger acids, *e.g.*, 0.1 *M* HCl or H_2SO_4, overcame the problem. Solution filtration before injection is recommended but is not necessary. When filtration is employed, silanized filters should be used to avoid adsorption losses (5–10%). Without filtration, no considerable column efficiency decrease was observed after the injection of several hundred serum extracts.

Extraction Recovery—Extraction recovery was evaluated by analyzing spiked serum samples. In these experiments, the internal standard was added after transfer of the organic phase. Calibration data were obtained by carrying out the same analysis, without extraction, of minocycline and internal standard solutions in ethyl acetate, starting from the evaporation step. The results (Table II) indicate reasonably constant extraction yields (84.8–93.8%) over the entire therapeutic range (0–2.8 μg/ml).

Linearity, Precision, and Sensitivity—A linear relationship was found over the 0–3-μg/ml range. Calibration data obtained on 6 consecutive days are summarized in Table III. Precision was evaluated by calculating variations on normalized peak height ratios (peak height ratio of each standard divided by the corresponding minocycline concentration). A pooled standard curve of mean peak height ratios *versus* concentrations based on all data was calculated by linear regression fitting ($y = 0.531x - 0.012$, $r = 0.9998$). Day-to-day variations (CV) on normalized peak height ratios for six concentrations ranged from 2.6 to 7.6% (Table IV).

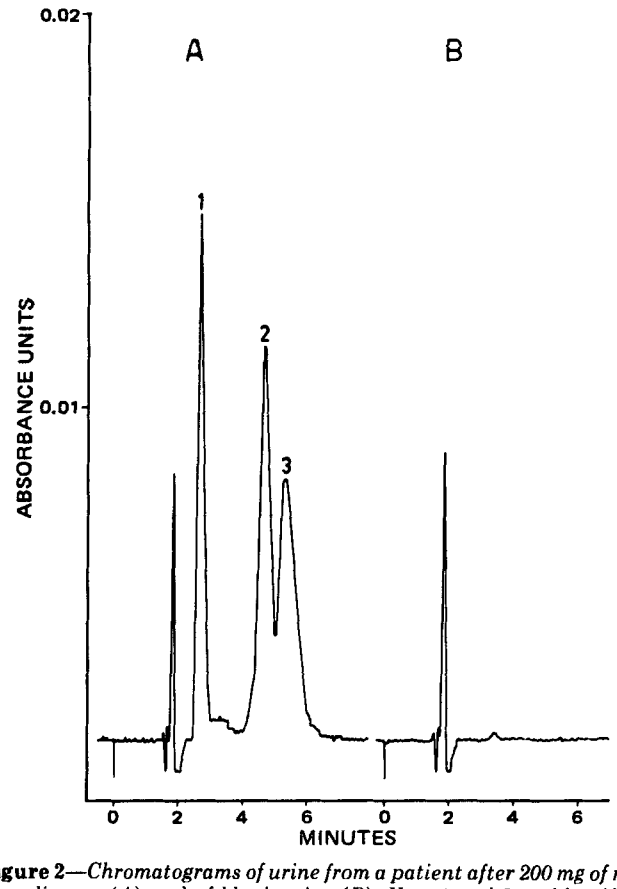

Figure 2—*Chromatograms of urine from a patient after 200 mg of minocycline po (A) and of blank urine (B). Key: 1 and 2, unidentified metabolites; and 3, minocycline. The flow rate was 0.5 ml/min, and the chart speed was 1 cm/min.*

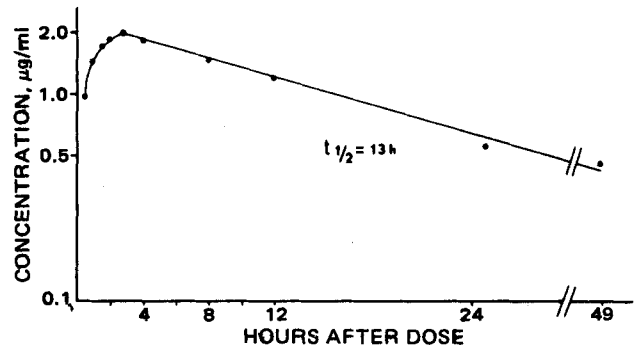

Figure 3—*Serum minocycline levels in a human volunteer following a single oral 200-mg dose.*

The detection limit with a 0.5-ml sample was ~50 ng/ml. This limit corresponds to a serum concentration resulting in a peak height equal to four times the signal-to-noise ratio.

Applicability—The overall procedure is very convenient for routine determinations because of its simplicity and speed (one analysis may be completed in <45 min). A typical chromatogram of a serum extract from a patient who received 200 mg of minocycline po is presented in Fig. 1A.

As shown by a blank serum chromatogram (Fig. 1B), no interfering peaks were observed. Two small additional peaks (1 and 2) eluted before minocycline. They possibly were associated with some polar metabolites. This assumption was supported by the analysis of a urine extract from the same patient (Fig. 2). Two large peaks with the same retention times were visible, representing >50% of the total drug content in the urine sample. Their isolation and identification are now under study.

As an illustration, serum minocycline levels as a function of time were studied in a human volunteer following a single oral 200-mg dose. Serum levels were plotted *versus* time and yielded the profile shown in Fig. 3. A peak serum level of 2.1 μg/ml was reached after 3 hr; 45 hr later, 0.22 μg/ml still could be measured accurately. A very small peak was detected 78 hr after dosage and corresponded to ~50 ng/ml, the detection limit.

REFERENCES

(1) C. R. Stephens, J. K. Beereboom, H. H. Rennhard, P. N. Gordon, K. Murai, R. K. Blackwood, and M. Schach von Wittenau, *J. Am. Chem. Soc.*, **85**, 2643 (1963).

(2) J. J. Hlavka, A. Schneller, H. Krazinski, and J. H. Boothe, *ibid.*, **84**, 1426 (1962).

(3) M. J. Martell and J. H. Boothe, *J. Med. Chem.*, **10**, 44 (1967).

(4) W. C. Barringer, W. Shultz, G. M. Sieger, and R. A. Nash, *Am. J. Pharm.*, **146**, 179 (1974).

(5) B. Bernard, E. Jong Yin, and H. J. Simon, *J. Clin. Pharmacol.*, **2**, 332 (1971).

(6) N. H. Steigbigel, C. W. Reed, and M. Finland, *Am. J. Med. Sci.*, **255**, 179 (1968).

(7) V. E. Del Bene and M. Rogers, *Antimicrob. Agents Chemother.*, **7**, 801 (1975).

(8) R. A. Frisk and G. Tunevall, *ibid.*, **1968**, 335.

(9) Data sheet on Minocin, Lederle Laboratories, Pearl River, N.Y.

(10) R. G. Kelly and L. A. Kanegis, *Toxicol. Appl. Pharmacol.*, **11**, 171 (1967).

(11) C. Simon, V. Malerckzyk, I. Preuss, K. Schmidt, and H. Grahmann, *Arzneim.-Forsch.*, **26**, 556 (1976).

(12) L. P. Garrod, H. P. Lambert, and F. O'Grady, "Antibiotics and Chemotherapy," Churchill Livingstone, Edinburgh, Scotland, 1973, p. 520.

(13) M. Lever, *Biochem. Med.*, **6**, 216 (1972).

(14) L. N. Ace and J. M. Jaffe, *ibid.*, **12**, 401 (1975).

(15) D. Hall, *Br. J. Clin. Pharmacol.*, **4**, 57 (1977).
(16) E. Ragazzi and G. Veronese, *Farmaco, Ed. Prat.*, **29**, 372 (1974).
(17) E. Ragazzi and G. Veronese, *J. Chromatogr.*, **132**, 105 (1977).
(18) A. G. Butterfield, D. W. Hughes, N. J. Pound, and W. L. Wilson, *Antimicrob. Agents Chemother.*, **4**, 11 (1973).
(19) G. D. Mack and R. B. Ashworth, *J. Chromatogr. Sci.*, **16**, 93 (1978).
(20) I. Nilsson-Ehle, T. T. Yoshikawa, M. C. Schotz, and L. B. Guze, *Antimicrob. Agents Chemother.*, **9**, 754 (1976).
(21) J. P. Sharma, E. G. Perkins, and R. F. Bevill, *J. Chromatogr.*, **134**, 441 (1977).
(22) J. P. Sharma, G. D. Koritz, E. G. Perkins, and R. F. Bevill, *J. Pharm. Sci.*, **66**, 1319 (1977).
(23) J. P. Sharma and R. F. Bevill, *J. Chromatogr.*, **166**, 213 (1978).
(24) A. P. De Leenheer and H. J. C. F. Nelis, *J. Pharm. Sci.*, **68**, 999 (1979).
(25) J. R. D. Mc. Cormick, S. M. Fox, L. L. Smith, B. A. Bitler, J. Reichenthal, V. E. Origoni, W. H. Muller, R. Winterbottom, and A. P. Doerschuk, *J. Am. Chem. Soc.*, **79**, 2849 (1957).
(26) A. P. De Leenheer and H. J. C. F. Nelis, *J. Chromatogr.*, **140**, 293 (1977).
(27) J. L. Colaizzi and P. R. Klink, *J. Pharm. Sci.*, **58**, 1184 (1969).
(28) N. E. Rigler, S. P. Bag, D. E. Leyden, J. L. Sudmeier, and C. N. Reilley, *Anal. Chem.*, **37**, 872 (1965).
(29) B. Scales and D. A. Assinder, *J. Pharm. Sci.*, **62**, 913 (1973).

ACKNOWLEDGMENTS

Supported in part by the National Research Foundation (NFWO).

The authors thank P. Schutyser, Lederle, Belgium, for supplying the minocycline standard and a compilation of its pharmacological and biological data. They are indebted to Dr. J. Gordts, Pfizer, Belgium, for the oxytetracycline hydrochloride. The helpful discussions of Dr. J. E. Sinsheimer, visiting professor (NFWO), are acknowledged gratefully.

Use of an Iodide-Specific Electrode to Study Lactoperoxidase-Catalyzed Iodination of *l*-Tyrosine

ROSE M. THREATTE *, MELVIN J. FREGLY ‡x, F. PETER FIELD *‡, and PATRICIA K. JONES ‡

Received March 16, 1979, from the **Department of Pharmaceutical Biology, College of Pharmacy, and the* ‡*Department of Physiology, College of Medicine, University of Florida, Gainesville, FL 32610.* Accepted for publication June 28, 1979.

Abstract □ An *in vitro* method employing an iodide-specific electrode for monitoring lactoperoxidase-catalyzed iodination is described. The method utilized lactoperoxidase, potassium iodide, and a glucose–glucose oxidase system for the generation of hydrogen peroxide and *l*-tyrosine. As iodination of *l*-tyrosine proceeded, the free iodide concentration in solution decreased and was monitored by an iodide-specific electrode. The iodide electrode was reliable when compared to a ^{131}I-method for measuring free iodide changes in solution. Increasing concentrations of resorcinol, a well-known inhibitor of thyroid peroxidase-catalyzed iodination, in the reaction mixture resulted in graded inhibition of the initial rate of lactoperoxidase-catalyzed *l*-tyrosine iodination. This *in vitro* system can be used to assess inhibitory activity of various antithyroid substances.

Keyphrases □ *l*-Tyrosine—iodination, lactoperoxidase catalysis, kinetics, *in vitro*, iodide-specific electrode □ Lactoperoxidase—*l*-tyrosine iodination, catalysis, kinetics, *in vitro* □ Resorcinol—inhibitory activity, kinetics, iodide-specific electrode □ Iodination—*l*-tyrosine, lactoperoxidase catalysis, kinetics, *in vitro*, iodide-specific electrode

Several recent investigations were conducted to study the kinetics of thyroid peroxidase-catalyzed iodination, the reaction responsible for thyroid hormone synthesis (1–4). Since thyroid peroxidase is not unique in its ability to catalyze iodination and thyroxine formation, *in vitro* iodination studies have employed a wide variety of peroxidases (5–10).

Numerous procedures have been utilized to study peroxidase-catalyzed iodination *in vitro* (7, 9, 11–15). The most widely used procedure involves isolation of the iodinated organic compounds and determination of the iodide incorporated into these products. Spectrophotometry is also used to monitor iodination *via* the changing spectral properties of the iodinated products (12, 13). A potentiometric procedure employing various substrates also has been used to follow the kinetics of iodination catalyzed by peroxidase (7, 9, 15).

The objective of the present study was to determine the optimal conditions for the use of an iodide-specific electrode for monitoring lactoperoxidase-catalyzed iodination of *l*-tyrosine. It was determined that lactoperoxidase is an acceptable peroxidase for investigating iodination kinetics (6, 10). Since several of the well-known antithyroid agents used clinically are general peroxidase inhibitors (6, 16–18), the present study also was intended to determine whether the iodide electrode could be used to study the inhibition kinetics of the antithyroid compound resorcinol.

EXPERIMENTAL

Procedure—An iodide-specific electrode[1], a pH expanded-scale millivolt meter[2], and a strip-chart recorder[3] were used to measure the free iodide concentration. As the peroxidase enzyme catalyzed the iodination of an appropriate iodide acceptor at a known initial iodide concentration, the iodide concentration decreased. The reduction in iodide concentration resulted in a potential change, which was related to the iodide-ion activity by the Nernst equation (19). To obtain the actual iodide concentration decrease per unit time (iodination rate), each millivolt change was converted to the corresponding iodide concentration by calibrating the iodide electrode in the concentration range of interest (1×10^{-5}–10×10^{-5} *M*), using appropriate dilutions of a 0.1 *M* sodium iodide standard solution[4].

Lactoperoxidase[5] was quantified by activity units; 1 unit of lactoper-

[1] Model 94-53A, Orion Research Inc., Cambridge, Mass.
[2] Model 12 research meter, Corning Scientific Instruments, Medfield, Mass.
[3] Beckman Instruments, Fullerton, Calif.
[4] Model 94-53-06, Orion Research Inc., Cambridge, Mass.
[5] Lot 430020 B grade, Calbiochem Chemical Works, Los Angeles, Calif.

0022-3549/79/1200-1530$01.00/0
© 1979, American Pharmaceutical Association

(15) D. Hall, *Br. J. Clin. Pharmacol.*, **4**, 57 (1977).
(16) E. Ragazzi and G. Veronese, *Farmaco, Ed. Prat.*, **29**, 372 (1974).
(17) E. Ragazzi and G. Veronese, *J. Chromatogr.*, **132**, 105 (1977).
(18) A. G. Butterfield, D. W. Hughes, N. J. Pound, and W. L. Wilson, *Antimicrob. Agents Chemother.*, **4**, 11 (1973).
(19) G. D. Mack and R. B. Ashworth, *J. Chromatogr. Sci.*, **16**, 93 (1978).
(20) I. Nilsson-Ehle, T. T. Yoshikawa, M. C. Schotz, and L. B. Guze, *Antimicrob. Agents Chemother.*, **9**, 754 (1976).
(21) J. P. Sharma, E. G. Perkins, and R. F. Bevill, *J. Chromatogr.*, **134**, 441 (1977).
(22) J. P. Sharma, G. D. Koritz, E. G. Perkins, and R. F. Bevill, *J. Pharm. Sci.*, **66**, 1319 (1977).
(23) J. P. Sharma and R. F. Bevill, *J. Chromatogr.*, **166**, 213 (1978).
(24) A. P. De Leenheer and H. J. C. F. Nelis, *J. Pharm. Sci.*, **68**, 999 (1979).
(25) J. R. D. Mc. Cormick, S. M. Fox, L. L. Smith, B. A. Bitler, J. Reichenthal, V. E. Origoni, W. H. Muller, R. Winterbottom, and A. P. Doerschuk, *J. Am. Chem. Soc.*, **79**, 2849 (1957).
(26) A. P. De Leenheer and H. J. C. F. Nelis, *J. Chromatogr.*, **140**, 293 (1977).
(27) J. L. Colaizzi and P. R. Klink, *J. Pharm. Sci.*, **58**, 1184 (1969).
(28) N. E. Rigler, S. P. Bag, D. E. Leyden, J. L. Sudmeier, and C. N. Reilley, *Anal. Chem.*, **37**, 872 (1965).
(29) B. Scales and D. A. Assinder, *J. Pharm. Sci.*, **62**, 913 (1973).

ACKNOWLEDGMENTS

Supported in part by the National Research Foundation (NFWO).

The authors thank P. Schutyser, Lederle, Belgium, for supplying the minocycline standard and a compilation of its pharmacological and biological data. They are indebted to Dr. J. Gordts, Pfizer, Belgium, for the oxytetracycline hydrochloride. The helpful discussions of Dr. J. E. Sinsheimer, visiting professor (NFWO), are acknowledged gratefully.

Use of an Iodide-Specific Electrode to Study Lactoperoxidase-Catalyzed Iodination of *l*-Tyrosine

ROSE M. THREATTE *, MELVIN J. FREGLY ‡x, F. PETER FIELD *‡, and PATRICIA K. JONES ‡

Received March 16, 1979, from the **Department of Pharmaceutical Biology, College of Pharmacy, and the* ‡*Department of Physiology, College of Medicine, University of Florida, Gainesville, FL 32610.* Accepted for publication June 28, 1979.

Abstract □ An *in vitro* method employing an iodide-specific electrode for monitoring lactoperoxidase-catalyzed iodination is described. The method utilized lactoperoxidase, potassium iodide, and a glucose–glucose oxidase system for the generation of hydrogen peroxide and *l*-tyrosine. As iodination of *l*-tyrosine proceeded, the free iodide concentration in solution decreased and was monitored by an iodide-specific electrode. The iodide electrode was reliable when compared to a ^{131}I-method for measuring free iodide changes in solution. Increasing concentrations of resorcinol, a well-known inhibitor of thyroid peroxidase-catalyzed iodination, in the reaction mixture resulted in graded inhibition of the initial rate of lactoperoxidase-catalyzed *l*-tyrosine iodination. This *in vitro* system can be used to assess inhibitory activity of various antithyroid substances.

Keyphrases □ *l*-Tyrosine—iodination, lactoperoxidase catalysis, kinetics, *in vitro*, iodide-specific electrode □ Lactoperoxidase—*l*-tyrosine iodination, catalysis, kinetics, *in vitro* □ Resorcinol—inhibitory activity, kinetics, iodide-specific electrode □ Iodination—*l*-tyrosine, lactoperoxidase catalysis, kinetics, *in vitro*, iodide-specific electrode

Several recent investigations were conducted to study the kinetics of thyroid peroxidase-catalyzed iodination, the reaction responsible for thyroid hormone synthesis (1–4). Since thyroid peroxidase is not unique in its ability to catalyze iodination and thyroxine formation, *in vitro* iodination studies have employed a wide variety of peroxidases (5–10).

Numerous procedures have been utilized to study peroxidase-catalyzed iodination *in vitro* (7, 9, 11–15). The most widely used procedure involves isolation of the iodinated organic compounds and determination of the iodide incorporated into these products. Spectrophotometry is also used to monitor iodination *via* the changing spectral properties of the iodinated products (12, 13). A potentiometric procedure employing various substrates also has been used to follow the kinetics of iodination catalyzed by peroxidase (7, 9, 15).

The objective of the present study was to determine the optimal conditions for the use of an iodide-specific electrode for monitoring lactoperoxidase-catalyzed iodination of *l*-tyrosine. It was determined that lactoperoxidase is an acceptable peroxidase for investigating iodination kinetics (6, 10). Since several of the well-known antithyroid agents used clinically are general peroxidase inhibitors (6, 16–18), the present study also was intended to determine whether the iodide electrode could be used to study the inhibition kinetics of the antithyroid compound resorcinol.

EXPERIMENTAL

Procedure—An iodide-specific electrode[1], a pH expanded-scale millivolt meter[2], and a strip-chart recorder[3] were used to measure the free iodide concentration. As the peroxidase enzyme catalyzed the iodination of an appropriate iodide acceptor at a known initial iodide concentration, the iodide concentration decreased. The reduction in iodide concentration resulted in a potential change, which was related to the iodide-ion activity by the Nernst equation (19). To obtain the actual iodide concentration decrease per unit time (iodination rate), each millivolt change was converted to the corresponding iodide concentration by calibrating the iodide electrode in the concentration range of interest (1×10^{-5}–10×10^{-5} *M*), using appropriate dilutions of a 0.1 *M* sodium iodide standard solution[4].

Lactoperoxidase[5] was quantified by activity units; 1 unit of lactoper-

[1] Model 94-53A, Orion Research Inc., Cambridge, Mass.
[2] Model 12 research meter, Corning Scientific Instruments, Medfield, Mass.
[3] Beckman Instruments, Fullerton, Calif.
[4] Model 94-53-06, Orion Research Inc., Cambridge, Mass.
[5] Lot 430020 B grade, Calbiochem Chemical Works, Los Angeles, Calif.

0022-3549/79/1200-1530$01.00/0
© 1979, American Pharmaceutical Association

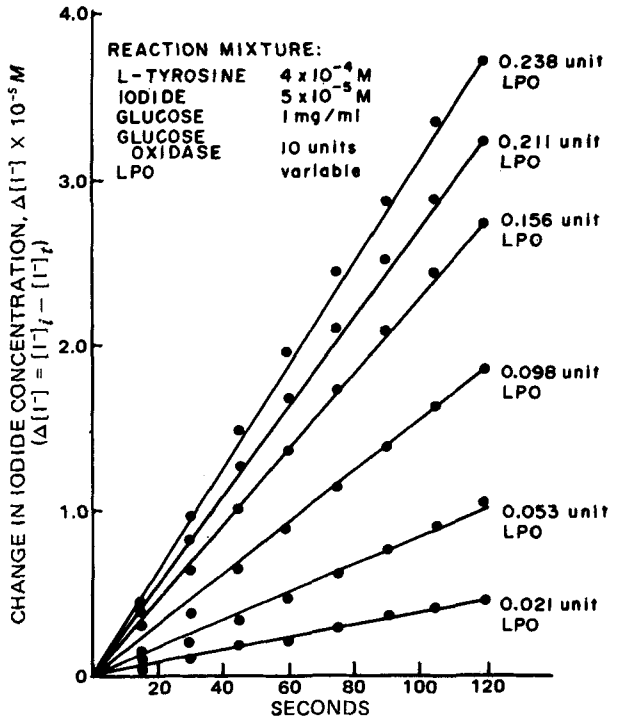

Figure 1—*Effect of varying the lactoperoxidase (LPO) concentration on the change in the initial iodide concentration with time.*

oxidase formed 1 mg of purpurogallin from pyrogallol in 20 sec at pH 6.0 and 20° (20). Hydrogen peroxide was generated in the reaction mixture by a glucose[6]-glucose oxidase[7] system in the presence of molecular oxygen and water. *l*-Tyrosine[8] was the iodide acceptor, while potassium iodide[9] served as the iodide donor.

A mixture of *l*-tyrosine, potassium iodide, and glucose was prepared (0.8:1:1), and 2.8 ml of this mixture (plus inhibitor, if any) was combined in a 50-ml reaction vessel with enough 0.06 *M* phosphate–edetic acid buffer, pH 6.0, to result in a final volume of 20 ml. The reaction vessel was transferred to a constant-temperature bath (37°), and the iodide electrode and single-junction reference electrode[10] were positioned in the reaction mixture. The reaction mixture was allowed to equilibrate for 6 min with constant stirring, and then the initial iodide concentration was measured. The strip-chart recorder was positioned at zero, and the chart speed was set at 2.54 cm/min. Glucose oxidase was added to the reaction mixture, and lactoperoxidase was added exactly 45 sec later. Iodination was allowed to proceed for 2 min.

The initial iodide concentration was calculated from the initial millivolt reading by the Nernst equation. The change in free iodide concentration, $\Delta[I_t]$, was calculated for each 15-sec interval up to 120 sec by calculating the iodide concentration for each cumulative time interval, $[I_t]$, and subtracting $[I_t]$ from $[I_i]$. The change in iodide concentration per unit time was linear over the first 120 sec. The initial iodination rate of *l*-tyrosine, $\Delta[I]$/sec, was determined by linear regression analysis, taking 15 sec as zero time (21).

Optimal Conditions—The effect of varying the lactoperoxidase amount on the iodination rate was investigated by conducting the assay with lactoperoxidase amounts ranging from 0.02 to 0.44 activity unit/reaction mixture. Ten determinations were made for each lactoperoxidase concentration.

The final *l*-tyrosine concentration (1×10^{-2} *M*, pH 10 stock solution) and the optimal pH for tyrosine iodination under these conditions were determined in the second group of studies. The reaction was conducted at pH 5.0, 6.0, 7.0, and 7.4. Four *l*-tyrosine concentrations, ranging from 2.5×10^{-4} to 1.0×10^{-3} *M*, were used in the assay, with all other components remaining constant. The assay was conducted for all four *l*-tyrosine concentrations at each pH. Six determinations of the iodination rate were made for each *l*-tyrosine concentration at each pH.

The effect of varying the initial iodide concentration was of interest in the third set of studies. The assay was conducted using initial iodide concentrations ranging from 1×10^{-5} to 1×10^{-3} *M* in the reaction mixture; six determinations were made for each initial iodide concentration used.

The fourth study investigated the effect of ionic strength on the iodination rate. Varying amounts of 2 *M* NaCl, 2.5×10^{-3}–2.0×10^{-1} *M* (giving rise to total ionic strengths of 0.097–0.297 *M*), were used to adjust the ionic strength of the reaction mixture.

Iodide Electrode Reliability—Iodine 131, 200 μl, was diluted with 5.0×10^{-5} *M* potassium iodide (1:282)[11]. At 30-sec intervals after initiation of the iodination reaction, 1-ml aliquots were removed and protein was precipitated with trichloroacetic acid. Millivolt readings were taken at the same time. The trichloroacetic acid-treated samples were applied to cation-exchange[12] columns (9 × 50 mm) and washed with deionized, distilled water. Both the eluates and the resin (bound ^{131}I-*l*-tyrosine) were counted in a counter with 4-π geometry (along with ^{131}I-standards). The percent of free iodide was calculated from both the ^{131}I-samples and the millivolt readings obtained from the iodide electrode.

Response of Iodination Reaction to Resorcinol—With a stock concentration of 2×10^{-5} *M* resorcinol[13], the effect of increasing resorcinol concentrations, ranging from 0 to 17.0×10^{-7} *M*, on the initial iodination rate was determined. Six determinations of the initial iodination rate for each resorcinol concentration were conducted.

RESULTS

Procedure—Calibration of the iodide-specific electrode with standard iodide solutions demonstrated that the iodide electrode response was

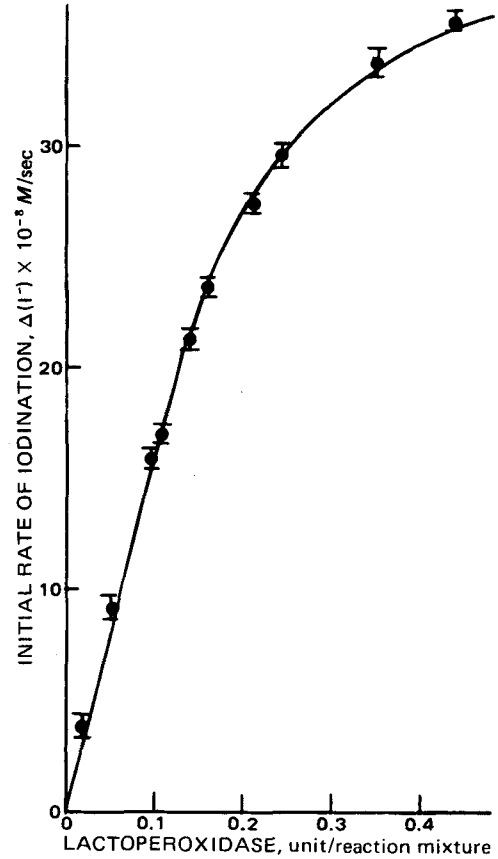

Figure 2—*Effect of varying the lactoperoxidase concentration on the initial iodination rate of* l*-tyrosine.*

[6] Dextrose, Mallinckrodt, St. Louis, Mo.
[7] Lot 501359 A grade, Calbiochem Chemical Works, Los Angeles, Calif.
[8] Lot 64619 A grade, Calbiochem Chemical Works, Los Angeles, Calif.
[9] Fisher Scientific Co., Fair Lawn, N.J.
[10] Model 90-01, Orion Research Inc., Cambridge, Mass.
[11] Na^{131}I (10 μCi/ml), New England Nuclear, Boston, Mass.
[12] Dowex 50X40, Dow Chemical Co., Midland, Mich.
[13] Sigma Chemical Co., St. Louis, Mo.

Table I—Effect of Varying Tyrosine Concentrations on the Iodination Rate [a] at Different pH Values [b]

pH	Tyrosine Concentration, M			
	2.5×10^{-4}	4.0×10^{-4}	5.0×10^{-4}	1.0×10^{-3}
5.0	17.35 ± 0.07[c]	17.41 ± 0.10	16.96 ± 0.10	16.68 ± 0.03
6.0	16.00 ± 0.04	16.14 ± 0.09	15.51 ± 0.02	15.05 ± 0.11
7.0	12.23 ± 0.02	11.53 ± 0.13	11.30 ± 0.09	10.28 ± 0.08
7.4	9.05 ± 0.03	8.60 ± 0.04	8.08 ± 0.04	7.12 ± 0.05

[a] Rate is expressed as $\Delta[I] \times 10^{-7}$ M/sec/lactoperoxidase unit. [b] Iodide concentration was 5×10^{-5} M. [c] Rate ± 1 SEM; $n = 6$.

linear with iodide concentration changes in the range defined by the equation, millivolts = 3.846 + 0.624 log [I^-] ($r = 1.00$). Thus, the iodide concentration could be determined for each millivolt change that occurred for any time, t, during the iodination of l-tyrosine.

Optimal Conditions—The result of varying the amount of lactoperoxidase from 0.021 to 0.238 activity unit in the reaction mixture on the iodide concentration change with time was such that as the amount of lactoperoxidase increased, the iodide concentration change increased. The iodide concentration change with time for each lactoperoxidase concentration was linear over the first 120 sec (Fig. 1). Increasing the lactoperoxidase from 0.021 to 0.156 unit in the reaction mixture resulted in a greater iodine concentration change with time than when lactoperoxidase was increased from 0.156 to 0.238 unit. Increasing the lactoperoxidase from 0.021 to 0.160 unit resulted in a greater change in the iodination rate relative to the change associated with increasing the lactoperoxidase from 0.160 to 0.440 unit (Fig. 2).

At pH 6.0, increasing the l-tyrosine concentration from 4.0×10^{-4} to 1.0×10^{-3} M resulted in an iodination rate decrease (Table I). This decrease also occurred at pH 5.0, 7.0, and 7.4. When the l-tyrosine concentration was 2.5×10^{-4} M, the iodination rate was either greater than, or not significantly different from, the rate observed at 4.0×10^{-4} M at all pH values tested. The iodination rate decreased as the pH increased at each l-tyrosine concentration.

Table II shows the effect of varying the iodide concentration on the l-tyrosine iodination rate at pH 6.0. From these data, it appeared that as the iodide concentration increased, the initial iodination rate of l-tyrosine increased as well.

The initial iodination rate was not affected appreciably by increasing the ionic strength from 0.097 to 0.197 M (Table III). When the ionic strength was increased to 0.297 M, however, the iodination rate decreased markedly.

Table IV—Comparison of the Iodide Electrode and the ^{131}I-Methods for Measuring Free Iodide Changes

Seconds	$I^- \times 10^{-5}$ M	Free Iodide, %	
		Iodide Electrode	^{131}I-Method
30	2.99	56.4	58.3
60	1.63	30.8	32.8
90	0.950	17.9	16.9
120	0.785	14.8	8.9

Iodide Electrode Reliability—A comparison of the iodide electrode with the ^{131}I-method for detecting changes in the iodide concentration as l-tyrosine iodination proceeded can be seen in Table IV. The sensitivity of the iodide electrode was comparable to that of the ^{131}I-method but was lower at a low iodide concentration (0.785×10^{-5} M).

Response of Iodination Reaction to Resorcinol—The iodide concentration change with time practically was linear over the first 120 sec for control (no inhibitor present) and in the presence of increasing resorcinol concentrations (Fig. 3). Therefore, the initial reaction rate could be calculated by applying linear regression analysis over the first 120 sec. By calculating the initial iodination rate in the presence of each resorcinol concentration, a log dose–inhibition curve was constructed (Fig. 4), in which the dose represented the resorcinol concentration and the response was the percent of the control rate (the initial iodination rate in the presence of resorcinol divided by the initial iodination rate in the absence of resorcinol).

DISCUSSION

The initial iodination rate of l-tyrosine changed in a biphasic manner with increasing lactoperoxidase concentrations (Fig. 2). The rate was dependent on the amount of lactoperoxidase present up to 0.16 activity unit. Between 0.16 and 0.44 unit, there was a slope change so that smaller increments in the rate occurred with large changes in lactoperoxidase concentration. Between 0.16 and 0.44 unit of lactoperoxidase, the generation of hydrogen peroxide and/or one substrate possibly became rate limiting as well. Use of 0.02–0.16 unit resulted in rates dependent on the lactoperoxidase amount present in the reaction mixture. Thus, all rates calculated in these studies were expressed in terms of the total number of lactoperoxidase units present so that the rate per lactoperoxidase unit was used for comparison, standardizing the rates obtained for all experiments.

Table II—Effect of Varying Iodide Concentrations on the Iodination [a] Rate [b]

Experiment	Iodide Concentration, M					
	10^{-5}	3.0×10^{-5}	5.0×10^{-5}	7.5×10^{-5}	10^{-4}	10^{-3}
1	6.24	14.10	16.25	17.24	19.13	53.88
2	6.23	14.10	16.43	18.29	19.11	45.39
3	6.28	14.09	16.12	17.56	18.90	57.17
4	6.27	14.11	16.12	17.72	19.10	47.77
5	6.27	14.22	16.20	17.60	18.95	59.75
6	6.25	13.85	16.12	18.28	18.88	52.88
$\bar{X}$[c]	6.26	14.08	16.20	17.78	19.01	52.79
S_x[d]	0.02	0.12	0.12	0.42	0.12	5.47
$S_{\bar{x}}$[e]	0.01	0.05	0.05	0.17	0.05	2.23

[a] Tyrosine concentration was 4×10^{-4} M. [b] Rate is expressed as $\Delta[I] \times 10^{-7}$ M/sec/lactoperoxidase unit. [c] Mean. [d] One standard deviation. [e] One standard error of the mean.

Table III—Effect of Ionic Strength on the Iodination [a] Rate [b]

Experiment	Total Ionic Strength, M					
	0.097	0.100	0.107	0.147	0.197	0.297
1	16.17	16.19	16.15	16.29	16.10	14.15
2	16.02	16.53	16.94	16.94	15.94	14.65
3	16.10	15.81	16.28	15.97	15.88	14.38
4	16.29	15.98	16.70	16.31	16.07	14.30
5	16.15	16.21	16.28	16.01	15.83	14.99
6	16.21	16.00	16.17	16.45	15.91	14.15
$\bar{X}$[c]	16.16	16.12	16.42	16.33	15.96	14.44
S_x[d]	0.09	0.25	0.33	0.35	0.11	0.33
$S_{\bar{x}}$[e]	0.04	0.10	0.13	0.14	0.05	0.13

[a] Tyrosine concentration was 4×10^{-4} M, and iodide concentration was 5×10^{-5} M. [b] Rate is expressed as $\Delta[I] \times 10^{-7}$ M/sec/lactoperoxidase unit. [c] Mean. [d] One standard deviation. [e] One standard error of the mean.

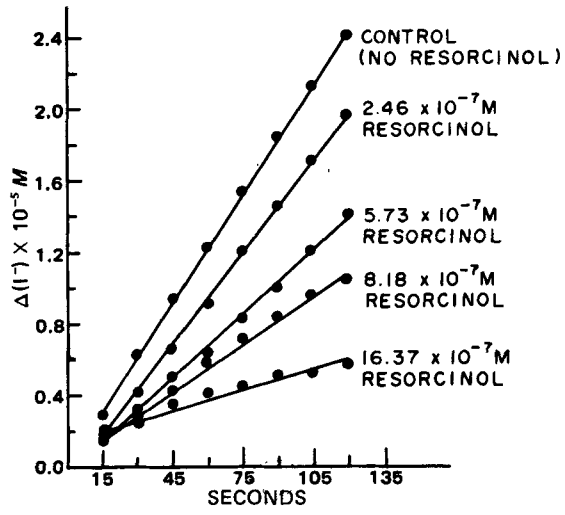

Figure 3—*Effect of increasing resorcinol concentration on the iodide concentration change with time.*

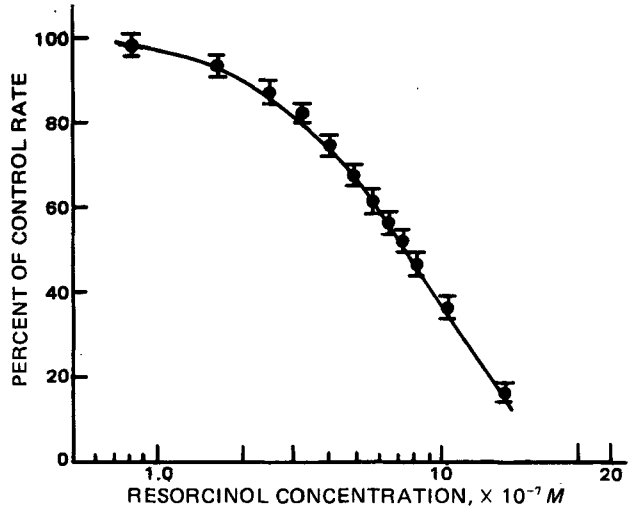

Figure 4—*Effect of graded resorcinol doses on the* l-*tyrosine iodination* (n = 6; *bars represent* ±SEM).

Although the iodination rates observed at pH 5.0, when the *l*-tyrosine concentration of the reaction mixture was varied, were greater than those observed at pH 6.0, the latter pH was chosen for this system since it was closer to physiological pH (Table I). A large reduction in the iodination rate was noted with all *l*-tyrosine concentrations at pH ≥7.0. The iodination rates obtained with *l*-tyrosine concentrations of 2.5×10^{-4} and 4.0×10^{-4} *M* at pH 6.0 were very similar; but as the *l*-tyrosine concentration was increased above 4.0×10^{-4} *M*, the rate decreased. This decrease was expected since adding enough of the alkaline stock *l*-tyrosine solution to the reaction mixture to produce 5.0×10^{-4} and 1.0×10^{-3} *M* resulted in a pH change of 0.2 and 0.5 unit, respectively. From these data, it was concluded that, at pH 6.0, an *l*-tyrosine concentration of 4.0×10^{-4} *M* should be used in subsequent studies since a satisfactory rate was achieved with only a minute pH change (0.05 unit).

When the iodide concentration was increased, the *l*-tyrosine iodination rate increased (Table II). A disproportionate rate increase was observed at very high iodide concentrations, and it was concluded that molecular iodine formation was occurring as well. This hypothesis was supported by previous observations that molecular iodine formation was favored at very high iodide concentrations (6, 22, 23). The iodide electrode, however, would not be able to distinguish between the two reactions since it was sensitive only to the total free iodide change. When the iodide concentration was increased from 3.0×10^{-5} to 1.0×10^{-4} *M*, the iodination rate increased. Any one of these concentrations appeared to be suitable for the assay. Therefore, the concentration used was 5.0×10^{-5} *M*.

The effect of the total ionic strength of the reaction mixture on the iodination system was investigated since ion activity is a function of ionic strength (19). Little change in the initial rate was demonstrated when the ionic strength was increased to 0.197 *M* (Table III). The ionic strength of the reaction mixture used for iodide electrode calibration was 0.097 *M*. The greatest contributor to this ionic strength was the phosphate buffer. Table V summarizes the reagents and their final concentrations to be used in subsequent studies in the *in vitro* model of thyroid peroxidase-catalyzed iodination.

Table V—Assay for Lactoperoxidase-Catalyzed Tyrosine Iodination at pH 6.0, 37°

Reagent	Stock Concentration	Reaction Mixture (20 ml) Volume, ml	Concentration
l-Tyrosine	10^{-2} *M*, pH 10	0.8	4×10^{-4} *M*
Potassium iodide	10^{-3} *M*	1.0	5×10^{-5} *M*
Glucose	20 mg/ml	1.0	1 mg/ml
Glucose oxidase	0.20 mg/ml (170 units/mg)	0.3	10 units total
Lactoperoxidase	0.20 mg/ml	0.05[a]	0.10–0.16 unit total
pH 6.0 buffer	0.06 *M* phosphate, 10^{-3} *M* edetic acid	To 20	No change

[a] Of a 1:4 dilution of stock.

The reliability of the iodide electrode for monitoring the free iodide concentration change as *l*-tyrosine iodination proceeded was comparable to that of a ^{131}I-method for monitoring iodination (Table IV). The iodide electrode accurately measured the free iodide change in the reaction, except that its reliability dropped slightly compared to the ^{131}I-method after a significant amount of *l*-tyrosine iodination had taken place. Since only the first 120 sec was of concern in these studies, this drop was not considered to be a serious problem.

The lactoperoxidase-catalyzed iodination of *l*-tyrosine at pH 6.0 appeared to be a good model for assessment of the inhibitory activity of resorcinol, a well-known inhibitor of thyroid peroxidase-catalyzed iodination *in vivo* and *in vitro* (6). Over a resorcinol concentration range of 0.8×10^{-7}–17.0×10^{-7} *M*, a sigmoidal log dose–inhibition curve was obtained (Fig. 4). The results were similar to those reported for a method for monitoring iodination without an iodide-specific electrode (6), in which the resorcinol concentration corresponding to 50% inhibition of the thyroid peroxidase-catalyzed iodination of bovine serum albumin was 7.10×10^{-7} *M*. In this study, the resorcinol concentration that produced 50% inhibition of lactoperoxidase-catalyzed iodination of *l*-tyrosine was 7.64×10^{-7} *M*.

It was concluded from these data that the iodide-specific electrode could be used to monitor the lactoperoxidase-catalyzed iodination of *l*-tyrosine. In addition, this potentiometric method is ideal for studying the kinetics of inhibition of lactoperoxidase-catalyzed iodination by known or suspected inhibitors of the thyroid peroxidase enzyme.

REFERENCES

(1) E. W. Dempsey, *Endocrinology*, **34**, 27 (1944).
(2) E. DeRobertis and R. Grasso, *ibid.*, **38**, 137 (1946).
(3) L. J. DeGroot, *Biochim. Biophys. Acta*, **136**, 364 (1967).
(4) L. J. DeGroot, J. E. Thompson, and A. D. Dunn, *Endocrinology*, **76**, 632 (1965).
(5) M. Morrison, *Ann. N.Y. Acad. Sci.*, **212**, 175 (1973).
(6) A. Taurog, *Rec. Prog. Horm. Res.*, **26**, 189 (1970).
(7) M. Morrison and G. S. Bayse, *Biochemistry*, **9**, 2995 (1970).
(8) A. Taurog and E. M. Howell, *J. Biol. Chem.*, **241**, 1329 (1966).
(9) M. Morrison, *Gunma. Symp. Endocrinol.*, **5**, 239 (1968).
(10) A. Taurog, M. L. Dorris, and L. Lamas, *Endocrinology*, **94**, 1286 (1974).
(11) J. Roche, S. Lissitzky, and R. Michel, *Methods Biochem. Anal.*, **1**, 243 (1954).
(12) I. Covelli and J. Wolff, *Biochemistry*, **5**, 860 (1966).
(13) L. P. Hager, D. R. Morris, F. S. Brown, and H. Eberwein, *J. Biol. Chem.*, **241**, 1769 (1966).
(14) J. A. Thomas and L. P. Hager, *Biochem. Biophys. Res. Commun.*, **35**, 444 (1969).
(15) M. Morrison, G. S. Bayse, and R. G. Webster, *Immunochemistry*, **8**, 289 (1971).

(16) A. Taurog, *Endocrinology*, **98**, 1031 (1976).
(17) M. L. Coval and A. Taurog, *J. Biol. Chem.*, **242**, 5510 (1967).
(18) D. R. Morris and L. P. Hager, *ibid.*, **241**, 3582 (1966).
(19) J. W. Ross, in "Solid-State and Liquid Membrane Ion Selective Electrodes," R. A. Durst, Ed., National Bureau of Standards Special Publication 314, Washington, D.C., 1969, pp. 57–88.
(20) B. Chance and A. C. Maehly, in "Methods in Enzymology," S. P. Colowick and N. O. Kaplan, Eds., Academic, New York, N.Y., 1955, pp. 773–775.
(21) W. Mendenhall, "Introduction to Probability and Statistics," 3rd ed., Duxbury, Belmont, Calif., 1971, pp. 264–280.
(22) A. Taurog, *Arch. Biochem. Biophys.*, **139**, 212 (1970).
(23) J. Pommier, L. Sokoloff, and J. Nunez, *Eur. J. Biochem.*, **38**, 497 (1973).

ACKNOWLEDGMENTS

Supported by Grant AG815 from the Florida Heart Association.
Dr. Threatte is a trainee of the National Institute of Arthritis and Metabolic Diseases, Institutional Training Grant AM 0714-04.

Sustained Drug Delivery Systems II: Factors Affecting Release Rates from Poly(ϵ-caprolactone) and Related Biodegradable Polyesters

COLIN G. PITT ˣ, MARGIT M. GRATZL, A. ROBERT JEFFCOAT, RUTH ZWEIDINGER, and ANTON SCHINDLER

Received November 7, 1978, from the *Research Triangle Institute, Research Triangle Park, NC 27709.* Accepted for publication June 22, 1979.

Abstract □ The release rates of several steroids from films and capsules of homopolymers and copolymers of ϵ-caprolactone, DL-lactic acid, and glycolic acid were measured *in vitro* and *in vivo* for up to 200 days. Relatively constant release rates from capsules (reservoir devices) were observed only under certain conditions. Factors that influence the drug release kinetics were evaluated. Release from poly(ϵ-caprolactone) and poly(ϵ-caprolactone-co-DL-lactic acid) was diffusion controlled. Release from poly(DL-lactic acid-co-glycolic acid) was associated with polymer degradation. Release from poly(DL-lactic acid) was very slow when diffusion controlled.

Keyphrases □ Polyesters, biodegradable—poly(ϵ-caprolactone), poly(DL-lactic acid), copolymers, steroid release, films, capsules □ Drug delivery systems—kinetics, biodegradation, diffusion, films, capsules □ Poly(ϵ-caprolactone)—homopolymers, copolymers, release rates, films, capsules □ Sustained-release systems—biodegradable polyesters, poly(ϵ-caprolactone), films, capsules

Polymer systems for sustained subdermal drug delivery may be based on principles of drug diffusion and/or polymer degradation. The diffusion coefficients of steroids in poly(ϵ-caprolactone) and poly(ϵ-caprolactone-co-DL-lactic acid) are comparable to values reported for poly(dimethylsiloxane) and, *a priori*, these polymers may be used in diffusion-controlled delivery systems that biodegrade after drug exhaustion (1, 2). In contrast, diffusion in poly(DL-lactic acid) is much slower (2); consequently, diffusion, leaching, and biodegradation may contribute to the drug delivery rates reported in studies of this polymer (3–5).

This paper describes the release rates of several steroids from films and capsules of homopolymers and copolymers of ϵ-caprolactone, DL-lactic acid, and glycolic acid *in vitro* and *in vivo* and factors that determine the observed kinetics.

EXPERIMENTAL

Synthesis—Poly(ϵ-caprolactone), poly(DL-lactic acid), their copolymers, and poly(DL-lactic acid-co-glycolic acid) were prepared by bulk polymerization of the purified monomers at 130° *in vacuo* in the presence of stannous octoate (50–500 ppm). The polymers were purified by precipitation from methylene chloride with methanol, followed by rapid and thorough washing with water in a blender[1]. Copolymer composition was determined by NMR spectroscopy.

Films were prepared by casting a common solution of the steroid and polymer in methylene chloride onto a glass plate and spreading with an adjustable applicator[2]. When a thickness greater than 100 μm was required, thinner films were stacked and compression molded at 100–130° to ensure even drug distribution. Sandwiched films, *i.e.*, a drug–polymer layer completely encased by drug-free polymer, were prepared by casting a polymer–drug solution on a drug-free polymer film. The resulting double-cast film was cut to leave smaller squares, over which a drug-free film was cast. The triple film then was cut between the squares.

Polymer tubing was prepared by melt extrusion or, when limited material was available, by rolling polymer film around a short polytef tube and annealing *in vacuo* while mechanically rotating the tube about its axis. Capsules were prepared by heat sealing the tubing with warm pliers. Steroids were micronized[3] (<5 μm) and dispersed in a vehicle using a tissue grinder (10 min) prior to capsule filling.

Release Rate Measurement—Films or capsules were immersed totally in distilled water (80–400 ml) at 37°. Mixing was accomplished using a rotating shaker[4] maintained at 135 rpm. Increasing the shaker speed to 195 rpm did not change the release rate. The aqueous reservoir was changed daily (capsules) or more frequently (films); where release rates were very fast, a flow system was used to keep the aqueous drug concentration low. In most cases, the frequency of solution change was such that the drug concentration did not exceed 10% of its aqueous solubility and typically was <1%. Drugs were either tritium or carbon 14 labeled, and release rates were determined by radioassay.

In vivo release rates were determined by radioassay of the feces and/or urine after subdermal implantation of the films or capsules in female New Zealand White rabbits or Charles River rats *via* incisions about the dorsal midline.

THEORETICAL

The diffusion-controlled release of a drug from a monolithic film or slab of unit area into an infinite aqueous sink may be described by Eqs. 1 and 2. Equation 1 applies when the drug is dissolved completely in the polymer (6); Eq. 2 applies when the drug solubility is exceeded and the

[1] Waring.
[2] Boston-Bradley.
[3] Wig-L-Bug, Crescent Dental Manufacturing.
[4] Eberbach.

0022-3549/79/1200-1534$01.00/0
© 1979, American Pharmaceutical Association

(16) A. Taurog, *Endocrinology*, **98**, 1031 (1976).
(17) M. L. Coval and A. Taurog, *J. Biol. Chem.*, **242**, 5510 (1967).
(18) D. R. Morris and L. P. Hager, *ibid.*, **241**, 3582 (1966).
(19) J. W. Ross, in "Solid-State and Liquid Membrane Ion Selective Electrodes," R. A. Durst, Ed., National Bureau of Standards Special Publication 314, Washington, D.C., 1969, pp. 57–88.
(20) B. Chance and A. C. Maehly, in "Methods in Enzymology," S. P. Colowick and N. O. Kaplan, Eds., Academic, New York, N.Y., 1955, pp. 773–775.
(21) W. Mendenhall, "Introduction to Probability and Statistics," 3rd ed., Duxbury, Belmont, Calif., 1971, pp. 264–280.
(22) A. Taurog, *Arch. Biochem. Biophys.*, **139**, 212 (1970).
(23) J. Pommier, L. Sokoloff, and J. Nunez, *Eur. J. Biochem.*, **38**, 497 (1973).

ACKNOWLEDGMENTS

Supported by Grant AG815 from the Florida Heart Association.
Dr. Threatte is a trainee of the National Institute of Arthritis and Metabolic Diseases, Institutional Training Grant AM 0714-04.

Sustained Drug Delivery Systems II: Factors Affecting Release Rates from Poly(ϵ-caprolactone) and Related Biodegradable Polyesters

COLIN G. PITT ˣ, MARGIT M. GRATZL, A. ROBERT JEFFCOAT, RUTH ZWEIDINGER, and ANTON SCHINDLER

Received November 7, 1978, from the *Research Triangle Institute, Research Triangle Park, NC 27709.* Accepted for publication June 22, 1979.

Abstract □ The release rates of several steroids from films and capsules of homopolymers and copolymers of ϵ-caprolactone, DL-lactic acid, and glycolic acid were measured *in vitro* and *in vivo* for up to 200 days. Relatively constant release rates from capsules (reservoir devices) were observed only under certain conditions. Factors that influence the drug release kinetics were evaluated. Release from poly(ϵ-caprolactone) and poly(ϵ-caprolactone-co-DL-lactic acid) was diffusion controlled. Release from poly(DL-lactic acid-co-glycolic acid) was associated with polymer degradation. Release from poly(DL-lactic acid) was very slow when diffusion controlled.

Keyphrases □ Polyesters, biodegradable—poly(ϵ-caprolactone), poly(DL-lactic acid), copolymers, steroid release, films, capsules □ Drug delivery systems—kinetics, biodegradation, diffusion, films, capsules □ Poly(ϵ-caprolactone)—homopolymers, copolymers, release rates, films, capsules □ Sustained-release systems—biodegradable polyesters, poly(ϵ-caprolactone), films, capsules

Polymer systems for sustained subdermal drug delivery may be based on principles of drug diffusion and/or polymer degradation. The diffusion coefficients of steroids in poly(ϵ-caprolactone) and poly(ϵ-caprolactone-co-DL-lactic acid) are comparable to values reported for poly(dimethylsiloxane) and, *a priori*, these polymers may be used in diffusion-controlled delivery systems that biodegrade after drug exhaustion (1, 2). In contrast, diffusion in poly(DL-lactic acid) is much slower (2); consequently, diffusion, leaching, and biodegradation may contribute to the drug delivery rates reported in studies of this polymer (3–5).

This paper describes the release rates of several steroids from films and capsules of homopolymers and copolymers of ϵ-caprolactone, DL-lactic acid, and glycolic acid *in vitro* and *in vivo* and factors that determine the observed kinetics.

EXPERIMENTAL

Synthesis—Poly(ϵ-caprolactone), poly(DL-lactic acid), their copolymers, and poly(DL-lactic acid-co-glycolic acid) were prepared by bulk polymerization of the purified monomers at 130° *in vacuo* in the presence of stannous octoate (50–500 ppm). The polymers were purified by precipitation from methylene chloride with methanol, followed by rapid and thorough washing with water in a blender[1]. Copolymer composition was determined by NMR spectroscopy.

Films were prepared by casting a common solution of the steroid and polymer in methylene chloride onto a glass plate and spreading with an adjustable applicator[2]. When a thickness greater than 100 μm was required, thinner films were stacked and compression molded at 100–130° to ensure even drug distribution. Sandwiched films, *i.e.*, a drug–polymer layer completely encased by drug-free polymer, were prepared by casting a polymer–drug solution on a drug-free polymer film. The resulting double-cast film was cut to leave smaller squares, over which a drug-free film was cast. The triple film then was cut between the squares.

Polymer tubing was prepared by melt extrusion or, when limited material was available, by rolling polymer film around a short polytef tube and annealing *in vacuo* while mechanically rotating the tube about its axis. Capsules were prepared by heat sealing the tubing with warm pliers. Steroids were micronized[3] (<5 μm) and dispersed in a vehicle using a tissue grinder (10 min) prior to capsule filling.

Release Rate Measurement—Films or capsules were immersed totally in distilled water (80–400 ml) at 37°. Mixing was accomplished using a rotating shaker[4] maintained at 135 rpm. Increasing the shaker speed to 195 rpm did not change the release rate. The aqueous reservoir was changed daily (capsules) or more frequently (films); where release rates were very fast, a flow system was used to keep the aqueous drug concentration low. In most cases, the frequency of solution change was such that the drug concentration did not exceed 10% of its aqueous solubility and typically was <1%. Drugs were either tritium or carbon 14 labeled, and release rates were determined by radioassay.

In vivo release rates were determined by radioassay of the feces and/or urine after subdermal implantation of the films or capsules in female New Zealand White rabbits or Charles River rats *via* incisions about the dorsal midline.

THEORETICAL

The diffusion-controlled release of a drug from a monolithic film or slab of unit area into an infinite aqueous sink may be described by Eqs. 1 and 2. Equation 1 applies when the drug is dissolved completely in the polymer (6); Eq. 2 applies when the drug solubility is exceeded and the

[1] Waring.
[2] Boston-Bradley.
[3] Wig-L-Bug, Crescent Dental Manufacturing.
[4] Eberbach.

0022-3549/79/1200-1534$01.00/0
© 1979, American Pharmaceutical Association

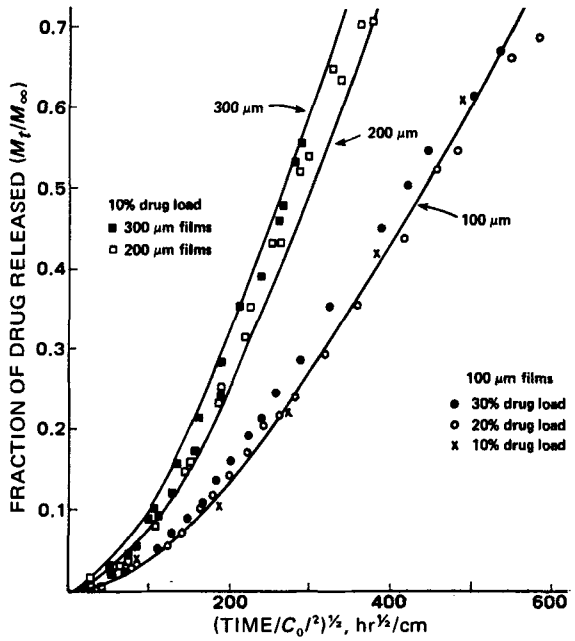

Figure 1—*Fraction of progesterone released from poly(ϵ-caprolactone) films with different thicknesses and drug loads, plotted as a function of* $(time/C_0l^2)^{1/2}$. *Solid lines were predicted from Eq. 3 using values for the constants listed in the text. The 100-μm films were cast; the 200- and 300-μm films were compression molded.*

solid drug particles are distributed uniformly in the film and are small relative to the average diffusion distance (7):

$$M_t/M_\infty = (4D_et/\pi l^2)^{1/2} \quad \text{for } M_t/M_\infty \leq 0.6 \quad \text{(Eq. 1a)}$$

$$M_t/M_\infty = 1 - 8\exp(-\pi^2 D_e t/l^2)/\pi^2 \quad \text{for } 0.4 \leq M_t/M_\infty \leq 1.0 \quad \text{(Eq. 1b)}$$

$$M_t/M_\infty = [4D_eC_st(2C_0 - C_s)/C_0^2l^2]^{1/2} \quad \text{for } C_0 > C_s \quad \text{(Eq. 2a)}$$

$$M_t/M_\infty = [8D_eC_st/C_0l^2]^{1/2} \quad \text{for } C_0 \gg C_s \quad \text{(Eq. 2b)}$$

where M_t is the cumulative drug released at time t, M_∞ is the total drug content (equals C_0l), C_s is the drug solubility in the polymer, C_0 is the initial drug concentration, l is the film thickness, and $D_e = D\epsilon/\tau$, where D_e is the effective diffusion coefficient and ϵ and τ are the volume fraction and the tortuosity of the polymer, respectively.

The case where the drug solubility in the polymer is exceeded, *i.e.*, $C_0 > C_s$, was expanded to include the effect of an aqueous boundary layer (8, 9). The modified kinetic expression is:

$$M_t/M_\infty = (A^2 + Bt)^{1/2} - A \quad \text{(Eq. 3)}$$

where A equals $2D_eh_aK/D_al$, B equals $8D_eC_s/C_0l^2$, K is the partition coefficient $(C_s/C_{aqueous})$, h_a is the aqueous boundary layer thickness, and D_a is the aqueous drug diffusion coefficient. At longer times, when $Bt \gg A$, Eq. 3 reduces to Eq. 2b.

In contrast to monolithic devices, diffusion-controlled drug release rates from a reservoir device are time invariant, provided the difference in drug concentrations (ΔC) on each side of the membrane remains constant. The latter condition is met when solid drug remains within the device and either a perfect sink or constant drug dissipation prevails outside. For a capsule (hollow cylinder) of unit length (centimeters), the drug diffusion rate through the walls (ends neglected) is given by (10):

$$dM/dt = 2\pi D_eK\,\Delta C/\ln(\text{o.d./i.d.}) = 2\pi D_eC_s/\ln(\text{o.d./i.d.}) \quad \text{(Eq. 4)}$$

RESULTS AND DISCUSSION

Poly(ϵ-caprolactone) Films—*In vitro* progesterone release rates were measured using different initial drug concentrations [C_0 = 10, 20, and 30% (w/w)] and film thicknesses (l = 100, 200, and 300 μm). Release was rapid, complete within 24 hr, and consistent with a diffusion-controlled process attenuated by an aqueous boundary layer (8, 9). Illustrative results are plotted in Fig. 1 as the drug fraction release (M_t/M_∞) *versus* $(t/C_0l^2)^{1/2}$ to normalize the effects of film thickness and drug concentration predicted by Eqs. 2a, 2b, and 3. The fact that the rates from the 100-μm films, C_0 = 10, 20, and 30% (w/w), conform to a single line when plotted in this manner shows that Eq. 1 is not valid, *i.e.*, $C_0 > C_s$. Although the crystallinity of poly(ϵ-caprolactone) prevented visual confirmation of undissolved progesterone, partition measurements showed that progesterone solubility in poly(ϵ-caprolactone) is only 1.69% (w/w) (2).

The initial curvature of the Fig. 1 plots (t < 15 min) is inconsistent with Eqs. 2a and 2b, unless it is associated with equilibration of the freshly immersed polymer film with the aqueous environment. It is probably the result of an aqueous diffusion barrier, and Eq. 3 is applicable. The experimental data with the 100-μm films could be reproduced by this equation (solid line, Fig. 1) using the following constants: $D_e = 8.3 \times 10^{-9}$ cm²/sec, $D_a = 7 \times 10^{-6}$ cm²/sec, $C_s = 1.69 \times 10^{-2}$ g/g, K = 1200, and h_a = 19 μm.

The value of D_a, the aqueous diffusion coefficient of progesterone, is estimated using the Sutherland–Einstein equation (11, 12); values of K and C_s are known (2), and h_a and D_e were chosen to fit the experimental data. The derived h_a value is comparable to estimates made in similar studies (8, 9, 11). The D_e value is only slightly greater than the value of 3.6×10^{-9} cm²/sec derived from diffusion cell measurements of the progesterone diffusion rate across an unloaded poly(ϵ-caprolactone) film (2).

The release rates from 200- and 300-μm films (10% drug load) were the same within experimental error when normalized for film thickness but significantly greater than the rate from 100-μm films (Fig. 1). The experimental results for the 200- and 300-μm films were reproduced by Eq. 3 using the given values of D_a, C_s, K, and h_a but with a higher D_e of 20.5 $\times 10^{-9}$ cm²/sec. This change in D_e with film thickness reflected different film preparation methods. For practical reasons, the thinner films were solvent cast and the 200- and 300-μm films were compression molded. When the 100-μm films also were compression molded, the estimated diffusion coefficient increased to the value observed with the thicker films (Fig. 2).

The dependence of D_e on the film preparation method is attributed to the fact that poly(ϵ-caprolactone) is a partially crystalline polymer (13). Thus, the film preparation method will affect the polymer morphology, which, in turn, can affect significantly the volume fraction, tortuosity, drug solubility, and intrinsic diffusivity of the polymer (14). The degree to which the experimental results conform to the theoretical model is surprisingly good in view of the assumptions made, particularly the assumption that the tortuosity and volume fraction are independent of C_0 and the drug fraction released.

In vivo progesterone release from poly(ϵ-caprolactone) films ($2 \times 1 \times 10^{-2}$ cm) was at least as fast as its excretion rate. Thus, when triplicate films containing 10% ^{3}H-progesterone were implanted in the dorsal area of two rabbits, the observed tritium urinary excretion rate was essentially identical to that observed when progesterone was injected subdermally as a sesame oil suspension: 16 hr, 49 ± 4%; 40 hr, 78 ± 4%. This result is consistent with the observed *in vitro* rates and shows that drug diffusion away from the polymer is not impaired by any foreign body reaction.

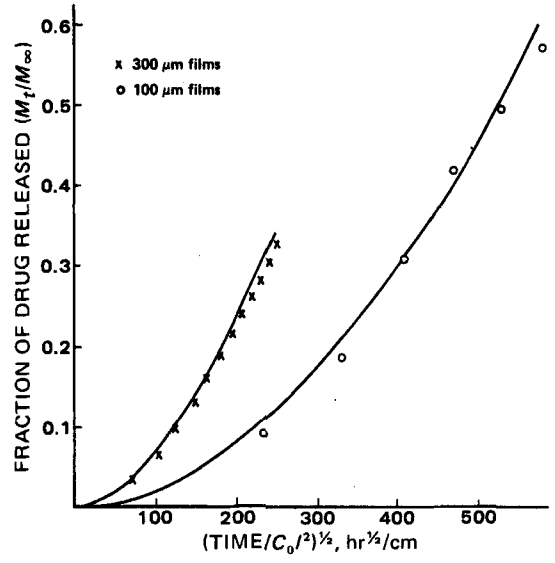

Figure 2—*Fraction of progesterone released from poly(ϵ-caprolactone) films, compression molded, 10% drug load. Solid lines were predicted from Eq. 3 using values for the constants listed in the text, except for* $D_e = 24.6 \times 10^{-9}$ *cm²/sec and* h_a = 34 μm.

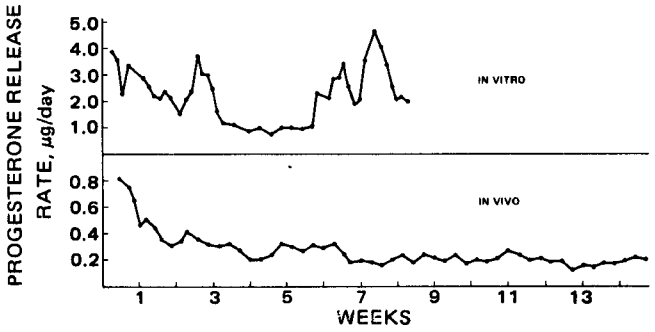

Figure 3—In vitro *and* in vivo *progesterone release rates from poly(DL-lactic acid) films, 100-μm thickness, 10% drug load.*

Poly(DL-lactic Acid) Films—Progesterone release from poly(DL-lactic acid) films was much slower and more erratic than from poly(ϵ-caprolactone) films. Figure 3 shows the daily progesterone release rate from poly(DL-lactic acid) films (C_0 = 10%, l = 100 μm) under both *in vitro* and *in vivo* conditions.

The much slower release from poly(DL-lactic acid) is consistent with the fact that both the solubility and diffusion coefficients of progesterone in this polymer are much lower (2): poly(DL-lactic acid), $D_e = 5.1 \times 10^{-12}$ cm²/sec and $C_s = 0.65 \times 10^{-3}$ g/g; and poly(ϵ-caprolactone), $D_e = 3.6 \times 10^{-9}$ cm²/sec and $C_s = 1.69 \times 10^{-2}$ g/g. However, the fact that the *in vitro* release rate from poly(DL-lactic acid) was so erratic and not proportional to $t^{1/2}$ suggested that leaching and/or polymer degradation might be largely responsible for the observed rate. To increase the contribution of diffusional release, the progesterone concentration was increased to 30% (w/w) and the films thickness was reduced to 3 μm. Since this thickness was no greater than the size of drug crystallites in the film, drug-free 3-μm films were cast on each side of the film to prevent leaching by direct contact between the undissolved drug and the aqueous reservoir.

With this film, the release rate was considerably more rapid, although it was still much slower than rates from 100-μm poly(ϵ-caprolactone) films. Plots of M_t *versus* $t^{1/2}$ were approximately linear after an induction period of 1 day *in vitro*, and similar results were obtained in *in vivo* monitoring of urinary excretion (Fig. 4). In this case, the induction period must be attributed to drug equilibration among the three layers of the sandwiched film. A simple calculation using Eq. 3 shows that the aqueous boundary layer can be neglected because of the time range covered. The smaller slope of the *in vivo* plot arises because drug release measurements were restricted to urinary excretion with no correction for metabolic losses by other routes.

Since the low permeability of poly(DL-lactic acid) is partly a reflection of its high glass transition temperature (57°), the effect of temperature on the release rate was of interest. When the *in vitro* temperature was raised from 37 to 60°, the progesterone release rate from the composite films increased 250-fold.

Copolymer Films—Progesterone release rates from films (100 μm,

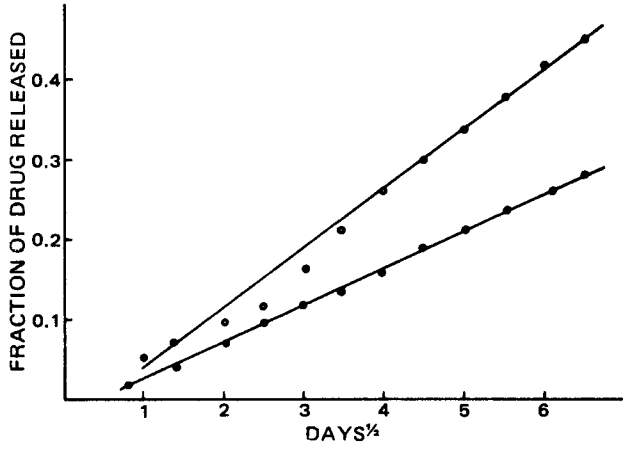

Figure 4—In vitro (○) *and* in vivo (●) *progesterone release rates from sandwiched poly(DL-lactic acid) films.*

Table I—Predicted Rates and Duration of Release of Steroids from Poly(ϵ-caprolactone) Capsules [a]

Drug	Release Rate, μg/day/cm 1.0-mm i.d.	Release Rate, μg/day/cm 2.0-mm i.d.	Duration, days 1.0-mm i.d.	Duration, days 2.0-mm i.d.
Progesterone	56	271	70	58
Testosterone	35	170	111	92
Norethindrone	9.3	45	422	352
Norgestrel	8.7	42	452	377

[a] Assumptions are: 2.4-mm o.d., 50% steroid in diluent, and D_e values derived from diffusion cell measurements (2).

10% drug load) of a 60:40 copolymer of ϵ-caprolactone and DL-lactic acid and a 90:10 copolymer of ϵ-caprolactone and glycolic acid were comparable to rates from poly(ϵ-caprolactone). In contrast, rates from copolymers of DL-lactic acid and glycolic acid were orders of magnitude slower. Four copolymers with 7, 14, 19, and 21 mole % of glycolic acid were evaluated *in vitro* as 100-μm films loaded with 10% progesterone. During the first 20 days, the cumulative drug released from each film was proportional to $t^{1/2}$ and, based on Eqs. 2*a* and 2*b*, the rates corresponded to DC_s values of 0.24×10^{-15}, 0.51×10^{-15}, 0.86×10^{-15}, and 1.08×10^{-15} g/cm/sec, respectively[5]. These values are essentially the same as those of poly(DL-lactic acid) determined from diffusion cell measurements (2).

After 20 and 30 days, the release rate from the two copolymers with the highest glycolic acid content (21 and 19 mole %) began to increase substantially until a new linear relationship between the drug fraction released and $t^{1/2}$ was established (Fig. 5). Since this transition coincided with the mechanical deterioration and fragmentation of the films, it can be attributed to polymer hydrolysis and exposure of a larger surface area. The linear relationship after fragmentation may well be fortuitous.

The copolymer films with less glycolic acid (7 and 14 mole %) were changed little during 50 days, and the initial progesterone release rate was essentially unchanged.

Since other studies (1) established that the bioerosion onset can be tailored by the choice of copolymer composition and molecular weight, poly(DL-lactic acid-co-glycolic acid) delivery systems with various kinetic

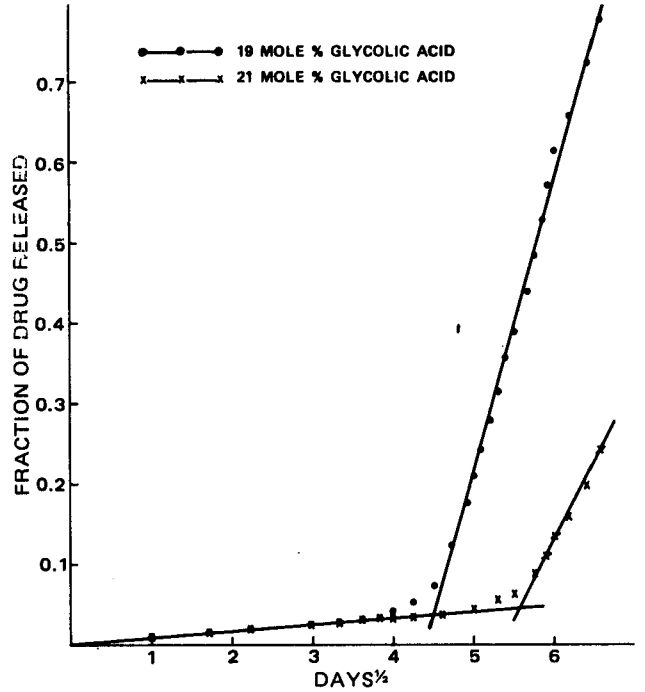

Figure 5—In vitro *progesterone release rates from poly(DL-lactic acid-co-glycolic acid) films, 100-μm thickness, 10% drug load.*

[5] The progesterone solubility in these copolymers was not determined, but the condition that $C_0 > C_s$ could be inferred from the progesterone solubility in the homopolymers.

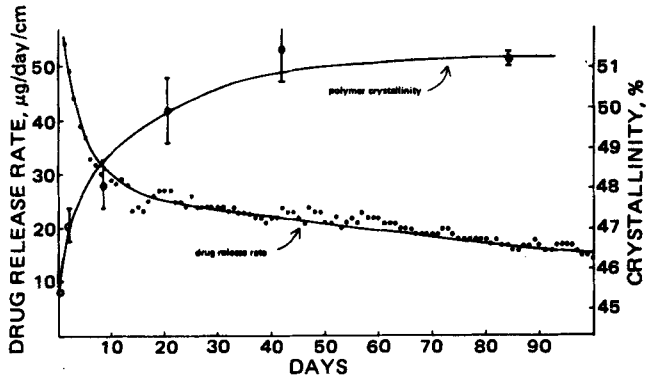

Figure 6—In vitro *norgestrel release rates from a poly(ϵ-caprolactone) capsule, o.d./i.d. = 2.41 mm/2.06 mm, and polymer crystallinity change under the same conditions.*

profiles probably can be designed by using copolymer blends.

Poly(ϵ-caprolactone) Capsules—*A priori*, the permeabilities of poly(ϵ-caprolactone) and its copolymers are such that diffusion-controlled delivery of efficacious amounts of a contraceptive agent for 1 year or longer is feasible. Table I summarizes rates and durations of release of four hormonal steroids from poly(ϵ-caprolactone) capsules, calculated from Eq. 4 using known (2) D_e and C_s values, two different inner diameters, and an outer diameter of 2.4 mm. An outer diameter of 2.4 mm was the maximum size compatible with subdermal insertion. It also was assumed that the drug was present as a 50% dispersion in an inert carrier. The carrier maximizes contact between the drug reservoir and the inner surface of the capsule and is necessary to maintain a constant concentration gradient and release rate (15).

The calculated rates fall within the range that is believed necessary for fertility control by sustained administration of the more potent progestins, *e.g.*, norethindrone and norgestrel (16). Furthermore, while the duration of release (load/rate) is independent of capsule length and not very sensitive to changes in the outside diameter–inside diameter ratio, manipulation of the percent dispersion provides a means of varying the duration from several months to years.

In practice, the higher steroid release rates in Table I could not be achieved for any significant period. Typically, the kinetics were characterized by a rapid and substantial rate decline during the first 20 days, followed by a much slower, smaller decline over the next 100–200 days. An example of this behavior *in vitro* is shown in Fig. 6. Two reasons for the failure to achieve a constant release rate seemed plausible: a permeability reduction produced by morphological changes in the polymer and, alternatively, a reduction in the concentration gradient across the polymer wall produced by a declining rate of steroid dissolution in the dispensing agent and/or polymer.

A declining drug dissolution rate might arise because of: (*a*) depletion

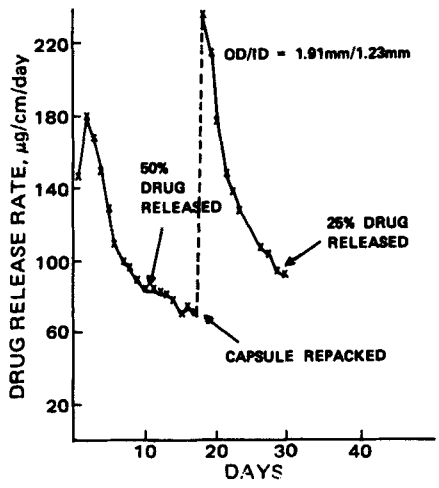

Figure 7—*Effect of repacking on release rate of ethinyl estradiol from poly(ϵ-caprolactone) capsules* in vitro.

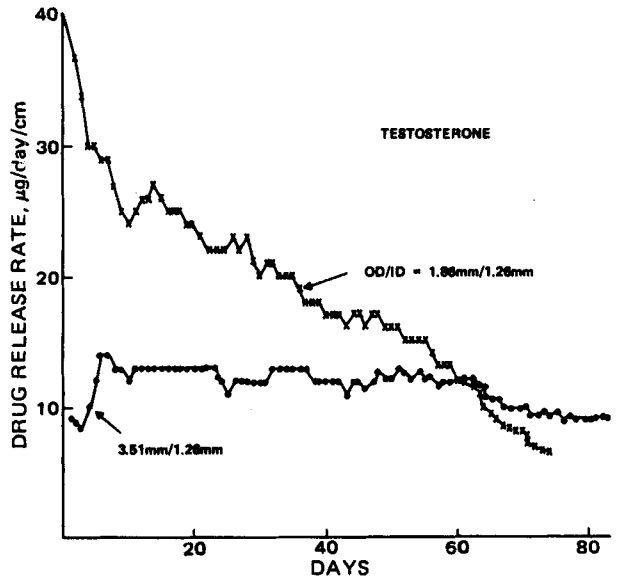

Figure 8—In vitro *testosterone release rates (15% dispersion in sesame oil) from poly(ϵ-caprolactone) capsules as a function of the ratio of the inner and outer diameters of the capsule.*

of the smaller drug particles during the initial time period, (*b*) aggregation of drug particles, or (*c*) drug recrystallization, producing an increase in the crystal size. A classical burst effect (10) was ruled out because the kinetics were unchanged if there was no time delay in immersing the freshly packed capsule in the aqueous reservoir. A series of experiments suggested that the larger release rate decline observed in the first 20 days was a reflection of a decreasing drug dissolution rate while the smaller, long-term decline was associated with a polymer crystallinity increase.

The larger decline was observed a second time when the partially depleted capsule was opened and repacked with freshly micronized drug, and the experiment was resumed (Fig. 7). On the other hand, the diffusion rates of progesterone and testosterone through a 100-μm poly(ϵ-caprolactone) membrane in water at 37° did not change when measured daily over 10 days using a diffusion cell and *efficient stirring*. Most importantly, it was possible to eliminate the initial release rate decline by increasing the capsule outside diameter–inside diameter ratio (Figs. 8 and 9). These results are consistent with the idea that dissolution of these steroids becomes slower and will determine the kinetics unless the outside diameter–inside diameter ratio is sufficiently large that diffusion through

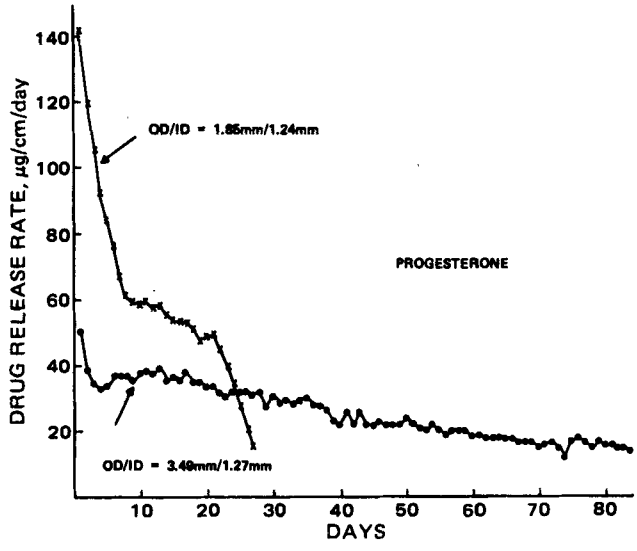

Figure 9—In vitro *progesterone release rates (15% dispersion in sesame oil) from poly(ϵ-caprolactone) capsules as a function of the ratio of the inner and outer diameters of the capsule.*

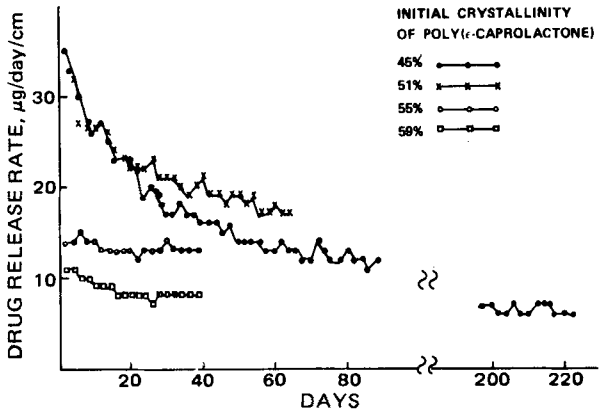

Figure 10—*Norgestrel release rates from capsules of poly(ε-caprolactone) with different degrees of crystallinity: untreated (45%), annealed (51%), and pretreated (55 and 59%).*

the polymer wall is the rate-determining step. Although increasing the outside diameter–inside diameter ratio eliminates the initial release rate drop, this result obviously is at the expense of the maximum rate.

Morphology is potentially relevant to the constancy of the release rate because poly(ε-caprolactone) is a semicrystalline polymer subject to slow hydrolysis *in vitro* and *in vivo* (1). The resulting molecular weight decrease, coupled with annealing, is associated with a considerable increase in crystallinity (Fig. 6), which, in turn, reduces polymer permeability. The significance of this finding was evaluated by determining the initial release rates of norgestrel from capsules with different crystallinities corresponding to increasing degrees of polymer hydrolysis. The release rate from capsules pretreated to increase the crystallinity to 51% was essentially the same as that observed with unannealed virgin capsules, 45% crystallinity, over 60 days (Fig. 10). This equality demonstrated that, despite a superficial correlation, the initial rapid decrease in release rate shown in Fig. 6 was not a manifestation of the crystallinity change but of drug dissolution. However, when the crystallinity was increased to 55%, the release rate was both lower and essentially constant (12–15 μg/day) for 60 days. Evidently, this increased crystallinity reduced the polymer permeability sufficiently so that drug diffusion, not dissolution, became the rate-determining process.

When the polymer crystallinity was increased to 59%, the release rate was even lower (6–7 μg/day). These release rate reductions with increasing crystallinity explain the longer term changes in release rates *in vitro* and *in vivo*. For example, after 220 days *in vitro*, the crystallinity of poly(ε-caprolactone) capsules increased from 45 to 58%. The norgestrel release rate after the same time had declined to 6–7 μg/day, which is the rate associated with a crystallinity of 58% (Fig. 10).

In conclusion, the rate and constancy of steroid release from poly(ε-caprolactone) capsules can be a function of both the steroid dissolution rate and the polymer crystallinity. The influence of steroid dissolution rates may be eliminated by appropriate choice of capsule dimensions. Methods of controlling the polymer crystallinity will be discussed in a later publication.

REFERENCES

(1) C. G. Pitt, D. Christensen, A. R. Jeffcoat, G. L. Kimmel, A. Schindler, M. E. Wall, and R. A. Zweidinger, "Biodegradable Polymers and Sustained Delivery of Contraceptive Drugs," in Proceedings Drug Delivery Systems, H. L. Gabelnick, Ed., DHEW Publication No. (NIH) 77-1238, Aug. 1976, pp. 141–192.

(2) C. G. Pitt, A. R. Jeffcoat, R. A. Zweidinger, and A. Schindler, *J. Biomed. Mater. Res.*, **13**, 497 (1979).

(3) J. H. R. Woodland, S. Yolles, D. A. Blake, M. Helrich, and M. J. Meyer, *J. Med. Chem.*, **16**, 897 (1973).

(4) T. M. Jackanicz, H. Nash, D. L. Wise, and J. B. Gregory, *Contraception*, **8**, 227 (1973).

(5) C. Thies, in "Development of Injectable Microcapsules for Use in the Treatment of Narcotic Addiction," National Institute of Drug Abuse Research Monograph No. 4, R. E. Willette, Ed., 1976.

(6) W. I. Higuchi, *J. Pharm. Sci.*, **51**, 802 (1962).

(7) T. Higuchi, *ibid.*, **50**, 874 (1961).

(8) T. J. Roseman and W. I. Higuchi, *ibid.*, **59**, 353 (1970).

(9) T. J. Roseman and S. H. Yalkowsky, *ibid.*, **63**, 1640 (1974).

(10) R. W. Baker and H. K. Lonsdale, in "Controlled Release of Biologically Active Agents," A. C. Tanquary and R. E. Lacey, Eds., Plenum, New York, N.Y., 1973, pp. 15–72.

(11) T. J. Roseman, *J. Pharm. Sci.*, **61**, 46 (1972).

(12) G. L. Flynn, N. F. H. Ho, S. Hwang, E. Owada, A. Molokhia, C. R. Behl, W. I. Higuchi, T. Yotsuyanagi, Y. Shah, and J. Park, in "Controlled Release Polymeric Formulations," D. R. Paul and F. W. Harris, Eds., ACS Symposium Series 33, American Chemical Society, Washington, D.C., 1976, pp. 87–122.

(13) H. Bittiger, R. H. Marchessault, and W. D. Niegisch, *Acta Crystallogr.*, **B26**, 1923 (1970).

(14) R. M. Barrer, in "Diffusion in Polymers," J. Crank and G. S. Park, Eds., Academic, New York, N.Y., 1968, pp. 165–219.

(15) R. W. Baker, M. E. Tuttle, H. K. Lonsdale, and J. W. Ayres, *J. Pharm. Sci.*, **68**, 20 (1979).

(16) M. J. K. Harper, in "Contraception—Retrospect and Prospect," E. Tucker, Ed., Birkhaüser AG, Basel, Switzerland, 1977, p. 306.

ACKNOWLEDGMENTS

Supported by the Contraceptive Development Branch, Center for Population Research, National Institute of Child Health and Human Development, National Institutes of Health, under Contract N01-ND-3-2741.

The authors are indebted to Dr. Henry Gabelnick, National Institute of Child Health and Human Development, for helpful discussions.

Antineoplastic Agents LXIV: 1,4-Bis(2′-chloroethyl)-1,4-diazabicyclo[2.2.1]heptane Dihydrogen Dimaleate

GEORGE R. PETTIT [x], DONALD P. GIESCHEN, and WILLIAM E. PETTIT

Received May 9, 1979, from the *Cancer Research Institute and Department of Chemistry, Arizona State University, Tempe, AZ 85281.* Accepted for publication June 12, 1979.

Abstract □ The 1,4-bis(2′-chloroethyl)-1,4-diazabicyclo[2.2.1]heptane dication (II) exhibits remarkable antineoplastic activity. Detailed evaluation of several dianion derivatives showed a curative response level against the murine P-388 lymphocytic leukemia, colon 26, CD8F$_1$ mammary, and the Walker 256 carcinosarcoma (rat) tumor systems. In addition, significant cancer chemotherapeutic activity was found against the murine L-1210 lymphoid leukemia, colon 38, and B16 melanocarcinoma tumor systems. The bicyclo dication (II) first was isolated, evaluated, and stored as the diperchlorate derivative (II*a*). Because of the promising anticancer activity of II*a*, procedures were developed for obtaining other anion derivatives for comparative biological purposes. Several naturally occurring substances were evaluated, and the dihydrogen dimaleate derivative (II*i*) obtained by an ion-exchange technique was the most suitable.

Keyphrases □ Antineoplastic agents—1,4-bis(2′ - chloroethyl) - 1,4-diazabicyclo[2.2.1]heptane cation, synthesis, diperchlorate and dihydrogen dimaleate salts □ 1,4-Bis(2′-chloroethyl)-1,4-diazabicyclo-[2.2.1]heptane cation—antineoplastic activity, synthesis, diperchlorate and dihydrogen dimaleate salts □ Heterocyclic anticancer agents—1,4-bis(2′-chloroethyl)-1,4-diazabicyclo[2.2.1]heptane cation, synthesis, diperchlorate and dihydrogen dimaleate salts

An early exploration of potential anticancer drugs in these laboratories led to the first 1,4-diazabicyclo[2.2.1]-heptane heterocyclic system. The facile preparation of 1,4-bis(2′-chloroethyl)-1,4 - diazabicyclo[2.2.1]heptane diperchlorate (II*a*, NSC 57198) from bis(2-chloroethyl)-amine (I) and formaldehyde has been reported (Scheme I) (1). Later, the structural elucidation (2), preparation of related substances (3), and confirmation of the structural assignment of II*a* by X-ray crystallography (4) were described. Meanwhile, II*a* has been evaluated against the National Cancer Institute's most important experimental tumor systems (Table I). Its promising antineoplastic activity encouraged the investigation of other presumably more suitable (7, 8) anions.

BACKGROUND

Initial isolation and structural investigations (1, 2) of diperchlorate II*a* emphasized that this heterocyclic system was very susceptible to nucleophilic attack, especially by hydroxyl ion, and this observation was confirmed by other investigators (9). As predicted, the very poor nucleophilicity of perchlorate is ideally suited to stabilizing the novel bridged heterocyclic system. Compound II*a* specimens prepared 17 years ago show no evidence of decomposition; II*a* has proven to be stable at temperatures up to 210–222° but burns violently when deliberately ignited. The corresponding dichloride derivative (II*b*), formed in the reaction of I with formaldehyde, was described previously (9). Attempts to improve its isolation (4% yield) and characterization, *e.g.*, by ion-exchange techniques, were not successful.

The objective of this investigation was to locate an anion such as that derived from ascorbic acid [vitamin C (10)] or another naturally occurring substance compatible with human use. The ascorbic acid derivative (II*e*) seemed attractive due to the possibility of increasing the immune response involved with interferon enhancement (11). Derivatives of the readily available maleic acid, a constituent of citrus and grape juices (12, 13), and D-tartaric acid also were considered. These three possibilities were inspected as part of a large series of anions of decreasing nucleophilicity derived from the following acids: acetic, pKa 4.74, II*c*; benzoic, 4.20, II*d*; ascorbic, 4.17, II*e*; salicylic, 2.97, II*f*; D-tartaric, 2.93, II*g*; saccharin, 1.60, II*h*; and maleic, 2.0, II*i*.

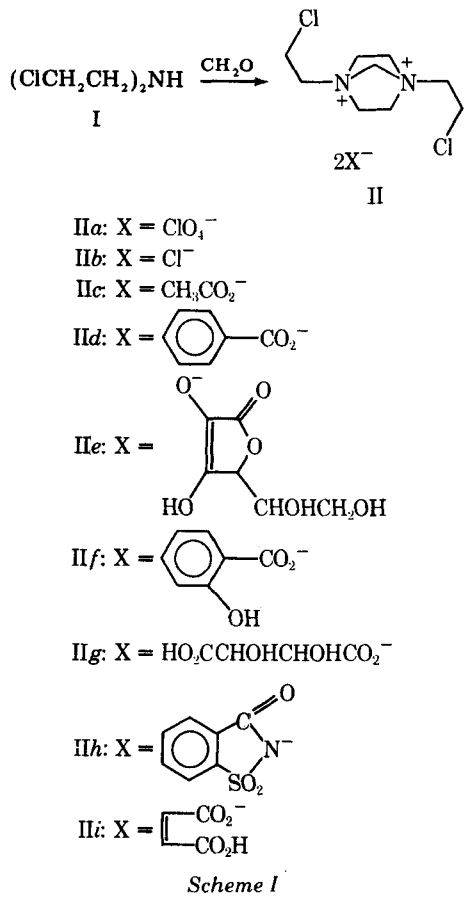

Scheme I

Two methods were found for displacing the perchlorate anions. The first procedure was based on the minimal solubility of potassium perchlorate in ethanol–acetonitrile mixtures and was workable except with maleic and D-tartaric acids since their corresponding potassium salts were not sufficiently soluble in this solvent. However, the nucleophilicity of the acetate, benzoate, and ascorbate anions was sufficient to cause decomposition of II*c*–II*e* during isolation. While disalicylate II*f* was stable only in the cold, disaccharin salt II*h* was obtained conveniently by this method and only slowly decomposed at ambient temperatures over 6 months. At this point, the potential bladder carcinogenic properties of saccharin became known; except for preliminary antineoplastic studies (Table I), II*h* was not considered further.

Ion-exchange chromatography was the alternative method utilized for displacing the perchlorate anions. Both ditartarate II*g* and dihydrogen dimaleate II*i* were synthesized by this method. However, II*g* was unstable at room temperature and could be maintained only at approximately −10°. Fortunately, II*i* has been maintained under normal conditions without any detectable change for over 3 years[1]. The well-established

[1] One important criterion for stabilizing cation II is an anion derived from an acid with a dissociation constant corresponding to pKa 2 or less.

0022-3549/79/1200-1539$01.00/0
© 1979, American Pharmaceutical Association

Table I—Tumor System (5, 6)

Compound	PS[a] Dose, mg/kg	PS[a] T/C, %[b]	PS[a] Cures, %	LE[c] Dose, mg/kg	LE[c] T/C, %	C8[d] Dose, mg/kg	C8[d] T/C, %	C6[e] Dose, mg/kg	C6[e] T/C, %	C6[e] Cures, %
II*a*	400	268	50	150	190	400	47	400	271	60
	200	190		100	189	200	62	200	272	89
	100	154		66.0	154			100	175	30
	50	145		44.0	140			50.0	129	
								25.0	128	
								12.5	120	
II*i*	200 (toxic)	192		200	180			200	186	20
	100	146		100	148	100	45	100	155	10
	50.0	123		50.0	120	50.0	44	50.0	133	10
	25.0	113		25.0	90	25.0	78	25.0	114	10
						12.5	84	12.5	102	10
II*h*	400	296	50					400		20
	200	240						200	171	30
	100	198						100	134	
	50.0	171						50.0	116	
								25.0	106	
III*a*	2.0 (toxic)			2.0	97					
	1.0	167		1.0	154					
	0.50	145		0.50						
	0.25	120		0.25	125					
	0.10	110		0.12	110					
III*b*	> 0.30 (toxic)									
	0.20	111		0.20	125					
	0.10	116		0.10	110					
	0.05	102		0.05	102					

Compound	CD[f] Dose, mg/kg	CD[f] T/C, %	B1[g] Dose, mg/kg	B1[g] T/C, %	LL[h] Dose, mg/kg	LL[h] T/C, %	RO[i] Dose, mg/kg	RO[i] T/C, %	WA[j] Dose, mg/kg	WA[j] T/C, %	WA[j] Cures, %
II*a*	400	6	100	146					80	562	100
	200	24	50.0	116					40	561	66
	100	44	25.0	136	100	136			20	237	33
	50.0	57							10	128	33
	25.0	104							5	128	
	12.5	65									
II*i*	400	0	100	138			200	121			
	200	4	50.0	130			100	124			
	100	19	25.0	129			50.0	110			
	50.0	78	12.5	128			25.0	94			
	25.0	85	6.25	117							
	12.5	16									
II*h*	600	12	200	143							
	400	43	100	120							
	200	43	50.0	117							
	100	93	25.0	108							
	50.0	67									
	25.0	75									
III*a*											
III*b*									0.15	39	
									0.075	85	
									0.037	78	

[a] P-388 lymphocytic leukemia. [b] Test/control. [c] L-1210 lymphoid leukemia. [d] Colon 38. [e] Colon 26. [f] $CD8F_1$ mammary tumor. [g] B16 melanocarcinoma. [h] Lewis lung carcinoma. [i] Ridgway osteogenic sarcoma. [j] Walker carcinosarcoma 256.

stability of II*i* seems consistent with the relatively poor nucleophilic properties expected for the hydrogen maleate anion. The relative instability observed with the saccharin anion may have a less obvious explanation and will be explored.

The stable diperchlorate (II*a*) and dihydrogen dimaleate (II*i*) salts showed substantial promise in key experimental tumor systems (Table I) and are being considered for clinical trial; II*a* had the more favorable therapeutic index. Biological data obtained with the disaccharin salt (II*h*) (prior to significant decomposition) also have been included. Comparison of these data with those obtained for piperazine III precludes the possibility that the high antineoplastic activity displayed by the 1,4-bis(2′-chloroethyl)-1,4-diazabicyclo[2.2.1]heptane dication is due significantly to production of this 2-chloroethylamine. The methylene-bridged diquaternary system II definitely is not a nitrogen mustard, and its mechanism of action appears to depend on *in vivo* formation and latent release of a substance(s) other than piperazine III. The *in vivo* production of a very reactive carbon–carbon or carbon–nitrogen bond-forming species (IV or V) derived from formaldehyde is an attractive prospect.

EXPERIMENTAL

Glass-distilled water was employed in the ion-exchange procedures. All other solvents were redistilled. Melting points were determined by the capillary method (oil bath) and are uncorrected. IR spectra[2] (potassium bromide) and PMR (^{1}H-NMR) spectra[3] (δ in parts per million with respect to tetramethylsilane or sodium 2,2-dimethyl-2-silapentane-5-sulfonate) were recorded. ^{13}C-NMR spectra (in parts per million downfield from the internal standard tetramethylsilane or *p*-dioxane, 67.4 ppm) also were measured[4] (at 22.6 MHz). NMR spectra were determined in deuterium oxide solution unless otherwise noted. Elemental microanalyses were performed[5].

Bis(2-chloroethyl)amine Hydrochloride (I-HCl)—Purification

[2] Perkin-Elmer 299 spectrophotometer.
[3] Varian Associates T-60A or XL-100.
[4] By Dr. J. Witschel, Jr., employing a Bruker WH-90 NMR spectrometer.
[5] Spang Microanalytical Laboratory, Eagle Harbor, Mich.

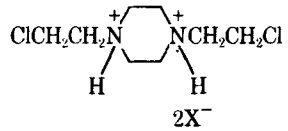

III

IIIa: X = Cl^-
IIIb: X = $HO_2CCH{=}CHCO_2^-$

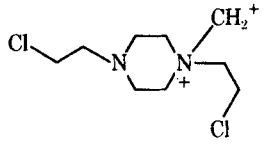

IV

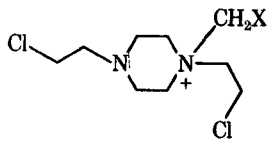

V

X = —NR_2, —OR, or —SR
R = H or alkyl

of currently available commercial bis(2-chloroethyl)amine hydrochloride, nitrogen mustard hydrochloride, is less efficient than the following improved (14, 15) synthesis. A solution of thionyl chloride (520 ml or 860 g) in chloroform (460 ml) was added slowly through a dropping funnel to a solution of 2,2′-iminodiethanol[6] (212 g) in 600 ml of chloroform. The reaction mixture was contained in a 5-liter, three-necked round-bottom flask equipped for efficient refluxing and rapid mechanical stirring and suspended in a cold water bath (for maintaining the reaction temperature at ~20°).

When the viscous material that formed on the stirring blade reached a constant mass, the remaining thionyl chloride was added rapidly. The water bath was heated, and the mixture was brought to reflux temperature slowly (to minimize foaming). After ~30 min, the yellow solution became clear and was allowed to cool. The crystalline product was collected and washed successively with chloroform (3 × 125 ml) and ether (200 ml) to yield I-HCl (250 g) as colorless crystals decomposing at 212–214°. Two recrystallizations from acetone–absolute ethanol (4:1) provided I-HCl (140 g) as needles decomposing at the same temperature; IR: 2975, 2760, 2440, 1595, 1460, 1445, 1355, 1305, 1050, 1000, 960, 885, 860, 840, 785, 755, 700, and 675 cm^{-1}. The ^{1}H-NMR data were reported previously (16).

Recrystallization of I-HCl obtained by this method was unnecessary for the preparation of II*a*.

1,4-Bis(2′-chloroethyl)-1,4-diazabicyclo[2.2.1]heptane Diperchlorate (II*a*)—The following procedure based on earlier studies (1, 2) is convenient and reliable for preparation of II*a*. A 10% NaOH solution (140 ml) was added in portions to I-HCl (50.0 g) in 100 ml of water. The mixture was extracted with ether (100 ml and 2 × 50 ml), and the combined extract was washed with saturated sodium chloride solution and dried (ice bath) over anhydrous magnesium sulfate. Solvent was removed by rotary evaporation (ice bath temperature) to afford the thermally unstable bis(2-chloroethyl)amine (I*a*) as a colorless oil.

Upon dissolution of the amine in absolute ethanol (150 ml), 37% formaldehyde solution (50 ml) was added quickly. After 1 day at room temperature, the mixture was cooled (ice bath) and 27 ml of 70% perchloric acid was added slowly. Crystallization of diperchlorate II*a* began within a few minutes; when completed, 32.2 g of II*a* was collected and recrystallized from water–ethanol to afford colorless crystals (24.2 g) decomposing at 222–223° [as found for the original elemental analytical sample (1)]; ^{13}C-NMR (deuterium oxide): 37.43 (-CH_2CH_2Cl), 59.73 (ring CH_2CH_2–), 60.05 (-CH_2CH_2Cl), and 83.39 (ring CH_2–). Other spectral and analytical data were reported earlier (2).

1,4-Bis(2′-chloroethyl)-1,4-diazabicyclo[2.2.1]heptane Disaccharin (II*h*)—Freshly prepared (from saccharin and potassium hydroxide in water) potassium saccharin (29.2 g) was dissolved in 95% ethanol (900 ml), and the hot solution was poured rapidly into a solution of diperchlorate II*a* (28.1 g) in acetonitrile (200 ml). After 2.25 hr, the potassium perchlorate precipitate was collected, the filtrate was concentrated to 150 ml, and potassium perchlorate was collected again. The remaining acetonitrile solution was concentrated to a yellow oil, which was dissolved in water and lyophilized to yield 37.4 g (96%) of disaccharin II*h* as pale-yellow flakes; IR: 3460, 3100, 1725, 1610, 1405, 1360, 1315, 1125, 1065, 1025, 880, 835, 770, 735, 705, 660, 610, and 585 cm^{-1}; PMR: δ 4.16–4.41 (m, 8H), 4.48 (s, 8H), 5.66 (s, 2H), and 7.85 (s, 4H).

Attempts to prepare a specimen for elemental analyses led to decomposition, precluding this characterization step. However, the IR and, especially, the ^{1}H-NMR spectra showing the methylene bridge signal at δ 5.66 were in complete accord with the assigned structure. When stored at ambient temperatures in a sealed container, II*h* underwent slow transformation. In approximately 6 months, the original substance remained in only a minor amount. The products are presently under investigation.

By employing the general procedure used to obtain disaccharin II*h*, the following reactions were attempted in hot ethanol–acetonitrile solutions. In each case, freshly prepared potassium acetate, benzoate, ascorbate, and salicylate were allowed to react separately with II*a*. The minimal solubilities of dipotassium D-tartarate and maleate in ethanol–acetonitrile mixtures precluded their use in these syntheses. The diacetate II*c* and dibenzoate II*d* were destroyed rapidly during the isolation. The diascorbate II*e* was transformed partially during isolation, and further characterization proved impractical.

Reaction between potassium salicylate (12.4 g in 250 ml of 95% ethanol) and diperchlorate II*a* (15.0 g) in acetonitrile (200 ml) provided nearly the theoretical amount of potassium perchlorate. Removal of solvent afforded disalicylate II*f* as a pale-yellow oil; PMR (acetonitrile-d_3): δ 4.0–4.8 (complex, 16H), 5.25 (s, H_2O), 5.95 (s, 2H), 6.7–7.1, 7.2–7.5, and 7.8–8.1 (complex, aromatic). Approaches to purifying II*f* led to its rapid destruction, which was monitered easily by observing the disappearance of the methylene bridge protons at δ 5.9 in the PMR spectra. Application of an ion-exchange technique (*cf.*, II*i*) to preparation of the acetate, benzoate, and salicylate derivatives also was unsuccessful[7].

1,4-Bis(2′-chloroethyl)-1,4-diazabicyclo[2.2.1]heptane Dihydrogen Dimaleate (II*i*)—In a typical experiment, a 100-ml volume of ion-exchange resin[8] (chloride form) in a chromatography column was treated with 40 volumes of 1 *N* NaOH/volume of resin. The resulting resin (hydroxide form) was washed with water until the eluate was neutral to pH paper[9]. The resin bimaleate was prepared by elution with 600 ml of 1 *N* maleic acid. The large maleic acid excess allowed conversion to II*i* rather than to the monomaleate derivative. Excess acid was removed by a final elution with 200 ml of water.

A solution of diperchlorate II*a* (20.0 g) in 1 liter of water was passed through the resin. Elution with an additional 0.5 liter of water and lyophilization of the combined fractions afforded 18.2 g (85%) of dihydrogen dimaleate II*i*. Three recrystallizations from ethanol provided an analytical specimen melting at 118–119° (slight decomposition); IR: ν_{max} 3440, 3010, 2920, 2850, 1580, 1495, 1385, 1365, 1195, 1110, 1070, 995, 875, 865, 750, and 695 cm^{-1}; PMR: δ 4.16–4.41 (m, 8H), 4.47 (s, 8H), 5.68 (s, 2H), and 6.32 (s, 2H).

Anal.—Calc. for $C_{17}H_{24}Cl_2N_2O_8$: C, 44.85; H, 5.31; Cl, 15.57; N, 6.15; O, 28.11. Found: C, 44.95; H, 5.36; Cl, 15.56; N, 6.14; O, 27.99.

The ion-exchange technique for obtaining II*i* was applied analogously to the preparation of the dihydrogen ditartarate II*g* from 20 g of II*a*. The 1.5-liter water eluate led to 20.2 g of glassy residue on lyophilization. The product was precipitated three times with ether from ethanol–water, and a water solution was relyophilized to yield II*g* as a pale-yellow powder; PMR: δ 4.16–4.41 (m, 8H), 4.47 (s, 8H), 4.83 (s, 2H), and 5.68 (s, 2H). Because of the persistent decomposition of this salt on further attempts at purification and relatively short storage at ambient temperatures, satisfactory elemental analyses were not obtained.

REFERENCES

(1) G. R. Pettit and J. A. Settepani, *Chem. Ind. (London)*, **1964**, 1805.

(2) G. R. Pettit, D. C. Fessler, and J. A. Settepani, *J. Org. Chem.*, **34**, 2978 (1969).

(3) D. C. Fessler, G. R. Pettit, and J. A. Settepani, *J. Med. Chem.*, **12**, 542 (1969).

(4) D. J. Abraham, R. D. Rosenstein, and G. R. Pettit, *ibid.*, **14**, 1141 (1971).

(5) G. R. Pettit, and G. C. Cragg, "Biosynthetic Products for Cancer Chemotherapy," vol. 2, Plenum, New York, N.Y., 1978.

(6) R. I. Geran, N. H. Greenbert, M. M. Macdonald, A. M. Schumacher, and B. J. Abbott, *Cancer Chemother. Rep. (part 3)*, **3**, 2 (1972).

[6] Aldrich Chemical Co.

[7] Experiments were performed by Mr. Scott D. Sucher.

[8] Mallinckrodt Amberlite IRA-400.

[9] Hydrion.

(7) J. C. Schumacher, "Perchlorates," Reinhold, New York, N.Y., 1960, pp. 65, 171–179.
(8) B. Blank, N. W. Di Tullio, A. J. Krog, and H. L. Saunders, *J. Med. Chem.*, **21**, 489 (1978).
(9) H. Böhme and H. Orth, *Arch. Pharm.*, **300**, 148 (1967).
(10) I. M. Sharman, *Endeavour*, **1**, 97 (1977).
(11) B. V. Siegel and J. I. Morton, *Experientia*, **33**, 393 (1977).
(12) E. P. Yufera, J. Sanchez, and J. Alberola, *Rev. Agroquim. Tecnol. Aliment.*, **5**, 121 (1965); through *Chem. Abstr.*, **63**, 12235e (1965).
(13) O. Colagrande, *Ann. Microbiol. Enzimol.*, **9**, 62 (1959); through *Chem. Abstr.*, **54**, 18681a (1960).
(14) F. G. Mann, *J. Chem. Soc.*, **1934**, 461.
(15) K. Ward, *J. Am Chem. Soc.*, **57**, 914 (1935).
(16) G. R. Pettit, J. A. Settepani, and R. A. Hill, *Can. J. Chem.*, **43**, 1792 (1965).

ACKNOWLEDGMENTS

Supported by Public Health Service Research Grant CA-16049-02-05 from the National Cancer Institute, the Fannie E. Ripple Foundation, Mrs. Mary Dell Pritzlaff, the Olin (Spencer T. and Ann W.) Foundation, Mr. Robert B. Dalton, the Phoenix Coca Cola Bottling Co., and the ARCS Foundation Phoenix Chapter.

The authors thank Dr. M. I. Suffness and Miss B. J. Abbott for undertaking these biological studies. Appreciation also is extended to Dr. J. D. Douros, Dr. R. Engle, Dr. K. Paull, and Dr. H. B. Wood for encouragement and assistance.

For Part LXIII of this series, see J. Polonsky, Z. Varon, C. Marazano, B. Arnoux, G. R. Pettit, J. M. Schmidt, and M. Ochi, *Experientia*, in press.

Tablet Position and Basket Type Effects in Spin-Filter Dissolution Device

STEPHEN A. HOWARD ˣ, JOHN W. MAUGER, AURWAN KHWANGSOPHA, and DEBORAH A. PASQUERELLI

Received December 18, 1978, from the *School of Pharmacy, West Virginia University, Morgantown, WV 26506.* Accepted for publication June 26, 1979.

Abstract □ The effects of stirring and basket placement on tablet dissolution using the previously developed Shah spin-filter device were investigated. Visualization of flow and dissolution patterns was possible by testing nondisintegrating colored tablets. Dissolution experiments were conducted on nondisintegrating double-layered tablets containing salicylic acid as the dissolving layer and ethylcellulose as an inert nondissolving layer. Visual observations revealed that color was drawn more rapidly from the tablet face resting on the bottom of the basket. Dissolution data from multilayered tablets revealed that when the salicylic acid face was resting on the bottom of the basket, the dissolution was appreciably more rapid than when it was facing up in the basket. This phenomenon was found for several stirring speeds.

Keyphrases □ Dissolution devices—spin filter, effects of tablet position and basket type, comparison to USP basket method □ Dissolution testing systems—spin filter compared to USP basket method, effects of tablet position and basket type □ Dosage forms—tablets, dissolution testing, spin filter compared to USP basket method, effects of tablet position and basket type

The dissolution profile of oral solid dosage forms is useful for controlling formulation and process variables that influence the bioavailability of the active ingredient.

An apparatus receiving acceptance by the scientific community is the spin-filter dissolution device developed by Shah *et al.* (1, 2). This apparatus provides a dynamic *in situ* microporous nonclogging rotating filter, which permits continuous and efficient filtration of the dissolution fluid. Furthermore, its relatively large filter area extends over most of the dissolution fluid, which permits representative sampling of the bulk dissolution medium. The smooth cylindrical surface of the rotating filter assembly without impeller blades and its agitation over a long vertical axis provide uniform, mild, laminar, nonturbulent, and reproducible stirring even at relatively high speeds.

In addition to a change in the stirring method from the USP apparatus (3), the basket mesh size was changed from the 40 mesh used in the USP basket to 12 mesh (1, 2). This change was made to prevent clogging of the basket pores by disintegrating tablets.

BACKGROUND

A study was undertaken to examine the spin-filter dissolution device hydrodynamically. Acceptance will probably increase since the spin filter was announced as acceptable for industrial dissolution testing by the Food and Drug Administration (4).

Several studies have been undertaken to examine dissolution devices hydrodynamically and to compare the spin-filter device to other dissolution devices (5–11). Skelly (12) and Grostic (13) highlighted the need for dissolution device standardization and suggested the use of nondisintegrating salicylic acid tablets as a calibrator to overcome device-to-device and laboratory-to-laboratory variations.

A carefully controlled study of the diffusion and hydrodynamic variables in the spin device seemed necessary. Nondisintegrating tablets were used so that hydrodynamic flow patterns rather than basket clogging or particle buildup would be the chief measurement parameter. Dye studies were initiated to measure visibly the large-scale flow patterns that would affect the dissolution of disintegrating as well as of nondisintegrating tablets. Nondisintegrating salicylic acid tablets were used (5) in this study, although special double-layered tablets were valuable for measuring position face as a variable. Direct correlation with nondisintegrating tablets may not be warranted, but such a study would provide valuable information in quantitating hydrodynamic effects and would apply directly to nondisintegrating dosage forms such as sustained-release products.

EXPERIMENTAL

All reported dissolution data were obtained using a device[1] reported by Shah *et al.* (1, 2) with the sample basket removed. The basic features

[1] Rotating filter dissolution device, courtesy of The Upjohn Co., Kalamazoo, Mich.

0022-3549/79/1200-1542$01.00/0
© 1979, American Pharmaceutical Association

(7) J. C. Schumacher, "Perchlorates," Reinhold, New York, N.Y., 1960, pp. 65, 171–179.
(8) B. Blank, N. W. Di Tullio, A. J. Krog, and H. L. Saunders, *J. Med. Chem.*, **21**, 489 (1978).
(9) H. Böhme and H. Orth, *Arch. Pharm.*, **300**, 148 (1967).
(10) I. M. Sharman, *Endeavour*, **1**, 97 (1977).
(11) B. V. Siegel and J. I. Morton, *Experientia*, **33**, 393 (1977).
(12) E. P. Yufera, J. Sanchez, and J. Alberola, *Rev. Agroquim. Tecnol. Aliment.*, **5**, 121 (1965); through *Chem. Abstr.*, **63**, 12235e (1965).
(13) O. Colagrande, *Ann. Microbiol. Enzimol.*, **9**, 62 (1959); through *Chem. Abstr.*, **54**, 18681a (1960).
(14) F. G. Mann, *J. Chem. Soc.*, **1934**, 461.
(15) K. Ward, *J. Am Chem. Soc.*, **57**, 914 (1935).
(16) G. R. Pettit, J. A. Settepani, and R. A. Hill, *Can. J. Chem.*, **43**, 1792 (1965).

ACKNOWLEDGMENTS

Supported by Public Health Service Research Grant CA-16049-02-05 from the National Cancer Institute, the Fannie E. Ripple Foundation, Mrs. Mary Dell Pritzlaff, the Olin (Spencer T. and Ann W.) Foundation, Mr. Robert B. Dalton, the Phoenix Coca Cola Bottling Co., and the ARCS Foundation Phoenix Chapter.

The authors thank Dr. M. I. Suffness and Miss B. J. Abbott for undertaking these biological studies. Appreciation also is extended to Dr. J. D. Douros, Dr. R. Engle, Dr. K. Paull, and Dr. H. B. Wood for encouragement and assistance.

For Part LXIII of this series, see J. Polonsky, Z. Varon, C. Marazano, B. Arnoux, G. R. Pettit, J. M. Schmidt, and M. Ochi, *Experientia*, in press.

Tablet Position and Basket Type Effects in Spin-Filter Dissolution Device

STEPHEN A. HOWARD ˣ, JOHN W. MAUGER, AURWAN KHWANGSOPHA, and DEBORAH A. PASQUERELLI

Received December 18, 1978, from the *School of Pharmacy, West Virginia University, Morgantown, WV 26506.* Accepted for publication June 26, 1979.

Abstract □ The effects of stirring and basket placement on tablet dissolution using the previously developed Shah spin-filter device were investigated. Visualization of flow and dissolution patterns was possible by testing nondisintegrating colored tablets. Dissolution experiments were conducted on nondisintegrating double-layered tablets containing salicylic acid as the dissolving layer and ethylcellulose as an inert nondissolving layer. Visual observations revealed that color was drawn more rapidly from the tablet face resting on the bottom of the basket. Dissolution data from multilayered tablets revealed that when the salicylic acid face was resting on the bottom of the basket, the dissolution was appreciably more rapid than when it was facing up in the basket. This phenomenon was found for several stirring speeds.

Keyphrases □ Dissolution devices—spin filter, effects of tablet position and basket type, comparison to USP basket method □ Dissolution testing systems—spin filter compared to USP basket method, effects of tablet position and basket type □ Dosage forms—tablets, dissolution testing, spin filter compared to USP basket method, effects of tablet position and basket type

The dissolution profile of oral solid dosage forms is useful for controlling formulation and process variables that influence the bioavailability of the active ingredient.

An apparatus receiving acceptance by the scientific community is the spin-filter dissolution device developed by Shah *et al.* (1, 2). This apparatus provides a dynamic *in situ* microporous nonclogging rotating filter, which permits continuous and efficient filtration of the dissolution fluid. Furthermore, its relatively large filter area extends over most of the dissolution fluid, which permits representative sampling of the bulk dissolution medium. The smooth cylindrical surface of the rotating filter assembly without impeller blades and its agitation over a long vertical axis provide uniform, mild, laminar, nonturbulent, and reproducible stirring even at relatively high speeds.

In addition to a change in the stirring method from the USP apparatus (3), the basket mesh size was changed from the 40 mesh used in the USP basket to 12 mesh (1, 2). This change was made to prevent clogging of the basket pores by disintegrating tablets.

BACKGROUND

A study was undertaken to examine the spin-filter dissolution device hydrodynamically. Acceptance will probably increase since the spin filter was announced as acceptable for industrial dissolution testing by the Food and Drug Administration (4).

Several studies have been undertaken to examine dissolution devices hydrodynamically and to compare the spin-filter device to other dissolution devices (5–11). Skelly (12) and Grostic (13) highlighted the need for dissolution device standardization and suggested the use of nondisintegrating salicylic acid tablets as a calibrator to overcome device-to-device and laboratory-to-laboratory variations.

A carefully controlled study of the diffusion and hydrodynamic variables in the spin device seemed necessary. Nondisintegrating tablets were used so that hydrodynamic flow patterns rather than basket clogging or particle buildup would be the chief measurement parameter. Dye studies were initiated to measure visibly the large-scale flow patterns that would affect the dissolution of disintegrating as well as of nondisintegrating tablets. Nondisintegrating salicylic acid tablets were used (5) in this study, although special double-layered tablets were valuable for measuring position face as a variable. Direct correlation with nondisintegrating tablets may not be warranted, but such a study would provide valuable information in quantitating hydrodynamic effects and would apply directly to nondisintegrating dosage forms such as sustained-release products.

EXPERIMENTAL

All reported dissolution data were obtained using a device[1] reported by Shah *et al.* (1, 2) with the sample basket removed. The basic features

[1] Rotating filter dissolution device, courtesy of The Upjohn Co., Kalamazoo, Mich.

0022-3549/79/1200-1542$01.00/0
© 1979, American Pharmaceutical Association

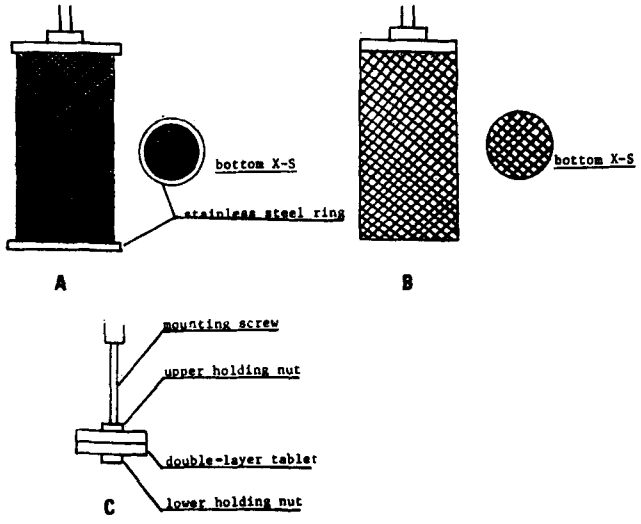

Figure 1—*Schematic diagram of the basket types and the suspended tablets used. Key: A, USP basket (40-mesh screen); B, Shah basket (12-mesh screen); and C, no basket, tablet suspended on the nut and bolt (used in System I).*

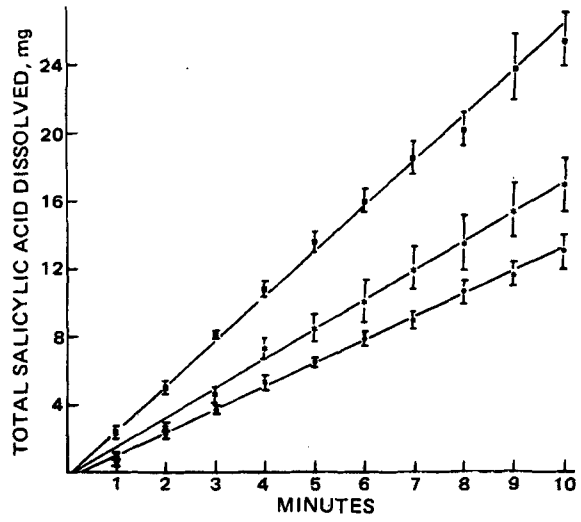

Figure 2—*Salicylic acid dissolution profiles demonstrating the effect of salicylic acid layer position on dissolution from the Shah basket at 300 rpm. Key (salicylic acid layer position): ●, faced up; *, faced down; and □, up–down.*

of this apparatus were a large volume fluid container, a rotating filter assembly, and an external, variable-speed magnetic stirrer. The rotating filter assembly provided a variable, mild, laminar liquid agitation and also functioned as an *in situ* nonclogging filter to permit efficient intermittent or continuous filtration of the dissolution fluid samples. A single dissolution cell with the temperature held at 37° was used for all studies.

The dissolution medium was an aqueous solution buffered at pH 7.2 with phosphate buffer USP (5). The assay was conducted spectrophotometrically at 296 nm using a flowcell with a sample flow rate of 100 ml/min. The tablet radius was 0.624 cm, and the average tablet thickness was 0.194 cm. Double-layered tablets of 0.624-cm radius consisted of 150 mg of salicylic acid and 150 mg of ethylcellulose. The ethylcellulose was compressed at 317 kg of pressure for 15 sec with a hydraulic press[2]. Salicylic acid powder was poured on the top of the compressed ethylcellulose in the die[3], and the two ingredients were compressed at 2268 kg for 15 sec. Single-layer, 300-mg salicylic acid tablets of 0.624-cm radius were compressed at 2268 kg for 15 sec. Nondisintegrating colored tablets made from polyethylene glycol 4000 USP and FD&C Red No. 3 were employed to demonstrate stirring effects and flow patterns for single-layer tablets in the dissolution medium.

Stirring speeds of 300 and 500 rpm were employed. The tablet was placed in the device using a 12-mesh basket (Shah basket), a 40-mesh screen basket (USP basket), or no basket (Fig. 1). When no basket was used, a nut and bolt assembly held the tablet in place (Fig. 1C); a hole was drilled in the tablet center, and a nut and bolt were used to connect the tablet to the holder assembly. All experiments were conducted in the same dissolution flask, thereby eliminating cell-to-cell variation.

Three tablet face positions were utilized. The "faced down" position utilized a double-layered tablet with the salicylic acid face resting on the bottom of the basket or on the bottom of the nut and bolt holder with no basket (Fig. 1). The "faced up" position utilized a double-layered tablet with the inert ethylcellulose layer resting on the bottom of the basket or on the nut and bolt holder (Fig. 1). In the "up–down" position, a single-layered pure salicylic acid tablet was utilized; thus, both tablet faces were active salicylic acid.

RESULTS AND DISCUSSION

An analytical methodology was developed to determine if the basket type, stirring speed, or tablet position in the basket would affect the dissolution rate of a nondisintegrating tablet. The systematic investigation of the tablet position effect on dissolution was begun with flow pattern visualization. Red polyethylene glycol tablets demonstrated that the color was drawn faster from the bottom than from the top of a tablet placed in the Shah basket. As a result of this demonstration and to show the quantitative effect of flow patterns on tablet dissolution in a basket, double-layered salicylic acid tablets were designed.

The salicylic acid dissolution profiles (Fig. 2) demonstrate the effect of the salicylic acid layer position on the salicylic acid dissolution rate from the Shah basket at 300 rpm. The y-axis in this plot is the total salicylic acid dissolved in milligrams, and the x-axis is the time in seconds. Each point is the average of three experiments, and the associated standard deviation is indicated by the vertical line. The slopes and intercepts are for least-squares lines for 10 min of data. In all three cases, the dissolution data were linear and highly reproducible, with correlation coefficients of ≥ 0.99. The dissolution profile for the up–down position was the most rapid, with the least-squares slope of 2.61. The dissolution rate for a double-layered salicylic acid tablet for the faced down position was much more rapid than for the faced up position.

To examine the differences among these three positions, an experiment with a 500-rpm stirring speed was performed. When compared with Fig. 2, Fig. 3 demonstrates that the dissolution profiles were affected more at 500 rpm than at 300 rpm. Again, the dissolution for the faced down

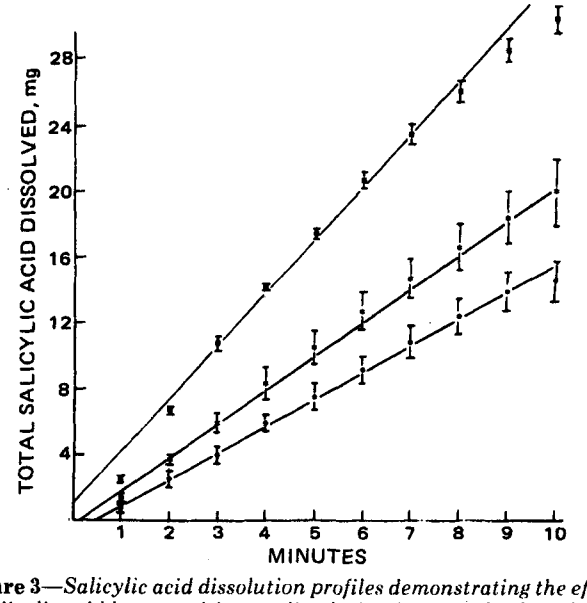

Figure 3—*Salicylic acid dissolution profiles demonstrating the effect of salicylic acid layer position on dissolution from the Shah basket at 500 rpm. Key (salicylic acid layer position): ●, faced up; *, faced down; and □, up–down.*

[2] Carver laboratory press model K, Fred S. Carver Inc., Summit, N.J.
[3] Beckman ACTA die model D-01, Beckman MIIC Ltd., Fife, Scotland.

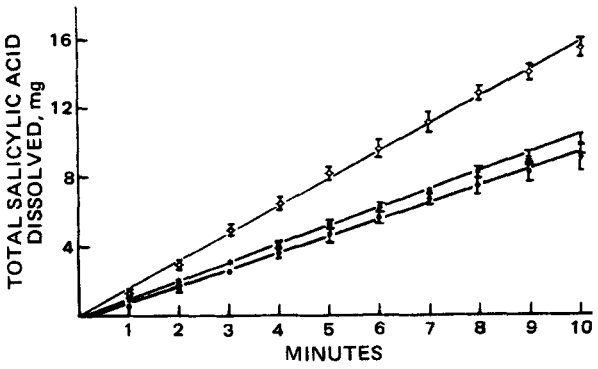

Figure 4—*Salicylic acid dissolution profiles demonstrating the effect of salicylic acid layer position on dissolution from the USP basket at 300 rpm. Key (salicylic acid layer position): ●, faced up; *, faced down; and O, up-down.*

position was much more rapid than for the faced up position. The dissolution profile for the up-down position was the most rapid, with a least-squares slope of 3.11, and was approximately equal to the summation of the faced up and faced down data. Therefore, the screening may interfere with the flow patterns around the salicylic acid layer tablet in the faced up position, increasing the effective diffusion layer. In contrast, the faced down tablet has a relatively higher dissolution rate because the salicylic acid layer in this position is in juxtaposition with the flow stream, which decreases the effective diffusion layer.

Since the USP dissolution basket is the most well known and commonly used, its effect on the dissolution rate was of interest. The dissolution medium flow pattern was visualized. The red color was being drawn again more from the bottom than from the top of the tablets but less dramatically than with the Shah basket.

The dissolution profile for the up-down position with the least-squares slope of 1.56 was the most rapid (Fig. 4). Even though the dissolution rate for the faced down position was slightly more rapid than the rate for the faced up position, the apparent difference between dissolution profiles was much less than for the Shah basket. The two dissolution profiles (Fig. 4) were close together, with least-squares slopes of 1.02 for the faced down and 0.95 for the faced up positions. The dissolution data for both positions at 500 rpm (Fig. 5) show that any apparent difference between the two positions was negligible. As expected, the dissolution profile for the up-down position was the most rapid.

One possible explanation for this phenomenon is that the USP basket has a stainless steel ring on the bottom, which is not present in the Shah basket. This ring should account for an increase in the stagnant layer at the bottom of the USP basket and for the decrease of salicylic acid dissolution in the faced down position.

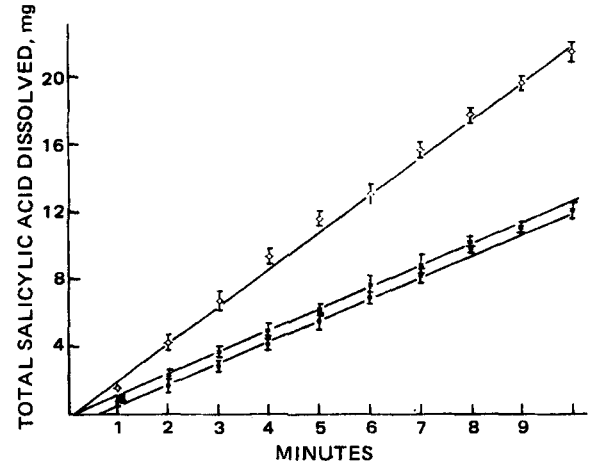

Figure 5—*Salicylic acid dissolution profiles demonstrating the effect of salicylic acid layer position on dissolution from the USP basket at 500 rpm. Key (salicylic acid layer position): ●, faced up; *, faced down; and O, up-down.*

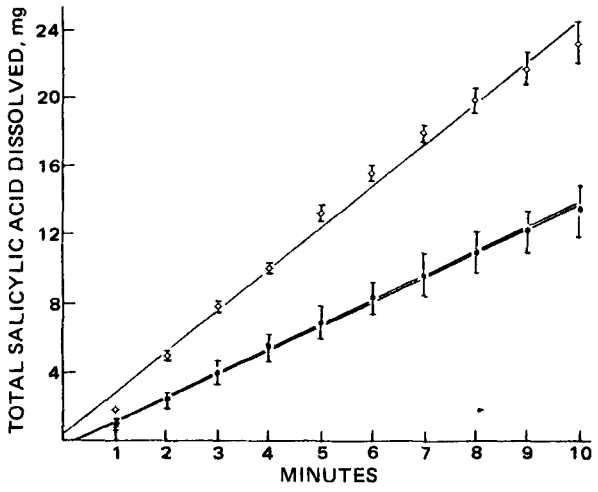

Figure 6—*Salicylic acid dissolution profiles demonstrating the effect of salicylic acid layer position on dissolution from the "no basket" system at 300 rpm. Key (salicylic acid layer position): ●, faced up; *, faced down; and O, up-down.*

All of the Shah basket dissolution rates were noticeably higher than the USP basket rates. Hence, the ratio of the Shah basket rates to those of the USP basket minus 1 was computed to show more clearly the differences in percentage.

According to the faced down comparison, the Shah basket was 76.5% faster at 300 rpm and 67.5% faster at 500 rpm than the USP basket. The faced up comparison shows that the Shah basket was 42.1% faster at 300 rpm and 27.5% faster at 500 rpm than the USP basket. With the faced down position, the dissolution data were affected more drastically by basket type. As mentioned, one possible explanation is that the stainless steel ring at the bottom of the USP basket yielded the significant dissolution rate decrease.

With the faced up position, this difference decreased 27.5% at 500 rpm. One possible explanation is that even though the wider screen size in the Shah basket seemed to yield more rapid dissolution than did the USP basket screen, at the faster stirring speed the flow stream is more capable of penetrating the USP basket screen than at lower speeds such as 300 rpm. The net result is a higher stirring speed effect with the USP basket.

The up-down data comparison shows differences of 67.3% at 300 rpm and 41.4% at 500 rpm. The resulting ratios were intermediate between the two other data sets. Although the slopes of the lines do not perfectly represent the rate, especially for the up-down dissolution data, they do excellently represent the effects of the baskets on the dissolution rate.

The stirring speed effect on the dissolution rate was determined by computing the ratio of the slopes at 500 to 300 rpm minus 1. The Shah basket dissolution data yielded percentages of 23.7% in the faced up position, 17.2% in the faced down position, and 19.1% in the up-down

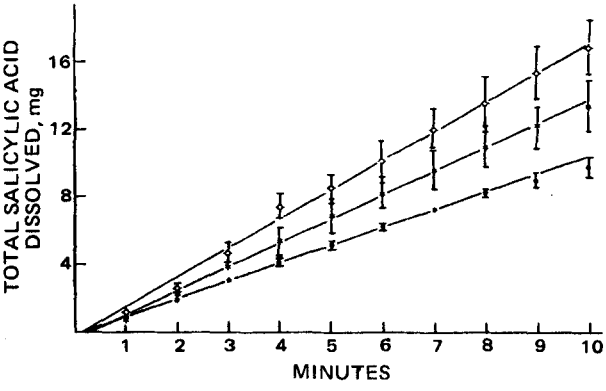

Figure 7—*Salicylic acid dissolution profiles demonstrating the effect of basket type on the dissolution of salicylic acid in the faced down position at 300 rpm. Key: O, Shah basket; ●, USP basket; and *, no basket.*

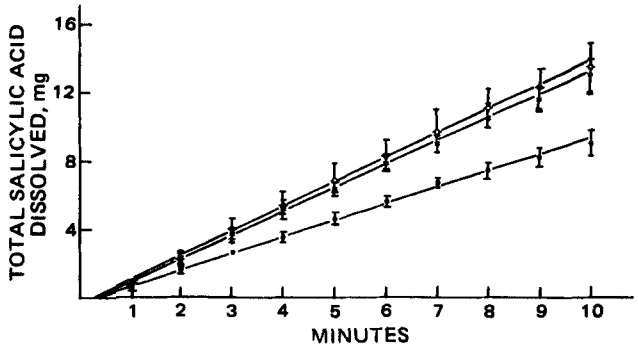

Figure 8—*Salicylic acid dissolution profiles demonstrating the effect of basket type on the dissolution of salicylic acid in the faced up position at 300 rpm. Key: *, Shah basket; ●, USP basket; and ○, no basket.*

position. With the USP basket, the dissolution rates yielded 37.9, 23.5, and 41.0%, respectively. These data suggest that the double-layered salicylic acid tablet was more affected by the stirring speed when placed in the USP basket than when placed in the Shah basket.

These experiments show that the basket screen, the stainless steel ring at the bottom of the USP basket, and the basket itself affected the dissolution rate of double-layered salicylic acid tablets. Therefore, to test the premise that the screen or the ring at the basket bottom in the direction of the flow stream caused the effect, the "no basket" condition was tested (Fig. 6).

The faced down and the faced up positions yielded almost identical dissolution profiles, with least-squares slopes of 1.42 and 1.43, respectively. When the tablet was suspended, there was no obstruction of the flow pattern, so the dissolution data for both positions were almost identical. The least-squares slope for the up–down position was 2.42 and was approximately equal to the summation of the two individual slopes.

The effects of position on dissolution rate were compared (Fig. 7). At 300 rpm, the faced down dissolution profile was faster for the Shah basket than for the no basket condition. The no basket dissolution was less rapid than expected. A possible explanation would be that the nut and bolt, present to suspend the tablet, took up ~10% of the total surface area and might have blocked the flow stream. As anticipated, the USP basket dissolution data were the slowest.

Figure 8 shows the faced up dissolution data at 300 rpm. The no basket dissolution rate was more rapid than the Shah basket dissolution rate. The no basket dissolution rate would have been expected to be much faster if the suspended tablet did not lose ~10% of the total surface area due to the nut and bolt. This figure seems to indicate that, in the faced up position, the mesh screen in the Shah basket interferes with the flow pattern, resulting in an increased stagnant layer and a decreased dissolution rate. The USP basket, with the finer mesh screen, had the slowest dissolution rate.

To demonstrate the effect of position on the dissolution rate, the ratio of slopes of the faced down to the faced up minus 1 were calculated. The percentage values were 33.3% at 300 rpm and 26.3% at 500 rpm for the Shah basket condition and 7.4% at 300 rpm and −3.8% at 500 rpm for the USP basket. The data indicate no significant position effect on dissolution from the USP basket. The effect was more drastic in the Shah basket. As expected for the no basket condition, position was not the important factor in determining tablet dissolution.

In summary, the dissolution data showed definite tablet position dependency effects when double-layered salicylic acid tablets were tested with a 12-mesh basket. This finding is potentially important in dissolution testing for tablets in general and for multilayered tablets in particular. Data from dissolution experiments with the finer 40-mesh USP basket compared with data with no basket present indicate that both screen size and basket design must be considered. Specifically, the support bar on the bottom of the USP basket appears to influence the measured dissolution rates.

The data support the idea that mechanical factors such as screen size and basket design play an important role in dissolution testing, especially with nondisintegrating tablets. Disintegrating tablets may yield different dependencies. Hydrodynamic characterization is important to tablet testing, to the establishment and understanding of procedures for optimum use of the device, and to the correct interpretation of test results.

REFERENCES

(1) A. C. Shah, C. B. Peot, and J. F. Ochs, *J. Pharm. Sci.*, **62**, 671 (1973).

(2) A. C. Shah and J. F. Ochs, *ibid.*, **63**, 110 (1974).

(3) "The United States Pharmacopeia," 18th rev., Mack Publishing Co., Easton, Pa., 1970, p. 934.

(4) B. E. Cabana and V. K. Prasad, presented at the APhA Academy of Pharmaceutical Sciences, Orlando, Fla., meeting, 1976.

(5) L. T. Grady, Academy Committee on Dissolution Methodology, "Collaborative Study By the Academy of Pharmaceutical Sciences," Academy of Pharmaceutical Sciences, The United States Pharmacopeia, Rockville, Md., 1976.

(6) M. Pernarowski, in "Dissolution Technology," L. Leeson and J. T. Carstensen, Eds., Industrial Pharmaceutical Technology Section, APhA Academy of Pharmaceutical Sciences, Washington, D.C., 1974, p. 102.

(7) R. J. Withey and A. J. Bowker, *J. Pharm. Pharmacol.*, **24**, 345 (1971).

(8) R. J. Withey, *ibid.*, **23**, 573 (1971).

(9) F. L. Underwood and D. E. Cadwallader, *J. Pharm. Sci.*, **65**, 697 (1976).

(10) J. D. Strum, J. C. Colaizzi, T. J. Goehl, J. M. Jaffe, W. H. Pitlick, V. P. Shah, and R. I. Poust, *ibid.*, **67**, 1399 (1978).

(11) J. T. Carstensen, T. Y. F. Lai, and U. K. Prasad, *ibid.*, **67**, 1303 (1978).

(12) J. P. Skelly, presented at the APhA Academy of Pharmaceutical Sciences, Montreal meeting, 1978.

(13) M. F. Grostic, *ibid.*

Rapid Compartment- and Model-Independent Estimation of Times Required to Attain Various Fractions of Steady-State Plasma Level during Multiple Dosing of Drugs Obeying Superposition Principle and Having Various Absorption or Infusion Kinetics

WIN L. CHIOU

Received March 6, 1979, from the *Clinical Pharmacokinetics Laboratory and Department of Pharmacy, College of Pharmacy, University of Illinois at the Medical Center, Chicago, IL 60612.* Accepted for publication June 22, 1979.

Abstract □ A new general equation based only on plasma data was derived for rapid estimation of the average plasma level and the mean fraction of the steady-state plasma level attained during any multiple-dosing interval. It can be applied to any complex absorption or infusion kinetics (*i.e.*, is not limited to zero-order or first-order kinetics) for drugs obeying linear disposition kinetic or superposition principles. The time, t, required to reach a certain mean fraction of the steady-state plasma level is equal to the time at which the plasma area from time zero to time t is equal to the same fraction of the plasma area from time zero to infinity ($AUC_{0\to\infty}$) following a single dose. No other pharmacokinetic parameters are necessary.

Keyphrases □ Plasma drug levels—rapid estimation of times required to attain various fractions of steady-state level, pharmacokinetics □ Drug absorption—estimation of times required to attain various fractions of steady-state level, pharmacokinetics □ Models, pharmacokinetic—times required to attain various fractions of steady-state plasma drug level

Accumulation profiles (times required to reach various mean fractions of the steady-state plasma level after multiple dosing) are important in drug therapy and animal and human toxicity studies. Most reported equations for predicting the accumulation profiles based on linear pharmacokinetics appear to be limited to classical one-compartment or two-compartment models with multiple (parallel) first-order absorption or with multiple intravenous bolus injection or short-time infusion (1–7). They usually require information such as the apparent volumes of distribution, the first-order intercompartmental distribution rate constants, the first-order elimination rate constant from the central compartment, the absorption rate constant, and the terminal first-order elimination rate constant. Equations will certainly become more complicated if more than a two-compartment open model is involved or if the absorption process cannot be described simply by zero-order or first-order equations.

The purpose of this article is to describe a novel compartment- and model-independent method for rapidly estimating the average plasma level and the times to obtain various mean fractions of the steady-state plasma level during multiple dosing. This method is based on the superposition principle (2, 3, 5, 8). It can be applied to any absorption or infusion kinetics, no matter how complex.

THEORETICAL

Following a single dose, the total area under the plasma level–time curve during each successive interval separated hypothetically by one dosing interval, T, is represented by $AUC_{0\to T}$, $AUC_{T\to 2T}$, $AUC_{2T\to 3T}$, . . . , $AUC_{(n-1)T\to nT}$. The cumulative area from time zero to time nT after a single dose is represented by $AUC_{0\to nT}$. The plasma area data after a single dose can be estimated by either the integration method or the linear or logarithmic trapezoidal rule methods (9, 10). The total areas under the plasma level–time curve during the first, second, third, . . . , nth dosing intervals after multiple dosing are denoted by AUC_{1T}, AUC_{2T}, AUC_{3T}, . . . , AUC_{nT}, respectively.

Based on the superposition principle, the total area during each interval after multiple dosing can be calculated by (2, 3, 5, 8):

$$AUC_{1T} = AUC_{0\to T} \quad \text{(Eq. 1)}$$

$$AUC_{2T} = AUC_{0\to T} + AUC_{T\to 2T} = AUC_{0\to 2T} \quad \text{(Eq. 2)}$$

$$AUC_{3T} = AUC_{0\to T} + AUC_{T\to 2T} + AUC_{2T\to 3T} = AUC_{0\to 3T} \quad \text{(Eq. 3)}$$

$$AUC_{nT} = AUC_{0\to T} + AUC_{T\to 2T} + \ldots + AUC_{(n-1)T\to nT} = AUC_{0\to nT} \quad \text{(Eq. 4)}$$

When n is large or approaching infinity, $AUC_{0\to nT}$ approaches $AUC_{0\to\infty}$, the total AUC from time zero to infinity obtained after a single (maintenance) dose. Therefore, the average steady-state plasma level, $\overline{C}_{pss}$, can be calculated by (2, 3, 5, 8):

$$\overline{C}_{pss} = \frac{AUC_{0\to\infty}}{T} \quad \text{(Eq. 5)}$$

and the average plasma level during the nth dosing interval of the multiple dosing should be equal to:

Table I—Hypothetical Plasma Level Data after a Single Oral Dose to a Subject

t, hr	Plasma Level, mg/liter	$AUC_{t1\to t2}$, hr mg/liter	$AUC_{0\to t}$, hr mg/liter	f^a
0	0	—	—	
0.5	0	0	0	0
1.0	2	0.5	0.5	0.0006
2.0	6	4.0	4.5	0.0054
3.0	10	8.0	12.5	0.0150
5.0	10	20.0	32.5	0.0390
10.0	9	47.5	80.0	0.0961
24.0	9	126.0	206.0	0.2475
48.0	8	204.0	410.0	0.4926
72.0	7	180.0	590.0	0.7088
96.0	3.5	121.2	711.2[b]	0.8544
120.0	1.75	60.6	771.8[b]	0.9272
144.0	0.875	30.3	802.1[b]	0.9636
∞		30.3	832.4[c]	1.0000

[a] $f = AUC_{0\to t}/AUC_{\infty}$. [b] Area estimated by the logarithmic trapezoidal rule method (11). [c] Area estimated by the extrapolation method using a half-life of 24 hr.

0022-3549/79/1200-1546$01.00/0
© 1979, American Pharmaceutical Association

$$\bar{C}_{pnT} = \frac{AUC_{0\to nT}}{T} \quad \text{(Eq. 6)}$$

Therefore, the mean fraction of the steady-state plasma level, f, achieved during the nth dosing interval should be equal to:

$$f = \frac{AUC_{0\to nT}}{AUC_{0\to\infty}} \quad \text{(Eq. 7)}$$

DISCUSSION

Equation 7 indicates that if a time of nT is needed to obtain an f fraction of $AUC_{0\to\infty}$ after a single dose, it also would take that long to obtain the same mean fraction of $\bar{C}_{pss}$ during the nth interval after multiple dosing. Equation 7 also indicates that the time to reach a certain mean fraction of $\bar{C}_{pss}$ is independent of the dosing interval. The terminal biological half-life of a drug *per se* does not affect the time required to reach a certain f value.

The major advantages of this new approach are simplicity, generality, and the elimination of many pharmacokinetic parameters commonly calculated after oral and intravenous administrations. The only information needed is the compartment- and model-independent plasma area data obtained after a single-dose study.

A hypothetical example illustrates the application of this new method. The hypothetical plasma level data after administration of a single oral dose to a subject and the data analyses based on Eq. 7 are summarized in Table I. The plasma level profile is very difficult, if not impossible, to describe by an equation. When the same dose is given every 12 hr, the average plasma levels between 60 and 72 hr and between 108 and 120 hr will be 70.88 and 92.72% of the steady-state plasma level, respectively (Table I). The steady-state plasma level should be equal to 69.37 mg/liter (*i.e.*, 832.4/12). On the other hand, the average plasma levels between 48 and 72 hr and between 96 and 120 hr will still be 70.88 and 92.72% of the steady-state plasma level, respectively, if the dose is given every 24 hr. The steady-state plasma level, however, will be reduced to only 50% of 69.37 mg/liter. This new method can also be applied when there is a lag time in absorption, as shown in the example.

For drugs obeying nonlinear pharmacokinetics, such as phenytoin, a new factor, the apparent volume of distribution, can also affect the times required to reach various fractions of the steady-state plasma level after multiple dosing (11).

REFERENCES

(1) G. A. Portmann, in "Current Concepts in the Pharmaceutical Sciences: Biopharmaceutics," Lea & Febiger, Philadelphia, Pa., 1970, chap. 1.

(2) M. Gibaldi and D. Perrier, "Pharmacokinetics," Dekker, New York, N.Y., 1975.

(3) J. G. Wagner, "Fundamentals of Clinical Pharmacokinetics," Drug Intelligence Publications, Hamilton Press, Hamilton, Ill., 1976.

(4) R. E. Notari, "Biopharmaceutics and Pharmacokinetics, An Introduction," 2nd ed., Dekker, New York, N.Y., 1976.

(5) W. A. Ritschel, "Handbook of Basic Pharmacokinetics," Drug Intelligence Publications, Hamilton Press, Hamilton, Ill., 1977, pp. 320–327.

(6) "Handbook of Experimental Pharmacology, Volume 47: Kinetics of Drug Action," J. M. van Rossum, Ed., Springer-Verlag, New York, N.Y., 1977.

(7) S. H. Curry, "Drug Disposition and Pharmacokinetics with a Consideration of Pharmacological and Clinical Relationship," 2nd ed., Blackwell Scientific Publications, Oxford, England, 1977, pp. 92, 148.

(8) J. S. Orr and J. Shimmins, *Lancet*, **2**, 771 (1969).

(9) W. L. Chiou, *J. Pharm. Pharmacol.*, **24**, 342 (1972).

(10) W. L. Chiou, *J. Pharmacokinet. Biopharm.*, **6**, 539 (1978).

(11) G. Lam and W. L. Chiou, *ibid.*, **7**, 227 (1979).

Determination of Ethylene Oxide, Ethylene Chlorohydrin, and Ethylene Glycol Residues in Ophthalmic Solutions at Proposed Concentration Limits

GERALD J. MANIUS

Received December 26, 1978, from the *Quality Control Department, Hoffmann-La Roche, Inc., Nutley, NJ 07110.* Accepted for publication May 24, 1979.

Abstract □ A GLC method was developed for the determination of ethylene oxide and its two reaction products, ethylene chlorohydrin and ethylene glycol, in ophthalmic solutions at the levels recently proposed by the Food and Drug Administration. The method requires no extractions, sample preparations, or elaborate trapping and concentrating techniques. All three components can be chromatographed on the same spiral glass column packed with a porous polymer adsorbent.

Keyphrases □ Ethylene oxide—analysis, GLC, ophthalmic solutions □ Ethylene chlorohydrin—analysis, GLC, ophthalmic solutions □ Ethylene glycol—analysis, GLC, ophthalmic solutions □ GLC—analysis, ethylene oxide, ethylene chlorohydrin, ethylene glycol, ophthalmic solutions

The Food and Drug Administration (FDA) recently published (1) proposed rules governing maximum residue limits for ethylene oxide (I) and its two reaction products, ethylene chlorohydrin (II) and ethylene glycol (III), in drugs and medical devices. These rules apply to ophthalmic solutions, for which maximum residue levels of 10, 20, and 60 ppm have been established for I, II, and III, respectively. These levels, proposed in conformance with current good manufacturing practices for finished pharmaceuticals, have been necessitated by the known toxicity and/or the mutagen potential of these compounds. Thus, while I is a highly effective sterilant, significant residues of it can be harmful. Its two reaction products, II, produced from ethylene oxide and free chloride ion, and III, an ethylene oxide hydrolysis product, also are harmful in significant amounts.

Ophthalmic solutions that are not treated with I but that contact treated package cap liners must be assayed for residue content according to the proposed specifications. This paper describes a successful attempt to satisfy this objective.

BACKGROUND

Extensive GLC work has been done on ethylene oxide (I) singly and in combination with its reaction products in various items including foods, fabrics, pharmaceuticals, medical and surgical devices, and plastics

0022-3549/79/1200-1547$01.00/0

© 1979, American Pharmaceutical Association

$$\bar{C}_{pnT} = \frac{AUC_{0\to nT}}{T} \quad \text{(Eq. 6)}$$

Therefore, the mean fraction of the steady-state plasma level, f, achieved during the nth dosing interval should be equal to:

$$f = \frac{AUC_{0\to nT}}{AUC_{0\to\infty}} \quad \text{(Eq. 7)}$$

DISCUSSION

Equation 7 indicates that if a time of nT is needed to obtain an f fraction of $AUC_{0\to\infty}$ after a single dose, it also would take that long to obtain the same mean fraction of $\bar{C}_{pss}$ during the nth interval after multiple dosing. Equation 7 also indicates that the time to reach a certain mean fraction of $\bar{C}_{pss}$ is independent of the dosing interval. The terminal biological half-life of a drug *per se* does not affect the time required to reach a certain f value.

The major advantages of this new approach are simplicity, generality, and the elimination of many pharmacokinetic parameters commonly calculated after oral and intravenous administrations. The only information needed is the compartment- and model-independent plasma area data obtained after a single-dose study.

A hypothetical example illustrates the application of this new method. The hypothetical plasma level data after administration of a single oral dose to a subject and the data analyses based on Eq. 7 are summarized in Table I. The plasma level profile is very difficult, if not impossible, to describe by an equation. When the same dose is given every 12 hr, the average plasma levels between 60 and 72 hr and between 108 and 120 hr will be 70.88 and 92.72% of the steady-state plasma level, respectively (Table I). The steady-state plasma level should be equal to 69.37 mg/liter (*i.e.*, 832.4/12). On the other hand, the average plasma levels between 48 and 72 hr and between 96 and 120 hr will still be 70.88 and 92.72% of the steady-state plasma level, respectively, if the dose is given every 24 hr. The steady-state plasma level, however, will be reduced to only 50% of 69.37 mg/liter. This new method can also be applied when there is a lag time in absorption, as shown in the example.

For drugs obeying nonlinear pharmacokinetics, such as phenytoin, a new factor, the apparent volume of distribution, can also affect the times required to reach various fractions of the steady-state plasma level after multiple dosing (11).

REFERENCES

(1) G. A. Portmann, in "Current Concepts in the Pharmaceutical Sciences: Biopharmaceutics," Lea & Febiger, Philadelphia, Pa., 1970, chap. 1.

(2) M. Gibaldi and D. Perrier, "Pharmacokinetics," Dekker, New York, N.Y., 1975.

(3) J. G. Wagner, "Fundamentals of Clinical Pharmacokinetics," Drug Intelligence Publications, Hamilton Press, Hamilton, Ill., 1976.

(4) R. E. Notari, "Biopharmaceutics and Pharmacokinetics, An Introduction," 2nd ed., Dekker, New York, N.Y., 1976.

(5) W. A. Ritschel, "Handbook of Basic Pharmacokinetics," Drug Intelligence Publications, Hamilton Press, Hamilton, Ill., 1977, pp. 320–327.

(6) "Handbook of Experimental Pharmacology, Volume 47: Kinetics of Drug Action," J. M. van Rossum, Ed., Springer-Verlag, New York, N.Y., 1977.

(7) S. H. Curry, "Drug Disposition and Pharmacokinetics with a Consideration of Pharmacological and Clinical Relationship," 2nd ed., Blackwell Scientific Publications, Oxford, England, 1977, pp. 92, 148.

(8) J. S. Orr and J. Shimmins, *Lancet*, **2**, 771 (1969).

(9) W. L. Chiou, *J. Pharm. Pharmacol.*, **24**, 342 (1972).

(10) W. L. Chiou, *J. Pharmacokinet. Biopharm.*, **6**, 539 (1978).

(11) G. Lam and W. L. Chiou, *ibid.*, **7**, 227 (1979).

Determination of Ethylene Oxide, Ethylene Chlorohydrin, and Ethylene Glycol Residues in Ophthalmic Solutions at Proposed Concentration Limits

GERALD J. MANIUS

Received December 26, 1978, from the *Quality Control Department, Hoffmann-La Roche, Inc., Nutley, NJ 07110.* Accepted for publication May 24, 1979.

Abstract □ A GLC method was developed for the determination of ethylene oxide and its two reaction products, ethylene chlorohydrin and ethylene glycol, in ophthalmic solutions at the levels recently proposed by the Food and Drug Administration. The method requires no extractions, sample preparations, or elaborate trapping and concentrating techniques. All three components can be chromatographed on the same spiral glass column packed with a porous polymer adsorbent.

Keyphrases □ Ethylene oxide—analysis, GLC, ophthalmic solutions □ Ethylene chlorohydrin—analysis, GLC, ophthalmic solutions □ Ethylene glycol—analysis, GLC, ophthalmic solutions □ GLC—analysis, ethylene oxide, ethylene chlorohydrin, ethylene glycol, ophthalmic solutions

The Food and Drug Administration (FDA) recently published (1) proposed rules governing maximum residue limits for ethylene oxide (I) and its two reaction products, ethylene chlorohydrin (II) and ethylene glycol (III), in drugs and medical devices. These rules apply to ophthalmic solutions, for which maximum residue levels of 10, 20, and 60 ppm have been established for I, II, and III, respectively. These levels, proposed in conformance with current good manufacturing practices for finished pharmaceuticals, have been necessitated by the known toxicity and/or the mutagen potential of these compounds. Thus, while I is a highly effective sterilant, significant residues of it can be harmful. Its two reaction products, II, produced from ethylene oxide and free chloride ion, and III, an ethylene oxide hydrolysis product, also are harmful in significant amounts.

Ophthalmic solutions that are not treated with I but that contact treated package cap liners must be assayed for residue content according to the proposed specifications. This paper describes a successful attempt to satisfy this objective.

BACKGROUND

Extensive GLC work has been done on ethylene oxide (I) singly and in combination with its reaction products in various items including foods, fabrics, pharmaceuticals, medical and surgical devices, and plastics

0022-3549/79/1200-1547$01.00/0

© 1979, American Pharmaceutical Association

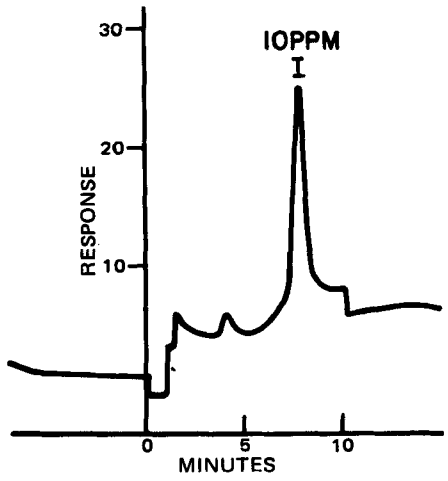

Figure 1—*Chromatogram of I reference standard at the 10-ppm level.*

(2–15). None of these studies applied to ophthalmic solutions specifically. Nearly all involved some type of extraction, recovery, and concentration such as solvent extractions (2, 6, 8), headspace sampling (4, 8, 12), co-sweep extractions (5, 6, 9), vacuum extractions and distillations, steam distillations (3, 7–11, 14), and chemical reactions (13).

Many of these techniques required a complex arrangement involving: (*a*) a heating system; (*b*) a combination of delivery systems such as solvent, gas, and vacuum; (*c*) a trapping device such as a coil or flask immersed in liquid nitrogen; and (*d*) a sample concentrator to improve the relative amounts of collected sample. A recent review article (16) discussed these procedures in detail. Needless to say, direct sample introduction is a distinct advantage, and ophthalmic solutions can be treated in this manner as if they were completely aqueous solutions, as in the investigation of Hartman and Bowman (15).

Additionally, a single chromatographic column was sought that could withstand the enormous deposits of sample components due to numerous injections without significantly changing and that could be used to analyze all three residues. Such a column was found and is suggested as a substitute for the two-column approach.

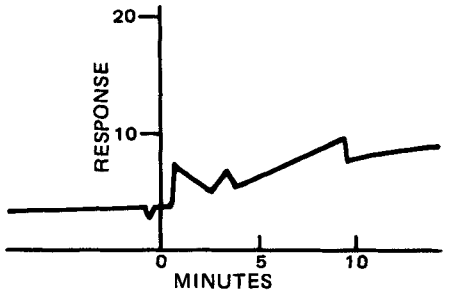

Figure 3—*Typical sample chromatogram in the analysis for I, showing none detected.*

EXPERIMENTAL

Instrument—The gas chromatograph[1] was equipped with a flame-ionization detector and a coiled glass column, 180 cm × 2 mm i.d., which was fitted for on-column injections. The column was packed with a porous polymer[2] (60–80 mesh). The column was conditioned at 200° under a nitrogen flow of 30 ml/min for 24 hr. For the analysis, this flow rate was maintained.

The column oven temperature was held isothermally at 100° for ethylene chlorohydrin (II) and ethylene glycol (III) determinations and at 50° for ethylene oxide (I) determinations. Injector temperatures were 150° for II and III and 100° for I. The detector was set at 200° and had gas flow rates of 30 ml/min for hydrogen and 300 ml/min for air. The instrument sensitivity range was 10^{-11}, and attenuation was 4× for II and III and 2× for I determinations.

Reagents—Compounds I–III, obtained from the same source[3], were used as received.

Standard Preparations—The I standard was prepared by pipetting 1 ml of cold I liquid (0–5°) into a 100-ml volumetric flask and diluting to volume with distilled water. This solution was diluted 100-fold to give

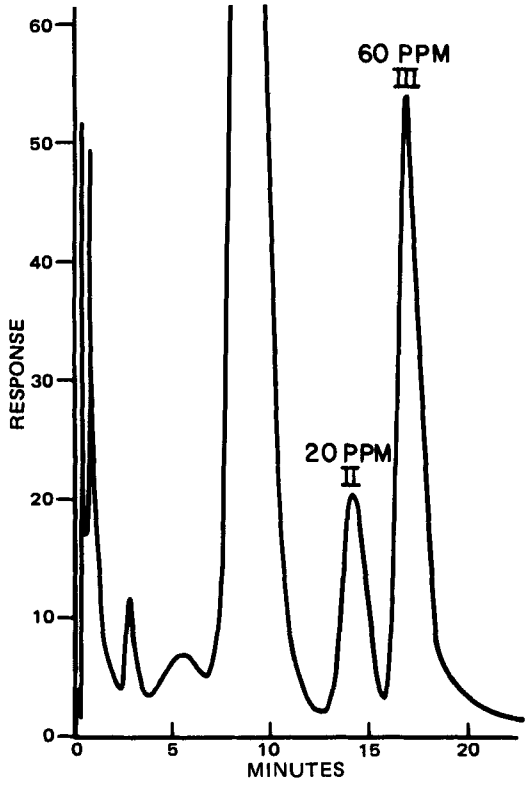

Figure 2—*Chromatogram of II and III reference standard at the 20- and 60-ppm levels, respectively.*

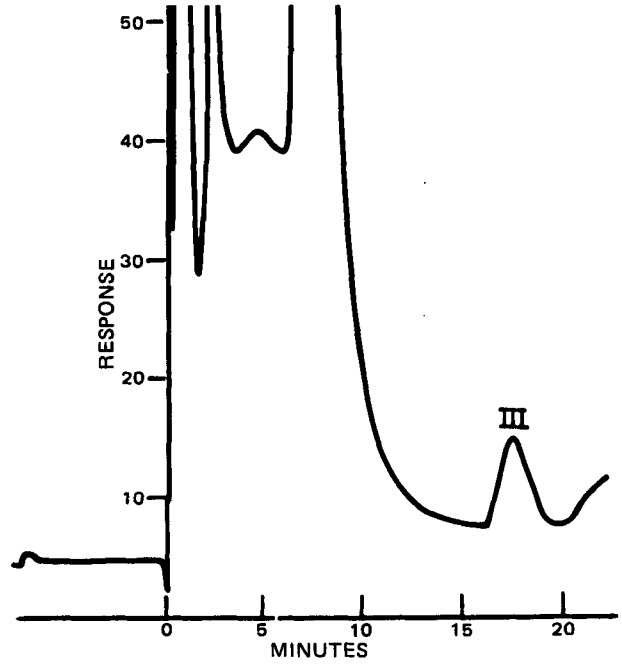

Figure 4—*Typical sample chromatogram in the analyses of II and III, showing some III.*

[1] Model 3700, Varian Instruments, Palo Alto, CA 94303.
[2] Tenax-GC, Applied Science Laboratories, State College, PA 16801.
[3] Eastman Organic Chemicals, Rochester, NY 14650.

Table I—Residue Levels in Ophthalmic Solutions

B	61	Cork and vinyl disk	0	0	26
C	59	Cork and vinyl disk	0	0	28
D	56	Cork and vinyl disk	0	2	0
E	54	Cork and vinyl disk	0	2	0
F	51	Cork and vinyl disk	0	4	23
G	18	Cork and vinyl disk	0	2	10
H	16	Cork and vinyl disk	0	2	0
I	15	Cork and vinyl disk	0	0	0
J	14	Cork and vinyl disk	0	0	0
K	11	Cork and vinyl disk	0	0	0
L	10	Polyethylene cone	0	0	0
M	8	Cork and vinyl disk	0	0	0
N	7	Cork and vinyl disk	0	0	0
O	6	Polyethylene cone	0	0	0
P	4	Polyethylene cone	0	0	0

a 100-ppm standard, which was finally diluted 10-fold to give the 10-ppm standard.

The combined II (20 ppm) and III (60 ppm) standard was prepared by transferring 20 μl of II and 60 μl of III to a 100-ml volumetric flask, diluting to volume with distilled water, and finally diluting 10-fold.

Sample Preparations—Ophthalmic solution in 15-ml bottles was hand shaken vigorously and allowed to stand in an inverted position for 10 days[4]. Prior to sampling, the bottle was reshaken. Ten-microliter aliquots were injected directly into the chromatograph.

Calculations—Quantitation was achieved by peak height measurements. Sample chromatograms were compared directly to the two standard chromatograms, showing peaks corresponding to 10, 20, and 60 ppm for I, II, and III, respectively[5].

RESULTS AND DISCUSSION

Chromatograms of the reference standards are shown in Figs. 1 and 2. Sample chromatograms are presented in Figs. 3 and 4. Elution of II was at 14 min, III eluted at 17 min, and I eluted at 7.5 min at its column temperature setting. Chromatographing all three components within the same chromatogram was impractical due to the large volatility differences between I and its two reaction products. Temperature programming resulted in extensive baseline climbing and increased ghosting distortions.

The ghosting phenomenon was the most troublesome problem encountered. Each successive injection of sample resulted in a continual buildup of peaks in both the III and I elution regions, although II remained unaffected. The first sample injection of the day barely showed these interferences, but they grew in intensity from injection to injection. The interferences became too great for meaningful interpretation of the later sample runs. By the following morning, the column (and septum) had corrected itself and sample runs could be made until the problem reoccurred.

Increasing oven temperatures for a considerable length of time to sweep away the interferences did not succeed. Fortunately, the problem was solved absolutely and completely merely by reducing injection port temperatures from an initial setting of 200 to 100° for I and to 150° for II and III. Although later eluters appeared (an additional 10-min wait is, therefore, recommended after the I region before injection of the next sample), interferences were eliminated. Other early eluting peaks (Fig. 2, excluding the desorption peak at 9 min) can be attributed to the water anomaly; although the hydrogen flame theoretically is insensitive to water, the disturbances caused by water do produce peaks (15). These extraneous peaks caused no problem in the assay.

In addition to the sample preparation described, another procedure was carried out. The cap liner, whether of vinyl with cork backing or of polyethylene, was removed, cut up, and immersed in the ophthalmic solution. The capped bottles were allowed to stand for up to 1 week, whereupon they were again sampled for residue content. No differences were observed between the chromatograms of these runs and those obtained without liner immersion (Table I).

[4] This time duration and bottle inversion were for investigational purposes only. Test results show that sampling and injection can be performed directly after shaking.

[5] Volumes were converted to weights by using the density of I at 0° and of II and III at 20°.

Table II—Recovery Data for Compound Additions to Control Ophthalmic Solution at Their Concentration Limits

I	8.9	8.5	96.0
II	23.9	23.6	98.7
III	66.8	76.4	114.4

None of the samples showed I, an indication that it readily converts to its two products. The I reference standard at the 10-ppm level did not change appreciably over a month. The most likely conversion was to III, as shown by the test data. The presence of II is mostly speculative. Some samples gave faint indications of it (miniscule blips in the II elution region), but none showed anything approaching the peak in the 20-ppm standard.

Linearity studies showed the response of the three components to be proportional to concentration within the range of 0.1–10 times the levels established as concentration limits (10, 20, and 60 ppm). Each compound could be detected at one-tenth of those levels (1, 2, and 6 ppm) at the same sensitivity settings used for the limits.

Recovery studies showed that when the three components were added at the 10-, 20-, and 60-ppm levels to a control sample of ophthalmic solution, they produced chromatograms with peak responses corresponding to those levels (Table II).

A most satisfying feature of this method has been the extraordinary longevity of the column. With between 75 and 100 sample injections already made, the column continues to function well and shows changes neither in retention time nor in sensitivity[6]. Since <2 g of packing is used per column and since no liquid phase must be coated on, the separation system described here is attractive. When one adds to that system the one-column operation and the fact that sample preparation is not necessary, it appears that this method should meet the new FDA requirements.

REFERENCES

(1) *Fed. Regist.*, **43**, No. 122, 27474 (June 23, 1978).

(2) H. D. Spitz and J. Weinberger, *J. Pharm. Sci.*, **60**, 271 (1971).

(3) J. E. Whitbourne, J. A. Mogenhan, and R. R. Ernst, *ibid.*, **58**, 1024 (1969).

(4) S. J. Romano, J. A. Renner, and P. M. Leitner, *Anal. Chem.*, **45**, 2327 (1973).

(5) J. Weinberger, *J. Pharm. Sci.*, **60**, 545 (1971).

(6) D. J. Brown, *J. Assoc. Off. Anal. Chem.*, **53**, 263 (1970).

(7) N. Adler, *J. Pharm. Sci.*, **54**, 735 (1965).

(8) S. J. Romano and J. A. Renner, *ibid.*, **64**, 1412 (1975).

(9) E. P. Ragelis, B. S. Fisher, B. A. Klimeck, and C. Johnson, *J. Assoc. Off. Anal. Chem.*, **51**, 709 (1968).

(10) J. A. Mogenhan, J. E. Whitbourne, and R. R. Ernst, *J. Pharm. Sci.*, **60**, 222 (1971).

(11) J. D. White and T. J. Bradley, *ibid.*, **62**, 1634 (1973).

(12) L. A. Zagar, *ibid.*, **61**, 1801 (1972).

(13) K. M. Brobst and H. Tai, *J. Assoc. Off. Anal. Chem.*, **54**, 1093 (1971).

(14) B. Warren, *J. Pharm. Pharmacol.*, **23**, 170S (1971).

(15) P. A. Hartman and P. B. Bowman, *J. Pharm. Sci.*, **66**, 789 (1977).

(16) P. B. Bowman and P. A. Hartman, in "GLC and HPLC Determination of Therapeutic Agents," part 2, K. Tsuji, Ed., Dekker, New York, N.Y., 1978, pp. 841–861.

ACKNOWLEDGMENTS

The author thanks Mr. R. Tscherne and Dr. S. Moros for reveiwing the manuscript.

[6] It would be beneficial, however, for the analyst to remove the inch or two of blackened residue from the inlet end of the column and to repack with fresh Tenax packing. This step might be done after a large number of samples (~50) has been run. Revitalizing the column in this manner should take a relatively short time.

Simple and Rapid High-Pressure Liquid Chromatographic Determination of Papaverine in Plasma

STEVEN L. PIERSON ˣ, JOHN J. HANIGAN, RICHARD E. TAYLOR, and JAMES E. McCLURG

Received March 1, 1979, from the *Biological Division, Harris Laboratories, Inc., Lincoln, NE 68501.* Accepted for publication June 12, 1979.

Abstract □ A rapid and sensitive high-pressure liquid chromatographic (HPLC) assay is described for the quantification of papaverine in plasma. A paired-ion, reversed-phase system was employed with detection at 254 nm. This procedure yielded reproducible results with a sensitivity of 2 ng/ml. Total extraction and quantification time was <1 hr. The suitability of this procedure for plasma sample analysis from a bioavailability study was demonstrated.

Keyphrases □ Papaverine—analysis, high-pressure liquid chromatography, human plasma, bioavailability □ Relaxants (smooth muscle)—papaverine, high-pressure liquid chromatographic analysis, human plasma, bioavailability □ High-pressure liquid chromatography—analysis, papaverine in human plasma, bioavailability

Papaverine, a smooth muscle relaxant, is used primarily as a peripheral vasodilator. *In vitro* studies implicated cyclic AMP as a mediator of the papaverine pharmacological effect (1). Its therapeutic effectiveness is limited by its rapid metabolism. The resultant necessity for frequent dosages has generated interest in the development of a dosage formulation to sustain therapeutic blood levels over longer dosage intervals (2–5).

Relatively few methods are available for the measurement of blood papaverine levels following oral administration. GLC methods require lengthy cleanup procedures and large sample volumes, which are cumbersome for the numerous samples generated by a bioequivalency study. In addition, the detection limits of these methods (generally in the 10-ng/ml range) are such that half-life determination of some formulations has been quite difficult (3, 6, 7). A recent GLC–mass spectroscopy procedure offers improved sensitivity (5 ng/ml) but requires lengthy extraction and expensive instrumentation (8).

Recently, the use of paired-ion, reversed-phase high-pressure liquid chromatography (HPLC) for quantitative drug analysis was demonstrated (9–11). This paper reports a simple, rapid, and highly sensitive HPLC method for papaverine determination in plasma.

EXPERIMENTAL

Chemicals and Reagents—1-Heptanesulfonic acid sodium[1] and papaverine hydrochloride[2] were used as received; all other chemicals and reagents were USP, NF, or ACS grade. Methanol and ether were distilled in glass prior to use.

HPLC System—A high-pressure liquid chromatograph[3] equipped with a valve injector[4], a guard column[5], a microparticulate reversed-phase HPLC column[6], a fixed-wavelength UV detector[7], and a potentiometric recorder[8] was used for separation and quantification. The system was operated at ambient temperature with a flow rate of 2.0 ml/min, and the detector was set at 254 nm.

The mobile phase consisted of 55% (v/v) methanol, 1% (v/v) acetic acid, and 0.005 *M* 1-heptanesulfonic acid sodium. Prior to use, the mobile phase was degassed by vacuum filtration through a 5-μm filter[9].

Procedure—An aliquot of plasma, 1.0 ml, in a 15-ml glass-stoppered centrifuge tube was spiked with 2 μg of chlorpheniramine maleate as the internal standard (100 μl of an aqueous solution) and vortexed. A 0.2-ml aliquot of 7 *N* NaOH and 10.0 ml of ether were added. The sample was shaken mechanically for 15 min and centrifuged to separate the phases.

The ether phase was transferred with a Pasteur pipet to another centrifuge tube and extracted with 0.2 ml of 0.3 *N* HCl by shaking and centrifuging as described previously. The ether phase was aspirated, and 100 μl of the aqueous phase was injected.

The ratio of the peak height of papaverine to that of the internal standard was used to calculate the papaverine concentration, based on a calibration curve prepared from spiked plasma samples.

Plasma Level Study—To demonstrate the applicability of this procedure to the determination of plasma papaverine levels from a bioavailability study, 150 mg of papaverine hydrochloride[10] was administered orally with 100 ml of water to two healthy male volunteers who had fasted overnight. Blood samples, 10 ml, were withdrawn from the cubital vein with heparinized evacuated tubes and centrifuged, and the plasma was transferred to screw-capped culture tubes before storage at −25°.

Table I—Standard Curve for Papaverine in Plasma [a]

Plasma Papaverine Concentration (as Free Base), ng/ml	Peak Height Ratio, Papaverine to Internal Standard	Response Factor[b]
5	0.054	10.8
10	0.119	11.9
25	0.304	12.2
50	0.591	11.8

[a] Linear regression equation: $y = 84.0813x + 0.0402$, $r = 0.9998$. [b] Peak height ratio divided by papaverine concentration in micrograms per milliliter.

Table II—Mean Coefficient of Variation Calculated from Duplicate Analyses of Samples

Number of Samples, *n*	Concentration (Range of Means), ng/ml	Mean *CV*, %
12	0–25	4.5
17	25–100	3.5
20	100–200	3.0
26	200–500	3.7
20	500–1000	1.5
12	1000–3000	3.0

RESULTS AND DISCUSSION

A UV scan of a solution of 1 μg of papaverine/ml in the mobile phase was performed to determine the optimum wavelength for detection. The absorption maximum was a broad band at ~250 nm, demonstrating the suitability of using a 254-nm fixed-wavelength UV detector.

The use of 10 ml of ether in the initial extraction, followed by back-extraction into dilute acid, yielded excellent recovery (~95–100%), which was independent of the concentration with essentially no interference

[1] Eastman Kodak, Rochester, N.Y.
[2] Marion Laboratories, Kansas City, Kans.
[3] Series 3, Perkin-Elmer, Norwalk, Conn.
[4] Model 7105, Rheodyne, Berkeley, Calif.
[5] CO:PELL ODS, Whatman, Clifton, N.J.
[6] Partisil 10-ODS, ISCO, Lincoln, Neb.
[7] Model 220, Chromatronix Inc., Berkeley, Calif.
[8] Omniscribe, Houston Instrument, Austin, Tex.
[9] FHUP 47 mm, Millipore Corp., Bedford, Mass.
[10] PAVABID Plateau CAPS, Marion Laboratories, Kansas City, Kans.

0022-3549/79/1200-1550$01.00/0
© 1979, American Pharmaceutical Association

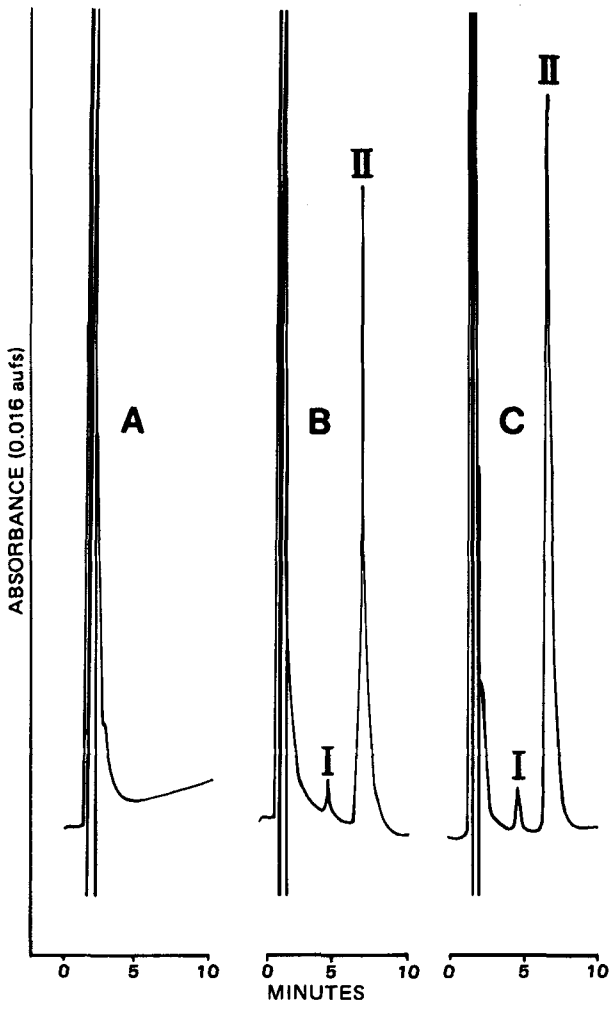

Figure 1—*Chromatogram of a human plasma blank (A), spiked plasma containing 5 ng of papaverine free base/ml and 2 μg of the internal standard/ml (B), and plasma from a dosed volunteer (1 hr) containing 6.0 ng of papaverine free base/ml and 2 μg of the internal standard/ml (C). Key: I, papaverine (free base); and II, internal standard.*

from the plasma. Good reproducibility is indicated by coefficients of variation (n = 12) of 4.0, 1.7, and 2.0% at 25, 75, and 500 ng of papaverine/ml, respectively.

Minor modifications in the extraction procedure (use of 4 μg of internal standard/ml and back-extraction into 1.5 ml of acid) were implemented in this laboratory for papaverine analysis in plasma obtained from multiple-dose bioavailability studies. These modifications facilitated the use of an autosampler[11], resulting in increased efficiency and reduced technician time.

Standard curves based on the ratio of the peak height of papaverine to that of the internal standard were linear over a wide range (2.0 ng/ml–1.0 μg/ml) and had intercepts near the origin. The data used to establish a typical standard curve for the plasma level study are summarized in Table I. The correlation coefficient of 0.9998 and the consistency of the response factors indicate the good linearity.

Daily standard curves showed a similar degree of linearity, reproducibility, and sensitivity. The average slope for seven standard curves using 2 μg of internal standard/ml was 0.01285 ± 0.00059 (mean ± *SD*), with an average correlation coefficient of 0.9997 ± 0.0003 (mean ± *SD*) and a detection limit (*i.e.*, three times baseline noise) of 2 ng/ml. Over 5 months with three different columns and various internal standard

[11] LC-420, Perkin-Elmer, Norwalk, Conn.

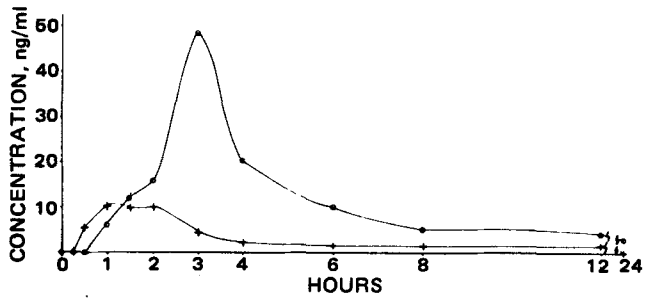

Figure 2—*Human plasma concentration of papaverine free base after administration of a single oral 150-mg dose of papaverine hydrochloride. Key: +, Subject 1; and O, Subject 2.*

concentrations, the average correlation coefficient was 0.9997 ± 0.0003 (mean ± *SD*, n = 24), demonstrating the linearity of this method over an extended period. In Table II, the mean coefficient of variation, as calculated from replicate samples from subjects in four bioavailability studies, indicates the reproducibility that may be expected from actual samples rather than from spiked plasma.

Typical chromatograms of blank human plasma, plasma spiked with papaverine and the internal standard, and plasma collected 60 min after administration of a 150-mg oral papaverine dose and spiked with internal standard are shown in Fig. 1. Papaverine and the internal standard were well resolved and eluted with retention times of 5.0 and 7.2 min, respectively.

The plasma papaverine time courses for the two subjects in the bioavailability study are shown in Fig. 2. The significant subject variability noted by others (3, 8) also was found in this study, as shown by the differences in the concentration maxima and time to peak values for the two subjects.

Current methods for papaverine analysis in plasma are time consuming and do not provide the sensitivity often required as demonstrated by the data for Subject 1 (Fig. 2). These problems were overcome with the present HPLC method, which has a detection limit of 2 ng/ml, response linearity over a wide range, and a simplified extraction procedure. Moreover, it uses only 1 ml of plasma and is adaptable to automatic sampling systems.

REFERENCES

(1) W. A. Ritschel and G. V. Hammer, *Int. J. Clin. Pharmacol.*, **15**, 227 (1977).

(2) B. Y. Lee, H. Sakamoto, F. Trainor, G. Brody, and Y. W. Cho, *ibid.*, **16**, 32 (1978).

(3) J. D. Arnold, J. Baldridge, B. Riley, and G. Brody, *ibid.*, **15**, 230 (1977).

(4) G. C. Maggi, D. Cerchiari, and G. Coppi, *Arzneim.-Forsch.*, **27**, 1211 (1977).

(5) R. B. Miller, S. T. Leslie, F. M. Black, and C. Boroda, *Br. J. Clin. Pharmacol.*, **5**, 51 (1978).

(6) D. E. Guttman, H. B. Kostenbauder, G. R. Wilkinson, and P. H. Dube, *J. Pharm. Sci.*, **63**, 1625 (1974).

(7) V. Bellia, J. Jacob, and H. T. Smith, *J. Chromatogr.*, **161**, 231 (1978).

(8) J. DeGraeve, J. Van Cantfort, and J. Gielen, *ibid.*, **133**, 153 (1977).

(9) "Paired Ion Chromatography," Bull. D61, Waters Associates, Milford, Mass., Dec. 1975.

(10) H. F. Proelss, H. J. Lohmann, and D. G. Miles, *Clin. Chem.*, **24**, 1948 (1978).

(11) J. L. Day, L. Tterlikkis, R. Niemann, A. Mobley, and C. Spikes, *J. Pharm. Sci.*, **67**, 1027 (1978).

ACKNOWLEDGMENTS

The authors thank Marion Laboratories for the gift of papaverine hydrochloride standard and Dale R. Bourg and Deanna Carter for assistance in conducting the plasma level study.

Competitive Inhibition between Folic Acid and Methotrexate for Transport Carrier in the Rat Small Intestine

VINOD S. CHUNGI, DAVID W. A. BOURNE, and LEWIS W. DITTERT *x

Received February 9, 1979, from the *College of Pharmacy, University of Kentucky, Lexington, KY 40506.* Accepted for publication June 1, 1979. *Present address: School of Pharmacy, University of Pittsburgh, Pittsburgh, PA 15261.

Abstract □ Folic acid absorption from the lumen of the rat small intestine *in situ* obeyed Michaelis–Menten kinetics. The values of V_{max} and K_m for absorption were 4.63×10^{-7} M/min and 1.21×10^{-6} M, respectively. Folic acid and methotrexate were mutual competitive inhibitors of absorption. Their K_i values were 1.28×10^{-6} and 1.9×10^{-5} M, respectively.

Keyphrases □ Folic acid—absorption, rat small intestine, competitive inhibition by methotrexate □ Methotrexate—absorption, rat small intestine, competitive inhibition by methotrexate □ Antineoplastic agents—methotrexate, absorption, rat small intestine, competitive inhibition by folic acid □ Intestinal absorption—folic acid, methotrexate, competitive inhibition, rats

Methotrexate absorption from the lumen of the rat small intestine *in situ* is a saturable process which obeys Michaelis–Menten kinetics (1). The values of V_{max} and K_m for this process were found to be 4.78×10^{-7} M/min and 1.49×10^{-5} M, respectively. Transport of methotrexate into various tumor cells and normal isolated murine intestinal cells *in vitro* has also been shown to be saturable (2–4). Furthermore, it was reported that folic acid uptake from the rat jejunum is a saturable process (5, 6). Since folic acid and methotrexate act on the same liver enzyme system (7), it was of interest to determine if they are transported by the same transport carrier in the small intestine.

The purposes of this study were to determine the Michaelis–Menten constants, V_{max} and K_m, for folic acid uptake from the rat small intestine *in situ* and to determine if folic acid and methotrexate are inhibitors of one another's transport in the rat small intestine.

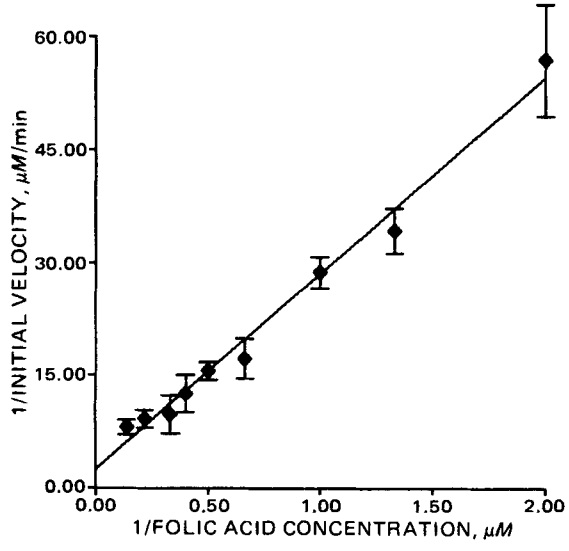

Figure 1—*Lineweaver–Burk plot (10) of absorption velocity* versus *folic acid concentration in the lumen of the rat small intestine* in situ *(mean of six animals ± SD).*

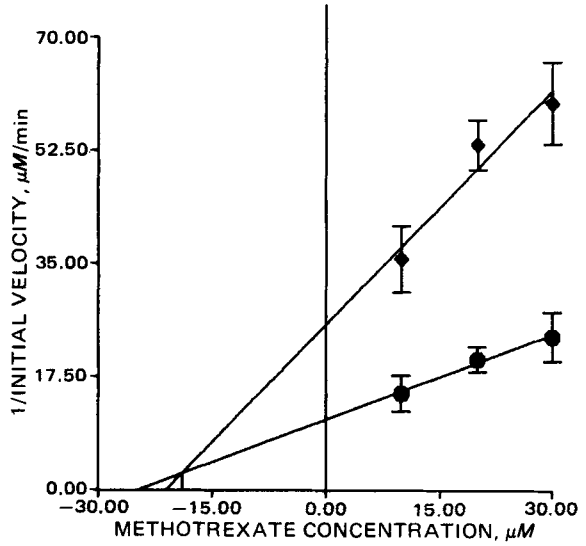

Figure 2—*Reciprocal of initial folic acid absorption velocity at 1×10^{-6} (●) and 2.5×10^{-6} (♦) M folic acid in the presence of 1×10^{-5}, 2×10^{-5}, and 3×10^{-5} M methotrexate (mean of four animals ± SD).*

EXPERIMENTAL

Male Sprague–Dawley rats[1], 200–250 g, were kept under observation for 7–10 days. Food was withdrawn 16–20 hr prior to the experiments, but water was allowed *ad libitum*. The rats were weighed and anesthetized with ketamine hydrochloride[2], 60 mg/kg im, and pentobarbital sodium[3], 21 mg/kg ip, as described previously (1).

Isolation and cannulation of the small intestine were carried out as described previously (8). The intestine was washed with normal saline. The drug solution was instilled, and 0.1-ml samples were collected every 5 min for 20 min.

Folic acid[4] and methotrexate[5] were prepared as 10^{-4} M stock solutions in 0.2% sodium bicarbonate and stored at 4° in flasks wrapped in aluminum foil. Although such solutions are stable for over 1 month (9), fresh stock solutions were prepared weekly. Stock solutions of 3′,5′,9(n)-^{3}H-methotrexate sodium salt[6] and of 2-^{14}C-folic acid potassium salt[6] in water were prepared such that 100 μl contained 0.1 μCi of radioactivity (2×10^{-11} M with respect to each drug). The radioactive stock solutions were frozen and stored in amber multidose containers under nitrogen.

Solutions for instillation into the intestine were prepared by diluting the nonradioactive stock solutions to the desired concentrations with normal saline and adding 100 μl of the respective radioactive stock solution. Thus, the radiolabeled drugs did not add significantly to the total concentrations of the solutions.

The disappearance of folic acid or methotrexate from the gut lumen was followed by removing 0.1-ml samples at 5-min intervals, diluting the

[1] Charles Rivers, Wilmington, Mass.
[2] Bristol Laboratories, Syracuse, N.Y.
[3] Abbott Laboratories, North Chicago, Ill.
[4] Sigma Chemical Co., St. Louis, Mo.
[5] Lederle Laboratories, Pearl River, N.Y.
[6] Amersham/Searle Corp., Arlington Heights, Ill.

0022-3549/79/1200-1552$01.00/0
© 1979, American Pharmaceutical Association

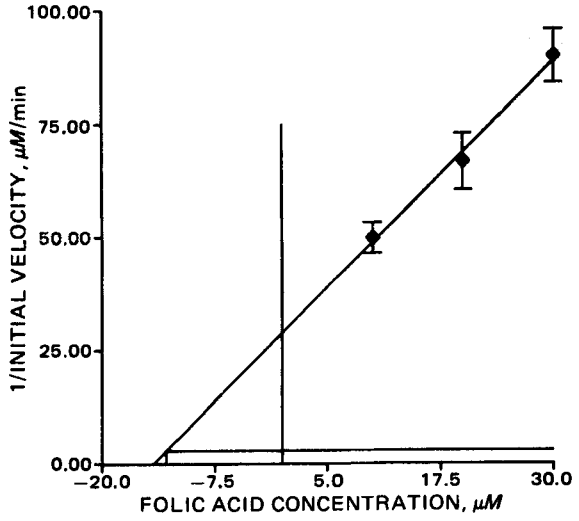

Figure 3—*Reciprocal of initial methotrexate absorption velocity at 8 × 10^{-6} M methotrexate in the presence of 1 × 10^{-5}, 2 × 10^{-5}, and 3 × 10^{-5} M folic acid (mean of four animals ± SD).*

samples in 15 ml of scintillation cocktail [2,5-diphenyloxazole[7] (4 g), 1,4-bis[2-(5-phenyloxazolyl)]benzene[7] (0.1 g), octoxynol[7] (360 g), and toluene[7] (*q.s.* to 1000 ml)], and counting on a scintillation counter[8]. Counting efficiencies were 26% for ^{3}H-methotrexate and 70% for 2-^{14}C-folic acid.

RESULTS AND DISCUSSION

A Lineweaver–Burk plot (10) of the reciprocal of the initial absorption velocity *versus* the reciprocal of the initial folic acid concentration in the lumen of the rat small intestine *in situ* is shown in Fig. 1. With the NONLIN program (11) and a digital computer[9], the data were fitted to (12):

$$V = \frac{(V_{max}C)}{(K_m + C)} \qquad \text{(Eq. 1)}$$

The values of V_{max} and K_m were 4.63 ± 0.3 × 10^{-7} M/min and 1.21 ± 0.21 × 10^{-6} M, respectively. These values were used to generate the solid line shown in Fig. 1.

The V_m values for methotrexate and folic acid (4.78 × 10^{-7} and 4.63 × 10^{-7} M/min) were quite similar; however, the K_m values obtained *in vivo* (1.49 × 10^{-5} and 1.21 × 10^{-6} M) were significantly different. This result is similar to earlier work by Sirotnak and coworkers (2–4) using isolated cell preparations, which also demonstrated differences in K_m with changes in chemical structure but relatively little change in V_m. In the present work, differences in transport rate apparently were due also to differences in the affinity of the drug for the transport carrier.

Figure 2 shows plots of the reciprocal of the initial folic acid absorption velocity at 1 × 10^{-6} and 2.5 × 10^{-6} M folic acid in the presence of 1 × 10^{-5}, 2 × 10^{-5}, and 3 × 10^{-5} M methotrexate. The plot shows typical competitive inhibition. The intersection of the least-squares lines in Fig. 2 gave a value of 1.9 × 10^{-5} M for the K_i of the methotrexate–transport carrier complex (13).

A plot of the reciprocal of the initial methotrexate absorption velocity at 8 × 10^{-6} M methotrexate in the presence of 1 × 10^{-5}, 2 × 10^{-5}, and 3 × 10^{-5} M folic acid is presented in Fig. 3. Since the competitive nature of the methotrexate inhibition of folic acid was already established, the method of Dixon (14) was used to determine the K_i for the folic acid–transport carrier complex. With the data in Fig. 3, this value was found to be 1.28 × 10^{-6} M.

These results show that methotrexate and folic acid mutually inhibit one another's absorption from the rat small intestine. If similar inhibition occurs in humans, the presence of certain foods, multivitamin preparations, and other sources of relatively large amounts of folic acid may significantly decrease the oral absorption of therapeutic methotrexate doses. Furthermore, oral methotrexate administration in frequent small doses may significantly decrease oral folic acid absorption from natural sources, resulting in an increase in the therapeutic activity and/or toxic side effects of methotrexate.

[7] Research Products International Corp., Elk Grove Village, Ill.
[8] Model 3375, Packard Instrument Co., Downers Grove, Ill.
[9] IBM 370/165.

REFERENCES

(1) V. S. Chungi, D. W. A. Bourne, and L. W. Dittert, *J. Pharm. Sci.*, **67**, 560 (1978).

(2) F. M. Sirotnak and R. C. Donsbach, *Cancer Res.*, **34**, 371 (1974).

(3) *Ibid.*, **36**, 1151 (1976).

(4) P. L. Chello, F. M. Sirotnak, D. M. Dorick, and R. C. Donsbach, *Cancer Res.*, **37**, 4297 (1977).

(5) C. H. Halstead, K. Bhanthumnarin, and E. Mezey, *J. Nutr.*, **104**, 1674 (1974).

(6) G. W. Hepner, *Br. J. Haematol.*, **16**, 241 (1969).

(7) I. H. Krakoff, in "Drill's Pharmacology in Medicine," 4th ed., J. R. DiPalma, Ed., McGraw-Hill, New York, N.Y., 1971, p. 1595.

(8) J. T. Doluisio, N. F. Billups, L. W. Dittert, E. T. Sugita, and J. V. Swintosky, *J. Pharm. Sci.*, **58**, 1196 (1969).

(9) J. M. Kinkade, W. R. Fogter, and P. G. Dayton, *Biochem. Med.*, **10**, 337 (1974).

(10) H. Lineweaver and D. Burk, *J. Am. Chem. Soc.*, **56**, 658 (1934).

(11) C. M. Metzler, G. L. Elfing, and A. J. McEwen, "A User's Manual for NONLIN and Associated Programs," Research Biostatistics, Upjohn Co., Kalamazoo, Mich., Apr. 1974.

(12) L. Michaelis and M. L. Menten, *Biochem. Z.*, **49**, 333 (1913).

(13) M. Dixon and E. C. Webb, "Enzymes," Academic, New York, N.Y., 1959, pp. 24, 25.

(14) M. Dixon, *Biochem. J.*, **55**, 170 (1953).

Effect of Dietary Lysine and Tryptophan Supplementation on Growth Rate and Toxicity of Barbiturates and Ethanol in Rats

LAWRENCE S. DUBROFF, CHARLES O. WARD *, and CHARLES I. JAROWSKI ˣ

Received August 12, 1974, from the *College of Pharmacy and Allied Health Professions, St. John's University, Jamaica, NY 11439.* Accepted for publication June 27, 1979. *Present address: Gulf Science and Technology Company, Medical and Health Resources Division, Pittsburgh, PA 15213.

Abstract □ Female Sprague–Dawley rats exhibited significantly improved growth after a 30-day feeding with lysine-supplemented rations. Supplementation with lysine and tryptophan led to improved growth in two of three experimental trials. Although increased weight gain was noted in male rats fed the supplemented rations, the results were significant in only one of three trials. The order of limiting amino acids and the supplementation level were calculated on the basis of the fasting plasma amino acid concentrations. After ethanol (6 g/kg po), animals fed either supplemented ration showed significant sleeping time reductions and significant increases in the onset of loss of the righting reflex. The ethanol LD_{50} value increased significantly only for the rats fed the ration supplemented with both amino acids. After pentobarbital (20 mg/kg po), the onset of loss of the righting reflex increased significantly in rats fed the lysine–tryptophan-supplemented ration. Effects on sleeping time and the LD_{50} were insignificant with rats fed either supplemented ration. Rats fed either supplemented ration showed significant sleeping time decreases and increases in the onset of loss of the righting reflex after hexobarbital (28 mg/kg po). No significant effect on the hexobarbital LD_{50} was observed with either supplemented ration.

Keyphrases □ Dietary supplements—effect of lysine and tryptophan on growth rate, barbiturate toxicity, ethanol toxicity, rats □ Essential amino acids—effect of dietary lysine and tryptophan supplementation on growth rate, barbiturate toxicity, ethanol toxicity □ Pentobarbital toxicity—effect of dietary lysine and tryptophan supplementation □ Hexobarbital toxicity—effect of dietary lysine and tryptophan supplementation □ Ethanol toxicity—effect of dietary lysine and tryptophan supplementation

The ability of rats to tolerate ethanol was shown to vary with the nature of their dietary protein (1). When rats were fed a diet that promoted better growth, they generally became less intoxicated as compared with rats fed a diet that was not as effective in growth promotion. Such reduced intoxication was observed after chronic administration. Among the natural protein mixtures studied (1), egg and milk proteins were more effective than those from cereal and other plant proteins. Milk protein and egg protein were equally effective in protecting the rats against ethanol toxicity. However, milk protein was considerably less effective against the inebriating effects of ethanol.

BACKGROUND

Pretreatment of mice with L-asparagine potentiated the depressant properties of ethanol and hexobarbital as measured by sleeping and immobility times (2). The LD_{50} values of intraperitoneal ethanol and hexobarbital were not affected; these values were 8.6 g/kg and 28 mg/kg, respectively.

Pretreatment of male Sprague–Dawley rats with L-tryptophan was reported to enhance the toxicities of pentobarbital, hexobarbital, and ethanol (3). The central nervous system (CNS) depressant effects of these barbiturates and ethanol also were enhanced, as shown by increased sleeping and immobility times. Ward *et al.* (4) showed that intraperitoneal or oral lysine administration 30 min prior to ethanol administration did not increase the LD_{50}. Pretreatment with intraperitoneal L-lysine significantly reduced the duration and prolonged the onset of sleeping time induced by ethanol.

Enzymatic activity in the liver was reported to decrease during fasting (5). Studies on hepatic enzyme concentrations showed a marked reduction after protein depletion. It is generally agreed that the principal ethanol oxidation site is in the liver. During fasting, the rat's ability to oxidize ethanol decreased (5). However, as soon as the weight of the animal became stationary after feeding, the rat's ability to oxidize ethanol returned to normal. The ethanol oxidation rate was proportional to the dose up to a maximum of 2.5–3 g/kg. At higher doses, the absolute rate in milligrams per kilogram of body weight per hour decreased (5).

Breglia *et al.* (6) demonstrated that there was no significant alteration of the ethanol LD_{50} with pretreatment or with simultaneous administration of selected amino acids. On the other hand, pretreatment with L-lysine, L-arginine, L-ornithine, or glycine counteracted the CNS effects of ethanol. Thus, sleeping time was reduced significantly, the onset of ataxia was prolonged, and the number of animals losing their righting reflex decreased. Ward *et al.* (4) prevented ethanol sleep induction by pretreatment with selected amino acids. These investigators used 30% ethanol, whereas Breglia *et al.* (6), employed 37.8% ethanol. Ethanol toxicity increased in relation to both concentration and dose in one study (7).

Hexobarbital metabolism increased in animals fed a high protein diet and decreased in those fed a low protein diet (8). These effects were much greater in male animals. Stimulation of microsomal enzymes was concluded to be much greater in rats fed a high protein diet. Hexobarbital, which is metabolized primarily in the liver, was reported to exert a greater depressant effect in fasting animals due to a decrease in hepatic microsomal oxidase activity (9).

Rats fed a rancid, biotin-deficient diet were more resistant to pentobarbital toxicity. This diet increased liver weight. Thus, a larger liver appeared to explain the ability of such animals to metabolize pentobarbital more effectively. When doses were calculated on the basis of liver weight, there was no increased resistance to pentobarbital (10).

Since supplemented rations were to be used, various procedures were considered for determining which of the essential amino acids in a ration was limiting. In addition, the calculation of the supplementation level was considered. Several procedures have been proposed for predicting the limiting amino acid; the chemical score method was used for a ration (11–13). The validity of this method rests on two important assumptions: (*a*) the estimated amino acid requirements are reasonably accurate, and (*b*) the amino acids in the ration are fully available.

Two methods, the plasma amino acid (PAA) score and the plasma amino acid ratio, were proposed for predicting the limiting amino acid in rations (14). In these procedures, the fasting plasma amino acid concentrations are compared with the plasma amino acid levels taken 6 hr after a test diet is fed. The modified plasma amino acid ratio (15) and the plasma amino acid score (16) can be calculated by:

$$\text{modified PAA} = \frac{\text{mean PAA level of test group} - \text{mean fasting PAA level}}{\text{animal's amino acid requirement}} \quad \text{(Eq. 1)}$$

$$\text{PAA score} = \frac{\text{mean PAA level of test group}}{\text{mean fasting PAA level}} \times 100 \quad \text{(Eq. 2)}$$

The fasting plasma profile equivalent (FPPE) concept was used to determine the limiting essential amino acid (17). The supplementation level can be calculated by Eq. 3 (the reported amino acid requirement of the animal is not needed for the calculation):

$$\text{FPPE} = \frac{\text{millimoles of amino acid/100 g of diet}}{\text{millimoles per liter in animal's fasting plasma}} \quad \text{(Eq. 3)}$$

Thus, for example, 100 g of ration[1] contains 10.8 mmoles of lysine. There is 0.389 mmole of lysine/liter in the fasting plasma of Sprague–Dawley

0022-3549/79/1200-1554$01.00/0
© 1979, American Pharmaceutical Association

Table I—Weight Increase of Sprague–Dawley Rats after 30 Days with a Control Ration in Comparison with a Lysine- and a Lysine–Tryptophan-Supplemented Ration

Ration	Average Starting Weight, g	Average Finishing Weight, g	Average Weight Gained ± *SD*, g	Weight Gained ± *SD*, %	Control *versus* Supplemented Rations (*p* Value)
			Males		
Experiment 1					
Control	86.1	204.9	118.8 ± 30.7	138 ± 36	—
Control + lysine	92.3	248.0	155.7 ± 28.1	169 ± 30	0.05
Control + lysine + tryptophan	80.4	220.0	139.6 ± 28.4	174 ± 35	<0.05
Experiment 2					
Control	94.7	227.9	133.2 ± 27.5	141 ± 29	—
Control + lysine	85.6	212.3	126.7 ± 31.6	148 ± 37	NS[a]
Control + lysine + tryptophan	93.5	231.5	138.0 ± 26.4	148 ± 28	NS
Experiment 3					
Control	131.6	221.5	89.9 ± 19.2	68 ± 15	—
Control + lysine	135.0	234.4	99.4 ± 18.4	74 ± 14	NS
Control + lysine + tryptophan	148.3	227.3	79.0 ± 17.1	53 ± 12	—
			Females		
Experiment 4					
Control	88.3	177.4	89.1 ± 19.3	101 ± 22	—
Control + lysine	80.9	184.3	103.4 ± 19.5	128 ± 24	<0.02
Control + lysine + tryptophan	86.9	180.5	93.6 ± 18.5	108 ± 21	NS
Experiment 5					
Control	114.2	196.1	81.9 ± 18.2	72 ± 16	—
Control + lysine	87.1	179.9	92.8 ± 19.2	107 ± 22	<0.001
Control + lysine + tryptophan	100.3	200.0	99.7 ± 17.1	99 ± 17	<0.01
Experiment 6					
Control	127.7	190.4	62.7 ± 17.7	50 ± 14	—
Control + lysine	125.7	218.5	92.8 ± 19.6	74 ± 16	<0.01
Control + lysine + tryptophan	120.5	206.1	85.6 ± 19.6	71 ± 16	<0.01

[a] Not significant; $p > 0.05$ (Student t test).

rats. Consequently, in the ration used, the fasting plasma profile equivalent of lysine is 27 (10.8/0.389). Since this value is the smallest fasting plasma profile equivalent value for the essential amino acids, lysine is considered to be limiting. The value for tryptophan is 29, and it is the next limiting amino acid.

The objective of this investigation was to determine the effect of lysine- and lysine–tryptophan-supplemented diets on the growth rate and on ethanol and barbiturate toxicity in Sprague–Dawley rats.

EXPERIMENTAL

Three groups of 10 Sprague–Dawley rats were fed three diets concurrently. The first group received the control ration[1]. The second group received the control ration supplemented with L-lysine monohydrochloride[2] (0.142 g added to 100 g of ration). This supplementation level made lysine and tryptophan equally limiting. The third group received the control ration supplemented with L-lysine monohydrochloride (0.995 g) and L-tryptophan[2] (0.132 g). In the latter supplemented ration, lysine, tryptophan, and threonine (the third limiting amino acid) were equally limiting.

The rats were fed for 30 days. Each day, a fresh 20-g portion of ration was placed in the feeding container. Water was provided *ad libitum*.

The diets were prepared as follows. The ration (1362 g) and povidone 400[3] (13.62 g) were placed in a mixer. A solution prepared by dissolving 1.93 g of L-lysine monohydrochloride in 1 liter of distilled water was distributed uniformly throughout the ration by paddle agitation. Ethanol (700 ml) was added to guard against mold growth during the drying step. The wet mass was passed through a No. 1 sieve. The granules were tray dried in an air-circulating oven at room temperature. In the preparation of the lysine–tryptophan-supplemented diet, 13.55 g of L-lysine monohydrochloride and 1.8 g of L-tryptophan were added to 1362 g of ration. The control diet was treated similarly in that distilled water and ethanol were added. The use of povidone 400 in the three rations favored the formation of homogeneous blends.

The effect on the growth rate was determined after 30 days by comparing the weight increase of the two test groups with that of the control group.

At the end of the 30-day feeding trial, the rats weighed between 175 and 200 g. These rats were used to determine the effect of the diet on the LD_{50}, loss of the righting reflex, and sleeping time after oral administration of ethanol, hexobarbital[4], and pentobarbital[4].

The LD_{50} values were determined by the Litchfield and Wilcoxon (18) method. The rats were fasted for 24 hr before being used in the LD_{50} determinations.

Sleeping time was defined as the total time elapsed from the initial loss of the righting reflex to its return without remission. Loss of the righting reflex was defined as the inability of the animal to right itself immediately when placed on its back.

The three concurrent feeding trials (control and two supplemented rations) were conducted six times. Three such studies each were carried out with male and female rats. The results represent averaged data points derived from 10 animals.

RESULTS AND DISCUSSION

The female rats showed significantly improved growth after the 30-day feeding trial with the lysine-supplemented rations (Table I). Supplementation with lysine and tryptophan led to improved growth in two of three feeding trials. Although increased weight gain was noted in male rats fed the supplemented rations, the results were significant in only one of three trials.

On the basis of the fasting plasma concentrations, lysine was calculated to be the first limiting essential amino acid in the commercial diet[1]. The second limiting amino acid in this ration was tryptophan. However, on the basis of whole egg protein, the first limiting essential amino acid in

[1] Rockland Farms mouse/rat diet.
[2] Sigma Chemical Co., St. Louis, Mo.
[3] Polyvinylpyrrolidone 400, Sigma Chemical Co., St. Louis, Mo.
[4] Merck and Co., Rahway, N.J.

Table II—Ethanol-Induced Toxicity and CNS Depression in Sprague–Dawley Rats Fed Lysine- and Lysine–Tryptophan-Supplemented Rations (Ethanol, 6 g/kg po)

Parameter	Male	Female	Combined Results	*p* Value
Control diet				
Sleeping time, min ± *SD*	273.0 ± 19.9	285.5 ± 18.5	279.2 ± 18.8	—
Loss of righting reflex, min ± *SD*	4.0 ± 1.4	4.3 ± 0.75	4.3 ± 1.1	—
LD_{50}, g/kg (range)	8.3 (7.54–9.13)	8.4 (7.6–9.2)	8.23 (7.88–8.53)	—
Control diet + lysine				
Sleeping time, min ± *SD*	230.0 ± 38.9	225.0 ± 46.9	227.5 ± 42.9	0.05
Loss of righting reflex, min ± *SD*	6.9 ± 1.9	6.0 ± 1.4	6.25 ± 1.7	0.05
LD_{50}, g/kg (range)	9.2 (8.37–10.12)	8.9 (7.9–9.3)	9.01 (8.53–9.54)	NS[a]
Control diet + lysine and tryptophan				
Sleeping time, min ± *SD*	190.0 ± 23.1	180.0 ± 20.2	185.0 ± 20.2	0.02
Loss of righting reflex, min ± *SD*	7.4 ± 2.3	7.6 ± 1.9	7.25 ± 2.1	0.03
LD_{50}, g/kg (range)	9.3 (8.68–9.85)	10.5 (8.9–12.6)	9.8 (9.3–10.09)	0.05

[a] Not significant.

Table III—Pentobarbital-Induced Toxicity and CNS Depression in Sprague–Dawley Rats Fed Lysine- and Lysine–Tryptophan-Supplemented Rations (Pentobarbital, 20 mg/kg po)

Parameter	Male	Female	Combined Results	*p* Value
Control diet				
Sleeping time, min ± *SD*	104.9 ± 6.5	106.7 ± 6.9	105.8 ± 6.7	—
Loss of righting reflex, min ± *SD*	7.4 ± 3.4	9.4 ± 6.3	8.4 ± 4.8	—
LD_{50}, mg/kg (range)	66.7 (55.9–77.8)	62.4 (51.2–74.4)	65.5 (58.0–76.1)	—
Control diet + lysine				
Sleeping time, min ± *SD*	92.8 ± 5.7	94.2 ± 5.9	93.5 ± 5.8	0.50
Loss of righting reflex, min ± *SD*	9.0 ± 3.4	10.4 ± 5.9	9.7 ± 4.7	0.50
LD_{50}, mg/kg (range)	68.8 (52.3–88.4)	65.8 (54.1–81.2)	67.8 (58.0–76.1)	0.50
Control diet + lysine and tryptophan				
Sleeping time, min ± *SD*	85.3 ± 5.0	87.3 ± 5.6	86.3 ± 5.3	0.10
Loss of righting reflex, min ± *SD*	16.9 ± 10.1	18.5 ± 11.5	17.7 ± 10.8	0.05
LD_{50}, mg/kg (range)	75.9 (68.2–82.5)	75.6 (68.2–82.5)	75.7 (68.2–82.5)	0.30

Table IV—Hexobarbital-Induced Toxicity and CNS Depression in Sprague–Dawley Rats Fed Lysine- and Lysine–Tryptophan-Supplemented Rations (Hexobarbital, 28 mg/kg po)

Parameter	Male	Female	Combined Results	*p* Value
Control diet				
Sleeping time, min ± *SD*	63.1 ± 13.7	72.0 ± 14.1	67.5 ± 13.9	—
Loss of righting reflex, min ± *SD*	16.0 ± 6.9	17.0 ± 6.9	16.5 ± 6.6	—
LD_{50}, mg/kg (range)	37.0 (32.1–42.5)	31.5 (27.4–36.3)	33.5 (29.1–39.4)	—
Control diet + lysine				
Sleeping time, min ± *SD*	43.1 ± 5.6	49.4 ± 13.9	46.7 ± 9.7	0.01
Loss of righting reflex, min ± *SD*	30.0 ± 16.8	29.1 ± 18.4	29.5 ± 17.1	0.01
LD_{50}, mg/kg (range)	37.5 (32.1–43.1)	32.0 (28.6–39.4)	34.75 (30.6–41.3)	0.50
Control diet + lysine and tryptophan				
Sleeping time, min ± *SD*	39.0 ± 5.0	40.2 ± 8.0	39.6 ± 6.5	0.005
Loss of righting reflex, min ± *SD*	32.0 ± 11.1	31.4 ± 9.3	31.7 ± 10.2	0.01
LD_{50}, mg/kg (range)	38.5 (32.1–44.9)	37.0 (31.1–42.9)	37.75 (32.3–43.3)	0.50

the commercial ration was methionine followed by tryptophan. The improved growth rates observed in rats fed the lysine-supplemented rations provide support for the fasting plasma profile concept.

A significant increase in the ethanol LD_{50} was shown by rats fed the lysine–tryptophan-supplemented ration (Table II). This reduction in toxicity can probably be attributed to an improvement in the biological value of the commercial ration by supplementation. As mentioned earlier (1), proteins that were more effective in growth promotion also were more effective in reducing ethanol toxicity and in counteracting its inebriating effects. Consequently, it was not unexpected that rats fed either supplemented ration would show significant sleeping time reductions and significant increases in time before loss of the righting reflex after ethanol administration.

Rats fed the supplemented rations showed no LD_{50} increase for pentobarbital (Table III) or for hexobarbital (Table IV). On the other hand, significant sleeping time reductions and increases in time before loss of the righting reflex were observed after hexobarbital administration in rats being fed either supplemented ration. In addition, rats fed either supplemented ration exhibited significant increases in time before loss of the righting reflex after pentobarbital administration. However, an

insignificant effect on sleeping time was observed.

Thus, strategic supplementation of a ration with essential amino acids to improve its biological value offers promise in reducing the toxicity of ethanol and selected barbiturates as well as in mitigating the CNS effects associated with such compounds.

REFERENCES

(1) C. C. Lucas, J. H. Ridout, and G. L. Lumchick, *Can. J. Physiol. Pharmacol.*, **46**, 475 (1968).

(2) R. B. Forney, F. W. Hughes, A. B. Richards, and G. W. Gates, *Toxicol. Appl. Pharmacol.*, **5**, 790 (1963).

(3) C. I. Jarowski and C. O. Ward, *ibid.*, **18**, 603 (1971).

(4) C. O. Ward, C. A. Lau-Cam, A. S. M. Tang, R. J. Breglia, and C. I. Jarowski, *ibid.*, **22**, 422 (1972).

(5) J. J. Vitalie and D. M. Hegsted, *J. Nutr.*, **53**, 533 (1954).

(6) R. J. Breglia, C. O. Ward, and C. I. Jarowski, *J. Pharm. Sci.*, **62**, 49 (1973).

(7) W. A. Hiestand, F. W. Stemler, and J. E. Wiebers, *Q. J. Stud. Alcohol*, **13**, 361 (1952).

(8) R. Kato, *Jpn. J. Pharmacol.*, **16**, 221 (1966).

(9) R. L. Dixon, R. W. Schultice, and J. P. Fonts, *Proc. Soc. Exp. Biol. Med.*, **103**, 333 (1960).

(10) B. Szepesi and R. A. Freeland, *J. Nutr.*, **94**, 463 (1968).

(11) R. J. Block and H. H. Mitchell, *Nutr. Abstr. Rev.*, **16**, 249 (1946).

(12) FAO Committee on Protein Requirements, "Protein Requirements," FAO Nutritional Studies No. 16, Food and Agriculture Organization of the United Nations, Rome, Italy, 1957, p. 1.

(13) P. B. R. Rao, H. W. Norton, and B. C. Johnson, *J. Nutr.*, **82**, 88 (1964).

(14) S. V. Rao, J. F. Noel, and M. J. Hogan, *Arch. Biochem. Biophys.*, **39**, 249 (1952).

(15) J. B. Longenecker and N. L. Hause, *ibid.*, **84**, 46 (1959).

(16) J. M. McLaughlan, *Can. J. Biochem.*, **42**, 1353 (1964).

(17) C. I. Jarowski and R. Pytelewski, *J. Pharm. Sci.*, **64**, 690 (1975).

(18) J. T. Litchfield, Jr., and F. Wilcoxon, *J. Pharmacol. Exp. Ther.*, **96**, 99 (1949).

Metabolic Effects of a New Hypolipidemic Agent, Ciprofibrate

AARON ARNOLD, JOHN P. McAULIFF, and ARTHUR L. BEYLER ˣ

Received February 2, 1979, from the *Sterling-Winthrop Research Institute, Rensselaer, NY 12144.* Accepted for publication June 6, 1979.

Abstract □ Ciprofibrate, a new orally effective hypolipidemic agent like clofibrate, suppressed tyloxapol-induced hypercholesterolemia in rats. Ciprofibrate at 10 mg/kg was effective. Clofibrate required a dosage of 180 mg/kg to suppress the tyloxapol effect. Norepinephrine-induced free fatty acid release was inhibited by clofibrate in rats in accordance with earlier findings. Ciprofibrate and lifibrate differed from clofibrate in that, at hypocholesterolemically effective doses, neither inhibited the hormone-sensitive lipase *in vivo*.

Keyphrases □ Ciprofibrate—hypolipidemic effects, effect on hormone-sensitive lipase, compared to clofibrate and lifibrate, rats □ Anticholesterolemic agents—ciprofibrate, effect on serum lipid levels, hormone-sensitive lipase, compared to clofibrate and lifibrate, rats

Evidence that hyperlipidemia is a major risk factor in coronary artery disease (1) has directed interest toward agents that can correct the lipid abnormality. One such agent is clofibrate, 2-(4-chlorophenoxy)-2-methylpropanoic acid ethyl ester, which serves as a model reference. Related agents are being sought that are more effective against hypercholesterolemia as well as against all types of hyperlipoproteinemia.

A previous report (2) presented evidence that ciprofibrate, 2-[4-(2,2-dichlorocyclopropyl)phenoxy]-2-methylpropanoic acid, is at least 100-fold as hypolipidemic in butter fat, cholesterol-fed hyperlipidemic rats as is clofibrate. In this discussion, additional comparisons between ciprofibrate and clofibrate are presented.

EXPERIMENTAL

Tyloxapol[1]-Induced Hypercholesterolemia—The tyloxapol treatment procedure followed that of Garattini *et al.* (3) and of Kariya *et al.* (4). Young adult Sprague–Dawley rats[2], averaging ~300 g each, were maintained on laboratory feed *ad libitum*. Based on preliminary trials, the test agents were given by intubation at one of the following dosages: ciprofibrate at 10 or 22.5 mg/kg/day or clofibrate at 90 or 180 mg/kg/day, each for 4 days. On the 4th day, the rats were each given tyloxapol at 200 mg/kg iv. Anticholesterolemic effects were evaluated on the basis of cholesterol levels in blood samples taken by cardiac puncture 20 hr later.

For analysis, the blood samples were centrifuged, and the serum was separated. Serum cholesterol was estimated colorimetrically according to the Liebermann–Burchard procedure, using a *p*-toluenesulfonic acid catalyst after Turner and Eales (5).

Inhibition of Hormone-Sensitive Lipase—Two studies were conducted in which the hypolipidemic agents were evaulated for their ability to inhibit the hormone-sensitive lipase. In one, clofibrate was compared with ciprofibrate. In the other, clofibrate was compared with lifibrate, bis(4-chlorophenoxy)acetic acid 1-methyl-4-piperidinyl ester (6).

Young adult Sprague–Dawley strain rats[2], averaging ~250–300 g each, were allocated into groups of nine. They were given one test agent at the following dosages: clofibrate at 150 mg/kg, ciprofibrate at 15 mg/kg, or lifibrate at 40 mg/kg. The test agents were given by intubation in a 1% aqueous gum tragacanth suspension (10 ml/kg) before *l*-norepinephrine (as the bitartrate). The vasoconstrictor effects of norepinephrine were inhibited with 100 mg of phenoxybenzamine/kg sc, 1 hr before norepinephrine was given.

Table I—Ciprofibrate and Clofibrate Effectiveness in Protecting Rats against Tyloxapol Hypercholesterolemia (Means ± *SE*)

Test Compound	Intragastric Dosage, mg/kg/day × 4	Tyloxapol[a]	*n*	Serum Cholesterol[b], mg/100 ml
None	None	−	12	75.2 ± 3.2
None	None	+	10	198.7 ± 16.3
Ciprofibrate	10	+	8	80.9 ± 7.9
	22.5		8	73.5 ± 5.7
Clofibrate	90	+	8	132.4 ± 23.7
	180		7	69.7 ± 4.4

[a] At 200 mg/kg iv on the 4th day of medication. [b] Blood taken 20 hr after tyloxapol.

[1] Triton WR-1339 or Triton A-20.
[2] Charles River.

0022-3549/79/1200-1557$01.00/0

© 1979, American Pharmaceutical Association

insignificant effect on sleeping time was observed.

Thus, strategic supplementation of a ration with essential amino acids to improve its biological value offers promise in reducing the toxicity of ethanol and selected barbiturates as well as in mitigating the CNS effects associated with such compounds.

REFERENCES

(1) C. C. Lucas, J. H. Ridout, and G. L. Lumchick, *Can. J. Physiol. Pharmacol.*, **46**, 475 (1968).

(2) R. B. Forney, F. W. Hughes, A. B. Richards, and G. W. Gates, *Toxicol. Appl. Pharmacol.*, **5**, 790 (1963).

(3) C. I. Jarowski and C. O. Ward, *ibid.*, **18**, 603 (1971).

(4) C. O. Ward, C. A. Lau-Cam, A. S. M. Tang, R. J. Breglia, and C. I. Jarowski, *ibid.*, **22**, 422 (1972).

(5) J. J. Vitalie and D. M. Hegsted, *J. Nutr.*, **53**, 533 (1954).

(6) R. J. Breglia, C. O. Ward, and C. I. Jarowski, *J. Pharm. Sci.*, **62**, 49 (1973).

(7) W. A. Hiestand, F. W. Stemler, and J. E. Wiebers, *Q. J. Stud. Alcohol*, **13**, 361 (1952).

(8) R. Kato, *Jpn. J. Pharmacol.*, **16**, 221 (1966).

(9) R. L. Dixon, R. W. Schultice, and J. P. Fonts, *Proc. Soc. Exp. Biol. Med.*, **103**, 333 (1960).

(10) B. Szepesi and R. A. Freeland, *J. Nutr.*, **94**, 463 (1968).

(11) R. J. Block and H. H. Mitchell, *Nutr. Abstr. Rev.*, **16**, 249 (1946).

(12) FAO Committee on Protein Requirements, "Protein Requirements," FAO Nutritional Studies No. 16, Food and Agriculture Organization of the United Nations, Rome, Italy, 1957, p. 1.

(13) P. B. R. Rao, H. W. Norton, and B. C. Johnson, *J. Nutr.*, **82**, 88 (1964).

(14) S. V. Rao, J. F. Noel, and M. J. Hogan, *Arch. Biochem. Biophys.*, **39**, 249 (1952).

(15) J. B. Longenecker and N. L. Hause, *ibid.*, **84**, 46 (1959).

(16) J. M. McLaughlan, *Can. J. Biochem.*, **42**, 1353 (1964).

(17) C. I. Jarowski and R. Pytelewski, *J. Pharm. Sci.*, **64**, 690 (1975).

(18) J. T. Litchfield, Jr., and F. Wilcoxon, *J. Pharmacol. Exp. Ther.*, **96**, 99 (1949).

Metabolic Effects of a New Hypolipidemic Agent, Ciprofibrate

AARON ARNOLD, JOHN P. McAULIFF, and ARTHUR L. BEYLER ˣ

Received February 2, 1979, from the *Sterling-Winthrop Research Institute, Rensselaer, NY 12144.* Accepted for publication June 6, 1979.

Abstract □ Ciprofibrate, a new orally effective hypolipidemic agent like clofibrate, suppressed tyloxapol-induced hypercholesterolemia in rats. Ciprofibrate at 10 mg/kg was effective. Clofibrate required a dosage of 180 mg/kg to suppress the tyloxapol effect. Norepinephrine-induced free fatty acid release was inhibited by clofibrate in rats in accordance with earlier findings. Ciprofibrate and lifibrate differed from clofibrate in that, at hypocholesterolemically effective doses, neither inhibited the hormone-sensitive lipase *in vivo*.

Keyphrases □ Ciprofibrate—hypolipidemic effects, effect on hormone-sensitive lipase, compared to clofibrate and lifibrate, rats □ Anticholesterolemic agents—ciprofibrate, effect on serum lipid levels, hormone-sensitive lipase, compared to clofibrate and lifibrate, rats

Evidence that hyperlipidemia is a major risk factor in coronary artery disease (1) has directed interest toward agents that can correct the lipid abnormality. One such agent is clofibrate, 2-(4-chlorophenoxy)-2-methylpropanoic acid ethyl ester, which serves as a model reference. Related agents are being sought that are more effective against hypercholesterolemia as well as against all types of hyperlipoproteinemia.

A previous report (2) presented evidence that ciprofibrate, 2-[4-(2,2-dichlorocyclopropyl)phenoxy]-2-methylpropanoic acid, is at least 100-fold as hypolipidemic in butter fat, cholesterol-fed hyperlipidemic rats as is clofibrate. In this discussion, additional comparisons between ciprofibrate and clofibrate are presented.

EXPERIMENTAL

Tyloxapol[1]-Induced Hypercholesterolemia—The tyloxapol treatment procedure followed that of Garattini *et al.* (3) and of Kariya *et al.* (4). Young adult Sprague–Dawley rats[2], averaging ~300 g each, were maintained on laboratory feed *ad libitum*. Based on preliminary trials, the test agents were given by intubation at one of the following dosages: ciprofibrate at 10 or 22.5 mg/kg/day or clofibrate at 90 or 180 mg/kg/day, each for 4 days. On the 4th day, the rats were each given tyloxapol at 200 mg/kg iv. Anticholesterolemic effects were evaluated on the basis of cholesterol levels in blood samples taken by cardiac puncture 20 hr later.

For analysis, the blood samples were centrifuged, and the serum was separated. Serum cholesterol was estimated colorimetrically according to the Liebermann–Burchard procedure, using a *p*-toluenesulfonic acid catalyst after Turner and Eales (5).

Inhibition of Hormone-Sensitive Lipase—Two studies were conducted in which the hypolipidemic agents were evaulated for their ability to inhibit the hormone-sensitive lipase. In one, clofibrate was compared with ciprofibrate. In the other, clofibrate was compared with lifibrate, bis(4-chlorophenoxy)acetic acid 1-methyl-4-piperidinyl ester (6).

Young adult Sprague–Dawley strain rats[2], averaging ~250–300 g each, were allocated into groups of nine. They were given one test agent at the following dosages: clofibrate at 150 mg/kg, ciprofibrate at 15 mg/kg, or lifibrate at 40 mg/kg. The test agents were given by intubation in a 1% aqueous gum tragacanth suspension (10 ml/kg) before *l*-norepinephrine (as the bitartrate). The vasoconstrictor effects of norepinephrine were inhibited with 100 mg of phenoxybenzamine/kg sc, 1 hr before norepinephrine was given.

Table I—Ciprofibrate and Clofibrate Effectiveness in Protecting Rats against Tyloxapol Hypercholesterolemia (Means ± *SE*)

Test Compound	Intragastric Dosage, mg/kg/day × 4	Tyloxapol[a]	*n*	Serum Cholesterol[b], mg/100 ml
None	None	−	12	75.2 ± 3.2
None	None	+	10	198.7 ± 16.3
Ciprofibrate	10	+	8	80.9 ± 7.9
	22.5		8	73.5 ± 5.7
Clofibrate	90	+	8	132.4 ± 23.7
	180		7	69.7 ± 4.4

[a] At 200 mg/kg iv on the 4th day of medication. [b] Blood taken 20 hr after tyloxapol.

[1] Triton WR-1339 or Triton A-20.
[2] Charles River.

0022-3549/79/1200-1557$01.00/0

© 1979, American Pharmaceutical Association

Table II—Comparison of Clofibrate, Ciprofibrate, and Lifibrate in Suppressing the *l*-Norepinephrine-Induced Increase in Serum Nonesterified Fatty Acids (NEFA) in the Unfasted Rat (Nine Rats per Group, Means ± *SE*)

	Trial 1						Trial 2					
	Control		Clofibrate[a]		Ciprofibrate[a]		Control		Clofibrate		Lifibrate[a]	
l-Norepinephrine Dosage, μg/kg ip	Serum NEFA, μEq/liter	Serum Cholesterol, mg/100 ml	Serum NEFA, μEq/liter	Serum Cholesterol, mg/100 ml	Serum NEFA, μEq/liter	Serum Cholesterol, mg/100 ml	Serum NEFA, μEq/liter	Serum Cholesterol, mg/100 ml	Serum NEFA, μEq/liter	Serum Cholesterol, mg/100 ml	Serum NEFA, μEq/liter	Serum Cholesterol, mg/100 ml
None	152 ± 23	70 ± 7					165 ± 31	60 ± 4				
10	185 ± 19	66 ± 5	134 ± 24	36 ± 2	180 ± 17	42 ± 2	216 ± 59	65 ± 4	215 ± 27	39 ± 2	211 ± 41	44 ± 3
30	351 ± 54	64 ± 2	164 ± 37	35 ± 1	349 ± 30	40 ± 2	332 ± 60	68 ± 3	217 ± 50	38 ± 2	324 ± 47	40 ± 2

[a] Test agent dosage: clofibrate, 150 mg/kg; ciprofibrate, 15 mg/kg; and lifibrate, 40 mg/kg; each given by intubation at 28, 20, and 2 hr before *l*-norepinephrine administration.

The rats were sedated with 55 mg of pentobarbital/kg sc 0.5 hr before norepinephrine. Norepinephrine was given at either 10 or 30 μg/kg ip 10 min before blood was taken by cardiac puncture. The blood was allowed to clot and was centrifuged, and the serum nonesterified fatty acids were estimated by the copper-soap procedure of Duncombe (7). The fatty acids were extracted with chloroform reacted with a copper–triethanolamine reagent, and color was developed with diethyldithiocarbamate for colorimetric estimation.

RESULTS

Tyloxapol-Treated Rats—In accordance with previous findings (3, 4), tyloxapol at 200 mg/kg doubled or more than doubled the normal blood cholesterol of the rats to nearly 200 mg of cholesterol/100 ml (Table I). Pretreatment with ≥10 mg of ciprofibrate/kg protected the rats from the hypercholesterolemic effects of tyloxapol. The rats also were protected from tyloxapol hypercholesterolemia by pretreatment with clofibrate at 180 mg/kg. At 90 mg/kg, clofibrate did not fully protect the rats. The clofibrate-pretreated rats had a serum cholesterol of 132.4 mg/100 ml, which was significantly above that of the normolipidemic control rats, 75.2 mg/100 ml. Accordingly, ciprofibrate may be judged to be ~18 times as effective as clofibrate in protecting rats against tyloxapol hypercholesterolemia.

Inhibition of Hormone-Sensitive Lipase—The control hormone-sensitive lipase findings (Table II) show that norepinephrine at 30 μg/kg doubled or more than doubled the serum nonesterified fatty acid level. The increases at 10 μg/kg were not significant.

In both trials, clofibrate inhibited the increase in the nonesterified fatty acid level that followed 30 μg of norepinephrine/kg. The serum nonesterified fatty acid levels of the clofibrate-pretreated rats given 10 μg of norepinephrine/kg were not significantly above control levels.

In both trials, the serum nonesterified fatty acid levels following ciprofibrate or lifibrate pretreatment were elevated to the same extent as in the control norepinephrine-treated rats. Thus, neither ciprofibrate nor lifibrate inhibited the hormone-sensitive lipase.

Serum cholesterol levels were significantly decreased by all of the hypolipidemic agents tested. The serum cholesterol levels following pretreatment with the hypolipidemic agents were all in the 35–44-mg/100 ml range, significantly less than control levels.

DISCUSSION

The hypercholesterolemic effects of tyloxapol were counteracted by pretreatment with 10 or 25 mg of ciprofibrate/kg daily or with 180 mg of clofibrate/kg daily. Pretreatment of the rats with 90 mg of clofibrate/kg daily did not protect the rats entirely from the effects of tyloxapol. This amount of clofibrate was similar to that found effective by Kariya *et al.* (4), 114 mg of clofibrate/kg (as the free acid from dietary agent at 0.25%). Thus, 10 mg of ciprofibrate/kg was approximately as protective as 180 mg of clofibrate/kg.

While ciprofibrate pretreatment was more effective in suppressing tyloxapol hypercholesterolemia than was clofibrate pretreatment, the two phenoxybutyrates were similar in that both exhibited inhibition. The protective effect noted for these agents is in accord with their ability to inhibit cholesterol biosynthesis (2, 8, 9) and with the findings that tyloxapol increases cholesterol and fatty acid synthesis in the liver (10, 11). In discussing the hyperlipidemic effects of tyloxapol, Schotz *et al.* (12) noted that tyloxapol may interfere with plasma lipoprotein catabolism.

In contrast to their similar hypocholesterolemic effects, ciprofibrate and clofibrate differed in inhibiting the hormone-sensitive lipase *in vivo*. Thorp (13) found that clofibrate (in combination with androsterone) suppressed the increase in plasma fatty acids that occurred in rats and in dogs following epinephrine administration. The findings on clofibrate are thus in accord with those of Thorp (13) in that clofibrate, at hypocholesterolemically effective doses, inhibits the norepinephrine-activated lipase.

In contrast to clofibrate, ciprofibrate and lifibrate, at hypocholesterolemically effective doses, did not inhibit the lipase. This result supports the view that ciprofibrate may be clinically similar to lifibrate rather than to clofibrate. Since lifibrate is effective in Type II hyperlipoproteinemic subjects (14), in contrast to clofibrate which is variably effective, the distinction may be therapeutically significant.

REFERENCES

(1) G. B. Kolata and J. L. Marx, *Science*, **194**, 509 (1976).

(2) A. Arnold, J. P. McAuliff, L. G. Powers, D. K. Phillips, and A. L. Beyler, *Atherosclerosis*, **32**, 155 (1979).

(3) S. Garattini, R. Paoletti, L. Bizzi, E. Grossi, and R. Vertua, in "Drugs Affecting Lipid Metabolism," S. Garattini and R. Paoletti, Eds., Elsevier, New York, N.Y., 1961, p. 144.

(4) T. Kariya, J. M. Grisar, N. L. Wiech, and T. R. Blohm, *J. Med. Chem.*, **15**, 659 (1962).

(5) T. J. Turner and L. Eales, *Scand. J. Clin. Lab. Invest.*, **9**, 210 (1957).

(6) A. R. Timms, L. A. Kelly, R. S. Ho, and J. H. Trapold, *Biochem. Pharmacol.*, **18**, 1861 (1969).

(7) W. G. Duncombe, *Clin. Chim. Acta*, **9**, 122 (1964).

(8) M. D. Best and C. H. Duncan, *J. Lab. Clin. Med.*, **64**, 634 (1964).

(9) D. R. Avoy, E. A. Swyryd, and R. G. Gould, *J. Lipid Res.*, **6**, 369 (1965).

(10) I. D. Frantz and B. T. Hinkelman, *J. Exp. Med.*, **101**, 225 (1955).

(11) S. Garattini, P. Paoletti, and R. Paoletti, *Experientia*, **15**, 33 (1959).

(12) M. C. Schotz, A. Scanu, and I. H. Page, *Am. J. Physiol.*, **188**, 399 (1957).

(13) J. M. Thorp, *J. Atheroscler. Res.*, **3**, 351 (1963).

(14) D. Berkowitz, *Circulation, Suppl. 3*, **40**, 44 (1969).

GLC Determination of *S*-2-(3-*tert*-Butylamino-2-hydroxypropoxy)-3-cyanopyridine in Human Plasma

S. VICKERS ˣ **and C. A. H. DUNCAN**

Received January 17, 1979, from the *Merck Institute for Therapeutic Research, West Point, PA 19486.* Accepted for publication June 22, 1979.

Abstract □ *S*-2-(3-*tert*-Butylamino-2-hydroxypropoxy)-3-cyanopyridine was recovered (~90%) from human plasma and detected by conversion to a diheptafluorobutyryl derivative for electron-capture GLC. A homolog served as an internal standard. The method measures plasma drug concentrations at the 5-ng/ml level and is suitable for plasma analysis from humans who receive a therapeutic oral dose.

Keyphrases □ *S*-2-(3-*tert*-Butylamino-2-hydroxypropoxy)-3-cyanopyridine—analysis, electron-capture GLC, diheptafluorobutyryl derivative, human plasma, antihypertensives □ Antihypertensives—*S*-2-(3-*tert*-butylamino-2-hydroxypropoxy)-3-cyanopyridine, analysis, electron-capture GLC, human plasma □ GLC, electron capture—*S*-2-(3-*tert*-butylamino-2-hydroxypropoxy)-3-cyanopyridine, human plasma

S-2-(3-*tert*-Butylamino-2-hydroxypropoxy)-3-cyanopyridine (I) hydrochloride is a potent antihypertensive β-adrenoceptor antagonist with peripheral vasodilating activity[1]. It lowers arterial pressure in spontaneously hypertensive rats and in hypertensive humans.

A sensitive and specific analytical method was required to measure I in human plasma. The use of electron-capture techniques to quantitate low drug levels in biological fluids was validated by many workers. A suitable derivatizing reagent sometimes must be used to impart electron-capturing properties to the assayed compound. Initial attempts at derivatization of I with either trifluoroacetic anhydride or pentafluoropropionic anhydride were unsuccessful because two products were formed.

A trifluoroacetic anhydride–trimethylamine mixture was used successfully for propranolol analysis (1); however, when applied to the analysis of I, the resultant derivative was not endowed with sufficient electron-capturing properties. Heptafluorobutyrylimidazole (III) is a reagent used in the analysis of indolealkylamines (2–4) and timolol maleate, another β-blocker (5). In the procedure reported here, I was extracted from plasma, derivatized to form the diheptafluorobutyryl analog, and determined by electron-capture GLC at concentrations as low as 5 ng/ml.

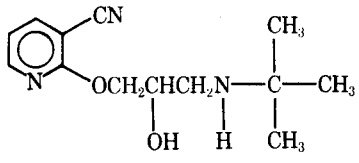

I

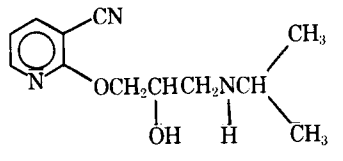

II

Table I—Reproducibility of the Electron-Capture GLC Assay for I

I, ng/ml	Peak Height Ratio ± *SD* (I/II) (*n* = 3)
100	1.08 ± 0.11
50	0.52 ± 0.01
25	0.31 ± 0.01
10	0.10 ± 0.01
5	0.055 ± 0.005

Table II—Major Ions in the Mass Spectrum of I Diheptafluorobutyryl Derivative

m/e	Ion	Fragment(s) Lost
626	M − 15⁺	CH_3
506	M − 135⁺	$C_6H_4N_2O + CH_3$
371	M − 270⁺	$C_4F_7O_2 + C_4H_9$

EXPERIMENTAL

Reagents—Hexane and toluene were nanograde quality. Ether (absolute) was ACS reagent grade. Compound III was obtained in 1-ml ampuls[2]. Compound I was used as the hydrochloride salt, and *S*-2-(3-isopropylamino-2-hydroxypropoxy)-3-cyanopyridine (II) served as the internal standard. All concentrations are expressed in terms of the free base.

Apparatus—GLC analysis was performed using a gas chromatograph[3] equipped with a ^{63}Ni-electron-capture detector (15 mCi) and a 122 × 0.64-cm (4 ft × 0.25 in.) column packed with 3% OV-1 on Gas Chrom Q[4] (60–80 mesh). The instrument was operated isothermally with the oven, detector, and injection port temperatures at 180, 300, and 250°, respectively. The carrier gas (5% methane in argon) flow rate was 78 ml/min. The pulse frequency was variable. Gas lines were fitted with filters containing molecular sieves (15 Å).

Procedure—Plasma, 1 ml, was mixed with II (50 μl of a 1-μg/ml solution of II in water) and 1 *N* NaOH (0.2 ml) and was then shaken with toluene–ether (4 ml of a 4:1 mixture) in a 13-ml glass-stoppered centrifuge tube for 10 min. After centrifugation, the organic layer was transferred as completely as possible to a 5-ml centrifuge tube containing 0.1 *N* HCl (0.3 ml). After being stoppered and shaken for 10 min, the tube contents were centrifuged, the organic layer was removed by aspiration, and the aqueous phase was mixed with 2 *N* NaOH (0.1 ml). Toluene–ether (1.5 ml of a 4:1 mixture) was added, and the tube was shaken for 10 min.

The organic phase was separated (after centrifugation), transferred to a 5-ml centrifuge tube, and evaporated under a nitrogen stream. Compound III, 25 μl, and hexane, 0.1 ml, were added to the residue. After heating at 90–100° for 1 hr, the tubes were allowed to cool, hexane (50 μl) and 0.1 *N* HCl (0.1 ml) were added, and the contents were agitated for 30 sec. The top hexane layer was analyzed by GLC on a 3% OV-1 column with electron-capture detection, using 1-μl aliquots/injection. The retention times of the derivatized internal standard and I were 4.8 and 6.8 min, respectively. GLC–mass spectrometry showed that the acylation products of these compounds are the diheptafluorobutyryl de-

[1] Dr. C. S. Sweet, Merck Institute for Therapeutic Research, West Point, Pa., unpublished results.

[2] Pierce Chemical Co.

[3] Hewlett-Packard model 5730A.

[4] Supelco.

0022-3549/79/1200-1559$01.00/0
© 1979, American Pharmaceutical Association

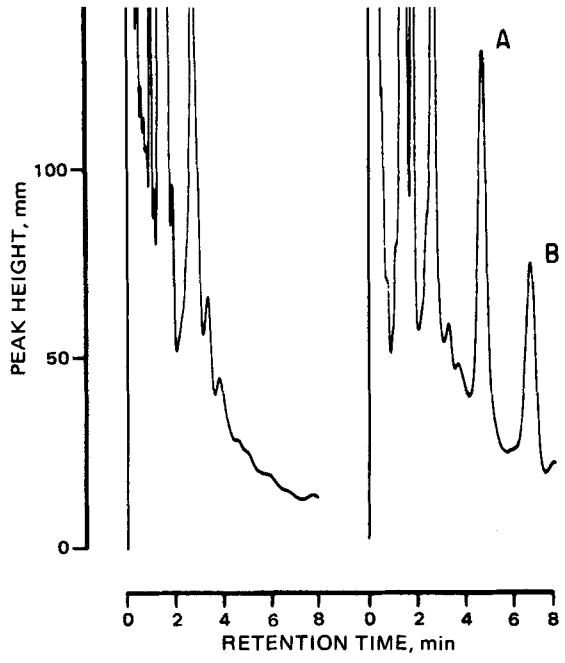

Figure 1—*Gas-liquid chromatograms (electron-capture detector) of human plasma extracts. Left: 0-hr human plasma. Right: 50 ng of II (as the diheptafluorobutyryl derivative A) and 50 ng of I (as the diheptafluorobutyryl derivative B) added to 1.0 ml of plasma.*

rivatives. A standard curve was constructed by analysis of control plasma samples containing known quantities of I and II.

Compound I in Human Plasma—Four normotensive human subjects each received a single 6-mg oral dose of ^{14}CN-I. Blood was collected in heparinized containers at intervals during the first 24 hr following the dose, and the plasma was harvested and frozen until assayed.

In a single-blind study, I was administered to five patients in a dosage range from 5 mg *sid* to 40 mg *bid* over a period ranging from several days to several weeks. On days when the daily dosage was increased, blood was drawn at 0, 1, 2, 4, 8, and 12 hr; the plasma was harvested for subsequent analysis.

RESULTS AND DISCUSSION

There was a linear relationship between the GLC peak height ratio, *i.e.*, I to II, and the plasma I concentration over a range of 5 ng to several micrograms. The method reproducibility was determined by analyzing plasma samples (1 ml) containing I, *e.g.*, 100, 50, 25, 10, and 5 ng/ml (Table I). To determine the recovery of I, the same procedure was used to extract ^{14}CN-I from human plasma. At 50 and 100 ng/ml, the radioactivity recoveries were 89.6 ± 4.1% (n = 3) and 88.4 ± 7.2% (n = 3), respectively. There was no radioactivity loss when the samples were evaporated to dryness prior to derivatization.

The reagent III was stored at −20° and subsequently was thawed and mixed with hexane for the derivatization reaction, which yielded the diheptafluorobutyryl derivative (Table II and Fig. 1). Substitution of hexane with the more polar solvent ethyl acetate did not give satisfactory results, contrary to published reports (5, 6). The derivatization had to be performed at 90–100°, although lower temperatures had been used (6) for a number of amines.

No interference was produced by plasma constituents. Occasionally, there was some day-to-day variation in the peak height ratio of I and its analog II. However, the assay of control samples at different times during a day indicated no fluctuation of this ratio over 8 hr.

Plasma I levels were measured in four humans who received an oral dose of ^{14}CN-I (see *Experimental*). Initially, I levels were similar to plasma radioactivity levels when the latter were expressed as I nanogram equivalents. A maximum I concentration (16 ± 2 ng/ml) was reached at 3 hr. At later times, there was a pronounced decrease in the plasma I levels, and the majority of the plasma radioactivity was apparently represented by ^{14}CN-I metabolites (Table III).

Table III—Mean Plasma I Levels in Four Normotensive Subjects after a Single Oral 6-mg Dose of ^{14}CN-I [a]

Hours after Dose	Plasma I ± *SD*, ng/ml: Radioactive Equivalents	Plasma I ± *SD*, ng/ml: I
0.25	<5	<5
0.5	11 ± 3 (n = 3)	7 ± 3 (n = 3)
1.0	16 ± 5 (n = 4)	12 ± 4 (n = 3)
1.5	20 ± 2 (n = 4)	10 ± 5 (n = 3)
2.0	21 ± 3 (n = 4)	15 ± 4 (n = 4)
3.0	22 ± 3 (n = 4)	16 ± 2 (n = 4)
4.0	22 ± 4 (n = 4)	8 ± 2 (n = 4)
5.0	19 ± 3 (n = 4)	7 ± 2 (n = 4)
6.0	18 ± 3 (n = 4)	7 ± 1 (n = 4)
7.0	16 ± 2 (n = 4)	6 ± 1 (n = 3)
8.0	14 ± 2 (n = 4)	6 ± 2 (n = 3)
12.0	9 ± 2 (n = 4)	<5
24.0	<5	<5

[a] Compound I had a specific activity of 8323 dpm/μg.

Table IV—Dependence of Plasma I Concentration on Dose in Five Subjects [a]

Hours	Dose, mg: 5[b]	10[b]	20	30	40
1	25 ± 11	17 ± 6	85 ± 26	131 ± 20	180 ± 72
2	12 ± 5	30 ± 8	75 ± 18	108 ± 35	169 ± 29
4	<5	19 ± 5	52 ± 18	97 ± 20	144 ± 47
8	<5	8 ± 3	23 ± 5	28 ± 24	74 ± 43
12	<5	<5	12 ± 2	24 ± 4	36 ± 19

[a] Values are mean and *SD* for five subjects. [b] n = 3.

The plasma I levels were dependent on the dose over a range of 5–40 mg (Table IV); *i.e.*, I did not display nonlinear pharmacokinetics with a therapeutic dosage regimen. This finding suggests that the I elimination routes are not easily saturated and that the drug metabolism enzymes are neither induced nor inhibited by I.

The GLC method reported here provides a sensitive assay for I in the plasma of humans following therapeutic doses. The use of an internal standard compensates for quantitation error during sample manipulation. The ^{14}C-tracer study indicated that the I metabolites present in human plasma are extremely water soluble (unlike the identified urinary metabolites of I[5]) and are not detectable under the electron-capture GLC assay conditions used. The assay is selective for I.

REFERENCES

(1) D. A. Saelens, T. Walle, and P. J. Privitera, *J. Chromatogr.*, **123**, 185 (1976).

(2) J. Vessman, A. M. Moss, M. G. Horning, and E. C. Horning, *Anal. Lett.*, **2**, 81 (1969).

(3) F. Benington, S. T. Christian, and R. D. Morin, *J. Chromatogr.*, **106**, 435 (1975).

(4) S. T. Christian, F. Benington, R. D. Morin, and L. Corbett, *Biochem. Med.*, **14**, 191 (1975).

(5) D. J. Tocco, F. A. deLuna, and A. E. W. Duncan, *J. Pharm. Sci.*, **64**, 1879 (1975).

(6) D. E. Bradway and T. Shafik, *J. Chromatogr.*, **15**, 322 (1977).

ACKNOWLEDGMENTS

The authors thank Dr. R. K. Ferguson and Dr. J. D. Arnold for the human plasma samples and Dr. A. G. Zacchei for mass spectral analysis of the I and II heptafluorobutyrylimidazole derivatives. Compounds I and II were synthesized by Dr. J. J. Baldwin and colleagues.

[5] Dr. S. Vickers, unpublished results.

Microencapsulation and Dissolution Parameters of Undecenovanillylamide: A Potential Coyote Deterrent

ANTHONY PALMIERI, III

Received April 2, 1979, from the *School of Pharmacy, University of Wyoming, Laramie, WY 82071.* Accepted for publication June 13, 1979.

Abstract □ The microencapsulation and dissolution of undecenovanillylamide (I), a potential coyote-aversive agent for use on sheep, were studied. While I has been shown to protect sheep, its short duration of action makes it economically unfeasible. Compound I microcapsules were prepared, and optimum conditions for encapsulation *via* complex coacervation were determined. Microcapsules that were hardened for 0.5, 1, and 2 hr, as well as I powder, were characterized according to their dissolution. Longer hardening times resulted in slower release, with all encapsulated I forms being released slower than the powder. The dissolution t_{50} for unencapsulated powder was less than 3 min; for microcapsules hardened for 30 min, the dissolution t_{50} was 7.3 min; for those hardened 60 min, the t_{50} was 17.7 min; and for those hardened 120 min, the t_{50} was 28 min. The encapsulated I would have a longer field life and, therefore, might be a viable economic and ecologic answer to coyote protection for sheep.

Keyphrases □ Undecenovanillylamide—coyote deterrent, microencapsulation, dissolution □ Coyote deterrents—undecenovanillylamide, microencapsulation, dissolution □ Microencapsulation—coyote deterrent, undecenovanillylamide, dissolution □ Dissolution—coyote deterrent, undecenovanillylamide, microencapsulation

Predator control has been a continual problem for Rocky Mountain area ranchers. This problem is compounded when the predator attacks sheep since almost all survival instinct has been bred out of the sheep to facilitate herding. While destruction of the coyote has been attempted, it is not an acceptable alternative to nondestructive control.

Recently, a chemical solution to this problem has shown promise[1]. Undecenovanillylamide (I) was shown to be an effective coyote deterrent when used as a spray or dip on sheep. Undecenovanillylamide, a pungent, hot-tasting chemical, is applied as a suspension in water or as a dilute isopropanol solution. When a sheep is attacked, the coyote usually discontinues the attack after taking a superficial bite; theoretically, a conditioning response has occurred. There are apparently no problems for the sheep except that I is useful for only 2 or 3 weeks and is not water resistant. The possibility of I encapsulation by complex coacervation was considered as a means of extending the effective I life (ideally for a summer season) and of decreasing the susceptibility of I to weather conditions.

Each possible encapsulation system has particular problems and specific microencapsulation requirements. Optimum encapsulation procedures for one chemical may be useless for a seemingly similar system. While many encapsulation methods exist, microencapsulation *via* complex coacervation was most applicable for I since the acacia–gelatin mixture imparts a stickiness to the microcapsules so that they adhere better to the wool.

EXPERIMENTAL

Microcapsule Preparation—All chemicals were used as supplied by the manufacturer. The basic procedure was previously reported (1); Scheme I shows the encapsulation procedure for I. The drug was passed through a No. 200 sieve before encapsulation. By varying the percent gelatin–acacia and the hardening time, microcapsules with different release rates were recovered.

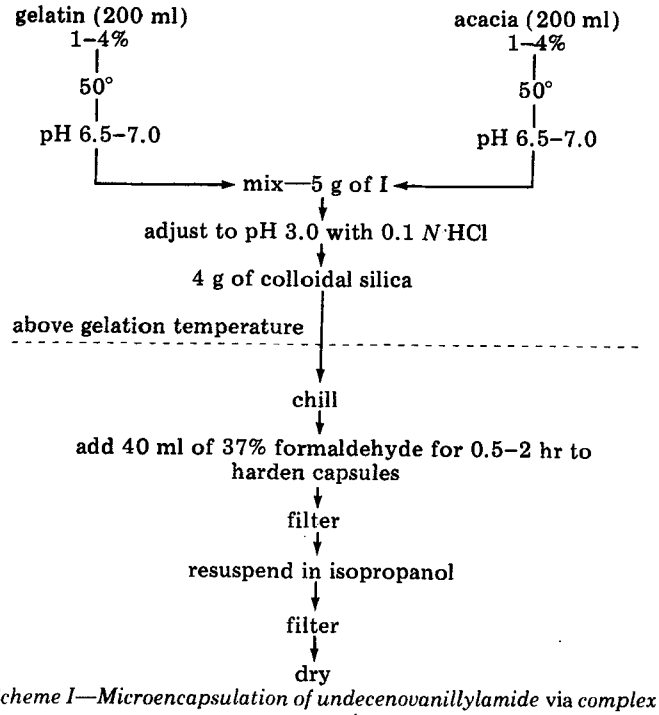

Scheme I—Microencapsulation of undecenovanillylamide via complex coacervation.

Dissolution Studies—The dissolution rate of pure I powder and microcapsules containing I was determined. The dissolution method was the flask method. A 500-ml round-bottom flask with a hole cut to allow stirrer insertion was filled with 300 ml of pH 6.5 buffer. A water bath maintained at 30° kept the dissolution medium at a constant temperature throughout dissolution. A flat, three-blade metal propeller with 2.5-cm blades was centered in the flask and immersed in the dissolution fluid to 35 mm. A constant-speed motor was calibrated to provide a 120-rpm stirring rate.

For all determinations, a known weight of I powder or microcapsules was added down the side of the flask. Samples of the dissolution fluid, 2 ml, were withdrawn at selected times with a pipet fitted with a glass wool

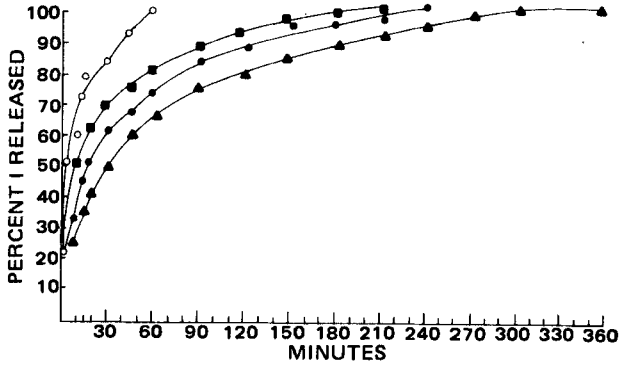

Figure 1—*Dissolution versus time profiles for undecenovanillylamide powder and microcapsules hardened for various times. Key:* ○, *powder;* ■, *microcapsules hardened for 0.5 hr;* ●, *microcapsules hardened for 1 hr; and* ▲, *microcapsules hardened for 2 hr.*

[1] R. J. McColloch and A. Palmieri, University of Wyoming, Laramie, Wyo., unpublished results.

0022-3549/79/1200-1561$01.00/0
© 1979, American Pharmaceutical Association

Table I—*In Vitro* Dissolution t_{50} *versus* Hardening Time for Undecenovanillylamide Microcapsules [a]

Hardening Time, min	*In Vitro* Dissolution t_{50}, min
Unencapsulated	<3
30	7.3
60	17.7
120	28.0

[a] $r = 0.98149$.

plug to ensure that undissolved drug was not included. An equivalent volume of fresh buffer and the glass wool plug were added to the flask after each withdrawal. The samples were then assayed spectrophotometrically at 280 nm after appropriate dilution with pH 6.5 buffer. Each determination was done at least in triplicate.

RESULTS AND DISCUSSION

Since encapsulation *via* complex coacervation occurs best at low colloid concentrations and when acacia and gelatin are employed in a 1:1 ratio (2), 1–4% concentrations were studied. There were no beneficial aspects at the higher concentration, so the 1% colloid concentrations were used to produce the least cohesive powder. The colloidal silica was added to aid in production and did, in fact, lead to easier microcapsule recovery as a dry, noncohesive powder.

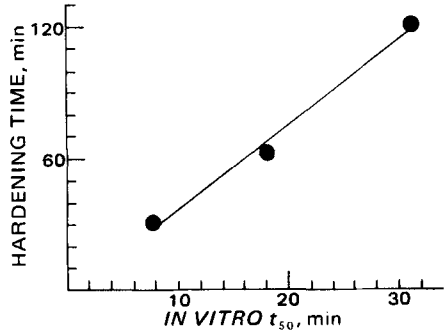

Figure 2—*Hardening time* versus in vitro t_{50} *for undecenovanillylamide microcapsules.*

The resuspension of the product in isopropanol for dehydration was successful with only 30% isopropanol. Lower concentrations did not result in a free-flowing powder, and higher concentrations destroyed the shell wall integrity.

Figure 1 shows the percent release *versus* time data for the various dosage forms studied. Each determination is the average of at least six dissolution profiles. Dissolution results for the powder and encapsulated forms of I indicate that the microencapsulated forms exhibited slower dissolution. The capsules hardened for 0.5 hr featured rapid initial release. This initial release may result from the soft shell and the large amount of unencapsulated I. The profiles in Fig. 1 are in rank order with hardening times; there was a definite delayed, sustained release for encapsulated I.

To explain the drug dissolution from the microcapsules, the release of the active ingredient through leaching or diffusion may be examined. For such release to occur, the dissolution medium must penetrate the wall to the nucleus, dissolve I, and then permeate out through the shell wall. Any of these processes may be rate limiting.

The effect of increased hardening times on the release profile is readily apparent. Since the dissolution t_{50} indicates the central tendency of the data, that point was chosen to compare release (Table I). There was a direct linear correlation ($r = 0.98149$) between microcapsule hardening time and the dissolution t_{50} values (Fig. 2).

REFERENCES

(1) A. Palmieri, *Drug Dev. Ind. Pharm.*, **3**, 309 (1977).

(2) L. A. Luzzi and R. J. Gerraughty, *J. Pharm. Sci.*, **56**, 634 (1967).

ACKNOWLEDGMENTS

Presented in part at the Basic Pharmaceutics Section, APhA Academy of Pharmaceutical Sciences, Anaheim meeting, April 1979.

Convenient Synthesis of *N*-Alkoxymethylbarbituric Acids and *N*-Alkoxymethylhydantoins

JOSEPH GAL

Received April 4, 1979, from the *Department of Pharmacology, Division of Clinical Pharmacology, School of Medicine, University of Colorado Medical Center, Denver, CO 80262.* Accepted for publication June 15, 1979.

Abstract □ A simple one-step method for the *N*-alkoxymethylation of barbituric acids and hydantoins is presented. The compounds are *N*-methoxymethylated or *N*-ethoxymethylated using phosphorus pentoxide and dimethoxymethane or diethoxymethane, respectively, in a chlorinated solvent. 1-Methoxymethyl-3-ethyl-5-phenylhydantoin showed significant anticonvulsant activity in the subcutaneous pentylenetetrazol test, while 1,3-bis(methoxymethyl)-5-ethyl-5-(*p*-tolyl)barbituric acid was inactive.

Keyphrases □ *N*-Alkoxymethylbarbituric acids—syntheses, anticonvulsant activity, structure-activity relationships □ *N*-Alkoxymethylhydantoins—syntheses, anticonvulsant activity, structure-activity relationships □ Anticonvulsants—*N*-alkoxymethylbarbituric acids and *N*-alkoxymethylhydantoins, syntheses, structure-activity relationships

N-Alkoxymethyl derivatives of barbituric acids and of hydantoins were recently synthesized, and several derivatives were shown to possess significant anticonvulsant activity in animal tests (1–4). One, 1,3-bis(methoxymethyl)phenobarbital (I), was studied in epileptic patients with promising results (5).

BACKGROUND

The original preparation of the *N*-alkoxymethyl derivatives involved alkylation of the barbituric acid or hydantoin alkali salt with chloromethyl methyl ether (II) (1–4). Since the latter reagent is a potent carcinogen (6–8), its use is highly restricted (9). Therefore, alternatives for the preparation of I have been sought, and two appeared in the patent literature. One method (10) is based on the preparation of 1,3-bis(chloromethyl)phenobarbital from phenobarbital, formaldehyde, acetyl chloride, hydrochloric acid, and a Lewis acid. These conditions are likely (11, 12) to result in the formation of bis(chloromethyl)ether (III), another, even more potent, carcinogen (8). 1,3-Bis(chloromethyl)phenobarbital was converted to I using sodium methoxide in methanol (10). The second

0022-3549/79/1200-1562$01.00/0
© 1979, American Pharmaceutical Association

Table I—*In Vitro* Dissolution t_{50} *versus* Hardening Time for Undecenovanillylamide Microcapsules [a]

Hardening Time, min	*In Vitro* Dissolution t_{50}, min
Unencapsulated	<3
30	7.3
60	17.7
120	28.0

[a] $r = 0.98149$.

plug to ensure that undissolved drug was not included. An equivalent volume of fresh buffer and the glass wool plug were added to the flask after each withdrawal. The samples were then assayed spectrophotometrically at 280 nm after appropriate dilution with pH 6.5 buffer. Each determination was done at least in triplicate.

RESULTS AND DISCUSSION

Since encapsulation *via* complex coacervation occurs best at low colloid concentrations and when acacia and gelatin are employed in a 1:1 ratio (2), 1–4% concentrations were studied. There were no beneficial aspects at the higher concentration, so the 1% colloid concentrations were used to produce the least cohesive powder. The colloidal silica was added to aid in production and did, in fact, lead to easier microcapsule recovery as a dry, noncohesive powder.

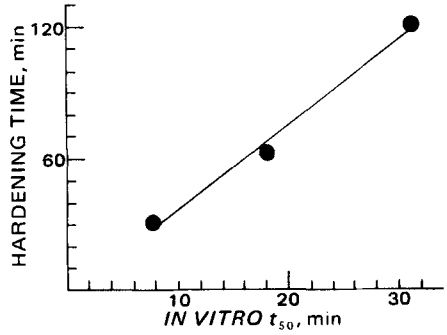

Figure 2—*Hardening time* versus in vitro t_{50} *for undecenovanillylamide microcapsules.*

The resuspension of the product in isopropanol for dehydration was successful with only 30% isopropanol. Lower concentrations did not result in a free-flowing powder, and higher concentrations destroyed the shell wall integrity.

Figure 1 shows the percent release *versus* time data for the various dosage forms studied. Each determination is the average of at least six dissolution profiles. Dissolution results for the powder and encapsulated forms of I indicate that the microencapsulated forms exhibited slower dissolution. The capsules hardened for 0.5 hr featured rapid initial release. This initial release may result from the soft shell and the large amount of unencapsulated I. The profiles in Fig. 1 are in rank order with hardening times; there was a definite delayed, sustained release for encapsulated I.

To explain the drug dissolution from the microcapsules, the release of the active ingredient through leaching or diffusion may be examined. For such release to occur, the dissolution medium must penetrate the wall to the nucleus, dissolve I, and then permeate out through the shell wall. Any of these processes may be rate limiting.

The effect of increased hardening times on the release profile is readily apparent. Since the dissolution t_{50} indicates the central tendency of the data, that point was chosen to compare release (Table I). There was a direct linear correlation ($r = 0.98149$) between microcapsule hardening time and the dissolution t_{50} values (Fig. 2).

REFERENCES

(1) A. Palmieri, *Drug Dev. Ind. Pharm.*, **3**, 309 (1977).

(2) L. A. Luzzi and R. J. Gerraughty, *J. Pharm. Sci.*, **56**, 634 (1967).

ACKNOWLEDGMENTS

Presented in part at the Basic Pharmaceutics Section, APhA Academy of Pharmaceutical Sciences, Anaheim meeting, April 1979.

Convenient Synthesis of *N*-Alkoxymethylbarbituric Acids and *N*-Alkoxymethylhydantoins

JOSEPH GAL

Received April 4, 1979, from the *Department of Pharmacology, Division of Clinical Pharmacology, School of Medicine, University of Colorado Medical Center, Denver, CO 80262.* Accepted for publication June 15, 1979.

Abstract □ A simple one-step method for the *N*-alkoxymethylation of barbituric acids and hydantoins is presented. The compounds are *N*-methoxymethylated or *N*-ethoxymethylated using phosphorus pentoxide and dimethoxymethane or diethoxymethane, respectively, in a chlorinated solvent. 1-Methoxymethyl-3-ethyl-5-phenylhydantoin showed significant anticonvulsant activity in the subcutaneous pentylenetetrazol test, while 1,3-bis(methoxymethyl)-5-ethyl-5-(*p*-tolyl)barbituric acid was inactive.

Keyphrases □ *N*-Alkoxymethylbarbituric acids—syntheses, anticonvulsant activity, structure-activity relationships □ *N*-Alkoxymethylhydantoins—syntheses, anticonvulsant activity, structure-activity relationships □ Anticonvulsants—*N*-alkoxymethylbarbituric acids and *N*-alkoxymethylhydantoins, syntheses, structure-activity relationships

N-Alkoxymethyl derivatives of barbituric acids and of hydantoins were recently synthesized, and several derivatives were shown to possess significant anticonvulsant activity in animal tests (1–4). One, 1,3-bis(methoxymethyl)phenobarbital (I), was studied in epileptic patients with promising results (5).

BACKGROUND

The original preparation of the *N*-alkoxymethyl derivatives involved alkylation of the barbituric acid or hydantoin alkali salt with chloromethyl methyl ether (II) (1–4). Since the latter reagent is a potent carcinogen (6–8), its use is highly restricted (9). Therefore, alternatives for the preparation of I have been sought, and two appeared in the patent literature. One method (10) is based on the preparation of 1,3-bis(chloromethyl)phenobarbital from phenobarbital, formaldehyde, acetyl chloride, hydrochloric acid, and a Lewis acid. These conditions are likely (11, 12) to result in the formation of bis(chloromethyl)ether (III), another, even more potent, carcinogen (8). 1,3-Bis(chloromethyl)phenobarbital was converted to I using sodium methoxide in methanol (10). The second

0022-3549/79/1200-1562$01.00/0
© 1979, American Pharmaceutical Association

Table I—Products of *N*-Alkoxymethylations

Starting Material	Product	Reaction Time[a]	Yield %	Product: Melting Point[b,c]	Product: NMR[d] Spectrum	Product: Mass Spectrum[e], *m/e* (relative intensity)
V	I	3	83	116–118°[f]	—[g]	—[h]
V[i]	VI	4	56	64–66°[j]	—[g]	—[g]
IX	VIII	3	51	114–115°[k]	—[g]	—[h]
XI	X	3 hr	71	74–76°[l]	7.44–7.22 (m, 5, C_6H_5), 4.64 (*AB* qt, 2, J_{AB} = 12 Hz, ν_A = 4.97, ν_B = 4.32, CH_2O), 3.38 (s, 3, OCH_3), 3.11 (s, 3, NCH_3), 2.89–2.00 (m, 2, CH_2CH_3), 0.96 (t, 3, J = 6 Hz, CH_2CH_3)	262 (1, M)[m], 233 (10), 203 (2), 118 (5), 117 (7), 91 (13), 77 (8), 45 (100), 44 (29)
XIII	XII[n,o]	6 hr	76	55–56°	7.67–7.00 (m, 5, C_6H_5), 4.67 (*AB* qt, 2, J_{AB} = 10 Hz, ν_A = 5.10, ν_B = 4.24, CH_2O), 5.05 (s, 1, CH), 3.64 (qt, 2, J = 6 Hz, CH_3CH_2), 3.33 (s, 3, OCH_3), 1.26 (t, 3, J = 6 Hz, CH_2CH_3)	248 (1, M), 233 (1), 217 (6), 216 (4), 146 (5), 132 (18), 118 (32), 117 (7), 91 (26), 90 (16), 77 (19), 76 (10), 51 (9), 45 (100), 44 (26)
XV	XIV[n,p]	3	87	139–141°	7.19 (s, 4, C_6H_4), 5.38 (*AB* qt, 4, J_{AB} = 10 Hz, ν_A = 5.44, ν_B = 5.29, NCH_2), 3.37 (s, 6, OCH_3), 2.46 (qt, 2, J = 7 Hz, CH_2CH_3), 2.31 (s, 3, $C_6H_4CH_3$), 0.98 (t, 3, J = 7 Hz, CH_2CH_3)	334 (3, M), 302 (10), 274 (11), 202 (9), 201 (6), 190 (15), 188 (17), 174 (5), 161 (15), 160 (100), 159 (14), 146 (6), 132 (26), 131 (26), 117 (57), 115 (17), 105 (12), 91 (18), 86 (29)
V	XVI	3	9	88–89°[q]	—[g]	—[g]

[a] In days, unless otherwise indicated. [b] Determined in a Fisher–Johns apparatus; values are uncorrected. [c] Product recrystallized from ethanol–water. [d] Determined with a Varian Associates EM-360 or EM-390 instrument, recorded in deuterochloroform; data are reported in parts per million (σ) downfield from tetramethylsilane internal standard. [e] Determined on Finnigan 1015 mass spectrometer, ionizing energy 70 ev. [f] Lit. (1) mp 116–118°. [g] Essentially identical to spectrum of same compound prepared *via* original procedure (1–4). [h] Essentially identical to published mass spectrum (16). [i] Diethoxymethane (VII) used in place of IV. [j] Lit. (1) mp 65–66°. [k] Lit. (3) mp 115–116°. [l] Lit. (4) mp 68.5–70.5°. [m] M = molecular ion. [n] Elemental analysis performed by Galbraith Laboratories, Knoxville, Tenn. [o] Calculated for $C_{13}H_{16}N_2O_3$: C, 62.89; H, 6.50; N, 11.28. Found: C, 62.95; H, 6.55; N, 11.25. [p] Calculated for $C_{17}H_{22}N_2O_5$: C, 61.07; H, 6.63; N, 8.38. Found: C, 60.89; H, 6.82; N, 8.25. [q] Melting point of sample prepared *via* previously published method (2): 88–89°.

alternative for the preparation of I involved the reaction of stannic chloride and dimethoxymethane (IV) with phenobarbital (V) (13). The presence of stannic chloride, a Lewis acid, in IV, however, carries the danger of generating chloromethyl methyl ether. Supporting this possibility is the facile conversion of IV to chloromethyl methyl ether in the presence of dry hydrogen chloride (14) or acetyl chloride (15).

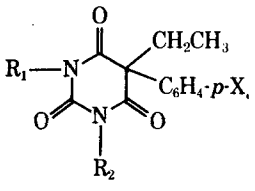

	R_1	R_2	X
I	CH_3OCH_2	CH_3OCH_2	H
V	H	H	H
VI	$CH_3CH_2OCH_2$	$CH_3CH_2OCH_2$	H
VIII	CH_3OCH_2	CH_3	H
IX	H	CH_3	H
XIV	CH_3OCH_2	CH_3OCH_2	CH_3
XV	H	H	CH_3
XVI	CH_3OCH_2	H	H

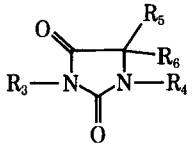

	R_3	R_4	R_5	R_6
X	CH_3	CH_3OCH_2	CH_2CH_3	C_6H_5
XI	CH_3	H	CH_2CH_3	C_6H_5
XII	CH_3CH_2	CH_3OCH_2	H	C_6H_5
XIII	CH_3CH_2	H	H	C_6H_5

YCH_2OCH_2Z

	Y	Z
II	H	Cl
III	Cl	Cl
IV	H	OCH_3
VII	CH_3	OCH_2CH_3

It appears, therefore, that an alternative method not involving carcinogenic halomethyl ethers is needed for the synthesis of *N*-alkoxymethyl derivatives of barbituric acids and hydantoins. Such a method is reported here.

EXPERIMENTAL

1,3-Bis(methoxymethyl)phenobarbital (I)—Phenobarbital (V, 500 mg, 2.2 mmoles), phosphorus pentoxide powder[1] (8 g), and methylene chloride (8 ml) were placed in a 125-ml, single-necked round-bottom flask. Compound IV (8 ml) was added, the flask was capped with a calcium chloride drying tube, and the mixture was stirred for 3 days. The flask was cooled in an ice bath while water (10 ml) was added. The flask was allowed to warm to room temperature, with occasional cooling in ice to control the reaction between water and phosphorus pentoxide.

Ether (10 ml) was added, and the mixture was transferred to a separator. The layers were separated after extraction, and the aqueous layer was further extracted with ether (2 × 10 ml). The combined organic extracts were washed with 1 *N* NaOH (2 × 10 ml) and with water (2 × 10 ml). The solution was dried (sodium sulfate), and the solvent was evaporated to obtain 579 mg of I. Further experimental details are listed in Table I.

Compounds VI, VIII, X, XII, and XIV also were prepared using this procedure, with some variation in experimental details (Table I).

1-Methoxymethylphenobarbital (XVI)—Phenobarbital (V, 2.0 g, 8.6 mmoles), methylene chloride (30 ml), and IV (30 ml) were combined in a 125-ml flask. The mixture was stirred magnetically while phosphorus pentoxide (20 g) was added in small portions. The flask was capped with a calcium chloride drying tube, and the mixture was stirred at room temperature for 3 days. The reaction flask was cooled in ice, and ice water (50 ml) was added with stirring until all of the phosphorus pentoxide had dissolved.

The mixture was extracted with ether (2 × 50 ml). The combined organic layers were extracted with 0.1 *N* NaOH (3 × 50 ml), and the combined alkaline aqueous layers were acidified to pH 4 with concentrated hydrochloric acid in an ice bath. The acidic solution was extracted with ether (3 × 50 ml). The combined organic extracts were washed with water (50 ml), dried with sodium sulfate, and concentrated *in vacuo*. The residue was kept at 4° for 3 days. The resulting crystalline material was recrystallized from ethanol–water (Table I).

Pharmacological Testing—Anticonvulsant activity was examined[2]

[1] Granular phosphorus pentoxide was much less effective.

[2] The testing was carried out by the Antiepileptic Drug Development Program, Epilepsy Branch, National Institute of Neurological and Communicative Disorders and Stroke, National Institutes of Health, Bethesda, MD 20014.

Table II—Anticonvulsant Activity and Neurotoxicity [a]

Compound	MES[b]		scMet[b]		Toxicity[b]	
	0.5 hr	4 hr	0.5 hr	4 hr	0.5 hr	4 hr
XII	+	–	++[c]	–	+	–
XIV	–	–	–	+[d]	–	–

[a] Assay methods are described under *Experimental*. [b] Activity and toxicity at 30, 100, or 300 mg/kg are represented by +++, ++, or +, respectively; – indicates no activity or toxicity observed. [c] Test repeated at 100 mg/kg: three of four animals protected. [d] Test repeated at 300 mg/kg: no animals protected.

in Screen 1 of the Anticonvulsant Screening Project Test Systems (17, 18). Three tests were performed in male mice[3]: the maximal electroshock seizure test (MES), the subcutaneous pentylenetetrazol seizure threshold test (scMet), and the rotorod test designed to detect neurotoxicity.

The compounds were tested at three dose levels (30, 100, and 300 mg/kg) at 30 min and 4 hr after their intraperitoneal administration. Four animals were injected with each dose, which was solubilized in 30% polyethylene glycol 400, and were examined 30 min later for toxicity in the rotorod test. Anticonvulsant activity was evaluated immediately thereafter by subjecting one mouse to the maximal electroshock seizure test and another to the subcutaneous pentylenetetrazol seizure threshold test. The same tests were repeated after 4 hr on the two remaining mice.

Anticonvulsant activity in the maximal electroshock seizure test is defined as abolition of the hindlimb tonic extensor component of the maximal electroshock seizure elicited with a 60-Hz alternating current of 50 mamp delivered for 0.2 sec *via* corneal electrodes. Activity in the subcutaneous pentylenetetrazol seizure threshold test is defined as failure to observe even a threshold seizure (a single episode of clonic spasms at least 5 sec in duration) at a pentylenetetrazol dose of 85 mg/kg. Neurologic toxicity is defined as failure of an animal to remain for at least 1 min on a 2.54-cm diameter, knurled plastic rod rotating at 6 rpm.

RESULTS AND DISCUSSION

The methoxymethylation of alcohols using IV and phosphorus pentoxide was described recently (19). With a related procedure, other investigators methoxymethylated phenols using IV and *p*-toluenesulfonic acid in the presence of molecular sieves (20). The applicability of these methods to the alkoxymethylation of barbituric acids and hydantoins was examined. While the latter procedure (20) failed to methoxymethylate any of the compounds studied, the former method (19) resulted in moderate to excellent yields of alkoxymethylated products (Table I).

Compounds I, VI, VIII, X, XII, XIV, and XVI were prepared. The melting point of X, 74–76°, differed slightly from the previously reported (4) value, 68.5–70.5°. This discrepancy may be because X was not recrystallized in the previous procedure (4). The NMR and mass spectra of X (Table I) were consistent with the proposed structure. Spectral data, melting points, and analytical data (for new compounds) also confirmed the structures of the other compounds. The methylene protons of the *N*-alkoxymethyl group in all of the compounds prepared gave rise to *AB* quartets in the NMR spectra. The reaction proceeded best in a halogenated solvent, *e.g.*, methylene chloride, chloroform, or ethylene dichloride. However, the reaction also was carried out successfully in other solvents. For example, I was prepared in ethyl acetate in a 77% yield.

The procedure also was useful in the preparation of 1-methoxymethylphenobarbital (XVI). Since XVI, an *N*-monosubstituted barbituric acid, could not be prepared by monomethoxymethylation of V with chloromethyl methyl ether (1), an alternative synthesis was developed (2) involving the *N,S*-bis(methoxymethyl) derivative of thiophenobarbital. The method uses chloromethyl methyl ether and is time consuming (2). The reaction described in the present report can be used to prepare XVI in moderate amounts in one safe, simple step.

Compounds XII and XIV, previously unreported, were tested for anticonvulsant activity (Table II). Compound XIV showed no anticonvulsant activity in the test system. This result is interesting when contrasted to the high activity (1) shown by I, a compound differing from XIV only in the lack of the *p*-methyl group on the phenyl ring. Compound XII, the 1-methoxymethyl derivative of ethotoin, showed activity at 100 mg/kg in the subcutaneous pentylenetetrazol test and at 300 mg/kg in the maximal electroshock seizure test at 30 min after administration. However, at 300 mg/kg, XII also had neurotoxic effects.

[3] Carworth Farms No. 1.

REFERENCES

(1) C. M. Samour, J. F. Reinhard, and J. A. Vida, *J. Med. Chem.*, **14**, 187 (1971).

(2) J. A. Vida, M. L. Hooker, C. M. Samour, and J. F. Reinhard, *ibid.*, **16**, 1378 (1973).

(3) J. A. Vida, M. L. Hooker, and J. F. Reinhard, *ibid.*, **16**, 602 (1973).

(4) J. A. Vida, M. H. O'Dea, C. M. Samour, and J. F. Reinhard, *ibid.*, **18**, 383 (1975).

(5) B. B. Gallagher, I. P. Braumel, S. G. Woodbury, and J. A. DiMicco, *Neurology*, **25**, 339 (1975).

(6) W. G. Figeroa, R. Raszkowski, and W. Weiss, *N. Engl. J. Med.*, **288**, 1096 (1973).

(7) S. M. Brown and S. Selvin, *ibid.*, **289**, 693 (1973).

(8) B. L. VanDuuren, A. Sivak, B. M. Goldschmidt, C. Katz, and S. Melchionne, *J. Natl. Cancer Inst.*, **43**, 481 (1969).

(9) *Fed. Regist.*, **39** (20), 3756 (Jan. 29, 1974).

(10) J. A. Vida (to Kendall Co.), U.S. pat. 3,947,443 (1976).

(11) G. J. Kallos and R. A. Solomon, *Am. Ind. Hyg. Assoc. J.*, **34**, 496 (1973).

(12) S. R. Buc, *Org. Syntheses, Coll. Vol.*, **4**, 202 (1963).

(13) J. A. Vida (to Bristol-Myers Co.), U.S. pat. 4,029,662 (1977).

(14) L. A. Ens (to Dow Chemical Co.), German Offen 2,431,778 (1975).

(15) M. J. Nattrass, *Natl. Inst. Metall. Repub. S. Afr., Rep.*, **1977**, 1853.

(16) J. Gal, B. J. Hodshon, and A. K. Cho, in "Proceedings of the 2nd International Conference on Stable Isotopes," E. R. Klein and P. D. Klein, Eds., United States Energy Research and Development Administration, CONF-751027, 1975, p. 177.

(17) R. L. Krall, J. K. Penry, B. G. White, H. J. Kupferberg, and E. A. Swinyard, *Epilepsia*, **19**, 409 (1978).

(18) Anticonvulsant Screening Project, Antiepileptic Drug Development Program, National Institutes of Health, DHEW Publication No. (NIH) 78-1093.

(19) K. Fuji, S. Nakano, and E. Fujita, *Synthesis*, **1975**, 276.

(20) J. P. Yardley and H. Fletcher, *ibid.*, **1976**, 244.

ACKNOWLEDGMENTS

Based in part on work carried out at the School of Pharmacy, University of Wisconsin, to whom the author is grateful for support.

Generous assistance by Ms. Toby N. Steinberger is deeply appreciated.

Colorimetric Determination of 1-(4′-Nitrophenyl)-2-aminopropane-1,3-diol with 2,4,6-Trinitrobenzenesulfonic Acid in the Presence of Chloramphenicol

P. G. PIETTA ˣ, D. AGNELLINI, and M. PACE

Received February 22, 1979, from the *Istituto di Chimica Organica ed Analitica, Via Celoria 2, 20133 Milan, Italy.* Accepted for publication June 25, 1979.

Abstract □ A colorimetric method based on the interaction between the chloramphenicol degradation product 1-(4′-nitrophenyl)-2-aminopropane-1,3-diol and the 2,4,6-trinitrobenzenesulfonic acid reagent was developed. Analytical solutions were reacted with the reagent at pH 9.1 for 20 min at room temperature, and the resulting color was measured at 340 nm. A linear relationship between absorbance and concentration occurred within the 5–25-μg/ml range under the conditions studied. Replicate analyses were in good agreement. An average recovery of 99.4 ± 0.4% was obtained for the synthetic mixtures.

Keyphrases □ Chloramphenicol degradation products—1-(4′-nitrophenyl)-2-aminopropane-1,3-diol, colorimetric analysis, in commercial chloramphenicol solutions □ 1-(4′-Nitrophenyl)-2-aminopropane-1,3-diol—colorimetric analysis, in commercial chloramphenicol solutions □ Colorimetry—analysis, chloramphenicol degradation products

Chloramphenicol solutions undergo hydrolysis (1–3), and one major degradation product is 1-(4′-nitrophenyl)-2-aminopropane-1,3-diol (I) (Scheme I). Since I has no antibiotic activity and is regarded as a contaminant in commercial drug preparations, its determination is important.

BACKGROUND

The interaction of I with 2,4,6-trinitrobenzenesulfonic acid reagent to give highly colored solutions led to the development of a new colorimetric method for I determination. This reagent previously was shown to be suitable for the colorimetric analysis of primary amino groups, amino acids, peptides, and proteins (4–7).

Existing analytical procedures for I include visible and UV spectrophotometry, polarography, and high-pressure liquid chromatography (HPLC) (6–9).

The standard colorimetric methods are based on the interaction of I with 1,2-naphthoquinone-4-sulfonate (10) and 1,4-naphthoquinone (11), but other chloramphenicol solution components (*e.g.*, chloramphenicol and acetate ions) can interfere with the reagents. Moreover, these procedures are not simple and involve the preparation of multireagent solutions.

This paper presents a new colorimetric method for the determination of microgram quantities of I in chloramphenicol solutions. At room temperature and pH 9.1, the procedure is not subject to chloramphenicol interference. This method has been applied successfully to the analysis of I in chloramphenicol dosage forms.

The synthesis and physicochemical properties of 2,4,6-trinitrophenyl-1-(4′-nitrophenyl)-2-aminopropane-1,3-diol (II) also are reported.

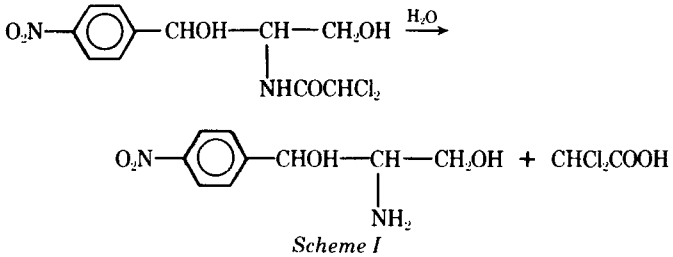

Scheme I

EXPERIMENTAL

Apparatus—Spectra and absorbance measurements were obtained by spectrophotometers[1–3] using matched quartz cells with a 1-cm optical path.

Reagents and Chemicals—2,4,6-Trinitrobenzenesulfonic acid was the chromogenic reagent. It was recrystallized before use according to a literature method (7). The 2,4,6-trinitrobenzenesulfonic acid reagent solution was prepared immediately prior to use by weighing accurately 100–500 mg of trinitrobenzenesulfonic acid and adding 0.1 ml of deionized water for each 100 mg of reagent.

Compound I was prepared quantitatively by acidic hydrolysis of chloramphenicol (12). The pKb value of the amino group was determined by acid–base titration to be 8.12.

Compound II was prepared by dissolving I (1 mmole), 2,4,6-trinitrobenzenesulfonic acid (200 mg), and sodium bicarbonate (200 mg) in water (10 ml); the solution became orange almost immediately, and the intensity increased over time. After 1 hr at room temperature, the solution was acidified to pH 2 and extracted with ethyl acetate. After washing with 1% $NaHCO_3$ and water, the solution was dried over sodium sulfate, the ethyl acetate was evaporated under vacuum, and the residue was crystallized from anhydrous ether–petroleum ether (275 mg, 65% yield, mp 85–88°).

TLC showed the product to be homogeneous in benzene–ethanol (9:1) and in *n*-butanol–acetic acid–water (4:1:1); IR (in mineral oil): 3360, 1620, 1590, 1570, 1515, and 1345 cm^{-1}; NMR: 3.6–3.8 (m, 1), 4.05 (d, 2), 7.45–7.7 (d, 2), 8.1–8.3 (d, 2), and 8.9–9.1 (d, 2). UV results are given in Fig. 1; log ε: 4.19 at 340 nm in 95% ethanol.

Anal.—Calc. for $C_{15}H_{13}N_5O_{10}$ (mol. wt. 423.20): C, 42.56; H, 3.09; N, 16.54. Found: C, 42.13; H, 3.12; N, 16.48.

The product was soluble in ethanol, methanol, ethyl acetate, and ether and was insoluble in carbon tetrachloride and chloroform.

Procedure—A sample of I was added to 2 ml of 0.1 *M* $Na_2B_4O_7$, and the volume was made up to 5.0 ml. Then 40 μl of trinitrobenzenesulfonic acid solution was added, and the solution was mixed rapidly.

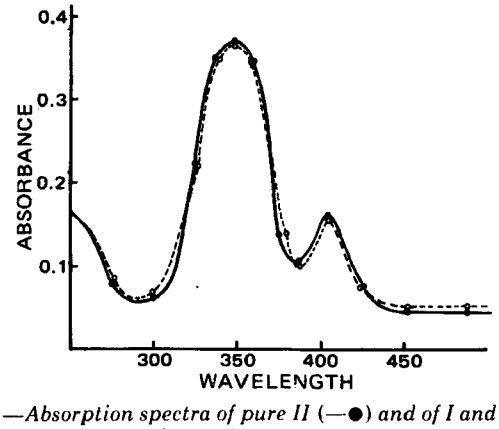

Figure 1—*Absorption spectra of pure II (—●) and of I and 2,4,6-trinitrobenzenesulfonic acid (– – ○).*

[1] Beckman Acculab 3.
[2] Beckman Acta III.
[3] Perkin-Elmer R 12, 60 MHz.

0022-3549/79/1200-1565$01.00/0
© 1979, American Pharmaceutical Association

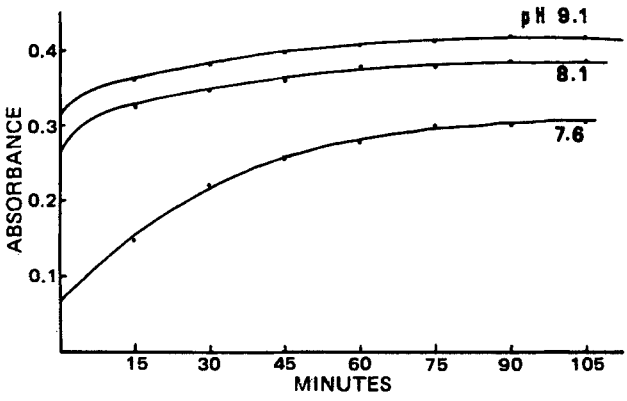

Figure 2—*Effect of pH on trinitrophenylation of I with 2,4,6-trinitrobenzenesulfonic acid and of coupling time on the final solution absorbance.*

After 20 min, the reaction was stopped by adding 5.0 ml of phosphate buffer (pH 4.5), and the absorbance at 340 nm was determined against a blank.

RESULTS AND DISCUSSION

When a I solution in 0.1 *M* $Na_2B_4O_7$ was added with 2,4,6-trinitrobenzenesulfonic acid, the solution became orange; the intensity increased during the initial 90 min at room temperature. A blank solution containing no amino compounds was pale yellow during this time. Upon acidification, the sample changed to a stable yellow while the blank became almost colorless. The UV–visible spectra of the acidified sample showed an absorption maximum at 340 nm (Fig. 1). No differences were found with pure synthetic II. This result indicated that the color was due exclusively to trinitrophenylation of the amino group.

The interaction between 2,4,6-trinitrobenzenesulfonic acid and I was affected by the pH and the reagent quantity. The higher the pH, the greater was the I reaction velocity with the reagent. However, in a strong alkaline solution, some decomposition of 2,4,6-trinitrobenzenesulfonic acid and II occurred. The optimum pH range for the trinitrophenylation was 8.1–9.1 at room temperature and fitted the amino group titration curve (pKb = 8.12, Fig. 2).

The reaction course was followed by the color development at 340 nm. Absorbance values increased through 120 min at room temperature and then stabilized. However, after 20 min at room temperature, the reaction was suitable for reproducible readings. Because the decomposition products absorbed less at acidic than at alkaline pH, the trinitrophenylation was stopped after 20 min by acidification with pH 4.5 phosphate buffer. The colors were stable for at least 2 hr, and the reference blank was unchanged under these conditions.

The color intensity also was affected by the 2,4,6-trinitrobenzenesulfonic acid concentration. Higher absorbances were obtained using up to a threefold reagent excess. Reagent quantities beyond this excess did not effectively increase the absorbance readings for I.

Standard curves, prepared by plotting absorbance *versus* I concentrations, showed a linear relationship up to 25 μg of I/ml.

The analysis is a semimicro procedure, and the sensitivity is in the range of 5 μg of I/ml. Reagent preparation is simple and rapid since 2,4,6-trinitrobenzenesulfonic acid is available commercially and is purified easily. The procedure requires ~20 min. The method is specific for I in the presence of chloramphenicol and normally employs components of chloramphenicol solutions (*e.g.*, *p*-oxybenzoates, sodium acetate, sodium borate, sodium chloride, and sodium phosphate).

A placebo was prepared containing chloramphenicol and some of the previously mentioned components; several weights of the components, each approximating the sample weight of commercial solutions, were spiked with a known amount of I and assayed. The average recovery was 99.4 ± 0.4%. Multiple analyses were performed on different commercial samples. Replicate analyses were in good agreement, and the samples assayed up to 35% of I.

Compound I in commercial chloramphenicol preparations is analyzed satisfactorily and rapidly by the described method.

REFERENCES

(1) T. Higuchi and C. D. Bias, *J. Am. Pharm. Assoc., Sci. Ed.*, **42**, 707 (1953).

(2) T. Higuchi and A. D. Marcus, *ibid.*, **43**, 530 (1954).

(3) I. K. Shih, *J. Pharm. Sci.*, **60**, 786 (1971).

(4) T. Okuyama and K. Satake, *J. Biochem. (Tokyo)*, **47**, 454 (1960).

(5) K. Satake, T. Okuyama, M. Ohashi, and T. Shinoda, *ibid.*, **47**, 654 (1960).

(6) R. B. Freeman and G. K. Radda, *Biochem. J.*, **108**, 383 (1968).

(7) R. Fields, *ibid.*, **124**, 581 (1971).

(8) S. L. Ali, *Pharm. Ztg.*, **122**, 1816 (1977).

(9) S. L. Ali, *J. Chromatogr.*, **154**, 103 (1978).

(10) A. Brunzell, *Sven. Farm. Tidskr.*, **46**, 129 (1957).

(11) H. J. Kallmayer, *Sci. Pharm.*, **42**, 85 (1974).

(12) M. C. Rebstock, H. M. Crooks, J. Controlius, and Q. R. Bartz, *J. Am. Chem. Soc.*, **71**, 2458 (1949).

ACKNOWLEDGMENTS

Supported by the Italian Ministry of Education, Grant 595-Div. XIV/CP, 1977.

The authors thank Dr. A. Jus for the NMR spectra.

Electron-Capture GLC Determination of Pseudoephedrine in Serum

SY-RONG SUN *x and MARY JO LEVEQUE

Received February 9, 1979, from the *Pharmaceutical Products Division, Abbott Laboratories, North Chicago, IL 60064.* Accepted for publication June 15, 1979. *Present address: United States Pharmacopeia, Rockville, MD 20852.

Abstract □ A GLC assay was developed for pseudoephedrine in serum using 3-methylamino-1-phenyl-1-propanol as an internal standard. After extraction from serum with benzene under alkaline conditions, pseudoephedrine was derivatized with pentafluorobenzyl bromide and quantitated by electron-capture GLC. The method has a detection limit of ~0.02 μg/ml of serum using 1-ml samples.

Keyphrases □ Pseudoephedrine—analysis, electron-capture GLC, human serum, bioavailability □ Vasoconstrictors (adrenergic)—pseudoephedrine, electron-capture GLC analysis, human serum, bioavailability □ GLC, electron capture—analysis, pseudoephedrine, human serum, bioavailability

Various analytical methods for pseudoephedrine (I) determination in biological fluids have been reported, including GLC methods with flame-ionization (1–3), electron-capture (4, 5), and nitrogen-specific (6) detection. The flame-ionization and nitrogen-specific detector procedures have low sensitivity, while the electron-capture procedure requires a time-consuming derivatization. Kuntzman *et al.* (7) prepared the acetyl derivative of pseudoephedrine with tritiated acetic anhydride and quantitated it by scintillation counting. However, this method lacks specificity.

The report describes a rapid and specific GLC method for pseudoephedrine determination in serum utilizing electron-capture detection of the pentafluorobenzyl derivative. The method is sufficiently sensitive for clinical pharmacokinetic evaluations after a single pseudoephedrine dose. Expected serum concentrations range from ~0.8 to 0.1 μg/ml during the 24-hr interval following oral ingestion of 180 mg of pseudoephedrine hydrochloride (7).

EXPERIMENTAL

Reagents and Materials—Pseudoephedrine hydrochloride[1], the internal standard[2], and pentafluorobenzyl bromide[3] were used as supplied. The other chemicals were analytical reagent grade.

Apparatus—The samples were extracted at 100 cpm on a two-speed reciprocating shaker[4] and centrifuged at 10° in a refrigerated centrifuge[5]. Sample solutions in test tubes were mixed by vortexing[6]. The pentafluorobenzyl derivatives were prepared at high temperature on a heating block[7].

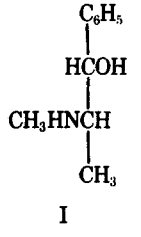

I

Table I—Assay Reproducibility of Serum Pseudoephedrine Concentration

Theoretical, μg/ml	Observed[a] Mean ± *SD*, μg/ml	*RSD*, %
0.05	0.055 ± 0.008	14.4
0.10	0.108 ± 0.009	8.1
0.20	0.218 ± 0.014	6.5
0.40	0.388 ± 0.015	3.8
0.60	0.552 ± 0.024	4.4
1.00	1.029 ± 0.060	5.8

[a] Mean of three determinations at each concentration.

GLC—A reporting gas chromatograph[8] equipped with a computing integrator[9], a ^{63}Ni-constant-current electron-capture detector[10], and an automatic sampler[11] were used. The 1.21-m (4-ft) × 4-mm i.d. glass column was packed with 5% OV-225[12] on Gas Chrom Q[12] (80–100 mesh). The column was conditioned at 250° for 16 hr with argon–methane (95:5)[13] at 20 ml/min before being connected to the detector. The carrier gas cylinder was fitted with an oxygen trap filter[14].

The samples were chromatographed using a carrier gas flow rate of 44 ml/min, with the injector, column oven, and detector maintained at 200, 190, and 300°, respectively.

Standards—A 100-μg/ml stock solution of pseudoephedrine was prepared by dissolving 24.4 mg of pseudoephedrine hydrochloride in 200 ml of distilled water. The 1-μg/ml working serum pseudoephedrine standard was prepared by diluting 1.0 ml of the stock solution to 100 ml with drug-free serum. Other serum standards were prepared by further diluting the 1-μg/ml serum standard with drug-free serum.

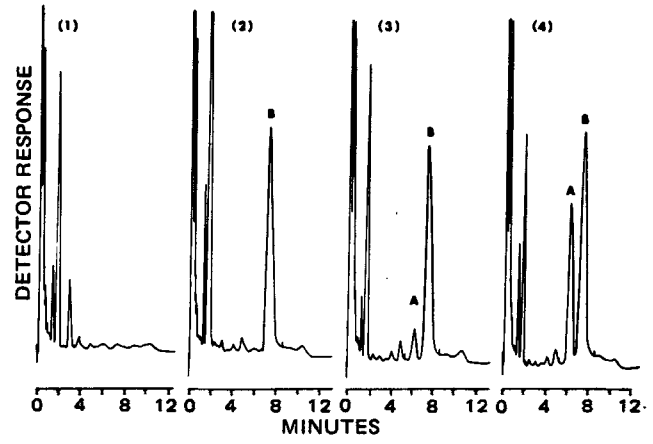

Figure 1—*Chromatograms of extracted serum samples. Key: 1, serum blank; 2, serum blank containing internal standard; 3, serum pseudoephedrine standard at 0.10 μg/ml; 4, serum pseudoephedrine standard at 0.60 μg/ml; A, pseudoephedrine; and B, internal standard.*

[1] NF reference standard.
[2] 3-Methylamino-1-phenyl-1-propanol, Abbott internal reference standard, A-10261, Abbott Laboratories, North Chicago, Ill.
[3] Pierce Chemical Co., Rockford, IL 61105.
[4] Eberbach Corp., Ann Arbor, Mich.
[5] Model RC-3, Sorvall, Newtown, Conn.
[6] Vortex Genie model K-550-GT, Scientific Industries, Springfield, Mass.
[7] Dri-block DB-3, Techne, Princeton, N.J.
[8] Hewlett-Packard model 5830A.
[9] Hewlett-Packard model 18850A.
[10] Hewlett-Packard model 18803A.
[11] Hewlett-Packard model 7671A.
[12] Applied Science Laboratories, State College, Pa.
[13] Matheson Gas Products, Elk Grove Village, Ill.
[14] Altech Associates, Arlington Heights, Ill.

0022-3549/79/1200-1567$01.00/0
© 1979, American Pharmaceutical Association

Table II—Assay Sensitivity

Serum Pseudoephedrine, μg/ml	Peak Area Ratio, Pseudoephedrine to Internal Standard
0.05	0.060
	0.072
	0.075
0.10	0.127
	0.125
	0.111
0.20	0.243
	0.219
	0.220
Linear Regression Parameters	
Number of points	9
Slope	1.057
y-Intercept	0.0158
Correlation coefficient	0.992
Calculated sensitivity[a], μg/ml	0.020

[a] Sensitivity was defined as the concentration calculated by linear regression analysis to give a peak area ratio greater than the y-intercept 95% of the time.

An internal standard stock solution, 100 μg/ml, was prepared by dissolving 20 mg of internal standard in 200 ml of methanol. The 1-μg/ml working internal standard was prepared by diluting 1 ml of the internal standard stock solution to 100 ml with distilled water.

Assay—To 1.0 ml of serum in 20-ml screw-capped test tubes fitted with polytef-lined caps were added 0.5 ml of the working internal standard, 1 ml of 0.1 *M* Na_3PO_4, and 6 ml of benzene. The samples were extracted by shaking at 100 cpm for 10 min. After centrifugation at 3000 rpm for 5 min, 5-ml aliquots of the organic phase were transferred to 15-ml screw-capped conical test tubes containing 1 ml of 0.1 *N* HCl. The pseudoephedrine and the internal standard were back-extracted into the acidic solution by shaking for 5 min.

Following centrifugation, the organic phase was removed by aspiration. The aqueous solution was alkalinized with 1 ml of 1 *N* NaOH and extracted with 2.5 ml of benzene for 5 min. Then 2 ml of the benzene extract was transferred to a screw-capped conical test tube and evaporated to dryness at 45° with filtered air[15]. To the residue were added 0.1 ml of 0.1 *M* K_2HPO_4, 0.1 ml of ethanol, and 0.1 ml of 2 mg of pentafluorobenzyl bromide/ml of ethanol. The mixture was capped after vortexing and reacted at 100° for 1 hr.

After the mixture had cooled to room temperature, 1 ml of 0.1 *M* K_2HPO_4 and 2.5 ml of benzene were added, and the solution was extracted for 5 min. Then 2 ml of the benzene extract was evaporated to dryness at 40° with filtered air to remove excess pentafluorobenzyl bromide. The residue was dissolved in 1 ml of benzene by vortexing, and a 2-μl aliquot was chromatographed.

Calculations—The peak area ratios of pseudoephedrine to the internal standard were plotted *versus* the pseudoephedrine concentration expressed as micrograms per milliliter of serum. Values for unknown pseudoephedrine concentrations in serum were calculated by the least-squares regression method from the calibration curve.

RESULTS AND DISCUSSION

Under the described assay conditions, derivation of pseudoephedrine and the internal standard with pentafluorobenzyl bromide yielded unique derivatives with GLC retention times of 6.3 and 7.5 min, respectively (Fig. 1). Pentafluorobenzyl derivatives of ephedrine and norephedrine have retention times of 5.1 and 21.8 min, respectively. The pseudoephedrine and internal standard derivatives were well resolved from coextracted endogenous compounds in serum.

[15] Air purifier, Koby Inc., Marlboro, Mass.

Table III—Assay Accuracy of Serum Pseudoephedrine Concentration

Unknown	Theoretical, μg/ml	Observed, μg/ml	Recovery, %
1	0.050	0.056	112.0
2	0	0	—
3	0.600	0.556	92.7
4	0.300	0.309	103.0
5	1.000	0.964	96.4
6	0.150	0.157	104.7
7	0.400	0.375	93.8
8	0.075	0.076	101.3
9	0.800	0.755	94.4
10	0.500	0.472	94.4
11	0.100	0.110	110.0
12	0.200	0.213	106.5
Average			100.8

Assay reproducibility was estimated by analyzing replicate standards (n = 3) ranging from 0.05 to 1.00 μg of pseudoephedrine/ml. Relative standard deviations (Table I) ranged from 14.4 to 3.8%, with the largest deviations associated with concentrations of <0.1 μg/ml. Assay sensitivity, defined as the pseudoephedrine concentration calculated by linear regression analysis that gave a peak area ratio response greater than the y-intercept 95% of the time, was ~0.02 μg/ml (Table II). The accuracy of the assay was estimated by analyzing serum samples containing known pseudoephedrine quantities under blind conditions. The average recovery was 100.8 ± 6.9% (n = 11) (Table III).

The extraction efficiency, compared to extraction of the standard in water, averaged 104.0 ± 2.2% (mean ± *SD*) for triplicate serum pseudoephedrine samples at 1 μg/ml. This value was calculated by dividing the peak area ratios of the extracted serum samples by the peak area ratios of the water samples.

This study indicated that the described GLC method can be employed to quantitate serum pseudoephedrine levels in a single-dose bioavailability study.

REFERENCES

(1) A. H. Beckett and G. R. Wilkinson, *J. Pharm. Pharmacol.*, **17**, 104S (1965).

(2) G. R. Wilkinson and A. H. Beckett, *J. Pharmacol. Exp. Ther.*, **162**, 139 (1968).

(3) V. F. Frosch, *Arzneim.-Forsch.*, **27**, 665 (1977).

(4) L. M. Cummins and M. J. Fourier, *Anal. Lett.*, **2**, 403 (1969).

(5) E. T. Lin, D. C. Brater, and L. Z. Benet, *J. Chromatogr.*, **140**, 275 (1977).

(6) C. Bye, H. M. Hill, D. T. D. Hughes, and A. W. Peck, *Eur. J. Clin. Pharmacol.*, **8**, 47 (1975).

(7) R. G. Kuntzman, I. Tsai, L. Brand, and L. C. Mark, *Clin. Pharmacol. Ther.*, **12**, 62 (1971).

ACKNOWLEDGMENTS

The authors thank Dr. S. Borodkin for helpful discussions.

Comparative Pharmacokinetics of Coumarin Anticoagulants XLIII: Concentration-Dependent Hepatic Uptake of Warfarin in Rats

KANJI TAKADA and GERHARD LEVY ˣ

Received May 31, 1979, from the *Department of Pharmaceutics, School of Pharmacy, State University of New York at Buffalo, Amherst, NY 14260.* Accepted for publication June 28, 1979.

Abstract □ The purpose of this study was to determine if hepatic warfarin uptake, which has a major quantitative effect on warfarin distribution in rats, is concentration dependent. Adult male rats received either 0.1 or 1.0 mg of racemic warfarin/kg iv and were killed 6 hr later. With increasing dose, the concentrations of free and total (free plus protein-bound) serum warfarin increased much more than proportionally, and the total warfarin concentration in the liver increased much less than proportionally. The liver to serum total warfarin concentration ratios 6 hr after injection of the 0.1- and 1.0-mg/kg doses were 11.3 ± 1.7 and 0.814 ± 0.222, respectively (mean ± *SD*, $n = 6$, $p < 0.001$). The ratio of the total drug concentration in the liver to the free drug concentration in serum (mean ± *SD*) was 866 ± 105 in animals that received the 0.1-mg/kg dose and 111 ± 42 in animals that received the 1.0-mg/kg dose ($p < 0.001$). It is concluded that hepatic warfarin uptake decreases with increasing drug concentration and that this may cause the apparent volume of distribution of warfarin to decrease with increasing dose in rats.

Keyphrases □ Coumarin anticoagulants—warfarin, hepatic uptake, concentration dependence, rats □ Warfarin—hepatic uptake, concentration dependence, rats □ Anticoagulants—warfarin, hepatic uptake, concentration dependence, rats □ Pharmacokinetics—anticoagulants, warfarin, hepatic uptake, rats

The pharmacokinetics of warfarin in rats provide a classical example of the effect of serum protein binding on the elimination of a drug with a hepatic clearance much lower than, and therefore independent of, the hepatic blood perfusion rate (1). Very large interindividual differences in total warfarin clearance by rats are associated with, and can be related to, corresponding differences in the serum free fraction of the drug (2). However, theoretical considerations suggest that the pharmacokinetic components of total clearance, *i.e.*, the apparent volume of distribution and β, are affected by changes in tissue binding of the drug, even though tissue binding should have no effect on the total clearance *per se* (3, 4).

Despite being bound extensively to serum proteins ($\simeq$ 99% in the pharmacologically realistic drug concentration range), warfarin concentrates in rat liver. In a previous study in this series, an average liver to serum concentration ratio of 2.5 was found in rats injected with a 0.6-mg/kg dose of warfarin and sacrificed when the serum warfarin concentration had declined to ~0.4 μg/ml (2). The rat livers contained nearly one-half the amount of warfarin in the bodies at the time of sacrifice. Whether caused by saturable binding to hepatic tissues or by a saturable transport process, this pronounced warfarin uptake by the liver could be drug concentration dependent. Such concentration dependence may have important effects on warfarin pharmacokinetics and was explored in this investigation.

EXPERIMENTAL

Twelve adult male Sprague–Dawley rats, 284–323 g, with unrestricted access to food and water received an intravenous injection of racemic ^{14}C-warfarin[1] (158 μCi/mg), about 3.5 μCi, together with sufficient nonradioactive warfarin to constitute a total dose of 0.1 or 1.0 mg/kg. Six rats received the low dose and six received the high dose. The drug was injected rapidly into the femoral vein. Six hours later, the animals were anesthetized with ether and exsanguinated from the aorta by syringe.

Serum was separated from the blood, and warfarin was extracted and separated from its metabolites by TLC to allow quantitation by scintillation spectrometry (5). The liver was excised, and the large left lobe was removed, weighed, and homogenized with two volumes of ice-cold 0.9% sodium chloride by means of a polytef pestle tissue grinder (30-ml chamber volume) at 2000 rpm for 5 min. Warfarin in the liver homogenate was extracted, separated from its metabolites, and assayed as described previously (2). Recovery of added warfarin from the liver homogenate was 88 ± 7% (mean ± *SD*, $n = 8$) and was concentration independent in the range of 0.2–22 μg/g wet weight of liver.

The free fraction of warfarin in serum was determined by equilibrium dialysis at 37° (2), without drug addition to either the buffer or the serum phase. The free warfarin fraction in the liver was calculated as described previously (6), based on the assumptions that the free warfarin concentrations in serum and in liver water are identical and that the liver contains 70% water.

Statistical significance of differences was determined by the Student t test (unpaired, two tailed).

RESULTS

The serum and liver drug concentrations were determined 6 hr after intravenous injection when serum warfarin concentrations were in the terminal exponential (β) phase (7). Injection of a 0.1-mg/kg dose of warfarin resulted in average total (free and bound) drug concentrations of 0.102 μg/ml in serum and 1.14 μg/g wet weight of liver (Table I). Upon injection of a 1.0-mg/kg dose, the average total concentrations were 4.65 μg/ml in serum and 3.58 μg/g of liver (Table II). Thus, a 10-fold increase in the warfarin dose produced a 46-fold increase in the total serum warfarin concentration but only a threefold increase of the concentration in the liver. Therefore, the average liver to serum concentration ratio of total warfarin decreased from 11.3 at the lower dose to only 0.814 at the higher dose.

The concentrations of free warfarin in serum (mean ± *SD*, $n = 6$) were 0.00133 ± 0.00016 and 0.0352 ± 0.0105 μg/ml in rats that received 0.1 and 1.0 mg/kg of warfarin, respectively, representing a 26-fold increase. The difference between the dose-normalized concentrations (*i.e.*, concentration/dose) of free drug is highly significant ($p < 0.001$).

Liver to serum warfarin concentration ratios at an average serum concentration intermediate between those observed in the present study were available from a previous investigation (2). However, the experimental conditions of the previous study were somewhat different in that the animals were older (body weight 400–450 g), the warfarin dose was 0.6 mg/kg, and the animals were killed when the total serum warfarin concentration had decreased to ~0.4 μg/ml. Therefore, the animals were killed after a period of time equal to about three times the biological half-life of the drug. The ratios of total liver drug concentration to total serum drug concentration (C_L^t/C_S^t) and total liver drug concentration to free serum drug concentration (C_L^t/C_S^f) obtained in the previous investigation and in this study are listed in Table III. Both ratios decreased strikingly with increasing serum warfarin concentration.

DISCUSSION

Direct *in vitro* equilibrium dialysis studies showed that rat liver ho-

[1] Amersham Corp., Arlington Heights, Ill.

0022-3549/79/1200-1569$01.00/0
© 1979, American Pharmaceutical Association

Table I—Free and Total Warfarin Concentrations in Rat Serum and Liver 6 hr after a 0.1-mg/kg iv Dose

Rat	Body Weight, g	Total Concentration, μg/ml or μg/g		Liver to Serum Total Concentration Ratio	Free Fraction × 100	
		Serum	Liver		Serum	Liver[a]
1 A	284	0.0985	1.13	11.5	1.21	0.0737
2 A	298	0.0981	1.10	11.2	1.53	0.0955
3 A	287	0.114	1.19	10.4	1.32	0.0888
4 A	295	0.110	1.04	9.45	1.13	0.0835
5 A	300	0.113	1.20	10.6	1.22	0.0805
6 A	298	0.0807	1.16	14.4	1.41	0.0688
Mean	293	0.102	1.14	11.3	1.30	0.0818
SD	7	0.010	0.06	1.7	0.15	0.0098

[a] Estimated by the method described in Ref. 6.

Table II—Free and Total Warfarin Concentrations in Rat Serum and Liver 6 hr after a 1.0-mg/kg iv Dose

Rat	Body Weight, g	Total Concentration, μg/ml or μg/g		Liver to Serum Total Concentration Ratio	Free Fraction × 100	
		Serum	Liver		Serum	Liver[a]
1 B	316	3.52	3.63	1.03	1.19	0.808
2 B	300	3.43	3.33	0.971	1.08	0.782
3 B	322	5.34	3.42	0.640	0.569	0.622
4 B	293	5.34	3.78	0.708	0.755	0.746
5 B	310	4.04	4.11	1.02	1.12	0.770
6 B	323	6.21	3.18	0.512	0.264	0.361
Mean	311	4.65[b]	3.58[c]	0.814[d]	0.830[e]	0.682[d]
SD	12	1.14	0.34	0.222	0.366	0.170

[a] Estimated by the method described in Ref. 6. [b] Significantly higher than the dose-normalized concentration 6 hr after a 0.1-mg/kg dose ($p < 0.001$). [c] Significantly lower than the dose-normalized concentration 6 hr after a 0.1-mg/kg dose ($p < 0.001$). [d] Significantly different from result obtained after injection of 0.1 mg/kg ($p < 0.001$). [e] Significantly different from result obtained after injection of 0.1 mg/kg ($p < 0.002$).

Table III—Relationship between Serum Concentration and Liver to Serum Concentration Ratio of Warfarin in Rats

Total Concentration, μg/ml or μg/g		Free Fraction in Serum × 100	Liver to Serum Total Concentration Ratio	Liver Total to Serum Free Concentration Ratio	Data Source
Serum	Liver				
0.102 ± 0.010[a]	1.14 ± 0.06	1.30 ± 0.15	11.3 ± 1.7	866 ± 105	This study; 0.1-mg/kg dose
0.397 ± 0.101	0.948 ± 0.156	0.956 (0.227–2.02)[b]	2.50 ± 0.59	451 ± 368	Reference 2
4.65 ± 1.14	3.58 ± 0.34	0.830 ± 0.366	0.814 ± 0.222[c]	111 ± 42[c]	This study; 1.0-mg/kg dose

[a] Mean ± *SD*. [b] Range (values not normally distributed). [c] Significantly different from the ratio obtained after the 0.1-mg/kg dose ($p < 0.001$).

mogenate binds warfarin (2). The results of this investigation demonstrate that *in vivo* warfarin uptake by the rat liver is drug concentration dependent, as reflected by a striking decrease in the liver to serum warfarin concentration ratio with increasing drug concentration (Table III). The more than proportional increase in the free and total serum warfarin concentrations with increasing dose (Tables I and II) may reflect a decrease in the apparent distribution volume, but this result can also be due to a dose-dependent change in the intrinsic drug clearance. Studies are now in progress to clarify this problem.

The free fraction of warfarin in serum of rats is concentration independent over a wide concentration range but exhibits considerable interanimal variation (2). The free warfarin fractions in serum and liver in any one rat are strongly correlated (2, 6). Consequently, the interindividual variation of the liver to serum warfarin concentration ratio at a given drug concentration is much smaller than the interindividual variation of free fraction values (6). The ratio of the total warfarin concentration in the liver to the free serum warfarin concentration during the β-phase is an unambiguous index of the hepatic warfarin uptake[2]. The fact that this ratio is very high (866 at 6 hr after a 0.1-mg/kg dose) and decreases markedly with increasing concentration suggests that warfarin is bound to saturable hepatic tissues and/or transported from plasma to the liver by a saturable process.

Kekki *et al.* (9) attempted to determine warfarin concentrations in rat plasma and liver as a function of time after intravenous injection of 1, 2, 8, and 40 mg/kg, using a spectrophotometric assay. They reported that assay difficulties prevented the determination of warfarin concentrations in the liver after the 1- and 2-mg/kg doses. The liver to plasma total concentration ratio 6 hr after injection of 8 mg/kg was ~0.2, and the plasma warfarin concentration was 38.4 ± 4.8 μg/ml (mean ± *SE*). These data are not inconsistent with those summarized in Table III. The liver to plasma total concentration ratio 6 hr after injection of 40 mg/kg was actually somewhat *higher* than that produced by the 8-mg/kg dose, apparently because of the threefold increase in the free fraction of warfarin in plasma at these very high and pharmacologically unrealistic concentrations.

Consideration of the results of this investigation together with those of Kekki *et al.* (9) indicates that a concentration-dependent warfarin uptake by the liver causes the liver to plasma warfarin concentration ratio to decrease with increasing concentration over the pharmacologically realistic concentration range (*i.e.*, in the range where synthesis of vitamin K-dependent clotting factors is inhibited or blocked) and that concentration-dependent plasma protein binding may reverse this trend at higher concentrations. Since the liver accounts for a major fraction of the total warfarin in the body of a rat following administration of a pharmacologically realistic dose (2), concentration-dependent hepatic drug uptake apparently may result in nonlinear (dose-dependent) warfarin pharmacokinetics in intact animals and particularly in a decrease in the apparent volume of distribution of the drug with increasing dose in the pharmacologically realistic dose range. Studies are now in progress to examine that possibility.

[2] The ratio of drug concentrations in the liver and in serum from blood obtained from the aorta is not necessarily identical to the ratio of drug concentrations in the liver and in serum from the hepatic venous outflow. With warfarin, a drug whose hepatic clearance is very much lower than the hepatic blood flow, the two ratios can be expected to be virtually identical on the basis of the criteria established by Chen and Gross (8).

REFERENCES

(1) G. Levy, in "The Effect of Disease States on Drug Pharmacokinetics," L. Z. Benet, Ed., American Pharmaceutical Association, Washington, D.C., 1976, chap. 9.

(2) A. Yacobi and G. Levy, *J. Pharm. Sci.*, **64**, 1660 (1975).

(3) M. Gibaldi, G. Levy, and P. J. McNamara, *Clin. Pharmacol. Ther.*, **24**, 1 (1978).

(4) P. J. McNamara, G. Levy, and M. Gibaldi, *J. Pharmacokinet. Biopharm.*, **7**, 195 (1979).

(5) A. Yacobi, L. B. Wingard, Jr., and G. Levy, *J. Pharm. Sci.*, **63**, 868 (1974).

(6) G. Levy, C.-M. Lai, and A. Yacobi, *ibid.*, **67**, 229 (1978).
(7) A. Yacobi and G. Levy, *ibid.*, **66**, 567 (1977).
(8) H.-S. G. Chen and J. F. Gross, *J. Pharmacokinet. Biopharm.*, **7**, 117 (1979).
(9) M. Kekki, R. J. K. Julkunen, and B. Wahlström, *Naunym-Schmiedebergs Arch. Pharmacol.*, **297**, 61 (1977).

ACKNOWLEDGMENTS

Supported in part by Grant GM 20852 from the National Institute of General Medical Sciences, National Institutes of Health.

Previous paper in this series: J. W. Crow, M. Gibaldi, and G. Levy, *J. Pharm. Sci.*, **68**, 1309 (1979).

COMMUNICATIONS

Pharmacokinetics of *cis*-Dichlorodiammine Platinum(II) in Rats Using an External Loop–Eigenfunction Expansion Technique

Keyphrases □ Pharmacokinetics—organometallic antineoplastic agents, external loop blood sampling techniques, eigenfunction expansion analysis, Fourier transform analysis □ External loop technique—blood collection, pharmacokinetics, eigenfunction expansion analysis □ Antineoplastic agents—organometallic, pharmacokinetics, external loop technique, eigenfunction expansion analysis

To the Editor:

An external loop technique for collecting many closely spaced blood concentration–time data points, early in an experiment when the concentration changes rapidly, was developed recently for compounds labeled with γ-emitting isotopes (1, 2). The large amount of accurate data collected at such frequent intervals allows the use of the more objective methods of Fourier transform or eigenfunction expansion analysis for the determination of pharmacokinetic parameters.

With conventional data collection methods, determination of the optimum number of exponentials necessary to describe adequately the time course of the drug is difficult. With a limited number of data points collected over a relatively short period (4–6 hr), a maximum of three exponentials has been suggested (3). For studies conducted over several days, it is possible to resolve more exponentials (4).

The external loop method permits continuous monitoring of radiopharmaceuticals and provides several advantages over traditional blood sampling techniques:

1. There is no sampling time error.
2. The number of samples is ~500 *versus* 40 since there is no blood volume loss to limit the sampling.
3. The sample volume does not change. Such a change affects both the compartment size and the loss of activity.
4. The continuous cumulative count of the analyzer gives an accurate average activity over the time interval.
5. The time interval may be varied or kept constant with a lower limit of less than a millisecond. This flexibility allows the collection of different data sets, thus enhancing numerical analysis by gaining more information at a crucial time.

The large amount of data collected permits the use of Fourier transform analysis to resolve the number of exponentials. Fourier transform analysis was used previously to analyze multicomponent exponential decay curves (5–8). By this method, it is possible to transform the raw data and obtain a plot of the transformed data *versus* the rate constants (λ). The major contributing rate constants can be determined as major peaks in this curve. Provencher (9) recently described a digital computer program for data analysis (9) that is described by a multiexponential equation using the Fourier transform method proposed by Gardner *et al.* (5, 6). Subsequently, an alternative method using an eigenfunction procedure was proposed (10).

cis-Dichlorodiammine platinum(II) (I) represents the first of a series of organometallic antineoplastic agents to be marketed. This compound is used clinically, particularly in the treatment of metastatic testicular carcinoma. Pharmacokinetic parameters for the platinum moiety from I were determined in the rat using traditional blood sampling techniques (4, 11) and an external loop method (2). As an initial step in further studies using I and related agents, we investigated the kinetics of I using an external loop and analyzed the data with an eigenfunction procedure[1].

Male Sprague–Dawley rats, 300–350 g, were prepared as previously described (1). Hexachloroplatinic acid containing platinum-195m[2] was used as the starting material

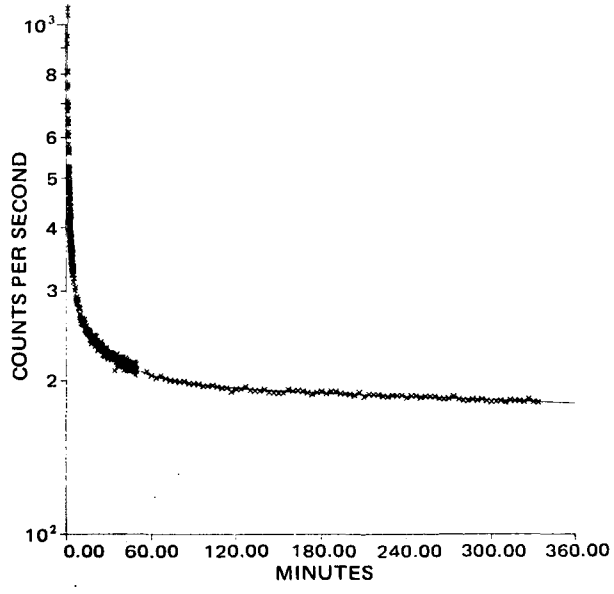

Figure 1—*Plot of counts per second* (×) versus *time measured in an external blood loop following intravenous administration of 1.1 mg of* cis*-dichlorodiammine platinum(II)/kg to Rat 1. The solid line was calculated using the equation that best fit the data.*

[1] A digitial computer program for performing the analysis was kindly provided by S. W. Provencher, Max-Planck-Institut fur Biophysikalische Chemie, D-3400 Gottingen-Nikolausberg, Federal Republic of Germany.
[2] Oak Ridge National Laboratory, Oak Ridge, Tenn.

0022-3549/79/1200-1571$01.00/0
© 1979, American Pharmaceutical Association

(6) G. Levy, C.-M. Lai, and A. Yacobi, *ibid.*, **67**, 229 (1978).
(7) A. Yacobi and G. Levy, *ibid.*, **66**, 567 (1977).
(8) H.-S. G. Chen and J. F. Gross, *J. Pharmacokinet. Biopharm.*, **7**, 117 (1979).
(9) M. Kekki, R. J. K. Julkunen, and B. Wahlström, *Naunym-Schmiedebergs Arch. Pharmacol.*, **297**, 61 (1977).

ACKNOWLEDGMENTS

Supported in part by Grant GM 20852 from the National Institute of General Medical Sciences, National Institutes of Health.

Previous paper in this series: J. W. Crow, M. Gibaldi, and G. Levy, *J. Pharm. Sci.*, **68**, 1309 (1979).

COMMUNICATIONS

Pharmacokinetics of *cis*-Dichlorodiammine Platinum(II) in Rats Using an External Loop–Eigenfunction Expansion Technique

Keyphrases □ Pharmacokinetics—organometallic antineoplastic agents, external loop blood sampling techniques, eigenfunction expansion analysis, Fourier transform analysis □ External loop technique—blood collection, pharmacokinetics, eigenfunction expansion analysis □ Antineoplastic agents—organometallic, pharmacokinetics, external loop technique, eigenfunction expansion analysis

To the Editor:

An external loop technique for collecting many closely spaced blood concentration–time data points, early in an experiment when the concentration changes rapidly, was developed recently for compounds labeled with γ-emitting isotopes (1, 2). The large amount of accurate data collected at such frequent intervals allows the use of the more objective methods of Fourier transform or eigenfunction expansion analysis for the determination of pharmacokinetic parameters.

With conventional data collection methods, determination of the optimum number of exponentials necessary to describe adequately the time course of the drug is difficult. With a limited number of data points collected over a relatively short period (4–6 hr), a maximum of three exponentials has been suggested (3). For studies conducted over several days, it is possible to resolve more exponentials (4).

The external loop method permits continuous monitoring of radiopharmaceuticals and provides several advantages over traditional blood sampling techniques:

1. There is no sampling time error.
2. The number of samples is ~500 *versus* 40 since there is no blood volume loss to limit the sampling.
3. The sample volume does not change. Such a change affects both the compartment size and the loss of activity.
4. The continuous cumulative count of the analyzer gives an accurate average activity over the time interval.
5. The time interval may be varied or kept constant with a lower limit of less than a millisecond. This flexibility allows the collection of different data sets, thus enhancing numerical analysis by gaining more information at a crucial time.

The large amount of data collected permits the use of Fourier transform analysis to resolve the number of exponentials. Fourier transform analysis was used previously to analyze multicomponent exponential decay curves (5–8). By this method, it is possible to transform the raw data and obtain a plot of the transformed data *versus* the rate constants (λ). The major contributing rate constants can be determined as major peaks in this curve. Provencher (9) recently described a digital computer program for data analysis (9) that is described by a multiexponential equation using the Fourier transform method proposed by Gardner *et al.* (5, 6). Subsequently, an alternative method using an eigenfunction procedure was proposed (10).

cis-Dichlorodiammine platinum(II) (I) represents the first of a series of organometallic antineoplastic agents to be marketed. This compound is used clinically, particularly in the treatment of metastatic testicular carcinoma. Pharmacokinetic parameters for the platinum moiety from I were determined in the rat using traditional blood sampling techniques (4, 11) and an external loop method (2). As an initial step in further studies using I and related agents, we investigated the kinetics of I using an external loop and analyzed the data with an eigenfunction procedure[1].

Male Sprague–Dawley rats, 300–350 g, were prepared as previously described (1). Hexachloroplatinic acid containing platinum-195m[2] was used as the starting material

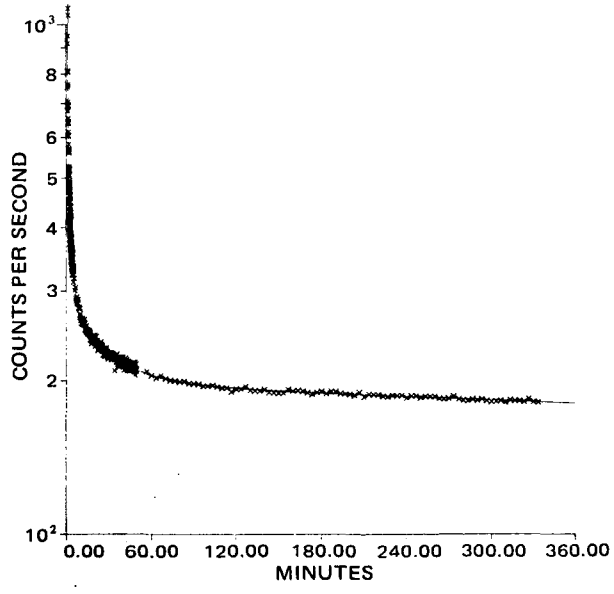

Figure 1—*Plot of counts per second* (×) versus *time measured in an external blood loop following intravenous administration of 1.1 mg of* cis*-dichlorodiammine platinum(II)/kg to Rat 1. The solid line was calculated using the equation that best fit the data.*

[1] A digitial computer program for performing the analysis was kindly provided by S. W. Provencher, Max-Planck-Institut fur Biophysikalische Chemie, D-3400 Gottingen-Nikolausberg, Federal Republic of Germany.
[2] Oak Ridge National Laboratory, Oak Ridge, Tenn.

0022-3549/79/1200-1571$01.00/0
© 1979, American Pharmaceutical Association

to prepare radiolabeled I using a modified literature method (12). Each rat received 1.1 mg of I/kg iv, corresponding to $\simeq 100$ μCi. Data were collected every 2 sec for the first 300 sec, every 20 sec for the next 3000 sec, and every 200 sec until the end of the study. Radioactivity measured in the loop was corrected for decay and background.

A typical plot showing the results obtained is shown in Fig. 1. The data were weighted inversely to the time interval of collection and analyzed by the program of Provencher[1]. The computer program automatically selected the best number of exponential terms required by the data according to an F test with a nonlinearity correction. The best-fit values for the rate constants were 7.90, 1.45, 2.96 $\times 10^{-1}$, 3.50 $\times 10^{-2}$, and 2.52 $\times 10^{-4}$ min^{-1} for Rat 1 and 4.18, 1.10, 2.69 $\times 10^{-1}$, 3.33 $\times 10^{-2}$, and 1.60 $\times 10^{-4}$ min^{-1} for Rat 2. The five-exponential equation that gave the best fit to the data for Rat 1 was used to calculate the solid line in Fig. 1. The fastest observed rate constant may be due to a mixing or rapid distribution within the animal; however, the remaining four exponentials are similar to the values obtained previously (2, 4).

(1) J. W. Triplett, D. W. A. Bourne, and R. B. Smith, *Int. J. Appl. Radiat. Isot.*, **29**, 189 (1978).

(2) W. Wolf and R. C. Manaka, *J. Clin. Hematol. Oncol.*, **7**, 79 (1977).

(3) R. F. Brown, F. R. Carson, L. Finkelstein, K. R. Godfrey, and R. P. Jones, *Med. Biol. Eng. Comput.*, **17**, 216 (1979).

(4) D. M. Taylor, *Biochimie*, **60**, 949 (1978).

(5) D. G. Gardner, J. C. Gardner, G. Laush, and W. W. Meinke, *J. Chem. Phys.*, **31**, 978 (1959).

(6) D. G. Gardner, *Ann. N.Y. Acad. Sci.*, **108**, 195 (1963).

(7) S. M. Pizer, A. B. Ashare, A. B. Callahan, and G. L. Brownell, in "Biomathematics," vol. I, "Concepts and Models of Biomathematics Simulation Technqiues and Methods," F. Heinmets, Ed., Dekker, New York, N.Y., 1969, p. 105.

(8) A. B. Callahan and S. M. Pizer, in "Natural Automata and Useful Simulations," H. Patter, Ed., Spartan, Washington, D.C., 1966, p. 149.

(9) S. W. Provencher, *Biophys. J.*, **16**, 27 (1976).

(10) S. W. Provencher, *J. Chem. Phys.*, **64**, 2772 (1976).

(11) C. L. Litterst, I. J. Torres, and A. M. Guarino, *J. Clin. Hematol. Oncol.*, **7**, 169 (1977).

(12) S. C. Dhara, *Indian J. Chem.*, **8**, 193 (1970).

D. W. A. Bourne ˣ
J. W. Triplett
College of Pharmacy
University of Kentucky
Lexington, KY 40506

T. L. Hayden
Department of Mathematics
University of Kentucky
Lexington, KY 40506

P. A. DeSimone
College of Medicine
University of Kentucky
Lexington, KY 40506

J. D. Hoeschele
Oak Ridge National Laboratory
Oak Ridge, TN 37830

Received June 8, 1979.
Accepted for publication September 14, 1979.
The authors thank J. D. Butts and L. K. McWhorter for technical assistance.

BOOKS

Terpenoids and Steroids, Vol. 8. Senior Reporter, J. R. HANSON. The Chemical Society, Burlington House, London W1V OBN, England. 1978. 301 pp. 15 × 22 cm. Price $50.00. (Available from Special Issues Sales, American Chemical Society, 1155 16th St., N.W., Washington, DC 20036.)

This book is the eighth volume on terpenoids and steroids in a valuable series initiated 8 years ago. The aim of each series of Specialist Periodical Reports is to provide a systematic, comprehensive, and critical review of progress in the major areas of chemical research. The various series, which now total 36, are published annually or biennially on such topics as Environmental Chemistry; Biosynthesis; Foreign Compound Metabolism in Mammals; The Alkaloids; Carbohydrate Chemistry; Amino-acids, Peptides, and Proteins; and Photochemistry.

This volume does not contain a subject index, but it is organized in a systematic manner which facilitates finding any desired information. The five pages in the Table of Contents outline this volume in detail. The chapters are divided into many sections, which are identified in bold type in the text as well as in the Table of Contents. These sections are divided into subsections. Chapter titles are found at the top of every other page of the text. The author index includes 3300 names and is helpful to anyone following the research of a given individual.

This review is illustrated with drawings of 1700 chemical structures. It is documented with 1650 references, most of which are listed at the bottom of the page where first used in a given chapter.

Part I covers the terpenoids and is divided into chapters that include Monoterpenoids, Sesquiterpenoids, Diterpenoids, Triterpenoids, and Carotenoids and Polyterpenoids. Part II, which covers steroids, is divided into two chapters entitled Physical Properties, and Steroid Reactions and Partial Syntheses. No compilation of references to review articles on subjects related to terpenoids or steroids is included in this volume as in many of the previous volumes.

The chapter on Steroid Reactions and Partial Syntheses is long and is divided into two sections. The first section is divided into subsections based on more common functional groups, a subsection on compounds of nitrogen, sulfur, and selenium, and subsections on such important topics as molecular rearrangements, functionalization of nonactivated positions, and photochemical reactions. The section on partial syntheses is divided into the following subsections: cholestane derivatives and analogs, vitamin D and its metabolites, pregnanes, androstones, cardenolides, secosteroids and cydosteroids, heterocyclic steroids, microbiological oxidations and reductions, and miscellaneous syntheses.

The editor and six reporters who prepared this volume are to be commended for maintaining the high standards set by the previous volumes in this series. Everyone interested in the chemistry of terpenoids and/or steroids should have access to this volume and others in the series. Many terpene and steroid chemists will want copies on their desk. This series is a great timesaver and a source of many ideas. I highly recommend it.

Reviewed by Norman J. Doorenbos
College of Science
Southern Illinois University at Carbondale
Carbondale, IL 62901

to prepare radiolabeled I using a modified literature method (12). Each rat received 1.1 mg of I/kg iv, corresponding to $\simeq 100$ μCi. Data were collected every 2 sec for the first 300 sec, every 20 sec for the next 3000 sec, and every 200 sec until the end of the study. Radioactivity measured in the loop was corrected for decay and background.

A typical plot showing the results obtained is shown in Fig. 1. The data were weighted inversely to the time interval of collection and analyzed by the program of Provencher[1]. The computer program automatically selected the best number of exponential terms required by the data according to an F test with a nonlinearity correction. The best-fit values for the rate constants were 7.90, 1.45, 2.96 $\times 10^{-1}$, 3.50 $\times 10^{-2}$, and 2.52 $\times 10^{-4}$ min^{-1} for Rat 1 and 4.18, 1.10, 2.69 $\times 10^{-1}$, 3.33 $\times 10^{-2}$, and 1.60 $\times 10^{-4}$ min^{-1} for Rat 2. The five-exponential equation that gave the best fit to the data for Rat 1 was used to calculate the solid line in Fig. 1. The fastest observed rate constant may be due to a mixing or rapid distribution within the animal; however, the remaining four exponentials are similar to the values obtained previously (2, 4).

(1) J. W. Triplett, D. W. A. Bourne, and R. B. Smith, *Int. J. Appl. Radiat. Isot.*, **29**, 189 (1978).

(2) W. Wolf and R. C. Manaka, *J. Clin. Hematol. Oncol.*, **7**, 79 (1977).

(3) R. F. Brown, F. R. Carson, L. Finkelstein, K. R. Godfrey, and R. P. Jones, *Med. Biol. Eng. Comput.*, **17**, 216 (1979).

(4) D. M. Taylor, *Biochimie*, **60**, 949 (1978).

(5) D. G. Gardner, J. C. Gardner, G. Laush, and W. W. Meinke, *J. Chem. Phys.*, **31**, 978 (1959).

(6) D. G. Gardner, *Ann. N.Y. Acad. Sci.*, **108**, 195 (1963).

(7) S. M. Pizer, A. B. Ashare, A. B. Callahan, and G. L. Brownell, in "Biomathematics," vol. I, "Concepts and Models of Biomathematics Simulation Technqiues and Methods," F. Heinmets, Ed., Dekker, New York, N.Y., 1969, p. 105.

(8) A. B. Callahan and S. M. Pizer, in "Natural Automata and Useful Simulations," H. Patter, Ed., Spartan, Washington, D.C., 1966, p. 149.

(9) S. W. Provencher, *Biophys. J.*, **16**, 27 (1976).

(10) S. W. Provencher, *J. Chem. Phys.*, **64**, 2772 (1976).

(11) C. L. Litterst, I. J. Torres, and A. M. Guarino, *J. Clin. Hematol. Oncol.*, **7**, 169 (1977).

(12) S. C. Dhara, *Indian J. Chem.*, **8**, 193 (1970).

D. W. A. Bourne ˣ
J. W. Triplett
College of Pharmacy
University of Kentucky
Lexington, KY 40506

T. L. Hayden
Department of Mathematics
University of Kentucky
Lexington, KY 40506

P. A. DeSimone
College of Medicine
University of Kentucky
Lexington, KY 40506

J. D. Hoeschele
Oak Ridge National Laboratory
Oak Ridge, TN 37830

Received June 8, 1979.
Accepted for publication September 14, 1979.
The authors thank J. D. Butts and L. K. McWhorter for technical assistance.

BOOKS

Terpenoids and Steroids, Vol. 8. Senior Reporter, J. R. HANSON. The Chemical Society, Burlington House, London W1V OBN, England. 1978. 301 pp. 15 × 22 cm. Price $50.00. (Available from Special Issues Sales, American Chemical Society, 1155 16th St., N.W., Washington, DC 20036.)

This book is the eighth volume on terpenoids and steroids in a valuable series initiated 8 years ago. The aim of each series of Specialist Periodical Reports is to provide a systematic, comprehensive, and critical review of progress in the major areas of chemical research. The various series, which now total 36, are published annually or biennially on such topics as Environmental Chemistry; Biosynthesis; Foreign Compound Metabolism in Mammals; The Alkaloids; Carbohydrate Chemistry; Amino-acids, Peptides, and Proteins; and Photochemistry.

This volume does not contain a subject index, but it is organized in a systematic manner which facilitates finding any desired information. The five pages in the Table of Contents outline this volume in detail. The chapters are divided into many sections, which are identified in bold type in the text as well as in the Table of Contents. These sections are divided into subsections. Chapter titles are found at the top of every other page of the text. The author index includes 3300 names and is helpful to anyone following the research of a given individual.

This review is illustrated with drawings of 1700 chemical structures. It is documented with 1650 references, most of which are listed at the bottom of the page where first used in a given chapter.

Part I covers the terpenoids and is divided into chapters that include Monoterpenoids, Sesquiterpenoids, Diterpenoids, Triterpenoids, and Carotenoids and Polyterpenoids. Part II, which covers steroids, is divided into two chapters entitled Physical Properties, and Steroid Reactions and Partial Syntheses. No compilation of references to review articles on subjects related to terpenoids or steroids is included in this volume as in many of the previous volumes.

The chapter on Steroid Reactions and Partial Syntheses is long and is divided into two sections. The first section is divided into subsections based on more common functional groups, a subsection on compounds of nitrogen, sulfur, and selenium, and subsections on such important topics as molecular rearrangements, functionalization of nonactivated positions, and photochemical reactions. The section on partial syntheses is divided into the following subsections: cholestane derivatives and analogs, vitamin D and its metabolites, pregnanes, androstones, cardenolides, secosteroids and cydosteroids, heterocyclic steroids, microbiological oxidations and reductions, and miscellaneous syntheses.

The editor and six reporters who prepared this volume are to be commended for maintaining the high standards set by the previous volumes in this series. Everyone interested in the chemistry of terpenoids and/or steroids should have access to this volume and others in the series. Many terpene and steroid chemists will want copies on their desk. This series is a great timesaver and a source of many ideas. I highly recommend it.

Reviewed by Norman J. Doorenbos
College of Science
Southern Illinois University at Carbondale
Carbondale, IL 62901

ERRATA

In the article titled "Potentiometric Titration on Monomeric and Micellar Acylcarnitines" (1), the following correction should be made:

On page 800, Table II, the pK value of Acetylcarnitine HCl should be 3.50 instead of 3.60.

(1) S. H. Yalkowsky and G. Zografi, *J. Pharm. Sci.*, **59,** 798 (1970).

In the article titled "Direct Spectrophotometric Assay of Quaternary Ammonium Compounds Using Bromthymol Blue" (1), the following correction should be made:

On page 111, column 1, under *Assay,* the first sentence should read: "In a 25-ml volumetric flask, 2.0 ml of hydroxyethylcellulose solution and 250 mg of sodium chloride were mixed with 5–10 ml of 0.05 *M* buffer solution, and 1.0 ml of dye solution was added by pipet."

(1) J. B. Lowry, *J. Pharm. Sci.*, **68,** 110 (1979).